

Q  
1  
S3  
V.83  
1980

# Physics Abstracts

PAMPHLET 60

Science Abstracts Series A  
July-December 1980

Subject Index (M - Z)

U.I.C.C.  
MAR 6 1981  
LIBRARY

# inspec

The Institution of

Electrical Engineers

## CONTENTS

Title page	i	Subject index	S2615
Abbreviations and acronyms	iii		

---

## SIX-MONTHLY INDEXES TO SCIENCE ABSTRACTS

Cumulative indexes to Science Abstracts are published twice a year covering the period January-June and July-December. They comprise author and subject indexes and some specialised or 'small' indexes. For Physics Abstracts and Electrical & Electronics Abstracts the Author Index and Subject Index are published as separate volumes. In this case the Small Indexes are included in the Author Index volume.

Cumulative author and subject indexes for preceding years are also available. For details please see inside back cover.

### Subject Index

The Subject index provides an alphabetical subject key to the articles included in the abstracts journal. Some general guidance on its use is given below:

1. Look in the index for the name of the specific subject in which you are interested. In most cases this name will be a heading in the index and you will find relevant articles listed under it. The majority of the subject headings fall into the following categories: property, phenomena, substance or named objects, instrument, device, theory, method, process, application, event.
2. Occasionally you will be directed from the subject heading chosen to a different heading under which the relevant or additional articles are listed.
3. If you do not find the subject heading you first chose, try a more general heading.
4. Each entry under the heading relates to an article appearing in the abstracts journal and gives the serial number of that article in the journal preceded by the last digit of the current year, e.g. 0-12345; i.e. Abstract number 12345 in the abstracts journal for 1980.

The language of the article, if it is not in English, is also indicated. e.g. digital frequency meter jamming, distribution function determ. (Russian) 0-41575.

Each entry starts with a Keyword or Keyphrase considered to be most relevant to the heading. On sorting these Keywords, the qualifying prefixes are usually ignored. (e.g.  $\alpha$ -brass, 5-sulphosalicylic, 31 Cygni, n-Ge are sorted under brass, sulphosalicylic, Cygni, Ge respectively).

There are three main Keyword lists; alphabetical A-Z, elementary particles, and chemical symbols (organic substances are written and not given as chemical formula). More than one Keyword list may be present under each subject heading.

For document on, say, 'photoemission of germanium' at least two access points 'photoemission' and 'Germanium' are provided. Under the heading 'photoemission' the Keyword will be 'Ge' and under 'germanium' the Keyword will be 'photoemission'.

In a case like this, it is advisable and quicker to use the heading 'photoemission' and go straight to the chemical symbol list for 'Ge'.

Intermetallic compounds are indexed under the appropriate alloy headings. The chemical formula is used as Keyword. However, it is important to realise in searching the chemical symbol list that, at present, alloys and intermetallic compounds are sorted separately. For example FeCo is sorted at the end of the Fe- list e.g. Fe-Al, ... Fe-Co, ... Fe-Si, ... Fe-Si-B, ... FeCo, ... FeSi and so on in this order.



# Physics Abstracts

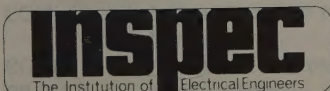
Science Abstracts Series A

July-December 1980

## Subject Index (M - Z)

Physics Abstracts is published twice monthly by the Institution of Electrical Engineers. Twice-yearly subject and author indexes covering the period January-June and July-December are included in the subscription. Printed by Unwin Brothers Ltd., Old Woking, Surrey, England. Second class postage paid at Piscataway, NJ 08854 USA. POSTMASTER: Send address changes to INSPEC/IEEE SERVICE CENTER, 445 Hoes Lane, Piscataway, NJ 08854

© 1981: THE INSTITUTION OF ELECTRICAL ENGINEERS







# Abbreviations and Acronyms

Abbreviations and acronyms are used in the modifiers in all INSPEC Cumulative Subject Indexes. Individual terms should be readily understood in the context of the subject headings. **Inorganic substances** are usually given by their chemical formulae. Iron and aluminium garnets appear in the formulae lists as MIG and MAG (where M is metal element, e.g. YIG and YAG);  $(\text{Pb},\text{La})(\text{Zr},\text{Ti})\text{O}_3$  and  $\text{Ce}_2\text{Mg}_3(\text{NO}_3)_{12}$  appear as PLZT and CMN respectively. **Organic substances** including **liquid crystals** are not given as formulae but common abbreviations are used.

ABS resin	acrylonitrile-butadiene-styrene	CRO	cathode ray oscilloscope
AC	alternating current	CRT	cathode ray tube
ACV	air cushion vehicle	CS	coupled states
A/D	analogue-to-digital	CSM	continuous slowing down models
ADP	administrative data processing	CTR	controlled thermonuclear reactor
AES	Auger electron spectra(oscopy)	CVD	chemical vapour deposition
AF	audio frequency	CW	continuous wave
AFC	automatic frequency control		
AFL	abstract family of languages		
AGC	automatic gain control	D/A	digital-to-analogue
AGR	advanced gas-cooled reactor	DBR	distributed Bragg reflector
AM	amplitude modulation	DC	direct current
ANS	Astronomical Netherlands Satellite	DDC	direct digital control
APACHE	accelerator for physics and chemistry of heavy elements	DDL	diode-diode logic
APR	acoustic paramagnetic resonance	DECENT	distribution of exact classical energy transfer
APS	appearance potential spectra(oscopy)	DESY	Deutsches Electron Synchrotron
APW	augmented plane wave	DF	Dirac-Fock
ATR	attenuated total reflection	DFB	distributed feedback
ATS	applications technology satellite	DH	double heterostructure
ATWS	anticipated transients without scram	DIL	dual-in-line
AVC	automatic volume control	DITE	divertor in torus experiment
		DLTS	deep level transient spectra(oscopy)
		DM	delta modulation
BARITT	barrier injection transit time	DMSO	dimethyl sulphoxide
BBEA	4-butoxybenzal-4'-ethylaniline	DMSS	Defence Meteorological Satellite System
BCC	body centred cubic	DOBAMBC	p-decyloxybenzylidene p'-amino 2-methyl butyl cinnamate
BCD	binary-code decimal		
BFO	beat-frequency oscillator	DODS	different orbitals for different spins
BWO	backward wave oscillator	DORIS	Dopple-ring-Speicher
BWR	boiling water reactor	DOVETT	double velocity transit time
BWT	backward wave tube	DP	data processing
		DPCM	differential pulse code modulation
		DPPH	diphenylpicrylhydrazyl
CAD	computer aided design	DPSK	differential phase shift keying
CAI	computer assisted instruction	DSC	differential scanning calorimetry
CARS	coherent antiStokes Raman scattering (spectra)	DTA	differential thermal analysis
CATV	community antenna TV	DV-X $\alpha$	discrete variational X $\alpha$ method
CB	citizen band		
CBOOA	cyanobenzylidene octyloxyaniline	E1,E2	electric dipole, quadrupole
C-CD	charge-coupled device	EAS	extensive air shower
CDI	collector diffusion isolation	EB	exponential Born
CDM	code division multiplexing	EBBA	4-ethoxybenzylidene-4'-n-butylniline
CDW	charge-density wave	EBR	experimental breeder reactor
CEM	channel electron multiplier	EBT	Elmo Bumpy Torus
CEPA	coupled electron-pair approximation	ECC	emergency core cooling
CERN	Conseil Européen pour la Recherche Nucléaire	ECELR	epithermal critical experiment laboratory reactor
CESR	conduction electron spin resonance	ECG	electrocardiography (-gram)
CGTO	contracted Gaussian-type orbital	EDA	ethylene diamine
CHF	coupled Hartree-Fock	EDP	electronic data processing
CI	configuration interaction	EDTA	ethylene diamine tetra-acetic acid
CIEH	charge iterated extended Huckel	EEBAC	ehtyl-4-(4'ethoxy-benzylidene-amino) cinnamate
CIHY	configuration interaction Hylleras		
CNDO	complete neglect of differential overlap	EEG	electroencephalography (-gram)
COC	cholesteryl oleyl carbonate	EELS	electron energy loss spectra
COM	computer output to microform (fiche or film)	EFM	extended Flygare method
COOB	4,4'-cyano-octyloxy-biphenyl	EHD	electrohydrodynamics
CP	charge, parity	EHF	extremely high frequency
CPA	coherent potential approximation	EHP	electron-hole potential method
CPSK	coherent phase shift keying	EHT	extended Huckel theory
CPT	charge, parity, time	EHV	extra high voltage
		ELDOR	electron electron double resonance



ELF	extremely low frequency	HOMO	highest occupied molecular orbitals
EM	electromagnetic	HORM	hybrid orbital rehybridisation method
EMC	electromagnetic compatibility	HTGR	high temperature gas-cooled reactor
EMF	electromotive force	HV	high voltage
EMG	electromyography(-gram)	HVEM	high voltage electron microscopy
ENDOR	electron nuclear double resonance	HWR	heavy water reactor
EOS	earth observatory satellite	IAEA	International Atomic Energy Authority
EPEN	empirical potential energy function based on interactions of electrons and nuclei	Agency	
EPMA	electron probe microanalysis	IBPBAC	isobutyl-4-(4'-phenylbenzylideneamino) cinnamate
EPR	electron paramagnetic resonance	IC	integrated circuit
ERG	electroretinography(-gram)	ICDF	intermediate coupling Dirac-Fock
ERPS	extramolecular relaxation polarisation shift	IDT	interdigital transducer
ERTS	earth resources technology satellite	IEPA	independent electron pair approximation
ESCA	electron spectroscopy for chemical analysis	IF	intermediate frequency
ESCAR	experimental superconducting accelerating ring	IGFET	insulated gate field effect transistor
ESFI	epitaxial silicon film on insulator	IKO	Institute v. Kernph. Ouder Amsterdam
ESS	electronic switching system	I <sup>2</sup> L	integrated injection logic
EUV	extreme ultraviolet	I <sup>3</sup> L	isoplanar I <sup>2</sup> L
EXAFS	extended X-ray absorption fine structure	ILS	instrument landing system
FBR	fast breeder reactor	IMPATT	impact avalanche transit time
FCC	face centred cubic	INDO	intermediate neglect of differential overlap
FDM	frequency division multiplex(ing)	INDOR	internuclear double resonance
FDNC	frequency dependent negative conductance	ING	intense neutron generator
FDNR	frequency dependent negative resistance	INO	iterative natural orbital
FEM	field emission microscopy	INTELSAT	international telecommunications satellite consortium
FET	field effect transistor	I/O	input/output
FFHR	fusion-fission hybrid reactor	IOC- $\omega$	inclusion of the overlap charges in the omega
FFT	fast Fourier transform	IR	infrared
FFTF	fast flux test facilities	IRDO	intermediate retention of differential overlap
FIM	field ion microscopy	ISABELLE	intersecting storage and acceleration
FM	frequency modulation	ISR	intersecting storage ring
FPT	finite perturbation theory	ISX	impurity study experiment
FSK	frequency-shift keying	ITEP	Institute of Theoretical and Experimental Physics
FSGO	floating spherical Gaussian orbitals	IU	Indiana University
FTR	fast test reactor	IVO	improved virtual orbitals
GAMBIT	gate modulated bipolar transistor	JET	Joint European torus
GANIL	grand accélérateur national a ions Lourds	JAERI	Japan Atomic Energy Research Institute
GARP	global atmospheric research programme	JINR	Joint Institute for Nuclear Research
GATE	GARP Atlantic tropical experiment	KEK	Japan National Laboratory for High Energy Physics
GCFR	gas-cooled fast breeder reactor	KKR	Korringa-Kohn-Rostoker
GCM	generator coordinate method	LAMPF	Los Alamos meson physics facility
GHF-NO-CI	generalised Hartree-Fock/natural orbital/configuration interactions	LC	inductance-capacitance
GIAO	gauge-invariant atomic orbitals	LCAO	linear combination of atomic orbitals
GO	Gaussian orbitals	LCBO	linear combinations of (semi-localised) band orbitals
GOO	generalised Overhauser orbitals	LCGO	linear combination of Gaussian orbitals
GPM	ground potential model	LCP	large coil program
GSO	general spin orbitals	LCRO	linear combination of Rydberg orbitals
GTO	Gaussian-type orbitals	LEC	liquid encapsulated Czochralski
GVB	generalised valence bond	LED	light emitting diode
HAM	hydrogenic atoms in molecules	LEED	low energy electron diffraction
HBAB	hexyloxybenzylidene-p' aminobenzonitrile	LEP	large electron positron
HBT	N-(p-hexyloxybenzylidene)-p-toluidene	LET	linear energy transfer
HCD	hypothetical core disruptive accident	LF	low frequency
HCP	hexagonal close packed	LMC	Large Magellanic Cloud
HEED	high energy electron diffraction	LMFBR	liquid metal fast breeder reactor
HF	high frequency or Hartree-Fock	LMTO	linear combination of muffin tin orbitals
HFB	Hartree-Fock-Bogoliubov	LOCA	loss of coolant accident
HFER	hot fuel examination facility	LOCE	loss of coolant experiment
HFIR	high flux isotope reactor	LOFT	loss of flow test facility
HFO	Hartree-Fock-Overhauser	LPE	liquid phase epitaxy
HFS	hyperfine structure	LSA	limited space charge accumulation
HLW	high level waste (radioactive)		
HMO	Huckel molecular orbitals		
HOAB	heptyloxazoxybenzene		
HOBHA	p-n-heptyloxy-benzylidene-p-n heptylaniline		



LSD	local spin density	ODMR	optical detection of magnetic resonance
LSI	large-scale integration	OER	oxygen enhancement ratio
LTE	local thermodynamic equilibrium	OGO	orbiting geophysical observatory
LUMO	lowest unoccupied molecular orbitals	OPHF	orbital polarised Hartree-Fock
LV	low voltage	OPW	orthogonal plane wave
LWR	light water reactor	OR	operations research
MADO	Mulliken approximation for differential overlap	ORELA	Oak Ridge electron linear accelerator
M1,M2	magnetic dipole, quadrupole	ORNL	Oak Ridge National Laboratory
MBBA	4-methoxybenzylidene-4'-n-butyl-aniline	OSO	orbiting solar observatory
MBE	molecular beam epitaxy	OTF	optical transfer function
MBPT	many body perturbation theory	PAA	paraazoxyanisole
MCD	magnetic circular dichroism	PABX	private automatic branch exchange
MCPESCF	multiconfiguration paired excitation SCF	PAC	perturbed angular correlation
MCZDO	multi-centre zero differential overlap	PAHR	post accident heat removal
MEDO	multipole expansion of diatomic overlap	PAM	pulse amplitude modulation
MESFET	metal-semiconductor field effect transistor	PAMPUS	photons for atomic and molecular processes and universal studies
MF	medium frequency	PAP	paraazoxyphenetole
MFP	mean free path	PBF	power bursts facility
MHD	magnetohydrodynamics	PBR	pebble bed reactor
MIC	microwave integrated circuit	PBX	private branch exchange
MIEHM	modified iterative extended Huckel method	PC	printed circuit
MIM	metal-insulator-metal	PCAC	partially conserved axial currents
MIS	metal-insulator-semiconductor or management information system	PCB	printed circuit board
MIT	Massachusetts Institute of Technology	PCGVB	pairwise correlated generalised valence bond
MMF	magnetomotive force	PCILOCC	perturbative configuration interaction using localised orbitals for crystal calculation
MNOS	metal-nitride-oxide-semiconductor	PCM	pulse code modulation
MO	molecular orbitals	PCX	plasma confinement experiment
MOCIC	molecular orbital constraint of interaction coordinates	PDX	poloidal divertor experiment
MODPOT	model potential	PEP	positron electron proton
MOS	metal-oxide-semiconductor	PETRA	positron electron tandem ringbeschleuniger anlage
MOSFET	metal-oxide-semiconductor field effect transistor	PF	power factor
MOST	metal-oxide-semiconductor transistor	PFM	pulse frequency modulation
MRD	multi-reference double excitation	PHWR	pressurised heavy water reactor
MRINDO	modified Rydberg INDO	PID(PI,PD)	proportional+integral+differential (derivative)
MSI	medium scale integration	PLA	phase locked arrays
MSR	molten salt reactor	PLC	programmable logic control
MSU	Michigan State University	PLL	phase locked loops
MTBF	mean-time between failures	PLT	Princeton Large Torus
MTF	modulation transfer function	PM	pulse modulation
MTX $\alpha$	muffin-tin X $\alpha$	PMMA	polymethylmethacrylate
MUF	maximum usable frequency	PMDR	phosphorescence microwave double resonance
MWH	Mulliken-Wolfsberg-Helmholz-semi-empirical method	PNDO	partial neglect of differential overlap
NAL	National Accelerator Laboratory	PNO-CI	pair natural orbital configuration interaction
NAND	not-and(logic)	POL	pair orthogonalised Lowdin
NC	numerical control	POP AE	protons on protons and electrons
NCMET	non-closed shell many electron theory	POPOP	phenyl-oxazolyI-phenyl-oxazolyI-phenyl
NDDO	neglect of diatomic differential overlap	POS	point of sale
NDT	nondestructive testing	PPDP/S	Pariser-Parr-Del Bene-Pople/Segal calculations
NEMO	non-empirical molecular orbitals	PPI	plan position indicator
NEVE	non-empirical valence-electron	PPM	pulse position modulation or parts per million
NIC	negative impedance converter	PPP	Pariser-Parr-Pople
NMR	nuclear magnetic resonance	PRDDO	partial retention of diatomic differential overlap
NNNDO	neglect of non-neighbour differential overlap	PRF	pulse recurrence (repetition) frequency
NOR	not-or(logic)	PROM	programmable read-only-memory or Pockels readout optical modulator
NPOST	non-perturbative open-shell theory	PS	proton synchrotron (CERN)
NPSO	non-paired spatial orbitals	PSK	phase shift keying
NQR	nuclear quadrupole resonance	PTFE	polytetrafluoroethylene
NRC	nuclear regulatory committee	PTM	pulse time modulation
NRM	natural remanent magnetisation	PVC	polyvinyl chloride
NTO	natural transition orbitals	PWM	pulse width modulation
OAQ	orbiting astronomical observatory	PWR	pressurised water reactor
OCR	optical character recognition		



QCD	quantum chromodynamics	TCR	temperature coefficient of resistance
QDMBPT	quasi-degenerate many-body perturbation theory	TDHF	time dependent Hartree-Fock
QED	quantum electrodynamics	TDM	time division multiplex(ing)
QPSK	quaternary phase shift keying	TDMA	time division multiple access
RAM	random access memory	TDPAC	time differential perturbed angular correlation
RBE	relative biological effectiveness	TE	transverse electric
RC	resistance-capacitance	TEA	transversely excited atmospheric
RCNDO	Rydberg CNDO	TEM	transverse electromagnetic or transmission electron microscopy
R & D	research and development	TEXT	Texas Experimental Tokamak
RF	radio frequency	TFTR	Tokamak fusion test reactor
RFI	radio frequency interference	TGFB	triglycine fluoroberyllate
RHEED	reflection high energy electron diffraction	TGS	triglycine sulphate
RINDO	Rydberg INDO	TGSe	triglycine selenate
RKKY	Rudermann-Kittel Kasuya-Yosida	TJS	transverse junction stripe
RLC	resistance-inductance-capacitance	TLD	thermoluminescent dosimeter(-ry)
RMS	root-mean-square	TM	transverse magnetic
ROM	read-only memory	TMMC	tetramethylammonium manganese chloride
RPA	random phase approximation	TOP	transient overpower accident
RPM	relaxation potential model	TNS	The next step
SAMO	simulated ab initio molecular orbitals	TRAPATT	trapped plasma avalanche triggered transit
SAS	small astronomy satellite	TREAT	transient reactor test facility
SAW	surface acoustic waves	TRM	thermoremanent magnetisation
SCF	self consistent field	TSC	thermally stimulated currents
SCL	space charge limited	TSEE	thermally stimulated exo-electron emission
SCPT	self consistent perturbation theory	TTF	tetrathiofulvalinium
SCR	silicon controlled rectifier	TTL	transistor transistor logic
SDM	space division multiplexing	TTT	tetrathiotetracene
SDO	shielded diatomic orbitals	TUCA	transient undercooling accident
SEHF	spin extended Hartree-Fock	TV	television
SEM	scanning electron microscope	TW	travelling wave
SFE	solar-flare effect	TWT	travelling wave tube
SGHWR	steam generating heavy water reactor	UCHF	uncoupled Hartree-Fock
SHF	superhigh frequency	UHF	ultra high frequency unrestricted Hartree-Fock
SHG	second harmonic generation	UHV	ultra high voltage
SIMS	secondary ion mass spectrometer	UKAEA	United Kingdom Atomic Energy Authority
SIN	Swiss Institute of Nuclear Research	ULF	ultra low frequency
SINDO	scaled INDO	UMD	united microwave devices
SISAM	spectrometer with interference selective amplitude modulation	UPS	ultraviolet photoelectron spectra
SMC	Small Magellanic Cloud	US	ultrasonic
SMS	synchronous meteorological satellite	UV	ultraviolet
S/N	signal-to-noise	VB	valence bond
SOG	strongly orthogonal geminal	VCR	video cassette recorder
SOS	silicon on sapphire	VDM	vector dominance model
SPA	separated pair approximation	VDU	visual display unit
SPC	stored program control	VHF	very high frequency
SPEAR	Stanford positron electron asymmetric ring	VLBI	very long base line interferometry
SPHF	spin polarised Hartree-Fock	VLF	very low frequency
SPIN-CIPSI	spin symmetry adapted generalisation of CIPSI	VLSI	very large scale integration
SPS	super proton synchrotron (CERN)	VOR	VHF omnidirectional range
SQUID	superconducting quantum interference device	VPE	vapour phase epitaxy
SRMCASE	symmetry-restricted-multiconfiguration annihilation of single excitations	VRC	visual record computer
SSB	single sideband	VRDDO	variable retention of diatomic differential
SSC	sudden storm commencement	VSB	vestigial sideband
SSI	supersonic transport	VSEPR	valence shell electron pair repulsion
STD	salinity-temperature-depth or subscriber trunk dialling	VSWR	voltage standing wave ratio
STEM	scanning transmission electron microscopy	VTOL	vertical take-off and landing
STO	Slater-type orbitals	VTR	voltage transformation ratio or video tape recorder
STOL	short take-off and landing	VUV	vacuum ultraviolet
STP	Slater-transfer Preuss	VVER	water moderated water cooled reactors
SUHFC	spin unrestricted Hartree-Fock with local approximation for correlations	WWER	water moderated water cooled reactors
SW	short wave	XPS	X-ray photoelectron spectra
SWR	standing wave ratio	ZEBRA	zero energy breeder reactor assembly
SXAPS	soft X-ray appearance potential spectrum	ZGS	zero gradient synchrotron
TBBA	terephthal-butylaniline	ZPPR	zero power plutonium reactor
TCNE	tetracyanoethylene		
TCNQ	tetracyanoquinodimethane		



# Subject Index

## M-centres

- laser, pulsed  $F_2$  centre, tunable in 1.1 to 1.26  $\mu\text{m}$  range, spectral characts. 0-91805
- GaP crystals, radiation defects, TSC obs. 0-65588
- KCl, additively coloured photochromic crystals, spectral sensitivity (*Russian*) 0-91871
- KCl:Li,  $(F_2^+)_A$  centres, optical props. 0-89026
- KCl:Li  $(F_2^+)_A$  centres, tunable CW laser action 0-87399
- KCl:Pb $^{2+}$ , pure and doped, electrolytically coloured, elec. cond. and optical absorpt. meas. 0-100668
- LiF, picosecond generation on  $F_2^+$  colour centres, induced mode synchronisation (*Russian*) 0-64033
- NaF,  $F_2^+$ -like colour centre, room temp. stable, CW laser, 0.99-1.22  $\mu\text{m}$  tunable 0-69399
- NaF, X-irrad., colour centres and thermolum. 0-84790

## M-regions see Sun

## Mach number

see also acoustic wave velocity; shock waves

- concave corners, Whitham theory of shock-wave diffr. 0-100012
- separated two-phase flow, pressure drop and sonic vel. 0-106840

## Mach principle see cosmology; space-time configurations

## machine bearings

- air bearing for precision linear displacement 0-105637
- elastomeric bearings, high-capacity, laminated, finite-element anal. 0-96197
- lubricant wear debris examination, oil anal. techniques, appl. to plain bearing materials study 0-97596
- lubricating oils, strength and damping coeffs., vibration diagnostics (*Russian*) 0-97592
- rotating mirror laser beam TV scanner, development programme (*Japanese*) 0-74369
- turbogenerator, with hybrid hydrostatic hydrodynamic lubrication, behaviour in laminar and turbulent conditions (*Italian*) 0-81208
- turbogenerator bearing oil film damping and stiffness coefficients determ. for dynamic behaviour stability study (*Italian*) 0-106762
- Al alloy-mica particle composite, cast prep. and mech. props., bearing appl. 0-71613

## machine insulation

- volts-per-bar and flashover, causal mechanisms and preventive measures 0-92408

## machine testing

- 200 kW vertical axis wind turbine, preliminary test results 0-66928
- electric equipment testing laboratory, movable, type ETL-35, design (*Russian*) 0-95088
- Savonius rotor, aerodynamic performance testing in wind tunnel 0-61266
- vertical axis wind turbines 0-66929

## machine theory

- viscous liquid flow through annular clearance over rotating inner cylinder 0-64626

## machine tools

see also numerical control

- acoustic noise, power press, relationship between force waveform and sound radiation 0-74596
- angle measurement, automatic testing of precision dividing heads (*German*) 0-82740
- chip geometry and cutting forces 0-93629
- diamond turning precision machine tool system 0-69568
- diffusive wear, effect of magnetic fields, cutting tools 0-60985
- grinding wheel life modelling, group method of data handling 0-58987
- hyperboloid lens manufacturing technique 0-96039
- position feedback by laser interferometer 0-73438
- spectral analysis of vibration data, failure prediction 0-79048

## machines, electric see electric machines

## machining

see also cutting; electrolytic machining; electrolytic polishing; electron beam machining; grinding; laser beam machining; spark machining

- alloys, machining damage, depth of surface layers determ. 0-85094
- diamond tool bit machining, comparison with conventional optical process 0-69569
- high strain rate processes, review 0-84864
- milling spherical surfaces 0-64222
- steel, stainless, smoothing for plastic pre-straining of material cut by turning (*Russian*) 0-60911
- tools, chip geometry and cutting forces 0-93629
- Fe-Cu-C sintered porous materials, machinability 0-66457
- Ti-Al-Cr-Mo, type VTZ-1, machinability, using different abrasive materials (*Russian*) 0-97593
- Ti-Al-Mo, type VT14, machinability, using different abrasive materials (*Russian*) 0-97593

## macromolecular configurations

- acetylcholine receptor protein structure 0-85339
- F-actin, struct. changes in living muscle fibres, polarised UV fluoresc. microscopy 0-67037
- albumin, adsorbed layers on polystyrene, contact angle meas. 0-61508
- bacteriorhodopsin, effect of high press. on absorpt. spectrum and isomeric composition 0-67041
- biological macromolecule, high resolution struct. determ. by electron microscopy 0-89717
- biological macromolecule observation using CTEM and STEM with negative staining 0-85561
- biological macromolecules, conformation studied by calorimetry, review 0-97870
- biopolymers, electro-optical changes, chem. and rotational contribs. 0-85352

## macromolecular configurations continued

- bis(methylthio)alkanes, model compounds of polythioethers, vibr. spectra 0-58430
- block copolymer chain conformations 0-69282
- butadiene styrene elastomers, cross-linked, mech. relax. behaviour (*German*) 0-84986
- Clq of human complement, neutron scatt. obs., conformational calcs. 0-81537
- chain mols., conformational transition kinetics 0-83339
- chaotic branched macromolecules, struct. simulation, parameters calcs. (*Russian*) 0-69283
- collagen, 3-dimens. struct., rel. to props. of connective tissue 0-67038
- collagen, polarisation, contribution of permanent and induced dipole moments, elec. birefringence 0-85351
- collagen molecular organisation and connective tissues props. 0-97858
- copolymer globule model, orientationally-ordered liq. cryst. state (*Russian*) 0-59389
- cytochrome c oxidase, macromolecular struct., electron microscopy and image anal. 0-89716
- cytochrome c oxidase, struct. of cytochrome  $a_3$ -Cu $_{23}$  couple, NO binding studies 0-67039
- dextran fractions, production, characterisation and solution properties 0-59368
- N,N-diethylacrylamide, cross-linked copolymer, improved mech. props. 0-61091
- DNA, B form conformations, double-helix and side-by-side models, X-ray diffraction 0-78735
- DNA, calf-thymus and superhelical PM2 aq. solns., electro-optic obs. of  $\gamma$ -irrad. damage 0-85452
- DNA, double-stranded,  $^{13}\text{C}$  NMR obs. 0-69281
- DNA, possible conformations calcs. 0-76705
- DNA, supercoiled torsional stress and local denaturation 0-72131
- DNA, torsionally stressed, transitions between B- and Z-conformations, theoretical anal. 0-94166
- DNA B-form, closer definition of struct. from X-ray diffr. and energetic criteria 0-81533
- DNA conformational fluctuations, internal motion correl. times,  $^{31}\text{P}$  NMR obs. 0-72135
- DNA in conc. solns. of neutral salts, conformational transitions 0-81531
- epoxy resin, plastic deform. mechanism 0-97534
- ferredoxin, *S. platensis* [2Fe-2S], struct. and evolution of chloroplast-type ferredoxins 0-94165
- fibrinogen, adsorbed layers on polystyrene, contact angle meas. 0-61508
- glutamine synthetase macromolecular struct., electron microscopy and image anal. 0-89716
- hydrate, struct. conversions of sugar phosphate chain and nitrogenous bases, IR spectra 0-81530
- hydrocarbon chains in a lipid bilayer conformational anal. 0-81532
- internal coordinates fluctuations, effect on dimensions 0-74266
- lanthanide complex, struct. and equilib. by time resolved Eu(III) spectrosc. 0-78736
- lanthanide ion bound to macromol., struct. and equilib. by time resolved Eu(III) spectrosc. 0-78736
- macromolecules, cluster expansion 0-106408
- medical polymers, chem. problems, conf., Prague, Czechoslovakia (Aug. 1977) 0-56996
- model polymer, conformation theory, correlated walk model 0-74268
- molecular structure, conformation and properties 0-63874
- myosin, struct. changes in living muscle fibres, polarised UV fluoresc. microscopy 0-67037
- nucleosomes and nucleosomal DNA, electro-optical props., relax. times and chain struct. 0-85350
- 3'-nucleotide, calcs. to assess rigidity 0-61506
- oxytocin, H bond linking ring and tail  $\beta$ -turns, biofunctional evaluation 0-61511
- poly(1,3-dioxepane), dipole moments, dielectric const. meas. 0-66099
- poly(2-vinyl pyridine), dil. solns., translational diffusion, chain conformation influence 0-103508
- poly(3,3-dimethyl oxetane), conform. energies and random-coil config. meas. 0-99590
- poly-4-vinylpyridine, electro-optic study of conformational changes induced by heavy metal ions 0-84725
- poly- $\gamma$ -benzyl-L(D)-glutamate, soln., liq. cryst. and pretransitional regions, optical rot. 0-66145
- poly-L-glutamic acid-Na, cooperativity parameter determ. from viscometry 0-75147
- poly-L-ornithine solution,  $^{15}\text{N}$  NMR, coil-helix transition, solvent effects and pH depend. 0-74275
- poly-p-chlorophenyl glycidyl ether, struct., tacticity and addition isomerism,  $^{13}\text{C}$  NMR 0-58427
- polyacetylene films, tensile props. and partial alignment 0-104210
- polyalkane imides, crystallisability, supermol. and crystalline structures 0-84100
- polyamide, aromatic, fibre, high modulus, mol. and supramol. struct. 0-79710
- polyaspartamides, soluble, fluorescent labelling 0-58426
- polycaprolactam, and copolymers, optical anisotropy and rigidity 0-88959
- polycyclohexanamide, and copolymers, optical anisotropy and rigidity 0-88959
- polydiacetylenes, visual conformational transitions, absorpt. and fluoresc. spectra, pH and electrolyte effect 0-102590
- polyheteroarenylenes, linear, conform. and struct., statistical calcs. (*Russian*) 0-69284
- polymer, cross-linked, on basis of oligodienedihydrazides and diepoxides, characts. (*Russian*) 0-58431
- polymer adhesion ability enhancement by block copolymer incorporation (*Russian*) 0-61065



**macromolecular configurations continued**

- polymer chain, direct renormalisation group procedure 0-91712  
 polymer chain statics and dynamics, Lennard-Jones interaction, calcs. 0-58425  
 polymer chains, Edwards' model, stochastic model 0-68140  
 polymer chains, zero component field (*French*) 0-69280  
 polymer coils, excluded volume parameters, light scatt. obs., graphical calcs. 0-89009  
 polymer conformation, correlated walk model calc. 0-78733  
 polymer liquid, entangled, phenomenological consequences of Doi-Edwards viscoelasticity theory 0-79250  
 polymer macromolecules, volume interactions, coil-globule transition, statistical physics, review 0-78737  
 polymer quantitative analysis by pyrolysis gas chromatography 0-61180  
 polymer structure elucidation, model construction and X-ray methods (*German*) 0-103267  
 polymer surface, supramol. struct. characterisation, use of C X-radiation 0-79705  
 polymeric chain with rigid side branches, intramol. phase transition of 1st kind (*Russian*) 0-58432  
 polymeric macromolecule containing mesogroups, phase diagrams (*Russian*) 0-58433  
 polymers, struct. determ. from elastostometric parameters 0-64923  
 polymers, topological entanglements, gauge description 0-99593  
 polymethacrylamide copolymer, soluble, mobility of spin label bonded to chain end 0-63873  
 polymethacrylic acid, stereoregular, synthesis,  $^{13}\text{C}$  NMR obs. 0-58422  
 polyoxadiazoles, cyclochain, conform. parameters calc. 0-78732  
 polypeptide, conformational change induced by strong elec. field 0-85336  
 polypeptides, comparison of conformational possibilities 0-94163  
 polypeptides, helix-coil transition dynamics, time correl. function theory 0-99591  
 polypeptides, ionic and non-ionic, electro-optical studies of conformation 0-71379  
 polypropylenes, iso- and syndio-tactic, Raman tacticity bands, vibr. spectrum 0-66193  
 polystyrene, atactic, structure elucidation, model construction and X-ray methods (*German*) 0-103267  
 polystyrene, conform. and near all-trans extended-chain model relevant in gels, X-ray diffr. patterns interpret. 0-79707  
 polystyrene, in solns., intrinsic viscosity rel. to mol. wt., unperturbed dimensions 0-65268  
 polystyrene, isotactic gel film, Fourier transform IR spectrum 0-104465  
 polystyrene, solns., sedimentation behaviour, branching effects determ. 0-66887  
 polystyrene, sulphonated, polyelectrolyte solution, correlations and dynamics 0-104446  
 polyurethanes, cross-linked, mol. mobility and struct., thermomechanical and NMR obs. (*Russian*) 0-69285  
 polyvinylidene chloride, crystalline, preferred chain conform., mol. models 0-79709  
 polyvinylidene chloride, normal vibr. analysis using conform. model 0-83529  
 protein, electron radiation damage on primary and secondary struct. level 0-89808  
 protein, structure and bonding, quantum theory, ab initio calcs. 0-61509  
 protein beta sheet structures, anal. and prediction by combinatorial approach 0-76710  
 protein molecular weight and ultrastruct. determ. in STEM 0-85562  
 proteins, conform. anal., algorithms and data structs. for array processing 0-83530  
 proteins, structure and bonding, modelling using aminoacetaldehyde 0-74273  
 proteins involved in active membrane transport, struct. review, book contrib. 0-108844  
 PTFE,  $\gamma$ -ray effects on 19 and 30°C phase transitions, Fourier transform IR spectroscopy 0-103387  
 PTFE grafted membranes, struct.-properties relationships, bifunctionality (*French*) 0-61137  
 PTFE grafted membranes, struct.-properties relationships (*French*) 0-61136  
 PTFE grafted membranes, struct.-properties relationships for poly-N-vinylpyrrolidone-containing membranes (*French*) 0-61138  
 purple membrane, orthorhombic 2D crystal form 0-85362  
 retinal chromophore, reson. Raman spectra obs. of struct. 0-94168  
 rhodopsin,  $\alpha$ -helix orientation, spectroscopic study 0-89711  
 RNA, conformational fluctuations, internal motion correl. times,  $^{31}\text{P}$  NMR obs. 0-72135  
 rubber, natural, crosslinked by dicumyl peroxide, modulus, swelling relations 0-59551  
 rubber mixtures in range of reversion, vulcanetry, cross-linking model (*German*) 0-104113  
 self-avoiding walks with span limitations, cubic lattice, mean square end-to-end distance 0-62568  
 short polymer chains, end-to-end vector, distrib. function 0-87254  
 solutions, electric field-induced optical rectification, rel. to electro-optic Kerr effect 0-84726  
 southern bean mosaic virus, struct. at 2.8 Å resolution 0-85334  
 valinomycin in its Ba complex, novel conformation 0-94167  
 viroid RNA, covalently closed circular mols., conform. states 0-85340

**macromolecular dynamics**

- ATPase,  $\text{Ca}^{2+}$ -activated, of sarcoplasmic reticulum, rot. motion and evidence for oligomeric structs. 0-72124  
 ATPase,  $\text{Ca}^{2+}$ -depend., struct. rearrangements during function 0-81527  
 bis(methylthio)alkanes, model compounds of polythioethers, vibr. spectra 0-58430  
 collagen fibril,  $^2\text{H}$  NMR of mol. motion 0-67034  
 conformational mobility, fluorescence obs. 0-63877  
 deoxyhaemoglobin,  $\text{Fe}(\text{II})\text{-N}(\text{His-F8})$  stretching freq. rel. to quaternary struct. 0-94160  
 dextran, aq. soln., conc., PMR (*Russian*) 0-71225  
 DNA, dye labelled elec. dichroism and birefringence, comparison with mol. props. from polarised fluoresc. 0-84785  
 DNA, Hg (II) and Ag (I) complexes in soln., theoret. interpret. of elec. dichroism obs. 0-85347  
 DNA, supercoiled torsional stress and local denaturation 0-72131  
 DNA, torsionally stressed, equilibrium statistical mechanics of helix coil transition 0-67032  
 DNA internal motions,  $^{31}\text{P}$  NMR and PMR 0-97855

**macromolecular dynamics continued**

- DNA solution, elec. birefringence, stabilised induced dipole behaviour 0-85349  
 dynamic living polymers, thermodynamic enhancement of oligomers, end-group interactions 0-58423  
 epoxides, dielectric relax. and deform props., cross-link density effect (*Russian*) 0-60942  
 ethylene-CO copolymer, dielec. absorpt. meas., permittivity (*French*) 0-103916  
 ferrocyclochrom c, mol. dynamics simulation 0-87255  
 flexible chain molecules, mutual interpenetration, fluorescence obs. 0-63877  
 fluorescence spectroscopic investigations of the dynamic properties of proteins, membranes and nucleic acids 0-101148  
 generalised polymer problems, Flory exponents 0-107039  
 haemoglobin, nanosec. probe of dynamics using time resolved reson. Raman scatt. 0-94162  
 high resolution NMR investig. 0-91708  
 librational motion effects on fluoresc. depolarisation and NMR relax. in macromols. and membranes 0-85324  
 lipid monolayer, simulation using mol. dynamics 0-108838  
 muscle proteins, rot. motions, saturation transfer EPR obs. 0-94151  
 myoglobin, refolding kinetics by diffusion-collision-adhesion model 0-94157  
 3'-nucleotide, calcs. to assess rigidity 0-61506  
 pancreatic trypsin inhibitor, bovine, macromol. dynamics, high resolution NMR investig. 0-91708  
 poly(3,3-dimethyl oxetane), conform. energies and random-coil config. meas. 0-99590  
 poly(spiro[2,4]hepta-4,6-diene) molecular characterisation, glassy state props. 0-64928  
 poly-4-vinylpyridine, intramol. mobility and local density in soln. spin mark method obs. (*Russian*) 0-70107  
 poly-4-vinylpyridine, mol. dynamics and local density in conc. soln., spin mark method obs. (*Russian*) 0-70108  
 polyspartamides, soluble, fluorescent labelling 0-58426  
 polydimethylsiloxanes, equilibrated, living oligomer distrib., end-group interactions 0-58423  
 polyelectrolytes, saturation of induced dipole moment, orientation mechanism and electro-optical effects 0-84785  
 polyethylene, mol. ultraslow rot. obs. using D probe spin alignment tech. 0-88890  
 polyheteroarenes, linear, conform. and struct., statistical calcs. (*Russian*) 0-69284  
 polymer chain, direct renormalisation group procedure 0-91712  
 polymer chain, linked rigid body, Brownian dynamics 0-74267  
 polymer chain dynamic critical index calcs. by renormalisation method 0-87256  
 polymer chain statics and dynamics, Lennard-Jones interaction, calcs. 0-58425  
 polymer chains, free rotating, depolarised light scatt. spectrum calcs. 0-78731  
 polymer chains, zero component field (*French*) 0-69280  
 polymer chains with rigid bonds, local relax. times, mol. dynamics study (*Russian*) 0-59373  
 polymer liquid, entangled, phenomenological consequences of Doi-Edwards viscoelasticity theory 0-79250  
 polymer solns., dynamic scaling theories at nonzero concs., tagged chain translational diffusion coeffs. 0-75143  
 polymer solution, diffusion of a chain, conc. effects 0-70103  
 polymeric chain with rigid side branches, intramol. phase transition of 1st kind (*Russian*) 0-58432  
 polymeric macromolecule containing mesogroups, phase diagrams (*Russian*) 0-58433  
 polymers, entanglement, topological theory, chain centre friction coeffs. 0-91709  
 polymethacrylamide copolymer, soluble, mobility of spin label bonded to chain end 0-63873  
 polynucleotide solution, elec. birefringence, stabilised induced dipole behaviour 0-85349  
 polynucleotide solution, elec. field induced orientation and effects 0-85348  
 polypeptides, helix-coil transition dynamics, time correl. function theory 0-99591  
 polypropylene glycol melt, mol. motion, dielectric and Kerr effect relax. obs. 0-60498  
 polystyrene, sulphonated, polyelectrolyte solution, correlations and dynamics 0-104446  
 polyurethanes, cross-linked, mol. mobility and struct., thermomechanical and NMR obs. (*Russian*) 0-69285  
 quantum many-body problem, polymer expansion 0-57181  
 rhodopsin and thermal intermediates, fast struct. fluctuations in protein component 0-72137  
 rigid symmetric top macromols., circular cylinder model, rot. dynamics 0-102591  
 rotational diffusion props., validity of general ellipsoid model 0-95751  
 self-organizing molecular system, dynamics 0-67028  
 short polymer chains, end-to-end vector, distrib. function 0-87254  
 siloxane, temp. transitions, linear dilatometry and X-ray diffr. obs. (*Russian*) 0-59404  
 solution, alternating elec. field light scatt., low angle approx. 0-84721  
 solution, dynamic light scatt. by flexible macromols. in fluctuating elec. field 0-84722  
 solution, rigid ellipsoidal macromols. in cond. soln. at low ionic strength, specific Kerr consts. 0-84718  
 solution, rot. diffusion coeff. calc. method w.r.t. mol. struct., elec. birefringence relax. time data interpret. 0-85331  
 solution, transient elec. birefringence in reversing fields of arbitrary strength and duration 0-84719  
 solutions and suspensions, polarised fluoresc. in elec. field, mol. props. deriv. 0-84785  
 telechelic, chain extension, qualitative aspects 0-95752

**macromolecular energy levels**

- infinite conjugated polymers,  $\pi$ -electron energy and energy gap, topological calcs. 0-91713  
 polynucleotide electron energy band studies 0-72132  
 protein, structure and bonding, quantum theory, ab initio calcs. 0-61509



**macromolecular spectra**

- see also *spectra of organic molecules and substances*  
 bis(methylthio)alkanes, model compounds of polythioethers, vibr. spectra 0-58430  
 cytochrome c, haeme-haeme mag. interaction, Mossbauer obs. 0-108836  
 cytochrome c, low freq. modes and excitation profiles, reson. Raman spectra 0-94428  
 DNA, dye labelled elec. dichroism and birefringence, comparison with mol. props. from polarised fluoresc. 0-84785  
 DNA, Hg (II) and Ag (I) complexes in soln., theoret. interpret. of elec. dichroism obs. 0-85347  
 fibrinogen, bovine, high energy-induced aggregation, time resolved spectra 0-61655  
 haemoglobin, low freq. modes and excitation profiles, reson. Raman spectra 0-94428  
 haemoglobin, nanosec. probe of dynamics using time resolved reson. Raman scatt. 0-94162  
 haemoglobin haem structure after photo-deligation, Raman spectra 0-61510  
 hydrate, struct. conversions of sugar phosphate chain and nitrogenous bases, IR spectra 0-81530  
 immunoglobulin, human, high energy-induced aggregation, time resolved spectra 0-61655  
 lanthanide complex, struct. and equil. by time resolved Eu(III) spectrosc. 0-78736  
 lanthanide ion bound to macromol., struct. and equil. by time resolved Eu(III) spectrosc. 0-78736  
 methaemoglobin, struct. change on addition of inositol hexaphosphate 0-72130  
 muscle proteins, rot. motions, saturation transfer EPR obs. 0-94151  
 Nylon-12 film, casting conditions effect on polymorphism 0-84903  
 pancreatic trypsin inhibitor, bovine, macromol. dynamics, high resolution NMR investig. 0-91708  
 poly-N-vinyl carbazole, pulsed laser excitation, time resolved fluoresc., 0-89041  
 poly-p-chlorophenyl glycidyl ether, struct., tacticity and addition isomerism,  $^{13}\text{C}$  NMR 0-58427  
 polyacrylamide gel and single chain in soln., laser light scatt. obs. near phase transitions 0-93808  
 polyethylene, vinyl group reactions during  $\gamma$ -irrad., crystallinity effect, absorbance obs. 0-81346  
 polymer chains, free rotating, depolarised light scatt. spectrum calcs. 0-78731  
 polymer chains with rigid bonds, local relax. times, mol. dynamics study (Russian) 0-59373  
 polymethacrylic acid, stereoregular, synthesis,  $^{13}\text{C}$  NMR obs. 0-58422  
 polyribonucleotides, dye tagged, aqueous solns., elec. induced fluoresc. changes 0-85346  
 polystyrene, epimerised isotactic, methylene C mag. resonance spectra 0-63878  
 polystyrene, isotactic gel film, Fourier transform IR spectrum 0-104465  
 polystyrene, uniaxially stretched atactic thin film, mol. orientation, polarized Raman study 0-103951  
 polystyrene latex spheres, characterisation using light scattering spectrom. 0-95753  
 polystyrene, benzene soln., characterisation using light scattering spectrom. 0-95753  
 retinal chromophore, reson. Raman spectra obs. of struct. 0-94168  
 rhodopsin,  $\alpha$ -helix orientation, spectroscopic study 0-89711  
 serum albumin, bovine, high energy-induced aggregation, time resolved spectra 0-61655

**macromolecules**

- see also *DNA; macromolecular configurations; macromolecular dynamics; macromolecular energy levels; macromolecular spectra; polymers; proteins*  
 bead-spring-type model in nonuniform vel. gradient, dil. soln. kinetic theory results 0-64628  
 biological, selection models, with time varying constraints 0-67029  
 biological, study by scanning microcalorimeters 0-61747  
 biological macromolecules, conformation studied by calorimetry, review 0-97870  
 birefringence kinetics in nonpolar mol. solns. 0-100648  
 charged macromolecules in external elec. field, spherical case 0-75145  
 chiral substances, electro-optical responses, Jones matrix, meas. system for rot. anisotropy 0-84723  
 conference, Mainz, Germany (Sept. 1979) 0-58429  
 dumbbells, nearly-Hookean, dilute soln., rheological equation of state 0-100321  
 electro-optics and dielectrics, conf., Uxbridge, England (Apr. 1978) 0-82577  
 heat capacity function, of macromolecular systems, statistical thermodynamic analysis 0-61514  
 linear, heat capacities, scanning calorimetry meas. 0-61134  
 macromolecules, cluster expansion 0-106408  
 molecular structure, conformation and properties 0-63874  
 nonlinear laser photomodification, radiation damage 0-61120  
 polyolefins, ultra-high modulus, production by tensile drawing and hydrostatic extrusion 0-81022  
 rodlike, gels, nonlinear elasticity in condensed state 0-104199  
 sedimentation, rapid, under gravity, basic theory and experimental demonstrations 0-66885  
 self-reproducing macromolecules, selection, controlled energy fluxes constraint 0-67027  
 thermal factor refinement procedure, restrained-parameter 0-79628  
 X-ray small-angle scattering, information content and error anal., Shannon sampling 0-59340  
 $\text{Li}_{3+2}\text{P}_2\text{O}_{3+1}$ , polyphosphate, melting and crystallisation 0-70376

**Madelung constant** see *lattice energy*

**magamps** see *magnetic amplifiers*

**Magellanic Clouds** see *galaxies*

**Maggi-Righi-Leduc effect** see *thermomagnetic effects*

**magnesium**

see also *nuclei with .....*

- $2p_{1/2}$  vacancy alignment in ion-atom collisions, electron capture role 0-83465  
 anomalous intensity ratios in H like  $\text{Li}$ , doublet in optically thick laser prod. plasmas 0-103186  
 atmosphere aerosols over tropical N.Atlantic Ocean, water-soluble K, Ca and Mg contents 0-72598

**magnesium continued**

- atom, 4sn autoionising states ejected electron spectra, low energy impact two electron excitation 0-83494  
 atom, approximate relativistic Hartree-Fock eqns., soln. using Slater-type functions 0-58168  
 atom, closed shell, Jastrow wave functions, var. calcs. 0-83249  
 atom, damping const. in acetylene-air flame, Lorentz collisions, mag. field effects 0-66805  
 atom, K-shell ionisation by ultrarelativistic electrons, density effect 0-99576  
 Auger spectra, KLL and KLV, screening effects and plasmon gains 0-80913  
 crystals, concentrated loads, 3-D anisotropic elasticity theory 0-83734  
 determination by activation anal. ( $\alpha, n$ ), ( $\alpha, p$ ) reacts. investig. 0-61206  
 dissolution of  $\text{H}_2$ , resistometric study under press. 0-70417  
 face, (0001), incipient oxidation, EELS and LEED studies 0-81237  
 films, struct. and props., X-ray diff. spectra anal. 0-80119  
 foil-excited ion, X-ray spectra and satellite classification 0-95567  
 forced-flow chromatography, detection by photometric method 0-71965  
 HCP, vacancy clusters and interstitials, computer simulation study 0-64992  
 HCP lattice, Huang diffuse scatt. from interstitials 0-88142  
 hydriding, Kirkendall marker movement 0-75385  
 inclusions, types and size distrib. (German, English) 0-97492  
 interstellar Mg lines in stellar spectra, rel. to existence of circumstellar clouds 0-94782  
 isoelectronic sequence, electron impact excitation of reson. transitions 0-63825  
 isotopic anomalies, role of  $^{26}\text{Al}$  synthesis in explosive H burning 0-85929  
 laser radiation absorption in craters on metal targets 0-97386  
 magnetic property volume depend., Knight shifts, electron spin response 0-88729  
 nucleosynthesis, isotopic yields from C and Ne zones in explosion of massive star 0-90406  
 plasma, heated by ruby laser pulses, X-ray emission spectrum 0-64781  
 quadrupole interaction of  $^{181}\text{Ta}$ , gamma-spectral study 0-80228  
 radioactive tracer for Pu nuclear fuel input accountability in reprocessing plants 0-73919  
 surface, rough, reflection loss for s and p polarised waves near surface plasmon freq. (French) 0-97225  
 XPS, plasmon gains as monitor of incomplete relax., interference effects and sudden to adiabatic limits transition 0-66390  
 $\alpha\text{-Al}_2\text{O}_3$  fibre FP reinforced Al and Mg composites, fabrication and props. 0-81004  
 InAs: Mg, ion implanted, photocond., photo-EMF, and optical absorpt. spectra 0-70763  
 KBr:  $\text{Mg}^{2+}$ , dopant aggregation and precipitation 0-107306  
 KCl:  $\text{Mg}^{2+}$ , dopant aggregation and precipitation 0-107306  
 K, MnF $_4$ : Mg, mag. effects of impurities 0-65869  
 K $_2$ MnF $_4$ : Zn(Mg)(Ni), local magnetisation, NMR and Green's function study 0-65870  
 LiF: Mg, dependence of optical absorpt. on temp. during X-ray irradi. 0-66237  
 LiF: Mg, flow stress changes during precipitation 0-92594  
 LiF: Mg, TLD-100, thermolum. phosphor, photolum. and absorpt. spectra, thermolum. mechanisms 0-97321  
 LiF: Mg, X-irrad., colour centres, ESR and UV absorpt. meas. 0-108069  
 LiF: Mg, X-irrad. induced sensitisation mechanism, optical absorpt. spectra 0-60637  
 LiF: Mg, Z $_r$  and associated Z-centres, elec. cond., ionic thermocurrent, and optical absorpt. meas. 0-107229  
 LiF: Mg, Ti, defect states, ESR and ionic cond. study 0-108058  
 LiF: Mg cryst., Mg electron colour centers 0-100229  
 LiF: Mg  $\gamma$ -irrad., phonon scatt. and interstitial clusters 0-70254  
 LiF: OH: Mg,  $\gamma$ -irrad. induced oxyhydril complexes 0-92555  
 Mg ( $\text{Mg}^+$ ), lifetime meas., beam foil spectra, comparison with numerical coulomb approx. calcs. 0-58367  
 Mg I and II in Sun, line profiles comparison with theoretical spectra, visible obs. 0-82320  
 Mg, I-XII, energy levels and optical spectra 0-87065  
 Mg II, UV line spectrum of active chromosphere star  $\epsilon$  Eridani, models 0-77394  
 Mg II 280 nm line in Persei, profile, calcs. and UV obs. 0-82421  
 Mg II h and k lines in cool giant star chromospheres, mass loss determ. 0-85935  
 Mg II lines in quasars and Seyfert galaxies, excitation and line strength 0-67896  
 Mg III-V, beam-foil spectra, 100-450 Å 0-83308  
 Mg isoelectronic sequence, static dipole quadrupole polarisabilities and shielding factors calc. using HF scheme 0-99450  
 Mg XI resonance lines, dielectronic satellite lines atomic parameters calcs. 0-78567  
 $\text{Mg}^+$ , shape resonances, shift potential, calcs. 0-69089  
 $\text{Mg}^+$  laser cooled ions bound in Penning trap, high-resolution optical spectra 0-102487  
 $\text{Mg}^{1+}$ , soft X-ray population inversion in laser plasmas, reson. photoexcitation, photon-assisted processes 0-87378  
 $\text{Mg}^{2+}$  atomic core states, antishielding effects calcs. 0-83299  
 $\text{Mg}^{2+}$ , second order correl. energy, Z depend. of irreducible-pair energies 0-91417  
 Mg-AgCl seawater battery, performance and EMF at great ocean depths 0-76623  
 Mg-Xe discharge and MgXe excimer band, emission intensities and excited-state densities meas. 0-92413  
 Mg+Ca, Ca metastable  $^3\text{P}$ -state, quenching reactions, fluoresc. meas. 0-102477  
 $\text{Mg}^+ + \text{He}(\text{Ne})$ , ns-np excitation, alignment and orientation, impact, parameter theory 0-91648  
 $\text{Mg}_2$ , ground state, multiple scatt. X $\alpha$  calcs. 0-58149  
 $\text{Mg}_2(\text{Mg}^{2+})$ , atomic clusters, electronic struct., LCAO-MO-SCF and HF calcs. 0-63880  
 MgNi $_4$ , four-layer, Friauf-Laves phases, stacking variants 0-96468  
 $^{24}\text{Mg}/^{26}\text{Mg}$ ,  $^{26}\text{Mg}$  of interplanetary dust particles 0-72879  
 NaCl: Mn $^{2+}$ ,  $\text{Mg}^{2+}$ , doubly doped, ionic thermocurrent study of linear di- $\text{SiO}_2$ -Mg-Cu powder compact, nitridation to form  $\text{Si}_3\text{ON}_2$  whiskers (Japanese) 0-93674

**magnesium alloys**

see also *magnesium compounds*

- Al-Zn-Mg (5.1 wt.%), decomp. process, TEM study 0-71660

**magnesium alloys continued**

- dilute, dynamic recryst. during creep, dislocation substruct., quartz comparison 0-109142  
 precipitate free zones, X-ray microanal. 0-108768  
 Ag-Mg (18.5 wt.%), solid soln., rheological study of crystallographic order on creep (*French*) 0-97548  
 AgMg, B2 intermediate phase, slip system, ordering energy and atomic size ratio depend. 0-59471  
 AgMg two phase bicrystal growth, orientation, interface struct. 0-60773  
 Ag<sub>3</sub>Mg, periodic antiphase boundaries, electron microscopy study (*French*) 0-59481  
 Al-Cu-Mg, type RR55, high strength, creep behaviour, effect rel. to anodic coatings, SEM study 0-97542  
 Al-Cu-Mg, type D16T, thin-wall cylinder cold rolling method 0-66535  
 Al-Cu-Mg (4, 1.5 wt.%), mica dispersed, wear charact. and bearing performance 0-108591  
 Al-Cu-Mg/mica particulate composite mech. props. 0-100919  
 Al-Cu-Mg-Li alloy extrusions, microstruct., embrittlement and fracture props. 0-60965  
 Al-Cu-Mg-Mn-Si-Fe, torsional vibrations decrement, deformed vol. effect 0-76326  
 Al-Cu-Si-Mg, deform. simulation using torsional test, elastoplastic constitutive eqn. 0-93594  
 Al-insulator-In<sub>1-x</sub>Mg<sub>x</sub> film tunnel junction, resistance zero-bias anomalies 0-107925  
 Al-Li-Mg-Be alloys, phase composition of surface films, oxidation protection mechanism (*Russian*) 0-65417  
 Al-Mg, alloy A5083-O, fatigue crack prop. and crack closure behaviour under plain strain conditions (*Japanese*) 0-81160  
 Al-Mg, comparison of liquid impact erosion and cavitation erosion 0-104302  
 Al-Mg, dil., ang. correlation of annihilation radiation from impurity trapped positrons 0-104010  
 Al-Mg, dil. binary alloy, planar interface stability during solidification (*Slovak*) 0-108424  
 Al-Mg, foil, oxidation in O<sub>2</sub> atm., TEM study 0-104356  
 Al-Mg, fracture resistance at low temps. 0-104284  
 Al-Mg, liquid impact erosion 0-108598  
 Al-Mg, low freq. internal friction during plastic deform. (*Chinese*) 0-103420  
 Al-Mg, oxidation control study, electron opt. techniques eval. 0-85089  
 Al-Mg, Si alloy, void form. under different precip. conditions, after Al ion irradi. 0-59529  
 Al-Mg, solidification, solid-liq. interface, solute conc. effects 0-59632  
 Al-Mg, type AMG6, pool metal solidification kinetics in welding with electromag. stirring 0-71636  
 Al-Mg, type A5083P-O effects of anisotropy in cutting mechanism (*Japanese*) 0-89232  
 Al-Mg 0-76244  
 Al-Mg (0.1 at.%), neutron damage, positron annihilation 0-65056  
 Al-Mg (0.3 wt.%) single cryst., dislocations obs. by high voltage electron microsc. 0-79796  
 Al-Mg (2 wt.%), hardening and fracture charact.,  $\beta$ -phase dissolution role 0-81178  
 Al-Mg (2.5wt.%) sheet, surface oxide state and weldability 0-59769  
 Al-Mg (4 wt.%), struct. and strengthening in hot working 0-84968  
 Al-Mg (7 wt.%), bare surface reaction rates in aq. solns. 0-101022  
 Al-Mg alloy, nitridation process study 0-61013  
 Al-Mg sheet, artificial stress raiser effect on strength and local plasticity of weld joint 0-81130  
 Al-Mg-Si, ageing sequence study by electron microdiff. 0-81068  
 Al-Mg-Si, STEM microdiff. obs. of precip. struct. 0-104167  
 Al-Mg-Li alloy, metastable S'-phase, struct. (*Russian*) 0-103291  
 Al-Mg-Si, cast, precip.-rich zones on grain boundaries, soln. heat treatment conditions effect on mech. props. 0-104176  
 Al-Mg-Si, type 6010, microstruct. charact. influence on formability, heat treatment 0-81090  
 Al-Mg-Si, type 6061-T6, 6063-T6, effective stress range factor in fatigue 0-100924  
 Al-Mg-Si alloy, Mg<sub>2</sub>Si dispersion hardened US waveguides, concentrators (*Polish*) 0-89237  
 Al-Mg-Si alloys, ductile intergranular fracture mechanisms, void formation and nucleation 0-108578  
 Al-Mg-Zn alloys, Al-rich, weld metal comp. effect on microsegregation and eutectic phase segregation (*German*) 0-108455  
 Al-Mg-Zn alloys, evaporation effect of alloying elements Mg and Zn in in-situ EM studies 0-103388  
 Al-Mg-Zn-Cu, type 7050, calorimetric study of fatigue induced microstructural changes 0-85034  
 Al-Mg(Cu)(Si), dimensional changes in heat treatment. 0-89271  
 Al-Mg(Cu)(Si), (5.0(4.5)(11.8 wt.%), ingots, vibr. effect during solidification on porosity formation 0-108426  
 Al-Mg(Zn-Mg), long term strength and creep 0-60925  
 Al-Zn-Mg, age-hardenable, precipitation and dissolution processes, positron annihilation and X-ray small-angle scattering comparison 0-89238  
 Al-Zn-Mg, atmosphere effect on fatigue crack prop. (*Japanese*) 0-81161  
 Al-Zn-Mg, crack-arrest markings on intergranular stress corrosion fracture surfaces 0-89405  
 Al-Zn-Mg, oriented growth of precipitates on dislocations, model 0-108448  
 Al-Zn-Mg, TEM and calorimetric study 0-76290  
 Al-Zn-Mg, TEM characteris. of precipitates 0-104166  
 Al-Zn-Mg, type 7075-T651 plate, thickness direction inhomogeneity of mech. props. and fracture toughness 0-100892  
 Al-Zn-Mg, type V-95, ultimate tensile strength for brief impact 0-70309  
 Al-Zn-Mg (3.6, 1.95 wt.%), ageing and plastic deform., effect on structure, electron microsc. and X-ray diff. study (*Russian*) 0-81108  
 Al-Zn-Mg (3.87, 1.79 wt.%), oriented growth of precipitates on dislocations, TEM obs. 0-108447  
 Al-Zn-Mg (91, 6, 3, wt.%), H embrittlement and trapping, HVEM obs. 0-76364  
 Al-Zn-Mg alloy, Ag addition and pre-precipitation treatment, influence on GP zone growth 0-71658  
 Al-Zn-Mg alloy AA-7039, stress corrosion cracking, SEM obs. 0-104323  
 Al-Zn-Mg alloys, grain boundary segregation, implications to stress corrosion cracking 0-84936  
 Al-Zn-Mg granules and bands rolled from them, heat treatment 0-100862  
 Al-Zn-Mg superplastic alloy, cavity growth under creep conditions 0-60940

**magnesium alloys continued**

- Al-Zn-Mg type 7N01-T4, weld, SCC in NaCl-H<sub>2</sub>O<sub>2</sub> soln. (*Japanese*) 0-108631  
 Al-Zn-Mg-Cu (6, 2.5, 1.5 wt.%), deform. simulation using torsional test, elastoplastic constitutive eqn. 0-93594  
 Al-Zn-Mg-Cu (6.2, xwt.%) type alloy, fatigue crack prop., Cu content and recryst. effect 0-60960  
 Al-Zn-Mg-Cu type 7075, heat treatment optimisation 0-60888  
 Al<sub>3</sub>Mg<sub>2</sub>, diffusionless phase transformation 0-104150  
 Al<sub>3</sub>Mg<sub>2</sub>, liquid alloys, vols. and entropies of mixing, calc. 0-75363  
 AuMg, B2 intermediate phase, slip system, ordering energy and atomic size ratio depend. 0-59471  
 Cd-Mg, selective dissolution, static samples 0-65228  
 Cd-Mg, selective dissolution, rotating ring disc electrode 0-65229  
 Cd<sub>1-x</sub>Mg<sub>x</sub>, energy spectrum pseudopotential calcs., mag. props., impurity scatt. (*Russian*) 0-65430  
 Ce-Mg-Fe master-alloy inoculated cast Fe, struct. and props. 0-100843  
 Fe, cast, grey, fracture surface after dynamic fracture, Mg conc. effect 0-100909  
 Gd-Mg amorphous films, spontaneous Hall effect and elec. resist. 0-80251  
 GdMg, noncollinear mag. struct., nonlinear band behaviour 0-75706  
 LaMg, Pauli paramagnet, mag. susceptibility, nonlinear band behaviour 0-75706  
 Li-Mg, Mathiessen's rule, elec. and thermal deviations, impurity scatt. 0-88536  
 Mg-Ag, ion implanted, recovery stage characterisation by electron irradi. 0-107295  
 Mg-Al-Zn (94.3, 3.9, 1.8 wt.%), precip. on dislocations, weak-beam TEM 0-76264  
 Mg-Al-Zn-Mn (8, 0.5, 0.3 wt.%) casting alloy, penetration resistance 0-100901  
 Mg-La(Ce)(mischmetal) alloys, appl. to H<sub>2</sub> storage 0-72093  
 Mg-MgNi<sub>2</sub>-Zn, diagram of state, Zn solubility, initial phase precipitation (*Russian*) 0-66478  
 Mg-Mn-Ce (1.5, 0.3 wt.%), superplasticity role of diffusional creep (*Russian*) 0-97528  
 Mg-Nd-Zn dilute alloy, metallography and precip. kinetics 0-71655  
 Mg-Tb(Dy)(Ho)(Tm), dil., macroscopic shape effect due to quadrupole orientation, magnetostriiction and thermal expansion meas. 0-60396  
 Mg-Zn (5 wt.%), age hardening, X-ray diff. anal. (*Chinese*) 0-104173  
 Mg-Zn alloy, aged, one dimensional transition phase  $\beta_2$ , crystallographic obs. (*Chinese*) 0-60865  
 MgAg, Auger spectra, 4d bandwidth effect 0-89093  
 Mg<sub>1.86</sub>Al<sub>1.67</sub>Si<sub>4.73</sub>O<sub>19.13</sub>N<sub>3.81</sub>, 12H polytype, intergranular phases and compositional variations 0-79645  
 MgCd wire, elongation during disorder-order transform. (*Russian*) 0-104148  
 Mg<sub>2</sub>Cu polycrystals, surface study by AES, XPES and X-ray induced AES 0-65346  
 Mg<sub>2</sub>Ni, magnetism and H<sub>2</sub> storage 0-70941  
 Mg<sub>2</sub>NiH<sub>4</sub>, solar energy storage by metal hydride 0-61455  
 MgZn<sub>2</sub>, two-layer, Friauf-Laves phases, stacking variants 0-96468  
 MgZn<sub>2</sub>-Mg<sub>2</sub>Ag, system, Friauf-Laves phases, stacking variants 0-96468  
 Ni-based superalloys, hot workability, effect of S, Ca, Mg, Y and Zr minor elements 0-66552  
 PrMg<sub>3</sub>, cryst. field study, inelastic neutron scatt. and sp. ht. meas. 0-59939  
 Sc-Mg, low-temp. heat capacity 0-75370  
 SnMg<sub>2</sub>, <sup>119</sup>Sn temp. depend. isomer shift, pseudopot. approach 0-84675  
 YMg, Pauli paramagnet, mag. susceptibility, nonlinear band behaviour 0-75706
- magnesium compounds**  
 see also magnesium alloys  
 cordierites, synthetic end members, variation of refr. index with water content 0-80739  
 dichlorophosphate complexes, cryst. struct. <sup>35</sup>Cl NQR obs. 0-108108  
 dolomite, powders sintering, decarbonisation cycle effect 0-104102  
 floating zone method growth, interface shapes 0-60775  
 magnesial refractory concretes, cast. props. 0-89306  
 magnesite, powders sintering, decarbonisation cycle effect 0-104102  
 magnesite artifacts, roasted, props., filler porosity effect 0-104099  
 magnesite refractories, unfired, by resin phosphate binding 0-104101  
 magnesite-dolomite refractories, tar bound, fracture and wear 0-104287  
 magnesium hexahydrate H<sub>2</sub>EDTA·VO<sup>2+</sup>, single cryst., ESR spectra and spin Hamiltonian parameters 0-75845  
 magnesium phthalocyanine, depletion layer studies, temp. depend. of LF capacitance 0-65617  
 MgAl<sub>2-x</sub>Fe<sub>x</sub>O<sub>4</sub> solid solution system, solid state properties study 0-93094  
 periclase refractories, props. after testing at over 2000°C 0-104317  
 silicate minerals, mantle related, thermodynamic props. at high press. and temp. 0-81874  
 steel, austenitic, type 316, in MgCl<sub>2</sub>, acidity and applied potential effect on stress corrosion cracking 0-85076  
 Ag<sub>2</sub>O-Al<sub>2</sub>O<sub>3</sub>-MgO-Na<sub>2</sub>O,  $\beta'$ -alumina, structure, X-ray determ. 0-107148  
 Ag<sub>2</sub>O-MgO-Al<sub>2</sub>O<sub>3</sub>, ionic cond. 0-107480  
 $\beta$ -Al<sub>1-x</sub>Mg<sub>x</sub>O<sub>16</sub>, X-ray diffuse scatt. obs. of struct. 0-107186  
 Al<sub>2</sub>O<sub>3</sub>-MgO, grain boundary segregation of Ca and Mg X-ray spectrosc. and STEM study 0-107269  
 Al<sub>2</sub>O<sub>3</sub>-MgTiO<sub>3</sub>, sintering temperature effect of titanate additions 0-60808  
 $\beta$ -Al<sub>2</sub>O<sub>3</sub>-K<sub>2</sub>O-MgO, cryst. struct., nonstoichiometry, ion-ion correlations 0-88129  
 Ba(PO<sub>3</sub>)<sub>2</sub>-AlF<sub>3</sub>-MgF<sub>2</sub>, glass, elec. cond. and IR spectra 0-89005  
 Ca-Mg-Ni hydrides, water form. on O<sub>2</sub> exposure 0-97727  
 CaF<sub>2</sub>-MgO, melts, elec. cond., surface tension, viscosity, density (*Russian*) 0-92758  
 CaF<sub>2</sub>-MgO-SiO<sub>2</sub>, melts, elec. cond., surface tension, viscosity, density (*Russian*) 0-92758  
 CaO-MgO-Cr<sub>2</sub>O<sub>3</sub>-Al<sub>2</sub>O<sub>3</sub>-ZrO<sub>2</sub>-SiO<sub>2</sub> system, subsolidus region charact. 0-97466  
 Cd<sub>1-x</sub>Mg<sub>x</sub>S, solid soln., phase equilib. diagrams 0-108412  
 (Ce<sub>0.9</sub>La<sub>0.1</sub>)<sub>2</sub>Mg<sub>2</sub>(NO<sub>3</sub>)<sub>12</sub>·24H<sub>2</sub>O, adiabatic demagnetisation temp., mag. entropy (*Russian*) 0-65892  
 Ce<sub>2</sub>Mg<sub>3</sub>(NO<sub>3</sub>)<sub>12</sub>, spin-lattice relax., dynamic susceptibility meas., liq. He contact effects 0-66011  
 Co-W alloy electrodeposition, influence of MgSO<sub>4</sub> and gum arabic additives (*Russian*) 0-80991  
 Co<sub>2</sub>Mg<sub>1-x</sub>O system, thermodynamic investigation, 1100 to 1300K (*German*) 0-107430  
 CoO-ZnO-MgO ternary systems, solid solns., struct. charact. 0-60629



## magnesium compounds continued

- CsMgBr<sub>3</sub>(I<sub>3</sub>), diamag. linear chain lattices, cryst. struct. 0-70172  
 FeMgBO<sub>3</sub> and FeMg<sub>2</sub>MO<sub>3</sub>, imperfect 1D mag. systems, Mossbauer expts. 0-60466  
 Fe<sub>2</sub>Mg<sub>1-x</sub>Cl<sub>2</sub>, metamagnet, mag. phase diagram by mag. induced light scatt. 0-65883  
 (Fe<sub>0.15</sub><sup>2+</sup>Mg<sub>0.85</sub><sup>2+</sup>Mn<sub>0.35</sub><sup>2+</sup>) [Fe<sub>1.87</sub><sup>3+</sup>Al<sub>1.13</sub><sup>3+</sup>O<sub>2</sub>]<sup>2-</sup>, influence of Fe<sup>2+</sup> ion substitution on electron hopping, Mossbauer study 0-71247  
 (Fe<sub>0.55</sub><sup>2+</sup>Mg<sub>0.32</sub><sup>2+</sup>Mn<sub>0.03</sub><sup>2+</sup>Cu<sub>0.10</sub><sup>2+</sup>) [Fe<sub>1.74</sub><sup>3+</sup>Al<sub>0.26</sub><sup>3+</sup>O<sub>2</sub>]<sup>2-</sup>, influence of Fe<sup>2+</sup> ion substitution on electron hopping, Mossbauer study 0-71247  
 Fe<sub>1-2</sub>Mg<sub>1-x</sub>Ti<sub>0.4</sub>O<sub>4</sub>, mag. ordering, Mossbauer effect in external mag. fields 0-71257  
 KMg<sub>2</sub>AlSi<sub>2</sub>O<sub>10</sub>F<sub>2</sub>, dislocations, subgrain boundaries, X-ray diffr. topography study (*Chinese*) 0-88149  
 KMgF<sub>3</sub>:Fe<sup>2+</sup>, anomalous acoustic relax. absorpt. and APR 0-88864  
 KMgF<sub>3</sub>:Ni<sup>2+</sup>, acoustic Faraday and Cotton-Mouton effects, theory 0-65987  
 K<sub>1.54</sub>Mg<sub>0.77</sub>Ti<sub>2.23</sub>O<sub>6</sub>, hollandite, one-dimens. superionic cond., transport model 0-107529  
 KMg<sub>2</sub>[AlSi<sub>2</sub>O<sub>10</sub>]F<sub>2</sub> with excess Al, synthetic fluorophlogopite, radiation-induced paramag. O<sup>-</sup> centres 0-60417  
 K<sub>2</sub>O-MgO-Al<sub>2</sub>O<sub>3</sub>, ionic cond. 0-107480  
 K<sub>2</sub>O-MgO-B<sub>2</sub>O<sub>3</sub>:Cu<sup>2+</sup>, micro-inhomogeneities, EPR and Raman study 0-84080  
 LaCrO<sub>3</sub>-MgO, LC20M electrode material in open cycle MHD systems, thermionic emission characters. 0-97394  
 LiMg, Σ<sup>+</sup> and Π states, mol. binding energy curves 0-58189  
 Li<sub>2</sub>O-MgO-Al<sub>2</sub>O<sub>3</sub> system, subsolidus phase equilibria 0-81036  
 Li<sub>2</sub>O-MgO-Al<sub>2</sub>O<sub>3</sub>-SiO<sub>2</sub> glass scintillator for pulsed neutron detection 0-87019  
 (Mg,Fe)<sub>2</sub>SiO<sub>4</sub>, dislocation recovery rate affected by high-pressure. 0-94515  
 Mg SiO<sub>3</sub> melt, instantaneous struct. simulated by mol. dynamics 0-84049  
 Mg-Si-Al-O-N ceramic, phase assemblages, relationships with props. 0-60848  
 MgAl<sub>2</sub>O<sub>4</sub> crystals, flux grown, artificial spinel twin form. by BeAl<sub>2</sub>O<sub>4</sub> addition 0-96542  
 MgAl<sub>2</sub>O<sub>4</sub>, faulted defect aggregates prod. by neutron-irrad. 0-107331  
 MgAl<sub>2</sub>O<sub>4</sub> film on Al-Li-Mg-Be alloy, phase composition, oxidation protection mechanism (*Russian*) 0-65417  
 MgAl<sub>2</sub>O<sub>4</sub>, γ-irradiated crystal, TSC, thermoelec. power, thermolum. and afterglow 0-75583  
 MgAl<sub>2</sub>O<sub>4</sub>, irradi. stability obs. using X-ray emission meas. (*Russian*) 0-66326  
 MgAl<sub>2</sub>O<sub>4</sub>, pure and Fe-doped spinel, elec. cond. 0-59702  
 MgAl<sub>2</sub>O<sub>4</sub>, radiation damage, optical absorpt., F-centres 0-64994  
 MgAl<sub>2</sub>O<sub>4</sub> spinel, anomalous thermal expansion, second order transition 0-84307  
 MgAl<sub>2</sub>O<sub>4</sub> spinel refractory, enthalpy and specific heat determs. 0-88334  
 MgAl<sub>2</sub>O<sub>4</sub>, strength-controlling fracture energy depend. on flaw-size to grain-size ratio 0-81152  
 Mg<sub>0.10</sub>Al<sub>0.44</sub>Mn<sub>0.89</sub>(SO<sub>4</sub>)<sub>2</sub>·8H<sub>2</sub>O, mooreite, X-ray cryst. struct. determ. and refinement 0-92488  
 3MgCO<sub>3</sub>·Mg(OH)<sub>2</sub>·3H<sub>2</sub>O, activation, for MgO sintering 0-89183  
 MgCa(CO<sub>3</sub>)<sub>2</sub>, dolomite, partial thermal decomp. into MgO and CaCO<sub>3</sub>, product cryst. growth 0-108706  
 Mg<sub>2</sub>Cd<sub>1-x</sub>Te, electroreflection spectra, comp. depend. 0-66230  
 MgCl<sub>2</sub> solution, Cl distrib. in oxide film on stainless steel, SIMS study (*French*) 0-108765  
 MgCl<sub>2</sub> solution, stress corrosion cracking of austenitic stainless steel, temp. effect (*Korean*) 0-93694  
 MgCl<sub>2</sub>-alkali metal chloride system, solid and molten states, struct. props., Raman spectra 0-76011  
 MgCl<sub>2</sub>·6NH<sub>3</sub>·MgCl<sub>2</sub>·2NH<sub>3</sub>, heating and cooling of solar energy storage system 0-81484  
 MgCr<sub>2</sub>O<sub>4</sub>, spinel refractory, enthalpy and specific heat determs. 0-88334  
 MgCr<sub>2</sub>O<sub>4</sub>-TiO<sub>2</sub>, porous ceramics, humidity-sensitive electrical conduction 0-107782  
 MgCr<sub>2</sub>O<sub>4</sub>-TiO<sub>2</sub>, porous ceramic humidity sensors 0-86325  
 MgF<sub>2</sub>, polycryst., quartz particle impacts no. effect on erosion in elastic-plastic response regime 0-81209  
 MgF<sub>2</sub>, <sup>4</sup>He<sup>+</sup> ion scatt. spectrometry below 5 keV 0-108313  
 MgF<sub>2</sub>, high temp. polymorphism and thermal props. 0-75199  
 MgF<sub>2</sub>, point defects study, cross relaxation processes, polarised β-active nuclei 0-60431  
 MgF<sub>2</sub>:Co(Ni), tunable transition-metal-doped solid state lasers 0-58549  
 MgF<sub>2</sub>:Li<sup>+</sup>, atom transport, diffusion and ionic cond. meas. 0-107492  
 MgF<sub>2</sub>-Na<sub>3</sub>AlF<sub>6</sub> thin film deposits, quenched ageing by chopping 0-97364  
 Mg<sub>2</sub>Fe<sub>1-x</sub>O<sub>4</sub>, diffusion of <sup>59</sup>Fe and elec. cond. 0-59700  
 Mg<sub>2</sub>Fe<sub>1-x</sub>O<sub>4</sub> crystals, first mag. anisotropy const., 7-295K 0-65855  
 Mg<sub>2</sub>Fe<sub>1-x</sub>O<sub>4</sub>, polycryst., Verwey type transition, resist., magnetisation, Mossbauer effect and permeability obs. 0-75764  
 Mg<sub>2</sub>GeO<sub>4</sub>-Mg<sub>2</sub>SiO<sub>4</sub> system, struct. similar solid soln. obs. and characters. 0-108403  
 MgH rotational temp. and solar photospheric models 0-62099  
 Mg<sup>2+</sup>(H<sub>2</sub>O)<sub>n</sub> (n=1,2,4,6), FSGO-pair-pot. calcs. (*German*) 0-74278  
 MgHPO<sub>3</sub>·3H<sub>2</sub>O and MgDPO<sub>3</sub>·3D<sub>2</sub>O, IR absorpt. and Raman spectra, vibr. assignments 0-97257  
 Mg(LO)<sub>3</sub>·4H<sub>2</sub>O, crystal struct., unit cell, X-ray study 0-59447  
 Mg(NH<sub>4</sub>)<sub>6</sub>(ClO<sub>4</sub>)<sub>3</sub>, phase transition, group theoretical anal. 0-65218  
 Mg(NH<sub>4</sub>)<sub>2</sub>(SO<sub>4</sub>)<sub>6</sub>H<sub>2</sub>O:VO(H<sub>2</sub>O)<sub>2</sub><sup>2+</sup> proton ENDOR meas. used to determine hyperfine coupling tensors 0-66075  
 Mg(NH<sub>4</sub>)<sub>2</sub>(SeO<sub>4</sub>)<sub>6</sub>H<sub>2</sub>O:Mn<sup>2+</sup>, EPR spectra 0-100608  
 Mg(NO<sub>3</sub>)<sub>2</sub>-RNO<sub>3</sub> (R=Li, Na, K), thermogravimetric anal. of dehydration processes (*Japanese*) 0-66791  
 MgNb<sub>2</sub>O<sub>6</sub>, force fields rel. to cryst. struct. (*French*) 0-107104  
 MgO, adsorption of acetonitrile, IR and TPD study 0-70528  
 MgO, atomic C anal. by <sup>13</sup>C(d,p) method 0-108766  
 MgO, atomic C anal. by laserflash induced mass spectrometry 0-108767  
 MgO, bonding, pressure effects in lower mantle 0-72491  
 MgO coated detector for SEM backscatter to secondary electron conversion 0-68332  
 MgO coated moderators, slow positron form. 0-62796  
 MgO, cohesive and thermophysical props., role of three-body interactions 0-92477  
 MgO containing Fe<sup>3+</sup> and Cr<sup>3+</sup>, EPR spectra obtained at room temp. and 1200°C 0-68233  
 MgO, crack tip dislocations and dislocation-free zones 0-96533  
 MgO crystal, contact damage obs. by cathodoluminesc. 0-71728  
 MgO crystal, yield strength and dislocation mobility 0-93601  
 MgO crystal cathodoluminescence, SEM analysis 0-97349

## magnesium compounds continued

- MgO crystals, dipolar defects, thermally stimulated depolarisation 0-66101  
 MgO crystals, geometrical-statistical parameters of dislocation interactions with point obstacles 0-103341  
 MgO crystals, plastic deform. activation parameters, rel. between macroscopic and in-situ HVEM expts. 0-103355  
 MgO crystals, radiation damage influence on deform. in HVEM 0-103391  
 MgO, deformed, cathodolum. obs. by STEM 0-76088  
 MgO doped powder phosphors, photo- and thermostimulated luminesc. obs. (*Russian*) 0-66263  
 MgO, electron irradiation damage, cryst. defects 0-107320  
 MgO, electronic transition strengths, shock tube meas. 0-87183  
 MgO, exoelectron emission, mean energy, temp. depend. 0-76160  
 MgO, fracture and crack tip plastic zones, in situ obs. 0-108686  
 MgO, Franck-Condon factors rot. depend. 0-58319  
 MgO, heated on W, thermal anal. using mass spectrometric, technique, vapourisation behaviour 0-79932  
 MgO, high temperature prestrain effect on plastic props., dislocation struct. 0-79866  
 MgO, inelastic electron tunnelling spectroscopy of adsorbates, Al<sub>2</sub>O<sub>3</sub> comparison 0-88686  
 MgO, ion sputter cleaning in EM 0-101895  
 MgO, photoluminesc. during mechanical deform. 0-60665  
 MgO polycrystals, mech. props., 900-1150°C (*French*) 0-104374  
 MgO powder, surface area determ. by adsorpt. of stearic acid and pyridine 0-107636  
 MgO, reduction by C, kinetics and mechanism (*Russian*) 0-93743  
 MgO role in Al<sub>2</sub>O<sub>3</sub> sintering 0-81010  
 MgO, semisintered, shear strength at high press. 0-76308  
 MgO single cryst., impact wear chars. 0-76374  
 MgO single cryst., impact wear damage 0-76375  
 MgO, single cryst., tensile creep, stress induced dislocation structs. 0-96539  
 MgO single crystals, impurity effects on cationic cond. (*French*) 0-65286  
 MgO single crystals, surface atomic steps obs. by electron microscopy, dark- and bright-field techniques 0-84040  
 MgO single crystals, dislocation processes, obs. by HVEM in-situ deform. 0-103340  
 MgO, sintered, refractories, props. after testing at over 2000°C 0-104317  
 MgO sintered-ceramic separator plate development, Li-Al/LiCl-KCl/FeS battery applications 0-61321  
 MgO sintering activator, effect on α-Al<sub>2</sub>O<sub>3</sub> mineralisation, alumina heat treatment 0-89186  
 MgO, sintering by activating 3MgCO<sub>3</sub>·Mg(OH)<sub>2</sub>·3H<sub>2</sub>O 0-89183  
 MgO, smoke particles, size distrib. 0-104471  
 MgO solubility products in molten NaCl-KCl, potentiometric determ. 0-76488  
 MgO, subgrain boundaries form. obs. by TEM, diffusion coeff. determ. 0-79817  
 MgO, substrate for <sup>4</sup>He film growth, vap. press. meas. 0-70499  
 MgO, thermally stimulated exoelectron emission (*German*) 0-66404  
 MgO, vacancy-dislocation interaction energies, atomistic model calcs. 0-59513  
 MgO, XPS valence bandstruct. 0-89117  
 MgO(Li), polycryst., internal friction (*German*) 0-59577  
 MgO:Al, and nominally pure single crystal, thermally stimulated luminesc. rel. to temp., and EPR (*Russian*) 0-84789  
 MgO:Co<sup>2+</sup>, ESR linewidths of Co<sup>2+</sup> 0-80596  
 MgO:Co<sup>2+</sup>, electronic and impurity-induced Raman scatt. 0-100659  
 MgO:Co<sup>2+</sup>, weak dynamic Jahn-Teller coupling, neutron inelastic scatt. obs. 0-59934  
 MgO:Cr, high resolution far IR spectroscopy of: lower energy levels of Cr<sup>2+</sup> 0-80822  
 MgO:Cr<sup>2+</sup>, APR under applied stress 0-88865  
 MgO:Cr<sup>2+</sup>(Fe<sup>2+</sup>), reson. relax. time for impurity electrons and localised phonons interaction, appl. to thermal cond. 0-59590  
 MgO:Cr<sup>2+</sup>(Mn<sup>3+</sup>)(V<sup>3+</sup>), HF phonon spectroscopy using supercond. tunnel junctions 0-65178  
 MgO:Cr<sup>3+</sup>, emission and excitation spectra 0-93387  
 MgO:Cr<sup>3+</sup>, ODMR, octahedral and orthorhombic site symm. 0-71243  
 MgO:Cr<sup>3+</sup>, ODMR study, Cr<sup>3+</sup> ions in tetragonal symm. sites 0-88892  
 MgO:Cr<sup>3+</sup>, optical excitation transfer 0-97325  
 MgO:Fe<sup>2+</sup>, shock compressed absorpt. spectrum, appl. to Earth mantle 0-90039  
 MgO:Fe<sup>2+</sup>, point defect complex-edge dislocation interaction energies, atomistic calc. 0-107314  
 MgO:Fe<sup>3+</sup>, spin-lattice relax. time, meas. 0-66020  
 MgO:Fe<sup>3+</sup>, single cryst., exchange energy 0-96834  
 MgO:Li, mech. deformed crystals, imprinting of slip bands using Li impurities 0-59473  
 MgO:Mn<sup>2+</sup>, spin-lattice relax. time, meas. 0-66020  
 MgO:Mo catalyst, adsorpt. of propylene, oxidation reactions, surface structs., IR absorpt. spectra obs. 0-66868  
 MgO:nAl<sub>2</sub>O<sub>3</sub> spinel, plastic deformation at T<1000°C, slip systems 0-108505  
 MgO:Ni, heavily doped, defect characterisation, rel. to use as laser material 0-65000  
 MgO:Ni, tunable transition-metal-doped solid state lasers 0-58549  
 MgO:Ni<sup>2+</sup>, near IR luminesc. from isolated and exchange-coupled Ni<sup>2+</sup> ion pairs, temp. depend. 0-93382  
 MgO:V<sup>2+</sup>, Jahn-Teller system, zero-phonon line broadening due to non-radiative transitions 0-108258  
 MgO-Al<sub>2</sub>O<sub>3</sub>-P<sub>2</sub>O<sub>5</sub> system glass, heat treatment of aluminium metaphosphate influence on thermolum. 0-108285  
 MgO-Al<sub>2</sub>O<sub>3</sub>-SiO<sub>2</sub>, sintered, cordierite, mineralogy and props. 0-60827  
 MgO-CaO-FeO-Fe<sub>2</sub>O<sub>3</sub>-SiO<sub>2</sub>-Cr<sub>2</sub>O<sub>3</sub>-Al<sub>2</sub>O<sub>3</sub> spinel refractories, physicochem. prod. conditions 0-89185  
 MgO-CdO, interface, coincidence-site-lattice relations 0-103588  
 MgO-MgF<sub>2</sub>, multilayer stack selective mirror with high reflectivity (*French*) 0-64131  
 MgO-NaCl refractory clinkers, Cr containing, densification, thermal treatment and phase composition effect (*French*) 0-76219  
 MgO-NiO, STEM microanal., absorpt. effects 0-80902  
 MgO-P<sub>2</sub>O<sub>5</sub> glass, US velocity rel. to elastic props. 0-103425  
 MgO-P<sub>2</sub>O<sub>5</sub> glass, ESR of VO<sup>2+</sup> ions 0-100610  
 MgO-Pd metal-ceramic reaction, micro/macro obs. 0-66467  
 MgO-TiO<sub>2</sub>-Al<sub>2</sub>O<sub>3</sub>-SiO<sub>2</sub> glass, γ-irrad., struct. position of Ti, EPR study 0-84644  
 MgOH (MgCl), mol. dissoc. energies calc. by high temp. mass spectrometer 0-83514



**magnesium compounds continued**

- MgOH, struct. and electronic props., ab initio calcs. 0-74113  
 Mg(OH)<sub>2</sub>, sintering, IR spectra, X-ray anal. 0-66452  
 MgO·1.1 Al<sub>2</sub>O<sub>3</sub> spinel, high temp. deform., cryst. orientation effect 0-107263  
 MgRb<sub>2</sub>(SeO<sub>4</sub>)<sub>2</sub>·6H<sub>2</sub>O·Mn<sup>2+</sup>, EPR spectra 0-100608  
 MgS·Ce<sup>3+</sup> phosphors, emission and excitation spectra (*French*) 0-93380  
 MgSb<sub>2</sub>O<sub>6</sub>, force fields rel. to cryst. struct. (*French*) 0-107104  
 Mg·SiO<sub>2</sub>·SiO<sub>2</sub>, elec. and dielec. props. 400-900°C 0-104953  
 Mg·SiO<sub>2</sub>, <sup>18</sup>O self-diffusion expts., high-temp. creep implications 0-81870  
 Mg·SiO<sub>4</sub> crystals, dislocations configuration and cleavage steps dissoln. 0-107250  
 Mg·SiO<sub>4</sub>, forsterite, O<sub>2</sub> self-diffusion coeffs. 0-70457  
 Mg·SiO<sub>4</sub>, temp. in high-pressure shock state 0-72490  
 Mg·SiO<sub>4</sub>·Tb, sensitized TLD phosphor, photon energy dependence 0-78498  
 Mg·SiO<sub>4</sub>·Tb, thermolum. phosphor, photolum. and absorpt. spectra, thermolum. mechanisms 0-97321  
 MgSiP<sub>2</sub>, electronic struct., X-ray spectroscopic investigation 0-108300  
 MgTa<sub>2</sub>O<sub>6</sub>, force fields rel. to cryst. struct. (*French*) 0-107104  
 MgTeMoO<sub>6</sub>, prep., cryst. struct., and catalytic props. 0-108709  
 Mg<sub>2</sub>TiO<sub>4</sub>·Cu(Ni), ESR of Cu<sup>2+</sup> and Ni<sup>2+</sup> 0-97131  
 Mg<sub>2</sub>TiO<sub>4</sub>·MgFe<sub>2</sub>O<sub>4</sub> mixed system, spinel, selective sublattice dilution, percolation problem 0-103850  
 MgUO<sub>4</sub>, energy transfer, cryst. struct. and chemical composition effect 0-108248  
 MgXe excimer bands, emission intensities and excited-state densities meas. 0-92413  
 Mg<sub>0.75</sub>Zn<sub>0.25</sub>Fe<sub>2</sub>O<sub>4</sub>, ferrite, DC cond., dielec. props., lattice consts. 0-80272  
 Mg·Zn<sub>1-x</sub>Te, band struct. refl. spectra meas. 0-80813  
 Mg·Zn<sub>1-x</sub>Te, comp. profile, second derivative wavelength modulation 0-103967  
 Mn<sub>1-x</sub>Mg<sub>x</sub>Se, mag. and struct. phase transitions, mag. susceptibility and X-ray diff. study 0-71022  
 Na<sub>2</sub>O·MgO·Al<sub>2</sub>O<sub>3</sub>, β"-alumina, high-resolution electron microscopy 0-75208  
 Na<sub>2</sub>O·MgO·Al<sub>2</sub>O<sub>3</sub>, ionic cond. 0-107480  
 Na<sub>2</sub>O·MgO·B<sub>2</sub>O<sub>3</sub>·Cu<sup>2+</sup>, micro-inhomogeneities, EPR and Raman study 0-84080  
 Na<sub>2</sub>O·MgO·SiO<sub>2</sub> glasses, elec. cond., room temp. to 450°C 0-107473  
 NiO·Cr<sub>2</sub>O<sub>3</sub>·MgSiO<sub>3</sub> methanation catalyst, S-resistant, IR and Raman spectra 0-93290  
 NiO·MgO solid solns., surface comp. study by XPS 0-104035  
 Pb<sub>2</sub>MgNb<sub>2</sub>O<sub>6</sub>, photoelectric states in real time spatial light modulators, photorefractive effect 0-80676  
 Pb(Z,Ti,Mg,W)O<sub>3</sub>, low-Q ceramics, props. and transducer appl. 0-75944  
 Si<sub>3</sub>N<sub>4</sub>·MgO, hot-pressed, linear thermal expansion rel. to MgO content 0-70430  
 SiO<sub>2</sub>·Al<sub>2</sub>O<sub>3</sub>·MgO·TiO<sub>2</sub> devitrificates, microstruct. and props. (*Polish*) 0-70141  
 SiO<sub>2</sub>·MgO porous catalysts, EPMA quantitative anal., new correction calc. method, modified ZAF method (*Japanese*) 0-93822  
 SiO<sub>2</sub>·MgO·BaO ceramic, steatite, glass-ceramics technology appl. 0-104097  
 SiO<sub>2</sub>·Na<sub>2</sub>O·CaO·MgO float glass, surface SnO<sub>2</sub> distrib., ellipsometry and XPS study 0-84346  
 Ti<sub>2</sub>O<sub>3</sub>·MgTi<sub>2</sub>O<sub>3</sub>, solid solubility, X-ray phase and optical microscopic exam. 0-59657  
 (Zn,Mg)<sub>2</sub>(PO<sub>3</sub>)<sub>2</sub>·Mn<sup>2+</sup>, cathodoluminescence obs. 0-71492  
 ZnS·MgF<sub>2</sub> mirror, dielectric, Rayleigh scatt. at 441.6 nm 0-97367

**magnetic aftereffect**

- automatic demagnetisation and measurement system for time decreasing permeability meas. 0-62696  
 ferromagnetic materials, review 0-88830  
 Permalloy-Mn film, diffusion aftereffect causing mag. state change (*Russian*) 0-103860  
 rare earth-Ag alloy, amorphous, model calcs., of mag. props. 0-84616  
 (Co,Fe)<sub>80</sub>B<sub>20</sub> glass, induced anisotropy and time changes of permeability 0-75815  
 Co<sub>70</sub>Fe<sub>40</sub>Si<sub>10</sub>B<sub>10</sub>, amorphous, mag. aftereffect spectra and annealing props. 0-88831  
 Dy(Co,Ni)<sub>2</sub>, intrinsic mag. aftereffect meas., domain wall motion 0-71121  
 α-Fe, cold work aftereffects 0-88830  
 Fe, mag. aftereffect meas., phenomenological description 0-88835  
 α-Fe, neutron irradiated, mobile C atom trapping, anelastic and magnetic relaxations 0-100306  
 Fe, pure and doped, electron irradi., mag. aftereffect 0-88838  
 Fe-Al(Ti), O containing, mag. aftereffect and disaccommodation meas., time depend., activation energy, and ageing props. 0-88836  
 Fe-Al(24.3 at.%)C alloy, magnetic permeability disaccommodation, 260-400K 0-93144  
 Fe-B, amorphous, mag. aftereffect, initial susceptibility time depend. 0-88829  
 Fe-B amorphous alloys, mag. aftereffect 0-65970  
 Fe-Co-Si(B), amorphous ferromagnet, mag. after effect on soft mag. props. 0-84626  
 Fe-Ni(Al), mag. aftereffect meas., phenomenological description 0-88835  
 Fe-Pd, magnetic after-effect of H isotopes 0-75817  
 Fe-Si (3 wt.%), power losses at extremely low freqs. 0-88815  
 (Fe-Ni-Mo)<sub>80</sub>(P-B)<sub>20</sub>, amorphous, mag. aftereffects and struct. instabilities 0-88833  
 Fe<sub>80</sub>B<sub>20</sub>, amorphous, mag. permeability aftereffect during annealing 0-88834  
 (Fe<sub>0.5</sub>Co<sub>0.5</sub>)<sub>75</sub>Si<sub>8</sub>B<sub>14</sub> amorphous ribbon, anomalous mag. aftereffect 0-100602  
 Fe<sub>40</sub>Ni<sub>40</sub>B<sub>20</sub> and Fe<sub>40</sub>Ni<sub>40</sub>P<sub>14</sub>B<sub>6</sub>, amorphous, mag. aftereffect spectra and annealing props. 0-88831  
 Fe<sub>40</sub>Ni<sub>40</sub>P<sub>14</sub>B<sub>6</sub>, amorphous, mag. permeability aftereffect during annealing 0-88834  
 Fe<sub>2</sub>O<sub>3</sub>, magnetite, mag. aftereffects, 4.35K 0-80571  
 Ni, diffusion and orientation aftereffects 0-88830  
 Ni-Fe, orientation aftereffect 0-88830  
 Ni-Fe, power losses at extremely low freqs. 0-88815  
 Ni-Fe, thermal fluctuation aftereffect meas. by pulse field method 0-88837  
 Ni<sub>2</sub>Fe, disaccommodation meas. after low temp. electron and neutron irradi. 0-88832  
 Ni<sub>88</sub>M<sub>2</sub>, M=impurity metal, formation of MH(D)-complexes 0-65236

**magnetic aftereffect continued**

- NiZn ferrites, V<sub>2</sub>O<sub>5</sub> induced mag. aftereffects 0-60379  
 R<sub>2</sub>In, R<sub>2</sub>In, R=Co, Tb, Dy, Ho, Nd, mag. props. 0-108009  
 SmCo<sub>5</sub>, sintered, mag. after-effect, expt. and model 0-75816  
 Tb-Fe amorphous thin films, magnetic after-effect, Kerr magneto-optic effect obs. 0-97123
- magnetic amplifiers**  
 No entries
- magnetic anisotropy**  
*see also induced anisotropy (magnetic)*  
 actinide mononitrides, anomalous mag. props., planar coupling theory 0-60245  
 aluminium copper tetrahalides, exchange, mag. anisotropy, and spin diffusion contribs. to EPR linewidth 0-80597  
 alloys, magnetic anisotropy, influence of local symmetry (*Russian*) 0-93109  
 amorphous magnet, random anisotropy axis model in the infinite-range limit 0-88761  
 amorphous magnets, random anisotropy axes, high-temp. expansion for sp. ht. 0-71041  
 amorphous thin films, struct. and mag. props., review 0-93148  
 anisotropic ferromagnet, one-dimensional Landau-Lifshits eqn. multi-soliton solutions (*Russian*) 0-71014  
 anisotropic Heisenberg chain, nonlinear excitations 0-70927  
 anisotropic spin-phonon coupling model, exact solutions (*Russian*) 0-100590  
 antiferromagnet, magnetic phases, spin configurations in external field 0-70955  
 antiferromagnet, two-dimensional, with easy-plane anisotropy, mag. excitations and two-magnon Raman scatt. 0-65839  
 antiferromagnet, two-sublattice Neel-type, stable spin configurations, external mag. field and single-ion orthorhombic anisotropy effects 0-60249  
 antiferromagnets, random, theory of mag. excitations, antiferromag. reson. 0-97146  
 cyclohexyl ammonium copper chloride, one dimensional spin 1/2 ferromag., mag. props. 0-71000  
 diethylammonium copper tetrabromide, mag. struct., NMR meas. 0-71192  
 dimethylammonium copper tetrabromide, quasi two-dimensional antiferromag., mag. behaviour 0-97098  
 dimethylammonium copper tetrachloride, ferromag., quasi two-dimensional, ordering temp., press. depend. 0-84601  
 dimethylammonium copper tetrachloride-tetrabromide mixed cryst., mag. transition 0-65874  
 dimethylammonium manganese trichloride: Cd(Cu), impurities in quasi-one-dimens. Heisenberg systems, anisotropy effect 0-80502  
 electrical steel sheet, determ. method and laboratory tests (*Polish*) 0-97071  
 exchange interactions, anisotropic, effect on singlet ground state system 0-65852  
 ferrite, hexagonal, with M, W and Y structures containing Fe<sup>2+</sup> and Fe<sup>3+</sup> mag. ions, saturation moment and anisotropy 0-71009  
 ferro- and ferrimagnets, anisotropy energy density 0-88742  
 ferromagnet, anisotropic, influence of spatially varying field on phase transitions 0-60339  
 ferromagnet, domain wall mobility, damping, dipole-dipole interaction 0-93140  
 ferromagnet, easy-plane, temp. and field depend., classical model 0-71008  
 ferromagnet, effects of biquadratic exchange and uniaxial anisotropy on T<sub>c</sub> 0-60329  
 ferromagnet, exact integration of nonlinear Landau-Lifshitz equation 0-80495  
 ferromagnet, one-dimens., algebraic soliton in mag. field directed along anisotropy axis 0-75785  
 ferromagnet, uniaxial two-sublattice, anisotropic, thermodynamic and mag. props. 0-65866  
 ferromagnet with easy-plane anisotropy, HF magnon energies, kinematic consistency 0-93097  
 ferromagnetic crystals, uniaxial anisotropy, first order magnetisation processes theory 0-60242  
 ferromagnetic Ising model, spin-one three dimensional, single-ion anisotropy, crit. behaviour 0-80540  
 ferromagnetic material, polycryst., magnetic texture anal. 0-108002  
 ferromagnetic metal, uniaxial, anisotropic spin fluctuations and anisotropic band struct. effects on resist. near T<sub>c</sub> 0-65543  
 ferromagnetic thin films parametric oscill. with biaxial anisotropy 0-103861  
 film, vertically suspended, torque curve meas., first-order calc. anal. 0-86354  
 film, with perpendicular anisotropy, stripe domain struct., theory (*Russian*) 0-65973  
 films, ferromagnetic, perpendicularly magnetised, surface and vol. magnetoelastic waves (*Russian*) 0-93151  
 garnet epitaxial film, stress induced magnetocrystalline anisotropy 0-71013  
 garnet epitaxial films, easy magnetisation axis orientation 0-60383  
 garnet films with orthorhombic anisotropy, domain wall motion 0-80580  
 garnets, large growth-induced anisotropy to preferential occupation of Fe sites 0-75754  
 garnets, superexchange operator and cryst. field interactions 0-59931  
 Heisenberg antiferromagnet, anisotropic, finite cell calcs. 0-60164  
 Heisenberg antiferromagnet, one-dimens., impure, mag. susceptibility 0-60168  
 Heisenberg ferromagnet, anisotropic, collective Green's function, dynamical RPA 0-70925  
 Heisenberg model, anisotropic spin system, S=1/2 frustration effects 0-65763  
 Ising chain, spin-1, sp. ht. in presence of impurities and mag. field 0-93128  
 Ising model, spin-one, bilinear and biquadratic interactions, phase diagram 0-75772  
 isopermalloy, permeability stability calc. rel. to texture (*Chinese*) 0-65959  
 linear electric field effects 0-65854  
 magnetic ordering, anisotropic, via combined spin and orbital exchange scatt. of conduction electrons 0-65863  
 magnetostriiction in terms of hexagonal and cubic harmonics up to degree 6 0-88856  
 manganese stearate, two-dimensional mag. struct. 0-108040



**magnetic anisotropy continued**

- metallic glass, micromag. calcs. and props. 0-80501  
 metallic magnets investigation, present state (*Polish*) 0-107987  
 Metglas 2605 ribbon, saturation magnetostriction meas. by small-angle magnetisation rot. 0-60391  
 Metglas 2826 ribbon, saturation magnetostriction meas. by small-angle magnetisation rot. 0-60391  
 neopentane adsorbed on graphite, quasi two-dimens. fluid, NMR 0-102525  
 NiWO<sub>4</sub>, antiferromag., low symmetry exhibited during spin-flop phase transition 0-60263  
 orthoferrite cryst. films, local coercivity of domains boundaries (*Russian*) 0-80578  
 paramagnet, anisotropic, spin dynamics, exchange-bond dilution effects 0-88763  
 Permalloy RF sputtered films, O effects in mag. and elec. props. 0-100603  
 Permalloy thin films, break-cross-tie wall energy 0-88842  
 Permalloy-Cu(Al) two-layer films, mag. anisotropy, grain boundary diffusion (*Russian*) 0-71122  
 Permalloy-Mn film, diffusion aftereffect causing mag. state change (*Russian*) 0-103860  
 phonon-induced temp. dependences of magnetocrystalline anisotropy consts. 0-65858  
 polycrystalline and amorphous strips, magnetostriction. consts. determ. method 0-86355  
 polycrystalline ferrites, anisotropy const. meas. 0-97090  
 porous anisotropic magnets, approach to mag. saturation 0-93146  
 pyridinium manganese chloride, anhydrous, quasi one-dimensional mag. behaviour, heat capacity meas. 0-80549  
 pyridinium nickel chloride, anhydrous, quasi one-dimensional mag. behaviour, heat capacity meas. 0-80549  
 quasi-two-dimensional planar spin system, mag. transition 0-65951  
 random anisotropy model in Ising model, Monte Carlo simulation 0-80546  
 rare earth alloys, amorphous, with random anisotropy axes, spin excitations in paramag. phase 0-80476  
 rare earth amorphous alloys, random anisotropy magnetism 0-65853  
 rare earth iron garnets, anisotropic, mag. props., high field and low temp. 0-75801  
 rare earth iron intermetallics, RFe<sub>2</sub>, magnetostrictive, book contrib. 0-75838  
 rare earth orthoferrites, hyperfine interaction anisotropy, NMR study (*Russian*) 0-66052  
 rare earth orthoferrites, mag. anisotropy in cryst. field approx. 0-60241  
 rare earth orthoferrites, Raman scatt. from magnons, anisotropy consts. determ. 0-66178  
 rare earth titanium oxides, RTiO<sub>3</sub> type, bulk mag. and struct. props., ferrimag. order 0-107993  
 rare earth-Ag alloys, amorphous, model calcs., of mag. props. 0-84616  
 spin glass materials, mag. field dependence of susceptibility peak 0-103840  
 spin-1/2 cubic lattice, with anisotropic exchange, configs. 0-65926  
 steel, alloy, corrugated texture perfection, mag. anal. 0-88745  
 surface states, theory, in spin wave resonance, review 0-84654  
 thermoelectret and magnoelectret states, diamag. anisotropy 0-97053  
 TMCC, linear antiferromag., mag. phase diagram, expt. and theoretical study 0-71038  
 torque method, vertically suspended specimen, field intensity effect 0-86353  
 transition metals, 3d, ferromag. props., book contrib. 0-75724  
 uniaxial ferromagnetic with intrinsic mag. field, domain struct. 0-93141  
 ytterbium ethyl sulphate, crystal field effects on mag. and hyperfine props. of Yb<sup>3+</sup> 0-97101  
 Au, resonant and nonresonant conduction-electron-spin transmission 0-75857  
 AuMn, mag. struct., phase transition, and magnon spectrum, random anisotropy effects 0-88722  
 Ba<sub>2</sub>Co<sub>0.65</sub>Fe<sub>0.35</sub><sup>2+</sup>Fe<sub>28</sub><sup>3+</sup>O<sub>46</sub>, temp.-mag. field phase diagram, torque method 0-60276  
 BaFe<sub>1-2x</sub>M<sub>x</sub>Ti<sub>2</sub>O<sub>9</sub> (M=Co, Ni, Zn), mag. props. determ. 0-75759  
 BaFe<sub>2</sub>O<sub>9</sub>, Ca<sup>2+</sup> substitution effect on hexaferrite lattice and mag. props. 0-60243  
 Ba<sub>2</sub>Zn<sub>2-2(x+y)</sub>Cu<sub>2</sub>Cd<sub>2</sub>Fe<sub>2</sub>O<sub>22</sub>, mag. props. and Mossbauer spectrum 0-75765  
 BaZn<sub>2</sub>Fe<sub>16-x</sub>M<sub>x</sub>O<sub>27</sub> (M=Al, Ga, In, Sc), mag. props. and Mossbauer effect 0-75766  
 Ba<sub>2</sub>Zn<sub>2</sub>Fe<sub>24</sub>O<sub>41</sub>, ferromag. reson., low power nonlinear effects 0-75861  
 Ca ferrite, composition and mag. props., anisotropy field, magnetisation 0-71109  
 Ca<sub>3</sub>Mn<sub>2</sub>Ge<sub>2</sub>O<sub>12</sub> garnet, metamagnetic transition, high anisotropy peculiarities (*Russian*) 0-60274  
 Ce monopnictides, anomalous mag. props., planar coupling theory 0-60245  
 Ce pnictides, unusual anisotropy mechanism due to virtual valence fluctuation 0-96828  
 CeB<sub>6</sub>, magnetostriction, US absorpt. and thermal expansion 0-66004  
 Co complex, Co(II)(1,2,4-triazole)<sub>2</sub>(NCS)<sub>2</sub> quasi two-dimens. canted S=1/2 antiferromag. 0-70976  
 Co film, mag. anisotropy study using NMR spin echo method 0-60384  
 Co-CoO films, evaporated, exchange anisotropy 0-88841  
 Co-Fe, dil., magnetocrystalline anisotropy anomalous temp. depend. 0-71007  
 Co-Fe, soft mag. props. rel. to metallurgical aspects 0-88810  
 Co-Gd-Mo films, sputtered, O effects on mag. props. during annealing 0-89374  
 Co-P, amorphous, domain struct., mag. anisotropy origin 0-80554  
 Co-P films with various preferred orientations, mag. props. 0-100604  
 Co-Si-B, amorphous ribbon, saturation magnetostriction meas. by small-angle magnetisation rot. 0-60391  
 CoCr<sub>2</sub>S<sub>4</sub>, ferrimag. semicond., magnetocrystalline anisotropy 0-71012  
 CoGa<sub>1-x</sub> alloys, cluster spin glass, host and impurity NMR and AC susceptibility 0-71194  
 (Co<sub>1-x</sub>Mn<sub>x</sub>)<sub>2</sub>B, magnetocrystalline anisotropy meas., 4.2-300K 0-71006  
 Co<sub>2</sub>(Ni<sub>0.5</sub>Cu<sub>0.5</sub>)<sub>1-x</sub>Fe<sub>2</sub>O<sub>4</sub> ferrite, relation between elec. cond. and mag. anisotropy 0-75548  
 CoP, and CoNiP, cylindrical amorphous electrodeposited layers, mag. props., torsion influence 0-88848  
 CoTiO<sub>3</sub>, antiferromag., mag. anisotropy, magnetisation meas. 0-65856  
 Cr, mag. struct., phase transition, and magnon spectrum, random anisotropy effects 0-88722

**magnetic anisotropy continued**

- Cr-Fe, dil., spin correlations and neutron scatt. near crit. conc., theory 0-60327  
 CsMn<sub>1-x</sub>Cu<sub>x</sub>Cl<sub>2</sub>·2H<sub>2</sub>O, impurities in quasi-one-dimens. Heisenberg systems, anisotropy effect 0-80502  
 CsMnF<sub>3</sub>, mag. struct., phase transition, and magnon spectrum, random anisotropy effects 0-88722  
 CsNiF<sub>3</sub>, anisotropic Heisenberg chain, nonlinear excitations 0-70927  
 CsNiF<sub>3</sub>, quasi-one-dimensional ferromagnet, subthreshold parallel pumping of magnons 0-75745  
 Cu ferrite films, Mn-, Ni- and Al-substituted, LPE growth 0-96752  
 Cu, resonant and nonresonant conduction-electron-spin transmission 0-75857  
 Cu:Co precipitates, mag. anisotropy, precipitate shape, coercive force 0-80500  
 Cu-Mn alloy spin glass, macroscopic mag. anisotropy, transverse susceptibility and zero field NMR enhancement 0-80525  
 Cu-Ni films, compositionally modulated, magnetic anisotropy, magnetisation curves 0-88840  
 CuCr(Fe)(Mn), dil., anisotropic hyperfine coupling, NMR study 0-65784  
 CuMn, hysteresis, spin orbit scattering effect on anisotropy in spin glass state 0-71095  
 Cu<sub>0.88</sub>Mn<sub>0.12</sub>, hysteresis loop development 0-65922  
 DyCo<sub>3</sub>, noncollinear mag. struct. appearance in mag. fields, magnetostriction meas. (*Russian*) 0-100607  
 DyFe<sub>7</sub>, domain structures and anisotropy constant. 0-93136  
 DyNi, crystal, basal plane anisotropy, torque meas. 0-65857  
 DyTb<sub>1-x</sub>Fe<sub>x</sub>, single cryst., torque meas. 0-65877  
 ErIG, high-field magnetisation, low temp. mag. anisotropy 0-75802  
 EuIG:Ga(Al), pure and doped, mag. anisotropy, magnetisation meas. 0-60240  
 (EuLu)<sub>3</sub>(FeAl)<sub>2</sub>O<sub>12</sub>, film epitaxial growth on Gd<sub>3</sub>GaO<sub>12</sub> substrate, mag. props. 0-65402  
 Fe group, mol. Jahn-Teller reson. states as possible antecedents to magnetism 0-75701  
 Fe pole pieces, in electromagnets, mag. anisotropy effect on mag. field homogeneity (*Japanese*) 0-93111  
 Fe, whisker single crystals, ferromag. reson. and surface anisotropy 0-71187  
 Fe-Co-Ni Perminvar, mag. props. singularities in region of mag. anisotropy (*Russian*) 0-84614  
 Fe-Cr-Co alloy, coercive force mechanism 0-71103  
 Fe-Ni, secondary recrystn. and mag. props. 0-89247  
 Fe-Ni (308-44.1 at.%) Invar alloys, anomalous mag. anisotropy and thermal expansion 0-75755  
 Fe-Ni alloy type YuNDK25B, anomalous magnetocaloric effect 0-60278  
 Fe-Pt Invar alloys, magnetocrystalline anisotropy const. determ. 0-65861  
 Fe-W-Cr-Mo system, mag. and mech. props. rel. to production methods (*Japanese*) 0-71107  
 Fe-Zn alloys, coercive force anisotropy after cold plastic deform. (*Bulgarian*) 0-75809  
 Fe<sub>0.5</sub>Co<sub>0.5-x</sub>Cr<sub>x</sub> films, vacuum-deposited cryst. and mag. struct. (*Russian*) 0-93081  
 (Fe<sub>1-x</sub>Co<sub>x</sub>)<sub>78</sub>Si<sub>10</sub>B<sub>12</sub>, amorphous, roll mag. anisotropy 0-75757  
 (Fe<sub>1-x</sub>Co<sub>x</sub>)<sub>78</sub>Si<sub>10</sub>B<sub>14</sub>, amorphous, saturation magnetostriction, strain modulated FMR obs. 0-75863  
 Fe<sub>40</sub>Ni<sub>38</sub>Mo<sub>2</sub>B<sub>18</sub>, amorphous, mag. anisotropy, Mossbauer study 0-65864  
 Fe<sub>40</sub>Ni<sub>38</sub>Mo<sub>2</sub>B<sub>18</sub>, amorphous, reversible enhancement of mag. directional ordering rate 0-103829  
 Fe<sub>40</sub>Ni<sub>40</sub>P<sub>14</sub>B<sub>6</sub> amorphous ribbon, mag. domains and anisotropy distrib. 0-108029  
 (Fe<sub>1-x</sub>Ni<sub>x</sub>)<sub>78</sub>Si<sub>10</sub>B<sub>12</sub> amorphous alloys, cold rolled and as-quenched, mag. anisotropy 0-97089  
 Fe<sub>2</sub>O<sub>4</sub> ferrofluids, spin glass behaviour 0-71120  
 Fe<sub>2</sub>O<sub>4</sub>, magnetocrystalline spin glass, anomalies in magnetostriction and elastic constants 0-60244  
 Fe<sub>2</sub>TiO<sub>6</sub>, anisotropic spin glass type behaviour 0-60296  
 Fe<sub>3-x</sub>Ti<sub>x</sub>O<sub>4</sub>, spin glass behaviour, susceptibility and hysteresis meas. 0-65917  
 Fe<sub>1-x</sub>Zn<sub>x</sub>F<sub>2</sub>, dil. antiferromag., electronic and mag. props., Raman scatt. and optical absorpt. study 0-108207  
 Fe<sub>1-x</sub>Zn<sub>x</sub>F<sub>2</sub>, electronic Raman scatt., mag. anisotropy 0-66184  
 (Gd,Tm,Y)<sub>3</sub>(Fe,Ga)<sub>2</sub>O<sub>12</sub> LPE garnet thin films, magnetocrystalline anisotropy 0-93147  
 Gd, magnetic crystalline anisotropy, Fermi level, electronic density of states 0-84596  
 Gd-Al(Cu)(Ga)(Ni)(Pd)(Rh) alloys, amorphous, mag. and elec. props. 0-80499  
 Gd-Ce(Eu)(Yb), magnetocrystalline anisotropy, magnetisation and torque curve meas. 0-65859  
 Gd-Co, amorphous films, mag. props. ferromag. reson. meas., 20-520°C (*Russian*) 0-97144  
 Gd-Co amorphous films, mag. struct., mag. bubbles, electron diff. study (*Chinese*) 0-71126  
 Gd-Co based amorphous sputtered films, microstruct. variability and mag. anisotropy, implanted ion effects 0-88459  
 Gd-Co(Ni)(Cu)(Rh)(Ru)(Pd)(Ga), amorphous, mag. props. and ferromag. reson. 0-75862  
 Gd-Fe amorphous films, stress contrib. to perpendicular anisotropy 0-75819  
 (Gd<sub>0.1</sub>-<sub>0.9</sub>)<sub>1-x</sub>Ar<sub>x</sub> amorphous films, effective anisotropy field, ferromag. reson. obs. 0-71123  
 GdCo<sub>5</sub>Ni<sub>5-5x</sub>, intrinsic coercivity, anisotropy, exchange and cryst. field interactions 0-75806  
 GdIG, local mag. anisotropy in stress field of single dislocation 0-88744  
 GdNi, single cryst., magnetocryst. anisotropy 0-88746  
 Gd<sub>70</sub>Tb<sub>30</sub>, magnetisation, AC susceptibility and microwave absorption meas. 0-60221  
 Ho,Tb<sub>1-x</sub>Co<sub>x</sub> laval phase compounds, elastic props., temp. and magnetic field dependence 0-60393  
 (Ho<sub>0.98</sub>Tb<sub>0.02</sub>Dy<sub>0.22</sub>)Fe<sub>2</sub>, microwave mag. props. 0-65860  
 K<sub>2</sub>CuF<sub>4</sub>, layered spin system, planar rotator symmetry, phase transition 0-65951  
 K<sub>2</sub>FeF<sub>4</sub>, antiferromagnet, two-dimensional, mag. excitations 0-80492  
 La ferrite, composition and mag. props., anisotropy field, magnetisation 0-71109  
 Li ferrites, porous, porosity effect on saturation of magnetisation 0-108036  
 Li<sub>2</sub>Fe<sub>2-5</sub>-Cr<sub>2</sub>O<sub>4</sub> press. depend. of anisotropy consts. 0-65865  
 LiTmF<sub>4</sub>, van-Vleck paramagnet, giant magnetostriction (*Russian*) 0-103872



**magnetic anisotropy continued**

- LuCrO<sub>3</sub>:Er<sup>3+</sup>, doping effect on <sup>53</sup>Cr NMR in domain walls 0-71219  
 Mg<sub>2</sub>Fe<sub>1-x</sub>O<sub>4</sub> crystals, first mag. anisotropy const., 7-295 K 0-65855  
 Mn(Br<sub>1-x</sub>Cl<sub>x</sub>)<sub>2</sub>·4H<sub>2</sub>O, antiferromagnetism, controllable anisotropy 0-93116  
 Mn<sub>2</sub>N, mag. struct. non-collinearity, neutron diffr. obs. 0-65796  
 MnO:Mn<sub>2</sub>O<sub>4</sub>, mag. props., susceptibility and magnetisation meas. 0-65824  
 MnSb, magnetic losses, ferromagnetic resonance and antiresonance 0-100618  
 MnZn ferrite, initial mag. permeability rel. to mag. anisotropy 0-80557  
 MnZn ferrous ferrite, initial mag. permeability second-order magnetocrystalline anisotropy influence 0-88820  
 MnZn ferrous ferrites, mag. permeability stress depend. 0-88822  
 MoS<sub>2</sub>, prep. and mag. props. (*French*) 0-93072  
 NdCo<sub>2</sub>, magnetocrystalline anisotropic props., torque meas. 0-108003  
 Ni, anisotropic magnetisation meas., 4-250 K 0-65862  
 Ni films, electronic struct. calc., effects of chemisorption; contact pot. and surface magnetisation 0-103734  
 Ni, stress induced crossover effect near Curie point (*German*) 0-103874  
 Ni-Fe, electronic struct. calc., effects of chemisorption; contact pot. and surface magnetisation 0-103734  
 Ni-Fe, soft mag. props. rel. to metallurgical aspects 0-88810  
 Ni-Ru ( $\leq 4$  at.%), influence of alloying on mag. anisotropy 0-71010  
 Ni<sub>1-x</sub>Cd<sub>x</sub>Fe<sub>2</sub>O<sub>4</sub>, mag. props. rel. to ionic struct. 0-75756  
 Ni<sub>2</sub>Co<sub>1-x</sub>Cl<sub>2</sub>·6H<sub>2</sub>O, mixed uniaxial planar antiferromag., magnetisation process 0-88788  
 NiFe, magnetising energy, anisotropic effects 0-88743  
 NiFe thin films, magnetoresistance, quasi-static characts. 0-107766  
 Ni<sub>2</sub>Fe, magnetocryst. anisotropy, annealing temp. depend. 0-103828  
 NiFe<sub>2</sub>O<sub>4</sub>, ferrite, mag. anisotropy compensation under neutron irradi. 0-75807  
 NiTiO<sub>3</sub>, antiferromag., mag. anisotropy, magnetisation meas. 0-65856  
 Ni<sub>0.85</sub>Zn<sub>0.15</sub>Fe<sub>2</sub>O<sub>4</sub>, ferrite, mag. anisotropy compensation under neutron irradi. 0-75807  
 Ni<sub>1-x</sub>Zn<sub>x</sub>Fe<sub>2</sub>O<sub>4</sub>, polycryst., domain wall energy rel. to anisotropy 0-71090  
 Pd-Fe, magnetic anisotropy near Curie point, quasi domain struct. (*Russian*) 0-65867  
 PrCo<sub>2-x</sub>, high field first order transitions, role of K<sub>2</sub> anisotropy const. 0-65879  
 PrFe<sub>2</sub>, Laves phase, mag. props., Mossbauer spectra, crystalline field mag. anisotropy 0-65851  
 Pt-Fe alloy, ordered, T-c phase diagram, antiferro- and ferromagnetism (*Russian*) 0-65871  
 Pt-Fe(Co)(Mn), dil., skew scatt. Hall effect, magnetoresist. and mag. anisotropy, orbital magnetism of impurity 0-70678  
 Rb<sub>2</sub>CrCl<sub>4</sub>, planar ferromag., spin waves 0-65835  
 Rb<sub>2</sub>FeF<sub>4</sub>, antiferromagnet, two-dimensional, mag. excitations 0-80492  
 (SN), supercond. polymer, mag. props. meas. 0-107953  
 SmCo<sub>5</sub>, mag. domains structure rel. to crystal defects, electron microscopy 0-103856  
 SmCo<sub>5</sub> permanent magnets, crystal texture effects on props. 0-100600  
 (SmLu)<sub>3</sub>(FeAl)<sub>5</sub>O<sub>12</sub>, film epitaxial growth on Gd<sub>3</sub>Ga<sub>5</sub>O<sub>12</sub> substrate, mag. props. lattice mismatch 0-65402  
 Sm<sub>0.4</sub>Y<sub>0.6</sub>Fe<sub>3</sub>Ga<sub>5</sub>O<sub>12</sub> epitaxial films, uniaxial mag. anisotropy, ferrimag. reson. study 0-80577  
 (SnBrO<sub>4</sub>)<sub>2</sub>, 0-107953  
 Sr<sub>2</sub>(Co<sub>1-x</sub>M<sub>x</sub>)<sub>17</sub>, M=Mn, Ti, Zr, powders, influence of substitutes on mag. props. 0-100601  
 SrCoO<sub>3-x</sub>, mag. and neutron diffr. study 0-65805  
 SrFe<sub>2</sub>O<sub>7</sub>, Ca<sup>2+</sup> additives effect on hexaferrite lattice and mag. props. 0-60243  
 TMMC, antiferromagnetic chain, 3-D ordering temp. controlled by solitons and defects, mag. field depend. 0-60275  
 Tb, magnetisation, AC susceptibility and microwave absorption meas. 0-60221  
 TbCo<sub>2</sub>, magnetocrystalline anisotropy and spontaneous magnetostriction 0-75831  
 TbCo<sub>5</sub>, sublattice magnetisation, temp. depend., neutron diffr. anal. (*Russian*) 0-103815  
 (Tb<sub>1-x</sub>Gd<sub>x</sub>)<sub>2</sub>Co, intermetallic cpd. mag. props., phase transform, and mag. hysteresis (*Russian*) 0-93113  
 UFe<sub>2</sub>, giant magnetoelastic deform. of cryst. struct. mag. props. (*Russian*) 0-93159  
 YCo<sub>3</sub> amorphous films, <sup>59</sup>Co spin echo study 0-80636  
 YCo<sub>3</sub>, uniaxial intermetallic, large magnetisation anisotropy 0-71011  
 YCrO<sub>3</sub>, bubble domain struct. temp. depend. 0-71137  
 Y<sub>2</sub>Fe<sub>3-x</sub>Co<sub>x</sub>Si<sub>2</sub>O<sub>12</sub>, spin reorientation, NMR and ferromag. reson. meas. 0-65890  
 YFeO<sub>3</sub>, mag. anisotropy in cryst. field approx. 0-60241  
 YGdG, with various domain wall orientations, natural spin reson. 0-66040  
 YIG: Si single crystals, mag. props. 0-107981  
 YIG-La(Ga) films, ferromagnetic resonance, ion implantation effect 0-97145  
 YIG:Sm<sup>3+</sup>, mag. anisotropy, effect of Sm<sup>3+</sup> ferromag. reson. study 0-80615  
 Y<sub>3-x</sub>La<sub>x</sub>Fe<sub>2</sub>O<sub>12</sub>, mag. props. rel. to ionic struct. 0-75756  
 Y<sub>1-x</sub>R<sub>x</sub>Co<sub>5</sub>, R=Gd,Tb,Nd, ferrimag., magnetisation, exchange interactions, mag. anisotropy 0-80565  
 (YSmLuCa)<sub>3</sub>(FeGe)<sub>5</sub>O<sub>12</sub>, epitaxial films, LPE grown, annealing effects on mag. anisotropy 0-66548  
 Zr(Fe<sub>1-x</sub>Al<sub>x</sub>)<sub>2</sub>, Curie temp., magnetisation, and cryst. struct., conc. depend. 0-75730

**magnetic annealing**

- see also induced anisotropy (magnetic)  
 ferromagnetic single crystal, mag. anisotropy induced by cold rolling (*Russian*) 0-84595  
 Permalloy-Cu(Al) two-layer films, mag. anisotropy, grain boundary diffusion (*Russian*) 0-71122  
 Co-P, electrodeposited amorphous alloys with high permeability, thermal treatment with and without field 0-89372  
 Co-Pt, ordering, study using X-ray scatt. (*Russian*) 0-81052  
 (Co<sub>0.85</sub>Fe<sub>0.15</sub>)<sub>72</sub>Mo<sub>2</sub>Si<sub>3</sub>B<sub>10</sub>, metallic glass, strain- and field-induced mag. anisotropy 0-108004  
 Co<sub>72</sub>Mo<sub>2</sub>Si<sub>3</sub>B<sub>10</sub>, metallic glass, strain- and field-induced mag. anisotropy 0-108004  
 Fe-B, amorphous, induced anisotropy, development by mag. annealing and under applied mech. stress 0-65868

**magnetic annealing continued**

- Fe-Co-Ni Perminvar, mag. props. singularities in region of mag. anisotropy (*Russian*) 0-84614  
 Fe-Co-Si-B, zero magnetostrictive amorphous alloy with high saturation induction, mag. annealing 0-60362  
 Fe-Cr-Co-Mo high energy permanent magnets, mag. props. 0-97119  
 Fe-Ni, secondary recrystn. and mag. props. 0-89247  
 Fe<sub>40</sub>Ni<sub>40</sub>B<sub>20</sub>, amorphous, RF annealing effects 0-108037  
 Ni-Co (25 wt.%), single crystals, mag. annealing effect on magnetostriction and magnetisation at high temps. 0-108047

**magnetic bays** see geomagnetic variations**magnetic bottles**

- see also magnetic mirrors  
 ring cusp, plasma width meas. 0-87927

**magnetic breakdown**

- Al, single crystals, high purity, anisotropy of apparent resist. in longit. mag. fields 0-75550  
 Cr, antiferromag., transverse magnetoresist., electron interference oscils. 0-65534  
 Fe, whisker, magnetoresistance, deviations from Kohler's rule 0-70673  
 LaB<sub>6</sub>, de Haas-van Alphen effect, low-field 0-75497  
 ReO<sub>3</sub>, mag. breakdown above compressibility collapse transition 0-103617

**magnetic bubble devices**

- ion milling fabrication process, string segment motion algorithm 0-71779  
 memories, rotational field coils winding turns counting, using moire system 0-73428  
 review of bubble material props. and prep. methods (*Rumanian*) 0-93149

**magnetic bubbles**

## see also magnetic bubble devices

- Bloch wall structure, horizontal, mag. bubble domains in implanted films 0-71131  
 bubble garnet film, saturation velocity, in-plane field effects 0-108041  
 bubbly dynamics and jump probability 0-65977  
 charged domain walls in implanted layers, theory 0-71130  
 dynamic measurements by rocking technique (*Chinese*) 0-65981  
 dynamic properties of magnetic domain walls and magnetic bubbles, review 0-88784  
 exchange vortices of magnetisation, micromagnetic bubble domains 0-71138  
 ferromagnetic film, heterogeneity influence on static and dynamic props. of domain walls (*Russian*) 0-65974  
 garnet film, non-implanted, surface mag. struct. 0-84628  
 garnet films with orthorhombic anisotropy, domain wall motion 0-80580  
 garnets, domain wall oscillations, bubble domain wall motion 0-108042  
 hard bubble formation due to bias pulse field (*Chinese*) 0-71127  
 interacting bubble domains, dynamics, theory 0-71132  
 light diffraction by domain gratings, and appl. 0-88970  
 magnetic film, bubble domains, magnetoelastic interactions 0-103865  
 magnetoelastic interactions 0-65976  
 micromagnetic method, bubble domain statics and dynamics 0-71081  
 rare earth iron garnets, Ca-Ge substituted, mag. loss and domain wall mobility 0-65980  
 review of bubble material props. and prep. methods (*Rumanian*) 0-93149  
 stationary circular motion 0-84629  
 T bar, domain wall study employing ferrofluid, rel. to magneto-optical Kerr effect meas. 0-60360  
 translational motion, mechanism for inertial effects 0-100606  
 twisted domain wall energy, thickness depend., simplified calc. (*Slovak*) 0-103862  
 two dimensional mag. domain wall, uniform magnetisation, effective force density of magnetostatic origin, mag. bubble motion anal. 0-100595  
 wall dynamics, review 0-75823  
 wall velocity depend. on bubble radial motion momentum 0-71136  
 Ba ferrite, FMR in uniaxial crystal plate with bubble domain lattice 0-93182  
 BaFe<sub>2</sub>O<sub>9</sub>, bubble and stripe lattice domain wall oscils. 0-97115  
 (BiTm)<sub>3</sub>(FeGa)<sub>5</sub>O<sub>12</sub> ion implanted epitaxial garnet film, bubble domains, cryst. struct. disorder 0-93150  
 (EuLu)<sub>3</sub>(FeAl)<sub>5</sub>O<sub>12</sub>, film epitaxial growth on Gd<sub>3</sub>Ga<sub>5</sub>O<sub>12</sub> substrate, mag. props. 0-65402  
 Gd-Co amorphous films, mag. struct., mag. bubbles, electron diffr. study (*Chinese*) 0-71126  
 PbFe<sub>2</sub>O<sub>9</sub>, bubble and stripe lattice domain wall oscils. 0-97115  
 (SmLu)<sub>3</sub>(FeAl)<sub>5</sub>O<sub>12</sub>, film epitaxial growth on Gd<sub>3</sub>Ga<sub>5</sub>O<sub>12</sub> substrate, mag. props. lattice mismatch 0-65402  
 (Y<sub>2</sub>SmCa)<sub>3</sub>(FeGe)<sub>5</sub>O<sub>12</sub> epitaxial films, mag. props., growth condition effects 0-97124  
 YCrO<sub>3</sub>, bubble domain struct. temp. depend. 0-71137  
 (YEuTm)<sub>3</sub>(GaFe)<sub>5</sub>O<sub>12</sub> ferrite garnet films, mag. bubbles, translational motion, mechanism for inertial effects 0-100606  
 Y<sub>2</sub>GdG film, amorphous, mag. bubbles obs. and structural transformation 0-75824  
 YGdTmFe<sub>4</sub>Ga<sub>0.7</sub>O<sub>12</sub> epitaxial films, bubble-domain lattices with specified parameters 0-60386  
 (YGdTm)<sub>3</sub>(FeGa)<sub>5</sub>O<sub>12</sub> epitaxial film, formation of lattice of cylindrical mag. domains from stripe domains (*Russian*) 0-80579  
 YIG, cylindrical mag. domains, translational motion 0-108043  
 (YLuSmCa)<sub>3</sub>(FeGe)<sub>5</sub>O<sub>12</sub> garnet film, bubble domain expansion, fuzzy wall struct. 0-71128  
 (YLuSmCa)<sub>3</sub>(GeFe)<sub>5</sub>O<sub>12</sub> garnet films, bubble expansion saturation vel., sampling optical photography 0-75820

**magnetic circuits**

- see also transformer magnetic circuits  
 transducer, matrix eddy-current, with magnetic circuit, design and construction 0-68228  
 Co permanent magnet material savings (*German*) 0-103851

**magnetic circular dichroism**

- (2,2) (2,6) azulenophanes, mag. circular dichroism and anomalous fluorescence spectra 0-83398  
 deoxyhaemoglobin, ferrous heme of high-spin type, MCD spectra in Soret, visible and near IR regions 0-94156  
 dichrograph for measuring dichroism in 200 to 850 nm region 0-101806  
 electronic spectra of molecules, pure elec. quadrupole transition polaris. 0-63691  
 matrix-isolated high-temp. molecules, apparatus for meas. of spectra 0-86356  
 nematic-chiral-dye mixture, circular dichroism, selective light scatt. (*Russian*) 0-103944



**magnetic circular dichroism continued**

- paramagnetic system with quadrupole splitting, magneto-optical effects, magnetic resonance saturation 0-60404  
recorder calibration at 10.6  $\mu\text{m}$  0-90876  
TiO in Ar matrix, meas. of MCD spectra 0-86356  
Bi, Faraday effect and magnetic circular dichroism 0-83399  
CaF<sub>2</sub>:U<sup>3+</sup>, anomalous magneto-optic props., optical detection of ESR and cross-relax. resonances 0-93287  
CdCr<sub>2</sub>Se<sub>4</sub>:Ag, magneto-optical effects in impurity spectral region 0-97313  
Cr(CO)<sub>6</sub>, MCD spectra, charge transfer transitions 0-95658  
CsI:Na, X-ray irradiated, optical and ESR studies in IR absorption band 0-80828  
Cs<sub>2</sub>ZrBr<sub>6</sub>:Os<sup>4+</sup>, intraconfig. absorpt. and MCD spectra 0-80776  
Cs<sub>2</sub>ZrCl<sub>6</sub>:Os<sup>4+</sup>, intraconfig. absorpt. and MCD spectra 0-80776  
KBr:Au<sup>-</sup>, optical absorpt. bands and MCD, electron-lattice interaction 0-108236  
KCl:Cu<sup>+</sup>, exciton bands, optical absorpt. and MCD spectra 0-80821  
KCl:Pb<sup>2+</sup>, X-ray irradiated, electron-trapped centres, Pb<sup>2+</sup> and Pb<sup>0</sup>, optical absorpt. spectra 0-71461  
Kl:Cu<sup>+</sup>, exciton bands, optical absorpt. and MCD spectra 0-80821  
K<sub>2</sub>NaGaF<sub>6</sub>:Cr<sup>3+</sup>, magneto-optical study of <sup>2</sup>T<sub>1g</sub>, <sup>4</sup>T<sub>2g</sub>, <sup>2</sup>E<sub>g</sub>, <sup>4</sup>A<sub>2g</sub> transitions 0-71384  
Mo(CO)<sub>6</sub>, MCD spectra, charge transfer transitions 0-95658  
NaI:F, electron-lattice coupling of F-centres, optical props. 0-60641  
Na<sub>3</sub>Pr(C<sub>4</sub>H<sub>9</sub>O<sub>3</sub>)<sub>2</sub>.2NaClO<sub>4</sub>.6H<sub>2</sub>O, absorpt., circular dichroism, and mag. circular dichroism spectra 0-97243  
RbCl:Au<sup>-</sup>, optical absorpt. bands and MCD, electron-lattice interaction 0-108236  
SiO<sub>2</sub>:Na<sub>2</sub>O-Nd<sub>2</sub>O<sub>3</sub> glass, magneto-optical props., absorpt. spectrum 0-88969  
SrCl<sub>2</sub>:Cu<sup>+</sup>, exciton bands, optical absorpt. and MCD spectra 0-80821  
U(BH<sub>4</sub>)<sub>4</sub>, in Hf(BH<sub>4</sub>)<sub>4</sub>, excited state assignments and E-symmetry ground state, near IR MCD obs. 0-66153  
Vl<sub>3</sub>, MCD spectra, interpretation rel. to mag. struct. 0-66222  
W(CO)<sub>6</sub>, MCD spectra, charge transfer transitions 0-95658  
YIG:Ru, optical absorpt. and MCD obs. of Ru<sup>4+</sup> site occupancy 0-71456  
YIG:Zr, near IR absorpt. and magnetic circular dichroism 0-60580

**magnetic cooling**

- (Ce,La<sub>1-x</sub>)<sub>2</sub>Mg<sub>3</sub>(NO<sub>3</sub>)<sub>12</sub>.24H<sub>2</sub>O, adiabatic demagnetisation temp., mag. entropy (Russian) 0-65892  
Fe-Cr-Co alloys, (5-9 wt.% Co), obtained by slow cooling under mag. field, permanent magnet prop. 0-75797  
HgCr<sub>2</sub>S<sub>4</sub>, cooling efficiency near 60K as mag. refrigerant 0-71034  
TmVO<sub>4</sub>, enhanced nuclear cooling and spin-lattice relax. time 0-80632

**magnetic cores**

- amorphous magnetic alloys, review, engineering magnetic props. and potential applications 0-71078  
complex mutual inductance concept for bioelectric impedance transformer bridge 0-63886  
DC permeameter for ring specimens 0-98954  
ferromagnets, cyclically remagnetised, discrete spectra of induction calcs., demagnetising factor 0-103859  
transformer, use of high permeability Fe-Si materials 0-88793  
Fe-Si, grain oriented transformer sheets, permeability and magnetostriction, tensile stress effects 0-88843  
Fe-Si, mag. props., stress and annealing effects 0-88844  
Fe-Si, stator core, grain-oriented and non-oriented, magnetic flux and loss distrib. 0-88798  
Li<sub>0.5</sub>Mn<sub>0.5</sub>Fe<sub>2.5</sub>O<sub>4</sub> ferrite cores with rectangular hysteresis loops, pulse parameters, effect of Fe<sub>2</sub>O<sub>3</sub> heat treatment 0-60370  
NiZnCo ferrites, voltage response under sinusoidal and pulse magnetisation effected by hydrostatic press. 0-88846

**magnetic devices**

- see also ferrite devices; magnetic amplifiers; magnetic lenses; magnetic thin film devices; magnetostrictive devices  
amorphous magnetic alloys, review, engineering magnetic props. and potential applications 0-71078  
defectoscopes, nonsinusoidal periodic currents meas. 0-104386  
eddy-current flaw detection of long ferromag. products, magnetizing device parameters 0-89447  
ferromagnetic material NDT, magnetising device, stabilization of Barkhausen discontinuities 0-89457  
magnetic soft and hard materials, garnets, magnetic properties and applications, structural props. 0-65760  
micromagnetic susceptibility with variable temp. 4.2K to 300K for small sample meas. 0-73395  
sector mag. analyzer, compact notation of second-order ion-optical coeffs. 0-63911  
steel 40 G, coercimeters with attached electromagnets used for quality control 0-108672

**magnetic dipoles** see magnetic moments**magnetic disc and drum storage**

- flexible disc/head interaction analysis 0-92093  
IR spectrophotometer, digital data acquisition/analysis system 0-73482

**magnetic disc storage** see magnetic disc and drum storage**magnetic domain walls**

- amorphous ribbons, twisted, magnetisation process, domain theory 0-71101  
antiferromagnet, interphase boundary dynamics, domain wall motion and scatt. (Russian) 0-108032  
antiferromagnets, magnetoacoustic resonance of domain boundaries (Russian) 0-65636  
antiferromagnets, nonlinear waves 0-84612  
Bloch wall displacement, rel. to rotational hysteresis in weak magnetic fields 0-75804  
Bloch wall structure, horizontal, mag. bubble domains in implanted films 0-71131  
Bloch walls, history 0-86065  
Bloch-Neel domain wall transition, discontinuity of limiting velocities (Russian) 0-75788  
bubble garnet film, saturation velocity, in-plane field effects 0-108041  
bubble wall dynamics, review 0-75823  
bubbles, stationary circular motion 0-84629  
charged domain walls in implanted layers, theory 0-71130  
dynamic properties of magnetic domain walls and magnetic bubbles, review 0-88784  
eddy current dominated domain wall dynamics and magnetisation losses 0-88778

**magnetic domain walls continued**

- exchange energy near singular points or lines 0-93106  
ferromagnetic Bloch wall oscills., viscosity coeffs. freq. depend., permeability and mag. losses 0-71094  
ferromagnet, domain wall mobility, damping, dipole-dipole interaction 0-93140  
ferromagnet, domain wall motion, pinning by lattice defects, magnetisation 0-71079  
ferromagnet, pinned domain wall motion, magnetic damping studies 0-65956  
ferromagnetic film, heterogeneity influence on static and dynamic props. of domain walls (Russian) 0-65974  
ferromagnetic thin film, direct determ. of mag. domain wall profiles, using split detector STEM 0-103867  
ferromagnets, spin waves in domain struct. 0-70993  
garnet films with orthorhombic anisotropy, domain wall motion 0-80580  
garnets, domain wall oscillations, bubble domain wall motion 0-108042  
Heisenberg ferromagnet, classical one-dimensional, transfer integral and collective coordinate results for free energy 0-93067  
interaction with strongly localised pinning centres, influence on hysteresis (Russian) 0-65961  
Ising ferromagnetic half-plane, surface, pinned domain wall, free energy and magnetisation profile 0-60361  
Ising model, nonlinear excitations and coherent states in transverse field 0-68143  
localised defect interactions, unidimensional flow of configs. (Russian) 0-65954  
magnetic bubbles, translational motion, mechanism for inertial effects 0-100606  
magnetic soft and hard materials, garnets, magnetic properties and applications, structural props. 0-65760  
motion, magneto-dipole EM wave radiation generation (Russian) 0-80555  
observation device for use with 1 MeV electron microscope 0-101882  
orthoferrite cryst. films, local coercivity of domains boundaries (Russian) 0-80578  
parade motion, low freq. (Russian) 0-103852  
particle capture 0-71093  
Permalloy film strip, unidirectional domain wall propag. with in-plane magnetisation 0-71134  
Permalloy thin films, break-cross-tie wall energy 0-88842  
Permalloy-Mn film, diffusion aftereffect causing mag. state change (Russian) 0-103860  
pinning on defects with finite radius of interaction, random pot. form effect on mag. hysteresis (Russian) 0-84611  
rare earth iron garnets, Ca-Ge substituted, mag. loss and domain wall mobility 0-65980  
rare earth orthoferrites, domain wall dynamics 0-65957  
spontaneous symmetry breaking and magnon-phonon spectra 0-65991  
steel, high-speed, low temp. mag. cycling effects, dislocation interactions with mag. domain walls 0-100928  
T bar, domain wall study employing ferrofluid, rel. to magneto-optical Kerr effect meas. 0-60360  
thickness, neutron small-angle scatt. meas. 0-71092  
twisted domain wall energy, thickness depend., simplified calc. (Slovak) 0-103862  
two dimensional mag. domain wall, uniform magnetisation, effective force density of magnetostatic origin, mag. bubble motion anal. 0-100595  
uniaxial ferromagnet with intrinsic mag. field, domain struct. 0-93141  
velocity dependence on bubble radial motion momentum 0-71136  
weak ferromagnet, domain wall dynamics, nonlinear waves, mag. solitons (Russian) 0-75793  
weak ferromagnets, Landau-Lifshitz eqn. solutions, moving domain walls, struct. (Russian) 0-100596  
BaFe<sub>2</sub>O<sub>9</sub>, bubble and stripe lattice domain wall oscills. 0-97115  
CdCr<sub>2</sub>Se<sub>4</sub>, magnetic semiconductor, photoinduced centre kinetics 0-71110  
(Co,Fe)<sub>80</sub>B<sub>20</sub> glass, induced anisotropy and time changes of permeability 0-75815  
Co film, mag. domain wall obs. by electron holography 0-80582  
Co<sub>90</sub>Zr<sub>10</sub>, ferromag. amorphous alloy, crystn. and domain struct. study 0-107056  
CrBr<sub>3</sub>, HF spectra, susceptibility, spin waves in domain walls (Russian) 0-80909  
CsCoCl<sub>3</sub>, spin dynamics, neutron scatt. study 0-80493  
CsMnCl<sub>3</sub>, antiferromagnetic resonance, parametric spin wave excitation (Russian) 0-93183  
Cu HCP film, uniaxial, mag. domain struct. 0-60385  
Dy(Co,Ni)<sub>2</sub>, intrinsic mag. aftereffect meas., domain wall motion 0-71121  
Dy,Fe<sub>2</sub>, domain structures and anisotropy constant. 0-93136  
EuS films, mag. and elec. props. rel. to stoichiometry and defects 0-97122  
Fe, 90° walls, stable orientations, theory and X-ray observations (Japanese) 0-60359  
Fe, high purity, magnetomechanical sampling, magnetic field variations 0-93156  
Fe thin layers, vacuum coated on PMMA, mag. behaviour during mech. stress cycles (German) 0-80581  
Fe-Cr-Co, magnetic domain walls, Lorentz microscopy 0-103854  
Fe-Si, single cryst., mag. domain wall motion, X-ray topography study 0-65953  
Fe-Si (3 wt.%), domain wall spacing and core loss, forsterite and stress coatings effect 0-88780  
Fe-Si (3 wt.%), grain-oriented, domain wall profiles throughout magnetisation cycle 0-88781  
Fe-Si (3 wt.%), grain-oriented, power loss and domain wall variation with lamination thickness 0-88814  
Fe-Si (3 wt.%), mag. domain wall contrast in synchrotron X-ray topographs 0-75792  
Fe-Si (3.25 wt.%) alloy, single cryst. with (007) planes, domain struct. influence on mag. torque 0-108034  
Fe<sub>2</sub>Co<sub>2</sub>B<sub>20</sub>, amorphous, magnetisation reversal and domain boundary configs. 0-88809  
Fe<sub>80</sub>Ni<sub>20</sub>B<sub>20-y</sub>P<sub>y</sub>, amorphous, Rayleigh region and coercive force 0-88806  
Fe<sub>40</sub>Ni<sub>40</sub>P<sub>14</sub>B<sub>6</sub>, Metglas 2826, amorphous ribbon under tension, mag. domain walls and pulsed magnetisation reversal 0-88825  
(Fe,Ni<sub>1-x</sub>)<sub>80</sub>P<sub>10</sub>B<sub>10</sub>, amorphous, magnetisation reversal and domain boundary configs. 0-88809  
FeSi picture frame single cryst., domain wall motion and magnetisation reversal, time-depend. neutron depolarisation study 0-88782  
FeV (2 at.%), NMR spin echoes, domain wall effects 0-75883



## magnetic domain walls continued

- Gd, mag. domain struct., 230-293K 0-88783  
 $Gd_2(MoO_4)_3$ , domain wall motion dynamics 0-108030  
 KCoF<sub>3</sub>, antiferromag. domain wall motion under external stress 0-80583  
 $LuCrO_3:Er^{3+}$ , doping effect on  $^{51}Cr$  NMR in domain walls 0-71219  
 MnBi, domain boundary inertia during mag. reversals (*Russian*) 0-88776  
 MnZn ferrite, initial mag. permeability rel. to mag. anisotropy 0-80557  
 Ni, 109° and 71° walls, stable orientations, theory and X-ray observations (*Japanese*) 0-60359  
 Ni-Fe film, thermally activated domain wall motion 0-88777  
 Ni-Fe films, energy change of Bloch wall with angle to easy axis, calc. (*Slovak*) 0-103863  
 Ni-Fe-Cr-Mo-Ti-Al, PE 16, thermally activated domain wall motion 0-88777  
 NiFe film, domain wall mass and relax. time from forced oscils. 0-71133  
 NiFe, mag. film, pulse switching at low temp. 0-103868  
 $Ni_{1-x}Zn_xFe_2O_4$ , polycryst., domain wall energy rel. to anisotropy 0-71090  
 $PbFe_{1-x}O_9$ , bubble and stripe lattice domain wall oscils. 0-97115  
 $SmCo_5$ , sintered, mag. after-effect, expt. and model 0-75816  
 Tb-Fe amorphous thin films, magnetic after-effect, Kerr magneto-optic effect obs. 0-97123  
 Tm ferrogarnet film, cylindrical mag. domain motions, domain boundary oscils. (*Russian*) 0-71140  
 Y-Sm ferrogarnet (*Russian*) 0-71140  
 (YEuTm)<sub>3</sub>(GaFe<sub>3</sub>)O<sub>12</sub>, ferrite garnet films, mag. bubbles, translational motion, mechanism for inertial effects 0-100606  
 $YFe_{2-x}Ga_xO_{12}$ , mag. domains and cryst. defects 0-75789  
 YFeO<sub>3</sub>, domain boundary inertia during mag. reversals (*Russian*) 0-88776  
 YFeO<sub>3</sub>, orthoferrite, crit. domain wall vel. 0-71135  
 YGdIG, with various domain wall orientations, natural spin reson. 0-66040  
 (YGdYbBi)<sub>3</sub>(FeAl)<sub>2</sub>O<sub>12</sub>, ferrite-garnet films, effect of in-plane field on dynamics of domain walls 0-65979  
 YIG, Bi-substituted, LPE, domain wall reson. 0-60387  
 YIG, Bloch line mass and mobility in a domain boundary (*Russian*) 0-93138  
 YIG, cylindrical mag. domains, translational motion 0-108043  
 YIG, domain wall mobility and mass meas. method (*Russian*) 0-108033  
 YIG, magnetic domain wall motion in high drive fields 0-65955  
 YIG, permeability, domain rot. and wall displacement contrib. 0-80564  
 YIG, polycryst., initial and reversible parallel susceptibilities, hydrostatic press. effects 0-75835  
 YIG:Co film, influence of stress induced anisotropy on domain struct. 0-100605  
 (YLuSmCa)<sub>3</sub>(GeFe)<sub>2</sub>O<sub>12</sub>, garnet films, bubble expansion saturation vel., sampling optical photography 0-75820

## magnetic domains

- see also magnetic bubbles; magnetic domain walls  
 dry colloid observation apparatus, 90K to 290K 0-73394  
 ellipsoid with domain struct., magnetostatic oscils., theory 0-93102  
 epitaxial ferrite-garnet films with inversion layers, behaviour of cylindrical mag. domains, visual tracking method 0-71139  
 ferric solution ferromagnetic liquid insulation in redox flow battery, quantum parameters separation 0-61338  
 ferromagnetic domain theory, quasi-dislocation theory appl. (*Japanese*) 0-60358  
 ferromagnetic metals, transport props., crit. behaviour 0-65522  
 ferromagnetic plate, domain struct. near first-order phase transition resembling second-order transition 0-93139  
 film, ferromag., dynamics near transition pt. from homogeneous to inhomogeneous magnetis. state 0-108038  
 film, mag. phase states when easy magnetisation axis is inclined rel. to film surface (*Russian*) 0-103864  
 film, with perpendicular anisotropy, stripe domain struct., theory (*Russian*) 0-65973  
 imaging by SEM, computer simulation 0-71091  
 lattice of transparent crystal regular birefr. regions, optical wave diff. divergence 0-102616  
 light diffraction by domain gratings, and appl. 0-88970  
 magnetic domain, SEM obs., method of removing fine magnetite particles from surface (*Japanese*) 0-108655  
 Neel ferrimagnets, phase transitions, field-induced spin-orientational 0-75767  
 neutron beam channelling and focusing in ferromagnets (*Russian*) 0-107351  
 neutron diff. study, symm. anal., polarisation effects 0-93083  
 nuclear magnetic ordering, domains, neutron diff. patterns, theory 0-100577  
 Permalloy films with band domain struct., thermomag. recording, resolving power (*Russian*) 0-75769  
 Permalloy thin-film head pole struct., domain configurations, SEM obs. 0-65975  
 rock magnetism, domain structure obs. by Lorentz electron microscopy 0-72502  
 screw spin structure, method of controlling the sense 0-70944  
 single domain grain assembly, theory for magnetisation processes 0-88828  
 soft magnetic materials, meas. methods, review 0-86345  
 spin glass, transitions, field-induced, masking effects 0-65943  
 spin-reorientation phase transition (*Russian*) 0-93122  
 steel, C, magnetomechanical acoustic emission for residual stress NDT 0-71149  
 steel, ferritic, magnetomechanical acoustic emission for residual stress NDT 0-71149  
 strip films, bulk and surface spin oscils., mag. reson. 0-97149  
 structure obs. by Kerr-magneto-optical effect, laser speckle suppression 0-85093  
 texture analysis, generalisation of dispersion theory 0-80556  
 thick layers with regular domain structure, magneto-optical diff. of light 0-108188  
 transversely heterogeneous magnetically uniaxial plates, non-through mag. domains (*Russian*) 0-93135  
 two-layer mag. structures, thermomag. recording 0-100588  
 uniaxial ferromagnet, domain struct. in mag. field 0-103853  
 uniaxial ferromagnet domain struct., phase transition (*Russian*) 0-108044  
 AuMn, mag. struct., phase transition, and magnon spectrum, random anisotropy effects 0-88722

## magnetic domains continued

- $BaFe_2O_9$  particles, magnetic domain study by colloid-SEM method 0-97120  
 $BaO.6Fe_2O_3$ , ferrite polycryst., depend. of domain width on sample thickness 0-108031  
 Co-CoO films, evaporated, exchange anisotropy 0-88841  
 Co-P, amorphous, domain struct., mag. anisotropy origin 0-80554  
 CoPd, single cryst., domain struct., temp. and field depend. 0-71085  
 Cr, antiferromagnetic, US attenuation and phase diagram 0-103831  
 Cr, mag. struct., phase transition, and magnon spectrum, random anisotropy effects 0-88722  
 CrBr<sub>3</sub>, ferromag. domains, using liq. He mag. specimen stage 0-103855  
 CrBr<sub>3</sub>, HF spectra, susceptibility, spin waves in domain walls (*Russian*) 0-80909  
 Cr<sub>2</sub>O<sub>3</sub>, dielec. const. in mag. field, nonlinear magnetoelec. effect in Neel pt. region 0-66006  
 CsMnF<sub>3</sub>, mag. struct., phase transition, and magnon spectrum, random anisotropy effects 0-88722  
 CsNiF<sub>3</sub>, quasielastic neutron scatt. around Neel-point 0-75768  
 Cu ferrite films, Mn-, Ni- and Al-substituted, LPE growth 0-96752  
 Cu:Co precipitates, mag. anisotropy, precipitate shape, coercive force 0-80500  
 Dy, domain effects near order-disorder and order-order ferromagnetic transitions 0-65886  
 Dy, magnetic domain structure, hysteresis, thermal modulation study 0-71082  
 DyCu film, amorphous, asperomagnetic domains, Barkhausen jumps in hysteresis loop 0-75822  
 Dy<sub>2</sub>Fe<sub>3</sub>, domain structures and anisotropy constant 0-93136  
 Dy<sub>0.5</sub>Ho<sub>0.5</sub>FeO<sub>3</sub> orthoferrite, domain struct., temp. depend. 0-71086  
 DyPO<sub>4</sub>, mag. transitions under hydrostatic press., neutron diff. study 0-71030  
 Fe, magnetomechanical acoustic emission for residual stress NDT 0-71149  
 Fe, stray mag. fields above stripe domains, electron microscope and  $\mu^*$ -tensor determ. 0-71089  
 Fe thin layers, vacuum coated on PMMA, mag. behaviour during mech. stress cycles (*German*) 0-80581  
 Fe-Al, domain struct. and magnetostriction, heat treatment effect 0-60398  
 Fe-B amorphous alloy, annealed, microstruct. and mag. domain changes 0-75790  
 Fe-P electrodeposited foil, amorphous, mag. domains 0-75821  
 Fe-Si (3 wt.%), ferromag. domains, imaging by neutron interferometry 0-71087  
 Fe-Si (3 wt.%), grain-oriented, domain struct. regulation and power loss reduction 0-88779  
 Fe-Si (3 wt.%), oriented, losses and domains, mech. stress effects 0-88852  
 Fe-Si (3 wt.%), stripe domain structure, dynamic behaviour at high max. induction values (*Russian*) 0-80553  
 Fe-Si (3 wt.%) laminations, magnetostriction behaviour associated with closure domain spikes 0-75834  
 Fe<sub>2</sub>Co<sub>0.5</sub>Cr<sub>1.5</sub> films, vacuum-deposited cryst. and mag. struct. (*Russian*) 0-93081  
 Fe<sub>40</sub>Ni<sub>40</sub>P<sub>10</sub>B<sub>10</sub> amorphous ribbon, mag. domains and anisotropy distrib. 0-108029  
 $\alpha$ -Fe<sub>2</sub>O<sub>3</sub>, single cryst., hematite, X-ray topographic obs. of domain struct. changes in external mag. field 0-88785  
 FeSi, single crystals, domain struct., temp. and field depend. 0-71085  
 Gd, domain effects near order-disorder and order-order ferromagnetic transitions 0-65886  
 GdBi single crystals, mag. behaviour and structure change at low temp. 0-71018  
 KNiF<sub>3</sub>,  $^{19}F$  spin-lattice relaxation 0-93211  
 MnAlGe film, mag. domains and amorphous to cryst. phase transition, electron microscopy obs. 0-71129  
 MnF<sub>2</sub>, antiferromag. and piezomag. domain struct., neutron topography study 0-71088  
 MnGaGe film, mag. domains and amorphous to cryst. phase transition, electron microscopy obs. 0-71129  
 Ni, stray mag. fields above stripe domains, electron microscope and  $\mu^*$ -tensor determ. 0-71089  
 Ni-Fe (36 to 50 wt.%), initial permeability, domain struct. model 0-88811  
 NiFe, single and multilayer thin films, strip domains, inplane magnetisation 0-103866  
 Ni<sub>3</sub>Fe, domain struct. after tensile deform., dislocation effects 0-71083  
 NiO, linear birefringence in S-domains near antiferromag. phase transition 0-60261  
 NiO, mag. struct., neutron Laue diff. method 0-70951  
 Pd-Fe, magnetic anisotropy near Curie point, quasi domain struct. (*Russian*) 0-65867  
 SmCo<sub>5</sub>, nucleation of reversed domains at Co-Sm; precip. 0-75791  
 SmCo<sub>5</sub>, rel. to crystal defects, electron microscopy 0-103856  
 Tb, ferromagnetic domain structures down to 95K 0-71080  
 Tm ferrogarnet film, cylindrical mag. domain motions, domain boundary oscils. (*Russian*) 0-71140  
 Y-Sm ferrogarnet (*Russian*) 0-71140  
 (YBiEr)<sub>3</sub>(FeGa)<sub>2</sub>O<sub>12</sub>, ferrite-garnet film, micron cylindrical mag. domains, high recording density 0-65978  
 Y<sub>3</sub>Fe<sub>5-x</sub>Al<sub>x</sub>O<sub>12</sub>, permeability spectra rel. to microstruct. 0-71100  
 YFe<sub>2</sub>Ga<sub>0.5</sub>O<sub>12</sub> domains, neutron depolarisation and Faraday rotation study 0-93137  
 Y<sub>2</sub>Fe<sub>4</sub>Ga<sub>0.5</sub>O<sub>12</sub>, domain struct., neutron depolarisation and Faraday rot. 0-71084  
 Y<sub>2</sub>Fe<sub>5-x</sub>Gd<sub>x</sub>O<sub>12</sub>, permeability spectra rel. to microstruct. 0-71100  
 (YGdYbTm)<sub>3</sub>(FeGa)<sub>2</sub>O<sub>12</sub> epitaxial film, formation of lattice of cylindrical mag. domains from stripe domains (*Russian*) 0-80579  
 (YGdYbBi)<sub>3</sub>(FeAl)<sub>2</sub>O<sub>12</sub> epitaxial garnet film, uniaxial ferromagnet domain struct., phase transition (*Russian*) 0-108044  
 YIG, permeability spectra rel. to microstruct. 0-71100  
 ZnCr<sub>2</sub>Se<sub>4</sub>, screw spin structure, method of controlling the sense, polarised neutron diff. study 0-70944



magnetic double refraction *see magneto-optical effects*

magnetic double resonance

*see also CIDEP; double nuclear magnetic resonance; dynamic nuclear polarisation; ELDOR; ENDOR; microwave-optical double resonance; nuclear polarisation*  
p-dichlorobenzene,  $^{35}\text{Cl}$  NQR line narrowing by nonreson. RF photon dressing 0-63662

$\text{LiYF}_4:\text{Pr}$ , NMR meas. of hyperfine const. of  $\text{Pr}^{3+}$  excited state 0-88895

magnetic drum storage *see magnetic disc and drum storage*

magnetic epitaxial layers

ferrite-garnet films with inversion layers, behaviour of cylindrical mag. domains, visual tracking method 0-71139

garnet epitaxial film, stress induced magnetocrystalline anisotropy 0-71013

garnet films, easy magnetisation axis orientation 0-60383

garnet films with orthorhombic anisotropy, domain wall motion 0-80580

Neel ferrimagnets, phase transitions, field-induced spin-orientational 0-75767

Co, even magneto-optical effects 0-76007

Cu ferrite films, Mn-, Ni- and Al-substituted, LPE growth 0-96752

$(\text{EuLu})_2(\text{FeAl})_2\text{O}_{12}$ , film epitaxial growth on  $\text{Gd}_3\text{Ga}_5\text{O}_{12}$  substrate, mag. props. 0-65402

Fe, even magneto-optical effects 0-76007

$\gamma\text{-Fe}$ , FCC film, epitaxial growth on CuAu (111) surfaces, strong ferromagnetism 0-70557

(Gd, Bi) $_2$ (Fe, Ga) $_2\text{O}_{12}$  magneto-optic LPE garnet films, high-energy heavy ion irradiat., props. 0-71390

(Gd,Tm,Y) $_3$ (Fe,Ga) $_2\text{O}_{12}$  LPE garnet thin films, magnetocrystalline anisotropy 0-93147

Ni, even magneto-optical effects 0-76007

$(\text{SmLu})_2(\text{FeAl})_2\text{O}_{12}$ , film epitaxial growth on  $\text{Gd}_3\text{Ga}_5\text{O}_{12}$  substrate, mag. props. lattice mismatch 0-65402

$\text{Sm}_{0.4}\text{Y}_{2.6}\text{Fe}_{3.8}\text{Ga}_{1.2}\text{O}_{12}$  epitaxial films, uniaxial mag. anisotropy, ferrimag. reson. study 0-80577

(Y,Sm,Ca) $_2$ (Fe,Ge) $_2\text{O}_{12}$  epitaxial films, mag. props., growth condition effects 0-97124

(Y,BiEr) $_2$ (FeGa) $_2\text{O}_{12}$  ferrite-garnet film, micron cylindrical mag. domains, high recording density 0-65978

$\text{YGdTmFe}_{4.5}\text{Ga}_{0.5}\text{O}_{12}$  epitaxial films, bubble-domain lattices with specified parameters 0-60386

$(\text{YGdTm})_2(\text{FeGa})_2\text{O}_{12}$  epitaxial film, formation of lattice of cylindrical mag. domains from stripe domains (Russian) 0-80579

$(\text{YGdYbBi})_2(\text{FeAl})_2\text{O}_{12}$  epitaxial garnet film, uniaxial ferromagnet domain struct., phase transition (Russian) 0-108044

YIG, Bi-substituted, LPE, domain wall reson. 0-60387

$\text{Y}_{2.85}\text{La}_{0.15}\text{Fe}_{3.75}\text{Ga}_{1.25}\text{O}_{12}$  LPE films, ion implantation effect on spin waves 0-71124

(YRBi) $_2$ (FeAl) $_2\text{O}_{12}$  films, R=Gd, Yb, Faraday effect in transverse mag. field, orientation depend. 0-88971

magnetic field effects

*see also biomagnetism; galvanomagnetic effects; magnetic levitation; magnetic properties of substances; magnetic separation; magneto-optical effects; magnetoacoustic effects; magnetocaloric effects; magnetoelectric effects; magnetohydrodynamics; magnetomechanical effects; particle optics; Scott effect; Senffleben-Beenakker effect; thermal magnetoresistance; thermomagnetic treatment*

acetylene-air flame,  $\text{Li}(\text{Na})(\text{K})(\text{Mg})(\text{Ca})$  damping consts., Lorentz collisions, mag. field effect 0-66805

behavioural sensitivity of a domestic bird to 60-Hz AC and to DC mag. fields 0-61622

benzophenone ketyl radical, in micelle, decay rate in mag. field, photolysis meas. 0-85154

bone stimulation devices, anal. of sinusoidal EM fields 0-108990

chlorodifluoromethane, IR multiphoton dissoc., mag. field effect 0-93772

electron beam, relativistic, propag. in strong mag. field (Japanese) 0-91737

electron cloud in equilib., mag. field effect, pot. and space charge distrib. 0-92410

electron gas, two-dimensional, in mag. field, polarisability 0-107888

glow discharge tube, EM MM-wave detection properties 0-70059

human beings, effects of elec. and mag. fields, HV lines to 800 kV (French, English) 0-72209

hyperthermia by magnetically induced currents, freq.-depth-penetration, comments and reply 0-108991

ionisation and breakdown of gases in crossed magnetic field 0-64805

isotropic medium, elastic waves, mag. field effects 0-58955

liquids, potential and flux conserving static equilibria in elec. or mag. fields, determ. 0-88399

magnetophosphenes, quantitative anal. of thresholds 0-72184

magnetophosphenes, quantitative determ. of thresholds 0-61620

metal, single crystal, dislocation loop formation, during deformation in quantising mag. fields (Russian) 0-103354

MHD channel, anisotropically conducting plasma in inhomogeneous elec. and mag. fields, current calc. (Russian) 0-74995

neutron dynamical diffraction, gravitational and mag. field effects 0-59345

Peierls transition in quantizing mag. field, possibility 0-103441

perfectly conducting elastic sphere, in vacuum, radial vibr. freq., mag. field effects 0-58955

plasma with strongly inhomogeneous magnetic field, linear echo 0-106919

plastic:Eu $^{3+}$ , Faraday rotation sign oscill. in very strong mag. fields (Russian) 0-88973

quantum magnetometers, effect of external sinusoidal magnetic fields on sensitivity (Russian) 0-90870

retardation of electrolytic mass transport in collinear electric-magnetic fields 0-104443

sparking potential in longit. mag. fields 0-106996

spatially modulated electron beam, parametric instability, periodic mag. field effect 0-87285

spherical cavity in infinite medium, radial vibr. freq., mag. field effects 0-58955

superdense glow discharge, effect of transverse magnetic field on ion concentration 0-87972

triode and diode guns, electron optics numerical determ. of beam profile 0-106435

triplet exciplexes, rapid rot., spin-selective depopulation of sublevels, heavy atom-induced mag. field effect 0-95552

triplet exciton annihilation rate, magnetic field depend. effect of spin-lattice relaxation 0-65459

magnetic field effects continued

vacuum polarisation by ambient mag. field, effects on Compton scatt. by unmagetised electrons 0-86631

vacuum polarisation by strong mag. field, effects of Thomson scatt. 0-86632

Ar gas, primary ionisation coeffs. in cross mag. field 0-83879

Bi, amorphous metal films, crystallisation with and without mag. field 0-70570

Ga, amorphous metal films, crystallisation with and without mag. field 0-70570

H bound states in strong mag. field 0-99438

H, effect of infinite magnetisation on spectrum and energy levels 0-77282

H, longit. excited states in intense mag. fields, rel. to pulsars 0-91469

H maser, frequency changes due to nonuniform magnetic field 0-99687

H, relativistic energy levels in strong mag. fields 0-102454

$\text{H}_2$ , ortho-para conversion, magneto-catalytic reaction, quantum formulation 0-108750

$\text{H}_2^+$ , bound states in strong mag. field 0-99438

$^3\text{He}$ - $^4\text{He}$  solution, periodic inhomogeneities, excitation in external mag. field parallel to temp. gradient 0-88392

NaK, liquid metal natural convection under transverse magnetic field 0-69827

Ne discharge in high press. narrow tube, Kadomtsev-Nedospasov instability 0-107004

Si, amorphous film, glow discharge deposition, rate enhancement by mag. field 0-65412

$\text{V}_2\text{O}_5$ , metal-insulator transition, external mag. field effects 0-92819

W, field emission, mag. field effects 0-93463

Yb, amorphous metal films, crystallisation with and without mag. field 0-70570

Zn, twinning, influence of dislocation drag. mag. field effects 0-59472

magnetic field measurement

*see also field plotting; fluxmeters; magnetometers*

absolute intensity of weak mag. field, use of RF biases SQUID 0-82794

alternating magnetic field amplitude meas. (French) 0-73332

brain, human, neural generator localisation underlying auditory evoked mag. fields 0-104703

bubble chamber, SKAT, main parameters and magnetic field meas. 0-69022

development review, 1980 status (French) 0-95114

eye, retina injuries, magnetoretiographic meas. using SQUID magnetometer 0-104702

gradiometers, unidirectional 0-68220

Hall effect probes, linearity improvement of type TLMK Hall probes (Slovak) 0-82795

induction meters, constants determ. using nutation teslameter 0-98946

isotropic RF electric/magnetic field strength meter, design 0-82751

Josephson element principles, applications to precision meas. of electric potential and magnetic flux at high freq. (Norwegian) 0-80447

lung, calc. of effect of changing parameters on two methods of meas. 0-104712

magnetic field diffr. meas. on axes of disks and apertures, Babinet principle, complex spirals 0-102599

magnetic heart vector components, simultaneous meas. with unipositional lead system 0-104697

magnetisation evaluation of magnetised structure via virtual magnetic charges 0-57341

MIS-3M magnetic measuring system (USSR), testing small permanent magnets 0-62699

NMR probe using single IC for HF head 0-62697

NMR radio spectrometers, meas. of field uniformities in gap of precision magnets 0-105683

optical and magnetic resonance studies, 3-axis computer controlled low field magnet 0-95113

optical fibre magnetic field sensors 0-69510

Permalloy magnetoresistive mag. field sensor, performance calc. 0-57342

plasma, hot, mag. field determ. using Faraday rot. (Rumanian) 0-87950

scanning electron microscope, two-dimensional stray microfields 0-86514

superconducting solenoids, automatic meas. using NMR 0-57344

toroidal controlled fusion poloidal mag. field meas. by far IR Faraday rotation 0-59303

weak, SQUIDS, review 0-86267

Wiegand module, magnetic field sensor (German) 0-62694

Al, thick-walled conducting shield in biomag. expts. 0-104845

Al thick-walled enclosure for LF biomag. meas. 0-62698

magnetic field variations, earth *see geomagnetic variations*

magnetic fields

*see also electromagnetic fields; geomagnetism; interplanetary magnetic fields; interstellar magnetic fields; magnetic field effects; magnetic field measurement; solar magnetism; superconducting critical field*

AC distribution in solid turns with skin effect, calc. (German) 0-69319

astronomical compact thermal sources, mag. fields determ. via linear polarisation spectrum (Russian) 0-90344

astrophysical plasmas in mag. and gravitational fields, MHD separation of high energy plasma 0-67547

brain, mag. evoked field mapping 0-104705

4C 32.69, quasar, discovery of ordered mag. field assoc. with radio jet 0-105375

calculation of magnetic field and force eqns., solns. using programmable calculator 0-91721

Cassiopeiae A, supernova remnant, mag. field origin 0-85989

charged particle interaction, mag. field energy, spatial distrib. of interaction contrib. 0-73625

conducting cylinders in field of conductors perpendicular to side surfaces (German) 0-106415

conducting fluid, two dims. motion, mag. field evolution, anti-dynamo theorem extension (Russian) 0-59127

crossed field plasma discharges characts. 0-100116

defect in medium, technical-saturation approx. 0-87262

eddy-current feed-through transducer, approx. calc. of mag. field, nonferromag. media 0-78746

electric machine end zone magnetic field calc. using approx. analytic method 0-106416

electron beam, magnetized, flowing through cavity, self-consistent potential calculation 0-91743

finite elements in electrical and magnetic field problems, book 0-62399

force-free field, new approach and appl. to solar active regions mag. field 0-62011



**magnetic fields continued**

- frequency/depth-penetration considerations in hyperthermia by magnetically induced currents 0-63887  
galactic magnetic field interaction with hot intergalactic gas, magnetosphere existence 0-67876  
Jupiter, bow shock and magnetosphere, Voyager 2 magnetometer obs. 0-77339  
Jupiter, effect on charged dust particles in ring, orbit changes 0-82273  
Jupiter, mag. field from 21 cm obs. of radiation belts 0-105195  
Jupiter, magnetic field similarities with pulsars, explanation for radio similarities (*Russian*) 0-77333  
Jupiter magnetic field, implications of radio emission polarisation obs. at 11 and 18 cm wavelength 0-67637  
magnetic multipole expansion, education 0-105456  
magnetic separator, drum-type with alternating polarity, analytical description of magnetic field (*Russian*) 0-99602  
Mars, magnetospheric interaction with solar wind 0-72835  
microtron electromagnet, mag. field distrib. using mag. scalar pot. 0-102597  
nonlinear magnetic field simulator for electromagnetic fields anal. (*Japanese*) 0-95756  
numerical analysis, fundamental equations and historical evolution (*Portuguese*) 0-78739  
particle acceleration near singular line of mag. field, energy spectrum (*Russian*) 0-90332  
plasma, infinitely conducting, pinch effect, dynamical accumulation towards neutral line of magnetic field 0-83977  
plasma, laser-produced, magnetic field generation 0-77818  
plasma, magnetic tape method obs. of self generated mag. fields 0-64775  
powers determination using direct analogue method (*Czech*) 0-69290  
protostellar cloud ang. momentum problem, mag. breaking 0-82342  
radio double sources (astronomical), beam and cloud stability, shear layers, two dimens. computations 0-67893  
radio sources, compact, extragalactic, mag. fields rel. to radio spectra interpretation 0-62299  
Saturn, cosmic ray cutoff rigidities in dipole mag. field 0-72873  
Saturn, dynamo precession model (*Russian*) 0-94752  
Saturn, Pioneer 11 obs. 0-82292  
Saturn magnetosphere, bowshock and magnetopause detect. by Pioneer 11, mag. field determ. 0-82283  
single-polepiece magnetic lens axial field distrib. 0-69317  
spheres and current carrying coils, integral representation of inductance 0-80469  
static field problems, numerical soln. algorithms 0-95757  
steady magnetic field from charges in arbitrary motion, education 0-105460  
steel, electrical, mag. hysteresis representation in numerical modelling of mag. fields 0-88813  
stochastic mag. field fluctuations, self-consistent model 0-100074  
straight-line current element, vector expression for mag. field 0-58440  
supernova remnant prod. 0-77474  
superstrong field production using implosion generator, solenoid for generation of initial mag. flux 0-105681  
time dependent vector field effects on mag. multipoles 0-99597  
toroidal field coils, EM parameters calcs. of current paths in homogeneous media (*Japanese*) 0-106155  
transverse magnetic field penetration through slits in ideal shield 0-78745  
two-dimensional numerical calc. of magnetic fields using summation method (*German*) 0-106414  
two-dimensional graph-theoretic model 0-87260  
uniformly magnetised body, mag. field strength invariance 0-58441  
Venus ionosphere, mag. flux ropes nature (*Russian*) 0-77313  
Venus magnetic tail field structure, role of unipolar induction effects 0-62060  
H<sub>2</sub> atoms trapping and thermal detection using superconducting magnet of low temp. 0-73396  
He, self-oscillating props. of discharge in mag. field 0-64814  
SiFe sheets, grain-oriented, stray field meas. 0-88775

**magnetic films** *see magnetic thin films***magnetic fluids**

- application in mineral microcrystal density determ. technique 0-85751  
barbotage and sedimentation, multivelocimetry model 0-61161  
behavioural props. (*German*) 0-61159  
bibliography 0-57021  
birefringence and dichroism, magnetically-induced, sign inversion 0-60548  
conductive, nonlinear magnetosonic waves 0-59121  
conference, Orlando, USA (Mar. 1980) 0-56995  
continuum mechanics, global balance law approach 0-60388  
dispersive magnetisable media, hydrodynamics including Brownian motion 0-59120  
ejecting force on nonuniform mag. bodies in ferromag. liq. 0-83855  
experimental study of mag., optical, and hydrodynamic props., review 0-60376  
ferric solution ferromagnetic liquid insulation in redox flow battery, quantum parameters separation 0-61338  
ferrofluid, dielec. behaviour in uniform mag. field 0-60390  
ferrofluid, nonlinear surface waves, bifurcation theory approach 0-58439  
ferrofluid, relax. in external mag. field, cubic cryst. case 0-71113  
ferrofluid, transverse heat transport in mag. field 0-59031  
ferrofluid behaviour in the presence of a rotating nonhomogeneous mag. field (*French*) 0-96313  
ferrofluid flow under influence of rotating mag. fields 0-59118  
ferrofluid seal against liq. 0-57270  
ferrofluid/lyotropic liq. cryst. combination, ferromagnetics and ferrocholesterics 0-59378  
ferrofluids, agglomeration, review 0-61162  
ferrofluids, appl. as acoustic transducer material 0-58877  
ferrofluids, conc. depend. mag. grain correls., small angle X-ray scatt. study 0-61160  
ferrofluids, dissipative process in non-homogeneous mag. field 0-59119  
ferrofluids, Landau and Lifshitz hydrostatic press., thought expts. 0-59111  
ferrofluids, phase diagrams and eqn. of state 0-60280  
ferromagnetic particle suspensions in non-conducting and metallic liqs., review 0-60372  
ferromagnetic suspension, residual magnetisation 0-84623  
ferromagnetic suspension serving as a liquid magnet 0-84622  
flow through porous medium with uniform mag. field oblique to interface 0-59107

**magnetic fluids continued**

- heat and mass transfer 0-59123  
instabilities, leading to rupture of continuity 0-59003  
light scattering and polarisation 0-60616  
optical birefr. and dichroism in mag. field 0-60547  
particle cluster configuration, Monte Carlo study 0-88827  
polariser for magnetising liquid, in NMR devices 0-57351  
response to mechanical, mag. and thermal forces 0-59122  
seals, high-speed cryogenic mag. fluid, for high-vacuum chambers 0-57314  
shaft seal, high-speed mag. fluid, heat dissipation 0-59032  
T bar, domain wall study employing ferrofluid, rel. to magneto-optical Kerr effect meas. 0-60360  
thermomechanics, mag. fluid as continuum with internal degrees of freedom 0-60377  
US attenuation, MHD approach 0-60389  
CoFe<sub>2</sub>O<sub>4</sub> mag. fluid particles, comp., struct., and mag. props. 0-60374  
Fe particles, dispersed in Hg, mag. props., aggregate form. 0-60375  
Fe<sub>3</sub>O<sub>4</sub> aqueous mag. fluids, dilution-stable, prep. by extended peptization techniques 0-60373  
Fe<sub>3</sub>O<sub>4</sub> ferrofluids, spin glass behaviour 0-71120  
Fe<sub>3</sub>O<sub>4</sub> mag. fluid particles, comp., struct., and mag. props. 0-60374  
Fe<sub>3</sub>O<sub>4</sub> particle suspensions in non-conducting and metallic liqs., review 0-60372  
NiFe<sub>2</sub>O<sub>4</sub> mag. fluid particles, comp., struct., and mag. props. 0-60374

**magnetic flux**

- see also flux creep; flux flow; flux-line lattice; flux pinning; fluxmeters; skin effect*  
ballistic galvanometer, error due to non-transient impulses, integral expression 0-86349  
cryogenics, magnetic flux-free environment creation 0-101797  
high-coercivity, magnetisation characteristic linearity determ. using flux controlling technique (*Russian*) 0-100597  
magnetocardiogram enhancement by applied mag. field 0-104701  
steel, electrical, mag. hysteresis representation in numerical modelling of mag. fields 0-88813  
Al superconducting film, order-parameter variations meas. 0-103797  
Fe-Si, loss meas. at high flux densities 0-88799  
Fe-Si, stator core, grain-oriented and non-oriented, magnetic flux and loss distrib. 0-88798  
Nb-Ti (50%), supercond., cryostat design for magnetisation study (*Spanish*) 0-75673

**magnetic flux jumping** *see Meissner-effect***magnetic glasses** *see spin glasses***magnetic hardness** *see ferromagnetic properties of substances***magnetic heads**

- Permalloy thin-film head pole struct., domain configurations, SEM obs. 0-65975  
vacuum-deposited layers formation, use of borosilicate glass intermediate layer 0-80979  
Fe-Si-Al ribbon-form Sendust alloy made by rapid roll quenching, mag. props., recording head appls. 0-81001  
Ni-Fe-Nb-Mo-Al, head material for mag. recording, DC and AC mag. props. 0-88812  
Ni-Zn ferrites, mag. head props., technical possibilities and limitations 0-88803

**magnetic hysteresis**

- Alnico type YuNDK25DA alloy permanent magnets, thermal mag. hysteresis 0-75818  
DC permeameter for ring specimens 0-98954  
domain boundaries, pinning on defects with finite radius of interaction, random pot. form effect on mag. hysteresis (*Russian*) 0-84611  
domain boundary with strongly localised pinning centres, influence on hysteresis (*Russian*) 0-65961  
ferromagnetic object inspection, method of higher harmonics, difference schemes 0-89444  
ferromagnetic solids, magnetomechanical effects, magnetostriction, hysteresis, stress, yielding, fatigue damage, crack growth (*Polish*) 0-71150  
ferromagnets, cyclically remagnetised, discrete spectra of induction calcs., demagnetising factor 0-103859  
hysteresisgraph with discontinuous sweep mode 0-86351  
induction meter testing, electromagnet reference measure from hysteresis effects 0-77817  
isomorphic transformation, characterisation of hysteresis processes (*Russian*) 0-80562  
metallic, glasses, soft-magnetic properties (*German*) 0-71108  
Permalloy, reference materials characts. obs., temperature effect 0-80563  
rare earth-Ag alloy, amorphous, model calcs., of mag. props. 0-84616  
rare earth-transition metal alloys, amorphous, electronic and mag. props. 0-93093  
rotational hysteresis in weak magnetic fields 0-75804  
soft mag. material representation 0-88787  
soft magnetic materials, meas. methods, review 0-86345  
steel, cold-rolled, isotropic, specific magnetic loss meas. at high frequency 0-101808  
steel, elect., mag. props. determ. with Epstein hysteresis tester 0-60364  
steel, electrical, mag. hysteresis representation in numerical modelling of mag. fields 0-88813  
steel, high-speed, low temp. mag. cycling effects on ferromag. struct. 0-100928  
steel strips, electrotechnical, mag. props. meas. using AC compensated permeameter 0-86352  
Al<sub>3</sub>Mn<sub>2</sub>Si<sub>2</sub>O<sub>12</sub>, amorphous insulating spin glass, susceptibility and magnetisation meas. 0-88765  
Au<sub>8</sub>Fe<sub>15</sub> and Au<sub>8</sub>Fe<sub>18</sub>, mag. props. 0-84592  
Ba hexaferrite, irradiated by fast neutrons, mag. props. 0-97116  
BaFe<sub>2</sub>O<sub>9</sub> microparticles, magnetisation reversal, hysteresis loop obs. 0-75813  
BaFe<sub>2</sub>O<sub>9</sub> powder, hysteresis of microwave absorpt. and magnetisation reversal 0-75814  
BaO-Mn<sub>2</sub>O<sub>3</sub>-B<sub>2</sub>O<sub>3</sub>, amorphous mag. oxide, field-cooling effect (*Japanese*) 0-84615  
Co-CoO films, evaporated, exchange anisotropy 0-88841  
Co-Fe amorphous alloys, worked, perminvar type mag. hysteresis loop, longit. Kerr effect obs. 0-65958  
Co-P, electrodeposited amorphous alloys with high permeability, thermal treatment with and without field 0-89372  
Co-W alloy electrodeposition, influence of MgSO<sub>4</sub> and gum arabic additives (*Russian*) 0-80991



**magnetic hysteresis continued**

- Co-W alloy electrolytic coatings, heat treatment effects on coercivity, hysteresis and structure (*Russian*) 0-60381  
 CoFe<sub>2</sub>O<sub>4</sub> mag. fluid particles, comp., struct., and mag. props. 0-60374  
 Cu-Mn alloy spin glass, macroscopic mag. anisotropy, transverse susceptibility and zero field NMR enhancement 0-80525  
 Cu-Mn-Al alloys, displaced hysteresis loop and microstructure obs. 0-84613  
 CuMn, hysteresis, spin orbit scattering effect on anisotropy in spin glass state 0-71095  
 Cu<sub>0.86</sub>Mn<sub>0.14</sub>, hysteresis loop development 0-65922  
 Dy, magnetic domain structure, hysteresis, thermal modulation study 0-71082  
 Dy-Cu, amorphous, mag. phase diagram, magnetisation and sp. ht. meas. 0-80532  
 DyCu film, amorphous, asperomagnetic domains, Barkhausen jumps in hysteresis loop 0-75822  
 DyPO<sub>4</sub>, mag. transitions under hydrostatic press., neutron diff. study 0-71030  
 (Fe,Co,Ni)-Si(B), amorphous mag. alloy, magnetostriction rel. to soft mag. props. 0-84633  
 Fe-Co-Ni Perminvar, mag. props. singularities in region of mag. anisotropy (*Russian*) 0-84614  
 Fe-Co-Si-B, amorphous soft ferromagnet with high mag. induction 0-84619  
 Fe-Co-Si(B), amorphous ferromagnet, mag. after effect on soft mag. props. 0-84626  
 Fe-Cr-Co alloys, (5-9 wt.% Co), obtained by slow cooling under mag. field, permanent magnet props. 0-75797  
 Fe-Si, (110) [001] oriented, mag. props., compressive stress effects 0-60392  
 Fe-Si, grain oriented sheet, AC hysteresis, surface struct. and elastic stress effects 0-88791  
 Fe-Si (3 wt.%), grain-oriented, stacking effect on power loss, mag. props. 0-88795  
 Fe-Si (6.5 wt%) filament, formation by modified Taylor technique, and mag. props. 0-75795  
 Fe-Si-B, magnetic metallic glasses, mag. props. 0-84620  
 Fe-Tb, magnetoelastic hysteresis, elastic stress and mag. field depend. (*Russian*) 0-65982  
 Fe-W-Cr-Mo system, mag. and mech. props. rel. to production methods (*Japanese*) 0-71107  
 Fe<sub>2</sub>Co<sub>2</sub>B<sub>20</sub>, amorphous, magnetisation reversal and domain boundary configs. 0-88809  
 Fe<sub>3</sub>Co<sub>3</sub>B<sub>20</sub>Si<sub>10</sub>Al<sub>3</sub>, stress-induced variation in magnetisation and dynamic magnetostrictive charact. 0-88855  
 (Fe<sub>0.05</sub>Co<sub>0.95</sub>)<sub>78</sub>Si<sub>2</sub>B<sub>14</sub> amorphous ribbon, anomalous mag. aftereffect 0-100602  
 (FeNi)<sub>80</sub>Bi<sub>17.5</sub>Al<sub>2</sub>Si<sub>0.5</sub>, stress-induced variation in magnetisation and dynamic magnetostrictive charact. 0-88855  
 (Fe,Ni)<sub>1-x</sub>80P<sub>10</sub>B<sub>10</sub>, amorphous, magnetisation reversal and domain boundary configs. 0-88809  
 Fe<sub>2</sub>O<sub>3</sub> mag. fluid particles, comp., struct., and mag. props. 0-60374  
 Fe<sub>80</sub>Si<sub>20</sub>, amorphous, soft mag. props. and potential uses 0-88807  
 Fe<sub>3-x</sub>Ti<sub>x</sub>O<sub>4</sub>, 0.5 ≤ x ≤ 1, mag. props. of antiferromag. phase 0-70960  
 Fe<sub>3-x</sub>Ti<sub>x</sub>O<sub>4</sub>, spin glass behaviour, susceptibility and hysteresis meas. 0-65917  
 (Gd,Tm,Y)<sub>3</sub>(Fe,Ga)<sub>2</sub>O<sub>12</sub> LPE garnet thin films, magnetocrystalline anisotropy 0-93147  
 GdBr<sub>3</sub> single crystals, mag. behaviour and structure change at low temp. 0-71018  
 Li<sub>0.5</sub>Mn<sub>0.15</sub>Fe<sub>2.35</sub>O<sub>4</sub> ferrite cores with rectangular hysteresis loops, pulse parameters, effect of Fe<sub>2</sub>O<sub>3</sub> heat treatment 0-60370  
 MnO:Mn<sub>2</sub>O<sub>3</sub>, mag. props., susceptibility and magnetisation meas. 0-65824  
 NiFe<sub>2</sub>O<sub>4</sub> mag. fluid particles, comp., struct., and mag. props. 0-60374  
 Ni(110), ferromag., surface magnetisation, polarised LEED expt. 0-97118  
 Pt-Fe alloy, ordered, T-c phase diagram, antiferro- and ferromagnetism (*Russian*) 0-65871  
 R<sub>2</sub>In, R<sub>2</sub>In, R=Gd, Tb, Dy, Ho, Nd, mag. props. 0-108009  
 SmCo<sub>5</sub>, sintered, hard mag. material, magnetisation behaviour 0-75805  
 SmCo<sub>5</sub>, coercive force depend. on annealing temp. 0-65964  
 (Tb<sub>1-x</sub>Gd<sub>x</sub>)<sub>2</sub>Co, intermetallic cpd. mag. props., phase transform, and mag. hysteresis (*Russian*) 0-93113  
 V (Ti), supercond., rotating discs, hysteresis losses and mag. phenomena 0-75695  
 Y(Fe,Co)<sub>1-x</sub>, x ≤ 0.2, mag. props. and Mossbauer meas. 0-75798

**magnetic impurity interactions**

- alloys, dil. mag., transport props. in mag. field, impurity-electron scatt. 0-65541  
 alloys, magnetic localisation and charge oscillations 0-75781  
 aluminoborate glass, Fe and Cr ion interaction, mag. and spectral props. 0-103883  
 antiferromagnet, impure, Heisenberg model, impurity banding and mag. reson., theory 0-93181  
 Baxter-Wu model, site impure modified crit. behaviour and crossover 0-60322  
 borosilicate glass, Fe and Cr ion interaction, mag. and spectral props. 0-103883  
 conduction electron-magnetic ion Coulomb interactions, unitary transform., spin angular momentum operators 0-84451  
 dilute magnetic alloys, electron sound absorpt., disordered mag. impurities, spin glasses (*Russian*) 0-80503  
 dimethyl ammonium manganese chloride, quasi one-dimensional mag. systems, impurity effects 0-71015  
 dimethylammonium manganese trichloride: Cd(Cu), impurities in quasi-one-dimens. Heisenberg systems, anisotropy effect 0-80502  
 ferromagnet, one-dimensional localised nuclear magnon modes 0-93098  
 ferromagnetic Fermi-liquid model, electron-impurity system hydrodynamics, elec. cond. 0-103835  
 ferromagnets, spin wave excitation due to parallel pumping, mag. impurity interactions (*Russian*) 0-84097  
 Heisenberg antiferromagnet, one-dimens., impure, mag. susceptibility 0-60168  
 Heisenberg magnet, impurity band resonance at 0K, theory 0-66041  
 Heisenberg model, randomly dilute, renormalisation group calcs. 0-60321  
 Ising chain, spin-1, sp. ht. in presence of impurities and mag. field 0-93128  
 Ising ferromagnet, randomly dilute, conc. expansion study 0-60315

**magnetic impurity interactions continued**

- Ising model, bond-dil. two-dimens., phase transition 0-60320  
 Kondo lattice, impurity interactions, ground state calc., impurity conc. effect 0-65782  
 manganese formate dihydrate, Zn- and Mg-substituted, anomalous crit. phenomena 0-60316  
 metals, hyperfine mag. fields at <sup>119</sup>Sn nuclei 0-60248  
 metals, Kondo effect, Anderson hamiltonian 0-60187  
 MIM tunnel junction, magnetically doped, hopping model of zero-bias tunnelling anomalies, comparison with expt. 0-65703  
 nonmagnetic metal, s-d exchange model exact solution, mag. susceptibility, mag. impurity interactions (*Russian*) 0-70943  
 one dimensional randomly dilute Ising ferromagnet, dynamics 0-70922  
 proximity systems with magnetic impurities, DC Josephson effect 0-100554  
 spherical model with layered impurities, critical behaviour 0-93124  
 spin XY one dimensional system containing impurities, static mag. props. (*Russian*) 0-65826  
 TMCC, one-dimens. magnet, local magnon modes 0-65829  
 Cd<sub>1-x</sub>Mg<sub>x</sub>, energy spectrum pseudopotential calcs., mag. props., impurity scatt. (*Russian*) 0-65430  
 Co-Fe, dil., hyperfine mag. fields, press. effect, Mossbauer meas. 0-71277  
 Cr-Fe, dil., magnetisation, Fe local moments 0-60215  
 Cr-Fe (6.5 wt.%), atomic clustering and mag. defects, mag. moments 0-60246  
 Cr-Si, dilute alloy, mag. susceptibility and Neel temp. meas. 0-71017  
 CsMnCl<sub>3</sub>·2H<sub>2</sub>O, quasi one-dimensional mag. systems, impurity effects 0-71015  
 CsMn<sub>1-x</sub>Cu<sub>x</sub>Cl<sub>3</sub>·2H<sub>2</sub>O, impurities in quasi-one-dimens. Heisenberg systems, anisotropy effect 0-80502  
 CsNiF<sub>3</sub>, one-dimens. magnet, local magnon modes 0-65829  
 Cu-Fe group, dil., NMR satellite data calc., struct. of mag. impurities 0-103894  
 Cu-Mn-Au(Pt) spin glasses, anisotropic exchange interactions, effect of nonmag. impurities 0-80534  
 CuCr(Fe)(Mn), dil., anisotropic hyperfine coupling, NMR study 0-65784  
 CuMn, hysteresis, spin orbit scattering effect on anisotropy in spin glass state 0-71095  
 Fe-P(Ga)(As)(Sb), dil., short range order, NMR study 0-71237  
 Fe-Sb-Ni(Cr), dil., short range order, NMR study 0-71237  
 Fe<sub>2</sub>Mn, antiferromag., NMR relax., impurity bonding 0-66061  
 Fe<sub>2</sub>Mn, antiferromag. reson. and local magnon mode, FIR laser study 0-66042  
 Fe<sub>2</sub>Mn, Heisenberg model, impurity band resonance at 0K, theory 0-66041  
 (Fe<sub>1-x</sub>Mn<sub>x</sub>)<sub>2</sub>Y(B), Mn effect on Fe mag. moments, Mossbauer and mag. meas. 0-71016  
 (Fe<sub>0.2</sub>Ni<sub>0.8</sub>)<sub>1-y</sub>(SiO)<sub>y</sub>, Permalloy material, magnetisation, temp. and impurity atom conc. depend., band model calcs. (*Russian*) 0-93088  
 Fe<sub>70</sub>P<sub>13</sub>B<sub>8</sub> amorphous alloys, sput cooled, Mn, Cr and V substituted, mag. and transport props. 0-84593  
 K<sub>2</sub>MnF<sub>4</sub>:Zn(Mg)(Ni), mag. effects of impurities 0-65869  
 K<sub>2</sub>MnF<sub>4</sub>:Zn(Mg)(Ni), local magnetisation, NMR and Green's function study 0-65870  
 MnO:Mn<sub>2</sub>O<sub>3</sub>, mag. props., susceptibility and magnetisation meas. 0-65824  
 Ni, paramag. region, Fe and Co impurity effects on susceptibility, Faraday obs. (*Russian*) 0-88731  
 Ni-Fe, dil., hyperfine mag. fields, press. effect, Mossbauer meas. 0-71277  
 Ni<sub>88</sub>M<sub>2</sub>, M=impurity metal, formation of MH(D)-complexes 0-65236  
 PrIn<sub>3</sub>, nucl. orientation of <sup>144</sup>Pm in singlet ground state, exchange interaction and cryst. field splitting obs. 0-71275  
 Si:Gd(Pr), photoconductivity anomalies due to mag. impurities (*Russian*) 0-103722  
 ZnMn, dil., magnetoresist. meas., temp. depend. anisotropy 0-65532

**magnetic inks see magnetic fluids****magnetic leakage**

- amorphous alloys, mag. props. rel to device appl. 0-88804  
 composite multifilamentary superconductor carrying DC transport currents, transient field losses 0-84551  
 errors, systematic and random, in wattmeter apparatus for measuring unit losses in electrical steel sheet 0-71858  
 ferrimagnetic Bloch wall oscills., viscosity coeffs. freq. depend., permeability and mag. losses 0-71094  
 ferrites, soft, production and props. 0-88801  
 ferromagnetic plates eddy current phenomena numerical computation method (*German*) 0-65952  
 form factor influence on measurement of losses in sheets (*Rumanian*) 0-68226  
 power loss meas. under sinusoidal flux conditions 0-86348  
 soft magnetic materials, meas. methods, review 0-86345  
 steel, B-Si, grain-oriented, high induction, Cu impurity effects 0-89366  
 steel, cold-rolled, isotropic, specific magnetic loss meas. at high frequency 0-101808  
 superconductor, multifilamentary, mag. props. effect on losses in variable mag. field 0-60136  
 Co-Fe-V-Ni, mag. and mech. props., heat treatment and stress effects 0-60363  
 Co<sub>3</sub>Fe<sub>2</sub>Ni<sub>10</sub>(Si<sub>2</sub>B)<sub>28</sub>, amorphous, soft mag. props., switched-mode power supply appls. 0-88850  
 Fe powder-plastic composite, soft mag. material, mag. and mech. props. 0-75812  
 Fe-B-C amorphous alloys with high saturation induction 0-84617  
 Fe-Ci (3 wt.%), local magnetisation losses, grain orientation effect 0-88817  
 Fe-Co-Ni Perminvar, mag. props. singularities in region of mag. anisotropy (*Russian*) 0-84614  
 Fe-Co-Si-B, amorphous soft ferromagnet with high mag. induction 0-84619  
 Fe-Ni-Mn, Invar, RF collapse and thermal effects, Mossbauer study 0-100624  
 Fe-Si, (110) [001] oriented, mag. props., compressive stress effects 0-60392  
 Fe-Si, grain oriented, misorientation effects on mag. props 0-88792  
 Fe-Si, grain-oriented sheets, high permeability, low losses, review 0-88790  
 Fe-Si, loss meas. at high flux densities 0-88799  
 Fe-Si, mag. props., stress and reannealing effects 0-88844



**magnetic leakage continued**

- Fe-Si, power loss and permeability meas. by means of Hall probes and stochastic ergodic correl. 0-86350  
 Fe-Si, stator core, grain-oriented and non-oriented, magnetic flux and loss distrib. 0-88798  
 Fe-Si (3 to 5 wt.%) sinters, mag. props., Si and Fe-Si additions effect 0-71104  
 Fe-Si (3 wt.%), domain wall spacing and core loss, forsterite and stress coatings effect 0-88780  
 Fe-Si (3 wt.%), grain-oriented, stacking effect on power loss, mag. props. 0-88795  
 Fe-Si (3 wt.%), grain-oriented, power loss and domain wall variation with lamination thickness 0-88814  
 Fe-Si (3 wt.%), high permeability, use in transformer cores 0-88793  
 Fe-Si (3 wt.%), losses, demagnetisation freq. and grain orientation depend. 0-88796  
 Fe-Si (3 wt.%), mag. loss and magnetostriction, DC flux alternation effects 0-88794  
 Fe-Si (3 wt.%), oriented, losses and domains, mech. stress effects 0-88852  
 Fe-Si (3 wt.%), power losses at extremely low freqs. 0-88815  
 Fe-Si (3 wt.%), stripe domain structure, dynamic behaviour at high max. induction values (*Russian*) 0-80553  
 Fe-Si (3 wt.%) laminations, grain oriented, plastically deformed, anomalous losses 0-88853  
 Fe-Si (6.5 wt.%) ribbon, splat-cooled, mag. props. 0-88805  
 Fe<sub>40</sub>B<sub>40</sub>P<sub>14</sub>B<sub>6</sub> and Fe<sub>40</sub>B<sub>30</sub>, Metglas 2826 and 2605, amorphous ribbon, power loss variation with freq. and applied stress 0-88849  
 Fe<sub>40</sub>Ni<sub>40</sub>B<sub>20</sub>, amorphous ribbon, power loss variation with freq. and applied stress 0-88849  
 Fe<sub>40</sub>Ni<sub>40</sub>(Mo,Si,B)<sub>20</sub>, amorphous, soft mag. props., switched-mode power supply appls. 0-88850  
 Fe<sub>80</sub>Si<sub>20</sub>B<sub>15</sub>, amorphous, soft mag. props. and potential uses 0-88807  
 MnSb, magnetic losses, ferromagnetic resonance and antiresonance 0-100618  
 Ni-Fe, power losses at extremely low freqs. 0-88815

**magnetic lenses**

see also aberrations

- aberration formulae, approximate 0-95781  
 aberrations, reduction by optimisation techniques 0-87290  
 design, finite element program improvement 0-69316  
 einzel lens, satisfying anastigmatic and achromatic conditions 0-87288  
 electron, min. spherical aberration 0-87287  
 electron gun, with electrostatic and electromagnetic lenses 0-99007  
 electron microscope spiral distortion correction double-lens system 0-68327  
 sextupole corrector limitations 0-102604  
 single-pole magnetic lens as condenser for field emission electron gun 0-68325  
 single-polepiece magnetic lens axial field distrib. 0-69317  
 single-polepiece objective and projector lenses for electron microscope 0-68326  
 spherical aberration, correction by foil lens, appl. to STEM 0-87294  
 superconducting lens, electron microscope appl. 0-86530  
 superconducting lens system for 500 kV electron microscope 0-68321

**magnetic levitation**

- electrodynamic suspension system, current coil interaction with semi-infinite superconducting sheet (*Russian*) 0-83539  
 fusion reactor, multipole fusion confinement with 2 MA levitated superconducting coil 0-106191

**magnetic lines of force** see magnetic flux**magnetic liquids** see magnetic fluids**magnetic losses** see magnetic leakage**magnetic materials**

- see also ferrites; garnets; magnetic fluids; magnetic thin films; permalloy; permanent magnets  
 conference, Munich, Germany (Sep. 1979) 0-56997  
 hard material demagnetisation curve evaluation 0-90869  
 magnetic anisotropy of electrical steel sheet, determ. method and laboratory tests (*Polish*) 0-97071  
 nonferromagnetic media, triple-layer, approx. calc. of mag. field of feed-through transducer 0-78746  
 prediction of existence using cybernetic computer learning methods 0-108048  
 soft, conf., Munster, Germany (Sept. 1979) 0-86032  
 Co permanent magnet material savings (*German*) 0-103851

**magnetic materials, amorphous** see magnetic properties of amorphous substances**magnetic mirrors**

- axisymmetric mirror machine, MHD stable confinement possibilities 0-83988  
 Beta II, field reversed expt., device description 0-91274  
 Beta-II, magnetised coaxial plasma gun mechanical design and construction 0-91271  
 electron and plasma stream reflection at a nonadiabatic mirror 0-87929  
 electron beam stabilised mirror confined gas, hot electron population study 0-100089  
 electron heating, ion cyclotron influence in min-B mirror trap 0-79521  
 field reversed mirror confinement, finite gyro-radius effects 0-83989  
 field reversed mirror neutral beam startup, hybrid plasma code simulation 0-99313  
 fusion reactors, Tokamak and tandem mirror reactors, neutral beam injection and superconducting magnets 0-63391  
 gas lasers with non-self-sustaining discharge, mag. mirrors (*Russian*) 0-106530  
 high density machines, critical lengths 0-64768  
 ion confinement increases, Joule heating 0-83985  
 loss suppression from mirror ends 0-83987  
 MFTF, BBC CQK 200-4 modulator tube for sustaining neutral beam power supply 0-99290  
 MFTF, cryogenic system 0-106163  
 MFTF, electrical systems, overview 0-91278  
 MFTF, end loss region high energy plasma gettering 0-102343  
 MFTF, exception handling control system 0-99325  
 MFTF, intense neutron environment, test cell side wall design, shielding materials 0-102318  
 MFTF, ion and neutral beams dumps, design 0-102317  
 MFTF, mag. cryostability 0-106198  
 MFTF, neutral beam accel power supply protection 0-102380

**magnetic mirrors continued**

- MFTF, neutral beam module component design and development 0-91270  
 MFTF, neutral beam source development 0-102368  
 MFTF, plasma buildup, contaminant control 0-95461  
 MFTF, plasma diagnostics system 0-95444  
 MFTF, plasma streaming system, description 0-91280  
 MFTF, power supply system, digital simulation using EMTF code 0-91286  
 MFTF, start up neutral beam power supply system 0-91281  
 MFTF, superconducting mag. quench vent rate 0-106197  
 MFTF, supervisory control and diagnostics system, database management system 0-99326  
 MFTF, supervisory control and diagnostics system, database management system, data structs. 0-99327  
 MFTF, supervisory control and diagnostics system software 0-99324  
 MFTF, sustaining neutral beam power supply, cct. anal. using ASTAP and EMTF codes 0-91284  
 MFTF, sustaining neutral beam power supply, shunt preconditioner, IBM-ASTAP anal. 0-102332  
 MFTF, sustaining neutral beam power supply system, modelling with ASTAP code 0-91285  
 mFTF plasma diagnostics Data Acquisition System 0-99319  
 MFTF superconducting mag. design and construction 0-101008  
 MFTF-B, full tandem extension, description 0-99294  
 Mirror Fusion Test Facility, superconductor core manufacturing and quality 0-93521  
 Mirror-Torus-System-1 with divertor mag. field, plasma density and depolarisation current 0-70022  
 multiple mirror, coil design and economic optimisation 0-99284  
 multiple mirror system, for high density confinement 0-92364  
 nonadiabatic leakage of particles from mag. mirror trap, multiple lifetimes 0-106968  
 nonlinear converging resonance cones in Princeton L-3 device 0-59262  
 particle stochastic motion in mirror machines 0-59264  
 picket-fence surface magnetic fields at end of magnetised plasma 0-87922  
 plasma confinement in mirror and cusp fields, Monte Carlo simulation 0-96379  
 plasma confinement time investigation using Monte Carlo simulation 0-64770  
 production of large-radius, high-beta, confined mirror plasma 0-87907  
 reversed field mirror reactors, startup using coaxial plasma guns, scaling laws 0-99279  
 SAFFIRE, Cat-D fueled, synthetic and fissile fuel prod. 0-99280  
 spheromak devices, magnetohydrostatic equilibrium config. 0-83965  
 tandem mirror plasmas, alpha particle dynamics 0-83986  
 Tandem Mirror Reactor, end plug mag. system design 0-102347  
 Tandem Mirror Reactor power plant, maintenance and handling economics 0-102311  
 Tandem Mirror Reactor startup and shutdown, simulation and control 0-99277  
 Tandem Mirror Reactor steady state, simulation and control 0-99278  
 TMX, config., liq. N<sub>2</sub> supply and operation of vacuum system 0-95448  
 TMX, injector system mech. design and installation 0-99393  
 TMX, installation and operation of cryoliner in vacuum system 0-95449  
 TMX, mag. control system 0-95442  
 TMX, magnet construction and alignment 0-91266  
 TMX, neutral beam control systems 0-99323  
 TMX, neutral beam system startup 0-99306  
 unneutralized electron cloud injection and containment in bumpy toroidal mag. field 0-64761  
 USA, mirror machine research progress 0-74016

**magnetic moments**

- see also atomic magnetic moment; hyperon magnetic moment; local moments in dilute systems; meson magnetic moment; molecular moments; nuclear magnetic moment; proton magnetic moment  
 actinide elements and compounds, mag. props., book contrib. 0-75727  
 amorphous ferromagnets, book contrib. 0-75743  
 anomalous magnetic moment, perturbative expansion divergence 0-78063  
 baryon, magnetic moments, ground-state, SU(6) symmetry 0-78064  
 baryons, b-quark, magnetic moments, broken SU(5) symmetry 0-95257  
 baryons, leptonic decays and mag. moments in nonlocal quark model (*Russian*) 0-86711  
 classical mag. moment system, antiferromag. phase transition, secular dipole interactions 0-80551  
 composite leptons and quarks, anomalous mag. moment, flavour as dynamical quantum number 0-105854  
 composite leptons and quarks, mag. moment 0-105896  
 composite quarks and leptons, mag. moments 0-91056  
 copper formate tetrahydrate, antiferromag. phase, neutron diff. study 0-93085  
 cyclohexyl ammonium copper chloride, one dimensional spin 1/2 ferromag., mag. props. 0-71000  
 electron anomalous magnetic moment, muon effects in QED 0-62899  
 ferrite, hexagonal, with M, W and Y structures containing Fe<sup>2+</sup> and Fe<sup>3+</sup> mag. ions, saturation moment and anisotropy 0-71009  
 ferromagnet, itinerant, mag. props., temp. depend., functional integral approach 0-60170  
 ferromagnet, tight binding model, surface magnetisation 0-103807  
 ferromagnet magnetisation, influence of high intensity longitudinal sound waves 0-103875  
 giant moments and spin glasses, order out of disorder (*Dutch*) 0-97107  
 hadron magnetic dipole transition, quark anomalous mag. moments (*Russian*) 0-82975  
 intermediate valence compounds, dynamic susceptibilities 0-70653  
 intrinsic semiconductors, indirect exchange interaction, finite temp., valence bands and energy gaps effect 0-59943  
 Kondon lattice, impurity interactions, ground state calc., impurity conc. effect 0-65782  
 liquid metals and alloys, mag. model 0-88719  
 magnetic multipole expansion, education 0-105456  
 manganese carboxylate, dodecanuclear mixed-valence, prep., struct., and mag. props. 0-107196  
 massive neutrinos, mag. moment and spin rotation 0-105895  
 metals, ground state of solids, spin density functional method, binding energy, compressibility 0-65477  
 metals, polar states and free electron gas, mag. moments (*Russian*) 0-84415



**magnetic moments continued**

- MIT bag model, charmed and b-flavoured hadron mag. moments 0-95271
- naive quark model predictions for meson mass and baryon mass and mag. moment 0-78036
- nuclear magnetism and ultralow temperature, review (*Japanese*) 0-86806
- polarisation and magnetisation of electronic matter 0-75929
- rare earth-Ag alloy, amorphous, model calcs., of mag. props. 0-84616
- rare earth-transition metal alloys,  $\text{RM}_2\text{Si}_2\text{-Ge}_2$  and  $\text{RM}_{4-x}\text{Al}_{8-x}$ , magnetism and hyperfine interactions, magnetisation and Mossbauer effect studies 0-75892
- rotation operators, time-depend. aspects, teaching 0-90634
- spatial distribution in single ground state systems with impurities 0-97074
- spin XY one dimensional system containing impurities, static mag. props. (*Russian*) 0-65826
- spinning charge, torsion contrib. to magnetic field 0-77676
- SU(2)XU(1) gauge model, muon anomalous mag. moment, charged Higgs boson contrib. 0-78011
- superconductor, mag. scatt. of neutrons 0-103819
- superconductor, magnetic, spin fluctuation and US attenuation 0-80445
- superparamagnetic particles, magnetic moment time development and discrete orientation model 0-60378
- texture analysis, generalisation of dispersion theory 0-80556
- transition metal 3d monoxides, specific vol. and mag. moment calcs. 0-65822
- transition metal alloys, amorphous, mag. props., chem. short-range order 0-75739
- transition metal alloys, amorphous, mag. props., structure and preparation 0-75737
- 3d-transition metal complexes, low spin-high spin paramag. transition, Ising model calc. 0-93073
- transition metal intermetallic cpds., H absorption and mag. props. 0-60224
- transition metals, paramagnetic state, itinerant electron model 0-65769
- uniaxial antiferromagnetic, phase diagram, spin flop transition (*Russian*) 0-100587
- bb baryons, mag. moment sum rules, in  $\text{Su}(S)$  0-78065
- $\chi$ - $\psi\gamma$ , charmonium E1 radiative transitions and quark mag. moments 0-86721
- e, anomalous magnetic moment, QED test 0-77996
- $\mu$ , anomalous magnetic moment, QED test 0-77996
- $\mu$  anomalous magnetic moment, free gluon mass, lower bound in integer-quark-charge model 0-78042
- $\nu$ , EM form factors and mag. moments, Weinberg-Salam model and extensions (*German*) 0-62904
- $\psi$ - $\chi\gamma$ , charmonium E1 radiative transitions and quark mag. moments 0-86721
- $\text{Au}_{85}\text{Fe}_{15}$ , and  $\text{Au}_{87}\text{Fe}_{13}$ , mag. props. 0-84592
- $\text{BaVS}_3$ , magnetisation and neutron study 0-84588
- $\text{Cd}_{1-x}\text{Ni}_x\text{Fe}_2\text{O}_4$ , solid soln., mag. and structural characterisation 0-103906
- $\text{CeIn}_3$ , mag. struct., neutron diffr. study 0-80481
- $\text{Ce}_2\text{Mg}_3(\text{NO}_3)_{12}\cdot 24\text{H}_2\text{O}$ , ground state with dipole-dipole and exchange interactions in external mag. field 0-84582
- $\text{CeNi}_3$ , and ternary hydride, mag. props. 0-108007
- $\text{Ce}_{(1-x)}\text{Fe}_x$ , mag. susceptibility and Mossbauer meas., lattice parameters 0-97068
- Co fine particles in Cu, interface magnetisation 0-88858
- Co-Mn alloys, ferromagnetic, high field mag. susceptibility meas. 0-75729
- Co-V, Co rich, ferromag. behaviour, mag. moments, Curie temp., and NMR spectrum 0-70964
- $\text{Co}_2\text{Ga}_{8-x}$ , NMR expts. interpretation 0-75870
- $\text{CoMnSi}_{1-x}\text{Ge}_x$ , amg. props. 0-60270
- $\text{Co}_{1-x}\text{Te}_x$ , fluctuating localised mag. moments, d band motion, Mossbauer study 0-65768
- CoV alloys, phase dependent MNR spectra 0-108114
- Cr, electronic struct., spin-density functional calcs. 0-88476
- Cr-Fe (6.5 wt.%), atomic clustering and mag. defects, mag. moments 0-60246
- Cr-Ge system, XPS, X-ray and neutron diffr. and mag. meas. to study chem. bonding and electronic struct. 0-60749
- $\text{Cr}_2\text{Mo}_{1-x}\text{O}_7$  ( $x \leq 0.5$ ), mag. moment rel. to Cr content 0-70177
- $\text{CrO}_2$ , particulate, proton donor adsorption effect on mag. moment, XPS anal. 0-71117
- $\text{CsMnF}_4$ , planar ferromag., cryst. and mag. struct., Jahn-Teller effect 0-75715
- $\text{CsNiF}_3$ , one-dimensional ferromagnet, optical absorpt. and static spin correlation functions 0-71415
- Cu-Ni, random ferromag. alloy, local mag. moment calc. 0-70974
- $\text{CuCr}_2\text{Se}_4$ , mag. moment distrib. by neutron diffr., Goodenough model 0-70945
- $\text{Cu}_{1-x}\text{Cr}_x\text{Se}_4$ , influence of excess Cu on physical props. 0-103836
- $\text{Cu}_2\text{Fe}_2\text{O}_7\cdot\text{ZnFe}_2\text{O}_4$ , cation distrib., mag. moment, Mossbauer spectra, chem. anal. 0-75210
- CuMn, spin glass, random moments time correl., zero field muon spin relax. meas. 0-60335
- $\text{Cu}_2\text{NiSi}_3\text{X}$ , X-ray cryst. struct. determ., mag. props. 0-107172
- Dy, visible spectra obs., hyperfine struct., mag. dipole and electric quadrupole interaction const. anal. 0-91698
- $\text{DyCo}_2$ - $\text{DyAl}_2$  system, mag. and structural studies 0-108006
- $\text{ErRh}_2\text{B}_4$ , superconducting, magnetic dilemma 0-75680
- $\text{ErTiO}_3$ , magnetic structure determination, neutron scatt. study 0-65809
- $\text{EuIrH}_5$ , prep., cryst. struct., mag. and elec. props. 0-88117
- $\text{EuS-Ga}_2\text{S}_3\text{-GeS}_2$ , chalcogenide glasses, conditions of form. of glassy prod. (*French*) 0-100325
- $\text{Eu}_{1-x}\text{Yb}_x\text{Te}$ , ( $0 < x < 1$ ), mag. semicond., elec., mag. and optical props. 0-97070
- $\gamma$ -Fe, FCC film, epitaxial growth on CuAu (111) surfaces, strong ferromagnetism 0-70557
- Fe film, nuclear spin system dynamics Mossbauer study in FMR conditions (*Russian*) 0-80651
- Fe group, mol. Jahn-Teller reson. states as possible antecedents to magnetism 0-75701
- Fe, magnetic moments, local short range order, high temp. effects 0-65902
- Fe-B, amorphous alloy, mag. props. 0-84618
- Fe-B-C, amorphous, effects of replacement of B by C on mag. props. 0-84621
- Fe-Cr, BCC, local moments in Mossbauer study 0-108125

**magnetic moments continued**

- Fe-Cr, random ferromag. alloys, local mag. moment calc. 0-70974
- Fe-Ni, magnetisation calc. method based on moments of density of states 0-65770
- Fe-Pd Invar alloys, elec. and mag. props. and thermal expansion 0-75732
- Fe-SiO multilayer films, interface magnetisation 0-88858
- $\text{Fe}_3\text{Al}(\text{Si})$ , electronic structure, magnetic moments 0-107695
- $\text{Fe}_{1-x}\text{B}_x$ , amorphous, hyperfine fields and local mag. moments, Mossbauer study 0-75895
- $\text{FeCl}_3$ , magnetic transition and sublattice mag. moment rotation nonequivalence (*Russian*) 0-100586
- $\text{FeCl}_2$ , reorientation of mag. moments under mech. stresses at 0K 0-93153
- $(\text{Fe}_{0.5}\text{Co}_{0.5})_{1-x}\text{B}_x$ , amorphous, hyperfine fields and local mag. moments, Mossbauer study 0-75895
- $(\text{Fe}_{93}\text{Cr}_7)_{79}\text{P}_{13}\text{B}_8$  and  $(\text{Fe}_{96}\text{Cr}_4)_{79}\text{P}_{13}\text{B}_8$ , amorphous, low temp. sp. ht., mag. contribs. 0-80552
- $(\text{Fe}_{1-x}\text{Mn}_x)_2\text{Y}(\text{B})$ , Mn effect on Fe mag. moments, Mossbauer and mag. meas. 0-71016
- $(\text{Fe}_{1-x}\text{Ni}_x)_{10}\text{B}_{20-x}\text{P}_x$ , amorphous, hyperfine fields and local mag. moments, Mossbauer study 0-75895
- $\text{Fe}_{1.6}\text{Ni}_{78.4}\text{B}_{10.0}$ , metallic glass, superparamag. behaviour, chem. inhomogeneities role 0-84625
- $(\text{Fe}_{1-x}\text{Ni}_x)_{80}\text{P}_{20}$ , amorphous, ferromagnetic alloys, mag. anomalies of Invar type (*Russian*) 0-93089
- $\text{Fe}_{79}\text{P}_{13}\text{B}_8$ , amorphous alloys, splat cooled, Mn, Cr and V substituted, mag. and transport props. 0-84593
- $\text{Fe}_{90}\text{P}_{20-x}\text{C}_x(\text{Si}_x)(\text{Ge}_x)$ , amorphous, size effect of metalloids on mag. props. 0-84594
- $\text{Fe}_{1-x}\text{Te}_x$ , fluctuating localised mag. moments, d band motion, Mossbauer study 0-65768
- $\text{Fe}_{90}\text{P}_{20-x}\text{C}_x(\text{Si}_x)(\text{Ge}_x)$ , amorphous, size effect of metalloids on mag. props. 0-84594
- Gd-Al(C)(Cu)(Ga)(Ni)(Pd)(Rh) alloys, amorphous, mag. and elec. props. 0-80499
- Gd $\text{Eu}_{1-x}\text{B}_6$ , solid solns., mag. susceptibility, 80 to 1000K (*Russian*) 0-88713
- GdIG, local mag. anisotropy in stress field of single dislocation 0-88744
- Gd $\text{La}_{1-x}\text{B}_6$ , solid solns., mag. susceptibility, 80 to 1000K (*Russian*) 0-88713
- GdMn $_2$ -GdAl $_3$  system, mag. and structural studies 0-108006
- GdRh $_2\text{B}_4$ , magnetic and electrostatic props., NMR study 0-93195
- $(\text{Gd}_x\text{Y}_{1-x})_2\text{Co}_3$ , Curie temp. and resist.-temp. curves, comp. depend. 0-71020
- HgCr $_2\text{S}_4$ , cooling efficiency near 60K as mag. refrigerant 0-71034
- $\text{HoCo}_2\text{Ge}_2$ , crystal and magnetic structure obs. 0-64976
- $\text{HoTiO}_3$ , magnetic structure determination, neutron scatt. study 0-65809
- $\text{K}_2\text{CuF}_4$ , magnon condensation obs. in quasi-2D planar ferromag. phase 0-60232
- La-Fe alloy, amorphous, sputtered at high rate, mag. props. 0-75753
- $(\text{La}_{0.9}\text{Ca}_{0.1})\text{MnO}_{3+y}$ , mag. props., Faraday method meas. 0-103832
- $\text{LaCoO}_3$ , Mott isolator, paramag. props., calc. 0-93071
- $\text{LaLiO}_5\text{FeO}_3$ , perovskite, prep. and mag. study 0-80486
- $\text{LaMnO}_3$ , phase diagram, mag. moments, neutron diffr. study 0-108414
- $\text{LuRh}_2\text{B}_4$ , magnetic and electrostatic props., NMR study 0-93195
- $\alpha$ -Mn, localised spin fluctuations, Knight shift obs. 0-60181
- $\delta$ -Mn, paramag., antiferromag. and ferromag., magnetic moment calcs. 0-60223
- Mn-Cu, micromagnetic props., neutron diffr. obs. 0-65906
- $\tau$ -MnAl, estimated theoretical limit of mag. moment 0-97072
- $\gamma$ -MnCu, Mn-rich, inclined spin axis, neutron diffr. study 0-75723
- $\text{Mn}_{1-x}\text{Sb}_x$ , Mn electronic state, neutron diffr. study 0-65806
- $\text{Na}_2(\text{Fe,Mg})_2\text{Si}_2\text{O}_7(\text{OH})_2$ , riebeckite, low temp. Mossbauer obs. of oriented single cryst. behaviour and mag. props. 0-84674
- $\text{NdAg}_3$ , low temp. mag. meas. 0-107989
- $\text{Nd}_{1-x}\text{Zn}_x$  system, solid soln., mag. susceptibility, 77 to 600K (*Russian*) 0-65776
- Ni (100) films, spin density by self-consistent linear APW method 0-65710
- Ni, ferromagnetic, electronic struct. by real space approach 0-65432
- Ni, paramag. region, Fe and Co impurity effects on susceptibility, Faraday obs. (*Russian*) 0-88731
- Ni-Cu, ferromag., mag. moment, local environment effects, HF CPA cluster calc. 0-65817
- Ni-Mn alloys, ferromagnetism-to-spin glass phase transition and strong mag. field effect 0-75773
- Ni-Pd, mag. moment distrib., one-mag.-species model calc. 0-65788
- Ni-Pd-Mn ternary alloys, mag. characs., use for thermosed 0-107995
- Ni-Pt alloys, magnetic-moment distrib. neutron study 0-97066
- Ni-Rh, mag. moment distrib., one-mag.-species model calc. 0-65788
- Ni-SiO multilayer films, interface magnetisation 0-88858
- NiBr $_2$ , commensurate and incommensurate mag. struct., neutron diffr. study 0-97067
- $\text{Ni}(\text{Fe,Cr})$  and  $\text{Ni}_2(\text{Fe,Cr})$ , electron states density model and mag. characs. calcs. (*Russian*) 0-92804
- $\text{NiFe}_2\text{O}_4$  ferrite, mag. props., neutron irradi. 0-103858
- $\text{Ni}_{1-x}\text{Te}_x$ , fluctuating localised mag. moments, d band motion, Mossbauer study 0-65768
- $\text{Ni}(001)$  surface states, surface magnetisation, electron spin polarisation 0-88612
- $\text{NpO}_2$ , mag. transition at 25K, Kramers doublet as cryst. field ground state 0-59936
- Pb superconducting slabs, magnetisation and migration field, reversible stage 0-65737
- $\text{PbMo}_6\text{S}_8\text{Fe}$ , elec. cond. anomalous temp. depend., mag. moments (*Russian*) 0-92878
- Pd, sd hybridisation, paramagnetic Curie temp. and susceptibility (*Russian*) 0-103808
- $\text{Pd}_{0.98}\text{Fe}_{0.01}$   $\text{Gd}_{0.01}$ , Pd-Gd exchange const., neutron diffuse scatt. meas. 0-71002
- $\beta$ -PdIn, electrical resistance, mag. susceptibility and IR freq. dispersion (*Russian*) 0-107759
- $\text{Pd}_{1-x}\text{MnSb}$  Heusler alloys, magnetic hyperfine fields on  $^{111}\text{Cd}$ , TDPAC and magnetisation meas. 0-93219
- PrAg $_3$ , low temp. mag. meas. 0-107989
- $\text{PrCo}_2\text{Ge}_2$ , crystal and magnetic structure obs. 0-64976
- Pt-Fe alloy, ordered, T-c phase diagram, antiferro- and ferromagnetism (*Russian*) 0-65871
- $\text{Pt}_3\text{Cr}$ , ferrimag., magnetisation density, polarised neutron diffr. meas. 0-60204



**magnetic moments continued**

- RbFeCl<sub>2</sub>·2H<sub>2</sub>O, pseudo-one-dimensional canted Ising antiferromag., spin-cluster excitations 0-70989  
 ScFe<sub>2</sub>, Mossbauer effect of <sup>57</sup>Fe 0-75903  
 ScFe<sub>2</sub>H<sub>2</sub>, Mossbauer effect of <sup>57</sup>Fe 0-75903  
 Sm<sub>2</sub>Mn<sub>23</sub>-Fe<sub>2</sub>, magnetic behaviour, temp. and comp. depend. 0-93090  
 SmZn, ferromag., cond. band antiparallel polarisation exceeding 4f moment 0-60207  
 Tb, neutron elastic scattering, high-angle, anal. 0-80480  
 TbCo<sub>2</sub>, magnetocrystalline anisotropy and spontaneous magnetostriction 0-75831  
 (Tb<sub>1-x</sub>Gd<sub>x</sub>)<sub>2</sub>Co, intermetallic cpd. mag. props., phase transform, and mag. hysteresis (*Russian*) 0-93113  
 TbP (As<sub>2</sub>)<sub>2</sub>(Sb)(Bi), mag. transitions, quadrupolar interaction effects 0-80512  
 Th-Dy, dil., type I superconductor, paramag. Dy moment relax., Mossbauer spectra study 0-65755  
 Ti-Fe, H storage material, Mossbauer surface studies, Fe clusters 0-97167  
 TiFe<sub>1-x</sub>Co<sub>x</sub>, electronic struct. and mag. moment calcs. 0-65821  
 (Ti<sub>1-x</sub>V<sub>x</sub>)<sub>2</sub>O<sub>3</sub>, 0 < x < 0.1, magnetisation and mag. moments 0-65772  
 TmSe, mag. ordering under press., neutron diff. obs. 0-70947  
 UFe<sub>2</sub>, giant magnetoelastic deform. of cryst. struct. mag. props. (*Russian*) 0-93159  
 U(Fe<sub>1-x</sub>Mn<sub>x</sub>)<sub>2</sub>, Curie temp. and saturation moment at 4.2K 0-70966  
 U<sub>2</sub>Zr<sub>1-x</sub>Fe<sub>x</sub>, Curie temp. and saturation moment at 4.2K 0-70966  
 V surface, spin fluctuations, finite temp. mag. props. study 0-107994  
 V<sub>2</sub>Se<sub>4</sub>, itinerant antiferromag., spin fluctuations, NMR study 0-75874  
 V<sub>2</sub>Se<sub>4</sub>, itinerant antiferromag., spin fluctuations, NMR study 0-75874  
 Y<sub>6</sub>(Fe<sub>1-x</sub>Mn<sub>x</sub>)<sub>23</sub>, Mn-rich compounds, Mossbauer effect study 0-71276  
 YIG:Tb garnet, Faraday effect in strong mag. field (*Russian*) 0-100651  
 Zr-3d Laves phase binary and pseudobinary intermetallics, mag. props. H absorb. effect 0-88821  
 Zr(Fe<sub>1-x</sub>Al<sub>x</sub>)<sub>2</sub>, Curie temp., magnetisation, and cryst. struct., conc. depend. 0-75730

**magnetic monopoles**

- Abelian self-dual multimonopoles, covariant Laplace operator Green function 0-77969  
 Bogomolny-Prasad-Sommerfield one-monopole soln. by Backlund transformation 0-99059  
 BPS one monopole generation by Backlund transform 0-77980  
 Dirac's monopoles and action-at-a-distance theory: classical dynamics 0-95210  
 dynamical groups, symmetries and constants of motion for electric and mag. charges 0-101945  
 electron+monopole, scatt. through small angles, Dirac-Schwinger monopole 0-68398  
 fundamental monopoles and multimonopole solutions for arbitrary simple gauge groups 0-77952  
 geometric configuration of mag. flux string and monopoles, compared to O(3) nonlinear  $\sigma$ -model 0-57527  
 grand unified theories, compatibility with big bang cosmology, superheavy monopoles 0-86647  
 grand unified theories, mag. monopoles and cosmological implications 0-86643  
 Higgs field zeros for axially symmetric multi-monopole configurations 0-82887  
 instantons and monopoles in Yang-Mills gauge field theories 0-91003  
 magnetically bound monopole pair, possible fermion struct. 0-86661  
 primordial magnetic monopoles in unified gauge theories 0-91035  
 relic monopoles from big bang, cosmological problem for standard unified theories 0-77532  
 singular state problems, monopole pair energy levels, charged monopole-electron system (*Chinese*) 0-101733  
 spin (10) grand unified theory, monopole mass 0-99080  
 static magnetic SU(2) Yang-Mills-Higgs system, static axial and mirror symmetric monopoles 0-90992  
 SU(2) Yang's monopole, quaternionic gauge fields on S<sup>2</sup> 0-57473  
 SU(3) colour gauge group, coloured monopoles 0-68360  
 SU(5) grand unification, spin from isospin, half integer spin charge monopoles 0-68406  
 SU(5) model, dyons and monopoles 0-82931  
 SU(5) monopoles, magnetic symmetry and confinement 0-99078  
 SU(S) based grand unified theory, monopoles and vector bosons, symmetry breaking 0-99079  
 two-potential formulation of electrodynamics with magnetic monopoles (*Russian*) 0-62893  
 Z(N) gauge theories, phase transitions 0-73609

**magnetic permeability**

- amorphous alloys, mag. props. rel. to device appl. 0-88804  
 amorphous ferromagnets, structural instabilities and mag. permeability relax., 77 to 400K 0-80559  
 ferrimagnetic Bloch wall oscils., viscosity coeffs. freq. depend., permeability and mag. losses 0-71094  
 ferrimagnetic magnetisation theoretical models, for uniparametric materials 0-65960  
 ferrites, soft, production and props. 0-88801  
 isopermalloy, permeability stability calc. rel. to texture (*Chinese*) 0-65959  
 magnetisation curves representation by cubic spline functions (*German*) 0-71112  
 metallic, glasses, soft-magnetic properties (*German*) 0-71108  
 non-magnetic material wear in presence of magnetic field 0-60982  
 nonuniform systems, effective conductivity from percolation and conduction theory 0-62597  
 Permalloy, 50NP, and 79NM, magnetic properties and structure, environment effect during annealing 0-60366  
 ring specimens, computer controlled mag. meas. system 0-86346  
 steel, B-Si, grain-oriented, high induction, Cu impurity effects 0-89366  
 steel, Si, grain-oriented, high permeability, dissoln. and precip. of AlN and MnS 0-89223  
 steel, Si, permeability change due to stress variation after demagnetization in Rayleigh region 0-88854  
 steels, high permeability grain oriented elec., and instrument current transformers 0-88824  
 unidirectional fibre composites, anisotropic constituents, effect elastic moduli and other props. 0-58911  
 CdCr<sub>2</sub>Se<sub>4</sub> magnetic semiconductor, photoinduced centre kinetics 0-71110  
 (Co,Fe)<sub>80</sub>B<sub>20</sub> glass, induced anisotropy and time changes of permeability 0-75815  
 Co-Fe, soft mag. props. rel. to metallurgical aspects 0-88810

**magnetic permeability continued**

- Co-Mn-Ni-Fe-Si-B amorphous alloys, mag. props., low magnetostriction 0-75832  
 Co-P, electrodeposited amorphous alloys with high permeability, thermal treatment with and without field 0-89372  
 Co<sub>2</sub>Z ferroxplana form. process peculiarities 0-89368  
 Fe powder-plastic composite, soft mag. material, mag. and mech. props. 0-75812  
 Fe-Al(24.3 at.%)C alloy, magnetic permeability disaccommodation, 260-400K 0-93144  
 Fe-Co-Si-B, zero magnetostrictive amorphous alloy with high saturation induction, mag. annealing 0-60362  
 Fe-Ni, Invar, Curie point, annealing effects and time depend. 0-80508  
 Fe-Ni, secondary recryst. and mag. props. 0-89247  
 Fe-Si, grain oriented transformer sheets, permeability and magnetostriction, tensile stress effects 0-88843  
 Fe-Si, grain-oriented sheets, high permeability, low losses, review 0-88790  
 Fe-Si (3 wt.%), grain-oriented, stacking effect on power loss, mag. props. 0-88795  
 Fe-Si (3 wt.%), high permeability, use in transformer cores 0-88793  
 Fe-Si (6.5 wt.%) filament, formation by modified Taylor technique, and mag. props. 0-75795  
 Fe-Si-Al, Sendust, ribbon-form, prep. by rapid quenching, mech. and mag. props. 0-71611  
 Fe-Si-Al (9.6, 5.4 wt.%), ribbon-form Sendust alloy, mag. props., annealing effects 0-88800  
 Fe-Si-B, high induction, hot rolling treatment 0-89266  
 Fe-Si-B glassy alloys, mag. props., comp. effects 0-88752  
 (Fe<sub>0.07</sub>Co<sub>0.93</sub>)<sub>75-x</sub>Cr<sub>2</sub>Si<sub>13</sub>B<sub>10</sub>, amorphous, disaccommodation of mag. permeability and induced anisotropy 0-88741  
 Fe<sub>80</sub>Si<sub>15</sub>, amorphous, soft mag. props. and potential uses 0-88807  
 Gd, coil noise due to permeability fluctuations at phase transition temp. 0-84598  
 Mg, Fe<sub>2-x</sub>O<sub>x</sub>, polycryst., Verwey type transition, resist., magnetisation, Mossbauer effect and permeability obs. 0-75764  
 Mn ferrite, magnetic permeability, photoinduced reduction (*Rumanian*) 0-75794  
 MnZn ferrite, initial mag. permeability rel. to mag. anisotropy 0-80557  
 MnZn ferrite, microstructure and initial permeability, presintering process effect 0-89367  
 MnZn ferrites, internal friction and  $\Delta E$  effect depend. on demagnetisation method 0-80584  
 MnZn ferrites, post sinter-cooling rates effects 0-89369  
 MnZn ferrous ferrite, initial mag. permeability second-order magnetocrystalline anisotropy influence 0-88820  
 MnZn ferrous ferrites, mag. permeability stress depend. 0-88822  
 Ni, ferromag. props., teaching expt. 0-82608  
 Ni-Fe, soft mag. props. rel. to metallurgical aspects 0-88810  
 Ni-Fe (36 to 50 wt.%), initial permeability, domain struct. model 0-88811  
 Ni-Fe-Nb-Mo-Al, head material for mag. recording, DC and AC mag. props. 0-88812  
 NiFe<sub>2</sub>O<sub>4</sub>, ferrite, mag. anisotropy compensation under neutron irradi. 0-75807  
 NiZn ferrite, ZrO<sub>2</sub> additions influence on sintering and physicochem. props. 0-108369  
 NiZn ferrites, density and mag. props., isostatic pressure effect 0-60816  
 NiZn ferrites, internal friction and  $\Delta E$  effect depend. on demagnetisation method 0-80584  
 NiZn ferrites, mag. head props., technical possibilities and limitations 0-88803  
 Ni<sub>0.85</sub>Zn<sub>0.15</sub>Fe<sub>2</sub>O<sub>4</sub>, ferrite, mag. anisotropy compensation under neutron irradi. 0-75807  
 Ni<sub>1-x</sub>Zn<sub>x</sub>Fe<sub>2</sub>O<sub>4</sub>, polycryst., domain wall energy rel. to anisotropy 0-71090  
 Y<sub>3</sub>Fe<sub>x</sub>-Al<sub>2</sub>O<sub>3</sub>, permeability spectra rel. to microstruct. 0-71100  
 Y<sub>3</sub>Fe<sub>x</sub>-Gd<sub>2</sub>O<sub>3</sub>, permeability spectra rel. to microstruct. 0-71100  
 YIG, permeability, domain rot. and wall displacement contrib. 0-80564  
 YIG, permeability spectra rel. to microstruct. 0-71100

**magnetic permeability measurement**

- automatic demagnetisation and measurement system for time decreasing permeability meas. 0-62696  
 calibration of permeability meters, short cct. coaxial lines as inductance standards 0-77816  
 DC permeameter for ring specimens 0-98954  
 ferrites, toroidal samples, apparatus for measurement of initial permeability as function of temp. 0-57346  
 Fe-Si, power loss and permeability meas. by means of Hall probes and stochastic ergodic correl. 0-86350

**magnetic pinch** see *pinch effect***magnetic properties of amorphous substances**

- alloy, indirect exchange interaction and paramag. Curie temp. 0-75752  
 alloys, Curie temp. comp. depend. 0-84597  
 alloys, mag. and nonmag., thermoelec. power, 15 to 580K 0-80255  
 alloys, mag. props. rel. to device appl. 0-88804  
 alloys and semiconductors, Mossbauer spectrometry (*French*) 0-80660  
 amorphous magnetic alloys, review, engineering magnetic props. and potential applications 0-71078  
 antiferromagnet, amorphous, spin waves, exchange fluctuations, calc. 0-65847  
 antiferromagnetism in amorphous Heisenberg magnet, ground state and frustration, theory 0-65766  
 bubble film, magnetoelectric interactions 0-65976  
 bubble materials, props. and prep. methods, review (*Rumanian*) 0-93149  
 easy plane amorphous wire, magnetisation, variational calc. 0-71098  
 ferromagnet, disordered, phase transitions, mol. field and Landau-Ginzburg theories 0-93118  
 ferromagnet, Landau-Ginzburg theory, magnetisation and Curie temp. 0-75700  
 ferromagnetic alloys, disordered cryst. and amorphous, mag. dipolar field distrib., computer simulation 0-65790  
 ferromagnets, book contrib. 0-75743  
 ferromagnets, hidden excitations, theory 0-75748  
 ferromagnets, structural instabilities and mag. permeability relax., 77 to 400K 0-80559  
 glass, magnetic susceptibility measurement, torsional reson. technique 0-82796  
 glasses, soft-magnetic properties (*German*) 0-71108



**magnetic properties of amorphous substances continued**

- Heisenberg amorphous ferromagnet, magnetisation and Curie temp., CPA calc. 0-75703  
 Heisenberg and Ising chains, thermodynamics 0-108022  
 ionic compounds, amorphous, exhibiting Mossbauer spectra, magnetic props. (*French*) 0-80490  
 ionic compounds, amorphous, Mossbauer study, frozen mag. state and hyperfine interaction (*French*) 0-80661  
 Ising antiferromagnetic model, frustration effects 0-103838  
 Ising model, computer simulation 0-60299  
 metallic glass, micromag. calcs. and props. 0-80501  
 metallic glass, prep. and phys. props. development 0-81003  
 metallic glass, splat cooled, mag. props. 0-80491  
 metallic glass ribbon, magnetostrictive stress depend. of longitudinal wave rel. 0-75825  
 metallic glasses, Brillouin-Mandelstam scattering from thermal and excited magnons 0-70980  
 metallic glasses, electronic structure rel. to elec. cond., supercond. and mag. props. 0-65429  
 metals, glassy, structure, transport props., magnetic behaviour, review 0-70138  
 metals, rapidly quenched, conf., Brighton, England (July 1978) 0-67934  
 metals and alloys, amorphous, exhibiting Mossbauer spectra, mean magnetic props. (*French*) 0-80489  
 Metglas 2605 ribbon, saturation magnetostriction meas. by small-angle magnetisation rot. 0-60391  
 Metglas 2826 ribbon, saturation magnetostriction meas. by small-angle magnetisation rot. 0-60391  
 polystyrene,  $\gamma$ -Fe<sub>2</sub>O<sub>3</sub> powder filled, mag. films, packing and particle orientation (*Japanese*) 0-104115  
 polyvinyl acetate,  $\gamma$ -Fe<sub>2</sub>O<sub>3</sub> powder filled, mag. films, packing and particle orientation (*Japanese*) 0-104115  
 polyvinyl butyral,  $\gamma$ -Fe<sub>2</sub>O<sub>3</sub> powder filled, mag. films, packing and particle orientation (*Japanese*) 0-104115  
 quenched free energy of mag. systems with random interactions, upper bounds 0-103845  
 random anisotropy axes, high-temp. expansion for sp. ht. 0-71041  
 random anisotropy axis model in the infinite-range limit 0-88761  
 rare earth alloy, amorphous, ferromag. state, non-axial elec. field gradient effect 0-75728  
 rare earth alloys, R<sub>99</sub>Ni<sub>1</sub>, amorphous, Curie temp., mag. susceptibility and coercive force, 4.2 to 300K 0-93092  
 rare earth alloys, with random anisotropy axes, spin excitations in paramag. phase 0-80476  
 rare earth amorphous alloys, random anisotropy magnetism 0-65853  
 rare earth-Ag alloy, model calcs. of mag. props. 0-84616  
 rare earth-Co, R<sub>99</sub>Co<sub>1</sub>, amorphous, mag. props. 0-84590  
 rare earth-transition metal alloys, amorphous, electronic and mag. props. 0-93093  
 rare earth-transition metal alloys, amorphous, ferrimag., spin arrangements in large fields 0-75718  
 ribbons, twisted, magnetisation process, domain theory 0-71101  
 spin glass-ferromagnetic phase, mean field theory 0-103841  
 spin waves in amorphous ferromagnets, asperomagnets and spin-glasses 0-75747  
 steels Kh18N(10-25), mag. susceptibility, 4.2 to 300K, and magnetoelasticity (*Russian*) 0-65812  
 thin films, struct. and mag. props., review 0-93148  
 transition metal alloys, amorphous, mag. props., chem. short-range order 0-75739  
 transition metal alloys, amorphous, mag. props., structure and preparation 0-75737  
 Al<sub>1</sub>Mn<sub>2</sub>Si<sub>2</sub>O<sub>12</sub>, amorphous insulating spin glass, susceptibility and magnetisation meas. 0-88765  
 B<sub>2</sub>O<sub>3</sub>-PbO-GeO<sub>2</sub>-Fe<sub>2</sub>O<sub>3</sub> glasses, mag. props. and Mossbauer spectra, speromag. order at low temps. 0-80530  
 BaO-Fe<sub>2</sub>O<sub>3</sub>-B<sub>2</sub>O<sub>3</sub>(Na<sub>2</sub>O) glasses, high Fe<sub>2</sub>O<sub>3</sub> content, micromagnetic props. 0-65916  
 BaO-Fe<sub>2</sub>O<sub>3</sub>(Na<sub>2</sub>O) glass, rapidly quenched, mag. and ferrimag. props. 0-75744  
 BaO-Mn<sub>2</sub>O<sub>3</sub>-B<sub>2</sub>O<sub>3</sub>, amorphous mag. oxide, field-cooling effect (*Japanese*) 0-84615  
 Ce<sub>80</sub>Al<sub>20</sub>, mag. ordering and cryst. field effects, speromagnetism 0-80531  
 (Co,Fe)<sub>80</sub>B<sub>20</sub> glass, induced anisotropy and time changes of permeability 0-75815  
 Co alloys, amorphous, effects of metalloids on mag. props. 0-75738  
 Co-(B-Cr) thin film glasses, mag. props. and corrosion resist. 0-80576  
 Co-Fe amorphous alloys, worked, perminvar type mag. hysteresis loop, longit. Kerr effect obs. 0-65958  
 Co-Fe-Si-B, ferromag., magneto-optical spectra in amorphous and cryst. states (*Russian*) 0-84749  
 Co-Mn-Ni-Fe-Si-B amorphous alloys, mag. props., low magnetostriction 0-75832  
 Co-P, domain struct., mag. anisotropy origin 0-80554  
 Co-P, electrodeposited amorphous alloys with high permeability, thermal treatment with and without field 0-89372  
 Co-Si-B, amorphous ribbon, saturation magnetostriction meas. by small-angle magnetisation rot. 0-60391  
 Co<sub>100-x</sub>B<sub>x</sub>, amorphous, mag. struct., mag. susceptibility meas. 0-80485  
 Co<sub>80</sub>B<sub>20</sub> hyperfine field distrib., <sup>59</sup>Co spin echo spectra 0-80635  
 (Co<sub>91</sub>Fe<sub>07</sub>)<sub>75-x</sub>Cr<sub>25</sub>B<sub>10</sub> amorphous alloy, thermal stability, Cr conc. effects, DTA expts. 0-59395  
 (Co<sub>85</sub>Fe<sub>11</sub>)<sub>72</sub>Mo<sub>2</sub>Si<sub>3</sub>B<sub>10</sub>, metallic glass, strain- and field-induced mag. anisotropy 0-108004  
 Co<sub>5</sub>Fe<sub>2</sub>Ni<sub>10</sub>(Si<sub>2</sub>B)<sub>78</sub>, amorphous, soft mag. props., switched-mode power supply apps. 0-88850  
 Co<sub>70-x</sub>Fe<sub>40-x</sub>Si<sub>10</sub>B<sub>10</sub>, amorphous, mag. aftereffect spectra and annealing props. 0-88831  
 Co<sub>71</sub>Mo<sub>2</sub>Si<sub>3</sub>B<sub>10</sub>, metallic glass, strain- and field-induced mag. anisotropy 0-108004  
 Co-P, and Co-NiP, cylindrical amorphous electrodeposited layers, mag. props., torsion influence 0-88848  
 Co<sub>90</sub>P<sub>10</sub> noncrystalline ferromagnet, electroless deposited, struct. and microscopic mag. props. 0-88063  
 Co<sub>80-x</sub>Pd<sub>20-x</sub>Si<sub>20</sub>, structural and mag. heterogeneities 0-80484  
 Co<sub>90</sub>Zr<sub>10</sub>, ferromag. amorphous alloy, crystn. and domain struct. study 0-107056  
 Dy-Cu, mag. phase diagram, magnetisation and sp. ht. meas. 0-80532  
 Dy-Cu film, asperomagnetic domains, Barkhausen jumps in hysteresis loop 0-75822

**magnetic properties of amorphous substances continued**

- (Fe,Co,Ni)-Si(B), amorphous mag. alloy, magnetostriction rel. to soft mag. props. 0-84633  
 Fe alloys, amorphous, effects of metalloids on mag. props. 0-75738  
 Fe alloys, amorphous, mag. saturation, spin wave stiffness, temp. depend. 0-75741  
 Fe alloys, amorphous, saturation magnetisation, Curie temp. and size effect 0-65815  
 Fe and Fe-Ni Metglas alloys, ohmic and Hall resist. 100-700K, mag. behaviour 0-80254  
 Fe sputtered film, amorphous, Mossbauer study and electron diff. obs. 0-75897  
 Fe-B, amorphous, induced anisotropy, development by mag. annealing and under applied mech. stress 0-65868  
 Fe-B, amorphous, induced anisotropy by heat treatment in mag. field and under applied mech. stress 0-75758  
 Fe-B, amorphous, mag. aftereffect, initial susceptibility time depend. 0-88829  
 Fe-B, amorphous ferromag., temp. depend. of resist., appl. of extended Ziman theory 0-59950  
 Fe-B, rapidly quenched, Curie temp., saturation magnetisation 0-84618  
 Fe-B amorphous alloy, annealed, microstruct. and mag. domain changes 0-75790  
 Fe-B amorphous alloys, mag. aftereffect 0-65970  
 Fe-B metallic glasses, struct., stability and crystn. 0-75173  
 Fe-B metallic ribbons, correl. between quenching temp. and mech. and mag. props. 0-89373  
 Fe-B ribbon, microhardness, and static coercive force, melt overheating effect 0-84978  
 Fe-B-C, effects of replacement of B by C on mag. props. 0-84621  
 Fe-B-C, formation, mag. props., thermal stability and density 0-75796  
 Fe-B-C amorphous alloys for use in power transformers 0-88808  
 Fe-B-C amorphous alloys with high saturation induction 0-84617  
 Fe-B-Cr(Mo), metallic glasses, mag. struct., and elec. props. 0-88751  
 Fe-B-Cr(Si) thin film glasses, mag. props. and corrosion resist. 0-80576  
 Fe-B-Si-C amorphous alloys, prep. and props. 0-88748  
 Fe-B-(Si), glassy, field-induced mag. anisotropy near eutectic comp. 0-93110  
 Fe-B(B) alloys, anomalous thermal expansion,  $\Delta E$  effect, Invar and Elinvar characts., delay time 0-80589  
 Fe-Co-Si-B, amorphous soft ferromagnet with high mag. induction 0-84619  
 Fe-Co-Si-B, zero magnetostrictive amorphous alloy with high saturation induction, mag. annealing 0-60362  
 Fe-Co-Si(B), mag. aftereffect on soft mag. props. 0-84626  
 Fe-Ni based metallic glass, Metglas 2826 MB, Mossbauer study 0-75897  
 Fe-Ni-B-Si, amorphous, mag. props., heat treatment effects 0-89370  
 Fe-Ni-B-(P), ferromag., magneto-optical spectra in amorphous and cryst. states (*Russian*) 0-84749  
 Fe-Ni-P-B, metallic glasses, struct. relax., annealing effects on mag. props. 0-89261  
 Fe-P electrodeposited foil, amorphous, mag. domains 0-75821  
 Fe-rare earth alloys, magnetoelasticity and moment rot., US vel. calc. and neutron scatt. meas. 0-65992  
 Fe-Sb amorphous films, Mossbauer effect study 0-75896  
 Fe-Si-B, magnetic metallic glasses, mag. props. 0-84620  
 Fe-Si-B glassy alloys, mag. props., comp. effects 0-88752  
 (Fe-Ni-Mo)<sub>80</sub>(P-B)<sub>20</sub>, amorphous, mag. aftereffects and struct. instabilities 0-88833  
 Fe<sub>1-x</sub>B<sub>x</sub>, amorphous, hyperfine fields and local mag. moments, Mossbauer study 0-75895  
 Fe<sub>100-x</sub>B<sub>x</sub>, amorphous, mag. struct., mag. susceptibility meas. 0-80485  
 Fe<sub>80</sub>B<sub>20</sub>, amorphous, Brillouin scatt. from magnons, ferromag. reson. 0-65844  
 Fe<sub>80</sub>B<sub>20</sub>, amorphous, mag. permeability aftereffect during annealing 0-88834  
 Fe<sub>80</sub>B<sub>20</sub>, amorphous ferromagnet, Mossbauer hyperfine fields, mag. struct. 0-75894  
 Fe<sub>80</sub>B<sub>20</sub> amorphous ribbon, initial susceptibility time lag 0-100579  
 Fe<sub>80</sub>B<sub>20</sub> film, amorphous metallic, standing spin waves, Brillouin scatt. obs. 0-97291  
 Fe<sub>80</sub>B<sub>20</sub> glass, magnetisation reorientation, Mossbauer effect 0-66092  
 Fe<sub>80</sub>B<sub>20</sub> metallic glass, crystn. and struct. relax., Mossbauer effect study 0-75182  
 Fe<sub>80</sub>B<sub>20</sub> metallic glasses, stability and transforms. 0-75174  
 Fe<sub>81-x</sub>B<sub>16.6</sub>, amorphous, mag. props. and microstruct., cooling rate and melt overheating effects 0-65965  
 Fe<sub>83-x</sub>B<sub>16.6</sub> amorphous, mag. props., melt overheating and cooling rate effects 0-89371  
 Fe<sub>40</sub>B<sub>40</sub>P<sub>14</sub>B<sub>6</sub> and Fe<sub>80</sub>B<sub>20</sub>, Metglas 2826 and 2605, amorphous ribbon, power loss variation with freq. and applied stress 0-88849  
 (Fe<sub>95</sub>Co<sub>5</sub>)<sub>1-x</sub>B<sub>x</sub>, amorphous, hyperfine fields and local mag. moments, Mossbauer study 0-75895  
 Fe<sub>2</sub>Co<sub>2</sub>B<sub>80</sub>, amorphous, magnetisation reversal and domain boundary configs. 0-88809  
 Fe<sub>35</sub>Co<sub>32</sub>B<sub>20</sub>Si<sub>10</sub>Al<sub>3</sub>, stress-induced variation in magnetisation and dynamic magnetostrictive charact. 0-88855  
 (Fe<sub>0.05</sub>Co<sub>0.95</sub>)<sub>78</sub>Si<sub>6</sub>B<sub>14</sub> amorphous ribbon, anomalous mag. aftereffect 0-100602  
 (Fe<sub>1-x</sub>Co<sub>x</sub>)<sub>78</sub>Si<sub>10</sub>B<sub>12</sub>, amorphous, roll mag. anisotropy 0-75757  
 (Fe,Co)<sub>1-x/3</sub>Si<sub>2/3</sub>B<sub>14</sub>, amorphous, saturation magnetostriction, strain modulated FMR obs. 0-75863  
 (Fe<sub>98</sub>Cr<sub>2</sub>)<sub>70</sub>P<sub>13</sub>B<sub>8</sub> and (Fe<sub>96</sub>Cr<sub>4</sub>)<sub>70</sub>P<sub>13</sub>B<sub>8</sub>, amorphous, low temp. sp. ht., mag. contribs. 0-80552  
 FeF<sub>2</sub>, types of magnetism and methods of study (*French*) 0-80490  
 FeF<sub>3</sub>, amorphous, mag. props. and Mossbauer spectra, speromagnetism and micromagnetism 0-75778  
 FeF<sub>3</sub>, amorphous, struct. and mag. props., computer model 0-96446  
 (Fe<sub>1-x</sub>Ni<sub>x</sub>)<sub>83</sub>B<sub>17</sub>, amorphous alloys ferromagnetic resonance 0-108080  
 Fe<sub>40</sub>Ni<sub>40</sub>B<sub>20</sub>, amorphous, RF annealing effects 0-108037  
 Fe<sub>40</sub>Ni<sub>40</sub>B<sub>20</sub>, amorphous ribbon, power loss variation with freq. and applied stress 0-88849  
 Fe<sub>40</sub>Ni<sub>40</sub>B<sub>20</sub> and Fe<sub>40</sub>Ni<sub>40</sub>P<sub>14</sub>B<sub>6</sub>, amorphous, mag. aftereffect spectra and annealing props. 0-88831  
 Fe<sub>40-x</sub>Ni<sub>40-x</sub>B<sub>20</sub> and Fe<sub>40-x</sub>Ni<sub>40-x</sub>P<sub>14</sub>B<sub>6</sub> amorphous alloys, microhardness correl. with mag. props. 0-88826  
 Fe<sub>2</sub>Ni<sub>80-x</sub>B<sub>20</sub> and Fe<sub>2</sub>Ni<sub>80-x</sub>P<sub>14</sub>B<sub>6</sub> metallic glasses, low temp. resist. and galvanomag. effects, mag. state influence 0-84461  
 Fe<sub>2</sub>Ni<sub>80-x</sub>B<sub>20</sub> glass, resist., magnetoresist., and thermoelec. power 0-70681



## magnetic properties of amorphous substances continued

- (Fe<sub>1-x</sub>Ni<sub>x</sub>)<sub>0.8</sub>B<sub>0.2-x</sub>P<sub>x</sub>, amorphous, hyperfine fields and local mag. moments, Mossbauer study 0-75895  
 Fe<sub>61</sub>Ni<sub>38</sub>B<sub>10</sub>P<sub>10</sub> metallic glass, superparamag. behaviour, chem. inhomogeneities role 0-84625  
 Fe<sub>90</sub>-Ni<sub>10</sub>B<sub>20-y</sub>P<sub>y</sub>, amorphous, Rayleigh region and coercive force 0-88806  
 (FeNi)<sub>80</sub>Al<sub>17.5</sub>Si<sub>0.5</sub>, stress-induced variation in magnetisation and dynamic magnetostriuctive charact. 0-88855  
 Fe<sub>20</sub>Ni<sub>40</sub>C<sub>14</sub>P<sub>6</sub>, amorphous film, dislocation and mag. struct., neutron diff. study 0-70956  
 Fe<sub>32</sub>Ni<sub>38</sub>Cr<sub>14</sub>P<sub>16</sub>B<sub>6</sub>, Metglas 2826A, EPR at 20 GHz 0-75848  
 Fe<sub>40</sub>Ni<sub>40</sub>(MoSiB)<sub>20</sub>, amorphous, soft mag. props., switched-mode power supply appls. 0-88850  
 Fe<sub>40</sub>Ni<sub>38</sub>MoB<sub>18</sub>, amorphous, mag. anisotropy, Mossbauer study 0-65864  
 Fe<sub>40</sub>Ni<sub>38</sub>MoB<sub>18</sub>, amorphous, reversible enhancement of mag. directional ordering rate 0-103829  
 Fe<sub>20</sub>Ni<sub>38</sub>MoB<sub>18</sub> and Fe<sub>70</sub>MoB<sub>20</sub> amorphous ribbons, magnetoelastic effects in as-quenched and stress-relieved states 0-80588  
 (Fe<sub>1-x</sub>Ni<sub>x</sub>)<sub>80</sub>P<sub>20</sub>, amorphous, ferromagnetic alloys, mag. anomalies of Invar type (Russian) 0-93089  
 Fe<sub>40</sub>Ni<sub>40</sub>P<sub>14</sub>B<sub>6</sub>, amorphous ferromagnet, Mossbauer hyperfine fields, mag. struct. 0-75894  
 Fe<sub>40</sub>Ni<sub>40</sub>P<sub>14</sub>B<sub>6</sub>, amorphous, mag. permeability aftereffect during annealing 0-88834  
 Fe<sub>40</sub>Ni<sub>40</sub>P<sub>14</sub>B<sub>6</sub>, amorphous ferromag., spin wave excitations 0-97079  
 Fe<sub>40</sub>Ni<sub>40</sub>P<sub>14</sub>B<sub>6</sub>, amorphous ribbon, mag. domains and anisotropy distrib. 0-108029  
 Fe<sub>40</sub>Ni<sub>40</sub>P<sub>14</sub>B<sub>6</sub>, mag. polarisation in approach to ferromag. saturation 0-80560  
 Fe<sub>40</sub>Ni<sub>40</sub>P<sub>14</sub>B<sub>6</sub>, Metglas 2826, amorphous ribbon under tension, mag. domain walls and pulsed magnetisation reversal 0-88825  
 (Fe,Ni)<sub>1-x</sub>80P<sub>10</sub>B<sub>10</sub>, amorphous, magnetisation reversal and domain boundary configs. 0-88809  
 Fe<sub>80</sub>Ni<sub>20</sub>P<sub>14</sub>B<sub>6</sub> glass, resist., magnetoresist., and thermoelec. power 0-70681  
 (Fe<sub>1-x</sub>Ni<sub>x</sub>)<sub>75</sub>Si<sub>10</sub>B<sub>15</sub>, amorphous, Landau-Ginzburg theory, magnetisation and Curie temp. 0-75700  
 (Fe<sub>1-x</sub>Ni<sub>x</sub>)<sub>75</sub>Si<sub>10</sub>B<sub>15</sub> amorphous alloys, cold rolled and as-quenched, mag. anisotropy 0-97089  
 Fe<sub>2</sub>O<sub>3</sub> amorphous layer on graphite, Mossbauer spectra, superparamag. props. 0-60474  
 Fe<sub>2</sub>O<sub>3</sub>, types of magnetism and methods of study (French) 0-80490  
 Fe<sub>2</sub>O<sub>3</sub>-BaO-B<sub>2</sub>O<sub>3</sub>, magnetic props. of Fe-rich amorphous oxide (French) 0-80511  
 Fe<sub>100-x</sub>P<sub>x</sub>, structural analysis of models for amorphous metallic alloys 0-103249  
 Fe<sub>20</sub>P<sub>13</sub>B<sub>8</sub>, amorphous alloys, splat cooled, Mn, Cr and V substituted, mag. and transport props. 0-84593  
 Fe<sub>80</sub>P<sub>20-x</sub>C<sub>x</sub>(Si<sub>1-x</sub>Ge<sub>x</sub>), amorphous, size effect of metalloids on mag. props. 0-84594  
 Fe<sub>80</sub>Pd<sub>20</sub>-Si<sub>20</sub>, structural and mag. heterogeneities 0-80484  
 Fe<sub>80</sub>Pd<sub>20</sub>-Si<sub>18</sub> metallic glass, long range interaction and spin wave interactions 0-65949  
 Fe<sub>80</sub>Si<sub>18</sub>, amorphous film, magneto-optic Kerr effect 0-66158  
 Fe<sub>80</sub>Si<sub>8</sub>B<sub>12</sub>, amorphous, soft mag. props. and potential uses 0-88807  
 (Fe<sub>1-x</sub>Si<sub>x</sub>)<sub>1-x</sub>By, metallic glass, mag. props., crystallisation 0-65885  
 Fe<sub>80</sub>Si<sub>18</sub>, amorphous film, struct. and mag. props. 0-65972  
 Fe<sub>80</sub>Pd<sub>20-x</sub>C<sub>x</sub>(Si<sub>1-x</sub>Ge<sub>x</sub>), amorphous, size effect of metalloids on mag. props. 0-84594  
 Gd-Al(Cu)(Ga)(Ni)(Pd)(Rh) alloys, mag. and elec. props. 0-80499  
 Gd-Co, amorphous films, mag. props. ferromag. reson. meas., 20-520°C (Russian) 0-97144  
 Gd-Co amorphous films, mag. struct., mag. bubbles, electron diff. study (Chinese) 0-71126  
 Gd-Co based amorphous sputtered films, microstruct. variability and mag. anisotropy, implanted ion effects 0-88459  
 Gd-Co(Ni)(Cu)(Rh)(Ru)(Pd)(Ga), mag. props. and ferromag. reson. 0-75862  
 Gd-Fe amorphous films, stress contrib. to perpendicular anisotropy 0-75819  
 Gd-Ti(V)(Cr)(Mg)(Nb)(Ge)(Si)(Au) amorphous films, spontaneous Hall effect and elec. resist. 0-80251  
 (GdCo)<sub>1-x</sub>(<sub>1-x</sub>)Ar, amorphous films, effective anisotropy field, ferromag. reson. obs. 0-71123  
 (Gd<sub>0.5</sub>Fe<sub>0.5</sub>)<sub>80</sub>B<sub>10</sub>, amorphous, mag. props., Mossbauer study 0-93093  
 GdFeBi, amorphous ferrimag. films, magneto-optical props., optical spectra 0-76008  
 (Ho<sub>0.2</sub>O<sub>0.194</sub>(Al<sub>0.227</sub>(Si<sub>0.279</sub>), amorphous, low temp. spin glass behaviour 0-60297  
 KFeF<sub>4</sub>, amorphous, mag. props. and Mossbauer spectra, speromagnetism and micromagnetism 0-75778  
 La-Fe alloy, amorphous, sputtered at high rate, mag. props. 0-75753  
 La<sub>30</sub>-Pr<sub>40</sub>Au<sub>30</sub>, mag. and supercond. props. 0-75713  
 Li<sub>2</sub>B<sub>2</sub>O<sub>7</sub>-LiFe<sub>2</sub>O<sub>4</sub>, borate glass, mag. props. of Fe<sup>3+</sup> cations 0-100599  
 Li<sub>2</sub>B<sub>2</sub>O<sub>7</sub>-LiFe<sub>2</sub>O<sub>4</sub> glass, rapidly quenched, mag. and ferrimag. props. 0-75744  
 MnAlGe film, mag. domains and amorphous to cryst. phase transition, electron microscopy obs. 0-71129  
 MnGaGe film, mag. domains and amorphous to cryst. phase transition, electron microscopy obs. 0-71129  
 MnO-Al<sub>2</sub>O<sub>3</sub>-SiO<sub>2</sub>, amorphous spin glass, AC susceptibility 0-80520  
 MnSi(Ge), spin glass transition, AC susceptibility meas. 0-75779  
 NaFeF<sub>4</sub>, amorphous, mag. props. and Mossbauer spectra, speromagnetism and micromagnetism 0-75778  
 α-Na<sub>2</sub>Fe<sub>2</sub>(PO<sub>4</sub>)<sub>3</sub> orthophosphate, cryst. and vitreous, Mossbauer spectroscopy and mag. susceptibility (French) 0-80657  
 Nd<sub>21</sub>Ag<sub>79</sub>, and Nd<sub>50</sub>Ag<sub>50</sub>, susceptibility and magnetisation 0-60182  
 Ni, electrodeposited film, thermal anal., occlusion of gases rel. to mag. props. 0-59823  
 Ni-B thin film glasses, mag. props. and corrosion resist. 0-80576  
 Ni-Fe based metallic glasses, Curie pt. anomalies 0-60256  
 Ni-P, electrodeposited film, thermal anal., occlusion of gases rel. to mag. props. 0-59823  
 Ni-S, electrodeposited film, thermal anal., occlusion of gases rel. to mag. props. 0-59823  
 Ni<sub>100-x</sub>B<sub>x</sub>, amorphous, mag. struct., mag. susceptibility meas. 0-80485  
 Ni<sub>32</sub>Fe<sub>32</sub>Cr<sub>14</sub>P<sub>12</sub>B<sub>6</sub> metallic glass, mech. props. and thermal stability 0-76362  
 (Ni<sub>99</sub>Fe<sub>1</sub>)<sub>70</sub>P<sub>13</sub>B<sub>8</sub>, amorphous, low temp. sp. ht., mag. contribs. 0-80552  
 (Ni<sub>1</sub>Fe<sub>1-x</sub>)<sub>80</sub>P<sub>10</sub>B<sub>10</sub>, Curie temp., press. effect 0-75833

## magnetic properties of amorphous substances continued

- Ni<sub>2</sub>Zr<sub>1-x</sub>, metallic glass, crystallisation kinetics, elec. resist. and mag. susceptibility meas. 0-103659  
 PbMnFeF<sub>3</sub> and PbMnFeF<sub>3</sub>, vitreous, insulating, evidence of spin-glass transition 0-97112  
 Pd<sub>35</sub>Zr<sub>65</sub>, mag. susceptibility meas. 0-75740  
 Pr<sub>21</sub>Ag<sub>79</sub>, amorphous, sp. ht. at low temp. 0-75780  
 Pr<sub>21</sub>Ag<sub>79</sub>, Pr<sub>50</sub>Ag<sub>50</sub>, Pr<sub>10</sub>Lu<sub>40</sub>Ag<sub>50</sub>, susceptibility and magnetisation 0-60182  
 Sm-Co, plasma-sprayed, role of Ar or H<sub>2</sub> atm. in mag. props. and crystn., rel. to H<sub>2</sub> storage 0-64898  
 Sm<sub>2</sub>Ag<sub>78</sub>, amorphous, sp. ht. at low temp. 0-75780  
 SmCo<sub>5</sub>, amorphous, supermag.-ferromag. transition and directional crystallisation 0-65891  
 Tb-Fe amorphous thin films, magnetic after-effect, Kerr magneto-optic effect obs. 0-97123  
 YCo<sub>2</sub> amorphous films, <sup>59</sup>Co spin echo study 0-80636  
 Y<sub>1-x</sub>Co<sub>x</sub>, amorphous, mag. props. 0-84590  
 Y<sub>1-x</sub>Fe<sub>x</sub>O<sub>1.2</sub>, types of magnetism and methods of study (French) 0-80490  
 Y-GdIG film, amorphous, mag. bubbles obs. and structural transformation 0-75824
- magnetic properties of dilute alloys** *see magnetic properties of dilute systems*
- magnetic properties of dilute systems**  
*see also local moments in dilute systems; magnetic impurity interactions*  
 anisotropic magnet, dil., crit. behaviour near percolation threshold 0-88767  
 anisotropic magnets, dil., scaling representation meas. percolation threshold 0-88766  
 antiferromagnet, itinerant, paramag. impurity effects on Neel temp., calc. 0-60257  
 CuCr, dil., specific heat, impurity contrib. Kondo temp. 0-65903  
 dilute magnetic alloys, electron sound absorpt., disordered mag. impurities, spin glasses (Russian) 0-80503  
 disordered binary alloys of ferromag. crystals, mag. dipole fields at interstitial sites 0-97176  
 Ising and Heisenberg, systems with competing interactions, mag. ordering, appl. to Eu<sub>2</sub>Si<sub>1-x</sub>S<sub>x</sub> 0-65914  
 transition metal alloys, dilute ferromagnetic, itinerant d-electron(hole) degenerate, spin stiffness constant 0-70930  
 transition metal alloys, spin glasses, mag. ordering, book contrib. 0-75787  
 transition metals, ferromag., dil. H electronic struct. 0-70638  
 AgCr, dil., specific heat, impurity contrib. Kondo temp. 0-65903  
 AgNi, dil., mag. susceptibility of isolated Ni atoms 0-65777  
 Au-Fe, dil., crit. dynamics 0-60325  
 Au-Fe (1 at.%), spin glass, specific heat 0-60355  
 CePd<sub>3</sub>-Er, dil., low field mag. susceptibility, electro-nuclear effects 0-60189  
 Ce<sub>0.08</sub>Y<sub>0.92</sub>Sb, dilute f-electron system in cluster regime, crystal field and exchange splittings 0-97062  
 Co-Fe, dil., magnetocrystalline anisotropy anomalous temp. depend. 0-71007  
 Co-W alloy electrodeposition, influence of MgSO<sub>4</sub> and gum arabic additives (Russian) 0-80991  
 CoMn(Cr)(V)(Ti), dil., low temp. specific heat and magnetisation 0-65925  
 Cr-Co, dil., antiferromag., elec. resist. min., press. and impurity effects 0-59970  
 Cr-Fe, dil., antiferromag., elec. resist. min., press. and impurity effects 0-59970  
 Cr-Fe, dil., spin correlations and neutron scatt. near crit. conc., theory 0-60327  
 Cr-Re (0.18 wt.%), mag. excitations in longitudinal and transverse SDW phases 0-70946  
 Cr-Si-V, (2, 0.1 at.%), paramag. to commensurate spin density wave transition 0-65875  
 (Eu, Sr<sub>1-x</sub>)<sub>2</sub>S, very dil., magnetisation dynamics 0-65915  
 Fe-Cr, dil., spin density wave under high press., neutron diff. study 0-65798  
 Fe<sub>1-x</sub>Zn<sub>x</sub>F<sub>2</sub>, dil. antiferromag., electronic and mag. props., Raman scatt. and optical absorpt. study 0-108207  
 (La,Y)Ce, dil., Kondo supercond., transition temp., susceptibility and resist. 0-65733  
 La<sub>80</sub>-Pr<sub>20</sub>Au<sub>30</sub>, amorphous, mag. and supercond. props. 0-75713  
 Pd-Co, breakdown of ferromag. order, magnetoresist. obs. 0-71046  
 Pt-Fe, breakdown of ferromag. order, magnetoresist. obs. 0-71046  
 Pt-Fe(Co)(Mn), skew scatt. Hall effect, magnetoresist. and mag. anisotropy, orbital magnetism of impurity 0-70678  
 Si-Cr, dil., spin density wave under high press., neutron diff. study 0-65798  
 Sm-Eu alloy, mag. and elec. hyperfine interac., TDPAD obs., paramag. behaviour, exchange integral 0-103908  
 Zn-Mn, Kondo-system, ion implantation as method for study 0-70241
- magnetic properties of fine particles**  
*see also superparamagnetism*  
 superparamagnetic particles, magnetic moment time development and discrete orientation model 0-60378  
 BaFe<sub>2</sub>O<sub>19</sub>, microparticles, magnetisation reversal, hysteresis loop obs. 0-75813  
 BaFe<sub>2</sub>O<sub>19</sub>, particles, magnetic domain study by colloid-SEM method 0-97120  
 BaFe<sub>2</sub>O<sub>19</sub> powder, hysteresis of microwave absorpt. and magnetisation reversal 0-75814  
 Co fine particles in Cu, interface magnetisation 0-88858  
 Co single domain particles, randomly oriented easy axes and particle size distrib., coercivity 0-71119  
 CoFe<sub>2</sub>O<sub>4</sub> mag. fluid particles, comp., struct., and mag. props. 0-60374  
 CrO<sub>2</sub> and CrO(OH), fine particle obs. of cryst. morphology and topotaxy 0-65969  
 CrO<sub>2</sub>, particulate, proton donor adsorption effect on mag. moment, XPS anal. 0-71117  
 Cu-Mn-Al, Heusler alloys, ferromag. inclusions, mag. props. and struct. study (Russian) 0-80570  
 Cu-Ni-Co, mag. props. of system of disperse ferromag. particles, 73 to 673K (Russian) 0-65968  
 Fe powder-plastic composite, soft mag. material, mag. and mech. props. 0-75812  
 Fe, spin collinearity, Mossbauer spectra study 0-71114  
 Fe<sub>2</sub>O<sub>4</sub> mag. fluid particles, comp., struct., and mag. props. 0-60374



**magnetic properties of fine particles continued**

NiFe<sub>2</sub>O<sub>4</sub> mag. fluid particles, comp., struct., and mag. props. 0-60374  
 Ni<sub>3</sub>Fe<sub>2-x</sub>O<sub>4</sub>, spinels, fine particles, magnetic properties obs. 0-71031

**magnetic properties of substances**

*see also antiferromagnetic properties of substances; demagnetisation; diamagnetic properties of substances; ferrimagnetic properties of substances; ferromagnetic properties of substances; magnetic permeability; magnetic properties of amorphous substances; magnetic properties of dilute systems; magnetic properties of fine particles; magnetic structure; magnetic surface phenomena; magnetic susceptibility; magnetic transitions; magnetisation; magnetocaloric effects; paramagnetic properties of substances*

conference, Munich, Germany (Sep. 1979) 0-56997  
 glasses, elec., mag., and optical props., conference, Troy, NY, USA (Aug. 1979) 0-105417  
 rare earth-Sn-X, X=Rh, Ir, Ru, Co, cryst. growth and cryst.-chem. invest, supercond./mag. ternary cpds. 0-100777  
 rare earths, light, stacking faults and magnetism, transform. effects 0-75840  
 solid state physics, book 0-101676  
 solid state physics, historical aspects, symposium, London, England (Apr.-May 1979) 0-56999  
 titanomagnetite sand from New Zealand, density, elec. and mag. prop 0-98311  
 wustite solid solns., props. connected with localised electron state 0-107734  
 Sn ternary intermetallic systems, new supercond./mag. cpds., X-ray powder diffr. data 0-100215

**magnetic read/write heads *see magnetic heads*****magnetic recording**

*see also tape recorders; thermomagnetic recording*  
 cinematography, magnetic sound records release print KMP-23 (Russian) 0-90918  
 time reference singal for tape recording, IRIG and NASA code formats 0-57262  
 Ni-Fe-Nb-Mo-Al, head material for mag. recording, DC and AC mag. props. 0-88812

**magnetic relaxation**

*see also ferromagnetic relaxation; magnetic resonance; spin-lattice relaxation; spin-spin relaxation*  
 amorphous ferromagnets, structural instabilities and mag. permeability relax., 77 to 400K 0-80559  
 antiferromagnet, easy-plane, antiferromag. reson. linewidth and relax., theory 0-71189  
 cross relaxation under action of 90° pulse trains, characts. 0-60402  
 Ising magnet, kinetic processes, 1-D chain, magnetic relaxation, quantum stat. mechs. 0-80471  
 Ising magnet, kinetic processes, reduction of statistical description of system during evolution 0-80470  
 CW Leonis (IRC+10216), IR C star, circumstellar dust orientation by paramag. relaxation rel. to intrinsic polarisation 0-67730  
 Mattis model, modified, mag. relax. 0-65947  
 paramagnetic crystal, magnetisation change by light pulse 0-70932  
 spin system, paramagnetic, two-level open system, kinetic theory of resonance and relaxation 0-88859  
 Au-Fe, spin glasses, alternating susceptibility 0-65912  
 Au-Fe (4 at.%), spin glass, magnetisation and energy relax. below T<sub>g</sub> 0-65921  
 CaH, spin doubling, SCF calcs. 0-95649  
 Cu-Mn, mag. viscosity below freezing temp. 0-65910  
 Cu-Mn, spin glasses, alternating susceptibility 0-65912  
 Fe<sub>2</sub>O<sub>4</sub>, magnetite, mag. aftereffects, 4.35K 0-80571  
<sup>3</sup>He, superfluid A-phase, longitudinal mag. relax. 0-59751  
 KM<sub>n</sub>Mg<sub>1-x</sub>F<sub>3</sub>, randomly diluted Heisenberg paramag. nucl. relax. 0-60444  
 Li-Zn ferrites, (Li, Zn, Ti, Cr substituted), Mossbauer spectrometry, effect of supertransferred hyperfine fields and relaxation (French) 0-80654  
 Ni-Co (25 wt.%), single crystals, mag. annealing effect on magnetostriction and magnetisation at high temps. 0-108047  
 Ni<sub>98</sub>M<sub>2</sub>, M=impurity metal, formation of MH(D)-complexes 0-65236

**magnetic resonance**

*see also acoustic magnetic resonance; antiferromagnetic resonance; atomic beam magnetic resonance; ferrimagnetic resonance; ferromagnetic resonance; laser magnetic resonance; magnetic double resonance; magnetic relaxation; molecular beam magnetic resonance; nuclear magnetic resonance; paramagnetic resonance*  
 angular velocity nonuniformity meas. (Russian) 0-62637  
 chlorophylls, mag. reson., site selected fluoresc. detection 0-69164  
 magnetic semiconductor, helicon wave propag., hyperfine interaction effect 0-80307  
 magnetism, conference, Munich, Germany (Sep. 1979) 0-56997  
 protochlorophyll, mag. reson., site selected fluoresc. detection 0-69164  
 spin system, paramagnetic, two-level open system, kinetic theory of resonance and relaxation 0-88859  
 YGdIG, with various domain wall orientations, natural spin reson. 0-66040  
 YIG, Bi-substituted, LPE, domain wall reson. 0-60387

**magnetic resonance spectrometers**

cross-polarisation <sup>13</sup>C NMR with magic angle spinning, appl. to fossil fuels and polymers 0-77819  
 EPR high-temperature cavity for easily oxidised fluorides 0-77831  
 EPR spectrometer attachment for studying materials in 120 to 350K. 1-10<sup>4</sup> atm. range 0-105686  
 EPR spectrometer with mag. field modulation in 10 Hz to 1 MHz range, 30 MHz IF amplifier 0-98955  
 Fourier transform, NMR spectrometer, magic-angle rot. 0-105688  
 Fourier transform NMR spectrometer, pulsed field gradient system 0-57353  
 high-temp. EPR spectrometer with CO<sub>2</sub> laser-heated sample holder 0-68233  
 low-temperature UHF detector, with low noise preamplifier based on n-type InSb 0-68230  
 microwave spin resonance spectrometer, influence of nonlinearity of microwave network characteristics 0-62707  
 NMR radio spectrometers, meas. of field uniformities in gap of precision magnets 0-105683  
 NMR radiospectrometers, calc. of optimal configuration of shims 0-73398  
 NMR signal enhancement by rod-induced convection 0-77823

**magnetic resonance spectrometers continued**

NMR spectrom., pulsed, 10 MHz, using solid state devices 0-86361  
 NMR spectrometer, FT, multipurpose, design and computer interfaces 0-86362  
 NMR spectrometers, SQUID-based sensitivity limit 0-98961  
 pulsed FT NQR spectrometer, automation for single crystal Zeeman studies 0-66066  
 pulsed NMR spectrometer, high-isolation duplexing switch 0-86363  
 pulsed NMR spectrometer, thyristor temp. regulator 0-105687  
 pulsed NMR spectrometer incorporating phase-splitting circuit 0-62704  
 RE-1306 radiospectrometer for crystals obs., using LF modulation of magnetic field 0-57350  
 RYa-2308 radiospectrometer, attachment for obs. of DNMR in <sup>31</sup>P 0-98957  
 single-coil triple-tuned NMR probe for simultaneous stimulation of <sup>1</sup>H, <sup>2</sup>H and <sup>13</sup>C resonances 0-86364  
 two-way EPR cavity, for Stark effect meas. on NO<sub>2</sub> 0-90872  
 XL-100 spectrometer, design of voltage-controlled oscillator 0-71211

**magnetic resonance spectroscopy**

l-alanine powder, short dipolar relaxation time meas. by saturation method 0-60441  
 computer programmable digital pulse generator for Fourier NMR spectroscopy 0-98959  
 cryostat for low-temp. EPR studies 0-86321  
 digitised EPR system, appln. to saturation transfer 0-77825  
 eigenvectors and eigenvalues from mag. reson. results, error estimation by linear data-fitting techniques 0-68018  
 EPR, elec. field modulated, appl. to study of ferroelectrics 0-75841  
 high power pulsed NMR, automation and control 0-86359  
 Lorentzian lineshapes and isotropic distrib. of molecules, analytical expressions derived for powder samples 0-60401  
 low field magnet, computer controlled, for optical and magnetic resonance studies 0-95113  
 microwave network characteristics, influence of nonlinearity on shape of mag. resonance spectra 0-62707  
 multinuclear magnetic resonance spectroscopy, universal referencing, solvent effects 0-73402  
 NMR, homonuclear selective population inversion in AB system 0-75865  
 NMR, population distribution to enhance sensitivity and allow decoupling of low gyromagnetic ratio nuclei 0-73399  
 NMR imaging rotating frame selective pulses 0-68232  
 NMR meas. at ultra-low temps, S/N ratio, appl. to thermometry 0-73400  
 NMR spectrometers, high freq. effects 0-77829  
 NMR spin imaging by mag. field modulation 0-90873  
 NMR spin-lattice relax. time meas., fast inversion-recovery technique 0-77826  
 NMR-ESR spectroscopy, miniature magnetic assembly, teaching 0-105467  
 NQR, bisymmetric Zeeman modulator 0-98960  
 NQR, electronics appls. 0-63668  
 NQR, pulsed spin locking technique, theory 0-98958  
 optogalvanic double-resonance spectroscopy 0-57385  
 proton 2D J spectra, phase-sensitive displays 0-77830  
 pulsed NMR, high resolution, adjusting conditions of pulse sequences 0-93184  
 quick access sample system for low temp. K-band ESR and ENDOR 0-57552  
 saturation transfer EPR spectroscopy detection system by Fourier transformation 0-86357  
 scaling of heteronuclear spin interactions by multipulse sequences 0-73405  
 solid materials, high resolution <sup>13</sup>C NMR spectroscopy 0-97150  
 spin-lattice relaxation time meas. using saturation, inversion and fast inversion expts. 0-57356  
 spin-lattice relaxation times meas., mathematical formulation 0-62703  
 successive oscillatory fields, molecular beam resonance method 0-91706  
 thymopoeitin active fragment in H<sub>2</sub>O, soln. conformation by DNMR spectroscopy 0-89710  
 Voigt lineshape, evaluation and characterisation 0-73401  
 yaRV-2 compact automatic nuclear resonance hygrometer 0-105657  
 zeugmographic imaging, gradient control device using microprocessor 0-89822  
 Ba, atomic beam and resonance spectroscopy 0-58180  
<sup>43</sup>Ca, atomic beam and resonance spectroscopy 0-58180

**magnetic screening *see magnetic shielding*****magnetic semiconductor materials *see magnetic semiconductors*****magnetic semiconductors**

conference, Montpellier, France (Sept. 79) 0-94916  
 doped semiconductors, local spin-density-functional method, appl. to metal-insulator transition 0-96789  
 electron spin-lattice relaxation in ferromag. metals and semiconds. (Russian) 0-103823  
 electronic properties, critical behaviour, theory 0-96861  
 EuSe, photocond. and photodiffusive voltage spectra 0-96940  
 exchange interaction, indirect, between localised moments 0-93079  
 ferromagnetic, doped, electron spin polarisation and conduction band struct. 0-65449  
 ferromagnetic, energy and mobility of spin polarons 0-70982  
 ferromagnetic, red shift effect, optical absorpt. edge calc. 0-66140  
 ferromagnetic, s-f interaction on conduction band, red shift effect theory 0-59872  
 ferromagnetic, surface localised low energy electron-magnon states (Russian) 0-88734  
 ferromagnetic multivalley anisotropic, electron autolocalisation (Russian) 0-92848  
 ferromagnetic semiconductor, localised magnon mode relax. theory 0-70986  
 ferromagnetic semiconductor, mag. polaron stability 0-96803  
 ferromagnetic semiconductor, polaron solitary waves 0-70625  
 ferromagnetic semiconductor, spectral density approach for s-f model quasiparticle concept 0-80173  
 ferromagnetic semiconductor, spin polaron props., effect on carrier scatt. 0-60233  
 ferromagnetic semiconductor, two-band s-d model hybridization 0-65446  
 ferromagnetic semiconductors, electronic quasiparticle spectrum 0-97051  
 ferromagnetic semiconductors, free carrier absorpt. of radiation 0-97227  
 ferromagnetic semiconductors, hot electron relax. time 0-59996  
 ferromagnetic semiconductors, short wavelength magnon generation 0-70987



## magnetic semiconductors continued

- ferromagnetic semiconductors with hot electrons, instability of coupled spin-helical waves 0-107841  
 helicon wave propag., hyperfine interaction effect 0-80307  
 indirect exchange interaction, mean free path effects 0-97088  
 intrinsic, indirect exchange interaction, finite temp., valence bands and energy gaps effect 0-59943  
 rare earth cpds., studies in Soviet Union, review 0-96875  
 small polaron form, and motion 0-96882  
 spin wave electron amplification theory 0-97083  
 TCNQ salt, dibenzo-TTF-TCNQCl<sub>2</sub>, one-dimens. mag. semicond., mag. and elec. props. 0-88601  
 CdCr<sub>2</sub>S<sub>4</sub> crystal growth, structural defects, physical properties 0-60759  
 CdCr<sub>2</sub>S<sub>4</sub>, ferromag. semicond., IR refl. spectra, phonon props. and dielec. function 0-66191  
 CdCr<sub>2</sub>S<sub>4</sub>, phototreshold changes below mag. ordering temp. 0-97406  
 CdCr<sub>2</sub>S<sub>4</sub>(Se<sub>4</sub>), thermoreflection, photoconductance, Raman scatt. near mag. phase transition 0-97298  
 CdCr<sub>2</sub>Se<sub>4</sub>, Crit. relax. processes, mag. reson. expts. 0-60425  
 CdCr<sub>2</sub>Se<sub>4</sub>, energy band struct. calc. by augmented plane wave method 0-103621  
 CdCr<sub>2</sub>Se<sub>4</sub>, energy structure, magnetooptic effects 0-71394  
 CdCr<sub>2</sub>Se<sub>4</sub>, ferromag. semicond., conc. anomalies rel. to red shift of absorpt. edge 0-70732  
 CdCr<sub>2</sub>Se<sub>4</sub> magnetic semiconductor, photoinduced centre kinetics 0-71110  
 CdCr<sub>2</sub>Se<sub>4</sub>, magnetisation, study of photoinduced charges 0-80567  
 CdCr<sub>2</sub>Se<sub>4</sub>, modulated piezoreflection spectra 0-97237  
 CdCr<sub>2</sub>Se<sub>4</sub>, Mott ferromagnetic semiconductor, optical absorption edge, critical behaviour 0-97226  
 CdCr<sub>2</sub>Se<sub>4</sub>Ag, magneto-optical effects in impurity spectral region 0-97313  
 CdCr<sub>2</sub>Se<sub>4</sub>Ga(In), photoconductivity, photomagnetoconductance near Curie point (Russian) 0-100485  
 CdCr<sub>2</sub>Se<sub>4</sub>In(Ga), elec. resist. and magnetoresist., 2 to 200K 0-96876  
 Cd<sub>1-x</sub>Mn<sub>x</sub>Te, exchange induced ionization of bound excitons, luminesc. meas. 0-97328  
 Cd<sub>1-x</sub>Mn<sub>x</sub>Te, indirect exchange interaction 0-97087  
 Cd<sub>1-x</sub>Mn<sub>x</sub>Te, semimagnetic, exchange interactions between localised and delocalised electrons 0-97245  
 CoCr<sub>2</sub>S<sub>4</sub>, ferrimag. semicond., magnetocrystalline anisotropy 0-71012  
 CoRhS<sub>4</sub>, mag. semicond., mag. and elec. props. 0-93121  
 CoS<sub>2</sub>, narrow-band ferromag., high press. effect on anomalous elec. resist. 0-70698  
 Co(S<sub>1-x</sub>Se<sub>x</sub>)<sub>2</sub>, galvanomag. effects, obs. and interpretation 0-70726  
 CuCr<sub>2</sub>Se<sub>4</sub>, influence of excess Cu on physical props. 0-103836  
 Cu<sub>2</sub>Cr<sub>2</sub>Se<sub>4-x</sub>Br<sub>x</sub>, ferromagnetic, Hall effect 0-60012  
 Eu chalcogenides, mag. polaron stability 0-96803  
 Eu chalcogenides, resonant Raman scattering model via magnetic exciton in ferromagnetic phase 0-93326  
 Eu chalcogenides, spin-dependent Raman scatt. from phonons 0-97274  
 Eu solid solutions with lanthanides, monosulfides, and oxides, vacant d states, X-ray absorpt. 0-103623  
 EuAl<sub>2</sub>S<sub>4</sub>, mag. susceptibility and EPR meas. 0-71173  
 EuB<sub>6</sub>, electronic struct., transport and mag. props. 0-96782  
 EuB<sub>6</sub>, ferromag., spin-polarised energy band struct., APW calc. 0-96779  
 EuB<sub>6</sub>, Hall effect and resistivity data, ferromagnetic ordering temp., pressure depend. 0-60010  
 EuB<sub>6</sub>, resist., Hall effect, and magnetoresist. under hydrostatic press., 4.2 to 300K 0-96879  
 EuGa<sub>2</sub>S<sub>4</sub>(Se<sub>4</sub>), mag. susceptibility and EPR meas. 0-71173  
 Eu<sub>2</sub>IrH<sub>4</sub>, prep., cryst. struct., mag. and elec. props. 0-88117  
 EuO, electronic struct. investigation by electron spectroscopy method 0-92812  
 EuO, ferromagnetic piezotransmission behaviour in magnetic field 0-97272  
 EuO, light scatt. from spin waves and magneto-optic hysteresis meas. 0-97244  
 EuO magnetic semiconductor, quasiparticle lifetimes, CPA study 0-65443  
 EuO nonstoichiometric film, ESR spectra and exchange interaction 0-93176  
 EuO, physical and physicochem. props., review 0-96875  
 EuO, transmission and resistivity, stress modulation effect near Curie temperature 0-96874  
 EuO:Gd, elec. cond. under hydrostatic press., Curie temp. 0-96881  
 EuO:Gd, ferromag. semicond., electron spin polarisation and conduction band struct. 0-65449  
 EuO:Gd, pure and doped, elec., mag., and optical props. rel. to electronic cond. 0-96880  
 EuO:Gd, surface mag. props. 0-71566  
 EuO:La(Gd), phototreshold changes below mag. ordering temp. 0-97406  
 EuO(S), ferromagnetic electronic structure, absorption, thermoreflection and thermotransmission spectra (French) 0-97300  
 EuO(S)(Se)(Te), spin order and fluctuations, Raman scatt. study 0-97273  
 EuO(Se), complex elec. cond. anomalies 0-107812  
 Eu<sub>1-x</sub>R<sub>x</sub>O<sub>1-x</sub> (R=Nd, Eu, Gd), lattice parameters, mag. and elec. props. 0-100578  
 EuS, ferromag. semicond., high field susceptibility, spin waves 0-75735  
 EuS films, mag. and elec. props. rel. to stoichiometry and defects 0-97122  
 EuS, light scatt. from spin waves and magneto-optic hysteresis meas. 0-97244  
 EuS, thin film, Brillouin scattering from spin waves 0-65843  
 EuS(Se)(Te), spin-assisted phonon Raman scatt., mag. phase depend. 0-71413  
 EuSe, VPE by hot-wall technique 0-80958  
 EuSe(Te), magnetic phase transitions, thermal modulation spectroscopy study (French) 0-97301  
 Eu<sub>2</sub>Sr<sub>1-x</sub>S<sub>x</sub>, magneto-optical redshift in absorpt. and photoluminesc., mag. short-range order 0-71388  
 EuTe, antiferromag. semicond., Raman scatt., spin-phonon interactions 0-66185  
 EuTe, magnetic impurity states, mag. and transport props. 0-96913  
 Eu<sub>1-x</sub>Yb<sub>x</sub>Te, (0<x<1), mag. semicond., elec., mag. and optical props. 0-97070  
 Fe<sub>0.5</sub>Co<sub>0.5</sub>S<sub>2</sub>, narrow-band ferromag., high press. effect on anomalous elec. resist. 0-70698  
 Fe<sub>1-x</sub>Co<sub>x</sub>Si solid solution, semiconductor-metal transition 0-103627

## magnetic semiconductors continued

- Fe<sub>0.5</sub>Co<sub>0.5</sub>Cr<sub>2</sub>S<sub>4</sub>, ESR spectra, elec. and mag. props., Curie temp. 0-97137  
 Fe<sub>0.9</sub>O, phototreshold changes below mag. ordering temp. 0-97406  
 α-Fe<sub>2</sub>O<sub>3</sub>, photochem. props. of sintered and doped samples for solar photoelectrochem. cell appls. 0-89651  
 FeRh<sub>2</sub>S<sub>4</sub>, mag. semicond., mag. and elec. props. 0-93121  
 Ga<sub>1-x</sub>Mn<sub>x</sub>Sb, elec. cond., mag. susceptibility, Hall const., and thermoelectric EMF, 80 to 1000K (Russian) 0-88549  
 Gd<sub>1-x</sub>□<sub>x</sub>S<sub>4</sub>, transport and mag. props., mag. Wigner localisation 0-97069  
<sup>3</sup>He, solid, as mag. semicond., analogy to Mott insulator 0-96720  
 HgCr<sub>2-x</sub>Al<sub>x</sub>Se<sub>4</sub> and HgCr<sub>2-x</sub>Ga<sub>x</sub>Se<sub>4</sub>, temp. depend. of ESR linewidth, 105-300K 0-71161  
 HgCr<sub>2</sub>Sd<sub>4-x</sub>Te<sub>x</sub>, ferromag. semicond., zero bandgap transition 0-96783  
 HgCr<sub>2</sub>Se<sub>4</sub>, electronic props. rel. to departure from stoichiometry 0-100472  
 HgCr<sub>2</sub>Se<sub>4</sub>, n-type ferromag. semicond., galvanomagnetic props. 0-70727  
 HgCr<sub>2</sub>Se<sub>4</sub>, thermoreflection, photoconductance, Raman scatt. near mag. phase transition 0-97298  
 Hg<sub>1-x</sub>Mn<sub>x</sub>Te, indirect exchange interaction 0-97087  
 Hg<sub>1-x</sub>Mn<sub>x</sub>Te, non-parabolic zero-gap semicond., indirect exchange interaction 0-80498  
 Hg<sub>1-x</sub>Mn<sub>x</sub>Te, semimagnetic, exchange interactions between localised and delocalised electrons 0-97245  
 Hg<sub>1-x</sub>Mn<sub>x</sub>Te, transverse magnetoresistance in quantised mag. fields 0-96922  
 HgTe, Γ<sub>8</sub> symm. acceptor centre hole mag. props. (Russian) 0-88733  
 Hg<sub>1-x</sub>Zn<sub>x</sub>Cr<sub>2</sub>Se<sub>4</sub>, magnetic struct., neutrographic and mag. investigation (Russian) 0-88726  
 La<sub>1-x</sub>Sr<sub>x</sub>CoO<sub>3</sub>, (0.5≤x≤0.9), ferromag., elec. props., itinerant electron model 0-107785  
 Mn<sub>2</sub>Cd<sub>1-x</sub>Te, phonons, Raman scatt. and IR absorpt. meas. (French) 0-97275  
 MnS, thermal cond., temp. depend., paramag.-antiferromag. transition effects 0-65321  
 Ni<sub>1-x</sub>Cr<sub>x</sub>S, elec. transport, mag. susceptibility and DTA meas. 0-96954  
 Ru<sub>2</sub>Ge<sub>3-x</sub>Sn<sub>x</sub> and Ru<sub>2</sub>Ge<sub>3-x</sub>Si<sub>x</sub>, diffusionless phase transitions, elec. and mag. props. 0-96871  
 SmB<sub>6</sub>, mixed valent semicond., transport props. and electronic struct., review 0-96877  
 Sm<sub>1-x</sub>La<sub>x</sub>S<sub>2</sub>, magnetoresist. in semicond. and metallic phases 0-96914  
 SmS, electron-phonon interaction, lattice dynamical model 0-96610  
 SmS<sub>1-x</sub>As<sub>x</sub>, magnetoresist. in semicond. and metallic phases 0-96914  
 Sm<sub>1-x</sub>Y<sub>x</sub>S<sub>2</sub>, magnetoresist. in semicond. and metallic phases 0-96914  
 Sn<sub>1-x</sub>Mn<sub>x</sub>Te, electronic struct., transport props., mag. ordering effects 0-65441  
 TmSe, Anderson lattice resist. for antiferromag. ordering 0-65556  
 TmSe, elec. resist. under press. at very low temp. 0-96878  
 TmSe-TmTe(EuSe), semiconductor-metal transitions 0-96953  
 UO<sub>2</sub>, 5f-magnetic semiconductor, spectroscopic data, review 0-97299  
 UO<sub>2</sub>, electronic transitions, crystal field effects and phonons, phase transition 0-97303  
 ZnCr<sub>2</sub>Se<sub>4</sub>, electroconductivity, thermoelectromotive force, Hall effect (Russian) 0-70694  
 ZnCr<sub>2</sub>Se<sub>4</sub>, screw spin structure, method of controlling the sense, polarised neutron diffr. study 0-70944  
 ZnCr<sub>2</sub>Se<sub>4</sub>, screw spin structure, magnetoelectric effect 0-75827  
 ZnCr<sub>2</sub>Se<sub>4</sub>In, magnetoresist. and elec. resist. above and below Neel temp. (Russian) 0-88576
- magnetic separation**  
 domain wall capture of mag. particles 0-71093  
 magnetic separator, drum-type with alternating polarity, analytical description of magnetic field (Russian) 0-99602  
 mineral microcrystals, mag. fluid technique for density determ. 0-85751  
 synovial fluid analysis by ferrography 0-101242  
 uniformly magnetised body, mag. field strength invariance 0-58441
- magnetic shielding**  
 alkanes, H<sup>+</sup> chemical shifts, extended Huckel calcs. with gauge in variant atomic orbitals 0-102449  
 benzene, H<sup>+</sup> chemical shifts, extended Huckel calcs. with gauge in variant atomic orbitals 0-102449  
 biomagnetic measurement facility installation in hospital environment, design criteria and procedure 0-104707  
 eddy current losses, estimation method, in large steel plate having one-phase excitation (Polish) 0-93145  
 ethylene compounds, H<sup>+</sup> chemical shifts, extended Huckel calcs. with gauge in variant atomic orbitals 0-102449  
 neutral beam source, cryopumping and mag. shielding, fabrication and operating cost 0-106229  
 SQUID magnetometers, geophysical dewar systems design 0-101462  
 superconductive helmet with SQUID for magnetoencephalography 0-104708  
 Al shielded room for biomag. meas. 0-104846  
 Al, thick-walled conducting shield in biomag. expts. 0-104845  
 Al thick-walled enclosure for LF biomag. meas. 0-62698  
 NH<sub>4</sub>H<sub>2</sub>(SeO<sub>3</sub>)<sub>2</sub>, single crystal, <sup>77</sup>Se magnetic shielding, chemical shift tensors 0-71207
- magnetic shielding, nuclear** see nuclear screening
- magnetic stars**  
 A<sub>1</sub> stars, Fe I photoionisation spectrum causing UV absorpt. 0-109437  
 adiabatic stability, of stars containing mixed poloidal and toroidal mag. fields 0-67706  
 Am and Ap-stars and high southern galactic latitude, four colour and Hβ obs. 0-82357  
 Am stars, τ Ursae Majoris and 15 Vulpeculae, energy distrib. from spectral obs. 0-85949  
 Am stars, evolved, search for photometric variability on lower part of Cepheid instability strip 0-62145  
 Am-type, binary stars, tidal interaction producing stable atm., evolution 0-67752  
 α Andromedae, HgMn star, evidence for Hg in thin atmospheric layer rel. to diffusion model 0-105243  
 Ap, Am stars, chemical differentiation and abundance spots prod. by diffusion 0-77381  
 Ap, Bp stars catalogue of photometric data rel. to surface mag. fields 0-85873  
 Ap and Bp stars, surface mag. field intensity rel. to Geneva photometry 0-105248  
 Ap stars, mag. fields meas. techniques and field geometries 0-82213



## magnetic stars continued

- Ap stars, new  $\Delta$ -photometry and evidence for two-component struct. of 5200 Å feature 0-67734  
 Ap stars broad flux depressions, comparison between synthetic spectra and spectrophotometry 0-67735  
 Ap stars in close detached binaries chem. anomalies surface distrib. 0-109475  
 Ap stars in spectroscopic binary systems, chemical anomalies surface distrib. 0-62140  
 $\delta_{1000}$ -Ap type stars, excess UV index, photometry obs. 0-72963  
 Ap-stars, mag. field obs. using photoelec. method, visible spectra obs. 0-82373  
 Ap-stars, spectral energy distrib., spectrophotometry in 3300 to 7100 Å region 0-85953  
 $\sigma$  Aquarii (A0 IVs), hot metallic-line star, abundance anal. from model atmosphere 0-90415  
 AR Aurigae, eclipsing binary Hg star, peculiar spectral var. during eclipse 0-98679  
 late B-type stars small  $v \sin i$  values, Ap star determ., visible spectra 0-77409  
 Bp-star (No.7) in cluster near IC 1805, photometry 0-62214  
 53 Camelopardalis, Ap star, Ca II K and H $\delta$  lines rapid vars. (*Russian*) 0-90458  
 53 Camelopardalis (AX Camelopardalis), Ap star, UVB photoelectric photometry and period of var. (*Italian*) 0-90448  
 $\alpha^2$  Canum Venaticorum, line blanketed model atmospheres of Ap-star 0-90440  
 XY Ceti, metallic line eclipsing binary, masses, radii and luminosities from revised photometric elements 0-109458  
 17 Comae A, Ap star, mag. field meas. and rot. period (*Russian*) 0-90457  
 convective stability in magnetic stars, theory 0-94781  
 $\beta$  Coronae Borealis, Ap star, Ca II K and H $\delta$  lines rapid vars. (*Russian*) 0-90458  
 $\alpha$  Coronae Borealis, Hg-Mn star, spectroscopic binary, visible spectra obs. 0-72983  
 $\beta$  Coronae Borealis, obs. with Zeeman analyzer system on McDonald 2.7 m telescope 0-62021  
 HD 101065, Przybylski's star, light variability freq. anal. 0-62152  
 HD 10783, Ap star, spectrophotometric obs. 0-98663  
 HD 129494, new pulsating  $\delta$  Delphini star, photometric obs. and luminosity 0-67750  
 HD 129708, bright short-period Cepheid with  $\delta$  Delphini tube spectrum, photometric obs. 0-67751  
 HD 153882, obs. with Zeeman analyzer system on McDonald 2.7 m telescope 0-62021  
 HD 187473, rare earths in Si star 0-98671  
 $\phi$  Herculis, Hg-Mn star, corona search, UV obs. 0-72986  
 HR 5049, Co II in spectrum of southern magnetic Ap-star 0-82384  
 HR 6127, chemically peculiar star, spectral lines and equivalent width lists, visible obs. 0-82387  
 HR 96, Ap-type star, atm. parameters and stellar comp., visible obs. 0-67740  
 $\mu$  Leporis, HgMn star, evidence for Hg in thin atmospheric layer rel. to diffusion model 0-105243  
 $\chi$  Lupi, HgMn star, evidence for Hg in thin atmospheric layer rel. to diffusion model 0-105243  
 metallic line stars, spectral energy distrib. (*Russian*) 0-72975  
 oscillations, nonradial mode splitting 0-77414  
 IW Persei, metallic-line close binary star, photometric and spectroscopic obs. 0-62186  
 polarity reversals, appl. of skin effect approx. 0-62010  
 41 Tauri, Ap star, Ca II K and H $\delta$  lines rapid vars. (*Russian*) 0-90458  
 upper main-sequence peculiar stars, chemical and physical props. rel. to radiatively driven diffusion theory 0-82374  
 $\tau$  Ursae Majoris, Am star, energy distrib. from spectral obs. 0-85949  
 $\tau$  Ursae Majoris, Am star, microturbulence and metal content determ. 0-82377  
 CU Virginis (HD 124224), Ap star, spectrophotometric obs. 0-98663  
 15 Vulpeculae, Am star, energy distrib. from spectral obs. 0-85949  
 He rich stars, intermediate and extreme, spectral atlas in 3700 to 4600 Å range 0-94806  
 He variable stars, IR excesses obs. 0-67733  
 Hg-Mn binary stars, inhibition of atmos. diffusion 0-62153  
 Mn stars, Hg II line oscillator strength determ., diffusion models implication 0-72966  
 Mn-Hg stars, surface gravity and stellar temp. derivation from uvby $\beta$  data, statistical anal. 0-82397

## magnetic storms

- see also micropulsations  
 1974 August to November, effects on nighttime electron content of mid-latit. plasmasphere 0-94642  
 1976 October 7, ground-based obs. of auroral zone elec. currents using two-dimensional magnetometer array 0-90245  
 1978 December 11, mini-substorm and long-period Pi 2 event obs. by Jikiken satellite (*Japanese*) 0-94653  
 1978 July 15, severe scintillation of VHF and GHz waves from geostationary satellites 0-109302  
 $A_1$ -index, 1964-1976, rel. to geomag. field and interplanetary field states 0-104866  
 airglow during magnetic storm, O I 7774 Å multiplet obs. 0-72663  
 auroral infrasonic waves in substorm area, source regions (*Japanese*) 0-85788  
 auroral substorm, ionospheric irregularities simultaneous rocket probe, scintillation and incoherent scatter radar obs. 0-94640  
 cleft region dynamics 0-101483  
 $D_1$  index, negative change assoc. with whistler ducts formation 0-94659  
 electrojet intensification by substorm 0-85796  
 electron precipitation during substorm, modulation by hydromagnetic waves 0-105113  
 F-layer electron density, mag. storm effects 0-61970  
 F-layer, anomalous decrease in equatorial  $f_o$  during strong storms 0-77197  
 F-region, total electron density content and peak electron vars., 140 MHz obs. 0-101471  
 gradual commencements, rel. to interplanetary mag. field intensity vars. (*Russian*) 0-105127  
 high-latitude substorms, characts. 0-109315  
 inner magnetosphere penetration by energetic particles 0-72716

## magnetic storms continued

- interplanetary shock and substorm activity, with increased solar wind energy deposition 0-77237  
 ion composition and origin, of high-altitude region during mag. storm 0-82144  
 ionosphere, elec. fields induced by ion drag and substorms 0-77199  
 ionosphere, geomag. field dependence of global absorpt. meas. on board ships 0-98500  
 ionosphere, mag. storm effect on struct. at low latitude, 406 kHz impedance obs. 0-67468  
 ionosphere, mag. storms rel. to radio waves winter absorpt. anomaly at middle latit. 0-67459  
 ionosphere disturbance assoc. with storm, electron density vars. with latitude 0-101474  
 ionosphere during auroral substorm expansion, riometer absorpt. spikes obs. 0-85799  
 isolated substorm over Scandinavia, 1st March 1977, ground-based obs. 0-105132  
 magnetic ULF waves over auroral arc during substorm event 0-72722  
 magnetosphere, charged particle fluxes obs. by JIKIKEN satellite rel. to mag. storms (*Japanese*) 0-94654  
 magnetosphere, connection with solar flare activity 0-72919  
 magnetosphere, elec. field in VLF to HF range, EXOS-B obs. 0-67478  
 magnetosphere substorm and simultaneous thunderstorm, elec. fields, electron precip. and VLF radiation 0-67392  
 magnetosphere substorm onset, coincidence with kilometric radiation enhancement, JIKIKEN (EXOS-B) satellite obs. (*Japanese*) 0-94648  
 magnetosphere substorms, cause of plasma sheet thinning 0-72705  
 nightglow from  $N_2^+$ , correl. to geomagnetic activity 0-72665  
 PiB magnetic pulsation during substorm 0-72723  
 plasma sheet dynamics and mag. storms, conceptual model 0-72736  
 plasma sheet thinning during substorms 0-105131  
 plasma stability during storm conditions, Alfvén waves and drift modes 0-82150  
 polar cap, mag. field perturbations compared to solar electron profile 0-72718  
 protonosphere depletion assoc. with mag. storm, and recovery 0-85784  
 Ps 6 magnetic disturbances, seasonal and diurnal var. 0-67477  
 ring current magnetic field characts., spherical harmonic analysis 0-101493  
 ring current particle origin, by inward displacement of trapped particles 0-72708  
 solar wind-magnetosphere dynamo, energy coupling function and substorms 0-105134  
 solar wind-magnetosphere energy coupling, geomag. disturbances 0-85821  
 substorm, definition of phenomena 0-82145  
 substorm variation field modeling, current system anal. 0-105130  
 substorms, assoc. variability of plasma sheet dynamics 0-98518  
 substorms, classical equiv. stream systems (*Russian*) 0-85806  
 substorms, electron flux vars. in inner radiation belt during substorms 0-67470  
 substorms, geomag. induction effects in central Australia 0-72424  
 sudden storm commencements, analytical study of ionospheric response (*Japanese*) 0-101490  
 synchronous orbit magnetosphere behaviour during nighttime substorm 0-85811  
 telluric currents, induced, in Alaska oil pipeline, meas. by gradient fluxgate and SQUID magnetometers 0-98231  
 upper atmosphere perturbations assoc. with mag. storms, review 0-98495  
 whistlers at low-latitude during mag. storm, equatorial elec. field 0-85817

## magnetic structure

- see also canted spin arrangements  
 actinide compounds, neutron scatt. studies 0-75716  
 actinide mononitrides, anomalous mag. props., planar coupling theory 0-60245  
 amorphous alloys and semiconductors, Mossbauer spectrometry (*French*) 0-80660  
 bubble garnet film, non-implanted, surface mag. struct. 0-84628  
 copper formate anhydrate, cryst. struct. and mag. props. 0-79768  
 copper formate tetrahydrate, antiferromag. phase, neutron diffr. study 0-93085  
 crystals, mag. struct., exchange multiplets 0-60202  
 diethylammonium copper tetrabromide, mag. struct., NMR meas. 0-71192  
 dimethylammonium copper tetrachloride-tetrabromide mixed cryst., mag. transition 0-65874  
 electron and magnetisation densities in molecules and crystals, Arles, France (Aug. 1978) 0-105428  
 electron-hole paired systems, ferromagnetic ordering phase diagram 0-97097  
 ferromagnet, electron capture spectroscopy, technique for surface science and ferromagnetism 0-92766  
 ferromagnetic alloys, disordered cryst. and amorphous, mag. dipolar field distrib., computer simulation 0-65790  
 harmonic rotor model, interactions, spirals and phase transitions with and without long range order 0-60350  
 Invar, magnetic structure, depend. on absorbed H, Stoner's band model calcs., Mossbauer spectra 0-65787  
 Invar film, superfine mag. struct. (*Russian*) 0-80572  
 ionic compounds, amorphous, exhibiting Mossbauer spectra, mag. props. (*French*) 0-80490  
 ionic compounds, amorphous, Mossbauer study, frozen mag. state and hyperfine interaction (*French*) 0-80661  
 Ising ferromagnet and antiferromagnet, two-dimens. square, ground state, apparent 3-spin interactions 0-88709  
 longitudinal static spin wave struct., magnetotropic interaction of light (*Russian*) 0-93285  
 magnetically ordered crystals, exchange symm., mag. struct. (*Russian*) 0-65785  
 neutron diffr. study, symm. anal., polarisation effects 0-93083  
 oxides,  $RCu_3Mn_2O_{12}$ ,  $R=La$  to  $Lu$ , Y, synthesis and mag. props. 0-75717  
 photoemission technique for meas. of magnetic order and spin depend. of electron scatt. 0-60748  
 pyridinium manganese chloride, anhydrous, quasi one-dimensional mag. behaviour, heat capacity meas. 0-80549  
 pyridinium nickel chloride, anhydrous, quasi one-dimensional mag. behaviour, heat capacity meas. 0-80549



**magnetic structure continued**

- rare earth intermetallic compounds, ferromag. props., book contrib. 0-75726
- rare earth intermetallics,  $\text{AlAl}_2$ , orbital and spin polarisations of cond. electrons 0-65791
- rare earth iron garnets, anisotropic, mag. props., high field and low temp. 0-75801
- rare earth metals, electronic sound attenuation anomalies at transition to helical phase, Fermi surface topology (*Russian*) 0-92807
- rare earth metals and alloys, ferromag. props., book contrib. 0-75725
- rare earth titanium oxides,  $\text{RTiO}_3$  type, bulk mag. and struct. props., ferrimag. order 0-107993
- rare earth-transition metal alloys, amorphous, ferrimag., spin arrangements in large fields 0-75718
- rare earth-transition metal alloys,  $\text{RM}_2\text{Si}_{2-x}\text{Ge}_x$  and  $\text{RM}_{4-x}\text{Al}_{x-2}$ , magnetism and hyperfine interactions, magnetisation and Mossbauer effect studies 0-75892
- screw spin structure, method of controlling the sense 0-70944
- submicron magnetic objects, mag. struct. study using magneto-optic micro-magnetometer 0-57349
- superconductor, helical ordering of spins 0-88669
- symmetry, wreath groups 0-88724
- transition metal complexes, electron densities, local orbital populations, polarised neutron diffraction 0-88725
- weak ferromagnets, Landau-Lifshitz eqn. solutions, moving domain walls, struct. (*Russian*) 0-100596
- $\text{AuMn}$ , mag. struct., phase transition, and magnon spectrum, random anisotropy effects 0-88722
- $\text{BaMnF}_4$ , magnetic neutron scatt. from structurally distorted cryst. 0-93086
- $\text{BaNi}_2(\text{PO}_4)_2$  and  $\text{BaNi}_2(\text{AsO}_4)_2$ , mag. props., neutron diff. and sp. ht. meas. 0-70948
- $\text{BiFeO}_3$ , ferroelec., antiferromag., cryst. and mag. struct., neutron diff. study 0-65786
- $\text{CaLaFeO}_4$ , two-dimens. mag. props. rel. to cryst. struct. 0-75776
- Ce mononitrides, anomalous mag. props., planar coupling theory 0-60245
- $\text{CeAl}_2$ , multiple- $q$  structure or coexistence of different mag. phases, neutron diff. study 0-107985
- $\text{CeIn}_3$ , mag. struct., neutron diff. study 0-80481
- CsB, antiferromag., first-order transitions, mag. phase diagram 0-60252
- CsN<sub>3</sub>, mixed valence cpd., electronic struct. and mag. props. 0-70649
- Co complex,  $\text{Co}(\text{II})(1,2,4\text{-triazole})_2(\text{NCS})_2$  quasi two-dimens. canted  $S=1/2$  antiferromag. 0-70976
- $\text{Co}_{100-x}\text{B}_x$ , amorphous, mag. struct., mag. susceptibility meas. 0-80485
- $\text{CoCO}_3$ , weakly ferromag., light absorpt. dichroism and mag. config. 0-66223
- $\text{CoMnP}$ , cryst. mag. struct., neutron diff. study (*French*) 0-59439
- Cr, antiferromagnetic structure, mag. field effect, spin density wave model (*Russian*) 0-70953
- Cr, mag. struct., phase transition, and magnon spectrum, random anisotropy effects 0-88722
- $(\text{CrF}_6)^{3-}$  6a AR-AT complexes, electron densities, local orbital populations, polarised neutron diffraction 0-88725
- $\text{Cr}_{0.995}\text{Pt}_{0.005}$  alloy, mag. struct., neutron diff. study 0-60198
- $\text{CsRb}_3$ , neutron diff. expts. at 300, 77 and 1.2K 0-107163
- $\text{CsCuCl}_3$ , helical mag. struct., neutron diffraction study 0-107983
- $\text{CsFeF}_6$ , mag. struct. and one-dimens. antiferromagnetism 0-60209
- $\text{CsMnF}_3$ , mag. struct., phase transition, and magnon spectrum, random anisotropy effects 0-88722
- $\text{CsMnF}_4$ , planar ferromag., cryst. and mag. struct., Jahn-Teller effect 0-75715
- $\text{CsNiF}_3$ , quasielastic neutron scatt. around Neel-point 0-75768
- Cu-Mn (8 to 75 at.%), spin correl., neutron polarisation anal. study 0-65905
- $\text{DyCo}_3$ , noncollinear mag. struct. appearance in mag. fields, magnetostriction meas. (*Russian*) 0-100607
- $\text{Dy}_2\text{O}_3\text{SO}_4$ , mag. ordering, magnetisation, AC susceptibility and Zeeman effect meas. 0-60205
- Er-La, HCP, mag. phase diagram, neutron diff. meas. 0-70950
- $\text{ErRh}_2\text{B}_4$ , superconducting, magnetic dilemma 0-75680
- $\text{ErTiO}_3$ , magnetic structure determination, neutron scatt. study 0-65809
- Fe, magnetism at high temps. 0-75721
- Fe particles, spin collinearity, Mossbauer spectra study 0-71114
- Fe-Ni (32.3 at.%), mag. struct. in commensurate approx., neutron diff. study 0-60212
- Fe-Ni (33-38 at.%), low-angle neutron diff., anomalous crit. scatt. (*Russian*) 0-60193
- Fe-Ni-Cr, mag. props. in weak mag. fields (*Russian*) 0-75771
- $\text{Fe}_{100-x}\text{B}_x$ , amorphous, mag. struct., mag. susceptibility meas. 0-80485
- $\text{Fe}_{80}\text{B}_{20}$ , amorphous ferromagnet, Mossbauer hyperfine fields, mag. struct. 0-75894
- $\text{Fe}_1\text{Co}_2\text{Cl}_2\text{H}_2\text{O}$ , random mixture with competing spin anisotropies, tetracrit. behaviour 0-60324
- $\text{Fe}_{0.5}\text{Co}_{0.5-x}\text{Cr}_x$  films, vacuum-deposited cryst. and mag. struct. (*Russian*) 0-93081
- $\text{FeMoS}_4$ , Mossbauer investigation, Neel point, superparamag. effects 0-97170
- $\text{Fe}_{1-x}\text{Mg}_x\text{Ti}_2\text{O}_4$ , mag. ordering, Mossbauer effect in external mag. fields 0-71257
- $(\text{Fe}_{0.45}\text{Nb}_{0.55})\text{O}_2$ , rutile, cation distrib. and mag. ordering (*German*) 0-107116
- $\text{Fe}_{40}\text{Ni}_{40}\text{C}_{14}\text{P}_6$  amorphous film, dislocation and mag. struct., neutron diff. study 0-70956
- $\text{Fe}_{65}\text{Ni}_{28}\text{Mn}_7$ , disordered, mag. struct. near ferro-antiferromagnetic transition 0-60211
- $\text{Fe}_{40}\text{Ni}_{40}\text{P}_{14}\text{B}_6$ , amorphous ferromagnet, Mossbauer hyperfine fields, mag. struct. 0-75894
- $(\text{Fe}_{0.5}\text{Ta}_{0.5})\text{O}_2$ , rutile, cation distrib. and mag. ordering (*German*) 0-107116
- $\text{FeTh}_2\text{S}_8$ , mag. struct. and props., neutron diff. and mag. meas. 0-60201
- Gd-Co amorphous films, mag. struct., mag. bubbles, electron diff. study (*Chinese*) 0-71126
- GdMg, noncollinear mag. struct., nonlinear band behaviour 0-75706
- GdNi, and  $\text{GdNi}_{1-x}\text{O}_x$ , mag. interactions 0-60218
- $\text{Hg}_{1-x}\text{Zn}_x\text{Cr}_2\text{Se}_4$ , magnetic struct., neutrographic and mag. investigation (*Russian*) 0-88726
- Ho-La, HCP, mag. phase diagram, neutron diff. meas. 0-70950
- $\text{HoCo}_2\text{Ge}_2$ , crystal and magnetic structure obs. 0-64976
- $\text{HoCu}_2$ , mag. struct. and elec. resist., neutron diff. obs. 0-60206

**magnetic structure continued**

- $\text{Ho}_2\text{O}_3\text{SO}_4$ , mag. ordering, magnetisation, AC susceptibility and Zeeman effect meas. 0-60205
- $\text{HoTiO}_3$ , magnetic structure determination, neutron scatt. study 0-65809
- $\text{KCrO}_2$ , two-dimens. mag. props. rel. to cryst. struct. 0-75776
- $\text{K}_2\text{FeF}_6$ , mag. struct. and one-dimens. antiferromagnetism 0-60209
- $(\text{La}_{0.9}\text{Ca}_{0.1})\text{MnO}_{3+y}$ , mag. props., Faraday method meas. 0-103832
- $\text{La}_2\text{MnFeS}_6$ , antiferromag., mag. props. and mag. struct., neutron diff. and magnetisation meas. 0-65801
- $\text{LiCrO}_2$ , two-dimens. mag. props. rel. to cryst. struct. 0-75776
- $\gamma\text{-Mn}$ , antiferromagnetic, self-consistent bandstructure calcs. 0-88475
- $\gamma\text{-Mn}$ , collinear spin structure stability 0-107984
- $\text{MnCr}_2\text{S}_4$ , mag. struct. under applied mag. field 0-97065
- $\text{MnCr}_2\text{S}_4$ , substituted, mag. struct. and transitions 0-65795
- $\gamma\text{-MnCu}$ , Mn-rich, inclined spin axis, neutron diff. study 0-75723
- $\text{MnF}_2$ , antiferromag., mag. space groups, Clebsch-Gordan coeff. calcs. 0-79731
- $\text{Mn}_3\text{Ga}_{1-x}\text{Mn}_x\text{N}$ , perovskite struct., phase transformations (*French*) 0-81048
- $\text{Mn}_3\text{Ga}_{1-x}\text{C}_x$ , perovskite struct., phase transformations (*French*) 0-81048
- $\text{Mn}_2\text{N}$ , mag. struct. non-collinearity, neutron diff. obs. 0-65796
- $\text{MnOOH}$ , mag. ordering, fine struct. and crit. behaviour, neutron diff. meas. 0-65800
- $\text{MnSO}_4$ , mag. struct. and phase transitions, neutron diff. study 0-60208
- $\text{MnSb-CrSb}$ , NiAs-type system, single crystals, neutron diff. studies 0-60200
- $\text{Mn}_2\text{SnS}_4$ , cryst. struct. refinement and mag. struct. determ. (*French*) 0-107131
- $\text{Mn}_{1-x}\text{Zn}_x\text{Fe}_2\text{O}_4$ , prepared by wet method, neutron diff. and high field Mossbauer expts. 0-75719
- $\text{NaCrO}_2$ , two-dimens. mag. props. rel. to cryst. struct. 0-75776
- $\alpha\text{-Na}_2\text{Fe}_2(\text{PO}_4)_3$  orthophosphate, cryst. and vitreous, Mossbauer spectroscopy and mag. susceptibility (*French*) 0-80657
- $\text{NaMnCl}_3$ , mag. struct. and spin-flip transition, powder neutron diff. exam. 0-60210
- $\text{NaMnCrF}_6$ , mag. struct., neutron Laue diff. method 0-70951
- Nd, mag. struct., 18.6K mag. phase transition 0-65799
- Nd, magnetic-structure, neutron and X-ray diff. study 0-60197
- Ni, paramagnetic, mag. form factors in Stoner-like model 0-97061
- Ni-Cu, ferromag., mag. moment, local environment effects, HF CPA cluster calc. 0-65817
- Ni-Mn (17-27 at.%), low-angle neutron diff., anomalous crit. scatt. (*Russian*) 0-60193
- Ni-Pt alloys, magnetic-moment distrib. neutron study 0-97066
- $\text{Ni}_{100-x}\text{B}_x$ , amorphous, mag. struct., mag. susceptibility meas. 0-80485
- $\text{NiBr}_2$ , commensurate and incommensurate mag. struct., neutron diff. study 0-97067
- $\text{NiBr}_2$ , low-temperature magnetic phase, incommensurate spin structure 0-93082
- $\text{NiCl}_2\text{6NH}_3$ , low temp. sp. ht. and mag. ordering 0-75784
- $\text{NiFe}_2\text{O}_4$  ferrite, mag. props., neutron irradi. 0-103858
- $\text{NiI}_2$  anhydrous, magnetic phase transition, neutron diff. study 0-71033
- $\text{NiMnGe}_{1-x}\text{Si}_x$ , mag. props., neutron diff. and magnetometric meas., 80-600K 0-65793
- NiO, mag. struct., neutron Laue diff. method 0-70951
- $\text{NpCo}_2\text{Si}_2$ , mag. struct., neutron diff. determ. 0-93084
- $\text{NpCu}_2\text{Si}_2$ , mag. struct., neutron diff. determ. 0-93084
- $\text{Pd}_{2-x}\text{MnSb}$ , struct., appl. as improved neutron polariser 0-60199
- $\text{Pr}_{1-x}\text{Ca}_x\text{MnO}_3$ , struct. and magnetisation study 0-65804
- $\text{PrCoGe}_2$ , crystal and magnetic structure obs. 0-64976
- $\text{Rb}_2\text{FeF}_5$ , mag. struct. and one-dimens. antiferromagnetism 0-60209
- $\text{SmZn}_2$ , ferromag., cond. band antiparallel polarisation exceeding 4f moment 0-60207
- $\text{SrCoO}_{3-x}$ , mag. and neutron diff. study 0-65805
- $\text{SrFe}_2\text{Ga}_2\text{O}_{19}$  ferrite, mag. struct., Mossbauer study 0-93087
- $\text{SrLaFeO}_4$ , two-dimens. mag. props. rel. to cryst. struct. 0-75776
- $(\text{Tb}_2\text{La}_{1-x})\text{Be}_{13}$ , mag. struct., cryst. field effects, neutron diff. study 0-65789
- $\text{Tb}_{0.26}\text{V}_{0.74}\text{Fe}_2\text{O}_{12}$  garnet, mag. transition, mag. props. anomaly 0-93120
- $(\text{Ti}_{1-x}\text{V}_x)_2\text{O}_3$ , metallic antiferromag. struct., neutron studies 0-65797
- Tm magnetic transitions, effect of  $\text{H}_2$  in solid solns., elec. resist. meas. 0-100585
- $\text{V}_1$ , MCD spectra, interpretation rel. to mag. struct. 0-66222
- $\text{V}_1$ , mag. struct., long- and short-range order and Mossbauer spectroscopy 0-65803
- $\text{V}_1$ , mag. superlattice, neutron oscill. and Weissenberg photography 0-65802
- $\text{ZnCr}_2\text{Se}_4$ , screw spin structure, method of controlling the sense, polarised neutron diff. study 0-70944
- $\text{ZnCr}_2\text{Se}_4$ , screw spin structure, magnetoelectric effect 0-75827
- $(\text{Zr}_{1-x}\text{Nb}_x)\text{Fe}_2$ , antiferromag. spin struct., Mossbauer effect study 0-66086

**magnetic surface phenomena**

- antiferromagnet, long-wavelength, surface spin-waves 0-88737
- bubble garnet film, non-implanted, surface mag. struct. 0-84628
- epitaxial ferrite-garnet films with inversion layers, behaviour of cylindrical mag. domains, visual tracking method 0-71139
- ferrofluid, nonlinear surface waves, bifurcation theory approach 0-58439
- ferromagnet, Brillouin light scatt. by spin waves 0-93359
- ferromagnet, surface and bulk nucl. spin waves, Green function formalism 0-70984
- ferromagnet, tight binding model, surface magnetisation 0-103807
- ferromagnetic alloys, surface spin waves, cluster Bethe lattice approach 0-70983
- ferromagnetic slab, finite thickness, spin correl. functions 0-80522
- ferromagnetic slab, light scattering from bulk and surface spin waves, theory 0-71389
- films, ferromagnetic, perpendicularly magnetised, surface and vol. magnetoelastic waves (*Russian*) 0-93151
- Heisenberg ferromagnet, surface magnetisation profile and localised magnons 0-70985
- Ising ferromagnetic half-plane, surface, pinned domain wall, free energy and magnetisation profile 0-60361
- Ising model, surface crit. behaviour, layer and local susceptibility 0-71058
- Ising model strips, scaling theory, wall effects in crit. systems 0-80539
- polarised electron scatt. study 0-93160
- spin wave resonance, theory of magnetic surface states, review 0-84654
- strip films, bulk and surface spin oscils., mag. reson. 0-97149



**magnetic surface phenomena continued**

- thin film alloys, surface magnetism props., Curie temp., Ising model 0-108039  
 transition metal, chemisorption of H, effect of surface spin fluctuations 0-75613  
 Co fine particles in Cu, interface magnetisation 0-88858  
 EuO:Gd, surface mag. props. 0-71566  
 Fe film, coated, interface magnetism by Mossbauer spectroscopy 0-75890  
 Fe, whisker single crystals, ferromag. reson. and surface anisotropy 0-71187  
 Fe-SiO multilayer films, interface magnetisation 0-88858  
 Ni-SiO multilayer films, interface magnetisation 0-88858  
 Ni(001) surface states, surface magnetisation, electron spin polarisation 0-88612  
 Ni(110), ferromag., surface magnetisation, polarised LEED expt. 0-97118  
 O<sub>2</sub> monolayers, on graphite, mag.  $\alpha$ -phase and  $\alpha$ - $\beta$ -phase transition 0-70530  
 V surface, spin fluctuations, finite temp. mag. props. study 0-107994  
 YIG, multiple mag. layer structures, magnetostatic surfacewave propag. 0-88839  
 Y<sub>3-x</sub>Sm<sub>x</sub>Fe<sub>2</sub>O<sub>12</sub>:<sup>57</sup>Fe film, ion implanted, Mossbauer conversion spectra study 0-80663

**magnetic susceptibility**

- see also molecular magnetic susceptibility; photomagnetic effect*  
 aluminium copper tetrahalides, exchange, mag. anisotropy, and spin diffusion contribs. to EPR linewidth 0-80597  
 alkali metals, magnetic property volume depend., Knight shifts, electron spin response 0-88729  
 alloys, d-metal, magnetic susceptibility and Knight shift meas. 0-66055  
 aluminoborate glass, Fe and Cr ion interaction, mag. and spectral props. 0-103883  
 aluminosilicate glass:Co (14.3 wt.%), AC susceptibility meas. 0-88771  
 amorphous magnet, random anisotropy axis model in the infinite-range limit 0-88761  
 Anderson model, orbitally degenerate, exchange coupling in atomic limit, rel. to two-site Hubbard model 0-108000  
 antiferroelectric ferrites, coupled magnetoelc. oscills. and high freq. susceptibility tensor (*Russian*) 0-93152  
 antiferromagnet, crit. fluctuation of staggered magnetisation, AC susceptibility meas. 0-60219  
 antiferromagnet, Ising model, two-dimens., mag. susceptibility calc. 0-60225  
 antiferromagnet, two-dimensional, expansion for susceptibilities 0-70963  
 antiferromagnetic triangular cactus tree, bond-diluted, ordered phase 0-101037  
 antiferromagnets, disordered spin flop, bicritical behaviour, critical experiments 0-65899  
 antiferromagnets, random, theory of mag. excitations, antiferromag. reson. 0-97146  
 Bloch electrons, nonlinear orbital magnetisation in weak mag. fields (*Russian*) 0-70931  
 borosilicate glass, Fe and Cr ion interaction, mag. and spectral props. 0-103883  
 coal, mag. susceptibility and Mossbauer meas. 0-60464  
 copper porphyrins, mag. susceptibility and EPR, sample grinding effects 0-60420  
 copper quaternary thiopins, mag. and elec. props. (*French*) 0-65771  
 4-cyanobenzoyloxy-4'-pentylstilbene, nematic, smectic A, and orthogonal smectic B phases 0-64890  
 dialkylammonium iron tetrachloride, antiferromag., mag. susceptibility meas. 0-60220  
 diisopropylammonium copper chloride, mag. interactions, susceptibility, 2-230K 0-60237  
 dimethylamine iron tetrachloride, antiferromag., mag. susceptibility meas. 0-60220  
 dimethylammonium copper tetrabromide, quasi two-dimensional antiferromag., mag. behaviour 0-97098  
 dimethylammonium copper tetrachloride, crit. slowing down and anomalous relax. near Curie temp. 0-71053  
 dimethylammonium copper tetrachloride, ferromag., quasi two-dimensional, ordering temp., press. depend. 0-84601  
 dimethylammonium copper tetrachloride, two-dimens. ferromag., saturation of parallel-pumped magnons 0-97147  
 dimethylammonium copper tetrahalide, layer compound (CH<sub>3</sub>NH<sub>2</sub>)<sub>2</sub>Cu(Cl,Br,I)<sub>4</sub>, antiferro- to ferromag. transition 0-108005  
 dipalmitoylphosphatidylcholine, changes in vol. mag. susceptibility at the phase transition 0-76770  
 dipropylammonium manganese tetrachloride, two-dimens. weak ferromagnet, AC susceptibility 0-65823  
 dithiocarbamate complexes of Cr, Mn, Sn and Pb IR, electronic and mass spectra, mag. susceptibility, cond. meas. 0-97270  
 electron fluid, adiabatic de Haas-van Alphen effect at low temp., Fermi fluid interaction and chem. pot. effects (*Russian*) 0-84442  
 electron gas, inhomogeneous, exchange effects and nonzero temps. 0-84444  
 ellipsoid with domain struct., magnetostatic oscills., theory 0-93102  
 ferrites type 1500 NMZ and 2000 NMI, mag. susceptibility depend. on heating (*Russian*) 0-108603  
 ferrofluids, mag., optical, and hydrodynamic props., expt. study, review 0-60376  
 ferromagnet, Ising model, diamond lattice, phase transition, crit. props. 0-93127  
 ferromagnet, itinerant, mag. props., temp. depend., functional integral approach 0-60170  
 ferromagnet, itinerant electron, magnetoelastic contribs. to US vel., elastic consts., and susceptibility 0-75829  
 ferromagnet, itinerant electron, magnon spectrum just below T<sub>c</sub>, theory 0-65833  
 ferromagnet, magnetic susceptibility, spin and charge density waves, Curie temp. (*Russian*) 0-100581  
 ferromagnetic metals, spin fluctuation theory, Curie temp., mag. susceptibility 0-65937  
 glass, magnetic susceptibility measurement, torsional reson. technique 0-82796  
 graphite, diamagnetism with quasilinear dispersion law, orbital susceptibility, valence bands (*Russian*) 0-80475  
 heavily doped semiconductor, n-type, disordered mag. system, hierarchy of exchange interactions 0-80235

**magnetic susceptibility continued**

- Heisenberg, ferromagnet, classical, with dipole-dipole interaction, renormalisation group and crit. exponents 0-60351  
 Heisenberg antiferromagnet, Green function theory 0-107975  
 Heisenberg antiferromagnet, one-dimens., impure, mag. susceptibility 0-60168  
 Heisenberg ferromagnet, anisotropic, collective Green's function, dynamical RPA 0-70925  
 intermediate valence compounds, dynamic susceptibilities 0-70653  
 ionic compounds, amorphous, exhibiting Mossbauer spectra, mag. props. (*French*) 0-80490  
 iron(II)-A-zeolites, reduction, mag. and Mossbauer study 0-71115  
 Ising antiferromagnet, nonlinear response to high freq. mag. field, quantum theory (*Russian*) 0-93066  
 Ising chain, double, transverse susceptibility (*Russian*) 0-88727  
 Ising chain, with next-nearest neighbour interactions, mag. responses to spin-Peierls transition 0-71054  
 Ising ferromagnet, two-dimens., order parameter and induced susceptibility 0-71036  
 Ising model, bond random, ferromagnetic-antiferromag. mixture, triangular cactus tree, statistical theory 0-75702  
 Ising model, critical temperature, modulated Pade approximant 0-84605  
 Ising model, max. susceptibility locus crit. behaviour 0-71040  
 Ising model, surface crit. behaviour, layer and local susceptibility 0-71058  
 Ising model, three-dimensional, with four-spin interaction, exact soln. 0-88711  
 Ising model, with transverse field, ferromagnetic and antiferromagnetic susceptibilities 0-60160  
 Ising spin glass, glass, Edwards-Anderson order parameter instability 0-71043  
 Ising spin glass, d-dimensional, frustration effect 0-108019  
 Ising spin glass, d-dimensional, frustration effect and dilution problems 0-108018  
 itinerant electron ferromagnets, magneto-volume effects 0-60397  
 itinerant electron model, susceptibility, local exchange approx. calc. 0-60169  
 itinerant-electron systems with narrow bands, single-site spin fluctuation theory 0-97049  
 Kapton, pyrolysed, cond. polymer, transport and mag. props. 0-96887  
 Kondo Hamiltonians diagonalisation, zero-temp. mag. susceptibility 0-93078  
 liquid crystals, prep. and phys. props., book 0-105444  
 liquid crystals, thermodynamic props. calc. 0-103464  
 magnetic fluids, particle cluster configuration, Monte Carlo study 0-88827  
 manganese acetate tetrahydrate, paramag. susceptibility, spin trimer model 0-97055  
 manganese carboxylate, dodecanuclear mixed-valence, prep., struct., and mag. props. 0-107196  
 manganese formate dihydrate, Zn- and Mg-substituted, anomalous crit. phenomena 0-60316  
 mesophase pitch, magnetically-oriented, phys. props., mol. struct. 0-64885  
 metal, indirect coupling between localised mag. moments by narrow band electrons 0-70942  
 metal-insulator transition, density-functional theory 0-75507  
 metallomacrocycles, mixed valent, cofacial assembly, cond. polymeric material 0-70143  
 metals and alloys, amorphous, exhibiting Mossbauer spectra, mean magnetic props. (*French*) 0-80489  
 MgAl<sub>2-x</sub>Fe<sub>x</sub>O<sub>4</sub> solid solution system, solid state properties study 0-93094  
 micromagnetic susceptometer with variable temp. 4.2K to 300K for small sample meas. 0-73395  
 mixed valence compounds, dynamic susceptibility, RPA study of Anderson lattice 0-97075  
 Ni-Pt-P, metallic glass, electronic structure, pulsed NMR study 0-75869  
 niobates, mixed metal, Eu oxidation state, mag. props., Mossbauer study 0-66080  
 nonmagnetic metal, s-d exchange model exact solution, mag. susceptibility, mag. impurity interactions (*Russian*) 0-70943  
 one dimensional randomly dilute Ising ferromagnet, dynamics 0-70922  
 organic conductors, quasi one-dimensional, low temp. mag. susceptibility 0-93069  
 organic liquids, diamagnetism, mass mag. suscept. meas., temp. depend. 0-97054  
 polyacetylene:AsF<sub>6</sub>, soliton doping mechanism, mag. susceptibility meas. 0-107979  
 polyparaphenylene:SbF<sub>6</sub>, pure and doped, metallic, absence of Pauli paramagnetism, mag. susceptibility meas. and ESR obs. 0-97060  
 Potts s-state model on Cayley tree Bethe-Peierls critical coupling 0-103844  
 random binary Ising system with transverse field, Curie temp., paramagnetic susceptibility 0-65938  
 rare earth alloys, R<sub>2</sub>Pt (R=Gd, Tb, Dy, Ho, Er), magnetic susceptibility meas., mag. transition obs. 0-60222  
 rare earth alloys, R<sub>48</sub>Ni<sub>11</sub>, amorphous, Curie temp., mag. susceptibility and coercive force, 4.2 to 300K 0-93092  
 rare earth alloys, RBe<sub>3</sub>, XPS, resist. and susceptibility study 0-71565  
 rare earth binary insulating compounds, exchange interactions, paramag. susceptibility expts. 0-60177  
 rare earth metals, heavy, liq., mag. susceptibility meas. 0-75740  
 rare earth metals and alloys, ferromag. props., book contrib. 0-75725  
 rare earth sesquioxides, exchange interactions, paramag. susceptibility expts. 0-60177  
 rare earth titanium oxides, RTiO<sub>3</sub> type, bulk mag. and struct. props., ferrimag. order 0-107993  
 rare earth-Pt, RPt<sub>3</sub>, low temp. mag. susceptibility 0-93075  
 rare earth-transition metal alloys, amorphous, electronic and mag. props. 0-93093  
 rare earth-transition metal alloys, RM<sub>2</sub>Si<sub>2-x</sub>Ge<sub>x</sub> and RM<sub>4-x</sub>Al<sub>8-x</sub>, magnetism and hyperfine interactions, magnetisation and Mossbauer effect studies 0-75892  
 rats, living, meas. meters 0-72391  
 ruthenates, ACu<sub>2</sub>Ru<sub>4</sub>O<sub>12</sub>, A=Na,Ca,Sr,Cd,La,Pr,Nd, synthesis, cryst. struct., mag. and elec. props. (*French*) 0-107151  
 semiconductor, tetrahedrally coordinated, temp. depend. of diamagnetic susceptibility (*Rumanian*) 0-88717  
 singlet-triplet system in paramag. phase, low-freq. response 0-60172  
 spin glass, dil., conc. expansions at zero temp., Ising model 0-60303  
 spin glass, Heisenberg mode, RPA approx. 0-65904



**magnetic susceptibility continued**

- spin glass, infinite range model, stability and susceptibility in Parisi's soln. 0-88762
- spin glass, infinite-ranged model, mean field theory hypothesis 0-97104
- spin glass, one dimens. ideal, dynamical susceptibility and relax. behaviour 0-65950
- spin glasses, free energy, order parameter expansion, random bond model 0-84609
- spin Hamiltonian, constant-coupling, higher-order, statics and dynamics 0-60262
- spin systems, randomly competing, random ordered phase, frustration, phenomenological theory 0-60349
- SQUID magnetometer with temp. control, spontaneous magnetisation and mag. susceptibility meas. 0-68221
- steels Kh18N(10-25), mag. susceptibility, 4.2 to 300K, and magnetoelasticity (*Russian*) 0-65812
- subdominant critical indices for the ferromagnetic susceptibility of the spin-1/2 Ising model 0-100574
- substitutional alloys of intermediate valence systems, static mag. susceptibility con. and temp. depend. 0-84586
- superconducting composites, granular, Ginzburg-Landau theory, props. 0-88673
- superconductor, magnetic, spin fluctuation and US attenuation 0-80445
- susceptibilities of  $S=1/2$  XY model on the square lattice at  $T=0$  0-88732
- susceptometer for biomedical meas., Fe stored in human tissue, in vivo 0-101245
- tantalates, mixed metal, Eu oxidation state, mag. props., Mossbauer study 0-66080
- TCNQ complexes, disordered, thermodynamics of random exchange models 0-103826
- TCNQ salt, dibenzo-TTF-TCNQCl<sub>2</sub>, one-dimens. mag. semicond., mag. and elec. props. 0-88601
- TCNQ salt, MeDABCO(TCNQ)<sub>2</sub>, optical, elec., and mag. props. 0-65539
- TCNQ salt, MEM(TCNQ)<sub>2</sub>, dielec. const. obs., DC and microwave cond. obs. 0-59963
- tetraethylammonium neptunium hexachloride, Mossbauer spectra and mag. susceptibility meas. 0-108140
- tetramethylammonium neptunium hexachloride, Mossbauer spectra and mag. susceptibility meas. 0-108140
- TMMC, crossover transition, effects on susceptibility and EPR shift 0-71047
- TMMC, linear antiferromag., mag. phase diagram, expt. and theoretical study 0-71038
- (TMTSF)<sub>2</sub>PF<sub>6</sub>, ESR g-factor, linewidth, spin susceptibility, metal-insulator transition 0-103887
- (TMTSF)<sub>2</sub>PF<sub>6</sub>, quasi-dimens. cond., diamagnetic AC susceptibility 0-103781
- (TMTSF)<sub>2</sub>X ( $X=PF_6^-, AsF_6^-, SbF_6^-, BF_4^-, NO_3^-$ ) highly conducting salts, props. 0-59969
- transition metal-noble metal spin glass films, mag. props. 0-60306
- transition metals, 3d, ferromag. props., book contrib. 0-75724
- transition metals, paramagnetic susceptibility, phonon instability, mixed localised-collective electron states 0-103811
- transverse dynamic susceptibility and spin waves in itinerant electron SPW states 0-97076
- trimethylammonium cobalt trichloride, metamagnet, AC susceptibility and exchange consts. 0-70961
- TTF-TCNQ, implications of amplitude solitons in incommensurate Peierls systems 0-92841
- TTF-TCNQ, quasi one-dimensional low temp. mag. susceptibility 0-93069
- TTF-TCNQ complex, trans-diethyl-dimethyl TTF-TCNQ, one-dimens. cond. 0-96853
- TTF-TCNQ low temp. mag. susceptibility, neutron irradi. effects 0-60311
- uniaxial ferromagnet, domain struct. in mag. field 0-103853
- Van Vleck compounds, LF dynamics, NMR linewidth, RKKY exchange mechanism role 0-103812
- Wolff model, thermodynamic props., local moments in dil. alloys, var. method 0-65781
- ytterbium ethyl sulphate, crystal field effects on mag. and hyperfine props. of Yb<sup>3+</sup> 0-97101
- Ag Animalu transition metal model pot. invest. 0-75711
- Ag-S(Se)(Te), liq., mag. susceptibility meas., electron localisation and chem. bonding 0-60178
- AgNi, dil., mag. susceptibility of isolated Ni atoms 0-65777
- Al, dynamic susceptibility, model pot. theory 0-75710
- Al<sub>2</sub>Mn<sub>2</sub>Si<sub>2</sub>O<sub>12</sub>, amorphous insulating spin glass, susceptibility and magnetisation meas. 0-88765
- Au, Animalu transition metal model pot. invest. 0-75711
- Au-Fe, spin glass, transition temp., freq. depend. 0-97113
- Au-Fe, spin glasses, alternating susceptibility 0-65912
- Au-Fe alloys, magnetism and atomic clustering 0-103810
- Au-Pd-Au sandwich, obs. of strongly enhanced mag. susceptibility 0-93076
- Au<sub>3</sub>Fe<sub>14</sub> and Au<sub>3</sub>Fe<sub>18</sub>, mag. props. 0-84592
- B<sub>2</sub>O<sub>3</sub>-PbO-GeO<sub>2</sub>-Fe<sub>2</sub>O<sub>3</sub> glasses, mag. props. and Mossbauer spectra, spin mag. order at low temps. 0-80530
- B<sub>2</sub>O<sub>3</sub>-Fe<sub>2</sub>O<sub>3</sub>-nMO, (n=2 or 4, M=Mg, Co, Ni, Cu), mag. props., transitions 0-75763
- Ba-CoS<sub>3</sub>, linear chain antiferromag., mag. susceptibility meas. and Mossbauer spectra 0-107992
- Ba-FeS<sub>3</sub>, linear chain antiferromag., mag. susceptibility meas. and Mossbauer spectra 0-107992
- BaLaMRuO<sub>6</sub>, (M=Mg, Fe, Co, Ni, Zn), cubic ordered perovskites, Mossbauer and mag. susceptibility meas. 0-75889
- Ba<sub>2</sub>MnS<sub>3</sub>, linear chain antiferromag., mag. susceptibility meas. and Mossbauer spectra 0-107992
- Ba<sub>2</sub>NbRuO<sub>6</sub> and Ba<sub>2</sub>TaRuO<sub>6</sub>, (Ru<sub>2</sub>O<sub>7</sub>)<sup>13-</sup> cluster obs. in presence of orbital degeneracy and spin-orbit coupling (*French*) 0-70655
- Ba<sub>2</sub>Ni<sub>2</sub>F<sub>10</sub>, cryst. struct. and antiferromag. props. 0-107153
- BaO-Fe<sub>2</sub>O<sub>3</sub>-(Na<sub>2</sub>O) glass, rapidly quenched, mag. and ferrimag. props. 0-75744
- BaVS<sub>3</sub>, magnetisation and neutron study 0-84588
- BaVS<sub>3</sub>:Fe, Mossbauer and mag. studies, electronic state of Fe 0-108130
- Be intermetallics, MB<sub>2</sub> (M=Y, La, Ce, Lu, Th), lattice spacings and susceptibilities 0-65778
- Be<sub>1-x</sub>Mn<sub>x</sub>, Be-rich, NMR and paramag. susceptibility 0-71206
- Bi-Sb(As), band struct., effects of Sb and As, mag. susceptibility meas. (*Russian*) 0-65775

**magnetic susceptibility continued**

- C chars, thermally activated paramagnetism, mag. susceptibility meas. 0-75709
- C<sub>2</sub>Br<sub>2</sub>Cl<sub>2</sub>, intercalate, crystallographic, elec., mag. props. 0-107184
- CS<sub>2</sub>, liq., diamagnetism, mass mag. suscept. meas., temp. depend. 0-97054
- Cd-Sn alloy, superconductivity and microstructure 0-107949
- CdCr<sub>2</sub>Se<sub>4</sub>, reactor radiation influence on ferromagnetic phase transform. (*Russian*) 0-75760
- CdHg alloy,  $\omega$  phase, mag. susceptibility anisotropy w.r.t. uniform compression (*Russian*) 0-71143
- Cd<sub>1-x</sub>Mg<sub>x</sub>, energy spectrum pseudopotential calcs., mag. props., impurity scatt. (*Russian*) 0-65430
- CdS, doped, amorphous antiferromagnet model, susceptibility and spin-flip Raman scatt. meas. 0-97057
- CdTe:Mn<sup>2+</sup>, exciton refl. spectra and mag. susceptibility 0-66253
- $\alpha$ -Ce, exchange-enhanced, elec. resist. T<sup>2</sup> depend., press. effect 0-96845
- Ce<sub>30</sub>Al<sub>20</sub>, metallic glass, mag. ordering and cryst. field effects, speromagnetism 0-80531
- CeB<sub>6</sub>, mag. and electronic props. 0-71048
- CeBe<sub>13</sub>, intermediate valence state, XPS, resist. and susceptibility study 0-71565
- CeC<sub>3</sub>, mag. props. 0-108008
- Ce<sub>2</sub>Dy<sub>1-x</sub>C<sub>2</sub>, solid solns., mag. props. 0-108008
- Ce(In, Sn)<sub>3</sub>, mag. susceptibility, temp. depend., intermediate valence 0-65779
- CeIn<sub>3</sub>-Sn, mixed valence system, low-temp. susceptibility, paramagnon study 0-97077
- Ce<sub>2</sub>Mg<sub>3</sub>(NO<sub>3</sub>)<sub>12</sub>, spin-lattice relax., dynamic susceptibility meas., liq. He contact effects 0-66011
- CeNi<sub>2</sub>-CePt, system, structural and mag. studies on valence behaviour of Ce 0-103809
- CeNi<sub>3</sub>, and ternary hydride, mag. props. 0-108007
- CeNi<sub>2</sub>Al, mag. susceptibility, H adsorption-desorption cycle effects 0-107990
- CePd<sub>2</sub>-Er, dil., low field mag. susceptibility, electro-nuclear effects 0-60189
- Ce<sub>1-x</sub>Sc<sub>x</sub>Pd<sub>3</sub>, intermediate valence of Ce, susceptibility, lattice const., ESR meas. 0-103648
- CeSn<sub>3</sub>, mixed valence cpd., electronic struct. and mag. props. 0-70649
- CeTi<sub>3</sub>, mag. susceptibility, magnetisation, neutron diff., elec. resist., and sp. ht. meas. 0-75733
- (Ce, Y<sub>1-x</sub>)Fe<sub>8</sub>, mag. susceptibility and Mossbauer meas., lattice parameters 0-97068
- Co complex, Co(II)(1,2,4-triazole)<sub>2</sub>(NCS)<sub>2</sub> quasi two-dimens. canted  $S=1/2$  antiferromag. 0-70976
- Co-Mn, FCC, micromagnetism, magnetisation and mag. susceptibility meas. 0-60310
- Co-Mn alloys, ferromagnetic, high field mag. susceptibility meas. 0-75729
- Co<sub>2</sub>(AsO<sub>4</sub>)Cl, temp. depend. of mag. susceptibility 0-70962
- Co<sub>100-x</sub>B<sub>x</sub>, amorphous, mag. struct., mag. susceptibility meas. 0-80485
- Co(C<sub>2</sub>H<sub>5</sub>NO)<sub>6</sub>(ClO<sub>4</sub>)<sub>2</sub> [(BF<sub>4</sub>)<sub>3</sub>], X-Y antiferromagnet, Neel temp., spin correlation functions 0-60345
- CoCO<sub>3</sub>, mag. props., microscopic level calcs. (*Russian*) 0-97078
- Co<sub>2</sub>Ga<sub>1-x</sub> alloys, cluster spin glass, host and impurity NMR and AC susceptibility 0-71194
- CoGa<sub>2-x</sub>Fe<sub>x</sub>O<sub>4</sub>, x=0.1-0.4, mag. susceptibility temp. depend. (*Russian*) 0-70957
- Co<sub>50</sub>Mn<sub>50</sub>Ga<sub>50-x</sub>, ordering and disordering phenomena, mag. study 0-70154
- Co<sup>2+</sup>Mo<sup>4+</sup>O<sub>3</sub>, defect spinel struct., elec. and mag. props. 0-70176
- CoO-ZnO-MgO ternary systems, solid solns., struct. charact. 0-60629
- Co<sub>2</sub>Pd<sub>90</sub>-Si<sub>10</sub>, amorphous, structural and mag. heterogeneities 0-80484
- Co<sub>2</sub>RhS<sub>4</sub>, mag. semicond., mag. and elec. props. 0-93121
- Co<sub>2</sub>Sm crystals, microstruct., homogeneous precip. and nucleation 0-104160
- Co<sub>2</sub>Sn, mag. polarisation and susceptibility (*German*) 0-104147
- Co<sub>2</sub>T<sub>2</sub>, fluctuating localised mag. moments, d band motion, Mossbauer study 0-65768
- CoTi<sub>1-x</sub>Al<sub>x</sub>, mag. and electronic props., ferromag. and paramag. state 0-65814
- Co<sub>2</sub>Zn<sub>1-x</sub>Rh<sub>x</sub>O<sub>4</sub>, mag. props., EPR spectra, antiferromag. order 0-75736
- Co(urea)<sub>2</sub>Cl<sub>2</sub>·2H<sub>2</sub>O, two-dimens. mag. props., cryst. struct., specific heat 0-75777
- Cr-Ge system, XPS, X-ray and neutron diff. and mag. meas. to study chem. bonding and electronic struct. 0-60749
- Cr-Si, dilute alloy, mag. susceptibility and Neel temp. meas. 0-71017
- Cr-Si-V, (2, 0.1 at.%), paramag. to commensurate spin density wave transition 0-65875
- CrBr<sub>3</sub>, HF spectra, susceptibility, spin waves in domain walls (*Russian*) 0-80909
- Cr<sub>2</sub>Mn<sub>1-x</sub>As<sub>x</sub>, mag. susceptibility anomaly at displacive phase transition 0-93091
- Cr<sub>2</sub>Se<sub>4</sub>, struct., elec. and mag. props. 0-107160
- Cr<sub>2</sub>Si, mag. susceptibility, 2 to 300K, rel. to electron energy spectrum 0-60185
- Cs-FeF<sub>3</sub>, mag. struct. and one-dimens. antiferromagnetism 0-60209
- CsGa<sub>2</sub>-Fe<sub>2</sub>S<sub>2</sub>, tetrahedrally coordinated Fe atoms in low spin state, mag. props. and neutron diff. study (*German*) 0-88714
- CsMgHfO<sub>6</sub> (M=Na, K, Rb), mag. behaviour (*German*) 0-65774
- CsMnCl<sub>3</sub>, antiferromagnetic resonance, parametric spin wave excitation (*Russian*) 0-93183
- Cs<sub>2</sub>NaErCl<sub>6</sub>, mag. susceptibility and IR and Raman spectra meas., crystal field splitting determ. 0-100652
- CsNiF<sub>3</sub>, longit. paramag. susceptibility, reaction field approx. 0-97059
- CsNiF<sub>3</sub>, quasielastic neutron scatt. around Neel-point 0-75768
- Cs<sub>2</sub>NpCl<sub>6</sub>, Mossbauer spectra and mag. susceptibility meas. 0-108140
- Cu, Animalu transition metal model pot. invest. 0-75711
- Cu complex, (4,4'-bipy H<sub>2</sub>)CuCl<sub>4</sub> with infinite linear chains of dimeric units, struct. and mag. susceptibility 0-96498
- Cu complex, Cu<sub>2</sub>Cl<sub>2</sub>(H<sub>2</sub>O)<sub>2</sub>·2 tetramethylsulphate, mag. interactions, susceptibility, 2-230K 0-60237
- Cu, dynamic susceptibility, model pot. theory 0-75710
- Cu-Al-Co liquid alloys, constant Co-content of 5 wt.%, mag. props. (*German*) 0-88720
- Cu-Al-Mn liq. alloys, susceptibility behaviour 0-93077
- Cu-Mn, spin glass, transition temp., freq. depend. 0-97113
- Cu-Mn, spin glasses, alternating susceptibility 0-65912
- Cu-Mn alloy spin glass, macroscopic mag. anisotropy, transverse susceptibility and zero field NMR enhancement 0-80525



## magnetic susceptibility continued

- Cu-Mn-Al, Heusler alloys, ferromag. inclusions, mag. props. and struct. study (*Russian*) 0-80570  
 Cu-Ni-Co, mag. props. of system of disperse ferromag. particles, 73 to 673K (*Russian*) 0-65968  
 $\text{Cu}_2(\text{AsO}_4)\text{Cl}$ , temp. depend. of mag. susceptibility 0-70962  
 CuCl, pressure depend. of structural, chemical, elec. and mag. props. 0-96596  
 $\text{Cu}_{1-x}\text{Cr}_x\text{Se}_4$ , influence of excess Cu on physical props. 0-103836  
 CuFe solid solns., quenched from vap. phase, mag. props. 0-60307  
 Cu(II)-DL-proline complex, ESR, magnetic susceptibility and optical absorption 0-93167  
 $\text{n-CuInS}_2$ , mag. props., obs. 0-70939  
 CuMn spin glass, AC susceptibility 0-60305  
 $\text{Cu}_{98}\text{Mn}_2\text{O}_{20}$ , spin glass, Heisenberg mode, RPA approx. 0-65904  
 $\text{Cu}_2\text{NiSi}_2\text{S}_7$ , X-ray cryst. struct. determ., mag. props. 0-107172  
 $\text{Cu}(\text{Rh}_{1-x}\text{Cr}_x)\text{S}_4$ , spinel system, susceptibility and metallic resistivity, anomalies due to s-d interaction 0-70958  
 $\text{Cu}_2\text{S}$ ,  $1 \leq x \leq 2$ , quantum temp. size effect and magnetism (*Russian*) 0-103764  
 $\text{Cu}_{2-x}\text{Se}$ , nonstoichiometric, diamag. and paramag. props., susceptibility meas. 0-70936  
 $\text{CuSe}_2\text{O}_5$ , strongly antiferromag. coupled Cu linear chain, orbital props. 0-100580  
 $\text{Cu}_2\text{U}_{13}(\text{Se}_{13})_3$ , cryst. struct. and magnetic props. (*French*) 0-96496  
 Dy, domain effects near order-disorder and order-order ferromagnetic transitions 0-65886  
 Dy, magnetic domain structure, hysteresis, thermal modulation study 0-71082  
 $\text{DyAsO}_4$ , phase transitions obs. 0-70412  
 $\text{DyCo}_2\text{Si}_2$ , mag. props. 0-107988  
 $\text{DyGa}_2\text{O}_{12}$ , dipolar magnet, sp. ht. and magnetisation meas. 0-60344  
 $\text{DyNi}_2\text{Si}_3$ , mag. props., 4.2-200K 0-84602  
 $\text{Dy}_2\text{O}_3\text{SO}_4$ , mag. ordering, magnetisation, AC susceptibility and Zeeman effect meas. 0-60205  
 $\text{DyVO}_4$ , phase transitions obs. 0-70412  
 $\text{ErCo}_2\text{Si}_2$ , mag. props. 0-107988  
 $\text{ErNi}_2\text{Si}_2$ , mag. props., 4.2-200K 0-84602  
 $\text{ErRh}_3\text{Sn}_{3.6}$ , synthesis, supercond. and mag. props. 0-100547  
 $\text{EuAl}_2\text{S}_6$ , mag. susceptibility and EPR meas. 0-71173  
 $\text{EuGa}_2\text{S}_4(\text{Se}_4)$ , mag. susceptibility and EPR meas. 0-71173  
 $\text{Eu}_{1-x}\text{Gd}_x\text{S}$  and  $\text{Eu}_{1-x}\text{Sr}_{1-x}\text{S}$ , spin glasses, transition temp., freq. depend. 0-97113  
 $\text{Eu}_2\text{IrH}_5$ , prep., cryst. struct., mag. and elec. props. 0-88117  
 EuO, magnetic susceptibility critical exponent, corrections to scaling 0-103846  
 $\text{Eu}_{1-x}\text{R}_x\text{O}_{1-x}$  ( $\text{R}=\text{Nd}, \text{Eu}, \text{Gd}$ ), lattice parameters, mag. and elec. props. 0-100578  
 $\text{EuS}$ , ferromag. semicond., high field susceptibility, spin waves 0-75735  
 $\text{EuS}$ , single cryst., high-field susceptibility meas., temp. range 2.5 to 16.5K 0-84589  
 $\text{Eu}_{1-x}\text{Sm}_x\text{S}$ , ESR, exchange interaction, susceptibility, elec. cond., thermoelectric power 0-93174  
 $\text{Eu}_2\text{Sn}_2\text{S}_7$ , mag. and thermodynamic props., metamagnetism 0-60273  
 $\text{Eu}_2\text{Sr}_{1-x}\text{S}$ , paramag. susceptibility, expt. and comparison with high temp. series expansion 0-60176  
 $\text{Eu}_2\text{Sr}_{1-x}\text{S}$ , spin glass to ferromag. transition, neutron scatt. and susceptibility meas. 0-60254  
 $(\text{Eu}_2\text{Sr}_{1-x}\text{S})_y$ , very dil., magnetisation dynamics 0-65915  
 Fe complex,  $\text{Fe}(\text{1,2,4-triazole})_2(\text{NCS})_2$ , quasi-2-dimens.  $S=1/2$  antiferromag., mag. props., hidden canting 0-107986  
 Fe complex (2, 9-dimethylphenanthroline) sulphate, mag. props., Mossbauer spectra 0-66081  
 $\text{Fe}$ , ferromag., dynamic susceptibility calc. 0-80488  
 $\text{Fe}$ , spin susceptibility, high-field, spin-density functional formalism 0-70959  
 $\text{Fe-Al}_2\text{O}_3$  granular films, superparamagnetism and relax. effects 0-71118  
 $\text{Fe-B}$ , amorphous, mag. aftereffect, initial susceptibility time depend. 0-88829  
 $\text{Fe-B}$ , liq., mag. susceptibility meas. 0-75740  
 $\text{Fe-Ni}$  Invar, magnetovolume coupling enhancement factor, temp. depend. 0-88851  
 $\text{Fe-Ni}$  Invar anomalies, explanation in terms of itinerant electron magnetism 0-75705  
 $\text{Fe-Pd}$  Invar alloys, elec. and mag. props. and thermal expansion 0-75732  
 $\text{Fe-Pt}$  Invar alloy, paramag. susceptibility 0-70940  
 $\text{Fe-Ti}$ , magnetism and  $\text{H}_2$  storage 0-70941  
 $\text{Fe}_{100-x}\text{B}_x$ , amorphous, mag. struct., mag. susceptibility meas. 0-80485  
 $\text{Fe}_{90}\text{B}_{10}$  amorphous ribbon, initial susceptibility time lag 0-100579  
 $\text{FeCl}_2(\text{pyrazole})_2$ , linear-chain cpd., low-temp. mag. behaviour 0-71253  
 $\text{Fe}_{0.5}\text{Cu}_{0.5}\text{Cr}_2\text{S}_4$ , ESR spectra, elec. and mag. props., Curie temp. 0-97137  
 $\text{FeF}_2$ , mag. sp. ht. near Neel temp. mag. susceptibility meas. 0-60341  
 $\text{FeF}_3$ , amorphous, mag. props. and Mossbauer spectra, speromagnetism and micromagnetism 0-75778  
 $\text{FeGa}_2\text{Se}_4$ , elec. cond., phase diagram 0-88301  
 $\text{Fe}_{1-x}\text{Mn}_x\text{Cl}_2$ , disordered, Raman scatt. from  $\text{Fe}^{2+}$  and Neel temp. 0-60579  
 $\text{Fe}_{80-x}\text{Ni}_{20-x}\text{P}_x$ , amorphous, Rayleigh region and coercive force 0-88806  
 $\text{Fe}_{2-x}\text{BaO-B}_2\text{O}_3$ , magnetic props. of Fe-rich amorphous oxide (*French*) 0-80511  
 $\text{Fe}_2\text{O}_4$  ferrofluids, spin glass behaviour 0-71120  
 $\text{Fe}_2(\text{PO}_4)_2$ , temp. depend. of mag. susceptibility 0-70962  
 $\text{Fe}_2\text{Pd}_{80-x}\text{Si}_{20-x}$ , amorphous, structural and mag. heterogeneities 0-80484  
 $\text{Fe}_2\text{Pd}_{82-x}\text{Si}_{18-x}$  metallic glass, mag. transitions, weak ferromagnetism 0-100583  
 $\text{Fe-Pt}$  Invar alloy, anomalous Curie const., susceptibility meas. 0-75731  
 $\text{FeRh}_2\text{S}_4$ , mag. semicond., mag. and elec. props. 0-93121  
 $\text{FeSO}_4 \cdot \text{H}_2\text{O}$  ( $n=1,4,5,7$ ),  $\text{Fe}^{2+}$  ion mag. interaction with crystallisation water protons, proton NMR obs. 0-60447  
 $\text{Fe}_{1-x}\text{Sb}_x$ , nonstoichiometry influence on mag. props. (*Russian*) 0-65813  
 $\text{Fe}(\text{Sb}_{1-x}\text{Te}_x)_3$  system cpds., prep., cryst. struct., elec. and mag. characteristics 0-108349  
 $\text{FeTaS}_2$ , metallic, mag. susceptibility at low temp. 0-70972  
 $\text{Fe}_{1-x}\text{Te}_x$ , fluctuating localised mag. moments, d band motion, Mossbauer study 0-65768  
 $\text{FeThS}_2$ , mag. struct. and props., neutron diff. and mag. meas. 0-60201  
 $\text{FeTi}$ , surface and mag. props., heat treatment and hydrogenation effects 0-75447  
 $\text{Fe}_2\text{TiO}_5$ , anisotropic spin glass type behaviour 0-60296

## magnetic susceptibility continued

- $\text{Fe}_3-x\text{Ti}_x\text{O}_4$ ,  $0.5 \leq x \leq 1$ , mag. props. of antiferromag. phase 0-70960  
 $\text{Fe}_{1-x}\text{Ti}_x\text{O}_4$ , spin glass behaviour, susceptibility and hysteresis meas. 0-65917  
 $\theta\text{-Fe}_2\text{V}_2\text{O}_5$ , spin glass and paramag. props., susceptibility, EPR and Mossbauer studies 0-75782  
 $\text{Ga}$ , magnetic susceptibility near melting point 0-60186  
 $\text{Ga}_{1-x}\text{Mn}_x\text{Sb}$ , elec. cond., mag. susceptibility, Hall const., and thermoelectric EMF, 80 to 1000K (*Russian*) 0-88549  
 $\text{Ga}_2\text{Se}_3\text{-FeSe}$ , phase diagram, elec. cond., mag. susceptibility 0-88301  
 Gd, domain effects near order-disorder and order-order ferromagnetic transitions 0-65886  
 $\text{Gd NiSi}_2$ , mag. props., 4.2-200K 0-84602  
 $\text{Gd-Al(C)(Cu)(Ga)(Ni)(Pd)(Rh)}$  alloys, amorphous, mag. and elec. props. 0-80499  
 $\text{Gd-Co(Ni)(Cu)(Rh)(Ru)(Pd)(Ga)}$ , amorphous, mag. props. and ferromag. reson. 0-75862  
 $\text{GdAlO}_3\text{-La}$ , antiferromag., random-field crit. and multicritical behaviour 0-65939  
 $\text{GdB}_2$  single crystals, mag. behaviour and structure change at low temp. 0-71018  
 $\text{Gd}_{1-x}\text{Ca}_x\text{Al}_2$ , mag. props. and phase relations 0-107991  
 $\text{GdCo}_2\text{Si}_2$ , mag. props. 0-107988  
 $\text{GdCu}$ , electrical resistivity and length changes with temp., hysteretic behaviour 0-97600  
 $\text{GdEu}_{1-x}\text{B}_x$ , solid solns., mag. susceptibility, 80 to 1000K (*Russian*) 0-88713  
 $\text{Gd(FeAl}_{1-x}\text{)}_2$ , magnetic behavior 0-108079  
 $\text{Gd}_2\text{Ga}_2\text{O}_{12}$ , mag. phase diagram, AC susceptibility meas. 0-60265  
 $\text{GdLa}_{1-x}\text{B}_x$ , solid solns., mag. susceptibility, 80 to 1000K (*Russian*) 0-88713  
 $\text{GdN}$ , mag. interaction and carrier conc. 0-71005  
 $\text{GdNi}_{1-x}\text{O}_x$ , magnetic interaction and carrier conc. 0-71005  
 $\text{Gd,Nd}_{1-x}\text{Zn}$ , ferromag., mag. susceptibility and magnetisation, temp. depend. 0-70975  
 $\text{GdRh}_2\text{B}_4$ , magnetic and electrostatic props., NMR study 0-93195  
 $\text{Gd}_{1-x}\text{S}_x$ , ferromag., elec. props. near Curie temp. 0-107788  
 $\text{Gd}_2\text{B}_{10}\text{B}_{30}$ , magnetisation, AC susceptibility and microwave absorption meas. 0-60221  
 $(\text{Gd}_x\text{Y}_{1-x})\text{Al}_2$ , ferromag. and spin glass like behaviour, magnetisation meas. 0-75734  
 $\text{Gd}_2\text{Y}_{1-x}\text{Zn}_x$ , ferromag., mag. susceptibility and magnetisation, temp. depend. 0-70975  
 $\text{Gd}_2\text{-}\square_2\text{S}_4$ , transport and mag. props., mag. Wigner localisation 0-97069  
 $\text{H}_2\text{-MoO}_3$ , electronic props., mag. susceptibility and spectra 0-80266  
 $\text{H}_2\text{O}$ , liquid, diamagnetism, temp. dependence, NMR chemical shift calcs., molecular interactions data 0-75707  
 $\text{H}_2\text{O}$ , liquid, equation for mag. susceptibility, electric polarisability 0-75708  
 $^3\text{He}$ , BCC solid, nucl. mag. order and paramag. susceptibility 0-59757  
 $^3\text{He}$ , liq., exchange model 0-88387  
 $\text{HgTe}$ ,  $1 \pm$  symm. acceptor centre hole mag. props. (*Russian*) 0-88733  
 $\text{HoAlO}_3$ , electronic and nucl. mag. ordering, mol. field approx. 0-60157  
 $\text{HoAu}_2$ , mag. phase diagram 0-75761  
 $\text{HoCo}_5\text{-Mn}_2(\text{Fe})_2(\text{Ni})_2(\text{Cu})_2$ , cryst. struct. and mag. props. 0-75800  
 $\text{HoCo}_2\text{Si}_2$ , mag. props. 0-107988  
 $\text{Ho(IrRh}_{1-x}\text{)}_4\text{B}_4$  pseudoternary system, supercond. and mag. ordering 0-70876  
 $\text{HoNiSi}_2$ , mag. props., 4.2-200K 0-84602  
 $(\text{Ho}_{0.3}\text{Al}_{0.194}\text{Al}_{0.227}\text{Si}_{0.257})_2$ , amorphous, low temp. spin glass behaviour 0-60297  
 $\text{Ho}_2\text{O}_3\text{SO}_4$ , mag. ordering, magnetisation, AC susceptibility and Zeeman effect meas. 0-60205  
 $\text{HoRh}_2\text{B}_4$ , low temp. mag. props. 0-88728  
 $\text{HoVO}_4$ , RF susceptibility below 1K, mag. sp. ht. 0-84585  
 $\text{Ho}_2\text{Y}_{1-x}\text{Sb}_x$  system, magnetisation, elec. resist., and sp. ht. meas. 0-60213  
 $\text{In-Se(Te)}$ , liq., mag. susceptibility meas., electron localisation and chem. bonding 0-60178  
 $\text{K}_2\text{CuF}_4$ , spin relax., crit. behaviour, high freq. susceptibility meas. 0-65936  
 $\text{K}_2\text{CuF}_4$ , two-dimens. ferromag., saturation of parallel-pumped magnons 0-97147  
 $\text{KFeF}_4$ , amorphous, mag. props. and Mossbauer spectra, speromagnetism and micromagnetism 0-75778  
 $\text{K}_2\text{FeF}_6$ , mag. struct. and one-dimens. antiferromagnetism 0-60209  
 $\text{K}[(\text{OH})_{0.42}(\text{O}_2)_{0.50}]$ , cubic solid soln., structural and mag. study (*French*) 0-107177  
 $(\text{La}_x\text{Y}_{1-x})\text{Ce}$ , dil., Kondo supercond., transition temp., susceptibility and resist. 0-65733  
 $(\text{La}_{0.8}\text{Ca}_{0.2})\text{MnO}_{3+y}$ , mag. props., Faraday method meas. 0-103832  
 $\text{LaCoO}_3$ , Mott isolator, paramag. props., calc. 0-93071  
 $\text{La}_2\text{CoO}_4$ , mag. behaviour obs. 0-70971  
 $\text{LaLiO}_3\text{-SrO}_3$ , perovskite, prep. and mag. study 0-80486  
 $\text{LaMg}$ , Pauli paramagnet, mag. susceptibility, nonlinear band behaviour 0-75706  
 $\text{LaNi}_3$  hydrides, 4.2K paramag. susceptibility 0-70934  
 $\text{LaNi}_5$ , magnetism and  $\text{H}_2$  storage 0-70941  
 $\text{LaNi}_{1-x}\text{Fe}_x\text{O}_3$ , magnetisation meas. and  $^{57}\text{Fe}$  Mossbauer studies 0-93217  
 $\text{La}_2\text{NiO}_4$ ,  $\text{La}_2\text{CuO}_4$ , magnetic properties obs. 0-70937  
 $\text{La}_{80-x}\text{Pr}_{20-x}\text{Au}_{20}$ , amorphous, mag. and supercond. props. 0-75713  
 $\text{La}_{2-x}\text{Sr}_x\text{CoO}_4$ , mag. behaviour obs. 0-70971  
 $\text{Li-Pt}$ , phase diagram for comp. range 0-40 at.% Pt, mag. and elec. props. (*German*) 0-84912  
 $\text{Li}_2\text{B}_2\text{O}_4\text{-LiFe}_2\text{O}_5$ , borate glass, mag. props. of  $\text{Fe}^{3+}$  cations 0-100599  
 $\text{Li}_2\text{B}_2\text{O}_4\text{-LiFe}_2\text{O}_5$  glass, rapidly quenched, mag. and ferrimag. props. 0-75744  
 $\text{LiHoF}_4$ , uniaxial dipolar ferromag., critical behaviour, mag. susceptibility meas. 0-80528  
 $\text{LiRF}_4$  ( $\text{R}=\text{Tb}, \text{Ho}, \text{Er}$ ), cryst. field parameters, mag. susceptibility meas., 0.3 to 100K 0-60214  
 $\text{LiTbF}_4$ , uniaxial dipolar ferromag., critical behaviour, mag. susceptibility meas. 0-80528  
 $\text{LiTb}_{0.5}\text{Y}_{0.5}\text{F}_4$ , uniaxial dipolar ferromag., critical behaviour, mag. susceptibility meas., effect of  $\text{Y}^{3+}$  dilution 0-80528  
 $\text{LuRh}_2\text{B}_4$ , magnetic and electrostatic props., NMR study 0-93195  
 $\text{LuRhO}_3$ , elec., mag. and photoelectrochemical props. 0-96925  
 $\text{Mg}_2\text{Ni}$ , magnetism and  $\text{H}_2$  storage 0-70941  
 $\text{Mn-Bi}$  micromagnetic alloy, mag., elec. and elastic props. (*Russian*) 0-108028



## magnetic susceptibility continued

- Mn-Ni, thermal expansion, mag. susceptibility, lattice consts. 0-100341  
 MnAs<sub>1-x</sub>P<sub>x</sub>, mag. susceptibility anomaly at displacive phase transition 0-93091  
 MnB<sub>2</sub>, polycryst., magnetoresist. and mag. props. (*Russian*) 0-92907  
 Mn(Br<sub>1-x</sub>Cl<sub>x</sub>)<sub>2</sub>·4H<sub>2</sub>O, antiferromagnetism, controllable anisotropy 0-93116  
 Mn<sub>2-x</sub>Fe<sub>x</sub>Si<sub>2</sub>, elec. resist. and mag. susceptibility, ferromag. to antiferromag. transition 0-80504  
 Mn<sub>1-x</sub>Mg<sub>x</sub>Se, mag. and struct. phase transitions, mag. susceptibility and X-ray diffr. study 0-71022  
 Mn<sup>2+</sup>Mo<sup>4+</sup>O<sub>3</sub>, defect spinel struct., elec. and mag. props. 0-70176  
 MnO:Mn<sub>2</sub>O<sub>4</sub>, mag. props., susceptibility and magnetisation meas. 0-65824  
 MnO-Al<sub>2</sub>O<sub>3</sub>-SiO<sub>2</sub>, amorphous spin glass, AC susceptibility 0-80520  
 MnP, Lifshitz point, transverse differential susceptibility meas. 0-84599  
 α-MnSe, mag. and struct. phase transitions, mag. susceptibility and X-ray diffr. study 0-71022  
 MnSi(Ge), amorphous, spin glass transition, AC susceptibility meas. 0-75779  
 Mo oxides, magnetic susceptibility meas., temp. effect 0-103822  
 Mo, plastically deformed single cryst., mag. susceptibility (*Russian*) 0-93074  
 Mo-Co Kondo alloy, Co impurity susceptibilities, Knight shift 0-88721  
 MoS<sub>2</sub>, prep. and mag. props. (*French*) 0-93072  
 N<sub>2</sub> complex, Ni(C<sub>2</sub>H<sub>4</sub>NO<sub>3</sub>)<sub>2</sub>, singlet ground-state systems, field induced mag. long range order 0-60266  
 NaA neolyte, Hg cluster transition to paramagnetic state due to mag. field (*Russian*) 0-60183  
 NaFeF<sub>4</sub>, amorphous, mag. props. and Mossbauer spectra, speromagnetism and micromagnetism 0-75778  
 α-Na<sub>2</sub>Fe<sub>2</sub>(PO<sub>4</sub>)<sub>3</sub> orthophosphate, cryst. and vitreous, Mossbauer spectroscopy and mag. susceptibility (*French*) 0-80657  
 NbSe<sub>3</sub>, mag. susceptibility, CDW effect 0-88716  
 NbSe<sub>3</sub>, superconducting transitions and diamagnetism 0-84526  
 Nb<sub>1-x</sub>V<sub>x</sub>Se<sub>2</sub>, elec. and mag. anomalies at CDW transition 0-107722  
 NdAg<sub>3</sub>, low temp. mag. meas. 0-107989  
 Nd<sub>2</sub>Ag<sub>20</sub> and Nd<sub>2</sub>Ag<sub>20</sub>, amorphous, mag. props. 0-60182  
 Nd<sub>2</sub>NiO<sub>4</sub>, Nd<sub>2</sub>CuO<sub>4</sub>, magnetic properties obs. 0-70937  
 Nd<sub>2</sub>Y<sub>1-x</sub>Zn<sub>x</sub> system, solid soln., mag. susceptibility, 77 to 600K (*Russian*) 0-65776  
 Ni ferrite, quenched, Neel temp. and initial susceptibility 0-75762  
 Ni, ferromag., dynamic susceptibility calc. 0-80488  
 Ni, paramag. region, Fe and Co impurity effects on susceptibility, Faraday obs. (*Russian*) 0-88731  
 Ni-Co, high-field susceptibility, spin-wave spectrum, CPA calc. 0-65818  
 Ni-Cu, high-field susceptibility, spin-wave spectrum, CPA calc. 0-65818  
 Ni-Fe, high-field susceptibility, spin-wave spectrum, CPA calc. 0-65818  
 Ni-Mn alloys, ferromagnetism-to-spin glass phase transition and strong mag. field effect 0-75773  
 Ni-Pd-P, metallic glass, electronic structure, pulsed NMR study 0-75869  
 Ni<sub>3</sub>Al(Ga), off-stoichiometric alloy, inverse mag. susceptibility rel. to defect conc. 0-60216  
 Ni<sub>100-x</sub>B<sub>x</sub>, amorphous, mag. struct., mag. susceptibility meas. 0-80485  
 Ni<sub>2</sub>Co<sub>2-x</sub>O<sub>4</sub>, composition depend antiferromagnetic-ferromagnetic ordering, mag. susceptibility meas. 0-70973  
 Ni<sub>1-x</sub>Cr<sub>x</sub>S, elec. transport, mag. susceptibility and DTA meas. 0-96954  
 NiMnGe<sub>1-x</sub>Si<sub>x</sub>, mag. props., neutron diffr. and magnetometric meas., 80-600K 0-65793  
 NiSe<sub>2</sub>, paramag. props., NMR, mag. susceptibility 0-60175  
 Ni<sub>1-x</sub>Te<sub>x</sub>, fluctuating localised mag. moments, d band motion, Mossbauer study 0-65768  
 NiZn ferrites, nonstoichiometric, initial susceptibility and microstruct. 0-84591  
 Ni<sub>2</sub>Zr<sub>1-x</sub>, metallic glass, crystallisation kinetics, elec. resist. and mag. susceptibility meas. 0-103659  
 PbMnFeF<sub>7</sub> and PbMnFeF<sub>6</sub>, vitreous, insulating, evidence of spin-glass transition 0-97112  
 Pb<sub>1-x</sub>Sn<sub>x</sub>Te, narrow gap semicond., theory of mag. susceptibility 0-93070  
 PbTe:Fe, single crystals, state and behaviour of Fe, mag. props. 0-93080  
 PbTe:In, mag. susceptibility, temp. depend., 4.2 to 200K 0-65773  
 Pd, sd hybridisation, paramagnetic Curie temp. and susceptibility (*Russian*) 0-103808  
 Pd, spin fluctuation model interpretation of mag. susceptibility 0-80477  
 β-PdIn, electrical resistance, mag. susceptibility and IR freq. dispersion (*Russian*) 0-107759  
 Pd<sub>1-x</sub>Mn<sub>x</sub>H<sub>2</sub>, alloy, spin glass, transition temp., susceptibility and EPR meas. 0-65930  
 Pd<sub>35</sub>Zr<sub>65</sub>, mag. susceptibility meas. 0-75740  
 PrAg<sub>3</sub>, low temp. mag. meas. 0-107989  
 Pr<sub>2</sub>Ag<sub>20</sub>, Pr<sub>2</sub>Ag<sub>20</sub>, and Pr<sub>10</sub>Lu<sub>10</sub>Ag<sub>20</sub>, amorphous, mag. props. 0-60182  
 Pr<sub>1-x</sub>Ca<sub>x</sub>Al<sub>3</sub>, mag. props. and phase relations 0-107991  
 PrCo<sub>2</sub>, strongly exchange-enhanced paramagnetism, susceptibility 0-60179  
 PrIr<sub>2</sub>(Pt<sub>3</sub>)(Rh<sub>3</sub>)(Ru<sub>3</sub>), sp. ht., differential susceptibility and elec. resist. meas., 1.4-40K 0-71063  
 PrNi<sub>2</sub>, LF dynamics and <sup>141</sup>Pr thermal relax., coupling parameter and RKKY exchange mechanism 0-103812  
 Pr<sub>2</sub>NiO<sub>4</sub>, Pr<sub>2</sub>CuO<sub>4</sub>, magnetic properties obs. 0-70937  
 Pt, spin fluctuation model interpretation of mag. susceptibility 0-80477  
 Pt-Co system, low temp. susceptibility 0-65920  
 Pt-Cr, disordered, atomic order-disorder transform. effect on resist. min. 0-65911  
 Pt-Fe alloy, ordered, T-c phase diagram, antiferro- and ferromagnetism (*Russian*) 0-65871  
 Pt-Fe ordered alloy, multiply mag. phase transitions 0-60264  
 PtCr, AC susceptibility near percolation limit, ordered and disordered alloy 0-65900  
 PtMn, spin glass, nonlinear susceptibility and sp. ht. 0-60304  
 R-In, R-In, R=Gd, Tb, Dy, Ho, Nd, mag. props. 0-108009  
 Rb-FeF<sub>3</sub>, mag. struct. and one-dimens. antiferromagnetism 0-60209  
 RbNiF<sub>3</sub> spin lattice, susceptibility, Heisenberg model (*Russian*) 0-65893  
 Ru<sub>2</sub>Ge<sub>2-x</sub>Sn<sub>x</sub> and Ru<sub>2</sub>Ge<sub>2-x</sub>Si<sub>x</sub>, diffusionless phase transitions, elec. and mag. props. 0-96871  
 Sb<sub>2</sub>Se<sub>3</sub> crystals, mag. and elec. props. 0-96873  
 ScAl<sub>2</sub>-Eu, intermediate valence on Eu ions, Mossbauer isomer shift 0-84587  
 p-Si, n-channel inversion layers, mag. susceptibility of electrons in presence of quantising mag. field. 0-75650

## magnetic susceptibility continued

- (SiTe)<sub>1-x</sub>(ATe)<sub>x</sub>, A=Ge, Sn, Pb, solid soln. with small substitution (*Russian*) 0-70933  
 Sm<sub>2</sub>CuO<sub>4</sub>, magnetic properties obs. 0-70937  
 Sm<sub>1-x</sub>La<sub>x</sub>B<sub>6</sub>, valence transition, lattice parameter and mag. susceptibility meas. 0-59929  
 Sm<sub>2</sub>Mn<sub>23-x</sub>Fe<sub>x</sub>, magnetic behaviour, temp. and comp. depend. 0-93090  
 Sm<sub>2</sub>Se<sub>4</sub>, valence fluctuation, mag. susceptibility meas. 0-97056  
 Sm<sub>1-x</sub>Yb<sub>x</sub>B<sub>6</sub>, valence transition, lattice parameter and mag. susceptibility meas. 0-59929  
 Sn-Se(Te), liq., mag. susceptibility meas., electron localisation and chem. bonding 0-60178  
 Sn<sub>1-x</sub>Mn<sub>x</sub>Te, electronic struct., transport props., mag. ordering effects 0-65441  
 SrF<sub>2</sub>:Ce<sup>3+</sup>, cryst. field energies 0-59941  
 Sr<sub>0.5</sub>La<sub>1.5</sub>Li<sub>0.5</sub>Fe<sub>0.5</sub>O<sub>3</sub>, high spin configuration stabilisation for Fe<sup>4+</sup> (*French*) 0-88519  
 TCNQ salts, Qn(TCNQ)<sub>2</sub> and N-propyl-Qn(TCNO)<sub>2</sub>, low temp. mag. susceptibility, neutron irradi. effects 0-60311  
 TaSe<sub>3</sub>, superconducting transitions and diamagnetism 0-84526  
 Tb, magnetisation, AC susceptibility and microwave absorption meas. 0-60221  
 Tb, magnetisation intensity in antiferromag. state and mag. field induced phase transforms. (*Russian*) 0-65811  
 TbAu<sub>3</sub>, mag. phase diagram 0-75761  
 TbCo<sub>2</sub>Si<sub>2</sub>, mag. props. 0-107988  
 TbFeO<sub>3</sub>, mag. susceptibility, temp. depend., effective field at Tb ion sites 0-75742  
 TbH<sub>2-x</sub>, TbD<sub>2-x</sub>, mag. susceptibility conc. depend. 0-70968  
 TbNi<sub>2</sub>Si<sub>2</sub>, mag. props., 4.2-200K 0-84602  
 TbPO<sub>3</sub>, zircon struct., cryst. field analysis 0-80232  
 Tb<sub>0.26</sub>Y<sub>0.74</sub>FeO<sub>3</sub>, garnet, mag. transition, mag. props. anomaly 0-93120  
 TeCr<sub>2</sub>O<sub>6</sub>, exchange interactions within binuclear entity (Cr<sub>2</sub>O<sub>10</sub>)<sup>4-</sup> 0-60236  
 Th<sub>2</sub>Co<sub>3</sub>, effect of absorbed H<sub>2</sub> on mag. behaviour 0-60184  
 Th<sub>2</sub>Ni<sub>3</sub>, effect of absorbed H<sub>2</sub> on mag. behaviour 0-60184  
 α-Ti alloys VT1 and VT5, struct. and phys. props., H<sub>2</sub> effect 0-108576  
 Ti-Nb-Zr-Fe, supercond. and paramag. props., effect of Fe additions (*Russian*) 0-65730  
 TiBe<sub>2-x</sub>Cu<sub>x</sub>, high press. study of Curie temp. and mag. susceptibility 0-84600  
 Ti(Fe, Co), off-stoichiometric alloy, inverse mag. susceptibility rel. to defect conc. 0-60216  
 (Ti<sub>1-x</sub>V<sub>x</sub>)<sub>2</sub>O<sub>3</sub>, spin glass, nonlinear susceptibility and sp. ht. 0-60304  
 (Ti<sub>1-x</sub>V<sub>x</sub>)<sub>2</sub>Se<sub>3</sub>, mag. susceptibility, 4.2-300K 0-60188  
 Ti<sub>2</sub>(Fe<sub>1-x</sub>Se<sub>x</sub>) mixtures, liq., electrical conductivity and mag. susceptibility 0-88715  
 TmNi<sub>2</sub>Si<sub>2</sub>, mag. props., 4.2-200K 0-84602  
 Tm<sub>2</sub>Si<sub>8</sub>, low temp. Mossbauer study and mag. susceptibility 0-80656  
 TmSe, intermediate valence cpd., susceptibility, single-ion approach 0-70935  
 TmVO<sub>4</sub>, enhanced nuclear cooling and spin-lattice relax. time 0-80632  
 U(Co<sub>1-x</sub>Fe<sub>x</sub>)<sub>2</sub>, ferromag. onset, susceptibility and resist. meas. 0-70967  
 U<sub>2</sub>Th<sub>1-x</sub>Sb<sub>x</sub>, valence change of U accompanied by singlet-ground-state ferromag. 0-70965  
 V, dynamic susceptibility, model pot. theory 0-75710  
 V, small particles, crystal structure, magnetic and superconducting props. 0-97121  
 V surface, spin fluctuations, finite temp. mag. props. study 0-107994  
 V-Pt, sp. ht. and mag. meas. in ordered and disordered phases 0-70422  
 V<sub>2</sub>(Hf,Zr), NMR and mag. susceptibility, density of states determ. (*Russian*) 0-66053  
 V<sub>2</sub>Hf<sub>2</sub>-Zr<sub>2</sub>, normal and supercond. state, transition temps., mag. susceptibility and specific heat determ. (*Russian*) 0-60132  
 V<sub>2-x</sub>Nb<sub>x</sub>Hf<sub>2</sub>, NMR of <sup>51</sup>V and mag. susceptibility, 20-300K (*Russian*) 0-93192  
 VO<sub>2</sub>, magnetic susceptibility in insulating and metallic phases, electron-electron and electron-lattice interactions 0-96788  
 V<sub>2</sub>O<sub>5</sub>-V<sub>2</sub>O<sub>3</sub>-BaZnO<sub>3</sub> glass, V ion states, mag. and elec. props. 0-88556  
 V<sub>2</sub>O<sub>5</sub>-Ti<sub>2</sub>O<sub>5</sub>, DTA, mag. susceptibility and X-ray diffr. study 0-70970  
 V<sub>2</sub>Se<sub>3</sub>:Fe, Mossbauer and mag. studies, electronic state of Fe 0-108130  
 V<sub>2</sub>Se<sub>3</sub>, itinerant antiferromag., spin fluctuations, NMR study 0-75874  
 V<sub>2</sub>Se<sub>3</sub>, itinerant antiferromag., spin fluctuations, NMR study 0-75874  
 VSe<sub>2-x</sub>S<sub>x</sub> (0<x<2) solid solutions, characterisation 0-88730  
 V<sub>2</sub>Si, magnetic susceptibility, density of states model for lattice transformation in A-15 compounds 0-65219  
 VTe, mag. and elec. transport props. 0-92897  
 W, plastically deformed single cryst., mag. susceptibility (*Russian*) 0-93074  
 WCr<sub>2</sub>O<sub>6</sub>, exchange interactions within binuclear entity (Cr<sub>2</sub>O<sub>10</sub>)<sup>4-</sup> 0-60236  
 WV<sub>2</sub>O<sub>6</sub>, exchange interactions within binuclear entity (V<sub>2</sub>O<sub>10</sub>)<sup>4-</sup> 0-60236  
 WV<sub>2</sub>O<sub>6</sub>, magnetic susceptibility, behaviour in terms of quasi-isolated binuclear units 0-97073  
 YCo<sub>2</sub>Si<sub>2</sub>, mag. props. 0-107988  
 YIG, Faraday effect, influence of mag. field on sublattice contributions 0-88975  
 YIG, polycryst., initial and reversible parallel susceptibilities, hydrostatic press. effects 0-75835  
 YIG: Si single crystals, mag. props. 0-107981  
 YMG, Pauli paramagnet, mag. susceptibility, nonlinear band behaviour 0-75706  
 YNi<sub>3</sub>, magnetism resurgence, neutron diffr. and mag. props. study 0-65819  
 Y<sub>1-x</sub>Tb<sub>x</sub>Pd<sub>3</sub>, magnetisation, magnetostriction, and inelastic neutron spectra 0-65998  
 YVO<sub>4</sub>:Nd<sup>3+</sup>, zircon struct., cryst. field analysis 0-80232  
 YbCuAl, mixed valence cpd., dynamic susceptibility, neutron inelastic scatt. 0-65807  
 YbGaG, mag. props. between 44-60 mK 0-80517  
 YbGa<sub>2</sub>O<sub>12</sub>, dipolar magnet, sp. ht. and magnetisation meas. 0-60344  
 YbMo<sub>2</sub>S<sub>8</sub>, low temp. Mossbauer study and mag. susceptibility 0-80656  
 f-YbSe<sub>3</sub>, mag. susceptibility and cryst. field parameters 0-65510  
 Yb<sub>1-x</sub>Y<sub>x</sub>CuAl, disordered extended Anderson model, CPA-alloy analogue treatment 0-65506  
 Zn<sup>2+</sup>Mo<sup>4+</sup>O<sub>3</sub>, defect spinel struct., elec. and mag. props. 0-70176  
 Zr, mag. susceptibility, plastic deform. effect (*Russian*) 0-65984  
 ZrCu, constitutional and struct. studies, by mag. susceptibility, metallography and X-ray diffr. 0-70166



**magnetic susceptibility continued**

- ZrV<sub>2</sub>, Knight shift vs. susceptibility plot 0-75712  
 ZrZn<sub>2</sub>, high press. study of Curie temp. and mag. susceptibility 0-84600  
**magnetic switching**  
 temperature measurement, using magnetically controlled reed switches (French) 0-57291  
 (Co,Fe)<sub>80</sub>B<sub>20</sub> glass, induced anisotropy and time changes of permeability 0-75815  
 NiZnCo ferrites, switching time and coeff., hydrostatic press. effect 0-88802

**magnetic tape recorders** *see tape recorders***magnetic tapes**

- flaws, calcs. of field reflections 0-104387  
 magnetic field diff. meas. on axes of disks and apertures, Babinet principle, complex spirals 0-102599  
 magnetographic inspection, determ. of magnetisation regimes 0-108665

**magnetic thin film devices**

- see also magnetic bubble devices*  
 magnetic soft and hard materials, garnets, magnetic properties and applications, structural props. 0-65760  
 Permalloy thin-film head pole struct., domain configurations, SEM obs. 0-65975  
 SQUID gradiometer, DC, design optimisation 0-89951

**magnetic thin films***see also magnetic epitaxial layers*

- alloys, surface magnetism props., Curie temp., Ising model 0-108039  
 amorphous, struct. and mag. props., review 0-93148  
 Bloch wall structure, horizontal, mag. bubble domains in implanted films 0-71131  
 bubble domain interactions, dynamics, theory 0-71132  
 bubble domain statics and dynamics, micromag. study 0-71081  
 bubble domains, magnetoelastic interactions 0-103865  
 bubble film, magnetoelastic interactions 0-65976  
 bubble garnet film, non-implanted, surface mag. struct. 0-84628  
 bubble garnet film, saturation velocity, in-plane field effects 0-108041  
 bubble materials, props. and prep. methods, review (Rumanian) 0-93149  
 charged domain walls in implanted layers, theory 0-71130  
 ferromagnet, heterogeneity influence on static and dynamic props. of domain walls (Russian) 0-65974  
 ferromagnetic, Brillouin scattering from spin waves 0-65843  
 ferromagnetic, direct determ. of mag. domain wall profiles, using split detector STEM 0-103867  
 ferromagnetic, dynamics near transition pt. from homogeneous to inhomogeneous magnetis. state 0-108038  
 ferromagnetic, parametric oscill. with biaxial anisotropy 0-103861  
 ferromagnetic, thick film, reson. transmission of EM energy via phonons 0-60382  
 garnets, meas. of Faraday effect and susceptibility using magneto-optical apparatus 0-105680  
 Invar film, superfine mag. struct. (Russian) 0-80572  
 magnetic soft and hard materials, garnets, magnetic properties and applications, structural props. 0-65760  
 manganese stearate, two-dimensional mag. struct. 0-108040  
 metallic glasses, Brillouin-Mandelstam scattering from thermal and excited magnons 0-70980  
 orthoferrite cryst. films, local coercivity of domains boundaries (Russian) 0-80578  
 Permalloy, mag. microstruct. obs. in nonlinear ripple magnetis. case (Russian) 0-65971  
 Permalloy film strip, unidirectional domain wall propag. with in-plane magnetisation 0-71134  
 Permalloy films with band domain struct., thermomag. recording, resolving power (Russian) 0-75769  
 Permalloy RF sputtered films, O effects in mag. and elec. props. 0-100603  
 Permalloy thin films, break-cross-tie wall energy 0-88842  
 Permalloy-Cu(Al) two-layer films, mag. anisotropy, grain boundary diffusion (Russian) 0-71122  
 Permalloy-Mn film, diffusion aftereffect causing mag. state change (Russian) 0-103860  
 perpendicularly magnetised, surface and vol. magnetoelastic waves (Russian) 0-93151  
 phase states when easy magnetisation axis is inclined rel. to film surface (Russian) 0-103864  
 rare earth iron garnets, Ca-Ge substituted, mag. loss and domain wall mobility 0-65980  
 strip films, bulk and surface spin oscills., mag. reson. 0-97149  
 stripe domain struct. of film, with perpendicular anisotropy, theory (Russian) 0-65973  
 surface states, theory, in spin wave resonance, review 0-84654  
 thickness meas. of ferromagnetic films of high conductivity using magnetic reluctance thickness gauge 0-68178  
 twisted domain wall energy, thickness depend., simplified calc. (Slovak) 0-103862  
 uniaxial ferromagnet domain struct., phase transition (Russian) 0-108044  
 vertically suspended, torque curve meas., first-order calc. anal. 0-86354  
 Au-Yb thin films, ESR spectra, strain effects 0-71172  
 (BiTm)(FeGa)<sub>2</sub>O<sub>12</sub> ion implanted epitaxial garnet film, bubble domains, cryst. struct. disorder 0-93150  
 Co film, mag. anisotropy study using NMR spin echo method 0-60384  
 Co film, mag. domain wall obs. by electron holography 0-80582  
 Co-Bi(Cr) thin film glasses, mag. props. and corrosion resist. 0-80576  
 Co-CoO films, evaporated, exchange anisotropy 0-88841  
 Co-Cr mag. film, crystallographic texture formation effects on props. (Russian) 0-108471  
 Co-Gd-Mo films, sputtered, O effects on mag. props. during annealing 0-89374  
 Co-Gd(Tb)(Sm), magneto-optic coeff. and refr. index, ellipsometric determ. 0-71501  
 Co-P films with various preferred orientations, mag. props. 0-100604  
 Co-W alloy electrolytic coatings, heat treatment effects on coercivity, hysteresis and structure (Russian) 0-60381  
 Cu HCP film, uniaxial, mag. domain struct. 0-60385  
 Cu/Ni coherent modulated structures, electronic struct. and magnetism 0-103620  
 Cu-Ni thin films, ferromag., Hall effect meas. 0-80428  
 DyCu film, amorphous, asperomagnetic domains, Barkhausen jumps in hysteresis loop 0-75822  
 EuEr<sub>2</sub>Ga<sub>8</sub>Fe<sub>2</sub>O<sub>12</sub>, garnet thin films, magnetisation orientation, temp. depend. 0-71125

**magnetic thin films continued**

- EuO film threshold characteristics in holographic and bit recording (Russian) 0-63944  
 EuO, light scatt. from spin waves and magneto-optic hysteresis meas. 0-97244  
 EuS films, mag. and elec. props. rel. to stoichiometry and defects 0-97122  
 EuS, light scatt. from spin waves and magneto-optic hysteresis meas. 0-97244  
 Fe, ferromag. film, surface states, surface magnetisation and electron spin polarisation 0-65648  
 Fe film, coated, interface magnetism by Mossbauer spectroscopy 0-75890  
 Fe films, ferromagnetic reson., photoacoustic detection 0-80613  
 Fe sputtered film, amorphous, Mossbauer study and electron diff. obs. 0-75897  
 Fe thin films, surface demagnetisation due to chemisorption, ferromagnetic reson. study 0-80616  
 Fe thin layers, vacuum coated on PMMA, mag. behaviour during mech. stress cycles (German) 0-80581  
 Fe-B-Cr(Si) thin film glasses, mag. props. and corrosion resist. 0-80576  
 Fe-Gd(Tb), magneto-optic coeff. and refr. index, ellipsometric determ. 0-71501  
 Fe-Ni, amorphous, martensite form. time and struct. 0-104159  
 Fe-Ni film, electrodeposited, struct. and mag. props. 0-107668  
 Fe-P electrodeposited foil, amorphous, mag. domains 0-75821  
 Fe-Sb amorphous films, Mossbauer effect study 0-75896  
 Fe-Si-Cr, sputtered, corrosion reduction, effect of Cr obs. 0-80573  
 Fe<sub>0.5</sub>Co<sub>0.5-x</sub>Cr<sub>x</sub> films, vacuum-deposited cryst. and mag. struct. (Russian) 0-93081  
 Fe<sub>40</sub>Ni<sub>40</sub>C<sub>14</sub>P<sub>6</sub> amorphous film, dislocation and mag. struct., neutron diff. study 0-70956  
 Fe<sub>3</sub>Si<sub>1-x</sub>, amorphous film, magneto-optic Kerr effect 0-66158  
 Fe<sub>2</sub>Sn<sub>1-x</sub>, amorphous film, struct. and mag. props. 0-65972  
 Gd-Co, amorphous films, mag. props. ferromag. reson. meas., 20-520°C (Russian) 0-97144  
 Gd-Co amorphous films, mag. struct., mag. bubbles, electron diff. study (Chinese) 0-71126  
 Gd-Co based amorphous sputtered films, microstruct. variability and mag. anisotropy, implanted ion effects 0-88459  
 Gd-Fe amorphous films, stress contrib. to perpendicular anisotropy 0-75819  
 Gd-Ti(V)(Cr)(Mg)(Nb)(Ge)(Si)(Au) amorphous films, spontaneous Hall effect and elec. resist. 0-80251  
 (Gd<sub>1-x</sub>Co<sub>x</sub>)<sub>1-x</sub>Ar, amorphous mag. film, elec. and mag. prop. depend. on Ar 0-80410  
 (Gd,Co<sub>1-x</sub>)<sub>1-x</sub>Ar, amorphous films, effective anisotropy field, ferromag. reson. obs. 0-71123  
 La-Fe alloy, amorphous, sputtered at high rate, mag. props. 0-75753  
 MnAlGe film, mag. domains and amorphous to cryst. phase transition, electron microscopy obs. 0-71129  
 MnBi films, prep. by ionised-cluster beam deposition technique, magneto-optical props. 0-100790  
 MnBi-Bi garnet film struct., thermomagnetic recording 0-100588  
 MnGaGe film, mag. domains and amorphous to cryst. phase transition, electron microscopy obs. 0-71129  
 MnSb<sub>1-x</sub>Sn<sub>x</sub> films, Faraday rotation, optical absorpt. coeffs. 0-97242  
 Ni (100) films, spin density by self-consistent linear APW method 0-65710  
 Ni, electrodeposited film, thermal anal., occlusion of gases rel. to mag. props. 0-59823  
 Ni, evaporated, for use as variable delay SAW device, magnetostrictive effects 0-71144  
 Ni, ferromag. film, surface states, surface magnetisation and electron spin polarisation 0-65648  
 Ni films, ferromagnetic reson., photoacoustic detection 0-80613  
 Ni, thin films, surface demagnetisation due to chemisorption, ferromagnetic reson. study 0-80616  
 Ni-B electrodeless-plated amorphous films, anomalous mag. temp. characts. 0-96757  
 Ni-B thin film glasses, mag. props. and corrosion resist. 0-80576  
 Ni-Fe film, thermally activated domain wall motion 0-88777  
 Ni-Fe films, energy change of Bloch wall with angle to easy axis, calc. (Slovak) 0-103863  
 Ni-P, electrodeposited film, thermal anal., occlusion of gases rel. to mag. props. 0-59823  
 Ni-S, electrodeposited film, thermal anal., occlusion of gases rel. to mag. props. 0-59823  
 NiFe film, domain wall mass and relax. time from forced oscills. 0-71133  
 NiFe, pulse switching at low temp. 0-103868  
 NiFe, single and multilayer thin films, strip domains, inplane magnetisation 0-103866  
 NiFe thin films, magnetoresistance, quasi-static characts. 0-107766  
 SmCo<sub>5</sub>, mag. domains structure rel. to crystal defects, electron microscopy 0-103856  
 SrFe<sub>2</sub>Al<sub>2</sub>O<sub>9</sub>, thin film LPE growth and mag. props. 0-80992  
 (Tb,Dy)-Fe amorphous films prep. by cosputtering, magnetoelastic props. 0-97429  
 Tb-Fe amorphous thin films, magnetic after-effect, Kerr magneto-optic effect obs. 0-97123  
 Tm ferromagnet film, cylindrical mag. domain motions, domain boundary oscills. (Russian) 0-71140  
 Y-Sm ferromagnet (Russian) 0-71140  
 YCo<sub>5</sub> amorphous films, <sup>59</sup>Co spin echo study 0-80636  
 (YEuTm)<sub>3</sub>(GaFe)<sub>2</sub>O<sub>12</sub> ferrite garnet films, mag. bubbles, translational motion, mechanism for inertial effects 0-100606  
 Y<sub>2-x</sub>Gd<sub>x</sub>GaFe<sub>2</sub>O<sub>12</sub> garnet thin films, magnetisation orientation, temp. depend. 0-71125  
 (YGdYbBi)<sub>3</sub>(FeAl)<sub>2</sub>O<sub>12</sub> ferrite-garnet films, effect of in-plane field on dynamics of domain walls 0-65979  
 (YGdYbBi)<sub>3</sub>(FeAl)<sub>2</sub>O<sub>12</sub> epitaxial garnet film, uniaxial ferromagnet domain struct., phase transition (Russian) 0-108044  
 YIG, cylindrical mag. domains, translational motion 0-108043  
 YIG film, magnetostatic surface wave propag. in nonuniform mag. field 0-80574  
 YIG film, periodically corrugated, insertion loss, reson. linewidth effect 0-80614  
 YIG, multiple mag. layer structures, magnetostatic surface wave propag. 0-88839  
 YIG sandwiched between grounded dielectric layers, magnetostatic bulk wave propagation 0-60380



**magnetic thin films continued**

- YIG thin film gyromag. waveguide, on GGG substrate, optical propag. props. Faraday effect 0-74513  
 YIG, thin films, magnetostatic modes at Q-band freq. 0-65828  
 YIG:Co film, influence of stress induced anisotropy on domain struct. 0-100605  
 YIG:La,Ga, film, LPE-grown, Ga incorporation, depend. of magnetisation on growth rate 0-84627  
 YIG:La(Ga) films, ferromagnetic resonance, ion implantation effect 0-97145  
 $Y_{2.85}La_{0.15}Fe_{3.85}Ga_{1.15}O_{12}$  garnet, mag. props., ion implantation effect, Mossbauer study 0-97166  
 $(YLuSmCa)_2(FeGe)_2O_{12}$  garnet film, bubble domain expansion, fuzzy wall struct. 0-71128  
 $Y_{3-x}Sm_xFe_2O_{7.5-x}$  Fe film, ion implanted, Mossbauer conversion spectra study 0-80663  
 $Y_{1.5}Tb_{1.5}Al_{0.85}Fe_{3.5}O_{12}$  garnet thin films, magnetisation orientation, depend. 0-71125

**magnetic transition temperature**

- see also Curie temperature; Morin temperature; Neel temperature  
 anisotropic magnet, dil., crit. behaviour near percolation threshold 0-88767  
 antiferroelectric ferrites, coupled magnetoelec. oscills. and high freq. susceptibility tensor (Russian) 0-93152  
 effective Hamiltonian approximation, quenched and annealed random systems 0-93125  
 Heisenberg antiferromagnet, Green function theory 0-107975  
 Heisenberg ferromagnet, transition temp., mean field upper bound 0-97048  
 Ising and Heisenberg inhomogeneous mixture, quenched system, critical temp. 0-88770  
 Ising spin glass, d-dimensional, frustration effect 0-108019  
 metamagnetic tricritical point, effective exponent  $\beta$  0-71045  
 spin glass, Sherrington-Kirkpatrick, white and weighted averages over solns. of Thouless-Anderson-Palmer eqns. 0-108012  
 spin-1/2 cubic lattice, with anisotropic exchange, configs. 0-65926  
 Au-Fe, spin glass, transition temp., freq. depend. 0-97113  
 $B_2O_3.Fe_2O_3.nMO$ , ( $n=2$  or 4,  $M=Mg, Co, Ni, Cu$ ), mag. props., transitions 0-75763  
 $CaLaFeO_4$ , two-dimens. mag. props. rel. to cryst. struct. 0-75776  
 Cr alloyed with d-transition elements, magnetic transformations, triple point (Russian) 0-88747  
 Cr, spin-flip transition temperature, press. depend. from elastic const. meas. 0-65944  
 Cu-Mn, spin glass, transition temp., freq. depend. 0-97113  
 EuB<sub>6</sub>, ferromag. and antiferromag. sp. ht meas., 1.8-77K 0-65948  
 $Eu_{1-x}Gd_xS$  and  $Eu_xSr_{1-x}S$ , spin glasses, transition temp., freq. depend. 0-97113  
 EuPt, compounds, partial valence change, <sup>151</sup>Eu Mossbauer and magnetisation obs. 0-70167  
 $Fe_2O_3$ , magnetocrystalline anisotropy, anomalies in magnetostriction and elastic constants 0-60244  
 $KCrO_2$ , two-dimens. mag. props. rel. to cryst. struct. 0-75776  
 $LiCrO_2$ , two-dimens. mag. props. rel. to cryst. struct. 0-75776  
 $NaCrO_2$ , two-dimens. mag. props. rel. to cryst. struct. 0-75776  
 Nd, mag. struct., 18.6K mag. phase transition 0-65799  
 $Pd_{1-x}Mn_xH$ , alloy, spin glass, transition temp., susceptibility and EPR meas. 0-65930  
 $Pt_{1-x}(Rh)_x(Rh)_{1-x}(Ru)_x$ , sp. ht., differential susceptibility and elec. resist. meas., 1.4-40K 0-71063  
 Rh borides,  $RRh_2B_2$  ( $R=rare\ earth$ ), supercond. and mag. props. 0-97028  
 Ru borides,  $RRu_2B_2$  ( $R=rare\ earth, Y, Th, or U$ ), supercond. and mag. props. 0-97028  
 $SrLaFeO_4$ , two-dimens. mag. props. rel. to cryst. struct. 0-75776  
 $(Tb_{1-x}Gd_x)_2Co$ , intermetallic cpd. mag. props., phase transform., and mag. hysteresis (Russian) 0-93113  
 $VI_2$ , mag. struct., long- and short-range order and Mossbauer spectroscopy 0-65803

**magnetic transitions**

- see also critical fluctuations; ferromagnetic-antiferromagnetic transitions; ferromagnetic-paramagnetic transitions; magnetic transition temperature; paramagnetic-antiferromagnetic transitions  
 actinide mononitrides, anomalous mag. props., planar coupling theory 0-60245  
 alkali hyperoxides, ionic  $\pi$ -electron systems, magnetogyration 0-93155  
 alloy, binary, magnetic, interface struct., Monte Carlo simulation 0-60317  
 amorphous Ising antiferromagnetic model, frustration effects 0-103838  
 anisotropic exchange interactions, effect on singlet ground state system 0-65852  
 anisotropic magnets, dil., scaling representation meas. percolation threshold 0-88766  
 anisotropic spin-phonon coupling model, exact solutions (Russian) 0-100590  
 antiferromagnet, FCC, Ising model, mag. phase diagram, ordering, Monte Carlo calc. 0-103833  
 antiferromagnet, Ising model, crit. props., calc. 0-65946  
 antiferromagnet, magnetic phases, spin configurations in external field 0-70955  
 antiferromagnet, quantum critical dynamics with mode coupling 0-108024  
 antiferromagnet, rhombohedral, spin-reorientation phase transition (Russian) 0-93122  
 antiferromagnet, two-sublattice Neel-type, stable spin configurations, external mag. field and single-ion orthorhombic anisotropy effects 0-60249  
 antiferromagnetic triangular cactus tree, bond-diluted, ordered phase 0-71037  
 antiferromagnets, Berezinski transition, effective temp. (Russian) 0-65889  
 antiferromagnets, disordered spin flop, bicritical behaviour, critical experiments 0-65899  
 Ashkin-Teller-Potts model, dil., crit. behaviour 0-65897  
 Baxter-Wu model, site impure modified crit. behaviour and crossover 0-60322  
 BCC crystal, anisotropic spin-pair correlation function, neutron mag. crit. scatt. cross-section 0-60194  
 biaxial Lifshitz point problem in 3-dimens., spin wave theory 0-88759  
 commensurate phases, spatially modulated, in simple Ising model 0-79909  
 compressible dilute Ising systems, critical behaviour 0-108017

**magnetic transitions continued**

- cubic lattices, fully frustrated, phase transitions, Gaussian and spherical model, free energy calcs. 0-60281  
 dimethylammonium copper tetrabromide, quasi two-dimensional antiferromag., mag. behaviour 0-97098  
 dimethylammonium copper tetrachloride-tetrabromide mixed cryst., mag. transition 0-65874  
 disordered spin systems, tricrit. behaviour 0-60319  
 dynamical plane rotator model, dynamical correl. functions in mol. field approx. 0-88758  
 Edwards-Anderson spin glass model in two dimensions, numerical results 0-97100  
 electron-hole paired systems, ferromagnetic ordering phase diagram 0-97097  
 equivalent neighbour model, generalised, derivation of high temp. lattice consts. 0-77721  
 extended defect system, phase transform., critical props. 0-103455  
 ferroelectric antiferromagnets, phase transformations (Russian) 0-93114  
 ferrofluids, phase diagrams and eqn. of state 0-60280  
 ferromagnet, anisotropic, in external mag. field, continuous phase transition existence 0-108011  
 ferromagnet, anisotropic, influence of spatially varying field on phase transitions 0-60339  
 ferromagnet, anisotropic, with external field, crit. pts. derivation 0-103837  
 ferromagnet, excitonic, zero-sound excitations, Fermi liq. model 0-93101  
 ferromagnet, Ising model, diamond lattice, phase transition, crit. props. 0-93127  
 ferromagnet, random quenched, crit. behaviour, effective exponents, renormalisation 0-60326  
 ferromagnetic crystals, uniaxial anisotropy, first order magnetisation processes theory 0-60242  
 ferromagnetic Ising model, spin-one three dimensional, single-ion anisotropy, crit. behaviour 0-80540  
 ferromagnetic plate, domain struct. near first-order phase transition resembling second-order transition 0-93139  
 ferromagnetic semiconductor, energy and mobility of spin polarons 0-70982  
 ferromagnetic systems, crit. experiments, field theory, Borel transform. 0-80541  
 ferromagnets, quantum critical dynamics with mode coupling 0-108023  
 first order instability in finite model system, computer simulation 0-65932  
 Gaussian-to-Heisenberg crossover, specific heat, renormalised perturbation theory 0-60356  
 harmonic rotor model, interactions, spirals and phase transitions with and without long range order 0-60350  
 Heisenberg bicritical points in antiferromagnets, universality tests 0-84604  
 Heisenberg chain, classical anisotropic, scaling theory 0-80515  
 Heisenberg ferromagnet, critical dynamics of impurity spin below  $T_c$  0-71076  
 Heisenberg metamagnet, collinear, mag. phase diagram 0-71035  
 Heisenberg model, disordered ferromag. states, random exchange integrals 0-80550  
 Heisenberg model, randomly dilute, renormalisation group calcs. 0-60321  
 Heisenberg multi-quadratic isotropic model, LRO, phase transf., exchange interactions (Chinese) 0-88756  
 Hubbard model, equivalent spin Hamiltonian, for phase transition studies 0-80474  
 Hubbard model, single band, magnetic phase diagram, cluster variational calc. 0-60340  
 Ising antiferromag. phase boundaries, hard-core lattice gas calcs. 0-80542  
 Ising antiferromagnet, FCC, nearest neighbour interactions, Monte Carlo method 0-80544  
 Ising chain, with next-nearest neighbour interactions, mag. responses to spin-Peierls transition 0-71054  
 Ising ferromagnet, comparison with plane rotor 0-60348  
 Ising ferromagnet, phase coexistence, translation invariance and stability 0-80513  
 Ising ferromagnet, randomly dilute, conc. expansion study 0-60315  
 Ising ferromagnet, two-dimens., order parameter and induced susceptibility 0-71036  
 Ising magnet, metastable, in negative field, near criticality 0-84608  
 Ising magnet coupled to isotropic elastic medium, first order transition, renormalisation method 0-68151  
 Ising model, bond random, ferromagnetic-antiferromag. mixture, triangular cactus tree, statistical theory 0-75702  
 Ising model, bond-dil., two-dimens., phase transition 0-60320  
 Ising model, constant-coupling approx., successive phase transitions 0-97108  
 Ising model, continuous-variable, real-space renormalisation group method 0-100589  
 Ising model, critical dynamics, time-dependent real-space renormalisation group 0-60282  
 Ising model, critical temperature, modulated Pade approximant 0-84605  
 Ising model, Devil's staircase and harmless staircase, oscillating interactions through elastic struts or other harmonic fields 0-88296  
 Ising model, quenched-bond disorder, cluster extension of effective-interaction approximation 0-93130  
 Ising model, spatially nonhomogeneous, correl. functions 0-60314  
 Ising model, spin-one, bilinear and biquadratic interactions 0-75772  
 Ising model, surface crit. behaviour, layer and local susceptibility 0-71058  
 Ising model, three-dimensional, with four-spin interaction, exact soln. 0-88711  
 Ising model, two-dimens., ferromagnet-spin glass transition, Monte Carlo calc. 0-60287  
 Ising model phase boundary, line of analytic singularities 0-60283  
 Ising model strips, scaling theory, wall effects in crit. systems 0-80539  
 Ising model with biquadratic interaction, phase transition, Monte Carlo method 0-60352  
 Ising model with competing interactions, critical properties and exact results 0-93129  
 Ising spin glass, d-dimensional, frustration effect and dilution problems 0-108018  
 Ising spin system, coupled to acoustic and optic lattice modes, critical behaviour 0-71044  
 Lifshitz point, phase diagrams and crit. behaviour 0-65928  
 Lifshitz points and Landau theory in presence of mag. field 0-60338



## magnetic transitions continued

magnetic alloys, binary, spinodal decomp., computer simulation study of interface behaviour 0-84913  
 magnetic order coexistence with charge density waves 0-97096  
 magnetically ordered cryst., dislocation drag, magnetoelastic waves 0-103332  
 metal-insulator transition, density-functional theory 0-75507  
 metamagnet, compressible, renormalisation group theory of pseudocritical point 0-60337  
 metamagnetic tricritical point, effective exponent  $\beta$  0-71045  
 mischmetal-Co system, thermomagnetic analysis of intermediate phases 0-93115  
 Neel ferrimagnets, phase transitions, field-induced spin-orientational 0-75767  
 $\text{NiWO}_4$ , antiferromag., low symmetry exhibited during spin-flop phase transition 0-60263  
 ordered magnetic cpds., selective sublattice dilution, percolation problem 0-103850  
 Permalloy-Mn film, diffusion aftereffect causing mag. state change (*Russian*) 0-103860  
 phase transitions with two order parameters, Landau theory, mag. reorientation 0-103456  
 planar magnets, quasi-two-dimensional, dynamics of vortices 0-71066  
 Potts model, three-state, first order phase transitions 0-60333  
 quantum compressible Ising model, critical behaviour 0-108016  
 quantum spin glass theory 0-103839  
 quantum spin model, appl. of projective renormalisation group 0-84607  
 quantum spin system, two-dimens., frustration, renormalisation group study 0-80535  
 quasi-one-dimensional systems, spin-lattice Peierls instabilities, static and dynamic aspects 0-71052  
 quasi-two-dimensional planar spin system, mag. transition 0-65951  
 random antiferromagnets, crit. and multicritical props. 0-60332  
 random ferromagnets, Ginzburg criterion, critical fluctuations 0-71032  
 random hierarchical model, crit. props. 0-71072  
 randomly disordered alloys, ferromagnetism onset, mag. inhomogeneity 0-75774  
 rare earth alloys,  $\text{R}_2\text{Pt}$  ( $\text{R}=\text{Gd}, \text{Tb}, \text{Dy}, \text{Ho}, \text{Er}$ ), magnetic susceptibility meas., mag. transition obs. 0-60222  
 rare earth compounds,  $\text{RCo}_2$ , metamagnetic transitions in internal fields 0-60272  
 rare earth intermetallic cpds., cryst. field effects rel. to mag. props. 0-59933  
 rare earth metals, electronic sound attenuation anomalies at transition to helical phase, Fermi surface topology (*Russian*) 0-92807  
 semiconductors, electronic properties, critical behaviour, theory 0-96861  
 spherical model, phase separation, symmetry breaking fields study 0-88760  
 spin glass, dil., conc. expansions at zero temp., Ising model 0-60303  
 spin glass, infinite range model, stability and susceptibility in Parisi's soln. 0-88762  
 spin glass, transitions, field-induced, masking effects 0-65943  
 spin glass transition, cumulant expansion of free energy of disordered systems 0-71067  
 spin glass transition, lower crit. dimensionality 0-60291  
 spin glasses, dilute, at zero temperature, low concentration series expansion 0-93131  
 spin glasses, free energy, order parameter expansion, random bond model 0-84609  
 spin glasses, random mixture of Ising systems, phase boundaries 0-60285  
 spin models planar, duality props. and phase diagrams 0-60286  
 spin-glass, obs. by DC Josephson effect 0-100594  
 spin-Peierls phase diagrams, obs. and models 0-60330  
 SQUID magnetometer with temp. control, spontaneous magnetisation and mag. susceptibility meas. 0-68221  
 structural and mag. phase transforms., integral rational basis of invariants (*Russian*) 0-62602  
 superconductor, helical ordering of spins 0-88669  
 surface magnetisation profile singularities near critical point 0-103843  
 systems far from thermodynamic equilb., dissipative structures, broken symm. equilb. phase transition theory 0-65827  
 TCNQ salt, dibenzo-TTF-TCNQCl<sub>2</sub>, one-dimens. mag. semicond., mag. and elec. props. 0-88601  
 TMMC, crossover transition, effects on susceptibility and EPR shift 0-71047  
 TMMC, linear antiferromag., mag. phase diagram, expt. and theoretical study 0-71038  
 3d-transition metal complexes, low spin-high spin paramag. transition, Ising model calc. 0-93073  
 transition metal pnictides, displacive and mag. transitions 0-59616  
 two-dimensional Ising system, crossing over to two-dimensional Heisenberg system 0-93123  
 two-spin correlation function, dipolar crossover 0-80516  
 uniaxial antiferromagnetic, phase diagram, spin flop transition (*Russian*) 0-100587  
 uniaxial ferromagnet, domain struct. in mag. field 0-103853  
 uniaxial ferromagnet domain struct., phase transition (*Russian*) 0-108044  
 X-Y model, biquadratic, spin one, variation of Curie temp. 0-97102  
 X-Y model, quantum effects and dynamics at low temps., path integral approach 0-84584  
 X-Y model,  $S=1/2$ , phase transitions at  $T=0$ , z-field renormalisation group method 0-71051  
 Au-Co, liquidus line determ. by mag. meas. 0-60250  
 Au-Fe, dil., crit. dynamics 0-60325  
 $\text{Ba}_2\text{Co}_{1-x}\text{Fe}_{2x}\text{F}_{12}$ ,  $\text{Fe}_{28}^{3+}\text{O}_{46}$ , temp.-mag. field phase diagram, torque method 0-60276  
 $\text{BaMnF}_6$ , magnetic neutron scatt. from structurally distorted cryst. 0-93086  
 $\text{BaVS}_3$ , mag. transition and hyperfine interaction, neutron spin-flip scatt. obs. 0-97093  
 $\text{CdCr}_2\text{Se}_4$ , reactor radiation influence on ferromagnetic phase transform. (*Russian*) 0-75760  
 Ce monochalcogenides, mag. ordering, expt. test for  $\epsilon$ -expansions with  $n=4$  0-60259  
 Ce mononitrides, anomalous mag. props., planar coupling theory 0-60245  
 $\text{CeAl}_2$ , magnetic ordering, 24 component Ginzburg-Landau model 0-97095  
 $\text{CeB}_6$ , anomalous sp. ht. intrinsic mag. phase transitions obs. 0-108027  
 Co-mischmetal system, phase relations, microstruct., mag. props. 0-104118

## magnetic transitions continued

$\text{CoBr}_2 \cdot 6(0.48\text{D}_2\text{O}, 0.52\text{H}_2\text{O})$  spin-flop system, intermediate phase existence, sublattice magnetisation reorientation 0-80510  
 $\text{CoBr}_2 \cdot 6(1-x)\text{H}_2\text{O} \cdot x\text{D}_2\text{O}$ , mag. intermediate phase, magnetisation and neutron scatt. meas. 0-60195  
 Cr alloyed with d-transition elements, magnetic transformations, triple point (*Russian*) 0-88747  
 Cr, antiferromagnetic, US attenuation and phase diagram 0-103831  
 Cr, hyperfine interactions on  $^{111}\text{Cd}$ -probe nuclei, TDPAC meas. 0-75904  
 Cr, mag. phase diagram, near, spin-flip temp., US attenuation 0-60267  
 Cr-Fe, dil., spin correlations and neutron scatt. near crit. conc., theory 0-60327  
 $\text{Cr}_2\text{Mn}_{1-x}\text{As}_x$ , mag. susceptibility anomaly at displacive phase transition 0-93091  
 $\text{CsMnCl}_2 \cdot 2\text{H}_2\text{O}$ , mag. phase diagram near bicritical point 0-71021  
 Cu, NMR study on nuclear ordering below  $1\text{ }\mu\text{K}$  0-93187  
 $\text{CuCl}_2$ , anhydrous, mag. phase transition 0-80506  
 $\text{Cu}_2\text{-}_x\text{Se}$ , nonstoichiometric, diamag. and paramag. props., susceptibility meas. 0-70936  
 Dy-Cu, amorphous, mag. phase diagram, magnetisation and sp. ht. meas. 0-80532  
 DyCo<sub>2</sub>-DyAl<sub>3</sub> system, mag. and structural studies 0-108006  
 DyCo<sub>3</sub>, noncollinear mag. struct. appearance in mag. fields, magnetostriction meas. (*Russian*) 0-100607  
 $\text{Dy}_{0.5}\text{Ho}_{0.5}\text{FeO}_3$ , orthoferrite, domain struct., temp. depend. 0-71086  
 $\text{Er}_{1-x}\text{Ho}_x\text{Rh}_2\text{B}_4$ , mag. and supercond. transitions, cryst. field effects 0-107950  
 $\text{Er}_{1-x}\text{Tm}_x\text{Rh}_2\text{B}_4$ , mag. and supercond. transitions, cryst. field effects 0-107950  
 $\text{Er}_2\text{Y}_{1-x}\text{Rh}_2\text{B}_4$ , mag. and supercond. transitions 0-70874  
 $\text{EuSe}(\text{Te})$ , magnetic phase transitions, thermal modulation spectroscopy study (*French*) 0-97301  
 $\text{EuSe}(\text{Te})$ , spin order and fluctuations, Raman scatt. study 0-97273  
 $\text{EuSr}_{1-x}\text{S}_x$ , spin glass to ferromag. transition, neutron scatt. and susceptibility meas. 0-60254  
 $\text{EuSr}_{1-x}\text{S}_x$ , spin-glass props. and mag. transition 0-97105  
 Fe, dynamic exponent, crossover obs., TDPAC Meas. 0-108021  
 Fe-Ni, Invar, Curie point, annealing effects and time depend. 0-80508  
 Fe-Pd Invar alloy, Young's modulus, magnetostriction, Curie temp. 0-65988  
 $\text{FeBO}_3$ , spin-reorientation phase transition (*Russian*) 0-93122  
 $\text{FeCl}_2$ , collinear metamag., mag. phase diagram 0-71035  
 $\text{FeCl}_2$ , logarithmic corrections to tricritical scaling 0-65940  
 $\text{Fe}_2\text{O}_3 \cdot \text{Co}_2\text{Cl}_2 \cdot 2\text{H}_2\text{O}$ , random mixture with competing spin anisotropies, tetracrit. behaviour 0-60324  
 $\text{Fe}_2\text{Cr}_{1-x}\text{S}_x$ , spin-wave evolution crossing from ferromag. to spin-glass regime 0-97080  
 $\text{Fe}_2\text{O}_3 \cdot \text{BaO} \cdot \text{B}_2\text{O}_3$ , magnetic props. of Fe-rich amorphous oxide (*French*) 0-80511  
 $\text{Fe}_2\text{O}_3$ , magnetite, and related Jente spinels, mag. crit. point behaviour 0-60342  
 $\text{Fe}_2\text{P}$ , spin wave excitations meas. 0-65831  
 $\text{Fe}_{50}\text{Pd}_{50}\text{-Si}_{18}$  metallic glass, mag. transitions, weak ferromagnetism 0-100583  
 $\theta\text{-Fe}_2\text{V}_2\text{O}_5$ , spin glass and paramag. props., susceptibility, EPR and Mossbauer studies 0-75782  
 Gd, ferromag., transport props., crit. behaviour 0-65522  
 $\text{GdAlO}_3\text{-La}$ , antiferromag., random-field crit. and multicritical behaviour 0-65939  
 $\text{GdAlO}_3\text{-La}$ , random antiferromagnets, crit. and multicritical props. 0-60332  
 $\text{Gd}_2\text{Ga}_2\text{O}_7$ , mag. phase diagram, AC susceptibility meas. 0-60265  
 $\text{GdMn}_2\text{-GdAl}$  system, mag. and structural studies 0-108006  
 $^3\text{He}$ , HCP, and adsorbed  $^3\text{He}$  with triangular lattice, exchange and mag. order 0-107606  
 $^3\text{He}$ , solid, mag. phase diagram from static magnetisation meas. 0-84342  
 Ho-Cu intermetallics, resist. and magnetoresist., mag. ordering obs. 0-70677  
 $\text{HoRh}_2\text{B}_4$ , low temperature magnetic properties 0-88728  
 $\text{HoSb}$ , mag. phase diagram, quadrupolar interactions 0-65820  
 $\text{La}_2\text{CoO}_4$ , mag. behaviour obs. 0-70971  
 $\text{La}_2\text{-}_x\text{Sr}_x\text{CoO}_4$ , mag. behaviour obs. 0-70971  
 $\text{LiHoF}_4$ , uniaxial dipolar ferromag., critical behaviour, mag. susceptibility meas. 0-80528  
 $\text{LiTbF}_4$ , uniaxial dipolar ferromag., critical behaviour, mag. susceptibility meas. 0-80528  
 $\text{LiTb}_{0.5}\text{Y}_{0.5}\text{F}_4$ , uniaxial dipolar ferromag., critical behaviour, mag. susceptibility meas., effect of  $\text{Y}^{3+}$  dilution 0-80528  
 $\text{MgFe}_{3-x}\text{O}_4$ , polycryst., Verwey type transition, resist., magnetisation, Mossbauer effect and permeability obs. 0-75764  
 Mn-Bi micromagnetic alloy, mag., elec. and elastic props. (*Russian*) 0-108028  
 $\text{MnAs}_{1-x}\text{P}_x$ , mag. susceptibility anomaly at displacive phase transition 0-93091  
 $\text{Mn}_{1.88}\text{Cr}_{0.12}\text{Sb}$ , antiferromag.-ferrimag. transition, neutron crit. scatt. and crossover effect 0-71023  
 $\text{Mn}_{1-x}\text{Mg}_x\text{Se}$ , mag. and struct. phase transitions, mag. susceptibility and X-ray diffr. study 0-71022  
 MnP, ferro-spiral transition, neutron scatt. studies 0-65876  
 MnP, Lifshitz point, transverse differential susceptibility meas. 0-84599  
 MnP, low field magnetoresistances, mag. phase diagram purity depend. 0-107816  
 $\alpha\text{-MnSe}$ , mag. and struct. phase transitions, mag. susceptibility and X-ray diffr. study 0-71022  
 $\text{N}_2$  complex,  $\text{Ni}(\text{C}_6\text{H}_5\text{NO})_2(\text{NO})_2$ , singlet ground-state systems, field induced mag. long range order 0-60266  
 $(\text{NH}_4)_2\text{ReCl}_4(\text{IrCl}_4)$ , proton relaxation near antiferromagnetic phase transitions 0-80640  
 $\text{NaMnCl}_3$ , mag. struct. and spin-flip transition, powder neutron diffr. exam. 0-60210  
 Ni dynamic exponent, crossover obs., TDPAC meas. 0-108021  
 Ni-Mn alloys, ferromagnetism-to-spin glass phase transition and strong mag. field effect 0-75773  
 $\text{NiBr}_2$ , commensurate and incommensurate mag. struct., neutron diffr. study 0-97067  
 $\text{Ni}_3\text{Fe}$ , compression induced magnetic anisotropy, annealing effect 0-93112  
 NiI, anhydrous, magnetic phase transition, neutron diffr. study 0-71033  
 NiO, antiferromag. ordering, mag. transition-state approach 0-80507  
 $\text{NiS}_2\text{-}_x\text{Se}_x$ , phase diagram, intermediate valence effects 0-103834



**magnetic transitions continued**

- NpO<sub>2</sub>, mag. transition at 25K, Kramers doublet as cryst. field ground state 0-59936
- Pd-Co, dil., breakdown of ferromag. order, magnetoresist. obs. 0-71046
- Pd-Co (0.1-45.7 at.%), thermo EMF at 4.2-300K (*Russian*) 0-92881
- Pd-Fe (0.54-8.0 at.%), thermo EMF at 4.2-300K (*Russian*) 0-92881
- Pd-Mn, ferromagnetism to spin glass behaviour transition 0-71062
- Pd-Ni (15-90 at.%), thermo EMF at 4.2-300K (*Russian*) 0-92881
- PrAg, low temp. mag. meas. 0-107989
- PrCo<sub>2</sub>, high field first order transitions, role of K<sub>2</sub> anisotropy const. 0-65879
- PrSn<sub>3</sub>, thermal expansion and transverse elastic const. near mag. phase transition 0-60394
- Pr<sub>2</sub>Ti, thermal expansion and transverse elastic const. near mag. phase transition 0-60394
- Pt-Fe, dil., breakdown of ferromag. order, magnetoresist. obs. 0-71046
- Pt-Fe alloy, ordered, T-c phase diagram, antiferro- and ferromagnetism (*Russian*) 0-65871
- PtMn, spin glass, non-linear susceptibility and sp. ht. 0-60304
- Rb<sub>2</sub>CrCl<sub>4</sub>, planar ferromag., spin waves 0-65835
- RbMnCl<sub>3</sub>, twinning struct., cryst. domains, orientation mag. transition (*Russian*) 0-107275
- Rb<sub>2</sub>MnCl<sub>4</sub>, quasi-2D-antiferromag., linear birefr. and optical absorpt. spectra 0-71385
- SmCo<sub>5</sub>, amorphous, supermag.-ferromag. transition and directional crystallisation 0-65891
- SmIG, mag. phase transitions, Mossbauer spectroscopy obs. 0-80509
- Tb<sub>0.76</sub>Y<sub>0.24</sub>Fe<sub>2</sub>O<sub>12</sub> garnet, mag. transition, mag. props. anomaly 0-93120
- TbZn, elec. resist., behaviour at mag. crit. points 0-65901
- (Ti<sub>1-x</sub>V<sub>x</sub>)<sub>2</sub>O<sub>3</sub>, spin glass, nonlinear susceptibility and sp. ht. 0-60304
- Tm magnetic transitions, effect of H<sub>2</sub> in solid solns., elec. resist. meas. 0-100585
- TmFeO<sub>3</sub>, acoustic vel. and attenuation shifts at spin reorientation phase transition 0-65986
- UAs, search for lattice distortions at low temps. 0-79759
- U<sub>3</sub>As<sub>4</sub>, ferromag., mag. field induced phase transitions 0-65887
- U<sub>3</sub>As<sub>4</sub>, heat capacity, 5-300K, ferromag. transition obs. 0-88769
- UF<sub>6</sub>, giant magnetoelastic deform. of cryst. struct. mag. props. (*Russian*) 0-93159
- UN-ZrN, Young's modulus antiferromagnetic anomaly 0-92583
- UNi<sub>3</sub>, mag. phase transition, elec. resist. meas. 0-97094
- U<sub>2</sub>Th<sub>1-x</sub>As<sub>x</sub>, mag. phase diagram, magnetisation meas. 0-60271
- (V<sub>1-x</sub>Cr<sub>x</sub>)<sub>2</sub>O<sub>3</sub>, Raman scatt. and phase transitions 0-71420
- (YGdYbBi)<sub>2</sub>(FeAl)<sub>2</sub>O<sub>12</sub>, epitaxial garnet film, uniaxial ferromagnet domain struct., phase transition (*Russian*) 0-108044

**magnetic traps**

- see also *magnetic bottles*
- ambipolar trap, ballooning effect in flute oscillations and plasma stability limits (*Russian*) 0-106955
- axially-symmetric ambipolar trap, flute oscills. stability limits (*Russian*) 0-103176
- closed poloidal heliotron, accelerated electron focusing (*Russian*) 0-106961
- cusp fields, plasma confinement time investigation using Monte Carlo simulation, collision effects 0-64770
- drift-mode stability analysis for the Tandem Mirror 0-64704
- EBT, toroidal MHD equilibrium 0-87871
- ELMO Bumpy Torus, microwave coupling 0-99328
- ELMO Bumpy Torus, ring power balance optimisation 0-99316
- ELMO Bumpy Torus Proof-of-Principle, proposed mag. system 0-99296
- EM confinement system, energy distributions of plasma electrons and ions 0-79542
- fusion reactor, neutral beam injector mag. cusp plasma source, design and fabrication 0-99377
- Jupiter-1 M, one slit EM open trap (*Russian*) 0-83970
- mirror machines, 2X11B neutral-beam-heated, extreme UV spectroscopy 0-74002
- moving plasmoid reactors using advanced fuel, modularisation 0-99312
- multipole confinement of laser plasma, radial and axial arrangement 0-83974
- neo-Z-pinch, mag. fusion appls. 0-103180
- nonlinear equilibrium state of wave-beam, kinetic theory (*Russian*) 0-106888
- plasma confinement in multislit EM trap, model description (*Russian*) 0-96382
- reverse loss-cone instability in ambipolar trap (*Russian*) 0-106893
- ripple trapping coefficient, poloidal variation 0-87923
- rippled trapped particles, depletion, in Alcator A Tokamak 0-87924
- spherical multipole magnetic trap, plasma containment 0-87937
- tandem mirror fusion reactors, axisymmetric sloshing-ion plugs 0-73998
- vacuum arc plasma flow in plasma-optical system (*Russian*) 0-106992

**magnetic variables control**

- high-coercivity, magnetisation characteristic linearity determ. using flux controlling technique (*Russian*) 0-100597

**magnetic variables measurement**

- see also *fluxmeters; magnetic field measurement; magnetic permeability measurement; magnetometers*
- circular dichroism in 200 to 850 nm region, construction of dichrograph 0-101806
- circular dichroism of matrix-isolated high-temp. molecules 0-86356
- coercimeter KIFM-1 with automatic measurement of the demagnetizing current 0-68229
- conference on precision EM meas., Braunschweig, Germany (Jun. 1980) 0-98903
- Curie temperature, determ. using magnetic pendulum (*Japanese*) 0-82797
- disaccommodation in ferromagnets, electronic device for automatic measurement (*Japanese*) 0-68227
- Faraday effect and susceptibility of garnet films, meas. using magneto-optical apparatus 0-105680
- film, vertically suspended, torque curve meas., first-order calc. anal. 0-86354
- flux density, electromagnetreference measure free from hysteresis effects for checking of meters 0-77817
- flux density using galvanometric 3-component mag. induction gauge 0-105682
- hard material demagnetisation curve evaluation 0-90869
- hysteresisgraph with discontinuous sweep mode 0-86351
- loss, form factor influence (*Rumanian*) 0-68226
- Permalloy, reference materials characs. obs., temperature effect 0-80563
- photomagnetic, SQUID magnetometer appl. 0-98950

**magnetic variables measurement continued**

- polycrystalline and amorphous strips, magnetostriction const. determ. method 0-86355
- power loss meas. under sinusoidal flux conditions 0-86348
- pulsed magnetic analyser, IMA-5 0-104399
- remance, weak, accurate meas. 0-68225
- ring specimens, computer controlled mag. meas. system 0-86346
- soft magnetic materials, meas. methods, review 0-86345
- SQUID biomedical appl., iron overloaded liver non-invasive diagnosis 0-101244
- SQUID system for low drift high sensitivity magnetisation meas. 0-86347
- steel, cold-rolled, isotropic, specific magnetic loss meas. at high frequency 0-101808
- steel, elect., mag. props. determ. with Epstein hysteresis tester 0-60364
- steel strips, electrotechnical, mag. props. meas. using AC compensated permeameter 0-86352
- susceptometer for biomedical meas., Fe stored in human tissue, in vivo 0-101245
- torque method, vertically suspended specimen, field intensity effect 0-86353
- very high field meas. of mag. materials 0-68224
- Si, on sapphire, Schottky magnetodiode, integrated mag. sensor 0-68223

**magnetic wells** see *magnetic traps***magnetisation**

- see also *Barkhausen effect; coercive force; demagnetisation; magnetic aftereffect; magnetic anisotropy; magnetic domains; magnetic hysteresis; magnetisation reversal; magnetostatic waves; remanence; spontaneous magnetisation*
- alloys, magnetisation calc. method based on moments of density of states 0-65770
- amorphous alloys, mag. props. rel to device appl. 0-88804
- amorphous ferromagnets, book contrib. 0-75743
- amorphous ferromagnets, hidden excitations, theory 0-75748
- analytical approx., accuracy investigation (*Bulgarian*) 0-71111
- anisotropic ferromagnet, one-dimensional Landau-Lifshits eqn. multi-soliton solutions (*Russian*) 0-71014
- anisotropy and ferromagnetic reson., linear electric field effects 0-65854
- antiferromagnet, crit. fluctuation of staggered magnetisation, AC susceptibility meas. 0-60219
- antiferromagnet, induced staggered magnetic fields, microscopic mech. 0-80527
- antiferromagnets, nonlinear waves 0-84612
- Bloch electrons, nonlinear orbital magnetisation in weak mag. fields (*Russian*) 0-70931
- caesium perfluorooctanoate/D<sub>2</sub>O system, <sup>2</sup>H NMR quantum orders, RF pulses 0-103892
- composite multifilamentary superconductor carrying DC transport currents, transient field losses 0-84551
- copper benzoate, low-dimensional Heisenberg antiferromag., high field magnetisation 0-80558
- copper formate tetrahydrate, antiferromag. phase, neutron diff. study 0-93085
- copper tetraamine sulphate, two-dimensional Heisenberg antiferromag., high field magnetisation 0-80558
- cross relaxation under action of 90° pulse trains, characs. 0-60402
- cubic spline functions representation of magnetisation curves (*German*) 0-71112
- current loops, thermodynamics, teaching 0-90633
- current transformer magnetisation curve, piece-wise linear, design method (*Russian*) 0-100598
- 1,8-dichlorooctane, quadrupolar relax. centres, limited spin diffusion 0-100649
- disordered Heisenberg spin model, magnetisation calc. 0-60167
- domain boundary parade motion, low freq. (*Russian*) 0-103852
- easy direction, meas. with aid of phase theory 0-65963
- easy plane amorphous wire, magnetisation, variational calc. 0-71098
- eddy-current flaw detection of long ferromag. products, magnetizing device parameters 0-89447
- electron and magnetisation densities in molecules and crystals, Arles, France (Aug. 1978) 0-105428
- exchange vortices of magnetisation, micromagnetic bubble domains 0-71138
- extended Hubbard model, ferromag. solns. 0-80473
- ferrite, regulation in expts. on self-acceleration of electron beam 0-63425
- ferrite spheres, magnetisation, resonance oscillation freq. determ. 0-71106
- ferrofluid, relax. in external mag. field, cubic cryst. case 0-71113
- ferromagnet, amorphous, Landau-Ginzburg theory, magnetisation and Curie temp. 0-75700
- ferromagnet, domain wall mobility, damping, dipole-dipole interaction 0-93140
- ferromagnet, domain wall motion, pinning by lattice defects, magnetisation 0-71079
- ferromagnet, Ising model, diamond lattice, phase transition, crit. props. 0-93127
- ferromagnet, itinerant, mag. props., temp. depend., functional integral approach 0-60170
- ferromagnet, nuclear magnetisation motion, hyperfine field microscopic inhomogeneity, NMR freq. shift (*Russian*) 0-80623
- ferromagnet, photoelectric effect rel. to saturation magnetisation 0-65618
- ferromagnet, tight binding model, surface magnetisation 0-103807
- ferromagnet magnetisation, influence of high intensity longitudinal sound waves 0-103875
- ferromagnetic Heisenberg chain, weakly bound magnon states (*Russian*) 0-100591
- ferromagnetic material NDT, magnetising device, stabilization of Barkhausen discontinuities 0-89457
- ferromagnetic metals, spin fluctuation theory, Curie temp., mag. susceptibility 0-65937
- ferromagnetic semiconductors, s-f interaction on conduction band, red shift effect theory 0-59872
- ferromagnetic superconductors, self-induced vortices, magnetisation, Gibbs free energy 0-70916
- ferromagnets, magnetisation stimulation by nonresonance AC mag. field (*Russian*) 0-65962
- ferromagnets, spin wave excitation due to parallel pumping, mag. impurity interactions (*Russian*) 0-80497
- film, ferromag., dynamics near transition pt. from homogeneous to inhomogeneous magnetis. state 0-108038



**magnetisation continued**

- film, mag. phase states when easy magnetisation axis is inclined rel. to film surface (*Russian*) 0-103864
- Heisenberg, ferromagnet, classical, with dipole-dipole interaction, renormalisation group and crit. exponents 0-60351
- Heisenberg amorphous ferromagnet, magnetisation and Curie temp., CPA calc. 0-75703
- Heisenberg ferromagnet, magnon renormalisation 0-65849
- Heisenberg ferromagnet, surface magnetisation profile and localised magnons 0-70985
- Heisenberg metamagnet, collinear, mag. phase diagram 0-71035
- hysteresis processes, characterisation by isomorphic transform method (*Russian*) 0-80562
- ionic compounds, amorphous, exhibiting Mossbauer spectra, magnetic props. (*French*) 0-80490
- Ising ferromagnet, gaussian fluctuations of mol. field, magnetisation and free energy 0-70918
- Ising model, one-dimensional transverse-field, in complex longitudinal field, real-space renormalization group method,  $T=0$  0-103806
- Ising model, two-dimensional semi-infinite, correlation functions, local magnetisation 0-71074
- Ising spins, disordered linear chain, relaxation, 1-D Glauber model, effect of disorder 0-65761
- isopermalloy, permeability stability calc. rel. to texture (*Chinese*) 0-65959
- isotropic ferromagnet, with two mutually orthogonal sinusoidal mag. intensities, planar cyclic remagnetisation (*Russian*) 0-80561
- magnetic domain wall motion, magneto-dipole EM wave radiation generation (*Russian*) 0-80555
- magnetic fluid as continuum with internal degrees of freedom 0-60377
- magnetisable and polarisable media with microstructure, models 0-88708
- magnetised structure evaluation via virtual magnetic charges 0-57341
- magnetographic inspection, determ. of magnetisation regimes 0-108665
- metal, indirect coupling between localised mag. moments by narrow band electrons 0-70942
- metal-insulator transition, density-functional theory 0-75507
- metallic ferromagnet, antiferromagnetic region, EM wave propag., Maxwells' eqns. soln. 0-66038
- metallic glass, splat cooled, mag. props. 0-80491
- metals, quantum magneto-dimensional effects, open Fermi surfaces, conduction electrons (*Russian*) 0-80487
- molybdenum chalcogenides, multicomponent, physical props. 0-84577
- nematic liquid crystals, orientation fluctuations in high mag. field, quenching, birefringence effects 0-64892
- NiWO<sub>4</sub>, antiferromag., low symmetry exhibited during spin-flop phase transition 0-60263
- one dimensional randomly dilute Ising ferromagnet, dynamics 0-70922
- one-dimensional Heisenberg magnet, in mag. field, dynamic correlations 0-70926
- paramagnetic crystal, magnetisation change by light pulse 0-70932
- Permalloy film, mag. microstruct. obs. in nonlinear ripple magnetis. case (*Russian*) 0-65971
- permeable specimen, magnetisation distribution, saturation approach 0-80566
- polarisation and magnetisation of electronic matter 0-75929
- polariser for magnetising liquid, in NMR devices 0-57351
- porous anisotropic magnets, approach to mag. saturation 0-93146
- proton synchrotrons, magnetisation of ferrites in tunable accelerating resonators 0-68983
- quinolinium (TCNQ)<sub>2</sub>, random exchange Neisenberg antiferromag. chain, intermediate field magnetisation meas. 0-103857
- random Glauber chain, relax. of magnetisation, numerical studies 0-60313
- rare earth alloy, amorphous, ferromag. state, non-axial elec. field gradient effect 0-75728
- rare earth garnets, RIG, (R=Tb, Dy, Ho, Er), spontaneous Faraday rot. rel. to sublattice magnetisation 0-66159
- rare earth iron garnets, anisotropic, mag. props., high field and low temp. 0-75801
- rare earth iron intermetallics, RFe<sub>2</sub>, (R=Sc, Lu, Y), mag. props., 80-1300K (*Russian*) 0-75750
- rare earth iron intermetallics, RFe<sub>2</sub>, magnetostrictive, book contrib. 0-75838
- rare earth-transition metal alloys, disordered, magnetisation behaviour 0-71099
- simple ferromagnets, crit. behaviour 0-60331
- single domain grain assembly, theory for magnetisation processes 0-88828
- spin-lattice relaxation time meas. using saturation, inversion and fast inversion expts. 0-57356
- spin-lattice relaxation times meas., mathematical formulation 0-62703
- spin-Peierls phase diagrams, obs. and models 0-60330
- SQUID system for low drift high sensitivity magnetisation meas. 0-86347
- steel, high speed tool, wear, effect of magnetisation on tool life 0-89361
- steel, martensitic, sp. ht. and magnetisation meas. 1.2 to 10K 0-71059
- superconducting cylinder, type II, magnetisation change induced by current near upper crit. field 0-70890
- superparamagnetic particles, magnetic moment time development and discrete orientation model 0-60378
- superpin in NMR, appl. to ABX system 0-60426
- surface magnetisation profile singularities near critical point 0-103843
- T bar, domain wall study employing ferrofluid, rel. to magneto-optical Kerr effect meas. 0-60360
- transition metal alloys, amorphous, mag. props., chem. short-range order 0-75739
- transition metal alloys, amorphous, mag. props., structure and preparation 0-75737
- transition metals, ferromag., dil. H electronic struct. 0-70638
- tridimensional numerical calc. of magnetic fields using summation method (*German*) 0-106414
- tube, magnetization with transverse field, approx. soln. 0-69321
- type I superconductor, magnetisation in thermodynamic and metastable phases 0-93027
- type II superconductor, bounded, intermediate state struct. form. near crit. field, role of surface 0-80465
- very high field meas. of mag. materials 0-68224
- weak ferromagnet, domain wall dynamics, nonlinear waves, mag. solitons (*Russian*) 0-75793
- weak ferromagnet, with easy plane anisotropy correl. functions and magnetisation, temp. depend. (*Russian*) 0-84581

**magnetisation continued**

- weak magnetic field, absolute intensity meas., use of RF biased SQUID 0-82794
- Ag, resonant and nonresonant conduction-electron-spin transmission 0-75857
- Au, resonant and nonresonant conduction-electron-spin transmission 0-75857
- Au-Co, liquidus line determ. by mag. meas. 0-60250
- Au-Fe (4.2 at.%), spin glass, DC magnetisation, field depend. 0-97103
- Au-Mn alloys, reversible and irreversible DC magnetisation in spin glass regime 0-65908
- Ba hexaferrite, irradiated by fast neutrons, mag. props. 0-97116
- BaO-Mn<sub>2</sub>O<sub>3</sub>-B<sub>2</sub>O<sub>3</sub>, amorphous mag. oxide, field-cooling effect (*Japanese*) 0-84615
- BaVS<sub>3</sub>, magnetisation and neutron study 0-84588
- Ba<sub>2</sub>WFe<sub>2</sub>O<sub>9</sub> and Ba<sub>2</sub>WFe<sub>2</sub>O<sub>8.42</sub>, crystallographic and mag. props., comparative study 0-103303
- Ba<sub>2</sub>Zn<sub>2-2(x+y)</sub>Cu<sub>2</sub>Cd<sub>2</sub>Fe<sub>12</sub>O<sub>22</sub>, mag. props. and Mossbauer spectrum 0-75765
- BaZn<sub>2</sub>Fe<sub>6-4x</sub>M<sub>2</sub>O<sub>27</sub> (M=Al, Ga, In, Sc), mag. props. and Mossbauer effect 0-75766
- Ca ferrite, composition and mag. props., anisotropy field, magnetisation 0-71109
- CdCr<sub>2</sub>Se<sub>4</sub>, study of photoinduced changes 0-80567
- Ce<sub>2</sub>Al<sub>11</sub>, competition between ferro- and antiferromag. interactions 0-60258
- Ce<sub>80</sub>Au<sub>20</sub>, metallic glass, mag. ordering and cryst. field effects, speromagnetism 0-80531
- CeBi, Sb<sub>1-x</sub>, mag. props. and press. effects 0-71026
- Ce<sub>2</sub>Co<sub>7</sub>, and ternary hydride, mag. props. 0-108007
- CeSb<sub>x</sub>As<sub>1-x</sub>, mag. props. and press. effects 0-71026
- CeTi<sub>3</sub>, mag. susceptibility, magnetisation, neutron diff., elec. resist., and sp. ht. meas. 0-75733
- (Ce<sub>2</sub>Y<sub>1-x</sub>)Fe<sub>2</sub>, mag. susceptibility and Mossbauer meas., lattice parameters 0-97068
- Co alloys, amorphous, effects of metalloids on mag. props. 0-75738
- Co fine particles in Cu, interface magnetisation 0-88858
- Co-Bi-(Cr) thin film glasses, mag. props. and corrosion resist. 0-80576
- Co-Mn, FCC, micromagnetism, magnetisation and mag. susceptibility meas. 0-60310
- Co-Mn alloys, ferromagnetic, high field mag. susceptibility meas. 0-75729
- Co-Mn-Ni-Fe-Si-B amorphous alloys, mag. props., low magnetostriction 0-75832
- CoBr<sub>2</sub>·6(0.48D<sub>2</sub>O, 0.52H<sub>2</sub>O) spin-flop system, intermediate phase existence, sublattice magnetisation reorientation 0-80510
- CoBr<sub>2</sub>·6[(1-x)H<sub>2</sub>O.xD<sub>2</sub>O], mag. intermediate phase, magnetisation and neutron scatt. meas. 0-60195
- CoCl<sub>2</sub>·2H<sub>2</sub>O, Ising antiferromag., high field transverse magnetisation meas. 0-93143
- Co<sub>0.54</sub>Ga<sub>0.46</sub>, frequency depend. magnetisation, superparamagnetic behaviour 0-84624
- Co<sub>2</sub>Ga<sub>1-x</sub>, NMR expts. interpretation 0-75870
- Co(GaTiV) alloys, ferromag. onset, electron conc. depend. 0-60203
- CoMn(Cr)(V)(Ti), dil., low temp. specific heat and magnetisation 0-65925
- Co<sub>30</sub>Mn<sub>70</sub>Ga<sub>50-x</sub>, ordering and disordering phenomena, mag. study 0-70154
- Co<sub>2</sub>(Ni<sub>0.5</sub>Cu<sub>0.5</sub>)<sub>1-x</sub>Fe<sub>2</sub>O<sub>4</sub> ferrite, relation between elec. cond. and mag. anisotropy 0-75548
- Co<sub>2</sub>Pd<sub>80-x</sub>Si<sub>20</sub>, amorphous, structural and mag. heterogeneities 0-80484
- CoTiO<sub>3</sub>, antiferromag., mag. anisotropy, magnetisation meas. 0-65856
- Co<sub>2</sub>Z ferroxplana form. process peculiarities 0-89368
- Co<sub>2</sub>Zn<sub>1-x</sub>Rh<sub>x</sub>O<sub>4</sub>, mag. props., EPR spectra, antiferromag. order 0-75736
- Cr, hyperfine interactions on <sup>111</sup>Cd-probe nuclei, TDPAC meas. 0-75904
- Cr-Fe, dil., magnetisation, Fe local moments 0-60215
- Cr<sub>1-x</sub>Se<sub>x</sub>, struct., elec. and mag. props. 0-107160
- CsMn<sub>1-x</sub>Co<sub>x</sub>Cl<sub>2</sub>H<sub>2</sub>O, random mag. mixture, oblique-antiferromag. phase obs. 0-93142
- CsNiF<sub>3</sub>, quasi-one-dimensional ferromagnet, subthreshold parallel pumping of magnons 0-75745
- Cu, resonant and nonresonant conduction-electron-spin transmission 0-75857
- Cu/Ni coherent modulated structures, electronic struct. and magnetism 0-103620
- Cu-Cr, dil., spin-density magnetisation near Cr atoms, NMR study 0-80626
- Cu-Mn, mag. viscosity below freezing temp. 0-65910
- Cu(Rh<sub>1-x</sub>Cr<sub>x</sub>)S<sub>2</sub>, spinel system, susceptibility and metallic resistivity, anomalies due to s-d interaction 0-70958
- DyAsO<sub>4</sub>, phase transitions obs. 0-70412
- DyBi, mag. behaviour 0-71025
- DyCo<sub>2</sub>DyAl<sub>2</sub> system, mag. and structural studies 0-108006
- DyCo<sub>3</sub>, noncollinear mag. struct. appearance in mag. fields, magnetostriction meas. (*Russian*) 0-100607
- Dy<sub>2</sub>Ga<sub>2</sub>O<sub>12</sub>, dipolar magnet, sp. ht. and magnetisation meas. 0-60344
- Dy<sub>2</sub>O<sub>3</sub>SO<sub>4</sub>, mag. ordering, magnetisation, AC susceptibility and Zeeman effect meas. 0-60205
- DyVO<sub>4</sub>, phase transitions obs. 0-70412
- Er, magnetisation, quantum jump 0-60369
- ErFe<sub>2</sub>-YFe<sub>2</sub>, and ErFe<sub>2</sub>-LuFe<sub>2</sub>, mag. props., 80-1300K (*Russian*) 0-75750
- ErRh<sub>2</sub>B<sub>4</sub>, superconducting thin films, critical mag. field 0-75693
- Er<sub>2</sub>Y<sub>1-x</sub>Rh<sub>x</sub>B<sub>4</sub>, mag. and supercond. transitions 0-70874
- EuB<sub>6</sub>, electronic struct., transport and mag. props. 0-96782
- EuEr<sub>2</sub>Ga<sub>2</sub>Fe<sub>4</sub>O<sub>12</sub>, garnet thin films, magnetisation orientation, temp. depend. 0-71125
- Eu<sub>1-x</sub>Gd<sub>x</sub>O, mag. props., transport meas. 0-97117
- EuO-Gd, elec. cond. under hydrostatic press., Curie temp. 0-96881
- EuO-Gd, pure and doped, elec., mag., and optical props. rel. to electronic conc. 0-96880
- EuO-Gd, surface mag. props. 0-71566
- Eu<sub>2</sub>Sn<sub>2</sub>S<sub>2</sub>, mag. and thermodynamic props., metamagnetism 0-60273
- (Eu<sub>2</sub>Sr<sub>1-x</sub>)S<sub>2</sub>, very dil., magnetisation dynamics 0-65915
- Fe alloys, amorphous, effects of metalloids on mag. props. 0-75738
- Fe alloys, amorphous, mag. saturation, spin wave stiffness, temp. depend. 0-75741
- Fe alloys, amorphous, saturation magnetisation, Curie temp. and size effect 0-65815
- Fe and Fe-Ni Metglas alloys, ohmic and Hall resist. 100-700K, mag. behaviour 0-80254



## magnetisation continued

- Fe complex,  $\text{Fe}(1,2,4\text{-triazole})_2(\text{NCS})_2$ , quasi-2-dimens.  $S=1/2$  antiferromag., mag. props., hidden canting 0-107986  
 Fe, ferromag. film, surface states, surface magnetisation and electron spin polarisation 0-65648  
 Fe garnets, sublattice magnetisation curves, Mossbauer study 0-75808  
 Fe,  $\text{H}_2$  embrittlement and  $\text{H}_2$  adsorption 0-89401  
 Fe particles, dispersed in Hg, mag. props., aggregate form. 0-60375  
 Fe whisker, magnetisation curve meas. using SQUID system 0-86347  
 Fe whiskers, inverse Wiedemann effect, torsional strain and azimuthal mag. field influence 0-108045  
 $\text{Fe-Al}_2\text{O}_3$  granular films, superparamagnetism and relax. effects 0-71118  
 Fe-B amorphous alloy, annealed, microstruct. and mag. domain changes 0-75790  
 Fe-B metallic glasses, struct., stability and crystn. 0-75173  
 Fe-B-C, amorphous, effects of replacement of B by C on mag. props. 0-84621  
 Fe-B-C amorphous alloy, formation, mag. props., thermal stability and density 0-75796  
 Fe-B-Cr(Si) thin film glasses, mag. props. and corrosion resist. 0-80576  
 Fe-B-Si-C amorphous alloys, prep. and props. 0-88748  
 Fe-Co-V(Ni), annealing effect on microstruct. rel. to mag. and mech. props. 0-89267  
 Fe-Cr-Co alloy, coercive force mechanism 0-71103  
 Fe-Ni alloy type YrNCK25B, anomalous magnetocaloric effect 0-60278  
 Fe-Ni Invar alloys, splat quenched, mag. props. 0-75799  
 Fe-Ni Invar anomalies, explanation in terms of itinerant electron magnetism 0-75705  
 Fe-Ni-Co-Cu-Ti YrNCKT alloys, impaired mag. props. with C and S additions 0-60368  
 Fe-Ni(35.4 at.%) Invar alloys,  $T^2$  term contribution to magnetisation 0-71096  
 Fe-Si, grain oriented, misorientation effects on mag. props. 0-88792  
 Fe-Si, non-oriented sheets, production and props. 0-88797  
 Fe-Si (3 wt.%), grain-oriented, domain wall profiles throughout magnetisation cycle 0-88781  
 Fe-Si (3 wt.%), nonoriented sheets, magnetisation, tensile stress effects 0-88845  
 Fe-Si (3 wt.%), stripe domain structure, dynamic behaviour at high max. induction values (Russian) 0-80553  
 Fe-Si (3 wt.%) laminations, magnetostriction behaviour associated with closure domain spikes 0-75834  
 Fe-Si (3.25 wt.%) alloy, single cryst. with (007) planes, domain struct. influence on mag. torque 0-108034  
 Fe-SiO multilayer films, interface magnetisation 0-88858  
 $\text{Fe}_3\text{B}_{10}$  glass, magnetisation reorientation, Mossbauer effect 0-66092  
 $\text{Fe}_{34}\text{B}_{16}$  amorphous, mag. props. and microstruct., cooling rate and melt overheating effects 0-65965  
 $\text{FeCl}_3$ , logarithmic corrections to tricritical scaling 0-65940  
 $\text{FeCl}_3$ , metamagnet, scaling props. of magnetisation and heat capacity, test of tricritical scaling 0-60336  
 $\text{FeF}_3$ , amorphous, mag. props. and Mossbauer spectra, speromagnetism and micromagnetism 0-75778  
 $\text{Fe}_{80-x}\text{Ni}_x\text{B}_{20}$  and  $\text{Fe}_{80-x}\text{Ni}_x\text{P}_{14}\text{B}_6$  amorphous alloys, microhardness correl. with mag. props. 0-88826  
 $\text{Fe}_{1-x}\text{Ni}_x\text{B}_{10}\text{P}_{10}$  metallic glass, superparamag. behaviour, chem. inhomogeneities role 0-84625  
 $\text{Fe}_3\text{Ni}_3\text{Mn}_3$ , disordered, mag. struct. near ferro-antiferromagnetic transition 0-60211  
 $\text{Fe}_2\text{Ni}_3\text{Mo}_2\text{B}_{18}$ , amorphous, mag. anisotropy, Mossbauer study 0-65864  
 $(\text{Fe}_{1-x}\text{Ni}_x)_2\text{P}_{20}$  amorphous, ferromagnetic alloys, mag. anomalies of Invar type (Russian) 0-93089  
 $\text{Fe}_2\text{Ni}_3\text{P}_{14}\text{B}_6$  amorphous, mag. polarisation in approach to ferromag. saturation 0-80560  
 $(\text{Fe}_{1-x}\text{Ni}_x)_2\text{Si}_{10}\text{B}_{10}$  amorphous, Landau-Ginzburg theory, magnetisation and Curie temp. 0-75700  
 $(\text{Fe}_{0.5}\text{Ni}_{0.5})_x(\text{SiO})_{1-x}$ , Permalloy material, magnetisation, temp. and impurity atom conc. depend., band model calcs. (Russian) 0-93088  
 $\alpha\text{-Fe}_2\text{O}_3$ , Mossbauer spectra near Neel temp., critical indices, magnetisation (Russian) 0-66094  
 $\text{Fe}_2\text{O}_3\text{-BaO-B}_2\text{O}_3$ , magnetic props. of Fe-rich amorphous oxide (French) 0-80511  
 $\text{Fe}_x\text{P}_{13}\text{B}_8$  amorphous alloys, splat cooled, Mn, Cr and V substituted, mag. and transport props. 0-84593  
 $\text{Fe}_{60-x}\text{Si}_{20}$  amorphous, structural and mag. heterogeneities 0-80484  
 $\text{Fe}_{60-x}\text{Si}_{20}$  metallic glass, long range interaction and spin wave interactions 0-65949  
 $\text{Fe}_x\text{Sb}_{1-x}$ , nonstoichiometry influence on mag. props. (Russian) 0-65813  
 $(\text{Fe}_{1-x}\text{Si}_x)_{1-y}\text{By}$ , metallic glass, mag. props., crystallisation 0-65885  
 $\text{Fe}_2\text{TiO}_5$ , spin glass system, cation distrib. Mossbauer spectra 0-71248  
 (Gd, Bi) $_2(\text{Fe, Ga})_2\text{O}_{12}$  magneto-optic LPE garnet films, high-energy heavy ion irradiat., props. 0-71390  
 Gd, meas. of easy direction of magnetisation with aid of phase theory 0-65963  
 Gd-Co(Eu)(Yb), magnetocrystalline anisotropy, magnetisation and torque curve meas. 0-65859  
 $\text{Gd}_{1-x}\text{Ca}_x\text{Al}_2$ , mag. props. and phase relations 0-107991  
 $(\text{Gd}_{1-x}\text{Co}_x)_{1-y}\text{Ar}_y$  amorphous mag. film, elec. and mag. prop. depend. on Ar 0-80410  
 GdIG, local mag. anisotropy in stress field of single dislocation 0-88744  
 GdMn-GdAl $_3$  system, mag. and structural studies 0-108006  
 GdN, and  $\text{GdN}_{1-x}\text{O}_x$ , mag. interactions 0-60218  
 GdN, mag. interaction and carrier conc. 0-71005  
 $\text{GdN}_{1-x}\text{O}_x$ , magnetic interaction and carrier conc. 0-71005  
 Gd,Nd $_x$ Zn, ferromag., mag. susceptibility and magnetisation, temp. depend. 0-70975  
 GdRh-H $_2$ , GdRu-H $_2$ , struct. and mag. props., Mossbauer and magnetisation meas. 0-71271  
 Gd $_3$ -S $_2$ , ferromag., elec. props. near Curie temp. 0-107788  
 GdTb, ferromag., magnetisation and microwave absorpt. 0-65816  
 Gd $_2\text{O}_3$ , magnetisation, AC susceptibility and microwave absorption meas. 0-60221  
 (Gd,Y $_x$ ) $_2\text{Al}_3$ , ferromag. and spin glass like behaviour, magnetisation meas. 0-75734  
 Gd,Y $_x$ Zn, ferromag., mag. susceptibility and magnetisation, temp. depend. 0-70975  
 Gd $_2$ □S $_2$ , transport and mag. props., mag. Wigner localisation 0-97069  
 H, spin-polarised, mag. eqn. of state 0-100374  
 He, FCC, vacancy induced spin polarons 0-59756  
 He, liq., polarisation effect on mag. ordering, melting curve 0-80021

## magnetisation continued

- He, solid, mag. phase diagram from static magnetisation meas. 0-84342  
 He, superflow, gap functions, critical currents, susceptibilities 0-103531  
 He, superfluid, nonlinear motion of magnetisation, parallel ringing 0-107597  
 He, superfluid, p-wave spin triplet pairing Hamiltonian, 5-D spin 0-75400  
 He superfluid A-phase, exptl. studies of solitons 0-88386  
 He, superfluid A-phase, longitudinal mag. relax. 0-59751  
 He-Z near A phase transition, collective oscill. hybridisation (Russian) 0-80020  
 Hg $_2$ -Zn,Cr-Se $_2$ , magnetic struct., neutrographic and mag. investigation (Russian) 0-88726  
 HoAu $_3$ , mag. phase diagram 0-75761  
 HoCo $_5$ -Mn $_2$ (Fe $_2$ )(Cu $_2$ ), cryst. struct. and mag. props. 0-75800  
 Ho-O-SO $_4$ , mag. ordering, magnetisation, AC susceptibility and Zeeman effect meas. 0-60205  
 HoRh $_2$ B $_4$ , low temperature magnetic properties 0-88728  
 HoSb, mag. phase diagram, quadrupolar interactions 0-65820  
 $(\text{Ho}_{0.98}\text{Tb}_{0.02}\text{Dy}_{0.02})\text{Fe}_2$ , microwave mag. props. 0-65860  
 Ho,Y $_x$ Sb system, magnetisation, elec. resist., and sp. ht. meas. 0-60213  
 In-Pb (7 at.%) alloy cylinder, magnetisation change induced by current near upper crit. field 0-70890  
 K-FeCl $_2$ (H $_2$ O), antiferromag., press. depend. on spin-flop transition 0-80505  
 KFeF $_4$ , amorphous, mag. props. and Mossbauer spectra, speromagnetism and micromagnetism 0-75778  
 K $_2$ FeF $_4$ , two dimensional easy plane antiferromag., neutron scatt. expts. 0-65838  
 K $_2$ MnF $_4$ :Zn(Mg)(Ni), mag. effects of impurities 0-65869  
 K $_2$ MnF $_4$ :Zn(Mg)(Ni), local magnetisation, NMR and Green's function study 0-65870  
 KNiF $_3$ ,  $^{19}\text{F}$  spin-lattice relaxation 0-93211  
 La ferrite, composition and mag. props., anisotropy field, magnetisation 0-71109  
 LaNi $_2$ , H $_2$  absorption in thin film hydriding alloys 0-65238  
 LaNi $_2$ , Fe $_2$ O $_3$ , magnetisation meas. and  $^{57}\text{Fe}$  Mossbauer studies 0-93217  
 La $_3$ -Tb $_2$ Al $_3$ , competing paramag. anisotropy from cryst. field and indirect quadrupolar coupling 0-60180  
 Li ferrites, porous, porosity effect on saturation of magnetisation 0-108036  
 Li $_2$ B $_2$ O $_7$ -LiFe $_2$ O $_4$ , borate glass, mag. props. of Fe $^{3+}$  cations 0-100599  
 Li $_2$ Fe $_2$ -Cr $_2$ O $_7$ , press. depend. of anisotropy consts. 0-65865  
 Li $_2$ Fe $_2$ O $_7$ , Ru substitution effect on struct. and mag. props., and max. solubility determ. 0-75364  
 LuFe $_2$ , ferromag., magnetisation density, neutron diff. study 0-60217  
 Mg,Fe $_2$ -O $_2$ , polycryst., Verwey type transition, resist., magnetisation, Mossbauer effect and permeability obs. 0-75764  
 $\gamma$ -Mn, antiferromagnetic, self-consistent bandstructure calcs. 0-88475  
 Mn-H $_2$ , hydride formation in high press. range 0-65235  
 MnAs $_2$ -P $_2$ , double exchange ferromag. coupling, magnetisation meas. 0-75751  
 MnB $_2$ , polycryst., magnetoresist. and mag. props. (Russian) 0-92907  
 Mn $_2$ -Cr $_2$ As $_2$ , double exchange ferromag. coupling, magnetisation meas. 0-75751  
 MnCr $_2$ S $_4$ , substituted, mag. struct. and transitions 0-65795  
 NaFeF $_4$ , amorphous, mag. props. and Mossbauer spectra, speromagnetism and micromagnetism 0-75778  
 Nb-Ti (50%), supercond., cryostat design for magnetisation study (Spanish) 0-75673  
 Nd $_2$ Ag $_2$  and Nd $_2$ Ag $_3$ , amorphous, mag. props. 0-60182  
 Ni(110), polarised LEED study of magnetism 0-71102  
 Ni, anisotropic magnetisation meas., 4-250K 0-65862  
 Ni, ferromag. film, surface states, surface magnetisation and electron spin polarisation 0-65648  
 Ni film, evaporated, for use as variable delay SAW device, magnetostrictive effects 0-71144  
 Ni-B thin film glasses, mag. props. and corrosion resist. 0-80576  
 Ni-Co (25 wt.%), single crystals, mag. annealing effect on magnetostriction and magnetisation at high temps. 0-108047  
 Ni-Cu-H systems, Curie temp. during phase transitions under high press. H $_2$  0-71029  
 Ni-Mn alloys, ferromagnetism-to-spin glass phase transition and strong mag. field effect 0-75773  
 Ni-Mn-H solid solutions, mag. props. 0-88753  
 Ni-Pd-Mn ternary alloys, mag. characts., use for thermosced 0-107995  
 Ni-Ru ( $\leq 4$  at.%), influence of alloying on mag. anisotropy 0-71010  
 Ni-SiO multilayer films, interface magnetisation 0-88858  
 Ni $_2$ Co $_2$ Cl $_2$ 6H $_2$ O, mixed uniaxial planar antiferromag., magnetisation process 0-88788  
 NiFe $_2$ O $_4$  ferrite, mag. props., neutron irradiat. 0-103858  
 Ni $_2$ Fe $_2$ O $_4$  spinels, fine particles, magnetic properties obs. 0-71031  
 Nil, anhydrous, magnetic phase transition, neutron diff. study 0-71033  
 NiMnGe $_2$ -Si $_2$ , mag. props., neutron diff. and magnetometric meas., 80-600K 0-65793  
 NiS $_2$ , weak ferro- and antiferromag., magnetisation and neutron diff. meas. 0-65794  
 NiTiO $_3$ , antiferromag., mag. anisotropy, magnetisation meas. 0-65856  
 NiZn ferrite, ZnO $_2$  additions influence on sintering and physicochem. props. 0-108369  
 NiZnCo ferrites, voltage response under sinusoidal and pulse magnetisation effected by hydrostatic press. 0-88846  
 Ni(001) surface states, surface magnetisation, electron spin polarisation 0-88612  
 Ni(110), ferromag., surface magnetisation, polarised LEED expt. 0-97118  
 Pb superconducting slabs, magnetisation and migration field, reversible stage 0-65737  
 Pd-Fe, magnetic anisotropy near Curie point, quasi domain struct. (Russian) 0-65867  
 Pd-Fe-Mn, ferromagnet-spin glass, thermal expansion forced, magnetostriction and magnetisation under high press. 0-65255  
 Pd-Mn, ferromagnetism to spin glass behaviour transition 0-71062  
 Pd,MnIn $_2$ -Sn, and Pd,MnIn $_2$ -Sb, Heusler alloys, mag. order, disorder effects 0-88723  
 Pd $_2$ -MnSb Heusler alloys, magnetic hyperfine fields on  $^{111}\text{Cd}$ , TDPAC and magnetisation meas. 0-93219  
 Pr $_2$ Ag $_2$ , Pr $_{50}\text{Ag}_{50}$ , and Pr $_{10}\text{Lu}_{90}\text{Ag}_{90}$ , amorphous, mag. props. 0-60182  
 Pr $_2$ -CaAl $_2$ , mag. props. and phase relations 0-107991  
 Pr $_2$ -Ca,MnO $_3$ , struct. and magnetisation study 0-65804



**magnetisation continued**

- PrCo<sub>5-23</sub>, high field first order transitions, role of K<sub>3</sub> anisotropy const. 0-65879  
 PrIr<sub>2</sub>(Pt<sub>1</sub>)(Rh<sub>2</sub>)(Ru<sub>2</sub>), hyperfine sp. ht. and magnetisation meas. at 4.2K 0-75775  
 Pr<sub>2</sub>Se<sub>3</sub>(S<sub>4</sub>), induced ferromagnet, mag. props. under hydrostatic press. 0-60395  
 Pt-Fe alloy, ordered, T-c phase diagram, antiferro- and ferromagnetism (Russian) 0-65871  
 Pt-Fe ordered alloy, multiply mag. phase transitions 0-60264  
 Pt<sub>2</sub>Cr, ferrimag., magnetisation density, polarised neutron diffr. meas. 0-60204  
 R<sub>2</sub>In, R=Gd, Tb, Dy, Ho, Nd, mag. props. 0-108009  
 RbMnCl<sub>3</sub>, twinning struct., cryst. domains, orientation mag. transition (Russian) 0-107275  
 (SN)<sub>2</sub>, supercond. polymer, mag. props. meas. 0-107953  
 (SNBr<sub>0.4</sub>)<sub>2</sub>, supercond. polymer, mag. props. meas. 0-107953  
 Sc-Gd, spin glasses, low temp. sp. ht. and magnetisation 0-65913  
 Sm-Co, amorphous, plasma-sprayed, role of Ar or H<sub>2</sub> atm. in mag. props. and crystn., rel. to H<sub>2</sub> storage 0-64898  
 SmCo<sub>5</sub>, H<sub>2</sub> absorption in thin film hydriding alloys 0-65238  
 SmCo<sub>5</sub>, sintered, hard mag. material, magnetisation behaviour 0-75805  
 Sr<sub>2</sub>(Co<sub>1-x</sub>M<sub>x</sub>)<sub>17</sub>, M=Mn, Ti, Zr, powders, influence of substitutes on mag. props. 0-100601  
 SrFe<sub>2</sub>Al<sub>2</sub>O<sub>9</sub>, thin film LE growth and mag. props. 0-80992  
 Tb, magnetisation, AC susceptibility and microwave absorption meas. 0-60221  
 Tb, magnetisation in basal plane, calc. 0-70969  
 Tb, magnetisation intensity in antiferromag. state and mag. field induced phase transforms. (Russian) 0-65811  
 TbAu<sub>3</sub>, mag. phase diagram 0-75761  
 TbCo<sub>3</sub>, sublattice magnetisation, temp. depend., neutron diffr. anal. (Russian) 0-103815  
 TbFeO<sub>3</sub>, mag. susceptibility, temp. depend., effective field at Tb ion sites 0-75742  
 (Tb<sub>1-x</sub>La<sub>x</sub>)Be<sub>13</sub>, mag. struct., cryst. field effects, neutron diffr. study 0-65789  
 Th<sub>2</sub>Co<sub>3</sub>, effect of absorbed H<sub>2</sub> on mag. behaviour 0-60184  
 Th<sub>2</sub>Ni<sub>3</sub>, effect of absorbed H<sub>2</sub> on mag. behaviour 0-60184  
 TiBe<sub>18</sub>Cu<sub>20</sub>, ferromag., magnetisation density 0-103817  
 Ti(Fe,Co)H<sub>2</sub>, mag. and <sup>57</sup>Fe Mossbauer studies 0-71272  
 (Ti<sub>1-x</sub>V<sub>x</sub>)<sub>2</sub>O<sub>7</sub>, 0<x<0.1, magnetisation and mag. moments 0-65772  
 TmSe, mag. props. 0-97086  
 U<sub>2</sub>As<sub>2</sub>, ferromag., mag. field induced phase transitions 0-65887  
 UTe, crit. exponents, neutron and magnetisation meas. 0-88823  
 U<sub>2</sub>Th<sub>1-x</sub>As<sub>2</sub>, mag. phase diagram, magnetisation meas. 0-60271  
 VO<sub>2</sub>, metal-insulator transition, external mag. field effects 0-92819  
 VSe<sub>2-x</sub>S<sub>x</sub> (0<x<0.2) solid solutions, characterisation 0-88730  
 W, resonant and nonresonant conduction-electron-spin transmission 0-75857  
 Y garnet, inhomogeneous collective magnon oscill. excited by RF field (Russian) 0-100582  
 Y-Gd, spin glasses, low temp. sp. ht. and magnetisation 0-65913  
 YFe<sub>2-x</sub>Al<sub>x</sub>O<sub>12</sub>, impurity redistrib. kinetics, temp. depend., vacancy effects 0-75263  
 Y<sub>3</sub>Fe<sub>5-x</sub>Al<sub>x</sub>O<sub>12</sub>, mixed garnet, cation distrib., temp. depend., magnetisation study 0-79831  
 YFe<sub>2-x</sub>Ga<sub>x</sub>O<sub>12</sub>, impurity redistrib. kinetics, temp. depend., vacancy effects 0-75263  
 Y<sub>3</sub>Fe<sub>5-x</sub>Ga<sub>x</sub>O<sub>12</sub>, mag. domains and cryst. defects 0-75789  
 Y<sub>3</sub>Fe<sub>5-x</sub>Ga<sub>x</sub>O<sub>12</sub>, mixed garnet, cation distrib., temp. depend., magnetisation study 0-79831  
 Y<sub>2-x</sub>Gd<sub>x</sub>O<sub>12</sub>, garnet thin films, magnetisation orientation, temp. depend. 0-71125  
 YIG, magnetic domain wall motion in high drive fields 0-65955  
 YIG, open die hot pressing, spin wave and FMR line width 0-89170  
 YIG, thermomag. anal. by electron diffr. 0-108035  
 YIG: Si single crystals, mag. props. 0-107981  
 YIG:La,Ga, film, LPE-grown, Ga incorporation, depend. of magnetisation on growth rate 0-84627  
 Y<sub>2.85</sub>La<sub>0.15</sub>Fe<sub>3.85</sub>Ga<sub>1.15</sub>O<sub>12</sub>, garnet, mag. props., ion implantation effect, Mossbauer study 0-97166  
 YNi<sub>3</sub>, magnetism resurgence, neutron diffr. and mag. props. study 0-65819  
 Y<sub>1-x</sub>R<sub>x</sub>Co<sub>5</sub>, R=Gd,Tb,Nd, ferrimag., magnetisation, exchange interactions, mag. anisotropy 0-80565  
 Y<sub>1-x</sub>Tb<sub>x</sub>Al<sub>0.65</sub>Fe<sub>4.35</sub>O<sub>12</sub>, garnet thin films, magnetisation orientation, temp. depend. 0-71125  
 Y<sub>1-x</sub>Tb<sub>x</sub>Pd<sub>3</sub>, magnetisation, magnetostriction, and inelastic neutron spectra 0-65998  
 YbCuAl, mixed-valent cpd., thermal expansion and magneto-volume effects 0-66005  
 YbGaG, mag. props. between 44-600 mK 0-80517  
 Yb<sub>2</sub>Ga<sub>2</sub>O<sub>7</sub>, dipolar magnet, sp. ht. and magnetisation meas. 0-60344  
 Zn<sub>2</sub>Fe<sub>3-x</sub>O<sub>4</sub>, ferrite, mag. struct., Mossbauer spectra and magnetisation study, 4.2K 0-103818  
 Zr-3d Laves phase binary and pseudobinary intermetallics, mag. props. H absorpt. effect 0-88821

**magnetisation reversal**

- Alnico type YuNDK25DA alloy permanent magnets, thermal mag. hysteresis 0-75818  
 amorphous ribbons, twisted, magnetisation process, domain theory 0-71101  
 BaFe<sub>2</sub>O<sub>19</sub>, microparticles, magnetisation reversal, hysteresis loop obs. 0-75813  
 BaFe<sub>2</sub>O<sub>19</sub>, powder, hysteresis of microwave absorpt. and magnetisation reversal 0-75814  
 Fe-Ci (3 wt.%), local magnetisation losses, grain orientation effect 0-88817  
 Fe-Cr-Co, magnetic domain walls, Lorentz microscopy 0-103854  
 Fe-Ni-Mn, Invar, RF collapse and thermal effects, Mossbauer study 0-100624  
 Fe<sub>2</sub>Co<sub>2</sub>B<sub>20</sub>, amorphous, magnetisation reversal and domain boundary configs. 0-88809  
 Fe<sub>80</sub>Ni<sub>20</sub>P<sub>10</sub>B<sub>10</sub>, Metglas 2826, amorphous ribbon under tension, mag. domain walls and pulsed magnetisation reversal 0-88825  
 (Fe,Ni<sub>1-x</sub>)<sub>80</sub>P<sub>10</sub>B<sub>10</sub>, amorphous, magnetisation reversal and domain boundary configs. 0-88809  
 FeSi picture frame single cryst., domain wall motion and magnetisation reversal, time-depend. neutron depolarisation study 0-88782

**magnetisation reversal continued**

- MnBi, domain boundary inertia during mag. reversals (Russian) 0-88776  
 SmCo<sub>5</sub>, sintered, hard mag. material, magnetisation behaviour 0-75805  
 YFeO<sub>3</sub>, domain boundary inertia during mag. reversals (Russian) 0-88776

**magnetism**

- see also *antiferromagnetism; antiferromagnetism; band model of magnetism; diamagnetism; electromagnetism; ferrimagnetism; ferromagnetism; geomagnetism; Heisenberg model; Ising model; magnetic moments; magnetic monopoles; metamagnetism; paramagnetism; rock magnetism; stellar magnetism; superparamagnetism; weak ferromagnetism; X-Y model*  
 conference, Munich, Germany (Sep. 1979) 0-56997  
 magnetic multipoles in time dependent fields 0-99597

**magneto-optical devices**

- electric current measurement, AC, using magneto-optical methods, principles and advantages (Polish) 0-105676  
 Faraday effect in lightguide, weak microwave field meas. 0-73463  
 Faraday rotator using low Verdet constant material 0-69520  
 Faraday rotators in fibre Raman lasers 0-58775  
 holographic platform, optical path stabilisation with magneto-optic periodic grating 0-99678  
 metal cryostat, optical meas. at 0.4K 0-73369  
 CdTe AC Faraday rotation devices for far IR laser intracavity polarisation modulation 0-58613  
 (Co,Cr,Fe)<sub>2</sub>O<sub>4</sub>, (Co,Rh,Fe)<sub>2</sub>O<sub>4</sub> film magneto-optical switches, for laser beam synchronisation 0-58615

**magneto-optical effects**

- see also *Faraday effect; Kerr magneto-optical effect; magnetic circular dichroism; magnetoabsorption; magnetorefractance; optical constants; Zeeman effect*  
 antiferromagnet, IR absorption on impurity excitations near upper edge of spin-wave band 0-80829  
 atomic spectra in intense mag. fields, theory and appl. to dense stars atmospheres 0-105160  
 Brillouin-Mandelstam scattering from thermal and excited magnons 0-70980  
 canted magnetic structured materials, exciton spectra, optical props. 0-70622  
 Cotton-Mouton effect in Jupiter ionosphere and magnetosphere, rel. to decametre radio emission modulation 0-67643  
 disordered system in mag. field, frequency dependence of conductivity tensor, theoretical investigation 0-70725  
 domain boundary parade motion, low freq. (Russian) 0-103852  
 domain lattice of transparent crystal regular birefr. regions, optical wave diffr. divergence 0-102616  
 EM waves polarisation, in magnetically ordered crystals 0-108189  
 ethylammoniumtetrachlorochromate, optical absorption intensity, short-range spin correlation 0-108185  
 ferromagnet, linear mag. birefr. (Russian) 0-93284  
 ferromagnet, surface, Brillouin light scatt. by spin waves 0-93359  
 ferromagnetic slab, light scattering from bulk and surface spin waves, theory 0-71389  
 ferromagnetic surface, spin fluctuations and light scatt. 0-84727  
 ferromagnetic thin films, Brillouin scattering from spin waves 0-65843  
 fluorophate glasses, containing rare earth ions, magneto-opt. characts. 0-64126  
 gapless semiconductor, magnetic field resonance states (Polish) 0-88508  
 garnets, IR refl., ATR, Voigt and Faraday expts. 0-66180  
 gas, inhomogeneous layer, transmission calc. for spectral line with Voigt profile 0-59164  
 gas, photon echo in a magnetic field at small areas of the exciting pulses 0-95961  
 gas laser, linearly polarized waves, interaction with longitudinal mag. field 0-95936  
 gas lasers, mode interactions in longit. mag. field, active medium dispersion effects 0-63967  
 gases, spectral line form. depth in mag. field (Chinese) 0-105159  
 graphite, suspensions, particle shape influence on light absorpt. in mag. field 0-60549  
 light diffraction by domain gratings, and appl. 0-88970  
 light diffraction in thick layers with regular domain structure 0-108188  
 longitudinal static spin wave struct., magnetotropic interaction of light (Russian) 0-93285  
 low-temperature investigations using flowthrough opt. cryostat with superconducting solenoid 0-105651  
 magnetic colloids, birefringence and dichroism, magnetically-induced, sign inversion 0-60548  
 magnetic fluids, light scattering and polarisation 0-60616  
 magnetic fluids, mag., optical, and hydrodynamic props., expt. study, review 0-60376  
 magnetic fluids, optical birefr. and dichroism in mag. field 0-60547  
 magnetic semiconductors, critical behaviour of electronic properties, theory 0-96861  
 methylammoniumtetrachlorochromate, optical absorption intensity, short-range spin correlation 0-108185  
 methylglyoxal, fluoresc. mag. field effect 0-102535  
 trans-p-n-octyloxy-α-methyl-p'-cyanophenyl cinnamate, mag. and elec. birefr. in isotropic phase 0-80744  
 paramagnetic ions in cubic crystals, in const. mag. field and variable EM field, adiabatic basis 0-88972  
 paramagnetic liquid, depolarized light scatt. in mag. field 0-80759  
 Raman scattering of Raman-inactive phonon polaritons 0-91843  
 Raman spectroscopy of chiral molecules in mag. fields 0-102532  
 rare earth orthoferrites, Raman scatt. from magnons, anisotropy const. determ. 0-66178  
 resonant light scattering from magnetic excitations, review 0-97290  
 ruby, luminescence, absorption of R and N lines, effect of mag. field 0-60550  
 semiconductor, submillimetric magneto-optical props., strip line technique 0-60554  
 submicron magnetic objects, mag. struct. study using magneto-optic micro-magnetometer 0-57349  
 Voigt profile measured over finite frequency range, parameters determ. 0-106870  
 Ag<sub>2</sub>O, exciton luminesc. spectra, mag. field influence 0-80860  
 Bi, EM wave dispersion and damping, Voigt configuration, non-local calcs. 0-100475  
 CaF<sub>2</sub>:Eu<sup>2+</sup>, photoluminesc. mag. circ. polaris. 0-89056



**magneto-optical effects continued**

- CdCr<sub>2</sub>S<sub>4</sub>(Se<sub>4</sub>), thermoreflectance, photoconductance, Raman scatt. near mag. phase transition 0-97298  
 CdCr<sub>2</sub>Se<sub>4</sub>, energy structure, magneto-optical effects 0-71394  
 Cd<sub>1-x</sub>Mn<sub>x</sub>Te, exchange induced ionization of bound excitons, luminesc. meas. 0-97328  
 CdS, doped, amorphous antiferromagnet model, susceptibility and spin-flip Raman scatt. meas. 0-97057  
 CdS electronic two- and one-photon Raman scatt. via biexcitons, stimulated-reflect. obs. mag. field shift 0-103963  
 CdTe:Mn<sup>2+</sup>, luminesc. and magneto-optic reson., mag. field effect 0-93390  
 Co, epitaxial films, even magneto-optical effects 0-76007  
 Co, thin films, optical and magneto-optical permittivities 0-66163  
 Co-Fe-Si-B, ferromag., magneto-optical spectra in amorphous and cryst. states (*Russian*) 0-84749  
 Co-Gd(Tb)(Sm) film, magneto-optic coeff. and refr. index, ellipsometric determ. 0-71501  
 CoCO<sub>3</sub>, Brillouin-Mandelstam light scatt. obs. of spin wave spectra 0-93358  
 CoCO<sub>3</sub>, LF exciton and Raman spectra, one-magnon and two-magnon scatt. 0-93333  
 CoCO<sub>3</sub>, light scatt. from magnons and phonons excited by microwave pumping 0-66213  
 CoCO<sub>3</sub>, linear magneto-optical effect, birefr. 0-66155  
 CoF<sub>2</sub>, linear magneto-optical effect, birefr. 0-66155  
 CsNiF<sub>3</sub>, 1D ferromag., optical absorption and spin dynamics 0-71417  
 Cu<sub>2</sub>O, exciton luminesc. spectra, mag. field influence 0-80860  
 DyVO<sub>4</sub>, cooperative Jahn-Teller phase transition, linear birefr. meas. 0-88960  
 Eu chalcogenides, resonant Raman scattering model via magnetic exciton in ferromagnetic phase 0-93326  
 EuO, ferromagnetic piezotransmission behaviour in magnetic field 0-97272  
 EuO, light scatt. from spin waves and magneto-optic hysteresis meas. 0-97244  
 EuO(S), ferromagnetic electronic structure, absorption, thermoreflection and thermotransmission spectra (*French*) 0-97300  
 EuO(S)(Se)(Te), spin order and fluctuations, Raman scatt. study 0-97273  
 EuS, light scatt. from spin waves and magneto-optic hysteresis meas. 0-97244  
 EuSe(Te), magnetic phase transitions, thermal modulation spectroscopy study (*French*) 0-97301  
 EuSr<sub>1-x</sub>S, magneto-optical redshift in absorpt. and photoluminesc., mag. short-range order 0-71388  
 EuTe, mag. 'Bragg' scatt. obs. through Raman scatt. 0-66179  
 Fe, epitaxial films, even magneto-optical effects 0-76007  
 Fe, ferromagnetic, partial circular polarisation of thermal emission in mag. field 0-71387  
 Fe garnet, optical radiation interaction with magnetostatic waves 0-76009  
 Fe, monocryst. and polycryst., thermal emission, magneto-optic circular polarisation obs. 0-70435  
 Fe-Gd(Tb) film, magneto-optic coeff. and refr. index, ellipsometric determ. 0-71501  
 Fe-Ni-B(P), ferromag., magneto-optical spectra in amorphous and cryst. states (*Russian*) 0-84749  
 Fe<sub>80</sub>B<sub>20</sub>, amorphous, Brillouin scatt. from magnons, ferromag. reson. 0-65844  
 FeBO<sub>3</sub>, mag. linear dichroism and absorpt. spectra, exciton-magnon absorpt. mechanism 0-66160  
 Fe<sub>2</sub>Co<sub>1-x</sub>Cl<sub>2</sub>, metamagnet, mag. phase diagram by mag. induced light scatt. 0-65883  
 FeF<sub>2</sub>, antiferromag., anomalous anti-Stokes/Stokes Raman scatt. intensity ratio 0-66177  
 FeI<sub>2</sub>, spin waves and two magnon bound states, mag. field IR absorption meas. 0-65840  
 Fe<sub>2</sub>Mg<sub>1-x</sub>Cl<sub>2</sub>, metamagnet, mag. phase diagram by mag. induced light scatt. 0-65883  
 Fe<sub>1-x</sub>Mn<sub>x</sub>Cl<sub>2</sub>, disordered, Raman scatt. from Fe<sup>2+</sup> and Neel temp. 0-60579  
 Fe<sub>2</sub>O<sub>4</sub>, IR refl., ATR, Voigt and Faraday expts. 0-66180  
 Fe<sub>2</sub>Zn<sub>1-x</sub>F<sub>2</sub>, Neel point and short range order, dilution effects, mag. birefr. obs. 0-71019  
 GaAs, excitons in arbitrary mag. fields 0-96798  
 p-GaP:ZnS, spin polarisation of donors and acceptors in mag. field, optical and microwave study 0-93393  
 Gd<sub>2</sub>Ga<sub>2</sub>O<sub>12</sub>, IR refl., ATR, Voigt and Faraday expts. 0-66180  
 GdI<sub>2</sub>, IR refl., ATR, Voigt and Faraday expts. 0-66180  
 Hg, Voigt profile, absorpt. line calcs. for the 396.5, 361.4, 318.7, 492.2, 587.6 and 447.1 nm lines 0-99471  
 He-Ne ring laser, nonreciprocal effects with transverse mag. field applied to active medium 0-91820  
 Hg<sub>0.77</sub>Cd<sub>0.23</sub>Te nonlinear optical IR generation 0-58642  
 HgCr<sub>2</sub>Se<sub>4</sub>, thermoreflectance, photoconductance, Raman scatt. near mag. phase transition 0-97298  
 p-InSb, photoexcited exciton spin-flip scatt. 0-74434  
 KCl:Ca(Yb), Z<sub>2</sub> and Z<sub>1</sub><sup>+</sup> centres, excited state, magneto-optical spectra 0-108233  
 KCl(Br), F-centre emission, mag. circular polarisation 0-108251  
 K<sub>2</sub>CoF<sub>4</sub>, 2-dimens. Ising antiferromag., mag. excitons, Raman scatt. obs. 0-66181  
 K<sub>2</sub>CoF<sub>4</sub>, two-dimens. Ising antiferromag., nearest neighbour correl. function, birefr. expts. 0-71386  
 KCuF<sub>3</sub>, linear chain Heisenberg antiferromag., nearest neighbour correl. function, birefr. expts. 0-71386  
 MgO:Cr, high resolution far IR spectroscopy of lower energy levels of Cr<sup>3+</sup> 0-80822  
 MnBi films, prep. by ionised-cluster beam deposition technique, magneto-optical props. 0-100790  
 Mn<sub>1-x</sub>Zn<sub>x</sub>F<sub>2</sub>, Neel point and short range order, dilution effects, mag. birefr. obs. 0-71019  
 MoSe<sub>2</sub>, exciton spectra 0-97296  
 NaBr(I), optically activated F→F' centre conversion in mag. field 0-108253  
 Ni, epitaxial films, even magneto-optical effects 0-76007  
 Ni, polycryst., thermal emission, magneto-optic circular polarisation obs. 0-70435  
 α-O<sub>2</sub>, antiferromagnetic polycrystal, splitting of exciton absorpt. lines in mag. field (*Russian*) 0-103943

**magneto-optical effects continued**

- RbCl(Br), F-centre emission, mag. circular polarisation 0-108251  
 RbCoF<sub>4</sub>, 2-dimens. Ising antiferromag., mag. excitons, Raman scatt. obs. 0-66181  
 Rb<sub>2</sub>CrCl<sub>4</sub>, optical absorption intensity, short-range spin correlation 0-108185  
 Rb<sub>2</sub>MnCl<sub>4</sub>, quasi-2D-antiferromag., linear birefr. and optical absorpt. spectra 0-71385  
 SiC, laser Raman spin-flip scatt. from excitons, luminesc. 0-80786  
 TbIG, [111] magnetoelastic props., rel. to Cotton-Mouton birefringence, 90-500K 0-103876  
 TlBr, resonant polaron coupling and excitons under mag. field 0-71383  
 V<sub>1</sub>, mag. 'Bragg' scatt. obs. through Raman scatt. 0-66179  
 V<sub>2</sub>O<sub>3</sub>, Raman scatt. and phase transitions 0-71420

**magnetoabsorption**

- metal-insulator-semiconductor struct., magneto-optic interband absorption by semicond. surface layer 0-93288  
 MIS, magneto-optic absorption by electron gas, optical phonon effects 0-97248  
 semiconductor, optically anisotropic, magnetoabsorpt., light freq. modulation effect 0-66162  
 CoCO<sub>3</sub>, two-sublattice noncollinear antiferromag., exciton-magnon light absorpt. mechanisms (*Russian*) 0-89017  
 CoCO<sub>3</sub>, weakly ferromag., light absorpt., dichroism and mag. config. 0-66223  
 Cu(II)-DL-proline complex, ESR, magnetic susceptibility and optical absorption 0-93167  
 Ge, internal Stark effect on impurity states, low-temp. magnet. absorption meas. 0-60636  
 HgSe, interband  $\Gamma_6 \rightarrow \Gamma_8$  magnetoabsorption, temp. study 0-76032  
 InSb, magnetoacoustic wave excitation by acoustic wave propagation 0-88597  
 p-In<sup>±</sup>, shift of fundamental absorpt. edge in crossed elec. and mag. fields 0-76034  
 PbTe, two photon magnetoabsorption (*Russian*) 0-60553  
 Rb<sub>2</sub>MnCl<sub>4</sub>, quasi-2D-antiferromag., linear birefr. and optical absorpt. spectra 0-71385

**magnetoacoustic effects**

see also *magnetoacoustic resonance*

- Barkhausen noise, appl. to residual stresses evaluation in welding 0-76436  
 defects in magnetized samples, magnetostrictive conversion of US waves into EM fields 0-66008  
 ferromagnet magnetisation, influence of high intensity longitudinal sound waves 0-103875  
 ferromagnetic, thick film, reson. transmission of EM energy via phonons 0-60382  
 ferromagnetic metals, ultrasound attenuation, EM generation 0-108046  
 itinerant electron ferromagnets, elastic props. and electronic struct. 0-66001  
 magnetic fluids, US attenuation, MHD approach 0-60389  
 magnetoelastic SAW velocity on magnetised ferrite substrate, non-reciprocity 0-80587  
 metal, Pippard sound-attenuation oscillating angular depend. (*Russian*) 0-103613  
 metallic films, ultrasound attenuation, size magnetoacoustic effect (*Russian*) 0-107869  
 metals, ferromag., max. in acoustic attenuation at low mag. fields 0-93158  
 piezoelectric nondegenerate semicond., magnetoacoustic effects of nonparabolic band struct. 0-96948  
 piezoelectric semiconductor-plasma, parametric excitation of helicon and acoustic waves 0-107837  
 rare earth metals, electronic sound attenuation anomalies at transition to helical phase, Fermi surface topology (*Russian*) 0-92807  
 semiconductor, planar acoustomagnetoelc. effect, theory 0-60052  
 semiconductors, heat pulse absorpt. in nonquantising mag. fields 0-60054  
 semiconductors, intervalley acoustoimpurity resonance 0-107868  
 sound attenuation in magnetic field at the 2<sup>1/2</sup>-order phase transition (*Russian*) 0-100487  
 Bi, gas-liquid type transform. and sound attenuation in strong mag. fields, electron-hole correl. effects 0-88598  
 Bi, giant quantum attenuation anomalies of sound waves at high mag. field, temp. and freq. depend. 0-70587  
 Bi, giant quantum attenuation anomalies of sound waves at high mag. field, extra attenuation peaks 0-70588  
 CeB<sub>6</sub>, magnetostriction, US absorpt. and thermal expansion 0-66004  
 Co-Pt ferromagnetic alloy, 6 T ultrasonic study of magnetoelastic coupling 0-93154  
 Cr, antiferromagnetic, US attenuation and phase diagram 0-103831  
 Cr, mag. phase diagram, near, spin-flip temp., US attenuation 0-60267  
 Fe-Ni-C, Invar, coated, Mossbauer spectra, effect of applied RF mag. field 0-80645  
 Fe-rare earth alloys, amorphous, magnetoelasticity and moment rot., US vel. calc. and neutron scatt. meas. 0-65992  
 Ge, electron-hole drag, interaction with thermal pulses 0-103631  
 InSb, magnetoacoustic wave excitation by acoustic wave propagation 0-88597  
 n-InSb, non-degenerate, linear longitudinal elc. cond., US wave effects in DC mag. field 0-88599  
 KMgF<sub>3</sub>:Ni<sup>2+</sup>, acoustic Faraday and Cotton-Mouton effects, theory 0-65987  
 TmFeO<sub>3</sub>, acoustic vel. and attenuation shifts at spin reorientation phase transition 0-65986

**magnetoacoustic resonance**

see also *ferroacoustic resonance*

- antiferromagnets, magnetoacoustic resonance of domain boundaries (*Russian*) 0-65636  
 He plasma, strongly inhomogeneous, magnetoacoustic reson. 0-69994

**magnetoacoustics** see *magnetoacoustic effects***magnetocaloric effects**

see also *magnetic cooling*; *thermomagnetic recording*; *thermomagnetic treatment*

- B-phase at equilib., formalism 0-88384  
 mischmetal-Co system, thermomagnetic analysis of intermediate phases 0-93115  
 Dy, magnetocaloric effect and mag. phase transitions, 80 to 300K 0-60279  
 Fe-Ni alloy type Y<sub>2</sub>NDK25B, anomalous magnetocaloric effect 0-60278



magnetocrystalline anisotropy *see magnetic anisotropy*

### magnetoelastic effects

alkali hyperoxides, ionic  $\pi$ -electron systems, magnetogyration 0-93155  
antiferromagnet, magnetoelastic soliton propag. 0-66003  
antiferromagnets, easy-plane, nucl. spin wave relax. 0-65850  
antiferromagnets, magnetoacoustic resonance of domain boundaries (*Russian*) 0-65636  
bubble materials, magnetoelastic interactions 0-65976  
Earth deformation, mag. field effects 0-109085  
ferrite window cores, magnetoelastic props., compressive stresses influence measurements using photo stress method (*Polish*) 0-93134  
ferromagnet, itinerant electron, magnetoelastic contribs. to US vel., elastic const., and susceptibility 0-75829  
ferromagnetic conductor, cylindrical, acoustic wave propag., EM field behaviour 0-88857  
ferromagnetic elastic solid, two coplanar Griffith cracks, singular stresses 0-65985  
ferromagnetic metals, ultrasound attenuation, EM generation 0-108046  
ferromagnets, hard, elastic, relaxation effects, vectorial internal variables, rational thermodynamics 0-75828  
itinerant electron ferromagnets, elastic props. and electronic struct. 0-66001  
itinerant ferromagnets, magnetoelastic props., thermodynamic aspects 0-66002  
magnetocrystalline anisotropy constants, phonon-induced temp. depend. 0-65858  
magnetostriction in terms of hexagonal and cubic harmonics up to degree 6 0-88856  
metal, ferromag., antiferromag., magnetoelastic coupling effect on magnetoel. reson. 0-75837  
metal rods, stress state and fracture in pulsed mag. field 0-81201  
porous anisotropic magnets, approach to mag. saturation 0-93146  
press. or stress induced, neutron scatt. obs. 0-65880  
rare earth compounds, multipolar interactions, evidence and origins 0-59935  
rare earth intermetallic compounds, quadrupolar interactions, parastriction 0-60400  
rare earth intermetallic cpds., cryst. field effects rel. to mag. props. 0-59933  
rare earth-Zn alloys, ferromag., parastriction and magnetoelastic coeffs. 0-65996  
semiconductors, magnetic, spin wave electron amplification theory 0-97083  
spin glass, parametric amplification of spin waves by elastic pumping (*Russian*) 0-65895  
spin-Peierls phase diagrams, obs. and models 0-60330  
spontaneous symmetry breaking and magnon-phonon spectra 0-65991  
steels Kh18N(10-25), mag. susceptibility, 4.2 to 300K, and magnetoelasticity (*Russian*) 0-65812  
transition metals, 3d, ferromag. props., book contrib. 0-75724  
viscoelastic medium, disturbances under transient tangential force and mag. field 0-92070  
 $\text{Al}_2\text{O}_3\text{V}^{3+}(\text{Fe}^{2+})$ , hyperfine splitting and magnetoelastic const., freq. crossing spectroscopy 0-107392  
Co-Pt ferromagnetic alloy, 6 T ultrasonic study of magnetoelastic coupling 0-93154  
CoP, and CoNiP, cylindrical amorphous electrodeposited layers, mag. props., torsion influence 0-88848  
ErFeO<sub>3</sub>, SAW meas. of magnetoelastic effects 0-75839  
Fe-B(P) amorphous alloys, anomalous thermal expansion,  $\Delta E$  effect, Invar and Elinvar characts., delay time 0-80589  
Fe-Ni(Pt) Invars, elastic and mag. props., magnetoelastic interaction effects (*Russian*) 0-84631  
Fe-rare earth alloys, amorphous, magnetoelasticity and moment rot., US vel. calc. and neutron scatt. meas. 0-65992  
Fe-Si (3 wt.%), oriented, losses and domains, mech. stress effects 0-88852  
Fe-Tb, magnetoelastic hysteresis, elastic stress and mag. field depend. (*Russian*) 0-65982  
FeBO<sub>3</sub>, magnetically tunable ultrasonic transducers for shear waves 0-74682  
FeBO<sub>3</sub>, parametric echo, magnetoelastic NMR excitation (*Russian*) 0-66072  
( $\text{Fe}_{1-x}\text{Ni}_x$ )<sub>83</sub>B<sub>17</sub>, amorphous alloys ferromagnetic resonance 0-108080  
Fe<sub>40</sub>Ni<sub>38</sub>Mo<sub>4</sub>B<sub>18</sub> and Fe<sub>70</sub>Mo<sub>2</sub>B<sub>20</sub> amorphous ribbons, magnetoelastic effects in as-quenched and stress-relieved states 0-80588  
Fe<sub>40</sub>Ni<sub>40</sub>P<sub>14</sub>B<sub>6</sub>, amorphous, mag. polarisation in approach to ferromag. saturation 0-80560  
GdIG, local mag. anisotropy in stress field of single dislocation 0-88744  
HoTb<sub>1-x</sub>Co<sub>x</sub> laval phase compounds, elastic props., temp. and magnetic field dependence 0-60393  
KCoF<sub>3</sub>, antiferromag. domain wall motion under external stress 0-80583  
KMgF<sub>3</sub>Fe<sup>2+</sup>, anomalous acoustic relax. absorpt. and APR 0-88864  
Ni<sub>2</sub>Fe, domain struct. after tensile deform., dislocation effects 0-71083  
NiZn ferrites, Villari effect 0-88847  
Pd-Fe, magnetic anisotropy near Curie point, quasi domain struct. (*Russian*) 0-65867  
PrSb, magnetic to nonmagnetic transition, press. or stress induced, neutron scatt. obs. 0-65880  
PrSn<sub>3</sub>, thermal expansion and transverse elastic const. near mag. phase transition 0-60394  
Pr<sub>2</sub>Ti<sub>3</sub>, thermal expansion and transverse elastic const. near mag. phase transition 0-60394  
TiFeCo<sub>1-x</sub>, thermal expansion and magnetoelastic effects 0-80585  
UFe<sub>2</sub>, giant magnetoelastic deform. of cryst. struct. mag. props. (*Russian*) 0-93159  
YIG, nonreciprocal attenuation of magnetoelastic Rayleigh waves 0-60399

### magnetoelastic waves

antiferromagnet, nuclear spin oscillations, interaction with lattice vibrs. 0-70996  
films, ferromagnetic, perpendicularly magnetised, surface and vol. magnetoelastic waves (*Russian*) 0-93151  
magnetic film, bubble domains, magnetoelastic interactions 0-103865  
magnetically ordered cryst., dislocation drag, magnetoelastic waves 0-103332  
metallic glass ribbon, magnetostrictive stress depend. of longitudinal wave vel. 0-75825  
SAW velocity on magnetised ferrite substrate, non-reciprocity 0-80587

### magnetoelastic waves continued

FeBO<sub>3</sub>, parametric echo, magnetoelastic NMR excitation (*Russian*) 0-66072  
YIG, magnetoelastic wave propagation time dispersion reduction 0-75836  
YIG, magnetoelastic wave propagation time dispersion reduction 0-75836  
YIG, nonreciprocal attenuation of magnetoelastic Rayleigh waves 0-60399  
**magnetolectric effects**  
antiferroelectric ferrites, coupled magnetoel. oscills. and high freq. susceptibility tensor (*Russian*) 0-93152  
ferroelectric and antiferroelectric phase transitions, magnetoel. effect 0-100637  
ferrofluid, dielec. behaviour in uniform mag. field 0-60390  
magnetoelctrets, possible mech. of mag. field effects 0-93157  
BaMn<sub>0.99</sub>Co<sub>0.01</sub>F<sub>4</sub>, magnetoel. phenomena, dielec. behaviour near Neel temp. 0-71151  
Cr<sub>2</sub>O<sub>3</sub>, dielec. const. in mag. field, nonlinear magnetoel. effect in Neel pt. region 0-66006  
Fe<sub>2</sub>O<sub>4</sub>, lattice parameters, NMR freqs., and magnetoel. pots. near 12K 0-71146  
Fe<sub>2</sub>O<sub>4</sub>, magnetite, magnetoel. effect temp. depend. obs. by mag. field rot. in a-c plane at 10K 0-71145  
ZnCr<sub>2</sub>Se<sub>4</sub>, screw spin structure, magnetoel. effect 0-75827

### magnetohydrodynamics *see magnetohydrodynamics*

### magnetogasdynamics *see magnetohydrodynamics*

### magnetohydrodynamic conversion

coal-fired MHD flow facility, development and operation 0-66982  
coal-fired MHD system, retrofitting to existing non-coal power stations 0-66983  
cylindrical plasma filament under axisymmetric perturbation, numerical anal. 0-106853  
fusion reactor, Tokamak, divertor mag. piston action, elec. AC power direct generation 0-102324  
thermonuclear fusion research, economic factors 0-73991  
H<sub>2</sub>-O<sub>2</sub> seeded system for MHD generator, elec. cond. 0-76642  
NO<sub>x</sub> emissions from coal-fired MHD power plants, simplified correlations for prediction 0-97842

### magnetohydrodynamic convertors

channel electrical characts., equivalent ccts. 0-75106  
conduction type with reciprocal motion of composite working element 0-84009  
dynamo, approx. design, equivalent circuit diagram 0-84008  
end effects in a MHD channel with diverging electrode walls 0-89657  
energy emitted by working medium of MHD generator, meas. 0-103078  
Faraday generators, longitudinal baffling 0-64790  
Faraday MHD generator-operating region 0-103132  
fossil fuels for use in MHD power stations 0-72074  
laminar flow, longitudinal dynamic effects determination for Na, Al, Sn, and Hg (*Rumanian*) 0-64792  
liquid metal piston dynamics, math. model (*Russian*) 0-74996  
open-cycle, supersonic flow of combustion products, nonequib. physico-chem. processes 0-103196  
plasma turbulence in combustion channel 0-75057  
power take-off design for diagonal-conducting-wall MHD channels 0-89656  
rare earth chromite based electrode material development for MHD generators 0-84893  
series generator, transition region geometry 0-84010  
simulated MHD combustion chamber working on natural gas and O<sub>2</sub> enriched air, NO formation investigation 0-106984  
steam, production of short bursts of power 0-64789  
test facility safety analysis methodology and documentation system 0-61388  
LaCrO<sub>3</sub>-MgO, LC20M electrode material in open cycle MHD systems, thermionic emission characts. 0-97394  
Na MHD generators, optimisation for maximum electrical efficiency, output and power factor (*Rumanian*) 0-64793  
ZrO<sub>2</sub> stabilised with lime, possible electrode material (*Rumanian*) 0-65575

### magnetohydrodynamic generators *see magnetohydrodynamic convertors*

### magnetohydrodynamic waves

Alfven nonlinear gravit. drift waves and  $\beta$  limitations in Tokamaks 0-92369  
Alfven wave scattering, integral eqns. 0-83848  
Alfven wave turbulence, interaction with whistler wave turbulence 0-64728  
Alfven waves, in stochastic mag. field, Khasminskii's theorem 0-59198  
Alfven waves, monochromatic non-WKB, normals evolution in solar wind 0-101521  
Alfven waves in Jupiter magnetosphere. rel. to Io interaction with plasma torus 0-98604  
Cassiopeia A, Alfven waves generation rel. to radio spectrum secular flattening 0-101637  
HF heating by MHD waves of finite press. plasma (*Russian*) 0-83950  
interplanetary medium, Alfven Mach number rel. to collisionless shock waves thickness 0-90314  
interplanetary medium, Alfven waves rel. to mean free path of low-rigidity cosmic rays 0-98524  
interstellar cloud, effect of nonlinear torsional Alfven waves on cloud rot. mag. braking during star form. 0-90493  
magnetisable fluid, conductive, nonlinear magnetosonic waves 0-59121  
nonlinear Alfven wave in an ultra-relativistic electron-positron plasma 0-106905  
nonlinear magnetostatic modes and twisting modes with magnetic islands 0-106900  
nonlinear sonic wave, excitation by quasi-monochromatic Alfven pumping 0-106649  
physiological aqueous solution, possibility of wave excitation 0-94246  
relativistic MHD growth and decay discontinuities 0-92280  
resistive drift Alfven waves in sheared mag. fields 0-64718  
shear Alfven waves, quasi-linear theory 0-64714  
shear flow stability and Alfven waves in magnetised plasma 0-96360  
simple waves and strong discontinuities in a magnetizable medium 0-69935  
solar corona, heating and wave generation by prominence turbulence 0-72907  
solar wind, accel. by Alfven wave flux from Sun 0-85923  
solar wind, dynamic mag. struct. of large amplitude Alfvenic vars. 0-72734



**magnetohydrodynamic waves continued**

- Sun, coronal thermal stability during fast mode wave heating 0-90397
- Sun, use of MHD pulses as diagnostic technique 0-109405
- ultra-relativistic electron-positron plasma, macroscopic wave behaviour 0-106904
- whistler-Alfvén turbulence interaction 0-75058
- Bi, EM wave dispersion and damping, Voigt configuration, non-local calcs. 0-100475

**magnetohydrodynamics**

- see also *magnetohydrodynamic conversion; magnetohydrodynamic converters; magnetohydrodynamic waves; plasma magnetohydrodynamics*
- air-Hg flow, stratified, co-current, in rectangular channel, interfacial wave structure 0-74955
- anisotropic explosion of magnetized spheroids 0-67532
- astrophysical plasma charged particle accel. by MHD shock waves 0-101532
- Bianchi universes, magnetic fields and fluids with conductivity 0-83864
- boundary layer similarity eqns. of MHD flow past a semi-infinite flat plate with heat transfer, exact numerical solns. 0-83861
- Cassiopeiae A, supernova remnant, mag. field origin 0-85989
- channel with uniform wall heat flux, heat transfer, Hall and ion-slip current effects 0-92230
- circle theorems for inviscid steady flows 0-59043
- combustor and channel temp. meas., microprocessor based Na reversal instrument 0-73364
- composite mixture, flow through porous medium, Rayleigh-Taylor instability 0-69912
- conducting fluid, two dims. motion, mag. field evolution, anti-dynamo theorem extension (*Russian*) 0-59127
- conducting fluid with spherical particle suspension oscillating flow in mag. field 0-79408
- constrained minimum energy problem in relativistic MHD 0-92238
- convection, magnetic, mean field approx., boundary layer method 0-69930
- convective flow through porous channel with Hall and wall conductance effects 0-74993
- cosmological models, perfect fluid, plane symmetry 0-82556
- Couette flow, Hall effect in rot. system 0-74991
- Couette flow, unsteady, between two plates when one subjected to random pulses 0-69938
- disc in electrically conducting fluid, hydromagnetic flow due to torsional oscillations about non-zero mean 0-74992
- discontinuity propagation along bi-characteristics 0-59125
- dispersive magnetisable media, hydrodynamics including Brownian motion 0-59120
- div B, nonzero, effect on numerical soln. 0-69939
- Earth core, dynamics of fluid core with inward growing boundaries 0-76934
- electrical potentials, uniqueness of solns. to extended class of elliptic boundary value problems 0-69937
- electrically conducting medium, rotation at exit of coaxial MHD channel 0-83853
- elliptic equations and systems, free-boundary problem solution method 0-69941
- energy emitted by working medium of MHD generator, meas. 0-103078
- equilibrium equations, convergence of iterative schemes 0-59115
- Fermi-accelerated cosmic rays mediation of shock front 0-85829
- ferrofluid behaviour in the presence of a rotating nonhomogeneous mag. field (*French*) 0-96313
- ferrofluid flow under influence of rotating mag. fields 0-59118
- ferrofluids, dissipative process in non-homogeneous mag. field 0-59119
- ferrofluids, Landau and Lifshitz hydrostatic press., thought expts. 0-59111
- ferromagnetic fluid, stability in vertical magnetic field, variational approach (*German*) 0-96316
- ferromagnetic suspension serving as a liquid magnet 0-84622
- film between porous circular discs with velocity slip 0-74997
- finite-amplitude thermal convection and geostrophic flow in a rotating magnetic system 0-87813
- force-free magnetic fields, variational approach and appl. to solar active regions mag. field 0-62011
- forced convection in channel bounded by plate and permeable bed, Hall effects 0-69934
- free convection heat transfer on a magnetic cylinder in a uniform magnetic field 0-83852
- gas dynamics, equatorial propagation of axisymmetric magneto-radiative shocks 0-79349
- generalised polar diagrams of plane-parallel stationary similarity flows, waves 0-96314
- glass industry, magneto-hydrodynamic phenomena, of mixing (*Polish*) 0-64647
- gravitating plasma polytropes in magnetostatic equilb., analytical solns. 0-94701
- Hartmann flow, nonlinear stability, monoharmonic analysis 0-83850
- heat transfer in MHD channel flow of rarefied gas, external circuit effects 0-83860
- hemisphere in MHD rotating stratified fluid 0-100039
- hemispherical container, flow induced by distributed current source and mag. field 0-92234
- hydromagnetic capillary instability of a liquid jet with an axial flow 0-74990
- induction pump, flow through helical channel, pressure field effect 0-87815
- induction pump, transverse and longitudinal fringe effects in channel 0-83854
- interplanetary medium, discontinuities, identification method 0-109322
- interstellar cloud rotation, mag. braking of aligned rotator during star form., exact time-depend. soln. 0-90493
- interstellar medium, equilb. configs. stability, hydromagnetic energy principle 0-82448
- interstellar nonrotating magnetic gas clouds collapse, numerical calcs. 0-105299
- jet, magnetisable liquid, stability 0-83831
- Kelvin-Helmholtz instability in supersonic and super-Alfvénic fluids 0-87816
- linear induction machine, MHD processes in channel 0-83859
- liquid metals laminar flow in curved channels, transversely applied mag. field, flow anal. 0-59116
- RR Lyrae stars, hydromagnetic processes as cause of period changes 0-105261

**magnetohydrodynamics continued**

- magnetic fluid, penetration through porous medium with uniform mag. field oblique to interface 0-59107
- magnetic fluid as continuum with internal degrees of freedom 0-60377
- magnetic fluids, conference, Orlando, USA (Mar. 1980) 0-56995
- magnetic fluids, heat and mass transfer 0-59123
- magnetic fluids, mag., optical, and hydrodynamic props., expt. study, review 0-60376
- magnetic fluids, response to mech., mag. and thermal forces 0-59122
- magnetic fluids, US attenuation, MHD approach 0-60389
- magnetic flux tubes, vibration modes, general dispersion relation 0-94706
- magnetically saturated fluid, continuum mechanics, global balance law approach 0-60388
- magnetogasdynamic parallel flows, inviscid stability 0-69933
- magnetogasdynamics, axially symmetric explosion 0-62007
- magnetosphere, field line MHD torsional oscill. rel. to mini-substorm and long-period Pi 2 event (*Japanese*) 0-94653
- magnetosphere, hydromag. energy spectra depend. on solar wind vel. and interplanetary mag. field direction 0-67476
- Maxwell fluids, immiscible, hydrodynamic flow through non-conducting rectangular channel 0-100038
- metals, liquid, duct flow, hot-film probe vel. meas. 0-75009
- MHD flow past accelerated plate, Hall effects 0-92275
- noncanonical Hamiltonian density formulation of perfect fluid 0-103010
- nonisothermal magnetisable fluid, thermal convective stability, modulated mag. field effects 0-64646
- one-dimensional isentropic flow, of ideal perfectly conducting fluid (*French*) 0-69936
- oscillating source flow of ducting fluid between parallel discs 0-99986
- particle acceleration by MHD shock turbulence 0-87894
- periodic MHD oscillations, stability, perturbation theory 0-83858
- piston, magnetic field effect, self-similar magnetogasdynamic problem with radiative heat transfer 0-64578
- plane wave-plane shock interaction in magnetofluid dynamics 0-69931
- porous straight channel, MHD flow 0-69932
- protostars, magnetic, quasistatic contraction due to mag. flux leakage 0-98662
- protostellar cloud ang. momentum problem, mag. breaking 0-82342
- pulsar, plasma coupling, boundary conditions 0-94823
- pulsar magnetosphere, relativistic particle curvature radiation 0-77434
- pulsars, finite force face cold plasma atm. models, plasma differential rot. 0-77378
- pulsating viscous flow superposed on steady laminar motion 0-92228
- radio sources, extragalactic, relativistic electron clouds rel. to variable radio emission temporal characs. (*Russian*) 0-62307
- radio sources, formation of knots in relativistic flows as model for compact synchrotron sources variability 0-105369
- relativistic invariant, magnetofluid dynamics, eqns. of motion for charged particle and charged fluid 0-87821
- relativistic magnetofluid and space-like conformal mappings 0-75001
- rotating gas, perfectly conducting compressible in mag. field under gravity, wave dispersion relations (*Chinese*) 0-77276
- self-gravitating gas masses containing axisymmetric mag. fields, equilb. structs. 0-94708
- separation of high energy plasma in mag. and gravitational fields 0-67547
- sink flow with transverse mag. field, boundary layer thickness 0-69940
- slowly spreading jets, MHD instability 0-87818
- small scale magnetic fields in turbulence, Saffman's approx. 0-106851
- solar atmosphere, acoustic waves interaction with mag. flux tubes 0-85911
- solar atmosphere, MHD fluctuations due to magnetosonic wave propag. in warm plasma 0-72775
- solar coronal arcades mag. instability, two ribbon flares origin 0-72911
- solar cosmic ray particles, accel. in expanding coronal mag. bottle 0-77244
- solar flares, force-free mag. fields evolution, nonequilb. states and preflare stage 0-105213
- solar hard X-ray bursts, thermal models 0-94766
- solar magnetic fields, floating-up time rel. to solar activity 11-year cycle 0-101580
- solar photosphere, hydrodynamic mag. pumping rel. to mag. fields fine struct. 0-98646
- solar surges, local mag. field strength rel. to dynamics of descending stage (*Chinese*) 0-105221
- solar wind, Alfvén waves, non-linear interaction with compressive fast magnetosonic waves 0-105142
- solar wind, dynamic mag. struct. of large amplitude Alfvénic vars. 0-72734
- solar wind, MHD turbulence props. 0-61977
- solar wind, plasmadynamical processes review (*German*) 0-109323
- solar wind turbulence 0-85834
- sphere, spinning, motion in conducting fluids, drag forces, Magnus transverse forces and dragging torque (*Russian*) 0-87817
- stability of hydromagnetic torques in a temperature field 0-92231
- star, magnetic flux tube, buoyancy and equilb. 0-109420
- stationary flow between porous rotating cylinders in a radial magnetic field 0-83857
- stationary waves at the surface of a magnetizable liquid in a stream impinging on a point barrier 0-83805
- Stokes' problem, mass transfer effects of MHD free convective flow 0-62003
- Stokes approximation for two-dims. flow in strong mag. fields 0-83849
- Stokes problem, hydromagnetic free convection flow for porous vertical limiting surface with const. suction 0-90328
- streamline flow round an array of profiles in a magnetic field perpendicular to the plane of the flow 0-83856
- suction effect near accelerated plate 0-92232
- Sun, dynamo action of mean flow from latitude depend. heat transport 0-90378
- supernovae, magnetorotational explosion in cylindrical model 0-101605
- thermal instability of layer of micropolar fluid, in transverse field 0-87812
- thermoelectric MHD, pipe end problem, boundary layers and rotation 0-69942
- turbulence, 2-D, hydrodynamic and plasma applications, dynamical eqns., diffusion, MHD, superfluidity, review 0-69769
- turbulence, development and generation (*French*) 0-79407
- turbulent free convection in mag. field, statistical characs., vortices 0-79310



**magnetohydrodynamics continued**

- unsteady hydromagnetic thermal boundary layer problem, numerical treatment 0-92227  
viscoelastic conducting fluid, MHD flow 0-92229  
viscous fluid, incompressible, hydromagnetic free convective flow past vertical porous wall, mass transfer 0-64645  
voltage losses near electrodes 0-103079  
white dwarf degenerate cores, thermomagnetic instability conditions 0-77395  
Ge, electron-hole liquid, MHD effects 0-80190  
Hg, transition and turbulent flow in curved channels under transverse mag. field 0-79396

**magnetomechanical effects**

- see also gyromagnetic effect; magnetoelastic effects; magnetoelastic waves; magnetostriction*  
cutting tools, diffusive wear, mag. field effect 0-60985  
dimethylammonium copper tetrachloride, ferromag., quasi two-dimensional, ordering temp., press. depend. 0-84601  
ferromagnet, pinned domain wall motion, magnetic damping studies 0-65956  
ferromagnetic metals, magneto-volume effect, Invar phenomena 0-66007  
garnet epitaxial film, stress induced magnetocrystalline anisotropy 0-71013  
magnetically saturated fluid, continuum mechanics, global balance law approach 0-60388  
non-magnetic material wear in presence of magnetic field 0-60982  
steel, C, magnetomechanical acoustic emission for residual stress NDT 0-71149  
steel, ferritic, magnetomechanical acoustic emission for residual stress NDT 0-71149  
steel, mild, fatigue softening and hardening detected from Barkhausen noise 0-76428  
steel, Si, permeability change due to stress variation after demagnetization in Rayleigh region 0-88854  
CdHg,  $\omega$  phase, mag. susceptibility anisotropy w.r.t. uniform compression (Russian) 0-71143  
CeAl<sub>2</sub>, multiple- $q$  structure or coexistence of different mag. phases, neutron diffraction study 0-107985  
Cr, Q-vector locking, press. induced hardening 0-103870  
Cr, spin density wave phases, domains 0-103871  
CrSb<sub>1-x</sub>As<sub>x</sub>, press. effect on Neel point 0-71147  
Cu-Ni-Fe, magnetic properties, heat treatment and compressive stress effects 0-60367  
EuB<sub>6</sub>, Hall effect and resistivity data, ferromagnetic ordering temp., pressure depend. 0-60010  
Fe, high purity, magnetic field variations 0-93156  
Fe, high purity, magnetomechanical sampling, magnetic field variations 0-93156  
Fe, magnetomechanical acoustic emission for residual stress NDT 0-71149  
Fe polycrystalline, two ferromag. methods for eval. of fatigue limit 0-89438  
Fe thin layers, vacuum coated on PMMA, mag. behaviour during mech. stress cycles (German) 0-80581  
Fe-B, amorphous, induced anisotropy, development by mag. annealing and under applied mech. stress 0-65868  
Fe-B, amorphous, induced anisotropy by heat treatment in mag. field and under applied mech. stress 0-75758  
Fe-B phase ferromag. amorphous alloys, stiffening below Curie temp., pole effect (Japanese) 0-84632  
Fe-Si, grain oriented, misorientation effects on mag. props 0-88792  
Fe-Si, grain oriented sheet, AC hysteresis, surface struct. and elastic stress effects 0-88791  
Fe-Si, grain oriented transformer sheets, permeability and magnetostriction, tensile stress effects 0-88843  
Fe-Si, mag. props., stress and reannealing effects 0-88844  
Fe-Si (3 wt.%), internal friction, instantaneous, depend. on phase of torsional oscils. (Russian) 0-71142  
Fe-Si (3 wt.%), mag. domain wall contrast in synchrotron X-ray topographs 0-75792  
Fe-Si (3 wt.%), magnetisation variation during bending oscils., rel. to  $\Delta E$  effect (Russian) 0-65983  
Fe-Si (3 wt.%), nonoriented sheets, magnetisation, tensile stress effects 0-88845  
Fe-Si (3 wt.%), oriented, losses and domains, mech. stress effects 0-88852  
Fe-Si (3 wt.%) laminations, grain oriented, plastically deformed, anomalous losses 0-88853  
Fe-Zn alloys, coercive force anisotropy after cold plastic deform. (Bulgarian) 0-75809  
Fe<sub>40</sub>B<sub>40</sub>P<sub>14</sub>B<sub>6</sub> and Fe<sub>80</sub>B<sub>20</sub>, Metglas 2826 and 2605, amorphous ribbon, power loss variation with freq. and applied stress 0-88849  
FeCl<sub>2</sub>, reorientation of mag. moments under mech. stresses at OK 0-93153  
Fe<sub>40</sub>Ni<sub>40</sub>B<sub>20</sub>, amorphous ribbon, power loss variation with freq. and applied stress 0-88849  
Fe<sub>40</sub>Ni<sub>40</sub>P<sub>14</sub>B<sub>6</sub>, Metglas 2826, amorphous ribbon under tension, mag. domain walls and pulsed magnetisation reversal 0-88825  
K<sub>2</sub>FeCl<sub>4</sub>(H<sub>2</sub>O), antiferromag., press. depend. on spin-flop transition 0-80505  
Li<sub>0.5</sub>Fe<sub>2.5-x</sub>Cr<sub>x</sub>O<sub>4</sub>, press. depend. of anisotropy consts. 0-65865  
MnF<sub>2</sub>, antiferromag. and piezomag. domain struct., neutron topography study 0-71088  
MnZn ferrites, internal friction and  $\Delta E$  effect depend. on demagnetisation method 0-80584  
MnZn ferrous ferrites, mag. permeability stress depend. 0-88822  
Ni, internal friction, instantaneous, depend. on phase of torsional oscils. (Russian) 0-71142  
Ni, stress induced cross-over effect near Curie point (German) 0-103873  
Ni, stress induced crossover effect near Curie point (German) 0-103874  
Ni-Mn, ordered and disordered, press. effect on Curie temp. 0-71148  
(Ni,Fe<sub>1-x</sub>)<sub>80</sub>P<sub>10</sub>B<sub>10</sub>, amorphous, Curie temp., press. effect 0-75833  
NiZn ferrites, internal friction and  $\Delta E$  effect depend. on demagnetisation method 0-80584  
NiZnCo ferrites, switching time and coeff., hydrostatic press. effect 0-88802  
NiZnCo ferrites, voltage response under sinusoidal and pulse magnetisation effected by hydrostatic press. 0-88846  
Pr<sub>3</sub>Se<sub>4</sub>(S<sub>2</sub>), induced ferromagnet, mag. props. under hydrostatic press. 0-60395

**magnetomechanical effects continued**

- Tb<sub>0.7</sub>Dy<sub>0.3</sub>Fe<sub>2</sub>, vertically zoned, magnetomechanical coupling and magnetostriction 0-65999  
TiBe<sub>2-x</sub>Cu<sub>x</sub>, high press. study of Curie temp. and mag. susceptibility 0-84600  
TmSe, mag. ordering under press., neutron diffraction obs. 0-70947  
U<sub>3</sub>P<sub>4</sub>, press. effects on elec. resist. and Curie temp. 0-75559  
YIG, polycryst., initial and reversible parallel susceptibilities, hydrostatic press. effects 0-75835  
Zr, mag. susceptibility, plastic deform. effect (Russian) 0-65984  
ZrZn<sub>2</sub>, high press. study of Curie temp. and mag. susceptibility 0-84600

**magnetometers**

- see also magnetic field measurement*  
automatic spinner magnetometer for rock specimens 0-101455  
Faraday magnetometer using Bitter coils 0-62695  
flux-gate magnetometer flight performance in Bhaskara satellite 0-72746  
fluxgate magnetometer on Pioneer Venus Orbiter, design and operation 0-67496  
geomagnetic field meas. with quartz H magnetometer, calc. of horiz. component 0-105062  
geomagnetic fluctuations meas. on sea-floor, ULF-ELF 0-77152  
gradient magnetometers, appl. to induced elec. currents meas. in Alaska oil pipeline 0-98231  
magnetocardiogram meas. first order gradiometer and DC-thin film SQUID 0-89877  
magnetoencephalography, sensitivity distrib. 0-101246  
magnetopneumography, analytic methods 0-104713  
MIS-3M magnetic measuring system (USSR), testing small permanent magnets 0-62699  
NMR, large-scale automation 0-57343  
quantum, effect of external sinusoidal magnetic fields on sensitivity (Russian) 0-90870  
quantum, optical pumping, alternating polarity modulating pulses, meas. errors (Russian) 0-90871  
RF SQUID magnetometer, synchronous demodulation, amplitude- and phase-sensitive detection 0-105679  
ring-core magnetometer, for mag. meas. in interplanetary space during Halley-Venus mission (Japanese) 0-94672  
ring-core magnetometer, high sensitivity, for balloons, high-altitude mag. meas. (Japanese) 0-94608  
ring-core magnetometer sensor for articulatory meas. of jaw movements 0-101243  
ring-core type magnetometer, for space vehicles, geomag. fluctuations high-sensitivity obs. (Japanese) 0-94671  
rotating sample magnetometer for contactless conductivity meas. 0-73391  
SQUID, 430 MHz, AC-biased, quantum limited 0-101809  
SQUID, AC-biased, classical to macroscopic quantum transition 0-98953  
SQUID, AC-biased, noise, slow rate and stability 0-98948  
SQUID, geophysical, dewar systems design 0-101462  
SQUID, magnetoretiographic meas. of retina injuries in eye 0-104702  
SQUID, meas. of magnetocardiogram and cardiac output 0-104709  
SQUID, optomagnetic meas. appl. 0-98950  
SQUID, with independent pumping 0-105685  
SQUID appl. to nuclear gyros and magnetometers, high stability and sensitivity 0-98949  
SQUID fluxgate magnetometers, magnetopneumographic meas. 0-104711  
SQUID gradiometer, DC, thin-film, design optimisation 0-98951  
SQUID magnetometer with temp. control, spontaneous magnetisation and mag. susceptibility meas. 0-68221  
SQUID magnetometers, AC-biased, macroscopically quantised, higher harmonics in Josephson effect 0-98952  
submicron magnetic objects, mag. struct. study using magneto-optic micro-magnetometer 0-57349  
superconductive gradiometers, for measuring magnetic effects of geophysical origin 0-101463  
susceptometer for biomedical meas., Fe stored in human tissue, in vivo 0-101245  
two-dimensional magnetometer array, for ground-based obs. of auroral zone elec. currents 0-90245  
vibrating reed magnetometer of high sensitivity for small ferromagnetic particles meas. 0-73397  
He Mz magnetometer, improving accuracy by reducing intensity of optical pumping 0-62700

**magneto-optics** *see magneto-optical effects***magnetoplasma** *see plasma***magnetoplasmadynamics** *see plasma magnetohydrodynamics***magnetorefractance**

- Cd<sub>1-x</sub>Hg<sub>x</sub>Te epitaxial graded gap layers, plasma reflection and magnetorefractance 0-71391  
Cd<sub>1-x</sub>Mn<sub>x</sub>Te, semimagnetic, exchange interactions between localised and delocalised electrons 0-97245  
CdTe, exciton magnetorefractance spectra, multicomponent polaritons, Zeeman splitting 0-88974  
Hg<sub>1-x</sub>Mn<sub>x</sub>Te, semimagnetic, exchange interactions between localised and delocalised electrons 0-97245  
PbTe, far IR magnetorefl., band struct. 0-76010

**magnetoresistance**

- see also Corbino effect*  
alkali metals, elec. and thermal cond. in weak mag. fields 0-65535  
Anderson model, ground state, var. trial function approach 0-59913  
asymmetric Anderson Hamiltonian, ground state, magnetoresist. calc. 0-65503  
clean metal magnetoresistance in solid and liquid phases (Russian) 0-107767  
conducting media, EPR line shape, magnetoresist. effect 0-84638  
crystal symmetry, cubic and non-cubic, distinguished by weak field galvanomagnetic meas. 0-60009  
cubic semiconductor with ellipsoidal valleys, magnetoresist. 0-80300  
double injection p-n structures in magnetic field 0-107899  
ferromagnet, itinerant electron, magnetoresist. and anomalous Hall effect due to electron-phonon interactions 0-70680  
gapless semiconductor, transport coeffs. in quantum limit 0-80302  
graphite, resistivity and magnetoresistance, 4.2 to 293K 0-100459  
graphite intercalated with AsF<sub>6</sub>, quantum oscillatory phenomena 0-107823  
graphite intercalation cpds., Fermi surface and transport props., LCAO model 0-80159  
graphite nitrates, elec. props. perpendicular to layers, resistance, magnetoresistance, charge transport mechanisms 0-80268



## magnetoresistance continued

- graphite-K intercalation compounds, electronic props., resistivity, Hall effect and magnetoresistance 0-75585  
 inflowing structure, Anderson localisation, elec. cond. temp. depend. (*Russian*) 0-103639  
 metal film, cond.-electron focusing by inhomogeneous mag. field (*Russian*) 0-70850  
 metals, compensated and uncompensated, effect of spherical voids on electrical magnetoresistivity 0-65531  
 metals, electron theory and cond. props., contrib. of Sir Rudolf Peierls, 1928-1935 0-57054  
 negative magnetoresistance, appl. to heavily doped superconductors 0-107818  
 normal-superconducting composites, magnetoresistance and Hall coeff., classical theory 0-84547  
 Permalloy magnetoresistive mag. field sensor, performance calc. 0-57342  
 pyrolytic graphite, magnetoresistance positive-negative transition (*Russian*) 0-96923  
 quasi-two dimensional conductor, galvanomagnetic props., optical analogy (*Russian*) 0-60108  
 random system, 2-D, spin-orbit interaction and magnetoresistance 0-70728  
 rare earth amorphous alloys, random anisotropy magnetism 0-65853  
 read head for magnetic tape recorders using magneto-resistance principle 0-87688  
 semiconductor, magnetophonon resonance oscills., peak shape, theory 0-107824  
 semiconductor, n-type, nonequilibrium photoelectron distrib. and absolute negative cond. in quantising mag. fields 0-65622  
 semiconductor, piezoelec., degenerate, transverse magnetoresist. in strong field, quantum effect 0-80299  
 semiconductor, zero-gap, magnetophonon oscills. of transverse magnetoresist. in strong elec. fields 0-96916  
 semiconductors, degenerate, energy band structure effect on transverse magnetoresistance 0-88580  
 spin-glass alloys, magnetoresistance, Boltzmann formalism calcs. 0-88540  
 thin film, magnetoresistance, specular reflectivity angular depend. (*Russian*) 0-100453  
 three-dimensional systems, negative magnetoresist. 0-75591  
 very high field meas. of mag. materials 0-86224  
 Al and dilute alloys with Ge and Zn, magnetoresist. depend. on temp., 4.2-70K 0-70682  
 Al, granular supercond., normal state cond. 0-88529  
 Al, magnetoresistance, path integral method calc. 0-65537  
 Al, single crystals, high purity, anisotropy of apparent resist. in longit. mag. fields 0-75550  
 Al, with linear lattice defects, temp. depend. of magnetoresist. and Matthiessen's rule departure (*Russian*) 0-84456  
 Au-Co, electron scatt., spin-orbit effects 0-65533  
 Au-Cu-Fe spin glass alloys, impurity mag. resist. meas. 0-59972  
 Au<sub>50-x</sub>Pd<sub>50-x</sub>Zn<sub>50-x</sub> (0 ≤ x ≤ 15.02), β'-phase, Hall effect and elec. cond. 0-107768  
 Au<sub>100-x</sub>Zn<sub>x</sub> (47 ≤ x ≤ 52), β-phase, Hall effect and elec. cond. 0-107768  
 Bi, charge carrier interaction with twinning planes in strong transverse mag. fields (*Russian*) 0-88577  
 Bi, deformation calculations, band struct. variation, electron phase transitions due to deform. (*Russian*) 0-65137  
 Bi, magnetoresistance, high temp. oscills., props. (*Russian*) 0-65606  
 Bi<sub>1-x</sub>Sb<sub>x</sub>, magnetophonon effect on hot electrons (*Russian*) 0-107814  
 Bi<sub>1-x</sub>Sb<sub>x</sub>, deformation calculations, band struct. variation, electron phase transitions due to deform. (*Russian*) 0-65137  
 Bi<sub>1-x</sub>Sb<sub>x</sub>, semiconducting alloy, band struct. study, Shubnikov-de Haas effect (*Russian*) 0-80181  
 Bi<sub>1-x</sub>Sb<sub>x</sub>, solid soln., temp. depend. of weak-field galvanomag. coeffs. (*Russian*) 0-70724  
 CdCr<sub>2</sub>S<sub>4</sub> crystal growth, structural defects, physical properties 0-60759  
 CdCr<sub>2</sub>Se<sub>4</sub>, ferromag. semicond., conc. anomalies rel. to red shift of absorpt. edge 0-70732  
 CdCr<sub>2</sub>Se<sub>4</sub>Ga(In), photoconductivity, photomagnetoresistance near Curie point (*Russian*) 0-100485  
 CdCr<sub>2</sub>Se<sub>4</sub>In(Ga), elec. resist. and magnetoresist., 2 to 200K 0-96876  
 p-CdSnAs<sub>2</sub>, Hall effect, thermo EMF, thermomagnetic effects 0-107822  
 p-CdSnAs<sub>2</sub>, heavily doped, elec. transport props. under elastic deformation 0-96915  
 CeB<sub>6</sub>, mag. and electronic props. 0-71048  
 Co<sub>2</sub>Ga<sub>1-x</sub>Fe<sub>x</sub>, elec. resist., temp. and mag. field depend., mag. contrib. 0-96846  
 Co<sub>2</sub>Ga<sub>2-x</sub>Fe<sub>x</sub>, mag. field depend. of resist., 5.80K 0-70676  
 CoS<sub>2</sub>, galvanomagnetic effect of single cryst. 0-96912  
 Co(S<sub>1-x</sub>Se<sub>x</sub>)<sub>2</sub>, galvanomag. effects, obs. and interpretation 0-70726  
 Cr, antiferromag., transverse magnetoresist., electron interference oscills. 0-65534  
 Cu and ilute Cu-Au alloy, magnetoresist. depend. on temp., 4.2-70K 0-70682  
 Cu, quenched, Hall coefficient, relaxation times, Fermi surface 0-84460  
 Cu wire, negative longitudinal magnetoresist. size effect 0-80252  
 CuH dilute alloy, Hall coefficient, relaxation times, Fermi surface 0-84460  
 Dy<sub>1-x</sub>Sm<sub>x</sub>, magnetoresist. of polycryst. specimens in fields up to 44 kOe (*Russian*) 0-92880  
 EuB<sub>2</sub>, electronic struct., transport and mag. props. 0-96782  
 EuB<sub>2</sub>, resist., Hall effect, and magnetoresist. under hydrostatic press., 4.2 to 300K 0-96879  
 EuTe, magnetic impurity states, mag. and transport props. 0-96913  
 Fe, irradiated with electrons then annealed, magnetoresistance at 20K (*French*) 0-103677  
 Fe, mag. breakdown and Hall resist., theory and model calcs. 0-75552  
 Fe thin layers, vacuum coated on PMMA, mag. behaviour during mech. stress cycles (*German*) 0-80581  
 Fe, whisker, deviations from Kohler's rule 0-70673  
 Fe-Al<sub>2</sub>O<sub>3</sub> granular films, superparamagnetism and relax. effects 0-71118  
 Fe<sub>1-x</sub>Ni<sub>x</sub>-B<sub>20</sub> and Fe<sub>1-x</sub>Ni<sub>x</sub>-P<sub>1-x</sub>B<sub>20</sub> metallic glasses, low temp. resist. and galvanomag. effects, mag. state influence 0-84461  
 Fe<sub>1-x</sub>Ni<sub>x</sub>-B<sub>20</sub> glass, resist., magnetoresist., and thermoelec. power 0-70681  
 Fe<sub>1-x</sub>Ni<sub>x</sub>-P<sub>1-x</sub>B<sub>20</sub> glass, resist., magnetoresist., and thermoelec. power 0-70681  
 Fe<sub>2</sub>O<sub>4</sub>, magnetite, magnetoresist., applied mag. field effects 0-80301  
 n-GaAs epitaxial film, magnetoresist. at low temp., geometric effect 0-93015

## magnetoresistance continued

- GaAs epitaxial films on strongly doped substrate, basic parameter meas. utilising magnetoresist. and SEM techniques under cathodoluminesc. conditions 0-65728  
 p-GaAs:Cr, semi-insulating, mobilities and carrier concentrations, temp. depend. 0-70702  
 GaAs-Al<sub>1-x</sub>Ga<sub>x</sub>-As heterojunction interface, two-dimensional hole gas obs., Shubnikov-de Haas meas. 0-80357  
 GaAs-Al<sub>1-x</sub>Ga<sub>x</sub>-As multilayers, two-dimens. transport at high mag. fields 0-65724  
 Ga<sub>1-x</sub>In<sub>x</sub>As, P<sub>1-y</sub>, electron effective mass, cyclotron reson. and magneto-phonon effect meas. 0-103618  
 Ge, magnetoresistance of electron-hole liq., percolation model 0-96920  
 p-Ge, negative magnetoresist. and Hall effect, press. and field depend. 0-70733  
 p-Ge, odd magnetoresist. under weak carrier heating conditions 0-96917  
 Hg, solid, resistivity ratio, 1.65 to 234K 0-59952  
 Hg<sub>0.82</sub>Cd<sub>0.18</sub>Te, electronic anomalous mass near reson. acceptor level, Shubnikov-de Haas meas. 0-80163  
 HgCr<sub>2</sub>Se<sub>4</sub>, n-type ferromag. semicond., galvanomagnetic props. 0-70727  
 Hg<sub>1-x</sub>Mn<sub>x</sub>Te, transverse magnetoresistance in quantised mag. fields 0-96922  
 HgSe, band struct. and spin splitting Shubnikov de Haas study 0-65445  
 Ho-Cu intermetallics, resist. and magnetoresist., mag. ordering obs. 0-70677  
 HoCu<sub>2</sub>, mag. struct. and elec. resist., neutron diffr. obs. 0-60206  
 InAs-GaSb superlattices, mag. field induced semimetal-semicond. transition 0-65656  
 In<sub>1-x</sub>Ga<sub>x</sub>As, P<sub>1-y</sub>, electron effective mass from Shubnikov-de Haas meas. 0-80298  
 In<sub>1-x</sub>Ga<sub>x</sub>P, As<sub>1-y</sub>, electron effective mass and Dingle temp., Shubnikov-de Haas oscills. 0-59859  
 n-InP, compensated, elec. props., space-charge effects 0-65569  
 InP, electron transport props., mag. field and temp. depend. 0-92888  
 InP epitaxial films, grown on heavily doped substrates, carrier mobility study, magnetoresist. meas. 0-60116  
 InSb, extrinsic and intrinsic, interaction of transverse magnetoresist. effects 0-65596  
 n-InSb, negative longit. magnetoresist., carrier conc. and mobility depend., 77K 0-60007  
 n-InSb, spin-magnetophonon resonance 0-96918  
 InSb, thin films, electrophysical props. obs. 0-103765  
 K, longitudinal elec. and thermal magnetoresistivities obs. 0-88541  
 LaB<sub>6</sub>, transverse magnetoresistance meas. 0-107764  
 MnB<sub>2</sub>, polycryst., magnetoresist. and mag. props. (*Russian*) 0-92907  
 MnP, high field magnetoresistance 0-107817  
 MnP, low field magnetoresistances, mag. phase diagram purity depend. 0-107816  
 n-Si, (111) inversion layers, valley splitting, Shubnikov de Haas oscills. 0-65698  
 NbSe<sub>2</sub>, CDW form., supercond. and Fermi surface determ., press. study 0-70891  
 NbSe<sub>2</sub>(2H), low field magnetoresist. and anomalous transport props. 0-65602  
 Nd, transport props., low temp., effect of mag. field 0-70679  
 Ni-Cu, magnetoresistivity anisotropy, spin mixing 0-88538  
 Ni-Si, magnetoresistivity anisotropy, spin mixing 0-88538  
 NiFe thin films, magnetoresistance, quasi-static characts. 0-107766  
 NiFe single crystals, longitudinal magnetoresist. meas. 0-70675  
 PbS, anomalous magnetoresist. 0-107813  
 Pb<sub>0.8</sub>Sn<sub>0.2</sub>Te: Cd, influence of Cd doping on high field magnetoresist. and Hall effect 0-75590  
 n-PbTe, noncubic (111) oriented epitaxial films, weak field magnetoresistance 0-75584  
 PbTe:In, Shubnikov-de Haas oscillatory effects, quasilocal impurity level 0-92912  
 Pd-Co, dil., breakdown of ferromag. order, magnetoresist. obs. 0-71046  
 Pd-Mn (1-10 wt.%), mag. ordering, influence on resistivity 0-75557  
 Pr, transport props., low temp., effect of mag. field 0-70679  
 Pt-Fe, dil., breakdown of ferromag. order, magnetoresist. obs. 0-71046  
 Pt-Fe(Co)(Mn), dil., skew scatt. Hall effect, magnetoresist. and mag. anisotropy, orbital magnetism of impurity 0-70678  
 Se-Gd, dil., reverse resist. anomaly and negative magnetoresist. 0-84459  
 Si, trigonal, transverse magnetoresistance meas., influence of illumination 0-65607  
 Si amorphous, negative magnetoresist., localised mag. states 0-70731  
 p-Si, odd magnetoresist. under weak carrier heating conditions 0-96917  
 Si on sapphire, residual strain effect on elec. props. (*Japanese*) 0-84522  
 Si on sapphire thin film, Hall effect, magnetoresistance (*French*) 0-65601  
 n-Si, size-induced magnetoresist. in strong elec. fields 0-65582  
 Si surface, MOS struct. band structure, minigaps, magnetoresistance, cond., space charge layers 0-92980  
 Si:P, polycryst. films, elec. props., EPR, defect states, doping effects 0-75660  
 Si-SiO<sub>2</sub> boundary, surface charge transport in valence band of Si 0-70789  
 Si-SiO<sub>2</sub> inversion layer, n-channel, anomalous magnetoresist., model 0-96996  
 Sm, magnetoresistivity and elec. resist., 4.2 to 300K (*Russian*) 0-88539  
 Sm, transport props., low temp., effect of mag. field 0-70679  
 Sm<sub>1-x</sub>La<sub>x</sub>S, magnetoresist. in semicond. and metallic phases 0-96914  
 SmS<sub>1-x</sub>As<sub>x</sub>, magnetoresist. in semicond. and metallic phases 0-96914  
 Sm<sub>1-x</sub>Y<sub>x</sub>S, magnetoresist. in semicond. and metallic phases 0-96914  
 Sn, galvanomagnetic props., temp. depend. meas. in single cryst. 0-96850  
 β-Sn, transverse magnetoresist., temp. depend. in mag. field (*Russian*) 0-107765  
 Ta<sub>1-x</sub>Ti<sub>x</sub>S<sub>2</sub> (1T), magnetoresistance in the Anderson localized states near the metal-nonmetal transition 0-88479  
 Ta<sub>1-x</sub>Ti<sub>x</sub>S<sub>2</sub> (1T), magnetoresist. near metal-nonmetal transition at ultra low temps. 0-88600  
 Te, impurity spectroscopy 0-65499  
 Te, two types of carriers 0-60013  
 Tm, Sm, magnetoresist. and Hall effect, stoichiometry effects 0-65597  
 Y-Gd, dil., reverse resist. anomaly and negative magnetoresist. 0-84459  
 ZnCr<sub>2</sub>Se<sub>4</sub>In, magnetoresist. and elec. resist. above and below Neel temp. (*Russian*) 0-88576  
 ZnMn, dil., magnetoresist. meas., temp. depend. anisotropy 0-65532  
 ZrC-C composite system, negative magnetoresist. 0-60008



magnetoresistance, thermal *see* thermal magnetoresistance

magnetoresistivity *see* magnetoresistance

# magnetosphere

*see also* magnetospheric electromagnetic wave propagation; radiation belts

A-index, 1964-1976, rel. to geomag. field and interplanetary field states 0-104866

auroral acceleration region, altitudinal double-layer criterion 0-94656

auroral arcs formation and V-potential double layers 0-103185

auroral arcs global formation, numerical simulation in three-dimensionally coupled ionosphere magnetosphere 0-67446

auroral convection over  $60^\circ \leq \Lambda \leq 75^\circ$ : Millstone Hill incoherent scatter obs. 0-67454

auroral particle dumping into ionosphere and magnetotail structure 0-109313

balloon and rocket programs, conf. Bournemouth, England (1980, Aug.) 0-105433

beam-plasma interaction experiment, using electron beam from JIKIKEN satellite (*Japanese*) 0-94655

Bernstein wave convective props. 0-90292

Birkeland current sheets in dayside polar region, rel. to interplanetary field 0-90289

Birkeland currents at high-latitude, suprathermal electron contrib. 0-90290

boundary layer, hydromagnetic waves driven by vel. shear 0-105133

boundary layer at low-latitude, fluid mech. model 0-85808

bow shock, backstreaming ions interaction with solar wind 0-101499

bow shock, collisionless shocks simulation and laboratory expts. 0-87893

bow shock, conference, Strasbourg, France (1978 August 31 to September 1) 0-82573

bow shock, DC mag. field obs. 0-90306

bow shock, first evidence and early studies, historical introduction 0-85816

bow shock, initial ISEE mag. field obs. 0-90307

bow shock, kinetic models of shocks in collisionless plasmas 0-90330

bow shock, nonlinear plasma processes in upstream solar wind 0-85833

bow shock, obs. of backstreaming protons in upstream solar wind 0-90309

bow shock, review of upstream energetic-particle meas. 0-90308

bow shock, satellite obs. of macroscopic struct. 0-85815

bow shock, solar wind interaction with backstreaming ions 0-90287

bow shock, solar wind upstream deceleration rel. to diffuse upstream ions origin 0-98528

bow shock, theory of magnetic shocks in collisionless plasma 0-85854

bow shock, three-dimensional shape 0-85832

bow shock, upstream particle events obs. close to shock and 200 R<sub>E</sub> upstream 0-77247

bow shock interaction, backstreaming ions and interplanetary mag. field 0-101500

bow shock plasma, possible generation mechanisms of low-freq. waves ( $\leq 50$  Hz) 0-90312

bow shock vicinity, low-freq. waves obs. 0-90311

charged particle fluxes, obs. by JIKIKEN scientific satellite (*Japanese*) 0-94654

cleft region dynamics 0-101483

configuration long-term changes, implications of auroral changes during 18th and 19th centuries 0-98498

convection, role in global scale electrodynamic coupling of ionosphere high and low latit. regions 0-77194

convection electric field, divergence rel. to auroral currents and elec. pots. and precip. generation 0-67453

convection in polar cap, after interplanetary mag. field becomes northward 0-94658

convection intensification, effect on mid-latitude ionosphere 0-105122

cusp region, precipitation and ion convection rel. to interplanetary mag. field 0-90288

cusp region on dayside, field line topography, precipitation implications 0-85822

cyclotron soliton theory of Earth's kilometric radiation 0-94657

daily mag. variations meas. in Alaska, atmos. current system 0-85590

disturbance, link with outer radiation belt electron intensity increase 0-77225

electric double layer, electron velocity distrib. on high pot. side 0-70010

electric field, influence on thermosphere N.Polar Cap winds 0-67445

electric field in VLF to HF range, EXOS-B obs. 0-67478

electric field on disturbed days, at mid-latitude 0-77230

electric fields, and currents, related geomag. vars., review 0-105121

electric fields parallel to mag. lines, studied by electron injection expts. 0-72702

electrical characteristics, rel. to field-aligned current sources in high-latit. ionosphere 0-72674

electrical coupling to lower atmos., quasi-static model 0-61865

electron beams, counterstreaming, at altitudes of 1 R<sub>E</sub> over auroral zone 0-67474

electron flux variations, in inner radiation belt 0-67470

electron intensity fluctuations meas. from Cosmos 484 satellite 0-72698

electron plasma oscillation bursts correl. with whistlers 0-72703

electron population regions, from magnetopause to ionosphere 0-77235

electron precipitation during substorm, modulation by hydromagnetic waves 0-105113

electrons, epithermal dumbbell distrib. Prognost 7 obs. following-shock wave 0-109321

electrons, evidence for trapped flux limit from pulsating aurorae 0-72666

electrostatic charge buildup on ATS 6 and 1976-059A 0-72744

electrostatic wave excited by current pulse in warm magnetoplasma, theory 0-77240

electrostatic waves near upper hybrid reson., free energy source 0-85805

ELF-VLF emissions, quasi-periodic, assoc. with Pc 3.4 mag. pulsations, geomag. conjugacy 0-67475

energetic particle penetration into inner magnetosphere during storms 0-72716

equatorial elec. field during storm, obs. of whistlers 0-85817

equatorial electric field at  $L=2.3$ , power density 0-82146

field aligned current above auroral arc, e<sup>-</sup> and H<sup>+</sup> precipitation obs. 0-77215

field aligned current distribution, from S<sub>p</sub> obs. in Alaska 0-85813

field-aligned electric currents, global distrib. of induced ionospheric fields and currents 0-109303

geomagnetic activity, cyclical nature due to interplanetary field 0-81813

geomagnetic activity, K-index 3-hr range, geophys. meaning 0-82143

# magnetosphere continued

geomagnetic bays rel. to geomagnetic activity and 1972 interplanetary magnetic field 0-105124

geomagnetic daily variations influenced by interplanetary field 0-85591

geomagnetic fluctuations, high sensitivity obs. by new space-borne ring-core type magnetometer (*Japanese*) 0-94671

geomagnetic transfer functions at pulsation periods 0-72417

geomagnetic variation field modeling during substorms, current system anal. 0-105130

geosynchronous satellite environment, ion contaminant cloud 0-72701

high-latit. magnetosphere, average parallel elec. field from perpendicular elec. field vars. below 8000 km 0-72706

hydromagnetic energy spectra, depend. on solar wind vel. and interplanetary mag. field direction 0-67476

hydromagnetic wave rotation between magnetosphere and ground 0-61969

induced elec. fields in ionosphere-magnetosphere system, review 0-94647

inner radiation belt electron precipitation, meas. 0-67452

inner radiation belt proton spectra from Kosmos 721 satellite 0-72699

International Sun-Earth Explorer (ISEE) mission, review 0-90320

interplanetary magnetic fields influencing atmos. elec. currents 0-105126

inverse loss cone electrons, temp. anisotropy quasi-linear relaxation due to interaction with electrostatic waves (*Russian*) 0-109314

ion beam experimental on Spacelab, source design 0-85840

ion beam injection from engines of proposed solar power satellites 0-82149

ion composition and origin, of high-altitude region during mag. storm 0-82144

ion counterstreaming of O<sup>+</sup> and H<sup>+</sup> in plasmasphere 0-72700

ion heating in auroral zone, by electrostatic ion cyclotron waves 0-72686

ionisation ducts, detect. via JIKIKEN (EXOS-B) satellite VLF Doppler shift meas. (*Japanese*) 0-94651

ionosphere electric fields induced by ion drag and substorms 0-77199

ionosphere field-aligned currents caused by magnetosphere convection 0-90278

ionosphere-magnetosphere current system, generating Pi ULF waves 0-85819

JIKIKEN (EXOS-B) scientific satellite, magnetosphere obs. (*Japanese*) 0-94674

kilometric radiation characts., initial results from JIKIKEN (EXOS-B) satellite obs. (*Japanese*) 0-94648

kilometric radiation from auroral zone, coherent nonlinear theory 0-101495

kilometric radiation from auroral zone, propagation direction 0-101497

kilometric radiation generation, inner magnetosphere auroral zone 0-105128

longitudinal currents, dynamic processes in turbulence development 0-67469

magnetic curl in front of magnetosphere boundary, laboratory expts. 0-85804

magnetic noise of low-freq., generated on auroral field lines 0-101494

magnetic-field-aligned elec. fields generation mechanisms 0-77233

magnetopause, energetic electron spectrum meas. from Prognost 3 0-72697

magnetopause and magnetotail particle burst obs. 0-85820

magnetopause wave-particle viscous effects, role of electrostatic flow shear instability 0-96359

magnetosheath, obs. of energetic electrons of magnetospheric origin 0-90310

magnetosheath, Prognost 4 obs. of  $\leq 2$  MeV electrons and cold plasma 0-90296

magnetosheath, turbulence rel. to solar wind ion injections in morning auroral oval 0-98502

magnetosheath burst of medium nuclei, obs. from Imp 8 (1974, Feb. 16) 0-101501

magnetosphere, characts. at 0840-1040 hours local time, satellite obs. 0-101498

magnetosphere boundary layer, field-aligned currents theory 0-67473

magnetosphere-ionosphere electrical coupling, two-dimens. model 0-61938

magnetotail, neutral sheet, particle accelerations 0-72696

magnetotail observing satellite GEOS-3, proposed mission 0-82163

magnetotail phenomena and auroral acceleration 0-85818

magnetotail plasma layer structure and auroral particle dumping into ionosphere 0-109313

magnetotail stretched configuration, dynamic evolution theory 0-72719

magnetotail structure, effect of interplanetary mag. field orientation 0-105131

material charging in space environment 0-109327

merging with interplanetary field, half-wave rectifier response 0-72710

MF duct formation and bubble initiation 0-72712

micropulsations near magnetopause, elec. field obs. 0-85814

mini-substorm and long-period Pi 2 event, 1978 December 11, Jikiken satellite obs. (*Japanese*) 0-94653

neutral sheet, shape and posn., statistical determ. 0-72717

open magnetic field lines near subsolar region, particle obs. 0-85810

OPEN program for investigation of origins of plasma in Earth's neighborhood 0-109318

particle radial diffusion, estimate from elec. & mag. field fluctuations 0-90293

Pc5 pulsations, model of magnetosphere and ionosphere elec. and mag. fields 0-77234

perturbations caused by mag. storms, review of obs. 0-98495

physics (*Chinese*) 0-82153

Pi 2 pulsations, equatorial, fine struct., rel. to magnetosphere cavity reson. 0-72721

Pi pulsation at high latitude, rel. to plasma convection 0-72726

plasma, collisionless, stability of contact discontinuity, solar wind and magnetosphere boundary appls. 0-62002

plasma, interaction of knowledge from astrophysical and lab. plasmas 0-59166

plasma convection in polar regions, model calcs. 0-82151

plasma drift in radial direction at nighttime, and coupling to ionosphere 0-77239

plasma populations, in simple open model 0-90295

plasma sheet, cause of thinning during magnetospheric substorms 0-72705

plasma sheet, magnetised plasma slow convection theory 0-109312

plasma sheet, plasma flows rel. to discrete auroras occurrence and lifetimes 0-67447

plasma sheet dynamics, variability assoc. with substorms 0-98518

plasma sheet dynamics and mag. storms, conceptual model 0-77236



**magnetosphere continued**

- plasma stability during storm conditions, Alfvén waves and drift modes 0-82150
- plasma waves, obs. during JIKIKEN (EXOS-B) satellite initial phase (Japanese) 0-94675
- plasma waves, stimulated, in magnetosphere, JIKIKEN (EXOS-B) satellite expts. (Japanese) 0-94649
- plasma pause, electron density profile meas. stimulated plasma wave results (Japanese) 0-94650
- plasma pause crossing by JIKIKEN (EXOS-B) satellite, detect. by VLF Doppler shift crossing (Japanese) 0-94651
- plasma sphere, magnetospheric and ionospheric elec. field simultaneous obs. 0-105110
- plasma sphere, mid-latitude, nighttime electron content, geophysical disturbance effects, 1974 August to November 0-94642
- plasma sphere, midlatitude thermal plasma affected by quiet time EM drifts 0-85807
- plasma sphere, wave-particle interactions, ELF-HF obs. from EXOS-B 0-67467
- polar cap, mag. field perturbations compared to solar electron profile 0-72718
- polar cap plasma flow entry region, longit. position 0-67472
- polar wind morphology in mag. quiet conditions 0-72713
- proportional counter, with thin mica windows, for low-energy particles 0-109260
- proton-cyclotron instabilities, in non-uniform loss-cone magnetospheric plasma 0-90286
- quadrupole shape 0-101492
- outer radiation belt, maximum fluxes of electrons with  $E > 1$  MeV (1958-1971) 0-61968
- radiation environment of space vehicles electronic components, laboratory simulation 0-94689
- radio waves, obs. during JIKIKEN (EXOS-B) satellite initial phase (Japanese) 0-94675
- ring current during quiet field variability, mid-latitude 0-72714
- ring current ion composition at  $L > 4$ , Prognost-7 obs. 0-98517
- ring current magnetic field at magnetically quiet geomagnetic equator 0-105123
- ring current magnetic field charact., spherical harmonic analysis 0-101493
- ring current of magnetic storm, origin by inward displacement of trapped particles 0-72708
- $S_a$  variation, magnetosphere or ionosphere dynamo? 0-109090
- shielding of atmosphere and evolution of life 0-104883
- solar wind compression, rel. to solar cycle var. in geomag. external spherical harmonic coeffs. 0-85592
- solar wind-magnetosphere dynamo, energy coupling function and substorms 0-105134
- solar wind-magnetosphere dynamo affected by IMF vector 0-85824
- solar wind-magnetosphere energy coupling, geomag. disturbances 0-85821
- spacecraft, charge neutralisation via electron emitter (Japanese) 0-94673
- substorm, definition of phenomena 0-82145
- synchronous orbit low energy ion flux, pitch angle distrib. 0-85812
- synchronous orbit magnetosphere behaviour during nighttime substorm 0-85811
- test particle in mag. field, pot. 0-106872
- trapped energetic particle spectra, effect of injection location 0-72711
- trapping of particles at  $90^\circ$  pitch angle for very long times 0-72709
- turbulent regions, rel. to ULF elec. field fluctuations in dayside auroral oval 0-98505
- ULF oscillation of ion flux during Pc 4, 5, ATS 6 obs. 0-72707
- VLF and magnetosphere structure, magnetic storms 0-72724
- VLF echoes excited by Isis 2 HF transmitter, theory of electrostatic wave excitation 0-72240
- VLF plasma waves, obs. and comparison with high energy electron flux by EXOS-B satellite (Japanese) 0-94652
- VLF wave events at  $L=4$  correl. to optical emission 0-101468
- VLF wave measurement at ground station, antenna pickup for vertical elec. field 0-105063
- VLF waves triggered by natural whistlers 0-98521
- wave-particle interactions satellite research review, Ariel 3, 4, Geos, ISEE satellites appl. 0-90317

**magnetospheric electromagnetic wave propagation**

- atmospherics propagation, simultaneous obs. made in Japan and Thailand 0-98520
- ATS-6 radio beacon data, rel. to geophysical disturbance effects on mid-lat. plasmasphere nighttime electron content 0-94642
- coherent VLF signal injection into magnetosphere, threshold power for growth 0-101496
- cosmic noise absorption during substorms 0-72727
- ELF-VLF emissions, quasi-periodic, interaction with Pc 3-4 mag. pulsations 0-67475
- kilometric radiation from auroral zone, propagation direction 0-101497
- layered plasma, use of Fuchsian differential eqns. 0-75060
- magneto-active plasma, group-vel. direction 0-59201
- magnetoactive collisional plasma, dielectric tensor, refl. index and attenuation 0-59202
- magnetoplasma, refr. index profiles in layered media, extraordinary mode 0-72723
- MF duct formation and bubble initiation 0-72712
- Pi propagation at nighttime, obs. on E-W axis 0-98519
- radio waves, obs. during JIKIKEN (EXOS-B) satellite initial phase (Japanese) 0-94675
- radio waves, propag. mode determ. using stimulated plasma wave results (Japanese) 0-94650
- radio window theory, transmission coeff. 0-61953
- riometer obs. during Pc 4-5, concurrent obs. in phase with magnetic data 0-82147
- side-band mutual interaction of whistler-mode waves 0-82148
- ULF wave propag., axisymmetric guided mode sources in magnetosphere model 0-72731
- VLF and magnetosphere structure, magnetic storms 0-72724
- VLF echoes excited by Isis 2 HF transmitter, theory of electrostatic wave excitation 0-72240
- VLF emission modulation freq. shift relative to geomagnetic pulsation freq. 0-72729
- VLF propagation, theory of rays and foci in magneto-ionic medium 0-105135
- VLF signals, Doppler shift meas. by JIKIKEN (EXOS-B) satellite (Japanese) 0-94651

**magnetospheric electromagnetic wave propagation continued**

- VLF whistler obs. of radial plasma drift and coupling to ionosphere 0-77239
- whistler ducting in plasmasphere, ray-trace study 0-72704
- whistler low-latitude coordinate observation system using direction finder and real-time analyser 0-67479
- whistler mode, interpretation of 6-component measurements 0-83921
- whistler precursor emissions and whistlers, ducted propagation 0-85809
- whistler propagation in magnetospheric plasma 0-90294
- whistlers, coherent nonlinear interaction dependent on wave amplitude 0-72715
- whistlers, duct struct. and formation 0-94659
- magnetostatic wave devices**
  - bulk wave propagation in multilayered structure 0-60380
- magnetostatic waves**
  - composite semiconductor-ferrite struct., surface magnetostatic spin wave interactions (Russian) 0-88739
  - ellipsoid with domain struct., magnetostatic oscills., theory 0-93102
  - films, ferromagnetic, perpendicularly magnetised, surface and vol. magnetoelastic waves (Russian) 0-93151
  - Fe garnet, optical radiation interaction with magnetostatic waves 0-76009
  - YIG film, magnetostatic surface wave propag. in nonuniform mag. field 0-80574
  - YIG, multilayer mag. layer structures, magnetostatic surface wave propag. 0-88839
  - YIG sandwiched between grounded dielectric layers, magnetostatic bulk wave propagation 0-60380
  - YIG, thin films, magnetostatic modes at Q-band freq. 0-65828

**magnetostriction**

- alkali hyperoxides, ionic  $\pi$ -electron systems, magnetostriction 0-93155
- antiferromagnets, magnetoacoustic resonance of domain boundaries (Russian) 0-65636
- cavitation corrosion of materials in molten metals on const. mag. field appl. (Russian) 0-60987
- defects in magnetized samples, magnetostrictive conversion of US waves into EM fields 0-66008
- ferrites, magnetostriction due to  $\text{Co}^{2+}$  ions, effect of excited states 0-65990
- ferromagnet, itinerant electron, magnetoelastic contribs. to US vel., elastic consts., and susceptibility 0-75829
- ferromagnetic bar, stressed, reverse magnetostrictive effect (Rumanian) 0-84630
- ferromagnetic domain theory, quasi-dislocation theory appl. (Japanese) 0-60358
- ferromagnetic solids, magnetomechanical effects, magnetostriction, hysteresis, stress, yielding, fatigue damage, crack growth (Polish) 0-71150
- hexagonal and cubic harmonics up to degree 6 0-88856
- itinerant electron ferromagnets, magneto-volume effects 0-60397
- itinerant ferromagnets, magnetoelastic props., thermodynamic aspects 0-66002
- martensitic transformation point shift, in strong mag. field, magnetostriction effect (Russian) 0-108440
- metallic-glass ribbon, stress dependences of longitudinal wave velocity 0-75825
- Metglas 2605 ribbon, saturation magnetostriction meas. by small-angle magnetisation rot. 0-60391
- Metglas 2826 ribbon, saturation magnetostriction meas. by small-angle magnetisation rot. 0-60391
- optical fibre magnetic field sensors 0-69510
- Permalloy films with band domain struct., thermomag. recording, resolving power (Russian) 0-75769
- phase transitions with two order parameters, Landau theory, mag. reorientation 0-103456
- polycrystalline and amorphous strips, magnetostriction consts. determ. method 0-86355
- rare earth-Fe, compounds, magnetoelast. props., book contrib. 0-75838
- rare earth-Zn alloys, ferromag., parastriction and magnetoelastic coeffs. 0-65996
- spontaneous symmetry breaking and magnon-phonon spectra 0-65991
- steel, structural, 34KhN3M, heat treatment effect on magnetostriction 0-104306
- transition metal, ferromag., band theory of linear magnetostriction 0-71141
- transition metals, 3d, ferromag. props., book contrib. 0-75724
- wheatstone bridge technique for magnetostriction measurements 0-57348
- $\text{CeB}_6$ , magnetostriction, US absorpt. and thermal expansion 0-66004
- Co-B-(Cr) thin film glasses, mag. props. and corrosion resist. 0-80576
- Co-Fe, soft mag. props. rel. to metallurgical aspects 0-88810
- Co-Fe amorphous alloys, worked, permivar type mag. hysteresis loop, longit. Kerr effect obs. 0-65958
- Co-Mn-Ni-Fe-Si-B amorphous alloys, mag. props., low magnetostriction 0-75832
- Co-Si-B, amorphous ribbon, saturation magnetostriction meas. by small-angle magnetisation rot. 0-60391
- $\text{Co}_2\text{Fe}_3\text{Ni}_{10}(\text{Si},\text{B})_{28}$ , amorphous, soft mag. props., switched-mode power supply apps. 0-88850
- Cr-Co, phase transformations and magnetostriction (Russian) 0-103869
- Cr-Ni-Mo 40KhN2MA, magnetostriction used in inspection after heat treatment 0-108673
- Cr-Re, phase transformations and magnetostriction (Russian) 0-103869
- $\text{DyCo}_5$ , noncollinear mag. struct. appearance in mag. fields, magnetostriction meas. (Russian) 0-100607
- $\text{DyFe}_3$  and  $\text{Dy}_2\text{Fe}_{23}$ , magnetostriction, room temp. to 80K 0-65993
- $\text{ErFe}_3$  and  $\text{Er}_2\text{Fe}_{23}$ , magnetostriction, room temp. to 80K 0-65993
- $\text{Er}_2\text{Fe}_{23}$ , magnetostriction, temp. depend., 20 to 350K 0-65994
- (Fe,Co,Ni)-(Si,B), amorphous mag. alloy, magnetostriction rel. to soft mag. props. 0-84633
- Fe, spontaneous volume magnetostriction 0-65989
- Fe-Al, domain struct. and magnetostriction, heat treatment effect 0-60398
- Fe-B-Cr(Si) thin film glasses, mag. props. and corrosion resist. 0-80576
- Fe-B(P) amorphous alloys, anomalous thermal expansion,  $\Delta E$  effect, Invar and Elinvar charact., delay time 0-80589
- Fe-Ni Invar, magnetovolume coupling enhancement factor, temp. depend. 0-88851
- Fe-Pd Invar alloy, Young's modulus, magnetostriction, Curie temp. 0-65988
- Fe-Si, (110) [001] oriented, mag. props., compressive stress effects 0-60392



**magnetostriction continued**

- Fe-Si, grain oriented transformer sheets, permeability and magnetostriction, tensile stress effects 0-88843  
 Fe-Si (3 wt.%), mag. loss and magnetostriction, DC flux alternation effects 0-88794  
 Fe-Si (3 wt.%) laminations, magnetostriction behaviour associated with closure domain spikes 0-75834  
 Fe<sub>80</sub>B<sub>20</sub> metallic glass, crystn. and struct. relax., Mossbauer effect study 0-75182  
 Fe<sub>3</sub>Co<sub>2</sub>B<sub>20</sub>Si<sub>10</sub>Al<sub>3</sub>, stress-induced variation in magnetisation and dynamic magnetostrictive charact. 0-88855  
 (Fe<sub>1-x</sub>Co<sub>x</sub>)<sub>70</sub>Si<sub>8</sub>B<sub>14</sub>, amorphous, saturation magnetostriction, strain modulated FMR obs. 0-75863  
 FeGe<sub>2</sub>, antiferromag., Fermi surface, stress effects, oscillatory magnetostriction and torque meas. 0-103616  
 Fe<sub>40</sub>-Ni<sub>60</sub>-P<sub>20</sub>-Y<sub>20</sub>, amorphous, Rayleigh region and coercive force 0-88806  
 (FeNi)<sub>80</sub>Bi<sub>17.5</sub>Al<sub>2</sub>Si<sub>0.5</sub>, stress-induced variation in magnetisation and dynamic magnetostrictive charact. 0-88855  
 Fe<sub>40</sub>Ni<sub>40</sub>(Mo<sub>10</sub>Si<sub>10</sub>B<sub>20</sub>), amorphous, soft mag. props., switched-mode power supply appls. 0-88850  
 Fe<sub>2</sub>O<sub>4</sub>, magnetocrystalline anisotropy, anomalies in magnetostriction and elastic constants 0-60244  
 Gd-Fe amorphous films, stress contrib. to perpendicular anisotropy 0-75819  
 Gd(Co<sub>1-x</sub>Ni<sub>x</sub>)<sub>2</sub> compounds, NMR and thermal expansion 0-66070  
 HoFe<sub>3</sub> and Ho<sub>2</sub>Fe<sub>23</sub>, magnetostriction, room temp. to 80K 0-65993  
 Ho<sub>2</sub>Fe<sub>23</sub>, magnetostriction, temp. depend., 20 to 350K 0-65994  
 HoRh<sub>2</sub>B<sub>4</sub>, low temperature magnetic properties 0-88728  
 KNiF<sub>3</sub>, magnetostriction, X-ray diffractometry and strain gauge meas. 0-65997  
 Li-Co ferrite, mag. anisotropy induced by thermomag. treatment, ionic order effect, magnetostriction meas. 0-103830  
 LiTmF<sub>4</sub>, van-Vleck paramagnet, giant magnetostriction (*Russian*) 0-103872  
 Mg-Tb(Dy)(Ho)(Tm), dil., macroscopic shape effect due to quadrupole orientation, magnetostriction and thermal expansion meas. 0-60396  
 Mn-Ni, thermal expansion, mag. susceptibility, lattice consts. 0-100341  
 NaFeF<sub>3</sub>, Mossbauer and low-temp. dilatometry study (*French*) 0-80662  
 Ni film, evaporated, for use as variable delay SAW device, magnetostrictive effects 0-71144  
 Ni, magnetostrictive vibr. obs. by laser interferometric technique 0-66000  
 Ni-B thin film glasses, mag. props. and corrosion resist. 0-80576  
 Ni-Co (25 wt.%), single crystals, mag. annealing effect on magnetostriction and magnetisation at high temps. 0-108047  
 Ni-Fe, soft mag. props. rel. to metallurgical aspects 0-88810  
 NiF<sub>2</sub>, thermal expansion and magnetostriction, 55K to room temp. 0-80586  
 NiFe, magnetising energy, anisotropic effects 0-88743  
 Ni<sub>2</sub>Fe<sub>3-x</sub>O<sub>4</sub>, magnetostriction, 80 to 300K, depend. on comp. and electron ordering on octahedral sites 0-65995  
 O<sub>2</sub> monolayers, on graphite, mag.  $\alpha$ -phase and  $\alpha$ - $\beta$ -phase transition 0-70530  
 Pd-Fe-Mn, ferromagnet-spin glass, thermal expansion forced, magnetostriction and magnetisation under high press. 0-65255  
 Pd-Ni, thermal expansion and magnetostriction meas. near crit. conc. for ferromagnetism 0-65881  
 Re, Fermi surface, Landau quantum oscill. meas. in magnetostriction, stress and strain derivatives 0-107691  
 SmFe<sub>2</sub> and Sm<sub>2</sub>Fe<sub>23</sub>, magnetostriction, room temp. to 80K 0-65993  
 (Tb,Dy)-Fe amorphous films prep. by cosputtering, magnetoelastic props. 0-97429  
 TbCo<sub>2</sub>, magnetocrystalline anisotropy and spontaneous magnetostriction 0-75831  
 Tb<sub>20</sub>Dy<sub>70</sub>Fe<sub>2</sub>, vertically zoned, magnetomechanical coupling and magnetostriction 0-65999  
 Tb<sub>3</sub>Dy<sub>70</sub>Fe<sub>2</sub>, prep. by powder metallurgy, magnetostrictive props. 0-75826  
 TbFe<sub>3</sub> and Tb<sub>2</sub>Fe<sub>3</sub>, magnetostriction, room temp. to 80K 0-65993  
 TbIG, [111] magnetoelastic props., rel. to Cotton-Mouton birefringence, 90-500K 0-103876  
 TmFe<sub>2</sub> and Tm<sub>2</sub>Fe<sub>23</sub>, magnetostriction, room temp. to 80K 0-65993  
 Y<sub>2</sub>Fe<sub>23</sub>, magnetostriction, temp. depend., 20 to 350K 0-65994  
 Y<sub>1-x</sub>Tb<sub>x</sub>Pd<sub>1-x</sub>, magnetisation, magnetostriction, and inelastic neutron spectra 0-65998  
 YbCuAl, mixed-valent cpd., thermal expansion and magneto-volume effects 0-66005  
 YbFe<sub>2</sub>, cryst. elec. field and exchange interac., <sup>170</sup>Yb Mossbauer obs., magnetostriction contrib. 0-108124  
 Zr(Fe<sub>1-x</sub>Co<sub>x</sub>)<sub>2</sub>, ferromag. and micromag., thermal expansion and forced volume magnetostriction 0-75830

**magnetostrictive devices**

- (Tb,Dy)-Fe amorphous films prep. by cosputtering, delay line characts. 0-97429

**magnetostrictive microphones** *see microphones***magnetostrictive transducers** *see magnetostrictive devices; transducers***magnetothermal effects** *see magnetocaloric effects***magnetrons**

- magnetic discharge cells with nonuniform periodic magnetic field 0-101799  
 mass spectrometer appl. using inverse magnetron and ion source on outside 0-57416

**magnets**

- see also electromagnets; permanent magnets; superconducting magnets*  
 ion optical system, magnet design for high current implantation or small isotope separators 0-68222  
 low field magnet, computer controlled, for optical and magnetic resonance studies 0-95113  
 non-superconducting magnet structures for near-term, large fusion experimental devices 0-86973  
 structural design features for commercial fusion power reactor magnet systems 0-86975  
 Sm-Co ring magnets for BWO, 110 to 170 GHz, design and appl. (*German*) 0-105684

**magnons***see also phonon-magnon interactions; spin waves*

- alkali hyperoxides, ionic  $\pi$ -electron systems, magnetogyration 0-93155  
 alloy, pseudobinary, ferromag., magnon energy derivation 0-107996  
 antiferromagnet, easy-plane, antiferromag. reson. linewidth and relax., theory 0-71189

**magnons continued**

- antiferromagnet, impure, Heisenberg model, impurity banding and mag. reson., theory 0-93181  
 antiferromagnet, neutron scatt. by magnons, modulated spin amplitudes 0-75722  
 antiferromagnet, two-dimensional, with easy-plane anisotropy, mag. excitations and two-magnon Raman scatt. 0-65839  
 antiferromagnets, exciton motion 0-70617  
 antiferromagnets, magnon damping in zero external mag. fields, magnon-magnon interactions 0-70988  
 $\alpha$ -bis (N-methylsalicylaldimino) copper II, one-dimens. spin-1/2 Heisenberg antiferromag., high-field spin dynamics 0-71224  
 Brillouin-Mandelstam scattering from thermal and excited magnons 0-70980  
 dimethylammonium copper tetrachloride, two-dimens. ferromag., saturation of parallel-pumped magnons 0-97147  
 disordered media, spin wave propagation, nonlinear magnon interactions (*Russian*) 0-80496  
 ethylammoniumtetrachlorochromate, optical absorption intensity, short-range spin correlation 0-108185  
 ferrimagnet, two sublattice, mag. polaritons 0-65845  
 ferrites, frequency tripling of spin waves due to longitudinal pumping excitation (*Russian*) 0-88740  
 ferromagnet, Heisenberg model, two-magnon reson. in absence of bound states, calc. 0-60423  
 ferromagnet, itinerant electron, magnon spectrum just below T<sub>c</sub>, theory 0-65833  
 ferromagnet, one dimensional, effect of biquadratic exchange on solitary waves 0-65836  
 ferromagnet, one-dimensional localised nuclear magnon modes 0-93098  
 ferromagnet magnetisation, influence of high intensity longitudinal sound waves 0-103875  
 ferromagnet with easy-plane anisotropy, HF magnon energies, kinematic consistency 0-93097  
 ferromagnetic Heisenberg chain, weakly bound magnon states (*Russian*) 0-100591  
 ferromagnetic semiconductor, surface localised low energy electron-magnon states (*Russian*) 0-88734  
 ferromagnetic semiconductors, free carrier absorpt. of radiation 0-97227  
 ferromagnetic slab, asymmetrical guided mag. polaritons 0-88738  
 ferromagnetic slab, light scattering from bulk and surface spin waves, theory 0-71389  
 ferromagnets, magnetisation stimulation by nonresonance AC mag. field (*Russian*) 0-65962  
 ferromagnets, spin wave excitation due to parallel pumping, mag. impurity interactions (*Russian*) 0-80497  
 Heisenberg amorphous ferromagnet, magnetisation and Curie temp., CPA calc. 0-75703  
 Heisenberg chain, classical, solitons and magnons 0-60161  
 Heisenberg chain, classical continuous, magnon-soliton phase shift 0-107998  
 Heisenberg continuous chain, quantum solitons as magnon bound states 0-60162  
 Heisenberg ferromagnet, cubic, with next nearest neighbour interactions, two-magnon bound states 0-70977  
 Heisenberg ferromagnet, linear, with applied mag. field, second-magnon like excitations 0-65837  
 Heisenberg ferromagnet, magnon renormalisation 0-65849  
 Heisenberg ferromagnet, surface magnetisation profile and localised magnons 0-70985  
 Heisenberg magnet, impurity band resonance at 0K, theory 0-66041  
 impurity relaxation in nonresonance field, phonon amplification (*Russian*) 0-100310  
 magnetically ordered cryst., indirect nuclear spin interactions 0-103847  
 magnon-photon interaction in ferromagnets, construct. and radiation effects 0-71188  
 metals, spin fluctuations, mag. field effect, electronic sp. ht. and elec. resist. 0-108026  
 methylammoniumtetrachlorochromate, optical absorption intensity, short-range spin correlation 0-108185  
 rare earth metals, magnon dispersions in ferromag. and screw structs., nonlinear s-f exchange interaction effect 0-75746  
 rare earth metals and alloys, ferromag. props., book contrib. 0-75725  
 rare earth orthoferrites, Raman scatt. from magnons, anisotropy consts. determ. 0-66178  
 rare earth systems, mag. excitations, review of neutron scatt. data 0-60227  
 resonant light scattering from magnetic excitations, review 0-97290  
 semiconductor, ferromag., localised magnon mode relax. theory 0-70986  
 semiconductor, ferromag., short wavelength magnon generation 0-70987  
 sine-Gordon chain, classical, low freq. dynamics 0-108020  
 TMMC, one-dimens. magnet, local magnon modes 0-65829  
 AuMn, mag. struct., phase transition, and magnon spectrum, random anisotropy effects 0-88722  
 CoCO<sub>3</sub>, Brillouin-Mandelstam light scatt. obs. of spin wave spectra 0-93358  
 CoCO<sub>3</sub>, LF exciton and Raman spectra, one-magnon and two-magnon scatt. 0-93333  
 CoCO<sub>3</sub>, light scatt. from magnons and phonons excited by microwave pumping 0-66213  
 CoCO<sub>3</sub>, spin excitation energies, quantum theory (*Russian*) 0-88735  
 CoCO<sub>3</sub>, two-sublattice noncollinear antiferromag., exciton-magnon light absorpt. mechanisms (*Russian*) 0-89017  
 Cr, mag. struct., phase transition, and magnon spectrum, random anisotropy effects 0-88722  
 CsCoBr<sub>3</sub>, ID Ising antiferromagnet, spin dependent Raman scattering from phonons and electronic excitations 0-103948  
 CsCoBr<sub>3</sub>, quasi ID Ising antiferromag., polarised Raman scatt. from mag. excitations 0-66182  
 CsCoCl<sub>3</sub> spin dynamics, neutron scatt. study 0-80493  
 CsMnCl<sub>2</sub>·2H<sub>2</sub>O, subthreshold two-magnon absorpt., depend. on freq., temp. and mag. field, exchange coupling const. (*Russian*) 0-71184  
 CsMnF<sub>3</sub>, antiferromag., variation of spin wave spectrum in interaction between magnons 0-65841  
 CsMnF<sub>3</sub>, exciton-magnon interactions in optical transition, absorpt. and emission spectra meas. 0-70981  
 CsMnF<sub>3</sub>, mag. struct., phase transition, and magnon spectrum, random anisotropy effects 0-88722  
 CsMnF<sub>3</sub>, parametric excitation of magnons, effect of RF modulation of mag. field 0-65842



**magnons continued**

- CsMnF<sub>3</sub>, parametric nuclear magnon excitation, mag. field modulation (*Russian*) 0-107999  
 CsNiF<sub>3</sub>, low frequency dynamics in external mag. field 0-108020  
 CsNiF<sub>3</sub>, one dimensional planar model with symm. breaking fields, thermodynamics, static props. 0-97111  
 CsNiF<sub>3</sub>, one-dimens. magnet, local magnon modes 0-65829  
 CsNiF<sub>3</sub>, quasi-one-dimensional ferromagnet, subthreshold parallel pumping of magnons 0-75745  
 CsNiF<sub>3</sub>, stochastic motion of Sine-Gordon-solitons, spin-correlation function 0-93105  
 CsNiF<sub>3</sub>, subthreshold parallel pumping of magnons and antiferromag. reson. 0-71185  
 Eu,Sr<sub>1-x</sub>S, Heisenberg spin glass system, excitations 0-84610  
 Fe<sub>2</sub> Pt, ordered ferromagnetic alloy, magnetic excitation obs. 0-70978  
 Fe<sub>80</sub>B<sub>20</sub>, amorphous, Brillouin scatt. from magnons, ferromag. reson. 0-65844  
 FeBO<sub>3</sub>, mag. linear dichroism and absorpt. spectra, exciton-magnon absorpt. mechanism 0-66160  
 FeF<sub>2</sub>, antiferromag., anomalous anti-Stokes/Stokes Raman scatt. intensity ratio 0-66177  
 FeF<sub>2</sub>:Mn, antiferromag. reson. and local magnon mode, FIR laser study 0-66042  
 FeF<sub>2</sub>:Mn, Heisenberg model, impurity band resonance at 0K, theory 0-66041  
 Fe<sub>1-x</sub>, spin waves and two magnon bound states, mag. field IR absorption meas. 0-65840  
 Fe<sub>1-x</sub>Mn<sub>x</sub>Cl<sub>2</sub>, disordered, Raman scatt. from Fe<sup>2+</sup> and Neel temp. 0-60579  
 Fe<sub>1-x</sub>Mn<sub>x</sub>Cl<sub>2</sub>, low-lying electronic excitations in antiferromag. and paramag. phases Raman scatt. study 0-71414  
 Fe<sub>1-x</sub>Zn<sub>x</sub>F<sub>2</sub>, dil. antiferromag., electronic and mag. props., Raman scatt. and optical absorpt. study 0-108207  
<sup>3</sup>He, normal liquid, elementary excitations, density and spin density, zero sound mode, press. depend. RPA model calcs. 0-59749  
 HoCo<sub>2</sub>, mag. excitations, neutron inelastic scatt. meas. 0-60231  
 K<sub>2</sub>CuF<sub>4</sub>, magnon condensation obs. in quasi-2D planar ferromag. phase 0-60232  
 K<sub>2</sub>CuF<sub>4</sub>, two-dimens. ferromag., saturation of parallel-pumped magnons 0-97147  
 K<sub>2</sub>FeF<sub>4</sub>, antiferromagnet, two-dimensional, mag. excitations 0-80492  
 K<sub>2</sub>FeF<sub>4</sub>, two-dimensional antiferromag., with easy-plane anisotropy, mag. excitations and two-magnon Raman scatt. 0-65839  
 K<sub>2</sub>MnF<sub>4</sub>, ordered quadratic-layer Heisenberg antiferromag., nucl. spin-magnon relax. 0-71217  
 K<sub>2</sub>MnF<sub>4</sub>, quadratic double layer antiferromag., two-magnon Raman scatt. 0-66183  
 KNiF<sub>3</sub>, <sup>19</sup>F spin-lattice relaxation 0-93211  
 K<sub>2</sub>NiF<sub>4</sub>, ordered quadratic-layer Heisenberg antiferromag., nucl. spin-magnon relax. 0-71217  
 K<sub>2</sub>Ni<sub>2</sub>F<sub>7</sub>, quadratic double layer antiferromag., two-magnon Raman scatt. 0-66183  
 MnCO<sub>3</sub>, parametric excitation of magnons, effect of RF modulation of mag. field 0-65842  
 MnCo<sub>3</sub>, parametric nuclear magnon excitation, mag. field modulation (*Russian*) 0-107999  
 Mn<sub>1-88</sub>Cr<sub>0.12</sub>Sb, antiferromag.-ferrimagnet, transition, neutron crit. scatt. and crossover effect 0-71023  
 MnF<sub>2</sub>, parallel pumping studies of magnon damping 0-70990  
 MnO, magnon-sideband lineshape, exciton-phonon interaction effects 0-65846  
 MnS, thermal cond., temp. depend., paramag.-antiferromag. transition effects 0-65321  
 α-O<sub>2</sub>, cryst., exciton, exciton-magnon, and biexciton absorpt. at 1.5K 0-84750  
 Pt<sub>0.75</sub>(Cr<sub>1-x</sub>Mn<sub>x</sub>)<sub>0.25</sub>, pseudobinary, magnon energy derivation 0-107996  
 Rb<sub>2</sub>CrCl<sub>4</sub>, optical absorption intensity, short-range spin correlation 0-108185  
 RbFeCl<sub>3</sub>·2H<sub>2</sub>O, pseudo-one-dimensional canted Ising antiferromag., spin-cluster excitations 0-70989  
 Rb<sub>2</sub>FeF<sub>4</sub>, antiferromagnet, two-dimensional, mag. excitations 0-80492  
 Rb<sub>2</sub>FeF<sub>4</sub>, two-dimensional antiferromag., with easy plane anisotropy, mag. excitations and two-magnon Raman scatt. 0-65839  
 Rb<sub>2</sub>MnCl<sub>4</sub>, quasi-2D antiferromag., linear birefr. and optical absorpt. spectra 0-71385  
 UAl<sub>2</sub>, spin fluctuations, mag. field effect, electronic sp. ht. and elec. resist. 0-108026  
 (V<sub>1-x</sub>Cr<sub>x</sub>)<sub>2</sub>O<sub>3</sub>, Raman scatt. and phase transitions 0-71420  
 Y garnet, inhomogeneous collective magnon oscill. excited by RF field (*Russian*) 0-100582  
 YIG, domain wall mobility and mass meas. method (*Russian*) 0-108033  
 YIG, one-magnon Raman scatt., Faraday rot. 0-66156

**Magnus effect** see fluid dynamics

**maintenance** see maintenance engineering

**maintenance engineering**

- accident at Three Mile Island, lessons learned 0-57929  
 electrical instruments in photometric laboratory 0-86283  
 fossil fuel utilisation, appls. 0-61234  
 fusion reactor, STARFIRE project, maintenance considerations 0-102346  
 fusion reactor, Tandem Mirror Reactor power plant, maintenance and handling economics 0-102311  
 fusion reactors, shielding and maintainability in an experimental Tokamak 0-99287  
 fusion reactors, Tokamaks, maintenance design requirements and economics 0-99285  
 power station, heat treatment, post weld, during construction and maintenance 0-93574  
 remote maintenance to comply with new legislation limiting occupational radiation exposure, in United States 0-106210  
 solar hotwater and heating systems, availability aspects 0-61314  
 turbogenerators, high capacity, heating reduction measures for enhanced reliability and interval between maintenance (*Russian*) 0-96175

**Majorana forces** see nuclear forces

**majority algebra** see algebra

**Malter effect** see secondary electron emission

**man-machine systems**

see also ergonomics

- nuclear power stations, control rooms, human factors design approaches, improvement of man-machine interface, error reduction 0-63327  
 nuclear power stations, human operator errors, analytical model 0-63329

**man-machine systems continued**

- voice communication, speech production mechanisms and models (*Spanish*) 0-87665  
 weather forecaster console for satellite data handling system 0-90205  
**management**  
 see also management science; research and development management  
 centralized management systems for Kagawa Prefecture irrigation-water system (*Japanese*) 0-89684  
 energy systems, logistic substitution model 0-89600  
 Indian scientists' role in policy making process, critical assessment 0-90653  
 water-resource development project design, optimal apportionment scheme appl. (*French*) 0-77019  
**management information systems**  
 see also database management systems; management science  
 steelworks computerised spectrometric analysis and management information system 0-89574  
 weather maps, structural description of contour maps 0-101419  
**management science**  
 see also critical path analysis  
 nuclear power plants, startup, staffing program, scope, tasks, resources, constraints, anal., implementation 0-63341  
**management techniques** see management science  
**Mandelstam representation**  
 hadronic targets, spin-1/2, Compton scatt., optimal sum-rule inequalities 0-105815  
 two-variable analyticity, phase-shift anal. 0-77987  
**manganese**  
 see also nuclei with .....  
 alkali chloride:Mn<sup>2+</sup>, spin Hamiltonian parameters, binding energies for cation vacancy complexes 0-96461  
 ammonium oxalate monohydrate:Mn<sup>2+</sup>, model for defect formation, EPR 0-103880  
 atom, collisional and radiative excited, lifetime meas. 0-91501  
 atom, fine struct. levels fitting, config. interaction effect, spin-orbit and electrostatic interaction parameters 0-69248  
 atom, nucl. quadrupole moments from laser-RF double reson. spectroscopy 0-57682  
 collinear spin structure of γ-phase, stability 0-107984  
 concentrations in NE-Pacific water 0-101384  
 film, elec. resist., deposition rate effect 0-97010  
 film, vacuum-evaporated, H(D) uptake kinetics and energetics 0-88430  
 K-shell ionisation cross sections, slow electron impact 0-83498  
 K-shell X-ray prod. by <sup>14</sup>N<sup>+</sup> bombardment 0-91482  
 laser, atomic, finely dispersed metal particle active medium 0-91777  
 lead acetate trihydrate:Mn<sup>2+</sup>, ESR, elec. cond. 0-93165  
 magnetic moment calcs., band struct. for paramag., antiferromag. and ferromag. states 0-60223  
 micronodules from NW Atlantic, SEM determination of morphology and chemistry 0-81869  
 n=2-2 transitions in XUV spectra, anal. 0-102472  
 spallogenic isotopes in Fe meteorites, radial distrib. 0-67488  
 thin film, DC resist., activation energy, thickness depend. 0-84518  
 thin films, vacuum deposited, in elec. field, resist., struct. 0-103761  
 tris-sarcosine calcium chloride:Mn<sup>2+</sup> ferroelec. dynamics, EPR and ENDOR study 0-75972  
 vapour, use in laser projection microscope with image-brightness amplifier 0-106541  
 X-ray absorpt., discontinuity, shape and extended fine struct. 0-66324  
 X-ray K-emission satellites, quasi-stationary states and origin 0-80903  
 Al<sub>2</sub>O<sub>3</sub>:Mn<sup>2+</sup>, Jahn-Teller Mn<sup>2+</sup> ions, phonon spectroscopy and thermal cond. meas. 0-88282  
 Al<sub>2</sub>O<sub>3</sub>:Mn<sup>2+</sup> under uniaxial stress, Jahn-Teller model 0-88521  
 BaMgF<sub>4</sub>:Mn<sup>2+</sup> ferroelec., EPR and ENDOR study, cryst. field tensor 0-71162  
 BaTiO<sub>3</sub> ceramic dielectric capacitor, processing prop. relations, hysteresis, permittivity 0-80730  
 CaF<sub>2</sub>:Mn, CaF<sub>2</sub>:Eu,Mn, single crystal predissociation phenomena, SEM cathodolum. obs. 0-59502  
 CaF<sub>2</sub>:Mn, EPR and optical absorpt. spectra 0-93171  
 CaF<sub>2</sub>:Mn, low temp. X-irrad., Mn centres, optical absorpt. and emission props. 0-60635  
 CaF<sub>2</sub>:Mn, X-irrad., impurity effects on defect prod. 0-92525  
 CaF<sub>2</sub>:Mn, X-irrad., thermolum. 0-60686  
 CdS:Mn, vacuum deposited film, Mn migration, EPR and X-ray study 0-65411  
 CdTe:Mn, introduction of elec. active defects 0-103647  
 CdTe:Mn, spin-lattice coeffs. of Mn<sup>2+</sup> 0-84646  
 CdTe:Mn<sup>2+</sup>, exciton refl. spectra and mag. susceptibility 0-66253  
 CdTe:Mn<sup>2+</sup>, luminesc. and magneto-optic reson., mag. field effect 0-93390  
 CsCaCl<sub>3</sub>:Mn, EPR, 4.2 to 450K, ferroelec. transition 0-60414  
 Cs<sub>2</sub>SiF<sub>6</sub>:Mn<sup>2+</sup>, IR absorpt. band, electron-vibr. effect 0-108238  
 Cu<sub>2</sub>O:Mn, photomemory mobility components, charged centre conc. 0-103725  
 FeF<sub>2</sub>:Mn, antiferromag., NMR relax., impurity bonding 0-66061  
 FeF<sub>2</sub>:Mn, antiferromag. reson. and local magnon mode, FIR laser study 0-66042  
 FeF<sub>2</sub>:Mn, Heisenberg antiferromag., impurity banding and mag. reson., theory 0-93181  
 FeF<sub>2</sub>:Mn, Heisenberg model, impurity band resonance at 0K, theory 0-66041  
 Ga<sub>1-x</sub>In<sub>x</sub>As:Mn grown by LPE, elect. props. 0-100541  
 Ge:Mn, Sb, recombination waves, convective instability development 0-70721  
 Ge:Mn, Sb 0-96906  
 Ge<sub>2</sub>S<sub>3</sub>:Mn, bond/struct. and character in Ge-S system, EPR obs. 0-66014  
 Ge<sub>40</sub>S<sub>60</sub>:Mn, bond struct. and character in Ge-S system, EPR obs. 0-66014  
 HgSe:Mn<sup>2+</sup>, temp. depend. of EPR of <sup>6</sup>S state ions 0-80593  
 InAs:Mn<sup>2+</sup>, Jahn-Teller effect for ion impurities 0-107753  
 (La<sub>2</sub>O<sub>3</sub>)<sub>1-x</sub>(CeO<sub>2</sub>)<sub>x</sub>:Mn, valence state of Mn, effect of annealing in H<sub>2</sub> atm., ESR obs. (*French*) 0-71164  
 (La<sub>2</sub>O<sub>3</sub>)<sub>0.95</sub>(CeO<sub>2</sub>)<sub>0.05</sub>:Mn<sup>2+</sup>, X-band EPR study 0-60409  
 Li<sub>2</sub>B<sub>4</sub>O<sub>7</sub>:Mn, thermolum. response to pions 0-101270  
 Li<sub>2</sub>B<sub>4</sub>O<sub>7</sub>:Mn<sup>2+</sup>, having inverse periodic struct., ENDOR study 0-97162  
 Mg(NH<sub>4</sub>)<sub>2</sub>(SeO<sub>4</sub>)<sub>2</sub>·6H<sub>2</sub>O:Mn<sup>2+</sup>, EPR spectra 0-100608  
 MgO:Mn<sup>2+</sup>, spin-lattice relax. time, meas. 0-66020



**manganese continued**

- MgO:Mn<sup>2+</sup>, HF phonon spectroscopy using supercond. tunnel junctions 0-65178  
 MgRb<sub>2</sub>(SeO<sub>4</sub>)<sub>2</sub>·6H<sub>2</sub>O:Mn<sup>2+</sup>, EPR spectra 0-100608  
 γ-Mn, antiferromagnetic, self-consistent bandstructure calcs. 0-88475  
 Mn [l]-lecithin lipid-water system, NMR and EPR obs. 0-61168  
 Mn<sup>2+</sup>, doped ion in divalent metal cpds., Szigeti charge and correl. with hyperfine coupling const. 0-96831  
 Mn<sup>2+</sup> ions in Scheelites, zero-field splittings 0-75531  
 Mn<sup>2+</sup>, zero-field splittings, correl. with axial site distortions, superposition model 0-93168  
 Mn-SiO<sub>2</sub>, annealed cermet films, elec. resist., composition depend. 0-97007  
 Mn-SiO<sub>2</sub> cermet thin film, DC resist., activation energy, thickness depend. 0-84518  
 Mn<sup>2+</sup>-oxalacetic acid-H<sub>2</sub>SO<sub>4</sub>-KBrO<sub>3</sub>, chaos type reactions anal. 0-85165  
 MnO, K X-ray absorpt. discontinuity, shape and extended fine struct. 0-66324  
 MnO<sub>2</sub>, K X-ray absorpt. discontinuity, shape and extended fine struct. 0-66324  
 Mn<sub>2</sub>O<sub>3</sub>, K X-ray absorpt. discontinuity, shape and extended fine struct. 0-66324  
 Mn<sub>3</sub>O<sub>4</sub>, K X-ray absorpt. discontinuity, shape and extended fine struct. 0-66324  
<sup>55</sup>Mn, variation of hyperfine splitting consts. with interatomic distance for 3d<sup>5</sup> ions 0-97133  
<sup>52</sup>Mn, new short-lived, generator-produced radionuclide, positron tomography appl. 0-109006  
 NaCl:Mn<sup>2+</sup>, Mg<sup>2+</sup>, doubly doped, ionic thermocurrent study of linear dimer 0-79977  
 NaCl:Mn<sup>2+</sup>, thermolum. spectra, mechanisms 0-80873  
 NaF:Mn, role of Mn<sup>2+</sup> in thermolum. 0-97353  
 Na<sub>2</sub>O-B<sub>2</sub>O<sub>3</sub>:Cu<sup>2+</sup>, Mn<sup>2+</sup> glasses, Cu<sup>2+</sup>-Mn<sup>2+</sup> interaction studied by ESR 0-93166  
 NaZnGeO<sub>4</sub>:Mn, electrolum., ionisation domains 0-84787  
 Si:Mn, impurity states, localised orbital approach 0-92851  
 Si:Mn, Bi, standard, doubly implanted, Rutherford backscattering meas. at MeV energies, screening corrections 0-88204  
 Si:Mn<sup>2+</sup>, spin-lattice relax. of Jahn-Teller centres, coexistence of minima with different symmetries 0-80602  
 SnO<sub>2</sub>-Cu, S-ZnS:Mn,Cu-Al<sub>2</sub>O<sub>3</sub>-Al, light-emitting struct., cond. and electrolum., heat treatment 0-97345  
 SnTe:Mn, NMR shift meas. 0-97154  
 SrS:Mn, Zr phosphor, photodielectric effect 0-107848  
 (Zn,Mg)<sub>2</sub>(PO<sub>4</sub>)<sub>2</sub>:Mn<sup>2+</sup>, cathodoluminescence obs. 0-71492  
 Zn(NH<sub>4</sub>)<sub>2</sub>(SeO<sub>4</sub>)<sub>2</sub>·6H<sub>2</sub>O:Mn<sup>2+</sup>, EPR spectra 0-100608  
 ZnRb<sub>2</sub>(SeO<sub>4</sub>)<sub>2</sub>·6H<sub>2</sub>O:Mn<sup>2+</sup>, EPR spectra 0-100608  
 ZnS:Cu, Cl, Mn film, AC electrolum. 0-60680  
 ZnS:Cu, Mn DC electroluminescent powder panels, bulk and junction effects 0-89068  
 ZnS:Mn, Cu, Cl films, AC electrolum. 0-60679  
 ZnS:Mn AC thin film devices, domain electrolum. 0-66303  
 ZnSe:Mn/n-GaAs low threshold thin film DC electrolum. cell, pulse-excited characts. 0-76081  
 ZnSe:Mn<sup>2+</sup>-n-Ge thin film electrolum. cell with low-threshold voltage 0-84786  
 Zn<sub>2</sub>SiO<sub>4</sub>:Mn, energy storage effect and retrieval 0-100684  
 ZnTe:Mn, spin-lattice coeffs. of Mn<sup>2+</sup> 0-84646  
 ZnTe:Mn<sup>2+</sup>, forbidden transitions of Mn<sup>2+</sup> induced by hyperfine interactions 0-60458  
 (ZrO<sub>2</sub>)<sub>0.9</sub>(Y<sub>2</sub>O<sub>3</sub>)<sub>0.1</sub>:Cr, Mn, stabilised single crystal, EPR of Mn<sup>2+</sup> and Cr<sup>3+</sup> obs. 0-66024

**manganese alloys**

see also *Elinvar*; *Invar*; *manganese compounds*

- Cu-Zn-Mn, de-alloying props. 0-104332  
 dilute alloys, amorphous, exhibiting Mossbauer effect, mean mag. props. (French) 0-80489  
 Heusler alloys, ferromag. alignment rel. to conduction electron polarisation 0-60235  
 Inconel 800, simulated, steam oxidation 0-76405  
 manganin foil like gauge calibration in planar shock wave expts. 0-95091  
 Permalloy-Mn film, diffusion aftereffect causing mag. state change (Russian) 0-103860  
 rare earth ternary alloys, RT<sub>2</sub>Al<sub>6</sub>, T=Cr, Mn, Fe, Cu, cryst. struct. 0-107110  
 steel, Cr-C-Mn, struct. prop. rel., design of struct. steels for high strength and toughness 0-97491  
 steel, Cr-Mn (13, 19 wt.%), elastic const. behaviour, anomalous, low temp. 0-97521  
 steel, Cr-Mo, Mn and Si effect on temper embrittlement, comp. and carbide precip. effects 0-85037  
 steel, Cr-Mu-W, carbide form., W effect 0-76259  
 steel, Cr-Ni-Mo-Mn, wetting of TiC, expt. planning investigation 0-60822  
 steel, high-strength, fatigue crack growth rate and crack tip shapes, cyclic bending (Russian) 0-71740  
 steel, low alloy, S and Mn influence on high temp. strength and ductility after solidification from melt (German) 0-81106  
 steel, low-Mn low-C, susceptibility to brittle fracture 0-76340  
 steel, Mn-Mo, castings, mech. props., Cu and Sn trace elements effect 0-66596  
 steel, Mn-Mo-Ni, embrittling effects of residual elements 0-66655  
 steel, Mn-Nb-Al-C, crack propag. and hot ductility during straightening concast strand 0-66646  
 steel, Mn-V reinforcing type, strain ageing characts. rel. to mech. props. 0-84969  
 Ag-Mn, conc. spin glasses, thermopower 0-65538  
 Ag-Mn, dil., valence and core level spectra, XPS study 0-84838  
 Al-(Mn), effects of Mn on electrode or free corrosion potentials 0-100942  
 Al-Cu-Mg-Mn-Si-Fe, torsional vibrations decrement, deformed vol. effect 0-76326  
 Al-Cu-Mn, long term strength and creep 0-60925  
 Al-Cu-Mn, type 2219, synchrotron radiation microradiography 0-85121  
 Al-Cu-Mn (1-5.2, 0-0.6 wt.%), N alloying and comp. effect on mech. props. (Bulgarian) 0-71719  
 Al-Cu-Si-Mn, type 2017S-T4, crack initiation at root of circumferential notch of round bar specimens (Japanese) 0-60947  
 Al-Li-Mn (2.8, 0.3 wt.%), recrystallised sheet, fracture behaviour, SEM and TEM study 0-97566

**manganese alloys continued**

- Al-Mn, dil., core and valence band spectra, XPS study 0-84837  
 Al-Mn, dil., supercond., nucl. spin relax. and quasiparticle excitations 0-88680  
 Al-Mn (1 wt.%), single crystals, rolled to (123)[412], recrystn. textures 0-104183  
 Al-Mn sheet, artificial stress raiser effect on strength and local plasticity of weld joint 0-81130  
 γ-Al-Mn-C, permanent magnetism and microstruct. 0-75811  
 Al-Zn-Mn, mech. props., Ti or Mn addition effect (Korean) 0-93613  
 Au-3d transition metal alloys, UPS study, localised states 0-93449  
 Au-Mn, conc. spin glasses, thermopower 0-65538  
 Au-Mn, UPS study, localised states 0-93449  
 Au-Mn alloys, reversible and irreversible DC magnetisation in spin glass regime 0-65908  
 AuMn, mag. struct., phase transition, and magnon spectrum, random anisotropy effects 0-88722  
 AuMn, ordered, vacuum deposited epitaxial films, orientation control by external stress 0-100426  
 Au<sub>11</sub>Mn<sub>4</sub> ordered phase formation, electron diff. and microscopy study 0-107418  
 Au<sub>3</sub>Mn thin films, electron diff. study 0-92793  
 Au<sub>4</sub>Mn, heat treated, short-range order, diffuse X-ray diff. study (German) 0-88092  
 Be<sub>1-x</sub>Mn<sub>x</sub>, Be-rich, NMR and paramag. susceptibility 0-71206  
 Bi-MnBi eutectic region, of Bi-Mn phase diagram 0-81034  
 Co-Mn, FCC, micromagnetism, magnetisation and mag. susceptibility meas. 0-60310  
 Co-Mn alloys, ferromagnetic, high field mag. susceptibility meas. 0-75729  
 Co-Mn-Ni-Fe-Si-B amorphous alloys, mag. props., low magnetostriction 0-75832  
 CoMn, dil., low temp. specific heat and magnetisation 0-65925  
 (Co<sub>1-x</sub>Mn<sub>x</sub>)<sub>2</sub>B, magnetocrystalline anisotropy meas., 4.2-300K 0-71006  
 Co<sub>50</sub>Mn<sub>50</sub>Ga<sub>50-x</sub>, ordering and disordering phenomena, mag. study 0-70154  
 CoMnP, cryst. mag. struct., neutron diff. study (French) 0-59439  
 CoMnSi<sub>1-x</sub>Ge<sub>x</sub>, amg. props. 0-60270  
 Cr-Fe(Co)-Mn, dil., antiferromag., elec. resist. min., press. and impurity effects 0-59970  
 Cu-Al-Mn liq. alloys, susceptibility behaviour 0-93077  
 Cu-Mn, de-alloying props. 0-104332  
 Cu-Mn, exchange-coupled localised moments, Korringa relaxation rate 0-75851  
 Cu-Mn, mag. viscosity below freezing temp. 0-65910  
 Cu-Mn, spin glass, transition temp., freq. depend. 0-97113  
 Cu-Mn, spin glass materials, mag. field dependence of susceptibility peak 0-103840  
 Cu-Mn, spin glasses, alternating susceptibility 0-65912  
 Cu-Mn, zero field ESR in spin glass state 0-66017  
 Cu-Mn (8 to 75 at.%), spin correl., neutron polarisation anal. study 0-65905  
 Cu-Mn alloy, manganin, hysteresis-corrected calibration under shock loading 0-74818  
 Cu-Mn spin glass, spin freezing and exchange narrowing of mag. reson. 0-60411  
 Cu-Mn-Al, Heusler alloys, ferromag. inclusions, mag. props. and struct. study (Russian) 0-80570  
 Cu-Mn-Al alloys, displaced hysteresis loop and microstructure obs. 0-84613  
 Cu-Mn-Al(Pt) spin glasses, anisotropic exchange interactions, effect of nonmag. impurities 0-80534  
 Cu-Ni-Mn, cast, strength and hot ductility, Mn, effect 0-66595  
 Cu-Ni-Zn-Mn fine grained precipitation-hardenable alloy, high strength and ductility 0-100805  
 Cu-Zn-Mn, steady-state diffusion of Zn and Mn 0-70445  
 r-CuMn, annealing ordered phase study by neutron diff. 0-89265  
 CuMn, dil., anisotropic hyperfine coupling, NMR study 0-65784  
 CuMn, hysteresis, spin orbit scattering effect on anisotropy in spin glass state 0-71095  
 CuMn spin glass, AC susceptibility 0-60305  
 CuMn spin glass, μ<sup>+</sup> zero-field spin relax. probe for spin dynamics 0-97177  
 CuMn, spin glass, random moments time correl., zero field muon spin relax. meas. 0-60335  
 CuMn spin glass, specific heat and entropy 0-60354  
 Cu<sub>0.86</sub>Mn<sub>0.14</sub>, hysteresis loop development 0-65922  
 Cu<sub>0.98</sub>Mn<sub>0.02</sub>, spin glass, Heisenberg mode, RPA approx. 0-65904  
 Cu<sub>2</sub>MnAl-Pd, MnAl mixed Heusler alloys, mag. props. 0-60269  
 Cu<sub>3-x</sub>Mn<sub>x</sub>Al, and Cu<sub>2</sub>Mn<sub>2-x</sub>Al<sub>x</sub>, Heusler alloys, order-disorder transitions 0-59619  
 Cu<sub>2</sub>MnAl<sub>1-x</sub>Sn<sub>x</sub>, Mossbauer effect study 0-60473  
 Cu<sub>2</sub>MnIn<sub>1-x</sub>Sn<sub>x</sub> alloy, compositional SRO, hyperfine interactions 0-71065  
 Cu<sub>1-x</sub>Pd<sub>x</sub>MnSb, mag. phase transition 0-60268  
 Fe-Mn, as cast, pseudo-composite struct. resulting from interdendritic segregation, cryogenic materials appl. (French) 0-93556  
 Fe-Mn, ε-martensite, preferred orientation and constitution, reverse pole figures (Russian) 0-104178  
 Fe-Mn, mechanical twinning of close-packed hexagonal ε-phase during plastic deform. (Russian) 0-60909  
 Fe-Mn (0.5 wt.%), Burgers vector of dislocation determ. by weak-beam image in HVEM 0-103351  
 Fe-Mn (1 at.%), strain age hardening 0-108472  
 Fe-Mn cast alloys, homogenisation annealing and chemical diffusion (Czech) 0-66551  
 Fe-Mn-B, B effect on intergranular embrittlement 0-108555  
 Fe-Mn-C, struct. superplasticity 0-76317  
 Fe-Mn-Zn, high-temperature phase diagram (German) 0-108390  
 Fe-MuS eutectics, unidirectional solidification (German) 0-100827  
 Fe-Ni-Mn (20, 5 wt.%), rel. orientation between adjacent martensite laths 0-76254  
 γ-Fe-Ni-Mn alloys, spin glass state, short and long range order investigation 0-65808  
 Fe-Sb-Mn, interactions and segregations, Mossbauer and X-ray diff. study 0-70415  
 Fe<sub>3-x</sub>Mn<sub>x</sub>Al, ordering of Fe atoms, X-ray diff. meas. and mid gamma reson. anal. (Russian) 0-96469  
 (Fe<sub>100-x</sub>Mn<sub>x</sub>)<sub>70</sub>P<sub>30</sub>, amorphous alloys, sput cooled, mag. and transport props. 0-84593  
 Fe<sub>1-x</sub>Mn<sub>x</sub>Sn, spin reorientation, Mossbauer study, 77 to 400K 0-97172



## manganese alloys continued

- Fe<sub>0.49</sub>Mn<sub>0.01</sub>Ti<sub>0.5</sub>H<sub>2</sub>, localised vibr., sp. ht. obs., room temp. 0-65248  
(Fe<sub>1-x</sub>Mn<sub>x</sub>)<sub>2</sub>Y(B), Mn effect on Fe mag. moments, Mossbauer and mag. meas. 0-71016  
Fe<sub>0.8</sub>Ni<sub>0.2</sub>Mn<sub>0.1</sub>, disordered, mag. struct. near ferro-antiferromagnetic transition 0-60211  
GdMn<sub>2</sub>-GdAl<sub>3</sub> system, mag. and structural studies 0-108006  
HoCo<sub>0.5-x</sub>Mn<sub>x</sub>, cryst. struct. and mag. props. 0-75800  
La<sub>0.9</sub>Eu<sub>0.1</sub>Ni<sub>0.4</sub>Mn<sub>0.4</sub>, absorption-desorption props. of H<sub>2</sub>, degradation mechanism, Mossbauer study 0-88431  
Li-Mn liquid alloys, form factor effects, pseudopotentials, resist. calc. 0-103608  
Mg-Al-Zn-Mn (8, 0.5, 0.3 wt.%) casting alloy, penetration resistance 0-100901  
Mg-Mn-Ce (1.5, 0.3 wt%), superplasticity role of diffusional creep (*Russian*) 0-97528  
Mn-Ag, XPS meas., Fermi level to 1000 eV below it 0-66389  
Mn-Al-C, ferromag. alloy, transform. kinetics 0-76229  
Mn-Al-C, fine-grained cast struct., remanence and coercive force 0-60365  
Mn-Al-C, metallic magnets investigations, present state (*Polish*) 0-107987  
Mn-Al-C (70, 29.5 wt.%) alloy magnet, Almax, anisotropic, mag. props. (*Japanese*) 0-60371  
Mn-bearing binary substitutional alloy systems, props., applicability of statistical thermodynamic approach 0-88336  
Mn-Bi micromagnetic alloy, mag., elec. and elastic props. (*Russian*) 0-108028  
Mn-Cr-Ti layers on low C steel, composite, residual stresses rel. to arc-spraying parameters (*German*) 0-104077  
Mn-Cu, micromagnetic props., neutron diff. obs. 0-65906  
γ-Mn-Cu (10 at.%), spin wave studies using neutron diffraction 0-70991  
Mn-Cu (25, 62 wt.%), elast. const., temp. depend., 170-300K (*Russian*) 0-81095  
Mn-Cu (25 wt.%) rod, transverse vibrations, energy dissipation, static longitudinal load effect 0-81099  
Mn-Cu (75, 25 wt.%), rod, coupled flexural and torsional vibr., energy dissipation 0-89281  
Mn-Ga system, X-ray struct. investigation, solubility (*Chinese*) 0-88084  
Mn-Ni, thermal expansion, mag. susceptibility, lattice const. 0-100341  
MnAg alloys, XPS meas. 0-60751  
r-MnAl, estimated theoretical limit of mag. moment 0-97072  
MnAlGe film, mag. domains and amorphous to cryst. phase transition, electron microscopy obs. 0-71129  
γ-MnAu, antiferromag., phase diagram, X-ray diff. and Young's modulus meas. 0-71024  
MnAu<sub>2</sub>, helical antiferromag., optical absorpt., density of states 0-66224  
MnBi, domain boundary inertia during mag. reversals (*Russian*) 0-88776  
MnBi film, electrical props., in situ annealing effect 0-65708  
Mn-Bi garnet film struct., thermomagnetic recording 0-100588  
Mn<sub>0.8</sub>Cr<sub>0.2</sub>Sb, antiferromag.-ferrimag. transition, neutron crit. scatt. and crossover effect 0-71023  
γ-MnCu crystals, antiferromag. Czochralski growth 0-97420  
γ-MnCu, Mn-rich, inclined spin axis, neutron diff. study 0-75723  
Mn<sub>0.5</sub>Fe<sub>0.5</sub>Si<sub>3</sub>, elec. resist. and mag. susceptibility, ferromag. to antiferromag. transition 0-80504  
MnGaGe film, mag. domains and amorphous to cryst. phase transition, electron microscopy obs. 0-71129  
Mn<sub>2</sub>GaN, sp. ht., 6 to 350K, mag. and crystallographic phase transitions 0-71060  
MnGe, amorphous, spin glass transition, AC susceptibility meas. 0-75779  
MnSb, magnetic losses, ferromagnetic resonance and antiresonance 0-100618  
Mn<sub>2</sub>Sb, spin-wave dispersion relations, exchange interactions, neutron inelastic scatt. 0-65832  
MnSb<sub>1-x</sub>Sn<sub>x</sub> films, Faraday rotation, optical absorpt. coeffs. 0-97242  
MnSi, amorphous, spin glass transition, AC susceptibility meas. 0-75779  
MnSi, electronic energy band struct., self-consistent APW calc. 0-65433  
MnSi-Si system, striations and cryst. struct. of matrix 0-103292  
MnSi<sub>1-1.3</sub>, crystal growth and characterisation 0-93474  
Mn<sub>2</sub>Si, electronic structure, X-ray spectra comparison with band struct. calcs. 0-97383  
Mn<sub>2</sub>ZnN, sp. ht., 6 to 350K, mag. and crystallographic phase transitions 0-71060  
Ni-Mn, dil., mag. moment distrib. and environmental effects, neutron scatt. obs. 0-60247  
Ni-Mn, ordered and disordered, press. effect on Curie temp. 0-71148  
Ni-Mn, permeability, diffusion and solubility of H 0-107573  
Ni-Mn (10-40 wt.%), γ solid soln., interdiffusion 0-100366  
Ni-Mn (17-27 at.%), low-angle neutron diff., anomalous crit. scatt. (*Russian*) 0-60193  
Ni-Mn alloys, ferromagnetism-to-spin glass phase transition and strong mag. field effect 0-75773  
Ni-Mn-H solid solutions, mag. props. 0-88753  
Ni-Pd-Mn ternary alloys, mag. characs., use for thermoseed 0-107995  
Ni<sub>3</sub>Mn, change of H<sub>2</sub> diffusivity with order-disorder transformation 0-59729  
Ni<sub>2</sub>Mn thin films, transmission spectra, structural order depend. 0-66318  
NiMnGe<sub>0.5</sub>Si<sub>0.5</sub>, mag. props., neutron diff. and magnetometric meas., 80-600K 0-65793  
Pd-Fe-Mn, ferromagnet-spin glass, thermal expansion forced, magnetostriiction and magnetisation under high press. 0-65255  
Pd-Mn, ferromagnetism to spin glass behaviour transition 0-71062  
Pd-Mn (1-10 wt.%), mag. ordering, influence on resistivity 0-75557  
(Pd<sub>0.996</sub>Fe<sub>0.003</sub>)<sub>1-x</sub>Mn<sub>x</sub>, mag. behaviour at Fe sites, Mossbauer effect meas. 0-66085  
Pd<sub>1-x</sub>Mn<sub>x</sub>H<sub>2</sub> alloy, spin glass, transition temp., susceptibility and EPR meas. 0-65930  
Pd<sub>2</sub>MnIn<sub>1-x</sub>Sn<sub>x</sub> and Pd<sub>2</sub>MnIn<sub>1-y</sub>Sb<sub>y</sub> Heusler alloys, mag. order, disorder effects 0-88723  
Pd<sub>1-x</sub>MnSb Heusler alloys, magnetic hyperfine fields on <sup>111</sup>Cd, TDPAC and magnetisation meas. 0-93219  
Pd<sub>2-x</sub>MnSb, struct., appl. as improved neutron polariser 0-60199  
Pd<sub>2</sub>MnV<sub>1-x</sub>Sn<sub>x</sub> Heusler alloy, structural disorder, Mossbauer study 0-80650  
Pt-Mn, dil., skew scatt. Hall effect, magnetoresist. and mag. anisotropy, orbital magnetism of impurity 0-70678  
Pt<sub>0.75</sub>(Cr<sub>1-x</sub>Mn<sub>x</sub>)<sub>0.25</sub>, pseudobinary, magnon energy derivation 0-107996  
PtMn, spin glass, nonlinear susceptibility and sp. ht. 0-60304  
Rh<sub>2</sub>Mn<sub>2</sub>Pb, hyperfine fields, ferromag., NMR and Mossbauer effect studies 0-71259

## manganese alloys continued

- Rh<sub>2</sub>MnSb, hyperfine fields, ferromag., NMR and Mossbauer effect studies 0-71259  
Sm<sub>2</sub>Mn<sub>23-x</sub>Fe<sub>x</sub>, magnetic behaviour, temp. and comp. depend. 0-93090  
Sr<sub>2</sub>(Co<sub>1-x</sub>Mn<sub>x</sub>)<sub>17</sub>, powders, influence of substitutes on mag. props. 0-100601  
TiC-(Mo-Cr-Ni-Mn) steel alloy, optimum comp. and manufacture conditions, Mn effect 0-84896  
TiCo<sub>1-x</sub>Mn<sub>x</sub>, H absorption-desorption characteristics 0-96735  
TiMn<sub>1.5</sub>, hydrogen storage appl. (*Japanese*) 0-61443  
Ti<sub>1-x</sub>Zr<sub>x</sub>M<sub>1-x</sub>Cr<sub>x</sub>V<sub>x</sub>, hydrogen storage appl. (*Japanese*) 0-61443  
U-Mn metallic glasses, glass form. and thermal stability 0-75183  
UMn<sub>2</sub>, transport props., influence of lattice distortion 0-100452  
Y<sub>2</sub>(Fe<sub>1-x</sub>Mn<sub>x</sub>)<sub>23</sub>, Mn-rich compounds, Mossbauer effect study 0-71276  
Y<sub>2</sub>Mn<sub>23</sub>, low temp. specific heat determ. 0-65896  
YMn<sub>2-x</sub>Fe<sub>x</sub>H<sub>2</sub>, mag. props., ordering temps. 0-71028  
Zn-Mn, Kondo-system, ion implantation as method for study 0-70241  
ZnMn, dil., magnetoresist. meas., temp. depend. anisotropy 0-65532  
ZrMn<sub>2</sub>, mag. props. H absorpt. effect 0-88821  
ZrMn<sub>2</sub>H<sub>2</sub>, proton NMR relax. time and Knight shifts, diffusional activation energies meas., sorption props. 0-75871  
Zr(Mn<sub>1-x</sub>M<sub>x</sub>)<sub>2</sub> (M=Fe, Co), H<sub>2</sub> absorpt. capacity 0-88433

## manganese compounds

- see also manganese alloys  
acetate tetrahydrate, paramag. susceptibility, spin trimer model 0-97055  
adipate dihydrate, cryst. struct., H-bonding and O atom coordination 0-96506  
dichlorophosphate complexes, cryst. struct. <sup>35</sup>Cl NQR obs. 0-108108  
diethylammonium manganese chloride, Heisenberg magnet, spin diffusion, EPR study 0-66019  
dimethylammonium copper manganese chloride, two-dimens. mixed magnet, EPR 0-66030  
dimethylammonium manganese tetrachloride, antiferromag. and spin-flop resonance obs., 70 to 100 GHz 0-71190  
dimethylammonium manganese trichloride: Cd(Cu), impurities in quasi-one-dimens. Heisenberg systems, anisotropy effect 0-80502  
dipropylammonium manganese tetrachloride, two-dimens. weak ferromagnet, AC susceptibility 0-65823  
ferrite, magnetic permeability, photoinduced reduction (*Rumanian*) 0-75794  
formate dihydrate, Zn- and Mg-substituted, anomalous crit. phenomena 0-60316  
manganese carboxylate, dodecanuclear mixed-valence, prep., struct., and mag. props. 0-107196  
oxide, catalysis of graphitisation C graphitisation 0-89166  
press. or stress induced, neutron scatt. obs. 0-65880  
stearate, Langmuir-Blodgett layers, high resolution X-ray diff. 0-80126  
stearate, quasi two-dimensional, dil. ESR line width 0-71155  
stearate, two-dimensional mag. struct. 0-108040  
TMCC, crossover transition, effects on susceptibility and EPR shift 0-71047  
TMCC, Cu-substituted, spin dynamics, neutron scatt. cross section 0-60312  
TMCC, low-symmetry spin distrib. effect on EPR line 0-66018  
TMCC, one-dimens. antiferromag., nonlinear dynamics 0-80521  
TMCC, one-dimens. magnet, local magnon modes 0-65829  
trimethylammonium manganese trichloride, Heisenberg antiferromag. chain, specific heat and EPR 0-65931  
X-ray absorption near edge structures in simple and complex tin compounds 0-104013  
Al<sub>2</sub>Mn<sub>2</sub>Si<sub>2</sub>O<sub>12</sub>, amorphous insulating spin glass, susceptibility and magnetisation meas. 0-88765  
BaO-Mn<sub>2</sub>O<sub>3</sub>-B<sub>2</sub>O<sub>3</sub>, amorphous mag. oxide, field-cooling effect (*Japanese*) 0-84615  
Ca-Mn-S-Se system, multicomponent solubilities 0-108416  
Ca<sub>3</sub>Mn<sub>2</sub>Ge<sub>2</sub>O<sub>12</sub> garnet, metamagnetic transition, high anisotropy peculiarities (*Russian*) 0-60274  
Cd<sub>1-x</sub>Mn<sub>x</sub>Se, fundamental optical props. 0-84751  
Cd<sub>1-x</sub>Mn<sub>x</sub>Te, exchange induced ionization of bound excitons, luminesc. meas. 0-97328  
Cd<sub>1-x</sub>Mn<sub>x</sub>Te, indirect exchange interaction 0-97087  
Cd<sub>1-x</sub>Mn<sub>x</sub>Te mixed crystals, Raman spectra 0-103961  
Cd<sub>1-x</sub>Mn<sub>x</sub>Te, semimagnetic, exchange interactions between localised and delocalised electrons 0-97245  
Co<sub>3-x</sub>Mo<sub>x</sub>O<sub>4</sub> films, prep., struct. and elec. characteris. 0-108353  
Cr<sub>2</sub>Mn<sub>1-x</sub>As<sub>x</sub>, mag. susceptibility anomaly at displacive phase transition 0-93091  
Cr<sub>1-x</sub>Mn<sub>x</sub>O<sub>2</sub>, hyperfine mag. fields at <sup>119</sup>Sn, Mossbauer study 0-71260  
CsMnCl<sub>3</sub>, antiferromagnetic resonance, parametric spin wave excitation (*Russian*) 0-93183  
CsMnCl<sub>3</sub>·2H<sub>2</sub>O, diagonal elastic const., thermal expansion coeffs., ultrasonic velocity meas. 0-79853  
CsMnCl<sub>3</sub>·2H<sub>2</sub>O, threshold two-magnon absorpt., depend. on freq., temp. and mag. field, exchange coupling const. (*Russian*) 0-71184  
CsMn<sub>1-x</sub>Co<sub>x</sub>Cl<sub>2</sub>·2H<sub>2</sub>O, random mag. mixture, oblique-antiferromag. phase obs. 0-93142  
CsMnF<sub>3</sub>, exciton migration, excitation and luminesc. study (*Russian*) 0-66264  
CsMnF<sub>3</sub>, parametric nuclear magnon excitation, mag. field modulation (*Russian*) 0-107999  
Cu-Mn ferrite films, LPE growth 0-96752  
(Fe<sub>0.19</sub><sup>2+</sup>Mg<sub>0.56</sub><sup>2+</sup>Mn<sub>0.25</sub><sup>2+</sup>)[Fe<sub>0.87</sub><sup>3+</sup>Al<sub>0.13</sub><sup>3+</sup>]<sub>4</sub>O<sub>4</sub><sup>2-</sup>, influence of Fe<sup>2+</sup> ion substitution on electron hopping, Mossbauer study 0-71247  
(Fe<sub>0.45</sub><sup>2+</sup>Mg<sub>0.32</sub><sup>2+</sup>Mn<sub>0.03</sub><sup>2+</sup>Cu<sub>0.10</sub><sup>2+</sup>)[Fe<sub>0.74</sub><sup>3+</sup>Al<sub>0.26</sub><sup>3+</sup>]<sub>4</sub>O<sub>4</sub><sup>2-</sup>, influence of Fe<sup>2+</sup> ion substitution on electron hopping, Mossbauer study 0-71247  
Fe<sub>1-x</sub>Mn<sub>x</sub>Cl<sub>2</sub>, disordered, Raman scatt. from Fe<sup>2+</sup> and Neel temp. 0-60579  
Fe<sub>1-x</sub>Mn<sub>x</sub>Cl<sub>2</sub>, low-lying electronic excitations in antiferromag. and paramag. phases Raman scatt. study 0-71414  
Ga<sub>1-x</sub>Mn<sub>x</sub>Sb, elec. cond., mag. susceptibility, Hall const., and thermo-EMF, 80 to 1000K (*Russian*) 0-88549  
Hg<sub>1-x</sub>Mn<sub>x</sub>Te, indirect exchange interaction 0-97087  
Hg<sub>1-x</sub>Mn<sub>x</sub>Te, non-parabolic zero-gap semicond., indirect exchange interaction 0-80498  
Hg<sub>1-x</sub>Mn<sub>x</sub>Te, semimagnetic, exchange interactions between localised and delocalised electrons 0-97245  
Hg<sub>1-x</sub>Mn<sub>x</sub>Te, transverse magnetoresistance in quantised mag. fields 0-96922  
KBr:MnO<sub>4</sub><sup>-</sup>, many-phonon impurity reson. Raman scatt. 0-60603



**manganese compounds continued**

- KBr:MnO<sub>2</sub>, model system, reson. Raman spectra, general behaviour obs. 0-60592  
 KMnF<sub>3</sub>, specific heat near Neel temp. (*Russian*) 0-100340  
 (Mn,Zn)Fe<sub>2</sub>O<sub>4</sub>:Si, Ca, Ti, second phase effect on elec. and mag. props. 0-60986  
 Mn complex, with 4-benzylpyridine hydrochloride, photoluminesc. props. 0-89044  
 Mn-Ge, thermophysical props., at elevated temp. 0-103493  
 Mn-H, hydride formation in high press. range 0-65235  
 Mn-Zn ferrites, grain boundary exam. using TEM and AES 0-107268  
 Mn<sub>2</sub>Al<sub>2</sub>Si<sub>2</sub>O<sub>12</sub>, amorphous, spin-glass, insulating, Mn<sup>2+</sup> mag. reson. 0-65918  
 MnAs<sub>0.95</sub>P<sub>0.05</sub>, anisotropy of elec. cond. and Hall effect 0-92908  
 MnAs<sub>1-x</sub>P<sub>x</sub>, double exchange ferromag. coupling, magnetisation meas. 0-75751  
 MnAs<sub>1-x</sub>P<sub>x</sub>, mag. susceptibility anomaly at displacive phase transition 0-93091  
 MnAs<sub>1-x</sub>P<sub>x</sub> mixed crystals, metallic magnetically ordered, Hall effect 0-65536  
 MnB<sub>2</sub>, polycryst., magnetoresist. and mag. props. (*Russian*) 0-92907  
 MnBi, problems for holographic recording (*Russian*) 0-91761  
 Mn(Br<sub>1-x</sub>Cl<sub>x</sub>)<sub>2</sub>·4H<sub>2</sub>O, antiferromagnetism, controllable anisotropy 0-93116  
 Mn(CN)<sub>3</sub>·(H<sub>2</sub>O)<sub>0.57</sub>, mag. interactions, theory 0-97085  
 MnCO<sub>3</sub>, parametric excitation of magnons, effect of RF modulation of mag. field 0-65842  
 Mn(CO), Br-Re(CO)<sub>3</sub>Br, polycryst., ν(CO) vibr. intermol. Raman intensity transfer 0-60564  
 Mn<sub>2</sub>Cd<sub>1-x</sub>Se single cryst., photoluminesc., composition depend. 0-80854  
 Mn<sub>2</sub>Cd<sub>1-x</sub>Te, lattice vibrs., Raman and IR spectra meas. 0-93311  
 Mn<sub>2</sub>Cd<sub>1-x</sub>Te, phonons, Raman scatt. and IR absorpt. meas. (*French*) 0-97275  
 MnCl<sub>2</sub>, cryst., self-consistent band struct., intersecting spheres model 0-75505  
 MnCl<sub>2</sub>, EXAFS amplitudes, many-body effects 0-97379  
 MnCl<sub>2</sub>, lattice dynamics, density of states and sp. ht. calc. 0-92624  
 Mn(ClO<sub>4</sub>)<sub>2</sub>/NaClO<sub>4</sub> in aq. soln., interaction between Mn<sup>2+</sup> and ClO<sub>4</sub><sup>-</sup>, NMR studies 0-71212  
 MnCl<sub>2</sub>·4H<sub>2</sub>O, antiferromag., low temp. thermal cond. 0-65320  
 MnCl<sub>2</sub>·6NH<sub>3</sub>, MnCl<sub>2</sub>·2NH<sub>3</sub>, solar energy storage system heating and cooling 0-81484  
 MnCO<sub>3</sub>, parametric nuclear magnon excitation, mag. field modulation (*Russian*) 0-107999  
 Mn<sub>1-x</sub>Cr<sub>x</sub>As, double exchange ferromag. coupling, magnetisation meas. 0-75751  
 MnCr<sub>2</sub>S<sub>4</sub>, mag. struct. under applied mag. field 0-97065  
 MnCr<sub>2</sub>S<sub>4</sub>, substituted, mag. struct. and transitions 0-65795  
 Mn<sup>2+</sup>F<sup>-</sup> and Mn<sup>2+</sup>F<sup>-</sup>Mn<sup>2+</sup> systems, transferred hyperfine interaction at F<sup>-</sup> site 0-70657  
 MnF<sub>2</sub>, antiferromag., mag. space groups, Clebsch-Gordan coeff. calcs. 0-79731  
 MnF<sub>2</sub>, antiferromag. and piezomag. domain struct., neutron topography study 0-71088  
 MnF<sub>2</sub>, high temp. polymorphism and thermal props. 0-75199  
 MnF<sub>2</sub>, parallel pumping studies of magnon damping 0-70990  
 MnF<sub>2</sub> spin wave lifetime, theory compared with expt. 0-60228  
 MnFe<sub>2</sub>O<sub>4</sub>, additional spin echo of <sup>55</sup>Mn nuclei 0-60455  
 Mn<sub>2</sub>Fe<sub>1-x</sub>O<sub>4</sub>, dielec. function and polar Kerr rotation, 0.5-3.6 eV 0-66221  
 Mn<sub>3</sub>Ga<sub>1-x</sub>Mn<sub>x</sub>N, perovskite struct., phase transformations (*French*) 0-81048  
 Mn<sub>3</sub>Ga<sub>1-x</sub>N<sub>1-x</sub>C<sub>x</sub>, perovskite struct., phase transformations (*French*) 0-81048  
 MnHPO<sub>4</sub>·3H<sub>2</sub>O and MnDPO<sub>4</sub>·3D<sub>2</sub>O, IR absorpt. and Raman spectra, vibr. assignments 0-97257  
 Mn<sub>1-x</sub>Mg<sub>x</sub>Se, mag. and struct. phase transitions, mag. susceptibility and X-ray diffr. study 0-71022  
 Mn<sup>2+</sup>Mo<sup>4+</sup>O<sub>3</sub>, defect spinel struct., elec. and mag. props. 0-70176  
 Mn<sub>2</sub>N, mag. struct. non-collinearity, neutron diffr. obs. 0-65796  
 MnNb<sub>2</sub>O<sub>6</sub>, force fields rel. to cryst. struct. (*French*) 0-107104  
 MnO, A<sup>6</sup>Σ<sup>+</sup>-X<sup>6</sup>Σ<sup>+</sup> electronic transition, rot. and hyperfine struct. 0-74134  
 MnO, antiferromag., temp. depend. of elastic consts., US study 0-79854  
 MnO, magnon-sideband lineshape, exciton-phonon interaction effects 0-65846  
 MnO, reduction by C, surface reactions, CO regeneration (*Russian*) 0-66772  
 MnO:Mn<sub>2</sub>O<sub>4</sub>, mag. props., susceptibility and magnetisation meas. 0-65824  
 MnO-Al<sub>2</sub>O<sub>3</sub>-SiO<sub>2</sub>, amorphous, remanent magnetisation short time depend. 0-65919  
 MnO-Al<sub>2</sub>O<sub>3</sub>-SiO<sub>2</sub>, amorphous spin glass, AC susceptibility 0-80520  
 MnO<sub>2</sub> (pyrolusite), UV irradiated, simulation of Viking gas exchange reaction on Mars 0-72831  
 MnO<sub>2</sub> additive for Pb(Zn<sub>1/3</sub>Nb<sub>2/3</sub>)<sub>3</sub>O<sub>3</sub>-PbTiO<sub>3</sub>-PbZrO<sub>3</sub> and Pb(Mg<sub>1/3</sub>Nb<sub>2/3</sub>)<sub>3</sub>O<sub>3</sub>-PbTiO<sub>3</sub>-PbZrO<sub>3</sub> ceramics, HF filters appl. (*Japanese*) 0-60507  
 MnO<sub>2</sub>, catalytic graphitization of nongraphitizable C 0-97440  
 MnO<sub>2</sub>, dispersion mode on Al<sub>2</sub>O<sub>3</sub> and SiO<sub>2</sub> powder supports, N adsorption obs. 0-81363  
 MnO<sub>2</sub>, doped, dry cell depolariser, hydrazine reduction kinetics 0-89603  
 MnO<sub>2</sub> porous powders, Al<sub>2</sub>O<sub>3</sub> and SiO<sub>2</sub> coated, changes in surface free energy for N adsorption 0-84363  
 MnO<sub>2</sub>, preparation and characterisation of doped samples for appl. as dry-battery depolarisers 0-89602  
 MnO<sub>2</sub>:Li(Mo)(V), Zn<sup>2+</sup> ion specific adsorpt. kinetics, <sup>65</sup>Zn γ-ray scintillation investig. 0-70529  
 Mn<sub>1-x</sub>O<sub>x</sub>, single cryst. growth by skull melting 0-84844  
 Mn<sub>2</sub>O<sub>3</sub>, cryst. growth using K<sub>2</sub>S<sub>2</sub>O<sub>8</sub> as flux material 0-71582  
 Mn<sub>2</sub>O<sub>3</sub>, hausmannite, tetragonal-cubic transform., X-ray anal. 0-103288  
 MnOOH, mag. ordering, fine struct. and crit. behaviour, neutron diffr. meas. 0-65800  
 MnO-Al<sub>2</sub>O<sub>3</sub>-SiO<sub>2</sub>, spin glass materials, mag. field dependence of susceptibility peak 0-103840  
 xMnO<sub>2</sub>(100-x)[19TeO<sub>3</sub>·PbO], EPR studies of Mn<sup>2+</sup> ion distribution 0-71167  
 MnP, ferro-spiral transition, neutron scatt. studies 0-65876  
 MnP, high field magnetoresistance 0-107817  
 MnP, Lifshitz point, transverse differential susceptibility meas. 0-84599

**manganese compounds continued**

- MnP, low field magnetoresistances, mag. phase diagram purity depend. 0-107816  
 MnP, spin polarised energy band struct., electronic specific heat, APW calcs. 0-65431  
 MnS, CVD crystal growth, role of Mn-Al-Cl complexes 0-84840  
 MnS, phase transform. at 200°C, diffusive and deformational mechanisms 0-65216  
 MnS solubility in Kh18N11 stainless steel, determ. method 0-84910  
 MnS, thermal cond., temp. depend., paramag.-antiferromag. transition effects 0-65321  
 MnS<sub>2</sub>, core-level and valence-band XPS 0-93450  
 MnSO<sub>4</sub>, mag. struct. and phase transitions, neutron diff. study 0-60208  
 MnSb-CrSb, NiAs-type system, single crystals, neutron diff. studies 0-60200  
 Mn<sub>1-x</sub>Sb<sub>x</sub>, Mn electronic state, neutron diffr. study 0-65806  
 MnSe, CVD crystal growth, role of Mn-Al-Cl complexes 0-84840  
 α-MnSe, mag. and struct. phase transitions, mag. susceptibility and X-ray diffr. study 0-71022  
 MnSe<sub>2</sub>, core-level and valence-band XPS 0-93450  
 α-MnSeO<sub>4</sub>, magnetic interactions, neutron inelastic scatt. study 0-107980  
 MnSi, weak itinerant magnetic compound, paramagnetic response function, polarised neutron scattering 0-107982  
 MnSi<sub>2</sub>, X=1.72 to 1.75, IR absorpt., transmission, refl., spectra 0-60600  
 Mn<sub>2</sub>Si<sub>3</sub>, elastic moduli, phase transitions, ultrasonic velocity 0-92589  
 Mn<sub>2</sub>SnS<sub>4</sub>, cryst. struct. refinement and mag. struct. determ. (*French*) 0-107131  
 MnTa<sub>2</sub>O<sub>6</sub>, force fields rel. to cryst. struct. (*French*) 0-107104  
 MnTe, CVD crystal growth, role of Mn-Al-Cl complexes 0-84840  
 MnZn ferrite, initial mag. permeability rel. to mag. anisotropy 0-80557  
 MnZn ferrite, microstructure and initial permeability, presintering process effect 0-89367  
 MnZn ferrite powder prep., wet method 0-89180  
 MnZn ferrite powders, reactive, mag. materials obtained by compaction 0-89182  
 MnZn ferrites, form. of comp. heterogeneity during high-temp. sintering 0-60818  
 MnZn ferrites, internal friction and ΔE effect depend. on demagnetisation method 0-80584  
 MnZn ferrites, post sinter-cooling rates effects 0-89369  
 MnZn ferrous ferrite, initial mag. permeability second-order magnetocrystalline anisotropy influence 0-88820  
 MnZn ferrous ferrites, mag. permeability stress depend. 0-88822  
 Mn<sub>2</sub>Zn<sub>1-x</sub>F<sub>2x</sub>, Neel point and short range order, dilution effects, mag. birefr. obs. 0-71019  
 Mn<sub>1-x</sub>Zn<sub>x</sub>Fe<sub>2</sub>O<sub>4</sub>, prepared by wet method, neutron diffr. and high field Mossbauer expts. 0-75719  
 (NH<sub>4</sub>)<sub>2</sub>SO<sub>4</sub>·MnO<sub>4</sub>, X-ray irradi. damage, optical absorpt. spectra study 0-66246  
 Pb<sub>1-x</sub>Mn<sub>x</sub>Te, photovoltaic effect, p-n junction, energy gap determ. 0-92931  
 RbMnCl<sub>3</sub>, specific heat near Neel temp. (*Russian*) 0-100340  
 RbMnCl<sub>3</sub>, twinning struct., cryst. domains, orientation mag. transition (*Russian*) 0-107275  
 RbMnF<sub>3</sub>, spin wave widths 0-97081  
 Sn<sub>1-x</sub>Mn<sub>x</sub>Te, electronic struct.; transport props., mag. ordering effects 0-65441  
 TiMnCl<sub>3</sub>, specific heat near Neel temp. (*Russian*) 0-100340

**manometers**

see also pressure measurement

- automated electromanometer, appl. for nuclear materials safeguarding 0-99211  
 constant pressure manometer with frequency read out, electrocapillary element appl. 0-73380  
 free-piston manometer comparison, weight relocation method 0-90831  
 glass membrane manometer for high-temperature measurement 0-86329  
 liquid, sensitivity, wetting hysteresis effect 0-98926  
 oscillatory flow in U-tube manometers, effect of drag reducing polymer additives 0-64584  
 variable pressure manometer, electrocapillary element appls. and properties 0-73379

**manufacture**

see also electronic equipment manufacture; steel manufacture

- fission reactors, VVER 440, design and engineering props., production and assembly 0-91207  
 fusion reactor, Heliotron E, vacuum chamber construction using electron beam welding 0-106180  
 fusion reactor, Large Coil Program, General Dynamics Convair/IGC manufacturing engineering 0-106169  
 fusion reactor, neutral beam ion source, core snubber network design, fabrication and testing 0-102378  
 fusion reactor, TEXT, toroidal field coil fabrication 0-91267  
 fusion reactor, TFTR, neutral beam injector prototype, construction and performance 0-99390  
 fusion reactor vacuum vessel, large, ultra high vacuum, design and manufacturing problems 0-99276  
 neutral beam, continuously operating, convectively cooled ion accelerator, mech. design and fabrication 0-102374  
 neutral beam source, cryopumping and mag. shielding, fabrication and operating cost 0-106229  
 neutral beam source manufacturing at Lawrence Livermore Laboratory 0-102377  
 vertical axis wind turbines 0-66929  
 Ag-Zn batteries, miniature, fabrication and characts. (*Polish*) 0-93866  
 Nb-Ti, multifilamentary, Mirror Fusion Test Facility, superconductor core manufacturing and quality 0-93521  
 Si photovoltaic industry, environmental control, economic and ecological requirements 0-94026

**manufacturing ADP** see manufacturing data processing

**manufacturing computer control**

see also manufacturing data processing; process computer control  
 polisher, computer controlled, efficiency 0-91938

**manufacturing data processing**

see also manufacturing computer control

- steelworks computerised spectrometric analysis and management information system 0-89574



**manufacturing processes**

see also *cold working; cutting; drawing (mechanical); extrusion; forging; forming processes; hot pressing; hot working; joining processes; machining; manufacture; rolling; sintering*  
fusion reactor, TFTR poloidal field coils, tooling and manufacture 0-91262  
polycarbonate styrene-acrylonitrile copolymer mixture, determ. of phase structure, electron microscopy 0-103272

**many-body problems**

see also *BCS theory; quantum statistical mechanics; renormalisation*  
3-body problem with one infinite mass particle, Schrodinger and integral eqn. soln. equivalence 0-77636  
atomic collisions, classical many-body collision model incorporating Heisenberg and Pauli principles 0-63511  
atomic many-body perturbation theory with radially restricted basis functions 0-78526  
binary dense gaseous mixtures, struct. and thermodynamic props., molecular dynamics study 0-64866  
binary liquid solutions, struct. and thermodynamic props., molecular dynamics study 0-64866  
boson condensate, dynamic eqn. functional formulation, many body theory 0-84334  
boundary conditions, spherical, for computer experiment 0-105597  
Chakravarty-Woo eqn., extension and appl. to liq.  $^4\text{He}$ , liq.  $^3\text{He}$ , and nucl. matter 0-68124  
cluster models, Faddeev-Yakubovskii coupling 0-105816  
composite particles, nonrelativistic many-body theory, foundations and statistical mechanics 0-82947  
configuration space basis state generation,  $U(n)$  matrix elements 0-86120  
contracted orbital formulation of many-body perturbation theory 0-87026  
core-hole processes, electronic Hamiltonian, many-body theory 0-91443  
Coulomb scattering, N-particle, cluster props. 0-73192  
crystal defects, functional eqn., Tamm Dancoff procedure, canonical transformation (German) 0-84448  
dielectric behaviour of materials undergoing dipole alignment transitions 0-88922  
Dirac particle+two Klein-Gordon particles, relativistic three-body wave equation, preon model 0-73574  
Eckart Hamiltonian, transformation approach 0-101726  
electron gas, interacting, local-field correction to dielectric constant, review 0-107731  
electron gas, uniform, electronic props. of H and He impurities 0-96807  
EXAFS amplitudes, many-body effects 0-97379  
Helmholtz equation, 1-D three-body problem, Sommerfeld Maluzhinetz transformation 0-62524  
isospectral matrices, finite transforms 0-105529  
kinetic few-body propagator by exact inversion 0-86123  
Klein-Gordon particles+Dirac particle, relativistic three-body wave equation, preon model 0-73574  
N interacting particle canonical distrib. from kinetic theory 0-105569  
neutron gas, crystallisation, zero-order, Bethe-Fermi homework potential 0-63117  
nuclear many body scattering, channel coupling array theory, wave function formalisms 0-78235  
nuclear scatt., variational principles for true three- and four-particle scatterings 0-78233  
nuclei, spherical, quasi-particle theory, modification of BCS basis 0-63109  
number operators for composite particles in nonrelativistic many-body theory 0-94982  
path integral approach to many-nucleon systems and time-dependent Hartree-Fock 0-78180  
polymer expansion for quantum many-body problem 0-57181  
power series soln. of coupled eqns. and three-body problem 0-86145  
quantised many-body problem, dissipative system wave eqn. 0-86104  
quantum field theory, multiloop, Fock-space technique, particle creation effects 0-77945  
quantum many-particle systems in curved spacetime 0-98751  
quantum systems, interacting particles, ground state energy per particle 0-68064  
quantum systems, mutual bonding of particles 0-101724  
quantum three particle system, action-angle variables 0-95708  
quantum-mechanical kinetic eqn. as measure of information in distribution 0-101725  
relativistic theory of many-electron atoms,  $H_+$  and  $h_+$  and related HF eqns. derivation 0-99458  
relaxational dynamics, renormalisation group anal., scaling fields and variables 0-105602  
resonance theory in indefinite metric spaces 0-101730  
scattering operator of few-body quantum mechanical system, sum of two-body potential operators 0-62516  
Schrodinger equation, three-body problem with hard cores, 1-D, reduction to 2-D Helmholtz eqn. 0-62523  
Schrodinger equation, three-body problem with hard cores, 1-D, eigenvalue lower bounds 0-68069  
Schrodinger equations, three-body problem, bound state eigenvalues lower bounds, upper bounds by Rayleigh-Ritz method 0-68068  
ten-electron systems, correl. energy, fourth order diagrammatic, many body Rayleigh Schrodinger perturbation theory 0-63556  
three-body problem in one dimension 0-82655  
three-body problem of two electron atoms 0-83286  
three-body scattering equations, nonsingular representation, partial-wave anal. 0-91021  
time inversion and mobility 0-101722  
two charged clusters collision, scatt. amplitudes and integral eqns. 0-68614  
two- and three-particle scatt. for relativistic systems in light front dynamics (Russian) 0-62892  
unitary group formulation of many-electron theory and quantum organic chemistry 0-106270  
vertex function and crossing symmetry 0-62515  
qq interactions and nonrelativistic quark model 0-73682  
 $H_+$ , many-body perturbation theory with radially restricted basis functions 0-78526  
 $H_2$ , four-body system, adiabatic representation 0-91530  
 $H_2O$ , many electron Green's function calcs. optical pot. 0-58126  
 $^3\text{He}$ , liq., binding energy, variational calcs. by Pandharipande's method 0-101752  
 $^4\text{He}$ , liq., binding energy, variational calcs. by Pandharipande's method 0-101752

**many-body problems continued**

$LiH$ , many electron Green's function calcs. optical pot. 0-58126  
 $Si$  MOSFET, surface quantum states, two-dimensionality of many-body effects 0-103740  
**many-particle systems** see *statistical mechanics*  
**many-valley semiconductor materials** see *many-valley semiconductors*  
**many-valley semiconductors**  
bound multi-exciton complexes, density-matrix functional approach 0-96794  
conductivity in heating electromag. wave 0-84483  
cubic, with ellipsoidal valleys, magnetoresist. 0-80300  
donor impurity levels and excitons, shallow-deep instabilities 0-75520  
ferromagnetic multivalley anisotropic, electron auto-localisation (Russian) 0-92848  
heavily doped scattering mechanisms resist. and Hall maxima 0-75586  
two-valley semiconductor, hot electron instability, intervalley scatt. (Russian) 0-92921  
two-valley semiconductors, carrier vel.-field characts. under high elec. field 0-70713  
n-AlSb, acoustoelectric effect due to piezoelectrically active wave 0-80331  
 $Bi_{1-x}Sb_x$ , solid soln., temp. depend. of weak-field galvanomag. coeffs. (Russian) 0-70724  
 $Ga_{1-x}Al_xAs$ , intervalley energy gaps, temp. junction, exptl. determ. 0-80179  
n-GaP, acoustoelectric effect due to piezoelectrically active wave 0-80331  
Ge, donor polarizability, multivalley effective mass calc. 0-96817  
n-Ge, Hall effect, uniaxial deform. effects 0-65605  
InSb, current-voltage characteristics at room temperature and high hydrostatic pressure 0-88560  
n-Si, (111) inversion layers, valley splitting, Shubnikov de Haas oscills. 0-65698  
Si, donor polarizability, multivalley effective mass calc. 0-96817  
n-Si, elec. cond. control by hot electron intervalley transfer 0-59993  
n-Si, multivalued Sasaki effect 0-107795  
Si, photovoltaic and photomagnetic effects, rel. to intervalley electron transfer 0-60034  
Si, uniaxially stressed, excitonic molecule emission spectra, electron valley degeneracy effects 0-60669  
**manybody problems** see *many-body problems*  
**map drawing** see *cartography*  
**marine systems**  
see also *ships*  
buoy for oceanographic and atmos. data acquisition, using Meteosat data transmission (German) 0-90224  
cosmic ray detector located in deep ocean 0-98522  
lift bag, salvage device for deep ocean 0-82107  
magnetometer for sea-floor mag. fluctuations, ULF-ELF 0-77152  
photometer for deep-sea work, using acoustic telemetering 0-98460  
radiocommunication buoy, antennas and operating freqs. (Russian) 0-109253  
submersibles for research work, remotely operated vehicles 0-82105  
windmills in North Sea, for 20% of UK's electricity demand 0-97759  
**mark scanning equipment**  
square-field scanned image construction time optimisation (Russian) 0-63933  
**marketing**  
fibre optics technology and connector systems, marketing 0-69522  
retail equity, NBS Standard Reference Materials 0-86249  
**Markov chains** see *Markov processes*  
**Markov processes**  
atmospheric precip.-time struct., daily precip. amounts modelling with Markov-I chain 0-101401  
Bernard convection, and linear fluctuation theory, Markovian processes and irreversibility 0-87766  
biological multistate systems, freq. of cyclic processes 0-108834  
boson field, damping superoperator eigenvalue problem, direct soln. 0-57180  
Brownian motion, generalised scalar case, computer simulation 0-77704  
characteristic function eqn. of Markov process, Langevin process applications 0-57192  
classical filtering model, optimal impulse control, separation theorem (French) 0-90659  
classical processes, nonequivalence to quantum mechanics 0-62583  
condensed phases, molecular roto-translation, single particle theory 0-64932  
decision processes, infinite-horizon, denumerable-state, finite-state approx. 0-68130  
derivation of equations for characteristic functionals 0-57197  
deterministic dynamics to probabilistic descriptions 0-68029  
direct solar energy, Markov chain simulation with one minute binning (French) 0-61293  
Dirichlet forms and Markov processes, book 0-73119  
earthquake recurrence, semi-Markov model 0-98247  
exponential growth of Markovian products of random matrices (French) 0-90656  
Gaussian Markov random fields, discrete parameter, generalised potential theory 0-57185  
generalised Feynman-Nelson model for free scalar field theory 0-105769  
geophysical data acquisition (Italian) 0-109254  
heavy ion reactions, 10-200 MeV/N, Markovian and non-Markovian effects in transition probabilities 0-102175  
hydrodynamic equations, stress tensor and local eqn. 0-82720  
hydrodynamic equations from constitutive equations 0-82721  
inhomogeneous Poisson flow with conductor function controlled by Markov chain, asymptotic behaviour 0-95032  
intramolecular dynamics, random coupling model, multiphoton excitation, kinetic eqns. 0-63700  
irreversibility, Onsager Casimir symmetry 0-62580  
Langevin equations, WKB-type expansion 0-86212  
lattice systems, attractive, global Markov property for + and - states 0-82725  
linear oscillator, nonstationary narrow band response and first passage probability, stochastic process 0-62465  
linear system with nondelta-correlated parameter fluctuations, statistical anal. 0-95036  
LMFBR cooling systems, reliability modelling appls. 0-57838  
minimal Markov process generated by second order differential operator, reversibility (Chinese) 0-68127



**Markov processes continued**

- molecular crystals, phononless exciton band lineshape, excitation transfer, stochastic models 0-107711
- molecular dissociation, RRKM formula correction by non Boltzmann character factors, Markov eqns. 0-71891
- molecular rotation and translation interaction 0-69262
- multistep compound cross section from Markovian processes 0-83090
- Nelson's stochastic field, tensor field quantisation 0-105574
- neural transformations of random signals, Wiener and of functionals of Markov chain 0-76727
- quantum field theory, Markovian homogeneous multicomponent Gaussian fields 0-77933
- rate processes in condensed media, master eqns. 0-77687
- regularisation by Dirichlet forms 0-86208
- resonance fluorescence in Markovian stochastic fields 0-83573
- semigroup, Markov, invariant measure and ergodic property (*Chinese*) 0-62578
- speech anal., reflection coefficient estimates based on Markov chain model 0-83710
- stochastic quantisation processes, review, Markov processes, Martingales, quantum dynamics 0-94969
- tuning fork oscillator internal random disturbances (*Russian*) 0-62459
- two-parameter process, Markov property (*French*) 0-68129
- velocity of light Markov process, Klein-Gordan quantum statistic, quantum mechanics 0-98808
- visual system of fly, giant neuron performance, spike generation 0-108886
- Weiner-Einstein processes, Markov, maxima and first-passage-time statistics 0-68134
- white noise, Gaussian and Poisson, Markov fields and local operators 0-57186
- Fe XV, line intensity and linewidths at high electron density, generalised population ratio 0-99481
- H II regions density fluctuations, statistical approach 0-77468

**Mars**

- active seismic exploration and liquid water in crust 0-67607
- astrometry with Danjon astrolabe at San Fernando Observatory (Jan. to Feb. 1978) (*French*) 0-94736
- atmosphere, general circulation model, including dust and topography 0-90354
- atmosphere, O I dayglow red emission at 630 nm 0-62063
- atmosphere, O spectral line shape following mol. dissociative excitation 0-105097
- atmosphere, radiative equilibrium temp. affected by O<sub>3</sub> 0-72827
- atmosphere, response to heat sources and perturbations (*Chinese*) 0-85748
- atmosphere boundary layer, momentum and heat turbulent flux, Viking 1 obs. 0-72810
- atmosphere dust affecting surface and atmos. heating 0-67625
- atmosphere pressure, annual cycle meas. by Viking landers 1 and 2 0-72812
- atmosphere relative humidity 0-72826
- chemical composition of interior, cosmochemical model 0-72813
- climate oscills., latitude depend. and oscill. spectra 0-90355
- cloud formations, reflectivity time var., visible photometry obs. 0-72840
- clouds over Tharsis volcanoes, diurnal props. 0-94738
- conference, Second International Colloquium on Mars, Pasadena (Jan. 1979) 0-62370
- crater count ages, ice and sand impact crater implications 0-67614
- crater depth study, evidence for subsurface volatiles 0-85878
- Deimos, loose material downslope movement obs. 0-94737
- Deimos, photometry from Viking orbiter images 0-72838
- desert features created by wind, Western Desert of Egypt compared with Mars 0-72815
- dune morphology and distrib., compared to Earth 0-72814
- dust storm, IR opacity of atmos. 0-72822
- dust storm of 1971, cloud form., multicolour TV photometry obs. 0-101546
- dust storms, opacity from Viking IR thermal mapping 0-82253
- dynamics obs. from Viking lander tracking data anal. 0-77314
- erosional processes and channelized water flows 0-67611
- feroxyhyte (6-FeOOH), possible occurrence on surface of Mars 0-85879
- fluidized crater morphology 0-67613
- gravity, twelfth degree and order spherical harmonic model 0-67608
- gravity anomalies and tectonics, review 0-98593
- hypometric curve construction and crust evolution model 0-77315
- igneous processes, impact crater and basin control 0-67615
- inert gases in atmosphere, accretion from protoplanetary nebula 0-109385
- ionosphere, ionic reactions in lab. and planetary atmospheres, probe data 0-59168
- lithosphere, possible S overabundance 0-72832
- lobate debris aprons and similar flows, distrib. 0-67619
- Lunae Planum—Chryse Planitia region, plains and channels 0-67612
- magnetic minerals, obs. by Viking extended mission 0-72830
- Maja and Kasei Valles, channel morphology 0-67610
- north polar cap, 1975-1978 photographic obs. 0-72823
- north polar cap, 1977-1978 regression obs. 0-72825
- Olympus Mons, subglacial origin and aureole deposits 0-67617
- Olympus Mons aureole and perimeter scarp, origin 0-77317
- orbit determination on basis of radar and visible observations 0-90323
- organic compound search by Viking, final conclusions 0-67627
- outflow channels erosion, implications of sediment transport modes in channelised water flows 0-98363
- permafrost, thermodynamics 0-67621
- Phobos, grooves distrib., morphology and possible origin 0-72837
- Phobos, orbital inclination evolution 0-67628
- Phobos, photometry from Viking orbiter images 0-72838
- Phoenicis Lacus and Coprates regions, tectonic trends inventory 0-77316
- pitted and fluted rock, compared with wind eroded Egyptian rock 0-72816
- polygonal troughs on Mars northern plains, origin 0-98590
- position determ. in 1978 using Double Zeiss Astrograph, Belgian obs. (*French*) 0-72809
- pseudocraters in Cydonia region 0-67618
- rotation period, determ. from transits of albedo stations across central meridian (1659 to 1971) 0-98588
- rough planar surfaces, radar, visual and thermal characts. 0-98589
- sand blown by wind, threshold windspeed laboratory expts. 0-72811
- sand sea (erg) in north polar region, wind patterns 0-67624

**Mars continued**

- satellites, crater density interpretation 0-82252
- satellites, effect of proximity to Roche limit on dynamical behaviour of ejecta 0-98592
- soil density map rel. to surface albedo, topography and geology 0-109388
- solar wind interaction, role of planetary ionosphere and magnetosphere 0-72835
- south polar cap, residual CO<sub>2</sub> frost in spring and summer 0-72820
- Soviet lunar and planetary exploration, handbook 0-62398
- surface, wave tilt sounding of multilayered structures 0-61926
- surface brine presence, Cl and sulphate abundance detect. 0-82254
- surface colour change at Viking landing site 0-72829
- surface composition from reflectance spectroscopy, summary 0-72834
- surface thermal properties, effect of nonideal surface 0-72819
- tectonic evolution 0-67606
- S. Tharsis, radar altimetry 0-98591
- thermal inertia, longit. var. rel. to var. of 2.8 cm brightness temp. 0-105191
- thermal map of northern equatorial and temperate latitudes 0-72818
- thermal maps of Chryse basin channel terrain 0-72817
- topography, photogrammetric portrayal 0-67609
- Valles Marineris, landslides 0-67620
- Viking, extended mission 0-67514
- Viking gas exchange reaction, simulation on UV irradiated MnO<sub>2</sub> substrate 0-72831
- Viking lander sample field obs., current status 0-67626
- Viking mission, review of planetary data 0-72839
- Viking mission results 0-82255
- Viking orbiters, radio occultation meas. of Mars atmosphere and topography and atmosphere 0-72836
- volcanic sulphate aerosol, formation and deposition 0-72828
- volcano-ice interactions, landforms 0-67616
- wind, crater generated lee waves 0-72824
- wind streaks, seasonal and secular var., Mariner 9 and Viking obs. 0-67622
- yardangs and wind erosion 0-67623
- CO<sub>2</sub> adsorption and capillary condensation on clays, significance for volatile storage and atmospheric history 0-72833
- CO<sub>2</sub> atmosphere, erosion by solar wind energetic atomic particles 0-72736
- CO<sub>2</sub> ice clouds, brightness temp. and radiative props. 0-105192
- CO<sub>2</sub> solid, optical properties in IR region 0-72821

**martensitic steel**

- ageing, effect of H<sub>2</sub> on stresses in process of  $\gamma \rightarrow \alpha$  transformation (*Russian*) 0-76252
- alloying element effect on coarsening behaviour of cementite particles in ferrite 0-66518
- ball bearing, fatigue damage, influence of dispersed phases in martensitic matrix 0-108549
- composite vessels, welded, glass fibre reinforced plastic wound, struct. strength 0-97552
- cutlery, pitting corrosion 0-100962
- etching technique, for revealing struct. inhomogeneities 0-61035
- fatigue life, low-cycle, temp. and strain rate effects 0-85056
- ferritic-martensitic steels, fatigue crack tip plastic zone (*Japanese*) 0-71738
- low Si, martensite struct. and mech. props. (*Korean*) 0-93614
- maraging steel, ageing kinetics and struct. of N12K7M5TYu, effect of high temp. deform. of austenite (*Russian*) 0-84960
- Ni-Cr-Mo, electroslag refined, fracture toughness and fatigue behaviour 0-81171
- plastic deformation influence in type N17K12M5T steel on mech. props. (*Russian*) 0-76305
- specific heat and magnetisation, 1.2 to 10K 0-71059
- stainless, in SO<sub>4</sub> solns., activation pH and susceptibility to H<sub>2</sub> assisted stress corrosion cracking 0-97619
- structural and mechanical props. of type Kh13N9D2MT martensitic aged steel (*Russian*) 0-93600
- thermal expansion, of heavily doped steels and alloys 0-103501
- Cr (12%), temper embrittlement 0-66650
- Cr-C (12, 0.15 wt.%) type AISI 410, role of C in embrittlement phenomena 0-93652
- Cr-Mn(Ni), Mn and Ni additions, effect on corrosion resistance and hardness 0-104342
- Cr-Mo, effect of Mo on high-temp. props. 0-85005
- Cr-Si-Mn-Ni-Mo-C, resist. to deform. and fracture, C effect 0-71757
- Fe-Ni-C martensite morphology, butterfly-lenticular transition temp., Cr addition effect (*Japanese*) 0-81053

**martensitic transformations**

- see also shape memory effects
- ageing, effect of H<sub>2</sub> on stresses in process of  $\gamma \rightarrow \alpha$  transformation (*Russian*) 0-76252
- alloys, phase transition premonitory phenomena, exam. by electron diffraction and microscopy (*French*) 0-59651
- brass, Cu-Zn (39/40 wt.%), shape memory effect and martensitic transform. depend. on heating-cooling cycles (*Russian*) 0-97482
- ceramics, transformation toughening, martensitic transforms. in crack-tip stress fields 0-104154
- crystal geometry, of martensitic transformations, electron microscopy study (*Russian*) 0-108441
- dislocation inheritance, crystallography, describable by nonuniform lattice strain (*Russian*) 0-81056
- dislocations and lattice transformations, book contrib. 0-107242
- elastic wave generation comparable to Bain deform., role of multiphonon processes (*Russian*) 0-84246
- ferroelectrics, domain structure as outcome state for poling procedure 0-80728
- lenticular martensite growth by transformation wave propag. 0-81055
- magnetostriiction effect, on martensite transformation point shift in strong mag. field (*Russian*) 0-108440
- memory alloy engine, efficiency 0-71648
- metals and alloys, shock wave effect on martensitic transform. (*Russian*) 0-96595
- $\beta$ -phase alloys, Landau theory 0-108444
- rare earths, light, stacking faults and magnetism, transform. effects 0-75840
- shape memory alloy, martensite boundaries, lattice imaging study 0-107359
- shape-memory alloys, shape recovery cycle thermal efficiency 0-108445



**martensitic transformations continued**

- single crystals under large loads, theoretical elastic behaviour, review and appl. 0-71681  
 steel, 35NiCr18, bainite transformation, study with aid of hot stage microscope 0-76253  
 steel, austenitic, quenched state, influence of austenite stability on impact strength (*Russian*) 0-81146  
 steel, austenitic stainless, unlubricated, friction, wear and microstruct. of types 304, 316 and Nitronic 60 0-108589  
 steel, austenitic stainless, welded explosively, induced martensites morphology 0-104153  
 steel, C, massive martensitic transformation kinetics 0-81060  
 steel, carburized and quenched, residual stresses (*Japanese*) 0-89262  
 steel, Cr-Mo-V pressure vessel, microstruct. parameters and yielding rel. to plastic deform. 0-89318  
 steel, high-speed, low temp. mag. cycling effects on ferromag. struct. 0-100928  
 steel, martensitic growth 0-108439  
 steel, Ni (17 wt.%), martensitic deform. temp., cryst. struct. effect (*Russian*) 0-66576  
 steel, stainless, austenitic, explosively welded, orientation relationship in martensitic transform. 0-104158  
 steel, stainless, austenitic type 304, acoustic emission identification, opt. microscopy obs. 0-81062  
 steel, stainless, martensite nucleation mechanisms, HVEM obs. 0-104157  
 steel, stainless, shock loaded, residual martensite obs. 0-104414  
 steel, stainless, wire, axial texture after electroplastic drawing, X-ray struct. investigation (*Russian*) 0-104177  
 steel, stress calcs, using statistical model (*Russian*) 0-93557  
 steel, TRIP, fatigue strength 0-108552  
 steel bearing, surface-ground, residual stress fatigue property comparison 0-60975  
 Co-Al alloy, multilayer martensite phases, illustration of polytype structures 0-84932  
 Cu, wire, axial texture after electroplastic drawing, X-ray struct. investigation (*Russian*) 0-104177  
 $\beta$ -Cu-Al-Ni (14, 3 wt.%), single cryst., thermal effect due to stress induced martensite formation 0-81059  
 Cu-Al-Ni Marmen alloys, rapid solidification and ageing 0-76245  
 Cu-Zn-Al martensite, lattice dynamics, neutron scatt. meas. 0-88286  
 $\beta$ -CuZn, acoustic emission rel. to stress induced martensitic transformation 0-81061  
 Fe, polycryst., influence of  $\alpha$ - $\gamma$  transform. on creep (*Russian*) 0-89289  
 Fe, splat-quenched, microhardness and martensite 0-76359  
 Fe-Cr-Ni (12, 15 wt.%) austenitic alloy,  $\text{Ni}^{60}$  irradiated, void swelling and phase stability, Si and Ti effects 0-65055  
 Fe-Cr-Ni (18,14 wt.%),  $\gamma$  to  $\alpha$  to  $\alpha'$  martensitic transform., external stress effect, double tensile deform. exam. 0-108438  
 Fe-Mn, as cast, pseudo-composite struct. resulting from interdendritic segregation, cryogenic materials appl. (*French*) 0-93556  
 Fe-Ni alloy, martensitic transform., influence of thermal and electron irradi. treatment of austenite (*Russian*) 0-66509  
 Fe-Ni film, amorphous, martensite form. time and struct. 0-104159  
 Fe-Ni Invar, magnetovolume coupling enhancement factor, temp. depend. 0-88851  
 Fe-Ni-C (25, 0.2 wt.%), strain-induced martensite (*Korean*) 0-71646  
 Fe-Ni-C (30, 0.5 wt.%) single cryst., stress induced martensitic transform. 0-60860  
 Fe-Ni-C (31.9,0.02 wt.%), determ. of number and size distrib. of martensitic plates 0-76255  
 Fe-Ni-Co-Ti, coherent particles effect inherited by martensite on  $\alpha$ - $\gamma$  transformation (*Russian*) 0-108443  
 Fe-Ni-Mn (20, 5 wt.%), rel. orientation between adjacent martensite laths 0-76254  
 Fe-Ni-Mo, annealing, influence on struct. of austenite (*Russian*) 0-81057  
 Fe-Ni(28 at.%), Mossbauer scattering, martensitic transformation, evidence of soft modes 0-93223  
 Fe-Pd (31.2 wt.%), thermoelastic FCC-FCT martensitic transformation 0-104156  
 Fe,Pt, atomic thermal vibr. anisotropy, martensitic transform. model (*French*) 0-70355  
 Fe,Pt austenites, ordering kinetics 0-104155  
 Fe,Pt austenitising conditions on  $M_s$  temp. 0-81088  
 Li single cryst., US attenuation and vel. measurements in vicinity of martensitic phase transformation 0-73558  
 Mn-Al-C, ferromag. alloy, transform. kinetics 0-76229  
 $\text{NH}_4\text{Br}$ , supercooled, polymorphic transform., struct. correspondences and mechanisms 0-107097  
 Nb<sub>3</sub>Sn, Young's modulus, 4.2-300K, behaviour near martensitic transition 0-66564  
 NiTi equiatomic alloy, single cryst. elastic constns. near martensitic transform. 0-75283  
 NiTi, premartensitic transformation of B2 phase, shape memory 0-84931  
 NiTi, shape memory effect, struct. characs., TEM  $2\frac{1}{2}$  D imaging obs. 0-108446  
 PbTiO<sub>3</sub>, phase transform., different kinetic types 0-71347  
 steels, Cr-C-Mn(Ni), struct. prop. rel., design of struct. steels for high strength and toughness 0-97491  
 Th-C-N system, existence of new  $\beta'$ -ThCN' phase, struct. and thermodynamic study (*French*) 0-92499  
 Ti alloys, reversibility of martensitic transformations (*Russian*) 0-108442  
 Ti-Al-Mo-Cr alloy weldment containing orthorhombic martensite, auto-tempering behaviour and alpha precip. strengthening 0-84976  
 Ti-Fe-Ni (67, 30, 3 wt.%), reversible shape alteration (*Russian*) 0-71647  
 Ti-Ni, monoclinic to triclinic phase (*Russian*) 0-81058  
 Ti-Ni, multiplicity of structural transitions, phase diagrams, elec. cond. meas. 0-71649  
 Ti-Ni-Fe, multiplicity of structural transitions, phase diagrams, elec. cond. meas. 0-71649  
 U-Nb (14 at.%), martensitic and polymorphic transformations 0-60861  
 U<sub>3</sub>Si, reversible twinning, in-situ obs. 0-104241  
 Zr-H formation, of  $\delta$ - $\gamma$  transformation 0-84929  
 Zr-H formation, the  $\delta$ - $\epsilon$  transformation 0-84930  
 ZrCu, constitutional and struct. studies, by mag. susceptibility, metallography and X-ray diff. 0-70166  
 ZrV<sub>2</sub>, anomalous softening at martensitic transform. 0-93630

**maser clocks** *see atomic clocks***masers**

- cosmic masers, collision-collisional pumping model (*Russian*) 0-90560  
 Dicke maser Hamiltonian,  $A^2$  term relevance 0-83577

**masers continued**

- Dicke maser model-van der Waals spin system thermodynamic equivalence 0-83572  
 electron cyclotron maser, fundamental mode, linear theory 0-58496  
 electron cyclotron maser, gyrotron, efficiency enhancement, nonlinear theory 0-91768  
 electron cyclotron maser device theory 0-58494  
 electron cyclotron maser in overmoded cavity, nonlinear multimode formulation 0-58495  
 formaldehyde maser in IRS 1 in NGC 7358, SHF band obs. 0-67822  
 frequency standard, thermal noise effect meas. on amplitude of oscillation 0-98898  
 gyromonotron, operating characteristics at 35 GHz 0-58497  
 gyromonotron design, 240 GHz, using supercond. magnet system 0-58498  
 interstellar H<sub>2</sub>O maser emission, new sources detect. 0-62298  
 interstellar OH and H<sub>2</sub>O masers, form. by thermal instability of radiative shock 0-67821  
 IRC+10374, IRC+10523, IR stars, H<sub>2</sub>O maser emission detect. 0-62298  
 microwave emission, by plasma produced electrons orbiting a positively charged wire 0-92272  
 multimegawatt gyrotron design for controlled thermonuclear reactor heating 0-59256  
 OH 205.1-14.1, unusual OH maser, new flare report and 1667 MHz line obs. 0-98734  
 OH masers, interstellar, obs. near Orion population stars 0-67716  
 Orion methanol masers, interferometric and multitransitional study 0-67891  
 paramagnetic crystal, quantum amplification and absorpt. of EM wave in moderating structure 0-87361  
 quantum frequency standard with pulsed optical pumping of Rb<sup>87</sup> vapours, performance factor 0-78823  
 Roberts 22, bipolar nebula with OH emission, visual, radio and IR obs. 0-94859  
 ruby maser, K-band, 500 MHz bandwidth 0-63966  
 Rydberg atom maser emission, heterodyne detection 0-78822  
 spectral line broadening mechanism of maser with beam of infling atoms 0-106503  
 stars, late supergiants and long period variables, radial vel. determ. 0-77410  
 successive oscillatory fields, molecular beam resonance method 0-91706  
 symbiotic stars, radio mol. maser line obs. 0-72960  
 two-level, population inversion, information approach, Maxwell demon 0-86241  
 two-resonator CRM oscillator with external feedback 0-87362  
 W3(OH), interstellar OH maser, struct. from VLBI synthesis obs. 0-105368  
 CO maser emission in evolved stars expanding envelopes, line profiles 0-82334  
<sup>133</sup>Cs, freq. standard, optimum conditions for population inversion for 0-0 transition 0-78824  
 Fe<sup>2+</sup>:TiO<sub>2</sub>, 86-88 GHz low-noise TW maser 0-69354  
 H, autotuning systems, theoretical anal. based on freq. or phase method 0-83575  
 H, frequency changes due to nonuniform magnetic field 0-99687  
 H, with automatically tuned resonators 0-95859  
 H<sub>2</sub> maser freq. standard using dual modulation 0-98900  
 H<sub>2</sub> maser wall shift and unperturbed hyperfine freq. of ground state of H<sub>2</sub> atom 0-98901  
 H<sub>2</sub>, multibeam collimator, used to stabilise maser frequency standard 0-91769  
 H<sub>2</sub>, temp. dependence of wall shift, 295 to 395K 0-83576  
 H<sub>2</sub>O maser source in Orion A, obs. of outburst (*Russian*) 0-105320  
 H<sub>2</sub>O maser sources in galactic plane, southern hemisphere survey 0-73054  
 H<sub>2</sub>O masers, 22 GHz galactic plane survey, 14 new sources 0-77464  
 H<sub>2</sub>O masers in NGC 6334, positions and spectra rel. to star form. 0-73025  
 H<sub>2</sub>O sources near Herbig-Haro objects 7-11, 22 GHz obs. 0-73019  
 OH astronomical maser sources OH 231.8+4.2, CY Canis Majoris, M1-92, UHF obs. 0-90550  
 OH main line emission from globular clusters, high sensitivity search 0-62207  
 OH main line maser in interstellar cloud, pumping mechanism 0-67824  
 OH maser emission, rot. excitation by H<sub>2</sub> at interstellar temps. 0-62232  
 OH maser in pulsating Mira type variables atm., IR line overlap pumping mechanism 0-72764  
 OH maser pumping efficiency of Mira variable stars 0-82379  
 OH maser source OH 351.78-0.54, UHF obs. (1980 August) 0-101644  
 Rb maser oscillator, freq. domain meas. of freq. stability 0-83574

**masking (acoustic)** *see hearing; speech intelligibility***masks**

- see also semiconductor device manufacture*  
 coherent optical pattern recognition using normalized invariant moments 0-99653  
 fibre-optic planar multimode coupling structure fabrication by ion exchange 0-64233  
 IC photomask and wafer linewidth meas. using optical spatial coherence 0-77850  
 ion milling, string segment motion algorithm 0-71779  
 MIS solar cells, etched slotted mask for direct deposition of metal contact pattern 0-97786  
 optical microscope, large field, for use in semiconductor manufacture 0-82812  
 Cr film, pattern generation by laser-induced oxidation 0-61009  
 Cr films, photoresist film on reverse gas plasma etching 0-97634  
 Fe<sub>2</sub>O<sub>3</sub> films, DC reactively sputtered, for selectively semitransparent photomasks, struct., mech. and chem. props. 0-59835  
 Fe<sub>2</sub>O<sub>3</sub> films, DC reactively sputtered, for selectively semitransparent photomasks, deposition conditions and optical props. 0-60782  
 Nb-Nb Josephson junctions, submicron, thermally recyclable, fabrication and characts. 0-100566  
 SiO<sub>2</sub>, masking film in alkaline etching 0-71771

**masonry dams** *see dams***mass**

- see also atomic mass; elementary particle mass; molecular weight*  
 Abell 399/Abell 401, X-ray binary galaxy cluster, mass 0-90546  
 Coma galaxy cluster, mass segregation and missing mass 0-98730  
 galaxies, elliptical, vel. dispersions rel. to mass to light ratios 0-98707



**mass continued**

- galaxies nonflat components (halo), mass limits 0-62291
- galaxy mass determination from binary galaxies, anal. of Turner's (1976) sample 0-67849
- globular clusters mass function, effects of tidal disruption by Galaxy 0-105294
- induced, equilateral triangular cylinder moving in an incompressible irrotational fluid 0-64237
- interstellar giant molecular clouds, gravit. field probing rel. to mass upper limits 0-62242
- ion scattering spectrometer for surface studies 0-98995
- NGC 1055, 681, 4594, galaxies, rot. curves and mass distrib. (*Russian*) 0-90541
- NGC 3115, S0 galaxy, rotation and mass of inner 5 kiloparsecs 0-105326
- Pluto+Charon system, mass and density from speckle obs. 0-109394

**mass analyzers** *see mass spectrometer components and accessories***mass differences**

- see also baryon mass; lepton mass; mass formulae; meson mass*
- hadron causality and EM mass shifts, remarks 0-73705
- $K^0 \rightarrow K^0$  transition in the standard SU(3) $\otimes$ SU(2) $\otimes$ U(1) scheme (*Russian*) 0-82951
- quark-gluon field coupling const., meson mass differences (*Russian*) 0-105898
- quarks, EM form factors in instanton fields 0-99102
- quarks, mass differences of up and down quarks, grand unification 0-62978
- C-quark, mass difference to be quark 0-78022
- $D^{*+}$  photoprod.,  $D^0$  mass difference 0-73720
- $e^+e^- \rightarrow$  hadrons, T, T', T'' states, mass differences, leptonic width ratio 0-68466
- $K_L-K_S$  mass differences, charged Higgs boson couplings 0-62917
- NM mass shifts, asymptotic bounds and causality conditions 0-73704
- $\pi$  EM mass shifts, asymptotic bounds and causality conditions 0-73704
- T and charmonium spectra, common pot. fit, T''-T mass difference 0-86712

**mass filters** *see mass spectrometer components and accessories***mass formulae**

- see also baryon mass; lepton mass; mass differences; meson mass*
- baryon mass relations in internal SU(6) symmetry 0-82962
- baryon spectrum and the forces between quarks 0-102004
- bottom hadrons, masses and allowed decays, SU(5) quark model 0-62954
- charged baryon mass and F/D ratio, colour magnetic interaction 0-62957
- charged hadrons, SU(4) mass-breaking, mass sum rules 0-62959
- distribution of masses of leptons and hadrons 0-99093
- fourth generation of quarks and leptons, mass formula 0-105876
- fundamental fermions, mass eigenvalues, rate of increase 0-105871
- hadron building blocks, pionic mass intervals in narrow and S-state resonances 0-105875
- lattice QCD, hadron mass spectrum, effective Hamiltonians, degenerate perturbation theory 0-102003
- light hadronic spectroscopy, expt. and quark model interpretations, review, book contrib. 0-68438
- meson and baryon mass formula, chromodynamics consideration (*Russian*) 0-91071
- $Q^0$  dibaryon resonances, orbitally excited mass spectrum, decays 0-73670
- SU(2) $_L \times$ U(1) with four flavours, relation between Cabibbo angle and quark masses 0-105872
- A<sub>1</sub> meson, mass formulas and selection rules in large SU(3) mixing 0-86700
- B meson, mass formulas and selection rules in large SU(3) mixing 0-86700
- $\Delta_{235}(1925)$  baryonic degrees of freedom, nonrelativistic, harmonic oscillator quark model mass formula 0-91066
- $\mu$ -e mass quotient, modified Weinberg-Salam model calcs. (*French*) 0-82926
- $Q_1(1280)$ , mass formulas and selection rules in large SU(3) mixing 0-86700
- $Q_1(1400)$ , mass formulas and selection rules in large SU(3) mixing 0-86700
- $qq(q\bar{q})^2$  mesons, mass formula 0-62958

**mass measurement**

- see also weighing*
- aerosol, single droplet, size and mass meas. using electrodynamic balance 0-89535
- air density effects, calc. from atm. variables 0-105615
- calibrations of multiples of the unit of mass, systematic search for orthogonal systems 0-82747
- high-accuracy (0.01%), developed for spacecraft appl. 0-73324
- measurement methods in Yugoslavia (*Croatian*) 0-105616
- microweighing in vacuum and controlled environments and use of beam microbalance, book 0-62401
- SI units fundamentals (*French*) 0-95059
- STEM methods and associated errors 0-73537
- substance amount, precise meas. and dosage 0-90819

**mass spectra**

- see also mass spectrometers; mass spectroscopic chemical analysis; mass spectroscopy; secondary ion mass spectra; time of flight mass spectra*
- acetaldehyde, multiphoton ionisation mass spectra 0-83436
- atmospheric negative ions, photodissoc. and photodetachment 0-69199
- azulene, multiphoton ionisation, mass spectra 0-63717
- benzaldehyde, photoionisation mass spectra formation by UV laser radiation (*Russian*) 0-93781
- benzene, mass spectra following reson. enhanced multiphoton ionisation 0-106362
- benzene, multiphoton ionisation fragmentation patterns, statistical theory 0-95693
- benzene, photoionisation mass spectra formation by UV laser radiation (*Russian*) 0-93781
- benzene, visible and UV photoionisation and fragmentation 0-69195
- benzene cation+benzene, trapped ion mass spectra 0-89470
- $Bo_2$ , 0-65252
- bromobenzene ion fragmentation, photoelectron-photoion coincidence spectra 0-95682
- 2-butene ion, fragmentation, angular momentum in ion-mol. reacts., RRKM calc. 0-66773
- chlorophyll-a, hydration, field desorp. mass spectral obs. 0-71936
- dibromalkanes, energy partitioning in mass spectrometric displacement reactions 0-89471

**mass spectra continued**

- formic acid ions, fragmentation, energy selected, photoelectron-photoion spectra 0-95676
- furan, resonantly enhanced multiphoton ionisation 0-106362
- hydrocarbon ions, mass spectra, H atom scrambling, delocalisation 0-81535
- inert gas Van der Waals dimers, electron impact ionis. 0-58400
- methanol, ionic dissoc., photoelectron-photoion coincidence spectroscopy 0-66774
- naphthalene, multiphoton ionisation, mass spectra 0-63717
- nucleotide base stacking interactions in vacuum, field mass spectrometry 0-81526
- perfluorobenzene, electron attachment, radiative and dissoc., negative ion lifetimes, ion cyclotron reson. spectra 0-74251
- perfluorocyclobutane, electron attachment, radiative and dissoc., negative ion lifetimes, ion cyclotron reson. spectra 0-74251
- perfluoromethylcyclohexane, electron attachment, radiative and dissoc., negative ion lifetimes, ion cyclotron reson. spectra 0-74251
- perfluorotoluene, electron attachment, radiative and dissoc., negative ion lifetimes, ion cyclotron reson. spectra 0-74251
- polyatomic molecules, visible and UV photoionisation and fragmentation 0-69195
- propynyl cation+propyne, reactant structure effects 0-89469
- pyrrole, resonantly enhanced multiphoton ionisation 0-106362
- rare earth hydrides, form. by rare earth reaction with H<sub>2</sub>O vapour 0-76504
- sputtered particles, energy and mass distrib. 0-84822
- steel, volatile products from reaction with H<sub>2</sub>O-CO<sub>2</sub>, high temp. 0-81233
- two photon absorptivity, ion cyclotron reson. photodissoc. spectra, CNDO/S-CI-perturbation theory 0-74123
- Al, thermal desorption of oxide film, influence of grain boundaries and recrystn. 0-61023
- Ar<sup>+</sup>, conversion to mol. ions, three body association coeffs. determ. using drift-tube mass spectrometer 0-108699
- Cl<sup>-</sup> hydration complexes, gas phase, electrostatic calcs. 0-100055
- CoO, desorp. of ions by low power laser beam 0-80092
- Er, vaporisation, heat of sublimation, meas. 0-103471
- ErD<sub>2</sub> thin film, degradation during film processing, investigation 0-101047
- H<sub>2</sub><sup>+</sup>, photodissoc., mass spectra 0-86489
- H<sub>2</sub>+D(O)(Cl)(Br), relax. and chem. reaction, time resolved IR fluorec. and mass spectrometry obs. 0-69177
- HCl+D(O)(Cl)(Br), relax. and chem. reaction, time resolved IR fluorec. and mass spectrometry obs. 0-69177
- H<sup>+</sup>(H<sub>2</sub>O)<sub>n</sub> ion-induced water clusters, mass spectra, IR continuum absorpt. 0-87257
- He<sup>+</sup>, conversion to mol. ions, three body association coeffs. determ. using drift-tube mass spectrometer 0-108699
- He<sup>+</sup>+H<sub>2</sub>(D<sub>2</sub>), dissociative charge transfer, 78-330K 0-61079
- I<sup>-</sup> hydration complexes, gas phase, electrostatic calcs. 0-100055
- InSb, undoped and Te-doped, anomalous impurity segregation, Hall and mass film meas. (*Chinese*) 0-59501
- Mo, Si, films, magnetron DC reactive sputtering, struct. and props. 0-80966
- Na<sub>2</sub>O-B<sub>2</sub>O<sub>3</sub>-GeO<sub>2</sub> vitreous melts, thermodynamic props. from mass spectra 0-65253
- Ne<sup>+</sup>, conversion to mol. ions, three body association coeffs. determ. using drift-tube mass spectrometer 0-108699
- Rh (111), chemisorption of acetylene and ethylene, EELS, LEED and thermal desorption mass spectrometry 0-80057
- Rh (111), co-adsorption of H<sub>2</sub> and CO segregation of co-adsorbed species 0-65361
- TeO<sub>1</sub>Cl<sub>2</sub> thermal decomposition, matrix isolation IR and mass spectra 0-81306
- XeF<sub>6</sub> seeded mol. beam, transverse ionisation, space charge, mass spectra and vel. 0-78725
- YC<sub>n</sub>+(n=2, 3, 4, 5, 6), atomisation energies, Knudsen cell mass spectrometric obs. 0-58409

**mass spectrometer applications**

- see also isotope separation; mass spectroscopic chemical analysis*
- biomedical continuous in vivo meas. (*Japanese*) 0-94309
- leak detection, probe with He-permeable membrane, domestic heating systems 0-98994
- leak detector range extension 0-73375
- metal clusters research, electronic time-of-flight mass spectrometer with separator 0-77907
- semiconductor packages, hermetically sealed, calibration and anal. of moisture by gas mass spectrometry 0-90928
- thin film sputter deposition, closed loop control using glow discharge mass spectroscopy 0-80973
- <sup>14</sup>C dating, high energy mass spectrometer appls. 0-101917

**mass spectrometer components and accessories**

- see also ion sources*
- A/D conversion system of wide dynamic range, gas chromatography mass spectrometry 0-62788
- dynamic mass analysers, charged particle motion in alternating elec. fields, scaling conditions 0-63903
- electric sector modifications, on Mattauch-Herzog mass. spectrometer, for ion kinetic energy meas. 0-62791
- electro-optical detector for spark source mass spectrometry, quantitative meas. 0-101868
- electron multiplier gains determ. for various ions by pulse counting method 0-57418
- filter, overall transmission of quadrupole spectrom. (*French*) 0-101877
- filter for RF spectrometer, background current elimination, expt. results (*Japanese*) 0-82844
- ion analyser enhancement based on MI-1305 mass spectrometer 0-105745
- ion cyclotron resonance detector-oscillator 0-86492
- ion source, electron bombardment type, for use with mass spectrom. 0-77909
- ion source cooling attachment using liquid M<sub>2</sub> for NI-1305 mass spectrometer 0-105744
- ion source for spark source mass spectrograph, modification to reduce residual gas effects 0-98996
- ion storage in a radio-frequency trap with semi-spherical electrodes 0-101869
- ion-field source emitter, influence of laser irradiation on ion current 0-101874



**mass spectrometer components and accessories continued**

- magnet design for high-current implanters or small isotope separators 0-68222  
 magnetic analyser constant current solid-state power unit 0-86499  
 quadrupole filter design, appln. of fundamental props. of Hill equation 0-95186  
 quadrupole ion store, spatial distribution of ions derived by phase space anal. 0-95185  
 quadrupole mass spectrometer, transmission of narrow ion beam, for SIMS studies (*French*) 0-105747  
 secondary ion emission, conf., Stanford, USA (Aug. 1979) 0-105419  
 separator for metal clusters research, electronic time-of-flight mass spectrometer 0-77907  
 tandem mass spectrometer with intermediate image, simultaneous angle and energy focusing 0-62793  
 uncoupled S systems, axial aberration free, general conditions for existence 0-62794  
 Wien filter, cluster ion beam mass anal. appl. 0-86493

**mass spectrometers**

- see also ion optics; mass spectra; mass spectroscopy*  
 Bennett ion mass spectrometers, on Pioneer Venus Bus and Orbiter 0-67499  
 Cherenkov, ninety channel, high energy electrons and gamma photons 0-91362  
 computer controlled photoionisation mass spectrometer 0-77905  
 computerized, technical aspects including data reduction and analysis 0-57417  
 fissile materials accounting, behaviour of the quadrupole mass spectrometer towards various noble gases 0-63300  
 He-jet fed online mass separator for recoil atom mass spectroscopic anal. 0-98998  
 ion energy and momentum spectrometer with high resolution 0-86495  
 ion optical props., aberration, crossed toroidal elec., mag. fields as mass spectrometer (*Chinese*) 0-82843  
 ion source for twin mass spectrometer, charge exchange of metal atoms 0-106215  
 ion-kinetic energy spectrometer, high resolution mass analysed, design and performance 0-101872  
 laser microprobe mass analyser, achievements and appls. 0-73536  
 magnetic analyser, wide-range reaction products of heavy ion beams 0-86491  
 magnetic analysis of charged particles,  $\alpha$ -,  $\beta$ - and mass spectrometers (*Russian*) 0-87011  
 magnetron, inverse, with ion source on outside 0-57416  
 Mattauch-Herzog, modification for ion kinetic energy meas. 0-62791  
 Mattauch-Herzog mass spectrometer, charge exchange 0-86486  
 N19302, for anal. of microscopic amounts of inert and chemically active gases 0-101873  
 N19302, static mode of operation 0-105743  
 neutral gas mass spectrometer expt., on Pioneer Venus Orbiter 0-67502  
 on-line mass separator for fission-produced alkali isotopes 0-98997  
 OSIRIS, target/ion source system for isotope separation in on-line mass separator, mol. ion prod. 0-99366  
 parallel detection system 0-86489  
 partial pressure measurement and gauges for ultrahigh vacuum meas. 0-57323  
 Pioneer Venus Bus neutral gas mass spectrometer 0-67513  
 Pioneer Venus Sounder Probe neutral gas mass spectrometer 0-67506  
 pulse-counting mass spectrometer for noble gas anal. 0-95187  
 quadrupole, transmission of narrow ion beam, for SIMS studies (*French*) 0-105747  
 QUISTOR, space charge and ion stability 0-86487  
 RF, background current elimination, using energy filter (*Japanese*) 0-82844  
 secondary ion emission, conf., Stanford, USA (Aug. 1979) 0-105419  
 spark source quadrupole mass spectrometry, development, appls. 0-62789  
 SSMS ion source modification, residual gas effects 0-98996  
 synchrocyclotron, in line, electrostatic filter 0-86490  
 tandem, for collision-induced dissoci. obs. 0-62790  
 tandem high-resolution system, sensitivity, mass range 0-90925  
 time of flight spectrometer using  $^{241}\text{Am}$  source for triggering pulses (*Japanese*) 0-90926  
 time-of-flight, comparison of TOF and stripping cell low-energy ion scattering methods 0-73522  
 time-of-flight, recording unit 0-73520  
 time-of-flight, separator for metal clusters 0-77907  
 vacuum materials, set up for meas. released gas 0-105746  
 ZGS, Effective Mass Spectrometer 0-91310  
 He desorption spectrometer, clustering of Kr in W (100) obs. 0-77908  
 He-jet online mass separator, improvements in total yield 0-98999

**mass spectrometry *see mass spectroscopy*****mass spectroscopic chemical analysis**

- see also atom probe field ion microscopy; ion microanalysis; ion microprobe analysis; isotope separation; mass spectra; secondary ion mass spectra; secondary ion mass spectroscopy*  
 acetic acid vapours, clustering, effect of supersonic mol. beam sampling, mass spectrometric study 0-104481  
 atomically clean surfaces, instruments for anal. and imaging 0-105749  
 benzophenone, laser spectroscopy by cascade photoionisation method in mass spectrometer 0-99496  
 benzoyl ions, collisional activation mass spectra, energy depend. 0-104482  
 biomedical laser microprobe mass analyser 0-98060  
 blood serum, rapid anal. by mass spectrometry/mass spectrometry 0-61173  
 butene, isomers, ion-mol. reactions, photoionisation mass spectra 0-81298  
 chromatography and mass spectrometry, conference, Carlsbad, Czechoslovakia (April 79) 0-73097  
 complex mixtures, rapid analysis by mass spectrometry/mass spectrometry 0-61173  
 computer controlled photoionisation mass spectrometer 0-77905  
 cyclohexane, rapid anal. by mass spectrometry/mass spectrometry 0-61173  
 digital isotope ratio meas. system, using programmable calculator with double collector mass spectrometer 0-63845  
 dithiocarbamate complexes of Cr, Mn, Sn and Pb IR, electronic and mass spectra, mag. susceptibility, cond. meas. 0-92720  
 electric arc, horizontal, in inhomogeneous mag. field, mass spectrometric anal. 0-79620

**mass spectroscopic chemical analysis continued**

- ethanol, H-bonding investigated with supersonic mol. beam using photoionisation quadrupole mass spectrometer 0-102543  
 F+dichloromethane, reaction products, modulated mol. beam mass spectrosc. obs. 0-97742  
 fissile materials accounting, behaviour of the quadrupole mass spectrometer towards various noble gases 0-63300  
 Freon 123, deuterium separation at high press. by ns  $\text{CO}_2$  laser multiple-photon dissoci. 0-91616  
 fusion reactor, DITE-II, neutral beam ion source particle beam identification 0-99397  
 gas, quantitative analysis, non-constant cracking patterns, press. depend. 0-61218  
 gas analysis, dynamic error determ., transfer function 0-61194  
 gas atmosphere quantitative analysis adsorption chamber 0-85234  
 gas mixture of air and propane, mixing ratio determ., using quadrupole mass spectrometer (*Japanese*) 0-81391  
 gas-phase reactions, anal. using computer interfaced time-of-flight mass spectrometer 0-71967  
 gaseous impurity microconcentrations, nonconducting materials 0-73518  
 GC/MS integrated systems, review of current techniques 0-68289  
 glass, excavation type, layers and profiles of  $\text{SiOH}$ ,  $\text{CaOH}$ , and  $\text{KOH}$  polyatomic ion groups special corrosion effect 0-81387  
 glass, gas content determ. by dynamic extraction method 0-61219  
 He-jet fed online mass separator for recoil atom mass spectroscopic anal. 0-98998  
 1-5-hexadiyne ion+neutral 1,5-hexadiyne, trapped-ion mass spectrometry 0-97694  
 histological section, high mass resolution by ionic analyser (*French*) 0-109069  
 human serum, definitive meas. of constituents 0-93818  
 hydroxonium complexes, produced by collisional dissoci. method, mass spectrometric study, dissoci. energies determ. 0-95707  
 implanted ion depth distrib., secondary ion mass spectra 0-79829  
 ion kinetic energy spectra, dish topped metastable peaks, rel. to field-free fragmentation regions 0-101871  
 ion reactivity arising from different region of translational energy release distribution, need for ang. collimation 0-104483  
 isotope detection in terrestrial and extraterrestrial samples, tandem accelerator appl. 0-61923  
 isotope dilution anal. by spark source mass spectrometry using electro-optical detector 0-101868  
 laser ion source, appl. in mass spectrometry 0-89564  
 LSI surface analytical techniques applied to electronic components [Si LSI chip inspection] 0-81392  
 MACS mass and charge analysis technique appl. 0-73521  
 mass peaks identification in SIMS using computer program 0-101867  
 methanol, dissoci. ionisation mechanism, correlation diagram approach, mass spectra obs., metastable processes 0-95728  
 methanol (-d), H-bonding investigated with supersonic mol. beam using photoionisation quadrupole mass spectrometer 0-102543  
 Microprobe Mole/plasma chromatograph system, for anal. of compounds on micron scale 0-101049  
 modulated-field linked-scan studies of metastable ions 0-77904  
 molecular ion formation on molecular cryst. surface UV laser irradi. (*Russian*) 0-71521  
 natural waters of Mt. Everest, mass spectrometric chem. anal. of D,  $^{17}\text{O}$  and  $^{18}\text{O}$  (*Chinese*) 0-77016  
 nuclear materials analysis using plasma desorption mass spectrometry isotope ratio determ. using TOF mass spectrometry 0-78375  
 organic mixture analysis by high-resolution mass spectrometry/mass spectrometry 0-104476  
 organic molecules, multiphoton ionisation mass spectra by ArF excimer laser 0-81381  
 organic surface contaminants, anal. by plasma chromatography-mass spectroscopy, and Raman microprobe technique 0-108773  
 PDX vacuum vessel, glow discharge conditioning 0-79607  
 peak matching for known mass difference ion unit mass determ. 0-77906  
 phenyl cation, struct., ion-molecule reactions studied by trapped ion mass spectroscopy 0-102586  
 polyacetylene, halogen doped, mass spectrometric anal. 0-108771  
 pyridine, deuterium substituted, Raman and IR vibr. spectra 0-84739  
 reactive gas mass spectrometric analysis with free-jet expansion sampling 0-89566  
 relative sensitivity factors in mass spectroscopy 0-86497  
 resin based mass spectroscopy for safeguarding Pu and U 0-73984  
 resonance ionization source for mass spectroscopy appl. isotope anal. and time of flight spectrometer 0-81380  
 second-generation ion microanalyser description and performance (*French*) 0-101055  
 secondary ion emission, conf., Stanford, USA (Aug. 1979) 0-105419  
 semiconductor materials, quantitative anal. 0-101052  
 SIMS, appl. to determ. of provenance of archaeological objects 0-61197  
 SIMS, depth profiling, automatic sequential mass analysis 0-108764  
 SIMS, one fitting parameter approach 0-108762  
 SIMS, quantitative, review 0-61195  
 solids, elemental anal. by SIMS 0-97748  
 spark source quadrupole mass spectrometry, development, appls. 0-62789  
 specimen charging control for SIMS and AES of insulators 0-101875  
 stainless steel, in  $\text{MgCl}_2$  solutions, Cl distrib. in oxide films, SIMS obs. (*French*) 0-108765  
 stainless steel, neutron dose determ., from isotope abundance ratio, mass spectra obs. 0-61220  
 surfaces and thin film studies by combined system of SIMS, AES and XPS 0-86536  
 tetrachlorodibenzo-p-dioxin determ. by low resolution gas chromatography-mass spectrometry 0-66893  
 thermal desorption mass spectroscopy, computer control, data acquisition, appls. 0-61181  
 time of flight atom probe, quantitative microanal., metallurgical appl. 0-86498  
 trifluoroethanol, H-bonding investigated with supersonic mol. beam using photoionisation quadrupole mass spectrometer 0-102543  
 Venus atmosphere, Pioneer Venus Orbiter neutral gas mass spectrometer expt. 0-67502  
 Venus ionosphere composition, meas. by ion mass spectrometers on Pioneer Venus Bus and Orbiter 0-67499  
 $\text{Al}_2\text{C}_3$ , vapor, thermodynamics, 1321-1607K 0-66859  
 $\text{AlF}_3\text{-MF}$  ( $\text{M}=\text{Li}, \text{Na}, \text{K}, \text{Rb}$  or  $\text{Cs}$ ), ion-molecule equilibria studied by mass spectrometric method, heats of dissoci. and form. calc. 0-104479  
 $\text{AlO}_2$  molecule, mass spectrometric study 0-89563



**mass spectroscopic chemical analysis continued**

- BF<sub>3</sub> radical, thermomechanical studies by mass spectrometry, enthalpy of form. and ionisation pot. determ., chem. bonds 0-81382  
 BeO, heated on W, thermal anal. using mass spectrometric, technique, vapourisation behaviour 0-79932  
<sup>10</sup>Be/<sup>9</sup>Be ratio meas. using electrostatic tandem accelerator 0-76579  
 CO, rapid anal. by mass spectrometry/mass spectrometry 0-61173  
 CO<sub>2</sub>+N<sub>2</sub>+He, glow discharge positive ion species identification (*Russian*) 0-84014  
 CS<sub>2</sub>, ionisation and fragmentation by monoenergetic electron impact, mass spectrometric study 0-102581  
 CaO, heated on W, thermal anal. using mass spectrometric, technique, vapourisation behaviour 0-79932  
 12CaO.7Al<sub>2</sub>O<sub>3</sub>, composition of gases released on heating, crystallisation (*Russian*) 0-93820  
 Cs-SiO<sub>2</sub>-Al<sub>2</sub>O<sub>3</sub> system interactions, getter development for radiocaesium 0-83208  
 Fe, purification, recrystn. temp. and elec. resistivity (*Japanese*) 0-100780  
 Ga<sub>2</sub>Se<sub>3</sub>-FeSe, phase diagram, elec. cond., mag. susceptibility 0-88301  
 GeO<sub>2</sub>-SiO<sub>2</sub>, glass, evaporation by high temp. mass spectrometry 0-79927  
 H+O<sub>2</sub>, reaction mechanism studied using photoionisation mass spectrometer, form. of O<sub>2</sub>(a<sup>1</sup>Δ<sub>g</sub>) 0-85168  
 HO<sub>2</sub>+ClO, free radical reaction rate consts. and products at 298K, discharge flow mass spectra 0-67391  
 He desorption spectrometer, clustering of Kr in W (100) obs. 0-77908  
 He-jet online mass separator, improvements in total yield 0-98999  
 He<sup>+</sup>+H<sub>2</sub>(D<sub>2</sub>), dissociative charge transfer, 78-330K 0-61079  
 Ir, chemisorption of H<sub>2</sub>, adsorption and desorption kinetics, struct. of overlayer 0-84367  
 LaB<sub>6</sub> crystals, zone refined, chem. characterisation 0-93821  
 LiCl, Li isotopic comp. determ. by mass spectrometry 0-66899  
 Li<sub>2</sub>O-SiO<sub>2</sub> glasses, Li self-diffusion, mass spectrometric method 0-79982  
 MgO, atomic C anal. by laserflash induced mass spectrometry 0-108767  
 MgO, heated on W, thermal anal. using mass spectrometric, technique, vapourisation behaviour 0-79932  
 NO<sub>2</sub>, laser spectroscopy by cascade photoionisation method in mass spectrometer 0-99496  
 NO<sub>3</sub>·(HNO<sub>3</sub>)<sub>n</sub> clusters, form. studied by mass spectrometer, thermodynamic functions, sol. struct., 0-95754  
 Na<sub>2</sub>O-B<sub>2</sub>O<sub>3</sub>-GeO<sub>2</sub> glass-forming melts, thermodynamic props. and vapourisation processes, mass spectrometric study 0-79926  
 Na<sub>2</sub>O-SiO<sub>2</sub> glass, evaporation by high temp. mass spectrometry 0-79927  
 Ni films, adsorption and decomp. of ethylene, coverage depend. meas. 0-96743  
 Ni-Cr(Fe)(Cu) alloy, matrix effect in SIMS anal. using O<sub>2</sub><sup>+</sup> primary beam 0-76576  
 O<sub>4</sub><sup>+</sup>(O<sub>3</sub><sup>+</sup>)(O<sub>6</sub><sup>+</sup>)(O<sub>2</sub><sup>+</sup>+H<sub>2</sub>O) 0-95707  
 Os, isotopic anomalies from different ore deposits, LAMMA determ. 0-61800  
 Pu, isotopic analysis by resin-bead mass spectrometry for materials safeguards 0-78392  
<sup>238</sup>Pu, alpha spectrometric determ. 0-81404  
<sup>241</sup>Pu half-life determ. by mass spectrometry 0-78232  
 Si, etching by CF<sub>4</sub>, plasma deposition reactor gas phase characts., mass spectra 0-70566  
 Si, etching in He-F<sub>2</sub> plasma, etch rates, mass spectra, direct ion sampling study 0-79510  
 SiO<sub>2</sub>, etching in He-F<sub>2</sub> plasma, etch rates, mass spectra, direct ion sampling study 0-79510  
 SnSe<sub>2</sub>, sublimation, temp. depend. of equilb. constants 0-88312  
 U, isotopic analysis by resin-bead mass spectrometry for materials safeguards 0-78392  
 U, isotopic composition, determ. using thermal ionisation spectrometry with automatic data eval. 0-66913  
 U, isotopic composition, determ. using thermal ionisation mass spectrometry 0-66914  
 UF<sub>6</sub>-MF (M=Na or K), ion-molecule equilibria, heat of form. and dissociation affinities determ. 0-104480  
<sup>235</sup>U burn-up determ. by mass spectrochemical anal. 0-71989  
<sup>235</sup>U/<sup>238</sup>U isotope ratio determ. in UF<sub>6</sub> samples using gas quadrupole mass spectrometry 0-78376  
 Uf<sub>6</sub>, mass spectrometric determ. of <sup>235</sup>U content 0-68961  
 W (100), clustering of Kr, He desorption spectrometry 0-77908

**mass spectroscopy**

- see also atom probe field ion microscopy; mass spectra; mass spectrometers; secondary ion mass spectrometry  
 alkali metal fluoroaluminates, dissociation enthalpies, mass spectrometric determ., heat of form. 0-97720  
 atomically clean surfaces, instruments for anal. and imaging 0-105749  
 benzene, multiphoton ionisation mass spectra 0-57420  
 cluster ion beams, mass anal. by Wien filter 0-86493  
 computerized, technical aspects including data reduction and analysis 0-57417  
 conference on nuclear physics, Mikolajki, Poland (2-14 Sept. 1979) 0-101662  
 cylindrical radiofrequency mass analyser, low resolution mass filter 0-73519  
 digital isotope ratio meas. system, using programmable calculator with double collector mass spectrometer 0-63845  
 education, advanced undergraduate expts. in vacuum physics and mass spectrometry 0-73153  
 electrostatic analyser with parabolic electrodes, particle energy distribution after traversing spectrometer 0-99000  
 field emission source preparation, metallic multi-point source 0-100758  
 Fourier transform ion cyclotron reson. mass spectroscopy, freq. sweep excitation 0-101810  
 gas chromatography-mass spectrometry, computerised, data-blocking cross-correlation peak detection 0-62725  
 GC/MS integrated systems, review of current techniques 0-68289  
 Hadamard transform appl. to beam spectroscopy 0-62741  
 ion cyclotron motion, Coriolis coupling of ion internal degrees of freedom 0-87246  
 ion cyclotron resonance phenomena, detection theory 0-95184  
 ion cyclotron resonance signal, broadband detection 0-62792  
 ion cyclotron resonance spectrometry, collisionally damped ion motion 0-57419  
 ion kinetic energy spectra, dish topped metastable peaks, rel. to field-free fragmentation regions 0-101871  
 ion-kinetic energy spectrometer, high resolution mass analysed, design and performance 0-101872

**mass spectroscopy continued**

- laser ion source, appl. in mass spectrometry 0-89564  
 liquid organic compound ionisation under atm. press. 0-86488  
 modulated-field linked-scan studies of metastable ions 0-77904  
 nuclei far from line of beta stability, mass spectroscopic anal. techniques, book contrib. 0-69014  
 photoplate processing, microcomputer based system 0-62787  
 relative sensitivity factors in mass spectroscopy 0-86497  
 resonance ionization source for mass spectroscopy appl. isotope anal. and time of flight spectrometer 0-81380  
 SEM microanalysis techniques, review 0-71995  
 SISAK 2, chemical separation method for short lived fission products in spectroscopic studies 0-74068  
 spark source quadrupole mass spectrometry, development, appls. 0-62789  
 tandem mass spectrometer, for collision-induced dissociation obs. 0-62790  
 tetrachlorodibenzo-p-dioxin determ. by low resolution gas chromatography-mass spectrometry 0-66893  
 transition metal-O bond energy in O<sub>2</sub> glow discharge, mass spectrometry obs. 0-64808  
 ultrasensitive mass spectrometry with tandem electrostatic accelerators 0-101876  
 Ar<sup>+</sup> ions, mobilities in He gas at 82K 0-75023  
 Au-O bond energy glow discharge, mass spectrometry obs. 0-64808  
 BaOH, (BaCl), mol. dissociation energies calc. by high temp. mass spectrometer 0-83514  
 BiLi, gas phase thermodynamics, Knudsen effusion mass spectrosc. 0-100057  
 CO<sub>3</sub><sup>-</sup>, laser photodissociation, tandem quadrupole study 0-81343  
 Ce, gettering of H, mass spectrometry and microgravimetry study, rel. to HTGR gas purification 0-73374  
 D<sub>2</sub>, sticking and accommodation on low-temp. substrate, mol. beam expts. 0-84368  
 F<sup>-</sup> ions in Kr and Xe; mobilities and diffusion determ. 0-100048  
 FeO, gas, thermochem. props., mass spectrosc. meas. 0-101034  
 FeOH, gas, thermochem. props., mass spectrosc. meas. 0-101034  
 H<sub>2</sub>, sticking and accommodation on low-temp. substrate, mol. beam expts. 0-84368  
 He-F(O)(N)(Ar) mixtures, RF discharge, mass spectroscopy, floating double probe meas. 0-84016  
<sup>129</sup>I, tandem accelerator mass spectrometry 0-86494  
 MgOH (MgCl), mol. dissociation energies calc. by high temp. mass spectrometer 0-83514  
 Na<sup>+</sup>, mobility and longit. diffusion coeffs. in Kr and Xe 0-106866  
 Ne<sup>+</sup> ions, mobilities in He gas at 82K 0-75023  
 O<sub>3</sub>+thiirane+olefin+SO<sub>2</sub>, excited neutral metastable SO<sub>2</sub> form. mass spectrometric study 0-83300  
 PbLi, gas phase thermodynamics, Knudsen effusion mass spectrosc. 0-100057  
 Rh, adsorption of CO and H<sub>2</sub>, on (111) surface, 2-dimens. phase separation 0-107634  
 SF<sub>6</sub> with gaseous contaminants, arc decomposition kinetics investigation by combined gas chromatograph-mass spectrometry methods 0-92250  
 SO<sub>2</sub>+active N<sub>2</sub>, excited neutral metastable SO<sub>2</sub> form. mass spectrometric study 0-83300  
 ScP, thermodynamics and high temp. vaporisation 0-88310  
 ScRh, gaseous, dissociation energies, high temp. mass spectrometric determ. 0-93790  
 SiBr<sub>n</sub> (n=1,2,3) heats of formation, mass spectrometric determ. 0-89511  
 ThC<sub>n</sub> (n=1 to 6), Knudsen effusion mass spectrometric investigations, enthalpies and heat of formation calcs. 0-66858  
 Ti, gettering of H, mass spectrometry and microgravimetry study, rel. to HTGR gas purification 0-73374  
 YRh, gaseous, dissociation energies, high temp. mass spectrometric determ. 0-93790  
 Zr, gettering of H, mass spectrometry and microgravimetry study, rel. to HTGR gas purification 0-73374  
 ZrO<sub>2-x</sub>(cubic)-ZrO<sub>2-x</sub>(cubic+tetragonal), phase boundary 0-81038

**mass standards see measurement standards****mass transfer**

- 2A0311-227, AM Herculis star, IR photometry and polarimetry rel. to mass accretion 0-77517  
 A-type supergiant stars, mass loss rates from UV reson. line profiles 0-90424  
 accreting neutron stars, He burning shell evolution 0-85968  
 accretion, spherical, buoyancy effect 0-109349  
 accretion disks, optically thick, pulsational instability to axially symm. oscils. 0-82190  
 accretion disks round neutron stars and white dwarfs, flux distrib. and colours 0-94778  
 accretion of gas onto intergalactic collapsed objects, source of cosmic X-ray background 0-90581  
 accretion onto compact gravitating object, hydrodynamic calcs. 0-67551  
 adiabatic accretion onto Schwarzschild black hole 0-77445  
 Algol type star, accretion and chem. struct., evolutionary calcs. 0-109481  
 Algol type stars, H I α obs. evidence for mass loss 0-109484  
 Algol type stars, mass loss and transfer 0-109480  
 R Aquarii (M7+pec), primary star mass loss rate from IUE obs. of circumstellar emission 0-82370  
 V603 Aquilae (Nova 1918), accretion disc eclipse model for periodic light vars. 0-82391  
 atmosphere, turbulent mass transfer in boundary layer, plume dispersion (*French*) 0-61850  
 T Aurigae (Nova 1891), old nova, cataclysmic binary model from photometric and spectroscopic obs. 0-90446  
 BD+33°2642, galactic halo blue star, mass loss determ. from IUE obs. 0-72947  
 benzoic acid, dissolution, mass transfer at vibr. spheres 0-57220  
 bibliography, heat and mass transfer, Polish works (1977-78) 0-57020  
 bibliography, Soviet works 0-94938  
 binary gaseous mixtures, transient heat conduction 0-64670  
 binary stars, detached, evolution to contact binaries involving mass flow 0-109477  
 binary stars, rapid mass accretion on to white dwarfs and extended envelope form. 0-67723  
 binary system, close, with mass and ang. momentum loss, period changes 0-72998  
 black hole, massive, accretion of gas debris of tidally disrupted star rel. to radiation spectrum 0-90467  
 black holes, supercritical accretion discs models 0-105272



## mass transfer continued

- boiling point drying by volumetric abs. of RF and MW EM energy, heat and mass transfer chars. 0-79130  
 boundary layer flow, unsteady, compressible, 3-D, near axisymmetric stagnation point 0-103011  
 boundary value problems, mixed and oblique derivative boundary conditions 0-69820  
 Z Camelopardalis, dwarf nova, mass transfer rates at standstill and in eruption 0-82366  
 UW Canis Majoris, eclipsing binary, mass flow anal. from UV spectrum 0-109429  
 $\zeta$  Capricorni, Ba star, white dwarf+giant, circumstellar gas mass transfer, UV obs. 0-105284  
 carboxy methyl cellulose solns., mass transfer from cylinders to power law fluids 0-83826  
 carboxy methyl cellulose solns., mass transfer from spheres to power law fluids 0-83825  
 carboxymethyl cellulose, aqueous soln., diffusion and mass transfer from rotating disc 0-83827  
 OY Carinae, white dwarf cataclysmic, eclipsing binary, parameter determ. 0-82385  
 carrier-mediated extraction, development 0-66870  
 cataclysmic binaries, circumstellar material geometrical and photometric parameters 0-109492  
 cataclysmic variables, period change due to mass transfer 0-82425  
 Centaurus X-3, neutron star accretion rel. to spin-up, and X-ray luminosity 0-101648  
 U Cephei, accretion discs obs. 0-82412  
 VW Cephei, W Ursae Majoris star, primary to secondary mass flow rel. to physical status 0-109495  
 9 Cephei (B2 Ib), circumstellar CO obs. and mass loss rate 0-94795  
 $\beta$  Cephei stars, effects of mass loss on instability strip 0-90436  
 VW Cephei W Ursae Majoris system, period and colour change mass transfer model 0-77453  
 Z Chamaeleontis, eruptive binary, accretion disc struct. rel. to photometric behaviour 0-72961  
 channel with porous walls, convective diffusion and mass transfer (French) 0-79305  
 chemically reacting system, coupled heat and mass transfer, finite element soln. 0-68153  
 close binaries, intermediate mass, mass transfer for different stars within evolutionary scheme 0-109476  
 close binary stars props. before and after mass transfer, obs. and theory comparison 0-62187  
 coefficients, concentration dependent diffusivities effect 0-98864  
 compressible fluid flow through annular orifices, computer-aided numerical anal. 0-87806  
 condensation heat transfer, nonequilib. temp. profiles, mass transfer engineering calc. 0-63227  
 contact binary star, mass loss rel. to dynamical evolution, idealised model (French) 0-62199  
 cool giant stars, chromosphere mass loss determ. from Mg II UV line obs. 0-85935  
 coupled heat and mass transfer, stability, inertial wave effects calcs. 0-105593  
 crystal growth, one-dimensional Stefan problem, expansions in time 0-64354  
 CH Cygni, symbiotic star, mass transferring binary model 0-62158  
 V1329 Cygni (HBV 475), symbiotic variable, accreting binary star model 0-62148  
 Czochralski crystal growth, heat, mass and fluid flow, computer simulation 0-104055  
 HR Delphini (Nova 1967), premaximum mass loss rate, H line anal. 0-82378  
 diethylphthalate layer, heated by radiant heat source, heat and mass transfer 0-74717  
 dissolved species, advection-diffusion eqn. in pulsating crack 0-96312  
 S Doradus, LMC star, evidence for circumstellar envelope and mass loss from IUE and optical obs. 0-101595  
 CX Draconis, binary Be star, UV obs. 0-82388  
 ducts, spanwise-periodic and corrugated, heat transfer and laminar flow 0-64547  
 early-type stars, mass loss from radio obs. at 6 cm 0-82347  
 eclipsing binary stars, near IR photometry rel. to mass transfer rates 0-67784  
 electrochemical, reactors, dimensioning, with three-dimensional electrodes (French) 0-71921  
 electrochemical mass transfer, drag-reducing polymers, effects, comparative study 0-76528  
 electrodes, sheet, mass transfer to continuous moving surface 0-69821  
 electrodes on vibrating sphere, mass transfer 0-61106  
 electrolyte, ionic mass transfer in narrow rectangular conduits 0-61105  
 filtration, plane, of underground waters, convective mass transfer, boundary problems (Russian) 0-83793  
 fixed-bed electrodes, three-dimensional, mass and charge transfer (French) 0-71920  
 flow round a sphere immersed in a fluidised bed (French) 0-92214  
 fractured medium, transient 2-D diffusion 0-106841  
 free interface film hydrodynamic and heat transfer characteristics 0-92140  
 Freon-12, annular mist flow in tube, wall film mass flow rate 0-69905  
 galactic disc, primordial gas inflow problem rel. to chemical evolution 0-62279  
 gas absorption, plastic packed column, mass transfer characteristics, proposal of packed column blood oxygenator 0-74968  
 gas flow, recirculating, in packed columns, mass transfer and mixing, cell model 0-69913  
 giant stars, mass loss before envelope ejection due to pulsational instability 0-72935  
 giant stars, Population I, mass loss during early evolution rel. to theoretical surface abundances 0-94796  
 glass melting process model, for flameheated tank furnace melting (Polish) 0-70380  
 hard spheres permeation through hard disc monolayers, interfacial mass transfer 0-107460  
 HD 153919 (=4U 1700-37), supergiant-neutron star, optical variability 0-82419  
 HD 192163, Wolf-Rayet star, mass loss rate 0-82386  
 HD 206267, exciting star in H II region IC 1396, stellar wind, role in cloud struct. 0-105316  
 HD 4174, symbiotic star, mass loss rel. to spectroscopic obs. 0-85945

## mass transfer continued

- HD 77581 (=Vela X-1), supergiant+neutron star, stellar wind mass transfer, spectral obs. 0-94892  
 heat and mass transfer bibliography—Soviet works 0-90618  
 Hercules X-1, neutron star in eclipsing binary, accretion, X-ray obs. 0-90580  
 hollow fibre dialyser, mass transfer 0-66873  
 HR 2142 and 7084, mass loss from UV spectra obs. 0-109485  
 $\epsilon$  Hydrae, dwarf nova, accretion disc dimensions from IR and optical light curves 0-67747  
 VW Hydri, dwarf nova, accretion disc dimensions from IR light curves 0-67747  
 immiscible incompressible fluids, interfacial convective instability, diffusional exchanges, adsorption-desorption processes 0-70504  
 impulsively started vertical plate, mass transfer and free convection currents 0-64567  
 incompressible fluid including heat and mass transfer, vel.-press. coupling treatment 0-69832  
 interstellar medium, mass accretion by stars from dense gas clouds (German) 0-109500  
 ionic, in open channels, electrolyte probe determ. 0-59110  
 IRC+30219, C star, mass loss interaction with extensive circumstellar envelope, visible spectra var. 0-90569  
 jets undergoing mass transfer, break-up effect of nonlinear concentration profiles 0-79371  
 laminar boundary layer, heat transfer, mass transfer and friction coeffs. (German) 0-74881  
 laminar falling liquid films, mass transfer with heat transfer and interfacial shear 0-80033  
 late-type stars mass loss 0-67755  
 layered porous medium transient 2-D diffusion 0-106841  
 liquid fluidised bed, mass transfer time fluctuations 0-79380  
 liquids, laminar flowing, concurrent, in horizontal cylindrical channel, mass transfer across interface of liquids 0-79397  
 magnetic fluids, heat and mass transfer 0-59123  
 massive stars, single and binaries, evolution review 0-82343  
 massive stars ( $M \geq 50 M_{\odot}$ ), binary star mass transfer model rel. to evolutionary status (Russian) 0-109425  
 melt reacting with gas jet, heat and mass transfer, mathematical modeling 0-87819  
 metallic membrane interface, mass transfer 0-81366  
 metals, atomic mobility under pulsed loading conditions (Russian) 0-96684  
 microwave heating with mass transfer using Luikov's system equations 0-106715  
 molar molecule heat and mass transfer phenomena, generalised variational principle 0-79104  
 N51D, giant filamentary shell in LMC, stellar wind driven 0-105343  
 naphthalene, sublimation, mass transfer at vibr. spheres 0-57220  
 neutron stars, accreting, thermonuclear bursts assoc. with chromosphere flares 0-98684  
 neutron stars, accreting magnetic, cyclotron line form. 0-90463  
 neutron stars, accretion disc interaction with rot. mag. field 0-62173  
 neutron stars, Eddington luminosity limit and supercritical accretion, time-independ. calcs. 0-67768  
 neutron stars, supercritical time-dependent accretion 0-85967  
 neutron stars plasma accretion, interaction with mag. field and accretion flow hydrodynamics 0-109452  
 non-Newtonian fluids, mass transfer from cylinders to power law fluids 0-83826  
 non-Newtonian fluids, mass transfer from spheres to power law fluids 0-83825  
 non-stationary heat and mass transfer, coupled, with convective motion and relaxation, variational principle 0-106797  
 nuclear materials safeguards, computerised chemical modelling of deviations, from mass transfer equilib. 0-83171  
 O-type binaries, anomalous mass ratios, evidence for mass loss 0-109478  
 O-type star, wind, effect on H II region evolution in mol. clouds 0-94846  
 O-type stars, mass loss rate from UV spectra 0-82346  
 OB stars, stellar wind mass loss determ., UV spectra obs. 0-94789  
 Of and O stars, reasons for difference in mass loss 0-90413  
 $\alpha$  Orionis, supergiant variable, mass loss, visible spectra obs. 0-67755  
 particles, spherical, interacting, different sizes and compositions transfer rate calc. by method of images 0-77729  
 perforated flat plate over porous medium, turbulence penetration, eddies, mass transfer 0-64528  
 RY Persei, eclipsing binary, effect of gas streams and envelope on spectrum 0-101618  
 $\beta$  Persei (Algol) eclipsing binaries, mass loss and mass transfer theory 0-62191  
 pipe inlets, turbulent local mass and heat transfer, swirling effects 0-64542  
 planetary satellite ejecta, effect of proximity to Roche limit on dynamics 0-98592  
 plates, vertical and inclined, mixed convection combined, heat and mass transfer 0-64552  
 polymer solutions, aqueous, diffusion and mass transfer from rotating disc 0-83827  
 porous structures for cooling laser reflectors, theoretical study 0-91809  
 power law fluids in fluidised beds 0-100032  
 $\zeta$  Puppis, of supergiant, mass flow var., visible and UV obs. 0-90431  
 $\zeta$  Puppis, Of type star, stellar wind model from UV line fit 0-72965  
 qualitative analysis of unsteady heat and mass transfer modes in a boundary layer with chemical reactions and intensive injections 0-69819  
 reacting particle in fluid, convective diffusion, nonlinear surface reaction kinetics 0-106854  
 rotating rods and plates, mass transfer and flow regimes 0-79326  
 WZ Sagittae, eruptive binary, accretion disc radius from hot spot eclipses anal. 0-72962  
 WZ Sagittae, recurrent nova, accretion disc models comparison with IUE obs. during outburst 0-109448  
 W Serpentis stars, long period eclipsing binaries, new class, accretion onto nondegenerate stars 0-109483  
 shear flow, linear, heat or mass transfer rate from freely suspended particle 0-79313  
 short crested waves, boundary layer vels. and mass transport 0-92169  
 slow novae and symbiotic stars, mass transfer from late-type components 0-94813  
 small particles suspended in turbulent fluid, convection, mass transfer 0-87793



**mass transfer continued**

- solid disperse systems, electro-osmotic mass transfer, surface cond. influence (*Russian*) 0-76546  
 solid particle systems, high Reynolds numbers, mass transfer, Karman-Pohlhausen method 0-79378  
 solid reacting particles, ordered system at high Peclet numbers, mass transfer, convection 0-69830  
 solid spheres, reacting, in periodic array, convective mass transfer in liq. laminar flow 0-96176  
 Soviet bibliography 0-77557  
 sphere in current carrying liq., convection mass transfer, num. anal. 0-83851  
 spherical accretion onto compact X-ray sources, luminosity thermal limit 0-82546  
 spherical cap bubble, mass transfer coeff. 0-79383  
 spherical droplet, evaporation and condensational growth, mass transport calcs. 0-97736  
 SS 433, relativistic beam interaction with interstellar matter, mass loss rate, visible obs. 0-101629  
 stars, mass flux fluctuation theory 0-72923  
 stars, massive, mass loss rates rel. to evolution 0-90416  
 stars, self-accreting winds 0-101588  
 stars in massive close binaries with OB components, evolution 0-90474  
 stars of galactic halo, mass loss during evolution from planetary nebulae nuclei props. 0-82344  
 stars of O and Of type, masses and mass loss 0-94793  
 steel, stainless 304, metallurgical factors on the corrosion and mass transfer in liq. Na (*Japanese*) 0-71804  
 stellar, winds, steady state transonic wind model, radiative cooling effects 0-77391  
 stellar accretion discs, steady, optically thick, convective vertical energy transport 0-62112  
 stellar accretion discs, viscosity determ. for Hercules X-1 and (SS 433) 0-62110  
 stellar gas accretion, thermodynamics and hydrodynamics 0-67696  
 Stokes' problem, mass transfer effects of MHD free convective flow 0-62003  
 submerged jets impinging on baffle, flow and mass transfer, polymer additive effects 0-92194  
 supernovae, explosive core overturn and mass ejection 0-72988  
 symbiotic stars, accretion rates rel. to subclasses 0-62144  
 symbiotic stars and slow novae, mass transfer from late-type components 0-94813  
 $\lambda$  Tauri, eclipsing binary star, mass loss from UV spectra obs. 0-109485  
 DR Tauri, T Tauri star, evidence for simultaneous mass infall and outflow from Balmer line profiles 0-101591  
 DR Tauri, T Tauri star, mass flow var. in envelope, visible spectra 0-85939  
 T Tauri star formation, stellar wind as dynamic input into dark mol. clouds 0-85980  
 T Tauri stars in dust cloud Lynds 134, mass loss causing cloud turbulence 0-94845  
 thin liquid films, break-up due to mass transfer intensity in absorption 0-80032  
 tube, cylindrical, coaxial, effect of array of spheres on mass transfer rate to tube wall 0-74884  
 turbulent boundary layer, mass transfer in viscous sublayer, statistical method (*Russian*) 0-87764  
 turbulent boundary layer with suction under nonisothermal conditions, heat and mass transfer 0-92125  
 turbulent pipe flow with suction or injection, high Prandtl no. heat and mass transfer 0-74857  
 two-phase multicomponent system interface, mass transfer relations (*German*) 0-74966  
 4U 1700-37 (HD 15319), high-energy X-ray obs. rel. to neutron stars accretion 0-86014  
 unsteady-state gas absorption/desorption, mass transfer product 0-79381  
 vertical cylinder, combined heat and mass transfer in natural convection 0-59027  
 vibrating spheres appls. 0-57220  
 viscous fluid, incompressible, hydromagnetic free convective flow past vertical porous wall, mass transfer 0-64645  
 water, annular mist flow in tube, wall film mass flow rate 0-69905  
 water evaporative cooling, convection and mass transfer, fog formation in boundary layers 0-79293  
 water evaporative cooling, heat and mass transfer coeffs., fog formation effects 0-79294  
 water layer, heated by radiant heat source, heat and mass transfer 0-74717  
 wear, entropy production model 0-74815  
 white dwarf in binary system, outer layer C and O enrichment from companion 0-109465  
 white dwarfs, mass accreting, evolution 0-77281  
 white dwarfs undergoing spherically symmetric steady-state accretion, stability 0-77402  
 Wolf-Rayet stars, Roche lobe overflow and stellar wind mass loss 0-105250  
 X-ray, burst sources, thermonuclear flashes in envelope of accreting neutron star 0-109455  
 X-ray binaries, mass transfer rel. to radio emission 0-62317  
 X-ray binaries, transient accretion model rel. to spin-up and spin-down timescales 0-109565  
 X-ray binary sources, pulsating, accretion from Keplerian disc rel. to spin-up 0-67904  
 young stars with mass accretion, evolution 0-101592  
 CO<sub>2</sub> laser amplifiers, porous tube generated flow field, heat and mass diffusion 0-63969  
 Fe(CN)<sub>6</sub><sup>4-</sup>-Fe(CN)<sub>6</sub><sup>3-</sup>, redox reactions, mass transfer at vibr. spheres 0-57220  
<sup>3</sup>He-<sup>3</sup>He normal solution, size effect influence on capillary mass transport (*Russian*) 0-70497

**master equation**

- atoms, superfluorescence initiation, master equation study, microscopic description 0-63577  
 biological multistate systems, freq. of cyclic processes 0-108834  
 characteristic function eqn. of Markov process, Langevin process applications 0-57192  
 chemical reaction diffusion systems, Chapman-Enskog development of multivariable master eqn. 0-81283

**master equation continued**

- chemical systems, single variable, master eqn. approximation by Fokker-Planck type eqns. 0-77702  
 collision processes, reduced phase space approach calcs. 0-83438  
 crystal growth, multi-component, master equations in lattice model 0-75194  
 discrete, continued fraction solns. not obeying detailed balance 0-101758  
 energy quanta, dissipation, linearly damped harmonic oscillator 0-68074  
 evolution systems, meas., rel. to master eqn., Bayesian anal. 0-90782  
 exciton motion in molecular crystals, Nakajima-Zwanzig generalised master eqn. 0-65462  
 excitonic annihilation phenomena in low dimensionality finite lattice, master eqn. 0-92821  
 Fokker-Planck eqn. expansion, weak diffusion, critical point 0-57228  
 gases, weakly ionised, electron motion, stochastic theory of homogeneous systems, review 0-77735  
 Glauber master equation, Ising spins, relaxation, 1-D Glauber model, effect of disorder 0-65761  
 heavy ion collisions, generalised master eqn., drift and diffusion coeffs. 0-106075  
 hopping conduction, master eqn. approach in presence of mag. field 0-103697  
 hopping transport kinetic theory, localised state separation, Pauli master eqn. 0-80276  
 intermicellar kinetics theory, stochastic approach, master equation for, irreversible reactions 0-76561  
 1 0-57221  
 limit cycle fluctuations near bifurcation point, Fokker Planck, Langevin eqn. calcs. 0-77709  
 molecular dissociation, RRKM formula correction by non Boltzmann character factors, Markov eqns. 0-71891  
 multivariate master equation for reaction-diffusion system 0-95045  
 non equilibrium systems, stochastic model, master eqns. (*Chinese*) 0-68126  
 nonequilibrium transition, stationary solns. 0-89466  
 nonlinear oscillator with fluctuating parameters, dynamics, thermal noise 0-101729  
 nuclear double resonance, theory of double spin flips 0-66076  
 rate processes in condensed media, master eqns. 0-77687  
 spin glasses, time translation, spatial scaling and nonexponential relaxation 0-97110  
<sup>3</sup>He, solid, phase separation of dil. <sup>4</sup>He impurities 0-88393

**matched filters**

- target discrimination methodology in remote sensing 0-58470

**materials**

- see also individual materials, e.g. ceramics  
 bitumens, oil sand, rheological props. 0-64506  
 enamelling by electrostatic frit powder spraying 0-97428  
 pitch and bitumen, viscosity, temp. depend. up to 500°C 0-92698  
 schist containing clay and sand, integrated normal emissivity with low heat conductivity coeffs. 0-103504  
 schist dust, integrated normal emissivity with low heat conductivity coeffs. 0-103504  
 semiconductor, diffusion length and lifetime meas. and assessment by SEM 0-96902  
 Shroud of Turin, IR reflectance spectrosc. and thermographic investigations 0-87578  
 Shroud of Turin, scientific investigation 0-87576  
 Shroud of Turin, spectral props. 0-87577  
 Shroud of Turin, UV-visible reflectance and fluoresc. spectra 0-87579  
 spacecraft materials in space environment, conf., Noordwijk, Netherlands (Oct. 1979) 0-67933  
 system concept in materials science 0-101003  
 vacuum system construction material selection and degassing 0-82783

**materials handling**

- see also crushing; fission reactor fuel preparation and reprocessing; fluidised beds; grinding; transportation; winding (process)  
 acoustic levitation devices of processing materials, limitations 0-74694  
 computer system for automatic inspection of fuel pellets 0-68795  
 granular material flow from parallel sided bins, thickness of shear zone 0-81279  
 hot cell, rigid hoist articulated grapple system development for enhanced remote maintenance 0-68968  
 hydraulic coal trunk pipeline transport systems, methods of improving economic effectiveness 0-106837  
 liquefied natural gas, nonsteady-state flow calculations in horizontal pipeline systems 0-106838  
 LWR spent fuel, head-end part of fuel reprocessing facility, unloading installations, handling and transfer techniques (*German*) 0-57939  
 plastics testing, automation 0-76443  
 pneumatic system for transferring radioactive samples at Savannah River Laboratory 0-68794  
 power, charged, electrostatic spark hazard identification and control 0-69291  
 radioactive materials, remote handling, history at Los Alamos 0-78417  
 radioactive waste, treatment and disposal methods (*German*) 0-57868  
 weighing, automatic, application in ceramics industry 0-95074  
<sup>3</sup>H, austenitic stainless steel embrittlement by He 0-102285  
 N<sub>2</sub>, liq., decanting siphon using self-opening valve 0-57310

**materials preparation**

- see also crystal growth; hot pressing; powder metallurgy; powder technology; sintering; vulcanisation  
 alloy colour and colour stability as alloy design criteria 0-101005  
 amorphous thin films, prep. from melt using roller-plate technique 0-71607  
 ceramics, development from organosilicon polymers by heat treatment 0-81014  
 ceramics, rare earth elements use as dopants (*Polish*) 0-97455  
 chaoite, a new allotropic form of carbon, produced by shock compression 0-80997  
 clay sample preparation for X-ray diff. anal. 0-97647  
 composites, advanced, design, applications and test methods 0-77550  
 crossed fields nitriding in air atm. 0-84867  
 diamond, synthesis (*Japanese*) 0-80994  
 ferrites, soft, production and props. 0-88801  
 fibre reinforced composites with high work of fracture 0-81029  
 glass, rare earth elements use as dopants (*Polish*) 0-97455  
 glass fibre, preparation, appl. in Portland cement reinforcement, alkali resistance 0-81019



## materials preparation continued

- granulation, by dehydration of sols. and suspensions in a fluidised bed 0-81373  
 graphite fibre epoxy laminates, low thermal expansivity, design considerations 0-81031  
 graphite fibre filled phthalocyanine composites, cure cycle investigation 0-81030  
 graphite intercalation cpds. with  $\text{AsF}_5$  and  $\text{SbF}_5$ , synthesis and elec. props. 0-70781  
 Hayes alloy no.716, Fe-Cr-Ni-Co-W-Mo-Si-C-B (26, 22, 12, 3.5, 3, 1.2, 1.1, 0.4 wt.%), hardfacing alloy 0-100802  
 heated porous body, impregnation with viscous liquid 0-79392  
 high pressure technology in materials development (*Japanese*) 0-84863  
 latex solids, agglomerating and dewatering 0-104470  
 liquid crystals, prep. and phys. props., book 0-105444  
 metal particles, small, characterisation and props., book contrib. 0-84417  
 methanol derivation from lignite, fuel appl. 0-61223  
 Nb, pure, production by carbothermic reduction-electron beam melting combination method 0-89177  
 opal glass, chemically toughened, prep. and mech. strength (*German*) 0-89191  
 plasma chemistry of heterogeneous systems 0-61100  
 PMMA, cross-linked positive electron resist, synthesis and props. 0-76221  
 polydifluoroacetylene, electronic struct., tight-binding LCAO-SCF-MO calcs., prep. 0-70591  
 polyester resin, cross-linked unsaturated, synthesis and fracture toughness 0-93634  
 polyethylene fibre prod. by surface growth method, mech. props. 0-104108  
 polyfluoroacetylene, electronic struct., tight-binding LCAO-SCF-MO calcs., prep. 0-70591  
 polypropylene fibrillated film reinforced cement matrix for low cost sheeting 0-80996  
 raw material acceptance testing for dielectric applications 0-97646  
 resin matrices and their contribution to composite properties 0-81028  
 rocket borne low-gravity programmes, conf., Bournemouth, England (Aug. 1980) 0-105433  
 sheet moulding compound, material, process and performance 0-81032  
 steel, austenitic (08KH18N10T), heat treatment and heavy plate prod. for fission reactor appls. 0-66454  
 steel, bar, and wire rod, small sample prep. and spectrometric anal. (*German*) 0-93704  
 $\text{Ag}_2\text{TeO}_2$  chem. prep. and cryst. struct. (*French*) 0-79755  
 Al alloy-mica particle composite, cast prep. and mech. props., bearing appl. 0-71613  
 $\text{Al}_2\text{O}_3$  compounds, shrink free, prod. method using slips made from clay, orthophosphoric acid 0-66460  
 $\alpha\text{-Al}_2\text{O}_3$  fibre FP, manufacture, strength and modulus 0-81013  
 $\alpha\text{-Al}_2\text{O}_3$  fibre FP reinforced Al and Mg composites, fabrication and props. 0-81004  
 $\beta\text{-Al}_2\text{O}_3\text{-D}_2\text{O}$ , anhydrous, prep. and struct. of  $\text{DAI}_2\text{O}_{17}$  0-107187  
 $\beta''\text{-Al}_2\text{O}_3\text{-Na}_2\text{O}$  tubes, fabrication from cast ceramic tape 0-60819  
 $\text{B}_2\text{O}_3$ -containing ceramic glaze, neutron probe anal. for control of prep. process (*Polish*) 0-97751  
 C fibre composite, aligned, prep. and theoretical strength agreement 0-84906  
 C fibre reinforced composites for spacecraft use, prep., props. and struct. 0-71625  
 C fibres, engineering applications, production requirements and mech. props. 0-89168  
 $\text{CaCeAl}_2\text{O}_7$ , melilite struct., prep. and props. 0-93524  
 $\text{CaO-SiO}_2$  glass prep. by gel method 0-100824  
 $\text{CaTiO}_3$ , prep. from film forming soln. 0-60811  
 CdS, rock-salt type high-pressure phase synthesis using metal sulphide additives 0-104084  
 $\text{CeO}_2\text{-Y}_2\text{O}_3$  solid soln. phases, synthesis 0-104132  
 Cr-Fe-C (28.4, 9.1 wt.%) prep. from  $\text{FeCr}_2\text{O}_4$  chromite 0-100804  
 $\text{Cr}_{1-x}\text{Fe}_x\text{OOH}$ ,  $0 \leq x \leq 10$ , prep., Mossbauer effect, Neel temp. 0-108134  
 $\text{CuF}_2\text{-H}_2\text{O}$ , synthesis, appl. for carrier-distillation emission spectroscopy 0-89164  
 $\text{Eu}_2\text{O}_3\text{-Y}_2\text{O}_3$  solid soln. phases, synthesis 0-104132  
 Fe-B(Si) alloy filaments produced by glass-coated melt spinning 0-76213  
 Fe-Si-Al, Sendust, ribbon-form, prep. by rapid quenching, mech. and mag. props. 0-71611  
 $\text{Fe}_2\text{O}_4$  aqueous mag. fluids, dilution-stable, prep. by extended peptization techniques 0-60373  
 $\text{HfF}_4\text{-BaF}_2\text{-LaF}_3$  glass system, IR transmitting, synthesis and props. 0-71623  
 $\text{HfF}_4\text{-BaF}_2\text{-ThF}_4\text{-(ZrF}_4\text{)}$  glass system, IR transmitting, synthesis and props. 0-71623  
 La-Si-As ternary cpd., synthesis, stoichiometry 0-104083  
 $\text{La}_{2-x}\text{Al}_{1+x}\text{Cu}_2\text{O}_{6-x/2}$  (A=Ca, Sr), synthesis and characterisation (*French*) 0-104085  
 $\text{La}_{76}\text{Au}_{24}$ , disordered ribbons, quenched samples production using arc furnace 0-71612  
 $\text{LaB}_6$  synthesis by heating BN with lanthanum citrate hydrate 0-100819  
 $\text{LaCrO}_3\text{-W(Mo)(Cr)}$  eutectics, prep. and microstruct. 0-108380  
 $\text{La}_{70}\text{Cu}_{30}$ , disordered ribbons, quenched samples production using arc furnace 0-71612  
 $\text{LaLiO}_3\text{-Ir}_2\text{O}_3$  perovskite, prep. and mag. study 0-80486  
 $\text{La}_2\text{S}_3\text{-Ag}_2\text{S-Ga}_2\text{S}_3$  glass system, prep., thermal and elec. props. (*French*) 0-89192  
 $\text{Li}_2\text{O}_2\text{SiO}_2$ , prep. from film forming soln. 0-60811  
 $\text{MoS}_3$ , prep. and mag. props. (*French*) 0-93072  
 $\text{MoS}_8$  Chevrel phases with group IIIa metals, Nb, Hg, Pb and Cu, synthesis, stability and characts. 0-71608  
 $\text{Na}_{5-x}\text{Li}_x\text{ErSi}_4\text{O}_{12}$ , solid electrolytes for Na/TiS<sub>2</sub> cells, synthesis, characts. and utilisation 0-107518  
 $\text{Na}_2\text{O-CaO}$  glass, abrasion-resistant, high strength 0-76369  
 $\text{Na}_2\text{O-SiO}_2$  glass, fusion process study, EMF meas. (*French*) 0-89190  
 $\text{Na}_2\text{O-SiO}_2$ , prep. from film forming soln. 0-60811  
 $\text{Na}_2\text{R(WNb)}_2\text{O}_7\text{F}_6$ , (R=Y, Nd, Eu, Gd, Dy, Lu), synthesis, cryst.-chem. and dielec. study (*French*) 0-108164  
 $\text{Na}_2\text{TeO}_3$ , chem. prep. and cryst. struct. (*French*) 0-79755  
 Nb-N(O)(C) system, specimen prep. for metallography (*German, English*) 0-89439  
 Nb<sub>2</sub>Si Al<sub>5</sub> struct., high press. synthesis (*Chinese*) 0-70917  
 $\text{Sb}_2\text{O}_3\text{-nH}_2\text{O}$  acid membranes, synthesis and characterisation 0-81027  
 Si solar cells, production process effect on fracture strength 0-93656

## materials preparation continued

- Si-Na-B-O-N glass, synthesis and characterisation 0-108381  
 SiC fibre, development from organosilicon polymers by heat treatment 0-81014  
 SiC fibre reinforced Al, synthesis by liquid pressing method 0-100816  
 $\text{Si}_3\text{N}_4$ , reaction-bonded, strength, effect of Si purity in production 0-100902  
 $\text{SiO}_2$  glass, formation by hydrolysis of  $\text{Si(OC}_2\text{H}_5)_4$  with  $\text{NH}_4\text{OH}$  and HCl soln., and characterisation 0-71622  
 $\text{SiO}_2\text{-NaAlSiO}_3$  glasses and devitrificates, prep. and vibr. spectroscopy study (*Polish*) 0-93530  
 $\text{SrTiO}_3$ , prep. from film forming soln. 0-60811  
 Ta-N(O)(C) system, specimen prep. for metallography (*German, English*) 0-89439  
 TiN formation, from  $\text{TiO}_2/\text{Si}_3\text{N}_4$  reaction in  $\text{N}_2$  atmosphere 0-71617  
 $\text{U}_2\text{O}_3\text{Cl}_2$ , prep. and cryst. struct. (*French*) 0-84150  
 V-N(O)(C) system, specimen prep. for metallography (*German, English*) 0-89439  
 $\text{VSe}_2\text{-S}_x$  ( $0 < x < 2$ ) solid solutions, characterisation 0-88730  
 W powder, prep. by  $\text{WO}_3$  reduction in H plasma jet (*Russian*) 0-76211  
 W-PVC composites, fabrication rel. to performance 0-76218  
 $\text{YCrO}_3\text{-W(Mo)(Cr)}$  eutectics, prep. and microstruct. 0-108380  
 ZnS, high purity, prep. from ZnO (*Rumanian*) 0-76206  
 $\text{ZrF}_4\text{-THF}_4\text{-BaF}_2$  glass, IR-transparent, synthesis using reactive atm. processing technique 0-100826  
 $\text{ZrO}_2\text{-SiO}_2\text{-(Na}_2\text{O)}$  glass fibres, prep. from metal alkoxides, resistance to NaOH soln. 0-97454  
 $\text{ZrSiO}_4$ , zircon yellow pigment, synthesis (*Polish*) 0-66466

## materials testing

- see also acoustic applications; corrosion testing; creep testing; dynamic testing; electron beam applications; fatigue testing; fracture toughness testing; hardness testing; insulation testing; mechanical testing; nondestructive testing; notch testing; ultrasonic materials testing  
 acoustic emission, amplitude distrib. anal. 0-66713  
 acoustic emission, unit for recording and reproduction of signals 0-79039  
 airframe material defectometry, quantitative test specifications (*German*) 0-89427  
 automatic inspection of materials using lasers 0-66734  
 bending test apparatus for high press., high temp. 0-85126  
 brass (37%Zn), workhardened thin specimens, fracture, anisotropy coeff. role (*French*) 0-104276  
 BWR containment vessels of prestressed concrete, pressure tests 0-81254  
 ceramic, proof testing 0-108654  
 ceramic building materials, high-temp. microscopy interpretation (*Polish*) 0-66743  
 ceramic layers on metallic substrates, mech. props. meas. (*French*) 0-104375  
 ceramics, bending test results processing 0-97672  
 ceramics, cracking characterisation by double torsion test (*French*) 0-104369  
 ceramics, mech. props. meas., apparatus for up to 1700°C (*French*) 0-104374  
 ceramics, mech. test apparatus for up to 2200°C (*French*) 0-104372  
 ceramics, surface cracks, acoustic surface wave meas. 0-61055  
 charcoal filters, NDT of residual adsorption capacity 0-89523  
 coke, metallurgical, microstruct., using refl. light microscopy and image anal. 0-66732  
 composite insulating materials, fatigue behaviour, influence of superposition of elec., mech. and environmental stresses 0-97590  
 composite laminates, proof test and fatigue study 0-93643  
 concrete, tensile testing device, axial 0-61054  
 concretes, further development of 2 point test for workability and extension of its range 0-66728  
 crack measurement, recording instrument 0-100984  
 defectoscopy of gamma-active objects in their natural radiation (*Bulgarian*) 0-71867  
 disperse system, plastoviscous, cone plastometer for strength props. determ. 0-76426  
 eddy-current transducers, double-ended, signal calc. for nonferromag. cylindrical products 0-89443  
 elastometric materials, friction testing using reciprocating friction and wear tester 0-76451  
 electrical conductivity meas., standard models 0-86343  
 electron microscope examination, feasibility and methodology of in situ experimentation (*French*) 0-68301  
 epoxy resin adhesives, capillary flow and bond strength 0-71883  
 FBR fuel pin safety expts. at SLSF, centerline fuel thermocouple performance 0-102283  
 ferromagnetic object inspection, method of higher harmonics, difference schemes 0-89444  
 FFTF, instrumented fuel test at the fuels open test assembly 0-102247  
 fibre reinforced composite, using burn-test apparatus 0-76441  
 fibreglass laminates, thermal NDT using liq. crystals 0-93709  
 fibrous materials, low-density, centrifugal method of studying mech. props. 0-71823  
 filaments, elastic, tensile test method, and treatment of expt. data 0-85111  
 fragile materials, mech. props. meas. using disc-shaped specimens (*French*) 0-104367  
 fuel pin rupture detection system using meas. of time differential of acoustic emissions 0-102282  
 Fusion Materials Irradiation Test facility initial target design 0-95410  
 fusion reactor first-wall performance under ion bombardment and cyclic stresses, in-reactor materials testing 0-104407  
 galvanic coatings, adhesion after strain hardening, test device 0-71837  
 galvanic coatings, tensile testing device 0-100988  
 glass fibre reinforced plastic, fatigue fracture kinetics studied by diffusion scatt. of luminous fluxes 0-76446  
 glass fibre reinforced plastics, shear characteristics of tubular specimens, strain gauge and clamp 0-85114  
 glasses and fragile materials, fracture energy, direct meas. (*French*) 0-104376  
 graphite, thermal shock resistance and fracture toughness during graphitising heat treatment (*Japanese*) 0-71843  
 graphite/epoxy laminate, T300/5208, proof testing under cyclic tension-tension fatigue 0-81249  
 high strain rate material behaviour and testing techniques, J.D. Campbell memorial lecture 0-82627  
 high strain rates, conf., Oxford, England (Mar. 79) 0-82575  
 implanted prosthesis failure analysis techniques and results 0-89906



**materials testing continued**

Inconel, steam generator tubing, mag. probe inspection 0-85119  
 indentation tester, vertical displacement, for compacted powders, plastics and foodstuffs 0-58988  
 inspection penetrants, evaluation 0-61056  
 insulating replacement gases for SF<sub>6</sub> 0-59313  
 interactive graphics system developed for NDT 0-66729  
 LMFBR fuel channels, measurement of irradiation creep in bending 0-104406  
 LMFBR fuel pin bundles in flowing Na, design and operation of SLSF test trains for safety tests 0-102281  
 LMFBR structural materials, development of an instrumented materials irradiation test for FFTF 0-57858  
 LMFBR structural materials, development of an instrumented materials irradiation test for FFTF 0-68797  
 load cell design and development 0-105628  
 lubricant testing, test machine 0-76452  
 LWR irradiated fuel assemblies, nondestructive exam. using  $\gamma$ -ray and neutron techniques 0-66760  
 metal, ductile, jet-impingement solid-particle erosion testing, halo effect 0-76376  
 metal, electronic work function under tension, 20 to 1200°C 0-76448  
 metal fatigue tests for plastic deformation (Hungarian) 0-97665  
 metal surfaces, radioactive contamination 0-68771  
 metallic wear debris, morphological anal. 0-76453  
 metallurgical coke, mech. behaviour charact. (French) 0-104371  
 metals, gas saturation, apparatus 0-61039  
 metals, hydrogen brittleness measurement 0-104291  
 metals and alloys, emissivity determ. using low-inertia opt. dilatometry 0-59684  
 microprocessor application for destructive examination of materials with data processing (German) 0-93714  
 natural rubber vulcanisate, network changes during physical testing 0-60936  
 nuclear materials, nondestructive neutron assay for accountability and criticality control 0-66759  
 nuclear steam generator tubes testing and evaluation, using CIS/DASIO system (Czech) 0-63301  
 phase change materials, thermal energy storage, cycle life tester 0-72090  
 planning and evaluation by statistical methods (German) 0-93725  
 plastics, auxiliary device for testing of property changes at high temps. (German) 0-66741  
 plastics testing, automation 0-76443  
 polycarbonate, bisphenol A, birefringent plates, cracks, stress intensity factors, refl. caustics method 0-93718  
 polycrystalline bodies, tensile test, uniaxial, for plastic deform. (Hungarian) 0-97657  
 polyethylene film, minimum running thickness, biaxial extensional flow study 0-100993  
 polyethylene terephthalate, shear compliances meas. of oriented sheet 0-104363  
 polymer based composites, mechanical test unit, with intense high-temp. heating 0-100987  
 polymers, photoresistor dilatometer design, with high stability and sensitivity 0-81251  
 polypropylene, oriented, microcracks diagnostics by paramag. probe method 0-66736  
 powders, brittle, shock wave disintegration test method 0-66744  
 PVC film gelling, auxiliary testing device, for prop. changes at high temps. (German) 0-66741  
 radioactive materials, package design, construction and testing for safe transportation 0-63412  
 raw material acceptance testing for dielectric applications 0-97646  
 refractories, hot-wire test, critical review and comparison with BS 1902 panel test 0-104409  
 refractories, strength and thermal properties, automated test system 0-100986  
 refractory concrete fracture strength, test apparatus simulating usage conditions 0-71824  
 rubber, crystallising, tensile test specimen prep. 0-71838  
 rubber, thermal defectoscopy study 0-89445  
 SEM, combined deformation/heating stage, acoustic emission rate meas. 0-101892  
 SEM analysis of object microrelief, metallurgy appls. 0-73319  
 semiconductors, cryst. growth and defects, appl. of analytical techniques for observation 0-73546  
 solar flat plate collector coatings, NBS standard 74-635 testing 0-61426  
 standard sample homogeneity evaluation, optimal obs. planning 0-93721  
 steel, alloy, dynamic stress intensity factor meas., possibilities and limits (German) 0-93719  
 steel, alloy, rolling wear study of misaligned cylindrical contacts 0-108590  
 steel, C, hardened by HF current, mech. testing method 0-61053  
 steel, C, hot plastic deform., vac. colour etching investigation 0-61036  
 steel, C, rolling wear study of misaligned cylindrical contacts 0-108590  
 steel, elect., mag. props. determ. with Epstein hysteresis tester 0-60364  
 steel, fatigue limit assessment, progressive load methods (German) 0-61058  
 steel, friction measuring test for use under conditions of high normal interfacial force 0-76454  
 steel, low C, dynamic stress intensity factor meas., possibilities and limits (German) 0-93719  
 steel, low C, nil ductility transition temp. 0-100896  
 steel, low C, welds, residual stresses, evaluation by Barkhausen noise meas. 0-76436  
 steel, martensitic-ageing, etching technique, for revealing struct. inhomogeneities 0-61035  
 steel, mild, 1019 AISI, acoustic emission generated during deform. 0-60921  
 steel, mild, fatigue crack propag. study using servohydraulic test system 0-76431  
 steel, stainless, 18Cr-2Mo-Ti, atmospheric corrosion 0-85078  
 steel, stainless, type 304, viscoplastic behaviour, strain rate sensitivity, creep, relaxation, tensile tests 0-66727  
 steel, stainless 304, explosive loading technique for uniform plastic expansion at high strain rates 0-81273  
 steel, stainless type SUS 304, diffusion welded joints, sound emission during tensile testing (German) 0-61062  
 steel, tuffrided, type S15CK, fatigue strength, estimation of size effect (Japanese) 0-81166  
 steel, wear characts. of burnished machined surfaces 0-108595

**materials testing continued**

steel sheet, hot and cold rolled, cold formability, notched tensile test and stretch bend test (German) 0-61031  
 strain and damage electrical measurement method (French) 0-71854  
 stress-intensity factor determ. by strain-gauge method 0-76445  
 surface potentials visualisation and meas., using SEM 0-68307  
 Swedish materials science expt. in Texus 1 and 2 sounding rockets 0-104362  
 tensile test, regulated, strength and deform. characteristic values, consistency (German) 0-93712  
 tensile test equipment and procedures for charact. value determ. (German) 0-93713  
 tensile testing, control of test cycles, data logging and data processing (German) 0-97648  
 tensile tests, standardization from metal physics viewpoint (German) 0-93711  
 texture goniometer alignment of Schulz reflection technique, method for testing 0-81272  
 thermoelastic phenomena in epoxy resin and glass microcircuitry elements (Polish) 0-93724  
 thermoplastic plates, strength meas. when supported by annular ring 0-81257  
 thermoplastic-based sheet materials, flexural anisotropy and stiffness assessment 0-76442  
 thin films, adhesion determination, electron and laser beam appls. 0-71833  
 wear, three-body abrasive, design of new tester 0-108682  
 wrought metals, plastic deform. testing, X-ray line profile anal. (Hungarian) 0-97663  
 Al alloys, types 1100 and 5454, long-time rupture tests 0-76434  
 Al, workhardened thin specimens, fracture, anisotropy coeff. role (French) 0-104276  
 Al-Cu, type 1100, synchrotron radiation microradiography 0-85121  
 Al-Cu-Mn, type 2219, synchrotron radiation microradiography 0-85121  
 Al-Cu-Si-Mg, deform. simulation using torsional test, elastoplastic constitutive eqn. 0-93594  
 Al-Zn-Mg-Cu (6, 2.5, 1.5 wt.%), deform. simulation using torsional test, elastoplastic constitutive eqn. 0-93594  
 Fe, cast with spherical graphite, SiC-Q apparatus for tensile strength meas. (German) 0-76450  
 Fe, pig, white, mech. props. meas. (French) 0-104370  
 Fe polycrystalline, two ferromag. methods for eval. of fatigue limit 0-89438  
 Mo, sintered, gas evolution and degassing 0-100814  
 Na<sub>2</sub>O-CaO-SiO<sub>2</sub>, proof testing 0-108654  
 Pd<sub>40</sub>Si<sub>20</sub> amorphous alloy, skid deform. and crit. shear stress, using tensile testing machine 0-89321  
 Pu, elastic constants at elevated temps., noncontact meas. tech. 0-104405  
 Si, near (111), fracture by painted indenter, SEM study 0-71734  
 Si semiconductor plates, control of quality of surface treatment, using Al spraying technique 0-60989  
 SiC heat-exchanger tubing, IR techniques for evaluation 0-76435  
 Si<sub>3</sub>N<sub>4</sub>, cracking characterisation by double torsion test (French) 0-104369

**mathematical analysis**  
*see also approximation theory; Bessel functions; calculus; catastrophe theory; differential equations; eigenvalues and eigenfunctions; Fourier analysis; integral equations; numerical analysis; series (mathematics); spectral analysis; transforms*  
 arc welding, molten pool solidification and bead formation 0-75341  
 asteroids orbital perturbations, analytical integration using regular proximities concept 0-72843  
 cosmology, relativistic, hierarchical, mathematical formalism and Einstein eqns. 0-82555  
 ferromagnetic systems, crit. experiments, field theory, Borel transform. 0-80541  
 modal analysis, general introduction for managers 0-91955  
 nuclear power station with VVER, for semi-peak load generation, mathematical model 0-68936  
 porous medium being dried, heat transfer and moisture flow, generalised model (Hungarian) 0-83839  
 strain energy of elastic prismatic bar, theorems (German) 0-79142  
 strain meas. by holographic interferometry, mathematical formulation (German) 0-78815  
 welding arcs, gas velocity fields modelling 0-75039

**mathematical logic** *see formal logic*

**mathematical programming**  
*see also dynamic programming; linear programming; nonlinear programming*  
 nuclear reactors, PWR core control, multistage mathematical programming 0-91227

**mathematics**  
*see also algebra; convergence; duality (mathematics); equations; formal logic; functions; geometry; mathematical analysis; probability; statistics; topology*  
 module, description and evaluation 0-86056  
 physics students, mathematics ability 0-77591  
 remedial work for university students in engineering courses 0-86054  
 teaching by computer, long division practice program 0-98775

**matrices** *see matrix algebra*

**matrix algebra**  
*see also S-matrix theory*  
 bending and nonuniform torsion of prismatic bar, matrix analysis 0-83736  
 Born's discovery of the quantum-mechanical matrix calculus 0-82615  
 colorimetry, appl. of matrix techniques 0-105690  
 configuration space basis state generation, U(n) matrix elements 0-86120  
 current transformers, oil insulated, parameters influencing heating assessment using sensibility matrix (Hungarian) 0-87708  
 decaying systems with degenerate livsic matrix 0-82629  
 eigenvalue determination by continued fraction 0-105490  
 ellipsometry, Mueller-Stokes calculus, conventions and formulas 0-102618  
 extreme eigensolution calculation method for high order real symmetric matrix 0-90703  
 geometrical optics teaching to engineers, numerical calc. methods 0-62415  
 isospectral matrices, finite transforms 0-105529  
 Kalamboukis tests of Davidson algorithm, comments, nuclear structure 0-86822



**matrix algebra continued**

- matrix function approximate factorisation algorithm 0-68022  
 nonsymmetrical optical system, matrix representation 0-64130  
 optical bare resonator eigenvalue analysis, matrix methods 0-78927  
 optics of anisotropic layered media,  $4 \times 4$  matrix algebra 0-106445  
 planar approximation for coupling  $N \times N$  matrices 0-62872  
 random matrix ensembles, joint eigenvalue distrib. 0-101748  
 residual spectra, general matrix approach 0-94947  
 residual spectra treatment appl. 0-68132  
 single eigenvalue distrib. for non-zero mean matrix ensembles, correct form 0-73198  
 spectral multiplication, props. as viewed in physical space, meteorological appls. 0-94607  
 transient electrical transport, general and unified treatment 0-59977  
 $U(2)_C^{2,2}$  representation theory, generalised Bessel functions 0-98818  
 $XY_0$  molecules,  $D_{3h}$  symm., U-, G-, F- and  $\Sigma$ -matrix determ. (French) 0-78599  
 $H_2$ , expressions for calc. Coulomb repulsion between electrons using adiabatic basis 0-91427

**matrix isolation spectra**

- see also *Shpolskii spectra*  
 5-acetyl-5H-benzobenzazole-5H-benz[b]carbazole, singlet-singlet energy transfer (German) 0-93402  
 acrolein, s-trans and s-cis, trapping from thermal mol. beams and UV-induced isomerisation in Ar matrices, enthalpy determ. 0-97688  
 9,10-anthraquinone, lower triplet states, interactions and position, matrix isolation spectra 0-63634  
 benzaldehyde in methylcyclohexane,  $n^* \pi^*$  spectra 0-63627  
 benzene radical cation in solid Ar, fluorescence spectra obs. 0-83382  
 benzyl radical, in solid Ar, absorption and photodissociation spectra 0-69156  
 chlorophyll, and related mols., in solid solns., fine-structured vibronic spectra under tunable dye laser excitation (Russian) 0-74164  
 dichloronaphthalenes, heavy atom effects on substrates of lowest triplet states, MDP obs. 0-91594  
 dye in polymer matrices, electrochromic props. and use as probe of matrix softening around  $T_g$  0-84724  
 2-fluoro ethanol, Ar matrix, induced conformational isomerisation by IR irradi. 0-101010  
 fluorobenzene radical cations in solid Ne, laser-induced fluoresc. spectra, vibr. struct. of excited and ground states 0-95671  
 formaldehyde dimers, matrix isolated, struct., IR spectra 0-99504  
 formaldehyde- $d_0$ -( $d_1$ )-( $d_2$ ), matrix isolated, IR spectra, monomer absorpt. 0-99503  
 free-base porphyrin, Zeeman shift meas. by photochem. hole-burning 0-83416  
 1,3,5-hexatriene radical cation, in Ne matrix, laser induced fluoresc. and emission spectra 0-87163  
 hydronaphthyl radicals embedded in naphthalene cryst., optical transition energies and ionisation energies 0-78595  
 inert gas crystal, lattice vibr. and radiative transitions of implanted ions (Russian) 0-69098  
 isopropyl radical, Ar matrix isolated, IR spectra and UV photolysis 0-66827  
 molecules, high temp., appl. of matrix isolation studies 0-57399  
 2(4)-monoxopyrimidines, gaseous, matrix, soln., tautomeric equilib., IR and UV absorpt. spectra 0-58256  
 naphthalene, phosphorescence spectra in rare gas matrices, multiplet struct. and pot. energy functions 0-106341  
 naphthalene in Ar matrix, geometry changes and multiplet struct., mol. fluoresc. and phosphoresc. obs. 0-95663  
 nitrocyclopropane, vibr. spectra struct. and bonding 0-102520  
 nitroxide radicals, q- and A-tensor components, rot. mobility 2 mm EPR spectrosc. determ. 0-102530  
 pentacene in naphthalene, triplet state, EPR study by electron spin-echo and laser flash excitation 0-58172  
 polyatomic molecules, radiationless transitions, Fermi resons. and quasisymmetric spectrum 0-95665  
 porphine- $d_4$ , vibronic transitions, polaris. determ. 0-63614  
 rhodamine 6G, in rigid matrix, conc. effects in spectra 0-83347  
 toluene cation in solid Ar, absorption and photodissociation spectra 0-69156  
 tropolone,  $\pi-\pi^*$  singlet state,  $H^+$  tunnelling dynamics and equilib. geometry 0-102539  
 xanthone, large zero-field splitting of lowest triplet state 0-58171  
 xanthone, in n-pentane, heat pulse induced delayed phosphorescence 0-83404  
 $Al_2Cl_6$ , matrix isolated, vibr. spectra, isotopic fine struct. and valence force field calcs. 0-58258  
 $BCl_3$ , in solid Ar, Kr, high resolution IR absorpt. spectra, isotopic splitting 0-87109  
 $BCl_3F$ , in solid Ar, Kr, high resolution IR absorpt. spectra, isotopic splitting 0-87109  
 $Bi_n$ , molecular clusters, laser fluoresc. spectrosc. 0-95755  
 Br matrix isolation ESR 0-106336  
 $Br_2$  in Ar matrix, reson. Raman scattering amplitude damping in discrete reson. limit 0-58262  
 $BrO$ , free radical, Ar matrix absorpt. spectra, mol. vibronic states obs., spectroscopic const. determ. 0-83387  
 $CO$ , lowest triplet state, Ar matrix isolation spectra 0-91569  
 $CF_3(FCI)(FBr)$ , matrix isolated IR and Raman spectra, assignments, force consts., isotope effects and thermodynamic props. 0-63631  
 $ClO$ , free radical, Ar matrix absorpt. spectra, mol. vibronic states obs., spectroscopic const. determ. 0-83387  
 $CsReO_4$ , IR matrix-isolation spectra 0-87108  
 Cu complex, Cu(II) bis(dithiocarbamate),  $^1H$  ENDOR 0-87154  
 $D_2$  IR spectra, mol. rot. and vibr. const. determ. 0-78617  
 $FCO$ , form. in Ar matrix, vibr. and electronic spectra, valence force potential determ., mol. photodissoc. obs. 0-85170  
 Fe monomers and dimers, in solid Ar, EXADS study 0-97381  
 $H+CF_3$ , IR matrix isolation spectra 0-97706  
 $H_2$ , IR spectra, mol. rot. and vibr. const. determ. 0-78617  
 $H_2O$ , Pt catalytic oxidation of  $H_2$  and  $D_2$ , matrix isolation and laser fluoresc. obs. of prods. 0-66865  
 $HgF_2(FCI)(FBr)$ , matrix isolated IR and Raman spectra, assignments, force consts., isotope effects and thermodynamic props. 0-63631  
 $^{13}C_2$ , frozen soln. in o- or p-xylene, Mossbauer effect obs. 0-78637  
 $^{17}O$ , in solid Ar, emission and excitation visible spectra at 12K 0-87137  
 $IO$ , free radical, Ar matrix absorpt. and emission spectra, mol. vibronic states obs., spectroscopic const. determ. 0-83387

**matrix isolation spectra continued**

- $LiReO_4$ , IR matrix-isolation spectra 0-87108  
 Na, matrix isolated in Ne, absorpt. and emission spectra 0-99465  
 $Ni_3$ , in solid Ar, reson. Raman spectra 0-63638  
 OH, Pt catalytic oxidation of  $H_2$  and  $D_2$ , matrix isolation and laser fluoresc. obs. of prods. 0-66865  
 Pt porphyrin in n-alkane single cryst.  $^3E_u-^1A_g$  transition, Zeeman expts. at 4.2K 0-78645  
 $RbReO_4$ , IR matrix-isolation spectra 0-87108  
 Ru(II) complex, carbonyl(pyridine)-phthalocyanatoruthenium(II), optical hole burning, matrix effects 0-102522  
 $S_2$ , matrix-isolated,  $B^1\Sigma_u^-$  predissoc., relax. processes 0-58329  
 $SBr_2$ ,  $SI_2$ , matrix isolated, IR spectra 0-58254  
 $Se_2$ , laser induced fluoresc. in inert gas matrix 0-87161  
 $SeF_6$ , in Kr matrix, temp. reversible IR spectral changes, site struct. dynamics 0-102505  
 $SiH_3$  radical, in  $Ar(Kr)(N_2)$  matrix, anisotropic ESR spectroscopic parameters 0-63687  
 $Sn_2$ , in Ar matrix, absorpt., fluoresc. and reson. Raman spectra 0-95640  
 $Te_2$ , laser induced fluoresc. in inert gas matrix 0-87161  
 $TeO_1Cl_2$ , thermal decomposition, matrix isolation IR and mass spectra 0-81306  
 Ti, and  $TiO$ , from sputtered Ti, sputtered ion fraction meas. using matrix isolation spectroscopy 0-60738  
 $Ti_2F_2(Cl_2)$ , assignment of vibr. Raman and IR spectra bands 0-58268  
 $TiReO_4$ , IR matrix-isolation spectra 0-87108  
 $UF_6$ , matrix isolated, vibronic fine struct. in fluoresc. spectrum 0-83406  
 $Zn+O_2$  matrix reactions, IR, Raman and visible spectra in Ar and  $N_2$  matrices 0-87110  
 $ZnF_2(FCI)(FBr)$ , matrix isolated IR and Raman spectra, assignments, force consts., isotope effects and thermodynamic props. 0-63631  
 Zr, and  $ZrO$ , from sputtered Zr, sputtered ion fraction meas. using matrix isolation spectroscopy 0-60738

**matrix isolation spectroscopy**

- fluorobenzenes in Ne matrices, molecular cation electronic absorption spectra, new photolytic technique 0-58415  
 frozen gas matrix, refr. index determ. by emission spectrosc. 0-90884  
 molecules high temp. appl. of IR isolation technique 0-57399  
 Raman spectroscopy, water pollution detect. appl. 0-108829  
 sputtered ion fraction meas. using matrix isolation spectroscopy 0-60738  
 $N_2$  matrix N-N stretching vibr., IR activation, guest mol. depend. 0-60570  
 $NaPO_3$ , mol. identification by matrix isolation IR spectrosc. 0-104485  
 $NaPO_3$ , mol. identification by matrix isolation IR spectrosc. 0-104485  
 $SF_6$ , matrix isolated, IR spectrosc., temp. reversible site structural changes 0-95613  
 $TiO_2:TeCl_3$  system, chem. vapour transport, matrix isolation IR studies 0-93755

**Matteucci effect**

No entries

**maxmin technique** see minimax techniques**Maxwell-Boltzmann distribution** see statistical mechanics**Maxwell effect** see flow birefringence**Maxwell equations** see electromagnetism**MBE** see molecular beam epitaxial growth**Mealy Moore machines** see finite automata**mean free path, carrier** see carrier mean free path**measurement**

- see also specific measurements, e.g. frequency measurement  
 see also instruments; measurement by laser beam; recording; testing; units (measurement)  
 automatic process-control measurement systems, meas. of characts., compound and element-by-element methods 0-62612  
 dimensions of physical quantities, use in metrology 0-77740  
 dynamic, problems and methods of overcoming them, reference standards 0-62613  
 fast processes, review of present methods in USSR, future prospects 0-57271  
 logical structure of meas. science (Japanese) 0-73299  
 matter under very high pressure (French) 0-90811  
 wet steam, high speed flows, drop dimensions meas. method 0-90817

**measurement by laser beam**

- see also laser velocimeters; plasma diagnostics by laser beam  
 airflow through cascade of turbine blades, laser anemometry 0-59146  
 atmospheric turbulence structural characts., meas. using spatially limited laser beam 0-98413  
 biological objects, electronic speckle pattern interferometry in vivo 0-109083  
 biomedical laser microprobe mass analyser 0-98060  
 biomedical measurements, review (Japanese) 0-94311  
 bonded interface defect testing by differential interferometric Stoneley wave meas. 0-76444  
 Brewster angle determ. by dithered laser beam synchronous detection 0-73422  
 calibration and measurement standard, high precision (German) 0-78862  
 conference, laser and electro-optical systems, San Diego, CA, USA (Feb. 1980) 0-62392  
 contactless laser interferometer sweep gauge for diamond-turned surfaces 0-73441  
 crystalline material optical absorption meas. 0-105718  
 dark-field surface inspection using total internal reflection 0-74519  
 diameter measurement of hot or cold objects, laser bar gauge system 0-105605  
 diffuse object real-time velocity meas. using laser speckle zero-crossings 0-77760  
 displacement, small, using three-mode laser, geodesic problems solution 0-77748  
 Doppler blood velocimetry (Japanese) 0-94310  
 dot matrix space-coded surface topographical mapping 0-98885  
 Earth strain measurement, He-Ne  $I_2$  stabilised laser reliability as interferometer source 0-106545  
 Earth surface deformation detect., 500-m base laser interferometer 0-105087  
 electro-optics, systems aspects, seminar, Huntsville, AL, USA (May 1979) 0-94921  
 electrostatic precipitator, particle velocity, laser Doppler anemometry study 0-59144  
 ellipsometric characts. of optical surfaces, determ. using nanosecond laser pulses 0-101822



## measurement by laser beam continued

ellipsometric technique using stabilised two-frequency laser 0-101820  
 end-standards and ruled scales using laser sources (*German*) 0-86251  
 erythrocyte distribution profiles during sedimentation as determ. by HeNe laser light 0-81563  
 fibre dispersion meas. with Nd:YAG laser at 1.06 to 1.6  $\mu\text{m}$  0-87555  
 flavins, meas. of sub ns fluoresc. decay by time-correl. photon counting and Ar laser 0-94429  
 flow, random, statistics analysed by photon correlation anemometry 0-64522  
 fluid meas. in mechanical engineering, conf., Johannesburg, South Africa, (Feb. 1979) 0-75016  
 fluid props. meas., by laser interferometry 0-75018  
 gas concentration meas. using Raman intensity depend. on giant pulse laser polarization 0-98986  
 gas detector, all-electric, using Stark cell 0-74417  
 geodesic interference distance meas. using semicond. lasers 0-77175  
 glass thickness automatic measurement by laser beam 0-82744  
 gravitational radiation detection, laser displacement sensor 0-101747  
 gyromagnetic ratio of proton and fine-structure constant redeterm., by meas. distance between wires 0-74253  
 hydrazine rocket fuel in ambient air, CO<sub>2</sub> laser absorption spectra and photoacoustic detection 0-104540  
 immunological reaction monitor using laser light scatt. 0-85463  
 interferometer systems, theory and application 0-73435  
 interferometers, AM and FM operation and applications (*German*) 0-86389  
 interferometry seminar, San Diego, CA, USA (Aug. 1979) 0-73096  
 IR laser interferometer operation and testing 0-73433  
 IR optical components and aspherics, 10.6  $\mu\text{m}$  interferometric testing 0-74523  
 IR spectrophotometer spectral slit width determ., method comparison 0-86472  
 length measurement with heterodyne interferometry (*German*) 0-68181  
 linear dimensions, measured on production line by optical techniques 0-82746  
 liquid, extinction coefficient meas. using coaxial dual channel laser system 0-73425  
 machine part, rotating, surface finish, laser method for determ. 0-89454  
 machine tool position feedback by laser interferometer 0-73438  
 metal surface, rough, hemispherical emittance 0-70434  
 microcomputer based laser interferometer for angular displacement meas. (*Polish*) 0-90816  
 microemulsions, heat transfer meas. by laser-induced thermal blooming 0-91833  
 monomode fibre dispersion and bandwidth meas. by mode-locked Q-switched Nd:YAG laser 0-91933  
 multichannel device structure and testing, for pulsed energies (*German*) 0-95933  
 nuclear track detectors, glass and plastic laser diff. appl. to determ. of etched track parameters 0-95499  
 optical fibre, PCVD, dispersion measurement by mode-locked synchronously-pumped dye laser 0-64191  
 optical glass, thermally tempered, surface stress meas. by crit. ray method 0-106766  
 optical surfaces, concave and convex, radii of curvature meas. 0-83654  
 parabolic mirror testing by vibration-insensitive laser unequal path interferometer 0-74537  
 parabolic mirror testing during fabrication by long-wavelength interferometer 0-74536  
 particle motion 3D sensing via multibeam laser system 0-83722  
 particle motion detection in transparent liquids, Fourier transform acousto-optical system performance 0-87680  
 particle size meter using laser light scatt. spectroscopy 0-77754  
 pathological samples, mol. microanal. in situ with laser-Raman microprobe 0-81683  
 power system current and voltage meas. using electro-optical effects (*Japanese*) 0-86342  
 Raman microprobe, microscopic samples molecular analysis, particle characts. determ. 0-57391  
 Raman microprobe analysis, principles and appl. 0-57390  
 Raman microprobe-microscope, molecular optical laser examiner appl. 0-62737  
 rangefinder and 3D object recognition algorithm 0-96016  
 refractometer laser detector for anal. of liquids 0-101830  
 retroreflector alignment, simple interferometric technique 0-95125  
 rough surface interferometry at 10.6  $\mu\text{m}$  0-86385  
 scanning laser acoustic microscopy, ceramic components nondestructive testing, comparison with SEM and optical microscopy results 0-58875  
 seismic microvibration frequency analysis by 50 m interferometer 0-109276  
 spectrophone, low-noise, using continuous laser beam 0-74418  
 spectroscopic light sources, far-IR, using tunable diode lasers, optical coupling arrangement 0-73481  
 sputtered particles, vel. meas. by Doppler-shift laser spectrometer 0-62638  
 Streptococcus mutans 10449, size determ. by laser light scatt. 0-109062  
 submarine periscope optical design for laser rangefinding compatibility 0-78987  
 temperature gradients in liquid, using laser microrefractometer 0-57362  
 thread grinder, high precision, laser interferometric auto-correcting system 0-90830  
 three-dimensional topographic mensuration, laser electro-optic system 0-99784  
 tracheal ciliary beat, improved device for freq. recording 0-109070  
 truss joint strain meas. by modified Michelson interferometer 0-74821  
 tunable IR solid-state laser characteristics and principles 0-87406  
 tunable laser interferometry, oscillator strength meas. 0-105697  
 turbulent mixing flow, velocity biasing resulting from non-uniform seeding 0-59143  
 two-colour length measurement scheme using CO<sub>2</sub> laser 0-99747  
 two-dimensional structure in-plane vibr., stress analysis by laser speckle method 0-103006  
 unequal path interferometer with electro-optical camera and minicomputer, fabrication/test appl. 0-77847  
 velocity gradients and laminar and turbulent diffusion, direct optical meas. 0-59132  
 vibration and small mechanical displacements measurement, heterodyning two laser beams 0-73309  
 vibrations of very small amplitude in US transducers using laser probe 0-73443

## measurement by laser beam continued

Al foil, deformation, laser optical scanning obs. 0-100995  
 Al plate, thermal strain meas. by one-beam laser speckle interferometry 0-103005  
 HO, detection by laser excited fluoresc., press. depend. of fluoresc. and photolytic interferences 0-95666  
 He-Ne 3.39  $\mu\text{m}$  laser interferometer, length and refr. index meas. 0-68172

**measurement errors**  
 acoustic noise meas. of elec. machines, errors (*Hungarian*) 0-96102  
 ampere, realization by means of current balance at NPL 0-105678  
 aquatic eyes, retinoscopy, refractive error considerations 0-61750  
 astrometry, astroclimatic influences on precision of photographic star positions obtained with wide-angle astrophotographs (*Russian*) 0-72748  
 astronomical optics testing by Hartmann method, estimation of reliability of results 0-67564  
 atmosphere 500 mb height, anal. error development, (1946 to 1969) 0-72615  
 atmosphere measurements by double theodolite technique, control of inherent uncertainties 0-77160  
 atmosphere temperature profiles, satellite retrieved, error due to aerosol particles effects 0-98449  
 atmosphere temperature sensors, humidity effects and sea salt contamination 0-82095  
 atmospheric precipitation acidity measurement, error anal. applied to indirect methods 0-72108  
 biomedical ECG recording, correction of timing errors due to tape speed variation 0-72354  
 blood perfusion rate estimation from diffusible indicator meas., sensitivity anal. 0-104803  
 blood pressure measurement with portable systems using Korotkov sounds, meas. accuracy 0-76855  
 blood pressure recording, simple method for fidelity improvement, Korotkov sounds 0-76811  
 body joints, centres and angles of rotation meas., errors and optimisation study 0-61604  
 catheter pressure meas., transducer smearing correction using microprocessor based discrete deconvolution 0-67275  
 cloudy atmospheric parameter determination using microwave radiometric method 0-67435  
 coatingZZ 0-77775  
 cometary orbits, reciprocal semimajor axes accuracy 0-62074  
 computerised tomography, gantry geometry rel. to aliasing and other geometry dependent errors 0-81695  
 concentricity, round parts, profile determ. (*German*) 0-57249  
 contact-type flowmeter working in thermal boundary layer, temp. error determination 0-103093  
 coordinate meas. uncertainty computation program (*German*) 0-86256  
 data acquisition systems, in steady and unsteady states, error determ. 0-95056  
 determination techniques, meas. of mass 0-57237  
 digital velocity meas. meter (*Russian*) 0-86266  
 digital voltmeter, automatic checking method 0-57240  
 digital voltmeter, instrumental error estimation technique 0-57239  
 dilatometric measurements, high-temp., systematic and fiducial error estimation 0-101796  
 dual-Doppler radar, meteorological, coverage area as function of meas. accuracy and spatial resolution 0-82093  
 dynamic, determ. and normalisation of meas. equipment characts. 0-62617  
 dynamic, of devices meas. turbulent temp. fluctuations, with detector dynamic response correction 0-77781  
 Earth induced polarisation (IP) sounding, effects of EM coupling in electrode arrays over uniform half-space 0-101324  
 Earth multifrequency EM sounding, topographic and misorientation effects study 0-101451  
 earthquake records, digitization errors and base line corrections 0-98245  
 electrical meas. devices, drift and additional errors, algorithms (*Russian*) 0-62615  
 electromagnetic meas., precision, conf., Braunschweig, Germany (Jun. 1980) 0-98903  
 evaluation, tendencies in the USSR 0-95052  
 exponential statistical distribution and aberrant values elimination (*Rumanian*) 0-68163  
 exposure meter errors during colour photographic printing 0-101818  
 film photon and electron absorbed-dose detector 0-91379  
 flowmeters, effect of hydrodynamic factors 0-96322  
 flowmeters, mobile weighing system 0-96326  
 frequency, probability anal. (*Russian*) 0-90823  
 frequency thermocoupler electrical correction (*Russian*) 0-57242  
 gas analysis, by mass spectrometer, dynamic error determ., transfer function 0-61194  
 gauge blocks, errors associated with checking by interferometric methods 0-105613  
 grating type monochromators, spectrophotometry and colorimetry errors caused by polarisation of meas. system (*Japanese*) 0-101815  
 gravitational wave interferometer, quantum mechanical radiation press. fluctuations 0-90770  
 gravity data, allowance for errors rel. to approximation of Stokes and Vening-Meinesz eqns. 0-101459  
 groundwater <sup>14</sup>C dating, errors from <sup>14</sup>C subsurface prod. 0-85690  
 gyromagnetic ratio of proton in weak mag. field at NPL 0-105678  
 high intensity local heat flow, anal. (*Russian*) 0-74865  
 hot-plate thermal conductivity meas., errors associated with imperfect surfaces 0-95098  
 impedance measurement, accuracy of electrode props. determ. 0-61108  
 IR spectrophotometers, meas. errors of polarising objects 0-86471  
 IR thermography, reflectance errors 0-62661  
 klirr-factor unit dimension, error in digital meas. 0-98873  
 laser Doppler anemometry, velocity and photomultiplier bias effects 0-59140  
 laser radiation spatial distribution determ., mode parameters 0-95055  
 least squares method, limit of applicability, modification for large errors in independent variable 0-73301  
 limits of reducibility of random measurement errors through statistical evaluation under consideration of input signal signal (*German*) 0-95057  
 linear displacement meas. accuracy meas. accuracy improvement under vibration 0-90815  
 magnetic defectoscopes, nonsinusoidal periodic currents meas. 0-104386  
 magnetic losses, form factor influence (*Rumanian*) 0-68226



**measurement errors continued**

- measurement and transmission system, relative error of analogue signal with bend for freq. band cut-off (*German*) 0-86242
- measurement techniques regarded as a subset of information techniques, error correction by computer programs and by networks (*German*) 0-68164
- metal, electron irradi., selfinterstitial atomic defect interaction radii, recovery expts. and error sources 0-65049
- methodic and instrumental, examples 0-57238
- moisture meters, representation as two series transducers, total error estimation 0-77792
- multichannel high resolution time analyser scale instability (*Russian*) 0-73326
- nonsinusoidal periodic current meas. using standard DC shunt with magnetic powder monitoring, frequency errors 0-104398
- nuclear decay data, need for uncertainties 0-87023
- nuclear materials safeguarding, measurement errors 0-73935
- optical attenuator metrological certification methods 0-91941
- optical constants meas. method using polarised light refl. coeffs., accuracy 0-73423
- optical density measurement accuracy by means of optical wedge 0-73416
- optical fibre attenuation meas. by backscattering method, effect of noise 0-102824
- optical instrument, target position meas., statistical model 0-101778
- optoelectronic angular meas. devices, anal. method (*Russian*) 0-95066
- palaeomagnetic meas., mag. declination and inclination errors in experimentally deposited specularite-bearing sand 0-90075
- passive sonar, range and bearing estimation, errors 0-79030
- pendulums, random interactions (*Russian*) 0-73313
- photodetector relative spectral sensitivity meas. method using two tandem monochromators (*Japanese*) 0-101840
- Photographic Zenith Tube at Tokyo Astron. Observatory, observational errors anal. 0-98547
- pneumatic feedback-monitoring instruments, pressure variation effects 0-77743
- polarisation resistance method, using 2 and 3 electrodes, error anal. in corrosion rates 0-100930
- position-sensitive detector, influence of discrete struct. on accuracy of coordinates determination 0-58076
- power transmission spectrometry, systematic error in calc. value of power absorpt. coeff. 0-98982
- probability distribution function determ. feasibility for various sample sizes 0-90806
- pycnometry, determ. density of liquid metals 0-73321
- quantum magnetometer with alternating polarity modulating pulses (*Russian*) 0-90871
- radio astronomy, influence of troposphere on radio-interferometric meas. of coordinates 0-67581
- random, of instruments under transient conditions, analysis based on instantaneous frequency response 0-77741
- ratemeters, with variable time const., error determ. 0-95507
- reactive power, three-phase two wattmeters, meas. errors (*Croatian*) 0-105677
- reflection dispersive Fourier interferometer window eliminating backlash error 0-57402
- refractive index of liquids, determ. with cell differential refractometer, prism wedge angle effect on meas. error 0-62715
- resistance thermometers, drift correct cct. 0-98912
- respirometric open systems, error anal. (*German*) 0-104782
- retroreflecting material metrology, errors in luminous refl., chromaticity meas. 0-68235
- retroreflector photometric and goniometric accuracy 0-86375
- retroreflector photometry, meas. error rel. to aperture size 0-73409
- rhograph linear-distortion estimation 0-85502
- RMS measurement errors quantified 0-57274
- roughness measurement, electrical stylus tip instrs. 0-90818
- SEASAT radar altimeter, resolution capability preliminary estimates 0-72645
- solar double-pass monochromator with automatic data processing, spectral lines recording error (*Russian*) 0-72777
- solar spectrum, photospheric lines damping const. determ. methods errors (*Russian*) 0-72899
- spinning analyser ellipsometer, meas. magneto-optic rotation and ellipticity (*Japanese*) 0-73419
- standards comparison, time and frequency, improved accuracy 0-95062
- stellar trigonometric parallaxes, freq. distrib. and systematic effects 0-94785
- STEM methods for mass measurement 0-73537
- stratosphere NO and ClO concs., effects of vars. at twilight on interpretation of solar occultation meas. 0-85756
- strip lines meas, dielectric, small standing wave ratio and losses meas. 0-77811
- stylus tip instrs. for surface roughness meas. (*German*) 0-101782
- superfluous, meas. elimination, precision evaluation 0-90805
- systematic duplicative, algorithm (*Russian*) 0-86245
- systematic uncertainties, randomisation and quantitative assessment 0-98869
- temperature measurement by thermocouple, avoiding errors 0-62664
- thermal EMF of semiconductors, thermal cell and copper blocks method, more accurate treatment of results 0-77812
- thermocouples principle, errors, due to windings heating (*German*) 0-95096
- thermogravimetry, balance inclination and specimen temp. error sources 0-98887
- thermometer thermoelectric, Pt-Rh, 1300 to 1700°C, errors obs. and analysis 0-77783
- thick planar films, transmission method for index meas., modal effects 0-102862
- time measurement, errors, accuracy of watches and clocks, time standard 0-90821
- transducers, dynamic, analysis using conversion factor 0-77770
- universal horizontal microscope, rational determ. of composite error on small micrometers 0-82742
- variational simulation of measuring equipment, machine-oriented description of the error determination and control process 0-95053
- vibration transducer, surface compliance of vibrating body (*Japanese*) 0-79046
- vibrational, using analogue photoelectric velocimeters, systematic errors determ. 0-79246

**measurement errors continued**

- wall impedance in Kundt's tube by means of FM transmitter signal (*German*) 0-102878
- Cs clocks made by Csilloquartz Company, investigation of metrological characts. 0-101787
- Cu alloys, molten, gas content meas., reduced pressure test (*Chinese*) 0-81390
- Pt resistance thermometers, effect of Pt oxidation 0-101794
- measurement standards**
- see also atomic clocks; temperature scales
- 600 MHz to 1 GHz coaxial thermal noise standard 0-98875
- atomic time and frequency standards development at Shanghai observatory, China 0-105617
- atomic time scale instability, contrib. of computation algorithm 0-98890
- automated time keeping system of Van Swinden Lab. 0-98891
- beta decay primary standard (*Rumanian*) 0-68603
- building heat loss diagnostics, IR image evaluation requirements 0-86424
- calibrations of multiples of the unit of mass, systematic search for orthogonal systems 0-82747
- capacitance, appl. of sensitivity criterion to Lampared-type electrostatic system 0-98942
- conference on metrology and fundamental constants, Varenna, Italy (July 1976) 0-105603
- cryoelectrics, computerised measurement instrumentation 0-98920
- dynamic measurement, time and measured-variable standards, problems and methods of overcoming them 0-62613
- EELS, standard for TEM, implanted Si 0-99017
- electrical standardising laboratory for developing countries 0-101774
- electromagnetic meas., precision, conf., Braunschweig, Germany (Jun. 1980) 0-98903
- electron probe X-ray microanalysis, P standards for ultrathin tissue sections 0-98193
- end-standards and ruled scales using laser sources (*German*) 0-86251
- fiber-optic measurements, using standards and instruments 0-74488
- frequency, clock error with a Wiener predictor and by numerical calculation 0-82748
- frequency, phase automatic freq. control parameters optimal values (*Russian*) 0-77814
- future prospects (*Japanese*) 0-73303
- gamma radiation detector, reference material, based on silicate glass 0-78454
- gas thermometer, 273.15 to 1337.58K range 0-77782
- GDR atomic time scale 0-98892
- gear tooth profile, portable meas. instrum. for large gears, interchangeable standard profiles 0-57259
- hierarchical systems, calibration errors influence on end item performance 0-98788
- inductance, calibration of permeability meters, short cct. coaxial lines 0-77816
- International Atomic Time Scale, problems of generation, quality and availability 0-98889
- ion laser,  $^{127}\text{I}_2$  stabilised, beat freq. intercomparisons at 514.5 nm 0-74338
- IR and millimetric waves and applications, conf., Miami Beach, USA (Dec. 1979) 0-57009
- IR and MM wave calibration standards requirements survey 0-57248
- Josephson voltage standard maintenance using standard cells combination with low temp. coeff. 0-101788
- klirr-factor unit dimension, error in digital meas. 0-98873
- laser, calibration and measurement standard, high precision (*German*) 0-78862
- laser low-level pulse meas. system at 1.064, transfer standards 0-86253
- length standard meas. procedures of GDR Bureau of Standards (*German*) 0-57246
- magnetic field induction meters, constants determ. using nutation teslameter 0-98946
- magneto-optical rotation, InSb and Ge, use in polarimeters 0-60551
- mass, air density effects, calc. from atm. variables 0-105615
- metal fixed points, limitations caused by trace impurities 0-105644
- methane triple point sealed cells using stainless steel envelope 0-95099
- metre, new definition proposal using 88 THz stabilised He-Ne laser 0-73304
- metrology standards and measurements laboratory, used by Matsushita Communication Industrial Co. Ltd. (*Japanese*) 0-82738
- monochromators for light scatt. and fluoresc. standard in colloid 0-57247
- monoenergetic fast neutron flux density measurements, international comparison 0-83138
- multijunction thermal convectors for AC-DC transfer standards 0-98874
- multijunction thermal converter AC/DC transfer, Thomson effect error reduction 0-103679
- neutron activation analysis, 14 MeV, standards, nonidentical samples, formalism 0-71980
- nuclear materials safeguard, role of standard reference materials in achieving measurement traceability 0-78371
- nuclear materials safeguarding, measurement standardisation 0-68812
- nuclear materials safeguards, prototype, reference materials for nondestructive assay 0-78372
- nuclear materials safeguards, reference materials and meas. traceability 0-78370
- nuclear materials safeguards and materials control, meas. tech. conf. Charleston, SC, USA (November 1979) 0-77544
- nuclear materials safeguards reference measurement system utilizing resonance neutron radiography for nondestructive assay meas. 0-78377
- optical density, NBS development of inverse fourth power photometric calibrator 0-73412
- optical fibre attenuation measurement comparison among USA manufacturers 0-58747
- phenoxylbenzene triple point cells, preparation and realization 0-105643
- photometric working standard establishment using photoreceptors (*Japanese*) 0-98964
- precision thermostat and capacitor enclose, maintaining the unit of capacitance 0-95063
- pressure, intercomparison for oil-operated pressure balances between NPL and LNE 0-98877
- pressure balance standards, international comparison over 1 to 10 MPa range 0-105671
- quantum frequency standard with pulsed optical pumping of  $\text{Rb}^{87}$  vapours, performance factor 0-78823
- radiance transfer, magnesium fluoride windowed deuterium discharge lamps, 115 nm to 370 nm 0-87451



## measurement standards continued

- radiation, test site suitability assessment for radiation measurements 0-82737
- radiation energy standards (*Japanese*) 0-62620
- radiation irradiance scales intercomparison, 90 to 250 nm wavelength range 0-98963
- radioactive waste management, US NBS proposals for measurement standards 0-102276
- reference radiations for radiation protection dose meter calibration (*French*) 0-57998
- reflective glass colour standards 0-90878
- retail equity, NBS Standard Reference Materials 0-86249
- retroreflectance measurements, unified coordinate system 0-73408
- retroreflector, NBS reference 0-73410
- solid density measurement, hydrostatic weighing 0-77758
- sound insulation between buildings, standard procedure 0-96108
- special nuclear materials, control and accounting, role of certified reference materials 0-68815
- specular gloss of paint, calibration of reference standards 0-95061
- specular reflectometer-spectrophotometer, NBS reference, mirror refl. meas. 0-68236
- specular sphere scatt. radiance matrix, refl. standard for polarised beam scatt. meas. 0-74299
- standard cells with low temp. coeff., characts. 0-101090
- standard sound sources, sound isolation tests of residential buildings, correlation with subjective privacy opinions 0-64323
- stellar absolute luminosity calibrations, consistency 0-62111
- stellar photometry, secondary standards spectrophotometric obs. rel. to Ap stars HD 10783 and CU Virginis 0-98663
- stellar spectral energy distribution in 3500 to 7500 Å region, absolute calibration 0-67710
- substrate uniformity, Kr vapour press. isotherms at 77K as standardized meas. 0-107657
- surface roughness, rel. to size tolerance 0-62634
- surface roughness standards for calibrating stylus tip instrums. (*German*) 0-101782
- synchrotron radiation as an absolute standard source for radiometry 0-90879
- temperature, lamps with W ribbon filaments 0-95102
- tensile force measurement instruments developed as first order reference standards (*German*) 0-105635
- terrestrial solar spectral irradiance distrib. variations, sensitivity of solar transmittance, reflectance and absorptance 0-82739
- thermal conductivity and expansion, appl. of fluorite 0-96704
- thermal expansion coeff. of steel gauge blocks (*German*) 0-68171
- thermal expansion reference data: 1-1000K 0-96669
- thermocouple calibrations, comparison, fixed point and melting wire methods 0-86252
- thermocouples and resistance thermometers, testing GDR standards (*German*) 0-90842
- thermodynamic temperature in range 0 to 1064°C, International Practical Temperature Scale revision 0-62669
- thermometry, review 0-86305
- time and freq. meas., users' manual 0-94934
- time and frequency errors in long-distance comparisons 0-95062
- time measurement, errors, accuracy of watches and clocks, time standard 0-90821
- transducers, alternating-voltage, analogue, checking and calibration methods in USSR 0-98872
- unit power standard for 53.57 to 78.33 GHz 0-90808
- USSR State Bureau of Standards, metrological resource programmes 0-90809
- Utrecht photometric system and adopted standard stars 0-62202
- vacuum standards intercomparison,  $8 \times 10^{-2}$  to  $8 \times 10^{-2}$  Pa 0-86333
- volt dissemination method and standard cell enclosure design 0-98876
- volt realization, method and equipment based on fundamental physical consts. and superconductivity phenomenon 0-98943
- voltage, Josephson-effect, at zero current bias 0-57245
- voltage standards, using Si reference diodes 0-62619
- X-ray and  $\gamma$ -ray spectra, National Bureau of Standards (USA) 0-90807
- n absorpt. power and equivalent dose 0-102351
- Ar triple point sealed cells using stainless steel envelope 0-95099
- CO<sub>2</sub> laser transitions, absolute freq. meas. by multiplication of CO<sub>2</sub> difference freq. 0-105618
- Ca 657.3 nm line saturated absorption spectroscopy, photon-recoil component resolution 0-86457
- D<sub>2</sub>O laser phase locking to freq. standard, CO<sub>2</sub>-OsO<sub>4</sub> laser freq. meas. 0-95080
- He vapour pressure scale determ. using paramag. salt thermometer and NPL-75 gas thermometer scale 0-95060
- He-Ne laser, <sup>127</sup>I<sub>2</sub> stabilised, length or freq. standard 0-106544
- He-Ne laser, methane-stabilized at 88 THz 0-73304
- He-Ne laser, stabilised by <sup>127</sup>I<sub>2</sub> saturated absorpt., wavelength international comparisons 0-95872
- He-Ne laser stabilised by methane E-component, reference source freq. reproducibility 0-106507
- NaCl high press. standard, eqn. of state to 32 kbar and 500°C, length change meas. 0-70361
- Si photodiode internal quantum efficiency basis for absolute radiometric standard 0-86410
- U<sub>3</sub>O<sub>8</sub> enrichment standards, gamma-ray spectra 0-78378

## measurement systems

- automated, general purpose, based on synchronous waveform digitisation under computer control, applications (*Portuguese*) 0-82753
- automatic differential variometer type equipment feasibility and preliminary design for big structure displacements remote measurements (*Italian*) 0-62623
- automatic for optical fibre for total loss spectra precision meas. 0-64169
- design, systematic 0-95094
- disturbed, estimation of signal parameters, autoregressive linear models (*German*) 0-68165
- ferrite materials and components, laboratory meas. automation (*Polish*) 0-101789
- human step length measurement apparatus 0-67271
- laser, multichannel device structure and testing, for pulsed energies (*German*) 0-95933
- semiconductor-insulator interface, microcomputer-aided interface-state analysis 0-80383
- solar collector-heat pump installations, meas. of efficiency under operational conditions (*German*) 0-101077

## measurement systems continued

- solar-radiation meter, automatic 0-89592
  - structures and functions (*Japanese*) 0-73300
  - thermovision flaw detector 'Stator-1', meas. channel 0-76449
  - throwing distance, for the Olympic Games, Moscow 0-82743
  - welding stresses on component surfaces, semi-automatic measuring device 0-68194
  - Cu alloys, molten, gas content meas., reduced pressure test (*Chinese*) 0-81390
- measurement theory**
- causality, macroscopic, Einstein correlation, CPT symmetry, decreasing probabilities, advanced waves, antiparticles 0-68073
  - conference Wroclaw, Poland, Sept. 1978 (*Hungarian*) 0-86247
  - data volume determ., based on risk for arbitrary volume of a priori data 0-95054
  - deparallelising method for cyclic calculation processes (*Russian*) 0-86246
  - double connecting channel model (*Russian*) 0-90804
  - engineering development trends (*German*) 0-86243
  - evolution systems, meas., rel. to master eqn., Bayesian anal. 0-90782
  - experimental data, anal. function optimisation meas. theory, appl. to spectrometry 0-62614
  - Feynman path, trajectories in Hilbert space connecting any two states, dense measurements 0-82678
  - linear state estimator design, updating budget 0-95058
  - local theories, probabilistic and deterministic, inequalities of Einstein locality 0-82656
  - maximising information, optimal initial state for indirect expts. 0-77744
  - nonlinear experimental design, information measures 0-62616
  - nonstationary, stochastic processes, probability characts. of mass flow rate meas. 0-73302
  - nuclear decay,  $\gamma$ -decay of coherent rotational states, random quantum meas. 0-73855
  - point-surface distance meas. adjustment, geometrical aspects (*German*) 0-86255
  - quantum observables, relative compatibility and joint distributions 0-105524
  - quantum system decay and reduction laws, repeated measurement perturbations 0-62496
  - roundness, reference criteria 0-62628
  - scales marking determination (*Russian*) 0-86244
  - transient input processes reconstruction, from output and dynamic props. 0-77742
  - unbiased clock variance calc. in uncalibrated atomic scale algorithms 0-105620

## mechanical birefringence

see also photoelasticity

- discs, doubly-connected, noncircular, full yielding at collapse, photoplastic verification 0-74756
- fibre, single-mode, pressure sensitivity meas. and limitation 0-106605
- fibre optic devices, single-mode, fractional wave devices and polarisation controllers 0-106606
- filter, single mode fibre birefringent 0-58713
- filter mechanical tuning techniques 0-102834
- fluorophosphate laser glasses, Nd doped, piezoelectric coeffs. meas. 0-99815
- glass, tempered, stress analysis, oblique incidence light scattering, birefringence (*Polish*) 0-71374
- opaque region, piezobirefringence anal. 0-60541
- optical fibre, single mode, bending induced birefringence 0-87537
- optical fibre, single-mode, for current meas. system, birefr. induced by bends and twists 0-99832
- optical fibre, single-polarisation single-mode, exposed cladding fabrication 0-58725
- optical fibres, single-mode, tension-coiled, high birefr. 0-99858
- optical glass, thermally tempered, surface stress meas. by crit. ray method 0-106766
- optical single mode CVD fibre, bend-induced birefringence obs. 0-58723
- phosphate laser glass, Nd doped, piezoelectric coeffs. meas. 0-99815
- photoelastic birefringent material stress determ. in single hologram exposure 0-106770
- 1,2-polybutadiene crosslinked in strain states; entanglement networks, stress-birefr. relations 0-66590
- polycarbonate, secondary flow and stress birefringence patterns in pressure hole 0-64590
- single mode fibre analysis and fabrication for low polarisation birefringence 0-58722
- stress measurement in birefringent medium by fast three-dimens. ellipsometry 0-101821
- KCl single cryst., stress birefr. 0-60542
- NaCl single cryst., stress birefr. 0-60542
- PLZT ceramics, elastooptic effect, stress induced birefr. 0-60543
- Si, piezobirefringence in opaque region 0-60541
- ZnS, reson. Brillouin scatt. and piezobirefringence 0-93348
- ZnSe, piezobirefringence in opaque region 0-60541

## mechanical contact

see also abrasion; friction; lubrication; wear

- abraded surfaces, topography rel. to contact area and abrasion mechanism 0-58986
- Barber boundary conditions for thermoelastic contact, heat flows 0-69745
- beam bending on Pasternak foundation, reciprocal variational inequalities 0-92091
- bodies with wavy surfaces, thermoelastic contact, heat conduction 0-64492
- bonded wedge shaped stamp apex singularity, Green's functions for elastic half space 0-64489
- bouncing of cantilever beam chattering against a stop, Bernoulli-Euler beam theory treatment 0-83752
- circular plate on elastic foundation, bending and contact problems 0-96235
- contact film absorption on plastic deform. of contacting bodies (*Russian*) 0-93596
- contact on a transversely isotropic half-space, or between two transversely isotropic bodies 0-64488
- cylindrical shell, contact problem with ribbed cylinder under axisymmetric loads 0-99974
- disc and coaxial ring, partial contact, loaded by external pressure (*Russian*) 0-74814
- disc inclusion, rigid, embedded in with transversely isotropic elastic medium 0-83763



**mechanical contact** continued

- elastic half space, rectangular cylinder penetration, contact problem, stress fields 0-64490
- friction, Coulomb, elast. solid with one-sided contact (*French*) 0-64485
- frictionless stamp impression in elastic half space, contact problem with semiunknown boundary of the contact region 0-69744
- magnetic flexible disc/head interface interaction analysis 0-92093
- metal surfaces, factors influencing contact behaviour 0-92092
- mirror/flaw-size relations, residual contact stresses effect 0-107363
- plate, rectangular with asymmetrically reinforcing beams, contact interaction 0-99975
- rigid indenter and elastic halfspace, dynamic contact with perfect adhesion and frictional slip 0-58980
- rigid punch bonded to elastic half plane, stress singularities 0-64491
- rigid stamp, elastic layer indentation under complete adhesion conditions 0-58979
- rough elastic bodies, plane and axisymmetric contact problems 0-74812
- rough spheres, elastic contact, anal. approx. 0-79240
- rough surface contact, review of expt. work 0-76377
- rubber covered rolls, contact and deformation nonlinear elastic problem, stress anal. 0-79239
- shear loaded interface crack, friction effects, contact zones, stress fields 0-79225
- shell, cylindrical, liquid and gas, breakaway from solid lodgement (*Russian*) 0-87744
- shell, high-shallow, with rib of equal resistance, contact interaction, tangential stress distrib. (*Russian*) 0-87745
- sliding contact, friction, wear, temp. anal. 0-93659
- sphere sliding on plane, transient thermoelastic contact 0-83765
- surface irregularities, deformation under static loads 0-58985
- tensionless contact without friction between elastic layer and elastic foundation 0-64487
- thermoelastic contact involving a sharp corner 0-83766
- thermoelastic transition from line to point contact 0-83768
- toroidal wheel, contact phenomena during curvilinear rolling, tangential stresses (*Russian*) 0-58983
- transversely isotropic half space, indentation anal. 0-92090
- two thick walled pipes, axisymmetric contact allowing for fitting surface roughness (*Russian*) 0-58982
- unilateral contact problem in linear elasticity 0-79238
- viscoelastic contact, aging 0-64486
- Fe, cast, contact deformation, reverse slipping effect (*Russian*) 0-97591
- LiF crystal, contact damage obs. by cathodoluminesc. 0-71728
- MgO crystal, contact damage obs. by cathodoluminesc. 0-71728
- W brittle alloy rolling, contact stresses (*Russian*) 0-93576

**mechanical engineering**

- fusion reactor, ISX-B, with bundle divertor, structural anal. 0-91254
- fusion reactor, ISX-B toroidal field coil finger joints, fatigue life, structural evaluation 0-91253
- fusion reactor, TFTR, neutron spectrometer mech. design 0-95498
- fusion reactors, Large Coil Program, superconducting mag. coil struct. design status 0-106189
- IR pyrometer performance parameters and applications (*German*) 0-86315

**mechanical engineering computing**

- see also computerised control
- crack simulation computer program for plate structures (*Japanese*) 0-79218
- fatigue crack growth testing, computer-controlled stress intensity gradient technique 0-76432
- fluid flow problems, incompressible, free surfaces 0-106774
- fusion reactor, compact toroidal ignition experiment, support struct. anal. by numerical code 0-106167
- fusion reactor, SLPX TF coil, stress anal. using COSMIC-NASTRAN 0-106168
- orientation angle calc. using image matrix transformation (*Russian*) 0-73314
- pendulum random interactions anal. (*Russian*) 0-73313
- random vibrations, statistical data digital processing method (*Japanese*) 0-64430
- rectangular laminated plate, free vibr., freq. and shape determ., complex boundary conditions 0-79203
- shells of revolution, computer program for linear and geometrically nonlinear static analysis (*Japanese*) 0-64500
- strength of materials and mechanical systems dynamics, based on three-dimensional models and finite element analysis (*German*) 0-58976
- US nondestructive inspection system, microprocessor utilization 0-71845

**mechanical impact** see impact (mechanical)**mechanical interfaces** see mechanical contact**mechanical organs** see artificial organs**mechanical permeability** see permeability**mechanical properties of liquids**

- see also elasticity of liquids
- water under tension monitoring, Berthelot-Bourdon tube method 0-88238

**mechanical properties of solids** see mechanical properties of substances**mechanical properties of substances**

- see also anelasticity; bending; brittleness; creep; deformation; elastic aftereffect; elastic moduli; elasticity; fracture; hardness; internal stresses; mechanical properties of liquids; mechanical strength; photoelasticity; photoplasticity; plasticity; slip; stress relaxation; stress/strain relations; tribology; viscoelasticity
- acrylic moulding formulations, optical and mech. props. 0-106582
- aorta, canine, mech. props. following hypercholesterolemia 0-104620
- ceramics, mech. props. meas., apparatus for up to 1700°C (*French*) 0-104374
- chitin (poly-N-acetyl-D-glucosamine), dynamic mech. behaviour, effect of water 0-97522
- chitosan (poly-D-glucosamine), dynamic mech. behaviour, effect of water 0-97522
- clay, mech. props. at high-pressure 0-76966
- N,N-diethylacrylamide, cross-linked copolymer, improved mech. props. 0-61091
- Estruder 31s, polyester moulding material (*Polish*) 0-66523
- ethylene vinyl alcohol copolymer, prep., props. and appls. (*German*) 0-89194
- fragile materials, mech. props. and fracture mech. (*French*) 0-104274
- fragile materials, mech. props. meas. using disc-shaped specimens (*French*) 0-104367

**mechanical properties of substances** continued

- glass characteristics, electromagnetic, mechanical and thermal props. 0-106587
- glass composition and props. for structural material 0-84944
- high strain rates, conf., Oxford, England (Mar. 79) 0-82575
- medical polymers, chem. problems, conf., Prague, Czechoslovakia (Aug. 1977) 0-56996
- metallic glasses, production and properties, technological appl. 0-71105
- metals, high temperature testing, MEITP-1 indentation system (USSR) 0-74820
- optical material physical props., seminar, San Diego, CA, USA (Aug. 79) 0-105423
- polyacrylic acid film, structuring and mech. props., EM obs. (*Russian*) 0-59406
- polyethylene fibre prod. by surface growth method, mech. props. 0-104108
- polymer structure and optical behaviour 0-106583
- rock salt from New Mexico Salado formation, mech. props. at high-pressure 0-72492
- sea ice, in-situ meas. of mech. props. using flatjack methods 0-69751
- sediments of United States Atlantic continental shelf, engineering props. 0-72511
- sheet moulding compound, material, process and performance 0-81032
- spinel single crystals, mech. props., 1350-1650°C (*French*) 0-104374
- steel, Cr-W-Mo-Co, high-speed, from atomised powders, mech. and cutting props. 0-66556
- steel, Ni-Mo-C (2.0, 0.2, 0.4 wt.%) sintered, struct. transforms. and mech. props. after quenching 0-66557
- UV and IR instrument material mech. and thermal props. 0-106584
- Al-Ti alloy for use in aircraft, work hardening (*French*) 0-97502
- C fibres, engineering applications, production requirements and mech. props. 0-89168
- Fe based alloy, amorphous, liq. quenched, struct., thermal stability and mech. props. 0-88059
- MgO polycrystals, mech. props., 900-1150°C (*French*) 0-104374
- Ni based alloy, amorphous, liq. quenched, struct., thermal stability and mech. props. 0-88059
- Pb(Zr, Ti)O<sub>3</sub> ceramics, low temp. sintering, elec. and mech. props. 0-71616
- SiO<sub>2</sub>-Al<sub>2</sub>O<sub>3</sub>-MgO-TiO<sub>2</sub> devitrificates, microstruct. and props. (*Polish*) 0-70141

**mechanical relaxation** see anelastic relaxation**mechanical strength**

- for fatigue strength, see fatigue; for creep strength see creep fracture
- see also bending strength; compressive strength; fracture toughness; impact strength; notch strength; shear strength; tensile strength; yield strength
- autotempered reinforcing wire, tempering under stress, effect on mech. props. and relaxation resistance 0-100861
- bone, demineralised dense human, strength props. nonuniformity 0-104611
- brittle fibre reinforced composite, static strength depend. on component separation boundaries (*Russian*) 0-76304
- cable design and testing, optical fibre 0-69551
- coke, metallurgical, microstruct., using refl. light microscopy and image anal. 0-66732
- composite glasses, high strength, prod. by overlayering 0-89193
- composite laminates, proof test and fatigue study 0-93643
- composite material, mechanical behaviour, book 0-94935
- composite materials, mech. props., theory, review 0-64392
- composite materials, stochastic fracture models, and strength test results statistical anal. 0-64470
- computing, based on three-dimensional models and finite element analysis (*German*) 0-58976
- concrete quality assessment, US pulse vel. meas. practical use 0-100991
- dispersion hardened alloys, strengthening theories 0-97498
- epoxides, dielectric relax. and deform props., cross-link density effect (*Russian*) 0-60942
- fibre reinforced composite aircraft materials, design allowables 0-81204
- fibre reinforced composites, micro- and macrocracks 0-65148
- fibre reinforced polymer matrix composites, space environmental effects 0-71721
- fusion reactor, TFTR, vacuum vessel bellows, strength and fatigue anal. 0-95455
- glass, devitrified opaque technical, microstrength and hardness 0-89312
- glass, mechanical destruction role of relaxation processes 0-89282
- glass, surface damage by abrasive contact, effect on strength 0-85066
- glass fibre reinforced plastic laminates, strength and deformability, artificial ageing effect 0-60893
- glass surfaces, cracked layer thickness determ., chemical method 0-64226
- granular materials, abrasive, failure and strength characts. in US field, test unit 0-85112
- graphites, strength and struct., conf., Bath, London, England (Apr. 1979) 0-82566
- heat resistant material, long term loss of strength 0-71751
- inorganic glass, effect of liq. medium on process of mechanical destruction 0-89283
- laminates, thin, optimal struct. and strength in two-dimens. stress state 0-64395
- leucosapphire, unique polishing features of hard crystals 0-64225
- lightguide fibre, ensuring mechanical reliability 0-79001
- low C steel, explosive-thermal treatment, sulphide cracking decrease, hydrogen embrittlement (*Russian*) 0-108477
- metal, pure, with max. of cryst. lattice distortion, struct. and strength props. (*Russian*) 0-89234
- metals, creep limit and long-term strength, parametric eval. method 0-100996
- metals, high temp. stress anal. by finite element method 0-96203
- mullite-corundum ceramics, thread-like crystals reinforced, props. 0-108525
- opal glass, chemically toughened, prep. and mech. strength (*German*) 0-89191
- optical fibres, mechanical strength reinforcing and reliability improvement methods of fabrication (*Japanese*) 0-87568
- optical high-strength fibre production and proof testing 0-64204
- organic textolite, long-term strength in plane stressed state 0-60930
- para-polyamide based fibres, struct. deform. props. 0-60928
- plexiglass composite, long term strength and durability 0-75294
- PMMA moist surface mech. strength reduced by electric charge (*Russian*) 0-60486



**mechanical strength continued**

- polyethylene, high-density unoriented, damage buildup kinetics under creep conditions, during prolonged loading 0-60932  
 polymers, long-term strength prediction, review 0-104226  
 refractory concrete fracture strength, test apparatus simulating usage conditions 0-71824  
 reinforced plastics, equations of state, taking account of mech. damage 0-97553  
 reinforced plastics, load-bearing capacity, effect of one-sided heating 0-81135  
 remaining creep life for components under stress at elevated temperatures 0-59566  
 rocks, dynamic and static strength rel. to criteria for impulsive fracture 0-85646  
 ruby, unique polishing features of hard crystals 0-64225  
 spheroplastics, mech. characts. calc. 0-60931  
 steel, alloy high-C, amorphous, mech. props. and thermal stability 0-76361  
 steel, alloy X8CrNiNb1613, creep limit and long-term strength, parametric eval. method 0-100996  
 steel, austenitic, ageing and plastic deform. effect on struct. and mech. props. of N15Kh5G3T3 (*Russian*) 0-71691  
 steel, austenitic, explosive-thermal treatment, sulphide cracking decrease, hydrogen embrittlement (*Russian*) 0-108477  
 steel, C, hardened by HF current, mech. testing method 0-61053  
 steel, Cr-Mo-(V), microstruct. effect on high-temp. props. (*Czech*) 0-89300  
 steel, Cr-Mo-V, strength and ductility in creep, purity influence 0-66598  
 steel, high strength, treatment effect on ductility and strength 0-60880  
 steel, low-C, hot deform., austenite strengthening and weakening 0-76282  
 steel, low Si, martensite struct. and mech. props. (*Korean*) 0-93614  
 steel, Ni-Co-Cr, high-strength medium C, Cr effect on props. 0-76339  
 steel, stainless, fixing pins for fractured bones, strength, ultrasound effect 0-71710  
 steel, type 12Kh1MF, dislocation struct. changes after thermomechanical treatment (*Russian*) 0-66545  
 steel, type Kh13N9D2MT martensitic aged, struct. and mech. props. (*Russian*) 0-93600  
 steel, type KVK, deform. strengthening of bayanite phase (*Russian*) 0-100851  
 steel, V-Nb and Cr-Mo-V-Nb, supercooled austenite isothermal decomp., struct., strength and fracture characts. 0-60966  
 steel composite vessels, martensitic welded, glass fibre reinforced plastic wound, struct. strength 0-97552  
 synthetic high strength material structures, mechanical strength, microstress levels (*Russian*) 0-76334  
 thermoplastic plates, strength meas. when supported by annular ring 0-81257  
 vertebrae, human, mech. props. 0-72206  
 viscoelastic body containing cracks, durability calcs. 0-79227  
 wire reinforced Al, stress-deformed state, elastic, strength props. (*Russian*) 0-76303  
 Al, stability and strength of FCC metal using Morse pot. 0-59430  
 Al-B fibre-D16 alloy welded composites, structure, strength and fracture props. (*Russian*) 0-108524  
 Al-Cu-Mn, long term strength and creep 0-60925  
 Al-Mg-(Zn-Mg), long term strength and creep 0-60925  
 AlN filamentary crystal reinforced mullite-corundum ceramics, filaments strength, eval. 0-104230  
 Al<sub>2</sub>O<sub>3</sub> bioceramic synthesis, for orthopedic purposes, props. (*Polish*) 0-66465  
 α-Al<sub>2</sub>O<sub>3</sub> filamentary crystal reinforced mullite-corundum ceramics, filaments strength, eval. 0-104230  
 β-Al<sub>2</sub>O<sub>3</sub>, hot isostatic press. 0-108377  
 β-Al<sub>2</sub>O<sub>3</sub>-Na<sub>2</sub>O, AC impedance, microstruct. and strength 0-100349  
 BaTiO<sub>3</sub>, ferroelectric ceramic, internal stress and strength, failure mechanism 0-66128  
 BaTiO<sub>3</sub>, ferroic materials, fracture processes 0-79869  
 Be, fracture and strength properties, dynamic ageing effects 0-81202  
 C fibres, mech. props., thermal stability up to 2000°C 0-60929  
 C, strength and struct., conf., Bath, London, England (Apr. 1979) 0-82566  
 Cu, microalloyed with B, elec. cond. and strength props. (*Polish*) 0-89285  
 Cu-Cu<sub>2</sub>S eutectic alloy, cast and directionally solidified, struct. and props. (*Russian*) 0-104138  
 Cu-Ni, cast, strength and hot ductility, alloying and residual elements effect 0-66595  
 Cu-Ni-Zn-Mn fine grained precipitation-hardenable alloy, high strength and ductility 0-100805  
 Fe, Armco, grain size and strength depend. on nonmetallic inclusions (*Russian*) 0-100894  
 Fe powders, cold-pressed, props., effect of air 0-100810  
 Fe-TiC pseudofused composite magnetoabrasive powders, props. 0-100926  
 Mo-Re(Os)(Ru), recovery after deform. and annealing, destrengthening mechanism (*Russian*) 0-97546  
 Na borosilicate glass microsphere material, sintering, struct., strength props. (*Russian*) 0-108383  
 NaCl, optical strength, effect of irradi. in mechanically stressed state 0-80695  
 Nb-O(N), dislocation pinning, impurity interactions, strengthening (*Russian*) 0-92532  
 Ni-Cr Nimonic alloys, mech. props., high-temp. irradi. effects 0-100885  
 Ni-Cr-Co-Al-W-Mo-Ti-Ta, heat resist. and struct., Ta effect 0-76312  
 Pb, strength loss in supercond. state, size factor effect (*Russian*) 0-88677  
 Pb-Sn(Bi)(Ni), strength loss in supercond. transition, nonmag. and paramag. impurities influence (*Russian*) 0-70875  
 PbIn films strengthening, by preventing formation of misfit dislocations 0-84858  
 Pb(Zr,Ti)O<sub>3</sub>, ferroic materials, fracture processes 0-79869  
 Si<sub>3</sub>N<sub>4</sub> reaction bonded, post-sintering, injection moulding applications 0-60807  
 SiO<sub>2</sub>-Al<sub>2</sub>O<sub>3</sub>-B<sub>2</sub>O<sub>3</sub> glass mech. strength increased by etching 0-97609  
 Ta-O(N), dislocation pinning, impurity interactions, strengthening (*Russian*) 0-92532  
 V-O dislocation pinning, impurity interactions, strengthening (*Russian*) 0-92532  
 Y, polycrystn., plastic deform. at different deform. speeds, dislocation glide (*Russian*) 0-93598

**mechanical strength continued**

- ZrN-Al<sub>2</sub>O<sub>3</sub> composites, strength rel. to solid-, liquid-phase sintering 0-100823  
 ZrO<sub>2</sub>, metastable, tetragonal, strengthening by surface grinding 0-71777  
 ZrO<sub>2</sub>, porous, sintered stabilised microspheres, strength and fracture studies 0-85019  
 ZrO<sub>2</sub>-CaO(Y<sub>2</sub>O<sub>3</sub>) ceramics with grainy structure, props., effect of heating to 2000°C 0-104194
- mechanical testing**  
 see also creep testing; dynamic testing; fatigue testing; fracture toughness testing; hardness testing; materials testing; mechanical variables measurement; notch testing  
 acoustic emission, amplitude distrib. anal. 0-66713  
 alkali silicate glass, isothermal mech. loss spectrum, appl. of Rheovibron 0-88260  
 apparatus for creep and long-term strength tests, with cyclic temp. var. 0-61046  
 capacitance type AC dilatometer for piezoelectric and electrostriction const. meas. 0-77747  
 coke, metallurgical, industrial strength meas. methods, critique 0-85117  
 composite laminates, proof test and fatigue study 0-93643  
 compression tests, device for centering specimens 0-61033  
 concretes, further development of 2 point test for workability and extension of its range 0-66728  
 deformation processes in complex profile shells, installation UDM-1 0-81261  
 disperse system, plastoviscous, cone plastometer for strength props. determ. 0-76426  
 elastometric materials, friction testing using reciprocating friction and wear tester 0-76451  
 fatigue crack growth investigation, testing equipment 0-81247  
 fatigue test data, statistical anal. (*Japanese*) 0-62452  
 fatigue test results, numerical expressions (*Japanese*) 0-62455  
 fatigue testing, in situ, devices for automatic emergency protecting of mill stands (*Russian*) 0-93717  
 fibrous structure, low-density, centrifugal method for mech. prop. obs. 0-71823  
 friction tester, variable speed 0-100990  
 glass fibre reinforced epoxy resin composites, fatigue behaviour, influence of superposition of elec., mech. and environmental stresses 0-97590  
 graphite fibre reinforced epoxy, US attenuation as an indicator of fatigue life 0-85118  
 high strain rate material behaviour and testing techniques, J.D. Campbell memorial lecture 0-82627  
 high strain rates, conf., Oxford, England (Mar. 79) 0-82575  
 internal friction test device for thin-walled tubular specimens 0-71836  
 low temperature, temp. control for tests in liquid coolant vapours 0-81260  
 metals, high temperature testing, MEITP-1 indentation system (USSR) 0-74820  
 metals and alloys, mech. props. electric current effect, test device for 4.2-300K 0-66719  
 microprocessor application for destructive examination of materials with data processing (*German*) 0-93714  
 plastic deformation, compression test method (*Hungarian*) 0-97658  
 plastic deformation, fatigue test method (*Hungarian*) 0-97665  
 plastic deformation, Griffith fracture test method (*Hungarian*) 0-97666  
 plastic deformation, hardness meas. test method (*Hungarian*) 0-97664  
 plastic deformation, internal friction test method (*Hungarian*) 0-97662  
 plastic deformation, stress relax. test method (*Hungarian*) 0-97661  
 plastic deformation, torsion test method (*Hungarian*) 0-97659  
 plastic deformation, uniaxial tensile test method (*Hungarian*) 0-97657  
 plastic deformation, X-ray line profile test method (*Hungarian*) 0-97663  
 polyethylene film, minimum running thickness, biaxial extensional flow study 0-100993  
 radioactive materials, package design, construction and testing for safe transportation 0-63412  
 sea ice, in-situ meas. of mech. props. using flatjack methods 0-69751  
 sheet material, method for strength meas. under biaxial tension 0-66717  
 SiC-Q apparatus, for tensile strength meas. of cast Fe (*German*) 0-76450  
 sliding contact, friction, wear, temp. anal. 0-93659  
 slippage in crystals, photogrammetric obs. method 0-100975  
 static tensile-compressive testing, smooth tubular specimens, grip for 0-66724  
 steel, Cr-Mo-Ni-V, dynamic stress intensity factor meas., possibilities and limits (*German*) 0-93719  
 steel, low C, dynamic stress intensity factor meas., possibilities and limits (*German*) 0-93719  
 steel, low C, mech. characts., specimen size and shape effects 0-66715  
 steel, Ni-Co-Mo, dynamic stress intensity factor meas., possibilities and limits (*German*) 0-93719  
 steel, stainless type SUS 304, diffusion welded joints, sound emission during tensile testing (*German*) 0-61062  
 steel, structural, wide plate tensile testing eval. (*German*) 0-100969  
 steel, tufted, type S15CK, fatigue strength, estimation of size effect (*Japanese*) 0-81166  
 strength of materials, empirical determ., cleavage fracture in plane waves 0-96225  
 stress relaxation test device, for variable temp. 0-85113  
 stress/strain, of fragile materials, at high temperatures, improved clamp for transducer attachment 0-73351  
 surface measurements in manufacturing processes, precise mechanical test method (*German*) 0-62624  
 tensile test, regulated, strength and deform. characteristic values, consistency (*German*) 0-93712  
 tensile test equipment and procedures for charact. value determ. (*German*) 0-93713  
 tensile testing, control of test cycles, data logging and data processing (*German*) 0-97648  
 tensile tests, standardization from metal physics viewpoint (*German*) 0-93711  
 thermoplastic plates, strength meas. when supported by annular ring 0-81257  
 thermoplastic-based sheet materials, flexural anisotropy and stiffness assessment 0-76442  
 thin films, adhesion, meas. device 0-66720  
 US plate testing equipment, computer controlled, working experience (*German*) 0-93720  
 volume stressed material under static or low-cycle load, testing device 0-71834



**mechanical testing continued**

- wear testing device, cyclic load and temp. var., to 800°C 0-66718
- Al alloys, types 1100 and 5454, long-time rupture tests 0-76434
- Fe polycrystalline, two ferromag. methods for eval. of fatigue limit 0-89438
- Pb(ZrTi)O<sub>3</sub> ceramic transducer for generation and detection of unipolar stress pulses 0-64328
- Pd<sub>3</sub>Si<sub>20</sub> amorphous alloy, slip deform. and crit. shear stress, using tensile testing machine 0-89321
- Si, near (111), fracture by painted indenter, SEM study 0-71734

**mechanical variables measurement**

- see also elastic moduli measurement; force measurement; pressure measurement; shock measurement; strain measurement; stress measurement; torque measurement; vibration measurement
- 200 kW Gedser windmill in Denmark, structural response meas. 0-61431
- friction, small mobile apparatus for meas. of floors 0-69747
- friction measuring test for use under conditions of high normal interfacial force 0-76454
- impact machines, pendulum, energy meas. using optical system 0-69746
- plastic deformation measurement, moire method (Polish) 0-69749
- porosimeter, continuous scan mercury type, pore pot. contrib. to hysteresis 0-77928
- surface measurements in manufacturing processes, precise mechanical test method (German) 0-62624

**mechanical waves** see elastic waves**mechanics**

- see also bending; biomechanics; celestial mechanics; classical mechanics; damping; density; dynamics; fluid mechanics; intermolecular mechanics; kinematics; momentum; relativistic mechanics; statics; statistical mechanics; wave mechanics
- dynamic interaction of moving vehicles and structures 0-64357
- frontal method for structural mechanics, algorithm for excluding unknowns 0-79157

**mechanics of fluids** see fluid mechanics**mechanoreception**

- acceleration effects, +Gz influence on semicircular canal function, air-craft appl. 0-94245
- afferent nerves from muscle spindles, signal interpretation method 0-101188
- balance in standing position on a mobile platform (French) 0-94244
- baroreceptor activation reactivity to noxious stimulation reduction, hypertension implications 0-61596
- blind aid, image conversion to a tactile presentation 0-94414
- cortex, human, no-stimulus, no-response, event-related pot., motosensory system obs. 0-108923
- cortical evoked potentials, math. model for source localisation, somatosensory stimulation 0-89774
- echolocation in bats and auditory system 0-108906
- evoked potentials, use in monitoring residual function of injured spinal cords 0-81747
- lumbo-sacral motoneuron pools, human, response patterns to distant somatosensory stimuli 0-108924
- maxillary gum trigeminal evoked pots. in humans 0-97948
- median nerve, transient responses to elec. stimulation, SQUID appl. to somatically evoked field meas. 0-104706
- midbrain, similarities between overlapping visual and tactile maps in mammals and reptiles 0-61550
- moment of inertia, human sensitivity, psychophysical study 0-72180
- neural conduction times, central and peripheral, in multiple sclerosis, somatosensory obs. 0-89773
- optical-to-tactile converter 0-57041
- oral mucosa, EMG registration of sensory thresholds (Croatian) 0-108925
- proprioception, input to horizontal oculomotor system of crayfish, expt. obs. 0-72181
- sensory neuron, second order, summation of excitation and inhibition by computer simulation 0-76769
- somatosensory evoked potentials, reduction during movement, cat extralemniscal pathways recordings 0-85421
- somatosensory evoked potentials, review of acquisition and anal. 0-101281
- somatosensory evoked potentials, short latency, in man following median nerve stimulation 0-94243
- somatosensory pathways, assessment of central conduction 0-97949
- somatosensory potentials following electroconvulsive therapy 0-97947
- somatosensory short latency pots. in humans 0-67099
- spider, web vibr. sensed by Argyrodes elavatus kleptoparasite 0-61595
- vestibular nuclei visual-vestibular convergence in cat 0-85420
- visual-vestibular interaction during body rotation in man, nonlinear model 0-76735

**medical administrative data processing**

- see also medical computing
- cardiac cellular electrophysiologic-clinical correlations using a relational data base 0-89890
- cardiac computing conf., Geneva, Switzerland, (Sept. 1979) 0-82582
- microprocessor systems for data acquisition, image processing, RIA anal., patient data retrieval 0-61670
- radiotherapy, tumour registration system 0-81710
- skin resistance measurements, collection and off-line processing (German) 0-67273

**medical computing**

- see also medical administrative data processing; medical diagnostic computing
- aortic valve replacement, computerised simultaneous press./vol. anal. before and after 0-85531
- biomedical surface mapping, interpolation methods, in FORTRAN 0-81750
- blood pulse measuring by computer (German) 0-104823
- brachytherapy program used with the Philips Treatment Planning System 0-81738
- cardiac cellular electrophysiologic-clinical correlations using a relational data base 0-89890
- cardiac computing conf., Geneva, Switzerland, (Sept. 1979) 0-82582
- cardiograms, image processing, cardiac function meas. (Japanese) 0-94354
- cardiovascular nuclear medicine, instrumentation and data processing, ventricular function evaluation 0-85481
- colonic contractile activity meas., pharmacological tests in dogs appl. 0-109068

**medical computing continued**

- conference on medicine and techniques, Zagreb, Yugoslavia, 1979 0-101667
- contour map production for electrophysiology 0-72340
- control signals and transducers for the control of upper extremities in plegic patients, computer controlled experiment (Slovak) 0-109061
- drug elimination interactions, physiological flow model in rat 0-81628
- ECG data reduction using a microcomputer (German) 0-81748
- ECG lead CAD 0-85526
- ECG telephone transmission, analogue and digital, errors and noise 0-94398
- ECGs, left ventricular hypertrophy study in borderline hypertensive young men 0-109050
- echocardiograms, left ventricular anal. (German) 0-81667
- echocardiograms, M-mode, microcomputer editing for semiautomatic anal. 0-94299
- EEG, automated monitoring of long-term implanted electrodes (Russian) 0-76857
- EEG, automatic interpretation, background activity anal. 0-85503
- EEG, real-time detection using two-component wave model 0-104788
- EEG, simple computer-generated dot-density topogram 0-94407
- EEG, syntactic anal. software system 0-104787
- ejection fraction rel. to ventricular vol., computer anal. 0-104599
- EMG, single motor unit action pots. identification 0-72343
- EMG processing for sleep research 0-67267
- ERG recording, computer assisted - standardised quantitative method 0-109048
- EVOQ: a system configurable for automatic simulation and recording of mean evoked potentials on a minicomputer (French) 0-85507
- eye motion kinetics in moving target pursuit, oculomotor abnormalities in neurological disorders detect. 0-108888
- heart fourth sound studied by FFT 0-94397
- heart relaxation parameters, digital anal. of isovolumic press. fall, dogs 0-94276
- image processing, introduction (Japanese) 0-81699
- image processing microprogrammed video display 0-72366
- long bone mechanics study under microprocessor control 0-76851
- lung, mag. field meas., comparison between two methods 0-104712
- magnetopneumography, analytic methods 0-104713
- moire contourography, computer-aided replication of human anatomy 0-67189
- multichannel analyser, microprocessor-controlled, transfer of blood pressures and neural activities for computer anal. 0-72356
- neuronal interspike intervals, meas., teleprocessing, anal. 0-85375
- nuclear medicine - computer software package for internal dose calc. 0-98139
- nuclear medicine, microprocessor systems for data acquisition, image processing, RIA anal., patient data retrieval 0-61670
- olfactory bulb, 55 counts/sec rhythm anal. and simulation 0-85422
- radiation therapy, external beam, planning using the Edinburgh algorithm 0-94316
- radiation treatment planning, accuracy 0-72328
- radioactive seed implants, computation of dose distrib. 0-101265
- radiographic equipment, computer-assisted quality assurance 0-89838
- radiographic image computer-controlled subtraction procedures 0-109014
- radiotherapy treatment planning, FORTRAN program for optimisation using complication probability factor 0-81686
- radiotherapy treatment planning for irregular fields 0-81739
- radiotherapy with fast electrons, computerised treatment planning, dose distrib. calc. 0-81740
- skin resistance measurements, collection and off-line processing (German) 0-67273
- SQUID fluxgate magnetometers, magnetopneumographic meas. 0-104711
- surface EMG, computer anal. during isometric exercise, muscle tension quantification 0-85505
- thyroid function radioimmunoassay, quality control, computer program (French) 0-94348
- ventricle, left, human, 3-D time-varying reconstruct error sources and magnitude estimation 0-85454
- <sup>137</sup>Cs gynecologic insertions, expt. derived algorithm for computer calc. dose rates 0-101264

**medical diagnostic computing**

- see also computerised signal processing
- 21-channel EEG monitor with real-time result colour display 0-72364
- cephalometric tracing processing system, software development (Japanese) 0-94409
- chest X-ray automated anal. 0-98098
- ECG diagnosis improvement by nonlinear feature extraction methods 0-85530
- ECG signals, diagnostical functions, effect of random noise (Croatian) 0-98169
- echocardiography, high-resolution, computerised US signal processing 0-76814
- hierarchical computer networks for processing data base generated by X-ray CT scanner 0-81732
- mandibular movements diagnosis, system for meas. and processing (Japanese) 0-101249
- orthogonal transforms program for medical scintigrams 0-72365
- radiographic image smoothing and edge enhancement 0-109015
- sinus rhythm, diagnosis by IBM ECG anal. program (Japanese) 0-67278
- tomosynthesis, flashing system, using simultaneously 25 X-ray tubes 0-81768

**medical effects of radiation** see biological effects of radiation**medical electronics** see biomedical electronics**medical information processing** see medical administrative data processing:**medical computing****medical sciences** see medicine**medicini**

- see also biomedical engineering; cardiology; health hazards; patient diagnosis; patient monitoring; patient treatment; physiology
- air flow patterns in the operating theatre 0-94439
- air flow patterns in the operating theatre 0-94440
- conference, Jerusalem, Israel (Aug. 1979) 0-98758
- conference, South Africa (Mar. 1979) 0-62366
- cyclotron, compact, clinical appl., isotope production (Japanese) 0-104757
- master's level graduate training in medical physics at the University of Colorado Health Sciences Center 0-82603
- nuclear medicine department, radiation safety 0-89868
- nuclear medicine laboratory, radiation safety 0-104772



## medicine continued

- radioactivity standards for medical use 0-67232  
 systems theory, importance and motivations (*Spanish*) 0-104549  
<sup>75</sup>Br, excitation functions for production, pot. nuclear medicine appls. 0-98135  
<sup>18</sup>F, prep. with an electron linear accelerator, medical and biological appls. 0-98136  
<sup>123</sup>I, prep. from gaseous TeF<sub>6</sub>, nuclear medicine appl. (*French*) 0-98137  
<sup>99m</sup>Tc generators, operational assessment by performance indices 0-94332

## Meissner effect

- SQUID, operating principles (*Hungarian*) 0-75686  
 superconductor Faraday effect obs. in polarising microscope 0-70892  
 (TMTSF)<sub>2</sub>PF<sub>6</sub>, quasi-dimens. cond., diamagnetic AC susceptibility 0-103781  
 CdS, flux exclusion, superconductivity at high temp. 0-97058  
 CeCu-Si<sub>2</sub>, collective phenomena 0-65933  
 Nb-V<sub>3</sub>Ga mixed state, Meissner effect investigation by muon method (*Russian*) 0-107954  
 NbSe<sub>2</sub>, CDW form., supercond. and Fermi surface determ., press. study 0-70891  
 Pb intermediate state, Meissner effect investigation by muon technique (*Russian*) 0-107954  
 V, small particles, crystal structure, magnetic and superconducting props. 0-97121

Meissner-Ochsenfeld effect *see* Meissner effect

## melting

- see also* melting point; zone melting  
 adsorbed film monolayer melting, dual symm. systems, periodic struct. (*Russian*) 0-107405  
 atomic and plastic crystals, melting transitions, thermodynamic props. 0-96452  
 benzene, phase transform. process, energy-dispersive X-ray diffractometry 0-96631  
 benzene adsorbed on graphite, melting and orientation, NMR study 0-100403  
 carbon tetrachloride, dual melting curves and metastability 0-92647  
 carbon tetrachloride, phase transform. process, energy-dispersive X-ray diffractometry 0-96631  
 cells, volumetric changes during freezing and thawing, thermodynamic model 0-108863  
 comet interiors, primordial radiogenic melting 0-67659  
 commensurate-incommensurate transition and melting in two-dimensions 0-75339  
 density changes during melting by X-ray absorption 0-103462  
 dislocation theory of melting 0-65198  
 dislocations and melting in two and three dimensions 0-103454  
 DNA derivate melting curves, automatic recorder using real time processing (*French*) 0-104833  
 Earth Mantle, partial melting, effect on elec. cond. 0-76936  
 education, Brownian motion, melting, surface tension and rubber networks, thermodynamic anal. 0-73132  
 entropy change on melting of simple substances, thermal expansion, configurational entropy 0-59630  
 fluorophosphate optical glass development 0-106588  
 glass, kinetic equation for interaction between grain material and liq. 0-84901  
 glass, melting in fire-heated tanks, modelling (*Polish*) 0-96633  
 glass, rare earth elements use as dopants (*Polish*) 0-97455  
 glass melting process model, for flameheated tank furnace melting (*Polish*) 0-70380  
 glass-metal composite, heat conduction, memory switching 0-96703  
 glassy alloy prod. using low temp. melt spinning device 0-100825  
 grain-boundary melting transition, in two-dimensional lattice-gas model 0-59634  
 hard sphere crystal, thermoelasticity in relation to melting 0-107353  
 heterogeneous system, US appl. to increase melting rate 0-74723  
 high-speed friction, intensity calc. 0-103416  
 ice, crystallisation and melting rate in laminar stream of liquid 0-100770  
 ice, upwelling in stratified ocean due to melting of glacier ice 0-81897  
 initial subcooling problems, heat balance integral appl. 0-96627  
 Invar, Fe-Ni (36 wt.%), alloy 36N, effect of melting conditions on thermal expansion coeff. 0-65256  
 ion impact induced shock processes in solids 0-89104  
 ionic salts, melting transition statistical model, dielectric const., surface tension 0-70378  
 laser annealing mechanisms, continuous and pulsed laser impact, melting 0-84964  
 lattice-gas model, modified, for gas-liquid-solid phase diagram 0-62591  
 liquid phase nuclei form. during bulk melting 0-88304  
 liquids, simple, corresponding states corrls. and triple point solid vol. 0-92649  
 metals, dislocations and shock compression, thermodynamics 0-100235  
 metals, EM levitation for melting without crucible (*Polish*) 0-89130  
 metals, melting temp., press. depend., vacancy mechanism 0-103460  
 metals, melting theory for small particles, Helmholtz free energy 0-59629  
 methane adsorbed submonolayer on graphite, structural transitions between epitaxially ordered phases 0-96740  
 minerals, dislocations and shock compression, thermodynamics 0-100235  
 molecular solids, melting curves, Lennard-Jones Devonshire theory 0-65201  
 monolayers, Lennard-Jones system, melting in external field 0-65362  
 multimode optical fibres, fusion splicing using gas flame heat source, development of splicing machine 0-102866  
 Nb, pure, production by cathodic reduction-electron beam melting combination method 0-89177  
 nonisothermal devitrification kinetics 0-92465  
 optical glass, melting, fining, surface tension, diffusion, nucleation in microgravity 0-81016  
 physisorbed monolayer on graphite, neutron scatt. studies 0-107655  
 polyethylene, flow-induced fibril form. from soln. 0-59402  
 polyethylene, low density, melting and crystallisation, DSC characterisation 0-64927  
 polyethylene, melt-crystallised fractions, surface and full-strand melting, small-angle X-ray scatt. obs. 0-84279  
 polyethylene fractions, quasi-binary systems, solidification and crystn. 0-84108  
 polyethylene melt, cryst. kinetics during cooling, nucleation density effect 0-100181

## melting continued

- polyethylene oxide-polystyrene-polyethylene oxide triblock copolymer, surface and full-strand melting, small-angle X-ray scatt. obs. 0-84279  
 polymer melting, theoretical aspects 0-59633  
 polymorphous material, Stefan problem, melting or freezing, interfacial boundaries 0-64350  
 radioactive waste, vitrification using in-can melting process 0-83204  
 radioactive waste immobilisation using continuous glass melter 0-83199  
 simple body melting time with convection boundary condition 0-99914  
 single crystal growth, techniques 0-108341  
 snow, melting prediction via radiometry in 3 to 60 mm wavelength region 0-72561  
 soft discs, two-dimens. melting, phase transition boundary 0-96629  
 solid-liquid interface free energy anisotropy clustering influence 0-80054  
 spherical solids melting in turbulent carrier fluid, deformation and breakup 0-92646  
 stainless steel, laser surface melting for corrosion protection 0-93698  
 steel, high speed, props. after electroslag remelting 0-104139  
 steel, high-strength tool steel D7KhFN, remelting effect on mech. props. 0-76284  
 steel, low C, HF oscillations during electron beam welding (*Russian*) 0-76273  
 steel, tool and high-speed, high freq. induction melting and centrifugal casting in instrumental anal. 0-84886  
 steel, W-Mo-Cr-V tool, laser surface melted, struct., heat treatment effect 0-76424  
 thermoelectric materials, B<sub>2</sub>C<sub>3</sub> and (B<sub>2</sub>Si)<sub>3</sub>C<sub>2</sub>, P-type LaS<sub>x</sub> N-type alloys, fabrication and thermoelectric props. 0-107771  
 thin absorbing films, laser-induced removal, two-phase mechanism 0-97384  
 Tokamak fusion test reactor, thermal response of first wall limiters 0-79585  
 two dimensional system, melting and condensation theory 0-57231  
 two-dimensional, dislocation-mediated theory predictions and consequences, light scatt. use as probe 0-92651  
 two-dimensional Lennard-Jones system, phase transitions, calc. 0-59621  
 Van der Waals film adsorbed on graphite, two-dimensional phase transitions 0-107653  
 vertical surface melting, heat transfer interferometric meas., convection effects 0-64339  
 Ag-Cu surface alloyed films, laser melt quenched, microstruct. 0-76423  
 Al, melting curve and Gruneisen coeff. at high press. 0-65200  
 Al<sub>2</sub>O<sub>3</sub>-Zr ceramic, elec. props., additives effect, and interaction with steel melt 0-104305  
 Al<sub>2</sub>O<sub>3</sub>-Y<sub>2</sub>O<sub>3</sub>, melting behaviour and metastability determ. by optical DTA 0-92648  
 Au, vacancy size effect, surface energy in small particles and bulk specimens 0-75223  
 Bi, effects of asymmetrical friction in piston-cylinder device on melting curve 0-86292  
 Bi, optical phonon anharmonicity and melting, light scatt. study 0-60621  
 Bi solid and liquid, positron annihilation temp. depend. 0-108296  
 Bi-Cd(Sn), eutectic, contact melting kinetics (*Russian*) 0-70377  
 C<sub>60</sub>(Eu)(Yb)(Ba) intercalation compounds, three dimensional continuous melting 0-59631  
 CdTe<sub>1-x</sub>Se<sub>x</sub>(Te<sub>4</sub>):Au, elec. cond., density, dielectric const., changes on fusion 0-88533  
 Cr, volt ampere characteristics during electron melting process (*Russian*) 0-75336  
 Cs, high press. melting curve maximum 0-75337  
 Eu, electrical resistivity of solid and liquid phases, thermopower, melting temp. 0-59955  
 Fe, EM levitation for melting without crucible (*Polish*) 0-89130  
 Fe meteorites of groups IAB and IIICD, origin by impact melting 0-109404  
 Fe, pure and alloyed, density and thermal expansion in liq. and solid states 0-96668  
 Fe, spreading behaviour of Al-Si melts 0-84345  
 Fe-Si, spreading behaviour of liq. Al 0-84345  
 Fe-Si system, melting equilibria study (*German*) 0-66473  
 Fe<sub>3</sub>Pt-Sn Invar alloy, Mossbauer shift temp. depend. 0-100626  
 Ga solid and liquid, positron annihilation temp. depend. 0-108296  
 GaAs, electrical conductivity and thermoelectric power charge due to melting 0-100490  
 Ge-Si, phase diagrams near melting point, Helmholtz free energy, heat of solution 0-70379  
 Ge-Si-S system, glass formation, transition temp., crystallisation and melting 0-100178  
 GeO<sub>2</sub> glass, nonisothermal devitrification kinetics 0-92465  
 GeSe<sub>2</sub>-As<sub>2</sub>Se<sub>3</sub>-Sb<sub>2</sub>Se<sub>3</sub>, elec. cond. over wide range of temp. 0-88564  
 He, room temp. melting at high-pressure 0-80025  
 He, sound transmission at liq. solid interface, probe of melting kinetics 0-92734  
<sup>3</sup>He, liq., polarisation effect on mag. ordering, melting curve 0-80021  
<sup>3</sup>He, solid, ordering obs. at melting press. in high mag. fields 0-84341  
<sup>3</sup>He, solid, spin ordered, melting press. and entropy 0-84340  
<sup>3</sup>He, solid-fluid, eqn. of state, melting props. under press. 0-96721  
<sup>3</sup>He, solid-superfluid interface, struct., surface tension 0-88380  
 HfC, pressing regime influence on high-temp. creep (*Russian*) 0-100852  
 Hg, melting line determ., pressures up to 1200 MPa 0-84281  
 In, effects of asymmetrical friction in piston-cylinder device on melting curve 0-86292  
 In, vacancy size effect, surface energy in small particles and bulk specimens 0-75223  
 InAs, electrical conductivity and thermoelectric power charge due to melting 0-100490  
 In<sub>2</sub>Bi, pre-melting absorption of sound 0-88277  
 KD<sub>2</sub>PO<sub>4</sub>, transparent dielec., thermal analysis of laser-induced damage 0-66336  
 KMg<sub>2</sub>LiSi<sub>4</sub>O<sub>10</sub>F<sub>2</sub>-NaMg<sub>2</sub>LiSi<sub>4</sub>O<sub>10</sub>F<sub>2</sub>, solid soln., solid solubility and swelling characts. 0-59660  
 K<sub>2</sub>O-PbO-SnO<sub>2</sub>, glass, effect of DC on corrosion of SnO<sub>2</sub> electrodes 0-85075  
 LiCl, microcrystal, melting, mol. dynamics simulation 0-65199  
 Mo, volt ampere characteristics during electron melting process (*Russian*) 0-75336  
 Mo-Al-Ge, phase equilibria, X-ray and microstructural anal. 0-93536  
 Mo<sub>2</sub>C<sub>2</sub>, pressing regime influence on high-temp. creep (*Russian*) 0-100852  
 Na, solid and liquid eqns. of state melting curve 0-103448



## melting continued

- NaF-SrF<sub>2</sub>-CrF<sub>3</sub> glass transition, crystn. and melting temps., optical transmission (*French*) 0-64910  
 Na<sub>2</sub>O-CaO-SiO<sub>2</sub> glass, redox phenomena evaluation in melting-fining process, SO<sub>2</sub> evolution 0-84900  
 Na<sub>2</sub>O-SiO<sub>2</sub> glass, bubble gas comp. change 0-79946  
 Na<sub>2</sub>O-SiO<sub>2</sub> glass, fusion process study, EMF meas. (*French*) 0-89190  
 Nb, volt ampere characteristics during electron melting process (*Russian*) 0-75336  
 NbC, pressing regime influence on high-temp. creep (*Russian*) 0-100852  
 Pb, changes in electron image contrast 0-100147  
 Pb, diffusion and saturation solubility of Pt, melting curve, conc. profiles 0-88365  
 Pd-Si, amorphous thin films, laser irradi., metastable phases 0-96622  
 Pt-Si, amorphous thin films, laser irradi., metastable phases 0-96622  
 R<sub>1</sub>-Co<sub>x</sub>, rare earth amorphous alloys, thermal stability, elec. cond. enthalpy 0-100172  
 Sb, optical phonon anharmonicity and melting, light scatt. study 0-60621  
 Se<sub>2</sub>O<sub>3</sub>, solid, enthalpy investig. at high temp. 0-103498  
 Si, amorphous and crystalline, heating by Q-switched laser radiation 0-84963  
 Si, impurity solubility limit after laser induced melting 0-107426  
 Si, ion implanted, self implanted, self annealing using high ion current density treatment 0-89254  
 Si, laser annealing mechanisms, disordered overlayers, crystalln. 0-84967  
 Si laser annealing of SiO<sub>2</sub> layers 0-97505  
 Si monocrystal peripheral fusion channelling under HF heating (*Russian*) 0-59627  
 Si:Sb vacuum deposited coating, p-n junction, pulsed electron beam annealing doping, diffusion 0-75480  
 Si:Te, laser melting, surface Te atom accumulation, profiles 0-100258  
 SiO<sub>2</sub>-Al<sub>2</sub>O<sub>3</sub>-CaO-BaO-SrO-ZnO-Na<sub>2</sub>O-K<sub>2</sub>O-B<sub>2</sub>O<sub>3</sub>, glaze effect of P<sub>2</sub>O<sub>5</sub> additions 0-60824  
 Ta(C,N)-Ni-VC, sintering behaviour, VC effect 0-93520  
 TaC, pressing regime influence on high-temp. creep (*Russian*) 0-100852  
 Te<sub>80</sub>Ge<sub>20</sub>-Sb<sub>x</sub>(Bi<sub>x</sub>), DSC studies of struct. phase transformation 0-66505  
 Ti<sub>3</sub>Te<sub>2</sub>-Ti<sub>4</sub>SnTe<sub>2</sub>-Ti<sub>4</sub>PbTe<sub>2</sub>, phase equilib., DTA, SPA and microhardness meas. 0-96628  
 V, volt ampere characteristics during electron melting process (*Russian*) 0-75336  
 W, volt ampere characteristics during electron melting process (*Russian*) 0-75336  
 Y, electrical resistivity of solid and liquid phases, thermopower, melting temp. 0-59955  
 YAlO<sub>3</sub>, melting behaviour and metastability determ. by optical DTA 0-92648  
 Zn, optical phonon anharmonicity and melting, light scatt. study 0-60621  
 ZrO<sub>2</sub> glass, melting depend. on minute components, surface crystallisation 0-84278

## melting point

- alkali halides, melting and boiling points vs. Coulomb pot., parabolic behaviour 0-70375  
 ceramics, lattice and grain boundary diffusion const., correls. 0-96679  
 disperse systems, solubility increase, phase composition, size effect calcs. 0-70418  
 F 0-100329  
 glass, melting in fire-heated tanks, modelling (*Polish*) 0-96633  
 ionic salts, melting transition statistical model, dielectric const., surface tension 0-70378  
 metal fixed points, limitations caused by trace impurities 0-105644  
 metals, entropies and heats of fusion 0-103458  
 metals, lattice and grain boundary diffusion const., correls. 0-96679  
 polyaryloxyphosphazene copolymers, thermal, morphological and rheological props. 0-103265  
 polydiphenylsiloxane, thermodynamics of fusion 0-84280  
 polyether-polyester elastomers, differential scanning calorimetry, crit. points (*Japanese*) 0-75344  
 polyethylene ribbons, flow-induced crystn. from melt, in dies fed by single screw extruder 0-84110  
 trans-1,4-polyisoprene crystals, press. effect on growth rate 0-88064  
 trans-1,4-polyisoprene crystals, press. effect on melting temp. and lamellar thickness, press. crystn. 0-88302  
 polymer films, Brillouin scatt. at transitions 0-70312  
 polypropylene, flow-induced crystn. from melt, in dies fed by single screw extruder 0-84110  
 rare earth germanates, R<sub>2</sub>O<sub>3</sub>-GeO<sub>2</sub> system cpds., physicochem. characts. 0-97469  
 rare earth oxyorthotitanates, crystallochem. classification 0-107142  
 transition metals, thermophysical data at high temps., submicrosecond-pulse-heating method 0-103459  
 Wigner solid, two-dimens., melting temp., quantum effects 0-88491  
 Wigner solid, two-dimens., melting temp. in strong mag. fields, quantum effects 0-88492  
 Al-Bi(Cd)(Pb)-Ti, containing low-melting pt. inclusions, mech. props. 0-93632  
 Au<sub>2</sub>P<sub>3</sub>, melting temp., Au<sub>2</sub>P<sub>3</sub>-Au eutectic temp. 0-59628  
 Ba, phase transitions under high press. 0-96641  
 Bi, Young's modulus and internal friction, 20°C to melting point (*Russian*) 0-89278  
 CaCeAl<sub>3</sub>O<sub>7</sub>, melilite struct., prep. and props. 0-93524  
 Cd, Young's modulus and internal friction, 20°C to melting point (*Russian*) 0-89278  
 Ce-In, phase equilibrium and cryst. struct. 0-66483  
 Ce-Ti, phase equilibrium and cryst. struct. 0-66483  
 CsSbF<sub>6</sub>, high press. phase relations, vibr. spectra, and cryst. chemistry 0-108200  
 Cu-Ni-Ti system, reactions with melt in Cu-rich region (*Japanese*) 0-89202  
 CuTiS, melting heat and melting entropy (*Russian*) 0-70374  
 D<sub>2</sub> 0-86338  
 D<sub>2</sub>, room temp. melting point, press. depend. calcs. 0-103463  
 Fe<sub>20</sub>Ni<sub>40</sub>P<sub>14</sub>B<sub>6</sub> glass, viscosity near T<sub>g</sub>, using rapid heating, and fusion characts. 0-70438  
 Ga, magnetic susceptibility near melting point 0-60186  
 H<sub>2</sub>, room temp. melting point, press. depend. calcs. 0-103463  
<sup>4</sup>He, room temp. melting point, press. depend. calcs. 0-103463  
<sup>4</sup>He, meas. using diamond-anvil cell 0-86338  
 Hf, liquid, viscosity at melting point, free energy (*Russian*) 0-92699

## melting point continued

- Hg-In (3, 15, 30, 45 at.%) amalgam, viscosity meas. near melting point 0-70441  
 I<sub>2</sub> liq., static structure factor, neutron diffraction 0-103236  
 K, liquid, interionic interaction theory, pseudopotential calcs. (*Russian*) 0-79675  
 KCl-CuCl eutectic fused salt, potential as intermediate temp. solar heat transfer and storage medium 0-101135  
 LiO<sub>2</sub>, melting point determ. for single crystal synthesis using vacuum fusion technique 0-71585  
 Li<sub>x+2</sub>P<sub>2</sub>O<sub>3x+1</sub>, polyphosphate, melting and crystallisation 0-70376  
 Li<sub>1+y</sub>Ta<sub>1-y</sub>Ti<sub>y</sub>O<sub>3</sub> (0≤y≤0.028), non-stoichiometric phase, crystallographic and dielec. props. 0-75212  
 Na liquid, interionic interaction theory, pseudopotential calcs. (*Russian*) 0-79675  
 Pb, ion bombardment-induced photon emission near melting point 0-100699  
 Pb, Young's modulus and internal friction, 20°C to melting point (*Russian*) 0-89278  
 Sm<sub>2</sub>O<sub>3</sub>-Ga<sub>2</sub>O<sub>3</sub> system, garnet-perovskite transform., phase diagram relationships 0-97460  
 Sm<sub>2</sub>O<sub>3</sub>-Ga<sub>2</sub>O<sub>3</sub> system, phase diagram relationships of garnet-perovskite transform. 0-97460  
 Sn, ion bombardment-induced photon emission near melting point 0-100699  
 Sn, Young's modulus and internal friction, 20°C to melting point (*Russian*) 0-89278  
 Sn-Te, molten, elec. cond. and phase diagram 0-84454  
 SrF<sub>2</sub>, vaporisation and sublimation thermodynamics (*German*) 0-81355  
 Th-based metal alloy fuels for FBRs, determ. of solidus temperature 0-104124  
 Ti, liquid, viscosity at melting point, free energy (*Russian*) 0-92699  
 UF<sub>4</sub>, vaporisation behaviour 0-84283  
 V, radiance temperature at melting point, surface roughness depend. 0-59683  
 YAG, melting behaviour and metastability determ. by optical DTA 0-92648  
 Zr, liquid, viscosity at melting point, free energy (*Russian*) 0-92699
- membranes**  
 see also biomembranes; lipid bilayers; osmosis  
 amperometric membrane probes for residual Cl determ. in saline cooling waters 0-82112  
 cable-band membrane, axisymmetric, interdependence between geometry and forces 0-96185  
 cellulose-acetate membrane, asymmetric, elec. and electroosmotic transport behaviour in dialysis-osmosis expts. 0-108745  
 cellulose acetate membrane, asymmetric, elec. and electroosmotic transport behaviour in hyperfiltration expts. 0-108746  
 cellulose diacetate membrane, diffusive permeability 0-104460  
 cellulose diacetate membranes, unilayer, transport phenomena, hydration and dialysis coeffs. 0-76556  
 chalcogenide ceramic membrane, Cu-selective electrode (*Chinese*) 0-81357  
 DECHEMA symposium, Tutzing, Germany, (Mar. 1978) 0-62373  
 dynamic response of a membrane with both curved and straight line boundaries 0-64440  
 filters as selective electrodes for synthetic penetrating ions 0-104821  
 hollow fibre dialyser, mass transfer 0-66873  
 hydrostatic pressure loaded membrane of revolution 0-64363  
 N-hydroxyethyl acrylamide-styrene(methyl methacrylate) copolymers, synthesis, anion active membrane transport appl. 0-61142  
 ion-exchange membrane, electroosmotic energy conversion efficiency 0-61430  
 ion-selective electrodes, Ag<sup>+</sup> and F<sup>-</sup> based ceramic materials appl. (*Japanese*) 0-61203  
 leaching from model porous bodies by reflection spectroscopy 0-100031  
 liquid membranes, emulsion-type, pertraction appls., comparison with double liq.-liq. extraction 0-66869  
 liquid membranes, separation and reaction appls. 0-66871  
 membrane surfaces, antibody association kinetics with spin-label haptens 0-66787  
 metallic, lifetime prediction and design 0-71752  
 metallic membrane interface, mass transfer 0-81366  
 Millipore-dioleophosphate model membrane, elec. current stimulus effects 0-67046  
 Nafion per fluorosulphonic acid ion exchange membranes, Mossbauer spectroscopy 0-80659  
 pH measurements using polarizable electrodes 0-76514  
 poly-N-vinylpyrrolidone-containing nonionisable membranes, equilib. props. struct. (*French*) 0-61138  
 polyester-hydrazide, aromatic, fibres and films, synthesis and props. (*Japanese*) 0-108387  
 polymeric film, variable-shape solar energy concentrator appl. 0-76645  
 preparative scale thin-film dialysis apparatus 0-101296  
 PTFE grafted membranes, struct.-properties relationships, bifunctionality (*French*) 0-61137  
 PTFE grafted membranes, struct.-properties relationships (*French*) 0-61136  
 PTFE grafted membranes, struct.-properties relationships for poly-N-vinylpyrrolidone-containing membranes (*French*) 0-61138  
 quantum model for transport through membranes 0-93796  
 ring, polymer, physical props, meas. and control appl. (*Slovak*) 0-61141  
 stability of nonlinear oscillations from Liapunov method 0-96212  
 steel, bimetal, alloy with austenitic stainless, H permeability 0-107572  
 strong acid types, with enhanced hydrophilicity 0-66872  
 surface water continuous analysis by NH<sub>4</sub><sup>+</sup>-sensitive plastic membrane electrode 0-89701  
 vibrating membrane speckle pattern analysis 0-106769  
 Nb, membrane, H permeation (*Japanese*) 0-100363  
 Pd, diffusion-cell for separation H<sub>2</sub> containing mixtures, solar furnace appl. 0-92245  
 Pd membrane, H atom interaction, superpermeability 0-81365  
 Pd, sorption of H<sub>2</sub>, adhesion and penetration probabilities, extreme values 0-101040  
 Sb<sub>2</sub>O<sub>3</sub>-nH<sub>2</sub>O acid membranes, synthesis and characterisation 0-81027

memories see digital storage

memory devices see storage devices

mendelevium

see also nuclei with .....

No entries



**mendelevium compounds**

No entries

**mercury (metal)**

see also nuclei with .....

adsorbed on W, thermal desorption kinetics, theory 0-59792  
 air-Hg flow, stratified, co-current, in rectangular channel, interfacial wave structure 0-74955  
 atom, 5d level open shell interactions, 304 Å photoelectron spectrum 0-87087  
 atom, <sup>199</sup>S, <sup>199</sup>P, <sup>199</sup>P states, dipole polarisabilities from compact variational trial functions 0-63568  
 atom, bright field image, on C support film, signal-to-noise enhancement by incoherent superposition 0-101906  
 atom, electron elastic scattering, 8 to 18 eV, electron spin polaris. 0-91669  
 atom, electron resonant elastic and inelastic scatt. (Russian) 0-78710  
 atom, Hanle resonance in radio-frequency fields 0-91508  
 atom, positron scatt. at low energy 0-91670  
 atom, two photon excitation, time resolved spectroscopy 0-87075  
 atoms, elastic electron scatt., relativistic effects 0-102568  
 atoms, electron binding energy and shift, core level XPS 0-87088  
 clusters in NaA neolyte, transition to paramagnetic state due to mag. field (Russian) 0-60183  
 condensation, two-dimensional, on W 0-107666  
 contact potential and charge exchange meas., at Hg-polymer interface 0-75642  
 discharge, high-pressure, NaI and TlI additives, line broadening and radiative transport 0-74199  
 discharge, low-freq. oscillation spectrum in weakly ionised plasma 0-87885  
 electric field gradients at different Be lattice sites, gamma-spectral study 0-80224  
 flow in curved channels under transverse mag. field, transition and turbulent flows 0-79396  
 gravity fed heat pipe for production of high purity fixed density of Hg atoms 0-69627  
 Laccadive Sea waters, total Hg concs. 0-104996  
 liquid, quadrupole relaxation rate temp. depend 0-88884  
 liquid, thermoelectric power, pseudopotential calc. 0-59959  
 liquid metal, electronic density of states, pseudopotential calcs. 0-70578  
 loss rate from contaminated estuarine sediments 0-85310  
 melting line, pressures up to 1200 MPa 0-84281  
 MHD duct flow, hot-film probe vel. meas. 0-75009  
 MHD laminar flow, longitudinal dynamic effects determination for Hg (Rumanian) 0-64792  
 optical properties by spectroscopic ellipsometry, review 0-103929  
 plasma, dense weakly ionised, thermo EMF, calc. 0-64686  
 positive column, electron energy distrib., numerical soln. of Boltzmann eqn. 0-87982  
 quadrupole interactions in Zn, lattice location, gamma spectral study 0-80227  
 reflection spectra, electronic density of states, calc. 0-66229  
 relaxation time constants meas. of optically pumped stored Hg ions 0-106287  
 solid, resistivity ratio, 1.65 to 234K 0-59952  
 static drop electrode, voltammetry appls. 0-97740  
 superconducting film, far IR and electrodynamic prop. meas. 0-103957  
 supercritical, elec. cond., four electrode method 0-62685  
 surface tension and width, density functional theory 0-103537  
 ultrathin metallic filaments, appearance of dielec. instability, coexistence with supercond. 0-103784  
 vapour, electron drift velocity at 573K 0-103103  
 vapour, electron momentum transfer cross section, from 0.1-5 eV 0-103104  
 vapour, line splitting on Tonks-Dattner reson. 0-59317  
 vapour, resonance line shape in presence of Hg(6<sup>3</sup>P<sub>1</sub>)-Hg(6<sup>1</sup>S<sub>0</sub>) interactions 0-78572  
 vapour discharges, high-press., e-beam initiated, laser absorpt. meas. 0-92412  
 vapour drag effect, McLeod gauge, capillary depression phenomena 0-98923  
 wetted reed switch, heat treatment variations effects on Fe-Ni alloys surface conditions and on switch behaviour 0-66547  
 wetting of GaAs surface, doping degree influence 0-92762  
 X-ray microanalysis, quantification of losses 0-85261  
 Ar-Hg-Cl<sub>2</sub>, elec. discharge, electron inelastic collision props. 0-79617  
 atom, resonance line, 253.7 nm for atomic absorpt. meas. 0-78556  
 Ge:Hg, impurity characterisation from thermal carrier meas. 0-65595  
 Ge:Hg, Sb, photoelec. props., 70 to 300K 0-65621  
 p-Ge:Hg, Au, Sb, radiation-defect form., Au influence 0-92911  
 He-Hg nuclear pumped laser, charge excitation pumping 0-63996  
 Hg II, 6p<sup>2</sup> and 6p<sup>1</sup>D levels, radiative lifetimes meas. 0-78576  
 Hg II line oscillator strength determ. in A-type stars, diffusion model implications 0-72966  
<sup>199</sup>Hg, 6<sup>1</sup>S<sub>0</sub>-6<sup>3</sup>P<sub>0</sub> forbidden transition absorpt. at 265.6 nm, A coeff. and self-press. broadening determ. 0-95562  
 Hg-InP Schottky-barrier diode, contact times, I-V characts. 0-96971  
 Hg-Tl-I discharges, 50 Hz, axial segregation effect on elec. field strength 0-59320  
 Hg-Xe vapour deposited films, cond. transitions, effect of disorder on supercond. 0-88659  
 Hg+benzene electronically excited, mol. fluoresc., vibr. relax. cross sections and equilibration rates determ. 0-87205  
 Hg+Cl<sub>2</sub>+hν→HgCl<sup>+</sup>+Cl, laser-induced harpooning reactions 0-83458  
 Hg+H<sub>2</sub>(CO)(NH<sub>2</sub>)<sub>2</sub>(ethylene), quenching rate constants determ. with nanosecond light pulser with Hg vapour 0-100111  
 Hg<sub>1-x</sub>Cd<sub>x</sub>Te:Hg, ion implanted, damage and lattice location study 0-103381  
 HgMn stars, evidence for Hg in thin atmospheric layer rel. to diffusion model 0-105243  
<sup>199</sup>Hg, atom-surface interaction, nucl. relax., temp. depend. 0-88886  
 Hg(6<sup>3</sup>P<sub>0</sub>)+Hg(6<sup>1</sup>P<sub>2</sub>), line excitation and population decay in afterglow 0-74242  
 Na-Hg high-press. discharge, Na reson. radiation, self-reversed maxima shifts 0-92411  
 Tl-Hg, excimer band emission from electron beam initiated discharge in TlI-Hg 0-78841

**Mercury (planet)**

cratered surface entropy 0-101541  
 exosphere simulation, Monte Carlo methods 0-67588

**Mercury (planet) continued**

exosphere simulation, Monte Carlo methods 0-67589  
 micrometeorite impact, ion emission 0-77362  
 morphological features of crust from Mariner 10 obs. 0-67603  
 plain formation, tectonic implications 0-101542  
 Hg II 3984 Å, variation during eclipse in eclipsing binary Hg star AR Aurigae 0-98679

**mercury alloys**

see also mercury compounds

Dispersalloy, Sn-Hg amalgam, γ<sub>2</sub> precip. suppression and gettering kinetics 0-71651  
 CdHg, ω phase, mag. susceptibility anisotropy w.r.t. uniform compression (Russian) 0-71143  
 Hg-In (3, 15, 30, 45 at.%) amalgam, viscosity meas. near melting point 0-70441  
 Hg-Tl, phase limits, determ. by enthalpy functions along liquidus (French) 0-84911  
 Hg-Tl amalgam, viscosity meas. 0-88349  
 Hg<sub>1-x</sub>Zn<sub>x</sub>Cr<sub>2</sub>Se<sub>4</sub>, magnetic struct., neutronographic and mag. investigation (Russian) 0-88726

**mercury compounds**

see also mercury alloys

benzyl mercury chloride, cryst. struct. and absorpt. calcs. 0-84166  
 eutectics, HgTe-PbTe and Au-PbTe, prep. and thermoelectric behaviour characts. 0-107774  
 HgCdTe/CdTe, limited diffusion volume photodiode, characterisation 0-75627  
 (Cd,Hg)Te epitaxial structures, comp. profile depend. on deposition parameters 0-100795  
 Cd<sub>1-x</sub>Hg<sub>x</sub>Te, elec. characts., impurity effects 0-92890  
 Cd<sub>1-x</sub>Hg<sub>x</sub>Se<sub>2</sub>S<sub>4</sub> solid solns., band structure, behaviour w.r.t. comp. (French) 0-107699  
 Cd<sub>1-x</sub>Hg<sub>x</sub>Se, phase transition and elastic const., US vel. study 0-75354  
 CdHgTe, anomalous avalanche breakdown 0-80284  
 CdHgTe photoelectromagnetic detector for 10.6 μm radiation, non-cooled, performance 0-82818  
 Cd<sub>0.175</sub>Hg<sub>0.825</sub>Te-Au(In) contacts, photo-effect in the 77-300K range, barrier height estimation 0-107850  
 Cd<sub>0.8</sub>Hg<sub>0.2</sub>Te, ion implantation doping for realisation of IR detectors, responsivity meas., ion range straggling 0-73452  
 Cd<sub>0.2</sub>Hg<sub>0.8</sub>Te recrystallisation for supercooled IR detector production (German) 0-86403  
 n-Cd<sub>0.2</sub>Hg<sub>0.75</sub>Te, excess generation-recombination noise 0-107880  
 n-Cd<sub>0.3</sub>Hg<sub>0.7</sub>Te, photoelec. props. at 78K, relax. time, minority carrier extraction 0-107864  
 Cd<sub>1-x</sub>Hg<sub>x</sub>Te, carrier lifetime, effect of comp. fluctuations and second-phase inclusions 0-80294  
 n-Cd<sub>1-x</sub>Hg<sub>x</sub>Te crystals, carrier recomb. in extrinsic conduction range 0-70722  
 Cd<sub>1-x</sub>Hg<sub>x</sub>Te crystals, donor compensation, low temp. cond. study 0-75571  
 Cd<sub>1-x</sub>Hg<sub>x</sub>Te, dislocation motion, effect of lattice defects on microhardness (Russian) 0-70220  
 Cd<sub>1-x</sub>Hg<sub>x</sub>Te epitaxial graded gap layers, plasma reflection and magnetoreflection 0-71391  
 Cd<sub>1-x</sub>Hg<sub>x</sub>Te, epitaxial growth from stoichiometric melt, crystn. and diffusion 0-75475  
 Cd<sub>1-x</sub>Hg<sub>x</sub>Te, epitaxial layer p-n junction, current-voltage characteristics of photovoltaic detectors, 1 to 15 μm 0-86407  
 Cd<sub>1-x</sub>Hg<sub>x</sub>Te films, growth by cathodic sputtering in Hg vapour plasma 0-97431  
 Cd<sub>1-x</sub>Hg<sub>x</sub>Te, graded gap epitaxial layers, spectral characts. of photoelectromagnetic effect 0-60022  
 Cd<sub>1-x</sub>Hg<sub>x</sub>Te, graded-gap layers, galvanomag. props. at low temp. and in weak mag. field 0-75664  
 Cd<sub>1-x</sub>Hg<sub>x</sub>Te layers, epitaxial graded-gap, nonlinear elec. effects 0-100468  
 Cd<sub>1-x</sub>Hg<sub>x</sub>Te, long term stability at 300K, rel. to device appl. 0-59978  
 n-Cd<sub>1-x</sub>Hg<sub>x</sub>Te, recombination due to surface excitation, photoconductivity, impurity states (Russian) 0-60042  
 Cd<sub>1-x</sub>Hg<sub>x</sub>Te, tunnelling effect in p-n junctions 0-75630  
 Cd<sub>1-x</sub>Hg<sub>x</sub>Te, vacancy electron states, acceptor behaviour, electron mobility 0-70193  
 CdTe/Hg<sub>1-x</sub>Cd<sub>x</sub>Te multilayers, LPE growth 0-80104  
 CdTe-HgTe superlattice on CdTe layers, evanescent states, tight binding calcs. 0-70611  
 Hg complex, DNA-Hg (II) in soln., theoret. interpret. of elec. dichroism obs. 0-85347  
 Hg complex, methylethynylmercury(II)-(d<sub>1</sub>-d<sub>3</sub>-d<sub>4</sub>), vibr. spectra and normal coord. calcs. 0-58259  
 Hg<sub>1-x</sub>AsF<sub>6</sub>, incommensurate crystal phases symmetry, incommensurate basic struct., superspace group approach 0-79727  
 Hg<sub>1-x</sub>AsF<sub>6</sub>, one-dimens. lattice dynamics, X-ray scatt. study 0-75317  
 HgBi<sub>2</sub>S<sub>4</sub>, X-ray cryst. struct. determ., rel. with pavonite homologous series 0-92487  
 HgBr+O<sub>2</sub>(N<sub>2</sub>)(H<sub>2</sub>)(He)(Ne)(Ar)(Kr)(Xe), vibr. relax., rate coeffs., fluoresc. obs. 0-63697  
 HgBr<sub>2</sub>, electronic struct. and photodissoc., effective core pots. and POL(1) CI wave function 0-63560  
 HgBr<sub>2</sub>, photofragment fluoresc. polarisation, press. depend. 0-63720  
 HgBr<sub>2</sub>, vac. UV absorpt. cross section 0-91574  
 HgBr<sub>2</sub>+inert gas metastable atom (N<sub>2</sub>(A<sup>3</sup>Σ<sub>u</sub><sup>+</sup>)), dissoci. excitation 0-63774  
 HgBr<sub>2</sub>+N<sub>2</sub><sup>\*</sup>, dissociative excitation, mol. fluoresc. obs. 0-91634  
 Hg<sub>2</sub>Br<sub>2</sub>, nonintrinsic ferroelastic, thermal expansion and thermodynamic potential 0-88344  
 Hg(CN)<sub>2</sub>, phonon freq. anomalous press. depend., mol. struct. distortion 0-88981  
 Hg(CN)<sub>2</sub><sup>-</sup> ion, CN and HgC stretching vibrations and HgCN bending vibration assignments 0-69140  
 HgCdTe, ion implantation, junction form. 0-100260  
 HgCdTe photodiodes formed by double-layer LPE 0-104078  
 HgCdTe reverse-biased photodiodes for wideband appls., excess noise 0-107876  
 HgCdTe solid solution photodiode for CO<sub>2</sub> laser active medium study 0-95868  
 HgCdTe-CdTe photodiode, 1.33 μm, grown by LPE, phys. props. 0-107892  
 Hg<sub>0.6</sub>Cd<sub>0.4</sub>Te LPE layer growth from Te-, Hg-, and HgTe-rich solns., comparison 0-76199



## mercury compounds continued

- (Hg<sub>0.6</sub>Cd<sub>0.4</sub>)<sub>1-x</sub>Te<sub>x</sub>, defect anal., intrinsic material parameters 0-75519  
 Hg<sub>0.74</sub>Cd<sub>0.26</sub>Te thin film deposition on Si substrates by RF triode-sputtering, large-area photodetector arrays 0-80965  
 Hg<sub>0.77</sub>Cd<sub>0.23</sub>Te nonlinear optical IR generation 0-58642  
 Hg<sub>0.8</sub>Cd<sub>0.2</sub>Te surface, sputter cleaning and dry oxidation, XPS and LEED study 0-108618  
 Hg<sub>0.82</sub>Cd<sub>0.18</sub>Te, electronic anomalous mass near reson. acceptor level, Shubnikov-de Haas meas. 0-80163  
 Hg<sub>1-x</sub>Cd<sub>x</sub>Te breakdown-limited MIS device, increased charge capacity using ramped gate voltage 0-103751  
 Hg<sub>1-x</sub>Cd<sub>x</sub>Te, degenerate four-wave mixing of 10.6  $\mu$ m radiation 0-95943  
 Hg<sub>1-x</sub>Cd<sub>x</sub>Te, Einstein relation for inversion layers 0-103706  
 Hg<sub>1-x</sub>Cd<sub>x</sub>Te, epitaxial layers, elec. properties in the range 4.2 to 300K (French) 0-65721  
 Hg<sub>1-x</sub>Cd<sub>x</sub>Te epitaxial layers, elec. props. 0-96910  
 Hg<sub>1-x</sub>Cd<sub>x</sub>Te, grown from melt, Kirkendall and Frenkel effects 0-100365  
 Hg<sub>1-x</sub>Cd<sub>x</sub>Te hot-electron photoconductive detection of near mm wave radiation 0-57377  
 Hg<sub>1-x</sub>Cd<sub>x</sub>Te, implanted with Hg, Al, damage and lattice location study 0-103381  
 Hg<sub>1-x</sub>Cd<sub>x</sub>Te, near band-gap photoluminesc., bound exciton luminesc. obs. 0-103973  
 Hg<sub>1-x</sub>Cd<sub>x</sub>Te, optical absorpt., quasilocal acceptor level effects, theory 0-92853  
 n-Hg<sub>1-x</sub>Cd<sub>x</sub>Te, optical phase conjugation 0-83644  
 Hg<sub>1-x</sub>Cd<sub>x</sub>Te photodiodes, long cutoff wavelength, effect of trap tunnelling on IR detector performance 0-73451  
 Hg<sub>1-x</sub>Cd<sub>x</sub>Te, recombination processes using impact ionization capture cross sections 0-75577  
 Hg<sub>1-x</sub>Cd<sub>x</sub>Te, segregation, compositional characterisation 0-107434  
 Hg<sub>1-x</sub>Cd<sub>x</sub>Te, semimetallic and semicond., Hall coeff., anomalous temp. depend., 4.2 to 70K 0-65604  
 Hg<sub>1-x</sub>Cd<sub>x</sub>Te, theory of optical absorpt., contribution by quasilocal acceptor levels (Russian) 0-71451  
 Hg<sub>1-x</sub>Cd<sub>x</sub>Te-In contact, diffusion of In 0-103520  
 Hg<sub>1-x</sub>Cd<sub>x</sub>Te-type semimetals, kinetic props., local acceptor level effects 0-65557  
 HgCl<sub>2</sub>, electronic struct. and photodissoc., effective core pots. and POL(1) CI wave function 0-63560  
 HgCl<sub>2</sub>, NQR freq., intermol. force effect 0-66065  
 HgCl<sub>2</sub>, vac. UV absorpt. cross section 0-91574  
 HgCl<sub>2</sub>, X-ray cryst. struct. redeterm. and refinement 0-107140  
 HgCl<sub>2</sub>, Zeeman NQR spectra obs. asymmetry parameters 0-80634  
 HgCl<sub>2</sub>, neutron and Raman scatt. studies, ferroelastic transitions 0-76015  
 Hg<sub>2</sub>Cl<sub>2</sub>, p-T phase diagram, pressure effect on phase transition 0-107370  
 HgCr<sub>2-x</sub>Al<sub>x</sub>Se<sub>4</sub> and HgCr<sub>2-x</sub>Ga<sub>x</sub>Se<sub>4</sub>, temp. depend. of ESR linewidth, 105-300K 0-71161  
 HgCr<sub>2</sub>Se<sub>4</sub>, cooling efficiency near 60K as mag. refrigerant 0-71034  
 HgCr<sub>2</sub>Se<sub>4-x</sub>Te<sub>x</sub>, ferromag. semicond., zero bandgap transition 0-96783  
 HgCr<sub>2</sub>Se<sub>4</sub>, electronic props. rel. to departure from stoichiometry 0-100472  
 HgCr<sub>2</sub>Se<sub>4</sub>, n-type ferromag. semicond., galvanomagnetic props. 0-70727  
 HgCr<sub>2</sub>Se<sub>4</sub>, spontaneous magnetisation temp. depend., nuclear resonance freq. depend. (French) 0-80483  
 HgCr<sub>2</sub>Se<sub>4</sub>, thermoreflectance, photoconductance, Raman scattering near magnetic phase transition 0-97298  
 HgF<sub>2</sub>(FCl)(FBr), matrix isolated IR and Raman spectra, assignments, force consts., isotope effects and thermodynamic props. 0-63631  
 Hg<sub>1-x</sub>Fe<sub>x</sub>Te, struct. invest. using X-ray diffr. and electron microscopy 0-75365  
 HgH, two-level laser system, discharge simulations 0-74351  
 HgI<sub>2</sub>, detectors for X-ray 0-89837  
 HgI<sub>2</sub>, IR lattice vibr. and dielec. dispersion 0-76018  
 HgI<sub>2</sub>, soln. grown crystals, low-energy gamma-ray cond. type detectors 0-97418  
 HgI<sub>2</sub>, vac. UV absorpt. cross section 0-91574  
 HgI<sub>2</sub>CdS binder layer photoreceptor, surface charge characts. thickness depend. 0-57409  
 Hg<sub>1-x</sub>Mn<sub>x</sub>Te, indirect exchange interaction 0-97087  
 Hg<sub>1-x</sub>Mn<sub>x</sub>Te, non-parabolic zero-gap semicond., indirect exchange interaction 0-80498  
 Hg<sub>1-x</sub>Mn<sub>x</sub>Te, semimagnetic, exchange interactions between localised and delocalised electrons 0-97245  
 Hg<sub>1-x</sub>Mn<sub>x</sub>Te, transverse magnetoresistance in quantised mag. fields 0-96922  
 Hg<sub>2</sub>Mo<sub>6</sub>S<sub>8</sub> Chevrel phase, synthesis, stability and characts. 0-71608  
 HgS, electrodeposition, using nonaqueous solvents 0-76200  
 $\alpha$ -HgS films, sputter-deposited in Hg vapour, growth and props. 0-75467  
 $\alpha$ -HgS, gas-phase and solid-state Hg 5d photoionisation processes, direct comparison 0-76149  
 HgS, habit variation of crystals of the C3<sub>2</sub>-C3<sub>2</sub> space group 0-107090  
 $\alpha$ -HgS, trapping parameters determ. by TSC meas. 0-59997  
 HgSe, band struct. and spin splitting Shubnikov de Haas study 0-65445  
 HgSe, elec. resist., high press. phase transform., band gap 0-70707  
 HgSe film, anomalous photocond., electron microscope study 0-65623  
 HgSe, interband  $\Gamma_6-\Gamma_8$  magnetoabsorption, temp. study 0-76032  
 HgSe, two-phonon resonant effect, far-infrared reflectivity 0-108203  
 HgSe:Mn<sup>2+</sup>, temp. depend. of EPR of <sup>5</sup>S state ions 0-80593  
 HgTe, 1.5 to 30K, thermal expansion and heat capacity meas. 0-59681  
 HgTe, energy bands and optical props. calcs., tight-bonding model with spin-orbit interaction 0-65448  
 HgTe, growth of epitaxial layers, activation by UV and IR radiation 0-71598  
 HgTe,  $\Gamma_8$  symm. acceptor centre hole mag. props. (Russian) 0-88733  
 HgTe, mobility of electrons and holes, 4 to 100K 0-107821  
 HgTe, phonon dispersion relations, neutron study 0-70340  
 HgTe surface, sputter cleaning and dry oxidation, XPS and LEED study 0-108618  
 HgTe, vacancy electron states, acceptor behaviour, electron mobility 0-70193  
 HgTl excimer laser, kinetics, optical excitation obs. 0-58527  
 HgX<sub>2</sub>+N<sub>2</sub>, A<sup>2</sup> $\Sigma_u^+$  state quenching obs. 0-108693  
<sup>199</sup>HgCl<sub>2</sub>, renal uptake meas., single tracer method for background subtraction 0-67217  
 K<sub>2</sub>Hg(CN)<sub>4</sub>, third order elastic consts. 0-84231  
 Pb<sub>1-x</sub>Hg<sub>x</sub>Si heterojunctions, elect. props. 0-100513  
 Pb<sub>0.97</sub>Hg<sub>0.03</sub>Te photovoltaic detector produced by Sb<sup>+</sup> ion implantation 0-82821

## mercury compounds continued

- Zn<sub>1-x</sub>Hg<sub>x</sub>Se, current carrier scattering mechanism 0-65546  
 Zn<sub>1-x</sub>Hg<sub>x</sub>Te, vacancy electron states, acceptor behaviour, electron mobility 0-70193  
**mercury lamps** see *mercury vapour lamps*  
**mercury vapour lamps**  
 dark film anal. in RF-excited lamps 0-92789  
 luminous colour control methods in pulsed arc discharges in Ne-Hg lamps (Japanese) 0-103214  
 nanosecond light pulser with Hg vapour, quenching rate constants determ. 0-100111  
 rapid-scan polarising Michelson interferometer and InSb detector calibration 0-59305  
 spectral power, appl. of microprocessor-controlled apparatus for pulsed spectra meas. 0-68261  
 Hg discharge, high-pressure, NaI and TlI additives, line broadening and radiative transport 0-74199  
**m.s.f.e.t.** see *Schottky gate field effect transistors*  
**mesic atoms**  
 atomic capture, mesic and muonic X-ray intensities effect, allotropic effect, relative capture rates 0-69277  
 deformed nuclei, absorption of slow  $\pi^-$ , mesic atoms 0-78321  
 exotic atoms, conf., Erice, Sicily, (1979) 0-67939  
 formation in mixtures of lightest elements 0-87252  
 kaon-nucleus reactions, low energy, nuclear density shape optical pot. kaonic atom level shifts 0-63213  
 kaonic atoms, quadrupole hyperfine structure 0-78726  
 negative mesons in H, atomic capture 0-69276  
 pionic atoms, Auger electron emission from C, N, O, Ag, Br (Russian) 0-69271  
 pionic atoms, electron screening and inner shell refilling, X-ray 0-78729  
 pionic atoms, quadrupole hyperfine structure 0-78726  
 prompt fission internal  $\gamma$ -ray conversion, fragment radiative transitions (Russian) 0-86944  
 K<sup>+</sup> p atom and  $\Lambda(1405)$ , KN interaction model 0-68479  
 $\pi$ -atomic states in  $\Lambda=12.52$ , nuclear structure influence, doorway processes 0-99588  
 $\pi^+$ He, liquid, K X-ray transition energies and Lorentzian widths 0-78727  
 H, atomic X-ray yields 1s and 2p level shifts and widths, cascades, calc. 0-78730  
<sup>1</sup>H, pionic, pion mass high accuracy meas. from transitions 0-106406  
 Ti, pionic, pion mass high accuracy meas. from transitions 0-106406  
**mesic molecules**  
 exotic atoms, conf., Erice, Sicily, (1979) 0-67939  
 hydrogenic mesomolecules and muon catalysed fusion 0-68719  
 mixtures, atomic capture prediction model 0-69277  
**mesomorphic state** see *liquid crystals*  
**meson absorption**  
 total pion absorption cross section, A depend., proton yields 0-106081  
 ( $\pi^+$ , X), absorption cross section in range 20 to 280 MeV for Al, Ti, Cu, Sn, Au nuclei 0-78327  
<sup>197</sup>Au( $\pi^-$ , X), X=d,t, <sup>3</sup>He, <sup>4</sup>He, particle emission following stopped pion absorption 0-91196  
<sup>59</sup>Co( $\pi^-$ , X), X=d,t, <sup>3</sup>He, <sup>4</sup>He, particle emission following stopped pion absorption 0-91196  
**meson-baryon interactions**  
 see also *kaon-baryon interactions; meson-baryon scattering; pion-baryon interactions*  
 N+vector meson, polarised deep inelastic collisions in nuclei (Russian) 0-102209  
**meson-baryon scattering**  
 see also *kaon-baryon scattering; meson-baryon interactions; pion-baryon scattering*  
 charmed particles, hadronic props., superconvergence sum rules 0-78043  
 large angle elastic scatt. calcs. 0-83002  
 resonance vertex functions and scatt. amplitudes resonance-nucleon scatt. p rescatt. (Russian) 0-105918  
 K<sup>+</sup>N, 70, 125, 175 GeV/c in Be, C, Al, Cu, Sn, Pb nuclei 0-83128  
 $\pi^+$ N, 70, 125, 175 GeV/c in Be, C, Al, Cu, Sn, Pb nuclei 0-83128  
**meson capture**  
 see also *mesic atoms; mesic molecules; radioactivity*  
 atomic capture, mesic and muonic X-ray intensities effect, allotropic effect, relative capture rates 0-69277  
 exotic atoms, conf., Erice, Sicily, (1979) 0-67939  
 ( $\pi^-$ , X), n and charged particle emission following  $\pi^-$  capture 0-73867  
 ( $\pi^+$ , X), 85 to 245 MeV, capture cross sections for Li, C, Al, Fe, Nb, Bi 0-73869  
**meson decay**  
 see also *kaon decay; meson hadronic decay; meson leptonic decay; pion decay*  
 bottom mesons, weak decays, strong correction meas. 0-82970  
 charmed mesons, lifetime measurement 0-73693  
 charmed mesons, semileptonic decays, charged weak current struct. 0-102042  
 charmonium decay, effective strong coupling constant for timelike Q<sup>2</sup> 0-99091  
 charmonium electromagnetic decay, relativistic eval. 0-68459  
 gluon and quark jets in a recursive model motivated by quantum chromodynamics, T decay 0-62936  
 heavy meson inclusive semileptonic decays, lifetime estimates, quark-parton model difficulties 0-86704  
 heavy meson weak decays, heavy quark decay, QCD corrections, real gluon role 0-57586  
 heavy quarkonium states, decay rate to lepton pairs, gluonic corrections 0-102043  
 light meson radiative decay, Zweig law (Russian) 0-102051  
 multi-channel baryonium and some peculiarities of its decays (Russian) 0-105857  
 neutral pseudoscalar meson radiative decays, K<sub>14</sub> decay in chiral quark model (Russian) 0-105900  
 perturbative QCD, renormalisation improvement, charmonium decay and scaling violations 0-101993  
 photocoupling in quark model 0-82954  
 QCD low energy tests, gluon non-zero effective mass,  $\psi$  decays 0-91054  
 tensor meson radiative decay in SU(6) $\times$ O(3) broken symmetry quark model 0-73710  
 top mesons, weak decays, strong correction meas. 0-82970  
 vector meson radiative decays, SU(3) symmetry viewpoint 0-95273  
 vector mesons, EM decay in broken SU(3) 0-82976



**meson decay continued**

- vector mesons, radiative decay, single parameter scheme 0-86720
- B meson, cascade decays, CP nonconservation 0-105811
- bb meson state lifetimes, R predictions above bottom threshold, quark model 0-99097
- $\bar{c}c$  qq states, decay, hadronic and photo-prod.,  $e^+e^-$  annihilation prod. 0-99092
- $\chi \rightarrow \psi\gamma$ , charmonium E1 radiative transitions and quark mag. moments 0-86721
- D $\rightarrow K^*\nu$ , charm-changing weak hadronic current, models 0-57585
- D-meson, charged Higgs boson couplings 0-62917
- D<sup>0</sup> lifetime difference from D<sup>+</sup> 0-91084
- $e^+e^- \rightarrow \gamma\gamma$ , 9.4-31.6 GeV, differential cross section,  $T \rightarrow \gamma\gamma$  decay limits 0-91073
- $e^+e^-$  initiated  $\gamma\gamma$  processes, charged pair prod.,  $f^0 \rightarrow \gamma\gamma$  width 0-91123
- $e^+e^- \rightarrow O$  particle, decay, mass, prod. from Zweig rule intermediate vector particle model (Chinese) 0-73697
- $\eta(\eta') \rightarrow \gamma\gamma$ , quark model tests 0-78067
- $\pi^- p \rightarrow \eta(\eta')n$ , 8.45 GeV/c, differential cross section ratio,  $\eta'$  decay branching 0-78094
- $\psi \rightarrow \eta(\eta')\gamma$ , quark model tests 0-78067
- $\psi' \rightarrow \chi\gamma$ , charmonium E1 radiative transitions and quark mag. moments 0-86721
- $\sigma \rightarrow 2\gamma$ , tensor-trace and triangle anomalies 0-73709
- T, production and decay in quark fusion model 0-102018
- pN, 350 GeV in Ne, D<sup>2</sup> prod. cross section and lifetime 0-68494

**meson detection and measurement**

No entries

**meson-deuteron interactions**

see also meson-deuteron scattering

- K<sup>-</sup>d $\rightarrow\pi^-\Lambda$ p, pole in <sup>3</sup>S<sub>1</sub> hyperon-nucleon scattering amplitudes 0-102068
- K<sup>-</sup>d $\rightarrow\Xi^-K^0p$ , 1.45, 1.65 GeV/c,  $\Xi^-p$  invariant mass enhancement 0-57639
- $\pi d$ , bound states, scatt. in light front field theory dynamics 0-68477
- K<sup>-</sup>d $\rightarrow(n,\Lambda)p$ , 13.2 GeV/c, pp forward low mass enhancement 0-86761
- $\pi^- d \rightarrow (\pi,\Lambda)p$ , 13.2 GeV/c, pp forward low mass enhancement 0-86761
- $\pi^+ d$ , 15 GeV, high-mass even-g states, broad dipion states beyond g(1680) 0-68487
- $\pi^+ d$ , 15 GeV, neutral three pion resonance prod., pure I=1 exchange 0-57644

**meson-deuteron scattering**

see also meson-deuteron interactions

- $\pi d$ , relativistic Faddeev calc. 0-102066
- $\pi d$  elastic scatt. in (3,3) resonance region, relativistic description 0-105923
- $\pi d$ , pion absorption effect from threshold to resonance 0-99193

**meson effects**

- K-electron ionisation in solids by relativistic heavy particles 0-84824

**meson field theory**

see also nuclear forces

- boson fields, massless, spontaneous symmetry breaking, and Goldstone theorem (Chinese) 0-62861
- collective excitations of nuclei in a relativistic mean-field theory 0-95300
- education, Schrodinger eqn. solns. using approximate nucleon-nucleon and A-nucleon pots. 0-62429
- energy-momentum tensor in the fermion-pairing model 0-62857
- extended phase space, unified meson fields 0-86551
- gravitational bubbles, radiative corrections to covariant massless quartically self-interacting meson theory 0-62826
- Hartree eqn., quasiclassical soliton soln., Newtonian interaction with screening 0-68569
- instantons, generation of meson mass spectrum, current algebra, mixing angles 0-86567
- nuclear field theory, phonon renormalisation, eigeneqns. and sum rules (Chinese) 0-102127
- nuclear field theory, schematic model functional approach, diagram rules 0-102128
- nuclear potential energy surfaces, folded Yukawa-plus-exponential model 0-86816
- Schwinger model, Ward identity, fermion axial vector current divergence, chiral invariant regulator field 0-57524
- static meson potentials 0-95219
- strong gravity, field equations, strong interactions, de Sitter microsphere idea of hadrons 0-68111
- SU(2) $\times$ U(1) unified model, universal Yukawa coupling 0-91032
- Yukawa<sub>2</sub> model, Schwinger functions, analyticity and Borel type summability (French) 0-73570
- Yukawa model with anomalous dimensionalities in four-dimensional space 0-101934
- Yukawa potentials, finite sum S-matrix 0-101940
- ed-ed, nucleon forces, meson exchange current effects, impulse approx., review 0-57603
- N form factor, isovector, meson field theory, pseudoscalar  $\pi N$  interaction 0-62986
- $\pi$  compositeness from wave function renormalisation constant 0-101997
- $\pi$  condensation in neutron matter, N-N interaction, critical density 0-57711
- $\pi$  condensed phase,  $\sigma$ -model, alternating-layer-spin struct. 0-83057
- $\pi\pi \rightarrow \pi\pi$ , self-interactions, nonperturbative, scatt. amplitudes containing only convergent integrals 0-68480
- <sup>12</sup>C( $\pi,\pi$ ), nonlinear meson dynamics and binding corrections, optical pots. 0-106080
- <sup>3</sup>H, EM form factors, 3-nucleon wave function calc. 0-95302
- <sup>3</sup>H<sub>A</sub>, binding energy, Faddeev equation in coord. space, Lambda-nucleon potential 0-63120
- <sup>3</sup>He, EM form factors, 3-nucleon wave function calc. 0-95302
- <sup>3</sup>He, nuclear charge form factor, two-boson exchange charge density  $\pi$ ,  $\rho$ ,  $\omega$  exchanges 0-63073
- <sup>16</sup>O( $\pi,\pi$ ), nonlinear meson dynamics and binding corrections, optical pots. 0-106080

**meson hadronic decay**

see also kaon hadronic decay

- bottom hadrons, masses and allowed decays, SU(5) quark model 0-62954
- bottom meson nonleptonic decay, many body final states, isospin-statistical models 0-62975
- charmed meson decays, soft hadron interaction effects on nonleptonic weak decays 0-86705
- charmed meson radiative decay, quark loop model, SU(3) splitting of quark masses 0-62990

**meson hadronic decay continued**

- dipion cascade decays, current algebra techniques, pole plus remainder model, chiral symmetry breaking and QCD 0-62972
- hadronic gauge couplings in meson decays 0-102037
- heavy quarkonium decays, renormalisation group approach, exclusive two meson and inclusive decays 0-82972
- heavy quarkonium states, hadronic transitions, QCD anomalies for T<sup>0</sup> and  $\psi'$  0-105888
- penguins in  $\Delta S=1$  nonleptonic weak decays 0-91086
- tensor meson decay, current algebra approach, symmetry-breaking Hamiltonian, chiral SU(3) $\times$ SU(3) or SU(4) $\times$ SU(4) 0-68450
- B(1235) $\rightarrow\omega\pi$ , many pion correlations from nonstrange mesonic resonances (Russian) 0-86708
- B $\rightarrow B^*\pi$ , contris. of B $\rightarrow B^*\gamma$  process 0-78066
- B<sup>0</sup>, B<sup>-</sup> hadronic decay modes, W boson exchange model clean test 0-57592
- B<sup>0</sup> $\rightarrow D^+X(F^+X)$ , W-exchange dominance, decay rates 0-86706
- c $\bar{c}g(\bar{c}qg)$ , exotic mesons, masses, decay widths, mixing matrix elements 0-62943
- D, mass and mean life from high energy cosmic ray data (Chinese) 0-102045
- D $\rightarrow K\pi$ , effective Hamiltonian in Kobayashi-Maskawa model 0-105887
- D $\rightarrow K\pi(K^*\pi)$ , nonleptonic decay rates, quark diagrams and pole approx. 0-86707
- D $\rightarrow K\pi(\pi)$ , current algebra relations and dual model amplitudes 0-82969
- D meson parity violating nonleptonic decays, vector meson dominance model 0-78058
- D nonleptonic decay rates and branching ratios, lifetimes 0-102047
- D-meson decay, hadronic, six-quark model, quark-mass dependence, final state interactions, mixing angle effects 0-62973
- D<sup>0</sup>, D<sup>+</sup> decays, gluon enhancements in charmed-meson decays 0-95265
- D<sup>0</sup> Cabibbo suppressed hadronic decays, Cabibbo universality fake violation, RH currents 0-73699
- D<sup>0</sup> decay enhancement mechanism, quark diagram with gluon prod. 0-105891
- D<sup>0</sup> hadronic decay modes, W boson exchange model clean test 0-57592
- D<sup>0</sup> $\rightarrow K^-\pi^+$ , quark total number conservation, D<sup>+</sup> lifetime longer than D<sup>0</sup> 0-57590
- D<sup>0</sup> $\rightarrow K^-\pi^+$ , role of free-quark pairs 0-78059
- D<sup>0</sup> $\rightarrow \bar{K}^0\pi^0$ ,  $\Delta T=1$  constraints and final state interactions 0-95267
- D<sup>0</sup> $\rightarrow \bar{K}^0\pi^0$ , quark total number conservation, D<sup>+</sup> lifetime longer than D<sup>0</sup> 0-57590
- D<sup>0</sup> $\rightarrow \bar{K}^0\pi^0$ , role of free-quark pairs 0-78059
- D<sup>0</sup> $\rightarrow \bar{K}^0\pi^0(K^-\pi^+)$ , weak interaction effects, K $\pi$  scatt. phase shifts 0-57591
- D<sup>0</sup> $\rightarrow \bar{K}^0\pi^0(\pi^+\pi^-)(K^+K^-)$ , phenomenological model for inclusive and exclusive decays 0-99098
- D<sup>0</sup> lifetime from  $\rho$  and  $\bar{\nu}$  interactions 0-105890
- D<sup>0</sup> nonleptonic decay, quark annihilation hypothesis test 0-102044
- D<sup>+</sup> $\rightarrow K^0\pi^+$ , quark total number conservation, D<sup>+</sup> lifetime longer than D<sup>0</sup> 0-57590
- D<sup>+</sup> $\rightarrow K^0\pi^+$ , role of free-quark pairs 0-78059
- D<sup>±</sup> nonleptonic and semileptonic decays, isospin selection rule tests 0-73700
- D<sup>±</sup>, charmed tensor meson, strong and EM decay modes 0-68451
- E(1420) $\rightarrow K^*K$ , correlation between A<sub>1</sub> parameters and Q data 0-82968
- E(1420) $\rightarrow \eta\pi\pi$ , correlation between A<sub>1</sub> parameters and Q data 0-82968
- $\eta \rightarrow \pi\pi\gamma$ , quark loop model, SU(3) splitting of quark masses 0-62990
- $\eta \rightarrow \rho\gamma(\gamma\gamma)$ , C-even meson radiative decay, SU(3), and VDM anal. (Russian) 0-68460
- $\eta' \rightarrow \eta\pi\pi$ , amplitude satisfying Adler conditions, relativistic quark pair creation model 0-95262
- $\eta' \rightarrow \pi\pi\pi$ ,  $\delta\eta/\pi$  and  $\delta\eta/\pi$  coupling constant ratio,  $\delta(980)$  quark content 0-82955
- $\eta' \rightarrow \pi\pi\pi(\pi^+\pi^-\gamma)$ , quark model description 0-62970
- F, nonleptonic decay rates and branching ratios, lifetimes 0-102047
- f(1270) $\rightarrow 4\pi$ , many pion correlations from nonstrange mesonic resonances (Russian) 0-86708
- F parity violating nonleptonic decays, vector meson dominance model 0-78058
- F-meson decay, hadronic, role of free-quark pairs 0-78059
- F<sup>±</sup> nonleptonic decay, quark annihilation hypothesis test 0-102044
- F<sup>±</sup> $\rightarrow \pi\eta$ , decay mode meas. for PCAC test 0-91018
- F<sup>±</sup> $\rightarrow \eta\pi$ , branching ratio in Faddeev  $\pi NN$  dynamics 0-105886
- F<sup>±</sup>, charmed tensor meson, strong and EM decay modes 0-68451
- g(1680) $\rightarrow \rho\rho$ , many pion correlations from nonstrange mesonic resonances (Russian) 0-86708
- K<sup>±</sup> $\rightarrow K\gamma$ , quark loop model, SU(3) splitting of quark masses 0-62990
- $\nu_e N$ , F<sup>±</sup>(2030) prod. and hadronic decay F<sup>±</sup> $\rightarrow \pi^+\pi^+\pi^-\pi^0$ , mass 0-91085
- $\phi$  decays, hadronic, asymptotic freedom, one-photon or three-gluon exchange 0-62971
- $\phi \rightarrow \eta\gamma$ , quark loop model, SU(3) splitting of quark masses 0-62990
- $\psi(4.03) \rightarrow DD(D^*D, DD^*, D^*D^*)$ , vector state strong decay 0-78057
- $\psi \rightarrow DD$  radial excitations of charmonium 0-102046
- $\psi$  decays, hadronic, asymptotic freedom, one-photon or three-gluon exchange 0-62971
- $\psi \rightarrow \eta\gamma$ , QCD, width, exclusive OZI violating radiative decay 0-68458
- $\psi'$ ,  $\psi$  decay branching ratios, isospin and flavour symmetry breaking 0-95264
- $\psi'$  and  $\psi$  decay ratios, composite particle matrix elements 0-95266
- $\psi \rightarrow \pi^0\psi$ , isospin isolating decay, branching ratio 0-57601
- $\psi \rightarrow \eta(\pi^0)$ , decay branching ratios 0-105889
- $\psi \rightarrow \psi\gamma\gamma$ ,  $\psi\gamma$  final state meas.,  $\psi \rightarrow \gamma\chi$ ,  $\chi \rightarrow \gamma\psi$  branching ratios 0-57601
- $(\bar{q}q) \rightarrow (\bar{q}'q')\gamma$ , width, exclusive OZI violating radiative decay 0-68458
- $\rho \rightarrow \pi\pi\gamma$ , radiative decay width from pion excitation anal. 0-57599
- s $\bar{s}$  vector mesons, hadronic decays and props., nonrelativistic quark model 0-105892
- t-quarkonium decay props. (Russian) 0-105856
- T(946) orthoquarkonium decay, jet profiles, three gluon structure 0-73698
- T(946) $\rightarrow$ hadrons, gluon spin and colour, QCD nontrivial test 0-82971
- T(944) $\rightarrow$ charmonium, quarkonium prod. via one gluon mechanism 0-95263
- T(954) decay modes from Zweig rule intermediate vector particle model (Chinese) 0-73697
- $\nu$  decays, hadronic, asymptotic freedom, one-photon or three-gluon exchange 0-62971



**meson interactions** see *lepton-hadron interactions; meson-baryon interactions; meson-deuteron interactions; meson-meson interactions; meson-nucleus reactions; photon-hadron interactions*

### meson leptonic decay

see also *kaon leptonic decay*  
 decay widths, relativistic formula, quark-pair creation effect estimate 0-105883  
 heavy vector meson annihilation to lepton pairs, hadronic corrections 0-68424  
 mass spectrum and Regge trajectories from relativistic quasipot. eqn. (Russian) 0-73690  
 meson-antimeson hadronic molecules, spectrum, leptonic and radiative decays (Russian) 0-57602  
 quark spinors in bound quark system, small component effects 0-73694  
 vector meson leptonic width, duality between vector mesons and perturbative QCD 0-57589  
 $D_s^\pm$  weak decay constant from bag model extension 0-62967  
 $e^+e^- \rightarrow e^+e^-$ ,  $T(946)$  electronic branching ratio and total width 0-86702  
 $e^+e^- \rightarrow FF(BB)$ ,  $\tau\nu$  decay signature for  $F^\pm$  and  $B^\pm$  detection 0-91099  
 $e^+e^- \rightarrow$  hadrons,  $T''$  observation at CESR, mass and leptonic width 0-86738  
 $e^+e^- \rightarrow$  hadrons ( $\mu^+\mu^-$ ),  $T(946)$  muonic branching ratio, total and leptonic width 0-86703  
 $e^+e^- \rightarrow \psi(3770)$ , cross section,  $\psi$  mass, total width and  $e^+e^-$  partial width 0-73696  
 $\eta \rightarrow \mu^+\mu^- \gamma$ , branching ratio and  $\eta$  EM form factor 0-105899  
 $F^+ \rightarrow \tau^+ \nu$ , gluon enhancements in charmed-meson decays 0-95265  
 $F^\pm$  weak decay constant from bag model extension 0-62967  
 $K^0 \rightarrow \mu e$ , flavour changing neutral current search 0-105836  
 $\mu N$ , 209 GeV,  $\psi$  diffractive prod. cross section,  $\psi \rightarrow \mu^+\mu^-$  decays 0-102054  
 $\mu N \rightarrow \mu TX$ , 209 GeV,  $T$  muon prod. limits from trimuon final states 0-105909  
 $\nu$  production, prompt sources, and axion decays and interactions, pN beam-dump experiment 0-63028  
 $P \rightarrow \gamma |1^-$ , EM characs. for pseudoscalar meson decay in nonlocal quark model (Russian) 0-102050  
 $pp$ , 53, 63 GeV, massive electron pair prod.,  $T$  ang. decay, scaling function 0-68495  
 $pp$ , 53, 63 GeV,  $T$  and  $\psi$  prod., dielectron decay angles 0-68496  
 $\psi$ , modified quark loop model, form factors, struct. functions, radiative decay 0-91088  
 $\pi \rightarrow e \nu \gamma$ , modified quark loop model, form factors, struct. functions, radiative decay 0-91088  
 $\pi \rightarrow e \nu \gamma$  and  $SU(3) \times SU(3)$   $\sigma$ -model 0-78054  
 $\pi$  p, 70 GeV/c, direct electron prod. from charm particle pair decay,  $e/\pi$  ratio 0-105928  
 $\pi$  p, 70 GeV/c, directly produced electrons from charmed D particle decay, cross sections 0-73755  
 $\psi \rightarrow \mu^+\mu^-$ , search for extra  $\mu$  in ( $\pi^-$ ,  $\psi$  CC), 225 GeV/c 0-82967  
 $T$ , vibrational states in string picture, mass and leptonic width 0-62949  
 $T(946)$ , leptonic branching ratio, from electronic width and muonic branching ratios 0-57588

### meson magnetic moment

$\gamma N \rightarrow \Delta \pi$ , mag. dipole photoexcitation, singular integral eqns., polynomial ambiguity 0-57608

### meson mass

bottom hadrons, masses and allowed decays,  $SU(5)$  quark model 0-62954  
 charmed hadrons,  $SU(4)$  mass-breaking, mass sum rules 0-62959  
 charmonium, mass in QCD 0-105867  
 hadron building blocks, pionic mass intervals in narrow and S-state resonances 0-105875  
 instantons, generation of meson mass spectrum, current algebra, mixing angles 0-86567  
 $M_\psi - M_{\psi(c)}$  and  $M_T - M_{T(b)}$  lower bounds, concave and convex pots. 0-91057  
 mass spectrum and Regge trajectories from relativistic quasipot. eqn. (Russian) 0-73690  
 meson and baryon mass formula, chromodynamics consideration (Russian) 0-91071  
 naive quark model predictions for meson mass and baryon mass and mag. moment 0-78036  
 nonperturbative QCD, large  $N_c$ , QCD bag model, instantons and  $\eta'$  mass 0-57559  
 QCD, hadron masses, behaviour of constituent quarks 0-57557  
 b-quark mesons, mass, quark model predictions 0-95256  
 c(qq)q, exotic mesons, masses, decay widths, mixing matrix elements 0-62943  
 D, mass and mean life from high energy cosmic ray data (Chinese) 0-102045  
 $D^{*+}$ , photoprod.,  $D^0$  mass difference 0-73720  
 $e^+e^- \rightarrow$  hadrons,  $T''$  observation at CESR, mass and leptonic width 0-86738  
 $e^+e^- \rightarrow O$  particle, decay, mass, prod. from Zweig rule intermediate vector particle model (Chinese) 0-73697  
 $e^+e^- \rightarrow \psi(3770)$ , cross section,  $\psi$  mass, total width and  $e^+e^-$  partial width 0-73696  
 $\eta$ , mass and other props, review from theoretical models 0-102025  
 $K_1-K_2$  mass differences, charged Higgs boson couplings 0-62917  
 $\mu N$ ,  $F^+$  (2030) prod. and hadronic decay  $F^+ \rightarrow \pi^+\pi^+\pi^-\pi^0$ , mass 0-91085  
 $\pi$  mass in improved static bag model 0-73667  
 $\pi \rightarrow (\pi^+\pi^-\pi^0)\Delta^{++}$ , 16 GeV/c, partial wave anal.,  $\omega^*$  and  $A_2^0$  0-63033  
 $\psi^*(3770)$ , mass width from quark model 0-73723  
 $q\bar{q}(q\bar{q})^2$  mesons, mass formula 0-62958  
 $q\bar{q}$  spectra, heavy systems, equaltime relativistic wave eqn. with confining potential 0-77977  
 $q\bar{q}$  systems, nonperturbative potential model 0-78040  
 t-quark mesons, mass, quark model predictions 0-95256  
 tt vector meson, proposed 40 GeV mass 0-62942  
 T, vibrational states in string picture, mass and leptonic width 0-62949  
 $T^H$ , pionic, pion mass high accuracy meas. from transitions 0-106406  
 Ti, pionic, pion mass high accuracy meas. from transitions 0-106406

### meson-meson interactions

see also *meson-meson scattering; pion-pion interactions*  
 BB annihilation process, simple geometrical picture 0-95291

### meson-meson scattering

see also *meson-meson interactions; pion-pion scattering*  
 charmed particles, hadronic props., superconvergence sum rules 0-78043  
 quark model asymptotic completeness for meson scatt. 0-73738

### meson-meson scattering continued

$K^*\gamma$ , QCD, one-gluon-exchange, resonating group method, soft-core approx. 0-63025  
 $\pi K$  scattering amplitude, analytic continuation, chiral symmetry breaking 0-63027  
 $\pi K$  scattering length, dispersion relation anal. of phase-shift 0-63026

### meson-nucleus reactions

for inelastic meson-nucleus scattering, see "meson-nucleus scattering"  
 see also *kaon-nucleus reactions; meson-baryon interactions; meson capture; pion-nucleus reactions*  
 $^{197}\text{Au}(\pi^+X)$ ,  $X=d,t$ ,  $^3\text{He}$ ,  $^4\text{He}$ , particle emission following stopped pion absorption 0-91196  
 $^{59}\text{Co}(\pi^+X)$ ,  $X=d,t$ ,  $^3\text{He}$ ,  $^4\text{He}$ , particle emission following stopped pion absorption 0-91196

### meson-nucleus scattering

see also *kaon-nucleus scattering; meson-baryon scattering; pion-nucleus scattering*  
 No entries

### meson photoproduction

[CC]  $^{12}\text{C}(\gamma,\pi^+)^{12}\text{B}$ , nuclear critical opalescence study 0-105988  
 high energy production, review 0-73719  
 $D^{*+}$ , photoprod.,  $D^0$  mass difference 0-73720  
 $\gamma N$ ,  $\pi^+$  photoprod., low energy, emission ang. depend. (Russian) 0-57769  
 $\gamma N \rightarrow \Delta \pi$ , mag. dipole photoexcitation, singular integral eqns., polynomial ambiguity 0-57608  
 $\gamma n \rightarrow \pi^+ p$ , 0.9-1.65 GeV, pol.  $\gamma$ , cross section asymmetry (Russian) 0-86728  
 $\gamma n \rightarrow \pi^+ p$ , 700 to 1200 MeV, recoil proton polarisation 0-78075  
 $\gamma N \rightarrow \pi^+ X$ , QCD cross sections 0-73715  
 $\gamma n \rightarrow \pi^+ p$ ,  $\pi^+ n$ ,  $\pi^+ p$ ,  $K^+ \Lambda$ ,  $K^+ \Sigma^0$  final state comparisons above resonance region 0-105906  
 $\gamma p$ , heavy quark particle photoprod., QCD model, vector dominance implications 0-86730  
 $\gamma p \rightarrow (pp)p$ , inclusive and exclusive pp photoprod. S(1936) prod. 0-86729  
 $\gamma p \rightarrow \pi^+ \pi^+$ , 340 MeV, pol. p, first resonance region,  $\pi^+$  photoprod., T-asymmetry (Russian) 0-62997  
 $\gamma p \rightarrow \pi^+ p$ , 0.6 to 1.8 GeV, backward angles,  $\eta$ -cusp 0-57609  
 $\gamma p \rightarrow \pi^+ p$ , 390-975 MeV, differential cross section 0-86725  
 $\gamma p \rightarrow \pi^+ p$ , 400 to 1142 MeV, recoil proton polarisation 0-82981  
 $\gamma p \rightarrow \pi^+ p$ , 450 to 800 MeV, proton polarisation, Walker-type anal.,  $P_{11}(1470)$ ,  $D_{13}(1470)$ ,  $S_{11}(1535)$  resonances 0-73721  
 $\gamma p \rightarrow \pi^+ p$ , high energies, semiempirical amplitude anal. dispersion relations and Regge poles 0-86726  
 $\gamma p \rightarrow \pi^+ n$ , 1.35-1.65 GeV, pol.  $\gamma$ , resonance energy region, cross section asymmetry (Russian) 0-86727  
 $\gamma p \rightarrow \pi^+ n$ ,  $\pi^+ n$ ,  $\pi^+ p$ ,  $K^+ \Lambda$ ,  $K^+ \Sigma^0$  final state comparisons above resonance region 0-105906  
 $\gamma p \rightarrow \pi^+ \pi^- \pi^0 p$ ,  $p'(1.6)$  production 0-102056  
 $\gamma p \rightarrow \pi^+ \pi^- \pi^+ \pi^- \pi^0 p$ ,  $p'$ , diffractive production, jet-like structure 0-57606  
 $\gamma p \rightarrow \pi^+ \pi^+ \pi^- \pi^- \pi^0 p$ ,  $p'(1.2)$  production 0-102056  
 $\gamma p \rightarrow \rho^+ \Delta^{++}$ , 2.8 to 4.8 GeV, cross-sections,  $\rho$  spin density matrices 0-62999  
 $\gamma p \rightarrow \rho^+ n$ , 2.8 to 4.8 GeV, cross-sections,  $\rho$  spin density matrices 0-62999  
 $\pi$  photoproduction amplitudes, Padé approximants and dispersion relation solns. 0-91096  
 $\pi^0$ , in  $^{12}\text{C}(\gamma, \pi^0 p)$  at 0.7-1.65 GeV, cross section asymmetry meas. (Russian) 0-63164  
 $^{12}\text{C}(\gamma, \pi^+)^{12}\text{N}$ , total cross section calc.,  $\Delta(1232)$  contrib. 0-91175  
 $\gamma p \rightarrow K^+ \Lambda(\Sigma^0)$ ,  $\pi^+ n$ ,  $\pi^+ p$ ,  $K^+ \Lambda$ ,  $K^+ \Sigma^0$  final state comparisons above resonance region 0-105906

### meson production

see also *kaon production; meson photoproduction; pion production*  
 bag model, meson and massive photon production 0-105850  
 charmed meson produced in  $e^+e^-$  annihilation 0-91106  
 cumulative hadron production, statistical bootstrap model with strangeness (Russian) 0-62948  
 $e^+e^- \rightarrow$  hadrons, 9.4-10.4 GeV, three T states, mass spacings, lepton pair widths 0-68465  
 electroproduction in correlating quark rearrangement model 0-86666  
 fast mesons as dressed quark fragmentation products, Kuti-Weisskopf model 0-91061  
 hadron-hadron inclusive interactions, charmed particle production,  $\eta_c$ ,  $\psi$  and other c $\bar{c}$  bound states 0-63036  
 heavy quark prod., nonperturbative gluon prod. versus perturbative QCD fusion models, B and  $\psi$  0-91058  
 high energy collisions, cumulative particle prod., parton recombination and quark-parton models 0-82956  
 high-transverse-momentum symmetric-particle-pair spectra and correlations 0-95250  
 inclusive vector meson production in fragmentation regions of meson at small  $P_T$  0-105931  
 nonperturbative gluon jet model, gluon fragments, meson prod. 0-68420  
 vector boson pair photoprod., theoretical cross sections 0-57610  
 $\bar{c}c$  qq states, decay, hadronic and photo-prod.,  $e^+e^-$  annihilation prod. 0-99092  
 $e^+e^-$  annihilation, CM energies 29.90-31.46 GeV, narrow resonance search upper limit 0-63003  
 $e^+e^-$  annihilation, gluon jets, multiplicity and ang. distrib. asymmetries 0-91105  
 $e^+e^-$  annihilation, narrow resonance search upper limit at PETRA, 29.90-31.46 GeV 0-57618  
 $e^+e^- \rightarrow$  charmed hadrons, quark mass effect on fragmentation functions 0-91098  
 $e^+e^- \rightarrow DD$ , above charm threshold at energy corresponding to  $\psi^*(3770)$  0-73723  
 $e^+e^- \rightarrow e^+e^- BB$ , cross-section from equivalent photon approx. 0-68467  
 $e^+e^- \rightarrow e^+e^- X_b$ , cross-section from equivalent photon approx. 0-68467  
 $e^+e^- \rightarrow e^+e^- \eta_b$ , cross-section from equivalent photon approx. 0-68467  
 $e^+e^- \rightarrow FF(BB)$ ,  $\tau\nu$  decay signature for  $F^\pm$  and  $B^\pm$  detection 0-91099  
 $e^+e^- \rightarrow \gamma X$ , obs. at DORIS 0-102058  
 $e^+e^- \rightarrow$  hadrons, fourth T state observation in annihilation events 0-86737  
 $e^+e^- \rightarrow$  hadrons, T,  $T'$ ,  $T''$  states, mass differences, leptonic width ratio 0-68466  
 $e^+e^- \rightarrow$  hadrons,  $T''$  observation at CESR, mass and leptonic width 0-86738  
 $e^+e^- \rightarrow VX$ , parton model, polarisation effects (Russian) 0-63002  
 $e^+e^- \rightarrow VX$ , polarisation states and differential cross sections for  $\pi A_1$  and  $\rho^0$  (Russian) 0-102059  
 $ep \rightarrow e p K^+ \pi^-$ , 1.8, 2.1, 2.5 GeV/c<sup>2</sup>, meson resonance observ. 0-82982



## meson production continued

- $e^+e^- \rightarrow \pi^+ \pi^- \pi^+ \pi^-$ , 1.8 GeV/c<sup>2</sup>, meson resonance observ. 0-82982  
 $\pi_c$  associated with gluon, hadronic prod. 0-105846  
 $\gamma p$ , 30-180 GeV,  $p$  and  $\phi$  elastic photoprod. cross sections 0-95278  
 $\gamma p$ , 40-70 GeV, inclusive  $D^0$  photoprod. cross sections, pair and associated prod. 0-91097  
 $\gamma p \rightarrow K^+ K^- p$ , 20-36 GeV,  $\Phi(1019)$  prod., cross sections 0-105907  
 $K p$ , 32 GeV/c, exclusive reaction anal. in terms of multiparticle variables (*Russian*) 0-86757  
 $K p \rightarrow A_1$ , 4.15 GeV/c, nondiffractive production, double-Regge model 0-78097  
 $K^- p \rightarrow B^- Y^{*+}(1385)$ , 8.25 GeV/c, quasi-two-body channel data 0-63023  
 $K^- p \rightarrow \rho^- Y^+ Y^+ \rightarrow \Sigma^+ \text{ or } Y^{*+}(1385)$ , 7 and 11.5 GeV/c, hyperon polarisation, vector meson decay angular distrib. 0-82997  
 $K_{s1}^0 p \rightarrow Q^0(Q^0)p$ , differential cross section slope, further Deck model anal. 0-73737  
 $\mu N$ , 209 GeV,  $\psi$  diffractive prod. cross section,  $\psi \rightarrow \mu^+ \mu^-$  decays 0-102054  
 $\mu N \rightarrow \mu^+ X$ , 209 GeV,  $T$  muoprod. limits from trimuon final states 0-105909  
 $(N,N,X)$ , shower proton and meson transverse momenta, intranuclear cascade model 0-102185  
 $NN \rightarrow (\pi, \rho, \omega, f)$ , statistical model 0-102028  
 $\nu_p N$ ,  $F^+$  (2030) prod. and hadronic decay  $F^+ \rightarrow \pi^+ \pi^+ \pi^- \pi^0$ , mass 0-91085  
 $p d$ , 355-1066 MeV/c, total and annihilation cross sections, S meson search 0-68473  
 $p p$ , 100 GeV/c, inclusive meson and strange particle prod., energy partition 0-95289  
 $p p$ , 355-1066 MeV/c, total and annihilation cross sections, S meson search 0-68473  
 $p p$ , 405 GeV/c,  $\rho^0$ ,  $f$ ,  $\phi$ ,  $h$  meson prod., cross sections 0-105930  
 $p p$ ,  $p p$ , 12-405 GeV, low  $p_T$  meson prod., quark-antiquark formation model 0-63056  
 $p p$ , probabilistic quark-model approach to  $p$  fragmentation 0-63049  
 $p p$ , secondary hadron absolute yield,  $L=1$  meson prod., quark model (*Chinese*) 0-99113  
 $p p$ -mesons, multimeson inclusive spectra and recombination model, multi-quark structure functions 0-73751  
 $\pi p \rightarrow \mu^+ X$ , 62 GeV,  $\psi$  and  $\gamma$  cross sections, scaling function 0-105932  
 $(\pi, \psi, CC)$ ,  $\psi \rightarrow \mu^+ \mu^-$ ,  $CC \rightarrow \mu^+ \nu X$ , 225 GeV/c, search for extra  $\mu$  0-82967  
 $\pi^- N \rightarrow \psi X$ , 225 GeV, bottom meson pair production limit 0-73750  
 $\pi^- p$ , 100 GeV/c, inclusive meson and strange particle prod., energy partition 0-95289  
 $\pi^- p$ , 150 GeV/c, leading particles and diffraction dissociation, 2-, 4- and 6-prong events 0-68486  
 $\pi^- p \rightarrow \eta n$ , Regge pole model with phenomenological residue functions 0-102077  
 $\pi^- p \rightarrow n e^+$ , 1.3 to 3.8 GeV/c, differential and total cross-sections 0-83000  
 $\pi\pi \rightarrow \pi\pi$ ,  $p$ -resonance production, quasipotential approach, linear  $\sigma$ -model 0-86755  
 $\psi$  associated with gluon, hadronic prod. 0-105846  
 $\psi \rightarrow \gamma \gamma$ , conflict with single parameter scheme for radiative decays of vector mesons 0-86720  
 $\psi$  production, gluon-gluon fusion model, gluon distrib.  $x$ -depend. 0-62922  
 $\rho^0$  (1600) meson resonance from 2- and 4-pion distrib. in photoproduction data 0-95279  
 $T$ , production and decay in quark fusion model 0-102018  
 $T$  production, photon-gluon fusion model, gluon distrib.  $x$ -depend. 0-62922  
 $Cu(\pi^+, \psi(3700))$ , 50 GeV, formation cross-sections (*Russian*) 0-106082

## meson resonances

- see also *D mesons; eta meson resonances; omega mesons; phi mesons; psi mesons; rho mesons*  
baryonium, geometrical approach 0-91065  
baryonium, ground state hyperfine splitting, harmonic oscillator potential anal. 0-68422  
baryonium, nuclear and quark confinement forces 0-68431  
baryonium states in QCD, review 0-102001  
bottom meson nonleptonic decay, many body final states, isospin-statistical models 0-62975  
bottomium, potential models, non-relativistic description 0-68426  
charm particle spectroscopy 0-73680  
charmonium, mass in QCD 0-105867  
charmonium, potential models, non-relativistic description 0-68426  
charmonium decay, effective strong coupling constant for timelike  $Q^2$  0-99091  
charmonium resonances above open charm threshold, nonrelativistic quark model 0-78039  
colour confining forces and effects saturation 0-73672  
Coulombic qq bound states, short range behaviour, quark mass 0-78033  
dibaryon resonances in NN scatt. 0-57605  
 $e^+e^-$ -hadrons, 9.4-10.4 GeV, three  $T$  states, mass spacings, lepton pair widths 0-68465  
four quark mesons, recoupled wave functions, phase inconsistency 0-68425  
ghost-pole subtraction and the  $\sigma$ -exchange NN potential 0-86819  
gluon and quark jets in a recursive model motivated by quantum chromodynamics,  $T$  decay 0-62936  
hadron induced multiparticle reactions, S-1500 GeV, resonance prod. correlations, jet model (*German*) 0-91118  
harmonically confined q q system, relativistic wave eqn. 0-95247  
heavy meson inclusive semileptonic decays, lifetime estimates, quark-parton model difficulties 0-86704  
heavy quark bound states of top quark and antiquark pairs, QCD test 0-68430  
heavy quark mesons, inclusive hadronic prod. (*Russian*) 0-86770  
heavy quark prod., nonperturbative gluoprod. versus perturbative QCD fusion models, B and  $\psi$  0-91058  
heavy quarkonium decays, renormalisation group approach, exclusive two meson and inclusive decays 0-82972  
heavy quarkonium states, hadronic transitions, QCD anomalies for  $T''$  and  $\psi'$  0-105888  
heavy quarks and new particles 0-73661  
heavy vector meson annihilation to lepton pairs, hadronic corrections 0-68424  
inclusive vector meson production in fragmentation regions of meson at small  $p_T$  0-105931  
 $M_{\psi} - M_{\psi(c)}$  and  $M_T - M_{T(b)}$  lower bounds, concave and convex pots. 0-91057

## meson resonances continued

- meson-antimeson hadronic molecules, spectrum, leptonic and radiative decays (*Russian*) 0-57602  
multi-channel baryonium and some peculiarities of its decays (*Russian*) 0-105857  
new particle discoveries since  $J/\psi$ , review 0-57018  
non-Abelian gauge theory with many flavours, high energy processes, asymptotical behaviour (*Russian*) 0-101935  
photoproduction, high energy review 0-73719  
 $QCD_s$ , qq bound state spectrum in leading  $1/N$  approx. 0-78031  
QCD, lifetime of QQ states, pseudoscalar charmonium and upion states 0-68429  
QCD, string constant, Regge slope and  $\Lambda$  parameter, empirical quarkonium approach 0-91053  
quarkonium, leptonic decay, quark spinors in bound quark system, small component effects 0-73694  
quarkonium systems, sum rules 0-68423  
radiative decays of vector mesons, single parameter scheme 0-86720  
Regge-pole approach to charmonium and bottomium 0-86697  
resonance vertex functions and scatt. amplitudes resonance-nucleon scatt.  $p$  rescatt. (*Russian*) 0-105918  
s-channel resonance model based on peripheral resonances, exotic peaks 0-91069  
SU(S) based grand unified theory, monopoles and vector bosons, symmetry breaking 0-99079  
T-baryonium system, four-body potential in multi-quark states 0-101996  
tensor meson radiative decay in  $SU(6) \times O(3)$  broken symmetry quark model 0-73710  
ultrarelativistic nuclear collisions, asymptotic hadron spectrum, hot hadronic matter 0-63118  
unitary symmetry in baryon-antibaryon systems (*Chinese*) 0-102000  
vector boson pair photoprod., theoretical cross sections 0-57610  
vector meson leptonic width, duality between vector mesons and perturbative QCD 0-57589  
vector meson radiative decays, SU(3) symmetry viewpoint 0-95273  
vector meson radiative decays, vector dominance model in broken SU(3) 0-73711  
vector mesons, EM decay in broken SU(3) 0-82976  
Wilson loop critical point behaviour in gauge and lattice gauge theories 0-90993  
Zweig forbidden processes, intermediate vector particle model, neutral vector mesons (*Chinese*) 0-62918  
 $A_1$ , Dalitz arrays from  $K^- p \rightarrow \pi^+ \pi^- \pi^+ \Sigma^-$  0-105924  
 $A_1$  meson, mass formulas and selection rules in large SU(3) mixing 0-86700  
 $A_2$ , Dalitz arrays from  $K^- p \rightarrow \pi^+ \pi^- \pi^0 \Lambda$  0-105924  
B, structure of hadrons containing heavy quark, MIT bag model 0-86672  
B(1235)  $\rightarrow \omega \pi$ , many pion correlations from nonstrange mesonic resonances (*Russian*) 0-86708  
B  $\rightarrow B^* \gamma$ , contribs. of B  $\rightarrow B^* \gamma$  process 0-78066  
B meson, cascade decays, CP nonconservation 0-105811  
B meson, mass formulas and selection rules in large SU(3) mixing 0-86700  
b-quark mesons, mass, quark model predictions 0-95256  
 $B^0$ , B<sup>-</sup> hadronic decay modes, W boson exchange model clean test 0-57592  
 $B^0 \rightarrow D^+ X(F^+ X)$ , W-exchange dominance, decay rates 0-86706  
bb meson state lifetimes, R predictions above bottom threshold, quark model 0-99097  
BB production in  $e^+e^-$  annihilation 0-68467  
 $CC \rightarrow \mu^+ \nu X$ , search for extra  $\mu$  in  $(\pi^-, \psi CC)$ , 225 GeV/c 0-82967  
cc qq states, decay, hadronic and photo-prod.,  $e^+e^-$  annihilation prod. 0-99092  
c $\bar{c}$  spectrum, equaltime relativistic wave eqn. with confining potential 0-77977  
c $\bar{c}g(c\bar{c}g)$ , exotic mesons, masses, decay widths, mixing matrix elements 0-62943  
 $x \rightarrow \psi \gamma$ , charmonium E1 radiative transitions and quark mag. moments 0-86721  
DD, DD\*, D\* $\bar{D}^*$ , charm molecules, dynamical model, light meson exchange 0-57572  
 $\delta$ (980) quark content from  $\eta' \rightarrow \eta \pi \pi$  0-82955  
 $\delta$  meson four quark nature (*Russian*) 0-101999  
E(1420)  $\rightarrow K^* K$ , correlation between  $A_1$  parameters and Q data 0-82968  
E(1420)  $\rightarrow \eta \pi \pi$ , correlation between  $A_1$  parameters and Q data 0-82968  
 $e^+e^-$  annihilation, CM energies 29.90-31.46 GeV, narrow resonance search upper limit 0-63003  
 $e^+e^-$  annihilation, narrow resonance search upper limit at PETRA, 29.90-31.46 GeV 0-57618  
 $e^+e^- \rightarrow e^+e^- T(9.46)$  electronic branching ratio and total width 0-86702  
 $e^+e^- \rightarrow FF(BB)$ ,  $\tau \nu$  decay signature for  $F^+$  and  $B^+$  detection 0-91099  
 $e^+e^- \rightarrow \gamma \gamma$ , 9.4-31.6 GeV, differential cross section,  $T \rightarrow \gamma \gamma$  decay limits 0-91073  
 $e^+e^-$ -hadrons, fourth T state observation in annihilation events 0-86737  
 $e^+e^-$ -hadrons, T, T', T'' states, mass differences, leptonic width ratio 0-68466  
 $e^+e^-$ -hadrons, T'' observation at CESR, mass and leptonic width 0-86738  
 $e^+e^-$ -hadrons ( $\mu^+ \mu^-$ ), T(9.46) muonic branching ratio, total and leptonic width 0-86703  
 $e^+e^-$  initiated  $\gamma \gamma$  processes, charged pair prod.,  $f^0 \rightarrow \gamma \gamma$  width 0-91123  
 $e^+e^- \rightarrow O$  particle, decay, mass, prod. from Zweig rule intermediate vector particle model (*Chinese*) 0-73697  
 $e^+e^- \rightarrow VX$ , parton model, polarisation effects (*Russian*) 0-63002  
 $e^+e^- \rightarrow \pi^+ \pi^- \pi^+ \pi^-$ , 1.8 GeV/c<sup>2</sup>, meson resonance observ. 0-82982  
 $e^+e^- \rightarrow K^+ K^- \pi^+$ , 1.8, 2.1, 2.5 GeV/c<sup>2</sup>, meson resonance observ. 0-82982  
F, nonleptonic decay rates and branching ratios, lifetimes 0-102047  
f(1270)  $\rightarrow 4\pi$ , many pion correlations from nonstrange mesonic resonances (*Russian*) 0-86708  
F parity violating nonleptonic decays, vector meson dominance model 0-78058  
F<sup>+</sup> nonleptonic decay, quark annihilation hypothesis test 0-102044  
F<sup>+</sup>  $\rightarrow \pi d$ , branching ratio in Faddeev  $\pi NN$  dynamics 0-105886  
g(1680)  $\rightarrow \rho \rho$ , many pion correlations from nonstrange mesonic resonances (*Russian*) 0-86708  
 $\gamma \rightarrow \gamma \pi \pi$ , current algebra techniques, pole plus remainder model, chiral symmetry breaking and QCD 0-62972  
 $\gamma d \rightarrow np$ , 400-650 MeV, proton polarisation and possible dibaryon resonances 0-105908  
 $\gamma N$ , exclusive photoprod. reactions, Okubo-Zweig-Iizuka rule 0-95277  
 $\gamma p \rightarrow (pp)$ , inclusive and exclusive pp photoprod. S(1936) prod. 0-86729



## meson resonances continued

- $\gamma p \rightarrow K^+ K^- p$ , 20-36 GeV,  $\Phi(1019)$  prod., cross sections 0-105907  
 $K^{*+}(890)$  produced in  $\pi^+ p \rightarrow K^+ V^+$ ,  $Y^+ = \Sigma^+$  or  $Y^{*+}(1385)$  0-82997  
 $K^{*+}(892)$  production in  $pp$  and  $\pi^+ p$  inclusive interactions 0-86765  
 $K^- p$ , 32 GeV/c, exclusive reaction anal. in terms of multiparticle variables (*Russian*) 0-86757  
 $K^- p \rightarrow A_1$ , 4.15 GeV/c, nondiffractive production, double-Regge model 0-78097  
 $K^- p \rightarrow B^- Y^{*+}(1385)$ , 8.25 GeV/c, quasi-two-body channel data 0-63023  
 $K^- p \rightarrow K_0^{*+} \pi^- n$ , 6 GeV/c,  $K^*$  and  $Q_2$  signals, partial wave anal. 0-86754  
 $K_1^0 p \rightarrow Q^0(Q^0)p$ , differential cross section slope, further Deck model anal. 0-73737  
 $\mu N \rightarrow \mu X$ , 209 GeV,  $T$  muoprod. limits from trimuon final states 0-105909  
 $NN$ , resonances and bound states, multichannel  $N/D$  formulation 0-78087  
 $NN \rightarrow (\pi, \rho, \omega, f)$ , statistical model 0-102028  
 $\nu$ , charmonium and strangeonium, linear+Coulomb pot. study, high  $\alpha_s$  regime 0-62935  
 $\nu N$ ,  $F^+$  (2030) prod. and hadronic decay  $F^+ \rightarrow \pi^+ \pi^+ \pi^- \pi^0$ , mass 0-91085  
 $pd$ , 355-1066 MeV/c, total and annihilation cross sections,  $S$  meson search 0-68473  
 $pd \rightarrow NX$ , <500 MeV/c, narrow  $NN$  state search 0-57627  
 $pN$ -charm particles, obs. in high resolution streamer chamber 0-73742  
 $pp$ , 355-1066 MeV/c, total and annihilation cross sections,  $S$  meson search 0-68473  
 $pp$ , 405 GeV/c,  $\rho^0$ ,  $f$ ,  $g^0$ ,  $h$  meson prod., cross sections 0-105930  
 $pp$ , 53, 63 GeV, massive electron pair prod.,  $T$  ang. decay, scaling function 0-68495  
 $pp$ , 53, 63 GeV,  $T$  and  $\psi$  prod., dielectron decay angles 0-68496  
 $pp$ ,  $D$ ,  $B$ ,  $K$  prod., QCD model for heavy flavour prod., two gluon annihilation 0-86744  
 $pp$ ,  $pp$ , 12-405 GeV, low  $p_T$  meson prod., quark-antiquark formation model 0-63056  
 $pp \rightarrow cX$ ,  $p\bar{c}$  exotic, triple-Regge formalism, Pomeron exchanges 0-63041  
 $pp \rightarrow \mu^+ \mu^- X$ , 62 GeV,  $\psi$  and  $\gamma$  cross sections, scaling function 0-105932  
 $pp \rightarrow \pi\pi$ , 1-2 GeV/c, Barrelet zero anal., resonant struct. 0-73735  
 $pp \rightarrow S \rightarrow pp$ ,  $S$  meson as baryonium state 0-62938  
 $\pi^+$  total cross-section, dibaryon resonant states, narrow peaks 0-63016  
 $\pi^+ d \rightarrow (n, p)pn$ , 13.2 GeV/c,  $pp$  forward low mass enhancement 0-86761  
 $\pi^+ d \rightarrow (p, p)pn$ , 13.2 GeV/c,  $pp$  forward low mass enhancement 0-86761  
 $\pi^+ d$ , 15 GeV, neutral three pion resonance prod., pure  $I=1$  exchange 0-57644  
 $\pi N$  interactions,  $N$  form factor, isovector, meson field theory, pseudoscalar  $\pi N$  interaction 0-62986  
 $\pi N$  scattering,  $\rho$  trajectory, finite-energy sum rules, three component duality 0-82996  
 $\pi^- p$ , 70 GeV/c, direct electron prod. from charm particle pair decay,  $e/\pi$  ratio 0-105928  
 $\pi^- p \rightarrow (pp)X^0$ , narrow  $pp$  state search 0-78102  
 $\pi^- p \rightarrow K^+ K^- \pi^+ n$ , 3.95 GeV/c,  $E(1420)$  quantum numbers and branching ratio 0-95286  
 $\pi^- p \rightarrow K^+ K^- n$ , 62 GeV, spin-5 boson resonance at 2300 MeV 0-102078  
 $\pi^+ p$ , 32 GeV/c,  $\pi$  and  $\rho^0$  inclusive prod.,  $f$  and  $\eta$  cross section estimates (*Russian*) 0-68499  
 $\pi^+ p \rightarrow (\pi^+ \pi^- \pi^0) \Delta^{++}$ , 16 GeV/c, partial wave anal.,  $\omega^*$  and  $A_2^0$  0-63033  
 $\pi^+ p \rightarrow \Delta_r^{++} pp$ , 9.8 GeV/c, narrow  $pp$  state search 0-57636  
 $\pi^+ p \rightarrow \Delta_r^{++} p$ , 15 GeV, high-mass even- $g$  states 0-68487  
 $Q_1(1280)$ , mass formulas and selection rules in large  $SU(3)$  mixing 0-86700  
 $Q_2(1400)$ , mass formulas and selection rules in large  $SU(3)$  mixing 0-86700  
 $QQ$ , bound system, dynamics 0-73676  
 $qq$  spectra, heavy systems, equaltime relativistic wave eqn. with confining potential 0-77977  
 $qq$  systems, nonperturbative potential model 0-78040  
 $qq\bar{q}\bar{q}$  diquonium states, production in  $e^+e^-$  processes 0-57615  
 $S(1936)$ , evidence against existence from  $pp$  interaction 0-78089  
 $S^*$  scalar meson, four-quark nature (*Russian*) 0-68432  
 $s\bar{s}$  vector mesons, hadronic decays and props., nonrelativistic quark model 0-105892  
 $\sigma \rightarrow 2\gamma$ , tensor-trace and triangle anomalies 0-73709  
 $T(2150)$ ,  $pp \rightarrow \pi^+ \pi^- (K^+ K^-)$  cross-sections, structure 0-68485  
 $t$ -quark mesons, mass, quark model predictions 0-95256  
 $t\bar{t}$  states,  $t$  threshold, potential model predictions 0-86682  
 $t\bar{t}$  vector meson, proposed 40 GeV mass 0-62942  
 $U(2310)$ ,  $pp \rightarrow \pi^+ \pi^- (K^+ K^-)$  cross-sections, structure 0-68485  
 $T$ , production and decay in quark fusion model 0-102018  
 $T$ , quarkonium spectroscopy in a potential model with vacuum-polarization corrections 0-78038  
 $T$ , vibrational states in string picture, mass and leptonic width 0-62949  
 $T(9.46)$ ,  $b\bar{b}$  bound state, bottom hadrons, masses and allowed decays,  $SU(5)$  quark model 0-62954  
 $T(9.46)$ , leptonic branching ratio, from electronic width and muonic branching ratios 0-57588  
 $T(9.46)$  orthoquarkonium decay, jet profiles, three gluon structure 0-73698  
 $T(9.4) \rightarrow \text{charmonium}$ , quarkonium prod. via one gluon mechanism 0-95263  
 $T(9.5)$  decay modes from Zweig rule intermediate vector particle model (*Chinese*) 0-73697  
 $T$  and charmonium spectra, common pot. fit,  $T^{*+}-T$  mass difference 0-86712  
 $T$  decays, hadronic, asymptotic freedom, one-photon or three-gluon exchange 0-62971  
 $T$  production, photon-gluon fusion model, gluon distrib.  $x$ -depend. 0-62922  
 $T$  spectrum, equaltime relativistic wave eqn. with confining potential 0-77977  
 $V \rightarrow \rho\mu^+ \mu^-$ , vector meson decay EM form factors in bag model (*Russian*) 0-62982  
 $KN(KN)$  scattering amplitudes, resonance region,  $t$ -channel couplings, hyperbolic dispersion relations 0-57643  
 $pp \rightarrow \pi^+ \pi^- (K^+ K^-)$ ,  $T$ ,  $U$  and  $V$  resonances 0-68485  
 $V(2480)$ ,  $pp \rightarrow \pi^+ \pi^- (K^+ K^-)$  cross sections, structure 0-68485

meson scattering see lepton-hadron scattering; meson-baryon scattering; meson-deuteron scattering; meson-meson scattering; meson-nucleus scattering; photon-hadron scattering

## meson spin and parity

$DD$ ,  $DD^*$ ,  $D^*D^*$ , charm molecules, dynamical model, light meson exchange 0-57572  
 $\pi^+ p \rightarrow (\pi^+ \pi^- \pi^0) \Delta^{++}$ , 16 GeV/c, partial wave anal.,  $\omega^*$  and  $A_2^0$  0-63033  
 $\psi(4.03)$ , isospin and  $G$ -parity, model independent prediction 0-86689

## mesonic atoms see mesic atoms

## mesonic molecules see mesic molecules

## mesons

for  $\mu$  mesons see muons

see also cosmic ray mesons; eta mesons; kaons; meson resonances; pions  
 bound state wave function, probability interpretation, form factors, Bethe-Salpeter eqn. (*Chinese*) 0-101930  
 charmed, hadronic props., superconvergence sum rules 0-78043  
 Green function, rainbow approach of scalar model (*Russian*) 0-68436  
 isospin classification, same finite group for mesons and baryons (*Chinese*) 0-62887  
 parton distrib. consistent with naive quark model and QCD 0-62937  
 properties, review from particle data group 0-67944  
 pseudoscalar mesons, charge radii and PCAC without soft current limit 0-99070  
 structure function in covariant parton model context 0-78020  
 superconductivity phase transition in meson states, quark quasiparticle model (*Chinese*) 0-102021  
 $qq$  systems, nonperturbative potential model 0-78040

## mesosphere

quasi 2-day wave in  $S$ -Hemisphere mesosphere, obs. 0-109207  
 aerosol, remote sensing techniques 0-109269  
 chemical composition, importance of energetic particle precip. 0-109213  
 eddy diffusion, models for mesosphere and lower thermosphere 0-109198  
 electron precipitation at high latitude, X-ray bremsstrahlung obs. 0-77205  
 energetics and thermal struct., theory 0-98412  
 equatorial, vertical vel. determ. from Diurnal Experiment 0-77047  
 gravity waves component in partial refl. drift obs. 0-81993  
 ionisation model of upper mesosphere, rel. to ionospheric reflecting layer below classical D-region 0-98508  
 light scatt. coeff. correl. to atmos. stratification (*Russian*) 0-105049  
 long-period waves in upper mesosphere, radar obs. 0-77056  
 mean meridional circulations of stratosphere and mesosphere, monthly mean planetary wave fluxes 0-109219  
 middle atmosphere, obs. from balloons, rockets and satellites, conference, London, England, (1978 December 12 to 13) 0-77540  
 neutral temperature from nightglow OH emission obs. 0-82121  
 noctilucent clouds, advances in space era, review 0-105095  
 noctilucent clouds over W.Europe (during 1979) 0-109289  
 planetary wave, radiatively damped, in middle atmosphere, interaction with zonally averaged circulation 0-109217  
 radar echo mechanisms, returns from clear air 0-90181  
 radar facility, MST radar at Poker Flat, Alaska 0-90254  
 radar for observing middle and upper atmosphere, Yaggi antenna array design 0-90255  
 radar studies at VHF and UHF freqs., review of obs. 0-90180  
 radar techniques (VHF and UHF) for dynamic struct. 0-105078  
 radiowave backscattering, depolarisation obs. at 50 MHz 0-85729  
 radiowave scattering of tropical latitude, VHF radar study 0-90193  
 satellite solar occultation sounding of the middle atmosphere 0-105079  
 semiannual oscillation in tropical middle atmosphere, review of observational evidence 0-109216  
 silver clouds, visible spectroscopic investig. from Salyut-4 orbit 0-82014  
 solar Mesosphere Explorer mission description (1981-2),  $O_3$  and related chemistry 0-105096  
 solar UV radiation, absorpt. in mesosphere and stratosphere 0-109248  
 spectral absorption, Lyman- $\alpha$  extinction by  $O_2$ , 0-77180  
 structure at Thumba from in situ UV absorpt. photometry obs. 0-105051  
 SURF storage ring calibrations for NASA stratosphere and climate programs 0-94721  
 temperature, obs. by satellite IR limb scanning method 0-105086  
 temperature diurnal variation, 25-65 km altitude equator region 0-82022  
 tides at meteor altitudes, CTOP radar obs. 0-77181  
 turbulent structure, spectral range (*Chinese*) 0-105092  
 Van der Waals molecules comp. of lower atmos. 0-85699  
 VHF radar obs. of struct. and dynamics 0-105032  
 wavelike struct. seen in radar obs. of vertical velocity 59-95 km altitude 0-90117  
 wind diurnal variation, 25-65 km altitude equator region 0-82022  
 wind in upper mesopause, diurnal variation of zonal and meridional components 0-109284  
 wind structure over Antarctica 0-81992  
 winds, mid-latitudes, mag. storm effects 0-61970  
 zonal mean circulation of middle atmosphere, numerical model 0-109218  
 H distribution, UV dayglow obs. 0-109290  
 NO, density profile from airglow obs., 72-120 km altitude 0-105094  
 O 2.53 mm line, Zeeman splitting rel. to geomagnetic field vars. 0-77124  
 O profile of mesosphere and lower thermosphere 0-72660  
 $O_3$  concentrations, meas. from 1.27  $\mu m$   $O_2$  airglow at middle latit. 0-72606  
 $O_3$  measurement by satellite IR limb scanning method 0-105086  
 $O_3$ , nighttime concentration (15-68 km), Nimbus 6 obs. comparison with OAQ-3 obs. 0-105016  
 $^{18}O^{16}O$ , photodissociation as source of atmospheric  $O_3$  0-94559

## metal castings see castings

## metal clusters

electronic time-of-flight mass spectrometer, separator for metal clusters research 0-77907  
 growth and props., appl. to catalysis and photographic processes, conf., Villeurbanne, France (Sep. '79) 0-105431  
 molecular clusters, UPS 0-80940  
 nucleation and mass spectra, clusters from 2 to 500 atoms 0-102596  
 TC, internal conversion, scattered-wave cluster technique 0-107696  
 transition metal clusters, carbonyls, fluxionality, collective oscills. and low energy spectra 0-87738  
 Ag, chemisorption of I, UPS obs. 0-84830  
 Ag clusters, latent image particles, electronic effects 0-82840  
 Ag-Au clusters, latent image particles, electronic effects 0-82840  
 Au, pentagonal symmetry, icosahedral struct. (*French*) 0-79729  
 Bi, 2 to 500 atoms, nucleation, mass spectra 0-102596  
 Cu<sub>2</sub> Zn clusters, electronic structures, SCF-X $\alpha$ -SW method 0-88468



**metal clusters continued**

- Cu<sub>4</sub> clusters, electronic structures, SCF-X $\alpha$ -SW method 0-88468  
 Mo<sub>2</sub>, one-dimens. condensation of Mo<sub>6</sub> octahedral clusters, prep. and struct. of Ti<sub>2</sub>Mo<sub>2</sub>S<sub>11</sub> and K<sub>2</sub>Mo<sub>2</sub>S<sub>11</sub> 0-107168  
 Ni clusters local densities of states 0-88466  
 Ni, metallic particles, stability and electronic struct. (French) 0-80155  
 Pb, 2 to 500 atoms, nucleation, mass spectra 0-102596  
 Pd, adsorption/desorption of CO, AES and thermal desorption meas. 0-75436  
 Ru-Cu clusters, EXAFS study 0-84804  
 Sb, 2 to 500 atoms, nucleation, mass spectra 0-102596  
 Sb discontinuous thin films, cluster shape models 0-100419  
 Ti-Fe, H storage material, Mossbauer surface studies, Fe clusters 0-97167  
 Zn<sub>4</sub> clusters, electronic structures, SCF-X $\alpha$ -SW method 0-88468

**metal corrosion** *see corrosion***metal-insulator boundaries**

- see also metal-insulator-metal structures*  
 charging polymer surfaces, injection times obs. 0-70796  
 electrification of polymers by metals, contact time effect obs. 0-70829  
 energy barrier, self-consistent theory 0-60087  
 frictional electrification of PVC contrib. of polymer mol. motion 0-70798  
 hexafluoropropylene-tetrafluoroethylene copolymer, surface component of vac. absorpt. and resorpt. currents, source of dielec. loss 0-70792  
 metal polymer contact, charge transfer and contact charge spectroscopy 0-65680  
 metal polymer contact, charge transfer and contact charge spectroscopy 0-65681  
 metal-dielectric interface, static point charge in dielec., pot. distrib. (Russian) 0-60088  
 metallic films, metal-dielectric boundary thermal resistance, nonlinear elec. resistance (Russian) 0-65530  
 polymers, surface component of vacuum absorpt. and resorpt. currents, surface charge accumulation 0-60063  
 polymers, surface component of vacuum absorpt. and resorpt. currents, origin and magnitude 0-70791  
 rubber-metal interface, adhesion mechanism, XPS study 0-65382  
 Al electrodes charge effects, on PET and SiO<sub>2</sub> films 0-75625  
 Al-SiO<sub>2</sub> interface in MOS capacitors, conductivity effects of oxidation temperatures 0-100518  
 Hg-polymer interface, contact potential and charge exchange meas. 0-75642  
 Pd-SiO<sub>2</sub>, work function changes due to adsorbed H<sub>2</sub>, surface and interface dipoles 0-96972  
 Si-SiO<sub>2</sub> inversion layer, n-channel, anomalous magnetoresist., model 0-96996

**metal-insulator-metal devices**

- point-contact diode harmonic generators and mixers 0-60105  
 Al-Al<sub>2</sub>O<sub>3</sub>-Au device in Cl<sub>2</sub> atmosphere, current-voltage characts., press. depend. 0-65704  
 W-Ni(Co) point-contact diodes as harmonic generators and mixers, DC bias dependence 0-75653

**metal-insulator-metal structures**

- barium stearate single-layer Langmuir films, elastic and inelastic tunnelling 0-80403  
 cadmium arachidate mixed with cyanine dyes, mol. layers, photoelec. props. 0-80401  
 calcium behenate monomolecular layers between Al electrodes, nonlinear dielec. props. 0-80405  
 cathode, local electron emission and electroluminescence patterns obs. 0-108327  
 cyanine dye monolayer assemblies with Al and Ba electrodes, photovolt., dark cond. and photocond. 0-80400  
 diodes, quantum noise at low temperature 0-103733  
 electron source, non-heated, review 0-84516  
 PMMA film in small area lateral MIMS device, cond., switching 0-97003  
 polyphenylene oxide thin films, electrochem. prep., impurity effects on cond., electroforming 0-88655  
 PVC films, soln. grown, DC cond. mechanisms, field and temp. depend. 0-97021  
 PVC in metal sandwich struct., switching props., voltage- and current-controlled negative resist. 0-103767  
 resonant tunnelling, IV characteristics, comments 0-70847  
 space charge limited cond. in MIM struct., transport eqns. 0-97002  
 stearic acid multilayers, dielec. props. 0-80404  
 TSC, space-charge layer model 0-93009  
 tunnel currents, closed-form approximation, analytical expressions 0-60064  
 tunnel junction, magnetically doped, hopping model of zero-bias tunnelling anomalies, comparison with expt. 0-65703  
 Ag:Al<sub>2</sub>O<sub>3</sub>:Al tunnel-junction struct., surface polariton mean free path, roughness 0-93008  
 Al/Al<sub>2</sub>O<sub>3</sub>/Al, dielec. props. 0-80404  
 Al/Al<sub>2</sub>O<sub>3</sub>/Al structures with organic monomolecular layer, cond. at high elec. fields 0-80402  
 Al-Al<sub>2</sub>O<sub>3</sub>-Dy thin junctions, Poole-Frenkel effect obs. and cause 0-80398  
 Al-Al<sub>2</sub>O<sub>3</sub>-Pb contacts, tunnelling spectroscopy, band struct. of Pb 0-80169  
 Al-AlF<sub>3</sub>-Al thin film structures, dielec. and elec. props. (Slovak) 0-100536  
 Al-Formvar-Sn coupled films, Ginzburg's excitonic supercond. model 0-97039  
 Al-insulator-In<sub>1-x</sub>Mg<sub>x</sub> film tunnel junction, resistance zero-bias anomalies 0-107925  
 Al-Si<sub>3</sub>N<sub>4</sub>-O-Al thin film cathode, physical model from expt. study 0-100535  
 Al-silicon oxynitride-Al cathode, LF noise sources and reduction 0-108328  
 Al-stearic acid-Al, low-loss thin film capacitor 0-71317  
 Al-Ta<sub>2</sub>O<sub>5</sub>-Al, healing of defects in dielec. film by anodisation 0-65406  
 Al-TbF<sub>3</sub>-Al structure, AC conduction in TbF<sub>3</sub> film 0-70868  
 Al-Y<sub>2</sub>O<sub>3</sub>-Au, electroforming props. in thin evaporated films 0-65705  
 AlN films, RF glow discharge deposited, current-voltage characts. 0-84515  
 Au-dye-amorphous SiO<sub>2</sub>-Au struct., dye-sensitised steady-state photocond. 0-107924  
 Bi<sub>2</sub>O<sub>3</sub>, thin film capacitor elec. props. under reduced press. 0-80397  
 CaF<sub>2</sub> thin films, partial ionic thermocurrent meas. 0-97018

**metal-insulator-metal structures continued**

- Pt-polymer-Au capacitor, electroforming, negative resist., electron emission 0-80406  
 SiO<sub>2</sub> thin film dielec., in MIM struct., interfacial props. rel. to non-stoichiometry 0-80399  
 Ta-Ta<sub>2</sub>O<sub>5</sub>-Ag junctions, polarity-depend. tunnelling cond. 0-70846  
 Tm<sub>2</sub>O<sub>3</sub> film, between Al electrodes, prep. and elec. props. 0-60103  
 Y-Y<sub>2</sub>O<sub>3</sub>-Au, electroforming props. in thin evaporated films 0-65705
- metal-insulator-semiconductor devices**  
*see also charge-coupled devices*  
 diode, C-V curve used to examine trapping level in semiconductors 0-65697  
 inversion layer solar cells, numerical modelling 0-81444  
 MOS, voltage ramp technique for meas. of lifetimes in damage gettered Si 0-75247  
 MOS capacitor, interface state parameter determ. by DLTS 0-65642  
 MOS diodes, tunnel-assisted transport at room temp. 0-92975  
 p-n-insulator metal switching devices, avalanche mode operation 0-70838  
 solar cells, automated surface states anal. 0-93966  
 solar cells, computer simulation studies rel. to interface state meas. 0-72048  
 solar cells, elliptic-align V-grooved hyperjunction thin film cell, MIS and SIS device apps. 0-94082  
 solar cells, effects of nonuniformity of insulating layer 0-104507  
 solar cells, electron beam evaporated Si films 0-93490  
 solar cells, etched slotted mask for direct deposition of metal contact pattern 0-97786  
 solar cells, fundamental mechanisms affecting performance of MOS-inversion layer cells 0-61377  
 solar cells, grating minority carrier, design and expt. results 0-81445  
 solar cells, interface problems, AES, SIMS and XPS study 0-89627  
 solar cells, inversion layer, surface passivation 0-101098  
 solar cells, inversion layer, two-dimensional model 0-89641  
 solar cells, Schottky barrier height change and current transport in presence of interfacial layer 0-61353  
 solar cells with diffused back surface field (BSF), and diffused junction solar cells with MIS BSF 0-94074  
 tunnel diode, minority-carrier, pot. barrier height 0-96998  
 tunnel structure, injection and extraction effects, self-consistent model 0-92996  
 Al-Si MIS solar cells, depth conc. profiles, elec. and optical props. of Al films 0-94076  
 Al-SiO<sub>2</sub>-p-Si solar cells, comparison of majority- and minority-carrier Si MIS cells 0-85280  
 Al-SiO<sub>2</sub>-Si MOS solar cells, open-cct. voltage var. with oxide layer thickness 0-81434  
 Al-SiO<sub>2</sub>-p-Si solar cells, comparison between MIS and SIS 0-81443  
 Au-SiO<sub>2</sub>-n-Si solar cells, comparison of majority- and minority-carrier Si MIS cells 0-85280  
 Cr-MIS solar cells, on polycryst. Si, grain boundary effect and conduction mech. 0-93894  
 Cr-MIS solar cells on p-type wacker poly-Si substrates, high efficiency design 0-93935  
 Cr-MIS solar cells on Si, revised process to increase active area efficiency and reproducibility 0-81462  
 Cr-SiO<sub>2</sub>-Si MIS solar cells, photovoltaic performance and interface states, nucl. radiation effects 0-94004  
 Cu<sub>2</sub>O MIS solar cell with SiO<sub>2</sub> interfacial layers, semi-transparent layers of Au, Cu, Ag and Al 0-93946  
 GaAs antireflecting MOS solar cells, epitaxial and polycryst. using OM-CVD techniques 0-94072  
 GaAs MIS solar cells, effects of thin oxide layers on characts. 0-89624  
 GaAs polycrystalline thin film solar cells, fabrication 0-94066  
 GaAs-Al<sub>0.5</sub>Ga<sub>0.5</sub>As MOS rib waveguide polariser, modulator and isolator 0-64217  
 n-InP, MOS solar cells, electrical and photovoltaic characteristics 0-85276  
 p-type InP/Langmuir film MIS diodes, characts. 0-80384  
 InP-SiO<sub>2</sub> interface, CVD problems, ESCA profiles 0-93497  
 InSb MIS diode, anodised, C-V characts., effect of high elec. field pulse 0-60092  
 Si based MOS device irradiation with  $\gamma$ -rays, minority carrier generation, CV characts. 0-88637  
 n-Si channel (100) inversion layer MOSFET, valley splitting, conductivity 0-70840  
 Si MIS grating solar cells on minority carrier blocking back surface field substrates 0-94078  
 Si MIS phototransistors, photoelec. props. at high illum. intensities 0-60101  
 Si MIS solar cells with Cr, Hf, Be, Sc and Y as barrier forming metals, expt. investigation 0-94077  
 Si MIS/inversion layer solar cells 0-94075  
 Si MOS back-surface-field solar cells, open-cct. voltage >700 mV, 20% conversion efficiencies 0-81435  
 Si minority carrier MIS solar cells, AM1 efficiencies 0-93975  
 Si, polycrystalline Czochralski-grown, MIS solar cell characterisation using scanned laser response exam. 0-93884  
 Si:H amorphous MIS solar cell, loss mechanisms and photovoltaic parameters, overview 0-93923  
 Si-SiO<sub>2</sub> in MOSFETs, inversion layer carrier mobility, theory 0-60094  
 Si-SiO<sub>2</sub> interface in MOS solar cells, operational characts. and struct. 0-93901  
 Si-SiO<sub>2</sub> MIS systems, dynamic props. of switching, appl. to charge transfer devices 0-92997  
 Si-SiO<sub>2</sub>-Al MOS surface channel influence on channel-to-contact diode charact. 0-92994  
 Si-SiO<sub>2</sub>-Au Schottky barrier solar cells, back-illuminated, theoretical performance 0-61345

**metal-insulator-semiconductor integrated circuits** *see field effect integrated circuits***metal-insulator-semiconductor structures**

- buried channel MOS structures, charge-handling capacity under hot electron conditions 0-80381  
 conductor-insulator-semiconductor. (CIS) solar cells, noncrystalline (poly and amorphous), interface importance 0-81466  
 conference, Durham, England (July 1979) 0-90612  
 dielectric layer, transient processes during charge trapping for injecting contact 0-70844  
 dielectric-semiconductor structures, surface ion migration, theoretical analysis 0-65700



**metal-insulator-semiconductor structures continued**

- Faraday rotation, far IR, 2D electron gas, carrier effective mass determ. 0-80389
- fast surface states density, photoelectric method of determ. 0-70835
- generation lifetime, surface generation velocity determ., linear sweep MOS-CV method (*Chinese*) 0-107916
- grain boundary diffusion, chemical reactions, contamination, AES and SIMS 0-72066
- hysteresis measurement, second order equivalent ccts. 0-57332
- III-V semiconductor based layered multielectronic systems, electronic process investig. survey (*Russian*) 0-107891
- III-V semiconductor-oxide interface states, photoemission obs. of energy levels induced by adsorpt. 0-93000
- inversion layer near electrode edge, pot. and charge density distribution 0-88642
- magnetodiode and magnetoconcentration effects, influence of field effect 0-107903
- magneto-optic absorption by electron gas, optical phonon effects 0-97248
- magneto-optic interband absorption by semicond. surface layer 0-93288
- metal-tunnel oxide-Si junctions, processing condition depend. 0-80380
- microelectronics, conf., Calcutta India (Jul. 79) 0-96755
- minority-carrier lifetime and surface generation velocity determ., hysteresis pulsed C-V method 0-70839
- MISIM struct. inversion layer, symmetrical, carrier conc. calc. 0-75651
- MNOS structure conductivity instability caused by passed charge 0-80394
- MNOS structures, electron-beam-irrad., interface defects, high temp. H<sub>2</sub> anneal 0-96745
- MOS capacitor, characterisation of surface states of HCl-grown oxides 0-65696
- MOS capacitor, direct current/voltage relns. as function of oxide doping 0-88635
- MOS capacitor formed over p-on-n semiconductor structure, G-V characts. 0-100532
- MOS interface states density, photoemission obs. using photocurrent and photocapacitance meas. 0-92990
- MOS inversion layers, freq. response of charge transfer 0-88638
- MOS pulsed capacitor, minority carrier lifetime meas. influence of Si-wafer surface state density 0-60098
- MOS space charge layer physics 0-92980
- MOS structure, semiconductor conductance and capacitance, extended AC conductance-bias method 0-96995
- MOS structure concentration profile numerical evaluation (*Slovak*) 0-65690
- MOS structure implanted with B ions, radiation defects and impurity activation 0-103757
- MOS structure Pt diffused, hysteresis and memory props. 0-96992
- MOS structure with highly doped region, relaxation processes at high voltages 0-70843
- MOS structure with nonuniformly doped semiconductors, heavy inversion, definition for onset 0-96994
- MOS structures, quasistatic and nonequilibrium phenomena with constant gate-current bias 0-80385
- MOS structures, radiation-induced positive charge, thermal annealing 0-75648
- MOS structures obtained by etching of Si and SiO<sub>2</sub> surfaces, props. 0-93671
- MOS structures of small-gap semicond., capacitance, effect of quantising mag. field 0-84513
- MOS-structure, with adjoining reversed biased p-n junction, charge pumping current and reverse current (*German*) 0-88636
- MOST structure modelling, using hybrid computer, Poisson partial differential equation solution (*Slovak*) 0-75643
- n-type capacitors, optically active interface states study 0-60096
- passivation by phosphosilicate glass layer, flat-band voltage, effect of growth conditions 0-107913
- photosensitive high resolution struct., spatial light modulation with liq. cryst. 0-96026
- photovoltaic technology, conf., San Diego, CA, USA (Jan. 1980) 0-86041
- solar cells appl. minority carrier MIS diodes (*Slovak*) 0-97792
- SOS MOST, electronic props. at Si-sapphire interface 0-96993
- surface depletion and inversion, arbitrary doping profile, theory 0-107912
- surface state density, determ. from surface saturation photo-EMF meas. 0-75652
- surface state spectrum meas. by pulsed C-V method 0-88641
- switching phenomena in thin-insulator MIS diodes, current-control-type negative resist. characts. 0-107915
- tunnel currents, closed-form approximation, analytical expressions 0-60064
- tunnel structure, injection and extraction effects, self-consistent model 0-92996
- tunnelling MIS structures, photovoltaic energy conversion, band struct. 0-92995
- Ag-In-S<sub>2</sub>-Si layered struct., Hall effect, I-V characts., surface states (*Russian*) 0-97001
- Al/SiO<sub>2</sub>/pSi MIS solar cells, stability 0-85287
- Al-Al<sub>2</sub>O<sub>3</sub>-GaAs backwall MIS Schottky barrier solar cell, anal. model 0-85289
- Al-Al<sub>2</sub>O<sub>3</sub>-Si structure, study of charge trapping 0-60097
- Al-Al<sub>2</sub>O<sub>3</sub>-SiO<sub>2</sub>-Si capacitors, physical and elec. props. of RF plasma grown Al<sub>2</sub>O<sub>3</sub> 0-100530
- Al-Al<sub>2</sub>O<sub>3</sub>-p-GaAs MOS diode, capacitance-voltage characts. 0-107914
- Al-AlN-SiO<sub>2</sub>-Si capacitors, physical and elec. props. of RF plasma grown AlN 0-100530
- Al-anodised Ta<sub>2</sub>O<sub>3</sub>/native oxide-n-GaAs MOS structure evaluation 0-84514
- Al-In-S<sub>2</sub>-Si layered struct., Hall effect, I-V characts., surface states (*Russian*) 0-97001
- Al-Si<sub>3</sub>N<sub>4</sub>-Ge, thermally stimulated depolarisation current meas. 0-88643
- Al-Si<sub>3</sub>N<sub>4</sub>-SiO<sub>2</sub>-Si, MNOS structures degradation under UV irradiation effect 0-107923
- Al-SiO<sub>2</sub> interface in MOS capacitors, conductivity effects of oxidation temperatures 0-100518
- Al-SiO<sub>2</sub>-Si, pyroelectricity 0-100524
- Al-SiO<sub>2</sub>-Si MOS structures, charge motion, TSC meas. 0-100534
- Al-SiO<sub>2</sub>-Si structures, minority carrier lifetime investigation in Si:Zn and Si:Co 0-80292
- Al-SiO<sub>2</sub>-(p)-Si barrier structs., minority carrier injection ratio meas., MIS solar cell model 0-93007
- Al<sub>2</sub>O<sub>3</sub> MIS Schottky structures, photovoltaic response 0-101115

**metal-insulator-semiconductor structures continued**

- Au/oxide/n-GaAs struct., photocurrent relax. 0-92978
- Au-oxide-GaAs, reverse bias influence on photocurrent 0-107921
- Au-SiO<sub>2</sub>-Si system, oxide film 16-36 Å thick, tunnel currents 0-70842
- Au-Ti/SiO<sub>2</sub>/p-Si MOS struct., interface state distrib., DC tunnelling spectra determ. 0-75611
- p-CdTe-Langmuir film interface, prep., characters. and MIS struct. 0-92998
- GaAs based MOS capacitors, scanning photovoltage investigation 0-80396
- GaAs films for solar cells appl., deposition and characterisation 0-84853
- GaAs MOS solar cells by anodisation in active region 0-101107
- GaAs MOS structures, leakage current for anodic oxide layers, space charge trapping effects 0-60091
- GaAs, native oxide growth by wet anodisation 0-70832
- GaAs oxide film form., ion implantation effects 0-100266
- GaAs, photocapacitive MIS IR detector, spectral response, noise characts. 0-75644
- GaAs, surface passivation using composite Al<sub>2</sub>O<sub>3</sub> and native oxide, MIS characts. 0-93004
- GaAs, surface passivation using Si<sub>3</sub>N<sub>4</sub>, interface characts. 0-93005
- GaAs, surface passivation using Ga<sub>x</sub>N<sub>y</sub> based multiple insulating layers 0-93006
- GaAs:Cr, deep levels, wavelength-modulated photocapacitance spectroscopy 0-76055
- GaAs-Al<sub>0.3</sub>Ga<sub>0.7</sub>As MOS rib waveguide polarizers 0-64207
- n-GaAs-SiO<sub>2</sub> interface, MOS capacitors, surface states from conductance and capacitance meas. 0-100533
- Ge-InAs based MIS struct., avalanche carrier multiplication 0-88566
- Hg<sub>1-x</sub>Cd<sub>x</sub>Te breakdown-limited MIS device, increased charge capacity using ramped gate voltage 0-103751
- InP, and In<sub>0.5</sub>Ga<sub>0.5</sub>As<sub>0.5</sub>P<sub>0.5</sub> binary and quaternary cpds., surface and dielec.-semicond. interface props. 0-93001
- InP, surface passivation using composite Al<sub>2</sub>O<sub>3</sub> and native oxide, MIS characts. 0-93004
- p-type InP/Langmuir film MIS diodes, characts. 0-80384
- n-InSb based MIS struct., carrier generation under nonequilibrium conditions 0-88640
- n-InSb, MIS diode, time-dependent photovoltaic effect 0-75601
- p-InSb MIS struct., field effect studies 0-80386
- InSb MIS structure, effect of room background on noise props. 0-103755
- InSb MOS struct., capacitance of n-channel inversion layers, elec. field effects 0-80393
- InSb MOS structs., energy spectrum of traps in oxide layer 0-107922
- n-InSb substrates, MIS struct. form. by reactive deposition of Si<sub>3</sub>N<sub>4</sub>, C/V meas. 0-103752
- LaF<sub>3</sub> superionic conductor insulating layer, used for photocapacitive detectors 0-92976
- MOS capacitor, photoionisation cross section and interface state density 0-92974
- Si based MIS negative barrier contact for induced back surface field solar cell 0-101101
- Si based MIS structure, photoelectric characts. carrier injection levels (*Russian*) 0-96946
- Si based MOS capacitors, scanning photovoltage investigation 0-80396
- Si MIS capacitors, C-V curves, outer oxide surface conditions effects 0-97000
- Si MIS-inversion layer solar cells 0-76632
- Si, MOS diode, dependence of minority carrier bulk generation on HCl concentration 0-88639
- Si p-channel MOS structure, stress effects on elec. props., press. transducer props. 0-100526
- Si, photocapacitive MIS IR detector, spectral response, noise characts. 0-75644
- Si, polycryst., energy distrib. of trapping states, from impedance of MOSS struct. 0-65691
- Si polycrystalline film resistivity reduction by Nd:YAG laser annealing 0-100539
- Si rich SiO<sub>2</sub>-SiO<sub>2</sub>-Si rich SiO<sub>2</sub> layers for dual electron injector struct. 0-96991
- Si solar cells using minority carrier MISS 0-101103
- Si, thermally oxidised surfaces, electron mobility in inversion and accumulation layers, MOS devices 0-103753
- Si:H, amorphous, surface states distribution using MOS tunnel junctions 0-103735
- Si:H, amorphous oxidised, Pt film growth AES and LEED study 0-88447
- Si-Cr<sub>2</sub>O<sub>3</sub>-Al, current-voltage characts., oxide film effects 0-70841
- Si-insulator interface, non-avalanche charge injection, expt. study, charge trapping effects 0-60099
- Si-Si<sub>3</sub>N<sub>4</sub> interface in MNS capacitors, surface state density investigation 0-60100
- Si-SiO<sub>2</sub>, MOS interface states density, meas. techniques and model development 0-92988
- n-Si-SiO<sub>2</sub>, MOS structures, radiation states 0-103758
- Si-SiO<sub>2</sub>, Si oxidation, solubility and transport behaviour of water, dissolution 0-93801
- Si-SiO<sub>2</sub>, thermal growth mechanisms of vitreous oxide layers on Si 0-93675
- Si-SiO<sub>2</sub> interface, barrier height in MOS tunnelling structures 0-88644
- Si-SiO<sub>2</sub> interface, doping depend. of interface states and charges 0-92992
- Si-SiO<sub>2</sub> interface, O<sub>2</sub> plasma effects on elec. props. 0-100523
- Si-SiO<sub>2</sub> interface, thermally grown, surface pot. inhomogeneities after stress ageing 0-92993
- Si-SiO<sub>2</sub> interface in MIS structs., effects of crystal defects on generation process 0-65702
- Si-SiO<sub>2</sub> interface in MOS structs. low-energy electron beam irradiation, charge accumulation process anal. 0-65701
- Si-SiO<sub>2</sub> interface in MOS capacitors, lateral diffusion of Na<sup>+</sup>, neutralisation 0-92986
- Si-SiO<sub>2</sub> interface states, deposition of H containing layers and annealing 0-92991
- Si-SiO<sub>2</sub> MIS systems, dynamic props. of switching, appl. to charge transfer devices 0-92997
- Si-SiO<sub>2</sub> MOS capacitors, relationship between trapped holes and interface states 0-70830
- Si-SiO<sub>2</sub> MOS interface, surface state density and minority carrier generation rate, meas. by DLTS, hot hole effect 0-100527
- Si-SiO<sub>2</sub> MOS interface states density, transient capacitance meas. eval. 0-92989



**metal-insulator-semiconductor structures continued**

- Si-SiO<sub>2</sub>-Al, interface barrier energies for tunnel oxides, internal photoemission meas. 0-84512  
 Si-SiO<sub>2</sub>-Al, internal photoemission, pot. barrier height determ. 0-65699  
 Si-SiO<sub>2</sub>-Al structures, SiO<sub>2</sub> thin dielec. film elec. props. with DC voltage (Slovak) 0-88634  
 Si-SiO<sub>2</sub>-Al with thick dielec. layer, photoelec. props. 0-92979  
 Si-SiO<sub>2</sub>-Mo-Si<sub>3</sub>N<sub>4</sub>-Al MNOS structures with metal grains, charge transport at SiO<sub>2</sub>-Si<sub>3</sub>N<sub>4</sub> interface 0-65693  
 Si-SiO<sub>2</sub>-Si thin film MOS structures, elec. props. with applied DC voltage (Slovak) 0-92977  
 Si-SiO<sub>2</sub>-Si<sub>3</sub>N<sub>4</sub> MNOS structure, chem. comp. and electronic states, Auger and energy loss spectra obs. 0-92999  
 Si-TiO<sub>2</sub>-Al, current-voltage characts., oxide film effects 0-70841  
 Si-V<sub>2</sub>O<sub>5</sub>-Al, current-voltage characts., oxide film effects 0-70841  
 Si<sub>3</sub>N<sub>4</sub> films, CVD in MNOS and MNS strucs., elec. resist. 0-97019  
 SiO<sub>2</sub>, As-implanted, electron trapping and detrapping characts. 0-65692  
 SiO<sub>2</sub> CVD layer, high current injection from Si rich SiO<sub>2</sub> film 0-80430  
 SiO<sub>2</sub> films in poly-oxide poly Si structures, elec. cond. and charge distrib. 0-92984  
 SiO<sub>2</sub> layer used for MOSFETs, electron trapping behaviour 0-92981  
 SiO<sub>2</sub> layers on Si, ionis. thresholds of electron traps 0-92983  
 SiO<sub>2</sub> MOS capacitor, defect current obs. 0-92987  
 SiO<sub>2</sub>, mobility and trapping of ions, Si-SiO<sub>2</sub> interface states 0-92985  
 SiO<sub>2</sub> tunnelling barrier asymmetry to electrons and holes in MOS struct., photocurrent 0-75645  
 SiO<sub>2</sub>:As<sup>+</sup> implanted layers in MOS struct., electron trapping and detrapping characts. 0-92982  
 Ta-Ta<sub>2</sub>O<sub>3</sub>-InP thin refractory MIS struct. deposition 0-75647  
 Ta<sub>2</sub>O<sub>5</sub> film on Al, Cu, Au, Ag electrode, electric strength of MIS system 0-96999  
 TiW-TiO<sub>2</sub>-InP thin refractory MIS struct. deposition 0-75647

**metal-insulator transition**

- see also electrical conductivity transitions; minimum metallic conductivity*  
 alloys, amorphous, exhibiting Mossbauer spectra, elec. props. (French) 0-80244  
 alloys, binary, 50-50, singularities at metal-insulator transition, CPA calc. 0-84428  
 Anderson transition, electron-electron interaction effects 0-65453  
 chemical mechanism, thermodynamics, vacancies 0-103626  
 density-functional theory 0-75507  
 disordered electronic systems, low-dimensionality, Anderson localisation, resist. 0-84491  
 energy bands, narrow, electron correlation, Gutzwiller variational method 0-84426  
 energy sub-bands in polar model of crystal (Russian) 0-80183  
 exciton insulators with spontaneous currents, impurity scatt. effect on phase transitions 0-80242  
 heavily doped semiconductor, n-type, disordered mag. system, hierarchy of exchange interactions 0-80235  
 Hubbard band, half-filled, in paramag. state 0-92817  
 Hubbard model, Poisson approx. to functional approach 0-96790  
 intermediate valency compounds, conduction processes, metal-insulator transition 0-96787  
 metal inhomogeneous granular, superconductivity 0-103795  
 Mott transition in Hubbard long range model, isostructural instability, thermodynamic props. (Russian) 0-65454  
 narrow band electron systems, unified theory of magnetism 0-70928  
 poly(p-phenylene), AsF<sub>5</sub> doped, highly cond. charge transfer complexes, elec. and optical props. 0-70778  
 polyacetylene:AsF<sub>5</sub>, soliton doping mechanism, mag. susceptibility meas. 0-107979  
 polyacetylene:SbF<sub>6</sub>, elec. cond. meas. 0-60055  
 polyacetylene, doped, elec. cond. and thermopower 0-96951  
 polyacetylene films, doping investigation, insulator-metal transition, optical transmission meas. 0-103729  
 semiconductor, doped, anal. 0-88478  
 semiconductor, n-type, donor-polarizability enhancement as the insulator-metal transition is approached from the insulating side 0-80184  
 semiconductors, doped, local spin-density-functional method, appl. to metal-insulator transition 0-96789  
 spatially disordered systems, Anderson localisation and metal-insulator transition 0-59926  
 spin-density functional approach to metal-insulator transition and local moment-formation 0-65451  
 superconductor, metal-insulator transition, electron pairing, effect on optical props. 0-60139  
 TCNQ ion radical salt, DECA(TCNQ)<sub>2</sub>, IR absorpt. spectra obs. of first-order transition 0-71397  
 tetramethylammonium(0), Li(CH<sub>3</sub>NH<sub>2</sub>)<sub>4</sub>, existence, conduction- and localised-electron spin reson. 0-66035  
 (TMTSF)<sub>2</sub>PF<sub>6</sub>, ESR g-factor, linewidth, spin susceptibility, metal-insulator transition 0-103887  
 (TMTSF)<sub>2</sub>X, (X=PF<sub>6</sub><sup>-</sup>, AsF<sub>6</sub><sup>-</sup>, SbF<sub>6</sub><sup>-</sup>, BF<sub>4</sub><sup>-</sup>, NO<sub>3</sub><sup>-</sup>) highly conducting salts, props. 0-59969  
 transition metal cpds., review 0-59874  
 TTF-TCNQ, CDW transition with tripling of period along chains 0-96805  
 TTF-TCNQ type crystals, Kolmogorov Arnold Moser theorems, appl. to struct. problems in condensed matter 0-59878  
 two-band model, Coulomb interactions, self consistent calcs. (Russian) 0-80185  
 valence transition, entropy and phase diagram 0-59877  
 Al, granular supercond., normal state cond. 0-88529  
 Au, Si<sub>1-x</sub>, amorphous films, phys. studies 0-75476  
 CaO, band struct. calc. rel. to high press. metallisation 0-84427  
 CdS, doped, amorphous antiferromagnet model, susceptibility and spin-flip Raman scatt. meas. 0-97057  
 Eu<sub>1-x</sub>Gd<sub>x</sub>O<sub>2</sub>, mag. props., transport meas. 0-97117  
 Eu<sub>1-x</sub>Nd<sub>x</sub>Fe<sub>2</sub>O<sub>7</sub>, lattice parameters, mag. and elec. props. 0-100578  
 FeTe, magnetic impurity states, mag. and transport props. 0-96913  
 Fe<sub>1-x</sub>Co<sub>x</sub>Si solid solution, semiconductor-metal transition 0-103627  
 Fe<sub>2</sub>O<sub>4</sub>, Verwey transition, cond. processes 0-96787  
 GaAs(P), semiconductor-metal transition, press. calibration above 100 kbars fixed points 0-77808  
 GaSe, press. induced metallic and supercond. state 0-75666  
 H<sub>2</sub>WO<sub>4</sub> bronzes, Anderson transition, XPS 0-107705  
<sup>3</sup>He, solid, as mag. semicond., analogy to Mott insulator 0-96720

**metal-insulator transition continued**

- Hg-Xe vapour deposited films, cond. transitions, effect of disorder on supercond. 0-88659  
 HgCr<sub>2</sub>Sd<sub>1-x</sub>Te<sub>x</sub>, ferromag. semicond., zero bandgap transition 0-96783  
 I, metallic, mol. and monatomic phase, elec. resist. at high press. and low temp. 0-65638  
 n-InP, impurity and minimum metallic cond. in mag. field 0-103731  
 In<sub>2</sub>Se<sub>3</sub>, transitions of high temp.  $\alpha$  form (French) 0-92473  
 Mg<sub>2</sub>Fe<sub>1-x</sub>O<sub>4</sub>, polycryst., Verwey type transition, resist., magnetisation, Mossbauer effect and permeability obs. 0-75764  
 Mo, field emission anomalies in mag. field (Russian) 0-93462  
 Nb, field emission anomalies in mag. field (Russian) 0-93462  
 Ni<sub>1-x</sub>Cr<sub>x</sub>S, elec. transport, mag. susceptibility and DTA meas. 0-96954  
 NiFe<sub>2</sub>O<sub>4</sub>, electronic phase transition 0-65640  
 NiS<sub>2</sub>-Se<sub>2</sub>, electronic struct., UPS and XPS study 0-80935  
 SMS, band struct. and semicond. metal phase transition 0-80180  
 Se, electronic struct. of cryst. phases and hydrostatic press. effects 0-59865  
 Si, static compression in [100] and [111] directions, elec. resist. obs. 0-65637  
 Si:Li, electron-phonon scatt., in intermediate conc. region 0-65180  
 Si:P, dielec. susceptibility meas., polarisation catastrophe at metal-insulator transition 0-59873  
 Si:P, thermal cond., electron-phonon interaction at low temps. 0-92730  
 Sm chalcogenides, semiconductor-metal transition, extended Fel'icov-Kimball model valcs. 0-70616  
 (Sm<sub>1-x</sub>Gd<sub>x</sub>)<sub>2</sub>S<sub>4</sub>, mixed valence compound, elec. cond. transition 0-70777  
 Sm<sub>1-x</sub>La<sub>x</sub>S, magnetoresist. in semicond. and metallic phases 0-96914  
 SmS, LO phonon freq. softening in semicond. and metallic phases 0-96619  
 SmS, trivalent rare earth substituted, stability of Sm<sup>2+</sup> 0-65508  
 SmS, valence transition, two band model 0-65507  
 SmS<sub>1-x</sub>As<sub>x</sub>, magnetoresist. in semicond. and metallic phases 0-96914  
 SmS<sub>1-x</sub>P<sub>x</sub>, valence changes, XPS and UPS study 0-97402  
 Sm<sub>1-x</sub>Y<sub>x</sub>S, magnetoresist. in semicond. and metallic phases 0-96914  
 TTTT<sub>1-x</sub> complex, influence of press. on metal-dielectric phase transition (Russian) 0-92818  
 Ta<sub>1-x</sub>Ti<sub>x</sub>S<sub>2</sub> (1T), magnetoresistance in the Anderson localized states near the metal-nonmetal transition 0-88479  
 Ta<sub>1-x</sub>Ti<sub>x</sub>S<sub>2</sub> (1T), magnetoresist. near metal-nonmetal transition at ultra low temps. 0-88600  
 Te, electronic struct. of cryst. phases and hydrostatic press. effects 0-59865  
 Te, Mossbauer spectra under press. up to 8000 MPa 0-80647  
 Te-Se liquid mixtures, sound vel. meas., adiabatic compressibility determ. 0-65161  
 Ti<sub>2</sub>Te-Tl liquid system, conc. fluctuation, time-of-flight quasielastic neutron scatt. obs. 0-88324  
 TmSe-TmTe(EuSe), semiconductor-metal transitions 0-96953  
 V oxides, change in phonon damping due to metal-insulator transition 0-103625  
 (V<sub>1-x</sub>Cr<sub>x</sub>)<sub>2</sub>O<sub>3+x</sub>, elec. props. and struct. 0-84494  
 VO<sub>2</sub>, ferroelastic metal-insulator transition, electronically triggered crystallographic phase transition 0-70614  
 VO<sub>2</sub>, magnetic susceptibility in insulating and metallic phases, electron-electron and electron-lattice interactions 0-96788  
 VO<sub>2</sub>, metal-insulator transition, electron correls. and spin dimerization, thermodynamical study 0-70615  
 VO<sub>2</sub>, metal-insulator transition and electronic struct., ion bombard. effects 0-92948  
 VO<sub>2</sub> thin films, light modulation appls., optical props. at metal-insulator transition 0-87547  
 VO<sub>2</sub>, V<sub>2</sub>O<sub>3</sub> and V<sub>2</sub>O<sub>5</sub>, film prep. under equil. conditions, struct. and elec. props. 0-108352  
 VO<sub>2(2n-1)/n</sub>, metal-semicond. transition temps. 0-59876  
 V<sub>2</sub>O<sub>5</sub>, impurity doping effects, elec. props. obs. 0-75609  
 V<sub>2</sub>O<sub>5</sub>, metal-insulator transition, external mag. field effects 0-92819  
 W, field emission anomalies in mag. field (Russian) 0-93462  
 Xe, condensed at high press., electron-band theory and fluid theory calcs. 0-59875  
 Xe, crystalline, lattice constant at insulator-metal transition 0-107706  
 ZnS(Se)(Te), thermal expansion and lattice dynamics under press. 0-100316  
 ZnTe(S), semiconductor-metal transition, press. calibration above 100 kbars fixed points 0-77808

**metal-oxide-semiconductor devices** *see metal-insulator-semiconductor devices*  
**metal-oxide-semiconductor field effect transistors** *see insulated gate field effect transistors*

**metal-oxide semiconductor structures** *see metal-insulator-semiconductor structures*

**metal-semiconductor boundaries** *see semiconductor-metal boundaries*

**metal semiconductor field effect transistors** *see Schottky gate field effect transistors*

**metal-semiconductor-metal structures**

- chromophore phospholipid Langmuir films, photoeffects 0-80409  
 magnesium phthalocyanine, depletion layer studies, temp. depend. of LF capacitance 0-65617  
 phthalocyanine layers, metal-free, between Ag and Al electrodes, switching effects 0-65706  
 polyacetylene films, AsF<sub>5</sub> doped, photocond. and junction props. 0-70770  
 tetraene, depletion layer studies, temp. depend. of LF capacitance 0-65617  
 Ag<sub>2</sub>Se, between metal electrodes, current-voltage characts (French) 0-97005  
 Ag<sub>2</sub>Se thin film, switching and Ag movement, point contact technique 0-60107  
 Al/As<sub>2</sub>Se<sub>3</sub>/Sb structures, rectifying effects 0-75654  
 Al-amorphous GeSe-Al junctions, electrical contact effects on properties (German) 0-93010  
 Au-amorphous GeSe-Au junctions, electrical contact effects on properties (German) 0-93010  
 Au-CdTe-Au structure, current transport props. 0-80408  
 Au-GeSe<sub>2</sub>-Al(Au) structures, photoconductance meas. in amorphous GeSe<sub>2</sub> layers 0-65632  
 BaTiO<sub>3</sub>:Nb, elec. props., contact material influence 0-70848  
 CdTe metal-semiconductor-metal  $\gamma$ -ray detector characts. 0-57451  
 Cr-phthalocyanine-Cr sandwich, I-V and C-V characts. 0-60106  
 Mo-amorphous GeSe-Mo junctions, electrical contact effects on properties (German) 0-93010  
 Mo-chalcogenide glass-Mo-Al struct., strong elec. field effects 0-97004



**metal-semiconductor-metal structures continued**

- Pb-CdS-Pb junctions, Josephson effect through 0-100558  
 Si amorphous films, switching, electrothermal model 0-80407

**metal theory**

see also *band structure of crystalline metals; electron gas; lattice dynamics of metallic crystals*

- adsorption potential in hydrodynamical model 0-100396  
 antiferromagnetic metal, thermoelec. power in mag. field 0-70686  
 atomic binding energy and surface energy rel. to prediction of physical props. 0-59434  
 atoms as structural components in metallurgy (*Dutch*) 0-96465  
 Boltzmann equation for electrons, solns., energy depend. 0-88537  
 classical plasma frequency in long-wavelength limit, quantum correction 0-107728  
 compressibility, local pseudopot. approach 0-65129  
 cyclotron resonance on open electron orbits (*Russian*) 0-88878  
 dielectric function, degenerate electron gas at metallic densities, nonlocal interactions, compressibility and dispersion 0-107730  
 doubly occupied Wannier functions, constructive definition 0-75492  
 education, deep one-dimens. periodic pot., zero energy gaps, Kronig-Penney model 0-62426  
 electron density behaviour near impurity charge 0-75518  
 electron fluid, adiabatic de Haas-van Alphen effect at low temp., Fermi fluid interaction and chem. pot. effects (*Russian*) 0-84442  
 electron theory, contrib. of Sir Rudolf Peierls 1928-1935 0-57054  
 electron theory, work at University of Bristol, 1930-37 0-57068  
 electron theory of metals, contrib. of Felix Bloch 0-57053  
 electron theory of metals and geometry, review 0-103611  
 electron-phonon interaction, contrib. of John Bardeen 0-57057  
 elements, metallic, core-level binding-energy shifts 0-88502  
 ellipsometry, metallic films and surfaces, nonlocal effects, theory 0-104006  
 equation of state of simple metals, non muffin-tin corrections (*French*) 0-59906  
 Fermi surface, electronic props., book 0-105445  
 ferromagnet, antiresonance region, EM wave propag., Maxwells' eqns. soln. 0-66038  
 ferromagnetic metal, exciton condensation effects on props., Hubbard model 0-60171  
 ground state energy, structural expansion, HF approx. 0-65420  
 ground state energy, structural expansion 0-88497  
 independent electron metal, soln. of X-ray edge problem, recoil spectrum of suddenly perturbed Fermi sea 0-80932  
 internal press. in electron theory of metals 0-92802  
 localised dynamic perturbations 0-73262  
 Morse potential appl. in molecular-metallic framework 0-79742  
 narrow-band metals, Auger line shape 0-60719  
 non-simple metals, dielectric matrix, analytic model 0-75512  
 oscillating dipole-metal surface interaction, jellium model and random phase approx. 0-92955  
 plasmon satellite struct. in (e,2e) process 0-96809  
 polar states and free electron gas (*Russian*) 0-84415  
 quantum mechanical electron theory develop., 1900-28 0-57065  
 quasiparticle props., density functional approx., electron gas calc. 0-96808  
 simple, density functional theory of chemisorption, book contrib. 0-107647  
 simple metals, compressibility, Harrison pot. calcs. 0-96460  
 simple metals, elastic moduli, chem. trends, pseudopot. method 0-107355  
 simple metals, model pseudopot. appl. to various props. 0-59845  
 small metal particles, thermodynamic props. of electrons 0-59844  
 solid state physics, 1925-33 0-57066  
 solid state physics, 1933-40, contrib. of Sir Nevill Mott 0-57055  
 solid state theory, 1926-33 0-57067  
 solidification of metals, variational formulation of stationary free boundary problem (*French*) 0-96626  
 spin fluctuations, mag. field effect, electronic sp. ht. and elec. resist. 0-108026  
 strained metals, interpolation functions for Fermi surface 0-65425  
 surface, adatom mobility, density functional approximation calc. 0-103577  
 surface, force on moving charge, spatial dispersion effects 0-65646  
 surface, gradient approx. anal. appl. 0-96810  
 surface, work function, pseudopot. calc. 0-96970  
 surface atom vibrations, self-consistent calc. in tight-binding model 0-103560  
 surface dipole barrier, calc. 0-96958  
 surface energy, exchange and correl. contrib., wave-vector decomp. 0-75615  
 surface impedance near anomalous skin-effect limit, electron-electron N processes 0-100497  
 surface region, electrostatic energy and screened charge interaction for different Fermi surface shape 0-70631  
 Thomas-Fermi-pseudopotential approach to static props. of simple metals 0-75514  
 tight-binding metals, electronic struct. and kinetic props. at high temp. 0-59848  
 transition, rare earth, and normal metals, electronic struct. and magnetism, review 0-70573  
 transition metals, correlation effects, perturb. treatment within Hubbard model 0-70582  
 unidimensional metals, plasmon freq., effect of nonuniform electron density profile (*Russian*) 0-59896  
 US attenuation, quantum oscils. with dislocations under pressure (*Russian*) 0-88273  
 vacancy-dislocation interaction, tight-binding calc. 0-92554  
 Ag, mag. susceptibility, Animalu model pot. calc. 0-75711  
 Al, dynamic susceptibility, model pot. theory 0-75710  
 Au, mag. susceptibility, Animalu model pot. calc. 0-75711  
 Au, self-consistent relativistic band struct. 0-75501  
 Cu, dynamic susceptibility, model pot. theory 0-75710  
 Cu, mag. susceptibility, Animalu model pot. calc. 0-75711  
 Fe, mag. breakdown and Hall resist., theory and model calcs. 0-75552  
 Na, BCC, doubly occupied Wannier functions, constructive definition 0-75492  
 Na, equilibrium struct. and phys. props., pseudopot. method 0-96778  
 Na, Fermi surface distortions, model pot. 0-80157  
 Ni, dielectric matrix, analytic model 0-75512  
 Ni, metallic particles, stability and electronic struct. (*French*) 0-80155  
 Pb, ab initio band struct. calcs. 0-75502

**metal theory continued**

- Tc, superconductivity and Fermi surface calcs. 0-70873  
 V, dynamic susceptibility, model pot. theory 0-75710

**metal vapour lamps**

- see also *mercury vapour lamps*  
 alkali metal vapour arc lamp, source for Nd<sup>3+</sup>:YAG laser pumping 0-78924

**metallic epitaxial layers**

- Ag (111), epitaxially grown on mica, surface defect struct., LEED study 0-80038  
 Ag, electron channeling pattern, large angle, generation and appl. 0-100296  
 Ag, epitaxial growth on Pd, AES and LEED obs. of growth modes and substrate influences (*French*) 0-84408  
 Ag, thin-film bicrystals, planar lattice defects and migrating grain boundaries interaction 0-79835  
 Ag, twin form., LEED detection 0-88442  
 Au, contrast from epitaxially sandwiched macromolecules in TEM 0-85565  
 Au, electron channeling pattern, large angle, generation and appl. 0-100296  
 Au/Cu, bilayers, interdiffusion phenomena, lattice dislocations, TEM obs. 0-59736  
 Au/Cu, initial epitaxial growth at room temp. 0-59829  
 Au/Mn alloy, ordered, vacuum deposited epitaxial films, orientation control by external stress 0-100426  
 Co vacuum deposited coatings on metal substrates, cryst. struct. and stability 0-75481  
 Cu, bicrystalline, characterisation of [001] tilt boundaries 0-75473  
 Cu on Fe (001) substrate, orientation relationship 0-65415  
 Cu, twin form., LEED detection 0-88442  
 CuAu alloy, ordered, vacuum deposited epitaxial films, orientation control by external stress 0-100426  
 Fe-Au bimetal epitaxial films, examination of interaction at temps.  $\geq 600^\circ\text{C}$  0-75482  
 Gd films, electrical props. correlation with microstructure 0-97009  
 Nb, film, epitaxy, struct. and supercond. props., on (001) surface of fluorophlogopite (*Russian*) 0-80101  
 Nb/Al film, electron-beam coevaporated, prep. and characts. 0-76187  
 Ni on Fe (001) substrate, orientation relationship 0-65415  
 Pb film, monocryst., heteroepitaxial growth, struct. defects, and elec. props. (*Russian*) 0-84403  
 Pb, underpotential adsorption, cathodic deposition, on Ag(111) and (100) (*German*) 0-108363  
 Pd/Si films on Si, lattice imaging obs. of structural details 0-103604  
 Te film, microstructure 0-103598  
 Tl, underpotential adsorption, cathodic deposition, on Ag(111) and (100) (*German*) 0-108363  
 Zn film deposition on Al, TEM and electron diffr. obs. 0-75460

**metallic glasses**

- amorphism, rapid quenching, techniques for determ. very short room temp. lifetimes 0-84981  
 amorphous alloys, thermal stability, crystn., DSC and elec. resist. study 0-107060  
 annealing behaviour, thermal stability and crystn. 0-75167  
 Bragg bubble glass, struct. and plastic flow 0-84091  
 Brillouin-Mandelstam scattering from thermal and excited magnons 0-70980  
 corrosion behaviour, metalloid elements influence 0-89421  
 crystallisation, thermosonometric investigation 0-75180  
 electrical resistivity, press. depend. 0-96841  
 electron transport theory, diff. model appl. 0-80245  
 electronic lifetime, noncumulative two-level model 0-103663  
 electronic structure rel. to elec. cond., supercond. and mag. props. 0-65429  
 eutectic alloy prod. using low temp. melt spinning device 0-100825  
 ferromagnets, book contrib. 0-75743  
 ferromagnets, structural instabilities and mag. permeability relax., 77 to 400K 0-80559  
 formation, stabilities, and props. 0-64912  
 formation and rapid quenching techniques 0-76214  
 friction coeff. determ. using sliding friction rig 0-89355  
 heat of crystn. and viscous behaviour 0-75166  
 local structure exam. by EXAFS 0-108301  
 magnetic, indirect exchange interaction and paramag. Curie temp. 0-75752  
 magnetic, soft-magnetic properties (*German*) 0-71108  
 magnetic and nonmag. amorphous alloys, thermoelec. power, 15 to 580K 0-80255  
 magnetostrictive metallic-glass ribbon, stress dependences of longitudinal wave velocity 0-75825  
 metal metal system, glass formation 0-64921  
 Metglas 2605 ribbon, saturation magnetostriction meas. by small-angle magnetisation rot. 0-60391  
 Metglas 2826 ribbon, saturation magnetostriction meas. by small-angle magnetisation rot. 0-60391  
 Metglas 2826 ribbon, voids formation during crystallisation 0-108428  
 micromagnetic calculations and props. 0-80501  
 preparation and phys. props. development 0-81003  
 production and properties, technological appl. 0-71105  
 rapidly quenched metals, conf., Brighton, England (July 1978) 0-67934  
 rare earth-transition metal alloys, amorphous, electronic and mag. props. 0-83093  
 rare earth-transition metal alloys, amorphous, ferromag., spin arrangements in large fields 0-75718  
 review 0-88051  
 spin waves in amorphous ferromagnets, asperomagnets and spin-glasses 0-75747  
 splat cooled, mag. props. 0-80491  
 stability, hole theory of liquids appl. 0-100174  
 stability 0-75184  
 structure, review of current exptl. data 0-88058  
 structure, transport props., magnetic behaviour, review 0-70138  
 structure model, structural changes 0-92462  
 superconducting metastable alloys, review of current work 0-81002  
 transition metal alloys, amorphous, mag. props., chem. short-range order 0-75739  
 transition metal alloys, amorphous, mag. props., structure and preparation 0-75737



## metallic glasses continued

- transition metal-metalloid glasses, short range order of dense-random-packing models 0-64907  
 transition metal-metalloid glasses, struct., compositional effects (*Japanese*) 0-84086  
 transition metal-metalloid glasses, struct. end plastic flow, review 0-84090  
 transition metal-nonmetal glasses, with defined local coordination, struct. model 0-84092  
 tunnelling states, struct. model 0-70137  
 tunnelling two-level system, Kondo-like state 0-88547  
 vapour quenching techniques, high-rate, use in amorphous phase prep. 0-80977  
 Al-Cu, superconducting amorphous films of high stability 0-70889  
 Al<sub>20</sub>Cu<sub>75</sub>Zr<sub>55</sub> metallic glass, inelastic deform., free energy spectra 0-71699  
 Au-Ge-Si, influence of struct. on elec. resist. of glass forming alloys 0-65518  
 Au<sub>77</sub>Ge<sub>13.5</sub>Si<sub>9.4</sub>, heat of crystn. and viscous behaviour 0-75166  
 Au<sub>35</sub>Si<sub>65</sub>, vacuum-deposited and liquid-quenched films, diffusion and crystn. 0-84094  
 Au<sub>31</sub>Si<sub>69</sub> amorphous films, phys. studies 0-75476  
 Ca<sub>0.65</sub>Mo<sub>0.35</sub>, glass transition temp., comp. depend. 0-79702  
 Ce<sub>80</sub>Au<sub>20</sub>, mag. ordering and cryst. field effects, speromagnetism 0-80531  
 (Co,Fe)<sub>80</sub>B<sub>20</sub>, induced anisotropy and time changes of permeability 0-75815  
 Co alloys, amorphous, effects of metalloids on mag. props. 0-75738  
 Co base amorphous alloys, alloying elements influence on corrosion behaviour, XPS obs. 0-89422  
 Co-B-Si amorphous alloy, liq. quenched, elec. resist. and cyclic deform. 0-59949  
 Co-B-(Cr) thin film glasses, mag. props. and corrosion resist. 0-80576  
 Co-Fe amorphous alloys, worked, permivar type mag. hysteresis loop, longit. Kerr effect obs. 0-65958  
 Co-Fe-B, amorphous, crystn. and thermal stability 0-107057  
 Co-Fe-Si-B, decomp. of amorphous state during annealing below recryst. temp. (*Russian*) 0-75164  
 Co-Fe-Si-B, ferromag., magneto-optical spectra in amorphous and cryst. states (*Russian*) 0-84749  
 Co-Mn-Ni-Fe-Si-B amorphous alloys, mag. props., low magnetostriction 0-75832  
 Co-Mo-B metallic glass ribbons, tensile strength, crystn. temp. 0-89173  
 Co-Ni-Mo-C, amorphous alloys, med. props. and thermal stability (*Japanese*) 0-85049  
 Co-P, domain struct., mag. anisotropy origin 0-80554  
 Co-P alloys, geometric struct. models and diffraction exam. techniques 0-79700  
 Co-Si-B, amorphous ribbon, saturation magnetostriction meas. by small-angle magnetisation rot. 0-60391  
 Co-Zr, amorphous phase form. in Zr-poor region, hardness and fracture strength (*Japanese*) 0-84914  
 Co<sub>100-x</sub>B<sub>x</sub>, amorphous, mag. struct., mag. susceptibility meas. 0-80485  
 Co<sub>61</sub>B<sub>39</sub>, hyperfine field distrib., <sup>59</sup>Co spin echo spectra 0-80635  
 Co<sub>67</sub>Er<sub>33</sub> amorphous alloy, sputtered, local order and amorphous struct. 0-88061  
 (Co<sub>93</sub>Fe<sub>0.07</sub>)<sub>75-x</sub>Cr<sub>3</sub>Si<sub>15</sub>B<sub>10</sub> amorphous alloy, thermal stability, Cr conc. effects, DTA expts. 0-59395  
 (Co<sub>89</sub>Fe<sub>0.11</sub>)<sub>72</sub>Mo<sub>2</sub>Si<sub>13</sub>B<sub>10</sub> metallic glass, strain- and field-induced mag. anisotropy 0-108004  
 Co<sub>57</sub>Fe<sub>3</sub>Ni<sub>10</sub>(Si<sub>3</sub>B)<sub>28</sub>, amorphous, soft mag. props., switched-mode power supply appls. 0-88850  
 Co<sub>70</sub>Fe<sub>25</sub>Si<sub>5</sub>B<sub>10</sub>, amorphous, crystn. and thermal stability 0-107057  
 Co<sub>70.4</sub>Fe<sub>4.6</sub>Si<sub>13</sub>B<sub>10</sub>, amorphous, mag. aftereffect spectra and annealing props. 0-88831  
 Co<sub>73</sub>Mo<sub>2</sub>Si<sub>7</sub>B<sub>10</sub>, metallic glass, strain- and field-induced mag. anisotropy 0-108004  
 CoP amorphous alloy, heat treatments influence on opt. props., struct. and DC resist. obs. 0-80892  
 Co<sub>90</sub>P<sub>10</sub>, noncrystalline ferromagnet, electrodeposited, struct. and microscopic mag. props. 0-88063  
 Co<sub>1-x</sub>P<sub>x</sub> amorphous alloy film, elec. resistance, temp. depend. (*Russian*) 0-103660  
 Co<sub>92</sub>P<sub>8</sub>, amorphous alloys, electronic struct.,  $\gamma$ -ray Compton scatt. study (*Japanese*) 0-84422  
 Co<sub>3</sub>Pd<sub>90</sub>, Si<sub>30</sub>, structural and mag. heterogeneities 0-80484  
 Co<sub>75</sub>Si<sub>15</sub>B<sub>10</sub>, amorphous, crystn. and thermal stability 0-107057  
 Co<sub>90</sub>Zr<sub>10</sub>, ferromag. amorphous alloy, crystn. and domain struct. study 0-107056  
 Cu-Ag-Ge, Hume-Rothery glass form. 0-96449  
 Cu-Ag-P(6-14, 11-14 wt.%) amorphous, crystn. and elec. props., X-ray diff., elec. resist. and DTA meas. (*Japanese*) 0-84088  
 Cu-Zr amorphous alloy, sput. cooled, local order and amorphous struct. 0-88061  
 Cu<sub>3</sub>La<sub>1-x</sub>, sput.-cooled, phase diagram and supercond. props. 0-70881  
 Cu<sub>40</sub>Zr<sub>60</sub>, Cu<sub>56</sub>Zr<sub>44</sub>, and Cu<sub>60</sub>Zr<sub>40</sub> metallic glass, inelastic deform., free energy spectra 0-71699  
 Cu<sub>0.57</sub>Zr<sub>0.43</sub> amorphous alloy, neutron diff. obs. of struct. 0-88060  
 Cu<sub>40</sub>Zr<sub>60</sub>, amorphous alloys, supercond. transition temp., press. depend. 0-84524  
 Cu<sub>60</sub>Zr<sub>40</sub>, amorphous, ductility and stress relief, low-temp. annealing effects 0-76296  
 Cu<sub>66</sub>Zr<sub>34</sub>, amorphous metallic glass, differences caused by preparation technique (*French*) 0-103247  
 (Fe,Co,Ni)-Si(B), amorphous mag. alloy, magnetostriction rel. to soft mag. props. 0-84633  
 Fe alloys, amorphous, effects of metalloids on mag. props. 0-75738  
 Fe alloys, amorphous, mag. saturation, spin wave stiffness, temp. depend. 0-75741  
 Fe and Fe-Ni Metglas alloys, ohmic and Hall resist. 100-700K, mag. behaviour 0-80254  
 Fe based alloy, amorphous, liq. quenched, struct., thermal stability and mech. props. 0-88059  
 Fe-(Co)-B and Fe-Ni-B(P), amorphous, crystn. 0-79704  
 Fe-B, amorphous, crystn., metal or metalloid exchange influence 0-75172  
 Fe-B, amorphous, induced anisotropy, development by mag. annealing and under applied mech. stress 0-65868  
 Fe-B, amorphous, induced anisotropy by heat treatment in mag. field and under applied mech. stress 0-75758  
 Fe-B, amorphous, mag. aftereffect, initial susceptibility time depend. 0-88829  
 Fe-B, amorphous alloy, mag. props. 0-84618

## metallic glasses continued

- Fe-B, amorphous ferromag., temp. depend. of resist., appl. of extended Ziman theory 0-59950  
 Fe-B, amorphous to cryst. transition 0-88048  
 Fe-B, compositional study on short-range struct. 0-84095  
 Fe-B, rapidly quenched, metastable phases 0-76234  
 Fe-B amorphous alloy, annealed, microstruct. and mag. domain changes 0-75790  
 Fe-B amorphous alloy, fast neutron and <sup>235</sup>U fission fragment irradiation 0-100288  
 Fe-B amorphous alloys, mag. aftereffect 0-65970  
 Fe-B amorphous ribbons formation, high-speed photography investigation 0-76216  
 Fe-B metallic glass, X-ray diff. meas., semi-empirical struct. model 0-107059  
 Fe-B metallic glasses, diffusion coeffs. from primary crystn. data 0-100345  
 Fe-B metallic glasses, struct., stability and crystn. 0-75173  
 Fe-B metallic ribbons, correl. between quenching temp. and mech. and mag. props. 0-89373  
 Fe-B phase ferromag. amorphous alloys, stiffening below Curie temp., pole effect (*Japanese*) 0-84632  
 Fe-B ribbon, microhardness, and static coercive force, melt overheating effect 0-84978  
 Fe-B-C, formation, mag. props., thermal stability and density 0-75796  
 Fe-B-C amorphous alloys for use in power transformers 0-88808  
 Fe-B-C amorphous alloys with high saturation induction 0-84617  
 Fe-B-Cr(Mo), mag., struct., and elec. props. 0-88751  
 Fe-B-Cr(Si) thin film glasses, mag. props. and corrosion resist. 0-80576  
 Fe-B-Si amorphous alloy, liq. quenched, elec. resist. and cyclic deform. 0-59949  
 Fe-B-Si-C amorphous alloys, prep. and props. 0-88748  
 Fe-B-(Si), glassy, field-induced mag. anisotropy near eutectic comp. 0-93110  
 Fe-B-(Si) alloy filaments produced by glass-coated melt spinning 0-76213  
 Fe-B(P) amorphous alloys, anomalous thermal expansion,  $\Delta E$  effect, Invar and Elinvar charact., delay time 0-80589  
 Fe-C-X, glasses and metastable cryst. phases, third element effect 0-75171  
 Fe-Co-Mo-C, amorphous alloys, med. props. and thermal stability (*Japanese*) 0-85049  
 Fe-Co-Si-B, amorphous soft ferromagnet with high mag. induction 0-84619  
 Fe-Co-Si-B, zero magnetostrictive amorphous alloy with high saturation induction, mag. annealing 0-60362  
 Fe-Co-Si(B), amorphous ferromagnet, mag. after effect on soft mag. props. 0-84626  
 Fe-Cr-Mo and Fe-Cr-Mo-Si alloys, amorphous films, corrosion resist. and ion plating use 0-89423  
 Fe-Mo-B metallic glass ribbons, tensile strength, crystn. temp. 0-89173  
 Fe-Ni based metallic glass, Metglas 2826 MB, Mossbauer study 0-75897  
 Fe-Ni film, amorphous, martensite form. time and struct. 0-104159  
 Fe-Ni-B glassy ribbons melt spinning, gas boundary layer effects 0-76217  
 Fe-Ni-B metallic glass, X-ray diff. meas., semi-empirical struct. model 0-107059  
 Fe-Ni-B-Mo, crystn. temp. and elec. cond. correl., Mo effect 0-75179  
 Fe-Ni-B-Si, amorphous, mag. props., heat treatment effects 0-89370  
 Fe-Ni-B-(P), ferromag., magneto-optical spectra in amorphous and cryst. states (*Russian*) 0-84749  
 Fe-Ni-Mo-C, amorphous alloys, med. props. and thermal stability (*Japanese*) 0-85049  
 Fe-Ni-P-B, amorphous, crystn. and struct. 0-75175  
 Fe-Ni-P-B, metallic glasses, struct. relax., annealing effects on mag. props. 0-89261  
 Fe-Ni-P-B amorphous ribbons, form. by melt spin technique 0-76215  
 Fe-Ni-P-B metallic glass, crystallisation temperature values from isothermal transformation times 0-59397  
 Fe-P electrodeposited foil, amorphous, mag. domains 0-75821  
 Fe-P-C, amorphous, crystn. and struct. 0-75175  
 Fe-Sb amorphous films, Mossbauer effect study 0-75896  
 Fe-Si-B, mag. props. 0-84620  
 Fe-Si-B amorphous alloys, Mossbauer spectroscopy (*French*) 0-80653  
 Fe-Si-B glassy alloys, mag. props., comp. effects 0-88752  
 Fe-Zr, amorphous phase form. in Zr-poor region, hardness and fracture strength (*Japanese*) 0-84914  
 (Fe-Ni-Mo)<sub>80</sub>(P-B)<sub>20</sub>, amorphous, mag. aftereffects and struct. instabilities 0-88833  
 Fe<sub>1-x</sub>B<sub>x</sub>, amorphous, hyperfine fields and local mag. moments, Mossbauer study 0-75895  
 Fe<sub>100-x</sub>B<sub>x</sub>, amorphous, mag. struct., mag. susceptibility meas. 0-80485  
 Fe<sub>75</sub>B<sub>25</sub> metallic glass, nonisothermal meas. evaluation, non-existence of dynamic correction term 0-107406  
 Fe<sub>80</sub>B<sub>20</sub>, amorphous, Brillouin scatt. from magnons, ferromag. reson. 0-65844  
 Fe<sub>80</sub>B<sub>20</sub>, amorphous, cold neutron scatt., local and extended defects 0-84089  
 Fe<sub>80</sub>B<sub>20</sub>, amorphous, crystn. 0-75187  
 Fe<sub>80</sub>B<sub>20</sub>, amorphous, mag. permeability aftereffect during annealing 0-88834  
 Fe<sub>80</sub>B<sub>20</sub>, amorphous ferromagnet, Mossbauer hyperfine fields, mag. struct. 0-75894  
 Fe<sub>80</sub>B<sub>20</sub>, amorphous struct., Mossbauer spectroscopy investigation 0-84677  
 Fe<sub>80</sub>B<sub>20</sub> amorphous wire, crystn. by annealing at 780°C 0-100177  
 Fe<sub>80</sub>B<sub>20</sub> film, amorphous metallic, standing spin waves, Brillouin scatt. obs. 0-97291  
 Fe<sub>80</sub>B<sub>20</sub> glass, magnetisation reorientation, Mossbauer effect 0-66092  
 Fe<sub>80</sub>B<sub>20</sub>, metallic glass, Doppler broadening of positron annihilation  $\gamma$ -radiation and elec. resist. 0-66321  
 Fe<sub>80</sub>B<sub>20</sub> metallic glass, crystn. and struct. relax., Mossbauer effect study 0-75182  
 Fe<sub>80</sub>B<sub>20</sub> metallic glass, crystn. kinetics 0-84083  
 Fe<sub>80</sub>B<sub>20</sub>, metallic glass, optical and magneto-optical props. 0-84728  
 Fe<sub>80</sub>B<sub>20</sub> metallic glasses, stability and transforms. 0-75174  
 Fe<sub>80</sub>B<sub>20</sub>, Metglas 2605, Young's modulus meas. using piezoelectric US composite oscillator technique 0-108656  
 Fe<sub>83.4</sub>B<sub>16.6</sub>, amorphous, mag. props. and microstruct., cooling rate and melt overheating effects 0-65965



## metallic glasses continued

- Fe<sub>34</sub>B<sub>66</sub>, amorphous, mag. props., melt overheating and cooling rate effects 0-89371
- Fe<sub>34</sub>B<sub>66</sub>, metallic glass, electrical resistivity and crystallisation 0-88526
- Fe<sub>34</sub>B<sub>66</sub>, metallic glass, ion implanted, UPS meas. 0-97411
- Fe<sub>40</sub>P<sub>14</sub>B<sub>46</sub> and Fe<sub>40</sub>B<sub>20</sub>, Metglas 2826 and 2605, amorphous ribbon, power loss variation with freq. and applied stress 0-88849
- Fe<sub>34</sub>B<sub>14</sub>Si<sub>4</sub>, chill block melt-spinning process, geometry depend. 0-97448
- Fe<sub>34</sub>B<sub>13</sub>Si<sub>3</sub>, metallic glass, electrical resistivity and crystallisation 0-88526
- Fe<sub>40</sub>(C<sub>1-x</sub>B<sub>x</sub>)<sub>20</sub>, amorphous alloy,  $\alpha$ -Fe crystn., morphology 0-70129
- (Fe<sub>0.3</sub>Co<sub>0.5</sub>)<sub>1-x</sub>B<sub>x</sub>, amorphous, hyperfine fields and local mag. moments, Mossbauer study 0-75895
- Fe<sub>40</sub>B<sub>20</sub>, amorphous, magnetisation reversal and domain boundary configs. 0-88809
- Fe<sub>1</sub>Co<sub>1-x</sub>B<sub>20</sub>Si<sub>10</sub>Al<sub>1</sub>, stress-induced variation in magnetisation and dynamic magnetostrictive charact. 0-88855
- (Fe<sub>1-x</sub>Co<sub>x</sub>)<sub>78</sub>Si<sub>10</sub>B<sub>12</sub>, amorphous, roll mag. anisotropy 0-75757
- (Fe<sub>0.9</sub>Co<sub>0.1</sub>)<sub>78</sub>Si<sub>10</sub>B<sub>12</sub>, amorphous, saturation magnetostriction, strain modulated FMR obs. 0-75863
- Fe<sub>14</sub>Cr<sub>12</sub>Ni<sub>14</sub>B<sub>12</sub>B<sub>6</sub>, amorphous X-ray absorpt. spectra, effective coordination charges 0-84805
- (Fe<sub>98</sub>Cr<sub>2</sub>)<sub>79</sub>P<sub>13</sub>B<sub>8</sub> and (Fe<sub>96</sub>Cr<sub>4</sub>)<sub>79</sub>P<sub>13</sub>B<sub>8</sub>, amorphous, low temp. sp. ht., mag. contribs. 0-80552
- Fe<sub>31-x</sub>M<sub>x</sub>B<sub>17</sub> and Fe<sub>78-x</sub>M<sub>x</sub>Si<sub>10</sub>B<sub>12</sub> (M=refractory metal), glass form. and thermal stability 0-79703
- Fe<sub>73</sub>Mo<sub>7</sub>B<sub>20</sub>, metallic glass, Doppler broadening of positron annihilation  $\gamma$ -radiation and elec. resist. 0-66321
- (Fe<sub>0.9</sub>Ni<sub>0.1</sub>)<sub>80-x</sub>B<sub>x</sub> and (Fe<sub>100-x</sub>Ni<sub>x</sub>)<sub>80</sub>B<sub>20</sub> amorphous alloys, X-ray diffr. struct. determ. 0-64906
- (Fe<sub>1-x</sub>Ni<sub>x</sub>)<sub>83</sub>B<sub>17</sub>, amorphous alloys ferromagnetic resonance 0-108080
- (Fe<sub>100-x</sub>Ni<sub>x</sub>)<sub>83</sub>B<sub>17</sub>, amorphous, crystn. 0-75176
- Fe<sub>60</sub>Ni<sub>40</sub>B<sub>20</sub>, amorphous, phase transforms., resistometric anal. 0-75538
- Fe<sub>60</sub>Ni<sub>40</sub>B<sub>20</sub>, amorphous, RF annealing effects 0-108037
- Fe<sub>60</sub>Ni<sub>40</sub>B<sub>20</sub>, amorphous ribbon, power loss variation with freq. and applied stress 0-88849
- Fe<sub>40</sub>Ni<sub>40</sub>B<sub>20</sub> and Fe<sub>40</sub>Ni<sub>40</sub>P<sub>14</sub>B<sub>6</sub>, amorphous, mag. aftereffect spectra and annealing props. 0-88831
- Fe<sub>60</sub>Ni<sub>40</sub>B<sub>20</sub>, chill block melt-spinning process, geometry depend. 0-97448
- Fe<sub>80-x</sub>Ni<sub>x</sub>B<sub>20</sub> and Fe<sub>80-x</sub>Ni<sub>x</sub>P<sub>14</sub>B<sub>6</sub> amorphous alloys, microhardness correl. with mag. props. 0-88826
- Fe<sub>81</sub>Ni<sub>19</sub>-x-B<sub>20</sub> and Fe<sub>81</sub>Ni<sub>19</sub>-x-P<sub>14</sub>B<sub>6</sub>, low temp. resist. and galvanomag. effects, mag. state influence 0-84461
- Fe<sub>81</sub>Ni<sub>19</sub>-x-B<sub>20</sub> glass, resist., magnetoresist., and thermoelec. power 0-70681
- (Fe<sub>1-x</sub>Ni<sub>x</sub>)<sub>80</sub>B<sub>20-x</sub>P<sub>x</sub>, amorphous, hyperfine fields and local mag. moments, Mossbauer study 0-75895
- Fe<sub>14</sub>Ni<sub>78</sub>B<sub>10</sub>P<sub>10</sub>, superparamag. behaviour, chem. inhomogeneities role 0-84625
- Fe<sub>62</sub>Ni<sub>38</sub>B<sub>20-x</sub>P<sub>x</sub>, local struct. and dynamic disorder of Fe and Ni, EXAFS obs. 0-89088
- Fe<sub>80-x</sub>Ni<sub>x</sub>B<sub>20-x</sub>P<sub>y</sub>, amorphous, Rayleigh region and coercive force 0-88806
- (FeNi)<sub>81</sub>B<sub>17-x</sub>Al<sub>1</sub>Si<sub>0.5</sub>, stress-induced variation in magnetisation and dynamic magnetostrictive charact. 0-88855
- Fe<sub>62</sub>Ni<sub>38</sub>C<sub>14</sub>P<sub>4</sub>, amorphous film, dislocation and mag. struct., neutron diffr. study 0-70956
- Fe<sub>73</sub>Ni<sub>36</sub>Cr<sub>14</sub>P<sub>12</sub>B<sub>6</sub>, metallic glass, Doppler broadening of positron annihilation  $\gamma$ -radiation and elec. resist. 0-66321
- Fe<sub>73</sub>Ni<sub>36</sub>Cr<sub>14</sub>P<sub>12</sub>B<sub>6</sub>, metallic glass, crystn. kinetics by TEM 0-75186
- Fe<sub>73</sub>Ni<sub>36</sub>Cr<sub>14</sub>P<sub>12</sub>B<sub>6</sub>, Metglas 2826A, EPR at 20 GHz 0-75848
- Fe<sub>73</sub>Ni<sub>36</sub>Cr<sub>14</sub>P<sub>12</sub>B<sub>6</sub>, Metglas, bending deform., shear band form., high-speed cinematographic obs. 0-89322
- Fe<sub>73</sub>Ni<sub>36</sub>Cr<sub>14</sub>P<sub>12</sub>B<sub>6</sub>, Metglas amorphous films, corrosion resist. and ion plating use 0-89423
- Fe<sub>73</sub>Ni<sub>36</sub>Cr<sub>14</sub>P<sub>12</sub>B<sub>6</sub>, metallic glass, effect of pre-ageing on glass transition temp. 0-100326
- Fe<sub>62</sub>Ni<sub>38</sub>(Mo,Si,B)<sub>20</sub>, amorphous, soft mag. props., switched-mode power supply appls. 0-88850
- Fe<sub>62</sub>Ni<sub>38</sub>Mo<sub>18</sub>, amorphous, mag. anisotropy, Mossbauer study 0-65864
- Fe<sub>62</sub>Ni<sub>38</sub>Mo<sub>18</sub>, amorphous, reversible enhancement of mag. directional ordering rate 0-103829
- Fe<sub>73</sub>Ni<sub>36</sub>Mo<sub>18</sub> and Fe<sub>73</sub>Mo<sub>7</sub>B<sub>20</sub> amorphous ribbons, magnetoelastic effects in as-quenched and stress-relieved states 0-80588
- (Fe<sub>1-x</sub>Ni<sub>x</sub>)<sub>80</sub>P<sub>20</sub>, amorphous, ferromagnetic alloys, mag. anomalies of Invar type (Russian) 0-93089
- Fe<sub>40</sub>Ni<sub>40</sub>P<sub>14</sub>, glass transition, viscous flow and differential scanning calorimetry meas. 0-96635
- Fe<sub>40</sub>Ni<sub>40</sub>P<sub>14</sub>B<sub>6</sub>, amorphous, resistometric study of short-range ordering rel. to heat treatment 0-70140
- Fe<sub>40</sub>Ni<sub>40</sub>P<sub>14</sub>B<sub>6</sub>, amorphous ferromagnet, Mossbauer hyperfine fields, mag. struct. 0-75894
- Fe<sub>40</sub>Ni<sub>40</sub>P<sub>14</sub>B<sub>6</sub>, amorphous alloy, temper embrittlement 0-76295
- Fe<sub>40</sub>Ni<sub>40</sub>P<sub>14</sub>B<sub>6</sub>, amorphous, steady-state creep rate, cryst. effect 0-81102
- Fe<sub>40</sub>Ni<sub>40</sub>P<sub>14</sub>B<sub>6</sub>, amorphous, mag. permeability aftereffect during annealing 0-88834
- Fe<sub>40</sub>Ni<sub>40</sub>P<sub>14</sub>B<sub>6</sub>, amorphous ribbon, mag. domains and anisotropy distrib. 0-108029
- Fe<sub>40</sub>Ni<sub>40</sub>P<sub>14</sub>B<sub>6</sub>, bending tests, evidence of ideal elastic-plastic deform. 0-97543
- Fe<sub>40</sub>Ni<sub>40</sub>P<sub>14</sub>B<sub>6</sub>, glass, viscosity near T<sub>g</sub>, using rapid heating, and fusion characs. 0-70438
- Fe<sub>40</sub>Ni<sub>40</sub>P<sub>14</sub>B<sub>6</sub>, mag. polarisation in approach to ferromag. saturation 0-80560
- Fe<sub>40</sub>Ni<sub>40</sub>P<sub>14</sub>B<sub>6</sub>, metallic glass, crystn. 0-70127
- Fe<sub>40</sub>Ni<sub>40</sub>P<sub>14</sub>B<sub>6</sub>, Metglas 2826, hot forming 0-84980
- Fe<sub>40</sub>Ni<sub>40</sub>P<sub>14</sub>B<sub>6</sub>, Metglas 2826, amorphous ribbon under tension, mag. domain walls and pulsed magnetisation reversal 0-88825
- (Fe<sub>1-x</sub>Ni<sub>x</sub>)<sub>80</sub>P<sub>10</sub>B<sub>10</sub>, amorphous, magnetisation reversal and domain boundary configs. 0-88809
- Fe<sub>81</sub>Ni<sub>19</sub>-x-P<sub>14</sub>B<sub>6</sub> glass, resist., magnetoresist., and thermoelec. power 0-70681
- Fe<sub>81</sub>Ni<sub>19</sub>-x-P<sub>14</sub>B<sub>6</sub>, metallic glass, low temp. sp. ht. for spin-glass and spin-cluster-glass regime 0-71071
- (Fe<sub>1-x</sub>Ni<sub>x</sub>)<sub>79</sub>P<sub>13</sub>B<sub>8</sub>, metallic glass, low temp. sp. ht. for spin-glass and spin-cluster-glass regime 0-71071
- (Fe<sub>65</sub>Ni<sub>35</sub>)<sub>77</sub>P<sub>14</sub>B<sub>6</sub>Al<sub>1</sub>, amorphous, crystn. temp., press. and heating rate depend. 0-70132
- (Fe<sub>1-x</sub>Ni<sub>x</sub>)<sub>77</sub>Si<sub>10</sub>B<sub>13</sub>, amorphous, Landau-Ginzburg theory, magnetisation and Curie temp. 0-75700
- (Fe<sub>1-x</sub>Ni<sub>x</sub>)<sub>77</sub>Si<sub>10</sub>B<sub>12</sub> amorphous alloys, cold rolled and as-quenched, mag. anisotropy 0-97089

## metallic glasses continued

- Fe<sub>1-x</sub>(P,B)<sub>x</sub>, amorphous and crystalline, photoemission and band structure 0-60754
- Fe<sub>100-x</sub>P<sub>x</sub>, structural analysis of models for amorphous metallic alloys 0-103249
- Fe<sub>75</sub>P<sub>25</sub>, amorphous alloy, atomic struct., computer simulation 0-88043
- Fe<sub>75</sub>P<sub>24</sub>, amorphous alloy, electronic struct., KKR calc. 0-96775
- Fe<sub>75</sub>P<sub>13</sub>B<sub>8</sub>, amorphous alloys, splat cooled, Mn, Cr and V substituted, mag. and transport props. 0-84593
- Fe<sub>80</sub>(P<sub>1</sub>C<sub>7</sub>)<sub>20</sub>-x<sub>2</sub>(Si<sub>1</sub>)<sub>2</sub>, density, microhardness, and crystn. temp., comp. depend. 0-84093
- Fe<sub>80</sub>P<sub>20</sub>-x<sub>2</sub>(Si<sub>1</sub>)<sub>2</sub>(Ge<sub>2</sub>), amorphous, size effect of metalloids on mag. props. 0-84594
- Fe<sub>80</sub>P<sub>20</sub>-x<sub>2</sub>Si<sub>20</sub>, structural and mag. heterogeneities 0-80484
- Fe<sub>82-x</sub>Si<sub>18</sub>, metallic glass, long range interaction and spin wave interactions 0-65949
- Fe<sub>82-x</sub>Si<sub>18</sub>, metallic glass, mag. transitions, weak ferromagnetism 0-100583
- Fe<sub>80</sub>Si<sub>18</sub>B<sub>15</sub>, amorphous, soft mag. props. and potential uses 0-88807
- (Fe<sub>1-x</sub>Si<sub>x</sub>)<sub>1-y</sub>By, metallic glass, mag. props., crystallisation 0-65885
- Fe<sub>81</sub>Ni<sub>19</sub>-x, amorphous film, struct. and mag. props. 0-65972
- Fe<sub>80</sub>B<sub>20-x</sub>C<sub>x</sub>(Si<sub>1</sub>)<sub>2</sub>(Ge<sub>2</sub>), amorphous, size effect of metalloids on mag. props. 0-84594
- Gd-Al(Cu)(Ga)(Ni)(Pd)(Rh) alloys, mag. and elec. props. 0-80499
- (Gd<sub>0.5</sub>Fe<sub>0.5</sub>)<sub>90</sub>B<sub>10</sub>, amorphous, mag. props., Mossbauer study 0-93093
- GdFeB<sub>1</sub>, amorphous ferrimag. films, magneto-optical props., optical spectra 0-76008
- Hf-Fe(Cu), amorphous, thermal stability, crystn., DSC and elec. resist. study 0-107060
- Hf<sub>1-x</sub>Fe<sub>x</sub>, amorphous alloys, formation, crystallisation and electrical resistivity 0-96838
- La-Al alloys, internal friction, relaxation process 0-92607
- La-Au, splat-quenched, Mossbauer effect and elec. resist., amorphous struct. 0-84676
- La<sub>2</sub>Ga<sub>2</sub>, amorphous, local symmetry around glass-former sites, elec. quadrupole effects, NMR 0-80618
- La<sub>80-x</sub>Pr<sub>x</sub>Au<sub>20</sub>, mag. and supercond. props. 0-75713
- Mo-based metallic glass development 0-89172
- Mo-Ru-(Si), amorphous superconductors, prep. by electron beam evaporation and liq. quenching, crit. temp. 0-103776
- Mo<sub>70</sub>B<sub>30</sub>, amorphous, local symmetry around glass-former sites, elec. quadrupole effects, NMR 0-80618
- Mo<sub>48</sub>Ru<sub>32</sub>B<sub>20</sub>, amorphous, local symmetry around glass-former sites, elec. quadrupole effects, NMR 0-80618
- (Mo<sub>0.9</sub>Ru<sub>0.1</sub>)<sub>80</sub>Si<sub>10</sub>B<sub>10</sub>, amorphous supercond. matrix, flux pinning by MoRu precip. 0-65756
- Mo<sub>70</sub>Si<sub>30</sub>B<sub>10</sub>, amorphous alloys obtained by liq. quenching, superconductivity 0-75670
- Nb-Ir(Rh) system glasses, form., crystn. and microhardness, resist. obs. 0-89178
- Nb-Ni, amorphous, thermal stability, crystn., DSC and elec. resist. study 0-107060
- Nb-Ni amorphous alloys, glass transition and ductility, O additions effect 0-75168
- Nb-Si-(V)(Zr)(Mo)(Ta)(W)(C)(B)(Ge), ductile amorphous, superconductivity 0-60131
- Nb<sub>5</sub>(Al,Ge) and Nb<sub>5</sub>(Al,Si), liq. quenched, supercond. props. 0-84580
- Nb<sub>40</sub>Fe<sub>40</sub>P<sub>14</sub>B<sub>6</sub>, Metglas 2826, explosive compaction, mech. props. 0-89176
- Nb<sub>73</sub>Ge(Si), amorphous films, thermally-activated internal friction peaks, structural obs. 0-80147
- Nb<sub>40</sub>Ni<sub>60</sub>, amorphous, produced by Ni<sup>+</sup> implantation, damage distrib. 0-107062
- Ni based alloy, amorphous, liq. quenched, struct., thermal stability and mech. props. 0-88059
- Ni-B thin film glasses, mag. props. and corrosion resist. 0-80576
- Ni-Cr-P, amorphous, corrosion behaviour, immersion tests and electrochem. meas. (Japanese) 0-85085
- Ni-Fe based, Curie pt. anomalies 0-60256
- Ni-Mo-B metallic glass ribbons, tensile strength, crystn. temp. 0-89173
- Ni-P, electrodeposited film, thermal anal., occlusion of gases rel. to mag. props. 0-59823
- Ni-P amorphous alloys, electrodeposited and melt-quenched atomic and electronic structures 0-88062
- Ni-Pd-P, electronic structure, pulsed NMR study 0-75869
- Ni-Pt-P, electronic structure, pulsed NMR study 0-75869
- Ni-Si-B, amorphous, thermal stability of ductility 0-76327
- Ni-Ta (70, 30 wt.%) metallic glass, struct. and crystn. (Russian) 0-70136
- Ni-Ti-P, amorphous, corrosion behaviour, immersion tests and electrochem. meas. (Japanese) 0-85085
- Ni-Zr, amorphous phase form. in Zr-poor region, hardness and fracture strength (Japanese) 0-84914
- Ni<sub>100-x</sub>B<sub>x</sub>, amorphous, mag. struct., mag. susceptibility meas. 0-80485
- Ni<sub>34</sub>Fe<sub>1</sub>Cr<sub>14</sub>P<sub>12</sub>B<sub>6</sub>, metallic glass, mech. props. and thermal stability 0-76362
- (Ni<sub>99</sub>Fe<sub>1</sub>)<sub>79</sub>P<sub>13</sub>B<sub>8</sub>, amorphous, low temp. sp. ht., mag. contribs. 0-80552
- (Ni<sub>1</sub>Fe<sub>0.9</sub>)<sub>80</sub>P<sub>10</sub>B<sub>10</sub>, Curie temp., press. effect 0-75833
- Ni<sub>78-x</sub>M<sub>x</sub>Si<sub>10</sub>B<sub>12</sub> (M=refractory metal), glass form. and thermal stability 0-79703
- NiP amorphous alloy, heat treatments influence on opt. props., struct. and DC resist. obs. 0-80892
- Ni<sub>3</sub>P<sub>10</sub>, amorphous alloys, electronic struct.,  $\gamma$ -ray Compton scatt. study (Japanese) 0-84422
- Ni<sub>78</sub>P<sub>14</sub>B<sub>8</sub>, amorphous, local symmetry around glass-former sites, elec. quadrupole effects, NMR 0-80618
- (Ni<sub>0</sub>Pd<sub>0.5</sub>)<sub>82</sub>P<sub>18</sub>, amorphous alloy, liquid-quenched, crystn. kinetics, effect of thermal history 0-100175
- (Ni<sub>0</sub>Pd<sub>0.5</sub>)<sub>82</sub>P<sub>18</sub>, amorphous alloy, liquid-quenched, crystn. kinetics, nucleation 0-100176
- Ni<sub>46</sub>Ti<sub>60</sub>, amorphous, chem. short-range-order, X-ray and neutron scatt. obs. 0-96447
- Ni<sub>3</sub>Zr<sub>1-x</sub>, crystallisation kinetics, elec. resist. and mag. susceptibility meas. 0-103659
- Pd-Au-Si, influence of struct. on elec. resist. of glass forming alloys 0-65518
- Pd-Cu-Si, glass form., crit. cooling rate 0-75169
- Pd-Si, amorphous, struct., crystn. and Hall effect meas. 0-75178
- Pd-Si, amorphous metallic glass, with defined local coordination, struct. model 0-84092
- Pd-Si, amorphous thin films, laser irradi., metastable phases 0-96622



## metallic glasses continued

- Pd-Si, compositional study on short-range struct. 0-84095  
 Pd-Si amorphous alloy, heat treated, low temp. lattice sp. ht. 0-75368  
 Pd-Si metallic glass, high-resolution electron microscopy 0-84097  
 Pd-Si-(Cu), amorphous, Hall effect meas. and electronic struct. 0-75551  
 Pd-Si-(Cu) amorphous ribbons, low temp. sp. ht., density of states trends 0-79957  
 (Pd<sub>80</sub>Au<sub>20</sub>Si<sub>13</sub>)/Fe<sub>30</sub>, compositionally modulated amorphous film, diffusion, struct. relax. 0-103518  
 Pd<sub>75</sub>Cu<sub>6</sub>Si<sub>16.5</sub>, heat of crystn. and viscous behaviour 0-75166  
 Pd<sub>75</sub>Cu<sub>6</sub>Si<sub>16.5</sub> metallic glass, glass transition temp., cooling rate depend. 0-75181  
 Pd<sub>50</sub>Si<sub>50</sub>, amorphous alloy, partial struct. functions, X-ray, electron and neutron diff. studies (*Japanese*) 0-88050  
 Pd<sub>50</sub>Si<sub>50</sub> amorphous alloy, skip deform. and crit. shear stress, using tensile testing machine 0-89321  
 Pd<sub>50</sub>Si<sub>50</sub>, deform. localisation, plastic instabilities and fracture 0-89320  
 Pd<sub>50</sub>Si<sub>50</sub> metallic glass, inelastic deform., free energy spectra 0-71699  
 Pd<sub>50</sub>Si<sub>50</sub>, tensile deform., shear band form., high-speed cinematographic obs. 0-89322  
 Pd<sub>3</sub>Si<sub>98</sub>, stress/strain rate depend. of homogeneous flow 0-71687  
 (Pd<sub>85</sub>Si<sub>15</sub>)<sub>61</sub>/(Fe<sub>85</sub>B<sub>15</sub>)<sub>39</sub>, compositionally modulated amorphous film, diffusion, struct. relax. 0-103518  
 PdSiCu, amorphous, US attenuation and vel. studies at low temps. 0-88278  
 Pd<sub>30</sub>Zr<sub>70</sub>, amorphous alloys, supercond. transition temp., press. depend. 0-84524  
 Pd<sub>4</sub>Zr<sub>65</sub>, mag. susceptibility meas. 0-75740  
 Pr-Ni, amorphous, thermal stability, crystn., DSC and elec. resist. study 0-107060  
 Pt-Si, amorphous thin films, laser irradi., metastable phases 0-96622  
 Ta-Ir(Rh) system glasses, form., crystn. and microhardness, resist. obs. 0-89178  
 Th-Cu, amorphous, thermal stability, crystn., DSC and elec. resist. study 0-107060  
 Ti-Nb-Si, amorphous alloy, supercond. props. and crystn. behaviour, TEM and DTA study (*Japanese*) 0-84536  
 Ti-Ni amorphous alloys, glass transition and ductility, O additions effect 0-75168  
 Ti-Si amorphous alloy, melt-quenched, transform. studies and mech. props. 0-100838  
 Ti<sub>60</sub>Be<sub>40</sub>Zr<sub>10</sub>, amorphous, crystn. temp., press. and heating rate depend. 0-70132  
 Ti<sub>70</sub>Co<sub>30</sub>B<sub>10</sub>, amorphous alloys, crystn. behaviour, TEM study (*Japanese*) 0-84087  
 Ti<sub>70</sub>Fe<sub>30</sub>B<sub>10</sub>, amorphous alloys, crystn. behaviour, TEM study (*Japanese*) 0-84087  
 Ti<sub>70</sub>Ni<sub>30</sub>B<sub>10</sub>, amorphous alloys, crystn. behaviour, TEM study (*Japanese*) 0-84087  
 U-Co(Ce)(Fe)(Mn)(Ni)(V) metallic glasses, glass form. and thermal stability 0-75183  
 W<sub>80</sub>Fe<sub>20</sub> glassy alloy, refractory, triode sputtered 0-75185  
 W<sub>77</sub>Si<sub>23</sub>B<sub>10</sub>, amorphous alloys obtained by liq. quenching, superconductivity 0-75670  
 Y-Fe(Co), amorphous, thermal stability, crystn., DSC and elec. resist. study 0-107060  
 Zr-Cu amorphous alloys, glass transition and ductility, O additions effect 0-75168  
 Zr-Cu(Ni)(Co)(Fe) metallic glasses, glass form. and thermal stability 0-75177  
 Zr-Ti-Be metallic glass, phase separation 0-97464  
 Zr<sub>70</sub>Co<sub>30</sub>, Zr<sub>70</sub>Fe<sub>30</sub>, Zr<sub>70</sub>Ni<sub>30</sub> and Zr<sub>70</sub>Pd<sub>30</sub> amorphous alloys, struct. factors and radial distrib. functions 0-84096  
 Zr<sub>0.475</sub>Cu<sub>0.475</sub>Mo<sub>0.05</sub>, glass transition temp., comp. depend. 0-79702

## metallic thin films

- see also discontinuous metallic thin films; electronic conduction in metallic thin films; metallic epitaxial layers; metallic glasses; metallisation
- 1/f noise, nonlinear mechanism 0-96955  
 anomalous optical props., interpretation (*French*) 0-60692  
 contact to Te film, time evolution of photovoltaic effect 0-65687  
 cyclotron resonance on open electron orbits (*Russian*) 0-88878  
 deposition by organometallic compound decomp. on surface 0-71599  
 electrical conductivity measurement, thickness dependence, quantum size effect (*German*) 0-86344  
 electron backscattering, empirical study 0-108310  
 ellipsometry, metallic films and surfaces, nonlocal effects, theory 0-104006  
 etching by conical beam of Ar ions (*Russian*) 0-76383  
 Everhart theory extension of backscattered electron energy spectra 0-108309  
 film, evaporated at oblique incidence, columnar grains inclination angle 0-75468  
 film characterisation technique, APFIM, time-of-flight spectroscopy 0-75138  
 film on Si substrate, eutectic point displacement on annealing (*Russian*) 0-100850  
 hot electron distribution function, nonlinear elec. resistance (*Russian*) 0-65717  
 interference filters, metal-dielec., in transmitted light 0-96013  
 ion beam milling, anomalous sputter yield behaviour 0-108624  
 layer thickness measurement using X-ray fluorescence principle (*German*) 0-93705  
 mass transport and assoc. failures 0-59694  
 metal-dielectric boundary thermal resistance, nonlinear elec. resistance (*Russian*) 0-65530  
 metallised coating on polyethylene terephthalate film, fracture under laser irradi. (*Russian*) 0-76333  
 overlayers, on mol. monolayers, IR absorpt. enhancement, ATR technique 0-88995  
 preheating as aid to laser recording 0-102753  
 rare earth metal silicide thin film formation on (100), (111)Si substrates, backscattering study 0-70542  
 resistivity strain coeff. calcs. 0-100449  
 SEM specimen preparation thin film coating techniques 0-68308  
 size effect in Landau diamagnetism, surface pot. effect (*Russian*) 0-93012  
 surface polariton motion in thin surface layer, nonstationary phenomenological theory (*German*) 0-88608

## metallic thin films continued

- surface region, electrostatic energy and screened charge interaction for different Fermi surface shape 0-70631  
 target preparation for stopping power meas. of channelled ions in low energy region 0-63431  
 thermal strains, effect of support, theory 0-88647  
 thermoelectric power, thermal stress effects, theory 0-65714  
 thermoelectric props. of conductor covered with electrolytic deposit, thermal flux meas. (*French*) 0-59961  
 thickness measurement, for single layer and multilayer systems, X-ray fluoresc. technique 0-68180  
 thickness measurement, using nondestructive radioisotopic technique 0-68179  
 3d transition metal films, EELS, anomalous L<sub>3</sub>/L<sub>2</sub> white-line ratios 0-93444  
 transition metals, BCC, films, vac. evaporated, optical cond. 0-76100  
 transition metals, on Si, silicide form. at interface, interface marker technique obs. 0-59734  
 transverse electric quantum wave spectrum (*Russian*) 0-84517  
 ultra-fine metal particle form., pulsed laser breakdown of carbonyl vapours 0-84881  
 ultrasound attenuation, size magnetoacoustic effect (*Russian*) 0-107869  
 vacuum deposition, ultra-high vac. technique 0-100791  
 vapourisation by laser, vapourisation front relativistic velocities (*Russian*) 0-66337  
 Ag, (111) surface electron microscopy 0-103556  
 Ag, adsorbed CO, enhanced Raman scatt. mechanism in ultrahigh vacuum 0-107645  
 Ag, conduction electron spin disorientation at surface 0-75855  
 Ag, defect density, thickness depend., elec. resist. obs. 0-70568  
 Ag, energy losses and straggling for H<sup>+</sup> and He<sup>+</sup> beams (*Russian*) 0-84226  
 Ag, film, chem. deposited, agglomeration, SEM and TEM obs. 0-59828  
 Ag film, ellipsometric response to CO adsorption 0-103571  
 Ag film, energy losses of electrons, microcalorimetric meas. 0-59543  
 Ag film, intrinsic stress meas. 0-71696  
 Ag film, on amorphous C and Si substrates, dispersion force contrib. to adhesion (*French*) 0-59842  
 Ag film, surface roughness, light scatt. meas. 0-107624  
 Ag film, vacuum deposition on Pb (111), substrate diffusion effects, RHEED, LEED, AES 0-65410  
 Ag film, void growth, TEM obs. 0-59833  
 Ag film deposition, thermal effects, influence on internal stress meas. 0-96767  
 Ag film for Ga liquid spreading, kinetic eqn. (*Russian*) 0-59376  
 Ag film growth on Pd substrate, interface cpd. form., AES study (*French*) 0-80131  
 Ag films, effect of Ar- and N-ion bombardment on texture (*Russian*) 0-107338  
 Ag foil, surface-plasmon resonance, roughness-induced wavelength corrections 0-108288  
 Ag, interaction with adsorbed dye mols., absorpt. and luminesc. 0-103981  
 Ag thin evaporated films, rel. between microstruct. and excess free energy, TEM 0-70427  
 Ag thin film, X-ray fluoresc. spectroscopy of surface using RHEED-solid state detector method 0-108760  
 Ag, thin film deposited on Si, work function (*French*) 0-80353  
 Ag, thin targets, electron transmission below 3 keV (*French*) 0-60725  
 Ag, vacuum deposited, orientation axis tilt rel. to vapour angle of incidence 0-88456  
 Ag-InP interface, Ag<sub>2</sub>P<sub>3</sub> formation during sintering 0-65309  
 Ag-Sn, double, high-speed superconducting bolometer appl. 0-57368  
 Ag-Te, thin film system, stress-relief appearance conditions 0-65416  
 Al, 1/f noise depend. on internal mech. stresses 0-65711  
 Al, deposited metallic thin films, H incorporation effects on stress and electromigration 0-80139  
 Al deposition using solar furnace 0-89148  
 Al, energy losses and straggling for H<sup>+</sup> and He<sup>+</sup> beams (*Russian*) 0-84226  
 Al film, deform. under He ion bombardment 0-65073  
 Al film, dislocation observation by electron microscope using convergent beam (*French*) 0-96532  
 Al film, electron transmission, calc. 0-60724  
 Al film, energy losses of electrons, microcalorimetric meas. 0-59543  
 Al film, etching in carbon tetrachloride plasmas 0-76407  
 Al film, intrinsic stress meas. 0-71696  
 Al film, lattice and bulk heat capacity meas. for normal and supercond. states 0-92684  
 Al film, on amorphous C and Si substrates, dispersion force contrib. to adhesion (*French*) 0-59842  
 Al film, wave front reversal, holography/applications (*Russian*) 0-58483  
 Al film and polished bulk specimens, initial stages of oxidation obs. using SIMS 0-81239  
 Al, film on Si(111) substrate, struct., props. depend. on vapour flow, ionisation (*Russian*) 0-75453  
 Al films, resistance changes due to bombardment by N, C, or Ar ions 0-103670  
 Al, on CdS, bonding and interdiffusion, XPS obs. 0-80000  
 Al, on polyethylene terephthalate, thickness determ. using photometry 0-62626  
 Al overlay film on quartz for temp. compensation, SAW device appl. 0-79043  
 Al, polycrystalline, trapping of <sup>3</sup>He and <sup>4</sup>He ions at room temp. 0-84221  
 Al surface, plasma cleaning and etching, removal of C 0-97645  
 Al thin conducting film, electromigration under superimposed DC and noise powers 0-107879  
 Al, thin film, thermal cond. meas., size effect 0-65715  
 Al, thin film deposited on Si, work function (*French*) 0-80353  
 Al thin film stripes, electromigration lifetimes width depend. 0-92799  
 Al thin films evaporated on rough quartz substrates, surface irregularity, light scattering measurements (*Polish*) 0-88450  
 Al/Cu thin film couples, TEM study of intermetallic nucleation at interface 0-65305  
 Al/Pd thin film couples, thermal reactions 0-59830  
 Al-Cr, thin film metal contact, sheet resistance changes 0-80356  
 Al-Li-Mg-Be alloys, phase composition of surface films, oxidation protection mechanism (*Russian*) 0-65417  
 Al-Zn thin film, prep. using Sn-Zn evaporant source 0-100789  
 Au (001), surface struct., high resolution TEM 0-100383  
 Au, (111) surface electron microscopy 0-103556



## metallic thin films continued

- Au, adsorbed CO, enhanced Raman scatt. mechanism in ultrahigh vacuum 0-107645  
 Au, bicrystal, diffraction effects from inclined grain boundaries 0-103362  
 Au, bicrystalline thin films, faceting of [001] grain boundaries 0-70222  
 Au, Co-hardened, characterisation by Mossbauer spectroscopy. Co precip. formation 0-80108  
 Au, diffusion barrier formation, at metal-semiconductor or metal-metal interface, using laser annealing 0-80373  
 Au, energy losses and straggling for  $H^+$  and  $He^+$  beams (Russian) 0-84226  
 Au, epitaxially grown bicrystalline thin films, preferred inclinations of (100) grain boundaries 0-103367  
 Au, evap., temp. change and gas adsorpt. effect on opt. const., ellipsometric obs. (German) 0-89081  
 Au film, Cr and Si low temp. diffusion, CO effect 0-100361  
 Au film, electron transmission, calc. 0-60724  
 Au film, energy losses of electrons, microcalorimetric meas. 0-59543  
 Au film, on amorphous C and Si substrates, dispersion force contrib. to adhesion (French) 0-59842  
 Au film, photoelectron emission, intershell interaction influence on 3d and 5d branching ratio 0-104038  
 Au film deposition, thermal effects, influence on internal stress meas. 0-96767  
 Au film electrodeposition, substrate effects on film props. 0-81329  
 Au film growth on Mo (110) surface, AES, LEED, thermal desorption study 0-80130  
 Au films, vac. condensed at oblique vapour incidence, oriented cryst. growth, electron diff. study 0-97432  
 Au, grain boundary structure, high resolution HVEM 0-103360  
 Au, integrated condensation coeff. on NaCl cleavage faces. Rutherford ion backscatt. obs. 0-59827  
 Au, interaction with adsorbed dye mols., absorpt. and luminesc. 0-103981  
 Au, ion bombarded, surface craters induced by displacement cascades 0-107344  
 Au, metallised coating on polyethylene terephthalate film, fracture under laser irradi. (Russian) 0-76333  
 Au, nonohmic characts. and electron emission 0-60066  
 Au, on CdS, bonding and interdiffusion, XPS obs. 0-80000  
 Au, on Si substrate, critical Au-film thickness obs. for room temp. interfacial reaction 0-75390  
 Au, on W substrates, interface struct., FIM obs. 0-65384  
 Au, optical props., dielec. function, void model, sample effects 0-76048  
 Au, overlay film on quartz for temp. compensation, SAW device appl. 0-79043  
 Au single cryst., thin films and bulk, anisotropic X-ray emission 0-108303  
 Au, spatial resolution of X-ray microanalysis 0-101065  
 Au, thin film, anomalous stopping power effects 0-65102  
 Au thin film, electromigration, adhesion layer effects 0-96685  
 Au, thin film, self-sustaining, electron mean free path meas. 0-92883  
 Au thin films, electron diff. investigation of Debye temp. 0-88420  
 Au thin layers, diffusion rate of  $H_2$ ,  $N_2$ , Ar,  $CO_2$ , air, and  $O_2$  0-100359  
 Au, twin boundary struct. and migration, atomic scale electron microscopy obs. 0-107276  
 Au/Al thin film, Al diffusion studied by attenuated total reflection method 0-92722  
 Au/Cu, double layer film, oxidation (Japanese) 0-61010  
 Au/Sn thin film couples, evaporated, TEM study 0-59832  
 Au-Pd-Au sandwich, obs. of strongly enhanced mag. susceptibility 0-93076  
 Au-refractory film interdiffusion obs., by combination of scattering techniques 0-65308  
 Au-Si thin film double layer, silicide form., electron diff. study 0-80005  
 Au-Ti<sub>0.5</sub>W<sub>0.5</sub>, thermal annealing study of metallisation on Si 0-80134  
 Au-Cu-Al thin film bilayer system, phase formation, backscattering spectra 0-96728  
 Au<sub>2</sub>Mn thin films, electron diff. study 0-92793  
 Ba getter, initial reaction probability with  $O_2$ , water, CO and  $CO_2$ , AES obs. 0-61153  
 Ba, semitransparent, opt. props. in 2-5.6 eV range, electronic transitions, thickness depend. (French) 0-108289  
 Be film, on W (110), growth mode, work function, thermal desorption, and struct. 0-75477  
 Bi, film, size effect of carrier heating, surface scatt. (Russian) 0-100474  
 Bi films, resistance changes due to bombardment by N, C, or Ar ions 0-103670  
 Bi, thin film, resistivity, rel. to thickness 0-107928  
 Cd, dry lubrication on C steel, tribological behaviour 0-89364  
 Cd films, struct. and props., X-ray diff. spectra anal. 0-80119  
 Co thin film, nuclear spin echo excitation on subharmonics, and multiple freq. (Russian) 0-60454  
 Co, thin films, optical and magneto-optical permittivities 0-66163  
 Co<sub>2</sub>Pd ordered, stacking fault obs. by TEM and interpret. using many-beam theory 0-107680  
 Cr containing Cr<sub>2</sub>O<sub>3</sub> film struct., oxide percentage determ. and temp. coeff. of resist. 0-103607  
 Cr film, 3p-3d intershell interaction, photoemission 0-80934  
 Cr film, evaporated, concurrent ion bombard. effects 0-80142  
 Cr film, obtained by thermo ionic precipitation, phase composition, lattice parameters (Russian) 0-96756  
 Cr film, pattern generation by laser-induced oxidation 0-61009  
 Cr film, trivalent, cathodic deposition, as bonding interface between Cu and polyethylene 0-76201  
 Cr films, photoresist film on reverse gas plasma etching 0-97634  
 Cr, on polycryst. CdS, thermal diffusion, 240-400°C 0-80001  
 Cr, preparation by decomp. of bis-arene cpds., struct. and phys. props. 0-60785  
 Cu, (111) surface electron microscopy 0-103556  
 Cu alloy, precipitation strengthened compositions with oxide particles, condensed, struct. criteria and thin layer possibilities (Russian) 0-89236  
 Cu, bulk and (001) films, extended tight-binding calcs. 0-70592  
 Cu electrodeposition in cylindrical pores by pulse plating 0-81330  
 Cu, energy losses and straggling for  $H^+$  and  $He^+$  beams (Russian) 0-84226  
 Cu film, diffuse optical scattering from variable roughness surfaces 0-100704  
 Cu film, electron transmission, calc. 0-60724  
 Cu film, Gorsky effect, internal friction maxima, atom diffusional mobility (Russian) 0-70446

## metallic thin films continued

- Cu film, on amorphous C and Si substrates, dispersion force contrib. to adhesion (French) 0-59842  
 Cu film, on Au substrate, oxidation and interfacial behaviour, ion scatt. spectroscopy study 0-66691  
 Cu film, optical const. deduced from surface EM wave propag. 0-60697  
 Cu film, photoelectron emission, intershell interaction influence on 3d and 5d branching ratio 0-104038  
 Cu film, vacuum deposition on Pb (111), substrate diffusion effects, RHEED, LEED, AES 0-65410  
 Cu film deposition, thermal effects, influence on internal stress meas. 0-96767  
 Cu films, resistance changes due to bombardment by N, C, or Ar ions 0-103670  
 Cu films, vac. condensed at oblique vapour incidence, oriented cryst. growth, electron diff. study 0-97432  
 Cu, interaction with adsorbed dye mols., absorpt. and luminesc. 0-103981  
 Cu, metallised coating on polyethylene terephthalate film, fracture under laser irradi. (Russian) 0-76333  
 Cu, oxidation, RMEED/SEM studies 0-100968  
 Cu, partially oxidised, EXAFS studies on superficial regions 0-75474  
 Cu surface, plasma cleaning and etching, removal of C 0-97645  
 Cu thin film, electromigration, adhesion layer effects 0-96685  
 Cu thin foils, intrinsic struct. in grain boundaries and boundary mobility 0-103368  
 Cu, thin targets, electron transmission below 3 keV (French) 0-60725  
 Cu, vacuum deposited layer, ion bombardment induced preferential orientation 0-100290  
 Cu-Al films, elec. cond. of vacuum condensates depend. on composition, annealing (Russian) 0-65709  
 Cu-Al thin film multistructure, Xe<sup>+</sup> ion beam cratering 0-66708  
 Cu-metal thin film couples, room temperature interactions 0-96699  
 Cu-Ni films, compositionally modulated, magnetic anisotropy, magnetisation curves 0-88840  
 Cu<sub>2</sub>Au thin films, fine-grained and disordered, low temp. ordering 0-97433  
 Fe, epitaxial growth on Au platelets, dislocations 0-96760  
 Fe, evaporated, adsorbed acetylacetone, XPS study 0-76133  
 Fe, ferromag. film, surface states, surface magnetisation and electron spin polarisation 0-65648  
 Fe film, nuclear spin system dynamics Mossbauer study in FMR conditions (Russian) 0-80651  
 Fe, thickness variations in extraordinary and spontaneous Hall coeffs. 0-97013  
 Fe, thin foil, extrinsic grain boundary dislocations, low C content influence 0-107273  
 Fe thin layers, vacuum coated on PMMA, mag. behaviour during mech. stress cycles (German) 0-80581  
 Fe vacuum deposits on Ni(Cu)(Ag) (111) FCC substrates, orientation relationships 0-59836  
 Fe-Ni film, electrodeposited, struct. and mag. props. 0-107668  
 FeNi amorphous films, fast phase transition investigation by TEM method 0-107029  
 Ga, amorphous metal films, crystallisation with and without mag. field 0-70570  
 Hg, condensation, two-dimensional, on W 0-107666  
 In-PbTe contacts, fabrication and props. 0-60078  
 In-P-Al interface struct., low temp. interaction, AES study 0-107661  
 Insular metal films, influence on crystn. of continuous films 0-88454  
 Mg films, struct. and props., X-ray diff. spectra anal. 0-80119  
 Mn film, vacuum-evaporated, (H/D) uptake kinetics and energetics 0-88430  
 Mo films, sputtered from cylindrical-post magnetron with Ne, Ar, Kr and Xe, compressive stress and presence of inert-gas obs. 0-80140  
 Mo, formation by reduction of MoCl<sub>5</sub>, influence of electric field 0-93491  
 Mo-Si film-substrate interface, reaction on heat treatment, silicide formation 0-79999  
 Nb electron beam deposited on Si surface 0-66862  
 Nb, thin-film SQUID working at 4.2K, fabrication and characterisation 0-100570  
 Nb/Cu layered ultrathin coherent struct. 0-80122  
 NbTi films, effect of Ar- and N-ion bombardment on texture (Russian) 0-107338  
 Ni (100) films, spin density by self-consistent linear APW method 0-65710  
 Ni alloy, precipitation strengthened compositions with oxide particles, condensed, struct. criteria and thin layer possibilities (Russian) 0-89236  
 Ni, amorphous layer covered, target prep. for channelled ion stopping power meas. 0-63431  
 Ni electrodeposition on Cu (001), three-dimens. epitaxial crystallites, TEM image contrast 0-88457  
 Ni, evaporated, adsorbed acetylacetone, XPS study 0-76133  
 Ni, ferromag. film, surface states, surface magnetisation and electron spin polarisation 0-65648  
 Ni film, interaction with  $O_2$ , AES, EELS, work function, and gravimetric meas. 0-75433  
 Ni film crystallisation on C fibres and sapphire crystals (Russian) 0-75455  
 Ni films, adhesion on graphite 0-80141  
 Ni films, self-supporting, electroplating method of prep. 0-66436  
 Ni, metallised coating on polyethylene terephthalate film, fracture under laser irradi. (Russian) 0-76333  
 Ni on Au substrate, interdiffusion, backscatt. study 0-79991  
 Ni/GaAs film contact system, alloying reaction 0-96747  
 Ni-B, film crystallisation on C fibres and sapphire crystals (Russian) 0-75455  
 Ni-Cr films implanted with N ions, electric properties (Russian) 0-107927  
 Ni-Cr(Fe)(Cu) alloy, matrix effect in SIMS anal. using  $O_2^+$  primary beam 0-76576  
 Ni(001) surface states, surface magnetisation, electron spin polarisation 0-88612  
 Pb, deposition on Au, quantitative Auger electron spectroscopy, substrate and instrumental effects 0-71523  
 Pb, film, thermal strain, strain relax. above room temp. 0-59841  
 Pb, grain boundary self diffusion, microtome serial sectioning anal. 0-79975  
 Pb, hillock formation by grain boundary sliding 0-107673  
 Pb, hillock growth upon cycling to cryogenic temps. 0-88448  
 Pb, on Ag electrode, anisotropy of optical props. 0-60534



**metallic thin films continued**

- Pb, silicon and polytextured thin films, band struct., tunnelling spectroscopy 0-80169  
 PbO, thin film, microstruct. and thermal stress, doping effects 0-88458  
 Pd, (111) surface electron microscopy 0-103556  
 Pd, electron beam deposited on Si surface, silicide formation using scanning CW laser beam 0-66862  
 Pd on Si substrate, epitaxial silicide growth, LEED and AES study 0-103590  
 Pd, work function changes due to adsorbed H<sub>2</sub>, surface and interface dipoles 0-96972  
 Pd-Ti on Si substrate, silicide form. 0-80006  
 Pt, electron beam deposited on Si surface, silicide formation using scanning CW laser beam 0-66862  
 Pt film, growth on amorphous Si:H, AES and LEED study 0-88447  
 Pt, polycrystalline, trapping of <sup>3</sup>He and <sup>4</sup>He ions at room temp. 0-84221  
 Pt thin-film temp. sensor (*Japanese*) 0-105645  
 Pt-Cr(Si) interface, low-temp. diffusion, ambient effects 0-100355  
 Pt-Si:As, silicide form. during laser irr., p-n junctions and ohmic contacts 0-84397  
 PtSi, formation by ion sputtering and annealing, form. and exam. problems 0-100782  
 Re film, prep. by laser melting 0-84859  
 Se thin films, obtained in vac. of 10<sup>-5</sup>-10<sup>-6</sup> Torr, struct. and elec. resist. 0-107931  
 Sn, anomalous transmittance of metal-insulator interface for thermally radiated phonons (*Russian*) 0-103664  
 Sn polycrystalline films, elec. props. and crystallite size, 4.2K to room temp. (*Russian*) 0-93011  
 Sn, vacuum deposited, substrate and substrate temp. effects on struct. 0-107677  
 Sn/Au thin film diffusion couples, Kirkendall void form. 0-96698  
 Sn/Cu electroplated bimetallic films, interfacial reaction 0-96765  
 (Tb,Dy)-Fe amorphous films prep. by cosputtering, magnetoelastic props. 0-97429  
 Te film, microstructure 0-103598  
 Ti thin films, H absorption and desorption, Tokamak gettering, Auger electron spectrosc. 0-75092  
 W, support film for electron microscopy, Fourier spectrum analysis of phase contrast 0-95199  
 W, vapour deposited, dislocation struct., rel. to texture (*Russian*) 0-65394  
 Yb, amorphous metal films, crystallisation with and without mag. field 0-70570  
 Zr, TEM, sources of background X-radiation 0-101908

**metallisation**

- see also electrodeposition*  
 ceramic/metal layer adhesion mechanism for metallization of electronic ceramics, elec. props. (*German*) 0-76381  
 corrosion, IR microscopy failure anal. 0-98976  
 diamond powders, Mo coated, X-ray diff. study 0-100936  
 electrets, metallised, mech. instabilities (*French*) 0-88906  
 glass fibre reinforced epoxy laminate, metallization by Cu and chem. treatment by H<sub>2</sub>CrO<sub>4</sub> (*German*) 0-93670  
 MIS solar cells, etched slotted mask for direct deposition of metal contact pattern 0-97786  
 solar cell metallisation using screen printing tech. 0-85291  
 solar cells, front- and back-surface metallisation patterns 0-93943  
 transition metal silicides, refractory for ICs, review 0-100820  
 VLSI Al and Al alloy metallisation sputter deposition 0-66429  
 Al, 1/f noise depend. on internal mech. stresses 0-65711  
 Al-n<sup>+</sup>Si ohmic contacts, metallisation structs. for very shallow n<sup>+</sup>/p junctions 0-60084  
 Au-refractory film interdiffusion obs., by combination of scattering techniques 0-65308  
 Au-Ti<sub>0.3</sub>W<sub>0.7</sub>, thermal annealing study of metallisation on Si 0-80134  
 Be-Au, ohmic contact to p-InP, low contact resist. 0-65677  
 Cr deposition as diffusion barrier layer, improved Cr-Zr source 0-76163  
 Cr, on polycryst. CdS, thermal diffusion, 240-400°C 0-80001  
 GaAs, alloying with Au and Au alloy ohmic contact metallisations, SEM and optical study 0-70820  
 GaAs/metal contacts, metallisation of defined surfaces (*French*) 0-107909  
 LiNbO<sub>3</sub>, optical waveguide surface, acoustooptical interaction for TE modes, metallisation effect 0-69541  
 Ni-Cr/Au films, interdiffusion processes and oxidation phenomena 0-59735  
 Si device metallisation, TiN and TaN as diffusion barriers 0-65304  
 Si solar cells, low cost, Ni contacts 0-94017  
 Si solar cells, low cost processes for fabrication 0-94013  
 Si solar cells, Ni-Cu conductor system 0-93991  
 Si solar cells with screen printed diffusion and metallisation 0-94015  
 Si terrestrial solar cells, stress tested, contact integrity testing 0-94018  
 Si/Al and Si/Al-Si(Cu), Si regrowth minimisation through overlying Al or Al alloy film 0-70569  
 p-Si-Al, ohmic contacts, Si dissoln. and recrystn. effects, computer calc. 0-103749  
 Si-Pd<sub>80</sub>Si<sub>20</sub>, amorphous, Pd<sub>2</sub>Si layer form., shallow contact 0-103586  
 Ta-Ta<sub>2</sub>O<sub>5</sub>-InP thin refractory MIS struct. deposition 0-75647  
 Ti/Cu/(Au) thin films thermocompression bonds degradation by thermal ageing 0-66546  
 TiW-TiO<sub>2</sub>-InP thin refractory MIS struct. deposition 0-75647

**metallising *see metallisation*****metallo-organic compounds *see organometallic compounds*****metallocenes *see organometallic compounds*****metallography**

- see also electron diffraction examination of materials; electron microscopy; optical microscopy*  
 adhesion in metal cutting, direct SEM obs. of frictional sliding 0-104412  
 Alnico 5 alloy, S and Ti additions effect rel. to non-metallic inclusions, coercive force and grindability 0-89375  
 convergent beam electron microscopy for materials science 0-107028  
 crack tip, plastic deform., metallographic anal. by recrystn. 0-85029  
 critical temperatures determination, elec. resist. method, IMASH-5S-69 installation 0-71827  
 electron metallography of material wear using SEM, TEM 0-76455  
 electron microscope examination, feasibility and methodology of in situ experimentation (*French*) 0-68301  
 electron microscopy on etched thin foils, comparative SEM, STEM and TEM analysis 0-100144

**metallography continued**

- EPIQUANT, assessment of post-hotforming recrystallization condition of 34Cr4 steel 0-84949  
 EPIQUANT, automatic structure analyser 0-85116  
 fine fragmented crystals, complex struct. analysis by electron microscopy 0-104416  
 Hastelloy-X, Ni-Cr-Fe-Mo, cyclic oxidation resist. improvement by high temp. etching treatment 0-97627  
 Inconel 617, creep, morphological changes of carbides, affect on creep props. 0-108509  
 interference microscopy, for colour development and phase separation 0-100976  
 ion-etching application, to metallography (*Japanese*) 0-93715  
 large parts, without taking specimens, portable grinding and polishing machine 0-61042  
 microfractography (*Japanese*) 0-71841  
 NEOPHOT 2, assessment of post-hotforming recrystallization condition of 34Cr4 steel 0-84949  
 Ni-base wrought superalloy, creep and stress rupture behaviour in air and vacuum 0-60918  
 porous materials, effects of different methods of prep. on reproducing surface 0-60995  
 sample preparation, procedures 0-57272  
 scanning optical microscope as new metallographic tool 0-71852  
 skeletonization in quantitative metallography 0-101002  
 spacecraft materials failure, metallurgical exam. 0-71868  
 steel, 0.7% C, welded zone, fatigue strength and microstruct. (*Japanese*) 0-89339  
 steel, 35NiCr18, bainite transformation, study with aid of hot stage microscope 0-76253  
 steel, (0.36 wt.% C) Ni-Cr-Mo, electroslog refined, fracture toughness and fatigue behaviour 0-81171  
 steel, austenitic 30KhGSA, white phases structure after heat treatment 0-76281  
 steel, austenitic stainless, creep props., effect of high temp. ageing, SEM 0-97516  
 steel, austenitic stainless, SUS 304, stress corrosion cracking in various environments, fractography (*Japanese*) 0-93690  
 steel, austenitic stainless, welded explosively, induced martensites morphology 0-104153  
 steel, Cr, cold roll, frictional heating surface damage 0-76289  
 steel, Cr-Mo:P (2.25, 1 wt.%), stress relief cracking, effect of P segregation 0-89324  
 steel, Cr-Mo, oxidised, mechanism of crack decoration of oxides by electrodeposition 0-97560  
 steel, Cr-Mo (10-14, 2-6 wt.%), heat-resist., creep-rupture strengths 0-104271  
 steel, Cr-Ni-Mn, adiabatic shear band determ. by surface obs. 0-97579  
 steel, En 24, Cr, V, deform. effect on decomp. of austenite, carbide precipitation 0-84938  
 steel, etchant for revealing austenite grain boundaries 0-85098  
 steel, Fe-V-C (1, 0.2 wt.%), austenite formation 0-84927  
 steel, ferritic and austenitic, microstruct. study by means of replicas taken from components at 100°C 0-81256  
 steel, ferritic Cr-Mo type, microanalysis of precipitates using TEM 0-108688  
 steel, HSLA, V and N effect on recovery and recrystn. during and after hot working 0-84973  
 steel, low C, type En3, high strain deform., struct. and props. 0-89301  
 steel, microalloyed, types V1599, V1600, V1286, NbCn precipitation in undeformed austenite 0-89230  
 steel, N determ. by track autoradiography 0-100979  
 steel, pearlitic structural, austenite grains, growth rate during heating 0-100860  
 steel, plain C having ferrite-martensite mixed structs., microstructural parameters effect on fatigue strength (*Japanese*) 0-71735  
 steel, stainless, austenitic type 304, martensite transform, acoustic emission identification, opt. microscopy obs. 0-81062  
 steel, stainless, Cr-Ni-Ti, metallographic detection of (Ti,Ni)<sub>6</sub>C 0-66721  
 steel, stainless, fixing pins for fractured bones, strength, ultrasound effect 0-71710  
 steel, stainless, type 316, low cycle fatigue props. in vac., fracture mode 0-85021  
 steel, structural, macroscopic and microscopic features of fracture 0-81179  
 steel, surface state influence on etching effect 0-81235  
 steel, type 34Cr4, post-hotforming recrystallisation condition, use of NEOPHOT 2 and EPIQUANT 0-84949  
 steel ball bearing, fatigued, phase changes, nomenclature 0-89198  
 steels, obs. and anal. of sulphides, using non-aqueous electrolyte-potentiostatic etching method (*Japanese*) 0-89433  
 steels ShKh15 and 12KhN3A, white phases structure after heat treatment 0-76281  
 STEM, low resolution imaging problems and soln. 0-108685  
 STEM microdiffraction use for misorientation between subgrains obs. 0-104415  
 subgrain imaging, in bulk specimens to study localised plasticity using SEM 0-66609  
 surface deformation and wear track obs. using analytical electron microscope 0-108687  
 two-surface analysis, of polished sections in scanning electron microscope 0-77912  
 white cast Fe, abrasive wear 0-108587  
 white Fe castings, morphology of eutectic M<sub>2</sub>C and M<sub>7</sub>C<sub>3</sub> 0-108427  
 Ag thin evaporated films, rel. between microstruct. and excess free energy, TEM 0-70427  
 Al alloy, FIM and microanalysis, developments 0-100155  
 Al, fracture mechanism 0-100903  
 Al-Ag, type-II superconductor, torque oscillations in mag. field (*Russian*) 0-103800  
 Al-Ag (7.27 wt.%), peculiarities exhibited during fatigue loading (*Chinese*) 0-71723  
 Al-Bi(Cd)(Pb)-Ti, containing low-melting pt. inclusions, mech. props. 0-93632  
 Al-Cu, high strength, type 2024-T3, crack growth, fatigue induced surface deform., holographic detect. 0-85120  
 Al-Mg-Si, type 6010, microstruct. chars. influence on formability, heat treatment 0-81090  
 Al-Ni (6 wt.%), fine-grained, deform. in tension and torsion 0-85008  
 Al-Ni(Cd)(Fe)(Si), cold worked, struct. and props. 0-71666



**metallography continued**

- Al-Si eutectic alloy, banded struct., SEM and optical microscopy 0-104144  
 Al-Zn alloys, interfacial stability of planar solid-liq. interface during solidification 0-104145  
 Co-CoAl, two phase, interaction between deform., fracture initiation and propag. 0-85006  
 Cu crystals, two-phase, recrystn. retardation, particle size, spacing effects 0-89242  
 Cu, polycrystn., strain localisation during hot deform. 0-104195  
 Cu single crystals, neutron irradiated, secondary slip 0-88161  
 Cu, single crysts., (110) oriented, tensile deformed, HVEM of recrystn., recrystallised state 0-89256  
 Cu single crystals., deformed, HVEM study of recrystn. texture 0-104179  
 Cu-Be (2 at.%), plastic deform. and dislocation substruct. 0-76307  
 Cu-Cr (0.75 wt.%), deformation characts., fully reversed cyclic strain with fatigue cracks and dislocation struct. 0-81148  
 Cu-Ni-Zn alloy, surface comp., outdoor exposure influence 0-59770  
 Cu-Sn alloy, surface comp., outdoor exposure influence 0-59770  
 Cu-Zn alloys, surface comp., outdoor exposure influence 0-59770  
 Fe, cast, austenitic grain size determ. 0-81255  
 Fe, cast, graphite content determ. by X-ray diff. method 0-100977  
 Fe, cast, grey, solidified in oscillatory and rotating moulds, metallographic study 0-89213  
 Fe, cast, white, high Cr, phase composition, B effect 0-104172  
 Fe, cast, with spheroidal graphite, crystn. (*German, English*) 0-97473  
 Fe, high purity, boriding with cryst. B powder 0-84951  
 Fe, pig, white, mech. props. meas. (*French*) 0-104370  
 Fe, sintered, influence of metallographic treatment on pore analysis 0-76417  
 Fe-Co-Ti-Al alloy type YuNDK magnets, metallographic method of distinguishing cracks 0-85096  
 Fe-Cr-Co alloy, spinodally decomposed, micro-twinning 0-92537  
 Fe-Cr(W)-M, (M=Si,Mo,Ni,Mn,P,Cr), cellular growth of S-pearlite formed by carburisation 0-108486  
 Fe-Ni, interference microscopy, for colour development and phase separation 0-100976  
 Fe-Ni-C (31.9, 0.02 wt.%) alloy, hardness of martensite-austenite mixtures 0-60959  
 Fe-Ni-Cr-Al-Y, oxidation mechanism, Y addition effect on kinetics and oxide adherence 0-97623  
 Fe-Ni-Mn (20, 5 wt.%), rel. orientation between adjacent martensite laths 0-76254  
 Fe-Ni-(Al) (Ti) (V)-(Cu), Cu addition strengthening at 77K, mech. props. 0-60875  
 Fe-Ti-C, rapidly quenched by splat-cooling 0-84923  
 Fe-X-C (X=Cr, Mo, W), quenched rapidly from melts, nonequilib. phases (*Japanese*) 0-71630  
 InBi single crystal, deform. mode under dynamic indentation 0-88163  
 LaNi<sub>4</sub>B<sub>6</sub>, H<sub>2</sub> absorpt. props. 0-88432  
 Mg-Nd-Zn dilute alloy, metallography and precip. kinetics 0-71655  
 Mn-Si-Si system, striations and cryst. struct. of matrix 0-103292  
 Mo powder, influence of powder reduction processes on props. 0-89175  
 Mo-(Zr+V+C) (1.1 wt.%) alloy, phase composition, carbide phase micro-hardness (*Russian*) 0-60834  
 N determination by track autoradiography 0-100979  
 Nb-Nb(O)(C) system, specimen prep. for metallography (*German, English*) 0-89439  
 Nb-Pd constitution diagram, metallographic and X-ray diff. anal. 0-89204  
 Ni alloys, cast, interference microscopy, for colour development and phase separation 0-100976  
 Ni, sintering kinetics, metallographic study 0-93519  
 Ni-(Co)-Cr, aluminide coating, microstruct. and chem. 0-76189  
 Ni-base superalloys, technique for replication of  $\gamma'$  0-79648  
 Ni-Cr-NbC eutectic composite, unidirectional solidification, thermal cycling, temp. range effect on microstructural degradation 0-89272  
 Ni-Fe-Cr superalloy 718, heat treatment effect on room temp. and elevated temp. fracture toughness response 0-100922  
 Ni<sub>2</sub>Ge-Fe<sub>2</sub>Ge solid soln., flow stress, transition from positive to negative temp. depend. 0-60906  
 NiH<sub>2</sub>, formation and decomp. studies 0-71626  
 Si-B system, DTA, X-ray diff. and metallographic study (*German*) 0-66484  
 Ta-Nb(O)(C) system, specimen prep. for metallography (*German, English*) 0-89439  
 (Ti,Ni)<sub>6</sub>C, metallographic detection in 12Kh18N10T steels 0-66721  
 Ti alloys, surface layers examination using vacuum UV spectrograph (*French*) 0-71987  
 Ti, surface layer, study using vac. UV spectrograph (*French*) 0-71987  
 Ti-Al-Sn-Zr-Mo (6,2,4,6 wt.%) fusion weldment, substruct. characts. 0-84183  
 Ti-Al-V-Sn (6,6,2 wt.%) fusion weldment, substruct. characts. 0-84183  
 $\beta$ -Ti-Mo-Zr-Sn (11.5, 6, 4, 5 wt.%), metastable phase III, microstruct. and age hardening response 0-84945  
 $\alpha$ -U, strain rate effect on flow and fracture 0-100887  
 $\alpha$ -U, strain rate effect on tensile flow and fracture 0-84992  
V, oxidation in low press. O<sub>2</sub> at high temp. (*Japanese*) 0-71807  
V-Nb(O)(C) system, specimen prep. for metallography (*German, English*) 0-89439  
W, deformed, surface layer struct. effect on polygonisation and recryst., X-ray diff. anal. and metallographic exam. (*Russian*) 0-84948  
W fibre reinforced Cu composites, correl. between thermal cycling-induced microstructural changes at interphase boundaries and tensile behaviour (*Japanese*) 0-71674  
Zr-H formation, of  $\delta$ - $\gamma$  transformation 0-84929  
Zr-H formation, the  $\delta$ - $\epsilon$  transformation 0-84930  
Zr<sub>3</sub>Al, ordered, oxidation, weight gain and metallography 0-89398  
ZrB<sub>2</sub>-Nb, reactions between components 0-100812  
ZrCu, constitutional and struct. studies, by mag. susceptibility, metallography and X-ray diff. 0-70166

**metallurgical industries**

- see also forging*  
 automatic barrel line type ATS closed system, small parts electroplating, after-treatment and drying (*German*) 0-84861  
 cast iron foundry, iron smelting, chemical composition and operation control using SiC-Q apparatus (*German*) 0-76450  
 electroplating, rack parts or bulk goods, in GTL-barrel units, Zn coating using acid electrolyte (*German*) 0-84862

**metallurgical industries continued**

- ore dressing X-ray spectrometric analysis centre 0-86541  
 vacuum metallurgy, using electron beam techniques, technical problems (*German*) 0-84850
- metallurgy**  
*see also ageing; alloys; crystal microstructure; deformation; electrical properties of substances; hardening; heat treatment; magnetic properties of substances; materials testing; mechanical properties of substances; metallography; metallurgical industries; metals; metalworking; phase diagrams; phase transformations; physical chemistry; powder metallurgy; precipitation; recrystallisation; surface treatment; zone refining*  
 applications of XPS, AES, and SIMS (*French*) 0-81253  
 electron microscopy, review 0-76458  
 hydro-metallurgy, dispersed three-dimensional electrodes appl. (*French*) 0-71919  
 thermophysical property research, metallurgical applications 0-97457
- metallurgical compounds** *see organometallic compounds*
- metals**  
*see also actinides; alkali metals; alkaline earth metals; aluminium; bimetallic; cadmium; gallium; indium; lattice dynamics of metallic crystals; lead; mercury (metal); metallic thin films; rare earth metals; thallium; thermoelectric effects in metals and alloys; tin; transition metals; zinc*  
 abrasive wear theory based on shear effects 0-89363  
 acoustic signal shape produced by high density electron fluxes 0-108674  
 adhesive bonds with polymers, shear resist., polymer crystn. effect 0-89462  
 adsorption, metal atoms on metallic substrate, enthalpy calc. 0-100406  
 adsorption of atoms on metals, Green's function formalism for studying electronic struct., local density of states calc. 0-107884  
 alkali metals, electron-electron scatt., thermal and elec. resistivity 0-59956  
 amorphous, superconducting properties rel. to ordering 0-65735  
 analysis of H ratios and profiling using nucl. techniques and Rutherford backscatt. 0-61202  
 atomic mobility under pulsed loading conditions (*Russian*) 0-96684  
 BCC, diffusion of H<sub>2</sub> and its isotopes, phonon-assisted quantum-mechanical tunnelling of interstitials 0-59730  
 BCC, effective valence, from phonon data, rel. to vacancy formation energies 0-79781  
 BCC, plastic deform., review 0-104213  
 BCC, struct. of tilt grain boundaries 0-84184  
 BCC, twin boundary and stacking fault structs., computer simulation 0-59485  
 BCC, under elastic stress, Snoek peak height determ. 0-65153  
 BCC lattice, crit. embrittlement temp., struct. parameters effect (*Russian*) 0-66618  
 bending test device for thin spring strip 0-61052  
 blister formation due to the ion irradi. 0-65072  
 brittle intercrystalline fracture, impurities effect 0-100915  
 carburising, surface-gaseous medium interaction laws 0-76411  
 ceramic/metal layer adhesion mechanism for metallization of electronic ceramics, elec. props. (*German*) 0-76381  
 CESR, cond. electron spin scatt. due to dislocations 0-75856  
 CESR, mm waves, surface effects 0-66036  
 chemicothermal treatment, mathematical modelling 0-100955  
 coated, IR surface wave interferometry 0-63913  
 coatings, electric field atomisation from melt 0-76174  
 compensated and uncompensated effect of spherical voids on electrical magnetoresistivity 0-65531  
 conduction band width calcs. 0-103619  
 conduction electron-magnetic ion Coulomb interactions, unitary transform., spin angular momentum operators 0-84451  
 conductivity, plasma model 0-80311  
 constitutive model at high strain-rate, shear modulus, yield strength 0-75292  
 corrosion, colloid chem. appls. 0-89541  
 crack resistance determination, cyclic loading, methodological instructions 0-108660  
 creep characteristics, multi-axial 0-64398  
 creep damage and cavity growth, assessment using density meas. 0-104217  
 creep limit and long-term strength, parametric eval. method 0-100996  
 creep loading, engineering approach for cumulative damage 0-58935  
 creep of metals and plastics under combined stresses. A review 0-59567  
 critical temperatures determination, elec. resist. method, IMASH-55-69 installation 0-71827  
 crystallites, characterisation by selected-zone and weak-beam dark field TEM 0-79654  
 crystallographic orientations distribution function, computer calc. for cubic metals 0-64827  
 cyclotron resonance depend. on surface, anomalous skin effect (*Russian*) 0-75860  
 deformation broaching of difficult-to-form metals 0-108473  
 deformation in quantizing mag. field, dislocation loop formation (*Russian*) 0-103354  
 deformation resistance, depend. on hot press. working speed (*Russian*) 0-65126  
 deformation structure during cutting, investigation by TEM (*Japanese*) 0-70086  
 density measurement, using X-ray total external reflect. and double crystal spectrometer 0-64831  
 diffusion constants, melting pt. diffusivity activation energy and volume corrls. 0-96679  
 diffusion welding, migration of oriented intergranular boundary with pores (*Russian*) 0-84943  
 dilatation centres and grain boundaries, induced elastic interaction (*Russian*) 0-84205  
 dislocation-core movement and frictional stress 0-92529  
 dislocations, research at Birmingham, (1945-55) 0-62444  
 dislocations and shock compression, thermodynamics 0-100235  
 dissolution of interstitial H<sub>2</sub> and D<sub>2</sub>, diffusion coeffs., reverse isotope effect (*Russian*) 0-88368  
 ductile, jet-impingement solid-particle erosion testing, halo effect 0-76376  
 edge dislocation screening in metals and superconductors, metal softening (*Russian*) 0-64997  
 elastic constants and moduli of axial textures 0-75286  
 electrical and thermal resistance, influence of static atomic displacements 0-103674  
 electrical conductivity, high pressure effects 0-92879



## metals continued

electrical resistance variations due to defects, one and two interstitial model 0-88143  
 electrolytic polishing and etching to reveal the structures of high melting point metals (*German, English*) 0-89417  
 electron irradiated, elastic point defect-dislocation interactions, defect dragging model extension 0-65050  
 electron irradiated, selfinterstitial atomic defect interaction radii, recovery expts. and error sources 0-65049  
 electron reflection from metal surfaces, surface roughness, IR absorpt. 0-71526  
 electron scattering, inelastic, plasma oscillations effect 0-100439  
 electron-deformation interaction, lattice contraction, Hubbard model calcs. (*Russian*) 0-59592  
 electron-phonon interaction effects on spin susceptibility 0-93108  
 electronic work function under tension, 20 to 1200°C 0-76448  
 EM generation of ultrasound, theory 0-103727  
 EM levitation for melting without crucible (*Polish*) 0-89130  
 emissivity determination, using low-inertia opt. dilatometry 0-59684  
 entropies and heats of fusion 0-103458  
 exotic atoms, conf., Erice, Sicily, (1979) 0-67939  
 facings, rubber-metal, vulcanisation degree determ.,  $\gamma$ -ray method 0-61043  
 failures analysis, structural for industrial appl. 0-76429  
 fatigue crack growth micromechanisms at high stress 0-108569  
 fatigue life distrib. theoretical obs. near fatigue limit 0-59569  
 fatigue lives, eval. using crack initiation model (*Japanese*) 0-104258  
 fatigue resistance, processes leading to failure 0-94907  
 fatigue test method using EM pulsator 0-89440  
 FCC, 'brass to copper' transition in rolling textures 0-76246  
 FCC, deformed single crystals, struct. evolution at heating 0-103337  
 FCC, dislocation barriers at coherent twin boundaries, anisotropic elasticity solns. 0-96522  
 FCC, dislocation behaviour at high strain rates, US detection method, data analysis basis 0-85136  
 FCC, interstitial diffusion, theory (*Russian*) 0-65296  
 FCC, misfit defect and extended screw dislocation anisotropic elastic interaction 0-96563  
 FCC, stacking faults, long-range oscillatory interactions and stability 0-65012  
 FCC, void volume, swelling, errors in determ. by TEM 0-84208  
 FCC anisotropic crystals, extended screw dislocation, (110) misfit defect elastic interactions 0-100232  
 FCC metal, dislocation dissociation 0-107235  
 ferromagnet, uniaxial, anisotropic spin fluctuations and anisotropic band struct. effects on resist. near  $T_c$  0-65543  
 ferromagnetic, electron spin-lattice relaxation (*Russian*) 0-103823  
 ferromagnetic, magneto-volume effect and Invar phenomena 0-66007  
 ferromagnetic, max. in acoustic attenuation at low mag. fields 0-93158  
 ferromagnetic, thermal oxidation rate determ. using nanowebermeters 0-61045  
 ferromagnetic, transport props., crit. behaviour 0-65522  
 fibre knitted gauze permeable materials, mech. props. 0-66607  
 foils, low energy heavy ion multiple scatt. in finite range potential 0-70283  
 fracture strain measurement at high strain rates, radial expansion technique 0-85134  
 granular, supercond. transition, increased resistance rel. to quasi-particle tunnelling 0-88689  
 granular superconductivity, instability 0-103796  
 ground state of solids, spin density functional method, binding energy, compressibility 0-65477  
 HCP, atom movement in twinning,  $\{10\bar{1}1\}$ ,  $\{10\bar{1}3\}$  twins  $\{10\bar{1}1\}$   $\{10\bar{1}2\}$  double twinning, new model 0-100252  
 HCP, stacking faults, long-range oscillatory interactions and stability 0-65012  
 heat content correlation under fast heating (*Russian*) 0-70426  
 heavy ion bombard., high density collision emission cascades 0-71531  
 HF wave dispersion for complex wave numbers, ordinary waves 0-70740  
 high strain rate material behaviour and testing techniques, J.D. Campbell memorial lecture 0-82627  
 hydrogen brittleness measurement 0-104291  
 hydrogen embrittlement, effect on props. 0-104290  
 individual atomic events on surfaces, quantitative examination 0-75409  
 indoor corrosion rates meas. 0-76404  
 inductive dislocation braking in mag. field (*Russian*) 0-79791  
 inelastic cyclic strain under nonuniform stress state conditions, residual stresses effect 0-81132  
 inhomogeneous granular, superconductivity 0-103795  
 interstitial loop growth, pulsed irradi. effects 0-88210  
 ion bombard., void conc., effect of implanted He (*Russian*) 0-88213  
 ion implantation damage, light element, review 0-88219  
 ion implanted H(D), interstitial positions and vibr. amplitudes, fast ion channelling study, review 0-79848  
 ion lasers, hollow cathode 0-99708  
 IR optical const., meas. by self-radiation method 0-84710  
 irradiated, containing pre-existing dislocations, interstitial loop form. kinetics 0-65040  
 irradiated, mechanism of formation of vacancy dislocation loops (*Russian*) 0-65053  
 Kondo effect, Anderson hamiltonian 0-60187  
 laser beam optimal heating in oxidising medium 0-69445  
 laser radiation absorption in craters on metal targets 0-97386  
 laser-photoinduced etching, photodissociation of dissolved complexed halogens in soln. 0-100929  
 lattice heating by radiation, plasma effects, degenerate electron gas calcs. 0-70742  
 light interstitials diffusion, multiphonon transition modes classification 0-70448  
 liquid, contactless resistivity meas., impedance change of a coil 0-73388  
 liquid, density meas. by pycnometry, errors 0-73321  
 liquidus and solidus temperatures, determ. by  $\gamma$ -ray method 0-65193  
 localised moments, ESR 0-71153  
 longitudinal flow velocity distribution in rolling (*Russian*) 0-93575  
 longitudinal weakly damped EM waves near cyclotron resonance 0-103890  
 magnetic localisation and charge oscillations 0-75781  
 mechanical properties, electric current effect, test device for 4.2-300K 0-66719  
 mechanical properties, meas. at high temperatures, MEITP-1 indentation system (USSR) 0-74820

## metals continued

melting temp., press. depend., vacancy mechanism 0-103460  
 melting theory for small particles, Helmholtz free energy 0-59629  
 membrane, lifetime prediction and design 0-71752  
 metal-H systems, temp. depend. of impurity resist. 0-65529  
 metals, cubic, heavily deformed, development of lattice curvature 0-81136  
 metals, radiation creep speed and swelling, self diffusion mechanisms (*Russian*) 0-92595  
 microinhomogeneous plastic deformation, rules 0-89307  
 monolayers, on metal cryst. surfaces, surface struct., review 0-80067  
 non-ferrous, recycling, effect on comp. 0-66455  
 nonstationary temperature fields due to moving heat sources, heat capacity, thermal cond. (*Russian*) 0-107448  
 notched, cyclic stress/strain behaviour, random fatigue life (*German*) 0-100907  
 optical materials, metallic and glass components compared 0-69473  
 optical properties by spectroscopic ellipsometry, review 0-103929  
 overbarrier states of H and D, subsystem heat capacity, equilibrium props. (*Russian*) 0-79998  
 oxide thick film growth, fund. theory 0-89391  
 oxidizable, laser heating in air by obliquely incident radiation 0-71815  
 particulate matter, graphite furnace atomic absorption spectrometry appl. 0-94134  
 Peierls transition in quantizing mag. field, possibility 0-103441  
 phonon-phonon scatt. role in lattice thermal cond., phonon drag, elec. cond. 0-70483  
 Pippard sound attenuation oscills., ang. depend. (*Russian*) 0-103613  
 plastic deform., time depend., thermodynamics model 0-76309  
 plastic deform. generalised constitutive eqns. 0-104219  
 plastic deformation, deform. resist. (*Bulgarian*) 0-88248  
 plastic yield criteria, interpolation scheme 0-64400  
 plasticity, theory extension to three dims. and appl. to geophysics 0-104955  
 plate, radioelectric effect 0-70744  
 point defect diffusion controlled reaction theory, book contrib. 0-103318  
 point defect dynamic props. and diffusion controlled reactions, book 0-101674  
 point defect dynamical props., book contrib. 0-103317  
 polycrystalline, relations between shear modulus, bulk modulus and Young's modulus 0-97540  
 polymer-metal sliding, wear eqn. in terms of fatigue and topography of sliding surfaces 0-108597  
 porous gauzes, hydraulic resist. in laminar filtration 0-100034  
 positive muon interactions 0-71284  
 positron trapping by defects influence of positron-phonon and electron-phonon interactions (*Russian*) 0-93425  
 powder, method for TEM study 0-84038  
 powder coatings, in metal finishing, review 0-104330  
 powder compact with polymer, cond. threshold, particle size ratio effect 0-80337  
 powder on piezoelec. substrate, dynamic SAW reflecting struct. 0-74565  
 pure, with max. of cryst. lattice distortion, struct. and strength props. (*Russian*) 0-89234  
 quantum magneto-dimensional effects, open Fermi surfaces, conduction electrons (*Russian*) 0-80487  
 quenched, vacancy cluster form. process 0-92706  
 radiation defect treatment at annealing stages V and VI (*Russian*) 0-71676  
 radiation induced vapourisation, press. behaviour 0-84288  
 rare earth metal impurity in metallic host, exchange interaction, electrical resistivity 0-84453  
 recycling, residual and additive elements control by specifications 0-66522  
 reflectance changes during laser irradi. 0-93261  
 reflection of light, nonlinear thermo-optic effect at high intensity 0-93289  
 reflectivity anomalous behaviour after 10.6  $\mu$  pulsed laser irradi. 0-93260  
 residual stress on drawing calcs. by stress state changes variational principle (*Russian*) 0-65125  
 residuals, impurities and props. 0-66521  
 reversible H embrittlement 0-104292  
 rheological interpretation of planar deformed state in extremal friction regime (*Russian*) 0-64385  
 rods, stress state and fracture in pulsed mag. field 0-81201  
 rolling, hot longitudinal, periodically charging sections with flash, pressures calc. (*Polish*) 0-89257  
 rolling moments, calc. for longit. rolling periodically changing sections (*Polish*) 0-89239  
 rolling theory, deformed and kinematic state eqns. using Gauss principle (*Russian*) 0-65124  
 saturation with gas, apparatus for 0-61039  
 SAW mode conversion by EM generation of ultrasound 0-84357  
 segregation, non-equilib., review 0-66516  
 segregation studies by imaging atom probe microscopy 0-66911  
 shell, explosive expansion, rupture behaviour 0-85063  
 shock wave effect on martensitic transform. (*Russian*) 0-96595  
 sintering analysis using sintering maps 0-93513  
 small metal particles, dielectric function and IR absorption 0-60607  
 small particles, characterisation and props., book contrib. 0-84417  
 solid electrolyte-metal interface adsorption layer capacitance calc. (*Russian*) 0-59697  
 sorption of H, multiplateau absorpt. isotherms, theory 0-103564  
 sound absorption and dispersion temp. depend. associated with Fermi surface plateaus (*Russian*) 0-65166  
 sound propagation, HF, nonlinear effects 0-88279  
 sound pulse spike like transport near acoustic cyclotron resonance (*Russian*) 0-100617  
 spacecraft materials failure, metallurgical exam. 0-71868  
 spacecraft thermal control materials, low-energy proton effects 0-70288  
 spin and charge polarisation around mag. impurities 0-75714  
 sputtering yield, energy depend., semiempirical formula 0-100736  
 strain rate history, endochronic theory of viscoplasticity 0-65122  
 stress analysis, at high temp. by finite element method 0-96203  
 strong, compressive stress/strain props. meas. at very high strain rates, modified Hopkinson bar system 0-85128  
 submicron particle heating in hot gas, plasma metallurgy 0-81092  
 submicroscopic defects, influence on HVEM in-situ expts. 0-103392  
 subsurface imaging with photoacoustics 0-74648  
 superconductivity studied by electron-phonon and Coulombian e-e coupling strength and quasi particle mass 0-88666  
 surface, approached by substrate, surface amplitude patterns 0-75620



**metals continued**

- surface, catalysed thermal desorption and dissoc. processes, microscopic theory 0-75439  
 surface, electrodynamics, optical refl. coeffs. and surface plasmon dispersion law 0-75619  
 surface, electron and photon stimulated desorption 0-75440  
 surface, enhanced Raman scatt. by adsorbates, including nonlocal metal response, nonradiative modes excitation 0-88994  
 surface, giant Raman scatt. by adsorbed mol., review 0-93343  
 surface, giant Raman scatt. by adsorbed mol., theory 0-93345  
 surface, heterogeneous cluster ion bombardment, secondary electron emission 0-60742  
 surface, ion beam induced desorption of overlayers 0-59786  
 surface, keV neutrals energy determ. method 0-89100  
 surface, mol. vibr. energy transfer, classical EM theory 0-96806  
 surface, plasma cleaning and etching, removal of C 0-97645  
 surface, rough, anomalous low-freq. Raman scatt. from localised acoustic vibrs. 0-93307  
 surface, rough, hemispherical emittance 0-70434  
 surface, rough, reflection loss for s and p polarised waves near surface plasmon freq. (French) 0-97225  
 surface, SHG, hydrodynamic theory of electron gas 0-87437  
 surface chemisorbed H<sub>2</sub>O molecule structure, interband angle 0-59787  
 surface chemisorption theory, electron localisation, surface interactions 0-84376  
 surface electrochemical smoothing, roughness, diffusional pre-electrode layer (Russian) 0-76401  
 surface laser beam irradi., effective absorpt. coeff., temp. field determ. (Russian) 0-76108  
 surface molecule enhanced Raman scatt., rough surface spheroidal model 0-84744  
 surface oxidation study, vacuum microbalance investigation 0-76552  
 surface positronium formation, stopping distance, positron-phonon interactions 0-96582  
 surface SHG, nonlinear response to optical fields 0-83645  
 surfaces, radioactive contamination 0-68771  
 surfaces, rough, characterisation by meas. of single roughness constant 0-86264  
 surfaces, shape and deformations, holographic contour immersion method (Polish) 0-62630  
 tenacity parameters 0-60973  
 textured cubic, residual stress evaluation 0-89435  
 textured specimens, with uniaxial symm. ellipsoidal model (Russian) 0-80100  
 thermal conductivity, pseudoharmonic effects of phonons, high temp. region 0-70326  
 thermal coupling of 2.8- $\mu$ m laser radiation to metal targets 0-76107  
 thermal expansion, positron response 0-84306  
 thickness meas. by backscatt.  $\gamma$  radiation 0-101781  
 thin-walled cylinder, elongation upon torsion 0-64386  
 trace element detection by atom probe microanalysis 0-66910  
 twinning, HCP struct., relative orientation of cryst. lattices 0-84181  
 unidirectional solidification, heat flow model 0-79914  
 US flaw detection of ingots, struct. effect 0-66722  
 US inspection, echo-mirror method with transform. of elastic waves 0-108663  
 vacuum heat treatment, efficiency 0-81089  
 void growth and time-lag, statistical theory 0-88208  
 wave movement, resonance phenomena in deformation zone during rolling (Russian) 0-65123  
 wear debris, morphological anal. 0-76453  
 wire reinforcing rolled glass 0-104107  
 X-ray absorption edges, exciton effects 0-108298  
 X-ray analysis of inhomogeneities, using STEM with field emission gun 0-59354  
 XPS, anomalous, frequency dependence of exponents 0-71563

**metalworking**

- see also bending; cold working; forging; hot working*  
 cutting tips, BN on Ti and WC-Co, contact reactions 0-61029  
 friction, role in metalworking, and energy saving in deep drawing 0-76271  
 tribology, material aspects in manufacturing processes 0-81210

**metamagnetism**

- compressible metamagnet, renormalisation group theory of pseudocritical point 0-60337  
 cyclohexyl ammonium copper chloride, one dimensional spin  $1/2$  ferromag., mag. props. 0-71000  
 disordered metamagnets, random field effects 0-60318  
 Heisenberg metamagnet, collinear, mag. phase diagram 0-71035  
 rare earth compounds, RCo<sub>2</sub> metamagnetic transitions in internal fields 0-60272  
 transition in absence of mag. field, model 0-97092  
 tricritical point, effective exponent 0-71045  
 trimethylammonium cobalt trichloride, AC susceptibility and exchange consts. 0-70961  
 two-dimensional, tricritical spinodal decomp., Monte Carlo study 0-93117  
 Ca<sub>2</sub>Mn<sub>2</sub>Ge<sub>2</sub>O<sub>12</sub> garnet, metamagnetic transition, high anisotropy peculiarities (Russian) 0-60274  
 Ce<sub>2</sub>Al<sub>11</sub>, competition between ferro- and antiferromag. interactions 0-60258  
 Ce<sub>2</sub>Mg<sub>3</sub>(NO<sub>3</sub>)<sub>12</sub>·24H<sub>2</sub>O, ground state with dipole-dipole and exchange interactions in external mag. field 0-84582  
 Co(S, Se)<sub>2</sub>, metamagnetic transitions in external fields 0-60272  
 Cr<sub>3-x</sub>Se<sub>4</sub>, struct., elec. and mag. props. 0-107160  
 DyPO<sub>4</sub>, mag. transitions under hydrostatic press., neutron diff. study 0-71030  
 EuSe, spin order and fluctuations, Raman scatt. study 0-97273  
 Eu<sub>2</sub>Sn<sub>2</sub>S<sub>12</sub>, mag. and thermodynamic props., metamagnetism 0-60273  
 Fe complex, Fe(1,2,4-triazole)<sub>2</sub>(NCS)<sub>2</sub>, quasi-2-dimens. S=1/2 antiferromag., mag. props., hidden canting 0-107986  
 FeBr<sub>2</sub>, metamagnet, unusual phase diagram, theory 0-93119  
 FeCl<sub>2</sub>, collinear metamag., mag. phase diagram 0-71035  
 FeCl<sub>2</sub>, logarithmic corrections to tricritical scaling 0-65940  
 FeCl<sub>2</sub>, metamagnet, scaling props. of magnetisation and heat capacity, test of tricritical scaling 0-60336  
 Fe<sub>2</sub>Co<sub>1-x</sub>Cl<sub>2</sub>, metamagnet, mag. phase diagram by mag. induced light scatt. 0-65883  
 Fe<sub>x</sub>Mg<sub>1-x</sub>Cl<sub>2</sub>, metamagnet, mag. phase diagram by mag. induced light scatt. 0-65883

**metamagnetism continued**

- FePt<sub>3</sub>, metamagnetic transitions in external fields 0-60272  
 GdN<sub>1-x</sub> and GdN<sub>1-x</sub>O<sub>x</sub>, mag. interactions 0-60218  
 GdN<sub>1-x</sub>O<sub>x</sub>, magnetic interaction and carrier conc. 0-71005  
 HoCu<sub>2</sub>, resist. and magnetoresist., mag. ordering obs. 0-70677  
 NiBr<sub>2</sub>, low-temperature magnetic phase, incommensurate spin structure 0-93082  
 TmSe, valence mixing, mag. props. obs. 0-70648

**meteor trails** *see* **meteors****meteorites**

*see also meteors; micrometeorites*

- Abec, C rich material with high volatile element content, implications 0-85908  
 Allende, <sup>26</sup>Al and inert gas composition 0-98620  
 Allende, I-Xe dating of inclusions 0-67666  
 Allende, mineralogy and petrology of isotopically unusual Ca-Al rich inclusion HAL 0-109399  
 Allende, primordial refractory metal particles 0-85906  
 Allende, S content, neutron capture gamma-ray spectroscopy 0-94728  
 Allende <sup>238</sup>U/<sup>235</sup>U ratio, early Solar System <sup>247</sup>Cm evidence 0-90347  
 Allende C3 chondrite, search for Xe fission fragment recoil 0-62083  
 Allende inclusion HAL, member of FUN family, O isotopic study 0-105211  
 Allende meteorite, <sup>40</sup>Ar-<sup>39</sup>Ar ages 0-98621  
 Allende mineral grain inclusion, excess <sup>129</sup>Xe meas., chronological information 0-67675  
 Antarctic C2 carbonaceous chondrite, meteoric origin, amino acid existence 0-67674  
 asteroid IR spectral obs. indicative of achondrite parent body, 349 and Vesta 0-98595  
 astrometres on Earth's surface, review 0-98324  
 Bereba, <sup>26</sup>Al and inert gas composition 0-98620  
 Bruderheim, L6 chondrite, U-Pb age and 500 Ma shock event in L-group meteorites parent body 0-98616  
 C2 chondrite meteorites, evidence for chemical fractionations 0-109400  
 carbonaceous chondrite Kr and Xe isotopes, studies of <sup>248</sup>Cm and <sup>250</sup>Cf spontaneous fission products 0-63215  
 carbonaceous chondrites, ion beam analysis 0-62089  
 chondrite classification and metamorphism based on metal phase composition 0-98619  
 chondrites, <sup>129</sup>I/<sup>127</sup>I early solar system chronometer 0-62043  
 chondrites, cosmogenic isotope radioactivity, galactic cosmic ray solar latitude variations 0-101507  
 chondrites, crystallisation of chondrules 0-77361  
 chondritic meteorites, search for U isotopic anomalies 0-85903  
 chondrules origin, chemical energy in cold-cloud aggregates 0-105210  
 chondrules textures, experimental reproduction 0-94763  
 chromite grains in Fe formation from Early Precambrian Isua supracrustal belt, W. Greenland, probable cosmic origin 0-72508  
 CM chondrite, age alteration inferred from matrix chem. 0-62084  
 Collescopoli meteorite, H-5 type, fusion crust glass fragments, electron microprobe obs. 0-67669  
 conference, 42nd Annual Meeting of Meteoritical Society, Heidelberg, Germany (1979 September 3 to 7) 0-62374  
 cosmic ray tracks to determine galactic cosmic nuclei time averaged abundance 0-101513  
 crater field formation, effects of meteoroid atmospheric breakup 0-94760  
 crater formation modelling, meteorite impact effects 0-90088  
 cratering processes, erosion of material layer which loses charact. props. during regolith reprocessing 0-62053  
 Darwin glass and crater, gravity survey 0-67365  
 Dehesa, Fe meteorite chem. classification 0-109403  
 Dhajala, India, cosmic radiation effects, fossil track studies 0-72733  
 East Anglian 'meteorite' of 1646, meteorological interpretation 0-68009  
 El Quemado, stone found near Acapulco, preliminary report 0-82318  
 enstatite chondrite, Bi and Pb microdistribution obs. 0-62085  
 enstatite chondrites, siderophile element fractionation 0-98617  
 Estherville meteorite, electron-optical obs. of ordered FeNi 0-62088  
 fall observations anal. 0-62090  
 glass formation by meteorite impact, EPR study 0-85659  
 Goat Paddock cryptoexplosion crater, W. Australia struct. and shocked rocks petrology 0-98322  
 H-type chondrites, noble gas-rich separates 0-85907  
 hexahedrites, shock transformed, sensitivity to grain boundary corrosion 0-72894  
 howardite, metal composition and origin 0-72888  
 IAB irons, <sup>40</sup>Ar-<sup>39</sup>Ar date of inclusions 0-62086  
 igneous lithic clasts from mesosiderites and howardites, petrography and chemistry compared with eucrites and diogenites 0-72890  
 impact craters, diameter to depth ratio dependence 0-94765  
 impact craters, modification by fallback ejecta 0-82317  
 impact structure, Gosses Bluff, Australia, gravity investigation 0-72520  
 isovaline radiocarbonization, cosmochemical implications 0-62087  
 Jilin, thermolumin. of IV-1 Nanlantu meteorite 0-90372  
 Jodzie howardite, CM xenoliths characterisation 0-62082  
 Juvinas, <sup>26</sup>Al and inert gas composition 0-98620  
 Kirin H5 chondrite, <sup>40</sup>Ar/<sup>39</sup>Ar age and thermal history 0-101567  
 Kirin meteorite, temp. gradient prod. in atm. passages, thermolum. obs. 0-67672  
 Krymka LL3 chondrite, myserite inclusions, electron microprobe study 0-85905  
 lunar highlands, effects of meteorite bombardment on primordial crust 0-109381  
 Marjalahti pallasite, cosmic ray induced <sup>53</sup>Mn production 0-72891  
 Mayfield chondrite, Cu alloy, Ni content determ. 0-67671  
 Melrose-b howardite, REE distrib. and pre-terrestrial Ce depletion 0-101566  
 Morasko, composition and origin 0-77359  
 Muchison, Si in metal grain from type 2 carbonaceous chondrite 0-77363  
 Murchison, organic polymer chem. composition of C2 chondrite 0-98622  
 Murchison C2 chondrite, presolar gas components, isotopic anomalies 0-85904  
 Murchison chondrite, s-process Kr comp. rel. to s-process neutron capture time scale 0-73080  
 Murray (C-2) carbonaceous chondrite, I-Xe age and trapped Xe components 0-98618  
 Naragh olivine-bronzite chondrite, composition and petrographic features, chem. anal. and X-ray fluoresc. obs. 0-67668



**meteorites continued**

- Netschaev, IIE iron, silicate inclusion age, I-Xe and Ar isotope ratios 0-77360  
 Niger (I) carbonaceous chondrite, origin of olivine grains in C2s 0-67667  
 olivines, cosmic ray nuclei groups  $Z \geq$  abundances, fossil tracks 0-105139  
 pinon, Fe meteorite, isotopically anomalous Ag discovery 0-85902  
 Pribram, pre-atmospheric size from spallation prods. and fossil cosmic ray tracks 0-82314  
 primitive meteorites thermal metamorphism, trace element loss from Allende heated to 1400°C 0-109401  
 primitive meteorites thermal metamorphism, trace element loss from Allende (C3V) heated to 1400°C 0-109402  
 pyroxenes from planetary basalt, silicate mineralogy study 0-72802  
 radioactivity, appl. to galactic cosmic ray solar modulation (*Bulgarian*) 0-72728  
 rare earth elements in solar nebula, fractionation 0-72796  
 Santa Catharina meteorite, Mossbauer spectra and X-ray diffr. of Fe-Ni phase 0-67673  
 Santa Clara, Fe meteorite, isotopically anomalous Ag discovery 0-85902  
 scattering ellipse after original meteoroid break up in atm. 0-77356  
 Shibayama chondrite, chem. composition, petrography and mineralogy 0-72892  
 Sikhote-Alin field craters, determ. of flight trajectory azimuth of original meteoroid 0-72893  
 St. Severin chondrite,  $^{53}\text{Mn}$  production due to nucl. spallation, depth-depend. 0-82316  
 St. Severin chondrite, U and Pu distrib. 0-72889  
 tektite and impact glass Li abundance 0-61799  
 tektite-like material in archaeological remains, Indonesia 0-101365  
 tektites, N.American strewn field assoc. with Earth ring system form. and Eocene terminal event 0-76890  
 Tenham, ringwoodite and majorite identification of cryst. dislocations 0-85909  
 thermobarometric chemistry of mineral inclusions (*Russian*) 0-104954  
 Tieschitz, H3 chondrite, Cd isotope fractionation in meteorite fractions 0-94764  
 Tieschitz un-equilibrated chondrite, taenite petrogenesis 0-82315  
 Weckeroo Station, IIE iron, silicate inclusion age, I-Xe and Ar isotope ratios 0-77360  
 Yamato-74 chondrites, crystallisation of chondrules 0-77361  
 Zhamsanin crater, age determ. by different methods 0-101568  
 $^{26}\text{Al}$  from red giant stars and decay to anomalous  $^{26}\text{Mg}$  0-67712  
 Fe meteorites, chem. classification 0-109403  
 Fe meteorites, composition from factor anal. 0-67670  
 Fe meteorites, radial distrib. of spallogenic K, Ca, Ti, V, Mn and Cr isotopes 0-67488  
 Fe meteorites of groups IAB and IIICD, origin 0-109404  
 Fe-Ni (25 to 50%), FCC, meteorites and thermodynamic equilib., Mossbauer and X-ray diffr. study 0-88087  
 Fe-Ni meteorite, STEM/X-ray microanalysis across  $\alpha/\gamma$  interface 0-10512  
 Mg isotope anomalies explained by  $^{26}\text{Al}$  form. in collapsing star (*Russian*) 0-77285  
 Mg isotopic anomalies, role of  $^{26}\text{Al}$  synthesis in explosive H burning 0-85929  
 $^{17}\text{O}$  and  $^{16}\text{O}$ , fractionation by chemical equilib. 0-89513

**meteoroids**

- see also meteorites; meteors  
 atmospheric breakup, effects on crater field form. 0-94760  
 bombardment of lunar rocks, Apollo samples obs. rel. to microcrater and accretionary grain populations 0-94732  
 bombardment of lunar rocks, microcrater and accretionary grain populations temporal development 0-94731  
 break up in Earth's atm. 0-77356  
 close encounters with Jupiter, mass distrib. throughout Solar System implications 0-77329  
 detector film penetration, lab. expts. on Al and parylene films 0-77292  
 Earth grazing fireball, eqns. of motion, vel., orbit and mass determ. 0-67663  
 flight trajectory azimuth from Sikhote-Alin field craters 0-72893  
 inner solar system micrometeoroids, orbital and physical characts. 0-77355  
 orbit determ., correl. with interplanetary dust, radio and photographic meteor obs. 0-101555  
 particle flux near Saturn, Pioneer 11 meteoroid obs. 0-82291  
 solar wind sputtering rate 0-85835  
 surface shielding by vaporised and refl. mols., theory of first collisions 0-77357

**meteorological instruments**

- see also anemometers; barometers; hygrometers  
 anemograph, digital, for wind direction and average speed meas. (*Czech*) 0-77174  
 dual-Doppler radar, coverage area as function of meas. accuracy and spatial resolution 0-82093  
 hygrometer with a heated electrolytic sensor 0-109262  
 hygrometer with  $\text{LiNbO}_3$  sensor (*Japanese*) 0-95103  
 interpretation device, for signals from meteorological radar equipment (*Russian*) 0-67432  
 METEOSAT data processing system (*Italian*) 0-109275  
 METEOSAT project, interactive image system 0-109330  
 psychrometer, portable differential system construction and operation 0-105072  
 pyrliometers of the UK Meteorological Office, and radiation reference scales 0-109206  
 rain sequential sampler, design, construction and operation 0-105090  
 rainfall instantaneous rate, meas. instrument and influence on high-voltage transmission lines 0-98471  
 raingauges, high density meas. of convective mean rainfall over small areas 0-77157  
 raingauges, tipping bucket type, digital recording system description and field testing 0-77161  
 satellite picture processor for TIROS-N series, visible and IR pictures 0-67439  
 temperature sensors, humidity effects and sea salt contamination 0-82095  
 wind direction meas. by vane, graphic recording and averaging 0-82098  
 wind vanes, wind direction meas. and motion 0-90264

**meteorological optics** see atmospheric optics**meteorology**

- see also climatology; wind  
 Aberdeenshire, mesoclimate of Upper Don Basin 0-61889

**meteorology continued**

- air pollution episodes in Venetian region, real-time forecasting via advection-diffusion model 0-77096  
 air pollution episodes in Venetian region, real-time forecasting via Kalman predictor 0-82046  
 air pollution meteorology, use of sodar acoustic echo sounder, low level stability and wind velocity monitors 0-108828  
 analysis of W.Europe network meteorology data, polynomial interpolation (*French*) 0-85710  
 asynchronous data from satellite, scheme for reduction to a common time 0-85735  
 asynchronous meteorological data interpretation 0-109271  
 N.Atlantic weather forecasting, multiday, for press. field 0-98417  
 atmospheric dynamics in quasistatic approximation, characterisation of approximation (*German*) 0-98383  
 atmospheric surface pressure measured using microwave signals transmitted from orbiting satellite 0-94581  
 automatic observation for atm. refr. determ. (*Japanese*) 0-82110  
 available potential energy in atm. in press. coords. (*Russian*) 0-109187  
 aviation, forecasting systems, TECAM '79 conf. 0-94569  
 baroclinic instability of short-wavelength two-layer Eady model 0-72593  
 barotropic model for N.hemisphere spectral integration 0-82027  
 W.Bay of Bengal, 1978 southwest monsoon effects. on wave characts. 0-109152  
 Beaufort Sea, mesoscale weather conditions rel. to August ice cover vars. 0-101366  
 Beijing, China, weather conditions effect on pollution (*Chinese*) 0-108825  
 boundary layer interacting with free atmos. (*Russian*) 0-77037  
 British Isles, poor summers and assoc. atmospheric conditions 0-109241  
 British National Meteorological Library, MOLARS automation 0-82068  
 British spring weather of 1979, compared with average climate 0-98427  
 California, spring rains correl. with Pacific Ocean December sea surface temps. 0-77064  
 Cape Verde Islands, hurricane form., general circulation from Meteosat 0-105042  
 NE.China, persistently low summer temp., causative circulation pattern (*Chinese*) 0-109235  
 climate data archiving and quality control by computer 0-61907  
 cold front, obs. of 3-D circulation, precipitation and wave motions 0-90142  
 cold front of midlatitude cyclone, cloud and precipitation struct. 0-109192  
 conference, on climatology, hydrology, atmospheric research and meteorology from space, Ajaccio, Corsica (1979 November 12 to 16) 0-62397  
 conference on air pollution, New Orleans, USA (March 1980) 0-90603  
 convective systems during Phase III of GATE 0-90153  
 cyclone at temperature latitude, water vap. and energy budget 0-85731  
 cyclone development along weak thermal fronts, model soln. 0-81994  
 Cyclone Joan 1975, wind and rain meas. over W.Australia by satellite microwave sensing 0-98485  
 data determination by weather satellites (*French*) 0-82019  
 digital data composition for satellite and radar imagery 0-67413  
 drought definitions 0-105010  
 drought effects on hydrological independent mixed models 0-81954  
 drought in streamflow series, statistical characts. 0-105009  
 dust haze of African Harmattan wind, 1962-1973 visibility obs. 0-61900  
 Earth observation programme of ESA 0-109250  
 East Anglian 'meteorite' of 1646, meteorological interpretation 0-68009  
 eddy fluxes of conserved quantities by small-amplitude waves 0-61858  
 electrical coupling to upper atmosphere, quasi-static model 0-61865  
 equatorial atmosphere zonal model, Coriolis force and stratification on stationary motions 0-77071  
 equatorial stationary zonal circulation, numerical calcs. 0-85732  
 equatorial trough zone, heat balance 0-81977  
 NW Europe, polar air outbreak, subsynoptic disturbance case study 0-101408  
 S.Far East, weather variability rel. to NW.Pacific currents 0-101417  
 first GARP Experiment (FGGE), formation of data sets from obs. 0-101437  
 floods of E.Australia catchments, freq. distrib. 0-105012  
 forced Rossby waves on a zonal shear flow, model 0-77072  
 forecast model, with boundary layer vertical eddy flux representation 0-61844  
 forecasting in atmosphere-ocean models, max. attainable accuracy 0-82036  
 forecasting max. and min. temp., use of probabilities 0-82020  
 forecasting model to determine meteorological elements effect on geopotential field 0-82033  
 forecasting nocturnal temperature, short-range model 0-109200  
 forecasting NW.Europe winter weather, time-mean atmos. study 0-77040  
 forecasting of local weather, numerical prediction models 0-67398  
 forecasting of sea-level press. with allowance for surface press. tendency 0-85738  
 forecasting solenoidal wind vel. component 0-82034  
 front formation over central Europe, internal processes 0-81979  
 front position, precise determination from temp. and press. field data 0-98426  
 frontogenesis, baroclinic instability of jet flow 0-61855  
 frontogenesis, Hoskins-Bretherton model and surface frontal zone anal. 0-94572  
 frontogenesis and warm sector formation affected by boundary layer vertical motion (*Russian*) 0-105027  
 G 0-72592  
 GATE aircraft measurements, their value 0-82071  
 GATE ship surface meas. systems, anal. or drift 0-82070  
 general circulation at mid-latitude, fluctuations seen in rawinsonde data 0-81980  
 general circulation by GLAS model, cumulus friction and Jan. Hadly circulation 0-72588  
 general circulation model, response time rel. to ocean surface temp. change 0-98422  
 general circulation model (NCAR), response to sea surface temp. change 0-98390  
 general circulation of midlatitude troposphere, NCAR and GFDL models 0-61856  
 general circulation of N.hemisphere in winter, horiz. transport by transient eddies 0-72589  
 general weather situation rel. to tropospheric  $\text{O}_3$  concs. 0-101397  
 geopotential height fluctuations, geographic variation of vertical struct. 0-90132



## meteorology continued

- SW.Germany, heavy rainfall from May 22 to 24 (1978) (*German*) 0-61869  
 Germany, weather forecast for New Year's Day 1978-9, moist baroclinic model (*German*) 0-77065  
 Global Weather Experiment, role played by geostationary meteorological satellites 0-77256  
 Global Weather Experiment, Second Special Observing Period 0-77119  
 Greenland, summer aerosols and trace gases 0-72609  
 NE. Gulf of Alaska, development of synoptic climatology 0-98405  
 hail cell detection, for cloud seeding criteria, radar method 0-90170  
 hang gliding and assoc. weather 0-105043  
 Hebei Plain, summer drought and flood rel. to atm. circulation seasonal var. 0-90203  
 N.Hemisphere transient motions, RMS 1000 and 500 mb geopotential height 0-90163  
 N. hemisphere winter circulation, general circulation model, comparison with obs. 0-109189  
 Himalaya, summer weather and climate 0-72620  
 Hunan and Zhejiang Provinces, rainy season, long range forecasting 0-90204  
 hurricane season activity analysis, N.Atlantic (1886-1974) 0-101427  
 India, westerly upper air troughs rel. to western disturbances development 0-90173  
 jet stream-frontal systems, pot. vorticity, role or turbulence 0-77044  
 Kashmir region, vars. of aerosols and snow chemical components with weather conditions 0-94594  
 Liege, Belgium, sixteenth century weather record (*French*) 0-82029  
 long-range weather forecasting, art and science 0-109184  
 Los Angeles, anal. of meteorological processes affecting oxidant and precursors in LARPP (operation 33) 0-61479  
 lunar tide in atmosphere, influence of local weather on solar modulation 0-94593  
 man-machine interface, weather forecaster console for satellite data handling system 0-90205  
 mesoscale convective systems, inertial instability 0-90131  
 mesosphere, meteorological fields rel. to eddy diffusion models 0-109198  
 METEOSAT 1 weather satellite pictures, amateur facsimile reception (*German*) 0-81982  
 Meteosat data-collection system, description and appl. 0-77122  
 Meteosat remote sensing equipment for atm. general circulation obs. 0-94595  
 Meteosat-1, research uses of early data, review 0-77257  
 Mohliner Feld (east of Basle), topoclimate investigations (*German*) 0-61890  
 monsoon, model of large scale seasonal struct. 0-98393  
 monsoon breaks, effects of surface press. 10 to 20-day westward propag. mode 0-94592  
 monsoon disturbances over India, quasi-geostrophic model 0-98394  
 monsoon driving mechanisms, model of seasonal struct. 0-98392  
 monsoon in winter over warm ocean current, heat and moisture budgets 0-72590  
 Montreal, rain estimation using geostationary satellite data 0-90244  
 Mount Kenya, condensation nuclei and weather obs. 0-82012  
 New York State, local climate trends in four cities 0-105044  
 NOAA library and information services, description 0-109180  
 numerical dynamic model atmosphere on a spherical Earth, used in forecasting 0-101416  
 ocean tide caused by meteorological conditions, energy transfer calc. (*Russian*) 0-76988  
 Pacific and E.Asia, average vertical circulation in winter 0-90199  
 NW.Pacific Ocean, relation between atmospheric press. and sea level 0-101415  
 W.Pacific subtropical high, summer, form. and struct. simulation (*Chinese*) 0-109233  
 pattern recognition theory methods, appl. to meteorological field anal. and forecasting 0-98421  
 photographic obs., cold front passage over Salt Lake Valley, Utah, obs. of orographic effects 0-98380  
 Po Valley, circulation driven by diurnal heating 0-85716  
 polar region, rawinsonde obs. from single station 0-81981  
 pollution long-range transport modeling review 0-108823  
 Port Moresby, Papua New Guinea, rainfall trend, (1945 to 1976) 0-98430  
 precip. time struct., daily precip. amounts modelling with Markov-I chain 0-101401  
 precipitation forecasting in Arizona, rel. to marine layer depth and moisture content at San Diego, California 0-101395  
 prediction of weather, normalised variance anal. for meteorological time series, F-distribution (*Chinese*) 0-67388  
 process computer appl., thermal balance recording methods 0-82044  
 pyrocumulus cloud over North Canterbury, New Zealand, effects of synoptic situation 0-109240  
 quasi-cycles in meteorology, anal. of evidence 0-109239  
 quasi-geostrophic flow over anisotropic mountain 0-61860  
 radar echoes from distributed targets, averaging of time, angle and range 0-109264  
 radar observation from aircraft, pulse Doppler method 0-85757  
 radiothermal sounding of press. and geopotential (*Russian*) 0-77038  
 rain measurement and forecasting in UK-using radar as part of integrated system, progress and plans 0-98490  
 rain measurement by dual-polarisation radar, drop size and fall rate 0-72650  
 rainfall, annual, stochastic anal. rel. to effects of urbanisation 0-98407  
 rainfall prediction for short response time hydrological basins 0-98491  
 rapid morning boundary-layer time transition, case study from Haswell, Colorado, expt. 0-81996  
 riming process, laboratory expts. 0-105037  
 Rossby neutral mode, secular stability 0-81983  
 Sahel drought, Africa, 1967 to 1974, Earth surface albedo vars, investigation 0-76981  
 severe local storms, automated 12 to 36 hour probability forecasts 0-77062  
 Shanghai plum rains, mid-range forecasting (*Chinese*) 0-109232  
 short-range numerical weather forecasting, effect of subjectively enhancing initial vorticity field 0-82008  
 Sierra Leone, climatic regime rel. to surface and soil temps. seasonal vars. 0-109242  
 snow prediction, using 10-level model 0-82025  
 sodar appl. to weather analysis and local forecasting 0-85713  
 solar flares influencing lower atmos. phenomena 0-109230

## meteorology continued

- Somali jet, planetary boundary layer model 0-72591  
 squall line at midlatitude, thermodynamic and kinematic struct. obs. 0-109191  
 St. Louis, Missouri, pollutant source strength-rainfall relationships investigation 0-77059  
 stationary mesoscale fields, method of calc. from remotely sensed data 0-85734  
 steam fog in Fenlands, obs. after heavy rain, (1979 May 1) 0-98431  
 stratosphere, generalised Lagrangian-mean description of wave/mean flow interaction 0-109214  
 stratosphere, southern hemisphere, temp. and press. field spring transformation anal. 0-98420  
 stratosphere, zonal mean winds vars. rel. to planetary wave props. and links with troposphere 0-109225  
 subtropical and polar front jet confluence, rawinsonde obs. 0-81981  
 Taiwan, weather connected with typhoons 0-90200  
 temp. in central England, 1660-1977, air temp. variability study 0-98437  
 troposphere, lower, meteorological quantities fields rel. to eddy diffusion models 0-109198  
 thunderstorms, automated 12 to 36 hour probability forecasts 0-77062  
 tidal motion on sphere, simulation by geodesic finite-difference method for curved domains 0-109153  
 TIROS satellite program 0-109328  
 transients eddies, synoptic-scale, observational study of upward sensible heat flux 0-94591  
 transmitting weather charts by facsimile for military appl. 0-90206  
 tropical E.Atlantic, press. and wind fields from TROPEX data 0-82040  
 tropical middle atmosphere, observational evidence of semiannual oscillation 0-109216  
 tropical weather prediction, multilevel primitive eqns. with press. wind adjustment 0-77070  
 Uccle, vertical ozone distrib., during polar front passage 0-94582  
 ultralong waves forced on cyclone scale, numerical expt. 0-61857  
 urban environment, cold air drainage effects on temp. fields, case study of topographical influence on climate 0-94555  
 urban microclimate of Alma-Ata, significant factors 0-101418  
 urban valley micrometeorology of N.Saskatchewan river valley 0-61843  
 visibility at ground level, two meas. methods 0-82078  
 vorticity response to IMF sector boundary crossing (southern hemisphere) 0-109199  
 S.Wales floods of late December 1979, meteorological anal. 0-98429  
 warm frontal clouds in midlatitude cyclones, air motion and precipitation 0-109193  
 warm frontal region, wind and precipitation struct., Doppler radar study 0-81995  
 weather forecast model, low-order spectral difference type 0-98415  
 weather forecasting, atmospheric prediction models, computing and numerical methods 0-77095  
 weather forecasting, conditional probabilities prediction method (*Chinese*) 0-109238  
 weather forecasting, satellite systems for local short-period forecasts 0-94558  
 weather forecasting, use of satellite imagery by the Meteorological Office (UK) 0-85714  
 weather forecasting for central Asia, for short-term press. field 0-98416  
 weather forecasting for N. hemisphere, six days ahead 0-82024  
 weather forecasting games at American Universities, survey 0-98770  
 weather forecasting numerical model, parameterisation of boundary layer 0-72572  
 weather forecasting processing of radar and satellite imagery data 0-109252  
 weather forecasts, impact of satellite temp. sounding data 0-77028  
 weather maps, structural description of contour maps 0-101419  
 weather prediction, short range numerical hemispheric model 0-81976  
 weather review (1978) for Belgium (*French*) 0-77069  
 western boundary currents and detached shear layers in rot. liq. 0-81984  
 wind, synoptic time scale vars. correl. with sea level changes on Scotian shelf 0-72531  
 wind measurement (absynoptic scale) using dual Doppler radar and vel. azimuth display 0-109263  
 wind power, meteorological aspects, resource assessment, site selection, US R and D program 0-76593  
 wind speed at sea, climatic comparisons of estimated and measured winds from ships 0-105020  
 wind-field analysis methods 0-105038  
 windchill maps of lowland Britain, calc. from instantaneous data 0-61893  
 Zambia, weather during rainy system rel. to upper westerly waves interaction with intertropical convergence zone 0-90175  
 CO<sub>2</sub> and global warming, effect on regional climate 0-77099

## meteors

- see also meteorites; meteoroids*  
 atoms, effective excitation cross-sections, var. with meteor vel. 0-101565  
 Earth grazing fireball, eqns. of motion, vel., orbit and mass determ. 0-67663  
 fireball of meteorite, deduction of props. from behav. in atoms 0-82311  
 Geminid stream, struct. from radar obs. 0-82310  
 historical meteors, Latin terminology 0-62437  
 hypersonic flow past disintegrating blunt bodies, radiative heating in H<sub>2</sub>-He atms. 0-69865  
 ionisation columns of bright meteors, initial radii meas. 0-94762  
 ionisation effects on LF radio navigational signals, meteor rate determ. 0-82309  
 ionosphere E<sub>2</sub>-layer, creation, effect of variable meteor particle sizes 0-105108  
 long-lived meteor train, IR brightness obs. 0-94629  
 metallic ions of meteor origin effect in VHF ionospheric forward scattering, contribution to sporadic E formation 0-67461  
 modelling of influx of meteoric matter with radar observations (*Russian*) 0-67664  
 New South Wales fireball, 7 April 1978, trajectory and ground track 0-82313  
 optical brightness rel. to ionised trail props. 0-77354  
 radar meteors rate depend. on geomag. activity and coronal activity 0-67662  
 recording frequency, influence of form and orientation of antenna directivity diagram (*Russian*) 0-67665  
 spectacular showers, possible assoc. nightglow 0-94761  
 sporadic radio-meteors, ionisation height meas., VHF obs. 0-82312  
 stratosphere, chem. of meteor trail metal ions 0-72580



**meteors continued**

- surface shielding by evaporating mols. 0-101564
- surface shielding by vaporised and refl. mols., theory of first collisions 0-77357
- thermal fracture, detached particles mean dia. 0-62081
- thermosphere, winter motions radar in S.hemisphere meteor region 0-109287
- trails, studies using large-aperture radio system 0-85870
- trajectories and orbits, visible obs. 0-72887
- Na enhancement in upper atmosphere possible meteoric origin, lidar obs. 0-101466

**metering**

- see also ammeters; electrometers; frequency meters; galvanometers; level meters; ohmmeters; phase meters; volt-ampere meters; voltmeters; watt-hour meters; wattmeters
- digital panel meters, characts. and appls. 0-68190
- isotropic RF electric/magnetic field strength meter, design 0-82751

**meters see metering****metrology see measurement****metrosils see varistors****MHD see magnetohydrodynamics****MHD convertors see magnetohydrodynamic convertors****mica**

- biotites, X-ray photoelectron diff., quantitative anal. 0-66912
- dispersed Al-Cu-Mg (4, 1.5 wt.%), wear characts. and bearing performance 0-108591
- dosimeters for visualisation of electron isodose curves in a medium 0-99349
- fluorophlogopite, synthetic, with excess Al, radiation-induced paramag. O<sup>-</sup> centres 0-60417
- muscovite, pulse electric breakdown under pressure, lamination effects 0-66110
- muscovite for high neutron fluence meas. using fission track technique 0-91395
- natural, high  $\gamma$ - and electron-irrad. doses effect on annealing behaviour, thermal decomp. resist. 0-60897
- nuclear track microfilters, prod. and props. 0-96574
- phlogopite, pulse electric breakdown under pressure, lamination effects 0-66110
- solid state particle track detectors, fission fragment ranges rel. to cryst. orientation 0-91408
- substrate, Pb<sub>1-x</sub>Sn<sub>x</sub>Te-PbTe heterostructures produced by MBE 0-88629
- Al alloy-mica particle composite, cast prep. and mech. props., bearing appl. 0-71613
- Al-Cu-Mg/mica particulate composite mech. props. 0-100919
- Fe rich micas, X-ray absorpt., heat treatment effects, chem. and struct. interpretation 0-84806
- Na<sub>2</sub>O-CaO glass phlogopite mica powders, composite fabrication, cellular struct. 0-84902

**Micelle systems see colloids****microcalorimeters see calorimeters****microchemical analysis see chemical analysis****microcircuits see integrated circuits****microcomputers**

- for microcomputer applications see under relevant applications e.g. computerised control; natural sciences computing
- see also microprocessor chips; personal computing
- bubble chamber pictures, SNOOP module CAMAC interface to 168/E microprocessor 0-58103
- microprocessor multichannel analyzer laboratory project 0-101685
- nuclear reactor guard line circuits dual microprocessor system, decision-making and self-testing 0-57901
- teaching, systems, appls. for chemistry CAI 0-57042

**microcopying see microphotography****microelectrodes**

- biological special purpose electrode (Japanese) 0-94426
- double-barrel ion-sensitive microelectrodes, extra thin tip diameters, intracellular meas. appl. 0-101298
- EM microelectrode holder for pulsating penetration of brain tissue 0-98199
- glass, open tip, influence of diffusion, double layer, and glass conduction on elec. resistance 0-67300
- histological marking with multiple thin-film electrode probe for intracortical recording 0-67297
- intracellular measuring production method micropipettes of very low resistance 0-61738
- intracortical recording of field pots., 16-fold semi-microelectrode 0-67298
- liquid-ion exchanger microelectrode estimates of epithelial cells Na<sup>+</sup> activity, resistive artifacts 0-89909
- microcircuit electrodes, extracellular, recording of action pots. from cultured neurons 0-72382
- moving cell microelectrode puller 0-67309
- multibarrel microelectrodes, 'piggy-back', simple technique for construction 0-85541
- photoelectrode for recording intracerebral cellular Ca<sup>2+</sup> transients 0-67307
- pipette electrode tips, beveled, non-destructive electron microscopic exam. 0-89915
- pipette electrodes, dry beveling 0-89914
- vibrating, excursion in tissue 0-104829
- voltage clamp, single electrode, design for neuroresearch 0-72385
- C-fibre microelectrodes, neurophysiology appl. 0-67314
- Ta-Al<sub>2</sub>O<sub>3</sub> microelectrode array, design and fabrication 0-76868

**microelectronics see integrated circuits****microfarad meters see capacitance measurement****microfilming see microphotography****microhardness see hardness****micromanometers see manometers****micrometeorites**

- element composition, neutron activation study, stratosphere collected particle 0-82319
- impact on atmosphereless planets, ion emission 0-77362
- impact on Io, form. of Na clouds and regolith 0-77330
- ionospheric sublayers in lower thermosphere caused by micrometeorites 0-61956
- lunar microcraters, diameter to depth ratio dependence 0-94765

**micrometeorites continued**

- lunar rocks, microcrater and accretionary grain populations under meteoroid and solar wind bombardment 0-94731
- lunar rocks, microcrater and accretionary grain populations from lunar surface and Apollo samples obs. 0-94732

**micrometeoroids see meteoroids****micrometers see micrometry****micrometry**

- see also interferometry; strain gauges
- coating thickness meas., 1979 status in USSR 0-77749
- micro-optics testing, width meas. of slit test objects 0-64223
- reflection dispersive Fourier interferometer window eliminating backlash error 0-57402
- reliability assessment method (Rumanian) 0-68175
- universal horizontal metroscope, rational determ. of composite error on small micrometers 0-82742

**microphones**

- artificial heads with stereophonic intensity signals, directional effects (German) 0-106701
- condenser, draft laboratory standard (Japanese) 0-79096
- condenser, pressure calibration, note concerning the implementation of IEC 327:1971 0-74686
- development and calibration accuracy, review 0-96167
- EL2 electret telephone transmitter, technology development 0-83723
- electret condenser, design for meas. purposes 0-79086
- high-impedance low quality microphone using small 8  $\Omega$  loudspeaker (Spanish) 0-96173
- meas., with prepolarized cartridges (electrets) 0-74649
- piezoelectric microphones with rigidly supported piezopolymer membranes 0-64330

**microphonics see microphones****microphotography**

- bone polychrome fluorescence labelling and photomicrography 0-89821
- exposure control, manual 0-98975
- holocamera for 3-D micrography of the alert human eye 0-98057
- photomicroscopes with automatic exposure control 0-86475

**microphotometers see densitometry; photometers****microprobe analysis, electron see electron probe analysis****microprobe analysis, ion see ion microprobe analysis****microprocessor chips**

- horological microprocessor, design and circuit architecture, functions (French) 0-90822
- speech synthesis microprocessor 0-91983
- US nondestructive inspection system, microprocessor utilization 0-71845

**microprocessor systems see microcomputers****microprocessors see microcomputers; microprocessor chips****microprogramming**

- microprocessor multichannel analyzer laboratory project 0-101685

**micropulsations**

- activity related to substorms and cosmic noise absorpt. 0-72727
- auroral luminosity rel. to geomag. field changes 0-77187
- boundary layer, hydromagnetic waves as origin of mag. pulsations 0-105133
- daylight hemisphere Pi at low latitude, coincident with Pi2 of local mid-night sector 0-77232
- frequency shift relative to modulated VLF emission 0-77229
- geomagnetic transfer functions at pulsation periods 0-72417
- interplanetary medium affecting pulsations 0-77228
- ion flux ULF oscillations during Pc 4, 5 0-72707
- ionosphere control of micropulsations obs. at ground 0-77207
- IPDP field fluctuations and proton precipitation, simultaneous obs. 0-77238
- latitude dependence of Pc pulsation periods 0-101502
- magnetic ULF waves over auroral arc during substorm event 0-72722
- nighttime Pi 1 and 2 obs. on E-W axis, propag. characts. 0-98519
- Pc5 pulsation theory, consequences of ionosphere Hall current 0-105129
- Pc5 pulsation theory, consequences of N. and S. hemispheres ionosphere electricity 0-109316
- Pc5 pulsations, model of magnetosphere and ionosphere elec. and mag. fields 0-77234
- Pc 1, classification of pulsation occurrence, and pulsation prediction 0-109317
- Pc 1 pearl event correl. with 4278 Å nightglow, Antarctic obs. 0-72664
- Pc 2-4 pulsation excitation, numerical study 0-77227
- Pc 3 pulsations in magnetosphere, obs. by new space-borne ring-core type magnetometer (Japanese) 0-94671
- Pc 3-4 pulsations, geomag. conjugacy with quasi-periodic ELF-VLF emissions 0-67475
- Pc 4-5 pulsation band, phase correl. of riometer and magnetometer data 0-82147
- peninsular method for ULF generation in iono- and magnetosphere 0-90247
- Pi 2, latitudinal profile from five-station synchronous records 0-105125
- Pi 2 and high-freq. enhancements, simultaneous ground and satellite obs. 0-105136
- Pi 2 event, long-period, assoc. with mini-substorm, 1978 December 11, Jikiken satellite obs. (Japanese) 0-94653
- Pi 2 pulsations, equatorial, fine struct. 0-72721
- Pi 2 pulsations, substorm-related, coincidence with kilometric radiation enhancement, JIKIKEN (EXOS-B) satellite obs. (Japanese) 0-94648
- Pi pulsation at high latitude, rel. to plasma convection 0-77226
- Pi ULF waves generated by magnetosphere-ionosphere current system 0-85819
- PiB magnetic pulsation during substorm 0-72723
- plasmopause region pulsations, elec. field obs. 0-85814
- Ps 6 magnetic disturbances, seasonal and diurnal var. 0-67477
- solar wind controlled micropulsations, origination region 0-85823
- ULF wave propag., axisymmetric guided mode sources in magnetosphere model 0-77231

**microrecording see microphotography****microreduction see microphotography****microscopes**

- see also acoustic microscopes; electron microscopes; ion microscopes; optical microscopes
- cryogenic scanning microscopy 0-79080
- intelligent microscopes, recent and near-future advances 0-98166



**microscopy**

- see also *electron microscopy*; *ion microscopy*; *optical microscopy*  
 bibliography, equipment, methods, applications and related topics 0-73124  
 bibliography 0-90619  
 bibliography of equipment, methods, appls. and related topics 0-105450  
 bibliography of microscopic equipment, methods, appls. and related topics 0-94941  
 bibliography of publications on microscopic equipment, methods and appls. 0-62406  
 ceramic building materials, high-temp. microscopy interpretation (*Polish*) 0-66743  
 IR light scattering, and absorpt. microscopy study of dislocations in GaAs 0-107249  
 polyethylene-polypropylene blend, size distribution determ. of spherical occlusions from photomicrographs (*Czech*) 0-89539  
 teaching, course at North Carolina State University 0-95135  
 X-ray, high resolution, with synchrotron radiation, for chem. microanal. 0-81416

**microstructure, crystal** see *crystal microstructure***microtomes** see *laboratory apparatus and techniques***microtrons**

- electron phase motion, accelerating field higher harmonics influence 0-106212  
 modulator, thyristor, circuit and construction 0-63422  
 NDT application in industrial products inspection 0-81267

**microwave acoustic devices** see *acoustic microwave devices***microwave antenna arrays**

- solar power satellites microwave power transmission system rectennas, Yagi-Uda receiving elements design, characteristics and economics 0-66938

**microwave antennas**

- see also *waveguide antennas*  
 biomedical system, invasive, for locally-induced hyperthermia for cancer therapy 0-67193  
 cancer treatment appl. of microwave arrays for localised tumour heating 0-94308  
 microstrip antenna for biomedical applications 0-89826  
 microstrip slot radiator for medical appls. 0-108994  
 plasma, focusing hog-horn antenna for microwave diagnostics in plasma machines 0-96395  
 transponder dipole antennas in and near three-layered body 0-98181

**microwave detectors**

- cm-wave radiometer, with enhanced long-term stability, for solar radio emission obs. 0-109361  
 Faraday effect in lightguide, weak microwave field meas. 0-73463  
 glow discharge tube, EM MM-wave detection properties in mag. field 0-70059  
 Josephson junctions, applications in plasma physics 0-103194  
 liquid crystals, thermooptical effects used to visualise EM fields 0-62723  
 MM wave detector using ohmic diode (*Japanese*) 0-73464  
 photon detector for subMM wavelengths using Rydberg atoms 0-77867  
 radiometer, microprocessor-based signal processing unit 0-77874  
 radiometer for rain attenuation measurements at X, K bands, communication appl. 0-68254  
 Rydberg atom microwave and far IR spectroscopy 0-63564  
 superconducting, space appl. 0-85836  
 superconductor-insulator-superconductor quasiparticle tunnel junctions, as microwave detectors 0-65744  
 thermophotoindicators based on cholesteric liquid crystals, analysis of diffuse light spectra 0-73457  
 TIROS-N microwave sounder unit for global temp. distribution meas. 0-90265  
 Ge and Ge-diamond bolometers operated at 4.2, 2.0, 1.2, 0.3, 0.1K, design and construction 0-77868  
 Hg<sub>1-x</sub>Cd<sub>x</sub>Te hot-electron photoconductive detection of near mm wave radiation 0-57377  
 In-In<sub>2</sub>O<sub>3</sub>-Pb, Josephson tunnel junction fabrication for MM-wave detector 0-100427  
 In-In<sub>2</sub>O<sub>3</sub>-Pb, tunnel junction fabrication for MM-wave detector 0-100427  
 InP Schottky-barrier diodes appl., operation in submm. wave region 0-105707

**microwave devices**

- see also *acoustic microwave devices*; *Gunn devices*; *masers*; *microwave parametric devices*; *solid-state microwave devices*; *waveguides*  
 cavities, Q-factor meas. by analytic method using reflection coeff. vs. freq. 0-98937  
 coaxial microwave cavity for improved EPR sensitivity with loss solvents 0-62705  
 conference, IR and MM waves and appls., Miami Beach, USA (Dec. 1979) 0-57009  
 diathermy applicator for irradi. of rat brain 0-94425  
 electron beam switch, microwave energy compression 0-96396  
 MM wave sensors, conf., London (Apr. 1980) 0-67441  
 p-i-n diode modulator, transient plasma instability meas. (*German*) 0-87942  
 remote sensing expt., operation in Spacelab 0-109332

**microwave filters**

- bandpass interference filters for 1-3 mm window 0-109368  
 low-pass interference filters for Tokamak plasma diagnostics 0-64783

**microwave generation**

- see also *microwave oscillators*; *relativistic electron beam tubes*  
 intense relativistic electron beam generation by foillless diodes, simulation 0-63438  
 CdS, subMM radiation excitation by N<sub>2</sub> laser pulse 0-60678

**microwave heaters** see *radiofrequency heating***microwave heating** see *radiofrequency heating***microwave holography**

- 3D image-construction technique and appl. to microwave diagnostics 0-83565  
 image reconstruction using computer tomography algorithm, numerical simulation and expt. 0-58484  
 long-wave imaging with super-resolution by wavelength diversity 0-102675  
 MM wave systems operating at 35, 70 and 140 GHz 0-63963

**microwave induced delayed phosphorescence** see *MIDP***microwave-infrared double resonance** see *optical double resonance***microwave integrated circuits**

see also *hybrid integrated circuits*

- Ca<sub>1-x</sub>Sr<sub>x/2</sub>Ba<sub>x/2</sub>Zr<sub>1-x</sub>Ti<sub>x</sub>O<sub>3</sub>, ceramic system, dielectric props., microwave resonator application 0-80674  
 GaAlAs injection DH laser and GaAs Schottky-gate FET, monolithic integration 0-58593

**microwave links**

- BWO appl., 110 to 170 GHz, using Sm-Co ring magnets (*German*) 0-105684  
 METEOSAT 1 weather satellite pictures, amateur facsimile reception (*German*) 0-81982  
 rain cell attenuation of Earth-space link 0-94586  
 space communications, Voyager project 0-77263  
 trans-horizon propagation path over sea, transmission loss due to ducting at 1.8 GHz 0-105041

**microwave measurement**

see also *microwave reflectometry*

- 3 GHz surface and lateral EM wave meas. 0-103742  
 air pollution, pollutant gases monitoring from space using passive microwave techniques 0-76690  
 AM active method for plasma density meas. 0-87948  
 atmosphere boundary layer temp. profile determ. from ground-based 60 GHz radiometry (*German*) 0-82097  
 atmosphere parameters, retrieval from scanning multichannel microwave radiometer obs. 0-90261  
 atmospheric surface pressure measured using microwave signals transmitted from orbiting satellite 0-94581  
 biological liquids, reflection meas. of complex dielectric const. 0-101309  
 biomeasurements using microwaves (*Japanese*) 0-94314  
 cloudy atmospheric parameter determination using radiometric method 0-67435  
 conference, IR and MM waves and appls., Miami Beach, USA (Dec. 1979) 0-57009  
 dielectric cylinders, microwave meas. of permittivity using retarded waves (*Czech*) 0-95111  
 dielectric props. of organic liquids in freq. range 400 MHz to 285 GHz, internat. comparison of meas. methods (*German*) 0-68168  
 dielectric relaxation of compressed water at 17.613 GHz using microwave refl. meas. method (*German*) 0-71306  
 dielectric relaxation spectroscopy of polar fluids in microwave region, double beam interferometry method (*German*) 0-71309  
 double electron-nuclear resonance obs. using 3 cm rectangular resonator, low-temp. 0-98956  
 electromagnetic meas., precision, conf., Braunschweig, Germany (Jun. 1980) 0-98903  
 extinction cross section for single particles at 100 GHz 0-82116  
 high surface vels. using K-band microwave interferometry 0-77761  
 imagery of isolated canine kidney, use of orthogonal polarisations 0-81783  
 in vivo probe measurement technique for determining dielectric properties at VHF through microwave frequencies 0-85542  
 moisture content determ. of cloudless atmosphere, microwave radiation meas. 0-94624  
 ocean surface parameters, retrieval from scanning multichannel microwave radiometer obs. 0-90261  
 permittivity meas. at microwave freqs., two coupler method modification 0-100632  
 pulmonary oedema diagnosis by a surgically noninvasive microwave technique 0-61659  
 remote sensing from satellites, appl. to meteorological meas. over W. Australia 0-98485  
 remote sensing technology for marine oil pollution surveillance (*Japanese*) 0-76685  
 sea surface waves, remote sensing using one and two freq. microwave techniques 0-94622  
 snow, parameters investigation by radiometry in 3 to 60 mm wavelength region 0-72561  
 snow, water equiv. of dry snowpack, active and passive microwave response 0-72563  
 snow wetness, active and passive microwave response 0-67382  
 superheterodyne tracking cct. for mm-wave measurements 0-59288  
 tubular dielectric, complex permittivity and loss angle meas. in X-band using H<sub>011</sub> cavity resonator method (*German*) 0-62690  
 unit power standard for 53.57 to 78.33 GHz 0-90808  
 using microwave O line splitting 0-77124  
 water pollution, dielectric props. and determ. of microwave emissivity 0-101142  
 NH<sub>3</sub> monitoring using Stark microwave cavity resonator 0-61500

**microwave-optical double resonance**

see also *PMDR*

- allylamine, laser-microwave double and triple reson. 0-83397  
 aniline, in p-xylene host cryst., phosphoresc. triplet state, ESR and MIDP obs. 0-66077  
 benzenoid aromatics, triplet zero field splitting parameters, ODMR obs., struct. effects 0-78636  
 p-diazines, polycyclic, T<sub>1</sub>( $\pi\pi^*$ ) $\rightarrow$ S<sub>0</sub> intersystem crossing, isotope effects, ODMR and phosphoresc. obs. 0-91586  
 double radiooptical resonance, signal propag. and shape 0-87360  
 EEDOR triplet state zero-field transition energy, spectral diffusion 0-88893  
 ethylene oxide, rot. relax., double reson. and Stark switching obs. 0-106340  
 fluoracetylene-d, Stark and microwave double reson. laser spectra 0-63690  
 II-VI semiconductors deep centres, ODMR (*French*) 0-60461  
 methyl acetate, microwave spectra and internal rot. 0-87100  
 methyl bromide, NQR and A<sub>1</sub>-A<sub>2</sub> splitting, RF spectrosc. inside laser cavity 0-91579  
 molecular triplet states under optical spin orientation conditions, microwave energy transfer 0-74187  
 propynal-d, in ground vibrational state, IR microwave double resonance spectra, rot. and centrifugal distortion const. determ. 0-83358  
 propynal-d, IR microwave double reson. spectroscopy 0-69172  
 pyrene solutions, radical ion pairs, pulse radiolysis, time resolved EPR spectra meas. by ODMR of fluoresc. 0-83395  
 slotted tube resonator, pulsed ESR and ODMR expts. 0-86360  
 1,2,4,5-tetrachlorobenzene, triplet excitons, zero field ODMR 0-88891



**microwave-optical double resonance** continued

- trifluoriodomethane, laser microwave double reson. spectroscopy with  $\text{CO}_2$  laser lines 0-87156  
 $\text{CaF}_2:\text{U}^{3+}$ , anomalous magneto-optic props., optical detection of ESR and cross-relax. resonances 0-93287  
 $\text{CaO}$ , obs. of dipolar induced spin dephasing, coherent optical-microwave spectroscopy 0-103900  
 $\text{CdTe}:\text{Mn}^{2+}$ , luminesc. and magneto-optic reson., mag. field effect 0-93390  
 $^{37}\text{ClO}_2$ ,  $\nu_1 = 1$  state, laser-microwave double reson. obs. 0-95657  
 $\text{p-GaP}:\text{ZnS}$ , spin polarisation of donors and acceptors in mag. field, optical and microwave study 0-93393  
 $\text{He}$  fine structure interval  $2^3\text{P}_0-2^3\text{P}_2$ , optical microwave atomic beam mag. resonance meas. 0-102585  
 $\text{MgO}:\text{Cr}^{3+}$ , ODMR, octahedral and orthorhombic site symm. 0-71243  
 $\text{MgO}:\text{Cr}^{3+}$ , ODMR study,  $\text{Cr}^{3+}$  ions in tetragonal symm. sites 0-88892  
NHD, rotational transitions, microwave optical double resonance obs. 0-58293  
 $\text{SiC}:\text{Al,N}$  (6H), ODMR for effective-mass-like acceptor 0-93213  
 $\text{ZnS}$ , ODMR of Zn vacancy obs. 0-108121

**microwave oscillators**

- see also Gunn oscillators; microwave parametric oscillators; tunnel diode oscillators*  
2.148 GHz SAW oscillator 0-74680  
BWO for 110 to 170 GHz, using Sm-Co using magnets, design and appl. (German) 0-105684  
IMPATT source, frequency-stabilised, 115 GHz 0-67573  
 $\text{Ca}_{1-x}\text{Sr}_{x/2}\text{Ba}_{x/2}\text{Zr}_{1-x}\text{Ti}_x\text{O}_3$ , ceramic system, dielectric props., microwave resonator application 0-80674

**microwave parametric amplifiers**

- Josephson parametric amplifiers, gain-dependent noise temp. 0-84552  
superconducting, space appl. 0-85836

**microwave parametric devices**

- see also microwave parametric amplifiers; microwave parametric oscillators*

No entries

**microwave parametric oscillators**

No entries

**microwave reflectometry**

- see also swept-frequency reflectometry; time-domain reflectometry*  
backscatter from ploughed soil, surface roughness meas. (French) 0-82072  
direct measures of small microwave signal reflections occurring on four-terminal networks and on dummy loads (Polish) 0-57334  
strip lines meas., dielectric, small standing wave ratio and losses meas. 0-77811

**microwave region** *see microwaves***microwave spectra**

- see also molecular rotation; molecular vibration; radiofrequency and microwave spectra of diatomic inorganic molecules; radiofrequency and microwave spectra of organic molecules and substances; radiofrequency and microwave spectra of polyatomic inorganic molecules*  
energy interval measurement by obs. Zeeman transition in microwave spectra 0-69274  
polyethylene, microwave photon echo 0-66330  
semiconductor, submillimetric magneto-optical props., strip line technique 0-60554  
 $\text{BaFe}_2\text{O}_{10}$  powder, hysteresis of microwave absorpt. and magnetisation reversal 0-75814  
 $\text{BrF}(\text{Cl})$ , rot. spectra in millimeter wave region, rot. transitions obs., equilib. const. determ. 0-78607  
CIF, rot. spectra in millimeter wave region, rot. transitions obs., equilib. const. determ. 0-78607  
 $\text{Cs}$   $n=15-17$  f-g interval meas. 0-91477  
 $\text{Cs}^+$  excited levels, hyperfine struct. and lifetimes 0-63590  
Ge, compensated, sub mm radiation absorpt., temp. depend. 0-66331  
Ge, impurity spectral linewidth meas., free electron effects 0-71463  
Ge:Be, P, absorption of radiation, 0.6-2.8 mm, 4.2 to 20K 0-66332  
 $\text{ICl}(\text{Br})$ , rot. spectra in millimeter wave region, rot. transitions obs., equilib. const. determ. 0-78607

**microwave spectrometers**

- see also magnetic resonance spectrometers*  
absorption, swept-freq. system for dielectric characterisation 0-104824  
bridge type superheterodyne microwave spectrometer, for transient effects investig. 0-91551  
Fourier transform spectrometer, double-pass rapid-scanning, for plasma diagnostics 0-103190  
Ku-band microwave Fourier transform spectrometer, construction, appls. 0-68265  
noise considerations in millimeter-wave spectrometers, air pollution detection appl. 0-57367  
pressure-scanning millimetric-wave dispersion spectrometer expt. 0-61904  
spin resonance spectrometer, influence of nonlinearity of microwave network characteristics 0-62707  
TWT prior to crystal detection for sensitivity increase 0-82822

**microwave spectroscopy**

- see also magnetic resonance spectroscopy; microwave spectrometers; paramagnetic resonance*  
dielectric props. of biological substances, physical meas. 0-94417  
millimetric/submillimetric coherent transient spectroscopy 0-58651  
network characteristics, influence of nonlinearity on shape of mag. resonance spectra 0-62707  
Rydberg atom microwave and far IR spectroscopy 0-63564  
successive oscillatory fields, molecular beam resonance method 0-91706

**microwave tubes**

- see also electron-wave tubes; relativistic electron beam tubes*  
gyrotron oscillator, TNS, electron cyclotron heating startup system, design 0-99330  
gyrotron oscillator for electron cyclotron heating expt. on ISX-B Tokamak 0-99329  
gyrotrons for electron cyclotron reson. heating of Tokamak power reactor 0-99331

**microwaves**

- auditory perception of microwaves, contrib. of middle-ear structs. 0-67097  
biological solids, resonant interactions, physical plasma 0-101222  
computed tomography with microwaves 0-104719  
hearing mechanism hypotheses, holographic assessment 0-72178

**microwaves** continued

- interaction of electron beams with microwave-frequency field, of planar gap 0-106431  
magnetic field diff. meas. on axes of disks and apertures, Babinet principle, complex spirals 0-102599  
mammalian nervous system, possible microwave mechs. 0-89738  
plant leaves, microwave photoconductivity obs. 0-104637  
power absorption differences between normal and malignant tissue 0-104640

**micromagnetism**

*see also spin glasses*

- $\text{B}_2\text{O}_3\text{-PbO-GeO}_2\text{-Fe}_2\text{O}_3$  glasses, mag. props. and Mossbauer spectra, speromagnetic order at low temps. 0-80530  
 $\text{BaO-Fe}_2\text{O}_3\text{-B}_2\text{O}_3(\text{Na}_2\text{O})$  glasses, high  $\text{Fe}_2\text{O}_3$  content, micromagnetic props. 0-65916  
 $\text{Ce}_{80}\text{Au}_{20}$ , metallic glass, mag. ordering and cryst. field effects, speromagnetism 0-80531  
Co-Mn, FCC, magnetisation and mag. susceptibility meas. 0-60310  
Cu-Mn (8 to 75 at.%), spin correl., neutron polarisation anal. study 0-65905  
 $\text{FeF}_3$ , amorphous, mag. props. and Mossbauer spectra, speromagnetism and micromagnetism 0-75778  
 $\text{Fe}_2\text{O}_3\text{-BaO-B}_2\text{O}_3$ , magnetic props. of Fe-rich amorphous oxide (French) 0-80511  
 $\text{KFeF}_4$ , amorphous, mag. props. and Mossbauer spectra, speromagnetism and micromagnetism 0-75778  
 $\text{LaNi}_{1-x}\text{Fe}_x\text{O}_3$ , magnetisation meas. and  $^{57}\text{Fe}$  Mossbauer studies 0-93217  
Mn-Bi, micromagnetic alloy, mag., elec. and elastic props. (Russian) 0-108028  
Mn-Cu, micromagnetic props., neutron diff. obs. 0-65906  
 $\text{NaFeF}_4$ , amorphous, mag. props. and Mossbauer spectra, speromagnetism and micromagnetism 0-75778  
 $\text{Y}(\text{Fe},\text{Co}_{1-x})_2$ ,  $x \leq 0.2$ , mag. props. and Mossbauer meas. 0-75798  
 $\text{Zr}(\text{Fe}_{1-x}\text{Co}_x)_2$ , thermal expansion and forced volume magnetostriction 0-75830

**MIDP**

- aniline, in p-xylene host cryst., phosphoresc. triplet state, ESR and MIDP obs. 0-66077  
p-bromochlorobenzene,  $T_1$  states, zero-field ODMR, MIDP and phosphorescence excitation spectra 0-74191  
p-dibromobenzene,  $T_1$  states, zero-field ODMR, MIDP and phosphorescence excitation spectra 0-74191  
dichloronaphthalenes, heavy atom effects on substrates of lowest triplet states, MIDP obs. 0-91594

**Mie theory** *see electromagnetic wave scattering***military administrative data processing** *see military computing***military ADP** *see military computing***military computing**

- battlefield smoke/dust cloud temporal analysis algorithm 0-98484

**military equipment**

- see also aircraft; military systems; ships*  
night vision goggles, military low-cost, design and development 0-78990  
staring IR sensors, space and reconnaissance appln. 0-86406

**military systems**

- see also military equipment*  
bandwidth compression effect on military target observers' detection and recognition performance 0-106844  
context-dependent automatic image screening system 0-95820  
electro-optics, systems aspects, seminar, Huntsville, AL, USA (May 1979) 0-94921  
holographic one-tube goggle system engineering 0-78988  
IR technology utilisation, symposium, San Diego, CA, USA (Aug. 79) 0-86037  
man-machine interfaces, weather forecaster console for satellite data handling system 0-90205  
near-millimetric wavelength military systems 0-86428  
optical long focal length aerial reconnaissance system response to thermal shock 0-78939  
optical system temperature effects and counter-measures 0-78938  
photodiode array integration with optical power spectral analysis 0-99645  
physics and arms race, physicists participation explored for general education students 0-57023  
submarine periscope optical design for laser rangefinding compatibility 0-78987  
weather chart transmission by facsimile 0-90206

**Milky Way** *see the Galaxy***milliameters** *see ammeters***m.i.m. devices** *see metal-insulator-metal devices***m.i.m. structures** *see metal-insulator-metal structures***MINDO calculations**

- alicyclic compounds, nucl. spin-spin coupling via nonbonded interactions,  $\gamma$ -substituent effects 0-69078  
aliphatic compounds, nucl. spin-spin coupling via nonbonded interactions,  $\gamma$ -substituent effects 0-69078  
alkanes, nucl. spin-spin coupling via nonbonded interactions, conformational and substituent effects 0-69077  
p-cyano-N,N-dimethylaniline in polar solvents, double fluorescence, theoretical model 0-58296  
formic acid, fragmentation, fragment structs. and energies calcs. 0-74124  
methane, mol. cations, struct., Jahn-Teller effect, MINDO/3 calcs. 0-74135  
organic molecules, small, harmonic force consts., vibr. freqs., integrated intensities, MINDO/3 method 0-58411  
spirohydrocarbons, strained, bond angles, interatomic distances, semiempirical and ab initio calcs. 0-95533  
triatomc inorganic mols., harmonic force consts., vibr. freqs., integrated intensities, MINDO/3 method 0-58411  
vinylidene +  $\text{H}_2$ , addition reaction, MINDO/3 study 0-108705

**mineral oil industry** *see petroleum industry***mineral processing industry**

- Colombian alluvial platina, processing historical account 0-86060  
ore dressing X-ray spectrometric analysis centre 0-86541

**mineralogy** *see minerals***minerals**

- see also lunar rocks and minerals; mineral processing industry*  
adsorption of Tc and I radioisotopes by minerals 0-83203  
Allende meteorite, mineralogy and petrology of isotopically unusual Ca-Al rich inclusion HAL 0-109399



## minerals continued

- amphiboles, high-resolution electron microscopy 0-75241  
 anorthite, thermal eqn. of state up to 120 GPa, appl. to Earth mantle 0-109136  
 apatite crystal growth in skeletal tissues 0-94181  
 apatite solubility in magma, laboratory expts. 0-72504  
 apatites, dipolar reorientations, TSD study 0-107068  
 babephite, cryst. struct. determ. using PI automatic diffractometer 0-107179  
 Baltic underwater coastal slope sand grain size and mineral composition (*Russian*) 0-76963  
 baryta, crystal gas-liquid inclusion meas. with microscope heating stage 0-76967  
 beryl, natural and synthetic, ion channelling transmission ratios 0-75277  
 beryls, optical absorpt. spectra in the near IR (900-2500 nm) 0-89004  
 biotite, Mossbauer and optical spectra,  $\text{Fe}^{2+}$ - $\text{Fe}^{3+}$  interactions 0-60470  
 biotites, Alpine, excess Ar evolution from  $^{40}\text{Ar}$ - $^{39}\text{Ar}$  anal. 0-94521  
 bornite, cathodolum. and AES, ionic diffusion obs. 0-71497  
 Burgers vector characterisation method using electron microscope contrast simulations 0-109141  
 calcite, deform. twinning mechanisms 0-79814  
 calcite, luminescence spectral anal. of polycyclic aromatic hydrocarbon impurities 0-71483  
 calcite dating, appl. of luminesc. under  $\text{N}_2$  laser excitation 0-60685  
 $\text{CaO}$ - $\text{SiO}_2$ - $\text{CO}_2$ , subsolidus and liquidus phase relationships to 30 kbar 0-85643  
 carbonate mineral identification by  $\text{CO}_2$  evolution on heating 0-90248  
 chabazitic tuff, a zeolitic rock for thermal storage of solar energy 0-94117  
 chalcopyrite, cathodolum. and AES, ionic diffusion obs. 0-71497  
 chalcopyrite, superficial degradation in air and water, XPS obs. (*French*) 0-89110  
 chemical analysis, energy dispersive X-ray spectrometry with Si (Li) diodes (*French*) 0-85251  
 chloritoid intergrown polytype identification by electron multiple scatt. 0-70184  
 chondrules, experimental reproduction of textures 0-94763  
 chromite grains in Fe formation from Early Precambrian Isua supracrustal belt, W. Greenland, probable cosmic origin 0-72508  
 chromite natural samples of Brazilian, Philippine origin, chem. comp., Mossbauer spectroscopy 0-103901  
 chromites, electron microscopy, high-resolution observations 0-75241  
 coal and mineral content characterisation by Fourier transform IR spectroscopy 0-104474  
 cordierite, evidence of giant halo radioactive inclusions 0-94524  
 crystalline minerals, elastic consts. rel. to surface waves propagation over liquid and crystalline layers 0-76924  
 crystalline minerals, surface waves propagation over liquid and crystalline layers 0-76925  
 crystallographic defects, high-resolution TEM obs. 0-72517  
 diaspore,  $\text{AlOOH}$ , cryst. struct. refinement and electron density distrib. 0-79758  
 dickite, unusual crystal habit, structural disorder 0-59445  
 dislocations and shock compression, thermodynamics 0-100235  
 dolomite, deform. twinning mechanisms 0-79814  
 Earth interior, mineral comp. prediction for rocks at great depths (*Russian*) 0-104956  
 emerald, artificial single crystal, distrib. of  $\text{Cr}^{3+}$  impurity 0-59505  
 erivanit based glass, granulation and briqueting 0-60823  
 fayalite, elec. cond. obs. under shock compression 0-81873  
 fayalite,  $\text{Fe}_2\text{SiO}_4$ , Czochralski growth under controlled  $\text{O}_2$  fugacity conditions 0-84843  
 ferroxhyte ( $\delta\text{-FeOOH}$ ), possible occurrence on surface of Mars 0-85879  
 fibre characterisation using energy dispersive X-ray spectrometry in TEM (*French*) 0-82857  
 fluid inclusions obs., Raman laser microprobe analysis appl. 0-57390  
 fluorite, crystal gas-liquid inclusion meas. with microscope heating stage 0-76967  
 fluorite, use of proton irradi. to reveal growth and deform. features 0-84216  
 fluorite mineralisation of carbonate bearing rocks, dynamic model 0-81876  
 fluorophlogopite, synthetic, with excess Al, radiation-induced paramag. O<sup>-</sup> centres 0-60417  
 forsterite,  $^{18}\text{O}$  self-diffusion expts., high-temp. creep implications 0-81870  
 forsterite,  $\text{O}^2$  self-diffusion coeffs. 0-70457  
 forsterite, temp. in high-pressure. shock state 0-72490  
 forsterite, with  $\text{SiO}_2$  impurity, elec. and dielec. props. at high temp. 0-104953  
 galena, superficial degradation in air and water, XPS obs. (*French*) 0-89110  
 garnet solid soln. series, elastic props. inferred from expts. on pyrope 0-76968  
 haematite, elec. resist. and phase transition under shock compression 0-72496  
 haematite, secondary, in Pliensbachian limestone sequence at Bakonycsérnye, effects on remanent magnetisation 0-90074  
 haematite in Jurassic silicic rocks from Nevada, USA, thermochemical remanent magnetisation 0-98310  
 hematite/magnetite transformation matrices, higher-order orientation relationships 0-100846  
 hemoilmenites, mag. anisotropy, torque balance obs. 0-98309  
 hilgardite,  $\text{Ca}_2[\text{B}_5\text{O}_{13}]\text{Cl}\cdot\text{H}_2\text{O}$ , PMR of water mol. 0-84655  
 hutnahorite, deform. twinning mechanisms 0-79814  
 hydrothermal alteration minerals, near IR spectra for remote sensing use 0-81871  
 hydrothermal deposit on Guaymas Basin spreading axis 0-101355  
 hydroxyllestadite, X-ray cryst. struct. determ. 0-96485  
 ilmenite upgrading, equil. phase data of  $\text{Fe}_{0.394}\text{-Ti}_{0.606}\text{-O-S}$  subsystem under reducing conditions 0-76240  
 in situ capture gamma analysis of large mineral samples 0-61215  
 inorganic gas chromatography for determ. of  $\text{H}_2\text{O}$  and  $\text{CO}_2$  in rocks and minerals 0-85767  
 jerrfisherite, X-ray cryst. struct. determ. 0-92512  
 jimthompsonite and anthophyllite from Swiss Alps, disordered intermediate minerals imaging 0-72518  
 kaolinite rare-earth complexes, relax., molar free energy of activation for dipole relax. 0-88919  
 lower mantle minerals, evaluation of finite strain eqns. of state using lattice models 0-96620  
 magnetite, magnetisation of immobilised particles, shape factors 0-72499

## minerals continued

- magnetite, single domain, weak field thermoremanent magnetisation intensity, cooling rate effect 0-109139  
 majorite, dislocation obs., Earth mantle implications 0-85909  
 metallic mineral deposits of Australia mag. induced polarisation survey results 0-98223  
 monazite,  $\alpha$ -spectra evidence for natural activity at 6.52 to 9.07 MeV 0-67363  
 monazite, from South Indian beach sand, superheavy element search, K X-ray fluoresc. anal. 0-61801  
 mooreite, X-ray cryst. struct. determ. and refinement 0-92488  
 nephrite, amphibole, planar defects termination, high resolu. electron microscopy 0-79772  
 neutron capture  $\gamma$ -ray borehole mineral anal., optimum neutron source size 0-61213  
 NQR analysis, appls. to mineralogy 0-67426  
 olivine, dislocation recovery rate affected by high-pressure. 0-94515  
 olivine, shock deform. expts., Hugoniot data implications 0-94497  
 olivine in Japanese peridotites, appl. to uppermost mantle differential stress lateral var. determ. 0-98275  
 olivines, cosmic ray nuclei groups  $Z \geq$  abundances, fossil tracks in meteorites 0-105139  
 oxides,  $\text{ABO}_4$  type, high press. phase transforms. and struct. types, cryst. chem. aspects 0-79940  
 paradumite,  $\text{Zn}_2(\text{AsO}_4)(\text{OH})$ , crystal struct., anisotropic temp. factors 0-84145  
 paulmooreite,  $\text{Pb}_2[\text{As}_2\text{O}_7]$ , crystal struct., dimeric arsenite groups 0-84143  
 pegmatites,  $\text{U}^{235}$  estimation by homogenised fission track anal. using solid state track detector 0-97719  
 penninite, one-layer triclinic chlorite, neutron diffraction study 0-84144  
 periclase, containing  $\text{Fe}^{2+}$ , visible absorpt. spectra and mantle radiative transfer 0-90039  
 pigeonite, antiphase domains exptl. coarsening 0-81886  
 pigeonite, inverted, from SW Norway, precipitation temp. estimation 0-72500  
 plagioclases, volcanic, thermoluminescence dating 0-98475  
 pyrite, superficial degradation in air and water, XPS obs. (*French*) 0-89110  
 pyrite layers in coal, rel. to anisotropic elec. props. 0-98312  
 pyrolusite ( $\text{MnO}_2$ ), UV irradiated, simulation of Viking gas exchange reaction on Mars 0-72831  
 pyrope, elasticity of single crystal, implications for garnets 0-76968  
 pyroxenes, antiphase domains, contrasting props. and behaviour 0-79813  
 quartz, c-axis fabrics anal. via photometric method 0-101456  
 quartz, dislocations fine structure under electron irradi. 0-70213  
 quartz, low, CC Si-O bond characteristics 0-84132  
 quartz, low, ionicity of Si-O bond 0-84133  
 $\alpha$ -quartz 0-72490  
 quartz grains in Moine thrust zone, deformation-induced microstructs. rel. to differential stress 0-85652  
 rectorite, stacking and ordered interstratification, high-resolution TEM obs. 0-109140  
 rhodochrosite, deform. twinning mechanisms 0-79814  
 riebeckite, low temp. Mossbauer obs. of oriented single cryst. behaviour and mag. props. 0-84674  
 ringwoodite, dislocation obs., Earth mantle implications 0-85909  
 rinneite, Rb-Sr dating of potash salt deposits 0-67429  
 rustumite, crystal structure, X-ray anal. 0-79766  
 rustumite, crystal structure determ. by X-ray diff. method 0-70182  
 scanning electron microscopy for mineralogy 0-82077  
 shock deformation of brittle solid, review of theory 0-72493  
 shungite, Ar degassing to form ancient atmos., isotope fractionation 0-85749  
 silicate, interstellar, porous grains, free-space equil. temps. calc., rel. to optical props. 0-62223  
 silicate, linear variation of secondary ion yield (*French*) 0-108763  
 silicate, microscopic samples molecular analysis, with Raman microprobe 0-57391  
 silicate HV high-resolution electron microscopy 0-70096  
 silicate minerals, X-ray photoelectron diff., quantitative anal. 0-66912  
 silicate smokes, vapour-condensed, 800 to 130 nm extinction and interstellar extinction curve 0-82180  
 silicates, layered, optical filtering of faulted areas in electron micrographs 0-84035  
 single domain grains, mag. blocking temps. during slow cooling 0-90082  
 sodium rare earth silicates, single cryst. data and ionic cond. 0-84158  
 specularite, in sandstone, exptl. evidence for primary depositional magnetisation 0-90075  
 sphalerite, superficial degradation in air and water, XPS obs. (*French*) 0-89110  
 spence, fission track annealing, fission track age-temp. relationship 0-98316  
 spinel, dislocation obs., Earth mantle implications 0-85909  
 spinel,  $\text{MgAl}_2\text{O}_4$ , anomalous thermal expansion, second order transition 0-84307  
 sputtering rates, implications for abundances of solar elements in lunar samples 0-61797  
 sulphide deposits from E. Pacific Rise near  $21^\circ\text{N}$ , mineralogy and geochemistry 0-101361  
 sulphide ore deposits in NW. Kola Peninsula, electric near zone field development method testing (*Russian*) 0-85761  
 surface interactions with organic solutes, groundwater vel. determ. 0-98492  
 talc, vibr. mode assignments, Raman microprobe spectra 0-88977  
 thermobarogeochemistry of inclusions (*Russian*) 0-104954  
 thermodynamic functions from eqns. of state for end members 0-90084  
 thermodynamic properties of mantle related substances at high press. and temp. 0-81874  
 titanomaghemite, identification in rock by mag. rot. hysteresis loss 0-67428  
 titanomagnetite, identification in rock by mag. rot. hysteresis loss 0-67428  
 titanomagnetites, exsolution microstructures, magnetic significance 0-98313  
 titanomagnetites, temp. depend. cation distrib., mag. prop. obs. 0-85647  
 tridymite, thermal expansion meas. 0-59682  
 ultrasonic damping due to internal friction, freq. depend. (*German*) 0-90078  
 vermiculite, fission track annealing and dating 0-81885



**minerals continued**

- xonotlite,  $\text{Ca}_2\text{Si}_6\text{O}_{17}(\text{OH})_2$ , polytype identification from electron diffraction patterns 0-72519  
 zircon, radiation defect centre, EPR obs. 0-75853  
 zircon, X-ray crystal structure, determination 0-92513  
 $\text{CaO}$ , solid, phase transition at high-pressure, lower mantle implications 0-79876  
 $\text{CaO}$ , tentative evidence for high pressure metallisation 0-84427  
 Fe ore, cold bound pellets, reduction using  $\text{H}_2$  gas, 700 to 900°C (Japanese) 0-71907  
 K concentration, electron probe analysis with low temperature sample holder (French) 0-85248  
 $\text{MgSiO}_3$  melt, instantaneous structure, simulated by molecular dynamics 0-84049  
 Mg-cordierites, synthetic end member, variation of refractive index with water content 0-80739  
 Mo oxides, low-grade, soda roasting study (Korean) 0-93508  
 Na concentration, electron probe analysis with low temperature sample holder (French) 0-85248  
 Na zeolites, electronic structure, quantum chemical study 0-69058  
 Na-rich plagioclase microstructure and exsolution 0-72501  
 Nb-Ta family minerals, crystal structure, X-ray powder diffraction study 0-107169  
 NiO ore, reduction of Ni in segregation roasting process (Japanese) 0-71908  
 $^{18}\text{O}$  isotopic anomalies from different ore deposits, LAMMA determination 0-61800

**mines (coal)** *see mining***mines (mineral)** *see mining***minicomputers**

- for minicomputer applications *see under relevant applications; administrative data processing; computerised control; natural sciences computing*  
*see also electronic calculators*  
 neurophysiological experiments, fast data acquisition and processing system, minicomputer application (Japanese) 0-85536  
 program-controlled electronic keyboard computers, application to oceanographic information analysis, automation 0-101439

**minimax techniques**

- elasticity, beam bending on Pasternak foundation, reciprocal variational inequalities 0-92091

**minimisation**

- see also minimisation of switching nets*  
 molecular geometry optimisations, invariance criteria, symmetry conservation rules 0-58406  
 spectrometer, IR, instrumental distortion computation without measuring apparatus function 0-95159

**minimisation of switching nets***see also logic design*

No entries

**minimum metallic conductivity**

- $\text{La}_{1-x}\text{Sr}_x\text{VO}_3$ , Anderson transition, electrical resistivity and thermopower measurements 0-100488  
 Si:H amorphous films, conductivity and temperature dependence of optical gap 0-100462

**mining***see also mineral processing industry*

- coal seam fault location 0-94613  
 coal seams fault indication using acoustic array processor 0-85778  
 mining tectonics forecast maps, geoelectric bed sounding method (Hungarian) 0-105075  
 opencast coal, principal environmental noise sources 0-81505  
 quarrying, use of electronic transient recorders for measurements, explosion noise and vibration 0-67023

**minimax technique** *see minimax techniques***minor planets** *see asteroids***minority carrier conduction** *see minority carriers***minority carriers**

- Auger recombination of carriers bound to centres involving phonons 0-107805  
 DLTS, photo-excited, minority carrier trap measurements 0-96816  
 electron beam depth profiling in semiconductors, using carrier collection models 0-70723  
 graphite, thermoelectric power, low temperature, anomaly related to phonon drag 0-65610  
 $\text{HgCdTe/CdTe}$ , limited diffusion volume photodiode, characterisation 0-75627  
 III-V semiconductor epitaxial structures as wide-gap substrates, minority carrier diffusion length determination, by photoluminescence 0-103992  
 injection in trap free semiconductor 0-96904  
 lifetime mapping by SEM 0-96903  
 minority carrier recombination 0-65591  
 MIS negative barrier contact for induced back surface field solar cell 0-101101  
 MIS solar cells with diffused back surface field (BSF), and diffused junction solar cells with MIS BSF 0-94074  
 MIS structure, hysteresis pulsed C-V method for minority-carrier lifetime and surface generation velocity determination 0-70839  
 MIS tunnel diode, minority-carrier, potential barrier height 0-96998  
 MOS pulsed capacitor, minority carrier lifetime measurements, influence of Si-wafer surface state density 0-60098  
 n-p junctions, determination of transport parameters of minority carriers using electron microscope 0-65665  
 p<sup>+</sup>-n, n<sup>+</sup>-p solar cell structures on polycrystalline material, performance 0-89640  
 p-n junction, magnetic injection of minority carriers 0-107900  
 Schottky barrier solar cell, doping density effect on efficiency 0-101100  
 semiconductor, n-type, inhomogeneous, nonequilibrium carrier diffusion and lifetime 0-60005  
 semiconductor, optical absorption coefficient, and minority-carrier diffusion length, differential photocurrent method of measurements 0-96896  
 semiconductor, SEM electron beam induced current images of dislocations and stacking faults, computer simulation 0-70198  
 semiconductors, exhibiting negative photoconductivity, photovoltaic effects 0-96943  
 Al-SiO<sub>2</sub>-(p)-Si barrier structures, minority carrier injection ratio measurements, MIS solar cell model 0-93007  
 BN glass transfer process 0-107459  
 n- $\text{Cd}_{0.9}\text{Hg}_{0.1}\text{Te}$ , photoelectric properties at 78K, relaxation time, minority carrier extraction 0-107864

**minority carriers continued**

- CdTe, minority carrier diffusion length from photocurrent measurements in semiconductor-electrolyte boundary 0-65584  
 CdTe-CdS thin film p-n solar cells, spectral response temperature dependence 0-93871  
 Cr-SiO<sub>2</sub>-Si MIS solar cells, photovoltaic performance and interface states, nuclear radiation effects 0-94004  
 Cu<sub>2</sub>O-Cu diode junction, Schottky barrier, electronic structure and minority carrier diffusion length (French) 0-65682  
 Cu<sub>2</sub>S/CdS heterojunction solar cells, diffusion length determination, using minority carrier SEM 0-61359  
 GaAs, electron beam induced current, minority carrier generation distribution 0-96900  
 GaAs, polycrystalline films, measurements of effective diffusion length by SEM 0-80424  
 GaAs solar cell polycrystalline conducting substrate, minority carrier diffusion length spatially-resolved measurements 0-94084  
 GaAs:Fe p-n junction minority carrier trap measurements, by photo-excited DLTS 0-96816  
 GaAs:Se cathodoluminescence decay observations, with SEM and streak camera, 90 to 300K 0-97348  
 GaAs:Te Schottky barrier solar cells, diffusion length determination, using minority carrier SEM 0-61359  
 GaAs-Ga<sub>1-x</sub>Al<sub>x</sub>As DH lasers, electron beam induced current microscopy 0-95899  
 p-GaSe, back wall Schottky barrier cells, diffusion length, RT spectral response measurements 0-107806  
 Ge-metal Schottky barrier photodetectors, near IR interband transitions and optical parameters 0-73449  
 In<sub>0.5</sub>Ga<sub>0.5</sub>As<sub>1-y</sub>P<sub>y</sub> epitaxial layers, characterisation and relation to lattice matching 0-100540  
 p-InSb, magnetoc concentration effect in extrinsic conduction, range 0-65593  
 MIS solar cells, comparison of majority- and minority carrier 0-85280  
 Si based MOS device irradiation with γ-rays, minority carrier generation, CV characteristics 0-88637  
 Si, carrier lifetime depth distribution, due to Ar ion implantation 0-70232  
 Si, float zone, measurements of deep levels by photovoltage spectroscopy 0-103723  
 Si, gettering by ion damage, minority carrier lifetime and backscattering study 0-100286  
 Si, heavily doped, minority-carrier transport parameters measurements 0-80291  
 Si junction diodes, fabrication by LPE on Si:B substrates, and characteristics 0-80363  
 Si large grain films on metallurgical Si substrates, diffusion length profile 0-61357  
 Si, MOS diode, dependence of minority carrier bulk generation on HCl concentration 0-88639  
 Si materials, advanced, preliminary evaluation for space solar cells 0-94006  
 Si, minority carrier lifetime improvement through laser damage gettering 0-65589  
 Si minority carrier MIS solar cells, design and experimental results 0-81445  
 Si minority carrier MIS solar cells, AM1 efficiencies 0-93975  
 Si p-n junction diodes and solar cells, minority carrier diffusion length 0-107894  
 Si, polycrystalline films, measurements of effective diffusion length, by surface photovoltage measurements 0-80424  
 Si, polycrystalline-metal contacts, minority carrier injection 0-103750  
 Si ribbon solar cells, variation of minority-carrier diffusion length with light intensity, heavy metal doping effects 0-93937  
 Si solar cell parameters, grain size dependence 0-94049  
 Si solar cells, inhomogeneities and their influence on cell performance 0-93967  
 Si solar cells, radiation damaged, origin of reverse annealing 0-76630  
 Si solar cells using minority carrier MIS 0-101103  
 Si wafers, Czochralski grown, minority carrier transport properties, laser beam scan for homogeneity analysis, photovoltaic cell applications 0-92905  
 Si:B photodiode front region collection efficiency models 0-96899  
 Si:B radiation damage and minority carrier lifetime, SEM-EBIC observations 0-96573  
 p-Si:B(Al), radiation defect formation and annealing study using Hall effect, conduction and carrier diffusion length 0-84214  
 Si:Co, minority carrier lifetime investigation 0-80292  
 Si:Zn, minority carrier lifetime investigation 0-80292  
 Si-SiO<sub>2</sub> boundary, relaxation of nonequilibrium capacitance in electrolyte in intense electric fields 0-70845  
 Si-SiO<sub>2</sub> MIS systems, dynamic properties of switching, application to charge transfer devices 0-92997  
 Si-SiO<sub>2</sub> MOS interface, surface-state density and minority carrier generation rate, measurements, by DLTS, hot hole effect 0-100527  
 Zn<sub>3</sub>P<sub>2</sub> thin polycrystalline films for solar photovoltaic cells 0-97797  
 ZnSe, minority carriers diffusion length by surface photovoltage method 0-60003

**mirages** *see atmospheric optics; light refraction***mirrors**

- adaptive deformable mirror system using polyvinylidene fluoride piezoelectric film 0-74455  
 annular aperture, light distribution, from diffraction, aberration correction using mirror lenses (German) 0-69325  
 annular HSURIA resonators, testing with CO<sub>2</sub> laser, polarisation effects 0-58599  
 aplanatic two mirror telescope from near-normal to grazing incidence, comparative performance analysis 0-58654  
 aplanatic waxicon insensitive to tilt errors, for high power laser beam transport 0-74460  
 astronomical optical surface shaping process automation 0-105169  
 asymmetric, with thin absorbing film, design 0-69493  
 automatic target alignment of Helios CO<sub>2</sub> laser system 0-74416  
 axisymmetric mirror class with uniform flux concentration, properties, along axes 0-95978  
 Bragg mirror, corner-reflector type, laser beam divergence reduction 0-91822  
 cassegrain solar concentrators for photovoltaics 0-61304  
 catoptric Schmidt telescope correcting mirrors, aspherisation by elastic relaxation (French) 0-62015  
 coelostat pointing method 0-90338  
 cold light mirror multilayer coating deposition 0-87464  
 complex aspheric mirror testing by phase measurements, interferometry 0-74467  
 concave paraboloidal mirror, production method, interferogram tests 0-58823



**mirrors continued**

conical optics for radiation conversion from laser with unstable resonator 0-91831  
 contact problems in optical surface shaping 0-74540  
 corner edge mirror, vector transform., object space to image space 0-95983  
 coronagraph objective component surface scatt. angular distrib. obs. 0-74463  
 cylindrical mirror and lens optical figure characterisation with conventional interferometer 0-78944  
 deflection effect of light reflected from moving mirror in ether theory 0-91749  
 deformable mirror design for wavefront correction in CO<sub>2</sub> laser fusion system 0-74427  
 deformable mirror for wavefront error correction in Gemini CO<sub>2</sub> laser fusion system 0-74426  
 deformable mirrors for wavefront error correction, piezoelectric material requirements 0-78928  
 diamond turned surface production, interferometric test repeatability 0-74538  
 dielectric, Rayleigh scatt. at 441.6 nm 0-97367  
 dielectric multilayer mirrors, reflectance under slight absorpt. conditions 0-83655  
 dual-grating direct-reading spectrograph mirror system design and performance 0-81397  
 electron microscopy, contrast form. 0-68299  
 electrostatic, resolution improvement method 0-78753  
 electrostatic energy filter, telescopic, with cylindrical mirror analysers 0-87296  
 ellipsoidal, detector system for cathodoluminescence SEM 0-101898  
 ellipsoidal mirror furnace for Czochralski growth 0-60766  
 facet surfaces of large mirror reflectors, approx. methods (*Russian*) 0-69564  
 far IR modular Fourier interferometer construction, very high resolution 0-57401  
 fiducial system compatible with computer-controlled polishing facility 0-74539  
 flat mirror multivalent solar concentrator 0-61420  
 glasses, high vol. low cost, as solar reflectors, compositions and weathering effects 0-106589  
 hazards to air traffic, photometric photography of dazzling heliostat mirrors (*French*) 0-61295  
 heat mirror on plastic sheet for radiation insulation of visible windows 0-95985  
 helenoid actuators applied to deformable mirrors 0-74454  
 heliostat solar collectors, meas. of performance characts. 0-85303  
 hemianopia, new mirror design for detect. 0-108992  
 holographic simulation for fabrication 0-87351  
 injection laser diode mode structure enhancement by backface plating 0-64056  
 interferometric examination of lenses, mirrors and optical systems, 3D display 0-69497  
 interferometry, multimode fibre optic, applications 0-86387  
 IR optical components and aspherics, 10.6  $\mu$ m interferometric testing 0-74523  
 isotropic dielectric mirror theory 0-102797  
 large-aperture holographic visual simulator 0-102679  
 laser, CW heterojunction, mirror surfaces degradation on 10000 hr. lifetime tests 0-106542  
 laser beam expander design corrected for Petzval curvature 0-74461  
 laser beam expander for short cavity dye laser 0-87532  
 laser grating mount, compact stepping motor design 0-87402  
 laser light source for spectroscopy, far-IR, optical coupling arrangements 0-73481  
 laser mirror birefringence, ellipsometric meas. using stabilised two-frequency laser 0-101820  
 laser resonator formed by 90° cone and mirror, misalignment characts. 0-99757  
 light-valve projectors, mirror system use (*Russian*) 0-78930  
 measuring projector, examination of recording heads 0-83657  
 meniscus collimator viewfinder, optimisation of mirror light transmission coeffs. 0-74469  
 metal oxide/fluoride mirror coatings, light scatt. and optical strength in UV range 0-106595  
 microscope, scanning mirror, with optical sectioning characts., ophthalmology appls. 0-85461  
 monochromator, telescopic, in CTEM, with cylindrical mirror analysers 0-87296  
 monochromator using concave holographic grating and plane mirror, imaging props. 0-99856  
 moving atmosphere simulation by rotating phase plate 0-79021  
 multidither hillclimbing adaptive optical system, secondary intensity maxima correction 0-106593  
 multilayer dielectric mirror, light scattering due to surface roughness 0-58460  
 multilayer dielectric mirrors, phase anisotropy, temp. depend., intracavity method, meas. 0-78931  
 nonaxisymmetric, fabrication by stressed mirror polishing 0-99885  
 nonlinear interference mirror, reflection of light 0-102761  
 nontracking solar collectors, wide-angle lenses and image collapsing subreflectors 0-76603  
 opaque surface, roughness determ., photometric method 0-95072  
 optical systems, entropy and negentropy (*French*) 0-102608  
 parabolic, 20 cm diam. f/3, null testing in modified scatterplate interferometer 0-79015  
 parabolic, TV large-screen virtual display, fabrication by rotational method 0-87465  
 parabolic mirror testing by vibration-insensitive laser unequal path interferometer 0-74537  
 parabolic mirror testing during fabrication by long-wavelength interferometer 0-74536  
 paraboloid, off-axis section, fabrication by stressed mirror polishing 0-99886  
 paraboloid mirror with coaxial linear source, intensity distribution 0-74456  
 phase conjugate mirror component for optical cavity, Gaussian transverse modes 0-58595  
 phase conjugate mirror forming optical cavity, Hermite-Gaussian higher-order reson. modes 0-58594  
 photovoltaic solar energy concentrators, image calcs. for an array of directable mirrors 0-76609

**mirrors continued**

plane, spatially separated, adjustment to coplanarity, interferometric technique 0-95974  
 polisher, computer controlled, efficiency 0-91938  
 porous structures for cooling laser reflectors, theoretical study 0-91809  
 production technology advances, seminar, London, England (April 1979) 0-67938  
 pyroceramic lightweight mirror blank fabrication using standard metal-working equip. 0-102871  
 quarter-wave mirrors, oblique incidence reflection coefficient, small absorption of layers effect 0-64140  
 resonator, annular, adaptive mirror effects on performance 0-58596  
 retroreflective array as resonator mirror 0-95973  
 ring laser, perturbed cavity calcs. 0-102739  
 rotating, laser beam TV scanner, development programme (*Japanese*) 0-74369  
 secondary mirror centering of Tingo telescope 0-101533  
 shadow methods for studying turbulence using reflection from a mirror in the medium 0-95801  
 single-point diamond-turned mirror performance before and after polishing 0-74466  
 solar collector with flat specular mirror, optimal tilt angles with seasonal variations 0-72081  
 solar energy concentrators, performance evaluation 0-87457  
 solar energy concentrators, segmented parabolic mirrors, optical performance anal. by THEK computer code (*French*) 0-61294  
 solar point focusing concentrators, effects of tracking errors on performance, statistical anal. of intercept factor 0-61302  
 solar thermal collector, internal cusp reflector, optical anal. 0-101127  
 spatial variables meas., Mekometer additional equipment design, manufacture and calibration for more complete utilisation (*Italian*) 0-64129  
 specular reflectance standards for visible and infrared region using thin Al film vacuum deposited on optical flats (*Japanese*) 0-102789  
 specular reflectometer-spectrophotometer, NBS reference, mirror refl. meas. 0-68236  
 stereoscope for viewing aerial photographs, interpretoskop optics, modifications 0-105081  
 stimulated Brillouin scatt. complex conjugate mirror for ruby laser 0-87438  
 stimulated Brillouin scatt. mirror, short high-power pulses obtained by wavefront reversal 0-99801  
 stratosphere trace molecule Fourier transform spectrometer optical design 0-82099  
 systematisation of mirror lenses according to extent of central obstruction (*German*) 0-102795  
 telescope, altazimuth mounted, primary mirror deflection and stress anal. 0-58659  
 telescope primary mirror manufacture, monitored null corrector 0-78946  
 telescopic system, unstable resonator calculation, laser operating on organic compound solution 0-58600  
 temperature-dependent absorbance, laser-induced thermal runaway 0-91882  
 testing using autocollimation method with multiple pendulum mirrors 0-102792  
 thermal blooming cell design for use in evaluating adaptive optics 0-102780  
 thermal imaging scanners, mirror rotation axis optimisation 0-86426  
 transverse structure of radiation from a laser with an additional mirror 0-58604  
 two-mirror pancratic system, extraneous image plane highlights elimination 0-87467  
 wide-angle concentric dome and shell production, double-pass null test 0-79022  
 Wolter lens component replication 0-95972  
 X-ray catoptrical crossed-mirror imaging at grazing incidence 0-77923  
 X-ray focusing mirror for synchrotron radiation 0-90961  
 X-ray imaging system, surface roughness and scatt. effects 0-77921  
 X-ray mirror profile meas. machine 0-69496  
 X-ray resonator based on successive refls. of surface wave 0-99021  
 XUV mirror reflectivities from 50-150 eV 0-90966  
 Ag mirror, Y<sub>2</sub>O<sub>3</sub> coated, for the 0.5 to 14  $\mu$ m region 0-87456  
 Al coating reflectivity in vacuum UV, heating effect 0-95981  
 CO<sub>2</sub> laser Anates fusion system, mirror quality specifications 0-74423  
 Cu-Sn(Al)(Ga) reflecting surface absorpt. coeffs. at 10.6  $\mu$ m 0-95984  
 MgO-MgF<sub>2</sub> multilayer stack selective mirror with high reflectivity (*French*) 0-64131  
 PbF<sub>2</sub>-ZnSe multilayer 16  $\mu$ m dichroic mirror, 16  $\mu$ m region, mech. stress compensation 0-74465

**m.i.s. devices** see metal-insulator-semiconductor devices

**m.i.s. integrated circuits** see field effect integrated circuits

**m.i.s. structures** see metal-insulator-semiconductor structures

**miscibility** see solubility

**missiles**

navigation, proportional, teaching exercises 0-82611

**mixed conductivity**

$\alpha$ -AgSbS<sub>2</sub> crystals, influence of external elec. field on elec. cond. 0-60056  
 coal dispersions, solvent refined, elec. props., surface characts. 0-80333  
 fast ionic transport in solid electrolytes and mixed conductors, material stability and chem. diffusion 0-65292  
 intercalation compound electrodes, thermodynamic and transport props. 0-66963  
 proton semiconductors, with H-bonds, quantum theory of proton cond. 0-65641  
 AgCNS, mixed conductor, elec. cond. props. 0-65639  
 AgI-Ag<sub>2</sub>O-MoO<sub>3</sub> glass glass superionic cond., struct. and transport props. 0-88602  
 AgN<sub>3</sub>, high-resist. explosive cpd., elec. and galvanomag. props., temp. depend. 0-103728  
 Al<sub>2</sub>O<sub>3</sub> polycrystalline, effects of space charge, grain-boundary segregation and mobility differences on conductivity 0-79979  
 As<sub>2</sub>S<sub>3</sub> glasses, DC elec. cond. and thermo-elec. power 0-96865  
 Ba<sub>2</sub>Sc<sub>2</sub>O<sub>9</sub>, Ba<sub>2</sub>Sc<sub>2</sub>WO<sub>9</sub> and Ba<sub>2</sub>ScTaO<sub>9</sub>, elec. cond. nature, depend. on comp. and medium thermodynamic parameters 0-70773  
 Cu-Cul-graphite secondary cell, transient ionic current obs. 0-108790  
 Cu-Cul-graphite secondary cell, steady state hole current obs. 0-108791  
 Cu<sub>2</sub>Mo<sub>2</sub>S<sub>8-x</sub>, mixed conductor, partial Cu ion cond. and chem. diffusion 0-84323  
 Cu<sub>2</sub>Mo<sub>2</sub>S<sub>8-x</sub>, mixed conductor, equilib. partial thermodynamic props. 0-85270



**mixed conductivity continued**

- p-Cu<sub>2</sub>VS<sub>4</sub>, mixed conduction due to cationic interstitials 0-70772  
 Cu<sub>2</sub>VS<sub>4</sub>, out of equil. mixed cond., electronic cond. decrease in ionic soln. 0-107874  
 Cu<sub>2</sub>VS<sub>4</sub>, out of equil. mixed cond., off-centre positions and order-disorder transition, ultrafast nucl. relax. obs. 0-108103  
 Cu<sub>2</sub>VS<sub>4</sub>, out of equil. mixed cond., chem. origin of mobile ions, spin-lattice relax. and NQR obs. 0-108104  
 D-T, liq., dielectric constant and elec. cond. 0-84680  
 IrO<sub>2</sub>, anodic films, electrochromism and ionic cond., model 0-59706  
 Li<sub>2</sub>FeP<sub>2</sub>(Se<sub>3</sub>), Li<sub>2</sub>MnPSe<sub>2</sub> and Li<sub>2</sub>NiPS<sub>2</sub>(Se<sub>3</sub>), NMR and neutron diff. obs., mag. props. 0-60433  
 Li<sub>2</sub>O-Al<sub>2</sub>O<sub>3</sub>, rapidly quenched glasses, Li ion cond., elec. cond. 0-100346  
 Li<sub>2</sub>O-Bi<sub>2</sub>O<sub>3</sub>, rapidly quenched glasses, Li ion cond., elec. cond. 0-100346  
 Li<sub>2</sub>O-Ga<sub>2</sub>O<sub>3</sub>, rapidly quenched glasses, Li ion cond., elec. cond. 0-100346  
 Li<sub>2</sub>Si<sub>3</sub>, cryst. struct. and electrochem. anal. (*German*) 0-88132  
 Nd<sub>2</sub>Zr<sub>1-x</sub>O<sub>2-x/2</sub>, elec. cond. of ceramic solid solutions 0-107554  
 Sb<sub>2</sub>S<sub>3</sub>, defect drift in elec. fields and bistable switching 0-92947  
 SiO<sub>2</sub>, thin dielectric films in MOS structures, elec. props. with DC voltage (*Slovak*) 0-88634  
 ThO<sub>2</sub>:Ce<sup>3+</sup>(Ce<sup>4+</sup>), mixed ionic and electronic transport 0-107875

**mixed state**

- see also flux creep; flux flow; flux-line lattice; flux pinning*  
 flux cutting in type-II superconductors, direct evidence 0-70915  
 hard superconductor, critical state stability and oscillations 0-107959  
 thin films, vortices, phase transitions, review 0-88698  
 two-dimensional superconductor, resistivity evidence in Monte Carlo studies 0-80434  
 Al, nonlinear conductivity of thin films in mixed state (*Russian*) 0-80464  
 Bi, superconducting amorphous film, <sup>1</sup>Kosterlitz-Thouless transition 0-88699  
 ErRh<sub>2</sub>B<sub>4</sub>, mag. supercond., NMR study of <sup>11</sup>B 0-107957  
 In, mixed state, two-dimensional effect study, destruction current (*Russian*) 0-93054  
 In-Bi, mixed state, pinning centre distrib. statistics, I-V characts. (*Russian*) 0-100571  
 Nb, hysteresis of US attenuation 0-84549  
 Nb, US attenuation, hysteresis near and below H<sub>c1</sub> 0-75676  
 Nb-V<sub>2</sub>Ga mixed state, Meissner effect investigation by muon method (*Russian*) 0-107954  
 Nb<sub>3</sub>Ge, bridge contact, Josephson effect 0-70906  
 Sn, nonlinear conductivity of thin films in mixed state (*Russian*) 0-80464  
 Sn-In, nonlinear conductivity of thin films in mixed state (*Russian*) 0-80464  
 V-Ti (42 at.%), ultrasonic vel. in mixed state 0-75689  
 V<sub>2</sub>Si bridge contacts, nonstationary props. 0-103793  
 V<sub>2</sub>Si, hysteresis in elastic characteristics (*Russian*) 0-103799  
 V<sub>2</sub>Si, supercond. mixed state, low temp. tetragonal-domain-reorientation phenomena, US expts. and thermal props. 0-60141

**mixed valence compounds**

- asymmetric Anderson Hamiltonian, ground state 0-65503  
 asymmetric Anderson model, ground state, perturbation approach 0-65504  
 conduction processes in magnetic and intermediate valency compounds 0-96787  
 Creutz-Taube complex, mixed valence, reson. Raman calcs. using vibronic coupling model 0-97249  
 diatomic molecule model 0-107751  
 disordered extended Anderson model, CPA-alloy analogue treatment 0-65506  
 dynamic susceptibilities 0-70653  
 dynamic susceptibility, RPA study of Anderson lattice 0-97075  
 electrical conductivity, periodic Anderson model, memory function approach 0-84458  
 electron-phonon coupling, theory 0-70343  
 entropy and phase diagram of valence transition 0-59877  
 Falicov-Kimball model at atomic limit 0-65505  
 IR absorption, anomalous, in fluctuating valence compounds 0-66210  
 local polaron model, appl. to intermediate valence systems 0-107717  
 localised description of valence fluctuations 0-80225  
 metallomacrocycles, mixed valent, cofacial assembly, cond. polymeric material 0-70143  
 niobates, mixed metal, Eu oxidation state, mag. props., Mossbauer study 0-66080  
 periodic Anderson Hamiltonian, alloy analogy treatment for mixed valence states 0-75527  
 properties and appearance conditions, review 0-103649  
 rare earth alloys and cpds., intermediate valence, models for anomalous systems 0-96827  
 rare earth compounds, mixed valence state, conduction band struct. 0-103624  
 rare earth cpds., RM<sub>2</sub>Sb<sub>2</sub> (R=La, Ce, Pr, Nd, Sm, Eu; M=Fe, Ru, Os), prep. and cryst. struct. 0-100211  
 rare earth systems with valence transitions, phonons 0-96611  
 spinless model, coherent-hybridisation states and virtual-bound states 0-107749  
 spinless model, isolated f-level problem 0-107750  
 substitutional alloys of intermediate valence systems, static mag. susceptibility con. and temp. depend. 0-84586  
 tantalates, mixed metal, Eu oxidation state, mag. props., Mossbauer study 0-66080  
 theory, electronic sp. ht. calc. 0-79956  
 Wolfram's red salt, mixed valence, reson. Raman calcs. using vibronic coupling model 0-97249  
 Ag<sub>2</sub>Na<sub>2-x</sub>Te<sub>2</sub><sup>IV</sup>Te<sub>2</sub><sup>VI</sup>O<sub>14</sub> (x=0.4), mixed tellurate, cryst. chem. and elec. cond. (*French*) 0-107150  
 Be intermetallics, MB<sub>2</sub> (M=Y, La, Ce, Lu, Th), lattice spacings and susceptibilities 0-65778  
 CaFe<sup>3+</sup>Fe<sub>2</sub><sup>2+</sup>(Si<sub>2</sub>O<sub>7</sub>)O(OH), ilvaite, electronic struct., press. and temp. depend. of <sup>57</sup>Fe Mossbauer spectrum 0-108129  
 CdCr<sub>2</sub>Se<sub>4</sub>(Se<sub>4</sub>), pure and Ag doped, electronic struct., mixed valence 0-70612  
 (Ce, La)In, heat capacity and elec. resist. 0-71049  
 Ce pnictides, unusual anisotropy mechanism due to virtual valence fluctuation 0-96828  
 CeAl<sub>2</sub>, resistivity and volumetric meas., phase diagrams, comparison with CeS 0-107789  
 CeBe<sub>3</sub>, intermediate valence state, XPS, resist. and susceptibility study 0-71565  
 Ce(In, Sn)<sub>3</sub>, heat capacity and elec. resist. 0-71049

**mixed valence compounds continued**

- Ce(In, Sn)<sub>3</sub>, mag. susceptibility, temp. depend., intermediate valence 0-65779  
 CeIn<sub>2</sub>-Sn, mixed valence system, low-temp. susceptibility, paramagnon study 0-97077  
 Ce<sub>0.92</sub>-La<sub>0.08</sub>, mixed valence state, static and dynamic mag. response 0-103816  
 CePd<sub>3</sub> fluctuating-valence compound, anomalous far IR absorption 0-66210  
 CePd<sub>3</sub>, mixed-valence, 3d and 4d core levels, XPS study 0-89111  
 CePd<sub>2</sub>-MPd<sub>3</sub> mixed valent systems, nonlinear conc. depend. of resist. 0-65528  
 CeS, resistivity and volumetric meas., phase diagrams, comparison with CeAl 0-107789  
 Ce<sub>1-x</sub>Sc<sub>x</sub>Pd<sub>3</sub>, intermediate valence of Ce, susceptibility, lattice const., ESR meas. 0-103648  
 CeSn<sub>3</sub>, electronic struct. and mag. props. 0-70649  
 CeSn<sub>3</sub>, intermediate valence cpd., search for phonon anomalies, inelastic neutron scatt. 0-100317  
 CsInCl<sub>3</sub>, mixed-valence cpd., structural phase transition (*German*) 0-70406  
 Cs<sub>2</sub>ZrBr<sub>6</sub>, PtBr<sub>2</sub><sup>2-</sup>-PtBr<sub>6</sub><sup>2-</sup> doped, mixed valence, absorpt. spectra, vibronic struct. 0-97308  
 CuCr<sub>2</sub>Se<sub>4</sub>(Se<sub>4</sub>), electronic struct., mixed valence 0-70612  
 EuCu<sub>2</sub>Si<sub>2</sub>, interconfiguration fluctuation, NMR expts. 0-66069  
 EuCu<sub>2</sub>Si<sub>2</sub>, mixed valence system, X-ray absorption spectroscopic study 0-80906  
 EuO, physical and physicochem. props., review 0-96875  
 K<sub>2</sub>Te<sup>2+</sup>Te<sub>3</sub><sup>3+</sup>O<sub>12</sub>, mixed tellurate, cryst. chem. and elec. cond. (*French*) 0-107150  
 (La<sub>2</sub>O<sub>3</sub>)<sub>1-x</sub>(CeO<sub>3</sub>)<sub>x</sub>:Mn, valence state of Mn, effect of annealing in H<sub>2</sub> atm., ESR obs. (*French*) 0-71164  
 La<sub>0.5</sub>Tm<sub>0.5</sub>Se, sp. ht. meas., 1.6 to 20K, mag. contrib. 0-65934  
 NiS<sub>2</sub>-Se<sub>2</sub> phase diagram, intermediate valence effects 0-103834  
 Pd and Pt mixed valence complex, [Pd(ethylenediamine)<sub>2</sub>Pt(ethylenediamine)<sub>2</sub>Cl<sub>2</sub>](ClO<sub>4</sub>)<sub>2</sub>, Raman spectra 0-84734  
 Pt-transition metal, dil., impurity resist. 0-92875  
 PtCu<sub>2</sub>Si<sub>2</sub>, mixed valence system, X-ray absorption spectroscopic study 0-80906  
 ScAl<sub>2</sub>-Eu, intermediate valence on Eu ions, Mossbauer isomer shift 0-84587  
 Sm, surface mixed valence, XPS study 0-60753  
 SmB<sub>6</sub>, crystal preparation, elec. resistance, phase transitions 0-97427  
 SmB<sub>6</sub>, intermediate valence, <sup>11</sup>B NMR study 0-93193  
 SmB<sub>6</sub>, mixed valent semicond., transport props. and electronic struct., review 0-96877  
 SmB<sub>6</sub>, resistivity press. variation, lattice consts. 0-100456  
 SmB<sub>6</sub>, surface mixed valence, XPS study 0-60753  
 Sm<sub>1-x</sub>B<sub>x</sub>S, valence transition induced by alloying 0-96829  
 Sm<sub>4</sub>Bi<sub>3</sub>, mixed valence system, X-ray absorption spectroscopic study 0-80906  
 (Sm<sub>1-x</sub>Gd<sub>x</sub>)<sub>3</sub>S<sub>4</sub>, mixed valence compound, elec. cond. transition 0-70777  
 Sm<sub>1-x</sub>La<sub>x</sub>B<sub>6</sub>, valence transition, lattice parameter and mag. susceptibility meas. 0-59929  
 Sm<sub>1-x</sub>La<sub>x</sub>S, magnetoresist. in semicond. and metallic phases 0-96914  
 SmS, intermediate valence, low lying states 0-96826  
 SmS, LO phonon freq. softening in semicond. and metallic phases 0-96619  
 SmS, physical and physicochem. props., review 0-96875  
 SmS, trivalent rare earth substituted, stability of Sm<sup>2+</sup> 0-65508  
 SmS type semiconductors, electronic struct., influence of point defects 0-70650  
 SmS, valence transition, two band model 0-65507  
 SmS<sub>1-x</sub>As<sub>x</sub>, magnetoresist. in semicond. and metallic phases 0-96914  
 Sm<sub>1-x</sub>P<sub>x</sub>, valence changes, XPS and UPS study 0-97402  
 Sm<sub>3</sub>Se<sub>4</sub>, valence fluctuation, mag. susceptibility meas. 0-97056  
 Sm<sub>0.75</sub>Y<sub>0.25</sub>S, mixed-valence, electron-lattice correlations, EXAFS studies 0-76103  
 Sm<sub>1-x</sub>Y<sub>x</sub>S, electron-phonon coupling, theory 0-70343  
 Sm<sub>1-x</sub>Y<sub>x</sub>S, magnetoresist. in semicond. and metallic phases 0-96914  
 Sm<sub>1-x</sub>Y<sub>x</sub>S, mixed valence, phonon softening and linewidths, calc. 0-75319  
 Sm<sub>1-x</sub>Y<sub>x</sub>B<sub>6</sub>, valence transition, lattice parameter and mag. susceptibility meas. 0-59929  
 Sn<sub>2</sub>S<sub>3</sub> mixed valence semiconductor, far IR refl. spectra 0-108191  
 Tm<sub>1-x</sub>Eu<sub>x</sub>Se, semicond. with valence instabilities, cryst. chem. considerations 0-100213  
 TmSe and its mixed crystals, valence instabilities, phase diagram 0-70651  
 TmSe, Anderson lattice resist. for antiferromag. ordering 0-65556  
 TmSe, first obs. of negative elastic const. 0-103409  
 TmSe, intermediate valence cpd., susceptibility, single-ion approach 0-70935  
 TmSe, mag. ordering under press., neutron diff. obs. 0-70947  
 TmSe, mixed valence, X-ray absorption study 0-76102  
 TmSe, valence mixing, mag. props. obs. 0-70648  
 Tm<sub>2</sub>Se, magnetoresist. and Hall effect, stoichiometry effects 0-65597  
 TmSe<sub>1-x</sub>Te<sub>x</sub>, semicond. with valence instabilities, cryst. chem. considerations 0-100213  
 U<sub>x</sub>Th<sub>1-x</sub>Sb, valence change of U accompanied by singlet-ground-state ferromag. 0-70965  
 Y<sub>0.8</sub>Tm<sub>0.2</sub>Se, sp. ht. meas., 1.6 to 20K, mag. contrib. 0-65934  
 Yb-Al mixed valent film form., XPS study 0-80943  
 YbAu<sub>2</sub>, valence transition at surface of Yb 0-70652  
 YbCuAl, mixed valence cpd., dynamic susceptibility, neutron inelastic scatt. 0-65807  
 YbCuAl, mixed-valent cpd., thermal expansion and magneto-volume effects 0-66005  
 YbCu<sub>2</sub>Si<sub>2</sub>, interconfiguration fluctuation, NMR expts. 0-66069  
 Yb<sub>1-x</sub>Y<sub>x</sub>CuAl, disordered extended Anderson model, CPA-alloy analogue treatment 0-65506  
 Zn<sub>1-x</sub>Ge<sub>x</sub>Fe<sub>2-x</sub><sup>3+</sup>Fe<sub>2x</sub><sup>2+</sup>O<sub>4</sub>, double exchange magnetism, Mossbauer study 0-66087

**mixers (circuits)**

- see also frequency converters; radio receivers*  
 MM point-contact diode harmonic generators and mixers 0-60105  
 MM wave radiometry conducted at Appleton Laboratory 0-67442  
 Schottky-barrier diode IR capacitive mixing and detect. at high, intermediate or modulation freqs. 0-77864  
 superconducting, space appl. 0-85836



**mixers (circuits)** continued

superconductor-insulator-superconductor quasiparticle mixers, conversion gain prediction 0-70901  
 W-Ni(Co) point-contact diodes as harmonic generators and mixers, DC bias dependence 0-75653

**mixes** *see mixtures***mixing**

*see also dissolving; heat of mixing; mixtures; solubility; solutions*  
 aerated systems, oblong, flow and mixing, transverse circulating flow of liquid, longitudinal dispersion 0-69900  
 alloy surface composition modification by high-power CW lasers 0-93699  
 atmosphere turbulent mixing, rel. to use of passive antenna system as cond. meas. device 0-85762  
 flow measurement, plane mixing layer vortex digital image processing 0-103095  
 fluidised system, heterogeneous, aerodynamic aspects of transfer processes, crit. state 0-79394  
 free turbulent mixing in streamwise press. gradients, linearised k- $\epsilon$  anal., wakes 0-59039  
 galaxy mergers, stellar populations mixing processes 0-67860  
 gas flow, recirculating, in packed columns, mass transfer and mixing, cell model 0-69913  
 glass, complex raw material, hydrothermal prep. 0-104106  
 homogeneous fluid, laboratory investigations of mixed layer evolution, appl. to ocean (*Russian*) 0-94529  
 Lennard-Jones mixture, binary, equimolar, static (dynamic) props., mol. dynamics calc. 0-64857  
 magmas, contrasted, commingling in plutonic environment, examples from Nain anorthositic complex 0-104959  
 magneto-hydrodynamic phenomena, of mixing in the glass industry (*Polish*) 0-64647  
 methanol-ethanol (n-propanol)(n-butanol) binary systems, excess vol. of mixing, dilatometric meas. 0-59656  
 molten alloys, compound-forming, vol. of mixing, conc. depend. 0-103484  
 upperocean mixed layer, temp. and salinity struct. during POLE expt. 0-72536  
 powder, ordered mixtures production, humidity effect 0-76208  
 propylene carbonate and dimethoxyethane mixed electrolyte solns., for high energy density batteries 0-76627  
 stars, main-sequence, mag. mixing rel. to CNO isotope abundances and  $\alpha$  Bootis (Arcturus) problem 0-105229  
 stars, massive, convective and semiconvective mixing 0-90405  
 stationary system, diffusion mixing model, approx. soln. 0-79410  
 stellar cores, heating and mixing by core He flash with two-dimensional convection 0-105230  
 stellar winds, turbulent mixing with interstellar gas 0-67701  
 thin polycrystalline films, rate of mixing depend. on grain boundary struct. 0-107578  
 turbulent mixing with react. of miscible reactant streams, simulation 0-64651  
 viscoplastic material, mixing process, Bingham model, two-dimens. flow (*German*) 0-92076  
 Al<sub>1</sub>Mg<sub>1-c</sub> liquid alloys, vols. and entropies of mixing, calc. 0-75363  
 CO<sub>2</sub> absorption in H<sub>2</sub>O, aq. solns. with interfacial turbulence due to microstirrers 0-64527  
 Ga-Ge-Zn ternary alloys, thermodynamic props., EMF meas. 0-81033  
 SiO<sub>2</sub>, three-component glass, liq. phase separation, with two oxide modifiers 0-103250

**mixing, heat of** *see heat of mixing***mixing circuits** *see mixers (circuits)***mixtures**

*see also critical mixtures; mixing; solutions*  
 acetone-toluene-tetrachloromethane, mol. interaction and thermodynamic props. 0-71935  
 acetonitrile-toluene-benzene, mol. interaction and thermodynamic props. 0-71935  
 air/water mixture mass flow meas. by drag devices and  $\gamma$  densitometer 0-79385  
 analysis of multicomponent by method of additions 0-61187  
 binary and ternary, activity coeffs. rel. to excess Gibbs free energies 0-96665  
 binary dense gaseous mixtures, struct. and thermodynamic props., molecular dynamics study 0-64866  
 binary homogeneous mixtures, motion in infinite rot. cylinder, generalised diffusion theory 0-79328  
 binary liquid, containing one rotational isomeric relaxing liquid, US absorption 0-70315  
 binary liquid, US evaluation of energy of vapourisation 0-65209  
 binary liquid solutions, struct. and thermodynamic props., molecular dynamics study 0-64866  
 binary liquid systems, thermodynamic and transport props. 0-92686  
 binary mixtures flowing through activated C, adsorpt. interference 0-107635  
 boson mixtures, binary, ground state configs. 0-105570  
 t-butyl alcohol, mixtures, assoc., thermodynamic study using 2-constant model 0-66789  
 chlorobenzene-cis-decalin, mixtures, dielec. const. and loss tangent in liq. and solid phases 0-100628  
 o-chlorophenol-acetone (ethyl methyl ketone), thermodynamic and transport props. 0-92686  
 cholesteric mixtures, quasithermal crystn. 0-92652  
 cholesteryl laurate-cholesteryl caprylate (75 wt.%), polymorphic behaviour, optical, elec. and dielec. meas. 0-65208  
 cholesteryl nonanoate, cyclohexanone admixture effect on mesophase order parameter, refr. index meas. 0-100165  
 COOB-cholesteric liq. cryst. mixtures, helix pitch, temp. depend. 0-64895  
 4-cyanobiphenyl/4-cyano-p-terphenyl liq. cryst. mixture, order parameters of dissolved dyes 0-100167  
 $\alpha$ -cyclodextrin and  $\alpha$ , $\beta$ -D-xylose, absorption mode spin-echo spectra appl. 0-78634  
 dextran T-10 and  $\alpha$ -cyclodextrin, absorption mode spin-echo spectra appl. 0-78634  
 dichloromethane-cyclohexane, liq. mixture, intermol. vibrational energy transfer, US study 0-70313  
 drop dynamics in mixture with uniform temp., thermal diffusion effects 0-103097  
 electric conductivity of dispersed mixtures containing high-conductivity components 0-92954  
 ellipsoidal aerosol particles in bina binary gas mixture, diffusophoresis under hydrodynamic conditions 0-66888

**mixtures** continued

fluid mixtures, asymmetric, Henry's constants and second virial coefficients from perturbed-hard-chain theory 0-96621  
 furan-cyclohexane, liq. mixture, intermol. vibrational energy transfer, US study 0-70313  
 gas, large-volume prep. technique based on compressibility ratio 0-59165  
 gas mixture, physical and chemical process modelling 0-71892  
 gas mixtures, detonating, symmetric piston motion 0-59073  
 gas mixtures, marginal comp., thermal diffusion column performance evaluation (*German*) 0-59157  
 gas mixtures, pumping in high vacuum region 0-95107  
 gas-liquid mixture, outflow from large container with a slit 0-74951  
 gas-oil mixtures trapped under ice, stable config. obs., energy meas. 0-108818  
 graphite-air mixture steady and oscill., mean heat transfer 0-89536  
 hard ion mixtures, Ornstein-Zernike eqn. and Yukawa closure 0-107031  
 HCl-inert gas mixtures, van der Waals molecules, far IR spectra 0-95610  
 n-heptane/3-pentanone mixture, vap. press. meas., thermodynamic functions calcs. 0-75345  
 n-hexane-perfluoro-n-hexane mixtures, US vel. and absorpt. mixtures 0-88281  
 n-hexane/3-pentanone(acetone) mixtures, vap. press. meas., thermodynamic functions calcs. 0-75345  
 inert gas, binary,  $\mu$ -capture, near 5 atm., X-ray yield 0-58419  
 inert gas mixture, dipole autocorrelation function, Lennard-Jones and exponential dipole pots., classical calc. 0-64665  
 ionic mixtures, phase separation 0-77279  
 isobutyric acid-water near-critical liquid mixture, nucleation 0-92664  
 isopropanol-n-propanol aq. mixtures, US relax., US absorpt. and vel. meas. (*French*) 0-103426  
 Lennard-Jones, liq., binary, equimolar, static (dynamic) props., mol. dynamics calc. 0-64857  
 liquid, binary, ultrasonic approach to interaction 0-79881  
 liquid, US propag. parameters, effective Debye temp. 0-79882  
 liquid binary mixtures, evaluation of excess internal pressure, Van der Waals' constant and ultrasonic velocity from flory's theory 0-70310  
 liquid crystal, binary mixtures, phase transition, entropy, relation to smectic plane tilt angle 0-65203  
 liquid mixture, surface tension theory 0-88404  
 liquid mixtures, showing phase splitting, modified Wilson eqn., phase equilib. prediction 0-96636  
 molten metal binary mixtures with wide immiscibility range, gravitational layering of components (*Russian*) 0-104092  
 monolithic materials for creating high pressures, anvil device with lune toroid 0-73377  
 natural gas mixtures, simulated, enthalpy and phase equil., correl. with modified Starling eqn. 0-61127  
 nematic liquid crystals, dielec. permittivity dispersion 0-88921  
 4-nitrophenyl-4-octyloxybenzoate/cholesteric liq. cryst. mixtures, helix pitch, temp. depend. 0-64895  
 non-equilibrium thermodynamics of simple mixtures 0-76543  
 nonracemic mixtures, theory of chirality functions, concept of qualitative completeness 0-69255  
 nonxyloxybenzoic acid/cholesteric liq. cryst. mixtures, helix pitch, temp. depend. 0-64895  
 organic mixture analysis by high-resolution mass spectrometry/mass spectrometry 0-104476  
 overstability in horizontal layer of binary liq. mixture with Soret effect 0-106782  
 perfluorocarbon-SF<sub>6</sub> mixtures, sparking C inhibition, decomp. product investig. 0-89478  
 perfluoromethylcyclohexane-methylcyclohexane, near-critical liquid mixture, nucleation 0-92664  
 polar liquids, binary mixtures, Sarma and Rao's rel. for dielectric relax. time 0-88914  
 polar solvent mixtures, solvated electron diffusion, 2-absorber model 0-85206  
 polydisperse, vapour-liquid mixtures, acoustic velocity, damping decrement 0-66881  
 polyethylene-polystyrene blends, crystn. characts. 0-103261  
 polymethylmethacrylate-polycarbonate blends, kneading characts. (*Japanese*) 0-104112  
 polystyrene-polyethylene-(polymethylmethacrylate) blends, kneading characts. (*Japanese*) 0-104112  
 porous media models using thermodynamics of mixtures 0-96184  
 powder, fine particle, morphological anal. 0-104087  
 purification of materials with overlapping absorpt. spectra 0-78452  
 solvent-rod mixture, two phase, interfacial free energies, quartic van der Waals theory 0-59377  
 steel, low C, dual-phase, law of mixtures, applicability 0-89346  
 surface segregation, nonequilibrium 0-88325  
 theory of constrained mixtures with multiple temperatures 0-62600  
 translational relaxation at shock wave front in gas mixture 0-74917  
 two-component, two photon isotope separation, dynamics 0-102584  
 vacancy solution theory of adsorption from gas mixtures 0-65357  
 vapour-liquid crit. props. for pure liqs. and mixtures 0-65213  
 vapour-liquid mixture, outflow from large container with a slit 0-74951  
 water-alcohol, US attenuation meas., method of streaming 0-88272  
 water-methanol mixtures, viscosity at 25°C, isotope substitution effects 0-92700  
 Ar-N<sub>2</sub> mixture, lasing at four lines 0-99713  
 BCl<sub>3</sub>-N<sub>2</sub>, thermodiffusion props., effect of resonant excitation of mol. vibr. by laser, isotope separation 0-100047  
 CO<sub>2</sub>-N<sub>2</sub> mixture, strongly excited, vibr. relax. 0-102555  
 CO<sub>2</sub>-N<sub>2</sub> mixture, temperature measurement by spectrum line reversal 0-73358  
 CO<sub>2</sub>-N<sub>2</sub> mixture gasdynamic laser, energy characts. 0-69362  
 CdI<sub>2</sub>-Cd(I) mixture, molten, nuclear spin relax. 0-88887  
 H/He mixtures in interiors of Jupiter and Saturn, condensed matter physics 0-77307  
 H<sup>+</sup>-He<sup>2+</sup> mixture, fully ionised, two-component plasma, mean spherical model 0-87854  
 H<sub>2</sub>-D<sub>2</sub> gas, thermal cond. meas., 2-36 MPa 0-64668  
 H<sub>2</sub>-He, thermal cond. meas., up to 14 MPa 0-64669  
 He-Xe, eqn. of state, Monte Carlo calcs. 0-59158  
 LiCl-KCl, molten mixture, struct., diffusion, cond., mol. dynamics calc. 0-64871  
 LiCl-RbCl, molten, Chemla effect, mol. dynamics simulation, self exchange vel. 0-79967



**mixtures continued**

- $\text{N}_2\text{-O}_2$  gas mixture, weakly ionised, electron transport coeffs. anal. (Japanese) 0-59184  
 $\text{O}_2\text{-N}_2$  mixture, attachment cooling, press. depend. 0-91663  
 $\text{S-benzene}$  systems, liq.-liq. phase separation 0-96658  
 $\text{SO}_2\text{-}^{18}\text{O}_2$  mixtures, IR laser pumped, intermol. vibr. energy transfer dynamics obs. 0-87207  
 $\text{SbCl}_3/\text{AlCl}_3$  molten mixtures, Raman spectra 0-93305  
 $\text{SeCl}_4\text{-SbCl}_3$  systems, Raman spectra (German) 0-93324  
 $\text{UF}_4\text{-LiF(KF)}$  molten binary mixtures, viscosity meas. 0-65270

**mm waves** *see* **microwaves****MO calculations** *see* **molecular orbitals calculations****mobile radio systems**

- microwave communications from outer planets, Voyager project 0-77263

**mobility, carrier** *see* **carrier mobility****modelling**

- see also* **brain models**; **catastrophe theory**; **identification**; **physiological models**; **semiconductor device models**; **simulation**  
 absorption refrigeration machine driven by solar heat for air conditioning, math. modelling 0-76651  
 adsorbed layers, general principles of construction of structural models 0-84351  
 air quality models development for limited wind fetch, method 0-104533  
 alloy melt, impurity conc. field model, growth by Czochralski method (Russian) 0-75191  
 annular two-phase, two-component flow, quasi-stationary model in three-group approx. (Bulgarian) 0-69911  
 atmosphere, mesoscale dispersion expts., trajectory-diffusion modelling 0-61837  
 binary alloy, solidification chemical inhomogeneity (Russian) 0-75335  
 binary alloys, two phase region calcs. in solidifying melt (Russian) 0-65195  
 binary image statistical modelling, enhancement and recognition (Russian) 0-63929  
 biomacromolecules, rigid, modelling approaches of hydrodynamic props. 0-61613  
 blood pressure automated control in dogs using microprocessor 0-81797  
 BWR LOCA analysis, jet pump modelling using RELAP4 0-68850  
 BWR long-term cooling, closed form analytical model 0-78355  
 clarinet, functional model of simplified version 0-96147  
 cloud formation and development, numerical convection model (Russian) 0-81987  
 coal conversion reactor environments, simulation 0-100831  
 concatenated fibre-optic cable, cumulative baseband frequency response models 0-78983  
 crack dislocation model 0-69741  
 creep damage and the remaining life concept 0-59574  
 creep modelling incorporating initial strain and ageing 0-58939  
 crystal growth, topological modelling techniques 0-59418  
 crystal growth models, attachment energy at habit controlling factor 0-59420  
 crystallisation, technical, modern trends, computer modelling 0-66406  
 current transformers, oil insulated, parameters influencing heating assessment using sensibility matrix (Hungarian) 0-87708  
 cyclic queue models of semiconductor noise and vehicle fleet operations 0-80336  
 Czochralski growth model, transient phenomena 0-84125  
 dislocation motion, lattice resist., effect of impurity interstitials 0-84170  
 disordered crystals., optical transforms 0-78783  
 disordered structures, two-dimensional, computer program for modelling (French) 0-59337  
 double connecting channel model (Russian) 0-90804  
 elastic-plastic transition, model for metallic materials (German) 0-75295  
 electrostatic discharges, energy determ. 0-70065  
 epoxy resin insulation, adapted models selection problems for electric ageing (German) 0-89365  
 failure, for cyclically hardenable metals and alloys, statistical model (Bulgarian) 0-70296  
 fatigue behaviour of fibre reinforced plastics, under random loadings (Japanese) 0-85032  
 fatigue crack growth, surface reaction and transport controlled, model 0-75299  
 fatigue crack propagation, rel. to cyclic plastic instability zone 0-71733  
 fatigue lives, in metals, eval. using crack initiation model (Japanese) 0-104258  
 fatigue-crack-growth-retardation model, based on critical damage approach 0-99960  
 fibre reinforced composite, single ply, thickness effect on percolation and conductivity 0-92953  
 fibre reinforced composites, fracture processes modelling, digital computer appl. 0-65147  
 field emission gun SEM column electron-optical performance obs. and model 0-68328  
 foundational studies, A. Mostowski, book 0-57014  
 foundational studies, A. Mostowski, book 0-57015  
 grinding wheel life modelling, group method of data handling 0-58987  
 ingots, cooling regime in conditions of minimal thermal stress, modelling (Russian) 0-65194  
 jet flow, three-dimensional, hydrodynamical model 0-79369  
 LMFBR, surface temp. distrib. of peripheral fuel elements, approx. thermal modelling 0-63237  
 LWR LOCA, modelling of press. and temp. changes in two-phase, two-component flow (Bulgarian) 0-68904  
 magnetic alloy, interface behaviour 0-84913  
 mathematical, influx of meteoric matter modelling with radar observations (Russian) 0-67664  
 mathematical, vibrational resonances of built-up structures, use of meas. data 0-69718  
 memory alloy, pseudoelastic, model for first-order phase transition 0-92642  
 metrological research on prospective measuring techniques, conf. Wroclaw, Poland, Sept. 1978 (Hungarian) 0-86247  
 MHD generator channel, liquid metal piston dynamics, math. model (Russian) 0-74996  
 natural terrain scenes, segmentation-based boundary-modelling processor 0-99661  
 nuclear materials safeguards, computerised chemical modelling of deviations, from mass transfer equilb. 0-83171  
 nuclear power reactor systems, dynamical behaviour modelling 0-91216

**modelling continued**

- nuclear power station with VVER, for semi-peak load generation, mathematical model 0-68936  
 offshore wind power model estimates 0-61244  
 once through steam generator, Na-heated, stability anal. nuclear reactor systems model 0-91218  
 optical component polishing process modelling (German) 0-87565  
 optical transfer function description, of photochromic hologram recording medium 0-78796  
 photoacoustic cell for liqs. and solids, one-dimens. model generalisation 0-82827  
 planet thermal radiation intensity field modelling; principles 0-62056  
 polymers, glassy, craze surface displacements, model 0-93651  
 polymorphic transformations kinetics model, computer modelling (Russian) 0-97478  
 PWR dynamical behaviour modelling in FORTRAN 0-91217  
 PWR pressuriser behaviour during operational transient, math. model 0-63230  
 radioactive waste, geologic disposal, modelling of radionuclide transport and decay products 0-78415  
 radioimmunoassay, fitting of general form of fundamental physical model 0-94150  
 radionuclide distribution in extended medium, qualitative and quantitative anal., mathematical modelling 0-71985  
 reactor fuel extraction processing of nuclear fuel fluxes, effect of flux oscill. on Pu accumulation, math. simulation 0-63355  
 riverbeds, channel deformations, hydraulic modelling 0-77024  
 signal-dependent film-grain noise, optimal image estimation 0-102659  
 solar cell life prediction using physical chemical failure progression modelling 0-61370  
 solar collectors, flat-plate, dynamic modelling and verification 0-66992  
 solar power station, tower-type, concentrating and receiving systems design modelling 0-91873  
 steel, electrical, mag. hysteresis representation in numerical modelling of mag. fields 0-88813  
 steel, stainless, type 316, modelling effects of fast neutron irradiation in mech. behaviour 0-84234  
 structural system, simulation anal. of reliability and maintenance (Japanese) 0-62453  
 thermoelectric cooling, single stage, finite element thermal stress anal. 0-108807  
 thermoelectric heat pumps, cross flow, anal. of operation and performance using mathematical model 0-107836  
 thin film condensates coalescence, influence on morphological changes, modelling 0-107676  
 three-stage birefringent filter, tuning over visible region 0-58667  
 transfer function with several inputs, model, math. methods of investigation identification 0-62451  
 two-dimensional random field model for image structural analysis (Russian) 0-63932  
 void growth modelling, in ICFR first walls 0-63377  
 void modelling, in FBR pins, porosity and crack effects on transient over-power anal. 0-71760  
 welding arcs, gas velocity fields modelling 0-75039  
 wind energy conversion systems, value to electric utility, economic model 0-61257  
 Au, atomic struct. of large angle [001] twist boundary, determ. by computer modelling and X-ray diffr. study 0-70162  
 $\text{CaF}_2$ , mol. dynamics studies of superionic conductors 0-107547  
 Fe, segregation of impurities, physico-chemical aspects (Czech) 0-60866  
 $\text{GaAs}_{1-x}\text{P}_x$  alloy, composition effects in growth by MBE 0-59816  
 HF, pulsed laser numerical modelling, rot. relax. 0-87388  
 $\text{InAs}_{1-x}\text{P}_x$  alloy, composition effects in growth by MBE 0-59816
- modelling, computer** *see* **computer-aided analysis**  
**models** *see* **modelling**  
**moderation (neutron)** *see* **neutron moderation**  
**moderators**  
*see also* **beryllium**; **graphite**; **heavy water**  
 $\text{BeH}_2$  as a moderator in minimum critical mass systems 0-83151  
 linear extrapolation distance for a black cylindrical control rod with the pulsed neutron method 0-68839  
 pressure tube-type reactors, moderator temp. coeffs. of reactivity meas. 0-57893  
 Au, moderator surface preparation for increased slow positron yield 0-61011  
 Eu-B-C ternary and binary boundary systems, preparation techniques, X-ray analysis 0-60840  
 MgO coated moderators, slow positron form. 0-62796
- modes, laser** *see* **laser modes**  
**modes, lattice vibrations** *see* **lattice dynamics**  
**modes, vibration** *see* **vibrations**  
**modular circuits** *see* **modules**  
**modulation**  
*see also* **amplitude modulation**; **demodulation**; **demodulators**; **modulation spectroscopy**; **modulators**; **optical modulation**; **pulse modulation**; **Schwarz-Hora effect**  
 acoustical communication theory, computation of modulation and carrier functions of an arbitrary audio signal 0-79064  
 application of communication theory to acoustics, separation of sound carrier and modulating signal 0-79063  
 Jupiter decametre radio emission, dynamic spectrum modulation lines origin 0-67643  
 pulse-phase, torquemeter comprising magnetically coupled pulse transducer with electronic phasemeter 0-74819  
 X-ray astronomy, automodulation collimator telescope (Russian) 0-62018
- modulation factor** *see* **modulation**  
**modulation index** *see* **modulation**  
**modulation spectroscopy**  
*see also* **appearance potential spectroscopy**; **electroabsorption**; **electroreflectance**; **magnetoabsorption**; **magnetorelectance**; **piezorelectance**; **thermoreflectance**  
 acousto-optic interaction in solids, appl. to high speed anal. of spectra (French) 0-95156  
 EPR, elec. field modulated, appl. to study of ferroelectrics 0-75841  
 fluorescence decay meas. via modulated gain spectroscopy, appl. to rhodamine B 0-63699  
 frequency crossing techniques appl. to high resolution phonon spectroscopy 0-107392  
 normalising amplifier, meas. and other automated systems appl. 0-73470



**modulation spectroscopy continued**

- photocapacitance spectra, wavelength modulated, deep level determ. 0-76055
- photon echo spectroscopy of crystals, review 0-83648
- saturation spectroscopy with multiple-frequency excitation 0-102774
- selective modulation interference spectrometer, far IR 0-57397
- semiconducting alloys, comp. profile, second derivative wavelength modulation 0-103967
- semiconductor, submillimetric magneto-optical props., strip line technique 0-60554
- semiconductors, dielec. function, modulation spectroscopy and elec. field effects book contrib. 0-80201
- solid-state circular dichroism spectra, phase modulation spectrosc. obs. 0-93271
- wavelength-modulating spectrometer implemented with photovoltaic photo-diodes, comments 0-98981
- Zeeman, line shape analysis 0-74197
- Cr complex,  $(-)_p$ -tris(ethylenediamine) chromium (III), solid-state circular dichroism spectra, phase modulation spectrosc. obs. 0-93271

**modulation transfer function** *see optical transfer function***modulators***see also demodulators; modulation*

- bisymmetric Zeeman modulator for NQR 0-98960
- fusion reactor, FTIR, neutral beam source, arc current modulator design 0-102379
- microcantilever electrostatic deflection system for transmission optical modulator array 0-87512
- microtrons, thyristor modulator circuit and construction 0-63422
- GaAs 400 MHz TW laser modulator 0-87541

**modules***see also CAMAC*

- IR detector balanced common module coolers 0-95142
- IR scanning system modular design, assembly and alignment 0-78989
- multifuel fluidised bed combustion packaged boiler to supply 10000 lb/h saturated steam at 100 psig 0-108779
- optical transmitter laser diode module description and performance 0-64069
- photovoltaic solar devices, modular system (German) 0-89629
- plastic encapsulated and hermetic, corrosion model 0-100937
- solar cell, transparent, with improved glass, adhesives and heat dissipation 0-76636
- surface meas. instrument, with indicator and strip recorder (German) 0-57283
- transducers of electrical variables, third-generation, individual and group arrangements (Czech) 0-62645
- PbS IR staring mosaic detector array module development 0-86413

**modulus, Young's** *see Young's modulus***moire fringes**

- aortic valve study, by holographic interferometry and shadow Moire methods 0-104613
- brittle solid, atomically sharp cracks, TEM study 0-71729
- computer generated moire for profile testing 0-105689
- contourgraphy, computer-aided replication of human anatomy 0-67189
- fluid flow studies using stretched membrane and moire fringes 0-64658
- holography, devel. and present status of moire topography 0-63960
- in-plane motion measurements with Fourier lensless holography 0-77746
- lattice distortion, X-ray moire pattern fine struct. study 0-79775
- linear displacement meas. accuracy meas. accuracy improvement under vibration 0-90815
- orthopaedics, grating-TV method, image evaluation using moire figures 0-67199
- plastic deformation measurement, moire method (Polish) 0-69749
- plate vibration analysis by time-averaged projection-moire method 0-79241
- topograms, real-time, video electronic generation 0-67198
- topographical mapping of the human face by Moire photography 0-85462
- vibration analysis by multiplied moire fringes holography, expansion of meas. limitation 0-64505
- vibration analysis using moire fringes holography, facilitation of fringes counting 0-64504
- winding terms counting 0-73428
- X-ray interferometer, LLL type, interfering beam phase rels. 0-90973
- X-ray mirror profile meas. machine 0-69496

**moistening** *see wetting***moisture***see also humidity*

- atmosphere, effect on acoustic backscatter in GATE 0-85709
- by TIROS-N operational vertical sounder 0-77132
- in coal, moisture content rel. to anisotropic elec. props. 0-98312
- flow in porous medium being dried, generalised model (Hungarian) 0-83839
- graphite fibre epoxy composites, eutectic coating moisture barriers 0-81228
- graphite fibre reinforced composites, damage by moisture, diffusion anal. 0-81227
- optical fibres,  $\text{GeO}_2\text{-B}_2\text{O}_3\text{-SiO}_2$ , ageing effects of moisture on fatigue and tensile strength 0-66539
- optical fibres, tensile strength and static fatigue, analysis using Weibull distribution for optimum design 0-80011
- PMMA moist surface mech. strength reduced by electric charge (Russian) 0-60486
- polyester-E glass composites, types SMC-25, SMC-65 and SMC-30EA, moisture absorpt. 0-93799
- snow, moisture content investigation by radiometry in 3 to 60 mm wavelength region 0-72561
- soil-atmosphere boundary, heat and moisture transport 0-77023
- NaCl:Ca crystals, surface recrystn., moisture effect 0-84950
- Si, polycryst., layer structure dependence on carrier gas moisture and  $\text{O}_2$  content (Bulgarian) 0-59811

**moisture content** *see moisture***moisture measurement***see also humidity measurement*

- cloudless atmosphere, microwave radiation meas. from on board aircraft 0-94624
- hygrometry testing scheme for the Soviet countries 0-57312
- semiconductor packages, hermetically sealed, calibration and anal. of moisture by gas mass spectrometry 0-90928
- soil beneath crop canopy, IR remote thermography 0-109147

**moisture measurement continued**

- soil moisture, basic hydrophys. charact., determ. method 0-85696
- soil moisture determination, soil drying procedure 0-82109
- total errors of moisture meters, representation as two series transducers 0-77792
- water-petroleum emulsions, mean particle diameter and conc. determ. by light scatt. 0-89538
- yaRV-2 compact automatic nuclear resonance hygrometer 0-105657

**molar volume** *see density***molecular alignment** *see molecular orientation***molecular beam electric resonance**

- dimer, partially deuterated, microwave spectra and struct. 0-74212
- Ramsey reson. obs. by linear laser spectroscopy 0-99514
- $\text{ArSO}_3$ , weakly bound complex, struct., MBER obs. 0-95701
- $\text{NO}$ , Zeeman spectrum, mol. beam elec. reson. spectrosc. 0-91621
- $\text{N}_2\text{SO}_3$ , weakly bound complex, dipole moments, MBER obs. 0-95701

**molecular beam epitaxial growth**

- $\text{Al}_x\text{Ga}_{1-x}\text{As}/\text{Al}_x\text{Ga}_{1-x}\text{As}$  heterostructure lasers, prep. characts., and CW reliability 0-58586
- epitaxial films, condensed from vapour or molecular ion beams, impurity distrib. 0-65032
- film, interfacial boundaries and transition regions (Russian) 0-103596
- nucleation kinetics, at high supersaturations on (111) faces of crystals with diamond struct. 0-84128
- semiconducting thin film manufacture 0-103593
- semiconductor device growth and precision doping 0-89156
- semiconductor film growth, multilayer systems, spectroscopic ellipsometry, review 0-103603
- thin films, deposition techniques, review 0-80964
- $\text{AlGaAs}$  DH laser, self-pulsations due to proton bombarded region self-annealing during ageing 0-99728
- $\text{Al}_x\text{Ga}_{1-x}\text{As}$  CW multiwavelength TJS laser, MBE, single-longitudinal modes 0-64049
- $\text{Al}_x\text{Ga}_{1-x}\text{As-Al}_x\text{Ga}_{1-x}\text{As}$  DH IR-visible (0.89-0.72  $\mu\text{m}$ ) MBE grown lasers 0-64058
- n-GaAs, MBE, correl. between electron traps and growth processes 0-65387
- p-GaAs, MBE grown,  $\text{As}_2$  and  $\text{As}_4$  effects on photolum. 0-103974
- GaAs, MBE of doped cryst., thermodynamics and kinetics interplay 0-70144
- GaAs, monocrystalline, lateral definition, prep. by MBE 0-108357
- n-GaAs:Ge, film, substrate temp. depend. of Ge incorporation during MBE 0-76196
- GaAs:Ge film, MBE grown, heavily doped, elec. props. rel. to growth parameters 0-100537
- GaAs:Ge MBE power FETs with Sn surface impurities 0-80374
- GaAs:Si, accelerated growth rate effect on MBE, Hall mobility and photolum. meas. 0-104067
- GaAs/metal contacts, recent developments in investigations of preparation and props. (French) 0-107909
- $\text{GaAs-Al}_{0.25}\text{Ga}_{0.75}\text{As}$  DH lasers grown by MBE, influence of growth conditions on threshold current density 0-58587
- $\text{GaAs-Al}_x\text{Ga}_{1-x}\text{As}$  transverse junction lasers with low threshold current prep. by MBE on semi-insulating substrates 0-58588
- $\text{GaAs-Al}_x\text{Ga}_{1-x}\text{As}$ , current transverse junction lasers, low threshold, MBE prep. 0-83614
- $\text{GaAs-Al}_x\text{Ga}_{1-x}\text{As}$  buried-heterostructure lasers, current injection confinement, MBE/LPE hybrid technique 0-74374
- $\text{GaAs-Al}_x\text{Ga}_{1-x}\text{As}$  DH laser, MBE grown, CW electro-optical props. 0-102725
- $\text{GaAs-GaAlAs-GaAs}$  rectifying semicond. struct., prep. by MBE and characts. 0-65657
- GaAs-Ge, heterostructure, zincblende-on-diamond type systems, MBE growth, (110) orientation as preferred orientation 0-80099
- $\text{GaAs-n-Al}_x\text{Ga}_{1-x}\text{As}$  heterojunctions, selectively doped, FET 0-80364
- $(\text{GaAs})_n(\text{AlAs})_m$  multilayers, MBE, interdiffusion, X-ray diff. study 0-70474
- $\text{GaAs-P}_{1-x}\text{As}_x$  alloy, composition effects in growth by MBE 0-59816
- $\text{GaIn}_{1-x}\text{As}_x\text{-InP}$ , MBE film growth, composition control obs. 0-84399
- $\text{GaP-Si}$ , heterostructure, zincblende-on-diamond type systems, MBE growth, (110) orientation as preferred orientation 0-80099
- $\text{InAs-P}_{1-x}\text{As}_x$  alloy, composition effects in growth by MBE 0-59816
- InP, MBE, substrate temp. related degradation mechanisms 0-65385
- InSb film, grown by MBE, RHEED study 0-100415
- $\text{NaCl}$  on Pt and Ir surfaces, adsorption kinetics 0-84393
- $\text{Pb}_{1-x}\text{Sn}_x\text{Te-PbTe}$  heterostructures, MBE produced on mica and  $\text{LiNbO}_3$ , elec. props. study 0-88629
- Si epitaxial layers, vacuum deposited, conditions for impurity migration from B, P, Sb doped sources (Russian) 0-107570
- Si epitaxial thin film growth on sapphire and spinel by MBE 0-76186
- Si film, MBE, cryst. defect props., substrate treatment effects 0-70551
- Si:As, MBE with simultaneous ion implant doping 0-66432
- Si:Sb, MBE film, doping technique 0-79821
- Si-CoSi<sub>2</sub>Si, double heteroepitaxy, solid phase and MBE 0-104063
- Te film, microstructure 0-103598
- ZnSe, MBE growth, elec. and optical props. 0-75462
- ZnTe, MBE growth, elec. and optical props. 0-75462

**molecular beam magnetic resonance**

- methane, rotational state, avoided-crossing molecular beam spectroscopy 0-63730
- successive oscillatory fields, molecular beam resonance method 0-91706
- $\text{GeH}_4$ , avoided-crossing molecular-beam spectroscopy, hyperfine and spin rot. const. and rot. g factors determ. 0-78671
- $\text{H}_2\text{-H}_2$  dimers, hyperfine struct. in zero mag. field 0-95700
- $\text{I}_2$ , laser fluoresc. state selected and detected mol. beam mag. reson., hyperfine transitions 0-63731
- $\text{I}_2$ , polarisability anisotropy, laser assisted mol. beam spectroscopy 0-78646
- $\text{SiH}_4$ , avoided-crossing molecular-beam spectroscopy, hyperfine and spin rot. const. and rot. g factors determ. 0-78671

**molecular beams***see also molecular beam electric resonance; molecular beam magnetic resonance; molecule-surface impact; particle velocity analysis*

- acetic acid vapours, clustering, effect of supersonic mol. beam sampling, spectrometric study 0-104481
- acetylene- $\text{d}_0$ -( $\text{d}_1$ )-( $\text{d}_2$ ) metastable state, mol. beam elec. deflection obs. 0-74137
- acrolein, s-trans and s-cis, trapping from thermal mol. beams and UV-induced isomerisation in Ar matrices, enthalpy determ. 0-97688



**molecular beams continued**

- benzene,  $S_0-S_1$  transitions, two-photon absorpt. spectra by nozzle beam-multiphoton ionisation method 0-63728  
 chlorobenzene,  $S_0-S_1$  transitions, two-photon absorpt. spectra by nozzle beam-multiphoton ionisation method 0-63728  
 cluster beam, multiple stage ioniser, spatial potential distribution and electron trajectory calcs. (*Japanese*) 0-99596  
 ethanol, H-bonding investigated with supersonic mol. beam using photoionisation quadrupole mass spectrometer 0-102543  
 fluorobenzene,  $S_0-S_1$  transitions, two-photon absorpt. spectra by nozzle beam-multiphoton ionisation method 0-63728  
 formaldehyde, molecular beam rotation temp. meas. (*French*) 0-78724  
 methane, optical Ramsey resonance, in three separated fields produced by corner reflector, theory 0-74166  
 methanol (-d), H-bonding investigated with supersonic mol. beam using photoionisation quadrupole mass spectrometer 0-102543  
 neutral molecule motion control by electron beams 0-99582  
 optical Ramsey resonance, in three separated fields produced by corner reflector, theory 0-74166  
 pulsed beam experiments employing electromechanical valve 0-63870  
 quantum state selected atomic and molecular beams production, developments in techniques 0-63871  
 reactive gas mass spectrometric analysis with free-jet expansion sampling 0-89566  
 sources, gasdynamic, use of lasers, time-of-flight and detection techniques 0-69264  
 structure and dynamics of mols. by pulsed mol. beams 0-102563  
 supersonic source, simple calibration method 0-82845  
 tetracene molecules in Ar clusters, excited state intramol. dynamics, laser-induced fluoresc. spectra obs. 0-78674  
 trifluoroethanol, H-bonding investigated with supersonic mol. beam using photoionisation quadrupole mass spectrometer 0-102543  
 Ar, calibration of supersonic mol. beam source 0-82845  
 Ar, supersonic molecular beam source, simple calibration method 0-82845  
 $Ba + Cl_2 \rightarrow BaCl^+ + Cl^-$ , chemi-ionis. reaction, mol. beam obs. 0-104434  
 $Ba + HF \rightarrow BaF^+ + H$ , dual mol. beam excitation difference spectroscopy, state-to-state vibr. resolved dynamics 0-89474  
 CO, rot. distrib. in supersonic beam, IR bolometry using tunable diode laser 0-63869  
 $CS_2^+ + CS_2 \rightarrow CS_3^+ + CS + e^-$ , chemiionisation, mol. beam photoionisation 0-76495  
 $D_2$ , sticking and accommodation on low-temp. substrate, mol. beam expts. 0-84368  
 $H_2$ , sticking and accommodation on low-temp. substrate, mol. beam expts. 0-84368  
 $H_2^+$  differential cross section rel. to charge exchange cross sections of fragments 0-78704  
 $K_2$ , supersonic mol. beam, isotope selective two-step photoionisation study 0-74203  
 Kr, calibration of supersonic mol. beam source 0-82845  
 Kr, supersonic molecular beam source, simple calibration method 0-82845  
 $N_2$ , calibration of supersonic mol. beam source 0-82845  
 $N_2$  jet, freely expanding, quantum effects in rot. relax. 0-58355  
 $O_2$ , calibration of supersonic mol. beam source 0-82845  
 $SF_6$ , laser pumping in collisional region of nozzle beam, internal excitation, time-of-flight anal. 0-95719  
 $SF_6$  multiphoton dissoci. by mol. beam method, energy distribution meas. by time-of-flight spectra, dissoci. dynamics 0-78670  
 $XeF_6$  seeded mol. beam, transverse ionisation, space charge, mass spectra and vel. 0-78725

**molecular biophysics**

- see also biomembrane transport; biomolecular effects of radiation; DNA; lipid bilayers; proteins*  
 acetate-ferrileghemoglobin, X-ray struct. anal., 3D refinement at resoln. of 2.0 Å 0-104554  
 N-acetyl-D-alloisoleucine, soln. struct., dynamics, proton relaxation mechanisms 0-76708  
 acetylcholine neurotransmitter, PCIO-INDO calcs. 0-58153  
 acetylcholine receptor protein structure 0-85339  
 F-actin, struct. changes in living muscle fibres, polarised UV fluoresc. microscopy 0-67037  
 adenine, hydroxy and methoxy derivatives, absorption UV spectroscopy and electronic struct. of ionic and tautomeric forms 0-74177  
 adenine, tautomeric forms protonation, ab initio HF Roothaan SCF calcs. 0-78534  
 agarose gel immunoelectrophoretic determination of molecular weights of tubulin antigens 0-67313  
 alarm pheromones, activity rel. to mol. similarity, electron density function meas. 0-91413  
 albumin, adsorbed layers on polystyrene, contact angle meas. 0-61508  
 $\alpha$ -amino acids, naturally occurring, in aq. soln., Kerr constants 0-85353  
 amphipathic apolipoprotein ApoC-III bound to phosphatidylcholine bilayers, lateral mobility 0-97884  
 apomyoglobin reconstituted with  $^{111}In(III)$ mesoporphyrin IX, rot. correl. time determ. 0-76698  
 ascorbic acid adduct model systems, SCF calc., rel. to protein internal charge transfer 0-69072  
 ATPase,  $Ca^{2+}$ -activated, of sarcoplasmic reticulum, rot. motion and evidence for oligomeric structs. 0-72124  
 ATPase,  $Ca^{2+}$ -depend., struct. rearrangements during function 0-81527  
 azo dyes, UV-visible spectrophotometric 0-61207  
 bacterio-opsin, changes in protonation state during reconstitution of bacteriorhodopsin 0-89707  
 bacteriorhodopsin radicals, role in primary charge separation of Rhodospseudomonas viridis 0-63688  
 bacteriophages T4B and T7, determ. of rotational diffusion coeff. by depolarised dynamic light scattering 0-85549  
 bacteriopheophytin b radicals, role in primary charge separation of Rhodospseudomonas viridis 0-63688  
 bacteriorhodopsin, effect of high press. on absorpt. spectrum and isomeric composition 0-67041  
 bacteriorhodopsin membrane preps. associated with lipid-water interface, form. of elec. pot. diff. 0-81551  
 bent molecular organic crystals, electron diff. intensities 0-100132  
 bioenergetics, H bonded chain theory 0-76699  
 biomolecules+chloranil, charge transfer interaction, equilib. const., enthalpy and entropy determ., mol. polarisability 0-89708

**molecular biophysics continued**

- biopolymers, chromophore aggregates in Frenkel exciton model, dynamic perturbation effects on circular dichroism intensity 0-93273  
 bovine serum albumin, conformational changes and mol. dynamics exam. by perturbed angular correl. 0-81538  
 Clq of human complement, neutron scatt. obs., conformational calcs. 0-81537  
 calcium oxalate hydrates, crystn. kinetics, comparison for mono-, di-, and trihydrates 0-81528  
 carotenoid molecules in living cells of chlorella, vibrational state population 0-97861  
 cartilage proteoglycan, association with hyaluronic acid, elec. birefringence obs. 0-85332  
 cell membranes, at mol. resoln., introduction 0-104841  
 cell surface anisotropic molecular motion 0-97883  
 cell surface component rotational diffusion, time-resolved phosphoresc. anisotropy 0-97885  
 cellulose, mobility of adsorbed water, NMR pulse obs. 0-108835  
 cerebrin, thermotropic and lyotropic mesomorphism 0-76703  
 ceruloplasmin, human, calc. of rotation function for tetragonal. cryst. at 10 Å resoln. 0-108843  
 chemical oscillators responding frequency switch 0-108837  
 chemical rectifiers, one-way catalysis 0-71901  
 chlorophyll a, cation radical formation by pulse radiolysis, oxidation and demetalation rate consts. 0-61505  
 chlorophyll-a, fluoresc. at low concs., noise reduction by low pass filter for DC signal 0-87249  
 cholesteric mixtures, quasithermal crystn. 0-92652  
 chromatin, low-angle X-ray and neutron diff., interparticle effects 0-72134  
 chromophores in membrane suspensions, determ. of orientational order, intensity depend. of flash-induced anisotropy 0-94177  
 coherent phonons and excitons in biological systems, Bose condensation 0-67042  
 collagen, 3-dimens. struct., rel. to props. of connective tissue 0-67038  
 collagen, polarisation, contribution of permanent and induced dipole moments, elec. birefringence 0-85351  
 collagen fibres, mech. props., role of struct. organisation 0-72207  
 collagen fibril,  $^2H$  NMR of mol. motion 0-67034  
 collagen molecular organisation and connective tissues props. 0-97858  
 collagen type supramolecular structs., 2 possible mechs. of formation 0-76702  
 conference, Crystal XII, Canberra, Australia (Jan.-Feb. 1980) 0-62388  
 cowpea chlorotic mottle virus packing in crystalline monolayers, electron microscopy 0-89922  
 cyanine dyes, excited electronic states, CNDO/S CI calc., visual pigment spectra appl. 0-85333  
 cyclophosphazene-DNA complex, spectrofluorometric and spectrophotometric investig. 0-95643  
 cytochrome  $c_3$ , anhydrous film, elec. cond., temp. and ambient press. depend. 0-85327  
 cytochrome  $c_3$ , haeme-haeme mag. interaction, Mossbauer obs. 0-108836  
 cytochrome  $c_3$ -hydrogenase, reduction kinetics, Mossbauer spectra 0-67031  
 cytochrome c, low freq. modes and excitation profiles, reson. Raman spectra 0-94428  
 cytochrome c, protein influence on haeme, Raman difference spectroscopy 0-72125  
 cytochrome c oxidase, Cu ENDOR 0-94170  
 cytochrome c oxidase, macromolecular struct., electron microscopy and image anal. 0-89716  
 cytochrome c oxidase, struct. of cytochrome  $a_3$ - $Cu_{a3}$  couple, NO binding studies 0-67039  
 cytosine, hydroxy and methoxy derivatives, absorption UV spectroscopy and electronic struct. of ionic and tautomeric forms 0-74177  
 deoxyhaemoglobin,  $Fe(II)-N_5(His-F8)$  stretching freq. rel. to quaternary struct. 0-94160  
 deoxyhaemoglobin, ferrous heme of high-spin type, MCD spectra in Soret, visible and near IR regions 0-94156  
 2,4-diamino-6-hydroxy-pyrimidine, IR absorption spectrum, vibr. anal., tautomerism 0-85253  
 1,2-dimyristoyl-sn-glycero-3-phosphoserine multilayers, phase transitions, temp. depend., ellipsometric study 0-108846  
 1,2-dipalmitoyl-sn-glycero-3-phosphocholine multilayers, phase transitions, temp. depend., ellipsometric study 0-108846  
 DNA,  $^{11}In$  bound, rot. correl. times, from  $\gamma$ -ray perturbed angular correl. 0-94152  
 DNA, calf-thymus Na-DNA aq. solns., dielec. behaviour in 5 kHz to 100 MHz range 0-85330  
 DNA, dye labelled elec. dichroism and birefringence, comparison with mol. props. from polarised fluoresc. 0-84785  
 DNA, electronic interaction with N-methyl-N-nitrosourea, ESR obs. and INDO calcs. 0-94154  
 DNA, Hg (II) and Ag (I) complexes in soln., theoret. interpret. of elec. dichroism obs. 0-85347  
 DNA, linear dichroism in pulsed elec. field, meas. apparatus 0-90875  
 DNA, phase transitions in water-ethanol solns. (*Japanese*) 0-89709  
 DNA, possible conformations calcs. 0-76705  
 DNA, proton radiationless transitions for hydrogen bonds (*Russian*) 0-97857  
 DNA, supercoiled torsional stress and local denaturation 0-72131  
 DNA, torsionally stressed, equilibrium statistical mechanics of helix coil transition 0-67032  
 DNA, torsionally stressed, transitions between B- and Z-conformations, theoretical anal. 0-94166  
 DNA and RNA fragments, selective laser multistep excitation, uses 0-61122  
 DNA B-form, closer definition of struct. from X-ray diff. and energetic criteria 0-81533  
 DNA compact form, tertiary struct., small angle X-ray scatt. 0-72129  
 DNA conformational fluctuations, internal motion correl. times,  $^{31}P$  NMR obs. 0-72135  
 DNA derivative melting curves, automatic recorder using real time processing (*French*) 0-104833  
 DNA helix destabilising protein cryst., electron microscopy 0-85338  
 DNA hydrate, struct. conversions of sugar phosphate chain and nitrogenous bases, IR spectra 0-81530  
 DNA in conc. solns. of neutral salts, conformational transitions 0-81531  
 DNA interactions with cations, UV difference spectrosc. and Marcus theory 0-94153  
 DNA internal motions,  $^{31}P$  NMR and PMR 0-97855



**molecular biophysics continued**

- DNA solution, elec. birefringence, stabilised induced dipole behaviour 0-85349
- DNA-lipid interaction, IR spectroscopic obs., DNA compactisation on disperse particles 0-104550
- DNA's, natural, hypochromism, dependence on content and sequence of nucleotides 0-76711
- DNA[Cu<sup>2+</sup>], <sup>111</sup>In bound, rot. correl. times, from  $\gamma$ -ray perturbed angular correl. 0-94152
- dopamine, thermal blooming spectroscopy 0-86441
- electric birefringence transient, of macromol. solns. in reversing fields of arbitrary strength and duration 0-84719
- electron transfer processes, system of differential eqns., certain evaluations of solns. 0-76694
- electron tunnelling, thermal and photoassisted, theory, fast charge separation in photosynthesis 0-89730
- enzyme-catalysed reactions, network thermodynamic modelling 0-89463
- enzymes, molecular struct. reconstruction from electron microscopy images 0-89715
- epithelial mucus, rheology and mol. organisation 0-97959
- ethidium bromide E-DNA, intercalated birefringent fibres, microspectrophotometric investg. (*German*) 0-57392
- factor VIII, native and modified, surface adsorption and mol. interactions, ellipsometric obs. 0-104555
- fatty acid monolayers, light scatt. meas. 0-89011
- ferredoxin, Fe atoms at active centre, exchange integral of antiferromag. interaction 0-76697
- ferredoxin, *S. platensis* [2Fe-2S], struct. and evolution of chloroplast-type ferredoxins 0-94165
- ferrocyclochrome c<sub>1</sub>, anhydrous, ionisation pot., UV photoelectron spectrosc. obs. 0-85328
- ferrous nitrosylhaemoglobin, NO binding, spin distrib., orbital model and mag. props. 0-81534
- fibrinogen, adsorbed layers on polystyrene, contact angle meas. 0-61508
- fibrinogen, native and modified, surface adsorption and mol. interactions, ellipsometric obs. 0-104555
- flavins, meas. of sub ns fluoresc. decay by time-correl. photon counting and Ar laser 0-94429
- fluorescence spectroscopic investigations of the dynamic properties of proteins, membranes and nucleic acids 0-101148
- fluorescently labelled molecules as probes of living cells struct. and function, review 0-67321
- glutamine synthetase macromolecular struct., electron microscopy and image anal. 0-89716
- guanine, tautomeric forms protonation, ab initio HF Roothaan SCF calcs. 0-78534
- haematoporphyrine, complexed with chloranil and tryptophane, energy spectra, transition moments and intermolecular distances 0-72127
- haemocyanin of *Limulus polyphemus*, quaternary struct. 0-85337
- haemoglobin, human, maleimide spin labeled, proton ENDOR spectra obs. 0-89719
- haemoglobin, Jahn-Teller pseudo effect rel. to Fe release and conformational changes 0-76701
- haemoglobin, low freq. modes and excitation profiles, reson. Raman spectra 0-94428
- haemoglobin, mutual and tracer diffusion coeffs., photon correl. obs. 0-72123
- haemoglobin, nanosec. probe of dynamics using time resolved reson. Raman scatt. 0-94162
- haemoglobin, quaternary struct., hydration and self-association, <sup>1</sup>H NMR obs. 0-67040
- haemoglobin equilibria in soln., surface free energy model 0-81535
- haemoglobin haem structure after photo-deligation, Raman spectra 0-61510
- haemoglobin macroporous particle study, photoacoustic spectrometry 0-85543
- heat capacity function, of macromolecular systems, statistical thermodynamic analysis 0-61514
- high density lipoprotein-3 macromolecule observation using CTM and STEM with negative staining 0-85561
- hormonal steroids, <sup>13</sup>C NMR spectra 0-81543
- human serum Cu, EPR spectrum obs. 0-91582
- hydrocarbon chains in a lipid bilayer conformational anal. 0-81532
- hydrodynamic properties of rigid macromolecules, modelling approaches 0-61613
- interstellar molecules in prebiological evolution 0-94726
- kinetic IR spectroscopy IR, appl. to biochem. systems 0-98178
- $\beta$ -lactam antibiotics, ab initio SCF-MO-LCAO calcs., amidic bond breaking, methoxy substitution effect 0-78533
- laser Raman scattering, mol. probe of contractile state of intact single muscle fibres 0-89718
- leghaemoglobin, thermal denaturing in cryst. and soln. 0-108849
- librational motion effects on fluoresc. depolarisation and NMR relax. in macromols. and membranes 0-85324
- light scattering, dynamic, by flexible macromols. in fluctuating elec. field 0-84722
- light scattering from macromolecular soln. in alternating elec. field, low angle approx. 0-84721
- lipid bilayer couple, cation-phospholipid-induced shape changes 0-108855
- lipid bilayer phase transition, cholesterol effect 0-85361
- lipid hydrocarbon chain, biomembrane, rot. motion and fluidity 0-76714
- lipid monolayer, simulation using mol. dynamics 0-108838
- lipid thermotropic clustering in *Tetrahymena* endoplasmic reticulum membranes 0-85363
- liver alcohol dehydrogenase, proton relay system, SCRF PCE theory, CNDO/2 calcs. 0-85325
- lysozyme, search for superconducting regions 0-101149
- lysozyme hydration, correl. of diverse types of meas. 0-61507
- macromolecular solution, rot. diffusion coeff. calc. method w.r.t. mol. struct., elec. birefringence relax. time data interpret. 0-85331
- macromolecule, high resolution struct. determ. by electron microscopy 0-89717
- macromolecules, biological, selection models, with time varying constraints 0-67029
- macromolecules, conformation studied by calorimetry, review 0-97870
- macromolecules, impurity action of transition metal ions in variable oxidation states 0-85329
- magnetic circular dichroism of biological molecules, review, book contrib. 0-109080
- membrane preparatory procedures, for electron microscopic anal., at mol. level resoln. 0-104843

**molecular biophysics continued**

- membranes, structural order of lipids and proteins, fluoresc. anisotropy data eval. 0-97873
- metalloenzymes, model for biological active sites, ab initio calcs. 0-104551
- metalloporphyrin, cation radical formation by pulse radiolysis, oxidation and demetalation rate consts. 0-61505
- metalloproteins, metal nuclei, biophysical appls. of NMR, review, book contrib. 0-109081
- methaemoglobin, struct. change on addition of inositol hexaphosphate 0-72130
- methotrexate-dihydrofolate reductase complex form., conform., laser Raman obs. 0-104553
- Mossbauer spectrometry of Fe in hepatic and splenic tissues 0-81544
- multi-enzyme complex carrying out electron transfer, asymptotic anal. of functioning 0-81523
- multistate systems, freq. of cyclic processes 0-108834
- muscle, contracting, dynamic structure, X-ray scatt., time resolved, rapid data collection systems 0-61740
- muscle, F-actin subunits of thin filaments, functional role of struct. non-equivalence 0-76704
- muscle, skeletal, water protons NMR relax. times anisotropy obs. 0-85341
- muscle chemo-mechanical energy transduction, mol. basis 0-72143
- muscle contraction, single, high-time resolution X-ray investigation method 0-81777
- muscle contraction process, 10 ms time resolution X-ray diff. 0-61741
- muscle cross bridge rotation during contraction, fluctuations in polarised fluoresc. 0-97856
- myoglobin, refolding kinetics by diffusion-collision-adhesion model 0-94157
- myoglobins, Fe-, Co-substituted, O<sub>2</sub> binding, comparisons, thermodynamic investg. 0-67030
- myosin, struct. changes in living muscle fibres, polarised UV fluoresc. microscopy 0-67037
- nerve action pot., lipid bilayer local phase transition 0-89744
- nicotinamide adenine dinucleotide, and reduced form, pH induced modification, Raman spectra 0-85343
- nitrosylhaemoglobin, electron spin distrib. 0-83528
- non-centrosymmetry, optical second harmonic generation 0-72133
- nonpolar molecules, adsorption into lipid bilayer membranes 0-61517
- nucleic acids, bases and base pairs, water struct. in soln., Monte Carlo simulation 0-76709
- nucleic acids, electron microscopy using basic protein film method 0-104844
- nucleic acids and their aggregates, optical activity, review, book contrib. 0-108847
- nucleic acids bases, excited state dipole moments and geometries 0-95738
- nucleosomes and nucleosomal DNA, electro-optical props., relax. times and chain struct. 0-85350
- 3'-nucleotide, calcs. to assess rigidity 0-61506
- nucleotide base stacking interactions in vacuum, field mass spectrometry 0-81526
- optically active molecule separation asymmetry by longitudinally polarised relativistic electrons (*Russian*) 0-94172
- oriented DNA, hydration, neutron scatt. obs. 0-89714
- origin of life, chem. evolution (bibliography) 0-90620
- origin of life, mol. biophys. basis 0-94158
- origins, autobiographical review 0-57052
- oxyhaemoglobin-hydrazine (dimethylhydrazine) interaction,  $\gamma$ -reson. spectroscopy 0-81525
- oxymyoglobin, evidence for conformational and diffusional mean square displacements 0-89713
- oxytocin, H bond linking ring and tail  $\beta$ -turns, biofunctional evaluation 0-61511
- pancreatic trypsin inhibitor, bovine, macromol. dynamics, high resolution NMR investg. 0-91708
- papain probes, active site  $\alpha$ -helix and ion pair stability 0-74265
- peptides, bradykinin-potentiating, spatial structs. 0-95736
- phosphatidylcholine bilayers, fluidity changes and phase transitions, intramol. excimer fluoresc. obs. 0-85342
- phospholipid bilayer, one- and two-component, main phase transition, Landau phenomenological theory 0-97872
- phospholipid bilayers, carbonyl groups dynamics, <sup>13</sup>C chem. shift anisotropy obs. 0-85326
- phospholipid bilayers, low temp. transition from fluid state 0-97871
- phosphoryl transfer enzymes, biophysical appls. of NMR, review, book contrib. 0-109081
- photoelectrochemical conversion, using bacteria reaction centre working on SnO<sub>2</sub> electrode 0-94092
- photosynthesis, analogue reaction in a porphyrin-quinone linked mol. 0-89720
- photosynthesis, electron transfer reactions in carrier mol. complexes, kinetics and thermodynamics 0-108859
- photosynthetic reaction centre chromophore organisation, high-resolution magnetophotoselection 0-97880
- photosynthetic systems, discovery of phase transitions 0-81539
- $\beta$ -phycocyanin crystals, twinned by merohedry, diff. data treatment 0-108845
- plant fibre temperature stability investigation, rotary diffusion, spin label obs. 0-81529
- polymers, electro-optical changes, chem. and rotational contribs. 0-85352
- polynucleotide electron energy band studies 0-72132
- polynucleotide solution, elec. birefringence, stabilised induced dipole behaviour 0-85349
- polypeptide, conformational change induced by strong elec. field 0-85336
- polypeptide chains, struct. of conduction and valence band 0-76700
- polypeptides, comparison of conformational possibilities 0-94163
- polypeptides, electronic struct., side-chain disorder effect 0-76706
- polypeptides, helix-coil transition dynamics, time correl. function theory 0-99591
- polyribonucleotides, dye tagged, aqueous solns., elec. induced fluoresc. changes 0-85346
- protein, structure and bonding, quantum theory, ab initio calcs. 0-61509
- protein adsorbed layers on field-emitter tips, removal by UV radiation 0-104836
- protein analysis using PIXE 0-61691
- protein beta sheet structures, anal. and prediction by combinatorial approach 0-76710
- protein, cryst. struct. analysis by electron diff., single scatt. approx., domains of validity 0-101150



# molecular biophysics continued

- protein internal charge transfer, ascorbic acid adduct model systems, SCF calc. 0-69072
- protein-peroxide radicals,  $^{17}\text{O}$ -labelled, EPR obs. 0-85345
- proteins,  $\alpha$ -helical, possible role in membrane charge transfer processes 0-81524
- proteins, amino acid neighbourhood relationships, breakdown into overlapping doublets, triplets, and quadruplets 0-67035
- proteins, conform. anal., algorithms and data structs. for array processing 0-83530
- proteins, globular, in water, proton NMR spin echo decay comparative investigation 0-81541
- proteins, representation, unique method 0-67036
- proteins involved in active membrane transport, struct. review, book contrib. 0-108844
- protoporphyrin IX, triplet states, flash photolysis, obs. 0-95555
- protoporphyrin IX dimethyl ester, triplet states, flash photolysis, obs. 0-95555
- purple membrane, orthorhombic 2D crystal form 0-85362
- purple membrane fragment suspensions, elec. dichroism obs., trimer model interpret. 0-89728
- pyrene, migration between lipid vesicles in aq. soln., fluoresc. stopped-flow obs. 0-85360
- pyrimidine nucleotides, UV reson. Raman excitation profiles 0-58265
- pyrimidines, substituted analogues, absorption UV spectroscopy and electronic struct. of ionic and tautomeric forms 0-74177
- pyrophosphatase, inorganic, of yeast, cryst. growth, derivatives formation, heavy atoms positions 0-108842
- quinacrine mustard, 2-step laser-induced photodamage 0-85198
- relaxation times in solid-state theory and one-dimensional molecular systems (Russian) 0-100640
- resonant interactions 0-72128
- retina, bovine, R2 component of early receptor pot. rel. to metarhodopsin II form. 0-97904
- retinal chromophore, reson. Raman spectra obs. of struct. 0-94168
- retinal photoreceptors, small angle X-ray data processing 0-81536
- Rhacopholus embryo yolk platelets, freeze fracture study of crystalline struct. 0-104552
- rhodopsin,  $\alpha$ -helix orientation, spectroscopic study 0-89711
- rhodopsin chromophore, and desmethyl analogues, theory 0-94169
- ribonuclease A, bovine, cryst. struct. determ. by X-ray and neutron diff. 0-108841
- ribonuclease A, microviscosity, mobility profile 0-91710
- ribosomal component, cryst. struct. at 2.6 Å resolution 0-97859
- RNA, conformational fluctuations, internal motion correl. times,  $^{31}\text{P}$  NMR obs. 0-72135
- sarcoplasmic reticulum membranes, small angle X-ray data processing 0-81536
- satellite tobacco necrosis virus struct., detect. and idealisation procedures of non-crystallographic symmetry with phase refinement appl. 0-108840
- scanning microcalorimeters for studying macromolecules 0-61747
- SCF-LCAO-ASMO and CI calcs. of low-lying multiplets and excited states 0-94155
- self-organizing molecular system, dynamics 0-67028
- self-reproducing macromolecules, selection, controlled energy fluxes constraint 0-67027
- serine, neutral and zwitterion, water solvation, Monte Carlo simulation 0-76707
- serum albumin, bovine, hydrated, dielec. and elec. props. 0-97854
- serum albumin, bovine, mutual and tracer diffusion coeffs., photon correl. obs. 0-72123
- serum low density lipoprotein, human, anomalous permittivity behaviour 0-81540
- solution X-ray scattering, review of recent developments, book contrib. 0-109077
- southern bean mosaic virus, struct. at 2.8 Å resolution 0-85334
- symmetry in systems 0-81519
- thiourea, struct., hydration, ab initio SCF calcs. 0-58142
- thymopietin active fragment in  $\text{H}_2\text{O}$ , soln. conformation by DNMR spectroscopy 0-89710
- tissues, normal and malignant, pulsed NMR obs. 0-94171
- triplet states in photosystem I of spinach chloroplasts and subchloroplast particles, EPR obs. 0-85344
- tRNA in soln., selected topics review, book contrib. 0-108839
- tryptophan residue in horse liver alcohol dehydrogenase, room-temp. phosphoresc., temp. and enzymic complex form. effects 0-61512
- $\text{N}_2$ -undecylmethylflavin, high resolution fluoresc. and excitation spectroscopy, vibronic transitions obs. 0-78639
- urea molecule, bond-length corrections for external and internal vibrs. 0-106402
- uric acid occurrence, growth morphology of  $\text{C}_3\text{H}_4\text{N}_4\text{O}_3$  anhydrous monoclinic modification 0-84123
- valinomycin in its Ba complex, novel conformation 0-94167
- viroid RNA, covalently closed circular mols., conform. states 0-85340
- vision, molecular basis 0-108876
- water localisation in a DNA mol. by differential Fourier synthesis 0-94164
- X-ray diffraction patterns of seed materials subjected to mag. field 0-89721
- x-ray diffraction studies of the heart, review, book contrib. 0-109079
- Be complexes, binding and orbital energies, biological systems ab initio calc. 0-102442
- $(\text{Be}(\text{OH})(\text{NH}_3)_2)^+$  model for biological active sites, ab initio calcs., comparison with Zn complex 0-104551
- CO-myoglobin, mol. tunnelling, isotope effect, time resolved IR Fourier transform obs. 0-72126
- CsDNA of T2 phase, in classical crystn. B form, struct., amplitudes, synchrotron radiation diffraction 0-85335
- $\text{H}_2\text{O}$  in biological samples, PMR, fast-exchange model interpretation via diffusional kinetics clarified 0-67033
- Li complexes  $(\text{C}_2\text{H}_2\text{X}_2)_2\text{Li}^+$  where  $\text{X}=\text{S}, \text{O}$ , binding and orbital energies, biological systems ab initio calc. 0-102442
- $(\text{Zn}(\text{OH})(\text{NH}_3)_2)^+$  model for biological active sites, ab initio calcs., comparison with Be complex 0-104551

# molecular bonds see bonds (chemical)

# molecular clusters

- acetic acid vapours, clustering, effect of supersonic mol. beam sampling, mass spectrometric study 0-104481
- admolecule association on conductor surfaces (Russian) 0-80078

# molecular clusters continued

- alkali metal hydroxide clusters in gas phase, high press. mass spectrometry, atmospheric implications 0-58436
- n-t-butanol in alkanes, molecular relaxation processes studied by  $^{13}\text{C}$  NMR 0-63654
- cluster beam, multiple stage ioniser, spatial potential distribution and electron trajectory calcs. (Japanese) 0-99596
- electron attachment to mol. and mol. clusters, electron-mol. collision, Rydberg electron exchange 0-63843
- electronic structure calcs. with double self-consistency-Bersuker's method 0-69289
- ethanol, H-bonding investigated with supersonic mol. beam using photoionisation quadrupole mass spectrometer 0-102543
- ethylene( $\text{d}_4$ ) clusters, IR photodissoc. 0-89506
- hydroxonium complexes, produced by collisional dissoc. method, mass spectrometric study, dissoc. energies determ. 0-95707
- ion cluster emission in SIMS, parity rule applies. (French) 0-63882
- ionic clusters, struct., thermodynamic functions, energy surfaces and SIMS 0-63881
- liquid organic compound ionisation under atm. press. 0-86488
- metal clusters, UPS 0-80940
- methanol ( $\text{d}$ ), H-bonding investigated with supersonic mol. beam using photoionisation quadrupole mass spectrometer 0-102543
- methyl( $\text{d}_3$ ) ions, association reactions, isotopic exchanges, SIFT study, review 0-58435
- polynuclear clusters, programs for calc. electronic struct. by Mulliken-Wolfsberg-Helmholtz method 0-69288
- serine, neutral and zwitterion, water solvation, Monte Carlo simulation 0-76707
- small clusters, formations, struct. and props. 0-58437
- styrene-sodium methacrylate copolymers, Raman spectra, ion clustering 0-71416
- tetracene molecules in Ar clusters, excited state intramol. dynamics, laser-induced fluoresc. spectra obs. 0-78674
- trifluoroethanol, H-bonding investigated with supersonic mol. beam using photoionisation quadrupole mass spectrometer 0-102543
- $\text{Al}^{3+}(\text{H}_2\text{O})_n$  ( $n=1,2,4,6$ ), FSGO-pair-pot. calcs. (German) 0-74278
- $\text{Be}^{2+}(\text{H}_2\text{O})_n$  ( $n=1,2,3,4,6$ ), FSGO-pair-pot. calcs. (German) 0-74277
- $\text{Bi}_n$  molecular clusters, laser fluoresc. spectrosc. 0-95755
- $\text{D}_3\text{O}^+(\text{H}_2\text{O})_{0.1,2}+\text{H}_2\text{O}$  reactions, SIFT studies, review 0-58435
- $\text{F}(\text{H}_2\text{O})_n(n=1,2)$ , FSGO-pair-pot. calcs. (German) 0-74278
- GaAs, eliminating  $\alpha$  exchange parameter in multiple scatt. method 0-103652
- $\text{H}_2\text{F}_2$  and  $\text{H}_3\text{F}_3$  clusters, molecular structures, ab initio calcs. 0-83532
- $\text{H}^+(\text{H}_2\text{O})_n$  ion-induced water clusters, mass spectra, IR continuum absorpt. 0-87257
- $\text{H}_2\text{O}$ , charged clathrates, model for formation and stabilisation 0-91714
- $\text{H}_2\text{O}-\text{H}_2\text{SO}_4$  ion aerosol particles, ultrafine, stratospheric form., ion-induced nucleation 0-72608
- $\text{H}_2\text{O}^+(\text{H}_2\text{O})_{0.1,2}+\text{D}_2\text{O}$  reactions, SIFT studies, review 0-58435
- $\text{Li}_n^{(n-1)+}$ , energy cluster expansion convergence 0-91715
- $\text{Li}^+(\text{H}_2\text{O})_n$  ( $n=1,2,3,4,6$ ), FSGO-pair-pot. calcs. (German) 0-74277
- $\text{Mg}^{2+}(\text{H}_2\text{O})_n$  ( $n=1,2,4,6$ ), FSGO-pair-pot. calcs. (German) 0-74278
- $\text{Mo}_x\text{S}_8$  cluster cpds. ( $\text{X}=\text{F}, \text{Cl}, \text{Br}, \text{I}$ ), SCF-SW-Xa calcs. 0-74276
- $\text{NO}_2$  hydrate clusters, ground-state HF pot., Monte Carlo simulation, energy surfaces and rot. barriers 0-106412
- $\text{NO}_3^-(\text{HNO}_3)_n$  clusters, form. studied by mass spectrometry, thermodynamic functions, sol. struct., 0-95754
- $\text{Na}^+(\text{H}_2\text{O})_n$  clusters, gas phase, high press. mass spectrometry, atmospheric implications 0-58436
- NaCl crystals, electronic and hole centres and surface, quantum-chemical calcs. 0-65489
- $\text{Na}^+(\text{H}_2\text{O})_n$  ( $n=1,2,4,6$ ), FSGO-pair-pot. calcs. (German) 0-74278
- $\text{NiO}$ , bulk props., initial state  $\text{MO Ni}_2\text{O}_4$  and  $\text{Ni}_3\text{O}_{14}$ , cluster model, lattice and force const., photoemission and CT absorpt. spectra 0-84828
- $\text{O}_4^+(\text{O}_4^+)(\text{O}_4^+)(\text{O}_2^+ \text{H}_2\text{O})$  0-95707
- $\text{Os}_8(\text{CO})_{18}$ , electronic struct., metal cluster carbonyls mol. orbital description obs. 0-63879
- Si, ambient effect of O precipitation, self interstitial mechanisms, IR spectra, TEM study 0-66510
- molecular collision processes** see elastic scattering of atoms and molecules; molecular inelastic collisions
- molecular configuration interactions** see molecular electron correlations
- molecular configurations**  
see also bond angles; bond lengths; inorganic molecule configurations; isomerism; macromolecular configurations; molecular orbitals calculations; organic molecule configurations; X-ray diffraction examination of molecular structure
- bound-state properties calcs., theoretical error estimates 0-102425
- bridge angle, vibr. behaviour, simplified and accurate calcs. 0-95735
- chemical bonding, antisymmetrised geminal power and simple correlated wave function 0-102423
- chemical bonding studied using scattering theory concepts 0-103289
- chemical reactivity, reliability of quantum mechanical predictions, config. of reaction prod., H-bonded species 0-108691
- clusters, small, formation, struct. and props. 0-58437
- direct CI calcs. with multiconfigurational reference state 0-63506
- excited states, variable metric optimisation of mol. geometry 0-58178
- gas linear molecules, symmetrised Liouville basis vectors, appl. to spectral linewidths 0-83457
- geometry optimisations, invariance criteria, symmetry conservation rules 0-58406
- influence of solvent struct. on conformations 0-91700
- intramolecular interactions effect on transferability props. of localised description of chemical groups 0-102424
- matrix isolated molecules, energy accumulation by migration to geometric trap configurations 0-78691
- molecules under static mag. field, gauge invariance 0-102587
- nonlinear molecules, tetrahedra, symmetry constraints on configurational props. 0-63854
- nonrigid molecule, sum of states, isometric group, symmetry no., thermodynamic functions 0-58186
- nonrigid molecules, dipolar relax. and nuclear Overhauser effects, fluctuating internuclear distances effect 0-91578
- optically active mols., coherent Raman scatt., quantum theory 0-69150
- optically active mols., Raman and Rayleigh scatt. angle anal. 0-69151
- PCIO-INDO method, theory and apps. 0-58153
- polyatomic molecule, atomic force correlation functions for determ. vibr. relax. rates, role of mol. symmetry 0-83337



**molecular configurations continued**

- polyatomic mols., vibr. total energy distrib. in terms of symm. coords., forces and momenta 0-69123  
 quantum mechanical aspects of the molecular structure hypothesis 0-102421  
 quantum mechanical view of molecular structure and shapes 0-102422  
 quantum theory, concept of mol. struct., interpretation problems 0-106248  
 quantum topology, theory of mol. struct. and its morphogenesis 0-106247  
 rigid XYX and nonrigid three-body systems, correlation diagram 0-69249  
 ring characterisation method 0-63853  
 similarity, electron density function meas. 0-91413  
 small molecules, localised charge densities calcs., bond length effects 0-83256  
 structure and dynamics of mols. by pulsed mol. beams 0-102563  
 symmetrical molecules, reorientation spectroscopic meas. models 0-58405  
 topological indices for branching of tree-like graphs 0-57076  
 topological spaces, structs. 0-91701  
 twisted conjugated molecule, zwitterionic excited states investig. 0-58179  
 two and three-centre molecules, periodicity and internal torsional conformers around single bond, symmetry analysis 0-69250  
 XY<sub>6</sub>(O<sub>8</sub>) octahedral system, F-(G)-matrix elements setting-up, transformation rules (*German*) 0-58242

**molecular conformations** *see molecular configurations***molecular dissociation**

- see also heat of dissociation; molecular dissociation energies; molecular electron impact dissociation; molecular photodissociation; molecular predissociation*  
 acetic acid, vapour, chem. reaction effect on speed of sound 0-103100  
 acetylene, reaction with Ni (100) and (110), room temp., UPS expts. 0-61151  
 alkyl halide and  $\sigma^*$  anion radicals, stability 0-89468  
 anthracenes, exciplex form. with amines, form. kinetics and luminesc. props. 0-66792  
 atom+diatomic molecule, restricted 2-D Morse oscillator model, semiclassical calcs. for mol. dissoci. 0-74222  
 2-butene ion, fragmentation, angular momentum in ion-mol. reacts., RRKM calc. 0-66773  
 clusters, small, formation, struct. and props. 0-58437  
 collision processes, angular correlations, summary of review papers 0-63757  
 collision-induced, tandem mass spectrometer obs. 0-62790  
 collisionally induced dissociation, struct. determ. 0-66357  
 cyclobutane decomposition, vibr. excitation transients using variable encounter method 0-61072  
 diatomic molecules, dissoci., vibr.-rot. excitation effects 0-102502  
 diatomic molecules at low press., dissociative instability, role of vibr. energy 0-74227  
 dibromoalkanes, energy partitioning in mass spectrometric displacement reactions 0-89471  
 electronic polarization in solids probed by dissociation of fast molecular ions 0-71530  
 ethane, unimol. decomp., energy transfer processes, Monte Carlo simulation 0-99555  
 ethyl acetate, gas, radiatively heated by CO<sub>2</sub> laser, cooling mechanism investig. 0-75021  
 ethylene, adsorption and decomposition on Ni films, coverage depend. meas. 0-96743  
 fast molecular ions, break-up on collision with solids 0-66353  
 fast molecular ions, collision induced fragmentation 0-66354  
 fluoriodomethane, vibr. excited, dissociation, trajectory calcs. using pot. energy surface parameters 0-76508  
 formic acid, fragmentation, fragment structs. and energies calcs. 0-74124  
 formic acid, on Ni surface, decomp., dipole interactions effects 0-61143  
 formic acid ions, fragmentation, energy selected, photoelectron-photoion spectra 0-95676  
 gases, radiatively heated by CO<sub>2</sub> laser, cooling mechanism investig. 0-75021  
 haemoglobin equilibria in soln., surface free energy model 0-81535  
 1,5-hexadiyne, time-depend. mass spectra, ionisation efficiency and breakdown curves 0-95747  
 hexanes, isomeric, unimol. decomp. processes following field ionisation, temp. depend. 0-95733  
 hydrazine, decomp. on Ir(111) surface, N<sub>2</sub> emission, ang. depend. 0-97731  
 hydrazine adsorbed on Al, decomp., XPS obs. 0-92783  
 hydrides, aq. dissoci., solvation, MINDO/S calcs. solvation theory 0-97708  
 indirect dissociative recomb., T-matrix element, Feshbach's projection operator technique 0-58114  
 methane-d<sub>0</sub>-(d<sub>4</sub>), unimol. decomp., energy transfer processes, Monte Carlo simulation 0-99555  
 methanol, ionic dissoci., photoelectron-photoion coincidence spectroscopy 0-66774  
 naphthylamines, abnormal fluorimetric titration behaviour, kinetic anal., fluoresc. quantum yields and lifetime meas. 0-89560  
 perfluorobenzene, electron attachment, radiative and dissoci., negative ion lifetimes, ion cyclotron reson. spectra 0-74251  
 perfluorocarbon-SF<sub>6</sub> mixtures, sparking C inhibition, decomp. product investig. 0-89478  
 perfluorocyclobutane, electron attachment, radiative and dissoci., negative ion lifetimes, ion cyclotron reson. spectra 0-74251  
 perfluoromethylcyclohexane, electron attachment, radiative and dissoci., negative ion lifetimes, ion cyclotron reson. spectra 0-74251  
 perfluorotoluene, electron attachment, radiative and dissoci., negative ion lifetimes, ion cyclotron reson. spectra 0-74251  
 RRKM formula correction by non Boltzmann character factors, Markov eqns. 0-71891  
 RX<sup>-</sup>, radical anion stability conditions, pot. energy diagrams 0-85161  
 Saha equation, elementary derivation, rel. to mol. dissoci. 0-82599  
 thermal desorption and dissociation catalyzed by a solid surface 0-108734  
 trifluoromethanesulphonic acid, and salts, electrochem. characts. in nonaqueous solvents 0-89499  
 unimolecular decomp. kinetics, rot. effects 0-81319  
 water molecule, photoassisted decomposition at SrTiO<sub>3</sub> surface 0-85202  
 BiLi, gas phase thermodynamics, Knudsen effusion mass spectrosc. 0-100057

**molecular dissociation continued**

- Br<sub>2</sub>+Ar collisions, dissociation reaction, trajectory study by ensemble method 0-66765  
 C-H, A<sup>2</sup> $\Delta$ -X<sup>2</sup> $\Pi$ , dissociative excitation, form. environment and parent mol. effects 0-78682  
 CH<sub>4</sub><sup>+</sup>, Jahn-Teller distortion, energy and angular distrib. of collisional dissociation fragment 0-66356  
 CO, chemisorbed on Mo (100), surface kinetics, photoemission study method 0-80941  
 CO<sub>2</sub> CW laser, vibr. temp., dissoci. and gain limitation determ., new technique 0-87369  
 CO<sub>2</sub> dissociation in a nonequilibrium plasma 0-87851  
 CO<sub>2</sub>, dissociation into CO and O<sub>2</sub>, H<sub>2</sub> production from CO+steam, fusion reactor heat 0-67014  
 CO<sub>2</sub> sealed high-pressure pulsed laser, gas equilibrium chemical comp. 0-63972  
 CO<sub>2</sub>+Ar\*, CO\* prod., use in laser systems 0-63824  
 CS<sub>2</sub>, shock heated, visible emission 0-58274  
 CaCl, X<sup>2</sup> $\Sigma$  pot. energy curves, polarisability and dissoci. 0-91629  
 D+HX (X=Cl, I), HX dissociative ionisation, H<sup>+</sup> signal origin, mol. beam obs. 0-66778  
 D<sub>2</sub><sup>+</sup>, dissociation on impact with mylar foil 0-67164  
 $\beta$ -FeOOH, dehydration 0-79767  
 H<sup>+</sup> form. by surface and vol. processes, neg. ion source appl., review 0-58375  
 H+D<sub>2</sub>, collinear motion, energy transfer and dissociation, collision dynamics 0-99563  
 H<sub>2</sub> adsorption on Ni (001) surface, mol. dissoci., calc. 0-101036  
 H<sub>2</sub><sup>+</sup> differential cross section rel. to charge exchange cross sections of fragments 0-78704  
 H<sub>2</sub><sup>+</sup>, dissoci. recombination, doubly excited Rydberg states 0-83506  
 H<sub>2</sub><sup>+</sup>, internuclear separations distrib. in 3.0 MeV collisions with C foils 0-71529  
 H<sub>2</sub><sup>+</sup>+Ar, low energy proton transfer reactions, crossed beam studies 0-108697  
 H<sub>2</sub><sup>+</sup>+methanol, dissoci. charge transfer reaction studied at rel. translational energies from 600 eV to 5000 eV 0-104432  
 HBr, fine struct. in dissociative attachment cross sections 0-87248  
 HCl dissociation for XeCl(B) formation in electron beam assisted Xe/HCl laser discharge 0-63988  
 HCl, dissociative electron attachment, differential cross section, Feshbach resons. 0-83508  
 HF, fine struct. in dissociative attachment cross sections 0-87248  
 H<sub>2</sub>O<sup>+</sup>, ab initio potential-energy surface study by CI techniques, equilibrium conform. determ., mol. dissoci. pathways 0-78550  
 H<sub>2</sub>O<sup>+</sup> (D<sub>2</sub>O<sup>+</sup>), plasma dissociative ion electron recomb., rate coeffs. 0-63747  
 He+H<sub>2</sub>, mol. energy transfer by quasiclassical trajectory methods, vibr. relax. and dissoci., rot. effect 0-99557  
 He<sup>+</sup>+H<sub>2</sub>(D<sub>2</sub>), dissociative charge transfer, 78-330K 0-61079  
 He<sup>+</sup>+methanol, dissoci. charge transfer reaction studied at rel. translational energies from 600 eV to 5000 eV 0-104432  
 He<sup>+</sup>+SO<sub>2</sub>, dissoci. charge transfer reaction, SO<sup>+</sup> (A<sup>2</sup> $\Pi$ -X<sup>2</sup> $\Pi$ ) emission 0-95659  
 He<sub>2</sub> high press. afterglows, reviews 0-64823  
 He<sub>2</sub>, high-order replacements inclusion in CI calc. 0-63504  
 (HeH)<sup>+</sup>, breakup in single dissociative collision, fragment charge states 0-74226  
 HeH<sup>+</sup> dissoci. on impact at C. foil, emitted light polarisation meas. 0-58361  
 HeH<sup>+</sup>, foil induced dissociation, H<sup>0</sup> prod. 0-66355  
 HeH<sup>+</sup>, internuclear separations distrib. in 3.0 MeV collisions with C foils 0-71529  
 HgBr<sub>2</sub>+inert gas metastable atom (N<sub>2</sub>(A<sup>3</sup> $\Sigma_u^+$ )), dissoci. excitation 0-63774  
 HgBr<sub>2</sub>+N<sub>2</sub><sup>\*</sup>, dissociative excitation, mol. fluoresc. obs. 0-91634  
<sup>129</sup>I<sub>2</sub>, energy levels near B-state dissoci. limit, two-photon spectrosc. obs. 0-106367  
 N<sub>2</sub>, electron impact dissoci., EELS, N<sup>-</sup> autoionisation 0-106397  
 N<sub>2</sub><sup>+</sup>+H<sub>2</sub>, collisional dissoci. cross-section, 2.4-24.3 keV 0-58373  
 N<sub>2</sub><sup>+</sup>+O<sub>2</sub>, collisional dissoci. cross-section, 2.4-24.3 keV 0-58373  
 NH radical formed in NH<sub>3</sub> dissoci., fluoresc. spectrum, rotational relaxation 0-58310  
 NH<sub>3</sub>, adsorption of Al surface, NH<sub>3</sub> decomp., XPS obs. 0-92783  
 NH<sub>3</sub>, chemisorption on Ni (111) and reaction, LEED, desorption and photoemission expts. 0-59799  
 NO<sub>2</sub>, shock heated, visible emission 0-58274  
 NO<sub>2</sub>(N<sub>2</sub>O<sub>2</sub>) surface decomposition, resonance and spontaneous Raman spectra 0-61144  
 O source with improved long term stability for chemiluminescence reaction, mol. dissoci. and recombination 0-93758  
 O<sub>2</sub>, two-dimensional adsorbed layer on graphite, props. calc. 0-103568  
 OH<sup>+</sup>, Coulomb explosion in 11.2 MeV collisions with C foils 0-66358  
 PbLi, gas phase thermodynamics, Knudsen effusion mass spectrosc. 0-100057  
 SO<sub>2</sub>, interaction with NiO (100) surface, electron diff. and Auger spectrosc. obs. (*French*) 0-97728  
 SO<sub>2</sub>, shock heated, visible emission 0-58274  
 SO<sub>2</sub> surface reaction and decomposition on zeolites, resonance Raman study 0-61145  
 SO<sub>2</sub>+Ar, dissoci. rate meas. behind shock wave, laser Schlieren method 0-81296  
 SeCl<sub>4</sub>-SbCl<sub>5</sub> systems, Raman spectra (*German*) 0-93324  
 Sr<sup>2</sup> dimer, photoassoc., photoluminesc., collisional dissoci. 0-58303  
 UO<sup>+</sup>+Ar, collision-induced dissoci. cross section and threshold 0-95706  
 UO<sub>2</sub><sup>+</sup>+Ar, collision-induced dissoci. cross section and threshold 0-95706  
 URu<sub>3</sub>, sublimation thermodynamics 0-97722  
 Xe+Cl<sub>2</sub>, classical trajectory calcs., energy threshold for collision induced dissoci. determ., 0-95709

**molecular dissociation energies**

- butyl cation, H-elimination, energy partitioning, transition state geometry calc. using MINDO/3 0-104430  
 diatomic molecules, spectrosc. determ., near-dissoc. expansions 0-83513  
 diatomic molecules, dissoci. energy determ., Simmons-Parr-Finlan pot. calcs. 0-58128  
 hydroxonium complexes, produced by collisional dissoci. method, mass spectrometric study, dissoci. energies determ. 0-95707  
 metals, atomic binding energy and surface energy rel. to prediction of physical props. 0-59434



**molecular dissociation energies continued**

- polyatomic mol. force consts. and heat of atomisation, approx. separable pot. function 0-78675  
 $\text{Al}_2\text{Cl}_6$ , matrix isolated, vibr. spectra, isotopic fine struct. and valence force field calcs. 0-58258  
 $\text{Ba}^+ + \text{D}_2 \rightarrow \text{D} + \text{BaD}^+$ , sequential impulse model, prod. bond dissoci. energy and cross section 0-81295  
 $\text{BaOH}$ , ( $\text{BaCl}$ ), mol. dissoci. energies calc. by high temp. mass spectrometer 0-83514  
 $\text{BeAr}^+(\text{X}^2\Sigma^+)$ , spectrosc. determ., near-dissoc. expansions 0-83513  
 $\text{C}_2(\text{C}_2^-)$  pot. energy curves calc. using SCF, MCSCF and CI methods, dissoci. energies, bond lengths, electron affinity 0-95523  
 $\text{CO}_2$ ,  $\text{CO}_2^+$  + ethylene, rate coeffs. and product distribution determ., dissoci. energy and heat of form. 0-97693  
 $\text{Ca}_2$ ,  $\text{A}^2\Sigma_u^+ - \text{X}_2\Sigma_g^+$  system, laser induced fluoresc., pot. energy curve and mol. consts. 0-58307  
 $\text{Ca}_2$ , ground state, multiple scatt.  $\text{X}\alpha$  calcs. 0-58149  
 $\text{CaO}$  dissoci. energy from  $\text{Ca} + \text{O}_2$  chemiluminesc. 0-97697  
 $\text{CeO}$ , dissoci. energy, rel. band strengths of  $\text{a}_2\text{-X}_2$  and  $\text{b}_2\text{-X}_2$  systems 0-99495  
 $\text{ClO}$ , dissoci. energy and bond length, CI calcs., bond function effects 0-102450  
 $\text{FeO}$ , gas, thermochem. props., mass spectrosc. meas. 0-101034  
 $\text{FeOH}$ , gas, thermochem. props., mass spectrosc. meas. 0-101034  
 $\text{HeCN}^+$ , SCF calcs., dissoci. energies, rot. and hyperfine const. determ. 0-95531  
 $\text{I}_2\text{Ar}^+$ , product state distrib. and binding energy 0-63857  
 $\text{I}_2\text{He}^+$ , product state distrib. and binding energy 0-63857  
 $\text{I}_2\text{Ne}^+$ , product state distrib. and binding energy 0-63857  
 $\text{Mg}_2$ , ground state, multiple scatt.  $\text{X}\alpha$  calcs. 0-58149  
 $\text{MgOH}$  ( $\text{MgCl}$ ), mol. dissoci. energies calc. by high temp. mass spectrometer 0-83514  
 $\text{NeCN}^+$ , SCF calcs., dissoci. energies, rot. and hyperfine const. determ. 0-95531  
 $\text{NiCu}$  molecule, electronic states determ. by ab initio HF and CI methods 0-69087  
 $\text{O}_2^+(\text{O}_2^+)(\text{O}_2^+)(\text{O}_2^+ + \text{H}_2\text{O})$  0-95707  
 $\text{Rb}^+$ , dissoci. energy from ionisation rate coeffs. of  $\text{Rb} + \text{Rb}$  0-58363  
 $\text{ScO}$ , pot. energy curves and dissoci. energy of  $\text{X}^2\Sigma$  state 0-69203  
 $\text{ScRh}$ , gaseous, dissociation energies, high temp. mass spectrometric determ. 0-93790  
 $\text{SiH}^+$ , oscillator strengths and dissoci. energy determ. from time resolved precision spectroscopy 0-58272  
 $\text{XeAr}^+$ , form. from  $\text{Xe}^+ + \text{Ar}$ , reaction equilib. and rate consts. 0-61071  
 $\text{YCn}^+$  ( $\text{n}=2, 3, 4, 5, 6$ ), atomisation energies, Knudsen cell mass spectrometric obs. 0-58409  
 $\text{YRh}$ , gaseous, dissociation energies, high temp. mass spectrometric determ. 0-93790

**molecular electron correlations**

- acetophenones, di- and trisubstituted,  $\pi^* - \pi$  systems, UV electronic absorpt. spectra 0-74132  
acetophenones, mono substituted, semi empirical II-electron calcs. 0-74131  
acetophenones, spectrosc. characts. using PPP SCF CI calcs. 0-102448  
acetylcholine neurotransmitter, PCIL0-INDO calcs. 0-58153  
allyl radical, restricted SCF and MC SCF calc. of  $\text{C}_{2v}$  and  $\text{C}_s$  structs. 0-83289  
benzene, excitation spectra, cluster configuration method appl. 0-78546  
Brillouin theorem, proof 0-91415  
butadiene, excitation spectra, cluster configuration method appl. 0-78546  
closed-shell linear molecules, relativistic Dirac-Fock multiconfig. SCF calcs. 0-99455  
closed-shell polyatomic molecules, relativistic Dirac-Fock multiconfig. SCF calcs. 0-99456  
closed-shell system, polarisability and mag. susceptibility calc. by SCF and CI method 0-99443  
complex molecular orbitals, pairing representation 0-91454  
cyanine dyes, excited electronic states, CNDO/S CI calcs., visual pigment spectra appl. 0-85333  
deoxyhaemoglobin, ferrous heme of high-spin type, MCD spectra in Soret, visible and near IR regions 0-94156  
deoxyhaemoglobin, porphyrin-Fe-imidazole system, SCF-LCAO-ASMO and CI calcs. of low-lying multiplets and excited states 0-94155  
diamagnetic susceptibilities and NMR chemical shifts in terms of localised MO's 0-106256  
diatomic isovalent systems, pot. curves, ab initio MRD-CI method 0-83293  
diatomic molecule, electron correlations, cryst. field interactions, Hubbard calc. 0-75530  
direct orbital optimisation for MC SCF theory by unitary transformations 0-87049  
dodecahexenes, sudden polarisation effect, ab initio and CI calcs. 0-58160  
 $\pi$ -electron systems, excitation spectra, cluster configuration method appl. 0-78546  
ethane cation, relative stability of  $^2\text{A}_{1g}$ ,  $^2\text{E}_g$  states 0-58140  
ethylene, pot. energy and dipole moment surfaces, polarisation effect, ab initio CI calcs. 0-106272  
ethylene, rot. around double bond, four orbital-four-electron model 0-95592  
ethylene ozonide, ab initio gradient and MC SCF calc., conformational anal. 0-83290  
ethylidene, rearrangement to ethylene, barriers, ab initio MO calcs. 0-104424  
excitation energies calc., using renormalised Green's function method (Japanese) 0-83295  
excited states, variable metric optimisation of mol. geometry 0-58178  
formaldehyde,  $^3\text{A}''$  state, zero-field splitting param., ab initio CI calcs. 0-99454  
formaldehyde, electronic struct., dipole moments, mol. polarisability, force fields, ab initio calcs. 0-78531  
formaldehyde anion radical, hyperfine coupling const., vibr. depend., ab initio calcs. 0-87150  
fourth order perturbation theory, triple substitutions to electron correl. energy 0-74133  
 $\text{H}_2\text{O}$ , CI calcs. using modified virtual orbitals 0-58163  
hexatriene, excitation spectra, cluster configuration method appl. 0-78546  
hydrocarbons, cyclic, non alternant, nonsingle instabilities of HF solns. 0-58164

**molecular electron correlations continued**

- hydronaphthyl radicals embedded in naphthalene cryst., optical transition energies and ionisation energies 0-78595  
 $\beta$ -hydroxy acrolein, lower excited states, electronic struct. and H-bonding, ab initio SCF and CI calcs., photochemical mechanism 0-83278  
many-electron theory, unitary group formulations and quantum organic chemistry 0-106270  
MCSCF and CI wave functions, two-particle density matrix and graphical unitary group approach 0-63558  
methane +  $\text{O}(\text{P})$ , barrier height and transition state geometry, POL-CI calc., H abstraction reaction 0-66782  
methane cation, photodissoc., ab initio RHF and MRD CI calcs. 0-95695  
methanol, dissoci. ionisation mechanism, correlation diagram approach, mass spectra obs., metastable processes 0-95728  
methyl radical, hyperfine coupling const., vibr. depend., ab initio calcs. 0-87150  
methylene peroxide, struct., energy levels, ab initio UHF and MRUHF NO CI calcs. 0-83287  
modified virtual orbitals, for config. interaction calc. 0-58163  
modified virtual orbitals, systematic CI procedure 0-83294  
multi-config. SCF super-CI calc., density matrix formulation 0-78547  
multiconfigurational Hartree-Fock procedure, second-order, 2-electron integral transformations 0-87045  
n-pitroanilines, intramol. charge transfer satellites, XPS 0-78650  
nucleic acids bases, excited state dipole moments and geometries 0-95738  
open-shell system, polarisability and mag. susceptibility calc. by SCF and CI method 0-99443  
organic compounds, excitation energies, CNDO/S-CI method calc. appls. (German) 0-106275  
oxirane cation, struct. rearrangement following vertical ionisation, ab initio CI calc. 0-58191  
oxoniomethylene cation, rearrangement to hydroxymethyl cation, barriers, ab initio MO calcs. 0-104424  
PCIL0-INDO method, theory and appls. 0-58153  
phthalic acid derivatives, excitation energies, CNDO/S-CI method calc. appls. (German) 0-106275  
n-propanol, preferred conformers, PCIL0 study 0-95542  
pyridines, monosubst.,  $\text{H}_2\text{O}$  complexes,  $n - \pi^*$  transitions, H bonding, MO theory 0-95550  
relativistic Dirac-Fock multiconfig. SCF calcs. 0-99455  
self consistent electron pair theory, perfect pairing valence bond generalisation 0-63532  
1,3-sigmatropic rearrangements, ab initio calcs., basis set and electron correl. effects 0-104428  
spin-coupled particle-hole excitation, general matrix element formulas 0-69086  
spin-free configuration interaction, representation matrix elements 0-91459  
spin-orbital eqns. for anal. derivatives of config. interaction energy including double substitutions 0-78549  
ten-electron systems, correl. energy, fourth order diagrammatic, many body Rayleigh Schrodinger perturbation theory 0-63556  
tetramethyl-p-benzoquinone, mol. struct., gas phase electron diff. obs. 0-58386  
thioformaldehyde, electronic struct., dipole moments, mol. polarisability, force fields, ab initio calcs. 0-78531  
three-electron bonds, strengths, ab initio LCAO MO CI calcs. 0-87046  
triatomic dihydride molecules, Walsh's rules and small bond angle states 0-106255  
twisted conjugated molecule, zwitterionic excited states investig. 0-58179  
two photon absorptivities, CNDO/S-CI calc. with second order time depend. perturbation eqns. 0-74122  
two photon absorptivity, ion cyclotron reson. photodissoc. spectra, CNDO/S-CI-perturbation theory 0-74123  
two-photon spectroscopy, dipole-forbidden transitions, double excited configurations, CNDO-CI methods 0-58332  
valence correlation energies, contributions of triply- and quadruply excited states determ. using perturbation theory 0-78545  
 $\text{Al}_2(\text{Al})_2^-(\text{Al})_2^+$  configurations, ab initio study, LCAO, STO, MO-SCF and CI calcs., binding energy (French) 0-91447  
 $\text{Ar}_2$  van der Waals dimer, intermol. pot., SCF CI ab initio calcs. 0-106274  
BF, diagrammatic perturbation theory, using universal even-tempered basis set 0-58131  
 $\text{BH}_3$ , Walsh's rules and small bond angle states 0-106255  
 $\text{BH}_3$ , electronic wave function determ., genealogical technique using Clebsch-Gordan coeff. 0-95529  
 $\text{BeO}$ , MCSCF and CI calcs. 0-95526  
 $\text{Be}_2(\Sigma_g^+)$ , binding energy, ab initio pot. curves, interacting correlated fragments method 0-63557  
 $\text{C}_2(\text{C}_2^-)$  pot. energy curves calc. using SCF, MCSCF and CI methods, dissoci. energies, bond lengths, electron affinity 0-95523  
 $\text{CCO}$  radical, heat of form. calc., geometries excitation energies and vibr. freq. calc. using POL-CI wave functions 0-89512  
CH radical, SCF theory, multiconfig., direct orbital optimisation 0-87049  
 $\text{CH}^+$ ,  $a^1\Pi - b^1\Sigma^+$  transition moment, ab initio calcs. 0-87047  
 $\text{CH}^+$ , excited states, pot. curves and transition moments determ. by ab initio CI methods 0-106286  
 $\text{CH}_2$ , CI calcs. using modified virtual orbitals 0-58163  
 $\text{CH}_2^+$ , Walsh's rules and small bond angle states 0-106255  
 $\text{CH}_3$ ,  $\text{CH}_2$  and CH deformation vibration group frequencies and MO electron densities, interaction force const. 0-87101  
 $\text{CN}^-$ , spectrosc. const. for ground and excited states, ab initio, CI calcs. 0-78551  
 $\text{CN}^+$  ion,  $^1\Sigma^+$  and  $^3\Pi$  states, multi-reference CI study 0-83288  
 $\text{CO}$ , polarisability derivatives, bond length depend., SCF and CI calcs. 0-58162  
 $\text{CO}_2$ , diagrammatic perturbation theory, using universal even-tempered basis set 0-58131  
 $\text{CO}_2$ , stretch-stretch interaction force const., electron correlation influence, ab initio CI study 0-58161  
 $\text{Cl}_2$ , one electron props. and polarisability, SCF and CI calcs. 0-58159  
 $\text{ClO}$ , dissoci. energy and bond length, CI calcs., bond function effects 0-102450  
Co, Auger spectrum, ab initio MO LCAO SCF CI calc. many electron contribs. 0-87169  
 $\text{CrOCl}_3$ , electronic structure and valence ionisation energies, obs. by ab initio and SW-X $\alpha$  methods 0-69073



**molecular electron correlations continued**

- CuNi molecule, electronic states determ. by ab initio HF and CI methods 0-69087
- F<sub>2</sub>O, geometry, electron spectrum, vert. ionis. pot. ab initio calc. 0-58187
- H<sub>4</sub>-methane, abstraction and exchange reaction, barrier height calc. using POL-CI wave functions 0-81304
- H<sup>+</sup>+H<sub>2</sub>, vibr. excitation, ab initio CI pot. energy surface calcs. 0-74228
- H<sup>+</sup>+H<sub>2</sub>, vibr.-rot. excitation, ab initio CI pot. energy surface calcs. 0-74229
- H<sub>2</sub>, electronic struct., valence bond orbital method appl. 0-106268
- H<sub>2</sub>, relativistic Dirac-Fock multiconfig. SCF calcs. 0-99455
- H<sub>2</sub>-H<sub>2</sub> intermol. pair pot., ab initio SCF-CI surface 0-91457
- HCN, Fermi and Coulomb correl. holes, SCF and CI wave functions 0-69085
- HCN, modified virtual orbitals, systematic CI procedure 0-83294
- HCN<sup>+</sup>, <sup>2</sup>Σ<sup>+</sup> and <sup>2</sup>Π states, SCF and CI calcs. for determ. optimum linear geometries, bond angles calc. 0-74114
- HCl, electrostatically interacting mol.s., CI multipole function calcs. convergence 0-91458
- HCl, one electron props. and polarizability, SCF and CI calcs. 0-58159
- HF, electrostatically interacting mol.s., CI multipole function calcs. convergence 0-91458
- HF, SCF theory, multiconfig., direct orbital optimisation 0-87049
- HF+Li<sup>+</sup>-LiF+H<sub>2</sub> pot. energy surface, SCF and CI calcs. 0-71904
- HNC<sup>+</sup>, <sup>2</sup>Σ<sup>+</sup> and <sup>2</sup>Π states, SCF and CI calcs. for determ. optimum linear geometries, bond angles calc. 0-74114
- HNO, isomerism, low lying electronic states, ab initio MRD-CI calcs. 0-83291
- HNO, low-lying states, pot. energy surfaces calcs. 0-102460
- H<sub>2</sub>O, ground state, CI calcs. on triply and quadruply excited configs., basis set effects 0-95549
- H<sub>2</sub>O, ground state, cond. energies, higher-order excitation contribs. 0-58166
- H<sub>2</sub>O, multi-root config. interaction calcs. 0-102451
- H<sub>2</sub>O, polarisability and mag. susceptibility calc. by SCF and CI method 0-99443
- H<sub>2</sub>O<sup>+</sup>, ab initio potential energy surface study by CI techniques, equilibrium conform. determ., mol. dissoci. pathways 0-78550
- H<sub>2</sub>O<sup>+</sup>, inversion barrier, high-order replacements inclusion in CI calcs. 0-63504
- HPN-HNP, isomerisation energies, ab initio MRD-CI calcs. 0-106271
- H<sub>2</sub>S<sup>+</sup>, <sup>2</sup>B<sub>1</sub>, <sup>2</sup>A<sub>1</sub> and <sup>2</sup>B<sub>2</sub> electronic states, pot. energy curves, CI calcs. 0-87048
- HSC-HOS, isomerisation energies, ab initio MRD-CI calcs. 0-106271
- HSIC-HCSI, isomerisation energies, ab initio MRD-CI calcs. 0-106271
- H<sub>2</sub>SiO, electronic struct., dipole moments, mol. polarisability, force fields, ab initio calcs. 0-78531
- He+H<sub>2</sub>, pot. energy surface, ab initio calcs., van der Waals const. determ. 0-106372
- HgBr<sub>2</sub>, electronic struct. and photodissoc., effective core pots. and POL(1) CI wave function 0-63560
- HgCl<sub>2</sub>, electronic struct. and photodissoc., effective core pots. and POL(1) CI wave function 0-63560
- Li<sub>3</sub>, electronic struct., SCF and SCF-CI calcs. 0-87044
- Li<sub>3</sub><sup>+</sup>, electronic struct., SCF and SCF-CI calcs. 0-87044
- Li<sub>3</sub><sup>+</sup>, electronic struct., SCF and SCF-CI calcs. 0-87044
- Li<sub>4</sub>, MCSCF and CI calcs. 0-95526
- LiH, electronic struct., valence bond orbital method appl. 0-106268
- LiH, relativistic Dirac-Fock multiconfig. SCF calcs. 0-99455
- N<sub>2</sub>, diagrammatic perturbation theory, using universal even-tempered basis set 0-58131
- N<sub>2</sub>, multi-config. SCF super-CI calc., density matrix formulation 0-78547
- NH<sub>2</sub>, pot. energy curves of X<sup>2</sup>B<sub>1</sub>, A<sup>2</sup>A<sub>1</sub>, <sup>2</sup>B<sub>2</sub> valence-shell and π<sub>u</sub><sup>2</sup>3s-type Rydberg states calc. by CI 0-74138
- NO<sub>2</sub><sup>+</sup>, gas phase equilb. geometry, force consts., vibr. freq., dipole moment function MCSCF/CI calcs. 0-78520
- NOH isomerism, low lying electronic states, ab initio MRD-CI calcs. 0-83291
- Ni complex, nickel-bis-dithiolene, pseudopot. MCSCF and limited CI calcs. 0-83292
- O<sub>2</sub>, <sup>3</sup>Π diatomic Rydberg states, ab initio CI calcs. 0-95554
- O<sub>2</sub>, <sup>3</sup>Σ<sup>-</sup> ground state, pot. energy curve, direct CI method appl. 0-58165
- O<sub>2</sub>, Rydberg states, <sup>3</sup>Σ<sup>-</sup>, <sup>3</sup>Σ<sub>u</sub><sup>+</sup>, <sup>3</sup>Π<sub>g</sub>, <sup>1</sup>Π<sub>g</sub>, <sup>1</sup>Σ<sub>g</sub><sup>+</sup> symm., ab initio CI study 0-99460
- O<sub>2</sub>, Schumann-Runge continuum, oscill. strength and electron impact excitation 0-69121
- O<sub>2</sub>, ab initio UHF and UHF-natural orbital CI studies 0-102452
- SiH<sub>3</sub> radical, hyperfine coupling consts., vibr. depend., ab initio calcs. 0-87150

**molecular electron impact dissociation**

- air, O<sub>3</sub> generation, macroscopic props. of field-accelerated electrons 0-61118
- alkali metal fluoroaluminate, dissoci. enthalpies, mass spectrometric determ., heat of form. 0-97720
- bromobenzene -d<sub>0</sub>(-d<sub>2</sub>) radical cation, electron impact dissoci., secondary isotope effect 0-63836
- collisional cross-sections determ. for low and intermediate energy processes 0-99579
- 5,5'-diethylbarbituric acid, EPR and INDO-MO study of radical formation after irradi. 0-93774
- electronic and at. collisions, conf., Kyoto, Japan (Aug.-Sept. 1979) 0-57011
- electronic and at. collisions, conference, Kyoto, Japan (Aug.-Sept. 1979) 0-62394
- ethynyl cation, dissociative recomb. cross section determ., merged beam obs. 0-78715
- halogen mol.s., electron dissociative attachment 0-91694
- methane, 25 to 40 eV electron dissoci. ionisation, proton formation 0-91690
- methanol, dissoci. ionisation mechanism, correlation diagram approach, mass spectra obs., metastable processes 0-95728
- phenylalanine, hydrated electron impact dissoci., laser flash photolytic investig. 0-58396
- protein, electron radiation damage on primary and secondary struct. level 0-89808
- vinyl cation, dissociative recomb. cross section determ., merged beam obs. 0-78715
- Ar:OCS, liq., dissoci. studies 0-78716

**molecular electron impact dissociation continued**

- C<sup>+</sup>, dissociative recomb. cross section determ., merged beam obs. 0-78715
- C<sub>2</sub>H<sub>2</sub><sup>+</sup>, dissociative recomb. cross section determ., merged beam obs. 0-78715
- Cu/CuCl double pulse laser, dissoci. pulse, afterglow, and laser pulse model 0-91775
- D<sub>2</sub>, electron impact dissoci. ionisation 0-83510
- F<sub>2</sub>, electron impact excitation, dissoci. of lowest electronic state 0-63839
- H<sub>2</sub>, electron dissociative attachment 0-91694
- H<sub>2</sub>, electron impact, H<sub>α</sub> and H<sub>β</sub> lines emission, intensity decay curves meas. 0-83505
- H<sub>2</sub>, electron impact dissoci. ionisation 0-83510
- H<sub>2</sub>, electron impact H<sup>+</sup> prod., kinetic energy, ang. distrib. 0-63838
- H<sub>2</sub>, electron scatt., elastic and inelastic, Glauber approx. 0-91695
- HD, electron impact dissoci. ionisation 0-83510
- H<sub>2</sub>O, electron impact dissoci., OH(A<sup>2</sup>Σ<sup>+</sup>→X<sup>2</sup>Π<sub>1</sub>) emission spectra, crossed-beam investigations 0-83504
- InBr, electron impact dissoci. ionis., In electron affinity meas. (French) 0-63849
- InI, electron impact dissoci. ionis., In electron affinity meas. (French) 0-63849
- N<sub>2</sub>, electron excitation of Birge-Hopfield bands (b<sup>1</sup>π<sub>u</sub>-X<sup>1</sup>Σ<sub>g</sub><sup>+</sup>) 0-95731
- N<sub>2</sub>, electron impact dissoci., EELS, N<sup>+</sup> autoionisation 0-106397
- N<sub>2</sub>, electron scatt., elastic and inelastic, Glauber approx. 0-91695
- N<sub>2</sub>, electron scatt., reson. excitation and dissoci. attachment, vibr. state depend. 0-78717
- O<sub>2</sub>, macroscopic props. of field-accel. electrons in pure gas (French) 0-59161
- O<sub>2</sub>, O<sub>3</sub> generation, macroscopic props. of field-accelerated electrons 0-61118
- TlBr, electron impact dissoci. ionis., Tl electron affinity meas. (French) 0-63849
- TlI, electron impact dissoci. ionis., Tl electron affinity meas. (French) 0-63849
- XeF laser performance, ground state population effect 0-63987
- molecular electron impact excitation**
- see also electron spectra
- ab initio methods for atomic and molecular processes 0-63550
- acetylene-d<sub>0</sub>(-d<sub>1</sub>)(-d<sub>2</sub>) metastable state, mol. beam elec. deflection obs. 0-74137
- biacetyl, triplet n→π\* and π→π\* transitions studied by low-energy electron diff. 0-83502
- collisional cross-sections determ. for low and intermediate energy processes 0-99579
- diatomic molecules, N<sub>2</sub> and CO nuclear pumped lasers, electron impact cross section meas. 0-63985
- electron attachment to mol. and mol. clusters, electron-mol. collision, Rydberg electron exchange 0-63843
- electron impact dissoci. ionisation 0-83510
- electron-collision cross-section data for atom or molecule, rel. to radiation physics 0-63829
- electronic and at. collisions, conf., Kyoto, Japan (Aug.-Sept. 1979) 0-57011
- electronic and at. collisions, conference, Kyoto, Japan (Aug.-Sept. 1979) 0-62394
- fluorophenol cations, emission and photoelectron spectra in gaseous phase 0-58316
- formyl ion, electron impact rot. excitation, Glauber approx. with Coulomb effect 0-63840
- gases, molecular, total scatt. cross sections for intermediate-energy positrons 0-91692
- glyoxal, triplet n→π\* and π→π\* transitions studied by low-energy electron diff. 0-83502
- indirect dissociative recomb., T-matrix element, Feshbach's projection operator technique 0-58114
- inner-shell electron impact excitation, developments in electron energy loss spectroscopy 0-63842
- laser field, photon correl. effects 0-83481
- methyl iodide, van der Waals mol., electron self-scavenging 0-95727
- multiple scatt. method, scatt. cross section calc. 0-63816
- nitromethane, variable angle electron-impact excitation, transitions in 7-12 eV energy-loss range 0-69244
- polar molecules, electron impact, elastic scatt. and vibr. excitation, effective range theory 0-83485
- resonant phenomena, complex stabilisation method 0-78515
- theory and calc. techniques 0-63841
- trifluorodimethylmercury, gas phase mol. struct., electron diff. and microwave spectra obs. 0-78609
- trifluoriodomethane nuclear pumped lasers, electron impact cross section meas. 0-63985
- CO, d<sup>3</sup>Δ state, low energy electron impact excitation and radiative decay 0-91691
- CO, ν=0-1 vibr. excitation, electron impact cross sections 0-83507
- CO, vibr. excitation via high-energy shape resonances 0-91693
- CO<sup>+</sup>, electron impact rot. excitation, Glauber approx. with Coulomb effect 0-63840
- CO-N<sub>2</sub> discharge, plasma characts. and vibr. kinetics anal. 0-59331
- CO<sub>2</sub>, electron elastic scatt. and vibr. excitation by 4, 10, 20 and 50 eV electrons 0-83484
- CS<sub>2</sub>, electron impact excitation and ionisation 0-63837
- F<sub>2</sub>, electron impact excitation, dissoci. of lowest electronic state 0-63839
- H<sub>2</sub>, elec. discharge, non-equilib. ionisation rate calcs. 0-59319
- H<sub>2</sub>, electron impact, H<sub>α</sub> and H<sub>β</sub> lines emission, intensity decay curves meas. 0-83505
- H<sub>2</sub>, electron impact dissoci. ionisation 0-83510
- H<sub>2</sub>, electron impact excitation, to high Rydberg states, by threshold energy collision 0-83509
- H<sub>2</sub>, electron impact excitation, low energy, distorted wave approx. cross-sections 0-83511
- H<sub>2</sub>, electron scatt., iterative approach to Schwinger variational principle 0-99580
- H<sub>2</sub>, optical polarisation following electron impact 0-63831
- H<sub>2</sub>, total cross sections meas. for electron scatt. at very low energies 0-58398
- H<sub>2</sub>+e<sup>-</sup>→H<sub>2</sub><sup>+</sup>+e<sup>-</sup>, Gaussian basis Glauber approx., elastic and vibrational excitation cross sections 0-58399
- HD, electron impact dissoci. ionisation 0-83510
- H<sub>2</sub>O, electron impact, vibr. excitation, effective range theory 0-83485



# molecular electron impact excitation continued

- KrF<sub>2</sub> electron beam pumped laser medium, time depend. fluoresc. spectrum in high current density range 0-78842  
N<sub>2</sub>, elastic and inelastic electron scatt., state to state cross section 0-78708  
N<sub>2</sub>, electron excitation of Birge-Hopfield bands ( $b^1\Pi_u-X^1\Sigma_g^+$ ) 0-95731  
N<sub>2</sub>, electron impact excitation, to high Rydberg states, by threshold energy collision 0-83509  
N<sub>2</sub>, electron scatt., reson. excitation and dissoc. attachment, vibr. state depend. 0-78717  
N<sub>2</sub>, excitation efficiency for rot. states 0-102557  
N<sub>2</sub>, IR laser transition, excitation process 0-87383  
N<sub>2</sub>, multiple scatt. method, scatt. cross section calc. 0-63816  
N<sub>2</sub>, first  $^2\Pi_u$  state form. and decay 0-58177  
NH<sub>3</sub>, electron impact, 35 keV, Bethe surface and Compton profile 0-87235  
N<sub>2</sub>H<sup>+</sup>, electron impact rot. excitation, Glauber approx. with Coulomb effect 0-63840  
O<sub>2</sub>, electron coincidence spectrosc., valence electron momentum distrib. and binding energies 0-102583  
O<sub>2</sub>, Schumann-Runge continuum, oscill. strength and electron impact excitation 0-69121  
O<sub>2</sub>, low energy elastic and inelastic electron scatt., rot. transitions, close coupling calc. 0-78706  
OCS, electron impact excitation and ionisation 0-63837  
SiH<sub>4</sub>, L<sub>2</sub>,MM Auger spectrum, line width and intensities 0-58325  
UF<sub>6</sub> nuclear pumped lasers, electron impact cross section meas. 0-63985  
XeF, direct pumping by electron beam pulses, gain and laser oscill. obs. in blue-green 0-102699  
XeF<sub>6</sub> molecules with Jahn-Teller pseudo-effect, ang. depend. of inelastic scatt. of electrons 0-69246  
XeF\* temp. dependent quenching rate constants 0-63701

# molecular electron impact ionisation

- see also electron spectra*  
chlorofluoromethanes, electron attachment, electron swarm method 0-69245  
collisional cross-sections determ. for low and intermediate energy processes 0-99579  
electron attachment to mol. and mol. clusters, electron-mol. collision, Rydberg electron exchange 0-63843  
electron coincidence spectroscopy, binding energy charge density meas. 0-63817  
electron scatt. and photoionisation, shape-resonance enhanced nuclear motion effects 0-63603  
electronic and at. collisions, conf., Kyoto, Japan (Aug.-Sept. 1979) 0-57011  
inert gas Van der Waals dimers, electron impact ionis. 0-58400  
organic molecular systems, polarisabilities, susceptibilities, electron impact ionis. cross-sections calcs. 0-63835  
phenyl cation, struct., ion-molecule reactions studied by trapped ion mass spectroscopy 0-102586  
CO, adsorbed layer, electron impact, electron impulsive ionisation spectroscopy obs. 0-60720  
CO<sub>2</sub> gas, electron impact ionisation, electronic fluoresc. spectra 0-95664  
CO<sub>2</sub>, electron impact ionisation, cross section obs. 0-58397  
CS<sub>2</sub>-N<sub>2</sub>-He-O<sub>2</sub> discharge mixture, three body electron attachment to O<sub>2</sub> 0-64779  
CS<sub>2</sub>, electron impact excitation and ionisation 0-63837  
CS<sub>2</sub>, ionisation and fragmentation by monoenergetic electron impact, mass spectrometric study 0-102581  
D<sub>2</sub>, electron impact dissociation 0-83510  
H<sub>2</sub>, electron impact dissociation 0-83510  
H<sub>2</sub>, electron impact H<sup>+</sup> prod., kinetic energy, ang. distrib. 0-63838  
H<sub>2</sub>, electron impact ionisation cross section 0-78718  
H<sub>2</sub>, statistical fluctuations in ionisation yield, rel. to electron degradation spectrum 0-99581  
HBr, electron impact ionisation, vibr. excitation spectra threshold peaks, negative ion effects 0-106322  
HD, electron impact dissociation 0-83510  
InBr, electron impact dissociation, In electron affinity meas. (French) 0-63849  
InI, electron impact dissociation, In electron affinity meas. (French) 0-63849  
N<sub>2</sub> gas, electron impact ionisation, electronic fluoresc. spectra 0-95664  
NH<sub>3</sub>, electron impact ionisation, total and partial cross sections meas. 0-95729  
NO, adsorbed layer, electron impact, electron impulsive ionisation spectroscopy obs. 0-60720  
NO<sub>2</sub>, single and double ionisation by electron impact, ionisation pot. determ. 0-95730  
N<sub>2</sub>O gas, electron impact ionisation, electronic fluoresc. spectra 0-95664  
N<sub>2</sub>\* ( $A^1\Sigma_g^+$ ), electron impact ionisation cross section 0-78718  
OCS, electron impact excitation and ionisation 0-63837  
SF<sub>6</sub>-N<sub>2</sub> mixture, electron swarm development, Boltzman eqn. anal. 0-87841  
TiBr, electron impact dissociation, Ti electron affinity meas. (French) 0-63849  
TiI, electron impact dissociation, Ti electron affinity meas. (French) 0-63849  
Xe<sup>2+</sup> (Xe<sup>3+</sup>)(Xe<sup>4+</sup>)(Xe<sup>5+</sup>), molecular electron impact ionisation 0-102582

**molecular electron scattering** *see elastic scattering of electrons by atoms and molecules; molecular electron impact dissociation; molecular electron impact excitation; molecular electron impact ionisation*

# molecular electronic states

- see also charge transfer states; molecular metastable states; triplet state*  
acetylene, excited state, photochem. and spectrosc. investig. 0-95553  
acetylene, higher excited states, electron energy loss spectra 0-91664  
N-acetylglycine, X-irrad., stable radical electronic and mol. struct., ENDOR and ESR 0-80637  
activated complexes, exp. obs., bonding MO LCAO states 0-76506  
adenine, hydroxy and methoxy derivatives, absorption UV spectroscopy and electronic struct. of ionic and tautomeric forms 0-74177  
alkali metal chlorides, photofragment spectra, bond energies and excited state symmetries 0-87190  
n-alkanes, mol. Rydberg S—S and S—T transitions, semi-empirical SCF MO calc. 0-91453  
alkyl benzenes, jet-cooled, vibr. relax., nanosecond time evolution 0-95584

# molecular electronic states continued

- alkynoyl cations, struct., charge distrib., ab initio population anal. calcs. 0-58407  
1H-alloxazine, and derivatives electronic struct., photoelectron spectrosc. and ab initio study 0-106261  
aromatic hydrocarbons, sequential coupling 0-58297  
azaaromatics, neutral and protonated, excited singlet and triplet states, charge densities, INDO calcs. 0-58152  
azacyclotetradienes, conjugated mols. electronic struct. and geometry, Hartree-Fock instability 0-69055  
1,2-benzanthracene, secondary reson. radiation and hot energy transfer, soln. luminesc. 0-87167  
benzene, dynamic polarisabilities, calcs., superposition method of excited config., nonstationary perturbation theory eqns. 0-69257  
benzene, excitation spectra, cluster configuration method appl. 0-78546  
benzene-Dewar benzene, lower excited states pot. energy surfaces for isomerisation 0-104429  
benzenes, substituted, electronic struct., ab initio calcs., photoelectron spectra 0-58314  
p-bromochlorobenzene, T<sub>1</sub> states, zero-field ODMR, MIDP and phosphorescence excitation spectra 0-74191  
p-bromofluorobenzene, UV electronic absorption spectrum, band shape and molecular geometry 0-87147  
trans-butadiene,  $B_{1u}$ -state dynamics in cooled supersonic expansion, electronic absorpt. spectra obs. 0-78629  
butadiene, excitation spectra, cluster configuration method appl. 0-78546  
butadiene, twisted zwitterionic excited states, SCF calcs. 0-58179  
carbenes, heterosubstituted, singlet-triplet splitting depend. on heteroatom electronegativity and conform. 0-63553  
 $\beta$ -carotene, excitation profile of  $\nu_2$  line in resonance Raman spectrum, solvent effects 0-74173  
chemically induced magnetic polarization by S-T<sub>±</sub> mixing in strong mag. field 0-83515  
chrysene, excited singlet and triplet state, CARS obs. 0-83374  
classical many-body collision model incorporating Heisenberg and Pauli principles 0-63511  
cluster systems, program for calc. electronic struct. with double self-consistency-Bersuker's method 0-69289  
Co<sub>2</sub>Sb<sub>2</sub>(CO)<sub>12</sub>, electronic struct. calc. (Russian) 0-58136  
core-hole processes, electronic Hamiltonian, many-body theory 0-91443  
coumarin 102, excited state interaction dynamics, picosec. time-resolved spectral shift obs. 0-78624  
cyanine dyes, excited electronic states, CNDO/S CI calc., visual pigment spectra appl. 0-85333  
p-cyano-N,N-dimethylaniline in polar solvents, double fluorescence, theoretical model 0-58296  
6-cyanobenzquinuclidine, intramol. electron-transfer excited state 0-58295  
cyclic 3- and 4-membered ring cpds., saturated, ab initio struct. anal. 0-58192  
cyclic ketones, electrochromism and electric dichroism for studying transitions to second excited singlet 0-63692  
cyclic molecules, localised electronic vacancies lifetimes 0-106264  
cyclopropane, IR spectra studied by tunable laser,  $\nu_{10}+\nu_{11}$  band anal. 0-95615  
cytosine, hydroxy and methoxy, derivatives, absorption UV spectroscopy and electronic struct. of ionic and tautomeric forms 0-74177  
decacyclene anion, photoexcited quartet state, transient EPR 0-78635  
deoxyhaemoglobin, ferrous heme of high-spin type, MCD spectra in Soret, visible and near IR regions 0-94156  
deoxyhaemoglobin, porphyrin-Fe-imidazole system, SCF-LCAO-ASMO and CI calcs. of low-lying multiplets and excited states 0-94155  
diatomic hydrides, quantum mechanically calculated observables, reliability determ. 0-63505  
diatomic isovalent systems, pot. curves, ab initio MRD-CI method 0-83293  
diatomic mol., vibr. rot. Hamiltonian expansion, Born Oppenheimer  $\kappa$ , explicit introduction 0-69118  
diatomic molecules, excited states, electronic transition probabilities and lifetimes, review 0-78658  
diatomic molecules, laser-induced predissoc., surface mag. field effect 0-106365  
diatomic molecules, optically pumped lasers, review 0-58519  
diatomic molecules, rotational Raman intensities and polarisability anisotropy change meas. with internuclear distance 0-63641  
diatomic molecules, shortening of energy relax. time of excited mol. vibr. in dense medium by form. of H-bonds 0-91553  
diatomic mols., electronegativity, bond charge and chemical pot. approach 0-91703  
p-dibromobenzene, T<sub>1</sub> states, zero-field ODMR, MIDP and phosphorescence excitation spectra 0-74191  
S<sub>1</sub>p-difluorobenzene, time resolved fluoresc. spectra, direct view of intramolecular vibr. redistribution 0-83341  
difluoroethene, cis- and trans-, photoelectron-photoion coincidence study, fluoresc. obs. 0-95678  
dihydroquinoxalinediones, conjugated mols. electronic struct. and geometry, Hartree-Fock instability 0-69055  
diphenylpolyene molecules, excited electronic states, vibronic mixing, wave functions, method of fragments anal. 0-63615  
DODCI in ethanol, DQOCI added, electronic energy transfer, real-time ps meas. 0-58311  
DODCI in ethanol, malachite green added, electronic energy transfer, real-time ps meas. 0-58311  
 $\pi$ -electron systems, excitation spectra, cluster configuration method appl. 0-78546  
electronic and at. collisions, conference, Kyoto, Japan (Aug.-Sept. 1979) 0-62394  
electronic degrees of freedom, classical models 0-63507  
electronic excitation functions by low electron impact spectroscopy, trapped electron restrictions 0-69184  
electronic spin orbit interaction, molecular Aharonov-Bohm effect 0-83303  
electronic structure calculations by fast accurate kinetic-energy method 0-83257  
ethane, photoionisation spectra, cond. hole model 0-58326  
ethane cation, relative stability of  $^2A_{1g}$ ,  $^2E_g$  states 0-58140  
ethylene, pot. energy and dipole moment surfaces, polarisation effect, ab initio CI calcs. 0-106272  
ethylene, twisted, intervalence charge transfer and reson., sudden polarisation effect 0-69230



## molecular electronic states continued

ethylene, valence states, effective Hamiltonian from canonical transformation 0-74130  
ethylene as singlet methylene dimer, nonempirical double zeta calculations, zwitterionic singlet excited states 0-83258  
excitation energies calc., using renormalised Green's function method (*Japanese*) 0-83295  
excited states, interpretation charge-transfer numbers 0-78530  
excited states, variable metric optimisation of mol. geometry 0-58178  
ferrous nitrosylhaemoglobin, NO binding, spin distrib., orbital model and mag. props. 0-81534  
fluorobenzene radical cations in solid Ne, laser-induced fluoresc. spectra, vibr. struct. of excited and ground states 0-95671  
fluorophenol cations, emission and photoelectron spectra in gaseous phase 0-58316  
fluorostyrene, UV Raman spectra, reson. effect in photoreactive states 0-106326  
formaldehyde, electronic struct., dipole moments, mol. polarisability, force fields, ab initio calcs. 0-78531  
formaldehyde, excited state vibr. freq. calcs. by method based on scaled ab initio force fields 0-87092  
formaldehyde, mol. Rydberg S<sub>1</sub>-S and S<sub>1</sub>-T transitions, semi-empirical SCF MO calc. 0-91453  
formaldehyde, sequential coupling 0-58297  
Franck-Condon factors, Wigner distrib. function 0-99520  
glyoxal, vapour, predissoc. in S<sub>1</sub> zero-point level states 0-102544  
ground state alkali molecules, mag. shielding and spin-rot. interaction 0-87186  
heavy ion+atom collisions, small impact parameters, K-vacancy prod., molecular theory 0-69229  
hexatriene, excitation spectra, cluster configuration method appl. 0-78546  
1,3,5-hexatriene radical cation, in Ne matrix, laser induced fluoresc. and emission spectra 0-87163  
hole burning, photophysical and photochemical theories 0-58322  
hydrocarbon ions, mass spectra, H atom scrambling, delocalisation 0-58135  
hydrocarbons, cyclic, non alternant, nonsingle instabilities of HF solns. 0-58164  
 $\beta$ -hydroxy acrolein, lower excited states, electronic struct. and H-bonding, ab initio SCF and CI calcs., photochemical mechanism 0-83278  
para-hydroxyaniline, mol. complex., electronic struct., basis set and correlation effects 0-91436  
inert gas nuclear pumped lasers, prod. efficiency of excited states 0-63998  
intramolecular dynamics, random coupling model, math. approach 0-58308  
intramolecular dynamics, random coupling model, multiphoton excitation, kinetic eqns. 0-63700  
10H-isoalloxazine, and derivatives electronic struct., photoelectron spectrosc. and ab initio study 0-106261  
lanthanide-porphyrin complexes, upper  $\pi\pi^*$  electronic states, fluoresc. 0-83410  
linear mols.,  $\pi$  orbital electron energy contrib. to reaction heat 0-76539  
malonic acid, and  $\alpha$ -alkyl derivatives, photoelectron spectra, lone-pair interactions 0-58315  
metalloporphyrins, two quantum fluoresc. excitation from higher excited electronic states 0-106350  
methanol, dissociation mechanism, correlation diagram approach, mass spectra obs., metastable processes 0-95728  
methoxy radical, LMR spectra anal. 0-63677  
methoxy species on Ni (111), photoelectron spectra, electronic struct. and orientation 0-83420  
methyl allenyl sulphide, UV absorpt. spectra, role of 3d valence-shell and 4s Rydberg-type atomic orbitals 0-83384  
methyl orange, aq. soln., reson. Raman spectra of D and <sup>14</sup>N isotopes 0-91566  
methylbenzenes, 3p Rydberg transitions, multiphoton ionis. spectrosc. obs. 0-95644  
methylene, <sup>1</sup>B<sub>1</sub>-<sup>1</sup>A<sub>1</sub> separation, ab initio 0-106251  
molecular polarisabilities calcs., superposition method of excited config., nonstationary perturbation theory eqn. 0-69257  
molecule core 1s and 1b, photoelectron bands, vibr. excitations, ab initio calc. 0-63543  
molecules containing heavy atoms, program for calc. electronic struct. by quasirelativistic method 0-69088  
molecules in degenerate electronic state, IR laser radiation effects 0-81351  
multicharged ions, transitions between energy levels in strong external field, relativistic calcs. (*Russian*) 0-63547  
N-electron system, Schrödinger eqn. soln. using antisymmetrisation 0-106246  
naphthalene in Ar matrix, geometry changes and multiplet struct., mol. fluoresc. and phosphoresc. obs. 0-95663  
naphthalenes, methyl substituted radical cations, UHF spin densities, additivity model calcs. 0-58139  
naphthol complexes, H-bonded, form. of ion pairs in presence of crown ethers, proton-transfer photoreactions 0-85199  
naphthyl group, excited singlet state, intramol. fluoresc. quenching by halogeno substituents 0-102537  
1- $\beta$ -naphthyl-2-N-piperidinoethane, intramol. exciplex form., ground state conform. control 0-102547  
nitrosobenzene, fluoresc. quantum yields, determ. from Raman scatt. 0-58294  
nonlinear oscillators, 1-D, intramolecular vibr. energy transfer, quantal, classical and statistical behaviour 0-91641  
pair energy, perturbative corrections, incomplete basis set problem 0-78507  
pentacene, first excited singlet state, butterfly motion studied by fluoresc. spectra 0-78615  
phenylnaphthalenes isomers, fluoresc. lifetime difference and mol. geometry 0-69176  
phthalocyanine compounds, XPS and charge transfer 0-95681  
pinacyanol in ethanol, electronic relax., analysing light ps spectroscopy 0-99517  
planar cyclic radicals, C-H proton isotropic hyperfine const., C hybridisation 0-95646  
polyatomic molecules, nonadiabatic transitions between electronic terms of identical symmetry 0-83265  
polynuclear clusters, programs for calc. electronic struct. by Mulliken-Wolfsberg-Helmholtz method 0-69288  
polypeptides, electronic struct., side-chain disorder effect 0-76706

## molecular electronic states continued

propylol chloride(-d), 357-333 nm absorpt. system 0-69161  
propylol fluoride(-d), 290 nm absorpt. system 0-87142  
pyridine-N-oxide, electronic struct. assignment, He I/He II intensities (*German*) 0-83423  
pyrimidines, substituted analogues, absorption UV spectroscopy and electronic struct. of ionic and tautomeric forms 0-74177  
quantum mechanical aspects of the molecular structure hypothesis 0-102421  
radiationless transitions, synchrotron radiation obs. 0-63706  
radiative transitions, proximity effects, role of vibronic coupling and static crystal field interactions model 0-69126  
resonant Raman spectra, overtone intensity distrib., effect of excited electronic state 0-87128  
resonant Rayleigh-type mixing spectroscopy using ps light pulses, ultrafast relax. study 0-91834  
rhodamine 6G dye laser, induced radiation spectral characts., effect of vibr. relax. 0-64008  
rigid symmetric top molecules, dynamic Stark effect spectrum 0-63621  
ruthenium tris-bipyridyl, excited state electron transfer quenching, H<sub>2</sub>O photoreduction mediators effects 0-102536  
ruthenium trisbipyridyl ions in surfactant solns., excited state decay kinetics 0-83407  
Rydberg transitions, correl. algorithms for Rydberg term values 0-83277  
scattering amplitude calculations, role of radiative crossings between potentials of dressed mol. 0-63642  
self-consistency accel. procedure 0-78529  
similarity, electron density function meas. 0-91413  
spiropyron solutions, nitro-substituted, electronic state participation in photochromy 0-81347  
stilbene anion radicals, photoinduced isomerisation, 77K 0-66818  
stilbenes, substituted, donor-acceptor interaction effects on excited singlet state polarity (*German*) 0-91470  
styrene, UV Raman spectra, reson. effect in photoreactive states 0-106326  
tetrafluoromethane, valence electron binding energies, molecular symmetry restrictions effect 0-63528  
tetramethyl-1,3-cyclobutanedithione-h<sub>12</sub> and -d<sub>12</sub>, visible spectra,  $\pi\pi^*$  transitions obs., mol. vibr. 0-97297  
thioformaldehyde, electronic struct., dipole moments, mol. polarisability, force fields, ab initio calcs. 0-78531  
thioxanthone, fluoresc. and internal conversion, rel. to proximity effects 0-91592  
time of flight spectroscopy, particles in excited state produced via IR laser excitation 0-74257  
3d-transition metal ions, s-doublet struct., appl. of exchange correlation mass operator approx. 0-106266  
triatomic dihydride molecules, Walsh's rules and small bond angle states 0-106255  
triatomic molecule, rot. vibr. electronic Hamiltonian, Born-Oppenheimer approx., breakdown 0-87097  
triatomic mols., Renner-Teller effect, orbital angular momentum 0-78513  
trifluoriodomethane, highly excited, intermol. vibr. energy transfer, transient UV absorpt. spectra 0-106381  
trioxane,  $\nu_1(E)=\nu_{20}(E)=1$  state, rot. spectrum assignment, microwave obs. 0-58248  
twisted conjugated molecule, zwitterionic excited states investig. 0-58179  
two-photon spectroscopy, dipole-forbidden transitions, double excited configurations, CNDO-CI methods 0-58332  
valence correlation energies, contributions of triply- and quadruply excited states determ. using perturbation theory 0-78545  
Al<sub>2</sub> (<sup>1</sup>A<sub>1</sub>), (<sup>1</sup>A<sub>1</sub>) configurations, ab initio study, LCAO, STO, MO-SCF and CI calcs., binding energy (*French*) 0-91447  
Ar+Na<sub>2</sub>, differential cross sections meas. for rot. energy transfer process, obs. of halos 0-91643  
ArH<sup>+</sup>, transition moments, perturbation calcs. 0-102542  
BF, isoelectronic sequence, Rydberg transitions, term value-ionisation pot. correl. 0-58276  
BH<sub>2</sub>, Walsh's rules and small bond angle states 0-106255  
BH<sub>3</sub>, electronic wave function determ., genealogical technique using Clebsch-Gordan coeff. 0-95529  
BO<sub>2</sub>,  $\Pi$  vibronic states, laser induced fluoresc. obs. 0-58301  
BaO, excited electronic states, lifetimes and transition moments 0-87177  
Be<sub>2</sub>, ground state, multiple scatt. X $\alpha$  calcs. 0-58149  
BeBH<sub>3</sub>, H bridged system, floating spherical Gaussian model 0-78518  
BeF, A<sup>2</sup> $\Pi$  state config., ab initio MO calcs. 0-95532  
BeH, <sup>2</sup> $\Sigma^+$  states, spin-coupled valence bond theory of molecular electronic struct. 0-83285  
BeO, MCSCF and CI calcs. 0-95526  
BeOH, struct. and electronic props., ab initio calcs. 0-74113  
Br<sub>2</sub>, long-lived A<sup>2</sup> $\Pi(1_u)$  state, quantum-resolved dynamics of excited states 0-69178  
Br<sub>2</sub>, Q branches of  $\Delta n=1$  profiles, calcs., rotation effect on scatt. amplitudes 0-63643  
BrF<sub>3</sub>, electronic struct. and ionisation pot., SCF DV X $\alpha$  method 0-69057  
BrF<sub>5</sub>, electronic struct. and ionisation pot., SCF DV X $\alpha$  method 0-69057  
C<sub>1</sub>, A<sup>2</sup> $\Pi_u$  state, orbital angular momentum 0-78514  
CF<sub>2</sub>, excitation by Hg 253.7 nm line, reson. fluoresc. spectra 0-63694  
CH radical, sputtered, rotational and vibrational excitation 0-69224  
CH<sup>+</sup>, excited states, pot. curves and transition moments determ. by ab initio CI methods 0-106286  
CH<sub>2</sub><sup>+</sup>, Walsh's rules and small bond angle states 0-106255  
CN, B<sup>2</sup> $\Sigma^+$ -A<sup>2</sup> $\Pi$  0-0 and 1-0 bands, laser excitation spectra 0-91588  
CN free radical, A<sup>2</sup> $\Pi$ -X<sup>2</sup> $\Sigma^+$  Red system, perturbation analysis 0-87247  
CN, internal energy distrib. following vinyl cyanide photodissoc., temp. depend. 0-78638  
CN<sup>+</sup>, spectrosc. const. for ground and excited states, ab initio, CI calcs. 0-78551  
CN<sup>+</sup> ion, <sup>2</sup> $\Sigma^+$  and <sup>3</sup> $\Pi$  states, multi-reference CI study 0-83288  
CO, (4+)<sup>+</sup> system, electronic transition probability 0-106332  
CO,  $\Delta$  state, low energy electron impact excitation and radiative decay 0-91691  
CO, Dunham vibration-rotation coefficients, isotope dependence 0-83518  
CO, electronic structure calcs., self-consistent, accelerating convergence of iterative process 0-87037  
CO, isoelectronic sequence, Rydberg transitions, term value-ionisation pot. correl. 0-58276  
CO, X<sup>2</sup> $\Sigma^+$ , vibr. levels, UPS electron attachment obs. 0-95683  
CO-N<sub>2</sub> discharge, plasma characts. and vibr. kinetics anal. 0-59331



## molecular electronic states continued

- CO<sub>2</sub>, high resolution UV photoelectron spectra 0-91603  
C<sub>2</sub>O<sub>2</sub>, semirigid bender, rot.-vibr. energy level separations obs., struct. and pot. functions determ. 0-83446  
COS, high resolution UV photoelectron spectra 0-91603  
CO(1)+CO( $\nu$ )-CO(0)+CO( $\nu+1$ ), vibr. energy accumulation, reaction rate anal. 0-78692  
CS, prompt emission and internal energy distrib. of X' $\Sigma^+$  state 0-106364  
CS<sub>2</sub>, high resolution UV photoelectron spectra 0-91603  
CS<sub>2</sub>, photodissoc., fragment energy distrib. 0-69200  
CS<sub>2</sub>, shock heated, visible emission 0-58274  
Ca<sub>2</sub>, ground state, multiple scatt. X $\alpha$  calcs. 0-58149  
CaF,  $\Sigma$  ground state, laser-RF double reson. spectrosc. 0-69171  
CaH, spin doubling, SCF calcs. 0-95649  
Cl<sub>2</sub>, inner shell excited states, X-ray absorpt. spectra, HF calcs. 0-78536  
CINO, ground state geometry, ab initio calcs. 0-106259  
<sup>37</sup>ClO<sub>2</sub>,  $\nu_3=1$  state, laser-microwave double reson. obs. 0-95657  
Cl<sub>2</sub>Si(CH<sub>3</sub>)<sub>4-m</sub>, <sup>35</sup>Cl NQR, geminal and vicinal interactions on substituents electronic effect 0-63663  
Cl<sub>2</sub>Si(OCH<sub>3</sub>)<sub>4-m</sub>, <sup>35</sup>Cl NQR, geminal and vicinal interactions on substituents electronic effect 0-63663  
Cr(NO)<sub>4</sub>, bonding, shake-up intensities and shake-up energies, SCF X $\alpha$  multiple scatt. calc. 0-74121  
CrO, A' $\Pi$ -X' $\Pi$  transition, rot. anal. laser induced fluoresc. and discharge emission spectra 0-69173  
Cs<sub>2</sub>, 4800 Å absorpt. band, classical method anal. 0-106330  
Cs<sub>2</sub><sup>+</sup>, interaction potential determ., comparison between all-electron frozen core and pseudo-potential results 0-69054  
Cs<sub>2</sub><sup>+</sup>, low-lying states, MC SCF+CI 0-69053  
CuCl<sub>2</sub>(Cl<sub>2</sub><sup>2-</sup>)(Cl<sub>4</sub><sup>4-</sup>), electronic struct. studies by SCF, MSX $\alpha$  and INDO methods 0-74119  
CuF<sub>2</sub>(F<sub>4</sub><sup>4-</sup>), electronic struct. studies by SCF, MSX $\alpha$  and INDO methods 0-74119  
CuH, UV absorpt. spectra 0-87143  
D<sub>3</sub>, emission spectra, rot. struct. obs. mol. const. determ., predissociation 0-106331  
DyO, UV emission spectrum, high resolution, band systems and isotopic shifts 0-87146  
F<sub>2</sub>, electron impact excitation, dissociation of lowest electronic state 0-63839  
F<sub>2</sub>O, geometry, electron spectrum, vert. ionis. pot. ab initio calc. 0-58187  
FeX<sub>4</sub> (X=F, Cl and Br), electronic struct. and isomer shift 0-63545  
GeH<sub>3</sub>, electronic struct., electron affinity, inversion barrier, ab initio SCF Gaussian basis calc. 0-63552  
H<sub>2</sub>, Bender-Wu formula, SO(4,2) dynamical group and Zeeman effect, perturbation coeffs. determ. 0-95674  
H<sub>2</sub>, E,F' $\Sigma_u^+$  state, collisional and radiative props. 0-58357  
H<sub>2</sub>, electron impact excitation, to high Rydberg states, by threshold energy collision 0-83509  
H<sub>2</sub>, electronic chemical pot., natural orbitals occupation numbers and electronegativity 0-63509  
H<sub>2</sub>, electronic struct., valence bond model, pairwise correlation 0-78543  
H<sub>2</sub>, lowest singlet and triplet states, interactions, electronic force calcs. 0-63742  
H<sub>2</sub>, singlet superexcited levels, radiative emission 0-83415  
H<sub>2</sub>, states velocity auto-correl. function, relax time, neutron scatt. obs. 0-58401  
H<sub>2</sub><sup>+</sup>, bound states in strong mag. field 0-99438  
H<sub>2</sub><sup>+</sup>, mol. electron density distrib., binding/antibinding anal. 0-95534  
H<sub>2</sub>-Ar, states velocity auto-correl. function, relax time, neutron scatt. obs. 0-58401  
H<sub>2</sub><sup>+</sup>+H<sub>2</sub>→H<sub>3</sub><sup>+</sup>+H, state-selected ion-molecule reactions threshold electron-secondary ion coincidence technique obs. 0-85166  
H<sub>3</sub>, emission spectra, rot. struct. obs. mol. const. determ., predissociation 0-106331  
HBr, fine struct. in dissociative attachment cross sections 0-87248  
HCN, photodissoc., photoabsorpt., photoemission and CN form. obs. 0-87141  
HCN<sup>+</sup>,  $\Sigma^+$  and  $\Pi$  states, SCF and CI calcs. for determ. optimum linear geometries, bond angles calc. 0-74114  
HCl, vibr. excitation in electric discharge 0-87978  
HD<sup>+</sup>, Hellmann-Feynman theorem anomaly 0-63510  
HF, fine struct. in dissociative attachment cross sections 0-87248  
HF+Li→LiF+H, pot. energy surface, SCF and CI calcs. 0-71904  
HNC<sup>+</sup>,  $\Sigma^+$  and  $\Pi$  states, SCF and CI calcs. for determ. optimum linear geometries, bond angles calc. 0-74114  
HNO A' $\Pi$  excited state dipole moment, optical-optical double reson. Stark spectrosc. obs. 0-106337  
HNO, isomerism, low lying electronic states, ab initio MRD-CI calcs. 0-83291  
HNO, low-lying states, pot. energy surfaces calcs. 0-102460  
H<sub>2</sub>O, ground state, CI calcs. on triply and quadruply excited configs., basis set effects 0-95549  
H<sub>2</sub>O, ground state, cond. energies, higher-order excitation contribs. 0-58166  
H<sub>2</sub>O, mol. Rydberg S<sub>u</sub>-S and S<sub>u</sub>-T transitions, semi-empirical SCF MO calc. 0-91453  
H<sub>2</sub>O, multiplet states, SCF theory 0-69062  
H<sub>2</sub>O<sup>+</sup>, spin and rot. fine struct., orbital angular momentum 0-83247  
H<sub>2</sub>O<sup>+</sup>, vibr. and rot. struct., intensity factors and orbital angular momentum 0-83246  
HPN-HNP, isomerisation energies, ab initio MRD-CI calcs. 0-106271  
HS<sub>n</sub><sup>+</sup>, n=1-4, electronic struct., ab initio Hartree-Fock-Slater calcs. 0-74107  
HS<sub>n</sub><sup>2+</sup>, n=1-4, electronic struct., ab initio Hartree-Fock-Slater calcs. 0-74107  
H<sub>2</sub>S<sup>+</sup>, <sup>2</sup>B<sub>1</sub>, <sup>2</sup>A<sub>1</sub> and <sup>2</sup>B<sub>2</sub> electronic states, pot. energy curves, CI calcs. 0-87048  
H<sub>2</sub>S<sub>2</sub>, rot. barriers, internal rot. and electronic struct., valence electron study 0-83344  
H<sub>2</sub>S<sub>2</sub>, n=1-4, electronic struct., ab initio Hartree-Fock-Slater calcs. 0-74107  
HSO radical, Doppler-limited dye laser excitation spectroscopy, rot., distortion and spin-rot. interaction const. determ. 0-83383  
HSO-HOS, isomerisation energies, ab initio MRD-CI calcs. 0-106271  
H<sub>2</sub>Se, rot. barriers, internal rot. and electronic struct., valence electron study 0-83344  
HSiC-HCSi, isomerisation energies, ab initio MRD-CI calcs. 0-106271  
H<sub>2</sub>SiO, electronic struct., dipole moments, mol. polarisability, force fields, ab initio calcs. 0-78531  
H<sub>2</sub>Te<sub>2</sub>, rot. barriers, internal rot. and electronic struct., valence electron study 0-83344

## molecular electronic states continued

- He, Padé type variational functions, appln. to ground state 0-87025  
He<sub>2</sub>, 600 Å emission continuum struct., in 700-900 Å region in glow discharge 0-95641  
He<sub>2</sub>, laser-driven transitions to high Rydberg states 0-106360  
He, optical absorpt. spectra and kinetic behaviour 0-95635  
HeH<sup>+</sup>, electronic momentum distribution, Coulomb shift and correl. coeffs. 0-83266  
HgBr+O<sub>2</sub>(N<sub>2</sub>)(H<sub>2</sub>)(He)(Ne)(Ar)(Kr)(Xe), vibr. relax., rate coeffs., fluorescence obs. 0-63697  
HgBr<sub>2</sub>, electronic struct. and photodissoc., effective core pots. and POL(1) CI wave function 0-63560  
HgCl<sub>2</sub>, electronic struct. and photodissoc., effective core pots. and POL(1) CI wave function 0-63560  
I<sub>2</sub> in Ar, emission spectrum interpretation 0-95634  
<sup>127</sup>I<sub>2</sub>, energy levels near B-state dissociation limit, two-photon spectrosc. obs. 0-106367  
IBr, B' $\Pi$ (O<sup>+</sup>) excited state, laser-induced fluoresc. 0-58309  
ICN, A-state photolysis, I(P<sub>1/2,3/2</sub>) branching ratio wavelength depend. 0-81335  
K<sub>2</sub>, absorpt. and relax. const. determ. by optical laser pumping method 0-102550  
KrCl, B and C states, energy ordering from temp. depend. of emission spectra 0-78837  
LaF<sup>+</sup>, electronic spectra, rot. anal. and orbital configurations 0-83240  
Li<sub>2</sub>, MCSCF and CI calcs. 0-95526  
Li<sub>3</sub>, electronic struct., SCF and SCF-CI calcs. 0-87044  
Li<sub>3</sub><sup>+</sup>, electronic struct., SCF and SCF-CI calcs. 0-87044  
Li<sub>3</sub><sup>+</sup>, electronic struct., SCF and SCF-CI calcs. 0-87044  
Li<sub>4</sub>, MCSCF and CI calcs. 0-95526  
LiBH<sub>4</sub>, H bridged system, floating spherical Gaussian model 0-78518  
LiBeH<sub>3</sub>, H bridged system, floating spherical Gaussian model 0-78518  
LiBe(Mg)(Ca),  $\Sigma^+$  and  $\Pi$  states, mol. binding energy curves 0-58189  
LiCH<sub>3</sub>, H bridged system, floating spherical Gaussian model 0-78518  
Mg<sub>2</sub>, ground state, multiple scatt. X $\alpha$  calcs. 0-58149  
MgO, electronic transition strengths, shock tube meas. 0-87183  
MgOH, struct. and electronic props., ab initio calcs. 0-74113  
MnO, A' $\Sigma^+$ -X' $\Sigma^+$  electronic transition, rot. and hyperfine struct. 0-74134  
N<sub>2</sub>, electron impact excitation, to high Rydberg states, by threshold energy collision 0-83509  
N<sub>2</sub>, electron scatt., reson. excitation and dissociation attachment, vibr. state depend. 0-78717  
N<sub>2</sub>, electronic structure calcs., self-consistent, accelerating convergence of iterative process 0-87037  
N<sub>2</sub>, isoelectronic sequence, Rydberg transitions, term value-ionisation pot. correl. 0-58276  
N<sub>2</sub><sup>+</sup>, first  $\Pi_u$  state form. and decay 0-58177  
N<sub>2</sub><sup>+</sup>, Meinel system, high resolution spectrum to 11 250 Å 0-99497  
N<sub>2</sub><sup>+</sup>, partial photoionisation cross section and photoelectron angular distribution for X' $\Sigma_u^+$  state determ. 0-83429  
N<sub>2</sub><sup>+</sup>, X' $\Sigma_u^+$ -state, vibr. states asymmetry parameter and photoelectron spectrum 0-95591  
N<sub>2</sub><sup>2+</sup>, low-lying electronic states, pot. energy curves calcs. by SCF technique, vibr. and ionisation consts. 0-69091  
N<sub>2</sub><sup>2+</sup>, recomb. energy determ. from pot. curves 0-58335  
Ne, He ion nuclear pumped lasers feasibility study and quenching 0-64001  
NH<sub>2</sub>, pot. energy curves of X<sup>2</sup>B<sub>1</sub>, A<sup>2</sup>A<sub>1</sub>, <sup>2</sup>B<sub>2</sub> valence-shell and  $\pi_u^*$  3s-type Rydberg states calc. by CI 0-74138  
NH<sub>2</sub>, spin and rot. fine struct., orbital angular momentum 0-83247  
NH<sub>2</sub>, vibr. and rot. struct., intensity factors and orbital angular momentum 0-83246  
NH<sub>3</sub>, expansion cooled, mol. photoionisation, rot. struct., rot. predissoc. of excited states 0-91611  
NH<sub>3</sub>, mol. Rydberg S<sub>u</sub>-S and S<sub>u</sub>-T transitions, semi-empirical SCF MO calc. 0-91453  
NH(ND) X' $\Sigma^+$ , in inert gas solid, vibr. relax., matrix and isotope effects 0-95713  
NH<sub>3</sub>(ND<sub>3</sub>) in solid Ar, UV absorption spectra, temp. depend. of matrix spectra 0-63652  
NO,  $\gamma$  and  $\beta$  system, electronic transition probability 0-106332  
NO,  $\gamma$  band lines, collisional broadening coeff. and optical collision diameter 0-63714  
NO,  $\gamma$ (0,0) band, collisional broadening parameters 0-63713  
NO, IR emission Fourier transform spectroscopy, mol. rot.-vibr., RKR potential curve calc. 0-95618  
NO, X' $\Pi$  state, vibr. relax., IR-UV double reson. obs. 0-106338  
NO, Zeeman spectrum, mol. beam elec. reson. spectrosc. 0-91621  
NO+O<sub>3</sub>, fs-states and rot. states, effect on reactivity 0-89473  
NO<sub>2</sub>, ground state pot. surface, ab initio LCAO MO SCF calcs. 0-102461  
NO<sub>2</sub>, shock heated, visible emission 0-58274  
N<sub>2</sub>O, photoelectron spectrum, vibronic interaction and autoionis. effects 0-95680  
NOH isomerism, low lying electronic states, ab initio MRD-CI calcs. 0-83291  
Na zeolites, electronic struct., quantum chemical study 0-69058  
Na<sub>2</sub>, absorpt. and relax. const. determ. by optical laser pumping method 0-102550  
Na<sub>2</sub> in free jet expansion, internal-state distribution 0-83403  
Na<sub>2</sub>, Rydberg state, two-step polarisation labelling 0-87053  
Na<sub>2</sub>, wave function and potential energy curves for lowest  $\Sigma_u^+$ ,  $\Sigma_u^+$ ,  $\Sigma_u^+$ ,  $\Pi_u$ ,  $\Pi_u$ ,  $\Pi_u$  and  $\Pi_u$  states 0-63738  
Ne<sup>+</sup>+D<sub>2</sub>, energy-loss scaling in 0.5-3.5 keV 0-63768  
Ne<sup>+</sup>+D<sub>2</sub>(H<sub>2</sub>), energy-loss scaling in 0.5-3.5 keV 0-63768  
NiCu molecule, electronic states determ. by ab initio HF and CI methods 0-69087  
O<sub>2</sub>,  $\Pi_u$  diabatic Rydberg states, ab initio CI calcs. 0-95554  
O<sub>2</sub>,  $\Sigma_u^+$  ground state, pot. energy curve, direct CI method appl. 0-58165  
O<sub>2</sub>, A' $\Delta_u$  state, inversion, presence in nightglow and discharges 0-63616  
O<sub>2</sub> b' $\Sigma_u^+$  state prod. and deactivation following O(<sup>1</sup>D<sub>2</sub>) quenching 0-76493  
O<sub>2</sub> electron coincidence spectrosc., valence electron momentum distrib. and binding energies 0-102583  
O<sub>2</sub>, Rydberg states,  $\Sigma_u^+$ ,  $\Sigma_u^+$ ,  $\Pi_u$ ,  $\Pi_u$ ,  $\Sigma_u^+$  symm., ab initio CI study 0-99460  
O<sub>2</sub>, A' $\Pi_u$  state pot. energy curve, MCSCF calcs. 0-63565  
O<sub>2</sub><sup>+</sup>,  $\Pi_u$  state, quasi-bound levels, predissociation, band rot. anal., photofragment kinetic energy anal. 0-63650



**molecular electronic states continued**

- O<sub>3</sub>, line and band strengths in IR spectra, variational calcs. 0-87112  
 OH in flames, laser excitation dynamics 0-74201  
 ONF, J transitions, rot. Zeeman effect 0-63707  
 PN, absorpt. and emission spectra, electronic transition and vibr. obs. 0-91573  
 Pd<sub>2</sub>, ab initio relativistic core pot. studies of metal-metal bonding 0-106257  
 PdH, ab initio relativistic core pot. studies of metal-H bonding 0-106257  
 Pt<sub>2</sub>, ab initio relativistic core pot. studies of metal-metal bonding 0-106257  
 PtH, ab initio relativistic core pot. studies of metal-H bonding 0-106257  
 Ru(II) complex, carbonyl(pyridine)-phthalocyaninoruthenium(II), optical hole burning, matrix effects 0-102522  
 SF<sub>6</sub>, IR multiphoton dissociation studies, inverse bottle-neck effect 0-87193  
 S<sub>2</sub>N<sub>2</sub>, photoelectron spectrum, interpretation, Green's function calcs. 0-87175  
 SO<sub>2</sub>, IR multiphoton excitation and inverse electronic relax., mol. vibr. and fluoresc. 0-106349  
 SO<sub>2</sub>, shock heated, visible emission 0-58274  
 SeH<sub>2</sub>, isotope effects, Rydberg levels-ground state transitions, rot. const., VUV spectra obs. 0-58279  
 Si<sub>2</sub>, electronic struct. and bonding, atomic effective pot. appl. 0-95745  
 Sn<sub>2</sub>, in Ar matrix, absorpt., fluoresc. and reson. Raman spectra 0-95640  
 SrI, low-lying electronic states, vibr. anal. 0-106315  
 Te<sub>2</sub>, B<sub>0</sub><sup>+</sup>-b<sub>2</sub><sup>+</sup> system, transition assignment, IR and visible spectra obs. 0-58298  
 ThF<sub>4</sub>(Cl<sub>4</sub>), electronic struct., MS-SCF-X $\alpha$  calcs. and VUV photoelectron spectra 0-63710  
 TiN, electronic absorpt. spectrum, rot. anal. 0-78601  
 UC, electronic struct., comparison with photoemission spectra 0-91450  
 UF<sub>6</sub>(Cl<sub>4</sub>), electronic struct., MS-SCF-X $\alpha$  calcs. and VUV photoelectron spectra 0-63710  
 UN, electronic struct., comparison with photoemission spectra 0-91450  
 Xe<sub>2</sub>, dispersion damping functions and interaction energy calcs. 0-78673  
 XeBr, B and C states, energy ordering from temp. depend. of emission spectra 0-78837  
 XeCl, B and C states, energy ordering from temp. depend. of emission spectra 0-78837  
 XeCl<sub>2</sub>, electronic structure, MSW-SCF-X $\alpha$  method 0-78539  
 XeF laser performance, ground state population effect 0-63987  
 XeF<sub>2</sub>,  $\chi=2, 4, 6$ , electronic structure, MSW-SCF-X $\alpha$  method 0-78539  
 XeF<sub>2</sub>(C) state lifetime, quenching rate consts., photolysis in inert gas atmospheres 0-66816  
 Xe(nf)+SF<sub>6</sub>, l-changing collisions obs. 0-91633  
 ZrO, singlet-triplet separation meas. 0-78623

**molecular electronic structure** *see molecular electronic states***molecular energy level calculations**

- see also molecular electron correlations; molecular orbitals calculations; molecular rotation calculations; molecular rotation-vibration calculations; molecular vibration calculations; VB calculations*  
 alkynyl cations, struct., charge distrib., ab initio population anal. calcs. 0-58407  
 aromatic systems, alternant, sign-alternation rule for triplet state 0-102420  
 chemical reactions, quantum chemical methods appls. 0-93752  
 coordinate rotation calcs., complex basis function appls. 0-95515  
 diatomic hydrides, quantum mechanically calculated observables, reliability determ. 0-63505  
 effective atomic charge distribution in mols., multiple scatt. calcs. 0-83244  
 electronic energies, homogeneity prop. 0-63539  
 general SCF coupling operators, arbitrariness 0-99439  
 geometry optimisations, invariance criteria, symmetry conservation rules 0-58406  
 graph theory, eigenvalues of graphs with threefold symmetry 0-58123  
 Kirkwood-Pople-Schofield method, appls. to polarisabilities calcs. 0-83272  
 methoxy, Jahn-Teller induced rovibronic effect, nuclear spin-electron spin hyperfine Hamiltonian 0-83298  
 microscopic description 0-102433  
 model calculations, matching with experiment through linear regression 0-58243  
 molecular duplexes, graph construction yields 0-106245  
 molecular quantum mechanically calculated observables, reliability determ. 0-63505  
 N-electron system, Schrodinger eqn. soln. using antisymmetrisation 0-106246  
 phase integral approximations, advantages over JWKB approx. 0-87027  
 phenol-phenyl complex, electrostatic mol. pot. contour maps, MODPOT and VRDDO calcs. 0-102463  
 stilbene aza-analogues, lowest excited states, INDO/S calcs. 0-95545  
 transition probability evaluation in double asymmetric pot. well 0-69120  
 trioxane <sup>13</sup>C(<sup>18</sup>O) substituted, mol. consts. and rot. spectra 0-87096  
 universal variational functionals of electron densities, first-order density matrices, and natural spin-orbitals and solution of the  $\nu$ -representability problem 0-95516  
 Cu complex, Cu(NH<sub>3</sub>)<sub>3</sub>(NCX)<sub>2</sub>, X=O, S, electronic struct., stereochem. 0-58156  
 H<sub>2</sub>, electron repulsion matrix elements, asymptotic form, adiabatic representation 0-87038  
 H<sub>3</sub>, relative magnitudes of direct and indirect exchange, Heitler-London calcs. 0-69069  
 (H<sub>2</sub>O)<sub>2</sub>, difference electrostatic mol. pot. contour maps, basis set superposition effect 0-102462  
 SeOCl<sub>2</sub>, Pr<sup>3+</sup>(Nd<sup>3+</sup>)(Er<sup>3+</sup>), SbCl<sub>5</sub> acidified, Racah and Judd-Ofelt parameters in laser liqs. 0-106516

**molecular energy levels**

- see also macromolecular energy levels; molecular electronic states; molecular energy level calculations; molecular fine structure; molecular hyperfine structure; molecular libration; molecular polarisability; molecular reorientation; molecular resonant states; molecular rotation; molecular rotation-vibration; molecular vibration; molecular vibronic states; nuclear screening*  
 anharmonic corrections in unimolecular theory, Monte Carlo calcs. 0-83441  
 aromaticity, reson. energy in graph theory 0-91412  
 Auger lineshape anal. of molecules and solids 0-76113

**molecular energy levels continued**

- chemical bonding, antisymmetrised geminal power and simple correlated wave function 0-102423  
 diatomic molecules with Coulomb forces, time dependent Born-Oppenheimer approximation 0-105518  
 electron pairwise interactions, energy depend. on occupation numbers 0-102427  
 ethane, internal rot. splittings, vibr.-rot.-torsion energy levels perturbations 0-91531  
 Faraday effect measurement in pulsed mag. field 0-80758  
 fractional parentage coefficient identities, atomic, molecular spectroscopy applications 0-69050  
 methylene peroxide, struct., energy levels, ab. initio UHF and MRUHF NO CI calcs. 0-83287  
 mixed-valence system, diatomic molecule model 0-107751  
 O K-emission spectra, electron struct. 0-87099  
 one-electron polynuclear systems, Dirac eqn., variational soln. 0-83242  
 point charge model of molecules, Mulliken population anal. 0-102429  
 polymethine dye lasers, optical absorpt. 0-64009  
 quantum chemistry, conf., Kyoto, Japan, 29 Oct.-3 Nov. 1979 0-101659  
 quantum mechanical aspects of the molecular structure hypothesis 0-102421  
 quantum topology, theory of mol. struct. and its morphogenesis 0-106247  
 reduced Bessel functions calcs. for multipole and overlap integrals 0-83250  
 rotations and translations in isospin space 0-102431  
 spin-density functional formalism, correl. energies calcs., appls. and corrections 0-91433  
 Tamm-Dancoff approximation, 2p-h, rel. to other self energy approximants 0-83243  
 transitions, excitation by monochromatic laser radiation, Doppler-broadened transitions 0-78582  
 triatomic mols., bound state, mol. Aharonov-Bohm effect 0-83302  
 unified theory of atoms and atomic aggregates, self consistent theory 0-102418  
 CO, energy levels for perturbed Morse oscillators 0-78676  
 CO, one-electron props., corrections, Moller-Plesset perturbation theory calc. 0-95519  
 Co complexes, Co(III) mixed complexes, orbital angular momentum reduction, <sup>57</sup>Co NMR chemical shift 0-58137  
 H<sub>2</sub>, electronic struct., valence bond orbital method appl. 0-106268  
 HCl, one-electron props., corrections, Moller-Plesset perturbation theory calc. 0-95519  
 H<sub>2</sub>O, relative ionisation energies, Tamm-Dancoff approx. calcs. 0-83243  
 LiH, electronic struct., valence bond orbital method appl. 0-106268  
 N<sub>2</sub>, relative ionisation energies, Tamm-Dancoff approx. calcs. 0-83243  
 Na<sub>2</sub> vapour, IR absorpt. bands 0-102507  
 O<sub>2</sub>, symmetry adapted wave function generation using group theoretical projection operators 0-102428  
 SO<sub>2</sub><sup>2-</sup>, SO<sub>2</sub><sup>2-</sup>, O K-emission spectra, electron struct. 0-87099  
 SeO<sub>2</sub><sup>2-</sup>, SeO<sub>4</sub><sup>2-</sup>, O K-emission spectra, electron struct. 0-87099  
 SiH<sub>4</sub>(SiF<sub>4</sub>), electron rearrangement after inner shell ionisation by heavy charge particle impact 0-87043  
 UF<sub>6</sub>, relativistic scattered wave calculations 0-63538

**molecular excitation** *see beam-foil spectra; chemical reactions; Davydov splitting; discharges (electric); molecular fluorescence; optical pumping; photoionisation; radiation quenching***molecular fine structure**

- 9,10anthraquinone, lower triplet states, interactions and position, matrix isolation spectra 0-63634  
 benzene, IR spectra, fine struct. of rot.-vibr. bands 0-102504  
 chlorophyll, and related mols., in solid solns., fine-structured vibronic spectra under tunable dye laser excitation (*Russian*) 0-74164  
 diacetylhydrazine, <sup>14</sup>N NQR lines fine structure 0-63667  
 diformylhydrazine, <sup>14</sup>N NQR lines fine structure 0-63667  
 formic acid ions, fragmentation, energy selected, photoelectron-photoion spectra 0-95676  
 4-pyridine carbaldehyde, microwave spectrum, rot. assignments, quadrupole coupling consts. 0-91548  
 CaF, A<sup>1</sup>II-X<sup>2</sup> transition, HFS and fine struct., intermodulated fluoresc. spectra obs. 0-63695  
 HBr, fine struct. in dissociative attachment cross sections 0-87248  
 HF, fine struct. in dissociative attachment cross sections 0-87248  
 H<sub>2</sub>O vapour, visible absorpt. spectrum, fine struct. acoustooptical determ. 0-86450  
 H<sub>2</sub>O<sup>+</sup>, spin and rot. fine struct., orbital angular momentum 0-83247  
 NH<sub>2</sub>, spin and rot. fine struct., orbital angular momentum 0-83247  
 NH<sub>3</sub>, IR spectra, fine struct. of rot.-vibr. bands 0-102504  
 Ni<sub>3</sub>, in solid Ar, reson. Raman spectra 0-63638  
 SF<sub>6</sub>, IR spectra, fine struct. of rot.-vibr. bands 0-102504  
 SO<sub>2</sub>, absorption spectrum, meas. using frequency doubled pulsed dye laser 0-87144  
 SO<sub>2</sub>, absorption spectrum, meas. using frequency doubled CW dye laser 0-87145

**molecular fluorescence**

- acetylene, vibr. relax. study using laser-induced fluoresc. 0-74219  
 acetylene+inert gas, vibr. relax. study using laser-induced fluoresc. 0-74219  
 acridine, temp. depend. of fluoresc. decay meas. using picosecond techniques 0-99518  
 acridine orange, fluoresc. decay meas. by high repetition rate gated photon counting 0-86402  
 acrylonitrile, IR multiphoton dissociation, prod. of CN(X<sup>2</sup> $\Sigma^+$ ) and C<sub>2</sub>(a<sup>1</sup> $\Pi_u$ ) radicals 0-63723  
 F-actin, struct. changes in living muscle fibres, polarised UV fluoresc. microscopy 0-67037  
 adsorbed molecules, Raman and fluoresc. enhancement by surface roughness 0-102511  
 aliphatic amines, tertiary, fluoresc. decay 0-91590  
 alkyl benzenes, jet-cooled, vibr. relax., nanosecond time evolution 0-95584  
 para-alkylanilines having optically active modes, vibr. relax. studied by absorpt. and fluoresc. spectra 0-83340  
 alkylbenzenes, jet-cooled, vibr. relax., absorpt. spectra 0-74236  
 alkylbenzenes, jet-cooled, vibr. relax., fluoresc. spectra 0-78694  
 4-amino-N-methylphthalimide in n-propanol, nanosecond laser fluorimetry 0-102721  
 2-aminopurine, in viscous soln., fluoresc. quenching, emission, intensity and reson. transfer (*German*) 0-91599



# molecular fluorescence continued

anthracene in polychlorinated alkanes photochemical study by rapid scanning fluoresc. spectroscopy 0-86440  
anthracenes, exciplex form. with amines, form. kinetics and luminesc. props. 0-66792  
anthraquinone-xanthone liq. soln., upper excited singlet state, delayed fluoresc. 0-106345  
antibunching phenomena on single-scatterer fluorescence in weak-field limit 0-63580  
antimalarial drugs, lifetime meas. via reiterative convolution using fluorescence decay curves 0-57380  
aromatic hydrocarbons, sequential coupling 0-58297  
(2,2) (2,6) azulenophanes, mag. circular dichroism and anomalous fluoresc. spectra 0-83398  
Bengal pink-anthracene, mixed annihilation delayed fluoresc. 0-74193  
1,2-benzanthracene, secondary reson. radiation and hot energy transfer, soln. luminesc. 0-87167  
benzene + Hg, electronically excited, mol. fluoresc., vibr. relax. cross sections and equilibration rates determ. 0-87205  
benzene radical cation in solid Ar, fluorescence spectra obs. 0-83382  
benzene-d<sub>6</sub> + N<sub>2</sub> + CO<sub>2</sub>, electronically excited, mol. fluoresc., vibr. relax. cross sections and equilibration rates determ. 0-87205  
benzophenone vapour, fluoresc. and phosphoresc., nonradiative transitions between triplet and singlet state obs. 0-99516  
benzoxazole, aromatic derivatives, spectral luminesc. and lasing props. rel. to electronic struct. 0-99519  
benzyl radicals, monomethyl- and dimethyl-substituted, electronic spectra and radical affinity 0-63618  
biomolecule and membrane dynamics, fluoresc. spectroscopy 0-101148  
biphenyl polyenes, vibronic states, quasi-linear spectra (*Russian*) 0-95598  
bromofluoromethylene radical, laser-induced fluoresc., <sup>1</sup>A'-<sup>1</sup>A' transition 0-91589  
bromomethane, IR multiphotonic excitation, depend. on cell geometry, mol. fluoresc. and decomp. obs. 0-83430  
cells, living, fluorescently labelled mols. as probes of struct. and function, review 0-67321  
cetyltrimethylammonium bromide-1-butanol system, micellar conc. meas. using fluoresc. probe study 0-85217  
chlorophyll, and related mols., in solid solns., fine-structured vibronic spectra under tunable dye laser excitation (*Russian*) 0-74164  
chlorophyll a, absorpt. and fluoresc. spectra, observance of Stepanov relation 0-81554  
chlorophyll-a, fluoresc. at low concs., noise reduction by low pass filter for DC signal 0-87249  
chlorophyllide fluorescence quantum yield during photochlorophyllide reduction in etiolated leaves 0-81542  
chlorophylls, mag. reson., site selected fluoresc. detection 0-69164  
cholesteric liquid cryst., guest mol. fluoresc. in scatt. state 0-63698  
cluster containing tetracene molecules, excited state intramol. dynamics, laser-induced fluoresc. spectra obs. 0-78674  
conformational mobility, fluorescence obs. 0-63877  
coumarin laser dyes, fluoresc. quantum yields and lifetimes, polar solvent effects 0-87054  
coumarin laser dyes, solvent effects on photophysical parameters 0-91598  
p-cyano-N,N-dimethylaniline in polar solvents, double fluorescence, theoretical model 0-58296  
6-cyanobenzquinuclidine, intramol. electron-transfer excited state 0-85295  
4-cyanobiphenyl and 4'-alkyl- or 4'-alkoxy-substituted liq. cryst. derivatives, soln., absorpt. and fluoresc. spectra 0-87164  
cyclophosphazene-DNA complex, spectrofluorometric and spectrophotometric investig. 0-95643  
decay measurement via modulated gain spectroscopy 0-63699  
deconvolution nomogram for single exponential fluoresc. decays 0-67290  
diacetyl vapour, fluoresc. and phosphoresc., nonradiative transitions between triplet and singlet state obs. 0-99516  
3,6-diaminophthalimide vapour, mol. electronic excitation energy degradation path depend. on pentane 0-74195  
dichloromethane-d<sub>2</sub>, vibr.-vibr. energy transfer, laser-induced fluoresc. obs. 0-78689  
3,3-diethyl thiadiazolopyranine iodide dye, stimulated fluoresc. and stimulated reson. Raman scatt. relationship 0-91853  
3,3'-diethylthiadicarbonyl iodine-rhodamine 6G, energy transfer with increased local conc., Forster mechanism 0-69220  
S,p-difluorobenzene, time resolved fluoresc. spectra, direct view of intramolecular vibr. redistribution 0-83341  
difluoroethene, cis- and trans-, photoelectron-photoion coincidence study, fluoresc. obs. 0-95678  
dimethyl-s-tetrazine, vapour, mol. fluoresc., photodissoc. product 0-81352  
2,5-diphenyl-1,3,4-oxadiazole, fluoresc. quantum efficiency, one-photon dissociation, temp. depends. 0-69180  
2,5-diphenyl-1,3,4-oxadiazole, vapour, spectral, fluoresc., photochem. and laser props. 0-106344  
2,5-diphenyl-1,3-oxazole vapour, spectral, fluoresc., photochem. and laser props. 0-106344  
9,10-diphenylanthracene, refr. index meas. of frozen gas matrices, fluoresc. method 0-90884  
2,5-diphenylfuran vapour, spectral, fluoresc., photochem. and laser props. 0-106344  
1,6-diphenylhexatriene, radiationless transitions and natural lifetimes, solvent effects 0-63622  
diphenylpolyene molecules, excited electronic states, vibronic mixing, wave functions, method of fragments anal. 0-63615  
DODCI in ethanol, DQOCI added, electronic energy transfer, real-time ps meas. 0-58311  
DODCI in ethanol, malachite green added, electronic energy transfer, real-time ps meas. 0-58311  
dye, Q quenching for surface flow visualisation 0-79422  
dye laser, nanosecond laser fluorometry 0-102721  
dye monomolecular layers, energy transfer between sensitizers and acceptors 0-80861  
dyes, fast mode-locking, IR fluoresc. and laser action obs. 0-102717  
N-ethylphthalimide + olefins, photochemical reaction, absorpt., fluoresc., phosphoresc. and triplet-triplet absorpt. spectra 0-85197  
fast fluorescence spectroscopy, nanosec. range, using synchrotron radiation 0-62736  
flavins, meas. of sub ns fluoresc. decay by time-correl. photon counting and Ar laser 0-94429  
flexible chain molecules, mutual interpenetration, fluorescence obs. 0-63877

# molecular fluorescence continued

fluorescein dye, halogen substituted, in dimethyl sulphoxide, spectral evidence for anion-counterion association 0-71909  
fluoroanthene in micelles soln., fluoresc., halide ion induced quenching and enhancement 0-95672  
fluorobenzene radical cations in solid Ne, laser-induced fluoresc. spectra, vibr. struct. of excited and ground states 0-95671  
fluoromethane + fluoromethane, collision induced mode selective energy transfer, fluoresc. obs. 0-69177  
formaldehyde, sequential coupling 0-58297  
formaldehyde S<sub>1</sub> levels, collisionless single rot. level lifetimes, elec. field depend. 0-63566  
formaldehyde-d<sub>6</sub> (-d<sub>7</sub>), S<sub>1</sub> single rot. level lifetimes, isotope, elec. field and vibr. state depend. 0-78655  
gasoline-air flame, laser induced fluorescence spectra obs. 0-91587  
glyoxal, vapour, predissoc. in S<sub>1</sub> zero-point level states 0-102544  
halobenzene cations, in solid Ne matrix, slow vibr. relax., fluoresc. obs. 0-74194  
heterocyclics, intramolecular, picosecond time-resolved fluorescence studies 0-83401  
1,3,5-hexatriene radical cation, in Ne matrix, laser induced fluoresc. and emission spectra 0-87163  
hydroxyethyl cellulose, polymer segments, fluoresc. depolarisation on conjugated spin lables 0-91711  
intrastate scrambling in large mol. bound level struct., appl. to tetracene 0-63696  
iodomethyl radical, vibr. excited, photofragmentation IR emission obs. 0-87162  
IR laser photolysis of polyat. mols. photochem. appls. 0-66835  
kerosene-air flame laser induced fluorescence spectra obs. 0-91587  
lanthanide-porphyrin complexes, upper  $\pi\pi^*$  electronic states, fluoresc. 0-83410  
librational motion effects on fluoresc. depolarisation and NMR relax. in macromols. and membranes 0-85324  
metalloporphyrins, two quantum fluoresc. excitation from higher excited electronic states 0-106350  
methane, V-V energy transfer 0-83469  
methine dyes, spectral props., solvent effects 0-69181  
methoxy prod. from methyl nitrite photolysis 0-85200  
methoxy radical and deuterate, vibronic level fluoresc. spectrum 0-58305  
methoxy radical prod. from 266 nm photolysis of methyl nitrite 0-76534  
methyl radical, vibr. excited, photofragmentation IR emission obs. 0-87162  
methylamine, photochemical conversion to HCN with ArF laser, mol. fluoresc. obs. 0-97710  
9-methylanthracene, solubilisation in water by hypercoiled polymethacrylic acid 0-91591  
methylglyoxal, fluoresc. mag. field effect 0-102535  
1-methylindole-n-butanol (ethyl acetate), soln., ground state complex form., fluoresc. spectra, Stoke's shift origin 0-58299  
 $\beta$ -methylumbelliferone in ethanol solns., spontaneous luminesc. kinetics 0-74192  
monochromators for light scatt. and fluoresc. standard in colloid 0-57247  
myosin, struct. changes in living muscle fibres, polarised UV fluoresc. microscopy 0-67037  
naphthalene in Ar matrix, geometry changes and multiplet struct., mol. fluoresc. and phosphoresc. obs. 0-95663  
naphthyl group, excited singlet state, intramol. fluoresc. quenching by halogeno substituents 0-102537  
 $\beta$ -naphthylamine, fluoresc. quenching and spectra, excited state reaction, red edge effect obs. 0-83400  
naphthylamines, abnormal fluorimetric titration behaviour, kinetic anal., fluoresc. quantum yields and lifetime meas. 0-89560  
nitrosobenzene, fluoresc. quantum yields, determ. from Raman scatt. 0-58294  
organic dyes, fluoresc. spectra calcs.,  $\beta$ -variation method (*German*) 0-69182  
organic gases, IR fluoresc. by CO<sub>2</sub> laser 0-78619  
organic scintillators, vap. phase dye laser media, photophysical parameters 0-95884  
2-oxyphenylbenzoxazol, proton intramolecular transfer, light absorpt. and emission, dichroism, polarised fluoresc. 0-87166  
2,2 paracyclophane, dimer vibration influence on emission spectrum 0-69133  
paraterphenyl, fluoresc. quantum efficiency, one-photon dissociation, temp. depends. 0-69180  
pentacene, first excited singlet state, butterfly motion studied by fluoresc. spectra 0-78615  
perylene crystal, molecular exciton system, resonance Raman and fluorescence studies, dynamical effects 0-66169  
2-phenylindole, in viscous soln., fluoresc., quenching, emission, intensity and reson. transfer (*German*) 0-91599  
phenylnaphthalenes isomers, fluoresc. lifetime difference and mol. geometry 0-69176  
phosphatidylcholine bilayers, fluidity changes and phase transitions, intramol. excimer fluoresc. obs. 0-85342  
phthalocyanine, free base, fluoresc. excitation spectrum, cooling in supersonic free jet 0-95670  
planar aromatic hydrocarbons in polymer films, polarisation data interpretation, photoselection spectroscopy appl. 0-58302  
polydiacetylenes, visual conformational transitions, absorpt. and fluoresc. spectra, pH and electrolyte effect 0-102590  
polyethylene oxide, polymer segments, fluoresc. depolarisation on conjugated spin lables 0-91711  
polymer film, proton intramolecular transfer, light absorpt. and emission, dichroism, polarised fluoresc. 0-87166  
polymethine dye nonequilib. protolytic forms, lasing, fluoresc. and nonradiative transitions 0-102722  
polymethine saturable absorbing dyes, dual component fluoresc. lifetime meas. 0-106359  
POPOP, fluoresc. quantum efficiency, one-photon dissociation, temp. depends. 0-69180  
POPOP vapour, spectral, fluoresc., photochem. and laser props. 0-106344  
porphin free base, vibr. and normal mode anal. 0-69122  
prolate molecules in solvents, anisotropic fluoresc. (*German*) 0-69183  
propynal, rovibronic populations, collisionless IR multiphoton spectra, energy deposition, photoacoustic determ. 0-83354  
protochlorophyll, mag. reson., site selected fluoresc. detection 0-69164  
pseudozulenes, anomalous fluoresc., radiationless transitions 0-91593  
pyrazine, vapour, fluoresc. quantum yields, rot. effects 0-95661



## molecular fluorescence continued

- pyrene, distinction of delayed fluorescences  $S_1 \rightarrow S_0$  and  $S_2 \rightarrow S_0$  by selective quenching of  $S_1 \rightarrow S_0$  0-69175
- pyrene, migration between lipid vesicles in aq. soln., fluoresc. stopped-flow obs. 0-85360
- pyrene excimer fluorescence, erythrocyte membrane fluidity changes after X-irrad. obs. 0-72262
- pyrimidine, vapour, fluoresc. quantum yields, rot. effects 0-95661
- quasi-linear spectra and vibronic states of molecules with end phenyl rings (*Russian*) 0-95597
- Quinacrine Mustard, time-resolved fluoresc. spectrum 0-87165
- Raman and fluorescent scattering by molecules embedded in dielectric spheroids 0-99507
- resonance Raman lineshapes and fluorescence in strong radiation fields 0-87074
- rhodamine 6G<sub>2</sub> molecules in solution, photoluminescence study, fluorescence decay time 0-80832
- rhodamine 6G, in ethanol, time-depend. fluoresc. spectrum, using synchrotron radiation 0-62736
- rhodamine 6G ethanol soln., absorpt. and luminesc. spectra using picosecond excitation 0-106351
- rhodamine 6G solution, absolute fluoresc. quantum yield determ. by calorimetric method 0-78851
- rhodamine B in ethylene glycol, fluoresc. decay meas. via modulated gain spectroscopy 0-63699
- rhodamines, 5G, 6G, B, 3B in ethanol soln., luminesc. quenching by photoradiation 0-87168
- rhodopsin and thermal intermediates, fast struct. fluctuations in protein component 0-72137
- ruthenium trisbipyridyl ions in surfactant solns., excited state decay kinetics 0-83407
- Shpol'skii multisite luminesc. spectrum deconvolution, vibr. struct. anal. 0-58304
- sodium dodecyl sulphate micelles- $\omega$ -( $\alpha$ -naphthyl) dodecanoic acid soln. fluoresc. decay obs. 0-61158
- solutions, photoluminesc. decay time, donor conc. effect 0-66299
- spherical particle, surface enhanced Raman scatt. by molecules 0-95629
- stilbene, cis and trans, transient spectra, radiative lifetimes and quantum yields 0-78640
- trans-stilbene, soln., lifetime and anisotropic fluoresc., viscosity effects (*German*) 0-106352
- stilbene aza-analogues, lowest excited states, INDO/S calcs. 0-95545
- stilbenes, prolate molecules in solvents, anisotropic fluoresc. (*German*) 0-69183
- p-terphenyl vapour, spectral, fluoresc., photochem. and laser props. 0-106344
- tetrachloromethane, UV laser photolysis 0-66826
- tetrachloromethane+Xe, excitation functions and rotational polarisation, chemiluminesc., crossed beam study 0-76491
- tetramethyl pyrazine in durene, phosphorescent mols., quantum beats in triplet states 0-58312
- thiocarbonyl chlorofluoride, second excited singlet state emission spectroscopy, resonance fluorescence obs. 0-69158
- thioxanthone, fluoresc. and internal conversion, rel. to proximity effects 0-91592
- tri-n-propylamine, fluoresc. decay 0-91590
- trichlorofluoromethane, UV laser photolysis 0-66826
- triethylamine, fluoresc. decay 0-91590
- trimethylamine, collision induced fluoresc. enhancement and quenching, relax. processes 0-83412
- trimethylamine, electronically excited isolated mol., relax. and intramol. processes 0-83411
- trimethylamine, fluoresc. decay 0-91590
- tris(bipyridine)ruthenium(II)dichloride, fluoresc. decay meas. by high repetition rate gated photon counting 0-86402
- tropolone,  $\pi$ - $\pi^*$  singlet state, H<sup>+</sup> tunnelling dynamics and equilib. geometry 0-102539
- N<sub>3</sub>-undecylfluorimyl, high resolution fluoresc. and excitation spectroscopy, vibronic transitions obs. 0-78639
- vinyl copolymers, containing fluorescent groups, optically active 0-102594
- X-ray spectra observation using 5 m grating spectrograph 0-86538
- xanthene dyes in n-alcohols (ethylene glycol) (glycerol), rot. relax., time-resolved fluoresc. depolaris. obs. 0-58300
- Ar-Kr-F<sub>2</sub> mixture, nucl. induced excimer fluoresc. for I laser excitation 0-78846
- Ar\*+Fe(CO)<sub>5</sub>, chemiionisation and chemiluminescence reactions, Penning ionisation and fluoresc. obs. 0-97689
- BCl<sub>3</sub>, visible fluorescence dynamics due to IR laser irrad. (*Chinese*) 0-102534
- BO<sub>2</sub>, II vibronic states, laser induced fluoresc. obs. 0-58301
- Ba+HBr, laser induced fluoresc. study at different collision energies 0-91632
- Ba+HCl, laser induced fluoresc. study at different collision energies 0-91632
- BaO, excited electronic states, lifetimes and transition moments 0-87177
- Bi<sub>2</sub>, radiative lifetime and self-quenching cross sections meas. from laser induced fluorescence expt. 0-69189
- Bi<sub>n</sub>, molecular clusters, laser fluoresc. spectrosc. 0-95755
- Br<sub>2</sub> in Ar matrix, reson. Raman scattering amplitude damping in discrete reson. limit 0-58262
- Br<sub>2</sub>, Kr ion laser-excited fluorescence, predissoc. 0-83414
- Br<sub>2</sub>, long-lived A<sup>2</sup>Π(1<sub>g</sub>) state, quantum-resolved dynamics of excited states 0-69178
- Br<sub>2</sub>, single rot. states, lifetimes and collisional quenching cross sections determ. by obs. fluoresc. decay 0-91595
- Br<sub>2</sub>+Xe, excitation functions and rotational polarisation, chemiluminesc., crossed beam study 0-76491
- BrCl laser induced fluoresc., quantum resolved level dynamics in B<sup>2</sup>Π(0<sup>+</sup>) state 0-74188
- C in molecule, K-shell fluoresc. yield, statistical scaling 0-78644
- C<sub>3</sub> production, vibr. relax., chem. kinetics, following IR multiphoton allene photolysis 0-66820
- CD<sup>+</sup>, in RF ion trap, laser induced fluoresc. spectrum, 0,0 vibr. band and rot. consts. 0-74189
- CF<sub>2</sub>, excitation by Hg 253.7 nm line, reson. fluoresc.-spectra 0-63694
- CH(A<sup>2</sup>Δ) radicals, electronically excited, lifetimes and quenching rate constants meas. 0-69188
- CHF radical, A<sup>1</sup>A<sup>+</sup>-X<sup>1</sup>A' transition, laser induced fluoresc. 0-95660
- CN, B<sup>2</sup>Σ<sup>+</sup>←A<sup>2</sup>Π 0-0 and 1-0 bands, laser excitation spectra 0-91588
- CN, internal energy distrib. following vinyl cyanide photodissoc., temp. depend. 0-78638
- molecular fluorescence continued
- CN\*, B<sup>2</sup>Σ<sup>+</sup> state, fluoresc. decay dynamics, collisional quenching and radiative lifetimes 0-58306
- <sup>12</sup>C<sup>16</sup>O+<sup>13</sup>C<sup>16</sup>O, vibr. energy transfer, laser-induced fluoresc. obs. 0-78690
- CO<sub>2</sub> gas, electron impact ionisation, electronic fluoresc. spectra 0-95664
- CO<sub>2</sub>, laser-induced fluoresc. obs. of N<sub>2</sub>\*+H<sub>2</sub>O(H<sub>2</sub>S)(methane) deactivation 0-63776
- CO<sub>2</sub>+polyatomic molecule, (00<sup>0</sup>1) mode deactivation, laser induced fluoresc. obs. 0-83453
- C<sub>2</sub>O+NO(O<sub>2</sub>)(isobutene), absolute reaction rate consts. meas. by laser induced fluoresc. 0-93738
- CO\* prod. from Ar\*+CO<sub>2</sub>, use in laser systems 0-63824
- CO<sub>2</sub>\*+SO<sub>2</sub>, near-reson. energy transfer, fluoresc. obs. 0-106348
- CS, prompt emission and internal energy distrib. of X<sup>1</sup>Σ<sup>+</sup> state 0-106364
- Ca<sub>2</sub>, A<sup>1</sup>Σ<sup>+</sup>+X<sup>2</sup>Σ<sup>+</sup> system, laser induced fluoresc., pot. energy curve and mol. consts. 0-58307
- CaF, A<sup>2</sup>Π-X<sup>2</sup>Σ<sup>+</sup> transition, HFS and fine struct., intermodulated fluoresc. spectra obs. 0-63695
- CaF, B<sup>2</sup>Σ<sup>+</sup>+X<sup>2</sup>Σ<sup>+</sup> system, rot. and vibr. anal. 0-74156
- ClF UV laser system 0-83597
- CrO, A<sup>2</sup>Π-X<sup>2</sup>Π transition, rot. anal. laser induced fluoresc. and discharge emission spectra 0-69173
- CrO<sub>2</sub>Cl<sub>2</sub>, multiphoton induced inverse electronic relax. 0-66836
- Cs-H<sub>2</sub> vapour, resonant character of laser induced formation of particles 0-89481
- Cs<sub>2</sub>, laser-induced fluoresc. spectrum, diffuse band anal. 0-106346
- Cu<sup>+</sup>, 1,5-dimethyl-2,4-hexadiene, fluoresc. quenching method for determ. binding const. 0-89530
- D<sub>2</sub>O, vibr. relax. rates 0-95717
- F+HCl(HBr)(DBr)(HI), H abstraction reactions, temp. depend., laser photolysis IR fluoresc. obs. 0-93744
- F<sub>2</sub> UV laser system 0-83597
- GeF, use in chemical lasers 0-64004
- H<sub>2</sub>, E,F<sup>2</sup>Σ<sup>+</sup> state, collisional and radiative props. 0-58357
- H<sub>2</sub> singlet superexcited levels, radiative emission 0-83415
- H<sub>2</sub>+D(O)(Cl)(Br), relax. and chem. reaction, time resolved IR fluoresc. and mass spectrometry obs. 0-69177
- HCl+D(O)(Cl)(Br), relax. and chem. reaction, time resolved IR fluoresc. and mass spectrometry obs. 0-69177
- HF+HF (methane)(methane-d<sub>4</sub>), collision relaxation rate constants and rot. equilibration time meas. 0-69213
- HN<sub>3</sub>, UV photolysis 0-101027
- HO detection by laser excited fluoresc., press. depend. of fluoresc. and photolytic interferences 0-95666
- HO radical form. from H<sub>2</sub>+N<sub>2</sub>O reaction on Pt surface, laser-induced fluoresc. obs. 0-108738
- H<sub>2</sub>O, Pt catalytic oxidation of H<sub>2</sub> and D<sub>2</sub>, matrix isolation and laser fluoresc. obs. of prods. 0-66865
- H<sub>2</sub>O+H<sub>2</sub>O(He)(Ar)(N<sub>2</sub>)(O<sub>2</sub>)(CO<sub>2</sub>), vibr. energy transfer temp. depend. 0-63763
- He+LiH, rot. inelastic collisions, state-to-state cross sections determ. 0-87210
- He<sup>+</sup>+N<sub>2</sub>, collisional excitation processes, visible emission, cross-sections 0-99571
- HgBr+O<sub>2</sub>(N<sub>2</sub>)(H<sub>2</sub>)(He)(Ne)(Ar)(Kr)(Xe), vibr. relax., rate coeffs., fluoresc. obs. 0-63697
- HgBr<sub>2</sub>, photofragment fluoresc. polarisation, press. depend. 0-63720
- HgBr<sub>2</sub>+inert gas metastable atom (N<sub>2</sub>(A<sup>3</sup>Σ<sub>u</sub><sup>+</sup>)), dissoci. excitation 0-63774
- HgBr<sub>2</sub>+N<sub>2</sub>\*, dissociative excitation, mol. fluoresc. obs. 0-91634
- HgTl excimer laser, kinetics, optical excitation obs. 0-58527
- I<sub>2</sub>, B-X fluoresc. band system, intensity and relative band strengths meas. 0-102540
- I<sub>2</sub>, fluorescence, CW dye laser emission wavelength locking by intracavity gain 0-99721
- I<sub>2</sub>, laser fluoresc. state selected and detected mol. beam mag. reson., hyperfine transitions 0-63731
- I<sub>2</sub> lines, Franck-Condon factors, Ar<sup>+</sup>, Kr<sup>+</sup> and He-Ne laser excitation 0-58320
- I<sub>2</sub>, polarisability anisotropy, laser assisted mol. beam spectroscopy 0-78646
- IBr, B<sup>2</sup>Π(0<sup>+</sup>) excited state, laser-induced fluoresc. 0-58309
- IF emission spectrum and form. kinetics in electron-beam-produced plasma 0-102533
- <sup>127</sup>I<sub>2</sub>, Doppler-free optoacoustic spectroscopy 0-57396
- <sup>127</sup>I<sub>2</sub>, rovibronic absorpt. lines, hyperfine struct. 0-78596
- <sup>129</sup>I<sub>2</sub>, rovibronic absorpt. lines, hyperfine struct. 0-78596
- I<sub>2</sub>\*+He, low energy collisions, energy redistrib. 0-63765
- K<sub>2</sub>, absorpt. and relax. const. determ. by optical laser pumping method 0-102550
- K<sub>2</sub>, ground state thermalisation speed, collision cross-sections meas. (*Russian*) 0-78723
- KrCl, B and C states, energy ordering from temp. depend. of emission spectra 0-78837
- KrF, electron beam pumped laser medium, time depend. fluoresc. spectrum in high current density range 0-78842
- LiH, state selected rot. transition integral cross section, laser fluoresc. obs. 0-63770
- <sup>7</sup>LiH+HCN, rot. inelastic collision, energy transfer 0-87211
- N<sub>2</sub>, desorbed after N atom recomb. on Fe, vibr. energy, electron beam induced fluoresc. 0-61149
- N<sub>2</sub> gas, electron impact ionisation, electronic fluoresc. spectra 0-95664
- N<sub>2</sub>+Ar, metastable atom excitation of C<sup>2</sup>Π<sub>u</sub> state, symmetry, propensity rules and alternation intensity, rot. spectrum 0-87135
- N<sub>2</sub><sup>+</sup>+He, N<sub>2</sub><sup>+</sup> selectively excited, collisional deactivation 0-83338
- NF+H(NF), electronically-excited free radical reactions 0-97707
- NF<sub>3</sub>+H(O)(N), electronically-excited free radical reactions 0-97707
- N-F<sub>3</sub>, mol. photodissoc. using CO<sub>2</sub>-laser radiation, rate const. meas., mol. fluoresc. and time-resolved UV spectra obs. (*German*) 0-83434
- N-F<sub>3</sub>, multiphoton excitation and vibr. energy flow, fluoresc. obs. 0-95673
- NH radical formed in NH<sub>3</sub> dissoci., fluoresc. spectrum, rotational relaxation 0-58310
- NH<sub>3</sub>+NH<sub>3</sub>(He)(Ar)(N<sub>2</sub>)(O<sub>2</sub>), vibr. energy transfer temp. depend. 0-63763
- NO electronically excited photofragment of VUV photodissoc. methylnitrite, identification and quantum yield 0-99527
- NO measurements in CH<sub>4</sub>-O<sub>2</sub>-N<sub>2</sub> flame by laser fluorescence 0-61178
- NO<sub>2</sub>, fluoresc. spectra and collisional quenching 0-102538
- N<sub>2</sub>O gas, electron impact ionisation, electronic fluoresc. spectra 0-95664



## molecular fluorescence continued

- $\text{N}_2\text{O} + \text{SF}_6$ , vibr.-vibr. energy transfer, fluoresc. 0-78688  
 $\text{Na}_2$ , absorpt. and relax. const. determ. by optical laser pumping method 0-102550  
 $\text{Na}_2$  in free jet expansion, internal-state distribution 0-83403  
 $\text{Na}_2 + \text{He}$ , rot. transitions differential cross sections, laser fluoresc. meas. 0-63771  
 $\text{NaK}$ , laser induced  ${}^1\Pi\text{-}^3\Sigma$  fluorescence, mol. vibr. 0-87160  
 $\text{NdO}$ , electronic spectrum, rotational struct. anal. 0-78643  
 $\text{Ne}^* + \text{Fe}(\text{CO})_5$ , chemionisation and chemiluminescence reactions, Penning ionisation and fluoresc. obs. 0-97689  
 $\text{O}$  in molecule, K-shell fluoresc. yield, statistical scaling 0-78644  
 $\text{O} + \text{CS}_2 \rightarrow \text{CS} + \text{SO}$ , vibrational distribution of  $\text{CS}$ , laser-induced fluoresc. meas. 0-71895  
 $\text{O} + \text{saturated hydrocarbon}$ , chem. reaction dynamics. OH prod. investig. 0-101016  
 $\text{O} + \text{saturated hydrocarbon} \rightarrow \text{OH} + \text{alkyl radical}$ , reaction dynamics, mol. beam-laser induced fluoresc. obs. 0-97695  
 $\text{O}_2$ , laser excited, quenching by  $\text{CO}_2$ ,  $\text{H}_2\text{O}$  and  $\text{I}_2$  0-99515  
 $\text{O}_2$ , UV absorpt. spectra, IR laser induced changes 0-83385  
 $\text{OCS}$ , vibr. energy transfer map 0-99560  
 $\text{OH } A^2\Sigma^+$  state, laser excited, vibr. energy transfer, flame thermometry appls. 0-58349  
 $\text{OH}$ , laser induced fluoresc. spectrosc. for flame temperature meas. 0-90839  
 $\text{OH}$ , Pt catalytic oxidation of  $\text{H}_2$  and  $\text{D}_2$ , matrix isolation and laser fluoresc. obs. of prods. 0-66865  
 $\text{OH} + \text{H}_2\text{O} \rightarrow \text{HO}_2 + \text{H}_2\text{O}$ , reaction rate const., laser induced fluoresc. 0-101017  
 $\text{OH} + \text{NO}(\text{NO}_2)(\text{O}_2)$ ,  $\text{OH}(\nu=1)$  relax., time resolved spectra 0-74240  
 $\text{OH}(\nu, \text{N})$  bimodal rot. distrib. from  $\text{O}({}^1\text{D}_2) + \text{NH}_3$  0-76501  
 $\text{S}_2$ , matrix-isolated,  $\text{B}^2\Sigma_g^-$  predissoc., relax. processes 0-58329  
 $\text{S}_2$  vapour,  $x=3$  to 8, UV absorption and fluorescence spectrosc., vibrational constants of  $\text{S}_2$  0-78631  
 $\text{SF}_6$ , IR multiphotonic excitation, depend. on cell geometry, mol. fluoresc. and decomp. obs. 0-83430  
 $\text{SO}^+ ({}^2\Pi\text{-}{}^2\Sigma^+)$  emission following  $\text{He}^+ + \text{SO}_2$  afterglow reaction 0-95659  
 $\text{SO}_2$ , IR multiphoton excitation and inverse electronic relax., mol. vibr. and fluoresc. 0-106349  
 $\text{SO}_2$ , single vibronic level fluoresc. spectra 0-91597  
 $\text{SO}_2$ , UV excitation spectra, mol. fluoresc. meas., mol. predissoc. obs. 0-83389  
 $\text{SO}_2\text{-}^{18}\text{O}$  mixtures, IR laser pumped, intermol. vibr. energy transfer dynamics obs. 0-87207  
 $\text{S}_2\text{O}$ , UV excitation spectra, mol. fluoresc. meas. 0-83389  
 $\text{SO}_2\text{F}$ , dye laser excitation of vibr. levels of upper electronic state, mol. fluoresc. meas. 0-83402  
 $\text{Se}_2$ , laser induced fluoresc. in inert gas matrix 0-87161  
 $\text{SeO}_2 + \text{Ar}(\text{N}_2)(\text{CO}_2)$ , radiative lifetime and quenching rates 0-95685  
 $\text{SiF}$ , use in chemical lasers 0-64004  
 $\text{Sn}_2$ , in Ar matrix, absorpt., fluoresc. and reson. Raman spectra 0-95640  
 $\text{SnF}$ , use in chemical lasers 0-64004  
 $\text{Sr}_2$  dimer, photoassoc., photoluminesc., collisional dissoc. 0-58303  
 $\text{Te}_2$ ,  $\text{BO}_2^+ \rightarrow \text{b}^2\Sigma_g^+$  system, transition assignment, IR and visible spectra obs. 0-58298  
 $\text{Te}_2$ , laser induced fluoresc. in inert gas matrix 0-87161  
 $\text{UF}_6$ , matrix isolated, vibronic fine struct. in fluoresc. spectrum 0-83406  
 $\text{UF}_6$  molecule dissociation in two-frequency IR laser field 0-66855  
 $\text{Xe}_2$  excimer laser, electron beam excitation, VUV fluoresc., lasing 0-87379  
 $\text{XeBr}$ , B and C states, energy ordering from temp. depend. of emission spectra 0-78837  
 $\text{XeCl}$ , B and C states, energy ordering from temp. depend. of emission spectra 0-78837  
 $\text{XeCl}$  laser, B-X, form. and quenching kinetics 0-74341  
 $\text{XeF}$  electron-beam-pumped laser, characts., 300-600K 0-78839  
 $\text{XeF}$  laser performance, ground state population effect 0-63987  
 $\text{XeF}^*$ ,  $\text{B}^2\Sigma^+$  and  $\text{C}^2\Pi_{3/2}$  states, fluoresc. decay dynamics, collisional quenching and radiative lifetimes 0-58306  
 $\text{XeI}^*$ , production via laser absorpt. processes at 193 nm, quenching kinetics 0-91466  
 $\text{ZrO}$ , B  ${}^2\Pi\text{-}X^1\Sigma$  intercombination transitions rel. to singlet-triplet separation 0-78623

## molecular force constants

see also Coriolis force

- acetylene(-d), Raman and vibr. spectra and force const. calcs. 0-108747  
 alkali metal halide dimers, mol. force const. and vibr. amplitudes calc. using electron gas model data 0-87245  
 aromatic compounds, out-of-plane mol. vibrs., force field approx. calcs. 0-91538  
 benzene, corrected valence force field, force constants calc. 0-63868  
 benzene, out-of-plane mol. vibrs., force field approx. calcs. 0-91538  
 borazines, substituted, Urey Bradley force field, pot. energy const. 0-78588  
 bridge angle, vibr. behaviour, simplified and accurate calcs. 0-95735  
 cis-1-cholobutadiene-1,3, microwave spectrum, struct., nuclear quadrupole coupling, distortion const., thermodynamic functions calc. 0-99500  
 diatomic mol. vibr. rot. Hamiltonian expansion, Born Oppenheimer  $\kappa$ , explicit introduction 0-69118  
 diatomic systems, nonadiabatic coupling matrix elements by Hellmann-Feynman theorem and HF 0-83263  
 1-10-dicarba-closo-decaborane (10), mol. struct., vibr. and shrinkage corrections calc. from force field 0-95739  
 dimethylphosphines, IR spectra, coupling between methyl rocking, PH bending, and PC stretching, force field interpretation 0-69141  
 ethane, inclusion of nonbonded interactions in vibr. freq. calcs. 0-95590  
 force field calcs., damped least-squares method 0-91533  
 formaldehyde, electronic struct., dipole moments, mol. polarisability, force fields, ab initio calcs. 0-78531  
 formaldehyde, excited state vibr. freq. calcs. by method based on scaled ab initio force fields 0-87092  
 formaldehyde, force field calcs., damped least-squares method 0-91533  
 formamide, force const. and dipole moment derivatives, ab initio MO calcs. 0-95521  
 formic acid (-d), microwave spectra and rot. const., astrophysical appl. 0-91550  
 formic acid dimer, vibr. spectra, CNDO/2 interpretation (French) 0-58155

## molecular force constants continued

- cis-formic acid geometry, force fields and fundamental vibr. freq., ab initio study 0-87040  
 formic acid- $\text{d}_2$ (- $\text{d}_1$ )(- $\text{d}_1$ )(- $\text{d}_2$ ), vibr. spectra, CNDO/2 interpretation (French) 0-58155  
 Group IV tetrabromides, intramol. force fields and mean vibr. amplitudes 0-106316  
 hexahalo ions, octahedral, mol. const. calcs. 0-106317  
 hexahaloanions of group IV A and V, mol. const. determ. 0-87093  
 hexaoxy ions, octahedral, mol. const. calcs. 0-106317  
 hydrides, first row, bending pot. calc. using MINDO approx., force const., equilb. geometry 0-95544  
 methyl fluoride, harmonic force field calcs. and exptl. configs. 0-63865  
 methyl halides, mol. force field at SCF ab initio levels, quantum-mechanical calc., LCAO-MO method 0-106319  
 methylene glycol(- $\text{d}_4$ )=formaldehyde(- $\text{d}_2$ ) +  $\text{H}_2\text{O}(\text{D}_2\text{O})$  Raman spectra and normal vibr. 0-58271  
 naphthalene, out-of-plane mol. vibrs., force field approx. calcs. 0-91538  
 organic molecules, small, harmonic force const., vibr. freqs., integrated intensities, MINDO/3 method 0-58411  
 organometallic amines, Raman and IR spectra, band intensity and assignment, force const. determ., vibr. props. (German) 0-87133  
 perovskites, ordered cubic, cationic effect on intramolecular forces, stretching force const. 0-88979  
 polyatomic force fields, Ohwada's pairwise interaction model 0-106321  
 polyatomic mol. force const. and heat of atomisation, approx. separable pot. function 0-78675  
 polyatomic molecule, intramolecular coord. relax., generalised classical theory 0-78589  
 pyramidal molecules and ions, bond polarisability and force constants 0-69260  
 pyridine(-d), force const. and vibr. spectra by CNDO/2 force method 0-95540  
 semicarbazide hydrochloride, vibr. spectra, normal coord. anal. 0-58255  
 semicarbazide- $\text{d}_6$ , - $\text{d}_4$ , vibr. spectra, normal coord. anal. 0-58255  
 terpenes, methyl groups internal rotation,  $^{13}\text{C}$  spin lattice relaxation times and force field calcs. 0-74255  
 tetrafluoromethane, mol. const. and mean vibr. amplitudes calcs. 0-106318  
 thioformaldehyde, electronic struct., dipole moments, mol. polarisability, force fields, ab initio calcs. 0-78531  
 triatomic inorganic mols., harmonic force const., vibr. freqs., integrated intensities, MINDO/3 method 0-58411  
 triatomic molecule, rot. vibr. electronic Hamiltonian, Born-Oppenheimer approx., breakdown 0-87097  
 trifluoroethene- $\text{d}_3$ , mol. struct., microwave and electron diff. obs. 0-58384  
 trigonal and triatomic molecules, orbital valency force field const. calcs. 0-78516  
 tris(trimethylstannyl)amine, gas phase electron diffraction 0-106401  
 uranyl complexes, IR spectra and bond distances 0-74167  
 valence force constants in planar and pyramidal  $\text{XY}_3$  molecules, effective nuclear charge model appln. 0-63864  
 vibrational intensity calcs., CNDO/2 method with extended basis set 0-91445  
 $\text{XY}_2$  bent symmetrical molecules, Coriolis coupling const., centrifugal distortion const. 0-58236  
 $\text{XY}_2$  linear symmetric mols., chem. perturbations, Green's function calcs. 0-63866  
 $\text{XY}_4$  molecules, force const. by modified Redington and Aljibury method 0-69261  
 $\text{XY}_6$  molecules,  $\text{D}_{3h}$  symm., U-, G-, F- and  $\Sigma$ -matrix determ. (French) 0-78599  
 $\text{Al}_2\text{Cl}_6$ , matrix isolated, vibr. spectra, isotopic fine struct. and valence force field calcs. 0-58258  
 $\text{ArHBr}$ ,  $\text{ArHCl}$  and isotopic forms, rot. spectra, mol. struct., mol. const. 0-58246  
 $\text{B}_2\text{O}_3$ , bipyramidal struct., stability, ab initio SCF-MO calcs. 0-99446  
 $\text{C}_3$ , ground state pot. surfaces, analytical functions 0-83304  
 $\text{CF}_3\text{S}$ , mol. const., kinetic const. method calcs. 0-58235  
 $\text{CF}_3\text{Se}$ , mol. const., kinetics const. method calcs. 0-58235  
 $\text{CH}_3$ ,  $\text{CH}_2$  and CH deformation vibration group frequencies and MO electron densities, interaction force const. 0-87101  
 $\text{CO}_2$ , dipole moment functions 0-87094  
 $\text{CO}_2$ , stretch-stretch interaction force const., electron correlation influence, ab initio CI study 0-58161  
 $^{13}\text{C}$ ,  $^{13}\text{C}$  spin-spin coupling const. and stretching force const., single and double bonds 0-63867  
 $\text{Ca}_2$ ,  $\text{A}^2\Sigma_u^+ \rightarrow \text{X}^2\Sigma_g^+$  system, laser induced fluoresc., pot. energy curve and mol. const. 0-58307  
 $\text{CdF}_2(\text{FCl})(\text{FBr})$ , matrix isolated IR and Raman spectra, assignments, force const., isotope effects and thermodynamic props. 0-63631  
 $\text{CrBr}_4$ , mol. const. and mean vibr. amplitudes calcs. 0-106318  
 $\text{CrCl}_4$ , mol. const. and mean vibr. amplitudes calcs. 0-106318  
 $\text{Cu}$  complex,  $\text{Cu}(\text{NH}_3)_2(\text{NCX})_2$ , X=O, S, electronic struct., stereochem. 0-58156  
 $\text{FCO}$ , form. in Ar matrix, vibr. and electronic spectra, valence force potential determ., mol. photodissoc. obs. 0-85170  
 $\text{FeCl}_3$ , intramolecular force fields, compliance const. and vibr. amplitudes 0-58234  
 $\text{Ga}$  trihalides, vibr. anal., pot. const. determ., mol., compliance and Coriolis coupling const. calc. 0-95579  
 $\text{GaCl}(\text{Br})(\text{I})_2$ , intramolecular force fields, compliance const. and vibr. amplitudes 0-58234  
 $\text{GaI}$ , rot. spectrum, EHF spectra obs. 0-58245  
 $\text{GeH}_3\text{X}$ , (X=F, Cl, Br, I), force fields and const., Redington's method calcs. 0-58130  
 $\text{HBF}_2$  and  $\text{DBF}_2$ , harmonic force field and ground-state average struct. determ. 0-83342  
 $\text{HCN}$ , ground state pot. surfaces, analytical functions 0-83304  
 $\text{HCP}$ , force fields and force const. of electronically excited states 0-69116  
 $\text{HD}^+$ , Hellmann-Feynman theorem anomaly 0-63510  
 $\text{H}_2\text{SiO}$ , electronic struct., dipole moments, mol. polarisability, force fields, ab initio calcs. 0-78531  
 $\text{Hg}$  complex, methylthynylmercury(II)(- $\text{d}_1$ ,- $\text{d}_3$ ,- $\text{d}_4$ ), vibr. spectra and normal coord. calcs. 0-58259  
 $\text{HgF}_2(\text{FCl})(\text{FBr})$ , matrix isolated IR and Raman spectra, assignments, force const., isotope effects and thermodynamic props. 0-63631  
 In trihalides, vibr. anal., pot. const. determ., mol., compliance and Coriolis coupling const. calc. 0-95579



**molecular force constants continued**

- $\text{InCl}_3$ , intramolecular force fields, compliance const. and vibr. amplitudes 0-58234  
 $\text{KrHBr}$ ,  $\text{KrCHI}$ , and isotopic forms, rot. spectra, mol. struct., mol. const. 0-58246  
 $\text{Li}_2\text{F}_2$ , struct., force fields and normal mode freqs., ab initio calcs. 0-83260  
 $\text{LiH}_2(\text{LiD})_2(\text{LiT})_2$ , pot. surfaces, fundamental freqs. and thermodynamic functions 0-69205  
 $\text{Li}_2\text{H}(\text{Li}_2\text{D})(\text{Li}_2\text{T})_2$ , pot. surfaces, fundamental freqs. and thermodynamic functions 0-69205  
 $\text{N}_2^+$ , high press. IR vibr. spectroscopy (*German*) 0-74170  
 $\text{NH}_2$  radical, mag. hyperfine interactions, zero-point vibr. effects 0-58167  
 $\text{NH}_3$ , vibr. excitation in soft X-ray emission and core ESCA spectra 0-69163  
 $\text{NH}_3^+$  radical, mag. hyperfine interactions, zero-point vibr. effects 0-58167  
 $\text{NH}_4^+$  mol. const. and mean vibr. amplitudes calcs. 0-106318  
 $\text{N}_2\text{H}_2^+$  radical, mag. hyperfine interactions, zero-point vibr. effects 0-58167  
 $\text{NO}_2^+$ , high press. IR vibr. spectroscopy (*German*) 0-74170  
 $\text{NO}_2^+$ , gas phase equilib. geometry, force const., vibr. freq., dipole moment function MCSCF/CI calcs. 0-78520  
 $\text{N}_2\text{O}$ , dipole moment functions 0-87094  
 $\text{N}_2\text{O}^+$  force fields and force const. of electronically excited states 0-69116  
 $\text{NiO}$ , bulk props., initial state  $\text{MO}$   $\text{Ni}_4\text{O}_4$  and  $\text{Ni}_3\text{O}_{14}$ , cluster model, lattice and force const., photoemission and CT absorpt. spectra 0-84828  
 $\text{OH}$ , optimum mol. const. and term values,  $\text{X}^2\Pi$  and  $\text{A}^2\Sigma^+$  states, vibr.-rot. and microwave freqs. 0-95577  
 $\text{Pt}$  complexes, INDO calcs. for predicting ground-state props., charge distributions and force const. determ. 0-83283  
 $\text{SO}_2$ , surface reaction and decomposition on zeolites, resonance Raman study 0-61145  
 $\text{SeH}$ , isotope effects, Rydberg levels-ground state transitions, rot. const., VUV spectra obs. 0-58279  
 $\text{SiHX}_3$  ( $\text{X}=\text{F}, \text{Cl}, \text{Br}, \text{I}$ ), force fields and const., Redington's method calcs. 0-58130  
 $\text{Te}_2^{2+}$ , pseudopot. SCF-MO calcs., spectrum assignments 0-83269  
 $\text{XeF}_2$ , pseudopotential SCF-MO studies, equil. struct., stretch-stretch interaction force const. 0-95525  
 $\text{XeF}_4$ , pseudopotential SCF-MO studies, equil. struct., stretch-stretch interaction force const. 0-95525  
 $\text{XeF}_5^+$ , pseudopot. SCF MO studies, steric aspects of struct. and force fields, Jahn-Teller effect 0-99444  
 $\text{XeF}_6$ , pseudopot. SCF MO studies, steric aspects of struct. and force fields, Jahn-Teller effect 0-99444  
 $\text{ZnF}_2(\text{FCl})(\text{FBr})$ , matrix isolated IR and Raman spectra, assignments, force const., isotope effects and thermodynamic props. 0-63631

**molecular force fields** *see molecular force constants***molecular hyperfine structure**

- azaphenanthrenes, lowest triplet state zero field splitting parameters calcs. 0-83391  
 benzenoid aromatics, triplet zero field splitting parameters, ODMR obs., struct. effects 0-78636  
 copper (II) complex, bis(dithiocarbamate), HF-Slater-LCAO calcs., mag. coupling parameters and optical spectrum 0-99447  
 cyclopropyl cyanide, high-resolution microwave spectra, quadrupole hyperfine struct. of rot. transitions anal. 0-95601  
 cytochrome  $c_3$ , haeme-haeme mag. interaction, Mossbauer obs. 0-108836  
 ethyldimine, pyrolysis product, microwave spectra, rot. distortion and electric quadrupole const. and rot. barriers determ. 0-78608  
 formaldehyde,  $\text{A}''$  state, zero-field splitting param., ab initio CI calcs. 0-99454  
 formaldehyde anion radical, hyperfine coupling const., vibr. depend., ab initio calcs. 0-87150  
 free radicals, hyperfine struct., EPR spectra method determ. 0-102531  
 hexafluorobenzene anion-radicals in squalene, ESR spectrum optical detection 0-95655  
 hexafluorobenzene radical anion,  $^{13}\text{C}$  hyperfine interaction, EPR obs. 0-83392  
 3-iodopropene, rot. spectra, quadrupole hyperfine struct. 0-91545  
 lowest triplet state zero field splitting parameters calcs. 0-83391  
 methane, rotational state, avoided-crossing molecular beam spectroscopy 0-63730  
 methoxy, Jahn-Teller induced rovibronic effect, nuclear spin-electron spin hyperfine Hamiltonian 0-83298  
 methyl bromide, NQR and  $\text{A}_1\text{-A}_2$  splitting, RF spectrosc. inside laser cavity 0-91579  
 methyl radical, hyperfine coupling const., vibr. depend., ab initio calcs. 0-87150  
 nitrosylhaemoglobin, electron spin distrib. 0-83528  
 pentacene in naphthalene, triplet state, EPR study by electron spin-echo and laser flash excitation 0-58172  
 phenanthrene, lowest triplet state zero field splitting parameters calcs. 0-83391  
 planar cyclic radicals, C-H proton isotropic hyperfine const., C hybridisation 0-95646  
 radical pairs recombination probability in liqs., HF mag. field, reson. effect 0-93737  
 tetramethyl pyrazine in durene, phosphorescent mols., quantum beats in triplet states 0-58312  
 trifluoriodomethane, laser microwave double reson. spectroscopy with  $\text{CO}_2$  laser lines 0-87156  
 xanthione, large zero-field splitting of lowest triplet state 0-58171  
 Ar-acetylene van der Waals molecule, radiofreq. spectroscopy and Stark effect meas., equil. struct. and props. 0-91543  
 $\text{CaF}_2$ ,  $^2\Sigma$  ground state, laser-RF double reson. spectrosc. 0-69171  
 $\text{CaF}$ ,  $\text{A}^2\Pi\text{-X}^2\Sigma^+$  transition, HFS and fine struct., intermodulated fluoresc. spectra obs. 0-63695  
 $\text{Cu}$  complex,  $\text{N,N}'$ -ethylenbis (salicylaldiminato) copper (II)-thiourea, in solns., bond strength and hyperfine linewidth, EPR 0-74186  
 $\text{Cu}$  complex,  $\text{N,N}'$ -o-phenylenebis (salicylaldiminato) copper (II)-thiourea, in solns., bond strength and hyperfine linewidth, EPR 0-74186  
 $\text{GeH}_4$ , avoided-crossing molecular-beam spectroscopy, hyperfine and spin rot. const. and rot. g factors determ. 0-78671  
 $\text{H}_2\text{-H}_2$  dimers, hyperfine struct. in zero mag. field 0-95700

**molecular hyperfine structure continued**

- $\text{HI}$  nuclear quadrupole HFS in IR spectrum, obs. using tunable diode laser 0-58412  
 $\text{HeCN}^+$ , SCF calcs., dissociation energies, rot. and hyperfine const. determ. 0-95531  
 $\text{I}_2$ , B-X transitions, rot.-vibr. hyperfine coupling const., extension to other levels 0-63625  
 $\text{I}_2$ , laser fluoresc. state selected and detected mol. beam mag. reson., hyperfine transitions 0-63731  
 $^{129}\text{I}_2$ , rovibronic absorpt. lines, hyperfine struct. 0-78596  
 $^{129}\text{I}_2$ , complete hyperfine spectrum obs. at 612 nm 0-95638  
 $^{129}\text{I}_2$ , rovibronic absorpt. lines, hyperfine struct. 0-78596  
 $\text{MnO}$ ,  $\text{A}^2\Sigma^+\text{-X}^2\Sigma^+$  electronic transition, rot. and hyperfine struct. 0-74134  
 $\text{NH}_2$  radical, mag. hyperfine interactions, zero-point vibr. effects 0-58167  
 $\text{NH}_3^+$  radical, mag. hyperfine interactions, zero-point vibr. effects 0-58167  
 $\text{N}_2\text{H}_2^+$  radical, mag. hyperfine interactions, zero-point vibr. effects 0-58167  
 $\text{NHD}$ , rotational transitions, microwave optical double resonance obs. 0-58293  
 $\text{NeCN}^+$ , SCF calcs., dissociation energies, rot. and hyperfine const. determ. 0-95531  
 $^{23}\text{SF}_6$ , point group symmetry breakdown, vibr.-rot. state, saturation spectroscopy 0-87116  
 $\text{SiH}_3$  radical, hyperfine coupling const., vibr. depend., ab initio calcs. 0-87150  
 $\text{SiH}_3$  radical, in  $\text{Ar}(\text{Kr})(\text{N}_2)$  matrix, anisotropic ESR spectroscopic parameters 0-63687  
 $\text{SiH}_4$ , avoided-crossing molecular-beam spectroscopy, hyperfine and spin rot. const. and rot. g factors determ. 0-78671

**molecular inelastic collisions**

- see also atom-molecule collisions; atom-molecule reactions; ion-molecule collisions; ionisation of molecules; molecular rotational-vibrational energy transfer; molecule-molecule reactions*  
 acetylene, triplet state quenching by foreign gases 0-91596  
 acetylene, vibr. relax. study using laser-induced fluoresc. 0-74219  
 angular correlations, summary of review papers 0-63757  
 benzene + bromomethane, microwave line width and quadrupole moments, perturbation theory 0-69190  
 benzene + OCS, microwave line width and quadrupole moments, perturbation theory 0-69190  
 chemical ionisation, classical description, complex interaction pot., exponential representation 0-99570  
 collisional dephasing in strong radiation fields, unified theory, Karplus-Schwinger formula 0-91635  
 compound state resonances, semiclassical calcs. 0-87031  
 cosmic masers, collision-collisional pumping model (*Russian*) 0-90560  
 diatom + diatom, effect on depolarised light scatt. linewidths 0-58321  
 diatomic molecular fluids, slow neutron scatt., models 0-83463  
 diatomic molecular fluids, slow neutron scattering, moment expansions 0-87201  
 diatomic molecule, neutron scatt. induced electronic transitions, tunnelling 0-63844  
 diatomic transition operators,  $\text{L}^2$  basis expansions 0-63519  
 distorted wave matrix elements for inverse power pots., approx. analytic evaluation 0-83442  
 electronic degrees of freedom, classical models 0-63507  
 ethylene, quadrupole moment tensor determ. by collision-induced absorpt. spectrum 0-91555  
 fluorobenzene, mol. reorientation and weak mol. interaction influence,  $^2\text{D}$  spin-lattice relax. obs. 0-106333  
 fluoromethane, vibrational-translational transfer rate, optoacoustic meas. using short pulse  $\text{CO}_2$  laser 0-74258  
 fluoromethane + fluoromethane, collision induced mode selective energy transfer, fluoresc. obs. 0-69177  
 fluoromethane +  $\text{SF}_6(\text{CS}_2)$ , fluoromethane laser, buffer gases collisional narrowing 0-99710  
 gas linear molecules, symmetrised Liouville basis vectors, appl. to spectral linewidths 0-83457  
 gas phase chemical reactions in IR laser field, collision-induced absorpt. spectra 0-76499  
 inert gas, dense, rotational relax. of solute molecules reln. with local anisotropy fluc. 0-58183  
 interaction anisotropy, small angle scatt., spectral evidence 0-78600  
 intermolecular spectroscopy and dynamical properties of dense systems, conf., Varenna, Italy (1978) 0-82581  
 isotropic molecular gases, binary collision-induced light scatt., rot. Raman scatt. 0-78660  
 isotropic molecular gases, binary collisions induced light scatt. 0-83428  
 in laser field, basis set selection and rotating-wave approx. 0-58341  
 in laser field, multiphoton vibrational excitation enhancement, semiclassical theory 0-58350  
 lasers, atomic and molecular, appl. to collision physics 0-63596  
 Lennard-Jones fluids, orientational and collision induced light scatt. 0-63644  
 linewidths and shifts determ. by convolution method 0-102541  
 methane, V-V energy transfer 0-83469  
 methane +  $\text{SF}_6$ , vibr.-vibr. relax 0-99537  
 methane- $\text{d}_4$ , vibr.-translational relax. 0-99537  
 methane- $\text{d}_4$  + methane, vibr. relaxation 0-99537  
 methyl iodide, vibrational dephasing by translational collision 0-87202  
 optically isotropic molecules, collision-induced scatt., many-body correls. 0-87127  
 potentials, anisotropic, from rotationally inelastic and elastic cross sections, direct inversion method 0-69090  
 quantum three particle system, action-angle variables 0-95708  
 R-matrix propag., amplitude density function and invariant bedding methods 0-91622  
 reduced phase space approach calcs. 0-83438  
 relaxation processes, symposium, London, England (Dec. 1976) 0-56993  
 semiclassical calculations using arithmetic mean of velocities associated with initial and final states 0-83460  
 state selected molecules, sudden approx. 0-106377  
 structure and dynamics of mols. by pulsed mol. beams 0-102563  
 superposition of reactive and nonreactive scattering amplitudes in the presence of a conical intersection 0-63733  
 tetrafluoromethane, collision-induced scatt., many-body correls. 0-87127



**molecular inelastic collisions continued**

- s-tetrazine, UV and vis. photodissoc., three-body half-collision dynamics 0-78664  
 trimethylamine, collision induced fluoresc. enhancement and quenching, relax. processes 0-83412  
 vibrational dephasing by translational collision 0-87202  
 vibrational-translational transfer rate, optoacoustic meas. using short pulse CO<sub>2</sub> laser 0-74258  
 Ar gas, primary ionisation coeffs. in cross mag. field 0-83879  
 BaO+CO<sub>2</sub>, in Ar flame, rot. and translational relax. by sub-Doppler optical-optical double reson. 0-95583  
 C<sub>2</sub>+acetylene, C<sub>2</sub> Swan band transition probabilities, collisional energy transfer effects 0-87214  
 C<sub>2</sub>+O<sub>2</sub>, C<sub>2</sub>(X<sup>2</sup> $\Sigma^+$ ) and C<sub>2</sub>(a<sup>3</sup> $\Pi_u$ ) intersystem crossing and free radical kinetics 0-95688  
 CO+H<sub>2</sub>, rot. excitation, rel. between tensorial cross sections 0-83454  
 CO<sub>2</sub> R-branch line intensities and press.-broadened line widths at 15  $\mu$ m 0-102508  
 CO<sub>2</sub>+polyatomic molecule, (00<sup>0</sup>1) mode deactivation, laser induced fluoresc. obs. 0-83453  
 Cs<sub>2</sub>+halogens(SnCl<sub>4</sub>)(MoF<sub>4</sub>)(UF<sub>6</sub>), ionisation reactions, absolute cross sections 0-99565  
 DCl+CO, V-V energy transfer 0-78695  
 DF, vibr. relax., isotope effect, quantum model 0-91460  
 D<sub>2</sub>O, vibr. relax. rates 0-95717  
 H<sub>2</sub>+D<sub>2</sub>, reactive and inelastic scatt., semiempirical pot. energy surfaces calcs. 0-74140  
 HB rot. relaxation, diffusion theory 0-106313  
 HCN+H<sub>2</sub>(CH<sub>3</sub>F), HCN excited vibr. state, T<sub>2</sub> meas. 0-102498  
 HCl, rot. relaxation, diffusion theory 0-106313  
 HF+HF (methane)(methane-d<sub>4</sub>), collision relaxation rate constants and rot. equilibration time meas. 0-69213  
 HgBr<sub>2</sub>+N<sub>2</sub>\*, dissociative excitation, mol. fluoresc. obs. 0-91634  
 K<sub>2</sub>, absorpt. and relax. const. determ. by optical laser pumping method 0-102550  
 K<sub>2</sub>, ground state thermalisation speed, collision cross-sections meas. (*Russian*) 0-78723  
 K<sub>2</sub>+halogens(SnCl<sub>4</sub>)(MoF<sub>4</sub>)(UF<sub>6</sub>), ionisation reactions, absolute cross sections 0-99565  
 N<sub>2</sub>, I<sup>-</sup> system bands, line broadening and shift 0-87138  
 N<sub>2</sub> structural second virial coeff., intermol. pot. and mag. scatt. 0-78678  
 NH<sub>3</sub>+CO<sub>2</sub>(N<sub>2</sub>), collisional broadening of NH<sub>3</sub> inversion spectrum lines 0-99521  
 NH<sub>3</sub>+H<sub>2</sub>, NH<sub>3</sub> inversion transition, linewidths and T<sub>1</sub>/T<sub>2</sub> ratio 0-99499  
 NO+CO<sub>2</sub> collisions in CO<sub>2</sub> gasdynamic laser, causing depopulation of lower active level 0-74336  
 N<sub>2</sub>\*+H<sub>2</sub>O(H<sub>2</sub>S)(methane), deactivation, from laser-induced CO<sub>2</sub> fluoresc. obs. 0-63776  
 Na<sub>2</sub>, absorpt. and relax. const. determ. by optical laser pumping method 0-102550  
 O<sub>2</sub>, laser excited, quenching by CO<sub>2</sub>, H<sub>2</sub>O and I<sub>2</sub> 0-99515  
 O<sub>2</sub> structural second virial coeff., intermol. pot. and mag. scatt. 0-78678  
 OCS, vibr. energy transfer map 0-99560  
 OH+H<sub>2</sub>O, OH linewidth rot. depend. on UV transitions 0-91606  
 OH+NO(NO<sub>2</sub>)(O<sub>3</sub>), OH( $\nu=1$ ) relax., time resolved spectra 0-74240  
 SF<sub>6</sub>, multiple photon absorption, laser pulse intensity and collisions influence 0-95699  
 SF<sub>6</sub>+H<sub>2</sub> chemical laser, electron beam pumping 0-91784  
 SeO<sub>2</sub>+N<sub>2</sub>(CO<sub>2</sub>), radiative lifetime and quenching rates 0-95685  
 Sr<sub>2</sub> dimer, photoassoc., photoluminesc., collisional dissociation 0-58303  
 XeCl+HCl, ground state destruction, quenching rate const. meas. 0-63758

**molecular internal conversion** *see nonradiative transitions***molecular internal mechanics** *see molecular vibration***molecular internal rotation** *see rotational isomerism***molecular intersystem crossing** *see nonradiative transitions***molecular libration***see also macromolecular dynamics*

- aniline, in p-xylene host cryst., phosphoresc. triplet state, ESR and MIDP obs. 0-66077  
 anthracene:tetracyanobenzene charge transfer complex, cryst. struct., temp. effects 0-96508  
 2-haloethanols, torsional interaction, IR spectra, ab initio calcs., 2-dimens. model 0-74160  
 impurity molecule in cryst. lattice, strong EM field effect on librational-rot. motion 0-80824  
 methane, solid, phase II, Raman spectrum, vol. and temp. depend. 0-97260  
 naphthalene, external mode one-density states, low freq. Raman scatt. spectra (*French*) 0-76012  
 pentacene in naphthalene (p-terphenyl), mol. mixed crystals, optical dephasing and vibronic relax. 0-95957  
 pyridine, adsorbed on Ag surface, Raman active librational modes 0-65359  
 triethylenediamine, Raman spectra study (*French*) 0-80768  
 TTF-TCNQ, Landau theory of phase transitions 0-92666  
 urea molecule, bond-length corrections for external and internal vibrs. 0-106402  
 CN<sup>-</sup>, on Ag surface, Raman active librational modes 0-65359  
 CO<sub>2</sub>, solid, high press. mol. libration calc. with Kihara core pots., Gruneisen parameter and lattice 0-65173  
 Ca<sub>10</sub>-Sr<sub>9</sub>(PO<sub>4</sub>)<sub>6</sub>(OH)<sub>2</sub>, continuous cation migration, IR spectra study 0-93297  
 $\alpha$ -LiIO<sub>3</sub>, pot. energy distrib. and force const. variations with temp. 0-79894  
 Li<sub>2</sub>SO<sub>4</sub>.H<sub>2</sub>O, far IR spectra, H<sub>2</sub>O flipping motion, lattice modes 0-84258  
 (NH<sub>4</sub>)<sub>2</sub>M(SO<sub>4</sub>)<sub>2</sub>.6H<sub>2</sub>O, M=Ni, Co, Mg, IR spectra 0-97280  
 Ni(NH<sub>3</sub>)<sub>2</sub>Cl<sub>2</sub>, phase transition and rot. excitation 0-96642  
 $\beta$ -O<sub>2</sub> crystal, thermodynamics of mol. libration motion (*Russian*) 0-70328

**molecular librational states** *see molecular libration***molecular magnetic susceptibility**

- benzene, ring currents hypersusceptibilities calcs. 0-102588  
 carboxyhaemoglobin, carp, variability of mag. moment 0-94159  
 closed-shell system, polarisability and mag. susceptibility calc. by SCF and CI method 0-99443  
 conjugated compounds, ring currents static octopole hyperpolarisabilities calcs. 0-102588  
 diamagnetic susceptibilities and NMR chemical shifts in terms of localised MO's 0-106256

**molecular magnetic susceptibility continued**

- diamotic molecules, diamag. susceptibility and second moments, intramol. charge transfer effects 0-78702  
 fulvene, ring currents hypersusceptibilities calcs. 0-102588  
 hydrocarbons, average elec. polarisabilities and mag. susceptibilities, ab initio valence electron calcs. 0-87033  
 methane, rotational state, avoided-crossing molecular beam spectroscopy 0-63730  
 methylamine, C-N and N-H bond nucl. mag. isoscreening line diagrams 0-78555  
 naphthalene, ring currents hypersusceptibilities calcs. 0-102588  
 open-shell system, polarisability and mag. susceptibility calc. by SCF and CI method 0-99443  
 organic molecular systems, polarisabilities, susceptibilities, electron impact ionis. cross-sections calcs. 0-63835  
 ozulene, ring currents hypersusceptibilities calcs. 0-102588  
 ring current theory 0-87240  
 small molecules, diamag. susceptibility and second moments, intramol. charge transfer effects 0-78702  
 tetra-glycine, cyclic, mol. polaris. and diamag. suscept. calcs. 0-63858  
 tetra-l-alanine, cyclic, mol. polaris. and diamag. suscept. calcs. 0-63858  
 vector potential variation method for calc. mag. props., effective selection of gradient transform. functions 0-69258  
 H<sub>2</sub>, mag. susceptibility calc., vector pot. variation method, effective selection of gradient transform. function 0-69258  
 HCl, second order mag. props., coupled Hartree-Fock perturbation theory 0-87042  
 H<sub>2</sub>O, liquid, diamagnetism, temp. dependence, NMR chemical shift calcs., molecular interactions data 0-75707  
 H<sub>2</sub>O, liquid, equations for mag. susceptibility, electric polarisability 0-75708  
 H<sub>2</sub>O, polarisability and mag. susceptibility calc. by SCF and CI method 0-99443  
 H<sub>2</sub>S, second order mag. props., coupled Hartree-Fock perturbation theory 0-87042  
 NO, Zeeman spectrum, mol. beam elec. reson. spectrosc. 0-91621  
 PH<sub>3</sub>, second order mag. props., coupled Hartree-Fock perturbation theory 0-87042  
 SiH<sub>4</sub>, second order mag. props., coupled Hartree-Fock perturbation theory 0-87042

**molecular mass** *see molecular weight***molecular metastable states**

- acetylene-d<sub>0</sub>-(d<sub>1</sub>)-(d<sub>2</sub>) metastable state, mol. beam elec. deflection obs. 0-74137  
 butyl cation, H-elimination, energy partitioning, transition state geometry calc. using MINDO/3 0-104430  
 dye lasers, metastable state relaxation time determ. 0-102719  
 electronic field effects 0-91465  
 mass spectra, modulated-field linked-scan studies of metastable ions 0-77904  
 multiphoton transition detection 0-58231  
 polymeric macromolecule containing mesogroups, phase diagrams (*Russian*) 0-58433  
 vibrational predissociation in hydrogen bonded complexes 0-61078  
 Ba<sup>2+</sup>, very long lived vibr. states, lifetimes, WKB calc. 0-78560  
 Cl<sub>2</sub> formaldehyde, photolysis, Fourier transform IR studies, metastable species detection 0-81293  
 GeF, use in chemical lasers 0-64004  
 H<sub>2</sub>+e<sup>-</sup>→H<sub>2</sub>\*+e<sup>-</sup>, Gaussian basis Glauber approx., elastic and vibrorotational excitation cross sections 0-58399  
 N<sub>2</sub>+Ar(Xe),  $\Delta^1\Sigma_u^+$  state energy pooling in flowing afterglow, Herman IR system 0-83503  
 N<sub>2</sub>\* (A<sup>3</sup> $\Sigma_u^+$ ), electron impact ionisation cross section 0-78718  
 N<sub>2</sub>\*+H<sub>2</sub>O→N<sub>2</sub>+H<sub>2</sub>O\* 0-87212  
 N<sub>2</sub>\*+HgBr<sub>2</sub>, dissociative excitation, mol. fluoresc. obs. 0-91634  
 O<sub>2</sub>  $\Delta_g$ , produced in HF low-press. plasma, use in organic compd. synthesis 0-61099  
 O<sub>3</sub>+thiirane+olefin+SO<sub>2</sub>, excited neutral metastable SO<sub>2</sub> form. mass spectrometric study 0-83300  
 O<sub>2</sub>(b<sup>3</sup> $\Sigma_u^+$ ), temp. dependent quenching, photochemical study by H<sub>2</sub>-VUV laser 0-63702  
 SO<sub>2</sub>+active N<sub>2</sub>, excited neutral metastable SO<sub>2</sub> form. mass spectrometric study 0-83300  
 SiF, use in chemical lasers 0-64004  
 SnF, use in chemical lasers 0-64004

**molecular moments**

- acetophenones, mono substituted, semi empirical  $\Pi$ -electron calcs. 0-74131  
 adsorbed molecules, Raman and fluoresc. enhancement by surface roughness 0-102511  
 alkali halide mols., electronic polarisability, ionic radii and repulsive pot. parameters, mol. const. 0-87242  
 alkyl halides, conform. energy calcs., polar bonds and polarisability, polaris. model appl. 0-58188  
 allylamine, N-cis lone electron pair trans isomer, total dipole moment, rel. orientation 0-69259  
 anisometric mol. liqs., Raman spectral components, vibr. reson. coupling and noncoincidence effect 0-69149  
 anthracene derivatives in solution, polarisability and dipole moments, emission and absorpt. spectra obs. 0-69256  
 aromatic butadienes, dipole moment and dielectric relax. meas. 0-83516  
 aromatic ethylenes, dipole moment and dielectric relax. meas. 0-83516  
 aromatic polyesters, with S atoms, configurational props. 0-74269  
 benzaldehyde, and isomeric phthalaldehydes, dipole moments meas., config., ab initio MO calc. 0-58410  
 benzene, quadrupole moments, elec. field-gradient birefringence method 0-95746  
 benzene+bromomethane, microwave line width and quadrupole moments, perturbation theory 0-69190  
 benzene+OCS, microwave line width and quadrupole moments, perturbation theory 0-69190  
 biomolecules+chloranil, charge transfer interaction, equilib. const., enthalpy and entropy determ., mol. polarisability 0-89708  
 biopolymers, electro-optical changes, chem. and rotational contribs. 0-85352  
 t-butyl acetate, rot. isomerism, dielect. and Raman spectra 0-106328  
 t-butyl formate, rot. isomerism, dielect. and Raman spectra 0-106328  
 carboxyhaemoglobin, carp, variability of mag. moment 0-94159  
 4-chloro, 3-nitrotoluene, partially aligned in elec. field, <sup>13</sup>C NMR, dipole moment determ. 0-78633



## molecular moments continued

- chloromethyl formate, conformation potential energy surfaces, ab initio calcs. 0-69065
- collagen, polarisation, contribution of permanent and induced dipole moments, elec. birefringence 0-85351
- cyclic ketones, electrochromism and electric dichroism for studying transitions to second excited singlet 0-63692
- Debye generalised fluid model, dielectric relax., depolarised dynamic light scatt. 0-108156
- diatomic molecular spectra, conventions for defining electric transition moment and rot. line intensity factors 0-83346
- diatomic molecules, diamag. susceptibility and second moments, intramol. charge transfer effects 0-78702
- dimethylamine-HCl systems, H-bonded complexes studied by ab initio MO method, dipole moments determ. 0-83253
- ethyl alcohol-d<sub>0</sub>-(d<sub>1</sub>)-(d<sub>2</sub>)-(d<sub>3</sub>), internal rot. and microwave rot. spectra 0-69128
- ethylene, quadrupole moment tensor determ. by collision-induced absorpt. spectrum 0-91555
- ethylidenimine, pyrolysis product, microwave spectra, rot. distortion and electric quadrupole const. and rot. barriers determ. 0-78608
- field-induced molecular multipoles, local polarisation theory 0-74141
- first row elements, split-valence basis set, mol. vibr. and mol. moment calcs. 0-69063
- 1-fluoro, 2,4-dinitrobenzene, partially aligned in elec. field, <sup>13</sup>C NMR, dipole moment determ. 0-78633
- fluoroacetylene-d, Stark and microwave double reson. laser spectra 0-63690
- fluoromethyl formate, conformation potential energy surfaces, ab initio calcs. 0-69065
- formaldehyde, <sup>3</sup>A'' state, zero-field splitting param., ab initio CI calcs. 0-99454
- formaldehyde, electronic struct., dipole moments, mol. polarisability, force fields, ab initio calcs. 0-78531
- formamide, force consts. and dipole moment derivatives, ab initio MO calcs. 0-95521
- formic acid (-d), microwave spectra and rot. consts., astrophysical appl. 0-91550
- ground state alkali molecules, mag. shielding and spin-rot. interaction 0-87186
- hexafluorobenzene, quadrupole moments, elec. field-gradient birefringence method 0-95746
- hexamethylbenzene, quadrupole moments, elec. field-gradient birefringence method 0-95746
- ice orientational correlation parameter, water mol. dipole moment 0-59407
- identical molecules, dispersion intermolecular pot. anomaly prod. by intense radiation field 0-58336
- intermolecular spectroscopy and dynamical properties of dense systems, conf., Varenna, Italy (1978) 0-82581
- ion+ polar molecules, long range dipole interaction effect 0-102558
- magnetic multipole moment integrals for Slater-type orbitals, analytic evaluation 0-58110
- methane, rotational state, avoided-crossing molecular beam spectroscopy 0-63730
- 2-methoxyethylamine, microwave spectra, H-bond, torsional motion and mol. vibr. obs., rot. isomerism, mol. moments determ. 0-95603
- methyl fluorofluoride, isomer conformation, CNDO and ab initio STO calcs. 0-58151
- methyl iodide, vibrational dephasing by translational collision 0-87202
- methylacetylene,  $\nu_3$  band, microwave and IR laser Stark spectrosc. 0-91558
- methylamine-HCl systems, H-bonded complexes studied by ab initio MO method, dipole moments determ. 0-83253
- methylpropylether, trans-trans isomer, microwave spectra, struct., dipole moment and rot. barriers calcs. 0-83348
- norbornane, microwave spectrum and dipole moments 0-78606
- nucleic acids bases, excited state dipole moments and geometries 0-95738
- organic molcs., relative Raman intensities, CNDO/2 INDO param. effect 0-95633
- paramagnetic liquid, depolarized light scatt. in mag. field 0-80759
- point charge model of molecules, Mulliken population anal. 0-102429
- polar tensors, compact formulation on bond moment hypothesis 0-58108
- pyrrole-acetonitrile, H-bonded complex, ab initio MO calcs. 0-102440
- RNA, molecular motions investigated by <sup>31</sup>P and <sup>13</sup>C NMR relaxation 0-63657
- rotamers, total dipole moment orientation calcs. 0-91705
- silyl acetylene, microwave spectra in ground and  $\nu_{10}$  vibr. state 0-78610
- small molecules, diamag. susceptibility and second moments, intramol. charge transfer effects 0-78702
- stilbenes, substituted, donor-acceptor interaction effects on excited singlet state polarity (German) 0-91470
- surface adsorbed molecules, internal optic modes, mol. dipole model 0-100395
- tetracyanoethylene in acetone-d<sub>6</sub>, anion solvation, electron spin echo modulation 0-63676
- tetracyanoethylene in dimethylsulphoxide-d<sub>6</sub>, anion solvation, electron spin echo modulation 0-63676
- tetracyanoethylene in methanol-d<sub>3</sub>(d<sub>1</sub>), anion solvation, electron spin echo modulation 0-63676
- thioformaldehyde, electronic struct., dipole moments, mol. polarisability, force fields, ab initio calcs. 0-78531
- 1,3,5-trifluorobenzene, quadrupole moments, elec. field-gradient birefringence method 0-95746
- trifluoromethyl bromide, microwave spectra, mol. rot., isotopic variation in bond lengths, Stark meas., dipole moments determ. 0-74165
- trifluoromethyl iodide, microwave spectra, mol. rot., isotopic variation in bond lengths, Stark meas., dipole moments determ. 0-74165
- 1,3,5-trimethylbenzene, quadrupole moments, elec. field-gradient birefringence method 0-95746
- vibrational dephasing by translational collision 0-87202
- AgI surface, adsorption of water, effective pair pot. model 0-100394
- BH, elec. polarisabilities and dipole moments, var. perturbation obs. 0-63527
- CH bond dipole calcs. 0-69067
- CN<sup>+</sup>, spectrosc. consts. for ground and excited states, ab initio, CI calcs. 0-78551
- CO, adsorbed on Pt, internal optic modes, mol. dipole model 0-100395
- CO<sub>2</sub>, collision-induced Raman spectrum, theoretical studies 0-63646
- CO<sub>2</sub>, dipole moment functions 0-87094
- CO<sub>2</sub>, IR band intensity 0-83425

## molecular moments continued

- CO<sub>2</sub>, induced absorpt. spectral moment, mol. calcs. 0-63737
- <sup>12</sup>C<sup>18</sup>O<sub>2</sub>,  $\nu_3$  band, IR single line strength 0-83370
- COF<sub>2</sub>, dipole moment from compact formulation of polar tensors on bond moment hypothesis 0-58108
- Cl<sub>2</sub>, quadrupole moment determ. by refr. index anisotropy meas. method 0-78722
- Co<sub>2</sub>, electrooptical consts.,  $2\nu_3$  band induced component 0-78626
- FCP, microwave spectrum, struct., dipole moment and vibr.-rot. props. obs. 0-91549
- HCl, electrostatically interacting molcs., CI multipole function calcs. convergence 0-91458
- HF, electrostatically interacting molcs., CI multipole function calcs. convergence 0-91458
- HNO  $\tilde{A}'A''$  excited state dipole moment, optical-optical double reson. Stark spectrosc. obs. 0-106337
- HNO, isomerism, low lying electronic states, ab initio MRD-CI calcs. 0-83291
- HO<sub>2</sub> free radical, dipole moments and Stark effects from microwave spectra 0-63623
- H<sub>2</sub>O-HF heterodimer, H bonding, microwave rot. spectrum, mol. geometry and moment 0-99501
- H<sub>2</sub>SiO, electronic struct., dipole moments, mol. polarisability, force fields, ab initio calcs. 0-78531
- I<sub>2</sub>(I<sub>2</sub><sup>+</sup>)(I<sub>2</sub><sup>-</sup>), HF and SCF calcs., pot. curves, electron affinity and quadrupole moment determ. 0-95527
- <sup>127</sup>I<sub>2</sub> rovibronic absorpt. lines, hyperfine struct. 0-78596
- <sup>129</sup>I<sub>2</sub> rovibronic absorpt. lines, hyperfine struct. 0-78596
- LiBr, pair pot., dipole moment, polarisability tensor, bond length depend., finite field SCF calcs. 0-58127
- LiH<sub>2</sub>PO<sub>3</sub>, P-H bond dipole direction, nonlinear optical coeffs. meas. 0-69253
- N<sub>2</sub>, electron excitation of Birge-Hopfield bands ( $b'_1\pi_u-X'_2\Sigma^+$ ) 0-95731
- N<sub>2</sub>, liq. and gas, induced absorpt. spectral moment, mol. calcs. 0-63737
- NH<sub>3</sub>, lone pair contributions to the IR intensities, ab initio calcs. 0-63630
- NO, Zeeman spectrum, mol. beam elec. reson. spectrosc. 0-91621
- N<sub>2</sub>O, dipole moment functions 0-87094
- N<sub>2</sub>O,  $\nu_3$  and  $2\nu_3$  IR bands, shape and dipole correl. functions 0-91560
- N<sub>2</sub>O isomerism, low lying electronic states, ab initio MRD-CI calcs. 0-83291
- N<sub>2</sub>SO<sub>3</sub>, weakly bound complex, dipole moments, MBER obs. 0-95701
- <sup>14</sup>NH<sub>3</sub>, ground state, microwave inversion lines 0-87098
- O<sub>2</sub>, atmospheric, electric quadrupole transitions detection in A band 0-85746
- O<sub>2</sub>, liq. and gas, induced absorpt. spectral moment, mol. calcs. 0-63737
- O<sub>2</sub>, line and band strengths in IR spectra, variational calcs. 0-87112
- ONF, J transitions, rot. Zeeman effect 0-63707

## molecular nuclear coupling

- acetonitrile-d<sub>3</sub>, <sup>2</sup>H NMR spectra, vibr. and asymmetry corrections to quadrupole coupling consts. 0-74184
- alicyclic compounds, nucl. spin-spin coupling via nonbonded interactions,  $\gamma$ -substituent effects 0-69078
- aliphatic compounds, nucl. spin-spin coupling via nonbonded interactions,  $\gamma$ -substituent effects 0-69078
- alkanes, nucl. spin-spin coupling via nonbonded interactions, conformational and substituent effects 0-69077
- benzene-d<sub>6</sub>, <sup>2</sup>H NMR spectra, vibr. and asymmetry corrections to quadrupole coupling consts. 0-74184
- cis-1-cholobutadiene-1,3, microwave spectrum, struct., nuclear quadrupole coupling, distortion const., thermodynamic functions calc. 0-99500
- 2-cyanoaziridine, microwave rot. spectrum, assignments 0-91546
- cyclopropyl cyanide, high-resolution microwave spectra, quadrupole hyperfine struct. of rot. transitions anal. 0-95601
- dimethyldichlorosilane, microwave spectrum, rot., centrifugal distortion and quadrupole coupling consts. 0-91547
- formaldehyde anion radical, hyperfine coupling consts., vibr. depend., ab initio calcs. 0-87150
- ground state alkali molecules, mag. shielding and spin-rot. interaction 0-87186
- imidazole, quadrupole coupling consts. interpretation, ab initio field gradient calcs. 0-58282
- methyl bromide, NQR and A<sub>1</sub>-A<sub>2</sub> splitting, RF spectrosc. inside laser cavity 0-91579
- methyl radical, hyperfine coupling consts., vibr. depend., ab initio calcs. 0-87150
- $\alpha$ -oxalic acid dihydrate, H<sub>2</sub>O proton shielding tensor, multiple pulse proton NMR obs. 0-63655
- planar cyclic radicals, C-H proton isotropic hyperfine consts., C hybridisation 0-95646
- 4-pyridine carbaldehyde, microwave spectrum, rot. assignments, quadrupole coupling consts. 0-91548
- second-row hydrides, nucl. spin-spin coupling consts., ab initio calcs. 0-95647
- spin-spin coupling constant calculations in mol. by CNDO/SP methods 0-74126
- spin-spin coupling constants, directly bonded C-C and C-H, CDOE/INDO LMO calcs. 0-95546
- ArHBr, ArHCl, and isotopic forms, rot. spectra, mol. struct., mol. consts. 0-58246
- As<sub>2</sub>I<sub>3</sub>, <sup>127</sup>I, <sup>75</sup>As NQR freqs. meas. 0-58285
- <sup>13</sup>C-<sup>13</sup>C spin-spin coupling const. and stretching force consts., single and double bonds 0-63867
- CaH, spin doubling, SCF calcs. 0-95649
- <sup>37</sup>ClO<sub>2</sub>,  $\nu_3=1$  state, laser-microwave double reson. obs. 0-95657
- Cu complex, Cu(II) bis(dithiocarbamate), <sup>1</sup>H ENDOR 0-87154
- GeH<sub>4</sub>, avoided-crossing molecular-beam spectroscopy, hyperfine and spin rot. const. and rot. g factors determ. 0-78671
- GeI<sub>2</sub>, <sup>127</sup>I NQR freqs. meas. 0-58285
- HD, spin-dipolar term, spin-spin coupling const. corrections, Fermi contact terms calcs. 0-99448
- HD, spin-spin coupling constant convergence, comparative study 0-63536
- KrHBr, KrCHl, and isotopic forms, rot. spectra, mol. struct., mol. consts. 0-58246
- Mo<sub>2</sub>Cl<sub>3</sub><sup>3-</sup> complexes, cluster exchange coupling consts. SCF-X $\alpha$ -SW calcs. 0-74120
- <sup>14</sup>N quadrupole coupling consts., ab initio calcs. 0-58283
- SiH<sub>3</sub> radical, hyperfine coupling consts., vibr. depend., ab initio calcs. 0-87150



**molecular nuclear coupling continued**

- SiH<sub>4</sub>, avoided-crossing molecular-beam spectroscopy, hyperfine and spin rot. const. and rot. g factors determ. 0-78671  
 SnI<sub>2</sub>, <sup>127</sup>I NQR freqs. meas. 0-58285  
 ZnCl<sub>2</sub>, <sup>35</sup>Cl NQR freqs. meas. 0-58285  
 ZnI<sub>2</sub>, <sup>127</sup>I NQR freqs. meas. 0-58285

**molecular orbitals** *see* molecular energy levels**molecular orbitals calculations**

*includes calculations of electronic and geometric molecular structure see also APW calculations; EHT calculations; GO calculations; GTO calculations; HMO calculations; KKR calculations; LCAO calculations; NDO calculations; OPW calculations; PNO calculations; PPP calculations; STO calculations*

- acetic acid, monomer and dimer, photoelectron spectrosc. 0-87172  
 acetophenones, di- and trisubstituted,  $\pi^*$ - $\pi$  systems, UV electronic absorpt. spectra 0-74132  
 acetophenones, mono substituted, semi empirical  $\Pi$ -electron calcs. 0-74131  
 alkali metalborates, vapour over heated solid, XPS, obs. 0-87171  
 n-alkanes, mol. Rydberg S-S and S-T transitions, semi-empirical SCF MO calc. 0-91453  
 alkenes, 1,1-, 1,2-disubstituted, fragmentation modes in perturbational MO anal. 0-58138  
 allyl radical, restricted SCF and MC SCF calc. of C<sub>2v</sub> and C<sub>s</sub> structs. 0-83289  
 aminoborolpolynes, intermolecular interaction through triple bonds, internal rot. 0-106370  
 aminopolynes, intermolecular interaction through triple bonds, internal rot. 0-106370  
 aromatic hydrocarbons, vibronic calcs. 0-58238  
 aromaticity, reson. energy in graph theory 0-91412  
 benzaldehyde, and isomeric phthalaldehydes, dipole moments meas., config., ab initio MO calc. 0-58410  
 benzene, dynamic polarisabilities, calcs., superposition method of excited config., nonstationary perturbation theory eqns. 0-69257  
 benzene derivatives, mol. electrostatic pot., approx. evaluation 0-58337  
 benzenes, substituted, electronic struct., ab initio calcs., photoelectron spectra 0-58314  
 bond bending, bond orbitals rel. to nucl. motion 0-95513  
 chelotropic reaction, intrinsic single and dual mol. orbital symmetry conservation 0-102419  
 chemical bonding studied using scattering theory concepts 0-103289  
 closed shell Hartree theory with orthonormal orbitals 0-69051  
 collision systems  $\alpha(Z_1 + Z_2) \geq 1$ , quasimolecular 1  $\sigma$  orbital, excitation and spectroscopy 0-87199  
 complex molecular orbitals, pairing representation 0-91454  
 compound state resonances, semiclassical calcs. 0-87031  
 conjugated molecules, electronic transitions,  $\Sigma$ - $\Pi$  separability 0-58124  
 correlated wave functions anal. gradients from two particle density matrix and unitary group 0-78548  
 cross section by complex basis function calcs. of resolvent matrix elements 0-78662  
 cyclopentanone, n- $\pi^*$  transition, vibr. band intensities 0-74116  
 deoxyhaemoglobin, porphyrin-Fe-imidazole system, SCF-LCAO-ASMO and CI calcs. of low-lying multiplets and excited states 0-94155  
 diamagnetic susceptibilities and NMR chemical shifts in terms of localised MO's 0-106256  
 diatomic transition operators, L<sup>2</sup> basis expansions 0-63519  
 dimethylamine-HCl systems, H-bonded complexes studied by ab initio MO method, dipole moments determ. 0-83253  
 direct orbital optimisation for MC SCF theory by unitary transformations 0-87049  
 electronic structure calculations by fast accurate kinetic-energy method 0-83257  
 ethylene, valence states, effective Hamiltonian from canonical transformation 0-74130  
 ethylene as singlet methylene dimer, nonempirical double zeta calculations, zwitterionic singlet excited states 0-83258  
 ethylene ozonide, ab initio gradient and MC SCF calc., conformational anal. 0-83290  
 ethylidene, rearrangement to ethylene, barriers, ab initio MO calcs. 0-104424  
 first row elements, split-valence basis set, mol. vibr. and mol. moment calcs. 0-69063  
 first-row atoms, SCF calcs. using cusped-Gaussian basis sets, polarisation effects 0-74118  
 formaldehyde, mol. Rydberg S-S and S-T transitions, semi-empirical SCF MO calc. 0-91453  
 formamide, force consts. and dipole moment derivatives, ab initio MO calcs. 0-95521  
 formamide-glyoxal, charge transfer theory, Mulliken population, ab initio calc., multiconfiguration scheme 0-106392  
 heavy ion collisions, electron EM field interaction, quantised field formalism 0-83478  
 hydronaphthyl radicals embedded in naphthalene cryst., optical transition energies and ionisation energies 0-78595  
 integrated spatial electron populations, evaluations for simple mols. 0-78524  
 intramolecular interactions effect on transferability props. of localised description of chemical groups 0-102424  
 intrinsic single and dual mol. orbital symmetry conservation 0-102419  
 $\beta$ -lactam antibiotics, ab initio SCF-MO-LCAO calcs., amidic bond breaking, methoxy substitution effect 0-78533  
 large molecules, mol. fragment basis, generalisation, for ab initio calcs. 0-91438  
 LCAS MS SCF method within Gaussian basis set 0-102438  
 localised orbital theories, cancellation effects 0-84445  
 magnetic susceptibility calc., vector pot., variation method, effective selection of gradient transform. function 0-69258  
 MCSF and CI wave functions, two-particle density matrix and graphical unitary group approach 0-63558  
 methane, energy quantities from localised charge densities, dependence on geometry and basis set 0-63525  
 methane, orbital relax. energy for single and double ionis. from valence shells 0-106253  
 methane, SCF calcs. including polaris. functions 0-87034  
 methane+O(<sup>3</sup>P), barrier height and transition state geometry, POL-CI calc., H abstraction reaction 0-66782  
 methoxide surface complexes on Li, He(I) photoelectron spectra, MO calcs. 0-83417

**molecular orbitals calculations continued**

- methyamine-HCl systems, H-bonded complexes studied by ab initio MO method, dipole moments determ. 0-83253  
 modified virtual orbitals, for config. interaction calc. 0-58163  
 molecular polarisabilities calcs., superposition method of excited config., nonstationary perturbation theory eqn. 0-69257  
 monochromatic wave perturbation, time depend. HF calcs. (French) 0-63516  
 multi-config. SCF super-CI calc., density matrix formulation 0-78547  
 multicentre molecular integrals evaluation over hydrogen like atomic orbitals (Russian) 0-63548  
 Nesbet equation for molecular calculations, appl. to Hubbard model 0-87029  
 nuclear spin-spin coupling constants, directly bonded C-C and C-H, CDOE/INDO LMO calcs. 0-95546  
 oxoniomethylene cation, rearrangement to hydroxymethyl cation, barriers, ab initio MO calcs. 0-104424  
 papain models, active site  $\alpha$ -helix and ion pair stability 0-74265  
 phase and population relax., semigroup formalism 0-78519  
 photoelectron spectra, localised and delocalised calcs. 0-63709  
 photoelectron spectra, self-consistent charge calcs. of core-electron binding energy shifts 0-69084  
 polarisabilities, average, empirical calc. method 0-63859  
 polyatomic ions, charge distributions, rel. with cohesive energies of ionic crystals 0-70161  
 polyynes, intermolecular interaction through triple bonds, internal rot. 0-106370  
 n-propanol, preferred conformers, PCIO study 0-95542  
 propionitriles (-O, NH, S), conformational investig., NMR, IR and semiempirical MO methods 0-95650  
 pseudopotential method, testing of arbitrariness and limits 0-91446  
 pyrrole-acetonitrile, H-bonded complex, ab initio MO calcs. 0-102440  
 relativistic self-consistent field theory for open-shell molecules 0-95518  
 Rydberg transitions, correl. algorithms for Rydberg term values 0-83277  
 semiconductor, defect electronic structure and lattice config., MO approaches 0-65495  
 semiempirical theory for ground and excited states, Fock operator expansion, STO-3G and CNDO/S calcs. 0-58154  
 shifted Hartree-Fock eigenvalues and Slater's transition-state concept 0-83261  
 SiH<sub>4</sub>, SCF calcs. including polaris. functions 0-87034  
 singlet-triplet energy difference and singlet generalised oscillator strength, Lassetre-Dillon relation 0-63508  
 Slater is orbital four centre mol. integrals, Fourier transforms 0-74104  
 Slater-type orbitals, expansion, electron-repulsion integrals evaluation 0-99451  
 small molecules, localised charge densities calcs., bond length effects 0-83256  
 spherical harmonics problems, identities 0-63515  
 spin-orbital eqns. for anal. derivatives of config. interaction energy including double substitutions 0-78549  
 spirohydrocarbons, strained, bond angles, interatomic distances, semiempirical and ab initio calcs. 0-95533  
 struct. and props. SCF calcs. 0-106260  
 supra-antarafacial cycloaddition intrinsic single and dual mol. orbital symmetry conservation 0-102419  
 TCNE-benzene, charge transfer theory, Mulliken population, ab initio calc., multiconfiguration scheme 0-106392  
 tetrabiomethane, electronic struct., X $\alpha$  SW calcs. 0-102447  
 tetrafluoromethane, electronic struct., X $\alpha$  SW calcs. 0-102447  
 time-dependent multiconfigurational Hartree-Fock theory 0-58117  
 topological model and orbital mapping for chemical systems 0-78512  
 total electronic energy, atoms and mols., SCF binding energy, Z<sup>-1</sup> perturbation theory 0-83268  
 trifluoroacetic acid, monomer and dimer, photoelectron spectrosc. 0-87172  
 trimethylamine, SCF calcs. including polaris. functions 0-87034  
 triphenylene derivatives, hexasubstituted, disc-like cpd., mol. conform. and arrangement, semiempirical calcs. 0-107048  
 two state two mode vibronic coupling model, Born-Oppenheimer and crude adiabatic perturbation methods 0-87036  
 two-centre charge distrib., Fourier transform, STO general expression derivation 0-58119  
 two-electron wave functions with monopole interaction, asymptotic forms 0-78528  
 UHF orbitals, ionisation energy calcs. appls. 0-58141  
 valence orbital studies using atomic Fues potential, homonuclear diatomics 0-78544  
 X $\alpha$  method with pseudopotentials 0-83282  
 Ag<sub>2</sub>, Harris-Pohl selected valence electron split-shell MO calcs. 0-91439  
 Al<sub>2</sub>(Al<sub>2</sub>)<sub>2</sub>(Al<sub>2</sub>)<sub>2</sub> configurations, ab initio study, LCAO, STO, MO-SCF and CI calcs., binding energy (French) 0-91447  
 Al<sup>3+</sup>(H<sub>2</sub>O)<sub>n</sub> (n=1,2,4,6), FSGO-pair-pot. calcs. (German) 0-74278  
 $\alpha$ -Al<sub>2</sub>O<sub>3</sub>, charge distribution determ., SCF calc., Slater-type orbitals, Madelung type const. 0-107100  
 Au<sub>2</sub>, Harris-Pohl selected valence electron split-shell MO calcs. 0-91439  
 BH<sub>3</sub>-ethylene complex, semiorthogonalised orbitals, integral approx. scheme 0-83262  
 B<sub>2</sub>O<sub>3</sub>, bipyramidal struct., stability, ab initio SCF-MO calcs. 0-99446  
 BaTiO<sub>3</sub>, photoelectron and optical spectra derived from self-consistent charge MO and band calcs. 0-96785  
 Be complexes, binding and orbital energies, biological systems ab initio calc. 0-102442  
 BeF, A <sup>2</sup> $\Pi$  state config., ab initio MO calcs. 0-95532  
 Be<sup>2+</sup>(H<sub>2</sub>O)<sub>n</sub> (n=1,2,3,4,6), FSGO-pair-pot. calcs. (German) 0-74277  
 CH bond dipole calcs. 0-69067  
 CH, one-centre integrals of semiempirical theories of valence, ab initio calcs. 0-102441  
 CH<sub>3</sub>, CH<sub>2</sub> and CH deformation vibration group frequencies and MO electron densities, interaction force const. 0-87101  
 CO, LCAO-X $\alpha$  method calcs., comparison with Hartree Fock and MS X $\alpha$  methods 0-95539  
 CO+H<sup>+</sup>, ground state pot. energy surface, ab initio SCF calc., protonated equilib. geometry 0-83301  
 CO+H<sup>+</sup>, vibr. excitation calc., close coupling and sudden approx. 0-78561  
 Cds,In, impurity resist., Matsubara-Toyozawa theory extension 0-80264  
 CIO radical, struct. and props. calcs. 0-74112  
 ClO<sub>2</sub><sup>+</sup>, ClO<sub>2</sub> and ClO<sub>2</sub><sup>-</sup> (n=1 to 3), ab initio calcs., localised MO and nature of Cl-O bond 0-69070  
 ClOO radical, struct. and props. calcs. 0-74112



## molecular orbitals calculations continued

- Co complex,  $O_2CoCl_4$  and  $O_2CoCl_4NH_3^{2-}$ , struct. and bonding model, CNDO-UHF calcs. 0-95541
- Co complexes, Co(III) mixed complexes, orbital angular momentum reduction,  $^{59}Co$  NMR chemical shift 0-58137
- CrOCl<sub>3</sub>, electronic structure and valence ionisation energies, obs. by ab initio and SW-Xa methods 0-69073
- Cu<sub>2</sub>, Harris-Pohl selected valence electron split-shell MO calcs. 0-91439
- CuNi molecule, electronic states determ. by ab initio HF and CI methods 0-69087
- FCO, radical, struct. and props. calcs. 0-74112
- F<sup>-</sup>(H<sub>2</sub>O)<sub>n</sub> (n=1,2), FSGO-pair-pot. calcs. (German) 0-74278
- FOO radical, struct. and props. calcs. 0-74112
- FSO (FOS), struct. and props., SCF calcs. 0-106260
- FSS, struct. and props., SCF calcs. 0-106260
- Fe<sup>2+</sup> and Fe<sup>3+</sup> hydrate clusters, aq. electron exchange reaction, ab initio RHF MO calc. of inner shell reorganisations, vibr. freq. 0-102564
- GeBr<sub>4</sub>, electronic struct., Xa SW calcs. 0-102447
- GeF<sub>4</sub>, electronic struct., Xa SW calcs. 0-102447
- GeH<sub>3</sub><sup>+</sup>, electronic struct., electron affinity, inversion barrier, ab initio SCF Gaussian basis calc. 0-63552
- H<sub>2</sub>, diatomic transition operators, L<sup>2</sup> basis expansions  $^1\Sigma$  and  $^3\Sigma$  state pots. 0-63519
- H<sub>2</sub>, expressions for calc. Coulomb repulsion between electrons using adiabatic basis 0-91427
- H<sub>2</sub>, mag. susceptibility vector pot. variational method, gradient transform. function selection 0-69258
- H<sub>2</sub><sup>+</sup>, free free absorpt. coeffs. dipole length formulation and two centre close coupling calc. 0-83345
- H<sub>3</sub>, relative magnitudes of direct and indirect exchange, Heitler-London calcs. 0-69069
- HCN-CO complex, charge transfer theory, Mulliken population, ab initio calc., multiconfiguration scheme 0-106392
- HCl, second order mag. props., coupled Hartree-Fock perturbation theory 0-87042
- HF, energy quantities from localised charge densities, dependence on geometry and basis set 0-63525
- HF, orbital relax. energy for single and double ionis. from valence shells 0-106253
- HO<sub>2</sub>, struct. and props., SCF calcs. 0-106260
- H<sub>2</sub>O, energy quantities from localised charge densities, dependence on geometry and basis set 0-63525
- H<sub>2</sub>O, mol. Rydberg S—S and S—T transitions, semi-empirical SCF MO calc. 0-91453
- H<sub>2</sub>O, orbital relax. energy for single and double ionis. from valence shells 0-106253
- H<sub>2</sub>O, SCF calcs. using cusped Gaussian basis sets, polarisation effects 0-74118
- H<sub>2</sub>O, separated electron pair theory, numerical calcs. 0-87049
- H<sub>2</sub>O<sup>+</sup>, ab initio potential energy surface study by CI techniques, equilibrium conform. determ., mol. dissociation pathways 0-78550
- H<sub>2</sub>PNH<sub>2</sub>, inversion-rot. mechanism, basis set and geometry optimisation effects 0-83273
- H<sub>2</sub>S, second order mag. props., coupled Hartree-Fock perturbation theory 0-87042
- HSS, struct. and props., SCF calcs. 0-106260
- HgBr<sub>2</sub>, electronic struct. and photodissoc., effective core pots. and POL(1) CI wave function 0-63560
- HgCl<sub>2</sub>, electronic struct. and photodissoc., effective core pots. and POL(1) CI wave function 0-63560
- K<sub>2</sub>NaGaF<sub>6</sub>:Cr<sup>3+</sup>, magneto-optical study of  $^2T_{1g}$ ,  $^4T_{2g}$ ,  $^2E_g$ ,  $^4A_{2g}$  transitions 0-71384
- Li complexes ((C<sub>2</sub>H<sub>5</sub>X<sub>2</sub>)<sub>2</sub>Li)<sup>n</sup> where X=S, O, binding and orbital energies, biological systems ab initio calc. 0-102442
- Li<sup>+</sup>-H<sub>2</sub>O complex, charge transfer theory, Mulliken population, ab initio calc., multiconfiguration scheme 0-106392
- LiBeF<sub>3</sub>, pot. energy surface, struct., stability and internuclear distances, ab initio calc. 0-58147
- LiH, direct optimisation of orbitals for multiconfiguration self-consistent field theory by unitary transformations 0-63544
- LiH, SCF calcs., undergraduate exercise 0-82597
- Li<sup>+</sup>(H<sub>2</sub>O)<sub>n</sub> (n=1,2,3,4,6), FSGO-pair-pot. calcs. (German) 0-74277
- Mg<sup>2+</sup>(H<sub>2</sub>O)<sub>n</sub> (n=1,2,4,6), FSGO-pair-pot. calcs. (German) 0-74278
- N<sub>2</sub>, ab initio MO-LCAO-SCF and Gordon-Kim intermolecular pot. for seven different orientations 0-95522
- N<sub>2</sub> SCF calcs. using cusped Gaussian basis sets, polarisation effects 0-74118
- NH<sub>2</sub>, pot. energy curves of X<sup>2</sup>B<sub>1</sub>, A<sup>2</sup>A<sub>1</sub>, <sup>2</sup>B<sub>2</sub> valence-shell and  $\pi_u^{23s}$ -type Rydberg states calc. by CI 0-74138
- NH<sub>3</sub>, energy quantities from localised charge densities, dependence on geometry and basis set 0-63525
- NH<sub>3</sub>, mol. Rydberg S—S and S—T transitions, semi-empirical SCF MO calc. 0-91453
- NH<sub>3</sub>, orbital relax. energy for single and double ionis. from valence shells 0-106253
- Na<sup>+</sup>(H<sub>2</sub>O)<sub>n</sub> (n=1,2,4,6), FSGO-pair-pot. calcs. (German) 0-74278
- NaNCO<sub>2</sub>, val. band electronic struct., XPS meas., MOC and INDO calcs. 0-95520
- Ni, extended basis set LCAO Xalpha treatment 0-95537
- NiH, extended basis set LCAO Xalpha treatment 0-95537
- NiO, bulk props., initial state MO Ni<sub>4</sub>O<sub>4</sub> and Ni<sub>3</sub>O<sub>4</sub>, cluster model, lattice and force consts., photoemission and CI absorpt. spectra 0-84828
- O<sub>2</sub>,  $^3\Sigma_g^-$  ground state, pot. energy curve, direct CI method appl. 0-58165
- O<sub>2</sub>,  $^1\Delta_g$  state pot. energy curve, MCSCF calcs. 0-63565
- O<sub>2</sub><sup>+</sup>, hypothetical, mol. self-consistent study, possible prep. method (French) 0-91717
- O<sub>3</sub>H<sup>+</sup>, isomeric structs. ab initio MO calcs. 0-83270
- Os<sub>8</sub>(CO)<sub>18</sub>, electronic struct., metal cluster carbonyls mol. orbital description obs. 0-63879
- PH<sub>3</sub>, second order mag. props., coupled Hartree-Fock perturbation theory 0-87042
- SeCl<sub>2</sub>, photoelectron spectra 0-69186
- Se<sub>2</sub>Cl<sub>2</sub>, photoelectron spectra 0-69186
- SiBr<sub>4</sub>, electronic struct., Xa SW calcs. 0-102447
- SiF<sub>4</sub>, electronic struct., Xa SW calcs. 0-102447
- SiH<sub>4</sub>, SCF calcs. including polaris. functions 0-87034
- SiH<sub>4</sub>, second order mag. props., coupled Hartree-Fock perturbation theory 0-87042
- (SiH<sub>3</sub>)<sub>3</sub>N, SCF calcs. including polaris. functions 0-87034

## molecular orbitals calculations continued

- TeF<sub>6</sub><sup>2+</sup>, pseudopot. SCF-MO calcs., spectrum assignments 0-83269
- ThF<sub>4</sub>(Cl<sub>4</sub>), electronic struct., MS-SCF-Xa calcs. and VUV photoelectron spectra 0-63710
- UC, electronic struct., comparison with photoemission spectra 0-91450
- UF<sub>6</sub>, relativistic scattered wave calculations 0-63538
- UF<sub>6</sub>(Cl<sub>4</sub>), electronic struct., MS-SCF-Xa calcs. and VUV photoelectron spectra 0-63710
- UN, electronic struct., comparison with photoemission spectra 0-91450
- XeF<sub>2</sub>, pseudopotential SCF-MO studies, equilib. struct., stretch-stretch interaction force const. 0-95525
- XeF<sub>4</sub>, pseudopotential SCF-MO studies, equilib. struct., stretch-stretch interaction force const. 0-95525
- molecular orientation**
- acetonitrile, dissolved in nematic EBBA, oriented CH<sub>3</sub> group relax., multiple quantum NMR 0-66057
- n-alkanes, anisotropic London dispersion forces, surface effects 0-74214
- p-alkoxybenzylidene-p-n-butylanilines, IR absorpt. spectra, elec. field effects, orientational order parameter determ. by IR dichroism 0-80778
- p-alkoxybenzylidene-p-aminoxyanilines, IR absorpt. spectra, elec. field effect, orientational order parameter determ. by IR dichroism 0-80777
- p-azoxyanisole, directed crystn. in elec. and mag. fields 0-107052
- benzene adsorbed on graphite, melting and orientation, NMR study 0-100403
- p-n-butyl-p'-heptanoyloxyazobenzene oriented on NaCl MgF<sub>2</sub> coated NaCl, surface phenomena and IR spectra 0-79678
- cholesteric systems, with nonmesogenic additives, Keating-Bottcher theory 0-84057
- cholesteryl nonanoate, cyclohexanone admixture effect on mesophase order parameter, refr. index meas. 0-100165
- cholesteryl nonanoate-MBBA, liq. cryst. mixture, two colour display device 0-70116
- COC, cholesteric liq. cryst., positron lifetimes and phase transitions 0-59383
- COOB-cholesteric liq. cryst. mixtures, helix pitch, temp. depend. 0-64895
- cyano-biphenyl series, nematogens and smectogens, props. characterised by even-odd effect 0-107046
- 4-cyanobiphenyl/4-cyano-p-terphenyl liq. cryst. mixture, order parameters of dissolved dyes 0-100167
- cyanobiphenyls molecular conformational mobility study by optical probing method (Russian) 0-92459
- dipalmitoyl lecithin bilayer, mol. tilt, X-ray diffraction obs. in gel phase 0-84059
- p-nodocycloxy benzylidene p-azophenyl aniline, smectic phases, mol. order, EPR study 0-79693
- dye activated CLC, distributed feedback, tunable radiation generation (Russian) 0-102720
- dye laser amplifier, DC elec. field effects 0-64006
- EBBA, IR absorpt. spectra, elec. field effects, orientational order parameter determ. by IR dichroism, bend elastic consts. 0-80778
- EBBA, nematic, orientational order, effect of hexa-n-alkoxy-triphenylene disc-like solutes 0-79682
- EBBA, orientational order in glassy and nematic phases, IR dichroism meas. 0-64891
- ethanol-d<sub>2</sub>(d<sub>3</sub>)(d<sub>5</sub>), glassy state, solvated electron geometry, electron spin echo modulation obs. 0-66009
- halobenzenes, in potassium laurate mesophase, NMR, proton distance ratios and order tensor elements calcs. 0-63672
- 4-n-heptyl-d<sub>15</sub>-oxybenzoic acid-d<sub>1</sub>, nematic and smectic phases, mol. and relative segmental order 0-96439
- heptyloxyazobenzene, filamentary structures 0-107051
- high speed rot., spin diffusion, NMR spin lattice relax. obs. of D 0-66056
- liquid crystals, orientational order parameter, optical birefr. meas., polarisation field problems 0-79688
- liquid crystal alignment films prod. by RF plasma beam technique 0-76198
- liquid crystal matrix, orientational distrib. coeffs. 0-92452
- liquid crystal surface, statistical thermodynamics, local order parameter 0-88023
- liquid crystals, mol. conformation and orientational order, NMR studies, review 0-75151
- MBBA, IR absorpt. spectra, elec. field effects, orientational order parameter determ. by IR dichroism, bend elastic consts. 0-80778
- MBBA, nematic, flexibility gradient of fatty acid spin labels, EPR study 0-71181
- MBBA, nematic, mol. alignment on SiO film, film thickness effects 0-59384
- MBBA, orientational order in glassy and nematic phases, IR dichroism meas. 0-64891
- mesophase pitch, magnetically-oriented, phys. props., mol. struct. 0-64885
- methane, melting transitions, thermodynamic props., positional disordering energies 0-96452
- methoxy species on Ni (111), photoelectron spectra, electronic struct. and orientation 0-83420
- molecular crystals, mol. orientation defects, effect on polarised IR and Raman spectra 0-88989
- monolayers, polycryst., IR determ. 0-80891
- nematic liquid cryst., orientational fluctuations effect on evanescent modes of transmitted EM wave 0-64889
- nematic liquid cryst. mixture, ZLI-207, nonideally oriented layers, Fredericksz transition dynamics 0-100163
- nematic liquid crystal, twist cell, dynamic props., voltage depend. 0-70117
- nematic liquid crystal reversely pretitled cell, conformation of molecular orientation 0-59388
- nematic liquid crystals, acoustic props., rotating mag. field study 0-88034
- nematic liquid crystals, orientation fluctuations in high mag. field, quenching, birefringence effects 0-64892
- nematic liquid crystals, paramagnetic, flexomagnetoec. effects 0-75158
- nematic liquid crystals, surface and anchoring energies, van der Waals contrib. 0-92455
- nematic liquid crystals, molecular alignment using alkoxysilanes, rel. to surface energy 0-100164
- nematic-chiral-dye mixture, circular dichroism, selective light scatt. (Russian) 0-103944
- 4-nitrophenyl-4-octyloxybenzoate/cholesteric liq. cryst. mixtures, helix pitch, temp. depend. 0-64895



**molecular orientation continued**

- p-n-nonyloxybenzoic acid, smectic C phase, electro-optical effect (*Russian*) 0-92458  
 nonyloxybenzoic acid/cholesteric liq. cryst. mixtures, helix pitch, temp. depend. 0-64895  
 nuclear quadrupole spin-lattice relax. due to mol. reorientation in cryst. 0-66062  
 Nylon 6 gut yarn, fine struct. change in twisting, annealing and untwisting, X-ray and electron microscopy obs. 0-84904  
 octyl-cyano-biphenyl, influence of laser light wave field on nematic phase (*Russian*) 0-92456  
 4-n-octyl-d<sub>11</sub>-oxybenzoic acid-d<sub>11</sub>, nematic and smectic phases, mol. and relative segmental order 0-96439  
 p-n-octyloxy benzyldiene-p-toluidine, mol. order, EPR VAAC probe 0-70114  
 optically active and inactive molecules, electric and mag. dispersion forces interaction 0-99533  
 orientational bistability, nematic storage effects 0-70112  
 2-oxyphenylbenzoxazol, proton intramolecular transfer, light absorpt. and emission, dichroism, polarised fluoresc. 0-87166  
 partially oriented molecules, uniaxial, two-photon processes, polarised spectrosc. 0-74209  
 pentacene in naphthalene, triplet state, EPR study by electron spin-echo and laser flash excitation 0-58172  
 4-n-pentyloxy-phenyl-4'-n-octyloxybenzoate, nematic, dielec. relax. and freq. depend. of threshold voltage 0-60497  
 PET, biaxial orientation, refr. index meas. by Raman and IR spectrosc. 0-60583  
 PET films, one-way drawn, constant strain effects, IR meas. 0-60584  
 plastic crystal, orientational disorder, group theory method 0-107091  
 plastic crystal, orientational dynamics, neutron scatt. data interpret. using functions derived from group theory 0-107092  
 poly-γ-benzyl-L-glutamate, soln., liquid crystal transitions anal. 0-65207  
 polymers, aliphatic and aromatic, mean mol. orientation factors, from IR spectra and acoustic method 0-70142  
 polymers, crystn. under mol. orientation, formation of stacked lamellar structs. 0-84109  
 porphyrin in n-octane Shpolskii matrix, defect props., Monte Carlo obs. 0-63533  
 N-p-propoxybenzylidene-p-pentylaniline, orientational order in glassy and nematic phases, IR dichroism meas. 0-64891  
 Schiff base azo dyes in nematic liq. cryst. hosts, order parameters, optical density meas. 0-84055  
 SLC, chiral structure in electric field, dielectric permeability, spontaneous polarisation (*Russian*) 0-75159  
 smectic C liq. cryst. film, mol. orientation fluctuations in two-dimens., light scatt. obs. 0-93355  
 smectic liquid crystals, ferroelec., submicrosecond bistable electro-optic switching 0-84051  
 solute orientation in stretched polymer matrix, dichroism anal. 0-75998  
 TBACA, chiral, smectic C\* and H\* phases, mol. orientational ordering, <sup>14</sup>N NQR study 0-75152  
 tolanes, molecular conformational mobility study by optical probing method (*Russian*) 0-92459  
 trichlorophosphazo compound, Cl<sub>3</sub>P:NCCl(CF<sub>3</sub>)<sub>2</sub>, nuclear quadrupole spin-lattice relax. 0-66062  
 twisted nematic display with cholesteric dopant, transmission characteristic temp. depend. compensation 0-103934  
 two-dimensional systems, order parameter from chemical shift anisotropy patterns 0-80624  
 BCl<sub>3</sub>NCO, soln., force fields and normal modes, vibr. spectra, IR and Raman obs. (*French*) 0-58266  
 BX<sub>2</sub>NCS (X=Cl, Br, I), soln., force fields and normal modes, vibr. spectra, IR and Raman obs. (*French*) 0-58266  
 Ce<sub>2</sub>(SO<sub>4</sub>)<sub>3</sub>·9H<sub>2</sub>O(D<sub>2</sub>O), polarised Raman spectra, vibr. props. and role of lattice H<sub>2</sub>O 0-66201  
 Co complex, triazene-1-oxide complexes, EPR spectra in frozen nematic liq. cryst. glass 0-88871  
 Cu complex, triazene-1-oxide complexes, EPR spectra in frozen nematic liq. cryst. glass 0-88871  
 InO<sub>3</sub>Sn transparent conducting films, homeotropic orientation of liquid crystals (*Russian*) 0-108181  
 N<sub>2</sub>, ab initio MO-LCAO-SCF and Gordon-Kim intermolecular pot. for seven different orientations 0-95522  
 NH<sub>4</sub>Br, NH<sub>4</sub><sup>+</sup> rot. motion, quasielastic neutron scatt. obs. 0-96492  
 O<sub>2</sub>, two-dimensional adsorbed layer on graphite, props. calc. 0-103568

**molecular photodissociation**

- acrylonitrile, IR multiphoton dissociation, prod. of CN(X<sup>2</sup>Σ<sup>+</sup>) and C<sub>2</sub>(a<sup>3</sup>Π<sub>u</sub>) radicals 0-63723  
 alkali metal chlorides, photofragment spectra, bond energies and excited state symmetries 0-87190  
 alkali metal halide, UV photodissoc., metal-atom resonance-line lasers 0-58529  
 alkenes, IR multiphoton dissociation, IR detection of H atoms 0-83356  
 atmospheric negative ions, photodissoc. and photodetachment 0-69199  
 bent triatomic mol., photodissoc. rot. distrib. 0-95694  
 benzaldehyde, photoionisation mass spectra formation by UV laser radiation (*Russian*) 0-93781  
 benzene, multiphoton ionisation fragmentation patterns, statistical theory 0-95693  
 benzene, photoionisation mass spectra formation by UV laser radiation (*Russian*) 0-93781  
 benzyl radical, in solid Ar, absorption and photodissociation spectra 0-69156  
 bromomethane, IR multiphoton dissociation, depend. on cell geometry, mol. fluoresc. and decomp. obs. 0-83430  
 bromotrifluoromethane, IR multiphoton selective dissociation, effect of acceptor radicals 0-66854  
 bromotrifluoromethane cation, photodissoc. by quasi-continuum single IR photon absorption 0-61124  
 bromotrifluoromethyl cation, IR photodissoc. 0-87188  
 chlorodifluoromethane, IR multiphoton dissociation, mag. field effect 0-93772  
 chlorodifluoromethane, unimol. reaction by IR radiation, rate consts. and prod. yield, fluence and intensity depend. 0-97713  
 chloropentafluoroethane, isotopically selective multiphoton dissociation, CO<sub>2</sub>-laser wavelength, pressure and additives effects 0-78666  
 chloropentafluoroethane-(He)(Xe)(O<sub>2</sub>)(H<sub>2</sub>)(NO), multiphoton dissociation, <sup>13</sup>C enrichment factor, CO<sub>2</sub> laser wavelength and fluence depend. 0-58331  
 chlorotrifluoromethane, multiphoton dissociation, <sup>13</sup>C enrichment (*French*) 0-91615

**molecular photodissociation continued**

- chlorotrifluoromethyl cation, IR photodissoc. 0-87188  
 comets neutral atmospheres, average random walk model for mol. phot. dissociation 0-77351  
 cyclobutane, absorpt. of pulsed IR radiation and decomp., joulemeter and opto-acoustic obs. 0-58328  
 dichlorofluoromethyl peroxyhydrate, UV absorpt., spectra, photodissoc. lifetime meas. 0-83386  
 dimethyl-s-tetrazine, vapour, mol. fluoresc., photodissoc. product 0-81352  
 2,5-diphenyl-1,3,4-oxadiazole, fluoresc. quantum efficiency, one-photon dissociation, temp. depends. 0-69180  
 dye laser deterioration, effect on performance 0-83602  
 energy deposition by multiple IR photon absorpt. 0-66833  
 ethanol, multiphoton absorpt. and dissociation 0-99530  
 ethylene-(d<sub>2</sub>) clusters, IR photodissoc. 0-89506  
 ferrocene, multiphoton dissociation and ionisation by tuneable dye lasers 0-99524  
 fluoroformaldehyde, pot. energy surface characts., substitution effect 0-89505  
 fluoromethane, deuterium separation at high press. by ns CO<sub>2</sub> laser multiphoton dissociation 0-91616  
 Freon 123, deuterium separation at high press. by ns CO<sub>2</sub> laser multiphoton dissociation 0-91616  
 glyoxal, vapour, predissoc. in S<sub>1</sub> zero-point level states 0-102544  
 group IIIA metal halide, UV photodissoc., metal-atom resonance-line lasers 0-58529  
 haemoglobin, nanosec. probe of dynamics using time resolved reson. Raman scatt. 0-94162  
 halogens, dissolved complexed in liq. soln., laser-induced photodissociation for etching 0-100929  
 bis(1,1,1,5,5,5-hexafluoropentane-2,4-dionato)dioxouranium (VI), isotope selective IR laser induced unimol. dissociation 0-69197  
 highly excited molecular systems, high energy photochem. 0-66831  
 hole burning, photophysical and photochemical theories 0-58322  
 homonuclear diatomic mols., Morse pot. and vibr. level field induced, shift and broadening 0-69117  
 intramolecular dynamics, random coupling model, multiphoton excitation, kinetic eqns. 0-63700  
 iodotrifluoromethane, high vibr. state excitation in high-power laser field, spectral characs. 0-91562  
 iodotrifluoromethane, IR multiphoton selective dissociation, effect of acceptor radicals 0-66854  
 ion kinetics in high-pressure laser plasmas 0-64002  
 IR laser photolysis of polyat. mols. photochem. appls. 0-66835  
 laser, optical excitation by photodissoc. wave propag. in dense gas 0-74352  
 laser-induced selective multistep processes: impact on nuclear physics, chemistry and biology 0-61122  
 methane cation, photodissoc., ab initio RHF and MRD CI calcs. 0-95695  
 methanol-(d<sub>3</sub>), multiphoton absorpt. and dissociation 0-99530  
 methyl alcohol, IR photodissoc., CH prod. 0-97690  
 methyl chloroform, vap., multiphoton dissociation by CO<sub>2</sub> laser beam 0-61123  
 methyl iodide photodissoc. laser, kinetic model, cross-section calcs. 0-58530  
 methyl peroxyhydrate, UV absorpt., spectra, photodissoc. lifetime meas. 0-83386  
 methylnitrite VUV photodissoc., NO electronically excited photofragment identification and quantum yield 0-99527  
 molecular laser, optical pumping in damped photodissoc. wave propag. in dense gas 0-99714  
 multiphoton IR decomposition, approx. model and exact soln. of energy grained master eqn. 0-66829  
 naphthalene molecular ion, two and four photon absorpt., dissociation 0-74210  
 nickelocene, multiphoton dissociation and ionisation by tuneable dye lasers 0-99524  
 organic scintillators, vap. phase dye laser media, photophysical parameters 0-95884  
 paraterphenyl, fluoresc. quantum efficiency, one-photon dissociation, temp. depends. 0-69180  
 photofragment distrib. in two-photon photochem., isotope separation appl. 0-81344  
 polyatomic ions, IR photodissoc. 0-87188  
 polyatomic molecule dissociation in IR laser field (*Chinese*) 0-106363  
 polyatomic molecules, cyclopropane, selective bond breaking by multiple IR photon absorption 0-66834  
 polyatomic molecules, multistage IR dissociation, collisionless energy-gathering process 0-99526  
 polyatomic molecules, photofragmentation obs. methods 0-63725  
 POPOP, fluoresc. quantum efficiency, one-photon dissociation, temp. depends. 0-69180  
 pulsed molecular beam experiments employing electromechanical valve 0-63870  
 recombination afterglow, quenching var., activator penetration to region inaccessible to quencher 0-64813  
 switched, for inversion of atomic and molecular species 0-74206  
 tetramethyldioxetane, multiphoton dissociation, collisional vibr. relax., rate eqns. model 0-63729  
 s-tetrazine, UV and vis. photodissoc., three-body half-collision dynamics 0-78664  
 time of flight spectroscopy, particles in excited state produced via IR laser excitation 0-74257  
 toluene cation in solid Ar, absorption and photodissociation spectra 0-69156  
 triatomic molecule, IR multiphoton dissociation, quantal and classical calcs. 0-83431  
 tricarboaniline, laser dyes, flashlamp-pumped, photochemical stability 0-83604  
 1,1,2-trichloro-2,2-difluoroethane, vac. UV photodecomp. 0-66828  
 trichloromethyl peroxyhydrate, UV absorpt., spectra, photodissoc. lifetime meas. 0-83386  
 2,2,2-trifluoroethanol, multiphoton absorpt. and dissociation 0-99530  
 trifluoriodomethane cation, photodissoc. by quasi-continuum single IR photon absorption 0-61124  
 trifluoriodomethyl cation, IR photodissoc. 0-87188  
 two photon absorptivity, ion cyclotron reson. photodissoc. spectra, CNDO/S-CI-perturbation theory 0-74123  
 unimolecular decomposition, photon catalysed, first-order rate constant 0-99528  
 vinyl cyanide, IR multiphoton dissociation, CN internal energy distrib., time depend. 0-78638



## molecular photodissociation continued

- Ar:N<sub>2</sub>O, O(<sup>1</sup>S) photodissociative prod., photoluminesc. excitation spectra, excitation energy transfer 0-89508  
 Ar:OCS, O(<sup>1</sup>S) and S(<sup>1</sup>S) photodissociative prod., photoluminesc. excitation spectra, excitation energy transfer 0-89508  
 Bi<sub>2</sub>, three photon excitation, Bi Rydberg series 0-106280  
 CH<sup>+</sup>, excited states, pot. curves and transition moments determ. by ab initio CI methods 0-106286  
 CH<sup>+</sup>, photodissociation to C<sup>+</sup> and H, wavelength depend. and photofragment kinetic energies, visible obs. 0-58275  
 CH<sub>3</sub>OH<sup>+</sup>, IR photodissoc., fluence depend., saturation effects 0-78663  
 CO<sub>2</sub> in comet comae, effect of solar photodissociative ionisation 0-90370  
 CO<sub>3</sub><sup>-</sup>, laser photodissociation, tandem quadrupole study 0-81343  
 CS<sub>2</sub>, 193 nm laser dissoc., prompt emission and internal energy distrib. of CS 0-106364  
 CS<sub>2</sub>, photodissoc., fragment energy distrib. 0-69200  
 Cr(CO)<sub>6</sub>, photodissoc., Cr prod. 0-95575  
 CrO<sub>2</sub>Cl<sub>2</sub>, multiphoton induced inverse electronic relax. 0-66836  
 Cs orientation in CsI photodissociation by UV light (*Russian*) 0-69201  
 Cs<sub>2</sub>, Cs Rydberg states, diamag. and collisional perturbations 0-58181  
 CsI, photodissoc., UV, Cs atom orientation (*Russian*) 0-69201  
 FCO, form. in Ar matrix, vibr. and electronic spectra, valence force potential determ., mol. photodissoc. obs. 0-85170  
 H<sup>+</sup> photofragments angular distribution, parity favoured electric dipole transitions 0-58330  
 H<sub>2</sub><sup>+</sup>, photodissoc., mass spectra 0-86489  
 HCN in neutral cometary atmospheres, photodissoc. rel. to CN prod. 0-82303  
 HCN, photodissoc., photoabsorpt., photoemission and CN form. obs. 0-87141  
 HNO<sub>3</sub>, VUV photodissoc., vibr. and rot. distrib. 0-87191  
 H<sub>2</sub>O, gaseous, photodecomposition over TiO<sub>2</sub> and TiO<sub>2</sub>-RuO<sub>2</sub> surfaces 0-85194  
 H<sub>2</sub>O, photodecomposition over Pt/TiO<sub>2</sub> catalysts 0-81337  
 H<sub>2</sub>O, photodissoc. resonances, converged 3-dimens. quantum mech. calcs. 0-106366  
 H<sub>2</sub>O photodissociation, OH(A<sup>2</sup>Σ<sup>+</sup> → X<sup>2</sup>Π<sub>2</sub>) yields 0-71927  
 H<sub>2</sub>O, VUV photodissoc., vibr. and rot. distrib. 0-87191  
 HOCl, photodissoc. rot. distrib. 0-95694  
 HO<sub>2</sub>NO, UV absorpt., spectra, photodissoc. lifetime meas. 0-83386  
 H<sub>2</sub>S(D<sub>2</sub>S) photodissoc., SH internal energy distribution 0-95697  
 He photofragments angular distribution, parity favoured electric dipole transitions 0-58330  
 HgBr<sub>2</sub>, electronic struct. and photodissoc., effective core pots. and POL(1) CI wave function 0-63560  
 HgBr<sub>2</sub>, photofragment fluoresc. polarisation, press. depend. 0-63720  
 HgCl<sub>2</sub>, electronic struct. and photodissoc., effective core pots. and POL(1) CI wave function 0-63560  
 I<sub>2</sub>, photodissoc., atomic He(I) photoelectron spectrum 0-83325  
 I<sub>2</sub>Ar<sup>+</sup>, product state distrib. and binding energy 0-63857  
 ICN, A-state photolysis, I(C<sup>2</sup>P<sub>1/2,3/2</sub>) branching ratio wavelength depend. 0-81335  
 I<sub>2</sub>He, van der Waals mol., photodissoc. 0-63765  
 I<sub>2</sub>He\*, product state distrib. and binding energy 0-63857  
 I<sub>2</sub>Ne\*, product state distrib. and binding energy 0-63857  
 Kr:OCS, O(<sup>1</sup>S) and S(<sup>1</sup>S) photodissociative prod., photoluminesc. excitation spectra, excitation energy transfer 0-89508  
 LiI UV photodissoc. cross section, reson. ionis. Li detection 0-63719  
 N<sub>2</sub>, multiphoton absorpt., spectroscopic evidence 0-63726  
 N<sub>2</sub>F<sub>4</sub>, collisionless dissociation kinetics in highpower IR radiation field 0-66853  
 N<sub>2</sub>F<sub>4</sub>, mol. photodissoc. using CO<sub>2</sub>-laserradiation, rate const. meas., mol. fluoresc. and time-resolved UV spectra obs. (*German*) 0-83434  
 N<sub>2</sub>O<sup>+</sup>, dissoc., threshold photoelectron-photoion coincidence obs. 0-87189  
 Na<sub>2</sub>, laser-induced dissoc., polarisation of atomic fluorescence obs. 0-78569  
 Na<sub>2</sub>, photodissoc., <sup>2</sup>P products, at. fine struct. anal. 0-78665  
 NaBr photodissoc., Na non-Gaussian line shape, level shifting and velocity inversion 0-58182  
 O<sub>2</sub> in stratosphere and mesosphere, photodissoc. through solar UV radiation absorpt. 0-109248  
 O<sub>2</sub><sup>+</sup>, f<sup>2</sup>Π<sub>g</sub> state, quasi-bound levels, predissociation, band rot. anal., photofragment kinetic energy anal. 0-63650  
 O<sub>3</sub>, atmospheric, annual var. of effects of diffuse solar radiation on photodissoc. 0-109210  
 O<sub>3</sub> in stratosphere and mesosphere, photodissoc. through solar UV radiation absorpt. 0-109248  
 O<sub>3</sub>, photodissoc., O(<sup>1</sup>S) yield at 1700-2000 Å 0-97714  
 O<sub>3</sub>, photodissoc. cross section, vibr. excitation effects obs. 0-95696  
 O<sub>3</sub>, photolysis at 248 nm, O(<sup>1</sup>P<sub>1</sub>) direct obs. 0-101028  
 OCS<sub>e</sub>, quantum yields for Se, <sup>1</sup>S<sub>0</sub>, <sup>1</sup>D<sub>2</sub>, and <sup>3</sup>P<sub>0,1,2</sub> atoms determ. in photolysis, lifetime and quenching rate meas. 0-97741  
<sup>18</sup>O<sup>16</sup>O, in atmosphere, photodissociation as source of atmospheric O<sub>3</sub> 0-94559  
 Pb salts, inorganic 0-77081  
 Pb<sub>2</sub>, three photon excitation, Pb Rydberg series 0-106280  
 PbBr<sub>2</sub>(L<sub>2</sub>) photodissociation, stimulated emission obs. on Pb 405.8, 368.3 and 364.0 nm lines 0-87387  
 Rb<sub>2</sub>, photodissoc., <sup>2</sup>P products, at. fine struct. anal. 0-78665  
 SF<sub>6</sub>, Doppler-limited spectroscopy, of 3<sub>v</sub> band 0-58244  
 SF<sub>6</sub>, Doppler-limited spectroscopy of 3<sub>v</sub> band, rot. const. and anharmonic parameters calcs., mol. photodissoc. 0-83361  
 SF<sub>6</sub>, IR multiphoton dissociation studies, inverse bottle-neck effect 0-87193  
 SF<sub>6</sub>, IR multiphotonic excitation, depend. on cell geometry, mol. fluoresc. and decomp. obs. 0-83430  
 SF<sub>6</sub>, multiphoton dissoc. by mol. beam method, energy distribution meas. by time-of-flight spectra, dissoc. dynamics 0-78670  
 SF<sub>6</sub>+Si(surface), IR laser induced reaction, mol. vibr. and mol. dissoc. obs. 0-93798  
 SO<sub>2</sub>-containing ions, photodestruction 0-63722  
 TiI, atomic fluorescence, D<sub>2</sub> pressure effect on width and shift 0-99475  
 TiI, photodissoc., Ti 535.0 nm line shift by H<sub>2</sub> perturber 0-91506  
 UF<sub>6</sub>, laser chemistry 0-69198  
 UF<sub>6</sub>, molecular dissociation by DF<sub>2</sub> laser radiation 0-91619  
 UF<sub>6</sub>, molecule dissociation in two-frequency IR laser field 0-66855  
 UF<sub>6</sub>, photodissoc. through light scatt. of UF<sub>6</sub> particles, influence of N<sub>2</sub> as collisional partner 0-95698  
 UF<sub>6</sub>, UF<sub>6</sub>-H<sub>2</sub> gas dissociation in pulsed IR and UV laser fields 0-91620  
 W(CO)<sub>6</sub>, photodissoc., W prod. 0-95575

## molecular polarisability

- see also molecular moments  
 alkali halide mols., electronic polarisability, ionic radii and repulsive pot. parameters, mol. consts. 0-87242  
 alkali metal halide, zero point Compton profile anisotropies and bond polarities, correl. 0-78659  
 alkyl halides, conform. energy calcs., polar bonds and polarisability, polaris. model appl. 0-58188  
 anisotropic, optical study (*Rumanian*) 0-74256  
 anisotropic atom point dipole interaction model calcs., involving electron repulsion 0-78521  
 anthracene derivatives in solution, polarisability and dipole moments, emission and absorpt. spectra obs. 0-69256  
 average, empirical calc. method 0-63859  
 benzene, dipole polarisability, finite-field SCF MO calcs. 0-83255  
 benzene, dynamic polarisabilities, calcs., superposition method of excited config., nonstationary perturbation theory eqns. 0-69257  
 biomolecules+chloranil, charge transfer interaction, equilb. const., enthalpy and entropy determ., mol. polarisability 0-89708  
 trans-butadiene, polarisability, nonlinear elec. susceptibility, SCF calcs. 0-95547  
 chemically induced magnetic polarization by S-T<sub>±1</sub> mixing in strong mag. field 0-83515  
 closed-shell system, polarisability and mag. susceptibility calc. by SCF and CI method 0-99443  
 colloids, electro-optic studies, stability 0-85222  
 coumarin laser dyes, solvent effects on photophysical parameters 0-91598  
 p-cyanophenyl p-n-alkyloxybenzoates, nematic, birefringence, polarisability and order parameter 0-100642  
 cyclic ketones, electrochromism and electric dichroism for studying transitions to second excited singlet 0-63692  
 diatomic molecules, rotational Raman intensities and polarisability anisotropy change meas. with internuclear distance 0-63641  
 dodecahexenes, sudden polarisation effect, ab initio and CI calcs. 0-58160  
 dynamic polarisabilities calcs., superposition method of excited config., nonstationary perturbation theory, eqn. 0-69257  
 electrostatic interactions in liquid state, effect on frontier orbitals and chem. reactivity 0-84046  
 ethene, dipole polarisability, finite-field SCF MO calcs. 0-83255  
 ethylene, polarisability, nonlinear elec. susceptibility, SCF calcs. 0-95547  
 ethylene, pot. energy and dipole moment surfaces, polarisation effect, ab initio CI calcs. 0-106272  
 ethylene, rot. around double bond, four orbital-four-electron model 0-95592  
 formaldehyde, electronic struct., dipole moments, mol. polarisability, force fields, ab initio calcs. 0-78531  
 free radical reaction, chemically induced dynamic polarisation in strong mag. field, radical rotation influence 0-76509  
 hexatriene, polarisability, nonlinear elec. susceptibility, SCF calcs. 0-95547  
 hydrocarbons, average elec. polarisabilities and mag. susceptibilities, ab initio valence electron calcs. 0-87033  
 hydrocarbons, on activated C, rel. between adsorption and polarizabilities 0-76558  
 intermolecular spectroscopy and dynamical properties of dense systems, conf., Varenna, Italy (1978) 0-82581  
 Kirkwood-Pople-Schofield method, appls. to polarisabilities calcs. 0-83272  
 Lennard-Jones fluids, orientational and collision induced light scatt. 0-63644  
 methane-(d<sub>4</sub>), liq., Brillouin scatt. and refr. index measurements 0-76035  
 molecular crystals, microscopic dielec. theory 0-97186  
 naphthalene, dipole polarisability, finite-field SCF MO calcs. 0-83255  
 nematic liquid crystals, polarisabilities, Lippincott δ-function pot. model 0-79686  
 nonpolar polarisable fluids, effective field of a dipole, rel. to mol. polaris. 0-79659  
 open-shell system, polarisability and mag. susceptibility calc. by SCF and CI method 0-99443  
 organic molecular systems, polarisabilities, susceptibilities, electron impact ionis. cross-sections calcs. 0-63835  
 organic mols., relative Raman intensities, CNDO/2 INDO param. effect 0-95633  
 polar molecules with fluctuating polarisability, dielec. theory 0-97178  
 polydisperse dilute suspensions, of rod-like particles, anisotropy of electric polarisability 0-85224  
 quinoxalines, enzyme inhibitory, structure-activity quantitative study 0-78540  
 Raman and fluorescent scattering by molecules embedded in dielectric spheroids 0-99507  
 sепiolite, electric polarisability, anisotropy, length depend. of ionic contrib. 0-85224  
 spherical tops, chiral discrimination 0-106314  
 static polarisability, ab initio SCF wave functions 0-74106  
 tetra-glycine, cyclic, mol. polaris. and diamag. suscept. calcs. 0-63858  
 tetra-l-alanine, cyclic, mol. polaris. and diamag. suscept. calcs. 0-63858  
 thioformaldehyde, electronic struct., dipole moments, mol. polarisability, force fields, ab initio calcs. 0-78531  
 unsaturated hydrocarbons, dipole polarisabilities, STO-4G calcs. 0-83255  
 van der Waals coeff., two-body combination rules 0-78677  
 BH, elec. polarisabilities and dipole moments, var. perturbation obs. 0-63527  
 C<sub>2</sub>N<sub>2</sub>, 2<sub>v</sub> band overtones, Raman intensities, bond polarisability theory 0-63639  
 CO, polarisability derivatives, bond length depend., SCF and CI calcs. 0-58162  
 CO<sub>2</sub>, collision-induced Raman spectrum, theoretical studies 0-63646  
 CaCl<sub>2</sub>, X<sup>2</sup>Σ<sup>+</sup> pot. energy curves, polarisability and dissoc. 0-91629  
 Cl<sub>2</sub>, one electron props. and polarisability, SCF and CI calcs. 0-58159  
 H<sub>2</sub>, dipole polarisability, coupled perturbed Hartree-Fock method improvement 0-58148  
 H<sub>2</sub>, dynamic dipole polarisabilities calcs. 0-74110  
 H<sub>2</sub>, dynamic polarisabilities, variation-perturbation calcs. 0-87243  
 H<sub>2</sub>, optical polarisation following electron impact 0-63831  
 H<sub>2</sub>, triplet state, molecular polarisability, ab initio calcs. 0-63860  
 HCN+He(H<sub>2</sub>)(CH<sub>3</sub>F), HCN excited vibr. state, T<sub>2</sub> meas. 0-102498  
 HCl, electron elastic scatt., exchange and polarisation 0-91668  
 HCl, one electron props. and polarizability, SCF and CI calcs. 0-58159  
 HCl, polar liqs. models, mol. polarisability effect 0-92444  
 HF, polar liqs. models, mol. polarisability effect 0-92444



**molecular polarisability continued**

- H<sub>2</sub>O, liquid, equations for mag. susceptibility, electric polarisability 0-75708  
 H<sub>2</sub>O, polarisability and mag. susceptibility calc. by SCF and CI method 0-99443  
 H<sub>2</sub>O, SCF calcs. using cusped Gaussian basis sets, polarisation effects 0-74118  
 H<sub>2</sub>SiO, electronic struct., dipole moments, mol. polarisability, force fields, ab initio calcs. 0-78531  
 HeH<sup>+</sup>, dynamic dipole polarisabilities calcs. 0-74110  
 I<sub>2</sub>, polarisability anisotropy, laser assisted mol. beam spectroscopy 0-78646  
 LiBr, pair pot., dipole moment, polarisability tensor, bond length depend., finite field SCF calcs. 0-58127  
 N<sub>2</sub>, SCF calcs. using cusped Gaussian basis sets, polarisation effects 0-74118  
 Ne<sub>2</sub>, collision induced Raman spectra and diatom polarisability 0-63647  
 SF<sub>6</sub>, pair polarisability anisotropy, point atom polarisability approx. calcs. 0-87244

**molecular positron scattering** *see elastic scattering of electrons by atoms and molecules; molecular electron impact dissociation; molecular electron impact excitation; molecular electron impact ionisation*

**molecular potentials** *see potential energy functions*

**molecular predissociation**

- diatomic molecules, laser-induced predissoc., surface mag. field effect 0-106365  
 diazonium salts in aqueous solns. and polymer matrices, IR absorpt. spectra 0-76030  
 glyoxal, vapour, predissoc. in S<sub>1</sub> zero-point level states 0-102544  
 highly excited molecular systems, high energy photochem. 0-66831  
 polyatomic molecules, photofragmentation obs. methods 0-63725  
 preionis. and predissoc., rel. to spectral line shape 0-63724  
 triatomic van der Waals mol., rot. predissoc. 0-63721  
 two-channel model, resonances with complex rot. method 0-58327  
 van der Waals mol. rot. predissociation study, complex coord. method 0-74205  
 vibrational predissociation in hydrogen bonded complexes 0-61078  
 ArH<sub>3</sub>, van der Waals mol., rot. predissoc. 0-63721  
 ArN<sub>3</sub>, van der Waals mol., rot. predissoc. 0-63721  
 Br<sub>2</sub>, B<sup>2</sup>II(O<sup>+</sup>) predissoc. rates, analytical interpretation 0-91617  
 Br<sub>2</sub>, Kr ion laser-excited fluorescence, predissoc. 0-83414  
 Br<sub>2</sub>, single rot. states, lifetimes and collisional quenching cross sections determ. by obs. fluoresc. decay 0-91595  
 BrCl laser induced fluoresc., quantum resolved level dynamics in B<sup>2</sup>II(O<sup>+</sup>) state 0-74188  
 CH<sup>+</sup>, photodissociation to C<sup>+</sup> and H, wavelength depend. and photofragment kinetic energies, visible obs. 0-58275  
 CuH, UV absorpt. spectra 0-87143  
 D<sub>3</sub>, emission spectra, rot. struct. obs. mol. const. determ., predissociation 0-106331  
 H<sub>2</sub>, predissoc., interference effects, lineshape obs. 0-83432  
 H<sub>2</sub>, preionis. and predissoc., rel. to spectral line shape 0-63724  
 H<sub>3</sub>, emission spectra, rot. struct. obs. mol. const. determ., predissociation 0-106331  
 HCN predissoc. Frank-Condon amplitudes 0-95694  
 HD, predissoc., interference effects, lineshape obs. 0-83432  
 HF, Feshbach resons., predissoc. investig. 0-83433  
 IBr, B<sup>2</sup>II(O<sup>+</sup>) excited state, laser-induced fluoresc. 0-58309  
 KrH<sub>3</sub>, van der Waals mol., rot. predissoc. 0-63721  
 N<sub>2</sub>, preionis. and predissoc., rel. to spectral line shape 0-63724  
 NH<sub>3</sub>, expansion cooled, mol. photoionisation, rot. struct., rot. predissoc. of excited states 0-91611  
<sup>15,14</sup>NO<sub>2</sub>, predissoc. rot. struct. in 2490 Å band 0-87192  
 N<sub>2</sub>O, preionis. and predissoc., rel. to spectral line shape 0-63724  
 NeH<sub>3</sub>, van der Waals mol., rot. predissoc. 0-63721  
 O<sub>2</sub><sup>+</sup>, I<sup>2</sup>Π<sub>g</sub> state, quasi-bound levels, predissociation, band rot. anal., photofragment kinetic energy anal. 0-63650  
 S<sub>2</sub>, matrix-isolated, B<sup>2</sup>Σ<sub>u</sub> predissoc., relax. processes 0-58329  
 SO<sub>2</sub>, UV excitation spectra, mol. fluoresc. meas., mol. predissoc. obs. 0-83389  
 S<sub>2</sub>O, UV excitation spectra, mol. fluoresc. meas. 0-83389

**molecular quadrupole moments** *see molecular moments*

**molecular relaxation** *see chemical reactions; molecular fluorescence; molecular inelastic collisions; molecular spectra; time resolved spectra*

**molecular reorientation**

*see also macromolecular dynamics*

- acetone, <sup>17</sup>O chemical shift and NMR linewidth meas., self-association equilib. const. determ., mol. reorientations obs. 0-87148  
 acetonitrile, <sup>13</sup>C relaxation times anal. using J-diffusion model of mol. reorientation 0-87149  
 acetonitrile, dissolved in nematic EBBA, oriented CH<sub>3</sub> group relax., multiple quantum NMR 0-66057  
 acetonitrile, IR and Raman spectra, vibr. and reorientational and energy transfer width separation, rot. const. determ. 0-87131  
 adamantane, plastic phase; C<sub>4</sub> rot. jumps, existence and uniqueness 0-88067  
 2-adamantanone, cryst. struct. in plastic phase 0-88065  
 alkali hyperoxides, ionic π-electron systems, magnetogyratation 0-93155  
 p-alkoxybenzylidene-p-aminocyanolines, IR absorpt. spectra, elec. field effect, orientational order parameter determ. by IR dichroism 0-80777  
 alkyl chains, <sup>13</sup>C longitudinal relax. times and nuclear Overhauser enhancement anal. 0-83390  
 anisotropic rotational diffusion studied by passage saturation transfer EPR 0-60403  
 anthracene:tetracyanobenzene charge transfer complex, cryst. struct., temp. effects 0-96508  
 anthracene dianions in dimethyl ether, rotational diffusion meas. 0-65262  
 apatites, dipolar reorientations, TSD study 0-107068  
 atomic and plastic crystals, melting transitions, thermodynamic props. 0-96452  
 benzene, liq., mol. motion at high press. 0-103509  
 t-butyl bromide, vibr. relax. in pure liq. and soln., Raman spectra 0-66167  
 t-butyl chloride, vibr. relax. in pure liq. and soln., Raman spectra 0-66167  
 carborane, ortho- and para- phase transition and mol. reorientation, isomer effects, PMR obs. 0-80628  
 collagen fibril, <sup>2</sup>H NMR of mol. motion 0-67034  
 condensed phases, molecular rototranslation, single particle theory 0-64932

**molecular reorientation continued**

- crystal orientational disordering, thermodynamic props., stat. mech. model 0-96453  
 4-cyanobiphenyl and 4'-alkyl- or 4'-alkoxy-substituted liq. cryst. derivatives, soln., absorpt. and fluoresc. spectra 0-87164  
 cyanomethane-d<sub>0</sub>-d<sub>3</sub>, soln., for IR spectra, band shape and moment anal. 0-58252  
 cyclohexane, in benzene soln., mol. motion, correl. functions 0-96431  
 decylammonium chloride micelles, <sup>13</sup>C longitudinal relax. times and nuclear Overhauser enhancement anal. 0-83390  
 dibenzenechromium-dibenzenevanadium, proton HFS data, ENDOR obs. 0-66073  
 dichloromethane-d<sub>0</sub>-d<sub>2</sub>, soln., far IR spectra, band shapes and moment anal. 0-58252  
 dichloromethane-d<sub>3</sub>, spectral densities determ. from spin-lattice relax. and spin-echo decay rates 0-75877  
 dipolar liquid time-variation of dispersion and absorption of third-order electric polarisation, mol. relax. times 0-60487  
 EBBA, NMR and Raman scatt. studies in nematic phase 0-100619  
 electronic spectra of molecules, pure elec. quadrupole transition polaris. 0-63691  
 ethane, solid, mol. reorientational motions, incoherent neutron scatt. studies 0-107070  
 ethanol, polymorphic forms, mol. motion, NMR obs. 0-88885  
 fluorobenzene, mol. reorientation and weak mol. interaction influence, <sup>2</sup>D spin-lattice relax. obs. 0-106333  
 n-heptyl-4-cyanobiphenyl, nematic phase, dielec. loss, diffusion equations 0-71305  
 hexamethylenetetramine, mol. ultraslow rot. obs. using D probe spin alignment tech. 0-88890  
 hexamethylenetetramine, ultraslow tetrahedral jumps, deuteron NMR spin alignment obs. 0-66046  
 hydroxyapatites, dipolar reorientations, TSC study 0-60491  
 ice orientational correlation parameter, water mol. dipole moment 0-59407  
 impurity molecule in cryst. lattice, strong EM field effect on librational-rot. motion 0-80824  
 intermolecular spectroscopy and dynamical properties of dense systems, conf., Varenna, Italy (1978) 0-82581  
 liquid memory functions for ang. motions 0-59358  
 liquids, collective molecular motion from depolarized light scatt. 0-60614  
 liquids, rotational relaxation, molecular hydrodynamics, long time tails 0-59357  
 MBBA, nematic liq. cryst., nonlinear optical amplification above Frederiks transition 0-95937  
 MBBA, NMR and Raman scatt. studies in nematic phase 0-100619  
 methane, phase II, nuclear spin-lattice relax. and site symm. 0-97155  
 methane, solid, phase II, Raman spectrum, vol. and temp. depend. 0-97260  
 methane-d<sub>4</sub>, solid, rot. tunnelling, neutron scatt. obs., isotope effect 0-92468  
 methane-d<sub>4</sub>, solid, tunnel splittings, heat capacity meas. 0-96451  
 p-methoxybenzoate-p'-n-pentyl benzene, slow non-critical mol. reorientation in isotropic phase 0-84062  
 methyl bromide, <sup>13</sup>C relaxation times anal. using J-diffusion model of mol. reorientation 0-87149  
 methyl groups, spin symmetry species, neutron scatt. transitions 0-92470  
 methyl iodide, <sup>13</sup>C relaxation times anal. using J-diffusion model of mol. reorientation 0-87149  
 methyl iodide, liq., mol. reorientation, dielec. and viscosity meas. 0-100157  
 4-methyl-2,6-di-tert-butylphenol, methyl group reorientation, classical dynamics, NMR relax. and inelastic neutron scatt. 0-88066  
 methyl-d groups, reorienting or tunnelling spin-lattice relax. 0-97156  
 motions in liquids, review and anal., hydrodynamics 0-59356  
 nitrobenzene, liquid and CCl<sub>4</sub> soln. shear waves and translation-rotation coupling obs. by depolarised Rayleigh scattering 0-71432  
 nitromethane, solid, tunnel states investig. 0-103274  
 nitroxide free radical spin label EPR spectra, determ. of rot. correl. time and HFS coupling 0-74260  
 nonlinear molecules, tetrahedra, symmetry constraints on configurational props. 0-63854  
 organic liquid systems, dielectric and dynamic Kerr-effect studies 0-60496  
 organic molecular crystals, use of atom-atom pots. in interpreting behaviour, book contrib. 0-84136  
 paramagnetic liquid, depolarized light scatt. in mag. field 0-80759  
 pentacene dianions in dimethyl ether, rotational diffusion meas. 0-65262  
 PMMA, effect of fillers on molecular motions, dielectric relax. meas. 0-80691  
 polar fluids, rigid, dielectric relaxation theory 0-60495  
 polydiethylsiloxane, mol. motion, NMR spin relax. data re-interpret. 0-84664  
 polymer chains with rigid bonds, local relax. times, mol. dynamics study (Russian) 0-59373  
 pyridine-water soln., reorientational relax. and activation energy of pyridine, depolarised Rayleigh scattering 0-76037  
 pyridinium iodide, order-disorder phase transition and reorientation fluctuations studied by Raman spectra 0-80764  
 relaxation processes, symposium, London, England (Dec. 1976) 0-56993  
 resonance Raman lineshape studies of vibrational and rotational relaxation in soln. 0-60560  
 rod-shaped molecules, restricted rot. diffusion, time correl. functions 0-79655  
 siloxane, temp. transitions, linear dilatometry and X-ray diffr. obs. (Russian) 0-59404  
 smectic phases, long mol. axis reorientation, LF dielec. dispersion 0-70124  
 solid, ultraslow mol. rot. obs. using D probe spin alignment tech. 0-88890  
 symmetrical molecules, reorientation spectroscopic meas. models 0-58405  
 tetracene dianions in dimethyl ether, rotational diffusion meas. 0-65262  
 tetrafluoromethane, liq., mol. reorientation 0-106320  
 tetramethylammonium octahydrotriborate, NMR study of proton and B dynamics 0-93200  
 thiourea-d<sub>4</sub>-ferrocene inclusion cpd. mol. motion, PMR spectrum 0-84656  
 toluene, in benzene soln., mol. motion, correl. functions 0-96431  
 bis-triazolopyridazines, deformation, rot. angles and intramolecular steric factors 0-69079  
 bis-triazolyls, deformation, rot. angles and intramolecular steric factors 0-69079



**molecular reorientation continued**

- 1,2,4-trichlorobenzene liq., mol. reorientation, translation and vibr. relax., Rayleigh and Raman spectra 0-95632  
 trichloromethane-d<sub>0</sub>-d<sub>1</sub>, soln., far IR spectra, band shape and moment anal. 0-58252  
 tunnelling molecular groups in solids, symmetry of rotor part of rotor-phonon interaction 0-84114  
 water, supercooled, sound vel. dispersion, struct. relax. effect, Brillouin scatt. obs. 0-107375  
 xanthene dyes in n-alcohols (ethylene glycol) (glycerol), rot. relax., time-resolved fluoresc. depolaris. obs. 0-58300  
 Al<sub>2</sub>Cl<sub>6</sub> molten, nuclear mag. relax., mol. rot. 0-71209  
 β-Al<sub>2</sub>O<sub>3</sub>-NH<sub>4</sub><sup>+</sup>, PMR relax. time obs. of ionic motion 0-71213  
 β-Al<sub>2</sub>O<sub>3</sub>-NH<sub>4</sub><sup>+</sup>, proton dynamics neutron scatt. study 0-59408  
 β-Al<sub>2</sub>O<sub>3</sub>-OH<sub>3</sub><sup>+</sup>, proton dynamics neutron scatt. study 0-59408  
 Fe cyclopentadienyl-dibenzenevanadium, coalescence temps., full proton HFS tensor, ENDOR obs. 0-66073  
 K+NaK collisions studied using circularly polarised laser fluorescence, molecular reorientation obs. 0-69215  
 KCN, inelastic neutron scatt. by coupled rot. and translational modes 0-79895  
 NH<sub>4</sub><sup>+</sup> ion rotation, quantum effect on spin-lattice relax. time 0-75875  
 N<sub>2</sub>H<sub>6</sub><sup>2+</sup> salts, NMR spin lattice relaxation study, <sup>14</sup>N-<sup>1</sup>H dipole-dipole contrib. to relax. 0-75878  
 NH<sub>4</sub>NO<sub>3</sub> crystals, NH<sub>4</sub><sup>+</sup> ion symmetry in phases II-V, Raman spectra obs. 0-66200  
 Ni(NH<sub>3</sub>)<sub>6</sub>I<sub>2</sub>, phase transition and rot. excitation 0-96642  
 SF<sub>6</sub>, vibr. coupling in collision-induced Raman scatt. 0-83373  
 Si biradical, six-coordinate, mol. mobility two-spin probe investig. 0-102529  
 SiCl<sub>4</sub> molecule, NMR relaxation expts. 0-63673  
 SiH<sub>3</sub> radical, in Ar(Kr)(N<sub>2</sub>) matrix, anisotropic ESR spectroscopic parameters 0-63687

**molecular reorientational states** *see molecular reorientation***molecular resonant states**

- see also Fermi resonance; molecular vibronic states*  
 adsorbed mols., effective reson. Raman spectra 0-97730  
 allylamine, laser-microwave double and triple reson. 0-83397  
 aromaticity, reson. energy in graph theory 0-91412  
 biomolecule resonant interactions 0-72128  
 compound state resonances, semiclassical calcs. 0-87031  
 ethylene, narrow resonances of multiple-photon IR absorpt. 0-99529  
 ethylene, twisted, intervalence charge transfer and reson., sudden polarisation effect 0-69230  
 furan, resonantly enhanced multiphoton ionisation 0-106362  
 hydrocarbons, non-alternant, reson. energies 0-106278  
 ionisation spectroscopy, reson. chem.-physics appls. 0-68259  
 laser field interaction, Floquet theory 0-63716  
 methyl iodide, van der Waals mol., electron self-scavenging 0-95727  
 N-methyl pyrrole, resonantly enhanced multiphoton ionisation 0-106362  
 multichannel threshold structures in scattering theory 0-58334  
 naphthalene mixed crystals, dimer reson. self-energy 0-99459  
 negative ions, Feshbach type reson. scatt., Glauber approx. calcs. 0-102570  
 polyatomic molecules, nonadiabatic transitions between electronic terms of identical symmetry 0-83265  
 potential surfaces, complex coord. calcs. in adiabatic approx. 0-102464  
 potential surfaces, complex coord. calcs. using stationarity condition 0-102465  
 predissociated two-channel model, resonances with complex rot. method 0-58327  
 pyrazine, reson. to the S<sub>2</sub>(π,π\*) state, Raman spectra calcs. 0-69147  
 pyrimidine nucleotides, UV reson. Raman excitation profiles 0-58265  
 pyrrole, resonantly enhanced multiphoton ionisation 0-106362  
 resonance eigenvalues, accuracy criteria 0-91423  
 twisted conjugated molecule, zwitterionic excited states investig. 0-58179  
 wavefunctions of complex coord. method 0-106282  
 Br<sub>2</sub> in Ar matrix, reson. Raman scattering amplitude damping in discrete reson. limit 0-58262  
 CO, vibr. excitation via high-energy shape resonances 0-91693  
 CO<sub>2</sub>, photoionisation, nuclear motion effects 0-58324  
 CO<sub>2</sub>, VV processes, estimation of almost resonant molecular energy transfer due to multiphoton pot. 0-91642  
 DF-HBr CW optical resonance transfer laser 0-64003  
 HCl, dissociative electron attachment, differential cross section, Feshbach resons. 0-83508  
 HF, Feshbach resons., predissoc. investig. 0-83433  
 HNCO, rot. spectrum, ground and vibr. state reson., centrifugal distortion coupling 0-83364  
 H<sub>2</sub>O, photodissoc. resonances, converged 3-dimens. quantum mech. calcs. 0-106366  
 N<sub>2</sub>, electron scatt., absolute total cross-sections 0-83486  
 O<sub>2</sub>, I and I' resonance series, vibr. level populations in autoionisation, photoelectron spectra, bond length determ. 0-91612  
 UF<sub>4</sub>, absorption spectrum indicating presence of resonantly localised continuum state 0-58173

**molecular rotation**

- see also macromolecular dynamics; molecular force constants; molecular reorientation; molecular rotation calculations; molecular rotational-vibrational energy transfer; molecular spectra; rotational isomerism*  
 α,β-β-trifluoroacetonitrile, liq.-liq. transition rel. to mol. motion, NMR study 0-70383  
 acetaldehyde, T<sub>2</sub>-relax. meas. press. depend. for rot. transitions, pulse spectrometer 0-78612  
 acetonitrile, IR and Raman spectra, vibr. and reorientational and energy transfer width separation, rot. const. determ. 0-87131  
 acrylonitrile, NMR and relax. props., liq.-liq. transition rel. to mol. motion 0-70382  
 alkali hydride molecules, pot. energy function, rot. const., vibr. const., and binding energy 0-99532  
 allylamine, laser-microwave double and triple reson. 0-83397  
 bent triatomic mol., photodissoc. rot. distrib. 0-95694  
 1-1-d<sub>2</sub>-but-1-ene skew form, microwave spectra, rot. const. and centrifugal distortion coefficients determ. 0-83351  
 chain mols., conformational transition kinetics 0-83339  
 chloromethyl formate, conformation potential energy surfaces, ab initio calcs. 0-69065  
 condensed phases, molecular rototranslation, single particle theory 0-64932

**molecular rotation continued**

- coumarin laser dyes, fluoresc. quantum yields and lifetimes, polar solvent effects 0-87054  
 p-cyano-N,N-dimethylaniline in polar solvents, double fluorescence, theoretical model 0-58296  
 2-cyanoaziridine, microwave rot. spectrum, assignments 0-91546  
 cyanocyclopentane, microwave spectral study of axial and equatorial conformers 0-95604  
 3-cyanothiophene-<sup>35</sup>S(-<sup>15</sup>N), partial r<sub>0</sub>-struct., microwave spectra 0-91552  
 cyclic 4-ring rotation-puckering, use of spherical coords. 0-58193  
 cyclohexane, liquid, density effect on transport properties 0-65264  
 cyclopentadienylhafniumdichloride, gaseous, far IR and Raman spectra 0-95624  
 cyclopentadienyltitanium dichloride, gaseous, far IR and Raman spectra 0-95624  
 cyclopentadienyltitaniumtrichloride, gaseous, far IR and Raman spectra 0-95624  
 cyclopentadienylzirconiumdichloride, gaseous, far IR and Raman spectra 0-95624  
 cyclopropyl cyanide, high-resolution microwave spectra, quadrupole hyperfine struct. of rot. transitions anal. 0-95601  
 diatom-surface scatt., rot. inelastic, impulsive collision limit calc. 0-104030  
 diatomic molecular spectra, conventions for defining electric transition moment and rot. line intensity factors 0-83346  
 diatomic molecules, rotational Raman intensities and polarisability anisotropy change meas. with internuclear distance 0-63641  
 dimethyldichlorosilane, microwave spectrum, rot., centrifugal distortion and quadrupole coupling consts. 0-91547  
 DNA, <sup>111</sup>In bound, rot. correl. times, from γ-ray perturbed angular correl. 0-94152  
 DNA, molecular motions, investigated by <sup>31</sup>P and <sup>13</sup>C NMR relaxation 0-63657  
 DNA[Cu<sup>2+</sup>], <sup>111</sup>In bound, rot. correl. times, from γ-ray perturbed angular correl. 0-94152  
 energy loss spectra, state-to-state rot. transition cross sections 0-91665  
 ethane, CH bond orbitals, internal rot. barriers, antisymmetrization effects 0-63529  
 ethane-1,1,1-d<sub>3</sub>, gas-phase IR spectra, rot. fine struct. obs. 0-83359  
 ethyl alcohol-d<sub>0</sub>(-d<sub>1</sub>)(-d<sub>2</sub>), internal rot. and microwave rot. spectra 0-69128  
 ethyl iodide, microwave spectra and internal rot. anal. 0-69130  
 ethylene, IR absorpt. spectra of ν<sub>1</sub>, ν<sub>10</sub> and ν<sub>4</sub> interacting band 0-83369  
 ethylene, rot. around double bond, four orbital-four-electron model 0-95592  
 fluorobenzene, mol. reorientation and weak mol. interaction influence, <sup>2</sup>D spin-lattice relax. obs. 0-106333  
 fluoromethyl formate, conformation potential energy surfaces, ab initio calcs. 0-69065  
 formaldehyde, molecular beam rotation temp. meas. (French) 0-78724  
 formaldehyde and its isotopic species, rot. spectra of ground vibr. state, rot. const. determ. 0-83350  
 formaldehyde S<sub>1</sub> levels, collisionless single rot. level lifetimes, elec. field depend. 0-63566  
 formaldehyde substituted with <sup>17</sup>O and <sup>18</sup>O, microwave spectra of ground vibr. states, rot. and distortion const. determ. 0-83349  
 formaldehyde-d<sub>0</sub>(-d<sub>2</sub>), S<sub>1</sub> single rot. level lifetimes, isotope, elec. field and vibr. state depend. 0-78655  
 formic acid, <sup>16</sup>C, <sup>18</sup>O, microwave spectra and centrifugal distortion consts. 0-83352  
 formyl ion, electron impact rot. excitation, Glauber approx. with Coulomb effect 0-63840  
 free radical reaction, chemically induced dynamic polarisation in strong mag. field, radical rotation influence 0-76509  
 ground state alkali molecules, mag. shielding and spin-rot. interaction 0-87186  
 identical molecules, dispersion intermolecular pot. anomaly prod. by intense radiation field 0-58336  
 inert gas, dense, rotational relax. of solute molecules reln. with local anisotropy fluc. 0-58183  
 interaction of molecular rotation and translation 0-69262  
 3-iodopropene, rot. spectra, quadrupole hyperfine struct. 0-91545  
 ion+polar molecule collision, low-energy, rot. state approach 0-74224  
 ion+polar molecules, long range dipole interaction effect 0-102558  
 ion cyclotron motion, Coriolis coupling of ion internal degrees of freedom 0-87246  
 isothiazole, rot. Zeeman effect, localised susceptibilities 0-91600  
 laser IR excited mols., excited fraction determ. 0-78661  
 lipid hydrocarbon chain, biomembrane, rot. motion and fluidity 0-76714  
 macromolecule rotational diffusion props., validity of general ellipsoid model 0-95751  
 methane, rotational state, avoided-crossing molecular beam spectroscopy 0-63730  
 methane-d<sub>1</sub>, high resolution spectra, line intensities, ground-state rot. const. determ. 0-83517  
 methanol laser, optically pumped, use of crystalline reflector in cavity 0-64080  
 methanol-d<sub>1</sub>, (CH<sub>3</sub>DOH), microwave torsional-rot. spectrum, rei. to interstellar search 0-99498  
 methyl acetate, microwave spectra and internal rot. 0-87100  
 methyl azidoformate, microwave rot. spectrum, satellite transitions 0-69127  
 methyl chloride, rot. anal. of IR absorpt. spectra, mol. vibr., rot. const. determ. 0-99505  
 methyl fluoroformate, isomer conformation, CNDO and ab initio STO calcs. 0-58151  
 N-methyl m-fluoroaniline, conformational anal., microwave spectra obs. 0-58247  
 methylacetylene, ν<sub>5</sub> band, microwave and IR laser Stark spectrosc. 0-91558  
 molecules, isolated, intersystem crossing, rot. motion effect 0-95669  
 molecules D<sub>2h</sub>, D<sub>3h</sub> and D<sub>3d</sub>, appln. of Aliev-Watson maxima-minima criteria for quartic centrifugal distortion const. 0-87132  
 nitroxide radicals, q- and A-tensor components, rot. mobility 2 mm EPR spectrosc. determ. 0-102530  
 nonrigid molecules, dipolar relax. and nuclear Overhauser effects, fluctuating internuclear distances effect 0-91578  
 nonspherical molecules, rot. diffusion tensors determ. from rot. friction tensor calcs. 0-63861  
 norbornane, microwave spectrum and dipole moments 0-78606  
 phenolic Mannich bases, dielec. relax. study 0-97196



## molecular rotation continued

- predissociated two-channel model, resonances with complex rot. method 0-58327
- prolate molecules in solvents, anisotropic fluoresc. (*German*) 0-69183
- propenal, IR-microwave double reson. and two-photon expts. 0-83396
- propenal-d, in ground vibrational state, IR microwave double resonance spectra, rot. and centrifugal distortion const. determ. 0-83358
- propenal-d, IR microwave double reson. spectroscopy 0-69172
- pulsed molecular beam experiments employing electromechanical valve 0-63870
- pyrazine, vapour, fluoresc. quantum yields, rot. effects 0-95661
- 4-pyridine carbaldehyde, microwave spectrum, rot. assignments, quadrupole coupling consts. 0-91548
- pyrimidine, vapour, fluoresc. quantum yields, rot. effects 0-95661
- quantum state selected atomic and molecular beams production, developments in techniques 0-63871
- reaction product initial rot. state distrib., pump and probe laser obs. 0-85158
- rigid YXX and nonrigid three-body systems, correlation diagram 0-69249
- rotations and translations in isospin space 0-102431
- spectra, unresolved rot. struct., use in flame temp. meas. 0-86300
- spherical tops, chiral discrimination 0-106314
- stilbenes, prolate molecules in solvents, anisotropic fluoresc. (*German*) 0-69183
- tetrafluoromethane,  $\nu_2 + \nu_4$  band, high resolution diode laser spectra 0-69138
- tetrafluoromethane, liq., mol. reorientation 0-106320
- thiazole, rot. Zeeman effect, localised susceptibilities 0-91600
- thioformaldehyde,  $\tilde{A}^1A_2 - \tilde{X}^1A_1$  IR absorpt. spectra 0-83362
- triatomic molecule, rot. vibr. electronic Hamiltonian, Born-Oppenheimer approx., breakdown 0-87097
- triatomic van der Waals mols., rot. predissoc. 0-63721
- trifluoroethene-d<sub>0</sub>d<sub>1</sub>, mol. struct., microwave and electron diffraction obs. 0-58384
- trifluoroiodomethane, laser microwave double reson. spectroscopy with CO<sub>2</sub> laser lines 0-87156
- trifluoromethyl bromide, microwave spectra, mol. rot., isotopic variation in bond lengths, Stark meas., dipole moments determ. 0-74165
- trifluoromethyl hydroperoxide(-d), CF<sub>3</sub> torsional vibr., low freq. Raman spectra 0-91565
- trifluoromethyl hypofluorite (hypochlorite), CF<sub>3</sub> torsional vibr., low freq. Raman spectra 0-91565
- trifluoromethyl iodide, microwave spectra, mol. rot., isotopic variation in bond lengths, Stark meas., dipole moments determ. 0-74165
- trifluoromethyl peroxyfluoride (peroxychloride), CF<sub>3</sub> torsional vibr., low freq. Raman spectra 0-91565
- trimethylbromosilane, microwave spectra, struct., chemical bonding 0-95602
- trinitromethane, microwave and rot. spectra, effect of twist of NO<sub>2</sub> groups, rot. and centrifugal distortion const. determ. 0-95605
- trioxane,  $\nu_{10}(E) = \nu_{20}(E) = 1$  state, rot. spectrum assignment, microwave obs. 0-58248
- trioxane <sup>13</sup>C(<sup>18</sup>O) substituted, mol. consts. and rot. spectra 0-87096
- two and three-centre molecules, periodicity and internal torsional conformers around single bond, symmetry analysis 0-69250
- unimolecular decomp. kinetics, rot. effects 0-81319
- van der Waals mol. rot. predissociation study, complex coord. method 0-74205
- AlH<sup>+</sup>, spectrum at 3632 Å, rot. anal. 0-78632
- AlS, B<sup>1</sup>Π-X<sup>2</sup>Σ<sup>+</sup> transition, assignment of UV bands, vibr. and rot. anal. 0-58278
- Ar+HCl, inelastic scatt. exponential perturbation theories 0-74217
- Ar+N<sub>2</sub>, inelastic scatt. exponential perturbation theories 0-74217
- ArH<sub>3</sub>, van der Waals mols., rot. predissoc. 0-63721
- ArHBr, ArHCl, and isotopic forms, rot. spectra, mol. struct., mol. consts. 0-58246
- ArN<sub>3</sub>, van der Waals mols., rot. predissoc. 0-63721
- Ba+HF, product rot. and vibr. distributions and reaction cross sections depend. on reagent translational energy 0-93745
- BaO, excited electronic states, lifetimes and transition moments 0-87177
- BaO+Ar(CO<sub>2</sub>), in Ar flame, rot. and translational relax. by sub-Doppler optical-optical double reson. 0-95583
- Br<sub>2</sub>, Q branches of Δn=1 profiles, calcs., rotation effect on scatt. amplitudes 0-63643
- Br<sub>2</sub>, single rot. states, lifetimes and collisional quenching cross sections determ. by obs. fluoresc. decay 0-91595
- BrF(Cl), rot. spectra in millimeter wave region, rot. transitions obs., equil. const. determ. 0-78607
- C-H, A<sup>2</sup>Δ-X<sup>2</sup>Π, dissociative excitation, form. environment and parent mol. effects 0-78682
- C<sub>2</sub>, interstellar, rot. fine-struct. lines obs. towards { Persei 0-67811
- C<sub>2</sub>, rotational temp. and solar photospheric models 0-62099
- C<sub>2</sub> vapour, Swan bands, oscillator strength 0-63712
- C<sub>3</sub>, A<sup>1</sup>Π<sub>u</sub> state, orbital angular momentum 0-78514
- CD<sup>+</sup>, in RF ion trap, laser induced fluoresc. spectrum, 0,0 vibr. band and rot. consts. 0-74189
- CH<sup>+</sup>, a<sup>1</sup>Π-b<sup>2</sup>Σ<sup>+</sup> transition moment, ab initio calcs. 0-87047
- CN, internal energy distrib. following vinyl cyanide photodissoc., temp. depend. 0-78638
- CO, centrifugal distortion calcs. by perturbed Morse oscillator model including Dunham parameters 0-63862
- CO, rot. distrib. in supersonic beam, IR bolometry using tunable diode laser 0-63869
- CO<sup>+</sup>, electron impact rot. excitation, Glauber approx. with Coulomb effect 0-63840
- <sup>13</sup>C<sup>16</sup>O<sup>+</sup> (2,0) band, comet-tail system, rot. anal. 0-74157
- CO-HBr, weakly bound, rot. spectra 0-91544
- CO-HCl, weakly bound, rot. spectra 0-91544
- CO-HF, weakly bound, rot. spectra 0-91544
- CO+H<sub>2</sub>, rot. excitation, rel. between tensorial cross sections 0-83454
- CO<sub>2</sub> lasers, optically pumped, use of crystalline reflector in cavity 0-64080
- CO<sub>2</sub> multi-rotational line TEA laser, theoretical model 0-69361
- CO<sub>2</sub> TEA laser, injection tuning and mode locking on low gain rot. lines 0-95928
- CS<sub>2</sub>, photodissoc., fragment energy distrib. 0-69200
- CaCl, B<sup>2</sup>Σ<sup>+</sup>-X<sup>2</sup>Σ<sup>+</sup> transitions, rot. anal. by laser spectroscopy 0-91536
- CaF, A<sup>2</sup>Π-X<sup>2</sup>Σ<sup>+</sup> transition, HFS and fine struct., intermodulated fluoresc. spectra obs. 0-63695
- CaF, B<sup>2</sup>Σ<sup>+</sup>-X<sup>2</sup>Σ<sup>+</sup> system, rot. and vibr. anal. 0-74156

## molecular rotation continued

- Cd+H<sub>2</sub>-CdH+H, product initial rot. state distrib., pump and probe laser obs. 0-85158
- ClF, rot. spectra in millimeter wave region, rot. transitions obs., equil. const. determ. 0-78607
- <sup>37</sup>ClO<sub>2</sub>,  $\nu_3 = 1$  state, laser-microwave double reson. obs. 0-95657
- CrO, A<sup>2</sup>Π-X<sup>2</sup>Π transition, rot. anal. laser induced fluoresc. and discharge emission spectra 0-69173
- CuCl, mol. emission spectrum, 5900-6800 angstrom, rot. anal. of A-X system 0-58273
- CuF from Cu+F<sub>2</sub> chemiluminesc. reactions, mol. beam study 0-97702
- D<sub>2</sub>, matrix isolated, IR spectra, mol. rot. and vibr. const. determ. 0-78617
- D<sub>3</sub>, emission spectra, rot. struct. obs. mol. const. determ., predissociation 0-106331
- DT, vibr. rot. Raman anal. 0-87126
- DyO, UV emission spectrum, high resolution, band systems and isotopic shifts 0-87146
- GaBr, rot. analysis of <sup>3</sup>Π<sub>0,1</sub>-X<sup>1</sup>Σ<sup>+</sup> transition 0-69129
- GaI, rot. spectrum, EHF spectra obs. 0-58245
- GeH<sub>4</sub>, avoided-crossing molecular-beam spectroscopy, hyperfine and spin rot. const. and rot. g factors determ. 0-78671
- <sup>74</sup>GeH<sub>4</sub> mol. vibr., IR and CARS spectra (*Russian*) 0-102509
- H<sup>+</sup>+H<sub>2</sub>, rot. and vibr. excitation, energy loss obs. 0-63773
- H<sub>2</sub>, CARS, optical Stark effect on vibr., and rot. transitions 0-99512
- H<sub>2</sub>, fluid, Raman meas., 0.2-630 kbar, at room temp. 0-58269
- H<sub>2</sub>, high resolution electron spectroscopy 0-62740
- H<sub>2</sub>, matrix isolated, IR spectra, mol. rot. and vibr. const. determ. 0-78617
- H<sub>2</sub> photoelectron spectra, rot. intensity distrib. 0-91605
- H<sub>2</sub>, stimulated Raman scatt. gain of Nd laser radiation by rot. levels 0-69464
- H<sub>2</sub><sup>+</sup>, rot. lines and rot. consts. 0-91605
- H<sub>2</sub>-H<sub>2</sub> dimers, hyperfine struct. in zero mag. field 0-95700
- H<sub>2</sub>+CO<sub>2</sub>, exponential gap relation, rot. inelasticity 0-78693
- H<sub>2</sub>+H, exponential gap relation, rot. inelasticity 0-78693
- H<sub>2</sub>+H<sub>2</sub>, exponential gap relation, rot. inelasticity 0-78693
- H<sub>2</sub>+He, exponential gap relation, rot. inelasticity 0-78693
- H<sub>2</sub>+Li, exponential gap relation, rot. inelasticity 0-78693
- H<sub>2</sub>+Li<sup>+</sup>, exponential gap relation, rot. inelasticity 0-78693
- H<sub>2</sub>+Ar, low energy proton transfer reactions, crossed beam studies 0-108697
- H<sub>3</sub>, emission spectra, rot. struct. obs. mol. const. determ., predissociation 0-106331
- HB rot. relaxation, diffusion theory 0-106313
- HCN predissoc. Frank-Condon amplitudes 0-95694
- HCN+He(H<sub>2</sub>)(CH<sub>3</sub>F), HCN excited vibr. state, T<sub>2</sub> meas. 0-102498
- HCl, rot. relaxation, diffusion theory 0-106313
- HCl+N<sub>2</sub>(O<sub>2</sub>)(D<sub>2</sub>)(H<sub>2</sub>), HCl  $\nu_2$ - $\nu_1$  band perturbations, linewidth and shifts calcs., IR spectra obs. (*French*) 0-58251
- HDSe, high resolution IR spectra, anal. of 2ν<sub>1</sub> band, rot. ground state const. determ. 0-95616
- HF+HF (methane)(methane-d<sub>4</sub>), collision relaxation rate constants and rot. equilibration time meas. 0-69213
- HNCO, rot. spectrum, ground and vibr. state reson., centrifugal distortion coupling 0-83364
- HNO A<sup>2</sup>Δ<sup>+</sup> excited state dipole moment, optical-optical double reson. Stark spectrosc. obs. 0-106337
- HNO<sub>3</sub>, VUV photodissoc., vibr. and rot. distrib. 0-87191
- H<sub>2</sub>O, electron impact dissociation, OH(A<sup>2</sup>Σ<sup>+</sup>-X<sup>2</sup>Π<sub>g</sub>) emission spectra, crossed-beam investigations 0-83504
- H<sub>2</sub>O, VUV photodissoc., vibr. and rot. distrib. 0-87191
- H<sub>2</sub>O<sup>+</sup>, spin and rot. fine struct., orbital angular momentum 0-83247
- H<sub>2</sub>O<sup>+</sup>, vibr. and rot. struct., intensity factors and orbital angular momentum 0-83246
- H<sub>2</sub>O-HF heterodimer, H bonding, microwave rot. spectrum, mol. geometry and moment 0-99501
- HOCl, photodissoc. rot. distrib. 0-95694
- H<sub>2</sub>S<sub>2</sub>, rot. barriers, internal rot. and electronic struct., valence electron study 0-83344
- H<sub>2</sub>S(D<sub>2</sub>S) photodissoc., SH internal energy distribution 0-95697
- H<sub>2</sub>O radical, Doppler-limited dye laser excitation spectroscopy, rot., distortion and spin-rot. interaction const. determ. 0-83383
- H<sub>2</sub>Se<sub>2</sub>, rot. barriers, internal rot. and electronic struct., valence electron study 0-83344
- H<sub>2</sub>Te<sub>2</sub>, rot. barriers, internal rot. and electronic struct., valence electron study 0-83344
- He+H<sub>2</sub>, inelastic scatt. exponential perturbation theories 0-74217
- He+H<sub>2</sub>, mol. energy transfer by quasiclassical trajectory methods, vibr. relax. and dissociation, rot. effect 0-99557
- He+LiH, rot. inelastic collisions, state-to-state cross sections determ. 0-87210
- He+Na<sub>2</sub>, rotational inelastic scatt., uniform semiclassical sudden approx. 0-99544
- HeCN<sup>+</sup>, SCF calcs., dissociation energies, rot. and hyperfine const. determ. 0-95531
- I<sub>2</sub>, B-X system, mol. consts. and Dunham expansion parameters 0-87095
- <sup>129</sup>I<sub>2</sub>, energy levels near B-state dissociation limit, two-photon spectrosc. obs. 0-106367
- ICl(Br), rot. spectra in millimeter wave region, rot. transitions obs., equil. const. determ. 0-78607
- K+CO, rotational inelastic scatt., uniform semiclassical sudden approx. 0-99544
- KrH, van der Waals mols., rot. predissoc. 0-63721
- KrHBr, KrCHI, and isotopic forms, rot. spectra, mol. struct., mol. consts. 0-58246
- LaF<sup>+</sup>, electronic spectra, rot. anal. and orbital configurations 0-83240
- LiF+Ar, polarisation cross section, close-coupling calcs. 0-69214
- LiH+He, rot. inelastic collisions, rigid shell models 0-99545
- MgH rotational temp. and solar photospheric models 0-62099
- MnO, A<sup>2</sup>Σ<sup>+</sup>-X<sup>2</sup>Σ<sup>+</sup> electronic transition, rot. and hyperfine struct. 0-74134
- N<sub>2</sub>, CARS, optical Stark effect on vibr., and rot. transitions 0-99512
- N<sub>2</sub>, elastic and inelastic electron scatt., state to state cross section 0-78708
- N<sub>2</sub>, excitation efficiency for rot. states 0-102557
- N<sub>2</sub> fluid, light scatt. orientational memory function at moderate density 0-102521
- N<sub>2</sub>, high energy electron spectroscopy techniques 0-62740
- N<sub>2</sub> laser 337.1 nm transition, rotational struct. variation 0-78836
- N<sub>2</sub>, pure rot. CARS obs. 0-99511



**molecular rotation continued**

- $N_2 + Ar$ , metastable atom excitation of  $C^3\Pi_u$  state, symmetry, propensity rules and alternation intensity, rot. spectrum 0-87135  
 NH radical formed in  $NH_3$  dissociation, fluoresc. spectrum, rotational relaxation 0-58310  
 $NH_3$ , spin and rot. fine struct., orbital angular momentum 0-83247  
 $NH_3$ , vibr. and rot. struct., intensity factors and orbital angular momentum 0-83246  
 $NH_3$ , expansion cooled, mol. photoionisation, rot. struct., rot. predissoc. of excited states 0-91611  
 $NH_3 + H_2$ ,  $NH_3$  inversion transition, linewidths and  $T_1/T_2$  ratio 0-99499  
 $NH_3 + He(Ne)(Ar)(Kr)$ , pure rot. line, press. broadening calcs. 0-78656  
 $N_2H^+$ , electron impact rot. excitation, Glauber approx. with Coulomb effect 0-63840  
 NHD, rotational transitions, microwave optical double resonance obs. 0-58293  
 $NH_3(ND_3)$  in solid Ar, UV absorption spectra, temp. depend. of matrix spectra 0-63652  
 NO,  $\gamma(0,0)$  band, collisional broadening parameters 0-63713  
 NO, Zeeman modulation spectroscopy, line shape analysis 0-74197  
 $NO + N_2(CO_2)(CO)(CH_3)(Ar)$ , NO  $\gamma(0,0)$  band, oscillator strength and line broadening 0-106356  
 $NO + O_3$ , fs-states and rot. states, effect on reactivity 0-89473  
 $NO_2$ , fluoresc. spectra and collisional quenching 0-102538  
 $^{15,14}NO_2$ , predissoc. rot. struct. in 2490 Å band 0-87192  
 $^{14}NH_3$ , ground state, microwave inversion lines 0-87098  
 NDO, electronic spectrum, rotational struct. anal. 0-78643  
 $NeCN^+$ , SCF calcs., dissociation energies, rot. and hyperfine const. determ. 0-95531  
 $NeH_2$ , van der Waals mols., rot. predissoc. 0-63721  
 Ni complex, nickel-bis-dithiolenes, pseudopot. MCSCF and limited CI calcs. 0-83292  
 $O + H_2O \rightarrow OH + OH$ , energy partitioning 0-101009  
 $O +$  saturated hydrocarbon  $\rightarrow OH +$  alkyl radical, reaction dynamics, mol. beam-laser induced fluoresc. obs. 0-97695  
 $O_2$ , pure rot. CARS obs. 0-99511  
 $O_2$ ,  $f^4\Pi_g$  state, quasi-bound levels, predissociation, band rot. anal., photofragment kinetic energy anal. 0-63650  
 $O_3$ , line position and intensities of  $2\nu_3$ ,  $\nu_1 + \nu_3$  bands 0-87181  
 OCS, millimeter wave rot. spectra, isotope shifts, freqs. and mol. consts. 0-78611  
 OH, (0,0) UV transitions, band oscill. strength 0-69162  
 $OH + H_2O$ , OH linewidth rot. depend. on UV transitions 0-91606  
 $OH(v,N)$  bimodal rot. distrib. from  $O(^1D_2) + NH_3$  0-76501  
 $PD^+$ , IR emission spectra, rot. anal. and mol. parameters 0-69134  
 $PH^+$ , IR emission spectra, rot. anal. and mol. parameters 0-69134  
 $PbO$ , laser excitation IR spectra, photoluminescence obs., rot. anal., rot. const. determ. 0-95619  
 $SF_6$ ,  $^9F$  NMR vibr. anharmonicity effects 0-91580  
 $SF_6$ , Doppler-limited spectroscopy, of  $3\nu_3$  band 0-58244  
 $SF_6$ , Doppler-limited spectroscopy of  $3\nu_3$  band, rot. const. and anharmonic parameters calcs., mol. photodissoc. 0-83361  
 $SeH_4$ , isotope effects, Rydberg levels-ground state transitions, rot. const., VUV spectra obs. 0-58279  
 Si biradical, six-coordinate, mol. mobility two-spin probe investig. 0-102529  
 $SiH_4$ , avoided-crossing molecular-beam spectroscopy, hyperfine and spin rot. const. and rot. g factors determ. 0-78671  
 $SiS$ , chemiluminescent flame spectra, electronic states and rot. struct. obs., vibr. assignments, Franck-Condon factors determ. 0-85179  
 $Te_2$ ,  $BO_2^+ - b^1\Sigma_g^+$  system, transition assignment, IR and visible spectra obs. 0-58298  
 TiN, electronic absorpt. spectrum, rot. anal. 0-78601  
 $^{90,92}ZrO^+$ , rot. anal. in near IR 0-74162

**molecular rotation calculations**

- formaldehyde-d ( $d_2$ ) submillimeter lasers, optically pumped, assignment of laser lines 0-58513  
 methane, quantum mech. rot. partition function 0-102501  
 polar mol. rot. relax., dielectric friction, Onsager cavity model 0-64664  
 Raman scattering, spontaneous and stimulated, by forbidden rotational and vibr.-rot. transitions in strong optical field 0-74174  
 sum rules for the turning forces of pure rotational transitions 0-78597  
 $CO + H^+$ , vibr. excitation calc., close coupling and sudden approx. 0-78561  
 CS, rotation analysis of  $d^3\Delta - a^3\Pi$  transition, IR spectra 0-78591  
 HNNN, substitution struct., rot. const. calcs. 0-91534  
 $LaO$ , Franck-Condon factors rot. depend. 0-58319  
 $MgO$ , Franck-Condon factors rot. depend. 0-58319  
 $O_3$ , low energy elastic and inelastic electron scatt., rot. transitions, close coupling calc. 0-78706  
 $SiO$ , Franck-Condon factors rot. depend. 0-58319  
 $TiO$ , Franck-Condon factors rot. depend. 0-58319  
 $ZrO$ , Franck-Condon factors rot. depend. 0-58319

**molecular rotation in solids** see *molecular reorientation; nuclear magnetic resonance; plastic crystals*

**molecular rotation-vibration**

- see also *macromolecular dynamics; molecular force constants; molecular rotation-vibration calculations*  
 ab initio methods for atomic and molecular processes 0-63550  
 acetylene, rot. vibr. anal., Raman spectra obs. 0-69146  
 acetylene- $d_2(d_1)$ , rot.-vibr. Raman spectra 0-83372  
 atom + polyatom systems, rotation-vibration symmetry correlation 0-61074  
 benzene, IR spectra, fine struct. of rot.-vibr. bands 0-102504  
 carbon tetrafluoride  $^{12}CF_4$  laser, Doppler-limited absorption spectroscopy 0-74347  
 carbon tetrafluoride laser,  $CF_4$  molecule  $\nu_3 + \nu_4$  band optical pumping 0-74349  
 cyanoacetylene,  $\nu_1$  vibr.-rot. band, diode laser spectrum 0-91563  
 cyclopropane- $d_6$ , high resolution IR spectra, vibr. rot. band anal. 0-95621  
 diatomic mol., vibr. rot. Hamiltonian expansion, Born Oppenheimer  $\kappa$ , explicit introduction 0-69118  
 diatomic molecule, Franck Condon factors, vibr. rot. interaction effect 0-74198  
 diatomic molecules, dissociation, vibr.-rot. excitation effects 0-102502  
 diatomic molecules, rotational Raman intensities and polarizability anisotropy change meas. with internuclear distance 0-63641  
 ethane, internal rot. splittings, vibr.-rot.-torsion energy levels perturbations 0-91531

**molecular rotation-vibration continued**

- intramolecular nonradiative transitions of gaseous small molecules, rovibronic level, lineshapes 0-95667  
 methane- $d_4$ , 4.5  $\mu m$  absorpt.,  $2\nu_2$  overtone band anal. 0-91557  
 methoxy, Jahn-Teller induced rovibronic effect, nuclear spin-electron spin hyperfine Hamiltonian 0-83298  
 methyl azidoformate, microwave rot. spectrum, satellite transitions 0-69127  
 methyl cyanide, far IR laser line assignments 0-69380  
 methylacetylene,  $\nu_5$  band, microwave and IR laser Stark spectrosc. 0-91558  
 molecules, isolated, intersystem crossing, rot. motion effect 0-95669  
 phosphine, IR spectrum,  $\nu_1$  and  $\nu_2$  band analysis 0-83366  
 propynal, rovibronic populations, collisionless IR multiphoton spectra, energy deposition, photoacoustic determ. 0-83354  
 spherically symmetric molecules, many-photon excitation in IR laser field 0-95596  
 triatomic molecule, rot. vibr. electronic Hamiltonian, Born-Oppenheimer approx., breakdown 0-87097  
 $Ar + HF$ , state-to-state cross sections for rot. to translational energy transfer determ. 0-91644  
 $Ar^+ + H$ , assoc. ionization, rovibronic struct. in electron energy spectrum 0-106380  
 $BaO + Ar(CO_2)$ , in Ar flame, rot. and translational relax. by sub-Doppler optical-optical double reson. 0-95583  
 $Br_2$ , long-lived  $A^3\Pi(1_u)$  state, quantum-resolved dynamics of excited states 0-69178  
 CN free radical,  $A^2\Pi - X^2\Sigma^+$  Red system, perturbation analysis 0-87247  
 CO, Dunham vibration-rotation coefficients, isotope dependence 0-83518  
 CO, laser, output characts. at high pump levels 0-58509  
 $C_3O_2$ , semirigid bender, rot.-vibr. energy level separations obs., struct. and pot. functions determ. 0-83446  
 $CaF$ ,  $B^2\Sigma^+ - X^2\Sigma^+$  system, rot. and vibr. anal. 0-74156  
 $Cl_2 +$  muonium ( $H(D)$ ), pot. energy surfaces, inversion calcs. 0-93734  
 $D_3^+$ , IR spectrum, vibr.-rot. assignment 0-95627  
 DT, vibr. rot. Raman anal. 0-87126  
 FCP, microwave spectrum, struct., dipole moment and vibr.-rot. props. obs. 0-91549  
 HCl, overtone vibr.-rot. bands, intracavity dye laser techniques meas. 0-91532  
 HCl- $l$ -ert gas, weak collisions, HCl spectral line broadening of IR spectra 0-74161  
 $HCl + N_2(O_2)(D_2)(H_2)$ , HCl  $\nu_2 - \nu_1$  band perturbations, linewidth and shifts calcs., IR spectra obs. (French) 0-58251  
 HF in absorption, anomalous dispersion meas. 0-95881  
 HF, vibr.-rot. band, absorpt. line self-broadening, rot. relax. 0-87213  
 $H^{14}N_3$ , rotational-vibrational Raman spectrum of  $\nu_2$  band 0-91564  
 $I_2$ , B-X transitions, rot.-vibr. hyperfine coupling consts., extension to other levels 0-63625  
 $IBr$ ,  $B^1\Pi(0^+)$  excited state, laser-induced fluoresc. 0-58309  
 $^{127}I_2$  rovibronic absorpt. lines, hyperfine struct. 0-78596  
 $^{129}I_2$  rovibronic absorpt. lines, hyperfine struct. 0-78596  
 $K_2$ , absorpt. and relax. const. determ. by optical laser pumping method 0-102550  
 $N_2$ , elastic and inelastic electron scatt., state to state cross section 0-78708  
 $N_2$ , liquid, vibrational dephasing, computer simulation, Raman spectra, pair potential effect 0-63863  
 $NH_3$ , IR spectra, fine struct. of rot.-vibr. bands 0-102504  
 NO, IR emission Fourier transform spectroscopy, mol. rot.-vibr., RKR potential curve calc. 0-95618  
 NO, selectively excited rovibrational states, multiphoton ionisation spectra 0-69202  
 $NO_2$ , fluoresc. spectra and collisional quenching 0-102538  
 $NO_2$ , absorpt. and relax. const. determ. by optical laser pumping method 0-102550  
 $Na_2$  in free jet expansion, internal-state distribution 0-83403  
 $Na_2$ , Rydberg state, two-step polarisation labelling 0-87053  
 $Ne^+ + H$ , assoc. ionization, rovibronic struct. in electron energy spectrum 0-106380  
 $O_3$ , line and band strengths in IR spectra, variational calcs. 0-87112  
 $O_3$ , line position and intensities of  $2\nu_3$ ,  $\nu_1 + \nu_3$  bands 0-87181  
 OH, optimum mol. consts. and term values,  $X^2\Pi$  and  $A^2\Sigma^+$  states, vibr.-rot. and microwave freqs. 0-95577  
 $SF_6$ , IR spectra, fine struct. of rot.-vibr. bands 0-102504  
 $SF_6$ , multiphoton-excitation due to vibr.-rot. transitions 0-102546  
 $Sc + NO_2$ , chemiluminescence, nonequilibrium product distrib. 0-101014  
 $SiH^+$ , rot.-vibr. consts. and dissociation energy determ. from time resolved precision spectroscopy 0-58272  
 YI, IR  $^1\Pi - ^1\Sigma$  system, Fourier spectrometry, rovibrational anal. 0-83360

**molecular rotation-vibration calculations**

- acetylene, relationships between higher-transition frequencies 0-69119  
 composite particle, vibr. amplitude and vibr. rot. anal. 0-74158  
 diatomic molecule, vibr.-rot. states, high accuracy wave functions and energies 0-74159  
 dipole moment matrix element for  $C_2$ , symmetry molecules 0-91537  
 formaldehyde-d ( $d_2$ ) submillimeter lasers, optically pumped, assignment of laser lines 0-58513  
 interaction anisotropy, small angle scatt., spectral evidence 0-78600  
 isolated molecules, vibration relax. theory, adiabatic approx. 0-58237  
 methane- $d_0(d_4)$  vibrational state rotational struct., CARS spectra (Russian) 0-99513  
 nonpolar molecules in degenerate vibr. states, pure rot. absorpt. spectra 0-78598  
 radiation escape kinetics, radiation captured by plane optically thick layer 0-95593  
 Raman scattering, spontaneous and stimulated, by forbidden rotational and vibr.-rot. transitions in strong optical field 0-74174  
 $Ca_2$ , vibr.-rot. states, high accuracy wave functions and energies 0-74159  
 ClH-dimethyl ether, vibr.-rot. IR spectra, quantum and classical mechanics 0-91561  
 $D_3^+$ , rot.-vibr. spectrum, ab initio calcs. 0-95595  
 $GeH_4$ , vibrational state rotational struct., CARS spectra (Russian) 0-99513  
 $H + H_2 \rightarrow H_2 + H$  three dimens. chem. reaction, distorted-wave calcs. 0-81294  
 $H_2 + e^- \rightarrow H_2^+ + e^-$ , Gaussian basis Glauber approx., elastic and vibrorotational excitation cross sections 0-58399  
 $H_3^+$ , rot.-vibr. spectrum, ab initio calcs. 0-95595  
 HCN, relationships between higher-transition frequencies 0-69119



**molecular rotation-vibration calculations continued**

HCl-inert gas rot.-vibr. line pressure broadening and shift calc. 0-69124  
 $K_2$ , ground state thermalisation speed, collision cross-sections meas. (*Russian*) 0-78723  
 $\text{OH}^+$ , rot.-vibr. bands, line positions, oscill. strengths transition probabilities 0-67828

**molecular rotational energy transfer** *see molecular rotational-vibrational energy transfer***molecular rotational states** *see molecular rotation***molecular rotational-vibrational coupling** *see molecular rotation-vibration***molecular rotational-vibrational energy transfer**

*see also atom-molecule reactions; molecule-molecule reactions*

acetonitrile, IR and Raman spectra, vibr. and reorientational and energy transfer width separation, rot. const. determ. 0-87131  
 alkylbenzenes, jet-cooled, vibr. relax., absorpt. spectra 0-74236  
 alkylbenzenes, jet-cooled, vibr. relax., fluoresc. spectra 0-78694  
 atom+diatom, sudden approx. of Cross, computational tests, cross section factorisation, scatt. phenomena 0-58352  
 atom+molecule, rotational rainbow maxima: a time dependent study 0-58353  
 atom-diatom kinetic cross section, ES, CS and IOS approx. with translational-internal coupling, viscomag. effect 0-63764  
 benzene+Hg, electronically excited, mol. fluoresc., vibr. relax. cross sections and equilibration rates determ. 0-87205  
 benzene- $d_6$ + $\text{N}_2$ + $\text{CO}_2$ , electronically excited, mol. fluoresc., vibr. relax. cross sections and equilibration rates determ. 0-87205  
 t-butyl bromide, vibr. relax. in pure liq. and soln., Raman spectra 0-66167  
 t-butyl chloride, vibr. relax. in pure liq. and soln., Raman spectra 0-66167  
 carbon tetrachloride, polarized light scatt., relaxation processes 0-60615  
 chlorobenzene, polarized light scatt., relaxation processes 0-60615  
 collisional relax. of highly excited states, laser-induced fluoresc. obs. 0-58205  
 cyclobutane decomposition, vibr. excitation transients using variable encounter method 0-61072  
 diatomic molecules at low press., dissociative instability, role of vibr. energy 0-74227  
 diazaphthalenes, excited state absorpt. spectra and intersystem crossing kinetics 0-74176  
 dichloromethane-cyclohexane, liq. mixture, intermol. vibrational energy transfer, US study 0-70313  
 dichloromethane- $d_2$ , vibr.-vibr. energy transfer, laser-induced fluoresc. obs. 0-78689  
 3,3'-diethylthiacyanobenzene iodine-rhodamine 6G, energy transfer with increased local conc., Forster mechanism 0-69220  
 ethane, unimol. decomp., energy transfer processes, Monte Carlo simulation 0-99555  
 ethylene oxide, rot. relax., double reson. and Stark switching obs. 0-106340  
 fast molecular ions, break-up on collision with solids 0-66353  
 fluorobenzene, polarized light scatt., relaxation processes 0-60615  
 fluoromethane+fluoromethane, collision induced mode selective energy transfer, fluoresc. obs. 0-69177  
 furan-cyclohexane, liq. mixture, intermol. vibrational energy transfer, US study 0-70313  
 gas, diatomic, spherical source expansion 0-58356  
 H+FH(FD), low barrier quantum model, vibr. deactivation 0-69216  
 halobenzene cations, in solid Ne matrix, slow vibr. relax., fluoresc. obs. 0-74194  
 halobenzenes, liquid, vibr. relaxation, Brillouin spectra 0-108219  
 hexafluorobenzene, IR multiphoton excitation, vibr. energy redistrib. and hot band spectrum 0-95656  
 hydrogen halides rot. relax. with inert buffer gas, comment 0-69221  
 hydrogen halides rot. relax. with inert buffer gas, reply 0-69222  
 intermolecular potential, rot. energy transfer, sensitivity anal. 0-63762  
 interstellar molecules collisional excitation by  $\text{H}_2$ , theory for linear mols. CO, OCS, SiO, HCN and  $\text{HC}_3\text{N}$  in  $\Sigma$  state 0-109508  
 isobutylene, liq., vibr. phase relax. and freq. shifts, density and temp. effects 0-74235  
 isolated molecules, vibration relax. theory, adiabatic approx. 0-58237  
 liquids, vibr. energy relax., nonMarkovian effects 0-74230  
 matrix isolated molecules, energy accumulation by migration to geometric trap configurations 0-78691  
 metal surface, mol. vibr. energy transfer, classical EM theory 0-96806  
 methane, harmonic and anharmonic matrix elements comparison, appl. to vibrational energy transfer 0-63760  
 methane, photoacoustic Raman spectroscopy under pulsed laser excitation 0-82825  
 methane+ $\text{SF}_6$ , vibr.-vibr. relax 0-99537  
 methane isotopic mixtures, enrichment of D using vibrationally sensitized reaction 0-76532  
 methane- $d_0$ (- $d_4$ ), unimol. decomp., energy transfer processes, Monte Carlo simulation 0-99555  
 methane- $d_4$ , vibr.-translational relax. 0-99537  
 methane- $d_4$ +Ar, vibr.-translational relax. 0-99537  
 methane- $d_4$ +methane, vibr. relaxation 0-99537  
 methanol 70 and 118  $\mu\text{m}$  laser line diagnostic expts. 0-69387  
 methyl fluoride, laser collision-induced energy absorpt. and vibr. excitation 0-74233  
 methyl halides, semiclassical theory for collision induced vibr.-rot. transitions 0-63767  
 methyl halides, vibr. energy relax., opto-acoustic obs. 0-95711  
 mixture, strongly excited, vibr. relax. 0-102555  
 Morse oscillator collinear collision, inelastic vibr. energy transfer, mol. continuum influence 0-106383  
 multiple photon photochemistry in low temp. matrices 0-76533  
 nitrobenzene, liquid and  $\text{CCl}_4$  soln. shear waves and translation-rotation coupling obs. by depolarised Rayleigh scattering 0-71432  
 non-adiabatic transitions induced by rotational coupling 0-106385  
 nonlinear oscillators, 1-D, intramolecular vibr. energy transfer, quantal, classical and statistical behaviour 0-91641  
 nonradiative transition of molecule in condensed medium, vibr. relax. effect 0-80848  
 polar mol. rot. relax., dielectric friction, Onsager cavity model 0-64664  
 polyatomic molecule, multiphoton excitation by two IR lasers 0-91607  
 polyatomic molecules, intramolecular vibr. relax., restricted quantum exchange theory 0-63610  
 polyatomic molecules, multistage IR dissoc., collisionless energy-gathering process 0-99526

**molecular rotational-vibrational energy transfer continued**

rhodamine 6G dye laser, induced radiation spectral characts., effect of vibr. relax. 0-64008  
 sudden rotational approximation, reactive and inelastic, body-fixed frame, exchange reaction extension 0-61073  
 tetramethyldioxetane, multiphoton dissoc., collisional vibr. relax., rate eqns. model 0-63729  
 trifluoro+OH(D), vibrational and rotational energy effect 0-76497  
 tolueniodomethane, highly excited, intermol. vibr. energy transfer, transient UV absorpt. spectra 0-106381  
 triiodomethane, polarized light scatt., relaxation processes 0-60615  
 1,3,5-trimethylbenzene+OH(D), vibrational and rotational energy effect 0-76497  
 xanthene dyes in n-alcohols (ethylene glycol) (glycerol), rot. relax., time-resolved fluoresc. depolaris. obs. 0-58300  
 Ar+HF, state-to-state cross sections for rot. to translational energy transfer determ. 0-91644  
 Ar+ $\text{Na}_2$ , differential cross sections meas. for rot. energy transfer process, obs. of halos 0-91643  
 Br $_2$ , kinetics of excited states using laser excitation, radiative lifetimes and collisional deactivation 0-74237  
 BrCl laser induced fluoresc., quantum resolved level dynamics in  $\text{B}^1\Pi(\text{O}^+)$  state 0-74188  
 C $_3$  production, vibr. relax., chem. kinetics, following IR multiphoton allene photolysis 0-66820  
 CH radical, sputtered, rotational and vibrational excitation 0-69224  
 $\text{CN}^+$ ,  $\text{B}^2\Sigma^+$  state, fluoresc. decay dynamics, collisional quenching and radiative lifetimes 0-58306  
 CO electric discharge lasers, vibr. kinetics, modelling and expts. 0-69374  
 CO lasers, scaling laws 0-95878  
 CO supersonic lasers, CW double elec. discharge performance 0-69416  
 CO+H $_2$ , rot. excitation, rel. between tensorial cross sections 0-83454  
 CO+H $^+$ , computed cross section vibr. threshold effects 0-63759  
 $^{12}\text{C}^{16}\text{O}+^{13}\text{C}^{16}\text{C}$ , vibr. energy transfer, laser-induced fluoresc. obs. 0-78690  
 CO $_2$  dissociation in a nonequilibrium plasma 0-87851  
 CO $_2$  laser amplifier multipulse energy extraction 0-78832  
 CO $_2$ , photoacoustic Raman spectroscopy under pulsed laser excitation 0-82825  
 CO $_2$ , VV processes, estimation of almost resonant molecular energy transfer due to multipolar pot. 0-91642  
 CO $_2$ -N $_2$  mixture, strongly excited, vibr. relax. 0-102555  
 CO $_2$ +H $_2$ , rot. transfer, ab initio intermol. pot. energy surface 0-58354  
 CO $_2$ +H $^+$  ( $\text{D}^+$ ), vibr. excitation, isotope and time effects 0-63773  
 CO $_2$ +He, translational-vibrational energy transfer, quantum dynamical study 0-63746  
 CO $_2$ +Ne, energy transfer rate consts., semiclassical method 0-91640  
 CO $_2$ +SO $_2$ , near-reson. energy transfer, fluoresc. obs. 0-106348  
 CO(1)+CO( $\nu$ )-CO(0)+CO( $\nu+1$ ), vibr. energy accumulation, reaction rate anal. 0-78692  
 Cl $^-$ +HBr(HI)-HCl+Br $^-$  ( $\text{I}^-$ ), vibr. product state distrib., IR chemiluminesc. obs. 0-81309  
 D+FD(FM), low barrier quantum model, vibr. deactivation on chemically reactive potential surfaces 0-69216  
 D $_2$ +D $_2$ , ladder operators in vibr.-vibr. and vibr.-translational transitions at high collisional energies 0-106382  
 D $_2$ +Ne(Ar)(HD), state-resolved  $\Delta j=2$  rot. transitions 0-63772  
 D $_2$ , compressed fluid, vibrational population relaxation time obs. 0-69219  
 H+H $_2$ , sudden rot. reactive scatt., 3-dimens., approx. quantum mech. calcs. 0-76498  
 H $^+$ +H $_2$ , rot. and vibr. excitation, energy loss obs. 0-63773  
 H $^+$ +H $_2$ , vibr. excitation, ab initio CI pot. energy surface calcs. 0-74228  
 H $^+$ +H $_2$ , vibr.-rot. excitation, ab initio CI pot. energy surface calcs. 0-74229  
 H $^+$ +H $_2$ (CO $_2$ ), vibr. excitation, 10-30 meV 0-58358  
 H $_2$ , E,F $\Sigma_g^+$  state, collisional and radiative props. 0-58357  
 H $_2$  in Ar, vibr. energy relax. 0-106384  
 p-H $_2$ + $^4\text{He}$ , vibr. relax., analytical approx. 0-63761  
 H $_2$ +CO $_2$ , exponential gap relation, rot. inelasticity 0-78693  
 H $_2$ +D(O)(Cl)(Br), relax. and chem. reaction, time resolved IR fluoresc. and mass spectrometry obs. 0-69177  
 H $_2$ +H, exponential gap relation, rot. inelasticity 0-78693  
 H $_2$ +H $_2$ , exponential gap relation, rot. inelasticity 0-78693  
 H $_2$ +H $_2$ , rot. relax. collision, scaling theory anal. 0-74232  
 H $_2$ +He, exponential gap relation, rot. inelasticity 0-78693  
 H $_2$ +Li, exponential gap relation, rot. inelasticity 0-78693  
 H $_2$ +Li $^+$ , exponential gap relation, rot. inelasticity 0-78693  
 H $_2^+$ +H $_2$ -H $_3^+$ +H, state-selected ion-molecule reactions threshold electron-secondary ion coincidence technique obs. 0-85166  
 HBr+CO(CO $_2$ )(N $_2$ O)(NO)(N $_2$ O)(O $_2$ ), rate consts. for vibr. energy transfer meas. using laser. induced fluorescence technique 0-87206  
 HCN+He, translational-vibrational energy transfer, quantum dynamical study 0-63746  
 HCl, liq., vibr. relax., IR double reson. 0-95712  
 HCl, vibr. emission from ClF-H $_2$  chem. laser 0-97709  
 HCl+D(O)(Cl)(Br), relax. and chem. reaction, time resolved IR fluoresc. and mass spectrometry obs. 0-69177  
 HCl+HBr, single quantum vibr. energy transfer 0-69223  
 HF, pulsed laser numerical modelling, rot. relax. 0-87388  
 HF, vibr.-rot. band, absorpt. line self-broadening, rot. relax. 0-87213  
 HF+H $_2$ (D $_2$ )(N $_2$ ), 200K and 295K vibr. relax. rates 0-63766  
 HF+HCl(CO $_2$ )(N $_2$ O)(CO)(N $_2$ O)(O $_2$ ), HF( $\nu=3$ ) relax. and rate consts. 0-61069  
 HF+HF, rot. relax. collision, scaling theory anal. 0-74232  
 H $_2$ O, harmonic and anharmonic matrix elements comparison, appl. to vibrational energy transfer 0-63760  
 H $_2$ O+H $_2$ O(He)(Ar)(N $_2$ )(O $_2$ )(CO $_2$ ), vibr. energy transfer temp. depend. 0-63763  
 H $_2$ S(D $_2$ S) photodissoc., SH internal energy distribution 0-95697  
 He-LiH, rot. inelastic collisions, ab initio pot. energy surface calcs. 0-87208  
 He+H $_2$ , mol. energy transfer by quasiclassical trajectory methods, vibr. relax. and dissoc., rot. effect 0-99557  
 He+H $_2$ , vibr. inelastic integral cross-sections, transitions to  $\nu=2$  level 0-99559  
 He+I $^*$ , low energy collisions, energy redistrib. 0-63765  
 He+LiH, rot. inelastic collisions, dynamics 0-87209  
 He+LiH, rot. inelastic collisions, state-to-state cross sections determ. 0-87210



**molecular rotational-vibrational energy transfer continued**

- HgBr+O<sub>2</sub>(N<sub>2</sub>)(H<sub>2</sub>)(He)(Ne)(Ar)(Kr)(Xe), vibr. relax., rate coeffs., fluoreosc. obs. 0-63697  
 I<sub>2</sub>, seeded in supersonic free jet, collision-induced rotational relax. 0-102556  
 I<sub>2</sub>, He, van der Waals mol., photodissoc. 0-63765  
 I<sub>2</sub>-He\* Van der Waals complex, vibr. relax. processes and decomposition 0-63765  
 I<sub>2</sub>\*+He(Ne), energy depend. of collision induced intramolecular energy transfer 0-83470  
 KrF, form., relax. and quenching 0-81314  
 Li<sup>+</sup>+CO<sub>2</sub>, collisional excitation, quasiclassical trajectory calcs. 0-83467  
 LiH, state selected rot. transition integral cross section, laser fluoreosc. obs. 0-63770  
<sup>7</sup>LiH+HCN, rot. inelastic collision, energy transfer 0-87211  
 N<sub>2</sub>, excitation efficiency for rot. states 0-102557  
 N<sub>2</sub> jet, freely expanding, quantum effects in rot. relax. 0-58355  
 N<sub>2</sub> plasma heating in electrodeless RF capacitive discharge, mechanism, impurity effect 0-59312  
<sup>14</sup>N<sub>2</sub>+CO, vibr.-vibr. energy transfer, long and short range pot. effect 0-99556  
<sup>15</sup>N<sub>2</sub>+CO, vibr.-vibr. energy transfer, long and short range pot. effect 0-99556  
 NH<sub>3</sub>+NH<sub>3</sub>(He)(Ar)(N<sub>2</sub>)(O<sub>2</sub>), vibr. energy transfer temp. depend. 0-63763  
 NH(ND) X<sup>3</sup>Σ<sup>-</sup>, in inert gas solid, vibr. relax., matrix and isotope effects 0-95713  
<sup>14</sup>N<sup>15</sup>N+CO, vibr.-vibr. energy transfer, long and short range pot. effect 0-99556  
 NO, X<sup>2</sup>Π state, vibr. relax., IR-UV double reson. obs. 0-106338  
 N<sub>2</sub>\*+H<sub>2</sub>O→N<sub>2</sub>+H<sub>2</sub>O\* 0-87212  
 Na<sub>2</sub>+He, rot. transitions differential cross sections, laser fluoreosc. meas. 0-63771  
 Na<sub>2</sub>+He, rotationally inelastic scatt., state-to-state differential cross sections 0-74234  
 Na<sub>2</sub>\*+Xe, rot. energy transfer, vel. depend. 0-95715  
 Na(3P), electronic to vibrational energy transfer in collisions with simple molecules 0-63769  
 Ne+D<sub>2</sub>, anisotropic inversion pot., rot. inelastic cross sections 0-78696  
 Ne+D<sub>2</sub>, energy-loss scaling in 0.5-3.5 keV 0-63768  
 Ne<sup>+</sup>+D<sub>2</sub>(H<sub>2</sub>), energy-loss scaling in 0.5-3.5 keV 0-63768  
 O<sub>2</sub>, UV absorpt. spectra, IR laser induced changes 0-83385  
 O<sub>2</sub>+He(D<sub>2</sub>)(H<sub>2</sub>), vibr. relax. rate consts. 0-74231  
 OCS, T<sub>2</sub> relax. meas. using budge-type superhet. microwave spectrometer 0-91551  
 OCS+He, translational-vibrational energy transfer, quantum dynamical study 0-63746  
 O<sub>2</sub>(Δ)+H<sub>2</sub>O, atmospheric, collisional emission rel. to new diffuse bands in twilight 0-72662  
 OH A<sup>2</sup>Σ<sup>+</sup> state, laser excited, vibr. energy transfer, flame thermometry appls. 0-58349  
 OH, interstellar, rot. excitation by H<sub>2</sub> rel. to maser emission 0-62232  
 SF<sub>6</sub>, laser pumping in collisional region of nozzle beam, internal excitation, time-of-flight anal. 0-95719  
 SF<sub>6</sub>, multiphoton dissociation by mol. beam method, energy distribution meas. by time-of-flight spectra, dissociation dynamics 0-78670  
 SF<sub>6</sub>+Li<sup>+</sup>(H<sup>+</sup>), mode selective vibr. excitation 0-58351  
 SF<sub>6</sub>+N<sub>2</sub>O, vibr.-vibr. energy transfer, fluoreosc. 0-78688  
 SO<sub>2</sub>, harmonic and anharmonic matrix elements comparison, appl. to vibrational energy transfer 0-63760  
 SO<sub>2</sub>, T<sub>2</sub> relax. meas. using budge-type superhet. microwave spectrometer 0-91551  
 SO<sub>2</sub>, vibr. relax., phase spectrophone method obs. 0-87059  
 SO<sub>2</sub>-<sup>18</sup>O<sub>2</sub> mixtures, IR laser pumped, intermol. vibr. energy transfer dynamics obs. 0-87207  
 Se<sub>2</sub>, laser induced fluoreosc. in inert gas matrix 0-87161  
 Te<sub>2</sub>, laser induced fluoreosc. in inert gas matrix 0-87161  
 U+molecule, collisional relax. of highly excited states, laser-induced fluoreosc. obs. 0-58205  
 Xe+Cl<sub>2</sub>, classical trajectory calcs., energy threshold for collision induced dissociation, determ., 0-95709  
 XeCl, form., relax. and quenching 0-81314  
 XeF, form., relax. and quenching 0-81314  
 XeF, ground state kinetics, multilevel model of energy transfer 0-99707  
 XeF\*, B<sup>2</sup>Σ<sup>+</sup> and C<sup>2</sup>Π<sub>3/2</sub> states, fluoreosc. decay dynamics, collisional quenching and radiative lifetimes 0-58306

**molecular rotational-vibrational states** see *molecular rotation-vibration*

**molecular spectra**

- see also *macromolecular spectra*; *molecular fluorescence*; *molecular rotation*; *molecular spectral line breadth*; *molecular vibration*; *multiphoton spectra*; *optical double resonance*; *radiative corrections*; *spectra of inorganic molecules*; *spectra of organic molecules and substances*  
 anharmonically coupled oscils., time depend. Hartree theory, susceptibility, absorpt. and Raman spectrum 0-58241  
 chemical reaction wave, propag. of coherent probe light pulse 0-61190  
 coherent and nonlinear optics, conf., Leningrad, USSR (Jun. 1978) 0-98753  
 diatomic molecular spectra, conventions for defining electric transition moment and rot. line intensity factors 0-83346  
 diatomic molecules, excited states, electronic transition probabilities and lifetimes, review 0-78658  
 electronic spectra of molecules, pure elec. quadrupole transition polaris. 0-63691  
 electronic-vibrational transitions in laser radiation field 0-99522  
 gas phase chemical reactions in IR laser field, collision-induced absorpt. spectra 0-76499  
 gases, nonuniform vols., IR emission calcs. 0-78657  
 high pressure effects, Morse potential formulation 0-63617  
 hook spectra, evaluation limitations 0-90905  
 intramolecular dynamics, random coupling model, math. approach 0-58308  
 intramolecular dynamics, random coupling model, multiphoton excitation, kinetic eqns. 0-63700  
 micelle formation model, relaxation spectra 0-71934  
 millimetric/submillimetric coherent transient spectroscopy 0-58651  
 model calculations, matching with experiment through linear regression 0-58243  
 molecule+molecule, enhancement by collision induced absorpt. of IR laser radiation 0-66798

**molecular spectra continued**

- nonpolar molecules in degenerate vibr. states, pure rot. absorpt. spectra 0-78598  
 optical properties in resonant low freq. laser radiation field (*Russian*) 0-78628  
 optogalvanic double-resonance spectroscopy 0-57385  
 photon emission from mol. and electronic transitions, quantum dynamics, semiclassical description 0-105466  
 polyatomic molecule, multiphoton excitation by two IR lasers 0-91607  
 polymer film, proton intramolecular transfer, light absorpt. and emission, dichroism, polarised fluoreosc. 0-87166  
 Raman microprobe analysis, principles and appl. 0-57390  
 Ramsey reson. obs. by linear laser spectroscopy 0-99514  
 resonant coherent Raman scatt. spectra of excited molecules 0-87129  
 resonant Raman spectra, overtone intensity distrib., effect of excited electronic state 0-87128  
 rotational spectra, doublet splittings caused by tunnelling, perturbation treatment 0-91541  
 shake-up and UV charge transfer transitions, comparison 0-102567  
 triatomic molcs., Renner-Teller effect, orbital angular momentum 0-78513  
 two-photon spectroscopy, dipole-forbidden transitions, double excited configurations, CNDO-CI methods 0-58332  
 unresolved rot. struct., use in flame temp. meas. 0-86300  
 Bi<sup>3+</sup>-HCl solution, metal cation influence on spectra and luminescence kinetics (*Russian*) 0-78627  
 C<sub>2</sub>+acetylene, C<sub>2</sub> Swan band transition probabilities, collisional energy transfer effects 0-87214  
 F<sub>2</sub>O, geometry, electron spectrum, vert. ionis. pot. ab initio calc. 0-58187  
 K<sub>2</sub>Pr(CN)<sub>4</sub>, muonic X-ray radiation anisotropy (*German*) 0-69267  
 S<sub>x</sub> vapour, x=3 to 8, UV absorption and fluorescence spectrosc., vibrational constants of S<sub>2</sub> 0-78631

**molecular spectral line breadth**

- acetone, IR and Raman spectra, vibr. and reorientational and energy transfer width separation, rot. const. determ. 0-87131  
 acetylene-air flame, Li(Na)(K)(Mg)(Ca) damping consts., Lorentz collisions, mag. field effect 0-66805  
 acetylene-d<sub>2</sub>(d<sub>1</sub>), rot.-vibr. Raman spectra 0-83372  
 benzene, liq., visible region absorpt. spectra, overtones meas. 0-78625  
 benzene+bromomethane, microwave line width and quadrupole moments, perturbation theory 0-69190  
 benzene+OCS, microwave line width and quadrupole moments, perturbation theory 0-69190  
 chloroform-d in soln., vibr. and reorientational relax., Raman study 0-63636  
 collisional dephasing in strong radiation fields, unified theory, Karplus-Schwinger formula 0-91635  
 cyanoacetylene, ν<sub>3</sub> vibr.-rot. band, diode laser spectrum 0-91563  
 cyanomethane-d<sub>0</sub>-d<sub>3</sub>, soln., for IR spectra, band shape and moment anal. 0-58252  
 cyclohexane-d<sub>12</sub>, Raman linewidth and molecular diameter meas. 0-69153  
 diatom+diatom, effect on depolarised light scatt. linewidths 0-58321  
 dichloromethane-d<sub>0</sub>-d<sub>2</sub>, soln., far IR spectra, band shapes and moment anal. 0-58252  
 Doppler line convolution by Gaussian instrument function, appl. to diode laser 0-82830  
 electronic transitions, band shape in multimode weak coupling limit, multidim. subspace theory 0-87178  
 energy loss spectra, state-to-state rot. transition cross sections 0-91665  
 ethylene, narrow resonances of multiple-photon IR absorpt. 0-99529  
 ethylene(-d<sub>4</sub>) clusters, IR photodissoc. 0-89506  
 formaldehyde, isolated Voigt line, off-peak spectral absorpt. coeff. 0-106355  
 formaldehyde+Ar(N<sub>2</sub>O), mol. isolated Voigt line, off-peak spectral absorpt. coeff. 0-106355  
 formic acid (-d), microwave spectra and rot. consts., astrophysical appl. 0-91550  
 gas linear molecules, symmetrised Liouville basis vectors, appl. to spectral linewidths 0-83457  
 gases, nonuniform vols., IR emission calcs. 0-78657  
 interaction anisotropy, small angle scatt., spectral evidence 0-78600  
 intramolecular nonradiative transitions of gaseous small molecules, rovibronic level, lineshapes 0-95667  
 iodomethane, P-line and ν<sub>6</sub> band spectra using CO<sub>2</sub> laser absorpt. 0-69142  
 iodomethane, Raman band shapes, mol. oscil. bands (*German*) 0-69154  
 isobutylene, liq., vibr. phase relax. and freq. shifts, density and temp. effects 0-74235  
 isotropic molecular gases, binary collision-induced light scatt., rot. Raman scatt. 0-78660  
 isotropic molecular gases, binary collisions induced light scatt. 0-83428  
 liquids, Maxwell effect relax. time and light scatt. line broadening 0-76040  
 Lorentzian lineshapes and isotropic distrib. of molecules, analytical expressions derived for powder samples 0-60401  
 Lorentzian Raman lines, eqn. for correcting finite slit width effect 0-63593  
 methane, Jovian line profiles near 1.1 μ as probe of cloud struct. and C/H ratio 0-62067  
 methane, optical Ramsey resonance, in three separated fields produced by corner reflector, theory 0-74166  
 methane-d<sub>1</sub>, high resolution spectra, line intensities, ground-state rot. const. determ. 0-83517  
 nickel-octaethylporphyrin, in benzene soln., reson. CARS and CSRS line shapes 0-74432  
 OH 1667 MHz, line width in unusual maser source OH 205.1-14.1 during flare 0-98734  
 optical Autler-Townes effect, time depend., finite bandwidth laser appl. theory 0-91499  
 optical Ramsey resonance, in three separated fields produced by corner reflector, theory 0-74166  
 organic molecules, C-H Raman stretching bands in soln., vibr. freqs. and linewidth 0-78622  
 organometallic amines, Raman and IR spectra, band intensity and assignment, force const. determ., vibr. props. (*German*) 0-87133  
 oxy-myoglobin, evidence for conformational and diffusional mean square displacements 0-89713  
 phase and population relax., semigroup formalism 0-78519  
 polyatomic molecules, intramolecular vibr. relax., restricted quantum exchange theory 0-63610



**molecular spectral line breadth continued**

- polynuclear aromatic hydrocarbons, synchronous excitation spectrofluorometry (*Japanese*) 0-86452  
 predissociated two-channel model, resonances with complex rot. method 0-58327  
 preionis. and predissoc., rel. to spectral line shape 0-63724  
 Ramsey reson. obs. by linear laser spectroscopy 0-99514  
 spectral line narrowing of triplet state, in laser excited experiments 0-63703  
 subnatural linewidth spectra by optical double reson. with two-photon pumping 0-74200  
 triatomic van der Waals mols., rot. predissoc. 0-63721  
 1,2,4-trichlorobenzene liq., mol. reorientation, translation and vibr. relax., Rayleigh and Raman spectra 0-95632  
 trichloromethane-d<sub>0</sub>-d<sub>1</sub>, soln., far IR spectra, band shape and moment anal. 0-58252  
 trichloromethane-d, Raman band shapes, mol. oscill. bands (*German*) 0-69154  
 trimethylcarbinol complexes in soln., weakly H-bonded, IR bandshapes 0-106354  
 triphenylcarbinol complexes in soln., weakly H-bonded, IR bandshapes 0-106354  
 two level system, homogeneously broadened, saturable absorpt., coherence effects 0-95958  
 van der Waals interaction, spectral line broadening, growth curves 0-102548  
 Ar<sub>2</sub>O<sub>2</sub> (6%) cryst., vibr. Raman spectra 0-60558  
 ArH<sub>2</sub>, van der Waals mols., rot. predissoc. 0-63721  
 ArN<sub>2</sub>, van der Waals mols., rot. predissoc. 0-63721  
 Br<sub>2</sub>, B<sup>2</sup>Π(O<sub>u</sub><sup>+</sup>) predissoc. rates, analytical interpretation 0-91617  
 CH, interstellar, in bright rimmed mol. clouds, line widths rel. to post-shock gas emission 0-62238  
 CO, P(6) line absorpt. coeff. and halfwidth, temp. depend. 0-78618  
 CO, thermal and maser emission lines profiles in evolved stars expanding envelopes 0-82334  
 CO<sub>2</sub>, IR band intensity 0-83425  
 CO<sub>2</sub>, IR bands transmission functions 0-106324  
 CO<sub>2</sub> laser, transitions, linewidth, temp. depend. 0-69360  
 CO<sub>2</sub>, R-branch line intensities and press.-broadened line widths at 15 μm 0-102508  
<sup>12</sup>C<sup>16</sup>O<sub>2</sub>, ν<sub>3</sub> band, IR single line strength 0-83370  
<sup>13</sup>C<sup>16</sup>O<sub>2</sub>, IR line strength 0-83371  
 CaF, B<sup>2</sup>Σ<sup>+</sup>-X<sup>2</sup>Σ<sup>+</sup> system, rot. and vibr. anal. 0-74156  
 H<sub>2</sub> photoelectron spectra, rot. intensity distrib. 0-91605  
 H<sub>2</sub>, predissoc., interference effects, lineshape obs. 0-83432  
 H<sub>2</sub>, preionis. and predissoc., rel. to spectral line shape 0-63724  
 HCl+I<sub>2</sub> gas, weak collisions, HCl spectral line broadening of IR spectra 0-74161  
 HCl+N<sub>2</sub>(O<sub>2</sub>)(D<sub>2</sub>)(H<sub>2</sub>), HCl ν<sub>2</sub>-ν<sub>1</sub> band perturbations, linewidth and shifts calcs., IR spectra obs. (*French*) 0-58251  
 HD, predissoc., interference effects, lineshape obs. 0-83432  
 HF, laser field interaction, Floquet theory, dynamic Stark shift, broadening 0-63716  
 HF, vibr.-rot. band, absorpt. line self-broadening, rot. relax. 0-87213  
 HNO<sub>3</sub>, IR spectra, 865.5-871.0 and 884.5-887.0 cm<sup>-1</sup> regions, equiv. width meas., atm. spectrum appl. (*French*) 0-87114  
 H<sub>2</sub>O vapour, IR bands transmission functions 0-106324  
 Hg discharge, high-pressure, NaI and TlI additives, line broadening and radiative transport 0-74199  
 I<sub>2</sub>, RF optically heterodyned saturation spectroscopy, reson. degenerate four-wave mixing 0-74211  
 IBr-benzene in n-decane soln., IR line broadening by chemical exchange 0-87111  
 KrH, van der Waals mols., rot. predissoc. 0-63721  
 N<sub>2</sub>, I<sup>-</sup> system bands, line broadening and shift 0-87138  
 β-N<sub>2</sub> cryst., vibr. Raman spectra 0-60558  
 N<sub>2</sub>, liquid, vibrational dephasing, computer simulation, Raman spectra, pair potential effect 0-63863  
 N<sub>2</sub>, preionis. and predissoc., rel. to spectral line shape 0-63724  
 N<sub>2</sub>-Ar(Kr)(O<sub>2</sub>)(CO)(CH<sub>4</sub>), liquid, high resolution CW CARS spectra 0-63635  
 NH<sub>3</sub>, inversion spectrum collisional line broadening, general theory 0-87184  
 NH<sub>3</sub><sup>+</sup>, two-mode Jahn-Teller effect calcs. 0-83297  
 NH<sub>3</sub>+CO<sub>2</sub>(N<sub>2</sub>), collisional broadening of NH<sub>3</sub> inversion spectrum lines 0-99521  
 NH<sub>3</sub>+H<sub>2</sub>, NH<sub>3</sub> inversion transition, linewidths and T<sub>1</sub>/T<sub>2</sub> ratio 0-99499  
 NH<sub>3</sub>+He(Ne)(Ar)(Kr), pure rot. line, press. broadening calcs. 0-78656  
 NO, γ band lines, collisional broadening coeff. and optical collision diameter 0-63714  
 NO, γ(0,0) band, collisional broadening parameters 0-63713  
 NO, Zeeman modulation spectroscopy, line shape analysis 0-74197  
 NO+N<sub>2</sub>(CO<sub>2</sub>)(CO)(CH<sub>4</sub>)(Ar), NO γ(0,0) band, oscillator strength and line broadening 0-106356  
 N<sub>2</sub>O, ν<sub>3</sub> and 2ν<sub>3</sub> IR bandshape and dipole correl. functions 0-91560  
 N<sub>2</sub>O, preionis. and predissoc., rel. to spectral line shape 0-63724  
 Na<sub>2</sub>, triplet satellite band obs. in self-broadened D-line very far blue wing 0-95688  
 NeH<sub>2</sub>, van der Waals mols., rot. predissoc. 0-63721  
 γ-O<sub>2</sub> cryst., vibr. Raman spectra 0-60558  
 OH+H<sub>2</sub>O, OH linewidth rot. depend. on UV transitions 0-91606  
 SiH<sub>4</sub>, L<sub>2,3</sub>MM Auger spectrum, line width and intensities 0-58325  
 TiO in sunspots, equiv. width meas. theoretical interpretation, line form. process 0-72902  
 ZrO, IR spectrum band strengths rel. to possible presence in S-type stars 0-62124

**molecular structure (electronic)** *see molecular electronic states*

**molecular structure (geometrical)** *see molecular configurations*

**molecular vibration**

- see also Fermi resonance; macromolecular dynamics; molecular force constants; molecular rotational-vibrational energy transfer; molecular spectra; molecular vibration calculations; molecular vibration in solids; potential energy curves and surfaces of molecules; potential energy functions*  
 absorption bands, vibronic intensification obs., floating-orbital method 0-63619  
 acetaldehyde, carbonyl addition, model transition states, vibr. anal. 0-71898  
 acetaldehyde, dichroic effects, computational expts. 0-83424

**molecular vibration continued**

- acetaldehyde, lowest Rydberg state, multiphoton ionisation spectra 0-83435  
 acetic acid, and derivatives, vibr. spectra in soln. 0-63633  
 acetone, absorption bands, vibronic intensification obs., floating-orbital method 0-63619  
 acetonitrile-d<sub>3</sub>, <sup>2</sup>H NMR spectra, vibr. and asymmetry corrections to quadrupole coupling consts. 0-74184  
 acetonitrile, IR and Raman spectra, vibr. and reorientational and energy transfer width separation, rot. const. determ. 0-87131  
 acetophenone, T<sub>1</sub>-S<sub>0</sub> intersystem crossing, nonradiative decay rate, excitation energy depend. 0-63609  
 acetophenones, spectrosc. characs. using PPP SCF CI calcs. 0-102448  
 acetylene, vibr. relax. study using laser-induced fluoresc. 0-74219  
 acetylene+inert gas, vibr. relax. study using laser-induced fluoresc. 0-74219  
 acid oxalate ion in aq. soln., vibr. studies, IR and Raman spectra 0-95589  
 alcohol H-complexes interactions, H-bond vibr. freq., anharmonic calcs. 0-99453  
 alkali hydride molecules, pot. energy function, rot. const., vibr. const., and binding energy 0-99532  
 alkali metal halide dimers, mol. force consts. and vibr. amplitudes calc. using electron gas model data 0-87245  
 alkanes, liq., mol. struct., selective deuteration and IR vibr. spectra 0-96432  
 alkyl benzenes, jet-cooled, vibr. relax., nanosecond time evolution 0-95584  
 alkyl halide+K potentially reactive collisions, electronic excitation 0-74239  
 alkyl metal carbonyls, phosphine monosubstituted, LF vibrs., IR and Raman spectra 0-95585  
 para-alkylanilines having optically active modes, vibr. relax. studied by absorpt. and fluoresc. spectra 0-83340  
 allylamine, laser-microwave double and triple reson. 0-83397  
 aminopyrazine, far IR spectra, barrier to planarity, pot. function and energy levels 0-69137  
 aniline-chlorophenol complexes, <sup>35</sup>Cl NQR, inter- and intramol. interactions 0-63666  
 anisometric mol. liqs., Raman spectral components, vibr. reson. coupling and noncoincidence effect 0-69149  
 anthracene, electronic vibr. spectra, stochastic description, numerical modeling, comparison with expt. 0-63620  
 atom+diatomic molecule, restricted 2-D Morse oscillator model, semiclassical calcs. for mol. dissociation 0-74222  
 benzaldehyde gas, nonradiative electronic transition 0-83413  
 benzaldehyde in methyleyclohexane, n<sup>π</sup>\* spectra 0-63627  
 benzene, deuterated and chemisorbed on glass, vibr. bands, Raman scatt. study 0-84737  
 benzene, liq., visible region absorpt. spectra, overtones meas. 0-78625  
 benzene+Hg, electronically excited, mol. fluoresc., vibr. relax. cross sections and equilibration rates determ. 0-87205  
 benzene chemisorbed on Raney Ni, struct., neutron inelastic spectroscopy study 0-101038  
 benzene radical cation in solid Ar, fluorescence spectra obs. 0-83382  
 benzene-d<sub>6</sub>(-d<sub>5</sub>), radiationless triplet decay, non-Condon effects 0-83405  
 benzene-d<sub>3</sub>, <sup>2</sup>H NMR spectra, vibr. and asymmetry corrections to quadrupole coupling consts. 0-74184  
 benzene-d<sub>6</sub>+N<sub>2</sub>+CO<sub>2</sub>, electronically excited, mol. fluoresc., vibr. relax. cross sections and equilibration rates determ. 0-87205  
 bicyclobutyl+methylene, products decomposition, competitive channels and vibr. relax. 0-83336  
 biomolecule resonant interactions 0-72128  
 bridge angle, vibr. behaviour, simplified and accurate calcs. 0-95735  
 bromoform, highly excited vibr. states, thermal lensing spectrosc. and local mode model 0-87140  
 bromotrifluoromethane cation, photodissoc. by quasi-continuum single IR photon absorption 0-61124  
 t-butyl acetate, rot. isomerism, dielect. and Raman spectra 0-106328  
 t-butyl formate, rot. isomerism, dielect. and Raman spectra 0-106328  
 3-buten-1-ol, vibr. spectra, assignments, rot. isomerism 0-58257  
 calcium oxalate monohydrate, IR and Raman spectra, vibrational studies 0-69139  
 carotenoid molecules in living cells of *Chlorella*, vibrational state population 0-97861  
 chemical reaction wave, propag. of coherent probe light pulse 0-61190  
 chloro(ethyl)silanes and its C derivatives, Raman spectra, mol. vibr. and rot. isomerism 0-87134  
 1-chloro-2,2-dimethylpropane, IR and Raman spectra, vibr. assignment 0-74169  
 1-chloro-2-methylpropane, IR and Raman spectra, vibr. assignment 0-74169  
 chloroanisoles, <sup>35</sup>Cl NQR, inter- and intramol. interactions 0-63666  
 chlorobenzaldehyde, a<sup>3</sup>A'→X<sup>1</sup>A' phosphoresc., conformations and ground state fundamentals 0-78642  
 chloroform, highly excited vibr. states, thermal lensing spectrosc. and local mode model 0-87140  
 chloroform-d in soln., vibr. and reorientational relax., Raman study 0-63636  
 chlorophenols, <sup>35</sup>Cl NQR, inter- and intramol. interactions 0-63666  
 cinnoline, prereson. Raman spectra, vibr. band intensities obs. 0-102515  
 collisions in laser field, multiphoton vibrational excitation enhancement, semiclassical theory 0-58350  
 coumarin dye molecules, CH stretching modes, population lifetime meas. 0-58185  
 α-cyanoacrylate adhesive in first monolayer on bulk Al surface, IR spectra, H-bond form., stretching vibr. 0-87119  
 cyanodiacetylene cation, gas phase, UV emission spectra of A(π<sup>-</sup>)→X(π<sup>-</sup>) band system 0-95636  
 cycloalkanones, carbonyl charact. freqs., kinematic and pot. energy effects 0-95578  
 cyclobutane(-d<sub>8</sub>), centrifugal distortion const. calc., rel. to struct. and mol. wt. 0-95580  
 cyclopentadienyldichloride, gaseous, far IR and Raman spectra 0-95624  
 cyclopentadienyltitanium dichloride, gaseous, far IR and Raman spectra 0-95624  
 cyclopentadienyltitaniumtrichloride, gaseous, far IR and Raman spectra 0-95624  
 cyclopentadienylzirconiumdichloride, gaseous, far IR and Raman spectra 0-95624

## molecular vibration continued

- cyclopentylamine, vibr. spectra and struct. 0-102516  
 cyclopropane, IR spectra studied by tunable laser,  $\nu_{10} + \nu_{11}$  band anal. 0-95615  
 cyclopropane-( $d_4$ ), centrifugal distortion const. and thermodynamic functions calc. 0-95582  
 cytochrome c, protein influence on haeme, Raman difference spectroscopy 0-72125  
 2,4-diamino-6-hydroxy-pyrimidine, IR absorption spectrum, vibr. anal., tautomerism 0-58253  
 diatomic molecules, shortening of energy relax. time of excited mol. vibr. in dense medium by form. of H-bonds 0-91553  
 diatomic mols., electronic transition probabilities, isoelectronic, isovalent corrs. for transition strength and vibr. consts. 0-87182  
 dibromomethane, highly excited vibr. states, thermal lensing spectrosc. and local mode model 0-87140  
 1-10-dicarba-closo-decarborane (10), mol. struct., vibr. and shrinkage corrections calc. from force field 0-95739  
 2,6-dichlorobenzamide, IR spectrum, vibr. assignment 0-95608  
 2,2-dichlorobutane, liquid and solid, vibr. spectra, IR and Raman obs. 0-60567  
 dichloromethane, highly excited vibr. states, thermal lensing spectrosc. and local mode model 0-87140  
 2,2-dichloropropane, normal coordinate calcs. 0-60567  
 dicyclopentadienyl  $Ti^{3+}$ - $N_2$  compound complexes, reson. Raman scatt. 0-99510  
 diethylaniline, vibrational Raman bands, excitation profiles (French) 0-83380  
 S,p-difluorobenzene, time resolved fluoresc. spectra, direct view of intramolecular vibr. redistribution 0-83341  
 1,1-difluoroethane, mol. struct., gas phase electron diff. obs. 0-58385  
 dimethoxymethane, vibr. spectra and rot. isomerism 0-106325  
 DNA, proton radiationless transitions for hydrogen bonds (Russian) 0-97857  
 double well damped motion, proton tunnelling, transfer rate temp. depend. (German) 0-87058  
 EBBA, NMR and Raman scatt. studies in nematic phase 0-100619  
 electron scatt. resons. near threshold, vibr. induced narrowing 0-91673  
 ethane, inclusion of nonbonded interactions in vibr. freq. calcs. 0-95590  
 ethane, unimol. decomp., energy transfer processes, Monte Carlo simulation 0-99555  
 ethane gas, local mode overtone bands 0-83444  
 ethyl-furan-2-carboxylate, skeletal vibr. of IR spectra, conformational props., solvent polarity effect 0-87118  
 ethylcyanodiacyetylene cation, gas phase, UV emission spectra of  $A(\pi^{-1}) \rightarrow X(\pi^{-1})$  band system 0-95636  
 ethylcyclopropane, solid, liquid, vapour phase, IR and Raman vibr. spectra 0-84740  
 ethylene, IR absorpt. spectra of  $\nu_1$ ,  $\nu_{10}$  and  $\nu_2$  interacting band 0-83369  
 ethyloxirane, solid, liquid, vapour phase, IR and Raman vibr. spectra 0-84740  
 excited mols., laser induced photochem., review 0-71925  
 2-fluoro ethanol, Ar matrix, induced conformational isomerisation by IR irradi. 0-101010  
 fluoroacetylene-d, Stark and microwave double reson. laser spectra 0-63690  
 fluorobenzene radical cations in solid Ne, laser-induced fluoresc. spectra, vibr. struct. of excited and ground states 0-95671  
 fluoroiodomethane, vibr. excited, dissociation, trajectory calcs. using pot. energy surface parameters 0-76508  
 fluoromethane+fluoromethane, collision induced mode selective energy transfer, fluoresc. obs. 0-69177  
 fluorophenol cations, emission and photoelectron spectra in gaseous phase 0-58316  
 fluorostyrene, UV Raman spectra, reson. effect in photoreactive states 0-106326  
 formaldehyde, excited state vibr. freq. calcs. by method based on scaled ab initio force fields 0-87092  
 formaldehyde and its isotopic species, rot. spectra of ground vibr. state, rot. const. determ. 0-83350  
 formaldehyde anion radical, hyperfine coupling consts., vibr. depend., ab initio calcs. 0-87150  
 formaldehyde substituted with  $^{17}O$  and  $^{18}O$ , microwave spectra of ground vibr. states, rot. and distortion const. determ. 0-83349  
 formaldehyde- $d_0$ -( $d_2$ ),  $S_1$  single rot. level lifetimes, isotope, elec. field and vibr. state depend. 0-78655  
 formamide, force consts. and dipole moment derivatives, ab initio MO calcs. 0-95521  
 formic acid,  $^{16}C$ ,  $^{18}O$ , microwave spectra and centrifugal distortion consts. 0-83352  
 formic acid dimer, vibr. spectra, CNDO/2 interpretation (French) 0-58155  
 trans-formic acid geometry, force fields and fundamental vibr. freq., ab initio study 0-87040  
 formic acid ions, fragmentation, energy selected, photoelectron-photoion spectra 0-95676  
 formic acid- $d_0$ -( $d_1$ )-( $d_2$ )-( $d_3$ ), vibr. spectra, CNDO/2 interpretation (French) 0-58155  
 furan, resonantly enhanced multiphoton ionisation 0-106362  
 furane, cryst., low freq. vibr. spectrum, temp. depend., 12 to 253K 0-84743  
 germylacetylene- $d_0$ -( $d_3$ ), centrifugal distortion const. and thermodynamic functions calc. 0-95581  
 haemoglobin, nanosec. probe of dynamics using time resolved reson. Raman scatt. 0-94162  
 halobenzenes, in potassium laurate mesophase, NMR, proton distance ratios and order tensor elements calcs. 0-63672  
 Henon-Heiles Hamiltonian system, vibr. energy levels in quasiperiodic and stochastic regimes, props. 0-91529  
 heterocyclic compounds, bond lengths, fifth overtone of C-H stretching vibr. obs. 0-91528  
 hexafluorocyclopropane, centrifugal distortion const. and thermodynamic functions calc. 0-95582  
 hexamethylbenzene in tetrachloromethane soln., local mode overtone bands 0-83444  
 1,3,5-hexatriene radical cation, in Ne matrix, laser induced fluoresc. and emission spectra 0-87163  
 homonuclear diatomic mols., Morse pot. and vibr. level field induced, shift and broadening 0-69117  
 1-indanone,  $T_1$ - $S_0$  intersystem crossing, nonradiative decay rate, excitation energy depend. 0-63609

## molecular vibration continued

- intermolecular spectroscopy and dynamical properties of dense systems, conf. Varenna, Italy (1978) 0-82581  
 intrastate scrambling in large mol. bound level struct., appl. to tetracene 0-63696  
 iodomethyl radical, vibr. excited, photofragmentation IR emission obs. 0-87162  
 iodo trifluoromethane, high vibr. state excitation in high-power laser field, spectral characts. 0-91562  
 isopropylcyclopropane, solid, liquid, vapour phase, IR and Raman vibr. spectra 0-84740  
 isotopic sum rules for frequencies, band intensities and Coriolis coupling constants 0-83343  
 laser-chemical reaction kinetic mechanism (Russian) 0-101007  
 liquid, Raman band profile, vibr. dephasing and intermolecular interactions 0-60556  
 local mode mols., normal mode spectra 0-95687  
 MBBA, NMR and Raman scatt. studies in nematic phase 0-100619  
 mesogenic materials, tails or smear effects in X-ray diff. photographs 0-96438  
 methane, IR anal. of  $\nu_2$  and  $\nu_4$  bands (French) 0-87113  
 methane, liq., pure vibr. Raman spectra 0-97262  
 methane, V-V energy transfer 0-83469  
 methane+ $SF_6$ , vibr.-vibr. relax 0-99537  
 methane- $d_0$ -( $d_4$ ), unimol. decomp., energy-transfer processes, Monte Carlo simulation 0-99555  
 methane- $d_4$ , vibr.-translational relax. 0-99537  
 methane- $d_4$ +Ar, vibr.-translational relax. 0-99537  
 methane- $d_4$ +methane, vibr. relaxation 0-99537  
 methane-d, 4.5  $\mu$ m absorpt.,  $2\nu_6$  overtone band anal. 0-91557  
 methanes,  $^{12}CH_4$  and  $^{13}CH_4$ , IR spectra obs., anal. of  $\nu_2 + \nu_3$  band 0-95614  
 methanol, aqueous, damped coupled oscillator model used to study Fermi resonance 0-69152  
 methanol-d, laboratory freqs. of J=2-1, a-type transitions 0-63624  
 p-methoxy benzonitrile, IR absorpt. spectra, vibr. assignments 0-95609  
 methoxydifluorophosphine- $d_0$  and - $d_3$ , IR and Raman spectra, mol. vibr. and struct. obs. 0-87103  
 2-methoxyethylamine, microwave spectra, H-bond, torsional motion and mol. vibr. obs., rot. isomerism, mol. moments determ. 0-95603  
 methyl alcohol- $d_3$ , Fermi resonance due to large amplitude vibr. 0-83519  
 methyl azidoformate, microwave rot. spectrum, satellite transitions 0-69127  
 methyl chloride, rot. anal. of IR absorpt. spectra, mol. vibr., rot. const. determ. 0-99505  
 methyl chloroform, vap., multiphoton dissoc. by  $CO_2$  laser beam 0-61123  
 methyl furan-2-carboxylate, skeletal vibr. of IR spectra, conformational props., solvent polarity effect 0-87118  
 methyl furan-2-thiocarboxylate, skeletal vibr. of IR spectra, conformational props., solvent polarity effect 0-87118  
 methyl halides, mol. force field at SCF ab initio levels, quantum-mechanical calc., LCAO-MO method 0-106319  
 methyl iodide, vibrational dephasing by translational collision 0-87202  
 N-methyl pyrrole, resonantly enhanced multiphoton ionisation 0-106362  
 methyl radical, hyperfine coupling consts., vibr. depend., ab initio calcs. 0-87150  
 methyl radical, vibr. excited, photofragmentation IR emission obs. 0-87162  
 methylacetylene,  $\nu_5$  band, microwave and IR laser Stark spectrosc. 0-91558  
 methylbicyclobutyl decomposition intramolecular vibr. relax., competitive channels 0-83336  
 methylcyanodiacyetylene cation, gas phase, UV emission spectra of  $A(\pi^{-1}) \rightarrow X(\pi^{-1})$  band system 0-95636  
 (+)-(3R)-methylcyclohexanone, vibr. optical activity, Raman obs. 0-102499  
 methylpyridine adsorbed on Ag, surface enhanced Raman spectra 0-83376  
 minimum energy reaction paths, reactive domains of energy hypersurfaces and stability 0-71893  
 mol. target internal motion 0-78697  
 molecular gas, vibr. instability on optical excitation (Russian) 0-100065  
 naphthalene, prereson. Raman spectra, vibr. band intensities obs. 0-102515  
 naphthalene- $d_0$ -( $d_8$ ), radiationless triplet decay, non-Condon effects 0-83405  
 neopentane liq., local mode overtone bands 0-83444  
 nicotinamide adenine dinucleotide, and reduced form, pH induced modification, Raman spectra 0-83343  
 nitrocyclopropane, vibr. spectra struct. and bonding 0-102520  
 organic gases, IR fluoresc. by  $CO_2$  laser 0-78619  
 organic molecules, C-H Raman stretching bands in soln., vibr. freqs. and linewidth 0-78622  
 organometallic amines, Raman and IR spectra, band intensity and assignment, force const. determ., vibr. props. (German) 0-87133  
 oxalate ion in aq. soln., vibr. study and Raman bands 0-95588  
 oxalic acid in aq. soln., vibr. studies, IR and Raman spectra 0-95589  
 2,2 paracyclophane, dimer vibration influence on emission spectrum 0-69133  
 phenazine, prereson. Raman spectra, vibr. band intensities obs. 0-102515  
 phenyl acetylene, liq., phase relax., vibr. dephasing, Raman spectra obs. 0-91567  
 phosphine, IR spectrum,  $\nu_1$  and  $\nu_2$  band analysis 0-83366  
 phthalazine, prereson. Raman spectra, vibr. band intensities 0-102514  
 phthalocyanine, free base, fluoresc. excitation spectrum, cooling in supersonic free jet 0-95670  
 polyatomic molecule, multiphoton excitation by two IR lasers 0-91607  
 polyatomic molecules, bond distribution functions, anharmonicity effects of electron diff. pattern 0-69234  
 polyatomic molecules, multistage IR dissoc., collisionless energy-gathering process 0-99526  
 polyatomic mols., vibr. total energy distrib. in terms of symm. coords., forces and momenta 0-69123  
 polyatomic mols. in liqs., vibr. energy relax. 0-63611  
 polyenes, electronic absorpt. spectra, charact. spectral band criteria 0-63651  
 porphyrin, hypersurface of adiabatic pot. calc. by CNDO/2 method, vibr. freqs., absorpt. spectra calc. 0-95543  
 porphyrin free base, vibr. and normal mode anal. 0-69122



## molecular vibration continued

- propanal, methyl torsional pot. functions, LF Raman and IR vibr. spectra 0-95612
- propiolyl chloride(-d), 357-333 nm absorpt. system 0-69161
- propiolyl fluoride(-d), 290 nm absorpt. system 0-87142
- propynal, IR-microwave double reson. and two-photon expts. 0-83396
- propynal-d, in ground vibrational state, IR microwave double resonance spectra, rot. and centrifugal distortion const. determ. 0-83358
- propynal-d, IR microwave double reson. spectroscopy 0-69172
- propyne-d<sub>0</sub>(-d<sub>3</sub>), absolute and integrated IR intensities of fundamental modes 0-87179
- pyrazine, prereson. Raman spectra, vibr. band intensities obs. 0-102515
- pyrazine, reson. to the S<sub>2</sub>( $\pi,\pi^*$ ) state, Raman spectra calcs. 0-69147
- pyridazine, prereson. Raman spectra, vibr. band intensities 0-102514
- pyridine, deuterium substituted, Raman and IR vibr. spectra 0-84739
- pyridine(-d), force consts. and vibr. spectra by CNDO/2 force method 0-95540
- pyridine-2,3,5,6-d<sub>4</sub>, vibr. spectra, IR and Raman, assignment 0-102519
- pyridine-3,4,5-d<sub>3</sub>, vibr. spectra, IR and Raman, H exchange rates meas. 0-102518
- pyridine-3,5-d<sub>2</sub>, vibr. spectra, IR and Raman, H exchange rates meas. 0-102518
- pyridine-d<sub>5</sub>, vibr. spectra, IR and Raman, assignment 0-102519
- pyrimidine, bi-exponential decay, methylation and vibr. excitation, proximity effects 0-78641
- pyrimidine, vapour, phosphoresc. 0-83408
- pyrrole, resonantly enhanced multiphoton ionisation 0-106362
- quinazoline, prereson. Raman spectra, vibr. band intensities obs. 0-102515
- quinoxaline, prereson. Raman spectra, vibr. band intensities 0-102514
- Raman scattering, pre-reson., by t-type mode near A $\rightarrow$ T electronic transition 0-58261
- Raman spectroscopy, of IR multiple-photon excited mols. 0-74207
- Raman spectroscopy of chiral molecules in mag. fields 0-102532
- rare earth oxyphosphates, IR and Raman spectra, vibr. assignments, cryst. struct. characts. 0-97258
- resonance Raman lineshape studies of vibrational and rotational relaxation in soln. 0-60560
- retinal chromophore, reson. Raman spectra obs. of struct. 0-94168
- rigid symmetric top molecules, dynamic Stark effect spectrum 0-63621
- semicarbazide hydrochloride, vibr. spectra, normal coord. anal. 0-58255
- semicarbazide-d<sub>0</sub>, -d<sub>6</sub>, vibr. spectra, normal coord. anal. 0-58255
- silane coupling agent deposited on E-glass fibre, hydrolysis and drying effect on siloxane bonds 0-85072
- silyl acetylene, microwave spectra in ground and  $\nu_{10}$  vibr. state 0-78610
- stilbene anion radicals, photoinduced isomerisation, 77K 0-66818
- styrene, UV Raman spectra, reson. effect in photoreactive states 0-106326
- 1,1,1,2-tetrafluoroethane, mol. struct. studied by gas-phase electron diff., vibr. amplitudes, bond angles and lengths calc. 0-95740
- tetrafluoromethane,  $\nu_2 + \nu_4$  band, high resolution diode laser spectra 0-69138
- tetrafluoromethane, liq., pure vibr. Raman spectra 0-97262
- tetramethyl-1,3-cyclobutanedione-h<sub>12</sub> and -d<sub>12</sub>, visible spectra,  $n\pi^*$  transitions obs., mol. vibr. 0-97297
- tetramethylbutane in hexachlorobutadiene soln., local mode overtone bands 0-83444
- 2-thio alkyl (allyl, benzyl) pyrimidines, IR and Raman spectra anal., mol. vibr. and symmetry (French) 0-87123
- thioformaldehyde,  $\bar{a}A_2 - X^1A_1$  IR absorpt. spectra 0-83362
- thiones, N-H-S weak and medium strong H bonds, IR spectra 0-69132
- thiouras, alkyl and phenyl groups trisubstituted, conformation, steric and stacking interaction 0-95587
- transition metal cluster carbonyls, fluxionality, collective oscils. and low energy spectra 0-78738
- transition probability evaluation in double asymmetric pot. well 0-69120
- trialkylthiouras, N-H stretching vibrs. and conformation 0-95586
- trichlorobenzene cation, selectively excited wavelength resolved emission spectra 0-87136
- 1,2,4-trichlorobenzene liq., mol. reorientation, translation and vibr. relax., Rayleigh and Raman spectra 0-95632
- trichlorosilane liquid, Si-H stretching mode vibr. dephasing, Raman study 0-84736
- trifluorobenzene cation, selectively excited wavelength resolved emission spectra 0-87136
- trifluoroethene-d<sub>0</sub>-d<sub>1</sub>, mol. struct., microwave and electron diff. obs. 0-58384
- trifluoroiodomethane, IR multi-photon excited mols. 0-74207
- trifluoroiodomethane, laser microwave double reson. spectroscopy with CO<sub>2</sub> laser lines 0-87156
- trifluoroiodomethane cation, photodissoc. by quasi-continuum single IR photon absorption 0-61124
- trifluoromethyl hydroperoxide(-d), CF<sub>3</sub> torsional vibrs., low freq. Raman spectra 0-91565
- trifluoromethyl hypochlorite, vibr. spectra and normal coord. anal. 0-102517
- trifluoromethyl hypofluorite, vibr. spectra and normal coord. anal. 0-102517
- trifluoromethyl hypofluorite (hypochlorite), CF<sub>3</sub> torsional vibrs., low freq. Raman spectra 0-91565
- trifluoromethyl peroxyfluoride (peroxychloride), CF<sub>3</sub> torsional vibrs., low freq. Raman spectra 0-91565
- trigonal and triatomic molecules, orbital valency force field const. calcs. 0-78516
- trimethyl-d<sub>3</sub>-vinylsilane, IR and Raman spectra, struct., vibr. assignment, barriers to internal rot. calc. 0-87102
- trimethylamine, collision induced fluoresc. enhancement and quenching, relax. processes 0-83412
- trimethylaminegallane, microwave, IR and Raman spectra, struct., vibr. assignment 0-95600
- trimethylvinylsilane, IR and Raman spectra, struct., vibr. assignment, barriers to internal rot. calc. 0-87102
- tropolone,  $\pi-\pi^*$  singlet state, H<sup>+</sup> tunnelling dynamics and equilib. geometry 0-102539
- N<sub>7</sub>-undecylumiflavin, high resolution fluoresc. and excitation spectroscopy, vibronic transitions obs. 0-78639
- urea molecule, bond-length corrections for external and internal vibrs. 0-106402
- ureas, alkyl and phenyl groups trisubstituted, conformation, steric and stacking interaction 0-95587
- vibrational dephasing by translational collision 0-87202

## molecular vibration continued

- vinylloxirane, Raman and IR vibr. spectra and conformations 0-83379
- water, coherent Raman ellipsometry, vibr. stretching region and liq. struct. obs. 0-93341
- Al<sub>2</sub>Cl<sub>6</sub>, matrix isolated, vibr. spectra, isotopic fine struct. and valence force field calcs. 0-58258
- AlS, B<sup>2</sup> $\Pi-X^2\Sigma^+$  transition, assignment of UV bands, vibr. and rot. anal. 0-58278
- BCl<sub>3</sub>-N<sub>2</sub> mixtures, thermodiffusion props., effect of resonant excitation of mol. vibr. by laser, isotope separation 0-100047
- BCl<sub>3</sub>NCO, soln., force fields and normal modes, vibr. spectra, IR and Raman obs. (French) 0-58266
- BX<sub>3</sub><sup>16</sup>NCS (X=Cl, Br, I), soln., force fields and normal modes, vibr. spectra, IR and Raman obs. (French) 0-58266
- Ba+HBr, laser induced fluoresc. study at different collision energies 0-91632
- Ba+HCl, laser induced fluoresc. study at different collision energies 0-91632
- Ba+HF, product rot. and vibr. distributions and reaction cross sections depend. on reagent translational energy 0-93745
- Ba+HF-BaF+H, dual mol. beam excitation difference spectroscopy, state-to-state vibr. resolved dynamics 0-89474
- Ba<sup>2+</sup>, very long lived vibr. states, lifetimes, WKB calc. 0-78560
- Ba<sub>3</sub>, excited electronic states, lifetimes and transition moments 0-87177
- Bi<sub>3</sub>, molecular clusters, laser fluoresc. spectrosc. 0-95755
- Br<sub>2</sub> in Ar, solvent effects on equilibrium props. 0-61128
- Br<sub>2</sub> in Ar matrix, reson. Raman scattering amplitude damping in discrete reson. limit 0-58262
- Br<sub>2</sub> in liq. Ar, effective intramol. pot. 0-69208
- BrCl laser induced fluoresc., quantum resolved level dynamics in B<sup>2</sup> $\Pi(O^+)$  state 0-74188
- BrF(Cl), rot. spectra in millimeter wave region, rot. transitions obs., equilib. const. determ. 0-78607
- BrO, free radical, Ar matrix absorpt. spectra, mol. vibronic states obs., spectroscopic const. determ. 0-83387
- C-H, A<sup>2</sup> $\Delta-X^2\Pi$ , dissociative excitation, form. environment and parent mol. effects 0-78682
- C<sub>3</sub> production, vibr. relax., chem. kinetics, following IR multiphoton allene photolysis 0-66820
- CD<sup>+</sup>, in RF ion trap, laser induced fluoresc. spectrum, 0,0 vibr. band and rot. consts. 0-74189
- CH<sup>+</sup>, a<sup>3</sup> $\Pi-b^3\Sigma^-$  transition moment, ab initio calcs. 0-87047
- CH<sub>3</sub>, CH<sub>2</sub>, and CH deformation vibration group frequencies and MO electron densities, interaction force const. 0-87101
- CO, (4+) system, electronic transition probability 0-106332
- CO chemisorbed on Fe, low energy vibr. modes studied by tunnelling spectroscopy 0-78590
- CO,  $\Delta$  state, low energy electron impact excitation and radiative decay 0-91691
- CO laser output power, active species and buffer He isotope effects (Russian) 0-63986
- CO, liq., pure vibr. Raman spectra 0-97262
- CO, photoelectron ang. distributions, wavelength and vibr. state depend., reson. effects, asymmetry parameters 0-91602
- CO room temperature nuclear pumped laser, parameter optimisation and spectral props. obs. 0-63995
- CO,  $v=0-1$  vibr. excitation, electron impact cross sections 0-83507
- CO, vibr. excitation via high-energy shape resonances 0-91693
- CO, X<sup>2</sup> $\Sigma^+$  vibr. levels, UPS electron attachment obs. 0-95683
- CO-N<sub>2</sub>, discharge, plasma characts. and vibr. kinetics anal. 0-59331
- CO-UF<sub>6</sub> nuclear pumped laser, expansion cooled, vibr. excitation distrib. 0-63997
- CO<sup>+</sup>+D<sub>2</sub>, state selected reaction cross-sections, coincidence technique obs. 0-66797
- CO<sub>2</sub><sup>0-1</sup>-10<sup>0</sup> transition in CO-N<sub>2</sub>O reacting gas mixture, gain 0-74337
- CO<sub>2</sub> CW laser, vibr. temp., dissociation and gain limitation determ., new technique 0-87369
- CO<sub>2</sub>, electron elastic scatt. and vibr. excitation by 4, 10, 20 and 50 eV electrons 0-83484
- CO<sub>2</sub>, high resolution UV photoelectron spectra 0-91603
- CO<sub>2</sub>, photoionisation, nuclear motion effects 0-58324
- <sup>12</sup>C<sup>18</sup>O<sub>2</sub>,  $\nu_2$  band, IR single line strength 0-83370
- CO<sub>2</sub>+H<sub>2</sub>, collinear atom-triatom transition probabilities for anharmonic triatom pots., quantum mech. calcs. 0-83455
- CO<sub>2</sub>+H<sup>+</sup> (D<sup>+</sup>), vibr. excitation, isotope and time effects 0-63773
- CO<sub>2</sub>+Kr, collinear atom-triatom transition probabilities for anharmonic triatom pots., quantum mech. calcs. 0-83455
- COS, high resolution UV photoelectron spectra 0-91603
- CO\* prod. from Ar<sup>+</sup>+CO<sub>2</sub>, use in laser systems 0-63824
- CS<sub>2</sub>, high resolution UV photoelectron spectra 0-91603
- CS<sub>2</sub>,  $\nu_2$  bending fundamental, high resolution IR spectrum 0-91559
- CS<sub>2</sub>, photodissoc., fragment energy distrib. 0-69200
- CaCl, B<sup>2</sup> $\Sigma-X^2\Sigma$  transitions, rot. anal. by laser spectroscopy 0-91536
- CaCl, X<sup>2</sup> $\Sigma$  pot. energy curves, polarisability and dissociation 0-91629
- CaF, B<sup>2</sup> $\Sigma-X^2\Sigma^+$  system, rot. and vibr. anal. 0-74156
- Cd complexes, Cd(II) mixed halide complex anions, Raman spectra 0-58270
- Cl+vinyl bromide-d<sub>3</sub> reaction, IR chemiluminesc. 0-102506
- ClF, rot. spectra in millimeter wave region, rot. transitions obs., equilib. const. determ. 0-78607
- CIO, free radical, Ar matrix absorpt. spectra, mol. vibronic states obs., spectroscopic const. determ. 0-83387
- Coll salen complexes, O binding, reson. Raman obs. 0-58267
- CsBrICN, Raman and IR vibr. spectra, struct. 0-102513
- CsClICN, Raman and IR vibr. spectra, struct. 0-102513
- CsI<sub>2</sub>CN, Raman and IR vibr. spectra, struct. 0-102513
- CuF from Cu+F<sub>2</sub> chemiluminesc. reactions, mol. beam study 0-97702
- D+H<sub>2</sub> reaction, transition state theory calculations, kinetic isotope effect explanation 0-66784
- D+H<sub>2</sub> rearrangement collision, vibr. excitation effects 0-71910
- D<sub>2</sub>, matrix isolated, IR spectra, mol. rot. and vibr. const. determ. 0-78617
- DCl+CO, V-V energy transfer 0-78695
- DF, vibr. relax., isotope effect, quantum model 0-91460
- DNSO, IR spectra obs., mole. vibr., anharmonicity constant determ. 0-83357
- D<sub>2</sub>O, vibr. relax. rates 0-95717
- DOD, vibr. intensities, ab initio and empirical calcs. 0-78592
- DOD, vibr. intensities, ab initio and empirical calcs., band strengths 0-78593



## molecular vibration continued

- F+ethylene (benzene) derivatives, deuterated, IR chemiluminesc. 0-102506  
 FCO, form. in Ar matrix, vibr. and electronic spectra, valence force potential determ., mol. photodissoc. obs. 0-85170  
 FO(X<sup>II</sup>) radical from F+O<sub>3</sub> reaction, VUV photoelectron spectra 0-104455  
 Fe<sup>2+</sup> and Fe<sup>3+</sup> hydrate clusters, aq. electron exchange reaction, ab initio RHF MO calc. of inner shell reorganisations, vibr. freq. 0-102564  
 FeCl<sub>2</sub>, internal motion, mol. vibr. calcs. 0-106323  
 FeCl<sub>3</sub>, internal motion, mol. vibr. calcs. 0-106323  
 Fe<sub>2</sub>Cl<sub>4</sub>, internal motion, mol. vibr. calcs. 0-106323  
 Fe<sub>2</sub>Cl<sub>6</sub>, internal motion, mol. vibr. calcs. 0-106323  
 Ga trihalides, vibr. anal., pot. const. determ., mol., compliance and Coriolis coupling const. calc. 0-95579  
<sup>74</sup>GeH<sub>4</sub> mol. vibr., IR and CARS spectra (Russian) 0-102509  
 H-bonded systems, frequency shift rel. to IR bandwidth 0-99502  
 H+D<sub>2</sub>, collinear motion, energy transfer and dissociation, collision dynamics 0-99563  
 H+D<sub>2</sub> reaction, transition state theory calculations, kinetic isotope effect explanation 0-66784  
 H<sup>+</sup>+H<sub>2</sub>, rot. and vibr. excitation, energy loss obs. 0-63773  
 H<sub>2</sub>, CARS, optical Stark effect on vibr., and rot. transitions 0-99512  
 H<sub>2</sub>, elec. discharge, non-equilib. ionisation rate calcs. 0-59319  
 H<sub>2</sub>, electron impact ionisation cross section 0-78718  
 H<sub>2</sub>, field ionisation under nonequilibrium conditions 0-74244  
 H<sub>2</sub>, fluid, Raman meas., 0.2-630 kbar, at room temp. 0-58269  
 H<sub>2</sub>, four-body system, adiabatic representation 0-91530  
 H<sub>2</sub>, matrix isolated, IR spectra, mol. rot. and vibr. const. determ. 0-78617  
 H<sub>2</sub> photoelectron spectra, rot. intensity distrib. 0-91605  
 H<sub>2</sub>+He, vibr. relax. cross section 0-99494  
 H<sub>2</sub><sup>+</sup>+H<sub>2</sub>, state selected reaction cross sections, coincidence technique obs. 0-66797  
 H<sub>3</sub><sup>+</sup>, IR spectrum,  $\nu_2$  band obs. 0-99506  
 HBr, electron impact ionisation, vibr. excitation spectra threshold peaks, negative ion effects 0-106322  
 HCN+He(H<sub>2</sub>)(CH<sub>3</sub>F), HCN excited vibr. state, T<sub>2</sub> meas. 0-102498  
 HCl, electron elastic scatt., exchange and polarisation 0-91668  
 HCl, from H+Cl<sup>-</sup>, vibr. state distrib. 0-66794  
 HCl, vibr. emission from Cl-F-H<sub>2</sub> chem. laser 0-97709  
 HCl, vibr. excitation in electric discharge 0-87978  
 HCl+Cl(Br)(H), vibr. relaxation and reaction rates determ. 0-108698  
 HD<sup>+</sup>, Hellmann-Feynman theorem anomaly 0-63510  
 HDSe, high resolution IR spectra, anal. of 2 $\nu_1$  band, rot. ground state const. determ. 0-95616  
 HF+HF (methane)(methane-d<sub>4</sub>), collision relaxation rate constants and rot. equilibration time meas. 0-69213  
 HF+Li—LiF+H, pot. energy surface, SCF and CI calcs. 0-71904  
 HNCO, rot. spectrum, ground and vibr. state reson., centrifugal distortion coupling 0-83364  
 HNF<sub>2</sub> and DNF<sub>2</sub>, photoelectron spectra, vibr. struct. obs, ionisation pot. determ., ab initio calcs. of ionic geometry 0-83418  
 HNO<sub>3</sub>, aqueous soln., reflectance and complex refractive index, IR spectra, vibr. modes 0-66168  
 HNO<sub>3</sub>, VUV photodissoc., vibr. and rot. distrib. 0-87191  
 H<sub>2</sub>O, electron impact dissoc., OH(A<sup>2</sup> $\Sigma^+$ →X<sup>2</sup> $\Pi$ ) emission spectra, crossed-beam investigations 0-83504  
 H<sub>2</sub>O, excited stretching vibr., quantum mechanics. 0-91535  
 H<sub>2</sub>O, multiplet states, SCF theory 0-69062  
 H<sub>2</sub>O, VUV photodissoc., vibr. and rot. distrib. 0-87191  
 H<sub>2</sub>O<sup>+</sup>, vibr. and rot. struct., intensity factors and orbital angular momentum 0-83246  
 H<sub>3</sub>O<sup>+</sup> (D<sub>3</sub>O<sup>+</sup>), plasma dissociative ion electron recomb., rate coeffs. 0-63747  
 HOD, vibr. intensities, ab initio and empirical calcs. 0-78592  
 HOD, vibr. intensities, ab initio and empirical calcs., band strengths 0-78593  
 HOT, vibr. intensities, ab initio and empirical calcs. 0-78592  
 HOT, vibr. intensities, ab initio and empirical calcs., band strengths 0-78593  
 He+H<sub>2</sub>, mol. energy transfer by quasiclassical trajectory methods, vibr. relax. and dissoc., rot. effect 0-99557  
 He+CS<sub>2</sub>, dissoc. charge-transfer, CS<sup>+</sup>(B<sup>2</sup> $\Sigma^+$ -A<sup>2</sup> $\Pi$ ) emission prod., Morse pot. Franck-Condon factors calc., vibr. anal. 0-99539  
 He+OCS, dissoc. charge-transfer, CS<sup>+</sup>(B<sup>2</sup> $\Sigma^+$ -A<sup>2</sup> $\Pi$ ) emission prod., Morse pot. Franck-Condon factors calc., vibr. anal. 0-99539  
 He, optical absorpt. spectra and kinetic behaviour 0-95635  
 HgBr+O<sub>2</sub>(N<sub>2</sub>)(H<sub>2</sub>)(He)(Ne)(Ar)(Kr)(Xe), vibr. relax., rate coeffs., fluorescence obs. 0-63697  
 Hg(CN)<sub>2</sub>, ion, CN and HgC stretching vibrations and HgCN bending vibration assignments 0-9140  
 I<sub>2</sub>, B-X fluoresc. band system, intensity and relative band strengths meas. 0-102540  
 I<sub>2</sub>, B-X system, mol. consts. and Dunham expansion parameters 0-87095  
 I<sub>2</sub>, energy levels near B-state dissoc. limit, two-photon spectrosc. obs. 0-106367  
 IBr, B<sup>2</sup> $\Pi$ (0<sup>+</sup>) excited state, laser-induced fluoresc. 0-58309  
 ICl(Br), rot. spectra in millimeter wave region, rot. transitions obs., equilib. const. determ. 0-78607  
 IO, free radical, Ar matrix absorpt. and emission spectra, mol. vibronic states obs., spectroscopic const. determ. 0-83387  
 I<sub>2</sub><sup>+</sup>+He(Ne), energy depend. of collision induced intramolecular energy transfer 0-83470  
 In trihalides, vibr. anal., pot. const. determ., mol., compliance and Coriolis coupling const. calc. 0-95579  
 K salt of  $\beta$ -ketoaldehyde, configurations of anions in solutions studied by IR spectroscopy, H-bond form. 0-87117  
 K+O<sub>2</sub>, mol. target internal motion 0-78697  
 KBr:CN<sup>-</sup>, neutron scatt. studies of (CN)<sup>-</sup> defects 0-92620  
 K<sup>+</sup>CF<sub>3</sub>SeO<sub>2</sub><sup>-</sup>, IR and Raman spectra, normal coordinate anal. for CF<sub>3</sub>SeO<sub>2</sub><sup>-</sup> anion 0-87122  
 Li salt of  $\beta$ -ketoaldehyde, configurations of anions in solutions studied by IR spectroscopy, H-bond form. 0-87117  
 Li<sub>2</sub>F<sub>2</sub>, struct., internuclear-distances and mean amplitude of vibr. determ. by electron diff. 0-69252  
 LiH<sub>2</sub>(LiD<sub>2</sub>)(LiT<sub>2</sub>), pot. surfaces, fundamental freqs. and thermodynamic functions 0-69205  
 Li<sub>2</sub>H(Li<sub>2</sub>D)(Li<sub>2</sub>T), pot. surfaces, fundamental freqs. and thermodynamic functions 0-69205  
 methane 2 $\nu_4$ - $\nu_4$  and  $\nu_2$ + $\nu_4$ - $\nu_2$  hot bands, difference bands 0-63632

## molecular vibration continued

- MgHPO<sub>4</sub>·3H<sub>2</sub>O and MgDPO<sub>4</sub>·3D<sub>2</sub>O, IR absorpt. and Raman spectra, vibr. assignments 0-97257  
 MnHPO<sub>4</sub>·3H<sub>2</sub>O and MnDPO<sub>4</sub>·3D<sub>2</sub>O, IR absorpt. and Raman spectra, vibr. assignments 0-97257  
 MnO, A<sup>2</sup> $\Sigma^+$ -X<sup>6</sup> $\Sigma^+$  electronic transition, rot. and hyperfine struct. 0-74134  
 N<sub>2</sub>, adsorbed on W(100), vibr. spectra, bonding struct., LEED study 0-84387  
 N<sub>2</sub>, CARS, optical Stark effect on vibr., and rot. transitions 0-99512  
 N<sub>2</sub>, desorbed after N atom recomb. on Fe, vibr. energy, electron beam induced fluoresc. 0-61149  
 N<sub>2</sub>, elastic and inelastic electron scatt., state to state cross section 0-78708  
 N<sub>2</sub>, electron scatt., reson. excitation and dissoc. attachment, vibr. state depend. 0-78717  
 N<sub>2</sub> in nonequilibrium gas-dynamic current, vibr.-level populations determ. by Raman scatt. 0-99509  
 N<sub>2</sub>, liq. pure vibr. Raman spectra 0-97262  
 N<sub>2</sub>, liquid, in Kr, methane, and CO, Raman scatt. parameters, high-resolution coherent active spectroscopy 0-66207  
 N<sub>2</sub>, liquid, vibrational depahing, computer simulation, Raman spectra, pair potential effect 0-63863  
 N<sub>2</sub><sup>-</sup>, first <sup>2</sup> $\Pi$ <sub>g</sub> state form. and decay 0-58177  
 N<sub>2</sub><sup>+</sup>, 1 NG emissions from proton aurora, anomalous vibr. distrib. 0-67448  
 N<sub>2</sub><sup>+</sup>, partial photoionisation cross section and photoelectron angular distribution for X<sup>2</sup> $\Sigma^+$  state determ. 0-83429  
 N<sub>2</sub><sup>+</sup> X<sup>2</sup> $\Sigma^+$  state, vibr. states asymmetry parameter and photoelectron spectrum 0-95591  
 N<sub>2</sub><sup>+</sup>+recomb. energy determ. from pot. curves 0-58335  
 N<sub>2</sub>+H<sub>2</sub>+N<sub>2</sub>H<sub>4</sub>, mixtures with nonthermal vibr. excitation of mol. N<sub>2</sub> 0-76545  
 N<sub>2</sub>+O<sub>2</sub>+NO, mixtures with nonthermal vibr. excitation of mol. N<sub>2</sub>, formula for calc. equil. const. 0-76545  
 N<sub>2</sub><sup>+</sup>+He, N<sub>2</sub><sup>+</sup> selectively excited, collisional deactivation 0-83338  
 N<sub>2</sub>F<sub>4</sub>, multiphoton excitation and vibr. energy flow, fluoresc. obs. 0-95673  
 NH<sub>2</sub> radical, mag. hyperfine interactions, zero-point vibr. effects 0-58167  
 NH<sub>2</sub>, vibr. and rot. struct., intensity factors and orbital angular momentum 0-83246  
 NH<sub>3</sub>, vibr. excitation in soft X-ray emission and core ESCA spectra 0-69163  
 NH<sub>3</sub><sup>+</sup> radical, mag. hyperfine interactions, zero-point vibr. effects 0-58167  
 NH<sub>3</sub><sup>+</sup> two-mode Jahn-Teller effect calcs. 0-83297  
 N<sub>2</sub>H<sub>2</sub><sup>+</sup> radical, mag. hyperfine interactions, zero-point vibr. effects 0-58167  
 NH<sub>4</sub><sup>+</sup>CF<sub>3</sub>SeO<sub>2</sub><sup>-</sup>, IR and Raman spectra, normal coordinate anal. for CF<sub>3</sub>SeO<sub>2</sub><sup>-</sup> anion 0-87122  
 NH<sub>4</sub>NO<sub>3</sub>, IR spectra and vibr. bands 0-69144  
 NO, Fourier transform spectra, intensity and self-broadening coeff. meas. 0-102503  
 NO,  $\gamma$  and  $\beta$  system, electronic transition probability 0-106332  
 NO vibr. overtone band, mag. rot. spectrosc. obs. 0-86446  
 NO<sub>2</sub>, fluoresc. spectra and collisional quenching 0-102538  
 N<sub>2</sub>O<sup>+</sup>, dissoc., threshold photoelectron-photoion coincidence obs. 0-87189  
 N<sub>2</sub><sup>+</sup> (A<sup>2</sup> $\Sigma^+$ ), electron impact ionisation cross section 0-78718  
 Na salt of  $\beta$ -ketoaldehydes, configurations of anions in solutions studied by IR spectroscopy, H-bond form. 0-87117  
 NaK, laser induced D<sup>2</sup> $\Pi$ -a<sup>2</sup> $\Sigma$  fluorescence, mol. vibr. 0-87160  
 Ni catalyst, chemisorption of benzene, Raman and vibr. spectra 0-108747  
 O+CS<sub>2</sub>→CS+SO, vibrational distribution of CS, laser-induced fluorescence meas. 0-71895  
 O+H<sub>2</sub>O→OH+OH, energy partitioning 0-101009  
 O-saturated hydrocarbon→OH+alkyl radical, reaction dynamics, mol. beam-laser induced fluoresc. obs. 0-97695  
 O<sub>2</sub>, <sup>3</sup> $\Pi_g$  diabatic Rydberg states, ab initio CI calcs. 0-95554  
 O<sub>2</sub>, electron attachment threshold photoelectron spectra, vibr. excitation 0-83422  
 O<sub>2</sub>, I and I' resonance series, vibr. level populations in autoionisation, photoelectron spectra, bond length determ. 0-91612  
 O<sub>2</sub>, liq. pure vibr. Raman spectra 0-97262  
 O<sub>2</sub>, Rydberg states, <sup>3</sup> $\Sigma_g^-$ , <sup>3</sup> $\Sigma_u^-$ , <sup>1</sup> $\Pi_g$ , <sup>1</sup> $\Sigma_g^+$  symm., ab initio CI study 0-99460  
 O<sub>3</sub>, line position and intensities of 2 $\nu_3$ ,  $\nu_1$ + $\nu_2$  bands 0-87181  
 O<sub>3</sub>, photodissoc. cross section, vibr. excitation effects obs. 0-95696  
 O<sub>3</sub>, UV absorpt. spectrum, Hartley continuum, IR laser induced changes 0-95639  
 OCS, vibr. energy transfer map 0-99560  
<sup>16</sup>O<sup>12</sup>C<sup>34</sup>S and <sup>18</sup>O<sup>13</sup>C<sup>34</sup>S, IR spectra,  $\nu_3$  band anal. 0-95620  
 OH, fundamental vibr. band, mag. rot. spectrosc. obs. 0-86446  
 OH+H<sub>2</sub>→H<sub>2</sub>O+H, reaction product vibr. distrib., quasiclassical trajectory, calcs. 0-85162  
 OH(A<sup>2</sup> $\Sigma^+$ →X<sup>2</sup> $\Pi$ ) yields from H<sub>2</sub>O photodissoc. 0-71927  
 ONCl, vibr. freq., anharmonic ab initio/empirical pot. energy functions 0-99457  
 OPBr<sub>3</sub>, mol. struct., electron diff. and spectroscopic vibr. amplitude 0-58387  
 PN, absorpt. and emission spectra, electronic transition and vibr. obs. 0-91573  
 Rb<sup>+</sup>CF<sub>3</sub>SeO<sub>2</sub><sup>-</sup>, IR and Raman spectra, normal coordinate anal. for CF<sub>3</sub>SeO<sub>2</sub><sup>-</sup> anion 0-87122  
 S<sub>2</sub>, matrix-isolated, B<sup>2</sup> $\Sigma_u^-$  predissoc., relax. processes 0-58329  
 S<sub>2</sub> vibrational constants, UV absorption and fluorescence spectrosc. of S<sub>x</sub> vapour, x=3 to 8 0-78631  
 SF<sub>6</sub>, Doppler-limited spectroscopy, of 3 $\nu_3$  band 0-58244  
 SF<sub>6</sub>, IR multiple-photon excited molecules, Raman spectroscopy 0-74207  
 SF<sub>6</sub>, multiphoton dissoc. by mol. beam method, energy distribution meas. by time-of-flight spectra, dissoc. dynamics 0-78670  
 SF<sub>6</sub>, partial saturation of  $\nu_3$  ladder in IR absorpt., rate process model 0-58645  
 SF<sub>6</sub>, vibr. coupling in collision-induced Raman scatt. 0-83373  
 SF<sub>6</sub>+Si(surface), IR laser induced reaction, mol. vibr. and mol. dissoc. obs. 0-93798  
 SO<sub>2</sub>, IR multiphoton excitations and inverse electronic relax., mol. vibr. and fluoresc. 0-106349  
 SPBr<sub>3</sub>, mol. struct., electron diff. and spectroscopic vibr. amplitude 0-58387



molecular vibration continued

Se<sub>2</sub>, b<sup>1</sup>Σ<sup>+</sup>→X<sup>2</sup>Σ<sup>+</sup> near IR emission obs. 0-91556  
SeF<sub>6</sub>, in Kr matrix, temp. reversible IR spectral changes, site struct. dynamics 0-102505  
SeO, b<sup>1</sup>Σ<sup>+</sup>→X<sup>2</sup>Σ<sup>+</sup> near IR emission obs. 0-91556  
SeS, b<sup>1</sup>Σ<sup>+</sup>→X<sup>2</sup>Σ<sup>+</sup> near IR emission obs. 0-91556  
Si<sub>4</sub>, integrated IR band intensities and transition moments 0-95611  
SiH<sub>4</sub>, radical, hyperfine coupling consts., vibr. depend., ab initio calcs. 0-87150  
SIS, chemiluminescent flame spectra, electronic states and rot. struct. obs., vibr. assignments, Franck-Condon factors determ. 0-85179  
SrI, low-lying electronic states, vibr. anal. 0-106315  
TOT, vibr. intensities, ab initio and empirical calcs. 0-78592  
TOT, vibr. intensities, ab initio and empirical calcs., band strengths 0-78593  
Te<sub>2</sub>, BO<sub>2</sub><sup>+</sup>→b<sup>1</sup>Σ<sub>g</sub><sup>+</sup> system, transition assignment, IR and visible spectra obs. 0-58298  
TeOCl<sub>2</sub>, from TeO<sub>2</sub>Cl<sub>2</sub> pyrolysis, normal coord. anal. 0-81306  
Ti<sub>2</sub>F<sub>2</sub>(Cl<sub>2</sub>), assignment of vibr. Raman and IR spectra bands 0-58268  
W (100), H adsorbate low energy electron vibrational excitation 0-84375  
Xe+Cl<sub>2</sub>, classical trajectory calcs., energy threshold for collision induced dissociation, 0-95709  
XeCl+HCl (inert gas atom), ground state destruction, quenching rate consts. meas. 0-63758  
Xe<sub>2</sub><sup>+</sup>, synchrotron radiation excited, time resolved spectroscopy 0-69092

molecular vibration calculations

anharmonically coupled oscills., time depend. Hartree theory, susceptibility, absorpt. and Raman spectrum 0-58241  
aromatic compounds, out-of-plane mol. vibrs., force field approx. calcs. 0-91538  
aromatic hydrocarbons, vibronic calcs. 0-58238  
benzene, out-of-plane mol. vibrs., force field approx. calcs. 0-58239  
borazines, substituted, Urey Bradley force field, pot. energy consts. 0-78588  
bound continuum vibr. transitions, Franck-Condon matrix elements calcs. 0-69191  
composite particle, vibr. amplitude and vibr.-rot. anal. 0-74158  
coupled oscillator system, SCF-state interaction method 0-58239  
cyclopentanone, n-π\* transition, vibr. band intensities 0-74116  
diatomic molecule, vibr. energies and functions, cubic splines method calcs. 0-78594  
diatomic molecules, dipole matrix elements for vibrational transitions, numerical calc. 0-95594  
diatomic molecules, r-centroid method appl. 0-102500  
energy deposition by multiple IR photon absorpt. 0-66833  
first row elements, split-valence basis set, mol. vibr. and mol. moment calcs. 0-69063  
Group IIIA metal tetrahalide ions, vibr. anal. 0-63608  
Group IV tetrabromides, intramol. force fields and mean vibr. amplitudes 0-106316  
harmonic and Morse oscillator freq. change influence on Franck-Condon factors 0-106312  
hexahalo ions, octahedral, mol. consts. calcs. 0-106317  
hexaoxy ions, octahedral, mol. consts. calcs. 0-106317  
intensity calcs., CNDO/2 method with extended basis set 0-91445  
intramolecular dynamics, random coupling model, math. approach 0-58308  
intramolecular dynamics, random coupling model, multiphoton excitation, kinetic eqns. 0-63700  
methane-d<sub>4</sub> (*Russian*) 0-91540  
methyl ethyl ether, charact. vibrs., isomer and isotope effects, rel. to reverse spectral problem 0-63613  
methylene glycol-(d<sub>4</sub>)=formaldehyde-(d<sub>2</sub>)+H<sub>2</sub>O(D<sub>2</sub>O) Raman spectra and normal vibr. 0-58271  
mol. consts. and mean vibr. amplitudes calcs. 0-106318  
naphthalene, out-of-plane mol. vibrs., force field approx. calcs. 0-91538  
organic molecules, small, harmonic force consts., vibr. freqs., integrated intensities, MINDO/3 method 0-58411  
phase and population relax., semigroup formalism 0-78519  
polyatomic excited molecules, vibrational energy exchange (*Russian*) 0-91539  
polyatomic force fields, Ohwada's pairwise interaction model 0-106321  
polyatomic molecule, atomic force correlation functions for determ. vibr. relax. rates, role of mol. symmetry 0-83337  
polyatomic molecule, intramolecular coord. relax., generalised classical theory 0-78589  
polyatomic molecule dissociation in IR laser field (*Chinese*) 0-106363  
polyvinylidene chloride, normal vibr. analysis using conform. model 0-83529  
predissociation, vibrational, in H-bonded complexes 0-61078  
quartic anharmonic oscillator, semiclassical and quasiclassical particle function 0-99434  
resonant Raman spectra, overtone intensity distrib., effect of excited electronic state 0-87128  
reverse spectral problem, charact. vibrs. effects calcs. 0-63613  
superposition state in regular and irregular spectrum, time evolution, intramolecular dynamics 0-83335  
tetra-glycine, cyclic, mol. polaris. and diamag. suscept. calcs. 0-63858  
tetra-L-alanine, cyclic, mol. polaris. and diamag. suscept. calcs. 0-63858  
tetrafluoromethane, mol. consts. and mean vibr. amplitudes calcs. 0-106318  
triatomic inorganic mols., harmonic force consts., vibr. freqs., integrated intensities, MINDO/3 method 0-58411  
XY<sub>2</sub> bent symmetrical molecules, Coriolis coupling consts., centrifugal distortion consts. 0-58236  
XY<sub>2</sub>(O<sub>2</sub>) octahedral system, F-(G-) matrix elements setting-up, transformation rules (*German*) 0-58242  
Ar, Hulburt-Hirschfelder pot. function 0-63612  
CCO radical, heat of form. calc., geometries excitation energies and vibr. freq. calc. using POL-CI wave functions 0-89512  
CF<sub>3</sub>S, mol. consts., kinetic consts. method calcs. 0-58235  
CF<sub>3</sub>Se, mol. consts., kinetics consts. method calcs. 0-58235  
C<sub>2</sub>H<sub>2</sub> species formed in chemisorption of ethylene on Pt, vibr. anal. 0-61150  
C<sub>2</sub>N<sub>2</sub>, 2ν<sub>2</sub> band overtones, Raman intensities, bond polarisability theory 0-63639  
CO, vibrational transitions dipole matrix elements, numerical calc. 0-95594  
CO+H<sup>+</sup>, vibr. excitation calc., close coupling and sudden approx. 0-78561

molecular vibration calculations continued

CrCl<sub>2</sub>, mol. consts. and mean vibr. amplitudes calcs. 0-106318  
Cu complex, Cu(NH<sub>3</sub>)<sub>2</sub>(NCX)<sub>2</sub>, X=O, S, electronic struct., stereochem. 0-58156  
HCP, force fields and force consts. of electronically excited states 0-69116  
Hg complex, methylethynylmercury(II)(-d<sub>1</sub>, -d<sub>3</sub>, -d<sub>4</sub>), vibr. spectra and normal coord. calcs. 0-58259  
Li<sub>2</sub>F<sub>2</sub>, struct., force fields and normal mode freqs., ab initio calcs. 0-83260  
N<sub>2</sub><sup>2+</sup>, low-lying electronic states, pot. energy curves calcs. by SCF technique, vibr. and ionisation consts. 0-69091  
NH<sub>3</sub>, inversion spectrum collisional line broadening, general theory 0-87184  
NH<sub>4</sub><sup>+</sup>, mol. consts. and mean vibr. amplitudes calcs. 0-106318  
N<sub>2</sub>O<sup>+</sup>, force fields and force const. of electronically excited states 0-69116  
NiCu molecule, electronic states determ. by ab initio HF and CI methods 0-69087  
SF<sub>6</sub>, gas, excited molecule vibr. translational relaxation, nonlinear processes (*Russian*) 0-91540  
Te<sub>4</sub><sup>2+</sup>, pseudopot. SCF-MO calcs., spectrum assignments 0-83269

molecular vibration in solids

L-alanine and DL-alanine, cryst., Raman band intensities of local group modes 0-93298  
alkali halides, molecular centre symm. groups, roto-vibronic spectra (*Russian*) 0-88283  
benzene-hexa-n-hexanoate, phase transitions and mesophase form., sp. ht. and IR spectra, 13 to 393K 0-79955  
bond anharmonicities, Gruneisen parameters and pressure-induced frequency shifts 0-107397  
calcium dipicolinate trihydrate, IR and Raman spectra, isotopic frequency shift, mol. vibr. obs., point groups determ. 0-89001  
chloro(ethyl)silanes and its C derivatives, solid, Raman spectra, mol. vibr. and rot. isomerism 0-87134  
trans-1,4-chlorobromocyclohexane, liquid, crystalline and amorphous state, conformation and vibr. spectra, IR obs. 0-60568  
trans-1,4-chloriodocyclohexane, liquid, crystalline and amorphous state, conformation and vibr. spectra, IR obs. 0-60568  
chlorophyll, and related mols., in solid solns., fine-structured vibronic spectra under tunable dye laser excitation (*Russian*) 0-74164  
condensed media, vibrational relaxation studied by picosecond or Raman spectrosc., review 0-80797  
cubic crystal, Jahn-Teller effect, soft mode influence 0-59937  
cyclopentylamine, vibr. spectra and struct. 0-102516  
dense media, absorpt. profiles of mol. transitions 0-59589  
diatomic molecule in crystal, rate of radiationless electronic transitions 0-93373  
diatomic molecules, shortening of energy relax. time of excited mol. vibr. in dense medium by form. of H-bonds 0-91553  
2,2-dichlorobutane, liquid and solid, vibr. spectra, IR and Raman obs. 0-60567  
m-dinitrobenzene, oriented film, intermol. vibr. coupling, polarised IR spectra 0-97264  
dipicolinic acid, IR and Raman spectra, isotopic frequency shift, mol. vibr. obs., point groups determ. 0-89001  
formic acid, cryst., H bonded, IR spectrum computer simulation 0-97253  
furan, cryst., low freq. vibr. spectrum, temp. depend., 12 to 253K 0-84743  
X-glycine, cryst., Raman band intensities of local group modes 0-93298  
graphite-HSO<sub>3</sub>F intercalation compound, Raman spectral study (*French*) 0-60581  
ice, O-H and O-D bond stretching vibrs., Raman spectra at atmospheric press. 0-66166  
intra-site vibration effects on elec. cond. in disordered Hubbard model 0-107775  
malononitrile, cryst., phase transitions, Raman and IR obs. 0-88980  
MBBA, Raman spectra in cryst., frozen glassy, and liq. cryst. states 0-60601  
metal surface, mol. vibr. energy transfer, classical EM theory 0-96806  
methanol-CO<sub>2</sub>-H<sub>2</sub>O-NH<sub>3</sub> solid mixture vibr. modes, IR spectra 0-90504  
methoxydifluorophosphine-d<sub>0</sub> and -d<sub>3</sub>, solid, IR and Raman spectra, mol. vibr. and struct. obs. 0-87103  
N-methylacetamide, solid, Fermi resons. 0-97266  
neopentane, diamond force const., rel. to crystal elastic consts., Raman freq., bulk compressibility and freq. assignments 0-65183  
nonradiative electron transitions in crystal, impurity molecule vibr. 0-103645  
phase and population relax., semigroup formalism 0-78519  
phenanthrene, two-photon excitation spectra, exciton-phonon and intramol. vibronic coupling 0-84774  
polar semiconductor crystalline thin films, surface vibr. states, IR absorpt. spectra obs. (*Russian*) 0-60606  
Polaroid K, oriented analogue of polyacetylene, reson. Raman spectroscopy 0-66208  
polyacetylene:I, pure and doped, reson. Raman spectroscopy 0-66208  
radical radiation formation in solid organic compounds 0-85201  
scheelite crystals, Davydov splitting of vibr. levels, short range interaction 0-71418  
semicarbazide hydrochloride, vibr. spectra, normal coord. anal. 0-58255  
semicarbazide-d<sub>0</sub>, -d<sub>2</sub>, vibr. spectra, normal coord. anal. 0-58255  
Shpol'skii multisite luminesc. spectrum deconvolution, vibr. struct. anal. 0-58304  
solid phase chemical reactions, low temp. and fast, mol. motion effect 0-97681  
talc, vibr. mode assignments, Raman microprobe spectra 0-88977  
TCNQ salt, n-methyl-n-ethylmorpholinium, unpaired electron states, IR refl. study 0-75491  
tetrabromomethane, monoclinic monocryst., polarised Raman spectra (*French*) 0-93302  
tetracene, unrelaxed fluoresc., direct picosecond obs. 0-89046  
tetramethyl-1,3-cyclobutanedione-h<sub>12</sub> and -d<sub>12</sub>, visible spectra, nπ\* transitions obs., mol. vibr. 0-97297  
Toda lattice, excitation spectrum, molecular dynamics study 0-105588  
toluene-sulphonate-diacyetylene, thermal polymerisation, near IR absorpt. and low lying states obs. 0-71399  
Ag<sub>2</sub>HgI<sub>4</sub>, Raman line shape and ionic cond., coupled mode model 0-66171  
Ar:O<sub>2</sub> (6%) cryst., vibr. Raman spectra 0-60558  
CO, solid, CO laser excited, strong vibr. population inversion 0-58547

**molecular vibration in solids continued**

- CO<sub>2</sub>, solid, Fermi reson. press. tuning, Raman spectra 0-93293  
 CS<sub>2</sub>, second order Raman spectrum in condensed phase 0-93299  
 Cs<sub>10</sub>-Sr(PO<sub>4</sub>)<sub>6</sub>(OH)<sub>2</sub>, continuous cation migration, IR spectra study 0-93297  
 Ce<sub>2</sub>(SO<sub>4</sub>)<sub>3</sub>·9H<sub>2</sub>O(D<sub>2</sub>O), polarised Raman spectra, vibr. props. and role of lattice H<sub>2</sub>O 0-66201  
 Co<sub>2</sub>SiO<sub>4</sub>, IR absorpt. spectra 0-60591  
 CsHg(CN)<sub>3</sub>, CN and HgC stretching vibrations and HgCN bending vibration assignments 0-69140  
 Cs<sub>2</sub>NaErCl<sub>6</sub>, mag. susceptibility and IR and Raman spectra meas., crystal field splitting determ. 0-100652  
 Cs<sub>2</sub>SiF<sub>6</sub>:Mn<sup>2+</sup>, IR absorpt. band, electron-vibr. effect 0-108238  
 FeCl<sub>3</sub>, intramolecular force fields, compliance const. and vibr. amplitudes 0-58234  
 FeSiO<sub>4</sub>, spinel, IR absorpt. spectra 0-60591  
 GaCl<sub>3</sub>(Br)<sub>3</sub>(I)<sub>3</sub>, intramolecular force fields, compliance const. and vibr. amplitudes 0-58234  
 B-Gd<sub>2</sub>O<sub>3</sub>, monoclinic single cryst., Raman spectrum 0-103953  
 p-H<sub>2</sub>, solid, time-resolved CARS, disorder effects on coherent vibr. states 0-93342  
 HAl<sub>11</sub>O<sub>17</sub>, H β-alumina, IR absorpt. study 0-100655  
 InCl<sub>3</sub>, intramolecular force fields, compliance const. and vibr. amplitudes 0-58234  
 KCN, dynamics of CN<sup>-</sup> ions near phase transitions at 83K 0-80717  
 KDy(MoO<sub>4</sub>)<sub>2</sub>, polarised IR and Raman struct., <sup>92</sup>Mo/<sup>100</sup>Mo isotope effect 0-108198  
 KTaO<sub>3</sub>:OH<sup>-</sup>(OD<sup>-</sup>)(OT<sup>-</sup>), IR spectra, spectrosc. const. 0-100671  
 Li<sub>2</sub>SO<sub>4</sub>·H<sub>2</sub>O, far IR spectra, H<sub>2</sub>O flipping motion, lattice modes 0-84258  
 Mn(CO)<sub>5</sub> Br-Re(CO)<sub>5</sub>Br, polycryst., ν(CO) vibr. intermol. Raman intensity transfer 0-60564  
 β-N<sub>2</sub> cryst., vibr. Raman spectra 0-60558  
 N<sub>2</sub> matrix N-N stretching vibr., IR activation, guest mol. depend. 0-60570  
 α-N<sub>2</sub>, solid, time-resolved CARS, disorder effects on coherent vibr. states 0-93342  
 α-N<sub>2</sub>, temp. depend. of IR spectra, Gruneisen parameters determ. 0-84730  
 ND<sub>2</sub>I, Raman spectrum, press. effects 0-97261  
 (NH<sub>4</sub>)<sub>2</sub>GeF<sub>6</sub>, cryst., highly bent H bonds, IR spectrosc. investig. 0-93292  
 NH<sub>4</sub>I, Raman spectrum, press. effects 0-97261  
 NH(ND) X<sup>2</sup>Σ<sup>-</sup>, in inert gas solid, vibr. relax., matrix and isotope effects 0-95713  
 NH<sub>3</sub>(ND<sub>3</sub>) in solid Ar, UV absorption spectra, temp. depend. of matrix spectra 0-63652  
 (NH<sub>4</sub>)<sub>2</sub>SiF<sub>6</sub>, cryst., highly bent H bonds, IR spectrosc. investig. 0-93292  
 (NH<sub>4</sub>)<sub>2</sub>SnF<sub>6</sub>, cryst., highly bent H bonds, IR spectrosc. investig. 0-93292  
 (NH<sub>4</sub>)<sub>2</sub>TiF<sub>6</sub>, cryst., highly bent H bonds, IR spectrosc. investig. 0-93292  
 NaF:U, luminesc. spectra, Vibr. struct. 0-80840  
 Na<sub>2</sub>O·Li<sub>2</sub>O·β-Al<sub>2</sub>O<sub>3</sub>·H<sub>2</sub>O, water mol. vibrs., IR and Raman spectra 0-89006  
 Na<sub>2</sub>SbS<sub>4</sub>, vibrational spectra, internal SbS<sub>4</sub> vibr. assignments 0-66199  
 Na<sub>2</sub>SbS<sub>4</sub>·9H<sub>2</sub>O(D<sub>2</sub>O), vibrational spectra, internal SbS<sub>4</sub> and H<sub>2</sub>O(D<sub>2</sub>O) vibr. assignments 0-66199  
 γ-O<sub>2</sub> cryst., vibr. Raman spectra 0-60558

**molecular vibrational energy transfer** *see molecular rotational-vibrational energy transfer***molecular vibrational relaxation** *see molecular rotational-vibrational energy transfer***molecular vibrational states** *see molecular vibration***molecular vibronic states**

- aromatic hydrocarbons, sequential coupling 0-58297  
 aromatic hydrocarbons, vibronic calcs. 0-58238  
 benzene, first-ionisation Rydberg spectrum assignment via Jahn-Teller splitting 0-69155  
 biphenyl polyenes, vibronic states, quasi-linear spectra (*Russian*) 0-95598  
 p-bromofluorobenzene, UV electronic absorption spectrum, band shape and molecular geometry 0-87147  
 β-carotene, excitation profile of ν<sub>2</sub> line in resonance Raman spectrum, solvent effects 0-74173  
 chlorophyll, and related mols., in solid solns., fine-structured vibronic spectra under tunable dye laser excitation (*Russian*) 0-74164  
 chloroquinolines, photoph. behaviour, substituent and solvent effects 0-106342  
 cyclopentanone, n-π\* transition, vibr. band intensities 0-74116  
 diphenylpolyene molecules, excited electronic states, vibronic mixing, wave functions, method of fragments anal. 0-63615  
 fluorobenzene, multiphoton ionisation spectrum in one-photon wavelength region 0-63727  
 formaldehyde, sequential coupling 0-58297  
 formaldehyde-d<sub>0</sub>(-d<sub>2</sub>), S<sub>1</sub> single rot. level lifetimes, isotope, elec. field and vibr. state depend. 0-78655  
 β-hydroxy acrolein, lower excited states, electronic struct. and H-bonding, ab initio SCF and CI calcs., photochemical mechanism 0-83278  
 metalloporphyrin, low symmetry environment, Raman excitation spectra and absorpt. spectrum 0-74172  
 methoxy, Jahn-Teller induced rovibronic effect, nuclear spin-electron spin hyperfine Hamiltonian 0-83298  
 methoxy radical and deuterate, vibronic level fluoresc. spectrum 0-58305  
 naphthalene molecule in durene and xylene crystals, vibronic interactions 0-84755  
 nickel-octaethylporphyrin, in benzene soln., reson. CARS and CSRS line shapes 0-74432  
 2,2 paracyclophane, dimer vibration influence on emission spectrum 0-69133  
 pentacene in naphthalene (p-terphenyl), mol. mixed crystals, optical dephasing and vibronic relax. 0-95957  
 phenanthrene, two-photon excitation spectra, exciton-phonon and intramol. vibronic coupling 0-84774  
 porphyrin free base, vibr. and normal mode anal. 0-69122  
 porphine-d<sub>4</sub>, vibronic transitions, polaris. determ. 0-63614  
 propenal, rovibronic populations, collisionless IR multiphoton spectra, energy deposition, photoacoustic determ. 0-83354  
 pyrimidine, bi-exponential decay, methylation and vibr. excitation, proximity effects 0-78641  
 quasi-linear spectra and vibronic states of molecules with end phenyl rings (*Russian*) 0-95597  
 radiationless transitions, synchrotron radiation obs. 0-63706  
 radiative transitions, proximity effects, role of vibronic coupling and static crystal field interactions model 0-69126

**molecular vibronic states continued**

- rhodamine 6G dye laser, induced radiation spectral characts., effect of vibr. relax. 0-64008  
 thiocarbonyl chlorofluoride, second excited singlet state emission spectroscopy, resonance fluorescence obs. 0-69158  
 thiophosgene, second excited singlet state emission spectroscopy, Franck-Condon anal. 0-69157  
 thiophosgene, vibronic anal. of electronic transition, inversion doubling splittings obs. 0-83388  
 triatomic mols., Renner-Teller effect, orbital angular momentum 0-78513  
 trichlorobenzene cation, selectively excited wavelength resolved emission spectra 0-87136  
 trichlorobenzene cations, Jahn-Teller distortions, quadratic and mode mixing effects., distortion geometry determ. 0-91462  
 symtrifluorobenzene cation, Jahn-Teller effects, intermode interactions and intensity anomalies 0-78553  
 sym-trifluorobenzene cation, Jahn-Teller effects, quadrupole coupling 0-78554  
 trifluorobenzene cation, selectively excited wavelength resolved emission spectra 0-87136  
 trifluorobenzene cations, Jahn-Teller distortions, quadratic and mode mixing effects., distortion geometry determ. 0-91462  
 two state two mode vibronic coupling model, Born-Oppenheimer and crude adiabatic perturbation methods 0-87036  
 N<sub>2</sub>-undecylumiflavin, high resolution fluoresc. and excitation spectroscopy, vibronic transitions obs. 0-78639  
 Ar<sup>+</sup>+H, assoc. ionis., rovibronic struct. in electron energy spectrum 0-106380  
 BO<sub>2</sub>, Π vibronic states, laser induced fluoresc. obs. 0-58301  
 BrO, free radical, Ar matrix absorpt. spectra, mol. vibronic states obs., spectroscopic const. determ. 0-83387  
 C<sub>3</sub>, A<sup>1</sup>Π<sub>u</sub> state, orbital angular momentum 0-78514  
 CHF radical, A<sup>1</sup>A''-X<sup>1</sup>A' transition, laser induced fluoresc. 0-95660  
 CN free radical, A<sup>2</sup>Π-X<sup>2</sup>Σ<sup>+</sup> Red system, perturbation analysis 0-87247  
 ClO, free radical, Ar matrix absorpt. spectra, mol. vibronic states obs., spectroscopic const. determ. 0-83387  
 CrO<sub>2</sub>Cl<sub>2</sub>, multiphoton induced inverse electronic relax. 0-66836  
 Cs<sub>2</sub>MX<sub>6</sub>(M=Se, Te, X=Cl, Br), Γ<sub>4</sub> (<sup>3</sup>T<sub>1g</sub>) state, Jahn-Teller effect, luminesc. obs. 0-60650  
 H<sub>2</sub>+e<sup>-</sup>→H<sub>2</sub><sup>+</sup>+e<sup>-</sup>, Gaussian basis Glauber approx., elastic and vibrorotational excitation cross sections 0-58399  
 HNO A<sup>1</sup>A'' excited state dipole moment, optical-optical double reson. Stark spectrosc. obs. 0-106337  
 H<sub>2</sub>O<sup>+</sup>, ab initio potential energy surface study by CI techniques, equilibrium conform. determ., mol. dissc. pathways 0-78550  
 H<sub>2</sub>O<sup>+</sup>-vibr. and rot. struct., intensity factors and orbital angular momentum 0-83246  
 HSO radical, Doppler-limited dye laser excitation spectroscopy, rot., distortion and spin-rot. interaction const. determ. 0-83383  
 IO, free radical, Ar matrix absorpt. and emission spectra, mol. vibronic states obs., spectroscopic const. determ. 0-83387  
 K<sub>2</sub>, supersonic mol. beam, isotope selective two-step photoionisation study 0-74203  
 NH<sub>2</sub>, vibr. and rot. struct., intensity factors and orbital angular momentum 0-83246  
 N<sub>2</sub>O, photoelectron spectrum, vibronic interaction and autoionis. effects 0-95680  
 Ne<sup>+</sup>+H, assoc. ionis., rovibronic struct. in electron energy spectrum 0-106380  
 α-O<sub>2</sub>, antiferromagnetic polycrystal, splitting of exciton absorpt. lines in mag. field (*Russian*) 0-103943  
 SO<sub>2</sub>, single vibronic level fluoresc. spectra 0-91597  
 SO<sub>2</sub>F, dye laser excitation of vibr. levels of upper electronic state, mol. fluoresc. meas. 0-83402  
 UF<sub>6</sub>, matrix isolated, vibronic fine struct. in fluoresc. spectrum 0-83406  
 XeF<sub>6</sub> molecules with Jahn-Teller pseudo-effect, ang. depend. of inelastic scatt. of electrons 0-69246

**molecular weight***see also mass spectra; molecular weight determination*

- adsorbed polymer chains, surface restricted self avoiding walks span, mol. weight depend. 0-65360  
 cellulose fibre, gamma-irrad., and storage effects on props. (*Russian*) 0-61121  
 dextran fractions, production, characterisation and solution properties 0-59368  
 distribution function, polynomial series expansion 0-58116  
 macromolecules, molecular structure, conformation and properties 0-63874  
 PMMA, neutron and gamma irradiation effects 0-66839  
 poly-4,4-diphenylphthalateinterphthalamide, mol. mass distrib., sedimentation and fractionation method meas. (*Russian*) 0-71957  
 polyacrylamide, aq. soln., thermodynamic props., light scatt. obs. (*Russian*) 0-71439  
 polyacrylamide, high mol. wt., prep. by electron beam irradiation 0-76222  
 polycarbonate, γ-irradiated, dielec. behaviour and glass transition 0-97182  
 polyethylene, high-density, solid-state coextrusion, mol. wt. distrib. effect 0-104212  
 polyethylene, linear, draw temp. and mol. wt. effect on draw ratio and Young's modulus 0-84998  
 polyheteroarylenes, linear, conform. and struct., statistical calcs. (*Russian*) 0-69284  
 polymer, molecular weight ratio, number-average: weight-average, polydispersity 0-74274  
 polymer, polydisperse, glass transition temp., mol. mass depend. 0-92656  
 polymer solution, sedimentation rates for low mol. wt. materials in dilute region 0-108756  
 polymer solutions, mod. wt. depend. of partial specific vol. 0-99594  
 polymer structure and optical behaviour 0-106583  
 polymers, adaptive control of molecular weight distribution 0-58434  
 polymers, multi-functional, mol. wt. distrib. 0-83531  
 polymers, polydisperse, mol. wt. distrib. correl. with props. (*Russian*) 0-69286  
 polymers in mixed solvents, preferential adsorpt. coeff. rel. to mol. dimens. 0-103237  
 polyolefine, liq., memory effect 0-103268  
 polyolefins, ultra-high modulus, production by tensile drawing and hydrostatic extrusion 0-81022  
 polypropylene, (Moplen) influence of temp. and mol. wt. on high speed fracture mechanics 0-76341



# molecular weight continued

polypropylene, ultrahigh modulus, tensile drawing, mol. wt. effect 0-104211  
 polystyrene, in solns., intrinsic viscosity rel. to mol. wt., unperturbed dimensions 0-65268  
 polystyrene in benzene or cyclohexane, zero shear-rate intrinsic viscosities 0-75376  
 polystyrene-methylcyclohexane, coexistence curve, comparison obs. and free energy calc. 0-88323  
 polystyrene-methylcyclohexane, coexistence curves, range of simple scaling and critical exponents 0-88322  
 polystyrene, neutron and gamma-irradiation effects 0-66839  
 polyvinylbutyral, elec. and dielec. props., mol. wt. effect on charge storage 0-97192

# molecular weight determination

*see also mass spectra*  
 agarose gel immunoelectrophoretic determination of molecular weights of tubulin antigens 0-67313  
 gel permeation chromatography, calibration, appl. to polycarbonate 0-58424  
 mass spectroscopy, peak matching for known mass difference ion unit mass determ. 0-77906  
 polycarbonate, bisphenol-A, mol. wt. determ. using gel permeation chromatography 0-58424  
 polyethylene, photodegradation mechanism, from yield strength, elongation and mol. wt. studies (*Japanese*) 0-76311  
 polymers, struct. determ. from elastomeric parameters 0-64923  
 polysulfonamide, optically active, synthesised by interfacial polycondensation, mol. wt. determ. 0-99595  
 protein molecular weight and ultrastruct. determ. in STEM 0-85562  
 proteins, mol. wt. determ. by monolayer surface press. meas. technique 0-89526

# molecule-atom collisions *see atom-molecule collisions*

# molecule-ion collisions *see ion-molecule collisions*

# molecule-ion reactions *see ion-molecule reactions*

# molecule-molecule reactions

*see also molecular rotational-vibrational energy transfer*  
 anthracenes, exciplex form. with amines, form. kinetics and luminesc. props. 0-66792  
 bicyclobutyl+methylene, products decomposition, competitive channels and vibr. relax. 0-83336  
 biomolecules+chloranil, charge transfer interaction, equilb. const., enthalpy and entropy determ., mol. polarisability 0-89708  
 cellulose fibre hydrolysability increase on gamma-irrad. (*Russian*) 0-61121  
 enhancement by collision induced absorpt. of IR laser radiation 0-66798  
 ethylene+HBr, low temp. chain hydrobromination, kinetics and mechanism 0-93735  
 formaldehyde+ClO radical, expt. showing no reactivity, stratospheric implications 0-90119  
 methoxy+NO, reaction rate upper limit, laser induced fluoresc. 0-85200  
 methoxy radical+NO, reaction rate meas. 0-76534  
 polyatomic excited molecules, vibrational energy exchange (*Russian*) 0-91539  
 R-matrix propag., amplitude density function and invariant bedding methods 0-91622  
 trifluoroacetophenone+dimethoxy benzene, in acetonitrile photoelectron, nuclear spin polarisation, criterion for triplet-Overhauser mechanism 0-69168  
 two component bimolecular reaction system, stable limit cycles, choice of chem. pot. differences 0-66779  
 $C_2+O_2$ ,  $C_2(X^2\Sigma^+)$  and  $C_2(a^1\Pi_u)$  intersystem crossing and free radical kinetics 0-95668  
 CCl(X<sup>2</sup>II)+methylhalosilanes, reaction rate const. determ. by kinetic absorpt. spectroscopy 0-97683  
 $CO^++NO \rightarrow CO_2^++N$ , crossed beam study 0-104436  
 $C_2O+NO(O_2)$  (isobutene), absolute reaction rate consts. meas. by laser induced fluoresc. 0-93738  
 $CO(1)+CO(v) \rightarrow CO(0)+CO(v+1)$ , vibr. energy accumulation, reaction rate anal. 0-78692  
 $CS_2^++CS_2 \rightarrow CS_3^++CS+e^-$ , chemiionisation, mol. beam photoionisation 0-76495  
 ClF+SF<sub>4</sub> (perfluoroethane)(Xe), thermal and photochem. reactions investig. 0-61117  
 CrO<sub>2</sub>Cl<sub>2</sub>+carbon tetrachloride+acetone, intermediate complex form., electronic spectra 0-61075  
 H<sub>2</sub>+CO<sub>2</sub>, exponential gap relation, rot. inelasticity 0-78693  
 H<sub>2</sub>+D<sub>2</sub>, reactive and inelastic scatt., semiempirical pot. energy surfaces calcs. 0-74140  
 H<sub>2</sub>+F<sub>2</sub>, branched chain reaction, role of thermally nonequilibrium atoms and molecules 0-76507  
 H<sub>2</sub>+H<sub>2</sub>, exponential gap relation, rot. inelasticity 0-78693  
 H<sub>2</sub>+N<sub>2</sub>O, HO radical form. on Pt surface, laser-induced fluoresc. obs. 0-108738  
 H<sub>2</sub>+H<sub>2</sub>, hexadecapolar U-branch transitions in IR fundamental band 0-91631  
 HBr+CO(CO<sub>2</sub>)(N<sub>2</sub>O)(NO)(N<sub>2</sub>O)(O<sub>2</sub>), rate consts. for vibr. energy transfer meas. using laser induced fluorescence technique 0-87206  
 HD(v=5)+HD(v=0)→H<sub>2</sub>+D<sub>2</sub>, mol. H<sub>2</sub> exchange, reaction mechanism 0-85167  
 HN<sub>3</sub>+NH(NH<sub>3</sub>), rate consts. from HN<sub>3</sub> UV photolysis data 0-101027  
 HO<sub>2</sub>+ClO, reaction product distrib. 0-72586  
 HO<sub>2</sub>+O<sub>3</sub>, reaction kinetics, laser mag. reson. obs. 0-102528  
 H<sub>2</sub>SO<sub>4</sub>+atmospheric species, collisional reaction probabilities rel. to H<sub>2</sub>SO<sub>4</sub> aerosols as tropospheric sinks 0-72612  
 He<sup>3</sup>, diatom, optical absorpt. spectra and kinetic behaviour 0-95635  
 HgBr<sub>2</sub>+N<sub>2</sub>(A<sup>2</sup>Σ<sup>+</sup>), dissoci. excitation 0-63774  
 I<sub>2</sub>+acetylene, laser-induced 1,2-diiodoethylene form., isomerisation 0-85157  
 N<sub>2</sub>+HgX<sub>2</sub> (X=halide), A<sup>2</sup>Σ<sup>+</sup>-state quenching obs. 0-108693  
 N<sub>2</sub>+methane, N<sub>2</sub> fixation, catalytic processes in non-equilibrium plasma chemical reactors (*French*) 0-89483  
 N<sub>2</sub>+methylmercury halides, A<sup>2</sup>Σ<sup>+</sup>-state quenching obs. 0-108693  
 N<sub>2</sub>+O<sub>2</sub>, N<sub>2</sub> fixation, catalytic processes in non-equilibrium plasma chemical reactors (*French*) 0-89484  
 N<sub>2</sub><sup>+</sup>+H<sub>2</sub>, collisional dissoci. cross-section, 2.4-24.3 keV 0-58373  
 N<sub>2</sub><sup>+</sup>+O<sub>2</sub>, collisional dissoci. cross-section, 2.4-24.3 keV 0-58373  
<sup>14</sup>N<sub>2</sub>+CO, vibr.-vibr. energy transfer, long and short range pot. effect 0-99556

# molecule-molecule reactions continued

<sup>15</sup>N<sub>2</sub>+CO, vibr.-vibr. energy transfer, long and short range pot. effect 0-99556  
 NH<sub>2</sub>+O<sub>3</sub>, reaction rate const., rel. to atmospheric processes 0-85155  
 NH<sub>3</sub>, inversion spectrum collisional line broadening, general theory 0-87184  
<sup>14</sup>N<sup>15</sup>N+CO, vibr.-vibr. energy transfer, long and short range pot. effect 0-99556  
 NO+O<sub>3</sub>, fs-states and rot. states, effect on reactivity 0-89473  
 O<sub>3</sub>+thiirane, autocatalytic reaction, stopped-flow study, reaction rate meas. 0-85152  
 OH+Br<sub>2</sub>, hydroxyl radicals reactive scatt. 0-85172  
 OH+H<sub>2</sub>→H<sub>2</sub>O+H, reaction product vibr. distrib., quasiclassical trajectory, calcs. 0-85162  
 OH+OCS(CS<sub>2</sub>), lower atmosphere chem. 0-61870  
 SO<sub>2</sub>+O<sub>2</sub>→SO+O<sub>2</sub>, gas phase reaction, rate coeffs. meas. 0-97704  
 SbF<sub>5</sub>+benzyl chloride, chemi-ionis. reaction, temp. depend., flow tube investig. 0-108701  
 SiO+F<sub>2</sub>, matrix reaction, OSiF<sub>2</sub> prod., IR spectra and force consts. calcs. (*German*) 0-97718  
 W, direct inelastic and trapping-desorpt. scatt. of N<sub>2</sub>, elementary steps in N<sub>2</sub> chemisorpt. 0-60737

# molecules

*see also excimers; hydrogen neutral molecules; macromolecules; mesic molecules; muonic molecules; quasimolecules*  
 No entries

# Mollier diagrams *see thermodynamic properties*

# molten metals *see liquid metals*

# molten polymers *see polymer melts*

# molybdenum

*see also nuclei with .....*  
 (110) surface, molecular adsorbed CO, electronic states, photoemission spectra 0-65363  
 adsorption of NH<sub>3</sub> on (111) planes, preferential nitriding, FEM study 0-66877  
 adsorption of O<sub>2</sub> and Cs, struct., emission props., thermal stability 0-66878  
 atom, X-ray spectra, Kα hypersatellites 0-63576  
 atoms, N<sub>2</sub>N<sub>3</sub>N<sub>4</sub>, super Coster Kronig processes 0-106303  
 chemisorbed CO on (100), surface kinetics, photoemission study method 0-80941  
 coated diamond powders, X-ray diff. study 0-100936  
 composite, sapphire fibre reinforced, strength at rupture 0-104286  
 condensation of Cu and Ag on (100), early stage comparison with W(100) 0-80072  
 core level binding energies 0-71564  
 corrosion behaviour in high temp. impure He gas 0-76402  
 creep deformed single crystals, subboundary struct. obs., dislocation sets 0-103348  
 diffuse electron scatt. (*Russian*) 0-103438  
 diffusion of H<sub>2</sub> enhanced by self-interstitial atoms, surface reaction const. determ. 0-75386  
 diffusion of Li, Cs, vacancy and divacancy mechanisms (*Russian*) 0-70472  
 dislocation structure, changes during work softening, HVEM 0-103336  
 dislocation structure evolution near electro-eroded crater (*Russian*) 0-100237  
 dislocation structure of diffusional welding zone (*Russian*) 0-96531  
 effective mass meas. and electron velocities 0-96773  
 electrical resistivity, quadratic contrib., 2 to 40K (*Russian*) 0-92874  
 electrode, Mo extraction grid for high power ion source 0-102372  
 electrode reactions with molten glass 0-85186  
 electron irradiated in HVEM, anisotropy of damage prod. 0-107322  
 electronics industry applications, prep. processing and props. 0-89171  
 extinction length  $\xi_{200}$  meas., electron energy influence 0-90935  
 fatigue of single crystals, dislocation struct. and strain localisation (*Russian*) 0-71741  
 Fermi surface vol. depend. of extremal cross sectional areas from de Haas-van Alphen meas. 0-70589  
 fibre reinforced Cu, rule of mixtures of deform. parameters in stage III 0-97532  
 fibre reinforced Cu with weak interfaces, stability of tensile deform. 0-97533  
 field emission anomalies in mag. field (*Russian*) 0-93462  
 film, evaporated, annealing behaviour, SEM obs. 0-65397  
 film, evaporated, grain size and resist. 0-88650  
 film, formation by reduction of MoCl<sub>5</sub>, influence of electric field 0-93491  
 film, sputtered, elec. resist., annealing and struct. effects 0-60109  
 film on sapphire substrate, orientational growth, epitaxial textures, nucleation textures (*Russian*) 0-74544  
 films, sputtered from cylindrical-post magnetron with Ne, Ar, Kr and Xe, compressive stress and presence of inert-gas obs. 0-80140  
 films, vac. evaporated, optical cond. 0-76100  
 fine tip cathode, field emission stability, rel. to passivation 0-100760  
 foil electrolytic perforation, surface film phase composition obs. (*Russian*) 0-61004  
 foils, device for electrolytic thinning from wire, for electron microscopy 0-85105  
 fracture and crack tip plastic zones, in situ obs. 0-108686  
 fusion reactor material, low energy ion erosion expts., Kaufman source appl. 0-68942  
 gamma irradiated defects, interaction with positrons (*Russian*) 0-97372  
 high temp. radiative props., expt. determ., spectral emissivities 0-74718  
 Hugoniot data, ultrahigh press. (TPa) shockwave from underground nuclear explosion 0-95980  
 implantation in Al and Al-Zn-Mg-Cu, effect on corrosion behaviour 0-71794  
 impurity flux, time resolved, in DITE Tokamak 0-63373  
 ion bombard., ion and photon yields, CO adsorption effect 0-89098

**molybdenum continued**

ion irradiated, defect anal., electron microscopy, appl. of theory of non-edge loop image contrast 0-70200  
 ion-plated orthopaedic En58J stainless steel, corrosion fatigue 0-66694  
 islet films, effect of external elec. field on electron emission 0-80952  
 ISSEC selection for fusion reactor 0-57950  
 laser induced dislocation struct. in single cryst. 0-70210  
 lattice dynamics, improved Fiekel model 0-59598  
 liquid, elec. resist., melting pt., to boiling pt., temp. depend. 0-96839  
 longwave dopplers, nonlocal Hall effect, surface impedance, size effect (Russian) 0-80253  
 luminescence characteristics of pure surfaces acted on by flux of field emission electrons 0-100695  
 mechanical properties, effect of exposure to high temp. He containing O<sub>2</sub>, room temp. study 0-93639  
 metallised amorphous GeSe junctions, electrical contact effects on properties (German) 0-93010  
 neutron irradiated, radiation anneal hardening mechanism 0-71678  
 neutron-bombarded, diffuse X-ray scattering (Russian) 0-92560  
 nonstationary temperature fields due to moving heat sources, heat capacity, thermal cond. (Russian) 0-107448  
 particle formation, ultrafine, via pulsed laser breakdown of MO(CO)<sub>6</sub> 0-84881  
 phonon dispersion relations, modified tensor force model 0-103428  
 plastically deformed single cryst., mag. susceptibility (Russian) 0-93074  
 polycrystals, grain misalignment, electron microscope determ. (Russian) 0-103358  
 proton-induced L-shell ionisation cross-sections 0-100707  
 radiation induced vacancies and D<sub>2</sub><sup>+</sup> implantation 0-65076  
 self-weldability in high temp Na (Japanese) 0-89392  
 shock deformation twinning, shock loaded BCC and FCC metals comparison 0-104413  
 single crystals, orientation and alloying effect on mech. (Russian) 0-71706  
 sintered, gas evolution and degassing 0-100814  
 spectrochemical analysis, atomic-absorption, tubes design with hollow cathode (Bulgarian) 0-85232  
 stray X-rays from Mo components in transmission electron microscope, reduction 0-73550  
 stress measurement, in single cryst., using  $\psi$ - $\phi$  goniometer 0-64837  
 substrate limiting temp. during vapourisation and condensation coating in vacuum (Russian) 0-100787  
 surface, adsorbed Ga and Sn, struct., FIM obs. 0-103576  
 surface, clean and gas covered, He\* impact, deexcitation, pot. energy transfer mechanism 0-60743  
 surface, low-temperature thermionic converter with an expanded-area collector 0-70045  
 surface, pulsed laser atom-probe FIM, expts. 0-66402  
 surface, rolled, H<sub>2</sub><sup>+</sup> ion bombard, large blister form. 0-75274  
 surface (001), clean and H chemisorbed, atomic displacements, LEED obs. 0-70514  
 surface (110), Au film growth, AES, LEED, thermal desorption study 0-80130  
 surface (111), electroluminescence in 200 to 630 nm range 0-103997  
 surface (111), work function temp. coeff. 0-100499  
 thermal conduct. of high-purity single crystals in temp. range 2-70K 0-75545  
 thermal fatigue test, quick heating, sintered, electron-beam melted, vac. arc melted, fusion reactor appl. (Japanese) 0-93716  
 thermophysical data at high temps., submicrosecond-pulse-heating method 0-103459  
 thin film deposition by high current ion beam sputtering, struct. and elec. props. 0-59837  
 trapping of <sup>3</sup>He and D and mutual replacement 0-59493  
 void containing, positron annihilation characts. 0-80898  
 volt ampere characteristics during electron melting process (Russian) 0-75336  
 wire, US inspection, immersion method 0-66757  
 X-ray absorption, discontinuities and limits, chem. combination effects 0-93435  
 X-ray emission spectra, detect. from Alcator-A Tokamak 0-92389  
 AlN-Mo cermets, ZrO<sub>2</sub> and mullite whisker reinforced, strength var. with temp. 0-104232  
 Al<sub>2</sub>O<sub>3</sub>-Mo cermets, ZrO<sub>2</sub> and mullite whisker reinforced, strength var. with temp. 0-104232  
 Ba<sub>3</sub>NaNb<sub>3</sub>O<sub>15</sub>:Fe,Mo, photorefractive mechanism and photoelec. props. 0-71381  
 BaO-P<sub>2</sub>O<sub>5</sub>:Mo<sup>5+</sup> glass, EPR spectra, computer simulation 0-88872  
 Bi<sub>2</sub>SiO<sub>20</sub>:Mo, Raman scatt. spectra, impurity effect 0-80795  
 MgO-Mo catalyst, adsorpt. of propylene, oxidation reactions, surface structs., IR absorpt. spectra obs. 0-66868  
 MnO<sub>2</sub>:Mo, Zn<sup>2+</sup> ion specific adsorpt. kinetics, <sup>65</sup>Zn  $\gamma$ -ray scintillation investig. 0-70529  
 Mo crystals, joined by compression during heating, structural changes (Russian) 0-108513  
 Mo electrode, corrosion rate in molten glass (Chinese) 0-66687  
 Mo polycrystn., cyclically deformed, dislocation arrangements 0-108506  
 Mo powder, influence of powder reduction processes on props. 0-89175  
 Mo wire, struct. and high-temp. creep, dopant elements influence 0-66603  
 Mo XIII-XVIII, spectrum 20 to 90 Å from laser-prod. plasma and low-inductance vac. spark 0-102473  
 Mo XIV to Mo XXIX, extreme UV spectra 0-87068  
 Mo-C (110) surface, segregation, precip. and desorpt. of C, AES and LEED study (French) 0-103480  
 Mo-chalcogenide glass-Mo-Al struct., strong elec. field effects 0-97004  
 Mo-Cu cathode, spot motion and nature in UHV 0-79597  
 Mo-Si, interface modification by ion implantation 0-70475  
 Mo-Si film-substrate interface, reaction on heat treatment, silicide formation 0-79999  
 Mo-Si sputtered contacts, contact resistance 0-92970  
 Mo-TiC lamellar eutectic composite, deformation and strength, room temp. to 2073K (Japanese) 0-71702  
 Mo<sub>12</sub> cluster, one-dimens condensation of Mo<sub>6</sub> octahedral clusters, prep. and struct. of Ti<sub>2</sub>Mo<sub>3</sub>S<sub>11</sub>, and K<sub>2</sub>Mo<sub>3</sub>S<sub>11</sub> 0-107168  
 Mo<sub>2</sub> metal-metal bond energy, SCF-X $\alpha$ -SW calcs. 0-78538  
 MoO<sub>3</sub> topotactic transform into MoO<sub>2</sub>, electron microscopy, X-ray anal. 0-107417  
 Mo<sub>70</sub>Si<sub>30</sub>B<sub>10</sub>, amorphous alloys obtained by liq. quenching, superconductivity 0-75670

**molybdenum continued**

<sup>99</sup>Mo, A=95, 97, nucl. quadrupole moments from laser-RF double reson. spectroscopy 0-57682  
 Si:Mo contaminated solar cells, POCl<sub>3</sub> gettering 0-94010  
 Si-SiO<sub>2</sub>-Mo-Si<sub>3</sub>N<sub>4</sub>-Al MNOS structures with metal grains, charge transport at SiO<sub>2</sub>-Si<sub>3</sub>N<sub>4</sub> interface 0-65693  
 TiO<sub>2</sub>:Mo<sup>5+</sup>, interstitial EPR, g-tensor and hyperfine tensor 0-84647

**molybdenum alloys**  
 see also molybdenum compounds  
 creep rate in vacuum, grain size effect, for TsM-6 0-108514  
 dilute, HVEM bombarded, neutron damage simulation, defect cluster and dislocation obs. 0-107330  
 Hastelloy, C-276, H transport rel. to ageing treatment 0-75384  
 Hastelloy, C-276, H-induced crack growth 0-71747  
 Hastelloy, H<sub>2</sub> embrittlement in H<sub>2</sub>S environments, impurity segregation effects 0-71724  
 Hastelloy-B-2, corroded surface, electron bombardment effect during Auger electron anal. 0-61014  
 Hastelloy-X, low cycle fatigue crack propagation at 25°C and 760°C 0-104270  
 Hastelloy-X, Ni-Cr-Fe-Mo, cyclic oxidation resist. improvement by high temp. etching treatment 0-97627  
 Hayes alloy no.716, Fe-Cr-Ni-Co-W-Mo-Si-C-B (26, 22, 12, 3.5, 3, 1.2, 1.1, 0.4 wt.%), hardfacing alloy 0-100802  
 Inconel 617, creep, morphological changes of carbides, affect on creep props. 0-108509  
 Inconel 625, electron yields under ion bombardment for clean and oxidised surfaces 0-66368  
 Inconel 718, grain growth during sintering 0-97449  
 Inconel hardfacing materials, friction characts. in high temp. Na (Japanese) 0-89356  
 intercryst. fracture in ductile-brittle transition region, local internal stresses effect 0-81200  
 metallic glass, Mo-based, development 0-89172  
 Nimonic PE16, irradiation creep data obtained in fast and thermal neutron spectra correlation with displacement cross-sections 0-84993  
 Nimonic PE-16, electron irradi. in HVEM, void growth, vacuum environment influence 0-107323  
 recrystallisation, crystallographic and structure texture of Mo alloy with dispersed HfN phase (Ukrainian) 0-71668  
 sphere, three-body abrasive wear with small size diamond abrasives 0-76373  
 steel, Al-Ti-(V)-Mo, Al-V-Mo and Al-Ti-Nb-Mo low-alloy, toughness improvement through Ti additions 0-66525  
 steel, Cr-Mo, effect of Mo on high-temp. props. 0-85005  
 steel, Cr-Mo, ferritic, grain boundary segregation, X-ray microanal. by STEM 0-66740  
 steel, Cr-Mo, H embrittlement in H<sub>2</sub>S environment, Mo effect 0-76415  
 steel, Cr-Mo and Ni-Cr-Mo-V low-alloy, additive remedy for temper brittleness 0-66659  
 steel, Cr-Mo weld metal, reheat cracking, residual elements and microstruct. influence 0-66553  
 steel, Cr-Mo weld metal, trace element embrittlement suppression by creep strength effects 0-66656  
 steel, Cr-Mo-(V) austenitic, creep resist., high-temp. props. residuals effect 0-66600  
 steel, Cr-Mo-V, strength and ductility in creep, purity influence 0-66598  
 steel, Cr-Mo-V low-alloy, high-temp. ductility and crack growth, impurities effect 0-66652  
 steel, Cr-Mo-V low-alloy, mech. props. and stress relief cracking, effects of impurities and deoxidation practice 0-66599  
 steel, Cr-Mo-V low-alloy, prior austenite grain boundary embrittlement by B 0-66657  
 steel, Cr-Mo-V low-alloy, stress relief cracking, impurity and alloy content effects 0-66654  
 steel, Cr-Mo-V low-alloy with high residual element content, cavitation control 0-66663  
 steel, Cr-Ni-Mo-Mn, wetting of TiC, expt. planning investigation 0-60822  
 steel, Cr-W-Mo-Co, high-speed, from atomised powders, mech. and cutting props. 0-66556  
 steel, Cu-Ni-Mo (2, 2, 0.25 wt.%), sintering, kinetic characts. 0-60805  
 steel, Mn-Mo, castings, mech. props., Cu and Sn trace elements effect 0-66596  
 steel, Mn-Mo-Ni, embrittling effects of residual elements 0-66655  
 steel, Ni-Mo-C (2.0, 0.2, 0.4 wt.%) sintered, struct. transforms. and mech. props. after quenching 0-66557  
 steel, Ni-Mo-Cr, embrittling effects of residual elements 0-66655  
 steel, W-Mo-Co, high-speed tool, struct. and props., cooling rate effect at primary crystn. temp. 0-76241  
 steel, W-Mo-Cr-V tool, laser surface melted, struct., heat treatment effect 0-76424  
 thermally degenerated Schottky diodes, resonant tunnelling 0-100503  
 TsM10VD, erosion, effect of ion bombardment dose and previous surface treatment 0-89419  
 TZM, blistering under He ion bombard. 0-92567  
 TZM-Mo alloy, mech. props., effect of exposure to high temp. He containing O<sub>2</sub>, room temp. study 0-93639  
 Co-Gd-Mo amorphous films, resist. and extraordinary Hall effect, thermal annealing effect 0-70852  
 Co-Gd-Mo films, sputtered, O effects on mag. props. during annealing 0-89374  
 Co-Mo, dendritic segregation 0-76260  
 Co-Mo-B metallic glass ribbons, tensile strength, crystn. temp. 0-89173  
 Co-Ni-Cr-Mo (35, 20, 10 wt.%), MP35N, TEM study of phase transformations 0-81054  
 Co-Ni-Mo-C, amorphous alloys, med. props. and thermal stability (Japanese) 0-85049  
 (Co<sub>0.89</sub>Fe<sub>0.11</sub>)<sub>72</sub>Mo<sub>5</sub>Si<sub>3</sub>B<sub>10</sub>, metallic glass, strain- and field-induced mag. anisotropy 0-108004  
 Co<sub>72</sub>Mo<sub>5</sub>Si<sub>3</sub>B<sub>10</sub>, metallic glass, strain- and field-induced mag. anisotropy 0-108004  
 Cr-Mo, elec. resist. and thermo-EMF, conc. depend., 4.2 to 1500K (Russian) 0-80247  
 Cr-Mo, electrical resistivity, spin density wave gap, Neel temp. 0-88534  
 Cr-Mo steel types JIS SCMV 2, SCMV 3 and SCMV 4, high-temp. high-cycle fatigue props., press. vessel appls. (Japanese) 0-93650  
 Cr-Mo-V-Nb, supercooled austenite isothermal decomp., struct., strength and fracture characts. 0-60966



**molybdenum alloys continued**

Cr-Nb-Mo system, comp. and temp. depend. alterations in mech. props., phase diagram interpret. (*Russian*) 0-85045  
 Fe-B-Mo metallic glasses, mag., struct., and elec. props. 0-88751  
 Fe-Co-Mo, phase relations in system at 1100°C 0-108392  
 Fe-Co-Mo-C, amorphous alloys, med. props. and thermal stability (*Japanese*) 0-85049  
 Fe-Co-Mo-Nb(Ta) semihard mag. alloy, mag. props., thermal expansion, elec. resistivity and hardness (*Japanese*) 0-88789  
 Fe-Cr-Co-Mo high energy permanent magnets, mag. props. 0-97119  
 Fe-Cr-Mo, white cast, optimising fracture toughness and abrasion resist. 0-85042  
 Fe-Cr-Mo alloy castings, thick-section, factors affecting 0-108374  
 Fe-Cr-Mo and Fe-Cr-Mo-Si, amorphous films, corrosion resist. and ion plating use 0-89423  
 Fe-Cr-Ti-Mo-TiO<sub>2</sub> (13, 3.5, 1.5, 2 wt.%) dispersion hardened, void swelling 0-65046  
 Fe-Mo (13-20 at.%) binary alloys, spinodal decomp. on ageing, TEM and X-ray diffr. study 0-97503  
 Fe-Mo system, thermomech. props. 0-89208  
 Fe-Mo-B metallic glass ribbons, tensile strength, crystn. temp. 0-89173  
 Fe-Mo-C (0 to 4, 1 wt.%), phase equilibria at 1143, 1198 and 1253K 0-60835  
 Fe-Mo-CaF<sub>2</sub> sintered composite, struct. and mech. props., heat treatment effect 0-66526  
 Fe-Mo-Ta, ternary Laves phase strengthening 0-108466  
 Fe-Mo(4.1 wt.%), steady state creep at high temps. 0-89316  
 Fe-Ni-B-Mo, crystn. temp. and elec. cond. correl., Mo effect 0-75179  
 Fe-Ni-Co-Mo (18.65, 8.99, 4.87 wt.%), ageing characts., 380-530°C 0-60876  
 Fe-Ni-Cr-Al-Ti-W-Mo (35, 15, 2.4, 2.3, 2.2 wt.%) wrought superalloy, freckles (*Chinese*) 0-104137  
 Fe-Ni-Mo, austenite, annealing effect on atom redistrib., Mossbauer anal. (*Russian*) 0-66529  
 Fe-Ni-Mo, martensitic transformation, annealing, influence on struct. of austenite (*Russian*) 0-81057  
 Fe-Ni-Mo, phase relations in system at 1100°C 0-108392  
 Fe-Ni-Mo-C, amorphous alloys, med. props. and thermal stability (*Japanese*) 0-85049  
 Fe-W-Cr-Mo system, mag. and mech. props. rel. to production methods (*Japanese*) 0-71107  
 (Fe-Ni-Mo)<sub>80</sub>(P-B)<sub>20</sub>, amorphous, mag. aftereffects and struct. instabilities 0-88833  
 Fe<sub>71</sub>Mo<sub>29</sub>B<sub>20</sub> amorphous ribbons, magnetoelastic effects in as-quenched and stress-relieved states 0-80588  
 Fe<sub>71</sub>Mo<sub>29</sub>B<sub>20</sub>, metallic glass, Doppler broadening of positron annihilation  $\gamma$ -radiation and elec. resist. 0-66321  
 Fe<sub>40</sub>Ni<sub>40</sub>(Mo,Si)<sub>20</sub>, amorphous, soft mag. props., switched-mode power supply appls. 0-88850  
 Fe<sub>40</sub>Ni<sub>38</sub>Mo<sub>4</sub>B<sub>18</sub> amorphous ribbons, magnetoelastic effects in as-quenched and stress-relieved states 0-80588  
 Fe<sub>40</sub>Ni<sub>38</sub>Mo<sub>4</sub>B<sub>18</sub>, amorphous, mag. anisotropy, Mossbauer study 0-65864  
 Fe<sub>40</sub>Ni<sub>38</sub>Mo<sub>4</sub>B<sub>18</sub>, amorphous, reversible enhancement of mag. directional ordering rate 0-103829  
 Mo-(Zr+V+C) (1.1 wt.%) alloy, phase composition, carbide phase microhardness (*Russian*) 0-60834  
 Mo-Al-Ge, phase equilibria, X-ray and microstructural anal. 0-93536  
 Mo-Be solid solutions, superconducting transition, temp. changing peculiarity due to press. (*Russian*) 0-70878  
 Mo-Co Kondo alloy, Co impurity susceptibilities, Knight shift 0-88721  
 Mo-Cr-V-P, load curves, structure states boundaries and strain hardening (*Russian*) 0-89241  
 Mo-HfC, eutectic formation of regular struct., crystn. (*Russian*) 0-66496  
 Mo-Mo<sub>2</sub>C, eutectic formation of regular struct., crystn. (*Russian*) 0-66496  
 Mo-N solid solution, thermodynamic props., 1618 to 1883K 0-65230  
 Mo-Nb (Re), thermoelec. power, 4.2 to 300K 0-70683  
 Mo-Nb-C, mech. props., effect of alloying and Mo cryst. orientation (*Russian*) 0-71706  
 Mo-Nb-Ti-N alloy, with dispersed second phase, ductile-brittle transition 0-93653  
 Mo-Re(Os)(Ru), recovery after deform. and annealing, destrengthening mechanism (*Russian*) 0-97546  
 Mo-Ru-(Si), amorphous superconductors, prep. by electron beam evaporation and liq. quenching, crit. temp. 0-103776  
 Mo-Sn-Se system, supercond. crit. temp. and cryst. struct. (*Russian*) 0-107947  
 Mo-Ti (3.5 wt.%), load curves, structure states boundaries and strain hardening (*Russian*) 0-89241  
 Mo-Ti-N alloy, with dispersed second phase, ductile-brittle transition 0-93653  
 Mo-Ti-Zr, TZM, corrosion behaviour in high temp. impure He gas 0-76402  
 Mo-TiC, eutectic formation of regular struct., crystn. (*Russian*) 0-66496  
 Mo-V, elec. resist. and thermo-EMF, conc. depend., 4.2 to 1500K (*Russian*) 0-80247  
 Mo-W (30 wt.%), wrought, fracture, characteristic features 0-104278  
 Mo-W alloy type MW25N, crystallisation form, globular dendrites, grain boundaries (*Russian*) 0-66494  
 Mo-W-N system, nitrided annealed samples, W replacement of Mo 0-76227  
 Mo-Zr, nucleation conditions, effect on formation of oxide phase during internal oxidation (*Russian*) 0-81064  
 Mo-Zr (0.15 wt.%), wrought, fracture, characteristic features 0-104278  
 Mo-Zr-Ti (0.5, 0.1%), adhesive wear polishing of 25 mm spheres 0-89397  
 Mo-ZrC, eutectic formation of regular struct., crystn. (*Russian*) 0-66496  
 Mo<sub>70</sub>B<sub>30</sub>, amorphous, local symmetry around glass-former sites, elec. quadrupole effects, NMR 0-80618  
 Mo<sub>3</sub>Ge, Al<sub>15</sub> cpd., normal state, low temp. resist. 0-107762  
 Mo<sub>3</sub>Pb<sub>5</sub> embedded in resin, composite supercond., high transition temp. 0-88660  
 Mo<sub>8</sub>Ru<sub>12</sub>B<sub>20</sub>, amorphous, local symmetry around glass-former sites, elec. quadrupole effects, NMR 0-80618  
 (Mo<sub>0.8</sub>Ru<sub>0.4</sub>)<sub>40</sub>(Si<sub>0.6</sub>B<sub>10</sub>)<sub>60</sub>, amorphous supercond. matrix, flux pinning by MoRu precip. 0-65756  
 Nb-Mo, AC loss minimum, pinning, flux distribution 0-84574  
 Nb-Mo, resistivity due to H incorporation 0-70666  
 Nb-Mo, specific heat enhancement and electron-phonon interaction 0-65242  
 Nb-Mo-Si, ductile amorphous, superconductivity 0-60131

**molybdenum alloys continued**

Nb-W-Mo-Zr (5, 2.1, 0.92 wt.%), creep resist., high temp. ageing in vacuum 0-71716  
 Ni-Al-Mo (12.7, 21.6 wt.%), directionally solidified eutectic composite, precipitation 0-108454  
 Ni-Co-Cr-Mo-Al-Ti (17.5, 15.1, 4.9, 4.15, 3.25 wt.%), creep and stress rupture behaviour in air and vacuum 0-60918  
 Ni-Co-Mo, phase relations in system at 1100°C 0-108392  
 Ni-Cr-Co-Al-W-Mo-Ti-Ta, heat resist. and struct., Ta effect 0-76312  
 Ni-Cr-Co-Ti-Mo-W-Al (14, 9.8, 5, 4, 3.9, 3 wt.%), low cycle fatigue, prior heat treatment effect 0-60962  
 Ni-Cr-Mo-W-Al-Ti, heat-resist., phase comp. 0-76250  
 Ni-Cr-W-Co-Mo, high-temp. sulphide corrosion 0-76408  
 Ni-Cr-W-Mo-Ti-Al, heat-resist., recovery and recrystn. 0-76268  
 Ni-Fe-Cr-Mo-Ti-Al, PE 16, thermally activated domain wall motion 0-88777  
 Ni-Fe-Nb-Mo-Al, head material for mag. recording, DC and AC mag. props. 0-88812  
 Ni-Mo-B metallic glass ribbons, tensile strength, crystn. temp. 0-89173  
 Ni-Mo-W, diagram of state, W solubility, dispersion hardening (*Russian*) 0-66477  
 Ti-Al-Mo, phase relations 0-108398  
 Ti-Al-Mo, type BT22, phase transformations under step-by-step heat treatment (*Russian*) 0-108436  
 Ti-Al-Mo-Cr, weldment containing orthorhombic martensite, auto-tempering behaviour and alpha precip. strengthening 0-84976  
 Ti-Al-Mo-Cr (4.5, 5, 1.5 wt.%), weld metal,  $\alpha/\beta$  interface sliding 0-108512  
 Ti-Al-Mo-V (8, 1, 1 wt.%), Widmanstätten colonies, fracture toughness 0-85031  
 Ti-Al-Mo-Zr, compressor disk, surface plastic deform., optimal method 0-60924  
 Ti-Al-Mo-Zr, type VT-9, creep eqns. rel. to extension and compression props. 0-100875  
 Ti-Al-Sn-Zr, Ti-680, O contamination under high temp. (*Chinese*) 0-66688  
 Ti-Al-Sn-Zr-Mo (6,2,4,6 wt.%) fusion weldment, substruct. characts. 0-84183  
 Ti-Mo, diffuse electron scatt. (*Russian*) 0-103438  
 Ti-Mo, metastable diffusionless equilibria, high press. conditions 0-71627  
 Ti-Mo, structure associated with BCC to omega transform. (*Russian*) 0-108432  
 $\beta$ -Ti-Mo, thermal instability, hardness and tensile deform. (*Japanese*) 0-71703  
 Ti-Mo (20 at.%), incommensurate struct., stacking soliton 0-107109  
 Ti-Mo (3 to 35 wt.%), high pressure influence on transition temp. to supercond. 0-107952  
 Ti-Mo alloy, thin anodic oxide, AES depth profile 0-71801  
 Ti-Mo alloys, structural stability under high-pressure soaking 0-104151  
 Ti-Mo-V-Al-Cr-Fe (4.8, 4.7, 5.2, 1.1, 1.0 wt.%), structural changes during heating up to 1000°C, DTA study (*Russian*) 0-93552  
 Ti-Mo-Zr-Sn (11.5, 6.0, 4.5 wt.%), mech. property, microstruct. relationships 0-84961  
 Ti-Mo-Zr-Sn (11.5, 6.0, 4.5 wt.%) alloy, struct. as affected by processing history 0-84972  
 $\beta$ -Ti-Mo-Zr-Sn(11.5, 6, 4.5 wt.%), metastable phase III, microstruct. and age hardening response 0-84945  
 Ti-Mo-Zr-(Al) (15, 5 (3) wt.%), quenched and aged metastable  $\beta$ -phase, crystallography, morphology and decomposition 0-76262  
 Ti-V-Cr-Mo, fracture resistance at low temps. 0-104284  
 TiC-(Mo-Cr-Ni-Mn) steel alloy, optimum comp. and manufacture conditions, Mn effect 0-84896  
 U-Mo (2 wt.%), depleted, effect of microstruct. on mech. props. 0-108497  
 V-Mo (25 wt.%), corrosion behaviour in high temp. impure He gas 0-76402  
 V<sub>2</sub>Si-SiO<sub>2</sub>-Mo<sub>2</sub>Re<sub>3</sub>, supercond. tunnel junctions 0-107961  
 Zr-Mo, Zr-Sn-Mo, creep characts., influence of Sn and Mo (*Czech*) 0-81119

**molybdenum compounds**

see also molybdenum alloys  
 chalcogenides, multicomponent, physical props. 0-84577  
 molybdates, alkaline earth, U activated, scheelite struct. luminesc. props. vibr. modes and quenching temp. 0-60651  
 oxide, catalysis of graphitisable C graphitisation 0-89166  
 oxide reduction by electron cyclotron reson. plasma of H, model study on discharge cleaning 0-76548  
 oxides, low-grade, soda roasting study (*Korean*) 0-93508  
 oxides, magnetic susceptibility meas., temp. effect 0-103822  
 rare earth cpds., RMo<sub>6</sub>S<sub>8</sub>(Se<sub>8</sub>), coexistence of supercond. and mag. ordering (*Russian*) 0-84542  
 superconducting ternary chalcogenides, structures and properties survey (*Czech*) 0-70870  
 ternary compounds, R<sub>2</sub>Sn<sub>2</sub>Mo<sub>2</sub>S<sub>8</sub> (R=La, Ce, Pr, Eu, Gd, Ho, Lu, Y, In, U), supercond. props. 0-97023  
 AgI-Ag<sub>2</sub>O-MoO<sub>3</sub> glass glass superionic cond., struct. and transport props. 0-88602  
 AgI-Ag<sub>2</sub>O-MoO<sub>3</sub> glass electrolyte galvanic cells 0-104513  
 Cu<sub>10</sub>Mo<sub>8</sub>S<sub>8</sub>, supercond. Chevrel phase, electron tunnelling spectroscopy expts. (*German*) 0-107966  
 Cu<sub>10</sub>Mo<sub>8</sub>S<sub>8-y</sub> electrodes, thermodynamic and transport props. 0-66963  
 K<sub>2</sub>Mo<sub>6</sub>S<sub>11</sub>, prep. and struct., Mo<sub>12</sub> cluster in Mo<sub>12</sub>S<sub>14</sub> unit 0-107168  
 LaCrO<sub>3</sub>-Mo eutectics, prep. and microstruct. 0-108380  
 Li<sub>10</sub>Mo<sub>8</sub>S<sub>8-y</sub> electrodes, thermodynamic and transport props. 0-66963  
 Mo-N, bond-strength bond-length relationships 0-91702  
 Mo-Si, film deposition by reactive sputtering, characteris. (*Japanese*) 0-93485  
 MoC, precipitates in Ni-base superalloy, STEM microanal. 0-81067  
 MoC<sub>2</sub>, pressing regime influence on high-temp. creep (*Russian*) 0-100852  
 Mo<sub>2</sub>C, cathodic needle growth, at lower electric fields from Mo(CO)<sub>6</sub> vapour 0-76161  
 Mo(CO)<sub>6</sub>, MCD spectra, charge transfer transitions 0-95658  
 Mo(CO)<sub>6</sub>, physisorption and reaction on  $\gamma$ -Al<sub>2</sub>O<sub>3</sub>, IR spectra obs. 0-80064  
 MoCl<sub>5</sub>, reduction by H<sub>2</sub>, influence of electric field on Mo film deposition 0-93491  
 Mo<sub>2</sub>Cl<sub>4</sub><sup>+</sup>, metal-metal bond energy, SCF-X $\alpha$ -SW calcs. 0-78538  
 Mo<sub>2</sub>Cl<sub>4</sub><sup>+</sup>, complexes, cluster exchange coupling consts. SCF-X $\alpha$ -SW calcs. 0-74120



**molybdenum compounds continued**

- MoF<sub>4</sub> + K<sub>2</sub>(Cs<sub>2</sub>), ionisation reactions, absolute cross sections 0-99565  
 MoF<sub>6</sub>, in Ar matrix, photolysis, MoF<sub>5</sub> form., IR spectrum 0-87115  
 MoF<sub>6</sub>, reduction by H in the presence of HF (*Russian*) 0-61076  
 MoO<sub>2</sub>Re(V), current carrier sign, Fermi surface cross section variations (*Russian*) 0-84420  
 MoO<sub>3</sub> smoke particles prepared by gas evap., morphology and coalescence growth 0-97738  
 MoO<sub>3</sub>, X-ray absorption, discontinuities and limits, chem. combination effects 0-93435  
 MoO<sub>3</sub> + Ni<sup>2+</sup> interaction on Al<sub>2</sub>O<sub>3</sub>, Raman spectrum 0-108742  
 Mo<sub>6</sub>-Rh, Te<sub>8</sub>, synthesis, struct., and elec. props. 0-92877  
 Mo<sub>6</sub>Ru<sub>2</sub>Se<sub>8</sub>(Te<sub>8</sub>), synthesis, struct., and elec. props. 0-92877  
 MoS<sub>2</sub>, homogeneity size estimation, stacking fault conc. effect 0-96661  
 MoS<sub>2</sub>, lattice images of defects and radiation damage applies. 0-107210  
 MoS<sub>2</sub>, molybdenite band structural props. rel. to supercond. and semicond. 0-96781  
 MoS<sub>2</sub>, molybdenite crystal, direct imaging of atom configuration projected onto the basal plane 0-64847  
 MoS<sub>2</sub>, prep. and mag. props. (*French*) 0-93072  
 MoS<sub>2</sub>, solid lubricant, antifiction and elec. props. depend. on oxidation temp., dopant influence 0-108584  
 Mo<sub>6</sub>S<sub>8</sub> Chevrel phases with group IIIa metals, Nb, Hg, Pb and Cu, synthesis, stability and characts. 0-71608  
 Mo<sub>6</sub>S<sub>8</sub>Sn, triple chalcogenide, NMR spectra in supercond. state (*Russian*) 0-93194  
 n-MoSe<sub>2</sub>, based liq. junction solar cell, nonaqueous electrolyte system employing Cl<sub>2</sub>/Cl<sup>-</sup> couple 0-81432  
 MoSe<sub>2</sub>, exciton spectra 0-97296  
 MoSe<sub>2</sub>, imperfections from TEM study 0-79800  
 Mo<sub>6</sub>Se<sub>8</sub>Sn, triple chalcogenide, NMR spectra in supercond. state (*Russian*) 0-93194  
 MoSi<sub>2</sub> film, elastic stiffness and thermal expansion coeffs. 0-107451  
 MoSi<sub>2</sub>, oxidation behaviour, Ge additions effect (*German*) 0-71782  
 MoSi<sub>2</sub> oxide film, dielec. props. and growth kinetics 0-81215  
 MoSi<sub>2</sub> refractory formation by As<sup>+</sup> ion beam bombardment 0-107286  
 Mo<sub>2</sub>Si<sub>3</sub>, layer electrotransfer of Si 0-92708  
 Mo<sub>2</sub>Si<sub>2</sub> films, magnetron DC reactive sputtering, struct. and props. 0-80966  
 Mo<sub>3</sub>W<sub>3</sub>Se<sub>8</sub> single cryst. vapour growth, characterisation 0-93466  
 Mo<sub>3</sub>X<sub>4</sub> cluster cpds. (X = F, Cl, Br, I), SCF-SW-Xα calcs. 0-74276  
 PbMo<sub>6</sub>S<sub>8</sub>, supercond. Chevrel phase, electron tunnelling spectroscopy expts. (*German*) 0-107966  
 PbMo<sub>6</sub>S<sub>8</sub> wire, powder processed, crit. current density and field 0-80466  
 PbMo<sub>6</sub>S<sub>8</sub>Fe, elec. cond. anomalous temp. depend., mag. moments (*Russian*) 0-92878  
 PbO-MoO<sub>3</sub>-MO system, M = Ca, Ba, Mg, Sr, perovskite type cpds. detection 0-108404  
 Sb<sub>0.20</sub>Mo<sub>0.40</sub>Mo<sub>0.31</sub>, synthesis, struct. and oxidation state (*French*) 0-64971  
 Sn<sub>2</sub>Mo<sub>6</sub>S<sub>8</sub>, struct. anal. supercond. props. 0-97023  
 Sn<sub>2</sub>Mo<sub>6</sub>O<sub>3</sub>-V<sub>2</sub>C<sub>5</sub>, phase comp. determ. using X-ray diffr., electron microscopy and DTA (*German*) 0-88046  
 Ti<sub>2</sub>Mo<sub>6</sub>S<sub>8</sub>, prep. and struct., Mo<sub>12</sub> cluster in Mo<sub>12</sub>S<sub>14</sub> unit 0-107168  
 TmO<sub>2</sub>S<sub>8</sub>, low temp. Mossbauer study and mag. susceptibility 0-80656  
 (W, Mo)C, hard-facing applications, effect of Mo on struct and hardness of WC 0-108474  
 YCrO<sub>3</sub>-Mo eutectics, prep. and microstruct. 0-108380  
 YbMo<sub>6</sub>S<sub>8</sub>, low temp. Mossbauer study and mag. susceptibility 0-80656

**moments (electric)** *see electric moments*

**moments (magnetic)** *see magnetic moments*

**moments (molecules)** *see molecular moments*

**momentum**

- see also angular momentum*  
 atmosphere, planetary wave heat and momentum fluxes rel. to stratosphere and mesosphere meridional circulations 0-109219  
 education, momentum flow as force, alternative conceptualisation for teaching mechanics 0-67993  
 quantisation and measurement of momentum observables 0-98815  
 theory, generalised formulation for transient phenomena 0-62474

**monitoring**

- see also patient monitoring; radiation monitoring*  
 air pollution, monitoring instrums. including chemiluminescent NO<sub>x</sub> monitor 0-72118  
 air pollution, pollutant gases monitoring from space using passive microwave techniques 0-76690  
 ambient air analysis, area survey and sampling mobile laboratory 0-104528  
 corrosion field testing, NBS program 0-76427  
 detonation deposition of coatings, monitoring method 0-60780  
 effluent tank contents anal. by HPLC 0-71982  
 electron emission spectroscopy based instrument applic. to rate controlled deposition of alloy films (*German*) 0-89152  
 Finnish river water pollution monitoring network 0-89686  
 gaseous criteria pollutant methodology and standards for USA Clean Air Act 0-94133  
 level of liquid N<sub>2</sub>, automatic, in Dewar flasks 0-57309  
 LMFBR, Na purification system, cold traps and plugging indicator 0-99209  
 nonsinusoidal periodic current meas. using standard DC shunt with magnetic powder monitoring, frequency errors 0-104398  
 plating line Co concentration monitoring, by automatic colorimeter 0-105691  
 pulsed magnetic analyser, IMA-5 0-104399  
 smoking pattern recorder, portable 0-94385  
 stress/duress automated detect. system 0-76852  
 surface water continuous analysis by NH<sub>4</sub><sup>+</sup>-sensitive plastic membrane electrode 0-89701  
 vacuum deposited layers, thickness monitoring techniques (*Japanese*) 0-60783  
 wind energy prospecting in Prince Edward Island, programme overview and status report 0-61243  
 Cl monitoring, TAGA 3000 mobile test unit 0-72114  
 H<sub>2</sub>SO<sub>4</sub> mist monitor, semicontinuous 0-61495  
 NH<sub>3</sub>, using Stark microwave cavity resonator 0-61500  
<sup>222</sup>Rn, atmospheric, two-filter continuous monitor 0-58097

**monitoring, computerised** *see computerised monitoring*

**monitors** *see monitoring*

**monochromators**

- see also X-ray monochromators*  
 automation of high-intensity monochromator using wavelength-scan and intensity-control system 0-86366  
 conical diffraction mounting for synchrotron radiation monochromators 0-91910  
 Czerny-Turner grating monochromator, Cary principle dynamic dispersion determ. 0-58666  
 double-grating monochromator, theory 0-58708  
 double-pass solar monochromator, with digital device for obs. and spectrum processing automation (*Russian*) 0-72777  
 dual toroidal grating XUV monochromator, performance 80 to 1280 Å 0-90941  
 dual-prism, scanning attachment, appl. to cytospectrofluorometric installation 0-101837  
 Ebert-Fastie, alignment using He-Ne laser and Fresnel diffraction pattern 0-99853  
 fluorescent materials, reflective radiance factor meas. by two-monochromator method (*Japanese*) 0-68237  
 Fourier transform spectrometer performance, instrumentation for assessment 0-95165  
 grating type monochromators, spectrophotometry and colorimetry errors caused by polarisation of meas. system (*Japanese*) 0-101815  
 high energy electron spectroscopy techniques 0-62740  
 high resolution double monochromator, for light scatt. and fluoresc. standard in colloid 0-57247  
 holographic concave grating monochromator, design (*Chinese*) 0-58676  
 imaging properties, monochromator using concave holographic grating and plane mirror 0-99856  
 IR spectrophotometer, digital data acquisition/analysis system 0-73482  
 mounting with ruled diff. grating at 45° off-plane 0-87479  
 multiple, construction (*Hungarian*) 0-102812  
 neutron, curved Cu comb 0-63427  
 normal incidence monochromator, 2m high throughput, for SURF II storage ring 0-90951  
 photodetector relative spectral sensitivity meas. method using two tandem monochromators (*Japanese*) 0-101840  
 single, appl. in modern spectroscopy (*Hungarian*) 0-91905  
 spectral slit width correction for precision energy measurements 0-96020  
 spectrophotometer for measuring small sharp absorption bands in solids at low temps. 0-86456  
 spectroscopic, 1980 state and selection criteria (*Hungarian*) 0-73469  
 synchrotron radiation, with three-wave Bragg diffr. 0-87993  
 telescopic, in CTEM, with cylindrical mirror analysers 0-87296  
 triple monochromator a spectrometer in Raman scatt. (*French*) 0-96007  
 trochoidal electron monochromator, optimization of parameters 0-86511  
 VUV 4 m normal incidence monochromator 0-90950  
 VUV monochromators, 10 to 300 Å for synchrotron radiation, evaluation 0-90907  
 VUV monochromators with toroidal holographic gratings, Strehl criterion 0-90949  
 NaCl curved crystal-monochromator, influence of elastic element area on reflecting surface relief (*Russian*) 0-64157

**monolayers**

- see also adsorbed layers*  
 acetylene adsorbed on Fe containing segregated C, hydrogenation, C-1s XPS spectra obs. 0-84366  
 acoustic phonons, obs. method using Brillouin scatt. in adsorbed monolayers 0-59804  
 adsorbed, Lennard-Jones system, melting in external field 0-65362  
 adsorbed film monolayer melting, dual symm. systems, periodic struct. (*Russian*) 0-107405  
 adsorbed monolayer parameter determ. by full current spectroscopy method (*Russian*) 0-70539  
 adsorption isotherms of partially localised, partially mobile, monolayer films, temp. depend., theory 0-107646  
 barium stearate film, low energy electron range meas. using radioisotope Auger electrons 0-70257  
 calcium behenate monomolecular layers between Al electrodes, nonlinear dielec. props. 0-80405  
 chlorophyll a, Langmuir-Blodgett films, deposition onto SnO<sub>2</sub> optically transparent electrode 0-80093  
 cobalt stearate, monomolecular multilayers, XPS escape length depend. on emission angle, elastic scatt. role (*Japanese*) 0-84833  
 α-cyanoacrylate adhesive in first monolayer on bulk Al surface, IR spectra, H-bond form., stretching vibr. 0-87119  
 dye, energy transfer between sensitizers and acceptors 0-80861  
 ellipsometry of clean surfaces, submonolayer and monolayer films, review 0-103546  
 ethylene, adsorption on Ag (111) surface, XPS and UPS investigation 0-103573  
 fatty acid monolayers, light scatt. meas. 0-89011  
 film-deposition model of correlated percolation 0-107679  
 gases on solid surfaces, mobile and localized adsorption, theory 0-65379  
 graphite on Ni (110) surface, oxidation mechanism 0-101037  
 insoluble, on water surface, meas. of temp. gradients in water during evaporation 0-88402  
 insoluble, surfactant adsorpt., Gibbs eqn. calcs. 0-59781  
 IR spectroscopy, reflection-absorption, of adsorbed layer systems, review, book contrib. 0-84747  
 Langmuir-Blodgett, monolayer to multilayer 0-80031  
 metal, on metal cryst. surfaces, surface struct., review 0-80067  
 methane-d<sub>4</sub> monolayer films on graphite, neutron diffr. studies of phases 0-96739  
 methanol adsorption on Cu(110), XPS, UPS and thermal desorpt. study 0-84388  
 molecular, IR absorpt. enhancement by thin metal overlayers, ATR technique 0-88995  
 one-dimensional, Frank-van der Merwe model, incommensurate-commensurate crossover, transfer integral method 0-88426  
 organic molecules in monolayers, reactivity 0-81367  
 pentadecanoic acid, insoluble monolayer, phase transition, simple lattice model 0-70527  
 physisorbed monolayer on graphite, neutron scatt. studies 0-107655  
 polycrystalline, mol. orientation, IR determ. 0-80891  
 pyrazine, electronic energy transfer to metal surface, classical image dipole theory 0-97318



**monolayers continued**

- pyrene dodecanoic acid, lateral diffusion at air-water interface, monomer excimer dynamics 0-92693  
 4-pyridinecarboxaldehyde, in inelastic electron tunnelling spectroscopy junctions, Raman scatt. 0-93344  
 Raman scattering, giant, by mols. adsorbed on metals, review 0-93343  
 Raman scattering, giant, by mols. adsorbed on metals, theory 0-93345  
 Raman spectroscopy of mol. monolayers in inelastic electron tunnelling spectroscopy junctions 0-93344  
 sphere crowded monolayer, multiple EM wave scatt., migration imaging film appl. 0-99627  
 surface pressure at air-water interface, meas. technique 0-89526  
 Ag, on rough Au surface, adsorbed pyridine giant Raman effect 0-63637  
 Au, adsorbed on graphite, overlayer-substrate spacing, LEED determ. 0-103579  
 BaO, monolayer on W (110), film struct. and electron state 0-100498  
 CN, on Ag surface, vibr. spectra, picosec. Raman gain technique 0-91859  
 H, on Sc (0001) and Ti (0001), geometric vs. electronic factor in surface electronic structure 0-70788  
 He monolayer, phase diagram, order-disorder transition 0-107604  
 Kr adsorbed on graphite, commensurate-incommensurate transitions, low temp. theory 0-103582  
 Kr adsorbed on graphite, overlayer-substrate spacing, LEED determ. 0-103579  
 Kr, on graphite, commensurate to incommensurate transition 0-80079  
 Kr submonolayer films on graphite, mol. dynamics simulation 0-88425  
 Mo:C (110) surface, segregation, precip. and desorpt. of C, AES and LEED study (*French*) 0-103480  
 N<sub>2</sub> adsorption on polycryst. W,  $\alpha$  and  $\beta$  adsorption states 0-100404  
 Na, on Cu (111), UPS study of surface electronic struct. 0-80350  
 Ni on TiO<sub>2</sub>, interface electronic props., struct., comp., chemical bonding 0-84499  
 O, half-monolayer on W (100), surface reconstruction kinetics 0-65375  
 O, on GaAs, influence of cleavage defects on interaction 0-66684  
 O<sub>2</sub>, on graphite, mag.  $\alpha$ -phase and  $\beta$ -phase transition 0-70530  
 O<sub>2</sub>, on graphite, partially localised, partially mobile monolayer films, adsorption isotherms 0-107646  
 Pb, deposition on Au, quantitative Auger electron spectroscopy, substrate and instrumental effects 0-71523  
 Pb monolayer, double layer with Sn, growth on Al (111), struct. 0-70567  
 S, adsorbed on Al (111), angle resolved UPS obs. of 2-dimens. band struct. 0-60059  
 Se, adsorbed on Al (111), angle resolved UPS obs. of 2-dimens. band struct. 0-60059  
 Se sphere monolayer, multiple EM wave scatt., migration imaging film appl. 0-99627  
 Sn, monolayer, double layer with Pb on Al (111), layer growth, struct. 0-70567  
 Te, adsorbed on Al (111), angle resolved UPS obs. of 2-dimens. band struct. 0-60059  
 W epitaxy on W(110) substrate, work function meas., LEED investigation 0-80103  
 Xe adsorbed on graphite (0001) surface, monolayer liquid and solid struct. 0-65400

**monolithic integrated circuits**

- see also bipolar integrated circuits; field effect integrated circuits; large scale integration*  
 capacitive pressure sensors for deep-body biomedical appls., pulse-period output 0-67274  
 custom IC fabrication for implantable multichannel neural stimulator 0-85534  
 gas-sensitive sensor with ultrafine particle film deposited on monolithic IC chip (*Japanese*) 0-105630  
 microminiature monolithic capacitive pressure sensor with pulse-period output electronics on same chip 0-81752  
 quasimonolithic and hybrid integrated optical circuits on Si substrates 0-64218  
 AlGaAs/GaAs monolithic series-connected solar cell arrays 0-97794  
 GaAlAs injection DH laser and GaAs Schottky-gate FET 0-58593  
 GaAs, semi-insulating substrates, monolithic integration of optical and electronic devices, review 0-58543

**monomers *see molecules*****monomolecular films *see monolayers*****monomolecular layers *see monolayers*****Monte Carlo methods**

- aerosol scattering indicatrices under clear sky conditions in 0.55 to 2.4  $\mu$  spectral range, determ. (*Russian*) 0-94600  
 AES, quantitative 0-84813  
 alloy, binary, magnetic, interface struct., Monte Carlo simulation 0-60317  
 ammonium halides, phase transitions by Monte Carlo method using cubic Ising model 0-70408  
 amorphous targets, energetic in transport, Monte Carlo program 0-102411  
 anharmonic corrections in unimolecular theory, Monte Carlo calcs. 0-83441  
 antiferromagnet, FCC, Ising model, mag. phase diagram, ordering, Monte Carlo calc. 0-103833  
 antiferromagnet, Ising model, crit. props., calc. 0-65946  
 atmospheric optics, book 0-77115  
 atom-atom recombinations, energy transfer mechanisms studied using trajectory calcs. and Monte Carlo method 0-66785  
 binary triangular lattice solution, phase stratification statistical modeling 0-65239  
 blackbody cavities, directional emissivity calc., Monte Carlo method 0-83729  
 blackness of cylindrical cavity containing gas, calcs. using Monte Carlo method 0-106711  
 bond percolation, 2D, cluster size crit. exponent 0-68144  
 Chakravarty-Woo eqn., extension and appl. to liq. <sup>4</sup>He, liq. <sup>3</sup>He, and nucl. matter 0-68124  
 circumstellar dust shells, polarisation by Mie scatt., Monte Carlo anal. 0-98650  
 classical harmonic oscillators, microcanonical ensemble, Monte Carlo sampling 0-102459  
 classical mag. moment system, antiferromag. phase transition, secular dipole interactions 0-80551  
 cobalt stearate, monomolecular multilayers, XPS escape length depend. on emission angle, elastic scatt. role (*Japanese*) 0-84833

**Monte Carlo methods continued**

- colloids, model, elastic moduli, Monte Carlo methods 0-108754  
 comets, orbital evolution of short-period objects, Monte Carlo simulations 0-62073  
 Coulombic systems, charged hard sphere system, rel. to restricted primitive model 0-64854  
 defective solids, Haven ratio in athermal lattice gas, Monte Carlo method 0-84313  
 dendrite development and growth in very small crystals, Monte Carlo study 0-107683  
 dense fluids, solvation forces between two solids 0-64855  
 depletion stabilisation and depletion flocculation, theory 0-89534  
 diamond-like semiconductor film epitaxial growth, computer simulation 0-70560  
 diffuse light scattering, mathematical modelling 0-106450  
 electric field calculation by floating random walk method 0-95760  
 electron beam, energy coupling to expanding thick-shelled target 0-96365  
 electron beam scattering, in organic specimen 0-100148  
 electron displacement damage simulation in HVEM irradi. 0-107325  
 electron gas, ground state, stochastic method calcs. 0-95031  
 electron scattering calculations in solids, high energy 0-96422  
 electron transport in solids, book contrib. 0-100458  
 elementary particle inclusive interactions, multiple production processes regularities, Monte Carlo model 0-102082  
 energy transfer models in solids 0-76074  
 ethane, unimol. decomp., energy transfer processes, Monte Carlo simulation 0-99555  
 exospheres of Moon and Mercury, Monte Carlo simulation methods 0-67588  
 exospheres of Moon and Mercury, Monte Carlo simulation methods 0-67589  
 FCC Blume-Capel model, Monte Carlo study 0-103453  
 ferromagnet, Ising model, diamond lattice, phase transition, crit. props. 0-93127  
 fission reactor safety, cooling system, fault tree anal. using Monte Carlo and anal. methods (*Spanish*) 0-57870  
 fluid, cavity-biased (T,V, $\mu$ ) Monte Carlo method, computer simulation 0-92434  
 fluid dynamics, Rayleigh-Benard convection, randomly forced 0-79314  
 fluid structure and dynamical props., computer simulation, using Monte Carlo and mol. dynamic methods (*German*) 0-69757  
 fusion reactor, FINTOR-D, T breeding blanket, Monte Carlo calcs. 0-99283  
 fusion reactors, TFTR test cell, calc. dose rates from induced activity 0-57967  
 galaxies in clusters, Monte-Carlo simulation of orientations 0-90528  
 galaxy correlation function evolution, N-body Monte Carlo model 0-62292  
 growing lattice animals and Monte-Carlo methods 0-57207  
 hard disc fluid, infinite dilution solute chemical pot. by Monte Carlo simulation 0-88009  
 hard spherocylinder fluid, Monte Carlo simulation, ang. correl. functions 0-75140  
 heat conduction, multimedia problems, Monte Carlo soln. method 0-74704  
 hopping conduction, random one-dimens. system, Monte Carlo computer simulation 0-80278  
 IR sensor noise reduction algorithms, Monte Carlo evaluation 0-95824  
 Ising antiferromagnet, FCC, nearest neighbour interactions, Monte Carlo method 0-80544  
 Ising chain, spin-1, sp. ht. in presence of impurities and mag. field 0-93128  
 Ising model, two-dimens., ferromagnet-spin glass transition, Monte Carlo calc. 0-60287  
 Ising model with biquadratic interaction, phase transition, Monte Carlo method 0-60352  
 Ising models, spatially modulated phase, with competing interactions 0-60334  
 Ising spin glass, three-dimensional mag. correlations 0-103849  
 liquid phase sintered systems, particle coalescence probability estimation 0-104086  
 liquids, diatomic, hard and soft core, free energy difference, Monte Carlo calcs. 0-92436  
 low-temperature plasma production by electron beam ionisation of gas mixture 0-87908  
 magnetic alloys, binary, spinodal decomp., computer simulation study of interface behaviour 0-84913  
 magnetic fluids, particle cluster configuration, Monte Carlo study 0-88827  
 magnetic model systems, computer simulations 0-65924  
 magnetic system, Lifshitz point, phase diagrams and crit. behaviour 0-65928  
 mammography, absorbed dose evaluation, Monte Carlo simulation studies 0-98143  
 Mattis model, modified, mag. relax. 0-65947  
 metal cylindrical wire, elec. resist., scatt. processes, Monte Carlo calc. 0-75560  
 metamagnet, two-dimens., tricritical spinodal decomp., Monte Carlo study 0-93117  
 methane, pot. energy curves, Monte Carlo and SCF LCAO MO calcs. 0-63526  
 methane-d<sub>0</sub>(-d<sub>4</sub>), unimol. decomp., energy transfer processes, Monte Carlo simulation 0-99555  
 monatomic gas, rarefied flows in axisymmetric expansion nozzle 0-92182  
 multi-parameter Monte Carlo computations, adaptive estimation procedures 0-105572  
 nematic liquid crystal, two-dimensional, Monte Carlo simulation 0-100168  
 nematics, uniaxial and biaxial, formed by non-cylindrical symm. mols., computer simulation 0-79680  
 neutrino energy equilibration models in supernova core collapse, Monte Carlo simulations 0-105265  
 neutron transport theory, reduction of computational time for point detector estimator 0-68724  
 NMR spin-lattice relax., effect of correlated atomic diffusion 0-107495  
 noise calc., in III-V semiconductors 0-75575  
 nonlinear radiation transport, soln. by renormalisation group method 0-67555  
 nonuniform one dimensional classical fluids, Lennard-Jones pot. interactions, Percus Yevick approx. and density functional calcs. 0-64864  
 nuclear materials safeguarding, isotopic inventory prediction employing a Monte Carlo Dancoff factor 0-73924

**Monte Carlo methods continued**

nuclear materials safeguards, Monte Carlo simulation of MUF distrib. 0-83170  
 nuclear reactions,  $^{40}\text{Ca}(^{40}\text{Ca},x)$ , relativistic, compression and pion distrib., Monte Carlo calc. 0-73853  
 nucleic acids, bases and base pairs, water struct. in soln., Monte Carlo simulation 0-76709  
 orbit evolution simulations for comets becoming asteroids 0-82261  
 ordered magnetic cpds., selective sublattice dilution, percolation problem 0-103850  
 oriented bond percolation, threshold probability and correlation length exponent calc. 0-68146  
 particle absorption rates at high cell concs., Monte Carlo simulation 0-94141  
 particle passage through thin layers, Monte Carlo calc. 0-100708  
 phase separation kinetics, percolation effects 0-65233  
 photon penetration, photon backscatt. incidence angle depend. 0-104008  
 plane rotator model, Monte Carlo simulation 0-73295  
 plasma, classical one-component, improved equation of state 0-83887  
 plasma confinement in mirror and cusp fields, Monte Carlo simulation 0-96379  
 plasma confinement time investigation using Monte Carlo simulation, for mag. mirror 0-64770  
 polar liqs. permittivity, computer simulation with hard sphere point dipole pot. 0-103911  
 polymer between planes, crossover between dimensionalities, Monte-Carlo study 0-74272  
 polymer chain statics and dynamics, Lennard-Jones interaction, calcs. 0-58425  
 polymer chains, scaling props., excluded-volume expansion 0-96435  
 polymer fluid, static bulk props., reptation Monte Carlo method, LJ pot. 0-64868  
 polystyrene, epimerised isotactic, methylene C mag. resonance spectra 0-63878  
 porous media, water circulation, models (*Rumanian*) 0-69917  
 porous solids, diffusion of gases, Monte Carlo simulation 0-65299  
 porphyrin in n-octane Shpolskii matrix, defect props., Monte Carlo obs. 0-63533  
 Potts model, three-state, first order phase transitions 0-60333  
 Potts models, q-state, two-dimens., Monte Carlo renormalisation-group studies 0-77727  
 primitive model electrolytes, grand canonical Monte Carlo calculations 0-92427  
 primitive model electrolytes, symmetrical, canonical Monte Carlo calcs. 0-92428  
 quantised SU(2) gauge theory, Monte Carlo study 0-77973  
 quasars, Comptonised spectrum, Monte Carlo simulation 0-90566  
 radiative transfer, inverse soln. by  $F_N$  and Monte Carlo methods 0-109352  
 radiotherapy treatment planning, inhomogeneity correction methods compared with Monte Carlo data 0-61698  
 random anisotropy model in Ising model, Monte Carlo simulation 0-80546  
 REBEL-3, code for dose calcs., phantom standing in dwelling room 0-94377  
 relativistic electron beam relaxation in dense gas, radiative energy transfer 0-69968  
 segmented calorimeter, high energy performance, Monte Carlo simulation 0-58029  
 semiconducting photocathodes, carrier transport simulation, Monte Carlo method 0-71575  
 semiconductor, lightly doped, compensated, percolation level, Monte Carlo calc. 0-59923  
 semiconductor, lightly doped compensated, electric fields at impurity centres (*Russian*) 0-84198  
 semiconductor detector active volume, determ. from gamma ray interactions, Monte Carlo method 0-63448  
 semiconductor laser, electron beam pumping efficiency, coating effect 0-91795  
 serine, neutral and zwitterion, water solvation, Monte Carlo simulation 0-76707  
 shadow device, characts., scattering medium effects, Monte Carlo calcs. 0-99630  
 simple fluid, struct. and thermodynamics, Monte Carlo calcs. 0-59365  
 simple liqs. with repulsive forces, thermodynamically selfconsistent theory 0-75139  
 solid-on-solid representation, planar model Monte Carlo simulation 0-96727  
 spent fuel waste products, delayed neutron nondestructive assay instrumentation, Monte Carlo calculational design 0-81271  
 spin glass, five-dimensional, Edwards-Anderson ordering possibility 0-60295  
 spin glasses, mag. props. of Sherrington-Kirkpatrick model 0-88774  
 spin glasses, time translation, spatial scaling and nonexponential relaxation 0-97110  
 square lattice site problem, percolating cluster, Monte Carlo study 0-77720  
 square well fluid, eqn. of state well width depend., Monte Carlo calc. 0-64853  
 structural system, simulation anal. of reliability and maintenance (*Japanese*) 0-62453  
 SU(2) theory, asymptotic freedom scales calc. using Monte Carlo methods 0-90988  
 SU(3) theory, asymptotic freedom scales calc. using Monte Carlo methods 0-90988  
 supersaturated vapour, critical clusters, theory and Monte Carlo simulation, review 0-82734  
 three body ion-ion recombination probability, Monte Carlo simulation 0-85160  
 tissue equivalent phantom, dose distrib. calc. using Monte Carlo programme 0-78457  
 transport phenomena calc., in semiconductor junction lasers 0-98766  
 two-dimensional superconductor, resistivity evidence in Monte Carlo studies 0-80434  
 water, Monte Carlo simulation of struct. and thermodynamic props. 0-88017  
 water irradiated by photons up to 2 MeV, initial energies of Compton electrons and photoelectrons 0-108320  
 X-ray spatial resolution, for SEM and STEM specimens 0-101066  
 XY Lifshitz point region, crit. exponents 0-65898  
 $Z_2$  lattice gauge Higgs theories, Monte-Carlo calcs. 0-86593

**Monte Carlo methods continued**

$e^+e^-$  jets, exclusive calcs. for QCD jets, Monte Carlo approach 0-105911  
 $K^+p \rightarrow \pi^+ \pi^+ X$ , 32 GeV/c, two-pion correlations, Monte Carlo model 0-83008  
 $\Lambda$  hyperon polarisation, meas. by hybrid Monte Carlo tech. 0-99431  
 Al alloys, fatigue crack initiation, computer simulation 0-100893  
 Ar, solid, equilib. props., uncorrel. pairs approx. 0-84303  
 Au, polycrystn., deformed, computer simulation of vacancy annihilation to dislocations (*Japanese*) 0-88205  
 Be, ion-implanted, impurity lattice location, channelling meas., Monte Carlo calc. 0-107291  
 BeF<sub>2</sub> glass transition, Monte Carlo study 0-75343  
 BeF<sub>2</sub>Eu<sup>3+</sup> glass, struct. and optical props. 0-84067  
 BeF<sub>2</sub>Eu<sup>3+</sup> glass, struct., Monte Carlo simulations 0-96448  
 Br<sub>2</sub> in liq. Ar, effective intramol. pot. 0-69208  
 $^A\text{Ca}(\pi^+, \pi^-N)$ , A=40, 44, 48, 291 MeV, quasielastic scatt., differential cross sections, Monte-Carlo data fit 0-68703  
 Cu( $\pi^-, \psi$  (3700)), 50 GeV, formation cross-sections (*Russian*) 0-106082  
 GaAs, carrier diffusion in transient response regime 0-103688  
 GaAs, circuit effects in time-of-flight diffusivity measurements 0-88563  
 GaAs, diffusion and power spectral density and correl. function of vel. fluctuation for electrons 0-65576  
 GaAs, self-scattering in Monte Carlo calcs. of transient dynamic response 0-103687  
 GaAs, transient dynamic response calculation by Monte Carlo techniques 0-107796  
 Ga, In, Sb, electron transport in RF field, Monte Carlo simulation 0-96932  
 H<sub>2</sub>, metallic, ground-state energies of liq. and solid phases, variational and Monte Carlo methods 0-70502  
 H<sub>2</sub>O, ST<sub>2</sub>, discrepancy between Monte Carlo and mol. dynamics calc. using truncated pot. anal., internal energy determ. 0-95702  
 He-He, Born Oppenheimer pot. using Hylleraas-type electronic wave functions 0-91442  
 He-Xe, eqn. of state, Monte Carlo calcs. 0-59158  
 He+2l<sub>1</sub>-l<sub>2</sub>+He, energy transfer mechanisms studied using trajectory calcs. and Monte Carlo method 0-66785  
<sup>3</sup>He gridded fast neutron ionisation chambers, Monte Carlo calc., of energy dependent efficiency 0-99417  
<sup>3</sup>He, ground state of polarised and unpolarised fluid, Monte Carlo calcs. 0-92748  
<sup>4</sup>He, liq., variational Monte Carlo calcs. with three body correl. 0-96711  
<sup>4</sup>He, liq. film and solid, hypernetted chain generalised eqn. optimal solns. 0-75396  
 I<sub>2</sub> liq., static structure factor, neutron diffraction 0-103236  
 InAs, transient dynamic response calculation by Monte Carlo techniques 0-107796  
 p-InP field-assisted photocathodes, quantum efficiency 0-84831  
 InSb, current-voltage characteristics at room temperature and high hydrostatic pressure 0-88560  
 n-InSb, hot electron noise temp., Monte Carlo calc. 0-107877  
 N<sub>2</sub> gas, electron energy degradation, Monte Carlo study 0-69969  
 NO<sub>2</sub> hydrate clusters, ground-state HF pot., Monte Carlo simulation, energy surfaces and rot. barriers 0-106412  
 Ne(<sup>3</sup>P), elastically scattered, metastable, ang. distrib., conventional rel. to Doppler shift methods 0-58418  
<sup>21</sup>Ne, strength function calcs. in many fermion systems, Monte-Carlo method 0-86820  
 Ni (111), O adlayer phases and binding sites 0-80069  
 O<sup>+</sup>+O<sub>2</sub>→O<sub>2</sub><sup>+</sup>+O, cross section kinetic energy depend., rate consts. meas. and Monte Carlo calcs. 0-78701  
 Se, liquid and amorphous, struct. modelling using Monte Carlo method 0-59391  
 Si, blistering due to 400 to 1800 keV <sup>4</sup>He<sup>+</sup> ions, modal range determ. 0-100289  
 Si, diffusion and power spectral density and correl. function of vel. fluctuation for electrons 0-65576  
 Si, electrical conductivity, inertia of electron heating, expt. and theory 0-65613  
 Si, electron beam annealing, beam voltage effect modeling 0-75275  
<sup>28</sup>Si, strength function calcs. in many fermion systems, Monte-Carlo method 0-86820  
 U, prospecting by active neutron logging, evaluation models 0-98480

**Moon**

see also *lunar seismology; lunar structure*  
 Babylonian lunar theory 0-94729  
 celestial mechanics, ELP soln. of Moon main problem (*French*) 0-62044  
 crater depth/diameter ratio, morphological characts. 0-62049  
 crater morphology from impact spacecraft imagery 0-62052  
 craters, image edge determ. algorithm 0-98581  
 density structure, max. entropy inversion 0-67602  
 differentiation processes of interior, trace elements as probes, review 0-98584  
 exosphere simulation, Monte Carlo methods 0-67588  
 exosphere simulation, Monte Carlo methods 0-67589  
 fission origin from Earth mantle, geosynchronous phase, consequences for Moon 0-101537  
 geosynchronous revolution and terrestrial continent form. 0-101348  
 gravitational field model, harmonic anal. 0-72799  
 gravity anomalies and tectonics, review 0-98593  
 gravity meas., gradiometer systems on polar orbiting satellite 0-94730  
 highlands crust 0-109381  
 main lunar problem, comparison between ELP and SALE (*French*) 0-85844  
 Mare Crisium, regolithic radioactivity 0-62045  
 Mare Serenitatis multiringed basin, struct. and selenology 0-77304  
 marginal zone, absolute elevations from stellar occultations 0-62047  
 megalithic lunar site a Callanish, Lewis 0-77300  
 micrometeorite impact, ion emission 0-77362  
 moment of inertia and gravity field, study of Earth-Moon system 0-105184  
 noise effects assessment, on satellite links (*Japanese*) 0-82239  
 occultation of Crab Nebula, obs. at decametre wavelengths 0-62248  
 occultation scans, object shape retrieval from new algorithms 0-105149  
 occultations, appl. of deconvolution method 0-105174  
 occultations of X-ray sources, first and last dates (1980 to 1985) 0-77513  
 Oceanus Procellarum, Ti rich basalt geology of Flamsteed region 0-105183



**Moon continued**

- origin, fission theory and geosynchronous release 0-101536  
 photometric anomalies from 1962 obs., possible transient phenomena 0-67587  
 positions, low-precision formulae 0-61990  
 radar contact in 1946 0-85866  
 radiogenic heat source content and cooling 0-90007  
 relief and selenoid deform., harmonic anal. 0-72800  
 rotation around centre of mass, historical development of understanding 0-57064  
 secular accel. rel. to Earth-Moon tidal friction, Earth moment of inertia change 0-81803  
 selenodetic reference network construction, choice of coordinate system (*Russian*) 0-72797  
 solar wind sputtering rate 0-85835  
 Soviet lunar and planetary exploration, handbook 0-62398  
 surface in-situ experiments, solar wind data review 0-77556  
 thermal history, present state and tectonics, fission origin model 0-98582  
 tidal evolution of Earth-Moon system 0-82240  
 tidal-friction theory of the Earth-Moon system 0-81802  
 transient lunar events, possible mechanisms 0-82238  
 transient phenomena observations, fourth list (1821 to 1978) 0-62038  
 translatory-rotatory motion, peculiarities caused by force function third and higher harmonics (*Russian*) 0-90349  
 Li abundance in Luna 24 soil samples 0-67590

**Moon structure** *see* lunar structure**moonquakes** *see* lunar seismology**Morin temperature***see also weak ferromagnetism*

- DyFeO<sub>3</sub>, spin reorientation transitions induced by magnetic fields, Mossbauer study 0-71246

**Morse potential***see also intermolecular mechanics; kinetic theory*

- anharmonic corrections in unimolecular theory, Monte Carlo calcs. 0-83441  
 atom+Morse oscillator, inelastic vibr. energy transfer, mol. continuum influence 0-106383  
 diamond, compressibility, appl. of Murnaghan eqn. of state, Morse pot. 0-79861  
 homonuclear diatomic mols., Morse pot. and vibr. level field induced, shift and broadening 0-69117  
 insulating materials, thermal expansion, Morse pot. model 0-107449  
 matrix elements for Morse oscillators 0-83451  
 metals, Morse potential appl. in molecular-metallic framework 0-79742  
 molecular electronic spectra, high pressure effects, Morse potential formulation 0-63617  
 molecular vibration frequency change influence on Franck-Condon factors 0-106312  
 polymers, breaking down of anharmonic chain, computer calc. 0-106410  
 radical radiation formation in solid organic compounds 0-85201  
 surface, adsorbed atoms thermal desorption, one dimens. microscopic model, weak binding case 0-96729  
 two body T matrices derived from strong potentials 0-63732  
 unimolecular decomp. kinetics, rot. effects 0-81319  
 XH-Y complexes, IR absorpt. spectra, intramol. coupling influence, pot. energy surfaces derivation 0-91624  
 Al, stability and strength of FCC metal using Morse pot. 0-59430  
 Ar, Hulburt-Hirschfelder pot. function 0-63612  
 Au, tilt boundary,  $\Sigma=11$ , simulated and observed struct., vibr. of individual atoms at grain boundary 0-88167  
 CO, centrifugal distortion calcs. by perturbed Morse oscillator model including Dunham parameters 0-63862  
 CO, energy levels for perturbed Morse oscillators 0-78676  
 CrOOH(D), barrier to proton or deuteron tunnelling 0-70156  
 Ge, self-diffusion, activation energy and entropy factors 0-88353  
 H+D<sub>2</sub>, collinear motion, energy transfer and dissociation, collision dynamics 0-99563  
 H<sub>2</sub>O, excited stretching vibrs., quantum mechanics. 0-91535  
 He+CO<sub>2</sub>, translational-vibrational energy transfer, quantum dynamical study 0-63746  
 He+HCN, translational-vibrational energy transfer, quantum dynamical study 0-63746  
 He+OCS, translational-vibrational energy transfer, quantum dynamical study 0-63746  
 He<sup>+</sup>+CS<sub>2</sub>, dissoci. charge-transfer, CS<sup>+</sup>(B<sup>2</sup> $\Sigma^+$ -A<sup>2</sup> $\Pi$ ) emission prod., Morse pot. Franck-Condon factors calc., vibr. anal. 0-99539  
 He<sup>+</sup>+OCS, dissoci. charge-transfer, CS<sup>+</sup>(B<sup>2</sup> $\Sigma^+$ -A<sup>2</sup> $\Pi$ ) emission prod., Morse pot. Franck-Condon factors calc., vibr. anal. 0-99539  
 LiF surface, diffractive scatt. of H atoms, meas., Debye temp. and Morse pot. determ. 0-76124  
 Ni perfect crystal, stability under various stresses 0-104208  
 Si, self-diffusion, activation energy and entropy factors 0-88353  
 Sr<sub>2</sub> dimer, photoassoc., photoluminesc., collisional dissoci. 0-58303

**m.o.s. devices** *see* metal-insulator-semiconductor devices**m.o.s. integrated circuits** *see* field effect integrated circuits**m.o.s. structures** *see* metal-insulator-semiconductor structures**mosaic structure (microstructure)**

- B<sub>2</sub>O<sub>3</sub>-Nb<sub>2</sub>O<sub>5</sub> system, phase equil. and phase struct. obs. by high resolution TEM 0-108419  
 KZnF<sub>2</sub>, single crystal growth, Czochralski method 0-97421  
 Pb film, monocryst., heteroepitaxial growth, struct. defects, and elec. props. (*Russian*) 0-84403  
 Pd-Si films on Si, lattice imaging obs. of structural details 0-103604  
 Si, epitaxial, on sapphire, characterisation, X-ray rocking curves 0-75458

**m.o.s.f.e.t.** *see* insulated gate field effect transistors**m.o.s.i.c.** *see* field effect integrated circuits**Mossbauer effect**

- absorption spectra, thickness and polarisation effects, line intensities of a multiple line absorber (*French*) 0-77924  
 absorption spectra variations induced by LF acoustic excitations 0-102904  
 amorphous alloys and semiconductors, Mossbauer spectrometry (*French*) 0-80660  
 amorphous materials props. and investigation methods (*French*) 0-80652  
 amorphous metals, geometric struct. models and diffraction exam. techniques 0-79700  
 atom in solid, mean square amplitude and velocity 0-62813  
 benzene-I<sub>2</sub>,  $\pi$ - $\sigma$  charge-transfer complex, frozen soln., Mossbauer spectra obs. 0-91655

**Mossbauer effect continued**

- biotic, Mossbauer and optical spectra, Fe<sup>2+</sup>-Fe<sup>3+</sup> interactions 0-60470  
 bubble garnet film, ion-implanted, mag. struct., conversion-electron Mossbauer spectroscopy 0-84628  
 chromite natural samples of Brazilian, Philippine origin, chem. comp., Mossbauer spectroscopy 0-103901  
 coal, mag. susceptibility and Mossbauer meas. 0-60464  
 complementary techniques: EXAFS, determ. of struct. of disordered regions (*French*) 0-80905  
 complementary techniques: positron annihilation, review of appls. (*French*) 0-80899  
 complementary techniques muon spin rotation appl. to physics of condensed matter (*French*) 0-80667  
 computerised analysis, collaboration collection report 0-73106  
 conversion electron Mossbauer spectroscopy, cryogenic proportional He counter 0-69010  
 cytochrome c<sub>3</sub>, haeme-haeme mag. interaction obs. 0-108836  
 cytochrome c<sub>3</sub>-hydrogenase, reduction kinetics, Mossbauer spectra 0-67031  
 dithioferrates (III), electronic struct. and hyperfine interactions, X $\alpha$  calcs. 0-100448  
 Doppler shift, second order, press. depend. 0-66088  
 elemental semiconductors, group IV, Mossbauer spectroscopy of defects, radiation damage and deep levels 0-59533  
<sup>57</sup>Fe, isomer-shift calibration by lifetime variations in electron capture decays of <sup>52</sup>Fe 0-75902  
 ferromagnet, shape of Mossbauer line 0-71251  
 function generator using IC, for Mossbauer effect work 0-68334  
 gamma-quantum coherent scatt. in field of US waves, kinematic theory 0-80649  
 gamma-ray source design, calibration and polarimeter 0-86535  
 glass: <sup>57</sup>Fe, 2-parameter distrib. analysis using general inversion method 0-66079  
 glasses, elec., mag., and optical props., conference, Troy, NY, USA (Aug. 1979) 0-105417  
 inelastic scattering intensity meas. of gamma quanta 0-71245  
 Invar, magnetic structure, depend. on absorbed H, Stoner's band model calcs., Mossbauer spectra 0-65787  
 ionic compounds, amorphous, Mossbauer study, frozen mag. state and hyperfine interaction (*French*) 0-80661  
 iron(II)-A-zeolites, reduction, mag. and Mossbauer study 0-71115  
 isomer shift cancellation with resonant detectors 0-80664  
 lattice atom interactions from resonance  $\gamma$ -ray fluoresc., theory 0-71278  
 lattice parameters, mag. and elec. props. 0-100578  
 line narrowing by resonant filter 0-77922  
 line-broadening of Mossbauer spectra 0-93221  
 Lorentzian function fitting using non-iterative method 0-93220  
 magnetic fluids, mag., optical, and hydrodynamic props., expt. study, review 0-60376  
 magnetic metals, hyperfine mag. fields at <sup>119</sup>Sn nuclei 0-60248  
 magnetism, conference, Munich, Germany (Sep. 1979) 0-56997  
 methylated benzene-I<sub>2</sub>,  $\pi$ - $\sigma$  charge transfer complex, frozen soln., Mossbauer spectra obs. 0-91655  
 myoglobin, atomic vibr. mean square displacement, Rayleigh scatt. of Mossbauer radiation meas. (*Russian*) 0-100665  
 Nafion per fluorosulphonic acid ion exchange membranes, Mossbauer spectroscopy 0-80659  
 niobates, mixed metal, Eu oxidation state, mag. props., Mossbauer study 0-66080  
 non-equilibrium phonon distrib., in cryst., spectral line shape theory 0-60530  
 nuclear energy level shift non-measurability due to pion diamagnetism in Mossbauer effect 0-73808  
 obsidian, Japanese, <sup>57</sup>Fe Mossbauer spectra of naturally occurring glasses 0-67364  
 optical isomer crystal, energy difference due to parity nonconservation (*Russian*) 0-106405  
 oxyhaemoglobin-hydrazine (dimethylhydrazine) interaction,  $\gamma$ -reson. spectroscopy 0-81525  
 oxymyoglobin, evidence for conformational and diffusional mean square displacements 0-89713  
 perovskite compound combination, Mossbauer spectroscopy study (*Russian*) 0-80666  
 pyridine-I<sub>2</sub>,  $n$ - $\sigma$  charge-transfer complex, frozen soln., Mossbauer spectra obs. 0-91655  
 rare earth-transition metal alloys, RM<sub>2</sub>Si<sub>2-x</sub>Ge<sub>x</sub> and RM<sub>4+x</sub>Al<sub>8-x</sub>, magnetism and hyperfine interactions, magnetisation and Mossbauer effect studies 0-75892  
 scattering spectra, numerical analysis 0-75899  
 silicate glasses of geologic interest: Mossbauer absorpt. of Fe III, effect of glass chem. comp. (*French*) 0-80658  
 spectra, effect of gate setting of recording apparatus on spectral parameters 0-90938  
 steel, high C, investigation of transformations during tempering by nuclear gamma resonance method (*Russian*) 0-76256  
 steel, W-Co-Mo-Cr-V-C (8.5, 8.1, 4.5, 3.5, 2.2, 1.02 wt.%), phase composition, struct. and props. 0-104163  
 superparamagnetic particles, magnetic moment time development and discrete orientation model 0-60378  
 tantalates, mixed metal, Eu oxidation state, mag. props., Mossbauer study 0-66080  
 tetraethylammonium neptunium hexachloride, Mossbauer spectra and mag. susceptibility meas. 0-108140  
 tetramethylammonium neptunium hexachloride, Mossbauer spectra and mag. susceptibility meas. 0-108140  
 tetramethyltin, adsorbed on graphite, nature of 2 D diffusion, Mossbauer meas. 0-84372  
 three-level Mossbauer gamma-ray lasers, two-stage pumping 0-78857  
 transition metal intermetallic cpds., H absorption and mag. props. 0-60224  
 triethylamine-I<sub>2</sub>,  $n$ - $\sigma$  charge-transfer complex, frozen soln., Mossbauer spectra obs. 0-91655  
 trimethyl tin chloride adsorbed on grafoil, Mossbauer study 0-80643  
 trinuclear exchange clusters, Dzyaloshinsky coupling effects in Mossbauer spectra (*Russian*) 0-108142  
 triphenyl tin chloride adsorbed on grafoil, Mossbauer study 0-80643  
 ultrarelativistic particle radiation in cryst.,  $\gamma$ - $\gamma$  correlations obs. 0-71274  
 ultrasonic sideband intensity depend. on acoustic field statistics 0-75905  
 Al-Fe, dil. solid soln., vacancy-trapped Mossbauer impurity Debye Waller factor 0-60468  
 Al-steel, cementite isolation, Mossbauer anal. 0-93225



## Mossbauer effect continued

- As-Se-Sb, crystallised glasses, struct. from Mossbauer spectra 0-64917  
 As<sub>2</sub>Se<sub>3</sub>:Pt, glass, effect of impurities on elec. props. 0-103699  
 Au, Co-hardened, characterisation by Mossbauer spectroscopy, Co precip. formation 0-80108  
 Au-Dy, dil., hyperfine interaction, Mossbauer study, Kramers quartets 0-66083  
 Au-Fe ion implanted alloy, Mossbauer conversion electron scatt. 0-88898  
 Au-transition metal alloys, <sup>197</sup>Au Mossbauer isomer shift cellular atomic model 0-84673  
 Ba<sub>2</sub>O<sub>3</sub>-PbO-GeO<sub>2</sub>-Fe<sub>2</sub>O<sub>3</sub> glasses, mag. props. and Mossbauer spectra, spero-mag. order at low temps. 0-80530  
 Ba<sub>2</sub>CoS<sub>3</sub>, linear chain antiferromag., mag. susceptibility meas. and Mossbauer spectra 0-107992  
 BaFe<sub>2</sub>O<sub>10</sub>, Ca<sup>2+</sup> substitution effect on hexaferrite lattice and mag. props. 0-60243  
 Ba, FeS<sub>2</sub>, linear chain antiferromag., mag. susceptibility meas. and Mossbauer spectra 0-107992  
 Ba, FeTa<sub>2</sub>O<sub>6</sub>, Mossbauer and X-ray diffr. studies 0-103905  
 BaLaMRuO<sub>6</sub>, (M=Mg, Fe, Co, Ni, Zn), cubic ordered perovskites, Mossbauer and mag. susceptibility meas. 0-75889  
 Ba<sub>2</sub>MnS<sub>3</sub>, linear chain antiferromag., mag. susceptibility meas. and Mossbauer spectra 0-107992  
 Ba<sub>3</sub>Ru<sub>2</sub>MO<sub>6</sub>, (M=Mg, Ca, Sr, Co, Ni, Cu, Zn, Ca), Mossbauer spectra 0-108136  
 BaSr<sub>1-x</sub>Ca<sub>1-x</sub>Fe<sub>2</sub>O<sub>8</sub>, substituted hexagonal ferrites, mag. split Mossbauer spectra obs. and X-ray struct. data 0-71250  
 BaTiO<sub>3</sub>, Mossbauer spectroscopy, sample prep. and results 0-66078  
 BaVS<sub>2</sub>:Fe, Mossbauer and mag. studies, electronic state of Fe 0-108130  
 Ba<sub>2</sub>Zn<sub>2-2(x+y)</sub>Cu<sub>2x</sub>Cd<sub>2y</sub>Fe<sub>12</sub>O<sub>22</sub>, mag. props. and Mossbauer spectrum 0-75765  
 BaZnFe<sub>16-2x</sub>M<sub>2x</sub>O<sub>27</sub> (M=Al, Ga, In, Sc), mag. props. and Mossbauer effect 0-75766  
 Be-Ir, dil., elec. field gradient, Mossbauer meas. 0-80665  
 CaCO<sub>3</sub>:Fe<sup>2+</sup>, Mossbauer spectra 0-108138  
 CaFe<sup>2+</sup>Fe<sup>2+</sup>(Si<sub>2</sub>O<sub>7</sub>)O(OH), ilvaite, electronic struct., press. and temp. depend. of <sup>57</sup>Fe Mossbauer spectrum 0-108129  
 Ca, Fe<sub>2</sub>Ge<sub>2</sub>O<sub>12</sub> garnet, light absorpt. spectral study 0-93322  
 CdCO<sub>3</sub>:Fe<sup>2+</sup>, Mossbauer spectra 0-108138  
 Cd<sub>1-x</sub>Ni<sub>x</sub>Fe<sub>2</sub>O<sub>4</sub>, solid soln., mag. and structural characterisation 0-103906  
 (Ce<sub>1-x</sub>Y<sub>x</sub>)Fe<sub>2</sub>, mag. susceptibility and Mossbauer meas., lattice parameters 0-97068  
 Co implantation in Al, replacement collision probability at 4.2K 0-70237  
 Co-Fe, dil., hyperfine mag. fields, press. effect, Mossbauer meas. 0-71277  
 Co-P alloys, geometric struct. models and diffraction exam. techniques 0-79700  
 CoFe<sub>2</sub>O<sub>4</sub> mag. fluid particles, comp., struct., and mag. props. 0-60374  
 CoFe<sub>2</sub>O<sub>4</sub> mag. hyperfine fields, Mossbauer spectra 0-108139  
 CoFe<sub>2</sub>O<sub>4</sub> ultrafine particles, prep. and mag. props. 0-71116  
 Co,HfAl, hyperfine fields of Fe impurities, Mossbauer spectra 0-71255  
 Co, Pd<sub>80-80</sub>Si<sub>20</sub>, amorphous, structural and mag. heterogeneities 0-80484  
 Co<sub>1-x</sub>Te<sub>x</sub>, fluctuating localised mag. moments, d band motion, Mossbauer study 0-65768  
 Co,TiAl, hyperfine fields of Fe impurities, Mossbauer spectra 0-71255  
 Co,VAI, hyperfine fields of Fe impurities, Mossbauer spectra 0-71255  
<sup>57</sup>Co, Mossbauer absorpt. and emission spectra, hyperfine struct. and relax. effects 0-71279  
 Cr-Co-Fe, low Co, phase separation, TEM and Mossbauer spectra obs. 0-71269  
 Cr<sub>1-x</sub>Fe<sub>x</sub>OOH, 0≤x≤10, prep., Mossbauer effect, Neel temp. 0-108134  
 Cr<sub>1-x</sub>Mn<sub>x</sub>O<sub>2</sub>, hyperfine mag. fields at <sup>119</sup>Sn, Mossbauer study 0-71260  
 Cs<sub>2</sub>Au<sub>2</sub>Cl<sub>6</sub>, electronic state of Au at high press., Mossbauer spectra 0-60467  
 CsFeCl<sub>3</sub>·2H<sub>2</sub>O, rectangular Ising cpd., Mossbauer meas. 0-71252  
 CsFeF<sub>3</sub>, mag. struct. and one-dimens. antiferromagnetism 0-60209  
 CsLi<sub>0.5</sub>(Al,Fe)<sub>0.5</sub>F<sub>6</sub> pyrochlore, Mossbauer contrib. to exam. of cationic order (*French*) 0-93224  
 CsLi<sub>0.5</sub>Fe<sub>0.5</sub>F<sub>6</sub> pyrochlore, Mossbauer contrib. to exam. of cationic order (*French*) 0-93224  
 CsNiFeF<sub>6</sub> pyrochlore, Mossbauer contrib. to exam. of cationic order (*French*) 0-93224  
 Cs<sub>2</sub>NpCl<sub>6</sub>, Mossbauer spectra and mag. susceptibility meas. 0-108140  
 Cu-Au-Fe, ferromag. ordering in FCC γ-Fe precipitates, Mossbauer study 0-71267  
 CuFe<sub>2</sub>O<sub>4</sub>, Jahn-Teller type crystal distortions 0-103904  
 Cu<sub>0.5</sub>Fe<sub>0.5</sub>O<sub>2</sub>-ZnFe<sub>2</sub>O<sub>4</sub>, cation distrib., mag. moment, Mossbauer spectra, chem. anal. 0-75210  
 Cu<sub>2</sub>MnAl<sub>1-x</sub>Sn<sub>x</sub>, Mossbauer effect study 0-60473  
 Cu<sub>2</sub>MnIn<sub>1-x</sub>Sn<sub>x</sub> alloy, compositional SRO, hyperfine interactions 0-71065  
 DyFeO<sub>3</sub>, field induced spin reorientation, Mossbauer spectroscopy 0-65878  
 DyFeO<sub>3</sub>, spin reorientation transitions induced by magnetic fields, Mossbauer study 0-71246  
 ErFeO<sub>3</sub>, field induced spin reorientation, Mossbauer spectroscopy 0-65878  
 ErRh<sub>2</sub>B<sub>4</sub>, superconducting, magnetic dilemma 0-75680  
 EuO:Gd, pure and doped, elec., mag., and optical props. rel. to electronic conc. 0-96880  
 EuPt<sub>2</sub> compounds, partial valence change, <sup>151</sup>Eu Mossbauer and magnetisation obs. 0-70167  
 β-FeOOH, Mossbauer spectra obs., chemical and thermal anal., X-ray diffr., saturation magnetisation 0-88896  
 Fe complex (2, 9-dimethylphenanthroline) sulphate, mag. props., Mossbauer spectra 0-66081  
 Fe film, coated, interface magnetism by Mossbauer spectroscopy 0-75890  
 Fe film, nuclear spin system dynamics Mossbauer study in FMR conditions (*Russian*) 0-80651  
 Fe garnets, sublattice magnetisation curves, Mossbauer study 0-75808  
 Fe, high purity, boriding with cryst. B powder 0-84951  
 Fe in hepatic and splenic tissues 0-81544  
 Fe, mag. hyperfine field at <sup>129</sup>I, press. depend., nucl. gamma reson. 0-71256  
 Fe particles, spin collinearity, Mossbauer spectra study 0-71114  
 Fe small, particle motion effect on Mossbauer spectra 0-84671  
 Fe sputtered film, amorphous, Mossbauer study and electron diffr. obs. 0-75897  
 α-Fe, uniaxial stress effect on Mossbauer spectrum 0-71244  
 Fe-As system, mag. props., Mossbauer study 0-88897

## Mossbauer effect continued

- Fe-B, rapidly quenched, metastable phases 0-76234  
 Fe-B metallic glasses, struct., stability and crystn. 0-75173  
 Fe-Cr, BCC, local moments in Mossbauer study 0-108125  
 Fe-Cr, hyperfine magnetic fields, Mossbauer spectra 0-97165  
 γ-Fe-Ni, local magnetisation of Fe atoms, Mossbauer effect meas. 0-75891  
 Fe-Ni (25 to 50%), FCC, meteorites and thermodynamic equilib., Mossbauer and X-ray diffr. study 0-88087  
 Fe-Ni (28 at.%), martensitic transformations, Mossbauer scattering evidence of soft modes 0-93223  
 Fe-Ni (6-8 at.%), 0-75888  
 Fe-Ni alloy, fluorination kinetics and fluoride film form., chem. nature obs. 0-101035  
 Fe-Ni based metallic glass, Meiglas 2826 MB, Mossbauer study 0-75897  
 Fe-Ni-C, Invar, coated, Mossbauer spectra, effect of applied RF mag. field 0-80645  
 Fe-Ni-Mn, Invar RF collapse and thermal effects, study 0-100624  
 Fe-Ni-Mo(Si), austenite, annealing effect on atom redistrib., Mossbauer anal. (*Russian*) 0-66529  
 Fe-Pd (1-2 wt.%), solution of <sup>119</sup>Sn, study by Mossbauer spectroscopy 0-75888  
 Fe-Sb amorphous films, Mossbauer effect study 0-75896  
 Fe-Sb-Ti(V)(Cr)(Mn)(Co)(Ni), interactions and segregations, Mossbauer and X-ray diffr. study 0-70415  
 Fe-Si (3 wt.%), grain-oriented, stacking effect on power loss, mag. props. 0-88795  
 Fe-Si (3 wt.%), texture, Mossbauer expts. 0-71262  
 Fe-Si-B amorphous alloys, Mossbauer spectroscopy (*French*) 0-80653  
 Fe<sub>1-x</sub>B<sub>x</sub>, amorphous, hyperfine fields and local mag. moments, Mossbauer study 0-75895  
 Fe<sub>30</sub>B<sub>70</sub>, amorphous, crystn. 0-75187  
 Fe<sub>30</sub>B<sub>70</sub>, amorphous ferromagnet, Mossbauer hyperfine fields, mag. struct. 0-75894  
 Fe<sub>30</sub>B<sub>70</sub>, amorphous struct., Mossbauer spectroscopy investigation 0-84677  
 Fe<sub>30</sub>B<sub>70</sub> glass, magnetisation reorientation, Mossbauer effect 0-66092  
 Fe<sub>30</sub>B<sub>70</sub> metallic glass, crystn. and struct. relax., Mossbauer effect study 0-75182  
 FeBO<sub>3</sub>, dynamical diffraction of gamma rays, enhanced nuclear reson. scatt. 0-108127  
 FeBO<sub>3</sub>, nuclear reaction suppression, Mossbauer spectra for Laue diffr. (*Russian*) 0-66093  
 FeBO<sub>3</sub>, suppression effect under hyperfine quadrupole splitting, Mossbauer study (*Russian*) 0-75906  
 FeCl<sub>2</sub>(pyrazole), linear-chain cpd., low-temp. mag. behaviour 0-71253  
 Fe<sub>3-x</sub>Co<sub>x</sub>Al, site preference and local environment effects, Mossbauer and NMR meas. 0-71264  
 (Fe<sub>0.5</sub>Co<sub>0.5</sub>)<sub>1-x</sub>B<sub>x</sub>, amorphous, hyperfine fields and local mag. moments, Mossbauer study 0-75895  
 Fe<sub>1-x</sub>Co<sub>x</sub>Cl<sub>2</sub>·2H<sub>2</sub>O, random mixture with competing spin anisotropies, tetraar. behaviour 0-60324  
 FeCr<sub>2</sub>S<sub>4</sub>, ionic distrib. and band struct., Mossbauer study 0-80646  
 FeF<sub>3</sub>, amorphous, mag. props. and Mossbauer spectra, speromagnetism and micromagnetism 0-75778  
 FeF<sub>3</sub>, amorphous, struct. and mag. props., computer model 0-96446  
 β-Fe<sub>2</sub>Ge<sub>2</sub>, formation in isothermal sintering, phase transition kinetics 0-89197  
 Fe(H<sub>2</sub>O)<sub>6</sub><sup>3+</sup> ion, amorphous frozen soln., Mossbauer study, hyperfine struct. 0-80644  
 FeLu<sub>2</sub>S<sub>4</sub>, structural study, X-ray diffr., Mossbauer spectroscopy 0-107159  
 (Fe<sub>1-x</sub>M<sub>x</sub>)<sub>2</sub>O<sub>3</sub>, yH<sub>2</sub>O, M=Cr,Cu,Ni, crystal growth, characterisation by Mossbauer spectroscopy, mag. meas. and electron microscopy (*French*) 0-80655  
 FeMo<sub>2</sub>S<sub>4</sub>, Mossbauer investigation, Neel point, superparamag. effects 0-97170  
 FeMgBO<sub>3</sub>, and FeMg<sub>2</sub>MO<sub>3</sub>, imperfect 1D mag. systems, Mossbauer expts. 0-60466  
 (Fe<sub>0.10</sub><sup>2+</sup>Mg<sub>0.90</sub><sup>2+</sup>Mn<sub>0.25</sub>) [Fe<sub>1.87</sub><sup>3+</sup>Al<sub>0.13</sub><sup>3+</sup>]O<sub>4</sub><sup>2-</sup>, influence of Fe<sup>2+</sup> ion substitution on electron hopping, Mossbauer study 0-71247  
 (Fe<sub>0.5</sub><sup>2+</sup>Mg<sub>0.5</sub><sup>2+</sup>Mn<sub>0.03</sub><sup>2+</sup>Cu<sub>0.10</sub><sup>2+</sup>) [Fe<sub>1.74</sub><sup>3+</sup>Al<sub>0.26</sub><sup>3+</sup>]O<sub>4</sub><sup>2-</sup>, influence of Fe<sup>2+</sup> ion substitution on electron hopping, Mossbauer study 0-71247  
 Fe<sub>1-x</sub>Mg<sub>x</sub>Ti<sub>0.4</sub>O<sub>4</sub>, mag. ordering, Mossbauer effect in external mag. fields 0-71257  
 Fe<sub>1-x</sub>Mg<sub>1-x</sub>-Zn<sub>1-x</sub>Ti<sub>0.4</sub>O<sub>4</sub> spinel system, X-ray diffraction study 0-88900  
 Fe<sub>2-x</sub>Mn<sub>x</sub>Al, ordering of Fe atoms, X-ray diffr. meas. and mid gamma reson. anal. (*Russian*) 0-96469  
 Fe<sub>1-x</sub>Mn<sub>x</sub>Sn, spin reorientation, Mossbauer study, 77 to 400K 0-97172  
 (Fe<sub>1-x</sub>Mn<sub>x</sub>)<sub>2</sub>Y(B), Mn effect on Fe mag. moments, Mossbauer and mag. meas. 0-71016  
 Fe(NH<sub>4</sub>)<sub>2</sub>(SO<sub>4</sub>)<sub>2</sub>·4H<sub>2</sub>O, rehydration kinetics, Mossbauer effect study 0-61081  
 Fe<sub>0.33</sub>NbS<sub>2</sub>, lattice dynamics and hyperfine interactions, Mossbauer spectra study 0-108135  
 Fe<sub>40</sub>Ni<sub>40</sub>B<sub>20</sub>, amorphous, RF annealing effects 0-108037  
 (Fe<sub>1-x</sub>Ni<sub>x</sub>)<sub>0.5</sub>B<sub>0.5</sub>-P<sub>x</sub>, amorphous, hyperfine fields and local mag. moments, Mossbauer study 0-75895  
 Fe<sub>63</sub>Ni<sub>23</sub>Mn<sub>14</sub>, disordered, mag. struct. near ferro-antiferromagnetic transition 0-60211  
 Fe<sub>40</sub>Ni<sub>30</sub>Mo<sub>10</sub>B<sub>10</sub>, amorphous, mag. anisotropy, Mossbauer study 0-65864  
 (Fe<sub>1-x</sub>Ni<sub>x</sub>)<sub>80</sub>P<sub>20</sub>, amorphous, ferromagnetic alloys, mag. anomalies of Invar type (*Russian*) 0-93089  
 Fe<sub>40</sub>Ni<sub>40</sub>P<sub>10</sub>B<sub>10</sub>, amorphous ferromagnet, Mossbauer hyperfine fields, mag. struct. 0-75894  
 Fe<sub>2</sub>O<sub>3</sub> amorphous layer on graphite, Mossbauer spectra, superparamag. props. 0-60474  
 α-Fe<sub>2</sub>O<sub>3</sub>, Mossbauer spectra near Neel temp., critical indices, magnetisation (*Russian*) 0-66094  
 Fe<sub>2</sub>O<sub>3</sub> ultrafine particles in PTFE matrix, EPR and Mossbauer study 0-100625  
 Fe<sub>2</sub>O<sub>3</sub>-BaO-B<sub>2</sub>O<sub>3</sub>, magnetic props. of Fe-rich amorphous oxide (*French*) 0-80511  
 α-Fe<sub>2</sub>O<sub>3</sub>-Cr<sub>2</sub>O<sub>3</sub> solid solution, Mossbauer effect studies 0-71249  
 Fe<sub>2</sub>O<sub>3</sub> mag. fluid particles, comp., struct., and mag. props. 0-60374  
 Fe(OH)<sub>3</sub> thin films, Mossbauer spectra obs., chemical and thermal anal., X-ray diffr., saturation magnetisation 0-88896  
 α-FeO<sub>2</sub>, asymmetric line shapes of Mossbauer spectra (*Chinese*) 0-103902  
 Fe<sub>2</sub>O(OH)<sub>2</sub>, Mossbauer spectra obs., chemical and thermal anal., X-ray diffr., saturation magnetisation 0-88896



## Mossbauer effect continued

- Fe<sub>71</sub>Pt<sub>29</sub>B<sub>8</sub> amorphous alloys, splat cooled, Mn, Cr and V substituted, mag. and transport props. 0-84593
- Fe<sub>50</sub>Pd<sub>50</sub>, order-disorder transition, Mossbauer study 0-71268
- Fe<sub>80</sub>Pd<sub>20</sub>-Si<sub>20</sub> amorphous, structural and mag. heterogeneities 0-80484
- Fe<sub>50</sub>Pt<sub>50</sub> Invar alloy, Mossbauer shift temp. depend. 0-100626
- Fe<sup>57</sup>(S) paramagnetisations, spin lattice relaxation Mossbauer study, dynamic spin Hamiltonian formalism 0-97173
- Fe<sub>0.54</sub>Sb, temperature effect on lattice const., Mossbauer spectra and density 0-88124
- Fe(Sb<sub>1-x</sub>Te<sub>x</sub>)<sub>2</sub> system cpds., prep., cryst. struct., elec. and mag. charact. 0-108349
- α-Fe<sub>1-x</sub>Si<sub>x</sub> vacancy ordering, cryst. stabilisation energy aspects 0-103325
- FeSiF<sub>6</sub> isotropy of Lamb-Mossbauer factor, Debye model 0-60465
- Fe<sub>3</sub>Sn<sub>1-x</sub> amorphous film, struct. and mag. props. 0-65972
- Fe<sub>1-x</sub>Te, fluctuating localised mag. moments, d band motion, Mossbauer study 0-65768
- Fe<sub>2</sub>TiO<sub>3</sub>, anisotropic spin glass type behaviour 0-60296
- Fe<sub>2</sub>TiO<sub>3</sub>, spin glass system, cation distrib. Mossbauer spectra 0-71248
- Fe<sub>2</sub>TiS<sub>2</sub> lattice dynamics and hyperfine interactions, Mossbauer spectra study 0-108135
- θ-Fe<sub>2</sub>V<sub>2</sub>O<sub>7</sub>, spin glass and paramag. props., susceptibility, EPR and Mossbauer studies 0-75782
- FeYb<sub>2</sub>S<sub>4</sub>, structural study, X-ray diff., Mossbauer spectroscopy 0-107159
- <sup>57</sup>Fe, hyperfine interactions in implanted metals, Mossbauer spectra 0-108141
- <sup>57</sup>Fe, Mossbauer absorpt. and emission spectra, hyperfine struct. and relax. effects 0-71279
- <sup>57</sup>Fe spectra, ferrous charact., cryst. field interactions 0-108133
- GaAs:Sn<sup>+</sup>, impurity-defect complex from <sup>119</sup>In implantation, Mossbauer study 0-59486
- GaP, complex <sup>119</sup>Sn impurity-defect, Mossbauer study 0-75898
- Gd(Al<sub>1-x</sub>Fe<sub>x</sub>)<sub>2</sub>, intermetallic compounds, pseudobinary, Mossbauer studies 0-75887
- GdAlO<sub>3</sub>, canted antiferromagnetic, Mossbauer meas. 0-97171
- (Gd<sub>0.5</sub>Fe<sub>0.5</sub>)<sub>90</sub>B<sub>10</sub>, amorphous, mag. props., Mossbauer study 0-93093
- GdRh<sub>2</sub>F<sub>10</sub>, GdRu<sub>2</sub>H<sub>8</sub>, struct. and mag. props., Mossbauer and magnetisation meas. 0-71271
- Ge:<sup>119</sup>Sn, impurity lattice dynamics, Mossbauer spectra, Debye temp. 0-84262
- Ge:Sn, ion implantation of radioactive <sup>119</sup>Sn 0-59495
- Hf-Ir, dil., elec. field gradient at <sup>193</sup>Ir, Mossbauer meas. 0-66090
- HoFeO<sub>3</sub>, field induced spin reorientation, Mossbauer spectroscopy 0-65878
- I, atoms, Mossbauer isotopes, isomer shift 0-78573
- <sup>129</sup>I<sub>2</sub>, frozen soln. in o- or p-xylene, Mossbauer effect obs. 0-78637
- Ir-Fe, dil., local magnetisation, Mossbauer meas. 0-66091
- <sup>193</sup>Ir, excited nuclei mean precession time depend. on γ-spectral width, g-factors (*Russian*) 0-78211
- KFeF<sub>4</sub>, amorphous, mag. props. and Mossbauer spectra, speromagnetism and micromagnetism 0-75778
- K<sub>2</sub>FeF<sub>4</sub>, two-dimensional antiferromag., cryst. field effects, Mossbauer spectroscopy 0-71254
- K<sub>2</sub>FeF<sub>5</sub>, mag. struct. and one-dimens. antiferromagnetism 0-60209
- K<sub>2</sub>FeF<sub>5</sub>, one-dimensional antiferromag. systems, Mossbauer studies 0-71266
- K<sub>2</sub>Fe<sub>2</sub>F<sub>7</sub>, two-dimensional antiferromag., cryst. field effects, Mossbauer spectroscopy 0-71254
- K<sub>2</sub>FeO<sub>4</sub>, crit. slowing down of spin fluctuations, Mossbauer spectra and relax. theory 0-65882
- KMnF<sub>3</sub>, gamma quanta scattering near 186K transition 0-108126
- K<sub>2</sub>O-B<sub>2</sub>O<sub>3</sub>-Fe<sub>2</sub>O<sub>3</sub>, γ-irrad., Mossbauer spectroscopic study 0-108132
- La-Au, splat-quenched, Mossbauer effect and elec. resist., amorphous struct. 0-84676
- La<sub>2</sub>Co<sub>2</sub>, mag. props. changes upon H<sub>2</sub> absorpt. 0-71270
- La<sub>2</sub>LiO<sub>3</sub>Co<sub>0.5</sub>O<sub>4</sub> phase, intermediate electronic configuration 0-80226
- La<sub>2</sub>MnO<sub>6</sub> (M=Mg, Co, Ni, Zn), cubic ordered perovskites Mossbauer obs. and absence of mag. order 0-75889
- LaNi<sub>1-x</sub>Fe<sub>x</sub>O<sub>3</sub>, magnetisation meas. and <sup>57</sup>Fe Mossbauer studies 0-93217
- Li-Zn ferrites (Li, Zn, Ti, Cr substituted), Mossbauer spectrometry, effect of supertransferred hyperfine fields and relaxation (*French*) 0-80654
- Li-B-O<sub>2</sub>-LiFe<sub>2</sub>O<sub>6</sub>, borate glass, mag. props. of Fe<sup>3+</sup> cations 0-100599
- LiNbO<sub>3</sub>:Fe, impurity charge states after UV irradiation 0-60462
- Lu-Ir, dil., elec. field gradient at <sup>193</sup>Ir, Mossbauer meas. 0-66090
- LuFe<sub>2</sub>, mag. props. changes upon H<sub>2</sub> absorpt. 0-71270
- Mg<sub>2</sub>Fe<sub>1-x</sub>O<sub>4</sub>, polycryst., Verwey type transition, resist., magnetisation, Mossbauer effect and permeability obs. 0-75764
- Mn<sub>1-x</sub>Zn<sub>x</sub>Fe<sub>2</sub>O<sub>4</sub>, prepared by wet method, neutron diff. and high field Mossbauer expts. 0-75719
- (NH<sub>4</sub>)<sub>2</sub>FeF<sub>5</sub>, one-dimensional antiferromag. systems, Mossbauer studies 0-71266
- N<sub>2</sub>H<sub>4</sub>FeF<sub>5</sub>, one-dimensional antiferromagnetism, Mossbauer study 0-65872
- NH<sub>4</sub>H<sub>2</sub>PO<sub>4</sub>:<sup>57</sup>Fe, Mossbauer study, Fe<sup>3+</sup> effect in habit 0-100627
- Na<sub>2</sub>(Fe,Mg)<sub>2</sub>Si<sub>2</sub>O<sub>7</sub>(OH)<sub>2</sub>, riebeckite, low temp. Mossbauer obs. of oriented single cryst. behaviour and mag. props. 0-84674
- Na<sub>2</sub>Fe(CN)<sub>5</sub>NO<sub>2</sub>H<sub>2</sub>O, absolute Mossbauer fraction of <sup>57</sup>Fe nuclei 0-80648
- NaFeF<sub>3</sub>, Mossbauer and low-temp. dilatometry study (*French*) 0-80662
- NaFeF<sub>3</sub>, amorphous, mag. props. and Mossbauer spectra, speromagnetism and micromagnetism 0-75778
- α-Na<sub>2</sub>Fe(PO<sub>4</sub>)<sub>2</sub> orthophosphate, cryst. and vitreous, Mossbauer spectroscopy and mag. susceptibility (*French*) 0-80657
- Na<sub>2</sub>O-3SiO<sub>2</sub>:Fe<sup>3+</sup>, Fe<sup>3+</sup> glasses, Mossbauer and ESR spectra and internal friction 0-100865
- Na<sub>2</sub>O-PbO-SiO<sub>2</sub>, glass-ceramic composite, directionally crystallised 0-107058
- 5Na<sub>2</sub>O.Fe<sub>2</sub>O<sub>3</sub>.8SiO<sub>2</sub>, glass crystallisation study by Fe<sup>3+</sup> EPR and Mossbauer spectra 0-64904
- NdFe<sub>2</sub>, high field Mossbauer study 0-75893
- Ni-Fe, dil., hyperfine mag. fields, press. effect, Mossbauer meas. 0-71277
- Ni-Fe Invar, thermal expansion and spontaneous magnetisation, Invar anomalies, low spin model 0-71001
- Ni<sub>3</sub>Fe<sub>1-x</sub>Cr<sub>1-x</sub>P<sub>1-x</sub>B<sub>6</sub> metallic glass, mech. props. and thermal stability 0-76362
- NiFe<sub>2</sub>O<sub>4</sub> mag. fluid particles, comp., struct., and mag. props. 0-60374
- Ni<sub>2</sub>Sb, temperature effect on lattice const., Mossbauer spectra and density 0-88124

## Mossbauer effect continued

- Ni<sub>1-x</sub>Te, fluctuating localised mag. moments, d band motion, Mossbauer study 0-65768
- Ni<sub>0.25</sub>Zn<sub>0.75</sub>Fe<sub>2</sub>O<sub>4</sub>, Mossbauer study, spin fluctuations 0-60471
- Ni<sub>0.25</sub>Zn<sub>0.75</sub>Fe<sub>2</sub>O<sub>4</sub>, Mossbauer study, noncollinear spin struct. 0-60472
- PbFe<sub>2</sub>O<sub>9</sub>, single crystal, Mossbauer spectra 0-84670
- PbMnFeF<sub>7</sub> and Pb<sub>2</sub>MnFeF<sub>9</sub>, vitreous, insulating, evidence of spin-glass transition 0-97112
- Pd concentration determ. by gamma-ray absorption from <sup>119</sup>Sn<sup>m</sup> 0-108123
- Pd-Fe, very dil., Mossbauer emission spectra, relax. effects 0-66084
- Pd-H, Mossbauer study of local environment of substitutional Co and Fe impurities 0-60475
- (Pd<sub>0.9965</sub>Fe<sub>0.0035</sub>)<sub>1-x</sub>Mn<sub>x</sub>, mag. behaviour at Fe sites, Mossbauer effect meas. 0-66085
- β-PdH<sub>2</sub>, diffusion-induced reduction of <sup>57</sup>Fe Mossbauer fraction 0-108131
- PdH<sub>2</sub>Fe<sub>0.003</sub>, Kondo system, local moments, hyperfine fields, Mossbauer study 0-80478
- Pd<sub>2</sub>Mn<sub>2</sub>V<sub>1-x</sub>Sn, Heusler alloy, structural disorder, Mossbauer study 0-80650
- Pd<sub>2</sub>Sn<sub>2</sub> (x=0.95, y=0.05; x=3, y=1), Mossbauer spectra, high press. effects, force const. 0-84669
- PrFe<sub>2</sub>, high field Mossbauer study 0-75893
- PrFe<sub>2</sub>, Laves phase, mag. props., Mossbauer spectra, crystalline field mag. anisotropy 0-65851
- Pt-Fe, very dil., Mossbauer emission spectra, relax. effects 0-66084
- RbFeCl<sub>2</sub>·2H<sub>2</sub>O, rectangular Ising cpd., Mossbauer meas. 0-71252
- Rb<sub>2</sub>FeF<sub>5</sub>, mag. struct. and one-dimens. antiferromagnetism 0-60209
- Rb<sub>2</sub>FeF<sub>5</sub>, one-dimensional antiferromag. systems, Mossbauer studies 0-71266
- Rh<sub>2</sub>Mn<sub>2</sub>Pb, hyperfine fields, ferromag., NMR and Mossbauer effect studies 0-71259
- Rh<sub>2</sub>Mn<sub>2</sub>Sb, hyperfine fields, ferromag., NMR and Mossbauer effect studies 0-71259
- Ru-Fe, dil., local magnetisation, Mossbauer meas. 0-66091
- Ru<sub>2</sub>FeSn, ferromag. Heusler alloys, hyperfine fields at nonmagnetic atoms in various sites, Mossbauer effect and NMR meas. 0-66089
- Sc-Fe(ru)(Au), dil., elec. field gradient, Mossbauer meas. 0-80665
- Sc-Ir, dil., elec. field gradient at <sup>193</sup>Ir, Mossbauer meas. 0-66090
- ScAl<sub>2</sub>-Eu, intermediate valence on Eu ions, Mossbauer isomer shift 0-84587
- ScFe<sub>2</sub>, Mossbauer effect of <sup>57</sup>Fe 0-75903
- ScFe<sub>2</sub>H<sub>2</sub>, Mossbauer effect of <sup>57</sup>Fe 0-75903
- Si:<sup>119</sup>Sn, impurity lattice dynamics, Mossbauer spectra, Debye temp. 0-84262
- Si:<sup>57</sup>Co(<sup>57</sup>Fe), implanted, Mossbauer spectra, study of dose dependence 0-75900
- Si-Fe, ion implanted, laser annealing studies using Mossbauer spectroscopy 0-79827
- SiSb, Mossbauer spectra of <sup>119</sup>Sn defect struct. 0-97174
- Si-Sn, Mossbauer study of defects due to <sup>119</sup>In implantation 0-80641
- Si-Pb heterojunction, RHEED, Mossbauer spectroscopy and I-V charact. 0-70828
- Si-Sn heterojunction, RHEED, Mossbauer spectroscopy and I-V charact. 0-70828
- SmI<sub>2</sub>, mag. phase transitions, Mossbauer spectroscopy obs. 0-80509
- α-Sn, ion implanted, defect struct., Mossbauer spectra 0-80214
- α-Sn:<sup>119</sup>Sn, impurity lattice dynamics, Mossbauer spectra, Debye temp. 0-84262
- SnBaO<sub>3</sub>, resonantly scatt. gamma radiation from <sup>119</sup>Sn, energy spectrum with time parameters 0-108122
- SnO<sub>2</sub> aerosols, Lamb-Mossbauer factor (*French*) 0-81375
- SnO<sub>2</sub> films, non-stoichiometric, DC reactively sputtered, elec. props. 0-80415
- Sn<sub>1-x</sub>Pb<sub>x</sub>Se(Te) films, of <sup>119</sup>Sn, spectral charact., conc. depend. 0-103903
- Sn<sub>1-x</sub>Pb<sub>x</sub>Se(Te) films, oxidation rel. to annealing temp. and time, Mossbauer spectra, X-ray and microstruct. obs. 0-104311
- SnTe, mechanochem. and thermal oxidation comparison 0-104310
- Sn temp. depend. isomer shift, pseudopot. approach 0-84675
- <sup>119</sup>Sn, total mass absorpt. coeff. of gamma quanta, chem. binding influence, determ. using Mossbauer effect 0-99467
- SrFe<sub>12-x</sub>Cr<sub>x</sub>O<sub>19</sub>, hexagonal ferrite series, Mossbauer study 0-71258
- SrFe<sub>6</sub>Ga<sub>6</sub>O<sub>19</sub> ferrite, mag. struct., Mossbauer study 0-93087
- SrFe<sub>2</sub>O<sub>19</sub>, Ca<sup>2+</sup> additives effect on hexaferrite lattice and mag. props. 0-60243
- Sr<sub>2</sub>FeTa<sub>2</sub>O<sub>9</sub>, Mossbauer and X-ray diff. studies 0-103905
- Sr<sub>0.5</sub>La<sub>0.5</sub>Fe<sub>0.5</sub>O<sub>4</sub>, high spin configuration stabilisation for Fe<sup>4+</sup> (*French*) 0-88519
- SiTiO<sub>3</sub>, Mossbauer spectroscopy, sample prep. and results 0-66078
- <sup>182</sup>Ta Mossbauer sources (*French*) 0-74064
- Tc-Fe, dil., local magnetisation, Mossbauer meas. 0-66091
- Te, Mossbauer spectra under press. up to 8000 MPa 0-80647
- Th-Dy, dil., type I superconductor, paramag. Dy moment relax., Mossbauer spectra study 0-65755
- Ti-Ir, dil., elec. field gradient at <sup>193</sup>Ir, Mossbauer meas. 0-66090
- Ti(Fe,Co)H<sub>2</sub>, mag. and <sup>57</sup>Fe Mossbauer studies 0-71272
- Tm-3d transition metal intermetallics, <sup>169</sup>Tm Mossbauer effect 0-71261
- TmAG, Mossbauer study of crystal field props. 0-66082
- Tm<sub>2</sub>Ga<sub>2</sub>O<sub>12</sub>, Mossbauer study of crystal field props. 0-66082
- Tm<sub>2</sub>O<sub>3</sub>, low temp. Mossbauer study and mag. susceptibility 0-80656
- TmZn<sub>2</sub>, Mossbauer effect meas. in antiferromag. and paramag. states 0-71265
- UFe<sub>3</sub>B<sub>2</sub>(B<sub>2</sub>), Mossbauer effect of <sup>57</sup>Fe nuclei, mag. props. 0-103907
- VI<sub>3</sub>, mag. struct., long- and short-range order and Mossbauer spectroscopy 0-65803
- V<sub>2</sub>Se<sub>2</sub>Fe, Mossbauer and mag. studies, electronic state of Fe 0-108130
- Y-Ir, dil., elec. field gradient at <sup>193</sup>Ir, Mossbauer meas. 0-66090
- Y(Fe,Co)<sub>x</sub>, x≤0.2, mag. props. and Mossbauer meas. 0-75798
- Y<sub>6</sub>(Fe<sub>1-x</sub>Mn<sub>x</sub>)<sub>23</sub>, Mn-rich compounds, Mossbauer effect study 0-71276
- YIG, vitreous electric-field-gradient distrib., Mossbauer quadrupole splitting temp. 0-75901
- Y<sub>2.85</sub>La<sub>0.15</sub>Fe<sub>3.85</sub>Ga<sub>1.15</sub>O<sub>12</sub> garnet, mag. props., ion implantation effect, Mossbauer study 0-97166
- Y<sub>3-x</sub>Sm<sub>x</sub>Fe<sub>2</sub>O<sub>12</sub>:<sup>57</sup>Fe film, ion implanted, Mossbauer conversion spectra study 0-80663
- YbFe<sub>2</sub>, cryst. elec. field and exchange interac., <sup>170</sup>Yb Mossbauer obs., magnetostriction contrib. 0-108124
- YbFe<sub>2</sub>, high field Mossbauer study 0-75893
- YbMo<sub>6</sub>S<sub>8</sub>, low temp. Mossbauer study and mag. susceptibility 0-80656

**Mossbauer effect continued**

- ZnCr<sub>2</sub>Fe<sub>2</sub>O<sub>4</sub>, Mossbauer spectra, quadrupole splitting, Debye temp. 0-93218  
 Zn<sub>2</sub>Fe<sub>3</sub>O<sub>4</sub> ferrite, mag. struct., Mossbauer spectra and magnetisation study, 4.2K 0-103818  
 Zn<sub>1-x</sub>Ge<sub>x</sub>Fe<sub>2-x</sub><sup>3+</sup>Fe<sub>2x</sub><sup>2+</sup>O<sub>4</sub>, double exchange magnetism, Mossbauer study 0-66087  
 ZnS:<sup>57</sup>Co Mossbauer sources, Fe<sup>3+</sup> transient charge state 0-108128  
 Zr-ir, dil., elec. field gradient at <sup>193</sup>Ir, Mossbauer meas. 0-66090  
 (Zr<sub>1-x</sub>Nb<sub>x</sub>)Fe<sub>2</sub>, antiferromag. spin struct., Mossbauer effect study 0-66086

**Mossbauer spectra** *see Mossbauer effect***motion picture photography** *see cinematography***motors, electric** *see electric motors***Mott insulator** *see localised electron states***movements, atmospheric** *see atmospheric movements***moving-coil instruments**

- chopping pyrometer for remote meas. below 200°C (*German*) 0-86313  
 cryogenics, linear variable differential transformer displacement transducer optimisation 0-86323  
 current and EMF meas. system, vel. control technique 0-98939  
 loudspeaker moving coil temp. meas. systems (*Hungarian*) 0-106698  
 microelectrode puller for biological appls. 0-67309

**moving coil microphones** *see microphones***MS SCF calculations** *see Xalpha calculations***MS Xalpha calculations** *see Xalpha calculations* **$\mu$ -mesons** *see muons***mud** *see sediments***muffin-tin potential**

- adsorption of atoms on metals, Green's function formalism for studying electronic struct., local density of states calc. 0-107884  
 crystal slab, 3-D, surface states, relativistic Green matrix method, muffin-tin potential 0-80345  
 decay state interactions, autoionisation bands (*Russian*) 0-75486  
 disordered alloys, electronic density of states in muffin tin model 0-88467  
 interband transition probabilities calc. based on muffin tin potential 0-104014  
 Lloyd formula and muffin-tin CPA local density of states 0-70577  
 local density of states for an arbitrary array of muffin-tin potentials 0-92805  
 metal, simple, non muffin-tin corrections to eqn. of state (*French*) 0-59906  
 metals, amorphous and liq., s-phase-shift model 0-88473  
 oriented orbitals, photoemission cross-sections, surface Green function formalism 0-93453  
 polyacetylene, electronic energy states and charge density contours studied muffin tin orbitals technique 0-80164  
 polyethylene, electronic energy states and charge density contours studied muffin tin orbitals technique 0-80164  
 PTFE, electronic energy states and charge density contours studied muffin tin orbitals technique 0-80164  
 solids, chemical bonding studied using scattering theory concepts 0-103289  
 transition metals, universal LCAO parameters 0-75503  
 ZnS-V<sup>2+</sup>, impurity states by Green's function method 0-92855  
 Be, eqn. of state, solid-state models, comparison 0-75332  
 Cs, Fermi-surface press. dependence 0-96772  
 EuMo<sub>2</sub>S<sub>8</sub>, Chevrel phase, mag. interactions, LMT0 energy band studies 0-70606  
 Li, cryst. wave function deter., muffin-tin method 0-65436  
 $\gamma$ -Mn, antiferromagnetic, self-consistent bandstructure calcs. 0-88475  
 Nb, electron-phonon interaction, relativistic, APW calc. 0-92837  
 Ni-Cu(Zn)(Ga)(Ge)(As)(Se)(Br)(Kr), dil., ferromagnetic, hyperfine field and relax. time obs. of impurity heavy nuclei 0-75533  
 Ni(001), reaction of CO and H<sub>2</sub>, extended muffin-tin orbital theory 0-76557  
 Rb, Fermi-surface press. dependence 0-96772  
 Si, semi-empirical APW calc. of band structure 0-84424  
 SnMo<sub>2</sub>S<sub>8</sub>, Chevrel phase, mag. interactions, LMT0 energy band studies 0-70606  
 Ta, electron-phonon interaction, relativistic, APW calc. 0-92837  
 TaN, energy band struct. calc., symmetrised APW method 0-96784  
 U compounds, NaCl struct. type, relativistic energy bands, LMT0 calcs. 0-65442

**multichannel analysers** *see pulse height analysers***multidimensional systems**

- gas chromatography, pressure balancing techniques 0-89576  
 oscillations of mechanical systems that do not become linear when the parameter vanishes 0-68032  
 Russian speech automatic recognition, deductive strategy 0-91997

**multigroup diffusion** *see neutron diffusion***multimeters**

- capacitance meter, using DVM and diode pump cct. 0-62656  
 digital, Avo DA117, overview of field servicing appls. 0-68210  
 enlarger exposure meter, using photodiode and multimeter 0-101857

**multiperipheral models**

- cluster model, multi-Regge, comparison with multiparticle transverse and longitudinal data 0-62952  
 hadron+hadron, cluster model, field theoretic, multiperipheral production, Feynman scaling violation 0-57576  
 hadron-nucleus, rapidity distrib., 22.8, 50, 400 and  $\geq 1000$  GeV in emulsion, multiperipheral models 0-91117  
 parton model, deep inelastic processes 0-82961  
 K p $\rightarrow$ 2 $\pi^+\pi^-\pi^+$ , 4.15 GeV/c, nondiffractive A<sub>1</sub> production, double-Regge model 0-78097  
 NN, 10<sup>12</sup> eV, rapidity gap distrib., Snider multiperipheral cluster model 0-73757  
 (P,X), 400 GeV, correlation strength, dependence on target size, multiplicity and cluster size 0-78287  
 pN, 67 GeV, multiperipheral cluster production 0-73689  
 pp $\rightarrow$ pp+N clusters, multiperipheral process, interference terms in transition, amplitudes, correlation expansions 0-62953

**multiphase flow***see also two-phase flow*

- cavitation and multiphase flow, conf., New Orleans, LA, USA, March 1980 0-105430

**multiphase flow continued**

- composite mixture, flow through porous medium, Rayleigh-Taylor instability 0-69912  
 detonation waves, heterogeneous, propagation and blast wave initiation 0-74915  
 hydraulic coal trunk pipeline transport systems, methods of improving economic effectiveness 0-106837  
 particles in dilute suspension in general flow, mass flow and density meas. 0-101784  
 perturbed flow, moisture form. kinetics 0-79387  
 pipeline systems, problems in fluid mechanics for hydraulic transport of solid materials 0-106836  
 power system equipment and components, multiphase flow prediction 0-64616

**multiphonons** *see phonons***multiphoton spectra***see also two-photon spectra*

- acetaldehyde, lowest Rydberg state, multiphoton ionisation spectra 0-83435  
 acetaldehyde, multiphoton ionisation mass spectra 0-83436  
 atom, resonance light scattering, intensity effects 0-91511  
 atoms, multiphoton ionisation, reson. effects, light coherence effects 0-58232  
 atoms, multiphoton ionisation processes, resonance and laser coherence effects 0-74208  
 benzene, multiphoton ionisation mass spectra 0-57420  
 bixcitons, nonlinear laser spectrosc., multiphoton transitions 0-84433  
 chloropentafluoroethane, isotopically selective multiphoton dissoci., CO<sub>2</sub>-laser wavelength, pressure and additives effects 0-78666  
 coumarin 1, multiphoton cross-section determination by means of luminescence experiments 0-93377  
 dimethyl POPOP, multiphoton cross-section determination by means of luminescence experiments 0-93377  
 energy deposition by multiple IR photon absorpt. 0-66833  
 ethanol, multiphoton absorpt. and dissoci. 0-99530  
 ethylene, narrow resonances of multiple-photon IR absorpt. 0-99529  
 fluorobenzene, multiphoton ionisation spectrum in one-photon wavelength region 0-63727  
 four-photon spectroscopy of condensed media, nonlinear spectroscopy developments 0-91860  
 four-wave mixing spectroscopy in crystals, nonlinear spectroscopy developments 0-91861  
 free electron-laser-multiphoton analysis 0-78826  
 gas, resonance four-photon shift, optimal focusing of high-power pumping 0-95574  
 metastable atomic or molecular species, multiphoton transition detection 0-58231  
 methanol-(d<sub>3</sub>), multiphoton absorpt. and dissoci. 0-99530  
 methyl isocyanide photoisomerisation, laser isotope separation, C-isotope enrichment by one-photon vibr. photochemistry 0-81336  
 methylbenzenes, 3p Rydberg transitions, multiphoton ionis. spectrosc. obs. 0-95644  
 molecule, IR laser radiation multiphoton absorpt. direct meas. by pyroelec. detector 0-102545  
 molecules excited by laser IR radiation, excited fraction determ. 0-78661  
 multimode radiation, many-photon atomic excitation 0-74154  
 n-photon resonance phenomena, finite laser bandwidth effect 0-58230  
 naphthalene molecular ion, two and four photon absorpt., dissoci. 0-74210  
 narrow band gap semiconductors, multiphoton absorption in crossed fields (*Russian*) 0-60553  
 optical Autler-Townes effect, time depend., finite bandwidth laser appl. theory 0-91499  
 optically pumped laser three-photon transition theory 0-102690  
 propynal, rovibronic populations, collisionless IR multiphoton spectra, energy deposition, photoacoustic determ. 0-83354  
 Raman spectroscopy, of IR multiple-photon excited mols. 0-74207  
 resonance light scattering, spectral props. and photon correl. 0-91510  
 semiconductors, four-photon transitions, perturbation theory calc. 0-96786  
 semiconductors, IR tunable laser (*French*) 0-82836  
 semiconductors, nonlinear optical props., book contrib. 0-78899  
 solid surface, mol. dynamic processes interaction with laser radiation 0-71943  
 spherically symmetric molecules, many-photon excitation in IR laser field 0-95596  
 tetrachloromethane, UV laser photolysis 0-66826  
 trichlorofluoroethane, UV laser photolysis 0-66826  
 2,2,2-trifluoroethanol, multiphoton absorpt. and dissoci. 0-99530  
 trifluoriodomethane, IR multi-photon excited mols. 0-74207  
 two level atom, coherent and Raman scatt. spectra, secondary emissions 0-69449  
 two-level atoms, multiphoton cooperative radiation, SCF approx. calcs. 0-95856  
 CdS, multiphoton cross-section determination by means of luminescence experiments 0-93377  
 Cr, multiphoton ionisation and absorpt. 0-95575  
 Cs<sub>2</sub>,  $\bar{a}^3\Sigma^-$ -state detect. by reson. enhanced multiphoton ionis. spectrosc. 0-95551  
 Ge, saturation of transmitted intensity of CO<sub>2</sub> laser pulses 0-64111  
 He, metastable, multiphoton transition detection, n<sup>3</sup>S-n<sup>3</sup>D splitting meas. 0-58231  
 He+NO, multiphoton ionisation spectra in supersonic expansion, laser entrained collisional effects 0-83459  
 I<sub>2</sub>, RF optically heterodyned saturation spectroscopy, reson. degenerate four-wave mixing 0-74211  
 K, atomic vapour, resonant interaction with laser, Vavilov-Cherenkov effect (*Russian*) 0-106573  
 N, ionisation, multiphoton absorpt., spectroscopic evidence 0-63726  
 N<sub>2</sub>, multiphoton absorpt., spectroscopic evidence 0-63726  
 NH<sub>3</sub>, expansion cooled, mol. photoionisation, rot. struct., rot. predissoc. of excited states 0-91611  
 NO nonlinear laser spectroscopy, VUV harmonic generation 0-74175  
 NO, selectively excited rovibrational states, multiphoton ionisation spectra 0-69202  
 Na atoms cooling by resonant laser radiation (*Russian*) 0-74155  
 Na, four- and six-photon resonance spectra (*Russian*) 0-91527  
 PbI<sub>2</sub>, multiphoton cross-section determination by means of luminescence experiments 0-93377  
 PbTe, two photon magnetoabsorption (*Russian*) 0-60553



**multiphoton spectra continued**

- SF<sub>6</sub>, IR laser radiation multiphoton absorpt. direct meas. by pyroelec. detector 0-102545  
 SF<sub>6</sub>, IR multiple-photon excited molecules, Raman spectroscopy 0-74207  
 SF<sub>6</sub>, multiphoton dissociation by mol. beam method, energy distribution meas. by time-of-flight spectra, dissociation dynamics 0-78670  
 SF<sub>6</sub>, multiphoton excitation due to vibr.-rot. transitions 0-102546  
 SF<sub>6</sub>, multiphoton-excited,  $\nu_2 + \nu_6$  absorption and emission 0-63626  
 SF<sub>6</sub>, multiple photon absorption, laser pulse intensity and collisions influence 0-95699  
 SO<sub>2</sub>, IR multiphoton excitation and inverse electronic relax., mol. vibr. and fluoresc. 0-106349  
 Sr atomic beam, time correlations between two sidebands of reson. fluoresc. triplet, multiphoton processes 0-95570  
 UF<sub>6</sub>, multiphoton irradiation, spectra and modeling of laser induced emission 0-69160  
 W, multiphoton ionisation and absorpt. 0-95575

**multiple processor systems** *see computer networks***multiple scattering SCF-X-alpha calculations** *see Xalpha calculations***multiple stars**

- see also binary stars*  
 $\alpha$  Crucis, improved spectroscopic orbit for  $\alpha^1$  Crucis 0-67792  
 QZ Carinae (HD 93206), O-type quadruple eclipsing system, spectroscopic and radial vel. study 0-105275  
 VW Cephei, W Ursae Majoris star, third component detect. from rot. line broadening function 0-109494  
 contact binary stars, role of third component in producing sudden period changes 0-109497  
 CPD -62° 1837 (HDE 308122), long-period variable member of triple 0-105260  
 SW Cygni, period changes, mass transfer and third body effects 0-62183  
 40 Eridani, X-ray and radio images, evidence of corona 0-105282  
 extra-solar planetary systems, detection by Space Telescope 0-109356  
 1 Geminorum, radial vel. determ. 0-73006  
 lunar occultations phototelec. obs. 0-72920  
 planetary systems, detection using space-borne interferometers 0-109357  
 planetary systems, IR interferometric search, cosmic ray Cherenkov radiation effects 0-98523  
 speckle interferometric observations, of spectroscopic and visual binary stars 0-90477  
 SS 433, beam models, energetics anal., possible triple system 0-90433  
 Trapezium type multiple systems, connection with associations, galactic clusters and emission nebulae 0-67781  
 Trapezium-type systems, UBVR photometry 0-82431  
 $\gamma$  Velorum, photometric obs. 0-90482

**multiplex transmission** *see multiplexing***multiplexers** *see multiplexing equipment***multiplexing**

- see also frequency division multiplexing; time division multiplexing*  
 epicardial excitation spread, method for registration (*German*) 0-76845  
 image coding, astronomical IR speckle interferometry appl. (*French*) 0-67580  
 low-background astronomical integrated IR detector array development 0-85860  
 optical, using phase modulation 0-95830  
 optical information processing and transmission in white light 0-95833  
 optical space-variant processing with polychromatic light 0-87342  
 remote multiplexing for nuclear reactor instrumentation and control circuits 0-57885

**multiplexing equipment**

- corrugated-waveguide optical demultiplexer mode couplings 0-64194  
 directional coupler, interference filter all-fibre for wavelength division multiplexing 0-91900  
 edge interference filters for WDM transmission over multimode opt. fibres 0-83677  
 EEG recording system, portable pulse-interval modulation telemetry/multiplexing system, home use 0-67261  
 frequency-channel multiplexer and four-channel integrated-optics coupler 0-91936  
 optical access couplers for single strand systems 0-58766  
 optical directional filter structure and characteristics for bidirectional transmission 0-58734  
 optical fibre communication line with spectral multiplexing in 1.3  $\mu$ m region 0-74504  
 optical multiplexer/demultiplexer, low-loss, using interf. filters 0-58728  
 optical subpicosecond gate, velocity-matched directional coupler 0-74512  
 optical wavelength division multiplexing transmission technology 0-58727  
 self-imaging multiplexer and branching couplers 0-106629  
 temperature multiplexers, types of unit and configurations 0-82757  
 wavelength division multiplexer using optical fibre pieces 0-91917  
 wavelength division multiplexing technology status and prospects 0-64203  
 wavelength multiplexer, single-mode-fibre 0-102816  
 LiNbO<sub>3</sub>/Ti phase-matched waveguide electro-optic TE $\rightleftharpoons$ TM mode converter 0-58749

**multiplier phototubes** *see photomultipliers***multipliers, electron** *see electron multipliers***multiprocessing systems**

- see also parallel processing; pipeline processing*  
 image processing microprogrammed video display 0-72366  
 nuclear events picture anal. multiprocessor system (*Italian*) 0-69047  
 speech synthesiser implementation 0-96143

**multivalley semiconductors** *see many-valley semiconductors***multivariable control systems**

- Tokamak plasma, construction and simulation study (*Japanese*) 0-100100  
**multivariable systems**  
*see also multivariable control systems*  
 nuclear reactor surveillance, pattern recognition techniques appl. 0-63351  
 reactor cooling channels, flow anomaly diagnosis, autoregressive model appl. (*Japanese*) 0-83146  
 visual information processing, multi-input system representation, polynomial algorithm properties 0-101145

**multivibrators**

- see also flip-flops*  
 integrated astable optical, Mach-Zehnder interferometric optical switches use 0-87560  
 timer, touch controlled, photography appls. (*Spanish*) 0-86478

**muon absorption**

No entries

**muon capture**

- see also muonic atoms; muonic molecules; radioactivity*  
 anomalous capture and conservation schemes 0-68654  
 exotic atoms, conf., Erice, Sicily, (1979) 0-67939  
 inert gas binary mixture,  $\mu$ -capture, near 5 atm., X-ray yield 0-58419  
 radiative muon capture, transition amplitude, PCAC test 0-83076  
 response tail to high threshold reaction 0-83075  
 $(\mu, n)$ , high energy neutron spectroscopy 0-73841  
 $\mu + p$ , elastic scattering cross section of muonic H atoms 0-69278  
<sup>12</sup>C( $\mu, \gamma$ )<sup>12</sup>B, polarisation studies, muon capture, weak interaction aspects 0-68655  
<sup>40</sup>Ca( $\mu, \gamma$ ), photon asymmetry, O(1/m<sup>2</sup>) and nuclear effects 0-78219  
 H<sub>2</sub>, liq., capture rate meas. 0-69275  
<sup>1</sup>H( $\mu, \nu\gamma$ ), radiative capture relativistic calcs., rate and photon spectrum 0-68605  
<sup>3</sup>He( $\mu, \gamma\nu$ ), transition amplitude, PCAC tests 0-102152  
<sup>3</sup>He( $\mu, \nu\gamma$ ), radiative capture relativistic calcs., rate and photon spectrum 0-68605  
<sup>14</sup>N<sub>g.s.</sub> partial muon capture, mesonic exchange currents, weak process microscopic treatment 0-57742  
 Ne, total muon capture rates using HF wave functions 0-63135  
<sup>237</sup>Np muonic, prompt fission, fragment atomic muon capture 0-95312  
<sup>237</sup>Np, muonic atom lifetimes from muon induced fission 0-69269  
<sup>A</sup>Pu, A=239,242, muonic, prompt fission, fragment atomic muon capture 0-95312  
<sup>A</sup>Pu, A=239,242, muonic atom lifetimes from muon induced fission 0-69269  
<sup>A</sup>U, A=235,238, muonic atom lifetimes from muon induced fission 0-69269

**muon decay**

- CPT, CP and T invariance from correlations and lifetimes 0-77996  
 SU(2)<sub>c</sub> XU(1) theory, radiative corrections, simple renormalisation framework 0-101973  
 weak and EM radiative corrections to low-energy processes 0-95274  
 $\mu^+ \rightarrow eee$ , flavour changing neutral current search 0-105836  
 $\mu^+$  decay from muonium 0-102086  
 $\mu^+ \rightarrow e^+ \gamma$ , upper limit for branching ratio 0-78051  
 $\mu^+ \rightarrow e^+ \bar{\nu}_\mu$ , pol. meas. 0-73760

**muon detection and measurement**

- detector response in EAS 0-63491  
 energy threshold of cosmic ray muon detectors 0-63489  
 Si detectors and Pb absorber plate, telescope structure, high energy muon flux measurement 0-58061

**muon interactions** *see lepton-hadron interactions; lepton-lepton interactions; muon-nucleon interactions; muon-nucleus reactions; photon-lepton interactions***muon-nucleon interactions**

- see also muon-nucleon scattering*  
 deep inelastic scatt., heavy lepton mixings, Weinberg-Salam model 0-62992  
 deep inelastic scattering, gluon jets 0-105862  
 $\mu$ N, 209 GeV,  $\psi$  diffractive prod. cross section,  $\psi \rightarrow \mu^+ \mu^-$  decays 0-102054  
 $\mu$ N $\rightarrow$ TX, 209 GeV, T muoprod. limits from trimuon final states 0-105909  
 $\mu^-$ N-hadron shower, charm-pair production effects 0-73748  
 $\mu^-$ N $\rightarrow$ Ne<sup>+</sup>, muon-electron conversion bounds in <sup>32</sup>S 0-91092  
 $\mu^-$ N in Fe, 280 GeV, dimuon prod. cross sections 0-91094  
 $\mu^-$ N in Fe, 280 GeV, trimuon event cross sections 0-99104  
 $\mu$ p, hadron prod. ang. distrib. and transverse momentum, QCD test 0-82980  
 $\mu$ p deep inelastic scatt., inclusive cross section, lepton pair EM prod. contrib. (*Russian*) 0-105904  
 $\mu$ p-K<sup>0</sup>X, 225 GeV, deep inelastic scatt., strange neutral particle prod. 0-105902  
 $\mu$ p- $\Lambda^0(\Lambda^0)$ X, 225 GeV, deep inelastic scatt., strange neutral particle prod. 0-105902  
 $\mu$ p- $\mu$ nW<sup>+</sup>, current algebra and sum rules high energy W<sup>+</sup> prod. 0-102039

**muon-nucleon scattering**

- see also muon-nucleon interactions*  
 polarised  $\mu$  scattering, elastic and deep inelastic, covariant formulation 0-78069  
 $\mu$ p, deep inelastic scatt., higher order asymptotic freedom corrections 0-105903

**muon-nucleus reactions**

- for inelastic muon-nucleus scattering, see "muon-nucleus scattering"*  
*see also muon capture; muon-nucleon interactions*  
 $(\mu^\pm, \mu^\pm XN)$ , A=12-203, muonintegration cross sections, PWBA anal. 0-68650  
 $(\mu, n)$ , high energy neutron spectroscopy 0-73841  
<sup>2</sup>H( $\mu, n$ )<sup>3</sup>He, muon catalysed fusion, neutron yield, muonic molecules 0-106095  
<sup>242</sup>Pu( $\mu, f$ ), radiationless muonic transition induced fission, fission dynamics probe, friction coeff. 0-78336  
<sup>32</sup>S( $\mu, e$ ), muon-electron conversion bounds 0-91092  
<sup>A</sup>U( $\mu, f$ ), A=235,238, prompt and delayed fission, absolute yields and lifetimes 0-78337

**muon-nucleus scattering***see also muon-nucleon scattering*

No entries

**muon probes**

- condensed matter, muon spin rot., comparison with Mossbauer spectroscopy (*French*) 0-80667  
 diamagnetic domains, study by positive muon method 0-60174  
 diffusion and trapping in solids 0-71283  
 disordered binary alloys of ferromag. crystals, mag. dipole fields at interstitial sites 0-97176  
 exotic atoms, conf., Erice, Sicily, (1979) 0-67939  
 interstitial site determ.,  $\mu$ SR technique 0-71287  
 metal studies by positive probes, review 0-103909  
 metals,  $\mu^+$  diffusion, LAMPF results 0-71285  
 metals, light interstitials diffusion, multiphonon transition modes classification 0-70448  
 metals, positive muon interactions 0-71284  
 quartz, quadrupole effects in spin precession of muonium 0-75910  
 rare earth orthoferrites, muon states, local mag. fields 0-75911  
 spin rotation method, review (*Polish*) 0-88901  
 AuFe spin glass,  $\mu^+$  zero-field spin relax. probe for spin dynamics 0-97177

**muon probes continued**

- Co, interstitial site determ.,  $\mu$ SR technique 0-71287  
 Cr, antiferromagnetic, muon diffusion, spin relax. and coherent motion 0-71281  
 Cr<sub>2</sub>O<sub>3</sub>, muon spin rotation expts. 0-71282  
 Cr<sub>2</sub>O<sub>3</sub>, muon states, local mag. fields 0-75911  
 Cu,  $\mu^+$  diffusion data anal., theory of incoherent direct and indirect muon transitions 0-70448  
 CuMn spin glass,  $\mu^+$  zero-field spin relax. probe for spin dynamics 0-97177  
 CuMn, spin glass, random moments time correl., zero field muon spin relax. meas. 0-60335  
 Dy, interstitial site determ.,  $\mu$ SR technique 0-71287  
 DyFeO<sub>3</sub>, weak ferromagnet,  $\mu$ SR study 0-93226  
 ErFeO<sub>3</sub>, weak ferromagnet,  $\mu$ SR study 0-93226  
 Fe, muon diffusion and relaxation studies 0-75913  
 Fe, positive muon diffusion, press. depend. 0-75907  
 Fe, quantum diffusion of positive muons, 3 to 300K 0-75909  
 $\alpha$ -Fe<sub>2</sub>O<sub>3</sub>, muon spin rotation expts. 0-71282  
 $\alpha$ -Fe<sub>2</sub>O<sub>3</sub>, muon states, local mag. fields 0-75911  
 Fe<sub>3</sub>O<sub>4</sub>, muon states, local mag. fields 0-75911  
 Gd, interstitial site determ.,  $\mu$ SR technique 0-71287  
 Ge, muonium relaxation rates 0-75912  
 Ge,  $\mu$ SR, spin Hamiltonian and anomalous muonium states 0-71286  
 Nb, electron irradiated, muon diffusion 0-80668  
 Nb-V<sub>2</sub> Ga mixed state, Meissner effect investigation by muon method (Russian) 0-107954  
 Ni, interstitial site determ.,  $\mu$ SR technique 0-71287  
 Ni, paramag., muon spin rot. Knight shift, 637 to 906K 0-75908  
 Ni, positive muon diffusion, press. depend. 0-75907  
 Ni-H, ferromag., H impurities and  $\mu$ SR, self-consistent calc. 0-84447  
 Pb intermediate state, Meissner effect investigation by muon technique (Russian) 0-107954  
 Pd, metallic, positive muon Knight shift 0-71280  
 Si,  $\mu$ SR, spin Hamiltonian and anomalous muonium states 0-71286

**muon production**

- bag model, meson and massive photon production 0-105850  
 Drell-Yan model at measured  $Q_T$ : asymptotic smallness of the one-loop corrections 0-105847  
 Drell-Yan muon prod., QCD correction uniqueness 0-78032  
 Drell-Yan process higher order corrections, QCD and parton model sum rules 0-95251  
 Drell-Yan processes, A-depend. of valence and sea quark contribs. 0-86684  
 Drell-Yan processes, asymptotic freedom corrections,  $Q^2$ -dependence 0-62933  
 higher-twist effects in QCD, deep inelastic scattering and the Drell-Yan process 0-102020  
 pair generation, nucleon cascade role 0-91120  
 spin dependent photon structure functions from Drell-Yan and  $e^+e^-$  reactions 0-82973  
 $e^+e^-$  annihilation, QCD and semilocal duality (hadrons/ $\mu^+\mu^-$ ) cross section ratio 0-78085  
 $e^+e^- \rightarrow e^+e^-(\mu^+\mu^-)(\gamma\gamma)$ , 12-31.6 GeV, QED test and Weinberg angle 0-91027  
 $e^+e^- \rightarrow$  hadrons ( $\mu^+\mu^-$ ),  $T(9.46)$  muonic branching ratio, total and leptonic width 0-86703  
 $e^+e^- \rightarrow \mu^+\mu^-$ ; radiative corrections around  $Z^0$ , Weinberg-Salam model 0-99103  
 $\gamma N \rightarrow \mu\mu X$ , QCD cross sections 0-73715  
 $K_L^0 \rightarrow \pi^+\mu^-\nu_\mu$ , transverse polarisation of  $\mu$ , violation of time-reversal invariance 0-68448  
 $K^+N \rightarrow \mu^+\mu^- X$ ,  $K^+/\pi^-$  structure function ratio using Drell-Yan process 0-86718  
 $\mu^+e^+$  pair production in  $\nu_e N$  interaction (Russian) 0-91076  
 $\mu N$ , 209 GeV,  $\psi$  diffractive prod. cross section,  $\psi \rightarrow \mu^+\mu^-$  decays 0-102054  
 $\mu N \rightarrow \mu TX$ , 209 GeV,  $T$  muoprod. limits from trimuon final states 0-105909  
 $\mu^+N$  in Fe, 280 GeV, dimuon prod. cross sections 0-91094  
 $\mu^+N$  in Fe, 280 GeV, trimuon event cross sections 0-99104  
 $\bar{\nu}$  induced dimuon events,  $V^0$  yield, possible beautiful baryon prod. 0-105882  
 $\nu(\bar{\nu})N \rightarrow \mu^+\mu^- X$ , dimuon rate and strange quark sea 0-62961  
 $\bar{\nu}_e e^- \rightarrow \nu_\mu \mu^-$ , exotic lepton number violation and neutrino Majorana masses, Higgs sector 0-86615  
 $\nu N \rightarrow \mu\mu X$ , neutral strange particle prod. in opposite sign dimuon events 0-57584  
 $\bar{\nu}_e N \rightarrow \mu^+ N$ , 2-30 GeV, deep inelastic interactions SKAT preliminary results 0-82963  
 $\bar{\nu} p \rightarrow \mu^+ p \pi^-$ , 5-70 GeV, cross section,  $l=1/2$  prod. amplitude 0-62962  
 $pp \rightarrow \mu^+ \mu^- X$ , 62 GeV,  $\psi$  and  $\gamma$  cross sections, scaling function 0-105932  
 $(\pi^-, \psi CC)$ ,  $\psi \rightarrow \mu^+\mu^-$ ,  $CC \rightarrow \mu^+\nu X$ , 225 GeV/c, search for extra  $\mu$  0-82967  
 $\pi^- N$ , 16, 22 GeV, dimuon prod. parton intrinsic transverse momentum, QCD perturbation 0-63037  
 $\pi^- N \rightarrow \mu^+\mu^- X$ ,  $K^+/\pi^-$  structure function ratio using Drell-Yan process 0-86718  
 $\pi p \rightarrow \mu^+\mu^- X$ , quark transverse momentum effect in bag model 0-86668  
 $\psi \rightarrow \mu^+\mu^-$ , search for extra  $\mu$  in  $(\pi^-, \psi CC)$ , 225 GeV/c 0-82967  
 $e^+e^-$  annihilation, 30 GeV, inclusive  $K^0$  prod.  $K^0 K^+/\mu^+\mu^-$  prod. ratio 0-91103  
 $e^+e^-$ , high energy interactions (Chinese) 0-78074

**muon scattering** see lepton-hadron scattering; lepton-lepton scattering; muon-nucleon scattering; muon-nucleus scattering; photon-lepton scattering

**muonic atoms**

- energy shifts and polarisability of deformed nuclei 0-86893  
 exotic atoms, conf., Erice, Sicily, (1979) 0-67939  
 inert gas binary mixture,  $\mu$ -capture, near 5 atm., X-ray yield 0-58419  
 X-ray emission, circular polarisation (German) 0-69266  
 X-ray emission polarisation (German) 0-69268  
 $\mu p + p$ , elastic scattering cross section of muonic H atoms 0-69278  
 B, muonic X-ray transitions, nuclear charge radii 0-99589  
 Be muonic X-ray transitions, nuclear charge radii 0-99589  
 C, muonic X-ray transitions, nuclear charge radii 0-99589  
 D+Y, muon transfer mechanism from free muonic deuterium 0-69218  
 $^A\text{Fe}(e)$ , 100-275 MeV,  $A=54,56,57$ , cross sections and muonic X-ray meas., charge distrib. systematics 0-86801  
 H, formation at extremely low press. 0-74263  
 H+Y, muon transfer mechanism from free muonic hydrogen 0-69218

**muonic atoms continued**

- $^A\text{H}$ ,  $A=1,2,3$ , muonic atoms, ground state energy levels from quasipot. eqn. 0-87251  
 He, hyperfine structure 0-69273  
 He, muonic, 3p-3d transitions calcs., energy splittings 0-87253  
 N, muonic X-ray transitions, nuclear charge radii 0-99589  
 Na, muonic,  $2s^1/2$  level decay channel concurrence, neutral current effects observation (Russian) 0-83526  
 $^A\text{Ni}(e)$ , 100-275 MeV,  $A=58,60,62,64$ , cross sections and muonic X-ray meas., charge distrib. systematics 0-86801  
 $^{237}\text{Np}$  muonic, prompt fission, fragment atomic muon capture 0-95312  
 $^{237}\text{Np}$ , muonic atom lifetimes from muon induced fission 0-69269  
 $^{204}\text{Pb}$ , muonic, first excited  $2^+$  state, isomer shift of E2 transition 0-99150  
 $^{207}\text{Pb}$ , muonic, octupole doublet isomer shifts, octupole vibr. 0-95750  
 $^{207}\text{Pb}$ , muonic isomer shifts, neutron hole anomalous moment contribs. 0-78728  
 $^A\text{Pu}$ ,  $A=239,242$ , muonic, prompt fission, fragment atomic muon capture 0-95312  
 $^A\text{Pu}$ ,  $A=239,242$ , muonic atom lifetimes from muon induced fission 0-69269  
 $^{294}\text{Pu}$ , muonic atom direct electroprod., finite nuclear size effects (Russian) 0-69272  
 $^A\text{U}$ ,  $A=235,238$ , muonic atom lifetimes from muon induced fission 0-69269  
 $^A\text{Zn}(e)$ , 100-275 MeV,  $A=64,66,68,70$ , cross sections and muonic X-ray meas., charge distrib. systematics 0-86801  
 $^{68}\text{Zn}$ , 2s-2p muonic X-ray transition obs. 0-74264  
 $^{68}\text{Zn}$  muonic atom, dynamical E0 excitation, E0 resonances, muonic X-rays 0-95749

**muonic molecules**

- exotic atoms, conf., Erice, Sicily, (1979) 0-67939  
 free radicals,  $\mu$ SR spectra obs. 0-69279  
 H<sub>2</sub>, liq., capture rate meas. 0-69275  
 $^2\text{H}(\mu, n)^4\text{He}$ , muon catalysed fusion, neutron yield, muonic molecules 0-106095  
 K<sub>2</sub>Pt(CN)<sub>4</sub>, muonic X-ray radiation anisotropy (German) 0-69267

**muonium**

- decay rate, taking into account bound electron 0-102086  
 exotic atoms, conf., Erice, Sicily, (1979) 0-67939  
 hyperfine structure of ground state, magnetic moments, muonium-antimuonium conversion, excited states 0-69273  
 intrasur muonium form. time scale 0-63872  
 muonium+Cl<sub>2</sub>, pot. energy surfaces, inversion calcs. 0-93734  
 quartz, quadrupolar effects in spin precession of muonium 0-75910  
 $(\mu^+\mu^-)$  atom, Coulomb disintegration, cross sections and energy spectra (Chinese) 0-102589  
 Ge, muonium relaxation rates 0-75912  
 Ge,  $\mu$ SR, spin Hamiltonian and anomalous muonium states 0-71286  
 Si,  $\mu$ SR, spin Hamiltonian and anomalous muonium states 0-71286

**muons**

see also cosmic ray muons; muon probes

- electron-muon symmetry of Callan-Symanzik function: two-lepton case 0-73627  
 fusion reactor, catalysis of d-t fusion 0-78438  
 g-factor, (g-2) expts., review, book contrib. 0-68403  
 magnetic moment, anomalous, free gluon mass, lower bound in integer-quark-charge model 0-78042  
 magnetic moments, anomalous, QED test 0-77996  
 muon-electron mass ratio in a semi-classical model 0-91072  
 SU(2) $\times$ U(1) gauge model, muon anomalous mag. moment, charged Higgs boson contrib. 0-78011

**muscle**

- actions, model for semi-quantitative studies 0-61605  
 adaptive control mechanisms for complex motor systems 0-81573  
 adaptive stiffness control in human movement 0-108947  
 afferent nerves from muscle spindles, signal interpretation method 0-101188  
 airway smooth muscle, contracted, hysteresis, dog expts. 0-81634  
 anatomical model, internal pressure effects 0-67103  
 antagonistic muscles, functional elec. stimulation optimisation, math. modelling, joint motion 0-61730  
 arm posture control, spring model and equivalent neural network 0-101196  
 biomechanics, cardiac muscle (Japanese) 0-72201  
 biopsy, semiautomatic image analyser 0-85466  
 cardiac, resting, activation monitored by intensity fluctuation spectroscopy 0-108953  
 cardiac muscle, passive, viscoelastic theory and obs. 0-94273  
 chemomechanical energy transduction, mol. basis 0-72143  
 colon EMG, use of autoregressive-modelling techniques for anal. 0-101146  
 colonic contractile activity meas., pharmacological tests in dogs appl. 0-109068  
 contractile system, sliding motion anal. 0-67104  
 contraction, single, high-time resolution X-ray investigation method 0-81777  
 cross bridge rotation during contraction, fluctuations in polarised fluore. 0-97856  
 cross-striated fibres, efficiency of light diff. under stretch and isometric contract 0-85440  
 data acquisition and anal. of striated muscle diffraction patterns, use of direct memory access microprocessor system 0-89918  
 diaphragm, canine, in vivo stiffness props., obs. and meas. system 0-97988  
 dolphin, lung collapse and intramuscular circulation during diving 0-81643  
 duodenal slow waves, human, anal. and modelling. 0-72146  
 dynamic structure, X-ray scatt., time resolved, rapid data collection systems 0-61740  
 electrically induced muscle contraction, meas. of suggestion effects (Slovenian) 0-81571  
 electrically stimulated, closed-loop control of force 0-76728  
 EMG, filter bank analyser for automatic anal. 0-98162  
 EMG, multichannel data acquisition system for the survey of intercostal muscle activity 0-81790  
 EMG, pulsed integrator for anal. 0-61719  
 EMG, rectified surface, time constant in low pass filtering 0-67266  
 EMG, simultaneous recordings of parts of pectoralis major muscles during swimming 0-72147



**muscle** continued

- EMG, single motor unit action pots. identification by computerised anal. 0-72343
- EMG, single pots., anal. by means of multivariate methods 0-98170
- EMG, surface, dT-dL anal. during muscle fatigue, left hand obs. 0-104576
- EMG, surface, dT-dL anal. during muscle fatigue, right hand obs. 0-104575
- EMG, surface, system for meas., recording and digital anal. (*German*) 0-76848
- EMG biofeedback in hemiplegic patient treatment, comparison of actual and simulated treatment 0-104806
- EMG investigations of gait in cerebral palsied children 0-72186
- EMG period-amplitude analysis, cat locomotion and jumping obs. 0-67057
- EMG processing for sleep research 0-67267
- EMG registration of sensory thresholds in the oral mucosa (*Croatian*) 0-108925
- EMG shimmer in patients with neuropathy and neurogenic atrophy 0-72149
- EMG silent period and muscle mechanics in human soleus muscle 0-67060
- EMG silent period measurement, automated system 0-89883
- extracellular potentials generated by curved fibres in a vol. conductor, modelling 0-97889
- F-actin subunits of thin filaments, functional role of struct. non-equivalence 0-76704
- fatigue, electrophysiological pattern in healthy humans, effects of artificially induced ischemia 0-97890
- fatigue in muscular dystrophy, electrophysiological pattern of development 0-97888
- fibre bundle tension development, action of regulatory light chains 0-94270
- force development, filament spacing effect on axial forces 0-61597
- force development, geometrical factors influencing radial forces 0-67102
- geomagnetic field sensitivity in animals, ferromag. coupling to muscle receptors as basis 0-72185
- heart, isolated, grass-snake, motor reactivity obs. 0-67100
- heart  $Ca^{2+}$  transients during excitation-contraction coupling 0-97896
- Hill equation, fitting to expt. data 0-89777
- hyperbaric hyperreflexia, tendon-jerk and Hoffman reflexes in Man, soleus muscle 0-61530
- intestinal myoelectrical models, pulse synchronisation expts. 0-67061
- laser Raman scattering, mol. probe of contractile state of intact single muscle fibres 0-89718
- motor output response to applied torque perturbations in man, nonlinearities evaluation 0-76771
- multifibre preparation, intercellular clefts influence on pot. and current distrib. 0-72145
- muscle fibres of *Leithocerus maximus*, temp. dependance of cross bridge parameters 0-61598
- muscle stiffness in hypertonic solns. 0-67140
- myoelectric signal processing, expt. demonstration of optimal myoprocessor performance 0-89882
- myoelectric signal processing, optimal myoprocessor derivation 0-89881
- myoelectric signals, improved processor 0-104800
- myoelectrically controlled systems, five-state, error rate obs. 0-72376
- neuromuscular block indicator, model INMB-1, EMG amplitude meas. 0-104785
- neuromuscular unit discharge during muscle fatigue, structural model anal. 0-67066
- oesophageal diaphragmatic EMG in humans, effects of electrode position 0-81753
- papillary muscle selection and testing, some mech. considerations 0-89919
- paralysed, treatment by elec. stimulation (*Slovenian*) 0-81771
- paraplegic patient muscles, provision of functional use by elec. stimulation, review 0-101289
- proteins, rot. motions, saturation transfer EPR obs. 0-94151
- quadriceps femoris, function under maximal concentric and eccentric contractions 0-97963
- reflex stiffness of man's anti-gravity muscles during knee bends while carrying extra weights 0-61601
- resistance strain gauge-meas. techniques in biomech. expts. (*German*) 0-104819
- semiconductor force transducer suitable for use with small muscles 0-72395
- skeletal, cat, force-vel. and fatigability obs. 0-81637
- skeletal, contracting, simulation studies of mech. stretch 0-94263
- skeletal, frog, active tension changes during and after mech. stimulation 0-94262
- skeletal, human, LF sounds from sustained contract. 0-61751
- skeletal, implanted stimulated electrodes of different materials, threshold meas., cat 0-101297
- skeletal, lumped and population stochastic models, implications and predictions 0-76724
- skeletal, water protons NMR relax. times anisotropy obs. 0-85341
- skeletal fibres, endogenous elec. field, dependency on  $Na^{+}$ - $K^{+}$  pump 0-108869
- spindle afferents identification during in vivo recordings in man, preamplifier 0-98155
- stapedius, reflex thresholds and HF audiometry in juvenile diabetics 0-85411
- stretch reflex system, math. model (*Japanese*) 0-67067
- striated, contraction, 10 ms time resolution X-ray diff. 0-61741
- surface EMG, computer anal. during isometric exercise, muscle tension quantification 0-85505
- surface EMG and fatigue, muscle temp. and blood flow 0-94199
- trachealis muscle, dog, spontaneous mech. activities in vivo 0-101203
- tryptophan fluorescence polarisation 0-97877
- upper extremity, eccentric-concentric contract. study 0-85432
- US shear velocity of muscle tissues, mech. props. determ. 0-108930
- uterine, isotropy and anisotropy during labour contract. 0-94257
- vestibular control of oculomotor and postural mechanisms 0-72151
- voluntary movements in man, force gradation and motor unit activity 0-97887
- work-effort ratio of a large muscle group, theoretical model 0-108949
- x-ray diffraction studies of the heart, review, book contrib. 0-109079

**muscovite** see mica**music**

- Pfield principle, Hi-Fi music reproduction (*German*) 0-87685
- production and perception, relationship with human communications 0-96110
- scale, 12-tone, tempered Fourier transform 0-87671
- symphonic, practical and aesthetic microphone techniques for recording and broadcasting, comments 0-79073
- visualisation of the even tempered arrangement, logarithmic graph 0-69606

**music, electronic** see electronic music**musical acoustics**

- bassoon finite amplitude self-vibration 0-69607
- bowed violin strings, investigation of oscillations (*German*) 0-64312
- brass instrums., acoustic principles and problems of performance 0-74646
- complex tone classification according to shape of spectrum envelope 0-102939
- complex tones, interval-based representations, teaching 0-101684
- concert hall design, lateral and ensemble reflection requirements 0-91964
- concert hall design for orchestral balance in seats behind stage 0-91963
- concert hall problem, coherence length and diffuse reflection formulation 0-91962
- concert hall sound system for touring quartet 0-92013
- concert halls, sound reinforcement system, Nippon Budokan Hall (*Japanese*) 0-64291
- consonance and dissonance of pairs of inharmonic sounds 0-74645
- design of music practice rooms, user requirements 0-74606
- medium-scale live concert sound reinforcement system requirements 0-92012
- mode transitions for sounding modes of flute 0-79072
- music stage design 0-74605
- outdoor classical music sound reinforcement systems compared 0-92011
- recording studios, shortcomings of apparently improved acoustic designs 0-69601
- resonant tubes, definition of quality factor, errors arising 0-69572
- retard analysis in motor music 0-106680
- singer and auditorium interactions 0-74604
- sound fields and acoustic design in rooms, review of subjective effects (*Japanese*) 0-64293
- speed of sound, meas. by clapping technique 0-82620
- teaching, to blind student 0-77584
- warm string tone in concert halls, factors necessary to attainment 0-74603

**musical instruments**

- bassoon finite amplitude self-vibration 0-69607
- brass, acoustic principles and problems of performance 0-74646
- clarinet, functional model of simplified version 0-96147
- education, vibrating string, tuning guitar by television 0-73134
- electronic 0-106682
- flute, transition between sounding modes 0-79072
- four-channel percussion synthesiser using 5700 type modules, construction details 0-106681
- guitar, simple model for LF function 0-106678
- harmonic generation in organ pipes, recorders, and flutes 0-106679
- horns, quasi-standing waves, computation of acoustic impedance 0-79071
- percussion and harp, use of dynamic support microphones 0-79073
- portable electronic organ 0-96148
- RE electronic piano, organ pedal cct. construction, tone cct. elements (*Dutch*) 0-99904
- stringed, resonant plates, use of synthetic materials 0-102937
- tone filters for electronic organs, tone spectra and source waveforms 0-106683

**N-body problems**

- see also celestial mechanics; many-body problems
- boundary conditions, spherical, for computer experiment 0-105597
- education, N-body disintegration theory, Maxwellian distrib., nuclear appls. 0-57033
- Euler's three-body problem, eqns. of motion 0-67953
- four-body systems, statistical theory for disruption 0-101531
- galaxy correlation function evolution, N-body Monte Carlo model 0-62292
- globular star cluster, relax. degree and evolution, appl. of N-body system numerical integration 0-67808
- Hill's equation, new exact method (*Chinese*) 0-105152
- Keplerian systems, numerical simulations of collisional evolution 0-109342
- microcosm and macrocosm, discrete modelling 0-82643
- nonlinear discrete systems, integrability 0-98858
- one-dimensional self-gravitating isothermal systems, stability 0-73008
- one-dimensional system, time evolution soln. 0-82635
- particle statistics from induced representations of a local current group 0-57129
- permutational symmetry of many particle states 0-57128
- Ray-Reid generalised systems, invariants derivation 0-101710
- restricted three-body, equilib. points in planar mag. binary problem 0-82178
- restricted three-body problem, appl. to dynamics of ejecta from satellites close to planets 0-98592
- scattering theory combinatorics, partitions, and many-body physics 0-62504
- six bodies in cluster, translational-rotational motion (*Russian*) 0-67528
- stability of constant Laplace solutions of the unrestricted three-body problem 0-68030
- three-body problem, restricted case secular post-Newtonian effects, Treder dynamics 0-72753
- three body problem, planar circular restricted case, stochastic behaviour, reson. overlap criterion 0-105150
- three rigid bodies problem, particular solns. for translational motion (*Russian*) 0-61999
- three-body problem, classical restricted, Coriolis asymm. and Jacobian integral 0-61994
- three-body problem, conditionally periodic solns., KAMo method 0-109343
- three-body problem, elliptical restricted case, Lagrangian soln. stability (*Russian*) 0-94695
- three-body problem, general, three-dimens., biparametric family of symm. periodic orbits 0-61995
- three-body problem, photogravitational restricted circular case, triangular libration points stability (*Russian*) 0-77272

**N-body problems continued**

- three-body problem, plane averaged restricted case, qualitative analysis 0-109345
- three-body problem, restricted, in resisting medium, particular solution (Italian) 0-90325
- three-body problem, restricted case, Sun-Jupiter case, doubly symm. periodic orbit determ. 0-77269
- three-body problem, restricted case, Titan-Hyperion reson. and close approaches 0-77347
- three-body problem, restricted case, u-type families of periodic orbits 0-101530
- three-body problem, restricted classical case, generalisation for radiation press. 0-85843
- three-body problem, spatial periodic orbit families 0-77271
- three-body problem, Sun-Jupiter-satellite system, three dims. orbit determ. 0-67526
- three-body problem, triple collision and tri-parabolic escape 0-67521
- two charged particles problem, Lagrangian and Hamiltonian up to fourth-order terms 0-91736
- two-body problem, generalisation of Kepler's eqn. 0-105151

**N/D method**

- NN, resonances and bound states, multichannel N/D formulation 0-78087

**narrow band gap semiconductor materials** *see narrow band gap semiconductors*

**narrow band gap semiconductors**

- carrier quasienergy spectrum in strong EM wave field 0-92922
- diamagnetic excitons in two-band Dirac model 0-59888
- epitaxial layer, growth, activation by UV and IR radiation 0-71598
- EPR line shape, magnetoresist. effect 0-84638
- ferromagnetic semiconductors, s-f interaction on conduction band, red shift effect theory 0-59872
- gapless, transport coeffs. in quantum limit 0-80302
- gapless semiconductor, magnetic field resonance states (Polish) 0-88508
- intrinsic, indirect exchange interaction, finite temp., valence bands and energy gaps effect 0-59943
- inversion layers in strong elec. field modification of Einstein relation 0-96959
- IV-VI semiconductor, ferroelec., vibronic model of lattice instability 0-80723
- MOS structures of small-gap semicond., capacitance, effect of quantising mag. field 0-84513
- multiphoton absorption in crossed fields (Russian) 0-60553
- photocarrier distrib. and photomagnetolectric effect near stimulated emission threshold 0-80320
- plasmon-phonon interaction effect on optical phonon dispersion 0-103435
- rare earth chalcobismuthites, RBiTe<sub>3</sub>, prep., elec. props., and crystallographic date 0-59981
- recombination instability under crossed elec. and mag. fields 0-70712
- recombination mechanisms, review 0-96905
- thin layer zero-gap semicond., dielec. response 0-103635
- zero-gap, magnetophonon oscils. of transverse magnetoresist. in strong elec. fields 0-96916
- zincblende-symmetry narrow-gap semicond., Fermi energy and Fermi-Dirac integrals 0-70604
- Ag<sub>2</sub>Re films, galvanomag. props. and quantum size effects, obs. 0-70866
- Cd<sub>1-x</sub>Hg<sub>x</sub>Te crystals, donor compensation, low temp. cond. study 0-75571
- CoS<sub>2</sub>, narrow-band ferromag., high press. effect on anomalous elec. resist. 0-70698
- Co(S<sub>1-x</sub>Se<sub>x</sub>)<sub>2</sub>, galvanomag. effects, obs. and interpretation 0-70726
- EuB<sub>6</sub>, electronic struct., transport and mag. props. 0-96782
- Fe<sub>0.2</sub>Co<sub>0.8</sub>S<sub>2</sub>, narrow-band ferromag., high press. effect on anomalous elec. resist. 0-70698
- Hg<sub>1-x</sub>Cd<sub>x</sub>Te, Einstein relation for inversion layers 0-103706
- HgCr<sub>2</sub>Sd<sub>4-x</sub>Te<sub>x</sub>, ferromag. semicond., zero bandgap transition 0-96783
- HgSe film, anomalous photocond., electron microscope study 0-65623
- HgSe, interband  $\Gamma_6$ - $\Gamma_8$  magnetooabsorption, temp. study 0-76032
- InAs, thermal oxidation, growth rate and chem. comp., temp. depend. 0-108619
- InSb, CESR at high mag. fields, scatt. mechanisms 0-93177
- InSb, Einstein relation for inversion layers 0-103706
- InSb MOS struct., capacitance of n-channel inversion layers, elec. field effects 0-80393
- Pb<sub>0.9</sub>Sn<sub>0.1</sub>Te: Cd, influence of Cd doping on high field magnetoresist. and Hall effect 0-75590
- Pb<sub>1-x</sub>Sn<sub>x</sub>Te, narrow gap semicond., theory of mag. susceptibility 0-93070
- PbTe, two photon magnetoabsorption (Russian) 0-60553
- PtSb<sub>3</sub>, high field elec. props., impact ionisation 0-96892
- Sb<sub>2</sub>Te<sub>3</sub>, thermoelectric properties and phase transition, under hydrostatic pressure up to 9 GPa 0-65609
- SnTe, structural phase transition threshold instability in strong EM field 0-103477

**natural gas technology**

- gas distribution equipment in hydrogen service 0-97818
- health risks of high-Btu gas pipeline and electric power transmission systems 0-104520
- simulated natural gas mixtures, enthalpy and phase equil., correl. with modified Starling eqn. 0-61127
- underground pipes, excitation of an elastic half-space by a buried line source of conical waves 0-64245
- H<sub>2</sub> distribution in natural gas equipment, operating, safety and material problems 0-61468

**natural resources**

- see also agriculture; dams; energy resources; mining; water supply*
- coal basin evaluation, appl. of gravity profile across Bonnet Plume Basin, Yukon Territory, Canada 0-76898
- groundwater, saline water and fresh water zones delineation using resistivity and induced polarisation (IP) survey 0-104867
- hydrocarbon gases, in sediments of United States Atlantic continental shelf 0-72511
- ocean energy potential 0-66956
- offshore resources exploration, remote sensing, appls. to oceanography and sea ice 0-77176
- ore bodies in Itapicuru greenstone belt, Bahia, Brazil 0-81879
- Turkey, karst water resource development 0-61821
- water-resource development project design, optimal apportionment scheme appl. (French) 0-77019
- U, exploration and prospecting methods 0-85768

**natural resources continued**

- U, geophysical prospecting, <sup>222</sup>Rn mapping using mat to avoid hole drilling 0-82087
  - U, National Uranium Resource Evaluation (NURE) aerial radiometric survey data interpretation via principal components anal. 0-101438
- natural rubber** *see rubber*
- naval engineering**  
*see also marine systems*  
submarine periscope optical test equipment 0-78943
- Navier-Stokes equations**  
anemometry, hot-wire, in very low velocity flow, calibration of probes 0-75008  
axisymmetric waves on the surface of viscous fluids 0-96266  
blood flow, finite element soln. 0-94269  
boundary layer, numerical soln. of linearised Navier-Stokes eqns., effect of cell Reynolds number 0-106780  
boundary layer problems, finite difference methods, nonuniform grid generation 0-83780  
bounded domain, global weak solution to time dependent Navier-Stokes eqns. 0-77621  
channel, fluid flow behind plate in channel, jet and velocity pulsations (Russian) 0-74979  
detached flows past a cylinder with a flat end, subsonic and transonic vels. 0-92187  
discretisation, splitting of linear operators, iterative methods applied to stationary Navier-Stokes eqn. 0-69755  
discs, eccentric, rotating at different speeds, flow between discs, inertia effects 0-92104  
driven cavitation flow, Navier-Stokes eqn. soln. numerical stability 0-92147  
ducts, axisymmetric, internal viscous flows at moderate to high Reynolds numbers 0-106844  
dusty gases, fully dispersed wave struct., Navier-Stokes eqns. 0-69875  
electroosmotic permeability coefficient in charged membrane model 0-108749  
elliptic cylinder about axis perpendicular to flow, autorotation 0-103033  
emulsion, dilute, straining motion, effect of inertia on dynamic viscosity 0-87797  
falling horizontal cylinder, low Reynolds number, horizontal plane boundary effect 0-87757  
finite difference approx. with second-order accuracy 0-87756  
finite element MAC scheme for 2-D incompressible Navier-Stokes flow 0-74824  
flow in curved tube, finite difference anal. method 0-106846  
fluid flow problems, incompressible, free surfaces 0-106774  
gas-solid flow in cyclone, turbulent swirl velocity, particle sizes and concentrations 0-69902  
gases with molecular viscosity, flow calc. in large particles method (Russian) 0-74826  
generalised representation, of physical situation, appl. to hydrodynamics (Russian) 0-69760  
high Reynolds number, vicinity of wall and of initial motion (French) 0-74823  
incompressible flow calcs. by splitting method (Russian) 0-74827  
incompressible viscous flow, restricted rot. invariance 0-92103  
instability, post-, in class of smooth functions, mathematical model 0-69649  
jets, laminar, vertical, round, weak buoyancy effects due to temp. differences (German) 0-64595  
light induced kinetic effects in gases (Russian) 0-92244  
Maxwellian molecule gas, heat transfer between parallel plates, Navier-Stokes eqns. 0-87839  
natural convection, Navier-Stokes eqn. soln. numerical stability 0-92147  
natural laminar convection about isothermal cylinder, Navier-Stokes eqn. soln. 0-92143  
nonreflecting outflow boundary condition for subsonic Navier-Stokes calculations 0-74828  
periodic capillary tube, two phase fluid flow and hysteresis 0-107615  
periodic capillary tube, two phase fluid flow and hysteresis 0-107616  
pipe flow, curved pipes, fully developed oscillatory flow 0-83846  
pipe flow, low Reynolds number, in vicinity of three dimensional obstacles 0-74981  
polymer solutions, transport properties, conc. effects 0-64875  
rotational effects avoidance in turbulent flow, numerical solns. (German) 0-59057  
shock propagation, multidimensional fluid dynamic calcs., artificial viscosity use, Navier-Stokes viscosity 0-92181  
stably stratified medium, plane free convection from local heat source 0-96253  
steady laminar flow through channel with symmetrical constriction in step form 0-100036  
steady State stefan problem with convection 0-69625  
supersonic flow, parabolic Navier-Stokes equations, implicit finite-difference method using fractional steps technique 0-69866  
transient free convection flow around two-dimensional or axisymmetric bodies 0-69817  
transonic flow, unsteady, turbulence modelling, compression waves developing into shock wave 0-74909  
turbulence, isotropic and homogeneous self-similar behaviour (French) 0-74838  
two dimensional, numerical soln. methods (Russian) 0-101718  
unsteady 3-dims. compressible flow, implicit finite difference simulations, transonic appl. 0-64576  
unsteady boundary layer on a two dimensional or axisymmetric body with higher order effects 0-92106  
variational principle for perfect and imperfect fluids in general relativity 0-90733  
viscous flow, unsteady, around elliptic cylinder, heat transfer, finite difference method (Japanese) 0-69831  
viscous flows with no-slip walls, incompressible Navier-Stokes eqns., pseudospectral method 0-69924  
viscous fluid, deform. of falling elastic particle 0-79149  
viscous fluid, laminar flow, Navier-Stokes eqns., central difference scheme 0-69762  
vortex flows, between rotating cylinders, axisymmetric Navier-Stokes equations 0-59044  
water at 4°C, unsteady free convection past infinite vertical plate 0-69822  
weak nonlinear waves in compressible fluid, higher order approx. 0-92165



**Navier-Stokes equations continued**

- Wedemeyer spin up model, Ekman compatibility conditions, Navier-Stokes eqns. 0-83802  
welding arcs, gas velocity fields modelling 0-75039  
HF laser with flow-through chem. active medium, pulsed-periodic regime realisation 0-106513

**navigation**

- see also *inertial navigation; radar applications; radionavigation; sonar; tracking*  
astrodynamics conf. (Provincetown, MA, USA, June 1979) 0-82583  
marine navigation, remote sensing appls. to oceanography and sea ice 0-77176  
proportional, teaching exercises 0-82611  
satellite navigation, Chebyshev approximations for compression of Ephemerides 0-61993  
spacecraft braking problem in Jupiter atmosphere, ballistic and navigation aspects 0-61981  
spatial pattern recognition by spectral feature classification and coherent optical correlation 0-99644  
stellar direction finder, Cardan point geometry (*Russian*) 0-73312

**NDO calculations**

- see also *CNDO calculations; INDO calculations; MINDO calculations*  
extended Huckel theory, rel. to NDO LCAO theories 0-95536  
hydrides, first row, bending pot. calc. using MINDO approx., force const., equilb. geometry 0-95544  
molecules containing 1st row atoms, K-shell binding energy shifts, NDDO MO calcs. 0-58413  
S-matrix power series expansion 0-69080  
ZDO all valence semiempirical theories, screening effect inconsistencies 0-58154

**nearly-free-electron approximation**

- alloys, indeterminacy of a priori pseudopots., effects on form factors 0-103608  
amorphous superconductor, Eliashberg function, tunnelling and crit. temp. anal. 0-80455

**nebulae**

- see also *galaxies; planetary nebulae; supernova remnants*  
AFGL 2789 (V645 Cygni), refl. nebula, perplexing spectrum 0-73066  
Bok globules, collapsing cloud models 0-62216  
3C 120, Seyfert galaxy, spectrophotometric obs. of assoc. nebulosity 0-67890  
California (NGC 1499), visual extinction uniformity across nebula 0-62225  
Carina Nebula, extinction determ. from open cluster UVB photometry obs. 0-90513  
Carina Nebula, O-type stars on line of sight, extinction law, photometry obs. 0-105240  
Chamaeleon dark cloud, embedded Be-star HD 97048, visible and IR obs. 0-85943  
charge transfer of  $C^+$  and  $S^+$  in diffuse nebulae 0-77463  
Chu's object in Perseus, refl. nebula assoc. with B-type star 0-62132  
dark clouds,  $^{13}C^{16}O/^{12}C^{16}O$  double ratio, isotopic fractionation, evidence 0-73017  
dark clouds, formaldehyde obs., 5 GHz survey 0-73028  
dark clumpy molecular clouds, dynamic model 0-85980  
dark nebulae in M31, catalogue 0-72787  
diffuse gaseous nebulae, H $\alpha$  photoelectric photometry (*French*) 0-62240  
30 Doradus nebula in LMC, optical obs. of bright core 0-67827  
30 Doradus nebular complex, chemical comp. and struct. obs. 0-62226  
DR15, H II region, optical emission assoc. with 408 to 2695 MHz radio sources 0-94881  
DR 21/W75 complex, detection of H $_2$  vibrationally excited 2  $\mu$ m lines 0-94853  
emission line spectra, automatic reduction 0-77294  
emission nebulae, association with Trapezium type multiple systems 0-67781  
emission-line nebulae misclassified as H planetary nebulae, catalogue 0-109378  
emission-line stars misclassified as H planetary nebulae, catalogue 0-109378  
gas clouds, equilb. states during cooling in gravitational fields 0-94862  
giant and supergiant shell nebulae in Magellanic Clouds, obs. 0-94858  
Herbig-Haro objects, 2 micron search for exciting stars 0-67720  
Herbig-Haro objects, stellar wind model 0-85985  
Herbig-Haro objects and surrounding dark clouds, NH $_3$  23 GHz obs. 0-72934  
IC 1396 (Sharpless 131), 2695 MHz continuum map 0-105310  
interstellar cloud, gravitating plasma polytropes in magnetostatic equilb. 0-94701  
IR sources, unidentified emission features, possible mechanism 0-82452  
Kleinmann-Low nebula, NH $_3$  obs. and hot core source 0-73016  
Lynds 134 dust cloud turbulence, formaldehyde obs. at 6 cm. 0-94845  
Lynds 1551, CO obs. of dark cloud and stellar wind driven shocks 0-105318  
Lynds 1630 dark cloud, OH 205.1-14.1 IR candidate 0-101630  
M1-92, bipolar nebula, OH maser source, UHF spectra obs. 0-90550  
molecular cloud complexes, origin, lifetimes and mass 0-82453  
molecular clouds, embedded supernova, spectra and luminosity, evolution 0-82399  
molecular clouds, embedded supernova remnant struct. and emission 0-82450  
N51D, bubble-like nebula in LMC, internal motions obs. 0-105295  
N70, giant filamentary shell in LMC, dynamics 0-90511  
NGC 1999, reflection nebula, optical polarisation map and struct. 0-94856  
NGC 2261, variable refl. nebula assoc. with R Monocerotis, rel. to stellar long period light vars. 0-82350  
NGC 2264 and 7000/IC 5070, new H $\alpha$  stars, slitless spectrographic search 0-62120  
NGC 3372 (Carina Nebula), embedded open clusters dist. determ. 0-85977  
NGC 6302, direct evidence for energetic stellar wind 0-67835  
NGC 6334, H $_2$ O masers mapping and star form. 0-73025  
NGC 6729, variable refl. nebula assoc. with R Coronae Austrinae, rel. to stellar long period light vars. 0-82350  
NGC 6888, filamentary nebula, optical spectra calc. 0-105304  
NGC 6888, ring nebula, central Wolf-Rayet star HD 192163, SHF obs. 0-82386  
NGC 6888, ring nebulae around Wolf-Rayet star HD 192163, spectra of filaments and smooth gas (*Russian*) 0-90515

**nebulae continued**

- NGC 7000 (North America Nebula), rocket UV imagery 0-82440  
NGC 7023, refl. nebula, optical and UV extinction of HD 200775 by dust 0-109515  
NGC 7023, reflection nebula, optical polarization and IR spectrum of HD 200775 possible protostar 0-85944  
OMC-2, detection of H $_2$  vibrationally excited 2  $\mu$ m lines 0-94853  
Omega Nebula (M17, W38, NGC 6618), S III, O III, N III, IR obs. 0-90495  
 $\rho$  Ophiuchi cloud, cosmic ray accel. by stellar winds 0-77512  
 $\rho$  Ophiuchi cloud, no assoc. with CG 353+16  $\gamma$ -ray source 0-94896  
 $\rho$  Ophiuchi dark cloud, late-type young stars, photometry obs. 0-72942  
Orion, C abundance from visible and IUE obs. 0-82451  
Orion, Herbig-Haro objects 0-77397  
Orion, macroscopic motions from atomic line vels. 0-62243  
Orion Molecular Cloud, HCN J=4-3 354 GHz transition detection 0-101636  
Orion Nebula, forbidden Cl II and forbidden Fe II near IR high resolution mapping 0-82217  
Orion Nebula, He ionisation struct. and abundance, SHF obs. 0-105315  
Orion Nebula, IUE obs. of UV continuous spectrum 0-90499  
Orion Nebula, radio obs. of nearby H I distrib. and vels. 0-105322  
Orion Nebula (NGC 1976), long-slit spectroscopy in rocket UV 0-105297  
Pelican Nebula (IC 5070=W80), CO obs. of expanding mol. shell surrounding H II region 0-105296  
proto-planetary nebulae, props. and comparison with planetary nebulae 0-109538  
protosolar nebula, dust grain motion time evolution 0-82234  
protostellar cloud, solar-type star form. with spherical symmetry 0-85930  
reflection nebulae, associated mol. clouds, CO emission, EHF obs. 0-82447  
ring-shaped nebulae in LMC, diameter rel. to number of embedded stars 0-77457  
Roberts 22, bipolar nebula with OH emission, visual, radio and IR obs. 0-94859  
S140, mol. cloud, continuum emission mapping at 89.6 GHz 0-94842  
S171 (W1), optical supernova remnant radial vel. field 0-62250  
Sanduleak's star in LMC, candidate symbiotic star, possibly compact high-excitation emission nebula 0-62139  
solar nebula, development, chemical and gravitational crystallization (*Hungarian*) 0-72795  
near SS 433, faint, highly-contorted nebular filament discovery 0-94855  
star formation regions, rel. to galactic spiral struct. in vicinity of Sun (*Russian*) 0-62290  
superassociations in spiral and irregular galaxies, brightest as distance indicators 0-62260  
T Tauri nebula, ionisation and emission line spectrum calc. 0-67820  
W50, supernova remnant, optical spectrum of faint filamentary nebula 0-90557  
H I emission-line spectrum 0-72759  
H II regions assoc. with interstellar dark clouds, radio continuum interferometry 0-98699  
O II, relative intensities and lifetimes in nebulae, conventional radiation theory 0-109513

**necking**

- bar, rectangular, necked, void growth, finite element anal. 0-64383  
corner theories, time-independent incremental behaviour at corner of yield surface 0-64388  
elastic-viscoplastic materials, strain rate effects on necking 0-58918  
fuel sheaths, neck growth during high temp. transients in steam 0-78396  
metallic shell, explosive expansion, deform. and rupture modes and mechanisms 0-85064  
1-nylon polymers, stress-strain curve 0-60938  
plastic instabilities and uniaxial tensile ductilities 0-79180  
polycarbonate, ductile, large strain cyclic deform. 0-85000  
polycarbonate, neck propaga., rel. to dry craze growth mechanism 0-59563  
polyethylene, high density, ductile, large strain cyclic deform. 0-85000  
polypropylene, ductile, large strain cyclic deform. 0-85000  
polypropylene, microstruct. changes during large strain cyclic deform. 0-66627  
punch stretching, localised necking, finite element anal. 0-102971  
steel, C, tensile props. in high press. H $_2$  at room temp. (*Japanese*) 0-108501  
steel, fibrous crack extension, micromechanisms 0-108563  
Mo fibre reinforced Cu with weak interfaces, stability of tensile deform. 0-97533

**Neel temperature**

- antiferromagnetic Fermi liquid, critical phenomena, neutron scatt., Neel point (*Russian*) 0-71077  
copper, benzoate, one-dimens. antiferromag., heat capacity, field-induced crossover of spin-dimensionality 0-97099  
copper formate tetrahydrate, antiferromag. phase, neutron diffr. study 0-93085  
dimethylammonium manganese trichloride: Cd(Cu), impurities in quasi-one-dimens. Heisenberg systems, anisotropy effect 0-80502  
ferrimagnetic Neel mode with helical mode, coupling energy study (*French*) 0-70999  
itinerant antiferromagnet, paramag. impurity effects on Neel temp., calc. 0-60257  
manganese formate dihydrate, Zn- and Mg-substituted, anomalous crit. phenomena 0-60316  
mixed valence compounds, dynamic susceptibility, RPA study of Anderson lattice 0-97075  
steel, Cr-Mn (13, 19 wt.%), elastic const. behaviour, anomalous, low temp. 0-97521  
TMCM, linear antiferromag., mag. phase diagram, expt. and theoretical study 0-71038  
weak ferromagnet, with easy plane anisotropy correl. functions and magnetisation, temp. depend. (*Russian*) 0-84581  
wustite solid solns., props. connected with localised electron state 0-107734  
BaLaMRuO $_6$  (M=Mg, Fe, Co, Ni, Zn), cubic ordered perovskites, Mossbauer and mag. susceptibility meas. 0-75889  
BaMn $_{0.99}$ Co $_{0.01}$ F $_4$ , magnetoelec. phenomena, dielec. behaviour near Neel temp. 0-71151  
BaMnF $_4$ , spectroscopy near ferroelec. transition, dielec. anomalies near mag. ordering temp. 0-75965

## Neel temperature continued

- BaSr<sub>1-x</sub>Ca<sub>x</sub>Fe<sub>2</sub>O<sub>7</sub>, substituted hexagonal ferrites, mag. split Mossbauer spectra obs. and X-ray struct. data 0-71250  
 Ca<sub>3</sub>Mn<sub>2</sub>Ge<sub>2</sub>O<sub>13</sub>, garnet, metamagnetic transition, high anisotropy peculiarities (Russian) 0-60274  
 Cd<sub>1-x</sub>Ni<sub>x</sub>Fe<sub>2</sub>O<sub>4</sub>, solid soln., mag. and structural characterisation 0-103906  
 CeBi<sub>1-x</sub>Sb<sub>x</sub>, mag. props. and press. effects 0-71026  
 CeS<sub>2</sub>, mag. props. 0-108008  
 Ce<sub>2</sub>Dy<sub>1-x</sub>C<sub>2</sub>, solid solns., mag. props. 0-108008  
 CeSb<sub>1-x</sub>As<sub>x</sub>, mag. props. and press. effects 0-71026  
 Co(C<sub>2</sub>H<sub>5</sub>NO)<sub>6</sub>(ClO<sub>4</sub>)<sub>2</sub> [(BF<sub>4</sub>)<sub>2</sub>], X-Y antiferromagnet, Neel temp., spin correlation functions 0-60345  
 CoCl<sub>2</sub>, antiferromag., phase diagram, heat capacity meas. 0-93126  
 Co<sub>2</sub>Zn<sub>1-x</sub>Rh<sub>x</sub>O<sub>4</sub>, mag. props., EPR spectra, antiferromag. order 0-75736  
 Cr alloys, Neel temp. of one dims. electron gas in spin density wave state 0-65884  
 Cr, hyperfine interactions on <sup>111</sup>Cd-probe nuclei, TDPAC meas. 0-75904  
 Cr, Neel temperature and Fermi energy, nonmag. impurity effects 0-65888  
 Cr-Mo, electrical resistivity, spin density wave gap, Neel temp. 0-88534  
 Cr-Si, dilute alloy, mag. susceptibility and Neel temp. meas. 0-71017  
 Cr<sub>1-x</sub>Fe<sub>x</sub>OOH, 0 ≤ x ≤ 10, prep., Mossbauer effect, Neel temp. 0-108134  
 Cr<sub>2</sub>O<sub>3</sub>, dielec. const. in mag. field, nonlinear magnetoelec. effect in Neel pt. region 0-66006  
 CrSb<sub>1-x</sub>As<sub>x</sub>, press. effect on Neel point 0-71147  
 CsCoBr<sub>3</sub>, quasi 1D Ising antiferromag., polarised Raman scatt. from mag. excitations 0-66182  
 CsLi<sub>0.5</sub>(Al,Fe)<sub>1.5</sub>F<sub>6</sub> pyrochlore, Mossbauer contrib. to exam. of cationic order (French) 0-93224  
 CsLi<sub>0.5</sub>Fe<sub>1.5</sub>F<sub>6</sub> pyrochlore, Mossbauer contrib. to exam. of cationic order (French) 0-93224  
 CsMn<sub>1-x</sub>Cu<sub>x</sub>Cl<sub>3</sub>·2H<sub>2</sub>O, impurities in quasi-one-dims. Heisenberg systems, anisotropy effect 0-80502  
 CsNiF<sub>6</sub>, quasielastic neutron scatt. around Neel-point 0-75768  
 CsNiFeF<sub>6</sub> pyrochlore, Mossbauer contrib. to exam. of cationic order (French) 0-93224  
 CuCl<sub>2</sub>·2D<sub>2</sub>O, cryst. struct., mag. and reson. props. 0-60424  
 Cu<sub>2</sub>NiSi<sub>2</sub>S<sub>7</sub>, X-ray cryst. struct. determ., mag. props. 0-107172  
 DyAsO<sub>4</sub>, phase transitions obs. 0-70412  
 DyBi, mag. behaviour 0-71025  
 DyCoSi<sub>2</sub>, mag. props. 0-107988  
 DyNiSi<sub>2</sub>, mag. props., 4.2-200K 0-84602  
 Dy<sub>1-x</sub>Sm<sub>x</sub>, magnetoresist. of polycryst. specimens in fields up to 44 kOe (Russian) 0-92880  
 DyVO<sub>4</sub>, phase transitions obs. 0-70412  
 ErCoSi<sub>2</sub>, mag. props. 0-107988  
 Eu<sub>1-x</sub>Yb<sub>x</sub>Te, (0 < x < 1), mag. semicond., elec., mag. and optical props. 0-97070  
 Fe-Cr, dil., spin density wave under high press., neutron diff. study 0-65798  
 Fe<sub>2</sub>As<sub>2</sub>, mag. props., Mossbauer study 0-88897  
 FeBr<sub>2</sub>, metamagnet, unusual phase diagram, theory 0-93119  
 FeF<sub>2</sub>, mag. sp. ht. near Neel temp. mag. susceptibility meas. 0-60341  
 FeMo<sub>2</sub>S<sub>8</sub>, Mossbauer investigation, Neel point, superparamag. effects 0-97170  
 Fe<sub>1-x</sub>Mn<sub>x</sub>Cl<sub>2</sub>, disordered, Raman scatt. from Fe<sup>2+</sup> and Neel temp. 0-60579  
 α-Fe<sub>2</sub>O<sub>3</sub>, Mossbauer spectra near Neel temp., critical indices, magnetisation (Russian) 0-66094  
 FeSO<sub>4</sub>, α- and β-forms, magnetic interactions, neutron inelastic scatt. study 0-107980  
 Fe<sub>1-x</sub>Sb<sub>x</sub>, nonstoichiometry influence on mag. props. (Russian) 0-65813  
 Fe<sub>1-x</sub>Zn<sub>x</sub>F<sub>2</sub>, dil. antiferromag., electronic and mag. props., Raman scatt. and optical absorpt. study 0-108207  
 Fe<sub>2</sub>Zn<sub>1-x</sub>F<sub>2</sub>, Neel point and short range order, dilution effects, mag. birefr. obs. 0-71019  
 Gd NiSi<sub>2</sub>, mag. props., 4.2-200K 0-84602  
 Gd-Y alloys, mag. crit. temp. gap 0-60260  
 GdBr<sub>3</sub>, single crystals, mag. behaviour and structure change at low temp. 0-71018  
 GdCoSi<sub>2</sub>, mag. props. 0-107988  
 GdN<sub>1-x</sub>O<sub>x</sub>, mag. interactions 0-60218  
 HoAu<sub>3</sub>, mag. phase diagram 0-75761  
 HoCoGe<sub>2</sub>, crystal and magnetic structure obs. 0-64976  
 HoCu<sub>2</sub>, mag. struct. and elec. resist., neutron diff. obs. 0-60206  
 Ho(Tr,Rh<sub>1-x</sub>)<sub>2</sub>B<sub>4</sub> pseudoternary system, supercond. and mag. ordering 0-70876  
 Ho<sub>1-x</sub>Sb<sub>x</sub> system, magnetisation, elec. resist., and sp. ht. meas. 0-60213  
 K<sub>2</sub>FeF<sub>6</sub>, one-dimensional antiferromag. systems, Mossbauer studies 0-71266  
 KMnF<sub>3</sub>, specific heat near Neel temp. (Russian) 0-100340  
 K<sub>2</sub>Mn<sub>2</sub>F<sub>7</sub>, crit. EPR line broadening near Neel temp. 0-71165  
 Li<sub>2</sub>FeP<sub>2</sub>(Se<sub>3</sub>), Li<sub>2</sub>MnPSe<sub>2</sub> and Li<sub>2</sub>NiPS<sub>2</sub>(Se<sub>3</sub>), NMR and neutron diff. obs., mag. props. 0-60433  
 Mn-Ni, thermal expansion, mag. susceptibility, lattice consts. 0-100341  
 MnAs<sub>1-x</sub>P<sub>x</sub>, mixed crystals, metallic magnetically ordered, Hall effect 0-65536  
 Mn(Br<sub>1-x</sub>Cl<sub>x</sub>)<sub>2</sub>·4H<sub>2</sub>O, antiferromagnetism, controllable anisotropy 0-93116  
 MnCr<sub>2</sub>S<sub>4</sub>, substituted, mag. struct. and transitions 0-65795  
 α-MnSeO<sub>4</sub>, magnetic interactions, neutron inelastic scatt. study 0-107980  
 Mn<sub>2</sub>Zn<sub>1-x</sub>F<sub>2</sub>, Neel point and short range order, dilution effects, mag. birefr. obs. 0-71019  
 (NH<sub>4</sub>)<sub>2</sub>FeF<sub>6</sub>, one-dimensional antiferromag. systems, Mossbauer studies 0-71266  
 N<sub>2</sub>H<sub>4</sub>FeF<sub>6</sub>, one-dimensional antiferromagnetism, Mossbauer study 0-65872  
 (NH<sub>4</sub>)<sub>2</sub>ReCl<sub>6</sub>(IrCl<sub>6</sub>), proton relaxation near antiferromagnetic phase transitions 0-80640  
 NaFeF<sub>3</sub>, Mossbauer and low-temp. dilatometry study (French) 0-80662  
 NdAg<sub>3</sub>, low temp. mag. meas. 0-107989  
 Ni ferrite, quenched, Neel temp. and initial susceptibility 0-75762  
 Ni-I single crystals, mag. and dielectric props. 0-93095  
 NiO, antiferromag. ordering, mag. transition-state approach 0-80507  
 Ni<sub>0.25</sub>Zn<sub>0.75</sub>Fe<sub>2</sub>O<sub>4</sub>, Mossbauer study, spin fluctuations 0-60471  
 Rb<sub>2</sub>CoF<sub>4</sub>, critical fluctuations near Neel temp., US attenuation study 0-108013  
 Rb<sub>2</sub>FeF<sub>6</sub>, one-dimensional antiferromag. systems, Mossbauer studies 0-71266

## Neel temperature continued

- RbMnCl<sub>3</sub>, specific heat near Neel temp. (Russian) 0-100340  
 Si-Cr, dil., spin density wave under high press., neutron diff. study 0-65798  
 TMMC, antiferromagnetic chain, 3-D ordering temp. controlled by solitons and defects, mag. field depend. 0-60275  
 TbAu<sub>3</sub>, mag. phase diagram 0-75761  
 TbNi<sub>2</sub>Si<sub>2</sub>, mag. props., 4.2-200K 0-84602  
 TbP<sup>+</sup>(As)(Sb)(Bi), mag. transitions, quadrupolar interaction effects 0-80512  
 (Ti<sub>1-x</sub>V<sub>x</sub>)<sub>2</sub>O<sub>3</sub>, metallic antiferromag. struct., neutron studies 0-65797  
 TiMnCl<sub>3</sub>, specific heat near Neel temp. (Russian) 0-100340  
 TmSe, mag. ordering under press., neutron diff. obs. 0-70947  
 UN-ZrN, Young's modulus antiferromagnetic anomaly 0-92583  
 VTe, mag. and elec. transport props. 0-92897  
 YIG, Neel point behaviour in stoichiometry vicinity 0-88750  
 ZnCr<sub>2</sub>Se<sub>4</sub>, screw spin structure, method of controlling the sense, polarised neutron diff. study 0-70944  
 ZnCr<sub>2</sub>Se<sub>4</sub>In, magnetoresist. and elec. resist. above and below Neel temp. (Russian) 0-88576
- negative feedback** see feedback
- negative feedback control systems** see closed loop systems
- negative ions**
- alkyl halide and σ\* anion radicals, stability 0-89468  
 anthracene ion in liqs., photoelectron emission and photocond. 0-75600  
 atmospheric negative ions, photodissoc. and photodetachment 0-69199  
 atomic, optimum pot. model used to generate numerical pot., energies and electron affinities determ. 0-99534  
 atomic collisions, negative ion electron detachment, zero range Fermi approach 0-63798  
 collisions with atoms and molecules, electron detachment for energies near threshold 0-63797  
 decacyclene anion, photoexcited quartet state, transient EPR 0-78635  
 electron impact detachment cross sections, classical scaling theory appls. 0-83492  
 enolate anion from acetone, gas phase, negative ion chemistry 0-87060  
 Feshbach type reson. scatt., Glauber approx. calcs. 0-102570  
 formaldehyde anion radical, hyperfine coupling consts., vibr. depend., ab initio calcs. 0-87150  
 formation by field ionisation 0-89123  
 Group IIIA metal tetrahalide ions, vibr. anal. 0-63608  
 halide ions, recombination, exciplex or excimer form. in plasma 0-75026  
 halogermane radical anions, ESR spectra and struct. 0-87153  
 hexafluorobenzene anion-radicals in squalane, ESR spectrum optical detection 0-95655  
 hexafluorobenzene radical anion, <sup>13</sup>C hyperfine interaction, EPR obs. 0-83392  
 hexahalo ions, octahedral, mol. consts. calcs. 0-106317  
 hexahaloanions of group IV A and V, mol. const. determ. 0-87093  
 hexaony ions, octahedral, mol. consts. calcs. 0-106317  
 MIN, negative ion injector, Na charge exchange cell 0-99386  
 nitrobenzene<sup>-</sup>, positive ion formation energetics by negative ion charge stripping 0-78700  
 perfluorobenzene, electron attachment, radiative and dissoc., negative ion lifetimes, ion cyclotron reson. spectra 0-74251  
 perfluorocyclobutane, electron attachment, radiative and dissoc., negative ion lifetimes, ion cyclotron reson. spectra 0-74251  
 perfluoromethylcyclohexane, electron attachment, radiative and dissoc., negative ion lifetimes, ion cyclotron reson. spectra 0-74251  
 perfluorotoluene, electron attachment, radiative and dissoc., negative ion lifetimes, ion cyclotron reson. spectra 0-74251  
 photoabsorption spectra, long-range field effect 0-91521  
 positive ion formation energetics by negative ion charge stripping 0-78700  
 RX<sup>-</sup>, radical anion stability conditions, pot. energy diagrams 0-85161  
 stable negative ions instability, Xalpha calcs. 0-99452  
 Al<sub>2</sub><sup>-</sup>, configurations, ab initio study, LCAO, STO, MO-SCF and CI calcs., binding energy (French) 0-91447  
 BH<sub>4</sub><sup>-</sup>, electron momentum distribution and Compton profiles, FSGO calcs. 0-87032  
 BH<sub>4</sub><sup>-</sup>, pot. energy surfaces and mol. deform. induced by external cation 0-106285  
 B<sub>2</sub>H<sub>6</sub><sup>-</sup>, electron momentum distribution and Compton profiles, FSGO calcs. 0-87032  
 Be<sup>-</sup>, <sup>2</sup>P shape resonances, shift potential calcs. 0-69089  
 C<sub>2</sub><sup>-</sup>, A<sup>2</sup>Π<sub>g</sub>-X<sup>2</sup>Σ<sub>g</sub><sup>+</sup> lines, obs. in carbon stars 0-98861  
 CH<sub>3</sub>OH<sup>-</sup>, IR photodissoc., fluence depend., saturation effects 0-78663  
 CN<sup>-</sup>, electron propagator theory, mol. electron affinities calcs. 0-83521  
 CN<sup>-</sup>, spectrosc. consts. for ground and excited states, ab initio, CI calcs. 0-78551  
 Cl<sup>-</sup>, atomic core states, antishielding effects calcs. 0-83299  
 Cl<sup>-</sup>, contracted Gaussian basis sets for mol. calcs. 0-83264  
 Cl<sup>-</sup>, formation by HCl dissociative electron attachment, differential cross section, Feshbach resons. 0-83508  
 Cl<sup>-</sup> hydration complexes, gas phase, electrostatic calcs. 0-100055  
 Cl<sup>-</sup> + HBr(HI) → HCl + Br<sup>-</sup> (I<sup>-</sup>), vibr. product state distrib., IR chemilumines. obs. 0-81309  
 Cl<sup>-</sup> + Xe<sup>+</sup> + Ne, three body ion-ion recombination probability, Monte Carlo simulation 0-85160  
 Cl<sub>2</sub><sup>-</sup>, electron propagator theory, mol. electron affinities calcs. 0-83521  
 D<sup>-</sup>, ion source for high voltage neutral beams for fusion reactors 0-99379  
 F<sup>-</sup> + Kr<sup>+</sup> + Ar, three body ion-ion recombination probability, Monte Carlo simulation 0-85160  
 GeH<sub>3</sub><sup>-</sup>, electronic struct., electron affinity, inversion barrier, ab initio SCF Gaussian basis calc. 0-63552  
 H<sup>-</sup>, classical many-body collision model incorporating Heisenberg and Pauli principles 0-63511  
 H<sup>-</sup>, DC Stark broadening of <sup>1</sup>P<sup>0</sup> shape reson. 0-63585  
 H<sup>-</sup>, form by surface and vol. processes, neg. ion source appl., review 0-58375  
 H<sup>-</sup>, formation by HCl dissociative electron attachment, differential cross section, Feshbach resons. 0-83508  
 H<sup>-</sup>, ion beam diagnostics using laser beam 0-95497  
 H<sup>-</sup>, many-body perturbation theory with radially restricted basis functions 0-78526  
 H<sup>-</sup>, photoabsorption spectra, long-range field effect 0-91521  
 H<sup>-</sup>, production in foil breakup of H<sub>2</sub><sup>+</sup>, inhibition effect 0-99549  
 H<sup>-</sup>, two-electron photodetachment threshold, blackbody radiation effects 0-91524



**negative ions continued**

- H<sup>+</sup>+H(He), electron detachment in adiabatic regime, mechanisms 0-63800  
 H<sup>+</sup>+He, electron detachment, theoretical obs. 0-63799  
 H<sup>+</sup>+inert gas, negative ion detachment cross section determ. 0-63796  
 H<sub>2</sub><sup>+</sup>, free free absorpt. coeffs. dipole length formulation and two centre close coupling calc. 0-83345  
 (H-He)<sup>+</sup>, ab initio calcs. 0-63799  
 HBr, electron impact ionisation, vibr. excitation spectra threshold peaks, negative ion effects 0-106322  
 HS<sub>n</sub><sup>-</sup>, n=1-4, electronic struct., ab initio Hartree-Fock-Slater calcs. 0-74107  
 HS<sub>n</sub><sup>2-</sup>, n=1-4, electronic struct., ab initio Hartree-Fock-Slater calcs. 0-74107  
 He<sup>-</sup>, inelastic Feshbach resons., quasi projection operator calc. 0-58395  
<sup>3</sup>He, negative ion mobility, theory 0-107598  
 Hg(CN)<sub>2</sub><sup>-</sup> ion, CN and HgC stretching vibrations and HgCN bending vibration assignments 0-69140  
 I<sup>-</sup>, 3d<sup>4</sup>4f config., collapse of 4f electron, X-ray spectral obs. (Russian) 0-58204  
 I<sup>-</sup> hydration complexes, gas phase, electrostatic calcs. 0-100055  
 I<sup>-</sup>, HF and SCF calcs., pot. curves, electron affinity and quadrupole moment determ. 0-95527  
 IO<sub>3</sub><sup>-</sup>, adsorption desorption by TiO<sub>2</sub> suspension, kinetics, relax. technique 0-93804  
 K<sup>-</sup>, photodetachment and at. polarisability 0-91522  
 K+H<sub>2</sub>(S<sub>2</sub>), collisional ionisation, positive and negative ion energy spectra obs. 0-63775  
 KTaO<sub>3</sub>:OH<sup>-</sup> (OD<sup>-</sup>) (OT<sup>-</sup>), IR spectra, spectrosc. consts. 0-100671  
 Li<sub>2</sub><sup>-</sup>, core excited bound states in beam foil expts., CI calcs. 0-78559  
 Li<sub>2</sub><sup>-</sup>, core-excited bound states 0-91468  
 Li<sub>3</sub><sup>-</sup>, electronic struct., SCF and SCF-CI calcs. 0-87044  
 Mg<sup>-</sup>, shape resonances, shift potential calcs. 0-69089  
 Mo<sub>2</sub>Cl<sub>6</sub><sup>-</sup>, metal-metal bond energy, SCF-X $\alpha$ -SW calcs. 0-78538  
 Mo<sub>2</sub>Cl<sub>6</sub><sup>-</sup> complexes, cluster exchange coupling consts. SCF-X $\alpha$ -SW calcs. 0-74120  
 N<sub>2</sub> in high press. air plasma, photodissoc. 0-64691  
 N<sub>2</sub><sup>-</sup>, first <sup>2</sup> $\Pi_u$  state form. and decay 0-58177  
 N<sub>2</sub><sup>-</sup>, high press. IR vibr. spectroscopy (German) 0-74170  
 NO<sub>2</sub><sup>-</sup>, high press. IR vibr. spectroscopy (German) 0-74170  
 Ne<sup>-</sup> scatt. electron spectra, distinction from neutral autoionising states 0-83482  
 Ne+H<sup>-</sup> (D<sup>-</sup>), electron detachment, dynamical phenomenon 0-106305  
 O<sup>-</sup>+O<sub>2</sub>→O<sub>2</sub><sup>-</sup>+O, cross section kinetic energy depend., rate consts. meas. and Monte Carlo calcs. 0-78701  
 O<sub>2</sub><sup>-</sup>, A<sup>2</sup> $\Pi_u$  state pot. energy curve, MCSCF calcs. 0-63565  
 O<sub>5</sub><sup>-</sup>, hypothetical, mol. self-consistent study, possible prep. method (French) 0-91717  
 O<sup>-</sup> (O<sub>2</sub><sup>-</sup>), optimum pot. model used to generate numerical pot., energies and electron affinities determ. 0-99534  
 P<sup>-</sup>, contracted Gaussian basis sets for mol. calcs. 0-83264  
 P<sup>-</sup>, contracted Gaussian basis sets for mol. calcs. 0-83264  
 S<sub>2</sub><sup>2-</sup>, structure investigation by ab initio calcs. 0-69066  
 SO<sub>2</sub>-containing ions, photodestruction 0-63722  
 SO<sub>2</sub><sup>2-</sup>, SO<sub>2</sub><sup>2-</sup>, O K-emission spectra, electron struct. 0-87099  
 SeO<sub>2</sub><sup>2-</sup>, SeO<sub>2</sub><sup>2-</sup>, O K-emission spectra, electron struct. 0-87099  
 TeO<sub>3</sub><sup>2-</sup>, TeO<sub>4</sub><sup>2-</sup>, O K-emission spectra, electron struct. 0-87099

**negative resistance**

- back diode amplifier, use at low temp. 0-57324  
 semiconductor, complex energy band under optical excitation, high-frequency negative cond. and population inversion 0-107858  
 Al-Al<sub>2</sub>O<sub>3</sub>-Au device in Cl<sub>2</sub> atmosphere, current-voltage characts., press. depend. 0-65704  
 ZnIn<sub>2</sub>S<sub>4</sub>, S-type negative resist. and switching effects 0-65581

**negative resistance effects**

see also Gunn effect

- MIS diode, thin-insulator, switching phenomena, current-control-type negative resist. characts. 0-107915  
 polyphenylene oxide thin films, electrochem. prep., impurity effects on cond., electroforming 0-88655  
 PVC in metal sandwich struct., switching props., voltage- and current-controlled negative resist. 0-103767  
 semiconductor, ambipolar hot-carrier size effect kinetics 0-107799  
 semiconductor, n-type, nonequilibrium photoelectron distrib. and absolute negative cond. in quantising mag. fields 0-65622  
 semiconductors, exhibiting negative photocond., photovoltaic effects 0-96943  
 thin film heterostructure, energy spectrum study 0-70787  
 tunnel junction, resonance differential negative resistance in the Fredkin-Wannier inhomogeneous field model 0-80355  
 (AlGa)As DH lasers, superlinear emission characts., negative resist. obs. 0-95895  
 Al-Au couple, electroformed, nonohmic characts. and electron emission 0-60066  
 As<sub>2</sub>Se<sub>3</sub>Ag, glassy semicond. film, prep. by photodiffusion of Ag, negative photocond. 0-92934  
 Au film, nonohmic characts. and electron emission 0-60066  
 CdCr<sub>2</sub>Se<sub>4</sub>, ferromag. semicond., conc. anomalies rel. to red shift of absorpt. edge 0-70732  
 GaAs, DC biased, filamentation of laser radiation 0-74428  
 GaAs:Fe, p-p-n-n struct., photoelec. props. 0-107862  
 GaAs:O p-p-n struct., injection current and negative photocond., saturation mechanism 0-92967  
 GaAs-Al<sub>0.1</sub>Ga<sub>0.9</sub>As heterostructures, real-space electron transfer by thermionic emission, analytical model 0-100512  
 Ga<sub>0.4</sub>In<sub>0.6</sub>Sb, electron transport in RF field, Monte Carlo simulation 0-96932  
 Ge, ambipolar hot-carrier size effect kinetics 0-107799  
 p-Ge, negative magnetoresist. and Hall effect, press. and field depend. 0-70733  
 InSb, current-voltage characteristics at room temperature and high hydrostatic pressure 0-88560  
 p-InSb, magnetoconcentration effect, negative differential conductance 0-70729  
 n-InSb, negative longit. magnetoresist., carrier conc. and mobility depend., 77K 0-60007  
 Nd, transport props., low temp., effect of mag. field 0-70679  
 Pr, transport props., low temp., effect of mag. field 0-70679  
 Pt-polymer/Au capacitor, electroforming, negative resist., electron emission 0-80406

**negative resistance effects continued**

- Si amorphous, ion implantation, negative magnetoresist., localised mag. states 0-70731  
 Sm, transport props., low temp., effect of mag. field 0-70679  
 V<sub>2</sub>O<sub>5</sub>-As<sub>2</sub>O<sub>3</sub>-RO, R=Ba, Ca, Pb, semicond. glass, electronic props. 0-88557  
 ZnS, prebreakdown electrolum., domain form. and negative resist. effects 0-84788  
 ZrC-C composite system, negative magnetoresist. 0-60008

**negative temperature coefficient thermistors** see thermistors**nematic liquid crystals**

- acetic acid-<sup>13</sup>C<sub>1</sub>, in nematic phase soln., dipole-dipole couplings, selective spin population transfer investig. 0-60427  
 acoustic field response, streaming component and instability 0-80747  
 acoustical properties, rotating mag. field study 0-88034  
 acousto-optic effect, acoustic streaming 0-88964  
 acousto-optical effect due to anisotropic attenuation, new developments and appls. 0-76002  
 4-alcanoyloxybenzoyloxy-4'-cyanoazobenzene series, influence of substituent on reentrant mesophases 0-88027  
 4-alcanoyloxybenzoyloxy-4'-cyanobiphenyl series, influence of substituent on reentrant mesophases 0-88027  
 4-alcanoyloxybenzoyloxy-4'-cyanostilbene series, influence of substituent on reentrant mesophases 0-88027  
 4-n-alkoxy benzoyloxybenzylidene 4'-cyanoaniline series, nematic reentrant mesophases, phase diagrams 0-103467  
 p-alkoxybenzylidene-p-n-butylanilines, IR absorpt. spectra, elec. field effects, orientational order parameter determ. by IR dichroism 0-80778  
 p-alkoxybenzylidene-p-aminocyananilines, IR absorpt. spectra, elec. field effect, orientational order parameter determ. by IR dichroism 0-80777  
 4,4'-n-alkoxybenzylideneamino-biphenyls, central Schiff's base linkage reversal effect on liq. cryst. props. 0-79683  
 4-alkoxyphenyl-4'-alkylbenzoates, mesomorphic props., terminal alkyl chain length effect 0-88024  
 5-alkyl-2-(4'-cyanophenyl)-1,3-dioxanes, synthesis and electro-optical characts. 0-88029  
 alkyl-cyanobiphenyl homologues, isotropic-nematic phase, optical Kerr effect 0-91866  
 1-4-n-alkylbenzoyloxyphenyl 2-(4'-cyanophenyl) ethane series, nematic reentrant mesophases, phase diagrams 0-103467  
 4-4-n-alkyloxybenzoyloxy-benzylidene-4'-cyanoanilines, reentrant nematic and smectic phases 0-88308  
 p-azobyanisole, directed crystn. in elec. and mag. fields 0-107052  
 p-azophenotole, single cryst., deuterated, phonon dispersion curves, inelastic neutron scatt. obs. 0-84261  
 binary mixtures, phase transitions, entropy, relation to smectic plane tilt angle 0-65203  
 CBNA, nematic-isotropic transition at high press., turbidity meas. 0-92655  
 colloidal solution, flow alignment, transition from isotropic to nematic phase 0-84060  
 COOB-cholesteric liq. cryst. mixtures, helix pitch, temp. depend. 0-64895  
 Couette flow, orientation instability for finite anchoring energies 0-74923  
 cyano compounds, liq. cryst. phases, incommensurate coexistent density fluctuations 0-79691  
 4-cyano-4'-n-pentylbiphenyl, refr. index meas. and isotropic-nematic phase transition study, surface plasmon technique 0-84282  
 4-cyano-4'-octylbiphenyl, dielectric relax. anal. in nematic and smectic phases 0-108153  
 cyano-biphenyl LC alignment on obliquely evaporated SiO<sub>2</sub> films 0-79677  
 cyano-biphenyl series, nematogens and smectogens, props. characterised by even-odd effect 0-107046  
 4-cyanobenzoyloxy-4'-pentylstilbene, nematic, smectic A, and orthogonal smectic B phases 0-64890  
 4-cyanobiphenyl and 4'-alkyl- or 4'-alkoxy-substituted liq. cryst. derivatives, soln., absorpt. and fluoresc. spectra 0-87164  
 4-cyanobiphenyl/4-cyano-p-terphenyl liq. cryst. mixture, order parameters of dissolved dyes 0-100167  
 cyanobiphenyls molecular conformational mobility study by optical probing method (Russian) 0-92459  
 p-cyanophenyl p-n-alkyloxybenzoates, birefringence, polarisability and order parameter 0-100642  
 cybotactic nematic mesophase, X-ray scatt. 0-92454  
 p,p'-dihexylytolan, flexoelec. coeff. in nematic phase, thermal depend. 0-79685  
 director in dielec. regime, dynamical behaviour, EHD instabilities (Japanese) 0-59387  
 dodecylate/dodecyltrimethylammonium micelles, type II mesophase, bilayer struct., NMR spectra study 0-75149  
 EABAC, smectic A, nematic, and isotropic phases, NMR and quasielastic neutron scatt. obs. 0-88022  
 EBBA, IR absorpt. spectra, elec. field effects, orientational order parameter determ. by IR dichroism, bend elastic consts. 0-80778  
 EBBA, mol. and cryst. struct., X-ray diff. study 0-88134  
 EBBA, nematic-isotropic transition at high press., turbidity meas. 0-92655  
 EBBA, NMR and Raman scatt. studies in nematic phase 0-100619  
 EBBA, orientational order, effect of hexa-n-alkoxy-triphenylene disc-like solutes 0-79682  
 EBBA, orientational order in glassy and nematic phases, IR dichroism meas. 0-64891  
 EBBA, Tsvetkov parameter, temp. depend. 0-88035  
 EBBA, nematic, EPR investig. 0-108077  
 effective ion mass and mobility calcs. (Russian) 0-79694  
 EHD instabilities, white noise effect 0-70115  
 EHD instability, nematic liquid crystal in contact with photoconductor 0-79695  
 elect. conduct. based on injection-contact phenomena theory (Russian) 0-107807  
 electro-optic switch, four-port, for unpolarized fibre light 0-58715  
 electrooptical characteristics of ZhK-440 controllable crystal transparency 0-78996  
 p-(p'-ethoxybenzylidene)amino-benzonitrile, cryst. struct. rel. to liq. crystallinity 0-100225  
 ferrofluid/lyotropic liq. cryst. combination, ferromagnetics and ferrocholesterics 0-59378  
 gigantic optical nonlinearity, self focusing in oriented mesophase (Russian) 0-64120

## nematic liquid crystals continued

- n-heptyl-4-cyanobiphenyl, nematic phase, dielec. loss, diffusion equations 0-71305
- p-p'-n-heptyl-cyanobiphenyl-isotropic solute systems, nematic-isotropic phase transformation, volumetric study 0-92653
- 4-n-heptyl-d<sub>15</sub>-oxybenzoic acid-d<sub>4</sub>, nematic and smectic phases, mol. and relative segmental order 0-96439
- heptyloxyazobenzene, filamentary structures 0-107051
- 4-n-heptyloxybenzylidene-4'-n-hexylaniline, nematic and smectic phases, long mol. axis reorientation, LF dielec. dispersion 0-70124
- 4-n-heptyloxybenzylideneamino-4'-cyanobiphenyl, reentrant nematic phase and low temp. smectic phases 0-88031
- 4-n-hexyloxybenzylidene-4'-n-hexylaniline, nematic and smectic phases, long mol. axis reorientation, LF dielec. dispersion 0-70124
- homeotropically oriented, spectral studies of acoustooptical interaction 0-88965
- hybrid field-effect liquid-crystal light valve, optical data processing performance 0-99860
- image transducer, performance effects of liquid crystal thickness 0-102838
- induced cholesteric order by chiral 2,2'-spirobiindane derivatives (*German*) 0-64884
- inelastic light scattering by order parameter biaxial and longitudinal fluctuations (*Russian*) 0-75160
- isotropic phase, pulse acoustic-optic modulator 0-95993
- light transmission meas. 0-88025
- MBBA, acousto-hydrodynamic effects when excited by 20 MHz US surface waves 0-76003
- MBBA, dielec. relax. in metastable modification of solid phase 0-84689
- MBBA, flexibility gradient of fatty acid spin labels, EPR study 0-71181
- MBBA, flexoelec. coeff. in nematic phase, thermal depend. 0-79685
- MBBA, fluorinated analogues, mesomorphic props. 0-70118
- MBBA, frozen nematic glass, EPR spectra of copper and cobalt triazene-1-oxide complexes 0-88871
- MBBA, IR absorpt. spectra, elec. field effects, orientational order parameter determ. by IR dichroism, bend elastic consts. 0-80778
- MBBA, nematic-isotropic transition at high press., turbidity meas. 0-92655
- MBBA, NMR and Raman scatt. studies in nematic phase 0-100619
- MBBA, nonlinear optical amplification above Fredericks transition 0-95937
- MBBA, orientational order in glassy and nematic phases, IR dichroism meas. 0-64891
- MBBA, positive space charge influence on texture, domain form. factor, polarised light study 0-88037
- MBBA, proton spin-lattice relax. in crit. regime 0-80631
- MBBA, Raman spectra in cryst., frozen glassy, and liq. cryst. states 0-60601
- MBBA, Tsvetkov parameter, temp. depend. 0-88035
- MBBA mol. alignment on SiO film, film thickness effects 0-59384
- MBBA-cholesteryl nonanoate, liq. cryst. mixture, two colour display device 0-70116
- MBBA-d<sub>13</sub>, <sup>1</sup>H spin-lattice relaxation, intermol. and intramol. contribs. 0-75873
- MBBA-d<sub>13</sub>, nematic phase, rot. frame spin-lattice relax. 0-84668
- MBBA-EBBA, controllable liq. cryst. transparency, electrooptical characts. 0-78996
- MBBA-n-heptane, nematic soln., lattice model, thermodynamic functions (*Russian*) 0-64896
- mesophase pitch, magnetically-oriented, phys. props., mol. struct. 0-64885
- p-methoxybenzoate-p-n-pentylbenzene, isotropic phase nematogen optical Kerr const. 0-78919
- p-methoxybenzoate-p'-n-pentyl benzene, slow non-critical mol. reorientation in isotropic phase 0-84062
- p-(p'-methoxybenzylidene)amino-phenyl acetate, cryst. struct. rel. to liq. crystallinity 0-100225
- p-methoxybenzylidene-cyanoaniline, mol. and cryst. struct., X-ray diffr. study 0-88134
- mixture, ZLI-207, nonideally oriented layers, Fredericksz transition dynamics 0-100163
- mixtures, dielec. permittivity dispersion 0-88921
- molecular alignment using alkoxysilanes, rel. to surface energy 0-100164
- molecular conformation and orientational order, NMR studies, review 0-75151
- molecular form and hydrodynamics connection, reactive coeff. (*Russian*) 0-64894
- monomer-dimer system with attractive interactions on square lattice, nematic ordering 0-79681
- multiplexed liquid cryst. display, use of cholesteric-nematic phase change 0-107408
- nematic-chiral-dye mixture, circular dichroism, selective light scatt. (*Russian*) 0-103944
- nematic-isotropic phase transition character, molecular bending fluctuations critical growth (*Russian*) 0-79919
- nematic-isotropic transition, thermodynamic props. calc. 0-103464
- 4-nitrophenyl-4-octyloxybenzoate/cholesteric liq. cryst. mixtures, helix pitch, temp. depend. 0-64895
- nonlinear reversible hydrodynamics, external mag. field influence 0-75156
- nonlinear stability of the motion of a nematic liquid crystal 0-83784
- octyl-cyano-biphenyl, influence of laser light wave field on nematic phase (*Russian*) 0-92456
- 4-n-octyl-d<sub>15</sub>-oxybenzoic acid-d<sub>4</sub>, nematic and smectic phases, mol. and relative segmental order 0-96439
- octyleyanobiphenyl, crit. heat. capacity near nematic-smectic A transition 0-100323
- p-n-octyloxy benzylidene-p-toluidine, mol. order, EPR VAAC probe 0-70114
- trans-p-n-octyloxy- $\alpha$ -methyl-p'-cyanophenyl cinnamate, mag. and elec. birefr. in isotropic phase 0-80744
- p,p'-octyloxycyanobiphenyl, flexoelec. coeff. in nematic phase, thermal depend. 0-79685
- octyloxycyanobiphenyl, nematic-smectic A transition, heat capacity study 0-88033
- 4-n-octyloxyphenyl 4-n-pentyloxybenzoate, permittivity, microwave dielectric relaxation 0-80671
- organic doublet radicals in nematic and smectic liq. crystals, ENDOR obs. 0-91585
- orientation fluctuations in high mag. field, quenching, birefringence effects 0-64892

## nematic liquid crystals continued

- orientational bistability, nematic storage effects 0-70112
- orientational fluctuations causing light intensity fluctuations, spectral anal. 0-60618
- orientational fluctuations effect on evanescent modes of transmitted EM wave 0-64889
- PAA, fluctuations near Rayleigh-Benard instability, real time obs. by neutron scatt. 0-59390
- PAA, nematic, NMR study of ordering, intramol. mobility 0-100162
- PAA, nonlinear soft mode at Rayleigh-Benard instability, neutron cond. spectrosc. obs. 0-79266
- PAA, Tsvetkov parameter, temp. depend. 0-88035
- PAA-di, nematic liquid crystal, NMR data, appl. of Landau-de Gennes theory 0-64893
- PAP, Tsvetkov parameter, temp. depend. 0-88035
- paramagnetic, flexomagnetoec. effects 0-75158
- PEBAB, nematic, EPR investig. 0-108077
- pentyl cyanobiphenyl, laser and electric field induced Kerr effect 0-84061
- pentyl-cyano-biphenyl, nematic, hydrodynamic parameters meas. with and without applied elec. field 0-100297
- 4-n-pentyloxy-phenyl-4'-n-octyloxybenzoate, nematic, dielec. relax. and freq. depend. of threshold voltage 0-60497
- 4-n-pentylphenyl (pentyloxyloxy)-3-chlorobenzoate, flexoelec. coeff. in nematic phase, thermal depend. 0-79685
- phase transition, smectic A-nematic, liq. cryst. binary mixture, birefringence study 0-59638
- phase V, host for porphyrins and zinc, pyrochlorophyllide, oriented photoexcited triplets, EPR study 0-84636
- 4-phenylbenzylidene-4'-n-alkoxyanilines, central Schiff's base linkage reversal effect on liq. cryst. props. 0-79683
- phenylene derivatives, effect of substitution on liq. crystalline props. 0-70113
- piezoelectric effect use as light modulator 0-83679
- polarisabilities, Lippincott  $\delta$ -function pot. model 0-79686
- poly- $\gamma$ -benzyl-L-glutamate, soln., liquid crystal transitions anal. 0-65207
- polydisperse solution of rodlike particles, isotropic-nematic phase transition, Onsager theory 0-100324
- polymer liquid-crystalline solns., struct. 0-103235
- potassium laurate-1-decanol-water mixtures, biaxial nematic phase obs. 0-107409
- N-p-propoxybenzylidene-p-pentylaniline, orientational order in glassy and nematic phases, IR dichroism meas. 0-64891
- re-entrant nematic phase, orientational order, electron reson. study 0-103242
- reflection, total internal, review 0-96445
- refractive index and birefringence by interference method 0-96440
- reversely pretitled cell, conformation of molecular orientation 0-59388
- Schiff base azo dyes in nematic liq. cryst. hosts, order parameters, optical density meas. 0-84055
- shearing, sinusoidal, and temporal sinusoidal standing twist wave 0-84053
- solvent-rod mixture, two phase, interfacial free energies, quartic van der Waals theory 0-59377
- surface, statistical thermodynamics, local order parameter 0-88023
- surface and anchoring energies, van der Waals contrib. 0-92455
- surface and bulk configurations, topology 0-59381
- TBBA, mesophase identification by X-ray diffr., review 0-100166
- tolanes, molecular conformational mobility study by optical probing method (*Russian*) 0-92459
- transducers, dynamic scatt., pre-excitation 0-88021
- tridimensional variational approximated model, existence, uniqueness and regularity of solns. 0-59379
- truxene derivatives, temp. inverted nematic-columnar sequence in disc-like mesogens 0-88032
- twisted, ang. and voltage depend of light transmission, two-layer model 0-76006
- twisted nematic cell, dynamic props., voltage depend. 0-70117
- twisted nematic display with cholesteric dopant, transmission characteristic temp. depend. compensation 0-103934
- two-dimensional, Monte Carlo simulation 0-100168
- uniaxial and biaxial, formed by non-cylindrically symm. mols., computer simulation 0-79680
- unified model for bulk smectic-A, nematic and isotropic phases 0-79692
- X-ray and light scattering obs., high resolution 0-92460
- X-ray diffr. studies, review 0-100166
- MBBA + optically active substance, pretransition optical rotation in isotropic phase (*Russian*) 0-92657
- Ni complexes, dithienes, nematic and smectic mesophases, synthesis and characts. 0-70120
- Ni dithiene complexes, mesomorphic props. 0-88026
- Pt complex, bis [4-(n-butyl)-styryl dithiolato] Pt nematic complex with strong IR absorption 0-88305
- Pt dithiene complexes, mesomorphic props. 0-88026

## neodymium

- see also nuclei with .....
- addition to Ni-Cr austenitic stainless steel, effect on heat resist. and comp. of non-metallic inclusions 0-76315
- basalt isotopic abundance, Earth struct. models 0-72475
- o-chlorobenzoic acid: Nd<sup>3+</sup>, solid, vibrational spectra 0-84758
- Earth mantle, Nd-Sr isotopic correl. and constraints on continental crust comp. and nature of lower crust 0-94498
- glass: Nd<sup>3+</sup>, resonantly enhanced four-wave mixing in absorbing media (*Chinese*) 0-102764
- glass: Nd<sup>3+</sup>, spectral props. (*Chinese*) 0-60645
- granitoid rocks, Nd-Sr isotopic relationship and continental crust development, chemical approach to orogenesis 0-94522
- laser, excited stimulated Mendelstam-Brillouin scatt. phase fluctuations (*Russian*) 0-89014
- laser glasses, phosphate and fluorophosphate, Nd doped, piezooptic coeffs. meas. 0-99815
- magnetic structure, 18.6K mag. phase transition 0-65799
- magnetic-structure, neutron and X-ray diffr. study 0-60197
- metaphosphate glass: Nd<sup>3+</sup>, Yb<sup>3+</sup> luminesc., energy transmission and migration between Nd<sup>3+</sup> and Yb<sup>3+</sup> 0-66297
- Nd-glass multichannel laser with plasma shutter 0-64088
- photoelectric cross sections at 52.4, 60, 72.2 and 84.4 keV 0-69187
- pulsed diode simulators of solid lasers Al<sub>x</sub>Ga<sub>1-x</sub>As and Ga<sub>x</sub>In<sub>1-x</sub>P<sub>1-y</sub>As, solid solns. 0-91816



## neodymium continued

- surface and volume props., flow props., surface layer thickness (*Russian*) 0-59760
- transport properties, low temp., effect of mag. field 0-70679
- $\text{CaF}_2\text{Nd}^{3+}$ ,  $^{19}\text{F}$  NMR studies 0-60429
- $\text{CaS:Nd}$  phosphors, X-ray powder diff. anal. 0-100204
- $\text{CaWO}_4\text{Nd}^{3+}$  absorpt. spectra, hypersensitivity of  $^4\text{I}_{9/2}$  to  $^4\text{G}_{5/2}$   $^2\text{G}_{7/2}$  transition 0-97309
- $\text{CdF}_2$ , Nd, ionic cond. investigation by complex admittance method 0-100352
- $\text{La}_2\text{Be}_2\text{O}_7\text{Nd}^{3+}$ , crystal growth, spectral and laser properties in  $^4\text{F}_{3/2} \rightarrow ^4\text{I}_{11/2}$  and  $^4\text{F}_{3/2} \rightarrow ^4\text{I}_{13/2}$  transitions 0-80853
- $\text{LiNbO}_3\text{Nd}$ , SHG, phase-matching temp., impurity influence 0-69463
- Nd,Cr:Li-La phosphate glass, Nd luminesc. quantum efficiency meas., Nd-Cr nonradiative transfer 0-66296
- Nd garnet ring laser, with return mirror, mode locking 0-99764
- Nd I, isotope shifts in energy levels of neutral Nd atom 0-69095
- Nd IV, 3d and 4f energy level parametrisation, Slater parameters and correl. corrections 0-87041
- Nd laser Mikron system, ultimate Xe pump lamp module operating conditions 0-91815
- Nd laser produced plasma, nonlinear scattering of laser radiation by fast ion waves in plasma 0-106916
- $\text{Nd}^{3+}$  ions in solids, radiationless decay processes, laser photoacoustic spectroscopy meas. 0-84766
- Nd:glass, comparative lasing characts. of silicate and phosphate laser glasses 0-74364
- Nd:glass, subnanosecond pulse oscillator, investigation by high-speed oscillography 0-74411
- Nd:glass laser, blue tunable picosecond pulse generation by synchronous mixing with sideband radiation in  $\text{NH}_4\text{H}_2\text{PO}_4$  0-87431
- Nd:glass laser, influence of neutron and  $\gamma$  irradi. on generating characts. (*Russian*) 0-69402
- Nd:glass laser, short pulse mode-locked, using prisms 0-83617
- Nd:glass laser, stable ultrashort light pulses generation (*German*) 0-91823
- Nd:glass laser, ultimate power characts. at high pulse repetition freqs. 0-64036
- Nd:glass laser in Tl vapour, output conversion from 1.06 micron to 388.1 nm 0-91850
- Nd:glass laser performance and reliability developments 0-78869
- Nd:glass laser rod, pumped, thermal relaxation 0-69397
- Nd:glass laser six beam system, output characts. (*Chinese*) 0-83612
- Nd:glass laser system, Thompson scattering diagnostics of low density plasmas 0-96388
- Nd:glass laser with active mode locking, ultrashort pulses 0-64087
- Nd:glass laser with numerical programmed control (*Russian*) 0-91811
- Nd:glass laser with US Q-switch 0-64034
- Nd:glass solid state laser, giant emission pulse prod. 0-91803
- Nd:glass telescopic small-signal amplifier with a Brillouin mirror 0-69420
- Nd:silicate glass, resonance laser excitation, inhomogeneously broadened emission spectra 0-66295
- Nd:YAG, electro-optical extraction of ps laser pulse (*German*) 0-87416
- Nd:YAG CW laser, mode locking, 30 W average power 0-87419
- Nd:YAG CW mode-locked laser, negative feedback power stabilization 0-69435
- Nd:YAG crystal, orientation influence on thermally induced birefringence (*Chinese*) 0-88958
- Nd:YAG giant pulse lasers, energy characts., superradiance effects 0-64031
- Nd:YAG laser, CW mode-locked and intracavity freq. doubled, anal. 0-58548
- Nd:YAG laser, intracavity freq. doubling by  $\text{LiIO}_3$  long pulse emission 0-102736
- Nd:YAG laser, Q-switched, pulse stretching using Pockels cell 0-95927
- Nd:YAG laser, Raman shifted, frequency conversion appl. 0-69451
- Nd:YAG laser, subnanosecond pulse generation at 100K 0-74397
- Nd:YAG laser as source for airborne lidar system for atmospheric expts. (*Italian*) 0-109278
- Nd:YAG laser integration into optical systems 0-78887
- Nd:YAG passively locked laser, pulse width meas. by SHG method (*Chinese*) 0-87432
- Nd:YAG pumped tunable sources, appl. to spectroscopy 0-58576
- Nd:YAG regenerative amplifier, expt. studies 0-95909
- Nd:YAG laser reflection resonator with hole coupling 0-58597
- $\text{Nd}^{3+}$ , glass laser for stimulated Raman scatt. Dewar cell 0-99799
- $\text{Nd}^{3+}$ ,  $\text{Gd}_2\text{Ga}_2\text{O}_7$  pulse-pumped laser action at  $1.054 \mu\text{m}$  0-64030
- $\text{Nd}^{3+}$ , glass luminesc. band profile deform. under free-oscillation conditions 0-71487
- $\text{Nd}^{3+}$ ,  $\text{LaCl}_3$ , laser-induced fluoresc., hyperfine structs. 0-100677
- $\text{Nd}^{3+}$ ,  $\text{LaCl}_3$ , laser-induced fluoresc. energy transfer effects 0-100678
- $\text{Nd}^{3+}$ , YAG, Q-switching mechanism by intracavity stimulated Brillouin scatt. 0-106552
- $\text{Nd}^{3+}$ , YAG CW laser, intensity fluctuations in single-freq. mode 0-91802
- $\text{Nd}^{3+}$ , YAG laser, high repetition rate electrooptic Q-switching, birefringence 0-69430
- $\text{Nd}^{3+}$ , YAG laser, pumping by alkali metal vapour arc discharge 0-78924
- $\text{Nd}^{3+}$ , YAG laser, stable periodic-pulse, with CW pump 0-74400
- $\text{Nd}^{3+}$ , YAG laser active element, linearly polarised light depolarisation due to thermally induced birefr. 0-106528
- $\text{Nd}^{3+}$ , YAG laser frequency stability improvement using active interferometer (*Russian*) 0-64043
- $\text{Nd}^{3+}$ , YAG multimode laser radiation noise 0-74366
- $\text{Nd}^{3+}$  +  $\text{UO}_2^{3+}$  solution, nuclear pumped liq. lasers, LASL program 0-64011
- $^{143}\text{Nd}/^{144}\text{Nd}$ , ratios in Cretaceous mid-ocean ridge basalt (MORB) from DSDP Holes 417D and 418A 0-94520
- $^{143}\text{Nd}/^{144}\text{Nd}$  in Bay of Islands ophiolite complex, rel. to midocean ridge basalts source evolution 0-85651
- $^{143}\text{Nd}/^{144}\text{Nd}$  in Kerguelen Islands igneous rocks, inferences on enriched oceanic mantle sources 0-98319
- $^{143}\text{Nd}/^{144}\text{Nd}$  in mantle xenoliths, equilibrated isotopic comp. meas. with unequilibrated Sr isotopes 0-98321
- $^{143}\text{Nd}/^{144}\text{Nd}$  in Norwegian eclogites, rel. to crustal origin 0-76978
- $^{143}\text{Nd}/^{144}\text{Nd}$  in Scottish Caledonian granites, isotopic evidence for crustal provenance 0-109146
- $\text{SeOCl}_2\text{Nd}^{3+}$ ,  $\text{SbCl}_5$  acidified, Racah and Judd-Ofelt parameters in laser liqs. 0-106516

## neodymium continued

- $\text{Y}_2\text{O}_3\text{Nd}$  single crystal growth, floating zone method with Xe arc lamp imaging furnace 0-60777
- $\text{Y}_2\text{O}_3\text{Nd}^{3+}$  absorpt. spectra, hypersensitivity of  $^4\text{I}_{9/2}$  to  $^4\text{G}_{5/2}$   $^2\text{G}_{7/2}$  transition 0-97309
- $\text{Y}_2\text{SiO}_5\text{Nd}^{3+}$ , EPR and spin-lattice relax. 0-108063
- $\text{YVO}_4\text{Nd}^{3+}$ , energy transfer processes, laser-excited time-resolved spectroscopy 0-84765
- $\text{YVO}_4\text{Nd}^{3+}$ , zircon struct., cryst. field analysis 0-80232
- $\text{ZnO:Nd}$ , electrolum. brightness, field strength and freq. depend. 0-100696
- neodymium alloys**
- ESR studies of pseudobinary rare earth intermetallic compounds 0-108064
- mischmetall-Co system, phase relations, microstruct., mag. props. 0-104118
- $\text{Gd}_2\text{Nd}_{1-x}\text{Zn}$ , ferromag., mag. susceptibility and magnetisation, temp. depend. 0-70975
- $(\text{La,Nd})\text{Sn}_3$ , reverse Kondo effect in presence of crystalline elec. field splitting 0-103684
- La alloys, supercond., Nd-doped, crystal field effects, tunnelling within mK range 0-70907
- Mg-Nd-Zn dilute alloy, metallography and precip. kinetics 0-71655
- $\text{NaAl}_2\text{Ga}_3$ , synthesis, NMR and X-ray absorpt. studies 0-108083
- $\text{NdAg}_x$ , low temp. mag. meas. 0-107989
- $\text{Nd}_2\text{Ag}_{79}$  and  $\text{Nd}_{50}\text{Ag}_{50}$ , amorphous, mag. props. 0-60182
- $\text{NdAl}_2$ , orbital and spin polarisations of cond. electrons 0-65791
- $\text{NdCo}_2$ , magnetocrystalline anisotropic props., torque meas. 0-108003
- $\text{Nd}_2\text{Co}_3$ , polymorphism of C subgroup alloys, eutectic decomposition (*Russian*) 0-66504
- $\text{NdFe}_2$ , high field Mossbauer study 0-75893
- $\text{NdIn}$ , mag. props. 0-108009
- $\text{NdIn}$ , mag. props. 0-108009
- $\text{NdIr}_2$ , cryst. struct. 0-96473
- $\text{NdOs}$ , cryst. struct. 0-96474
- $\text{NdPt}_5$ , low temp. mag. susceptibility 0-93075
- $\text{NdRh}_1\text{Sn}_{11}$ , new supercond./mag. cpds., X-ray powder diff. data 0-100215
- $\text{NdSn}_3$ , elec. cond., cryst. field effect, spin disorder contrib. 0-65540
- $\text{Nd}_2\text{Y}_{1-x}\text{Zn}$  system, solid soln., mag. susceptibility, 77 to 600K (*Russian*) 0-65776
- $\text{Y}_{1-x}\text{Nd}_x\text{Co}_5$ , ferrimag., magnetisation, exchange interactions, mag. anisotropy 0-80565
- neodymium compounds**
- see also neodymium alloys
- $\text{BaO-Nd}_2\text{O}_3\text{-TiO}_2\text{-Bi}_2\text{O}_3$  system ceramics, high stability low loss dielectric preparation 0-81008
- $\alpha\text{-CsNd(PO}_3)_4$ , single cryst. struct. and spectral-luminescent props. 0-96490
- $\text{Eu}_{1-x}\text{Nd}_x\text{O}_{1-x}\text{N}_x$ , lattice parameters, mag. and elec. props. 0-100578
- $\text{LiNdP}_4\text{O}_{12}$  laser, relaxation oscillations and mode spectra, high density pumping effect 0-69396
- $\text{Nd-H(D)}$ , lattice parameters 0-64982
- $\text{NdAsO}_4$ , ferroelectricity, dielec. meas. 0-60515
- $\text{NdCO}_3\text{Y}^{3-}$ , ( $\text{Y} = \text{ethylenediaminetetracetate ion}$ ), formation constants (*French*) 0-104458
- $\text{Nd}_{1-x}\text{Ca}_x\text{VO}_3$ , solid solutions, elec. props. 0-96866
- $\text{NdCl}_3$ , anhydrous,  $\text{Nd}^{3+}$  absorption spectra and quantum states (*Chinese*) 0-89032
- $\text{Nd}_2\text{CuO}_4$ , magnetic properties obs. 0-70937
- $\text{NdCu}_2\text{Ru}_4\text{O}_{12}$ , synthesis, cryst. struct., mag. and elec. props. (*French*) 0-107151
- $\text{NdF}_3$ , enthalpy of formation 0-93789
- $\text{Nd}_2\text{Ga}_2\text{O}_{12}$ , floating zone method growth, interface shapes 0-60775
- $\text{Nd}_2\text{Ga}_2\text{O}_{12}\text{Nd}^{3+}$ , radiationless decay processes, laser photoacoustic spectroscopy meas. 0-84766
- $\text{NdH}_{2.57262}$ , optical vibr. spectra of H, inelastic neutron scatt. study 0-107391
- $\text{NdN}$ , miscibility with UC (*German*) 0-96654
- $\text{Nd(NO}_3)_3$ , aqueous soln., single photon absorpt. band struct., electronic resons. coherent ellipsometry 0-90881
- $\text{NdNbO}_4$ , room temp. form., symmetry determ. by convergent beam electron diff. 0-79723
- $\text{Nd}_2\text{NiO}_4$ , magnetic properties obs. 0-70937
- $\text{NdO}$ , electronic spectrum, rotational struct. anal. 0-78643
- $\text{Nd}_2\text{O}_3$ , cryst. struct., X-ray powder diff. and electron diff. study 0-107161
- $\text{Nd}_2\text{O}_3$ , EELS, low loss peak due to plasmon 0-79953
- $\text{Nd}_2\text{O}_3$ , electrostatic cryst. field parameters including induced dipole contrs. 0-80233
- $\text{Nd}_2\text{O}_3\text{-Y}_2\text{O}_3$  film, segregation obs. by EELS 0-79953
- $\text{Nd(OH)}_3$ , dynamical effects of interaction between 4f electrons and optical phonons 0-108196
- $\text{Nd(OH)}_3$ , heat capacity from 10 to 350K, lattice and Schottky contrs. 0-84300
- $\text{Nd}_2\text{O}_3\text{S}$ , electrostatic cryst. field parameters including induced dipole contrs. 0-80233
- $\text{NdOs}_2\text{Sb}_{12}$ , prep. and cryst. struct. 0-100211
- $\text{NdP}_2\text{O}_{14}$ , ferroelastic, hydrostatic press. effect on phase transition temp. 0-70293
- $\text{NdP}_2\text{O}_{14}$ , fluoresc. lifetime meas., IR and photoacoustic spectroscopy 0-60652
- $\text{Nd}_2\text{PO}_7$ , IR and Raman spectra, vibr. assignments, cryst. struct. characts. 0-97258
- $\text{Nd}_2\text{R}_{1-x}\text{P}_2\text{O}_{14}$  ( $\text{R} = \text{La, Y}$ :  $0.1 < x < 1$ ), laser quality cryst. growth, morphology 0-66412
- $\text{NdRu}_2\text{Sb}_{12}$ , prep. and cryst. struct. 0-100211
- $\text{Nd}_2\text{S}_3$ , optical props. and electronic struct. in fund. absorpt. region 0-80817
- $\text{Nd}_2\text{S}_3$ , vibr. spectra, factor-group anal. 0-80793
- $\text{Nd}_2\text{Ti}_2\text{O}_7$ , ferroelec., layer type struct., cryst. growth 0-108348
- $\text{NdTiO}_3$ , layered ferroelectric, anomalous photovoltaic effect, photovoltaic current 0-75603
- $\text{Nd}_2\text{Y}_{1-x}\text{P}_2\text{O}_{14}\text{Nd}^{3+}$ , radiationless decay processes, laser photoacoustic spectroscopy meas. 0-84766
- $\text{Nd}_2\text{Zr}_{1-x}\text{O}_{2-x/2}$ , elec. cond. of ceramic solid solutions 0-107554
- $\text{Nd}_2\text{Zr}_{1-x}\text{O}_{2-x/2}$ , fluorite and pyrochlore solid solutions, electrical conductivity meas. 0-65287
- $\text{Pb}_{1-x}\text{Nd}_x\text{Ge}_2\text{O}_{11}$ , ferroelec. props. 0-75960



**neodymium compounds continued**

- $\text{SiO}_2\text{-Na}_2\text{O-Nd}_2\text{O}_3$  glass, magneto-optical props., absorpt. spectrum 0-88969  
 $\text{U}_{1-x}\text{Nd}_x\text{S}$ , mag. phase diagram 0-71027  
 $\text{ZrF}_4\text{-BaF}_2\text{-NdF}_3$ , vitreous phases, network formers, modifiers and stabilisers (French) 0-64909  
 $\text{ZrF}_4\text{-BaF}_2\text{-NdF}_3$   $\text{F}^-$  ion cond. glasses, cond. process 0-107477

**neon**

see also nuclei with .....

- atom,  $1s_2$  metastable, velocity-changing collisions, study by time resolved saturated absorption 0-82832  
 atom,  $(2p^3p)$  states, radiative lifetimes, collisional deactivation rate consts. 0-69107  
 atom, approximate relativistic Hartree-Fock eqns., soln. using Slater-type functions 0-58168  
 atom, closed shell, Jastrow wave functions, var. calcs. 0-83249  
 atom, correl. contrs. to dipole polarisability, coupled HF-perturbation theory 0-106269  
 atom, correl. energy, fourth order diagrammatic, many body Rayleigh Schrodinger perturbation theory 0-63556  
 atom, dipole dynamic polarisabilities and two-photon photoionisation cross section calc., R-matrix approach 0-102444  
 atom, electron impact excitation of  $2s2p^3s$  and  $2s2p^3p$  configs., energy loss obs. 0-91685  
 atom, first excited config., intermediate coupling coeff. 0-83450  
 atom, metastable electronic states, electron impact excitation, time of flight spectra 0-106411  
 atom, temp. perturbed Thomas Fermi eqn., variational principle 0-69074  
 atoms, classical many-body collision model incorporating Heisenberg and Pauli principles 0-63511  
 atoms, Compton profiles, Xalpha wavefunctions 0-106265  
 atoms, electron energy loss spectra, Compton defect characterised by shift and asymmetry parameters 0-95723  
 atoms, even-parity levels, double excited energy levels, frozen-core superposition, config. calcs. 0-106273  
 Auger electron emission due to ion collisions with solid targets (French) 0-104031  
 beam source, high-flux 0-58416  
 [C] He-Ne laser scanning system, for video record player, information identification (German) 0-106557  
 Clausius-Mossotti second virial coefficient 0-79426  
 discharge, high-freq., excited atoms concentration determ., Ne or Ar, using spectral method (German) 0-70053  
 discharge, high-freq., excited atoms concentration determ., using spectral method (German) 0-70053  
 discharge in high press. narrow tube, Kadomtsev-Nedospasov instability 0-107004  
 discharges, HF and glow, excited atoms concentration determ. (Russian) 0-70050  
 electron Coulomb profile beyond impulse approx. 0-87083  
 electron impact K-shell excitation, EELS 0-106396  
 embryo  $\text{C3H10T1/2}$  cells, mouse, high-energy neon particle irradi., viral transformation enhancement 0-104668  
 excited atom + molecules reactions, electronically excited atoms and alkali metal atoms analogy 0-76490  
 explosive burning in supernovae 0-94780  
 frozen gas matrix, laser beam waveguide propag. 0-64168  
 gas, compressed, Rayleigh-Brillouin spectrum, hydrodynamic region 0-100063  
 gas, compressed, Rayleigh-Buillouin spectrum, scaling 0-100062  
 gas atoms, electron thermalization time and position distribution meas. 0-93771  
 hollow cathode discharge tube, spectral line intensities, rise time 0-103212  
 impact on W surface, tangential momentum accommodation coeff. meas. by acoustic vel. and absorpt. obs. 0-66867  
 implantation in Fe, effect on corrosion by  $\text{H}_2\text{SO}_4$  soln. 0-71793  
 ion, energy and ang. distrib. in passing through C, Cu, Ag films 0-100292  
 ion mobilities in He gas at 82K 0-75023  
 isoelectronic sequence, X-ray spectra 0-87071  
 isoelectronic series, second order correl. energy, Z depend. of irreducible-pair energies 0-91417  
 isotope separation by cathoporesis in DC gas discharge 0-103213  
 laser, discharge pumped multiwavelength (Chinese) 0-102703  
 Lennard Jones- (12,6) pot. distance parameter, transport props. calc. 0-79423  
 liquid, comparison on interaction induced light scatt. and IR absorption 0-60561  
 low press. discharge, electron free streaming waves expansion 0-79595  
 momentum eigenfunctions in complex momentum plane, Hartree Fock functions 0-63517  
 negative ions, scatt. electron spectra, distinction from neutral autoionising states 0-83482  
 nuclear induced plasma, simulated 0-64786  
 plasma, electron collision ionisation, electron kinetic behaviour during elec. field perturbation (German) 0-64676  
 plasma, photon reabsorption attenuated radiation emission 0-64776  
 positive column plasmas, metastable atom density meas. by improved self absorpt. method 0-87968  
 pulsed transverse discharge, spectrosc. absorpt. investig. with nanosec. time resolution (Russian) 0-64782  
 recoil ion, highly charged, K X-ray emission 0-91649  
 solid, bulk excitons, expt. 0-92827  
 solid, bulk excitons, theory 0-92826  
 solid, energy bands, depend. on choice of exchange-correlation pot. 0-70607  
 solid, hole band struct., Bratsev wave function calcs. (Russian) 0-65437  
 thermal conductivity, at high press. 0-103099  
 vertical valence ionisation potential calc. by perturbation, CI and CPA techniques 0-69263  
 X-ray line shift for high density laser produced plasma diagnostics 0-64778  
 Ar-Ne, liquid solution, dielectric props., intermolecular interactions (Russian) 0-88904  
 D, lamps, influence of Ne and Ar on spectral parameters 0-86460  
 D-Ne capillary-arc lamp, optimum parameters 0-95971  
 He-Ne, laser, scheme for automatic fine frequency tuning along the Lamb depression 0-74385

**neon continued**

- He-Ne  $^{127}\text{I}_2$  stabilised laser source for Michelson interferometer, optical feedback obs. 0-106545  
 He-Ne 3.39  $\mu\text{m}$  laser, FM eliminated  $\text{CH}_4$  locked freq. stabilisation in dual feedback control 0-99772  
 He-Ne  $\text{CH}_4$  locked laser, freq. stability meas. 0-87422  
 He-Ne dual mode laser, injection modulation in coupled laser oscillators 0-99773  
 He-Ne gas lasers, 2 mW and 5 mW, reliability 0-95913  
 He-Ne laser,  $^{127}\text{I}_2$  stabilised, length or freq. standard 0-106544  
 He-Ne laser, 6328  $\text{\AA}$  power fluctuations due to striation noise 0-78834  
 He-Ne laser, beat freq., high displacement sensitivity meas. 0-95926  
 He-Ne laser, cavity losses, phase polarisation method in lasing regime 0-87413  
 He-Ne laser, compact, transverse microwave discharge, energy characts. 0-64064  
 He-Ne laser, methane-stabilized at 88 THz 0-73304  
 He-Ne laser, operating on 0.63, 3.39  $\mu\text{m}$  coupled transitions, intensity modulation 0-69365  
 He-Ne laser, stabilised by  $^{127}\text{I}_2$  saturated absorpt., wavelength international comparisons 0-95872  
 He-Ne laser model LG-10, design (Rumanian) 0-87407  
 He-Ne laser stabilisation,  $\text{I}_2$  absorption cell power densities 0-99767  
 He-Ne laser stabilisation by  $\text{I}_2$  612 nm saturated absorption 0-99765  
 He-Ne laser stabilisation by  $\text{I}_2$  611.8 nm-saturated absorption 0-99766  
 He-Ne laser stabilised by methane E-component, reference source freq. reproducibility 0-106507  
 He-Ne laser wavelength drift 0-67978  
 He-Ne lasers, in hollow Cu cathode, 632.8 nm output characts. 0-63975  
 He-Ne lasers, transverse microwave freq. gas-discharge pumping 0-74339  
 He-Ne low-gain laser amplifier, phase control 0-64059  
 He-Ne methane system, narrow nonlinear resonances in three level system (Russian) 0-78898  
 He-Ne mixture, cathaporetic gas separation in DC glow discharge with end volumes 0-79428  
 He-Ne ring laser, 6328  $\mu\text{m}$ , self-pulsing conditions 0-87414  
 He-Ne ring laser, methane stabilised, nonlinear resonance freq. shift due to back scatt. (Russian) 0-78874  
 He-Ne ring laser, nonlinear spectroscopic technique 0-91819  
 He-Ne ring laser, nonreciprocal effects with transverse mag. field applied to active medium 0-91820  
 He-Ne/ $\text{CH}_4$  FM eliminated laser, freq. stability meas. 0-87423  
 He-Ne-Xe ion lasers, hollow cathode, CW operation and excitation mechanism 0-69363  
 He-Ne-methane ring laser, power resonances 0-99761  
 He-Ne-methane ring laser, freq. synchronisation interval for oppositely directed waves 0-99762  
 He+ $\text{He}^+$ (Ne), tensor polarisabilities of  $1snd$   $^1D$  level, fluoresc. depolarisation obs. 0-69099  
 Na+Ne, potential curves from a model potential (French) 0-78685  
 Ne II 12.81  $\mu\text{m}$  forbidden line obs. of G333.6-0.2 H II region 0-85983  
 Ne $^+$ , absolute electron impact ionisation cross section 0-83496  
 Ne $^+$ , conversion to mol. ions, three body association coeffs. determ. using drift-tube mass spectrometer 0-108699  
 Ne $^{10+}$ , microdosimetric measurements of pretherapeutic heavy ion beams 0-72337  
 Ne-H, exciton states and  $L_{\alpha}$  emission 0-93372  
 Ne-Al large diameter hollow cathode discharge, near IR Al II laser transitions 0-102715  
 Ne- $\text{CO}(\text{CO}_2)$ , C nuclear pumped lasers, energy storage 0-63996  
 Ne- $\text{H}_2$  liq. mixtures, phase equilb. effects, thermodynamic perturb. theory (Russian) 0-92663  
 Ne-like atoms and ions, gradient expansion of atomic kinetic energy functional 0-95530  
 Ne-N $_2$ , atomic N nuclear pumped lasers, surface effects 0-63996  
 Ne-N $_2$  AC discharge, pulse to continuous mode transition, Ne metastable effects (German) 0-84011  
 Ne-Na, non-Lorentzian spectral line shape 0-106297  
 Ne-Xe, equilibrium of coexisting phases 0-87197  
 Ne+ $\text{Ne}^+$ , optical transition excitation function and cross sections 0-63787  
 Ne+acetylene, vibr. relax. study using laser-induced fluoresc. 0-74219  
 Ne+ $\text{Be}^+$ , 180 degree phase jumps for  $\text{Be}^+(2s-2p)$  excitation amplitudes, coherence obs. 0-63793  
 Ne+ $\text{Be}^+$ , Be II  $2^2P$  excitation, alignment and orientation 0-91647  
 Ne+ $\text{Be}^+(\text{Mg}^+)$ , ns-np excitation, alignment and orientation, impact, parameter theory 0-91648  
 Ne+ $\text{C}^{n+}(\text{N}^{n+})(\text{O}^{n+})$ , charge exchange contribution to K-vacancy production 0-102553  
 Ne+ $\text{CO}_2$ , energy transfer rate consts., semiclassical method 0-91640  
 Ne+ $\text{CS}_2$ , metastable atoms, energy transfer processes 0-83466  
 Ne+ $\text{CO}_2$ , intermol. pot. in repulsive short-range region, ab initio 0-69204  
 Ne+ $\text{D}_2$ , anisotropic inversion pot., rot. inelastic cross sections 0-78696  
 Ne+ $\text{D}_2$ , anisotropic potentials, direct inversion methods calcs. 0-69090  
 Ne+ $\text{D}_2$ , energy-loss scaling in 0.5-3.5 keV 0-63768  
 Ne+ $\text{D}_2$ , state-resolved  $\Delta j=2$  rot. transitions 0-63772  
 Ne+H, electron energy loss 0-87217  
 Ne+ $\text{H}^-(\text{D}^-)$ , electron detachment, dynamical phenomenon 0-106305  
 Ne+He,  $2s_0$ -level excitation, rate const., temp. depend. 0-87218  
 Ne+ $\text{He}^+$ , He( $3^1P$ ) level excitation, total emission cross section, fast oscils. obs. 0-58362  
 Ne+ $\text{He}(2^1S, 2^3S)$ , transition probs., pots. 0-58371  
 Ne+heavy ion, highly charged very slow Ne recoil ions, K X-ray transition 0-91649  
 Ne+ $\text{I}_2^+$ , energy depend. of collision induced intramolecular energy transfer 0-83470  
 Ne+Kr, collision induced microwave absorpt. spectra 0-74216  
 Ne+ $\text{Li}^+$ , collisions, vel. dependence of Ne 2s and 2p, vacancy production, electron spectroscopy 0-58344  
 Ne+ $\text{Li}^+(2^2P)$ , collision induced fine struct. transition 0-74220  
 Ne+ $\text{NH}_3$ , pure rot. line, press. broadening calcs. 0-78656  
 Ne+Na,  $3^3P$ - $3^3D$  line broadening obs. 0-78684  
 Ne+Na( $3P_{1/2}$ ), vel.-changing collisions, effect on 2 photon and stepwise absorpt. line shape 0-87221  
 Ne+Ne, (He) low pressure broadening and shift of Ne line, Lennard-Jones pot. 0-102554  
 Ne+proton, charge transfer, target K-shell electron capture, impact parameter depend. 0-102552  
 Ne+U, collisional relax. of highly excited states, laser-induced fluoresc. obs. 0-58205



**neon continued**

- Ne+Xe, quenching of excited Xe\*(<sup>3</sup>P<sub>2</sub>, <sup>3</sup>P<sub>1</sub>, <sup>1</sup>P<sub>1</sub>) 0-63578  
 Ne+Xe<sup>+</sup>+Cl<sup>-</sup>, three body ion-ion recombination probability, Monte Carlo simulation 0-85160  
 Ne<sup>+</sup>+2He, three body reaction, rate coeffs., temp. depend., 100 to 300K 0-108703  
 Ne<sup>+</sup>+Ar integral elastic scatt., repulsive potentials derivation 0-63744  
 Ne<sup>+</sup>+D<sub>2</sub>(H<sub>2</sub>), energy-loss scaling in 0.5-3.5 keV 0-63768  
 Ne<sup>+</sup>+Ar(Kr)(Xe), single electron capture excitation, photon emission, VUV spectroscopy 0-58379  
 Ne<sup>+</sup>+H<sub>2</sub>(N<sub>2</sub>)(O<sub>2</sub>)(CO)(CO<sub>2</sub>)(methane), charge transfer reactions, rate coeffs. and product-ion distributions meas. 0-104431  
 Ne<sup>+</sup>+inert gas, low energy reactions, SIFT and drift tube obs. 0-97705  
 Ne<sup>+</sup>+Li, electron capture excitation, VUV spectroscopy 0-63810  
 Ne<sup>+</sup>+Xe, electron capture collisions, 15 to 50 keV, excitation 0-102566  
 Ne<sub>2</sub>, collision induced Raman spectra and diatom polarisability 0-63647  
 Ne<sub>2</sub><sup>+</sup>+atom (molecule), bimolecular and termolecular reaction rate coeffs. 0-81308  
 Ne(P<sub>0</sub>)<sub>2</sub>+Ne, differential cross sections 0-58370  
 Ne(P<sub>2</sub>) elastically scattered, metastable, ang. distrib., conventional rel. to Doppler shift methods 0-58418  
<sup>22</sup>Ne as neutron source for solar systems s-process, difficulty 0-72926  
<sup>22</sup>Ne nucleosynthesis in novae and supernovae outbursts 0-62143  
 Ne\* 5882 Å line, Doppler free spectra, press. broadening and shifts, saturation spectroscopy 0-78565  
 Ne\*-He\*, Penning ionisation of metastable He\* 0-83472  
 Ne<sup>+</sup>+Ar, associative ionisation studied by merging-beams technique 0-91646  
 Ne<sup>+</sup>+Ar\*, Penning ionisation studied by merging-beams technique 0-91646  
 Ne<sup>+</sup>+Fe(CO)<sub>5</sub>, chemiionisation and chemiluminescence reactions, Penning ionisation and fluoresc. obs. 0-97689  
 Ne<sup>+</sup>+H, assoc. ionis., rovibronic struct. in electron energy spectrum 0-106380  
 Ne<sup>+</sup>+H<sub>2</sub>O, pot. energy surfaces, MO and CI calcs., Penning ionisation electron spectra 0-106376  
 Si:Ne, ion implanted, nature of defect reverse annealing 0-88875

**neon compounds**

- NeCN<sup>+</sup>, SCF calcs., dissoc. energies, rot. and hyperfine const. determ. 0-95531  
 NeH<sub>3</sub>, van der Waals mols., rot. predissoc. 0-63721  
 NeO, nonadiabatic coupling matrix elements by Hellmann-Feynman theory and HF 0-83263

**nephelometry** *see turbidimetry***Neptune**

- albedo and brightness temp., 5 µm IR obs. 0-82300  
 atmosphere, ammonia and water vapour contents 0-90366  
 atmospheric VHF refraction 0-98608  
 limb brightening in 7300 Å methane band, photometry obs. 0-82297  
 magnetic field, hydromagnetic dynamo in core 0-90365  
 observations by Galileo, (1612 and 1613) 0-105485  
 polar moment of inertia determ. 0-94694  
 positions, reduction of 19th century obs., method comparison 0-94691  
 ring, observational evidence in 1846-7 from Lassell and Challis 0-67652  
 rotation, equatorial flow theory 0-67653  
 rotation period, correction, photometric and spectroscopic results comparison 0-82301  
 stellar recultation, 1980 August 21, obs. 0-109395  
 structure and evolution in three-layer interior model 0-72877  
 UV albedo, meas. 0-82295

**neptunium**

- see also nuclei with .....*  
 LaBr<sub>3</sub>:Np<sup>3+</sup>, energy level anal., polarised absorpt. and fluoresc. spectra 0-76056  
 LaCl<sub>3</sub>:Np<sup>3+</sup>, energy level anal., polarised absorpt. and fluoresc. spectra 0-76056  
 LaCl<sub>3</sub>:Np<sup>3+</sup>, phonon-induced relax. in excited optical states, linewidth temp. depend. meas. 0-100688  
<sup>235</sup>Np, radioactive waste, sorption in igneous rocks 0-95367  
 U<sup>238</sup>Np, muonic atom lifetimes from muon induced fission 0-69269  
 U<sup>238</sup>Pu-<sup>237</sup>Np GCRF fuel cycle to produce isotopically denatured Pu for LWR 0-78427

**neptunium compounds**

- NpO<sub>2</sub>, mag. transition at 25K, Kramers doublet as cryst. field ground state 0-59936  
 NpO<sub>2</sub>, single crystal growth, gas phase chemical transport method (French) 0-60760

**Nernst effect** *see thermomagnetic effects***Nernst-Ettingshausen effect** *see thermomagnetic effects***network analysis (management)** *see management science***network equalisers** *see equalisers***network parameters**

- see also S-parameters*  
 four-terminal, x-y recorder sweep generator, sweep speed dependent on transfer charact. 0-62649

**network synthesis**

- filter, Kalman, digital, with a priori uncertainty of data, phasemeter appl. 0-98934

**network theory** *see circuit theory***networks** *see networks (circuits)***networks (circuits)**

- see also specific network and circuit headings e.g. communication networks, pulse circuits, oscillators*  
 education, linear programming, introduction and appl. to simple cct. 0-73136  
 electronics for the physicist with applications, book 0-62403

**Neumann algebra** *see algebra***neural nets**

- see also brain models*  
 alpha-rhythm, neural vet model 0-76719  
 anthozoans, pennatulacea, colonial coordination 0-94197  
 arm posture control, spring model and equivalent neural network 0-101196  
 EEG waves, neural basis 0-108868  
 finger tapping by both hands, coordinated, two coupled oscillators as model 0-101163  
 holographic models of neural struets., optical system (Russian) 0-76878  
 Leaky-Integrator Neuron Model, input-output relationship 0-72152

**neural nets continued**

- neocognitron, self-organising neural network model, pattern recognition mechanism unaffected by shift in position 0-76745  
 neuron electronic model (Spanish) 0-104580  
 neuron model as component of neural network, hardware realisation 0-61534  
 neuron soma model with high reliability and low power consumption 0-72392  
 oscillatory neural networks in the rabbit hippocampus 0-89743  
 pattern separability in random neural net with inhibitory connections 0-76726  
 photosensitive neuron in crayfish caudal ganglion, properties, expt. (French) 0-89705  
 self-organising nerve nets, fundamental theory, developmental plasticity anal. 0-67062  
 synchronous oscillation in idealised neuronal circuit with recurrent inhibition (Japanese) 0-101164  
 tightly coupled two layer random nerve net with inhibitory mechanism, pattern separability 0-61533  
 two-terminal electronic circuit neuron model 0-61526

**neuristor networks** *see neural nets***neuron models** *see neural nets***neurophysiology***see also brain; neural nets*

- 40 Hz activity in sigmoid gyrus, nucleus accumbens and amygdala, cross correl. anal. 0-76730  
 acetylcholine, diffusion in synaptic cleft of normal and myasthenia gravis human endplates 0-94198  
 action pot., lipid bilayer local phase transition 0-89744  
 action potential propagation, effects of cellular geometry on current flow 0-94196  
 action potentials from cultured neurons, recording by extracellular micro-circuit electrodes 0-72382  
 afferent nerves from muscle spindles, signal interpretation method 0-101188  
 Alopec process: Visual receptive fields by response feedback, trigger features 0-61546  
 alpha-rhythm, neural vet model 0-76719  
 amblyopia, human, differences in neural basis, effect of mean luminance 0-72156  
 anthozoans, pennatulacea, colonial coordination 0-94197  
 auditory brainstem frequency, response to waveform envelope periodicity 0-61590  
 auditory cortex unit response to synthesized formants, cat 0-67098  
 auditory nerve fibre model 0-94227  
 auditory primary neurons, comparative physiology 0-94224  
 auditory-nerve fibre encoding of 2-tone approximations to steady-state vowels 0-61582  
 auditory-nerve fibre responses to bandlimited noise, nonlinearities 0-61583  
 autoradiographic visualisation of rat brain dopaminergic nerve endings, test of technique 0-61742  
 autorhythmicity and entrainment in excitable membranes 0-108866  
 averaged multiple unit activity as estimate of local neuronal activity changes, vol. conducted pots. 0-89917  
 axonal transport, theoretical approach to anal. 0-67064  
 axons, giant, squid, interaction of Ba<sup>2+</sup> with K<sup>+</sup> channels 0-85379  
 binocular vision, frog ipsilateral retino-tectal pathways 0-85401  
 biomagnetic fields and cellular current flow 0-101192  
 brain, caudate nucleus, neurotransmitter activity transient alterations after irradi., rat expts. 0-72267  
 brain, human, neural generator localisation underlying auditory evoked mag. fields 0-104703  
 brain, mag. evoked field mapping 0-104705  
 brain, magnetoencephalogram power spectrum estimation 0-104704  
 brain activities, synchronous, spatio-temporal filter approach 0-61503  
 brain research, computed transaxial tomography, ring detector positron camera system 0-61739  
 brainstem population responses, inhibitory influence 0-104595  
 brightness perception and retinal rivalry in binocular vision, integrated model 0-101180  
 cerebellar model, spatial freq. characts. (Japanese) 0-67068  
 chemoreceptor afferents from aortic and carotid bodies, relative latency of responses 0-101189  
 cochlear fibre responses in guinea pigs with well defined cochlear lesions 0-94226  
 colour sensitive neural networks, reaction to intensity and colour steps (German) 0-76737  
 conditioning auditory stimuli and the cutaneous eyeblink reflex, human obs. 0-67090  
 conduction times, central and peripheral, in multiple sclerosis, somatosensory obs. 0-89773  
 conductivity monitor for isolated nerve preparation expts. 0-67301  
 cone outer segments, light-induced changes in membrane current, tiger salamander and turtle 0-108899  
 EEG, automated monitoring of long-term implanted electrodes (Russian) 0-76857  
 EEG, decision P350, waveform and neural mechanism, auditory click and elec. finger stimuli 0-61528  
 EEG theta rhythm, dipole-like neuronal sources, anesthetized rat obs. 0-61527  
 EEG waves, neural basis 0-108868  
 electrocyte stacks of torpedine ray, assembly for quick-freezing tissues 0-67316  
 EMG shimmer in patients with neuropathy and neurogenic atrophy 0-72149  
 encoder, adaptive model 0-97897  
 endogenous and exogenous activity in molluscan neurone, identification by spike train anal. 0-89735  
 epidural neurostimulation, percutaneous, histological reaction, short and long term study results 0-67285  
 excitation properties of the squid axon membrane and model systems with current stimulation 0-67054  
 external geniculate body, cat, geometric props. of space of description of images 0-94203  
 extracellular potentials generated by curved fibres in a vol. conductor, modelling 0-97889  
 eye and hand motor systems, optimal response in pointing at a visual target 0-61567



## neurophysiology continued

- eye movements control, effects of frontal eye field and superior colliculus ablations 0-72154
- fibre membrane analogue-code conversion, ionic mechanisms 0-81575
- fibre membrane Na permeab. reversible blockage by increase in temp. of medium above 45°C 0-81576
- finger tapping by both hands, coordinated, two coupled oscillators as model 0-101163
- glial smooth endoplasmic reticulum acid phosphatase transport into damaged axons, role of microtubules 0-85381
- glycoproteins, fast axonal transport in guinea pig auditory neurons 0-104573
- hippocampal burst-firing neurons, slow inward current, voltage clamp obs. 0-94194
- Hodgkin-Huxley standard model, squid axons in reduced external  $\text{Ca}^{2+}$  0-94188
- holographic models of neural structs., optical system (*Russian*) 0-76878
- impulse conduction, modulation along the axonal tree, review, book contrib. 0-108872
- impulse conduction along a myelinated fibre, math. model 0-94195
- impulse data treatment for comparison with theory 0-97893
- inferior colliculus neurons, cat, response to binaural beat stimuli obs. 0-72179
- influx current of edible snail neurons, dependence on  $\text{Ca}^{2+}$  conc. and membrane pot. 0-108865
- intellectual activity, classification of normal and anomalous forms, quantised-wave theory of coherent brain appl. (*Russian*) 0-76722
- intellectual activity, psychoheuristic relationship of psychotism structs. and giftedness structs. introduction, quantised wave theory of coherent brain appl. (*Russian*) 0-76723
- intertrial spiking, spontaneous, awake kindred rat 0-67058
- interspike intervals, meas. teleprocessing, anal. 0-85375
- lateral geniculate cells, functional organisation after visual cortex removal in newborn kittens 0-81587
- Limulus ommatidia, resonant response of neural model to double freq. stimulation 0-76734
- locus coeruleus neurons, impulse activity in awake rats and monkeys 0-104581
- lumbo-sacral motoneuron pools, human, response patterns to distant somatosensory stimuli 0-108924
- mammalian nervous system, possible microwave mechs. 0-89738
- median nerve, transient responses to elec. stimulation, SQUID appl. to somatically evoked field meas. 0-104706
- medullary respiratory neuron activity, rel. to tonic and phasic REM sleep 0-97891
- membrane conductance channels, current-induced coupling, multi-channel interaction and mean field cond. 0-67063
- membrane process field potentials anal. and synthesis, computer system 0-85374
- memory neuron, synapse microchem. for memory component of neuroconnective brain model 0-104579
- micropipettes of very low resistance for intracellular meas., production method 0-61738
- microtubules in optic nerves of temperature acclimated goldfish, electron microscopy 0-85395
- minicomputer application for fast expt. data acquisition and processing (*Japanese*) 0-85536
- Molluscan branched neuron, location of spike-initiating or spike entry zones 0-61536
- motor neuron activity patterns of *Drosophila*, anal. with neural analogues 0-108870
- movement detection, performance of a wide-field element in the blowfly visual system 0-89763
- movement-detecting neurons, fly, contrast sensitivity obs. 0-72163
- multibarrel microelectrodes, 'piggy-back', simple technique for construction 0-85541
- multipath neural systems, statistical anal. 0-101162
- myelinated nerve fibre, response to short duration biphasic stimulating currents 0-85373
- Nephrops norvegicus (L.), circadian rhythmicity, neurohumoral basis 0-108889
- nerve cell membrane detection of HF EM fields, possibility discussion (*Russian*) 0-76785
- nerve excitation, gating currents and dipole transitions 0-67056
- nerve fibre counting by pipeline minicomputer image processing 0-109013
- nerve fields, topographic organisation 0-89742
- nerve impulse encoding, elec. processes 0-76718
- nerve membrane, excitability, genetic alteration, temp.-sensitive paralytic *Drosophila* mutants 0-97895
- nerve signals derivation from contrast flash data 0-108885
- nerve trunk multifibre activity quantitation 0-76853
- neural pulse wave analysis, microprocessor-based instrument 0-104791
- neural system, one-dimensional, numerical investigation of kinetic neuron equations 0-76725
- neural transformations of random signals, Wiener and of functionals of Markov chain 0-76727
- neuromagnetic fields sources location, using SQUID system, comparison with electrical method 0-101190
- neuromuscular block indicator, model INMB-1, EMG amplitude meas. 0-104785
- neuromuscular junction, frog, electrostatic screening of neurotransmitter release 0-89741
- neuron electronic model (*Spanish*) 0-104580
- neuron input current, *Helix pomatia*, rel. to membrane pot. and extracellular  $\text{Sr}$  and  $\text{Ca}$  ion concs. 0-81577
- neuron membrane, design of a single electrode voltage clamp 0-72385
- neuron membrane, electrostatic plasma probe physical analogue 0-79573
- neuron model as component of neural network, hardware realisation 0-61534
- neuron soma model with high reliability and low power consumption 0-72392
- neurons, electrical behaviour, general input-output relations 0-85378
- neurons, single, rapid killing by irradiation of intracellularly injected dye 0-81795
- neurostimulation automatic triggering as function of several EEG parameters, apparatus 0-98203
- nexus, evidence for fixed charge, permeability, obs. 0-94193
- octopus, *Eledone cirrhosa*, electrophysiology of isolated central nervous system 0-104577
- olfactory bulb, 55 counts/sec rhythm anal. and simulation 0-85422

## neurophysiology continued

- optic tectum, goldfish, fine struct. 0-85396
- optic tract fibres, physiologically characterised, projection patterns, cat obs. 0-101167
- oscillatory neural networks in the rabbit hippocampus 0-89743
- pain control in man, medial thalamic permanent electrodes, electrophysiological and clinical study 0-67282
- peripheral nerve, generation of unidirectionally propagated action pots. by brief stimuli 0-85546
- photoelectrode for recording intracerebral cellular  $\text{Ca}^{2+}$  transients 0-67307
- photoreceptor membrane interfacial pots., light-induced 0-72161
- photosensitive neuron in crayfish caudal ganglion, properties, expt. (*French*) 0-89705
- photostimulator, LED fibre optic, for research on visual nervous integration 0-67302
- picture distortions compensation of moving patterns typical for time filters 0-76731
- presynaptic receptors, occurrence and role (*German*) 0-76729
- pupil response during mental activity, link with intelligence 0-61532
- refractory period measurements, dependence on conduction distance, computer simulation anal. 0-67065
- retina, frog, morphometric anal. of internal horizontal cells 0-108892
- retina, Limulus, oscillatory responses 0-101166
- retina, serial reconstruct. of adjacent ganglion cells 0-89749
- retinal ganglion cell layer, cat, newly identified presumptive microneurons population 0-67077
- retinal ganglion cells, class I, in the toad, *Bufo spinulosus* 0-85393
- retinal ganglion cells in the galago, size and topographic arrangement 0-67078
- retinal neuron firing rates, lack of predictability from interspike interval statistics 0-67075
- rods, toad, spontaneous quantal events induced by pigment bleaching 0-108895
- sciatic nerves, frog, isolated, effects of microwave irradiation on vitality 0-108959
- screening-pigment migration in retinula cells of crayfish, spectral sensitivity 0-72165
- section embedding technique for sequential light and electron microscopic exam. 0-67317
- self-organising nerve nets, fundamental theory, developmental plasticity anal. 0-67062
- sensory neuron, second order, summation of excitation and inhibition by computer simulation 0-76769
- signal recording using implantable electrode and telemetry system, awake animals (*Japanese*) 0-94427
- signals, dipole theory of interactions 0-81574
- single unit activity from foetal pig brains, recording method 0-67315
- skeletal muscle, lumped and population stochastic models, implications and predictions 0-76724
- somatosensory pathways, assessment of central conduction 0-97949
- spike train data, adaptive filtering 0-67265
- spike trains, interleaved, in a noisy channel, separation system 0-94424
- spinal cord to axilla, F-wave conduction vel. 0-97894
- sterotaxic method for recording from single neurons in the cat eye 0-89913
- striate cortex, cat, movement direction detect. and contrast reversal effects, cell response obs. 0-72155
- stuttering, articulatory behaviours, cinefluorographic anal. 0-94240
- stuttering model, movement disorder 0-94241
- supraoptic neurons, rat hypothalamus, osmosensitivity obs. 0-104578
- sympathetic ganglia stimulated in vitro, effect of temp. on coated vesicle form, in presynaptic terminals, cat 0-85380
- synaptic slow responses, props. and possible underlying mechs., review, book contrib. 0-108873
- synaptic vesicles and synaptosomal membranes, electrokinetic props. 0-67055
- synchronous oscillation in idealised neuronal circuit with recurrent inhibition (*Japanese*) 0-101164
- thermoregulation of rabbit head, facial vein myogenic mech. 0-97869
- tightly coupled two layer random nerve net with inhibitory mechanism, pattern separability 0-61533
- transport of substances in nerve cells 0-89745
- two-terminal electronic circuit neuron model 0-61526
- unit activity rel. to movement, photographic technique for anal. 0-67310
- vertebrate retina modelling and simulation, extended networks 0-108884
- vertebrate retina neuronal activities modelling and simulation 0-85386
- vertebrate retinas, outer segment layer, light-induced  $\text{Ca}$  fluxes 0-94207
- vestibular control of oculomotor and postural mechanisms 0-72151
- vision, gloss perception, model using binocular cells in lateral geniculate body 0-72167
- vision, luminance flicker enhancement by colour-opponent mechanisms, monkey obs. 0-61549
- vision, pattern recognition functional mechanisms in humans 0-81609
- vision, receptive fields in area 17 of cat visual cortex, linear and nonlinear properties 0-104583
- vision, spatial frequency channels, inhibition between, complex gratings adaptation 0-72160
- vision, spectral sensitivity in goldfish, photochem. and neural correlates 0-81599
- vision, transient mechanism in the human system, spatiotemporal characterisation 0-72159
- visual cortical neurons, optimality of bar and grating stimuli 0-85391
- visual flicker-induced asymmetries, separate neural systems for darkness, brightness perception 0-67083
- visual system of fly, giant neuron performance, spike generation 0-108886
- visual-vestibular convergence in the vestibular nuclei of the cat 0-85420
- visually evoked potentials and sensory dimensions 0-61548
- walking, connections between different legs, quantitative model 0-101161
- walking, individual leg control, model 0-101160
- C-fibre microelectrodes, neurophysiology appl. 0-67314
- $\text{K}^+$  channel in axonal membrane of mammals (myelinated fibres) 0-61538
- $\text{K}^+$  conductance absence in central myelinated axons 0-108871
- $\text{K}^+$  currents in squid axons, single channel recordings 0-76721

## neural currents

- atoms, Hüller-Sucher-Feinberg identity, generalisation, accuracy for approx. wavefunctions 0-63512
- canonical neural-current predictions from the weak-electromagnetic gauge group  $\text{SU}(3) \times \text{U}(1)$  0-95242



**neutrino currents continued**

- droplet model and neutral currents, operator form 0-91043  
 $E_7$  grand unification, neutral currents problem in  $SU(2) \otimes [U(1)]^3$  gauge theory (*Russian*) 0-62913  
 flavor-changing effective neutral-current couplings in the Weinberg-Salam model 0-86649  
 flavour changing neutral current search in leptonic and semileptonic decays 0-105836  
 flavour changing neutral currents with b quarks and/or  $\tau$  leptons 0-73656  
 fundamental constituents of matter and unification of weak and electromagnetic interactions 0-62940  
 grand unification from neutral currents in gauge models 0-78009  
 Higgs flavour-changing, suppression in  $SU(2)_L \times SU(2)_R \times U(1)$  left-right symmetric gauge theory 0-78016  
 high energy lepton pair prod. with pol. hadrons, P and C violations 0-99068  
 left-right symmetric gauge models, parameter constraints from neutral current data 0-86588  
 MIT bag model, static electroweak props., PCAC 0-73645  
 neutral-current weak interaction without electroweak unification 0-105835  
 parity nonconservation in heavy atoms and weak magnetism in neutral currents (*Russian*) 0-82932  
 PETRA QED tests, implications for weak neutral current struct. 0-86657  
 $\sin^2 \theta_w$ , grand unified gauge theories and proton decay 0-73634  
 strength limit at PETRA energies 0-105839  
 $SU(2)_L \times U(1) \times U(1)_R$  model, chiral symmetry and weak neutral currents 0-101980  
 $SU(2) \times U(1)$  model, fermion and Higgs multiplet structure, universality 0-62909  
 $SU(2) \otimes U(1)$  standard and  $SU(5)$  grand unification models, neutral current data implications 0-78000  
 $SU(3) \times U(1)$  gauge theory, electro-weak interaction, helicity mixed representation 0-78013  
 $SU(5)$ , unification of weak, EM and strong interactions, review 0-105814  
 $SU(5) \times U(1)$  unified theory, neutral current anal. 0-73647  
 torsion potential, coupling strength, experimental bounds 0-73249  
 unconfined colour quark models, weak interactions and neutral currents (*Russian*) 0-105841  
 unified gauge theories, electroweak mixing angle, renormalisation 0-86651  
 unified gauge theories, electroweak mixing angle, sequential triplets scheme of fermions 0-86650  
 weak current interactions, review 0-73654  
 weak interactions, lepton-hadron symmetry, CP violation and  $\Delta I = 1/2$  rule 0-82934  
 weak neutral currents unveiled 0-73658  
 Weinberg-Salam model and extensions,  $\nu$  EM form factors and mag. moments, neutral currents, astrophysics applies. (*German*) 0-62904  
 Weinberg-Salam model Yang-Mills theory of electro-weak interactions 0-73638  
 $D^0$ - $\bar{D}^0$  mixing, flavour-changing Higgs bosons 0-62915  
 $e^+e^-$ ,  $SU(2)_L \times U(1)$  and  $SU(2)_R \times SU(2)_L \times U(1)$  predictions at high  $Q^2$ , neutral currents, Z-bosons 0-63029  
 $e^+e^- \rightarrow \gamma^* \rightarrow \gamma$ , neutral current effects around vector resonances, polarisation 0-105878  
 $e^+e^- \rightarrow q\bar{q}$ , gluon bremsstrahlung, neutral current and beam polarisation effects 0-99106  
 $eN \rightarrow eX$ ,  $SU(2)_L \times U(1)$  gauge theory distinguished from  $SU(2)_L \times SU(2)_R \times U(1)$ , neutral currents, z-bosons 0-62908  
 $eN$  elastic scatt. in nuclei, P violating asymmetry due to weak neutral currents 0-73713  
 $en \rightarrow en\pi$ , pol. e, P-odd asymmetry and cross sections,  $SU(2) \times U(1)$ ,  $SU(3) \times U(1)$  calcs. (*Russian*) 0-62998  
 $e^-N \rightarrow e^- \Delta(3/2, 3/2)$ , P-odd asymmetry, P nonconserving neutral current interaction 0-57611  
 $\gamma$  circular polarisation, neutral current effect in bremsstrahlung and pair production 0-73655  
 $K^+ \rightarrow \pi^+ e^+ e^-$ , neutral-current process, strong interaction corrections 0-62968  
 $K^0 \rightarrow K^0$ , weak neutral current diagonality, mixing amplitude, multi-quark gauge model (*Russian*) 0-68414  
 $\nu(\bar{\nu})p$ , 2 GeV elastic scatt., charged current/neutral current event ratio 0-57582  
 $\nu N$ , charged and neutral current interactions, cross sections and scaling variable distribts. 0-57581  
 $\nu N$ , charmed particle prod. due to neutral weak currents (*Russian*) 0-68447  
 $\nu n \rightarrow \nu p \pi^-$ , neutral current process, excitation function, cross section ratio 0-78053  
 $\nu N \rightarrow \nu X$ ,  $SU(2)_L \times U(1)$  gauge theory distinguished from  $SU(2)_L \times SU(2)_R \times U(1)$ , neutral currents, z-bosons 0-62908  
 $\nu N \rightarrow \nu X$ , neutral current  $\psi$  prod.,  $Z^0$ -gluon fusion model 0-78015  
 $\bar{\nu} p$ , 1.1 GeV, charged and neutral current events, strangeness changing currents, charm prod. 0-57583  
 $\bar{\nu} p$ ,  $\bar{\nu} p$ ,  $SU(2)_L \times U(1)$  and  $SU(2)_L \times SU(2)_R \times U(1)$  predictions at high  $Q^2$ , neutral currents, Z-bosons 0-63029  
 $\bar{\nu} p \rightarrow e^+ e^-$  annihilation, weak neutral current effects (*Russian*) 0-105837  
 $Cs$  cell, laser beam excitation, multipass, optical pumping and weak neutral current parity violation 0-58207  
 $D^0 \rightarrow D^0$ , weak neutral current diagonality, mixing amplitude, multi-quark gauge model (*Russian*) 0-68414  
 $Na$ , muonic,  $2s_{1/2}$  level decay channel concurrence, neutral current effects observation (*Russian*) 0-83526

**neutrino detection and measurement**

- coherent low energy neutrino detector, design reanal. with neutrino interaction model 0-58096  
 Converse hodoscope combined with steamer chamber 0-63455  
 flash chambers for neutrino detection, construction and performance 0-58026  
 undersea detection system, located in deep ocean 0-98522  
 water Cherenkov neutrino detector, construction and performance 0-91397

**neutrino-electron interactions**

- see also *neutrino-electron scattering*  
 $\bar{\nu}e$  annihilation in Weinberg-Salam model, number of quarks and leptons (*Russian*) 0-102041

**neutrino-electron interactions continued**

- $\nu_e e \rightarrow \mu^- \bar{\nu}_e$ , inverse muon decay rate 0-82965  
 $\bar{\nu}_e e \rightarrow \nu_\mu \mu^-$ , exotic lepton number violation and neutrino Majorana masses, Higgs sector 0-86615  
**neutrino-electron scattering**  
 see also *neutrino-electron interactions*  
 supernovae core collapse, neutrino energy equilibration models 0-105265  
 weak and EM radiative corrections to low-energy processes 0-95274  
 $\nu_e e \rightarrow \nu_e e$ , cross section meas. 0-73692  
**neutrino interactions**  
 see also *neutrino-electron interactions*; *neutrino-neutrino interactions*; *neutrino-nucleon interactions*; *neutrino scattering*  
 $\beta$ -active nuclei, neutrino exchange and long range interactions 0-73826  
 coherent low energy neutrino detector, design reanal. with neutrino interaction model 0-58096  
 deep inelastic scatt., inclusive observables and hard gluon emission 0-99094  
 dilepton charge production cross section for  $\nu$  and  $\bar{\nu}$ , parton model 0-62966  
 errors on ratios of small numbers of events 0-105879  
 low and high energy expts. 0-91083  
 multilepton production in neutrino expts. 0-91081  
 narrow band beam expts. at SPS 0-91082  
 neutrino oscillations in  $\nu_e, \nu_\mu, \nu_\tau$  system 0-82964  
 physics of neutrino beams 0-91077  
 semi-leptonic neutrino interactions at the CERN proton synchrotron and related topics 0-91078  
 stellar dense cores, time-dependent neutrino transport 0-94783  
 $SU(2)_L \times U(1)$  theory, radiative corrections, simple renormalisation framework 0-101973  
 total cross section meas. using bubble chambers 0-91080  
 weak interactions, summer school, Varenna, Italy (Jul. 1977) 0-90597  
 $D^0$  lifetime from  $\nu$  and  $\bar{\nu}$  interactions 0-105890  
 $\bar{\nu}$  induced dimuon events,  $V^0$  yield, possible beautiful baryon prod. 0-105882  
**neutrino-neutrino interactions**  
 see also *neutrino-neutrino scattering*  
 No entries  
**neutrino-neutrino scattering**  
 see also *neutrino-neutrino interactions*  
 No entries  
**neutrino-nucleon interactions**  
 see also *neutrino-nucleon scattering*  
 charged and neutral current interactions, cross sections and scaling variable distribts. 0-57581  
 charged current  $\nu$  and  $\bar{\nu}$  interaction cross sections, bubble chamber expt. 0-62965  
 deep inelastic scatt., quark-parton model with logarithmic scaling violation 0-78071  
 Nachtmann moments of  $F_2^{\nu N}(x, Q^2)$  and energy momentum sum rule 0-57580  
 structure functions of deep inelastic scatt., QCD test, high-twist contribs. 0-57579  
 b-quark production,  $SU(2) \times SU(2) \times U(1)$  gauge group mixing angles 0-68445  
 $\nu(\bar{\nu})N$ , pol.N, deep inelastic processes from valence straton distrib. functions (*Chinese*) 0-99095  
 $\nu(\bar{\nu})N \rightarrow N' \gamma e(\bar{e})$ , current algebras and high energy  $\gamma$ -prod., sum rules 0-102039  
 $\nu(\bar{\nu})N \rightarrow \mu^+ \mu^- X$ , dimuon rate and strange quark sea 0-62961  
 $\nu(\bar{\nu})N$ , heavy lepton prod. and decay, differential cross sections (*Russian*) 0-105940  
 $\nu N$ , charmed particle prod. due to neutral weak currents (*Russian*) 0-68447  
 $\bar{\nu} N$ ,  $K^0$  and  $\pi^-$  prod. rates,  $SU(3)$  symmetry violation in quark jet 0-82966  
 $\nu n \rightarrow \nu p \pi^-$ , neutral current process, excitation function, cross section ratio 0-78053  
 $\bar{\nu} N$  deep inelastic scatt., net charge in current fragmentation region, quark fragmentation 0-62964  
 $\nu N$ -hadron shower, charm-pair production effects 0-73748  
 $\nu N \rightarrow \mu^- p$ , Higgs boson exchange effects on second-class currents 0-91075  
 $\nu N \rightarrow \mu \mu X$ , neutral strange particle prod. in opposite sign dimuon events 0-57584  
 $\nu N \rightarrow \nu X$ ,  $SU(2)_L \times U(1)$  gauge theory distinguished from  $SU(2)_L \times SU(2)_R \times U(1)$ , neutral currents, z-bosons 0-62908  
 $\nu n \rightarrow \nu p \pi^-$ , expt. results comparison to theory 0-102038  
 $\nu N \rightarrow \nu \psi X$ , neutral current  $\psi$  prod.,  $Z^0$ -gluon fusion model 0-78015  
 $\nu N$ , 4-30 GeV,  $\mu^- e^+$  pair production (*Russian*) 0-91076  
 $\bar{\nu}_\mu N$ ,  $F^+(2030)$  prod. and hadronic decay  $F^+ \rightarrow \pi^+ \pi^+ \pi^0$ , mass 0-91085  
 $\bar{\nu}_\mu N \rightarrow \mu^- N$ , 2-30 GeV, deep inelastic interactions SKAT preliminary results 0-82963  
 $\bar{\nu} p$ , 1.1 GeV, charged and neutral current events, strangeness changing currents, charm prod. 0-57583  
 $\bar{\nu} p$ , multiple production processes regularities, Monte Carlo model 0-102082  
 $\bar{\nu} p$  charged current interaction, inclusive  $\rho^0$  prod. 0-62963  
 $\bar{\nu} p$  charged current interactions, quark fragmentation, quark-parton model test 0-68444  
 $\bar{\nu} p \rightarrow$  charm quarks 0-102040  
 $\bar{\nu} p \rightarrow \mu^- p K^+ \pi^+ \pi^0$ ,  $Z_s^+$  prod. and decay 0-86710  
 $\bar{\nu} p \rightarrow \mu^- n$ , Higgs boson exchange effects on second-class currents 0-91075  
 $\bar{\nu} p \rightarrow \mu^+ \pi^-$ , 5-70 GeV, cross section,  $I=1/2$  prod. amplitude 0-62962  
 t-quark production,  $SU(2) \times SU(2) \times U(1)$  gauge group mixing angles 0-68445  
**neutrino-nucleon scattering**  
 see also *neutrino-nucleon interactions*  
 valence quark clusters in nucleon structure functions from neutrino scatt. 0-95252  
 $\nu(\bar{\nu})p$ , 2 GeV elastic scatt., charged current/neutral current event ratio 0-57582  
**neutrino-nucleus reactions**  
 for inelastic *neutrino-nucleus scattering*, see "*neutrino-nucleus scattering*"  
 see also *neutrino-nucleon interactions*  
 charmed baryon production, mass and F/D ratio, colour magnetic interaction 0-62957  
 $^{12}C(\nu, p)^{11}B$ , occurrence in stellar C layer 0-82337  
 $^2H(\bar{\nu}_e, p)n$ , antineutrino spectrum 0-102150  
 $^{26}Mg(\nu_e, e^-)$ ,  $^{26}Al$  prod. in stellar collapsed core (*Russian*) 0-77285

**neutrino-nucleus scattering**

see also *neutrino-nucleon scattering*

${}^7\text{Li}$  ( $\bar{\nu}_e$ ,  $\bar{\nu}_e$ ), antineutrino spectrum 0-102150

**neutrino production**

neutrino pair bremsstrahlung and number of lepton generations 0-101978  
nuclear neutrino pair photoprod. in strong mag. field, pulsar neutrino luminosity (*Russian*) 0-68648  
prompt sources, and axion decays and interactions, pN beam-dump experiment 0-63028  
stellar dense cores, time-dependent neutrino transport 0-94783  
white dwarfs, neutrino cooling rel. to evolution 0-82356  
 $e^+e^- \rightarrow \gamma\nu\bar{\nu}$ , neutrino counting,  $e^+e^- \rightarrow 3\gamma$  background 0-68441  
 $K_1^0 \rightarrow \pi^+ \mu^- \nu_\mu$ , transverse polarisation of  $\mu$ , violation of time-reversal invariance 0-68448

**neutrino scattering**

see also *neutrino-electron scattering*; *neutrino interactions*; *neutrino-neutrino scattering*; *neutrino-nucleon scattering*  
elastic and inelastic, coherent interaction of neutrinos with dense matter, astrophysics role (*Russian*) 0-68446  
neutrino current, lepton-hadron symmetry, CP violation and  $\Delta I = 1/2$  rule 0-82934  
weak elastic scattering 0-91079

**neutrinos**

see also *cosmic ray neutrinos*

Bianchi-V cosmological space-time, Einstein-Weyl equations, neutrino currents 0-86023  
big bang, helium synthesis, neutrino flavors, and cosmological implications 0-73084  
cosmological  $\nu$  sea, EM wave propagation, torsionic background 0-77283  
 $E_\nu$  model of unified interactions, asymptotically free, mass relations and interactions 0-73642  
emission from blackbody, thermodynamic laws, teaching 0-105451  
emission from cylindrically symmetric cluster of many gravitating masses 0-94707  
gauge hierarchy and neutrino mass problem 0-90989  
heavy Majorana particles, cosmological and astrophysical implications 0-90331  
helicity from  ${}^{12}\text{C}$   $\mu^-$  capture 0-68655  
horizontal symmetries dynamical symmetry breaking and neutrino masses 0-105830  
local B-L symmetry of electroweak interactions, Majorana neutrinos, and neutron oscillations 0-73643  
massive neutrinos, mag. moment and spin rotation 0-105895  
minimal  $O(10)$  grand unification,  $\nu$  mass 0-57546  
neutron stars, neutrino energy loss rel. to cooling 0-77443  
nonzero rest mass effect on cosmological  ${}^4\text{He}$  production 0-105413  
oscillations, eigenstates of weak interactions 0-105825  
oscillations, Majorana and Dirac mass mixing 0-101969  
oscillations, mass and mixing scales 0-105823  
oscillations in  $\nu_e$ ,  $\nu_\mu$ ,  $\nu_\tau$  system 0-82964  
oscillations in weak interaction model 0-78014  
Pontecorvo neutrino oscillations for Dirac and Majorana masses, CP non-conservation 0-105829  
properties and experimental neutrino astrophysics, review, book contrib. 0-72769  
rest mass, effects on Universe density perturbations spectrum and microwave background small-scale fluctuations (*Russian*) 0-109576  
rest mass, implications for Universe density perturbations evolution and galaxy clusters hidden mass (*Russian*) 0-105414  
rest mass of electron neutrinos, implications for mass density and age of Universe (*Russian*) 0-109575  
solar, detection problem 0-101585  
solar neutrino problem, implications of solar oscill. obs. for Sun internal struct. 0-105226  
stellar degenerate C ignition, neutrino losses rel. to core implosion 0-77390  
stellar dense cores, time-dependent neutrino transport 0-94783  
stellar evolved C cores, neutrino energy dissipation rel. to core collapse and C detonation 0-82339  
 $\text{SU}(2)_c \otimes \text{SU}(2)_L \otimes \text{U}(1)$  weak model,  $\nu$  mass and spontaneous P nonconservation 0-62884  
supernovae, effect of core Rayleigh-Taylor convective overturn on neutrino release and explosion 0-77429  
supernovae, neutrino mediated shocks 0-94818  
supernovae core collapse, neutrino energy equilibration models 0-105265  
trapping in collapsing stars, effect on nucl. dissoc. 0-90407  
unified theories, neutrino number and isotropy of Universe 0-85852  
Weinberg-Salam model and extensions,  $\nu$  EM form factors and mag. moments, neutral currents, astrophysics appls. (*German*) 0-62904  
Weyl neutrino, nonlocal position and momentum operators 0-73586  
 $\bar{\nu}_e$  mass from  ${}^3\text{H}$   $\beta$ -decay spectrum (*Russian*) 0-91159  
 $\nu_e$  mass from  ${}^3\text{H}$   $\beta$ -spectrum in valine molecule 0-91158  
 $\nu_\tau$  mass from  $\tau$  decay 0-63057  
 $\bar{\nu}_e e^- \rightarrow \mu^+ \mu^-$ , exotic lepton number violation and neutrino Majorana masses, Higgs sector 0-86615  
 ${}^{239}\text{Pu}(n, \gamma)$ , thermal, fission product  $\bar{\nu}_e$  spectrum,  $\beta$ -decay characts. 0-78340  
 ${}^{235}\text{U}(n, \gamma)$ , thermal, fission product  $\bar{\nu}_e$  spectrum,  $\beta$ -decay characts. 0-78340

**neutron absorption**

BWR spent fuel element storage, neutron physical aspects 0-68841  
in-reactor measurement of neutron absorber performance 0-73951  
KERMA values, consistent set for H, C, N, and O for neutrons from 10 to 80 MeV 0-68967  
measurement standard for units of absorpt. power 0-102351  
porcelain, neutron-retardation behaviour for continual moisture determ. (*German*) 0-105660  
radiometric testing of materials, review 0-71860  
reactor physics, control poison optimisation, depletion calcs. 0-57906  
slow neutron action on glasses and vitreous ceramic and cryst. materials (*Spanish*) 0-57816  
ultracold neutrons, lifetime in traps, film-substrate model calcs. 0-106098  
 $\text{B}_4\text{C}$ , thermophysical props. and neutron absorpt. 0-103488  
 $\text{Eu}_2\text{O}_3$ , thermophysical props. and neutron absorpt. 0-103488  
Ta, thermophysical props. and neutron absorpt. 0-103488  
 $\text{UO}_2$  low enriched fuel rods, storage and transportation, critical separation in water with fixed neutron poisons 0-73918

**neutron activation analysis**

$1/\text{E}^{1+\alpha}$  epithermal neutron spectra, resonance integral correction, effective resonance energy 0-71978

**neutron activation analysis continued**

$1/\text{E}^{1+\alpha}$  epithermal neutron spectrum,  $\alpha$ -determ. methods, accuracy 0-71977  
 $1/\text{E}^{1+\alpha}$  epithermal neutron spectrum,  $\alpha$ -determ. without Cd cover 0-71976  
biological materials, anal. by monostandard method 0-72398  
conferences, quantitative study of participants, session titles 0-62361  
criticality accidents, dosimetry using activations of blood and hair 0-89857  
cyclic instrumental, optimum timing parameters for determ. of short-lived nuclides, computer program 0-61211  
dead time correction for short and long lived nuclide mix. 0-93825  
epithermal neutron fields in nuclear geophysics (*Russian*) 0-85658  
faecal samples, Ca determ. method using instrumental fast neutron activation anal. 0-104733  
halogen content of ultramafic nodules, determ. by gamma-ray spectroscopy and radioactivity meas. 0-76945  
lunar regolith samples from Luna-24, element abundance determ., neutron activation obs. 0-67597  
lunar soil samples from Luna-24,  $\text{N}_2$  abundance, neutron activation obs. 0-67594  
milk, trace elements, comparison of cows' milk, infant formulae and human milk 0-61210  
milk, trace elements, comparison of cows' milk, infant formulae and human milk 0-71996  
neutron capture  $\gamma$ -ray borehole mineral anal., optimum neutron source size 0-61213  
radioisotopes, X-ray characteristics in neutron activation anal. at 14 MeV 0-93827  
reactor fuel anal. using radioactive thermal neutron capture gamma rays 0-61214  
self-shielding by neutron flux 0-93835  
standards, nonidentical samples, formalism 0-71980  
steel, Al semikilled, ( $\text{Fe}, \text{Mn}, \dots$ ) $\text{O}, \text{Al}_2\text{O}_3$  inclusions, deoxidation, thermodynamic conditions 0-60830  
 $\gamma$ -ray counting, simultaneous use of Ge(Li) semiconductor and NaI(Tl) scintillation spectrometer 0-78485  
Al, simultaneous determ. with Si in atmospheric aerosols by neutron activation anal. 0-72116  
Al-Sc, elec. resist. determ. 0-92876  
 $\text{B}_2\text{O}_3$ -containing ceramic glaze, neutron probe anal. for control of prep. process (*Polish*) 0-97751  
Cd conc. in kidney and liver, neutron activation anal., organ depth determ. 0-72321  
Cd, organ tissue levels, in vivo meas. system 0-67224  
Fe, purification, recrystn. temp. and elec. resistivity (*Japanese*) 0-100780  
Fe utilisation studies by stable tracer  ${}^{58}\text{Fe}$  technique 0-61734  
 $\text{H}_2\text{O}$ , determ. of selected elements and heavy metals 0-76580  
Nb, O impurity distrib. determ. by neutron activation anal. (*Russian*) 0-70243  
P in sheep bone, transportable system for determ. 0-109066  
 ${}^{75}\text{Se}$ , anal. using coincidence counting, orchard leaves, bovine liver, root samples (*Japanese*) 0-97750  
Si crystal, impurities determ. and resistivity after reactor neutron irradi. 0-65563  
Si, purity for semicond. appls., neutron activation anal. 0-71979  
Si, simultaneous determ. with Al in atmospheric aerosols by neutron activation anal. 0-72116  
Si-Fe, solubility study by EPR and neutron activation anal. 0-75361  
Si-P, measurement techniques for determining P densities 0-75262  
U, assay of natural samples, meas. of gamma- or neutron activity of short-lived fission products 0-61179  
U in Hueco and Guadalupe Mountain Indian ceramics, delayed neutron activation analysis 0-85230

**neutron angular distribution**

see also *neutron spectra*

( $\alpha, \text{xn}$ ), 640, 710 MeV, n ang. and energy distrib., intranuclear cascade model 0-83109

**neutron beam effects** see *neutron effects***neutron detection and measurement**

see also *neutron spectrometers*

0-99428  
albedo neutron dosimetry, advances 0-57982  
calibration of neutron detectors, simple recipes for ground scatt. 0-106231  
calibration of zero-angle direction for neutron detector 0-91185  
corrected calibration of Andersson and Braun type rem counter for divergently incident Am-Be neutrons 0-74031  
correction for air scattering in front of detector 0-102226  
detector for determ. of transuranic element comp. of nuclear fuel cladding hulls 0-63471  
dose and quality factor meas. by tissue equivalent proportional counters 0-58079  
dosimeter for pulsed neutron dose rate meas., portable, microcomputer-based 0-86991  
dosimetry at JINR synchrocyclotron 0-57983  
dosimetry system, based on fission counter for fuel processing plant 0-57981  
failed fuel element detection, delayed neutrons meas. (*Polish*) 0-73952  
fast neutron criticality monitor, response to prompt critical bursts 0-63398  
fission counters, high sensitivity, neutron spectroscopy and dosimetry appl. (*French*) 0-58078  
fission track spark counting method for neutron monitoring 0-58080  
fission track technique using mica muscovite for high neutron fluence meas. 0-91395  
high energy neutron spectrometry using cellulose nitrate nuclear track detectors 0-91394  
high neutron fluence meas. using mica muscovite as track detector 0-106237  
LR115 cellulose nitrate detector system for personal dosimetry near high energy accelerators 0-58081  
LWR irradiated fuel assemblies, nondestructive exam. using  $\gamma$ -ray and neutron techniques 0-66760  
LWR spent fuel, non-destructive anal. using inherent and induced neutron radiation (*Russian*) 0-68805  
LWR spent fuel, nondestructive meas. and verification for materials safeguards 0-78420  
medical dosimetry problems rel. to incorrect composition of tissue-equivalent gas 0-81743



**neutron detection and measurement continued**

- methane-based tissue equivalent gas,  $W_n$  and neutron kerma 0-104769  
 multiaxis neutron diffractometer automation 0-102417  
 neutron monitor calibration, standard fields at Physikalisch-Technische Bundesanstalt 0-57999  
 non-destructive assay techniques for irradiated fissile material in extended configurations 0-71872  
 nondestructive neutron assay for nuclear materials accountability and criticality control 0-66759  
 nuclear accident dosimetry system, Czechoslovakia 0-57978  
 nuclear materials accountability, U and P NDA of crated waste by gamma-ray and neutron coincidence counting 0-83166  
 passive personnel portal detectors for nuclear materials diversion protection using gamma-ray and neutron detectors 0-78389  
 personnel dosimeters, European comparisons 0-57980  
 personnel neutron dosimeters, calibration for use in different neutron fields 0-58001  
 polycarbonate fast neutron dosimeter, development and comparison with conventional emulsion dosimeter 0-86990  
 position sensitive thermal neutron detector, large area, high precision position readout 0-58063  
 position-sensitive proportional counter 0-63459  
 prompt neutron multiplicity distrib. meas. from  $^{242}\text{Cm}$  spontaneous fission 0-83131  
 proportional counter, position-sensitive, direct position and time digitizer 0-58090  
 pulse shape analyser, effect of pulse pile-up on discrimination between neutrons and gamma rays 0-91402  
 Q-factor measurements of Oak Ridge National Labs. Dosimetry Appls. Research Facility 0-83237  
 radiometers testing standardisation, Soviet method 0-99405  
 reactor material safeguards, unirradiated fuel control in BOR-60 fuel assemblies (*Russian*) 0-68809  
 relativistic calculations, importance in proton recoil telescope efficiencies 0-102225  
 scintillation detectors with nanosecond time resolution 0-69029  
 scintillation neutron counter, photomultiplier noise characteristics 0-74077  
 self powered detectors, neutron response, epithermal component 0-58073  
 self-powered neutron detectors, calc. of activation component of response to thermal and epithermal neutrons 0-63470  
 semiconductor counter with ion implantation 0-69030  
 solid dielectric detectors with breakdown phenomena and their applications in radioprotection 0-91388  
 solid state nuclear track detectors, reactor neutron fluence meas. using Au and In foils 0-69035  
 solid state nuclear track detectors for fast neutron meas. 0-91393  
 solid-state track recorder applications in U.S. nuclear reactor energy programs 0-95506  
 special nuclear materials, assay and accountability using neutron correlation meas. tech. 0-69015  
 thermal neutron coincidence counting, correction for variable moderation and multiplication 0-69045  
 thermoluminescent detectors, fast neutron sensitivities 0-102413  
 time of flight single crystal diffractometer using a position sensitive detector 0-99404  
 track etch detectors, neutron energy depend. and threshold energy 0-61703  
 transit-time spectrometry, detector containing  $^3\text{He}$  0-63441  
 ultra-cold neutron scintillation detectors, optimisation 0-74090  
 A hyperon polarisation, meas. by hybrid Monte Carlo tech. 0-99431  
 Ag-activated Geiger counter calibration for neutron yield determ. in Frascati plasma focus expt. 0-99409  
 BF<sub>3</sub> detector assembly for photofission and photoneutron studies 0-63484  
 $^3\text{He}$  gridded fast neutron ionisation chambers, Monte Carlo calc., of energy dependent efficiency 0-99417  
 $^3\text{He}$  ionisation chamber, improved time resolution in n- $\gamma$  coincidence meas. 0-99416  
 $^3\text{He}$  proportional counters, thermal neutron detection performance, temp. depend. 0-58071  
 Li<sub>2</sub>O-MgO-Al<sub>2</sub>O<sub>3</sub>-SiO<sub>2</sub> glass scintillator for pulsed neutron detection 0-70191  
 Na(Tl) scintillator detectors for neutron-gamma discrimination 0-102386  
 polarised neutrons, 2.50 MeV, meas. of small angle scattering ( $<1^\circ$ ) 0-99432  
 Pu fallout detection using fission tracks prod. with neutron irradiation spectra 0-95479  
 Rh self powered neutron detectors, influence of Rh burnup on sensitivity 0-63462  
 U, assay of natural samples, meas. of gamma- or neutron activity of short-lived fission products 0-61179  
 U, prospecting by active neutron logging, evaluation models 0-98480

**neutron diffraction**

- see also neutron diffraction crystallography; neutron diffraction examination of materials*  
 interference, gravity and inertial effects, principle of equivalence at quantum level 0-77669  
 zone plate, appl. of diffraction to neutrons imaging and focusing 0-106433

**neutron diffraction crystallography**

- see also crystal atomic structure*  
 cold, and ultracold neutrons, production by a moving crystal lattice 0-79640  
 copolymer, semicryst. random, characterisation by small angle neutron and X-ray scatt. 0-75189  
 cryorefrigerator, double-stage for cooling to 10K on a 4-circle diffractometer 0-98919  
 diffracting crystals, neutron anomalous flight time 0-87995  
 diffractometer, transit-time, for structural investigations of monocrystals 0-64840  
 dynamical diffraction of neutrons, gravitational and mag. field effects 0-59345  
 electron and magnetisation densities in molecules and crystals, Arles, France (Aug. 1978) 0-105428  
 equilibrium and nonequilibrium phonons, excitons, and polaritons, inelastic neutron scatt. 0-84032  
 extinction correction, in white X-ray and neutron diffr. 0-100120  
 Heisenberg magnet, random one-dimens., classical, spin dynamics, neutron scatt. cross section 0-60312  
 inelastic neutron scatt., use of spin echo property (*French*) 0-64842

**neutron diffraction crystallography continued**

- inelastic scattering, optimisation of struct. studying conditions (*Russian*) 0-79641  
 lineshapes in pulsed neutron powder diffraction 0-64841  
 mosaic crystals, multiple Bragg-reflected neutrons 0-100129  
 organic molecular crystals, inelastic neutron scatt., exciton creation 0-70084  
 small-angle neutron scattering instrument, at ORNL using position sensitive area detector 0-79639  
 texture analysis, quantitative, time of flight vs. conventional method on drawn steel wire 0-81078  
 time-depend. phenomena studies using time-of flight neutron diffraction (*Japanese*) 0-70083  
 valence electron distribution, in crystals, diffr. data processing 0-92418

**neutron diffraction examination of materials**

- see also neutron diffraction crystallography*  
 actinide compounds, neutron scatt. studies 0-75716  
 adamantane, plastic phase, C<sub>4</sub> rot. jumps, existence and uniqueness 0-88067  
 adsorbed molecular, surfaces, and interfaces, neutron scatt., review, book contrib. 0-84394  
 aerosol OT-n-heptane-water, reversed micellar solution; addition of electrolyte, neutron small angle scattering 0-104468  
 alkali metal acid osalates, neutron inelastic scatt. spectra in 2200-200 cm<sup>-1</sup> range 0-70327  
 4-aminopyridine hemiperchlorate, struct. determ. by neutron diffr. and IR spectra 0-92515  
 amorphous metals, geometric struct. models and diffraction exam. techniques 0-79700  
 antiferromagnet, neutron scatt. by magnons, modulated spin amplitudes 0-75722  
 p-azoxyphenetole, single cryst., deuterated, phonon dispersion curves, inelastic neutron scatt. obs. 0-84261  
 BCC crystal, anisotropic spin-pair correlation function, neutron mag. crit. scatt. cross-section 0-60194  
 benzene chemisorbed on Raney Ni, struct., neutron inelastic spectroscopy study 0-101038  
 Bloch wall thickness, neutron small-angle scatt. meas. 0-71092  
 Clq of human complement, neutron scatt. obs., conformational calcs. 0-81537  
 carbon tetrabromide, disordered phase, neutron, diffuse scatt. 0-79717  
 carbon tetrabromide, disordered phase, neutron diffuse scattering 0-79716  
 chromatin, low-angle X-ray and neutron diffr., interparticle effects 0-72134  
 copper acetate, deuterated, dimeric, single crystals, inelastic neutron scatt. 0-92867  
 copper formate anhydrate, cryst. struct. and mag. props. 0-79768  
 copper formate tetrahydrate, antiferromag. phase, neutron diffr. study 0-93085  
 dense fluid, collective modes and neutron scatt. 0-92442  
 diatomic molecular fluids, slow neutron scatt., models 0-83463  
 diatomic molecular fluids, slow neutron scattering, moment expansions 0-87201  
 p-dibromo-tetrafluorobenzene mol. cryst., in commensurate phase, quasielastic neutron scatt. 0-107386  
 EABAC, smectic A, nematic, and isotropic phases, NMR and quasielastic neutron scatt. obs. 0-88022  
 ethane, solid, mol. reorientational motions, incoherent neutron scatt. studies 0-107070  
 ferroelectrics, improper and incommensurate phase transitions, neutron scatt. studies 0-75974  
 ferromagnet, itinerant electron, magnon spectrum just below T<sub>c</sub>, theory 0-65833  
 film adsorbed on graphite, two-dimensional phase transitions 0-107653  
 ice, Ih, elastic diffuse neutron scattering due to D-D correlation functions 0-96493  
 intermediate valence compounds, dynamic susceptibilities 0-70653  
 ionic crystal with vacancies, coherent neutron scatt., calc. 0-59346  
 ionic liquids, structural props., review 0-96430  
 magnetic soft and hard materials, garnets, magnetic properties and applications, structural props. 0-65760  
 magnetic structure, neutron diffr. study, symm. anal., polarisation effects 0-93083  
 magnetic superconductors, mag. scatt. of neutrons 0-103819  
 metal-H system, inelastic neutron scattering meas. of optical vibr. freq. distrib. 0-59605  
 metals, BCC and FCC, H-diffusion and trapping 0-70447  
 methane-d<sub>4</sub>, solid, rot. tunnelling, neutron scatt. obs., isotope effect 0-92468  
 methane-d<sub>4</sub> monolayer films on graphite, neutron diffr. studies of phases 0-96739  
 methyl groups, spin symmetry species, neutron scatt. transitions 0-92470  
 4-methyl-2,6-ditertiarybutylphenol, methyl group reorientation, classical dynamics, NMR relax. and inelastic neutron scatt. 0-88066  
 nuclear magnetic ordering, domains, neutron diffr. patterns, theory 0-100577  
 organic molecular crystals, intermolecular interactions, spectroscopic studies, review 0-103958  
 oriented DNA, hydration, neutron scatt. obs. 0-89714  
 oxides, RCu<sub>3</sub>Mn<sub>4</sub>O<sub>12</sub>, R=La to Lu, Y, synthesis and mag. props. 0-75717  
 PAA, fluctuations near Rayleigh-Benard instability, real time obs. by neutron scatt. 0-59390  
 penninite, one-layer triclinic chlorite, neutron diffraction study 0-84144  
 physisorbed monolayer on graphite, neutron scatt. studies 0-107655  
 plastic crystal, orientational dynamics, neutron scatt. data interpret. using functions derived from group theory 0-107092  
 polyethylene, chlorinated, semicryst. random, characterisation by small angle neutron and X-ray scatt. 0-75189  
 polyisoprene, small angle neutron scatt., single chain form factors 0-107038  
 polymer protonated and deuterated mixtures, partial miscibility 0-107037  
 polystyrene, sulphonated, polyelectrolyte solution, correlations and dynamics 0-104446  
 quartz, acoustic activity, inelastic neutron scatt. obs. (*French*) 0-103431  
 rare earth intermetallics, AlAl<sub>2</sub>, orbital and spin polarisations of cond. electrons 0-65791  
 rare earth systems, mag. excitations, review of neutron scatt. data 0-60227

**neutron diffraction examination of materials continued**

- ribonuclease A, bovine, cryst. struct. determ. by X-ray and neutron diffr. 0-108841
- spin-Peierls phase diagrams, obs. and models 0-60330
- squaric acid, antiferroelec., struct. phase transition mechanism 0-75969
- steel, drawn wire, quantitative texture anal., neutron diffr. studies 0-81078
- tetramethylammonium perfluorooctanoate-water, lamellar lyotropic liq. cryst., neutron diffr. struct. obs. 0-64888
- tetramethylammonium tetrachlorocuprate, incommensurate phase, neutron diffr. study 0-79935
- TGS, crit. behaviour of thermal expansion, neutron diffr. study 0-75371
- TGS, electrostrictive and dielec. coeffs., neutron diffr. study 0-75943
- thiourea, incommensurate phase, soft modes, condensation of even-order harmonics 0-103313
- thiourea, incommensurate phase transition, X-ray and neutron scatt. study 0-75963
- TMMC, Cu-substituted, spin dynamics, neutron scatt. cross section 0-60312
- transition metal, BCC, neutron spectroscopy of fast H diffusion 0-59731
- transition metal complexes, electron densities, local orbital populations, polarised neutron diffraction 0-88725
- transition metal-metalloid glasses, struct. and plastic flow, review 0-84090
- transition metal-nonmetal glasses, with defined local coordination, struct. model 0-84092
- 1,3,5-trioxane-1, 3-dioxolane copolymer, semicryst. random, characterisation by small angle neutron and X-ray scatt. 0-75189
- AgBi(Cr<sub>2</sub>O<sub>7</sub>), cryst. struct. determ. by X-ray and neutron diffr. (French) 0-92492
- $\alpha$ -AgI, cond. mechanisms in superionic phases 0-59714
- $\alpha$ -AgI, diffusion dynamics, quasielastic neut. scatt. expt. 0-107484
- $\beta$ -Ag<sub>2</sub>S, cond. mechanisms in superionic phases 0-59714
- Al, liq. and polycryst., density fluctuations, neutron scatt. anal. 0-70349
- Al-Fe (49 at.%) quenched alloy, neutron diffuse scatt., diffuse  $\omega$  phase obs. 0-84141
- $\beta$ -Al<sub>2</sub>O<sub>3</sub>-Al<sub>2</sub>O<sub>3</sub>O(D<sub>2</sub>O)(NH<sub>4</sub><sup>+</sup>) 0-107512
- $\beta$ -Al<sub>2</sub>O<sub>3</sub>-Al<sub>2</sub>O<sub>3</sub>O(K<sub>2</sub>O)(Li<sub>2</sub>O)(Na<sub>2</sub>O)(Rb<sub>2</sub>O), single cryst. Raman scatt., cond. mechanism and cryst. struct. 0-66209
- $\beta$ -Al<sub>2</sub>O<sub>3</sub>-D<sub>2</sub>O, anhydrous, prep. and struct. of DAL<sub>1</sub>O<sub>17</sub> 0-107187
- $\beta$ -Al<sub>2</sub>O<sub>3</sub>-H<sub>2</sub>O (Na<sub>2</sub>O), struct. basis for superionic cond. 0-107498
- $\beta$ -Al<sub>2</sub>O<sub>3</sub>-NH<sub>4</sub><sup>+</sup> proton dynamics neutron scatt. study 0-59408
- $\beta$ -Al<sub>2</sub>O<sub>3</sub>-OH<sub>3</sub><sup>+</sup> proton dynamics neutron scatt. study 0-59408
- (As<sub>0.5</sub>Se<sub>0.5</sub>)<sub>100-100-x</sub>Cu<sub>x</sub>, glassy, struct. and elec. cond. study 0-59399
- Au-Fe alloys, spin correlations, neutron diffr. meas. 0-80482
- BaMnF<sub>4</sub>, magnetic neutron scatt. from structurally distorted cryst. 0-93086
- BaMnF<sub>4</sub>, spectroscopy near ferroelec. transition, dielec. anomalies near mag. ordering temp. 0-75965
- Ba<sub>2</sub>NbNb<sub>2</sub>O<sub>15</sub>, incommensurate refls. near ferroelastic transition, neutron and X-ray precession obs. 0-70395
- BaNi<sub>2</sub>(PO<sub>4</sub>)<sub>2</sub> and BaNi<sub>2</sub>(AsO<sub>4</sub>)<sub>2</sub>, mag. props., neutron diffr. and sp. ht. meas. 0-70948
- BaVS<sub>3</sub>, mag. transition and hyperfine interaction, neutron spin-flip scatt. obs. 0-97093
- BaVS<sub>3</sub>, magnetisation and neutron study 0-84588
- BaWO<sub>4</sub>, slow neutron inelastic scatt. spectra, Debye temp. calcs. (Russian) 0-59347
- BiFeO<sub>3</sub>, ferroelec., antiferromag., cryst. and mag. struct., neutron diffr. study 0-65786
- C<sub>2</sub>Rb, intercalated graphite, order struct. determ. by neutron scatt. 0-107143
- CSe<sub>2</sub>, liq., partial struct. factor, neutron diffraction meas. 0-79672
- CaF<sub>2</sub>, anion motion at high temps., quasielastic neutron scatt. obs. 0-59715
- CaWO<sub>4</sub>, slow neutron inelastic scatt. spectra, Debye temp. calcs. (Russian) 0-59347
- $\gamma$ -Ce, FCC, localised vibration of interstitial H impurities 0-75322
- CaAl<sub>2</sub>, multiple- $q$  structure or coexistence of different mag. phases, neutron diffr. study 0-107985
- CeIn<sub>3</sub>, mag. struct., neutron diffr. study 0-80481
- Co<sub>0.9-x</sub>La<sub>x</sub>Th<sub>0.1</sub>, mixed valence state, static and dynamic mag. response 0-103816
- CeSb, antiferromag., first-order transitions, mag. phase diagram 0-60252
- CeSn<sub>3</sub>, intermediate valence cpd., search for phonon anomalies, inelastic neutron scatt. 0-100317
- CeTi<sub>3</sub>, mag. susceptibility, magnetisation, neutron diffr., elec. resist., and sp. ht. meas. 0-75733
- Co<sub>0.08</sub>Y<sub>0.92</sub>Sb, dilute f-electron system in cluster regime, crystal field and exchange splittings 0-97062
- Co complex, Co(II)(1,2,4-triazole)<sub>2</sub>(NCS)<sub>2</sub> quasi two-dimens. canted S=1/2 antiferromag. 0-70976
- Co fine particles in Cu, interface magnetisation 0-88858
- Co-P alloys, geometric struct. models and diffraction exam. techniques 0-79700
- CoBr<sub>2</sub>.6(0.48D<sub>2</sub>O, 0.52H<sub>2</sub>O) spin-flop system, intermediate phase existence, sublattice magnetisation reorientation 0-80510
- CoBr<sub>2</sub>.6(1-x)H<sub>2</sub>O.xD<sub>2</sub>O, mag. intermediate phase, magnetisation and neutron scatt. meas. 0-60195
- CoF<sub>2</sub>, antiferromag. crit. props., neutron scatt. obs. 0-88749
- Co(GaTiV) alloys, ferromag. onset, electron conc. depend. 0-60203
- CoMnP, cryst. mag. struct., neutron diffr. study (French) 0-59439
- Co<sub>1-x</sub>Zn<sub>x</sub>F<sub>2</sub>, antiferromag. crit. props., neutron scatt. obs. 0-88749
- Cr-Fe, dil., spin correlations and neutron scatt. near crit. conc., theory 0-60327
- Cr-Ge system, XPS, X-ray and neutron diffr. and mag. meas. to study chem. bonding and electronic struct. 0-60749
- Cr-Re (0.18 wt.%), mag. excitations in longitudinal and transverse SDW phases 0-70946
- (CrF<sub>6</sub>)<sup>3+</sup>6a AR-AT complexes, electron densities, local orbital populations, polarised neutron diffraction 0-88725
- Cr<sub>4</sub>(OH)<sub>6</sub>(NH<sub>3</sub>)<sub>2</sub>Cl<sub>6</sub>4H<sub>2</sub>O, exchange coupled mol. Cr<sup>3+</sup> tetramers, inelastic neutron scatt. 0-65792
- Cr<sub>0.995</sub>Pt<sub>0.005</sub> alloy, mag. struct., neutron diffr. study 0-60198
- CsCN, inelastic neutron scatt. by coupled rotational and translational modes 0-70333
- CsCoCl<sub>3</sub>, spin dynamics, neutron scatt. study 0-80493
- CsCrI<sub>3</sub>, neutron diffr. expts. at 300, 77 and 1.2K 0-107163
- CsCuCl<sub>3</sub>, helical mag. struct., neutron diffraction study 0-107983
- CsFeCl<sub>3</sub>, pseudo-one-dimens. singlet ground state ferromag., mag. excitations, neutron scatt. study 0-97064

**neutron diffraction examination of materials continued**

- Cs<sub>2</sub>FeF<sub>6</sub>, mag. struct. and one-dimens. antiferromagnetism 0-60209
- CsGa<sub>2</sub>-Fe<sub>2</sub>S<sub>2</sub>, tetrahedrally coordinated Fe atoms in low spin state, mag. props. and neutron diffr. study (German) 0-88714
- CsH<sub>2</sub>PO<sub>4</sub>, ferroelec. transition, neutron diffr. study 0-93247
- CsMnF<sub>4</sub>, planar ferromag., cryst. and mag. struct., Jahn-Teller effect 0-75715
- CsNiF<sub>3</sub>, nonlinear excitations, 1D-ferromag., neutron scatt. 0-70949
- CsNiF<sub>3</sub>, quasielastic neutron scatt. around Neel-point 0-75768
- CsPbCl<sub>3</sub>, nucl. smearing functions, multipole analysis 0-88097
- Cs<sub>2</sub>PbCu(NO<sub>2</sub>)<sub>6</sub>, incommensurate Jahn-Teller transition, Huang scatt. 0-70401
- Cs<sub>2</sub>PbCu(NO<sub>2</sub>)<sub>6</sub>, low-temp.  $\gamma$ -modification, struct., powder neutron diffr. study, 160K 0-84151
- Cu-Be solid solutions, local oscill. conc. depend., impurity bands (Russian) 0-75318
- Cu-Mn (8 to 75 at.%), spin correl., neutron polarisation anal. study 0-65905
- Cu-Pt system, phonon dispersion relations, force constant disorder effect 0-84263
- Cu-Zn-Al martensite, lattice dynamics, neutron scatt. meas. 0-88286
- CuBr<sub>2</sub>(Cl<sub>2</sub>), aq. soln., structural transition, neutron diffr. study 0-64872
- CuCr<sub>2</sub>Se<sub>4</sub>, mag. moment distrib. by neutron diffr., Goodenough model 0-70945
- r-CuMn, annealing ordered phase study by neutron diffr. 0-89265
- Cu<sub>2</sub>MnAl-Pd, MnAl mixed Heusler alloys, mag. props. 0-60269
- Cu<sub>2</sub>P<sub>2</sub>Br<sub>2</sub>, cryst. struct. at 293 and 473K, thermal parameters 0-59450
- Cu<sub>1-x</sub>Pd<sub>x</sub>MnSb, mag. phase transition 0-60268
- CuSO<sub>4</sub>.5H<sub>2</sub>O, EXAFS, rel. between Debye-Waller factor and thermal parameters meas. by neutron diffr. 0-84803
- Cu<sub>0.57</sub>Zn<sub>0.43</sub> amorphous alloy, neutron diffr. obs. of struct. 0-88060
- D<sub>2</sub>O.ClO<sub>4</sub>, solid, neutron powder diffr. study 0-107176
- Dy<sub>2</sub>Ga<sub>2</sub>O<sub>7</sub>, induced staggered mag. fields, neutron diffr. study 0-60196
- DyPO<sub>4</sub>, mag. transitions under hydrostatic press., neutron diffr. study 0-71030
- Er-La, HCP, mag. phase diagram, neutron diffr. meas. 0-70950
- ErCo<sub>2</sub>(Fe<sub>2</sub>), mag. excitations, RPA theory 0-65830
- ErMo<sub>2</sub>Se<sub>8</sub>, mag. supercond., neutron scatt. obs. 0-70952
- ErRh<sub>1-x</sub>Sn<sub>x</sub>, synthesis, supercond. and mag. props. 0-100547
- ErTiO<sub>3</sub>, magnetic structure determination, neutron scatt. study 0-65809
- Eu<sub>0.4</sub>Sr<sub>0.6</sub>S, spin glass, spin dynamics, neutron scatt. study 0-65907
- Eu<sub>2</sub>Sr<sub>1-x</sub>S, spin glass to ferromag. transition, neutron scatt. and susceptibility meas. 0-60254
- Fe complex, Fe(1,2,4-triazole)<sub>2</sub>(NCS)<sub>2</sub>, quasi-2-dimens. S=1/2 antiferromag., mag. props., hidden-canting 0-107986
- Fe, ferromag., dynamic susceptibility calc., neutron scatt. intensity calc. 0-80488
- Fe-B, amorphous alloys, compositional study on short-range struct. 0-84095
- Fe-Cr, dil., spin density wave under high press., neutron diffr. study 0-65798
- Fe-Ge, amorphous, atomic struct., neutron diffr. study 0-59392
- Fe-Ni (32.3 at.%), mag. struct. in commensurate approx., neutron diffr. study 0-60212
- Fe-Ni (33-38 at.%), low-angle neutron diffr., anomalous crit. scatt. (Russian) 0-60193
- Fe-rare earth alloys, amorphous, magnetoelasticity and moment rot., US vel. calc. and neutron scatt. meas. 0-65992
- Fe-Si (3 wt.%), ferromag. domains, imaging by neutron interferometry 0-71087
- Fe-SiO multilayer films, interface magnetisation 0-88858
- Fe<sub>2</sub>Pt, ordered ferromagnetic alloy, magnetic excitation obs. 0-70978
- Fe<sub>90</sub>B<sub>10</sub>, amorphous, cold neutron scatt., local and extended defects 0-84089
- Fe<sub>1-x</sub>Co<sub>x</sub>Cl<sub>2</sub>.2H<sub>2</sub>O, random mixture with competing spin anisotropies, tetra-crit. behaviour 0-60324
- Fe,Cr<sub>1-x</sub>, spin-wave evolution crossing from ferromag. to spin-glass regime 0-97080
- (Fe<sub>0.4</sub>Nb<sub>0.5</sub>)O<sub>2</sub>, rutile, cation distrib. and mag. ordering (German) 0-107116
- Fe<sub>65</sub>Ni<sub>28</sub>Mn<sub>7</sub>, disordered, mag. struct. near ferro-antiferromagnetic transition 0-60211
- Fe<sub>40</sub>Ni<sub>40</sub>P<sub>14</sub>B<sub>6</sub>, amorphous ferromag., spin wave excitations 0-97079
- Fe<sub>1-x</sub>O, wustite, defect struct. 0-107216
- Fe<sub>2</sub>O<sub>3</sub>, neutron diff. fusc. due to molecular polarons 0-88488
- FeSO<sub>4</sub>,  $\alpha$ - and  $\beta$ -forms, magnetic interactions, neutron inelastic scatt. study 0-107980
- FeSi picture frame single cryst., domain wall motion and magnetisation reversal, time-depend. neutron depolarisation study 0-88782
- (Fe<sub>0.5</sub>Ta<sub>0.5</sub>)O<sub>2</sub>, rutile, cation distrib. and mag. ordering (German) 0-107116
- FeTh<sub>2</sub>S<sub>8</sub>, mag. struct. and props., neutron diffr. and mag. meas. 0-60201
- FeTiD(H),  $\gamma$ -phase, neutron and electron diffr. 0-84156
- FeTiD<sub>2</sub>(O $\leq$ x $\leq$ 1.9), neutron diffr. struct. anal. 0-75447
- Fe<sub>2</sub>TiO<sub>4</sub>, cooperative Jahn-Teller phase transition, crit. diffuse scatt. 0-59930
- Fe<sub>2</sub>TiO<sub>4</sub>, anisotropic spin glass type behaviour 0-60296
- Gd<sub>2</sub>Mo<sub>2</sub>Se<sub>8</sub>, coexistence of supercond. and long range antiferromag. order 0-84534
- p-H<sub>2</sub>, solid, neutron diffr. studies up to 5 kbar 0-59436
- H<sub>2</sub>, states velocity auto-correl. function, relax time, neutron scatt. obs. 0-58401
- H<sub>2</sub>-Ar, states velocity auto-correl. function, relax time, neutron scatt. obs. 0-58401
- He, liq., multiphonon boundary of excitation spectrum, neutron and inelastic light scatt. 0-92740
- <sup>3</sup>He liquid, zero sound lifetime, neutron inelastic scatt. study 0-65329
- <sup>4</sup>He, liq., static struct. factor and pair  $\omega$ -correls., neutron diffr. study, 1.00 to 4.27K 0-80010
- <sup>4</sup>He, liq., static structure factor and pair correlation function, at saturated vapour press. 0-64878
- <sup>4</sup>He, normal liq., collective excitations, neutron inelastic scatt. study 0-107590
- <sup>4</sup>He, superfluid, elementary excitations,  $\mu$ eV resolution study by neutron spin echo 0-65327
- <sup>4</sup>He, superfluid, neutron spin-echo study of excitations 0-80014
- HfV<sub>2</sub>D<sub>4</sub>, disordered solid solution, order-disorder transition 0-88321
- Hg<sub>2</sub>Cl<sub>2</sub>, neutron and Raman scatt. studies, ferroelastic transitions 0-76015
- HgTe, phonon dispersion relations, neutron study 0-70340
- Ho-La, HCP, mag. phase diagram, neutron diffr. meas. 0-70950



## neutron diffraction examination of materials continued

- $\text{HoCo}_2$ , mag. excitations, neutron inelastic scatt. meas. 0-60231  
 $\text{HoCo}_2\text{Ge}_2$ , crystal and magnetic structure obs. 0-64976  
 $\text{HoCu}_2$ , mag. struct. and elec. resist., neutron diff. obs. 0-60206  
 $\text{HoMo}_2\text{S}_6(\text{Se}_6)$ , mag. supercond., neutron scatt. obs. 0-70952  
 $\text{HoTiO}_3$ , magnetic structure determination, neutron scatt. study 0-65809  
 $\text{I}_2$ , liq., static structure factor, neutron diffraction 0-103236  
 $\text{KAgF}_5$ , superionic phase transition, dynamical and crit. pt. props. 0-107535  
 $\text{KBr}$ , molten, solutions of K, conc. fluctuations, small angle neutron scatt. study 0-92448  
 $\text{KBr}:\text{CN}^-$ , neutron scatt. studies of  $(\text{CN})^-$  defects 0-92620  
 $\text{KBr}_{1-x}(\text{CN})_x$ , mixed mol. cryst., coupled rot. and translational modes 0-84267  
 $\text{KCN}$ , inelastic neutron scatt. by coupled rot. and translational modes 0-79895  
 $\text{KCaF}_3$ , struct. phase transitions, DSC, birefr., and neutron powder diff. obs. 0-70149  
 $\text{KCuF}_3$ , one-dimens. antiferromag., spin waves, neutron scatt. study 0-65848  
 $\text{K}_2\text{CuF}_4$ , magnon condensation obs. in quasi-2D planar ferromag. phase 0-60232  
 $\text{KD}_2\text{PO}_4$ , neutron scattering from coupled polar-elastic waves 0-92623  
 $\text{KD}_2\text{PO}_4$ , phase transitions study, role of cryst. struct. determ. 0-75197  
 $\text{KD}_2(\text{SeO}_4)_2$ , phase transition, neutron scatt. study 0-75351  
 $\text{K}_2\text{FeF}_4$ , two dimensional easy plane antiferromag., neutron scatt. expts. 0-65838  
 $\text{K}_2\text{FeF}_5$ , mag. struct. and one-dimens. antiferromagnetism 0-60209  
 $\text{KH}_2\text{PO}_4$ , phase transitions study, role of cryst. struct. determ. 0-75197  
 $\text{KH}_2\text{PO}_4$ , single crystal neutron diffraction study at high pressure 0-92497  
 $\text{KMn}_{1-x}\text{Ni}_x\text{F}_3$ , antiferromag. crit. props., neutron scatt. obs. 0-88749  
 $\text{K}_2\text{PbCu}(\text{NO}_3)_6$ , incommensurate Jahn-Teller transition, Huang scatt. 0-70401  
 $\text{K}_2\text{SO}_4$ , longitudinal-acoustic soft mode in phase transition 0-75326  
 $\text{K}_2\text{SeO}_4$ , incommensurate to ferroelec. transition, hydrostatic press. effects, neutron scatt. study 0-108166  
 $\text{K}_2\text{SnCl}_6$ , elastic const., inelastic neutron scatt. and US meas. 0-59553  
 $\text{K}[(\text{OH})_{0.42}(\text{O}_2)_{0.50}]$ , cubic solid soln., structural and mag. study (French) 0-107177  
 $\text{LaAgIn}_{1-x}$ , phonon dispersion, elastic const. and struct. instability, soft mode behaviour 0-103436  
 $\text{La}(\text{Co}_{1-x}\text{Ni}_x)_2$ , distrib. of Co and Ni atoms, neutron diff. obs. (Russian) 0-64954  
 $\text{LaD}_3$ , stoichiometric, structural phase transform., neutron diffraction evidence 0-88319  
 $\text{La}_2\text{Li}_2\text{Co}_2\text{O}_4$ , neutron diffraction data 0-80226  
 $\text{La}_2\text{MnFeS}_8$ , antiferromag., mag. props. and mag. struct., neutron diff. and magnetisation meas. 0-65801  
 $\text{LaMnO}_3$ , phase diagram, mag. moments, neutron diff. study 0-108414  
 $\text{Li}$ , anharmonicity and low temp. phase struct., neutron diff. study 0-107105  
 $\text{LiAlSiO}_4$ ,  $\beta$ -eucryptite one-dimens. fast ion cond., temp. depend. of cryst. struct. 0-107191  
 $\text{Li}_2\text{FePS}_3(\text{Se}_3)$ ,  $\text{Li}_2\text{MnPS}_3$  and  $\text{Li}_2\text{NiPS}_3(\text{Se}_3)$ , NMR and neutron diff. obs., mag. props. 0-60433  
 $\text{LiH}_2(\text{SeO}_4)_2$ , ferroelec., absolute atomic arrangement and spontaneous polarisation, neutron diff. study 0-59442  
 $\text{LiNO}_3 \cdot 3\text{H}_2\text{O}$ , neutron diff. studies at 120 and 295K, H bond studies 0-88099  
 $(\text{LiO}_6)_x(\text{NaO}_3)_y\text{O}_2 \cdot 2\text{SiO}_2$ , short range struct. by pulsed neutron scatt. 0-59396  
 $\text{Li}_2\text{O} \cdot \text{Al}_2\text{O}_3 \cdot \text{SiO}_2$ , phase separation of initial stages of sitallisation 0-88053  
 $\text{Li}_2\text{O} \cdot \text{LiX} \cdot \text{B}_2\text{O}_3$  glass, X=halogen, high anionic cond. of new solid electrolytes 0-107546  
 $\text{Li}_2\text{O} \cdot 2\text{SiO}_2$ , short range struct. by pulsed neutron scatt. 0-59396  
 $\text{Li}_2\text{SO}_4$  based solid electrolytes, FCC phase transport mechanism studies and uses 0-107525  
 $\text{Li}_2\text{SO}_4$ , fast ion conductors, X-ray diff., neutron diff., and Brillouin scatt. study 0-107170  
 $\text{Li}_2\text{SO}_4$ , high temp. fast ion cond. phases, neutron diff. obs. of struct. 0-107512  
 $\text{Li}_8\text{Fe}_4\text{S}_{14}$ , antiferromag., neutron diff. study 0-70954  
 $\text{LuFe}_2$ , ferromag., magnetisation density, neutron diff. study 0-60217  
 $\text{MgO} \cdot \text{Co}^{2+}$ , weak dynamic Jahn-Teller coupling, neutron inelastic scatt. obs. 0-59934  
 $\text{Mn-Cu}$ , micromagnetic props., neutron diff. obs. 0-65906  
 $\gamma\text{-Mn-Cu}$  (10 at.%), spin wave studies using neutron diffraction 0-70991  
 $\text{Mn}_{1.88}\text{Cr}_{0.12}\text{Sb}$ , antiferromag.-ferrimag. transition, neutron crit. scatt. and crossover effect 0-107023  
 $\gamma\text{-MnCu}$  crystals, antiferromag. Czochralski growth 0-97420  
 $\gamma\text{-MnCu}$ , Mn-rich, inclined spin axis, neutron diff. study 0-75723  
 $\text{MnF}_2$ , antiferromag. and piezomag. domain struct., neutron topography study 0-71088  
 $\text{Mn}_2\text{Ga}_{1-x}\text{Mn}_x\text{N}$ , perovskite struct., phase transformations (French) 0-81048  
 $\text{Mn}_2\text{Ga}_{1-x}\text{C}_x$ , perovskite struct., phase transformations (French) 0-81048  
 $\text{Mn}_2\text{N}$ , mag. struct. non-collinearity, neutron diff. obs. 0-65796  
 $\text{MnO}$ , order-disorder mag. transition, press. or stress induced, neutron scatt. obs. 0-65880  
 $\text{MnOOH}$ , mag. ordering, fine struct. and crit. behaviour, neutron diff. meas. 0-65800  
 $\text{MnP}$ , ferro-spiral transition, neutron scatt. studies 0-65876  
 $\text{MnSO}_4$ , mag. struct. and phase transitions, neutron diff. study 0-60208  
 $\text{MnSb-CrSb}$ , NiAs-type system, single crystals, neutron diff. studies 0-60200  
 $\text{Mn}_{1-x}\text{Sb}$ , Mn electronic state, neutron diff. study 0-65806  
 $\text{Mn}_2\text{Sb}$ , spin-wave dispersion relations, exchange interactions, neutron inelastic scatt. 0-65832  
 $\alpha\text{-MnSeO}_4$ , magnetic interactions, neutron inelastic scatt. study 0-107980  
 $\text{MnSi}$ , weak itinerant magnetic compound, paramagnetic response function, polarised neutron scattering 0-107982  
 $\text{Mn}_2\text{SnS}_4$ , cryst. struct. refinement and mag. struct. determ. (French) 0-107131  
 $\text{Mn}_{1-x}\text{Zn}_x\text{Fe}_2\text{O}_4$ , prepared by wet method, neutron diff. and high field Mossbauer expts. 0-75719  
 $(\text{ND}_4)_2\text{D}_2\text{IO}_6$ , neutron diff. study 0-88098  
 $\text{NH}_4\text{Ag}_2\text{I}_5$ , superionic phase transition, dynamical and crit. pt. props. 0-107535

## neutron diffraction examination of materials continued

- $(\text{NH}_4)_2\text{BeF}_4$ , paraelec. phase, X-ray and neutron diff. cryst. struct. anal. 0-84159  
 $\text{NH}_4\text{Br}$ ,  $\text{NH}_4^+$  rot. motion, quasielastic neutron scatt. obs. 0-96492  
 $(\text{NH}_4)_2\text{H}_2\text{IO}_6$ , neutron diff. study 0-88098  
 $\text{NH}_4\text{NO}_3$ , phase III, cryst. struct., neutron powder diffractometer study 0-107134  
 $\text{Na}$ , atomic jump processes, quasi-elast. neutron scatt. study 0-84317  
 $\text{Na-K}$  liquid alloys, struct., X-ray and neutron diff. meas. 0-107041  
 $\text{NaClO}_4$ , acoustic activity, inelastic neutron scatt. obs. (French) 0-103431  
 $\text{NaClO}_4$ , lattice vibrations and sp. ht., neutron spectroscopic study 0-107388  
 $\text{NaH}_2(\text{SeO}_3)_2$ , ferroelec., proton motion within H bonds, neutron scatt. study 0-75986  
 $\text{NaMnCl}_3$ , mag. struct. and spin-flip transition, powder neutron diff. exam. 0-60210  
 $\text{NaMnCrF}_6$ , mag. struct., neutron Laue diff. method 0-70951  
 $\text{NaNO}_3$ , lattice vibration neutron diffusion study (French) 0-103429  
 $\text{NaOD}$  solution in  $\text{D}_2\text{O}$ , collective excitations in liquid and amorphous state, 77 to 300K 0-92636  
 $\text{Na}_2\text{O} \cdot 2\text{SiO}_2$ , short range struct. by pulsed neutron scatt. 0-59396  
 $\text{Na}_2\text{PO}_4$ , high temp. fast ion cond. phases, neutron diff. obs. of struct. 0-107512  
 $\text{NaTaO}_3$ , high temp. struct., neutron powder diff., comparison with  $\text{SrZrO}_3$  and  $\text{NaNbO}_3$  0-88094  
 $\text{Nb}$ , pure and N doped, neutron diffuse-scatt. intensities 0-59597  
 $\text{Nb-H(D)}$ , H ordering, review 0-60850  
 $\text{NbD}_{0.85}$ , localised D vibr., temp. depend., neutron inelastic scatt. study 0-107395  
 $\text{NbH}_{0.82}$ , localised H vibr., temp. depend., neutron inelastic scatt. study 0-107395  
 $\text{NbN}$  single crystal preparation, zone melting and nitriding techniques 0-60776  
 $\text{Nd}$ , mag. struct., 18.6K mag. phase transition 0-65799  
 $\text{Nd}$ , magnetic-structure, neutron and X-ray diff. study 0-60197  
 $\text{Ni}$  catalysts, chemisorption of  $\text{H}_2(\text{H}_2\text{O})$ , dynamics, neutron spectrosc. obs. 0-59778  
 $\text{Ni}$ , ferromag., dynamic susceptibility calc., neutron scatt. intensity calc. 0-80488  
 $\text{Ni}$ , ferromag., exchange integral maximisation, neutron scatt. obs. and ten-fold degenerate Hubbard model comparison 0-71004  
 $\text{Ni}$ , magnetic neutron scattering by dislocations, temp. depend. 0-103820  
 $\text{Ni-Cu}$ , electron-irrad., neutron-scatt. studies 0-75268  
 $\text{Ni-Ge}$ , amorphous, atomic struct., neutron diff. study 0-59392  
 $\text{Ni-Mn}$ , dil., mag. moment distrib. and environmental effects, neutron scatt. obs. 0-60247  
 $\text{Ni-Mn}$  (17-27 at.%), low-angle neutron diff., anomalous crit. scatt. (Russian) 0-60193  
 $\text{Ni-P}$  amorphous alloys, electrodeposited and melt-quenched atomic and electronic structures 0-88062  
 $\text{Ni-Pt}$  alloys, magnetic-moment distrib. neutron study 0-97066  
 $\text{Ni-SiO}$  multilayer films, interface magnetisation 0-88858  
 $\text{NiBr}_2$ , commensurate and incommensurate mag. struct., neutron diff. study 0-97067  
 $\text{NiBr}_2$ , low-temperature magnetic phase, incommensurate spin structure 0-93082  
 $\text{NiCl}_2$ , aq. soln., structural transition, neutron diff. study 0-64872  
 $\text{Ni}_{0.89}\text{Cr}_{0.11}$ , phonons with disorder caused by force const., neutron diff. obs. and CPA calc. 0-96602  
 $\text{NiMnGe}_{1-x}\text{Si}_x$ , mag. props., neutron diff. and magnetometric meas., 80-600K 0-65793  
 $\text{Ni}(\text{NH}_3)_6\text{I}_2$ , phase transition and rot. excitation 0-96642  
 $\text{NiO}$ , mag. struct., neutron Laue diff. method 0-70951  
 $\text{NiS}_2$ , weak ferro- and antiferromag., magnetisation and neutron diff. meas. 0-65794  
 $\text{Ni}_{40}\text{Ti}_{60}$ , amorphous, chem. short-range-order, X-ray and neutron scatt. obs. 0-96447  
 $\text{Ni}_{0.25}\text{Zn}_{0.75}\text{Fe}_2\text{O}_4$ , structural phase transition, X-ray and neutron diff. study 0-79735  
 $\text{NpCo}_2\text{Si}_2$ , mag. struct., neutron diff. determ. 0-93084  
 $\text{NpCu}_2\text{Si}_2$ , mag. struct., neutron diff. determ. 0-93084  
 $p\text{-O}_2$ , solid, slow neutron scatt. into external radiation field (Russian) 0-59348  
 $\text{Pb}$ , liq., collective excitations, neutron inelastic scatt. obs. 0-75148  
 $\text{Pb}_{1-x}\text{Bi}_x\text{F}_{2+x}$ , solid soln., struct. and ionic cond. correl., neutron diff. study (French) 0-84324  
 $\text{PbF}_2$ , anion disorder at high temps. 0-59614  
 $\text{PbF}_2$ , fast ion conductor, phonon freq. distrib., temp. variation 0-84264  
 $\text{PbHPO}_4$ , phase transitions study, role of cryst. struct. determ. 0-75197  
 $\text{PbI}_2$ , 2H polytype, optical mode inversion hear M-critical point, neutron scatt. mass 0-103432  
 $\text{Pb}_3(\text{P}_{0.95}\text{V}_{0.05}\text{O}_4)_2$ , ferroelastic transition, soft mode, inelastic neutron scatt. study 0-70357  
 $\text{PbZrO}_3$ , ferroelec. solid solns., atom shifts, polarisation and Curie temps. 0-100636  
 $\text{Pd-Si}$ , amorphous, compositional study on short-range struct. 0-84095  
 $\text{Pd-Si}$ , amorphous metallic glass, with defined local coordination, struct. model 0-84092  
 $\text{PdD}_{0.73}$ , (1, 1/2, 0)-superlattice reflection splitting near 50K, neutron diff. studies 0-70168  
 $\beta\text{-PdDx}$  ( $x=0.710, 0.742, 0.754, 0.780$ ), structural changes in temp. region of 50K anomaly 0-100131  
 $\text{Pd}_{0.98}\text{Fe}_{0.02}$ , Gd<sub>0.01</sub>, Pd-Gd exchange const., neutron diffuse scatt. meas. 0-71002  
 $\text{PdH}_x$ , inelastic neutron scattering meas. of optical vibr. freq. distrib. 0-59605  
 $\text{PdH}_x$ , local, soft modes, superconductivity thermal neutron inelastic scatt. (Chinese) 0-70331  
 $\text{Pd}_2\text{MnIn}_{1-x}\text{Sn}$ , and  $\text{Pd}_2\text{MnIn}_{1-y}\text{Sb}$ , Heusler alloys, mag. order, disorder effects 0-88723  
 $\text{Pd}_{2-x}\text{MnSb}$ , struct., appl. as improved neutron polariser 0-60199  
 $\text{Pd}_2\text{P}_{0.8}$ , pure and deuterated, cryst. struct., neutron diff. study 0-84152  
 $\text{Pd}_{80}\text{Si}_{20}$ , amorphous alloy, partial struct. functions, X-ray, electron and neutron diff. studies (Japanese) 0-88050  
 $o\text{-P}_2$ , solid, slow neutron scatt. into external radiation field (Russian) 0-59348  
 $\text{Pr}_{1-x}\text{Ca}_x\text{MnO}_3$ , struct. and magnetisation study 0-65804  
 $\text{PrCo}_2\text{Ge}_2$ , crystal and magnetic structure obs. 0-64976  
 $\text{PrMg}$ , cryst. field study, inelastic neutron scatt. and sp. ht. meas. 0-59939



**neutron diffraction examination of materials continued**

- PrSb, magnetic to nonmagnetic transition, press. or stress induced, neutron scatt. obs. 0-65880
- Pt/Cr, ferrimag., magnetisation density, polarised neutron diff. meas. 0-60204
- RbAg<sub>4</sub>I<sub>5</sub>, single particle excitations, inelastic neutron scatt. obs. 0-59599
- RbAg<sub>4</sub>I<sub>5</sub>, superionic phase transition, dynamical and crit. pt. props. 0-107535
- Rb<sub>2</sub>Co<sub>2</sub>Mg<sub>1-x</sub>F<sub>4</sub> mag.-nonmag. two-dimens. antiferromag. Ising system, spin fluctuations 0-80545
- Rb<sub>2</sub>CrCl<sub>4</sub>, 2D-ferromag., renormalisation of long wavelength spin waves, neutron scatt. 0-60229
- RbFeCl<sub>3</sub>, pseudo-one-dimens. singlet ground state ferromag., mag. excitations, neutron scatt. study 0-97064
- Rb<sub>2</sub>FeF<sub>6</sub>, mag. struct. and one-dimens. antiferromagnetism 0-60209
- RbH<sub>2</sub>PO<sub>4</sub>, phase transitions study, role of cryst. struct. determ. 0-75197
- RbNO<sub>3</sub>, struct., high temp. phases, neutron diff. study 0-79756
- Rb<sub>2</sub>PbCu(NO<sub>2</sub>)<sub>6</sub>, incommensurate Jahn-Teller transition, Huang scatt. 0-70401
- Rb<sub>2</sub>WO<sub>3</sub>, low lying phonon dispersion curves, neutron scatt. study 0-92622
- Rb<sub>2</sub>[C<sub>2</sub>O<sub>4</sub>].D<sub>2</sub>O<sub>2</sub>, neutron profile refinement at 5K 0-88103
- Si, amorphous, hydrogenated and deuterated, struct. 0-103245
- Si:H film, amorphous, plasma-deposited, small angle X-ray and neutron scatt. studies 0-59826
- Si-Cr, dil., spin density wave under high press., neutron diff. study 0-65798
- SiO<sub>2</sub>, hydroxylated amorphous, small-particle dynamics, neutron scatt. 0-79899
- SmZn, ferromag., cond. band antiparallel polarisation exceeding 4f moment 0-60207
- SnF<sub>2</sub>, second order  $\beta \rightarrow \gamma$  transition, neutron diff. and NMR obs. 0-107095
- SrCl<sub>2</sub>, anion disorder at high temps. 0-59614
- SrCl<sub>2</sub>, anion motion at high temps., quasielastic neutron scatt. obs. 0-59715
- SrCoO<sub>3-x</sub>, mag. and neutron diff. study 0-65805
- SrTiO<sub>3</sub>, heavily reduced, soft mode behaviour 0-71409
- SrTiO<sub>3</sub>, semiconductor, soft modes, zone boundary mode 0-71357
- SrWO<sub>4</sub>, slow neutron inelastic scatt. spectra, Debye temp. calcs. (Russian) 0-59347
- Tf-TCNQ, high press. structural transitions, neutron scatt. study 0-96647
- Ta-H(D), H ordering, review 0-60850
- Ta<sub>2</sub>S<sub>2</sub>H electrodes, topotactic reduction mechanism, neutron diff. obs. and intercalation cpd. form. 0-108748
- Ta<sub>2</sub>(NH<sub>3</sub>) and Ta<sub>2</sub>(NH<sub>3</sub>)<sub>1/3</sub>(H<sub>2</sub>O)<sub>2/3</sub>, incoherent inelastic neutron spectra 0-84163
- Tb, neutron elastic scattering, high-angle, anal. 0-80480
- TbCo<sub>5</sub>, sublattice magnetisation, temp. depend., neutron diff. anal. (Russian) 0-103815
- (Tb<sub>1-x</sub>La<sub>x</sub>)Be<sub>13</sub>, mag. struct., cryst. field effects, neutron diff. study 0-65789
- TeO<sub>2</sub>-P<sub>2</sub>O<sub>5</sub> system, glass struct., neutron diff. study 0-70128
- ThCo<sub>0.063</sub>, cryst. struct. and lattice dynamics 0-88088
- TiBe<sub>1.8</sub>Cu<sub>0.2</sub>, ferromag., magnetisation density 0-103817
- TiN<sub>0.33</sub>H<sub>0.19</sub>, cryst. struct., neutron diff. anal. (Russian) 0-64965
- (Ti<sub>1-x</sub>V<sub>x</sub>)<sub>2</sub>O<sub>3</sub>, metallic antiferromag. struct., neutron studies 0-65797
- Ti<sub>2</sub>PSe<sub>4</sub>, phonon dispersion temp. depend. 0-96600
- Ti<sub>2</sub>PbCu(NO<sub>2</sub>)<sub>6</sub>, incommensurate Jahn-Teller transition, Huang scatt. 0-70401
- Tl<sub>2</sub>Te-Tl liquid system, conc. fluctuation, time-of-flight quasielastic neutron scatt. obs. 0-88324
- TmSe, mag. ordering under press., neutron diff. obs. 0-70947
- UBr<sub>3</sub>, cryst. field levels, neutron scatt. determ. 0-65509
- UO<sub>2</sub>, single-cryst. neutron diff. data, reanal. using third cumulants 0-100130
- UTe, crit. exponents, neutron and magnetisation meas. 0-88823
- V-H(D), hydrogen ordering, review 0-60850
- $\alpha$ -VD<sub>0.7</sub>, vibrations of interstitial D, coherent neutron scatt. 0-96612
- VI<sub>2</sub>, mag. superlattice, neutron oscill. and Weissenberg photography 0-65802
- $\alpha$ -V<sub>0.99</sub>O<sub>0.01</sub> solid soln., impurity vibr., inelastic neutron scatt. study 0-92635
- Y(Co<sub>1-x</sub>Ni<sub>x</sub>)<sub>5</sub>, distrib. of Co and Ni atoms, neutron diff. obs. (Russian) 0-64954
- YD<sub>1.96</sub>, cryst. struct. by neutron diff. 0-70179
- YFe<sub>2</sub>Ga<sub>0.12</sub> domains, neutron dpolarisation and Faraday rotation study 0-93137
- YH<sub>1.98</sub>, cryst. struct. by neutron diff. 0-70179
- YNi<sub>3</sub>, magnetism resurgence, neutron diff. and mag. props. study 0-65819
- Y<sub>1-x</sub>Tb<sub>x</sub>Pd<sub>3</sub>, magnetisation, magnetostriction, and inelastic neutron spectra 0-65998
- YbCuAl, mixed valence cpd., dynamic susceptibility, neutron inelastic scatt. 0-65807
- Zn, mean square displacement of atoms in cryst. lattice, rel. to sp. ht. (German) 0-79902
- ZnCl<sub>2</sub>, aq. soln., structural transition, neutron diff. study 0-64872
- ZnCr<sub>2</sub>Se<sub>4</sub>, screw spin structure, method of controlling the sense, polarised neutron diff. study 0-70944
- ZnS, cubic, thermal vibr. temp. depend., anharmonic models 0-92618
- ZrCr<sub>2</sub>D<sub>2</sub>, site occupation modes and cryst. struct., neutron diff. study 0-59440
- ZrV<sub>2</sub>D<sub>2</sub>(H<sub>2</sub>), site occupation modes and cryst. struct., neutron diff. study 0-59440

**neutron diffusion**

- see also *neutron flux*; *neutron transport theory*
- analytical angular integration technique for generating multigroup transfer matrices 0-68722
- BWR core calculations using improved coarse mesh methods 0-68849
- code comparison for LMFBRs 0-95337
- double criticality of uniform-power-reflected reactors 0-57828
- FBR, nonstationary prompt-neutron diffusion, multigroup treatment 0-86956
- FBR analysis, general multigroup nodal procedure based on response matrix principles [for FBR analysis] 0-57827
- fission reactor theory, relationship among the various anisotropic diffusion coefficients for periodic lattices 0-57826
- fission reactors, fluidised bed concept, diffusion theory 0-68729

**neutron diffusion continued**

- fission reactors, seed-blanket calcs., 2-D, one-channel synthesis method, transport and diffusion 0-73876
- graphite, pulsed neutron wave propagation expt. using electron LINAC (Japanese) 0-78345
- LWR core, few group 2-D diffusion eqns. in hexagonal geometry, HEXAB-II-30E code (Bulgarian) 0-68765
- multigroup charged-particle transport calcs., temp. effects on cross sections 0-57818
- one-group equations, finite element soln. tech. using imaginary nodal points and element subdivision 0-68721
- PBR fission reactors, neutron flux distrib. in multisphere configs., diffusion-theoretical model (German) 0-73875
- PWR core analysis, transport-to-diffusion theory for gadolinia-loaded fuel pins 0-57908
- thermal reactor assemblies, effective neutron diffusion parameters 0-73874
- transport codes DOT and TWOTRAN as standards for diffusion in pebble bed reactors 0-68750
- neutron economy** see *neutron flux*
- neutron effects**
- see also *irradiation induced creep*
- brain tumour, rat, RBE of cyclotron fast neutrons rel. to <sup>60</sup>Co  $\gamma$ -rays 0-76797
- carbonaceous matrix materials for HTGK fuel rods, irradiation-induced dimensional changes 0-65052
- cell neoplastic transformation and dose fractionation, role of damage repair 0-72242
- ceramic nuclear fuels, irradi. induced rare gas diffusion 0-59524
- cervical spinal cord, rhesus monkey, effects of 50 MeV (d-Be) neutron irradi. 0-101228
- chromosomally aberrant cells, Japanese A-bomb survivors, dose-response relationship of neutrons and  $\gamma$ -rays 0-94295
- creep and growth, radiation induced, fundamental mechanisms 0-92596
- Demokritos research reactor, fast neutron irradi. facility 0-99270
- deoxyribonuclease I in aq. soln., inactivation by thermal neutrons 0-104664
- E. coli, value of photoreactivable component after exposure to ionising radiation 0-72224
- E. coli strains differing in DNA repair capability, survival after fission-spectrum neutrons irradi. 0-98031
- fast neutron induced DNA strand breaks and repair obs., cultured mammalian cells 0-61651
- ferroelectric ceramic, polycryst., elasticity props., neutron bombardment effects 0-79856
- fuel pins, fast breeder, fuel-cladding mech. interaction, obs. and anal. 0-86959
- Fusion Materials Irradiation Test Facility 0-91361
- fusion reactor, MFTF, intense neutron environment, test cell side wall design, shielding materials 0-102318
- fusion reactor, neutron irradiation effects on organic insulators at 5K for superconducting magnets 0-107336
- glassy-C, irradiation induced dimensional changes 0-65052
- graphite, electron-spectroscopic analysis of neutron-irradiated pyrographite 0-63261
- graphite, neutron irradiation effects on thermal shock resist. and fracture toughness (Japanese) 0-66622
- liver, RBE of cyclotron fast neutrons and  $\gamma$ -rays for late hepatic injury in rats 0-108975
- lung epithelial cells, type 2, proliferative response after X-rays and fission neutrons 0-108974
- lung tumour induction in RFM mice after localised X- or neutron irradi. 0-72260
- lymphocytes, human, RBE for d(42 MeV)-Be neutrons based on chromosome-type aberrations 0-104663
- lymphocytes, human, variation in neutron RBE values compared to X-rays 0-101229
- lymphoma, murine, effect of synchrony on survival of L5178Y cells after neutron irradi. 0-72227
- malignant melanoma, thermal neutron capture therapy, in vitro radiobiological anal. 0-104657
- mammalian cells, lethally damaged, proliferation obs. after irradi. by various particles 0-108971
- metals, irradi., mechanism of formation of vacancy dislocation loops (Russian) 0-65053
- mixed fluoride crystals, nucl. radiation effects 0-80831
- mixed oxide fuels, SEM obs. of gas bubble morphology 0-57843
- nuclear fuels, radiation enhanced kinetics in the fuel lattice 0-59522
- optical fibre, neutron and gamma induced transient absorpt. and luminesc. 0-58763
- optical fibre, step-index, pulse dispersion, neutron irradi. effects 0-91897
- optical fibre attenuation and pulse dispersion 0-58730
- optical fibres, glass and plastic, neutron irradiated, optical absorpt. spectra 0.7 to 1.1  $\mu$ m 0-58762
- oxide nuclear fuel, fission gas release and swelling, simple operational model 0-92565
- PMMA, neutron and gamma irradiation effects 0-66839
- PMMA, reactor irradi., growth of macroscopic radiolytic gas bubbles, diffusion model 0-65058
- polystyrene, neutron and gamma-irradiation effects 0-66839
- pyrocarbon, irradiation-induced dimensional changes 0-65052
- pyrocarbon coating, isotropic, gas permeability, neutron irradiation effect (French) 0-63260
- pyrographite, initial stress state, neutron irradi. effect 0-97555
- quartz, crystal structure rearrangement due to neutron irradi. 0-64981
- quartz, surface damage by X-rays,  $\gamma$ -rays, neutrons, SEM study 0-79837
- rice, M<sub>1</sub> damage, RBE of thermal neutrons 0-104649
- sapphire, F-centre, fluorescence decay below 75K 0-60664
- sapphire, neutron bombard., F-centre fluorescence, photoluminescence 0-100676
- semiconductor p-n junctions voltage-current characts., fast neutron irradi. effects (Russian) 0-65659
- slow neutron action on glasses and vitreous ceramic and cryst. materials (Spanish) 0-57816
- spermatogonial stem cells, mouse, survival after split-dose irradi. with fission neutrons 0-72244
- squamous-cell carcinoma, spontaneous, in mice, comparison of neutron- and X-irradi. effects 0-98033
- stainless steel, neutron dose determ., from isotope abundance ratio, mass spectra obs. 0-61220



# neutron effects continued

steel, alloy A533B1, neutron irradi., flow growth characts. by acoustic monitoring 0-100918  
steel, austenitic stainless, Cr-Ni, resist. damage rate during neutron irradi. at 23K 0-96571  
steel, austenitic stainless, fatigue crack propagation, effect of neutron irradiation 0-97583  
steel, austenitic stainless, fatigue crack propagation, influence of neutron irradiation 0-97584  
steel, austenitic stainless, neutron dose rate depend. of swelling in fission reactors 0-104233  
steel, austenitic-ferritic stainless, radiation swelling in fission reactors 0-65063  
steel, low alloy, 15Kh2MFA and 15Kh2NMFA, neutron irradi. embrittlement, effect of P, Sb and Sn impurities 0-85055  
steel, stainless, 304, bend test ductility of irradi. specimens for LMFBR appls. 0-104235  
steel, stainless, EBR-II reflector assembly irradi. induced bowing, implications for core restraint design 0-104234  
steel, stainless, fatigue props. of low-fluence neutron irradi. samples 0-97585  
steel, stainless, low-cycle fatigue characteristics of neutron irradi. samples 0-97586  
steel, stainless, Type 316, irradi. effects on tensile props. and microstruct. 0-65059  
steel, stainless, type 316, modelling effects of fast neutron irradiation in mech. behaviour 0-84234  
steel, stainless, type 4301, radiation enhanced permeation of H<sub>2</sub> 0-59732  
steel, stainless 316, fatigue behaviour of materials containing significant amounts of irradi.-induced He 0-100917  
steel, stainless type 316, irradi. induced nuclear cladding swelling, empirical development of design equation 0-59527  
steels, irradiated pressure vessel, reference fracture toughness curves 0-100921  
TCNQ salts, TSF-TCNQ, and HMTSF-TCNQ, low temp. fast neutron irradiation, elec. cond. meas. 0-59964  
testes, mice, comparative effects of various radiations on weight loss and spermatogenic stem-cell survival 0-108976  
TTF-TCNQ, low temp. fast neutron irradiation, elec. cond. meas. 0-59964  
TTF-TCNQ low temp. mag. susceptibility, neutron irradi. effects 0-60311  
tumour incidence and longevity in neutron and  $\gamma$ -irradi. rabbits, RBE assess. 0-104661  
Vicia faba growth reduction, RBE of d(50)-Be neutrons and 650-MeV He<sup>2+</sup> 0-98025  
weld metal, submerged arc irradiated, reference fracture toughness curves 0-100921  
Zircaloy, annealed, neutron irradiated, inhomogeneous deform. behaviour 0-85014  
Zircaloy fuel cladding, irradiation-induced in-reactor corrosion in CANDU reactors 0-104352  
Zircaloy-2, irradi. damage, TEM characts. 0-107332  
Zircaloy-2, irradiation growth, reaction rate theory calcs. 0-88212  
Zircaloy-2, irradiation growth, shape and volume changes 0-92562  
Zircaloy-2 pressure tube elongation, neutron induced creep and growth, meas. and anal. 0-93628  
Al, neutron damage, positron annihilation 0-65056  
Al, shock compression at high press., neutron irradi. (Russian) 0-88264  
Al-Cu (4 wt.%) alloy, irradi., weak-beam dark-field obs. of dislocations near  $\theta'$  precipitates 0-107333  
Al-Mg (0.1 at.%), neutron damage, positron annihilation 0-65056  
 $\alpha$ -Al<sub>2</sub>O<sub>3</sub>, polarised luminescence in neutron- and proton-irradiated single crystals 0-66271  
Ba hexaferrite, irradiated by fast neutrons, mag. props. 0-97116  
C-fibres, irradiation-induced dimensional changes 0-65052  
CdCr<sub>2</sub>Se<sub>4</sub>, reactor radiation influence on ferromagnetic phase transform. (Russian) 0-75760  
Cu, dislocation pinning rate, neutron and electron irradi., meas. by internal friction method 0-96570  
Cu, neutron and electron irradi., interstitial formation, dislocation pinning, internal friction meas. 0-100284  
Cu single crystals, neutron irradiated, secondary slip 0-88161  
Cu, single crystals, neutron irradiated, stresses and secondary slip between overlapping and dislocation arrays 0-88162  
Cu-Fe (1.5 wt.%) alloy, void form. during irradi. in HVEM, reactor irradi. simulation and ageing effects 0-107327  
Cu<sub>3</sub>Au, irradi., displacement cascades, direct obs. method 0-107335  
Fe base superalloy, type A-286, elevated temp. fracture toughness testing of thin section irradi. materials 0-61063  
 $\alpha$ -Fe, neutron irradiated, mobile C atom trapping, anelastic and magnetic relaxations 0-100306  
Fe-Al (40 at.%) and Fe-Al (50.5 at.%) ordered alloys, 20K neutron irradi. effects, stoichiometry depend., resist. obs. (French) 0-84215  
Fe-B amorphous alloy, fast neutron and <sup>235</sup>U fission fragment irradi. 0-100288  
GaAs, semi-insulating and n-type, doping by neutron transmutation 0-96553  
GaAs, electroluminescent study of irradi. induced struct. damage, athermal annealing 0-108280  
GaAs Schottky barrier diode, under high neutron fluence, current transport 0-65679  
Ge detector, high purity, fast neutron damage 0-59526  
Ge detector, high purity, fast neutron damage, hole trapping and detrapping 0-63463  
Ge, neutron irradi., absorpt. edge 0-93320  
Ge, neutron-irradiated, positron lifetime 0-97374  
Ge(Li) detector, fast neutron damage 0-59525  
InSb, neutron irradi., defect cluster form., effect on elec. props. 0-65062  
LiF:OH, neutron irradi., interstitial H-centres, ESR obs. 0-93175  
Li<sub>2</sub>O, neutron irradi. effects, optical absorpt. spectra 0-75271  
Li<sub>2</sub>O pellets, neutron irradiated, temp. distrib. 0-86968  
Li<sub>2</sub>O pellets, sintered; neutron irradiated, ESR study 0-92566  
MgAl<sub>2</sub>O<sub>4</sub>, faulted defect aggregates prod. by neutron-irradi. 0-107331  
MgAl<sub>2</sub>O<sub>4</sub>, radiation damage, optical absorpt., F-centres 0-64994  
Mo alloys, dil., HVEM bombarded, neutron damage simulation, defect cluster and dislocation obs. 0-107330  
Mo, neutron irradi., radiation anneal hardening mechanism 0-71678  
Mo, neutron-bombarded, diffuse X-ray scattering (Russian) 0-92560  
Mo, void containing, positron annihilation characts. 0-80898  
NaReO<sub>4</sub>, EPR spectra of paramag. centres and free radicals 0-108072  
Nb, neutron irradiated, radiation anneal hardening (Japanese) 0-89243

# neutron effects continued

Nb, neutron-irradiated, positron annihilation ang. correl. meas. 0-93430  
Nb-Zr (3 wt.%), neutron-irradiated, positron annihilation ang. correl. meas. 0-93430  
Nb<sub>3</sub>Al, supercond. props. and lattice parameter, comp. and neutron irradi. effects 0-70880  
NbC, supercond. critical temp., neutron irradi. effect 0-80433  
Nb(CN), supercond. critical temp., neutron irradi. effect 0-80433  
Nb<sub>3</sub>Ge, low temperature electron, neutron irradi. effects on critical temp. (French) 0-75669  
Nb<sub>3</sub>Sn, supercond. props., effect of neutron irradi. 0-80463  
Nd:glass laser, influence of neutron and  $\gamma$  irradi. on generating characts. (Russian) 0-69402  
Ni-Cr Nimonic alloys, mech. props., high-temp. irradi. effects 0-100885  
Ni<sub>3</sub>Fe, disaccommodation meas. after low temp. electron and neutron irradi. 0-88832  
NiFe<sub>2</sub>O<sub>4</sub>, ferrite, mag. anisotropy compensation under neutron irradi. 0-75807  
NiFe<sub>2</sub>O<sub>4</sub> ferrite, mag. props., neutron irradi. 0-103858  
Ni<sub>0.85</sub>Zn<sub>0.15</sub>Fe<sub>2</sub>O<sub>4</sub>, ferrite, mag. anisotropy compensation under neutron irradi. 0-75807  
Pb(Zr,Ti)O<sub>3</sub>, piezoelectric ceramics, low fluence neutron irradi. effects 0-92564  
Pt, neutron damage, positron annihilation 0-65056  
Pt, recovery spectrum after thermal neutron irradi., resist. obs., Au addition effect and defect conc. depend. 0-65057  
S, allotropic modifications and activity distrib. 0-70255  
Si, annealed, neutron-irradiated, EPR centre (S=1), characts. 0-71177  
Si crystal, impurities determ. and resistivity after reactor neutron irradi. 0-65563  
Si, neutron and electron bombard., radiation defect recomb., photoelec. props. meas. 0-60039  
Si, neutron transmutation doping, impediments to use in power device fabrication 0-96560  
Si, p-n junctions, voltage-current characts., fast neutron irradi. effects (Russian) 0-65659  
Si, phonon-phonon relaxation investigation for conventional and neutron doped crystals 0-96927  
Si:In extrinsic IR detector material with high responsivity compensated by neutron transmutation, float-zone growth 0-75597  
Si:P, homogeneous nuclear transmutation technique, thyristors appl. 0-70236  
Si:P, neutron transmutation doping, elec. props. rel. to neutron fluence 0-96555  
Si:P, neutron transmutation doping, resist. homogeneity rel. to compensation ratio 0-96556  
SiO<sub>2</sub>, amorphous, very small angle X-ray scatt. before and after thermal neutron irradi. 0-75270  
TCNQ salts, Qn(TCNQ), and N-propyl-Qn(TCNO)<sub>2</sub>, low temp. mag. susceptibility, neutron irradi. effects 0-60311  
Ta<sub>2</sub>S<sub>5</sub>, IT and IH polytypes, fast neutron irradi., defect prod., effects on resist. and charge density waves 0-65060  
Ti, characterization of dislocation loops 0-88155  
Ti, fast neutron irradi., twinning deform. at room temp. 0-65061  
Ti, twinning deformation, neutron irradiation effects 0-75236  
TiN, supercond. critical temp., neutron irradi. effect 0-80433  
U abundance in Himalayan plants, fission track determ. 0-101305  
U, irradiation growth during fission fragment and proton bombard. 0-92568  
UC, nuclear fuels, irradi. induced kinetics, diffusion and fission gas resoln. 0-59523  
UO<sub>2</sub>, high burnup nuclear fuels, relation between fission product release and fuel microstruct. 0-57845  
UO<sub>2</sub> nuclear fuel, sputtering by thermal neutrons, depend. of ejection coeff. on neutron flux 0-83157  
UO<sub>2</sub> nuclear fuels, distribution and size of intragranular fission gas bubbles 0-57840  
UO<sub>2</sub> nuclear fuels, irradi. induced kinetics, diffusion and fission gas resoln. 0-59523  
UO, volatilization pot. of metallic inclusions in irradi. nuclear fuel during LOF overheating transients 0-57895  
UO<sub>2</sub>-PuO<sub>2</sub> fuel pin, hyperstoichiometric, post irradiation examination 0-63258  
V<sub>3</sub>Si, neutron irradi., grain boundary pinning, field-depend. change of crit. current density 0-65759  
V<sub>3</sub>Si, supercond. props., effect of neutron irradi. 0-80463  
Zn, electron momentum distrib., neutron-induced defects, positron annihilation study, for single cryst. 0-71508  
Zr alloys, irradiation growth, influence of microstructure and test conditions 0-92561  
Zr and alloys, irradi. at 573 to 923K, damage struct. 0-107334  
Zr, foil bending by in situ irradi., neutron damage simulation, room temp. oxide growth 0-107342  
Zr, irradiation growth, influence of microstructure and test conditions 0-92561  
Zr, irradiation growth, reaction rate theory calcs. 0-88212  
Zr-Al (8.6 wt.%), dimensional stability struct. and mech. props, effects of neutron irradi. 0-92563  
Zr-Al (8.6 wt.%), fast neutron irradiated, tensile props. and fracture toughness 0-84994  
Zr-Nb (2.5 wt.%), nuclear fuel channels, neutron effects on ultimate fracture strength, 293 to 573K 0-85054

# neutron flux

1/E<sup>1+ $\alpha$</sup>  epithermal neutron spectra, resonance integral correction, effective resonance energy 0-71978  
1/E<sup>1+ $\alpha$</sup>  epithermal neutron spectrum,  $\alpha$ -determ. without Cd cover 0-71976  
associated particle counting tech. for abs. monitoring of DD and DT neutron fluences 0-99428  
epithermal neutron field for <sup>10</sup>B neutron capture therapy, prod. using FBR 0-61692  
fast monoenergetic, international comparison of meas. 0-83138  
FBR, nonstationary prompt-neutron diffusion, multigroup treatment 0-86956  
fission reactor thermal power determ. using neutron flux density meas. 0-73955  
fission reactors, reactivity reserve and K<sub>eff</sub> estimation (Russian) 0-73913  
fusion reactors, molten-salt blanket, effect of Pb and Bi neutron multiplication zones on the fission rates of <sup>232</sup>Th and <sup>235</sup>U 0-99272



## neutron flux continued

- high neutron fluence meas. using mica muscovite as track detector 0-106237  
 HWR TV-O, active core neutron spectrometry using Bonner spheres (Czech) 0-73948  
 kinematics of neutron producing reactions 0-86862  
 LMFBR, Na boiling detection, power spectral density surveillance systems 0-68740  
 LWR, thermal neutron disadvantage factors for  $\text{PuO}_2\text{-UO}_2$  and  $\text{UO}_2$  lattices 0-73945  
 moderation, quasi-asymptotic neutron flux attenuation constant in a moderator with a cylindrical cavity (Bulgarian) 0-68725  
 neutral beam injector penetrations, limiting neutron streaming, neutron flux calc. 0-95400  
 noise analysis in PWR and BWR power reactors 0-86964  
 nonlinear reactor noise anal., appl. of Langevin eqn. with system-size expansion 0-68727  
 nuclear pumped lasers, thermal neutron traps description 0-64041  
 PB-HTGR, control-rod induced flux perturbations, numerical anal. using out-of-force instrumentation (German) 0-83179  
 PBR fission reactors, neutron flux distrib. in multisphere configs., diffusion-theoretical model (German) 0-73875  
 PWR, neutron density noise variation during core life 0-99201  
 PWR, neutron noise diagnostics of 2-D control rod vibr. 0-68840  
 reaction and neutron leakage rates for a large thorium metal assembly surrounding a DT neutron source 0-106099  
 reactivity coefficients, perturbation effects from point-kinetics model (Hungarian) 0-78346  
 reactor critical facility, fast neutron spectrum meas. using (n,  $\alpha$ ) and (n, p) reactions 0-78403  
 reactor noise, AR-MA anal. hidden state variables 0-73944  
 relativistic calculations, importance in proton recoil telescope efficiencies 0-102225  
 $S_N$  transport method for calc. of anisotropic transmission problems 0-68720  
 solid state nuclear track detectors, reactor neutron fluence meas. using Au and In foils 0-69035  
 transmission probability method for calculation of neutron flux distributions in hexagonal geometry 0-106101  
 $^3\text{H}(d,n)^4\text{He}$ , neutron fluence and energy transfer standard 0-102194  
 $\text{UO}_2$  nuclear fuel, sputtering by thermal neutrons, depend. of ejection coeff. on neutron flux 0-83157

## neutron flux density see neutron flux

## neutron interactions see kaon-nucleon interactions; lepton-nucleon interactions; neutron-nucleus reactions; nucleon-nucleon interactions; photon-nucleon interactions; pion-nucleon interactions

## neutron moderation

- see also neutron transport theory  
 fission reactors, fluidised bed concept, diffusion theory 0-68729  
 pulsed neutron wave propagation expt. using electron LINAC (Japanese) 0-78345  
 quasi-asymptotic neutron flux attenuation constant in a moderator with a cylindrical cavity (Bulgarian) 0-68725  
 spent nuclear fuel storage, supercriticality through optimum moderation 0-57896  
 thermal neutron coincidence counting, correction for variable moderation and multiplication 0-69045  
 THERMOS spectrum code, accurate reduced mesh model for neutron thermalisation 0-57829  
 ultracold neutrons, multilayer ferromag. shutter 0-91354  
 $\text{UO}_2$  low enriched fuel rods, storage and transportation, critical separation in water with fixed neutron poisons 0-73918

## neutron-nucleus reactions

- for inelastic neutron-nucleus scattering, see "neutron-nucleus scattering"  
 see also neutron radiative capture; nucleon-nucleon interactions  
 compound neutron absorption processes, optical pots., one particle vibr. state effects (Russian) 0-105956  
 SAIPS information determination system, algorithms for spectra determ. w.r.t. measured reaction rates (Russian) 0-102416  
 UCN, quasibound states in matter, reson. positions and widths 0-73833  
 (n, 2n),  $\Sigma\Sigma$  spectrum, integral cross section meas. 0-68672  
 (n,  $\alpha$ ),  $\Sigma\Sigma$  spectrum, integral cross section meas. 0-68672  
 (n,  $\alpha$ ) with resonance neutrons, properties of highly-excited states of nuclei (Russian) 0-106053  
 (n, f), intermediate struct. line fitting, subthreshold fission resonances 0-102214  
 (n, f), thermal, parity violation from opposite parity rot. states 0-95303  
 (n,  $\gamma$ ), A=19-207, neutron scattering resonance radiative widths 0-99146  
 (n, p),  $\Sigma\Sigma$  spectrum, integral cross section meas. 0-68672  
 (n, p) charge exchange scatt., 190-590 MeV, differential cross section and ang. distrib. 0-57775  
 (n, X) X=p, 2n, 3n, precompound and compound emission mechanisms 0-102176  
 $^{27}\text{Al}(n, \alpha)$ , 14.8 MeV, expt. and statistical model determ. of  $\alpha$ -prod. in fusion reactors 0-95397  
 $^{241}\text{Am}(n, f)$ , 2.5 MeV neutrons, absolute cross section meas. (1.98  $\pm$  0.07 b) 0-73872  
 $^{241}\text{Am}(n, f)$ , 14.8 MeV, cross-section meas. using mica track detectors 0-95330  
 $^{197}\text{Au}(n, xn)$ , 20.6 MeV, neutron yield cross sections and spectra (Russian) 0-91188  
 $^{10}\text{B}(n, \alpha)^7\text{Li}$ , appl. to anal. of fusion reactor materials, archeometry, and nuclear spectroscopy 0-61200  
 $^{136}\text{Ba}(n, 2n)^{135}\text{Ba}^m$ , 14.2 MeV, neutron activation cross sections 0-91180  
 $^{138}\text{Ba}(n, \alpha)^{135}\text{Ce}^m$ , 14.2 MeV, neutron activation cross sections 0-91180  
 $^{138}\text{Ba}(n, p)$ , 14.2 MeV, neutron activation cross sections 0-91180  
 $^{209}\text{Bi}(n, xn)$ , fission high energy neutrons (Russian) 0-106091  
 $^{209}\text{Bi}(n, xn)$ , 20.6 MeV, neutron yield cross sections and spectra (Russian) 0-91188  
 $\text{CC } ^{93}\text{Nb}(n, 2n)$ , 14 MeV, cross section compilation 0-91181  
 $^{40}\text{Ca}(n, X)$ , local approximation to a non-local potential 0-91182  
 $^{243}\text{Cm}(n, f)$ , thermal neutron fission cross section and fission-resonance integral 0-86942  
 $^{245}\text{Cm}(n, f)$ , thermal, charge distrib.,  $^{135}\text{I}$  and  $^{190}\text{Ba}$  fractional cumulative yields 0-63074  
 $^{59}\text{Co}(n, 2n)$ , 14 MeV, cross section compilation 0-91181  
 $^{4}\text{Cr}(n, 2n)$ , A=50, 52, 54, 14 MeV, cross section compilation 0-91181  
 $^{64}\text{Cu}(n, \alpha)$ , A=63, 65, 14.8 MeV, expt. and statistical model determ. of  $\alpha$ -prod. in fusion reactors 0-95397

## neutron-nucleus reactions continued

- $^A\text{Fe}(n, 2n)$ , A=54, 56, 14 MeV, cross section compilation 0-91181  
 $^A\text{Fe}(n, xn)$ , 20.6 MeV, neutron yield cross sections and spectra (Russian) 0-91188  
 $^1\text{H}(n, p)^0\text{H}$ , differential cross sections for 470-590 MeV, ang. distrib. 0-57628  
 $^2\text{H}(n, nn)p$ , 25 MeV, neutron-neutron effective range 0-83041  
 $^2\text{H}(n, 2n)p$ , in thick targets, n-n scatt. length determ., computer expt. 0-57776  
 $^2\text{H}(n, n)$ , (n, p), 24 MeV, quasifree scatt., n-n effective range, Monte Carlo anal. 0-68554  
 $^2\text{H}(n, \pi^-)$ , 400-580 MeV, differential cross sections and ang. distrib. 0-86906  
 $^2\text{H}(n, \pi^-)^3\text{He}$ , 400 to 580 MeV at backward pion angles 0-73847  
 $^A\text{H}(n, X)$ , 60 keV-80 MeV, A=1, 2, 3 total cross section and scatt. length 0-99176  
 $^3\text{He}(n, p)\text{T}$ , appl. to anal. of fusion reactor materials, archeometry and nuclear spectroscopy 0-61200  
 $^A\text{He}(n, X)$ , local approximation to a non-local potential 0-91182  
 $^6\text{Li}(n, \alpha)^3\text{H}$ , 2.7 MeV triton recoil range, reaction in  $\text{Li}_2\text{O}$  single cryst. 0-63372  
 $^6\text{Li}(n, \alpha)^3\text{H}$ , radiolysis of Co III-EDTA soln. 0-93788  
 $^6\text{Li}(n, \alpha)\text{T}$ , appl. to anal. of fusion reactor materials, archeometry, and nuclear spectroscopy 0-61200  
 $^{55}\text{Mn}(n, 2n)$ , 14 MeV, cross section compilation 0-91181  
 $^{55}\text{Mn}(n, \alpha)^{52}\text{V}$ , neutron activation anal., Ge(Li) and NaI(Tl) detector  $\gamma$ -ray spectrometer 0-78485  
 $^A\text{Mo}$ , A=92, 95, 96, 97, 98, 100, (n, p), (n, n'p), (n,  $\alpha$ ), (n, n' $\alpha$ ), ( $n^3\text{He}$ ) prod. cross sections at 14 MeV 0-93829  
 $^A\text{Mo}(n, 2n)$ , A=92, 100, 14 MeV, cross section compilation 0-91181  
 $^{14}\text{N}(n, p)^{14}\text{C}$ , subsurface production of  $^{14}\text{C}$ , groundwater dating 0-85690  
 $^{23}\text{Na}(n, X\gamma)$ , 0.2 to 20 MeV, reaction cross sections 0-99172  
 $^{93}\text{Nb}$ , (n, p), (n, n'p), (n,  $\alpha$ ), (n, n' $\alpha$ ), ( $n^3\text{He}$ ) prod. cross sections at 14 MeV 0-93829  
 $^{58}\text{Ni}(n, 2n)$ , 14 MeV, cross section compilation 0-91181  
 $^{58}\text{Ni}(n, 2n)$ , 14 MeV, cross section compilation 0-91181  
 $^{237}\text{Np}(n, f)$ , thermal neutron sub-barrier fission  $^{134}\text{I}$  and  $^{135}\text{Xe}$  yields 0-86935  
 $^{17}\text{O}(n, \alpha)^{14}\text{C}$ , subsurface production of  $^{14}\text{C}$ , groundwater density 0-85690  
 $^{207}\text{Pb}(n, p)$  reaction, isobar analogue state excitation (Russian) 0-102124  
 $^A\text{Pu}(n, f)$  A=239, 242, 244, 14.8 MeV, cross-section meas. using mica track detectors 0-95330  
 $^A\text{Pu}(n, f)$  A=240, 241, 14.8 MeV, meas. of reaction parameters using solid state nuclear track detectors 0-91201  
 $^{230}\text{Pu}(n, f)$ , fission-fragment yields of neutron fission in FBR 0-83102  
 $^{239}\text{Pu}(n, f)$ , slow polarised neutrons, product separation asymmetry (Russian) 0-106088  
 $^{239}\text{Pu}(n, \gamma)$ , thermal, fission product  $\bar{\nu}_e$  spectrum,  $\beta$ -decay characts. 0-78340  
 $^{147}\text{Sm}(n, \alpha)^{144}\text{Nd}$ , 2 keV, statistical model anal. 0-102186  
 $^{181}\text{Ta}(n, 2n)^{180}\text{Ta}^m$ , 14.68 MeV, cross section 0-68659  
 $^{230}\text{Th}(n, f)$ , 0.68-1.10 MeV, fission fragment ang. distrib., resonance and moment of inertia 0-102219  
 $^{232}\text{Th}(n, 2n)$ , ratio to (n,  $\gamma$ ) in fast reactor, direct meas. 0-102233  
 $^{232}\text{Th}(n, f)$ , 2-8 MeV, fission product yields and mass distrib. 0-86939  
 $^{46}\text{Ti}(n, 2n)$ , 14 MeV, cross section compilation 0-91181  
 $^A\text{U}(n, f)$ , A=233, 235, ejection fission products angular depend. on thermally polarised neutron capture (Russian) 0-86941  
 $^A\text{U}(n, f)$ , A=235, 238, fission-fragment yields of neutron fission in FBR 0-83102  
 $^{233}\text{U}(n, f)$ , thermal polarised neutrons, neutron emission P-odd asymmetry (Russian) 0-78338  
 $^{235}\text{U}(n, f)$  slow polarised neutrons, product separation asymmetry (Russian) 0-106088  
 $^{235}\text{U}(n, f)$  thermal 3 MeV,  $^{136}\text{I}$  isomeric ratio (French) 0-68709  
 $^{235}\text{U}(n, f)$ , symmetric fission, proton scatt. by fission fragments in neck area 0-83130  
 $^{235}\text{U}(n, f)$ , thermal, fragment ionisation, charge distrib., stat. and instant perturbation theory (Russian) 0-63219  
 $^{235}\text{U}(n, \gamma)$ , thermal, d, t, He emission probabilities from stable core model (Russian) 0-68713  
 $^{235}\text{U}(n, \gamma)$ , thermal, fission product  $\bar{\nu}_e$  spectrum,  $\beta$ -decay characts. 0-78340  
 $^{235}\text{U}(n, \gamma f)$ , X-ray yield fluctuations,  $\gamma$ -transitions in  $^{236}\text{U}$  0-106085  
 $^{238}\text{U}(n, f)$ , 5 eV-2.5 MeV, fission cross section, fission barrier second well parameters, resonances 0-63217  
 $^{51}\text{V}(n, p)^{50}\text{Ti}$ , neutron activation anal., Ge(Li) and NaI(Tl) detector  $\gamma$ -ray spectrometer 0-78485  
 $^{90}\text{Zr}(n, X)$ , 10-20 MeV, multipole giant resonance contrib. to optical pot. imaginary part 0-78241  
 $^{90}\text{Zr}(n, \alpha)^{87}\text{Sr}$ , fast n, fission spectrum averaged cross section 0-63177

## neutron-nucleus scattering

- see also nucleon-nucleon scattering  
 elastic, angular distrib. of diff. cross sections, recording and anal., Legendre polynomial expansions 0-91185  
 neutron elastic removal cross sections, interference effect of strong scattering resonances in LMFBR 0-68658  
 non-elastic scatt. cross section at 14.2 MeV meas. method 0-73843  
 parity violation effects in neutron scattering and capture 0-105808  
 spin  $\pm 1/2$  polarised neutrons, differential scatt. by chiral systems, coupled oscill. model 0-102177  
 (n, n), A=90 region, elastic, inelastic and total cross section, statistical model calcs. 0-68674  
 (n, n'), 14 MeV, continuous spectra, multi-step direct reaction anal. 0-78258  
 (n, n'), 14.6 MeV, ang. distrib., preequil. and equil. neutron emission, unified model 0-86891  
 $^A\text{H}(n, pn)$ , 63.1 MeV, differential cross section 0-63186  
 $^{75}\text{As}(n, n)$ , slow n coherent scatt. length, free cross section, bound states 0-86909  
 $^{197}\text{Au}(n, xn)$ , 20.6 MeV, neutron yield cross sections and spectra (Russian) 0-91188  
 $^1\text{B}(n, n)$ , 2.6-8 MeV,  $^{12}\text{B}$  levels, J $^\pi$  and diff. cross sections, R-matrix anal. 0-78151  
 $^{209}\text{Bi}(n, n)$ , 1.2 to 4.5 MeV total and differential cross sections 0-86903  
 $^{209}\text{Bi}(n, xn)$ , 20.6 MeV, neutron yield cross sections and spectra (Russian) 0-91188  
 $^{12}\text{C}(n, n\gamma)^{12}\text{C}$ ,  $^{12}\text{C}$  gamma line Doppler broadening at 4438 keV 0-91147  
 $^{12}\text{C}(n, n)$ , spin-flip probability to first  $2^+$  level 0-78288  
 $\text{Cu}(n, X)$  0-68673



neutron-nucleus scattering continued

- <sup>56</sup>Fe(n,n'), 14.6 MeV, maximum excitation state  $\gamma$ -decay, cross section (Russian) 0-68586  
 Fe(n,xn), 20.6 MeV, neutron yield cross sections and spectra (Russian) 0-91188  
 H(n,n), 16.9 MeV, anal. power, F-wave contribs. 0-63158  
 H(n,n), pol. n, 13.5-16.9 MeV, anal. power and spin-orbit phase parameters 0-78269  
 H(n,n), pol. n, 50 MeV, anal. power 0-68639  
 H(n,pn), pol. np, 50 MeV, spin correlation parameter  $A_{yy}(\theta)$ , phase shift anal. 0-68530  
 H(n,n), (n,p), 24 MeV, quasifree scatt., n-n effective range, Monte Carlo anal. 0-68554  
 H(n,n), scatt. length, 4-nucleon problem, integral eqn. approach 0-91183  
 H(n,n), zero energy total cross section and scatt. lengths 0-57778  
 He(n,n), <sup>4</sup>He continuum microscopic calcs. cross sections and levels 0-57702  
 He(n,n), scatt. length, 4-nucleon problem, integral eqn. approach 0-91183  
 Li(n,n')<sup>7</sup>Li\* (0.478 MeV) cross-section meas. from 0.5 to 5.0 MeV 0-68661  
<sup>100</sup>Mo(n,n'), fast n, gamma transitions, level energies and scheme 0-73822  
<sup>204</sup>Pb(n,n'), 1.5-3.1 MeV, levels, J<sup>π</sup>, excitation functions and mixing ratios 0-102123  
<sup>208</sup>Pb(n,n'), <sup>209</sup>Pb excited states, 3/2<sup>-</sup> resonances from shell model 0-78240  
 polarised neutrons, 2.50 MeV, meas. of small angle scattering (<1°) 0-99432  
 Rb(n,n'), 550-2100 keV, A=85.87, levels, excitation functions, J<sup>π</sup>, Hauser-Feshbach anal. 0-105982  
<sup>3</sup>Si(n,n'), 13.9 MeV, 2<sup>+</sup> (2.23 MeV) excitation, spin flip probab., deexcitation  $\gamma$ -rays 0-86853  
<sup>3</sup>Si(n,n), 25-1100 keV, total cross section, multilevel anal., strength functions, optical parameters 0-78298  
<sup>3</sup>Si(n,n), spin-flip probability to first 2<sup>+</sup> level 0-78288  
 Se(n,n), A=76-78, 80, 82, slow n coherent scatt. length, free cross section, bound states 0-86909  
<sup>28</sup>Si(n,n), spin-flip probability to first 2<sup>+</sup> level 0-78288  
 Si(n,n), A=116, 118, 120, 122, 124, 11 MeV, levels, deformation parameters, isospin effects, optical parameters 0-57679  
 Sn(n,n'), A=116, 118, 120, 122, 11 MeV, octupole vibr. states, diff. cross section, deformation length, DWBA anal. 0-102092  
 Sn(n,n), 11-26 MeV, A=116, 118, 120, 122, 124, differential and total cross sections, optical pots. 0-78293  
<sup>124</sup>Sn(n,n), pol. thermal, parity violation near resonance, DWBA calcs. 0-68528  
<sup>8</sup> Sr(n,n'), 11 MeV, octupole vibr. states, diff. cross section, deformation length, DWBA anal. 0-102092  
 Ta(n,X), slow and ultracold total and inelastic cross sections 0-68673  
<sup>90</sup>Zr(n,n'), 11 MeV, octupole vibr. states, diff. cross section, deformation length, DWBA anal. 0-102092

neutron polarisation

- monochromatic thermal neutron polarisation crossed mag. field method 0-78477  
 Pd<sub>2</sub>, MnSb, struct., appl. as improved neutron polariser 0-60199

neutron production

- cold, and ultracold neutrons, production by a moving cryst. lattice 0-79640  
 neutral beam source of neutrons for shielding design criteria for fusion program 0-99387  
 nuclear neutron producing reaction kinematics 0-86862  
 photoneutron yield from electron-irradiated thick targets in giant-resonance region, calc. of photon track length 0-82983  
 stellar gravitational collapse, neutronisation and lepton escape rel. to hydrodynamics 0-77388  
 e<sup>+</sup>d-e<sup>-</sup>np, polarised, parity violating asymmetry 0-78080  
 ( $\gamma$ ,n), 45-160 MeV, cross sections in quasi-deuteron model for direct reactions 0-63170  
 $\gamma$ d $\rightarrow$ np, 300 MeV, dibaryon resonance manifestation, pseudo-independent amplitude elimination (Russian) 0-57612  
 $\gamma$ d $\rightarrow$ pn, 250 to 800 MeV, differential cross-section and proton polarisation, theoretical models 0-78081  
 $\gamma$ d $\rightarrow$ pn, proton polarisation energy depend., 400-700 MeV (Russian) 0-63000  
 pp $\rightarrow$ nX, baryonium exchange, triple-Regge couplings 0-86763  
 pp $\rightarrow$ ppn'( $\pi$ n $\pi^+$ )( $\pi$ n $\pi^-$ ), 8.8 GeV/c, one pion prod. cross sections, Deck model anal. 0-105919  
 $\pi^-$ N, in C, 5 GeV/c,  $\pi^0$  and n inclusive spectra, cascade model (Russian) 0-68490  
<sup>9</sup>Be(d,n)<sup>10</sup>B use of neutrons for meas. of full cross sections (Russian) 0-69008  
<sup>209</sup>Bi (n, xnf), fission high energy neutrons (Russian) 0-106091  
<sup>242</sup>Cm, spontaneous fission, prompt neutron multiplicity distrib. meas. 0-93131  
<sup>166</sup>Er(<sup>40</sup>Kr,X), 5.1-7.9 MeV/N, deep inelastic neutron emission, pre-equilibrium effects search 0-63200  
<sup>10</sup>O( $\gamma$ ,n<sub>0</sub>), 21.6-25.7 MeV, ground state photoneutron polarisation ang. distrib. 0-57765  
 Ti-T target system for production of 14 MeV neutrons, improvements 0-63433  
 UO<sub>2</sub>, burnup determ. in PWR and BWR using NDA of neutron emission rates 0-83148  
<sup>233</sup>U(n,f), thermal polarised neutrons, neutron emission P-odd asymmetry (Russian) 0-78338  
 W-D<sub>2</sub>O with 10 MeV electron beams 0-83231

neutron-proton interactions

- see also neutron-proton scattering  
 inelastic charge exchange, quark interchange 0-86759  
 np $\rightarrow$  $\pi^+\pi^-$ , 1.73GeV/c effective mass spectrum ( $\pi^+\pi^-$ ), narrow enhancements 0-86741  
 np $\rightarrow$ px, baryonium exchange, triple-Regge couplings 0-86763  
 np $\rightarrow$  $\pi^0$ d, differential cross sections for 470-590 MeV, ang. distribs. 0-76228  
 pn $\rightarrow$ x $\pi$ , temperature parameter for thermal-like emission spectra, fluctuations 0-68482

neutron-proton scattering

- see also neutron-proton interactions  
 dipole pomeron model, 70 to 400 GeV/c 0-105927

neutron-proton scattering continued

- dual absorptive model and np elastic scatt. at high energies 0-102072  
 polarisation phenomena in close-to-forward scatt., intermediate energy region 0-78086  
 preasymptotic effects in large angle elastic scatt. amplitudes, quasipot. scatt. (Russian) 0-57631  
 np elastic scatt., 70-400 GeV/c, cross sections, simple Regge pole model 0-63032

neutron radiative capture

- $\Sigma\Sigma$  spectrum, integral cross section meas. 0-68672  
 average resonance neutron capture, completeness in nuclear spectroscopy 0-106006  
 common doorway resonance, decay amplitude phase relation from (n, $\gamma$ ) reactions 0-57758  
 giant dipole resonance intermediate struct. using (n, $\gamma$ ) and ( $\gamma$ , n), Brink hypothesis test 0-63150  
 parity violation effects in neutron scattering and capture 0-105808  
 radiative nucleon capture, pure resonance model, direct-semidirect model, pure semidirect model 0-78257  
 s-process nucleosynthesis, neutron capture time scale from s-process Kr in meteorite 0-73080  
 thermal neutron capture  $\gamma$ -ray meas. using neutron guide tube 0-58099  
 total radiative width and degree of freedom, statistical model calcs. 0-57732  
 (n, $\gamma$ ), polarized space parity nonconservation, optical pot. and GDR parameters (Russian) 0-86803  
 (n, $\gamma$ ) gamma ray study at Tehran nuclear research centre 0-57735  
 (n, $\gamma$ ), (n, $\gamma$ ), low energy  $\gamma$ -transitions between compound states, statistical theory 0-57737  
<sup>107</sup>Ag(n, $\gamma$ ), 16.3 eV, <sup>108</sup>Ag levels and  $\gamma$ -transitions, population-spin correlation 0-63097  
<sup>109</sup>Ag(n, $\gamma$ ), <sup>110</sup>Ag 118.718 keV isomer, low lying states and transitions, coincidence study 0-73806  
<sup>27</sup>Al(n, $\gamma$ ), pol. Al and n, 0.017 eV, <sup>28</sup>Al levels, transitions and spin 0-78153  
<sup>13</sup>C(n, $\gamma$ )<sup>14</sup>C, subsurface production of <sup>14</sup>C, groundwater dating 0-85690  
<sup>40</sup>Ca(n, $\gamma$ ), direct-semidirect and compound nucleus contribs. to cross sections 0-68662  
<sup>40</sup>Ca(n, $\gamma$ ), fast n, <sup>41</sup>Ca E2 resonance, cross sections and  $\gamma$ -spectrum 0-57759  
<sup>140</sup>Ce(n, $\gamma$ ), <sup>141</sup>Ce collective M1 excitation effects on  $\gamma$ -ang. distribs., direct semidirect model 0-57733  
<sup>35</sup>Cl(n, $\gamma$ ), <sup>36</sup>Cl anomalous M1/E1 strength ratio and doorway states 0-57730  
<sup>133</sup>Cs(n, $\gamma$ ), <sup>134</sup>Cs 176.403 keV isomer, populating  $\gamma$ -rays, low lying levels 0-78200  
 Dy(n, $\gamma$ ), thermal, <sup>162,164</sup>Dy gamma to ground band transitions;  $\gamma$ - $\gamma$  directional correlations 0-68579  
<sup>151</sup>Eu(n, $\gamma$ ), <sup>152</sup>Eu 89.8488 keV isomeric state feeding, delayed coincidence meas., level scheme 0-63126  
<sup>153</sup>Eu(n, $\gamma$ ), <sup>154</sup>Eu low lying levels, bands, transitions 0-57694  
<sup>54</sup>Fe(n, $\gamma$ ), 1-18 keV, <sup>55</sup>Fe resonances, levels, J<sup>π</sup>, valence capture  $\gamma$ -ray spectrum 0-68652  
<sup>56</sup>Fe(n, $\gamma$ ), <sup>57</sup>Fe anomalous M1/E1 strength ratio and doorway states 0-57730  
<sup>58</sup>Fe(n, $\gamma$ ), <sup>59</sup>Fe resonances, primary  $\gamma$ -intensities, E1-M1 correlation 0-57740  
 Fe(n, $\gamma$ ), thermal, <sup>57,59</sup>Fe levels, J<sup>π</sup> and transition branching ratio 0-105976  
<sup>152</sup>Gd(n, $\gamma$ ), <sup>153</sup>Gd levels and  $\gamma$ -ray spectra 0-57736  
<sup>154</sup>Gd(n, $\gamma$ ), thermal, <sup>155</sup>Gd, vibr. state, level scheme,  $\gamma$  and conversion electron spectra 0-57696  
 H(n, $\gamma$ ), thermal, consistency between pion exchange currents and NN pot., cross sections 0-68556  
<sup>6</sup>Li(n, $\gamma$ ), cross section and spectroscopic factors from direct capture pot. model 0-99171  
<sup>55</sup>Mn(n, $\gamma$ ), pol. Mn and n, 0.017 eV, <sup>56</sup>Mn levels, transitions and spins 0-78154  
 Mn(n, $\gamma$ ), primary transitions using focused 24 keV filtered neutron beam 0-63436  
<sup>100</sup>Mo(n, $\gamma$ ), <sup>101</sup>Mo levels,  $\gamma$ -rays and p-wave resonance partial radiative widths 0-57739  
 Na(n, $\gamma$ ), thermal, <sup>24</sup>Na<sup>m</sup>, polarised,  $\beta$ -decay asymmetry and mag. moment 0-91157  
<sup>58</sup>Ni(n, $\gamma$ ), direct-semidirect and compound nucleus contribs. to cross sections 0-68662  
<sup>59</sup>Ni(n, $\gamma$ ), thermal, <sup>60</sup>Ni level scheme and  $\gamma$ -rays 0-63099  
 Ni(n, $\gamma$ ), primary transitions using focused 24 keV filtered neutron beam 0-63436  
<sup>192</sup>Os(n, $\gamma$ ), 2 keV, <sup>193</sup>Os level scheme and transitions, Coriolis coupled Nilsson states 0-57698  
<sup>206</sup>Pb(n, $\gamma$ ), <50 keV, <sup>207</sup>Pb p-wave resonances, enhanced primary M1 transitions 0-57728  
<sup>206</sup>Pb(n, $\gamma$ ), direct-semidirect and compound nucleus contribs. to cross sections 0-68662  
<sup>108</sup>Pd(n, $\gamma$ ), <sup>109</sup>Pd low spin odd parity states, rot. aligned model, Coriolis calc. 0-57695  
<sup>108</sup>Pd(n, $\gamma$ ), thermal, resonance, <sup>109</sup>Pd low spin odd parity levels,  $\gamma$ -rays, particle-rotor comparison 0-73805  
<sup>244</sup>Pu(n, $\gamma$ ) resonance integral meas. 0-73846  
<sup>28</sup>Si(n, $\gamma$ ), 2.7-6.2 MeV, <sup>29</sup>Si doorway state neutron capture, levels and  $\gamma$ -spectra 0-57729  
<sup>28</sup>Si(n, $\gamma$ ), 565, 813 keV, resonance  $\gamma$ , spectra, valence model test 0-63124  
<sup>30</sup>Si(n, $\gamma$ )<sup>31</sup>Si, thermal neutron cross-section determ. 0-95321  
<sup>144</sup>Sm(n, $\gamma$ ), <sup>145</sup>Sm primary  $\gamma$ -rays, direct capture and neutron separation energy, (d,p) correlation 0-57738  
<sup>150</sup>Sm(n, $\gamma$ ), <sup>151</sup>Sm low energy levels from expt. and Coriolis mixing calcs. 0-57697  
<sup>130</sup>Te(n, $\gamma$ ), thermal, <sup>131</sup>Te  $\gamma$ -transitions, spectroscopic factors and reduced transition intensities 0-91143  
<sup>230</sup>Th(n, $\gamma$ ), <sup>231</sup>Th excited states and bands, spins,  $\gamma$ -transitions 0-57699  
<sup>232</sup>Th(n, $\gamma$ ), ratio to (n,2n) in fast reactor, direct meas. 0-102233  
<sup>169</sup>Tm(n, $\gamma$ ), capture cross section from 10<sup>-5</sup> eV to 2×10<sup>7</sup> eV, statistical model 0-63189  
<sup>89</sup>Y(n, $\gamma$ ), direct-semidirect and compound nucleus contribs. to cross sections 0-68662  
<sup>4</sup>Zr(n, $\gamma$ ), A=64, 66, 67, 68, 70, 2.8-500 keV, capture cross sections 0-57780

**neutron radiography**see also *nondestructive testing*

computed axial tomography, using filtered neutron beams 0-101258  
 contrast enhancement using gaseous  $^3\text{He}$  penetrant 0-93707  
 imaging systems, MTFs and resolution capabilities 0-66758  
 nondestructive testing, nuclear engineering appl. (Slovak) 0-76430  
 nuclear materials safeguards reference measurement system utilizing resonance neutron radiography for nondestructive assay meas. 0-78377  
 simulated neutron tomography for nondestructive assays 0-99218  
 solid state nuclear track detectors 0-97671  
 $^{235}\text{U}$ -fission track micromapping, exam. of U mobilisation processes in Precambrian sediments 0-98477

**neutron reflection**

image formation with ultracold-neutron waves 0-78752

**neutron scattering** see *kaon-nucleon scattering; lepton-nucleon scattering; neutron-nucleus scattering; nucleon-nucleon scattering; photon-nucleon scattering; pion-nucleon scattering***neutron scattering (crystallography)** see *neutron diffraction; neutron diffraction crystallography; neutron diffraction examination of materials***neutron sources**

3 ns pulsed beam-target, thermonuclear neutron burst simulation 0-87008  
 absorption medium random, neutron source mean strength (French) 0-74057  
 Bratislava 14 MeV source, design concept 0-99362  
 electrostatic low energy, high current accelerator for 14 MeV neutron production 0-99353  
 engineering test facility as an intense pulsed neutron source or time-of-flight neutron source 0-57831  
 epithermal neutron field for  $^{10}\text{B}$  neutron capture therapy, prod. using FBR 0-61692  
 fast neutron beam for medical use, production and definition (French) 0-69003  
 fast neutron facilities for radiobiological irradiation 0-109064  
 Fusion Materials Irradiation Test Facility 0-91361  
 future nuclear power technology, impact of nuclear research in India 0-95345  
 monochromatic thermal neutron polarisation crossed mag. field method 0-78477  
 neutron capture  $\gamma$ -ray borehole mineral anal., optimum neutron source size 0-61213  
 remote handling design for the intense pulsed-neutron source 0-69006  
 stainless steel, reduction of H by Ar glow discharge, rel. to ultra cold neutron storage 0-104459  
 subcritical cyclostationary nuclear reactor, neutron counting statistics, sinusoidally modulated neutron source 0-99203  
 synchrocyclotron, Leningrad Institute of Nuclear Physics 0-87003  
 thermal-neutron-driven 14-MeV neutron generator 0-95496  
 ultracold neutron accumulation, above-barrier neutron effects, lifetime determ. 0-102227  
 $^9\text{Be}(d,n)^{10}\text{B}$  use of neutrons for meas. of full cross sections (Russian) 0-69008  
 $\text{D}_2\text{O}$ , secondary photoneutron effects on thermalisation experiments 0-99364  
 $^6\text{Li}$ , new material for polarised targets for pol. neutron prod. (French) 0-68987  
 $\text{W-D}_2\text{O}$  with 10 MeV electron beams 0-83231

**neutron spectra**see also *neutron spectrometers*

$1/\text{E}^{1+\alpha}$  epithermal neutron spectra, resonance integral correction, effective resonance energy 0-71978  
 $1/\text{E}^{1+\alpha}$  epithermal neutron spectrum,  $\alpha$ -determ. methods, accuracy 0-71977  
 $1/\text{E}^{1+\alpha}$  epithermal neutron spectrum,  $\alpha$ -determ. without Cd cover 0-71976  
 electron beam fusion, pellet and pellet-blanket neutronics and photonics 0-74006  
 fast neutron spectra transmitted through iron and sodium slabs 0-73873  
 FBR, neutron spectra in the MeV range in fast critical assemblies 0-83210  
 fission neutron spectra, light water-moderated, depth-dose characts. 0-106205  
 health physics research reactor, neutron spectra meas., various shielding conditions 0-63396  
 high energy neutron spectrometry using cellulose nitrate nuclear track detectors 0-91394  
 lineshapes in pulsed neutron powder diffraction 0-64841  
 Nimonic PE16, irradiation creep data obtained in fast and thermal neutron spectra correlation with displacement cross-sections 0-84993  
 nuclear far from  $\beta$ -stability, delayed neutron energy spectra, structure effects 0-78226  
 PAA, nonlinear soft mode at Rayleigh-Benard instability, neutron cond. spectrosc. obs. 0-79266  
 Q-factor for charged particle recoils rel. to neutron energy 0-63397  
 reactor critical facility, fast neutron spectrum meas. using (n,  $\alpha$ ) and (n, p) reactions 0-78403  
 SAIPS, information determination system, algorithms for spectra determ. w.r.t. measured reaction rates (Russian) 0-102416  
 steel, austenitic, types M316, FV548, 304, irradiation creep data obtained in fast and thermal neutron spectra correlation with displacement cross-sections 0-84993  
 ( $\alpha, \text{xn}$ ), 640, 710 MeV, n ang. and energy distrib., intranuclear cascade model 0-83109  
 ( $\gamma, \text{n}$ ), preequilibrium exciton model with evaporative component, photoneutron spectra, giant resonances 0-57762  
 (n,n'), 14 MeV, continuous spectra, multi-step direct reaction anal. 0-78258  
 $^{197}\text{Au}(^{132}\text{Xe}, \text{X})$ , neutron multiplicities 0-57797  
 $^3\text{H}(d,n)^4\text{He}$ , neutron fluence and energy transfer standard 0-102194  
 $^{235}\text{U}$ , quantitative determ. of unauthorised removal of nuclear materials, using changes in spectral indices (Russian) 0-63294  
 $^{181}\text{W}$  level density, n spectra and ang. correl., direct and nonequilibrium processes from  $^{181}\text{Ta}(p,n)$  (Russian) 0-68631

**neutron spectrometers**

cold neutron time of flight spectrometer at Studsvik, Sweden 0-63444  
 diffractometer, transit-time, for structural investigations of monocrystals 0-64840  
 fast, based on electrostatic charge-exchange accelerator 0-63440  
 fission counters, high sensitivity, neutron spectroscopy and dosimetry appl. (French) 0-58078

**neutron spectrometers continued**

Fourier time-of-flight spectroscopy, higher-harmonics contamination in slow-neutron spectra, theory 0-74072  
 fusion reactor, TFTR, neutron spectrometer mech. design 0-95498  
 inelastic spectrometer using resonance detector, energy transfer values in the order of 1 eV 0-74067  
 portable microprocessor controlled neutron spectrometer, NE213 organic scintillator 0-58022  
 pulse shape analyzer, effect of pulse pile-up on discrimination between neutrons and gamma rays 0-91402  
 resolution function of constant Q spectrometer 0-63443  
 reverse neutron time of flight method, slow neutron spectrometry with Fourier beam choppers 0-106230  
 TKS-420, triple axis neutron spectrometer, resolution. functions 0-69011  
 transit-time, detector containing  $^3\text{He}$  0-63441

**neutron stars**see also *pulsars*

accreting neutron stars, cyclotron line emissivity 0-90463  
 accretion disc, interaction with rot. mag. field 0-62173  
 accretion process giving rise to X-ray emission 0-90459  
 in binary systems, accretion disk flux distrib. and colours 0-94778  
 Centaurus X-3, neutron star characts. from correlated spin-up and X-ray luminosity meas. 0-101648  
 composition of outer crust, influence of mag. field 0-101610  
 Compton scattering by unmagnetised electrons in ambient mag. field, vacuum polarisation effects 0-86631  
 conservation of energy equation from scale covariant gravitation theory 0-73216  
 cooling, effects of pion condensate form. 0-77443  
 core, phase transition between nucl. and quark matter 0-67771  
 Crab pulsar, magnetized cracks in crust rel. to matter flow, radio, X-ray and optical emissions 0-72990  
 crust, torsional oscills., period determ. 0-90464  
 degenerate relativistic electron gas, electron collisions, thermal conductivity 0-109355  
 dense neutron matter physics, implications for neutron star props. 0-77277  
 Eddington luminosity limit and supercritical accretion, time-independ. calcs. 0-67768  
 electrodynamics in curved space, theory 0-90465  
 electrodynamics of disk accretion onto magnetic neutron star 0-85973  
 evolution of neutron star immersed in blue supergiant envelope 0-98689  
 expansion of neutron star matter and its final nuclear composition 0-67769  
 formation, from evolution of mass-accreting white dwarfs 0-77281  
 formation, role of stellar degenerate C ignition 0-77390  
 formation from core collapse, electron neutrino and antineutrino emission, spectral calcs. 0-109454  
 formation through stellar core collapse, effects of eqn. of state on mass 0-85928  
 gravitational collapse of stellar core, secondary indications 0-62177  
 gravitational lens effect, EM wave diff. in Schwarzschild space-time 0-90750  
 gravitational lens effect, focusing by slowly rotating relativistic spherical mass 0-105155  
 HD 153919 (=4U 1700-37), supergiant-neutron star, optical variability 0-82419  
 HD 77581 (=Vela X-1), supergiant+neutron star, stellar wind mass transfer, spectral obs. 0-94892  
 Hercules X-1 (HZ Herculis), X-ray continuum and Fe line emission during X-ray low state 0-105393  
 HZ Herculis (Hercules X-1), Ariel V X-ray spectra 0-90580  
 magnetic fields, strengths and props. of stellar condensed matter 0-82187  
 magnetic fields and related effects 0-72991  
 magnetic poles, pair formation and electric field boundary conditions 0-101613  
 magnetospheres, pair annihilation in superstrong magnetic fields 0-85847  
 masses, upper limit determ. from dense stellar matter physics 0-101611  
 massive spheres with an isothermal core 0-82405  
 micropulses, drifting subpulses and nonradial oscils. 0-67766  
 model with trapped neutrinos, implications for stellar collapse 0-90407  
 model within general relativity, mass evaluation 0-101612  
 N49, vibr. neutron star as source of March 1979  $\gamma$ -ray burst 0-105270  
 nonequilibrium shells, role in X-ray emission and nucleosynthesis, review 0-67774  
 nuclear and neutron matter with isobars, transition pot. model, neutron stars 0-68573  
 oscillations, junction conditions across perturbed contact discontinuities 0-94787  
 plasma accretion, interaction with mag. field and accretion flow hydrodynamics 0-109452  
 plasma coupling, boundary conditions 0-94823  
 pulsars emission mechanism, AC Josephson effect hypothesis 0-82404  
 pulsation damping due to interior weak interaction processes 0-77439  
 QCD and superdense matter, quark and gluon plasma, hadronic structure, neutron stars, hadron collisions, review 0-73683  
 quark beta decay and cooling 0-82406  
 radial perturbations of slowly rotating neutron stars, stability 0-98685  
 radiation source form. mechanism, mag. annihilation (Chinese) 0-77440  
 radiative transfer, in surface layers of neutron stars with mag. fields 0-94826  
 rotating, elec. field anal., effect on accretion and radio pulsar model 0-109453  
 rotating neutron stars, form of quantum vortex filaments 0-67770  
 rotating neutron stars, props. in bi-metric theory of gravitation 0-90466  
 rotational energy loss, slowing down index and time derivs. 0-67762  
 spectra of magnetic dense stars, theoretical anal. of atomic spectra 0-105160  
 SS 433, beam models, energetics anal., possible triple system 0-90433  
 SS 433, massive black hole and pulsar models rel. to precessional motion origin of 164 $\mu$  period 0-62138  
 SS 433, spectral features interpreted a precessing neutron star with jets, possible binary 0-90447  
 structure, determ. from pulsars and compact X-ray sources 0-77442  
 supercritical time-dependent accretion, theory 0-85967  
 superdense celestial bodies, theory 0-67773  
 superfluid neutron matter,  $^3\text{P}_2$  pairing, mag. field effects, vortices 0-62174  
 superfluid phase transition for neutron star matter 0-101607



neutron stars continued

superfluidity in neutron stars, theory 0-77441  
thermonuclear bursts assoc. with chromosphere flares 0-98684  
thermonuclear flashes in envelope of accreting neutron star, theory rel. to X-ray burst sources 0-109455  
thermonuclear flashes in envelopes of accreting objects 0-67772  
Thomson scattering in strong mag. field, vacuum polarisation effects 0-86632  
4U 1223-62 (GX 301-2, WRA 977), binary star orbit determ. from X-ray obs. 0-90570  
4U 1700-37 (=HD 153919), eclipsing binary, secondary neutron star, X-ray obs. 0-86016  
4U 1700-37 (HD 15319), high-energy X-ray obs. rel. to neutron stars accretion 0-86014  
X-ray binary sources, pulsating, spin-up due to accretion from Keplerian disc 0-67904  
X-ray emission models 0-62175  
X-ray sources, compact, radio emission origin 0-62317  
X-ray sources, pulsating, accretion disc mag. field calc. for oblique mag. dipole configuration 0-94895  
X-ray spectra from accretion column, optically thick region inc. 0-67767  
He burning shell evolution in accreting stars 0-85968

neutron transport theory

see also neutron diffusion; neutron moderation  
AMPX code for coupled multigroup n- $\gamma$  cross section sets 0-68741  
analytical angular integration technique for generating multigroup transfer matrices 0-68722  
anisotropic source flux iteration techniques, interpolation schemes 0-99200  
Boltzmann eqn.,  $P_1$  and diffusion eqn. asymptotic equivalence 0-95334  
BWR in-core neutron detector sensitivity to control rod vibr. using neutron noise anal. 0-57910  
CACTUS, a characteristics solution to the neutron transport equations in complicated geometries 0-95336  
discrete ordinates calculations of the importance factor of a neutron source using ANISN code 0-68723  
fast neutron spectra transmitted through iron and sodium slabs 0-73873  
FBR, nonstationary prompt-neutron diffusion, multigroup treatment 0-86956  
FBR analysis, general multigroup nodal procedure based on response matrix principles [for FBR analysis] 0-57827  
fission reactor theory, relationship among the various anisotropic diffusion coefficients for periodic lattices 0-57826  
fission reactors,  $\omega$  mode transport eqn., asymptotic soln. 0-102231  
fission reactors, fluidised bed concept, diffusion theory 0-68729  
fission reactors, seed-blanket calcs., 2-D, one-channel synthesis method, transport and diffusion 0-73876  
group cross sections, adjustment of fitting integral meas. 0-86951  
hybrid reactor analysis, separation technique for transport eqn. and sensitivity theory 0-57823  
integrals, quadrature sums, Gaussian, orthogonal polynomial method 0-83139  
inverse eigenvalue problem for a finite multiplying slab 0-86228  
Monte Carlo code, reduction of computational time for point detector estimator 0-68724  
multigroup charged-particle transport calcs., temp. effects on cross sections 0-57818  
multigroup criticality condition for a space-independent multiplying assembly via the Chapman-Kolmogorov equation 0-86949  
nonuniform lattice problems, 2-D constrained finite element anal. 0-86952  
nuclear constants, determ. as an inverse problem in radiation transport 0-83140  
nuclear reactors, HCDA, neutronics and hydrodynamics equations, energy release, DISCAL code 0-68842  
one-group diffusion equations, finite element soln. tech. using imaginary nodal points and element subdivision 0-68721  
PBR fission reactors, neutron flux distrib. in multisphere configs., diffusion-theoretical model (German) 0-73875  
PWR core analysis, transport-to-diffusion theory for gadolinia-loaded fuel pins 0-57908  
radiative transfer calculations, appln. of multiband method 0-95333  
reactor dynamics, localised, P, approx. to Boltzmann eqn. 0-78347  
reactor physics, transport theoretic  $P_N$  approximation 0-57830  
reactor resons. absorpt characts. 0-86955  
 $S_N$  transport method for calc. of anisotropic transmission problems 0-68720  
self-shielding factors, discrepancies between ETOX and TMS codes 0-68744  
semi-infinite medium, time depend. monoenergetic neutron transport eqn. soln. 0-95335  
SHETAN—a three-dimensional integral transport code for reactor analysis 0-63238  
shielding benchmark calcs. by Discrete Ordinates and Monte Carlo methods 0-73886  
slab with finite reflector, critical problem,  $F_N$  method 0-63221  
slabs and spheres, criticality problems 0-57817  
slowing down and propagation in gravity field, approx. theory 0-99199  
space dependent stochastic neutron kinetics with Gaussian parametric excitation 0-63223  
space independent low power model, multigroup energy formalism for reactor stochastic eqns. 0-63224  
stainless steel, reduction of H by Ar glow discharge, rel. to ultra cold neutron storage 0-104459  
thermal reactor assemblies, effective neutron diffusion parameters 0-73874  
thermodynamics and distrib. function of neutron gas system in stationary power reactor with decoupling 0-86950  
three-dimensional, integro-differential equations discrete ordinate solution 0-63222  
transmission probability method for calculation of neutron flux distributions in hexagonal geometry 0-106101  
ultracold neutron accumulation, above-barrier neutron effects, lifetime determ. 0-102227  
unified neutron transport theory for reactor analysis 0-63246  
BeO, neutron wave propag., space and angle depend. study 0-106096

neutrons

see also cosmic ray neutrons; delayed neutrons  
bound multineutron system, 8 and 20 neutrons, existence probability 0-68570

neutrons continued

clinical beams, light-ion flux mixed with collimated fast-neutron beams 0-81723  
cross-sections and kerma values for C, N and O from 20 to 50 MeV 0-101217  
decay, weak interaction meas., coincidence type ion electron converter detector obs. 0-58100  
disintegration, concepts of leptons and quarks, unified field theory (French) 0-91038  
electric charge, optical instrument for determining upper limit 0-63501  
electric dipole moment, CP violation in gauge theories 0-91041  
electric dipole moment using ultracold neutrons 0-82974  
electric polarisability, from photoabsorption cross-section 0-57597  
grand unification, neutron oscillations and massive neutral Majorana leptons, baryon number 0-91033  
local B-L symmetry of electroweak interactions, Majorana neutrinos, and neutron oscillations 0-73643  
mean lifetime meas. using EM trap 0-73703  
neutron-antineutron oscills., proton instability (Russian) 0-101948  
oscillation phenomenology in gauge model with spontaneously broken B-L symmetry 0-90996  
quasibound states in matter, reson. positions and widths 0-73833  
structure function nonsinglet moments from deep inelastic lepton scatt., QCD 0-62980  
SU(5) invariant theory, B-L nonconservation and neutron oscillation 0-78005  
ultra cold, thermomagnetic gates, accumulation in closed vessels 0-87005  
ultracold neutron accumulation, above-barrier neutron effects, lifetime determ. 0-102227  
n $\rightarrow\bar{n}$  oscillations in nuclei, detectable annihilation rate, grand unification 0-101966

Newtonian fluids see fluids

nickel

see also nuclei with .....  
(001) surface, electronic struct. of ordered S overlayers 0-84835  
(001) surface N adsorption due to ion beam irradi., surface struct. LEED study (Chinese) 0-84364  
(001) surface states, surface magnetisation, electron spin polarisation 0-88612  
(100) oxidised surface structure anal., extended appearance potential fine struct. study. 0-75411  
(111), chemisorption and reaction of  $\text{NH}_3$ , LEED, desorption and photoemission expts. 0-59799  
adsorbed H on (111) surface, angle-resolved and variable impact energy electron vibr. excitation spectroscopy 0-76119  
adsorbed  $\text{c}(2\times 2)$ -CO on (001), struct. by LEED, self-consistent scatt. pot. 0-70536  
adsorbed  $\text{H}_2$ , CO, and methanol, interaction on (100) surface, temp. programmed desorption study 0-66876  
adsorbed methoxy species, photoelectron spectra, electronic struct. and orientation 0-83420  
adsorbed Na and Te on (001), photoelectron diffr. effects in core-level photoemission 0-76144  
adsorption, of  $\text{O}_2$ , oxidation 0-108730  
adsorption of acetic acid and ethylenediamine, XPS study 0-76132  
adsorption of  $\text{N}_2$ , photoemission and electronic struct., cluster calcs. 0-97403  
adsorption of  $\text{N}_2$  on (001) surface,  $\text{c}(2\times 2)$  struct. form 0-80083  
adsorption of  $\text{O}_2$  on (100) surface and reduction of surface oxide by  $\text{H}_2$  0-108741  
adsorption residual C removal by electron beam irradi. and heat treatment (Chinese) 0-88421  
air electrode, bifunctional, for Fe-air batteries 0-72028  
anisotropic magnetisation meas., 4-250K 0-65862  
anodic oxidation, role of oxide defects 0-76403  
anodic passive film form. in NaOH soln., refl. and ellipsometric study 0-104447  
atmospheric corrosion, moisture adsorption and indoor corrosion rates 0-71799  
atom,  $\text{M}_{1111}$  spectrum, ab initio calculation 0-83276  
atom, X-ray transitions in laser produced plasma 0-100093  
atom+ $\text{H}^+$  ( $\text{D}^+$ ), K shell ionisation, nuclear Coulomb effect 0-91650  
band struct., angle-resolved photoemission meas. 0-71569  
band struct., cryst. pot. anisotropy effect (Russian) 0-88474  
band structure and multielectron excitations, angle-resolved photoemission determ. 0-76147  
Brillouin spectra, light scatt. cross section for surface ripples 0-71434  
Brillouin-Mandelstam scattering from thermal and excited magnons 0-70980  
carbonyl powder, dislocation density sintering 0-108372  
catalyst, chemisorption of ethylene-(d), Raman and vibr. spectra 0-108747  
catalyst, diamond synthesis by graphitisation of carbon materials at high press. and temp. 0-60795  
catalysts, chemisorption of  $\text{H}_2(\text{H}_2\text{O})$ , dynamics, neutron spectrosc. obs. 0-59778  
cavity coalescence following  $^4\text{He}^+$  irradi. 0-70272  
chemisorption, dissociative, and mol. adsorption of NO 0-65373  
chemisorption of CO on (001) surface, back donation in chemisorption bond, UPS study 0-107642  
chemisorption of O on (111), adlayer phases and binding sites 0-80069  
chemisorption of S on  $\text{Al}_2\text{O}_3$ -supported surface, thermodynamic parameters meas. 0-88424  
coated C fibre, coating struct., SEM study 0-97605  
coatings, detonation powder spray deposition 0-61028  
cold-rolled anomalous effects during X-ray stress meas. (German) 0-104184  
contacts for low cost Si solar cells 0-94017  
content in Cu alloy of Mayfield chondritic meteorite 0-67671  
core-electron excitation edges 0-66345  
correlation effects, perturb. treatment within Hubbard model 0-70582  
correlation effects, perturbation treatment 0-59897  
corrosion, high temp.,  $\text{SO}_4$  induced, studied at 900°C in  $\text{O}_2$ +4.2%  $\text{SO}_2$  0-97639  
corrosion, indoor, rate meas. 0-76404  
corrosion and passivation in phosphate soln., pH depend., ellipsometric study 0-104448  
corrosion due to  $\text{V}_2\text{O}_5$  melts (Japanese) 0-93691  
creep, irradi. induced with 17 MeV deuterons 0-93607  
creep, substruct. and internal stresses (Russian) 0-97527

## nickel continued

- creep, variation in dislocation density, determ. by X-ray diffr. analysis (*Russian*) 0-76302
- creep at 77, 295K, formation of five struct. 0-60926
- creep rate at low stresses, effect of grain size 0-71707
- creep rates, stress depend. and activation energies, constant stress tests, comparison with dislocation creep theory 0-71708
- determination using laser excited atomic fluoresc. spectrosc. 0-93811
- dielectric matrix, analytic model 0-75512
- diffusion and solubility of S (*Russian*) 0-70465
- diffusion of H and trapping 0-70447
- diffusion welding, migration of oriented intergranular boundary with pores (*Russian*) 0-84943
- dislocation structure evolution after hydroextrusion (*Russian*) 0-96530
- dislocations gliding on (001) planes, bright field and weak-beam images 0-107266
- dissolution kinetics and diffusion coefficients in molten Al 0-59666
- domain walls, 109 and 71°, stable orientations, theory and X-ray observations (*Japanese*) 0-60359
- ductility and fracture, nonmetallic inclusions effect 0-104221
- dynamic exponent, crossover obs., TDPAC meas. 0-108021
- electrochemical behaviour, in molten  $V_2O_5$  (*Japanese*) 0-89498
- electrocrystallisation, reaction mechanism, appl. of impedance meas. (*French*) 0-103597
- electrode reactions with molten glass 0-85186
- electrodeposited film, thermal anal., occlusion of gases rel. to mag. props. 0-59823
- electrodeposition, on to Al, Ga, ... Sb solid soln. 0-93505
- electrodeposition, structure-internal stress relationship 0-70561
- electrodeposition on Cu (001), three-dimens. epitaxial crystallites, TEM image contrast 0-88457
- electron irradiated in HVEM, interstitial loop growth 0-107326
- electron tunnelling into ferromagnetic metals 0-60104
- electron-phonon coupling, point contact spectroscopy obs. (*Russian*) 0-70342
- electronic structure, photoelectron spectra, theory 0-80168
- energy band dispersion and mag. exchange splitting, angle-resolved photoemission meas. 0-71567
- energy loss of heavy nonrelativistic ions in matter, semiclassical theory 0-84224
- energy loss spectra of  $C^{2+}$  ions in Ni targets 0-65114
- epitaxial films, even magneto-optical effects 0-76007
- erosive wear mechanisms, combined TEM and SEM obs. 0-108601
- exchange splitting of 3d bands, angle-resolved photoemission meas. 0-71568
- FCC(111) substrate, orientation relationship with Fe vac. deposits 0-59836
- Fermi surface under press., de Haas-van Alphen effect meas. 0-75499
- ferromagnet, dynamic susceptibility calc. 0-80488
- ferromagnet, itinerant, spin waves, surface effects, RPA calc. 0-60226
- ferromagnetic, diffusion and orientation aftereffects 0-88830
- ferromagnetic, electronic struct. and hyperfine field of nonmag. impurities, calc. 0-70658
- ferromagnetic, electronic struct. by real space approach 0-65432
- ferromagnetic, exchange integral maximisation, neutron scatt. obs. and ten-fold degenerate Hubbard model comparison 0-71004
- ferromagnetic, hyperfine field and relax. time obs. of impurity heavy nuclei 0-75533
- ferromagnetic, struct. in nucl. spin echoes 0-60453
- ferromagnetic film, surface states, surface magnetisation and electron spin polarisation 0-65648
- ferromagnetic metals, spin fluctuation theory, Curie temp., mag. susceptibility 0-65937
- ferromagnetic metals, ultrasound attenuation, EM generation 0-108046
- ferromagnetic properties, book contrib. 0-75724
- film, amorphous layer covered, target prep. for channelled ion stopping power meas. 0-63431
- film, EELS, anomalous  $L_3/L_2$  white-line ratios 0-93444
- film, evaporated, adsorbed acetylacetone, XPS study 0-76133
- film, evaporated, chemisorpt. of CO, ellipsometric investig. (*German*) 0-61156
- film, evaporated, elec. resist. and galvanomagnetic props. 0-80411
- film, evaporated, for use as variable delay SAW device, magnetostrictive effects 0-71144
- film, interaction with  $O_2$ , AES, EELS, work function, and gravimetric meas. 0-75433
- film, thickness meas., using nondestructive radioisotopic technique 0-68179
- film characterisation technique, APFIM, time-of-flight spectroscopy 0-75138
- film crystallisation on C fibres and sapphire crystals (*Russian*) 0-75455
- film on steel, type AISI 316, thermal passivation in controlled vacuum 0-76276
- films, (100), spin density by self-consistent linear APW method 0-65710
- films, adhesion on graphite 0-80141
- films, adsorption of ethylene, decomposition, coverage depend. meas. 0-96743
- films, electronic struct. calc., effects of chemisorption; contact pot. and surface magnetisation 0-103734
- films, ferromagnetic reson., photoacoustic detection 0-80613
- films, self-supporting, electroplating method of prep. 0-66436
- foil electrolytic perforation, surface film phase composition obs. (*Russian*) 0-61004
- galvanic oxidation in borate buffer soln. 0-100948
- grain boundary defect structure, hardening effects, TEM 0-103365
- grain boundary internal friction, B solid solubility as function of grain size 0-60903
- hardness after-effect studied by anelastic relaxation 0-66570
- internal friction, and rigidity modulus, strain amplitude-depend. (*Japanese*) 0-92606
- internal friction, instantaneous, depend. on phase of torsional oscills. (*Russian*) 0-71142
- internal friction peak, H-induced in cold worked Ni 0-107368
- interstitial site determ.,  $\mu$ SR technique 0-71287
- ion bombard., ion and photon yields, CO adsorption effect 0-89098
- ion irradiated with 20 and 500 keV  $^4He^+$ , depth distrib. of cavities and dislocation damage 0-107346
- ion irradiated with heavy ions, defect cluster obs. 0-107341
- ion irradiated with rare gas ions, in situ electron microscopy obs. of cluster creation 0-107343

## nickel continued

- ion plated onto Nb and Ta, prep.,  $H_2$  absorption and desorption rate (*Japanese*) 0-108358
- itinerant electron ferromagnet, magnetovolume effects 0-60397
- K-shell X-ray prod. by  $^{14}N^+$  bombardment 0-91482
- kinetics of C deposition from adsorbed CO on (100) surface 0-76553
- laser irradiation effect, virgin and ion-implanted Ni 0-108306
- liquid, Hall effect, band struct. and exchange scatt. 0-80250
- liquid, N solubility depend. on added elements, mechanism (*Russian*) 0-65223
- luminescence characteristics of pure surfaces acted on by flux of field emission electrons 0-100695
- magnetic neutron scattering by dislocations, temp. depend. 0-103820
- magnetoelastic contribs. to US vel., elastic consts., and susceptibility 0-75829
- magnetostrictive vibr. obs. by laser interferometric technique 0-66000
- Medicus matrix cathode, surface characts. 0-66378
- metallic particles, stability and electronic struct. (*French*) 0-80155
- metallised coating on polyethylene terephthalate film, fracture under laser irradi. (*Russian*) 0-76333
- microcrack propagation and plastic strain 0-81187
- multilayer Ni deposits, simultaneous thickness and electrochemical potential determination for individual layers 0-71813
- $n=2-2$  transitions in XUV spectra, anal. 0-102472
- NMR study of metal precipitated onto a cathode (*Russian*) 0-93185
- optical components, electroless Ni coated Be, comparison with glass 0-69473
- oriented bicrystal, sintering prod. technique 0-108371
- oxidation, high temp., effect of C on cavity form., SEM study 0-97638
- oxidation kinetics, influence of intermediate annealing treatment 0-89412
- oxide films, metal and  $O_2$  transport, AES and inert marker, techniques 0-97641
- oxidised surface, oxidising conditions effect on thermally stimulated exoelectron emission (*Japanese*) 0-89127
- N.Pacific, trace metal vertical profiles 0-67381
- paramagnetic, Fe and Co impurity effects on susceptibility, Faraday obs. (*Russian*) 0-88731
- paramagnetic, mag. form factors in Stoner-like model 0-97061
- paramagnetic, muon spin rot. Knight shift, 637 to 906K 0-75908
- paramagnetic state, itinerant electron model 0-65769
- particle formation by evap., electron microscopy obs. of interaction processes 0-104053
- particles, vibrations associated with twins 0-100253
- phonon density of states determ. from thermodynamic functions 0-96616
- photoacoustic effect from thermally thin solid 0-75304
- photoelectric cross sections at 52.4, 60, 72.2 and 84.4 keV 0-69187
- photoemission spectra, valence band and core level satellite due to excitation of d electron 0-97408
- photon emission due to  $Ar^+$  ion bombard., adsorbed and recoil-implanted O effect 0-80872
- pinned domain wall motion, magnetic damping studies 0-65956
- plasma arc spraying, chem. reaction with plasma gases 0-66427
- plastic deformation, cyclically deformed, HVEM in-situ study 0-103339
- plastically deformed, positron trapping rate, temp. depend. 0-71507
- plating, electroless, of Fe powder 0-61026
- plating C steel nails, barrel plating efficiency 0-100964
- PLEED results for W (100) using appl. of GaAs spin-polarized electron source 0-69000
- polarised, ferromag., evidence for K-shell polarisation of  $^{12}C$  ions via mol. orbital promotion 0-71273
- polycrystalline, strain hardening, dislocation length model 0-84953
- positive muon diffusion, press. depend 0-75907
- positron lifetime meas., 4.2 to 1700K, monovacancy form. enthalpy 0-97370
- precipitates, isothermal annealing influence on structural state, X-ray diffr. anal. (*Russian*) 0-100849
- proton-induced L-shell ionisation cross-sections 0-100707
- push-pull fatigued polycrystals, point defects, elec. excess resist. meas. 0-100910
- quasi-particle energies, two-hole XPS satellite 0-66399
- Raney Ni surface, chemisorbed benzene struct., neutron inelastic spectroscopy study 0-101038
- range distributions for 25-200 keV  $^{14}N^+$  ions 0-103405
- reaction kinetics of liquid with  $B_2C$  0-84344
- recycling, effect on comp. 0-66455
- rubbing of cast Fe, surface temperature effect on dry sliding wear 0-60983
- self implantation damaged, crit. behaviour, perturbed ang. distrib. meas. anal. 0-60476
- single crystal, compressed, strengthening and dislocation cells (*German*) 0-66536
- sintered, pressed, plasticity as function of porosity (*Russian*) 0-75290
- sintered permeable materials with bidisperse structure, pore-forming additions effect 0-84885
- sintering kinetics, metallographic study 0-93519
- slip character, H effect 0-89287
- small clusters, local densities of states 0-88466
- sputtering yields, ang. distrib. and differential, for low-energy light-ion irradi. 0-71527
- stability under various stresses of perfect Ni crystal 0-104208
- stopping power for  $^{107}Ag$ ,  $^{109}Ag$  and  $^{150}Sm$  0-70284
- stray mag. fields above stripe domains, electron microscope and  $\mu^*$ -tensor determ. 0-7108<sup>2</sup>
- stress corrosion susceptibility, S segregation effect, Auger spectrosc. study 0-61019
- stress induced cross-over effect near Curie point (*German*) 0-103873
- stress induced crossover effect near Curie point (*German*) 0-103874
- stress relaxation, in-reactor study at low temps. 0-93588
- structural changes, creep mechanism, multiple dislocation cross slip (*Russian*) 0-59476
- substrate, Sn autocatalytic deposition 0-100965
- surface, (100) and (100) with O overlayer, crystallographic effects in low energy ion scatt., local ion-atom neutralisation 0-84377
- surface, (001), adsorbed  $c(2 \times 2)CO$  layer, struct. 0-88428
- surface, (001), Ar ion bombarded, enhancement of oxidation, AES study 0-97644
- surface, (001),  $H_2$  dissociative adsorption, calc. 0-101036
- surface, (001), reaction of CO and  $H_2$ , extended muffin-tin orbital theory 0-76557
- surface, (100), adsorbed Na, photoelectron diffr. aximuthal patterns, struct. sensitivity 0-107644



## nickel continued

surface, (100), reson. behaviour of interband excitations in photoelectron spectra 0-104043  
 surface, (110), adsorbed H, adatom configuration, He diffr. study 0-103569  
 surface, (110), ferromag., surface magnetisation, polarised LEED expt. 0-97118  
 surface, (110), graphitic monolayer, oxidation mechanism 0-101037  
 surface, (110), mag. exchange splitting of electronic surface states 0-88610  
 surface, (110), O<sub>2</sub> adsorption, LEED and ion scatt. study 0-84386  
 surface, (110), polarised LEED study of magnetism 0-71102  
 surface, (110) and (111), two-photon photoemission 0-76150  
 surface, (110) clean, low energy ion scatt. 0-104026  
 surface, (111), chemisorbed CO, bond energies 0-100398  
 surface, adsorbed CO, N<sub>2</sub>, valence band photoemission, SCF MO CNDO calc. 0-100754  
 surface, adsorbed formic acid decomp., dipole interactions effects 0-61143  
 surface, clean and with adsorbed Na, photoemission, directional memory effects 0-100753  
 surface, CO chemisorpt., mol. cluster calc. 0-100407  
 surface, location of adsorbed atoms, surface channelling meas. 0-84373  
 surface, positronium emission 0-80897  
 surface, single-atom self-diffusion FIM study 0-103548  
 surface (001), azimuthal anisotropies of ejected dimer ions, SIMS expt. 0-60730  
 surface (100), ang. resolved Auger emission and LEED Kikuchi intensities at 850 eV 0-66340  
 surface (100), coadsorption of Sn on Pb, P or O contaminated surface, AES study 0-88437  
 surface (100), electronic struct., self-consistent local orbital calc. 0-65649  
 surface (100) and (110), reaction of acetylene, room temp., UPS expts. 0-61151  
 surface (110), damage induced by bombard. with 3-30 keV noble gas ions 0-60728  
 surface (111) and (110), laser-induced charge transfer to adsorbed CO, photoemission expts. 0-59798  
 surface vibrations, chemisorbed O influence 0-84361  
 thermal emission, magneto-optic circular polarisation obs. 0-70435  
 thin films, surface demagnetisation due to chemisorption, ferromagnetic reson. study 0-80616  
 thin-walled cylinder, elongation upon torsion 0-64386  
 US torsional vibrations in metals, measurement of absorpt. 0-58856  
 vacuum deposited epitaxial layer on Fe (001) substrate, orientation relationship 0-65415  
 volume changes and defect healing due to plastic deform. (*Russian*) 0-81139  
 X-ray intensity reson. near 2p threshold 0-60717  
 X-ray K-emission satellites, quasi-stationary states and origin 0-80903  
 X-ray spectra, L<sub>III</sub>-binding energy, absolute determ. from self-absorpt. meas. 0-71519  
 X-ray stress meas., anomalous effects in cold-rolled specimen (*German*) 0-104184  
 Au/Ni, interdiffusion, backscatt. study 0-79991  
 BP/Ni pillar crystal growth from vapour 0-60758  
 C/Ni, X-ray photoemission studies 0-76138  
 CaF<sub>2</sub>/Ni crystals, X-irradiated, EPR study of Ni<sup>2+</sup> and Ni<sup>3+</sup> 0-75849  
 CaF<sub>2</sub>/Ni, X-irrad., impurity effects on defect prod. 0-92525  
 CaF<sub>2</sub>/Ni, X-irrad., optical absorpt. spectra and dichroism meas. 0-108239  
 CaF<sub>2</sub>/Ni, X-irrad., thermolum. 0-60686  
 CaF<sub>2</sub>/Ni, X-irradiated, optical and EPR meas. 0-108235  
 CdS/Ni, nonradiative recomb., photocond. spectra 0-70764  
 CdS/Ni<sup>2+</sup>, Zeeman effect at Ni impurities 0-60633  
 Cr<sub>3</sub>C<sub>2</sub>-(Ni-Cr), self-weldability in high temp Na (*Japanese*) 0-89392  
 Cu/Ni coherent modulated structures, electronic struct. and magnetism 0-103620  
 electroless plating on Zn-Al alloys, baths and activating solns. (*Japanese*) 0-71604  
 GaAs/Ni, intra d-shell excitations of acceptors 0-84757  
 GaAs/Ni, substitutional impurity elec. struct. 0-88513  
 GaP/Ni, multivalence impurity, EPR and optical absorpt. meas. 0-75844  
 GaP/Ni, photolum. excitation spectroscopy 0-80841  
 GaP/Ni, positron annihilation meas. rel. to deep levels study 0-60712  
 Ge/Ni, gamma ray effects on impurity states 0-96822  
 Ge/Ni, Sb 0-96906  
 n-Ge/Ni p<sup>+</sup>-n-n<sup>+</sup> structs., double-injection current-voltage characts. 0-60074  
 KMgF<sub>2</sub>/Ni<sup>2+</sup>, acoustic Faraday and Cotton-Mouton effects, theory 0-65987  
 K<sub>2</sub>MnF<sub>4</sub>/Ni, mag. effects of impurities 0-65869  
 K<sub>2</sub>MnF<sub>4</sub>/Zn(Mg)(Ni), local magnetisation, NMR and Green's function study 0-65870  
 LiF/Ni, dislocation behaviour in diffusion zone, Cottrell clouds (*Russian*) 0-70212  
 LiNbO<sub>3</sub>/Ni optical absorpt. spectra 0-71450  
 MgO/Ni, heavily doped, defect characterisation, rel. to use as laser material 0-65000  
 MgO/Ni<sup>2+</sup>, near IR luminesc. from isolated and exchange-coupled Ni<sup>2+</sup> ion pairs, temp. depend. 0-93382  
 Mg<sub>2</sub>TiO<sub>4</sub>/Ni, ESR of Ni<sup>2+</sup> 0-97131  
 Ni IX to Ni XII, wavelengths of transitions between lower configurations 0-99474  
 NH<sub>4</sub>Cl/Ni<sup>2+</sup>, EPR spectrum, spin Hamiltonian, zero-field splitting effects 0-97135  
 Na<sub>2</sub>O-B<sub>2</sub>O<sub>3</sub>-SiO<sub>2</sub> glass-Ni compact, indented, strength and fracture toughness 0-93636  
 Ni catalyst, chemisorption of benzene, Raman and vibr. spectra 0-108747  
 Ni, cold-worked, rel. between dislocation and ferromag. damping 0-107369  
 Ni I, UV lines, oscillator strengths from hook method and absorpt. meas. in furnace 0-83319  
 Ni I isotope shift for stable isotopes, nuclear charge radii 0-99484  
 Ni I solar photosphere from oscillator strength obs. 0-98625  
 Ni passivation, S influence study by Auger and electron spectroscopy 0-65347  
 Ni XII, XIII, XIV, XV, 3s-3p and 3p-3d transitions, oscillator strengths and energy levels calcs. 0-83251

## nickel continued

Ni XII-XVIII solar 3s<sup>2</sup>3p<sup>6</sup>-3s3p<sup>n+1</sup> transition arrays, UV spectra classification 0-63570  
 Ni XVII transition probabilities and collision strengths 0-78562  
 Ni<sup>2+</sup> bombardment of stainless steels, effect on stress corrosion cracking and microhardness 0-85087  
 Ni<sub>2</sub>In, He, lattice defect struct., PAC meas. 0-70190  
 Ni<sub>2</sub>MgF<sub>2</sub>, tunable transition-metal-doped solid state lasers 0-58549  
 Ni<sub>2</sub>MgO, tunable transition-metal-doped solid state lasers 0-58549  
 Ni<sub>2</sub>O, single crystal, <sup>18</sup>O<sup>+</sup> ion implantation in channelling directions, expt. conditions and range profile obs. 0-65022  
 Ni<sub>2</sub>O single crystal, <sup>18</sup>O<sup>+</sup> ions implantation in channelling directions, stopping power meas. from max. range 0-65078  
 Ni/Al<sub>2</sub>O<sub>3</sub> catalysts, coprecipitated methanation type, metal-support interaction, XPS obs. 0-80936  
 Ni/GaAs film contact system, alloying reaction 0-96747  
 Ni/Pt/Si(111) Schottky diodes, current-voltage characts. and comp. profiles 0-84508  
 Ni-Cd batteries, button and cylinder types, self discharge behaviour during storage (*German*) 0-66960  
 Ni-Cd sealed battery electrode performance meas. 0-66962  
 Ni-ceramic coating structure, influence of micropowder inclusion (*Russian*) 0-59820  
 Ni-Cu conductor system for Si solar cells 0-93991  
 Ni-Fe thermocouple, appl. to surface temperature measurement 0-62668  
 Ni-ferriite powders, form. in presence of Li<sub>2</sub>SO<sub>4</sub>-Na<sub>2</sub>SO<sub>4</sub> molten salts, prep. and characts. 0-84869  
 Ni-H system, energy and electron density of states, improvements to theory 0-70636  
 Ni-H system, phase diagram and thermodynamic properties calcs. 0-66480  
 Ni-P undercoat, effect on struct. form. in sintered electrophoretic Cr<sub>3</sub>C<sub>2</sub> alloy coatings 0-61027  
 Ni-SiC coating adhesion to Al alloy, metal interdiffusion (*Russian*) 0-66697  
 Ni-SiO multilayer films, interface magnetisation 0-88858  
 Ni-Si(111), interface, reactivity and struct., ion channelling meas. 0-92788  
 Ni<sup>2+</sup>+H<sub>2</sub>(HD)(D<sub>2</sub>), endothermic reactions, investig. 0-97692  
 Ni<sup>16+</sup>+Ne, highly charged very slow Ne recoil ions, K X-ray transition 0-91649  
 Ni<sup>2+</sup>+MoO<sub>3</sub> catalyst on Al<sub>2</sub>O<sub>3</sub>, Raman spectrum 0-108742  
 Ni<sub>3</sub>, extended basis set LCAO Xalpha treatment 0-95537  
 Ni<sub>3</sub> in solid Ar, reson. Raman spectra 0-63638  
 NiVI, sixth spectrum analysis 220-335 and 890-1325 Å regions 0-95565  
 Si/Ni, Stoneley waves at (001) interface between cubic symm. cryst. 0-100388  
 SrF<sub>2</sub>/Ni, X-irrad., optical absorpt. spectra and dichroism meas. 0-108239  
 SrO/Ni<sup>2+</sup>, EPR line splitting rel. to Jahn-Teller coupling and soft localised mode 0-66022  
 SrO/Ni<sup>2+</sup>, ionic thermocurrent meas. 0-108148  
 SrO/Ni<sup>2+</sup>, linear Stark effect for zero-phonon optical absorpt. line 0-80830  
 TiO<sub>2</sub>-Ni (100) interface, electronic props., struct., comp., chemical bonding 0-84499  
 Zn(BF<sub>4</sub>)<sub>2</sub>·6H<sub>2</sub>O/Ni, phase transition study, EPR of diluted Ni<sup>2+</sup>, 98-298K 0-75846  
 ZnCl<sub>2</sub>-KCl-NaCl, molten system, containing Ni<sup>2+</sup> ions, appl. to electrorefining, polarographic study 0-66810  
 ZnO/Ni<sup>2+</sup>, Zeeman effect at Ni impurities 0-60633  
 ZnS/Ni, IR luminesc. and absorpt. spectroscopy 0-108261  
 ZnS/Ni<sup>2+</sup>, Zeeman effect at Ni impurities 0-60633  
 ZnS(Se)/Ni, optical absorpt., impurity ionisation, optical phonon coupling 0-88505  
 ZnSe/Ni, photolum. excitation spectroscopy 0-80841

## nickel alloys

see also Elinvar; Invar; nickel compounds; Permalloy  
 adhesive wear under unlubricated conditions 0-108593  
 Alnico 5 alloy, S and Ti additions effect rel. to non-metallic inclusions, coercive force and grindability 0-89375  
 Alnico 8, permanent magnetic alloy, topography of precipitate phase (*Chinese*) 0-66512  
 Alnico type YuNDK25DA alloy permanent magnets, thermal mag. hysteresis 0-75818  
 amorphous, liq. quenched, struct., thermal stability and mech. props. 0-88059  
 Carpenter 20 Cb-3 alloy, pitting resist. in low salinity geothermal brines 0-93681  
 Colmonoy, self-weldability in high temp Na (*Japanese*) 0-89392  
 Colmonoy hardfacing materials, friction characts. in high temp. Na (*Japanese*) 0-89356  
 composite, Cr<sub>3</sub>C<sub>2</sub> fibre reinforced, oxidation and creep, Y additions effect 0-66685  
 constructional, KhN56VMKYu, creep, viscosity, resist. to inelastic deform. 0-89309  
 corrosion behaviour in reducing environment of coal fired MHD generator 0-104322  
 creep transients, friction stress and recovery, dislocation substruct. 0-60933  
 cyclic oxidation, Ni base alloys, role of thermal shock 0-97640  
 dilute, hyperfine field distribns., DPAC meas. 0-93222  
 dilute, implant profiles modification by radiation enhanced diffusion and segregation 0-88217  
 embrittlement in high-pressure hydrogen, protection by Cu electroplating, aerospace engine appl. 0-76416  
 fatigue and cyclic plasticity rel. to struct. inhomogeneity 0-81184  
 Hastelloy, C-276, H transport rel. to ageing treatment 0-75384  
 Hastelloy, C-276, H-induced crack growth 0-71747  
 Hastelloy, H<sub>2</sub> embrittlement in H<sub>2</sub>S environments, impurity segregation effects 0-71724  
 Hastelloy alloy, G and C-276, pitting resist. in low salinity geothermal brines 0-93681  
 Hastelloy B-2, corroded surface, electron bombardment effect during Auger electron anal. 0-61014  
 Hastelloy-X, low cycle fatigue crack propagation at 25°C and 760°C 0-104270  
 Hastelloy-X, Ni-Cr-Fe-Mo, cyclic oxidation resist. improvement by high temp. etching treatment 0-97627  
 Hayes alloy no.716, Fe-Cr-Ni-Co-W-Mo-Si-C-B (26, 22, 12, 3.5, 3, 1.2, 1.1, 0.4 wt.%), hardfacing alloy 0-100802

## nickel alloys continued

- Haynes alloy 20 Mod, pitting resist. in low salinity geothermal brines 0-93681  
 heat resistant, fatigue limit comparison in torsion and tension-compression 0-81181  
 heat resistant El437B and El929, surface condition, air stream effect 0-76409  
 HYCSOS chemical heat pump, low grade heat enhancement using  $\text{LaNi}_{5-x}\text{Al}_x$  0-61467  
 Incoloy 800, clean and steam oxidised,  $T_p$  permeation 0-88364  
 Incoloy 800, nuclear grade boiling tubing superalloy, Co and C content anal. 0-78397  
 Incoloy 800, steam oxidised, oxide coating anal. 0-89399  
 Incoloy 800, stress corrosion cracking in NaOH solns., electrochem. aspects, peening treatment 0-97618  
 Incoloy 901, foil prep. for TEM exam. 0-88001  
 Inconel, caustic stress corrosion cracking resistance, processing variables effect 0-71796  
 Inconel, fusion reactors Li cooling system, corrosion inhibition by Al additions 0-108646  
 Inconel, steam generator tubing, mag. probe inspection 0-85119  
 Inconel 600, nuclear grade boiling tubing superalloy, Co and C content anal. 0-78397  
 Inconel 600, small bore tubing, crevice corrosion 0-60999  
 Inconel 600, stress corrosion cracking in NaOH solns., electrochem. aspects, peening treatment 0-97618  
 Inconel 600, thermal treatment, grain boundary microstruct. and SCC resistance 0-71675  
 Inconel 600 alloys, stress corrosion cracking, prediction in 10% NaOH soln. at 315°C 0-97616  
 Inconel 600 safe-end cracking failure at Duane Arnold reactor 0-104295  
 Inconel 617, creep, morphological changes of carbides, affect on creep props. 0-108509  
 Inconel 625, electron yields under ion bombardment for clean and oxidised surfaces 0-66368  
 Inconel 625, organic contamination removal by plasma cleaning and etching 0-97645  
 Inconel 625, pitting resist. in low salinity geothermal brines 0-93681  
 Inconel 718, grain growth during sintering 0-97449  
 Inconel 800, simulated, steam oxidation 0-76405  
 Inconel hardfacing materials, friction characts. in high temp. Na (Japanese) 0-89356  
 Inconel X-750, deform. and fracture characts., 24-816°C 0-108551  
 Kovar-silicon oxynitride-aluminium cathode, local electron emission and electroluminescence patterns obs. 0-108327  
 liquation cracking during welding, comp. influence 0-66645  
 manganin foil like gauge calibration in planar shock wave expts. 0-95091  
 Metglas 2826 ribbon, saturation magnetostriction meas. by small-angle magnetisation rot. 0-60391  
 Metglas 2826 ribbon, voids formation during crystallisation 0-108428  
 Ni-Co,  $\text{H}_2$  embrittlement, heat treatment and impurities effect 0-76331  
 Ni-Pd-P, metallic glass, electronic structure, pulsed NMR study 0-75869  
 Nimonic, irradiated, void nucleation, numerical evaluation 0-70252  
 Nimonic 105, creep and stress rupture props., trace elements influence 0-66602  
 Nimonic 80A, creep rupture under non-proportional loading 0-108518  
 Nimonic 80A, order hardening, comparison between revised theory and expt. 0-93565  
 Nimonic 80A superalloy, contrast from cavities in HVEM 0-79780  
 Nimonic PE16, irradiation creep data obtained in fast and thermal neutron spectra correlation with displacement cross-sections 0-84993  
 Nimonic PE 16, corrosion behaviour in high temp. impure He gas 0-76402  
 Nimonic PE-16, electron irradi. in HVEM, void growth, vacuum environment influence 0-107323  
 p 0-88364  
 plasticity, heat treatment effect 0-76277  
 powder alloy  $\text{ZrHfSbU}$ , US method of porosity detection 0-71828  
 rare earth alloys,  $\text{R}_{60}\text{Ni}_{40}$ , amorphous, Curie temp., mag. susceptibility and coercive force, 4.2 to 300K 0-93092  
 recrystallisation and grain growth, influence of alloying (Russian) 0-81071  
 Rene 80, dislocation behaviour during plastic deform. (Japanese) 0-108504  
 spring alloys, microplastic deform. and endurance limit 0-81197  
 steel, austenitic (03KH18N10T), heat treatment for fission reactor appls. 0-66454  
 steel, austenitic stainless Ni-Cr, heat resist. and comp. of non-metallic inclusions, effect of La, Nd, Pr and Ce 0-76315  
 steel, Cr-C-Ni, struct. prop. rel., design of struct. steels for high strength and toughness 0-97491  
 steel, Cr-Ni, pendant drop melt extracted, struct. and props. 0-76242  
 steel, Cr-Ni-Mo-Mn, wetting of TiC, expt. planning investigation 0-60822  
 steel, Cu-Ni-Mo (2, 2, 0.25 wt.%), sintering, kinetic characts. 0-60805  
 steel, high-strength, fatigue, interaction effects between trace impurities and environment 0-66651  
 steel, Mn-Mo-Ni, embrittling effects of residual elements 0-66655  
 steel, Ni, high-strength, impact fatigue strength, heat treatment conditions effect 0-76285  
 steel, Ni (17 wt.%), martensitic deform. temp., cryst. struct. effect (Russian) 0-66576  
 steel, Ni-Co-Cr, high-strength medium C, Cr effect on props. 0-76339  
 steel, Ni-Cr, anodic dissoln. in NaCl solns. at high current densities (Russian) 0-76396  
 steel, Ni-Cr-Mo-V low-alloy, additive remedy for temper brittleness 0-66659  
 steel, Ni-Mo-C (2.0, 0.2, 0.4 wt.%) sintered, struct. transforms. and mech. props. after quenching 0-66557  
 steel, Ni-Mo-Cr, embrittling effects of residual elements 0-66655  
 steel, stainless, Cr-Ni-Ti, metallographic detection of (Ti,Ni) $_6\text{C}$  0-66721  
 steel, stainless type 316, fusion reactor Li cooling system, corrosion inhibition by Al additions 0-108646  
 STEM microanal. of precipitates and their nuclei 0-81067  
 stress corrosion cracking test machine, design and construction, appl. to Fe-Cr-Ni alloys 0-97649  
 stress relaxation, in-reactor study at low temps. 0-93588  
 superalloy, rapid solidification, use in gas turbine engines 0-84888  
 superalloy, STEM microanalysis of precipitates 0-104492  
 superalloy Nimonic 80A, microstruct. anal. by high-resolution electron microscopy 0-76459

## nickel alloys continued

- superalloys, hot workability, effect of S, Ca, Mg, Y and Zr minor elements 0-66552  
 superalloys, powder metallurgical, creep-rupture at intermediate temps. 0-97568  
 Ag-Cd-Ni, internally oxidised, oxide particle size control (Japanese) 0-89480  
 Ag-Ni (10 wt.%) wire, plastically deformed, fracture struct. (German) 0-71744  
 Ag-Ni supersaturated metastable solid solns. formed by ion beam mixing 0-107425  
 AgNi, dil., mag. susceptibility of isolated Ni atoms 0-65777  
 Al-Al $_3$  eutectic, temp. gradients, microstructural changes 0-84971  
 Al-Al $_3$  eutectic alloy, electrolytic prep. of Al $_3$ Ni fibres, SEM and anodic polarisation studies 0-100817  
 Al-Ni, dil., core and valence band spectra, XPS study 0-84837  
 Al-Ni, rapid quenching, struct. and decomp. 0-76244  
 Al-Ni (3-18wt.%), gun-quenched from melt, struct. 0-76225  
 Al-Ni (6 wt.%), fine-grained, deform. in tension and torsion 0-85008  
 Al-Ni (6 wt.%) misorientation between subgrains, second-phase particles role, STEM microdiff. obs. 0-104415  
 Al-Ni multiphase system, simultaneous diffusion in cylindrical symm. (Russian) 0-100357  
 Al-Ni solid, liquid mixture, diffusion processes (Russian) 0-107563  
 Al-Ni(Cd)(Fe)(Si), cold worked, struct. and props. 0-71666  
 Al-Ni(Pt)(Zn), rapidly solidified, twinned dendrites 0-70572  
 AlCu-NiCo (5 at.%),  $\theta'$  hardened, creep mechanism 0-85013  
 Al $_4$ (Ni, Co) $_3$  ternary phase in Al-Ni-Co system, cryst. struct., vacancy controlled phase (Chinese) 0-70164  
 Al $_3$ Ni, cryst., theoretical morphology and comparison with observed habits (French) 0-79732  
 Al $_2\text{O}_3$ -NiCr composite, plasma sputtering of electroheating coatings, elec. props. (Russian) 0-108350  
 Au-Ni-P, interdiffusion, backscatt. study 0-79991  
 Au-Ge-Ni/GaAs metal-semiconductor thermoelectric coolers, effects of contact resist. and dopant conc. 0-81481  
 Au-Ni, dil., valence and core level spectra, XPS study 0-84838  
 Au-Ni, surface segregation, strain effects 0-80042  
 Au-Ni, UPS study, localised states 0-93449  
 Au $_3\text{Ni}_{55}$ , vapour quenched amorphous alloy, atomic arrangements 0-100173  
 Be-Ni, plastic deform., flow stresses, fracture (Russian) 0-108496  
 BeNi, dil., electronic struct., NMR study 0-108085  
 CC Fe-Ni-Cr (35, 15 wt.%): Nb(Ti)(Mo), corrosion in HTGR He environment 0-61021  
 CaNi $_2$ , Hauke compounds, low temp. heat capacity, Debye temp. 0-96663  
 CeNi $_2$ -CePt, system, structural and mag. studies on valence behaviour of Ce 0-103809  
 CeNi $_3$ , and ternary hydride, mag. props. 0-108007  
 CeNi $_3$ , sorption at press. up to 1500 atm. 0-97819  
 CeNi $_4$ Al, mag. susceptibility, H adsorption-desorption cycle effects 0-107990  
 CeNi $_5$ (Si $_2$ ) $_4$ , X-ray cryst. struct. determ. 0-88089  
 Co-Fe-V-Ni, mag. and mech. props., heat treatment and stress effects 0-60363  
 Co-Mn-Ni-Fe-Si-B amorphous alloys, mag. props., low magnetostriction 0-75832  
 Co-Ni, dendritic segregation 0-76260  
 Co-Ni-Cr-Mo (35, 20, 10 wt.%), MP35N, TEM study of phase transformations 0-81054  
 Co-Ni-Cr-Nb (40, 18, 1.8 wt.%), precipitation behaviour of NbC, effect of ageing temp. on morphology 0-89227  
 Co-Ni-Mo-C, amorphous alloys, med. props. and thermal stability (Japanese) 0-85049  
 Co-Ni-Zn, diagram of state, crystalline lattice consts., microhardness (Russian) 0-66479  
 Co $_5$ Fe $_2$ Ni $_3$ (Si,B) $_2$ , amorphous, soft mag. props., switched-mode power supply appls. 0-88850  
 CoNi, Hall effect, anomalous, residual coeff. calcs. using coherent pot. method (Russian) 0-80249  
 CoNiP, cylindrical amorphous electrodeposited layers, mag. props., torsion influence 0-88848  
 Co $_3$ P $_3$  noncrystalline ferromagnet, electroless deposited, struct. and microscopic mag. props. 0-88063  
 25Cr-20Ni stainless steel dendritic solidification, growth morphology and solute redistrib. (Japanese) 0-81045  
 Cr-Fe-Ni,  $\gamma$ -solid soln., thermodynamic activity determ. at 1500K 0-108397  
 Cr-Fe-Ni alloys, claddings, chemical compatibility with UC nuclear fuels, thermodynamic model 0-63263  
 Cr-Fe-Ni-Si, ternary phase equilibria for Cr-Fe-Ni rich portion, lattice stabilities. 0-71628  
 Cr-Ni compressor disk, surface plastic deform., optimal method 0-60924  
 Cr-Ni-Fe, ternary phase diagrams, interactive computer program 0-71629  
 Cr-Ni-Nb steel, oxidation in CO $_2$ , charged-particle nuclear techniques 0-61022  
 Cr $_2$ C $_2$ /Ni-Cr, self-weldability in high temp Na (Japanese) 0-89392  
 Cr $_2$ C $_2$ /Ni-Cr hardfacing materials, friction characts. in high temp. Na (Japanese) 0-89356  
 Cu/Sn-Ni/Au tricomplex, electrodeposited, interdiffusion obs. 0-84331  
 $\beta$ -Cu-Al-Ni (14, 3 wt.%), single cryst., thermal effect due to stress induced martensite formation 0-81059  
 Cu-Al-Ni (14.1, 3 wt.%), autooscillations and nonlinear anelasticity 0-70307  
 Cu-Al-Ni Marmen alloys, rapid solidification and ageing 0-76245  
 Cu-Ni, adsorption of H $_2$ +CO on (110) surface, TDS and UPS obs. 0-80052  
 Cu-Ni, cast, strength and hot ductility, alloying and residual elements effect 0-66595  
 Cu-Ni, crystallisation temp., overcooling temp. (Russian) 0-97472  
 Cu-Ni, density of states of d-electrons, tight binding approx. calcs. 0-59863  
 Cu-Ni, dil., screening charge density round  $\Delta Z = -1$  impurities, vacancies, NQR study 0-103897  
 Cu-Ni, dil., valence and core level spectra, XPS study 0-84838  
 Cu-Ni, evaporation limited segregation 0-70513  
 Cu-Ni, galvanic corrosion in sulphide modified seawater 0-100953  
 Cu-Ni, liq., surface conc. profile and surface energy 0-84350  
 Cu-Ni, random ferromag. alloy, local mag. moment calc. 0-70974



## nickel alloys continued

- Cu-Ni, rubbing contact with cast Fe, surface temperature effect on dry sliding wear 0-60983  
 Cu-Ni, sintering, Kirkendall effect 0-93518  
 Cu-Ni (10 at.%), creep, substruct. and internal stresses (*Russian*) 0-97527  
 Cu-Ni (10 at.%), hardening, recovery, and struct. changes during high temp. creep (*Russian*) 0-89288  
 Cu-Ni (110), adsorption of CO and H<sub>2</sub>, UPS, thermal desorption, AES, and LEED study 0-80087  
 Cu-Ni (30-90 wt.%), elect. resist. rel. to cold working and heat treatment 0-71765  
 Cu-Ni (4 at.%), anneal hardening mechanism 0-60879  
 Cu-Ni alloy,  $\alpha$ -phase, lattice sp. ht. calcs. 0-65246  
 Cu-Ni alloys, chemical interdiffusion under uniaxial stress 0-65307  
 Cu-Ni films, compositionally modulated, magnetic anisotropy, magnetisation curves 0-88840  
 Cu-Ni thin films, ferromag., Hall effect meas. 0-80428  
 Cu-Ni/Au-Ni multilayer films, ohmic behaviour, use as strain gauge 0-65713  
 Cu-Ni-Al (5, 2.5 at.%), precip. hardening (*Japanese*) 0-71663  
 Cu-Ni-Co, mag. props. of system of disperse ferromag. particles, 73 to 673K (*Russian*) 0-65968  
 Cu-Ni-Fe, magnetic properties, heat treatment and compressive stress effects 0-60367  
 Cu-Ni-Nb (30, 0.9 at.%), precipitate free zones, X-ray microanal. 0-108768  
 Cu-Ni-S, molten, thermodynamic props. 0-104122  
 Cu-Ni-Sn (10, 6 wt.%), spinodal decomposition, X-ray and electron diff. study 0-81063  
 Cu-Ni-Sn (15, 8 wt.%), prior deform. effect on spinodal age hardening 0-108465  
 Cu-Ni-Sn (9, 2 wt.%), surface comp., Auger electron spectroscopy study, manufacture and storage influence 0-65348  
 Cu-Ni-Ti, ordering within precipitates, TEM obs. 0-108461  
 Cu-Ni-Ti system, phase equilibria in Cu rich region and Cu-T quasi-binary constitution (*Japanese*) 0-89203  
 Cu-Ni-Ti system, reactions with melt in Cu-rich region (*Japanese*) 0-89202  
 Cu-Ni-Zn (18, 27 wt.%), surface comp., Auger electron spectroscopy study, manufacture and storage influence 0-75240  
 Cu-Ni-Zn alloy, surface comp., outdoor exposure influence 0-59770  
 Cu-Ni-Zn-Mn fine grained precipitation-hardenable alloy, high strength and ductility 0-100805  
 Cu-Sn alloy, surface comp., outdoor exposure influence 0-59770  
 Cu-Ti-Ni, wetting of Al<sub>2</sub>O<sub>3</sub>, alloying effects 0-107617  
 Cu<sub>2</sub>Au-Ni, antiphase domains morphology 0-108460  
 Cu<sub>2</sub>NiSn, Heusler alloy, elec. resist., 4.2 to 300K 0-75547  
 Cu<sub>2</sub>NiZn, comparison between different theories predicting stacking fault energy from extended nodes 0-75240  
 Cu<sub>2</sub>NiZn, stacking fault energy determ. from extended nodes 0-10780  
 Dy(Co,Ni)<sub>2</sub>, intrinsic mag. aftereffect meas., domain wall motion 0-71121  
 DyNi<sub>3</sub> crystal, basal plane anisotropy, torque meas. 0-65857  
 ErNi<sub>3</sub>, sorption at press. up to 1500 atm. 0-97819  
 (Fe,Co,Ni)<sub>2</sub>(Si,B), amorphous mag. alloy, magnetostriction rel. to soft mag. props. 0-84633  
 Fe-Co-Ni Perminvar, mag. props. singularities in region of mag. anisotropy (*Russian*) 0-84614  
 Fe-Co-Ni-C, activity coeff. of C at 1273K 0-96667  
 Fe-Co-V-Ni, annealing effect on microstruct. rel. to mag. and mech. props. 0-89267  
 Fe-Cr-Ni, corrosion behaviour in hot conc. NaOH soln. (*Japanese*) 0-85082  
 Fe-Cr-Ni, foil, in situ oxidation in HVEM 0-104354  
 Fe-Cr-Ni (12, 15 wt.%) austenitic alloy, Ni<sup>61</sup> irradiated, void swelling and phase stability, Si and Ti effects 0-65055  
 Fe-Cr-Ni (18, 14 wt.%),  $\gamma$  to  $\epsilon$  to  $\alpha$  martensitic transform., external stress effect, double tensile deform. exam. 0-108438  
 Fe-Cr-Ni (19, 13 wt.%), austenitic, Ni<sup>+</sup> ion irradiated, multiple dislocation loops (*French*) 0-65064  
 Fe-Cr-Ni based alloys, surface oxides at high temps., backscattering Raman spectroscopy 0-93291  
 Fe-M, dil., M=transition metal, impurity electronic struct., multiple scatt. approach 0-92856  
 Fe-Mn-Ni-V-C (0.5, 3.0, 1.0, 0.2 wt.%), austenite decomp., isothermal transform. characts. 0-97477  
 Fe-Ni, crystallisation temp., overcooling temp. (*Russian*) 0-97472  
 Fe-Ni, dilute, irradiation softening effect on yield stress 0-76319  
 Fe-Ni, elinvar comp., props. of materials used in electromechanical filter resonators (*Czech*) 0-76318  
 Fe-Ni, grain boundary segregation, X-ray microanal. by STEM 0-66740  
 Fe-Ni, Hall effect, anomalous, residual coeff. calcs. using coherent pot. method (*Russian*) 0-80249  
 Fe-Ni, interference microscopy, for colour development and phase separation 0-100976  
 Fe-Ni, itinerant electron ferromagnet, magnetovolume effects 0-60397  
 Fe-Ni, lenticular martensite growth by transformation wave propag. 0-81055  
 $\gamma$ -Fe-Ni, local magnetisation of Fe atoms, Mossbauer effect meas. 0-75891  
 Fe-Ni, mag. aftereffect meas., phenomenological description 0-88835  
 Fe-Ni, magnetisation calc. method based on moments of density of states 0-65770  
 Fe-Ni, reverse martensitic transform., shape deform. reversibility 0-66506  
 Fe-Ni, secondary recrystallisation singularities (*Russian*) 0-66528  
 Fe-Ni, secondary recrystn. and mag. props. 0-89247  
 Fe-Ni, sintered, porosity determ. by US attenuation and sound vel. meas. (*German*) 0-76437  
 Fe-Ni (25 to 50%), FCC, meteorites and thermodynamic equilb., Mossbauer and X-ray diff. study 0-88087  
 Fe-Ni (28 at.%), martensitic transformations, Mossbauer scattering evidence of soft modes 0-93223  
 $\alpha$ -Fe-Ni (3-12 wt.%), structure and  $\gamma$ - $\alpha$  polymorphic transform. kinetics 0-71645  
 Fe-Ni (32 wt.%), EMF appearance during  $\gamma$ - $\alpha$  transform. (*Russian*) 0-89215  
 Fe-Ni (32.3 at.%), mag. struct. in commensurable approx., neutron diff. study 0-60212

## nickel alloys continued

- Fe-Ni (33-38 at.%), low-angle neutron diff., anomalous crit. scatt. (*Russian*) 0-60193  
 Fe-Ni (4 wt.%), extrinsic grain boundary dislocations, low C content influence 0-107273  
 Fe-Ni (50 wt.%), surface comp. and oxide film thickness after various surface treatments, AES study 0-66693  
 Fe-Ni (6-8 wt.%), solution of <sup>119</sup>Sn, study by Mossbauer spectroscopy 0-75888  
 Fe-Ni alloy, martensitic transform., influence of thermal and electron irradi. treatment of austenite (*Russian*) 0-66509  
 Fe-Ni alloy type YuNDK25B, anomalous magnetocaloric effect 0-60278  
 Fe-Ni alloys, heat treatment variations effect on surface conditions and on Hg wetted switch behaviour 0-66547  
 Fe-Ni based metallic glass, Metglas 2826 MB, Mossbauer study 0-75897  
 Fe-Ni film, amorphous, martensite form. time and struct. 0-104159  
 Fe-Ni films, on glass substrate, thermolec. effect 0-107769  
 Fe-Ni fluorination kinetics and fluoride film form., chem. nature obs. 0-101035  
 Fe-Ni Metglas type, ohmic and Hall resist., 100-700K, mag. behaviour obs. 0-80254  
 Fe-Ni-Al-Co-Cu-Ti YuNDK type, S effect on mech. props. 0-60927  
 Fe-Ni-Al-(Cu) (12, 0.5, 0.5 to 3 wt.%), Cu addition strengthening at 77K, mech. props. 0-60875  
 Fe-Ni-B glassy ribbons melt spinning, gas boundary layer effects 0-76217  
 Fe-Ni-B metallic glass, X-ray diff. meas., semi-empirical struct. model 0-107059  
 Fe-Ni-B-Mo, crystn. temp. and elec. cond. correl., Mo effect 0-75179  
 Fe-Ni-B-Si, amorphous, mag. props., heat treatment effects 0-89370  
 Fe-Ni-B-(P), ferromag., magneto-optical spectra in amorphous and cryst. states (*Russian*) 0-84749  
 Fe-Ni-C, intercrystalline embrittlement in tempered martensite, elimination by reautenitization (*Slovak*) 0-108548  
 Fe-Ni-C, quenched martensite, annealing during cathodic hydrogenation, 200°C (*French*) 0-93573  
 Fe-Ni-C (25, 0.2 wt.%), strain-induced martensite (*Korean*) 0-71646  
 Fe-Ni-C (30, 0.5 wt.%) single cryst., stress induced martensitic transform. 0-60860  
 Fe-Ni-C (31.9, 0.02 wt.%) alloy, hardness of martensite-austenite mixtures 0-60959  
 Fe-Ni-C (31.9, 0.02 wt.%), determ. of number and size distrib. of martensitic plates 0-76255  
 Fe-Ni-C alloy with single-component martensite texture,  $\alpha$ - $\gamma$  transform., changes in shape (*Russian*) 0-104152  
 Fe-Ni-C austenitic alloy, banded struct. formed by deform. 0-71713  
 Fe-Ni-C martensite morphology, butterfly-lenticular transition temp., Cr addition effect (*Japanese*) 0-81053  
 Fe-Ni-Co-Cu-Ti YuNDK alloys, impaired mag. props. with C and S additions 0-60368  
 Fe-Ni-Co-Ti, coherent particles effect inherited by martensite on  $\alpha$ - $\gamma$  transformation (*Russian*) 0-108443  
 Fe-Ni-Co-W(Mo) (18.65, 8.99, 4.87 wt.%), ageing characts., 380-530°C 0-60876  
 Fe-Ni-Cr, carbide form. by C diffusion, precip. distrib. and morphology 0-104164  
 Fe-Ni-Cr, heavy ion irradi., defect cluster obs. 0-107341  
 Fe-Ni-Cr, mag. props. in weak mag. fields (*Russian*) 0-75771  
 Fe-Ni-Cr (30.6, 21.3 wt.%), Alloy 800, high temp. oxidation at low O<sub>2</sub> press., SEM, AES and electron probe microanal. study 0-93688  
 Fe-Ni-Cr (35, 15 wt.%) superalloy, stress rupture and tensile props., C and B additions effect (*Chinese*) 0-104244  
 Fe-Ni-Cr (44, 17 wt.%), nuclear microprobe methods for investigating oxidative corrosion 0-71787  
 Fe-Ni-Cr based alloy, KHN35VTy, temp. depend. of energy of fracture, influence of  $\gamma$  phase (*Russian*) 0-81147  
 Fe-Ni-Cr-Al-Ti-W-Mo (35, 15, 2.4, 2.3, 2.2 wt.%) wrought superalloy, freckles (*Chinese*) 0-104137  
 Fe-Ni-Cr-Al-Y, oxidation mechanism, Y addition effect on kinetics and oxide adherence 0-97623  
 Fe-Ni-Cr-Ti-Al, with thermoelastic control coeff., comp. and heat treatment influence on props. (*French*) 0-81074  
 Fe-Ni-Cr-Y, Y addition effect on selective oxidation/diffusion phenomena relationship (*French*) 0-108623  
 Fe-Ni-Mn (20, 5 wt.%), rel. orientation between adjacent martensite laths 0-76254  
 $\gamma$ -Fe-Ni-Mn alloys, spin glass state, short and long range order investigation 0-65808  
 Fe-Ni-Mo, martensitic transformation, annealing, influence on struct. of austenite (*Russian*) 0-81057  
 Fe-Ni-Mo, phase relations in system at 1100°C 0-108392  
 Fe-Ni-Mo-C, amorphous alloys, med. props. and thermal stability (*Japanese*) 0-85049  
 Fe-Ni-Mo(Si), austenite, annealing effect on atom redistrib., Mossbauer anal. (*Russian*) 0-66529  
 Fe-Ni-P-B, amorphous, crystn. and struct. 0-75175  
 Fe-Ni-P-B, metallic glasses, struct. relax., annealing effects on mag. props. 0-89261  
 Fe-Ni-P-B amorphous ribbons, form. by melt spin technique 0-76215  
 Fe-Ni-P-B metallic glass, crystallisation temperature values from isothermal transformation times 0-59397  
 Fe-Ni-Ti, preaged martensite, shear strain magnitude, X-ray diff. method 0-93592  
 Fe-Ni-Ti-(Cu) (12, 0.25, 2 wt.%), Cu addition strengthening at 77K, mech. props. 0-60875  
 Fe-Ni-V-(Cu) (12, 2, 2 wt.%), Cu addition strengthening at 77K, mech. props. 0-60875  
 Fe-Ni-(Cu) (12, 0.5 to 3 wt.%), Cu addition strengthening at 77K, mech. props. 0-60875  
 Fe-Ni-(P), phase diagram determ., 700 to 300°C 0-108399  
 Fe-Sb-Ni, dil., short range order, NMR study 0-71237  
 Fe-Sb-Ni, interactions and segregations, Mossbauer and X-ray diff. study 0-70415  
 (Fe,Ni-Mo)<sub>80</sub>(P-B)<sub>20</sub>, amorphous, mag. aftereffects and struct. instabilities 0-88833  
 Fe<sub>36</sub>Cr<sub>32</sub>Ni<sub>14</sub>B<sub>12</sub>B<sub>6</sub>, amorphous X-ray absorpt. spectra, effective co-ordination charges 0-84805  
 FeNi amorphous films, fast phase transition investigation by TEM method 0-107029  
 (Fe<sub>0.6</sub>Ni<sub>0.4</sub>)<sub>100-x</sub>B<sub>x</sub> and (Fe<sub>100-x</sub>Ni<sub>x</sub>)<sub>80</sub>B<sub>20</sub> amorphous alloys, X-ray diff. struct. determ. 0-64906



## nickel alloys continued

- (Fe<sub>1-x</sub>Ni<sub>x</sub>)<sub>83</sub>B<sub>17</sub>, amorphous alloys ferromagnetic resonance 0-108080  
 (Fe<sub>100-x</sub>Ni<sub>x</sub>)<sub>83</sub>B<sub>17</sub>, amorphous, crystn. 0-75176  
 Fe<sub>40</sub>Ni<sub>60</sub>B<sub>20</sub>, amorphous, phase transforms, resistometric anal. 0-75538  
 Fe<sub>40</sub>Ni<sub>60</sub>B<sub>20</sub>, amorphous, RF annealing effects 0-108037  
 Fe<sub>40</sub>Ni<sub>60</sub>B<sub>20</sub>, amorphous ribbon, power loss variation with freq. and applied stress 0-88849  
 Fe<sub>40</sub>Ni<sub>60</sub>B<sub>20</sub> and Fe<sub>40</sub>Ni<sub>60</sub>P<sub>10</sub>B<sub>10</sub>, amorphous, mag. aftereffect spectra and annealing props. 0-88831  
 Fe<sub>80-x</sub>Ni<sub>x</sub>B<sub>20</sub> and Fe<sub>80-x</sub>Ni<sub>x</sub>P<sub>14</sub>B<sub>6</sub>, amorphous alloys, microhardness correl. with mag. props. 0-88826  
 Fe<sub>2</sub>Ni<sub>80-x</sub>B<sub>20</sub> and Fe<sub>2</sub>Ni<sub>80-x</sub>P<sub>14</sub>B<sub>6</sub>, metallic glasses, low temp. resist. and galvanomag. effects, mag. state influence 0-84461  
 Fe<sub>2</sub>Ni<sub>80-x</sub>B<sub>20</sub> glass, resist., magnetoresist., and thermoelec. power 0-70681  
 (Fe<sub>1-x</sub>Ni<sub>x</sub>)<sub>0.8</sub>Al<sub>0.2-x</sub>P<sub>x</sub>, amorphous, hyperfine fields and local mag. moments, Mossbauer study 0-75895  
 Fe<sub>1.6</sub>Ni<sub>78.4</sub>B<sub>10</sub>P<sub>10</sub>, metallic glass, superparamag. behaviour, chem. inhomogeneities role 0-84625  
 Fe<sub>40</sub>Ni<sub>60</sub>B<sub>20-x</sub>P<sub>x</sub>, amorphous, mag. saturation, spin wave stiffness, temp. depend. 0-75741  
 Fe<sub>40</sub>Ni<sub>60</sub>B<sub>20-x</sub>P<sub>x</sub>, metallic glasses, local struct. and dynamic disorder of Fe and Ni, EXAFS obs. 0-89088  
 Fe<sub>80-x</sub>Ni<sub>x</sub>B<sub>20-x</sub>P<sub>x</sub>, amorphous, Rayleigh region and coercive force 0-88806  
 (FeNi)<sub>80</sub>B<sub>17.5</sub>Al<sub>2</sub>Si<sub>0.5</sub>, stress-induced variation in magnetisation and dynamic magnetostrictive charact. 0-88855  
 Fe<sub>31</sub>Ni<sub>36</sub>Cr<sub>14</sub>P<sub>19</sub>B<sub>6</sub>, metallic glass, Doppler broadening of positron annihilation  $\gamma$ -radiation and elec. resist. 0-66321  
 Fe<sub>32</sub>Ni<sub>36</sub>Cr<sub>14</sub>P<sub>19</sub>B<sub>6</sub>, metallic glass, crystn. kinetics by TEM 0-75186  
 Fe<sub>32</sub>Ni<sub>36</sub>Cr<sub>14</sub>P<sub>19</sub>B<sub>6</sub>, Metglas 2826A, EPR at 20 GHz 0-75848  
 Fe<sub>32</sub>Ni<sub>36</sub>Cr<sub>14</sub>P<sub>19</sub>B<sub>6</sub>, Metglas, bending deform., shear band form., high-speed cinematographic obs. 0-89322  
 Fe<sub>32</sub>Ni<sub>36</sub>Cr<sub>14</sub>P<sub>19</sub>B<sub>6</sub>, Metglas amorphous films, corrosion resist. and ion plating use 0-89423  
 Fe<sub>32</sub>Ni<sub>36</sub>Cr<sub>14</sub>P<sub>19</sub>B<sub>6</sub>, metallic glass, effect of pre-ageing on glass transition temp. 0-100326  
 Fe<sub>65</sub>Ni<sub>28</sub>Mn<sub>1</sub>, disordered, mag. struct. near ferro-antiferromagnetic transition 0-60211  
 Fe<sub>40</sub>Ni<sub>40</sub>(Mo,Si,B)<sub>20</sub>, amorphous, soft mag. props., switched-mode power supply appls. 0-88850  
 Fe<sub>40</sub>Ni<sub>38</sub>Mo<sub>4</sub>B<sub>18</sub>, amorphous ribbons, magnetoelastic effects in as-quenched and stress-relieved states 0-80588  
 Fe<sub>40</sub>Ni<sub>38</sub>Mo<sub>4</sub>B<sub>18</sub>, amorphous, mag. anisotropy, Mossbauer study 0-65864  
 Fe<sub>40</sub>Ni<sub>38</sub>Mo<sub>4</sub>B<sub>18</sub>, amorphous, reversible enhancement of mag. directional ordering rate 0-103829  
 (Fe<sub>1-x</sub>Ni<sub>x</sub>)<sub>80</sub>P<sub>20</sub>, amorphous, ferromagnetic alloys, mag. anomalies of Invar type (Russian) 0-93089  
 (FeNi)PB amorphous wires, surface oxidation and annealing influence on induced anisotropy 0-100957  
 Fe<sub>40</sub>Ni<sub>40</sub>P<sub>14</sub>B<sub>6</sub>, amorphous, resistometric study of short-range ordering rel. to heat treatment 0-70140  
 Fe<sub>40</sub>Ni<sub>40</sub>P<sub>14</sub>B<sub>6</sub>, amorphous ferromagnet, Mossbauer hyperfine fields, mag. struct. 0-75894  
 Fe<sub>40</sub>Ni<sub>40</sub>P<sub>14</sub>B<sub>6</sub>, amorphous alloy, temper embrittlement 0-76295  
 Fe<sub>40</sub>Ni<sub>40</sub>P<sub>14</sub>B<sub>6</sub>, amorphous, mag. polarisation in approach to ferromag. saturation 0-80560  
 Fe<sub>40</sub>Ni<sub>40</sub>P<sub>14</sub>B<sub>6</sub>, amorphous, steady-state creep rate, cryst. effect 0-81102  
 Fe<sub>40</sub>Ni<sub>40</sub>P<sub>14</sub>B<sub>6</sub>, amorphous, mag. permeability aftereffect during annealing 0-88834  
 Fe<sub>40</sub>Ni<sub>40</sub>P<sub>14</sub>B<sub>6</sub>, amorphous ferromag., spin wave excitations 0-97079  
 Fe<sub>40</sub>Ni<sub>40</sub>P<sub>14</sub>B<sub>6</sub>, amorphous ribbon, mag. domains and anisotropy distrib. 0-108029  
 Fe<sub>40</sub>Ni<sub>40</sub>P<sub>14</sub>B<sub>6</sub>, glass, viscosity near T<sub>g</sub>, using rapid heating, and fusion characts. 0-70438  
 Fe<sub>40</sub>Ni<sub>40</sub>P<sub>14</sub>B<sub>6</sub>, metallic glass, crystn. 0-70127  
 Fe<sub>40</sub>Ni<sub>40</sub>P<sub>14</sub>B<sub>6</sub>, metallic glass, glass transition, viscous flow and differential scanning calorimetry meas. 0-96635  
 Fe<sub>40</sub>Ni<sub>40</sub>P<sub>14</sub>B<sub>6</sub>, metallic glass, bending tests, evidence of ideal elastic-plastic deform. 0-97543  
 Fe<sub>40</sub>Ni<sub>40</sub>P<sub>14</sub>B<sub>6</sub>, Metglas 2826, hot forming 0-84980  
 Fe<sub>40</sub>Ni<sub>40</sub>P<sub>14</sub>B<sub>6</sub>, Metglas 2826, amorphous ribbon under tension, mag. domain walls and pulsed magnetisation reversal 0-88825  
 (Fe<sub>1-x</sub>Ni<sub>x</sub>)<sub>80</sub>P<sub>10</sub>B<sub>10</sub>, amorphous, magnetisation reversal and domain boundary configs. 0-88809  
 Fe<sub>2</sub>Ni<sub>80-x</sub>P<sub>14</sub>B<sub>6</sub> glass, resist., magnetoresist., and thermoelec. power 0-70681  
 Fe<sub>2</sub>Ni<sub>80-x</sub>P<sub>14</sub>B<sub>6</sub>, metallic glass, low temp. sp. ht. for spin-glass and spin-cluster-glass regime 0-71071  
 (Fe<sub>1-x</sub>Ni<sub>x</sub>)<sub>70</sub>P<sub>13</sub>B<sub>8</sub>, metallic glass, low temp. sp. ht. for spin-glass and spin-cluster-glass regime 0-71071  
 (Fe<sub>65</sub>Ni<sub>35</sub>)<sub>75</sub>P<sub>16</sub>B<sub>9</sub>Al<sub>1</sub>, amorphous, crystn. temp., press. and heating rate depend. 0-70132  
 (Fe<sub>1-x</sub>Ni<sub>x</sub>)<sub>77</sub>Si<sub>10</sub>B<sub>13</sub>, amorphous, Landau-Ginzburg theory, magnetisation and Curie temp. 0-75700  
 (Fe<sub>1-x</sub>Ni<sub>x</sub>)<sub>78</sub>Si<sub>10</sub>B<sub>12</sub>, amorphous alloys, cold rolled and as-quenched, mag. anisotropy 0-97089  
 Gd-Ni, amorphous, mag. and elec. props. 0-80499  
 Gd-Ni, amorphous, mag. props. and ferromag. reson. 0-75862  
 Gd-Ni, ferromag., elec. resist. temp. depend. 0-96843  
 Gd(Co<sub>1-x</sub>Ni<sub>x</sub>)<sub>2</sub>, compounds, NMR and thermal expansion 0-66070  
 GdCo<sub>2</sub>Ni<sub>1-x</sub>, intrinsic coercivity, anisotropy, exchange and cryst. field interactions 0-75806  
 Gd<sub>1-x</sub>Dy<sub>x</sub>Ni, FeB-CrB type stacking variations, cryst. struct. 0-64952  
 GdNi, single cryst., magnetocrystn. anisotropy 0-88746  
 GdNi<sub>x</sub>, (x=3, 3.5, 8.5), ferrimag., mag. reson. above and below Curie temp. 0-97148  
 Gd<sub>2</sub>Ni<sub>17-x</sub>Al<sub>x</sub>, EPR of Gd<sup>3+</sup> ions 0-97139  
 Gd<sub>1-x</sub>Y<sub>x</sub>Ni, FeB-CrB type stacking variations, cryst. struct. 0-64952  
 HoCo<sub>5-x</sub>Ni<sub>x</sub>, cryst. struct. and mag. props. 0-75800  
 La(Co<sub>1-x</sub>Ni<sub>x</sub>)<sub>3</sub>, distrib. of Co and Ni atoms, neutron diff. obs. (Russian) 0-64954  
 La<sub>0.9</sub>Eu<sub>0.1</sub>Ni<sub>4.6</sub>Mn<sub>0.4</sub>, absorption-desorption props. of H<sub>2</sub>, degradation mechanism, Mossbauer study 0-88431  
 LaNi<sub>5</sub>, H<sub>2</sub> absorpt. kinetics (Chinese) 0-103561  
 LaNi<sub>5</sub>, H<sub>2</sub> absorption in thin film hydriding alloys 0-65238  
 LaNi<sub>5</sub>, Haucke compounds, low temp. heat capacity, Debye temp. 0-96663  
 LaNi<sub>5</sub> hydrides, 4.2K paramag. susceptibility 0-70934  
 LaNi<sub>5</sub>, magnetism and H<sub>2</sub> storage 0-70941  
 LaNi<sub>5</sub>/H system, thermodynamics of H trapping 0-107444

## nickel alloys continued

- LaNi<sub>5</sub>, sorption at press. up to 1500 atm. 0-97819  
 LaNi<sub>4</sub>Al, solubility and sorption props. of H<sub>2</sub>, effect of Al 0-103482  
 LaNi<sub>5-x</sub>Al<sub>x</sub>, use in hydride conversion and storage system chemical heat pump 0-72077  
 LaNi<sub>4.6</sub>B<sub>0.6</sub>, H<sub>2</sub> absorpt. props. 0-88432  
 LaNi<sub>4</sub>Fe, H<sub>2</sub> absorpt. cracking, acoustic emission characts. (Japanese) 0-66631  
 LaNi<sub>4</sub>H<sub>6</sub>, solar energy storage by metal hydride 0-61455  
 Mg-MgNi<sub>2</sub>-Zn, diagram of state, Zn solubility, initial phase precipitation (Russian) 0-66478  
 MgNi<sub>2</sub>, four-layer, Friauf-Laves phases, stacking variants 0-96468  
 Mg<sub>2</sub>Ni, magnetism and H<sub>2</sub> storage 0-70941  
 Mg<sub>2</sub>NiH<sub>4</sub>, solar energy storage by metal hydride 0-61455  
 Mn-Ni, thermal expansion, mag. susceptibility, lattice consts. 0-100341  
 Nb-Ni, amorphous, thermal stability, crystn., DSC and elec. resist. study 0-107060  
 Nb-Ni amorphous alloys, glass transition and ductility, O additions effect 0-75168  
 Nb<sub>40</sub>Ni<sub>60</sub>, amorphous, produced by Ni<sup>+</sup> implantation, damage distrib. 0-107062  
 Ni alloy, precipitation strengthened compositions with oxide particles, condensed, struct. criteria and thin layer possibilities (Russian) 0-89236  
 Ni alloys, aluminising, thermodynamic anal. of phase transforms. 0-76413  
 Ni based Rene 80 superalloy, initial stages of pack aluminisation 0-76188  
 Ni-(Co)-Cr, aluminide coating, microstruct. and chem. 0-76189  
 Ni-Al, (2 and 6 wt.%), oxidation,  $\alpha$ -Al<sub>2</sub>O<sub>3</sub> growth, microstruct., precip. 0-108626  
 Ni-Al, order hardening, comparison between revised theory and expt. 0-93565  
 Ni-Al, solid soln., rheological study of crystallographic order on creep (French) 0-97548  
 Ni-Al (12.8 at.%) foil, ion irradi., surface effects on precip. morphology 0-104168  
 $\gamma$ -Ni-Al system, solid soln., interdiffusion (Japanese) 0-70476  
 Ni-Al-Cr<sub>2</sub>Cr<sub>3</sub>, eutectic alloy, directionally solidified, oxidation resistance, influence of Y 0-89409  
 Ni-Al-Mo (12.7, 21.6 wt.%), directionally solidified eutectic composite, precipitation 0-108454  
 Ni-Al-Nb ternary system, electron microprobe analysis of nickel-rich region at 1473K 0-71631  
 Ni-Al-Ta dendritic monocrystals, directionally solidified, coarsening kinetics 0-108425  
 Ni-Al-(Si), diffusion, lattice parameter, microhardness, and constitution, effect of Si additions (Russian) 0-84316  
 Ni-Al(Pd)(Cu) itinerant electron ferromagnet, magnetovolume effects 0-60397  
 Ni-B, film crystallisation on C fibres and sapphire crystals (Russian) 0-75455  
 Ni-B, grain boundary internal friction, B solid solubility as function of grain size 0-60903  
 Ni-B electroless-plated amorphous films, anomalous mag. temp. characts. 0-96757  
 Ni-B thin film glasses, mag. props. and corrosion resist. 0-80576  
 Ni-base superalloys, emission spectral anal. with fixed time integration technique (Japanese) 0-71974  
 Ni-base superalloys, technique for replication of  $\gamma$  0-79648  
 Ni-based TaC eutectic, directionally solidified, elastic moduli 0-84984  
 Ni-Co, dil., optical absorpt., electronic struct. 0-108227  
 Ni-Co, high-field susceptibility, spin-wave spectrum, CPA calc. 0-65818  
 Ni-Co (25 wt.%), single crystals, mag. annealing effect on magnetostriction and magnetisation at high temps. 0-108047  
 Ni-Co-Al alloys, continuous precip., SEM, TEM, X-ray diff. study 0-89220  
 Ni-Co-C solid solution, C precipitation, Ni<sub>3</sub>Co ordering, Ni-Co lattice parameter meas. (Czech) 0-60867  
 Ni-Co-Cr TEM foils, white band contrast 0-75134  
 Ni-Co-Cr/Al<sub>2</sub>O<sub>3</sub> catalyst, IR spectra of adsorption and interaction with pyridine 0-71946  
 Ni-Co-Cr-Mo-Al-Ti (17.5, 15.1, 4.9, 4.15, 3.25 wt.%), creep and stress rupture behaviour in air and vacuum 0-60918  
 Ni-Co-Mo, phase relations in system at 1100°C 0-108392  
 Ni-Co-W, electrodeposition, surface morphology and cryst. struct. 0-71602  
 Ni-containing alloys, hot workability after reheating using S-containing fuel 0-108483  
 Ni-Cr, (30 wt.%), collective dislocation movements, in situ study 0-100243  
 Ni-Cr, anodic dissoln. in NaCl solns. at high current densities (Russian) 0-76396  
 Ni-Cr, degradation after exposure to 1% H<sub>2</sub>S/H<sub>2</sub> gas mixture at 1000°C 0-89408  
 Ni-Cr, heat-resist., high-temp. ductility and embrittlement 0-76314  
 Ni-Cr, heavy ion irradi., defect cluster obs. 0-107341  
 Ni-Cr, high temp. thermomech. treatment effect on tensile diagrams of KhN77YuR (Russian) 0-60884  
 Ni-Cr, low short-term creep resist. at 700°C 0-76313  
 Ni-Cr, partial dislocation, stacking fault TEM study (Chinese) 0-84174  
 Ni-Cr, self-weldability in high temp Na (Japanese) 0-89392  
 Ni-Cr (33 at.%), plastic deformation, HVEM study (French) 0-66605  
 Ni-Cr (70 wt.%), oxidation behaviour, 1073-1473K 0-89416  
 Ni-Cr alloy KhN70MVYu wire, recrystn., optimum heat treatment 0-76278  
 Ni-Cr alloys, creep crack growth, environmental sensitivity 0-85030  
 Ni-Cr austenitic alloy, oxidation mechanism, intergranular diffusion effect (French) 0-81229  
 Ni-Cr films implanted with N ions, electric properties (Russian) 0-107927  
 Ni-Cr Nimonic alloys, mech. props., high-temp. irradi. effects 0-100885  
 Ni-Cr superalloy, interactions between creep and low cycle fatigue (Chinese) 0-66572  
 Ni-Cr/Al<sub>2</sub>O<sub>3</sub> films, interdiffusion processes and oxidation phenomena 0-59735  
 Ni-Cr-Al (20, 4 wt.%), tensile stress effect on high temp. oxidation (Japanese) 0-89393  
 Ni-Cr-Al sintered alloy, hot vac. pressure, fracture and mech. characts. 0-66667  
 Ni-Cr-Al<sub>2</sub>O<sub>3</sub> powder targets for plasma-ion spray deposition of resistance films 0-84897



## nickel alloys continued

- Ni-Cr-Al-TaC, eutectic composite, microstructure, fatigue props. 0-85038  
 Ni-Cr-Al-Ti, stress corrosion cracking, factors influencing susceptibility 0-97617  
 Ni-Cr-Co based alloy, IN-738 turbine blades, hot isostatically pressed investment castings, effect of heat treatment on grain boundary struct. 0-89270  
 Ni-Cr-Co superalloy, combined TEM, FIM, atom probe microanalysis of precipitates and carbide phase comp. 0-100844  
 Ni-Cr-Co-Al super alloy, IN-738, creep failure criteria 0-65150  
 Ni-Cr-Co-Al-W-Mo-Ti-Ta, heat resist. and struct., Ta effect 0-76312  
 Ni-Cr-Co-Ti-Mo-W-Al (14, 9.8, 5, 4, 3.9, 3 wt.%), low cycle fatigue, prior heat treatment effect 0-60962  
 Ni-Cr-Fe, radiation enhanced precip. and dissolution of precipitates, point defect kinetics and dislocation obs. 0-108467  
 Ni-Cr-Fe, stress corrosion cracking, factors influencing susceptibility 0-97617  
 Ni-Cr-Mo-W-Al-Ti, heat-resist., phase comp. 0-76250  
 Ni-Cr-NbC eutectic composite, unidirectional solidification, thermal cycling, temp. range effect on microstructural degradation 0-89272  
 Ni-Cr-P, amorphous, corrosion behaviour, immersion tests and electrochem. meas. (Japanese) 0-85085  
 Ni-Cr-Ta system, phase equilib. of Ni rich region at 1523 and 1273K 0-93541  
 Ni-Cr-Ta-Ti-Si, EP557 precipitation hardening alloy, mech. props., heat treatment effect 0-60877  
 Ni-Cr-Ti rapidly solidified superalloys, surface segregation 0-76263  
 Ni-Cr-W, oxidation behaviour in air at 1000-1250°C 0-89407  
 Ni-Cr-W-Co granules type ZHS6U, EP741, hot hydrostatic pressing 0-60796  
 Ni-Cr-W-Co-Ti, thermal fatigue, effects of inclusions 0-81183  
 Ni-Cr-W-Co-(Al)(Ti)(Mo), high-temp. sulphide corrosion 0-76408  
 Ni-Cr-W-Mo-Ti-Al, heat-resist., recovery and recryst. 0-76268  
 Ni-Cr-Zr, degradation after exposure to 1% H<sub>2</sub>S/H<sub>2</sub> gas mixture at 1000°C 0-89408  
 Ni-Cr(Fe)(Cu) alloy, matrix effect in SIMS anal. using O<sub>2</sub><sup>+</sup> primary beam 0-76576  
 Ni-Cu, electron-irrad., neutron-scatt. studies 0-75268  
 Ni-Cu, ferromag., mag. moment, local environment effects, HF CPA cluster calc. 0-65817  
 Ni-Cu, high-field susceptibility, spin-wave spectrum, CPA calc. 0-65818  
 Ni-Cu, implantation damaged, crit. behaviour, perturbed ang. distrib. meas. anal. 0-60476  
 Ni-Cu, magnetoresistivity anisotropy, spin mixing 0-88538  
 Ni-Cu, surface segregation, computerised atom-probe FIM study 0-75412  
 Ni-Cu-H systems, Curie temp. during phase transitions under high press. H<sub>2</sub> 0-71029  
 Ni-Cu-X (X=Sn, Nb, Ti), spinodal decomp. alloys, linear expansion coeff. influence on morphological anisotropy (Japanese) 0-70431  
 Ni-Cu(Zn)(Ga)(Ge)(As)(Se)(Br)(Kr), dil., ferromagnetic, hyperfine field and relax. time obs. of impurity heavy nuclei 0-75533  
 Ni-Fe, adsorption of O<sub>2</sub>, oxidation 0-108730  
 Ni-Fe, dil., hyperfine mag. fields, press. effect, Mossbauer meas. 0-71277  
 Ni-Fe, dil., optical absorpt., electronic struct. 0-108227  
 Ni-Fe, electronic struct. calc., effects of chemisorption; contact pot. and surface magnetisation 0-103734  
 Ni-Fe, high-field susceptibility, spin-wave spectrum, CPA calc. 0-65818  
 Ni-Fe, orientation aftereffect 0-88830  
 Ni-Fe, power losses at extremely low freqs. 0-88815  
 Ni-Fe, soft mag. props. rel. to metallurgical aspects 0-88810  
 Ni-Fe, thermal fluctuation aftereffect meas. by pulse field method 0-88837  
 Ni-Fe (19 wt.%), mag. anisotropy induced by cold rolling (Russian) 0-84595  
 Ni-Fe (36 to 50 wt.%), initial permeability, domain struct. model 0-88811  
 Ni-Fe based metallic glasses, Curie pt. anomalies 0-60256  
 Ni-Fe film, thermally activated domain wall motion 0-88777  
 Ni-Fe films, energy change of Bloch wall with angle to easy axis, calc. (Slovak) 0-103863  
 Ni-Fe-Co-Ti, electron microscopy and mag. meas. 0-71097  
 Ni-Fe-Cr superalloy type 718, heat treatment effect on room temp. and elevated temp. fracture toughness response 0-100922  
 Ni-Fe-Cr-Mo-Ti-Al, PE 16, thermally activated domain wall motion 0-88777  
 Ni-Fe-H and Ni-Co-H, hydride formation in high press. range 0-65235  
 Ni-Fe-Nb-Al (11.2, 8.09, 79.66 wt.%), modulated struct. growth process rel. to ageing (Chinese) 0-66541  
 Ni-Fe-Nb-Mo-Al, head material for mag. recording, DC and AC mag. props. 0-88812  
 Ni-Ge, amorphous, atomic struct., neutron diff. study 0-59392  
 Ni-Ge binary system, phase diagram rel. to that of Co-Ge (French) 0-97463  
 Ni-Ge-Au evaporated contacts on GaAs, TEM obs. 0-75449  
 Ni-H, ferromag., H impurities and GMR, self-consistent calc. 0-84447  
 Ni-H system, energy and electron density of states, improvements to theory 0-70636  
 Ni-In, implantation damaged, crit. behaviour, perturbed ang. distrib. meas. anal. 0-60476  
 Ni-Mn, dil., mag. moment distrib. and environmental effects, neutron scatt. obs. 0-60247  
 Ni-Mn, ordered and disordered, press. effect on Curie temp. 0-71148  
 Ni-Mn, permeability, diffusion and solubility of H 0-107573  
 Ni-Mn (10-40 wt.%),  $\gamma$  solid soln., interdiffusion 0-100366  
 Ni-Mn (17-27 at.%), low-angle neutron diff., anomalous crit. scatt. (Russian) 0-60193  
 Ni-Mn alloys, ferromagnetism-to-spin glass phase transition and strong mag. field effect 0-75773  
 Ni-Mn-H solid solutions, mag. props. 0-88753  
 Ni-Mo-B metallic glass ribbons, tensile strength, crystn. temp. 0-89173  
 Ni-Mo-W, diagram of state, W solubility, dispersion hardening (Russian) 0-66477  
 Ni-Nb-C, obtained by liq. quenching, superconductivity 0-75699  
 Ni-NbC (10 wt.%) eutectic alloy, directional solidification and struct. (Russian) 0-84922  
 Ni-Ni<sub>3</sub>B eutectic, high temp. X-ray anal. 0-71639  
 Ni-P, amorphous, low P, struct. study using high-angle X-ray diff. 0-107055  
 Ni-P, amorphous, prod. by ion implantation 0-75257

## nickel alloys continued

- Ni-P, electrodeposited film, thermal anal., occlusion of gases rel. to mag. props. 0-59823  
 Ni-P amorphous alloys, electrodeposited and melt-quenched atomic and electronic structures 0-88062  
 Ni-Pd, high mag. field effects, mag. isotherms near Curie point, exchange splitting energies 0-60272  
 Ni-Pd, mag. moment distrib., one-mag.-species model calc. 0-65788  
 Ni-Pd-Mn ternary alloys, mag. characts., use for thermocouple 0-107995  
 Ni-Pt alloys, magnetic-moment distrib. neutron study 0-97066  
 Ni-Pt-P, metallic glass, electronic structure, pulsed NMR study 0-75869  
 Ni-refractory metal/Si interactions, phase separation 0-65303  
 Ni-Rh, mag. moment distrib., one-mag.-species model calc. 0-65788  
 Ni-Ru ( $\leq 4$  at.%), influence of alloying on mag. anisotropy 0-71010  
 Ni-S, electrodeposited film, thermal anal., occlusion of gases rel. to mag. props. 0-59823  
 Ni-S, phase diagram calc. and thermodynamic props. of liq. phase 0-108401  
 Ni-S solid solns., residual elec. resist. (Russian) 0-70465  
 Ni-Si, magnetoresistivity anisotropy, spin mixing 0-88538  
 Ni-Si (12.7 at.%) foil, ion irrad., surface effects on precip. morphology 0-104168  
 Ni-Si melt refining by electric fields, ionic conduction of Ni, Si (Russian) 0-65273  
 Ni-Si-B, amorphous, thermal stability of ductility 0-76327  
 Ni-Sn intermetallic phase growth kinetics at liq. Sn-solid Ni interface 0-71638  
 Ni-Ta (70, 30 wt.%) metallic glass, struct. and crystn. (Russian) 0-70136  
 Ni-Th (1 at.%), surface comp., temp. and O<sub>2</sub> exposure effects, AES study 0-80914  
 Ni-Ti, dil., optical absorpt., electronic struct. 0-108227  
 Ni-Ti, heavily doped, linear expansion meas. 0-103501  
 Ni-Ti (12 wt.%), early stages of transformation 0-76251  
 Ni-Ti/Cu composite, plastic deform. influence on internal friction (Russian) 0-100871  
 Ni-Ti-Al superalloy, pendant drop melt extracted, struct. and props. 0-76242  
 Ni-Ti-P, amorphous, corrosion behaviour, immersion tests and electrochem. meas. (Japanese) 0-85085  
 Ni-V, dil., optical absorpt., electronic struct. 0-108227  
 Ni-V, solid soln., diffusion and thermodynamic props. 0-65278  
 Ni-Y, amorphous, elec. resist., press. depend. 0-96841  
 Ni-Zn, implantation damaged, crit. behaviour, perturbed ang. distrib. meas. anal. 0-60476  
 Ni-Zn, physical-chemical metallurgy (German) 0-108390  
 Ni-Zr, amorphous phase form. in Zr-poor region, hardness and fracture strength (Japanese) 0-84914  
 Ni<sub>3</sub>(Al, Nb) single crystal, yield stress, orientation and temp. depend. 0-108511  
 $\gamma$ -Ni<sub>3</sub>(Al,Ti), single crystal, dislocation movement, HVEM obs. (Japanese) 0-108503  
 $\beta$ -NiAl, electronic struct. and optical props. 0-97228  
 NiAl, nonstoichiometric, interstitial defect cluster obs. 0-107226  
 $\beta$ -NiAl, ordered, hardness after-effect studied by anelastic relaxation 0-66570  
 $\beta$ -NiAl, oxidation,  $\alpha$ -Al<sub>2</sub>O<sub>3</sub> growth and microstruct. 0-108627  
 $\beta$ -NiAl, oxide films, metal and O<sub>2</sub> transport, AES and inert marker, techniques 0-97641  
 Ni<sub>3</sub>Al, off-stoichiometric alloy, inverse mag. susceptibility rel. to defect conc. 0-60216  
 Ni<sub>100-x</sub>B<sub>x</sub>, amorphous, mag. struct., mag. susceptibility meas. 0-80485  
 Ni<sub>0.89</sub>Cr<sub>0.11</sub>, phonons with disorder caused by force consts., neutron diff. obs. and CPA calc. 0-96602  
 NiCu molecule, electronic states determ. by ab initio HF and CI methods 0-69087  
 Ni(Fe,Cr), electron states density model and mag. characts. calcs. (Russian) 0-92804  
 Ni<sub>3</sub>(Fe,Cr), electron states density model and mag. characts. calc. (Russian) 0-92804  
 NiFe film, domain wall mass and relax. time from forced oscills. 0-71133  
 NiFe, magnetising energy, anisotropic effects 0-88743  
 NiFe, single and multilayer thin films, strip domains, inplane magnetisation 0-103866  
 NiFe thin films, magnetoresistance, quasi-static characts. 0-107766  
 Ni<sub>2</sub>Fe, change of H<sub>2</sub> diffusivity with order-disorder transformation 0-59729  
 Ni<sub>2</sub>Fe, compression induced magnetic anisotropy, annealing effect 0-93112  
 Ni<sub>2</sub>Fe, disaccommodation meas. after low temp. electron and neutron irrad. 0-88832  
 Ni<sub>2</sub>Fe, domain struct. after tensile deform., dislocation effects 0-71083  
 Ni<sub>2</sub>Fe, low-temperature specific heat, long and short range order effects 0-100339  
 Ni<sub>2</sub>Fe, magnetocryst. anisotropy, annealing temp. depend. 0-103828  
 Ni<sub>2</sub>Fe, mono- and polycryst., strain hardening, test temp. effects (Russian) 0-66531  
 Ni<sub>2</sub>Fe, polycrystalline alloy evolution of slip-line pattern during straining 0-107362  
 Ni<sub>2</sub>Fe single crystals, longitudinal magnetoresist. meas. 0-70675  
 Ni<sub>36</sub>Fe<sub>23</sub>Cr<sub>14</sub>P<sub>12</sub>B<sub>6</sub> metallic glass, mech. props. and thermal stability 0-76362  
 Ni<sub>3</sub>(Fe<sub>1-x</sub>Nb<sub>x</sub>), temp. and conc. depend. of anomalous Hall effect (Russian) 0-70674  
 (Ni<sub>95</sub>Fe<sub>5</sub>)<sub>70</sub>P<sub>10</sub>B<sub>10</sub>, amorphous, low temp. sp. ht., mag. contribs. 0-80552  
 (Ni<sub>2</sub>Fe<sub>1-x</sub>)<sub>80</sub>P<sub>10</sub>B<sub>10</sub>, amorphous, Curie temp., press. effect 0-75833  
 NiFe, mag. film, pulse switching at low temp. 0-103868  
 Ni<sub>2</sub>Ga, off-stoichiometric alloy, inverse mag. susceptibility rel. to defect conc. 0-60216  
 Ni<sub>2</sub>Ge-Fe<sub>2</sub>Ge solid soln., flow stress, transition from positive to negative temp. depend. 0-60906  
 Ni<sub>2</sub>Ge<sub>3</sub>, amorphous and cryst. films, opt. props. in interband absorpt. region 0-66315  
 NiH<sub>2</sub>, formation and decomp. studies 0-71626  
 Ni<sub>98</sub>M<sub>2</sub>, M=impurity metal, formation of MH(D)-complexes 0-65236  
 Ni<sub>78-x</sub>M<sub>2</sub>Si<sub>16</sub>B<sub>12</sub> (M=refractory metal), glass form. and thermal stability 0-79703  
 Ni<sub>3</sub>Mn, change of H<sub>2</sub> diffusivity with order-disorder transformation 0-59729  
 Ni<sub>3</sub>Mn thin films, transmission spectra, structural order depend. 0-66318

**nickel alloys continued**

- NiMnGe<sub>1-x</sub>Si<sub>x</sub>, mag. props., neutron diffr. and magnetometric meas., 80-600K 0-65793  
 NiP amorphous alloy, heat treatments influence on opt. props., struct. and DC resist. obs. 0-80892  
 Ni<sub>81</sub>P<sub>19</sub>, amorphous alloys, electronic struct.,  $\gamma$ -ray Compton scatt. study (Japanese) 0-84422  
 Ni<sub>78</sub>P<sub>22</sub>, amorphous, local symmetry around glass-former sites, elec. quadrupole effects, NMR 0-80618  
 (Ni<sub>0.5</sub>Pd<sub>0.5</sub>)<sub>82</sub>P<sub>18</sub> amorphous alloy, liquid-quenched, crystn. kinetics, effect of thermal history 0-100175  
 (Ni<sub>0.5</sub>Pd<sub>0.5</sub>)<sub>82</sub>P<sub>18</sub> amorphous alloy, liquid-quenched, crystn. kinetics, nucleation 0-100176  
 NiPt, quenched, ordering kinetics and domain struct. form. during isothermal tempering (Russian) 0-66502  
 Ni<sub>3</sub>Pt, change of H<sub>2</sub> diffusivity with order-disorder transformation 0-59729  
 Ni<sub>0.98</sub>Sn<sub>0.04</sub>, surface segregation, XPS and AES obs. 0-76135  
 NiSi<sub>2</sub>, substrate ion implantation, channelled, through metal silicide film 0-70231  
 NiTaC, eutectic alloys, chem. incompatibility of ceramic nitrides for directionally solidifying 0-81046  
 NiTaC eutectic superalloy, casting, furnace atm. effects 0-84880  
 NiTi alloy single cryts., ferromag. reson., g-value and linewidth 0-71186  
 NiTi equiatomic alloy, single cryst. elastic const. near martensitic transform. 0-75283  
 NiTi martensite, shape memory effect, struct. characts., TEM 2<sup>1</sup>/<sub>2</sub> D imaging obs. 0-108446  
 NiTi, premartensitic transformation of B2 phase, shape memory 0-84931  
 Ni<sub>40</sub>Ti<sub>60</sub>, amorphous, chem. short-range-order, X-ray and neutron scatt. obs. 0-96447  
 Ni<sub>10.5</sub>Ta<sub>89.5</sub>, conservative domain struct., TEM study 0-79776  
 Ni<sub>2</sub>Zn with  $\gamma$ -brass struct., superstructures and defect obs. 0-107284  
 Ni<sub>2</sub>Zr<sub>1-x</sub> metallic glass, crystallisation kinetics, elec. resist. and mag. susceptibility meas. 0-103659  
 Pb-Ni, creep, low-temp., thermal heating and quantum mechanisms, supercond. transition effects 0-79868  
 Pb-Ni, strength loss in supercond. transition, nonmag. and paramag. impurities influence (Russian) 0-70875  
 Pd-Ni, dilute ferromagnets, press. effect on Curie temp. 0-65873  
 Pd-Ni, normal Hall effect (Russian) 0-103676  
 Pd-Ni, spin fluctuation alloy, thermopower peak diffusion origin 0-88542  
 Pd-Ni, thermal expansion and magnetostriction meas. near crit. conc. for ferromagnetism 0-65881  
 Pd-Ni (15-90 at.%), thermo EMF at 4.2-300K (Russian) 0-92881  
 Pd-Ni-H, hydride formation in high press. range 0-65235  
 Pd-Ni-Si amorphous alloys, crystn. process during isothermal ageing 0-89275  
 PdNi (4.7 at.%), effect of alloying on activation energy of H<sub>2</sub> diffusion 0-107571  
 Pr-Ni, amorphous, thermal stability, crystn., DSC and elec. resist. study 0-107060  
 PrNi<sub>2</sub>, LF dynamics and <sup>141</sup>Pr thermal relax., coupling parameter and RKKY exchange mechanism 0-103812  
 PrNi<sub>2</sub>-Gd, dil., single crystal, ESR study 0-75850  
 PrNi<sub>2</sub>, sorption at press. up to 1500 atm. 0-97819  
 Pt-Ni vacuum condensates on Si and SiO<sub>2</sub>, thermally treated, X-ray anal. (Russian) 0-70559  
 Sn-Ni electrodeposited equiatomic alloy, cryst. struct., X-ray, electron diffr. anal. 0-79748  
 Ta(C,N)-Ni-VC, sintering behaviour, VC effect 0-93520  
 ThNi<sub>3</sub>, Hauke compounds, low temp. heat capacity, Debye temp. 0-96663  
 ThNi<sub>3</sub>, effect of absorbed H<sub>2</sub> on mag. behaviour 0-60184  
 Ti-Fe-Ni (67, 30, 3 wt.%), reversible shape alteration (Russian) 0-71647  
 Ti-Ni, internal friction and US props. (Russian) 0-84247  
 Ti-Ni, martensitic transform., monoclinic to triclinic phase (Russian) 0-81058  
 Ti-Ni, multiplicity of structural transitions, phase diagrams, elec. cond. meas. 0-71649  
 Ti-Ni (48 to 53 at.%), heat treatment and deviation from stoichiometry 0-104192  
 Ti-Ni amorphous alloys, glass transition and ductility, O additions effect 0-75168  
 Ti-Ni-Co, constitution diagram, isothermal section, interdiffusion coeffs. (Russian) 0-89200  
 Ti-Ni-Fe, multiplicity of structural transitions, phase diagrams, elec. cond. meas. 0-71649  
 TiC-(Mo-Cr-Ni-Mn) steel alloy, optimum comp. and manufacture conditions, Mn effect 0-84896  
 Ti<sub>70</sub>Ni<sub>20</sub>B<sub>10</sub>, amorphous alloys, crystn. behaviour, TEM study (Japanese) 0-84087  
 U-Ni metallic glasses, glass form. and thermal stability 0-75183  
 UNi<sub>2</sub>, mag. phase transition, elec. resist. meas. 0-97094  
 V-Ni sigma phase alloys, NMR and electric-field gradients 0-108109  
 W-Ni-Fe system, reduction kinetics and alloy form. 0-60801  
 W-Ni(Co) point-contact diodes as harmonic generators and mixers, DC bias dependence 0-75653  
 WC-Ni hard alloy composite, sintered, void healing 0-60821  
 Y(Co<sub>1-x</sub>Ni<sub>x</sub>)<sub>2</sub>, distrib. of Co and Ni atoms, neutron diffr. obs. (Russian) 0-64954  
 YNi<sub>3</sub>, magnetism resurgence, neutron diffr. and mag. props. study 0-65819  
 YNi<sub>3</sub>, Hauke compounds, low temp. heat capacity, Debye temp. 0-96663  
 Zr-Ni, amorphous and crystalline, d-band struct., alloying effects 0-59862  
 Zr-Ni metallic glasses, glass form. and thermal stability 0-75177  
 Zr-Sn-Fe-Ni (1.5, 0.1, 0.15 wt.%), electron irradiation damage, direct obs. 0-84212  
 Zr-Sn(Fe)(Ni) (0.15 wt.%), electron irradiation damage, direct obs. 0-84212  
 Zr<sub>70</sub>Ni<sub>30</sub> amorphous alloys, struct. factors and radial distrib. functions 0-84096

**nickel compounds**

see also nickel alloys

- ferrite, quenched, Neel temp. and initial susceptibility 0-75762  
 halides, XPS, multiplet struct. and multielectron excitations, in 3 p and 2p shells 0-78649  
 intercalation, electron microscopy 0-84164

**nickel compounds continued**

- NiWO<sub>4</sub>, antiferromag., low symmetry exhibited during spin-flop phase transition 0-60263  
 oxide reduction by electron cyclotron reson. plasma of H, model study on discharge cleaning 0-76548  
 3p photoelectron spectra, light-induced changed in multiplet satellites 0-80946  
 polyphosphinate, bulk compressibility meas. to 30 kbar 0-76306  
 reduced Ni oxide, H absorption 0-76529  
 Tulton salts, cryst. field spectra in visible and near IR regions, solid dilution effect 0-100666  
 Ba<sub>2</sub>Ni<sub>3</sub>F<sub>10</sub>, cryst. struct. and antiferromag. props. 0-107153  
 BaNi<sub>2</sub>(PO<sub>4</sub>)<sub>2</sub> and BaNi<sub>2</sub>(AsO<sub>4</sub>)<sub>2</sub>, mag. props., neutron diffr. and sp. ht. meas. 0-70948  
 Ca-Mg-Ni hydrides, water form. on O<sub>2</sub> exposure 0-97727  
 Ca<sub>2</sub>Ni<sub>1-x</sub>Fe<sub>x</sub>O<sub>4</sub>, X-ray struct. anal., determ. of lattice constant and interplanar distances (French) 0-96487  
 Cd<sub>1-x</sub>Ni<sub>x</sub>Fe<sub>0.4</sub>O<sub>4</sub>, solid soln., mag. and structural characterisation 0-103906  
 Co<sub>2</sub>(Ni<sub>0.5</sub>Cu<sub>0.5</sub>)<sub>1-x</sub>Fe<sub>x</sub>O<sub>4</sub> ferrite, relation between elec. cond. and mag. anisotropy 0-75548  
 Co<sub>2</sub>Ni<sub>1-x</sub>Fe<sub>x</sub>O<sub>4</sub>, induced mag. anisotropy const., conc. and temp. depend. 0-108001  
 CsNiCl<sub>3</sub>, noncollinear magnetic order and spin wave spectrum in presence of competing exchange interactions 0-65834  
 CsNiF<sub>6</sub>, anisotropic Heisenberg chain, nonlinear excitations 0-70927  
 CsNiFeF<sub>6</sub> pyrochlore, Mossbauer contrib. to exam. of cationic order (French) 0-93224  
 Cu-Ni ferrite films, LPE growth 0-96752  
 DyNi<sub>2</sub>Si<sub>2</sub>, mag. props., 4.2-200K 0-84602  
 ErNi<sub>2</sub>Si<sub>2</sub>, mag. props., 4.2-200K 0-84602  
 Fe<sub>2</sub>C-Cr<sub>2</sub>C-NiC<sub>2</sub>, stainless steel carbide, solar selective surface, fabrication, magnetron sputtering system description 0-80967  
 Fe<sub>2</sub>C-Cr<sub>2</sub>C-NiC<sub>2</sub>, stainless steel carbide, graded solar selective surface, magnetron sputtered 0-81485  
 Fe<sub>2</sub>C-Cr<sub>2</sub>C-NiC<sub>2</sub>, stainless steel carbide, sputtered solar selective surface, grading profile 0-81486  
 Fe<sub>40</sub>Ni<sub>40</sub>Cu<sub>20</sub>P<sub>0</sub> amorphous film, dislocation and mag. struct., neutron diffr. study 0-70956  
 (Fe<sub>1-x</sub>Ni<sub>x</sub>)<sub>2</sub>O, yH<sub>2</sub>O crystal growth, characterisation by Mossbauer spectroscopy, mag. meas. and electron microscopy (French) 0-80655  
 (Fe<sub>1-x</sub>Ni<sub>x</sub>)<sub>2</sub>P, Curie temp., press. depend. meas. 0-97091  
 Gd Ni<sub>2</sub>Si<sub>2</sub>, mag. props., 4.2-200K 0-84602  
 HoNi<sub>2</sub>Si<sub>2</sub>, mag. props., 4.2-200K 0-84602  
 InSb-NiSb, photovolt. effects rel. to theory of semicond. with internal elec. short circuits 0-65620  
 KNiCl<sub>3</sub>, disorder as observed by electron diffr. 0-75213  
 KNiF<sub>3</sub>, <sup>19</sup>F spin-lattice relaxation 0-93211  
 MgO-NiO, STEM microanal., absorpt. effects 0-80902  
 N<sub>2</sub> complex, NiC(C<sub>2</sub>H<sub>3</sub>NO)<sub>2</sub>(NO)<sub>2</sub>, singlet ground-state systems, field induced mag. long range order 0-60266  
 Na<sub>2</sub>O-B<sub>2</sub>O<sub>3</sub>-NiO melts, NiO activity and solubility meas. by EMF method (Japanese) 0-92677  
 Na<sub>3</sub>PO<sub>4</sub>-Ni<sub>3</sub>(PO<sub>4</sub>)<sub>2</sub> system, phase equilibrium diagrams, crystallographic study, double orthophosphates (French) 0-93546  
 Ni complex, 2,6-N,N-diacetyldiaminopyridine-Ni(II) elec. cond.,  $\gamma$  dose and temp. (303-363K) effects 0-103696  
 Ni complex, 2,6-N,N-dibenzyldiaminopyridine-Ni(II) elec. cond.,  $\gamma$  dose and temp. (303-363K) effects 0-103696  
 Ni complex, diaquo-bis(acetylacetonate) nickel (II), cryst. struct. 0-100205  
 Ni complex, nickel-bis-dithiolene, pseudopot. MCSCF and limited CI calcs. 0-83292  
 Ni complexes, dithienic, nematic and smectic mesophases, synthesis and characts. 0-70120  
 Ni complexes hexamethylamine nickel halides, Ni<sup>2+</sup> EPR in high pulsed mag. field, zero field splitting parameters 0-71160  
 Ni dithiene complexes, mesomorphic props. 0-88026  
 Ni II acetylacetonate, XPS 0-74196  
 Ni-Ge-SiO, solar selective absorber surfaces, optical behaviour at high temp. 0-101130  
 Ni-I single crystals, mag. and dielectric props. 0-93095  
 Ni-Pt silicide Schottky diodes, current-voltage characts. and comp. profiles 0-84508  
 Ni-S incongruently subliming system, SEM and TEM obs. of high temp. transitions, temp.-comp. diagrams 0-104136  
 Ni-Zn-Co ferrites, synthesis from solid solns. of schoenite-type salts 0-93511  
 Ni<sub>3</sub>B<sub>2</sub>O<sub>7</sub>Br, boracite single cryst., nucleation control density growth 0-80955  
 Ni<sub>3</sub>B<sub>2</sub>O<sub>7</sub>Br, cubic, approx. nonlinear optical susceptibility 0-78904  
 Ni<sub>3</sub>B<sub>2</sub>O<sub>7</sub>Br, ferroelec. 43m-mm2 phase transition, molar heat capacity meas. 0-93249  
 NiBr boracite single crystals, dielectric, pyroelectric props., vapour phase transport growth 0-80673  
 NiBr<sub>2</sub>, aq. solns., EXAFS meas. 0-60714  
 NiBr<sub>2</sub>, commensurate and incommensurate mag. struct., neutron diffr. study 0-97067  
 NiBr<sub>2</sub>, low-temperature magnetic phase, incommensurate spin structure 0-93082  
 Ni(CO)<sub>4</sub>, form. on single Ni cryst., reaction kinetics and induced surface faceting 0-71948  
 Ni(CO)<sub>4</sub>, form. reaction rate, substrate mag. phase depend. 0-108737  
 Ni<sub>1-x</sub>Cd<sub>x</sub>Fe<sub>0.4</sub>O<sub>4</sub>, mag. props. rel. to ionic struct. 0-75756  
 NiCl<sub>2</sub>, aq. soln., structural transition, neutron diffr. study 0-64872  
 NiCl<sub>2</sub>, aq. solns., EXAFS meas. 0-60714  
 NiCl<sub>2</sub>, cryst., self-consistent band struct., intersecting spheres model 0-75505  
 NiClO<sub>4</sub>, neutron activated, radiation annealing 0-93569  
 NiCl<sub>2</sub>6NH<sub>3</sub>, low temp. sp. ht. and mag. ordering 0-75784  
 Ni<sub>2</sub>Co<sub>1-x</sub>Cl<sub>2</sub>6H<sub>2</sub>O, mixed uniaxial planar antiferromag., magnetisation process 0-88788  
 Ni<sub>2</sub>Co<sub>2-x</sub>O, composition depend antiferromagnetic-ferromagnetic ordering, mag. susceptibility meas. 0-70973  
 Ni<sub>1-x</sub>Co<sub>x</sub>S<sub>2</sub>, elec. cond., thermoelec. power and optical meas. 0-59986  
 Ni<sub>1-x</sub>Cr<sub>x</sub>S<sub>2</sub>, elec. transport, mag. susceptibility and DTA meas. 0-96954  
 NiF<sub>2</sub> film preparation and characterisation 0-59815  
 NiF<sub>2</sub>, high temp. polymorphism and thermal props. 0-75199  
 NiF<sub>2</sub>, thermal expansion and magnetostriction, 55K to room temp. 0-80586



## nickel compounds continued

- NiFe ferrite, prep. of single crystal by chem. transport with  $\text{TeCl}_4$  0-104051  
 NiFe<sub>2</sub>O<sub>4</sub>, electronic phase transition 0-65640  
 NiFe<sub>2</sub>O<sub>4</sub>, ferrite, mag. anisotropy compensation under neutron irradiation 0-75807  
 NiFe<sub>2</sub>O<sub>4</sub> ferrite, mag. props., neutron irradiation 0-103858  
 NiFe<sub>2</sub>O<sub>4</sub> mag. fluid particles, comp., struct., and mag. props. 0-60374  
 NiFe<sub>2</sub>O<sub>4</sub> milled ferrite powder, substract. and sinterability 0-84894  
 NiFe<sub>2</sub>-O<sub>4</sub>, DC and low freq. cond. and influence of microstruct. 0-70699  
 Ni<sub>3</sub>Fe<sub>1-x</sub>O<sub>4</sub>, magnetostriction, 80 to 300K, depend. on comp. and electron ordering on octahedral sites 0-65995  
 Ni<sub>3</sub>Fe<sub>1-x</sub>O<sub>4</sub>, spinels, fine particles, magnetic properties obs. 0-71031  
 NiH, extended basis set LCAO Alpha treatment 0-95537  
 NiI, anhydrous, magnetic phase transition, neutron diffraction study 0-71033  
 NiMoO<sub>4</sub>+TeO<sub>2</sub>, solid state reaction 0-108709  
 Ni<sub>3</sub>Mo<sub>2</sub>S<sub>2</sub>O<sub>7</sub>, O-containing Chevrel phases, synthesis and props. 0-108368  
 Ni(NH<sub>3</sub>)<sub>6</sub>(BF<sub>4</sub>)<sub>3</sub>, phase transition, group theoretical anal. 0-65218  
 Ni(N<sub>2</sub>H<sub>4</sub>)<sub>2</sub>B<sub>2</sub>H<sub>4</sub>, development, effect on photosensitivity of paper (*Russian*) 0-73509  
 Ni(NH<sub>3</sub>)<sub>6</sub>(ClO<sub>4</sub>)<sub>2</sub>, phase transition, group theoretical anal. 0-65218  
 Ni(NH<sub>3</sub>)<sub>6</sub>Cl<sub>2</sub>, phase transition and rot. excitation 0-96642  
 Ni(NH<sub>3</sub>)<sub>6</sub><sup>2+</sup>, photographic developer, potentiodynamic polarisation curves for Ag-less development (*Russian*) 0-90921  
 NiNb<sub>2</sub>O<sub>6</sub>, force fields rel. to cryst. struct. (*French*) 0-107104  
 NiO (001) surface, chemisorption of H<sub>2</sub>, surface and second-layer defect effects 0-65369  
 NiO (100) surface, LEED expt. and calc. down to 60 eV 0-92767  
 NiO, (100) surface interaction with SO<sub>2</sub>, electron diffraction and Auger spectroscopy obs. (*French*) 0-97728  
 NiO, (100) coincidence twist boundaries energy 0-107270  
 NiO, antiferromag. ordering, mag. transition-state approach 0-80507  
 NiO, bulk props., initial state MO Ni<sub>2</sub>O<sub>4</sub> and Ni<sub>3</sub>O<sub>4</sub>, cluster model, lattice and force consts., photoemission and CT absorpt. spectra 0-84828  
 NiO, cryst. growth using K<sub>2</sub>S<sub>2</sub>O<sub>7</sub> as flux material 0-71582  
 NiO, diffusion of <sup>35</sup>S by two different modes 0-59720  
 NiO, diffusion of ion-implanted <sup>18</sup>O 0-107494  
 NiO, dipole orientation from bound polaron hopping 0-84437  
 NiO, doped and undoped, elec. props. and surface characts. 0-65571  
 NiO, Hall effect anomaly, sign reversal at 600K 0-100471  
 NiO, isoelectric point meas. 0-88609  
 NiO, linear birefringence in S-domains near antiferromag. phase transition 0-60261  
 NiO, mag. struct., neutron Laue diffraction method 0-70951  
 NiO, nonstoichiometric, near-surface and bulk chem. diffusion 0-80035  
 NiO ore, reduction of Ni in segregation roasting process (*Japanese*) 0-71908  
 NiO, powder pressed disc, oxidising conditions effect on thermally stimulated exoelectron emission (*Japanese*) 0-89127  
 NiO, prepared by thermal decomp. of Ni(OH)<sub>2</sub>, microporosity and irreversible water vapour adsorption 0-80060  
 NiO promoted CuAl<sub>2</sub>O<sub>4</sub> catalyst, surface oxidation state and comp., XPS study 0-76134  
 NiO samples, colour difference, X-ray line broadening study 0-100206  
 NiO, single cryst. cleavage plane, oxidising conditions effect on thermally stimulated exoelectron emission (*Japanese*) 0-89127  
 NiO, stress relief and plastic flow in temp. range 1323-1473K 0-89302  
 NiO, undoped and Al doped, Ni self-diffusion, vacancy-impurity complex effects 0-107493  
 NiO-Al<sub>2</sub>O<sub>3</sub> reaction at film-substrate interface, Rutherford backscatt. obs. 0-59733  
 NiO-Cr<sub>2</sub>O<sub>3</sub>-MgSiO<sub>3</sub> methanation catalyst, S-resistant, IR and Raman spectra 0-93290  
 NiO-Fe<sub>2</sub>O<sub>3</sub>, isoelectric point meas. 0-88609  
 NiO-MgO solid solns., surface comp. study by XPS 0-104035  
 NiO-P<sub>2</sub>O<sub>5</sub> glass, ESR of VO<sup>2+</sup> ions 0-100610  
 NiPS<sub>3</sub>, layered semiconductors, optical and electronic props. 0-70761  
 NiPtCl<sub>6</sub>·6H<sub>2</sub>O, singlet-ground-state magnets, ESR at low temps. 0-97132  
 NiS, electrodeposition, using nonaqueous solvents 0-76200  
 NiS inclusions in glass, microcracking, fracture mech. description 0-89333  
 NiS, thermodynamic study of  $\alpha \rightleftharpoons \beta$  transition (*French*) 0-60854  
 NiS<sub>2</sub>, core-level and valence-band XPS 0-93450  
 NiS<sub>2</sub>, weak ferro- and antiferromag., magnetisation and neutron diffraction meas. 0-65794  
 Ni<sub>2</sub>S<sub>3</sub>, hazelwoodite, X-ray cryst. struct. determ. 0-88105  
 NiSO<sub>4</sub>, photographic developer, potentiodynamic polarisation curves for Ag-less development (*Russian*) 0-90921  
 NiS<sub>2</sub>-Se<sub>x</sub>, elec. cond., thermoelec. power and Hall effect meas. 0-65561  
 NiS<sub>2</sub>-Se<sub>x</sub>, first-order Raman scattering 0-108206  
 NiS<sub>2</sub>-Se<sub>x</sub>, phase diagram, intermediate valence effects 0-103834  
 NiS<sub>2</sub>(Se<sub>2</sub>), electronic struct., UPS and XPS study 0-80935  
 NiSb, bandstructure and density of states calc. 0-70580  
 Ni<sub>1-x</sub>Sb<sub>x</sub>, temperature effect on lattice consts., Mossbauer spectra and density 0-88124  
 NiSb<sub>2</sub>O<sub>6</sub>, force fields rel. to cryst. struct. (*French*) 0-107104  
 NiSe<sub>2</sub>, core-level and valence-band XPS 0-93450  
 NiSe<sub>2</sub>, paramag. props., NMR, mag. susceptibility 0-60175  
 NiSi, parallel contacts, Schottky barrier height meas. 0-96965  
 NiSiF<sub>6</sub>, dilute, single-spin cross-relax. calcs. 0-97129  
 NiSiF<sub>6</sub>·6H<sub>2</sub>O, non-Kramers system, spin-lattice relaxation at strong fields 0-100612  
 NiSnCl<sub>6</sub>·6H<sub>2</sub>O, singlet-ground-state magnets, ESR at low temps. 0-97132  
 NiTa<sub>2</sub>O<sub>6</sub>, force fields rel. to cryst. struct. (*French*) 0-107104  
 Ni<sub>1-x</sub>Te<sub>x</sub>, fluctuating localised mag. moments, d band motion, Mossbauer study 0-65768  
 NiTiO<sub>3</sub>, antiferromag., mag. anisotropy, magnetisation meas. 0-65856  
 NiWO<sub>4</sub>, AC elec. conductivity, thermoelec. power and dielec. const. 0-70736  
 NiZn ferrite, dielec. props., Jahn-Teller ion effects 0-97181  
 NiZn ferrite, prep. of single crystal by chem. transport with  $\text{TeCl}_4$  0-104051  
 NiZn ferrite, ZrO<sub>2</sub> additions influence on sintering and physicochem. props. 0-108369  
 NiZn ferrites, density and mag. props., isostatic pressure effect 0-60816  
 NiZn ferrites, internal friction and  $\Delta E$  effect depend. on demagnetisation method 0-80584

## nickel compounds continued

- NiZn ferrites, mag. head props., technical possibilities and limitations 0-88803  
 NiZn ferrites, nonstoichiometric, initial susceptibility and microstruct. 0-84591  
 NiZn ferrites, V<sub>2</sub>O<sub>5</sub> induced mag. aftereffects 0-60379  
 NiZnCo ferrites, switching time and coeff., hydrostatic press. effect 0-88802  
 NiZnCo ferrites, voltage response under sinusoidal and pulse magnetisation effected by hydrostatic press. 0-88846  
 Ni<sub>0.25</sub>Zn<sub>0.75</sub>Fe<sub>2</sub>O<sub>4</sub>, Mossbauer study, spin fluctuations 0-60471  
 Ni<sub>0.25</sub>Zn<sub>0.75</sub>Fe<sub>2</sub>O<sub>4</sub>, Mossbauer study, noncollinear spin struct. 0-60472  
 Ni<sub>0.25</sub>Zn<sub>0.75</sub>Fe<sub>2</sub>O<sub>4</sub>, structural phase transition, X-ray and neutron diffraction study 0-79735  
 Ni<sub>0.5</sub>Zn<sub>0.5</sub>Fe<sub>2</sub>O<sub>4</sub>, coarse grain polycryst. ferrite, diffusional creep (*Japanese*) 0-104238  
 Ni<sub>0.85</sub>Zn<sub>0.15</sub>Fe<sub>2</sub>O<sub>4</sub>, ferrite, mag. anisotropy compensation under neutron irradiation 0-75807  
 Ni<sub>1-x</sub>Zn<sub>x</sub>Fe<sub>2</sub>O<sub>4</sub>, polycryst., domain wall energy rel. to anisotropy 0-101090  
 Ni(s, l) + NiO(s) + NiX<sub>2</sub>O<sub>4</sub> (X = Al, Ga), chem. potential and solubility of O<sub>2</sub> 0-92679  
 RbNiCl<sub>3</sub>, noncollinear magnetic order and spin wave spectrum in presence of competing exchange interactions 0-65834  
 S-Ni-Fe system containing monosulphide solid soln., elec. and struct. relations 0-90038  
 SnO<sub>2</sub>-NiO, activated sintering mechanism 0-60810  
 TbNi<sub>2</sub>Si<sub>2</sub>, mag. props., 4.2-200K 0-84602  
 TmNi<sub>2</sub>Si<sub>2</sub>, mag. props., 4.2-200K 0-84602  
 WO<sub>3</sub>-NiCO<sub>3</sub>-Fe<sub>2</sub>O<sub>3</sub>, reduction alloy form. 0-60801
- night airglow** see *nightglow*
- night sky**  
 see also *nightglow*; *twilight*  
 brightness, Mitaka, Japan (*Japanese*) 0-82067  
 integrated starlight, synthetic spectrum between 3000 and 10000 Å, discussion 0-62200  
 interstellar UV radiation field, obs. from S2/68 sky-survey telescope 0-77523  
 He I, interstellar, UV emission, obs. and implications 0-62234
- nightglow**  
 meteoric nightglow, review of historical obs. 0-94761  
 Pc 1 pearl event correl. with 4278 Å nightglow, Antarctic obs. 0-72664  
 VLF wave events at L=4 correl. to optical emission 0-101468  
 N<sub>2</sub><sup>+</sup>, first negative band system correl. to mag. storm 0-72665  
 Na enhancement and nightglow, spaced lidar obs. 0-101466  
 Na I D doublet, excitation, Na abundance 0-98497  
 NaD, nightglow spectral intensity changes, correl. with O<sub>2</sub> spectra 0-61932  
 O I 7774 Å multiplet obs. over Arecibo during magnetic storm 0-72663  
 O<sub>2</sub>, A<sup>+</sup>Δ<sub>g</sub> state, inversion, presence in nightglow and discharges 0-63616  
 O<sub>2</sub>, atmospheric system, rocket meas. of 7619 Å band (*Japanese*) 0-94631  
 O<sub>2</sub>, nightglow spectral intensity changes correl. with NaD spectra 0-61932  
 OH emission, photometric obs. to find mesosphere neutral temp. 0-82121  
 OH Meinel bands, rocket meas. of 6863 Å band (*Japanese*) 0-94631
- Nilsson's model** see *nuclear shell model*
- niobium**  
 see also *nuclei with .....*  
 adsorbed H distrib., electron-stimulated desorption ion imaging 0-103572  
 adsorption of H, sticking coeff. calc. 0-59803  
 annealing, of single crystals, for tunnel meas., ultra high vac. device (*German*) 0-89169  
 atoms, N<sub>2</sub>N<sub>3</sub>N<sub>4</sub> super Coster Kronig processes 0-106303  
 BCC, interaction energy between self-interstitial and screw dislocation, calc. 0-70248  
 blisters due to He irradiation, proton backscatt. study 0-75273  
 chemisorption of H, photoemission studies 0-76145  
 chemisorption of H, two-state model kinetics 0-75438  
 core level binding energies 0-71564  
 creep rate in vacuum, grain size effect 0-108514  
 critical current density, deviation from critical state model 0-84578  
 deformed polycrystalline, γ-peak obs. and interpret. in internal friction, 300-500K 0-81098  
 diffuse electron scatter. (*Russian*) 0-103438  
 diffusion of H<sub>2</sub>, isotope effects, crystal field stabilisation 0-59728  
 diffusion of H(D), role of tunnelling, reson./nonreson. approaches 0-59718  
 diffusion of H and trapping 0-70447  
 diffusion of O and N, statistical calcs. on Arrhenius lines 0-59722  
 dislocation damping, amplitude depend. 0-59469  
 electrical resistivity due to interstitial H (D) 0-96848  
 electron bombardment, high-energy, secondary electron emission 0-80917  
 electron energy losses due to H, obs. by scanning TEM 0-79850  
 electron irradiated, muon diffusion 0-80668  
 electron-phonon interaction, relativistic, APW calc. 0-92837  
 electronic structure, thermoreflectance studies 0-76047  
 enthalpy meas., by levitation calorimetry 0-103499  
 Fermi surface, electron mass enhancement, orthonormal function enhancement 0-96777  
 fibre glass composite, new technique for producing fine metal fibres 0-108384  
 field emission anomalies in mag. field (*Russian*) 0-93462  
 film, critical mag. fields and currents, temp. depend. (*Russian*) 0-103798  
 film, epitaxy, struct. and supercond. props., on (001) surface of fluorophlogopite (*Russian*) 0-80101  
 film, struct. and electrophys. props. at 4.2K 0-80436  
 film, thin, microbridge, video detection of far IR radiation (*Japanese*) 0-97038  
 film on sapphire substrate, orientational growth, epitaxial textures, nucleation textures (*Russian*) 0-75454  
 films, oxidation, XPS study 0-80944  
 films, vac. evaporated, optical cond. 0-76100  
 granular films, ratio of supercond. transition temps. 0-84529  
 granulated film, critical current temp. depend. (*Russian*) 0-103803  
 high temp. radiative props., expt. determ., spectral emissivities 0-74718  
 impurity distribution, O determ. by neutron activation anal. (*Russian*) 0-70243  
 ion bombard. by 5 keV Ar<sup>+</sup>, sub-surface damage 0-103399  
 ion implanted, He blistering, large swelling meas., gas press., model 0-88218

**niobium** continued

ion plated with Pd and Ni, prep.,  $H_2$  absorption and desorption rate (Japanese) 0-108358  
 ion-implanted bridge with thick Pb banks, fabrication and characterisation of film parameters 0-100569  
 ISSEC selection for fusion reactor 0-57950  
 lattice dynamics, local frequency spectrum, mean thermal displacement of H 0-59604  
 layer, ion bombarded, supercond. props. and struct. 0-88671  
 liquid Nb, enthalpy meas. by levitation calorimetry 0-103499  
 luminescence characteristics of pure surfaces acted on by flux of field emission electrons 0-100695  
 membrane, H permeation (Japanese) 0-100363  
 muon diffusion, LAMPF results 0-71285  
 Nb, pure, production by carbothermic reduction-electron beam melting combination method 0-89177  
 neutron diffuse-scatt. intensities 0-59597  
 neutron irradiated, positron annihilation ang. correl. meas. 0-93430  
 neutron irradiated, radiation anneal hardening (Japanese) 0-89243  
 oxidation mechanism, 673 to 823K 0-108644  
 phonon dispersion curves, extended screened-shell model 0-96601  
 projected range distrib. of 5-25 keV  $He^+$  0-65094  
 proximity electron tunnelling spectroscopy 0-107964  
 solute trapping of H, symmetry of O-H pair 0-108488  
 SQUID, low-noise DC type, with 1  $\mu$ m tunnel junctions 0-80450  
 superconducting, peak effect due to vortex pinning in subsurface layer (Russian) 0-93060  
 superconducting, single crysts., fluxoid pinning by small nitride precip. 0-70913  
 superconducting, thermodynamic props. 0-107955  
 superconducting, US attenuation, hysteresis near and below  $H_{c1}$  0-75676  
 superconducting granular films as weak link in Josephson devices 0-88685  
 superconducting microbridges, vertical type, fabrication and DC characts. 0-103788  
 superconducting mixed state, hysteresis of US attenuation 0-84549  
 superconducting point contact, singularities of I-V curve and voltage fluctuations 0-93044  
 superconducting state influence on dislocation motion (Russian) 0-70208  
 superconductive transition point as reference temp. 0-107943  
 superconductor, effect of changes in  $\alpha^2(\Omega)F(\Omega)$  on the zero-temp. energy gap 0-97025  
 superconductor, upper crit. field, temp. depend. and anisotropy 0-80462  
 surface, scatt.  $H^{2+}$ , polarised Balmer radiation, adsorbed  $O_2$  effects 0-99569  
 swelling correlation with local gas concentration following He irradiation 0-70271  
 thin-film Josephson tunnel junctions, fabrication and props., in situ ellipsometric meas. 0-65749  
 thin-film SQUID working at 4.2K, fabrication and characterisation 0-100570  
 voids, TEM, elastic side band imaging 0-75219  
 volt ampere characteristics during electron melting process (Russian) 0-75336  
 X-ray emission L-spectra, influence of temp., liq.  $N_2$  temps. (Russian) 0-80907  
 BaTiO<sub>3</sub>:Nb, elec. props., contact material influence 0-70848  
 Nb films, ion beam sputtered, supercond., laser annealing effects 0-97024  
 Nb, mono- and polycrystn., crystallographic orientation, etching technique determ. 0-71814  
 Nb XIII, energy levels, spectrum obs. 0-63571  
 Nb:He, mech. props. and microstruct. 0-85003  
 Nb:N, neutron diffuse-scatt. intensities 0-59597  
 Nb/Cu, layered ultrathin coherent struct., supercond. props. 0-84525  
 Nb/Cu layered ultrathin coherent struct. 0-80122  
 Nb/In composite superconductor, transport props. 0-88658  
 Nb-Al, tunnelling expts. on normal metal backed by Al 0-65751  
 Nb-Al superimposed metallic layers, ionic movements during anodization, Rutherford backscatt. and nuclear microanal. 0-71913  
 Nb-Cu-Nb junctions, Josephson effect meas., critical current, temp. depend. 0-93041  
 Nb-Nb Josephson junctions, submicron, thermally recyclable, fabrication and characts. 0-100566  
 Nb-Nb<sub>2</sub>O<sub>5</sub>-Pb Josephson junction formed on Nb film edge 0-107960  
 Nb-Nb<sub>2</sub>O<sub>5</sub>-Pb(In) Josephson junctions, props. of Nb<sub>2</sub>O<sub>5</sub> thermally grown tunnel barriers 0-100568  
 Nb-Nb<sub>2</sub>O<sub>5</sub>-Pb Josephson junction current-biased on Fiske steps, mag. field depend. 0-84567  
 Nb-NbO<sub>2</sub>-Pb Josephson junctions with high current densities, critical current 0-100552  
 Nb-NbO<sub>2</sub>-Pb superconductive tunnel junctions, oxide tunnelling barriers, ESCA characterisation 0-65745  
 Nb-NbO<sub>2</sub>-Pb tunnel junction, temp. depend. of effective Nb energy gap 0-80454  
 Nb-Pb supercond. tunnel junction proximity effect, theory 0-65752  
 Nb-Pb tunnel junction, crit. Josephson current, proximity effect model 0-93047  
 Nb-Ta superimposed metallic layers, ionic movements during anodization, Rutherford backscatt. and nuclear microanal. 0-71913  
 Nb-Ta-Pb Josephson junctions, prep. and props. 0-65754  
 Nb-Pb Josephson junctions, magnetic field behaviour of zero field steps 0-100561  
 Pb-Nb-Pb bridged, variable thickness, ion implant, coherent vortex motion props. obs. 0-100562  
 Pb<sub>0.94-x/2</sub>Nb<sub>0.06-x/2</sub>Zr<sub>1-x/2</sub>O<sub>3</sub>, Nb dopant morphology effect on microstructure 0-81005  
 Pb(Zr,Ri)O<sub>3</sub>:Ni-silicon rubber flexible composite pyroelectric, dielectric props. 0-80704  
 Pb(Zr,Ti)O<sub>3</sub>:Fe(Nb) ceramic, elec. and electromechanical props., depend. on dopants 0-81212  
 n-TiO<sub>2</sub> photoelectrochemical electrodes, effect of Nb doping on quantum efficiency 0-101121  
 TiO<sub>2</sub>:Nb semicond. electrodes, electroreduction process kinetics, cathodic dark current meas. 0-66807

**niobium alloys**

see also niobium compounds

Inconel 625, electron yields under ion bombardment for clean and oxidised surfaces 0-66368  
 Inconel 718, grain growth during sintering 0-97449

**niobium alloys** continued

magnetic susceptibility and Knight shift meas., d-metal alloys 0-66055  
 steel, Al-Ti-(Mo), Al-Ti-V-(Mo), Al-Ti-Nb-(Mo) and Al-V-(Mo) low-alloy, toughness improvement through Ti additions 0-66525  
 steel, high-strength, fatigue crack growth rate and crack tip shapes, cyclic bending (Russian) 0-71740  
 steel, microalloyed, hot-rolled, Nb(C,N) precip. and austenite recrystn. 0-97513  
 steel, Mn-Nb-Al-C, crack progag. and hot ductility during straightening concast strand 0-66646  
 steel, Nb(V), (Al), hot-rolling, laboratory simulation, recrystn. of austenite 0-97512  
 steel, V-Nb, supercooled austenite isothermal decomp., struct., strength and fracture characts. 0-60966  
 CC NbTi, pool cooling superconducting test coil, Japanese design for fusion reactor large coil task 0-99340  
 Co-Nb-C, obtained by liq. quenching, superconductivity 0-75699  
 Co-Ni-Cr-Nb (40, 18, 1.8 wt.%), precipitation behaviour of NbC, effect of ageing temp. on morphology 0-89227  
 Cr-Mo-V-Nb, supercooled austenite isothermal decomp., struct., strength and fracture characts. 0-60966  
 Cr-Nb-Mo system, comp. and temp. depend. alterations in mech. props., phase diagram interpret. (Russian) 0-85045  
 Cr-Ni-Nb steel, oxidation in CO<sub>2</sub>, charged-particle nuclear techniques 0-61022  
 Cu-Nb alloy, chill casting, consumable arc melting, ingot prep. techniques 0-84879  
 Cu-Nb multifilamentary composite, dislocation resistivity 0-70671  
 Cu-Nb<sub>2</sub>Sn multifilamentary tapes, in situ formed, crit. current density anisotropy 0-84576  
 Cu-Ni-Nb (30, 0.9 at.%), precipitate free zones, X-ray microanal. 0-108768  
 Cu<sub>40</sub>Nb<sub>30</sub>X<sub>30</sub> (X=Ti, Zr, Hf), superconductors with metastable ordered structs. 0-108484  
 Fe-Co-Mo-Nb semihard mag. alloy, mag. props., thermal expansion, elec. resistivity and hardness (Japanese) 0-88789  
 Fe-Nb-V-C-N, equilibrium comp. and solubility in steels, model of ideal solns. (Russian) 0-60832  
 Gd-Nb amorphous films, spontaneous Hall effect and elec. resist. 0-80251  
 Mo-Nb, thermoelec. power, 4.2 to 300K 0-70683  
 Mo-Nb-C, mech. props., effect of alloying and Mo cryst. orientation (Russian) 0-71706  
 Mo-Nb-Ti-N alloy, with dispersed second phase, ductile-brittle transition 0-93653  
 Nb-Al-C, phase diagram and lattice constants, X-ray diffr. method 0-89207  
 Nb-Al-Ge-Cu, rapidly quenched, comp. and phase equilib. 0-76235  
 Nb-Al(Ga, Si, Ge, Sn)-Cu, rapidly quenched, comp. and phase equilib. 0-76235  
 Nb-Ga, A15 phase, chem. deposition on Hastelloy substrate, for superconducting tape (German) 0-104071  
 Nb-Ga-Sc, superconducting transition temp., X-ray, microscopic and microprobe anal. (Ukrainian) 0-75667  
 Nb-Ge, amorphous supercond. alloy, resistivity, transition temp. 0-60126  
 Nb-Ge, compounds with A15 structure, films, TEM study (French) 0-80135  
 Nb-Ge-Si, compounds with A15 structure, films, TEM study (French) 0-80135  
 Nb-H system, accommodation effects during hydride precipitation, TEM 0-89218  
 Nb-H system, phase diagram and transforms., struct. obs. of various phases 0-104125  
 Nb-H(D)(T) system, BCC, US vel. changes caused by H isotope dissolution 0-65117  
 Nb-Ir(Rh) system glasses, form., crystn. and microhardness, resist. obs. 0-89178  
 Nb-Mo, resistivity due to H incorporation 0-70666  
 Nb-Mo, specific heat enhancement and electron-phonon interaction 0-65242  
 Nb-N(O)(C) system, specimen prep. for metallography (German, English) 0-89439  
 Nb-Ni, amorphous, thermal stability, crystn., DSC and elec. resist. study 0-107060  
 Nb-Ni amorphous alloys, glass transition and ductility, O additions effect 0-75168  
 Nb-O system, solid soln. hardening and softening 0-71665  
 Nb-Pd constitution diagram, metallographic and X-ray diffr. anal. 0-89204  
 Nb-Rh,  $\sigma$ -phase alloy, superconductivity and resistance behaviour 0-70882  
 Nb-Si, compounds with A15 structure, films, TEM study (French) 0-80135  
 Nb-Si-(V)(Zr)(Mo)(Ta)(W)(C)(B)(Ge), ductile amorphous, superconductivity 0-60131  
 Nb-Ta, resistivity due to H incorporation 0-70666  
 Nb-Ta alloys, H diffusion at 296K 0-84329  
 Nb-Th, eutectic composition 0-100828  
 Nb-Ti, multifilamentary, Mirror Fusion Test Facility, superconductor core manufacturing and quality 0-93521  
 Nb-Ti, pinning curves, high field  $J_c$  and scaling behaviour 0-93064  
 Nb-Ti, resistivity due to H incorporation 0-70666  
 Nb-Ti, superconductor optimisation for 12 Tesla toroidal field coils 0-91272  
 Nb-Ti (50%), supercond., cryostat design for magnetisation study (Spanish) 0-75673  
 Nb-Ti multifilaments, effect of mech. and thermal treatments of supercond. props. 0-104197  
 Nb-Ti superconducting coils, for thermonuclear fusion (French) 0-95399  
 Nb-Ti superconducting single layered multifilamentary coil, eddy current loss depend. on demagnetisation 0-97040  
 Nb-Ti-Ta, pinning curves, high field  $J_c$  and scaling behaviour 0-93064  
 Nb-Ti-Ta, superconductor optimisation for 12 Tesla toroidal field coils 0-91272  
 Nb-Ti-Zr ternary system, high-field supercond. 0-97045  
 Nb-Ti(Mo), AC loss minimum, pinning, flux distribution 0-84574  
 Nb-V, resistivity due to H incorporation 0-70666  
 Nb-V system,  $H_2$  absorpt. 0-59808  
 Nb-V<sub>2</sub>Ga mixed state, Meissner effect investigation by muon, method (Russian) 0-107954



**niobium alloys continued**

- Nb-W-Mo-Zr (5, 2.1, 0.92 wt.%), creep resist., high temp. ageing in vacuum 0-71716  
 Nb-W-Zr-N alloy, with dispersed second phase, ductile-brittle transition 0-93653  
 Nb-W-Zr-Ta (90, 4.5, 3.5, 2 wt.%) creep and creep limit in super vac. at 1100°C, heat treatment effect 0-81133  
 Nb-Zr, crit. current, flow-flow resist. depend., allowance for superheating (*Russian*) 0-93061  
 Nb-Zr, thermoelec. power, 4.2 to 300K 0-70683  
 Nb-Zr (1 wt.%), corrosion behaviour in high temp. impure He gas 0-76402  
 Nb-Zr (3 wt.%), neutron-irradiated, positron annihilation ang. correl. meas. 0-93430  
 Nb-Zr alloy, BCC- $\omega$  phase transition, electronically driven nature 0-103433  
 Nb-Zr-C welding solid solutions, ageing kinetics, influence of inclusion elements (*Russian*) 0-100853  
 Nb-Zr-N biphasal alloy, recrystallization annealing 0-104180  
 Nb<sub>2</sub>/Sn-Cu composites, in situ processed, supercond. props. 0-75698  
 Nb<sub>2</sub>(AlGe) and Nb<sub>2</sub>(AlSi), liq. quenched, supercond. props. 0-84580  
 Nb<sub>2</sub>Al, A-15 struct., converted from cold worked BCC struct., crit. currents 0-75697  
 Nb<sub>2</sub>Al, A15 cpd., normal state, low temp. resist. 0-107762  
 Nb<sub>2</sub>Al, complex refractive index meas. 0-93264  
 Nb<sub>2</sub>Al film, electron-beam coevaporated, prep. and characts. 0-76187  
 Nb<sub>2</sub>Al, prep. by reduction of Nb<sub>2</sub>O<sub>5</sub> and Al<sub>2</sub>O<sub>3</sub> by CaH<sub>2</sub>, thermodynamic calc. 0-100809  
 Nb<sub>2</sub>Al, supercond. props. and lattice parameter, comp. and neutron irradi. effects 0-70880  
 Nb<sub>2</sub>Al, temp-depend. of elec. resist. 0-103675  
 Nb<sub>2</sub>Al(Ga), NQR freq. temp. depend., supercond. transition temp. 0-93207  
 Nb<sub>2</sub>Fe<sub>2</sub>P<sub>14</sub>B<sub>6</sub>, metallic glass, explosive compaction, mech. props. 0-89176  
 Nb<sub>73</sub>Ga<sub>25</sub>, A 15 phase high transition temp., sp. ht. determ. 0-60140  
 Nb<sub>2</sub>Ga, temp-depend. of elec. resist. 0-103675  
 Nb<sub>2</sub>Ga with structure A15, apparatus for rapid hardening from liquid state 0-76275  
 Nb<sub>2</sub>Ge, A15 cpd., normal state, low temp. resist. 0-107762  
 Nb<sub>2</sub>Ge, amorphous film, supercond., flux flow resist., vortex pair dissoc. 0-88701  
 Nb<sub>2</sub>Ge, amorphous films, thermally-activated internal friction peaks, structural obs. 0-80147  
 Nb<sub>2</sub>Ge, bridge contact, Josephson effect 0-70906  
 Nb<sub>2</sub>Ge coevaporated film, high supercond. transition temp., nucleation and growth 0-76185  
 Nb<sub>2</sub>Ge film, high-temp. supercond. phase stabilisation w.r.t. prep. conditions (*Russian*) 0-70871  
 Nb<sub>2</sub>Ge film, superconductivity, relevance of mag. interactions, EPR study 0-100545  
 Nb<sub>2</sub>Ge, low temperature electron, neutron irradi. effects on critical temp. (*French*) 0-75669  
 Nb<sub>2</sub>Ge, sputtered on Cu, film-substrate interface obs. by electron microscopy 0-65398  
 Nb<sub>2</sub>Ge, supercond. film, amorphous content, X-ray diffr. study, rel. to transition temp. 0-75668  
 Nb<sub>2</sub>GeAl<sub>1-x</sub>, ternary supercond. alloys, comp. variations 0-97022  
 Nb<sub>2</sub>Ge(Si), RF sputtered films, amorphous atomic scale struct. 0-84064  
 $\beta$  NbH<sub>0.82</sub>, fracture, TEM obs. 0-108519  
 NbH<sub>x</sub>, coherent  $\alpha$ - $\alpha'$  phase transition 0-71641  
 Nb<sub>2</sub>Nb<sub>1-x</sub>Si<sub>x</sub>(Ge)<sub>x</sub>, impurity stabilised A15 supercond., transition temp., lattice consts., specific heat 0-93026  
 Nb<sub>40</sub>Ni<sub>60</sub>, amorphous, produced by Ni<sup>+</sup> implantation, damage distrib. 0-107062  
 NbSe<sub>3</sub>, freq. depend. conductivity 0-107838  
 Nb<sub>2</sub>Si A15 phase from amorphous Nb-Si alloys, high-pres. synthesis 0-93516  
 Nb<sub>2</sub>Si A15 struct., high pres. synthesis (*Chinese*) 0-70917  
 Nb<sub>2</sub>Si, amorphous films, thermally-activated internal friction peaks, structural obs. 0-80147  
 Nb<sub>2</sub>Si, substituted, splat cooling influence on supercond. T<sub>c</sub> and stoichiometry 0-80439  
 Nb<sub>2</sub>Sn A15 composite superconductors; hydrostatic extrusion (*French*) 0-104090  
 Nb<sub>2</sub>Sn, A15 cpd., normal state, low temp. resist., disorder effects 0-107762  
 Nb<sub>2</sub>Sn based multifilamentary superconductors, bronze process fabrication, voids growth obs., via hot stage SEM 0-70089  
 Nb<sub>2</sub>Sn bronze process, flux pinning scaling law depend. on strain 0-75696  
 Nb<sub>2</sub>Sn, coherence parameter, nonlinear high temp. supercond. elements with A-15 lattice (*Russian*) 0-60127  
 Nb<sub>2</sub>Sn composite, superconducting transition depend. on non-hydrostatic stress 0-107948  
 Nb<sub>2</sub>Sn, composite superconducting wire, critical current-bend strain relationships 0-93063  
 Nb<sub>2</sub>Sn, effect of changes in  $\alpha^2(\Omega)F(\Omega)$  on the zero-temp. energy gap 0-97025  
 Nb<sub>2</sub>Sn, filaments in Cu matrix, thermal strain effects on superconducting critical temp. 0-93032  
 Nb<sub>2</sub>Sn film formation, solubility, precipitating processes (*Russian*) 0-92792  
 Nb<sub>2</sub>Sn, flux density gradient determ. by Faraday effect 0-107969  
 Nb<sub>2</sub>Sn forced flow superconducting test coil, Westinghouse design for fusion reactor large coil program 0-99337  
 Nb<sub>2</sub>Sn, hot isostatically pressed, plastic deform. 0-108510  
 Nb<sub>2</sub>Sn microfilamentary superconducting composite, critical currents, fracture props. 0-107970  
 Nb<sub>2</sub>Sn, monofilaments, radiation-enhanced diffusion growth, crit. current density 0-65758  
 Nb<sub>2</sub>Sn, multifilamentary coils for Lawrence Livermore Laboratory superconducting High Field Test Facility 0-90834  
 Nb<sub>2</sub>Sn multifilamentary composite supercond. wires, transverse sections prep., ion milling, TEM obs. of grain size 0-101000  
 Nb<sub>2</sub>Sn multifilamentary supercond. composites, crystallographic texturing 0-71669  
 Nb<sub>2</sub>Sn, multifilamentary superconductor preparation by 'in situ' and cold powder methods, review 0-93522  
 Nb<sub>2</sub>Sn, on LiNbO<sub>3</sub> substrate, US attenuation of SAW in applied mag. field 0-75678

**niobium alloys continued**

- Nb<sub>2</sub>Sn, powder metallurgically produced, microstruct. characts. 0-89233  
 Nb<sub>2</sub>Sn, softening of surface phonons in (100) plane 0-107627  
 Nb<sub>2</sub>Sn, supercond. composite, residual stress state, crit. currents 0-80468  
 Nb<sub>2</sub>Sn, supercond. props., effect of neutron irradi. 0-80463  
 Nb<sub>2</sub>Sn, superconductor for Large Coil Program, low temp. stability, joints, design method 0-106195  
 Nb<sub>2</sub>Sn, Young's modulus, 4.2-300K, behaviour near martensitic transition 0-66564  
 Nb<sub>2</sub>Sn-Cu multifilamentary composite wire, Nb<sub>2</sub>Sn filament morphology and grain size 0-100855  
 Nb<sub>2</sub>Sn<sub>47</sub>, effects of hydrostatic pressure on changes in elastic consts. caused by addition of H 0-75287  
 NbTi filaments for position-sensitive superconducting detector of ionizing particles 0-63460  
 NbTi films, effect of Ar- and N-ion bombardment on texture (*Russian*) 0-107338  
 NbTi, forced flow superconducting test coil, EURATOM design for fusion reactor Large Coil Task 0-99339  
 NbTi forced flow superconducting test coil, Swiss design for fusion reactor Large Coil Task 0-99341  
 NbTi monofilamentary wire in current sharing state, supercond. temp. sensor use 0-57288  
 NbTi, superconducting test coil, General Dynamics Convair Division, Intermagnetics General Corp. design for fusion reactor Large Coil Program 0-99338  
 NbTi superconducting test coil, General Electric design and manufacture program, for fusion reactors 0-102319  
 NbTi/In composite superconductor, transport props. 0-88658  
 NbTi-Cu, composite superconductor, acoustic emission 0-84546  
 NbTi-Cu, supercond. composite, use in temp. and heat transfer coeff. meas. 0-77780  
 NbTi-In granular supercond. composites, mag. field-induced dissipation 0-84545  
 (Nb<sub>0.99</sub>Ti<sub>0.01</sub>)<sub>1-x</sub>Ge<sub>x</sub>, high T<sub>c</sub> resist. meas. 0-88531  
 Nb<sub>20</sub>Zr<sub>80</sub>, supercond. and normal, sp. ht. meas., 2-20K 0-70893  
 (Nb<sub>0.99</sub>Zr<sub>0.01</sub>)<sub>3</sub>Sn, AC power losses in parallel AC and DC mag. fields 0-97041  
 Ni-Al-Nb ternary system, electron microprobe analysis of nickel-rich region at 1473K 0-71631  
 Ni-Cu-X (X=Sn, Nb, Ti), spinodal decomp. alloys, linear expansion coeff. influence on morphological anisotropy (*Japanese*) 0-70431  
 Ni-Fe-Nb-Al (11.2, 8.09, 79.66 wt.%), modulated struct. growth process rel. to ageing (*Chinese*) 0-66541  
 Ni-Fe-Nb-Mo-Al, head material for mag. recording, DC and AC mag. props. 0-88812  
 Ni-Nb-C, obtained by liq. quenching, superconductivity 0-75699  
 Ni-NbC (10 wt.%) eutectic alloy, directional solidification and struct. (*Russian*) 0-84922  
 Ni<sub>3</sub>(Al, Nb) single crystal, yield stress, orientation and temp. depend. 0-108511  
 Ni<sub>3</sub>(Fe<sub>1-x</sub>Nb<sub>x</sub>), temp. and conc. depend. of anomalous Hall effect (*Russian*) 0-70674  
 P+Nb, dil. alloy, NMR obs. of <sup>93</sup>Nb 0-71203  
 steel, Nb, deform., recrystn. and precip. interaction 0-97515  
 Ta<sub>20</sub>Nb<sub>80</sub>, Abrikosov vortex formation kinetics (*Russian*) 0-93055  
 Ti-Nb, diffuse electron scatt. (*Russian*) 0-103438  
 Ti-Nb (4.32 wt.%), high temp. oxidation kinetics under 1 bar pressure, 1255-1471K 0-89410  
 Ti-Nb-Si, amorphous alloy, supercond. props. and crystn. behaviour, TEM and DTA study (*Japanese*) 0-84536  
 Ti-Nb-Zr-Fe, supercond. and paramag. props., effect of Fe additions (*Russian*) 0-65730  
 Ti-Nb-Zr-Ta, superconducting props. comp. depend., stress effects and precipitation behaviour, X-ray scatt. 0-93059  
 U-Nb (14 at.%), martensitic and polymorphic transformations 0-60861  
 V-Nb-Ti-N alloy, with dispersed second phase, ductile-brittle transition 0-93653  
 V<sub>2-x</sub>Nb<sub>x</sub>Hf, NMR of <sup>51</sup>V and mag. susceptibility, 20-300K (*Russian*) 0-93192  
 Zr-Nb, structure associated with BCC to omega transform. (*Russian*) 0-108432  
 Zr-Nb (0.1, 2.5 wt.%), foil, dislocation loop nucleation and growth during 1 MeV electron irradi. 0-88152  
 Zr-Nb (2.5 wt.%), channel tubes, in-reactor creep and irradi. growth 0-93604  
 Zr-Nb (2.5 wt.%), cold-worked, pressure tubing, metallography and mech. props. 0-89269  
 Zr-Nb (2.5 wt.%), high temp. oxidation in flowing O<sub>2</sub>, 873-1173K 0-93687  
 Zr-Nb (2.5 wt.%), hydride precipitation and growth at crack tips, electron optical obs. 0-108449  
 Zr-Nb (2.5 wt.%), neutron irradi. at 573 to 923K, damage struct. 0-107334  
 Zr-Nb (2.5 wt.%), nuclear fuel channels, neutron effects on ultimate fracture strength, 293 to 573K 0-85054  
 Zr-Nb (2.5 wt.%), pressure tubes, irradi. creep and growth, anisotropy factors 0-97536  
 Zr-Nb (2.5 wt.%) pipe, fracture resistance, hydrogenation effect 0-104279  
 Zr-Nb (2.5 wt.%) pressure type rel. between stress intensity factor, crack opening displacement and J-integral 0-100920  
 Zr-Nb (97.5, 2.5 wt.%) nuclear reactor pressure tube material, H embrittlement study by TEM 0-76363  
 Zr-Nb-Sn (3.0, 1.0 wt.%), high temp. oxidation in flowing O<sub>2</sub>, 873-1173K 0-93687  
 ZrB<sub>2</sub>-Nb, reactions between components 0-100812  
 (Zr<sub>1-x</sub>Nb<sub>x</sub>)Fe<sub>2</sub>, antiferromag. spin struct., Mossbauer effect study 0-66086

**niobium compounds**

- see also niobium alloys  
 carbides, diffuse, production and superconductive props. (*Bulgarian*) 0-80467  
 chalcogenides and chalcogenide halides, geometrical struct. and metal-metal bonding 0-80172  
 minerals, cryst. struct., X-ray powder diffr. study 0-107169  
 nitrides, diffuse, production and superconductive props. (*Bulgarian*) 0-80467  
 PbO-Nb<sub>2</sub>O<sub>5</sub> system, X-ray and electron microscopic phase and struct. determ. (*French*) 0-92508



## niobium compounds continued

- B<sub>2</sub>O<sub>3</sub>-Nb<sub>2</sub>O<sub>5</sub> system, phase equil. and phase struct. obs. by high resolution TEM 0-108419  
 Ba<sub>2</sub>NbRu<sub>2</sub>O<sub>12</sub> (Ru<sub>2</sub>O<sub>12</sub>)<sup>13-</sup> cluster obs. in presence of orbital degeneracy and spin-orbit coupling (*French*) 0-70655  
 Cu-NbTi, composite conductor, acoustic emission 0-97032  
 Fe<sub>0.33</sub>NbS<sub>2</sub>, lattice dynamics and hyperfine interactions, Mossbauer spectra study 0-108135  
 Fe<sub>2</sub>NbSe<sub>2</sub>, transport props. and mag. ordering 0-65527  
 Y-Z LiNbO<sub>3</sub>, acoustic effects of filamentary defects 0-75314  
 Y-Z LiNbO<sub>3</sub>, filamentary defects visualisation at wafer inspection stage 0-75315  
 LiNbO<sub>3</sub>, temp. coeff. of freq. determ. 0-75316  
 (Nb,Ta)<sub>2</sub>N<sub>2</sub>O, cryst. struct. determ. (*German*) 0-107145  
 Nb complexes, <sup>93</sup>Nb quadrupole coupling tensors form EPR meas. 0-88866  
 Nb-D-H, equil. H/D separation factors 0-59668  
 Nb-H(D), H ordering, review 0-60850  
 Nb-N, superconducting layers, sputtering in high vacuum apparatus (*German*) 0-89147  
 Nb-Nb<sub>2</sub>O<sub>5</sub>-Pb Josephson junction formed on Nb film edge 0-107960  
 Nb-Nb<sub>2</sub>O<sub>5</sub>-Pb(In) Josephson junctions, props. of Nb<sub>2</sub>O<sub>5</sub> thermally grown tunnel barriers 0-100568  
 Nb-Nb<sub>2</sub>O<sub>5</sub>-Pb Josephson junction current-biased on Fiske steps, mag. field depend. 0-84567  
 Nb-NbO<sub>2</sub>-Pb Josephson junctions with high current densities, critical current 0-100552  
 Nb-NbO<sub>2</sub>-Pb superconductive tunnel junctions, oxide tunnelling barriers, ESCA characterisation 0-65745  
 Nb-NbO<sub>2</sub>-Pb tunnel junction, temp. depend. of effective Nb energy gap 0-80454  
 Nb-O(N), dislocation pinning, impurity interactions, strengthening (*Russian*) 0-92532  
 Nb-Ti-O, phase equilibria 0-96624  
 NbC, band struct. and X-ray emission spectra, APW and X<sub>α</sub> calc. 0-70605  
 NbC, electronic structure, PES study 0-70594  
 NbC, etchant for revealing microstructure 0-85097  
 NbC, pressing regime influence on high-temp. creep (*Russian*) 0-100852  
 NbC, rock salt struct., surface energy bands, Shockley surface states, bonding 0-92956  
 NbC single cryst., Vickers microhardness, slip mechanism 0-71732  
 NbC, supercond. critical temp., neutron irradiation effect 0-80433  
 NbC, vacuum condensate, struct. and mech. props., second phase effect (*Russian*) 0-71705  
 NbC<sub>x</sub>, supercond. transition temp., light element implantation effect 0-107951  
 Nb(CN)<sub>x</sub>, supercond. critical temp., neutron irradiation effect 0-80433  
 Nb<sub>2</sub>O<sub>3</sub>, x+y=0.73 to 0.88, thermal expansion coefficients 0-103502  
 NbCl<sub>3</sub>, nuclear electric hexadecapole interactions 0-65513  
 NbD<sub>0.85</sub>, localised D vibrs., temp. depend., neutron inelastic scatt. study 0-107395  
 NbGa<sub>2</sub>O<sub>4</sub>, O stabilised cpd., struct. determ. 0-103301  
 NbH<sub>0.2</sub>, localised H vibrs., temp. depend., neutron inelastic scatt. study 0-107395  
 NbH<sub>2</sub>, structural transform. rel. to order-disorder transform. 0-60858  
 Nb<sub>2</sub>Mo<sub>2</sub>S<sub>8</sub> Chevrel phase, synthesis, stability and charact. 0-71608  
 NbN, band structure, nonorthogonality and tight-binding fit 0-59852  
 NbN embedded in resin, composite supercond., high transition temp. 0-88660  
 NbN granular films, supercond., crit. props. 0-88661  
 NbN granular microbridges, Josephson effects 0-84556  
 NbN, granulated film, critical current temp. depend. (*Russian*) 0-103803  
 NbN, γ- and δ-forms, cryst. growth and supercond. transition temp. 0-107946  
 NbN single crystal preparation, zone melting and nitriding techniques 0-60776  
 NbN, supercond. granular films as weak link in Josephson devices 0-88685  
 NbN, supercond. RF reactively sputtered films, deposition parameter effects on props. 0-80972  
 NbN weak links, granular, Josephson behaviour 0-75681  
 Nb<sub>2</sub>N, supercond. props. and structural phase transform. induced by C<sup>+</sup> and N<sup>+</sup> implantation 0-107942  
 NbN<sub>0.7</sub>C<sub>0.3</sub>, cryst. growth and supercond. transition temp. 0-107946  
 4NbO<sub>0.76</sub> thin film, FCC cell struct. investigation 0-92796  
 NbO<sub>2</sub>, Lifshitz point behaviour 0-70402  
 NbO<sub>2</sub>, on-state decay rel. to recomb. and nonlinear props. 0-84492  
 Nb<sub>2</sub>O<sub>3</sub> and Al<sub>2</sub>O<sub>3</sub> simultaneous reduction by CaH<sub>2</sub>, Nb<sub>2</sub>Al prep. 0-100809  
 Nb<sub>2</sub>O<sub>3</sub>-PbO, acoustooptic props. from comp. and density 0-76000  
 Nb<sub>2</sub>O<sub>3</sub>-V<sub>2</sub>O<sub>5</sub>-P<sub>2</sub>O<sub>5</sub>, glasses and glass ceramics, elec. cond., struct. 0-84466  
 Nb<sub>2</sub>O<sub>3</sub>-WO<sub>3</sub> system complex cpds. with TTB type subcells, HV superhigh resolution electron microscopy obs. of struct. 0-103311  
 3Nb<sub>2</sub>O<sub>7</sub>·8WO<sub>3</sub>, circular diffuse scattering studied by 1 MV high resolution electron microscopy 0-59350  
 Nb<sub>2</sub>P, precipitates, obs. in austenitic stainless steel (*Japanese*) 0-89221  
 Nb<sub>2</sub>Pb superconducting film, prep., vac. deposition 0-89149  
 Nb<sub>2</sub>Pt<sub>2</sub>O, R phase of Nb-Pt|O system, cryst. struct. 0-96495  
 NbS<sub>2</sub>, intercalate with tetraalkylammonium hydroxide, prep. and struct. 0-79752  
 NbS<sub>2</sub>-(pyridine)<sub>1/2</sub> intercalation complex, superlattice struct., NMR meas. 0-70180  
 NbS<sub>3</sub>, electronic struct. and predicted cond. props. 0-92815  
 Nb<sub>2</sub>S<sub>4</sub>, electronic struct. and predicted cond. props. 0-92815  
 NbS<sub>2</sub>-Cl<sub>2</sub>(Br<sub>2</sub>)(I<sub>2</sub>), absorpt. edge spectrum, fine struct. 0-66219  
 NbSe<sub>2</sub> (2H), scattering effects on CDW transition temperature 0-107720  
 NbSe<sub>2</sub> (2H), Raman scatt. from supercond. gap excitations 0-93340  
 NbSe<sub>2</sub> (2H), Raman scatt. by supercond. gap excitations, coupling to CDWs 0-103956  
 NbSe<sub>2</sub>, experimental data, upper critical field theory fit 0-75692  
 NbSe<sub>2</sub> pure and intercalated with ethylenediamine, positron annihilation study 0-84801  
 NbSe<sub>2</sub> solid lubricant, antifriction and elec. props. depend. on oxidation temp., dopant influence 0-108584  
 NbSe<sub>2</sub>, upper crit. fields and reduced dimensionality 0-70910  
 NbSe<sub>2</sub>, CDW form., supercond. and Fermi surface determ., press. study 0-70891  
 NbSe<sub>3</sub>, CDW noise, temp. and freq. depend. 0-103681

## niobium compounds continued

- NbSe<sub>3</sub>, depinning props. of lower CDW, weak pinning model (*French*) 0-70630  
 NbSe<sub>3</sub>, electronic struct., chem. interpret. of geom. deform., oxidation state formalism 0-107690  
 NbSe<sub>3</sub> interference effects of CDW motions 0-88544  
 NbSe<sub>3</sub>, mag. susceptibility, CDW effect 0-88716  
 NbSe<sub>3</sub>, superconducting transitions and diamagnetism 0-84526  
 NbSe<sub>2</sub>(2H), low field magnetoresist. and anomalous transport props. 0-65602  
 Nb<sub>3</sub>Sn monofilamentary composite superconductor, tensile stress influence on critical current 0-97046  
 Nb<sub>3</sub>Sn, thin film, TEM microanalysis 0-104491  
 Nb<sub>1-x</sub>V<sub>x</sub>Se<sub>2</sub>, elec. and mag. anomalies at CDW transition 0-107722  
 Pb<sub>0.95</sub>Sn<sub>0.05</sub>(Zr<sub>x</sub>, Ti<sub>1-x</sub>)O<sub>3</sub>-Nb<sub>2</sub>O<sub>5</sub>, phase coexistence range, lattice const. 0-92680  
 PbZr<sub>1-x</sub>Ti<sub>x</sub>O<sub>3</sub>-Nb<sub>2</sub>O<sub>5</sub> ceramic, ferroelec. transitions, polarisation meas. (*French*) 0-66124  
 RbCrCl<sub>3</sub> crystals, β-γ structural phase transition, lattice dynamical anal. 0-84291  
 Rb<sub>2</sub>ZnBr<sub>4</sub>, incommensurate phase, <sup>87</sup>Rb NMR lineshape 0-93191  
 SnO<sub>2</sub>-Nb<sub>2</sub>O<sub>5</sub>, activated sintering mechanism 0-60810  
 V-H(D), anelasticity due to long-range diffusion 0-60904  
 V<sub>2</sub>O<sub>5</sub>-P<sub>2</sub>O<sub>5</sub>-Nb<sub>2</sub>O<sub>5</sub> glasses, switching 0-88604  
 4.26ZrO<sub>2</sub>·Nb<sub>2</sub>O<sub>5</sub>, elec. cond. meas. 0-100463
- nitrogen**  
 see also nuclei with .....  
 abundance anomalies in QSO Q0353-383, UV and visible spectral obs. 0-82532  
 abundance in B-type stars in associations and general field 0-67702  
 abundance in globular cluster NGC 6752 first giant branch 0-67719  
 abundance in lunar soil samples from Luna-24, neutron activation obs. 0-67594  
 adsorbed on Ni, valence band photoemission, SCF MO CNDO calc. 0-100754  
 adsorbed on W(100), vibr. spectra, bonding struct., LEED study 0-84387  
 adsorbent mesopores, capillary evaporation and struct. 0-107614  
 adsorption on CaHPO<sub>4</sub> powder and granules with starch mucilage binder, surface area obs. on compression 0-80998  
 adsorption on MnO<sub>2</sub> coated Al<sub>2</sub>O<sub>3</sub> and SiO<sub>2</sub> powder supports, dispersion mode obs. 0-81363  
 adsorption on MnO<sub>2</sub> porous powders, Al<sub>2</sub>O<sub>3</sub> and SiO<sub>2</sub> coated, surface free energy changes 0-84363  
 adsorption on Ni (001), c(2×2) struct. form 0-80083  
 adsorption on polycryst. W, α and β adsorption states 0-100404  
 adsorption on pure and SiO<sub>2</sub>-coated TiO<sub>2</sub>, 77.4K, microcalorimetry obs. 0-80062  
 adsorption on W (001), effect on LEED electron spin polarisation and intensity profiles 0-65377  
 adsorption on Zr, dissociation and diffusion 0-80085  
 afterglow decay, radiation escape kinetics, radiation captured by plane optically thick layer 0-95593  
 atom, (2S<sub>1/2</sub>), kinetic study by time resolved atomic resonance fluorescence 0-95557  
 atom, ab initio effective valence shell Hamiltonian for neutral and ionic valence states 0-74117  
 atom, associative ionisation, merging beams experiment 0-63789  
 atom, electron impact excitation, near threshold, cross-sections for (2s<sup>2</sup>2p<sup>3</sup>3s)<sup>4</sup>P and (2s2p<sup>4</sup>)<sup>4</sup>P states 0-91684  
 atom, spectra in Ar inductively coupled plasma 0-91474  
 atomic spectra of aurora, UV obs. of N(<sup>2</sup>P) metastable state 0-77185  
 atoms, far vac. UV spectra, oscillator strengths for 3s, 4s, 5s, 3d and 4d <sup>4</sup>P<sub>3/2</sub>-2p<sup>3</sup> <sup>4</sup>S<sub>3/2</sub> 0-74178  
 auroral collision processes of metastable N(<sup>2</sup>P) 0-72658  
 boiling heat transfer from structured surfaces to liquid nitrogen (*German*) 0-99919  
 broad beam ion source used for sputtering and etching 0-69002  
 concentration in thermosphere, depend. on solar activity 0-77178  
 critical heat flux in horizontal tube, up to critical press. (*German*) 0-99921  
 dense vapour, electron localisation 0-87840  
 determination by activation anal. (α,n), (α,p) reacts, investig. 0-61206  
 diamond, N, vacancy enhanced aggregation of N 0-70245  
 diffusion in Fe, Fe<sub>2</sub>N growth kinetics (*Korean*) 0-93540  
 diffusion in group V refractory metals, statistical calculations on Arrhenius lines 0-59722  
 diffusion rate in Au thin layers 0-100359  
 diffusion with CO in chamber and formed coke (*German*) 0-100356  
 emission from Ir(111) surface, following decomp. of hydrazine, ang. struct. 0-97731  
 ethylene-O<sub>2</sub>-N<sub>2</sub>-Al particle mixture, two-phase detonation and combustion (*French*) 0-61097  
 filament lamps, Kr-Ag-N gas mixture, thermal conduction coefficient calculational methods (*Russian*) 0-96335  
 film, on metal or sapphire substrates, luminescence and nonradiative energy transfer to surfaces 0-97350  
 flowing N spark gaps, electric breakdown study, improved method 0-64821  
 fluid, high density behaviour, extrapolated PρT surfaces and critical density 0-87834  
 gas, electron energy degradation, Monte Carlo study 0-69969  
 gas, pure rotational CARS obs. 0-99511  
 gas, weakly ionised, electron transport coeffs., Boltzmann eqn. anal. (*Japanese*) 0-59183  
 glow discharge, volt-ampere charact. in gas flow (*Russian*) 0-106991  
 glow discharges surface coronas and photopreionisation stability, demonstration 0-105475  
 high intensity arcs, anode contraction region modeling 0-103210  
 high power discharge laser excited through high dielectric constant ceramic materials 0-58572  
 injection into liquid through porous plate, squeezing out of liq. 0-64622  
 ion laser, travelling wave excitation 0-91774  
 ion pair creation by high-energy ions, meas. of average energy required 0-103105  
 ion source, HF, proton yield increase, influence of various admixtures to H<sub>2</sub> obs. 0-57422  
 jet, freely expanding, quantum effects in rot. relax. 0-58355  
 KERMA values, consistent set for H, C, N, and O for neutrons from 10 to 80 MeV 0-68967  
 laser, 406 nm emission on C-B band 0-64047



nitrogen continued

laser, appl. of pulsed transversally excited discharge (*French*) 0-107009  
laser, construction and properties, axial or cross-field discharge 0-69418  
laser, helical TE, tube geometry simplification 0-69406  
laser, multi-stage TEA type 0-95912  
laser, rotational struct. variation in 337.1 nm transition 0-78836  
laser, UV TEA, with Blumlein pulse generator, fabrication (*Japanese*) 0-69417  
laser pulsed, construction and theoretical explanation (*Slovak*) 0-95874  
laser transition, IR, excitation process 0-87383  
liquid, ang. distrib. of stimulated Raman scatt. following excitation by two coherent beams 0-106571  
liquid, atom pair pots., X-ray diff. 0-100158  
liquid, automatic level monitoring, in Dewar flasks 0-57309  
liquid, decanting siphon using self-opening valve 0-57310  
liquid, dielec. breakdown, press. depend. of polarity effect 0-75936  
liquid, high repetition rate stimulated Raman scatt., thermal blooming 0-91865  
liquid, in Kr, methane, and CO, Raman scatt. parameters, high-resolution coherent active spectroscopy 0-66207  
liquid, laser sonolum. at elevated hydrostatic press. 0-71498  
liquid, photoacoustic and photorefractive detect. of small absorpts., electrostrictive limits 0-108171  
liquid, pressure transmitting medium in low-temperature optical chamber 0-57358  
liquid, pure vibr. Raman spectra 0-97262  
liquid, solubility of light alkanes, IR spectroscopy obs. 0-59654  
liquid, vibrational dephasing, computer simulation, Raman spectra, pair potential effect 0-63863  
matrix for  $O_3 + Zn(Cd)$  matrix reactions, IR, Raman and visible spectra 0-87110  
matrix N-N stretching vibr., IR activation, guest mol. depend. 0-60570  
methane- $N_2$ -isobutane gas mixture composition by Raman spectra 0-87124  
mixing ratio in Saturn troposphere 0-94748  
mixtures, marginal comp., thermal diffusion column performance evaluation (*German*) 0-59157  
molecular sieves, adsorpt. of atmospheric gases, comparison of 13X and 4A at low temp., press. (*German*) 0-88423  
molecule,  $I^-$  system bands, line broadening and shift 0-87138  
molecule, asymmetry parameter, angle resolved photoelectron spectra, multiple scatt. method 0-63708  
molecule, CARS, optical Stark effect on vibr., and rot. transitions 0-99512  
molecule, diagrammatic perturbation theory, using universal even-tempered basis set 0-58131  
molecule, elastic and inelastic electron scatt., state to state cross section 0-78708  
molecule, electron excitation of Birge-Hopfield bands ( $b^1\pi_u-X^1\Sigma_g^+$ ) 0-95731  
molecule, electron impact excitation, to high Rydberg states, by threshold energy collision 0-83509  
molecule, electron multiple scatt. method, scatt. cross section calc. 0-63816  
molecule, electron scatt., absolute total cross-sections 0-83486  
molecule, electron scatt., elastic and inelastic, Glauber approx. 0-91695  
molecule, electron scatt., local exchange pot. comparison 0-78707  
molecule, electron scatt., low energy, multichannel variational calcs., static exchange approx. 0-83483  
molecule, electron scatt., reson. excitation and dissociation, attachment, vibr. state depend. 0-78717  
molecule, first positive system, electronic transition probabilities 0-78603  
molecule, fluid, light scatt. orientational memory function at moderate density 0-102521  
molecule, gas, electron impact ionisation, electronic fluoresce. spectra 0-95664  
molecule, liq. and gas, induced absorpt. spectral moment, mol. calcs. 0-63737  
molecule, multi-config. SCF super-CI calc., density matrix formulation 0-78547  
molecule, multiphoton absorpt., spectroscopic evidence 0-63726  
molecule, nonadiabatic coupling matrix elements by Hellmann-Feynman theory and HF 0-83263  
molecule, photoelectron asymmetry parameters 0-95684  
molecule, photoionisation cross section and asymmetry parameters calc. in UV region using static pot. 0-95692  
molecule, preionisation, and predissoc., rel. to spectral line shape 0-63724  
molecule, relative ionisation energies, Tamm-Dancoff approx. calcs. 0-83243  
molecule, SCF calcs. using cusped Gaussian basis sets, polarisation effects 0-74118  
molecule, second virial coeffs. 0-83440  
molecule, stimulated scattering investigation, 1-4 atm press. range 0-91568  
molecule, structural second virial coeff., intermol. pot. and mag. scatt. 0-78678  
molecule, vertical valence ionis. pot. calc. by perturbation, CI and CPA techniques 0-69263  
molecules, ab initio MO-LCAO-SCF and Gordon-Kim intermolecular pot. for seven different orientations 0-95522  
molecules, excitation efficiency for rot. states 0-102557  
molecules, isoelectronic sequence, Rydberg transitions, term value-ionisation pot. correl. 0-58276  
muonic X-ray transitions, nuclear charge radii 0-99589  
NGC 5236, spiral galaxy, N abundance radial var. and central N overabundance 0-82497  
nonequilibrium plasma, thermocouple diagnostics 0-103188  
nuclear pumped lasers, electron impact cross section meas. 0-63985  
oxidation resistance improvement of low-alloy steel 0-66706  
physisorbed monolayer on graphite, neutron scatt. studies 0-107655  
ponic, Auger electron emission (*Russian*) 0-69271  
planetary nebulae, abundances of He, Ne, Ar, N, and Cl 0-109532  
planetary nebulae in Magellanic Clouds, He, N and O abundances, effects of excitation class 0-109519  
plasma decay under constant voltage (*Russian*) 0-106988  
plasma heating in electrodeless RF capacitive discharge, mechanism, impurity effect 0-59312  
plasma jet, normally-impinging, heat transfer rates to flat plate 0-75061  
pure gas, enthalpy, Carlson-Thodos van der Waals eqn. calcs. 0-83878  
reactive N in unpolluted troposphere, stratospheric source 0-94561

nitrogen continued

scattering, inelastic and trapping desorpt., from W, elementary steps in chemisorpt. 0-60737  
solid,  $\alpha$ -phase, time-resolved CARS, disorder effects on coherent vibr. states 0-93342  
solid, exciton-phonon coupling in strong coupling limit, temp. depend. 0-92616  
solid, melting curves, Lennard-Jones Devonshire theory 0-65201  
solubility in Fe-Cr alloys (*Russian*) 0-92675  
steel, austenitic, Cr-Mn-N, plastic deformation influence on internal friction, relaxation processes (*Russian*) 0-100870  
steel, austenitic stainless, N-alloyed 0-108490  
steel, austenitic stainless, stacking fault energy, effect of N 0-107279  
superfluorescent UV laser, demonstration 0-105475  
supersonic molecular beam source, simple calibration method 0-82845  
thermal conductivity, corresponding states model 0-69964  
thermosphere, at N composition, seasonal and diurnal variation 0-85782  
thermosphere  $N_2$  composition, seasonal-latitudinal tidal struct. and mass density 0-101467  
track autoradiography for N detect. 0-100979  
W50, supernova remnant, N overabundance from optical spectrum 0-90557  
Ar- $N_2$  liquid soln., selective adsorption by plane homogenous surface and C atoms, mol. dynamics calc. 0-59806  
Ar- $N_2$  mixture, electron beam pumped, lasing obs. at 337, 358, 380 and 406 nm 0-102700  
Ar- $N_2$  mixture, lasing at four lines 0-99713  
BN,  $^{15}N$  zero point vibr. energy from nuclear photon scattering 0-59593  
C-N bond in methylamine, nucl. mag. isoscreening line diagrams 0-78555  
CO- $N_2$  discharge, plasma characts. and vibr. kinetics anal. 0-59331  
CO $_2$ -He- $N_2$ , absorpt. coeff. for 10.6  $\mu m$  CO $_2$  laser radiation, 295 to 650 K 0-92252  
CO $_2$ - $N_2$  electroionisation laser mixture, ionisation instability of semi self-maintaining discharge 0-63971  
CO $_2$ - $N_2$  fast-flow laser with unstable resonator, self-oscillation instability 0-95870  
CO $_2$ - $N_2$  mixture, strongly excited, vibr. relax. 0-102555  
CO $_2$ - $N_2$  mixture, temperature measurement by spectrum line reversal 0-73358  
CO $_2$ - $N_2$  mixture gasdynamic laser, energy characts. 0-69362  
CO $_2$ - $N_2$ -H $_2$ O fast flow discharge laser, output power time depend. 0-99697  
CO $_2$ - $N_2$ -He, pulse-periodic operation of electron-beam-controlled discharges, energy characts. changes 0-102695  
CO $_2$ - $N_2$ -He electroionisation laser, freq. mode, lasing conditions 0-63970  
CO $_2$ - $N_2$ -He laser media excitation by electron beams admitted through gasdynamic windows 0-99694  
CO $_2$ - $N_2$ -He-O $_2$  discharge mixture, three body electron attachment to O $_2$  0-64779  
CO $_2$ + $N_2$ +He, glow discharge positive ion species identification (*Russian*) 0-84014  
C $^{12}I_2$ , effective lifetime 0-102704  
Cd+N $_2$  vap., creation of inverse population of atomic Cd 6 $^3S$  and 5 $^3P_2$  levels 0-58219  
Cl $_2$ +N $_2$  mixture, Raman laser optical excitation, electron phototransition theory (*Russian*) 0-99711  
D $^{++}$ +N $_2$  fast collisions, impulse approx. 0-106281  
Fe, liquid, N solubility depend. on added elements, mechanism (*Russian*) 0-65223  
Fe surface hardening, ion-carbo-nitriding in CO- $N_2$ -H $_2$  gas mixtures, expt. (*Japanese*) 0-71670  
 $\alpha$ -Fe-N, valency effect of interstitials 0-65502  
 $\alpha$ -Fe-N, supersaturated solid solns., N atom precip. kinetics, resist. meas. 0-60864  
Ga $_{1-x}$ Al $_x$ P:N epitaxial films, ion implanted, cathodoluminescence study 0-60684  
Ga(As,P):N, isoelectronic impurity states, long-range, short-range model 0-75524  
GaAs:N, extended Huckel theory appl. 0-59916  
GaAs $_{1-x}$ P $_x$ :N, photolum. and electrolum. study of N isoelectronic traps 0-89061  
GaP:Bi:N, photoluminesc., electroluminesc., 4.2 to 300K, excitons and hole traps 0-108275  
GaP:N, bound exciton absorpt. line asymmetry, electroabsorption spectra 0-71459  
GaP:N, extended Huckel theory appl. 0-59916  
GaP:N LED structures, local dopant conc. determ. using SEM cathodolum. spectra 0-101057  
GaP $_x$ As $_{1-x}$ :N, luminesc. of N bound state excitons, local-environment effects 0-100691  
H+B $^{q+}$ (C $^{q+}$ )(N $^{q+}$ )(O $^{q+}$ ), (2 $\leq q\leq 4, 5$ ), cross sections at keV energies 0-78705  
H $^0$ +N $^{3+}$ , electron loss cross section 0-63805  
HF+H $_2$ (D $_2$ )(N $_2$ ), 200K and 295K vibr. relax. rates 0-63766  
He-N mixture, RF discharge, mass spectroscopy, floating double probe meas. 0-84016  
HgBr $_2$ +N $_2$ (A $^2\Sigma^+_g$ ), dissociation excitation 0-63774  
In $_0.3$ Ga $_{0.7}$ P:N ion implanted, photoluminescence study 0-97322  
liquid N $_2$  for stimulated Raman scatt. Dewar cell, 1.06 to 1.4  $\mu m$  Q-switched laser pulse conversion 0-99799  
Mo-N solid solution, thermodynamic props., 1618 to 1883K 0-65230  
molecules in nonequilibrium gas-dynamic current, vibr.-level populations determ. by Raman scatt. 0-99509  
N, detect. in Venus upper atmosphere 0-77310  
N I 5200 Å airglow, anal. of consistency of ground-based obs. with satellite results 0-98496  
N II, electron impact excitation cross sections, rel. to solar corona abundance 0-58391  
N II homologous ions series, Stark broadening trends 0-105157  
N III forbidden lines in Omega Nebula (W38, M17, NGC 6618), IR spectral obs. 0-90495  
N ion +Au, L-shell X-ray production and subshell ionisation cross sections meas. 0-91637  
N, ionisation, multiphoton absorpt., spectroscopic evidence 0-63726  
N V, hot interstellar gas diagnostic, IUE obs. 0-101634  
N $^-$  autoionisation from N $_2$  electron impact dissociation, EELS 0-106397  
N $^{+}$ , electronic stopping power in solids, range distrib. energy depend. 0-92575  
 $^{14}N$  II, 2p $^3$   $^1P_1$ , hyperfine struct. after ion beam surface impact at grazing incidence 0-58403



## nitrogen continued

- N-Fe solid soln. in equilibrium with N<sub>2</sub> gas, partial molar enthalpy and excess entropy 0-60838  
 N-H bond in methylamine, nucl. mag. isoscreening line diagrams 0-78555  
 N-O mixtures, positive glow corona in quasi-uniform fields 0-100104  
 N+Al(Sn), inner-shell multiple ionisation systematics, X-ray obs. 0-63790  
 N+H<sub>2</sub>SO<sub>4</sub>, atmosphere chemistry, collisional reaction probabilities 0-90168  
 N+H(2S), excitation and ionisation contributions to sum-rule Born cross sections 0-99551  
 N+NF<sub>2</sub>, electronically-excited free radical reactions 0-97707  
 N<sup>+</sup>+H<sub>2</sub>, electron capture and ion-loss cross-section, 2.4-24.3 keV 0-58373  
 N<sup>+</sup>+H<sub>2</sub>(N<sub>2</sub>), reactant ion electronic states, effect on charge transfer cross sections 0-63809  
 N<sup>+</sup>+O<sub>2</sub>, branching ratio kinetic energy depend. 0-97703  
 N<sup>+</sup>+O<sub>2</sub>, electron capture and ion-loss cross-section, 2.4-24.3 keV 0-58373  
 N<sup>3+</sup>+H, multicharged ion thermal charge exchange reaction, rel. to astrophysics 0-63815  
 N<sup>n+</sup>+H, charge transfer cross sections, oscillatory behaviour in low-energy collisions 0-63806  
 N<sup>n+</sup>+Ne, charge exchange contribution to K-vacancy production 0-102553  
 N<sub>2</sub>, adsorption on Ni, photoemission and electronic struct., cluster calcs. 0-97403  
 β-N<sub>2</sub> cryst., vibr. Raman spectra 0-60558  
 N<sub>2</sub>, desorbed after N atom recomb. on Fe, vibr. energy, electron beam induced fluoresc. 0-61149  
 N<sub>2</sub>, electron impact dissoci., EELS, N<sup>-</sup> autoionisation 0-106397  
 N<sub>2</sub>, electronic structure calcs., self-consistent, accelerating convergence of iterative process 0-87037  
 N<sub>2</sub>, high energy electron spectroscopy techniques 0-62740  
 N<sub>2</sub> in high press. air plasma, photodissoc. 0-64691  
 N<sub>2</sub> influence on photodissociation of UF<sub>6</sub> 0-95698  
 α-N<sub>2</sub>, mol. cryst., theory of time evolution of exciton coherence 0-65455  
 N<sub>2</sub>, molecular fluid, Rayleigh and Raman light scatt. props., orientational and collision induced effects 0-63644  
 N<sub>2</sub>, N<sub>2</sub><sup>+</sup>, discharge pumped multiwavelength lasers (*Chinese*) 0-102703  
 N<sub>2</sub> reduction in solar nebula, kinetic inhibition 0-85875  
 N<sub>2</sub>, rotational Raman intensities and polarisability anisotropy change meas. with internuclear distance 0-63641  
 α-N<sub>2</sub>, temp. depend. of IR spectra, Gruneisen parameters determ. 0-84730  
 N<sub>2</sub>, total scatt. cross sections for intermediate-energy positrons 0-91692  
 N<sub>2</sub><sup>+</sup>, first <sup>2</sup>Π<sub>g</sub> state form. and decay 0-58177  
 N<sub>2</sub><sup>+</sup> 1 NG emissions from proton aurora, anomalous vibr. distrib. 0-67448  
 N<sub>2</sub><sup>+</sup>, auroral Meinel band excitation rel. to pulsating structs. extreme thinness 0-72667  
 N<sub>2</sub><sup>+</sup> Meinel system, high resolution spectrum to 11 250 Å 0-99497  
 N<sub>2</sub><sup>+</sup>, partial photoionisation cross section and photoelectron angular distribution for X<sub>2</sub><sup>+</sup> state determ. 0-83429  
 N<sub>2</sub><sup>+</sup> spectrum, appl. air arc temp. meas. 0-59314  
 N<sub>2</sub><sup>+</sup>, X<sub>2</sub><sup>+</sup> state, vibr. states asymmetry parameter and photoelectron spectrum 0-95591  
<sup>14</sup>N<sub>2</sub>, Fourier spectrometry and IR emission spectra 0-83368  
 N<sub>2</sub><sup>2+</sup>, low-lying electronic states, pot. energy curves calcs. by SCF technique, vibr. and ionisation consts. 0-69091  
 N<sub>2</sub><sup>2+</sup>, recomb. energy determ. from pot. curves 0-58335  
 N<sub>2</sub>-Ar(Kr)(O<sub>2</sub>)(CO)(CH<sub>4</sub>), liquid, high resolution CW CARS spectra 0-63635  
 N<sub>2</sub>-BCl<sub>3</sub> mixture, thermodiffusion props., effect of resonant excitation of mol. vibr. by laser, isotope separation 0-100047  
 N<sub>2</sub>-Cu arc plasma, transport coeffs. 0-96344  
 N<sub>2</sub>-H<sub>2</sub> arc, bent and rot., flow mechanism 0-70047  
 N<sub>2</sub>-He ion nuclear pumped lasers feasibility study and quenching 0-64001  
 N<sub>2</sub>-He plasma, laser produced, high press. amplified stimulated emission 0-78843  
 N<sub>2</sub>-methane, rapidly developing discharge, streak camera records interpretation 0-59280  
 N<sub>2</sub>-O<sub>2</sub> gas mixture, weakly ionised, electron transport coeffs. anal. (*Japanese*) 0-59184  
 N<sub>2</sub>-O<sub>2</sub> mixture transient discharges, RF techniques 0-70067  
 N<sub>2</sub>-SF<sub>6</sub> pulsed discharge laser with CW X-ray preionisation 0-95910  
 N<sub>2</sub>+Ar, inelastic scatt. exponential perturbation theories 0-74217  
 N<sub>2</sub>+Ar, metastable atom excitation of C<sup>2</sup>Π<sub>u</sub> state, symmetry, propensity rules and alternation intensity, rot. spectrum 0-87135  
 N<sub>2</sub>+Ar, molecular fluid mixtures, equilibrium props. 0-64867  
 N<sub>2</sub>+Ar, short-range intermol. pots., combined interatomic pots. calcs. 0-87198  
 N<sub>2</sub>+Ar(Xe), A<sup>3</sup>Σ<sub>g</sub><sup>+</sup> state energy pooling in flowing afterglow, Herman IR system 0-83503  
 N<sub>2</sub>+Br<sup>-</sup>, total electron detachment cross sections for energies around threshold 0-99550  
 N<sub>2</sub>+CO<sub>2</sub>+benzene, electronically excited, mol. fluoresc., vibr. relax. cross sections and equilibration rates determ. 0-87205  
 N<sub>2</sub>+Cl<sup>-</sup>, total electron detachment cross sections for energies around threshold 0-99550  
 N<sub>2</sub>+H<sub>2</sub>, collisional coherent excitation, meas. of Lyman α-photons 0-99552  
 N<sub>2</sub>+H<sub>2</sub>+N<sub>2</sub>H<sub>4</sub>, mixtures with nonthermal vibr. excitation of mol. N<sub>2</sub> 0-76545  
 N<sub>2</sub>+H<sup>+</sup> collision, total ionis. cross section and stopping power for protons 0-69228  
 N<sub>2</sub>+HCl, HCl ν<sub>0</sub>-ν<sub>1</sub> band perturbations, linewidth and shifts calcs., IR spectra obs. (*French*) 0-58251  
 N<sub>2</sub>+HF, HF(ν=3) relax. and rate consts. 0-61069  
 N<sub>2</sub>+He, rot. inelastic scatt., appl. of sudden approx. 0-95705  
 N<sub>2</sub>+He<sup>+</sup>, 0.7-2 MeV, charge-changing collisions, electron capture 0-58372  
 N<sub>2</sub>+HgBr, vibr. relax., rate coeffs., fluoresc. obs. 0-63697  
 N<sub>2</sub>+HgX<sub>2</sub> (X=halide), A<sup>3</sup>Σ<sub>g</sub><sup>+</sup> state quenching obs. 0-108693  
 N<sub>2</sub>+Kr<sup>+</sup>, charge transfer reactions, rate coeffs. and product-ion distributions meas. 0-104431  
 N<sub>2</sub>+Li(2p), Li(2p) excitation, alignment and orientation obs. 0-63794  
 N<sub>2</sub>+methane, N<sub>2</sub> fixation, catalytic processes in non-equilibrium plasma chemical reactors (*French*) 0-89483

## nitrogen continued

- N<sub>2</sub>+methylmercury halides, A<sup>3</sup>Σ<sub>g</sub><sup>+</sup> state quenching obs. 0-108693  
 N<sub>2</sub>+NH<sub>3</sub>, collisional broadening of NH<sub>3</sub> inversion spectrum lines 0-99521  
 N<sub>2</sub>+Ne<sup>2+</sup>, charge transfer reactions, rate coeffs. and product-ion distributions meas. 0-104431  
 N<sub>2</sub>+O<sub>2</sub>, molecular fluid mixtures, equilibrium props. 0-64867  
 N<sub>2</sub>+O<sub>2</sub>, N<sub>2</sub> fixation, catalytic processes in non-equilibrium plasma chemical reactors (*French*) 0-89484  
 N<sub>2</sub>+O<sub>2</sub>+NO, mixtures with nonthermal vibr. excitation of mol. N<sub>2</sub>, formula for calc. equil. const. 0-76545  
 N<sub>2</sub>+O<sup>+</sup>, charge exchange collision, rate coeff. and ionosphere implications 0-87224  
 N<sub>2</sub>+O<sup>+</sup>(<sup>2</sup>D), thermal rate coeff., products and branching ratios in ionosphere 0-82117  
 N<sub>2</sub><sup>+</sup>+H<sub>2</sub>, collisional dissoci. cross-section, 2.4-24.3 keV 0-58373  
 N<sub>2</sub><sup>+</sup>+He, ion loss cross-section, 2.4-24.3 keV 0-58373  
 N<sub>2</sub><sup>+</sup>+He, N<sub>2</sub><sup>+</sup> selectively excited, collisional deactivation 0-83338  
 N<sub>2</sub><sup>+</sup>+O<sub>2</sub>, collisional dissoci. cross-section, 2.4-24.3 keV 0-58373  
 N<sub>2</sub><sup>+</sup>+O<sub>2</sub>, electron capture and ion loss cross-section, 2.4-24.3 keV 0-58373  
 N<sub>2</sub><sup>+</sup>+Re(metal), reaction dynamics studied by XPS and thermal desorpt. spectrometry 0-93797  
<sup>14</sup>N<sub>2</sub>+CO, vibr.-vibr. energy transfer, long and short range pot. effect 0-99556  
<sup>15</sup>N<sub>2</sub>+CO, vibr.-vibr. energy transfer, long and short range pot. effect 0-99556  
 (N<sub>2</sub>)<sub>2</sub>, Van der Waals molecule, struct. and internal rot. barriers determ., interaction pot. from ab initio calcs. 0-91626  
 N<sub>3</sub>, high press. IR vibr. spectroscopy (*German*) 0-74170  
 N<sub>2</sub>(B<sup>2</sup>Σ<sub>g</sub><sup>+</sup>), N<sub>2</sub>(C<sup>2</sup>Π<sub>g</sub>) and N<sub>2</sub>(C<sup>2</sup>Π<sub>u</sub>) molecules, emissions obs. in yellow N<sub>2</sub> afterglow 0-63649  
 N(<sup>2</sup>D,<sup>2</sup>P) metastable production by electron collisions in DC glow discharge 0-59274  
 NH<sub>4</sub>Cl, <sup>15</sup>N zero point vibr. energy from nuclear photon scattering 0-59593  
<sup>14</sup>N<sup>15</sup>N+CO, vibr.-vibr. energy transfer, long and short range pot. effect 0-99556  
 NO+N<sub>2</sub>, NO γ(0,0) band, oscillator strength and line broadening 0-106356  
 N<sub>2</sub>(X<sup>3</sup>Σ<sub>g</sub><sup>+</sup>)+O<sup>+</sup>(<sup>4</sup>S)→NO<sup>+</sup>(X<sup>2</sup>Σ<sup>+</sup>)+N(<sup>4</sup>S), MCSCF potential energy surface for collinear <sup>4</sup>Σ pathway 0-63540  
<sup>13</sup>N labelled NH<sub>3</sub> production for medical appl. 0-72327  
<sup>15</sup>N, spin-lattice relax. time, quantum effect of NH<sub>4</sub><sup>+</sup> ion rot. 0-75875  
<sup>15</sup>N/<sup>14</sup>N ratio in lunar microbreccias indicating ancient solar wind composition 0-62046  
<sup>15</sup>N<sub>2</sub>, solid struct., and thermodynamic props. (*Russian*) 0-88083  
 N<sub>2</sub><sup>+</sup>(A<sup>2</sup>Σ<sub>g</sub><sup>+</sup>), electron impact ionisation cross section 0-78718  
 N<sub>2</sub><sup>+</sup>+H<sub>2</sub>O(H<sub>2</sub>S)(methane), deactivation, from laser-induced CO<sub>2</sub> fluoresc. obs. 0-63776  
 N<sub>2</sub><sup>+</sup>+H<sub>2</sub>O-N<sub>2</sub>+H<sub>2</sub>O\* 0-87212  
 N<sub>2</sub><sup>+</sup>+HgBr<sub>2</sub>, dissociative excitation, mol. fluoresc. obs. 0-91634  
 N<sub>2</sub>(active)+SO<sub>2</sub>, excited neutral metastable SO<sub>2</sub> form. mass spectrometric study 0-83300  
 Nb:N, neutron diffuse-scatt. intensities 0-59597  
 Ne-N<sub>2</sub>, atomic N nuclear pumped lasers, surface effects 0-63996  
 Ne-N<sub>2</sub>, AC discharge, pulse to continuous mode transition, Ne metastable effects (*German*) 0-84011  
 Ni(001) surface N adsorption due to ion beam irradi., surface struct. LEED study (*Chinese*) 0-84364  
 O<sup>+</sup>+N<sub>2</sub>, excited ion reactions, charge transfer coeffs. at thermal energy 0-95721  
 O<sub>2</sub>-N<sub>2</sub> mixture, attachment cooling, press. depend. 0-91663  
 O<sup>+</sup>(<sup>2</sup>D)+N<sub>2</sub> charge exchange, rate coeff. temp. depend. 0-77179  
 O<sup>+</sup>+N<sub>2</sub>, metastable ion reactions, rate consts. and ion mobility at 300K 0-95722  
 reactant ion electronic states, effect on charge transfer cross sections 0-63809  
 S<sub>2</sub>+N<sub>2</sub>, (*Russian*) 0-99711  
 SF<sub>6</sub>-N<sub>2</sub> mixture, electron swarm development, Boltzman eqn. anal. 0-87841  
 SF<sub>6</sub>-N<sub>2</sub> mixtures, attachment coeffs. and ionic mobilities, 1.2-4 eV 0-96338  
 SeO<sub>2</sub>+N<sub>2</sub>, radiative lifetime and quenching rates 0-95685  
 Si, commercial, nitridation, effect of BaF<sub>2</sub> 0-81359  
 Si:N, high energy ion implantation of buried insulating layers 0-88188  
 Si:N, implantation at high doses, annealing conditions for homogeneous buried insulating layer (*French*) 0-59498  
 Si:N, ion implanted, IR transmission and rel. spectra study 0-108244  
 Si:N, ion implanted, nature of defect reverse annealing 0-88875  
 Si:N, ion implanted, oxidation characts. 0-89385  
 Si:N, laser-annealed, Jahn-Teller distorted donor, EPR meas. 0-84642  
 Si:N wafers, Si<sub>3</sub>N<sub>4</sub> layer growth by high dose implantation and annealing, elec. props. 0-70227  
 Si:AlN (6H), ODMR for effective-mass-like acceptor 0-93213  
 SiO<sub>2</sub> film, on GaP substrate, N ion implantation, optical refl. and EPR meas. 0-84197

## nitrogen compounds

see also ammonia; ammonium compounds

- chloropentafluoroethane-NO, multiphoton dissoci., <sup>13</sup>C enrichment factor, CO<sub>2</sub> laser wavelength and fluence depend. 0-58331  
 ESCA shifts and effective charges 0-78648  
 interstellar cloud gas phase chemistry 0-105319  
 methoxy+NO, reaction rate upper limit, laser induced fluoresc. 0-85200  
 nitrate determ. in atmosphere using HNO<sub>3</sub> collection on NaCl impregnated filters 0-81509  
 nitrates, gaseous, in atmosphere, investigations in urban and rural area 0-94123  
 nitroxide free radical spin label EPR spectra, determ. of rot. correl. time and HFS coupling 0-74260  
 nitroxide groups in crystals, H bonds and short intermolecular contacts 0-63855  
 oxides, formation in enriched MHD combustion chamber working on natural gas and O<sup>-</sup> ionized air, investigation 0-106984  
 positronium nitrate, [NO<sub>3</sub><sup>-</sup>;e<sup>+</sup>], existence, Hartree-Fock-Roothaan calcs. 0-83254  
 positronium nitrite, [NO<sub>2</sub><sup>-</sup>;e<sup>+</sup>], existence, Hartree-Fock-Roothaan calcs. 0-83254  
 Ar:N<sub>2</sub>O, O(<sup>1</sup>S) photodissociative prod., photoluminesc. excitation spectra, excitation energy transfer 0-89508



## nitrogen compounds continued

- CO-N<sub>2</sub>O reacting gas mixture, gain due to CO<sub>2</sub> 00<sup>0</sup>1-10<sup>0</sup> transition 0-74337  
CO<sup>+</sup>+NO→CO<sub>2</sub><sup>+</sup>+N, crossed beam study 0-104436  
FNNF, mol. struct., cis effect 0-91434  
HNO<sub>3</sub>, aqueous soln., reflectance and complex refractive index, IR spectra, vibr. modes 0-66168  
N-Fe solid soln. in equilibrium with N<sub>2</sub> gas, partial molar enthalpy and excess entropy 0-60838  
N<sub>2</sub>+HBr, rate consts. for vibr. energy transfer meas. using laser. induced fluorescence technique 0-87206  
NC+H, bimolecular exchange reactions, dynamical-statistical method calcs. 0-104435  
NCl<sub>3</sub>, bond polarisability and force constants 0-69260  
ND, singlet-triplet transitions, high resolution spectrosc. with new emission source (*French*) 0-57383  
NF+H(NF), electronically-excited free radical reactions 0-97707  
NF<sub>2</sub>+H(O)(N), electronically-excited free radical reactions 0-97707  
NF<sub>3</sub>, nuclear resonance, effects of intermolecular interactions and intramolecular dynamics 0-63658  
N<sub>2</sub>F<sub>4</sub>, collisionless dissociation kinetics in highpower IR radiation field 0-66853  
N<sub>2</sub>F<sub>4</sub>, mol. photodissoc. using CO<sub>2</sub>-laserirradiation, rate const. meas., mol. fluoresc. and time-resolved UV spectra obs. (*German*) 0-83434  
N<sub>2</sub>F<sub>4</sub>, multiphoton excitation and vibr. energy flow, fluoresc. obs. 0-95673  
NH, atmospheric, IR emission studied using Fourier spectroscopy 0-95628  
NH radical formed in NH<sub>3</sub> dissoc., fluoresc. spectrum, rotational relaxation 0-58310  
NH, singlet-triplet transitions, high resolution spectrosc. with new emission source (*French*) 0-57383  
NH<sup>2+</sup>, pot. energy curves, model pot. method, orbiting and reson. effects 0-63815  
NH+HN<sub>3</sub> rate consts. from HN<sub>3</sub> UV photolysis data 0-101027  
NH<sub>2</sub>,  $\nu_2$  band, laser mag. reson. 0-83523  
NH<sub>2</sub>, pot. energy curves of X<sup>2</sup>B<sub>1</sub>, A<sup>2</sup>A<sub>1</sub>, <sup>2</sup>B<sub>2</sub> valence-shell and  $\pi_u$ 2s-type Rydberg states calc. by CI 0-74138  
NH<sub>2</sub> radical, mag. hyperfine interactions, zero-point vibr. effects 0-58167  
NH<sub>2</sub>, spin and rot. fine struct., orbital angular momentum 0-83247  
NH<sub>2</sub>, vibr. and rot. struct., intensity factors and orbital angular momentum 0-83246  
NH<sub>2</sub>+HN<sub>3</sub>, rate consts. from HN<sub>3</sub> UV photolysis data 0-101027  
NH<sub>2</sub>+O<sub>3</sub>, reaction mechanism, flash photolysis obs. 0-104425  
NH<sub>2</sub>+O<sub>3</sub>, reaction rate const., rel. to atmospheric processes 0-85155  
(NH<sub>2</sub>)<sub>2</sub>, <sup>15</sup>N quadrupole coupling consts., ab initio calcs. 0-58283  
NH<sub>3</sub>, radical, mag. hyperfine interactions, zero-point vibr. effects 0-58167  
N<sub>2</sub>H<sup>+</sup>, electron impact rot. excitation, Glauber approx. with Coulomb effect 0-63840  
N<sub>2</sub>H<sub>2</sub>, intercalation of layer structures, charge density waves or artefacts 0-100221  
N<sub>2</sub>H<sub>2</sub><sup>+</sup> radical, mag. hyperfine interactions, zero-point vibr. effects 0-58167  
N<sub>2</sub>H<sub>2</sub>-H<sub>2</sub>O, isolation of singular component for heat capacities of supercooled H<sub>2</sub>O 0-107437  
N<sub>2</sub>H<sub>2</sub>+H<sub>2</sub>+H<sub>2</sub>, mixtures with nonthermal vibr. excitation of mol. N<sub>2</sub>, formula for calc. equilib. const. 0-76545  
N<sub>2</sub>H<sub>2</sub><sup>2+</sup> salts, NMR spin lattice relaxation study, <sup>14</sup>N-<sup>1</sup>H dipole-dipole contrib. to relax. 0-75878  
NH<sub>2</sub>Br, dislocation influence on phase transition and light scatt. (*Russian*) 0-59648  
NHD, rotational transitions, microwave optical double resonance obs. 0-58293  
N<sub>2</sub>H<sub>2</sub>FeF<sub>4</sub>, one-dimensional antiferromagnetism, Mossbauer study 0-58272  
NH(ND) X<sup>2</sup>Σ<sup>+</sup>, in inert gas solid, vibr. relax., matrix and isotope effects 0-95713  
NH(NH<sub>2</sub>) obs. in laser photolysis of methylamine, fluoresc. obs. 0-97710  
NO, adsorbed layer, electron impact, electron impulsive ionisation spectroscopy obs. 0-60720  
NO, adsorption and reactivity on Co (0001), LEED, AES, and thermal desorption study 0-80090  
NO, adsorption on Pt (111), EELS, thermal desorption, LEED, and AES study 0-80086  
NO, adsorption on Re(0001), XPS, UPS and temp. programmed desorption 0-71574  
NO, adsorption on SiO<sub>2</sub>-supported Pt or Pt-Pd, IR spectrosc. obs. 0-92780  
NO, adsorption on W, FEM obs. 0-84390  
NO, adsorption on Zr, dissoc. and diffusion 0-80085  
NO and NO<sub>2</sub> mixing ratio profiles of stratosphere from IR sunset spectra 0-94563  
NO, Auger peak kinetic energy compared to Cr(NO)<sub>4</sub>, complex bonding 0-58317  
NO concentration in thermosphere, depend. on solar activity 0-77178  
NO density enhancement on winter anomalous day at S. Uist 0-82130  
NO, density profile from airglow obs., 72-120 km altitude 0-105094  
NO dissociative chemisorption and mol. adsorption on Ni (100) 0-65373  
NO, electrocatalytic decomp. on electrochem. reduced zirconia surface 0-61113  
NO electronically excited photofragment of VUV photodissoc. methylnitrite, identification and quantum yield 0-99527  
NO, Fourier transform spectra, intensity and self-broadening coeff. meas. 0-102503  
NO,  $\gamma$  and  $\beta$  system, electronic transition probability 0-106332  
NO,  $\gamma$  band lines, collisional broadening coeff. and optical collision diameter 0-63714  
NO,  $\gamma$ (0,0) band, collisional broadening parameters 0-63713  
NO, IR emission Fourier transform spectroscopy, mol. rot.-vibr., RKR potential curve calc. 0-95618  
NO impurity in N plasma, effect on heating in RF discharge 0-59312  
NO in middle atmosphere, role of eddy diffusion in mesosphere and lower thermosphere 0-109198  
NO in middle atmosphere, prod. by energetic particle precip. 0-109213  
NO, in stratosphere, conc. vars. at twilight rel. to interpretation of solar occultation meas. 0-85756  
NO, laser stimulation optimisation for intracavity spectroscopy 0-77881  
NO measurements in CH<sub>4</sub>-O<sub>2</sub>-N<sub>2</sub> flame by laser fluorescence 0-61178

## nitrogen compounds continued

- NO nonlinear laser spectroscopy, VUV harmonic generation 0-74175  
NO photometric process analyser using resonance absorption method 0-57360  
NO, prod. in Venus atmosphere by thunderstorms 0-98587  
NO, production by lightning, shock and channel heating methods 0-72581  
NO, relative Raman scatt. cross section 0-100061  
NO, selectively excited rovibrational states, multiphoton ionisation spectra 0-69202  
NO synthesis in DC plasma jet 0-61099  
NO, thermosphere composition and UV spectral absorpt. 0-85781  
NO, thermosphere radiative cooling 0-72656  
NO vibr. overtone band, mag. rot. spectrosc. obs. 0-86446  
NO, X<sup>2</sup>H state, vibr. relax., IR-UV double reson. obs. 0-106338  
NO, Zeeman modulation spectroscopy, line shape analysis 0-74197  
NO, Zeeman spectrum, mol. beam elec. reson. spectrosc. 0-91621  
NO<sup>+</sup> cluster ion formation in D-region, temp. control by ion obs. 0-61931  
NO+C<sub>2</sub>, IR laser photolysis of polyat. mols. photochem. appls. 0-66835  
NO+C<sub>2</sub>, laser-induced chemilum. reaction 0-61101  
NO+C<sub>2</sub>O, absolute reaction rate consts. meas. by laser induced fluoresc. 0-93738  
NO+C<sub>3</sub>, reaction kinetics, laser induced fluoresc. obs. of allene photolysis 0-66820  
NO+C<sub>3</sub> collisions in CO<sub>2</sub> gasdynamic laser, causing depopulation of lower active level 0-74336  
NO+Cd(<sup>5</sup>P<sub>0,1</sub>), absolute quenching cross section, phase-shift method 0-58340  
NO+Cl<sup>+</sup>, reactions at room temp. 0-93749  
NO+HBr, rate consts. for vibr. energy transfer meas. using laser. induced fluorescence technique 0-87206  
NO+He, multiphoton ionisation spectra in supersonic expansion, laser entranced collisional effects 0-83459  
NO+methoxy radical, reaction rate meas. 0-76534  
NO+N<sub>2</sub>(CO)<sub>2</sub>(CO)(CH<sub>3</sub>)<sub>2</sub>(Ar), NO  $\gamma$ (0,0) band, oscillator strength and line broadening 0-106356  
NO+O<sub>2</sub>+N<sub>2</sub>, mixtures with nonthermal vibr. excitation of mol. N<sub>2</sub>, formula for calc. equilib. const. 0-76545  
NO+O<sub>3</sub>, fs-states and rot. states, effect on reactivity 0-89473  
NO+OH, OH( $\nu$ =1) relax., time resolved spectra 0-74240  
NO<sub>2</sub>, adsorption on W, FEM obs. 0-84390  
NO<sub>2</sub>, atmospheric abundance meas. using solar absorpt. method (*Japanese*) 0-94556  
NO<sub>2</sub> concentration in stratosphere, simultaneous inference using inversion algorithm 0-82000  
NO<sub>2</sub>, discrete reson. CARS emission, temporal and spectral props. 0-95630  
NO<sub>2</sub> fluoresc. spectra and collisional quenching 0-102538  
NO<sub>2</sub>, ground state pot. surface, ab initio LCAO MO SCF calcs. 0-102461  
NO<sub>2</sub> in stratosphere, conc. var. during total solar eclipse 0-105017  
NO<sub>2</sub> in stratosphere, obs. rel. to instantaneous global O<sub>3</sub> balance 0-109211  
NO<sub>2</sub>, laser spectroscopy by cascade photoionisation method in mass spectrometer 0-99496  
NO<sub>2</sub> mixing ratio profiles from IR solar spectra obs., in stratosphere 0-105015  
NO<sub>2</sub> on Cu, ultrahigh vacuum ESR studies 0-97729  
NO<sub>2</sub>, relative Raman scatt. cross section 0-100061  
NO<sub>2</sub>, shock heated, visible emission 0-58274  
NO<sub>2</sub>, single and double ionisation by electron impact, ionisation pot. determ. 0-95730  
NO<sub>2</sub>, stratospheric, ground based obs. 0-85697  
NO<sub>2</sub>, high press. IR vibr. spectroscopy (*German*) 0-74170  
NO<sub>2</sub>, hydrate clusters, ground-state HF pot., Monte Carlo simulation, energy surfaces and rot. barriers 0-106412  
NO<sub>2</sub> ion in nitrite salt cryst., <sup>13</sup>B<sub>1</sub>→<sup>1</sup>A<sub>1</sub> transition spectra, reasons for diffuseness 0-97276  
NO<sub>2</sub><sup>+</sup>, gas phase equilib. geometry, force consts., vibr. freq., dipole moment function MCSCF/CI calcs. 0-78520  
<sup>15</sup>N<sub>2</sub>, predissoc. rot. struct. in 2490 Å band 0-87192  
NO<sub>2</sub>-NaCl, atmospheric reaction, in situ TEM studies 0-104544  
NO<sub>2</sub>+acetylperoxy radicals, absorpt. spectrum and reaction kinetics 0-91571  
NO<sub>2</sub>+OH, OH( $\nu$ =1) relax., time resolved spectra 0-74240  
NO<sub>3</sub>, detect. in polluted troposphere by differential optical absorpt. 0-77036  
NO<sub>3</sub> in troposphere, obs. of content in mountain air 0-72582  
NO<sub>3</sub>, effect on spectral distribution and intensity of sonoluminescence of Ar saturated solutions 0-76091  
NO<sub>3</sub> chemiluminescent monitor for air pollution investigations 0-72118  
NO<sub>x</sub> emissions from coal-fired MHD power plants, simplified correlations for prediction 0-97842  
NO<sub>x</sub> removal from atmosphere, using MARTZCLEAN reagents based on NaClO<sub>2</sub> and K<sub>2</sub>CO<sub>3</sub> (*Japanese*) 0-61147  
NO<sub>x</sub>, Stark effect investig., using two-way EPR cavity system 0-90872  
N<sub>2</sub>O, <sup>14</sup>N quadrupole coupling consts., ab initio calcs. 0-58283  
N<sub>2</sub>O, 12<sup>1</sup> band lines, precise meas. with compact vacuum IR spectrometer 0-95157  
N<sub>2</sub>O adsorption on Cu (100) surface, reaction with CO 0-103583  
N<sub>2</sub>O, atmos. warming due to N<sub>2</sub>O release from fertiliser 0-94579  
N<sub>2</sub>O, determ. in water using electron capture detection gas chromatography, multiple equilib. 0-76566  
N<sub>2</sub>O, dipole moment functions 0-87094  
N<sub>2</sub>O, electronic autoionisation branching 0-91614  
N<sub>2</sub>O, gas 0-95664  
N<sub>2</sub>O in stratosphere, height profile meas. at several latits. 0-72601  
N<sub>2</sub>O in tropical E.Pacific Ocean, meas. in sea water and marine air 0-94542  
N<sub>2</sub>O laser as IR pump for obtaining far IR emissions in NH<sub>3</sub> 0-74345  
N<sub>2</sub>O,  $\nu_3$  and 2 $\nu_3$  IR bandshape and dipole correl. functions 0-91560  
N<sub>2</sub>O, photoelectron spectrum, vibronic interaction and autoionis. effects 0-95680  
N<sub>2</sub>O, preionis. and predissoc., rel. to spectral line shape 0-63724  
N<sub>2</sub>O, satellite struct. and momentum distrib., binary ( $\epsilon$ , $\epsilon$ ) spectroscopy 0-69125  
N<sub>2</sub>O<sup>+</sup>, dissoc., threshold photoelectron-photoion coincidence obs. 0-87189  
N<sub>2</sub>O<sup>+</sup>, force fields and force const. of electronically excited states 0-69116  
N<sub>2</sub>O+Cl<sup>+</sup>, reactions at room temp. 0-93749

**nitrogen compounds continued**

- N<sub>2</sub>O+formaldehyde, mol. isolated Voigt line, off-peak spectral absorpt. coeff. 0-106355  
 N<sub>2</sub>O+Ge, chemiluminesc. reaction, HTFFR kinetics study 0-76496  
 N<sub>2</sub>O+H<sub>2</sub>, HO radical form. on Pt surface, laser-induced fluoresc. obs. 0-108738  
 N<sub>2</sub>O+HBr, rate consts. for vibr. energy transfer meas. using laser. induced fluorescence technique 0-87206  
 N<sub>2</sub>O+HF, HF( $v=3$ ) relax. and rate consts. 0-61069  
 N<sub>2</sub>O+SF<sub>6</sub>, vibr.-vibr. energy transfer, fluoresc. 0-78688  
 N<sub>2</sub>O<sub>4</sub>, fission reactor coolant, heat transfer on condensation (Russian) 0-57860  
 N<sub>2</sub>O<sub>4</sub>, turbulent dissoc. flow, along heated tubes, heat transfer 0-63225  
 N<sub>2</sub>O<sub>4</sub>, viscosity and thermal cond., approx. polynomials (Russian) 0-59739  
 N<sub>2</sub>O<sub>4</sub>, gaseous, integrated band intensity data, stratospheric detection implications 0-58250  
 NOCl laser, for 16  $\mu$ m range, review (Rumanian) 0-87408  
 NOH isomerism, low lying electronic states, ab initio MRD-CI calcs. 0-83291  
 NO<sub>2</sub>(N<sub>2</sub>O<sub>4</sub>) surface decomposition, resonance and spontaneous Raman spectra 0-61144  
 NO<sub>2</sub>(SO<sub>2</sub>)<sub>2</sub>, photodestruction 0-63722  
 NO<sub>2</sub>(SO<sub>2</sub>)<sub>2</sub>, photodestruction 0-63722  
 NO<sub>2</sub><sup>-</sup>(HNO<sub>3</sub>)<sub>n</sub> clusters, form. studied by mass spectrometer, thermodynamic functions, sol. struct., 0-95754  
 N<sub>2</sub>P<sub>2</sub>Br<sub>6</sub>, <sup>81</sup>Br NQR, conformation investig. 0-63665  
 N<sub>2</sub>SO<sub>4</sub>, weakly bound complex, dipole moments, MBER obs. 0-95701  
 NSi+H, bimolecular exchange reactions, dynamical-statistical method calcs. 0-104435  
 NaOH:NO<sub>2</sub>, electron tunnelling, pulse radiolysis 0-108722  
 NiSi<sub>3</sub>, epitaxial film on (111) Si substrate, interfacial order, backscatter, channelling study 0-65390  
 O<sub>2</sub>+NO(NO<sub>2</sub>), rate constants determ. as function of relative kinetic energy 0-81292  
 ONF, J transitions, rot. Zeeman effect 0-63707  
 S-N system, inorganic, electronic struct. obs. by photoemission XPS and UPS, CNDO calcs. 0-78653  
 Sc+NO<sub>2</sub>, chemiluminesc., nonequib. product distrib. 0-101014

**NMR line breadth**

- acetone, <sup>17</sup>O chemical shift and NMR linewidth meas., self-association equil. const. determ., mol. reorientations obs. 0-87148  
 L-alanine, <sup>17</sup>O NMR chemical shifts and linewidths, pH dependence 0-80625  
 cholesteryl myristate, cholesterogenic, blue phase, D NMR obs. 0-97151  
 cholesteryl nonanoate, cholesterogenic, blue phase, D NMR obs. 0-97151  
 cytochrome c, PMR, eight-ring current model heme ring, conformation depend. shifts 0-74185  
 p-dichlorobenzene, <sup>35</sup>Cl NQR line narrowing by nonreson. RF photon dressing 0-63662  
 dipolar linewidth in asymmetrically broadened NQR spectra 0-71230  
 dipole NMR line width red. under magic angle conditions 0-60435  
 ethanol, polymorphic forms, mol. motion, NMR obs. 0-88885  
 glycine, <sup>17</sup>O NMR chemical shifts and linewidths, pH dependence 0-80625  
 heteronuclear system, line narrowing in many-pulse NMR expts. 0-71200  
 hexamethylenetetramine, ultraslow tetrahedral jumps, deuteron NMR spin alignment obs. 0-66046  
 lysine, aq. solns., H<sup>+</sup>(D<sup>+</sup>) exchange rates, <sup>17</sup>O NMR linewidths, pH depend. 0-91661  
 noise reduction filter in resolution enhancement 0-73403  
 NQR, inhomogeneous line narrowing by RF pulse sequence 0-93206  
 paramagnetic contribs. calcs. 0-58286  
 PMR, delayed Fourier transformation technique for resolution enhancement 0-74181  
 polymer, glassy state, <sup>13</sup>C NMR (German) 0-93188  
 solid-state NMR lineshapes, method for separating homonuclear and heteronuclear broadening 0-77828  
 Van Vleck compounds, LF dynamics, NMR linewidth, RKKY exchange mechanism role 0-103812  
 AgBr:Na<sup>+</sup>(Li<sup>+</sup>), correlated diffusion of impurities, nuclear spin relax. meas. 0-108094  
 (AgI)<sub>2</sub>(Ag<sub>2</sub>O<sub>2</sub>B<sub>2</sub>O<sub>7</sub>)<sub>2</sub>, amorphous superionic compound, <sup>11</sup>B lineshape and relaxation 0-108107  
 AgNa(NO<sub>2</sub>)<sub>2</sub>, <sup>23</sup>Na elec. field gradient tensor from NMR satellite lines near phase transition 0-71191  
 $\beta$ -Al<sub>2</sub>O<sub>3</sub>(NaLi)<sub>2</sub>O, NMR, Raman and IR spectra, and X-ray diffr., heat treatment induced changes 0-107508  
 $\beta$ -Al<sub>2</sub>O<sub>3</sub>(NaLi)<sub>2</sub>O solid electrolyte, Li motion and activation obs. using <sup>7</sup>Li NMR 0-108100  
 $\beta$ -Al<sub>2</sub>O<sub>3</sub>-NH<sub>4</sub><sup>+</sup> and  $\beta''$ -Al<sub>2</sub>O<sub>3</sub>-NH<sub>4</sub><sup>+</sup>-H<sub>2</sub>O, single cryst. PMR and proton motion 0-108101  
 $\beta$ -Al<sub>2</sub>O<sub>3</sub>-Na<sub>2</sub>O, <sup>23</sup>Na NQR and two-dimens. diffusion, model analysis 0-108111  
 $\beta$ -Al<sub>2</sub>O<sub>3</sub>-Na<sub>2</sub>O, <sup>27</sup>Al NMR obs., Na motion and cond. characts. 0-108096  
 $\beta''$ -Al<sub>2</sub>O<sub>3</sub>-Na<sub>2</sub>O, absorbed water effect on NMR lineshape and spin-lattice relax. time 0-108098  
 $\beta$ -Al<sub>2</sub>O<sub>3</sub>-Na<sub>2</sub>O, anomalous Na behaviour obs. using pulsed and CW NMR 0-108095  
 2,4-C<sub>2</sub>H<sub>2</sub>, polyhedral, spin coupled <sup>11</sup>B-<sup>1</sup>H systems, 2-dimens. correl. NMR 0-69166  
 CeAl<sub>3</sub>, antiferromag. ordering and Kondo behaviour, <sup>27</sup>Al NQR study 0-71231  
 Cu, NMR study on nuclear ordering below 1  $\mu$ K 0-93187  
 D<sub>2</sub>O, H<sup>+</sup>(D<sup>+</sup>) exchange rates, <sup>17</sup>O NMR linewidths, pH depend. 0-91661  
 Dy<sub>1-x</sub>Gd<sub>x</sub>Al<sub>3</sub>, ordered alloys, hyperfine field, anomalous con. depend. NMR 0-75868  
 HIO<sub>3</sub>, PMR spectra, homonuclear and heteronuclear broadening separation 0-77828  
 H<sub>2</sub>MoO<sub>4</sub> and H<sub>1.7</sub>MoO<sub>3</sub> bronzes, NMR relax. obs. at 77<T<450K, H diffusion 0-108089  
 H<sub>1.6</sub>MoO<sub>3</sub> bronze, proton shift tensors PMR meas. 0-71202  
 H<sub>2</sub>O, H<sup>+</sup>(D<sup>+</sup>) exchange rates, <sup>17</sup>O NMR linewidths, pH depend. 0-91661  
<sup>3</sup>He, superfluid A-phase, spin relax. and zero sound attenuation at low temp. 0-107595  
 KB<sub>2</sub>H<sub>8</sub>, NMR study of proton and boron dynamics 0-71210  
<sup>138,139</sup>La, Fourier transform NMR 0-57354

**NMR line breadth continued**

- LiCd intermetallic cpd., temp. depend. 0-75537  
 Li<sub>3</sub>N, diffusion processes and struct. NMR study 0-108090  
 Li<sub>3</sub>N layer structure with fast ion cond., <sup>6</sup>Li NMR obs. of diffusion 0-108102  
 Li<sub>2</sub>O-B<sub>2</sub>O<sub>3</sub> glasses, low Li<sub>2</sub>O content, <sup>7</sup>Li NMR study 0-84657  
 Li<sub>2</sub>(SO<sub>4</sub>), cation diffusion NMR investigation up to 800°C 0-108092  
 LuCrO<sub>3</sub>:Er<sup>3+</sup>, doping effect on <sup>53</sup>Cr NMR in domain walls 0-71219  
 NaCl, electric field gradients near dislocations, resulting NMR lineshapes 0-75225  
 NaNO<sub>2</sub>, <sup>23</sup>Na elec. field gradient tensor from NMR satellite lines near phase transition 0-71191  
 NaNO<sub>3</sub>, double quantum nuclear magnetic resonance of <sup>23</sup>Na by double resonance, line shape 0-75886  
 Na<sub>2</sub>(SO<sub>4</sub>), cation diffusion NMR investigation up to 800°C 0-108092  
 P+Nb, dil. alloy, NMR obs. of <sup>93</sup>Nb 0-71203  
 PbF<sub>2</sub>:Mn, mag. tagging of ion diffusion, <sup>19</sup>F NMR meas. 0-108106  
 PbNb, dilute, NMR obs. of <sup>93</sup>Nb 0-71203  
 PrNi<sub>2</sub>, LF dynamics and <sup>141</sup>Pr thermal relax., coupling parameter and RKKY exchange mechanism 0-103812  
 PtV, dil. alloys, NMR obs. of <sup>51</sup>V 0-71203  
 Rb<sub>2</sub>ZnBr<sub>4</sub>, incommensurate phase, <sup>87</sup>Rb NMR lineshape 0-93191  
 SmB<sub>6</sub>, intermediate valence, <sup>11</sup>B NMR study 0-93193  
 SnF<sub>2</sub>, second order  $\beta=\gamma$  transition, neutron diffr. and NMR obs. 0-107095  
 TaSe<sub>2</sub> (2H), CDW and discommensurations, <sup>77</sup>Se NMR study 0-88883  
 TI complex of lasalocid (X-537A), <sup>203</sup>Tl NMR study 0-58288  
<sup>89</sup>Y spin-spin relaxation times, pH depend. 0-66059  
 ZnS, <sup>67</sup>Zn and <sup>33</sup>S nuclear magnetic shielding, chemical shifts and linewidths 0-60434  
 ZnSe, <sup>67</sup>Zn nuclear magnetic shielding, chemical shifts and linewidths 0-60434  
 ZnTe, <sup>67</sup>Zn nuclear magnetic shielding, chemical shifts and linewidths 0-60434
- nobelium**  
 No entries
- nobelium compounds**  
 No entries
- noble gases** see inert gases
- noctilucent clouds** see clouds
- noise**  
 see also acoustic noise; atmospheric; electron device noise; interference; random noise; white noise  
 atomic absorpt. flame spectrometry, noise level meas., single and double beam instrum. comparison 0-76584  
 bilaterally distorted image linear restoration using Wiener filters 0-83557  
 biomagnetic measurement facility installation in hospital environment, design criteria and procedure 0-104707  
 biomembrane flexural fluctuations and non-equilib. noise 0-76712  
 cavitating orifice under reattached flow conditions, noise and vibration characteristics 0-83829  
 chemisorption kinetics, determ. from substrate current fluctuations 0-84833  
 coherent line-frequency noise in evoked pot. recordings, cancellation 0-98161  
 colour film archival storage, white light processing technique 0-99637  
 computerized tomography scanners, survey of noise, dose and contrast detectability and resolution 0-104750  
 dye laser, mode-locked, synchronously pumped, pulse-width stabilization 0-83622  
 ECG telephone transmission, analogue and digital, errors and noise 0-94398  
 electron micrograph, 500 kV, atomic resolution, computer image processing 0-100149  
 electron microscopy, correlation analysis of radiation damage 0-100282  
 electrophotography, noise perception and level of graininess 0-62753  
 external noise effect on transition to turbulent convection 0-96263  
 flaw detection system, noise immunity 0-104385  
 flow-detection apparatus, noise immunity, sounding signal freq. modulation 0-98441  
 Fourier transform spectrometer, SNR enhancement by elec. filter compensation of slide velocity errors 0-95151  
 gamma-Lorentzian intensity fluctuations, integrated, statistics 0-102685  
 gas lasers, low frequency noise 0-69364  
 heterodyne optical radar S/N ratio in atmospheric turbulence 0-106558  
 high-speed optical systems at 0.85  $\mu$ m, modal noise and optical feedback 0-87323  
 imagery, 2-D sampled, aliasing and blurring effects 0-99635  
 ion-cyclotron noise in topside ionosphere 0-101470  
 IR spectroscopy, computerised, noise props. 0-86466  
 Josephson parametric amplifiers, gain-dependent noise temp. 0-84552  
 laser, multimode, containing saturable absorbers, bistable operation 0-91862  
 LF fluctuation, dissipation and relaxation properties, universality 0-84687  
 medical imaging systems, information capacity considerations 0-98090  
 Michelson laser interferometers, noise limitations 0-82808  
 neutron counter, scintillation, photomultiplier noise characteristics 0-74077  
 NMR meas. at ultra-low tapes, S/N ratio, appl. to thermometry 0-73400  
 nonlinear holography, multiple-reference-beam, intermodulation background noise suppression appl. 0-99674  
 optical communication systems, nonlinear distortions and noise due to fibre connectors 0-96001  
 optical correlation detection, optimization by prewhitening 0-95802  
 optical fibre attenuation meas. by backscattering method, effect of noise 0-102824  
 optical fibres, multimode, freq. depend. of modal noise, speckle theory 0-102817  
 optical fibres, step-index, modal-noise probability distrib. meas. and anal. 0-99859  
 optical imager, linearly degraded, iterative restoration 0-95807  
 optical images, linearly degraded, iterative restoration, reblurring procedure 0-99640  
 optical noise and temporal coherence 0-102611  
 optical resolution, S/N ratio and meas. precision, revised numerical results 0-95806  
 optical waveguides, multichannel, cross-talk noise anal. 0-91922  
 pattern selection in non-equilib. processes, marginal stability theory, eutectic solidification model 0-60852



**noise continued**

- photophoretic spectroscopy, broadband 0-86469  
 polarimetry, noise suppression by polarization-plane rotation-angle amplification 0-68241  
 pseudocolour density encoding, white-light, using contrast reversal 0-83560  
 pulsar timing noise anal. 0-77431  
 radiographic granularity, of screen-film systems, assessment by entropy method 0-98070  
 radiography, medical diagnosis, information storage requirements 0-98086  
 random walk timing noise anal. for pulsar timing 0-77432  
 regularized object restoration, resolution beyond the diff. limit 0-87324  
 RF SQUID, hysteretic, input noise 0-70905  
 scalar diffraction, inverse theory, eigenvalue formulation 0-102613  
 speckle, dynamic props., zero-crossing study 0-63923  
 spectroscopy, noise reduction by low pass filter for DC signal, appl. chlorophyll-a fluoresc. 0-87249  
 target discrimination methodology in remote sensing 0-58470  
 temporal frequency dependence of modal noise in fibres [optical] 0-58687  
 thermal electrostatic noise in solar wind, LF obs. from ISEE 3 0-101519  
 Vibroseis deconvolution method, noise effects 0-90232  
 vision, conditions for motion flow in dynamical visual noise 0-72174  
 white light processing using diff. grating method 0-106470  
 X-ray backscattering, interface co-ordinate determ., signal-noise ratio 0-77925  
 Al shielded room for biomag. meas. 0-104846  
 n-Cd<sub>0.2</sub>Hg<sub>0.8</sub>Te, excess generation-recombination noise 0-107880  
 InSb MIS structure, effect of room background on noise props. 0-103755  
 La-Gd (8 at.%), FCC, under hydrostatic pressure, resistivity meas., comparison with positive-J spin glasses 0-59958  
 LiNbO<sub>3</sub>, holographic storage and retrieval 0-99669  
 Nd<sup>3+</sup>:YAG multimode laser radiation noise 0-74366  
 Si photodiode, avalanche, n<sup>+</sup>pp<sup>+</sup>-type, primary photocurrent anal. by noise measurements (French) 0-88624  
 Si, with dislocations, noise spectrum 0-107881  
 VO<sub>2</sub> single cryst., noise in presence of current filament 0-92952

**noise abatement**

- see also acoustic wave absorption*  
 absorbers, dimensioning of facings for acoustically effective structural elements (German) 0-74600  
 acoustic insulating material complex elastic modulus meas. and transfer function theory (Hungarian) 0-106765  
 active sound absorption, duct carrying uniformly flowing fluid 0-74556  
 aircraft, Siemens airport noise monitoring systems 0-99895  
 aircraft, the Netherlands, legal and economic factors 0-72112  
 baffles in closed spaces, dependence of effectiveness on nature of closed space, economic and annoyance factors 0-67019  
 computer simulation of traffic flows, car following theory, intersections having traffic lights 0-72109  
 critical tendencies in subjective assessment of environmental noise 0-72111  
 Demey metro station, noise level increase due to echoes from passing vehicles (French) 0-69600  
 diesel, engine exhaust noise, single monopole very low freq. noise source in air duct 0-64282  
 diesel engine noise generation, diagnosis and control 0-58857  
 diesel engine powered installations, noise reduction programme 0-96106  
 diesel-engined ships, noise in cabins and engine room, reduction by abatement at source (Japanese) 0-79052  
 domestic roofing sound insulation, expt. facilities of meas. laboratory, test details 0-79058  
 ear protectors, use of sound levels for assessing adequacy 0-104771  
 elastic floor coverings, effect of thickness and hardness on impact sound insulation props. (Japanese) 0-79053  
 electric machines, acoustic noise meas. errors (Hungarian) 0-96102  
 factories appl., computer simulation technique 0-64285  
 fan noise reduction by single- and double-wall barriers 0-87648  
 fanjet engines, discrete freq. noise reduction modelling 0-106652  
 helicopter environmental noise impact obs. and evaluation 0-104539  
 highway noise barriers, optimum weight with respect to effectiveness and cost 0-67021  
 highway traffic noise, noise screening elements in highway design (Hungarian) 0-106662  
 induction motors in air/air heat-exchangers for ventilation (Hungarian) 0-102923  
 industrial process burners, suppression methods 0-74597  
 low frequency noise breakout from air conditioning ducts 0-74594  
 noise control system design, panel systems 0-87649  
 noise transmission through stiffened panels 0-102922  
 oil-fired boilers, noise reduction by casing (Hungarian) 0-106663  
 opencast coalmining, principal noise sources 0-81505  
 outdoor noise of coal-fired power plants, possible controls 0-76683  
 pipeline under hydraulic impact 0-102927  
 propeller fans, noise reduction measures (Japanese) 0-64284  
 quarrying, use of electronic transient recorders for meas. explosion noise and vibration 0-67023  
 railways, meas. on noise protection screens (German) 0-102916  
 road traffic, control of noise level of moving vehicles 0-99894  
 road traffic, highway noise barrier perceived benefit 0-102920  
 road traffic, noise propag. characts. identification under different conditions, Kalman filter theory appl. (German) 0-99896  
 road traffic, reduction by correct building placement, noise emitted by single source in open space 0-87647  
 road traffic, use of sloped barriers for noise abatement 0-102925  
 road traffic noise, meas. radiating height of cars and lorries, effectiveness of sound barriers 0-64325  
 road traffic noise prediction, use of theoretical and empirical models (French) 0-67020  
 schoolroom acoustic insulation check allowing for boundary absorption (Hungarian) 0-106664  
 sonic boom, pressures inside room with open window 0-69602  
 sound absorption, perforated facings on porous backings, calculation of specific normal impedance 0-64281  
 sound isolation tests of residential buildings, correlation with subjective privacy opinions, standard sound source requirements 0-64323  
 sound-absorbing wedge design, reflection characts., materials and dims. (Japanese) 0-64322

**noise abatement continued**

- steam turbines, 200 MW, with accessories, noise reduction research and development 0-91958  
 surface effect vehicles, design problems 0-74598  
 transport systems, natural rubber for vibration insulation 0-96099  
 USA Quiet Communities Act (1978), implementation by Environmental Protection Agency 0-72113  
 wall insulation, prediction of output probability distribution of noise level, road traffic noise 0-69593  
 window-glasses, most effective window configurations 0-87655  
**noise control (acoustic)** *see noise abatement*  
**noise control (interference)** *see interference suppression*  
**noise elimination** *see interference suppression*  
**noise generators**  
 600 MHz to 1 GHz coaxial thermal noise standard 0-98875  
**noise levels, acoustic** *see acoustic noise*  
**noise measurement**  
*see also acoustic noise measurement; electric noise measurement; optical noise measurement*  
 VHF noise field strength at 95 MHz over India, meas. techniques and obs. 0-109294  
 X-ray image intensifier noise evaluation, digital method 0-98097  
**nomenclature and symbols**  
*see also units (measurement)*  
 asteroids, new names for 26 objects 0-77325  
 asteroids, new names on Minor Planet Circulars 5249-5286 for 48 objects 0-67632  
 asteroids, new names on Minor Planet Circulars 5423-5454 for 26 objects 0-98599  
 carbohydrate nomenclature, digital representation, chemistry education 0-62435  
 electrical quantities, units, symbols and definitions (German) 0-86248  
 graphic symbols denoting types and methods of NDT 0-86042  
 heliotechnics, basic values, symbols, units and definitions (Rumanian) 0-57243  
 measurement units, historical review and current systems in use (German) 0-68166  
 p-n junction photodiode terminology 0-70800  
 six-membered rings, conformation, nomenclature 0-78721  
 steel ball bearing, fatigued, phase changes, nomenclature 0-89198  
**nomograms**  
*see also graphs*  
 deconvolution nomogram for single exponential fluoresc. decays 0-67290  
 dew point temp. change with pressure, calc. 0-77607  
 gratings, ruled, lamellar and holographic, equivalence in const. deviation mountings 0-87474  
 steel, pearlitic structural, austenite grains, growth rate during heating 0-100860  
**nomographs** *see nomograms*  
**non-Newtonian flow**  
*see also non-Newtonian fluids*  
 a boundary layer theory for non-Newtonian fluids 0-83818  
 anisotropic liquid, axially symmetric flow 0-103050  
 annulus with negligible diffusion, laminar non-Newtonian flow, residence time distrib. 0-79357  
 blood flow in artery, pulsatile flow 0-106845  
 bubble rupture between two solid walls, effect of drag-reducing polymers on cavitation 0-106822  
 bubble translational motion in a viscoelastic liquid, retarded motion approx. 0-83777  
 buoyancy-thermocapillary convection layers with free surface, energy stability theory 0-87768  
 carboxy methyl cellulose solns., mass transfer from cylinders to power law fluids 0-83826  
 carboxy methyl cellulose solns., mass transfer from spheres to power law fluids 0-83825  
 classification criteria for rigid motions, viscometric flow and elongational flow 0-69881  
 cooperative phenomenon, theory 0-69878  
 Cosserat fluids, radial flow in convergent channels 0-74988  
 duct, rectangular, laminar non-Newtonian flow, vel. profiles 0-92217  
 elastico-viscous liquid flow in axisymmetric pipe of slowly varying cross-section 0-83774  
 elasto-hydrodynamic lubrication, non-Newtonian effects of volume relaxation 0-103009  
 exit flow through capillaries, effect of vibrations 0-79358  
 finite element routine using mixed method 0-103045  
 force multiple moments for a spherically symmetric particle in solution 0-92185  
 forced heat convection of linear flow of non-Newtonian fluids through rectangular channels 0-92141  
 hydrodynamic calculations for container pipeline systems with non-Newtonian liquids 0-106817  
 inelastic power-law fluid, unsteady flow in circular tube; implicit finite difference anal. 0-83821  
 inertial effects of liquid flow with an anisotropic viscosity tensor 0-83820  
 jet, flat submerged, in non-Newtonian liq. with power-law behaviour 0-59078  
 mass transfer from cylinders to power law fluids 0-83826  
 mass transfer from spheres to power law fluids 0-83825  
 mass transfer to power law fluids in fluidised beds 0-100032  
 Maxwell fluid, diffusion of vortex line in stagnation point flow 0-74892  
 Maxwell fluids, immiscible, hydrodynamic flow through non-conducting rectangular channel 0-100038  
 MHD flow of a viscoelastic conducting fluid 0-92229  
 micropolar fluid, heat transfer in stagnation point flow 0-79356  
 micropolar fluid, steady incompressible flow, linear steady-state system of eqns. 0-83819  
 micropolar fluid movement in presence of orientable particles, numerical study (French) 0-74924  
 micropolar fluid theory, Stokes flow existence and uniqueness 0-69877  
 micropolar fluids, potentials and Green's functions 0-96286  
 nematic liquid crystals, Couette flow, orientation instability for finite anchoring energies 0-74923  
 orientable polymer fluid, Ericksen's anisotropic fluids theory extension 0-79359  
 pipeline systems, problems in fluid mechanics for hydraulic transport of solid materials 0-106836  
 polyacrylamide Separan MG200, aq. soln., rheological props. 0-64507



**non-Newtonian flow continued**

- polymer solns., dilute, extensional and sink flow in channel 0-74925  
 polymer solutions, diffusion of ionic species, meas. by diffusion controlled electrolysis 0-74920  
 polymer solutions, liquid cryst., rheo-optics of shear and elongational flow, quiescent and flow birefringent charact. 0-83773  
 polystyrene, ordered monodisperse latexes, viscoelasticity and flow props. 0-58992  
 polystyrene melts, flame-retardant high-impact, shear viscosity-temp.-shear rate relationships 0-59691  
 pseudoplastic fluid, nonlinear singular boundary value problem 0-79362  
 PVC plastisol, flow behaviour at high shear rate (*German*) 0-92186  
 round tubes, non-Newtonian fluid transition and turbulent flow regions (*Russian*) 0-59077  
 second-order fluid, rectilinear flow, pressure error, boundary integral approach 0-59081  
 simple fluids, small strain oscillatory squeeze film flow, polymeric liquids 0-92765  
 slip phenomena, thermodynamic approach 0-59083  
 third grade fluids, viscometric flows 0-69883  
 turbulent jets, influence of drag reducing polymers on cavitation inception 0-106823  
 turbulent pipe flow, use of eddy viscosity expressions for vel. profiles in Newtonian, non-Newtonian and drag-reducing flows 0-83789  
 viscoelastic boundary layer flow, second order, at stagnation point, heat transfer 0-103025  
 viscoelastic boundary-layer flow past a parabola and a paraboloid 0-83817  
 viscoelastic droplet break-up, in nonuniform shear flow 0-64588  
 viscoelastic fluid, free surface between cylinders rotating at different speeds 0-59082  
 viscoelastic fluid, motion of rigid particles 0-103044  
 viscoelastic fluid, stability of steady shearing flows, energy method and parabolic maximum principle 0-74926  
 viscoelastic fluid lubrication, slider-bearing config., non-Newtonian normal stresses 0-69753  
 viscoelastic laminar flow, combined generalised measure approach, pseudo-plasticity 0-64586  
 viscoelastic liquid, boundary-layer flow past symmetric wedge or right circular cone 0-64513  
 viscoelastic liquids, Poiseuille flow, hole-press. meas., computer model 0-59080  
 viscoelastic tube, pulsatile flow, non-Newtonian effects (*French*) 0-59113  
 viscoelastic fluid velocity profiles at annulus inlet 0-64583  
 viscous fluid under cyclic deform., self-heating, hydrodynamic thermal explosion 0-58993  
 viscous incompressible, finite element method, Bingham fluid 0-92184  
 TiO<sub>2</sub> suspension in glycerine, Bingham plastic flow through annuli 0-64521

**non-Newtonian fluids**

- see also colloids; polymer melts; polymer solutions; rheology  
 channel, cylindrical, arbitrary cross section, nonlinearly viscous medium motion 0-69928  
 Cosserat continuum, kinetic energy, linear and angular momentum densities, invariance 0-74829  
 elastohydrodynamic traction, non-Newtonian thermo-viscoelastic, from combined slip and spin 0-103043  
 hydrodynamic calculations for container pipeline systems with non-Newtonian liquids 0-106817  
 incompressible viscoelastic fluid, Rayleigh-Taylor instability 0-79363  
 kaolin suspensions, aq., flocculated and dispersed, rheological behaviour in pipe flow 0-64510  
 liquid mixture separation by thermal diffusion in parasitic convection 0-64587  
 Maxwell fluid, die swell, finite element anal. 0-83822  
 micropolar fluid layer subject to magnetic field, thermal instability 0-64585  
 micropolar fluids, thermodynamical aspects, non-linear approach 0-105598  
 peristaltic transport, long wavelength, stream function and pressure field solns. 0-74922  
 polymer solution rheology based on a finitely extensible bead-spring chain model 0-83775  
 polymer solutions, dilute, normal stress difference and shear rate 0-83776  
 Rivlin-Ericksen fluid, dispersion medium on rheological behaviour of dilute suspension of dipolar dumbbells, viscoelastic props. 0-99983  
 simple fluid shear depend. viscosity, central force interactions 0-79970  
 thermoviscous fluid, steady slow motion through a circular tube 0-74921  
 turbulent flow in absence of anomalous wall effects 0-69880

**noncrystalline state structure**

- see also amorphous state; vitreous state  
 Agave cantala natural fibre, small-angle X-ray scatt. of densely packed colloidal system, scatt. inhomogeneities 0-76565  
 alkali germanate crystals and glasses, struct. and stability, IR spectra meas. 0-64911  
 alkali silicate glasses, high temp. relax. mechanisms 0-70134  
 alkali silicate glasses, struct. and thermal props. 0-84075  
 alloys, amorphous, exhibiting Mossbauer spectra, elec. props. (*French*) 0-80244  
 amagnetic thin films, amorphous, struct. and mag. props., review 0-93148  
 amorphous alloys, struct. determ. by energy dispersive X-ray diffraction 0-84063  
 amorphous solid, structural defects, computer simulation study 0-88040  
 B<sub>2</sub>O<sub>3</sub>-Li<sub>2</sub>O-LiCl, ionic conductor, IR refl. Raman study 0-66173  
 bis-(p-toluene-sulphonate) of 2,4 hexadiene 1,6 diol, X-ray scattering obs. of polymerisation mechanism and phase transition (*French*) 0-70399  
 borate glass, ESR study of effect of glass composition on symmetry of Cr complexes 0-88052  
 Bragg bubble glass, struct. and plastic flow 0-84091  
 ceramics, glassy, struct. and electron beam sensitivity 0-79841  
 cyclohexanol, glassy cryst., diffuse X-ray scatt. study 0-100171  
 elastic amorphous medium, relax. by defect diffusion 0-58925  
 epoxides, dielectric relax. and deform props., cross-link density effect (*Russian*) 0-60942  
 ethylene-vinyl acetate copolymers, extrusion and heavy duty films, radiation crosslinking, struct. effect 0-66844  
 ethylene-vinyl alcohol copolymer, drawn samples, annealing effect around T<sub>g</sub> temps. on shrinkage and mol. orientation 0-79712  
 glass: <sup>57</sup>Fe, 2-parameter distrib. analysis using general inversion method 0-66079

**noncrystalline state structure continued**

- glass, homogeneity by Christiansen filter method 0-84066  
 glass, isobaric thermal behaviour during heating and cooling, rate of recovery, one-parameter model 0-75165  
 glass local structure exam. by EXAFS 0-108301  
 glass struct. study using small-angle X-ray scatt. 0-84071  
 glass structure, isobaric variation, phenomenological theory (*French*) 0-59393  
 glasses, inorganic, struct. by X-ray scatt. diff. obs. 0-84069  
 glasses and ceramics, characterisation with analytical electron microscope 0-84068  
 ice orientational correlation parameter, water mol. dipole moment 0-59407  
 lithium polyisoprene, struct. regularity and crystn. 0-103269  
 metallic glass, prep. and phys. props. development 0-81003  
 metallic glass, review of current exptl. data 0-88058  
 metallic glasses, electronic structure rel. to elec. cond., supercond. and mag. props. 0-65429  
 metallic glasses, review 0-88051  
 metallomacrocycles, mixed valent, cofacial assembly, cond. polymeric material 0-70143  
 metals, amorphous, structure model, structural changes 0-92462  
 metals, glassy, structure, transport props., magnetic behaviour, review 0-70138  
 metals, rapidly quenched, conf., Brighton, England (July 1978) 0-67934  
 microparacrystals, struct., theory (*German*) 0-59545  
 Nafion, densities and expansion coeffs. as function of various parameters 0-79711  
 Nylon 6 film, prior high-press. treatment effects, weight swelling, density, IR crystallinity, X-ray and viscosity obs. 0-81025  
 Nylon 6 gut yarn, fine struct. change in twisting, annealing and untwisting, microbeam X-ray obs. 0-81026  
 Nylon 6 gut yarn, fine struct. change in twisting, annealing and untwisting, X-ray and electron microscopy obs. 0-84904  
 opal glasses, phosphate opacified, phase comp. and struct. 0-64919  
 optical fibres, UV radiation-induced losses rel. to colour centre form. 0-87517  
 oxide glasses,  $\gamma$ -irrad., CuO effects on EPR 0-84645  
 phosphate glasses, non-alkaline, transition states, phys. effects of fluors, phase diagrams and optical effects (*German*) 0-88045  
 phosphate glasses, optical breakdown rel. to microscopic inhomogeneous struct. 0-102784  
 poly(p-phenylene), AsF<sub>5</sub> doped, highly cond. charge transfer complexes, elec. and optical props. 0-70778  
 poly-arylate-dimethyl siloxane, polyblock copolymers, struct., thermodynamic stability (*Russian*) 0-64931  
 poly-m-toluenylsilsesquioxane mesomorphic struct., form. during polymerisation (*Russian*) 0-61095  
 polyacetylene, AsF<sub>5</sub> doped, X-ray absorpt. meas., 5K to room temp. 0-71516  
 polyacrylic acid film, structurisation and mech. props., EM obs. (*Russian*) 0-59406  
 polyalkane imides, crystallisability, supermol. and crystalline structures 0-84100  
 polyamide, aromatic, fibre, high modulus, mol. and supramol. struct. 0-79710  
 1,2-polybutadiene, crosslinked in states of strain, entanglement networks, swelling anisotropy obs. 0-79666  
 polybutadiene-poly- $\alpha$ -methylstyrene copolymers, struct. obs., prep. (*French*) 0-59401  
 polybutylene terephthalate, melt crystallised, solvent crystallised films and moulded bars, morphological obs. 0-84101  
 polycarbonate, bisphenol A, WAXS pattern, temp. effect and thermal history 0-93583  
 polydioxolan, crystn. kinetics, dilatometric analysis and microscopy obs. 0-79706  
 polyethylene, flow-induced fibril form. from soln. 0-59402  
 polyethylene, high press. phase, US, DTA, and X-ray diff. study 0-75188  
 polyethylene, linear, melt-crystallised sharp fraction, lamellar morphology, electron microscopy obs. 0-84099  
 polyethylene, low density, morphology and props. 0-64926  
 polyethylene, single crystal, fold domain boundaries, TEM 0-107065  
 polyethylene, stretched, birefringence rel. to struct. changes 0-84714  
 polyethylene, vinyl group reactions during  $\gamma$ -irrad., crystallinity effect, absorbance obs. 0-81346  
 polyethylene lattice, inclusion of chain defects, stat. approach 0-75190  
 polyethylene oxide, nascent and annealed, X-ray study of crystal structure 0-64922  
 polyethylenes, extrusion and heavy duty films struct. parameters influence on cross-linking by radiation 0-66844  
 polymer, dielec. breakdown theories, mol. and morphological features rel. to elec. strength, review (*Japanese*) 0-60501  
 polymer blends, selective staining method for TEM obs. of morphology 0-84103  
 polymer mech. or elec. props., struct. recovery (*French*) 0-59393  
 polymer structure and optical behaviour 0-106583  
 polymers, aliphatic and aromatic, mean mol. orientation factors, from IR spectra and acoustic method 0-70142  
 polymers, amorphous, struct. rel. to mech. props. 0-79713  
 polymers, struct. determ. from elastooosmometric parameters 0-64923  
 polypropylene, isothermal crystn., effect of contact with fibrous substrates 0-79708  
 polystyrene, conform. and near all-trans extended-chain model relevant in gels, X-ray diff. patterns interpret. 0-79707  
 polystyrene-b-isoprene-b-styrene, struct. regularity and crystn. 0-103269  
 polyurethane, segmented, domain struct., deform. effect 0-93623  
 polyvinylidene chloride, crystalline, preferred chain conform., mol. models 0-79709  
 polyvinylidene fluoride, cryst., struct. phase transition theory, free energy, uniaxial stress 0-64924  
 PVC, rigid resin, TEM studies of morphology, processing effects 0-108385  
 Pyrex, ion bombardment, form. of cpds., IR spectrosc. exam. (*German*) 0-88173  
 rheology of glassy state and highly viscous liq. 0-70130  
 semiconductors, amorphous, short-range order, theory and probes 0-79698  
 semiconductors, glassy, damage, photostructural changes, mechanism 0-92557  
 silicate glass, hydrated, proton and <sup>23</sup>Na wide-line NMR study 0-84659



## noncrystalline state structure continued

- silicate glasses, local order around Fe, exam. using X-ray absorpt. spectrometry 0-79701
- silicate glasses, longit. and transverse elastic wave vel., temp. and comp. variations 0-88258
- siloxane, temp. transitions, linear dilatometry and X-ray diffr. obs. (*Russian*) 0-59404
- superconducting metastable alloys, review of current work 0-81002
- transition metal alloys, amorphous, mag. props., structure and preparation 0-75737
- transition metal-metalloid glasses, short range order of dense-random-packing models 0-64907
- transition metal-metalloid glasses, struct., compositional effects (*Japanese*) 0-84086
- transition metal-metalloid glasses, struct. and plastic flow, review 0-84090
- transition metal-nonmetal glasses, with defined local coordination, struct. model 0-84092
- vibrational spectra and glass structure 0-84732
- vinylidene fluoride-trifluoroethylene film, cryst. phase transition 0-66120
- window glass, knots and cords, EPMA characterisation 0-84085
- AgI-Ag<sub>2</sub>O-MoO<sub>3</sub> glass glass superionic cond., struct. and transport props. 0-88602
- AlF<sub>3</sub> based glasses, chem., thermal and optical props. (*French*) 0-70139
- AlF<sub>3</sub>-M<sub>2</sub>F glasses, M=alkaline earth, density-of-states and structural forms, Raman spectra study 0-97255
- As-S-Tl, glass, viscosity and elastic props. 0-100180
- As-Se amorphous system, Raman scatt. 0-88984
- As-Se-Sb, crystallised glasses, struct. from Mossbauer spectra 0-64917
- As<sub>2</sub>S<sub>3</sub>, glassy, photoinduced defects, EPR and absorpt. spectra 0-59398
- As<sub>2</sub>S<sub>3</sub>, amorphous, struct., vibr. and electronic spectra 0-64908
- As<sub>2</sub>S<sub>100-x</sub> amorphous films, optical props. and photoinduced changes 0-60700
- As<sub>2</sub>S<sub>100-x</sub> glasses, Raman spectrum and structure 0-60593
- (As<sub>2</sub>O<sub>3</sub>)<sub>100-x</sub>Cu<sub>x</sub> glassy, struct. and elec. cond. study 0-59399
- As<sub>2</sub>Sb<sub>2</sub>Se<sub>9</sub> glassy semiconductors, electronic props. 0-103712
- As<sub>2</sub>Se<sub>3</sub> glass, mol. struct. model 0-100179
- Au film, discontinuous, centre-to-centre particle distrib. determ. 0-96761
- Au-Ge-Si, influence of struct. on elec. resist. of glass forming alloys 0-65518
- Au<sub>2</sub>Si<sub>65</sub> amorphous vacuum-deposited and liquid-quenched films, diffusion and crystn. 0-84094
- B<sub>2</sub>O<sub>3</sub> and alkali borate glasses, Raman study at high temps. 0-93306
- B<sub>2</sub>O<sub>3</sub>, vitreous, struct. study using <sup>10</sup>B NMR 0-84658
- BaB<sub>2</sub>O<sub>7</sub>-RF<sub>2</sub>, R=Mg, Ca, Sr, Ba, glass form., struct. and props. 0-84077
- BaO-WO<sub>3</sub>-P<sub>2</sub>O<sub>5</sub> glass, struct. and IR spectra 0-64914
- Ba(PO<sub>3</sub>)<sub>2</sub>-fluoride glass, elec. cond., struct. 0-88056
- BeF<sub>2</sub> glass transition, Monte Carlo study 0-75343
- BeF<sub>2</sub>-Eu<sup>3+</sup> glass, struct. and optical props. 0-84067
- BeF<sub>2</sub>-Eu<sup>3+</sup> glass, struct., Monte Carlo simulations 0-96448
- BeF<sub>2</sub>-KF-CaF<sub>2</sub>-AlF<sub>3</sub>-EuF<sub>3</sub> fluoroberyllate glass, Eu<sup>3+</sup> fluoresc. linewidth 0-66285
- CaO-Al<sub>2</sub>O<sub>3</sub>-SiO<sub>2</sub> glasses, density-of-states and structural forms, Raman spectra study 0-97255
- Co-B-Si amorphous alloy, liq. quenched, rel. to elec. resist. and cyclic deform. 0-59949
- Co-Fe-Si-B, decomp. of amorphous state during annealing below recryst. temp., electron microscope study (*Russian*) 0-75164
- Co-P alloys, geometric struct. models and diffraction exam. techniques 0-79700
- Co-Zr, amorphous phase form. in Zr-poor region, hardness and fracture strength (*Japanese*) 0-84914
- Co<sub>67</sub>Er<sub>33</sub> amorphous alloy, sputtered, local order and amorphous struct. 0-88061
- (Co<sub>93</sub>Fe<sub>07</sub>)<sub>75-x</sub>Cr<sub>25</sub>Si<sub>15</sub>B<sub>10</sub> amorphous alloy, thermal stability, Cr conc. effects, DTA expts. 0-59395
- CoP amorphous alloy, heat treatments influence on opt. props., struct. and DC resist. obs. 0-80892
- Co<sub>90</sub>P<sub>10</sub>, noncrystalline ferromagnet, electroless deposited, struct. and microscopic mag. props. 0-88063
- Cu-Ag-Ge, Hume-Rothery glass form. 0-96449
- Cu-Ag-P(6-14, 11-14 wt.%) amorphous, crystn. and elec. props., X-ray diffr., elec. resist. and DTA meas. (*Japanese*) 0-84088
- Cu-Sb-I system, glass form., struct. and IR spectra 0-64915
- Cu-Zr amorphous alloy, splat cooled, local order and amorphous struct. 0-88061
- CuInSe<sub>2</sub> amorphous thin film, flash evaporation, struct., stoichiometry 0-89150
- Cu<sub>0.57</sub>Zr<sub>0.43</sub> amorphous alloy, neutron diffr. obs. of struct. 0-88060
- Cu<sub>57</sub>Zr<sub>43</sub> amorphous alloy, computer simulation of atomic structure 0-70125
- Cu<sub>66</sub>Zr<sub>34</sub> amorphous metallic glass, differences caused by preparation technique (*French*) 0-103247
- EuS-Ga<sub>2</sub>S<sub>3</sub>-GeS<sub>2</sub>, chalcogenide glasses, conditions of form. of glassy prod. (*French*) 0-100325
- Fe based alloy, amorphous, liq. quenched, struct., thermal stability and mech. props. 0-88059
- Fe-B, amorphous alloys, compositional study on short-range struct. 0-84095
- Fe-B amorphous alloy, annealed, microstruct. and mag. domain changes 0-75790
- Fe-B metallic glass, X-ray diffr. meas., semi-empirical struct. model 0-107059
- Fe-B metallic glasses, struct., stability and crystn. 0-75173
- Fe-B-Si amorphous alloy, liq. quenched, rel. to elec. resist. and cyclic deform. 0-59949
- Fe-B(Si) alloy filaments produced by glass-coated melt spinning 0-76213
- Fe-Ge, amorphous, atomic struct., neutron diffr. study 0-59392
- Fe-Ni-B metallic glass, X-ray diffr. meas., semi-empirical struct. model 0-107059
- Fe-Ni-P-B, amorphous, crystn. and struct. 0-75175
- Fe-P-C, amorphous, crystn. and struct. 0-75175
- Fe-Zr, amorphous phase form. in Zr-poor region, hardness and fracture strength (*Japanese*) 0-84914
- Fe<sub>80</sub>B<sub>20</sub> amorphous, cold neutron scatt., local and extended defects 0-84089
- Fe<sub>80</sub>B<sub>20</sub> amorphous struct., Mossbauer spectroscopy investigation 0-84677

## noncrystalline state structure continued

- Fe<sub>80</sub>B<sub>20</sub> metallic glass, crystn. and struct. relax., Mossbauer effect study 0-75182
- Fe<sub>83.4</sub>B<sub>16.6</sub> amorphous, mag. props. and microstruct., cooling rate and melt overheating effects 0-65965
- Fe<sub>83.4</sub>B<sub>16.6</sub> amorphous, mag. props., melt overheating and cooling rate effects 0-89371
- FeF<sub>3</sub>, amorphous, struct. and mag. props., computer model 0-96446
- (Fe<sub>0.6</sub>Ni<sub>0.4</sub>)<sub>100-x</sub>B<sub>x</sub> and (Fe<sub>100-x</sub>Ni<sub>x</sub>)<sub>80</sub>B<sub>20</sub> amorphous alloys, X-ray diffr. struct. determ. 0-64906
- Fe<sub>40</sub>Ni<sub>40</sub>B<sub>20</sub>-P<sub>2</sub> metallic glasses, local struct. and dynamic disorder of Fe and Ni, EXAFS obs. 0-89088
- Fe<sub>40</sub>Ni<sub>40</sub>P<sub>14</sub>B<sub>6</sub> amorphous, resistometric study of short-range ordering rel. to heat treatment 0-70140
- Fe<sub>40</sub>Ni<sub>40</sub>P<sub>14</sub>B<sub>6</sub> Metglas 2826, hot forming 0-84980
- Fe(OH)<sub>2</sub> thin films, elec. cond. var. with temp., amorphous struct. 0-75566
- Fe<sub>100-x</sub>P<sub>x</sub>, structural analysis of models for amorphous metallic alloys 0-103249
- Fe<sub>75</sub>T<sub>25</sub> amorphous alloy, atomic struct., computer simulation 0-88043
- FePC molten and amorphous alloys, struct. factors 0-79674
- Gd-Co based amorphous sputtered films, microstruct. variability and mag. anisotropy, implanted ion effects 0-88459
- Ge amorphous film, bright-field hollow cone images 0-75136
- Ge amorphous films, structural relaxation and crystallisation 0-100170
- Ge:O, Cu, amorphous thin film, impurity effects on struct. 0-107054
- Ge-Ga amorphous alloy, co-evaporated elec. and optical props. 0-70860
- Ge-P-S glass system, EPR of intrinsic and Mn<sup>2+</sup> impurity centres 0-88870
- GeO<sub>2</sub> particles used for optical fibre fabrication, struct. props. 0-89167
- GeO<sub>2</sub>, vitreous, struct., contrasted with EXAFS obs. of ZnCl<sub>2</sub> liq. and glass struct. 0-70133
- GeO<sub>2</sub>-K<sub>2</sub>O(Na<sub>2</sub>O)(Li<sub>2</sub>O), glass, Raman spectra, struct. and crystn. 0-92463
- Ge<sub>2</sub>S<sub>3</sub> glass form. and characterisation (*German*) 0-64913
- Ge<sub>25</sub>S<sub>75</sub>Mn, bond struct. and character in Ge-S system, EPR obs. 0-66014
- Ge<sub>40</sub>S<sub>60</sub>Mn (Ag)(Cu), bond struct. and character in Ge-S system, EPR obs. 0-66014
- Ge<sub>2</sub>Se<sub>3</sub> glass form. and characterisation (*German*) 0-64913
- H<sub>5n-2</sub>UO<sub>2</sub>(IO<sub>6</sub>)<sub>n</sub>·4H<sub>2</sub>O, n=0.5 to 2.0, high proton cond. 0-107562
- K<sub>2</sub>O-Al<sub>2</sub>O<sub>3</sub>-P<sub>2</sub>O<sub>5</sub>-TiO<sub>2</sub>, structural role of Ti, kinetic study of chem. destruction 0-88055
- K<sub>2</sub>O-B<sub>2</sub>O<sub>3</sub>-Fe<sub>2</sub>O<sub>3</sub>, γ-irrad., Mossbauer spectroscopic study 0-108132
- K<sub>2</sub>O-MgO-B<sub>2</sub>O<sub>3</sub>-Cu<sup>2+</sup>, micro-inhomogeneities, EPR and Raman study 0-84080
- La-Au, splat-quenched, Mossbauer effect and elec. resist., amorphous struct. 0-84676
- (Li<sub>0.63</sub>Na<sub>0.37</sub>)<sub>2</sub>O·2SiO<sub>2</sub>, short range struct. by pulsed neutron scatt. 0-59396
- LiO<sub>2</sub>-Al<sub>2</sub>O<sub>3</sub>-SiO<sub>2</sub> glass containing ZrO<sub>2</sub>, cryst. process 0-103253
- Li<sub>2</sub>O-Al<sub>2</sub>O<sub>3</sub>-SiO<sub>2</sub>, phase separation of initial stages of sialisation 0-88053
- Li<sub>2</sub>O-B<sub>2</sub>O<sub>3</sub> glass struct. study using <sup>10</sup>B NMR 0-84658
- Li<sub>2</sub>O-LiF-B<sub>2</sub>O<sub>3</sub>-Li<sub>2</sub>SO<sub>4</sub> glasses, DC cond. and secondary struct. relax. 0-107469
- Li<sub>2</sub>O-TiO<sub>2</sub>-Al<sub>2</sub>O<sub>3</sub>-SiO<sub>2</sub> glass, γ-irrad., struct. position of Ti, EPR study 0-84644
- Li<sub>2</sub>O·2SiO<sub>2</sub>, short range struct. by pulsed neutron scatt. 0-59396
- Li<sub>2</sub>S-GeS<sub>2</sub> glass forming region, struct. and ionic cond. 0-88358
- MgO-TiO<sub>2</sub>-Al<sub>2</sub>O<sub>3</sub>-SiO<sub>2</sub> glass, γ-irrad., struct. position of Ti, EPR study 0-84644
- Na<sub>2</sub>O-Ag<sub>2</sub>O-B<sub>2</sub>O<sub>3</sub> glass, Ag<sup>+</sup> ion distrib., X-ray diffr. study 0-84076
- Na<sub>2</sub>O-B<sub>2</sub>O<sub>3</sub> glass struct. study using <sup>10</sup>B NMR 0-84658
- Na<sub>2</sub>O-B<sub>2</sub>O<sub>3</sub>-Bi<sub>2</sub>O<sub>3</sub> glass with metallic Bi granules, elec. cond. 0-84493
- Na<sub>2</sub>O-MgO-B<sub>2</sub>O<sub>3</sub>-Cu<sup>2+</sup>, micro-inhomogeneities, EPR and Raman study 0-84080
- Na<sub>2</sub>O-P<sub>2</sub>O<sub>5</sub>-SiO<sub>2</sub> glass, metastable liquid immiscibility 0-100331
- Na<sub>2</sub>O-SiO<sub>2</sub>, ion bombardment, form. of cpds., IR spectrosc. exam. (*German*) 0-88173
- Na<sub>2</sub>O-SiO<sub>2</sub> glass, bridging to non-bridging ratio and correl. to glass density and refr. index, ESCA study 0-84832
- Na<sub>2</sub>O-SiO<sub>2</sub> glass, internal and surface struct. by X-ray scatt. 0-84074
- Na<sub>2</sub>O-SiO<sub>2</sub> glass, OH<sup>-</sup> content effect on mech. and other props. 0-89337
- Na<sub>2</sub>O-TiO<sub>2</sub>-Al<sub>2</sub>O<sub>3</sub>-SiO<sub>2</sub> glass, γ-irrad., struct. position of Ti, EPR study 0-84644
- Na<sub>2</sub>O-TiO<sub>2</sub>-SiO<sub>2</sub> glass, co-ordination of Ti, X-ray emission spectra study 0-84072
- Na<sub>2</sub>O·2SiO<sub>2</sub>, short range struct. by pulsed neutron scatt. 0-59396
- Na<sub>2</sub>S-P<sub>2</sub>S<sub>3</sub> glass forming region, struct. and ionic cond. 0-88358
- Na<sub>2</sub>S-SiS<sub>2</sub>(GeS<sub>2</sub>)(P<sub>2</sub>S<sub>5</sub>), synthesis, structure and ionic conduction (*French*) 0-65291
- Na<sub>2</sub>S-XS<sub>2</sub>, X=Si, Ge, glass forming region, struct. and ionic cond. 0-88358
- Nb<sub>2</sub>Ge(Si), amorphous films, thermally-activated internal friction peaks, structural obs. 0-80147
- Nb<sub>2</sub>Ge(Si), RF sputtered films, amorphous atomic scale struct. 0-84064
- Nb<sub>2</sub>O<sub>5</sub>-V<sub>2</sub>O<sub>5</sub>-P<sub>2</sub>O<sub>5</sub> glasses and glass ceramics, elec. cond., struct. 0-84466
- Ni based alloy, amorphous, liq. quenched, struct., thermal stability and mech. props. 0-88059
- Ni-Cr-P, amorphous, corrosion behaviour, immersion tests and electrochem. meas. (*Japanese*) 0-85085
- Ni-Ge, amorphous, atomic struct., neutron diffr. study 0-59392
- Ni-P, amorphous, low P, struct. study using high-angle X-ray diffr. 0-107055
- Ni-P amorphous alloys, electrodeposited and melt-quenched atomic and electronic structures 0-88062
- Ni-Ta (70, 30 wt.%) metallic glass, struct. and crystn. (*Russian*) 0-70136
- Ni-Ti-P, amorphous, corrosion behaviour, immersion tests and electrochem. meas. (*Japanese*) 0-85085
- Ni-Zr, amorphous phase form. in Zr-poor region, hardness and fracture strength (*Japanese*) 0-84914
- NiP amorphous alloy, heat treatments influence on opt. props., struct. and DC resist. obs. 0-80892
- Ni<sub>40</sub>Ti<sub>60</sub> amorphous, chem. short-range-order, X-ray and neutron scatt. obs. 0-96447
- P, amorphous, prepared by chem. transport in low-pres. H<sub>2</sub> plasma, radial distrib. function 0-64899



**noncrystalline state structure continued**

- P, amorphous, struct. by electron microscopy 0-84065  
 PbO-B<sub>2</sub>O<sub>3</sub> glass-forming melt, specific volume and viscosity, temp. depend. 0-84073  
 PbO-B<sub>2</sub>O<sub>3</sub>-Bi<sub>2</sub>O<sub>3</sub>, glass with metallic Bi granules, elec. cond. 0-84493  
 PbO-GeO<sub>2</sub>, glass, structure of anionic network, IR spectra 0-103256  
 PbO-SiO<sub>2</sub> glasses, density-of-states and structural forms, Raman spectra study 0-97255  
 Pd-Au-Si, influence of struct. on elec. resist. of glass forming alloys 0-65518  
 Pd-Cu-Si, glass form., crit. cooling rate 0-75169  
 Pd-Si, amorphous, compositional study on short-range struct. 0-84095  
 Pd-Si, amorphous, struct., crystn. and Hall effect meas. 0-75178  
 Pd-Si, amorphous metallic glass, with defined local coordination, struct. model 0-84092  
 Pd-Si metallic glass, high-resolution electron microscopy 0-84097  
 (Pd<sub>80</sub>Au<sub>10</sub>Si<sub>10</sub>)/Fe<sub>30</sub>, compositionally modulated amorphous film, diffusion, struct. relax. 0-103518  
 Pd<sub>80</sub>Si<sub>20</sub>, amorphous alloy, partial struct. functions, X-ray, electron and neutron diff. studies (*Japanese*) 0-88050  
 (Pd<sub>85</sub>Si<sub>15</sub>)<sub>61</sub>/(Fe<sub>85</sub>Bi<sub>15</sub>)<sub>39</sub>, compositionally modulated amorphous film, diffusion, struct. relax. 0-103518  
 R<sub>1-2</sub>Co<sub>x</sub>, rare earth amorphous alloys, thermal stability, elec. cond. enthalpy 0-100172  
 (SN)<sub>x</sub>, brominated, X-ray absorpt. meas., 5K to room temp. 0-71516  
 (SN)<sub>x</sub>, halogenated, struct. behaviour, TEM obs. 0-70126  
 Sb-O-Cl(Br)(I), glass-forming regions 0-88057  
 Se, amorphous, elec. cond., activation energy, density, cryst. Se effect 0-65548  
 Se, amorphous and liquid state, Raman spectra, crystn. processes 0-60608  
 Se, amorphous film, highly disordered, UPS study 0-76148  
 Se, amorphous film, photocond., dark cond., rel. to crystn. 0-88596  
 Se, glassy, structural excitation energies of defects, pseudopot. approach 0-107061  
 Se, liquid and amorphous, struct. modelling using Monte Carlo method 0-59391  
 Se, mol. structure, local atomic arrangement at intrinsic bonding defects 0-59374  
 Se, trigonal and amorphous, electronic struct. and nonempirical calc. of struct. props. 0-59866  
 Se<sub>0.95</sub>Te<sub>0.05</sub>, glass crystallisation, effect of an alternating electric field 0-88054  
 Se<sub>1-x</sub>Te<sub>x</sub>, amorphous film, photo-crystallisation 0-59839  
 Se<sub>1-x</sub>Te<sub>x</sub>, amorphous, structural relaxation and crystallisation kinetics study by DTA 0-59394  
 Si, amorphous, hydrogenated and deuterated, struct. 0-103245  
 Si, amorphous layers, recrystallisation, pulsed laser annealing 0-65404  
 Si, effect of disorder on H content 0-75258  
 Si, noncrystalline film, struct., interatomic distances, SRO 0-107053  
 a-Si:H, electronic states and bonding config. 0-64900  
 Si:H amorphous films, IR spectrum and struct. 0-97277  
 Si<sub>1-x</sub>H<sub>x</sub>, noncrystalline film, struct., interatomic distances, SRO 0-107053  
 Si<sub>3</sub>N<sub>4</sub>-Al<sub>2</sub>O<sub>3</sub>-SiO<sub>2</sub> systems, glass forming regions 0-84070  
 SiO<sub>2</sub>, amorphous, very small angle X-ray scatt. before and after thermal neutron irradi. 0-75270  
 SiO<sub>2</sub> films, Si-rich, amorphous Si region obs. 0-84400  
 SiO<sub>2</sub>, fused, broken bond defect generation mechanisms 0-88044  
 SiO<sub>2</sub>, gel, internal and surface struct. by X-ray scatt. 0-84074  
 SiO<sub>2</sub> glass, formation by hydrolysis of Si(OC<sub>2</sub>H<sub>5</sub>)<sub>4</sub> with NH<sub>4</sub>OH and HCl soln., and characterisation 0-71622  
 SiO<sub>2</sub>, ion bombardment, form. of cpds., IR spectrosc. exam. (*German*) 0-88173  
 SiO<sub>2</sub>, vitreous, paramag. centres associated with bonding defects 0-80609  
 SiO<sub>2</sub>-B<sub>2</sub>O<sub>3</sub> glass system, gel hot pressing synthesis and characterisation (*French*) 0-66468  
 SiO<sub>2</sub>-B<sub>2</sub>O<sub>3</sub> glasses, Brillouin scattering meas. of attenuation and vel. of hypersounds 0-100309  
 SiO<sub>2</sub>-Li<sub>2</sub>O-Li<sub>2</sub>SO<sub>4</sub>, glass-forming region, struct. and ionic cond. 0-84320  
 Te, Raman spectra, crystn. processes 0-60608  
 Te, trigonal and amorphous, electronic struct. and nonempirical calc. of struct. props. 0-59866  
 Te<sub>80</sub>Ge<sub>20-x</sub>Sb<sub>x</sub>(Bi<sub>x</sub>), DSC studies of struct. phase transformation 0-66505  
 TeO<sub>2</sub>-MoO<sub>3</sub>-V<sub>2</sub>O<sub>5</sub>, phase comp. determ. using X-ray diffr., electron microscopy and DTA (*German*) 0-88046  
 TeO<sub>2</sub>-P<sub>2</sub>O<sub>5</sub> system, glass struct., neutron diff. study 0-70128  
 TlAsS<sub>2</sub>, glass, crystallisation, effect of an alternating electric field 0-88054  
 ZnB<sub>2</sub>O<sub>4</sub>-RF<sub>2</sub>, R=Mg, Ca, Sr, Ba, glass form., struct. and props. 0-84077  
 ZnCl<sub>2</sub>, glassy and liq, EXAFS obs. of struct., comparison with vitreous GeO<sub>2</sub> 0-70133  
 Zr-Ti-Be metallic glass, phase separation 0-97464  
 Zr<sub>70</sub>Co<sub>30</sub>, Zr<sub>70</sub>Fe<sub>30</sub>, Zr<sub>70</sub>Ni<sub>30</sub> and Zr<sub>70</sub>Pd<sub>30</sub> amorphous alloys, struct. factors and radial distribution functions 0-84096

**nondestructive testing**

- see also crack detection; ultrasonic materials testing; X-ray fluorescence analysis*  
 accountability, nondestructive assay using neutron counting, calorimetry and gamma spectrometry 0-63266  
 acoustic-emission pulse distrib., statistical investigation 0-87638  
 acoustical imaging, US visualization and characterization, conf., vol.8, Key Biscayne, FL, USA (May-June 1978) 0-83720  
 airframe material defectometry, quantitative test specifications (*German*) 0-89427  
 alloys, machining damage, depth of surface layers determ. 0-85094  
 amorphous layer thickness meas. by electron back scattering method 0-100721  
 automatic inspection of materials using lasers 0-66734  
 autoradiographic inventory methods for nondestructive assay of reactor fuels and fuel assemblies 0-71875  
 axisymmetric transducers, with various boundary conditions, single integral computer method for Green's function 0-87591  
 biomedical scattered radiation grids, method for testing 0-81717  
 bonded interface defect testing by differential interferometric Stoneley wave meas. 0-76444  
 brass, nondestructive determ. of in-depth profile 0-93836

**nondestructive testing continued**

- calorimetric nondestructive assay for in-field meas. of Pu-bearing materials 0-71874  
 ceramic components scanning laser acoustic microscopy, appl., comparison with SEM and optical microscopy results 0-58875  
 charcoal filters, NDT of residual adsorption capacity 0-89523  
 coherential KIFM-1 with automatic measurement of the demagnetizing current 0-68229  
 complex shape product inspection, local eddy current transducer 0-108671  
 composite materials, damage studying by NDT 0-66735  
 device for checking airtightness by parameter changes in object and medium 0-104404  
 dielectric material, NDT using Kirlian effect, high freq. technique 0-66749  
 eddy current testing of wire and bar 0-71819  
 eddy current transducer with electrical commutation of excitation field, NDT 0-105633  
 eddy currents in non-magnetic tubular conductors, NDT appl. (*French*) 0-83541  
 eddy-current feed-through transducer, approx. calc. of mag. field, nonferromag. media 0-78746  
 electrographic porosity test, reclassification as nondestructive method (*German*) 0-97652  
 equipment, calibration using reference materials for fissile material assay 0-71880  
 feed through eddy current transducer, numerical anal. or operating mode during ferromagnetic rod inspection 0-108670  
 ferromagnetic metals, thermal oxidation rate determ. using nanowebermeters 0-61045  
 ferromagnetic object inspection, method of higher harmonics, difference schemes 0-89444  
 ferromagnetic round bar, high energy alternating field stray flux testing technique 0-100972  
 ferromagnets, cyclically remagnetised, discrete spectra of induction calcs., demagnetising factor 0-103859  
 fibre composite structure, thermal field techniques for NDT 0-66737  
 fibreglass laminates, thermal NDT using liq. crystals 0-93709  
 flaw dimensions in direction of irradiation determ. from radiographs with aid of defectometer 0-71863  
 flexible scanning industrial X-ray fluoroscopic inspection 0-100971  
 flexible scanning industrial X-ray/fluoroscopic inspection 0-89459  
 fragile materials, mech. props. meas. using disc-shaped specimens (*French*) 0-104367  
 glass fibre reinforced plastics, exposed to liq. media, dynamic high-speed Young's modulus determ. (*German*) 0-85123  
 graphic symbols denoting types and methods of NDT 0-86042  
 heat treatment, electromagnetic quality inspection with specified intensity of internal field 0-108677  
 high-resolution photoacoustic spectroscopy for dopant depth profiling 0-77883  
 Inconel, steam generator tubing, mag. probe inspection 0-85119  
 industrial X-ray installation, spectroscopic anal. (*German*) 0-97668  
 interactive graphics system developed for NDT 0-66729  
 IR non-destructive testing of bonded materials, theory and practice 0-93708  
 IR techniques for evaluation of SiC heat-exchanger tubing 0-76435  
 irradiated fissile materials in extended configurations, nondestructive assay 0-71872  
 kevlar-epoxy composites pressure vessels, holographic nondestructive eval. 0-81275  
 laboratory and field equipment in India 0-108650  
 laminates, exposed to liq. media, dynamic high-speed Young's modulus determ. (*German*) 0-85123  
 linear wave motions study using FFT, NDT appl. 0-92038  
 LWR irradiated fuel assemblies, nondestructive exam. using  $\gamma$ -ray and neutron techniques 0-66760  
 LWR spent fuel, nondestructive meas. and verification for materials safeguards 0-78420  
 magnetic defectoscopes, nonsinusoidal periodic currents meas. 0-104386  
 magnetic particle inspection, nature of magnetic inks and powders 0-100974  
 magnetizing device for inspection of products of ferromagnetic materials according to parameters of Barkhausen discontinuity 0-89457  
 magnetographic inspection, determ. of magnetisation regimes 0-108665  
 medium with large no. of cracks, direct elec. current calcs. 0-96233  
 metal parts, large, without taking specimens, portable grinding and polishing machine 0-61042  
 metallic objects with complex shape, eddy-current inspection 0-89446  
 micropipette electrode tips, beveled, non-destructive electron microscopic exam. 0-89915  
 microtrons, appl. in nondestructive inspection of industrial products 0-81267  
 mobile nondestructive assay system for nuclear materials safeguarding 0-71876  
 multifrequency eddy current inspection with continuous wave methods 0-71844  
 neutron absorption radiometric testing of materials, review 0-71860  
 neutron radiography, contrast enhancement using gaseous <sup>3</sup>He penetrant 0-93707  
 neutron radiography, nuclear engineering appl. (*Slovak*) 0-76430  
 noncontact material testing using laser energy deposition and interferometry 0-71846  
 nonsinusoidal periodic current meas. using standard DC shunt with magnetic powder monitoring, frequency errors 0-104398  
 nuclear fuel shell inspection, mag. method for detecting ferromag. particles 0-66746  
 nuclear fuels, nondestructive measurement of U and Th conc. and quantities using XFA and gamma spectrometry 0-71877  
 nuclear material safeguarding, nondestructive meas. 0-76457  
 nuclear materials, neutron assay for accountability and criticality control 0-66759  
 nuclear materials, nondestructive element and isotope assay of Pu and U 0-71870  
 nuclear materials, results of international collaboration in the ESARDA working group 0-71879  
 nuclear materials accountability, U and P NDA of crated waste by gamma-ray and neutron coincidence counting 0-83166  
 nuclear materials safeguarding, nondestructive measurements of irradiated fuel assemblies at a reprocessing facility 0-95392



**nondestructive testing continued**

nuclear materials safeguards, assay of dissolver solns. by totally sampled wavelength dispersive X-ray fluorescence 0-83160  
 nuclear materials safeguards, collection and analysis of measured fission product data 0-95354  
 nuclear materials safeguards, mathematical simulation of calorimeters used for rapid nuclear fuel assay 0-95355  
 nuclear materials safeguards, nondestructive, energy-dispersive, X-ray fluorescence analysis of product-stream concentrations from reprocessed nuclear fuels 0-83163  
 nuclear materials safeguards, prototype, reference materials for nondestructive assay 0-78372  
 nuclear materials safeguards reference measurement system utilizing resonance neutron radiography for nondestructive assay meas. 0-78377  
 nuclear power station heat exchangers, eddy current probe for nondestructive testing of transfer tubes (*Japanese*) 0-81246  
 nuclear reactor components, NDT using acoustic emission (*Spanish*) 0-58781  
 optical fibre characterisation techniques compared 0-64202  
 optical fibre preform core diameter and Ge doping profile meas., X-ray nondestructive method 0-64231  
 optical fibre preform rod, refractive index profile meas. by transverse differential interferogram 0-64141  
 photometric calibrator appl., inverse fourth power, NBS development 0-73412  
 pipes, hot-rolled, automatic mag. quality control on prod. line 0-108661  
 prosthesis wear, holographic studies using optical contouring 0-67288  
 pulsed magnetic analyser, IMA-5 0-104399  
 PVF<sub>2</sub> transducers for NDT 0-76476  
 radio wave inspection with one sided access to object, conditions of coating and compensation 0-108679  
 radiographic inspection method, productivity 0-71861  
 radiographic testing equipment, device characts. (*German*) 0-76438  
 radiography gamma ray source, choice for welded joint monitoring 0-104396  
 review, nondestructive evaluation 0-71855  
 rubber-metal facings, vulcanisation degree determ.,  $\gamma$ -ray method 0-61043  
 sapphire and Si surfaces, using IR and UV specular reflectance meas. 0-108684  
 SAW generation using CW laser, NDT appl. 0-87683  
 simulated neutron tomography for nondestructive assays 0-99218  
 special nuclear materials, assay and accountability using neutron correlation meas. tech. 0-69015  
 special nuclear materials, nondestructive assay techniques for control and accountability 0-81270  
 spectral nuclear materials, control and accountability, reliability of nondestructive assay techniques 0-76456  
 spent fuel subassemblies, nondestructive assay, comparison of calcs. and meas. 0-78421  
 spent fuel waste products, delayed neutron nondestructive assay instrumentation, Monte Carlo calculational design 0-81271  
 steel, electrical, sheet, systematic and random errors, in wattmeter apparatus for measuring unit losses 0-71858  
 steel, ferritic, magnetomechanical acoustic emission for residual stress NDT 0-71149  
 steel, monitoring with pulsed magnetic analyser, IMA-5 0-104399  
 steel, neutron quasioalbedo thickness meas. of single layer product, optimization 0-105611  
 steel, nitrided layer depth, electroinduction meas. method 0-104379  
 steel, positron meas., for trapping mechanism detection 0-84798  
 steel, stainless type SUS 304, diffusion welded joints, sound emission during tensile testing (*German*) 0-61062  
 steel, structural ties, NDT by eddy current transducer, optimum parameters and capabilities 0-108669  
 steel case depth after quench hardening, inspection using coercimeters 0-104377  
 steels, heat treatment of 30KhN2MFA and 40Kh, nondestructive mag. quality control method 0-108662  
 strain and damage electrical measurement method (*French*) 0-71854  
 structural material analysis by computerized tomography 0-101001  
 structural stress distrib. determ. by remote IR thermometry 0-87749  
 surface topography quantitative determ. by Nomarski differential interference contrast microscopy 0-73318  
 survey assay meter developments at BNL for nuclear materials safeguarding appls. 0-69038  
 thermal, vortex tube appl. 0-89453  
 thin crystals and films, nondestructive microhardness testing of near-surface layers 0-71829  
 tomography, computerized, NDT appls. (*German*) 0-76439  
 transducer, matrix eddy-current, with magnetic circuit, design and construction 0-68228  
 transducer, straight-through screened circular primary, between multilayer cylinder and tube, EM field 0-71856  
 transducer orientation system in screen methods of NDT 0-66745  
 tube, magnetization with transverse field, approx. soln. 0-69321  
 weld inspection system for Space Shuttle external fuel tank, automatic, interim report 0-76463  
 welds, residual stresses, evaluation by Barkhausen noise meas. 0-76436  
 welds and castings, differential method of balancing out thickness-variation effects in radiography 0-66748  
 X-radiography, microfocus projection, scattering effect on contrast 0-100973  
 X-ray beam, half-value layer determ., analytic method 0-66747  
 X-ray flash methods and equipment (*German*) 0-97669  
 X-ray integration method, extension of  $\sin^2\psi$  method (*German*) 0-92420  
 X-ray line profile test method, for plastic deform. (*Hungarian*) 0-97663  
 X-ray stress meas., computer-aided system (*Japanese*) 0-104366  
 Al foil, deformation, laser optical scanning obs. 0-100995  
 Al-Cu, high strength, type 2024-T3, crack growth, fatigue induced surface deform., holographic detect. 0-85120  
 Al<sub>1</sub>Ga<sub>1-x</sub>As-GaAs heterostruct., varizional, parameter determ. by photoluminescence method (*Russian*) 0-108291  
 CdS thin films on brass substrates, nondestructive resistivity meas. tech. 0-93898  
 Fe, magnetomechanical acoustic emission for residual stress NDT 0-71149  
 Fe polycrystalline, two ferromag. methods for eval. of fatigue limit 0-89438  
 Pb-Sn (20wt.%), eddy current study of solidification 0-104141

**nondestructive testing continued**

Pu, accountability and control, field nondestructive assay measurements as applied to process inventories 0-63265  
 Pu, assay of large samples using portable neutron coincidence counter 0-69041  
 Pu nondestructive analysis, calibration by calorimetric assay 0-71878  
 Pu, nondestructive assay of large samples using passive neutron coincidence counting and gamma spectrometry 0-71871  
 Pu passive assay using Euratom variable dead-time neutron counter 0-69042  
 Pu safeguards, nondestructive assay using automated in-line instrumentation 0-95353  
 Pu safeguards, product soln. gamma-ray NDA using K-absorption edge densitometer 0-83162  
 Pu safeguards accountability, gamma-ray meas. of Pu and Am in molten salt residues 0-83165  
 Pu safeguards assay, isotopic meas. by gamma ray spectrometry using two-detector method 0-83161  
 Si monocrystal peripheral fusion channelling under HF heating (*Russian*) 0-59627  
 Si, polycrystalline Czochralski-grown, MIS solar cell characterisation using scanned laser response exam. 0-93884  
 Si polycrystalline film, effect of defects/grain boundaries on photovoltaic mech. 0-93883  
 SiC-ceramic, nondestructive evaluation, scanning photoacoustic microscopy 0-85115  
 Si<sub>3</sub>N<sub>4</sub>-ceramic, nondestructive evaluation, scanning photoacoustic microscopy 0-85115  
 steel, C, magnetomechanical acoustic emission for residual stress NDT 0-71149  
 (U,Pu)O<sub>2</sub>, nondestructive active assay of <sup>235</sup>U and <sup>239</sup>Pu 0-71873  
 U assay, experimental comparison of the active well coincidence counter with the random driver 0-78503  
 U, nuclear fuel conversion plant, nondestructive assay 0-66761  
 U/Pu fuel reprocessing solutions, NDA using X-ray L-edge densitometer for materials safeguards 0-83167  
 UO<sub>2</sub>, PuO<sub>2</sub>, fuel pellets, porosity meas. methods (*German*) 0-73915  
<sup>235</sup>U safeguards, expt. nondestructive assay using a random driver 0-83164  
<sup>235</sup>U, nondestructive assay, appl. to decommissioning of fuel reprocessing facility 0-81269

**nonelectric sensing devices**  
 fibre optics sensors for measurement and control appls. 0-58780  
 fluidic temperature sensors 0-73342  
 membranes appl., silicone rubber, physical props. (*Slovak*) 0-61141  
 optical sensor using optical fibres (*Japanese*) 0-78997  
 passive optical rotation sensors using guided waves, developments 0-58781  
 Permalloy magnetoresistive mag. field sensor, performance calc. 0-57342  
 viscosimeter solar radiation tracking sensor 0-86295

**nonleptonic decays**  
*see also baryon hadronic decay; meson hadronic decay*  
 bottom mesons, weak decays, strong correction meas. 0-82970  
 top mesons, weak decays, strong correction meas. 0-82970  
 $\Sigma^\pm$  lifetimes, decay asymmetry and nonleptonic decay branching ratio,  $|\Delta I|=1/2$  rule 0-78061

**nonlinear acoustics**  
 atmosphere acoustic and radio acoustic exploration, effects of sound nonlinear absorpt. (*Russian*) 0-94567  
 backward waves and acoustic scanning, nonlinear interaction of vol. and surface waves 0-79040  
 broadband parametric array with Gaussian primary directivity patterns 0-96066  
 caster oil, calculation of nonlinearity parameters thermodynamic method 0-79880  
 cavitation threshold meas. for polyalkylene glycol and castor oil 0-107374  
 closed tube, nonlinear resonant acoustic oscillators, finite rate theory 0-92171  
 dispersive waves, characterization using freq. approach 0-87606  
 gas bubbles in liquid, propag. of disturbances 0-59104  
 Gaussian beam propag. 0-87609  
 HF sound propagation, non-linear effects in tubes 0-87614  
 HF sound propagation in metals and semiconduction 0-88279  
 inhomogeneity of medium, determination by means of sound signals 0-87610  
 interaction of determinate packet with random noise, in Burgers' equation 0-106650  
 noise spectrum evolution, Gaussian, intensive, plane wave in lossless fluids 0-69581  
 nonlocal diffusion theory of wave propagation in highly viscous liquids 0-102897  
 parametric acoustic array, effect of finite aperture 0-106648  
 parametric acoustic arrays with intermediate directivity in water, expt. study 0-74569  
 parametric acoustic receiving array response to transducer vibration 0-74570  
 parametric arrays, beam pattern and propag. curve for air (*Japanese*) 0-83693  
 parametric sound generation, liquid containing gas bubbles 0-87615  
 piezosemiconductors, second harmonics of acoustoelectric current 0-80329  
 polyvinylidene fluoride films, SH and Lamb waves propag. 0-75948  
 propag. of sound beams with uniform amplitude distrib. 0-102896  
 propagation of plane harmonic waves, infinite isotropic medium having embedded doubly periodic array of cylindrical fibres 0-87607  
 pulsation noise damping from small air bubbles in water 0-64253  
 pulsed radiolysis, nonlinear radiation-acoustic phenomena 0-79029  
 radiation patterns of acoustical arrays with quantized time delays 0-74566  
 radiation pressure on rigid sphere in spherical wave field 0-64251  
 Rayleigh wave interaction in LiNbO<sub>3</sub>-CdS system, expt. investigation 0-102946  
 reflection from obstacle in one-dimens. medium with random inhomogeneities 0-58839  
 resonator cavity, influence of depth on acoustical props. 0-58838  
 SAW and anomalous sound absorpt. for fluid-fluid interface 0-74562  
 SAW elastic convolver, degenerate, nonlinear interactions 0-64254  
 SAW propag., photographs on TV images of travelling waves using strobed electron beam 0-102894



**nonlinear acoustics continued**

- SAWs of finite amplitude excited by monochromatic line source, propag. characs. 0-96091  
 second-harmonic generation in resonator of multilayered interference filter type 0-58840  
 semiconductor-piezoelectric structure, vol. acoustic wave excitation in nonlinear interaction with surface waves 0-69582  
 sonic wave, excitation by quasi-monochromatic Alfvén pumping 0-106649  
 sound field of plane radiator with arbitrary contour shape 0-79028  
 streaming in vicinity of plate possessing propagating longitudinal strain wave 0-87758  
 suppression of finite-amplitude primary wave attenuation, parametric acoustic arrays, use of bubbles 0-74563  
 surface charge on unapodized periodic ID1 0-91947  
 TGS, ferroelec. single crystal, low freq. nonlinear effects 0-84490  
 transonic gas flow, optical excitation of intense acoustic waves 0-74564  
 US nonlinearity parameter for solids, relationship with Grüneisen parameter 0-74561  
 US wave in cavitating liquids, optical visualisation 0-106651  
 wave propagation on turbulent jets using organ pipe flue 0-91946  
 $\text{KH}_2\text{PO}_4$  electro-optic modulator crystals, piezoelec. induced acoustic transients 0-70316  
 $\text{LiNbO}_3$ , parametric phonon echo obs. 0-59588

**nonlinear differential equations**

- Boltzmann equation, nonlinear, for internal state and Maxwell models 0-77733  
 Boltzmann equation, nonlinear, solns. of Krook-Tjon-Wu model, Laguerre expansion of distrib. function 0-68157  
 Boltzmann equation, nonlinear, with soft potential, spatially periodic problems 0-77731  
 Boltzmann equations for internal state and Maxwell models, similarity solutions 0-86231  
 Bose gas, impenetrable, one particle reduced density matrix, Painlevé-type eqn. 0-62576  
 Boussinesq equation, similarity solutions and Backlund transformation 0-68056  
 Boussinesq equation, group theoretical approach 0-82914  
 convection flow, free, between heated vertical parallel plates, quasi-linearization 0-92148  
 counterflow processes, nonlinear modelling using weighted residual methods 0-69754  
 coupled bilinear eqns., exact one- and two-periodic wave soln. 0-68050  
 cylindrical KdV equations, soln. asymptotic behaviour (in  $t$ ), Cauchy problem 0-98803  
 deflagration waves, heterogeneous, flame model for gas phase, nonlinear differential eqn. 0-81326  
 diffusion equation, nonlinear, invariance props., Lie-Backlund groups 0-62596  
 diffusion equation, stable profile evolution 0-82731  
 Duffing's equation, steady and chaotic motions 0-77616  
 Duffing's equation, strange attractors, explosion, chaotic behaviour 0-77617  
 elastoplastic thin vertical columns, postbuckled, deflections 0-87728  
 Ermakov systems generalized, nonlinear superposition law 0-86074  
 evolution eqns., conservation laws, group theoretical derivation 0-57520  
 evolution equations, connection to P-type differential eqs. 0-57078  
 evolution equations, nonlinear, connection with Painlevé type ordinary differential eqns., inverse scatt. transform 0-62486  
 evolution equations, nonlinear, inverse spectral transform, generalisation of Klein-Gordon problem 0-68055  
 evolution equations, reverse scattering method, Hamilton's structure and Backlund's transformations (Russian) 0-86090  
 evolution equations, symplectic operators and hereditary symmetries 0-82650  
 evolution equations and conservation laws, spectral transform method 0-62488  
 extension of nonlinear evolution equations of the K-dV (mK-dV) type to higher orders 0-105508  
 filtering, nonlinear, conditional laws, smoothness, stochastic calculus of variations (French) 0-68128  
 fins, nonlinear problems, 1-D conduction, initial value problem 0-83726  
 fluctuations, random, moment behaviour of soln. processes for nonlinear stochastic differential eqns. (Japanese) 0-95039  
 fluid dynamics, small-disturbance transonic flow, nonlinear mixed elliptic-hyperbolic eqn., finite element anal. 0-83814  
 friction, stochastic quantisation, nonlinear wave eqn. 0-98825  
 functional differential equation, compactness of bounded trajectories of dynamical systems 0-82636  
 Hartree equations, time-dependent, global solutions, and nonlinear Schrödinger eqn. 0-73193  
 heat and mass transfer, finite element soln., for chemically reacting system 0-68153  
 heat transfer and evaporation from cooled surfaces, nonlinear eqns. numerical soln. (German) 0-58893  
 heat-pulse experiments, nonlinear effects, theory 0-96182  
 Heisenberg chain, classical, solitons and magnons 0-60161  
 Heisenberg spin chain, operator equation, nonlinear differential form, auxiliary constraint 0-65762  
 higher order Korteweg-de Vries eqn., Backlund transform 0-105510  
 higher order modified KdV eqns., bilinearisation 0-105509  
 integrable nonlinear evolution equation, soliton soln. from inverse scatt. method 0-73186  
 inverse method for solving differential-difference and difference-difference eqns. 0-105513  
 KdV equation, perturbative expansion and initial value problem 0-62487  
 kidney model, numerical soln. by multiple shooting 0-104609  
 Klein-Gordon eqn., nonlinear interactions of counter-travelling waves 0-77627  
 Klein-Gordon equation, inverse spectral transform 0-68055  
 Korteweg-de Vries eqn., second modified, exact multi-soliton soln. 0-73180  
 Korteweg-de Vries eqn., bilinearization of nonlinear evolution equations 0-90654  
 Korteweg-de Vries eqn., generalised, conserved quantities 0-68054  
 Korteweg-de Vries eqn. and 2nd Painlevé transcendent, boundary value problem in plasma theory 0-69971  
 Korteweg-de Vries soliton solutions, perturbations 0-105511  
 Korteweg-de Vries type eqns., group-theoretical interp. 0-77624  
 magnetic domain boundary, interacting with localised defects, unidimensional flow of configs. (Russian) 0-65954

**nonlinear differential equations continued**

- Mathieu equation with damping, variational anal. 0-57079  
 monodromy- and spectrum-preserving deformations. I, soln. of nonlinear differential eqns. 0-98802  
 multi-soliton solutions of a derivative nonlinear Schrödinger equation 0-105528  
 nerve fields, topographic organisation 0-89742  
 nonlinear field eqn. and differential Schrödinger eqn. correction (French) 0-77637  
 nonlinear mechanical systems, constraint simulation 0-62461  
 nuclear reactor dynamics, numerical integration using real integrating factors 0-68730  
 open dynamic subsystem, nonlinear eqn. with fluctuating parameters derivation 0-94991  
 oscillation equation, single particle analogue of field equations of chiral Lagrangian theories of pion interactions, soln. 0-62470  
 partial, special multi-soliton solns. 0-105763  
 plasma wave propagation, nonlinear Schrödinger equation, modified Zakharov-Shabat inverse scatt. problem 0-59200  
 prolongation structure for a nonlinear equation with explicit space dependence 0-82664  
 radiation defect production, exact solns. of models for continuous and pulsed irradi., implications for stability and fluctuations 0-65041  
 random behaviour 0-77706  
 Schrödinger equation, classical systems with infinite set of conservation laws 0-86102  
 Schrödinger equation, nonlinear, constrained harmonic motion 0-77625  
 sine-Gordon eqn., inverse method for solving differential-difference and difference-difference eqns. 0-105513  
 sine-Gordon equation, 3 and 4 dimens., exact solns. 0-86091  
 sine-Gordon equation, Backlund transform., physical space-time solitons 0-77629  
 sine-Gordon equation, Backlund transformations and Dirac factorisation 0-73185  
 sine-Gordon equation, double, multidimensional multi-soliton kink solutions 0-73184  
 sine-Gordon equation, intrinsic geometry 0-86553  
 sine-Gordon equation, nonlinear, constrained harmonic motion 0-77625  
 $\text{SU}(2)$  gauge field theory, nonlinear scalar field eqn., spherical symmetric exact solns. (Chinese) 0-62886  
 symmetry approach to exactly solvable evolution equations 0-82648  
 Toda lattice, generalised eqn., solitons 0-95040  
 Toda lattice equation, nonlinear, constrained harmonic motion 0-77625  
 two dimensional, nonlinear partial difference eqns., two point function 0-101762  
 two-dimensional infiltration in unsaturated soils, nonlinear diffusion eqn. numerical soln. 0-69918  
 viscoelastic circular membrane, nonlinear, large axisymmetric deform. under its own weight 0-64380  
 wave equation, periodic solutions 0-73188  
 wave evolution, nonlinear, in free shear layers, effects of critical layer structure 0-83809

**nonlinear equations**

- see also nonlinear differential equations  
 background ensembles, nonlinear modeling 0-95037  
 Backlund transformations, canonical struct. 0-86141  
 chemical reaction diffusion equation, nearly degenerate bifurcations, mode interactions 0-85149  
 chemically reacting system with physical interactions, nonlinear eqns. 0-81288  
 convex analysis and variational inequalities (Japanese) 0-77606  
 cosmology, Friedmann model, expanding Universe, nonlinear acoustic effects (French) 0-67921  
 diffusion eqn., with nonlinear terms, Fourier transform 0-103514  
 electron cyclotron maser in overmoded cavity, nonlinear multimode formulation 0-58495  
 fluid dynamics, free boundary flow, surface tension effects, finite element fluid flow simulators 0-82647  
 fluid dynamics, pseudoplastic non-Newtonian fluid, nonlinear singular boundary value problem 0-79362  
 Hartree eqn., quasiclassical soliton soln., Newtonian interaction with screening 0-68569  
 Ising model correlation quadratic identities, discrete-time Toda eqn. 0-105582  
 nondissipative medium, boundary problem soln. with surface discontinuity (Russian) 0-101716  
 plasma nonlinear theory of unstable plane waves and solitons 0-87888  
 plates, circular, variable thickness, numerical solution for flexure 0-99951  
 pumpdown time eqn. and system selection 0-82785  
 reaction-diffusion systems, bifurcation theory, classification 0-108713  
 solitons, review of concepts and methods in theory (Polish) 0-68057  
 stochastic integral equations, nonlinear, mixed type, existence, uniqueness and stability of solutions 0-68131  
 uniaxial crystals, refl. ellipsometry nonlinear eqn. inversion 0-95120  
 XY one dimensional model, transverse correlations, eqns. of motion of finite temp. 0-105581

**nonlinear field theory**

- 1/N expansion, classical dynamics in large N limit 0-101923  
 1/N expansion and the theory of composite particles 0-73604  
 $\lambda\phi^4$  theory, dynamical mass generation in  $\text{S}^1 \times \text{R}^3$  0-99046  
 $\lambda\phi^4$  theory, trial wave function renormalisation using effective pot. 0-105791  
 $\nu$ -dimensional Yang-Mills and ( $\nu$ -1)-dimens. nonlinear  $\sigma$ -model connection, quark confinement, dual strings 0-90978  
 $\sigma$  model, supersymmetric chiral field, 1/N perturbation theory and quantum conservation laws 0-68373  
 $\sigma$  model, two and four-dimens., classical solns., instantons and merons 0-86548  
 $\sigma$  models of nonlinear evolution equations 0-57487  
 $\sigma$ -model, classical solns., stability props. 0-77954  
 $\sigma$ -model, generally covariant 4-dimens., dimensionless coupling upper bound 0-86584  
 $\sigma$ -model, nonlinear, curved space, spontaneous compactification, Grassmann manifold 0-57467  
 $\sigma$ -model, nonlinear, n-component, on lattice of arbitrary dimensions, 1/n expansion 0-73576  
 $\sigma$ -model, nonlinear, order-parameter relaxation from renormalisation group 0-57504  
 $\sigma$ -model, nonlinear, supersymmetric, Ricci-flat Kahler manifolds and supersymmetry 0-90994



**nonlinear field theory continued**

$\sigma$ -model,  $U(N,r)$ , supersymmetric, and  $O(2)$  extended supersymmetry 0-82878  
 $\sigma$ -model, UV infinity suppression in gravity modified field theories 0-105787  
 $\sigma$ -model supersymmetric dynamics on pre-QCD level with elementary quarks and composite gluons 0-82886  
 $\sigma$ -model supersymmetric extensions, dynamical conservation laws, symmetric space valued fields 0-95227  
 $\sigma$ -models, conservation laws, infinite series, differential geometric content 0-62841  
 $\sigma$ -models, non-linear, and universality in 3-D, scaling limit, and critical behaviour, chirality 0-62824  
 $\sigma$ -models, nonlinear, generalisation with gauge invariance 0-57469  
 $\sigma$ -models, nonlinear, supersymmetric, nonlocal conserved currents and instanton-like solutions 0-86544  
 $\sigma$ -models, supersymmetric, Kahler geometry and renormalisation 0-105789  
 $\sigma$ -models, two-dimens., nonlocal invariance and hidden symmetry 0-86596  
 $\tau$ -vacuum for  $\phi^4$  and sine-Gordon theories, stationary solitons (*Chinese*) 0-101932  
 $(\phi^3)_6$  theory, composite particle form factor, asymptotic behaviour 0-86595  
 $\phi^4$  model, strong coupling and infrared struct., renormalisation 0-101921  
anisotropic nonlinear  $\sigma$ -model, two dimensions, instanton quantum fluctuations (*Russian*) 0-86600  
Backlund transformation in the classical massive Thirring model 0-57456  
Backlund transformations in four-dimensional space-time 0-105768  
bagged complex scalar field, EM interaction, fine struct. const., possible dynamic origin 0-86635  
bell's inequalities from the field concept in general relativity 0-105771  
Bogomolny-Prasad-Sommerfield one-monopole soln. by Backlund transformation 0-99059  
chiral Gross-Neveu model embedded in  $U(1)$  gauge theory, fractional winding 0-86569  
colour geometrodynamics, eightfold way, review 0-95243  
condensation of the vortex solitons in a 2+1 dimensional Abelian Higgs model 0-99048  
conformal and chiral anomalies, anomalous Ward-Takahashi identities 0-86612  
conformally invariant  $\sigma$ -model in four dimensions, instantons 0-95215  
coupled non-linear field eqns., soliton solns. 0-68338  
covariant derivatives without gauge fields 0-73584  
 $CP^2$  model, classical real configuration quantisation 0-73606  
 $CP^2$  vierbien singularities in half integral spin fields with EM background 0-73572  
 $CP^{N-1}$  model, (2+1) dimensions, supersymmetric, supersymmetry algebra and central charge 0-86568  
 $CP^{n-1}$  model, embeddings of classical solns. of  $O(2p+1)$  nonlinear  $\sigma$ -models, instantons 0-86562  
 $CP^{N-1}$  model, instanton and large- $N$  methods, QCD similarity 0-77963  
 $CP^{n-1}$  model, pair prod. absence up to 3rd order perturbation theory 0-90990  
 $CP^{n-1}$  model with non-Abelian gauge symmetry, generalisation in 2+ $\epsilon$  dimensions 0-77953  
 $CP^{n-1}$  model with unconstrained variables, Lagrangian and Hamiltonian formulations 0-105780  
 $CP^{n-1}$  supersymmetric model, central charge, superalgebra and Dirac brackets 0-99044  
 $CP^{n-2}$  models in more than 2-dimens., confinement props. 0-86570  
 $CP^N$   $\sigma$ -models, 2-dimens., local conserved currents, conservation laws 0-86579  
 $CP^N$  model, generalisation with gauge invariance 0-57469  
 $CP(N)$  ( $N \geq 2$ ) chiral theory, 2-dimens., non-selfdual instantons 0-86585  
Dirac field, self-interacting, Coulomb-like potential, localised solns. 0-68351  
driven sine-Gordon chain, periodic and solitary states 0-82881  
Dyon solutions, existence, rigorous results 0-73595  
effective-potential approach to the quantization of the sine-Gordon theory in 1+1 dimensions 0-73608  
EM field, charged particle config., stability 0-57109  
Euclidean space, spherically symmetric self-dual eqns., representation theory and integration 0-77936  
factorised completely  $X$  symmetric  $S$ -matrix characterisation, multicomponent field theories 0-105800  
fermionic solitons in gauge theories and their quantum corrections 0-101927  
fermions, quantum field theory, large order perturb. theory, more than one coupling constant 0-77940  
 $g\bar{\psi}\psi\phi$  theory, trial wave function renormalisation using effective pot. 0-105791  
gauge ambiguities and nonlinear  $\sigma$ -model relations in Yang-Mills vacuum sector 0-105767  
Gel'fand-Levitan method as a generalized Jordan-Wigner transformation 0-77962  
gravitation, Newton constant's role 0-90761  
gravitational fields, stationary, axis-symmetric, soliton solutions 0-73253  
gravitational instantons and their interactions 0-90766  
Gross-Neveu model, chiral invariant,  $S$ -matrix direct calc. 0-68362  
group theoretical construction of two-dimensional models with infinite sets of conservation laws 0-99056  
Heisenberg Klein Gordon eqn., soln. in space time of const. curvature 0-62829  
Hopf fibrations of the sphere-constraints in the non-linear  $\sigma$  models 0-86573  
hydrodynamics, quantum relativistic, nonlinear generalised equations 0-68380  
instanton statistical mechanics in QCD 0-57567  
instantons,  $\theta$ -vacua, confinement in 1+1 Abelian Higgs model 0-77979  
instantons and monopoles in Yang-Mills gauge field theories 0-91003  
instantons in the presence of a fixed density of massless fermions in two dimensions 0-62853  
kink theories, approximately straight 0-82871  
kinks and cobordism in field theories, general relativity fermions 0-98835  
Korteweg-de Vries system, Lax representation, conservation laws 0-82893  
Korteweg-de Vries theory, Hamiltonian structures and Miura like transformation 0-95216  
lattice gauge theories, chiral symmetry dynamical breaking 0-99061  
linearisation program for nonlinear field eqns., Lie groups 0-105784  
linearization of relativistic nonlinear wave equations 0-62837

**nonlinear field theory continued**

magnetic fields, flux string and monopole, geometric configuration, compared to  $O(3)$  nonlinear  $\sigma$ -model 0-57527  
massive  $CP^n$  sigma models, topological struct., finite action configurations 0-57476  
massless Euclidean Thirring field, four point Schwinger function, Lorentz group invariant forms (*German*) 0-90980  
massless Wess-Zumino model in 4-dimens., asymptotic estimates 0-82877  
massless  $[g\phi^4]_4$  theory, functional integrals, complex instantons, and asymptotic perturbation series 0-86571  
membrane models and generalized  $Z_2$  gauge theories, renormalisation props. 0-86587  
meron pair, introduction, motivation and formalism 0-82861  
meron pairs, bare activity 0-82862  
Minkowski-space formulation of two-pseudoparticle processes 0-95220  
multi-soliton solutions of nonlinear partial differential eqns. 0-105763  
multidimensional nonlinear eqns.,  $N$ -soliton solns. by Hirota's method 0-105797  
nonpolynomial scalar interactions in four dimensions, bounded interactions 0-82895  
nonpolynomial scalar interactions in four dimensions, quartic interaction 0-82894  
 $O(2N)$  Gross-Neveu model,  $O(8)$  Dynkin diagram  $P_3$  symmetry 0-77968  
 $O(3)$  nonlinear  $\sigma$ -model, mass generation in dense instanton gas approx. 0-82880  
 $O(N)$  invariant  $(\phi^2)^2$  model, chiral field model and universality in 3-dimens. space 0-105796  
 $O(N)$  model, dynamical mass generation in  $S^1 \times R^3$  0-99046  
one-dimensional solitary-wave-bearing scalar fields, statistical mechanics, ideal-gas phenomenology 0-105792  
order, disorder and generalized statistics 0-99055  
particle stability in nonlinear scalar field theory 0-91004  
phase transitions, structural, first order, anharmonic oscillator model in (1+1) dimensions 0-86239  
planar diagrams,  $SU(N)$  asymmetric model, semiclassical approach 0-77957  
QCD, effective Lagrangian, possible  $\sigma$ -model 0-86679  
quarks, fermion field, nonlinear, origin of four quark flavours, quantum numbers, isosymmetry breaking 0-62920  
radiation damping force, 1-D, new mechanics 0-82632  
scattering operator, analyticity in nonlinear relativistic classical and quantised field theories 0-73611  
Schrödinger equation, nonlinear field equations, quantum inverse scattering transform method, 2-D ice and ferroelectric lattices 0-68348  
sine Gordon model, quantum inverse problem method 0-68377  
sine-Gordon theory, Hamiltonian structures and Miura like transformation 0-95216  
sine-Gordon chain, displacement fluctuations, long-time behaviour and dynamic scaling props. 0-101764  
sine-Gordon eqn. as nonlinear scalar field model in Duffin-Kemmer formalism (*Russian*) 0-86599  
sine-Gordon equation, Backlund transform., physical space-time solitons 0-77629  
sine-Gordon equation, discrete, on  $SU(2)$  lattice, group theory aspects 0-57486  
sine-Gordon equation, intrinsic geometry 0-86553  
sine-Gordon equation, nonlinear field equations, quantum inverse scattering transform method, 2-D ice and ferroelectric lattices 0-68348  
sine-Gordon equation, rotationally symmetric breather-like solns. 0-77955  
sine-Gordon equation, supersymmetric, prolongation struct. inverse scatt. formalism 0-99032  
sine-Gordon system, Lax representation, conservation laws 0-82893  
singular potentials in non-relativistic quantum theory, review (*Russian*) 0-68345  
solitary wave transport, nontrivial example soln., numerical method 0-77971  
soliton, extended particle, quantisation, degeneracy of eigenstates 0-73594  
soliton solutions, renormalisation and quantum corrections 0-82884  
solitons, charged, stability, relativistic complex scalar field, direct Lyapunov method 0-62827  
solitons, solution of nonlinear Liouville equation 0-68374  
spinor models, integrability in two-dimens. space-time 0-77935  
Stiefel manifolds, 2-dimens. nonlinear  $\sigma$ -model,  $S$ -matrix regularities 0-86576  
strongly interacting Higgs bosons, gauged nonlinear  $\sigma$ -model,  $SU(2)_L \times U(1)$  extension 0-86656  
 $SU_N/Z_N$  gauge invariant theory, phase factor operators and soliton fields 0-77947  
 $SU(2,1;1)$  nonlinear invariant  $\sigma$  model, superconformal group and curved fermionic twistor space 0-62831  
 $SU(2)$  gauge field theory, nonlinear scalar field eqn., spherical symmetric exact solns. (*Chinese*) 0-62886  
 $SU(2n)$  principle models for integrable nonlinear systems, current constraints, conservation laws 0-86619  
 $SU(N)$  Higgs theory, two-dimens., instanton approach 0-99053  
super  $(\phi^3)_4$  model, large order perturbation theory 0-82876  
super sine-Gordon eqn., supergroup geometrical interpretation, supersymmetric extension 0-57475  
Thirring model, chiral,  $CP^{n-1}$  and  $SU_n$ , exact  $S$ -matrix 0-90985  
topological solitons and duality (*German*) 0-91010  
wave functionals, soliton sector and asymptotic vacuum states, Creutz quantisation method 0-68340  
Weiss-Zumino model, three loop  $\beta$ -function for superfield techniques 0-99043  
Yang-Mills multi-instantons, quantum fluctuations, Seeley coeffs. 0-77934  
 $Z(2)$  and  $Z(3)$  cyclic symmetric vector field theories, 1-dimens. solitons 0-77950  
 $\phi^4$  model, free energy, spontaneous symmetry breaking 0-101925  
 $\phi^4$ -field model with image mass, spontaneous coherent state transition 0-99057  
 $\pi$  condensed phase,  $\sigma$ -model, alternating-layer-spin struct. 0-83057  
 $\pi \rightarrow e\nu\gamma$ , isospin-breaking, chiral limit, conserved-vector-current violation,  $\sigma$  model 0-62988

**nonlinear optical susceptibility**

Doppler-free two-photon dispersion problem 0-106562  
four-photon spectroscopy of condensed media, nonlinear spectroscopy developments 0-91860



**nonlinear optical susceptibility continued**

- four-wave mixing spectroscopy, coherent cancellation of background 0-91842  
 four-wave mixing spectroscopy in crystals, nonlinear spectroscopy developments 0-91861  
 ionic crystals, centrosymmetric, stimulated excitation of second harmonic, microscopic theory 0-91849  
 liquid crystal, isotropic phase, self-focusing stability of laser beam 0-99812  
 magneto-optic Raman scattering of Raman-inactive phonon polaritons 0-91843  
 rectification effect and meas. appls. 0-91835  
 resonant Rayleigh-type mixing spectroscopy using ps light pulses, ultrafast laser, study 0-91834  
 semiconductors, mixed and binary, nonlinear polarisability, self-action effects 0-99786  
 semiconductors, nonlinear optical props., book contrib. 0-78899  
 tendon, rat-tail, coherent optical SHG 0-89796  
 three-level system, narrow nonlinear resonances (*Russian*) 0-78898  
 CdSe 16  $\mu\text{m}$  parametric amplification with HF laser pumping 0-78910  
 $\text{Cr}_2\text{B}_2\text{O}_7\text{Cl}$ , cubic, approx. nonlinear optical susceptibility 0-78904  
 $\text{Cu}_3\text{B}_2\text{O}_7\text{Cl}$ , cubic, approx. nonlinear optical susceptibility 0-78904  
 $\text{Fe}_2\text{B}_2\text{O}_7\text{I}$ , cubic, approx. nonlinear optical susceptibility 0-78904  
 Ge, nonlinear susceptibility, 10  $\mu\text{m}$ , determ. by time resolved ellipse rotation 0-83633  
 Ge, phase conjugation of 4  $\mu\text{m}$  for single line and multiline radiation 0-83641  
 $\text{Hg}_{1-x}\text{Cd}_x\text{Te}$ , degenerate four-wave mixing of 10.6  $\mu\text{m}$  radiation 0-95943  
 $\text{n-Hg}_{1-x}\text{Cd}_x\text{Te}$ , optical phase conjugation 0-83644  
 $\text{I}_2$ , molecular vapour, saturable absorpt., self-focusing and nonlinear susceptibility 0-83647  
 n-InSb, cond. electron spectra in quantised mag. field, impurity resonance scatt. (*Russian*) 0-93178  
 Kr gas, nonlinear susceptibility meas. via third harmonic generation, Lyman- $\alpha$  1216  $\text{\AA}$  source 0-95947  
 $\text{NH}_3$ , phase conjugation via degenerate four-wave mixing 0-106566  
 NO nonlinear laser spectroscopy, VUV harmonic generation 0-74175  
 $\text{Nd}(\text{NO}_3)_3$ , aqueous soln., single photon absorpt. band struct., electronic resons. coherent ellipsometry 0-90881  
 $\text{Ni}_3\text{B}_2\text{O}_7\text{Br}$ , cubic, approx. nonlinear optical susceptibility 0-78904  
 Rb vapour, Doppler-free two-photon dispersion and optical bistability 0-95940  
 Te, SHG under two-photon reson. conditions, third-order nonlinear susceptibility 0-99803

**nonlinear optics**

- see also *nonlinear optical susceptibility; optical coherent transients; optical frequency conversion; optical parametric devices; optical phase conjugation; optical saturation; optical self-focusing; self-induced transparency; stimulated scattering*  
 absorptive optical bistability, transmitted light spectrum and dynamic response function 0-99789  
 absorptive optical bistability, two-level atom system, photon antibunching 0-58486  
 absorptive optical bistability transient, local relax., quantum statistical treatment 0-91838  
 active medium in Gaussian random optical field, stimulated emission statistics 0-58488  
 adaptive focusing of light in inhomogeneous nonlinear medium, interf. criteria 0-99633  
 anharmonic oscillator model for dispersive optical bistability 0-58623  
 applied solid state physics, book 0-94936  
 aqueous aerosol cloud containing medium, light beam propag., thermal self-interaction 0-91750  
 atmosphere radiative transfer, nonlinear propag. effects, conference, San Diego, California (1979 August 29 to 30) 0-62376  
 atomic collisions, nonlinear optical phenomena 0-99788  
 background ensembles, nonlinear modeling 0-95037  
 benzene, liquid, polarised light two photon thermal blooming near UV spectra 0-66216  
 biexcitons, nonlinear laser spectrosc., multiphoton transitions 0-84433  
 bistability, absorptive and dispersive, in Fabry-Perot and ring-cavity geometries 0-95942  
 bistability, exact semiclassical treatment of ring cavity 0-58627  
 bistability in bad cavity limit, Fokker Planck eqn. approach 0-64116  
 bistability in optical cavity filled with Kerr dielectric, nonlinear effect of powerful laser radiation field 0-99787  
 bistable nonlinear Fabry-Perot resonator switching speed and energy calc. 0-64095  
 bistable optical device development from integrated two-arm interferometer, appls. (*French*) 0-69555  
 bistable optical devices: an overview 0-58625  
 bistable optical devices, overshoot and alternate switching, subharmonic generation 0-99790  
 bistable optical devices, overshoot switching 0-58776  
 cavity, optical bistability, long-time behaviour 0-78892  
 chalcopyrite crystals, refractive index, temp. depend., appl. to nonlinear devices 0-60555  
 coherent and nonlinear optics, conf., Leningrad, USSR (Jun. 1978) 0-98753  
 conference, basic optical props. of materials, Gaithersburg, MD, USA (May 1980) 0-101668  
 continuum self-phase modulation and stimulated Raman scatt., combined effects 0-69460  
 convolution of ps optical signals 0-58629  
 degenerate four-wave mixing, hysteresis and optical bistability 0-69446  
 density matrix, time evolution, graphical representation 0-64097  
 dihydroxyanthraquinone, light-induced proton transfer, photochem. hole-burning obs. 0-76535  
 DNA light induced diffusion in solutions due to laser cutting (*Russian*) 0-81646  
 dynamic self-diffraction of coherent light beams, review 0-102777  
 electrooptic crystals, holographic recording, photogalvanic effect mechanism of nonlinear wave interaction 0-102672  
 empirical relationship for a nonlinear index coefficient 0-74445  
 exponential transformation using film nonlinearity for optical homomorphic filtering 0-58467  
 Fabry-Perot cavity, absorptive bistability, mean-field approx., truncated Bloch hierarchy 0-83631  
 Fabry-Perot cavity, dispersive optical bistability 0-78889  
 Fabry-Perot cavity, optical bistability, spatial effects 0-83632

**nonlinear optics continued**

- Fabry-Perot cavity, optical bistability, standing wave effects 0-91837  
 Fabry-Perot interferometer, optical bistability, inhomogeneous broadening, mean field approx. 0-90885  
 Fabry-Perot nonlinear interferometer, beam profile hysteresis variations 0-86393  
 four counterpropagating wave interaction in medium with cubic nonlinearity, dynamic holography concepts 0-91839  
 four wave interaction, light induced crit. behaviour in nonlinear system 0-95941  
 free atoms and molecules, nonlinear optics, book 0-73111  
 glass:  $\text{Nd}^{3+}$ , resonantly enhanced four-wave mixing in absorbing media (*Chinese*) 0-102764  
 holography, image contrast changes during recording in nonlinear media with local response 0-69346  
 homogeneously broadened medium, absorption spectra of optical bistability with dispersion 0-102757  
 homogeneously broadened medium with dispersion, optical bistability 0-83630  
 image processing, analogue and digital, feedback, review 0-102639  
 inhomogeneity influence on nonlinear cryst. effective length 0-106568  
 IR and FIR tunable coherent sources utilising modulational instability 0-95967  
 laser beam propagating in liquid, polarization, DC elec. field influence 0-91828  
 laser focus movement, nonlinear optical technique 0-74446  
 lasers for industrial chemistry, thermal lensing effect 0-87427  
 light wave diff. by complex spectral composition US 0-95939  
 limited light beam, nonlinear reflections and transmission 0-58624  
 luminescence quenching at high pumping levels, microscopic theory 0-89040  
 materials for nonlinear optical appls., review 0-74450  
 MBBA, nematic liq. cryst., nonlinear optical amplification above Fredericks transition 0-95937  
 metal, light refl., nonlinear thermo-optic effect at high intensity 0-93289  
 methyl iodide mol. nonlinear resonant interaction with pulsed subMM radiation (*Russian*) 0-99523  
 microemulsions, heat transfer meas. by laser-induced thermal blooming 0-91833  
 mirror, nonlinear interf., reflection of light 0-102761  
 model equation in dispersive medium, wave interactions, self-precession and freq. shift 0-78900  
 multiphoton cross-section determination by means of luminescence experiments 0-93377  
 multiphoton detectors of laser radiation, statistical characts. 0-86408  
 non-classical effects in the statistical properties of light, review 0-99686  
 nonlinear coherent coupler, new optical logic device 0-58630  
 nonlinear crystals, interference of optical harmonics 0-64102  
 optical bistability with dispersion 0-78893  
 optical communication systems, nonlinear distortions and noise due to fibre connectors 0-96001  
 optical fibre, soliton pulse propag. 0-58759  
 optical multistability, light self-modulation in double resonance (*Russian*) 0-106560  
 optical resonators, radiation excitation, review 0-69462  
 organic compounds usable as solvents in laser saturable absorber, nonlinear refr. index meas. 0-102758  
 organic laser dyes, nonlinear transmission including stimulated emission influence 0-99720  
 paramagnetic centre crystals, nonlinear optical Faraday effect 0-99811  
 partial spatial coherence blur correction by postdetection image processing 0-78792  
 phase compensation of thermal defocusing of light beams 0-64121  
 phase-switching of a dispersive non-linear interferometer 0-82810  
 photoelectric current in case of nonlinear interference of EM fields 0-80324  
 plane-parallel absorbing layer, in strong laser light field 0-58631  
 quantum electronics, conf., New York, USA (Jun. 1980) 0-90614  
 quasiequilibrium sample, light scatt. and thermal radiation, phenomenological approach 0-91840  
 radiation self-synchronisation during stimulated Raman scatt. in external resonator (*Russian*) 0-102772  
 Raman amplification, high-efficiency narrow-linewidth, spectral compression 0-102770  
 real time processing 0-87338  
 rectification effect and meas. appls. 0-91835  
 resonance light scattering, spectral props. and photon correls. 0-91510  
 resonant media, pulse counterpropagation and nonlinear interaction, transverse effect computation 0-106563  
 ring cavity, chaotic behaviour of transmitted light, optical turbulence 0-102760  
 ring dye laser, optical bistability and first order phase transition 0-95918  
 self pulsing in absorptive optical bistability, analytical description 0-78891  
 self pulsing in dispersive optical bistability in ring cavity 0-78890  
 self-imaging, light-optical experiments (*German*) 0-63938  
 semiconductor, IR switching, ultrafast optically controlled 0-58626  
 semiconductor, noncoherent interaction of a light pulse 0-106561  
 semiconductor etalon, optical bistability and ns modulation 0-64096  
 semiconductor, free carrier optical props., book contrib. 0-80738  
 semiconductors, mixed and binary, nonlinear polarisability, self-action effects 0-99786  
 semiconductors and insulators, nonequib. electron Coulomb collisions during optical pulse interband interaction 0-76049  
 solid under excitonic state reson. conditions, laser pulse propag. theory 0-87430  
 spectroscopy, solvent formalism appl. (*Japanese*) 0-82833  
 spin oscillators, optically pumped, orientation depend. of oscill. freq. 0-78896  
 thermal blooming, continuum-lens model 0-78918  
 thermal blooming cell design for use in evaluating adaptive optics 0-102780  
 thermal blooming in a diagonal wind 0-95965  
 thermal blooming in axial pipe flow: comment [and reply] 0-95966  
 thermal blooming spectroscopy for enzymatic anal. 0-86441  
 thermal defocusing of light beams, phase conjugation compensation method 0-64123  
 thermal lens, pulsed source 0-95968  
 thermal self-action problems and their compensation 0-106579  
 three level atoms, coherent nonlinear. mechanism for optical bistability 0-102756



**nonlinear optics continued**

- three-level system, narrow nonlinear resonances (*Russian*) 0-78898  
 turbulent absorbing liq. medium, laser radiation thermal self-interaction 0-91868  
 turbulent medium, pulsed laser radiation intensity fluctuations during thermal selfinteraction 0-102781  
 two level atom, coherent and Raman scatt. spectra, secondary emissions 0-69449  
 two-level Doppler-broadened medium in Fabry-Perot, optical bistability 0-102759  
 two-photon double-beam optical bistability 0-64113  
 ultrashort consecutive light pulse four-wave interaction in media (*Russian*) 0-78897  
 wave rectification, quantum limit 0-83634  
 wavefront rotation for light beam nonlinear deformation compensation (*Russian*) 0-64094  
 waveguides, optical, nonlinear pulse propag. theory 0-83669  
 AgGaSe<sub>2</sub>, two-photon absorpt. and short pulse stimulated recombination 0-89054  
 Al<sub>0.42</sub>Ga<sub>0.58</sub>As-GaAs-Al<sub>0.42</sub>Ga<sub>0.58</sub>As, etalon, optical bistability and modulation 0-58628  
 Bi<sub>12</sub>SiO<sub>20</sub>, photorefractive medium, real-time image processing via four-wave mixing 0-95944  
 CO<sub>2</sub> laser pulse, nonlinear propag. characts., computer simulation 0-106575  
 CdGeP<sub>2</sub>, thermo-optic coefficient, dispersion 0-71396  
 CdP<sub>2</sub>, 442 class gyrotropic crysts., self-induced rot. of light polarisation plane 0-99810  
 CdS, nonlinear self-action effect and absolute two-photon absorption coeff. 0-83649  
 CdS thermo-optic coefficient, dispersion 0-71396  
 CdSe thermo-optic coefficient, dispersion 0-71396  
 CoCl<sub>2</sub>·6H<sub>2</sub>O solution in ethanol, thin absorbing film, nonlinear optical props., Q-switch appl. 0-91836  
 CuGaS<sub>2</sub>, thermo-optic coefficient, dispersion 0-71396  
 GaAs, DC biased, filamentation of laser radiation 0-74428  
 p-Ge modulation of 3.39  $\mu$ m abs. by CO<sub>2</sub> laser irr. (*Japanese*) 0-74410  
 I<sub>2</sub>, Doppler-free optoacoustic spectroscopy 0-57396  
 InSb, nonlinear transmission of picosecond 10.6  $\mu$ m pulses 0-106559  
 KH<sub>2</sub>PO<sub>4</sub>, KD<sub>2</sub>PO<sub>4</sub> crystals, photoresponse under laser irr., nonlinear optical rectification 0-100479  
 LiH<sub>2</sub>PO<sub>4</sub>, P-H bond dipole direction, nonlinear optical coeffs. meas. 0-69253  
 $\alpha$ -LiIO<sub>3</sub>, two-photon absorption spectra, energy struct. anal. 0-99785  
 LiNbO<sub>3</sub>, two-photon absorption spectra, energy struct. anal. 0-99785  
 LiNbO<sub>3</sub>:Ti waveguide, ps signal processing with planar, nonlinear integrated optics 0-64208  
 InBIO<sub>3</sub>:Ti crystals and waveguides, absorption loss and photorefractive index changes 0-58787  
 Rb vapour, Doppler-free two-photon dispersion and optical bistability 0-95940  
 Rb vapour, Gaussian pulse propag. under two-photon near reson. conditions 0-87441  
 SF<sub>6</sub>, soln., cryosystem, vibr. relax. times, pulsed IR absorpt. spectral obs. 0-66188  
 ZnGeP<sub>2</sub>, thermo-optic coefficient, dispersion 0-71396  
 ZnP<sub>2</sub>, 442 class gyrotropic crysts., self-induced rot. of light polarisation plane 0-99810

**nonlinear programming**

- nuclear power stations, optimal size and location in energy parks 0-95489  
 SAW filter design using optimisation technique 0-74671

**nonlinear symmetries**

- dissipative classical systems, time-depend. canonical transforms. 0-62885

**nonlinear systems**

- biological membrane, electrically excited, nonlinear dynamic models for simulation 0-94178  
 dynamical system, limit cycles and symmetries 0-62462  
 neural transformations of random signals, Wiener and of functionals of Markov chain 0-76727  
 nonlinear experimental design, information measures 0-62616  
 oscillators, planar, nonlinear, stability of modes 0-74790  
 oscillators, weakly nonlinear, system with slowly varying parameters, resonance 0-62463  
 second order system, eigenfunction expansion solutions of Fokker Planck eqn. 0-73172  
 stochastic stability of dynamic multi-nonlinearity systems, action of white noise 0-68135  
 vibrating systems, nonlinear, multi-degree-of-freedom, harmonic excitation, instability 0-73162

**nonparametric statistics**

- EEG automatic classification, decision rules comparison 0-109054  
 speech quality parametric objective measures correlated with subjective results 0-91980

**nonradiative transitions**

- acetophenone, T<sub>1</sub>-S<sub>0</sub> intersystem crossing, nonradiative decay rate, excitation energy depend. 0-63609  
 aromatic hydrocarbons, sequential coupling 0-58297  
 benzaldehyde gas, nonradiative electronic transition 0-83413  
 benzene-d<sub>6</sub>-(d<sub>8</sub>), radiationless triplet decay, non-Condon effects 0-83405  
 benzophenone vapour, fluoresc. and phosphoresc., nonradiative transitions between triplet and singlet state obs. 0-99516  
 chalcogenide glasses, Luminescence, temp. depend. rel. to nonradiative transitions 0-71485  
 chloroquinolines, photophys. behaviour, substituent and solvent effects 0-106342  
 coumarin laser dyes, solvent effects on photophysical parameters 0-91598  
 diacetyl vapour, fluoresc. and phosphoresc., nonradiative transitions between triplet and singlet state obs. 0-99516  
 3,6-diaminophthalimide vapour, mol. electronic excitation energy degradation path depend. on pentane 0-74195  
 diatomic molecule, neutron scatt. induced electronic transitions, tunnelling 0-63844  
 diatomic molecule in crystal, rate of radiationless electronic transitions 0-93373  
 diazanaphthalenes, excited state absorpt. spectra and intersystem crossing kinetics 0-74176  
 p-diazines, polycyclic, T<sub>1</sub>( $\pi\pi^*$ ) $\rightarrow$ S<sub>0</sub> intersystem crossing, isotope effects, ODMR and phosphoresc. obs. 0-91586

**nonradiative transitions continued**

- 1,6-diphenylhexatriene, radiationless transitions and natural lifetimes, solvent effects 0-63622  
 DNA, proton radiationless transitions for hydrogen bonds (*Russian*) 0-97857  
 enhanced Raman scattering by adsorbates on metals, including nonlocal metal response, nonradiative modes excitation 0-88994  
 formaldehyde, sequential coupling 0-58297  
 glasses, non-radiative recombination at valence-alternation pairs 0-89048  
 glyoxal, singlet-triplet radiationless processes in mag. field 0-106347  
 impurity molecule in crystal 0-103645  
 l-indanone, T<sub>1</sub>-S<sub>0</sub> intersystem crossing, nonradiative decay rate, excitation energy depend. 0-63609  
 intermolecular energy transfer and high energy excitations, in condensed phase 0-66269  
 intramolecular dynamics, random coupling model, math. approach 0-58308  
 intramolecular dynamics, random coupling model, multiphoton excitation, kinetic eqns. 0-63700  
 intramolecular nonradiative transitions of gaseous small molecules, vibronic level, lineshapes 0-95667  
 intrastate scrambling in large mol. bound level struct., appl. to tetracene 0-63696  
 ionic crystal, exciton mechanism model for defect form. 0-80187  
 molecule located in condensed medium, vibr. relax. effect 0-80848  
 molecules, isolated, intersystem crossing, rot. motion effect 0-95669  
 naphthalene molecule in durene and xylene crystals, vibronic interactions 0-84755  
 naphthalene-d<sub>6</sub>-(d<sub>8</sub>), radiationless triplet decay, non-Condon effects 0-83405  
 non-equilibrium phonon distrib., in cryst., spectral line shape theory 0-60530  
 phenol biradical prod. from O+benzene-(d), crossed mol. beam investig. 0-71902  
 photoacoustic spectroscopy, freq. and time-domain, relax. time meas. condensed phases 0-82826  
 pinacyanol in ethanol, electronic relax., analysing light ps spectroscopy 0-99517  
 polyatomic molecules, radiationless transitions, Fermi resons. and quasisdiscrete spectrum 0-95665  
 polymethine dye nonequilibrium, protolytic forms, lasing, fluoresc. and nonradiative transitions 0-102722  
 pseudoazulenes, anomalous fluoresc., radiationless transitions 0-91593  
 pyrimidine, bi-exponential decay, methylation and vibr. excitation, proximity effects 0-78641  
 radical radiation formation in solid organic compounds 0-85201  
 ruby, energy transfer between different emitters and spatial diffusion 0-103978  
 solutions, photoluminesc. decay time, donor conc. effect 0-66299  
 stilbene aza-analogues, lowest excited states, INDO/S calcs. 0-95545  
 synchrotron radiation obs. 0-63706  
 synchrotron radiation techniques for studying atomic physics 0-63583  
 s-tetrazine, vapour, reson. CARS spectrosc., radiationless relax. rate 0-78614  
 thioxanthone, fluoresc. and internal conversion, rel. to proximity effects 0-91592  
 triphenylmethane dye soln., electronic relax., viscosity-depend., using picosec. flash photolysis 0-66258  
 triplet exciplexes, rapid rot., spin-selective depopulation of sublevels, heavy atom-induced mag. field effect 0-95552  
 AlGaAs heterojunctions, nonradiative recomb. vel. estimate from edge luminesc. props. 0-65668  
 Al<sub>2</sub>O<sub>3</sub>:Cr<sup>3+</sup>, Jahn-Teller system, zero-phonon line broadening due to non-radiative transitions 0-108258  
 C in molecule, K-shell fluoresc. yield, statistical scaling 0-78644  
 C<sub>2</sub>+O<sub>2</sub>, C<sub>2</sub>(X<sup>3</sup> $\Sigma_u^+$ ) and C<sub>2</sub>(a<sup>3</sup> $\Pi_u$ ) intersystem crossing and free radical kinetics 0-95668  
 CaF<sub>2</sub>:Eu<sup>2+</sup>, Sm<sup>3+</sup>, relaxed resonance acoustic phonons in vibronic anti-Stokes luminescence (*Russian*) 0-93404  
 CdS:In(Cl) concentration quenching mechanism of luminescence 0-97336  
 Cs<sub>2</sub>NaYCl<sub>6</sub>:Bi<sup>3+</sup>, luminescence props., emission and excitation spectra 0-108262  
 EuNa<sub>2</sub>Mg<sub>2</sub>(VO<sub>4</sub>)<sub>3</sub>, disordered, thermal quenching of luminesc. 0-71472  
 FeVIII-XXVI energy level tables and Grotrian diagrams 0-74142  
 GaAs,  $\gamma$ - and electron irradiation, influence on recomb. characts. near surface 0-71478  
 KCl, F-centre formation at highly excited triplet states of self-trapped excitons 0-76066  
 KI:Ti, decay of fast component of impurity luminesc. excitation in A-absorption band (*Russian*) 0-84767  
 Li-La phosphate glass, Nd, Cr activated, Nd luminesc. quantum efficiency meas., Nd-Cr nonradiative transfer 0-66296  
 MgO:V<sup>2+</sup>, Jahn-Teller system, zero-phonon line broadening due to non-radiative transitions 0-108258  
 N<sub>2</sub> film, on metal or sapphire substrates, luminescence and nonradiative energy transfer to surfaces 0-97350  
 Nd<sup>3+</sup> ions, in solids, radiationless decay processes, laser photoacoustic spectroscopy meas. 0-84766  
 O in molecule, K-shell fluoresc. yield, statistical scaling 0-78644  
 POCl<sub>3</sub>:Pr<sup>3+</sup>, fluoresc. and lifetimes of excited states 0-71466  
 Pb<sub>1-x</sub>Sn<sub>x</sub>Se epitaxial layers, radiative and nonradiative recomb. processes 0-60670  
 Pb<sub>0.78</sub>Sn<sub>0.22</sub>Te, Pb<sub>0.91</sub>Sn<sub>0.09</sub>Se, radiative and nonradiative recombination 0-80849  
 RbMnF<sub>6</sub>:Er<sup>3+</sup>, absorption, emission, excitation and lifetime meas. 0-71460  
 Re(CO)<sub>5</sub>Br-Mn(CO)<sub>5</sub>Br, polycryst.,  $\mu$ (CO) vibr. intermol. Raman intensity transfer 0-60564  
 SF<sub>6</sub>, partial saturation of  $\nu_3$  ladder in IR absorpt., rate process model 0-58645  
 Se<sub>2</sub>, laser induced fluoresc. in inert gas matrix 0-87161  
 Si, phonon-assisted Auger recomb., direct calc. of overlap integrals 0-107808  
 Te<sub>2</sub>, laser induced fluoresc. in inert gas matrix 0-87161  
 Ti atoms sputtered from Ti, Ti oxides, photon emission, nonradiative transition effects 0-58208

**normalising**

- stainless steel, laser surface melting for corrosion protection 0-93698  
 steel (*German*) 0-100869

**notch brittleness**

- composites, single fibre-brittle zone model, fracture behaviour 0-97570  
 PMMA, ductile glassy, notch brittleness under plane strain 0-100900  
 polycarbonate, ductile glassy, notch brittleness under plane strain 0-100900  
 PVC, ductile glassy, notch brittleness under plane strain 0-100900  
 steel, tempered, notched, impact bending tests, cold brittleness curves 0-71758  
 Fe, cast, grey, fracture kinetics, surface hardening effect 0-76354

**notch ductility**

- steel, Cr-Mo-V, stress rupture, notch influence, temp. depend. (German) 0-60945  
 steel, low C, crack initiation at root of circumferential notch of round bar specimens (Japanese) 0-60947  
 steel, tempered, notched, impact bending tests, cold brittleness curves 0-71758  
 Al notched bars, deform. behaviour and strength having biaxial state of stress at notch root (Japanese) 0-81116  
 Al-Cu-Si-Mn, type 2017S-T4, crack initiation at root of circumferential notch of round bar specimens (Japanese) 0-60947  
 Fe, cast flake and nodular, rupture strength, circumferential notch (Japanese) 0-93649

**notch sensitivity** *see* **notch strength****notch strength**

- see also* **fracture toughness**  
 $\alpha$ -brass, plane stress ductile fracture, prestrain effects 0-108532  
 fibre reinforced plastic, props., implications for structural design 0-81174  
 graphite, notch sensitivity, 20 to 2800°C 0-76353  
 graphite ring, eccentric, under radial thermal load, stress state 0-76351  
 metal, notched, cyclic stress/strain behaviour, random fatigue life (German) 0-100907  
 polymer, crack tip failure mechanism modelling 0-108565  
 powder metallurgy, fatigue strength significance (German) 0-60946  
 PVC, rigid plate, notching method effect on Charpy impact values, fractographic considerations (Japanese) 0-108541  
 steel, austenitic stainless, type SUS 304, low cycle fatigue strength reduction factor (Japanese) 0-104259  
 steel, austenitic stainless type SUS 316, low cycle fatigue tests, freq. effect on notch sensitivity at elevated temps. (Japanese) 0-104260  
 steel, C, crack initiation and propagation life under repeated impact tensile loads (Japanese) 0-104264  
 steel, C, type SFVVI, low cycle fatigue strength reduction factor (Japanese) 0-104259  
 steel, Cr-Mo-V, stress rupture, notch influence, temp. depend. (German) 0-60945  
 steel, hot forging die type, fractography (Japanese) 0-108547  
 steel, low and medium C, fatigue strength, small defect effect 0-104255  
 steel, mild, transgranular stress corrosion cracking in  $H_2SO_4$ -KI soln. 0-71797  
 steel, Ni-Cr-Mo and Cr-Cu-Mo and sintered, ductile fracture, microvoid effects (Japanese) 0-108542  
 steel (French) 0-66670  
 Al alloy 2024-T4, ductile fracture, microvoid effects (Japanese) 0-108542  
 Al notched bars, deform. behaviour and strength having biaxial state of stress at notch root (Japanese) 0-81116  
 Al-Mg sheet, artificial stress raiser effect on strength and local plasticity of weld joint 0-81130  
 Al-Mn sheet, artificial stress raiser effect on strength and local plasticity of weld joint 0-81130  
 $Al_2O_3$ , fracture toughness determ. using four-point-bend specimens 0-108536  
 B fibre reinforced epoxy composites, notched, tensile strength and failure modes 0-81205  
 Fe, cast flake and nodular, rupture strength, circumferential notch (Japanese) 0-93649  
 $Si_3N_4$ , hot-pressed, fracture toughness determ. using specimens with chevron and straight through notches 0-108538

**notch testing**

- see also* **fracture toughness testing**  
 brittle materials, crack size and effective specific work for failure determ. 0-85108  
 chevron notched short bar specimens, compliance and stress intensity coefficients 0-96232  
 device for producing fatigue cracks in specimens 0-61051  
 epoxy resin microcircuitry elements, thermoelastic phenomena testing (Polish) 0-93724  
 fatigue life estimates 0-100999  
 fracture toughness reference curve development 0-97588  
 glass microcircuitry element thermoelastic phenomena testing (Polish) 0-93724  
 nuclear power engineering materials certification testing for safety and reliability 0-78360  
 plates, V-notched elastic, symm. loaded, stress intensity factors, caustic method 0-83770  
 PMMA, crack size and effective specific work for failure determ. 0-85108  
 steel, C, fatigue crack propagation in sheet, influence of struct. of ferrite-pearlite bands (French) 0-76338  
 steel, Charpy type bars of AISI 4340, varying notch root radii, fracture initiation and propag. at notch root 0-85050  
 steel, Cr-Mn, low-cycle fatigue at 20 and -196°C 0-81196  
 steel, low C, impact strength and crit. brittleness temp., sample thickness and notch radius influence 0-85018  
 steel, pearlitic constructional,  $K_{IIC}$  expt. determ. 0-100985  
 steel, S45C notched specimens, Charpy impact tests, notch angle effects (Japanese) 0-85124  
 steel sheet, hot and cold rolled, cold formability, notched tensile test and stretch bend test (German) 0-61031  
 steels, wide plate and V-notch bending tests evaluation on basis of materials mechanics (German) 0-66571  
 strip with semicircular notches, tensile load conditions at end, interf. effects obs. 0-64455  
 Al alloy AK4-1, crack growth rate prediction under creep conditions 0-85107  
 $\alpha$ -U, mech. props. at very high strain rates, double-notch shear test use 0-85131

**novae**

- see also* **supernovae**  
 AE Aquarii, cataclysmic variable, IUE satellite UV obs. 0-72985

**novae continued**

- AE Aquarii, spectroscopic binary variable, X-ray source, orbital element determ. 0-105288  
 Aquilae 1891 (T Aurigae), spectrophotometry of shell 0-72955  
 Aquilae 1918 (V603 Aquilae), IUE obs. of periodic light vars. 0-105251  
 Aquilae 1918 (V603 Aquilae), old nova, eclipses obs. 0-90476  
 Aquilae 1918 (V603 Aquilae), periodic light vars. detect. 0-82391  
 Aquilae 1975 (V1301 Aquilae), dust grain IR emission model 0-105254  
 Aurigae 1891 (T Aurigae), old nova, photometric and spectroscopic obs. 0-90446  
 Z Camelopardalis, dwarf nova, spectrophotometry at standstill and in eruption 0-82366  
 TX Canum Venaticorum, cataclysmic variable, P Cygni type, visible spectral obs. 0-105249  
 OY Carinae, white dwarf cataclysmic, eclipsing binary, parameter determ. 0-82385  
 cataclysmic binaries, circumstellar material geometrical and photometric parameters 0-109492  
 cataclysmic binaries, role of white dwarf component 0-82356  
 cataclysmic variables, period change due to mass transfer 0-82425  
 cataclysmic variables, XUV emission (German) 0-109372  
 cataclysmic variables in globular clusters, preliminary report 0-109505  
 Z Chamaeleontis, eruptive binary, model from photoelectric data anal. 0-72961  
 Z Chamaeleontis, gravitational waves from eclipsing cataclysmic binary 0-90439  
 EM Cygni, cataclysmic variable, red and white dwarf binary, period change, B photometry 0-90434  
 SS Cygni, dwarf nova, rapid optical oscills. phase variability 0-85947  
 SS Cygni, spectroscopic binary variable, X-ray source, orbital element determ. 0-105288  
 Cygni 1975 (V1500 Cygni), Balmer line emission profiles evolution in early decline phase 0-82371  
 Cygni 1975 (V1500 Cygni), distance and temp., visible spectral obs. (Chinese) 0-85955  
 Cygni 1975 (V1500 Cygni), emission line vars. rel. to struct. of central object 0-82367  
 Cygni 1975 (V1500 Cygni), luminosity and distance, light curve obs. 0-72981  
 Cygni 1975 (V1500 Cygni), periodicity investigation at 21 cm 0-82529  
 Cygni 1975 (V1500 Cygni), radio obs. and analysis 0-67726  
 Cygni 1978 (V1668 Cygni), multifilter photometry and polarimetry 0-90454  
 Cygni 1978 (V1668 Cygni), optical light curve, uvby photometry 0-62154  
 Cygni 1978 (V1668 Cygni), post-max. short period oscills., photoelectric photometry 0-82380  
 Cygni 1978 (V1668 Cygni), spectroscopic and photometric obs., (1978 to 1979) (Russian) 0-109444  
 Delphini 1967 (HR Delphini), premax. outflow 0-82378  
 Delphini 1967 (HR Delphini), short period light vars. from UVB photometry 0-67744  
 Delphini 1967 (HR Delphini), simultaneous X-ray, UV and optical obs. 0-109440  
 dust formation and ionisation in nova envelopes, theory 0-98678  
 dust grains surrounding source, effect on nova model 0-105324  
 evolution from white dwarf binary system 0-109465  
 fast nova occurrence, mechanism for envelope C enhancement 0-85936  
 U Geminorum, dwarf nova, visual magnitudes during outburst, (1980 May 6 to 9) 0-72978  
 U Geminorum, visual magnitude estimates during outburst (1980 Oct.) 0-109439  
 AH Herculis, dwarf nova outburst, rapid oscills. evolution 0-94805  
 Herculis 1934 (DQ Herculis), eclipsing binary, emission line eclipse phenomena 0-94800  
 Herculis 1934 (DQ Herculis), white dwarf rot. period rel. to nova remnant shape 0-105244  
 historical novae, Latin terminology 0-62437  
 EX Hydrae, dwarf nova, IR and optical light curves 0-67747  
 EX Hydrae, dwarf nova lightcurve, periodic and secular vars. 0-77413  
 EX Hydrae, spectra of dwarf nova 0-98670  
 VW Hydri, dwarf nova, IR light curves 0-67747  
 KUV09313+4052, variable UV excess object and possible dwarf nova, discovery 0-62159  
 light curves, as manifestation of nonuniform stellar wind 0-62160  
 outburst, equatorial belt formation, plasma current rings model, double adiabatic MHD 0-67757  
 outbursts, effect of binary companion 0-82394  
 AG Pegasi, symbiotic binary system, UV and optical spectrum rel. to nature of components 0-109449  
 piston problem, one-dimensional, in non-ideal gas, time-dependent soln. 0-82185  
 remnants shapes, effects of white dwarf rotation 0-105244  
 WZ Sagittae, 1978-9 outburst of dwarf nova, spectra 0-94801  
 WZ Sagittae, eclipsing binary, outburst of December 1978, UV obs. 0-72982  
 WZ Sagittae, eruptive binary, model from hot spot eclipses anal. 0-72962  
 WZ Sagittae, image-tube spectroscopic obs. of 1978 Dec. outburst 0-72958  
 WZ Sagittae, recurrent nova, IUE obs. in outburst 0-109448  
 WZ Sagittae, recurrent nova, spectroscopic obs. and model for superhump phenomena 0-82368  
 VY Sculptoris, novalike variable, precise position 0-101597  
 Serpens 1970 (FH Serpens), dust grain IR emission model 0-105254  
 Serpens 1978, evolution of dust shell 0-90430  
 slow deflagration front stability at degenerate star surface 0-67729  
 slow novae and symbiotic stars, late-type components spectral classifications 0-94813  
 slow recurrent novae, relationship to type II symbiotic stars 0-62144  
 surface nucl. reactions and origin of mag. fields 0-101616  
 RW Trianguli, nova-like eclipsing binary radial vels., dimens. from visible spectra 0-82418  
 EK Trianguli Australis, SU Ursae Majoris dwarf nova, superhumps, light curve UVB obs. 0-105255  
 SU Ursae Majoris, soft X-ray halo around dwarf nova 0-98677  
 SU Ursae Majoris stars, important sub-group of dwarf novae, photometric props. 0-101596  
 Vulpecula, novalike object, 1980 May-June spectra and magnitudes 0-82392



**novae** continued

- Vulpecula, novalike object, UV decline and expanding cooling photosphere 0-67741
- Vulpecula, novalike object visual magnitude estimates (1980 February 2 to May 9) 0-72980
- Vulpecula novalike object, photometry, June 1980, and spectral classification 0-94807
- white dwarfs, He flash and nova evolution 0-72938
- <sup>26</sup>Al, synthesis in explosive H burning 0-85929
- <sup>22</sup>Ne and <sup>26</sup>Al nucleosynthesis in novae and supernovae outbursts 0-62143

**novoids** see *novae*

**nozzles**

- accelerating two-phase nozzle/diffuser flows, virtual mass effects on numerical stability 0-92204
- air bubbles, production, pulsation and damping, in dil. polymer solns. 0-69879
- axisymmetric afterbodies, separated turbulent flows, wakes, exhaust plume effects 0-74885
- chemical laser, low pressure, line-shape flattening resulting from hypersonic nozzle wedge flow 0-91783
- choked foam flow in convergent-divergent nozzle 0-74940
- circular impinging jet, heat transfer characts., stagnation point, boundary layers 0-79303
- compressible gas flow through exhaust valve, analytical calc. using flux analysis method (*Japanese*) 0-69896
- convergent nozzles, swirl effects on mass flux and thrust 0-74936
- CW supersonic chemical laser, porous nozzle, chemically reacting boundary layer 0-100022
- degeneration of supersonic flow due to interaction of centered compression and rarefaction waves 0-69864
- different jet regimes, internal and external flows, separation and wakes 0-100023
- dispersed supersonic two-phase flow, shock characts., droplet size depend. at nozzle 0-106815
- dispersive compressible fluid, transonic nozzle flows 0-69895
- drop formation hydrodynamics, macroencapsulation 0-64603
- duct, supersonic flow downstream oscillations from abrupt cross section increase, nozzles 0-74976
- flange tap orifice flowmeters, Stolz and ASME-AGA orifice eqns., lab. data comparison 0-64604
- gas jet blowing into supersonic flow without 3-dimens. boundary layer separation, nozzle shape 0-100009
- hypersonic flow from high enthalpy supersonic flow 0-74937
- injector with distrib. multijet liquid supply, efficiency and performance 0-74939
- internal profiling of the nozzles of model systems 0-92198
- jets, two-dimensional water, sensitive to sound, behaviour (*Japanese*) 0-79376
- Laval two-dimensional supersonic nozzles, numerical construction method 0-92197
- Ludwig tube, steady flow duration extension, reservoir orifice method, variable opening area effect 0-64579
- Mach wave radiation of hot supersonic jets 0-69894
- monatomic gas, rarefied flows in axisymmetric expansion nozzle 0-92182
- nonequilibrium gas relaxation in supersonic nozzle, analysis method 0-74941
- pipes and bends, structure-borne sound behind a jet nozzle (*German*) 0-87804
- rotating hollow gas jets, nozzle exit flow angle and pressure forces effects (*German*) 0-69887
- shear layer instability noise produced by various jet nozzle configurations 0-69791
- sound pulsation noise damping from small air bubbles in water 0-64253
- sound spectra radiated by gas jets, influence of closely located solid surfaces 0-69800
- spherical nozzles of high-temperature heaters, heat transfer calcs. 0-103022
- steam, 2-D two-phase flow, nucleating and wet steam, time-marching method 0-69906
- superheated liquid discharge from nozzle, pressure calc. 0-92199
- supersonic, pulsed jet wave struct. in nonstationary flow stage 0-59094
- supersonic and sonic annular jets, 0-100019
- supersonic molecular beam nozzle, use of pulse valve 0-100045
- swirl spray atomising nozzle, coefficient of discharge and spray cone angle 0-64602
- turbojet nozzle model used for investigating internal noise of turbojet engine 0-87644
- two-phase nozzle flows from separate phase model 0-74938
- water vapour expansion with condensation, nozzle flow at high pressure 0-106828
- Ar, cluster formation and homogeneous nucleation, comparison of expt. and theory, for supersonic nozzle flow 0-79925
- Ar, supersonic pulsed flow from conical nozzle 0-103056
- N<sub>2</sub> gas jet injection into Hg, interaction at submerged orifice 0-59102

**NTC thermistors** see *thermistors*

**ν (neutrino)** see *neutrinos*

**nuclear acoustic resonance** see *acoustic nuclear magnetic resonance*

**nuclear alignment** see *nuclear polarisation*

**nuclear binding energy**

see also *nuclear forces*

- <sup>206</sup>Pb, high spin pot. energy surfaces, fission barrier, α-, γ-decay half lives, yrast spectrum 0-73764
- Bloch density for nonlocal pots., h-expansion partial resummation, average binding energies 0-86797
- compressible nuclei, surface energy 0-83031
- generalised vibrational rule 0-105971
- infinite system of nucleons and Δ resonances, pot. energy, neutron stars 0-86836
- many body problem in Lee model, NN scatt. and matter binding energy 0-63116
- nuclear matter, hypernetted chain approx., impurity ground state energy 0-83055
- orbital excitation of the hyperon in hypernuclei 0-106001
- pairing correlation treatment, single particle levels, binding energy, spectra, branching ratios (*Chinese*) 0-102107
- polarised nuclear matter, binding energy, spin energies, relativistic calc. 0-102134
- saturation in finite nuclei, nuclear matter density and binding energy 0-83029

**nuclear binding energy** continued

- sd-shell nuclei heavy-ion reaction resonances, low level density regions, shell model 0-57757
- single-particle response and ground-state properties, Hartree-Fock theories 0-105997
- spherical nuclei, Hartree-Fock-Bogolyubov calcs., D1 effective interaction, nuclear matter, binding energies 0-63105
- symmetry effects on nuclear binding energy and rest mass of constituents (*French*) 0-63068
- Woods-Saxon potential spectrum, pairing force strength, Nilsson model comparison 0-57704
- (K.K.), isobar doorway model, optical pot., A-nuclear matter binding energy 0-106079
- AN distrib. function, A-binding to nuclear matter, Fermi hypernetted chain approx. 0-78131
- ANN correlations and A binding in nuclear matter 0-106000
- <sup>n</sup> binding energy, calc. from <sup>3</sup>H, <sup>3</sup>He, <sup>4</sup>H, <sup>4</sup>He and <sup>4</sup>Li ground-state properties 0-83044
- <sup>n</sup> system, bound state, Faddeev eqn. calc. 0-105989
- <sup>n</sup> binding energy, calc. from <sup>3</sup>H, <sup>3</sup>He, <sup>4</sup>H, <sup>4</sup>He and <sup>4</sup>Li ground-state properties 0-83044
- NNN bound state problems, hyperspherical harmonic expansion, review 0-91136
- (π,π), Weinberg chiral Lagrangian nonlinear terms, nuclear binding, optical pot. 0-78329
- Ba, charge radii and binding energy per nucleon, linear relationship evidence 0-68520
- <sup>252</sup>Fm, pot. energy surface, liquid model, deformation energy formulae (*Chinese*) 0-102106
- <sup>2</sup>H D-state probability lower bound, binding energy, quadrupole moment 0-91137
- <sup>3</sup>H binding energy, relativistic calc., Bethe Salpeter eqn. 0-68519
- <sup>3</sup>H realistic wave function, energy and density distrib. 0-86794
- <sup>3</sup>He, binding energy, Faddeev equation in coord. space, Lambda-nucleon potential 0-63120
- <sup>4</sup>H, A=2,3, binding energy from Brillouin-Wigner perturbation method, strong short ranged interactions 0-86796
- <sup>4</sup>He, ground state level determ. 0-99136
- <sup>4</sup>He Coulomb energy from configuration space Faddeev calcs. 0-102131
- <sup>4</sup>He binding energy, 4-nucleon problem, integral eqn. approach 0-91183
- <sup>4</sup>He(π,π), single scatt. optical pot., Pauli principle and binding effects on cross section 0-86933
- <sup>3</sup>He, A-N pot. Majorana component on B<sub>1</sub> value, overbinding 0-99144
- <sup>10</sup>Li neutron binding energy from Li(t, <sup>3</sup>Li)H (*Russian*) 0-105961
- <sup>10</sup>O, A=16, 17, valence-core self-consistency, wave functions, binding energy, levels, spectra 0-63123
- <sup>16</sup>O ground-state energy, nonunitary model operator approach 0-83030
- Ru, even isotopes, potential energy surfaces and ground state equilib. deformation 0-73789
- <sup>32</sup>S α-cluster struct., ground and first excited states, energies, radii and moments 0-102122
- <sup>145</sup>Sm primary γ-rays, direct capture and neutron separation energy, (d,p),(n,γ) correlation 0-57738
- Sr, even isotopes, potential energy surfaces and ground state equilib. deformation 0-73789
- <sup>93</sup>Sr neutron binding energy from transitions and β-delayed neutron defined level correspondences 0-63070
- <sup>23</sup>U, pot. energy surface, liquid model, deformation energy formulae (*Chinese*) 0-102106
- Xe, charge radii and binding energy per nucleon, linear relationship evidence 0-68520
- Zr, even isotopes, potential energy surfaces and ground state equilib. deformation 0-73789

**nuclear bombardment targets**

see also *nuclear reactions and scattering*

- amorphous targets, energetic in transport, Monte Carlo program 0-102411
- electron spectroscopy, target sources, centrifuge method of prep. 0-74060
- frozen spin target, horizontal dilution refrigerator with high cooling power 0-73372
- heating by ion beam, thermal characts. (*Japanese*) 0-99374
- laser fusion cryogenic target characterisation by wavefront shearing interferometer 0-74008
- metal target preparation for stopping power meas. of channelled ions in low energy region 0-63431
- polarised targets and cryogenics at Laboratori Nazionali di Legnaro 0-106219
- projected inertial confinement fusion reactor target evaluation by buoyancy analysis 0-78442
- remotely controlled target transport system for cyclotron irradiations 0-69005
- ZGS, polarised targets 0-91309
- H<sub>2</sub>, thin liquid target for low energy nuclear physics expts. 0-78471
- <sup>6</sup>LiD, new material for polarised targets for pol. neutron prod. (*French*) 0-68987
- <sup>6</sup>LiD, polarised target material, DNP 0-87007
- T gas targets, pressure monitoring system 0-99370
- Ti-T target system for production of 14 MeV neutrons, improvements 0-63433

**nuclear branching and mixing ratios**

- A=134-144, fission yields from spectroscopic meas., γ-branching and half-lives 0-78213
- A=163, nuclear data sheets to April 1979 0-98762
- linear polarisation mixing coeffs. for mixed dipole and quadrupole γ-radiations, Compton polarimeter 0-73110
- pairing correlation treatment, single particle levels, binding energy, spectra, branching ratios (*Chinese*) 0-102107
- XX <sup>126</sup>Xe, 2<sub>2</sub><sup>+</sup> transition multipole mixing ratio 0-78198
- <sup>Δ</sup>Al, A=25,26,27 levels, resonances, γ-ray branching ratios from Mg(p,γ) 0-86875
- <sup>26</sup>Al T=1 states, resonances, J<sup>π</sup> and transitions from <sup>25</sup>Mg(p,γ) 0-99131
- <sup>27</sup>Al isobaric analogue resonances, spectroscopic factors and γ-rays from (p,p), (p,γ) 0-86873
- <sup>27</sup>Al levels, resonances, J<sup>π</sup>, branching and mixing ratios from <sup>26</sup>Mg(p,γ) 0-99132
- <sup>Δ</sup>Ba, A=142,144,146, transition γ-γ ang. correlations, levels, J<sup>π</sup>, mixing ratios 0-73823
- <sup>142</sup>Ba, γγ ang. correlations, levels, spins and mixing ratios from <sup>142</sup>Cs decay 0-57734

**nuclear branching and mixing ratios continued**

- <sup>14</sup>C first excited 0<sup>+</sup> state, lifetime and E<sup>0</sup> decay from (d,p), (<sup>13</sup>C,p) 0-102145  
<sup>59</sup>Co level energies, branching ratios lifetimes and spins from (p,p'),(α,pγ) 0-63093  
<sup>63</sup>Co, A=142, 144, 146, low lying levels, J<sup>π</sup>, mixing ratios and γ-γ ang. correlations 0-102119  
<sup>63</sup>Cu(p,p') negative parity level excitation, gamma ray obs., test for core excitation model 0-68534  
<sup>19</sup>F(p,p'), 1459-110 keV transition, E2/M1 mixing ratio 0-106013  
<sup>56</sup>Fe, A=57, 59, levels, J<sup>π</sup> and transition branching ratio from Fe(n,γ) 0-105976  
<sup>56</sup>Fe low lying levels, J<sup>π</sup>, γ-γ coincidences, internal conversion from <sup>56</sup>Co β<sup>+</sup>-decay 0-86815  
<sup>3</sup>H(π<sup>+</sup>, γ)3n, rest π, resonance branching ratio, bound state upper limit 0-99162  
<sup>41</sup>In, A=119, 121, unified model description, vibr. multiplet yrast struct., branching ratios 0-105953  
<sup>11</sup>In low lying levels, transitions, T<sub>1/2</sub>, multipolarities and mixing ratios from <sup>112</sup>Cd(p,nγ) 0-68545  
<sup>191</sup>Ir, A=189, 191, levels, J<sup>π</sup>, transitions and mixing ratios from Pt decay 0-68602  
<sup>84</sup>Kr levels, γ-cascades, J<sup>π</sup>, mixing ratios and correlations from <sup>84</sup>Br decay 0-63134  
<sup>11</sup>Li beta decay, γ activity 0-106018  
<sup>23</sup>Np, absolute meas. of branching ratio for the 277.6 keV line 0-86854  
<sup>188</sup>Os, A=188, 189, levels, J<sup>π</sup>, transitions and mixing ratios from Ir decay 0-68602  
<sup>30</sup>P T=1 state decay, lifetimes and branching ratios, analogue E2 transitions from <sup>29</sup>Si(p,γ) 0-68598  
<sup>208</sup>Pb(n,n'), 1.5-3.1 MeV, levels, J<sup>π</sup>, excitation functions and mixing ratios 0-102123  
<sup>208</sup>Pb γγ directional correlations, multipole mixing ratios, transition strength limits from <sup>208</sup>Bi decay 0-86849  
<sup>101</sup>Pd nonyrast rotational states, transitions, T<sub>1/2</sub>, branching and mixing ratios from <sup>92</sup>Zr(<sup>12</sup>C,3n) 0-105950  
<sup>76</sup>Se high spin states, bands, J<sup>π</sup>, transitions and T<sub>1/2</sub> from <sup>71</sup>Ga(<sup>6</sup>Li,2n) 0-105951  
<sup>48</sup>Sm, A=147, 149, levels, J, γ-transitions and multipole mixing ratios, γγ correlations from Eu EC decay 0-106012  
<sup>84</sup>Sr, A=94,96 direct and skip cascades, γγ ang. correlations, levels, mixing ratios from Rb decay 0-86851  
<sup>92</sup>Sr γγ ang. correlations, levels, J<sup>π</sup>, mixing ratios from <sup>92</sup>Rb decay 0-57725  
<sup>180</sup>Ta<sup>+</sup>, β<sup>-</sup> and EC branching ratios, K-internal conversion coeff., γ-intensities, T<sub>1/2</sub> 0-68601  
<sup>126</sup>Te(p,n), 2<sub>2</sub><sup>+</sup>→2<sub>1</sub><sup>+</sup> transition multipole mixing ratio 0-78198  
<sup>167</sup>Tm rotational bands, J<sup>π</sup>, γ-transitions and branching ratios from <sup>167</sup>Ho(α,2nγ) 0-86781  
<sup>235</sup>U shape isomer, γ branch upper limit, γ-yields from <sup>235</sup>U(d,p) 0-99145  
<sup>132</sup>Xe level struct., J<sup>π</sup>, transitions and multipole mixing ratio from <sup>132</sup>I decay 0-91134

**nuclear charge**

- see also form factors (nuclear)*  
 deep inelastic heavy ion reactions, high multipole isovector modes and charge fluctuations 0-57793  
 heavy ion fusion reactions, charge density asymmetry liquid drop model 0-63220  
 light natural elements, muonic X-ray transitions, nuclear charge radii 0-99589  
 low energy fission, charge distrib., quantum mechanical phenomenon of GDR 0-86945  
 neutron rich nuclei; β<sup>-</sup>-emitters, deformation and spectroscopy 0-78223  
 Ba, charge radii and binding energy per nucleon, linear relationship evidence 0-68520  
 Ba, neutron deficient, charge radii, moments, transitions and isomers, atomic beam laser spectroscopy 0-102141  
<sup>209</sup>Bi(<sup>56</sup>Fe,X), damped collisions, fast A/Z equilibration and correlated nucleon exchange 0-86798  
<sup>12</sup>C(e,e), 25-115 MeV, ground state charge distrib. and RMS charge radius 0-57672  
<sup>4</sup>Ca, A=40 to 46,48, nuclear charge distrib., from isotope shift of 6573 angstrom line 0-57674  
<sup>41</sup>Ca, E2 core polarisation charge, Woods-Saxon shell model compared to harmonic oscillator model 0-63072  
<sup>136</sup>Cf(e, e'), 116, 194 MeV, A=35, 37, charge distrib. and RMS charge radius 0-102109  
<sup>245</sup>Cm (n,f), thermal, charge distrib., <sup>135</sup>I and <sup>190</sup>Ba fractional cumulative yields 0-63074  
 Cs, ground state spins, moments, charge radii by laser spectroscopy 0-78147  
<sup>166</sup>Er(<sup>86</sup>K,X), deep inelastic collision, charge drift and dispersion calc., thermal eqn. model based on shell model 0-57798  
<sup>100</sup>Fe(e,e), 100-275 MeV, A=54,56,57, cross sections and muonic X-ray meas., charge distrib. systematics 0-86801  
<sup>2</sup>H charge operator, retardation, quasipot. eqns. and rel. corrections 0-99122  
<sup>3</sup>H, EM form factors, 3-nucleon wave function calc. 0-95302  
<sup>3</sup>He, EM form factors, 3-nucleon wave function calc. 0-95302  
<sup>3</sup>He, nuclear charge form factor, two-boson exchange charge density π, ρ, ω exchanges 0-63073  
<sup>4</sup>He nuclear charge density determ. using form factor analyticity 0-63077  
<sup>4</sup>He, A=3, 4, charge structure, effect of neutron charge 0-105963  
 Li charge form factor with resonating group wave function, quad. moment, charge radius 0-102110  
<sup>206</sup>Pb hexadecapole moments, quadrupole deformation effects, E4 effective charge, valence polarisation 0-78142  
 Ni mean square charge radii from isotope shifts 0-99484  
<sup>100</sup>Ni(e,e), 100-275 MeV, A=58,60,62,64, cross sections and muonic X-ray meas., charge distrib. systematics 0-86801  
 Rb, ground state spins, moments, charge radii by laser spectroscopy 0-78147  
<sup>48</sup>Sm, A=144-154, mean square nuclear charge radius, laser atomic beam spectroscopy 0-102468  
<sup>232</sup>Th(p,f), 29-97 MeV, Rb, In and Cs relative indep. yields, charge division 0-102218  
<sup>235</sup>U(n,f), thermal, fragment ionisation, charge distrib., stat. and instant perturbation theory (Russian) 0-63219

**nuclear charge continued**

- <sup>238</sup>U(p,p'), 11-29 GeV, three dims. charge dispersion curves, isobaric yields 0-102111  
 Xe, charge radii and binding energy per nucleon, linear relationship evidence 0-68520  
<sup>66</sup>Zn(e,e), 100-275 MeV, A=64,66,68,70, cross sections and muonic X-ray meas., charge distrib. systematics 0-86801
- nuclear chemistry**  
*see also chemical effects of nuclear reactions and scattering; radiation chemistry; radiochemistry*  
<sup>18</sup>F+hexafluoropropylene nonequilibrium effects in moderated nuclear recoil experiments 0-89509  
<sup>18</sup>F+methane, nonequilibrium effects in moderated nuclear recoil experiments 0-89509  
<sup>16</sup>O ions, mag. hyperfine interactions, PAC meas. 0-95734
- nuclear cluster model**  
 α-clustering in heavy nuclei, pre-equil. model, nuclear matter NN, No interactions 0-63111  
 A=50 to 150, even-even, odd-even, odd-odd, cluster vibr. model 0-68567  
 Brueckner theory, unification with HFB theory 0-105995  
 cluster systems, normalisation kernels, SU(3) prop., generator coordinate theory 0-73814  
 deuteron form factors and spectroscopic factors in heavy spherical nuclei, shell model (Russian) 0-63078  
 Pauli principle in multiple scatt. theory, exact eqns., cluster exchange 0-106024  
 resonating group method alternative, comments, many body Lippmann-Schwinger eqns., cluster approx. 0-83052  
 two charged clusters collision, scatt. amplitudes and integral eqns. 0-68614  
 (α,<sup>12</sup>C), 90.3 MeV, multi-α-cluster transfer and direct pickup cross sections 0-57760  
 (d,<sup>6</sup>Li), A=144-238, alpha-cluster transfer from alpha-decaying nuclei 0-91166  
 (γ,d), odd-Z light nuclei, from (e,e'd), cross section, E2 transistors giant resonance and clusters 0-63169  
 (n, α) with resonance neutrons, properties of highly-excited states of nuclei (Russian) 0-106053  
 (P,X), 400 GeV, correlation strength, dependence on target size, multiplicity and cluster size 0-78287  
<sup>16</sup>(γ,X), bremsstrahlung weighted cross section, two-body correlations effects, linked cluster expansion 0-106047  
<sup>4</sup>Ag, A=105-109, negative parity states, vibr. versus rot. descriptions 0-73781  
<sup>193</sup>Au levels, three holes cluster vibr. and particle asymmetric rotor descriptions 0-57668  
<sup>8</sup>Be high spatial symmetry excited states, resonances, rot. band from (d,αt), (p,αt) 0-86780  
<sup>9</sup>Be low lying spectrum, 3-body molecular description, adiabatic one level approx. 0-78150  
<sup>12</sup>C, alpha cluster in Hartree Fock calcs. 0-63110  
<sup>12</sup>C(p,α), 45.2 MeV, cross sections, finite range DWBA anal., cluster form factors 0-68666  
<sup>40</sup>Ca composite system, heavy ion resonances from <sup>24</sup>Mg+<sup>16</sup>O, <sup>28</sup>Si+<sup>12</sup>C 0-86874  
 Ga, odd, single particle and collective degrees of freedom, clustering, shell model anal. 0-68510  
 Ge, odd, single particle and collective degrees of freedom, clustering, shell model anal. 0-68510  
<sup>4</sup>He(α,α), nuclear separable plus Coulomb interaction 0-83106  
<sup>4</sup>He(α,α), size change of α effect on phase shift, generator coordinate and variational methods (Chinese) 0-68683  
<sup>4</sup>He(d,d), low energy, resonating group method anal. with distortion effect 0-73851  
<sup>6</sup>Li, transition probabilities between cluster structure states and r.m.s. radius, double well-cluster model (Chinese) 0-63128  
<sup>6</sup>Li(d,X) system, resonating group method, single channel approx., cluster states 0-57782  
<sup>6</sup>Li(e,e'), 102, 123 MeV, excitation form factor, <sup>3</sup>H-<sup>3</sup>He cluster model 0-78190  
<sup>6</sup>Li(p,pd), 670 MeV, large angle quasifree scatt., spectroscopic factor, momentum distrib., cluster model 0-63184  
<sup>7</sup>Li, photodisintegration, cluster model wave function, bremsstrahlung weighted cross section 0-63163  
<sup>24</sup>Mg K=2 band and alpha cluster model state point symmetry 0-105946  
<sup>14</sup>N(d, α), pol.d, 1.5-3 MeV, vector anal. capacity for two α-particle groups 0-78266  
<sup>16</sup>O, 3 α forces, ground state energy and form factor 0-86817  
<sup>16</sup>O α-cluster states, widths and resonances, optical model, direct transfer in <sup>12</sup>C(<sup>6</sup>Li,d) 0-105975  
<sup>16</sup>O, cluster expansions for normalisation integral calc. 0-86831  
<sup>208</sup>Pb(<sup>6</sup>Li,d), 90 MeV, alpha-cluster transfer from alpha-decaying nuclei 0-91166  
<sup>85</sup>Rb levels, J<sup>π</sup> and transitions from Kr<sup>m-8</sup>, Sr<sup>m-8</sup> decay, cluster-vibr. model 0-78162  
<sup>32</sup>S α-cluster struct., ground and first excited states, energies, radii and moments 0-102122  
<sup>28</sup>Si, highly excited <sup>12</sup>C-<sup>12</sup>C molecular state, symmetrical decay (Russian) 0-86861  
<sup>48</sup>Sm, A=146,147, excited states, energy levels, spin, parity, shell and cluster-vibration models, from (α,xn) and (<sup>4</sup>He,xn) 0-57683
- nuclear collective model**  
*see also nuclear cranking model; nuclear liquid drop model*  
 A=12-240, even-even, dynamic deformation theory, B(E2) values, quadrupole and mag. moments 0-68591  
 A=158-176, 'extension of variable moment of inertia model to high spins', comments 0-86791  
 A=50 to 150, even-even, odd-even, odd-odd, truncated quadrupole phonon model 0-68567  
 A=50 to 150, shell, dynamical deformation and interacting boson models, limitations 0-68563  
 A~150, yrast states, deformed oscillator Hamiltonian calcs. 0-78126  
 algebraic formulation, collective and intrinsic submanifolds 0-73811  
 band crossing in interacting boson model, E2 transition probabilities and g-factors 0-102101  
 basis states for rotational and vibrational limits 0-86775  
 Bohr collective Hamiltonian and interacting boson model relationship 0-86825  
 collective 0<sup>+</sup> state, sum rules and breathing mode 0-86778



**nuclear collective model continued**

- cranked Hartree-Fock-Bogoliubov theory extension 0-105996  
eigenvalue distribution in scalar space for noninteracting and interacting bosons 0-78177  
energy dissipation, into internal energy superfluid wall formula 0-63108  
even-even nuclei, spectra calcs., interacting boson model 0-68590  
giant monopole vibrs., RPA and collective field description, surface compressibility 0-102100  
giant resonances in nuclear reactions, microscopic theory of intermediate struct. 0-99161  
governor model for asymmetric deformed nuclei, band anal. 0-86776  
interacting boson approx. and Frankfurt model, collective model confrontation 0-57706  
interacting boson approx. s.bosons, exact calcs. and fermion pair description 0-57707  
interacting boson model, monopole and quadrupole pairing 0-73812  
interacting boson model classical limits 0-86826  
l-azimuthal spherical harmonics in collective models 0-91139  
large amplitude collective motion in a nontrivial schematic model 0-73816  
level density of interacting bosons 0-105974  
low lying states in collective nuclei, boson expansion theory 0-78118  
many-body problem, classical hydrodynamics and collective motion approx. 0-83027  
microscopic theory for large amplitude collective motion in soft nuclei 0-86824  
moment map and collective motion, Hamiltonian action of Lie group 0-91138  
O(5)×SU(1,1) symmetric irreducible representations, orthonormal basis, interacting boson model appl. 0-78178  
octupole vibration, collective, wave functions, spherical harmonics 0-68532  
odd nuclei, soft and deformed, rotor plus quasiparticle approach, moments, transition probabilities 0-78214  
odd-A nuclei, O(6) spectra, interacting boson-fermion model, new coupling scheme 0-57727  
odd-A nuclei collective states, interacting boson-fermion model 0-95296  
particle-rotor model, pairing interaction treatment, yrast and yrare bands 0-83028  
particle-vibrator model, microscopic foundation 0-78179  
perturbative treatment of nuclear rots., two-dimens. rotor, bands, moments of inertia 0-78111  
spherical nuclei, fragmentation of hole states in quasiparticle-phonon model 0-83020  
spherical nuclei, quasi-particle theory, modification of BCS basis 0-63109  
spherical nuclei, quasiparticle-phonon model, iterative method 0-68566  
spin rotation, high angular velocity, collective aspects of heavy ion collisions 0-78309  
symplectic collective model, irreducible U(3) tensor interactions 0-83048  
two-phonon states, effect of Pauli principle 0-68565  
vibrational nuclei, variable moment of inertia model, relation to interacting boson model 0-83051  
<sup>4</sup>Ag, A=105-109, negative parity states, vibr. versus rot. descriptions 0-73781  
<sup>4</sup>Ag, A=105-109, negative parity states, EM props. from particle-asymmetric rotor model 0-102097  
<sup>103</sup>Ag collective excitation and J<sup>π</sup> following <sup>94</sup>Mo(<sup>12</sup>C,p2nγ), rotor-plus-particle model 0-86782  
<sup>193</sup>Au levels, three holes cluster vibr. and particle asymmetric rotor descriptions 0-57668  
<sup>8</sup>Be collective excitation spectra from generalised hyperspherical functions method (Russian) 0-91133  
<sup>12</sup>C(K<sup>+</sup>,K<sup>+</sup>), form factors, cross sections, interior probing capability 0-73866  
<sup>12</sup>C(p,p'), 20-40 MeV, pol. p, anal. powers, imaginary spin-orbit pot., coupled channels anal. 0-102179  
<sup>42</sup>Ca, collective states, quasi-degenerate intrinsic Hamiltonian, variational methods 0-68505  
Cd 2<sub>1</sub><sup>+</sup> excitation, α-spectroscopic factors in IBA model from Sn(d,<sup>6</sup>Li) 0-105967  
<sup>103</sup>Cd levels, J<sup>π</sup> and positive parity decoupled band, rotor anal. of <sup>94</sup>Mo(<sup>12</sup>C, 3nγ) 0-102096  
<sup>104</sup>Cd quasirot. ground state band and γ-transition from <sup>102</sup>Pd(α,2nγ) 0-105955  
<sup>127</sup>Cs collective quadrupole dynamics, band struct., transitions, collective model anal. from <sup>127</sup>I(α,4n) 0-78112  
<sup>166</sup>Er(γ,γ), 14.4-16.6 MeV, γ-vibr. band head transitions, dynamic collective model 0-57662  
<sup>57</sup>Fe, rot. band mixing microscopic theory using modified Kuo-Brown interaction 0-68513  
<sup>152</sup>Gd, vibrational states, B(E2) branching rates and interband transitions, pairing plus quadrupole calcs. 0-78127  
<sup>175</sup>Hf, three- and five-quasiparticle isomers, rotational bands and residual interactions from <sup>170</sup>Er(<sup>2</sup>Be, 4n) 0-83022  
Kr even-even isotopes, collective states and transitions, interacting boson approx. 0-73773  
<sup>78</sup>Kr bands, lifetimes and E2 transitions from interacting boson model and (<sup>16</sup>O,p2n), (<sup>19</sup>Fe,α2n) 0-73771  
<sup>4</sup>Mg, A=24,26, second order nonspherical quadrupole phonon effects 0-86790  
<sup>24</sup>Mg, low spin rotational states, energy props., extended deformation model 0-86785  
<sup>24</sup>Mg, triaxial nuclei rots., extended cranked shape consistent oscillator model 0-102133  
<sup>26</sup>Mg(<sup>3</sup>He,<sup>3</sup>He)<sup>+</sup>, 4<sup>+</sup> states, B(E2) values, and band mixing, rot.-vibr. model 0-83019  
<sup>96</sup>Mo vibration-rotation struct. and yrast levels from variable moment of inertia model 0-73778  
<sup>23</sup>Na, particle-rotor model with s-d shell pairing, BCS approx. 0-57705  
Nd, even-even, E2 transition probabilities from multiple Coulomb excitation, IBA comparison 0-78212  
<sup>147</sup>Nd low spin states ns lifetimes, particle rotor model interpretation 0-78207  
<sup>148</sup>Nd, vibrational states, B(E2) branching rates and interband transitions, pairing plus quadrupole calcs. 0-78127  
<sup>26</sup>Ne collective motion, B(E2) rates, algebraic formulation in symplectic shell model 0-83015  
<sup>16</sup>O(<sup>16</sup>O,<sup>16</sup>O), 10-41 MeV, molecular resonances γ-yield, band crossing model 0-106032

**nuclear collective model continued**

- <sup>16</sup>O(p,p'), 20-40 MeV, pol. p, anal. powers, imaginary spin-orbit pot., coupled channels anal. 0-102179  
Os even-even isotopes, excitation energies and EM props. from interacting boson model 0-106005  
<sup>4</sup>Os, A=186,188, levels and transitions from Re decay, triaxial rotor model 0-91155  
<sup>4</sup>Os, A=186-194, collective levels, transitions, mag. and quadrupole moments, boson expansion theory 0-105954  
Pb pairing vibr. band, microscopic struct. and wave functions from (p,t), (t,p) 0-91126  
Pb region, forbidden charge exchange collective modes, β- and γ-decay processes 0-86784  
<sup>208</sup>Pb monopole vibr. vel. field, asymptotic form 0-78115  
Pd, even-even, collective states, B(E2), branching ratios and moments, boson expansion method 0-102099  
<sup>109</sup>Pd low spin odd parity levels, γ-rays, particle-rotor comparison from <sup>108</sup>Pd(n,γ) 0-73805  
<sup>145</sup>Pm level struct., J<sup>π</sup> and lifetimes, cluster-vibr. model anal. of <sup>146</sup>Nd(p,2n) 0-91125  
<sup>149</sup>Pm levels, bands, transitions, in-beam spectroscopy, particle-rotor anal. from <sup>150</sup>Nd(p,2nγ) 0-78125  
Pt even-even isotopes, excitation energies and EM props. from interacting boson model 0-106005  
<sup>4</sup>Pt, A=188-198 collective levels, transitions, mag. and quadrupole moments, boson expansion theory 0-105954  
<sup>4</sup>Pt, A=190,192,194, state struct. in interacting boson model 0-83047  
Rb odd-even isotopes, collective states and transitions, interacting boson approx. 0-73773  
<sup>4</sup>Re, A=186,188, β-decay, weak magnetism effects, triaxial rotor model 0-91155  
Ru, even-even, collective states, B(E2), branching ratios and moments, boson expansion method 0-102099  
<sup>4</sup>Ru, A=104,106,108, level scheme and transitions, collective model anal. of Tc decay 0-78166  
Sb, neutron rich nuclei, IBM and shell model approaches, collective modes 0-78129  
<sup>4</sup>Si(e,e'), 126-293 MeV, A=28,29, levels and form factors, particle-phonon coupling anal. 0-105977  
<sup>150</sup>Sm, vibrational states, B(E2) branching rates and interband transitions, pairing plus quadrupole calcs. 0-78127  
Sn 2<sub>1</sub><sup>+</sup> excitation, α-spectroscopic factors in IBA model from Te(d,<sup>6</sup>Li) 0-105967  
Sn, even isotopes, collective states and transitions from simple phenomenological model 0-73787  
<sup>46</sup>Ti(γ,n), 15-27.5 MeV, giant dipole resonance splitting, dynamic collective model 0-57755  
<sup>238</sup>U collective and deformation props., general collective model 0-86827  
<sup>166</sup>Yb multiple band crossing, (gSS'S'') system gamma correlation patterns 0-106008
- nuclear collective motion** *see nuclear collective model*
- nuclear collective states and giant resonances**  
*see also isobaric analogue resonances*  
<sup>116</sup>Xe quasi-rotational bands, levels J<sup>π</sup> and T<sub>1/2</sub> from <sup>116</sup>Cs decay 0-83021  
<sup>208</sup>114, high spin pot. energy surfaces, fission barrier, α-, γ-decay half lives, yrast spectrum 0-73764  
A=12-208, adiabatic TDHF approx. isoscalar quadrupole collective motion, cranking mass 0-68507  
A=158-176, 'extension of variable moment of inertia model to high spins', comments 0-86791  
A=70, heavy-ion induced fission-evaporation reactions, magnetic substrate distrib., nuclear alignment 0-73857  
A=90 region, core pol. effects and giant quadrupole resonances, HF and macroscopic calcs. 0-57756  
A~150, yrast states, deformed oscillator Hamiltonian calcs. 0-78126  
A~90 nuclei, isomeric states, spin polarisation, M4 transitions and giant resonances 0-63157  
actinide nuclei, cranking model, collective inertia parameters 0-57665  
adiabatic TDHF approx., mass parameters, single collective variable, theoretical aspects 0-73765  
asymmetric nuclear matter, isospin waves, IAS and giant Gamow-Teller resonance 0-91142  
backbending nuclei, HFB cranking wave functions 0-83049  
band crossing in interacting boson model, E2 transition probabilities and g-factors 0-102101  
coherent rotational states, alpha decay, α-emission probability 0-102155  
collective 0<sup>+</sup> state, sum rules and breathing mode 0-86778  
collective excitations of nuclei in a relativistic mean-field theory 0-95300  
collective motion, basis states for rotational and vibrational limits 0-86775  
collective parameter dynamics, monopole vibrs., variational principles 0-95298  
compound neutron absorption processes, optical pots., one particle vibr. state effects (Russian) 0-105956  
conference on medium heavy nuclei structure, Rhodes, Greece (May 1979) 0-67935  
deformed nuclei, yrast level ground state correlations, RPA anal. 0-86777  
doorway states, energy dependence of inelastic cross-section, shell model, coupled channel anal. 0-73854  
doubly closed shell nuclei, isovector giant monopole resonances, sum rule approach 0-78244  
doubly even deformed nuclei, excited states, Pauli principle effects, quasi-particle-phonon model 0-63094  
doubly even nuclei, yrast band B(E2) values, hydrodynamical model and CAP effect 0-86793  
electric multipole modes in the fluid-dynamical approximation 0-106029  
even-even nuclei, yrast band backbending mechanism criteria 0-91128  
giant dipole resonance decoupling and threshold states in schematic and shell models 0-78245  
giant dipole resonance intermediate struct. using (n,γ) and (γ, n), Brink hypothesis test 0-63150  
giant monopole electro-excitation, energy-weighted isoscalar sum rules 0-63174  
giant monopole vibrs., RPA and collective field description, surface compressibility 0-102100  
giant resonance production mechanisms (French) 0-78243  
giant resonances in many particle systems, microscopic derivation of classical eqns. of motion 0-102199



## nuclear collective states and giant resonances continued

- giant resonances in nuclear reactions, microscopic theory of intermediate struct. 0-99161  
governor model for asymmetric deformed nuclei, band anal. 0-86776  
growth points in nuclear physics, book 0-94928  
heavy ion fusion reactions, statistical yrast line 0-86948  
heavy nuclei tensor forces, unnatural parity excitations, high momentum collectivity 0-63065  
high spin rot. motion, TDHF cranking model and RPA descript. 0-102091  
low energy fission, charge distrib., quantum mechanical phenomenon of GDR 0-86945  
low lying states in collective nuclei, boson expansion theory 0-78118  
many-body problem, classical hydrodynamics and collective motion approx. 0-83027  
multipole phonon states,  $G_2$  group shift operator properties 0-99139  
multipole phonon states,  $R(7)$  group shift operators 0-99140  
multipole residual interaction strength, radial depend. in RPA 0-83026  
 $N=5$  shell, deformed odd-neutron nuclei, band ordering and spectrum 0-83018  
 $N=82$  region, high spin isomers, cranked HF calcs., deformation shapes, excitation energies 0-99121  
 $N=82$  region, high spin isomers, deformation energy surface, shape constrained cranked HF theory 0-57666  
neutron rich transitional fission fragments, spectroscopy,  $0^+$  states and octupole vibr. 0-78204  
nuclear field theory, phonon renormalisation, eigeneqns. and sum rules (Chinese) 0-102127  
odd-A nuclei collective states, interacting boson-fermion model 0-95296  
odd-odd fission products, level schemes, rot. bands, shell model states 0-78167  
particle-rotor model, pairing interaction treatment, yrast and yrare bands 0-83028  
particle-vibration coupling form factor from simple model 0-57663  
perturbative treatment of nuclear rots., two-dimens. rotor, bands, moments of inertia 0-78111  
pre-actinide nuclei, fission barriers, level density collective effects (Russian) 0-106092  
quadrupole oscillation wave functions, multiplicity factor (Chinese) 0-102103  
rare earth deformed nuclei, high spin region excited rot. bands, RPA calcs. 0-78108  
rare earth nuclei, cranking model, collective inertia parameters 0-57665  
rare earth nuclei, high spin isomer  $\alpha$ -decay search 0-102158  
rotating nuclei, current distrib., cranked HF model 0-63059  
rotation, inertial parameters in microscopic theory 0-91132  
rotational nuclei, high-spin, variable moment of inertia model, microscopic-macroscopic approach 0-63058  
rotational states, coherent,  $\gamma$ -decay, random quantum meas. 0-73855  
S and ground band interaction in cranked HFB model 0-95299  
spin rotation, high angular velocity, collective aspects of heavy ion collisions 0-78309  
superband and ground band ang. momentum difference (Chinese) 0-102102  
vibrational nuclei, variable moment of inertia model, relation to interacting boson model 0-83051  
(d,d'),  $A=40$  to 208, 108 MeV, giant monopole resonance excitation and ang. distrib. 0-102164  
(e,e'), 70 MeV, 1p shell nuclei, shell model cross sections, giant M2, transversal E1 resonances 0-63143  
( $\gamma$ ,d), odd-Z light nuclei, from (e,d), cross section, E2 transistors giant resonance and clusters 0-63169  
( $\gamma$ ,n), preequilibrium exciton model with evaporative component, photon-neutron spectra, giant resonances 0-57762  
(n,f), thermal, parity violation from opposite parity rot. states 0-95303  
(n, $\gamma$ ), polarized space parity nonconservation, optical pot. and GDR parameters (Russian) 0-86803  
(p,n), anomalous optical potential for sub-Coulomb barrier protons, 2 particle 1 hole states 0-105948  
( $\pi$ , $\pi$ ), intermediate energies, collective isobaric resonance 0-63208  
 $\pi$  absorption at rest, high spin state excitation,  $\pi$ -condensation and  $\Delta^{++}$  (Russian) 0-86927  
 $^A$ Ag,  $A=105-109$ , negative parity states, vibr. versus rot. descriptions 0-73781  
 $^A$ Ag,  $A=105-109$ , negative parity states, EM props. from particle-asymmetric rotor model 0-102097  
 $^{103}$ Ag collective excitation and  $J^\pi$  following  $^{94}\text{Mo}(^{12}\text{C}, p, 2n\gamma)$ , rotor-plus-particle model 0-86782  
 $^{103}$ Ag high spin states, bands transitions, intermediate deformation Coriolis coupling from ( $^3\text{He}$ ,  $xn\gamma$ ) 0-105944  
 $^{104}$ Ag levels,  $J^\pi$ ,  $T_{1/2}$ , bands and transitions from  $^{103}\text{Rh}(\alpha, 3n\gamma)$  0-102093  
 $^A$ Al,  $A=24, 25, 26$ , giant M1 strength, comparison with cross sections from  $\text{Mg}(p, n)$  0-86878  
 $^{27}\text{Al}(\gamma, X)$ , 3-30 MeV, photoabsorption cross section, giant dipole resonances 0-78254  
 $^{60}\text{As}$  1306 keV state mag. moment, g-factor, rot. aligned band 0-86807  
 $^{193}\text{Au}$  levels, three holes cluster vibr. and particle asymmetric rotor descriptions 0-57668  
 $^{12}\text{B}$  analogue states at 4.5 MeV giant resonance region, strong spin-isospin model, from  $^{12}\text{C}(e, e'\pi^+) 0-78250$   
 $^A$ Ba,  $A=135, 137$ , Coulomb excitation, transition probabilities,  $\gamma$ -rays and level collectivity from ( $^{16}\text{O}$ ,  $^{18}\text{O}$ ), ( $\alpha, \alpha'$ ) 0-78201  
 $^B$ Be collective excitation spectra from generalised hyperspherical functions method (Russian) 0-91133  
 $^B$ Be fission mode, large amplitude collective motion, adiabatic TDHF calcs. 0-86786  
 $^B$ Be high spatial symmetry excited states, resonances, rot. band from (d, $\alpha$ ), (p, $\alpha$ ) 0-86780  
 $^{208}\text{Bi}$  M1 isobaric analogue resonances and giant spinflip resonances from  $^{208}\text{Pb}(p, n)$  0-106030  
 $^{209}\text{Bi}(\gamma, X)$ , 3-30 MeV, photoabsorption cross section, giant dipole resonances 0-78254  
CC  $^{20}\text{Ne}$   $8^+$  level radiative width, resonance strength from  $^{16}\text{O}(\alpha, \gamma)$  0-83065  
 $^{12}\text{C}(\gamma, \gamma)$ , 23.5-39 MeV, cross sections and giant resonances, E2 strength 0-63122  
 $^{12}\text{C}(\gamma, n\alpha)$  Be, electric quadrupole transition cross-sections, behind giant resonance (Russian) 0-78281  
 $^{12}\text{C}(\gamma, p)^{11}\text{B}$ , electric quadrupole transition cross-sections, behind giant resonance (Russian) 0-78281

## nuclear collective states and giant resonances continued

- $^{12}\text{C}(\gamma, p\alpha)^{11}\text{Li}$ , electric quadrupole transition cross-sections, behind giant resonance (Russian) 0-78281  
 $^{12}\text{C}(p, 2p)$ , asymmetric energy-sharing mode, half distorted-wave formalism, intermediate giant resonance 0-68656  
 $^{12}\text{C}(p, p)$ , 14-45 MeV, differential cross section and spin-flip probabilities, giant resonances 0-73850  
 $^A$ Ca,  $A=40$  to 48, giant multipole resonances, mass dependence of energy weighted sums 0-63144  
 $^A$ Ca(p,p), pol. p,  $A=40, 48, 800$  MeV, diff. cross sections, anal. powers, DWIA anal., high spin levels 0-83067  
 $^{40}\text{Ca}$ , magic nuclei at collective excitations, energy spectrum and shape (Russian) 0-106015  
 $^{40}\text{Ca}(^2\text{Be}, ^2\text{Be})$ , 45, 60 MeV, low lying collective states, ang. distrib., DWBA double folding pot. anal. 0-78113  
 $^{40}\text{Ca}(p, p')$ , isovector dipole strength excitation in giant resonance region 0-83066  
 $^{40}\text{Ca}(p, p')$ , 800 MeV, high energy octupole giant resonance, ang. distrib. 0-86879  
 $^{41}\text{Ca}$  E2 resonance, cross sections and  $\gamma$ -spectrum from  $^{40}\text{Ca}(n, \gamma)$  0-57759  
 $^{41}\text{Ca}$ , spin and parity from  $^{38}\text{Ar}(\alpha, n\gamma)$  angular distrib. and linear polarisation of  $\gamma$  0-63079  
 $^{42}\text{Ca}$ , collective states, quasi-degenerate intrinsic Hamiltonian, variational methods 0-68505  
Cd even-even nuclei, low lying collective states, two-photon character 0-57667  
 $^A$ Cd,  $A=112, 114, 0_2^+$  and  $0_3^+$  states, E0, E2 transitions and collectivity 0-102144  
 $^A$ Cd( $^{16}\text{O}$ ,  $^{16}\text{O}$ ), 44 MeV,  $A=112, 114, 0_2^+, 0_3^+$  state collectivity, E0 and E2 decay,  $T_{1/2}$  0-73784  
 $^{102}\text{Cd}$  levels,  $J^\pi$  and positive parity decoupled band, rotor anal. of  $^{94}\text{Mo}(^{12}\text{C}, 3n\gamma)$  0-102096  
 $^{104}\text{Cd}$  quasirot. ground state band and  $\gamma$ -transition from  $^{102}\text{Pd}(\alpha, 2n\gamma)$  0-105955  
 $^{14}\text{Ce}$  collective M1 excitation effects on  $\gamma$ -ang. distrib., direct semidirect model of  $^{140}\text{Ce}(n, \gamma)$  0-57733  
 $^{250}\text{Cf}$  low spin states, bandheads,  $J^\pi$  and transitions from  $^{250}\text{Es}$  EC decay 0-105952  
 $^A$ Cs,  $A=119-133$  odd isotopes, collective props., bands and transitions from heavy ion reactions 0-68512  
 $^{127}\text{Cs}$  collective quadrupole dynamics, band struct., transitions, collective model anal. from  $^{127}\text{I}(\alpha, n)$  0-78112  
Dy deformed nuclei, particle ang. momentum alignment effects 0-68522  
Dy,  $N=85$  isotones, bands and transitions from  $\alpha$  and HI excitation, in-beam study 0-78123  
 $^A$ Dy,  $A=161, 163$ , Nilsson state  $\Delta N=2$  mixing, rot. bands from (d,t), (d,p) 0-95295  
 $^A$ Dy,  $A=161, 163$ , rotational bands, coupled-channels Born approx. anal. of  $^{162,164}\text{Dy}(d, t)$  0-83104  
 $^A$ Dy,  $A=162, 164$ , gamma to ground band transitions,  $\gamma$ - $\gamma$  directional correlations from (n, $\gamma$ ) 0-68579  
 $^{127}\text{Dy}$ , high spin state populations from  $^{124}\text{Sn}(^{32}\text{S}, 4n)$  0-57660  
 $^{127}\text{Dy}$  yrast isomers,  $\gamma$ -rays from compound nuclei 0-86789  
 $^{134}\text{Dy}$   $N=88$  nuclei quasirot. bands and  $J^\pi$  from beta-decay 0-83025  
Er, deformed nuclei, particle ang. momentum alignment effects 0-68522  
Er rotational nuclei, transition energy correlations, very high ang. momentum 0-86787  
 $^A$ Er,  $A=159, 160$ , energy levels, deexcitation  $\gamma$ -rays, g-factors and hyperfine interaction from  $^{28}\text{Si}(^{136}\text{Xe}, xn)$  0-102114  
 $^A$ Er,  $A=165, 167$ , rotational bands, coupled-channels Born approx. anal. of  $^{166,168}\text{Er}(d, t)$  0-83104  
 $^{156}\text{Er}$   $N=88$  nuclei quasirot. bands and  $J^\pi$  from EC decay 0-83025  
 $^{164}\text{Er}$  high spin props. in multiple band crossing region from ( $^{18}\text{O}, 4n\gamma$ ), ( $\alpha, 4n\gamma$ ), ( $^{136}\text{Xe}, ^{136}\text{Xe}\gamma$ ) 0-83023  
 $^{166}\text{Er}(\gamma, \gamma)$ , 14.4-16.6 MeV,  $\gamma$ -vibr. band head transitions, dynamic collective model 0-57662  
 $^{168}\text{Er}$   $\gamma$ -vibr. band, M1 admixtures in intra-band transitions 0-99149  
 $^{172}\text{Er}$  levels, bands,  $J^\pi$  and transitions from  $^{170}\text{Er}(t, p)$  0-83038  
 $^{145}\text{Eu}$  high spin levels, isomers and in-beam  $\gamma$ -spectroscopy from  $^{144}\text{Sm}(\alpha, 2np)$  0-78124  
 $^{146}\text{Eu}$   $9^+$  isomer,  $\gamma$ -decay, high spin particle-hole multiplet population from  $^{147}\text{Sm}(p, 2n)$  0-63066  
 $^{151}\text{Eu}$  narrow band and pickup strength, shape coexistence from (d,t) 0-86799  
 $^{153}\text{Eu}$   $5/2^+$  ground state rot. band,  $J^\pi$ , shape coexistence from (d,p) 0-86799  
 $^{154}\text{Eu}$  low lying levels, bands, transitions from  $^{153}\text{Eu}(n, \gamma)$  0-57694  
 $^A$ Fe( $p, \gamma$ )Co,  $A=54, 56$ , giant dipole resonance splitting, direct-semidirect capture model anal. 0-106055  
 $^{54}\text{Fe}$   $8^+$  and  $10^+$  level spin assignments and lifetimes from ( $^{16}\text{O}, 2p$ ), ( $^6\text{Li}$ , pn) 0-68531  
 $^{56}\text{Fe}(e, e')$ , Coulomb form factor for  $0^+ \rightarrow 4^+$  transition, collective  $4^+$  states, shell model 0-57664  
 $^{57}\text{Fe}$ , rot. band mixing microscopic theory using modified Kuo-Brown interaction 0-68513  
Ga, odd, single particle and collective degrees of freedom, clustering, shell model anal. 0-68510  
 $^A$ Ga,  $A=65, 67$ , high spin states and transitions from  $\text{Fe}+^{12}\text{C}(^{14}\text{N})$  0-68516  
 $^A$ Ga high spin states,  $J^\pi$  and transitions, triaxial struct. from ( $^{12}\text{C}, \alpha p$ ), ( $^{12}\text{Li}, Zn$ ) 0-63062  
Gd,  $N=85$  isotones, bands and transitions from  $\alpha$  and HI excitation, in-beam study 0-78123  
 $^A$ Gd,  $A=144, 146, 147, 148$ , high spin isomer g-factors yrast traps from ( $^{28}\text{Si}$ ,  $^{28}\text{Si}$ ), ( $\alpha, \alpha'$ ) 0-78146  
 $^{152}\text{Gd}$   $\beta$ - and octupole bands, downbending moments of inertia from  $^{150}\text{Sm}(\alpha, 2n)$  0-91131  
 $^{152}\text{Gd}$   $N=88$  nuclei quasirot. bands and  $J^\pi$  from EC decay and ( $\alpha, xn\gamma$ ) 0-83025  
 $^{152}\text{Gd}$ , vibrational states, B(E2) branching rates and interband transitions, pairing plus quadrupole calcs. 0-78127  
 $^{154}\text{Gd}$  levels, bands,  $J^\pi$ , DWBA anal. of  $^{152}\text{Gd}(t, p)$  0-78110  
 $^{154}\text{Gd}$ , vibr. state, level scheme,  $\gamma$  and conversion electron spectra from  $^{154}\text{Gd}(n, \gamma)$  0-57696  
 $^{159}\text{Gd}$ , rotational bands, coupled-channels Born approx. anal. of  $^{166}\text{Gd}(d, t)$  0-83104  
Ge, odd, single particle and collective degrees of freedom, clustering, shell model anal. 0-68510  
 $^A$ Ge,  $A=66, 69, 70$ , negative parity high spin states, spin and lifetimes from HI reactions 0-73768



## nuclear collective states and giant resonances continued

- <sup>16</sup>Ge excited state, J, mean lifetimes and transitions from <sup>64</sup>Za(<sup>7</sup>Li,p)  
<sup>19</sup>Ge excited state, J, mean lifetimes and transitions 0-68517  
<sup>60</sup>Ge high spin states, J assignment, decay scheme from <sup>55</sup>Mn(<sup>16</sup>O,pn)  
 0-68518  
<sup>4</sup>He( $\alpha,\alpha$ ), large amplitude collective motion, adiabatic TDHF calcs.  
 0-86786  
<sup>175</sup>Hf, three- and five-quasiparticle isomers, rotational bands and residual  
 interactions from <sup>170</sup>Er(<sup>4</sup>Be,4n) 0-83022  
<sup>178</sup>Hf, energy levels, K-forbidden decays, M4 decay of yrast state  
 0-68506  
<sup>190</sup>Hg, 21 ns isomer ( $\nu_{1/2}^{+2}$ ) interpretation from g-factor meas. 0-105945  
<sup>149</sup>Ho low lying yrast states from <sup>122</sup>Te(<sup>32</sup>S,X), <sup>121</sup>Sb(<sup>32</sup>S,X) 0-91151  
<sup>1</sup>I, A=115-127 odd isotopes, collective props., bands and transitions from  
 heavy ion reactions 0-68512  
<sup>1</sup>In, A=119, 121, unified model description, vibr. multiplet yrast struct.,  
 branching ratios 0-105953  
<sup>108</sup>In high spin struct., in-beam spectroscopy, conversion electrons from  
<sup>98</sup>Mo(<sup>13</sup>N,4ny) 0-73782  
<sup>109</sup>In high spin states,  $\gamma$ -transitions, ang. distrib. from <sup>108</sup>Cd( $\alpha,2n$ )  
 0-73783  
<sup>111</sup>In 21/2<sup>+</sup> isomeric state g-factor and relaxation time from <sup>109</sup>Ag( $\alpha,2n\gamma$ )  
 0-73794  
 Kr even-even isotopes, collective states and transitions, interacting boson  
 approx. 0-73773  
<sup>1</sup>Kr, A=79, 81, high spin E2 bands, J<sup>\*</sup>, transitions from Ge(<sup>10,11</sup>B,  $\chi\gamma$ )  
 0-63061  
<sup>78</sup>Kr bands, lifetimes and E2 transitions from interacting boson model and  
 (<sup>16</sup>O,p2n), (<sup>19</sup>Fe, $\alpha,2n$ ) 0-73771  
<sup>1</sup>La, A=125, 127, collective props., bands and transitions from heavy ion  
 reactions 0-68512  
<sup>139</sup>La(e,p), 15-25 MeV, T<sub>0</sub>+1 giant dipole resonance and characteristic  
 decay mode 0-78247  
<sup>1</sup>Mg, A=24,26, second order nonspherical quadrupole phonon effects  
 0-86790  
<sup>1</sup>Mg(p, p'), A=24, 26, isovector dipole strength excitation in giant resonance  
 region 0-83066  
<sup>24</sup>Mg ground and  $\gamma$ -bands, direct and multistep processes from ( $\alpha$ ,<sup>6</sup>He),  
 (p,t), (<sup>16</sup>O, <sup>16</sup>O) 0-102094  
<sup>26</sup>Mg K=2 band and alpha cluster model state point symmetry  
 0-105946  
<sup>26</sup>Mg, low spin rotational states, energy props., extended deformation  
 model 0-86785  
<sup>24</sup>Mg rotational band collectivity, shell model excitation in Sp(4, R) sym-  
 metry 0-102095  
<sup>24</sup>Mg, triaxial nuclei rots., extended cranked shape consistent oscillator  
 model 0-102133  
<sup>24</sup>Mg(p,p), 14-45 MeV, differential cross section and spin-flip probabili-  
 ties, giant resonances 0-73850  
<sup>26</sup>Mg(<sup>2</sup>He,<sup>3</sup>He), 4<sup>+</sup> states, B(E2) values, and band mixing, rot.-vibr.  
 model 0-83019  
<sup>98</sup>Mo vibration-rotation struct. and yrast levels from variable moment of  
 inertia model 0-73778  
<sup>13</sup>N giant dipole resonance population amplitude and phase, E1 reaction  
 amps. from <sup>12</sup>C(p, $\gamma_0$ ), pol. p 0-63145  
<sup>23</sup>N high spin states, excitation functions, nonstatistical effects,  
 Hauser-Feshbach anal. of <sup>12</sup>C(<sup>13</sup>N, $\alpha$ ) 0-106041  
<sup>96</sup>Nb giant particle hole resonances, Gamow-Teller strength from  
<sup>90</sup>Zr(p,n) 0-86877  
 Nd, N=85 isotones, bands and transitions from  $\alpha$  and HI excitation,  
 in-beam study 0-78123  
<sup>140</sup>Nd, A=138,139, high spin states, isomers and  $\gamma$ -cascade from <sup>140</sup>Cd( $\alpha$ ,  
 xzn) 0-78120  
<sup>140</sup>Nd, A=138,139, high spin states, J<sup>\*</sup>,  $\gamma$ -cascades and shape transition  
 from <sup>140</sup>Ce( $\alpha$ , xn) 0-102090  
<sup>140</sup>Nd Ns isomers and yrast isomers,  $\gamma$ -transitions from <sup>128</sup>Te(<sup>16</sup>O,4n)  
 0-78121  
<sup>148</sup>Nd, vibrational states, B(E2) branding rates and interband transitions,  
 pairing plus quadrupole calcs. 0-78127  
<sup>26</sup>Ne collective motion, B(E2) rates, algebraic formulation in symplectic  
 shell model 0-83015  
<sup>26</sup>Ne giant E1 resonance intermediate struct. from <sup>19</sup>F(p, $\gamma$ ), pol. and  
 unpol. 0-78251  
<sup>26</sup>Ne with backbending, first excited 4<sup>+</sup> state g-factor 0-78144  
<sup>51</sup>Ni high spin yrast cascade, decay modes J assignment from <sup>54</sup>Fe( $\alpha,n\gamma$ )  
 0-68514  
<sup>60</sup>Ni high spin states, J<sup>\*</sup>, T<sub>1/2</sub>, ang. distrib. and polarisations from  
<sup>56</sup>Fe(<sup>7</sup>Li, p2n $\gamma$ ) 0-99116  
<sup>237</sup>Np(e,f), 10-34 MeV, electrofission cross section, E2 transition mode  
 and giant resonances 0-106084  
<sup>16</sup>O, magic nuclei at collective excitations, energy spectrum and shape  
 (Russian) 0-106015  
<sup>16</sup>O, rotational band collectivity, shell model excitation in Sp(4, R) sym-  
 metry 0-102095  
<sup>16</sup>O(<sup>16</sup>O,<sup>16</sup>O), 10-41 MeV, molecular resonances  $\gamma$ -yield, band crossing  
 model 0-106032  
<sup>1</sup>O( $\gamma$ ,p)<sup>15</sup>N, electric quadrupole transition cross-sections, behind giant  
 resonance (Russian) 0-78281  
<sup>16</sup>O(e,e'), 80-165.7 MeV, giant dipole and quadrupole resonances, form  
 factors 0-102168  
<sup>1</sup>Os, A=182, 184, 186, high spin yrast states, back-bending 0-86802  
<sup>1</sup>Os, A=186-194, collective levels, transitions, mag. and quadrupole  
 moments, boson expansion theory 0-105954  
 Pb even isotopes, two quasiparticle 2<sup>+</sup> state coupling to T=0 giant quad-  
 rupole resonance 0-68618  
 Pb pairing vibr. band, microscopic struct. and wave functions from (p,t),  
 (t,p) 0-91126  
 Pb region, forbidden charge exchange collective modes,  $\beta$ - and  $\gamma$ -decay  
 processes 0-86784  
 Pb region, particle-vibration multiplet spectra, self-consistent framework  
 0-102089  
<sup>207</sup>Pb, muonic, octupole doublet isomer shifts, octupole vibr. 0-95750  
<sup>208</sup>Pb (e,e'), 2<sup>+</sup> giant resonance twist mode excitation, B(M2) values, form  
 factors 0-78246  
<sup>208</sup>Pb breathing model transition density, single particle and collective  
 state dynamical coupling 0-106007  
<sup>208</sup>Pb giant monopole and quadrupole resonances, multiple excitations  
 from ( $\alpha$ , $\alpha'$ )(d,d') 0-106031  
<sup>208</sup>Pb, magnetic high spin states, microscopic struct. 0-95297  
<sup>208</sup>Pb monopole vibr. vel. field, asymptotic form 0-78115  
<sup>208</sup>Pb(<sup>14</sup>N,<sup>14</sup>N'), 266 MeV, giant resonance excitation 0-78253

## nuclear collective states and giant resonances continued

- <sup>208</sup>Pb(<sup>208</sup>Pb, X), giant resonance polarisation pots. from nucleus-nucleus  
 effective pot. 0-78248  
<sup>208</sup>Pb( $\alpha,\alpha$ ), 172 MeV, giant resonance structures 0-91163  
<sup>208</sup>Pb(e,e'), 70-335 MeV, natural parity, high spin state excitation  
 0-63060  
<sup>208</sup>Pb(p,p'), 135 MeV, normal parity level excitation, J<sup>\*</sup>, differential cross  
 sections 0-57690  
<sup>208</sup>Pb(p,p'), 135 MeV, normal parity excitations, microscopic description,  
 NN interaction shape 0-57691  
<sup>208</sup>Pb(p,p'), 800 MeV, high energy octupole giant resonance, ang. distrib.  
 0-86879  
 Pd, even-even, collective states, B(E2), branching ratios and moments,  
 boson expansion method 0-102099  
<sup>101</sup>Pd nonyrast rotational states, transitions, T<sub>1/2</sub>, branching and mixing  
 ratios from <sup>92</sup>Zr(<sup>12</sup>C,3n) 0-105950  
<sup>141</sup>Pm medium spin states, J<sup>\*</sup>, transitions and shape from (p,2n), (<sup>3</sup>He,3n),  
 ( $\alpha$ ,4n) 0-86779  
<sup>145</sup>Pm level struct., J<sup>\*</sup> and lifetimes, cluster-vibr. model anal. of  
<sup>146</sup>Nd(p,2n) 0-91125  
<sup>149</sup>Pm levels, bands, transitions, in-beam spectroscopy, particle-rotor anal.  
 from <sup>150</sup>Nd(p,2n $\gamma$ ) 0-78125  
<sup>153</sup>Pm 5/2<sup>-</sup> h<sub>11/2</sub> dominated band, anomalous ang. distrib., CCBA calcs.  
 for <sup>154</sup>Sm(t, $\alpha$ ) 0-86788  
<sup>139</sup>Pr medium spin states, J<sup>\*</sup>, transitions and shape from (p,2n), (<sup>3</sup>He,3n),  
 ( $\alpha$ ,4n) 0-86779  
<sup>141</sup>Pr(e,p), 15-25 MeV, T<sub>0</sub>+1 giant dipole resonance and characteristic  
 decay mode 0-78247  
<sup>1</sup>Pt, A=188-198 collective levels, transitions, mag. and quadrupole  
 moments, boson expansion theory 0-105954  
 Pu, even isotopes, K=0<sup>+</sup>, 0<sup>-</sup> bands, energies, inverse moments of inertia  
 0-63063  
 Ra, even isotopes, K=0<sup>+</sup>, 0<sup>-</sup> bands, energies, inverse moments of inertia  
 0-63063  
 Rb odd-even isotopes, collective states and transitions, interacting boson  
 approx. 0-73773  
<sup>1</sup>Rb, A=79, 81, decoupled g<sub>9/2</sub> bands, level lifetimes and E2 transi-  
 tions from (<sup>16</sup>O, 2n)(<sup>19</sup>F, p2n) 0-73772  
<sup>83</sup>Rb band struct., spin assignments and transitions from (<sup>6</sup>Li,3n),  
 (<sup>16</sup>O,p2n), ( $\alpha$ ,2n) 0-73774  
<sup>83</sup>Rb high spin states, J $\pi$  and transitions from HI and  $\alpha$  reactions  
 0-105949  
<sup>83</sup>Rb high spin states, yrast cascade, J<sup>\*</sup>,  $\gamma$ -transitions from <sup>82</sup>Se(Li,xn $\gamma$ )  
 0-73775  
<sup>1</sup>Re, A=181,182,187, rotational struct., spin polarization 0-83016  
 Rn, even isotopes, K=0<sup>+</sup>, 0<sup>-</sup> bands, energies, inverse moments of inertia  
 0-63063  
 Ru, even-even, collective states, B(E2), branching ratios and moments,  
 boson expansion method 0-102099  
<sup>97</sup>Ru high spin states, band like structs., transitions from <sup>88</sup>Sr(<sup>12</sup>C,3n $\gamma$ )  
 0-73779  
<sup>33</sup>Si(p,p), 14-45 MeV, differential cross section and spin-flip probabilities,  
 giant resonances 0-73850  
 Sb, neutron rich nuclei, IBM and shell model approaches, collective modes  
 0-78129  
<sup>1</sup>Sb, A=113-175, odd isotopes, collective props., bands and transitions  
 from heavy ion reactions 0-68512  
<sup>125</sup>Sb high spin levels, gamma transition energies and intensities from  
<sup>125</sup>Sn $\gamma$ , decay 0-73819  
<sup>42</sup>Sc, J<sup>\*</sup>=19/2<sup>-</sup> isomer, high-spin precursors, from <sup>28</sup>Si(<sup>16</sup>O,pn) 0-57656  
<sup>48</sup>Sc spin-flip isovector giant resonance, T<sub>1</sub>, Gamow-Teller strength from  
<sup>48</sup>Ca(p,n) 0-106019  
<sup>1</sup>Se, A=74, 76, vibr. states and transition from dynamic deformation  
 theory 0-73770  
<sup>72</sup>Se side band struct., negative parity states and transitions from  
<sup>58</sup>Ni(<sup>16</sup>O,2p) 0-73769  
<sup>76</sup>Se high spin states, bands, J<sup>\*</sup>, transitions and T<sub>1/2</sub> from <sup>71</sup>Ga(<sup>7</sup>Li,2n)  
 0-105951  
<sup>25</sup>Si(p,p), 14-45 MeV, differential cross section and spin-flip probabilities,  
 giant resonances 0-73850  
<sup>25</sup>Si(<sup>7</sup>Be, <sup>7</sup>Be'), 45, 60 MeV, low lying collective states, ang. distrib.,  
 DWBA double folding pot. anal. 0-78113  
<sup>28</sup>Si( $\gamma$ ,p), 18.1-29 MeV, photoproton energy spectra, contribs. to giant  
 dipole resonance 0-78242  
<sup>28</sup>Si(p, p'), isovector dipole strength excitation in giant resonance region  
 0-83066  
<sup>28</sup>Si rot.-vibr. coupling effects, excitation spectrum and ang. distrib. from  
<sup>28</sup>Si(d, p) 0-57661  
 Si(<sup>208</sup>Pb,<sup>208</sup>Pb), giant multipole resonance region, optical model anal.  
 0-57719  
<sup>142</sup>Sm ns isomers and yrast isomers,  $\gamma$ -transitions from (<sup>24</sup>Mg,4n), (<sup>19</sup>F,4n)  
 0-78121  
<sup>150</sup>Sm, vibrational states, B(E2) branding rates and interband transitions,  
 pairing plus quadrupole calcs. 0-78127  
<sup>1</sup>Sm ground and  $\gamma$ -bands, direct and multistep processes from ( $\alpha$ ,<sup>6</sup>He),  
 (p,t), (<sup>16</sup>O,<sup>16</sup>O) 0-102094  
<sup>152</sup>Sm, giant multipole reson. fragmentation among two-phonon states  
 0-78238  
 Sn, even isotopes, collective states and transitions from simple phenome-  
 nological model 0-73787  
<sup>1</sup>Sn, A=106-108, yrast levels and transitions from <sup>54</sup>Fe(<sup>58</sup>Ni, X)  
 0-105957  
<sup>1</sup>Sn, A=112-124 even isotopes, 0<sup>+</sup> state collectivity, E0 and E2 transition  
 rates 0-73785  
<sup>1</sup>Sn(n,n'), A=116, 118, 120, 122, 11 MeV, octupole vibr. states, diff.  
 cross section, deformation length, DWBA anal. 0-102092  
<sup>112</sup>Sn 6<sup>+</sup> isomeric state g-factor and relaxation time from Cd( $\alpha,2n\gamma$ )  
 0-73794  
<sup>116</sup>Sn( $\alpha,\alpha'$ ), 96, 129 MeV, giant resonance excitation, isoscalar breathing  
 mode state, nuclear incompressibility 0-68620  
<sup>116</sup>Sn(p,p'), 800 MeV, high energy octupole giant resonance, ang. distrib.  
 0-86879  
<sup>1</sup>Sr, A=81, 83, yrast and high spin states of neutron deficient isotopes  
 from Kr( $\alpha$ ,xn) 0-73776  
<sup>1</sup>Sr, A=98, 100 rot. struct. sudden onset, gamma transitions from Rb  
 decay 0-73777  
<sup>84</sup>Sr( $\gamma$ , $\gamma$ ), 14 MeV, highly excited spin-1 resonances, spin and radiative  
 widths 0-86876  
<sup>84</sup>Sr(n,n'), 11 MeV, octupole vibr. states, diff. cross section, deformation  
 length, DWBA anal. 0-102092

**nuclear collective states and giant resonances continued**

- <sup>98</sup>Sr very low lying  $0^+$  state, shape coexistence bands,  $T_{1/2}$ , transitions from <sup>98</sup>Rb decay 0-78148
- <sup>17</sup>Ta, rotational struct., spin polarization 0-83016
- <sup>18</sup>Ta( $\gamma$ ,X), 3-30 MeV, photoabsorption cross section, giant dipole resonances 0-78254
- <sup>183</sup>Ta single proton states and rot. bands,  $J^\pi$  from <sup>186</sup>W( $t,\alpha$ ), pol. t 0-91130
- <sup>93</sup>Tc,  $J=17/2$  doublet, parity mixing, weak NN interaction 0-73791
- <sup>97</sup>Te high spin states, spins and transitions from <sup>94</sup>Zr( $^6$ Li,3n $\gamma$ ) 0-73780
- <sup>94</sup>Te,  $A=122,124,126$  yrast band double backbending, possible mechanisms (Chinese) 0-99120
- <sup>120</sup>Te quasi-rot. band based on proton 4p-2h state, level scheme, transitions from <sup>118</sup>Sn( $\alpha,2n\gamma$ ) 0-78119
- <sup>125</sup>Te low lying negative parity high spin states multistep induced population from (d,t)(<sup>4</sup>He, $\alpha$ ) 0-57657
- <sup>127</sup>Te, M1, giant resonance and radiative strength functions 0-57731
- Th, even isotopes,  $K=0^+$ ,  $0^-$  bands, energies, inverse moments of inertia 0-63063
- <sup>23</sup>Th excited states and bands, spins,  $\gamma$ -transitions from <sup>230</sup>Th(n, $\gamma$ ) 0-57699
- <sup>232</sup>Th( $\gamma$ ,X) 5-18.3 MeV, photoneutron and photofission cross sections, giant resonance and deformations 0-68712
- Ti(<sup>12,13</sup>C,X) 45, 46 MeV, particle-gamma coincidences, isotope assignment for yrast spectroscopy 0-68593
- <sup>48</sup>Ti( $\gamma$ ,n), 15-27.5 MeV, giant dipole resonance splitting, dynamic collective model 0-57755
- <sup>167</sup>Tm, energy level scheme from <sup>165</sup>Ho( $\alpha,2n\gamma$ ) (German) 0-68576
- <sup>167</sup>Tm, levels and transitions from <sup>165</sup>Ho( $\alpha,2n$ ) 0-73766
- <sup>167</sup>Tm rotational bands,  $J^\pi$ ,  $\gamma$ -transitions and branching ratios from <sup>165</sup>Ho( $\alpha,2n\gamma$ ) 0-86781
- U, even isotopes,  $K=0^+$ ,  $0^-$  bands, energies, inverse moments of inertia 0-63063
- <sup>A</sup>U( $\gamma$ ,X),  $A=235, 236, 238, 5-18.3$  MeV, photoneutron and photofission cross sections, giant resonance and deformations 0-68712
- <sup>238</sup>U collective and deformation props., general collective model 0-68627
- uncorrelated target, optical pot. unitary content, DWIA and Glauber theory from ( $\alpha,\alpha$ )( $\gamma$ ) 0-105947
- <sup>A</sup>W,  $A=170-182$ , even isotopes, yrast states, spectra and quad. moments, variation formulation 0-99119
- <sup>180</sup>W octupole vibr. states,  $J^\pi$  and transitions from <sup>180</sup>Re decay 0-83024
- <sup>181</sup>W levels (neutron and collective) and  $J^\pi$ , ang. distrib. from <sup>183</sup>W(p,t) 0-78160
- <sup>89</sup>Y, giant reson. pionic excitation 0-73834
- <sup>160</sup>Yb yrast levels, 2nd and 3rd backbending, cranked HFB calcs. 0-63064
- <sup>160</sup>Yb multiple band crossing, (gSS'S $^*$ S $^*$ ) system gamma correlation patterns 0-106008
- <sup>172</sup>Yb levels, bands,  $J^\pi$  and  $T_{1/2}$  from <sup>170</sup>Er( $\alpha,2n$ ) 0-91127
- <sup>A</sup>Zn( $\alpha,\alpha'$ ),  $A=64, 66, 129$  MeV, isoscalar giant monopole resonances, nuclear incompressibility 0-83083
- <sup>64</sup>Zn high spin states,  $J^\pi$ ,  $T_{1/2}$ ,  $\gamma$ -decays from ( $\alpha,n\gamma$ ), (<sup>11</sup>B,p2n $\gamma$ ) 0-73767
- <sup>66</sup>Zn negative parity high spin states, spin and lifetimes from HI reactions 0-73768
- <sup>85</sup>Zr yrast and high spin states of neutron deficient isotopes from Sr( $\alpha,xn$ ) 0-73776
- <sup>90</sup>Zr( $\alpha,\alpha'$ ), 96, 129 MeV, giant resonance excitation, isoscalar breathing mode state, nuclear incompressibility 0-68620
- <sup>90</sup>Zr( $e,e'$ ), 2- giant resonance twist mode excitation, B(M2) values, form factors 0-78246
- <sup>90</sup>Zr( $\gamma,\alpha$ ) statistical and pre-equilibrium cross sections and multipolarities from ( $e,\alpha$ ) 0-68646
- <sup>90</sup>Zr( $n,X$ ), 10-20 MeV, multiple giant resonance contrib. to optical pot. imaginary part 0-78241
- <sup>90</sup>Zr( $n,n'$ ), 11 MeV, octupole vibr. states, diff. cross section, deformation length, DWBA anal. 0-102092
- <sup>90</sup>Zr( $\pi,\pi'$ ), 226 MeV, giant reson. examination 0-73871

**nuclear coupling, molecular see molecular nuclear coupling****nuclear cranking model**

- <sup>29</sup>14, high spin pot. energy surfaces, fission barrier,  $\alpha$ -,  $\gamma$ -decay half lives, yrast spectrum 0-73764
- $A=12-208$ , adiabatic TDHF approx. isoscalar quadrupole collective motion, cranking mass 0-68507
- actinide nuclei, cranking model, collective inertia parameters 0-57665
- adiabatic TDHF approx., mass parameters, single collective variable, theoretical aspects 0-73765
- backbending nuclei, HFB cranking wave functions 0-83049
- band crossing anomalies, large angular momentum fluctuation 0-73815
- high spin rot. motion, TDHF cranking model and RPA descript. 0-102091
- N=82 region, high spin isomers, cranked HF calcs., deformation shapes, excitation energies 0-99121
- N=82 region, high spin isomers, deformation energy surface, shape constrained cranked HF theory 0-57666
- rare earth nuclei, cranking model, collective inertia parameters 0-57665
- rotating nuclei, current distrib., cranked HF model 0-63059
- rotational nuclei, high-spin, variable moment of inertia model, microscopic-macroscopic approach 0-63058
- S and ground band interaction in cranked HFB model 0-95299
- Woods-Saxon potential spectrum, pairing force strength, Nilsson model comparison 0-75704
- <sup>24</sup>Mg, triaxial nuclei rots., extended cranked shape consistent oscillator model 0-102133
- <sup>20</sup>Ne, moment of inertia from cranked HF method 0-102098

**nuclear decay schemes see radioactive decay schemes****nuclear decay theory**

- see also alpha decay theory; beta decay theory
- gamma transitions and coincidences, construction of decay schemes, SMUDLA code 0-83063
- rotational states, coherent,  $\gamma$ -decay, random quantum meas. 0-73855
- $t_{-dn}$  vertex constant from Faddeev eqn. (Russian) 0-83079
- <sup>28</sup>Si, highly excited <sup>12</sup>C- $\alpha$ -<sup>12</sup>C molecular state, symmetrical decay (Russian) 0-86861

**nuclear deformation see nuclear shape****nuclear density**

- kaon-nucleus reactions, low energy, nuclear density shape optical pot. kaonic atom level shifts 0-63213
- nuclear matter density determ., HF versus droplet model 0-68574

**nuclear density continued**

- oscillations, from semi-infinite nuclear matter calc., Regge type oscillation comparison 0-57671
- saturation in finite nuclei, nuclear matter density and binding energy 0-83029
- $\pi$  condensation in neutron matter, N-N interaction, critical density 0-57711
- <sup>A</sup>Ca,  $A=40, 48$ , nuclear matter density distrib., saturation effect, optical potential from ( $\alpha,\alpha$ ) 0-63115
- <sup>A</sup>Ca( $\alpha,\alpha'$ ),  $A=40, 42, 44, 48, 104$  MeV nuclear size and density distrib. from folding model anal. 0-68525
- <sup>3</sup>H realistic wave function, energy and density distrib. 0-86794

**nuclear electric moment**

- see also molecular nuclear coupling
- $A=12-240$ , even-even, dynamic deformation theory, B(E2) values, quadrupole and mag. moments 0-68591
- E0-conversion, reduced probability, quadrupole moment effect 0-78138
- even-even nuclei, static quadrupole moments of arbitrary excited states, sum rule approach 0-91135
- fission isomers, spectrosc. props. 0-105966
- laser-RF double reson. spectroscopy of nucl. quadrupole moments, <sup>55</sup>Mn and <sup>20</sup>V 0-57682
- octupole vibration, collective, wave functions, spherical harmonics 0-68532
- short living nuclear states, optical orientation,  $\gamma$ -spectrum anisotropy, lifetime, moments (Russian) 0-63090
- stable odd-mass sd nuclei, EM multipole moments of ground states 0-102116
- <sup>11</sup>B, quadrupole transitions from <sup>12</sup>C( $\gamma,p$ ) (Russian) 0-78281
- Ba, neutron deficient, charge radii, moments, transitions and isomers, atomic beam laser spectroscopy 0-102141
- <sup>4</sup>Ca,  $A=41, 43, 45$ , quadrupole moments, from hyperfine struct. splitting of <sup>45</sup>Ca<sup>3+</sup>P<sub>1</sub> 0-57674
- <sup>A</sup>Ca,  $A=47, 49$ , single particle states lifetimes calcs. 0-105943
- (d,d),  $A=24-54$ , pol. d, 20 MeV, quadrupole transition amplitudes 0-99148
- <sup>A</sup>Dy,  $A=156-164$ , deformation hexadecapole moments, Hartree-Fock calcs. (Russian) 0-63081
- <sup>A</sup>Er,  $A=162-170$ , deformation hexadecapole moments, Hartree-Fock calcs. (Russian) 0-63081
- <sup>A</sup>Gd,  $A=152-160$ , deformation hexadecapole moments, Hartree-Fock calcs. (Russian) 0-63081
- <sup>2</sup>H D-state probability lower bound, binding energy, quadrupole moment 0-91137
- <sup>A</sup>H,  $A=1, 2$ ; nuclear electric dipole moments from P nonconserving atomic transitions 0-57681
- <sup>A</sup>He,  $A=176-180$ , deformation hexadecapole moments, Hartree-Fock calcs. (Russian) 0-63081
- <sup>129</sup>He time depend. quadrupole interactions,  $\gamma$ - $\gamma$  correlations from <sup>129</sup>Te<sup>m+g</sup> decay 0-78145
- <sup>186,188,190</sup>Ir in Re crystal, electric quadrupole orientation, elec. field gradient 0-78140
- <sup>47</sup>K, single particle states lifetimes calcs. 0-105943
- <sup>138,139</sup>La, Fourier transform NMR 0-57354
- <sup>7</sup>Li charge form factor with resonating group wave function, quad. moment, charge radius 0-102110
- <sup>A</sup>Mo,  $A=95, 97$ , nucl. quadrupole moments from laser-RF double reson. spectroscopy 0-57682
- <sup>15</sup>N, quadrupole transitions from <sup>16</sup>O( $\gamma,p$ ) (Russian) 0-78281
- <sup>20</sup>Ne hexadecapole moments, quadrupole deformation effects, E4 effective charge, valence polarisation 0-78142
- <sup>A</sup>Os,  $A=182, 184, 186$ , high spin yrast states, back-bending 0-86802
- <sup>A</sup>Os,  $A=186-194$ , collective levels, transitions, mag. and quadrupole moments, boson expansion theory 0-105954
- Pd, even-even, collective states, B(E2), branching ratios and moments, boson expansion method 0-102099
- <sup>A</sup>Pt,  $A=188-198$  collective levels, transitions, mag. and quadrupole moments, boson expansion theory 0-105954
- Ru, even-even, collective states, B(E2), branching ratios and moments, boson expansion method 0-102099
- <sup>107</sup>Ru(<sup>16</sup>O,<sup>16</sup>O), 38-42 MeV, Coulomb excitation, 2<sup>+</sup> state electric quadrupole moment 0-73793
- <sup>107</sup>Ru( $\alpha,\alpha'$ ), 8.5, 9.0 MeV, Coulomb excitation, 2<sup>+</sup> state electric quadrupole moment 0-73793
- <sup>32</sup>S  $\alpha$ -cluster struct., ground and first excited states, energies, radii and moments 0-102122
- <sup>49</sup>Sc, single particle states lifetimes calcs. 0-105943
- <sup>A</sup>W,  $A=170-182$ , even isotopes, yrast states, spectra and quad. moments, variation formulation 0-99119
- <sup>A</sup>W,  $A=182-186$ , deformation hexadecapole moments, Hartree-Fock calcs. (Russian) 0-63081
- <sup>A</sup>Yb,  $A=168-176$ , deformation hexadecapole moments, Hartree-Fock calcs. (Russian) 0-63081

**nuclear electric shielding see nuclear screening****nuclear electromagnetic transitions see nuclear energy level transitions****nuclear electron capture**

- see also beta-decay
- internal bremsstrahlung in s-electron capture 0-63133
- radioactive decay constants, constancy limits 0-78217
- <sup>195</sup>Au decay, K-shell capture fractions, internal conversion electrons, coincidence techniques 0-57743
- <sup>206</sup>Pb EC decay, <sup>206</sup>Pb  $\gamma$  directional correlations, multipole mixing ratios, transition strength limits 0-86849
- <sup>207</sup>Pb EC decay, <sup>207</sup>Pb, 569.65-1063.63 keV cascade  $\gamma$ - $\gamma$  ang. correl. meas. 0-86847
- <sup>129</sup>Cs decay, <sup>129</sup>Xe excited state lifetimes,  $\gamma$ -transitions 0-78205
- <sup>250</sup>Es EC decay, <sup>250</sup>Cf low spin states, bandheads,  $J^\pi$  and transitions 0-105952
- <sup>A</sup>Eu EC decay,  $A=147, 149, 147, 149$  Sm levels,  $J$ ,  $\gamma$ -transitions and multipole mixing ratios,  $\gamma$ - $\gamma$  correlations 0-106012
- <sup>152</sup>Eu decay, <sup>152</sup>Sm  $\gamma$ -transition energy and intensity meas. 0-73818
- <sup>153</sup>Eu decay, Gd L<sub>2,3</sub> subshell X-ray fluorescence and Coster-Kronig yields 0-69102
- <sup>1</sup>H, capture probabilities for 4.25 and 61.8 MeV protons in a neutron beam facility 0-78222
- <sup>123</sup>I production from <sup>123</sup>Xe formed in spallation reactions by 660 MeV protons, medical appls. 0-85494
- Ir decay, oriented nuclei, <sup>188,189</sup>Os levels,  $J^\pi$ , transitions and mixing ratios 0-68602



**nuclear electron capture continued**

- <sup>169</sup>Lu decay, <sup>169</sup>Yb  $\gamma\gamma$  ang. correlations, levels and spins (*Russian*) 0-83069  
<sup>172</sup>Lu decay, identification of  $\gamma$ -spectra unplaced energies by delayed coincidence meas. 0-78221  
 Pt decay, oriented nuclei, <sup>189,191</sup>Ir levels,  $J^\pi$ , transitions and mixing ratios 0-68602  
<sup>180</sup>Re decay, <sup>180</sup>W octupole vibr. states,  $J^\pi$  and transitions 0-83024  
<sup>85</sup>Sr<sup>m,8</sup> decay, <sup>85</sup>Rb levels,  $J^\pi$  and transitions 0-78162  
<sup>180</sup>Ta<sup>m</sup>,  $\beta^-$  and EC branching ratios, K-internal conversion coeff.,  $\gamma$ -intensities, T 1/2 0-68601  
<sup>140</sup>Tb decay and T<sub>1/2</sub>, <sup>140</sup>Gd lowest 2<sup>+</sup> state,  $J^\pi$  and transitions 0-105979  
<sup>152</sup>Tb decay, <sup>152</sup>Gd N=88 nuclei quasirot. bands and  $J^\pi$  0-83025  
<sup>160</sup>Tb-<sup>160</sup>Dy,  $\gamma$ -transitions and angular distributions 0-83060  
<sup>156</sup>Tm decay, <sup>156</sup>Er N=88 nuclei quasirot. bands and  $J^\pi$  0-83025

**nuclear emulsions see nuclear track emulsions****nuclear energy see nuclear power****nuclear energy level lifetimes**

- <sup>116</sup>Xe quasi-rotational bands, levels  $J^\pi$  and T<sub>1/2</sub> from <sup>116</sup>Cs decay 0-83021  
<sup>298</sup>114, high spin pot. energy surfaces, fission barrier,  $\alpha$ -,  $\gamma$ -decay half lives, yrast spectrum 0-73764  
 A=134-144, fission yields from spectroscopic meas.,  $\gamma$ -branching and half-lives 0-78213  
 measurement using on-line computer and registration time shift compensation 0-68577  
 measurement using recoil distance method expts. 0-73825  
 short living nuclear states, optical orientation,  $\gamma$ -spectrum anisotropy, lifetime, moments (*Russian*) 0-63090  
<sup>104</sup>Ag levels,  $J^\pi$ , T<sub>1/2</sub>, bands and transitions from <sup>103</sup>Rh( $\alpha$ , 3n $\gamma$ ) 0-102093  
<sup>^</sup>As, A=71, 73, levels,  $J^\pi$ , transitions, T<sub>1/2</sub> from Se decay, Ge(<sup>3</sup>He,d), (p,xn $\gamma$ ) 0-57684  
<sup>21</sup>At levels,  $J^\pi$ , transitions and lifetimes from <sup>208</sup>Pb(<sup>7</sup>Li,X) 0-68542  
<sup>^</sup>Ba, A=135,137, Coulomb excitation, transition probabilities,  $\gamma$ -rays and level collectivity from (<sup>16</sup>O,<sup>16</sup>O), ( $\alpha,\alpha'$ ) 0-78201  
<sup>76</sup>Br<sup>m</sup> decay props., half life and  $\gamma$ -transitions, level scheme 0-83071  
<sup>14</sup>C first excited 0<sup>+</sup> state, lifetime and E<sub>0</sub> decay from (d,p), (<sup>13</sup>C,p) 0-102145  
<sup>^</sup>Ca, A=47, 49, single particle states lifetimes calcs. 0-105943  
<sup>^</sup>Ca parity doublet gamma lifetimes, 3/2 levels, parity mixing from <sup>40</sup>Ca(d,p $\gamma$ ) 0-78209  
<sup>^</sup>Cd(<sup>16</sup>O,<sup>16</sup>O), 44 MeV, A=112, 114, 0<sub>2</sub><sup>+</sup>, 0<sub>3</sub><sup>+</sup> state collectivity, E<sub>0</sub> and E<sub>2</sub> decay, T<sub>1/2</sub> 0-73784  
<sup>59</sup>Co, energy levels, lifetimes, deexcitation following (n,n' $\gamma$ ) studies 0-83059  
<sup>59</sup>Co level energies, branching ratios lifetimes and spins from (p,p'), ( $\alpha$ ,p $\gamma$ ) 0-63093  
<sup>51</sup>Cr, EM properties, lifetimes of 749 and 777 keV levels, E2/M1 mixing ratio 0-63127  
<sup>^</sup>Cu A=29,63, Doppler shift attenuation factors, level lifetimes, resonances from Ni(p, $\gamma$ ) 0-57741  
<sup>63</sup>Cu low excitation states, level struct. and lifetimes from <sup>60</sup>Ni( $\alpha$ ,p $\gamma$ ) 0-86813  
<sup>^</sup>Dy, A=159,161, lifetimes of low excited states, delayed e- $\gamma$  and  $\gamma\gamma$  coincidences (*Russian*) 0-68596  
<sup>152</sup>Dy 60 ns isomer deexcitation E<sub>2</sub> x- (or $\Delta$ ) transition, half life,  $\gamma\gamma$ -coincidence from <sup>152</sup>Gd( $\alpha$ ,4n) 0-86859  
<sup>151</sup>Er, lifetimes of excited states, delayed e- $\gamma$  coincidences (*Russian*) 0-68597  
<sup>18</sup>F 1.04 MeV state lifetime and  $\gamma$ -transition polarisation from <sup>18</sup>O(p,n) 0-106016  
<sup>54</sup>Fe 8<sup>+</sup> and 10<sup>+</sup> level spin assignments and lifetimes from (<sup>16</sup>O,2p), (<sup>^</sup>Li, pn) 0-68531  
<sup>68</sup>Fe low lying state mean lifetimes and transitions from <sup>64</sup>Zn(<sup>7</sup>Li,p2n) 0-68599  
<sup>140</sup>Gd, 0<sub>2</sub><sup>+</sup> state EM decay, T<sub>1/2</sub> and monopole strength 0-95310  
<sup>^</sup>Ge, A=66,69,70, negative parity high spin states, spin and lifetimes from HI reactions 0-73768  
<sup>19</sup>Ge excited state, J, mean lifetimes and transitions from <sup>64</sup>Za(<sup>7</sup>Li,p) 0-68517  
<sup>19</sup>Ge excited state, J, mean lifetimes and transitions 0-68517  
<sup>66</sup>Ge levels, lifetimes,  $J^\pi$  and transitions from <sup>58</sup>Ni(<sup>10</sup>B,pn $\gamma$ ) 0-73799  
<sup>17</sup>Hf, three- and five-quasiparticle isomers, rotational bands and residual interactions from <sup>170</sup>Er(<sup>4</sup>He, 4n) 0-83022  
<sup>15</sup>Ho, lifetimes of excited states, delayed e- $\gamma$  coincidences (*Russian*) 0-68597  
<sup>107</sup>In nucleus and K shell excitation, lifetime meas. from <sup>106</sup>Cd(p,p')<sup>106</sup>Cd 0-63130  
<sup>111</sup>In 21/2<sup>+</sup> isomeric state g-factor and relaxation time from <sup>109</sup>Ag( $\alpha$ ,2n $\gamma$ ) 0-73794  
<sup>112</sup>In low lying levels, transitions, T<sub>1/2</sub>, multipolarities and mixing ratios from <sup>112</sup>Cd(p,n $\gamma$ ) 0-68545  
<sup>191</sup>Ir, excited nuclei mean precession time depend. on  $\gamma$ -spectral width, g-factors (*Russian*) 0-78211  
<sup>^</sup>K(p,p $\gamma$ ), 1.58 MeV, parity doublet gamma lifetimes, 3/2 levels, parity mixing 0-78209  
<sup>44</sup>K excited levels,  $J^\pi$ , transitions and lifetimes from <sup>48</sup>Ca(p, $\alpha$ n) 0-68544  
<sup>^</sup>K, single particle states lifetimes calcs. 0-105943  
<sup>78</sup>Kr bands, lifetimes and E<sub>2</sub> transitions from interacting boson model and (<sup>16</sup>O,p2n), (<sup>18</sup>Fe, $\alpha$ 2n) 0-73771  
<sup>174</sup>Lu isomeric levels,  $\gamma$ -spectra, T 1/2 and decay modes from <sup>176</sup>Yb(p,3n) 0-99151  
<sup>171</sup>Lu excited state lifetimes,  $\gamma$ -transitions from  $\beta$ -decay transitions 0-78205  
<sup>89</sup>Mo<sup>0</sup> levels, transitions and half life from <sup>93</sup>Mo(p,p'3n) 0-86858  
<sup>23</sup>Na 0<sup>+</sup> level mean life, isovector mag. dipole transition from <sup>19</sup>F( $\alpha$ ,n) 0-68595  
<sup>141</sup>Nd low spin states ns lifetimes, particle rotor model interpretation from <sup>146</sup>Nd(d,p $\gamma$ ) 0-78207  
<sup>^</sup>Ni high spin states,  $J^\pi$ , T<sub>1/2</sub>, ang. distrib. and polarisations from <sup>56</sup>Fe(<sup>7</sup>Li, p2n $\gamma$ ) 0-99116  
<sup>20</sup>O first excited state, g-factor and lifetime from <sup>3</sup>H(<sup>18</sup>O, p $\gamma$ ) 0-102115  
<sup>30</sup>P T=1 state decay, lifetimes and branching ratios, analogue E<sub>2</sub> transitions from <sup>29</sup>Si(p, $\gamma$ ) 0-68598  
<sup>210</sup>Pb levels,  $J^\pi$ , transitions and lifetimes from <sup>208</sup>Pb(<sup>7</sup>Li,X) 0-68542  
<sup>10</sup>Pd nonyrast rotational states, transitions, T<sub>1/2</sub>, branching and mixing ratios from <sup>92</sup>Zr(<sup>12</sup>C,3n) 0-105950  
<sup>145</sup>Pm level struct.,  $J^\pi$  and lifetimes, cluster-vibr. model anal. of <sup>146</sup>Nd(p,2n) 0-91125

**nuclear energy level lifetimes continued**

- <sup>218</sup>Po, levels,  $J^\pi$ , transitions and lifetimes from <sup>208</sup>Pb+<sup>7</sup>Li 0-68542  
<sup>^</sup>Rb, A=79, 81, decoupled g<sub>9/2</sub> bands, level lifetimes and E<sub>2</sub> transitions from (<sup>16</sup>O, 2n), (<sup>19</sup>F, p2n) 0-73772  
<sup>94</sup>Rh,  $\gamma$ -spectrum and half-lives 0-83062  
<sup>21</sup>Rn, shell model states, semiempirical calcs. half lives, mag. moments, excitation functions 0-63083  
<sup>43</sup>Sc,  $J^\pi=19/2^-$  isomer, high-spin precursors, from <sup>29</sup>Si(<sup>16</sup>O,pn) 0-57656  
<sup>^</sup>Sc levels,  $J^\pi$ , transitions and lifetimes from (p,p')(<sup>^</sup>He,<sup>3</sup>He')( $\alpha,\alpha'$ ) 0-63091  
<sup>49</sup>Sc, single particle states lifetimes calcs. 0-105943  
<sup>76</sup>Se high spin states, bands,  $J^\pi$ , transitions and T<sub>1/2</sub> from <sup>71</sup>Ga(<sup>7</sup>Li,2n) 0-105951  
<sup>28</sup>Si 4<sup>+</sup> state lifetime by blocking effect method from <sup>27</sup>Al(p, $\alpha$ ) (*Russian*) 0-91152  
<sup>142</sup>Sm isomers, lifetimes and transitions from <sup>142</sup>Nd( $\alpha$ ,4n) 0-78122  
<sup>112</sup>Sn 6<sup>+</sup> isomeric state g-factor and relaxation time from Cd( $\alpha$ ,2n $\gamma$ ) 0-73794  
<sup>132</sup>Sn levels, isomers, lifetimes and transition probabilities from fission 0-78163  
<sup>98</sup>Sr very low lying 0<sup>+</sup> state, shape coexistence bands, T<sub>1/2</sub>, transitions from <sup>98</sup>Rb decay 0-78148  
<sup>100</sup>Tc  $\mu$ s isomers, isomeric transitions and mean lives from <sup>100</sup>Mo(p,n) 0-73803  
<sup>120</sup>Te quasi-rot. band based on proton 4p-2h state, level scheme, transitions from <sup>118</sup>Sn( $\alpha$ ,2n $\gamma$ ) 0-78119  
<sup>45</sup>V level scheme,  $\gamma$ -rays, level lifetimes, internal conversion from <sup>40</sup>Ca(Li,xn) 0-63085  
<sup>129</sup>Xe excited state lifetimes,  $\gamma$ -transitions from <sup>129</sup>Cs decay 0-78205  
<sup>172</sup>Yb levels, bands,  $J^\pi$  and T<sub>1/2</sub> from <sup>170</sup>Er( $\alpha$ ,2n) 0-91127  
<sup>64</sup>Zn high spin states,  $J^\pi$ , T<sub>1/2</sub>,  $\gamma$ -decays from ( $\alpha$ ,n $\gamma$ ), (<sup>11</sup>B,p2n $\gamma$ ) 0-73767  
<sup>66</sup>Zn negative parity high spin states, spin and lifetimes from HI reactions 0-73768

**nuclear energy level transitions**

- see also internal conversion; Mossbauer effect; nuclear branching and mixing ratios; nuclear energy level lifetimes*  
<sup>298</sup>114, high spin pot. energy surfaces, fission barrier,  $\alpha$ -,  $\gamma$ -decay half lives, yrast spectrum 0-73764  
 A=120-150, levels and EM props., recent results 0-68592  
 A=12-240, even-even, dynamic deformation theory, B(E2) values, quadrupole and mag. moments 0-68591  
 A=134-144, fission yields from spectroscopic meas.,  $\gamma$ -branching and half-lives 0-78213  
 A=135-143, odd A fission products, delayed n, decay studies and Q<sub>B</sub> meas. 0-78227  
 A=184, 194, 200, 208, pygmy resonance, E1 transition probabilities, BCS wave functions, spin-isospin oscillation (*Chinese*) 0-63087  
 A=18-38, inelastic scatt. E4 transition probabilities in the 0d, 1s shell 0-78210  
 A=1-257, nuclear excitation by atomic electron transitions, nuclear levels 0-78191  
 A=54-82, ground state transition strengths from (p,t) reactions 0-95305  
 A=73, nuclear data sheets, levels,  $J^\pi$  and transitions 0-101673  
 A=77, nuclear data sheets, levels,  $J^\pi$  and transitions 0-105439  
 A=7-40, EM transition strength distrib. (*Russian*) 0-86855  
 A~90 nuclei, isomeric states, spin polarisation, M4 transitions and giant resonances 0-63157  
 actinide nuclei, even-even, E<sub>2</sub> transitions from 2<sup>+</sup> state of gamma-vibrational band 0-91150  
 average resonance neutron capture, completeness in nuclear spectroscopy 0-106006  
 B(E<sub>2</sub>) values of gamma-ray cascades and empirical relation 0-91145  
 band crossing in interacting boson model, E<sub>2</sub> transition probabilities and g-factors 0-102101  
 common doorway resonance, decay amplitude phase relation from (n, $\gamma$ ) reactions 0-57758  
 conference on medium heavy nuclei structure, Rhodes, Greece (May 1979) 0-67935  
 conference on nuclear spectroscopy of fission products, Grenoble, France (May 1979) 0-77546  
 decay scheme construction from gamma transitions and coincidences, SMUDLA code 0-83063  
 deep inelastic heavy ion reactions, high multipole isovector modes and charge fluctuations 0-57793  
 doubly even nuclei, yrast band B(E<sub>2</sub>) values, hydrodynamical model and CAP effect 0-86793  
 E1 transition selection rule, light nuclei transition strengths 0-106014  
 electric dipole sum rule in correlated nuclear matter 0-83056  
 even-even neutron-rich fission products, de-excitation spectra,  $\beta$ -decay, deformation 0-78203  
 even-even nuclei, spectra calcs., interacting boson model 0-68590  
 excited nuclear levels, polarisation induced by  $\alpha$  orientation 0-91144  
 generalised vibrational rule 0-105971  
 giant dipole resonance intermediate struct. using (n, $\gamma$ ) and ( $\gamma$ , n), Brink hypothesis test 0-63150  
 half life measurements for 35 radioisotopes 0-83070  
 heavy ion reactions, 10-200 MeV/n, Markovian and non-Markovian effects in transition probabilities 0-102175  
 hole excitation spectrum in finite Fermi system, many body field theory 0-102105  
 I-forbidden M1 transitions, shell effects, reduced transition probabilities 0-68594  
 level density in large spectroscopic spaces, statistical spectroscopic methods 0-86814  
 light deformed nuclei, Skyrme interaction spin components, spectra, projected HF theory 0-73820  
 linear polarisation mixing coeffs. for mixed dipole and quadrupole  $\gamma$ -radiations, Compton polarimeter 0-73110  
 magic and doubly magic nuclei, A=129, 131, 133 chains, 0<sup>+</sup> states, spectroscopy 0-78165  
 mesoatoms, prompt fission internal  $\gamma$ -ray conversion, fragment radiative transitions (*Russian*) 0-86944  
 muonic atoms, energy shifts and polarisability of deformed nuclei 0-86893  
 N=5 shell, deformed odd-neutron nuclei, band ordering and spectrum 0-83018  
 N=82 region, high spin isomers, cranked HF calcs., deformation shapes, excitation energies 0-99121

## nuclear energy level transitions continued

- neutron capture, total radiative width and degree of freedom, statistical model calcs. 0-57732
- neutron rich nuclei;  $\beta^-$ -emitters, deformation and spectroscopy 0-78223
- neutron rich transitional fission fragments, spectroscopy,  $0^+$  states and octupole vibr.: 0-78204
- nuclei far from stability,  $\beta$ -decay energies,  $\gamma$ -rays,  $Q_\beta$  values and masses 0-78225
- odd nuclei, soft and deformed, rotor plus quasiparticle approach, moments, transition probabilities 0-78214
- odd-A nuclei,  $O(6)$  spectra, interacting boson-fermion model, new coupling scheme 0-57727
- pairing correlation treatment, single particle levels, binding energy, spectra, branching ratios (*Chinese*) 0-102107
- radionuclide decay, computer simulation, levels, transitions, internal conversion 0-63136
- rare earth nuclei, even-even,  $E_2$  transitions from  $2^+$  state of gamma-vibrational band 0-91150
- rotational states, coherent,  $\gamma$ -decay, random quantum meas. 0-73855
- short living nuclear states, optical orientation,  $\gamma$ -spectrum anisotropy, lifetime, moments (*Russian*) 0-63090
- spherical nuclei, compound state  $\gamma$ -transitions, reduced  $\gamma$ -widths, Wigner stat. matrix method (*Russian*) 0-68587
- XX  $^{136}\text{Xe}$ ,  $2_2^+ \rightarrow 2_1^+$  transition multipole mixing ratio 0-78198
- (d,d'),  $A=40$  to 208, 108 MeV, giant monopole resonance excitation and ang. distrib. 0-102164
- (d,Li),  $A=60, 116$ ,  $L=0$  transitions, cross sections, microscopic anal. 0-78189
- (e,e'), light and medium nuclei, high energy approx. anal., transition densities and probabilities (*Russian*) 0-63129
- ( $\gamma$ ,d), odd-Z light nuclei, from (e,e'd), cross section, E2 transistors giant resonance and clusters 0-63169
- ( $\gamma$ , $\gamma$ ), 2.5-3.5 MeV, level photoexcitation 0-78193
- (n, $\gamma$ ) gamma ray study at Tehran nuclear research centre 0-57735
- (n, $\gamma$ ), (n, $\gamma$ ), low energy  $\gamma$ -transitions between compound states, statistical theory 0-57737
- (n,n $\gamma$ ),  $A=19$ -207, neutron scattering resonance radiative widths 0-99146
- (p,d), 51.9 MeV, forbidden transition ang. distrib., CCBA and DWBA anal. 0-86848
- $\pi$ - and  $\rho$ -exchange pots., influence on mag. resonances, mag. moments, and transition probabs. 0-99133
- $\pi$  absorption at rest, high spin state excitation,  $\pi$ -condensation and  $\Delta^{++}$  (*Russian*) 0-86927
- $^{18}\text{O}(\gamma,\sigma_0)$ , 19-32 MeV, E1 and E2 cross section, E1-E2 phase difference 0-63172
- $^{230}\text{Ac}$  levels,  $J^\pi$  and transitions, Nilsson assignments from  $^{230}\text{Ra}$  decay 0-68543
- $A_\pi$ ,  $A=105$ -109, negative parity states, EM props. from particle-asymmetric rotor model 0-102097
- $^{103}\text{Ag}$  collective excitation and  $J^\pi$  following  $^{94}\text{Mo}(^{12}\text{C},p2n\gamma)$ , rotor-plus-particle model 0-86782
- $^{103}\text{Ag}$  high spin states, bands transitions, intermediate deformation Coriolis coupling from ( $^{3,4}\text{He}$ , xn $\gamma$ ) 0-105944
- $^{104}\text{Ag}$  levels,  $J^\pi$ ,  $T_{1/2}$ , bands and transitions from  $^{103}\text{Rh}(\alpha, 3n\gamma)$  0-102093
- $^{106}\text{Ag}$  low-lying excited states from  $^{103}\text{Rh}(\alpha,n\gamma)$  and  $^{104}\text{Pd}(\alpha,n\gamma)$  0-57693
- $^{108}\text{Ag}$  levels and  $\gamma$ -transitions, population-spin correlation from  $^{107}\text{Ag}(n,\gamma)$  0-63097
- $^{110}\text{Ag}$ , 118.718 keV isomer, low lying states and transitions, coincidence study from  $^{109}\text{Ag}(n,\gamma)$  0-73806
- $A_{\text{M}}$ ,  $A=24, 25, 26$ , giant M1 strength, comparison with cross sections from  $\text{Mg}(p,n)$  0-86878
- $A_{\text{M}}$ ,  $A=25, 26, 27$  levels, resonances,  $\gamma$ -ray branching ratios from  $\text{Mg}(p,\gamma)$  0-86875
- $^{24}\text{Al}$ , effective M3 matrix elements and transitions from shell model 0-102143
- $^{26}\text{Al}$   $T=1$  states, resonances,  $J^\pi$  and transitions from  $^{25}\text{Mg}(p,\gamma)$  0-99131
- $^{27}\text{Al}$  isobaric analogue resonances, spectroscopic factors and  $\gamma$ -rays from (p,p), (p, $\gamma$ ) 0-86873
- $^{27}\text{Al}$  levels, resonances,  $J^\pi$ , branching and mixing ratios from  $^{26}\text{Mg}(p,\gamma)$  0-99132
- $^{27}\text{Al}(e,e')$ , 70-340 MeV, odd parity state electroexcitation, form factors, transition probabs. 0-78208
- $^{28}\text{Al}$  levels, transitions and spin from  $^{27}\text{Al}(n,\gamma)$ , pol. Al and n 0-78153
- $^{35}\text{Ar}$  levels, transitions and  $\beta$ -delayed protons from  $^{35}\text{K}$  decay 0-91156
- $^{36}\text{Ar}$  deduced levels from  $^{36}\text{K}$  beta-delayed particle emission 0-83074
- As isotopes, levels and spectra from broken pair model 0-73801
- As excited states, excitation functions and decays ang. distrib., cross sections from  $^{76}\text{Ge}(p,n\gamma)$  (*Russian*) 0-63089
- $^{209}\text{At}$ ,  $\gamma$ -transition, multipolarities, level scheme following  $^{208}\text{Rn}$  decay 0-83072
- $^{213}\text{At}$  levels,  $J^\pi$ , transitions and lifetimes from  $^{208}\text{Pb}(^7\text{Li},X)$  0-68542
- $^9\text{B}$  complex system, excitation functions for 17.19 and 17.64 MeV levels from  $^4\text{Li}+^3\text{He}$  0-78188
- Ba, neutron deficient, charge radii, moments, transitions and isomers, atomic beam laser spectroscopy 0-102141
- $A_{\text{Ba}}$ ,  $A=132, 134, 136$ , negative parity states,  $J^\pi$ , transitions, DWBA anal. of Ba(p, t) 0-86810
- $A_{\text{Ba}}$ ,  $A=135, 137$ , Coulomb excitation, transition probabilities,  $\gamma$ -rays and level collectivity from ( $^{16}\text{O}$ ,  $^{16}\text{O}$ ), ( $\alpha,\alpha'$ ) 0-78201
- $A_{\text{Ba}}$ ,  $A=142, 144, 146$ , transition  $\gamma$ - $\gamma$  ang. correlations, levels,  $J^\pi$ , mixing ratios 0-73823
- $^{133}\text{Ba}$ , 12.34 keV M1 transition 0-106004
- $^{142}\text{Ba}$ ,  $\gamma\gamma$  ang. correlations, levels, spins and mixing ratios from  $^{142}\text{Cs}$  decay 0-57734
- $^7\text{Be}$  effective for charge exchange analogues of Gamow-Teller transitions from  $^7\text{Li}(p,n)$  0-57726
- $^8\text{Be}$  collective excitation spectra from generalised hyperspherical functions method (*Russian*) 0-91133
- $^9\text{Be}$  low lying spectrum, 3-body molecular description, adiabatic one level approx. 0-78150
- $^{10}\text{Be}$ , excited states and spectra, continuum effects calcs. 0-57720
- $^{208}\text{Bi}$ ,  $0^+$  IAS, spreading width and isospin impurity, isovector monopole state influence 0-78155
- $^{209}\text{Bi}$  energy and transition probability convergence in Dyson's boson expansion 0-78206
- $^{76}\text{Bi}$  decay props., half life and  $\gamma$ -transitions, level scheme 0-83071
- CC  $^{20}\text{Ne}$   $8^+$  level radiative width, resonance strength from  $^{16}\text{O}(\alpha,\gamma)$  0-83065

## nuclear energy level transitions continued

- $^{12}\text{C}$   $1^-(T=1, 15.1 \text{ MeV})$  state excitational pionic modes, M1 form factor for (p,p'), (e,e') 0-78195
- $^{12}\text{C}$  gamma line Doppler broadening in  $^{12}\text{C}(n,n'\gamma)^{12}\text{C}$  and  $^9\text{Be}(\alpha,n\gamma)^{12}\text{C}$ , 4438 keV 0-91147
- $^{12}\text{C}$  isovector M1 excitations, current and spin contribs. from (e,e'), (p,n) 0-68582
- $^{12}\text{C}+^{12}\text{C}$  gross struct. resonances in excitation functions from  $^{12}\text{C}(^{12}\text{C}, ^{10,11}\text{B})$  0-102167
- $^{12}\text{C}(^{12}\text{C},\alpha)$ , 7-15 MeV, excitation function statistical anal., nonstatistical features 0-99167
- $^{12}\text{C}(^{14}\text{N},\alpha)$ , 10.1-15.9 MeV, forward angle excitation function structure, nonstatistical struct. 0-86885
- $^{12}\text{C}(^{16}\text{O},^{16}\text{O})$ , elastic and inelastic, 23-32 MeV, strong absorption region resonances, excitation functions 0-86884
- $^{12}\text{C}(^{16}\text{O},\alpha)$ ,  $^{24}\text{Mg}$  low spin resonances, excitation functions and ang. distrib. 0-63151
- $^{12}\text{C}(^{28}\text{Si},\alpha X)$ , 87-91.5 MeV,  $\alpha$ -HI angular correlations, excitation functions, statistical anal. 0-86915
- $^{12}\text{C}(K^+, K^+)$ , form factors, cross sections, interior probing capability 0-73866
- $^{12}\text{C}(\gamma,\gamma)$ , 23.5-39 MeV, cross sections and giant resonances, E2 strength 0-63122
- $^{12}\text{C}(\gamma,\gamma)$ , total photoabsorption and elastic cross sections, spectroscopic information (*Russian*) 0-83095
- $^{12}\text{C}(p,p')$ , 122 MeV, level excitation, cross sections, effective NN interaction, DWIA anal. 0-78197
- $^{12}\text{C}(p,p')$ , 22-27 MeV,  $1^+$  state de-excitation  $\gamma$ -ray ang. distrib., tensor force effects, DWBA anal. 0-68580
- $^{12}\text{C}(p,p')$ , pol. p, 800 MeV, unnatural parity states excitation, anal. powers and isospin 0-68538
- $^{12}\text{C}(\pi,\pi^*)$ ,  $A^*$  excitation,  $A^*$  model unified description 0-102205
- $^{13}\text{C}(^{12}\text{C},^{12}\text{C})$ , molecular neutron orbit formation,  $1/2^+$  state excitation, coupled channels calcs. 0-78156
- $^{13}\text{C}(\alpha,\alpha')$ , 22, 36 MeV, resonant state line shapes 0-91148
- $^{13}\text{C}(\gamma,n)$ , 6.5-9.3 MeV, ang. distrib., E1, M1 and E2 excitations, resonance radiative widths 0-68581
- $^{14}\text{C}$  first excited  $0^+$  state, lifetime and  $E^0$  decay from (d,p), ( $^{13}\text{C},p$ ) 0-102145
- $^{14}\text{Ca}$ ,  $A=44, 46$  excited states and transition ang. distrib. from  $\text{Ti}(^{14}\text{C},^{16}\text{O})$  0-93308
- $^{14}\text{Ca}(e,e')$ , backward scatt.,  $A=40, 42, 44, 48$ , mag. dipole ground state transition search 0-106009
- $^{14}\text{Ca}(p,p')$ , pol. p,  $A=40, 48$ , 800 MeV, diff. cross sections, anal. powers, DWIA anal., high spin levels 0-83067
- $^{40}\text{Ca}$ , magic nuclei at collective excitations, energy spectrum and shape (*Russian*) 0-106015
- $^{40}\text{Ca}(^6\text{Be},^6\text{Be})$ , 45, 60 MeV,  $1^-$  state excitation Frahn scaling formula for cross section 0-102136
- $^{40}\text{Ca}(d,d)$ , 4.5-5.4 MeV, excited states, excitation functions and ang. distrib., statistical anal. 0-57686
- $^{40}\text{Ca}(p, p')$ , isovector dipole strength excitation in giant resonance region 0-83066
- $^{40}\text{Ca}(p,p,\gamma)$ , 6.25 MeV, triple ang. correlation,  $3^-$  exit channel, resonances, single particle states 0-68626
- $^{40}\text{Ca}(p,p')$ , DWIA test in Glauber theory, transition density 0-99173
- $^{40}\text{Ca}$ , E2 core polarisation charge, Woods-Saxon shell model compared to harmonic oscillator model 0-63072
- $^{40}\text{Ca}$ , E2 resonance, cross sections and  $\gamma$ -spectrum from  $^{40}\text{Ca}(n,\gamma)$  0-57759
- $^{41}\text{Ca}$  excited states, excitation functions and ang. distrib., statistical anal. from  $^{40}\text{Ca}(d,p)$  0-57686
- $^{41}\text{Ca}$ , spin and parity from  $^{38}\text{Ar}(\alpha,n\gamma)$  angular distrib. and linear polarisation of  $\gamma$  0-63079
- $^{45}\text{Ca}$  levels, excitation functions and  $J^\pi$  from  $^{45}\text{K}$   $\beta$ -decay 0-105978
- $\text{Cd } 2^+$  excitation,  $\alpha$ -spectroscopic factors in IBA model from  $\text{Sn}(d,^6\text{Li})$  0-105967
- $^{112}\text{Cd}$ ,  $A=112, 114, 0_2^+$  and  $0_3^+$  states, E0, E2 transitions and collectivity 0-102144
- $^{112}\text{Cd}(^{16}\text{O},^{16}\text{O})$ , 44 MeV,  $A=112, 114, 0_2^+, 0_3^+$  state collectivity, E0 and E2 decay,  $T_{1/2}$  0-73784
- $^{103}\text{Cd}$  levels,  $J^\pi$  and positive parity decoupled band, rotor anal. of  $^{94}\text{Mo}(^{12}\text{C}, 3n\gamma)$  0-102096
- $^{104}\text{Cd}$  quasirot. ground state band and  $\gamma$ -transition from  $^{102}\text{Pd}(\alpha,2n\gamma)$  0-105955
- $^{111}\text{Cd}$ , 1330 keV level excitation cross section from positron annihilation 0-68583
- $^{112}\text{Cd}$ , E0 transition from  $0_1^+$  state following  $^{112}\text{In}$  beta decay 0-68578
- $^{141}\text{Ce}$  collective M1 excitation effects on  $\gamma$ -ang. distrib., direct semidirect model of  $^{140}\text{Ce}(n,\gamma)$  0-57733
- $^{250}\text{Cf}$  low spin states, bandheads,  $J^\pi$  and transitions from  $^{250}\text{Es}$  EC decay 0-105952
- $^{37}\text{Cl}$ ,  $A=34, 38$ , effective M3 matrix elements and transitions from shell model 0-102143
- $^{36}\text{Cl}$  anomalous M1/E1 strength ratio and doorway states from  $^{35}\text{Cl}(n,\gamma)$  0-57730
- $^{59}\text{Co}$ ,  $A=55, 59$ , energy levels from  $\text{Ni}(p_{\text{pp}},\alpha)$  0-68663
- $^{59}\text{Co}$  state alignment,  $\gamma$ -transitions and ang. distrib. from  $^{56}\text{Fe}(p,\gamma)$  0-73797
- $^{59}\text{Co}$ , energy levels, lifetimes, deexcitation following (n,n' $\gamma$ ) studies 0-83059
- $^{59}\text{Co}(\alpha,xnp)$ , 20-172.5 MeV, cross sections excitation functions, hybrid model, preequilib. effects 0-57784
- $^{49}\text{Cr}$  levels, transitions, and Gamow-Teller matrix elements from  $^{49}\text{Mn}$ ,  $\beta^+$ -decay 0-57746
- $\text{Cs}$ , fission fragment, delayed neutron branches from  $\gamma$ -spectroscopy 0-78230
- $^{137}\text{Cs}$ ,  $A=119$ -133 odd isotopes, collective props., bands and transitions from heavy ion reactions 0-68512
- $^{137}\text{Cs}$ ,  $A=142, 144, 146$ , low lying levels,  $J^\pi$ , mixing ratios and  $\gamma$ - $\gamma$  ang. correlations 0-102119
- $^{123}\text{Cs}(^{123}\text{mCs})$ , gamma and conversion electron radiation 0-106017
- $^{123}\text{Cs}$  collective quadrupole dynamics, band struct., transitions, collective model anal. from  $^{127}\text{In}(\alpha,n)$  0-78112
- $^{134}\text{Cs}$  176.403 keV isomer, populating  $\gamma$ -rays, low lying levels from  $^{133}\text{Cs}(n,\gamma)$ ,  $^{134}\text{Cs}$  176.403 keV isomer, populating  $\gamma$ -rays, low lying levels 0-78200
- $^{64}\text{Cu}$ ,  $A=29, 63$ , Doppler shift attenuation factors, level lifetimes, resonances from  $\text{Ni}(p,\gamma)$  0-57741
- $^{63}\text{Cu}$  levels, transitions and ang. distrib. from  $\alpha$ -transfer in  $^{59}\text{Co}(^6\text{Li},d)$  0-73798



nuclear energy level transitions continued

<sup>63</sup>Cu low excitation states, level struct. and lifetimes from <sup>60</sup>Ni( $\alpha$ , $\gamma$ ) 0-86813  
<sup>63</sup>Cu state alignment,  $\gamma$ -transitions and ang. distrib. from <sup>62</sup>Ni( $p$ , $\gamma$ ) 0-73797  
<sup>63</sup>Cu( $p$ , $p'$ ) negative parity level excitation, gamma ray obs., test for core excitation model 0-68534  
(d,d), A=24-54, pol.d., 20 MeV, quadrupole transition amplitudes 0-99148  
Dy K-shell internal conversion yields, gamma transition multipolarities from ( $\alpha$ ,xn), (<sup>12</sup>C,xn) 0-78215  
Dy, N=85 isotones, bands and transitions from  $\alpha$  and HI excitation, in-beam study 0-78123  
<sup>A</sup>Dy A=162, 164, gamma to ground band transitions,  $\gamma$ - $\gamma$  directional correlations from (n, $\gamma$ ) 0-68579  
<sup>152</sup>Dy 60 ns isomer deexcitation E2 x- (or $\Delta$ ) transition, half life,  $\gamma$ - $\gamma$  coincidence from <sup>152</sup>Gd( $\alpha$ ,n) 0-86859  
<sup>152</sup>Dy yrast isomers,  $\gamma$ -rays from compound nuclei 0-86789  
<sup>160</sup>Dy,  $\gamma$  transitions following <sup>160</sup>Tb decay 0-83060  
Er  $\gamma$ -multiplicities and cross sections, neutron evaporation from <sup>130</sup>Te(<sup>3</sup>S,X), (<sup>16</sup>,<sup>18</sup>O,X) 0-73824  
Er rotational nuclei, transition energy correlations, very high ang. momentum 0-86787  
<sup>A</sup>Er, A=159,160, energy levels, deexcitation  $\gamma$ -rays, g-factors and hyperfine interaction from <sup>28</sup>Si(<sup>136</sup>Xe, xn) 0-102114  
<sup>164</sup>Er high spin props. in multiple band crossing region from (<sup>18</sup>O,4n $\gamma$ ), ( $\alpha$ ,4n $\gamma$ ), (<sup>136</sup>Xe,<sup>136</sup>Xe $\gamma$ ) 0-83023  
<sup>164</sup>Er( $\gamma$ , $\gamma$ ), 14.4-16.6 MeV,  $\gamma$ -vibr. band head transitions, dynamic collective model 0-57662  
<sup>168</sup>Er, 80 and 1094 keV states, g-factors from ang. correlation methods 0-83035  
<sup>168</sup>Er  $\gamma$ -vibr. band, M1 admixtures in intra-band transitions 0-99149  
<sup>172</sup>Er levels, bands, J $^{\pi}$  and transitions from <sup>170</sup>Er(t,p) 0-83038  
<sup>145</sup>Eu high spin levels, isomers and in-beam  $\gamma$ -spectroscopy from <sup>144</sup>Sm( $\alpha$ ,2np) 0-78124  
<sup>146</sup>Eu 9 $^{+}$  isomer,  $\gamma$ -decay, high spin particle-hole multiplet population from <sup>147</sup>Sm( $p$ ,2n) 0-63066  
<sup>152</sup>Eu 89.848 keV isomeric state feeding, delayed coincidence meas., level scheme from <sup>151</sup>Eu(n, $\gamma$ ) 0-63126  
<sup>153</sup>Eu, EM transitions, multipole, internal conversion coeffs. (Russian) 0-63121  
<sup>154</sup>Eu low lying levels, bands, transitions from <sup>153</sup>Eu(n, $\gamma$ ) 0-57694  
<sup>18</sup>F 1.04 MeV state lifetime and  $\gamma$ -transition polarisation from <sup>18</sup>O(p,n) 0-106016  
<sup>18</sup>F resonances,  $\alpha$ -widths, isospin and parity mixing, R-matrix anal. of <sup>14</sup>N( $\alpha$ , $\alpha$ ) 0-91162  
<sup>19</sup>F( $p$ , $\gamma$ ), 1459-110 keV transition, E2/M1 mixing ratio 0-106013  
<sup>A</sup>Fe, A=57, 59, levels, J $^{\pi}$  and transition branching ratio from Fe(n, $\gamma$ ) 0-105976  
<sup>A</sup>Fe( $p$ , $p'$ ), pol. p., 800 MeV, diff. cross sections, anal. powers, DWIA anal. 0-83067  
<sup>56</sup>Fe resonances, levels, J $^{\pi}$ , valence capture  $\gamma$ -ray spectrum from <sup>54</sup>Fe(n, $\gamma$ ) 0-86852  
<sup>56</sup>Fe, fp shell model calcs., spectra and spectroscopic factors 0-68588  
<sup>56</sup>Fe isobaric analogue resonance levels, branching ratios, from <sup>55</sup>Mn( $p$ , $\gamma$ ) 0-68617  
<sup>56</sup>Fe low lying levels, J $^{\pi}$ ,  $\gamma$ - $\gamma$  coincidences, internal conversion from <sup>56</sup>Co  $\beta$ -decay 0-86815  
<sup>56</sup>Fe(e,e'), Coulomb form factor for O $^{+}$  $\rightarrow$ 4 $^{+}$  transition, collective 4 $^{+}$  states, shell model 0-57664  
<sup>56</sup>Fe(n,n' $\gamma$ ), 14.6 MeV, maximum excitation state  $\gamma$ -decay, cross section (Russian) 0-68586  
<sup>56</sup>Fe anomalous M1/E1 strength ratio and doorway states from <sup>56</sup>Fe(n, $\gamma$ ) 0-57730  
<sup>58</sup>Fe levels, J $^{\pi}$ , anal. powers and cross sections from <sup>58</sup>Fe(t,p) pol.t. 0-68539  
<sup>58</sup>Fe resonances, primary  $\gamma$ -intensities, E1-M1 correlation from <sup>58</sup>Fe(n, $\gamma$ ) 0-57740  
<sup>68</sup>Fe low lying state mean lifetimes and transitions from <sup>64</sup>Zn(<sup>7</sup>Li,p2n) 0-68599  
<sup>A</sup>Ga, A=65,67, high spin states and transitions from Fe+<sup>12</sup>C(<sup>14</sup>N) 0-68516  
<sup>63</sup>Ga high spin states, J $^{\pi}$  and transitions, triaxial struct. from (<sup>12</sup>C,ap),(<sup>7</sup>Li,Zn) 0-63062  
<sup>69</sup>Ga state alignment,  $\gamma$ -transitions and ang. distrib. from <sup>68</sup>Zn( $p$ , $\gamma$ ) 0-73797  
Gd, N=85 isotones, bands and transitions from  $\alpha$  and HI excitation, in-beam study 0-78123  
<sup>A</sup>Gd A=144,146,147,148, high spin isomer g-factors yrast traps from (<sup>28</sup>Si,<sup>28</sup>Si'), ( $\alpha$ , $\alpha'$ ) 0-78146  
<sup>A</sup>Gd, A=152, 154,  $\gamma$ -transition energy and intensity meas. from Eu decay 0-73818  
<sup>145</sup>Gd levels, J $^{\pi}$  and transitions, neutron hole coupling to <sup>146</sup>Gd core from <sup>144</sup>Sm( $\alpha$ ,3n) 0-78164  
<sup>146</sup>Gd lowest 2 $^{+}$  state, J $^{\pi}$  and transitions from <sup>146</sup>Tb decay 0-105979  
<sup>146</sup>Gd, O $_{2}^{+}$  state EM decay, T $_{1/2}$  and monopole strength 0-95310  
<sup>146</sup>Gd region, proton subshell effects from  $\alpha$ -decay and spectroscopy, self-consistent study 0-57748  
<sup>152</sup>Gd, vibrational states, B(E2) branching rates and interband transitions, pairing plus quadrupole calcs. 0-78127  
<sup>153</sup>Gd levels and  $\gamma$ -ray spectra from <sup>152</sup>Gd(n, $\gamma$ ) 0-57736  
<sup>155</sup>Gd, vibr. state, level scheme,  $\gamma$  and conversion electron spectra from <sup>154</sup>Gd(n, $\gamma$ ) 0-57696  
Ge, even-even nuclei,  $\gamma$ -spectroscopy, exptl. results and models 0-68589  
<sup>A</sup>Ge, A=68, 70,72,74, level excitation, n-p interaction role from  $\alpha$ -transfer in Zn(<sup>6</sup>Li,d) 0-73821  
<sup>A</sup>Ge(t,p), pol.t., A=70,72, octupole oscillations modes from anal. powers, 3 $_{1}^{-}$  octupole transition 0-102142  
<sup>68</sup>Ge excited state, J, mean lifetimes and transitions from <sup>64</sup>Za(<sup>7</sup>Li,ph) 0-73821  
<sup>19</sup>Ge excited state, J, mean lifetimes and transitions 0-68517  
<sup>66</sup>Ge levels, lifetimes, J $^{\pi}$  and transitions from <sup>58</sup>Ni(<sup>10</sup>B,pn $\gamma$ ) 0-73799  
<sup>66</sup>Ge high spin states, J assignment, decay scheme from <sup>55</sup>Mn(<sup>16</sup>O,pn) 0-68518  
<sup>A</sup>H( $\pi^{+}$ ,  $\pi^{+}$ ), A=1,2, 130-280 MeV, 180 $^{\circ}$  excitation function, dibaryon resonance signals 0-68619  
<sup>A</sup>He( $\alpha$ ,nd), 119 MeV, excited states, J $^{\pi}$  and  $\gamma$ -ang. correlations 0-86809  
<sup>178</sup>Hf, energy levels, K-forbidden decays, M4 decay of yrast state 0-68506  
<sup>A</sup>Ho low lying yrast states from <sup>122</sup>Te(<sup>32</sup>S,X), <sup>121</sup>Sb(<sup>32</sup>S,X) 0-91151  
<sup>A</sup>I, A=115-127 odd isotopes, collective props., bands and transitions from heavy ion reactions 0-68512

nuclear energy level transitions continued

<sup>129</sup>I time depend. quadrupole interactions,  $\gamma$ - $\gamma$  correlations from <sup>129</sup>Te $m^{+}g$  decay 0-78145  
<sup>132</sup>I isomer and gamma-ray spectrum from <sup>133</sup>Cs( $\pi^{-}$ p) 0-78199  
<sup>133</sup>I yield and  $\gamma$ -ray spectra from <sup>133</sup>Cs( $\pi^{-}$ p) 0-86857  
<sup>136</sup>I, isomeric ratio,  $\gamma$ -spectra thermal neutron and 3 MeV fission of <sup>235</sup>U (French) 0-68709  
<sup>A</sup>In, A=119, 121, unified model description, vibr. multiplet yrast struct., branching ratios 0-105953  
<sup>108</sup>In high spin struct., in-beam spectroscopy, conversion electrons from <sup>98</sup>Mo(<sup>18</sup>N,4n $\gamma$ ) 0-73782  
<sup>109</sup>In high spin states,  $\gamma$ -transitions, ang. distrib. from <sup>108</sup>Cd( $\alpha$ ,2np) 0-73783  
<sup>112</sup>In low lying levels, transitions, T $_{1/2}$ , multipolarities and mixing ratios from <sup>112</sup>Cd(p,n $\gamma$ ) 0-68545  
<sup>A</sup>Ir, A=189, 191, levels, J $^{\pi}$ , transitions and mixing ratios from Pt decay 0-68602  
<sup>191</sup>Ir 129 keV transition, atomic screening, time reversal violation 0-106011  
<sup>191</sup>Ir, excited nuclei mean precession time depend. on  $\gamma$ -spectral width, g-factors (Russian) 0-78211  
<sup>K</sup>, effective M3 matrix elements and transitions from shell model 0-102143  
<sup>K</sup> excited levels, J $^{\pi}$ , transitions and lifetimes from <sup>48</sup>Ca(p, $\alpha$ n) 0-68544  
Kr even-even isotopes, collective states and transitions, interacting boson approx. 0-73773  
<sup>A</sup>Kr, A=79, 81, high spin E2 bands, J $^{\pi}$ , transitions from Ge(<sup>10</sup>,<sup>11</sup>B,  $x\gamma$ ) 0-63061  
<sup>78</sup>Kr bands, lifetimes and E2 transitions from interacting boson model and (<sup>16</sup>O,p2n), (<sup>19</sup>Fe, $\alpha$ 2n) 0-73771  
<sup>79</sup>Kr, low lying levels from <sup>79</sup>Br(p,n $\gamma$ ) 0-105972  
<sup>84</sup>Kr levels,  $\gamma$ -cascades, J $^{\pi}$ , mixing ratios and correlations from <sup>84</sup>Br decay 0-63134  
<sup>A</sup>La, A=125, 127, collective props., bands and transitions from heavy ion reactions 0-68512  
<sup>(6</sup>Li,d), A=60,116, L=0 transitions, cross sections, microscopic anal. 0-78189  
<sup>6</sup>Li, transition probabilities between cluster structure states and r.m.s. radius, double well-cluster model (Chinese) 0-63128  
<sup>6</sup>Li $_{\alpha}$ , supermultiplet struct. and decay props. of hypernuclear 1 $^{+}$  resonances from (K, $\pi^{-}$ ) 0-78186  
<sup>6</sup>Li(e,e'), 102, 123 MeV, excitation form factor, <sup>3</sup>H-<sup>3</sup>He cluster model 0-78190  
<sup>6</sup>Li(e,e'), 76-141 MeV, form factors, appl. to ( $\pi^{-}$ , $\gamma$ ), phenomenological model 0-83068  
<sup>8</sup>Li possible  $\gamma$ -transition from <sup>9</sup>Be(K $^{-}$ , $\pi^{-}$ p) 0-106002  
<sup>A</sup>Li, A=6,7, excited states and spectra, continuum effects calcs. 0-57720  
<sup>A</sup>Lu, A=158, 159, alpha decay and gamma transitions 0-73827  
<sup>174</sup>Lu isomeric levels,  $\gamma$ -spectra, T 1/2 and decay modes from <sup>176</sup>Yb(p,3n) 0-99151  
<sup>175</sup>Lu delayed transitions from <sup>176</sup>Yb(p,3n) 0-99151  
<sup>177</sup>Lu excited state lifetimes,  $\gamma$ -transitions from  $\beta$ -decay transitions 0-78205  
<sup>A</sup>Mg(p, p'), A=24, 26, isovector dipole strength excitation in giant resonance region 0-83066  
<sup>23</sup>Mg resonances through  $\gamma$ -decay excitation functions from <sup>12</sup>C(<sup>12</sup>C,n) 0-63148  
<sup>24</sup>Mg ground and  $\gamma$ -bands, direct and multistep processes from ( $\alpha$ ,<sup>6</sup>He), (p,t), (<sup>16</sup>O, <sup>16</sup>O) 0-102094  
<sup>24</sup>Mg intermediate struct. correlations, elastic and reaction channel excitation functions from <sup>12</sup>C(<sup>12</sup>C,X) 0-68625  
<sup>24</sup>Mg isovector M1 excitations, current and spin contr. from (e,e'), (p,n) 0-58582  
<sup>24</sup>Mg rotational band collectivity, shell model excitation in Sp(4, R) symmetry 0-102095  
<sup>24</sup>Mg, triaxial nuclei rots., extended cranked shape consistent oscillator model 0-102133  
<sup>24</sup>Mg(<sup>12</sup>C,<sup>12</sup>C), 35 MeV, 2 $^{+}$ , population probab., spin-flip and spin orbit pots., coupled channel anal. 0-99125  
<sup>24</sup>Mg(<sup>16</sup>O,<sup>16</sup>O), 24-40 MeV, backward angles, excitation functions, ang. distrib. and resonant behaviour 0-68622  
<sup>26</sup>Mg transition strength n and p components,  $\pi^{-}$  inelastic scatt. comparison, shell model 0-68585  
<sup>26</sup>Mg(<sup>3</sup>He,<sup>3</sup>He), 4 $^{+}$  states, B(E2) values, and band mixing, rot.-vibr. model 0-83019  
<sup>52</sup>Mn fragmented g $_{9/2}$  isobaric analogue resonance,  $\gamma$ -spectra and excitation functions from <sup>52</sup>Cr(p, $\gamma$ ) 0-68627  
<sup>50</sup>Mn levels, transitions and spins from <sup>55</sup>Mn(n, $\gamma$ ), pol. Mn and n 0-78154  
Mn(n, $\gamma$ ), primary transitions using focused 24 keV filtered neutron beam 0-63436  
<sup>A</sup>Mo, A=98,102, anal. powers, transitions, shape coexistence states, DWBA anal. of Mo(t,p), pol.t. 0-86895  
<sup>89</sup>Mo $m^{+}$  levels, transitions and half life from <sup>93</sup>Mo(p,p' $^{3}$ n) 0-86858  
<sup>100</sup>Mo(n,n' $\gamma$ ), fast n, gamma transitions, level energies and scheme 0-73822  
<sup>101</sup>Mo levels,  $\gamma$ -rays and p-wave resonance partial radiative widths from <sup>100</sup>Mo(n, $\gamma$ ) 0-57739  
Mo(p,p' $\gamma$ ), odd isotopes, excited d-states from analogue resonances and  $p$ - $\gamma$  correlations 0-68546  
<sup>13</sup>N giant dipole resonance population amplitude and phase, E1 reaction amps. from <sup>12</sup>C( $\gamma$ , $\gamma$ ), pol. p. 0-63145  
<sup>14</sup>N levels and excitation energies, kinematically complete investigation from <sup>16</sup>O( $\pi^{-}$ , 2n) 0-99128  
<sup>14</sup>N(p,p'), 122 MeV, level excitation, cross sections, effective NN interaction, DWIA anal. 0-78197  
<sup>17</sup>N three particle states at high excitation energies, J $^{\pi}$ , selective population from <sup>12</sup>C(<sup>7</sup>Li,  $\alpha$ ) 0-99129  
<sup>22</sup>Na 0 $^{+}$  level mean life, isovector mag. dipole transition from <sup>19</sup>F( $\alpha$ ,n) 0-68595  
<sup>23</sup>Na high spin states, excitation functions, nonstatistical effects, Hauser-Feshbach anal. of <sup>14</sup>C(<sup>13</sup>N, $\alpha$ ) 0-106041  
<sup>23</sup>Na resonances through  $\gamma$ -decay excitation functions from <sup>12</sup>C(<sup>12</sup>C,p) 0-63148  
<sup>24</sup>Na, effective M3 matrix elements and transitions from shell model 0-102143  
Nd, even-even, E2 transition probabilities from multiple Coulomb excitation, IBA comparison 0-78212  
Nd, N=85 isotones, bands and transitions from  $\alpha$  and HI excitation, in-beam study 0-78123



## nuclear energy level transitions continued

- <sup>140</sup>Nd, A=138,139, high spin states, isomers and  $\gamma$ -cascade from <sup>140</sup>Cd( $\alpha$ , xzn) 0-78120
- <sup>140</sup>Nd, A=138,139, high spin states, J<sup>π</sup>,  $\gamma$ -cascades and shape transition from <sup>140</sup>Ce( $\alpha$ , xn) 0-102090
- <sup>140</sup>Nd ns isomers and yrast isomers,  $\gamma$ -transitions from <sup>128</sup>Te(<sup>16</sup>O,  $\alpha$ n) 0-78121
- <sup>148</sup>Nd, vibrational states, B(E2) branching rates and interband transitions, pairing plus quadrupole calcs. 0-78127
- <sup>26</sup>Ne 13482 keV level, parity violating effects in two resonance interference from <sup>19</sup>F(p,  $\alpha$ ) pol. p 0-83033
- <sup>26</sup>Ne 2<sup>+</sup>→0<sup>+</sup> transition from <sup>12</sup>C(<sup>16</sup>O, <sup>16</sup>O) 0-63125
- <sup>26</sup>Ne collective motion, B(E2) rates, algebraic formulation in symplectic shell model 0-83015
- <sup>26</sup>Ne resonances through  $\gamma$ -decay excitation functions from <sup>12</sup>C(<sup>12</sup>C,  $\alpha$ ) 0-63148
- <sup>26</sup>Ne(<sup>12</sup>C, X), 24-42 MeV, complete fusion, total cross section, excitation function 0-68717
- Ni, fp shell model calcs., spectra and spectroscopic factors 0-68588
- <sup>60</sup>Ni, A=60, 62, 66, levels, J<sup>π</sup>, anal. powers and cross sections from Ni(t,p)pol. t 0-68539
- <sup>57</sup>Ni high spin yrast cascade, decay modes J assignment from <sup>54</sup>Fe( $\alpha$ , n $\gamma$ ) 0-68514
- <sup>58</sup>Ni(d, d'), 10 MeV, diff. cross sections and d- $\gamma$  ang. correlations, multi-shell coupled channel calcs. 0-83064
- <sup>60</sup>Ni, Coulomb contributions to nuclear radii and energies 0-68515
- <sup>60</sup>Ni high spin states, J<sup>π</sup>, T<sub>1/2</sub>, ang. distrib. and polarisations from <sup>50</sup>Fe(<sup>11</sup>Li, p2n $\gamma$ ) 0-99116
- <sup>60</sup>Ni level scheme and  $\gamma$ -rays from <sup>59</sup>Ni(n,  $\gamma$ ) 0-63099
- Ni(e,  $\alpha$ ), E2 strength in resonance regions statistical decay 0-91146
- Ni(n,  $\gamma$ ), primary transitions using focused 24 keV filtered neutron beam 0-63436
- <sup>23</sup>Np electron transition excitation following K-shell photoionisation, deexcitation  $\gamma$ -rays 0-78196
- <sup>23</sup>Np(e, f), 10-34 MeV, electrofission cross section, E2 transition mode and giant resonances 0-106084
- <sup>16</sup>O, A=16, 17, valence-core self-consistency, wave functions, binding energy, levels, spectra 0-63123
- <sup>16</sup>O 3<sup>+</sup>→0<sup>+</sup> gamma transition from <sup>12</sup>C(<sup>16</sup>O, <sup>16</sup>O) 0-63125
- <sup>16</sup>O 4<sup>+</sup> state nonstatistical population in compound nucleus calcs. of <sup>12</sup>C(<sup>6</sup>Li, d) 0-102137
- <sup>16</sup>O  $\alpha$ -cluster states, widths and resonances, optical model, direct transfer in <sup>12</sup>C(<sup>6</sup>Li, d) 0-105975
- <sup>16</sup>O level excitation functions, resonances from <sup>12</sup>C(<sup>16</sup>O, <sup>12</sup>C) 0-63146
- <sup>16</sup>O, magic nuclei at collective excitations, energy spectrum and shape (Russian) 0-106015
- <sup>16</sup>O, rotational band collectivity, shell model excitation in Sp(4, R) symmetry 0-102095
- <sup>16</sup>O(<sup>16</sup>O, <sup>16</sup>O), 10-41 MeV, molecular resonances  $\gamma$ -yield, band crossing model 0-106032
- <sup>16</sup>O( $\gamma$ ,  $\gamma$ ), total photoabsorption and elastic cross sections, spectroscopic information (Russian) 0-83095
- <sup>18</sup>O 6p-4h states and composite spectra from <sup>12</sup>C(<sup>18</sup>O, <sup>12</sup>C) 0-63096
- <sup>18</sup>O, transition strength n and p components,  $\pi^+$  inelastic scatt. comparison, shell model 0-68585
- <sup>18</sup>O(e, e'), isovector mag. dipole and quadrupole transitions, analogues, ( $\pi^+$   $\gamma$ ) relation 0-106010
- Os even-even isotopes, excitation energies and EM props. from interacting boson model 0-106005
- <sup>186</sup>Os, A=186,188, levels and transitions from Re decay, triaxial rotor model 0-91155
- <sup>186</sup>Os, A=186-194, collective levels, transitions, mag. and quadrupole moments, boson expansion theory 0-105954
- <sup>186</sup>Os, A=188, 189, levels, J<sup>π</sup>, transitions and mixing ratios from Ir decay 0-68602
- <sup>193</sup>Os level scheme and transitions, Coriolis coupled Nilsson states from <sup>192</sup>Os(n,  $\gamma$ ) 0-57698
- <sup>30</sup>P level width isospin depend., excitation functions, statistical anal. of <sup>29</sup>Si(p,  $\alpha$ ) 0-78152
- <sup>30</sup>P positive parity states, transitions and spectroscopic strengths, DWBA anal. of <sup>29</sup>Si(<sup>3</sup>He, d) 0-102138
- <sup>30</sup>P T=1 state decay, lifetimes and branching ratios, analogue E2 transitions from <sup>29</sup>Si(p,  $\gamma$ ) 0-68598
- Pb region, forbidden charge exchange collective modes,  $\beta$ - and  $\gamma$ -decay processes 0-86784
- Pb region, particle-vibration multiplet spectra, self-consistent framework 0-102089
- <sup>197</sup>Pb, A=197,198, low energy  $\gamma$ -transitions 0-83058
- <sup>197</sup>Pb, A=202, 204, spectra from multistep shell model method 0-78194
- <sup>208</sup>Pb, muonic, first excited 2<sup>+</sup> state, isomer shift of E2 transition 0-99150
- <sup>208</sup>Pb(n, n $\gamma$ ), 1.5-3.1 MeV, levels, J<sup>π</sup>, excitation functions and mixing ratios 0-102123
- <sup>208</sup>Pb  $\gamma\gamma$  directional correlations, multipole mixing ratios, transition strength limits from <sup>206</sup>Bi decay 0-86849
- <sup>208</sup>Pb 569.65-1063.63 keV cascade,  $\gamma\gamma$  ang. correl. meas. from <sup>207</sup>Bi decay 0-86847
- <sup>208</sup>Pb, muonic, octupole doublet isomer shifts, octupole vibr. 0-95750
- <sup>208</sup>Pb muonic isomer shifts, neutron hole anomalous moment contribs. 0-78728
- <sup>207</sup>Pb p-wave resonances, enhanced primary M1 transitions from <sup>206</sup>Pb(n,  $\gamma$ ) 0-57728
- <sup>207</sup>Pb(n, p) reaction, isobar analogue state excitation (Russian) 0-102124
- <sup>207</sup>Pb (e, e'), 2<sup>+</sup> giant resonance twist mode excitation, B(M2) values, form factors 0-78246
- <sup>208</sup>Pb breathing model transition density, single particle and collective state dynamical coupling 0-106007
- <sup>208</sup>Pb giant monopole and quadrupole resonances, multipole excitations from ( $\alpha$ ,  $\alpha'$ )(d, d') 0-106031
- <sup>208</sup>Pb region, mag. transition strength, core polarisation effects, form factor shape 0-86850
- <sup>208</sup>Pb(<sup>12</sup>C, <sup>11</sup>B), 77 MeV, bound and continuum state excitation, direct and two step processes 0-63205
- <sup>208</sup>Pb(<sup>14</sup>N, <sup>14</sup>N), 266 MeV, giant resonance excitation 0-78253
- <sup>208</sup>Pb( $\alpha$ ,  $\alpha'$ ), levels, B(E3), transition density and nuclear pol., folding model anal. 0-86812
- <sup>208</sup>Pb(e, e'), 70-335 MeV, natural parity high spin state excitation 0-63060
- <sup>208</sup>Pb(p, p'), 135 MeV, normal parity level excitation, J<sup>π</sup>, differential cross sections 0-57690

## nuclear energy level transitions continued

- <sup>208</sup>Pb(p, p'), 135 MeV, normal parity excitations, microscopic description, NN interaction shape 0-57691
- <sup>210</sup>Pb levels, J<sup>π</sup>, transitions and lifetimes from <sup>208</sup>Pb(<sup>2</sup>Li, X) 0-68542
- Pb, even-even, collective states, B(E2), branching ratios and moments, boson expansion method 0-102099
- <sup>100</sup>Pd levels and  $\gamma$ -transitions from <sup>100</sup>Ag<sup>6.8m</sup> decay 0-83077
- <sup>100</sup>Pd nonyrast rotational states, transitions, T<sub>1/2</sub>, branching and mixing ratios from <sup>92</sup>Zr(<sup>12</sup>C,  $\alpha$ n) 0-105950
- <sup>102</sup>Pd(p, p $\gamma$ ), long lived O<sup>+</sup> state, E0 transitions 0-73804
- <sup>106</sup>Pd, E0 transition from 0<sup>+</sup> state following <sup>106</sup>Rh beta decay 0-68578
- <sup>109</sup>Pd low spin odd parity levels,  $\gamma$ -rays, particle-rotor comparison from <sup>108</sup>Pd(n,  $\gamma$ ) 0-73805
- <sup>109</sup>Pd low spin odd parity states, rot. aligned model, Coriolis calc. of <sup>108</sup>Pd(n,  $\gamma$ ) 0-57695
- <sup>140</sup>Pm, A=143, 145, proton states and transitions, stripping strength, shell model anal. from Nd(<sup>3</sup>He, d) 0-68508
- <sup>147</sup>Pm medium spin states, J<sup>π</sup>, transitions and shape from (p, 2n), (<sup>3</sup>He, 3n), ( $\alpha$ , 4n) 0-86779
- <sup>147</sup>Pm, level scheme and transitions following <sup>147</sup>Nd 0-83073
- <sup>147</sup>Pm levels, bands, transitions, in-beam spectroscopy, particle-rotor anal. from <sup>150</sup>Nd(p, 2n $\gamma$ ) 0-78125
- <sup>206</sup>Po,  $\gamma$ -rays, conversion electron spectra,  $\gamma\gamma$  coincidences 0-83061
- <sup>212</sup>Po, levels, J<sup>π</sup>, transitions and lifetimes from <sup>208</sup>Pb+<sup>7</sup>Li 0-68542
- <sup>139</sup>Pr medium spin states, J<sup>π</sup>, transitions and shape from (p, 2n), (<sup>3</sup>He, 3n), ( $\alpha$ , 4n) 0-86779
- <sup>140</sup>Pr isobaric analogue resonances, de-excitation cascade, K-shell ionisation, spin depend. from <sup>140</sup>Ce(p, n) 0-78202
- <sup>141</sup>Pr, positive parity levels, gamma-ray yields and ang. distrib. 0-105962
- Pt even-even isotopes, excitation energies and EM props. from interacting boson model 0-106005
- <sup>187</sup>Pt, A=188-198 collective levels, transitions, mag. and quadrupole moments, boson expansion theory 0-105954
- <sup>187</sup>Pt, A=190,192,194, state struct. in interacting boson model 0-83047
- <sup>244</sup>Pu level structure and  $\gamma$ -transitions from <sup>245</sup>Cm decay 0-105980
- <sup>244</sup>Pu(n,  $\gamma$ ) resonance integral meas. 0-73846
- <sup>230</sup>Ra levels, J<sup>π</sup> and transitions, Nilsson assignments from <sup>230</sup>Ac decay 0-68543
- Rb, fission fragment, delayed neutron branches from  $\gamma$ -spectroscopy 0-78230
- Rb odd-even isotopes, collective states and transitions, interacting boson approx. 0-73773
- <sup>85</sup>Rb, A=79, 81, decoupled  $\gamma$ -bands, level lifetimes and E2 transitions from (<sup>16</sup>O, 2n)(<sup>19</sup>F, p2n) 0-73772
- <sup>85</sup>Rb(n, n $\gamma$ ), 550-2100 keV, A=85,87, levels, excitation functions, J<sup>π</sup>, Hauser-Feshbach anal. 0-105982
- <sup>83</sup>Rb band struct., spin assignments and transitions from (<sup>6</sup>Li, 3n), (<sup>16</sup>O, p2n), ( $\alpha$ , 2n) 0-73774
- <sup>83</sup>Rb high spin states, J $\pi$  and transitions from HI and  $\alpha$  reactions 0-105949
- <sup>85</sup>Rb high spin states, yrast cascade, J<sup>π</sup>,  $\gamma$ -transitions from <sup>82</sup>Se(Li, xn $\gamma$ ) 0-73775
- <sup>85</sup>Rb levels, J<sup>π</sup> and transitions from Kr<sup>m.s.</sup>, Sr<sup>m.s.</sup> decay, cluster-vibr. model 0-78162
- <sup>94</sup>Rh,  $\gamma$ -spectrum and half-lives 0-83062
- <sup>97</sup>Rh levels and  $\gamma$ -transitions, 3QP model anal. of <sup>97</sup>Pd  $\beta^+$ -decay 0-102120
- <sup>208</sup>Rn→<sup>208</sup>At,  $\gamma$ -ray, conversion electron spectra 0-83072
- <sup>210</sup>Rn, shell model states, semiempirical calcs. half lives, mag. moments, excitation functions 0-63083
- Ru, even-even, collective states, B(E2), branching ratios and moments, boson expansion method 0-102099
- <sup>104</sup>Ru, A=104,106,108, level scheme and transitions, collective model anal. of Tc decay 0-78166
- <sup>104</sup>Ru, A=106, 108, levels, transitions, J<sup>π</sup> and shape from Tc decay 0-57744
- <sup>97</sup>Ru high spin states, band like structs., transitions from <sup>88</sup>Sr(<sup>12</sup>C, 3n $\gamma$ ) 0-73779
- <sup>32</sup>S resonances and excitation functions, Hauser Feshbach anal. of <sup>20</sup>Ne(<sup>12</sup>C, X), X=p, d,  $\alpha$  0-78249
- <sup>32</sup>S(n, n $\gamma$ ), 13.9 MeV, 2<sup>+</sup> (2.23 MeV) excitation, spin flip probab., deexcitation  $\gamma$ -rays 0-86853
- <sup>125</sup>Sb, A=113-175, odd isotopes, collective props., bands and transitions from heavy ion reactions 0-68512
- <sup>125</sup>Sb high spin levels, gamma transition energies and intensities from <sup>125</sup>Sn<sup>9</sup> decay 0-73819
- <sup>43</sup>Sc, J<sup>π</sup>=19/2<sup>+</sup> isomer, high-spin precursors, from <sup>29</sup>Si(<sup>16</sup>O, p $\alpha$ ) 0-57656
- <sup>45</sup>Sc levels, J<sup>π</sup>, transitions and lifetimes from (p, p')(<sup>3</sup>He, <sup>3</sup>He)( $\alpha$ ,  $\alpha'$ ) 0-63091
- <sup>45</sup>Sc( $\pi^+$ , X), stopped  $\pi^+$ , yields and  $\gamma$ -rays 0-86857
- <sup>48</sup>Sc proton single particle states, spectroscopic factors, DWBA anal. of <sup>48</sup>Ca(d, n) 0-99118
- Se, even-even nuclei,  $\gamma$ -spectroscopy, exptl. results and models 0-68589
- <sup>78</sup>Se, A=74, 76, vibr. states and transition from dynamic deformation theory 0-73770
- <sup>72</sup>Se side band struct., negative parity states and transitions from <sup>58</sup>Ni(<sup>16</sup>O, 2p) 0-73769
- <sup>78</sup>Se transition energy correlations in  $\gamma$ -continuum from <sup>64</sup>Ni(<sup>16</sup>O,  $\alpha$ 2n) 0-95309
- <sup>76</sup>Se high spin states, bands, J<sup>π</sup>, transitions and T<sub>1/2</sub> from <sup>71</sup>Ga(<sup>7</sup>Li, 2n) 0-105951
- <sup>79</sup>Se, 96 keV transition, conversion coeff.,  $\gamma$ -spectrum 0-63131
- <sup>28</sup>Si excitation functions, ang. distrib. and resonant behaviour from <sup>24</sup>Mg(<sup>16</sup>O, <sup>12</sup>C) 0-68622
- <sup>28</sup>Si excitation functions, ang. distrib., resonance spin assignments from <sup>24</sup>Mg(<sup>16</sup>O, <sup>12</sup>C) 0-68623
- <sup>28</sup>Si isovector M1 excitations, current and spin contribs. from (e, e'), (p, n) 0-68582
- <sup>28</sup>Si(n,  $\gamma$ ), 565, 813 keV, resonance  $\gamma$ , spectra, valence model test 0-63124
- <sup>28</sup>Si(p, p'), isovector dipole strength excitation in giant resonance region 0-83066
- <sup>29</sup>Si 3/2<sup>+</sup> and 5/2<sup>+</sup> states population, (d, p) and (p,  $\pi^+$ ) comparison 0-95307
- <sup>29</sup>Si doorway state neutron capture, levels and  $\gamma$ -spectra from <sup>28</sup>Si(n,  $\gamma$ ) 0-57729
- <sup>29</sup>Si, low lying energy level structure, from <sup>28</sup>Si(d<sub>pol</sub>,  $\gamma$ ) and multi-step reaction calcs. 0-68537
- <sup>29</sup>Si rot-vibr. coupling effects, excitation spectrum and ang. distrib. from <sup>28</sup>Si(d, p) 0-57661



## nuclear energy level transitions continued

- <sup>29</sup>Si(d,p), 1.1-2.1 MeV, excitation functions, statistical fluctuations anal. 0-95322
- <sup>30</sup>Si(p,γ), pol.p., 6.4-15.0 MeV, cross section and anal. power ang. distrib. 0-99168
- <sup>4</sup>Sm, A=147, 149, levels, J, γ-transitions and multipole mixing ratios, γγ correlations from Eu EC decay 0-106012
- <sup>142</sup>Sm isomers, lifetimes and transitions from <sup>142</sup>Nd(α,n) 0-78122
- <sup>42</sup>Sm ns isomers and yrast isomers, γ-transitions from (<sup>24</sup>Mg,4n), (<sup>19</sup>F,4n) 0-78121
- <sup>145</sup>Sm primary γ-rays, direct capture and neutron separation energy, (d,p),(n,γ) correlation 0-57738
- <sup>147</sup>Sm(n,α)<sup>144</sup>Nd, 2 keV, statistical model anal. 0-102186
- <sup>150</sup>Sm, vibrational states, B(E2) branching rates and interband transitions, pairing plus quadrupole calcs. 0-78127
- <sup>151</sup>Sm low energy levels from expt. and Coriolis mixing calcs. of <sup>151</sup>Sm(n,γ) 0-57697
- <sup>152</sup>Sm ground and γ-bands, direct and multistep processes from (α,<sup>6</sup>He), (p,t), (<sup>16</sup>O,<sup>16</sup>O) 0-102094
- <sup>152</sup>Sm, γ-transition energy and intensity meas. from <sup>152</sup>Eu decay 0-73818
- Sn 2<sup>+</sup> excitation, α-spectroscopic factors in IBA model from Te(d,<sup>6</sup>Li) 0-105967
- Sn isotopes, levels and spectra from broken pair model 0-73801
- <sup>4</sup>Sn, A=106-108, yrast levels and transitions from <sup>54</sup>Fe(<sup>28</sup>Ni, X) 0-105957
- <sup>4</sup>Sn, A=112-124 even isotopes, 0<sup>+</sup> state collectivity, E0 and E2 transition rates 0-73785
- <sup>4</sup>Sn, A=118,120,122, deep hole states, excitation energies and ang. distrib. from Sn(p,t) 0-86792
- <sup>116</sup>Sn(α,α'), 96, 129 MeV, giant resonance excitation, isoscalar breathing mode state, nuclear incompressibility 0-68620
- <sup>132</sup>Sn levels, isomers, lifetimes and transition probabilities from fission 0-78163
- <sup>4</sup>Sr, A=94,96 direct and skip cascades, γγ ang. correlations, levels, mixing ratios from Rb decay 0-86851
- <sup>4</sup>Sr, A=98, 100 rot. struct. sudden onset, gamma transitions from Rb decay 0-73777
- <sup>88</sup>Sr(γ,γ), 14 MeV, highly excited spin-1 resonances, spin and radiative widths 0-86876
- <sup>92</sup>Sr γγ ang. correlations, levels, J<sup>π</sup>, mixing ratios from <sup>92</sup>Rb decay 0-57725
- <sup>92</sup>Sr neutron binding energy from transitions and β-delayed neutron defined level correspondences 0-63070
- <sup>96</sup>Sr very low lying 0<sup>+</sup> state, shape coexistence bands, T<sub>1/2</sub>, transitions from <sup>96</sup>Rb decay 0-78148
- <sup>180</sup>Ta<sup>m</sup>, β<sup>-</sup> and EC branching ratios, K-internal conversion coeff., γ-intensities, T<sub>1/2</sub> 0-68601
- <sup>160</sup>Tb-<sup>160</sup>Dy, γ-transitions and angular distributions 0-83060
- <sup>97</sup>Tc, energy levels, low-lying, decay properties 0-63084
- <sup>97</sup>Tc high spin states, spins and transitions from <sup>94</sup>Zr(<sup>6</sup>Li,3nγ) 0-73780
- <sup>97</sup>Tc 14 μs isomer, low lying levels and transitions from <sup>98</sup>Mo(p,n) 0-73802
- <sup>100</sup>Tc μs isomers, isomeric transitions and mean lives from <sup>100</sup>Mo(p,n) 0-73803
- <sup>102</sup>Tc decay scheme and γ-intensities from <sup>102</sup>Mo fission product decay 0-78229
- <sup>120</sup>Te quasi-rot. band based on proton 4p-2h state, level scheme, transitions from <sup>118</sup>Sn(α,2nγ) 0-78119
- <sup>123</sup>Te low lying negative parity high spin states multistep induced population from (d,t)(<sup>3</sup>He,α) 0-57657
- <sup>126</sup>Te, M1, giant resonance and radiative strength functions 0-57731
- <sup>126</sup>Te(p,n), 2<sub>2</sub><sup>+</sup>→2<sub>1</sub><sup>+</sup> transition multipole mixing ratio 0-78198
- <sup>131</sup>Te γ-transitions, spectroscopic factors and reduced transition intensities from <sup>130</sup>Te(n,γ) 0-91143
- <sup>231</sup>Th excited states and bands, spins, γ-transitions from <sup>230</sup>Th(n,γ) 0-57699
- Ti(<sup>12,13</sup>C,X) 45, 46 MeV, particle-gamma coincidences, isotope assignment for yrast spectroscopy 0-68593
- <sup>4</sup>Ti, A=44, 48, ang. distrib. for transitions, DWBA anal., spectroscopic strengths from Ca(Li,t) 0-68584
- <sup>4</sup>Ti, A=48,50, excited states and transition ang. distrib. from Cr(<sup>14</sup>C,<sup>16</sup>O) 0-95308
- <sup>4</sup>Ti, weak E1 transitions examined using γ-ray, γ-γ coincidence and n-γ coincidence techniques 0-57724
- <sup>167</sup>Tm, energy level scheme from <sup>165</sup>Ho(α,2nγ) (German) 0-68576
- <sup>167</sup>Tm, levels and transitions from <sup>165</sup>Ho(α,2n) 0-73766
- <sup>167</sup>Tm rotational bands, J<sup>π</sup>, γ-transitions and branching ratios from <sup>165</sup>Ho(α,2nγ) 0-86781
- <sup>167</sup>Tm(HI,xnγ), ang. distrib., multipolarities (French) 0-68575
- <sup>236</sup>U γ-transitions from <sup>235</sup>U(n,γ,t) 0-106085
- <sup>236</sup>U shape isomer, γ branch upper limit, γ-yields from <sup>235</sup>U(d,p) 0-99145
- uncorrelated target, optical pot. unitary content, DWIA and Glauber theory from (α,α)(α,γ) 0-105947
- <sup>45</sup>V level scheme, γ-rays, level lifetimes, internal conversion from <sup>40</sup>Ca(Li,xn) 0-63085
- <sup>51</sup>V(p,p'), 6 MeV, levels, spins and EM props., shell model anal. 0-63092
- <sup>4</sup>W, A=170-182, even isotopes, yrast states, spectra and quad. moments, variation formulation 0-99119
- <sup>180</sup>W octupole vibr. states, J<sup>π</sup> and transitions from <sup>180</sup>Re decay 0-83024
- <sup>184</sup>W(<sup>12</sup>C,<sup>12</sup>C'), 70 MeV, 4<sup>+</sup> state excitation ang. distrib., hexadecapole deformation length effects 0-68521
- <sup>129</sup>Xe excited state lifetimes, γ-transitions from <sup>129</sup>Cs decay 0-78205
- <sup>132</sup>Xe level struct., J<sup>π</sup>, transitions and multipole mixing ratio from <sup>132</sup>I decay 0-91134
- <sup>137</sup>Xe neutron unbound states, high energy X-rays from <sup>137</sup>I decay 0-86856
- <sup>4</sup>Y<sup>m</sup>, A=86, 87, isomeric yield ratios and γ-spectra from <sup>93</sup>Nb(π<sup>-</sup>,X) 0-86857
- <sup>87</sup>Y level struct., γ-spectroscopy and J<sup>π</sup> from (p,2nγ), (α,2nγ) 0-83040
- <sup>89</sup>Y gamma transitions, microscopic finite-range anal. of <sup>92</sup>Zr(p,α) 0-63181
- <sup>4</sup>Yb, A=158, 159, alpha decay and gamma transitions 0-73827
- <sup>4</sup>Yb A=160-163, γ-transitions from Lu decay 0-102146
- <sup>166</sup>Yb multiple band crossing, (gSS'S/S'') system gamma correlation patterns 0-106008
- <sup>169</sup>Yb 7/2<sup>+</sup>→7/2<sup>+</sup>[633] transition ft value from <sup>169</sup>Lu allowed hindered β<sup>-</sup> decay 0-102148
- <sup>169</sup>Yb γγ ang. correlations, levels and spins from <sup>169</sup>Lu decay (Russian) 0-83069
- <sup>173</sup>Yb, γ-transitions from 7/2, 7/2<sup>-</sup> [514] 636 keV level 0-78187

## nuclear energy level transitions continued

- <sup>4</sup>Zn, A=64, 66 levels and primary E1 transition strength functions from Cu(p,γ) 0-91149
- <sup>62</sup>Zn ang. distrib. for transitions, DWBA anal., spectroscopic strengths from <sup>58</sup>Ni(<sup>7</sup>Li,t) 0-68584
- <sup>64</sup>Zn high spin states, J<sup>π</sup>, T<sub>1/2</sub>, γ-decays from (α,nγ), (<sup>11</sup>B,p2nγ) 0-73767
- <sup>4</sup>Zr, A=92, 96, first excited 0<sup>+</sup> state transition strength from (<sup>6</sup>Li,<sup>8</sup>B), (d,<sup>6</sup>Li) correlation 0-78260
- <sup>90</sup>Zr(<sup>4</sup>He,t)<sup>90</sup>Nb, 18.5 MeV resonance, isovector dipole and Gamow-Teller transitions 0-86881
- <sup>90</sup>Zr(α,α'), 96, 129 MeV, giant resonance excitation, isoscalar breathing mode state, nuclear incompressibility 0-68620
- <sup>90</sup>Zr(e,e'), 2<sup>-</sup> giant resonance twist mode excitation, B(M2) values, form factors 0-78246
- Zr(p,pγ), odd isotopes, excited d-states from analogue resonances and p-γ correlations 0-68546

## nuclear energy levels

- see also isobaric analogue states; nuclear collective states and giant resonances; nuclear resonances; nuclear spectroscopic factors
- A=120-150, levels and EM props., recent results 0-68592
- A=1-257, nuclear excitation by atomic electron transitions, nuclear levels 0-78191
- A=24-108, level widths in charged particle induced reactions, stat. anal. 0-68535
- A=73, nuclear data sheets, levels, J<sup>π</sup> and transitions 0-101673
- A=77, nuclear data sheets, levels, J<sup>π</sup> and transitions 0-105439
- average resonance neutron capture, completeness in nuclear spectroscopy 0-106006
- conference on medium heavy nuclei structure, Rhodes, Greece (May 1979) 0-67935
- deep hole states observed in particle transfer reactions 0-68511
- deformed nuclei, effect on Coriolis interaction, Nilsson model and Woods-Saxon pot. calcs. 0-63071
- deformed nuclei, single particle level blocking in BCS approx. 0-99117
- densities, shell effects and pairing effects, SCF theory of statistical thermodynamics (Chinese) 0-63088
- doubly even deformed nuclei, excited states, Pauli principle effects, quasi-particle-phonon model 0-63094
- even-even neutron-rich fission products, de-excitation spectra, β-decay, deformation 0-78203
- generalised vibrational rule 0-105971
- growth points in nuclear physics, book 0-94928
- heavy ion stripping and pickup reactions on closed shell nuclei, level shifts, DWBA 0-91168
- hole excitation spectrum in finite Fermi system, many body field theory 0-102105
- large deformations, single particle levels, self-consistent field rearrangement, HF method 0-78107
- level density in large spectroscopic spaces, statistical spectroscopic methods 0-86814
- level density of interacting bosons 0-105974
- level shift non-measurability due to pion diamagnetism in Mossbauer effect 0-73808
- magic and doubly magic nuclei, A=129, 131, 133 chains, 0<sup>+</sup> states, spectroscopy 0-78165
- neutron capture, total radiative width and degree of freedom, statistical model calcs. 0-57732
- neutron rich fission fragments, excited state spin assignment, various methods 0-78506
- neutron rich transitional fission fragments, spectroscopy, 0<sup>+</sup> states and octupole vibr. 0-78204
- nuclear matter momentum distrib., single particle orbitals, Fermi hypernetted chain theory 0-86841
- nuclear matter with neutron excess, thermal props. and level density parameter 0-91141
- odd mass nuclei, 1g<sub>7/2</sub><sup>+</sup> shell region, low lying states, anharmonic effects 0-57687
- odd-odd fission products, level schemes, rot. bands, shell model states 0-78167
- pairing correlation treatment, single particle levels, binding energy, spectra, branching ratios (Chinese) 0-102107
- particle-hole conjugation and protection theorems (Chinese) 0-73796
- pole expansions for resonance functions, scatt. amplitudes and continuum states (Russian) 0-86871
- radionuclide decay, computer simulation, levels, transitions, internal conversion 0-63136
- rare earth nuclei, modified oscillator pot. parameters, single particle levels 0-68509
- sd-shell nuclei heavy-ion reaction resonances, low level density regions, shell model 0-57757
- short living nuclear states, optical orientation, γ-spectrum anisotropy, lifetime, moments (Russian) 0-63090
- short-lived isotopes, laser spectroscopy in fast atomic beams and resonance cells 0-57700
- single particle pots., Lehmann representation discrete and continuous energy spectra (Chinese) 0-102104
- single particle states, discrete expansions of continuum wave functions, convergence props. 0-57659
- single-particle states in nuclear matter and in finite nuclei 0-78117
- spherical nuclei, fragmentation of hole states in quasiparticle-phonon model 0-83020
- spherical nuclei, level density rel. to eqn. of state at subnuclear densities 0-77278
- stable odd-mass sd nuclei, EM multipole moments of ground states 0-102116
- (γ,γ), 2.5-3.5 MeV, level photoexcitation 0-78193
- (p,n), anomalous optical potential for sub-Coulomb barrier protons, 2 particle 1 hole states 0-105948
- (p,p'), single neutron states, two step process and effective interaction 0-78290
- (p,p'), unnatural parity states excitation, π-condensate instability effects, DWBA anal. 0-78168
- (π<sup>+</sup>,π<sup>+</sup>), π<sup>-</sup> nuclear response enhancement, continuum effects, stretched state isospin mixing 0-86929
- <sup>207</sup>(e,e'), transverse scatt. amplitude suppression, form factors, neutron hole states 0-91129
- <sup>230</sup>Ac levels, J<sup>π</sup> and transitions, Nilsson assignments from <sup>230</sup>Ra decay 0-68543

## nuclear energy levels continued

- <sup>4</sup>Ag, A=105-109, negative parity states, EM props. from particle-asymmetric rotor model 0-102097
- <sup>106</sup>Ag low-lying excited states from <sup>103</sup>Rh( $\alpha, n\gamma$ ) and <sup>104</sup>Pd( $\alpha, p\gamma$ ) 0-57693
- <sup>108</sup>Ag levels and  $\gamma$ -transitions, population-spin correlation from <sup>107</sup>Ag( $n, \gamma$ ) 0-63097
- <sup>110</sup>Ag 118.718 keV isomer, low lying states and transitions, coincidence study from <sup>109</sup>Ag( $n, \gamma$ ) 0-73806
- <sup>1</sup>Al, A=25, 26, 27 levels, resonances,  $\gamma$ -ray branching ratios from Mg( $p, \gamma$ ) 0-86875
- <sup>26</sup>Al  $1^+T=0$  states, isobaric analogue state, spin-isospin effective interaction from <sup>26</sup>Mg( $p, n$ ) 0-68553
- <sup>26</sup>Al excited states, isobaric analogues, spins, DWBA anal. of <sup>27</sup>Al(<sup>3</sup>He,  $\alpha$ ) 0-105981
- <sup>26</sup>Al long lived nucl. isomeric states, thermalization in stars 0-85846
- <sup>26</sup>Al T=1 states, resonances, J<sup>\*</sup> and transitions from <sup>25</sup>Mg( $p, \gamma$ ) 0-99131
- <sup>27</sup>Al levels, resonances, J<sup>\*</sup>, branching and mixing ratios from <sup>26</sup>Mg( $p, \gamma$ ) 0-99132
- <sup>27</sup>Al(e, e'), 70-340 MeV, odd parity state electroexcitation, form factors, transition probs. 0-78208
- <sup>28</sup>Al levels, transitions and spin from <sup>27</sup>Al( $n, \gamma$ ), pol. Al and n 0-78153
- <sup>35</sup>Ar levels, transitions and  $\beta$ -delayed protons from <sup>35</sup>K decay 0-91156
- <sup>36</sup>Ar deduced levels from <sup>36</sup>K beta-delayed particle emission 0-83074
- <sup>As</sup> isotopes, levels and spectra from broken pair model 0-73801
- <sup>As</sup>, A=71, 73, levels, J<sup>\*</sup>, transitions, T1/2 from Se decay, Ge(<sup>3</sup>He, d), (p, xny) 0-57684
- <sup>76</sup>As excited states, excitation functions and decays ang. distrib., cross sections from <sup>76</sup>Ge( $p, n\gamma$ ) (Russian) 0-63089
- <sup>79</sup>As levels, J<sup>\*</sup> and ang. distrib. from <sup>76</sup>Ge( $\alpha, p$ ) 0-78161
- <sup>208</sup>At,  $\gamma$ -transition, multipolarities, level scheme following <sup>208</sup>Rn decay 0-83072
- <sup>212</sup>At excitation functions and isomer ratios from <sup>209</sup>Bi( $\alpha, n$ ) 0-83039
- <sup>213</sup>At levels, J<sup>\*</sup>, transitions and lifetimes from <sup>208</sup>Pb(<sup>7</sup>Li, X) 0-68542
- <sup>B</sup> complex system, excitation functions for 17.19 and 17.64 MeV levels from <sup>6</sup>Li+<sup>3</sup>He 0-78188
- <sup>10</sup>B levels and differential cross sections PWBA and coupled channel anal. of ( $\alpha, t$ ) 0-102121
- <sup>12</sup>B levels, J<sup>\*</sup> and diff. cross sections, R-matrix anal. of <sup>11</sup>B( $n, n$ ) 0-78151
- <sup>12</sup>Ba, A=132, 134, 136, negative parity states, J<sup>\*</sup>, transitions, DWBA anal. of Ba( $p, t$ ) 0-86810
- <sup>12</sup>Ba, A=142, 144, 146, transition  $\gamma$ - $\gamma$  ang. correlations, levels, J<sup>\*</sup>, mixing ratios 0-73823
- <sup>12</sup>Ba,  $\gamma\gamma$  ang. correlations, levels, spins and mixing ratios from <sup>142</sup>Cs decay 0-57734
- <sup>7</sup>Be effective for charge exchange analogues of Gamow-Teller transitions from <sup>7</sup>Li( $p, n$ ) 0-57726
- <sup>7</sup>Be  $1^+$  and  $1^-$  levels, expt. and shell model calcs. from <sup>7</sup>Li( $p, \gamma$ ) 0-63095
- <sup>8</sup>Be, energy levels deduced from <sup>6</sup>Li(<sup>6</sup>Li,  $\alpha$ ) reaction mechanism 0-83113
- <sup>9</sup>Be low lying spectrum, 3-body molecular description, adiabatic one level approx. 0-78150
- <sup>9</sup>Be( $\alpha, \alpha'$ ), 65 MeV, levels and differential cross sections, optical anal. 0-102121
- <sup>10</sup>Be levels and differential cross sections DWBA and coupled channel anal. of ( $\alpha, ^3$ He) 0-102121
- <sup>9</sup>Be, excited states and spectra, continuum effects calcs. 0-57720
- <sup>209</sup>Bi energy and transition probability convergence in Dyson's boson expansion 0-78206
- <sup>209</sup>Bi levels and spectroscopic factors, <sup>210</sup>Bi(9<sup>-</sup>) parentage from <sup>210</sup>Bi<sup>m</sup>(d, t) 0-78158
- <sup>209</sup>Bi single particle levels, ang. distrib., spectroscopic factors, DWBA anal. of <sup>208</sup>Pb(<sup>7</sup>Li, Me) 0-63067
- <sup>76</sup>Br<sup>m</sup> decay props., half life and  $\gamma$ -transitions, level scheme 0-83071
- <sup>C</sup>( $p, \pi^-$ ), A=12, 13, 200 MeV, analogue and nonanalogue state cross sections 0-99130
- <sup>12</sup>C  $2^+$  level, transverse EM form factor, convection current contrib. 0-63076
- <sup>12</sup>C( $\alpha, \alpha'$ ), generator coordinate multichannel calc., levels and resonances 0-78149
- <sup>12</sup>C( $p, p'$ ), 122 MeV, level excitation, cross sections, effective NN interaction, DWIA anal. 0-78197
- <sup>12</sup>C( $p, p'$ ), 22-27 MeV,  $1^+$  state de-excitation  $\gamma$ -ray ang. distrib., tensor force effects, DWBA anal. 0-68580
- <sup>12</sup>C( $p, p'$ ), 800 MeV, 15.11 MeV state diff. cross section, nuclear critical opalescence search 0-105984
- <sup>12</sup>C( $p, p'$ ), pol. p, 800 MeV, unnatural parity states excitation, anal. powers and isospin 0-68538
- <sup>12</sup>C( $p, p'$ ), 23.5-27 MeV,  $1^+$  state spin flip meas. DWBA anal., cross sections 0-68529
- <sup>13</sup>C(<sup>12</sup>C, <sup>12</sup>C), molecular neutron orbit formation, 1/2<sup>+</sup> state excitation, coupled channels calcs. 0-78156
- <sup>14</sup>C first excited 0<sup>+</sup> state, lifetime and E<sup>0</sup> decay from (d, p), (<sup>13</sup>C, p) 0-102145
- <sup>Ca</sup>, A=40, 48, single particle levels, rms charge radius, Wood-Saxon pot. 0-63106
- <sup>Ca</sup>, A=44, 46, excited states and transition ang. distrib. from Ti(<sup>14</sup>C, <sup>16</sup>O) 0-95308
- <sup>Ca</sup>, A=47, 49, single particle states lifetimes calcs. 0-105943
- <sup>40</sup>Ca(<sup>8</sup>Be, <sup>9</sup>Be<sup>-</sup>), 45, 60 MeV,  $1^-$  state excitation Frahn scaling formula for cross section 0-102136
- <sup>40</sup>Ca(d, d), 4.5-5.4 MeV, excited states, excitation functions and ang. distrib., statistical anal. 0-57686
- <sup>40</sup>Ca( $p, \gamma$ ), 6.25 MeV, triple ang. correlation, 3<sup>-</sup> exit channel, resonances, single particle states 0-68626
- <sup>41</sup>Ca excited states, excitation functions and ang. distrib., statistical anal. from <sup>40</sup>Ca(d, p) 0-57686
- <sup>41</sup>Ca parity doublet gamma lifetimes, 3/2 levels, parity mixing from <sup>40</sup>Ca(d, p $\gamma$ ) 0-78209
- <sup>45</sup>Ca levels, excitation functions and J<sup>\*</sup> from <sup>45</sup>K  $\beta$ -decay 0-105978
- <sup>Cd</sup>, A=104-116, low lying level scheme, mass excess from: Cd( $p, t$ ) 0-73807
- <sup>111</sup>Cd, 1330 keV level excitation cross section from positron annihilation 0-68583
- <sup>57</sup>Co state alignment,  $\gamma$ -transitions and ang. distrib. from <sup>56</sup>Fe( $p, \gamma$ ) 0-73797
- <sup>59</sup>Co, energy levels, lifetimes, deexcitation following (n, n' $\gamma$ ) studies 0-83059
- <sup>59</sup>Co level energies, branching ratios lifetimes and spins from (p, p'), ( $\alpha, p\gamma$ ) 0-63093

## nuclear energy levels continued

- <sup>45</sup>Cr ground analogue state fine struct., l=3 states differential cross section from <sup>52</sup>Cr( $p, d$ ) 0-63152
- <sup>49</sup>Cr levels, transitions, and Gamow-Teller matrix elements from <sup>49</sup>Mn,  $\beta^+$ -decay 0-57746
- <sup>51</sup>Cr levels, spectroscopic function and analogue states, PWBA anal. of <sup>52</sup>Cr(<sup>3</sup>He,  $\alpha$ ) 0-68547
- <sup>Ac</sup>, A=142, 144, 146, low lying levels, J<sup>\*</sup>, mixing ratios and  $\gamma$ - $\gamma$  ang. correlations 0-102119
- <sup>134</sup>Cs 176.403 keV isomer, populating  $\gamma$ -rays, low lying levels from <sup>133</sup>Cs( $n, \gamma$ ), <sup>134</sup>Cs 176.403 keV isomer, populating  $\gamma$ -rays, low lying levels 0-78200
- <sup>A</sup>Cu A=29, 63, Doppler shift attenuation factors, level lifetimes, resonances from Ni( $p, \gamma$ ) 0-57741
- <sup>63</sup>Cu levels, transitions and ang. distrib. from  $\alpha$ -transfer in <sup>59</sup>Co(<sup>6</sup>Li, d) 0-73798
- <sup>63</sup>Cu low excitation states, level struct. and lifetimes from <sup>60</sup>Ni( $\alpha, p\gamma$ ) 0-86813
- <sup>63</sup>Cu state alignment,  $\gamma$ -transitions and ang. distrib. from <sup>62</sup>Ni( $p, \gamma$ ) 0-73797
- <sup>63</sup>Cu( $p, p'$ ) negative parity level excitation, gamma ray obs., test for core excitation model 0-68534
- <sup>A</sup>Dy, A=159, 161, lifetimes of low excited states, delayed e- $\gamma$  and  $\gamma\gamma$  coincidences (Russian) 0-68596
- <sup>157</sup>Er, lifetimes of excited states, delayed e- $\gamma$  coincidences (Russian) 0-68597
- <sup>168</sup>Er, 80 and 1094 keV states, g-factors from ang. correlation methods 0-83035
- <sup>172</sup>Er levels, bands, J<sup>\*</sup> and transitions from <sup>170</sup>Er( $t, p$ ) 0-83038
- <sup>A</sup>Eu, A=153, 155, single proton hole states in pickup reactions from (p,  $\alpha$ ) 0-78128
- <sup>152</sup>Eu 89.8488 keV isomeric state feeding, delayed coincidence meas., level scheme from <sup>151</sup>Eu( $n, \gamma$ ) 0-63126
- <sup>152</sup>Eu low lying levels, bands, transitions from <sup>153</sup>Eu( $n, \gamma$ ) 0-57694
- <sup>18</sup>F 1.04 MeV state lifetime and  $\gamma$ -transition polarisation from <sup>18</sup>O(p, n) 0-106016
- <sup>A</sup>Fe, A=57, 59, levels, J<sup>\*</sup> and transition branching ratio from Fe( $n, \gamma$ ) 0-105976
- <sup>55</sup>Fe levels, J<sup>\*</sup>, spectroscopic factors, DWBA anal. of <sup>56</sup>Fe(<sup>3</sup>He,  $\alpha$ ) 0-99127
- <sup>55</sup>Fe resonances, levels, J<sup>\*</sup>, valence capture  $\gamma$ -ray spectrum from <sup>54</sup>Fe( $n, \gamma$ ) 0-86852
- <sup>56</sup>Fe low lying levels, J<sup>\*</sup>,  $\gamma$ - $\gamma$  coincidences, internal conversion from <sup>56</sup>Co  $\beta^+$ -decay 0-86815
- <sup>58</sup>Fe levels, J<sup>\*</sup>, anal. powers and cross sections from <sup>56</sup>Fe( $t, p$ ) pol. t 0-68539
- <sup>68</sup>Fe low lying state mean lifetimes and transitions from <sup>64</sup>Zn(<sup>7</sup>Li, p $n$ ) 0-68599
- Ga, odd, single particle and collective degrees of freedom, clustering, shell model anal. 0-68510
- <sup>69</sup>Ga state alignment,  $\gamma$ -transitions and ang. distrib. from <sup>68</sup>Zn( $p, \gamma$ ) 0-73797
- <sup>73</sup>Ga, levels, J<sup>\*</sup> and ang. distrib. from <sup>70</sup>Zn( $\alpha, p$ ) 0-78161
- <sup>146</sup>Gd levels, J<sup>\*</sup> and transitions, neutron hole coupling to <sup>146</sup>Gd core from <sup>144</sup>Sm( $\alpha, 3n$ ) 0-78164
- <sup>146</sup>Gd lowest 2<sup>+</sup> state, J<sup>\*</sup> and transitions from <sup>146</sup>Tb decay 0-105979
- <sup>146</sup>Gd, O<sub>2</sub><sup>+</sup> state EM decay, T<sub>1/2</sub> and monopole strength 0-95310
- <sup>153</sup>Gd levels and  $\gamma$ -ray spectra from <sup>152</sup>Gd( $n, \gamma$ ) 0-57736
- <sup>154</sup>Gd levels, bands, J<sup>\*</sup>, DWBA anal. of <sup>153</sup>Gd( $t, p$ ) 0-78110
- <sup>154</sup>Gd, vibr. state, level scheme,  $\gamma$  and conversion electron spectra from <sup>154</sup>Gd( $n, \gamma$ ) 0-57696
- Ge, even-even nuclei,  $\gamma$ -spectroscopy, exptl. results and models 0-68589
- Ge, odd, single particle and collective degrees of freedom, clustering, shell model anal. 0-68510
- <sup>A</sup>Ge, A=68, 70, 72, 74, level excitation, n-p interaction role from  $\alpha$ -transfer in Zn(<sup>6</sup>Li, d) 0-73821
- <sup>A</sup>Ge, A=72, 74, 0<sup>+</sup> levels, struct. transition between N=40 and 42 from Ga( $\alpha, p$ ) 0-73800
- <sup>66</sup>Ge levels, lifetimes, J<sup>\*</sup> and transitions from <sup>58</sup>Ni(<sup>10</sup>B, p $n\gamma$ ) 0-73799
- <sup>3</sup>H, ground state energy, second order Brueckner-Baranger approx. 0-63082
- <sup>3</sup>He, ground state level determ. 0-99136
- <sup>3</sup>He (e, e'pp) reaction cross-section and ground state shell model calcs. (Russian) 0-78283
- <sup>3</sup>He broad level search from <sup>3</sup>H(d, n) 0-102117
- <sup>3</sup>He continuum microscopic calcs. cross sections and levels from <sup>3</sup>He+n, <sup>3</sup>H+p channels 0-57702
- <sup>3</sup>He, ground state energy, second order Brueckner-Baranger approx. 0-63082
- <sup>4</sup>He, T=1 excited negative parity state struct. 0-57688
- <sup>4</sup>He( $\alpha, \alpha'$ ), 119 MeV, excited states, J<sup>\*</sup> and  $\gamma$ -ang. correlations 0-86809
- <sup>A</sup>Hg, A=190-200, even, phase transition and possible triaxial shape, energy levels 0-63098
- <sup>157</sup>Ho, lifetimes of excited states, delayed e- $\gamma$  coincidences (Russian) 0-68597
- <sup>I</sup>  $\beta^+$  decay force function resonance struct., level populations (Russian) 0-102154
- <sup>112</sup>In low lying levels, transitions, T<sub>1/2</sub>, multipolarities and mixing ratios from <sup>112</sup>Cd( $p, n\gamma$ ) 0-68545
- <sup>A</sup>Ir, A=189, 191, levels, J<sup>\*</sup>, transitions and mixing ratios from Pt decay 0-68602
- <sup>41</sup>K( $p, \gamma$ ), 1.58 MeV, parity doublet gamma lifetimes, 3/2 levels, parity mixing 0-78209
- <sup>44</sup>K excited levels, J<sup>\*</sup>, transitions and lifetimes from <sup>48</sup>Ca( $p, \alpha$ ) 0-68544
- <sup>46</sup>K levels, J<sup>\*</sup> and tensor anal. powers from <sup>48</sup>Ca(d,  $\alpha$ ), pol. d 0-102113
- <sup>K</sup>, single particle states lifetimes calcs. 0-105943
- <sup>84</sup>Kr levels,  $\gamma$ -cascades, J<sup>m</sup>, mixing ratios and correlations from <sup>84</sup>Br decay 0-63134
- <sup>61</sup>Li excited states, final state interactions, three-body force effects from <sup>7</sup>H( $\alpha, ap$ ) 0-57692
- <sup>A</sup>Li, A=6, 7, excited states and spectra, continuum effects calcs. 0-57720
- <sup>Lu</sup>  $\beta^+$  decay force function resonance struct., level populations (Russian) 0-102154
- <sup>177</sup>Lu excited state lifetimes,  $\gamma$ -transitions from  $\beta$ -decay transitions 0-78205
- <sup>24</sup>Mg, low spin rotational states, energy props., extended deformation, model 0-86785
- <sup>54</sup>Mn low lying 2p-4h states, J<sup>\*</sup> from tensor anal. powers of <sup>56</sup>Fe(d,  $\alpha$ ), pol. d 0-99124



## nuclear energy levels continued

- <sup>55</sup>Mn levels, transitions and spins from <sup>55</sup>Mn(n,γ), pol. Mn and n 0-78154
- <sup>56</sup>Mo, A=98,102, anal. powers, transitions, shape coexistence states, DWBA anal. of Mo(t,p), pol. 0-86895
- <sup>89</sup>Mo<sup>m</sup> levels, transitions and half life from <sup>93</sup>Mo(p,p') 0-86858
- <sup>100</sup>Mo(n,n'), fast n, gamma transitions, level energies and scheme 0-73822
- <sup>100</sup>Mo levels, γ-rays and p-wave resonance partial radiative widths from Mo(n,γ) 0-57739
- <sup>100</sup>Mo(p,p'), odd isotopes, excited d-states from analogue resonances and p-γ correlations 0-68546
- <sup>14</sup>N levels and excitation energies, kinematically complete investigation from <sup>16</sup>O(π<sup>+</sup>, 2n) 0-99128
- <sup>14</sup>N(p,p'), 122 MeV, level excitation, cross sections, effective NN interaction, DWBA anal. 0-78197
- <sup>14</sup>N(p,p'), 25-40 MeV, level cross sections, optical parameters, DWBA anal., tensor effective interaction 0-68555
- <sup>15</sup>N three particle states at high excitation energies, J<sup>π</sup>, selective population from <sup>12</sup>C(Li, α) 0-99129
- <sup>23</sup>Na 0<sup>+</sup> level mean life, isovector mag. dipole transition from <sup>19</sup>F(α,n) 0-68595
- <sup>92</sup>Nb low lying multiplets, DWBA anal. for spectroscopic factors from <sup>91</sup>Zr(α,t) 0-57685
- <sup>14</sup>Nd, A=145, 147, 149, single neutron hole states spectroscopic factors, DWBA anal. of (d,t), (<sup>2</sup>He,α) 0-78109
- <sup>145</sup>Nd energy levels from <sup>144</sup>Nd(d,p) and <sup>146</sup>Nd(d,t), DWBA calcs. 0-68533
- <sup>147</sup>Nd low spin states ns lifetimes, particle rotor model interpretation from <sup>146</sup>Nd(d,p) 0-78207
- <sup>20</sup>Ne 13482 keV level, parity violating effects in two resonance interference from <sup>19</sup>F(p,α) pol. p 0-83033
- <sup>20</sup>Ne ground state level calc., maximum method 0-73795
- <sup>20</sup>Ne low lying levels and intermediate structure J<sup>π</sup> from <sup>16</sup>O(<sup>12</sup>C, <sup>8</sup>Be) 0-102166
- <sup>20</sup>Ne, quartet states from <sup>19</sup>F(p,α) <sup>16</sup>O 0-105973
- <sup>20</sup>Ne deduced spectroscopic factors, levels and anal. powers from <sup>20</sup>Ne(d<sub>pol</sub>,p) 0-83087
- <sup>41</sup>Ni, A=60, 62, 66, levels, J<sup>π</sup>, anal. powers and cross sections from Ni(t,p) pol. t 0-68539
- <sup>58</sup>Ni(<sup>6</sup>Li, <sup>6</sup>Li), 71 MeV, excited states deformation lengths, DWBA and coupled channels anal. 0-68541
- <sup>59</sup>Ni levels, cross section and vector anal. power, ang. distrib. from <sup>58</sup>Ni(<sup>7</sup>Li, <sup>6</sup>Li), pol. <sup>7</sup>Li 0-106044
- <sup>60</sup>Ni level scheme and γ-rays from <sup>59</sup>Ni(n,γ) 0-63099
- <sup>237</sup>Np electron transition excitation following K-shell photoionisation, deexcitation γ-rays 0-78196
- <sup>16</sup>O, A=16, 17, valence-core self-consistency, wave functions, binding energy, levels, spectra 0-63123
- <sup>16</sup>O, 3 α forces, ground state energy and form factor 0-86817
- <sup>16</sup>O 4<sup>+</sup> state nonstatistical population in compound nucleus calcs. of <sup>12</sup>C(<sup>4</sup>Li, d) 0-102137
- <sup>16</sup>O α-cluster states, widths and resonances, optical model, direct transfer in <sup>12</sup>C(<sup>4</sup>Li, d) 0-105975
- <sup>16</sup>O ground state energy and low odd parity states, correlated basis function method 0-57689
- <sup>16</sup>O level excitation functions, resonances from <sup>12</sup>C(<sup>16</sup>O, <sup>12</sup>C) 0-63146
- <sup>16</sup>O(γ,π), total cross section, Δ-hole states damping, π<sup>0</sup>, π exchange, Δ isobar hole model 0-91174
- <sup>16</sup>O 6p-4h states and composite spectra from <sup>12</sup>C(<sup>18</sup>O, <sup>12</sup>C) 0-63096
- <sup>20</sup>O first excited state, g-factor and lifetime from <sup>1</sup>H(<sup>18</sup>O, p) 0-102115
- <sup>18</sup>Os, A=186,188, levels and transitions from Re decay, triaxial rotor model 0-91155
- <sup>18</sup>Os, A=188, 189, levels, J<sup>π</sup>, transitions and mixing ratios from Ir decay 0-68602
- <sup>193</sup>Os level scheme and transitions, Coriolis coupled Nilsson states from <sup>192</sup>Os(n,γ) 0-57698
- <sup>28</sup>P, nucleon unbound states, spin, parity, partial width, from <sup>28</sup>Si(d,pn) 0-102118
- <sup>30</sup>P level width isospin depend., excitation functions, statistical anal. of <sup>29</sup>Si(p,α) 0-78152
- <sup>30</sup>P positive parity states, transitions and spectroscopic strengths, DWBA anal. of <sup>29</sup>Si(<sup>3</sup>He, d) 0-102138
- <sup>30</sup>P T=1 state decay, lifetimes and branching ratios, analogue E2 transitions from <sup>29</sup>Si(p,γ) 0-68598
- <sup>31</sup>P high E<sub>x</sub> states, J<sup>π</sup>, DWBA anal. <sup>29</sup>Si(<sup>3</sup>He, p) 0-68536
- Pb even isotopes, two quasiparticle 2<sup>+</sup> state coupling to T=0 giant quadrupole resonance 0-68618
- <sup>204</sup>Pb, muonic, first excited 2<sup>+</sup> state, isomer shift of E2 transition 0-99150
- <sup>204</sup>Pb(n,n'), 1.5-3.1 MeV, levels, J<sup>π</sup>, excitation functions and mixing ratios 0-102123
- <sup>206</sup>Pb γγ directional correlations, multipole mixing ratios, transition strength limits from <sup>206</sup>Bi decay 0-86849
- <sup>207</sup>Pb muonic isomer shifts, neutron hole anomalous moment contribs. 0-78728
- <sup>208</sup>Pb breathing model transition density, single particle and collective state dynamical coupling 0-106007
- <sup>208</sup>Pb, magnetic high spin states, microscopic struct. 0-95297
- <sup>208</sup>Pb single particle and hole states, renormalisation, core polarisation, spectroscopic factors 0-57658
- <sup>208</sup>Pb(<sup>12</sup>C, <sup>1</sup>B), 77 MeV, bound and continuum state excitation, direct and two step processes 0-63205
- <sup>208</sup>Pb(α,α'), levels, B(E3), transition density and nuclear pot., folding model anal. 0-86812
- <sup>208</sup>Pb(p,p'), 135 MeV, normal parity level excitation, J<sup>π</sup>, differential cross sections 0-57690
- <sup>208</sup>Pb(p,p'), 135 MeV, normal parity excitations, microscopic description, NN interaction shape 0-57691
- <sup>209</sup>Pb excited states, 3/2<sup>-</sup> resonances from shell model of <sup>208</sup>Pb(n,n) 0-78240
- <sup>210</sup>Pb levels, J<sup>π</sup>, transitions and lifetimes from <sup>208</sup>Pb(<sup>7</sup>Li, X) 0-68542
- <sup>100</sup>Pd levels and γ-transitions from <sup>100</sup>Ag<sup>m</sup> decay 0-83077
- <sup>102</sup>Pd(p,p'), long lived 0<sup>+</sup> state, E0 transitions 0-73804
- <sup>109</sup>Pd low spin odd parity levels, γ-rays, particle-rotor comparison from <sup>108</sup>Pd(n,γ) 0-73805
- <sup>109</sup>Pd low spin odd parity states, rot. aligned model, Coriolis calc. of <sup>108</sup>Pd(n, γ) 0-57695
- <sup>14</sup>Pm, A=143, 145, proton states and transitions, stripping strength, shell model anal. from Nd(<sup>2</sup>He, d) 0-68508

## nuclear energy levels continued

- <sup>14</sup>Pm, A=147,149,151 single proton hole states in pickup reactions from Sm(p,α) 0-78128
- <sup>14</sup>Pm, A=149,151, shape coexistence, deformed states from Nd decay 0-78135
- <sup>147</sup>Pm, level scheme and transitions following <sup>147</sup>Nd 0-83073
- <sup>149</sup>Pm levels, bands, transitions, in-beam spectroscopy, particle-rotor anal. from <sup>150</sup>Nd(p,2n) 0-78125
- <sup>211</sup>Po excitation functions and isomer ratios from <sup>208</sup>Pb(α,n) and <sup>209</sup>Bi(α,np) 0-83039
- <sup>212</sup>Po excitation functions and isomer ratios from <sup>209</sup>Bi(α,p) 0-83039
- <sup>212</sup>Po, levels, J<sup>π</sup>, transitions and lifetimes from <sup>208</sup>Pb+<sup>4</sup>Li 0-68542
- <sup>191</sup>Pt, A=190,192,194, state struct. in interacting boson model 0-83047
- <sup>193</sup>Pt low lying negative parity states and shape from <sup>193</sup>Pt(p,t) 0-68540
- <sup>241</sup>Pu level structure and γ-transitions from <sup>241</sup>Cm decay 0-105980
- <sup>230</sup>Ra levels, J<sup>π</sup> and transitions, Nilsson assignments from <sup>230</sup>Ac decay 0-68543
- <sup>8</sup>Rb(n,n'), 550-2100 keV, A=85.87, levels, excitation functions, J<sup>π</sup>, Hauser-Feshbach anal. 0-105982
- <sup>84</sup>Rb levels, J<sup>π</sup> and transitions from Kr<sup>m</sup>, Sr<sup>m</sup> decay, cluster-vibr. model 0-78162
- <sup>9</sup>Rh levels and γ-transitions, 3QP model anal. of <sup>97</sup>Pd β<sup>+</sup>-decay 0-102120
- <sup>112</sup>Rn, shell model states, semiempirical calcs. half lives, mag. moments, excitation functions 0-63083
- <sup>101</sup>Ru, A=104,106,108, level scheme and transitions, collective model anal. of Tc decay 0-78166
- <sup>101</sup>Ru, A=106, 108, levels, transitions, J<sup>π</sup> and shape from Tc decay 0-57744
- <sup>94</sup>Ru level structure, spin and parity, from beta decay of <sup>94</sup>Rh isomers 0-57747
- <sup>102</sup>Ru(<sup>16</sup>O, <sup>16</sup>O), 38-42 MeV, Coulomb excitation, 2<sup>+</sup> state electric quadrupole moment 0-73793
- <sup>102</sup>Ru(α,α), 8.5, 9.0 MeV, Coulomb excitation, 2<sup>+</sup> state electric quadrupole moment 0-73793
- <sup>32</sup>S α-cluster struct., ground and first excited states, energies, radii and moments 0-102122
- <sup>32</sup>S(n,n'), 13.9 MeV, 2<sup>+</sup> (2.23 MeV) excitation, spin flip probab., deexcitation γ-rays 0-86853
- <sup>4</sup>Sc levels, J<sup>π</sup>, transitions and lifetimes from (p,p')(<sup>3</sup>He,<sup>3</sup>He)(α,α') 0-63091
- <sup>48</sup>Sc proton single particle states, spectroscopic factors, DWBA anal. of <sup>48</sup>Ca(d,n) 0-99118
- <sup>48</sup>Sc, single particle states lifetimes calcs. 0-105943
- Se, even-even nuclei, γ-spectroscopy, exptl. results and models 0-68589
- <sup>8</sup>Si(e,e'), 126-293 MeV, A=28,29, levels and form factors, particle-phonon coupling anal. 0-105977
- <sup>28</sup>Si 12.291 MeV level width, axial blocking meas. from <sup>27</sup>Al(p,α) 0-63086
- <sup>28</sup>Si 4<sup>+</sup> state lifetime by blocking effect method from <sup>27</sup>Al(p,α) (Russian) 0-91152
- <sup>28</sup>Si 3/2<sup>+</sup> and 5/2<sup>+</sup> states population, (d,p) and (p,π<sup>+</sup>) comparison 0-95307
- <sup>28</sup>Si doorway state neutron capture, levels and γ-spectra from <sup>28</sup>Si(n,γ) 0-57729
- <sup>28</sup>Si levels, J<sup>π</sup>, spectroscopic factor, DWBA anal. of <sup>28</sup>Si(<sup>3</sup>He, <sup>2</sup>He) 0-86811
- <sup>28</sup>Si levels and ang. distrib., DWBA anal. of <sup>27</sup>Al(α,d) 0-78157
- <sup>29</sup>Si, low lying energy level structure, from <sup>28</sup>Si(d<sub>pol</sub>,p) and multi-step reaction calcs. 0-68537
- <sup>29</sup>Si, nucleon unbound states, spin, parity, partial width, from <sup>28</sup>Si(d,pn) 0-102118
- <sup>147</sup>Sm, A=146,147, excited states, energy levels, spin, parity, shell and cluster-vibration models, from (α,xn) and (<sup>3</sup>He,xn) 0-57683
- <sup>147</sup>Sm, A=147, 149, levels, J, γ-transitions and multipole mixing ratios, γγ correlations from Eu EC decay 0-106012
- <sup>151</sup>Sm low energy levels from expt. and Coriolis mixing calcs. of <sup>150</sup>Sm(n,γ) 0-57697
- Sm(p,t), even isotopes, high energy neutron pairing strength, two neutron holes, resonances 0-78116
- Sn isotopes, levels and spectra from broken pair model 0-73801
- <sup>118</sup>Sn, A=118,120,122, deep hole states, excitation energies and ang. distrib. from Sn(p,t) 0-86792
- <sup>118</sup>Sn(n,n'), A=116, 118, 120, 122, 124, 11 MeV, levels, deformation parameters, isospin effects, optical parameters 0-57679
- <sup>115</sup>Sn weak coupling neutron hole states from <sup>116</sup>Sn(<sup>3</sup>He,α) 0-73786
- <sup>132</sup>Sn levels, isomers, lifetimes and transition probabilities from fission 0-78163
- <sup>8</sup>Sr, A=94,96 direct and skip cascades, γγ ang. correlations, levels, mixing ratios from Rb decay 0-86851
- <sup>8</sup>Sr 1<sub>g9/2</sub> neutron distrib. radial size, states, differential cross sections from <sup>86</sup>Sr(<sup>18</sup>O, <sup>17</sup>O) 0-95301
- <sup>92</sup>Sr γγ ang. correlations, levels, J<sup>π</sup>, mixing ratios from <sup>92</sup>Rb decay 0-57725
- <sup>98</sup>Sr very low lying 0<sup>+</sup> state, shape coexistence bands, T<sub>1/2</sub>, transitions from <sup>98</sup>Rb decay 0-78148
- <sup>185</sup>Ta single proton states and rot. bands, J<sup>π</sup> from <sup>186</sup>W(t,α), pol. t 0-91130
- <sup>97</sup>Tc, energy levels, low-lying, decay properties 0-63084
- <sup>98</sup>Tc 14 μs isomer, low lying levels and transitions from <sup>98</sup>Mo(p,n) 0-73802
- <sup>100</sup>Tc μs isomers, isomeric transitions and mean lives from <sup>100</sup>Mo(p,n) 0-73803
- <sup>231</sup>Th excited states and bands, spins, γ-transitions from <sup>230</sup>Th(n,γ) 0-57699
- <sup>4</sup>Ti, A=48,50, excited states and transition ang. distrib. from Cr(<sup>14</sup>C, <sup>16</sup>O) 0-95308
- <sup>204</sup>Tl neutron hole states, J<sup>π</sup> and spectroscopic factors from <sup>205</sup>Tl(p,d) 0-86783
- <sup>167</sup>Tm, energy level scheme from <sup>165</sup>Ho(α,2n) (German) 0-68576
- <sup>45</sup>V level scheme, γ-rays, level lifetimes, internal conversion from <sup>44</sup>Ca(Li,xn) 0-63085
- <sup>51</sup>V(p,p'), 6 MeV, levels, spins and EM props., shell model anal. 0-63092
- <sup>181</sup>W, A=178, 180, 182, 184, levels and J<sup>π</sup>, ang. distrib. from W(p,t) 0-78159
- <sup>181</sup>W level density, n spectra and ang. correl., direct and nonequilibrium processes from <sup>181</sup>Ta(p,n) (Russian) 0-68631
- <sup>181</sup>W levels (neutron and collective) and J<sup>π</sup>, ang. distrib. from <sup>183</sup>W(p,t) 0-78160
- <sup>184</sup>W(<sup>12</sup>C, <sup>12</sup>C), 70 MeV, 4<sup>+</sup> state excitation ang. distrib., hexadecapole deformation length effects 0-68521

**nuclear energy levels continued**

- <sup>135</sup>Xe excited state lifetimes,  $\gamma$ -transitions from <sup>129</sup>Cs decay 0-78205  
<sup>132</sup>Xe level struct., J<sup>π</sup>, transitions and multipole mixing ratio from <sup>132</sup>I decay 0-91134  
<sup>137</sup>Xe neutron unbound states, high energy X-rays from <sup>137</sup>I decay 0-86856  
<sup>87</sup>Y level struct.,  $\gamma$ -spectroscopy and J<sup>π</sup> from (p,2n $\gamma$ ), ( $\alpha$ ,2n $\gamma$ ) 0-83040  
<sup>90</sup>Y low lying multiplets, DWBA anal. for spectroscopic factors from <sup>91</sup>Zr(d,<sup>3</sup>He) 0-57685  
<sup>169</sup>Yb  $\gamma\gamma$  ang. correlations, levels and spins from <sup>169</sup>Lu decay (Russian) 0-83069  
<sup>173</sup>Yb,  $\gamma$ -transitions from 7/2, 7/2<sup>-</sup> [514] 636 keV level 0-78187  
<sup>Δ</sup>Zn, A=64, 66 levels and primary E1 transition strength functions from Cu(p, $\gamma$ ) 0-91149  
<sup>6</sup>Zn states, pseudo LS coupling model 0-68548  
<sup>Δ</sup>Zr, A=92, 96, first excited 0<sup>+</sup> state transition strength from (<sup>6</sup>Li,<sup>4</sup>B), (d,<sup>6</sup>Li) correlation 0-78260  
<sup>Δ</sup>Zr(<sup>35</sup>Cl,<sup>35</sup>Cl<sup>+</sup>), 90 MeV, A=92, 94, 2<sub>1</sub><sup>+</sup> levels mag. moments 0-105968  
<sup>92</sup>Zr levels, J<sup>π</sup>, cross sections, vector anal. power, optical parameters from <sup>91</sup>Zr+pol. d 0-78268  
Zr(p,p' $\gamma$ ), odd isotopes, excited d-states from analogue resonances and p- $\gamma$  correlations 0-68546

**nuclear engineering**

see also fission reactors

- fusion reactor, MFTF, sustaining neutral beam power supply, shunt preconditioner, IBM-ASTAP anal. 0-102332  
fusion reactor, PHIBEX, poloidal field power supply for ignition, computer based cct. anal. 0-102329  
heavy water dielectric constant meas. over temp. range 473K to 643K 0-103912  
power station development in Soviet Union, problems and solution 0-102290

**nuclear engineering computing**

see also computerised control; computerised instrumentation

- ALMOS, BWR plant model, appl. to turbine trip transient analysis (German) 0-83177  
AMPX code, operating experience 0-68743  
AMPX code for coupled multigroup n- $\gamma$  cross section sets 0-68741  
AMPX code implementation problems at KFA Jülich 0-68742  
analogue simulation for continuous gas flow control, nuclear fuel production (German) 0-78416  
BABEL, multigroup neutron library for fast reactor, shielding design studies 0-68745  
BWR, TRAB transient analysis program for pressure vessel and subsystems 0-73978  
BWR LOCA analysis, jet pump modelling using RELAP4 0-68850  
CACTUS, a characteristics solution to the neutron transport equations in complicated geometries 0-95336  
CANDU-PHW 600 MWe reactors, channel power mapping and calibration routing 0-57892  
clad failure prediction during FBR overpower transiency, JANE 0-78363  
COBRA, fuel bundles, thermal-hydraulic anal., comparison of computational techniques in COBRA-IIIC and COBRA-IIIP (Japanese) 0-95374  
conference, Berlin, Germany (Aug. 1979) 0-77539  
cost comparison of PWR and PHWR nuclear power plants in Korea using ORCOST and POWERCO-50 0-78281  
CRISIS code for LWR critical heat flux calc., anal. of empiric relations (Bulgarian) 0-68766  
CRNL NOS/BE I.3 system, dynamic core allocation 0-78425  
digital computer applications in reactor instrumentation and control 0-106134  
DISCAL, HCDA, neutronics and hydrodynamics equations, energy release 0-68842  
DOT 3.5, use in fast power reactor shield configuration calcs. 0-68749  
dynamic analysis facility at Chalk River National Laboratory 0-58106  
ENDF/B-V uncertainty data processing into multigroup covariance matrices 0-68752  
EULFCI code for numerical anal. of LMFBR HCDA fuel-coolant interaction 0-68733  
EURDYN, nonlinear transient dynamics programs for fast reactor safety 0-91234  
EURDYN-1M, safety studies on LMFBR, computer program 0-99267  
failure location algorithm for complex networks 0-99228  
FAPMAN-IC program module for LWR power stations, incremental fuel cost calcs. 0-95356  
fast breeder test reactor operator training simulator model development 0-91219  
FASTA, fuel performance modelling, pellet-cladding interaction 0-63264  
FASTA, fuel preconditioning, power shock anal. and sipping 0-63358  
FBR, space dependent simulation of transient behaviour using KINTIC-2 code (German) 0-83182  
FBR containment code, structural deform., SEURBNUK-2 0-78404  
FBR containment code validation program, SEURBNUK 0-78405  
fission gas release from high burn-up oxide fuel, predictions in ELESIM code 0-57864  
FLAIR-CENSOR, PWR core power manoeuvres, fuel duties and fuel preconditioning 0-63337  
fuel bundles, thermal-hydraulic anal., comparison of computational techniques in COBRA-IIIC and COBRA-IIIP (Japanese) 0-95374  
fuel element codes, structural anal. 0-78362  
fuel performance modelling, pellet-cladding interaction, FASTA 0-63264  
fuel preconditioning, power shock anal. and sipping, POSHA and FASTA 0-63358  
fusion reactor, compact toroidal ignition experiment, support struct. anal. by numerical code 0-106167  
fusion reactor, low power Tokamak experimental fusion power plant, scoping studies with empirical scaling, SISYFUS code 0-102309  
fusion reactor, magnetic confinement, structural anal., combined interactive/batch computer environment 0-91255  
fusion reactor, PDX Tokamak, finite element anal. using computer graphics 0-95424  
fusion reactor, SLPX TF coil, stress anal. using COSMIC-NASTRAN 0-106168  
GAM library data formation in energy groups, PWR appl. 0-68746  
guard line circuits dual microprocessor system, decision-making and self-testing 0-57901  
HCDA, neutronics and hydrodynamics equations, energy release, DISCAL code 0-68842

**nuclear engineering computing continued**

- HEATUP-R/AEP analysis of PWR LOCA reflood, effect of low containment press. on peak cladding temp. 0-57897  
HEXAB-II-30E code for few group 2-D diffusion eqns. in hexagonal geometry, LWR core calcs. (Bulgarian) 0-68765  
HTR spent fuel reprocessing facility, real-time data acquisition and processing system (German) 0-106148  
in-reactor fuel temperature, transient response of centreline thermocouples, appl. to fuel modelling 0-95372  
ISUNE-4 code for transient pellet-cladding interaction, in LWR 0-91228  
JANE, clad failure prediction during FBR overpower transiency 0-78363  
JET, control system, communications, diagnostics, data storage and anal., NORD computers 0-68943  
KINTIC-2, space dependent simulation of transient behaviour of FBR (German) 0-83182  
Large Coil Test Facility, instrumentation system design 0-95446  
LMFBR HCDA analysis, uncertainty in accident consequences calculated by large codes due to uncertainties in input 0-78413  
LMFBR intersubassembly transient heat transfer code, TCLUSTI 0-63231  
LMFBR subassembly, fuel coolant interaction anal.model and computer code SAMI 0-106136  
LOCA, data analysis using computer-aided models (Czech) 0-73949  
LOCA analysis in small compact reactors using RELAP4/MOD5 thermal hydraulic code 0-68852  
LWR code analysis, qualification of SIMULATE against the Hatch-1 end-of-cycle 1 gamma scan 0-57921  
LWR core, few group 2-D diffusion eqns. in hexagonal geometry, HEXAB-II-30E code (Bulgarian) 0-68765  
LWR critical heat flux calc., anal. of empiric relations using CRISIS code (Bulgarian) 0-68766  
LWR design codes EPRI-CELL and CPM, implementation 0-68751  
LWR fuel rod, transient pellet-cladding interaction, ISUNE-4 computer anal. 0-91228  
LWR power stations, incremental fuel cost calcs. using FAPMAN-IC program module 0-95356  
magnetic field and force eqns., solns. using programmable calculator 0-91721  
MARC finite element program, PWR piping, circumferential cracks, opening and extension 0-78364  
microprocessor controlled multitrack recorder with graphical video output for reactor core temperatures 0-57873  
microprocessor for nuclear reactor instrumentation 0-83147  
microprocessor-based fuel wire evaluation and anal. system 0-63353  
MORSE continuous weights code 0-68748  
MWPC, cylindrical, event triggers, correlation of wire addresses 0-58092  
neutron diffusion code comparison for LMFBRs 0-95337  
NOTUNG, anal. of ECCS dynamic procedures in SNR-300 LMFBR (German) 0-83185  
particle detectors, high speed data processing, histogram and tape writing 0-58101  
POSHA, fuel preconditioning, power shock anal. and sipping 0-63358  
PROFIP 3, PWR fuel clad failure characterisation based on fission product activity 0-95365  
protection system software validation, quality assurance experience 0-57886  
Porex process, first extraction, Pu accumulation, computer simulation, SEPHIS code 0-68907  
PWR, three loop, simulation in advanced recycle methodology program 0-68856  
PWR core analysis, methods and data validation 0-57924  
PWR core analysis, steady-state core physics and thermal-hydraulic reload design calcs. 0-57923  
PWR core analysis using EPRI ARMP program, calc. and meas. reactor physics parameters 0-57925  
PWR core analysis verification, reactivity rundown and power distrib. accuracy 0-57922  
PWR core power manoeuvres, fuel duties and fuel preconditioning, FLAIR-CENSOR 0-63337  
PWR dynamical behaviour modelling in FORTRAN 0-91217  
PWR engineered safety features actuation system follow-up system logic 0-57879  
PWR fuel clad failure characterisation based on fission product activity, PROFIP 3 code 0-95365  
PWR LOCA reflood, effect of low containment press. on peak cladding temp., HEATUP-R/AEP anal. 0-57897  
PWR piping, circumferential cracks, opening and extension, MARC finite element program 0-78364  
REACT/THERMIX, eval. of graphite (German) 0-83181  
reactor core energy distribution, algorithm for extremal control 0-83209  
reactor dynamics, numerical integration using real integrating factors 0-68730  
RELAP4, jet pump modelling in BWR LOCA anal. 0-68850  
RETRAN model analysis of TMI-2 accident 0-102263  
SDX cell homogenisation code validation for ZPPR pin geometry 0-86962  
seed-blanket calcs., 2-D, one-channel synthesis method, transport and diffusion 0-73876  
self-shielding factors, discrepancies between ETOX and TIMS codes 0-68744  
SEPHIS, Pu accumulation in Porex process, first extraction 0-68907  
SETS, shutdown heat removal system failure, fault tree, common-cause anal. 0-63334  
SEURBNUK, FBR containment code validation program 0-78405  
SEURBNUK-2, FBR containment code, structural deform. 0-78404  
shielding benchmark calcs. by Discrete Ordinates and Monte Carlo methods 0-73886  
shutdown heat removal system failure, fault tree, common-cause anal., SETS 0-63334  
SIMULATE qualification against the Hatch-1 end of cycle gamma scan 0-57921  
SNR-300 LMFBR, ECCS, decay heat removal during heat sink failure, accident anal. using NOTUNG code (German) 0-83185  
symbiotic system economic evaluation using SYMECON 0-106177  
TCLUSTI, LMFBR intersubassembly transient heat transfer code 0-63231  
TMI-2 accident analysis using two-loop RETRAN model 0-102263  
transport codes DOT and TWOTRAN as standards for diffusion in pebble bed reactors 0-68750  
UNCLE finite element scheme, input specification 0-95512



**nuclear engineering computing continued**

WIMSD performance in cell parameters calculation for  $\text{UO}_2\text{-D}_2\text{O}$  systems 0-68747  
 Yankee reactor physics method verification 0-63323

**nuclear explosions**

see also weapons

axially symmetric explosion in magnetogasdynamics 0-62007  
 fallout from atmospheric test as possible explanation of Ural contamination disaster 0-76666  
 thermonuclear microexplosion, use of black-body radiation as inertial confinement fusion driver 0-91241  
 ultrahigh press. (TPa) shockwave from underground nuclear explosion for solid Hugoniot data 0-59580  
 underground explosions, hydrophone recordings of mantle-refracted P-waves 0-98257  
 $^{14}\text{C}$  contamination of Atlantic from weapons tests 0-89683  
 $^{240}\text{Pu}$ , effect of spontaneous fission on energy release in a nuclear explosive 0-95464

**nuclear fission** see fission**nuclear fission of plutonium** see fission of plutonium**nuclear fission of uranium** see fission of uranium**nuclear fission piles** see fission reactors**nuclear fission products** see fission products**nuclear forces**

see also binding energy; meson field theory; nuclear binding energy  
 $\alpha$ -clustering in heavy nuclei, pre-equil. model, nuclear matter NN,  $N\alpha$  interactions 0-63111  
 $A=18$ , shell-model spectra, one-boson-exchange potential 0-68550  
 $A=42$ , multiple scattering formalism for the effective interaction 0-102126  
 CC  $^{12}\text{C}(\gamma, \pi^+)^{12}\text{B}$ , nuclear critical opalescence study 0-105988  
 double stripping core independ. 2-nucleon transfer, Tang-Herdon effective interactions,  $(\alpha, d)$ ,  $(t, p)$  0-73836  
 education, Schrodinger eqn. solns. using approximate nucleon-nucleon and  $A$ -nucleon pots. 0-62429  
 effective mass and exchange current effects in finite nuclei 0-78171  
 effective NN interaction and exchange current vel. depend., dipole sum rule enhancement 0-63100  
 effective potentials for heavy-ion scattering derived from channel coupling 0-57794  
 few nucleus correlations from high energy scatt., review (Russian) 0-68549  
 finite nuclei,  $\Delta$ -resonance self energy, Fermi broadening,  $\pi$ -nucleus optical pot. 0-68707  
 force on nucleus in non-stationary state, definition and anal. 0-105526  
 four-body system, Efimov effect and three-body effective pot. 0-86865  
 ghost-pole subtraction and the  $\sigma$ -exchange NN potential 0-86819  
 growth points in nuclear physics, book 0-94929  
 Hartree eqn., quasiclassical soliton soln., Newtonian interaction with screening 0-68569  
 heavy ion optical potential, real part, folding technique 0-73830  
 heavy nuclei tensor forces, unnatural parity excitations, high momentum collectivity 0-63065  
 hypernuclei, NN tensor force effect on  $\Lambda$  separation energy 0-86845  
 infinite system of nucleons and  $\Delta$  resonances, pot. energy, neutron stars 0-86836  
 many body problem in Lee model, NN scatt. and matter binding energy 0-63116  
 microscopic effective interactions in correlated model space, eqn. of motion method 0-86818  
 multipole residual interaction strength, radial depend. in RPA 0-83026  
 neutron rich nuclei stability, HF calcs. (Russian) 0-78181  
 nuclear energy level shift non-measurability due to pion diamagnetism in Mossbauer effect 0-73808  
 nuclear field theory, phonon renormalisation, eigeneqns. and sum rules (Chinese) 0-102127  
 nuclear field theory, schematic model functional approach, diagram rules 0-102128  
 nuclear matter, iterative isobar process role, effective NN interaction 0-99143  
 nuclear matter, S-wave  $\pi$ N interactions and PCAC 0-78185  
 nuclear matter, spin-isospin and pion condensation phase transitions, eqn. of state 0-86843  
 nuclear proximity interaction from HF functional with Skyrme interactions 0-83043  
 nucleon-nucleon interaction as derived from the De Rujula, Georgi, Glashow phenomenological quark-quark potential 0-78172  
 off shell form factor model, NN scatt. appl. 0-86800  
 PETRA results for fluons, nuclear forces, t-quarks and quark-lepton symmetry 0-86731  
 pion condensation precursor, quasi-elastic peak softening 0-78170  
 pion spectrum and polariz. operator in nuclear medium in heavy nuclei collisions (Russian) 0-68558  
 potential energy surfaces, folded Yukawa-plus-exponential model 0-86816  
 QCD and superdense matter, quark and gluon plasma, hadronic structure, neutron stars, hadron collisions, review 0-73683  
 s-d shell, two nucleon effective interaction, intruder state, RPA correlation 0-57701  
 S-wave  $\pi$ N interaction role in combined pion condensation 0-105998  
 S-wave nucleon-nucleon interaction, energy-dependent separable potential 0-68551  
 single-particle response and ground-state properties, Hartree-Fock theories 0-105997  
 spherical nuclei, Hartree-Fock-Bogolyubov calcs., D1 effective interaction, nuclear matter, binding energies 0-63105  
 spin rotation, high angular velocity, collective aspects of heavy ion collisions 0-78309  
 strongly bound pion states in nuclei, optical model 0-68557  
 Thomas-Fermi kinetic-energy density with gradient corrections 0-91169  
 three-body force from  $2\pi$ ,  $\pi\rho$ , and  $2\rho$  exchanges 0-78169  
 three-body force from kinematical effects in the three-nucleon system 0-105986  
 UCN, quasibound states in matter, reson. positions and widths 0-73833  
 Woods-Saxon potential spectrum, pairing force strength, Nilsson model comparison 0-57704  
 $(\alpha, \alpha)$ , local density dependence of NN interaction, double-folding calcs. 0-83114  
 $(d, x)$  deuteron break-up, dependence of differential cross section on n-p potential form (Russian) 0-78173

**nuclear forces continued**

ed-ed, nucleon forces, meson exchange current effects, impulse approx., review 0-57603  
 $\Lambda$ N distrib. function,  $\Lambda$ -binding to nuclear matter, Fermi hypernetted chain approx. 0-78131  
 $\Lambda$ NN correlations and  $\Lambda$  binding in nuclear matter 0-106000  
 $N^*(1688)$  resonance effects on nuclear reaction, NN scatt. phase parameters 0-105987  
 $\bar{N}N$  and  $\pi\bar{N}N$ ,  $\pi\bar{N}N$  bound states from  $\bar{N}N$  potentials 0-62951  
 $\bar{N}N \rightarrow B_1\pi$ ,  $B_1$  are  $\bar{N}N$  quasineuclei 0-57624  
 $\bar{N}N$  dynamics at medium energies, elastic and inelastic scatt., unitary model 0-63101  
 $\bar{N}N$  dynamics at medium energies, phase parameters, one pion exchange model 0-63102  
 $\bar{N}N$  forward scatt., two and three pion cut contribs., nucleon exchange model 0-63103  
 $\bar{N}N\bar{N}$  bound state problems, hyperspherical harmonic expansion, review 0-91136  
 $\bar{N}N\pi$  system, phenomenological relativistic quantum mechanics, scatt. theory 0-83082  
 $(p, p')$ , single neutron states, two step process and effective interaction 0-78290  
 $(p, p')$ , unnatural parity states excitation,  $\pi$ -condensate instability effects, DWBA anal. 0-78168  
 $(\pi, 2\pi)$ , possible probe for pion condensation precursor phenomena 0-78330  
 $(\pi, \pi)$ , Weinberg chiral Lagrangian nonlinear terms, nuclear binding, optical pot. 0-78329  
 $(\pi, X)$ , effective S-wave  $\pi\bar{N}N$  interaction, effects in nuclear matter 0-105985  
 $\pi$  condensation in neutron matter, N-N interaction, critical density 0-57711  
 $\pi$  condensed phase,  $\sigma$ -model, alternating-layer-spin struct. 0-83057  
 $\pi$ - and  $\rho$ -exchange pots., influence on mag. resonances, mag. moments, and transition probs. 0-99133  
 $\pi^-$  absorption at rest, high spin state excitation,  $\pi$ -condensation and  $\Delta^{++}$  (Russian) 0-86927  
 $\pi$ N elastic scatt., nonstatic model for nuclear reactions 0-102125  
 $\pi\bar{N}N$ -NN coupled problem, unitary model 0-99135  
 $\pi\bar{N}N$ -NN coupled systems theory, relativistic extensions 0-63104  
 $^{26}\text{Al } 1^+T=0$  states, isobaric analogue state, spin-isospin effective interaction from  $^{26}\text{Mg}(p, n)$  0-68553  
 $\text{Be}$ , neutron forces in relativistic electron radiation field in crystal, channelling (Russian) 0-70287  
 $^7\text{Be}$  effective for charge exchange analogues of Gamow-Teller transitions from  $^7\text{Li}(p, n)$  0-57726  
 $\text{Be}(\gamma, p)X$ , 180-420 MeV, quasifree NN system photodisintegration, p spectrum 0-106049  
 $^{20}\text{Bi}(\text{He}, d)$ , 30 MeV, effective residual interaction matrix elements, spectroscopic factors, cross sections 0-99134  
 $^{20}\text{Bi}(\alpha, t)$ , 40 MeV, effective residual interaction matrix elements, spectroscopic factors, cross sections 0-99134  
 $^A\text{C}$ ,  $A=12, 13$ , nuclear critical opalescence, M1 form factor, pion field and condensation 0-73809  
 $^{12}\text{C } 1^+(T=1, 15.1 \text{ MeV})$  state excitational pionic modes, M1 form factor for  $(p, p')$ ,  $(e, e')$  0-78195  
 $^{12}\text{C}$  M1 form factor, pion field critical opalescence,  $\rho$  role, polarisation phenomena 0-68552  
 $^{12}\text{C}(p, p')$ , 122 MeV, level excitation, cross sections, effective NN interaction, DWIA anal. 0-78197  
 $^{12}\text{C}(p, p')$ , 22-27 MeV,  $1^+$  state de-excitation  $\gamma$ -ray ang. distrib., tensor force effects, DWBA anal. 0-68580  
 $^{12}\text{C}(p, p')$ , 800 MeV, 15.1 MeV state diff. cross section, nuclear critical opalescence search 0-105984  
 $^{14}\text{C}_{\text{g.s.}}$   $\beta$ -decay, mesonic exchange currents, weak process microscopic treatment 0-57742  
 $^{40}\text{Ca}(^{16}\text{O}, X)$ , ion-ion interaction pot., imaginary part, effective interaction 0-68692  
 $^A\text{Ge}$ ,  $A=68, 70, 72, 74$ , level excitation, n-p interaction role from  $\alpha$ -transfer in  $\text{Zn}(^6\text{Li}, d)$  0-73821  
 $(\text{HI}, \text{HI})$ , local density dependence of NN interaction, double-folding calcs. 0-83114  
 $^1\text{H}(\gamma, \pi^+)$ , 3.4-18 GeV,  $\pi\bar{N}N$  form factor and differential cross sections, one pion exchange 0-68526  
 $^1\text{H}(n, \gamma\gamma)$ , thermal, consistency between pion exchange currents and NN pot., cross sections 0-68556  
 $^2\text{H}$  charge operator, retardation, quasipot. eqns. and rel. corrections 0-99122  
 $^2\text{H}(e, e')$ , 56.4 MeV, cross sections, form factors, meson exchange current contrib. 0-68649  
 $^2\text{H}(e, e)$ , form factors, tensor pol., and two-nucleon force calcs. 0-106045  
 $^2\text{H}(n, nn)p$ , 25 MeV, neutron-neutron effective range 0-83041  
 $^2\text{H}(n, n)$ ,  $(n, p)$ , 24 MeV, quasifree scatt., n-n effective range, Monte Carlo anal. 0-68554  
 $^2\text{H}(\pi, \pi)$ , 140-260 MeV,  $(3, 3)$  region, tensor force, cross sections, pol. parameters 0-68641  
 $^2\text{H}(\pi, \pi)$ , pion absorption effect from threshold to resonance 0-99193  
 $^2\text{H}(\pi, \pi)$ , scatt. length, exchange current contrib. 0-78328  
 $^2\text{H}(\pi, \pi)$ , multiple scatt. corrections, off-shell rescatt. effects, effective range 0-83127  
 $^2\text{H}(\pi^+, p)$ ,  $p, p$   $\pi$  exchange current effects on pion absorption, cross section enhancement 0-57803  
 $^3\text{H}$ , meson exchange currents, effect on charge form factors 0-105990  
 $^3\text{H}_{\text{g.s.}}$  short range repulsion, separation energy, K-harmonics calcs. 0-86846  
 $^A\text{H}$ ,  $A=2, 3$ , binding energy from Brillouin-Wigner perturbation method, strong short ranged interactions 0-86796  
 $^3\text{He}$ , meson exchange currents, effect on charge form factors 0-105990  
 $^3\text{He}(e, e'p)$ , cross-section, Fadeev technique, nucleon-nucleon interaction (Russian) 0-73842  
 $^3\text{He}(\pi, \pi)$ , 1 GeV, backward scatt., nonstable meson-nucleon interaction cross section, resonance (Russian) 0-68559  
 $^4\text{He}$ , four-nucleon bound state with realistic NN interaction, hyperspherical harmonics (Russian) 0-83045  
 $^6\text{He}_{\text{g.s.}}$  short range repulsion, separation energy, K-harmonics calcs. 0-86846  
 $^{17}\text{F}$ , three- and five-quasiparticle isomers, rotational bands and residual interactions from  $^{170}\text{Er}(^7\text{Be}, 4n)$  0-83022  
 $^{39}\text{K}(^{39}\text{K}, X)$ ,  $\pi^0$  condensation, spin-isospin instabilities, TDHF calcs. 0-83042

**nuclear forces continued**

- <sup>6</sup>Li excited states, final state interactions, three-body force effects from <sup>6</sup>H( $\alpha, \pi$ ) 0-57692  
<sup>15</sup>N<sub>g.s.</sub> partial muon capture, mesonic exchange currents, weak process microscopic treatment 0-57742  
<sup>15</sup>N(p,p), 122 MeV, level excitation, cross sections, effective NN interaction, DWIA anal. 0-78197  
<sup>15</sup>N(p,p), 25-40 MeV, level cross sections, optical parameters, DWBA anal., tensor effective interaction 0-68555  
<sup>15</sup>N(<sup>15</sup>N,X),  $\pi^0$  condensation, spin-isospin instabilities, TDHF calcs. 0-83042  
<sup>20</sup>Ne hexadecapole moments, quadrupole deformation effects, E4 effective charge, valence polarisation 0-78142  
<sup>14</sup>O<sub>g.s.</sub>  $\beta$ -decay, mesonic exchange currents, weak process microscopic treatment 0-57742  
<sup>16</sup>O, 3  $\alpha$  forces, ground state energy and form factor 0-86817  
<sup>16</sup>O ground-state energy, nonunitary model operator approach 0-83030  
<sup>16</sup>O( $\gamma, \pi$ ), total cross section,  $\Delta$ -hole states damping,  $\pi^0, \rho$  exchange,  $\Delta$  isobar hole model 0-91174  
<sup>208</sup>Pb(<sup>208</sup>Pb, X), giant resonance polarisation pots. from nucleus-nucleus effective pot. 0-78248  
<sup>208</sup>Pb(<sup>3</sup>He,d), 30 MeV, effective residual interaction matrix elements, spectroscopic factors, cross sections 0-99134  
<sup>208</sup>Pb( $\alpha, t$ ), 40 MeV, effective residual interaction matrix elements, spectroscopic factors, cross sections 0-99134  
<sup>28</sup>Si(e,e'), 6 T=1 resonance form factor, mag. strength quenching, meson exchange currents 0-86882  
<sup>93</sup>Tc, J=17/2 doublet, parity mixing, weak NN interaction 0-73791

**nuclear fusion**

see also nuclear explosions; nuclear reactions involving few nucleon systems

- 1p and 2s1d shell nuclei, fusion cross sections, entrance channel versus compound nucleus limitations 0-78343  
 A=70, heavy-ion induced fission-evaporation reactions, magnetic substrate distrib., nuclear alignment 0-73857  
 chain reactions, kinetics, high electron temps., interactions with D-T plasma 0-68945  
 composite nucleus scission, fusion and strongly damped collisions, rot. energy, boundary diffuseness 0-102224  
 conference on nuclear physics, Mikolajki, Poland (2-14 Sept. 1979) 0-101662  
 heavy ion fusion and damped reactions, rolling friction, nuclear pots., classical trajectories 0-78312  
 heavy ion fusion reactions, charge density asymmetry liquid drop model 0-63220  
 heavy ion fusion reactions, statistical yrast line 0-86948  
 heavy ion induced, fusion cross sections 0-86913  
 laser thermonuclear power plant, conceptual design study 0-78441  
 light heavy-ion systems, fusion cross section variations, nuclear proximity pot. 0-57815  
 muon catalysed fusion and hydrogenic mesomolecules 0-68719  
 neo-Z-pinch, mag. fusion appls. 0-103180  
 nuclear astrophysics, introduction to form. and evolution of matter in Universe, book 0-105447  
 probability games, modelling stellar evolution and fusion 0-77590  
 social aspects (Dutch) 0-106153  
 stellar evolved C cores, nuclear energy generation rates and energy dissipation 0-82339  
 stellar interiors, high energy particle excess, effect on secondary reaction rates (Russian) 0-77393  
 superconductor coils appls., based on Nb-Ti (French) 0-95399  
 thermonuclear reaction rates, target meas. 0-73108  
 ( $\alpha, X$ ), complete fusion barrier and evaporation from <sup>198</sup>Hg 0-68715  
 (p,X), complete fusion barrier and evaporation from <sup>198</sup>Hg 0-68715  
<sup>21</sup>Al(<sup>15</sup>N,X), 27-70 MeV, complete fusion, total fusion cross section, entrance channel effects 0-68716  
<sup>197</sup>Au(<sup>16</sup>O,X), colliding heavy ion interface, nucleon emission, fusion and strongly damped collisions 0-86922  
<sup>9</sup>Be(<sup>16</sup>O,X), 1.8-6.7 MeV, total fusion and transfer cross sections <sup>19</sup>O, <sup>21</sup>Ne, <sup>24</sup>Ne, <sup>28</sup>Na, <sup>28</sup>Mg prod. 0-91205  
 D-T compression, explosion-induced, cylindrical system with heavy inertial layer, neutron yield 0-68944  
<sup>58</sup>Fe(<sup>52</sup>Cr, X), entrance channel mass asymmetry effects on reaction mechanism, fission and fusion 0-106077  
<sup>160</sup>Gd(<sup>12</sup>C,  $\alpha n$ )<sup>168</sup>Er, particle fragmentation accompanied by incomplete fusion, two step model 0-86947  
<sup>2</sup>H(<sup>3</sup>H,n)<sup>4</sup>He, muon catalysis kinetics (Russian) 0-91206  
<sup>2</sup>H( $\nu, \mu$ )<sup>4</sup>He, muon catalysed fusion, neutron yield, muonic molecules 0-106095  
<sup>3</sup>H(<sup>3</sup>H,n)<sup>4</sup>He, chain carriers in fusion reaction kinetics 0-86969  
<sup>3</sup>H(d,n)<sup>4</sup>He, neutron fluence and energy transfer standard 0-102194  
<sup>92</sup>Mo(<sup>16</sup>O,X), entrance channel mass asymmetry effects on reaction mechanism, fission and fusion 0-106077  
<sup>146</sup>Nd(<sup>16</sup>O,X), 142 MeV, narrow window for incomplete fusion 0-95325  
<sup>206</sup>Ne(<sup>12</sup>C,X), 24-42 MeV, complete fusion, total cross section, excitation function 0-68717  
<sup>16</sup>O(<sup>16</sup>O, X), fusion limiting ang. momenta, from evaporation, mass distrib. stat. model fit 0-68714  
<sup>28</sup>Si+<sup>6</sup>Li(<sup>6</sup>Be)<sup>12</sup>C, fusion and strong absorption from elastic scatt. optical pot. 0-102222  
<sup>28</sup>Si(<sup>28</sup>Si,X), 60 MeV,  $\alpha\alpha$  correlations to probe fusion low ang. momentum window 0-106094  
<sup>28</sup>Si(<sup>7</sup>Be,<sup>7</sup>Be), 121-201.6 MeV, strong absorption dominance, global optical model anal., fusion barrier 0-83116  
<sup>28</sup>Si(<sup>7</sup>Be,X), 30-60 MeV, total fusion cross section, evaporation residues, optical model 0-78344  
<sup>28</sup>Si(<sup>7</sup>Be,X), X=p,d, $\alpha$ , energy dependence, angular distrib. of spectra, optical and statistical model anal. 0-68710  
<sup>4</sup>Sm(<sup>16</sup>O,X), 60-75 MeV, A=148,150,152,154, fusion cross section, evaporation residues 0-83137  
<sup>4</sup>Sm(<sup>40</sup>Ar,X) A=144, 148, 154, 3.6-4.5 MeV/A, sub-barrier fusion, evaporation residue cross section, deformation 0-68718  
<sup>159</sup>Tb(<sup>1</sup>B,X), 51 MeV, fusion and deep inelastic, quantised frictional motion calcs. 0-102223  
<sup>159</sup>Tb(<sup>15</sup>N,X), 140 MeV, incomplete fusion reactions, sum rule model 0-95332  
 Ti(<sup>16</sup>O,X), 310 MeV, fusion, upper limit to compound nucleus formation 0-78315  
<sup>40</sup>Ti(p, $\gamma$ ), 0.74-3.25 MeV, cross section and thermonuclear reaction rates, nucleosynthesis, IAR effects 0-102187

**nuclear fusion continued**

- <sup>40</sup>Ti(p,n), 0.74-3.25 MeV, cross section and thermonuclear reaction rates, nucleosynthesis 0-102187  
<sup>235</sup>U fission fragment thermonuclear superheavy nuclei synthesis, prod. cross sections 0-95331
- nuclear fusion reactors** see fusion reactors
- nuclear giant resonances** see nuclear collective states and giant resonances
- nuclear induction** see nuclear magnetic resonance
- nuclear instrumentation**  
 see also angular correlation techniques; beam handling equipment; counters; counting circuits; nuclear reactor instrumentation; particle accelerators; particle detectors; particle track visualisation  
 analog mean-timer circuit for use with large-volume scintillation counters 0-63477  
 combustion system for liquid scintillation wastings (Japanese) 0-63503  
 conference, nuclear power systems, San Francisco, CA, USA (Oct. 1979) 0-56994  
 dynamic analysis facility at Chalk River National Laboratory 0-58106  
 electronic systems based on the Harwell 6000 series 0-106242  
 fusion reactor, MFTF, electrical systems, overview 0-91278  
 high rate liquid Ar calorimeter electronic systems, design and operating experience 0-58087  
 hot cell extension optical profilometer 0-68789  
 microcomputer-based data acquisition system 0-63500  
 multichannel radiometer automatic channel separating system (Russian) 0-58094  
 multiprocessor system for nucl. event picture anal. (Italian) 0-69047  
 optical fibres, low-loss multimode, characterisation for nuclear diagnostics 0-78501  
 optical instrument for determining upper limit of neutron charge 0-63501  
 preamplifier, charge sensitive, loop phase shift and delays 0-58089  
 SQUID appl. to nuclear gyros and magnetometers, high stability and sensitivity 0-98949  
 vapourisation apparatus for liquid scintillation wasting (Japanese) 0-63502
- nuclear interactions** see nuclear reactions and scattering
- nuclear internal conversion** see internal conversion
- nuclear isobaric analogue resonances** see isobaric analogue resonances
- nuclear isobaric analogue states** see isobaric analogue states
- nuclear isomerism**  
 see also nuclear energy levels  
<sup>116</sup>Xe quasi-rotational bands, levels J $\pi$  and T<sub>1/2</sub> from <sup>116</sup>Cs decay 0-83021  
 A=90 nuclei, isomeric states, spin polarisation, M4 transitions and giant resonances 0-63157  
 alkali metal radioisotopes, hyperfine spectroscopy, nucl. props. 0-57677  
 fission isomers, spectrosc. props. 0-105966  
 N=82 region, high spin isomers, cranked HF calcs., deformation shapes, excitation energies 0-99121  
 N=82 region, high spin isomers, deformation energy surface, shape constrained cranked HF theory 0-57666  
 rare earth nuclei, high spin isomer  $\alpha$ -decay search 0-102158  
 short-lived isotopes, laser spectroscopy in fast atomic beams and resonance cells 0-57700  
 spin rotation, high angular velocity, collective aspects of heavy ion collisions 0-78309  
 unthermalised isomeric states, effect on red giant star s-branching ratios 0-90410  
<sup>94</sup>Rh isomers, beta decay, <sup>94</sup>Ru level structure, spin and parity 0-57747  
<sup>100</sup>Ag<sup>m</sup> decay, <sup>100</sup>Pd levels and  $\gamma$ -transitions 0-83077  
<sup>106</sup>Ag low-lying excited states from <sup>103</sup>Rh( $\alpha, n\gamma$ ) and <sup>104</sup>Pd( $\alpha, p n\gamma$ ) 0-57693  
<sup>110</sup>Ag 118.718 keV isomer, low lying states and transitions, coincidence study from <sup>109</sup>Ag( $n, \gamma$ ) 0-73806  
<sup>26</sup>Al long lived nucl. isomeric states, thermalization in stars 0-85846  
<sup>212</sup>At, A=198m, 198g, 199, alpha branching ratios 0-99154  
<sup>212</sup>At excitation functions and isomer ratios from <sup>209</sup>Bi( $\alpha, n$ ) 0-83039  
 Ba, neutron deficient, charge radii, moments, transitions and isomers, atomic beam laser spectroscopy 0-102141  
 Ba, radioisotopes, at. beam laser spectroscopy, hyperfine struct., nucl. moments and radii 0-57678  
<sup>136</sup>Ba(n,2n)<sup>135</sup>Ba<sup>m</sup>, 14.2 MeV, neutron activation cross sections 0-91180  
<sup>138</sup>Ba(n, $\alpha$ )<sup>135</sup>Xe<sup>m</sup>, 14.2 MeV, neutron activation cross sections 0-91180  
<sup>210</sup>Bi<sup>m</sup>(d,t), 17 MeV, <sup>209</sup>Bi levels and spectroscopic factors, <sup>210</sup>Bi(9 $^{-}$ ) parentage 0-78158  
<sup>76</sup>Br<sup>m</sup> decay props., half life and  $\gamma$ -transitions, level scheme 0-83071  
<sup>134</sup>Cs 176.403 keV isomer, populating  $\gamma$ -rays, low lying levels from <sup>133</sup>Cs(n, $\gamma$ ), <sup>134</sup>Cs 176.403 keV isomer, populating  $\gamma$ -rays, low lying levels 0-78200  
<sup>152</sup>Dy 60 ns isomer deexcitation E2 x- (or $\Delta$ ) transition, half life,  $\gamma\gamma$ -coincidence from <sup>152</sup>Gd( $\alpha, 4n$ ) 0-86859  
<sup>152</sup>Dy, high spin state populations from <sup>124</sup>Sn(<sup>32</sup>S,4n) 0-57660  
<sup>152</sup>Dy yrast isomers,  $\gamma$ -rays from compound nuclei 0-86789  
<sup>145</sup>Eu high spin levels, isomers and in-beam  $\gamma$ -spectroscopy from <sup>144</sup>Sm( $\alpha, 2p$ ) 0-78124  
<sup>146</sup>Eu 9 $^{+}$  isomer,  $\gamma$ -decay, high spin particle-hole multiplet population from <sup>147</sup>Sm(p,2n) 0-63066  
<sup>152</sup>Eu 89.848 keV isomeric state feeding, delayed coincidence meas., level scheme from <sup>151</sup>Eu(n, $\gamma$ ) 0-63126  
<sup>152</sup>Eu, isomeric state struct. 0-83017  
<sup>146</sup>Gd A=144,146,147,148, high spin isomer g-factors yrast traps from (<sup>28</sup>Si,<sup>28</sup>Si'), ( $\alpha, \alpha'$ ) 0-78146  
<sup>4</sup>He, T=1 excited negative parity state struct. 0-57688  
<sup>175</sup>Hf, three- and five-quasiparticle isomers, rotational bands and residual interactions from <sup>170</sup>Er(Be, 4n) 0-83022  
<sup>178</sup>Hf, energy levels, K-forbidden decays, M4 decay of yrast state 0-68506  
<sup>190</sup>Hg, 21 ns isomer ( $i_{13/2}^{2}$ ) interpretation from g-factor meas. 0-105945  
<sup>4</sup>Ho, A=152,160, isomeric state struct. 0-83017  
<sup>157</sup>Ho,<sup>157</sup>Dy decay, internal conversion electron spectra and  $\epsilon\gamma$  coincidences (Russian) 0-68604  
<sup>132</sup>I isomer and gamma-ray spectrum from <sup>133</sup>Cs( $\pi^{-}p$ ) 0-78199  
<sup>111</sup>In 21/2 $^{+}$  isomeric state g-factor and relaxation time from <sup>109</sup>Ag( $\alpha, 2n\gamma$ ) 0-73794  
<sup>85</sup>K<sup>m</sup> decay, <sup>85</sup>Rb levels, J $\pi$  and transitions 0-78162  
<sup>174</sup>Lu isomeric levels,  $\gamma$ -spectra, T 1/2 and decay modes from <sup>176</sup>Yb(p,3n) 0-99151  
<sup>89</sup>Mo<sup>m</sup> levels, transitions and half life from <sup>93</sup>Mo(p,3p $^{+}$ n) 0-86858  
<sup>24</sup>Na<sup>m</sup>, polarised,  $\beta$ -decay asymmetry and mag. moment from Na(n, $\gamma$ ) 0-91157



**nuclear isomerism continued**

- <sup>240m</sup>Na, laser induced nuclear orientation 0-57680  
<sup>140</sup>Nd, A=138,139, high spin states, isomers and  $\gamma$ -cascade from <sup>140</sup>Cd( $\alpha$ ,xn) 0-78120  
<sup>140</sup>Nd ns isomers and yrast isomers,  $\gamma$ -transitions from <sup>128</sup>Te(<sup>16</sup>O,4n) 0-78121  
<sup>204</sup>Pb, muonic, first excited 2<sup>+</sup> state, isomer shift of E2 transition 0-99150  
<sup>207</sup>Pb, muonic, octupole doublet isomer shifts, octupole vibr. 0-95750  
<sup>211</sup>Po excitation functions and isomer ratios from <sup>208</sup>Pb( $\alpha$ ,n) and <sup>209</sup>Bi( $\alpha$ ,np) 0-83039  
<sup>212</sup>Po excitation functions and isomer ratios from <sup>209</sup>Bi( $\alpha$ ,p) 0-83039  
<sup>242</sup>Pu isomeric state non-existence 0-105983  
<sup>199</sup>Rn and <sup>199</sup>Rn<sup>m</sup> alpha decay signatures from <sup>169</sup>Tm(<sup>35</sup>Cl,5n) 0-68610  
<sup>135</sup>S shape isomeric state from unconstrained variation 0-95306  
<sup>44</sup>Sc, A=44m,46,47,48, fragment emission, two-step model applicability from <sup>338</sup>U(p,X) 0-99177  
<sup>42</sup>Sc, J<sup>+</sup>=19/2<sup>+</sup> isomer, high-spin precursors, from <sup>29</sup>Si(<sup>16</sup>O,pn) 0-57656  
<sup>142</sup>Sm isomers, lifetimes and transitions from <sup>142</sup>Nd( $\alpha$ ,4n) 0-78122  
<sup>142</sup>Sm ns isomers and yrast isomers,  $\gamma$ -transitions from (<sup>14</sup>Mg,4n), (<sup>19</sup>F,4n) 0-78121  
<sup>112</sup>Sn 6<sup>+</sup> isomeric state g-factor and relaxation time from Cd( $\alpha$ ,2n $\gamma$ ) 0-73794  
<sup>132</sup>Sn levels, isomers, lifetimes and transition probabilities from fission 0-78163  
<sup>85</sup>Sr<sup>m</sup>g decay, <sup>85</sup>Rb levels, J<sup>+</sup> and transitions 0-78162  
<sup>180</sup>Ta mass, 10<sup>13</sup> y naturally occurring isomer state 0-57670  
<sup>180</sup>Ta<sup>m</sup>,  $\beta^-$  and EC branching ratios, K-internal conversion coeff.,  $\gamma$ -intensities, T 1/2 0-68601  
<sup>181</sup>Ta(n,2n)<sup>180</sup>Ta<sup>m</sup>, 14.68 MeV, cross section 0-68659  
<sup>98</sup>Tc 14  $\mu$ s isomer, low lying levels and transitions from <sup>98</sup>Mo(p,n) 0-73802  
<sup>100</sup>Tc vs isomers, isomeric transitions and mean lives from <sup>100</sup>Mo(p,n) 0-73803  
<sup>129</sup>Te<sup>m</sup>g decay, <sup>129</sup>I time depend. quadrupole interactions,  $\gamma$ - $\gamma$  correlations 0-78145  
<sup>141</sup>U<sup>m</sup>, A=236,238, isomeric to prompt fission ratios; fission fragments from (d,pf), (d,pnf) 0-86940  
<sup>235</sup>U internal conversion from 1/2<sup>+</sup> isomeric state, U<sup>4+</sup> electron configuration 0-58146  
<sup>236</sup>U isomeric and prompt fission, nuclear superfluidity evidence from <sup>235</sup>U(d,pf) 0-68711  
<sup>236</sup>U shape isomer,  $\gamma$  branch upper limit,  $\gamma$ -yields from <sup>235</sup>U(d,p) 0-99145  
<sup>14</sup>Y<sup>m</sup>g, A=86, 87, isomeric yield ratios and  $\gamma$ -spectra from <sup>93</sup>Nb( $\pi^-$ ,X) 0-86857  
<sup>87</sup>Y 14 ms 8<sup>+</sup> isomeric state, g-factor from <sup>87</sup>Rb( $\alpha$ ,3n) 0-63080

**nuclear isospin**

- A=200 region, macroscopic fission barriers, isospin depend., liquid drop model 0-57811  
 asymmetric nuclear matter, isospin waves, IAS and giant Gamow-Teller resonance 0-91142  
 nuclear matter, polarised, thermal props., temp., spin isospin and spin-isospin pressure 0-102135  
 nuclear matter, spin-isospin and pion condensation phase transitions, eqn. of state 0-86843  
 ( $\pi^+$ ,  $\pi^-$ ) A=9-32, 180 MeV 0-105960  
 ( $\pi^+$ ,  $\pi^-$ )  $\pi^-$  nuclear response enhancement, continuum effects, stretched state spin-isospin mixing 0-86929  
<sup>26</sup>Al 1<sup>+</sup>T=0 states, isobaric analogue state, spin-isospin effective interaction from <sup>26</sup>Mg(p,n) 0-68553  
<sup>208</sup>Bi, 0<sup>+</sup> IAS, spreading width and isospin impurity, isovector monopole state influence 0-78155  
<sup>13</sup>C(d,d'), isospin violating direct reaction, Coulomb interaction role 0-102170  
<sup>13</sup>C(p,p'), pol. p, 800 MeV, unnatural parity states excitation, anal. powers and isospin 0-68538  
<sup>13</sup>C(d,d',He), isospin violating direct reaction, Coulomb interaction role 0-102170  
<sup>13</sup>C(d,t), isospin violating direct reaction, Coulomb interaction role 0-102170  
<sup>18</sup>F resonances,  $\alpha$ -widths, isospin and parity mixing, R-matrix anal. of <sup>14</sup>N( $\alpha$ , $\alpha'$ ) 0-91162  
<sup>4</sup>Fe(\gamma)Co, A=54,56, giant dipole resonance splitting, direct-semidirect capture model anal. 0-106055  
<sup>16</sup>O, 4<sup>+</sup> particle-hole states, isospin mixing 0-99123  
<sup>16</sup>O isospin mixing matrix elements, three level model 0-78136  
<sup>30</sup>P level width isospin depend., excitation functions, statistical anal. of <sup>29</sup>Si(p, $\alpha$ ) 0-78152  
<sup>208</sup>Pb, isobaric analogue states, effects of Coulomb isospin coupling, random-phase method (Russian) 0-68608  
<sup>4</sup>Sn(n,n'), A=116, 118, 120, 122, 124, 11 MeV, levels, deformation parameters, isospin effects, optical parameters 0-57679  
<sup>4</sup>Te, A=122,124,126 yrast band double backbending, possible mechanisms (Chinese) 0-99120

**nuclear liquid drop model**

- A=200 region, macroscopic fission barriers, isospin depend., liquid drop model 0-57811  
 binary fission saddle points, shape parametrization for liquid-drop studies 0-106086  
 deformed and superdeformed nuclei from heavy ion reactions,  $\alpha$ -decay amplification 0-102156  
 ellipsoidal, liquid-drop model, irrotational incompressible hydrodynamic flow 0-83050  
 fissionability, target mass depend. for  $\pi$ ,  $\gamma$ ,  $\alpha$ , p, cascade-evaporation and liquid drop calcs. (Russian) 0-106089  
 fissioning nucleus, deformation process mass parameter, liquid drop model 0-102221  
 heavy ion collisions, hot compressed zone stability and temp., liquid drop model 0-78316  
 heavy ion fusion reactions, charge density asymmetry liquid drop model 0-63220  
 moment map and collective motion, Hamiltonian action of Lie group 0-91138  
 nuclear matter density determ., HF versus droplet model 0-68574  
 potential energy surfaces, folded Yukawa-plus-exponential model 0-86816  
<sup>20</sup>Ni from HI reactions, superdeformed nucleus decay,  $\alpha$ -decay amplification 0-68608  
<sup>149</sup>Tb from HI reactions, superdeformed nucleus decay,  $\alpha$ -decay amplification 0-68608

**nuclear magnetic acoustic resonance** *see acoustic nuclear magnetic resonance***nuclear magnetic moment**

- see also gyromagnetic ratio; molecular nuclear coupling; nuclear magnetic resonance*  
 A=12-240, even-even, dynamic deformation theory, B(E2) values, quadrupole and mag. moments 0-68591  
 band crossing in interacting boson model, E2 transition probabilities and g-factors 0-102101  
 effective NN interaction and exchange current vel. depend., dipole sum rule enhancement 0-63100  
 magnetic multipole expansion, education 0-105456  
 short living nuclear states, optical orientation,  $\gamma$ -spectrum anisotropy, lifetime, moments (Russian) 0-63090  
 stable odd-mass sd nuclei, EM multipole moments of ground states 0-102116  
 $\pi^-$  and  $\rho$ -exchange pots., influence on mag. resonances, mag. moments, and transition probs. 0-99133  
<sup>242</sup>Am, reduced E0 conversion due to mag. moment effects 0-83034  
<sup>69</sup>As 1306 keV state mag. moment, g-factor, rot. aligned band 0-86807  
 Ba, neutron deficient, charge radii, moments, transitions and isomers, atomic beam laser spectroscopy 0-102141  
<sup>12</sup>C, M1 form factor, pion field, rho meson role 0-105970  
<sup>152</sup>Er, A=159,160, energy levels, deexcitation  $\gamma$ -rays, g-factors and hyperfine interaction from <sup>28</sup>Si(<sup>136</sup>Xe, xn) 0-102114  
<sup>168</sup>Er, 80 and 1094 keV states, g-factors from ang. correlation methods 0-83035  
<sup>147</sup>Gd A=144,146,147,148, high spin isomer g-factors yrast traps from (<sup>28</sup>Si,<sup>28</sup>Si'), ( $\alpha$ , $\alpha'$ ) 0-78146  
<sup>190</sup>Hg, 21 ns isomer ( $\nu_{1/2}$ )<sup>2</sup> interpretation from g-factor meas. 0-105945  
<sup>166</sup>Ho<sup>m</sup> in HoVO<sub>4</sub>, nuclear orientation study below 1K 0-88899  
<sup>11</sup>In 21/2<sup>+</sup> isomeric state g-factor and relaxation time from <sup>109</sup>Ag( $\alpha$ ,2n $\gamma$ ) 0-73794  
<sup>111</sup>In, nucl. orientation coeffs., nucl. mag. moment 0-97168  
<sup>138,139</sup>La, Fourier transform NMR 0-57354  
<sup>24</sup>Na<sup>m</sup>, polarised,  $\beta$ -decay asymmetry and mag. moment from Na(n, $\gamma$ ) 0-91157  
<sup>20</sup>Ne with backbending, first excited 4<sup>+</sup> state g-factor 0-78144  
<sup>20</sup>O first excited state, g-factor and lifetime from <sup>3</sup>H(<sup>18</sup>O, p $\gamma$ ) 0-102115  
<sup>18</sup>Os, A=186-194, collective levels, transitions, mag. and quadrupole moments, boson expansion theory 0-105954  
<sup>183</sup>Os 9/2<sup>+</sup> [624] ground state g-factor from NMR 0-83037  
 Pd, even-even, collective states, B(E2), branching ratios and moments, boson expansion method 0-102099  
 PrIn<sub>3</sub>Gd, indirect nuclear exchange interactions, ESR-linewidth meas., sp. ht. determ. 0-103825  
<sup>4</sup>Pt, A=188-198 collective levels, transitions, mag. and quadrupole moments, boson expansion theory 0-105954  
<sup>212</sup>Rn, shell model states, semiempirical calcs. half lives, mag. moments, excitation functions 0-63083  
 Ru, even-even, collective states, B(E2), branching ratios and moments, boson expansion method 0-102099  
<sup>9</sup>Ru ground state g-factor, relaxation time 0-83036  
<sup>120</sup>Sn(<sup>21</sup>Cl,<sup>35</sup>Cl'), 108 MeV, A=112-124 even isotopes, 2<sub>1</sub><sup>+</sup> mag. moments and shell model struct. 0-86805  
<sup>112</sup>Sn 6<sup>+</sup> isomeric state g-factor and relaxation time from Cd( $\alpha$ ,2n $\gamma$ ) 0-73794  
<sup>180</sup>Ta nuclear spin and mag. dipole moment from laser resonance fluorescence 0-78143  
<sup>182</sup>Ta, in Fe-Ta, nuclear mag. moment, NMR-ON study 0-78139  
<sup>88</sup>Y 14 ms 8<sup>+</sup> isomeric state, g-factor from <sup>87</sup>Rb( $\alpha$ ,3n) 0-63080  
<sup>4</sup>Zr(<sup>35</sup>Cl,<sup>35</sup>Cl'), 90 MeV, A=92, 94, 2<sub>1</sub><sup>+</sup> levels mag. moments 0-105968

**nuclear magnetic resonance**

- see also acoustic nuclear magnetic resonance; chemical shift; double nuclear magnetic resonance; ENDOR; Knight shift; molecular nuclear coupling; NMR line breadth; nuclear quadrupole resonance; nuclear spin-lattice relaxation; proton magnetic resonance; spin echo (NMR); spin-spin relaxation*  
<sup>31</sup>P spectroscopic zeugmatography 0-76872  
 $\alpha,\beta$ -trifluoroacetonitrile, liq.-liq. transition rel. to mol. motion, NMR study 0-70383  
 absolute meas. of ampere 0-98941  
 acetic acid-<sup>13</sup>C<sub>1</sub>, in nematic phase soln., dipole-dipole couplings, selective spin population transfer investig. 0-60427  
 acetonitrile-d<sub>3</sub>, <sup>2</sup>H NMR spectra, vibr. and asymmetry corrections to quadrupole coupling consts. 0-74184  
 acetonitrile, dissolved in nematic EBBA, oriented CH<sub>3</sub> group relax., multiple quantum NMR 0-66057  
 N-acetyl-D-alloisoleucine, <sup>13</sup>C NMR, soln. struct., dynamics, proton relaxation mechanisms 0-76708  
 acrylonitrile, NMR and relax. props., liq.-liq. transition rel. to mol. motion 0-70382  
 adamantane, derivatives in solution, mol. motion and methyl group rot. barriers from <sup>13</sup>C NMR relax. times 0-74179  
 alkali halides, matter transport rel. to point defect parameters 0-107488  
 alkyl chains, <sup>13</sup>C longitudinal relax. times and nuclear Overhauser enhancement anal. 0-83390  
 4-amino-2,2,6,6-tetramethylpiperidine-N-oxyl and deuterated derivatives, mag. resonance study 0-63686  
 analytical chemistry appls., conf., Denver, CO, USA (Aug. 1979) 0-90598  
 atomic systems, coherent transients theorem 0-99808  
 ATP, <sup>31</sup>P spectroscopic zeugmatography 0-76872  
 benzene adsorbed on graphite, melting and orientation, NMR study 0-100403  
 benzene-d<sub>3</sub>, <sup>2</sup>H NMR spectra, vibr. and asymmetry corrections to quadrupole coupling consts. 0-74184  
 benzenes, monosubstituted, high resolution, automated anal. by computer program DAVINS appl. 0-63669  
 biological imaging, review (Japanese) 0-94312  
 biomedical whole-body imaging system design 0-98064  
 biomembrane, water transport determ. methods (Rumanian) 0-94435  
 bis-methylidgermyl chalcogenide, <sup>1</sup>H and <sup>13</sup>C NMR study, chemical shifts 0-71201  
 bis-methylidgermyl chalcogenide, <sup>1</sup>H and <sup>13</sup>C NMR study, chemical shifts 0-71201  
 bistrifluoromethylmercury, scalar coupling between rare spins 0-66047  
 n,t-butanol in alkanes, molecular relaxation processes studied by <sup>13</sup>C NMR 0-63654  
 caesium perfluoro-octanoate/D<sub>2</sub>O system, <sup>2</sup>H NMR quantum orders, RF pulses 0-103892



**nuclear magnetic resonance continued**

4-chloro, 3-nitrotoluene, partially aligned in elec. field,  $^{13}\text{C}$  NMR, dipole moment determ. 0-78633  
 cholesteryl myristate, cholesterogenic, blue phase, D NMR obs. 0-97151  
 cholesteryl nonanoate, cholesterogenic, blue phase, D NMR obs. 0-97151  
 collagen fibril,  $^1\text{H}$  NMR of mol. motion 0-67034  
 CP,  $^{31}\text{P}$  spectroscopic zeugmatography 0-76872  
 cross-polarisation  $^{13}\text{C}$  NMR with magic angle spinning, appl. to fossil fuels and polymers 0-77819  
 cyclopropane, liq., mol. dynamics, Raman and NMR studies of orientational motion 0-93296  
 decylammonium chloride micelles,  $^{13}\text{C}$  longitudinal relax. times and nuclear Overhauser enhancement anal. 0-83390  
 diethylammonium copper tetrabromide, mag. struct., NMR meas. 0-71192  
 dimethylformamide, intramolecular exchange rate determ. from  $^{13}\text{C}$  spin-lattice relax. times 0-69169  
 diplosporin derived from (1,2- $^{13}\text{C}$ )acetate,  $^{13}\text{C}$ - $^{13}\text{C}$  coupling assignment using DANTE excitation 0-80617  
 DNA, double-stranded,  $^{13}\text{C}$  NMR obs. 0-69281  
 DNA, molecular motions, investigated by  $^{31}\text{P}$  and  $^{13}\text{C}$  NMR relaxation 0-63657  
 DNA conformational fluctuations, internal motion correl. times,  $^{31}\text{P}$  NMR obs. 0-72135  
 DNA internal motions,  $^{31}\text{P}$  NMR and PMR 0-97855  
 dodecanate/decyltrimethylammonium micelles, type II mesophase, bilayer struct., NMR spectra study 0-75149  
 double quantum transitions, heteronuclear excitation and detection in solids, cross polaris. appls. 0-97153  
 doubly tuned oscillator configuration, nonlinear mode interactions, freq. jump effects 0-77824  
 EABAC, smectic A, nematic, and isotropic phases, NMR and quasielastic neutron scatt. obs. 0-88022  
 EBBA, NMR and Raman scatt. studies in nematic phase 0-100619  
 electric quadrupole interactions measured by nuclear orientation and NMR on oriented nuclei, review 0-92868  
 ferroelectrics, order-disorder, pseudo-one-dimens. kinetic Ising model 0-71333  
 ferromagnet, nuclear magnetisation motion, hyperfine field microscopic inhomogeneity, NMR freq. shift (*Russian*) 0-80623  
 flow-rate meas. for liquids, pulse-compensation method based on NMR 0-103088  
 1-fluoro, 2,4-dinitrobenzene, partially aligned in elec. field,  $^{13}\text{C}$  NMR, dipole moment determ. 0-78633  
 Fourier transform, NMR spectrometer, magic-angle rot. 0-105688  
 Fourier transform NMR spectroscopy, review 0-104486  
 FT NMR, digitisation and data processing 0-95115  
 gramicidin single-channel currents, rate theory calc. using NMR-derived rate consts. 0-94186  
 graphite intercalation compounds with Br, K,  $^{13}\text{C}$  NMR spectra 0-66048  
 4-n-heptyl-d<sub>5</sub>-oxybenzoic acid-d<sub>1</sub>, nematic and smectic phases, mol. and relative segmental order 0-96439  
 high frequency effects in NMR spectrometers 0-77829  
 high resolution, automated anal., principles and computational strategy 0-58287  
 high resolution, automated anal. by computer program DAVINS appl. 0-63669  
 hippuric acid, solid, second moment meas. by wide-line NMR 0-108081  
 homonuclear selective population inversion in AB system 0-75865  
 hormonal steroids,  $^{13}\text{C}$  NMR spectra 0-81543  
 hybrid relaxation and multiple pulse methods for studying chemical, physical and spin exchange 0-80629  
 imaging, selective irradi. line scan techniques 0-77822  
 ionic crystal defects, mag. reson. studies 0-108066  
 lactams, N-methylated, cis-trans isomerism,  $^1\text{H}$  and  $^{13}\text{C}$  NMR obs. 0-106335  
 librational motion effects on fluoresc. depolarisation and NMR relax. in macromols. and membranes 0-85324  
 liquid crystals, mol. conformation and orientational order, NMR studies, review 0-75151  
 low field magnet, computer controlled, for optical and magnetic resonance studies 0-95113  
 low-noise broadband transmit/receive circuit for NMR 0-62706  
 macromolecular dynamics, high resolution NMR investig. 0-91708  
 macromolecule, microconformation by fast exchange NMR spectra 0-102593  
 magnetic metals, hyperfine mag. fields at  $^{119}\text{Sn}$  nuclei 0-60248  
 magnetically ordered cryst., indirect nuclear spin interactions 0-103847  
 magnetometer large-scale automation 0-57343  
 MBBA, NMR and Raman scatt. studies in nematic phase 0-100619  
 medical imaging, conference, San Diego, USA (Aug. 1979) 0-94919  
 metalloproteins, metal nuclei, biophysical appls. of NMR, review, book contrib. 0-109081  
 metals, BCC and FCC, H-diffusion and trapping 0-70447  
 molecules, diamagnetic susceptibilities and NMR chemical shifts in terms of localised MO's 0-106256  
 molecules, physisorbed on homogeneous surfaces, NMR study 0-97732  
 motion induced NMR spin relax. times in low temp. HF limit 0-60443  
 multidimensional space and time signal processing in biology and medicine 0-85493  
 neopentane adsorbed on graphite, quasi two-dimens. fluid, NMR 0-102525  
 NMR-ESR spectroscopy, miniature magnetic assembly, teaching 0-105467  
 noise reduction filter in resolution enhancement 0-73403  
 nonrigid molecules, dipolar relax. and nuclear Overhauser effects, fluctuating internuclear distances effect 0-91578  
 norbornane, derivatives in solution, mol. motion and methyl group rot. barriers from  $^{13}\text{C}$  NMR relax. times 0-74179  
 nuclear echo formation in spin systems with dynamic freq. shift to NMR 0-93208  
 nuclear magnetic shielding density 0-63559  
 nuclear magnetism and ultralow temperature, review (*Japanese*) 0-86806  
 4-n-octyl-d<sub>17</sub>-oxybenzoic acid-d<sub>1</sub>, nematic and smectic phases, mol. and relative segmental order 0-96439  
 organic molecular crystals, intermolecular interactions, spectroscopic studies, review 0-103958  
 $\beta$ -oxy butyric acid ethyl ester, scaled spectra using three joined pulse sequences 0-73405  
 PAA, nematic, NMR study of ordering, intramol. mobility 0-100162

**nuclear magnetic resonance continued**

PAA-di, nematic liquid crystal, NMR data, appl. of Landau-de Gennes theory 0-64893  
 pancreatic trypsin inhibitor, bovine, macromol. dynamics, high resolution NMR investig. 0-91708  
 pentachlorotoluenes, positional isomers,  $^{13}\text{C}$  Fourier transform NMR spectroscopy, struct. and compositional anal. 0-91576  
 phenylphosphines, and derivatives,  $^1\text{H}$ ,  $^{13}\text{C}$  and  $^{31}\text{P}$  NMR studies 0-87152  
 phospholipid bilayers, carbonyl groups dynamics,  $^{13}\text{C}$  chem. shift anisotropy obs. 0-85326  
 phosphorus metabolites,  $^{31}\text{P}$  spectroscopic zeugmatography 0-76872  
 phosphoryl transfer enzymes, biophysical appls. of NMR, review, book contrib. 0-109081  
 PMMA, syndiotactic, solns. in toluene, NMR obs. of struct. and dynamics of associates 0-75867  
 polarised  $\beta$ -active nuclei, cross-relaxation processes 0-60431  
 polariser design, for magnetising liquid in NMR devices 0-57351  
 poly-L-ornithine solution,  $^{15}\text{N}$  NMR, coil-helix transition, solvent effects and pH depend. 0-74275  
 poly-p-chlorophenyl glycidyl ether, struct., tacticity and addition isomerism,  $^{13}\text{C}$  NMR 0-58427  
 polyacetylene-1, NMR struct. investigation 0-108082  
 polybutadiene, hexafluoro acetone substituted, H-NMR and  $^{19}\text{F}$ -NMR spectroscopy (*German*) 0-103893  
 polymethacrylic acid, stereoregular, synthesis,  $^{13}\text{C}$  NMR obs. 0-58422  
 polypropylene, isomeric, microconformation from slow exchange  $^{13}\text{C}$ -NMR spectra of low mol. wt. cmpds. 0-102592  
 polystyrene, epimerised isotactic, methylene C mag. resonance spectra 0-63878  
 polyurethanes, cross-linked, mol. mobility and struct., thermomechanical and NMR obs. (*Russian*) 0-69285  
 population distribution to enhance NMR sensitivity and allow decoupling of low gyromagnetic ratio nuclei 0-73399  
 potassium laurate-1-decanol-water mixtures, biaxial nematic phase obs. 0-107409  
 potassium palmitate-water solution, deuterated, NMR asymmetry parameter 0-88882  
 powders, high speed rot., spin diffusion, NMR spin lattice relax. obs. of D 0-66056  
 prepolymers, H-NMR and  $^{19}\text{F}$ -NMR spectroscopy (*German*) 0-103893  
 principles, introduction to basics 0-77820  
 propionitriles (-O, NH, S), conformational investig., NMR, IR and semiempirical MO methods 0-95650  
 propylene-butene copolymers, PB centred tetrad  $^{13}\text{C}$  NMR spectra assignment 0-58428  
 pulse programmer for single and double resonance expts. 0-57347  
 pulsed NMR experiments, microprocessor-controlled pulse sequencer 0-68231  
 pulsed NMR technique for meas. radiation effects in polymer 0-66051  
 PVC-vinylchloride system, glass transition, nuclear mag. relax. obs. (*German*) 0-79917  
 quadrupolar nuclei in solids, enhanced resolution NMR interferometric correl. of shifts 0-57355  
 radiofrequency pulse sequences which compensate their own imperfections, appl. to population inversion 0-77827  
 radiospectrometers, calc. of optimal configuration of shims 0-73398  
 rare earth intermetallic compounds, NMR anal. of indirect mag. interactions 0-71193  
 rare earth orthoferrites, hyperfine interaction anisotropy, NMR study (*Russian*) 0-66052  
 relaxation, electron spectral densities calcs. 0-60436  
 ring current theory 0-87240  
 RNA, conformational fluctuations, internal motion correl. times,  $^{31}\text{P}$  NMR obs. 0-72135  
 RNA, molecular motions investigated by  $^{31}\text{P}$  and  $^{13}\text{C}$  NMR relaxation 0-63657  
 rotating frame demagnetisation, J-ordered magnetic states production 0-73404  
 rotating frame selective pulses in NMR imaging 0-68232  
 scaling of heteronuclear spin interactions by multipulse sequences 0-73405  
 sigma phase alloys, NMR and electric-field gradients 0-108109  
 signal enhancement by rod-induced convection 0-77823  
 silicate glass, hydrated, proton and  $^{23}\text{Na}$  wide-line NMR study 0-84659  
 sodium dodecyl sulphate:  $\text{Gd}^{3+}$ , micellar system, chain folding,  $^{13}\text{C}$  NMR obs. 0-61158  
 solid electrolytes and solid soln. electrodes, review 0-60432  
 solid materials, high resolution  $^{13}\text{C}$  NMR spectroscopy 0-97150  
 solid polymers, review 0-88888  
 solid state physics applications (*Chinese*) 0-80622  
 solids, high resolution pulsed NMR, adjusting conditions of pulse sequences 0-93184  
 spectra, computer-aided interpretation, minicomputer based file search system 0-62702  
 spectra, computer-aided interpretation using artificial intelligence system 0-62701  
 spectrometers, SQUID-based, sensitivity limit 0-98961  
 spectroscopy, high power pulsed, automation and control 0-86359  
 spin imaging by mag. field modulation 0-90873  
 spin-lattice relax., effect of correlated atomic diffusion 0-107495  
 SQUID detection, low temp., NMR imaging improvement towards mol. kinetic meas. 0-104723  
 styrenes, 4-substituted, NMR substituent parameters, pattern recognition interpretation 0-58284  
 substituent parameters, pattern recognition interpretation 0-58284  
 superconducting solenoids fields meas., automatic 0-57344  
 superspin, appl. to ABX system 0-60426  
 techniques (*Chinese*) 0-80621  
 tetramethylammonium octahydrotriborate, NMR study of proton and B dynamics 0-93200  
 meso-tetraphenylporphine,  $\text{NH H}^+$  tunnelling rate 0-97158  
 thermometer, for multinuclear Fourier transform NMR 0-57292  
 thiourea, polycryst., mol. dynamics under hydrostatic press., NMR study 0-80619  
 thiourea-d<sub>4</sub>-ferrocene inclusion cpd. mol. motion, PMR spectrum 0-84656  
 titanocene, alkyl-substituted  $^{13}\text{C}$  and  $^1\text{H}$  NMR, chemical shifts prediction 0-63671  
 TMNC, quasi one dimensional planar ferromag., low temp. NMR study im mag. field 0-97157



**nuclear magnetic resonance continued**  
(TMTSF)<sub>x</sub> (X=PF<sub>6</sub><sup>-</sup>, AsF<sub>6</sub><sup>-</sup>, SbF<sub>6</sub><sup>-</sup>, BF<sub>4</sub><sup>-</sup>, NO<sub>3</sub><sup>-</sup>) highly conducting salts, props. 0-59969  
transition metal tetrahedral complex ions, F NMR chem. shifts, outer sphere cation effects 0-102527  
two-dimensional systems, order parameter from chemical shift anisotropy patterns 0-80624  
ultra-low temperature meas. of S/N ratio, appl. to thermometry 0-73400  
vinyl copolymers, containing fluorescent groups, optically active 0-102594  
zeolite, hydrated Na-Y, <sup>23</sup>Na pulsed NMR free induction decay 0-84660  
zeugmatographic imaging, gradient control device using microprocessor 0-89822  
zeugmatography by reconstruction from projections 0-77821  
zirconocene dichlorides, alkyl-substituted, <sup>13</sup>C and <sup>1</sup>H NMR, chemical shifts prediction 0-63671  
Ag halides, matter transport rel. to point defect parameters 0-107488  
AgBF<sub>4</sub>, ionic radii and chem. shifts, correl. with electronegativity 0-66054  
AgF(AgI, AgBr, AgCl), NMR chemical shifts 0-74180  
Al-Cu (4 wt.%) alloy, reversion process of Guinier-Preston zones, <sup>63</sup>Cu NMR obs. 0-60871  
Al<sub>2</sub>O<sub>3</sub>-H<sub>2</sub>O<sup>+</sup>, β and β' phases, protonic, conductance and spectroscopy 0-70450  
β-Al<sub>2</sub>O<sub>3</sub>-Na<sub>2</sub>O, protonic, conductance and spectroscopy 0-70450  
α-Al<sub>2</sub>O<sub>3</sub>-V<sub>2</sub>O<sub>5</sub>, NMR of <sup>51</sup>V 0-71232  
B<sub>2</sub>O<sub>3</sub>, vitreous, struct. study using <sup>10</sup>B NMR 0-84658  
BeF<sub>2</sub>, aqueous solns., mag. and quadrupole relax. 0-71226  
2,4-C<sub>6</sub>H<sub>3</sub>, polyhedral, spin coupled <sup>1</sup>B-<sup>1</sup>H systems, 2-dimens. correl. NMR 0-69166  
CO, adsorbed on Rh dispersed on Al<sub>2</sub>O<sub>3</sub>, <sup>13</sup>C NMR obs. of adsorbed states 0-96733  
<sup>13</sup>C, 2D NMR spectra, off-resonance decoupling 0-74182  
<sup>13</sup>C, CIDNP, obs. in reactions of organic and inorganic radicals during pulse radiolysis 0-63660  
<sup>13</sup>C, NMR spectra, transition intensities, off-resonance proton spin decoupling influence 0-74183  
CaF<sub>2</sub>, heteronuclear mag. spin system relaxation in many pulse NMR expts. 0-93203  
CaF<sub>2</sub>:Nd<sup>3+</sup> (Dy<sup>3+</sup>)(Ho<sup>3+</sup>)(Tm<sup>3+</sup>), <sup>19</sup>F NMR studies 0-60429  
CdCr<sub>2</sub>S<sub>4</sub>(Se<sub>4</sub>), spontaneous magnetisation temp. depend., nuclear resonance freq. depend. (French) 0-80483  
Co complexes, Co(III) mixed complexes, orbital angular momentum reduction, <sup>59</sup>Co NMR chemical shift 0-58137  
Co<sub>2</sub>Ga<sub>1-x</sub> alloys, cluster spin glass, host and impurity NMR and AC susceptibility 0-71194  
Cr complexes, NMR study <sup>31</sup>P chemical shift, substituents electronegativity steric hindrance and π-bonding effect 0-95651  
CrB<sub>2</sub>, itinerant antiferromag., spin fluctuations, NMR study 0-108119  
CsBF<sub>4</sub>, ionic radii and chem. shifts, correl. with electronegativity 0-66054  
CsD<sub>2</sub>PO<sub>4</sub>, pseudo-one-dimens. ferroelec. transition, DMR and relax. study 0-71223  
CsNiF<sub>4</sub>, quasi one dimensional planar ferromag., low temp. NMR study im mag. field 0-97157  
Cu, nuclear antiferromagnetism, low temp. NMR study 0-66049  
Cu, nuclear ordering below 1 μK, NMR study 0-93187  
Cu<sup>2+</sup> systems, magnetic, nuclear spin Hamiltonians (Japanese) 0-60430  
Cu-Fe group, dil., NMR satellite data calc., struct. of mag. impurities 0-103894  
Cu-Mn alloy spin glass, macroscopic mag. anisotropy, transverse susceptibility and zero field NMR enhancement 0-80525  
CuCr(Fe)(Mn), dil., anisotropic hyperfine coupling, NMR study 0-65784  
Er<sub>1-x</sub>Gd<sub>x</sub>Al<sub>2</sub>, effective mol. field at <sup>167</sup>Er, NMR meas. 0-71197  
ErRh<sub>2</sub>B<sub>4</sub>, mag. supercond., NMR study of <sup>115</sup>B 0-107957  
ethanol-water system, complex dielec. permitt. in UHF region and NMR spectra (Japanese) 0-100620  
EuI<sub>2</sub>H<sub>3</sub>, transferred hyperfine fields at Eu nuclei, NMR meas. 0-71195  
EuSe<sub>2</sub>Te<sub>2</sub>, transferred hyperfine fields at Eu nuclei, NMR meas. 0-71195  
(Eu,Sr)<sub>1-x</sub>S<sub>2</sub>, transferred hyperfine fields, NMR 0-71196  
Fe, BCC, high field Knight shift and hyperfine anisotropy of <sup>57</sup>Fe 0-71205  
Fe-<sup>48</sup>Ni, nucl. orientation of <sup>48</sup>Ni, γ-ray anisotropy obs. and NMR meas. 0-97169  
Fe-Ta, nuclear mag. moment of <sup>182</sup>Ta NMR-ON study 0-78139  
Fe<sub>2-x</sub>Co<sub>x</sub>Al, site preference and local environment effects, Mossbauer and NMR meas. 0-71264  
FeF<sub>2</sub>:Mn, antiferromag., NMR relax., impurity bonding 0-66061  
Fe<sub>2</sub>O<sub>3</sub>, lattice parameters, NMR freqs., and magnetoec. pots. near 12K 0-71146  
Fe<sub>80</sub>P<sub>13</sub>C<sub>7</sub>, amorphous and crystalline, electrochemical and semicond. behaviour (Russian) 0-101021  
θ-Fe<sub>0.35</sub>V<sub>2</sub>O<sub>5</sub>, NMR of <sup>51</sup>V 0-71232  
Gd(Co<sub>1-x</sub>Ni<sub>x</sub>)<sub>2</sub> compounds, NMR and thermal expansion 0-66070  
H<sub>2</sub>, adsorbed on Rh-TiO<sub>2</sub> catalyst, surface states, NMR spectrosc. invest. 0-103891  
H<sub>2</sub>, single crystals, NMR, dynamic effects 0-107608  
H<sub>2</sub>, solid, glass phase, use of NMR (French) 0-93190  
H<sub>2</sub>, D<sub>2</sub>Se(n=0, 1 and 2), <sup>77</sup>Se NMR on XL-100 spectrometer, isotope effects and spin-lattice relaxation 0-71211  
<sup>2</sup>H nuclei, spin-1 particle, eight-dimensional spin space determ. 0-60428  
He film, adsorbed, NMR measurements 0-107605  
<sup>3</sup>He, adsorbed monolayers, nuclear magnetic relaxation for two dimensional systems 0-103534  
<sup>3</sup>He, superfluid, A-phase, dissipation of flow, NMR study 0-92745  
<sup>3</sup>He, superfluid, A-phase, helical textures, NMR response 0-70496  
<sup>3</sup>He, superfluid, transport parameters, Kubo formulae and BCS-Green's functions 0-88382  
<sup>3</sup>He superfluid A-phase, exptl. studies of solitons 0-88386  
<sup>3</sup>He, superfluid A-phase, longitudinal mag. relax. 0-59751  
HgCr<sub>2</sub>Se<sub>4</sub>, spontaneous magnetisation temp. depend., nuclear resonance freq. depend. (French) 0-80483  
<sup>19</sup>Ir orientated in Fe and Ni, nuclear mag. resonance 0-84661  
KMnF<sub>3</sub>:Rb, phase transition and atomic motions, NMR study 0-75872  
K<sub>2</sub>MnF<sub>4</sub>:Zn(Mg)(Ni), local magnetisation, NMR and Green's function study 0-65870  
<sup>138,139</sup>La, Fourier transform NMR 0-57354  
LaF<sub>3</sub>, <sup>19</sup>F NMR study, relaxation times meas. 0-108093  
LaF<sub>3</sub>, ionic transport, NMR and cond. studies 0-107555  
La<sub>2</sub>Ga<sub>2</sub>, amorphous, local symmetry around glass-former sites, elec. quadrupole effects, NMR 0-80618

**nuclear magnetic resonance continued**  
Li, Knight shift volume depend. 0-84663  
Li<sup>+</sup>-ligand complexes, <sup>7</sup>Li chemical shifts, expt. and ab initio studies 0-63670  
LiF, cross relaxation of β-active <sup>8</sup>Li nuclei (Russian) 0-103895  
LiF, heteronuclear mag. spin system relaxation in many pulse NMR expts. 0-93203  
Li<sub>2</sub>FeP<sub>2</sub>(Se<sub>2</sub>), Li<sub>2</sub>MnPSe<sub>2</sub> and Li<sub>2</sub>NiP<sub>2</sub>(Se<sub>2</sub>), NMR and neutron diff. obs., mag. props. 0-60433  
Li<sub>2</sub>O-B<sub>2</sub>O<sub>3</sub> glass struct. study using <sup>10</sup>B NMR 0-84658  
Li<sub>2</sub>O-LiX-B<sub>2</sub>O<sub>3</sub> glass, X=halogen, high anionic cond. of new solid electrolytes 0-107546  
Mn II-lecithin lipid-water system, NMR and EPR obs. 0-61168  
Mn(ClO<sub>4</sub>)<sub>2</sub>/NaClO<sub>4</sub> in aq. soln., interaction between Mn<sup>2+</sup> and ClO<sub>4</sub><sup>-</sup>, NMR studies 0-71212  
Mo<sub>70</sub>B<sub>30</sub>, amorphous, local symmetry around glass-former sites, elec. quadrupole effects, NMR 0-80618  
Mo<sub>48</sub>Ru<sub>12</sub>B<sub>20</sub>, amorphous, local symmetry around glass-former sites, elec. quadrupole effects, NMR 0-80618  
N<sub>2</sub> complex, Ni(C<sub>2</sub>H<sub>5</sub>NO)<sub>2</sub>(NO)<sub>2</sub>, singlet ground-state systems, field induced mag. long range order 0-60266  
NF<sub>3</sub>, nuclear resonance, effects of intermolecular interactions and intramolecular dynamics 0-63658  
N<sub>2</sub>H<sub>4</sub><sup>2+</sup> salts, NMR spin lattice relaxation study, <sup>14</sup>N-<sup>1</sup>H dipole-dipole contrib. to relax. 0-75878  
NH<sub>4</sub>BF<sub>4</sub>, ionic radii and chem. shifts, correl. with electronegativity 0-66054  
NH<sub>4</sub>Fe(SeO<sub>3</sub>)<sub>2</sub>, single crystal, <sup>77</sup>Se magnetic shielding, chemical shift tensors 0-71207  
NaClO<sub>4</sub>/Mn(ClO<sub>4</sub>)<sub>2</sub> in aq. soln., interaction between Mn<sup>2+</sup> and ClO<sub>4</sub><sup>-</sup>, NMR studies 0-71212  
Na<sub>2</sub>O-B<sub>2</sub>O<sub>3</sub> glass struct. study using <sup>10</sup>B NMR 0-84658  
β-Na<sub>0.33</sub>V<sub>2</sub>O<sub>5</sub>, quasi-one-dimensional conductor, NMR studies 0-93204  
Na<sub>2</sub>WO<sub>3</sub>, 0.22<x<0.84, low temp. struct., press. effects, NMR study 0-59443  
<sup>23</sup>Na in heterogeneous system, nuclear mag. relaxation time determ., rel. with dimensions of colloidal particles 0-75876  
NbS<sub>2</sub>(pyridine)<sub>2</sub>, intercalation complex, superlattice struct., NMR meas. 0-70180  
Ni, NMR study of metal precipitated onto a cathode (Russian) 0-93185  
Ni<sub>72</sub>P<sub>12</sub>B<sub>8</sub>, amorphous, local symmetry around glass-former sites, elec. quadrupole effects, NMR 0-80618  
<sup>18</sup>O isotope shift in <sup>13</sup>C NMR, struct. depend. 0-69165  
P+Nb, dil. alloy, NMR obs. of <sup>93</sup>Nb 0-71203  
PCl<sub>5</sub>, sublimed phase studied by <sup>31</sup>P NMR, Raman spectra and X-ray diff. 0-100209  
PF<sub>3</sub>, nuclear resonance, effects of intermolecular interactions and intramolecular dynamics 0-63658  
PF<sub>3</sub>, nuclear resonance, effects of intermolecular interactions and intramolecular dynamics 0-63658  
POF<sub>3</sub>, nuclear resonance, effects of intermolecular interactions and intramolecular dynamics 0-63658  
<sup>31</sup>P NMR of the perfused heart 0-77534  
<sup>31</sup>P-NMR spectra of chicken erythrocyte nucleosomes, temp. dependence 0-94280  
Pb<sub>0.9</sub>Sb<sub>0.1</sub>F<sub>2</sub>, NMR study of F atom motion (French) 0-100622  
Rb<sub>2</sub>NaHoF<sub>6</sub>, NMR spectra of <sup>155</sup>Ho, 1.6 to 13K 0-80620  
Rb<sub>2</sub>NaTbF<sub>6</sub>, NMR spectra of <sup>155</sup>Tb, 1.6 to 13K 0-80620  
Rb<sub>2</sub>ZnCl<sub>4</sub>, incommensurate phase transition, <sup>87</sup>Rb NMR study 0-75967  
Rh<sub>2</sub>MnPt<sub>6</sub>, hyperfine fields, ferromag., NMR and Mossbauer effect studies 0-71259  
Rh<sub>2</sub>MnSb<sub>6</sub>, hyperfine fields, ferromag., NMR and Mossbauer effect studies 0-71259  
Ru<sub>2</sub>FeSn, ferromag. Heusler alloys, hyperfine fields at nonmagnetic atoms in various sites, Mossbauer effect and NMR meas. 0-66089  
SF<sub>6</sub>, <sup>19</sup>F NMR vibr. anharmonicity effects 0-91580  
SiCl<sub>4</sub> liquid, angular momentum relaxation, effective collision numbers 0-64873  
SiCl<sub>4</sub> molecule, NMR relaxation expts. to study molecular reorientation 0-63673  
<sup>117</sup>Sn, <sup>119</sup>Sn, low temp. NMR thermometry 0-82775  
TGS, ferroelectric phase transition, high resolution NMR study 0-97214  
Tb<sub>1-x</sub>Gd<sub>x</sub>Al<sub>2</sub>, effective mol. field at <sup>159</sup>Tb, NMR meas. 0-71197  
γ-TiH<sub>3</sub>, interstitial H diffusion mechanism, NMR spin-lattice relax. study 0-103515  
TiO<sub>2</sub>, rutile, superficial constitutive water, NMR study 0-88881  
Ti complex of lasaloid (X-537A), <sup>205</sup>Ti NMR study 0-58288  
Ti+Cs, Ti 6<sup>2</sup>P<sub>3/2</sub>-state relax., NMR obs. 0-95653  
V-Ni sigma phase alloys, NMR and electric-field gradients 0-108109  
V<sub>2</sub>(Hf,Zr), NMR and mag. susceptibility, density of states determ. (Russian) 0-66053  
VO<sub>2</sub>, <sup>51</sup>V NMR studies, microscopic mag. props. 0-108086  
V<sub>2</sub>Se<sub>3</sub>, itinerant antiferromag., spin fluctuations, NMR study 0-75874  
V<sub>2</sub>Se<sub>3</sub>, itinerant antiferromag., spin fluctuations, NMR study 0-75874  
<sup>89</sup>V spin-spin relaxation times, pH depend. 0-66059  
Zn-nucleotide, triphosphate complexes, <sup>35</sup>Cl NMR obs. 0-63661  
Zr and its alloys, H diffusion, NMR study 0-108088  
ZrF<sub>4</sub>-BaF<sub>2</sub>-ThF<sub>4</sub>(LaF<sub>3</sub>)(NdF<sub>3</sub>)(PrF<sub>3</sub>), F ion cond. glasses, cond. process 0-107477  
Zr(V<sub>1-x</sub>Co<sub>x</sub>)<sub>2</sub>, pseudobinary intermetallic compound, relation between electronic struct. and H<sub>2</sub> storing props. 0-76662

**nuclear magnetic shielding** see nuclear screening

# nuclear mass

see also atomic mass  
A=12-208, adiabatic TDHF approx. isoscalar quadrupole collective motion, cranking mass 0-68507  
adiabatic TDHF approx., mass parameters, single collective variable, theoretical aspects 0-73765  
conference on nuclear spectroscopy of fission products, Grenoble, France (May 1979) 0-77546  
dilute Fermi gas, self energy, momentum distrib., and effective mass, nuclear matter 0-63119  
effective mass and exchange current effects in finite nuclei 0-78171  
fissioning nucleus, deformation process mass parameter, liquid drop model 0-102221  
Franzini-Radicati mass relationship in isobars, Wigner SU(4) supermultiplet 0-105958  
mass fitting and averaging, correction due to one particle Hamiltonian symmetry (Russian) 0-83032

**nuclear mass continued**

- momentum and mass distrib., form factors, short range correlation effects 0-105959  
 nuclei far from stability,  $\beta$ -decay energies,  $\gamma$ -rays,  $Q_\beta$  values and masses 0-78225  
 $Z=37-43$ , neutron rich fission products, mass energy surface, decay props. 0-78228  
 $(\pi^+, \pi^-)$   $A=9-32$ , 180 MeV 0-105960  
 $^{140}\text{Ac}$ ,  $A=209-214$ , 216, deduced mass from Fr direct mass meas. 0-78130  
 $\text{Ag}(p,f)$ , 1 GeV, binary fission, possible mass instability of correlated fragments 0-83133  
 $^{140}\text{At}$ ,  $A=200-206$ , 208, deduced mass from Fr direct mass meas. 0-78130  
 $^{197}\text{Au}(p,X)$ , 0.2-6.0 GeV, product cross sections, mass yields, spallation products 0-83088  
 $^{209}\text{Bi}$ ,  $A=196-202$ , 204, deduced mass from Fr direct mass meas. 0-78130  
 $^{209}\text{Bi}(^{56}\text{Fe}, X)$ , damped collisions, fast  $A/Z$  equilibration and correlated nucleon exchange 0-86798  
 $^{110}\text{Cd}$ ,  $A=104-116$ , low lying level scheme, mass excess from  $\text{Cd}(p,t)$  0-73807  
 $\text{Cs}$ , neutron rich isotopes,  $Q_\beta$  and direct mass meas. 0-78132  
 $^{140}\text{Fr}$ ,  $A=201-203$ , alpha decay, branching ratios, mass excess and half life 0-99154  
 $^{140}\text{Fr}$ ,  $A=204-210$ , 212, 224-228, direct mass meas. 0-78130  
 $^{140}\text{Gd}$ ,  $A=146, 147$ , mass and  $Z=64$  shell closure from  $^{144}\text{Sm}(^{12}\text{C}, ^9\text{Be})$  0-57669  
 $^{11}\text{In}$  mass difference from  $Q$  values of  $\text{Cd}(^3\text{He}, d)$  0-63069  
 $^{16}\text{O}$ ,  $\Lambda$ - $N$  residual interactions,  $\Lambda$  spin-orbit splitting and effective mass 0-57722  
 $^{140}\text{Pa}$ ,  $A=215-218$ , deduced mass from Fr direct mass meas. 0-78130  
 $\text{Rb}$ , neutron rich isotopes,  $Q_\beta$  and direct mass meas. 0-78132  
 $(^{25}\text{X})$ ,  $A=59-89$ , double differential cross section, mass asymmetry, transport model 0-102203  
 $^{24}\text{Si}$ ,  $Q$  value and mass excess from  $^{28}\text{Si}(\alpha, ^8\text{He})$  0-86795  
 $^{180}\text{Ta}$  mass,  $10^{13}$  y naturally occurring isomer state 0-57670  
 $^{232}\text{Th}(n,f)$ , 2-8 MeV, fission product yields and mass distrib. 0-86939  
 $^{197}\text{Tl}$ , deduced mass from Fr direct mass meas. 0-78130

**nuclear matter**

- $\alpha$ -clustering in heavy nuclei, pre-equil. model, nuclear matter  $NN$ ,  $N\alpha$  interactions 0-63111  
 $\nu_e$  semirealistic model, variational theory accuracy and convergence 0-57712  
 abnormal occupation, two body correlations and plane wave HF energy 0-86844  
 asymmetric nuclear matter, isospin waves, IAS and giant Gamow-Teller resonance 0-91142  
 asymmetric semi-infinite nuclear matter, HF calcs., surface symmetry props., finite range forces 0-57713  
 baryonic inclusive spectra in hadron-, photon- and HI-nucleus collisions, fireball model 0-86892  
 binding energy, hypernetted chain approx., impurity ground state energy 0-83055  
 binding energy and rest mass of constituents, total symmetry effects (French) 0-63068  
 bound multinucleon system, 8 and 20 neutrons, existence probability 0-68570  
 Chakravarty-Woo eqn., extension and appl. to liq.  $^4\text{He}$ , liq.  $^3\text{He}$ , and nucl. matter 0-68124  
 colliding ion system, projectile nucleon mean free path, nuclear matter approach, Pauli blocking 0-86920  
 compressible nuclei, surface energy 0-83031  
 correlated nuclear matter, electric dipole sum rule 0-83056  
 dense matter physics, conference, Paris, France (1979 September 17 to 21) 0-73094  
 dense neutron matter physics, implications for neutron star props. 0-77277  
 dense plasmas and nuclear reactions, astrophysical appls. 0-77281  
 density determ., HF versus droplet model 0-68574  
 density fluctuation in nuclear matter 0-86838  
 density oscillations, from semi-infinite nuclear matter calc., Regge type oscillation comparison 0-57671  
 dilute Fermi gas, self energy, momentum distrib., and effective mass, nuclear matter 0-63119  
 effective  $NN$  interaction and exchange current vel. depend., dipole sum rule enhancement 0-63100  
 ellipsoidal, liquid-drop model, irrotational incompressible hydrodynamic flow 0-83050  
 equation of state at subnuclear densities, theory 0-77278  
 equation of state at ultrahigh densities and the speed of sound 0-57716  
 finite quark mass effects on superdense quarkion configurations 0-105852  
 fluid theory, universality in short range struct. in simple classical fluids 0-75141  
 generalised Fermi sea for plane wave HF theory, 3-dimens. semi-realistic interactions 0-105999  
 hadron matter physics, determ. from pulsars and compact X-ray sources 0-77442  
 hadronic interiors, meas. and charge distrib., hadronic diffraction scatt. 0-73817  
 head on heavy ion collisions, compression and temp. extremes, nuclear matter phase changes (Russian) 0-83121  
 heavy ion relativistic collisions, pion bremsstrahlung and critical phenomena, nuclear matter phases 0-86919  
 infinite system of nucleons and  $\Delta$  resonances, pot. energy, neutron stars 0-86836  
 ion beams, heavy, uses in nuclear physics (French) 0-78182  
 iterative isobar process rule, effective  $NN$  interaction 0-99143  
 leptoproduced high energy particles, nuclear attenuation, hadronisation time 0-102182  
 many body problem in Lee model,  $NN$  scatt. and matter binding energy 0-63116  
 massive star core collapse, core processes 0-82335  
 mean field near Fermi surface, energy dependence, single-particle quantities, Brueckner-Hartree-Fock calcs. 0-68572  
 momentum distrib., Fermi-hypernetted-chain theory 0-82716  
 momentum distrib., single particle orbitals, Fermi hypernetted chain theory 0-86841  
 multihadron production in nuclear matter and hadron struct., space-time description, review (Russian) 0-68571  
 neutron and nuclear matter with isobars, transition pot. model, neutron stars 0-68573

**nuclear matter continued**

- neutron excess, thermal props. and level density parameter 0-91141  
 neutron gas, crystallisation, zero-order, Bethe-Fermi homework potential 0-63117  
 neutron matter, hypernetted chain calcs. with the Paris pot. 0-57714  
 neutron matter-quark matter phase transition, QCD and extended Higgs model, instantons 0-91062  
 neutron star core, phase transition between nucl. and quark matter 0-67771  
 neutron star cores, AC Josephson effect rel. to pulsars emission 0-82404  
 neutron stars, superfluidity 0-77441  
 phase transition to abnormal nuclear matter at finite temperature and finite baryon density 0-86840  
 pion condensate, structures for symmetric nuclear matter 0-86839  
 pion condensation precursor, quasi-elastic peak softening 0-78170  
 pion spectrum and polariz. operator in nuclear medium in heavy nuclei collisions (Russian) 0-68558  
 polarised, thermal props., temp., spin isospin and spin-isospin pressure 0-102135  
 polarised nuclear matter, binding energy, spin energies, relativistic calc. 0-102134  
 pulsars outer crust, influence of mag. field on comp. 0-101610  
 quark-nucleon phase diagram and quantum chromodynamics 0-105855  
 Rayleigh and whispering gallery waves excited by heavy ion elastic and inelastic scatt. 0-91164  
 relativistic central heavy ion collisions, spherical and linear fluid dynamical models 0-86926  
 relativistic composite system, light-front wave functions 0-73592  
 relativistic condition of pion condensation 0-86837  
 S-wave  $\pi N$  interaction role in combined pion condensation 0-105998  
 S-wave  $\pi N$  interactions and PCAC 0-78185  
 saturation in finite nuclei, nuclear matter density and binding energy 0-83029  
 single-particle response and ground-state properties, Hartree-Fock theories 0-105997  
 single-particle states in nuclear matter and in finite nuclei 0-78117  
 spherical nuclei, Hartree-Fock-Bogolyubov calcs., D1 effective interaction, nuclear matter, binding energies 0-63105  
 spin-isospin and pion condensation phase transitions, eqn. of state 0-86843  
 stellar dense matter, nuclear size effect rel. to neutron stars limiting mass 0-101611  
 superdense celestial bodies, theory 0-67773  
 superfluid neutron matter,  $^3\text{P}_2$  pairing, mag. field effects, vortices 0-62174  
 supernovae, thermodynamic of nucleon, lepton, photon mixture, quantum mechanical calcs. 0-77273  
 thermonuclear explosions in stars 0-72766  
 three-body force from  $2\pi$ ,  $\pi\rho$ , and  $2\rho$  exchanges 0-78169  
 transport coefficient temperature dependence 0-78184  
 UCN, quasisub states in-matter, reson. positions and widths 0-73833  
 ultrarelativistic nuclear collisions, asymptotic hadron spectrum, hot hadronic matter 0-63118  
 valence nucleons, radial wave functions 0-73788  
 $(K,K)$ , isobar doorway model, optical pot.,  $\Lambda$ -nuclear matter binding energy 0-106079  
 $\Lambda NN$  correlations and  $\Lambda$  binding in nuclear matter 0-106000  
 $n$  distribution from 1 GeV  $p$  scattering (French) 0-78183  
 $^3n$  binding energy, calc. from  $^3\text{H}$ ,  $^3\text{He}$ ,  $^4\text{H}$ ,  $^4\text{He}$  and  $^4\text{Li}$  ground-state properties 0-83044  
 $^4n$  binding energy, calc. from  $^3\text{H}$ ,  $^3\text{He}$ ,  $^4\text{H}$ ,  $^4\text{He}$  and  $^4\text{Li}$  ground-state properties 0-83044  
 $(\bar{p}, X)$ ,  $\bar{p}$  annihilation on heavy nuclei, nuclear matter props. 0-63185  
 $(\pi, X)$ , effective S-wave  $\pi NN$  interaction, effects in nuclear matter 0-105985  
 $\pi$  condensation in neutron matter,  $N$ - $N$  interaction, critical density 0-57711  
 $\pi$  condensed phase,  $\sigma$ -model, alternating-layer-spin struct. 0-83057  
 $\pi^0 \rightarrow 2\gamma$ , decay width as signal for nuclear matter phase transition, Primakoff effect 0-86842  
 $(^{12}\text{C}, X)$ , in emulsion, 3.6 GeV/N, high energy multiply charged particle emission, nuclear shock waves (Russian) 0-86923  
 $^{12}\text{C}(^{12}\text{C}, X)$ , optical potential, nuclear matter approach 0-57801  
 $^{12}\text{C}(p,p')$ , 122 MeV, precritical phenomena 0-83089  
 $^{12}\text{C}(p,p')$ , 800 MeV, 15.11 MeV state diff. cross section, nuclear critical opalescence search 0-105984  
 $^{140}\text{Ca}$ ,  $A=40, 48$ , nuclear matter density distrib., saturation effect, optical potential from  $(\alpha, \alpha)$  0-63115  
 $^{40}\text{Ca}(^{16}\text{O}, ^{16}\text{O})$ , optical pot., nuclear matter approach, energy density matter [-] 0-83112  
 $^{40}\text{Ca}(^{40}\text{Ca}, ^{40}\text{Ca})$ , optical pot., nuclear matter approach, energy density matter [-] 0-83112  
 $^{40}\text{Ca}(^{40}\text{Ca}, X)$ , relativistic, compression and pion distrib., Monte Carlo calc. 0-73853  
 $^4\text{He}$ ,  $A=3, 4$ , charge structure, effect of neutron charge 0-105963  
 $^{39}\text{K}(^{39}\text{K}, X)$ ,  $\pi^0$  condensation, spin-isospin instabilities, TDHF calcs. 0-83042  
 $^{15}\text{N}(^{15}\text{N}, X)$ ,  $\pi^0$  condensation, spin-isospin instabilities, TDHF calcs. 0-83042  
 $^{58}\text{Ni}(^{58}\text{Ni}, X)$ , optical potential, nuclear matter approach 0-57801  
 $^A O(\pi, \pi^-)$ ,  $A=16, 18$ , resonance region, proton and neutron distrib. 0-91195  
 $^{16}\text{O}(^{16}\text{O}, ^{16}\text{O})$ , optical pot., nuclear matter approach, energy density matter [-] 0-83112  
 $^{208}\text{Pb}(\alpha, \alpha')$ , levels,  $B(E3)$ , transition density and nuclear pot., folding model anal. 0-86812  
 $\text{U}(\text{Ne}, X)$ , 250, 400, 800 MeV/N, nuclear matter collective sideward flow, nuclear fluid dynamics 0-57715

**nuclear models**

- see also nuclear cluster model; nuclear collective model; nuclear reaction and scattering models; nuclear shell model  
 $^{63}\text{Cu}(p,p')$  negative parity level excitation, gamma ray obs., test for core excitation model 0-68534

**nuclear moment of inertia**

- $A=158-176$ , 'extension of variable moment of inertia model to high spins', comments 0-86791  
 actinide nuclei, cranking model, collective inertia parameters 0-57665  
 even-even nuclei, yrast band backbending mechanism criteria 0-91128  
 fission isomers, spectrosc. props. 0-105966



# nuclear moment of inertia continued

- perturbative treatment of nuclear rots., two-dimens. rotor, bands, moments of inertia 0-78111
- rare earth nuclei, cranking model, collective inertia parameters 0-57665
- rotating nuclei, current distribts., cranked HF model 0-63059
- rotation, inertial parameters in microscopic theory 0-91132
- rotational nuclei, high-spin, variable moment of inertia model, microscopic-macroscopic approach 0-63058
- Woods-Saxon potential spectrum, pairing force strength, Nilsson model comparison 0-57704
- Er rotational nuclei, transition energy correlations, very high ang. momentum 0-86787
- <sup>152</sup>Gd  $\beta$ - and octupole bands, downbending moments of inertia from <sup>150</sup>Sm( $\alpha$ , 2n) 0-91131
- <sup>20</sup>Ne, moment of inertia from cranked HF method 0-102098
- <sup>58</sup>Ni(<sup>16</sup>O, X), 70 MeV, compound nuclei charged particle evaporation, moment of inertia 0-57785
- Pu, even isotopes, K=0<sup>+</sup>, 0<sup>-</sup> bands, energies, inverse moments of inertia 0-63063
- Ra, even isotopes, K=0<sup>+</sup>, 0<sup>-</sup> bands, energies, inverse moments of inertia 0-63063
- Rn, even isotopes, K=0<sup>+</sup>, 0<sup>-</sup> bands, energies, inverse moments of inertia 0-63063
- Th, even isotopes, K=0<sup>+</sup>, 0<sup>-</sup> bands, energies, inverse moments of inertia 0-63063
- <sup>238</sup>Th(n,f), 0.68-1.10 MeV, fission fragment ang. distribts., resonance and moment of inertia 0-102219
- U, even isotopes, K=0<sup>+</sup>, 0<sup>-</sup> bands, energies, inverse moments of inertia 0-63063
- <sup>172</sup>Yb levels, bands, J<sup>π</sup> and T<sub>1/2</sub> from <sup>170</sup>Er( $\alpha$ ,2n) 0-91127

# nuclear moments

- see also nuclear electric moment; nuclear magnetic moment; nuclear moment of inertia
- odd nuclei, soft and deformed, rotor plus quasiparticle approach, moments, transition probabilities 0-78214
- Ba, radioisotopes, at. beam laser spectroscopy, hyperfine struct., nucl. moments and radii 0-57678
- Ca, stable and radioisotopes, hfs, isotope shifts, dye laser saturation spectroscopy, beam expt. 0-58169
- Cs, ground state spins, moments, charge radii by laser spectroscopy 0-78147
- <sup>2</sup>H(e,e), EM form factors, relativistic formulae, moment corrections 0-63075
- Rb, ground state spins, moments, charge radii by laser spectroscopy 0-78147
- <sup>151</sup>Sm(p,p'), 0.8 GeV, ang. distribts. and multipole moments, DWBA and coupled channel anal. 0-105969
- <sup>176</sup>Yb(p,p'), 0.8 GeV, ang. distribts. and multipole moments, DWBA and coupled channel anal. 0-105969

# nuclear muon capture see muon capture

# nuclear optical model

- compound neutron absorption processes, optical pots., one particle vibr. state effects (*Russian*) 0-105956
- coupled channel optical model calc. improvement (*Chinese*) 0-99159
- doorway states, energy dependence of inelastic cross-section, shell model, coupled channel anal. 0-73854
- elastic two fragment collisions, Pauli principle and optical pot. 0-63153
- finite nuclei,  $\Delta$ -resonance self energy, Fermi broadening,  $\pi$ -nucleus optical pot. 0-68707
- fragment elastic scattering, unitarity and optical pot. 0-106028
- hadron-nucleus reactions, optical pot. eqns. for low and moderate energies (*Russian*) 0-63214
- hadronic interiors, meas. and charge distrib., hadronic diffraction scatt. 0-73817
- heavy ion+nucleus scattering, Regge pole contrib., forward- and backward-angle, Coulomb and nuclear scatt. functions 0-57788
- heavy ion deep inelastic collision processes, optical model description, statistical considerations 0-68687
- heavy ion elastic scattering 0-73858
- heavy ion optical potential, real part, folding technique 0-73830
- heavy ion-light particle angular correlation, forward peaked, light particle emission from l-windows 0-63142
- kaon-nucleus reactions, low energy, nuclear density shaped optical pot. kaonic atom level shifts 0-63213
- kaonic atoms, quadrupole hyperfine structure 0-78726
- nucleon spin-orbit optical pot., energy depend. 0-68616
- nucleus-nucleus interaction pot., transition from light to heavy ions, optical pots 0-63197
- OPTY, universal optical model code for elastic scatt. 0-73832
- phase-amplitude method for a separable non-local optical potential 0-78237
- pion-nucleus, single charge exchange and inelastic scatt. cross sections relationship 0-102204
- pionic atoms, quadrupole hyperfine structure 0-78726
- quasi elastic nucleus-nuclear scatt. differential cross section (*Russian*) 0-68696
- stellar environment, nucl. struct. and reactions 0-72765
- strongly bound pion states in nuclei, optical model 0-68557
- theory of energy-dependent nuclear optical-model potentials 0-102163
- uncorrelated target, optical pot. unitary content, DWIA and Glauber theory 0-99160
- ( $\alpha$ , $\alpha$ ), folding potentials, Woods-Saxon and squared Woods-Saxon parametrisations 0-102195
- ( $\alpha$ , $\alpha$ ), local density dependence of NN interaction, double-folding calcs. 0-83114
- (d,d), A=27-238, 12-90 MeV, global optical model pot. 0-78305
- (d,d), optical model analyses (*German*) 0-68676
- (d,d), pol. d, 56 MeV, A=16-208, cross sections, optical parameters, anal. powers 0-78270
- (d,d), pol.d, 52 MeV, A=12-197, vector anal. power and optical parameters 0-57764
- (d,d) medium heavy nuclei, optical model anal., cross sections, anal. powers 0-73839
- (e,e'), cross section near quasielastic maximum, shell and optical models (*Russian*) 0-91179
- ( $\gamma$ , $\pi$ ), photopion reaction sensitivity to optical pot. 0-78278
- (K,K), isobar doorway model, optical pot., A-nuclear matter binding energy 0-106079
- (n, $\gamma$ ), polarized space parity nonconservation, optical pot. and GDR parameters (*Russian*) 0-86803

# nuclear optical model continued

- (n,n), A=90 region, elastic, inelastic and total cross section, statistical model calcs. 0-68674
- (p,n), A=89-130, anomalous optical pot. for sub-Coulomb protons 0-102190
- (p,n), A=89-130, sub-Coulomb protons, anomalous optical pot. 0-102191
- (p,n), A=90 region, reaction cross section, statistical model calcs. 0-68674
- (p,n), anomalous optical potential for sub-Coulomb barrier protons, 2 particle 1 hole states 0-105948
- (p,p), 0.1-1 GeV, optical pot., vol. integrals and root mean square radii 0-106054
- ( $\pi^-$ , NN), low energy pion absorption,  $\sigma+\omega$  model, optical pots., real  $\rho^2(r)$  pot. 0-83125
- ( $\pi$ ,  $\pi$ ), lowest order optical pot. containing  $\pi$  emission and absorption effects 0-73865
- ( $\pi$ , $\pi$ ), Weinberg chiral Lagrangian nonlinear terms, nuclear binding, optical pot. 0-78329
- <sup>107</sup>Ag(p,p'), pol.p, 6.06 MeV, anal. powers, large absorption pot., optical model 0-83092
- <sup>27</sup>Al(<sup>6</sup>Li, <sup>6</sup>Li), 90 MeV, real optical pot. continuous ambiguity 0-102200
- <sup>197</sup>Au(<sup>14</sup>N,n), DWBA anal. above Coulomb barrier 0-86917
- <sup>9</sup>Be( $\alpha$ ,  $\alpha'$ ), 65 MeV, levels and differential cross sections, optical anal. 0-102121
- <sup>209</sup>Bi( $\alpha$ ,n), excitation functions and isomer ratios of <sup>212</sup>At 0-83039
- <sup>209</sup>Bi( $\alpha$ ,np), excitation functions and isomer ratios of <sup>211</sup>Po 0-83039
- <sup>209</sup>Bi( $\alpha$ ,p), excitation functions and isomer ratios of <sup>212</sup>Po 0-83039
- <sup>12</sup>C(<sup>12</sup>C,X), optical potential, nuclear matter approach 0-57801
- <sup>12</sup>C(<sup>16</sup>O,X), transparency to i=9 partial wave in 14.7 MeV resonance region 0-78314
- <sup>12</sup>C(p,X), reaction and scatt. dynamics, optical and coupled channel anal. 0-78297
- <sup>12</sup>C(p,p'), 20-40 MeV, pol. p, anal. powers, imaginary spin-orbit pot., coupled channels anal. 0-102179
- <sup>12</sup>C(p,p), radial sensitivity of optical pot. 0-86869
- <sup>12</sup>C( $\pi^+$ , $\pi^+$ ), nonlinear meson dynamics and binding corrections, optical pots. 0-106080
- <sup>12</sup>C( $\pi^+$ ,  $\pi^+$ ), 0-300 MeV, cross sections, pion-nucleus optical pot. including nuclear Hamiltonian 0-68706
- <sup>13</sup>C( $\pi^+$ ,  $\pi^+$ ), 0-300 MeV, cross sections, pion-nucleus optical pot. including nuclear Hamiltonian 0-68706
- <sup>4</sup>Ca, A=40, 48, nuclear matter density distrib., saturation effect, optical potential from ( $\alpha$ , $\alpha$ ) 0-63115
- <sup>4</sup>Ca( $\alpha$ , $\alpha$ ), A=40, 42, 44, 48, 104 MeV, cross sections and optical pots., nuclear size 0-68524
- <sup>4</sup>Ca( $\alpha$ , $\alpha$ ), A=40, 42, 44, 48, 104 MeV nuclear size and density distrib. from folding model anal. 0-68525
- <sup>4</sup>Ca( $\pi$ , $\pi$ ), A=40,48, 40-241 MeV, first and second order optical pots., resonance behaviour 0-68624
- <sup>40</sup>Ca(<sup>11</sup>B,<sup>10</sup>B), 51.5 MeV, n stripping, DWBA anal. with Woods-Saxon and double folding optical pots. 0-102171
- <sup>40</sup>Ca(<sup>11</sup>B,<sup>12</sup>C), 32, 68 MeV, single proton pickup, DWBA anal., optical pot. 0-106037
- <sup>40</sup>Ca(<sup>11</sup>B,<sup>12</sup>C), 51.5 MeV, p pickup, DWBA anal. with Woods-Saxon and double folding optical pots. 0-102171
- <sup>40</sup>Ca(<sup>13</sup>C,<sup>14</sup>N), 40, 68 MeV, single proton pickup, DWBA anal., optical pot. 0-106037
- <sup>40</sup>Ca(<sup>16</sup>O,<sup>16</sup>O), complex heavy ion optical pot., microscopic BHF derivation 0-106067
- <sup>40</sup>Ca(<sup>16</sup>O,<sup>16</sup>O), optical pot., nuclear matter approach, energy density matter [-] 0-83112
- <sup>40</sup>Ca(<sup>40</sup>Ca,<sup>40</sup>Ca), optical pot., nuclear matter approach, energy density matter [-] 0-83112
- Ca(<sup>8</sup>Be, <sup>8</sup>Be), 45, 60 MeV, low lying collective states, ang. distribts., DWBA double folding pot. anal. 0-78113
- <sup>40</sup>Ca(p,p), 30 MeV, optical pot. imaginary part calcs. 0-86868
- <sup>40</sup>Ca(p,p), absorbing optical pot., Coulomb correction term 0-73831
- <sup>44</sup>Ca(Li, <sup>7</sup>Li), 34 MeV, ang. distribts., cross sections, double folding model anal. 0-78313
- <sup>48</sup>Ca(<sup>16</sup>O, <sup>15</sup>N), <sup>15</sup>N excitation contrib. in optical pot., DWBA grazing peak shift 0-86921
- Ca(p,n), nucleon optical potential from Lane model 0-83097
- <sup>56</sup>Fe(p,p), 6 MeV, elastic and inelastic, quadrupole deformation, IAR excitation, optical pots. (*Russian*) 0-63149
- <sup>58</sup>Fe(<sup>7</sup>Li, <sup>7</sup>Li), 34 MeV, ang. distribts., cross sections, double folding model anal. 0-78313
- (HI,HI), local density dependence of NN interaction, double-folding calcs. 0-83114
- <sup>1</sup>H(p,X), elastic, inelastic and charge exchange cross sections in optical model 0-68665
- <sup>2</sup>H scattering, deformed tensor interactions, folding model 0-57783
- <sup>2</sup>H( $\pi^+$ ,p,p), pionic disintegration, absorptive  $\pi$ -nucleus optical pot., microscopic model 0-99191
- <sup>3</sup>He(e,e), relationship to <sup>3</sup>He( $\pi^-$ ,  $\pi^-$ ) 0-78323
- <sup>3</sup>He( $\pi$ , $\pi$ ), optical potential in momentum representation 0-78324
- <sup>3</sup>He( $\pi^-$ ,  $\pi^-$ ), 145, 180 and 195 MeV, relationship to <sup>3</sup>He(e,e) 0-78323
- <sup>3</sup>He( $\pi^-$ ,  $\pi^-$ ), H, optical potential in momentum representation 0-78324
- <sup>4</sup>He(p,p), 788 MeV, back angle diffraction struct., Dirac, eqn. optical model 0-68667
- <sup>4</sup>He( $\pi$ , $\pi$ ), single scatt. optical pot., Pauli principle and binding effects on cross section 0-86933
- H(p,x), direct and charge transfer scattering processes, second quantisation 0-78289
- (<sup>6</sup>Li,<sup>6</sup>Li), 30, 88 MeV, M3Y folding model eval., model indep. anal. 0-78317
- (<sup>6</sup>Li, <sup>7</sup>Li), 99 MeV, A=12-208, ang. distribts. from double folding model pots. 0-106074
- <sup>14</sup>N( $\gamma$ , $\pi^-$ ), DWIA anal., wave function and  $\pi$  optical pot. effects on cross section 0-63168
- <sup>14</sup>N(p,p'), 25-40 MeV, level cross sections, optical parameters, DWBA anal., tensor effective interaction 0-68555
- <sup>21</sup>Ne deduced spectroscopic factors, levels and anal. powers from <sup>20</sup>Ne(d,poly,p) 0-83087
- <sup>20</sup>Ni(<sup>7</sup>Li, <sup>7</sup>Li), A=58, 60, 34 MeV, ang. distribts., cross sections, double folding model anal. 0-78313
- <sup>58</sup>Ni(<sup>28</sup>Ni,X), optical potential, nuclear matter approach 0-57801
- <sup>58</sup>Ni(<sup>6</sup>Li,<sup>6</sup>Li), elastic and inelastic, 74 MeV, folding optical model parameters 0-102201
- <sup>58</sup>Ni( $\alpha$ , $\alpha$ ), radial sensitivity of optical pot. 0-86869

**nuclear optical model continued**

- <sup>58</sup>Ni( $\alpha$ , $\alpha$ ), 50.2 MeV, composite particle optical pot. discrete ambiguities, partly Pauli-forbidden states 0-86870
- <sup>58</sup>Ni(p,p), 800 MeV, elastic and inelastic, cross section, deformation lengths, optical and DWBA anal. 0-68664
- <sup>10</sup>O( $\pi^-$ ,  $\pi^-$ ),  $A=16, 18$ , resonance region, proton and neutron distrib. 0-91195
- <sup>16</sup>O( $^{16}$ O), M3Y folding model eval., model indep. anal. 0-78317
- <sup>16</sup>O  $\alpha$ -cluster states, widths and resonances, optical model, direct transfer in <sup>12</sup>C( $^{16}$ O,d) 0-105975
- <sup>16</sup>O( $^{16}$ O, $^{16}$ O), optical pot., nuclear matter approach, energy density matter [-] 0-83112
- <sup>16</sup>O(p,p), 20-40 MeV, pol. p, anal. powers, imaginary spin-orbit pot., coupled channels anal. 0-102179
- <sup>16</sup>O(p<sub>opt</sub>,2p), cross section, analysing power, energy sharing spectra, distorted wave impulse approx. 0-78291
- <sup>16</sup>O( $\pi$ , $\pi$ ), nonlinear meson dynamics and binding corrections, optical pots. 0-106080
- <sup>16</sup>O( $\pi$ , $\pi$ ) optical pot., local field correction 0-68705
- <sup>208</sup>Pb( $^{40}$ Ca,  $^{40}$ Ca), optical model anal., strong absorption radius (*Russian*) 0-68697
- <sup>208</sup>Pb( $^{48}$ Ar,  $^{40}$ Ar), optical model anal., strong absorption radius (*Russian*) 0-68697
- <sup>208</sup>Pb( $^{48}$ Ti,  $^{48}$ Ti), optical model anal., strong absorption radius (*Russian*) 0-68697
- <sup>208</sup>Pb( $^{6}$ Li, $^{6}$ Li), elastic and inelastic, 74 MeV, folding optical model parameters 0-102201
- <sup>208</sup>Pb( $\alpha$ , $\alpha$ ), levels, B(E3), transition density and nuclear pot., folding model anal. 0-86812
- <sup>208</sup>Pb( $\alpha$ ,n), excitation functions and isomer ratios of <sup>211</sup>Po 0-83039
- <sup>208</sup>Pb(p,n), nucleon optical potential from Lane model 0-83097
- <sup>208</sup>Pb(p,p), 0.8 GeV, cross sections, optical anal. np RMS radius difference,  $\Delta r_{np}$  0-63187
- <sup>208</sup>Pb(p,p), 30 MeV, optical pot. imaginary part calcs. 0-86868
- <sup>32</sup>S(n,n), 25-1100 keV, total cross section, multilevel anal., strength functions, optical parameters 0-78298
- <sup>28</sup>Si-<sup>6</sup>Li( $^{12}$ C), fusion and strong absorption from elastic scatt. optical pot. 0-102222
- <sup>28</sup>Si( $^{16}$ O, $^{16}$ O), radial sensitivity of optical pot. 0-86869
- <sup>28</sup>Si( $^{6}$ Li, $^{6}$ Li), 154 MeV, differential cross section ang. distrib., optical anal. 0-63201
- <sup>28</sup>Si( $^{9}$ Be,  $^{9}$ Be), 45, 60 MeV, low lying collective states, ang. distrib., DWBA double folding pot. anal. 0-78113
- <sup>28</sup>Si( $^{9}$ Be, $^{9}$ Be), 121-201.6 MeV, strong absorption dominance, global optical model anal., fusion barrier 0-83116
- <sup>28</sup>Si( $^{9}$ Be,X), 30-60 MeV, total fusion cross section, evaporation residues, optical model 0-78344
- <sup>28</sup>Si( $^{9}$ Be,X), X=p,d, $\alpha$ , energy dependence, angular distrib. of spectra, optical and statistical model anal. 0-68710
- Si(p<sub>opt</sub>,p<sub>opt</sub>), giant multipole resonance region, optical model anal. 0-57779
- <sup>48</sup>Sn(n,n'),  $A=116, 118, 120, 122, 124, 11$  MeV, levels, deformation parameters, isospin effects, optical parameters 0-57679
- <sup>48</sup>Sn(n,n), 11-26 MeV,  $A=116, 118, 120, 122, 124$ , differential and total cross sections, optical pots. 0-78293
- <sup>124</sup>Sn( $^{6}$ Li, $^{6}$ Li), elastic and inelastic, 74 MeV, folding optical model parameters 0-102201
- Sn(p,n), even isotopes, 4-10 MeV, cross sections, optical parameters and nuclear radius A-depend. 0-57773
- Sn(p,p), pol.p, 6.77-8.8 MeV, cross sections, optical parameters and nuclear radius A-depend. 0-57773
- <sup>90</sup>Ti( $\alpha$ , $\alpha$ ), 140 MeV, model independent description limits from local optical pots. 0-102196
- <sup>169</sup>Tm(n, $\gamma$ ), capture cross section from  $10^{-5}$  eV to  $2 \times 10^7$  eV, statistical model 0-63189
- <sup>90</sup>Zr( $^{6}$ Li, $^{6}$ Li), elastic and inelastic, 74 MeV, folding optical model parameters 0-102201
- <sup>90</sup>Zr( $\alpha$ , $\alpha$ ), form factor, coupling between real and imaginary optical potential 0-68680
- <sup>90</sup>Zr(n,X), 10-20 MeV, multipole giant resonance contrib. to optical pot. imaginary part 0-78241
- <sup>90</sup>Zr(p,n), nucleon optical potential from Lane model 0-83097
- <sup>90</sup>Zr levels, J $^{\pi}$ , cross sections, vector anal. power, optical parameters from <sup>91</sup>Zr + pol. d 0-78268

**nuclear orientation** see nuclear polarisation**nuclear Overhauser effect**

- acetone-trile, <sup>13</sup>C relaxation times anal. using J-diffusion model of mol. reorientation 0-87149
- alkyl chains, <sup>13</sup>C longitudinal relax. times and nuclear Overhauser enhancement anal. 0-83390
- decylammonium chloride micelles, <sup>13</sup>C longitudinal relax. times and nuclear Overhauser enhancement anal. 0-83390
- DNA, molecular motions, investigated by <sup>31</sup>P and <sup>13</sup>C NMR relaxation 0-63657
- methyl bromide, <sup>13</sup>C relaxation times anal. using J-diffusion model of mol. reorientation 0-87149
- methyl iodide, <sup>13</sup>C relaxation times anal. using J-diffusion model of mol. reorientation 0-87149
- methylene chloride, in EBBA-d<sub>23</sub>, intermol. dipolar random field cross-relax. term obs. 0-60438
- nonrigid molecules, dipolar relax. and nuclear Overhauser effects, fluctuating internuclear distances effect 0-91578
- RNA, molecular motions investigated by <sup>31</sup>P and <sup>13</sup>C NMR relaxation 0-63657

**nuclear particle track visualisation** see particle track visualisation**nuclear photoeffect** see photon-nucleus reactions**nuclear physics**

- see also fission; fission reactors; nuclear bombardment targets; nuclear decay theory; nuclear explosions; nuclear reactions and scattering; nuclear structure; radioactivity
- annual review book 0-67940
- laser applications in nucleus physics, review, book contrib. 0-68504
- Soddy, F., nuclear science, economics and social responsibility, holistic approach 0-90640

**nuclear polarisation**

- see also dynamic nuclear polarisation; magnetic double resonance; nuclear polarisation in liquids and solids
- $A=70$ , heavy-ion induced fission-evaporation reactions, magnetic substrate distrib., nuclear alignment 0-73857

**nuclear polarisation continued**

- $A=90$  region, core pol. effects and giant quadrupole resonances, HF and macroscopic calcs. 0-57756
- $A \sim 90$  nuclei, isomeric states, spin polarisation, M4 transitions and giant resonances 0-63157
- deformed nuclei, polarisation, and energy shifts in muonic atoms 0-86893
- laser induced nuclear orientation, <sup>24m</sup>Na appl. 0-57680
- nuclear matter, polarised, thermal props., temp., spin isospin and spin-isospin pressure 0-102135
- short living nuclear states, optical orientation,  $\gamma$ -spectrum anisotropy, lifetime, moments (*Russian*) 0-63090
- spin exchange and polarisation changes, RPA breakdown from HF connection 0-99142
- <sup>12</sup>B, aligned,  $\beta$ -ang. distrib. asymmetry coeffs., pseudotensor interaction, T=1 isospin triplet decay 0-106021
- <sup>12</sup>B spin polarisation in <sup>100</sup>Mo(<sup>14</sup>N,<sup>12</sup>B) 0-63160
- <sup>12</sup>B spin polarisation in <sup>232</sup>Th(<sup>14</sup>N,<sup>12</sup>B) 0-63161
- <sup>12</sup>C,  $A=12, 13$ , nuclear critical opalescence, M1 form factor, pion field and condensation 0-73809
- <sup>12</sup>C M1 form factor, pion field critical opalescence,  $\rho$  role, polarisation phenomena 0-68552
- <sup>12</sup>C, M1 form factor, pion field, rho meson role 0-105970
- <sup>60</sup>Co polarised nuclei,  $\beta$ -ray emission, directional distrib. and asymmetry factor 0-95315
- <sup>12</sup>N, aligned,  $\beta$ -ang. distrib. asymmetry coeffs., pseudotensor interaction, T=1 isospin triplet decay 0-106021
- Ne hexadecapole moments, quadrupole deformation effects, E4 effective charge, valence polarisation 0-78142
- <sup>208</sup>Pb region, mag. transition strength, core polarisation effects, form factor shape 0-86850
- <sup>208</sup>Pb single particle and hole states, renormalisation, core polarisation, spectroscopic factors 0-57658
- nuclear polarisation in liquids and solids**
- see also dynamic nuclear polarisation
- cross-relaxation processes, polarised  $\beta$ -active nuclei 0-60431
- electric quadrupole interactions measured by nuclear orientation and NMR on oriented nuclei, review 0-92868
- fluorene crystal, doped, photochemical hydrogen abstraction, proton hyperfine structure via optical nuclear polarisation 0-63659
- intermediate state perturbation in low temperature nuclear orientation 0-97168
- optical coherence storage in stimulated optically induced nucl. spin polaris. 0-58649
- semiconductor, nuclear polarisation due to anisotropic size effect in weak elec. field 0-71199
- <sup>111</sup>Cd, nucl. orientation coeffs. with axially symm. elec. field gradient 0-97168
- Co-<sup>48</sup>V, nucl. orientation of <sup>48</sup>V,  $\gamma$ -ray anisotropy obs. 0-97169
- Fe-<sup>48</sup>V, nucl. orientation of <sup>48</sup>V,  $\gamma$ -ray anisotropy obs. and NMR meas. 0-97169
- HoAlO<sub>3</sub>, electronic and nucl. mag. ordering, mol. field approx. 0-60157
- HoVO<sub>4</sub>, below 1K, nuclear orientation study of Van Vleck enhanced nuclear antiferromagnet 0-88899
- <sup>111</sup>In, nucl. orientation coeffs., nucl. mag. moment 0-97168
- PrIn<sub>3</sub>, nucl. orientation of <sup>141</sup>Pr in singlet ground state, exchange interaction and cryst. field splitting obs. 0-71275

**nuclear power**

- alternative versus conventional energy sources, advantages of controlled nuclear fusion (*German*) 0-72002
- American Nuclear Society proceedings (conf. Las Vegas, NV, June 1980) 0-94920
- China, R and D (*German*) 0-68971
- conference, Berlin, Germany (Aug. 1979) 0-77539
- energy supply, future tasks for nuclear energy 0-61317
- energy supply, transition from fossil fuel to nuclear and regenerative sources, technical, economic and ecological aspects 0-66955
- environmental effects, some practical issues 0-94121
- environmental impact, review 0-101143
- European thermonuclear fusion programme, role of technology 0-86982
- fusion energy, appl. to thermochemical H<sub>2</sub> production 0-76658
- HTGR and alternative nuclear strategies (*Chinese*) 0-78353
- international symbiotic nuclear energy parks using breeders and advanced convertors, economic feasibility 0-57825
- long-term nuclear energy strategies, role of fission and fusion 0-78354
- nonproliferation, nuclear fuel cycles and radiation damage 0-68934
- nuclear energy importance and developments in Great Britain (*German*) 0-99198
- option as long term investment 0-99351
- quality assurance, international standardisation, FORATOM 0-58008
- risk assessment in European Community 0-106135
- South Africa, industry development, book 0-73105
- US energy policy 0-81426
- US energy policymaking, suggested revision of production/consumption patterns 0-66954
- H<sub>2</sub> production using high temp. reactors 0-97814
- H<sub>2</sub> thermochemical production, plasmachemical H<sub>2</sub>O decomposition using nuclear energy source 0-61436

**nuclear power stations**

- 840 MW Loviisa-1 Nuclear Power Station, in Finland, two years' operating experience (*Russian*) 0-106151
- accident at Three Mile Island, lessons learned 0-57929
- accidents, Three Mile Island nuclear power station, viewpoint of member of Commission of Enquiry 0-83190
- accumulation ponds cooling possibility analysis (*Slovenian*) 0-91208
- aerodynamic and thermodynamic effects on environment (*German*) 0-61469
- aircraft impact, structural response, reaction-time and impact area-time curves 0-78407
- aseismic bearing foundation system for power station earthquake protection 0-83206
- Biblis nuclear power station, waste production, storage and disposal 0-68903
- boiler inlet temps. and corrosion product deposits, water chemistry effects 0-89528
- CANDU power stations, fuel safeguards scheme 0-63291
- CANDU-OCR power station options and costs 0-73989
- capital cost considerations, optimum plant size 0-63416
- containment building, Mark III, advantages, Grand Gulf Nuclear Station project 0-106122
- contamination monitoring station of Zarnowice plant (*Polish*) 0-74033



# nuclear power stations continued

control and instrumentation designs beyond the 1980s 0-57872  
control guidelines 0-106119  
control rooms, human factors design approaches, improvement of man-machine interface, error reduction 0-63327  
cost comparison of PWR and PHWR nuclear power plants in Korea 0-57821  
current nuclear power plant safety issues, 1980 conf. preview 0-95360  
Czechoslovak Research Institute activities, safety, waste disposal and personnel training (*Slovak*) 0-83188  
design basis R and D of power stations to cut costs and schedules 0-99204  
design management, plant replication for low-cost nuclear power, Philippines National Power Corp. 0-63242  
development in Soviet Union, problems and solution 0-102290  
engineering materials certification for safety and reliability testing 0-78360  
environment protection problems during construction (*French*) 0-76663  
environmental protection, reactor safety and waste handling (*Hungarian*) 0-91224  
environmental protection in Hungary (*Hungarian*) 0-91225  
environmental research data implementation (*French*) 0-74037  
environmental studies organisation (*French*) 0-76664  
FBR, electric power generation, research, development and demonstration, risk and timing 0-57837  
Grand Gulf, BWR designed for improved operation 0-106121  
Grand Gulf contributes to growth in the sunbelt 0-106150  
heat exchangers, eddy current probe for nondestructive testing of transfer tubes (*Japanese*) 0-81246  
HTGR development and its process heat, steam-cycle and gas turbine apps. 0-63250  
HTGR risk assessment, operator actions, event and fault tree anal. 0-63330  
human factors, normal operation and emergency procedures, errors, safety, maintenance, working conditions 0-63328  
hydrobiological studies, conception and data obtained (*French*) 0-76665  
improved radiation shielding using packed mixed size Pb particles, nuclear plant maint. apps. (*Japanese*) 0-106207  
industrial activities nearby causing hazards, deterministic and probabilistic studies 0-78408  
integrated fusion-fission nuclear energy system with fuel self-sufficiency, thermal-electric conversion efficiency decrement 0-57907  
international symbiotic nuclear energy parks using breeders and advanced converters, economic feasibility 0-57825  
Isar BWR power station, transient expts. during startup and initial operation (*German*) 0-83187  
laser thermonuclear power plant, conceptual design study 0-78441  
licensing procedure, public participation under Atomic Energy Act (*German*) 0-102256  
LMFBR, pool type, natural circulation cooling 0-102289  
LMFBR power stations, electric power generation and fuel fabrication 0-57928  
load factors and availability achieved with light water and heavy water reactors (*Slovenian*) 0-68843  
Lovisa Nuclear Power Station, in Finland, guarantee testing for output and efficiency (*Russian*) 0-102291  
Lovisa-1 Nuclear Power Station, in Finland, safety during design, building, and operating stages (*Russian*) 0-106128  
LWR, human operator errors, analytical model 0-63329  
LWR power stations, design features and instrumentation for materials safeguards (*Russian*) 0-63278  
LWR power stations, R and D for improving seismic safety 0-99231  
Maine Yankee power station update history 0-73967  
operation, socio-economic effects on demography, finance and local activities of region (*French*) 0-74038  
operator performance and response time, stress degradation, Poisson model 0-63415  
operator training simulator, design characteristics (*Spanish*) 0-58007  
optimal size and location in energy parks 0-95489  
photon radiation meas. in nuclear power stations 0-63403  
piping system design, rationalisation of power plant pipe break criteria 0-99205  
primary and secondary water chemistry of PWR power stations, European experience 0-106110  
principles underlying IAEA nuclear safety programme 0-95361  
probabilistic sitting analysis, atmospheric releases, health effects 0-106130  
PWR, heating, ventilating and air conditioning systems (*Japanese*) 0-91213  
PWR, ice condenser system (*Japanese*) 0-91214  
PWR, vibrations due to cooling medium flow, meas. and evaluation (*Hungarian*) 0-63304  
PWR accident prevention, extra instrumentation for Ringhals 2 station, Sweden 0-63369  
PWR boiler tubes, denting type corrosion, control by use of neutralisers 0-106109  
PWR design and plant layout, safety criteria 0-102288  
PWR power station secondary water chemistry study, progress report 0-106108  
radioactive pollution, population dose in the Northern Hemisphere 0-104779  
radioactive waste treatment and disposal (*French*) 0-99221  
radwaste evaporator improvement 0-91232  
reliability analysis, unavailability of systems under periodic test and maintenance 0-95368  
remote maintenance to comply with new legislation limiting occupational radiation exposure, in United States 0-106210  
safety, availability of redundant safety systems with common-mode and undetected failures 0-91230  
safety, West German policy (*German*) 0-57865  
safety analysis, methodology and apps. of probabilistic risk assessment 0-63352  
safety analysis and regulations in France, probabilistic methods 0-106123  
safety and influence upon environment (*Croatian*) 0-81492  
safety aspects (*Portuguese*) 0-68844  
safety assessment in Germany probabilistic methods 0-106124  
safety equipment qualification for dynamic loads 0-99233  
saturated steam parameters in reactor containments with escape of coolant, simplified calc. 0-68764  
seismic qualification of Class IE eqpt. 0-99234  
seismic qualification tests of elect. eqpt., damage severity factor concept 0-99235

# nuclear power stations continued

seismic safety margins research program of the US Nuclear Regulatory Commission 0-99229  
seismic safety of mechanical eqpt., R and D program 0-99232  
site selection, pragmatic pairwise group-decision approach 0-102356  
siting criteria, population density limits proposed in NUREG-0625 0-102357  
spent fuel storage and disposal and plant building and operating legislation (*German*) 0-99223  
startup, conduct of operations, organisation and personnel 0-63340  
startup, staffing program, scope, tasks, resources, constraints, anal., implementation 0-63341  
structural reliability, conference, Berlin, Germany (Aug. 1979) 0-105422  
Super-Phenix fast reactor power station, in France (*French*) 0-86967  
Thailand's first nuclear power plant, radiation monitoring programme 0-57996  
thermal efficiency, CO<sub>2</sub> fund. condensation cycles, performance characts. 0-63368  
thermonuclear power station based on theta-pinch reactor with cumulating liner, engineering level and economic charact. (*Russian*) 0-68951  
Three Mile Island, accident, malfunction development, prevention (*Hungarian*) 0-68846  
Three Mile Island accident, <sup>133</sup>Xe in plume 0-89696  
TMI, the need for evacuation to protect public safety 0-99352  
TMI-2 accident, cause, radiological consequences, NRC action 0-102262  
TMI-2 accident analysis using two-loop RETRAN model 0-102263  
VVER, for semi-peak load generation, mathematical model 0-68936  
VVER-400 reactor, primary circuit coolant pressure and quantity control (*Polish*) 0-91231  
waste management principles modifications (*German*) 0-102255  
Westinghouse power plants, uprating capacity 0-68878  
worldwide ISO standards for nuclear technology safety 0-102266  
Cl<sup>-</sup> ions in nuclear reactor water coolant, determination by flow-type porous metallic Ag electrode 0-89577  
SO<sub>2</sub>, ground-level conc. calcs. near a nuclear facility 0-97823

# nuclear pumped lasers

conference, Orsay, France (May 1978) 0-62393  
diatomic molecules, N<sub>2</sub> and CO nuclear pumped lasers, electron impact cross section meas. 0-63985  
gas nuclear pumped laser simulation experiments 0-64042  
hybrid nuclear reactor apps. for fission neutron energy recirculation 0-95408  
inert gas nuclear pumped lasers, electron impact cross section meas. 0-63985  
inert gas nuclear pumped lasers, prod. efficiency of excited states 0-63998  
ion kinetics in high-pressure laser plasmas 0-64002  
large volume multiple pass nucl. pumped laser, output energy, laser media vol. effects 0-63982  
plasma, <sup>3</sup>He and <sup>23</sup>UF<sub>6</sub> nucl. excitation, spectra obs. 0-83997  
power supply, gaseous and plasma U fueled fission reactors 0-63247  
thermal neutron traps description 0-64041  
trifluoriodomethane nuclear pumped lasers, electron impact cross section meas. 0-63985  
Ar-Kr-F<sub>2</sub> nuclear pumped laser, high energy beam deposition 0-63999  
C nuclear pumped lasers employing Ne(He)-CO(CO<sub>2</sub>) mixtures, energy storage 0-63996  
CO laser, cooled electroionisation type, in nucl. reactor active zone 0-64066  
CO nuclear pumped laser, fission fragment excited with gas cooling, performance obs. 0-63997  
CO room temperature nuclear pumped laser, parameter optimisation and spectral props. obs. 0-63995  
CO-<sup>3</sup>He nuclear pumped laser, optimisation with 2 MeV protons 0-64000  
CO-He nuclear pumped laser, high energy beam deposition 0-63999  
Eu<sup>3+</sup>+UO<sub>2</sub><sup>3+</sup> solution, nuclear pumped liq. lasers, LASL program 0-64011  
HF/UF<sub>6</sub>-H<sub>2</sub> nuclear pumped laser, characts. 0-78847  
He-Hg nuclear pumped laser, charge exchange pumping 0-63996  
He-Sr laser, possibility of nucl. pumping, 4305 Å Sr II transition 0-58518  
<sup>3</sup>He-Ar (Xe)(Kr)(Cl), volume pumped nuclear laser, survey of lasing 0-63979  
<sup>3</sup>He-Ar volumetric nucl. pumped laser, dominating processes and reaction physics 0-63981  
<sup>3</sup>He-Ar(Xe)(Kr)(Cl), nucl. lasing, population inversion mechanism 0-63980  
<sup>3</sup>He-Xe nuclear pumped laser, small signal gain coeff. and power output, theory comparison with expt. 0-63983  
<sup>3</sup>He-Xe nuclear pumped laser, electron distrib. function role 0-63984  
I, photodissociated by nucl. induced excimer fluoresc. 0-78846  
KrF\* nuclear pumped lasers, excited state prod. rate and fission power pulse shape matching 0-63998  
N<sub>2</sub>-He ion nuclear pumped lasers feasibility study and quenching 0-64001  
Nd<sup>3+</sup>+UO<sub>2</sub><sup>3+</sup> solution, nuclear pumped liq. lasers, LASL program 0-64011  
Ne-N<sub>2</sub>, atomic N nuclear pumped lasers, surface effects 0-63996  
Pm<sup>3+</sup>+UO<sub>2</sub><sup>3+</sup> solution, nuclear pumped liq. lasers, LASL program 0-64011  
Th<sup>3+</sup>+UO<sub>2</sub><sup>3+</sup> solution, nuclear pumped liq. lasers, LASL program 0-64011  
UF<sub>6</sub>, nucl. lasing, population inversion mechanism 0-63980  
UF<sub>6</sub> nuclear pumped lasers, electron impact cross section meas. 0-63985  
XeF\* nuclear pumped laser obs. 0-63996

nuclear quadrupole moments see nuclear electric moment

# nuclear quadrupole resonance

amidinium salts, <sup>14</sup>N NQR spectra, H<sup>+</sup> relax. times 0-60448  
aniline-chlorophenol complexes, <sup>35</sup>Cl NQR, inter- and intramol. interactions 0-63666  
bismetric Zeeman modulator for NQR 0-98960  
bromocyclotriphosphazatrienes, <sup>81</sup>Br NQR, conformation investig. 0-63665  
bromomethane derivatives, NQR frequency of Br, substituent group effects 0-95648  
chloranisoles, <sup>35</sup>Cl NQR, inter- and intramol. interactions 0-63666  
chloronitroloenes, <sup>35</sup>Cl NQR temp. depend. 0-106334  
chlorophenols, <sup>35</sup>Cl NQR, inter- and intramol. interactions 0-63666

**nuclear quadrupole resonance continued**

- coherent two-photon NMR, standard-basis operators, coherent averaging 0-82798
- crystals, NMR quadrupolar effects, RF energy absorpt., relaxation times (*Russian*) 0-71235
- diacetylhydrazine,  $^{14}\text{N}$  NQR lines fine structure 0-63667
- p-dichlorobenzene,  $^{35}\text{Cl}$  NQR line narrowing by nonreson. RF photon dressing 0-63662
- p-dichlorobenzene-naphthalene alloys, solid solns., NQR study 0-66063
- diformylhydrazine,  $^{14}\text{N}$  NQR lines fine structure 0-63667
- dipolar linewidth in asymmetrically broadened NQR spectra 0-71230
- geophysical techniques, use of  $^{27}\text{Al}$  as probe nucleus 0-67426
- halogen NQR spectra, struct. information for  $\text{R}_2\text{MX}_6$  compounds 0-71228
- imidazole, quadrupole coupling consts. interpretation, ab initio field gradient calcs. 0-58282
- inhomogeneous NQR line narrowing by RF pulse sequence 0-93206
- liquid, nuclear quadrupole relaxation of non centre symm. mols. (*Russian*) 0-88889
- methyl bromide, NQR and  $\text{A}_1\text{-A}_2$  splitting, RF spectrosc. inside laser cavity 0-91579
- molecular crystals, NQR freq., intermol. force effect 0-66065
- molecular reorientation in crystal, nuclear quadrupole spin-lattice relax. 0-66062
- monochloroacetic acid single crystal, Zeeman and  $^{35}\text{Cl}$  NQR investig. 0-66066
- organic molecular crystals, intermolecular interactions, spectroscopic studies, review 0-103958
- paradichlorobenzene, NQR freq., intermol. force effect 0-66065
- paradichlorobenzene, NQR study of the lattice dynamics (*Russian*) 0-97160
- pulsed spin locking technique, theory 0-98958
- spectroscopy, electronics appls. 0-63668
- spin echo, two-frequency action, amplification and modulation 0-108116
- TBACA, chiral, smectic  $\text{C}^*$  and  $\text{H}^*$  phases, mol. orientational ordering,  $^{14}\text{N}$  NQR study 0-75152
- tetramethylammonium hydrogen bis-trichloroacetate ( $-\text{d}_n$ ),  $^{35}\text{Cl}$  NQR study 0-66064
- trichlorophosphazene compound,  $\text{Cl}_3\text{P:NCCl}(\text{CF}_3)_2$ , nuclear quadrupole spin-lattice relax. 0-66062
- $\text{Al}_2\text{Cl}_6$  molten, nuclear mag. relax., mol. rot. 0-71209
- $\beta\text{-Al}_2\text{O}_3\text{-(Na,Li)}_2\text{O}$ , first-order quadrupole NMR obs. of cation distrib. and ion motion 0-108113
- $\beta\text{-Al}_2\text{O}_3\text{-Na}_2\text{O}$ ,  $^{23}\text{Na}$  NQR and two-dimens. diffusion, model analysis 0-108111
- $\beta\text{-Al}_2\text{O}_3\text{-Na}_2\text{O}$ , low-temp.  $^{23}\text{Na}$  satellite spectra, Na ion motion 0-108112
- $\beta''\text{-Al}_2\text{O}_3\text{-Na}_2\text{O}$ , of  $^{23}\text{Na}$ , elec. quad. interaction, 185 to 419K, ion motion obs. 0-108110
- $\theta\text{-Al}_2\text{O}_3\text{-V}_2\text{O}_5$ , NMR of  $^{51}\text{V}$  0-71232
- As metal, electric field gradient, temp. and press. variation 0-93205
- $\text{As}_2\text{I}_4$ ,  $^{127}\text{I}$ ,  $^{75}\text{As}$  NQR freqs. meas. 0-58285
- $\text{BrF}(\text{Cl})$ , rot. spectra in millimeter wave region, rot. transitions obs., equilib. const. determ. 0-78607
- Ca dichlorophosphate complexes, cryst. struct.  $^{35}\text{Cl}$  NQR obs. 0-108108
- $\text{CeAl}_2$ , antiferromag. ordering and Kondo behaviour,  $^{27}\text{Al}$  NQR study 0-71231
- ClF, rot. spectra in millimeter wave region, rot. transitions obs., equilib. const. determ. 0-78607
- $\text{Cl}_2\text{Si}(\text{CH}_3)_4$ ,  $^{35}\text{Cl}$  NQR, geminal and vicinal interactions on substituents electronic effect 0-63663
- $\text{Cl}_2\text{Si}(\text{OCH}_3)_4$ ,  $^{35}\text{Cl}$  NQR, geminal and vicinal interactions on substituents electronic effect 0-63663
- Co complexes,  $\text{Co}(\text{en})_2\text{Cl}_2\cdot\text{Cl}\cdot\text{HCl}\cdot 2\text{H}_2\text{O}$ , temp. dependence of NQR frequencies 0-66068
- $\text{Cs}_2\text{CuBr}_4$ , struct. phase transitions, NQR study 0-71343
- $\text{CsCuCl}_3$ , phase transition, refr. index, electrooptic coeff., pyroelec. signal, and NQR meas. 0-70386
- Cu, electron-irradiated, monovacancy migration during stage III annealing, NQR study 0-107576
- Cu, screening charge density round  $\Delta Z = -1$  impurities, vacancies, NQR study 0-103897
- $\text{Cu-Ni}(\text{Pd})(\text{Pt})$ , dil., screening charge density round  $\Delta Z = -1$  impurities, vacancies, NQR study 0-103897
- $\text{CuFeS}_2$ , antiferromag., NQR local mag. field effects 0-71234
- $\text{Cu}_2\text{V}_4\text{S}_4$ , out of equil. mixed cond., chem. origin of mobile ions, spin-lattice relax. and NQR obs. 0-108104
- $\text{EuCu}_2\text{Si}_2$ , interconfiguration fluctuation, NMR expts. 0-66069
- $\text{FeBO}_3$ , suppression effect under hyperfine quadrupole splitting, Mossbauer study (*Russian*) 0-75906
- $\theta\text{-FeO}_{3/2}\text{-V}_2\text{O}_5$ , NMR of  $^{51}\text{V}$  0-71232
- $\text{GeI}_2$ ,  $^{127}\text{I}$  NQR freqs. meas. 0-58285
- HCl and HCl-DCl, ferroelec. transition,  $^{35}\text{Cl}$  NQR study 0-71233
- HI nuclear quadrupole HFS in IR spectrum, obs. using tunable diode laser 0-58412
- Hg liquid, quadrupole relaxation rate temp. depend 0-88884
- $\text{HgCl}_2$ , NQR freq., intermol. force effect 0-66065
- $\text{HgCl}_2$ , Zeeman NQR spectra obs. asymmetry parameters 0-80634
- $\text{ICI}(\text{Br})$ , rot. spectra in millimeter wave region, rot. transitions obs., equilib. const. determ. 0-78607
- $\text{KClO}_3$ ,  $^{35}\text{Cl}$  NQR appl. in thermometry below 77K 0-66067
- $\text{KH}_2\text{AsO}_4$ , ferroelec. phase,  $^{75}\text{As}$  NQR, press. and temp. depend. 0-71227
- $\text{KH}_2\text{AsO}_4$ , ferroelectric phase transition under high hydrostatic press., mol. dynamics, NQR study 0-75880
- $\text{K}_2\text{OsCl}_6$ , Cl NQR spectra by Fourier transform methods 0-75879
- $\text{K}_2\text{OsCl}_6$ , impurity  $\text{H}^+$  ion motion,  $^{35}\text{Cl}$  NQR obs., 77 and 298K 0-60451
- $\text{K}_2\text{ZnCl}_4$ ,  $^{35}\text{Cl}$  NQR study of incommensurate phase transition 0-60450
- $\text{K}_2\text{ZnCl}_4$ , incommensurate phase transitions,  $^{35}\text{Cl}$  NQR study 0-75968
- La-D, phase transition, NMR meas. 0-66508
- La-H, ordered struct. near  $\text{LaH}_{2.65}$  at 250K, NMR 0-66508
- Mg dichlorophosphate complexes, cryst. struct.  $^{35}\text{Cl}$  NQR obs. 0-108108
- Mn dichlorophosphate complexes, cryst. struct.  $^{35}\text{Cl}$  NQR obs. 0-108108
- $(\text{NH}_4)_2\text{ZnCl}_4$ , commensurate-incommensurate phase transition,  $^{35}\text{Cl}$  NQR study 0-75966
- $\text{N}_3\text{PBr}_6$ ,  $^{81}\text{Br}$  NQR, conformation investig. 0-63665
- $\text{NaClO}_3$ ,  $^{35}\text{Cl}$  NQR appl. in thermometry below 77K 0-66067
- $\text{NaNO}_2$ , ferroelec. nuclear quadrupole coupling const. and spontaneous polarisation 0-71229
- $\beta\text{-Na}_{0.33}\text{V}_2\text{O}_5$ , quasi-one-dimensional conductor, NMR studies 0-93204

**nuclear quadrupole resonance continued**

- $\text{Nb}_3\text{Al}(\text{Ga})$ , NQR freq. temp. depend., supercond. transition temp. 0-93207
- $^{17}\text{O}$ , naturally abundant, fine struct. obs. 0-75881
- $\text{Pb}_{1-x}\text{Li}_x(\text{As})(\text{Ag})(\text{In})(\text{Sn})(\text{Sb})(\text{Te})(\text{Au})(\text{Ti})(\text{Bi})$ , liquid alloys, local fluctuations and quadrupolar relaxation 0-66060
- $\text{Rb}_2\text{ZnCl}_4$ , commensurate-incommensurate phase transition,  $^{35}\text{Cl}$  NQR study 0-75966
- $\text{Rb}_2\text{ZnCl}_4$ , incommensurate phase transitions,  $^{35}\text{Cl}$  NQR study 0-75968
- $^{99,101}\text{RuO}_2$ , NQR spectroscopy 0-63664
- $\text{SnCl}_2\cdot 1.5\text{H}_2\text{O}$  single cryst.,  $^{35}\text{Cl}$  NQR, cryst. struct. 0-60449
- $\text{SnI}_2$ ,  $^{127}\text{I}$  NQR freqs. meas. 0-58285
- V-CO sigma phase alloys, NMR and electric-field gradients 0-108109
- V-Ni sigma phase alloys, NMR and electric-field gradients 0-108109
- VB, nuclear quadrupole parameters 0-103896
- $\text{YbCu}_2\text{Si}_2$ , interconfiguration fluctuation, NMR expts. 0-66069
- $\text{ZnCl}_2$ ,  $^{35}\text{Cl}$  NQR freqs. meas. 0-58285
- $\text{ZnCr}_2\text{Fe}_{1-x}\text{O}_4$ , Mossbauer spectra, quadrupole splitting, Debye temp. 0-93218
- $\text{ZnI}_2$ ,  $^{127}\text{I}$  NQR freqs. meas. 0-58285
- $\text{ZrB}_2$ , self-consistent band struct., XPS, reflectance, NQR, Hall effect and density of states meas. 0-107689
- nuclear radius** see nuclear size
- nuclear reaction and scattering models**  
see also nuclear optical model
- heavy ion reactions, central, spectator-participant model 0-73861
- leading particle spectra on nuclear targets and multi-chain model 0-73829
- Lee model use in pion-nucleon scatt. theory testing 0-78325
- solitons as model for nuclear potential 0-83081
- threshold phenomena in weak coupling and memory loss models 0-106026
- weakly absorbed particles, modified Austern-Blair theory, DWBA 0-86867
- $^4\text{He}(\text{d,d})$ , distortion effects, orthogonality condition model 0-63190
- nuclear reaction and scattering theory**  
see also nuclear reaction and scattering models; statistical theory of nuclear reactions and scattering
- 1p and 2s1d shell nuclei, fusion cross sections, entrance channel versus compound nucleus limitations 0-78343
- central high energy heavy ion collisions, possible finite particle number effects, p spectra 0-99181
- channel averages and energy averaged cross section relation 0-68634
- coherent pion prod. in high energy heavy ion collisions, pion laser 0-73856
- colliding ion system, projectile nucleon mean free path, nuclear matter approach, Pauli blocking 0-86920
- composite nucleus scission, fusion and strongly damped collisions, rot. energy, boundary diffuseness 0-102224
- conference on nuclear physics, Mikolajki, Poland (2-14 Sept. 1979) 0-101662
- coupled channel optical model calc. improvement (*Chinese*) 0-99159
- cross-section adjustment and evaluation, finite element basis in data adjustment 0-68612
- deep inelastic heavy ion reactions, fast light particles and heavy ejectile ang. correlation 0-57791
- deep inelastic reaction, neutron excess degree of freedom relaxation model (*Chinese*) 0-102202
- dissipative heavy-ion collisions, doorway concept and relative motion 0-86925
- doorway states, fragmented, micro-resonances, strength functions, K-matrix width 0-57754
- double stripping core independ. 2-nucleon transfer, Tang-Herdon effective interactions, ( $\alpha,\text{d}$ ), ( $\text{t,p}$ ) 0-73836
- DWBA integrals, evaluating strategies for computation 0-86863
- education, N-body disintegration theory, Maxwellian distrib., nuclear appls. 0-57033
- effective potentials for heavy-ion scattering derived from channel coupling 0-57794
- Faddeev eqns., adiabatic limit for particle exchange, three-body scatt. 0-68613
- Feshbach-Villars formalism and pion-nucleon scattering, relativistic scatt. theory, T-matrix 0-63211
- four nucleon system, reactions and scatt. using K-matrix formalism, differential cross sections (*Russian*) 0-106027
- four-body system, Efimov effect and three-body effective pot. 0-86865
- fragment elastic scattering, unitarity and optical pot. 0-106028
- giant resonances in nuclear reactions, microscopic theory of intermediate struct. 0-99161
- hadron + nucleus, multi-chain model, recoil nucleon effect 0-83124
- half-off-shell quasiphasings of nonlocal interactions from on-shell phase functions 0-106023
- heavy ion + nucleus, orbiting quasimolecular system, nuclear-surface-wave interpretation 0-86914
- heavy ion collisions, critical electron state wave function calc. 0-57796
- heavy ion collisions, perturbed stationary state method, low energy collision and mol. resons. 0-78320
- heavy ion deep inelastic collisions, dissipative processes, Feynman's influence functional method treatment 0-57789
- heavy ion elastic scatt., internal S-matrix dynamics and internal deflection function 0-78307
- heavy ion fusion and damped reactions, rolling friction, nuclear pots., classical trajectories 0-78312
- heavy ion inclusive reactions, fragment momentum distrib., from Glauber approx. (*Chinese*) 0-99185
- heavy ion inelastic reactions, differential cross section from helicity representation (*Russian*) 0-86924
- heavy ion inelastic scatt., coupled channels calcs. for direct reactions, long range Coulomb coupling 0-83117
- heavy ion inelastic scatt., direct reactions, coupled channel calcs., coupled radial eqns. 0-83118
- heavy ion reactions, exact finite range DWBA overlap integral parameterization 0-68693
- heavy ion reactions, two-particle transfer, overlap functions, DWBA anal. 0-73862
- heavy ion relativistic collisions, pion bremsstrahlung and critical phenomena, nuclear matter phases 0-86919
- heavy ion scattering, Coulomb barrier top energies, WKB calc. 0-86918
- heavy ion stripping and pickup reactions on closed shell nuclei, level shifts, DWBA 0-91168



nuclear reaction and scattering theory continued

heavy ion transfer reactions, closed form description based on distorted waves theory 0-68691  
(HI,X), rare earths, deeply inelastic transfer reactions, kinematic anal. 0-99186  
high energy heavy ion collisions, single nucleon knockout, DWIA formalism 0-99165  
high energy scattering from a bound nucleon: unitarity and closure approximation 0-78236  
ion-ion interaction pot., real part energy depend., antisymmetrization effects, Fermi gas model 0-83120  
Lee model use in pion-nucleus scatt. theory testing 0-78325  
light heavy-ion systems, fusion cross section variations, nuclear proximity pot. 0-57815  
low energy fission, charge distrib., quantum mechanical phenomenon of GDR 0-86945  
many body scattering, channel coupling array theory, wave function formalisms 0-78235  
many particle systems, microscopic derivation of classical eqns. of motion 0-102199  
Marchenko eqn. extension to nonHermitian differential systems 0-83080  
matrix elements between arbitrary single particle wavefunctions, generator coordinate method 0-57751  
multistep compound processes, autocorrelation function, average fluctuation cross section, different theoretical approaches 0-78234  
N-body scattering equation approach using pole decomposition of Green's function 0-62540  
neutron producing reactions, kinematics 0-86862  
nonlinear dynamics reaction theory, S-matrix TDHF theory 0-86834  
nonlocal Hamiltonians, scatt. solns. in terms of generalised Bessel Neumann series 0-57752  
nuclear matter, leptoproducted high energy particles, nuclear attenuation, hadronisation time 0-102182  
nucleon-nucleus cross sections, Glauber theory and N-N inelasticity 0-68669  
nucleus-nucleus multiple scatt., high energies, profile function, approx. descripts. 0-106022  
nucleus-nucleus total cross section energy depend. 0-106071  
partition permuting array approach to few-body Hamiltonian models of nuclear reactions 0-86864  
Pauli principle in multiple scatt. theory, exact eqns., cluster exchange 0-106024  
pion electroproduction from the nucleon near threshold 0-68651  
pion spectrum and polariz. operator in nuclear medium in heavy nuclei collisions (*Russian*) 0-68558  
pole expansions for resonance functions, scatt. amplitudes and continuum states (*Russian*) 0-86871  
QCD and short range nuclear phenomena 0-91060  
quasi-free scatt. data anal. in the impulse approx. 0-68615  
radiative nucleon capture, pure resonance model, direct-semidirect model, pure semidirect model 0-78257  
Rayleigh and whispering gallery waves excited by heavy ion elastic and inelastic scatt. 0-91164  
relativistic heavy ion collisions, d prod. mechanism, three models, fireball rate eqns. 0-63198  
relativistic heavy ion collisions, fragmentation cross sections, abrasion-ablation model, factorisation 0-78261  
relativistic nuclear collisions, K prod. in multiple collision model 0-99157  
resonant states in the presence of Coulomb interactions, Schrodinger eqn. 0-91161  
review of reaction theory for nuclear engineers (*Japanese*) 0-99155  
scattering by singular potentials of the general type at high energies 0-63141  
stellar environment, strong interactions and nucl. struct. 0-72765  
t-matrix Lippmann-Schwinger type scatt. eqns., iterative solns., off shell matrix elements 0-86866  
three body problem, connected kernel method failure 0-106025  
three body problem with pairwise interactions, Baer-Kouri-Levin-Tobocman and Faddeev eqns. 0-99158  
three-body scatt., two pot. formula, distorted Faddeev eqns. integral form 0-57753  
time-dependent intranuclear cascade model 0-63140  
time-dependent mean-field approximation for nuclear dynamical problems 0-63113  
time-dependent-S-matrix Hartree-Fock theory of complex reactions 0-63112  
total pion absorption cross section, A depend., proton yields 0-106081  
trans-uranium nuclei, fission barrier and (neutron width-fission width), nucleon contents depend. (*Russian*) 0-106093  
truncated pion-nucleon amplitudes and pion-nucleus interactions 0-68708  
two charged clusters collision, scatt. amplitudes and integral eqns. 0-68614  
ultra-high energy nuclear interaction event with large transverse momentum at 445 TeV (*Chinese*) 0-105140  
ultrarelativistic nuclear collisions, asymptotic hadron spectrum, hot hadronic matter 0-63118  
uncorrelated target, optical pot. unitary content, DWIA and Glauber theory 0-99160  
variational principles for true three- and four-particle scatterings 0-78233  
very heavy ion-nucleus collisions, struct. effects in dissipative collisions 0-57795  
virtual excitations in the scattering of complex particles by nuclei 0-99156  
weakly absorbed particles, modified Austern-Blair theory, DWBA 0-86867  
( $\alpha, 2\alpha$ ), A=9, 12, 16, 20, 22 0-68629  
( $\alpha, \alpha$ ), internal S-matrix dynamics and internal deflection function 0-78307  
( $\alpha, \alpha'$ ), inelastic interaction cascade model for Z=3-13, 29-82 0-106064  
( $\alpha, ^3\text{He}$ ), composite particle scatt. breakup mechanism 0-83105  
( $\alpha, \alpha_n$ ), 640, 710 MeV, n ang. and energy distrib., intranuclear cascade model 0-83109  
(d,<sup>3</sup>Li), A=60,116, L=0 transitions, cross sections, microscopic anal. 0-78189  
(d,p), composite particle scatt. breakup mechanism 0-83105  
(d,p), role of  $\Delta N=2$  interaction, differential cross sections, DWBA anal. 0-91189  
(d,t), role of  $\Delta N=2$  interaction, differential cross sections, DWBA anal. 0-91189  
(e,e), c.m. motion effects in oscillator shell model 0-106050

nuclear reaction and scattering theory continued

(e,e'), light and medium nuclei, high energy approx. anal., transition densities and probabilities (*Russian*) 0-63129  
( $\gamma, \gamma$ ), 412, 468, 662 keV, elastic scatt. cross sections, Rayleigh scattering anal. 0-86898  
( $\gamma, n$ ), 45-160 MeV, cross sections in quasi-deuteron model for direct reactions 0-63170  
( $\bar{K}, \bar{K}$ ), isobar doorway model, optical pot.,  $\Lambda$ -nuclear matter binding energy 0-106079  
( $\mu^+, \mu^+$ ;  $\pi N$ ), A=12-203, muonintegration cross sections, PWBA anal. 0-68650  
(N, $\alpha$ ), microscopic finite-range anal. 0-63181  
(n,f), intermediate struct. line fitting, subthreshold fission resonances 0-102214  
(n, $\gamma$ ), polarized space parity nonconservation, optical pot. and GDR parameters (*Russian*) 0-86803  
(N,N' $\pi$ ), shower proton and meson transverse momenta, intranuclear cascade model 0-102185  
(n,X) X=p,2n,3n, precompound and compound emission mechanisms 0-102176  
N\*(1688) resonance effects on nuclear reaction, NN scatt. phase parameters 0-105987  
NN $\pi$  system, phenomenological relativistic quantum mechanics, scatt. theory 0-83082  
(p,2p), backward inclusive prod. mech. probing, differential cross section 0-68668  
(p,d), 51.9 MeV, forbidden transition ang. distrib., CCBA and DWBA anal. 0-86848  
(p,d), pol. p. 65 MeV, A=12-94, differential cross sections and anal. powers, pickup 0-91172  
(p,d'), inclusive cross section, constituent-constituent multiple scatt. model for dependence on atomic number 0-83101  
(p,n), 1 GeV, A=7-212, charge exchange scatt., Glauber diffractive theory anal. (*Russian*) 0-83103  
(p,n), anomalous optical potential for sub-Coulomb barrier protons, 2 particle 1 hole states 0-105948  
(p,n), pion exchange at intermediate energy 0-63179  
(p,p), 1 GeV elastic and inelastic scatt., diff. minima filling mechanism (*Russian*) 0-86907  
(p,p), <100 MeV, Coulomb corrections to NN coupled states, nonrelativistic scatt. theory 0-78114  
(p,p), small distances, new electrodynamics approach 0-63180  
(p,p), statistical significance of spreading widths for doorway states, reply to comments 0-63147  
(p,p'), 800 MeV, cross sections, quasifree knockout mechanisms, PWIA calcs. 0-78294  
(p,p'), single neutron states, two step process and effective interaction 0-78290  
(p,p'), unnatural parity states excitation,  $\pi$ -condensate instability effects, DWBA anal. 0-78168  
(p,p') inelastic spectra in high energy continuum, single and multiple scatt. mechanisms 0-57777  
(p,p'), quasifree scatt., break-up cross section at high energies 0-99174  
(p,X), 400 GeV/c, deuteron prod. mechanism, pick up reactions 0-83096  
(p,X), high energy, Glauber anal., produced particle-A relation (*Chinese*) 0-102192  
( $\bar{p}, X$ ), multi-chain model, charged particle distrib. 0-83098  
pp bremsstrahlung, 730 MeV,  $\gamma$ -energies of <300 MeV, differential cross section 0-99108  
( $\pi^-, NN$ ), low energy pion absorption,  $\sigma+\omega$  model, optical pots., real  $\rho^2(r)$  pot. 0-83125  
( $\pi, \pi$ ), elastic scatt. relativistic kinematics, differential cross sections 0-63210  
( $\pi, \pi$ ), (3,3) resonance region, Brown-Rho bag model descript. 0-57806  
( $\pi, \pi$ ) single and double charge exchange in resonance region, geometrical limit 0-86930  
( $\pi^+, \pi^+$ ),  $\pi^-$  nuclear response enhancement, continuum effects, stretched state isospin mixing 0-86929  
( $\pi, X$ ), effective S-wave  $\pi NN$  interaction, effects in nuclear matter 0-105985  
 $\pi N$  elastic scatt., nonstatic model for nuclear reactions 0-102125  
 $\pi NN$ -NN coupled problem, unitary model 0-99135  
 $^1\text{H}(d,d)$ , 5-45 MeV deuteron wave function asymptotic D- to S-state normalisation, anal. power 0-78304  
Al(Ne,X), proton inclusive spectra, direct plus thermal model 0-57799  
<sup>26</sup>Al excited states, isobaric analogues, spins, DWBA anal. of <sup>27</sup>Al(<sup>4</sup>He, $\alpha$ ) 0-105981  
<sup>27</sup>Al(d,p,X) 80 MeV, inclusive proton spectra, d break-up, DWBA anal. 0-91190  
<sup>27</sup>Al(e,e'), 70-340 MeV, odd parity state electroexcitation, form factors, transition probs. 0-78208  
<sup>27</sup>Al( $\pi^+, \pi^+ N$ ), 180-255 MeV, quasilastic pion scatt. coincidence expt. interpretation, impulse approx. 0-68704  
(<sup>40</sup>Ar,X), 222-340 MeV, A=116-197, charged particle emission, early collision evolution, fission and evaporation cross sections 0-106072  
<sup>197</sup>Au(<sup>16</sup>O,X), colliding heavy ion interface, nucleon emission, fusion and strongly damped collisions 0-86922  
<sup>197</sup>Au(<sup>20</sup>Ne, spallation), 8.0 GeV, cross sections and target residues, model comparison 0-68630  
<sup>197</sup>Au(d,p,X), 80 MeV, inclusive proton spectra, d break-up, DWBA anal. 0-91190  
<sup>8</sup>B  $\beta^-$ -decay,  $\beta$ - $\alpha$  angular correlations, final state energy depend., current test 0-102151  
<sup>10</sup>B levels and differential cross sections PWBA and coupled channel anal. of ( $\alpha, t$ ) 0-102121  
<sup>10</sup>B(d,p)<sup>11</sup>B, 2.5 to 21.0 MeV, angular distrib., DWBA analysis 0-68675  
<sup>10</sup>B(t,d)<sup>11</sup>B, 5.5 MeV, angular distrib., DWBA analysis 0-68675  
<sup>12</sup>B levels, J $\pi$  and diff. cross sections, R-matrix anal. of <sup>11</sup>B(n,n) 0-78151  
<sup>12</sup>Ba, A=132, 134, 136, negative parity states, J $\pi$ , transitions, DWBA anal. of Ba(p,t) 0-86810  
<sup>9</sup>Be(<sup>10</sup>B,<sup>10</sup>B), 9.5-14.2 MeV, ang. distrib., cross sections, elastic p transfer 0-78318  
<sup>9</sup>Be(e, $\pi^+$ ), 1848 MeV, virtual photon spectrum, virtual photon theory test 0-102183  
<sup>10</sup>Be levels and differential cross sections DWBA and coupled channel anal. of ( $\alpha, ^3\text{He}$ ) 0-102121  
<sup>201</sup>Bi ( $\alpha, f$ ), 23-140 MeV,  $I_{\text{crit}}$  from fragment ang. distrib. anal. 0-106087  
<sup>201</sup>Bi single particle levels, ang. distrib., spectroscopic factors, DWBA anal. of <sup>208</sup>Pb(Li,<sup>6</sup>He) 0-63067  
<sup>209</sup>Bi(<sup>136</sup>Xe,X), 940 MeV bombarding energy depend., fragment deformation, sequential fission 0-86938



## nuclear reaction and scattering theory continued

- <sup>209</sup>Bi(<sup>36</sup>Fe,X), damped collisions, fast A/Z equilibration and correlated nucleon exchange 0-86798
- <sup>209</sup>Bi( $\gamma$ ,f), 40-65 MeV, absolute total photofission cross section, compound nucleus form. 0-86934
- <sup>12</sup>C(<sup>12</sup>C, <sup>12</sup>C), shape resonance energy and widths, projection operator method 0-78255
- <sup>12</sup>C(<sup>12</sup>C,  $\gamma$ ), 11.8-20.0 MeV, total cross section resonant and average behaviour 0-106069
- <sup>12</sup>C(<sup>12</sup>C, <sup>12</sup>C), 10-30 MeV, projection operator method, Feshbach doorways, intermediate structure 0-68695
- <sup>12</sup>C(<sup>12</sup>C, <sup>12</sup>C), 10-30 MeV, molecular structure, projection operator anal., differential cross sections 0-106033
- <sup>12</sup>C(<sup>12</sup>Li,d), <sup>16</sup>O-<sup>12</sup>C+ $\alpha$ , reaction mechanism from ang. correlations, direct transfer 0-78319
- <sup>12</sup>C(K<sup>+</sup>,K<sup>+</sup>), 100-1000 MeV, differential and total cross sections, nucleon motion 0-102206
- <sup>12</sup>C( $\alpha$ , $\alpha$ ), 1.37 GeV, S-matrix expansion from Glauber multiple scatt. theory 0-91191
- <sup>12</sup>C(d,d), 1.69 GeV/c, Coulomb interference region, Glauber theory anal. 0-99178
- <sup>12</sup>C( $\gamma$ , $\pi$ ), final state interaction, distorted and plane wave momentum distrib. 0-78275
- <sup>12</sup>C(p,X), reaction and scatt. dynamics, optical and coupled channel anal. 0-78297
- <sup>12</sup>C(p,p), asymmetric energy-sharing mode, half distorted-wave formalism, intermediate giant resonance 0-68656
- <sup>12</sup>C(p, $\alpha$ ), 45.2 MeV, cross sections, finite range DWBA anal., cluster form factors 0-68666
- <sup>12</sup>C(p,n), 144 MeV, charge exchange, one pion exchange and PCAC tests 0-78299
- <sup>12</sup>C(p,p), 122 MeV, level excitation, cross sections, effective NN interaction, DWIA anal. 0-78197
- <sup>12</sup>C(p,p), 22-27 MeV, 1<sup>+</sup> state de-excitation  $\gamma$ -ray ang. distrib., tensor force effects, DWBA anal. 0-68580
- <sup>12</sup>C(p,p' $\gamma$ ), 23.5-27 MeV, 1<sup>+</sup> state spin flip meas. DWBA anal., cross sections 0-68529
- <sup>12</sup>C(p,p), 20-40 MeV, pol. p, anal. powers, imaginary spin-orbit pot., coupled channels anal. 0-102179
- <sup>12</sup>C(p,p), pol. p, 14.23 MeV resonance broadening, nuclear recoil, atomic excitation effects 0-102165
- <sup>12</sup>C( $\pi$ ,X), Kalinkin-Shmonin model, expt. data 0-86931
- <sup>12</sup>C( $\pi$ , $\pi$ ), A\* excitation, A\* model unified description 0-102205
- <sup>12</sup>C( $\pi$ , $\pi$ ), 260 MeV, short range correlations from Glauber multiple diffraction theory (Chinese) 0-102210
- <sup>12</sup>C( $\pi$ , $\pi$ ), 40 GeV, semi-coherent elastic scatt., angular distrib. 0-68701
- <sup>12</sup>C( $\pi$ , $\pi$ ), 100, 180 MeV, knock out reaction, cross section and pion distortion in DWIA 0-91167
- <sup>12</sup>C( $\pi$ , $\pi$ ), 291 MeV, quasielastic scatt., differential cross sections, Monte-Carlo data fit 0-68703
- <sup>12</sup>C( $\pi$ , $\pi$ ), 180-255 MeV, quasielastic pion scatt. coincidence expt. interpretation, impulse approx. 0-68704
- <sup>12</sup>C(<sup>12</sup>C, <sup>12</sup>C), molecular neutron orbit formation, 1/2<sup>+</sup> state excitation, coupled channels calcs. 0-78156
- <sup>13</sup>C(<sup>16</sup>O, <sup>17</sup>O)<sup>12</sup>C, non-orthogonality of channel states 0-83115
- <sup>13</sup>C(<sup>9</sup>Be,X), 11.6 MeV, p,t,d, $\alpha$ , <sup>8</sup>Be ang. distrib., Hauser-Feshbach and DWBA anal. 0-91193
- <sup>13</sup>C( $\alpha$ , $\alpha$ ), 22, 36 MeV, resonant state line shapes 0-91148
- <sup>13</sup>C( $\pi$ , $\pi$ ), 120-226 MeV, inelastic scatt. and charge exchange, coupled channels calcs. 0-57804
- <sup>16</sup>C(<sup>12</sup>Li,<sup>4</sup>He), 62 MeV, Gamow-Teller sum rules and ground state wave function 0-106073
- Ca(Ca,X), 400 MeV, classical eqns. of motion calcs., central collisions, thermal models 0-106070
- <sup>4</sup>Ca( $\alpha$ , $\alpha$ ), 24,29 MeV, A=40,42,44,48 backward ang. distrib. anomaly, coupled and channel anal. 0-86911
- <sup>4</sup>Ca(p,p), pol. p, A=40,48, 800 MeV, diff. cross sections, anal. powers, DWIA anal., high spin levels 0-83067
- <sup>4</sup>Ca( $\pi$ , $\pi$ ), A=40, 44, 48, 291 MeV, quasielastic scatt., differential cross sections, Monte-Carlo data fit 0-68703
- <sup>40</sup>Ca composite system, heavy ion resonances from <sup>24</sup>Mg+<sup>16</sup>O, <sup>28</sup>Si+<sup>13</sup>C 0-86874
- <sup>40</sup>Ca(<sup>11</sup>B,<sup>10</sup>B), 51.5 MeV, n stripping, DWBA anal. with Woods-Saxon and double folding optical pots. 0-102171
- <sup>40</sup>Ca(<sup>11</sup>B,<sup>12</sup>C), 32, 68 MeV, single proton pickup, DWBA anal., optical pot. 0-106037
- <sup>40</sup>Ca(<sup>11</sup>B,<sup>12</sup>C), 51.5 MeV, p pickup, DWBA anal. with Woods-Saxon and double folding optical pots. 0-102171
- <sup>40</sup>Ca(<sup>13</sup>C,<sup>14</sup>N), 40, 68 MeV, single proton pickup, DWBA anal., optical pot. 0-106037
- <sup>40</sup>Ca(<sup>16</sup>O,<sup>16</sup>O), optical pot., nuclear matter approach, energy density matter [-] 0-83112
- <sup>40</sup>Ca(<sup>16</sup>O,X), ion-ion interaction pot., imaginary part, effective interaction 0-68692
- <sup>40</sup>Ca(<sup>40</sup>Ca,<sup>40</sup>Ca), optical pot., nuclear matter approach, energy density matter [-] 0-83112
- <sup>40</sup>Ca(<sup>9</sup>Be,<sup>9</sup>Be), 45, 60 MeV, low lying collective states, ang. distrib., DWBA double folding pot. anal. 0-78113
- <sup>40</sup>Ca(<sup>9</sup>Be,<sup>9</sup>Be), 45, 60 MeV, 1<sup>+</sup> state excitation Frahn scaling formula for cross section 0-102136
- <sup>40</sup>Ca( $\alpha$ , $\alpha$ ), 1.37 GeV, S-matrix expansion from Glauber multiple scatt. theory 0-91191
- <sup>40</sup>Ca( $\mu$ , $\gamma$ ), photon asymmetry, O(1/m<sup>2</sup>) and nuclear effects 0-78219
- <sup>40</sup>Ca(n,X), local approximation to a non-local potential 0-91182
- <sup>40</sup>Ca(p,p), DWIA test in Glauber theory, transition density 0-99173
- <sup>42</sup>Ca(p,t) form factor, hole and continuum contribs. for pick-up reactions 0-78256
- <sup>48</sup>Ca(<sup>16</sup>O, <sup>14</sup>C), two nucleon sequential transfer, on-shell anal., cross sections 0-99180
- <sup>48</sup>Ca(<sup>16</sup>O, <sup>15</sup>N), <sup>15</sup>N excitation contrib. in optical pot., DWBA grazing peak shift 0-86921
- <sup>48</sup>Ca(<sup>16</sup>O, <sup>16</sup>O), two nucleon sequential transfer, on-shell anal., cross sections 0-99180
- <sup>48</sup>Ca(t,p), exact finite range DWBA calcs., realistic triton and nuclear wave functions 0-63191
- <sup>252</sup>Cf scission point configuration,  $\alpha$ -ang. distrib., trajectory calcs. for LRA fission 0-83134
- Cl(Ar,X), proton inclusive spectra, direct plus thermal model 0-57799
- <sup>59</sup>Co( $\alpha$ ,nyp), 20-172.5 MeV, cross sections excitation functions, hybrid model, preequilib. effects 0-57784

## nuclear reaction and scattering theory continued

- <sup>59</sup>Co(e,e), magnetic e scatt., exchange current effects, plane wave Born approx. 0-78282
- C(p, $\pi$ ) 240 MeV inclusive pion production (Russian) 0-86908
- C( $\pi$ , $\pi$ ),  $\pi$ -X, X=He or d, 170 MeV, cross sections and ang. distrib., direct knockout mechanism (Russian) 0-86887
- <sup>A</sup>Cr(p,p), A=50, 52, 6 MeV, elastic and inelastic differential cross sections, spin flip probability (Russian) 0-91187
- <sup>51</sup>Cr levels, spectroscopic function and analogue states, PWBA anal. of <sup>52</sup>Cr(<sup>3</sup>He, $\alpha$ ) 0-68547
- Cu(p, $\pi$ ) 240 MeV inclusive pion production (Russian) 0-86908
- <sup>A</sup>Dy(d,t), A=162, 164, coupled-channels Born approx. anal. 0-83104
- <sup>A</sup>Er(d,t), A=166, 168, coupled-channels Born approx. anal. 0-83104
- <sup>151</sup>Eu  $\pi$  row band and pickup strength, shape coexistence from (d,t) 0-86799
- <sup>153</sup>Eu 5/2<sup>+</sup> ground state rot. band, J<sup>+</sup>, shape coexistence from (d,p) 0-86799
- <sup>18</sup>F resonances,  $\alpha$ -widths, isospin and parity mixing, R-matrix anal. of <sup>14</sup>N( $\alpha$ , $\alpha$ ) 0-91162
- <sup>54</sup>Fe(<sup>3</sup>He,p), <sup>56</sup>Co particle-hole states, T=1, zero DWBA anal. 0-78308
- <sup>54</sup>Fe(p,p'), pol. p, 800 MeV, diff. cross sections, anal. powers, DWIA anal. 0-83067
- <sup>55</sup>Fe(<sup>52</sup>Cr, X), entrance channel mass asymmetry effects on reaction mechanism, fission and fusion 0-106077
- <sup>56</sup>Fe(e, $\alpha$ ), E2 isoscalar resonance sum rule, DWBA anal. 0-68621
- <sup>56</sup>Fe levels, J<sup>+</sup>, anal. powers and cross sections from <sup>56</sup>Fe(t,p) pol. 0-68539
- <sup>154</sup>Gd levels, bands, J<sup>+</sup>, DWBA anal. of <sup>152</sup>Gd(t,p) 0-78110
- <sup>160</sup>Gd(<sup>12</sup>C,  $\alpha$ nn) <sup>168</sup>-<sup>171</sup>Er, particle fragmentation accompanied by incomplete fusion, two step model 0-86947
- <sup>160</sup>Gd(d,t) <sup>159</sup>Gd, coupled-channels Born approx. anal. 0-83104
- <sup>1</sup>H( $\mu$ , $\gamma$ ), radiative capture relativistic calcs., rate and photon spectrum 0-68605
- <sup>1</sup>H(n, $\gamma$ ), thermal, consistency between pion exchange currents and NN pot., cross sections 0-68556
- <sup>1</sup>H(n,n), 16.9 MeV, anal. power, F-wave contribs. 0-63158
- <sup>1</sup>H(n,p), pol. n,p, 50 MeV, spin correlation parameter A<sub>yy</sub>( $\theta$ ), phase shift anal. 0-68530
- <sup>1</sup>H(p,p), 6.141 MeV, anal. power, Paris pot. predictions 0-63156
- <sup>1</sup>H(p,p), pol. p, 9.57 MeV, spin correlation parameter, phase shift anal. 0-102112
- <sup>1</sup>H(t,dn), 2.5 GeV/c, 4 $\pi$  geometry, pole approx. description 0-68678
- <sup>2</sup>H( $\pi$ , $\pi$ ), low energies, Coulomb interaction (Russian) 0-83129
- <sup>2</sup>H(d,n), pol.d, anal. power and polarisations in R-matrix methodology, comparison with (d,p) 0-78273
- <sup>2</sup>H(d,p), pol.d, anal. power and polarisations in R-matrix methodology, comparison with (d,n) 0-78273
- <sup>2</sup>H(e,e), EM form factors, relativistic formulae, moment corrections 0-63075
- <sup>2</sup>H( $\gamma$ , $\pi$ )nn, n-n final state interaction effects 0-102181
- <sup>2</sup>H( $\gamma$ , $\pi$ ), 210-700 MeV, total and differential cross sections from impulse approx. 0-68647
- <sup>2</sup>H(n,n), (n,p), 24 MeV, quasifree scatt., n-n effective range, Monte Carlo anal. 0-68554
- <sup>2</sup>H(p,p), 19 GeV/c, Thomas Reiche Kuhn sum rule appl., mean energy losses 0-91192
- <sup>2</sup>H(p,p), back angle elastic cross sections in Kerman-Kisslinger model, inelasticity corrections 0-106060
- <sup>2</sup>H(p,p), tensor asymmetries, deuteron D-wave and non-eikonal effects, Glauber model 0-78296
- <sup>2</sup>H(p,p) large angle elastic scatt., d form factor at large q<sup>2</sup> 0-102189
- <sup>2</sup>H( $\pi$ ,p), cross sections, Faddeev like eqns., absorption effects for scatt. 0-86928
- <sup>2</sup>H( $\pi$ ,p) in resonance region, theoretical models 0-83123
- <sup>2</sup>H( $\pi$ , $\pi$ ), pole terms and absorption in p-wave  $\pi$ d interaction 0-86932
- <sup>2</sup>H( $\pi$ , $\pi$ ), 140-260 MeV, (2,3) region, tensor force, cross sections, pol. parameters 0-68641
- <sup>2</sup>H( $\pi$ , $\pi$ ), high energies, total cross sections from refined Glauber model 0-78322
- <sup>2</sup>H( $\pi$ , $\pi$ ), scatt. length, exchange current contrib. 0-78328
- <sup>2</sup>H( $\pi$ , $\gamma$ n), multiple scatt. corrections, off-shell rescatt. effects, effective range 0-83127
- <sup>2</sup>H( $\pi$ , $\pi$ ), p,p,  $\pi$  exchange current effects on pion absorption, cross section enhancement 0-57803
- <sup>2</sup>H( $\pi$ , $\pi$ ), 49 MeV, P-wave dispersive contrib.  $\pi$  and  $\rho$  rescatt. 0-78331
- <sup>3</sup>H(n,n), scatt. length, 4-nucleon problem, integral eqn. approach 0-91183
- <sup>A</sup>H( $\gamma$ , $\pi$ ), A=1, 2, 1-10 MeV, photprod. yields, DWIA anal., dipole photprod. amplitudes 0-68645
- <sup>3</sup>He(e,e), nuclear high momentum components and y scaling 0-106051
- <sup>3</sup>He(e,e), charge formfactors, second Born approx. and pole model 0-78133
- <sup>3</sup>He( $\gamma$ ,2p), 80-120 MeV, proton energy distrib., diff. cross sections, direct breakup 0-86897
- <sup>3</sup>He( $\gamma$ , $\pi$ )<sup>3</sup>H cross section near threshold, 0-83093
- <sup>3</sup>He( $\mu$ , $\gamma$ ), radiative capture relativistic calcs., rate and photon spectrum 0-68605
- <sup>3</sup>He(n,n), scatt. length, 4-nucleon problem, integral eqn. approach 0-91183
- <sup>3</sup>He( $\pi$ , $\pi$ ), 68-154 MeV, single and double collision differential cross section calcs. (Russian) 0-106083
- <sup>3</sup>He( $\pi$ , $\pi$ ), form factor sensitivity in Glauber multiple scatt. formalism 0-105964
- <sup>4</sup>He( $\pi$ , $\pi$ ), 5 GeV/c, quasielastic scatt., cross section, form factor, final state interactions 0-99190
- <sup>4</sup>He photodisintegration, total, dipole, and quadrupole cross sections, sum rules (Russian) 0-83094
- <sup>4</sup>He( $\pi$ , $\pi$ ), elastic data inconsistencies and dispersion relations above 33 resonance 0-68700
- <sup>4</sup>He( $\alpha$ , $\alpha$ ), 4.5 GeV/c, Thomas Reiche Kuhn sum rule appl., mean energy losses 0-91192
- <sup>4</sup>He( $\alpha$ , $\alpha$ ), 4.32, 5.07 GeV/c, Glauber multiple scatt. theory comparisons 0-63192
- <sup>4</sup>He( $\alpha$ , $\alpha$ ), nuclear separable plus Coulomb interaction 0-83106
- <sup>4</sup>He( $\gamma$ ,X), X=p,n, 50-150 MeV, total cross sections, quasiparticle formalism calcs. 0-78277
- <sup>4</sup>He( $\gamma$ ,pn)<sup>3</sup>H, three particle photodisintegration, pole mechanism contrib. (Russian) 0-91176
- <sup>4</sup>He(n,X), local approximation to a non-local potential 0-91182



nuclear reaction and scattering theory continued

<sup>4</sup>He(p, p), 1.05 GeV, cross sections and polarisations, correlation effects calcs. 0-57774  
<sup>4</sup>He( $\pi$ ,  $\pi$ ), single scatt. optical pot., Pauli principle and binding effects on cross section 0-86933  
<sup>4</sup>He( $\gamma$ ,  $\pi^0$ ), A=3, 4, 1-10 MeV, photoprod. yields, DWIA anal., dipole photoprod. amplitudes 0-68645  
K(Ar,X), proton inclusive spectra, direct plus thermal model 0-57799  
<sup>6</sup>Li(X), 156 MeV, projectile breakup in continuous particle spectra, cross section, fragmentation 0-86889  
<sup>6</sup>Li(d, d), A=20 to 68, DWBA reduction, ground state  $\alpha$ -transfer strengths 0-106068  
<sup>6</sup>Li(d, d), A~60, 116, L=0 transitions, cross sections, microscopic anal. 0-78189  
<sup>6</sup>Li(<sup>3</sup>He, <sup>3</sup>He), phase shifts, cross sections, resonating group calcs., odd-even features, resonances 0-68681  
<sup>6</sup>Li(d, X) system, resonating group method, single channel approx., cluster states 0-57782  
<sup>6</sup>Li(e, e'), 76-141 MeV, form factors, appl. to ( $\pi^-$ ,  $\gamma$ ), phenomenological model 0-83068  
<sup>6</sup>Li(e, e), charge formfactors, second Born approx. and pole model 0-78133  
<sup>6</sup>Li(p, n), 144 MeV, charge exchange, one pion exchange and PCAC tests 0-78299  
<sup>6</sup>Li(p, p), 670 MeV, large angle quasifree scatt., spectroscopic factor, momentum distrib., cluster model 0-63184  
<sup>7</sup>Li(t, <sup>7</sup>Li), near threshold anomaly, S-matrix formalism, <sup>10</sup>Li neutron binding energy (*Russian*) 0-105961  
<sup>7</sup>Li  $\beta^-$  decay,  $\beta$ - $\alpha$  angular correlations, final state energy depend., current test 0-102151  
<sup>7</sup>Li( $\pi$ ,  $\pi$ ), A=6, 7, 75, 175 MeV, diffential cross sections, reaction mechanisms 0-78332  
<sup>8</sup>Mg(d, <sup>4</sup>Li), 80 MeV, A=24, 26,  $\alpha$ -spectroscopic factors and ang. distrib., DWBA anal. 0-99126  
<sup>24</sup>Mg(<sup>13</sup>C, <sup>13</sup>C), 35 MeV, 2<sup>+</sup> population probab., spin-flip and spin orbit pots., coupled channel anal. 0-99125  
<sup>40</sup>Ar, A=98, 102, anal. powers, transitions, shape coexistence states, DWBA anal. of Mo(t, p), pol. t 0-86895  
<sup>90</sup>Mo(<sup>16</sup>O, X), entrance channel mass asymmetry effects on reaction mechanism, fission and fusion 0-106077  
<sup>96</sup>Mo(t, p), pol. t, cross section and anal. powers, struct. depend., DWBA anal. 0-78272  
<sup>100</sup>Mo(<sup>14</sup>N, <sup>12</sup>B), 90 MeV, spin alignment of products, semi-classical model calcs. 0-73859  
<sup>14</sup>N( $\gamma$ ,  $\pi^-$ ), DWIA anal., wave function and  $\pi$  optical pot. effects on cross section 0-63168  
<sup>14</sup>N(p, n), 144 MeV, charge exchange, one pion exchange and PCAC tests 0-78299  
<sup>14</sup>N(p, p'), 122 MeV, level excitation, cross sections, effective NN interaction, DWIA anal. 0-78197  
<sup>14</sup>N(p, p'), 25-40 MeV, level cross sections, optical parameters, DWBA anal., tensor effective interaction 0-68555  
<sup>91</sup>Nb low lying multiplets, DWBA anal. for spectroscopic factors from <sup>91</sup>Zr( $\alpha$ , t) 0-57685  
<sup>91</sup>Nb(d, p, X), 80 MeV, inclusive proton spectra, d breakup, DWBA anal. 0-91190  
<sup>91</sup>Nb(e, e), magnetic e scatt., exchange current effects, plane wave Born approx. 0-78282  
<sup>4</sup>Nd, A=145, 147, 149, single neutron hole states spectroscopic factors, DWBA anal. of (d, t), (<sup>3</sup>He,  $\alpha$ ) 0-78109  
Ne(Ne, X), 117-800 MeV, classical eqns. of motion calcs., central collisions, thermal models 0-106070  
<sup>26</sup>Ne 13482 keV level, parity violating effects in two resonance interference from <sup>19</sup>F(p,  $\alpha$ ) pol. p 0-83033  
<sup>4</sup>Ni, A=60, 62, 66, levels, J $\pi$ , anal. powers and cross sections from Ni(t, p)pol. t 0-68539  
<sup>4</sup>Ni(e, p), (e,  $\alpha$ ), A=58, 60, 62, electrodisintegration cross sections, E1, E2 absorption, DWBA anal. 0-106052  
<sup>4</sup>Ni(p, xy), 80-164 MeV, A=58, 60, 62, 64, prod. cross sections, pre-equilibrium phase 0-78301  
<sup>58</sup>Ni(<sup>3</sup>He,  $\alpha$ ), 130 MeV, selected transition, DWBA anal., cross sections 0-83086  
<sup>58</sup>Ni(<sup>3</sup>Li, <sup>4</sup>Li<sup>2</sup>), 71 MeV, excited states deformation lengths, DWBA and coupled channels anal. 0-68541  
<sup>58</sup>Ni(d,  $\alpha$ ), <sup>56</sup>Co particle-hole states, T=1, zero DWBA anal. 0-78308  
<sup>58</sup>Ni(d, d'), 10 MeV, diff. cross sections and d- $\gamma$  ang. correlations, multi-shell coupled channel calcs. 0-83064  
<sup>58</sup>Ni(p, p), 800 MeV, elastic and inelastic, cross section, deformation lengths, optical and DWBA anal. 0-68664  
Ni(d, d), 13-80 MeV, second order breakup corrections in DWBA 0-86910  
N( $\pi^\pm$ ,  $\pi^\pm$  X), X=He or d, 170 MeV, cross sections and ang. distrib., direct knockout mechanism (*Russian*) 0-86887  
<sup>4</sup>O( $\pi^+$ ,  $\pi^-$ ), A=16, 18, cross section and ang. distrib., Glauber and coherent fluctuation models (*Chinese*) 0-102211  
<sup>16</sup>O(X), A=54-208, direct transfer to discrete and continuum states, DWBA diffraction model 0-78262  
<sup>12</sup>O 4<sup>+</sup> state nonstatistical population in compound nucleus calcs. of <sup>12</sup>C(<sup>12</sup>Li, d) 0-102137  
<sup>12</sup>C(<sup>12</sup>C, <sup>12</sup>C), 18-26 MeV, molecular structure, projection operator anal., differential cross sections 0-106033  
<sup>16</sup>O(<sup>16</sup>O, <sup>16</sup>O), elastic scatt., l-window formalism 0-68684  
<sup>16</sup>O(<sup>16</sup>O, <sup>16</sup>O), optical pot., nuclear matter approach, energy density matter J- 0-83112  
<sup>16</sup>O(d, X), X=d or N, elastic scatt. and stripping, three body calcs. 0-91165  
<sup>16</sup>O(e,  $\pi^+$ ), 180.4 MeV, virtual photon spectrum, virtual photon theory test 0-102183  
<sup>16</sup>O( $\gamma$ ,  $\pi^+$ ), 200-350 MeV, cross sections, DWIA anal. 0-106048  
<sup>16</sup>O( $\gamma$ ,  $\pi$ ), total cross section,  $\Delta$ -hole states damping,  $\pi^0$ ,  $\rho^0$  exchange,  $\Delta$  isobar hole model 0-91174  
<sup>16</sup>O(p, p'), 20-40 MeV, pol. p, anal. powers, imaginary spin-orbit pot., coupled channels anal. 0-102179  
<sup>16</sup>O(p, t), exact finite range DWBA calcs., realistic triton and nuclear wave functions 0-63191  
<sup>16</sup>O(p, t), finite range DWBA anal. with realistic triton wave function 0-78300  
O( $\pi^\pm$ ,  $\pi^\pm$  X), X=He or d, 170 MeV, cross sections and ang. distrib., direct knockout mechanism (*Russian*) 0-86887  
<sup>30</sup>P positive parity states, transitions and spectroscopic strengths, DWBA anal. of <sup>28</sup>Si(<sup>3</sup>He, d) 0-102138

nuclear reaction and scattering theory continued

<sup>31</sup>P high E, states, J $\pi$ , DWBA anal. <sup>28</sup>Si(<sup>3</sup>He, p) 0-68536  
<sup>208</sup>Pb (e, e'), 2<sup>-</sup> giant resonance twist mode excitation, B(M2) values, form factors 0-78246  
<sup>208</sup>Pb giant monopole and quadrupole resonances, multipole excitations from ( $\alpha$ ,  $\alpha'$ )(d, d') 0-106031  
<sup>208</sup>Pb(<sup>12</sup>C, <sup>12</sup>B), 77 MeV, bound and continuum state excitation, direct and two step processes 0-63205  
<sup>208</sup>Pb(<sup>208</sup>Pb, X), giant resonance polarisation pots. from nucleus-nucleus effective pot. 0-78248  
<sup>208</sup>Pb(<sup>208</sup>Ne, X), 400 MeV/N, inclusive p, d, t, <sup>3</sup>He cross sections from sequential scatt. model 0-57792  
<sup>208</sup>Pb(p, t), finite range DWBA anal. with realistic triton wave function 0-78300  
<sup>208</sup>Pb( $\pi^\pm$ ,  $\pi^\pm$  N), 180-255 MeV, quasielastic pion scatt. coincidence expt. interpretation, impulse approx. 0-68704  
<sup>106</sup>Pd(t, p), pol. t, cross section and anal. powers, struct. depend., DWBA anal. 0-78272  
<sup>153</sup>Pm 5/2<sup>-</sup> h<sub>11/2</sub> dominated band, anomalous ang. distrib., CCBA calcs. for <sup>154</sup>Sm(t,  $\alpha$ ) 0-86788  
<sup>242</sup>Pu( $\mu$ , f), radiationless muonic transition induced fission, fission dynamics probe, friction coeff. 0-78336  
<sup>232</sup>Sr(X), A=59-89, double differential cross section, mass asymmetry, transport model 0-102203  
<sup>32</sup>S(n, n), 25-1100 keV, total cross section, multilevel anal., strength functions, optical parameters 0-78298  
<sup>4</sup>Sc, A=44m, 46, 47, 48, fragment emission, two-step model applicability from <sup>238</sup>U(p, X) 0-99177  
<sup>4</sup>Sc proton single particle states, spectroscopic factors, DWBA anal. of <sup>4</sup>Ca(d, n) 0-99118  
<sup>74</sup>Se transition energy correlations in  $\gamma$ -continuum from <sup>64</sup>Ni(<sup>16</sup>O,  $\alpha$ n) 0-95309  
<sup>74</sup>Si(<sup>10</sup>B, <sup>3</sup>He), unique l=1 reaction, ang. distrib. wave number depend., DWBA anal. 0-63204  
<sup>74</sup>Si(<sup>3</sup>He, <sup>3</sup>He'), 45, 60 MeV, low lying collective states, ang. distrib., DWBA double folding pot. anal. 0-78113  
<sup>28</sup>Si(e, e'), 6<sup>-</sup> T=1 resonance form factor, mag. strength quenching, meson exchange currents 0-86882  
<sup>28</sup>Si(n,  $\gamma$ ), 565, 813 keV, resonance  $\gamma$ , spectra, valence model test 0-63124  
<sup>28</sup>Si levels, J $\pi$ , spectroscopic factor, DWBA anal. of <sup>28</sup>Si(<sup>3</sup>He, <sup>2</sup>He) 0-86811  
<sup>28</sup>Si levels and ang. distrib., DWBA anal. of <sup>27</sup>Al( $\alpha$ , d) 0-78157  
<sup>28</sup>Si(<sup>16</sup>O, <sup>7</sup>O), <sup>28</sup>Si, non-orthogonality of channel states 0-83115  
<sup>4</sup>Sm(p, p'), 0.8 GeV, ang. distrib. and multipole moments, DWBA and coupled channel anal. 0-105969  
<sup>4</sup>Sn(n, n'), A=116, 118, 120, 122, 11 MeV, octupole vibr. states, diff. cross section, deformation length, DWBA anal. 0-102092  
<sup>120</sup>Sn(p, n), statistical multistep direct emission, p-h and DWBA calcs. 0-106035  
<sup>124</sup>Sn(n, n), pol. thermal, parity violation near resonance, DWBA calcs. 0-68528  
<sup>87</sup>Sr(e, e), magnetic e scatt., exchange current effects, plane wave Born approx. 0-78282  
<sup>87</sup>Sr(n, n'), 11 MeV, octupole vibr. states, diff. cross section, deformation length, DWBA anal. 0-102092  
<sup>181</sup>Ta(<sup>28</sup>Ne, spallation), 8.0 GeV, cross sections and target residues, model comparison 0-68630  
<sup>185</sup>Ta single proton states and rot. bands, J $\pi$  from <sup>186</sup>W(t,  $\alpha$ ) pol. t 0-91130  
<sup>159</sup>Tb(<sup>12</sup>B, X), 51 MeV, fusion and deep inelastic, quantised frictional motion calcs. 0-102223  
<sup>159</sup>Tb(<sup>4</sup>N, X), 140 MeV, incomplete fusion reactions, sum rule model 0-95332  
<sup>125</sup>Te low lying negative parity high spin states multistep induced population from (d, t)(<sup>3</sup>He,  $\alpha$ ) 0-57657  
<sup>126</sup>Te(t, p), pol. t, cross section and anal. powers, struct. depend., DWBA anal. 0-78272  
<sup>4</sup>Ti, A=44, 48, ang. distrib. for transitions, DWBA anal., spectroscopic strengths from Ca(Li, t) 0-68584  
<sup>4</sup>Ti(e, e), magnetic e scatt., exchange current effects, plane wave Born approx. 0-78282  
<sup>50</sup>Ti( $\alpha$ ,  $\alpha$ ), 140 MeV, model independent description limits from local optical pots. 0-102196  
U(Ne, X), proton inclusive spectra, direct plus thermal model 0-57799  
<sup>235</sup>U fission fragment thermonuclear superheavy nuclei synthesis, prod. cross sections 0-95331  
<sup>235</sup>U(n, f), thermal, fragment ionisation, charge distrib., stat. and instant perturbation theory (*Russian*) 0-63219  
<sup>235</sup>U(n,  $\gamma$ ), thermal, d, t, He emission probabilities from stable core model (*Russian*) 0-68713  
<sup>238</sup>U subbarrier photofission, cross section and half-life, double hump model 0-102217  
<sup>51</sup>V(<sup>3</sup>He, dp), <sup>3</sup>He breakup, DWBA calcs. for strongly absorptive projectiles 0-68682  
<sup>51</sup>V(e, e), magnetic e scatt., exchange current effects, plane wave Born approx. 0-78282  
<sup>90</sup>Y low lying multiplets, DWBA anal. for spectroscopic factors from <sup>91</sup>Zr(d, <sup>3</sup>He) 0-57685  
<sup>91</sup>Zr(d, <sup>3</sup>He), 0.8 GeV, ang. distrib. and multipole moments, DWBA and coupled channel anal. 0-105969  
<sup>62</sup>Zn ang. distrib. for transitions, DWBA anal., spectroscopic strengths from <sup>38</sup>Ni(<sup>3</sup>Li, t) 0-68584  
<sup>90</sup>Zr(e, e'), 2<sup>-</sup> giant resonance twist mode excitation, B(M2) values, form factors 0-78246  
<sup>90</sup>Zr( $\gamma$ ,  $\alpha$ ), above GDR region, cross sections, DWBA anal. 0-63173  
<sup>90</sup>Zr(n, n'), 11 MeV, octupole vibr. states, diff. cross section, deformation length, DWBA anal. 0-102092  
<sup>90</sup>Zr(t, p), exact finite range DWBA calcs., realistic triton and nuclear wave functions 0-63191

nuclear reactions and scattering

see also alpha particle-nucleus reactions; alpha particle-nucleus scattering; chemical effects of nuclear reactions and scattering; cosmic ray-nucleus reactions; cosmic ray-nucleus scattering; deuteron-nucleus reactions; deuteron-nucleus scattering; direct nuclear reactions and scattering; electron-nucleus reactions; electron-nucleus scattering; fission; form factors (nuclear); hadron-nucleus reactions; hadron-nucleus scattering; heavy ion-nucleus reactions; heavy ion-nucleus scattering; helium 3-nucleus reactions; helium 3-nucleus scattering; muon-nucleus reactions; muon-nucleus scattering; neutrino-nucleus reactions; neutrino-nucleus scattering



**nuclear reactions and scattering continued**

scattering; nuclear fusion; nuclear reaction and scattering theory; nuclear reactions involving few nucleon systems; nuclear resonance reactions and scattering; nuclear scattering involving few nucleon systems; nuclear spallation; nuclear spectroscopic factors; nucleosynthesis; photon-nucleus reactions; photon-nucleus scattering; polarisation in nuclear reactions and scattering; triton-nucleus reactions; triton-nucleus scattering conference, general congress, Societe Francaise de Physique, Toulouse, France (June 1979) 0-77536  
growth points in nuclear physics, book 0-94929  
lepton collisions, cascade model, space-time model, tests and predictions 0-68633

**nuclear reactions involving few nucleon systems**

for nuclear inelastic scattering involving few nucleon systems see "nuclear scattering involving few nucleon systems"  
four nucleon system, reactions and scatt. using K-matrix formalism, differential cross sections (Russian) 0-106027  
 $^1\text{H}(\alpha,\alpha')X$ , 1.74, 2.57 GeV, low mass  $\pi\text{N}$  enhancement, cross section t-depend. 0-63193  
 $^1\text{H}(\pi,\gamma\gamma)$ , thermal, consistency between pion exchange currents and NN pot., cross sections 0-68556  
 $^1\text{H}(\text{t,dn})$ , 2.5 GeV/c,  $4\pi$  geometry, pole approx. description 0-68678  
 $^2\text{H}(\text{H,n})^3\text{He}$ , muon catalysis kinetics (Russian) 0-91206  
 $^2\text{H}(\text{d,n})$ , 18-26 MeV, differential cross sections, ang. distrib.,  $^4\text{He}$  broad level search 0-102117  
 $^2\text{H}(\text{n,nn})p$ , 25 MeV, neutron-neutron effective range 0-83041  
 $^2\text{H}(\text{n,2n})p$ , in thick targets, n-n scatt. length determ., computer expt. 0-57776  
 $^2\text{H}(\text{n},\pi^-)^3\text{He}$ , 400 to 580 MeV at backward pion angles 0-73847  
 $^2\text{H}(p,2p)n$ , 22.7 MeV, proton analysing power 0-78302  
 $^2\text{H}(p,\gamma)^3\text{He}$ , 450, 550 MeV, differential cross sections, inverse reaction comparison 0-86904  
 $^3\text{H}(\text{d,n})^4\text{He}$ , neutron fluence and energy transfer standard 0-102194  
 $^3\text{H}(p,n)$ , 1.24, 1.8 GeV, differential cross section, spin indep. Glauber model interpretation 0-63183  
 $^4\text{H}(\text{n,X})$ , 60 keV-80 MeV,  $A=1,2,3$  total cross section and scatt. length 0-99176  
 $^3\text{He}(p,\pi^+)^4\text{He}$ , 415 MeV, angular distrib., microscopic description, generalisation of  $(\pi,\pi)$  (Chinese) 0-63188

**nuclear reactor fuel see fission reactor fuel****nuclear reactor instrumentation**

BWR, computer based systems 0-83211  
BWR in-core neutron detector sensitivity to control rod vibr. using neutron noise anal. 0-57910  
conference, nuclear power systems, San Francisco, CA, USA (Oct. 1979) 0-56994  
control and instrumentation designs beyond the 1980s 0-57872  
control and instrumentation test loop diagrams 0-68890  
coolant pressure boundary leakage detection system 0-63306  
digital computer applications in reactor instrumentation and control 0-106134  
directional fully encapsulated gamma detector for in-core reactor meas. 0-63307  
EBR II, reactor subassembly removal using gripper device 0-57942  
FBR fuel pin safety expts. at SLSF, centerline fuel thermocouple performance 0-102283  
fluid velocity profile meas. by nonintrusive transaxial tomography 0-99268  
fuel rod gas pressure meas. during LOFT, sensor description 0-57876  
fuel thermocouples and liquid-level probes for core monitoring 0-99239  
fusion reactor, Doublet III, neutral beam injector system, instrumentation and control 0-99322  
high voltage instrument cables for 650°C, in-vessel breeder reactor service 0-57878  
high-temperature reactor structural displacement and strain analysis by picture processing (Japanese) 0-78352  
liquid level detector based on level sensitive transducer for PWR environment 0-57874  
LMFBR, Na purification system, cold traps and plugging indicator 0-99209  
LMFBR, safeguards system for monitoring of fissile material inventory 0-63293  
LMFBR coolant flow rate meas. using electromagnetic convertor 0-73887  
LOFT drag disc turbine meter rakes for two-phase flow measurement 0-102260  
LWR power stations, design features and instrumentation for materials safeguards (Russian) 0-63278  
mass flow instrumentation performance, during LOFT nonuclear test series 0-69952  
materials safeguarding, containment and surveillance devices 0-63349  
materials safeguarding, development of containment and surveillance measures for IAEA safeguards 0-63350  
materials safeguarding, fuel assembly identification using US signatures, statistical aspects 0-69620  
materials safeguarding, remote-controlled and long-distance unique identification of reactor fuel elements or assemblies using US signature equipment 0-63296  
materials safeguarding, VACOSS electronic sealing system 0-63348  
materials safeguards, ultrasonically identified security seals for CANDU safeguard systems 0-63297  
microprocessor appl. 0-83147  
microprocessor controlled multipoint recorder with graphical video output for reactor core temperatures 0-57873  
multiaxis neutron diffractometer automation 0-102417  
period meter, digital, microprocessor controlled, hardware and software 0-63473  
plant diagnostics—the integrated approach 0-68899  
portal monitors for detecting and safeguarding special nuclear materials 0-63406  
power density limitation system development 0-68884  
primary coolant flowmeter 0-73912  
PWR components, vibrations meas. using correlation techniques (German) 0-79247  
PWR with wide vessel to concrete air gaps, ex-core detector sensitivity studies 0-73970  
remote multiplexing for nuclear reactor instrumentation and control circuits 0-57885  
safeguarding of critical facilities to detect diversion of nuclear materials 0-68808

**nuclear reactor instrumentation continued**

solid-state track recorder applications in U.S. nuclear reactor energy programs 0-95506  
spent fuel bundle counter for 600 MW CANDU reactor 0-63269  
spent fuel bundle counters for CANDU reactors, appl. of safeguards design principles 0-63347  
steam fraction determ. in flowing air/stream mixtures by meas. of IR rad. attenuation 0-75010  
TAPIRO fast research reactor, computerised protection system 0-63308  
teleoperator systems for reactor maintenance, technology assessment 0-68872  
thermocouples, 2200°C fuel centerline for LOFT program 0-57877  
TMI-2 accident, nuclear reactor safety, role of instrumentation and control (Japanese) 0-73947  
track-etch monitor for reactor power anal., evaluation 0-78418  
two-phase-flow instrumentation development at Brookhaven National Laboratory 0-102261  
US thermometry appls. 0-73365  
US viewing system for reactor fuel assemblies under liquid Na 0-57875  
Be convertor/neutron counter apparatus for determ. of relative fission density release of fuel elements (Russian) 0-73973  
platinum self-powered in-core detectors for PWR core power distrib. monitoring 0-73971

**nuclear reactor materials see fission reactor materials****nuclear reactor operation see fission reactor operation****nuclear reactor theory and design see fission reactor theory and design****nuclear reactors see fission reactors****nuclear resonance reactions and scattering****see also nuclear resonances**

average resonance neutron capture, completeness in nuclear spectroscopy 0-106006  
giant resonance production mechanisms (French) 0-78243  
heavy ion+ nucleus, orbiting quasispherical system, nuclear-surface-wave interpretation 0-86914  
neutron elastic removal cross sections, interference effect of strong scattering resonances in LMFBR 0-68658  
radiative nucleon capture, pure resonance model, direct-semidirect model, pure semidirect model 0-78257  
Rayleigh and whispering gallery waves excited by heavy ion elastic and inelastic scatt. 0-91164  
(n,  $\alpha$ ) with resonance neutrons, properties of highly-excited states of nuclei (Russian) 0-106053  
(n,n $\gamma$ ),  $A=19-207$ , neutron scattering resonance radiative widths 0-99146  
 $^1\text{B}(\gamma,\gamma)$ , resonance scatt., molecular orientation effects 0-78252  
 $^{12}\text{C}(^{12}\text{C}, \gamma)$ , 11.8-20.0 MeV, total cross section resonant and average behaviour 0-106069  
 $^{12}\text{C}(^{14}\text{N}, \alpha)$ , 10.1-15.9 MeV, forward angle excitation function structure, nonstatistical struct. 0-86885  
 $^{12}\text{C}(^{16}\text{O}, ^{16}\text{O})$ , elastic and inelastic, 23-32 MeV, strong absorption region resonances, excitation functions 0-86884  
 $^{12}\text{C}(^{16}\text{O}, X)$ , transparency to  $l=9$  partial wave in 14.7 MeV resonance region 0-78314  
 $^{12}\text{C}(\text{d,p})^{13}\text{C}$ , 0.5 to 2.5 MeV, excitation functions and angular distrib., possible doorway state (Chinese) 0-68679  
 $^{12}\text{C}(\gamma,\pi^0)$ , pionic and EM  $A^*$  resonance excitation 0-91160  
 $^{243}\text{Cm}(\text{n,f})$ , thermal neutron fission cross section and fission-resonance integral 0-86942  
 $^2\text{H}(p,p)$ , pol.p, spin rot. and depolarisation, NN amplitude double spin flip part 0-78271  
 $^3\text{H}(\pi^-, \gamma)^3\text{n}$ , rest  $\pi$ , resonance branching ratio, bound state upper limit 0-99162  
 $^7\text{Li}(\text{e,e}')$  at first  $\pi\text{N}$  resonance, cross section longitudinal and transverse components (Russian) 0-86901  
 $^{54}\text{Mn}(p,\gamma)$ ,  $^{56}\text{Fe}$  isobaric analogue resonance levels, branching ratios 0-68617  
 $^{15}\text{N}(\gamma,\gamma)$ , 6.324 MeV, resonance scatt. cross section temp. depend. in BN,  $\text{NH}_4\text{Cl}$  0-57767  
 $\text{Ni}(\text{e},\alpha)$ , E2 strength in resonance regions statistical decay 0-91146  
 $^{40}\text{O}(\pi^{\pm}, \pi^{\pm})$ ,  $A=16, 18$ , resonance region, proton and neutron distrib. 0-91195  
 $^{16}\text{O}(^{12}\text{C}, \alpha X)$ , 140 MeV, fast  $\alpha$  prod. and molecular resonance search 0-106066  
 $^{244}\text{Pu}(\text{n},\gamma)$  resonance integral meas. 0-73846  
 $^{28}\text{Si}$  doorway state neutron capture, levels and  $\gamma$ -spectra from  $^{28}\text{Si}(\text{n},\gamma)$  0-57729  
 $^{124}\text{Sn}(\text{n,n})$ , pol. thermal, parity violation near resonance, DWBA calcs. 0-68528  
 $^{88}\text{Sr}(\gamma,\gamma)$ , 14 MeV, highly excited spin-1 resonances, spin and radiative widths 0-86876  
 $^{90}\text{Zr}(^7\text{He,t})^{90}\text{Nb}$ , 18.5 MeV resonance, isovector dipole and Gamow-Teller transitions 0-86881

**nuclear resonances****see also isobaric analogue resonances; nuclear collective states and giant resonances**

$A=184, 194, 200, 208$ , pygmy resonance, E1 transition probabilities, BCS wave functions, spin-isospin oscillation (Chinese) 0-63087  
 $A=7-40$ , EM transition strength distrib. (Russian) 0-86855  
common doorway resonance, decay amplitude phase relation from (n, $\gamma$ ) reactions 0-57758  
doorway states, fragmented, micro-resonances, strength functions, K-matrix width 0-57754  
heavy ion reactions, coherence angle and cross section fluctuations correlation function, resonances 0-57790  
neutron resonance data, statistical anal. method 0-102174  
pole expansions for resonance functions, scatt. amplitudes and continuum states (Russian) 0-86871  
resonant states in the presence of Coulomb interactions, Schrodinger eqn. 0-91161  
sd-shell nuclei heavy-ion reaction resonances, low level density regions, shell model 0-57757  
UCN, quasisub states in matter, reson. positions and widths 0-73833  
(n,f), intermediate struct. line fitting, subthreshold fission resonances 0-102214  
 $\pi$ - and  $p$ -exchange pots., influence on mag. resonances, mag. moments, and transition probabs. 0-99133  
 $^4\text{Al}$ ,  $A=25,26,27$  levels, resonances,  $\gamma$ -ray branching ratios from  $\text{Mg}(p,\gamma)$  0-86875  
 $^{26}\text{Al}$  T=1 states, resonances, J $^\pi$  and transitions from  $^{25}\text{Mg}(p,\gamma)$  0-99131



**nuclear resonances continued**

- <sup>27</sup>Al levels, resonances, J<sup>π</sup>, branching and mixing ratios from <sup>26</sup>Mg(p,γ) 0-99132
- <sup>12</sup>B levels, J<sup>π</sup> and diff. cross sections, R-matrix anal. of <sup>11</sup>B(n,n) 0-78151
- <sup>8</sup>Be high spatial symmetry excited states, resonances, rot. band from (d,α), (p,α) 0-86780
- <sup>20</sup>Ne 8<sup>+</sup> level radiative width, resonance strength from <sup>16</sup>O(α,γ) 0-83065
- <sup>12</sup>C+<sup>12</sup>C gross struct. resonances in excitation functions from <sup>12</sup>C(<sup>12</sup>C,<sup>10,11</sup>B) 0-102167
- <sup>12</sup>C+<sup>12</sup>C system resonant structs., J<sup>π</sup> assignments, true <sup>24</sup>Mg states from <sup>12</sup>C(<sup>12</sup>C,<sup>16</sup>O) 0-99163
- <sup>12</sup>C(<sup>12</sup>C,<sup>12</sup>C), shape resonance energy and widths, projection operator method 0-78255
- <sup>12</sup>C(<sup>12</sup>C,<sup>12</sup>C), 18.5-32.8 MeV, spin alignment and possible molecular resonances 0-86804
- <sup>12</sup>C(<sup>12</sup>C,<sup>12</sup>C), 10-30 MeV, projection operator method, Feshbach doorways, intermediate structure 0-68695
- <sup>12</sup>C(<sup>12</sup>C,<sup>12</sup>C), 10-30 MeV, molecular structure, projection operator anal., differential cross sections 0-106033
- <sup>12</sup>C(α,α'), generator coordinate multichannel calc., levels and resonances 0-78149
- <sup>12</sup>C(p,p), pol. p, 14.23 MeV resonance broadening, nuclear recoil, atomic excitation effects 0-102165
- <sup>12</sup>C(α,α'), 22, 36 MeV, resonant state line shapes 0-91148
- <sup>12</sup>C(γ,n), 6.5-9.3 MeV, ang. distrib., E1, M1 and E2 excitations, resonance radiative widths 0-68581
- <sup>4</sup>Ca(π,π), A=40,48, 40-241 MeV, first and second order optical pots., resonance behaviour 0-68624
- <sup>40</sup>Ca composite system, heavy ion resonances from <sup>24</sup>Mg+<sup>16</sup>O, <sup>28</sup>Si+<sup>12</sup>C 0-86874
- <sup>40</sup>Ca(p,p'), 6.25 MeV, triple ang. correlation, 3<sup>-</sup> exit channel, resonances, single particle states 0-68626
- <sup>35</sup>Cl anomalous M1/E1 strength ratio and doorway states from <sup>35</sup>Cl(n,γ) 0-57730
- <sup>4</sup>Cr(p,p), A=50, 52, 6 MeV, elastic and inelastic differential cross sections, spin flip probability (Russian) 0-91187
- <sup>63</sup>Cu A=29.63, Doppler shift attenuation factors, level lifetimes, resonances from Ni(p,γ) 0-57741
- <sup>18</sup>F resonances, α-widths, isospin and parity mixing, R-matrix anal. of <sup>18</sup>N(α,α) 0-91162
- <sup>56</sup>Fe(p,p'), A=54, 56, 6 MeV, resonances, spin flip and cross section depends., Hauser Feshbach anal. (Russian) 0-83084
- <sup>56</sup>Fe resonances, levels, J<sup>π</sup>, valence capture γ-ray spectrum from <sup>54</sup>Fe(n,γ) 0-68652
- <sup>56</sup>Fe(α,α), E2 isoscalar resonance sum rule, DWBA anal. 0-68621
- <sup>56</sup>Fe anomalous M1/E1 strength ratio and doorway states from <sup>56</sup>Fe(n,γ) 0-57730
- <sup>56</sup>Fe resonances, primary γ-intensities, E1-M1 correlation from <sup>58</sup>Fe(n,γ) 0-57740
- <sup>4</sup>H(π<sup>+</sup>, π<sup>+</sup>), A=1,2, 130-280 MeV, 180° excitation function, dibaryon resonance signals 0-68619
- <sup>3</sup>He(π,π), 1 GeV, backward scatt., nonstable meson-nucleon interaction cross section, resonance (Russian) 0-68559
- <sup>4</sup>He 2<sup>+</sup> resonance evidence at 40 MeV from <sup>4</sup>He(e,<sup>3</sup>H), and <sup>3</sup>H(p,γ) 0-68880
- <sup>1</sup>B<sup>+</sup> decay force function resonance struct., level populations (Russian) 0-102154
- <sup>6</sup>Li<sub>1</sub>, supermultiplet struct. and decay props. of hypernuclear 1<sup>+</sup> resonances from (K<sup>+</sup>, π<sup>+</sup>) 0-78186
- <sup>6</sup>Li(<sup>3</sup>He,<sup>3</sup>He), phase shifts, cross sections, resonating group calcs., odd-even features, resonances 0-68681
- <sup>151</sup>Lu β<sup>+</sup> decay force function resonance struct., level populations (Russian) 0-102154
- <sup>24</sup>Mg resonances through γ-decay excitation functions from <sup>12</sup>C(<sup>12</sup>C,n) 0-63148
- <sup>24</sup>Mg intermediate struct., correlations, elastic and reaction channel excitation functions from <sup>12</sup>C(<sup>12</sup>C,X) 0-68625
- <sup>24</sup>Mg(<sup>16</sup>O,<sup>16</sup>O), 24-40 MeV, backward angles, excitation functions, ang. distrib., and resonant behaviour 0-68622
- <sup>100</sup>Mo levels, γ-rays and p-wave resonance partial radiative widths from <sup>100</sup>Mo(n,γ) 0-57739
- <sup>23</sup>Na resonances through γ-decay excitation functions from <sup>12</sup>C(<sup>12</sup>C,p) 0-63148
- <sup>20</sup>Ne 13482 keV level, parity violating effects in two resonance interference from <sup>19</sup>F(p,α) pol. p 0-83033
- <sup>20</sup>Ne low lying levels and intermediate structure J<sup>π</sup> from <sup>16</sup>O(<sup>12</sup>C, <sup>8</sup>Be) 0-102166
- <sup>20</sup>Ne resonances through γ-decay excitation functions from <sup>12</sup>C(<sup>12</sup>C,α) 0-63148
- <sup>16</sup>O α-cluster states, widths and resonances, optical model, direct transfer in <sup>12</sup>C(<sup>4</sup>Li,d) 0-105975
- <sup>16</sup>O level excitation functions, resonances from <sup>12</sup>C(<sup>16</sup>O,<sup>12</sup>C) 0-63146
- <sup>16</sup>O(<sup>12</sup>C,α,X), 140 MeV, fast α prod. and molecular resonance search 0-106066
- <sup>16</sup>O(<sup>12</sup>C,<sup>12</sup>C), 18-26 MeV, molecular structure, projection operator anal., differential cross sections 0-106033
- <sup>16</sup>O(<sup>16</sup>O,<sup>16</sup>O), 10-41 MeV, molecular resonances γ-yield, band crossing model 0-106032
- <sup>16</sup>O(<sup>16</sup>O,X), cross sections, energy dependence, nuclear molecular resonances, band crossing model 0-68686
- <sup>208</sup>Pb p-wave resonances, enhanced primary M1 transitions from <sup>206</sup>Pb(n,γ) 0-57728
- <sup>208</sup>Pb excited states, 3/2<sup>-</sup> resonances from shell model of <sup>208</sup>Pb(n,n) 0-78240
- <sup>208</sup>Pb resonances and excitation functions, Hauser Feshbach anal. of <sup>20</sup>Ne(<sup>12</sup>C,X), X=p,d,α 0-78249
- <sup>40</sup>Ca 2p-1h intermediate struct. resonances, anal. powers, J<sup>π</sup> from <sup>40</sup>Ca(p,p') 0-86883
- <sup>28</sup>Si alpha doorway states from <sup>12</sup>C(<sup>16</sup>O,<sup>12</sup>C) 0-63146
- <sup>28</sup>Si excitation functions, ang. distrib., and resonant behaviour from <sup>24</sup>Mg(<sup>16</sup>O,<sup>12</sup>C) 0-68622
- <sup>28</sup>Si excitation functions, ang. distrib., resonance spin assignments from <sup>24</sup>Mg(<sup>16</sup>O,<sup>12</sup>C) 0-68623
- <sup>28</sup>Si resonance wave functions from differential cross sections of <sup>27</sup>Al(p,X), X=p,n,α 0-78239
- <sup>28</sup>Si(e,e'), 6<sup>-</sup> T=1 resonance form factor, mag. strength quenching, meson exchange currents 0-86882
- <sup>28</sup>Si(n,γ), 565, 813 keV, resonance γ, spectra, valence model test 0-63124

**nuclear resonances continued**

- Sm(p,t), even isotopes, high energy neutron pairing strength, two neutron holes, resonances 0-78116
  - <sup>230</sup>Th(n,f), 0.68-1.10 MeV, fission fragment ang. distrib., resonance and moment of inertia 0-102219
  - <sup>238</sup>U subbarrier photofission, cross section and half-life, double hump model 0-102217
  - <sup>238</sup>U(n,f), 5 eV-2.5 MeV, fission cross section, fission barrier second well parameters, resonances 0-63217
  - <sup>66</sup>Zn muonic atom, dynamical E0 excitation, E0 resonances, muonic X-rays 0-95749
- nuclear scattering see nuclear reactions and scattering**
- nuclear scattering involving few nucleon systems**
- four nucleon system, reactions and scatt. using K-matrix formalism, differential cross sections (Russian) 0-106027
  - <sup>1</sup>H(d,d), 5-45 MeV deuteron wave function asymptotic D- to S-state normalisation, anal. power 0-78304
  - <sup>1</sup>H(n,p), 63.1 MeV, differential cross section 0-63186
  - <sup>1</sup>H(n,n), 16.9 MeV, anal. power, F-wave contribs. 0-63158
  - <sup>1</sup>H(n,n), pol. n, 13.5-16.9 MeV, anal. power and spin-orbit phase parameters 0-78269
  - <sup>1</sup>H(n,n), pol. n, 50 MeV, anal. power 0-68639
  - <sup>1</sup>H(n,p), pol. n,p, 50 MeV, spin correlation parameter A<sub>yy</sub>(θ), phase shift anal. 0-68530
  - <sup>1</sup>H(p,p), 1-3 GeV/c, pol. p, spin parameters A and A<sub>nn</sub> 0-95304
  - <sup>1</sup>H(p,p), 6.141 MeV, anal. power, Paris pot. predictions 0-63156
  - <sup>1</sup>H(p,p), pol.p, 9.57 MeV, spin correlation parameter, phase shift anal. 0-102112
  - <sup>2</sup>H(n,n), (n,p), 24 MeV, quasifree scatt., n-n effective range, Monte Carlo anal. 0-68554
  - <sup>2</sup>H(p,p), 800 MeV, differential cross sections and anal. powers 0-83091
  - <sup>2</sup>H(p,p), pol.p, spin rot. and depolarisation, NN amplitude double spin flip part 0-78271
  - <sup>2</sup>H(p,p), tensor asymmetries, deuteron D-wave and non-eikonal effects, Glauber model 0-78296
  - <sup>2</sup>H(p,p) large angle elastic scatt., d form factor at large q<sup>2</sup> 0-102189
  - <sup>2</sup>H(p,γ), elastic cross sections, bremsstrahlung, threshold and Coulomb effects 0-91186
  - <sup>3</sup>H(n,n), scatt. length, 4-nucleon problem, integral eqn. approach 0-91183
  - <sup>3</sup>H(n,n), zero energy total cross section and scatt. lengths 0-57778
  - <sup>3</sup>H(p,p), 1.24 GeV, differential cross section, spin indep. Glauber model interpretation 0-63183
  - <sup>3</sup>He(<sup>3</sup>He, <sup>3</sup>He), 120 MeV, continuum energy spectra bump struct., cross sections 0-83108
  - <sup>3</sup>He(n,n), scatt. length, 4-nucleon problem, integral eqn. approach 0-91183
  - <sup>4</sup>He(α,α), nuclear separable plus Coulomb interaction 0-83106
  - <sup>4</sup>He(α,α), s-wave, Coulomb amplitudes from generator coordinate theory 0-83107
  - <sup>4</sup>He(α,α), size change of α effect on phase shift, generator coordinate and variational methods (Chinese) 0-68683
  - <sup>4</sup>He(d,d), distortion effects, orthogonality condition model 0-63190
  - <sup>4</sup>He(d,d), low energy, resonating group method anal. with distortion effect 0-73851
  - <sup>4</sup>He(p,p), 200-500 MeV, differential cross section and anal. power 0-68640
  - <sup>4</sup>He(p,p), 788 MeV, back angle diffraction struct., Dirac, eqn. optical model 0-68667
- nuclear screening**
- atomic quadrupole shielding factors calc. using elec. field variant orbitals 0-106276
  - atoms in molecules, diamag. shieldings rel. to electronegativity 0-102524
  - cation rad. verification using screened nucl. charge model 0-59944
  - Coulomb gas 2-D, interaction potential, screening length, critical temp. 0-62571
  - finite ligand size and the Sternheimer antishielding factor γ<sub>∞</sub> 0-103653
  - ionic crystals, Sternheimer quadrupole shielding-antishielding function for F<sup>-</sup>, Cl<sup>-</sup>, Br<sup>-</sup>, and I<sup>-</sup> 0-80236
  - line broadening theory, screening process dynamics (Russian) 0-69988
  - methane, nucl. elec. shielding tensor calcs. 0-83296
  - methane, rotational state, avoided-crossing molecular beam spectroscopy 0-63730
  - 3-methyl lumiflavin, in soln., absorpt. spectrum 0-58277
  - methylamine, C-N and N-H bond nucl. mag. isoscreening line diagrams 0-78555
  - nuclear magnetic shielding density 0-63559
  - pair production near threshold screening effects, partial wave calc., energy shift screening theory 0-57768
  - picnic atoms, electron screening and inner shell refilling, X-ray 0-78729
  - Slater's calculations, improved screening-loss parameter calc. 0-83271
  - CO, nucl. elec. shielding tensor calcs. 0-83296
  - Cl<sup>-</sup>, atomic core states, antishielding effects calcs. 0-83299
  - H<sub>2</sub>O, nucl. elec. shielding tensor calcs. 0-83296
  - <sup>197</sup>Ir 129 keV transition, atomic screening, time reversal violation 0-106011
  - Li<sup>+</sup>-ligand complexes, NMR appl. <sup>7</sup>Li chemical shifts, expt. and ab initio studies 0-63670
  - Mg<sup>2+</sup> atomic core states, antishielding effects calcs. 0-83299
  - NH<sub>3</sub>, nucl. elec. shielding tensor calcs. 0-83296
  - Na<sup>+</sup>, atomic core states, antishielding effects calcs. 0-83299
  - Sn, internal conversion coeffs. for inner shells of atomic ions and relativistic ionic potentials 0-68600
  - ZnS, <sup>67</sup>Zn and <sup>33</sup>S nuclear magnetic shielding, chemical shifts and linewidths 0-60434
  - ZnSe, <sup>67</sup>Zn nuclear magnetic shielding, chemical shifts and linewidths 0-60434
  - ZnTe, <sup>67</sup>Zn nuclear magnetic shielding, chemical shifts and linewidths 0-60434
- nuclear shape**
- see also nuclear collective states and giant resonances; nuclear energy levels; nuclear resonances*
- A=12-240, even-even, dynamic deformation theory, B(E2) values, quadrupole and mag. moments 0-68591
  - actinide nuclei, cranking model, collective inertia parameters 0-57665
  - actinide nuclei, even-even, E<sub>2</sub> transitions from 2<sup>+</sup> state of gamma-vibrational band 0-91150
  - binary fission saddle points, shape parametrization for liquid-drop studies 0-106086
  - collective model, two-phonon states, effect of Pauli principle 0-68565

**nuclear shape continued**

- conference on medium heavy nuclei structure, Rhodes, Greece (May 1979) 0-67935
- conference on nuclear physics, Mikolajki, Poland (2-14 Sept. 1979) 0-101662
- decoupling model for fission fragment transitional nuclei, odd-odd and even mass 0-78174
- deformation, large amplitude collective motion in a nontrivial schematic model 0-73816
- deformed and superdeformed nuclei from heavy ion reactions,  $\alpha$ -decay amplification 0-102156
- deformed nuclei, absorption of slow  $\pi^-$ , mesic atoms 0-78321
- deformed nuclei, constrained HF energies, two-step iterative method 0-83053
- deformed nuclei, effect on Coriolis interaction, Nilsson model and Woods-Saxon pot. calcs. 0-63071
- deformed nuclei, improved parametrisation of Woods-Saxon pot. 0-86823
- deformed nuclei, polarisation, and energy shifts in muonic atoms 0-86893
- deformed nuclei, single particle level blocking in BCS approx. 0-99117
- deformed nuclei, yrast level ground state correlations, RPA anal. 0-86777
- doubly even deformed nuclei, excited states, Pauli principle effects, quasi-particle-phonon model 0-63094
- ellipsoidal, liquid-drop model, irrotational incompressible hydrodynamic flow 0-83050
- even-even neutron-rich fission products, de-excitation spectra,  $\beta$ -decay, deformation 0-78203
- fissioning nucleus, deformation process mass parameter, liquid drop model 0-102221
- governor model for asymmetric deformed nuclei, band anal. 0-86776
- growth points in nuclear physics, book 0-94928
- large deformations, single particle levels, self-consistent field rearrangement, HF method 0-78107
- light deformed nuclei, Skyrme interaction spin components, spectra, projected HF theory 0-73820
- N=5 shell, deformed odd-neutron nuclei, band ordering and spectrum 0-83018
- N=82 region, high spin isomers, deformation energy surface, shape constrained cranked HF theory 0-57666
- neutron rich nuclei;  $\beta^-$ -emitters, deformation and spectroscopy 0-78223
- neutron rich transitional fission fragments, spectroscopy,  $0^+$  states and octupole vibr. 0-78204
- odd nuclei, soft and deformed, rotor plus quasiparticle approach, moments, transition probabilities 0-78214
- potential energy surfaces, folded Yukawa-plus-exponential model 0-86816
- radial wave functions of valence nucleons 0-73788
- rare earth deformed nuclei, high spin region excited rot. bands, RPA calcs. 0-78108
- rare earth nuclei, cranking model, collective inertia parameters 0-57665
- rare earth nuclei, even-even,  $E_2$  transitions from  $2^+$  state of gamma-vibrational band 0-91150
- rare earth nuclei, modified oscillator pot. parameters, single particle levels 0-68509
- rare earths, nuclear deformation, Coulomb displacement energy depend., shell model 0-102108
- spherical nuclei, fragmentation of hole states in quasiparticle-phonon model 0-83020
- spherical nuclei, quasi-particle theory, modification of BCS basis 0-63109
- spherical nuclei, quasiparticle-phonon model, iterative method 0-68566
- Woods-Saxon potential spectrum, pairing force strength, Nilsson model comparison 0-57704
- $^{103}\text{Ag}$  high spin states, bands transitions, intermediate deformation Coriolis coupling from ( $^3\text{He}$ , xny) 0-105944
- $\text{Au}$ , odd isotones, deformation pot. energy from Nilsson model 0-57676
- $^{40}\text{Ca}$ , magic nuclei at collective excitations, energy spectrum and shape (Russian) 0-106015
- $^{59}\text{Co}$ , deformation effect from fast neutron transmission in 0.8 to 20 MeV range 0-57675
- $^{51}\text{Cr}$ , EM properties, lifetimes of 749 and 777 keV levels, E2/M1 mixing ratio 0-63127
- $^{4}\text{Cs}$ , A=142, 144, 146, low lying levels,  $J^\pi$ , mixing ratios and  $\gamma$ - $\gamma$  ang. correlations 0-102119
- Dy deformed nuclei, particle ang. momentum alignment effects 0-68522
- Er, deformed nuclei, particle ang. momentum alignment effects 0-68522
- $^{151}\text{Eu}$  narrow band and pickup strength, shape coexistence from (d,t) 0-86799
- $^{151}\text{Eu}$   $5/2^+$  ground state rot. band,  $J^\pi$ , shape coexistence from (d,p) 0-86799
- $^{56}\text{Fe}$ (p,p), 6 MeV, elastic and inelastic, quadrupole deformation, IAR excitation, optical pots. (Russian) 0-63149
- $^{252}\text{Fm}$ , pot. energy surface, liquid model, deformation energy formulae (Chinese) 0-102106
- Ge isotopes, shape transition and quadrupole softness, Hartree Bogoliubov calc. 0-68527
- $^{\text{H}}$  scattering, deformed tensor interactions, folding model 0-57783
- $^{\text{Hg}}$ , A=190-200, even, phase transition and possible triaxial shape, energy levels 0-63098
- Ir, odd isotones, deformation pot. energy from Nilsson model 0-57676
- MO, onset of deformation at A~100 0-73790
- $^{24}\text{Mg}$ , low spin rotational states, energy props., extended deformation model 0-86785
- $^{24}\text{Mg}$ , triaxial nuclei rots., extended cranked shape consistent oscillator model 0-102133
- $^{\text{Mo}}$ , A=98,102, anal. powers, transitions, shape coexistence states, DWBA anal. of Mo(t,p), pol. t 0-86895
- $^{\text{Nd}}$ , A=138,139, high spin states,  $J^\pi$ ,  $\gamma$ -cascades and shape transition from  $^{140}\text{Ce}$ ( $\alpha$ , xn) 0-102090
- $^{20}\text{Ne}$  hexadecapole moments, quadrupole deformation effects, E4 effective charge, valence polarisation 0-78142
- $^{56}\text{Ni}$  from HI reactions, superdeformed nucleus decay,  $\alpha$ -decay amplification 0-68608
- $^{58}\text{Ni}$  ( $^7\text{Li}$ ,  $^7\text{Li}$ ), 14.22 MeV, alignment axis orientation depend. of cross section, mass quadrupole moment alignment 0-68638
- $^{58}\text{Ni}$ ( $^6\text{Li}$ ,  $^6\text{Li}$ ), 71 MeV, excited states deformation lengths, DWBA and coupled channels anal. 0-68541
- $^{58}\text{Ni}$ (p,p), 800 MeV, elastic and inelastic, cross section, deformation lengths, optical and DWBA anal. 0-68664
- $^{16}\text{O}$ , magic nuclei at collective excitations, energy spectrum and shape (Russian) 0-106015
- $^{\text{Os}}$ , A=182, 184, 186, high spin yrast states, back-bending 0-86802

**nuclear shape continued**

- $^{\text{Pm}}$ , A=149,151, shape coexistence, deformed states from Nd decay 0-78135
- $^{141}\text{Pm}$  medium spin states,  $J^\pi$ , transitions and shape from (p,2n), ( $^3\text{He}$ ,3n), ( $\alpha$ ,4n) 0-86779
- $^{139}\text{Pr}$  medium spin states,  $J^\pi$ , transitions and shape from (p,2n), ( $^3\text{He}$ ,3n), ( $\alpha$ ,4n) 0-86779
- $^{195}\text{Pt}$  low lying negative parity states and shape from  $^{195}\text{Pt}$ (p,t) 0-68540
- Re, odd isotones, deformation pot. energy from Nilsson model 0-57676
- Ru, even isotopes, potential energy surfaces and ground state equilib. deformation 0-73789
- $^{\text{Ru}}$ , A=106, 108, levels, transitions,  $J^\pi$  and shape from Tc decay 0-57744
- $^{32}\text{S}$  shape isomeric state from unconstrained variation 0-95306
- $^{\text{Sm}}$ ( $^{\text{Ar}}$ ,X) A=144, 148, 154, 3.6-4.5 MeV/A, sub-barrier fusion, evaporation residue cross section, deformation 0-68718
- $^{\text{Sn}}$ (n,n'), A=116, 118, 120, 122, 124, 11 MeV, levels, deformation parameters, isospin effects, optical parameters 0-57679
- $^{\text{Sn}}$ (n,n'), A=116, 118, 120, 122, 11 MeV, octupole vibr. states, diff. cross section, deformation length, DWBA anal. 0-102092
- Sr, even isotopes, potential energy surfaces and ground state equilib. deformation 0-73789
- $^{79}\text{Sr}$ , mass excess values from beta and gamma spectra from  $^{32}\text{S}+^{46}\text{Fe}$ ( $^{58}\text{Ni}$ ) 0-63137
- $^{88}\text{Sr}$ (n,n'), 11 MeV, octupole vibr. states, diff. cross section, deformation length, DWBA anal. 0-102092
- $^{90}\text{Sr}$  very low lying  $0^+$  state, shape coexistence bands,  $T_{1/2}$ , transitions from  $^{90}\text{Rb}$  decay 0-78148
- $^{149}\text{Tb}$  from HI reactions, superdeformed nucleus decay,  $\alpha$ -decay amplification 0-68608
- $^{232}\text{Th}$ ( $\gamma$ ,X) 5-18.3 MeV, photoneutron and photofission cross sections, giant resonance and deformations 0-68712
- Ti, odd isotones, deformation pot. energy from Nilsson model 0-57676
- $^{\text{U}}$ ( $\gamma$ ,X), A=235, 236, 238, 5-18.3 MeV, photoneutron and photofission cross sections, giant resonance and deformations 0-68712
- $^{235}\text{U}$ , pot. energy surface, liquid model, deformation energy formulae (Chinese) 0-102106
- $^{236}\text{U}$  shape isomer,  $\gamma$  branch upper limit,  $\gamma$ -yields from  $^{235}\text{U}$ (d,p) 0-99145
- $^{238}\text{U}$  collective and deformation props., general collective model 0-86827
- $^{\text{W}}$ (e,f), A=182,184,186, 35-55 MeV, fission barriers, pairing strength deformation depend., stat. anal. 0-57810
- $^{184}\text{W}$ ( $^{12}\text{C}$ , $^{12}\text{C}$ ), 70 MeV,  $4^+$  state excitation ang. distrib., hexadecapole deformation length effects 0-68521
- $^{\text{Y}}$ , A=82, 83, mass excess values from beta and gamma spectra from  $^{32}\text{S}+^{46}\text{Fe}$ ( $^{58}\text{Ni}$ ) 0-63137
- Zr, even isotopes, potential energy surfaces and ground state equilib. deformation 0-73789
- Zr, onset of deformation at A~100 0-73790
- $^{90}\text{Zr}$ (n,n'), 11 MeV, octupole vibr. states, diff. cross section, deformation length, DWBA anal. 0-102092

**nuclear shell model**

- A=18, shell-model spectra, one-boson-exchange potential 0-68550
- A=42, multiple scattering formalism for the effective interaction 0-102126
- A=50 to 150, shell, dynamical deformation and interacting boson models, limitations 0-68563
- A=90 region, N=50, shell model calcs. 0-68564
- analogue states and resonances in semimicroscopic shell model (Russian) 0-86872
- deformed nuclei, effect on Coriolis interaction, Nilsson model and Woods-Saxon pot. calcs. 0-63071
- deformed nuclei, improved parametrisation of Woods-Saxon pot. 0-86823
- deformed nuclei, polarisation, and energy shifts in muonic atoms 0-86893
- deuteron form factors and spectroscopic factors in heavy spherical nuclei, shell model (Russian) 0-63078
- doorway states, energy dependence of inelastic cross-section, shell model, coupled channel anal. 0-73854
- eigenvalue distribution in scalar space for noninteracting and interacting bosons 0-78177
- energy level densities, shell effects and pairing effects, SCF theory of statistical thermodynamics (Chinese) 0-63088
- giant dipole resonance decoupling and threshold states in schematic and shell models 0-78245
- heavy ion reactions, two-particle transfer, overlap functions, DWBA anal. 0-73862
- interacting boson model, monopole and quadrupole pairing 0-73812
- Kalamoukis tests of Davidson algorithm, comments, nuclear structure 0-86822
- l-forbidden M1 transitions, shell effects, reduced transition probabilities 0-68594
- mean field near Fermi surface, energy dependence, single-particle quantities, Brueckner-Hartree-Fock calcs. 0-68572
- neutron gas, crystallisation, zero-order, Bethe-Fermi homework potential 0-63117
- odd mass nuclei,  $1g_{7/2}^+$  shell region, low lying states, anharmonic effects 0-57687
- odd-odd fission products, level schemes, rot. bands, shell model states 0-78167
- rare earths, nuclear deformation, Coulomb displacement energy depend., shell model 0-102108
- sd-shell nuclei heavy-ion reaction resonances, low level density regions, shell model 0-57757
- spin rotation, high angular velocity, collective aspects of heavy ion collisions 0-78309
- stable odd-mass sd nuclei, EM multipole moments of ground states 0-102116
- symplectic collective model, irreducible U(3) tensor interactions 0-83048
- two nucleon reduced widths, symm. two-centre shell model 0-105994
- two-nucleon reduced widths in the asymmetric two-center shell model 0-63107
- valence nucleons, radial wave functions 0-73788
- Woods-Saxon potential for  $^{40}\text{Ca}$  and  $^{48}\text{Ca}$  0-63106
- ( $\alpha$ ), folding potentials, Woods-Saxon and squared Woods-Saxon parametrisations 0-102195
- (e,e),  $^{41}\text{Ti}$ ,  $^{51}\text{V}$ ,  $^{59}\text{Co}$ ,  $^{87}\text{Sr}$ ,  $^{93}\text{Nb}$  nuclei, exchange current effects, plane wave Born approx. 0-78282
- (e,e), c.m. motion effects in oscillator shell model 0-106050
- (e,e'), 70 MeV, 1p shell nuclei, shell model cross sections, giant M2, transversal E1 resonances 0-63143



nuclear shell model continued

(e,e'), cross section near quasielastic maximum, shell and optical models (Russian) 0-91179  
21Al, effective M3 matrix elements and transitions from shell model 0-102143  
26Al, sd-shell nuclei, stellar weak interaction rates, appl. to supernovae 0-82336  
243Am(n,f), low energy, far-out asymmetric mass distrib. 0-83132  
Au, odd isotones, deformation pot. energy from Nilsson model 0-57676  
8Be 1+ and 1- levels, expt. and shell model calcs. from 7Li(p,γ) 0-63095  
209Bi(136Xe,X), deeply inelastic collisions, mass transport, shell effects 0-99188  
4Ca, A=40 to 48, giant multipole resonances, mass dependence of energy weighted sums 0-63144  
4Ca, A=47, 49, single particle states lifetimes calcs. 0-105943  
4Ca, E2 core polarisation charge, Woods-Saxon shell model compared to harmonic oscillator model 0-63072  
4Ca, collective states, quasi-degenerate intrinsic Hamiltonian, variational methods 0-68505  
232Cf fission, spontaneous, far-out asymmetric mass distrib. 0-83132  
51Cl, A=34, 38, effective M3 matrix elements and transitions from shell model 0-102143  
4Dy, A=161, 163, Nilsson state ΔN=2 mixing, rot. bands from (d,t), (d,p) 0-95295  
166Er(86Kr,X), deep inelastic collision, charge drift and dispersion calc., thermal eqn. model based on shell model 0-57798  
54Fe(He,p), 56Co particle-hole states, T=1, zero DWBA anal. 0-78308  
56Fe, fp shell model calcs., spectra and spectroscopic factors 0-68588  
56Fe(e,e'), Coulomb form factor for O+→4+ transition, collective 4+ states, shell model 0-57664  
Ga, odd, single particle and collective degrees of freedom, clustering, shell model anal. 0-68510  
4Gd, A=146,147, mass and Z=64 shell closure from 144Sm(12C,910Be) 0-57669  
146Gd region, proton subshell effects from α-decay and spectroscopy, self-consistent study 0-57748  
Ge, odd, single particle and collective degrees of freedom, clustering, shell model anal. 0-68510  
4He (e,pp) reaction cross-section and ground state shell model calcs. (Russian) 0-78283  
4He(α,α), size change of α effect on phase shift, generator coordinate and variational methods (Chinese) 0-68683  
Ir, odd isotones, deformation pot. energy from Nilsson model 0-57676  
3K, effective M3 matrix elements and transitions from shell model 0-102143  
4K, single particle states lifetimes calcs. 0-105943  
6Li, supermultiplet struct. and decay props. of hypernuclear 1+ resonances from (K-,π-) 0-78186  
6Li(e,e), elastic and inelastic charge form factors from shell model wave functions 0-68523  
24Mg, low spin rotational states, energy props., extended deformation model 0-86785  
24Mg rotational band collectivity, shell model excitation in Sp(4, R) symmetry 0-102095  
24Mg transition strength n and p components, π+ inelastic scatt. comparison, shell model 0-68585  
24Na, effective M3 matrix elements and transitions from shell model 0-102143  
26Ne collective motion, B(E2) rates, algebraic formulation in symplectic shell model 0-83015  
Ni, fp shell model calcs., spectra and spectroscopic factors 0-68588  
56Ni(d,α), 56Co particle-hole states, T=1, zero DWBA anal. 0-78308  
4Np(n,f), A=234, 235, low energy, far-out asymmetric mass distrib. 0-83132  
4O, A=16, 17, valence-core self-consistency, wave functions, binding energy, levels, spectra 0-63123  
16O independent particle shell model momentum density distrib., short range correlations 0-78176  
16O, rotational band collectivity, shell model excitation in Sp(4, R) symmetry 0-102095  
18O, transition strength n and p components, π+ inelastic scatt. comparison, shell model 0-68585  
19Os level scheme and transitions, Coriolis coupled Nilsson states from 19Os(n,γ) 0-57698  
4Pb, A=202, 204, spectra from multistep shell model method 0-78194  
208Pb shell structure, effect on magicity of superheavy nuclei 0-78175  
209Pb excited states, 3/2- resonances from shell model of 208Pb(n,n) 0-78240  
4Pm, A=143, 145, proton states and transitions, stripping strength, shell model anal. from Nd(He,d) 0-68508  
4Pm, A=143-153, odd-A, spectroscopic factors, shell model anal. from pickup and stripping reactions 0-78137  
239Pu(n,f), far-out asymmetric mass distrib. 0-83132  
Re, odd isotones, deformation pot. energy from Nilsson model 0-57676  
212Rn, shell model states, semiempirical calcs. half lives, mag. moments, excitation functions 0-63083  
96Ru level structure, spin and parity, from beta decay of 94Rh isomers 0-57747  
Sb, neutron rich nuclei, IBM and shell model approaches, collective modes 0-78129  
4Sc, single particle states lifetimes calcs. 0-105943  
4Sm, A=146,147, excited states, energy levels, spin, parity, shell and cluster-vibration models, from (α,xn) and (He,xn) 0-57683  
4Sn(135Cl), 108 MeV, A=112-124 even isotopes, 2+ mag. moments and shell model struct. 0-86805  
Ti, odd isotones, deformation pot. energy from Nilsson model 0-57676  
4U(n,f), A=235, 238, low energy, far-out asymmetric mass distrib. 0-83132  
238U(238U,X), 7.42 MeV/N, mass transport, shell effects, anharmonic pots. 0-99187  
238U(238U,X) deeply inelastic collisions, mass transport, shell effects 0-99188  
238U(84Kr,X), mass fragmentation, dynamical theory, two centre shell model, binary decay process 0-68628  
51V(p,p'), 6 MeV, levels, spins and EM props., shell model anal. 0-63092

nuclear size

alkali metal radioisotopes, hyperfine spectroscopy, nucl. props. 0-57677  
growth points in nuclear physics, book 0-94928

nuclear size continued

light natural elements, muonic X-ray transitions, nuclear charge radii 0-99589  
potential energy surfaces, folded Yukawa-plus-exponential model 0-86816  
short-lived isotopes, laser spectroscopy in fast atomic beams and resonance cells 0-57700  
stellar dense matter, nuclear size effect rel. to neutron stars limiting mass 0-101611  
Ba, radioisotopes, at. beam laser spectroscopy, hyperfine struct., nucl. moments and radii 0-57678  
Ca, stable and radioisotopes, hfs, isotope shifts, dye laser saturation spectroscopy, beam expt. 0-58169  
4Ca, A=40, 48, single particle levels, rms charge radius, Wood-Saxon pot. 0-63106  
4Ca, A=40 to 46,48, nuclear charge distrib., from isotope shift of 6573 angstrom line 0-57674  
4Ca(α,α), A=40, 42, 44, 48, 104 MeV, cross sections and optical pots., nuclear size 0-68524  
4Ca(α,α), A=40, 42, 44, 48, 104 MeV nuclear size and density distrib. from folding model anal. 0-68525  
4Cl(e, e'), 116, 194 MeV, A=35, 37, charge distrib. and RMS charge radius 0-102109  
6Li, transition probabilities between cluster structure states and r.m.s. radii, double well-cluster model (Chinese) 0-63128  
Ni mean square charge radii from isotope shifts 0-99484  
60Ni, Coulomb contributions to nuclear radii and energies 0-68515  
4O(π+,π+), A=16, 18, resonance region, proton and neutron distrib. 0-91195  
28P, nucleon unbound states, spin, parity, partial width, from 28Si(d,pn) 0-102118  
294Pu, muonic atom direct electroprod., finite nuclear size effects (Russian) 0-69272  
32S α-cluster struct., ground and first excited states, energies, radii and moments 0-102122  
28Si, nucleon unbound states, spin, parity, partial width, from 28Si(d,pn) 0-102118  
4Sm, A=144-154, mean square nuclear charge radius, laser atomic beam spectroscopy 0-102468  
Sn(p,n), even isotopes, 4-10 MeV, cross sections, optical parameters and nuclear radius A-depend. 0-57773  
Sn(p,p), pol.p. 6.77-8.8 MeV, cross sections, optical parameters and nuclear radius A-depend. 0-57773  
87Sr 1 g9/2 neutron distrib. radial size, states, differential cross sections from 86Sr(18O,17O) 0-95301  
232Th(γ,X) 5-18.3 MeV, photoneutron and photofission cross sections, giant resonance and deformations 0-68712  
4U(γ,X), A=235, 236, 238, 5-18.3 MeV, photoneutron and photofission cross sections, giant resonance and deformations 0-68712  
68Zn(He,He), elastic and inelastic scatt. angular distrib. fine struct. 0-106063

**nuclear spallation**  
A=23 to 127, photospallation, 0.1 to 1 GeV, mass yield distrib. 0-73835  
St. Severin chondrite, 55Mn production due to nucl. spallation, depth-depend. 0-82316  
(p, spallation), 480 MeV, medium to heavy mass targets, deep spallation products 0-83085  
197Au(20Ne, spallation), 8.0 GeV, cross sections and target residues, model comparison 0-68630  
197Au(p,X), 0.2-6.0 GeV, product cross sections, mass yields, spallation products 0-83088  
C(π,πp), 170 MeV, two stage and knock out contribs., π+,π- spallation differences (Russian) 0-68632  
123I production from 123Xe formed in spallation reactions by 660 MeV protons, medical apps. 0-85494  
N(π,πp), 170 MeV, two stage and knock out contribs., π+,π- spallation differences (Russian) 0-68632  
O(π,πp), 170 MeV, two stage and knock out contribs., π+,π- spallation differences (Russian) 0-68632  
181Ta(20Ne, spallation), 8.0 GeV, cross sections and target residues, model comparison 0-68630

**nuclear spectroscopic factors**  
deuteron form factors and spectroscopic factors in heavy spherical nuclei, shell model (Russian) 0-63078  
double stripping core independ. 2-nucleon transfer, Tang-Herndon effective interactions, (α,d), (t,p) 0-73836  
fission isomers, spectrosc. props. 0-105966  
(α,2α), A=9, 12, 16, 20, 22 0-68629  
(d,He), A=144-238, alpha-cluster transfer from alpha-decaying nuclei 0-91166  
27Al isobaric analogue resonances, spectroscopic factors and γ-rays from (p,p), (p,γ) 0-86873  
209Bi levels and spectroscopic factors, 210Bi(9-) parentage from 210Bi(m,d,t) 0-78158  
209Bi single particle levels, ang. distrib., spectroscopic factors, DWBA anal. of 208Pb(He,He) 0-63067  
209Bi(He,d), 30 MeV, effective residual interaction matrix elements, spectroscopic factors, cross sections 0-99134  
209Bi(α,t), 40 MeV, effective residual interaction matrix elements, spectroscopic factors, cross sections 0-99134  
40Ca(11B,10B), 51.5 MeV, n stripping, DWBA anal. with Woods-Saxon and double folding optical pots. 0-102171  
40Ca(11B,12C), 51.5 MeV, p pickup, DWBA anal. with Woods-Saxon and double folding optical pots. 0-102171  
Cd 2+ excitation, α-spectroscopic factors in IBA model from Sn(d,He) 0-105967  
56Co, (3/2+ state), anomalous analyzing power, DWBA calc. from 56Ni(p,α) 0-86894  
51Cr levels, spectroscopic function and analogue states, PWBA anal. of 52Cr(He,α) 0-68547  
55Fe levels, Jπ, spectroscopic factors, DWBA anal. of 56Fe(He,α) 0-99127  
56Fe, fp shell model calcs., spectra and spectroscopic factors 0-68588  
4In, A=119, 121, unified model description, vibr. multiplet yrast struct., branching ratios 0-105953  
6Li(n,γ), cross section and spectroscopic factors from direct capture pot. model 0-99171  
6Li(p,γ), cross section and spectroscopic factors from direct capture pot. model 0-99171  
6Li(p,pd), 670 MeV, large angle quasifree scatt., spectroscopic factor, momentum distrib., cluster model 0-63184

**nuclear spectroscopic factors continued**

- <sup>8</sup>Mg(d,<sup>4</sup>Li), 80 MeV, A=24,26,  $\alpha$ -spectroscopic factors and ang. distrib., DWBA anal. 0-99126
- <sup>92</sup>Nb low lying multiplets, DWBA anal. for spectroscopic factors from <sup>91</sup>Zr( $\alpha$ ,t) 0-57685
- <sup>4</sup>Nd, A=145, 147, 149, single neutron hole states spectroscopic factors, DWBA anal. of (d,t), (<sup>3</sup>He, $\alpha$ ) 0-78109
- Ni, fp shell model calcs. spectra and spectroscopic factors 0-68588
- <sup>18</sup>O  $\alpha$ -cluster states, widths and resonances, optical model, direct transfer in <sup>17</sup>C(<sup>6</sup>Li,d) 0-105975
- <sup>30</sup>P positive parity states, transitions and spectroscopic strengths, DWBA anal. of <sup>28</sup>Si(<sup>3</sup>He,d) 0-102138
- <sup>208</sup>Pb single particle and hole states, renormalisation, core polarisation, spectroscopic factors 0-57658
- <sup>208</sup>Pb(<sup>3</sup>He,d), 30 MeV, effective residual interaction matrix elements, spectroscopic factors, cross sections 0-99134
- <sup>208</sup>Pb(<sup>6</sup>Li,d), 90 MeV, alpha-cluster transfer from alpha-decaying nuclei 0-91166
- <sup>208</sup>Pb( $\alpha$ ,t), 40 MeV, effective residual interaction matrix elements, spectroscopic factors, cross sections 0-99134
- <sup>4</sup>Pm, A=143-153, odd-A, spectroscopic factors, shell model anal. from pickup and stripping reactions 0-78137
- <sup>48</sup>Sc proton single particle states, spectroscopic factors, DWBA anal. of <sup>47</sup>Ca(d,n) 0-99118
- <sup>28</sup>Si levels, J<sup>+</sup>, spectroscopic factor, DWBA anal. of <sup>28</sup>Si(<sup>3</sup>He, <sup>2</sup>He) 0-86811
- Sn <sub>2,1</sub><sup>+</sup> excitation,  $\alpha$ -spectroscopic factors in IBA model from Te(d,<sup>4</sup>Li) 0-105967
- <sup>131</sup>Te  $\gamma$ -transitions, spectroscopic factors and reduced transition intensities from <sup>130</sup>Te(n, $\gamma$ ) 0-91143
- <sup>4</sup>Ti, A=44, 48, ang. distrib. for transitions, DWBA anal., spectroscopic strengths from Ca(<sup>7</sup>Li,t) 0-68584
- <sup>204</sup>Tl neutron hole states, J<sup>+</sup> and spectroscopic factors from <sup>205</sup>Tl(p,d) 0-86783
- <sup>90</sup>Y low lying multiplets, DWBA anal. for spectroscopic factors from <sup>91</sup>Zr(d,<sup>3</sup>He) 0-57685
- <sup>62</sup>Zn ang. distrib. for transitions, DWBA anal., spectroscopic strengths from <sup>58</sup>Ni(<sup>7</sup>Li,t) 0-68584

**nuclear spin and parity**

see also nuclear isospin

- <sup>116</sup>Xe quasi-rotational bands, levels J<sup>+</sup> and T<sub>1/2</sub> from <sup>116</sup>Cs decay 0-83021
- A=73, nuclear data sheets, levels, J<sup>+</sup> and transitions 0-101673
- A=77, nuclear data sheets, levels, J<sup>+</sup> and transitions 0-105439
- A~90 nuclei, isomeric states, spin polarisation, M4 transitions and giant resonances 0-63157
- light deformed nuclei, Skyrme interaction spin components, spectra, projected HF theory 0-7820
- neutron rich fission fragments, excited state spin assignment, various methods 0-78506
- nuclear matter, polarised, thermal props., temp., spin isospin and spin-isospin pressure 0-102135
- nuclear matter, spin-isospin and pion condensation phase transitions, eqn. of state 0-86843
- parity nonconservation in heavy atoms and weak magnetism in neutral currents (*Russian*) 0-82932
- polarised nuclear matter, binding energy, spin energies, relativistic calc. 0-102134
- spin exchange and polarisation changes, RPA breakdown from HF condensation 0-99142
- (n,f), thermal, parity violation from opposite parity rot. states 0-95303
- (n, $\gamma$ ), polarized space parity nonconservation, optical pot. and GDR parameters (*Russian*) 0-86803
- <sup>230</sup>Ac levels, J<sup>+</sup> and transitions, Nilsson assignments from <sup>230</sup>Ra decay 0-68543
- <sup>103</sup>Ag collective excitation and J<sup>+</sup> following <sup>94</sup>Mo(<sup>12</sup>C,p2n $\gamma$ ), rotor-plus-particle model 0-86782
- <sup>104</sup>Ag levels, J<sup>+</sup>, T<sub>1/2</sub>, bands and transitions from <sup>103</sup>Rh( $\alpha$ , 3n $\gamma$ ) 0-102093
- <sup>26</sup>Al 1<sup>+</sup>T=0 states, isobaric analogue state, spin-isospin effective interaction from <sup>26</sup>Mg(p,n) 0-68553
- <sup>26</sup>Al excited states, isobaric analogues, spins, DWBA anal. of <sup>27</sup>Al(<sup>3</sup>He, $\alpha$ ) 0-105981
- <sup>26</sup>Al T=1 states, resonances, J<sup>+</sup> and transitions from <sup>25</sup>Mg(p, $\gamma$ ) 0-99131
- <sup>27</sup>Al levels, resonances, J<sup>+</sup>, branching and mixing ratios from <sup>26</sup>Mg(p, $\gamma$ ) 0-99132
- <sup>28</sup>Al levels, transitions and spin from <sup>27</sup>Al(n, $\gamma$ ), pol. Al and n 0-78153
- <sup>4</sup>As, A=71, 73, levels, J<sup>+</sup>, transitions, T<sub>1/2</sub> from Se decay, Ge(<sup>3</sup>He,d), (p,xn $\gamma$ ) 0-57684
- <sup>76</sup>As levels, J<sup>+</sup> and ang. distrib. from <sup>76</sup>Ge( $\alpha$ ,p) 0-78161
- <sup>213</sup>At levels, J<sup>+</sup>, transitions and lifetimes from <sup>208</sup>Pb(<sup>7</sup>Li,X) 0-68542
- <sup>12</sup>B levels, J<sup>+</sup> and diff. cross sections, R-matrix anal. of <sup>11</sup>B(n,n) 0-78151
- <sup>4</sup>Ba, A=132, 134, 136, negative parity states, J<sup>+</sup>, transitions, DWBA anal. of Ba(p,t) 0-86810
- <sup>4</sup>Ba, A=142,144,146, transition  $\gamma$ - $\gamma$  ang. correlations, levels, J<sup>+</sup>, mixing ratios 0-73823
- <sup>142</sup>Ba,  $\gamma$  $\gamma$  ang. correlations, levels, spins and mixing ratios from <sup>142</sup>Cs decay 0-57734
- <sup>12</sup>C isovector M1 excitations, current and spin contribs. from (e,e'), (p,n) 0-68582
- <sup>12</sup>C, residual interactions, current conserving RPA calculations 0-57710
- <sup>12</sup>C+<sup>12</sup>C system resonant structs., J<sup>+</sup> assignments, true <sup>24</sup>Mg states from <sup>12</sup>C(<sup>12</sup>C, <sup>16</sup>O) 0-99163
- <sup>12</sup>C(<sup>12</sup>C,<sup>12</sup>C'), 18.5-32.8 MeV, spin alignment and possible molecular resonances 0-86804
- <sup>12</sup>C(n,n), spin-flip probability to first 2<sup>+</sup> level 0-78288
- <sup>12</sup>C(p,p $\gamma$ ), 23.5-27 MeV, 1<sup>+</sup> state spin flip meas. DWBA anal., cross sections 0-68529
- <sup>12</sup>C(p,p), 14-45 MeV, differential cross section and spin-flip probabilities, giant resonances 0-73850
- <sup>4</sup>Ca(p,p'), pol. p, A=40,48, 800 MeV, diff. cross sections, anal. powers, DWIA anal., high spin levels 0-83067
- <sup>40</sup>Ca, residual interactions, current conserving RPA calculations 0-57710
- <sup>40</sup>Ca parity doublet gamma lifetimes, 3/2 levels, parity mixing from <sup>40</sup>Ca(d,p $\gamma$ ) 0-78209
- <sup>40</sup>Ca, spin and parity from <sup>38</sup>Ar( $\alpha$ ,n $\gamma$ ) angular distrib. and linear polarisation of  $\gamma$  0-63079
- <sup>45</sup>Ca levels, excitation functions and J<sup>+</sup> from <sup>45</sup>K  $\beta$ -decay 0-105978
- <sup>103</sup>Cd levels, J<sup>+</sup> and positive parity decoupled band, rotor anal. of <sup>104</sup>Mo(<sup>12</sup>C, 3n $\gamma$ ) 0-102096
- nuclear spin and parity continued**
- <sup>250</sup>Cf low spin states, bandheads, J<sup>+</sup> and transitions from <sup>250</sup>Es EC decay 0-105952
- <sup>59</sup>Co level energies, branching ratios lifetimes and spins from (p,p'), ( $\alpha$ ,p $\gamma$ ) 0-63093
- <sup>4</sup>Cr(p,p'), A=50, 52, 6 MeV, elastic and inelastic differential cross sections, spin flip probability (*Russian*) 0-91187
- Cs, ground state spins, moments, charge radii by laser spectroscopy 0-78147
- <sup>4</sup>Cs, A=142, 144, 146, low lying levels, J<sup>+</sup>, mixing ratios and  $\gamma$ - $\gamma$  ang. correlations 0-102119
- <sup>63</sup>Cu(p,p') negative parity level excitation, gamma ray obs., test for core excitation model 0-68534
- <sup>152</sup>Dy, high spin state populations from <sup>124</sup>Sn(<sup>32</sup>S,4n) 0-57660
- <sup>154</sup>Dy N=88 nuclei quasirot. bands and J<sup>+</sup> from beta-decay 0-83025
- <sup>156</sup>Er N=88 nuclei quasirot. bands and J<sup>+</sup> from EC decay 0-83025
- <sup>172</sup>Er levels, bands, J<sup>+</sup> and transitions from <sup>170</sup>Er(t,p) 0-83038
- <sup>153</sup>Eu 5/2<sup>+</sup> ground state rot. band, J<sup>+</sup>, shape coexistence from (d,p) 0-86799
- <sup>18</sup>F resonances,  $\alpha$ -widths, isospin and parity mixing, R-matrix anal. of <sup>14</sup>N( $\alpha$ , $\alpha$ ) 0-91162
- <sup>54</sup>Fe 8<sup>+</sup> and 10<sup>+</sup> level spin assignments and lifetimes from (<sup>16</sup>O,2p), (<sup>6</sup>Li, pn) 0-68531
- <sup>54</sup>Fe levels, J<sup>+</sup>, spectroscopic factors, DWBA anal. of <sup>56</sup>Fe(<sup>3</sup>He, $\alpha$ ) 0-99127
- <sup>54</sup>Fe resonances, levels, J<sup>+</sup>, valence capture  $\gamma$ -ray spectrum from <sup>54</sup>Fe(n, $\gamma$ ) 0-86852
- <sup>56</sup>Fe low lying levels, J<sup>+</sup>,  $\gamma$ - $\gamma$  coincidences, internal conversion from <sup>56</sup>Co  $\beta^+$ -decay 0-86815
- <sup>56</sup>Fe levels, J<sup>+</sup>, anal. powers and cross sections from <sup>56</sup>Fe(t,p) pol.t 0-68539
- <sup>64</sup>Ga high spin states, J<sup>+</sup> and transitions, triaxial struct. from (<sup>12</sup>C, $\alpha$ p), (<sup>7</sup>Li,Zn) 0-63062
- <sup>70</sup>Ga levels, J<sup>+</sup> and ang. distrib. from <sup>70</sup>Zn( $\alpha$ ,p) 0-78161
- <sup>145</sup>Gd levels, J<sup>+</sup> and transitions, neutron hole coupling to <sup>146</sup>Gd core from <sup>144</sup>Sm( $\alpha$ ,3n) 0-78164
- <sup>146</sup>Gd lowest 2<sup>+</sup> state, J<sup>+</sup> and transitions from <sup>146</sup>Tb decay 0-105979
- <sup>152</sup>Gd N=88 nuclei quasirot. bands and J<sup>+</sup> from EC decay and ( $\alpha$ ,xn $\gamma$ ) 0-83025
- <sup>154</sup>Gd levels, bands, J<sup>+</sup>, DWBA anal. of <sup>152</sup>Gd(t,p) 0-78110
- <sup>4</sup>Ge, A=66,69,70, negative parity high spin states, spin and lifetimes from HI reactions 0-73768
- <sup>19</sup>Ge excited state, J, mean lifetimes and transitions from <sup>64</sup>Zn(<sup>7</sup>Li,ph) 0-68517
- <sup>19</sup>Ge excited state, J, mean lifetimes and transitions 0-68517
- <sup>66</sup>Ge levels, lifetimes, J<sup>+</sup> and transitions from <sup>58</sup>Ni(<sup>10</sup>B,pn $\gamma$ ) 0-73799
- <sup>69</sup>Ge high spin states, J assignment, decay scheme from <sup>55</sup>Mn(<sup>16</sup>O,pn) 0-68518
- <sup>1</sup>H(n,p)n, pol. n.p, 50 MeV, spin correlation parameter A<sub>yy</sub>( $\theta$ ), phase shift anal. 0-68530
- <sup>1</sup>H(p,p), 1-3 GeV/c, pol. p, spin parameters A and A<sub>nn</sub> 0-95304
- <sup>1</sup>H(p,p), pol.p, 9.57 MeV, spin correlation parameter, phase shift anal. 0-102112
- <sup>2</sup>H( $\gamma$ ,np), parity violation expts. review, weak NN interaction 0-73792
- <sup>2</sup>H(p,p), pol.p, spin rot. and depolarisation, NN amplitude double spin flip part 0-78271
- <sup>4</sup>H, A=1, 2, nuclear electric dipole moments from P nonconserving atomic transitions 0-57681
- <sup>4</sup>He, T=1 excited negative parity state struct. 0-57688
- <sup>4</sup>He( $\alpha$ ,d), 119 MeV, excited states, J<sup>+</sup> and  $\gamma$ -ang. correlations 0-86809
- <sup>175</sup>Hf, three- and five-quasiparticle isomers, rotational bands and residual interactions from <sup>170</sup>Er(<sup>3</sup>Be, 4n) 0-83022
- <sup>165</sup>Ho(<sup>165</sup>Ho,X), deep inelastic, spin and transferred ang. momentum alignment 0-106043
- <sup>4</sup>Ir, A=189, 191, levels, J<sup>+</sup>, transitions and mixing ratios from Pt decay 0-68602
- <sup>4</sup>K(p,p $\gamma$ ), 1.58 MeV, parity doublet gamma lifetimes, 3/2 levels, parity mixing 0-78209
- <sup>4</sup>K excited levels, J<sup>+</sup>, transitions and lifetimes from <sup>48</sup>Ca(p, $\alpha$ n) 0-68544
- <sup>46</sup>K levels, J<sup>+</sup> and tensor anal. powers from <sup>48</sup>Ca(d, $\alpha$ ), pol.d 0-102113
- <sup>4</sup>Kr, A=79, 81, high spin E2 bands, J<sup>+</sup>, transitions from Ge(<sup>10</sup>B,  $\chi$  $\gamma$ ) 0-63061
- <sup>79</sup>Kr, low lying levels from <sup>77</sup>Br(p,n $\gamma$ ) 0-105972
- <sup>84</sup>Kr levels,  $\gamma$ -cascades, J<sup>+</sup>, mixing ratios and correlations from <sup>84</sup>Br decay 0-63134
- <sup>2</sup>Mg isovector M1 excitations, current and spin contribs. from (e,e'), (p,n) 0-68582
- <sup>2</sup>Mg(<sup>12</sup>C,<sup>12</sup>C'), 35 MeV, 2<sup>+</sup> population probab., spin-flip and spin orbits., coupled channel anal. 0-99125
- <sup>2</sup>Mg(p,p), 14-45 MeV, differential cross section and spin-flip probabilities, giant resonances 0-73850
- <sup>56</sup>Mn low lying 2p-4h states, J<sup>+</sup> from tensor anal. powers of <sup>56</sup>Fe(d, $\alpha$ ), pol.d 0-99124
- <sup>55</sup>Mn levels, transitions and spins from <sup>55</sup>Mn(n, $\gamma$ ), pol. Mn and n 0-78154
- <sup>15</sup>N three particle states at high excitation energies, J<sup>+</sup>, selective population from <sup>12</sup>C(<sup>7</sup>Li,  $\alpha$ ) 0-99129
- <sup>91</sup>Nb low lying multiplets, DWBA anal. for spectroscopic factors from <sup>91</sup>Zr( $\alpha$ ,t) 0-57685
- <sup>4</sup>Nd, A=138,139, high spin states, J<sup>+</sup>,  $\gamma$ -cascades and shape transition from <sup>140</sup>Ce( $\alpha$ , xn) 0-102090
- <sup>12</sup>Ne parity mixing meas. extension review 0-73792
- <sup>20</sup>Ne 13482 keV level, parity violating effects in two resonance interference from <sup>19</sup>F(p, $\alpha$ ) pol. p 0-83033
- <sup>20</sup>Ne low lying levels and intermediate structure J<sup>+</sup> from <sup>16</sup>O(<sup>12</sup>C, <sup>8</sup>Be) 0-102166
- <sup>2</sup>Ne deduced spectroscopic factors, levels and anal. powers from <sup>20</sup>Ne(d,pol.p) 0-83087
- <sup>4</sup>Ni, A=60, 62, 66, levels, J<sup>+</sup>, anal. powers and cross sections from <sup>4</sup>Ni(t,p)pol.t 0-68539
- <sup>54</sup>Ni high spin yrast cascade, decay modes J assignment from <sup>54</sup>Fe( $\alpha$ ,n $\gamma$ ) 0-68514
- <sup>58</sup>Ni(<sup>16</sup>O, X), 70 MeV, compound nuclei charged particle evaporation, moment of inertia 0-57785
- <sup>60</sup>Ni high spin states, J<sup>+</sup>, T<sub>1/2</sub>, ang. distrib. and polarisations from <sup>56</sup>Fe(<sup>7</sup>Li, p2n $\gamma$ ) 0-99116
- <sup>16</sup>O, residual interactions, current conserving RPA calculations 0-57710
- <sup>4</sup>Os, A=188, 189, levels, J<sup>+</sup>, transitions and mixing ratios from Ir decay 0-68602
- <sup>2</sup>P, nucleon unbound states, spin, parity, partial width, from <sup>28</sup>Si(d,pn) 0-102118
- <sup>31</sup>P high E<sub>x</sub> states, J<sup>+</sup>, DWBA anal. <sup>29</sup>Si(<sup>3</sup>He,p) 0-68536



**nuclear spin and parity continued**

- <sup>208</sup>Pb(n,n'), 1.5-3.1 MeV, levels, J<sup>π</sup>, excitation functions and mixing ratios 0-102123
- <sup>208</sup>Pb(p,p'), 135 MeV, normal parity level excitation, J<sup>π</sup>, differential cross sections 0-57690
- <sup>210</sup>Pb levels, J<sup>π</sup>, transitions and lifetimes from <sup>208</sup>Pb(<sup>7</sup>Li,X) 0-68542
- <sup>141</sup>Pr medium spin states, J<sup>π</sup>, transitions and shape from (p,2n), (<sup>3</sup>He,3n), (α,4n) 0-86779
- <sup>145</sup>Pr level struct., J<sup>π</sup> and lifetimes, cluster-vibr. model anal. of <sup>146</sup>Nd(p,2n) 0-91125
- <sup>212</sup>Po, levels, J<sup>π</sup>, transitions and lifetimes from <sup>208</sup>Pb+<sup>7</sup>Li 0-68542
- <sup>139</sup>Pr medium spin states, J<sup>π</sup>, transitions and shape from (p,2n), (<sup>3</sup>He,3n), (α,4n) 0-86779
- <sup>140</sup>Pr isobaric analogue resonances, de-excitation cascade, K-shell ionisation, spin depend. from <sup>140</sup>Ce(p,n) 0-78202
- <sup>141</sup>Pr, positive parity levels, gamma-ray yields and ang. distrib. 0-105962
- <sup>230</sup>Ra levels, J<sup>π</sup> and transitions, Nilsson assignments from <sup>230</sup>Ac decay 0-68543
- Rb, ground state spins, moments, charge radii by laser spectroscopy 0-78147
- <sup>87</sup>Rb(n,n'), 550-2100 keV, A=85,87, levels, excitation functions, J<sup>π</sup>, Hauser-Feshbach anal. 0-105982
- <sup>83</sup>Rb band struct., spin assignments and transitions from (<sup>6</sup>Li,3n), (<sup>16</sup>O,p2n), (α,2n) 0-73774
- <sup>83</sup>Rb high spin states, J<sup>π</sup> and transitions from HI and α reactions 0-105949
- <sup>85</sup>Rb high spin states, yrast cascade, J<sup>π</sup>, γ-transitions from <sup>82</sup>Se(Li,xnγ) 0-73775
- <sup>85</sup>Rb levels, J<sup>π</sup> and transitions from Kr<sup>m.s.</sup>, Sr<sup>m.s.</sup> decay, cluster-vibr. model 0-78162
- <sup>186</sup>Re, A=181,182,187, rotational struct., spin polarization 0-83016
- <sup>186</sup>Ru, A=106, 108, levels, transitions, J<sup>π</sup> and shape from Tc decay 0-57744
- <sup>94</sup>Ru level structure, spin and parity, from beta decay of <sup>94</sup>Rh isomers 0-57747
- <sup>32</sup>S(n,n), spin-flip probability to first 2<sup>+</sup> level 0-78288
- <sup>32</sup>S(p,p), 14-45 MeV, differential cross section and spin-flip probabilities, giant resonances 0-73850
- <sup>41</sup>Sc 2p-1h intermediate struct. resonances, anal. powers, J<sup>π</sup> from <sup>40</sup>Ca(p,γ) 0-86883
- <sup>40</sup>Sc, J<sup>π</sup>=19/2<sup>-</sup> isomer, high-spin precursors, from <sup>29</sup>Si(<sup>16</sup>O,pn) 0-57656
- <sup>45</sup>Sc levels, J<sup>π</sup>, transitions and lifetimes from (p,p')(<sup>3</sup>He,<sup>3</sup>He)(α,α') 0-63091
- <sup>186</sup>Se(d,p,d), A=76,78,80,82, 12 MeV, two-step scatt. process via J<sup>π</sup>=2<sup>+</sup> excited states 0-57781
- <sup>76</sup>Se high spin states, bands, J<sup>π</sup>, transitions and T<sub>1/2</sub> from <sup>71</sup>Ga(<sup>7</sup>Li,2n) 0-105951
- <sup>28</sup>Si(p,p), 14-45 MeV, differential cross section and spin-flip probabilities, giant resonances 0-73850
- <sup>28</sup>Si excitation functions, ang. distrib., resonance spin assignments from <sup>24</sup>Mg(<sup>16</sup>O,<sup>12</sup>C) 0-68623
- <sup>24</sup>Mg isovector M1 excitations, current and spin contribs. from (e,e'), (p,n) 0-68582
- <sup>28</sup>Si(n,n), spin-flip probability to first 2<sup>+</sup> level 0-78288
- <sup>28</sup>Si, nucleon unbound states, spin, parity, partial width, from <sup>28</sup>Si(d,pn) 0-102118
- <sup>152</sup>Sm, A=146,147, excited states, energy levels, spin, parity, shell and cluster-vibration models, from (α,xn) and (<sup>3</sup>He,xn) 0-57683
- <sup>152</sup>Sm, A=147, 149, levels, J, γ-transitions and multipole mixing ratios, γγ correlations from Eu EC decay 0-106012
- <sup>124</sup>Sn(n,n), pol. thermal, parity violation near resonance, DWBA calcs. 0-68528
- <sup>84</sup>Sr, A=94,96 direct and skip cascades, γγ ang. correlations, levels, mixing ratios from Rb decay 0-86851
- <sup>88</sup>Sr(γγ), 14 MeV, highly excited spin-1 resonances, spin and radiative widths 0-86876
- <sup>92</sup>Sr γγ ang. correlations, levels, J<sup>π</sup>, mixing ratios from <sup>92</sup>Rb decay 0-57725
- <sup>177</sup>Ta, rotational struct., spin polarization 0-83016
- <sup>180</sup>Ta nuclear spin and mag. dipole moment from laser resonance fluorescence 0-78143
- <sup>183</sup>Ta single proton states and rot. bands, J<sup>π</sup> from <sup>186</sup>W(t,α),pol.t 0-91130
- <sup>93</sup>Tc, J=17/2 doublet, parity mixing, weak NN interaction 0-73791
- <sup>97</sup>Tc high spin states, spins and transitions from <sup>94</sup>Zr(<sup>6</sup>Li,3nγ) 0-73780
- <sup>231</sup>Th excited states and bands, spins, γ-transitions from <sup>230</sup>Th(n,γ) 0-57699
- <sup>204</sup>Tl neutron hole states, J<sup>π</sup> and spectroscopic factors from <sup>205</sup>Tl(p,d) 0-86783
- <sup>167</sup>Tm rotational bands, J<sup>π</sup>, γ-transitions and branching ratios from <sup>165</sup>Ho(α,2nγ) 0-86781
- <sup>238</sup>U(n,f), A=233,235, ejection fission products angular depend. on thermally polarised neutron capture (*Russian*) 0-86941
- <sup>233</sup>U(n,f), thermal polarised neutrons, neutron emission P-odd asymmetry (*Russian*) 0-78338
- <sup>51</sup>V(p,p'), 6 MeV, levels, spins and EM props., shell model anal. 0-63092
- <sup>184</sup>W, A=178, 180, 182, 184, levels and J<sup>π</sup>, ang. distrib. from W(p,t) 0-78159
- <sup>180</sup>W octupole vibr. states, J<sup>π</sup> and transitions from <sup>180</sup>Re decay 0-83024
- <sup>181</sup>W levels (neutron and collective) and J<sup>π</sup>, ang. distrib. from <sup>183</sup>W(p,t) 0-78160
- <sup>132</sup>Xe level struct., J<sup>π</sup>, transitions and multipole mixing ratio from <sup>132</sup>I decay 0-91134
- <sup>87</sup>Y level struct., γ-spectroscopy and J<sup>π</sup> from (p,2nγ), (α,2nγ) 0-83040
- <sup>91</sup>Y low lying multiplets, DWBA anal. for spectroscopic factors from <sup>91</sup>Zr(d,<sup>3</sup>He) 0-57685
- <sup>169</sup>Yb γγ ang. correlations, levels and spins from <sup>169</sup>Lu decay (*Russian*) 0-83069
- <sup>172</sup>Yb levels, bands, J<sup>π</sup> and T<sub>1/2</sub> from <sup>170</sup>Er(α,2n) 0-91127
- <sup>64</sup>Zn, A=64, 66 levels and primary E1 transition strength functions from Cu(p,γ) 0-91149
- <sup>64</sup>Zn high spin states, J<sup>π</sup>, T<sub>1/2</sub>, γ-decays from (α,nγ), (<sup>11</sup>B,p2nγ) 0-73767
- <sup>66</sup>Zn negative parity high spin states, spin and lifetimes from HI reactions 0-73768
- <sup>92</sup>Zr levels, J<sup>π</sup>, cross sections, vector anal. power, optical parameters from <sup>91</sup>Zr+pol. d 0-78268

**nuclear spin-lattice relaxation**

- α,β-trifluoroacetonitrile, liq.-liq. transition rel. to mol. motion, NMR study 0-70383
- acetonitrile, <sup>13</sup>C relaxation times anal. using J-diffusion model of mol. reorientation 0-87149
- N-acetyl-D-alloisoleucine, <sup>13</sup>C NMR, soln. struct., dynamics, proton relaxation mechanisms 0-76708
- acoustic, liquids 0-97128
- acrylonitrile, NMR and relax. props., liq.-liq. transition rel. to mol. motion 0-70382
- adamantane, derivatives in solution, mol. motion and methyl group rot. barriers from <sup>13</sup>C NMR relax. times 0-74179
- adamantane powder, dipolar relaxation, short time behaviour, pulse method meas. 0-84667
- l-alanine powder, short dipolar relaxation time meas. by saturation method 0-60441
- alkali halides, dislocation dynamics studied by nucl. spin relax. meas. 0-108091
- amidinium salts, <sup>14</sup>N NQR spectra, H<sup>+</sup> relax. times 0-60448
- biomembrane, water transport determ. methods (*Rumanian*) 0-94435
- α-bis (N-methylsalicylaldiminato) copper II, one-dimens. spin-1/2 Heisenberg antiferromag., high-field spin dynamics 0-71224
- n-t-butanol in alkanes, molecular relaxation processes studied by <sup>13</sup>C NMR 0-63654
- capronate, proton spin-lattice relaxation in various phases (*Russian*) 0-97163
- carbonyl groups, spin-lattice relax. mechanism, mathematical relaxation model (*German*) 0-80633
- carborane, ortho- and para-, phase transition and mol. reorientation, isomer effects, PMR obs. 0-80628
- cyclopropane, liq., mol. dynamics, Raman and NMR studies of orientational motion 0-93296
- cytochrome c<sub>3</sub>, haeme-haeme mag. interaction, Mossbauer obs. 0-108836
- 1,8-dichlorooctane, quadrupolar relax. centres, limited spin diffusion 0-100649
- DNA, molecular motions, investigated by <sup>31</sup>P and <sup>13</sup>C NMR relaxation 0-63657
- ethanol, polymorphic forms, mol. motion, NMR obs. 0-88885
- ethylene oxide, rot. relax., double reson. and Stark switching obs. 0-106340
- fast inversion-recovery technique for spin-lattice relax. meas., modified version 0-77826
- fluid near critical point, spin-lattice relaxation time 0-80630
- fluorobenzene, mol. reorientation and weak mol. interaction influence, <sup>2</sup>D spin-lattice relax. obs. 0-106333
- formate, proton spin-lattice relaxation in various phases (*Russian*) 0-97163
- Ga,Al<sub>1-x</sub>As, optically oriented electron, nuclei spin instability (*Russian*) 0-70660
- glassy polymers double NMR, appl. of cross relaxation dynamics in modulated systems 0-71242
- hexamethylethane, <sup>13</sup>C,<sup>13</sup>C dipolar interaction, NMR longit. cross relax. 0-93196
- hybrid relaxation and multiple pulse methods for studying chemical, physical and spin exchange 0-80629
- LF fluctuation, dissipation and relaxation properties, universality 0-84687
- liquid crystals, NMR spin-lattice relax. time near phase transitions 0-71222
- MBBA, proton spin-lattice relax. in crit. regime 0-80631
- MBBA-d<sub>3</sub>, <sup>1</sup>H spin-lattice relaxation, intermol. and intramol. contribs. 0-75873
- MBBA-d<sub>13</sub>, nematic phase, rot. frame spin-lattice relax. 0-84668
- methane, phase II, nuclear spin-lattice relax. and site symm. 0-97155
- methyl ammonium aluminium sulphate, ferroelec., proton spin-lattice relax. time anomaly 0-60440
- methyl bromide, <sup>13</sup>C relaxation times anal. using J-diffusion model of mol. reorientation 0-87149
- methyl group, proton tunnelling reson. at low temp. HF limit 0-108087
- methyl iodide, <sup>13</sup>C relaxation times anal. using J-diffusion model of mol. reorientation 0-87149
- 4-methyl-2,6-di-tert-butylphenol, methyl group reorientation, classical dynamics, NMR relax. and inelastic neutron scatt. 0-88066
- methyl-d groups, reorienting or tunnelling spin-lattice relax. 0-97156
- methylene chloride, in EBBA-d<sub>3</sub>, intermol. dipolar random field cross-relax. term obs. 0-60438
- molecular reorientation in crystal, nuclear quadrupole spin-lattice relax. 0-66062
- motion induced NMR spin relax. times in low temp. HF limit 0-60443
- neopentane adsorbed on graphite, quasi two-dimens. fluid, NMR 0-102525
- Ni-Pt-P, metallic glass, electronic structure, pulsed NMR study 0-75869
- NMR spin-lattice relax., effect of correlated atomic diffusion 0-107495
- norbornane, derivatives in solution, mol. motion and methyl group rot. barriers from <sup>13</sup>C NMR relax. times 0-74179
- organic free radicals, solid, selective pulse NMR expts. 0-60452
- organic glasses, low temp. mol. mobility, NMR T<sub>1</sub> meas. 0-60439
- paradichlorobenzene, NQR study of the lattice dynamics (*Russian*) 0-97160
- polarised β-active nuclei, cross relaxation processes 0-60431
- polyatomic molecules, intramolecular vibr. relax., restricted quantum exchange theory 0-63610
- polydiethylsiloxane, mol. motion, NMR spin relax. data re-interpret. 0-84664
- polyurethanes, cross-linked, mol. mobility and struct., thermomechanical and NMR obs. (*Russian*) 0-69285
- population inversion, spin-lattice relax. meas., composite 180° pulse effect 0-77827
- Portland cement, absorbed H<sub>2</sub>O, pulsed NMR study 0-84665
- powders, high speed rot., spin diffusion, NMR spin lattice relax. obs. of D 0-66056
- pyridine-H-bond donors, D spin-lattice relax. meas., mol. interactions anal. (*French*) 0-87151
- quinolinium (TCNQ)<sub>2</sub>, charge transport, proton spin-lattice relaxation 0-88545
- RNA, molecular motions investigated by <sup>31</sup>P and <sup>13</sup>C NMR relaxation 0-63657
- smectic-A liquid crystals, nucl. spin relax. by translational self diffusion 0-60442
- sodium dodecyl sulphate: Gd<sup>3+</sup>, micellar system, chain folding, <sup>13</sup>C NMR obs. 0-61158
- solid electrolytes and solid soln. electrodes, review 0-60432



**nuclear spin-lattice relaxation continued**

- solid polymers, NMR, review 0-88888  
 stearate, proton spin-lattice relaxation in various phases (*Russian*) 0-97163  
 sulpholan, molecular solid, laboratory frame and rotating frame spin-lattice relax., pulsed NMR meas., phase transitions obs. 0-93197  
 tetramethylammonium octahydrotriborate, NMR study of proton and B dynamics 0-93200  
 tetramethylgermanium, Zeeman spin-lattice relaxation rate maxima 0-84666  
 meso-tetraphenylporphine, NH<sup>+</sup> tunnelling rate 0-97158  
 thylakoid membranes of wheat chloroplasts, proton spin-lattice relax. time, -8°C phase transition 0-108853  
 TMMC, antiferromag., nuclear spin-lattice relax. by solitons 0-97159  
 translational diffusion mechanism, reciprocal-space formalism, mean-field theory 0-71208  
 trichlorophosphazene compound, Cl<sub>3</sub>P:NCCl(CF<sub>3</sub>)<sub>2</sub>, nuclear quadrupole spin-lattice relax. 0-66062  
 TTF-CuBDT, inter- and intra-chain exchange couplings, proton spin-lattice relax. time meas. 0-71220  
 water, liq., proton spin-lattice relax. by slow proton exchange 0-60437  
 AgBr:Na<sup>+</sup>(Li<sup>+</sup>), correlated diffusion of impurities, nuclear spin relax. meas. 0-108094  
 AgF, diffusion, elec. cond. and <sup>19</sup>F relax. T<sub>1</sub> meas. 0-92718  
 Ag<sub>2</sub>F, NMR of <sup>109</sup>Ag and <sup>19</sup>F, modified Korringa relation in two-dimens. metal 0-93199  
 (AgI)<sub>2</sub>(Ag<sub>2</sub>O B<sub>2</sub>O<sub>3</sub>)<sub>1-33</sub>, amorphous superionic compound, <sup>11</sup>B lineshape and relaxation 0-108107  
 Al particles, small supercond., nuclear spin-lattice relax. meas. 0-88681  
 Al, superconducting band gap anisotropy and Fermi surface anisotropy (*Spanish*) 0-84544  
 Al-Mn(Cr)(V), dil., supercond., nucl. spin relax. and quasiparticle excitations 0-88680  
 AlCl<sub>3</sub>, aq. soln., HCl additive effects on <sup>27</sup>Al spin-lattice relax. 0-66058  
 Al<sub>2</sub>Cl<sub>6</sub> molten, nuclear mag. relax., mol. rot. 0-71209  
 β-Al<sub>2</sub>O<sub>3</sub>-(Na,Li)<sub>2</sub>O, NMR, Raman and IR spectra, and X-ray diffr., heat treatment induced changes 0-107508  
 β-Al<sub>2</sub>O<sub>3</sub>-(Na,Li)<sub>2</sub>O, ionic motion obs. using NMR and internal friction 0-108099  
 β-Al<sub>2</sub>O<sub>3</sub>-(Na,Li)<sub>2</sub>O solid electrolyte, Li motion and activation obs. using <sup>7</sup>Li NMR 0-108100  
 β-Al<sub>2</sub>O<sub>3</sub>-Li<sub>2</sub>O-Na<sub>2</sub>O, spin-lattice relaxation and Li motion 0-70451  
 β-Al<sub>2</sub>O<sub>3</sub>-NH<sub>4</sub><sup>+</sup>, PMR relax. time obs. of ionic motion 0-71213  
 β-Al<sub>2</sub>O<sub>3</sub>-NH<sub>4</sub><sup>+</sup> and β"-Al<sub>2</sub>O<sub>3</sub>-NH<sub>4</sub><sup>+</sup>-H<sub>2</sub>O, single cryst. PMR and proton motion 0-108101  
 β"-Al<sub>2</sub>O<sub>3</sub>-Na<sub>2</sub>O, <sup>23</sup>Na NMR obs. of ionic diffusion, 180 to 800K, attempt freq. 0-108097  
 β-Al<sub>2</sub>O<sub>3</sub>-Na<sub>2</sub>O, <sup>23</sup>Na NQR and two-dimens. diffusion, model analysis 0-108111  
 β-Al<sub>2</sub>O<sub>3</sub>-Na<sub>2</sub>O, <sup>27</sup>Al NMR obs., Na motion and cond. characts. 0-108096  
 β-Al<sub>2</sub>O<sub>3</sub>-Na<sub>2</sub>O, AC ionic cond., dielec. and NMR relax. 0-59713  
 β"-Al<sub>2</sub>O<sub>3</sub>-Na<sub>2</sub>O, absorbed water effect on NMR lineshape and spin-lattice relax. time 0-108098  
 β-Al<sub>2</sub>O<sub>3</sub>-Na<sub>2</sub>O, anomalous Na behaviour obs. using pulsed and CW NMR 0-108095  
 Au-Fe, dil., crit. dynamics 0-60325  
 Be, electronic struct., NMR study 0-108085  
 BeF<sub>2</sub> aqueous solns., mag. and quadrupole relax. 0-71226  
 Be<sub>1-x</sub>Mn<sub>x</sub>, Be-rich, NMR and paramag. susceptibility 0-71206  
 BeNi, dil., electronic struct., NMR study 0-108085  
 CdI<sub>2</sub>-Cd(II) mixture, molten, nuclear spin relax. 0-88887  
 CeAl<sub>2</sub>, antiferromag. ordering and Kondo behaviour, <sup>27</sup>Al NQR study 0-71231  
 Co-<sup>48</sup>V, nucl. orientation of <sup>48</sup>V, γ-ray anisotropy obs. 0-97169  
 CrB<sub>2</sub>, itinerant antiferromag., spin fluctuations, NMR study 0-108119  
 Cs-Au liq. alloy, formation of localised electronic states, NMR obs. 0-93201  
 CsD<sub>2</sub>PO<sub>4</sub>, pseudo-one-dimensional ferroelectric transition, <sup>31</sup>P chemical shift and relaxation study 0-66123  
 CsD<sub>2</sub>PO<sub>4</sub>, pseudo-one-dimens. ferroelec. transition, DMR and relax. study 0-71223  
 CsH<sub>2</sub>PO<sub>4</sub> and CsD<sub>2</sub>PO<sub>4</sub>, pseudo one-dimens. ferroelec. ordering dynamics, <sup>31</sup>P NMR study 0-75971  
 (Cu,Zn)C<sub>2</sub>(SO<sub>4</sub>)<sub>2</sub>·6(H<sub>2</sub>O) Tutton salt, proton spin-lattice relax. time, proton conc. depend. and spin diffusion rate 0-71221  
 Cu<sub>3</sub>VS<sub>4</sub>, out of equil. mixed cond., off-centre positions and order-disorder transition, ultrafast nucl. relax. obs. 0-108103  
 Cu<sub>3</sub>VS<sub>4</sub>, out of equil. mixed cond., chem. origin of mobile ions, spin-lattice relax. and NQR obs. 0-108104  
 ErRh<sub>2</sub>B<sub>4</sub>, mag. supercond., NMR study of <sup>11</sup>B 0-107957  
 Fe-<sup>48</sup>V, nucl. orientation of <sup>48</sup>V, γ-ray anisotropy obs. and NMR meas. 0-97169  
 Fe-Co, 3d ferromagnet nuclear spin-lattice relaxation 0-80627  
 FeF<sub>2</sub>:Mn, antiferromag., NMR relax., impurity bonding 0-66061  
 FeSO<sub>4</sub>·n H<sub>2</sub>O (n=1,4,5,7), Fe<sup>2+</sup> ion mag. interaction with crystallisation water protons, proton NMR obs. 0-60447  
 H, gaseous, high-resolution mag. reson. study, 1 to 1.3K 0-95560  
 H<sub>2</sub>, single crystals, NMR, dynamic effects 0-107608  
 H<sub>2</sub>-D<sub>2</sub>Se(n=0, 1 and 2), <sup>77</sup>Se NMR on XL-100 spectrometer, isotope effects and spin-lattice relaxation 0-71211  
 H<sub>0.36</sub>MoO<sub>3</sub> and H<sub>1.37</sub>MoO<sub>3</sub> bronzes, NMR relax. obs. at 77<T<450K, H diffusion 0-108089  
 H<sub>2</sub>O in biological samples, PMR, fast-exchange model interpretation via differential kinetics clarified 0-67033  
<sup>3</sup>He:<sup>3</sup>He, HCP, solid, nucl. spin-lattice relax., <sup>4</sup>He impurity effects 0-88396  
 HFV<sub>2</sub>H<sub>2</sub>, proton NMR relax. time and Knight shifts, diffusional activation energies meas., sorption props. 0-75871  
 KB<sub>3</sub>H<sub>8</sub>, NMR study of proton and boron dynamics 0-71210  
 KCoF<sub>3</sub>, antiferromag., with residual orbital moment, nucl. mag. relax. 0-71215  
 KMg<sub>1-x</sub>Mn<sub>x</sub>F<sub>3</sub>, disordered paramagnet, <sup>19</sup>F NMR study 0-71216  
 K<sub>2</sub>MnF<sub>4</sub>, ordered quadratic-layer Heisenberg antiferromag., nucl. spin-magnon relax. 0-71217  
 KNiF<sub>3</sub>, <sup>19</sup>F spin-lattice relaxation 0-93211  
 K<sub>2</sub>NiF<sub>4</sub>, ordered quadratic-layer Heisenberg antiferromag., nucl. spin-magnon relax. 0-71217  
 K<sub>2</sub>OsCl<sub>6</sub>, Cl NQR spectra by Fourier transform methods 0-75879  
 KTaO<sub>3</sub>:Li, ferroelec. transition and atomic motions, <sup>7</sup>Li NMR study 0-75872

**nuclear spin-lattice relaxation continued**

- LaF<sub>3</sub>, <sup>139</sup>La NMR study, relaxation times meas. 0-108093  
 LaF<sub>3</sub>, ionic transport, NMR and cond. studies 0-107555  
 LaF<sub>3</sub>:Pr<sup>3+</sup>, optical meas. of spin-lattice relaxation of dilute nuclei 0-93212  
 Li<sub>3</sub>N, diffusion processes and struct. NMR study 0-108090  
 Li<sub>3</sub>N, ionic hopping model, NMR relax. data anal. 0-92714  
 Li<sub>3</sub>N layer structure with fast ion cond., <sup>6</sup>Li NMR obs. of diffusion 0-108102  
 Li<sub>2</sub>S(O), cation diffusion NMR investigation up to 800°C 0-108092  
 Mn(ClO<sub>4</sub>)<sub>2</sub>/NaClO<sub>4</sub> in aq. soln., interaction between Mn<sup>2+</sup> and ClO<sub>4</sub><sup>-</sup>, NMR studies 0-71212  
 (ND<sub>2</sub>)<sub>2</sub>BeF<sub>4</sub> and (NH<sub>4</sub>)<sub>2</sub>BeF<sub>4</sub>, incommensurate phase, <sup>9</sup>Be NMR study 0-75973  
 N<sub>2</sub>H<sub>2</sub><sup>2+</sup> salts, NMR spin lattice relaxation study, <sup>14</sup>N-<sup>1</sup>H dipole-dipole contrib. to relax. 0-75878  
 (NH<sub>4</sub>)<sub>2</sub>ReCl<sub>6</sub>(IrCl<sub>6</sub>), proton relaxation near antiferromagnetic phase transitions 0-80640  
<sup>15</sup>N, spin-lattice relax. time, quantum effect of NH<sub>4</sub>-ion rot. 0-75875  
 NaClO<sub>4</sub>/Mn(ClO<sub>4</sub>)<sub>2</sub> in aq. soln., interaction between Mn<sup>2+</sup> and ClO<sub>4</sub><sup>-</sup>, NMR studies 0-71212  
 Na<sub>2</sub>O-B<sub>2</sub>O<sub>3</sub>:Cu<sup>2+</sup>, Mn<sup>2+</sup> glasses, Cu<sup>2+</sup>-Mn<sup>2+</sup> interaction studied by ESR 0-93166  
 Na<sub>2</sub>S(O), cation diffusion NMR investigation up to 800°C 0-108092  
 Na<sub>2</sub>Y<sub>2</sub>Zr<sub>2</sub>S<sub>2</sub>, S<sub>2</sub> ionic cond. and NMR mobility obs., comp. depend. (*French*) 0-70459  
 Na<sub>2</sub>Zr<sub>2</sub>PSi<sub>2</sub>O<sub>12</sub>, NASICON, <sup>23</sup>Na NMR obs. of ionic diffusion, 180 to 800K 0-108097  
 Ni, ferromagnetic, electronic struct. and hyperfine field of nonmag. impurities, calc. 0-70658  
 Ni-Cu(Zn)(Ga)(Ge)(As)(Se)(Br)(Kr), dil., ferromagnetic, hyperfine field and relax. time obs. of impurity heavy nuclei 0-75533  
 Ni-Pd-P, metallic glass, electronic structure, pulsed NMR study 0-75869  
 NbS<sub>2</sub>, paramag. props., NMR, mag. susceptibility 0-60175  
 P+Nb, dil. alloy, NMR obs. of <sup>93</sup>Nb 0-71203  
 PbF<sub>2</sub>:Mn, mag. tagging of ion diffusion, <sup>19</sup>F NMR meas. 0-108106  
 PbNb, dilute, NMR obs. of <sup>93</sup>Nb 0-71203  
 PtV, dil. alloys, NMR obs. of <sup>51</sup>V 0-71203  
 RbAg<sub>4</sub>S<sub>4</sub>, static and dynamic NMR effects at 208K and 122K phase transitions 0-108105  
 RbCaF<sub>3</sub>, cubic to tetragonal phase transition, <sup>87</sup>Rb NMR study 0-70392  
 Rb<sub>2</sub>CuBr<sub>4</sub>·2H<sub>2</sub>O, dynamic props. in paramag. state, spin-lattice relax. time meas. 0-71214  
 Rb<sub>2</sub>ZnCl<sub>4</sub>, incommensurate phase transition, <sup>87</sup>Rb NMR study 0-75967  
 Sb<sub>2</sub>O<sub>3</sub>·H<sub>2</sub>O, crystalline, <sup>1</sup>H NMR study of proton transport 0-60446  
 Se, solid, chemical shift and nucl. spin-lattice relax., high temp behaviour 0-60445  
 Si:H film, amorphous, H-associated disorder modes, PMR spin-lattice relax. time meas. 0-93202  
 SiCl<sub>4</sub> molecule, NMR relaxation expts. to study molecular reorientation 0-63673  
<sup>117</sup>Sn, <sup>119</sup>Sn, low temp. NMR thermometry 0-82775  
 ThC<sub>2</sub>N<sub>2</sub>, NMR, Knight shift and spin-lattice relax. 0-100621  
 γ-TiH<sub>3</sub>, interstitial H diffusion mechanism, NMR spin-lattice relax. study 0-103515  
 TmVO<sub>4</sub>, enhanced nuclear cooling and spin-lattice relax. time 0-80632  
 V<sub>2</sub>(Hf,Zr), NMR and mag. susceptibility, density of states determ. (*Russian*) 0-66053  
 V<sub>2-x</sub>Nb<sub>x</sub>Hf, NMR of <sup>51</sup>V and mag. susceptibility, 20-300K (*Russian*) 0-93192  
 V<sub>2</sub>S<sub>5</sub> and V<sub>2</sub>S<sub>6</sub>, itinerant antiferromag. spin fluctuations, NMR studies 0-93198  
 V<sub>2</sub>Se<sub>4</sub>, itinerant antiferromag., spin fluctuations, NMR study 0-75874  
 V<sub>2</sub>Se<sub>5</sub>, itinerant antiferromag., spin fluctuations, NMR study 0-75874  
<sup>89</sup>Y spin-spin relaxation times, pH depend. 0-66059  
 Zr and its alloys, H diffusion, NMR study 0-108088  
 ZrMn<sub>2</sub>H<sub>2</sub>, proton NMR relax. time and Knight shifts, diffusional activation energies meas., sorption props. 0-75871

**nuclear spin-spin relaxation** *see spin-spin relaxation***nuclear structure**

- see also form factors (nuclear); nuclear binding energy; nuclear charge; nuclear density; nuclear energy level transitions; nuclear energy levels; nuclear forces; nuclear isomerism; nuclear isospin; nuclear matter; nuclear moments; nuclear polarisation; nuclear shape; nuclear size; nuclear spectroscopic factors; nuclear spin and parity; nuclear structure theory*  
 A=112, experimental nuclear structure data to January 1979 0-98763  
 A=123, experimental nuclear structure data to June 1979 0-94931  
 A=145, experimental nuclear structure data to August 1979 0-94932  
 A=163, nuclear data sheets to April 1979 0-98762  
 A=213, nuclear structure data sheets (July 1979) 0-67942  
 A=217, nuclear structure data sheets (July 1979) 0-67943  
 A=63, nuclear structure data sheets (July 1979) 0-67941  
 data sheets, 1979 recent references, cumulation 0-94930  
 growth points in nuclear physics, book 0-94928  
 ion-nucleus collisions, transfer reactions, study of nuclear structure (*French*) 0-78310  
 NN dynamics at medium energies, phase parameters, one pion exchange model 0-63102

**nuclear structure theory**

- see also generator coordinate method; HF calculations; nuclear models; nuclear reaction and scattering theory; RPA calculations*  
 A=42, multiple scattering formalism for the effective interaction 0-102126  
 A=50 to 150, shell, dynamical deformation and interacting boson models, limitations 0-68563  
 A=90 region, core pol. effects and giant quadrupole resonances, HF and macroscopic calcs. 0-57756  
 adiabatic TDHF approx., mass parameters, single collective variable, theoretical aspects 0-73765  
 analytic observables in nuclear physics 0-105993  
 Bloch density for nonlocal pots., h-expansion partial resummation, average binding energies 0-86797  
 bound multineutron system, 8 and 20 neutrons, existence probability 0-68570  
 Brueckner theory, unification with HFB theory 0-105995  
 collective excitations of nuclei in a relativistic mean-field theory 0-95306  
 collective parameter dynamics, monopole vibr., variational principles 0-95298



**nuclear structure theory continued**  
conference on medium heavy nuclei structure, Rhodes, Greece (May 1979) 0-67935  
constrained Hartree-Fock and quasi-spin projection 0-99141  
decoupling model for fission fragment transitional nuclei, odd-odd and even mass 0-78174  
deformed nuclei, constrained HF energies, two-step iterative method 0-83053  
deformed nuclei, single particle level blocking in BCS approx. 0-99117  
density oscillations, from semi-infinite nuclear matter calc., Regge type oscillation comparison 0-57671  
dilute Fermi gas, self energy, momentum distrib., and effective mass, nuclear matter 0-63119  
doubly closed shell nuclei, isovector giant monopole resonances, sum rule approach 0-78244  
doubly even deformed nuclei, excited states, Pauli principle effects, quasi-particle-phonon model 0-63094  
dynamical Bose-Fermi supersymmetries in complex nuclei 0-57703  
E1 transition selection rule, light nuclei transition strengths 0-106014  
effective mass and exchange current effects in finite nuclei 0-78171  
effective NN interaction and exchange current vel. depend., dipole sum rule enhancement 0-63100  
EM isovector form factors of bound nucleons 0-78134  
equilibration process, master eqn. and closed form approaches 0-99166  
even-even nuclei, static quadrupole moments of arbitrary excited states, sum rule approach 0-91135  
even-even nuclei, yrast band backbending mechanism criteria 0-91128  
Franzini-Radicati mass relationship in isobars, Wigner SU(4) supermultiplet 0-105958  
generalised Fermi sea for plane wave HF theory, 3-dimens. semi-realistic interactions 0-105999  
harmonic oscillator ground state, Faddeev eqn. exact soln. 0-86821  
Hartree eqn., quasiclassical soliton soln., Newtonian interaction with screening 0-68569  
hole excitation spectrum in finite Fermi system, many body field theory 0-102105  
large deformations, single particle levels, self-consistent field rearrangement, HF method 0-78107  
light deformed nuclei, Skyrme interaction spin components, spectra, projected HF theory 0-73820  
many body problem in Lee model, NN scatt. and matter binding energy 0-63116  
Marchenko eqn. extension to nonHermitian differential systems 0-83080  
mass fitting and averaging, correction due to one particle Hamiltonian symmetry (Russian) 0-83032  
matrix elements between arbitrary single particle wavefunctions, generator coordinate method 0-57751  
medium heavy nuclei, equations of motion appl. to pairing correlations, spurious states 0-73810  
microscopic effective interactions in correlated model space, eqn. of motion method 0-86818  
momentum and mass distrib., form factors, short range correlation effects 0-105959  
multipole phonon states,  $G_2$  group shift operator properties 0-99139  
multipole phonon states,  $R(7)$  group shift operators 0-99140  
multipole-phonon state classification by shift operator techniques 0-86828  
multipole-phonon states, classification, quadrupole shift operator eigenvalues 0-86829  
multipole-phonon states,  $O_4$  quadrupole phonon eigenstates 0-86830  
 $N=5$  shell, deformed odd-neutron nuclei, band ordering and spectrum 0-83018  
neutron matter, hypernetted chain calcs. with the Paris pot. 0-57714  
neutron rich nuclei stability, HF calcs. (Russian) 0-78181  
nuclear and neutron matter with isobars, transition pot. model, neutron stars 0-68573  
nuclear far from  $\beta$ -stability, delayed neutron energy spectra, structure effects 0-78226  
nuclear field theory, phonon renormalisation, eigeneqns. and sum rules (Chinese) 0-102127  
nuclear field theory, schematic model functional approach, diagram rules 0-102128  
nuclear matter,  $\nu_k$  semirealistic model, variational theory accuracy and convergence 0-57712  
nuclear matter, abnormal occupation, two body correlations and plane wave HF energy 0-86844  
nuclear matter, iterative isobar process role, effective NN interaction 0-99143  
nuclear matter, spin-isospin and pion condensation phase transitions, eqn. of state 0-86843  
nuclear matter binding energy, hypernetted chain approx., impurity ground state energy 0-83055  
nuclear matter momentum distrib., single particle orbitals, Fermi hypernetted chain theory 0-86841  
nucleon-nucleon interaction as derived from the De Rujula, Georgi, Glashow phenomenological quark-quark potential 0-78172  
number operators for composite particles-in nonrelativistic many-body theory 0-94982  
odd mass nuclei,  $1g_{7/2}^+$  shell region, low lying states, anharmonic effects 0-57687  
pairing correlation treatment, single particle levels, binding energy, spectra, branching ratios (Chinese) 0-102107  
pairing rotation and intrinsic Hamiltonian, RPA theory 0-57708  
particle-vibration coupling form factor from simple model 0-57663  
path integral approach to many-nucleon systems and time-dependent Hartree-Fock 0-78180  
Pauli principle test, particle stability  $e$  and  $N$  indistinguishability 0-105992  
pole expansions for resonance functions, scatt. amplitudes and continuum states (Russian) 0-86871  
pseudo Nilsson quantum numbers, goodness in asymptotic limit 0-99138  
quadrupole oscillation wave functions, multiplicity factor (Chinese) 0-102103  
quasi-particle theory modification in spherical nuclei, pairing model 0-105991  
rare earth nuclei, modified oscillator pot. parameters, single particle levels 0-68509  
resonant states in the presence of Coulomb interactions, Schrodinger eqn. 0-91161  
rotation, inertial parameters in microscopic theory 0-91132  
saturation in finite nuclei, nuclear matter density and binding energy 0-83029

**nuclear structure theory continued**  
self consistent pseudopots. in thermodynamic limit, state depend. one body field, HF calcs. 0-83054  
self-consistent quasiparticle RPA in nuclear structure theory 0-86835  
short-lived isotopes, laser spectroscopy in fast atomic beams and resonance cells 0-57700  
single particle pots., Lehmann representation discrete and continuous energy spectra (Chinese) 0-102104  
single particle states, discrete expansions of continuum wave functions, convergence props. 0-57659  
single-particle states in nuclear matter and in finite nuclei 0-78117  
Sp(3,R) matrix elements, recursion formula 0-62878  
spherical nuclei, compound state  $\gamma$ -transitions, reduced  $\gamma$ -widths, Wigner stat. matrix method (Russian) 0-68587  
spherical nuclei, Hartree-Fock-Bogolyubov calcs., D1 effective interaction, nuclear matter, binding energies 0-63105  
static Hartree Fock problem, imaginary time step method 0-86832  
static self-consistent HF problems, alternative methods 0-68568  
stellar environment, nucl. reactions and strong interactions 0-72765  
Sturmian expansion method for bound state problems 0-68561  
superband and ground band ang. momentum difference (Chinese) 0-102102  
TDHF equations of motion for algebraic Hamiltonians in a coherent state representation 0-57709  
TDHF with two-body dissipation 0-91140  
Thomas-Fermi kinetic-energy density with gradient corrections 0-91169  
three-body force from  $2\pi$ ,  $\pi\rho$ , and  $2\rho$  exchanges 0-78169  
three-body force from kinematical effects in the three-nucleon system 0-105986  
time-dependent mean-field approximation for nuclear dynamical problems 0-63113  
time-dependent mean-field theory and quantized bound states, Lipkin model 0-63114  
time-dependent-S-matrix Hartree-Fock theory of complex reactions 0-63112  
NN dynamics at medium energies, elastic and inelastic scatt., unitary model 0-63101  
NN forward scatt., two and three pion cut contribs., nucleon exchange model 0-63103  
 $\pi$ - and  $\rho$ -exchange pots., influence on mag. resonances, mag. moments, and transition probabs. 0-99133  
 $\pi$ NN-NN coupled systems theory, relativistic extensions 0-63104  
 $\Sigma$ -hypernuclear state width, model estimation 0-57719  
Ag nuclei, highly excited, disintegration, photographic emulsion, quark model theory comparison 0-68560  
As isotopes, levels and spectra from broken pair model 0-73801  
 $^{12}\text{B}$ , aligned,  $\beta$ -ang. distrib. asymmetry coeffs., pseudotensor interaction,  $T=1$  isospin triplet decay 0-106021  
 $^{208}\text{Bi}$ ,  $0^+$  IAS, spreading width and isospin impurity, isovector monopole state influence 0-78155  
 $^{209}\text{Bi}$  energy and transition probability convergence in Dyson's boson expansion 0-78206  
Br nuclei, highly excited, disintegration, photographic emulsion, quark model theory comparison 0-68560  
 $^{12}\text{C}$  M1 form factor, pion field critical opalescence,  $\rho$  role, polarisation phenomena 0-68552  
 $^{12}\text{C}$ , residual interactions, current conserving RPA calculations 0-57710  
 $^{14}\text{C}_{g.s.}$   $\beta$ -decay, mesonic exchange currents, weak process microscopic treatment 0-57742  
 $^{40}\text{Ca}$ , magic nuclei at collective excitations, energy spectrum and shape (Russian) 0-106015  
 $^{40}\text{Ca}$ , residual interactions, current conserving RPA calculations 0-57710  
Cd even-even nuclei, low lying collective states, two-photon character 0-57667  
Dy deformed nuclei, particle ang. momentum alignment effects 0-68522  
 $^{152}\text{Dy}$  yrast isomers,  $\gamma$ -rays from compound nuclei 0-86789  
Er, deformed nuclei, particle ang. momentum alignment effects 0-68522  
 $^{168}\text{Er}$   $\gamma$ -vibr. band, M1 admixtures in intra-band transitions 0-99149  
Ge, even-even nuclei,  $\gamma$ -spectroscopy, exptl. results and models 0-68589  
 $^2\text{H}$  bound state, relativistic quasipot. wave eqn. soln. 0-102132  
 $^2\text{H}$  charge operator, retardation, quasipot. eqns. and rel. corrections 0-99122  
 $^2\text{H}$  D-state probability, three lower bounds 0-102129  
 $^2\text{H}$  D-state probability lower bound, binding energy, quadrupole moment 0-91137  
 $^2\text{H}$  nucleus wave function momentum contribution from QCD diagrams (Russian) 0-68562  
 $^2\text{H}(e,e)$ , EM form factors, relativistic formulae, moment corrections 0-63075  
 $^2\text{H}(e,e)$ , form factors, tensor pol., and two-nucleon force calcs. 0-106045  
 $^2\text{H}(\gamma,n)p$ , parity violation expts. review, weak NN interaction 0-73792  
 $^3\text{H}$  binding energy, relativistic calc., Bethe Salpeter eqn. 0-68519  
 $^3\text{H}$ , ground state energy, second order Brueckner-Baranger approx. 0-63082  
 $^3\text{H}$  ground state props. from configuration space Faddeev calcs. 0-102130  
 $^3\text{H}$  realistic wave function, energy and density distrib. 0-86794  
 $^3\text{H}_{A_1}$ , short range repulsion, separation energy, K-harmonics calcs. 0-86846  
 $^4\text{H}$ ,  $A=2.3$ , binding energy from Brillouin-Wigner perturbation method, strong short ranged interactions 0-86796  
 $^3\text{He}$  Coulomb energy from configuration space Faddeev calcs. 0-102131  
 $^3\text{He}$ , totally antisymmetric wave function with generalised Faddeev eqn. 0-83046  
 $^4\text{He}$  binding energy, 4-nucleon problem, integral eqn. approach 0-91183  
 $^4\text{He}$ , four-nucleon bound state with realistic NN interaction, hyperspherical harmonics (Russian) 0-83045  
 $^4\text{He}$ , ground state energy, second order Brueckner-Baranger approx. 0-63082  
 $^4\text{He}$  nuclear charge density determ. using form factor analyticity 0-63077  
 $^5\text{He}_{A_1}$ , A-N pot. Majorana component on  $B_A$  value, overbinding 0-99144  
 $^5\text{He}_{A_1}$ , short range repulsion, separation energy, K-harmonics calcs. 0-86846  
 $^4\text{He}$ ,  $A=190$ -200, even, phase transition and possible triaxial shape, energy levels 0-63098  
 $^4\text{In}$ ,  $A=119$ , 121, unified model description, vibr. multiplet yrast struct., branching ratios 0-105953  
 $^6\text{Li}(d,X)$  system, resonating group method, single channel approx., cluster states 0-57782



**nuclear structure theory continued**

- <sup>7</sup>Li charge form factor with resonating group wave function, quad. moment, charge radius 0-102110
- <sup>7</sup>Li- $\alpha$  virtual decay vertex constant from (d,t), (p, $\alpha$ ) 0-78231
- <sup>12</sup>N, aligned,  $\beta$ -ang. distrib. asymmetry coeffs., pseudotensor interaction, T=1 isospin triplet decay 0-106021
- <sup>14</sup>N<sub>g.s.</sub> partial muon capture, mesonic exchange currents, weak process microscopic treatment 0-57742
- <sup>14</sup>Nb, A=90,92,94, Gamow-Teller strength distrib., RPA calcs. 0-78218
- <sup>20</sup>Ne ground state level calc., maximum method 0-73795
- <sup>21</sup>Ne, strength function calcs. in many fermion systems, Monte-Carlo method 0-86820
- <sup>60</sup>Ni, Coulomb contributions to nuclear radii and energies 0-68515
- <sup>16</sup>O, A=16, 17, valence-core self-consistency, wave functions, binding energy, levels, spectra 0-63123
- <sup>16</sup>O<sub>g.s.</sub>  $\beta$ -decay, mesonic exchange currents, weak process microscopic treatment 0-57742
- <sup>16</sup>O ground state energy and low odd parity states, correlated basis function method 0-57689
- <sup>16</sup>O ground-state energy, nonunitary model operator approach 0-83030
- <sup>16</sup>O isospin mixing matrix elements, three level model 0-78136
- <sup>16</sup>O, magic nuclei at collective excitations, energy spectrum and shape (Russian) 0-106015
- <sup>16</sup>O, residual interactions, current conserving RPA calculations 0-57710
- Pb even isotopes, two quasiparticle 2<sup>+</sup> state coupling to T=0 giant quadrupole resonance 0-68618
- Pb region, particle-vibration multiplet spectra, self-consistent framework 0-102089
- <sup>208</sup>Pb breathing model transition density, single particle and collective state dynamical coupling 0-106007
- <sup>208</sup>Pb region, mag. transition strength, core polarisation effects, form factor shape 0-86850
- <sup>208</sup>Pb single particle and hole states, renormalisation, core polarisation, spectroscopic factors 0-57658
- <sup>208</sup>Pb(p,p'), 135 MeV, normal parity excitations, microscopic description, NN interaction shape 0-57691
- <sup>109</sup>Pd low spin odd parity states, rot. aligned model, Coriolis calc. of <sup>109</sup>Pd(n, $\gamma$ ) 0-57695
- <sup>97</sup>Rh levels and  $\gamma$ -transitions, 3QP model anal. of <sup>97</sup>Pd  $\beta$ -decay 0-102120
- <sup>32</sup>S shape isomeric state from unconstrained variation 0-95306
- Se, even-even nuclei,  $\gamma$ -spectroscopy, exptl. results and models 0-68589
- <sup>134</sup>Se, A=74, 76, vibr. states and transition from dynamic deformation theory 0-73770
- <sup>28</sup>Si, strength function calcs. in many fermion systems, Monte-Carlo method 0-86820
- <sup>28</sup>Si rot.-vibr. coupling effects, excitation spectrum and ang. distrib. from <sup>28</sup>Si(d, p) 0-57661
- <sup>151</sup>Sm low energy levels from expt. and Coriolis mixing calcs. of <sup>150</sup>Sm(n, $\gamma$ ) 0-57697
- Sn isotopes, levels and spectra from broken pair model 0-73801
- <sup>126</sup>Te, A=122,124,126 yrast band double backbending, possible mechanisms (Chinese) 0-99120
- <sup>126</sup>Te, M1, giant resonance and radiative strength functions 0-57731
- <sup>176</sup>Yb, A=170-182, even isotopes, yrast states, spectra and quad. moments, variation formulation 0-99119
- <sup>61</sup>Zn states, pseudo LS coupling model 0-68548

**nuclear track emulsions**

- anomalous tracks observed in uranium loaded nuclear emulsions 0-99410
- CR-39 plastic, electrochem. etching, optimum conditions 0-95505
- detection and measurement of very short flight paths in nuclear emulsions 0-102389
- electrochemical etching of fast neutron induced recoil tracks in cellulose triacetate 0-91406
- heavy charged particle specific energy losses meas. using densitometric method (Russian) 0-63482
- laser plasma, 5-20 keV X-ray emission spectrum investigation using nucl. emulsions 0-92392
- lithium and <sup>6</sup>Li analysis with the nuclear track technique 0-95504
- mica solid state particle track detectors, fission fragment ranges rel. to cryst. orientation 0-91408
- solid state track detectors, critical angles for fission fragment registration 0-91407
- track struct. and particle identification 0-91383
- track width, filar micrometer meas. for low-energy heavy ions 0-91403
- Ag nuclei, highly excited, disintegration, photographic emulsion, quark model theory comparison 0-68560
- Br nuclei, highly excited, disintegration, photographic emulsion, quark model theory comparison 0-68560
- <sup>222</sup>Rn gas detection using Track Etch system for U exploration 0-98488
- Si(Li)-emulsion shower counter for cosmic ray electron obs. 0-58033
- U glass, fission track dating, error analysis 0-95503

**nucleation**

- see also crystal growth; crystallisation
- aerosol formation measurements from gas in coal fired power station plumes 0-81502
- alkali-halide crystals, two-dimens. nucleation and hole nucleation, mol. beam method (German) 0-93499
- alloys, spinodal decomposition, review 0-96657
- amorphous semiconductor film, laser induced nucleation, long wavelength instability 0-84126
- anthraquinone, UV light effect on nucleation during crystallisation on anthracene surface 0-75478
- anthrone, UV light effect on nucleation during crystallisation on anthracene surface 0-75478
- apatite crystal growth in skeletal tissues 0-94181
- attachment energy as habit controlling factor, growth models 0-59420
- binary liquid mixtures, spinodal decomposition, review 0-96657
- binary mixtures, near critical, metastable, phase separation and nucleation and drop growth, rate eqns. 0-65232
- bulk melting, liq. phase nuclei form. 0-88304
- cell wall and lattice misorientation origin during deform. 0-71712
- cloud, ice nucleation by aerosol particles 0-61864
- cloud chamber, thermal diffusion, unsteady state, supersaturation profile 0-63449
- cloud droplet nucleation, expts. with monodisperse NaCl aerosols 0-82003
- condensation from small nuclei, modified Mayer theory 0-79924
- creep damage and the remaining life concept 0-59574

**nucleation continued**

- crystal frequency distribution, simulation taking nuclei distrib. into account 0-100184
- decanoic acid, associated vapours, homogeneous nucleation 0-96638
- fatigue crack nucleation at particles in Al alloys, computer simulation 0-100893
- ferroelectrics, domain structure as outcome state for poling procedure 0-80728
- film defect growth and nucleation, electron microscopy and diffraction exam. (French) 0-59824
- fine particles aggregation, mechanism and rate at uniform shear field 0-101046
- glass, crystallisation and nucleation of reheating 0-84078
- glass forming melts, crystn. kinetics processes 0-64905
- glass forming systems, induced crystallisation, transient heterogeneous nucleation 0-64903
- glass-ceramics, transient heterogeneous nucleation of glass-forming systems 0-88042
- glasses, spinodal decomposition, review 0-96657
- heptanoic acid, associated vapours, homogeneous nucleation 0-96638
- ice disc growth from vapour, cryst. habit change mechanism 0-84117
- ice nucleation on AgI, exptl. verification of ice-forming activity theory 0-101406
- ice nucleation on AgI, influence of aerosol particle size, struct. 0-61164
- ion solvation, correlation of total and partial enthalpies, vel. to nucleation energy barrier 0-89514
- island films, statistical model 0-92795
- isobutyric acid-water near-critical liquid mixture, nucleation 0-92664
- magnetic alloy, interface behaviour 0-84913
- metal cluster growth and props., photography and catalysis appl., conf., Villeurbanne, France (Sep. '79) 0-105431
- metal clusters, 2 to 500 atoms, nucleation, mass spectra 0-102596
- metal colloids in ionic cryst., preparation, optical, mag. resonance, elec. props. 0-59459
- metal films, nucleation on alkali halide crystals, effect of ionisation of condensing flux 0-107675
- myristic acid, associated vapours, homogeneous nucleation 0-96638
- naphthalene crystal nucleation on anthracene microcrystals suspended in vapour-gas stream 0-76165
- n-nitroaniline, UV light effect on nucleation during crystallisation on anthracene surface 0-75478
- nucleation theory and first order phase transition dynamics near critical points 0-84284
- optical glass, melting, fining, surface tension, diffusion, nucleation in microgravity 0-81016
- ordered alloys with periodic struct., decomp. invest. (Russian) 0-93558
- perfluoromethylcyclohexane-methylcyclohexane, near-critical liquid mixture, nucleation 0-92664
- PET, crystallization, lamellar growth kinetics and thickness 0-103266
- phase boundaries in first-order phase transitions, dynamics stability 0-107403
- photographic development, nucleation and growth phenomena 0-101858
- polyethylene, flow-induced fibril form. from soln. 0-59402
- polyethylene melt, cryst. kinetics during cooling, nucleation density effect 0-100181
- trans-1,4-polyisoprene crystals, press. effect on growth rate 0-88064
- polystyrene, isotactic, spherulite radial growth retardation by SiO<sub>2</sub> nucleation 0-107066
- quasi-stationary approximation of nucleation kinetics at high supersaturations on (111) faces of cryst. with diamond struct. 0-84128
- rate of formation of condensation nuclei in two component metastable media 0-79930
- single crystals, growth simulation 0-88069
- spherulite primary nucleation, determ. from spherulite shapes in bulk samples 0-70359
- statistical mechanical theory of the kinetics of phase transitions, review, book contrib. 0-73270
- stearic acid homogeneous vapour phase nucleation, diffusion cloud chamber obs. 0-79923
- steel, austenitic stainless, irrad. creep of type 316 in HVEM 0-97523
- steel, ball bearing, fatigue damage, influence of dispersed phases in martensitic matrix 0-108549
- steel, Cr, lower bainite transform., significance of carbide precip. 0-97476
- steel, Cr-W(Mo), quenched, carbide reactions during tempering 0-89229
- steel, hardenability, role of B and P segregation 0-97486
- steel, stainless, ferrite to austenite decomp. 0-93554
- substitutional solid solutions, new phase nucleation mechanism 0-61135
- supersaturated soln., shape stability of growing cylindrical particle due to diffusion and interface kinetics 0-79720
- supersaturated vapour, critical clusters, theory and Monte Carlo simulation, review 0-82734
- supersaturated vapour, equilib. press. depend. on nucleating drop radius 0-69960
- thin film condensates coalescence, influence on morphological changes, modelling 0-107676
- thin films, kinetics under complete condensation conditions 0-88453
- thin films, precipitation and nuclei form. in presence of condensation centres, thermodynamic model 0-103594
- transients in cryst. growth rate 0-84118
- vapour-liquid-solid growth mechanism (Russian) 0-107074
- void swelling, nucleation theory 0-65038
- water droplets, ebullition under steady-state superheated conditions 0-74928
- water droplets, ebullition under transient superheated conditions 0-74929
- water vapour expansion with condensation, nozzle flow at high pressure 0-106828
- Ag film growth on Si (111), nucleation and growth modes, SEM study 0-100423
- Ag speck nucleation and phase formation in latent image 0-97716
- Ag-Al (26 at.%), massive transform,  $\beta \rightarrow \delta$ , crystallography and morphology 0-97475
- AgBr layer, sensitised, topography of developed centres 0-73491
- AgCl crystal growth in gelatin soln. 0-64942
- AgI aerosol, ice forming activity, UV irrad. effect 0-71950
- Al/Cu thin film couples, TEM study of intermetallic nucleation at interface 0-65305
- Al-Cu (2.5 wt.%), precipitation total surface influence on resistivity (French) 0-71650
- Al-Mg-Si alloys, ductile intergranular fracture mechanisms, void formation and nucleation 0-108578



**nucleation continued**

- Al-Zn, grain boundary reaction sites, determ. of struct. aspects, by electron microscopy 0-103359  
 Al<sub>2</sub>O<sub>3</sub> ultrafine gel particle form. from NH<sub>3</sub>-AlCl<sub>3</sub> solution 0-93807  
 Al<sub>2</sub>O<sub>3</sub>-TiO<sub>2</sub> powder, plasma-prepared, morphology and phase constitution 0-100833  
 AlSb, laser pulse annealing, induced nucleation, crystal growth 0-84966  
 Ar, cluster formation and homogeneous nucleation, comparison of expt. and theory 0-79925  
 Ar, nonequilibrium condensation and surface tension in supersonic jet flow (*Russian*) 0-65210  
 B, closed system CVD, deposition rate and rate-limiting steps 0-93492  
 Ba, silicates, solid state reactions, thermodynamics and kinetics (*German*) 0-76236  
 CaCO<sub>3</sub> crystallisation from aqueous solutions, kinetic study 0-59419  
 Ca<sub>10</sub>(PO<sub>4</sub>)<sub>6</sub>(OH)<sub>2</sub> dissolution kinetics, nucleation-controlled 0-59659  
 Cd<sub>3</sub>As<sub>2</sub> films, nucleation processes, on NaCl substrates 0-59813  
 CdS, epitaxial growth and nucleation, on monocryst. ZnS, substrate real struct. influence 0-88455  
 CdS single cryst., vaporization and form. of negative whiskers 0-92659  
 Co<sub>2</sub>Sm crystals, microstruct., homogeneous precip. and nucleation 0-104160  
 Cu crystals, two-phase, recrystn. retardation, particle size, spacing effects 0-89242  
 Cu, electrochem. nucleation and growth on Te and Al, TEM 0-104451  
 Cu electrocrystallisation on graphite electrodes, nucleation 0-93504  
 Cu, electrolytic epitaxial nucleation and growth, on (111) Ag 0-104081  
 Fe-C-Si, high purity, vacuum melted, nodular graphite form. 0-108452  
 Fe-Mo (13-20 at.%) binary alloys, spinodal decomp. on ageing, TEM and X-ray diffr. study 0-97503  
 Fe-Ni (28 at.%), martensitic transformations, Mossbauer scattering evidence of soft modes 0-93223  
 Fe<sub>2</sub>B<sub>3</sub>O<sub>13</sub>l, boracite single cryst., nucleation control density growth 0-80955  
 Fe<sub>30</sub>(C<sub>1-x</sub>B<sub>x</sub>)<sub>70</sub> amorphous alloy,  $\alpha$ -Fe crystn., morphology 0-70129  
 $\alpha$ -Fe<sub>2</sub>O<sub>3</sub> crystal flux growth, solubility and relative supersaturation in Fe<sub>2</sub>O<sub>3</sub>-PbO-V<sub>2</sub>O<sub>5</sub> fluxed melt system 0-64934  
 Gd<sub>3</sub>Ga<sub>2</sub>O<sub>12</sub>, flux growth and nucleation temp. determ. (*Chinese*) 0-60761  
 Ge, exciton condensation, electron-hole drop investigation in UHF field, nucleation (*Russian*) 0-80193  
 Ge, laser pulse annealing, induced nucleation, crystal growth 0-84966  
 H<sub>2</sub>O droplets, subcooled, nucleation in Ar-H<sub>2</sub>O vapour mixture, rate const. 0-61131  
 H<sub>2</sub>O-H<sub>2</sub>SO<sub>4</sub>-ion aerosol particles, ultrafine, stratospheric form., ion-induced nucleation 0-72608  
 H<sub>2</sub>SO<sub>4</sub>-H<sub>2</sub>O aerosols nucleation rate in presence of ionisation source 0-104464  
<sup>3</sup>He, solid, phase separation of dil. <sup>4</sup>He impurities 0-88393  
<sup>4</sup>He crystals, nucleation and orientation 0-84339  
<sup>4</sup>He, superfluid, vortex nucleation inhibition by strong electric fields 0-92735  
 Hg, condensation, two-dimensional, on W 0-107666  
 KCl, two-dimens. nucleation rate on the (100) surfaces, mol. beam method, 289-343°C (*German*) 0-93500  
 KCl:Ba<sup>2+</sup>, localised stress relaxation in excess vacancy system, prismatic loops (*Russian*) 0-88160  
 KH<sub>2</sub>PO<sub>4</sub> single crystal evidence for spiral growth on pyramidal faces 0-84120  
 Li<sub>2</sub>O-2SiO<sub>2</sub> glass, DTA study, Kissinger plot 0-84084  
 Li<sub>x-2</sub>P<sub>2</sub>O<sub>3x+1</sub>, polyphosphate, melting and crystallisation 0-70376  
 Mo, film on sapphire substrate, orientational growth, epitaxial textures, nucleation textures (*Russian*) 0-75454  
 Mo-Zr, nucleation conditions, effect on formation of oxide phase during internal oxidation (*Russian*) 0-81064  
 NH<sub>4</sub>Cl, submicron particles, density, morphology 0-61166  
 NH<sub>4</sub>Cl-H<sub>2</sub>O, solidification microstructs., effect of reduced gravity 0-96632  
 NH<sub>4</sub>H<sub>2</sub>PO<sub>4</sub> single crystal evidence for spiral growth on pyramidal faces 0-84120  
 Na<sub>2</sub>O-2CaO-3SiO<sub>2</sub> glass, cryst. nucleation and growth, viscosity, thermodynamic props. 0-84079  
 Na<sub>2</sub>O-Al<sub>2</sub>O<sub>3</sub>-SiO<sub>2</sub> glass, nucleation, crystn., ceramic form. 0-84082  
 Na<sub>2</sub>O-BaO-Al<sub>2</sub>O<sub>3</sub>-SiO<sub>2</sub> glass, nucleation, crystn., ceramic form. 0-84082  
 2Na<sub>2</sub>O-CaO-3SiO<sub>2</sub> glass, cryst. nucleation rate, viscosity, heat treatment 0-84081  
 Na<sub>2</sub>O-SiO<sub>2</sub>:Au+CeO<sub>2</sub>, Au particle nucleation 0-81066  
 Nb, film on sapphire substrate, orientational growth, epitaxial textures, nucleation textures (*Russian*) 0-75454  
 Nb<sub>3</sub>Ge coevaporated film, high supercond. transition temp., nucleation and growth 0-76185  
 Ni (100), adsorption of O<sub>2</sub> and reduction of surface oxide by H<sub>2</sub> 0-108741  
 Ni crystallisation, on reinforced fibres (*Russian*) 0-75455  
 Ni-B film, crystn. on reinforced fibres (*Russian*) 0-75455  
 Ni<sub>3</sub>B<sub>2</sub>O<sub>3</sub>Br, boracite single cryst., nucleation control density growth 0-80955  
 (Ni<sub>0.9</sub>Pd<sub>0.1</sub>)<sub>82</sub>P<sub>18</sub> amorphous alloy, liquid-quenched, crystn. kinetics, nucleation 0-100176  
 Pb, underpotential adsorption, cathodic deposition, on Ag(111) and (100) (*German*) 0-108363  
 Se<sub>0.9</sub>Te<sub>0.05</sub> glass crystallisation, effect of an alternating electric field 0-88054  
 Se<sub>1-x</sub>Te<sub>x</sub> amorphous film, photo-crystallisation 0-59839  
 Se<sub>2</sub>Te<sub>1-x</sub> growth of single crystals by Czochralski method 0-66423  
 Si, (111) surface structure phase transform, screw dislocations RHEED study 0-88153  
 Si, Czochralski grown crystal, O precip., nucleation behaviour and dislocation loop form. (*Japanese*) 0-59664  
 Si, slip dislocation nucleation during laser annealing 0-84179  
 Si-Al-Al<sub>2</sub>O<sub>3</sub> system, solid phase Si regrowth on sapphire 0-100413  
 Ta, film on sapphire substrate, orientational growth, epitaxial textures, nucleation textures (*Russian*) 0-75454  
 Te, growth of single crystals by Czochralski method 0-66423  
 Te, vacuum deposited on NaCl, crystallite growth and morphology, electron microscopy 0-65401  
 Ti, pit nucleation in bromide media, ion beam anal. 0-93683  
 Ti-Ag (10 to 17.5 wt.%), eutectoid system,  $\beta$ - $\alpha_m$  transform., nucleation kinetics 0-97474  
 Ti-Au, (9.9 wt.%), eutectoid system,  $\beta$ - $\alpha_m$  transform., nucleation kinetics 0-97474

**nucleation continued**

- Ti-Mo-Zr-Sn (11.5, 6.0, 4.5 wt.%) alloy, struct. as affected by processing history 0-84972  
 TiD<sub>2</sub>, nucleation and growth in D<sub>3</sub><sup>+</sup>-implanted Ti, TEM study 0-97717  
 TiO<sub>2</sub> brookite synthesis from Ti in NaF or Ti compounds, form. mechanism (*Japanese*) 0-93529  
 Tl, underpotential adsorption, cathodic deposition, on Ag(111) and (100) (*German*) 0-108363  
 TiAs<sub>2</sub>, glass, crystallisation, effect of an alternating electric field 0-88054  
 V, film on sapphire substrate, orientational growth, epitaxial textures, nucleation textures (*Russian*) 0-75454  
 W, film on sapphire substrate, orientational growth, epitaxial textures, nucleation textures (*Russian*) 0-75454  
 Zn, electrolytic deposition, on Pt single crystal spheres, critical overvoltage 0-104080

**nuclei see nucleus****nuclei with mass number 1 to 5**

- big bang, helium synthesis, neutrino flavors, and cosmological implications 0-73084  
 charge structure, effect of neutron charge 0-105963  
<sup>2</sup>n binding energy, calc. from <sup>3</sup>H, <sup>3</sup>He, <sup>4</sup>H, <sup>4</sup>He and <sup>4</sup>Li ground-state properties 0-83044  
<sup>2</sup>n system, bound state, Faddeev eqn. calc. 0-105989  
<sup>4</sup>n binding energy, calc. from <sup>3</sup>H, <sup>3</sup>He, <sup>4</sup>H, <sup>4</sup>He and <sup>4</sup>Li ground-state properties 0-83044  
 t-dn vertex constant from Faddeev eqn. (*Russian*) 0-83079  
<sup>2</sup>H(d,d), 5-45 MeV deuteron wave function asymptotic D- to S-state normalisation, anal. power 0-78304  
<sup>2</sup>H(n,p)n, 63.1 MeV, differential cross section 0-63186  
<sup>2</sup>H( $\alpha$ ,X), 1.74, 2.57 GeV, low mass  $\pi$ N enhancement, cross section t-depend. 0-63193  
<sup>2</sup>H( $\gamma$ , $\pi^+$ ), 3.4-18 GeV,  $\pi$ NN form factor and differential cross sections, one pion exchange 0-68526  
<sup>2</sup>H( $\mu$ , $\nu\gamma$ ), radiative capture relativistic calcs., rate and photon spectrum 0-68605  
<sup>2</sup>H(n, $\gamma\gamma$ ), thermal, consistency between pion exchange currents and NN pol., cross sections 0-68556  
<sup>2</sup>H(n,n), 16.9 MeV, anal. power, F-wave contribs. 0-63158  
<sup>2</sup>H(n,n), pol. n, 13.5-16.9 MeV, anal. power and spin-orbit phase parameters 0-78269  
<sup>2</sup>H(n,n), pol. n, 50 MeV, anal. power 0-68639  
<sup>2</sup>H(n,p)n, pol. n,p, 50 MeV, spin correlation parameter A<sub>yy</sub>( $\theta$ ), phase shift anal. 0-68530  
<sup>2</sup>H(n, $\pi^0$ )<sup>2</sup>H, differential cross sections for 470-590 MeV, ang. distribs. 0-57628  
<sup>2</sup>H(p,X), elastic, inelastic and charge exchange cross sections in optical model 0-68665  
<sup>2</sup>H(p,p), 1-3 GeV/c, pol. p, spin parameters A and A<sub>nn</sub> 0-95304  
<sup>2</sup>H(p,p), 6.14 MeV, anal. power, Paris pot. predictions 0-63156  
<sup>2</sup>H(p,p), pol.p, 9.57 MeV, spin correlation parameter, phase shift anal. 0-102112  
<sup>2</sup>H(p, $\pi^+$ )<sup>2</sup>H, pol. p, total cross section, ang. distribs. and asymmetry parameters 0-63182  
<sup>2</sup>H( $\pi^+$ , $\pi^+$ ), 269, 298, 324 MeV, radiative scatt. cross section, internal emission and recoil corrections 0-57805  
<sup>2</sup>H(d,n), 2.5 GeV/c,  $4\pi$  geometry, pol. approx. description 0-68678  
<sup>2</sup>H( $\pi^+$ , $\pi^+$ ), low energies, Coulomb interaction (*Russian*) 0-83129  
<sup>2</sup>H bound state, relativistic quasipot. wave eqn. soln. 0-102132  
<sup>2</sup>H charge operator, retardation, quasipot. eqns. and rel. corrections 0-99122  
<sup>2</sup>H nucleus wave function momentum contribution from QCD diagrams (*Russian*) 0-68562  
<sup>2</sup>H(<sup>2</sup>H,n)<sup>4</sup>He, muon catalysis kinetics (*Russian*) 0-91206  
<sup>2</sup>H(d,n), 18-26 MeV, differential cross sections, ang. distribs., <sup>4</sup>He broad level search 0-102117  
<sup>2</sup>H(d,n), pol.d, anal. power and polarisations in R-matrix methodology, comparison with (d,p) 0-78273  
<sup>2</sup>H(d,p), pol.d, anal. power and polarisations in R-matrix methodology, comparison with (d,n) 0-78273  
<sup>2</sup>H( $\delta$ , $\pi^0$ ), multiple scatt. contrib. to threshold photoprod. 0-73718  
<sup>2</sup>H(e,e'), 56.4 MeV, cross sections, form factors, meson exchange current contrib. 0-68649  
<sup>2</sup>H(e,e') 1180 MeV electrons, proton distribution, neutron momentum distribution (*Russian*) 0-68652  
<sup>2</sup>H(e,e), EM form factors, relativistic formulae, moment corrections 0-63075  
<sup>2</sup>H(e,e), form factors, tensor pol., and two-nucleon force calcs. 0-106045  
<sup>2</sup>H( $\gamma$ ,n), 20.3 MeV, linearly pol.  $\gamma$ , neutron yield and cross section 0-91171  
<sup>2</sup>H( $\gamma$ ,n)<sup>2</sup>H, 400-700 MeV, p polarisation (*Russian*) 0-106046  
<sup>2</sup>H( $\gamma$ ,n)p, 375-650 MeV, proton polarisation energy depend. at CMS angle 90° (*Russian*) 0-63159  
<sup>2</sup>H( $\gamma$ ,n)p, parity violation exps. review, weak NN interaction 0-73792  
<sup>2</sup>H( $\gamma$ , $\pi^+$ )nn, n-n final state interaction effects 0-102181  
<sup>2</sup>H( $\gamma$ , $\pi$ ), 210-700 MeV, total and differential cross sections from impulse approx. 0-68647  
<sup>2</sup>H(n, nn)p, 25 MeV, neutron-neutron effective range 0-83041  
<sup>2</sup>H(n,2n)p, in thick targets, n-n scatt. length determ., computer expt. 0-57776  
<sup>2</sup>H(n,n), (n,p), 24 MeV, quasifree scatt., n-n effective range, Monte Carlo anal. 0-68554  
<sup>2</sup>H(n, $\pi^+$ ), 400-580 MeV, differential cross sections and ang. distribs. 0-86906  
<sup>2</sup>H(n, $\pi^+$ )<sup>3</sup>He, 400 to 580 MeV at backward pion angles 0-73847  
<sup>2</sup>H( $\nu_e$ , $\bar{\nu}_e$ )n,p, antineutrino spectrum 0-102150  
<sup>2</sup>H( $\nu_e$ , $\gamma$ )<sup>2</sup>He, 450, 550 MeV, differential cross sections, inverse reaction comparison 0-86904  
<sup>2</sup>H(p,p), 800 MeV, differential cross sections and anal. powers 0-83091  
<sup>2</sup>H(p,p), back angle elastic cross sections in Kerman-Kisslinger model, inelasticity corrections 0-106060  
<sup>2</sup>H(p,p), pol.p, spin rot. and depolarisation, NN amplitude double spin flip part 0-78271  
<sup>2</sup>H(p,p), tensor asymmetries, deuteron D-wave and non-eikonal effects, Glauber model 0-78296  
<sup>2</sup>H(p,p) large angle elastic scatt., d form factor at large q<sup>2</sup> 0-102189  
<sup>2</sup>H(p,py), elastic cross sections, bremsstrahlung, threshold and Coulomb effects 0-91186  
<sup>2</sup>H(p, $\pi^+$ ), 400-470 MeV, backward  $\pi$  differential cross sections and anal. power 0-86905

## nuclei with mass number 1 to 5 continued

- $^2\text{H}(\pi, p)p$ , cross sections, Faddeev like eqns., absorption effects for scatt. 0-86928  
 $^2\text{H}(\pi, p)p$  in resonance region, theoretical models 0-83123  
 $^2\text{H}(\pi, \pi)$ , pole terms and absorption in p-wave  $\pi d$  interaction 0-86932  
 $^2\text{H}(\pi, \pi)$ , 140-260 MeV, (3,3) region, tensor force, cross sections, pol. parameters 0-86641  
 $^2\text{H}(\pi, \pi)$ , 142, 256 MeV, form factor-backward scatt. correlation, tensor polarisation 0-99189  
 $^2\text{H}(\pi, \pi)$ , high energies, total cross sections from refined Glauber model 0-78322  
 $^2\text{H}(\pi, \pi)$ , low energy scatt. absorption effects, cross sections, Faddeev like equations 0-86928  
 $^2\text{H}(\pi, \pi)$ , pion absorption effect from threshold to resonance 0-99193  
 $^2\text{H}(\pi, \pi)$ , relativistic Faddeev calc. 0-102066  
 $^2\text{H}(\pi, \pi)$ , scatt. length, exchange current contrib. 0-78328  
 $^2\text{H}(\pi, n)n$ , multiple scatt. corrections, off-shell rescatt. effects, effective range 0-83127  
 $^2\text{H}(\pi^+, p)p$ ,  $\pi\pi$  exchange current effects on pion absorption, cross section enhancement 0-57803  
 $^2\text{H}(\pi^+, \pi^+)$ , 49 MeV, P-wave dispersive contrib.  $\pi$  and  $\rho$  rescatt. 0-78331  
 $^2\text{H}(\pi^+, p)^3\text{H}$ , total cross section, ang. distrib. and asymmetry parameters 0-63182  
 $^2\text{H}(\pi^+, p)p$ , pionic disintegration, absorptive  $\pi$ -nucleus optical pot., microscopic model 0-99191  
 $^2\text{H}(\pi^+, \pi^+)$ , 130 to 350 MeV,  $180^\circ$  scatt. 0-78335  
 $^2\text{H}(\pi^+, \pi^+)$ , 140-260 MeV, backward scatt., differential cross sections 0-99194  
 $^2\text{H}(\mu, \mu)^4\text{He}$ , muon catalysed fusion, neutron yield, muonic molecules 0-106095  
 $^2\text{H}$  binding energy, relativistic calc., Bethe Salpeter eqn. 0-68519  
 $^2\text{H}$   $\beta$ -decay spectrum,  $\bar{\nu}_e$  mass (Russian) 0-91159  
 $^2\text{H}$  decay, electron spectra rel. to neutrino rest mass and astronomical consequences (Russian) 0-109575  
 $^2\text{H}$ , EM form factors, 3-nucleon wave function calc. 0-95302  
 $^2\text{H}$ , ground state energy, second order Brueckner-Baranger approx. 0-63082  
 $^2\text{H}$  ground state props. from configuration space Faddeev calcs. 0-102130  
 $^2\text{H}$ , meson exchange currents, effect on charge form factors 0-105990  
 $^2\text{H}$  realistic wave function, energy and density distrib. 0-86794  
 $^2\text{H}$ , short range repulsion, separation energy, K-harmonics calcs. 0-86846  
 $^2\text{H}(d, n)^3\text{He}$ , neutron fluence and energy transfer standard 0-102194  
 $^2\text{H}(e, np)$ , disintegration and Coulomb excitation cross sections in channelled nuclei 0-59539  
 $^2\text{H}(n, n)$ , scatt. length, 4-nucleon problem, integral eqn. approach 0-91183  
 $^2\text{H}(n, n)$ , zero energy total cross section and scatt. lengths 0-57778  
 $^2\text{H}(p, n)$ , 1.24, 1.8 GeV, differential cross section, spin independ. Glauber model interpretation 0-63183  
 $^2\text{H}(p, n)^3\text{He}$  charge exchange reaction, multifold diffr. scatt. theory (Russian) 0-78303  
 $^2\text{H}(p, p)$ , 1.24 GeV, differential cross section, spin independ. Glauber model interpretation 0-63183  
 $^2\text{H}(\pi, \gamma)^3\text{H}$ , rest  $\pi$ , resonance branching ratio, bound state upper limit 0-99162  
 $^4\text{H}$ ,  $A=1, 2$ , nuclear electric dipole moments from P nonconserving atomic transitions 0-57681  
 $^4\text{H}$ ,  $A=1, 2, 3$ , ang. and vel. distrib. from  $\text{Pb}(\alpha, X)$  (Russian) 0-63194  
 $^4\text{H}$ ,  $A=2, 3$ , binding energy from Brillouin-Wigner perturbation method, strong short ranged interactions 0-86796  
 $^4\text{H}(\gamma, \pi^0)$ ,  $A=1, 2, 1-10$  MeV, photoprod. yields, DWIA anal., dipole photoprod. amplitudes 0-68645  
 $^4\text{H}(n, X)$ , 60 keV-80 MeV,  $A=1, 2, 3$  total cross section and scatt. length 0-99176  
 $^4\text{H}(\pi, \pi)$ ,  $A=1, 2$ , intermediate energies, collective isobaric resonance 0-63208  
 $^4\text{H}(\pi^+, \pi^+)$ ,  $A=1, 2, 130-280$  MeV,  $180^\circ$  excitation function, dibaryon resonance signals 0-68619  
 $^4\text{He}$ , ground state level determ. 0-99136  
 $^4\text{He}(e, e)$  energy weighted sum rules (Russian) 0-86900  
 $^4\text{He}$  breakup, DWBA calcs. for strongly absorptive projectiles in  $^3\text{V}(^4\text{He}, d)p$  0-68682  
 $^4\text{He}$  Coulomb energy from configuration space Faddeev calcs. 0-102131  
 $^4\text{He}$ , EM form factors, 3-nucleon wave function calc. 0-95302  
 $^4\text{He}$ , liquid, pionic K X-ray transition energies and Lorentzian widths 0-78727  
 $^4\text{He}$ , meson exchange currents, effect on charge form factors 0-105990  
 $^4\text{He}$ , nuclear charge form factor, two-boson exchange charge density  $\pi$ ,  $\rho$ ,  $\omega$  exchanges 0-63073  
 $^4\text{He}$ , one-body charge form factor computer code listing 0-57673  
 $^4\text{He}$ , totally antisymmetric wave function with generalised Faddeev eqn. 0-83046  
 $^3\text{He}(^3\text{He}, ^3\text{He})$ , 120 MeV, continuum energy spectra bump struct., cross sections 0-83108  
 $^3\text{He}(e, e)$ , nuclear high momentum components and  $y$  scaling 0-106051  
 $^3\text{He}(e, p)$ , cross-section, Faddeev technique, nucleon-nucleon interaction (Russian) 0-73842  
 $^3\text{He}(e, e)$ , charge formfactors, second Born approx. and pole model 0-78133  
 $^3\text{He}(e, e)$ , relationship to  $^3\text{He}(\pi^-, \pi^-)$  0-78323  
 $^3\text{He}(\gamma, 2p)n$ , 80-120 MeV, proton energy distrib., diffr. cross sections, direct breakup 0-86897  
 $^3\text{He}(\gamma, \pi^+)^3\text{H}$  cross section near threshold, 0-83093  
 $^3\text{He}(\mu, \gamma\gamma)$ , transition amplitude, PCAC tests 0-102152  
 $^3\text{He}(\mu, \gamma\gamma)$ , radiative capture relativistic calcs., rate and photon spectrum 0-68605  
 $^3\text{He}(n, n)$ , scatt. length, 4-nucleon problem, integral eqn. approach 0-91183  
 $^3\text{He}(n, p)T$ , appl. to anal. of fusion reactor materials, archeometry, and nuclear spectroscopy 0-61200  
 $^3\text{He}(p, \pi^+)^4\text{He}$ , 415 MeV, angular distrib., microscopic description, generalisation of  $(\pi, \pi)$  (Chinese) 0-63188  
 $^3\text{He}(\pi, \pi)$ , 1 GeV, backward scatt., nonstable meson-nucleon interaction cross section, resonance (Russian) 0-86559  
 $^3\text{He}(\pi, \pi)$ , 68-154 MeV, single and double collision differential cross section calcs. (Russian) 0-106083  
 $^3\text{He}(\pi, \pi)$ , elastic interactions in JINR high press. streamer chamber, triggering system 0-102400

## nuclei with mass number 1 to 5 continued

- $^3\text{He}(\pi, \pi)$ , elastic interactions in JINR high press. streamer chamber, selection criteria 0-102401  
 $^3\text{He}(\pi, \pi)$ , optical potential in momentum representation 0-78324  
 $^3\text{He}(\pi^-, \pi^-)$ , 145, 180 and 195 MeV, relationship to  $^3\text{He}(e, e)$  0-78323  
 $^3\text{He}(\pi^-, \pi^0)$ , form factor sensitivity in Glauber multiple scatt. formalism 0-105964  
 $^3\text{He}(\pi^-, \pi^0)^3\text{H}$ , optical potential in momentum representation 0-78324  
 $^4\text{He}$  2 $^+$  resonance evidence at 40 MeV from  $^4\text{He}(e, ^3\text{H})$ , and  $^3\text{H}(p, \gamma)$  0-86880  
 $^4\text{He}(e, e'pp)$  reaction cross-section and ground state shell model calcs. (Russian) 0-78283  
 $^4\text{He}(\pi^-, \pi^+ p)$ , 5 GeV/c, quasielastic scatt., cross section, form factor, final state interactions 0-99190  
 $^4\text{He}$  binding energy, 4-nucleon problem, integral eqn. approach 0-91183  
 $^4\text{He}$  broad level search from  $^2\text{H}(d, n)$  0-102117  
 $^4\text{He}$  continuum microscopic calcs. cross sections and levels from  $^3\text{He}+n$ ,  $^3\text{H}+p$  channels 0-57702  
 $^4\text{He}$ , four-nucleon bound state with realistic NN interaction, hyperspherical harmonics (Russian) 0-83045  
 $^4\text{He}$ , ground state energy, second order Brueckner-Baranger approx. 0-63082  
 $^4\text{He}$  nuclear charge density determ. using form factor analyticity 0-63077  
 $^4\text{He}$  photodisintegration, pair correlation study (Russian) 0-86899  
 $^4\text{He}$  photodisintegration, total, dipole, and quadrupole cross sections, sum rules (Russian) 0-83094  
 $^4\text{He}$  production, nonzero neutrino rest mass effects 0-105413  
 $^4\text{He}$ ,  $T=1$  excited negative parity state struct. 0-57688  
 $^4\text{He}(\pi, \pi)$ , elastic data inconsistencies and dispersion relations above 33 resonance 0-68700  
 $^4\text{He}(\alpha, \alpha)$ , 4.32, 5.07 GeV/c, Glauber multiple scatt. theory comparisons 0-63192  
 $^4\text{He}(\alpha, \alpha)$ , large amplitude collective motion, adiabatic TDHF calcs. 0-86786  
 $^4\text{He}(\alpha, \alpha)$ , nuclear separable plus Coulomb interaction 0-83106  
 $^4\text{He}(\alpha, \alpha)$ , s-wave, Coulomb amplitudes from generator coordinate theory 0-83107  
 $^4\text{He}(\alpha, \alpha)$ , size change of  $\alpha$  effect on phase shift, generator coordinate and variational methods (Chinese) 0-68683  
 $^4\text{He}(\alpha, \alpha)$ , 119 MeV, excited states,  $J^\pi$  and  $\gamma$ -ang. correlations 0-86809  
 $^4\text{He}(d, d)$ , distortion effects, orthogonality condition model 0-63190  
 $^4\text{He}(d, d)$ , low energy, resonating group method anal. with distortion effect 0-73851  
 $^4\text{He}(\gamma, X)$ ,  $X=p, n$ , 50-150 MeV, total cross sections, quasiparticle formalism calcs. 0-78277  
 $^4\text{He}(\gamma, pn)^3\text{H}$ , three particle photodisintegration, pole mechanism contrib. (Russian) 0-91176  
 $^4\text{He}(n, X)$ , local approximation to a non-local potential 0-91182  
 $^4\text{He}(p, p)$ , 1.05 GeV, cross sections and polarisations, correlation effects calcs. 0-57774  
 $^4\text{He}(p, p)$ , 200-500 MeV, differential cross section and anal. power 0-68640  
 $^4\text{He}(p, p)$ , 788 MeV, back angle diffraction struct., Dirac, eqn. optical model 0-68667  
 $^4\text{He}(p, p)$ , differential cross-section, multifold diffr. scatt. theory (Russian) 0-78303  
 $^4\text{He}(\pi, X)$ , 120, 145, 165 MeV, total and differential cross sections 0-78326  
 $^4\text{He}(\pi, \pi)$ , elastic interactions in JINR high press. streamer chamber, selection criteria 0-102401  
 $^4\text{He}(\pi, \pi)$ , single scatt. optical pot., Pauli principle and binding effects on cross section 0-86933  
 $^3\text{He}$ , A-N pot. Majorana component on  $B_1$  value, overbinding 0-99144  
 $^4\text{He}$ ,  $A=3, 4$ , charge structure, effect of neutron charge 0-105963  
 $^4\text{He}(\gamma, \pi^0)$ ,  $A=3, 4, 1-10$  MeV, photoprod. yields, DWIA anal., dipole photoprod. amplitudes 0-68645  
 $^4\text{He}(\pi, \pi)$ ,  $A=3, 4$ , intermediate energies, collective isobaric resonance 0-63208  
 $^4\text{He}(\pi^+, \pi^+)$ ,  $A=3, 4, 260$  to 310 MeV, differential cross sections 0-99192  
 $^4\text{H}(p, A^0)$ , inclusive cross section, constituent-constituent multiple scatt. model for dependence on atomic number 0-83101  
 $^4\text{H}(p, X)$ , direct and charge transfer scattering processes, second quantisation 0-78289

## nuclei with mass number 6 to 19

- $A=18$ , shell-model spectra, one-boson-exchange potential 0-68550  
 $A=18-38$ , inelastic scatt. E4 transition probabilities in the Od, 1s shell 0-78210  
 $^{12}\text{C}(\gamma, \pi^+)^{12}\text{B}$ , nuclear critical opalescence study 0-105988  
stable odd-mass sd nuclei, EM multipole moments of ground states 0-102116  
 $^{18}\text{O}(\gamma, \sigma_0)$ , 19-32 MeV, E1 and E2 cross section, E1-E2 phase difference 0-63172  
 $B$ , muonic X-ray transitions, nuclear charge radii 0-99589  
 $B$   $\beta^+$ -decay,  $\beta$ - $\alpha$  angular correlations, final state energy depend., current test 0-102151  
 $B$  complex system, excitation functions for 17.19 and 17.64 MeV levels from  $^6\text{Li}+^3\text{He}$  0-78188  
 $^6\text{B}(p, \pi^+)$ ,  $A=10, 11, 200$  MeV, pion energy spectra for discrete final states, cross sections 0-106057  
 $B$  levels and differential cross sections PWBA and coupled channel anal. of  $(\alpha, t)$  0-102121  
 $^{10}\text{B}(d, p)^{11}\text{B}$ , 2.5 to 21.0 MeV, angular distrib., DWBA analysis 0-68675  
 $^{10}\text{B}(\gamma, d)$ , from  $(e, e'd)$ , cross section, E2 transistors giant resonance and clusters 0-63169  
 $^{10}\text{B}(n, \alpha)^7\text{Li}$ , appl. to anal. of fusion reactor materials, archeometry, and nuclear spectroscopy 0-61200  
 $^{10}\text{B}(d, t)^{11}\text{B}$ , 5.5 MeV, angular distrib., DWBA analysis 0-68675  
 $^{11}\text{B}$ , neutrino-induced prod. in stellar C layer 0-82337  
 $^{11}\text{B}(\gamma, \gamma)$ , resonance scatt., molecular orientation effects 0-78252  
 $^{11}\text{B}(p, n)^{11}\text{C}$ , steel B depth distrib. meas. using time of flight method 0-71986  
 $^{11}\text{B}(p, ^7\text{Li})^4\text{Li}$ , 51.9 MeV, five nucleon transfer mechanisms, DWBA calcs. 0-73845  
 $^{12}\text{B}$ , aligned,  $\beta$ -ang. distrib. asymmetry coeffs., pseudotensor interaction,  $T=1$  isospin triplet decay 0-106021  
 $^{12}\text{B}$  analogue states at 4.5 MeV giant resonance region, strong spin-isospin mode, from  $^{12}\text{C}(e, e'\pi^+)$  0-78250  
 $^{12}\text{B}$  spin polarisation in  $^{100}\text{Mo}(^{12}\text{B}, ^{12}\text{B})$  0-63160



## nuclei with mass number 6 to 19 continued

- <sup>12</sup>B spin polarisation in <sup>132</sup>Th(<sup>14</sup>N,<sup>12</sup>B) 0-63161  
 Be muonic X-ray transitions, nuclear charge radii 0-99589  
 Be, neutron forces in relativistic electron radiation field in crystal, channelling (*Russian*) 0-70287  
 Be, 477.6 keV, Analytic fitting of full-energy peaks in Ge(Li) spectra at high count rates 0-99147  
 Be as a tracer for helio-geophysical phenomena 0-98525  
 Be effective for charge exchange analogues of Gamow-Teller transitions from <sup>7</sup>Li(p,n) 0-57726  
 Be(p, $\gamma$ ), low energy cross section from direct, capture potential model 0-102184  
 Be <sup>1+</sup> and <sup>1-</sup> levels, expt. and shell model calcs. from <sup>7</sup>Li(p, $\gamma$ ) 0-63095  
 Be collective excitation spectra from generalised hyperspherical functions method (*Russian*) 0-91133  
 Be, energy levels deduced from <sup>6</sup>Li(<sup>4</sup>Li, $\alpha$ ) $\alpha$  reaction mechanism 0-83113  
 Be fission mode, large amplitude collective motion, adiabatic TDHF calcs. 0-86786  
 Be high spatial symmetry excited states, resonances, rot. band from (d, $\alpha$ t), (p, $\alpha$ t) 0-86780  
 Be low lying spectrum, 3-body molecular description, adiabatic one level approx. 0-78150  
 Be(<sup>10</sup>B,<sup>10</sup>B), 9.5-14.2 MeV, ang. distrib., cross sections, elastic p transfer 0-78318  
 Be(K<sup>-</sup>,  $\Pi^-$ ), 720 MeV/c, Sigma hypernuclei prod., missing mass spectrum 0-57721  
 Be( $\alpha$ ,  $\alpha'$ ), 65 MeV, levels and differential cross sections, optical anal. 0-102121  
 Be( $\alpha$ , $\alpha$ ), 140 MeV, quasifree knockout, DWIA anal. spectroscopic factors 0-68629  
 Be(d,n)<sup>10</sup>B use of neutrons for meas. of full cross sections (*Russian*) 0-69008  
 Be(e, $\pi^+$ ), 1848 MeV, virtual photon spectrum, virtual photon theory test 0-102183  
 Be( $\gamma$ , $\gamma$ ), 32 MeV, energy spectra, d prod. process (*Russian*) 0-91177  
 Be, distrib. in geophysical samples, meas. using tandem van de Graaf accelerator 0-61924  
 Be levels and differential cross sections DWBA and coupled channel anal. of ( $\alpha$ , <sup>3</sup>He) 0-102121  
 Be, excited states and spectra, continuum effects calcs. 0-57720  
 Be( $\gamma$ ,X), photoabsorption cross-section, Levinger's factor, mass number dependence 0-63165  
 Be( $\gamma$ ,p)X, 180-420 MeV, quasifree NN system photodisintegration, p spectrum 0-106049  
 Be(x,x), x= $\pi^+$ , K<sup>+</sup>, p,  $\bar{p}$  70, 125, 175 GeV/c 0-83128  
 (C,X), light relativistic ion-target interactions, particle emission 0-102193  
 C ( $\pi^-$  p) 1.5-5 GeV/c, cumulative proton polarisation (*Russian*) 0-86896  
 C, muonic X-ray transitions, nuclear charge radii 0-99589  
 C(<sup>12</sup>C,X), 4.5 GeV/c, emission of short range particles (R<100 mkm) (*Russian*) 0-63202  
 A<sup>+</sup>C, A=12, 13, nuclear critical opalescence, M1 form factor, pion field and condensation 0-73809  
 A<sup>+</sup>C( $\pi^+$ ), A=12,13, 200 MeV, pion energy spectra for discrete final states, cross sections 0-106057  
 A<sup>+</sup>C( $\pi^+$ ), A=12,13, 200 MeV, analogue and nonanalogue state cross sections 0-99130  
 C, forbidden transition ang. distrib., CCBA and DWBA anal. of (p,d) 0-86848  
 C <sup>1+</sup>(T=1, 15.1 MeV) state excitational pionic modes, M1 form factor for (p,p'), (e,e') 0-78195  
 C <sup>2+</sup> level, transverse EM form factor, convection current contrib. 0-63076  
 C, alpha cluster in Hartree Fock calcs. 0-63110  
 C gamma line Doppler broadening in <sup>12</sup>C(n,n' $\gamma$ )<sup>12</sup>C and <sup>9</sup>Be( $\alpha$ ,n $\gamma$ )<sup>12</sup>C, 4438 keV 0-91147  
 C isovector M1 excitations, current and spin contribs. from (e,e'), (p,n) 0-68582  
 C M1 form factor, pion field critical opalescence,  $\rho$  role, polarisation phenomena 0-68552  
 C, M1 form factor, pion field, rho meson role 0-105970  
 C,  $\pi^+$  absorption in flight, cross section, 91-143 MeV 0-63212  
 C, residual interactions, current conserving RPA calculations 0-57710  
 C transfer spectra direct contrib. from <sup>208</sup>Pb(<sup>16</sup>O,X) projectile fragmentation 0-63155  
 C+<sup>12</sup>C gross structure, resonances in excitation functions from <sup>12</sup>C(<sup>12</sup>C,<sup>10</sup>B) 0-102167  
 C+<sup>12</sup>C system resonant strucs., J<sup>+</sup> assignments, true <sup>24</sup>Mg states from <sup>12</sup>C(<sup>12</sup>C,<sup>10</sup>O) 0-99163  
 C(<sup>12</sup>C,<sup>12</sup>C), shape resonance energy and widths, projection operator method 0-78255  
 C(<sup>12</sup>C, $\gamma$ ), 11.8-20.0 MeV, total cross section resonant and average behaviour 0-106069  
 C(<sup>12</sup>C,<sup>12</sup>C), 10-30 MeV, projection operator method, Feshbach doorways, intermediate structure 0-68695  
 C(<sup>12</sup>C,<sup>12</sup>C), 10-30 MeV, molecular structure, projection operator anal., differential cross sections 0-106033  
 C(<sup>12</sup>C,<sup>12</sup>C), perturbed stationary state method, low energy collision and mol. resons. 0-78320  
 C(<sup>12</sup>C,X), collective potentials and inertia parameters, adiabatic time dependent HF calcs. quasimolecular resonances 0-63195  
 C(<sup>12</sup>C,X), optical potential, nuclear matter approach 0-57801  
 C(<sup>12</sup>C,X), two fireball model, pp correlations and inclusive pion spectrum 0-68694  
 C(<sup>12</sup>C, $\alpha$ ), 7-15 MeV, excitation function statistical anal., nonstatistical features 0-99167  
 C(<sup>14</sup>N, $\alpha$ ), 10.1-15.9 MeV, forward angle excitation function structure, nonstatistical struct. 0-86885  
 C(<sup>16</sup>O,<sup>16</sup>O), elastic and inelastic, 23-32 MeV, strong absorption region resonances, excitation functions 0-86884  
 C(<sup>16</sup>O,X), transparency to l=9 partial wave in 14.7 MeV resonance region 0-78314  
 C(<sup>28</sup>Si, $\alpha$ X), 87-91.5 MeV,  $\alpha$ -HI angular correlations, excitation functions, statistical anal. 0-86915  
 C(<sup>12</sup>Li,X), 156 MeV, projectile break up in continuous particle spectra, cross section, fragmentation 0-86889  
 C(<sup>12</sup>Li,d)<sup>16</sup>O-<sup>12</sup>C+ $\alpha$ , reaction mechanism from ang. correlations, direct transfer 0-78319  
 C(K<sup>-</sup>,K<sup>+</sup>), form factors, cross sections, interior probing capability 0-78366

## nuclei with mass number 6 to 19 continued

- <sup>12</sup>C(K<sup>+</sup>,K<sup>+</sup>), 100-1000 MeV, differential and total cross sections, nucleon motion 0-102206  
 C( $\alpha$ ,X), a=p,d,<sup>4</sup>He,<sup>12</sup>C, 4.2 GeV/c, multitudes of secondary negative particles, momentum distrib. ratios (*Russian*) 0-63178  
 C( $\alpha$ , $\alpha$ ), 140 MeV, quasifree knockout, DWIA anal. spectroscopic factors 0-68629  
 C( $\alpha$ , $\alpha'$ ), generator coordinate multichannel calc., levels and resonances 0-78149  
 C( $\alpha$ , $\alpha$ ), 1.37 GeV, S-matrix expansion from Glauber multiple scatt. theory 0-91191  
 C(d, d'), isospin violating direct reaction, Coulomb interaction role 0-102170  
 C(d,d), 1.69 GeV/c, Coulomb interference region, Glauber theory anal. 0-99178  
 C(d,p)<sup>13</sup>C, 0.5 to 2.5 MeV, excitation functions and angular distrib., possible doorway state (*Chinese*) 0-68679  
 C(e,e'), cross sections, shadowing effect at small four momentum transfer 0-63176  
 C(e,e'), role of two-particle scatt. (*Russian*) 0-91178  
 C(e,e), 25-115 MeV, ground state charge distrib. and RMS charge radius 0-57672  
 C( $\gamma$ ,  $\pi^0$ p), 0.7-1.65 GeV, cross section asymmetry of  $\pi^0$  photoprod. (*Russian*) 0-63164  
 C( $\gamma$ , $\gamma$ ), 23.5-39 MeV, cross sections and giant resonances, E2 strength 0-63122  
 C( $\gamma$ , $\gamma$ ), total photoabsorption and elastic cross sections, spectroscopic information (*Russian*) 0-83095  
 C( $\gamma$ ,n $\alpha$ )<sup>7</sup>Be, electric quadrupole transition cross-sections, behind giant resonance (*Russian*) 0-78281  
 C( $\gamma$ ,p)<sup>11</sup>B, electric quadrupole transition cross-sections, behind giant resonance (*Russian*) 0-78281  
 C( $\gamma$ ,p $\alpha$ )<sup>7</sup>Li, electric quadrupole transition cross-sections, behind giant resonance (*Russian*) 0-78281  
 C( $\gamma$ , $\pi^-$ )<sup>12</sup>N, total cross section calc.,  $\Delta(1232)$  contrib. 0-91175  
 C( $\gamma$ , $\pi^-$  p), final state interaction, distorted and plane wave momentum distrib. 0-78275  
 C( $\mu^-$ ,  $\nu$ )<sup>12</sup>B, polarisation studies, muon capture, weak interaction aspects 0-68655  
 C(n,n), spin-flip probability to first <sup>2+</sup> level 0-78288  
 C(p, X), pol. p, 65 MeV, continuum spectra anal. powers 0-102178  
 C(p,X), 50 MeV, effective cross sections 0-78284  
 C(p,X), reaction and scatt. dynamics, optical and coupled channel anal. 0-78297  
 C(p,2p), asymmetric energy-sharing mode, half distorted-wave formalism, intermediate giant resonance 0-68656  
 C(p, $\alpha$ ), 45.2 MeV, cross sections, finite range DWBA anal., cluster form factors 0-68666  
 C(p,n), 144 MeV, charge exchange, one pion exchange and PCAC tests 0-78299  
 C(p,p'), 122 MeV, level excitation, cross sections, effective NN interaction, DWIA anal. 0-78197  
 C(p,p'), 122 MeV, precritical phenomena 0-83089  
 C(p,p'), 22-27 MeV, <sup>1+</sup> state de-excitation  $\gamma$ -ray ang. distrib., tensor force effects, DWBA anal. 0-68580  
 C(p,p'), 800 MeV, 15.11 MeV state diff. cross section, nuclear critical opalescence search 0-105984  
 C(p,p'), pol. p, 800 MeV, unnatural parity states excitation, anal. powers and isospin 0-68538  
 C(p,p' $\gamma$ ), 23.5-27 MeV, <sup>1+</sup> state spin flip meas. DWBA anal., cross sections 0-68529  
 C(p,p'), 20-40 MeV, pol. p, anal. powers, imaginary spin-orbit pot., coupled channels anal. 0-102179  
 C(p,p), 14-45 MeV, differential cross section and spin-flip probabilities, giant resonances 0-73850  
 C(p,p), bremsstrahlung near 1.7 MeV resonance 0-68670  
 C(p,p), pol. p, 14.23 MeV resonance broadening, nuclear recoil, atomic excitation effects 0-102165  
 C(p,p), radial sensitivity of optical pot. 0-86869  
 C( $\pi$ ,X), Kalinkin-Shmonin model, expt. data 0-86931  
 C( $\pi$ , $\pi$ ), A\* excitation, A\* model unified description 0-102205  
 C( $\pi$ , $\pi$ ), 260 MeV, short range correlations from Glauber multiple diffraction theory (*Chinese*) 0-102210  
 C( $\pi$ , $\pi$ ), intermediate energies, collective isobaric resonance 0-63208  
 C( $\pi$ , $\pi$ ), nonlinear meson dynamics and binding corrections, optical pots. 0-106080  
 C( $\pi^-$ , X), 40 GeV/c, cumulative pions and nucleus total disintegration probability (*Russian*) 0-57807  
 C( $\pi^-$ ,  $\pi^-$ ), 40 GeV, semi-coherent elastic scatt., angular distrib. 0-68701  
 C( $\pi^-$ ,  $\pi^+$ p), 100, 180 MeV, knock out reaction, cross section and pion distortion in DWIA 0-91167  
 C( $\pi^+$ X), 85-245 MeV, true absorption and scatt. in (3,3) resonance region 0-102207  
 C( $\pi^+$ , $\pi^+$ ), 0-300 MeV, cross sections, pion-nucleus optical pot. including nuclear Hamiltonian 0-68706  
 C( $\pi^+$ , $\pi^+$ p), 100, 130 MeV, quasi-elastic scatt. cross section 0-102208  
 C(<sup>12</sup>C, $\pi^+$ N), 291 MeV, quasiselastic scatt., differential cross sections, Monte-Carlo data fit 0-68703  
 C( $\pi^+$ , $\pi^+$ N), 180-255 MeV, quasiselastic pion scatt. coincidence expt. interpretation, impulse approx. 0-68704  
 C( $\pi^+$ , $\pi^+$ p)<sup>11</sup>B, 180 MeV,  $\pi^+$  to  $\pi^-$  cross-section ratio 0-73868  
 C(<sup>12</sup>C,<sup>12</sup>C), molecular neutron orbit formation, 1/2<sup>+</sup> state excitation, coupled channels calcs. 0-78156  
 C(<sup>16</sup>O,<sup>16</sup>O), non-orthogonality of channel states 0-83115  
 C(<sup>9</sup>Be,X), 11.6 MeV, p,t,d, $\alpha$ , <sup>9</sup>Be ang. distrib., Hauser-Feshbach and DWBA anal. 0-91193  
 C(d, <sup>3</sup>He), isospin violating direct reaction, Coulomb interaction role 0-102170  
 C(d, t), isospin violating direct reaction, Coulomb interaction role 0-102170  
 C( $\gamma$ ,n), 6.5-9.3 MeV, ang. distrib., E1, M1 and E2 excitations, resonance radiative widths 0-68581  
 C( $\pi$ , $\pi$ ), elastic and inelastic near  $\pi$ N(3,3) reson. 0-73870  
 C( $\pi^+$ ,  $\pi^+$ o $\pi^0$ ), 120-226 MeV, inelastic scatt. and charge exchange, coupled channels calcs. 0-57804  
 C( $\pi^+$ , $\pi^0$ ), 0-300 MeV, cross sections, pion-nucleus optical pot. including nuclear Hamiltonian 0-68706  
 C first excited 0<sup>+</sup> state, lifetime and E<sup>0</sup> decay from (d,p), (<sup>13</sup>C,p) 0-102145

## nuclei with mass number 6 to 19 continued

- <sup>14</sup>C in groundwater, possible subsurface prod. rel. to dating 0-85690  
<sup>14</sup>C in wines, abundance vars. with 11-year solar cycle, (1909 to 1952) 0-109249  
<sup>14</sup>C<sub>gs</sub>,  $\beta$ -decay, mesonic exchange currents, weak process microscopic treatment 0-57742  
<sup>14</sup>C(<sup>Li</sup>,<sup>He</sup>), 62 MeV, Gamow-Teller sum rules and ground state wave function 0-106073  
<sup>14</sup>C( $\pi^+$ , $\pi^-$ ) 240 MeV inclusive pion production (*Russian*) 0-86908  
<sup>14</sup>C( $\pi^+$ ,X), charged heavy particle emission after pion capture (*Russian*) 0-69271  
<sup>14</sup>C( $\pi^+$ , $\pi^-$ ), X=He or d, 170 MeV, cross sections and ang. distrib., direct knockout mechanism (*Russian*) 0-86887  
<sup>14</sup>C( $\pi$ , $\pi$ ), 170 MeV, two stage and knock out contribs.,  $\pi^+$ , $\pi^-$  spallation differences (*Russian*) 0-68632  
<sup>14</sup>C(x,x), x= $\pi^+$ , K<sup>+</sup>, p,p, 70, 175 GeV/c 0-83128  
<sup>17</sup>F, muonic, energy shifts during atomic EM cascade, and polarisability of deformed nuclei 0-86893  
<sup>18</sup>F 1.04 MeV state lifetime and  $\gamma$ -transition polarisation from <sup>18</sup>O(p,n) 0-106016  
<sup>18</sup>F, prep. with an electron linear accelerator, medical and biological appls. 0-98136  
<sup>18</sup>F resonances,  $\alpha$ -widths, isospin and parity mixing, R-matrix anal. of <sup>14</sup>N( $\alpha$ , $\alpha$ ) 0-91162  
<sup>19</sup>F neutron scattering resonance radiative widths 0-99146  
<sup>19</sup>F, nuclear dealignment of multiply ionised 3 and 6 MeV atoms recoiling in gases 0-78267  
<sup>19</sup>F(p,p $\gamma$ ), 1459-110 keV transition, E2/M1 mixing ratio 0-106013  
<sup>6</sup>He<sub>gs</sub>, short range repulsion, separation energy, K-harmonics calcs. 0-86846  
<sup>6</sup>He, A=6, 8, neutron excess isotope prod. in fragmentation reactions (*Russian*) 0-86888  
<sup>6</sup>Li( $\gamma$ ,X), photoabsorption cross-section, Levinger's factor, mass number dependence 0-63165  
<sup>6</sup>Li(<sup>Li</sup>,<sup>Li</sup>), 30, 88 MeV, M3Y folding model eval., model indep. anal. 0-78317  
<sup>6</sup>Li(X), 156 MeV, projectile break up in continuous particle spectra, cross section, fragmentation 0-86889  
<sup>6</sup>Li, <sup>6</sup>Li, 99 MeV, A=12-208, ang. distrib. from double folding model pots. 0-106074  
<sup>6</sup>Li excited states, final state interactions, three-body force effects from <sup>2</sup>H( $\alpha$ , $\alpha$ ) 0-57692  
<sup>6</sup>Li, transition probabilities between cluster structure states and r.m.s. radius, double well-cluster model (*Chinese*) 0-63128  
<sup>6</sup>Li<sub>1</sub>, supermultiplet struct. and decay props. of hypernuclear 1<sup>+</sup> resonances from (K, $\pi^-$ ) 0-78186  
<sup>6</sup>Li(<sup>He</sup>,<sup>He</sup>), phase shifts, cross sections, resonating group calcs., odd-even features, resonances 0-68681  
<sup>6</sup>Li(<sup>Li</sup>, $\alpha$ ), 36 to 46 MeV, reaction mechanism 0-83113  
<sup>6</sup>Li(d,X) system, resonating group method, single channel approx., cluster states 0-57782  
<sup>6</sup>Li(e,e'), 102, 123 MeV, excitation form factor, <sup>3</sup>H-<sup>3</sup>He cluster model 0-78190  
<sup>6</sup>Li(e,e'), 76-141 MeV, form factors, appl. to ( $\pi^-$ , $\gamma$ ), phenomenological model 0-83068  
<sup>6</sup>Li(e,e), charge formfactors, second Born approx. and pole model 0-78133  
<sup>6</sup>Li(e,e), elastic and inelastic charge form factors from shell model wave functions 0-68523  
<sup>6</sup>Li( $\gamma$ ,X), X=n,p, 10.2-15.4 MeV bremsstrahlung, photoreaction mechanisms 0-68644  
<sup>6</sup>Li( $\gamma$ ,d), from (e,e'd), cross section, E2 transistors giant resonance and clusters 0-63169  
<sup>6</sup>Li(n, $\alpha$ )H, 2.7 MeV triton recoil range, reaction in Li<sub>2</sub>O single cryst. 0-63372  
<sup>6</sup>Li(n, $\alpha$ )T, appl. to anal. of fusion reactor materials, archeometry, and nuclear spectroscopy 0-61200  
<sup>6</sup>Li(n, $\gamma$ ), cross section and spectroscopic factors from direct capture pot. model 0-99171  
<sup>6</sup>Li(p, $\gamma$ ), cross section and spectroscopic factors from direct capture pot. model 0-99171  
<sup>6</sup>Li(p,n), 144 MeV, charge exchange, one pion exchange and PCAC tests 0-78299  
<sup>6</sup>Li(p,pd), 670 MeV, large angle quasifree scatt., spectroscopic factor, momentum distrib., cluster model 0-63184  
<sup>7</sup>Li ( $\bar{\nu}_e$ ,  $\bar{\nu}_e$ ), antineutrino spectrum 0-102150  
<sup>7</sup>Li charge form factor with resonating group wave function, quad. moment, charge radius 0-102110  
<sup>7</sup>Li electric quadrupole moment, from Coulomb scatt. of aligned <sup>7</sup>Li ions 0-78141  
<sup>7</sup>Li, photodisintegration, cluster model wave function, bremsstrahlung weighted cross section 0-63163  
<sup>7</sup>Li(e,e') at first  $\pi$ N resonance, cross section longitudinal and transverse components (*Russian*) 0-86901  
<sup>7</sup>Li( $\gamma$ , $\gamma$ ), 32 MeV, energy spectra, d prod. process (*Russian*) 0-91177  
<sup>7</sup>Li(n, $\gamma$ )Li\* (0.478 MeV) cross-section meas. from 0.5 to 5.0 MeV 0-68661  
<sup>7</sup>Li(t,<sup>Li</sup>)H, near threshold anomaly, S-matrix formalism, <sup>10</sup>Li neutron binding energy (*Russian*) 0-105961  
<sup>7</sup>Li $\rightarrow\alpha$ t virtual decay vertex constant from (d,t), (p, $\alpha$ ) 0-78231  
<sup>7</sup>Li ang. distrib. from <sup>9</sup>Be( $\pi^-$ , $\pi$ N) 0-106036  
<sup>8</sup>Li  $\beta^-$ -decay,  $\beta$ - $\alpha$  angular correlations, final state energy depend., current test 0-102151  
<sup>8</sup>Li, possible  $\gamma$ -transition from <sup>9</sup>Be(K<sup>+</sup>, $\pi^-$ ) 0-106002  
<sup>8</sup>Li, A=7, 8, 9, 11, neutron excess isotope prod. in fragmentation reactions (*Russian*) 0-86888  
<sup>8</sup>Li( $\pi$ ), A=6, 7, 75, 175 MeV, diffialt cross sections, reaction mechanisms 0-78332  
<sup>10</sup>Li neutron binding energy from <sup>7</sup>Li(t,<sup>9</sup>Li)H (*Russian*) 0-105961  
<sup>11</sup>Li beta decay,  $\gamma$  activity 0-106018  
<sup>11</sup>Li, A=6,7, excited states and spectra, continuum effects calcs. 0-57720  
<sup>11</sup>Li( $\gamma$ ,x), photoabsorption cross-section, Levinger's factor, mass number dependence 0-63165  
<sup>11</sup>Li, A=10, 11, double hypernuclei, prod. and decay from (K<sup>+</sup>,X), emulsion 0-57718  
<sup>11</sup>N, muonic X-ray transitions, nuclear charge radii 0-99589  
<sup>11</sup>(<sup>12</sup>C,X), 4.5 GeV/c, emission of short range particles (R<100 mkm) (*Russian*) 0-63202  
<sup>12</sup>N, aligned,  $\beta$ -ang. distrib. asymmetry coeffs., pseudotensor interaction, T=1 isospin triplet decay 0-106021

## nuclei with mass number 6 to 19 continued

- <sup>13</sup>N giant dipole resonance population amplitude and phase, E1 reaction amps. from <sup>12</sup>C(p, $\gamma$ ), pol. p 0-63145  
<sup>14</sup>N levels and excitation energies, kinematically complete investigation from <sup>16</sup>O( $\pi^-$ , 2n) 0-99128  
<sup>14</sup>N quadrupole coupling const., ab initio calcs. 0-58283  
<sup>14</sup>N<sub>gs</sub>, partial muon capture, mesonic exchange currents, weak process microscopic treatment 0-57742  
<sup>14</sup>N+<sup>27</sup>Al, 100 MeV, energy relaxation and mass transfer (*French*) 0-95327  
<sup>14</sup>N(d,  $\alpha$ ), pol.d., 1.5-3 MeV, vector anal. capacity for two  $\alpha$ -particle groups 0-78266  
<sup>14</sup>N( $\gamma$ ,d), from (e,e'd), cross section, E2 transistors giant resonance and clusters 0-63169  
<sup>14</sup>N( $\gamma$ , $\gamma$ ), 32 MeV, energy spectra, d prod. process (*Russian*) 0-91177  
<sup>14</sup>N( $\gamma$ , $\pi$ )<sup>12</sup>C, cross-section and <sup>12</sup>C distrib., quasi-deuteron mechanism 0-63166  
<sup>14</sup>N( $\gamma$ , $\pi^-$ ), DWIA anal., wave function and  $\pi$  optical pot. effects on cross section 0-63168  
<sup>14</sup>N( $\gamma$ , $\pi^-$ ), anomalous <sup>14</sup>N<sub>gs</sub> $\rightarrow$ <sup>14</sup>C<sub>gs</sub> transition, Kroll Ruderman terms 0-63167  
<sup>14</sup>N(p,X), 50 MeV, effective cross sections 0-78284  
<sup>14</sup>N(p,n), 144 MeV, charge exchange, one pion exchange and PCAC tests 0-78299  
<sup>14</sup>N(p,p'), 122 MeV, level excitation, cross sections, effective NN interaction, DWIA anal. 0-78197  
<sup>15</sup>N excitation contrib. in optical pot., DWBA grazing peak shift for <sup>48</sup>Ca(<sup>16</sup>O,<sup>15</sup>N) 0-86921  
<sup>15</sup>N three particle states at high excitation energies, J<sup>+</sup>, selective population from <sup>12</sup>C(<sup>Li</sup>,  $\alpha$ ) 0-99129  
<sup>15</sup>N transfer spectra direct contrib. from <sup>208</sup>Pb(<sup>16</sup>O,X) projectile fragmentation 0-63155  
<sup>15</sup>N(<sup>13</sup>N,X),  $\pi^0$  condensation, spin-isospin instabilities, TDHF calcs. 0-83042  
<sup>15</sup>N( $\gamma$ , $\gamma$ ), 6.324 MeV, resonance scatt. cross section temp. depend. in BN, NH<sub>4</sub>Cl 0-57767  
<sup>15</sup>N( $\gamma$ , $\gamma$ ), zero point vibr. energy in BN and NH<sub>4</sub>Cl 0-59593  
<sup>16</sup>Ne ground state masses in isospin quintet from ( $\pi^+$ , $\pi^-$ ) 0-105960  
<sup>16</sup>N( $\pi^-$ ,X), charged heavy particle emission after pion capture (*Russian*) 0-69271  
<sup>16</sup>N( $\pi$ , $\pi$ ), 170 MeV, two stage and knock out contribs.,  $\pi^+$ , $\pi^-$  spallation differences (*Russian*) 0-68632  
<sup>16</sup>N( $\pi^+$ , $\pi^-$ ), X=He or d, 170 MeV, cross sections and ang. distrib., direct knockout mechanism (*Russian*) 0-86887  
<sup>16</sup>O(<sup>12</sup>C,X), 4.5 GeV/c, emission of short range particles (R<100 mkm) (*Russian*) 0-63202  
<sup>16</sup>O, A=16, 17, valence-core self-consistency, wave functions, binding energy, levels, spectra 0-63123  
<sup>16</sup>O( $\pi^+$ , $\pi^-$ ), A=16,18, cross section and ang. distrib., Glauber and coherent fluctuation models (*Chinese*) 0-102211  
<sup>16</sup>O( $\pi^+$ , $\pi^+$ ), A=16, 18, resonance region, proton and neutron distrib. 0-91195  
<sup>16</sup>O ground state masses in isospin quintet from ( $\pi^+$ , $\pi^-$ ) 0-105960  
<sup>16</sup>O<sub>gs</sub>,  $\beta$ -decay, mesonic exchange currents, weak process microscopic treatment 0-57742  
<sup>16</sup>(<sup>16</sup>O), M3Y folding model eval., model indep. anal. 0-78317  
<sup>16</sup>(<sup>16</sup>O,X), 2 GeV/N, anomalous nuclei among relativistic projectile fragments 0-106034  
<sup>16</sup>O, 3  $\alpha$  forces, ground state energy and form factor 0-86817  
<sup>16</sup>O 3 $\rightarrow$ 0 $\gamma$  gamma transition from <sup>12</sup>C(<sup>16</sup>O,<sup>16</sup>O) 0-63125  
<sup>16</sup>O, 4 $\alpha$  particle-hole states, isospin mixing 0-99123  
<sup>16</sup>O 4 $\alpha$  state nonstatistical population in compound nucleus calcs. of <sup>12</sup>C(<sup>6</sup>Li,d) 0-102137  
<sup>16</sup>O  $\alpha$ -cluster states, widths and resonances, optical model, direct transfer in <sup>12</sup>C(<sup>6</sup>Li,d) 0-105975  
<sup>16</sup>O, cluster expansions for normalisation integral calc. 0-86831  
<sup>16</sup>O fragmentation at intermediate energies, statistical fluctuation, fragment momentum distrib. 0-78263  
<sup>16</sup>O ground state energy and low odd parity states, correlated basis function method 0-57689  
<sup>16</sup>O ground-state energy, nonunitary model operator approach 0-83030  
<sup>16</sup>O independent particle shell model momentum density distrib., short range correlations 0-78176  
<sup>16</sup>O isospin mixing matrix elements, three level model 0-78136  
<sup>16</sup>O level excitation functions, resonances from <sup>12</sup>C(<sup>16</sup>O,<sup>12</sup>C) 0-63146  
<sup>16</sup>O, magic nuclei at collective excitations, energy spectrum and shape (*Russian*) 0-106015  
<sup>16</sup>O, residual interactions, current conserving RPA calculations 0-57710  
<sup>16</sup>O, rotational band collectivity, shell model excitation in Sp(4, R) symmetry 0-102095  
<sup>16</sup>O<sub>gs</sub>, A-N residual interactions,  $\Lambda$  spin-orbit splitting and effective mass 0-57722  
<sup>16</sup>O(<sup>12</sup>Li,C,X), 140 MeV, fast  $\alpha$  prod. and molecular resonance search 0-106066  
<sup>16</sup>O(<sup>12</sup>C,<sup>12</sup>C), 18-26 MeV, molecular structure, projection operator anal., differential cross sections 0-106033  
<sup>16</sup>O(<sup>12</sup>C,<sup>12</sup>C), perturbed stationary state method, low energy collision and mol. reons. 0-78320  
<sup>16</sup>O(<sup>16</sup>O, X), fusion limiting ang. momenta, from evaporation, mass distrib. stat. model fit 0-68714  
<sup>16</sup>O(<sup>16</sup>O,<sup>16</sup>O), 10-41 MeV, molecular resonances  $\gamma$ -yield, band crossing model 0-106032  
<sup>16</sup>O(<sup>16</sup>O,<sup>16</sup>O), elastic scatt., l-window formalism 0-68684  
<sup>16</sup>O(<sup>16</sup>O,<sup>16</sup>O), optical pot., nuclear matter approach, energy density matter [-] 0-83112  
<sup>16</sup>O(<sup>16</sup>O,<sup>16</sup>O), perturbed stationary state method, low energy collision and mol. reons. 0-78320  
<sup>16</sup>O(<sup>16</sup>O,X), 55 MeV 0-83110  
<sup>16</sup>O(<sup>16</sup>O,X), collective potentials and inertia parameters, adiabatic time dependent HF calcs. quasimolecular resonances 0-63195  
<sup>16</sup>O(<sup>16</sup>O,X), cross sections, energy dependence, nuclear molecular resonances, band crossing model 0-68686  
<sup>16</sup>O(<sup>27</sup>Al,X), 105, 145 MeV, backward angle cross sections, evaporation residues, Z=6-9 yields 0-68688  
<sup>16</sup>O(<sup>12</sup>C), 90.3 MeV, multi- $\alpha$ -cluster transfer and direct pickup cross sections 0-57760  
<sup>16</sup>O( $\alpha$ , $\alpha$ ), 140 MeV, quasifree knockout, DWIA anal. spectroscopic factors 0-68629  
<sup>16</sup>O( $\alpha$ , $\alpha'$ ), hyperfine dynamic mag. field effects 0-68689  
<sup>16</sup>O(d,X), X=d or n, elastic scatt. and stripping, three body calc. 0-91165



## nuclei with mass number 6 to 19 continued

- $^{16}\text{O}(e,e')$ , 799, 996, 1178 MeV, cross sections (*Russian*) 0-68653  
 $^{16}\text{O}(e,\pi^+)$ , 180.4 MeV, virtual photon spectrum, virtual photon theory test 0-102183  
 $^{16}\text{O}(\gamma,\gamma)$ , total photoabsorption and elastic cross sections, spectroscopic information (*Russian*) 0-83095  
 $^{16}\text{O}(\gamma,n_0)$ , 21.6-25.7 MeV, ground state photoneutron polarisation ang. distrib. 0-57765  
 $^{16}\text{O}(\gamma,p)^{15}\text{N}$ , electric quadrupole transition cross-sections, behind giant resonance (*Russian*) 0-78281  
 $^{16}\text{O}(\gamma,\pi^-)$ , 200-350 MeV, cross sections, DWIA anal. 0-106048  
 $^{16}\text{O}(\gamma,\pi)$ , total cross section,  $\Delta$ -hole states damping,  $\pi^0\rho$  exchange,  $\Delta$  isobar hole model 0-91174  
 $^{16}\text{O}(p,^{11}\text{Li})^{11}\text{C}$ , 51.9 MeV, five nucleon transfer mechanisms, DWBA calcs. 0-73845  
 $^{16}\text{O}(p,X)$ , 50 MeV, effective cross sections 0-78284  
 $^{16}\text{O}(p,p')$ , 20-40 MeV, pol. p, anal. powers, imaginary spin-orbit pot., coupled channels anal. 0-102179  
 $^{16}\text{O}(p_{\text{pol}},2p)$ , cross section, analysing power, energy sharing spectra, distorted wave impulse approx. 0-78291  
 $^{16}\text{O}(\pi,\pi)$ , intermediate energies, collective isobaric resonance 0-63208  
 $^{16}\text{O}(\pi,\pi)$ , nonlinear meson dynamics and binding corrections, optical pots. 0-106080  
 $^{16}\text{O}(\pi,\pi)$  optical pot., local field correction 0-68705  
 $^{16}\text{O}(\pi,\pi p)$ , 163 MeV, coincidence expt. 0-78334  
 $^{16}\text{O}(\pi^+, \pi^-)$ , 240 MeV, integrated and doubly differential cross sections 0-68702  
 $^{16}\text{O}(t,n)^{18}\text{F}$ , 2.73 MeV, triton recoil and  $^{18}\text{F}$  yields 0-68677  
 $^{17}\text{O}$ , muonic, energy shifts during atomic EM cascade, and polarisability of deformed nuclei 0-86893  
 $^{18}\text{O}$  6p-4h states and composite spectra from  $^{12}\text{C}(^{18}\text{O},^{12}\text{C})$  0-63096  
 $^{18}\text{O}$ , transition strength n and p components,  $\pi^\pm$  inelastic scatt. comparison, shell model 0-68585  
 $^{18}\text{O}(e,e')$ , 80-165.7 MeV, giant dipole and quadrupole resonances, form factors 0-102168  
 $^{18}\text{O}(e,e')$ , isovector mag. dipole and quadrupole transitions, analogues,  $(\pi^-\gamma)$  relation 0-106010  
 $^{18}\text{O}(p,t)$ , exact finite range DWBA calcs., realistic triton and nuclear wave functions 0-63191  
 $^{18}\text{O}(p,t)$ , finite range DWBA anal. with realistic triton wave function 0-78300  
 $^{19}\text{O}$  total fusion and transfer cross sections from  $^9\text{Be}(^{18}\text{O},X)$  0-91205  
 $\text{O}(\alpha,n)$ , exam. of neutron yield 0-86912  
 $\text{O}(\gamma,X)$ , photoabsorption cross-section, Levinger's factor, mass number dependence 0-63165  
 $\text{O}(\pi^-, X)$ , charged heavy particle emission after pion capture (*Russian*) 0-69271  
 $\text{O}(\pi^\pm, \pi^\pm X)$ ,  $X=\text{He}$  or  $d$ , 170 MeV, cross sections and ang. distrib., direct knockout mechanism (*Russian*) 0-86887  
 $\text{O}(\pi,\pi p)$ , 170 MeV, two stage and knock out contribs.,  $\pi^+\pi^-$  spallation differences (*Russian*) 0-68632

## nuclei with mass number 20 to 38

- $A=18$ -38, inelastic scatt. E4 transition probabilities in the  $0d$ ,  $1s$  shell 0-78210  
 photospallation, 0.1 to 1 GeV, mass yield distrib. 0-73835  
 stable odd-mass sd nuclei, EM multipole moments of ground states 0-102116  
 $\text{Al}(\text{Ne},X)$ , proton inclusive spectra, direct plus thermal model 0-57799  
 $^{24}\text{Al}$ ,  $A=24,25,26$ , giant M1 strength, comparison with cross sections from  $\text{Mg}(p,n)$  0-86878  
 $^{24}\text{Al}$ ,  $A=25,26,27$  levels, resonances,  $\gamma$ -ray branching ratios from  $\text{Mg}(p,\gamma)$  0-86875  
 $^{24}\text{Al}$ , effective M3 matrix elements and transitions from shell model 0-102143  
 $^{26}\text{Al}$   $1^+T=0$  states, isobaric analogue state, spin-isospin effective interaction from  $^{26}\text{Mg}(p,n)$  0-68553  
 $^{26}\text{Al}$  excited states, isobaric analogues, spins, DWBA anal. of  $^{27}\text{Al}(^2\text{He},\alpha)$  0-105981  
 $^{26}\text{Al}$ ,  $\gamma$ -ray line detect. at Earth, constraint for stellar nucleosynthesis 0-94780  
 $^{26}\text{Al}$  in primordial comet interiors, contrib. to radiogenic melting 0-67659  
 $^{26}\text{Al}$  nucleosynthesis, long lived nucl. isomeric states, thermalization in stars 0-85846  
 $^{26}\text{Al}$  production at stellar core collapse from  $^{26}\text{Mg}(\nu_e, e^-)$  (*Russian*) 0-77285  
 $^{26}\text{Al}$ , sd-shell nuclei, stellar weak interaction rates, appl. to supernovae 0-82336  
 $^{26}\text{Al}$ , synthesis in explosive H burning 0-85929  
 $^{26}\text{Al}$   $T=1$  states, resonances,  $J^\pi$  and transitions from  $^{25}\text{Mg}(p,\gamma)$  0-99131  
 $^{26}\text{Al}$ , yield from C and Ne shells of exploding massive star 0-90406  
 $^{27}\text{Al}$  isobaric analogue resonances, spectroscopic factors and  $\gamma$ -rays from  $(p,p)$ ,  $(p,\gamma)$  0-86873  
 $^{27}\text{Al}$  levels, resonances,  $J^\pi$ , branching and mixing ratios from  $^{26}\text{Mg}(p,\gamma)$  0-99132  
 $^{27}\text{Al}$  neutron scattering resonance radiative widths 0-99146  
 $^{27}\text{Al}(^{15}\text{N},X)$ , 27-70 MeV, complete fusion, total fusion cross section, entrance channel effects 0-68716  
 $^{27}\text{Al}(^6\text{Li}, ^6\text{Li})$ , 90 MeV, real optical pot. continuous ambiguity 0-102200  
 $^{27}\text{Al}(d,\alpha)^{25}\text{Mg}$ , nuclear microanalysis of Al impurities in Si epitaxial layers 0-61193  
 $^{27}\text{Al}(d,pX)$  80 MeV, inclusive proton spectra, d break-up, DWBA anal. 0-91190  
 $^{27}\text{Al}(e,e')$ , 70-340 MeV, odd parity state electroexcitation, form factors, transition probs. 0-78208  
 $^{27}\text{Al}(e,e')$ , cross sections, shadowing effect at small four momentum transfer 0-63176  
 $^{27}\text{Al}(e,e)$  multipole operators in semileptonic weak and electromagnetic interactions 0-73840  
 $^{27}\text{Al}(e,X)$ , electrodisintegration charged particle yield,  $\alpha$  to t cross section ratio (*Russian*) 0-86902  
 $^{27}\text{Al}(\gamma,X)$ , 3-30 MeV, photoabsorption cross section, giant dipole resonances 0-78254  
 $^{27}\text{Al}(n,\alpha)$ , 14.8 MeV, expt. and statistical model determ. of  $\alpha$ -prod. in fusion reactors 0-95397  
 $^{27}\text{Al}(p,n)^{27}\text{Si}$ , cross sections and thermonuclear reaction rates 0-73852  
 $^{27}\text{Al}(p,X)$ ,  $X=\alpha, \tau, ^7\text{Li}$ , spectra and angular distrib. 0-68660  
 $^{27}\text{Al}(\pi^+, \pi^-N)$ , 180-255 MeV, quasielastic pion scatt. coincidence expt. interpretation, impulse approx. 0-68704  
 $^{28}\text{Al}$  levels, transitions and spin from  $^{27}\text{Al}(n,\gamma)$ , pol. Al and n 0-78153
- nuclei with mass number 20 to 38 continued  
 $\text{Al}(\gamma,X)$ , photoabsorption cross-section, Levinger's factor, mass number dependence 0-63165  
 $\text{Al}(X,x)$ ,  $X=\pi^\pm$ ,  $K^\pm$ ,  $p,p$ , 70, 125, 175 GeV/c 0-83128  
 $^{32}\text{Ar}$  ground state masses in isospin quintet from  $(\pi^+, \pi^-)$  0-105960  
 $^{35}\text{Ar}$  levels, transitions and  $\beta$ -delayed protons from  $^{35}\text{K}$  decay 0-91156  
 $^{36}\text{Ar}$  deduced levels from  $^{36}\text{K}$  beta-delayed particle emission 0-83074  
 $^{36}\text{Ar}$   $20\text{Ne } 8^+$  level radiative width, resonance strength from  $^{16}\text{O}(\alpha,\gamma)$  0-83065  
 $^{12}\text{C}+^{12}\text{C}$  gross struct. resonances in excitation functions from  $^{12}\text{C}(^{12}\text{C}, ^{10,11}\text{B})$  0-102167  
 $^{12}\text{C}+^{12}\text{C}$  system resonant structs.,  $J^\pi$  assignments, true  $^{24}\text{Mg}$  states from  $^{12}\text{C}(^{12}\text{C}, ^{16}\text{O})$  0-99163  
 $^{12}\text{C}(^{16}\text{O}, \alpha)$ ,  $^{24}\text{Mg}$  low spin resonances, excitation functions and ang. distrib. 0-63151  
 $\text{Cl}(\text{Ar},X)$ , 0.4-1.8 GeV/u, multipion prod. energy depend. 0-106065  
 $\text{Cl}(\text{Ar},X)$ , 800 MeV/N, single particle spectra from high multiplicity events 0-99184  
 $\text{Cl}(\text{Ar},X)$ , proton inclusive spectra, direct plus thermal model 0-57799  
 $^{35}\text{Cl}$ ,  $A=34, 38$ , effective M3 matrix elements and transitions from shell model 0-102143  
 $^{35}\text{Cl}(e, e')$ , 116, 194 MeV,  $A=35, 37$ , charge distrib. and RMS charge radius 0-102109  
 $^{35}\text{Cl}$  anomalous M1/E1 strength ratio and doorway states from  $^{35}\text{Cl}(n,\gamma)$  0-57730  
 $^{35}\text{K}$  decay,  $^{35}\text{Ar}$  levels, transitions and  $\beta$ -delayed protons 0-91156  
 $^{36}\text{K}$ , beta delayed emission of protons and  $\alpha$ -particles 0-83074  
 $^{38}\text{K}$ , effective M3 matrix elements and transitions from shell model 0-102143  
 $^{24}\text{Mg}$ ,  $A=24,26$ , second order nonspherical quadrupole phonon effects 0-86790  
 $^{24}\text{Mg}(\alpha,^{12}\text{C})$ ,  $A=24, 26, 90.3$  MeV, multi- $\alpha$ -cluster transfer and direct pickup cross sections 0-57760  
 $^{24}\text{Mg}(d,^4\text{Li})$ , 80 MeV,  $A=24,26$ ,  $\alpha$ -spectroscopic factors and ang. distrib., DWBA anal. 0-99126  
 $^{24}\text{Mg}(p, p')$ ,  $A=24, 26$ , isovector dipole strength excitation in giant resonance region 0-83066  
 $^{23}\text{Mg}$ , forbidden transition ang. distrib., CCBA and DWBA anal. of  $(p,d)$  0-86848  
 $^{23}\text{Mg}$  resonances through  $\gamma$ -decay excitation functions from  $^{12}\text{C}(^{12}\text{C},n)$  0-63148  
 $^{24}\text{Mg}$  ground and  $\gamma$ -bands, direct and multistep processes from  $(\alpha,^4\text{He})$ ,  $(p,t)$ ,  $(^{16}\text{O}, ^{16}\text{O})$  0-102094  
 $^{24}\text{Mg}$  intermediate struct. correlations, elastic and reaction channel excitation functions from  $^{12}\text{C}(^{12}\text{C},X)$  0-68625  
 $^{24}\text{Mg}$  isovector M1 excitations, current and spin contribs. from  $(e,e')$ ,  $(p,n)$  0-68582  
 $^{24}\text{Mg}$   $K=2$  band and alpha cluster model state point symmetry 0-105946  
 $^{24}\text{Mg}$ , low spin rotational states, energy props., extended deformation model 0-86785  
 $^{24}\text{Mg}$  neutron scattering resonance radiative widths 0-99146  
 $^{24}\text{Mg}$  rotational band collectivity, shell model excitation in  $\text{Sp}(4, R)$  symmetry 0-102095  
 $^{24}\text{Mg}$ , triaxial nuclei rots., extended cranked shape consistent oscillator model 0-102133  
 $^{24}\text{Mg}(^{13}\text{C},^{13}\text{C})$ , 35 MeV,  $2^+$  population probab., spin-flip and spin orbit pots., coupled channel anal. 0-99125  
 $^{24}\text{Mg}(^{16}\text{O}, ^{16}\text{O})$ , 24-40 MeV, backward angles, excitation functions, ang. distrib. and resonant behaviour 0-68622  
 $^{24}\text{Mg}(\alpha,n)^{27}\text{Si}$ , cross sections and thermonuclear reaction rates 0-73852  
 $^{24}\text{Mg}(d,d)$ , pol.d, 20 MeV, quadrupole transition amplitudes 0-99148  
 $^{24}\text{Mg}(p,p)$ , 14-45 MeV, differential cross section and spin-flip probabilities, giant resonances 0-73850  
 $^{25}\text{Mg}$  total fusion and transfer cross sections from  $^9\text{Be}(^{18}\text{O},X)$  0-91205  
 $^{25}\text{Mg}(p,\gamma)^{26}\text{Al}$ , reaction rate in explosive H burning 0-85929  
 $^{25}\text{Mg}(p,n)^{26}\text{Al}$ , cross sections and thermonuclear reaction rates 0-73852  
 $^{26}\text{Mg}$  transition strength n and p components,  $\pi^\pm$  inelastic scatt. comparison, shell model 0-68585  
 $^{26}\text{Mg}(^4\text{He}, ^4\text{He})$ ,  $4^+$  states,  $B(E2)$  values, and band mixing, rot.-vibr. model 0-83019  
 $^{26}\text{Mg}(p, p')$ , pol.p, 5.5-17.5 MeV, cross sections and anal. powers, autocorrelations 0-106042  
 $^{26}\text{Mg}(p,n)^{26}\text{Al}$ , 5.2-6.9 MeV, cross section via accelerator mass spectrometry 0-99175  
 $^{26}\text{Mg}(\pi^+, \pi^\pm)$ , pion spectra, absolute cross section 0-78333  
 $^{26}\text{Na}$ ,  $A=24, 25$ , total fusion and transfer cross sections from  $^9\text{Be}(^{18}\text{O},X)$  0-91205  
 $^{26}\text{Na}$ ,  $A=30,31,32$ , beta-delayed two-neutron emission 0-95316  
 $^{22}\text{Na } 0^+$  level mean life, isovector mag. dipole transition from  $^{19}\text{F}(\alpha,n)$  0-68595  
 $^{23}\text{Na}$  high spin states, excitation functions, nonstatistical effects, Hauser-Feshbach anal. of  $^{12}\text{C}(^{13}\text{N},\alpha)$  0-106041  
 $^{23}\text{Na}$ , particle-rotor model with s-d shell pairing, BCS approx. 0-57705  
 $^{23}\text{Na}$  resonances through  $\gamma$ -decay excitation functions from  $^{12}\text{C}(^{12}\text{C},p)$  0-63148  
 $^{23}\text{Na}(n,X\gamma)$ , 0.2 to 20 MeV, reaction cross sections 0-99172  
 $^{24}\text{Na}$ , effective M3 matrix elements and transitions from shell model 0-102143  
 $^{24}\text{Na}$  half-life determ.,  $T_{1/2}=(14.964\pm0.015)$  h 0-95311  
 $^{24}\text{Na}^m$ , polarised,  $\beta$ -decay asymmetry and mag. moment from  $\text{Na}(n,\gamma)$  0-91157  
 $^{24m}\text{Na}$ , laser induced nuclear orientation 0-57680  
 $\text{Ne}$ , total muon capture rates using HF wave functions 0-63135  
 $\text{Ne}(\text{Ne},X)$ , 117-800 MeV, classical eqns. of motion calcs., central collisions, thermal models 0-106070  
 $^{20}\text{Ne}$ ,  $A=21, 22, 23$ , total fusion and transfer cross sections from  $^9\text{Be}(^{18}\text{O},X)$  0-91205  
 $^{12}\text{Ne}$  parity mixing meas. extension review 0-73792  
 $^{12}\text{Ne}$  13482 keV level, parity violating effects in two resonance interference from  $^{19}\text{F}(p,\alpha)$  pol. p 0-83033  
 $^{20}\text{Ne } 2^+ \rightarrow 0^+$  transition from  $^{12}\text{C}(^{16}\text{O}, ^{16}\text{O})$  0-63125  
 $^{20}\text{Ne}$  collective motion,  $B(E2)$  rates, algebraic formulation in symplectic shell model 0-83015  
 $^{20}\text{Ne}$  giant E1 resonance intermediate struct. from  $^{19}\text{F}(p,\gamma)$ , pol. and unpol. 0-78251  
 $^{20}\text{Ne}$  ground state level calc., maximum method 0-73795  
 $^{20}\text{Ne}$  hexadecapole moments, quadrupole deformation effects, E4 effective charge, valence polarisation 0-78142  
 $^{20}\text{Ne}$  low lying levels and intermediate structure  $J^\pi$  from  $^{16}\text{O}(^{12}\text{C}, ^8\text{Be})$  0-102166



## nuclei with mass number 20 to 38 continued

- <sup>20</sup>Ne, moment of inertia from cranked HF method 0-102098  
<sup>20</sup>Ne, quartet states from <sup>19</sup>F(p,α)<sup>16</sup>O 0-105973  
<sup>20</sup>Ne resonances through γ-decay excitation functions from <sup>12</sup>C(<sup>12</sup>C,α) 0-63148  
<sup>20</sup>Ne with backbending, first excited 4<sup>+</sup> state g-factor 0-78144  
<sup>20</sup>Ne(<sup>12</sup>C,X), 24-42 MeV, complete fusion, total cross section, excitation function 0-68717  
<sup>20</sup>Ne(<sup>12</sup>C,X), 66.5 MeV, evaporation residue ang. and energy distrib. from statistical model anal. 0-83110  
<sup>20</sup>Ne(α,α'), 140 MeV, quasifree knockout, DWIA anal. spectroscopic factors 0-68629  
<sup>21</sup>Ne deduced spectroscopic factors, levels and anal. powers from <sup>20</sup>Ne(d,pol,p) 0-83087  
<sup>21</sup>Ne, strength function calcs. in many fermion systems, Monte-Carlo method 0-86820  
<sup>22</sup>Ne as neutron source for solar systems s-process, difficulty 0-72926  
<sup>22</sup>O first excited state, g-factor and lifetime from <sup>1</sup>H(<sup>16</sup>O, pγ) 0-102115  
<sup>28</sup>P, nucleon unbound states, spin, parity, partial width, from <sup>28</sup>Si(d,pn) 0-102118  
<sup>30</sup>P level width isospin depend., excitation functions, statistical anal. of <sup>29</sup>Si(p,α) 0-78152  
<sup>30</sup>P positive parity states, transitions and spectroscopic strengths, DWBA anal. of <sup>29</sup>Si(<sup>3</sup>He,d) 0-102138  
<sup>30</sup>P T=1 state decay, lifetimes and branching ratios, analogue E2 transitions from <sup>29</sup>Si(p,γ) 0-68598  
<sup>31</sup>P high E, states, J<sup>π</sup>, DWBA anal. <sup>28</sup>Si(<sup>3</sup>He,p) 0-68536  
<sup>32</sup>S α-cluster structure, ground and first excited states, energies, radii and moments 0-102122  
<sup>32</sup>S resonances and excitation functions, Hauser Feshbach anal. of <sup>20</sup>Ne(<sup>12</sup>C,X), X=p,α 0-78249  
<sup>32</sup>S shape isomeric state from unconstrained variation 0-95306  
<sup>32</sup>S(α,<sup>12</sup>C), 90.3 MeV, multi-α-cluster transfer and direct pickup cross sections 0-57760  
<sup>32</sup>S(d,d), pol.d., 20 MeV, quadrupole transition amplitudes 0-99148  
<sup>32</sup>S(γ,d), below 30 MeV, photodeuteron yield and cross section, meas. and statistical calcs. 0-63171  
<sup>32</sup>S(n,n'), 13.9 MeV, 2<sup>+</sup> (2.23 MeV) excitation, spin flip probab., deexcitation γ-rays 0-86853  
<sup>32</sup>S(n,n), 25-1100 keV, total cross section, multilevel anal., strength functions, optical parameters 0-78298  
<sup>32</sup>S(n,n), spin-flip probability to first 2<sup>+</sup> level 0-78288  
<sup>32</sup>S(p,p), 14-45 MeV, differential cross section and spin-flip probabilities, giant resonances 0-73850  
<sup>34</sup>Si(e,e'), 126-293 MeV, A=28,29, levels and form factors, particle-phonon coupling anal. 0-105977  
<sup>34</sup>Si ground state masses in isospin quintet from (π<sup>+</sup>, π<sup>-</sup>) 0-105960  
<sup>34</sup>Si, Q value and mass excess from <sup>28</sup>Si(α,He) 0-86795  
<sup>34</sup>Si(p,p), 14-45 MeV, differential cross section and spin-flip probabilities, giant resonances 0-73850  
<sup>34</sup>Si, forbidden transition ang. distrib., CCBA and DWBA anal. of (p,d) 0-86848  
<sup>34</sup>Si, 12.291 MeV level width, axial blocking meas. from <sup>27</sup>Al(p,α) 0-63086  
<sup>36</sup>Si 4<sup>+</sup> state lifetime by blocking effect method from <sup>27</sup>Al(p,α) (Russian) 0-91152  
<sup>36</sup>Si (p, X), pol.p., 65 MeV, continuum spectra anal. powers 0-102178  
<sup>36</sup>Si alpha doorway states from <sup>12</sup>C(<sup>16</sup>O,<sup>12</sup>C) 0-63146  
<sup>36</sup>Si excitation functions, ang. distrib. and resonant behaviour from <sup>24</sup>Mg(<sup>16</sup>O,<sup>12</sup>C) 0-68622  
<sup>36</sup>Si excitation functions, ang. distrib., resonance spin assignments from <sup>24</sup>Mg(<sup>16</sup>O,<sup>12</sup>C) 0-68623  
<sup>36</sup>Si, highly excited <sup>12</sup>C-α-<sup>12</sup>C molecular state, symmetrical decay (Russian) 0-68661  
<sup>36</sup>Si isovector M1 excitations, current and spin contribs. from (e,e'), (p,n) 0-68582  
<sup>36</sup>Si, neutron scattering resonance radiative widths 0-99146  
<sup>36</sup>Si resonance wave functions from differential cross sections of <sup>27</sup>Al(p,X), X=p,n,α 0-78239  
<sup>36</sup>Si, strength function calcs. in many fermion systems, Monte-Carlo method 0-86820  
<sup>36</sup>Si + <sup>12</sup>C(<sup>9</sup>Be,<sup>12</sup>C), fusion and strong absorption from elastic scatt. optical pot. 0-102222  
<sup>36</sup>Si(<sup>10</sup>B,<sup>9</sup>Be), unique l=1 reaction, ang. distrib. wave number depend., DWBA anal. 0-63204  
<sup>36</sup>Si(<sup>16</sup>O,<sup>16</sup>O), radial sensitivity of optical pot. 0-86869  
<sup>36</sup>Si(<sup>28</sup>Si,X), 60 MeV, α-α correlations to probe fusion low ang. momentum window 0-106094  
<sup>36</sup>Si(<sup>12</sup>C,X), 135 MeV, multi-particle prod., two fragment reactions, kinematical anal. 0-83111  
<sup>36</sup>Si(<sup>6</sup>Li, <sup>6</sup>Li), 154 MeV, differential cross section ang. distrib., optical anal. 0-63201  
<sup>36</sup>Si(<sup>9</sup>Be, <sup>9</sup>Be'), 45, 60 MeV, low lying collective states, ang. distrib., DWBA double folding pot. anal. 0-78113  
<sup>36</sup>Si(<sup>9</sup>Be,<sup>9</sup>Be), 121-201.6 MeV, strong absorption dominance, global optical model anal., fusion barrier 0-83116  
<sup>36</sup>Si(<sup>9</sup>Be,X), 30-60 MeV, total fusion cross section, evaporation residues, optical model 0-78344  
<sup>36</sup>Si(<sup>9</sup>Be,X), X=p,d,α, energy dependence, angular distrib. of spectra, optical and statistical model anal. 0-68710  
<sup>36</sup>Si(α,<sup>12</sup>C), 90.3 MeV, multi-α-cluster transfer and direct pickup cross sections 0-57760  
<sup>36</sup>Si(α,n)<sup>31</sup>S, cross sections and thermonuclear reaction rates 0-73852  
<sup>36</sup>Si(d,d), pol.d., 20 MeV, quadrupole transition amplitudes 0-99148  
<sup>36</sup>Si(d,pn), <sup>29</sup>P and <sup>29</sup>Si nucleon unbound states, spin, parity, partial width 0-102118  
<sup>36</sup>Si(e,e'), 6<sup>+</sup> T=1 resonance form factor, mag. strength quenching, meson exchange currents 0-86882  
<sup>36</sup>Si(γ,p), 18.1-29 MeV, photoproton energy spectra, contribs. to giant dipole resonance 0-78242  
<sup>36</sup>Si(n,γ), 565, 813 keV, resonance γ, spectra, valence model test 0-63124  
<sup>36</sup>Si(n,n), spin-flip probability to first 2<sup>+</sup> level 0-78288  
<sup>36</sup>Si(p, p'), isovector dipole strength excitation in giant resonance region 0-83066  
<sup>36</sup>Si(p,p(d)X), pol. p., 65 MeV, anal. powers of continuum energy spectra 0-68637  
<sup>36</sup>Si 3/2<sup>+</sup> and 5/2<sup>+</sup> states population, (d,p) and (p,π<sup>+</sup>) comparison 0-95307  
<sup>36</sup>Si doorway state neutron capture, levels and γ-spectra from <sup>28</sup>Si(n,γ) 0-57729

## nuclei with mass number 20 to 38 continued

- <sup>28</sup>Si levels, J<sup>π</sup>, spectroscopic factor, DWBA anal. of <sup>28</sup>Si(<sup>3</sup>He, <sup>2</sup>He) 0-86811  
<sup>28</sup>Si levels and ang. distrib., DWBA anal. of <sup>27</sup>Al(α,d) 0-78157  
<sup>28</sup>Si, low lying energy level structure, from <sup>28</sup>Si(d,pol,py) and multi-step reaction calcs. 0-68537  
<sup>28</sup>Si, nucleon unbound states, spin, parity, partial width, from <sup>28</sup>Si(d,pn) 0-102118  
<sup>28</sup>Si rot-vibr. coupling effects, excitation spectrum and ang. distrib. from <sup>28</sup>Si(d, p) 0-57661  
<sup>28</sup>Si(<sup>16</sup>O,<sup>16</sup>O)<sup>28</sup>Si, non-orthogonality of channel states 0-83115  
<sup>28</sup>Si(d,p), 1.1-2.1 MeV, excitation functions, statistical fluctuations anal. 0-95322  
<sup>30</sup>Si(n,γ)<sup>31</sup>Si, thermal neutron cross-section determ. 0-95321  
<sup>30</sup>Si(p,γ), pol.p., 6.4-15.0 MeV, cross section and anal. power ang. distrib. 0-99168  
<sup>31</sup>Si, half life determined from varved Gulf of California sediment core 0-91153  
<sup>31</sup>Si half life from tandem accelerator mass spectrometry 0-95313  
<sup>31</sup>Si half life via accelerator mass spectrometry 0-95314  
<sup>31</sup>Si(pol,pol), giant multipole resonance region, optical model anal. 0-57779  
uncorrelated target, optical pot. unitary content, DWIA and Glauber theory from (α,α)(α,γ) 0-105947
- nuclei with mass number 39 to 58
- A=42, multiple scattering formalism for the effective interaction 0-102126  
A=54-82, ground state transition strengths from (p,t) reactions 0-95305  
photospallation, 0.1 to 1 GeV, mass yield distrib. 0-73835  
<sup>40</sup>Ar + <sup>27</sup>Al, 340 MeV, energy relaxation and mass transfer (French) 0-95327  
Ca(Ca,X), 400 MeV, classical eqns. of motion calcs., central collisions, thermal models 0-106070  
<sup>40</sup>Ca, A=40, 48, nuclear matter density distrib., saturation effect, optical potential from (α,α) 0-63115  
<sup>40</sup>Ca, A=40, 48, single particle levels, rms charge radius, Wood-Saxon pot. 0-63106  
<sup>40</sup>Ca, A=40 to 46,48, nuclear charge distrib., from isotope shift of 6573 angstrom line 0-57674  
<sup>40</sup>Ca, A=40 to 48, giant multipole resonances, mass dependence of energy weighted sums 0-63144  
<sup>40</sup>Ca, A=41,43,45, quadrupole moments, from hyperfine struct. splitting of 4s4p<sup>2</sup>P, 0-57674  
<sup>40</sup>Ca, A=43, 45, spectra, particle-hole conjugation and protection theorems (Chinese) 0-73796  
<sup>40</sup>Ca, A=44,46 excited states and transition ang. distrib. from Ti(<sup>14</sup>C,<sup>16</sup>O) 0-95308  
<sup>40</sup>Ca, A=47, 49, single particle states lifetimes calcs. 0-105943  
<sup>40</sup>Ca(α,α'), 24,29 MeV, A=40,42,44,48 backward ang. distrib. anomaly, coupled and channel anal. 0-86911  
<sup>40</sup>Ca(α,α), A=40, 42, 44, 48, 104 MeV, cross sections and optical pots., nuclear size 0-68524  
<sup>40</sup>Ca(α,α), A=40, 42, 44, 48, 104 MeV nuclear size and density distrib. from folding model anal. 0-68525  
<sup>40</sup>Ca(e,e'), backward scatt., A=40, 42, 44, 48, mag. dipole ground state transition search 0-106009  
<sup>40</sup>Ca(p,p'), pol. p., A=40,48, 800 MeV, diff. cross sections, anal. powers, DWIA anal., high spin levels 0-83067  
<sup>40</sup>Ca(π,π), A=40,48, 40-241 MeV, first and second order optical pots., resonance behaviour 0-68624  
<sup>40</sup>Ca(π<sup>+</sup>, π<sup>-</sup>N), A=40, 44, 48, 291 MeV, quasielastic scatt., differential cross sections, Monte-Carlo data fit 0-68703  
<sup>39</sup>Ca, forbidden transition ang. distrib., CCBA and DWBA anal. of (p,d) 0-86848  
<sup>40</sup>Ca composite system, heavy ion resonances from <sup>24</sup>Mg + <sup>16</sup>O, <sup>28</sup>Si + <sup>13</sup>C 0-86874  
<sup>40</sup>Ca, magic nuclei at collective excitations, energy spectrum and shape (Russian) 0-106015  
<sup>40</sup>Ca, residual interactions, current conserving RPA calculations 0-57710  
<sup>40</sup>Ca(<sup>11</sup>B,<sup>10</sup>B), 51.5 MeV, n stripping, DWBA anal. with Woods-Saxon and double folding optical pots. 0-102171  
<sup>40</sup>Ca(<sup>11</sup>B,<sup>12</sup>C), 32, 68 MeV, single proton pickup, DWBA anal., optical pot. 0-106037  
<sup>40</sup>Ca(<sup>11</sup>B,<sup>12</sup>C), 51.5 MeV, p pickup, DWBA anal. with Woods-Saxon and double folding optical pots. 0-102171  
<sup>40</sup>Ca(<sup>13</sup>C,<sup>14</sup>N), 40, 68 MeV, single proton pickup, DWBA anal., optical pot. 0-106037  
<sup>40</sup>Ca(<sup>16</sup>O,<sup>16</sup>O), complex heavy ion optical pot., microscopic BHF derivation 0-106067  
<sup>40</sup>Ca(<sup>16</sup>O,<sup>16</sup>O), optical pot., nuclear matter approach, energy density matter [-] 0-83112  
<sup>40</sup>Ca(<sup>16</sup>O,X), ion-ion interaction pot., imaginary part, effective interaction 0-68692  
<sup>40</sup>Ca(<sup>40</sup>Ca,<sup>40</sup>Ca), optical pot., nuclear matter approach, energy density matter [-] 0-83112  
<sup>40</sup>Ca(<sup>40</sup>Ca,X), relativistic, compression and pion distrib., Monte Carlo calc. 0-73853  
<sup>40</sup>Ca(<sup>9</sup>Be, <sup>9</sup>Be'), 45, 60 MeV, low lying collective states, ang. distrib., DWBA double folding pot. anal. 0-78113  
<sup>40</sup>Ca(<sup>9</sup>Be,<sup>9</sup>Be'), 45, 60 MeV, 1<sup>-</sup> state excitation Frahn scaling formula for cross section 0-102136  
<sup>40</sup>Ca(α,<sup>12</sup>C), 90.3 MeV, multi-α-cluster transfer and direct pickup cross sections 0-57760  
<sup>40</sup>Ca(α,α), 1.37 GeV, S-matrix expansion from Glauber multiple scatt. theory 0-91191  
<sup>40</sup>Ca(d,d'), 108 MeV, giant monopole resonance excitation and ang. distrib. 0-102164  
<sup>40</sup>Ca(d,d), 4.5-5.4 MeV, excited states, excitation functions and ang. distrib., statistical anal. 0-57686  
<sup>40</sup>Ca(μ,γ), photon asymmetry, O(1/m<sup>2</sup>) and nuclear effects 0-78219  
<sup>40</sup>Ca(n,X), local approximation to a non-local potential 0-91182  
<sup>40</sup>Ca(n,γ), direct-semidirect and compound nucleus contribs. to cross sections 0-68662  
<sup>40</sup>Ca(p, p'), isovector dipole strength excitation in giant resonance region 0-83066  
<sup>40</sup>Ca(p,p'), 800 MeV, high energy octupole giant resonance, ang. distrib. 0-86879  
<sup>40</sup>Ca(p,γ), 6.25 MeV, triple ang. correlation, 3<sup>-</sup> exit channel, resonances, single particle states 0-68626  
<sup>40</sup>Ca(p,p), 30 MeV, optical pot. imaginary part calcs. 0-86868



## nuclei with mass number 39 to 58 continued

- <sup>40</sup>Ca(p,p), absorbing optical pot., Coulomb correction term 0-73831  
<sup>40</sup>Ca(p,p), DWIA test in Glauber theory, transition density 0-99173  
<sup>41</sup>Ca, E2 core polarisation charge, Woods-Saxon shell model compared to harmonic oscillator model 0-63072  
<sup>41</sup>Ca E2 resonance, cross sections and  $\gamma$ -spectrum from <sup>40</sup>Ca(n, $\gamma$ ) 0-57759  
<sup>41</sup>Ca excited states, excitation functions and ang. distrib., statistical anal. from <sup>40</sup>Ca(d,p) 0-57686  
<sup>41</sup>Ca, muonic, energy shifts during atomic EM cascade, and polarisability of deformed nuclei 0-86893  
<sup>41</sup>Ca parity doublet gamma lifetimes, 3/2 levels, parity mixing from <sup>40</sup>Ca(d,p $\gamma$ ) 0-78209  
<sup>41</sup>Ca, spin and parity from <sup>38</sup>Ar( $\alpha$ ,n $\gamma$ ) angular distrib. and linear polarisation of  $\gamma$  0-63079  
<sup>42</sup>Ca, collective states, quasi-degenerate intrinsic Hamiltonian, variational methods 0-68505  
<sup>42</sup>Ca( $\alpha$ ,n)<sup>45</sup>Ti, reaction rates in stars 0-82183  
<sup>42</sup>Ca(p, $\gamma$ )<sup>43</sup>Sc, reaction rates in stars 0-82183  
<sup>42</sup>Ca(p,t) form factor, hole and continuum contribs. for pick-up reactions 0-78256  
<sup>42</sup>Ca(<sup>7</sup>Li, <sup>7</sup>Li), 34 MeV, ang. distrib., cross sections, double folding model anal. 0-78313  
<sup>42</sup>Ca(p,n)<sup>44</sup>Sc, reaction rates in stars 0-82183  
<sup>42</sup>Ca levels, excitation functions and J $\pi$  from <sup>45</sup>K  $\beta$ -decay 0-105978  
<sup>42</sup>Ca(<sup>16</sup>O, <sup>14</sup>C), two nucleon sequential transfer, on-shell anal., cross sections 0-99180  
<sup>42</sup>Ca(<sup>16</sup>O, <sup>15</sup>N), <sup>15</sup>N excitation contrib. in optical pot., DWBA grazing peak shift 0-86921  
<sup>42</sup>Ca(<sup>18</sup>O, <sup>16</sup>O), two nucleon sequential transfer, on-shell anal., cross sections 0-99180  
<sup>42</sup>Ca(e,e), 757.5 MeV, elastic cross section 0-63175  
<sup>42</sup>Ca(p,n), nucleon optical potential from Lane model 0-83097  
<sup>42</sup>Ca(p,t)<sup>46</sup>Ca(0 $^+$ g.s.), 20 and 40 MeV, two step process, deuteron break-up effect 0-73844  
<sup>42</sup>Ca(t,p), exact finite range DWBA calcs., realistic triton and nuclear wave functions 0-63191  
<sup>42</sup>Ca( $\gamma$ ,X), photoabsorption cross-section, Levinger's factor, mass number dependence 0-63165  
<sup>53</sup>Co, energy levels from Ni(p $\nu$ , $\alpha$ ) 0-68663  
<sup>53</sup>Co  $\beta^+$ -decay, <sup>56</sup>Fe low lying levels, J $\pi$ ,  $\gamma$ - $\gamma$  coincidences, internal conversion 0-86815  
<sup>53</sup>Co, gamma-ray intensities, precision meas. 0-102139  
<sup>53</sup>Co in Type II supernovae, decay rel. to supernova light curves 0-77427  
<sup>53</sup>Co particle-hole states, T=1, zero DWBA anal. of <sup>54</sup>Fe(<sup>3</sup>He,p) and <sup>58</sup>Ni(d, $\alpha$ ) 0-78308  
<sup>53</sup>Co (3/2 $^+$  state), anomalous analyzing power, DWBA calc. from <sup>60</sup>Ni(p, $\alpha$ ) 0-86894  
<sup>53</sup>Co state alignment,  $\gamma$ -transitions and ang. distrib., from <sup>56</sup>Fe(p, $\gamma$ ) 0-73797  
<sup>43</sup>Cr(n,2n), A=50, 52, 54, 14 MeV, cross section compilation 0-91181  
<sup>43</sup>Cr(p,p), A=50, 52, 6 MeV, elastic and inelastic differential cross sections, spin flip probability (Russian) 0-91187  
<sup>43</sup>Cr, forbidden transition ang. distrib., CCBA and DWBA anal. of (p,d) 0-86848  
<sup>43</sup>Cr ground analogue state fine struct., l=3 states differential cross section from <sup>50</sup>Cr(p,d) 0-63152  
<sup>43</sup>Cr levels, transitions, and Gamow-Teller matrix elements from <sup>49</sup>Mn,  $\beta^+$ -decay 0-57746  
<sup>43</sup>Cr, EM properties, lifetimes of 749 and 777 keV levels, E2/M1 mixing ratio 0-63127  
<sup>43</sup>Cr levels, spectroscopic function and analogue states, PWBA anal. of <sup>52</sup>Cr(<sup>3</sup>He, $\alpha$ ) 0-68547  
<sup>43</sup>Cr(d,d), pol.d, 20 MeV, quadrupole transition amplitudes 0-99148  
<sup>43</sup>Cr, neutron rich nuclide from <sup>238</sup>U(<sup>40</sup>Ar,X) at 340 MeV 0-57802  
<sup>43</sup>Fe(X), 1.9 GeV/N, in emulsion, mean free paths, and fragmentation parameters 0-102197  
<sup>43</sup>Fe group elements, prod. in supernova outburst (Russian) 0-62167  
<sup>43</sup>Fe nuclei in galactic cosmic rays, isotopic comp. 0-72729  
<sup>43</sup>Fe, A=57, 59, levels, J $\pi$  and transition branching ratio from Fe(n, $\gamma$ ) 0-105976  
<sup>43</sup>Fe(e,e), 100-275 MeV, A=54,56,57, cross sections and muonic X-ray meas., charge distrib. systematics 0-86801  
<sup>43</sup>Fe(n,2n), A=54, 56, 14 MeV, cross section compilation 0-91181  
<sup>43</sup>Fe(p, $\gamma$ )Co, A=54,56, giant dipole resonance splitting, direct-semidirect capture model anal. 0-106055  
<sup>43</sup>Fe(p,p'), A=54, 56, 6 MeV, resonances, spin flip and cross section depends., Hauser Feshbach anal. (Russian) 0-83084  
<sup>43</sup>Fe 8 $^+$  and 10 $^+$  level spin assignments and lifetimes from (<sup>16</sup>O,2p), (<sup>6</sup>Li, pn) 0-68531  
<sup>43</sup>Fe(<sup>3</sup>He,p), <sup>56</sup>Co particle-hole states, T=1, zero DWBA anal. 0-78308  
<sup>43</sup>Fe(p,p'), pol. p, 800 MeV, diff. cross sections, anal. powers, DWIA anal. 0-83067  
<sup>43</sup>Fe levels, J $\pi$ , spectroscopic factors, DWBA anal. of <sup>56</sup>Fe(<sup>3</sup>He, $\alpha$ ) 0-99127  
<sup>43</sup>Fe resonances, levels, J $\pi$ , valence capture  $\gamma$ -ray spectrum from <sup>54</sup>Fe(n, $\gamma$ ) 0-86852  
<sup>43</sup>Fe(<sup>32</sup>Cr, X), entrance channel mass asymmetry effects on reaction mechanism, fission and fusion 0-106077  
<sup>43</sup>Fe(X), 0.5-2 GeV/N, on emulsion, secondary mean multiplicities and ang. distrib. (Russian) 0-106076  
<sup>43</sup>Fe(X), 2 GeV/N, anomalous nuclei among relativistic projectile fragments 0-106034  
<sup>43</sup>Fe, fp shell model calcs., spectra and spectroscopic factors 0-68588  
<sup>43</sup>Fe isobaric analogue resonance levels, branching ratios, from <sup>55</sup>Mn(p, $\gamma$ ) 0-68617  
<sup>43</sup>Fe low lying levels, J $\pi$ ,  $\gamma$ - $\gamma$  coincidences, internal conversion from <sup>56</sup>Co  $\beta^+$ -decay 0-86815  
<sup>43</sup>Fe, neutron scattering resonance radiative widths 0-99146  
<sup>43</sup>Fe(e, $\alpha$ ), E2 isoscalar resonance sum rule, DWBA anal. 0-68621  
<sup>43</sup>Fe(e $^+$ ), Coulomb form factor for O $^{+4}$  transition, collective 4 $^+$  states, shell model 0-57664  
<sup>43</sup>Fe(e $^+$ ), longitudinal and transverse inelastic response functions and cross sections 0-57771  
<sup>43</sup>Fe(n,n' $\gamma$ ), 14.6 MeV, maximum excitation state  $\gamma$ -decay, cross section (Russian) 0-68586  
<sup>43</sup>Fe(p,p), 6 MeV, elastic and inelastic, quadrupole deformation, IAR excitation, optical pots. (Russian) 0-63149  
<sup>43</sup>Fe anomalous M1/E1 strength ratio and doorway states from <sup>56</sup>Fe(n, $\gamma$ ) 0-57730

## nuclei with mass number 39 to 58 continued

- <sup>57</sup>Fe, rot. band mixing microscopic theory using modified Kuo-Brown interaction 0-68513  
<sup>58</sup>Fe levels, J $\pi$ , anal. powers and cross sections from <sup>56</sup>Fe(t,p) pol.t 0-68539  
<sup>58</sup>Fe(<sup>7</sup>Li, <sup>7</sup>Li), 34 MeV, ang. distrib., cross sections, double folding model anal. 0-78313  
<sup>58</sup>Fe(n,n), 20.6 MeV, neutron yield cross sections and spectra (Russian) 0-91188  
<sup>58</sup>K(Ar,X), 0.4-1.8 GeV/u, multipion prod. energy depend. 0-106065  
<sup>58</sup>K(Ar,X), 800 MeV/N, single particle spectra from high multiplicity events 0-99184  
<sup>58</sup>K(Ar,X), proton inclusive spectra, direct plus thermal model 0-57799  
<sup>59</sup>K(<sup>39</sup>K,X),  $\pi^0$  condensation, spin-isospin instabilities, TDHF calcs. 0-83042  
<sup>41</sup>K nucleus 11.36 MeV analog state total angular momentum from <sup>40</sup>Ar(p,p) reaction (Russian) 0-102169  
<sup>41</sup>K(p, $\gamma$ ), 1.58 MeV, parity doublet gamma lifetimes, 3/2 levels, parity mixing 0-78209  
<sup>41</sup>K excited levels, J $\pi$ , transitions and lifetimes from <sup>48</sup>Ca(p, $\alpha$ n) 0-68544  
<sup>41</sup>K  $\beta$ -decay, <sup>45</sup>Ca levels, excitation functions and J $\pi$  0-105978  
<sup>41</sup>K levels, J $\pi$  and tensor anal. powers from <sup>48</sup>Ca(d, $\alpha$ ), pol.d 0-102113  
<sup>41</sup>K, single particle states lifetimes calcs. 0-105943  
<sup>49</sup>Mn,  $\beta^+$ -decay superallowed branch, <sup>49</sup>Cr levels, transitions, and Gamow-Teller matrix elements 0-57746  
<sup>53</sup>Mn fragmented  $g_{9/2}$  isobaric analogue resonance,  $\gamma$ -spectra and excitation functions from <sup>52</sup>Cr(p, $\gamma$ ) 0-68627  
<sup>53</sup>Mn, spectra, particle-hole conjugation and protection theorems (Chinese) 0-73796  
<sup>54</sup>Mn low lying 2p-4h states, J $\pi$  from tensor anal. powers of <sup>56</sup>Fe(d, $\alpha$ ), pol.d 0-99124  
<sup>55</sup>Mn, nucl. quadrupole moments from laser-RF double reson. spectroscopy 0-57682  
<sup>55</sup>Mn(n,2n), 14 MeV, cross section compilation 0-91181  
<sup>55</sup>Mn(n, $\alpha$ )<sup>52</sup>V, neutron activation anal., Ge(Li) and NaI(Tl) detector  $\gamma$ -ray spectrometer 0-78485  
<sup>55</sup>Mn levels, transitions and spins from <sup>55</sup>Mn(n, $\gamma$ ), pol. Mn and n 0-78154  
<sup>55</sup>Mn(n, $\gamma$ ), primary transitions using focused 24 keV filtered neutron beam 0-63436  
<sup>55</sup>Ni, fp shell model calcs., spectra and spectroscopic factors 0-68588  
<sup>55</sup>Ni mean square charge radii from isotope shifts 0-99484  
<sup>55</sup>Ni(<sup>3</sup>He, p), 8, 10 MeV, A=58, 60, 62, p spectra compound nucleus contrib., odd-even effect 0-106061  
<sup>55</sup>Ni(<sup>7</sup>Li, <sup>7</sup>Li), A=58, 60, 34 MeV, ang. distrib., cross sections, double folding model anal. 0-78313  
<sup>55</sup>Ni(d,X), A=58, 64, 7.6 GeV/c, isotopic cross section ratios, He, Li fragments isotopic effects (Russian) 0-63154  
<sup>55</sup>Ni(e,e), 100-275 MeV, A=58,60,62,64, cross sections and muonic X-ray meas., charge distrib. systematics 0-86801  
<sup>55</sup>Ni(e,p)(e, $\alpha$ ), A=58, 60, 62, electrodisintegration cross sections, E1, E2 absorption, DWBA anal. 0-106052  
<sup>55</sup>Ni(p,X), A=58, 64, 7.6 GeV/c, isotopic cross section ratios, He, Li fragments isotopic effects (Russian) 0-63154  
<sup>55</sup>Ni(p, $\gamma$ ), 80-164 MeV, A=58, 60, 62, 64, prod. cross sections, pre-equilibrium phase 0-78301  
<sup>56</sup>Ni from HI reactions, superdeformed nucleus decay,  $\alpha$ -decay amplification 0-68608  
<sup>56</sup>Ni, nucleosynthesis in Type I supernovae rel. to radioactive excitation source model for late time spectra 0-105264  
<sup>56</sup>Ni high spin yrast cascade, decay modes J assignment from <sup>54</sup>Fe( $\alpha$ ,n $\gamma$ ) 0-68514  
<sup>56</sup>Ni (<sup>7</sup>Li, <sup>7</sup>Li), 14.22 MeV, alignment axis orientation depend. of cross section, mass quadrupole moment alignment 0-68638  
<sup>56</sup>Ni(<sup>16</sup>O, X), 70 MeV, compound nuclei charged particle evaporation, moment of inertia 0-57785  
<sup>56</sup>Ni(<sup>3</sup>He, $\alpha$ ), 130 MeV, selected transition, DWBA anal., cross sections 0-83086  
<sup>56</sup>Ni(<sup>40</sup>Ar,X), 280 MeV, deep inelastic, light fragments, thermal equil., ang. momentum transfer 0-63203  
<sup>56</sup>Ni(<sup>58</sup>Ni,X), optical potential, nuclear matter approach 0-57801  
<sup>56</sup>Ni(<sup>6</sup>Li, <sup>6</sup>Li $^2$ ), 71 MeV, excited states deformation lengths, DWBA and coupled channels anal. 0-68541  
<sup>56</sup>Ni(<sup>6</sup>Li,<sup>6</sup>Li), elastic and inelastic, 74 MeV, folding optical model parameters 0-102201  
<sup>56</sup>Ni( $\alpha$ ), radial sensitivity of optical pot. 0-86869  
<sup>56</sup>Ni( $\alpha$ ), 50.2 MeV, composite particle optical pot. discrete ambiguities, partly Pauli-forbidden states 0-86870  
<sup>56</sup>Ni(d, d'), 108 MeV, giant monopole resonance excitation and ang. distrib. 0-102164  
<sup>56</sup>Ni(d, $\alpha$ ), <sup>56</sup>Co particle-hole states, T=1, zero DWBA anal. 0-78308  
<sup>56</sup>Ni(d,d'), 10 MeV, diff. cross sections and d- $\gamma$  ang. correlations, multi-shell coupled channel calcs. 0-83064  
<sup>56</sup>Ni(n,2n), 14 MeV, cross section compilation 0-91181  
<sup>56</sup>Ni(n, $\gamma$ ), direct-semidirect and compound nucleus contribs. to cross sections 0-68662  
<sup>56</sup>Ni(p, X), pol.p, 65 MeV, continuum spectra anal. powers 0-102178  
<sup>56</sup>Ni(p,p'(d)X), pol. p, 65 MeV, anal. powers of continuum energy spectra 0-68637  
<sup>56</sup>Ni(p,p), 800 MeV, elastic and inelastic, cross section, deformation lengths, optical and DWBA anal. 0-68664  
<sup>56</sup>Ni(p $\nu$ , $\alpha$ ), 22 MeV, analysing power and cross sections, Co proton-hole states 0-68663  
<sup>56</sup>Sc, A=44,46-48, fragment ang. distrib. from <sup>238</sup>U(p,X), 0.8-400 GeV 0-83099  
<sup>56</sup>Sc, A=44m,46,47,48, fragment emission, two-step model applicability from <sup>238</sup>U(p,X) 0-99177  
<sup>41</sup>Sc 2p-1h intermediate struct. resonances, anal. powers, J $\pi$  from <sup>40</sup>Ca(p, $\gamma$ ) 0-86883  
<sup>41</sup>Sc, muonic, energy shifts during atomic EM cascade, and polarisability of deformed nuclei 0-86893  
<sup>43</sup>Sc, J $\pi$ =19/2 $^-$  isomer, high-spin precursors, from <sup>29</sup>Si(<sup>16</sup>O,pn) 0-57656  
<sup>43</sup>Sc levels, J $\pi$ , transitions and lifetimes from (p,p')(<sup>3</sup>He,<sup>3</sup>He)( $\alpha$ , $\alpha$ ) 0-63091  
<sup>43</sup>Sc(p, X), pol.p, 65 MeV, continuum spectra anal. powers 0-102178  
<sup>43</sup>Sc( $\pi^+$ , X), stopped  $\pi^+$ , yields and  $\gamma$ -rays 0-86857  
<sup>43</sup>Sc spin-flip isovector giant resonance, T $_1$  Gamow-Teller strength from <sup>42</sup>Ca(p,n) 0-106019  
<sup>43</sup>Sc proton single particle states, spectroscopic factors, DWBA anal. of <sup>48</sup>Ca(d,n) 0-99118  
<sup>43</sup>Sc, single particle states lifetimes calcs. 0-105943



## nuclei with mass number 39 to 58 continued

- Ti( $^{16}\text{O},\text{X}$ ), 310 MeV, fusion, upper limit to compound nucleus formation 0-78315  
 $^{48}\text{Ti}$ , A=44, 48, ang. distrib. for transitions, DWBA anal., spectroscopic strengths from Ca( $^{11}\text{Li}$ ,t) 0-68584  
 $^{48}\text{Ti}$ , A=48,50, excited states and transition ang. distrib. from Cr( $^{12}\text{C},^{16}\text{O}$ ) 0-95308  
 $^{48}\text{Ti}$ , weak E1 transitions examined using  $\gamma$ -ray,  $\gamma$ - $\gamma$  coincidence and n- $\gamma$  coincidence techniques 0-57724  
 $^{48}\text{Ti}(n,n)$ , 14 MeV, cross section compilation 0-91181  
 $^{48}\text{Ti}(n,n)$ , 15-27.5 MeV, giant dipole resonance splitting, dynamic collective model 0-57755  
 $^{48}\text{Ti}(e,e)$ , magnetic e scatt., exchange current effects, plane wave Born approx. 0-78282  
 $^{48}\text{Ti}(p,\gamma)$ , 0.74-3.25 MeV, cross section and thermonuclear reaction rates, nucleosynthesis, IAR effects 0-102187  
 $^{48}\text{Ti}(p,n)$ , 0.74-3.25 MeV, cross section and thermonuclear reaction rates, nucleosynthesis 0-102187  
 $^{50}\text{Ti}(\alpha,\alpha)$ , 140 MeV, model independent description limits from local optical pots. 0-102196  
 $^{50}\text{Ti}$ , neutron rich nuclide from  $^{238}\text{U}(^{40}\text{Ar},\text{X})$  at 340 MeV 0-57802  
 $^{48}\text{Ti}(^{3}\text{He},\text{xn})^{48}\text{Cr}$ , production of  $^{48}\text{Cr}$  for life sciences appls. 0-94367  
 $^{48}\text{Ti}$ , level scheme,  $\gamma$ -rays, level lifetimes, internal conversion from  $^{40}\text{Ca}(\text{Li},\text{xn})$  0-63085  
 $^{50}\text{V}$ , nucl. quadrupole moments from laser-RF double reson. spectroscopy 0-57682  
 $^{51}\text{V}$ , Spectra, particle-hole conjugation and protection theorems (*Chinese*) 0-73796  
 $^{51}\text{V}(^3\text{He},\text{dp})$ ,  $^3\text{He}$  breakup, DWBA calcs. for strongly absorptive projectiles 0-68682  
 $^{51}\text{V}(e,e)$ , magnetic e scatt., exchange current effects, plane wave Born approx. 0-78282  
 $^{51}\text{V}(n,p)^{51}\text{Ti}$ , neutron activation anal., Ge(Li) and NaI(Tl) detector  $\gamma$ -ray spectrometer 0-78485  
 $^{51}\text{V}(p,X)$ ,  $X=\gamma$  or  $n$ , 0.93-4.47 MeV, cross sections, competition effects, Hauser-Feshbach calcs. 0-91184  
 $^{51}\text{V}(p,p')$ , 6 MeV, levels, spins and EM props., shell model anal. 0-63092  
 $^{56}\text{V}$ , neutron rich nuclide from  $^{238}\text{U}(^{40}\text{Ar},\text{X})$  at 340 MeV 0-57802

## nuclei with mass number 59 to 89

- A=54-82, ground state transition strengths from (p,t) reactions 0-95305  
 A=63, nuclear structure data sheets (July 1979) 0-67941  
 A=70, heavy-ion induced fission-evaporation reactions, magnetic substrate distrib., nuclear alignment 0-73857  
 A=73, nuclear data sheets, levels,  $J^\pi$  and transitions 0-101673  
 A=77, nuclear data sheets, levels,  $J^\pi$  and transitions 0-105439  
 A=90 region, N=50, shell model calcs. 0-68564  
 A~90 nuclei, isomeric states, spin polarisation, M4 transitions and giant resonances 0-63157  
 composite nucleus scission, fusion and strongly damped collisions, rot. energy, boundary diffuseness 0-102224  
 photospallation, 0.1 to 1 GeV, mass yield distrib. 0-73835  
 (d, $^3\text{Li}$ ), A~60,116, L=0 transitions, cross sections, microscopic anal. 0-78189  
 (p,n), A=89-130, sub-Coulomb protons, anomalous optical pot. 0-102191  
 As isotopes, levels and spectra from broken pair model 0-73801  
 $^{73}\text{As}$ , A=71, 73, levels,  $J^\pi$ , transitions, T1/2 from Se decay, Ge( $^3\text{He},\text{d}$ ), (p,xn $\gamma$ ) 0-57684  
 $^{73}\text{As}$  1306 keV state mag. moment, g-factor, rot. aligned band 0-86807  
 $^{75}\text{As}(n,n)$ , slow n coherent scatt. length, free cross section, bound states 0-86909  
 $^{75}\text{As}$  excited states, excitation functions and decays ang. distrib., cross sections from  $^{76}\text{Ge}(p,n\gamma)$  (*Russian*) 0-63089  
 $^{75}\text{As}$  levels,  $J^\pi$  and ang. distrib. from  $^{76}\text{Ge}(\alpha,p)$  0-78161  
 Br nuclei, highly excited, disintegration, photographic emulsion, quark model theory comparison 0-68560  
 Br( $^{12}\text{C},\text{X}$ ), 4.5 GeV/c, emission of short range particles (R<100 mkm) (*Russian*) 0-63202  
 $^{79}\text{Br}$ , A=89-91, delayed neutron emission probabilities,  $\beta$ -decay half-lives 0-83078  
 $^{79}\text{Br}$ , excitation functions for production, pot. nuclear medicine appls. 0-98135  
 $^{79}\text{Br}^m$  decay props., half life and  $\gamma$ -transitions, level scheme 0-83071  
 $^{79}\text{Br}(^{32}\text{S},\text{X})$ , double differential cross section, mass asymmetry, transport model 0-102203  
 $^{84}\text{Br}$  decay,  $^{84}\text{Kr}$  levels,  $\gamma$ -cascades,  $J^\pi$ , mixing ratios and correlations 0-63134  
 Br( $\pi^-,X$ ), charged heavy particle emission after pion capture (*Russian*) 0-69271  
 $^{59}\text{Co}$ , deformation effect from fast neutron transmission in 0.8 to 20 MeV range 0-57675  
 $^{59}\text{Co}$ , energy levels, lifetimes, deexcitation following (n,n $\gamma$ ) studies 0-83059  
 $^{59}\text{Co}$ , energy levels from Ni( $p_{\text{pol}},\alpha$ ) 0-68663  
 $^{59}\text{Co}$  level energies, branching ratios lifetimes and spins from (p,p'), ( $\alpha,\text{p}\gamma$ ) 0-63093  
 $^{59}\text{Co}(^{32}\text{S},\text{X})$ , double differential cross section, mass asymmetry, transport model 0-102203  
 $^{59}\text{Co}(\alpha,\text{xn})$ , 20-172.5 MeV, cross sections excitation functions, hybrid model, preequil. effects 0-57784  
 $^{59}\text{Co}(e,e)$ , magnetic e scatt., exchange current effects, plane wave Born approx. 0-78282  
 $^{59}\text{Co}(n,n)$ , 14 MeV, cross section compilation 0-91181  
 $^{59}\text{Co}(p,X)$ ,  $X=\alpha, \tau, \gamma$ , 72 MeV, spectra and angular distrib. 0-68660  
 $^{59}\text{Co}(p^-,X)$ ,  $X=\text{d}, t, ^3\text{He}, ^4\text{He}$ , particle emission following stopped pion absorption 0-91196  
 $^{60}\text{Co}$  polarised nuclei,  $\beta$ -ray emission, directional distrib. and asymmetry factor 0-95315  
 Co(p, $^3\text{He}$ ), 72 MeV, pre-equilibrium emission (*German*) 0-68657  
 Co(p, $\alpha$ ), 72 MeV, pre-equilibrium emission (*German*) 0-68657  
 $^{59}\text{Cr}$ , neutron rich nuclide from  $^{238}\text{U}(^{40}\text{Ar},\text{X})$  at 340 MeV 0-57802  
 Cu( $n,X$ ) 0-68673  
 Cu( $p,\pi^+$ ) 240 MeV inclusive pion production (*Russian*) 0-86908  
 $^{63}\text{Cu}$ , A=29,63, Doppler shift attenuation factors, level lifetimes, resonances from Ni(p, $\gamma$ ) 0-57741  
 $^{63}\text{Cu}(n,\alpha)$ , A=63,65, 14.8 MeV, expt. and statistical model determ. of  $\alpha$ -prod. in fusion reactors 0-95397  
 $^{63}\text{Cu}$  levels, transitions and ang. distrib. from  $\alpha$ -transfer in  $^{59}\text{Co}(^6\text{Li},\text{d})$  0-73798  
 $^{63}\text{Cu}$  low excitation states, level struct. and lifetimes from  $^{60}\text{Ni}(\alpha,\text{p}\gamma)$  0-86813
- nuclei with mass number 59 to 89 continued  
 $^{63}\text{Cu}$  state alignment,  $\gamma$ -transitions and ang. distrib. from  $^{62}\text{Ni}(p,\gamma)$  0-73797  
 $^{63}\text{Cu}(p,p')$  negative parity level excitation, gamma ray obs., test for core excitation model 0-68534  
 $^{65}\text{Cu}(^{25}\text{S},\text{X})$ , double differential cross section, mass asymmetry, transport model 0-102203  
 Cu( $\gamma,X$ ),  $X=\text{p}, \text{d}, ^3\text{He}, ^4\text{He}$ , cascade-evaporation 0-57770  
 Cu( $\pi^-,X$ ), stopped pions, radioactive product yields 0-83126  
 Cu( $\pi^-,p$ ) 1.5-5 GeV/c, cumulative proton polarisation (*Russian*) 0-86896  
 Cu( $x,x$ ),  $x=\pi^+, K^+, p, p$ , 70, 175 GeV/c 0-83128  
 $^{64}\text{Fe}$ , A=57, 59, levels,  $J^\pi$  and transition branching ratio from Fe(n, $\gamma$ ) 0-105976  
 $^{64}\text{Fe}$ , A=63, 64, neutron rich nuclide from  $^{238}\text{U}(^{40}\text{Ar},\text{X})$  at 340 MeV 0-57802  
 $^{59}\text{Fe}$  resonances, primary  $\gamma$ -intensities, E1-M1 correlation from  $^{58}\text{Fe}(n,\gamma)$  0-57740  
 $^{68}\text{Fe}$  low lying state mean lifetimes and transitions from  $^{64}\text{Zn}(^7\text{Li},\text{p}n)$  0-68599  
 Ga, odd, single particle and collective degrees of freedom, clustering, shell model anal. 0-68510  
 $^{69}\text{Ga}$ , A=65,67, high spin states and transitions from Fe+ $^{12}\text{C}(^{14}\text{N})$  0-68516  
 $^{69}\text{Ga}$  high spin states,  $J^\pi$  and transitions, triaxial struct. from ( $^{12}\text{C},\alpha$ ), ( $^{12}\text{Li},\text{Zn}$ ) 0-63062  
 $^{69}\text{Ga}$  state alignment,  $\gamma$ -transitions and ang. distrib. from  $^{68}\text{Zn}(p,\gamma)$  0-73797  
 $^{73}\text{Ga}$ , levels,  $J^\pi$  and ang. distrib. from  $^{70}\text{Zn}(\alpha,p)$  0-78161  
 Ge, even-even nuclei,  $\gamma$ -spectroscopy, exptl. results and models 0-68589  
 Ge isotopes, shape transition and quadrupole softness, Hartree Bogoliubov calc. 0-68527  
 Ge, odd, single particle and collective degrees of freedom, clustering, shell model anal. 0-68510  
 $^{66}\text{Ge}$ , A=66,69,70, negative parity high spin states, spin and lifetimes from H1 reactions 0-73768  
 $^{66}\text{Ge}$ , A=68, 70,72,74, level excitation, n-p interaction role from  $\alpha$ -transfer in Zn( $^{14}\text{Li},\text{d}$ ) 0-73821  
 $^{66}\text{Ge}$ , A=72, 74,  $0_2^+$  levels, struct. transition between N=40 and 42 from Ga( $\alpha,p$ ) 0-73800  
 $^{66}\text{Ge}(t,p)$ , pol. t, A=70,72, octupole oscillations modes from anal. powers,  $3_1^-$  octupole transition 0-102142  
 $^{19}\text{Ge}$  excited state, J, mean lifetimes and transitions from  $^{64}\text{Za}(^7\text{Li},\text{ph})$   
 $^{19}\text{Ge}$  excited state, J, mean lifetimes and transitions 0-68517  
 $^{66}\text{Ge}$  levels, lifetimes,  $J^\pi$  and transitions from  $^{58}\text{Ni}(^{10}\text{B},\text{pn}\gamma)$  0-73799  
 $^{69}\text{Ge}$  high spin states, J assignment, decay scheme from  $^{55}\text{Mn}(^{16}\text{O},\text{pn})$  0-68518  
 $^{74}\text{Ge}(^{32}\text{S},\text{X})$ , double differential cross section, mass asymmetry, transport model 0-102203  
 Ge( $\gamma^+e^-$ ), cross section near threshold, atomic electron screening effects 0-78279  
 Kr even-even isotopes, collective states and transitions, interacting boson approx. 0-73773  
 $^{84}\text{Kr}$ , A=79, 81, high spin E2 bands,  $J^\pi$ , transitions from Ge( $^{10}\text{B},\text{x}\gamma$ ) 0-63061  
 $^{78}\text{Kr}$  bands, lifetimes and E2 transitions from interacting boson model and ( $^{16}\text{O},\text{p}n$ ), ( $^{19}\text{Fe},\alpha,\text{p}n$ ) 0-73771  
 $^{79}\text{Kr}$ , Kr low lying levels from  $^{79}\text{Br}(p,n\gamma)$  0-105972  
 $^{84}\text{Kr}$  levels,  $\gamma$ -cascades,  $J^\pi$ , mixing ratios and correlations from  $^{84}\text{Br}$  decay 0-63134  
 $^{85}\text{Kr}^m$  decay,  $^{85}\text{Rb}$  levels,  $J^\pi$  and transitions 0-78162  
 $^{86}\text{Kr}$  in meteorite, s-process nucleosynthesis and s-process neutron capture time scale 0-73080  
 Kr(p,xn) $^{81,82\text{m}}\text{Rb}$ ,  $^{81,82\text{m}}\text{Rb}$  prod. for positron emission tomography 0-98068  
 ( $^6\text{Li},\text{d}$ ), A~60,116, L=0 transitions, cross sections, microscopic anal. 0-78189  
 $^{61}\text{Mn}$ , neutron rich nuclide from  $^{238}\text{U}(^{40}\text{Ar},\text{X})$  at 340 MeV 0-57802  
 $^{89}\text{Mo}^m$  levels, transitions and half life from  $^{92}\text{Mo}(p,p_3n)$  0-86858  
 $^{60}\text{Ni}$ , A=60, 62, 66, levels,  $J^\pi$ , anal. powers and cross sections from Ni(t,p)pol. t 0-68539  
 $^{60}\text{Ni}(^6\text{He}, p)$ , 8, 10 MeV, A=58, 60, 62, p spectra compound nucleus contrib., odd-even effect 0-106061  
 $^{60}\text{Ni}(^6\text{Li}, ^7\text{Li})$ , A=58, 60, 34 MeV, ang. distrib., cross sections, double folding model anal. 0-78313  
 $^{60}\text{Ni}(d,X)$ , A=58, 64, 7.6 GeV/c, isotopic cross section ratios, He, Li fragments isotopic effects (*Russian*) 0-63154  
 $^{60}\text{Ni}(e,e)$ , 100-275 MeV, A=58,60,62,64, cross sections and muonic X-ray meas., charge distrib. systematics 0-86801  
 $^{60}\text{Ni}(e,p)$ , (e, $\alpha$ ), A=58, 60, 62, electrodisintegration cross sections, E1, E2 absorption, DWBA anal. 0-106052  
 $^{60}\text{Ni}(p,X)$ , A=58, 64, 7.6 10 GeV/c, isotopic cross section ratios, He, Li fragments isotopic effects (*Russian*) 0-63154  
 $^{60}\text{Ni}(p,\text{x}\gamma)$ , 80-164 MeV, A=58, 60, 62, 64, prod. cross sections, pre-equilibrium phase 0-78301  
 $^{60}\text{Ni}(p_{\text{pol}},\alpha)$ , A=60, 62, 22 MeV, analysing power and cross sections, Co proton-hole states 0-68663  
 $^{59}\text{Ni}$  levels, cross section and vector anal. power, ang. distrib. from  $^{59}\text{Ni}(^6\text{Li}, ^7\text{Li})$ , pol.  $^7\text{Li}$  0-106044  
 $^{59}\text{Ni}(n,n)$ , 14 MeV, cross section compilation 0-91181  
 $^{60}\text{Ni}$ , Coulomb contributions to nuclear radii and energies 0-68515  
 $^{60}\text{Ni}$  high spin states,  $J^\pi$ , T $_{1/2}$ , ang. distrib. and polarisations from  $^{56}\text{Fe}(^7\text{Li}, \text{p}n\gamma)$  0-99116  
 $^{60}\text{Ni}$  level scheme and  $\gamma$ -rays from  $^{59}\text{Ni}(n,\gamma)$  0-63099  
 $^{60}\text{Ni}(^6\text{Li},X)$ , 156 MeV, projectile break up in continuous particle spectra, cross section, fragmentation 0-86889  
 $^{60}\text{Ni}(p,\alpha)^{57}\text{Co}(3/2^-)$ , anomalous analyzing power, DWBA calc. 0-86894  
 Ni(d,d), 13-80 MeV, second order breakup corrections in DWBA 0-86910  
 Ni(e, $\alpha$ ), E2 strength in resonance regions statistical decay 0-91146  
 Ni(n, $\gamma$ ), primary transitions using focused 24 keV filtered neutron beam 0-63436  
 Rb, fission fragment, delayed neutron branches from  $\gamma$ -spectroscopy 0-78230  
 Rb, ground state spins, moments, charge radii by laser spectroscopy 0-78147  
 Rb, neutron rich isotopes,  $Q_\beta$  and direct mass meas. 0-78132  
 Rb odd-even isotopes, collective states and transitions, interacting boson approx. 0-73773  
 Rb relative independ. yield from  $^{232}\text{Th}(p,f)$  0-102218



nuclei with mass number 59 to 89 continued

<sup>81</sup>Rb, A=79, 81, decoupled  $g_{9/2}$  bands, level lifetimes and E2 transitions from (<sup>16</sup>O, 2n) (<sup>18</sup>F, p2n) 0-73772  
<sup>81</sup>Rb(n,n $\gamma$ ), 550-2100 keV, A=85,87, levels, excitation functions, J $\pi$ , Hauser-Feshbach anal. 0-105982  
<sup>81</sup>Rb-<sup>81</sup>Kr generators, aspects of production, elution and automation, medical appls. 0-61696  
<sup>83</sup>Rb band structure, spin assignments and transitions from (<sup>6</sup>Li,3n), (<sup>16</sup>O,p2n), ( $\alpha$ ,2n) 0-73774  
<sup>83</sup>Rb high spin states, J $\pi$  and transitions from HI and  $\alpha$  reactions 0-105949  
<sup>85</sup>Rb high spin states, yrast cascade, J $\pi$ ,  $\gamma$ -transitions from <sup>82</sup>Se(Li,xn $\gamma$ ) 0-73775  
<sup>85</sup>Rb levels, J $\pi$  and transitions from Kr<sup>m.s.</sup>, Sr<sup>m.s.</sup> decay, cluster-vibr. model 0-78162  
<sup>85</sup>Rb, proton induced nuclear reactions, excitation functions, medical appls. 0-78286  
<sup>85</sup>Rb(<sup>22</sup>Si, Z), double differential cross section, mass asymmetry, transport model 0-102203  
Se, even-even nuclei,  $\gamma$ -spectroscopy, exptl. results and models 0-68589  
<sup>76</sup>Se, A=74, 76, vibr. states and transition from dynamic deformation theory 0-73770  
<sup>76</sup>Se(d,pol,d), A=76,78,80,82, 12 MeV, two-step scatt. process via J $\pi$ =2 $_1^+$  excited states 0-57781  
<sup>76</sup>Se(n,n), A=76-78, 80, 82, slow n coherent scatt. length, free cross section, bound states 0-86909  
<sup>72</sup>Se side band structure, negative parity states and transitions from <sup>58</sup>Ni(<sup>16</sup>O,2p) 0-73769  
<sup>74</sup>Se transition energy correlations in  $\gamma$ -continuum from <sup>64</sup>Ni(<sup>16</sup>O, $\alpha$ 2n) 0-95309  
<sup>76</sup>Se high spin states, bands, J $\pi$ , transitions and T $_{1/2}$  from <sup>71</sup>Ga(<sup>7</sup>Li,2n) 0-105951  
<sup>76</sup>Se, 96 keV transition, conversion coeff.,  $\gamma$ -spectrum 0-63131  
Sr, even isotopes, potential energy surfaces and ground state equilib. deformation 0-73789  
<sup>81</sup>Sr, A=81, 83, yrast and high spin states of neutron deficient isotopes from Kr( $\alpha$ ,xn) 0-73776  
<sup>79</sup>Sr, mass excess values from beta and gamma spectra from <sup>32</sup>S+<sup>54</sup>Fe(<sup>38</sup>Ni) 0-63137  
<sup>85</sup>Sr, 514.0 keV, Analytic fitting of full-energy peaks in Ge(Li) spectra at high count rates 0-99147  
<sup>85</sup>Sr<sup>m.s.</sup> decay, <sup>85</sup>Rb levels, J $\pi$  and transitions 0-78162  
<sup>87</sup>Sr 1  $g_{9/2}$  neutron distrib. radial size, states, differential cross sections from <sup>86</sup>Sr(<sup>16</sup>O,<sup>1</sup>O) 0-95301  
<sup>87</sup>Sr(e,e), magnetic e scatt., exchange current effects, plane wave Born approx. 0-78282  
<sup>88</sup>Sr( $\gamma$ , $\gamma$ ), 14 MeV, highly excited spin-1 resonances, spin and radiative widths 0-86876  
<sup>88</sup>Sr(n,n $\gamma$ ), 11 MeV, octupole vibr. states, diff. cross section, deformation length, DWBA anal. 0-102092  
<sup>81</sup>Y, A=82, 83, mass excess values from beta and gamma spectra from <sup>32</sup>S+<sup>54</sup>Fe(<sup>38</sup>Ni) 0-63137  
<sup>81</sup>Y<sup>m.s.</sup>, A=86, 87, isomeric yield ratios and  $\gamma$ -spectra from <sup>93</sup>Nb( $\pi^-$ ,X) 0-86857  
<sup>87</sup>Y level struct.,  $\gamma$ -spectroscopy and J $\pi$  from (p,2n $\gamma$ ), ( $\alpha$ ,2n $\gamma$ ) 0-83040  
<sup>88</sup>Y 14 ms 8 $^+$  isomeric state, g-factor from <sup>87</sup>Rb( $\alpha$ ,3n) 0-63080  
<sup>88</sup>Y, gamma-ray intensities, precision meas. 0-102139  
<sup>89</sup>Y, giant reson. pionic excitation 0-73834  
<sup>89</sup>Y(<sup>3</sup>S,X), double differential cross section, mass asymmetry, transport model 0-102203  
<sup>89</sup>Y(n, $\gamma$ ), direct-semidirect and compound nucleus contribs. to cross sections 0-68662  
<sup>89</sup>Y(p,n), sub-Coulomb optical pot. 0-102190  
<sup>89</sup>Zn, A=64, 66 levels and primary E1 transition strength functions from Cu(p, $\gamma$ ) 0-91149  
<sup>89</sup>Zn( $\alpha$ ,  $\alpha'$ ), A=64, 66, 129 MeV, isoscalar giant monopole resonances, nuclear incompressibility 0-83083  
<sup>89</sup>Zn(e,e), 100-275 MeV, A=64,66,68,70, cross sections and muonic X-ray meas., charge distrib. systematics 0-86801  
<sup>61</sup>Zn states, pseudo LS coupling model 0-68548  
<sup>61</sup>Zn ang. distrib. for transitions, DWBA anal., spectroscopic strengths from <sup>58</sup>Ni(<sup>7</sup>Li,t) 0-68584  
<sup>64</sup>Zn high spin states, J $\pi$ , T $_{1/2}$ ,  $\gamma$ -decays from ( $\alpha$ ,n $\gamma$ ), (<sup>11</sup>B,p2n $\gamma$ ) 0-73767  
<sup>62</sup>Zn negative parity high spin states, spin and lifetimes from HI reactions 0-73768  
<sup>62</sup>Zn\* composite particle emission, ang.-distrib., exciton-coalescence model from (d,X), (<sup>3</sup>He,X), ( $\alpha$ ,X) 0-78265  
<sup>62</sup>Zn muonic atom, dynamical E0 excitation, E0 resonances, muonic X-rays 0-95749  
<sup>64</sup>Zn(<sup>3</sup>He,<sup>3</sup>He), elastic and inelastic scatt. angular distrib. fine struct. 0-106063  
<sup>4</sup>Zr(n, $\gamma$ ), A=64; 66, 67, 68, 70, 2.8-500 keV, capture cross sections 0-57780  
<sup>85</sup>Zr yrast and high spin states of neutron deficient isotopes from Sr( $\alpha$ ,xn) 0-73776

nuclei with mass number 90 to 149

<sup>116</sup>Xe quasi-rotational bands, levels J $\pi$  and T $_{1/2}$  from <sup>116</sup>Cs decay 0-83021  
A=112, experimental nuclear structure data to January 1979 0-98763  
A=120-150, levels and EM props., recent results 0-68592  
A=123, experimental nuclear structure data to June 1979 0-94931  
A=134-144, fission yields from spectroscopic meas.,  $\gamma$ -branching and half-lives 0-78213  
A=135-143, odd A fission products, delayed n, decay studies and Q $\beta$  meas. 0-78227  
A=145, experimental nuclear structure data to August 1979 0-94932  
A=90 region, core pol. effects and giant quadrupole resonances, HF and macroscopic calcs. 0-57756  
A=90 region, N=50, shell model calcs. 0-68564  
A~150, yrast states, deformed oscillator Hamiltonian calcs. 0-78126  
A~90 nuclei, isomeric states, spin polarisation, M4 transitions and giant resonances 0-61517  
charge radii and binding energy per nucleon, linear relationship evidence 0-68520  
doubly even nuclei, yrast band B(E2) values, hydrodynamical model and CAP effect 0-86793  
even-even neutron-rich fission products, de-excitation spectra,  $\beta$ -decay, deformation 0-78203

nuclei with mass number 90 to 149 continued

(HI,X), rare earths, deeply inelastic transfer reactions, kinematic anal. 0-99186  
magic and doubly magic nuclei, A=129, 131, 133 chains, 0 $^+$  states, spectroscopy 0-78165  
N=82 region, high spin isomers, cranked HF calcs., deformation shapes, excitation energies 0-99121  
N=82 region, high spin isomers, deformation energy surface, shape constrained cranked HF theory 0-57666  
odd-odd fission products, level schemes, rot. bands, shell model states 0-78167  
photospallation, 0.1 to 1 GeV, mass yield distrib. 0-73835  
rapid automated nuclear chemistry, short lived fission products, reactor safety 0-81353  
rare earth deformed nuclei, high spin region excited rot. bands, RPA calcs. 0-78108  
rare earth nuclei, modified oscillator pot. parameters, single particle levels 0-68509  
rare earths, nuclear deformation, Coulomb displacement energy depend., shell model 0-102108  
XX <sup>136</sup>Xe, 2 $^-$   $\rightarrow$  2 $^-$  transition multipole mixing ratio 0-78198  
Z=37-43, neutron rich fission products, mass energy surface, decay props. 0-78228  
(d,<sup>3</sup>Li), A~60,116, L=0 transitions, cross sections, microscopic anal. 0-78189  
(n,n), A=90 region, elastic, inelastic and total cross section, statistical model calcs. 0-68674  
(p,n), A=89-130, anomalous optical pot. for sub-Coulomb protons 0-102190  
(p,n), A=89-130, sub-Coulomb protons, anomalous optical pot. 0-102191  
(p,n), A=90 region, reaction cross section, statistical model calcs. 0-68674  
(p,n), anomalous optical potential for sub-Coulomb barrier protons, 2 particle 1 hole states 0-105948  
<sup>4</sup>Si(d,X), A=112, 124, 7.6 GeV/c, isotopic cross section ratios, He, Li fragments isotopic effects (*Russian*) 0-63154  
Ag nuclei, highly excited, disintegration, photographic emulsion, quark model theory comparison 0-68560  
Ag(<sup>12</sup>C,X), 4.5 GeV/c, emission of short range particles (R<100 mkm) (*Russian*) 0-63202  
<sup>103</sup>Ag, A=105-109, negative parity states, vibr. versus rot. descriptions 0-73781  
<sup>103</sup>Ag, A=105-109, negative parity states, EM props. from particle-asymmetric rotor model 0-102097  
<sup>100</sup>Ag<sup>m.s.</sup> decay, <sup>100</sup>Pd levels and  $\gamma$ -transitions 0-83077  
<sup>103</sup>Ag collective excitation and J $\pi$  following <sup>94</sup>Mo(<sup>12</sup>C,p2n $\gamma$ ), rotor-plus-particle model 0-86782  
<sup>103</sup>Ag high spin states, bands transitions, intermediate deformation Coriolis coupling from (<sup>3</sup>He,xn $\gamma$ ) 0-105944  
<sup>103</sup>Ag  $\rightarrow$  <sup>103</sup>Pd,  $\beta$ -ground state feedings and branchings 0-102147  
<sup>104</sup>Ag levels, J $\pi$ , T $_{1/2}$ , bands and transitions from <sup>103</sup>Rh( $\alpha$ , 3n $\gamma$ ) 0-102093  
<sup>106</sup>Ag low-lying excited states from <sup>103</sup>Rh( $\alpha$ ,n $\gamma$ ) and <sup>104</sup>Pd( $\alpha$ ,pn $\gamma$ ) 0-57693  
<sup>107</sup>AgZZ 0-95329  
<sup>108</sup>Ag levels and  $\gamma$ -transitions, population-spin correlation from <sup>107</sup>Ag(n, $\gamma$ ) 0-63097  
<sup>109</sup>Ag(<sup>40</sup>Ar,X), fusion reactions, charge density asymmetry liquid drop model 0-63220  
<sup>109</sup>Ag(p,p'), pol.p, 6.06 MeV, anal. powers, large absorption pot., optical model 0-83092  
<sup>110</sup>Ag 118.718 keV isomer, low lying states and transitions, coincidence study from <sup>108</sup>Ag(n, $\gamma$ ) 0-73806  
<sup>110</sup>Ag, decay period, least square fitting, pocket calculator program with variable precision 0-67976  
<sup>110m</sup>Ag, gamma-ray intensities, precision meas. 0-102139  
Ag( $\gamma$ ,X), X=p,d,t,<sup>3</sup>He,<sup>4</sup>He, cascade-evaporation 0-57770  
Ag( $\gamma$ , $\gamma$ ), 412, 468, 662 keV, elastic scatt. cross sections, Rayleigh scattering anal. 0-86898  
Ag(p,f), 1 GeV, binary fission, possible mass instability of correlated fragments 0-83133  
Ag( $\pi^-$ ,X), charged heavy particle emission after pion capture (*Russian*) 0-69271  
Ba, charge radii and binding energy per nucleon, linear relationship evidence 0-68520  
Ba, neutron deficient, charge radii, moments, transitions and isomers, atomic beam laser spectroscopy 0-102141  
Ba, radioisotopes, at. beam laser spectroscopy, hyperfine struct., nucl. moments and radii 0-57678  
<sup>4</sup>Ba, A=132, 134, 136, negative parity states, J $\pi$ , transitions, DWBA anal. of Ba(p,t) 0-86810  
<sup>4</sup>Ba, A=135,137, Coulomb excitation, transition probabilities,  $\gamma$ -rays and level collectivity from (<sup>16</sup>O,<sup>3</sup>O $\alpha'$ ) ( $\alpha$ , $\alpha'$ ) 0-78201  
<sup>4</sup>Ba, A=142,144,146, transition  $\gamma$ - $\gamma$  ang. correlations, levels, J $\pi$ , mixing ratios 0-73823  
<sup>133</sup>Ba, 12.34 keV M1 transition 0-106004  
<sup>136</sup>Ba(n,2n)<sup>135</sup>Ba<sup>m</sup>, 14.2 MeV, neutron activation cross sections 0-91180  
<sup>138</sup>Ba(n, $\alpha$ )<sup>135</sup>Xe<sup>m.s.</sup>, 14.2 MeV, neutron activation cross sections 0-91180  
<sup>138</sup>Ba(n,p), 14.2 MeV, neutron activation cross sections 0-91180  
<sup>139</sup>Ba,  $\gamma$ -ray emission probabilities and half-life obs. 0-57723  
<sup>140</sup>Ba, fractional cumulative yield from <sup>245</sup>Cm(n,f) 0-63074  
<sup>42</sup>Ba,  $\gamma$  $\gamma$  ang. correlations, levels, spins and mixing ratios from <sup>142</sup>Cs decay 0-57734  
Ba( $\gamma$ , $\gamma$ ), 412, 468, 662 keV, elastic scatt. cross sections, Rayleigh scattering anal. 0-86898  
<sup>4</sup>Br, A=89-91, delayed neutron emission probabilities,  $\beta$ -decay half-lives 0-83078  
CC <sup>93</sup>Nb(n,2n), 14 MeV, cross section compilation 0-91181  
Cd 2 $^+$  excitation,  $\alpha$ -spectroscopic factors in IBA model from Sn(d,<sup>6</sup>Li) 0-105967  
Cd even-even nuclei, low lying collective states, two-photon character 0-57667  
<sup>4</sup>Cd, A=104-116, low lying level scheme, mass excess from Cd(p,t) 0-73807  
<sup>4</sup>Cd, A=112, 114, 0 $_2^+$  and 0 $_3^+$  states, E0, E2 transitions and collectivity 0-102144  
<sup>4</sup>Cd(<sup>16</sup>O,<sup>16</sup>O), 44 MeV, A=112, 114, 0 $_2^+$ , 0 $_3^+$  state collectivity, E0 and E2 decay, T $_{1/2}$  0-73784  
<sup>103</sup>Cd levels, J $\pi$  and positive parity decoupled band, rotor anal. of <sup>94</sup>Mo(<sup>12</sup>C, 3n $\gamma$ ) 0-102096  
<sup>103</sup>Cd  $\rightarrow$  <sup>103</sup>Ag,  $\beta$ -ground state feedings and branchings 0-102147

## nuclei with mass number 90 to 149 continued

- <sup>104</sup>Cd quasirot. ground state band and  $\gamma$ -transition from <sup>102</sup>Pd( $\alpha$ ,2n $\gamma$ ) 0-105955  
<sup>111</sup>Cd, 1330 keV level excitation cross section from positron annihilation 0-68583  
<sup>111</sup>Cd, nucl. orientation coeffs. with axially symm. elec. field gradient 0-97168  
<sup>112</sup>Cd, E0 transition from  $\alpha_1^+$  state following <sup>112</sup>In beta decay 0-68578  
Cd( $\gamma$ , $\gamma$ ), 412, 468, 662 keV, elastic scatt. cross sections, Rayleigh scattering anal. 0-86898  
<sup>138</sup>Ce(<sup>57</sup>Fe,X), fusion reactions, charge density asymmetry liquid drop model 0-63220  
<sup>141</sup>Ce collective M1 excitation effects on  $\gamma$ -ang. distrib., direct semidirect model of <sup>140</sup>Ce(n, $\gamma$ ) 0-57733  
Cs, fission fragment, delayed neutron branches from  $\gamma$ -spectroscopy 0-78230  
Cs, ground state spins, moments, charge radii by laser spectroscopy 0-78147  
Cs, neutron rich isotopes,  $Q_\beta$  and direct mass meas. 0-78132  
Cs radioisotopes, hyperfine spectroscopy, nucl. charge radius, ground and isomeric states 0-57677  
Cs relative independ. yield from <sup>232</sup>Th(p,f) 0-102218  
<sup>A</sup>Cs, A=119-133 odd isotopes, collective props., bands and transitions from heavy ion reactions 0-68512  
<sup>A</sup>Cs, A=142, 144, 146, low lying levels,  $J^\pi$ , mixing ratios and  $\gamma$ - $\gamma$  ang. correlations 0-102119  
<sup>116</sup>Cs decay, <sup>116</sup>Xe quasi-rotational bands, levels  $J^\pi$  and  $T_{1/2}$  0-83021  
<sup>123</sup>Cs(<sup>123m</sup>Cs), gamma and conversion electron radiation 0-106017  
<sup>127</sup>Cs collective quadrupole dynamics, band struct., transitions, collective model anal. from <sup>127</sup>I( $\alpha$ ,4n) 0-78112  
<sup>129</sup>Cs decay, <sup>129</sup>Xe excited state lifetimes,  $\gamma$ -transitions 0-78205  
<sup>134</sup>Cs 176.403 keV isomer, populating  $\gamma$ -rays, low lying levels from <sup>133</sup>Cs(n, $\gamma$ ), <sup>134</sup>Cs 176.403 keV isomer, populating  $\gamma$ -rays, low lying levels 0-78200  
<sup>134</sup>Cs, gamma-ray intensities, precision meas. 0-102139  
<sup>134</sup>Cs decay, <sup>142</sup>Ba,  $\gamma\gamma$  ang. correlations, levels, spins and mixing ratios 0-57734  
<sup>143</sup>Cs, delayed neutrons, energy spectra 0-99153  
<sup>A</sup>Eu EC decay, A=147, 149, <sup>147,149</sup>Sm levels,  $J^\pi$ ,  $\gamma$ -transitions and multipole mixing ratios,  $\gamma\gamma$  correlations 0-106012  
<sup>147</sup>Eu high spin levels, isomers and in-beam  $\gamma$ -spectroscopy from <sup>146</sup>Sm( $\alpha$ ,2np) 0-78124  
<sup>146</sup>Eu 9<sup>+</sup> isomer,  $\gamma$ -decay, high spin particle-hole multiplet population from <sup>147</sup>Sm(p,2n) 0-63066  
<sup>A</sup>Gd A=144,146,147,148, high spin isomer g-factors yrast traps from (<sup>28</sup>Si,<sup>28</sup>Si'), ( $\alpha$ , $\alpha'$ ) 0-78146  
<sup>A</sup>Gd, A=146,147, mass and Z=64 shell closure from <sup>144</sup>Sm(<sup>12</sup>C,<sup>9,10</sup>Be) 0-57669  
<sup>145</sup>Gd levels,  $J^\pi$  and transitions, neutron hole coupling to <sup>146</sup>Gd core from <sup>144</sup>Sm( $\alpha$ ,3n) 0-78164  
<sup>146</sup>Gd lowest 2<sup>+</sup> state,  $J^\pi$  and transitions from <sup>146</sup>Tb decay 0-105979  
<sup>146</sup>Gd, O<sub>2</sub><sup>+</sup> state EM decay,  $T_{1/2}$  and monopole strength 0-95310  
<sup>Gd</sup> region, proton subshell effects from  $\alpha$ -decay and spectroscopy, self-consistent study 0-57748  
<sup>147</sup>Ho low lying yrast states from <sup>122</sup>Te(<sup>32</sup>S,X), <sup>121</sup>Sb(<sup>32</sup>S,X) 0-91151  
I  $\beta^+$  decay force function resonance struct., level populations (*Russian*) 0-102154  
<sup>A</sup>I, A=115-127 odd isotopes, collective props., bands and transitions from heavy ion reactions 0-68512  
<sup>A</sup>I, A=139-141, delayed neutron emission probabilities,  $\beta$ -decay half-lives 0-83078  
<sup>123</sup>I, prep. from gaseous TeF<sub>6</sub>, nuclear medicine appl. (*French*) 0-98137  
<sup>123</sup>I prod. from <sup>127</sup>(p,5n)<sup>123</sup>Xe-<sup>123</sup>I, at 58 MeV 0-94369  
<sup>123</sup>I production from <sup>123</sup>Xe formed in spallation reactions by 660 MeV protons, medical appls. 0-85494  
<sup>121</sup>I time depend. quadrupole interactions,  $\gamma$ - $\gamma$  correlations from <sup>129</sup>Te<sup>m+8</sup> decay 0-78145  
<sup>132</sup>I decay <sup>132</sup>Xe level struct.,  $J^\pi$ , transitions and multipole mixing ratio 0-91134  
<sup>132</sup>I isomer and gamma-ray spectrum from <sup>133</sup>Cs( $\pi^-$ ,p) 0-78199  
<sup>133</sup>I yield and  $\gamma$ -ray spectra from <sup>133</sup>Cs( $\pi^-$ ,p) 0-86857  
<sup>134</sup>I fractional independ. yield from <sup>238</sup>U( $\gamma$ ,f) 0-57814  
<sup>134</sup>I yield from <sup>237</sup>Np(n,f) 0-86935  
<sup>134</sup>I, fractional cumulative yield from <sup>245</sup>Cm(n,f) 0-63074  
<sup>136</sup>I, isomeric ratio,  $\gamma$ -spectra thermal neutron and 3 MeV fission of <sup>235</sup>U (*French*) 0-68709  
<sup>137</sup>I beta delayed neutrons, <sup>137</sup>Xe neutron unbound states, high energy X-rays 0-86856  
In relative independ. yield from <sup>232</sup>Th(p,f) 0-102218  
<sup>A</sup>In, A=119, 121, unified model description, vibr. multiplet yrast struct., branching ratios 0-105953  
<sup>107</sup>In nucleus and K shell excitation, lifetime meas. from <sup>106</sup>Cd(p,p')<sup>106</sup>Cd 0-63130  
<sup>108</sup>In high spin struct., in-beam spectroscopy, conversion electrons from <sup>98</sup>Mo(<sup>14</sup>N,4n $\gamma$ ) 0-73782  
<sup>109</sup>In high spin states,  $\gamma$ -transitions, ang. distrib. from <sup>108</sup>Cd( $\alpha$ ,2np) 0-73783  
<sup>111</sup>In 21/2<sup>+</sup> isomeric state g-factor and relaxation time from <sup>109</sup>Ag( $\alpha$ ,2n $\gamma$ ) 0-73794  
<sup>111</sup>In, nucl. orientation coeffs., nucl. mag. moment 0-97168  
<sup>111</sup>In-<sup>109</sup>In mass difference from  $Q$  values of Cd(<sup>4</sup>He,d) 0-63069  
<sup>111</sup>In low lying levels, transitions,  $T_{1/2}$ , multipolarities and mixing ratios from <sup>112</sup>Cd(p,n $\gamma$ ) 0-68545  
<sup>138,139</sup>La, Fourier transform NMR 0-57354  
<sup>A</sup>La, A=125, 127, collective props., bands and transitions from heavy ion reactions 0-68512  
<sup>137</sup>La(e,p), 15-25 MeV,  $T_0+1$  giant dipole resonance and characteristic decay mode 0-78247  
(<sup>6</sup>Li,d), A=60,116, L=0 transitions, cross sections, microscopic anal. 0-78189  
MO, onset of deformation at A~100 0-73790  
<sup>A</sup>Mo, A=103, 104, <sup>252</sup>Cf fission fragment  $\beta$ -decay, X-ray- $\beta$  particle coincidence technique 0-74094  
<sup>A</sup>Mo, A=92, 95, 96, 97, 98, 100, (n,p), (n,n'), (n, $\alpha$ ), (n,n' $\alpha$ ), (n,<sup>3</sup>He) prod. cross sections at 14 MeV 0-93829  
<sup>A</sup>Mo, A=95, 97, nucl. quadrupole moments from laser-RF double reson. spectroscopy 0-57682  
<sup>A</sup>Mo, A=98,102, anal. powers, transitions, shape coexistence states, DWBA anal. of Mo(t,p), pol.t 0-86895  
<sup>A</sup>Mo(n,2n), A=92, 100, 14 MeV, cross section compilation 0-91181

## nuclei with mass number 90 to 149 continued

- <sup>92</sup>Mo(<sup>16</sup>O,X), entrance channel mass asymmetry effects on reaction mechanism, fission and fusion 0-106077  
<sup>96</sup>Mo vibration-rotation struct. and yrast levels from variable moment of inertia model 0-73778  
<sup>96</sup>Mo(t,p), pol.t, cross section and anal. powers, struct. depend., DWBA anal. 0-78272  
<sup>100</sup>Mo(<sup>4</sup>N,<sup>3</sup>B), 200 MeV, <sup>12</sup>B spin polarisation in deep inelastic collision 0-63160  
<sup>100</sup>Mo(<sup>14</sup>N,<sup>12</sup>B), 90 meV, spin alignment of products, semi-classical model calcs. 0-73859  
<sup>108</sup>Mo(n,n' $\gamma$ ), fast n, gamma transitions, level energies and scheme 0-73822  
<sup>100</sup>Mo levels,  $\gamma$ -rays and p-wave resonance partial radiative widths from <sup>100</sup>Mo(n, $\gamma$ ) 0-57739  
<sup>102</sup>Mo fission product decay, <sup>102</sup>Tc decay scheme and  $\gamma$ -intensities 0-78229  
Mo(p,p' $\gamma$ ), odd isotopes, excited d-states from analogue resonances and p- $\gamma$  correlations 0-68546  
<sup>A</sup>Nb, A=90,92,94, Gamow-Teller strength distrib., RPA calcs. 0-78218  
<sup>90</sup>Nb giant particle hole resonances, Gamow-Teller strength from <sup>90</sup>Zr(p,n) 0-86877  
<sup>92</sup>Nb low lying multiplets, DWBA anal. for spectroscopic factors from <sup>91</sup>Zr( $\alpha$ ,t) 0-57685  
<sup>93</sup>Nb, (n,p), (n,n'), (n, $\alpha$ ), (n,n' $\alpha$ ), (n,<sup>3</sup>He) prod. cross sections at 14 MeV 0-93829  
<sup>93</sup>Nb(<sup>14</sup>N,X), 210 MeV, deep inelastic, particle-particle correlations for Li, Be, B, C 0-63206  
<sup>93</sup>Nb(d,p,X), 80 MeV, inclusive proton spectra, d break-up, DWBA anal. 0-91190  
<sup>93</sup>Nb(e,e), magnetic e scatt., exchange current effects, plane wave Born approx. 0-78282  
<sup>93</sup>Nb(p, X), pol.p, 65 MeV, continuum spectra anal. powers 0-102178  
Nd decay, <sup>A</sup>Pm, A=149,151, shape coexistence, deformed states 0-78135  
Nd, even-even, E2 transition probabilities from multiple Coulomb excitation, IBA comparison 0-78212  
Nd, N=85 isotones, bands and transitions from  $\alpha$  and HI excitation, in-beam study 0-78123  
<sup>A</sup>Nd, A=138,139, high spin states, isomers and  $\gamma$ -cascade from <sup>140</sup>Cd( $\alpha$ ,xn) 0-78120  
<sup>A</sup>Nd, A=138,139, high spin states,  $J^\pi$ ,  $\gamma$ -cascades and shape transition from <sup>140</sup>Ce( $\alpha$ ,xn) 0-102090  
<sup>A</sup>Nd, A=145, 147, 149, single neutron hole states spectroscopic factors, DWBA anal. of (d,t), (<sup>3</sup>He, $\alpha$ ) 0-78109  
<sup>140</sup>Nd ns isomers and yrast isomers,  $\gamma$ -transitions from <sup>128</sup>Te(<sup>16</sup>O,4n) 0-78121  
<sup>142</sup>Nd(<sup>84</sup>Kr,X), fusion reactions, charge density asymmetry liquid drop model 0-63220  
<sup>142</sup>Nd(<sup>6</sup>Ni,X), fusion reactions, charge density asymmetry liquid drop model 0-63220  
<sup>142</sup>Nd energy levels from <sup>144</sup>Nd(d,p) and <sup>146</sup>Nd(d,t), DWBA calcs. 0-68533  
<sup>142</sup>Nd(<sup>16</sup>O,X), 142 MeV, narrow window for incomplete fusion 0-95325  
<sup>147</sup>Nd,  $\beta$  decay, <sup>147</sup>Pm level scheme 0-83073  
<sup>147</sup>Nd low spin states ns lifetimes, particle rotor model interpretation from <sup>146</sup>Nd(d,p $\gamma$ ) 0-78207  
<sup>148</sup>Nd, vibrational states, B(E2) branching rates and interband transitions, pairing plus quadrupole calcs. 0-78127  
<sup>237</sup>Np(n,f), thermal neutron sub-barrier fission <sup>134</sup>I and <sup>135</sup>Xe yields 0-86935  
Pd, even-even, collective states, B(E2), branching ratios and moments, boson expansion method 0-102099  
<sup>97</sup>Pd  $\beta^+$ -decay, <sup>97</sup>Rh levels and  $\gamma$ -transitions, 3QP model anal. 0-102120  
<sup>100</sup>Pd levels and  $\gamma$ -transitions from <sup>100</sup>Ag<sup>em</sup> decay 0-83077  
<sup>100</sup>Pd nonyrast rotational states, transitions,  $T_{1/2}$ , branching and mixing ratios from <sup>92</sup>Zr(<sup>12</sup>C,3n) 0-105950  
<sup>102</sup>Pd(p,p' $\gamma$ ), long lived O<sub>1</sub><sup>+</sup> state, E0 transitions 0-73804  
<sup>106</sup>Pd, E0 transition from O<sub>1</sub><sup>+</sup> state following <sup>106</sup>Rh beta decay 0-68578  
<sup>106</sup>Pd(t,p), pol.t, cross section and anal. powers, struct. depend., DWBA anal. 0-78272  
<sup>107</sup>Pd low spin odd parity levels,  $\gamma$ -rays, particle-rotor comparison from <sup>107</sup>Pd(n, $\gamma$ ) 0-73805  
<sup>109</sup>Pd low spin odd parity states, rot. aligned model, Coriolis calc. of <sup>107</sup>Pd(n, $\gamma$ ) 0-57695  
<sup>A</sup>Pm, A=143, 145, proton states and transitions, stripping strength, shell model anal. from Nd(<sup>4</sup>He,d) 0-68508  
<sup>A</sup>Pm, A=143-153, odd-A, spectroscopic factors, shell model anal. from pickup and stripping reactions 0-78137  
<sup>A</sup>Pm, A=147,149,151 single proton hole states in pickup reactions from Sm(p, $\alpha$ ) 0-78128  
<sup>A</sup>Pm, A=149,151, shape coexistence, deformed states from Nd decay 0-78135  
<sup>147</sup>Pm medium spin states,  $J^\pi$ , transitions and shape from (p,2n), (<sup>3</sup>He,3n), ( $\alpha$ ,4n) 0-86779  
<sup>145</sup>Pm level struct.,  $J^\pi$  and lifetimes, cluster-vibr. model anal. of <sup>146</sup>Nd(p,2n) 0-91125  
<sup>147</sup>Pm, level scheme and transitions following <sup>147</sup>Nd 0-83073  
<sup>147</sup>Pm levels, bands, transitions, in-beam spectroscopy, particle-rotor anal. from <sup>152</sup>Nd(p,2n $\gamma$ ) 0-78125  
<sup>139</sup>Pr medium spin states,  $J^\pi$ , transitions and shape from (p,2n), (<sup>3</sup>He,3n), ( $\alpha$ ,4n) 0-86779  
<sup>140</sup>Pr isobaric analogue resonances, de-excitation cascade, K-shell ionisation, spin depend. from <sup>140</sup>Ce(p,n) 0-78202  
<sup>141</sup>Pr, positive parity levels, gamma-ray yields and ang. distrib. 0-105962  
<sup>141</sup>Pr(e,p), 15-25 MeV,  $T_0+1$  giant dipole resonance and characteristic decay mode 0-78247  
Rb decay, <sup>A</sup>Sr, A=98, 100 rot. struct. sudden onset, gamma transitions 0-73777  
Rb decay, <sup>94,96</sup>Sr direct and skip cascades,  $\gamma\gamma$  ang. correlations, levels, mixing ratios 0-86851  
<sup>A</sup>Rb, A=93,94,95, delayed neutrons, energy spectra 0-99153  
<sup>92</sup>Rb decay, <sup>92</sup>Sr  $\gamma\gamma$  ang. correlations, levels,  $J^\pi$ , mixing ratios 0-57725  
<sup>98</sup>Rb decay, <sup>98</sup>Sr very low lying O<sup>+</sup> state, shape coexistence bands,  $T_{1/2}$ , transitions 0-78148  
<sup>94</sup>Rh,  $\gamma$ -spectrum and half-lives 0-83062  
<sup>94</sup>Rh levels and  $\gamma$ -transitions, 3QP model anal. of <sup>97</sup>Pd  $\beta^+$ -decay 0-102120  
<sup>103</sup>Rh(p,n), sub-Coulomb optical pot. 0-102190  
Ru, even isotopes, potential energy surfaces and ground state equilib. deformation 0-73789



## nuclei with mass number 90 to 149 continued

- Ru, even-even, collective states, B(E2), branching ratios and moments, boson expansion method 0-102099
- <sup>94</sup>Ru, A=104,106,108, level scheme and transitions, collective model anal. of Tc decay 0-78166
- <sup>94</sup>Ru, A=106, 108, levels, transitions, J<sup>π</sup> and shape from Tc decay 0-57744
- <sup>94</sup>Ru level structure, spin and parity, from beta decay of <sup>94</sup>Rh isomers 0-57747
- <sup>94</sup>Ru ground state g-factor, relaxation time 0-83036
- <sup>94</sup>Ru high spin states, band like structs., transitions from <sup>88</sup>Sr(<sup>12</sup>C,3nγ) 0-73779
- <sup>102</sup>Ru(<sup>16</sup>O,<sup>16</sup>O), 38-42 MeV, Coulomb excitation, 2<sup>+</sup> state electric quadrupole moment 0-73793
- <sup>102</sup>Ru(α,α), 8.5, 9.0 MeV, Coulomb excitation, 2<sup>+</sup> state electric quadrupole moment 0-73793
- Sb, neutron rich nuclei, IBM and shell model approaches, collective modes 0-78129
- <sup>125</sup>Sb, A=113-175, odd isotopes, collective props., bands and transitions from heavy ion reactions 0-68512
- <sup>125</sup>Sb high spin levels, gamma transition energies and intensities from <sup>125</sup>Sn<sup>+</sup>, decay 0-73819
- <sup>147</sup>Sm, A=144-154, mean square nuclear charge radius, laser atomic beam spectroscopy 0-102468
- <sup>147</sup>Sm, A=146,147, excited states, energy levels, spin, parity, shell and cluster-vibration models, from (α,xn) and (<sup>2</sup>He,xn) 0-57683
- <sup>147</sup>Sm, A=147, 149, levels, J, γ-transitions and multipole mixing ratios, γγ correlations from Eu EC decay 0-106012
- <sup>147</sup>Sm(<sup>16</sup>O,X), 60-75 MeV, A=148,150,152,154, fusion cross section, evaporation residues 0-83137
- <sup>147</sup>Sm(<sup>40</sup>Ar,X) A=144, 148, 154, 3.6-4.5 MeV/A, sub-barrier fusion, evaporation residue cross section, deformation 0-68718
- <sup>142</sup>Sm isomers, lifetimes and transitions from <sup>142</sup>Nd(α,4n) 0-78122
- <sup>142</sup>Sm ns isomers and yrast isomers, γ-transitions from (<sup>24</sup>Mg,4n), (<sup>19</sup>F,4n) 0-78121
- <sup>145</sup>Sm primary γ-rays, direct capture and neutron separation energy, (d,p), (n,γ) correlation 0-57738
- <sup>147</sup>Sm(n,α)<sup>44</sup>Nd, 2 keV, statistical model anal. 0-102186
- Sm(p,t), even isotopes, high energy neutron pairing strength, two neutron holes, resonances 0-78116
- Sn 2<sup>+</sup> excitation, α-spectroscopic factors in IBA model from Te(d,<sup>6</sup>Li) 0-105967
- Sn, deep hole states observed in particle transfer reactions 0-68511
- Sn, even isotopes, collective states and transitions from simple phenomenological model 0-73787
- Sn, internal conversion coeffs. for inner shells of atomic ions and relativistic ionic potentials 0-68600
- Sn isotopes, levels and spectra from broken pair model 0-73801
- <sup>120</sup>Sn, A=106-108, yrast levels and transitions from <sup>54</sup>Fe(<sup>58</sup>Ni, X) 0-105957
- <sup>120</sup>Sn, A=112-124 even isotopes, 0<sup>+</sup> state collectivity, E0 and E2 transition rates 0-73785
- <sup>120</sup>Sn, A=118,120,122, deep hole states, excitation energies and ang. distrib. from Sn(p,t) 0-86792
- <sup>120</sup>Sn(<sup>35</sup>Cl,<sup>35</sup>Cl<sup>+</sup>), 108 MeV, A=112-124 even isotopes, 2<sub>1</sub><sup>+</sup> mag. moments and shell model struct. 0-86805
- <sup>120</sup>Sn(n,n), A=116, 118, 120, 122, 124, 11 MeV, levels, deformation parameters, isospin effects, optical parameters 0-57679
- <sup>120</sup>Sn(n,n'), A=116, 118, 120, 122, 11 MeV, octupole vibr. states, diff. cross section, deformation length, DWBA anal. 0-102092
- <sup>120</sup>Sn(n,n), 11-26 MeV, A=116, 118, 120, 122, 124, differential and total cross sections, optical pots. 0-78293
- <sup>120</sup>Sn(p,X), A=112, 124, 7.6, 10 GeV/c, isotopic cross section ratios, He, Li fragments isotopic effects (*Russian*) 0-63154
- <sup>120</sup>Sn 6<sup>+</sup> isomeric state g-factor and relaxation time from Cd(α,2nγ) 0-73794
- <sup>115</sup>Sn weak coupling neutron hole states from <sup>116</sup>Sn(<sup>3</sup>He,α) 0-73786
- <sup>116</sup>Sn(<sup>40</sup>Ar,X), 222-340 MeV, charged particle emission, early collision evolution, fission and evaporation cross sections 0-106072
- <sup>116</sup>Sn(α,α'), 96, 129 MeV, giant resonance excitation, isoscalar breathing mode state, nuclear incompressibility 0-68620
- <sup>116</sup>Sn(p,p'), 800 MeV, high energy octupole giant resonance, ang. distrib. 0-86879
- <sup>120</sup>Sn(<sup>6</sup>Li,X), 156 MeV, projectile break up in continuous particle spectra, cross section, fragmentation 0-86889
- <sup>120</sup>Sn(d,d'), 108 MeV, giant monopole resonance excitation and ang. distrib. 0-102164
- <sup>120</sup>Sn(p,n), statistical multistep direct emission, p-h and DWBA calcs. 0-106035
- <sup>124</sup>Sn(<sup>6</sup>Li,<sup>6</sup>Li), elastic and inelastic, 74 MeV, folding optical model parameters 0-102201
- <sup>124</sup>Sn(n,n), pol. thermal, parity violation near resonance, DWBA calcs. 0-68528
- <sup>125</sup>Sn, <sup>125</sup>Sb high spin levels, gamma transition energies and intensities 0-73819
- <sup>123</sup>Sn levels, isomers, lifetimes and transition probabilities from fission 0-78163
- Sn(p,n), even isotopes, 4-10 MeV, cross sections, optical parameters and nuclear radius A-depend. 0-57773
- Sn(p,p), pol.p., 6.77-8.8 MeV, cross sections, optical parameters and nuclear radius A-depend. 0-57773
- Sn(x,x), x=π<sup>2</sup>, K<sup>2</sup>, p,p, 70, 175 GeV/c 0-83128
- <sup>87</sup>Sr, A=94,96 direct and skip cascades, γγ ang. correlations, levels, mixing ratios from Rb decay 0-86851
- <sup>87</sup>Sr, A=98, 100 rot. struct. sudden onset, gamma transitions from Rb decay 0-73777
- <sup>87</sup>Sr γγ ang. correlations, levels, J<sup>π</sup>, mixing ratios from <sup>92</sup>Rb decay 0-57725
- <sup>87</sup>Sr neutron binding energy from transitions and β-delayed neutron defined level correspondences 0-63070
- <sup>96</sup>Sr very low lying 0<sup>+</sup> state, shape coexistence bands, T<sub>1/2</sub>, transitions from <sup>96</sup>Rb decay 0-78148
- <sup>146</sup>Tb decay and T<sub>1/2</sub>, <sup>146</sup>Gd lowest 2<sup>+</sup> state, J<sup>π</sup> and transitions 0-105979
- <sup>149</sup>Tb from HI reactions, superdeformed nucleus decay, α-decay amplification 0-68608
- Tc decay <sup>104,106,108</sup>Ru level scheme and transitions, collective model anal. 0-78166
- Tc decay <sup>106,108</sup>Ru levels, transitions, J<sup>π</sup> and shape 0-57744
- <sup>93</sup>Tc, J=17/2 doublet, parity mixing, weak NN interaction 0-73791
- <sup>97</sup>Tc, energy levels, low-lying, decay properties 0-63084

## nuclei with mass number 90 to 149 continued

- Tc high spin states, spins and transitions from <sup>94</sup>Zr(<sup>6</sup>Li,3nγ) 0-73780
- <sup>98</sup>Tc 14 μs isomer, low lying levels and transitions from <sup>98</sup>Mo(p,n) 0-73802
- <sup>100</sup>Tc μs isomers, isomeric transitions and mean lives from <sup>100</sup>Mo(p,n) 0-73803
- <sup>102</sup>Tc decay scheme and γ-intensities from <sup>102</sup>Mo fission product decay 0-78229
- <sup>99m</sup>Tc, in hexahalogen complexes, decay const. determ. 0-106020
- <sup>126</sup>Te, A=122,124,126 yrast band double backbending, possible mechanisms (*Chinese*) 0-99120
- <sup>126</sup>Te quasi-rot. band based on proton 4p-2h state, level scheme, transitions from <sup>118</sup>Sn(α,2nγ) 0-78119
- <sup>125</sup>Te low lying negative parity high spin states multistep induced population from (d,t)(<sup>3</sup>He,α) 0-57657
- <sup>126</sup>Te, M1, giant resonance and radiative strength functions 0-57731
- <sup>126</sup>Te(p,n), 2<sub>1</sub><sup>+</sup>→2<sub>1</sub><sup>+</sup> transition multipole mixing ratio 0-78198
- <sup>126</sup>Te(p,p), pol.t, cross section and anal. powers, struct. depend., DWBA anal. 0-78272
- <sup>125</sup>Te μs decay, <sup>129</sup>I time depend. quadrupole interactions, γ-γ correlations 0-78145
- <sup>130</sup>Te double β-decay, lepton charge conservation (*Russian*) 0-102153
- <sup>131</sup>Te γ-transitions, spectroscopic factors and reduced transition intensities from <sup>130</sup>Te(n,γ) 0-91143
- <sup>129</sup>Xe excited state lifetimes, γ-transitions from <sup>129</sup>Cs decay 0-78205
- <sup>132</sup>Xe level struct., J<sup>π</sup>, transitions and multipole mixing ratio from <sup>132</sup>I decay 0-91134
- <sup>135</sup>Xe, direct meas. of absolute and fractional indep. yields from <sup>238</sup>U(γ,f) 0-78341
- <sup>137</sup>Xe neutron unbound states, high energy X-rays from <sup>137</sup>I decay 0-86856
- <sup>89</sup>Y gamma transitions, microscopic finite-range anal. of <sup>92</sup>Zr(p,α) 0-63181
- <sup>90</sup>Y low lying multiplets, DWBA anal. for spectroscopic factors from <sup>91</sup>Zr(d,<sup>3</sup>He) 0-57685
- <sup>93</sup>Y(p,n), sub-Coulomb optical pot. 0-102190
- Zr, deep hole states observed in particle transfer reactions 0-68511
- Zr, even isotopes, potential energy surfaces and ground state equilib. deformation 0-73789
- Zr, onset of deformation at A~100 0-73790
- <sup>92</sup>Zr, A=92, 96, first excited 0<sup>+</sup> state transition strength from (<sup>6</sup>Li,<sup>8</sup>B), (d,<sup>6</sup>Li) correlation 0-78260
- <sup>92</sup>Zr(<sup>35</sup>Cl,<sup>35</sup>Cl<sup>+</sup>), 90 MeV, A=92, 94, 2<sub>1</sub><sup>+</sup> levels mag. moments 0-105968
- <sup>90</sup>Zr(<sup>3</sup>He,t)<sup>90</sup>Nb, 18.5 MeV resonance, isovector dipole and Gamow-Teller transitions 0-86881
- <sup>90</sup>Zr(<sup>6</sup>Li,<sup>6</sup>Li), elastic and inelastic, 74 MeV, folding optical model parameters 0-102201
- <sup>90</sup>Zr(<sup>6</sup>Li,X), 156 MeV, projectile break up in continuous particle spectra, cross section, fragmentation 0-86889
- <sup>90</sup>Zr(α,α'), 96, 129 MeV, giant resonance excitation, isoscalar breathing mode state, nuclear incompressibility 0-68620
- <sup>90</sup>Zr(α,α), form factor, coupling between real and imaginary optical potential 0-68680
- <sup>90</sup>Zr(d,d'), 108 MeV, giant monopole resonance excitation and ang. distrib. 0-102164
- <sup>90</sup>Zr(e,e'), 2<sup>+</sup> giant resonance twist mode excitation, B(M2) values, form factors 0-78246
- <sup>90</sup>Zr(γ, α), above GDR region, cross sections, DWBA anal. 0-63173
- <sup>90</sup>Zr(γ,α) statistical and pre-equilibrium cross sections and multipolarities from (e,α) 0-68646
- <sup>90</sup>Zr(n,X), 10-20 MeV, multipole giant resonance contrib. to optical pot. imaginary part 0-78241
- <sup>90</sup>Zr(n,n'), 11 MeV, octupole vibr. states, diff. cross section, deformation length, DWBA anal. 0-102092
- <sup>90</sup>Zr(p,n), nucleon optical potential from Lane model 0-83097
- <sup>90</sup>Zr(p,x), x=α,τ, 72 MeV, spectra and angular distrib. 0-68660
- <sup>90</sup>Zr(π,π'), 226 MeV, giant reson. examination 0-73871
- <sup>90</sup>Zr(t,p), exact finite range DWBA calcs., realistic triton and nuclear wave functions 0-63191
- <sup>92</sup>Zr levels, J<sup>π</sup>, cross sections, vector anal. power, optical parameters from <sup>91</sup>Zr+pol.d 0-78268
- <sup>94</sup>Zr(n,α)<sup>91</sup>Sr, fast n, fission spectrum averaged cross section 0-63177
- Zr(p,p,γ), odd isotopes, excited d-states from analogue resonances and p-γ correlations 0-68546

## nuclei with mass number 150 to 189

- A=120-150, levels and EM props., recent results 0-68592
- A=158-176, 'extension of variable moment of inertia model to high spins', comments 0-86791
- A=163, nuclear data sheets to April 1979 0-98762
- A~150, yrast states, deformed oscillator Hamiltonian calcs. 0-78126
- doubly even nuclei, yrast band B(E2) values, hydrodynamical model and CAP effect 0-86793
- (HI,X), rare earths, deeply inelastic transfer reactions, kinematic anal. 0-99186
- N=5 shell, deformed odd-neutron nuclei, band ordering and spectrum 0-83018
- N=82 region, high spin isomers, cranked HF calcs., deformation shapes, excitation energies 0-99121
- N=82 region, high spin isomers, deformation energy surface, shape constrained cranked HF theory 0-57666
- rare earth deformed nuclei, high spin region excited rot. bands, RPA calcs. 0-78108
- rare earth nuclei, modified oscillator pot. parameters, single particle levels 0-68509
- rare earths, nuclear deformation, Coulomb displacement energy depend., shell model 0-102108
- (γ,X), A=154-209, 7-20 MeV, total photoabsorption cross section 0-57766
- (p, spallation), 480 MeV, medium to heavy mass targets, deep spallation products 0-83085
- <sup>185</sup>Bi alpha decay half lives 0-57749
- Dy deformed nuclei, particle ang. momentum alignment effects 0-68522
- Dy, high spin isomer α-decay search 0-102158
- Dy K-shell internal conversion yields, gamma transition multipolarities from (α,xn), (<sup>12</sup>C,xn) 0-78215
- Dy, N=85 isotones, bands and transitions from α and HI excitation, in-beam study 0-78123
- <sup>161</sup>Dy, A=156-164, deformation hexadecapole moments, Hartree-Fock calcs. (*Russian*) 0-63081

## nuclei with mass number 150 to 189 continued

- <sup>14</sup>Dy, A=161, 163, Nilsson state  $\Delta N=2$  mixing, rot. bands from (d,t), (d,p) 0-95295
- <sup>14</sup>Dy, A=162, 164, gamma to ground band transitions,  $\gamma\gamma$  directional correlations from (n, $\gamma$ ) 0-68579
- <sup>14</sup>Dy(d,t), A=162, 164, coupled-channels Born approx. anal. 0-83104
- <sup>152</sup>Dy 60 ns isomer deexcitation E2 x- (or $\Delta$ ) transition, half life,  $\gamma\gamma$ -coincidence from <sup>152</sup>Gd( $\alpha$ ,n) 0-86859
- <sup>152</sup>Dy, high spin state populations from <sup>124</sup>Sn(<sup>32</sup>S,4n) 0-57660
- <sup>152</sup>Dy yrast isomers,  $\gamma$ -rays from compound nuclei 0-86789
- <sup>152</sup>Dy N=88 nuclei quasirot. bands and J<sup>\*</sup> from beta-decay 0-83025
- <sup>159</sup>Dy, lifetimes of low excited states, delayed e- $\gamma$  and  $\gamma\gamma$  coincidences (Russian) 0-68596
- <sup>160</sup>Dy,  $\gamma$  transitions following <sup>160</sup>Tb decay 0-83060
- <sup>160</sup>Dy, lifetimes of low excited states, delayed e- $\gamma$  and  $\gamma\gamma$  coincidences (Russian) 0-68596
- <sup>162</sup>Dy, static quadrupole moments of arbitrary excited states, sum rule approach 0-91135
- <sup>164</sup>Dy(<sup>40</sup>Ar,X), 222-340 MeV, charged particle emission, early collision evolution, fission and evaporation cross sections 0-106072
- Er, deformed nuclei, particle ang. momentum alignment effects 0-68522
- Er,  $\gamma$ -multiplicities and cross sections, neutron evaporation from <sup>130</sup>Te(<sup>32</sup>S,X), (<sup>16,18</sup>O,X) 0-73824
- Er, high spin isomer  $\alpha$ -decay search 0-102158
- Er rotational nuclei, transition energy correlations, very high ang. momentum 0-86787
- <sup>16</sup>Er, A=159,160, energy levels, deexcitation  $\gamma$ -rays, g-factors and hyperfine interaction from <sup>28</sup>Si(<sup>36</sup>Xe, xn) 0-102114
- <sup>16</sup>Er, A=162-170, deformation hexadecapole moments, Hartree-Fock calcs. (Russian) 0-63081
- <sup>16</sup>Er(d,t), A=166, 168, coupled-channels Born approx. anal. 0-83104
- <sup>156</sup>Er N=88 nuclei quasirot. bands and J<sup>\*</sup> from EC decay 0-83025
- <sup>157</sup>Er, lifetimes of excited states, delayed e- $\gamma$  coincidences (Russian) 0-68597
- <sup>162</sup>Er compound nucleus fission at high ang. momentum, fragments from <sup>30</sup>Si(<sup>132</sup>Xe,f) 0-99196
- <sup>164</sup>Er high spin procs. in multiple band crossing region from (<sup>18</sup>O,4n $\gamma$ ), ( $\alpha$ ,4n $\gamma$ ), (<sup>136</sup>Xe,<sup>36</sup>Xe $\gamma$ ) 0-83023
- <sup>166</sup>Er transverse form factors from projected HF approach 0-105965
- <sup>166</sup>Er(<sup>8</sup>K,X), deep inelastic collision, charge drift and dispersion calc., thermal eqn. model based on shell model 0-57798
- <sup>166</sup>Er(<sup>8</sup>Kr,X), 5.1-7.9 MeV/N, deep inelastic neutron emission, pre-equilibrium effects search 0-63200
- <sup>166</sup>Er( $\gamma$ , $\gamma$ ), 14.4-16.6 MeV,  $\gamma$ -vibr. band head transitions, dynamic collective model 0-57662
- <sup>166</sup>Er(p,X), pol.p. 65 MeV, continuum spectra anal. powers 0-102178
- <sup>168</sup>Er, 80 and 1094 keV states, g-factors from ang. correlation methods 0-83035
- <sup>168</sup>Er  $\gamma$ -vibr. band, M1 admixtures in intra-band transitions 0-99149
- <sup>172</sup>Er levels, bands, J<sup>\*</sup> and transitions from <sup>170</sup>Er(t,p) 0-83038
- <sup>16</sup>Eu, A=152,154, gamma-ray intensities, precession meas. 0-102140
- <sup>16</sup>Eu, A=153,155, single proton hole states in pickup reactions from (p, $\alpha$ ) 0-78128
- <sup>151</sup>Eu narrow band and pickup strength, shape coexistence from (d,t) 0-86799
- <sup>152</sup>Eu 89,848 keV isomeric state feeding, delayed coincidence meas., level scheme from <sup>151</sup>Eu(n, $\gamma$ ) 0-63126
- <sup>152</sup>Eu, isomeric state struct. 0-83017
- <sup>153</sup>Eu 5/2<sup>+</sup> ground state rot. band, J<sup>\*</sup>, shape coexistence from (d,p) 0-86799
- <sup>153</sup>Eu, EM transitions, multipole, internal conversion coeffs. (Russian) 0-63121
- <sup>154</sup>Eu low lying levels, bands, transitions from <sup>153</sup>Eu(n, $\gamma$ ) 0-57694
- Gd, high spin isomer  $\alpha$ -decay search 0-102158
- Gd, N=85 isotones, bands and transitions from  $\alpha$  and HI excitation, in-beam study 0-78123
- <sup>14</sup>Gd, A=152, 154,  $\gamma$ -transition energy and intensity meas. from Eu decay 0-73818
- <sup>14</sup>Gd, A=152-160, deformation hexadecapole moments, Hartree-Fock calcs. (Russian) 0-63081
- <sup>152</sup>Gd  $\beta$ - and octupole bands, downbending moments of inertia from <sup>150</sup>Sm( $\alpha$ ,2n) 0-91131
- <sup>152</sup>Gd N=88 nuclei quasirot. bands and J<sup>\*</sup> from EC decay and ( $\alpha$ ,xn $\gamma$ ) 0-83025
- <sup>152</sup>Gd, vibrational states, B(E2) branching rates and interband transitions, pairing plus quadrupole calcs. 0-78127
- <sup>154</sup>Gd levels and  $\gamma$ -ray spectra from <sup>152</sup>Gd(n, $\gamma$ ) 0-57736
- <sup>154</sup>Gd levels, bands, J<sup>\*</sup>, DWBA anal. of <sup>152</sup>Gd(t,p) 0-78110
- <sup>155</sup>Gd, vibr. state, level scheme,  $\gamma$  and conversion electron spectra from <sup>154</sup>Gd(n, $\gamma$ ) 0-57696
- <sup>160</sup>Gd(<sup>12</sup>C,  $\alpha$ xn)<sup>168-8</sup>Er, particle fragmentation accompanied by incomplete fusion, two step model 0-86947
- <sup>160</sup>Gd(d,t) <sup>159</sup>Gd, coupled-channels Born approx. anal. 0-83104
- Gd( $\alpha$ ,xn)Dy, K-shell ionisation cross-sections meas. 0-78687
- <sup>16</sup>Hf, A=176-180, deformation hexadecapole moments, Hartree-Fock calcs. (Russian) 0-63081
- <sup>172</sup>Hf, three- and five-quasiparticle isomers, rotational bands and residual interactions from <sup>170</sup>Er(<sup>6</sup>Be, 4n) 0-83022
- <sup>178</sup>Hf, energy levels, K-forbidden decays, M4 decay of yrast state 0-68506
- <sup>16</sup>Hg, A=182-184, alpha decay branching ratio 0-57749
- Ho, high spin isomer  $\alpha$ -decay search 0-102158
- <sup>157</sup>Ho, lifetimes of excited states, delayed e- $\gamma$  coincidences (Russian) 0-68597
- <sup>157</sup>Ho-<sup>157</sup>Dy decay, internal conversion electron spectra and e $\gamma$  coincidences (Russian) 0-68604
- <sup>165</sup>Ho transverse form factors from projected HF approach 0-105965
- <sup>165</sup>Ho(<sup>165</sup>Ho,X), deep inelastic, spin and transferred ang. momentum alignment 0-106043
- <sup>165</sup>Ho( $\alpha$ ,2n)<sup>167</sup>Tm, levels and transitions 0-73766
- <sup>165</sup>Ho(p,X), pol.p. 65 MeV, continuum spectra anal. powers 0-102178
- <sup>166</sup>Ho<sup>m</sup> in HoVO<sub>4</sub>, nuclear orientation study below 1K 0-88899
- <sup>186,188</sup>Ir in Re crystal, electric quadrupole orientation, elec. field gradient 0-78140
- Ir decay, oriented nuclei, <sup>188,189</sup>Os levels, J<sup>\*</sup>, transitions and mixing ratios 0-68602
- <sup>16</sup>Ir, A=189, 191, levels, J<sup>\*</sup>, transitions and mixing ratios from Pt decay 0-68602
- Lu  $\beta^+$  decay force function resonance struct., level populations (Russian) 0-102154
- <sup>16</sup>Lu, A=158, 159, alpha decay and gamma transitions 0-73827

## nuclei with mass number 150 to 189 continued

- <sup>16</sup>Lu, A=160-163, decay and T<sub>1/2</sub><sup>160-163</sup>Yb transitions 0-102146
- <sup>169</sup>Lu allowed hindered  $\beta^+$  decay, <sup>169</sup>Yb  $7/2^+ [404] \rightarrow 7/2^+ [633]$  transition ft value 0-10248
- <sup>169</sup>Lu decay, <sup>169</sup>Yb  $\gamma\gamma$  ang. correlations, levels and spins (Russian) 0-83069
- <sup>172</sup>Lu decay, identification of  $\gamma$ -spectra unplaced energies by delayed coincidence meas. 0-78221
- <sup>174</sup>Lu isomeric levels,  $\gamma$ -spectra, T 1/2 and decay modes from <sup>176</sup>Yb(p,3n) 0-99151
- <sup>175</sup>Lu delayed transitions from <sup>176</sup>Yb(p,3n) 0-99151
- <sup>177</sup>Lu excited state lifetimes,  $\gamma$ -transitions from  $\beta$ -decay transitions 0-78205
- Nd decay,  $\Delta$ pm, A=149,151, shape coexistence, deformed states 0-78135
- Nd, even-even, E2 transition probabilities from multiple Coulomb excitation, IBA comparison 0-78212
- <sup>16</sup>Os, A=182, 184, 186, high spin yrast states, back-bending 0-86802
- <sup>16</sup>Os, A=186-188, levels and transitions from Re decay, triaxial rotor model 0-91155
- <sup>16</sup>Os, A=186-194, collective levels, transitions, mag. and quadrupole moments, boson expansion theory 0-105954
- <sup>16</sup>Os, A=188, 189, levels, J<sup>\*</sup>, transitions and mixing ratios from Ir decay 0-68602
- <sup>183</sup>Os 9/2<sup>+</sup> [624] ground state g-factor from NMR 0-83037
- <sup>16</sup>Pb, A=183,184, alpha decay half lives 0-57749
- <sup>16</sup>Pm, A=143-153, odd-A, spectroscopic factors, shell model anal. from pickup and stripping reactions 0-78137
- <sup>16</sup>Pm, A=147,149,151 single proton hole states in pickup reactions from Sm(p, $\alpha$ ) 0-78128
- <sup>16</sup>Pm, A=149,151, shape coexistence, deformed states from Nd decay 0-78135
- <sup>153</sup>Pm 5/2<sup>+</sup> h<sub>1/2</sub> dominated band, anomalous ang. distrib., CCBA calcs. for <sup>153</sup>Sm(t, $\alpha$ ) 0-86788
- Pt decay, oriented nuclei, <sup>189,191</sup>Ir levels, J<sup>\*</sup>, transitions and mixing ratios 0-68602
- <sup>16</sup>Pt, A=178,179, alpha decay branching ratio 0-57749
- <sup>16</sup>Pt, A=188-198 collective levels, transitions, mag. and quadrupole moments, boson expansion theory 0-105954
- Re, odd isotones, deformation pot. energy from Nilsson model 0-57676
- <sup>16</sup>Re, A=181,182,187, rotational struct., spin polarization 0-83016
- <sup>180</sup>Re decay, <sup>180</sup>W octupole vibr. states, J<sup>\*</sup> and transitions 0-83024
- Sm, deep hole states observed in particle transfer reactions 0-68511
- <sup>16</sup>Sm, A=144-154, mean square nuclear charge radius, laser atomic beam spectroscopy 0-102468
- <sup>16</sup>Sm(<sup>16</sup>O,<sup>16</sup>O), A=150, 152, hyperfine dynamic mag. field effects 0-68689
- <sup>16</sup>Sm(<sup>16</sup>O,X), 60-75 MeV, A=148,150,152,154, fusion cross section, evaporation residues 0-83137
- <sup>16</sup>Sm(<sup>32</sup>S,<sup>32</sup>S), A=150, 152, hyperfine dynamic mag. field effects 0-68689
- <sup>16</sup>Sm(<sup>40</sup>Ar,X) A=144, 148, 154, 3.6-4.5 MeV/A, sub-barrier fusion, evaporation residue cross section, deformation 0-68718
- <sup>150</sup>Sm, vibrational states, B(E2) branching rates and interband transitions, pairing plus quadrupole calcs. 0-78127
- <sup>151</sup>Sm low energy levels from expt. and Coriolis mixing calcs. of <sup>150</sup>Sm(n, $\gamma$ ) 0-57697
- <sup>152</sup>Sm ground and  $\gamma$ -bands, direct and multistep processes from ( $\alpha$ ,<sup>6</sup>He), (p,t), (<sup>16</sup>O,<sup>16</sup>O) 0-102094
- <sup>152</sup>Sm,  $\gamma$ -transition energy and intensity meas. from <sup>152</sup>Eu decay 0-73818
- <sup>152</sup>Sm, static quadrupole moments of arbitrary excited states, sum rule approach 0-91135
- <sup>154</sup>Sm, giant multipole reson. fragmentation among two-phonon states 0-78238
- <sup>154</sup>Sm(<sup>40</sup>Ar,X), 222-340 MeV, charged particle emission, early collision evolution, fission and evaporation cross sections 0-106072
- <sup>154</sup>Sm(p,p'), 0.8 GeV, ang. distrib. and multipole moments, DWBA and coupled channel anal. 0-105969
- <sup>172</sup>Ta, rotational struct., spin polarization 0-83016
- <sup>180</sup>Ta mass, 10<sup>13</sup> y naturally occurring isomer state 0-57670
- <sup>180</sup>Ta nuclear spin and mag. dipole moment from laser resonance fluorescence 0-78143
- <sup>180</sup>Ta<sup>m</sup>,  $\beta^-$  and EC branching ratios, K-internal conversion coeff.,  $\gamma$ -intensities, T 1/2 0-68601
- <sup>181</sup>Ta transverse form factors from projected HF approach 0-105965
- <sup>181</sup>Ta(<sup>20</sup>Ne, spallation), 8.0 GeV, cross sections and target residues, model comparison 0-68630
- <sup>181</sup>Ta( $\alpha$ ,X), a=p,d,<sup>6</sup>He, <sup>12</sup>C, 4.2 GeV/c, multitudes of secondary negative particles, momentum distrib. ratios (Russian) 0-63178
- <sup>181</sup>Ta( $\gamma$ ,X), 3-30 MeV, photoabsorption cross section, giant dipole resonances 0-78254
- <sup>181</sup>Ta(n,2n)<sup>180</sup>Ta<sup>m</sup>, 14.68 MeV, cross section 0-68659
- <sup>181</sup>Ta(p,n)<sup>181</sup>W, multi-step compound and direct reactions, statistical theory 0-57761
- <sup>182</sup>Ta, Fe-Ta, nuclear mag. moment, NMR-ON study 0-78139
- <sup>185</sup>Ta single proton states and rot. bands, J<sup>\*</sup> from <sup>186</sup>W(t, $\alpha$ ), pol.t 0-91130
- Ta(n,X), slow and ultracold total and inelastic cross sections 0-68673
- Ta( $\pi^-$ ,X), stopped pions, radioactive product yields 0-83126
- Tb, high spin isomer  $\alpha$ -decay search 0-102158
- <sup>157</sup>Tb, fission barrier at 28.5 MeV 0-91202
- <sup>159</sup>Tb transverse form factors from projected HF approach 0-105965
- <sup>159</sup>Tb(<sup>6</sup>B,X), 51 MeV, fusion and deep inelastic, quantised frictional motion calcs. 0-102223
- <sup>159</sup>Tb(<sup>14</sup>N,X), 140 MeV, incomplete fusion reactions, sum rule model 0-95332
- <sup>159</sup>Tb(<sup>14</sup>N,X), 95 MeV, fast  $\alpha$ -particle ang. distrib. 0-63207
- <sup>160</sup>Tb-<sup>160</sup>Dy,  $\gamma$ -transitions and angular distributions 0-83060
- <sup>160</sup>Tm, energy level scheme from <sup>165</sup>Ho( $\alpha$ ,2n $\gamma$ ) (German) 0-68576
- <sup>167</sup>Tm, levels and transitions from <sup>165</sup>Ho( $\alpha$ ,2n) 0-73766
- <sup>167</sup>Tm rotational bands, J<sup>\*</sup>,  $\gamma$ -transitions and branching ratios from <sup>165</sup>Ho( $\alpha$ ,2n $\gamma$ ) 0-86781
- <sup>167</sup>Tm(HI,xn $\gamma$ ), ang. distrib., multiplicities (French) 0-68575
- <sup>169</sup>Tm(n, $\gamma$ ), capture cross section from 10<sup>-5</sup> eV to 2x10<sup>7</sup> eV, statistical model 0-63189
- <sup>16</sup>W, A=170-182, even isotopes, yrast states, spectra and quad. moments, variation formulation 0-99119
- <sup>16</sup>W, A=178, 180, 182, 184, levels and J<sup>\*</sup>, ang. distrib. from W(p,t) 0-78159
- <sup>16</sup>W, A=182-186, deformation hexadecapole moments, Hartree-Fock calcs. (Russian) 0-63081



## nuclei with mass number 150 to 189 continued

- <sup>150</sup>W(<sup>12</sup>C,f), A=182, 183, 184, 186, 80 to 115 MeV, lifetime meas. by crystal-blocking tech. 0-91198  
<sup>150</sup>W(<sup>16</sup>O,f), A=182, 183, 184, 186, 80 to 115 MeV, lifetime meas. by crystal-blocking tech. 0-91198  
<sup>150</sup>W(<sup>19</sup>F,f), A=182, 183, 184, 186, 80 to 115 MeV, lifetime meas. by crystal-blocking tech. 0-91198  
<sup>150</sup>W(e,f), A=182,184,186, 35-55 MeV, fission barriers, pairing strength deformation depend., stat. anal. 0-57810  
<sup>180</sup>W octupole vibr. states, J<sup>π</sup> and transitions from <sup>180</sup>Re decay 0-83024  
<sup>181</sup>W level density, γ spectra and ang. correls., direct and nonequilibrium processes from <sup>181</sup>Ta(p,n) (*Russian*) 0-68631  
<sup>181</sup>W levels (neutron and collective) and J<sup>π</sup>, ang. distrib. from <sup>183</sup>W(p,t) 0-78160  
<sup>184</sup>W, pygmy resonance, E1 transition probabilities, BCS wave functions, spin-isospin oscillation (*Chinese*) 0-63087  
<sup>184</sup>W(<sup>12</sup>C,<sup>12</sup>C'), 70 MeV, 4<sup>+</sup> state excitation ang. distrib., hexadecapole deformation length effects 0-68521  
W(γ,γ), 412, 468, 662 keV, elastic scatt. cross sections, Rayleigh scattering anal. 0-86898  
<sup>184</sup>Yb, A=158, 159, alpha decay and gamma transitions 0-73827  
<sup>184</sup>Yb, A=160-163, γ-transitions from Lu decay 0-102146  
<sup>184</sup>Yb, A=168-176, deformation hexadecapole moments, Hartree-Fock calcs. (*Russian*) 0-63081  
<sup>160</sup>Yb yrast levels, 2nd and 3rd backbending, cranked HFB calcs. 0-63064  
<sup>166</sup>Yb multiple band crossing, (gS'S'S''<sub>n</sub>) system gamma correlation patterns 0-106008  
<sup>169</sup>Yb <sup>1/2<sup>+</sup></sup>[404]-<sup>7/2<sup>+</sup></sup>[633] transition ft value from <sup>169</sup>Lu allowed hindered β<sup>+</sup> decay 0-102148  
<sup>169</sup>Yb γγ ang. correlations, levels and spins from <sup>169</sup>Lu decay (*Russian*) 0-83069  
<sup>172</sup>Yb levels, bands, J<sup>π</sup> and T<sub>1/2</sub> from <sup>170</sup>Er(α,2n) 0-91127  
<sup>173</sup>Yb, γ-transitions from 7/2<sup>+</sup>, 7/2<sup>-</sup> [514], 636 keV level 0-78187  
<sup>176</sup>Yb(p,p'), 0.8 GeV, ang. distributions and multipole moments, DWBA and coupled channel anal. 0-105969

## nuclei with mass number 190 to 219

- A=200 region, macroscopic fission barriers, isospin depend., liquid drop model 0-57811  
A=213, nuclear structure data sheets (July 1979) 0-67942  
A=217, nuclear structure data sheets (July 1979) 0-67943  
A≥208, pygmy resonance, E1 transition probabilities, BCS wave functions, spin-isospin oscillation (*Chinese*) 0-63087  
effective residual interaction matrix elements, spectroscopic factors, cross sections 0-99134  
even-even nuclei, E<sub>2</sub> transitions from 2<sup>+</sup> state of gamma-vibrational band 0-91150  
(γ,X), A=154-209, 7-20 MeV, total photoabsorption cross section 0-57766  
(p, spallation), 480 MeV, medium to heavy mass targets, deep spallation products 0-83085  
<sup>207</sup>(e,e'), transverse scatt. amplitude suppression, form factors, neutron hole states 0-91129  
<sup>208</sup>Ac, A=209-214, 216, deduced mass from Fr direct mass meas. 0-78130  
<sup>208</sup>Ac, A=198m,198g,199, alpha branching ratios 0-99154  
<sup>208</sup>Ac, A=200-206, 208, deduced mass from Fr direct mass meas. 0-78130  
<sup>209</sup>At, γ-transition, multipolarities, level scheme following <sup>208</sup>Rn decay 0-83072  
<sup>211</sup>At heavy product range and ang. distrib. from <sup>209</sup>Bi(HI,X) 0-83119  
<sup>212</sup>At excitation functions and isomer ratios from <sup>209</sup>Bi(α,n) 0-83039  
<sup>213</sup>At levels, J<sup>π</sup>, transitions and lifetimes from <sup>208</sup>Pb(<sup>12</sup>Li,X) 0-68542  
Au, odd isotones, deformation pot. energy from Nilsson model 0-57676  
Au(HI,X), fission fragment backscattering corrections to absolute fission counting rate measurements 0-68685  
<sup>147</sup>Au(<sup>40</sup>Ar, f), 340 MeV, H and He emission, rapid energy equil., to ang. distrib. 0-86936  
<sup>193</sup>Au levels, three holes cluster vibr. and particle asymmetric rotor descriptions 0-57668  
<sup>195</sup>Au decay, K-shell capture fractions, internal conversion electrons, coincidence techniques 0-57743  
<sup>197</sup>AuZr 0-95329  
<sup>197</sup>Au(<sup>132</sup>Xe,X), neutron multiplicities 0-57797  
<sup>197</sup>Au(<sup>14</sup>N,n), DWBA anal. above Coulomb barrier 0-86917  
<sup>197</sup>Au(<sup>16</sup>O,X), colliding heavy ion interface, nucleon emission, fusion and strongly damped collisions 0-86922  
<sup>197</sup>Au(<sup>16</sup>O,p,X), 315 MeV, high energy p emission, fireball and preequilibrium anal. 0-91194  
<sup>197</sup>Au(<sup>20</sup>Ne, spallation), 8.0 GeV, cross sections and target residues, model comparison 0-68630  
<sup>197</sup>Au(<sup>20</sup>Ne,X), exactly central heavy-ion collisions by nuclear hydrodynamics 0-68690  
<sup>197</sup>Au(<sup>22</sup>Ne, f), 178 MeV, α-particles and fission fragments, spectra and cross sections (*Russian*) 0-91203  
<sup>197</sup>Au(<sup>22</sup>Ne,α,X), 178 MeV, max. α-particle energy at forward angles 0-68698  
<sup>197</sup>Au(<sup>40</sup>Ar, X), deep inelastic reaction, neutron excess degree of freedom relaxation model (*Chinese*) 0-102202  
<sup>197</sup>Au(<sup>40</sup>Ar,X), 222-340 MeV, charged particle emission, early collision evolution, fission and evaporation cross sections 0-106072  
<sup>197</sup>Au(d,f), 80 MeV, post neutron emission fission products 0-83136  
<sup>197</sup>Au(d,p,X), 80 MeV, inclusive proton spectra, d break-up, DWBA anal. 0-91190  
<sup>197</sup>Au(n,xn), 20.6 MeV, neutron yield cross sections and spectra (*Russian*) 0-91188  
<sup>197</sup>Au(p,<sup>3</sup>He x), 72 MeV, pre-equilibrium emission (*German*) 0-68657  
<sup>197</sup>Au(p,X), 0.2-6.0 GeV, product cross sections, mass yields, spallation products 0-83088  
<sup>197</sup>Au(p,αx), 72 MeV, pre-equilibrium emission (*German*) 0-68657  
<sup>197</sup>Au(p,X), x=α, τ, 72 MeV, spectra and angular distrib. 0-68660  
<sup>197</sup>Au(π<sup>+</sup>,X), X=d,t,<sup>3</sup>He,<sup>4</sup>He, particle emission following stopped pion absorption 0-91196  
Au(γ,X), X=p,d,t,<sup>3</sup>He,<sup>4</sup>He, cascade-evaporation 0-57770  
<sup>201</sup>Bi, A=196-202, 204, deduced mass from Fr direct mass meas. 0-78130  
<sup>201</sup>Bi(α,f), 23-140 MeV, l<sub>crit</sub> from fragment ang. distrib. anal. 0-106087  
<sup>206</sup>Pb decay, <sup>206</sup>Pb γγ directional correlations, multipole mixing ratios, transition strength limits 0-86849  
<sup>207</sup>Pb EC decay, <sup>207</sup>Pb, 569.65-1063.63 keV cascade γ-γ ang. correl. meas. 0-86847  
<sup>207</sup>Pb, gamma-ray intensities, precision meas. 0-102139

## nuclei with mass number 190 to 219 continued

- <sup>208</sup>Bi, 0<sup>+</sup> IAS, spreading width and isospin impurity, isovector monopole state influence 0-78155  
<sup>208</sup>Bi M1 isobaric analogue resonances and giant spinflip resonances from <sup>208</sup>Pb(p,n) 0-106030  
<sup>208</sup>Bi(n, nfn), fission high energy neutrons (*Russian*) 0-106091  
<sup>209</sup>Bi energy and transition probability convergence in Dyson's boson expansion 0-78206  
<sup>209</sup>Bi levels and spectroscopic factors, <sup>210</sup>Bi(9<sup>-</sup>) parentage from <sup>210</sup>Bi<sup>π</sup>(d,t) 0-78158  
<sup>209</sup>Bi single particle levels, ang. distrib., spectroscopic factors, DWBA anal. of <sup>208</sup>Pb(<sup>7</sup>Li,<sup>6</sup>Me) 0-63067  
<sup>209</sup>BiZZ 0-95329  
<sup>209</sup>Bi(<sup>136</sup>Xe,X), 940 MeV bombarding energy depend., fragment deformation, sequential fission 0-86938  
<sup>209</sup>Bi(<sup>136</sup>Xe,X), deeply inelastic collisions, mass transport, shell effects 0-99188  
<sup>209</sup>Bi(<sup>4</sup>He,d), 30 MeV, effective residual interaction matrix elements, spectroscopic factors, cross sections 0-99134  
<sup>209</sup>Bi(<sup>26</sup>Fe,X), 464 MeV, damped collision, actinide spontaneous fission activities 0-86937  
<sup>209</sup>Bi(<sup>26</sup>Fe,X), damped collisions, fast A/Z equilibration and correlated nucleon exchange 0-86798  
<sup>209</sup>Bi(<sup>7</sup>Li,5n)<sup>211</sup>Rn, 38-60 MeV, excitation function 0-95323  
<sup>209</sup>Bi(HI,X), quasi-elastic transfer, heavy product range and ang. distrib. 0-83119  
<sup>209</sup>Bi(α,t), 40 MeV, effective residual interaction matrix elements, spectroscopic factors, cross sections 0-99134  
<sup>209</sup>Bi(γ,X), 3-30 MeV, photoabsorption cross section, giant dipole resonances 0-78254  
<sup>209</sup>Bi(γ,f), 40-65 MeV, absolute total photofission cross section, compound nucleus form. 0-86934  
<sup>209</sup>Bi(n,n), 1.2 to 4.5 MeV total and differential cross sections 0-86903  
<sup>209</sup>Bi(n,xn), 20.6 MeV, neutron yield cross sections and spectra (*Russian*) 0-91188  
<sup>209</sup>Bi(p,X), pol.p, 65 MeV, continuum spectra anal. powers 0-102178  
<sup>209</sup>Bi(p,p')(d,X), pol. p, 65 MeV, anal. powers of continuum energy spectra 0-68637  
<sup>209</sup>Fr, A=201-203, alpha decay, branching ratios, mass excess and half life 0-99154  
<sup>209</sup>Fr, A=204-210, 212, 224-228, direct mass meas. 0-78130  
<sup>210</sup>Hg, A=190-200, even, phase transition and possible triaxial shape, energy levels 0-63098  
<sup>190</sup>Hg, 21 ns isomer (*v*<sub>1/2</sub>)<sup>2</sup> interpretation from g-factor meas. 0-105945  
<sup>194</sup>Hg, α evaporation spectrum 0-68715  
Ir, odd isotones, deformation pot. energy from Nilsson model 0-57676  
<sup>189</sup>Ir, A=189, 191, levels, J<sup>π</sup>, transitions and mixing ratios from Pt decay 0-68602  
<sup>190</sup>Ir in Re crystal, elec. quadrupole orientation, elec. field gradient 0-78140  
<sup>191</sup>Ir 129 keV transition, atomic screening, time reversal violation 0-106011  
<sup>191</sup>Ir, excited nuclei mean precession time depend. on γ-spectral width, g-factors (*Russian*) 0-78211  
<sup>191</sup>Ir, gamma-ray intensities, precision meas. 0-102140  
Os even-even isotopes, excitation energies and EM props. from interacting boson model 0-106005  
<sup>190</sup>Os, A=186-194, collective levels, transitions, mag. and quadrupole moments, boson expansion theory 0-105954  
<sup>193</sup>Os level scheme and transitions, Coriolis coupled Nilsson states from <sup>192</sup>Os(n,γ) 0-57698  
<sup>194</sup>Pb, A=215-218, deduced mass from Fr direct mass meas. 0-78130  
Pb(γ,γ), 344-1408 keV <sup>152</sup>Eu γ rays, differential cross sections 0-99170  
Pb even isotopes, two quasiparticle 2<sup>+</sup> state coupling to T=0 giant quadrupole resonance 0-68618  
Pb pairing vibr. band, microscopic struct. and wave functions from (p,t), (t,p) 0-91126  
Pb region, forbidden charge exchange collective modes, β- and γ-decay processes 0-86784  
Pb region, particle-vibration multiplet spectra, self-consistent framework 0-102089  
Pb(Ar,X), 800 MeV/N, single particle spectra from high multiplicity events 0-99184  
Pb(<sup>12</sup>C,X), 1-2 GeV/n, central collision threshold phenomena, pion prod. 0-95326  
<sup>208</sup>Pb, A=197,198, low energy γ-transitions 0-83058  
<sup>208</sup>Pb, A=202, 204, spectra from multistep shell model method 0-78194  
<sup>208</sup>Pb, muonic, first excited 2<sup>+</sup> state, isomer shift of E2 transition 0-99150  
<sup>204</sup>Pb(n,n'), 1.5-3.1 MeV, levels, J<sup>π</sup>, excitation functions and mixing ratios 0-102123  
<sup>208</sup>Pb γγ directional correlations, multipole mixing ratios, transition strength limits from <sup>208</sup>Pb decay 0-86849  
<sup>208</sup>Pb(n,γ), direct-semidirect and compound nucleus contribs. to cross sections 0-68662  
<sup>207</sup>Pb 569.65-1063.63 keV cascade, γ-γ ang. correl. meas. from <sup>207</sup>Pb decay 0-86847  
<sup>207</sup>Pb, muonic, octupole doublet isomer shifts, octupole vibr. 0-95750  
<sup>207</sup>Pb muonic isomer shifts, neutron hole anomalous moment contribs. 0-78728  
<sup>207</sup>Pb, neutron scattering resonance radiative widths 0-99146  
<sup>206</sup>Pb p-wave resonances, enhanced primary M1 transitions from <sup>206</sup>Pb(n,γ) 0-57728  
<sup>207</sup>PbZZ 0-95329  
<sup>206</sup>Pb(n,p) reaction, isobar analogue state excitation (*Russian*) 0-102124  
<sup>208</sup>Pb(<sup>208</sup>Pb,f) 1539 MeV, exam. of four-pronged double sequential fission events using mica track detectors 0-95328  
<sup>208</sup>Pb(e,e'), 2<sup>+</sup> giant resonance twist mode excitation, B(M2) values, form factors 0-78246  
<sup>208</sup>Pb breathing model transition density, single particle and collective state dynamical coupling 0-106007  
<sup>208</sup>Pb giant monopole and quadrupole resonances, multipole excitations from (α,α')(d,d') 0-106031  
<sup>208</sup>Pb, isobaric analogue states, effects of Coulomb isospin coupling, random-phase method (*Russian*) 0-86808  
<sup>208</sup>Pb, magnetic high spin states, microscopic struct. 0-95297  
<sup>208</sup>Pb monopole vibr. vel. field, asymptotic form 0-78115  
<sup>208</sup>Pb region, mag. transition strength, core polarisation effects, form factor shape 0-86850  
<sup>208</sup>Pb shell structure, effect on magicity of superheavy nuclei 0-78175



## nuclei with mass number 190 to 219 continued

- <sup>208</sup>Pb single particle and hole states, renormalisation, core polarisation, spectroscopic factors 0-57658  
<sup>208</sup>Pb(<sup>12</sup>C,<sup>11</sup>B), 77 MeV, bound and continuum state excitation, direct and two step processes 0-63205  
<sup>208</sup>Pb(<sup>14</sup>N,<sup>14</sup>N'), 266 MeV, giant resonance excitation 0-78253  
<sup>208</sup>Pb(<sup>208</sup>Pb, H), 7-7.5 MeV/N, product energy and element distrib., fission probab., energy losses 0-86916  
<sup>208</sup>Pb(<sup>208</sup>Pb, X), giant resonance polarisation pots. from nucleus-nucleus effective pot. 0-78248  
<sup>208</sup>Pb(<sup>208</sup>Pb,X), exactly central heavy-ion collisions by nuclear hydrodynamics 0-68690  
<sup>208</sup>Pb(<sup>20</sup>Ne,X), 400 MeV/N, inclusive p, d, t, <sup>3</sup>He cross sections from sequential scatt. model 0-57792  
<sup>208</sup>Pb(<sup>3</sup>He,d), 30 MeV, effective residual interaction matrix elements, spectroscopic factors, cross sections 0-99134  
<sup>208</sup>Pb(<sup>40,48</sup>Ca, <sup>40,48</sup>Ca), optical model anal., strong absorption radius (*Russian*) 0-68697  
<sup>208</sup>Pb(<sup>40</sup>Ar, <sup>40</sup>Ar), optical model anal., strong absorption radius (*Russian*) 0-68697  
<sup>208</sup>Pb(<sup>48</sup>Ti, <sup>48</sup>Ti), optical model anal., strong absorption radius (*Russian*) 0-68697  
<sup>208</sup>Pb(<sup>6</sup>Li,<sup>6</sup>Li), elastic and inelastic, 74 MeV, folding optical model parameters 0-102201  
<sup>208</sup>Pb(<sup>6</sup>Li,X), 156 MeV, projectile break up in continuous particle spectra, cross section, fragmentation 0-86889  
<sup>208</sup>Pb(<sup>6</sup>Li,d), 90 MeV, alpha-cluster transfer from alpha-decaying nuclei 0-91166  
<sup>208</sup>Pb( $\alpha,\alpha'$ ), levels, B(E3), transition density and nuclear pot., folding model anal. 0-86812  
<sup>208</sup>Pb( $\alpha,\alpha'$ ), 172 MeV, giant resonance structures 0-91163  
<sup>208</sup>Pb( $\alpha$ , d'), 108 MeV, giant monopole resonance excitation and ang. distrib. 0-102164  
<sup>208</sup>Pb(d,p), tensor analyzing power, deuteron wave functions 0-99137  
<sup>208</sup>Pb(e,e'), 70-335 MeV, natural parity high spin state excitation 0-63060  
<sup>208</sup>Pb(p,n), nucleon optical potential from Lane model 0-83097  
<sup>208</sup>Pb(p,p'), 135 MeV, normal parity level excitation, J<sup>π</sup>, differential cross sections 0-57690  
<sup>208</sup>Pb(p,p'), 135 MeV, normal parity excitations, microscopic description, NN interaction shape 0-57691  
<sup>208</sup>Pb(p,p'), 800 MeV, high energy octupole giant resonance, ang. distrib. 0-86879  
<sup>208</sup>Pb(p,p), 0.8 GeV, cross sections, optical anal. np RMS radius difference,  $\Delta r_{np}$  0-63187  
<sup>208</sup>Pb(p,p), 30 MeV, optical pot. imaginary part calcs. 0-86868  
<sup>208</sup>Pb(p,t), finite range DWBA anal. with realistic triton wave function 0-78300  
<sup>208</sup>Pb(p,x),  $x=\alpha$ ,  $\tau$ , 72 MeV, spectra and angular distrib. 0-68660  
<sup>208</sup>Pb( $\pi^+$ ,  $\pi^-$ N), 180-255 MeV, quasilastic pion scatt. coincidence expt. interpretation, impulse approx. 0-68704  
<sup>209</sup>Pb excited states, 3/2<sup>+</sup> resonances from shell model of <sup>208</sup>Pb(n,n) 0-78240  
<sup>210</sup>Pb determination in sediment core from ocean floor off Californian coast 0-72101  
<sup>210</sup>Pb levels, J<sup>π</sup>, transitions and lifetimes from <sup>208</sup>Pb(<sup>7</sup>Li,X) 0-68542  
<sup>210</sup>Pb( $\alpha$ ,X), 3.6 GeV/N, secondary particle ang. and vel. distrib.,  $\pi$ ,p,d,t prod. (*Russian*) 0-63194  
<sup>210</sup>Pb(p,d), 9 GeV, nuclear emulsion expt. 0-78292  
<sup>210</sup>Pb( $\pi^-$ , p) 1.5-5 GeV/c, cumulative proton polarisation (*Russian*) 0-86896  
<sup>210</sup>Pb(x,x),  $x=\pi^+$ ,  $K^+$ , p,  $\bar{p}$ , 70, 125, 175 GeV/c 0-83128  
<sup>210</sup>Po  $\alpha$ ,  $\gamma$ -rays, conversion electron spectra,  $\gamma\gamma$  coincidences 0-83061  
<sup>210</sup>Po heavy product range and ang. distrib. from <sup>209</sup>Pb(HI,X) 0-83119  
<sup>210</sup>Po, nucl. alpha decay, electron inner shell vacancy creation, semi quantal approach 0-68607  
<sup>211</sup>Po excitation functions and isomer ratios from <sup>208</sup>Pb( $\alpha$ ,n) and <sup>209</sup>Bi( $\alpha$ ,np) 0-83039  
<sup>212</sup>Po excitation functions and isomer ratios from <sup>209</sup>Bi( $\alpha$ ,p) 0-83039  
<sup>212</sup>Po, levels, J<sup>π</sup>, transitions and lifetimes from <sup>208</sup>Pb+<sup>4</sup>Li 0-68542  
<sup>212</sup>Pt decay, oriented nuclei, <sup>189,191</sup>Ir levels, J<sup>π</sup>, transitions and mixing ratios 0-68602  
<sup>212</sup>Pt even-even isotopes, excitation energies and EM props. from interacting boson model 0-106005  
<sup>212</sup>Pt, A=188-198 collective levels, transitions, mag. and quadrupole moments, boson expansion theory 0-105954  
<sup>212</sup>Pt, A=190,192,194, state struct. in interacting boson model 0-83047  
<sup>213</sup>Pt low lying negative parity states and shape from <sup>193</sup>Pt(p,t) 0-68540  
<sup>194</sup>Pt, static quadrupole moments of arbitrary excited states, sum rule approach 0-91135  
<sup>213</sup>Pt( $\gamma,\gamma$ ), 412, 468, 662 keV, elastic scatt. cross sections, Rayleigh scattering anal. 0-86898  
<sup>199</sup>Rn and <sup>199</sup>Rn<sup>m</sup> alpha decay signatures from <sup>169</sup>Tm(<sup>35</sup>Cl,5n) 0-68610  
<sup>208</sup>Rn-<sup>208</sup>At,  $\gamma$ -ray, conversion electron spectra 0-83072  
<sup>211</sup>Rn heavy product range and ang. distrib. from <sup>209</sup>Bi(HI,X) 0-83119  
<sup>212</sup>Rn, shell model states, semiempirical calcs. half lives, mag. moments, excitation functions 0-63083  
<sup>213</sup>Tl odd isotones, deformation pot. energy from Nilsson model 0-57676  
<sup>197</sup>Tl, deduced mass from Fr direct mass meas. 0-78130  
<sup>204</sup>Tl  $\beta$ -decay, K-shell autoionisation accompanying internal bremsstrahlung 0-57745  
<sup>204</sup>Tl neutron hole states, J<sup>π</sup> and spectroscopic factors from <sup>205</sup>Tl(p,d) 0-86783  
<sup>205</sup>Tl(p,n)<sup>201</sup>Pb-<sup>201</sup>Tl, yields and excitation functions for Pb radioactivities, medical appls. 0-67249

## nuclei with mass number 220 or higher

- A<500, magicity, extrapolation of <sup>208</sup>Pb Woods-Saxon potential parameters 0-78175  
 even-even nuclei, E<sub>2</sub> transitions from 2<sup>+</sup> state of gamma-vibrational band 0-91150  
 fission isomers, spectrosc. props. 0-105966  
 magicity of superheavy nuclei, extrapolation of <sup>208</sup>Pb Woods-Saxon potential parameters up to A=500 0-78175  
 trans-uranium nuclei, fission barrier and (neutron width-fission width), nucleon contents depend. (*Russian*) 0-106093  
<sup>232</sup>UZZ 0-95329  
<sup>248</sup>Cm, spontaneous fission Xe and Kr daughter isotope ratios 0-63215  
<sup>230</sup>Ac decay, <sup>230</sup>Ra levels, J<sup>π</sup> and transitions, Nilsson assignments 0-68543  
<sup>230</sup>Ac levels, J<sup>π</sup> and transitions, Nilsson assignments from <sup>230</sup>Ra decay 0-68543

## nuclei with mass number 220 or higher continued

- <sup>248</sup>Am, A=240,244 actinide spontaneous fission activities from <sup>209</sup>Bi(<sup>56</sup>Fe,X) 0-86937  
<sup>241</sup>Am(n,f), 2.5 MeV neutrons, absolute cross section meas. (1.98±0.07) b 0-73872  
<sup>241</sup>Am(n,f), 14.8 MeV, cross-section meas. using mica track detectors 0-95330  
<sup>244</sup>Am, reduced E0 conversion due to mag. moment effects 0-83034  
<sup>244</sup>Am half life and  $\alpha$ -activity 0-102159  
<sup>244</sup>Am(n,f), low energy, far-out asymmetric mass distrib. 0-83132  
<sup>244</sup>Cf, A-234,238, actinide spontaneous fission activities from <sup>209</sup>Bi(<sup>56</sup>Fe, X) 0-86937  
<sup>250</sup>Cf low spin states, bandheads, J<sup>π</sup> and transitions from <sup>250</sup>Es EC decay 0-105952  
<sup>250</sup>Cf, spontaneous fission Xe and Kr daughter isotope ratios 0-63215  
<sup>252</sup>Cf fission, neutron deficient fragments, search for positron activity (*Russian*) 0-63218  
<sup>252</sup>Cf fission, spontaneous, far-out asymmetric mass distrib. 0-83132  
<sup>252</sup>Cf scission point configuration,  $\alpha$ -ang. distrib., trajectory calcs. for LRA fission 0-83134  
<sup>252</sup>Cf spontaneous fission, fission product  $\beta$  spectra (*Russian*) 0-91204  
<sup>252</sup>Cf spontaneous fission, prompt  $\gamma$ -ray differential angular distrib. 0-102220  
<sup>254</sup>Cf spontaneous fission, neutron-rich fragments, even-even products 0-78342  
<sup>254</sup>Cm, spontaneous fission, prompt neutron multiplicity distrib. meas. 0-83131  
<sup>254</sup>Cm(n,f), thermal neutron fission cross section and fission-resonance integral 0-86942  
<sup>254</sup>Cm(n,f), thermal, charge distrib., <sup>135</sup>I and <sup>190</sup>Ba fractional cumulative yields 0-63074  
<sup>254</sup>Cm decay, <sup>241</sup>Pu level structure and  $\gamma$ -transitions 0-105980  
<sup>250</sup>Es EC decay, <sup>250</sup>Cf low spin states, bandheads, J<sup>π</sup> and transitions 0-105952  
<sup>250</sup>Fm, A=242-246, actinide spontaneous fission activities from <sup>209</sup>Bi(<sup>56</sup>Fe, X) 0-86937  
<sup>250</sup>Fm, pot. energy surface, liquid model, deformation energy formulae (*Chinese*) 0-102106  
<sup>250</sup>Fr, A=204-210, 212, 224-228, direct mass meas. 0-78130  
<sup>252</sup>Fr-<sup>224</sup>Ra,  $\gamma$ rays, internal conversion,  $\epsilon\gamma$  coincidence spectra meas. 0-78216  
<sup>254</sup>Np(n,f), A=234, 235, low energy, far-out asymmetric mass distrib. 0-83132  
<sup>235</sup>Np, fission lifetime from <sup>235</sup>U(d,f) reaction 0-63216  
<sup>237</sup>Np, prompt fission, excitation following K-shell photoionisation, deexcitation  $\gamma$ -rays 0-78196  
<sup>237</sup>Np muonic, prompt fission, fragment atomic muon capture 0-95312  
<sup>237</sup>Np(e,f), 10-34 MeV, electrofission cross section, E2 transition mode and giant resonances 0-106084  
<sup>237</sup>Np(n,f), intermediate struct. line fitting, subthreshold fission resonances 0-102214  
<sup>237</sup>Np(n,f), thermal neutron sub-barrier fission <sup>134</sup>I and <sup>135</sup>Xe yields 0-86935  
<sup>237</sup>Np(p,f), 11-26 MeV, product yield 0-91197  
<sup>239</sup>Np, absolute meas. of branching ratio for the 277.6 keV line 0-86854  
<sup>239</sup>Pu, even isotopes, K=0<sup>+</sup>, 0<sup>-</sup> bands, energies, inverse moments of inertia 0-63063  
<sup>239</sup>Pu<sup>39</sup>, product separation asymmetry in fission by slow polarised neutrons (*Russian*) 0-106088  
<sup>240</sup>Pu(n,f), A=239,242,244, 14.8 MeV, cross-section meas. using mica track detectors 0-95330  
<sup>240</sup>Pu, A=239,242, muonic, prompt fission, fragment atomic muon capture 0-95312  
<sup>240</sup>Pu(n,f), A=240,241, 14.8 MeV, meas. of reaction parameters using solid state nuclear track detectors 0-91201  
<sup>230</sup>Pu(n,f), fission-fragment yields of neutron fission in FBR 0-83102  
<sup>238</sup>Pu(n,f), intermediate struct. line fitting, subthreshold fission resonances 0-102214  
<sup>239</sup>Pu, fission product beta decay,  $\bar{\nu}$  spectra 0-102150  
<sup>239</sup>Pu( $\gamma$ ,f), 15-55 MeV, photofission symmetric and asymmetric yields 0-83135  
<sup>239</sup>Pu(n,f), far-out asymmetric mass distrib. 0-83132  
<sup>239</sup>Pu(n, $\gamma$ ), thermal, fission product  $\bar{\nu}_e$  spectrum,  $\beta$ -decay characts. 0-78340  
<sup>241</sup>Pu half life from  $\alpha$ -spectrometry and <sup>241</sup>Am ingrowth 0-68609  
<sup>241</sup>Pu half-life determ. by mass spectrometry 0-78232  
<sup>241</sup>Pu isomeric state non-existence 0-105983  
<sup>241</sup>Pu level structure and  $\gamma$ -transitions from <sup>245</sup>Cm decay 0-105980  
<sup>241</sup>Pu( $\mu$ ,f), radiationless muonic transition induced fission, fission dynamics probe, friction coeff. 0-78336  
<sup>244</sup>Pu(n, $\gamma$ ) resonance integral meas. 0-73846  
<sup>294</sup>Pu, muonic atom direct electroprod., finite nuclear size effects (*Russian*) 0-69272  
<sup>248</sup>Ra, even isotopes, K=0<sup>+</sup>, 0<sup>-</sup> bands, energies, inverse moments of inertia 0-63063  
<sup>230</sup>Ra decay, <sup>230</sup>Ac levels, J<sup>π</sup> and transitions, Nilsson assignments 0-68543  
<sup>230</sup>Ra levels, J<sup>π</sup> and transitions, Nilsson assignments from <sup>230</sup>Ac decay 0-68543  
<sup>230</sup>Rn, even isotopes, K=0<sup>+</sup>, 0<sup>-</sup> bands, energies, inverse moments of inertia 0-63063  
<sup>220</sup>Rn decay products attachment to flowing aerosols using centrifuge 0-61167  
<sup>222</sup>Rn, props. and behaviour of short lived daughter nuclides in the atmos. (*Japanese*) 0-72339  
<sup>224</sup>Rn-<sup>224</sup>Fr±<sup>224</sup>Ra,  $\gamma$ -rays, internal conversion,  $\epsilon\gamma$  coincidence spectra meas. 0-78216  
<sup>230</sup>Th, even isotopes, K=0<sup>+</sup>, 0<sup>-</sup> bands, energies, inverse moments of inertia 0-63063  
<sup>230</sup>Th alpha-decay half life from specific activity method 0-102157  
<sup>230</sup>Th(n,f), 0.68-1.10 MeV, fission fragment ang. distrib., resonance and moment of inertia 0-102219  
<sup>231</sup>Th excited states and bands, spins,  $\gamma$ -transitions from <sup>230</sup>Th(n, $\gamma$ ) 0-57699  
<sup>232</sup>Th(<sup>14</sup>B,<sup>12</sup>B), 129 MeV, <sup>12</sup>B spin polarisation 0-63616  
<sup>232</sup>Th(<sup>40</sup>Ar, X), deep inelastic reaction, neutron excess degree of freedom relaxation model (*Chinese*) 0-102202  
<sup>232</sup>Th(<sup>63</sup>Cu, X), deep inelastic reaction, neutron excess degree of freedom relaxation model (*Chinese*) 0-102202  
<sup>232</sup>Th( $\gamma$ ,X) 5-18.3 MeV, photoneutron and photofission cross sections, giant resonance and deformations 0-68712



**nuclei with mass number 220 or higher continued**

- <sup>232</sup>Th( $\gamma, f$ ), 15-55 MeV, photofission symmetric and asymmetric yields 0-83135
- <sup>232</sup>Th( $n, n$ ), ratio to ( $n, \gamma$ ) in fast reactor, direct meas. 0-102233
- <sup>232</sup>Th( $n, f$ ), 2-8 MeV, fission product yields and mass distrib. 0-86939
- <sup>232</sup>Th( $n, \gamma$ ), ratio to ( $n, n$ ) in fast reactor, direct meas. 0-102233
- <sup>232</sup>Th( $p, f$ ), 29-97 MeV, Rb, In and Cs relative indep. yields, charge division 0-102218
- <sup>232</sup>Th( $p, p'f$ ), 52.5 MeV, fission probability 0-99195
- <sup>232</sup>Th( $p, x$ ),  $x = \alpha, \tau, \gamma$ , 72 MeV, spectra and angular distrib. 0-68660
- U, even isotopes,  $K = 0^+$ ,  $0^-$  bands, energies, inverse moments of inertia 0-63063
- U<sup>233</sup>, product separation asymmetry in fission by slow polarised neutrons (*Russian*) 0-106088
- U(Ne, X), 250, 400, 800 MeV/N, nuclear matter collective sideward flow, nuclear fluid dynamics 0-57715
- U(Ne, X), proton inclusive spectra, direct plus thermal model 0-57799
- <sup>A</sup>U, A=235, 238, fission product beta decay,  $\bar{\nu}$  spectra 0-102150
- <sup>A</sup>U<sup>m</sup>, A=236, 238, isomeric to prompt fission ratios; fission fragments from (d, pf), (d, pnf) 0-86940
- <sup>A</sup>U( $\gamma, X$ ), A=235, 236, 238, 5-18.3 MeV, photoneutron and photofission cross sections, giant resonance and deformations 0-68712
- <sup>A</sup>U( $\gamma, f$ ), A=235, 238, 15-55 MeV, photofission symmetric and asymmetric yields 0-83135
- <sup>A</sup>U( $\mu, f$ ), A=235, 238, prompt and delayed fission, absolute yields and lifetimes 0-78337
- <sup>A</sup>U( $n, f$ ), A=233, 235, ejection fission products angular depend. on thermally polarised neutron capture (*Russian*) 0-86941
- <sup>A</sup>U( $n, f$ ), A=235, 238, fission-fragment yields of neutron fission in FBR 0-83102
- <sup>A</sup>U( $n, f$ ), A=235, 238, low energy, far-out asymmetric mass distrib. 0-83132
- <sup>233</sup>U, half-life determ. 0-57750
- <sup>233</sup>U( $n, f$ ), thermal polarised neutrons, neutron emission P-odd asymmetry (*Russian*) 0-78338
- <sup>233</sup>U( $\rho, f$ ), alpha-particle angular and energy spectra, cross-section anisotropy 0-57809
- <sup>234</sup>U under barrier photofission, 4-5.7 MeV, fragment ang. distrib. (*Russian*) 0-106090
- <sup>234</sup>U( $n, f$ ), intermediate struct. line fitting, subthreshold fission resonances 0-102214
- <sup>235</sup>U, decay product radioactive accumulation, FORTRAN program 0-68611
- <sup>235</sup>U fission fragment thermonuclear superheavy nuclei synthesis, prod. cross sections 0-95331
- <sup>235</sup>U internal conversion from  $1/2^+$  isomeric state, U<sup>4+</sup> electron configuration 0-58146
- <sup>235</sup>U, pot. energy surface, liquid model, deformation energy formulae (*Chinese*) 0-102106
- <sup>235</sup>U, radioactive series decay, computer simulation 0-102160
- <sup>235</sup>U( $n, f$ ), symmetric fission, proton scatt. by fission fragments in neck area 0-83130
- <sup>235</sup>U( $n, f$ ), thermal, fragment ionisation, charge distrib., stat. and instant perturbation theory (*Russian*) 0-63219
- <sup>235</sup>U( $n, f$ ), thermal neutron induced fission, nuclear charge distribution in fission products 0-57808
- <sup>235</sup>U( $n, \gamma$ ), thermal, d, t, He emission probabilities from stable core model (*Russian*) 0-68713
- <sup>235</sup>U( $n, \gamma$ ), thermal, fission product  $\bar{\nu}_e$  spectrum,  $\beta$ -decay characts. 0-78340
- <sup>235</sup>U( $n, \gamma, f$ ), X-ray yield fluctuations,  $\gamma$ -transitions in <sup>236</sup>U 0-106085
- <sup>236</sup>U  $\gamma$ -transitions from <sup>235</sup>U( $n, \gamma, f$ ) 0-106085
- <sup>236</sup>U isomeric and prompt fission, nuclear superfluidity evidence from <sup>235</sup>U(d, pf) 0-68711
- <sup>236</sup>U shape isomer,  $\gamma$  branch upper limit,  $\gamma$ -yields from <sup>235</sup>U(d, p) 0-99145
- <sup>236</sup>U collective and deformation props., general collective model 0-86827
- <sup>238</sup>U, decay product radioactive accumulation, FORTRAN program 0-68611
- <sup>238</sup>U, radioactive series decay, computer simulation 0-102160
- <sup>238</sup>U subbarrier photofission, cross section and half-life, double hump model 0-102217
- <sup>238</sup>UZZ 0-95329
- <sup>238</sup>U(<sup>16</sup>O, x),  $x = p, d, t$ , 315 MeV, energy spectra in coalescence model 0-99183
- <sup>238</sup>U(<sup>238</sup>U, X), 7.42 MeV/N, mass transport, shell effects, anharmonic pots. 0-99187
- <sup>238</sup>U(<sup>238</sup>U, X) deeply inelastic collisions, mass transport, shell effects 0-99188
- <sup>238</sup>U(<sup>238</sup>U, f), 1785 MeV, exam. of multiprong events due to multiple sequential fission using solid state track detectors 0-91199
- <sup>238</sup>U(<sup>32</sup>S, X), deep inelastic reaction, neutron excess degree of freedom relaxation model (*Chinese*) 0-102202
- <sup>238</sup>U(<sup>40</sup>Ar, X), 263 MeV, deep inelastic reaction, neutron excess degree of freedom relaxation model (*Chinese*) 0-102202
- <sup>238</sup>U(<sup>40</sup>Ar, X), 340 MeV, production of neutron rich nuclides <sup>54</sup>Ti, <sup>56</sup>V, <sup>58, 59</sup>Cr, <sup>61</sup>Mn, <sup>63, 64</sup>Fe 0-57802
- <sup>238</sup>U(<sup>84</sup>Kr, X), mass fragmentation, dynamical theory, two centre shell model, binary decay process 0-68628
- <sup>238</sup>U(<sup>84</sup>Kr, f), 806 MeV, exam. of multiprong events due to multiple sequential fission using solid state track detectors 0-91199
- <sup>238</sup>U( $\gamma, f$ ), <sup>135</sup>Xe, direct meas. of absolute and fractional indep. yields 0-78341
- <sup>238</sup>U( $\gamma, f$ ), neutron capture  $\gamma$ -rays,  $\Gamma_{\gamma}/\Gamma_f$  meas. 0-57813
- <sup>238</sup>U( $\gamma, f$ ), neutron capture  $\gamma$ -rays,  $\Gamma_{\gamma}/\Gamma_f$  fractional indep. yield 0-57814
- <sup>238</sup>U( $n, f$ ), 5 eV-2.5 MeV, fission cross section, fission barrier second well parameters, resonances 0-63217
- <sup>238</sup>U(p, X), 0.8-400 GeV 0-83099
- <sup>238</sup>U(p, f), 11-29 GeV, three dims. charge dispersion curves, isobaric yields 0-102111
- U( $\gamma, \gamma$ ), 0.1-1.5 MeV, Delbruck and Rayleigh scatt., differential cross sections 0-102180
- U( $\gamma, \gamma$ ), 412, 468, 662 keV, elastic scatt. cross sections, Rayleigh scattering anal. 0-86898

**nucleic acids see macromolecules**

**nucleon interactions see hyperon-nucleon interactions; kaon-nucleon interactions; lepton-nucleon interactions; muon-nucleon interactions; neutrino-nucleon interactions; nucleon-nucleon interactions; nucleon-nucleus reactions; photon-nucleon interactions; pion-nucleon interactions**

**nucleon-nucleon interactions**

- see also nucleon-nucleon scattering; proton-proton interactions education, Schrodinger eqn. solns. using approximate nucleon-nucleon and  $\Lambda$ -nucleon pots. 0-62429
- effective NN interaction and exchange current vel. depend., dipole sum rule enhancement 0-63100
- hadron interactions, effective radius quantum number depend., quark sum rules (*Russian*) 0-102062
- heavy meson exchange effect on <sup>1</sup>D<sub>2</sub> and <sup>3</sup>F<sub>3</sub> N-N partial waves, dibaryon resonances 0-105874
- kinematic singularity free helicity amplitudes, crossing matrix anal. props. 0-95285
- muons pair generation, nucleon cascade role 0-91120
- NN, 10<sup>12</sup> eV, rapidity gap distrib., Snider multiperipheral cluster model 0-73757
- NN, resonances and bound states, multichannel N/D formulation 0-78087
- NN $\rightarrow$ ( $\pi, \rho, \omega, f$ ), statistical model 0-102028
- NN $\rightarrow$ B $\pi$ , B $\pi$  are NN quasinuclei 0-57624
- NN $\rightarrow$ NN $\pi$ , polarization analysis of reactions with four spin-1/2 particles 0-86745
- NN $\rightarrow$  $\pi\pi$ , off-shell terms of  $\pi$ N scatt. matrix 0-73739
- $\nu$  production, prompt sources, and axion decays and interactions, pN beam-dump experiment 0-63028
- p(p)N, 50-200 GeV/c, multiparticle production, multiplicities, cross sections and ang. distrib. 0-86768
- pN, 22.6 GeV in emulsion, cluster size in pionisation region 0-78099
- pN, 400 GeV, in emulsion, two-particle rapidity correlation 0-63054
- pN, 67 GeV, multiperipheral cluster production 0-73689
- pN, 67 GeV, rapidity dispersion and cluster production 0-78104
- pN, 67 GeV/c, in Be, Al, Cu, inclusive  $\pi^+$ , K<sup>+</sup>, p,  $\bar{p}$  prod. cross sections (*Russian*) 0-86769
- pN, 67 GeV/c, nuclear targets,  $\pi^+$ , K<sup>+</sup>, p,  $\bar{p}$  yields (*Russian*) 0-68501
- pN, 70 GeV in emulsion, pion cluster obs. 0-86762
- PN, 70 GeV/c, inelastic interaction, planarity effect at accelerator energy 0-83006
- pN $\rightarrow$ charm particles, obs. in high resolution streamer chamber 0-73742
- pN $\rightarrow$ hadron shower, charm-pair production effects 0-73748
- pN in emulsion, 200, 400 GeV/c, multiparticle prod., azimuthal and rapidity effects 0-63035
- pN in Fe, 400 GeV/c,  $\psi(3100)$  prod. 0-57650
- Pn $\rightarrow$ l<sup>+</sup>X, scaling predictions, Drell-Yan model 0-73756
- pN $\rightarrow$ A<sup>0</sup>X, inclusive cross section, constituent-constituent multiple scatt. model for dependence on atomic number 0-83101
- $\pi$  condensation in neutron matter, N-N interaction, critical density 0-57711
- pN, 350 GeV in Ne, D<sup>+</sup> prod. cross section and lifetime 0-68494

**nucleon-nucleon scattering**

- see also neutron-proton scattering; nucleon-nucleon interactions; proton-proton scattering
- bounds on the moduli for scatt. amplitudes 0-86742
- dibaryon resonances in NN scatt. 0-57605
- many body problem in Lee model, NN scatt. and matter binding energy 0-63116
- spin dependence, quark exchange evidence 0-102074
- NN dynamics at medium energies, elastic and inelastic scatt., unitary model 0-63101
- NN dynamics at medium energies, phase parameters, one pion exchange model 0-63102
- NN forward scatt., two and three pion cut contribs., nucleon exchange model 0-63103
- NN large angle elastic scatt., spin-spin asymmetries and flavour depend., quark interchange 0-86743
- NN scattering in the nonrelativistic quark model, total elastic cross section (*Russian*) 0-68475
- pN, 2-15 GeV/c, in Ge, Si, influence of channelling on scattering 0-73729
- pN, 70, 125, 175 GeV/c in Be, C, Al, Cu, Sn, Pb nuclei 0-83128

**nucleon-nucleus reactions**

- for inelastic nucleon-nucleus scattering, see 'nucleon-nucleus scattering'
- see also neutron-nucleus reactions; nucleon-nucleon interactions; proton-nucleus reactions
- cross sections, Glauber theory and N-N inelasticity 0-68669
- total reaction cross sections, microscopic description 0-95318
- (N, N'), shower proton and meson transverse momenta, intranuclear cascade model 0-102185
- (N, X), disintegration by high energy nucleons,  $\alpha$ -prod. mechanism from pre-equilibrium fluctuations (*Russian*) 0-106059

**nucleon-nucleus scattering**

- see also neutron-nucleus scattering; nucleon-nucleon scattering; proton-nucleus scattering
- No entries

**nucleon scattering see hyperon-nucleon scattering; kaon-nucleon scattering; lepton-nucleon scattering; muon-nucleon scattering; neutrino-nucleon scattering; nucleon-nucleon scattering; nucleon-nucleus scattering; photon-nucleon scattering; pion-nucleon scattering**

**nucleons**

- see also neutrons; protons
- charge radii, parton model 0-91064
- decay, symmetry relations, effective Hamiltonian and inclusive decay rates, kinship hypothesis 0-78060
- EM mass shifts, asymptotic bounds and causality conditions 0-73704
- form factor, isovector, meson field theory, pseudoscalar  $\pi$ N interaction 0-62986
- form factors, weak, asymptotic behaviour within QCD dipole and triple-pole formulae 0-62987
- properties in relativistic quark model with strong binding 0-102023
- structure functions, overview of measurable types 0-73706
- N structure function model from hard consistent quark interactions, scaling violations 0-86719

**nucleosynthesis**

- cosmological and stellar nucleosynthesis, review 0-62359
- cosmological He and D abundances 0-62356

**nucleosynthesis continued**

- galactic chemical evolution rel. to stellar evolution and nucleosynthesis 0-67847  
 light element reactions in stars 0-101585  
 neutron stars, nonequilibrium shells, role in X-ray emission and nucleosynthesis, review 0-67774  
 NGC 7027, planetary nebula, evidence for CNO and  $3\alpha$  processing of nebular material 0-82459  
 nuclear astrophysics, introduction to form. and evolution of matter in Universe, book 0-105447  
 primordial He production within scale covariant cosmology 0-105412  
 probability games, modelling stellar evolution and fusion 0-77590  
 r-nuclei prod. sites in Galaxy 0-72932  
 s-process, difficulty with  $^{22}\text{Ne}$  as neutron source 0-72926  
 s-process nucleosynthesis, effects of unthermalised isomeric states and time-varying neutron flux on branching ratios 0-90410  
 s-process nucleosynthesis, neutron capture time scale from s-process Kr in meteorite 0-73080  
 supernovae,  $^{56}\text{Co}$  synthesis from light curves analytic solns. 0-77427  
 supernovae, Fe group elements prod. through e-process nucleosynthesis, relative abundances (*Russian*) 0-62167  
 Al isotopes, yield from C and Ne zones of massive star supernova 0-90406  
 $^{26}\text{Al}$  in stars, long lived nucl. isomeric states, thermalization 0-85846  
 $^{26}\text{Al}$ , synthesis in explosive H burning 0-85929  
 $^{27}\text{Al(p,n)}^{27}\text{Si}$ , cross sections and thermonuclear reaction rates 0-73852  
 Ar, galactic nucleosynthesis rel. to low Ar abundances in three halo planetary nebulae 0-82443  
 $^1\text{B}$ , neutrino-induced prod. in stellar C layer 0-82337  
 C shell burning to Fe core collapse, evolution of 15  $\text{M}_{\odot}$  star 0-72937  
 Fe, nucleosynthesis rel. to galactic cosmic ray Fe nuclei isotopic comp. 0-72729  
 H and He flashes in envelopes of accreting neutron stars 0-67772  
 Mg isotopes, yield from C and Ne zones of massive star supernova 0-90406  
 $^{24}\text{Mg}(\alpha,n)^{27}\text{Si}$ , cross sections and thermonuclear reaction rates 0-73852  
 $^{27}\text{Mg(p,n)}^{25}\text{Al}$ , cross sections and thermonuclear reaction rates 0-73852  
 Na in M13 red giants 0-82439  
 Ne explosive burning in supernovae isotope production 0-94780  
 $^{22}\text{Ne}$  and  $^{26}\text{Al}$  nucleosynthesis in novae and supernovae outbursts 0-62143  
 $^{56}\text{Ni}$ , nucleosynthesis in Type I supernovae rel. to radioactive excitation source model for late time spectra 0-105264  
 O, enrichment rate in Galaxy determ. from planetary nebulae O/H ratios age depend. 0-105328  
 Sc production in stars,  $^{42}\text{Ca(p,\gamma)}$  and  $^{44}\text{Ca(p,n)}$  reaction rates 0-82183  
 $^{28}\text{Si}(\alpha,n)^{31}\text{S}$ , cross sections and thermonuclear reaction rates 0-73852  
 $^{28}\text{Ti}$  production in star,  $^{42}\text{Ca}(\alpha,n)$  reaction rate 0-82183  
 $^{49}\text{Ti(p,\gamma)}$ , 0.74-3.25 MeV, cross section and thermonuclear reaction rates, nucleosynthesis, IAR effects 0-102187  
 $^{49}\text{Ti(p,n)}$ , 0.74-3.25 MeV, cross section and thermonuclear reaction rates, nucleosynthesis 0-102187

**nucleus**

- see also hypernuclei; nuclei with mass number 150 to 189; nuclei with mass number 190 to 219; nuclei with mass number 1 to 5; nuclei with mass number 20 to 38; nuclei with mass number 220 or higher; nuclei with mass number 39 to 58; nuclei with mass number 59 to 89; nuclei with mass number 6 to 19; nuclei with mass number 90 to 149  
 No entries

**numerical analysis**

- see also approximation theory; curve fitting; difference equations; error analysis; finite element analysis; function approximation; functional analysis; functional equations; interpolation; iterative methods; Monte Carlo methods  
 accelerating two-phase nozzle/diffuser flows, virtual mass effects on numerical stability 0-92204  
 air pollution, photochemical, potential form. in United Kingdom, numerical estimation method. 0-76682  
 air pollution episodes in Venetian region, real-time forecasting via advection-diffusion model 0-77096  
 air pollution episodes in Venetian region, real-time forecasting via Kalman predictor 0-82046  
 alloy melt, impurity conc. field model, growth by Czochralski method (*Russian*) 0-75191  
 alloy melt, temperature distribution during cryst. growth by Czochralski method (*Russian*) 0-75192  
 Archaean tectonism, numerical models of vertical tectonism in greenstone belts 0-81861  
 atmosphere, middle, numerical model of zonal mean circulation 0-109218  
 atmosphere, urban, numerical simulation of mixing depths 0-105024  
 atmosphere thermals, laboratory and numerical models rel. to self-similarity soln. 0-109228  
 atmospheric movements, spatial problem on influence of orography with Coriolis force included (*Russian*) 0-94565  
 atom + diatom, sudden approx. of Cross, computational tests, cross section factorisation, scatt. phenomena 0-58352  
 atomic resonant states, wavefunctions of complex coord. method 0-106282  
 auroral arcs global formation, numerical simulation 0-67446  
 binary alloys, two phase region calcs. in solidifying melt (*Russian*) 0-65195  
 ceramics, fracture-mirror boundary formation, criteria 0-70297  
 channel with blocked branch, laminar flow, nonregular domain transformation into rectangular domain 0-64635  
 closed-end cylindrical shell under line load along a generator, elastic anal. based on discrete element method and Vlasov eqns. 0-69675  
 coiled tubes, laminar flow and heat transfer, efficient numerical procedure 0-64633  
 compressible fluid flow through annular orifices, computer-aided numerical anal. 0-87806  
 computational methods in physics, computer appls. 0-62456  
 crack extension angle, influence of specimen's geometry 0-99965  
 crystal growth, cubic, from soln., numerical soln. 0-88074  
 crystal growth, cylindrical pores growth, numerical calcs. 0-92471  
 cylinder, hollow with internal circular crack, axially symmetric torsion determ., numerical results for boundary value anal. 0-64456  
 diatomic molecules, vibrational transitions dipole matrix elements, numerical calc. 0-95594  
 discharges in gases, pulsed, theoretical and expt. study 0-92416  
 duct flow development, step-by-step anal. for laminar flow 0-64634

**numerical analysis continued**

- Earth EM sounding, boundary conditions for EM field above two-dimensional inhomogeneous struct. 0-85595  
 elastico-viscous liquid flow in axisymmetric pipe of slowly varying cross-section 0-83774  
 elastoplasticity, 2-D, boundary element method, initial stress approach 0-74762  
 electrons, field-accelerated, in dry air and pure  $\text{O}_2$ , macroscopic props. comparison (*French*) 0-59161  
 EM remote sensing of inhomogeneities in ground 0-77165  
 fatigue results, numerical expressions (*Japanese*) 0-62455  
 FBR thermal hydraulics, sensitivity theory for general systems of nonlinear equations 0-86954  
 flexible structures, dynamic simulation by substructure synthesis 0-87733  
 fluid dynamics, viscoelastic boundary layer flow, second order, at stagnation point, heat transfer 0-103025  
 fracture analysis, 2D linear, elastic, finite element anal. vs. the edge function method 0-99963  
 fracture dynamics, in glass fibre reinforced plastics 0-100906  
 impacted solids, compression and shear wave propag., modelling 0-83755  
 inelastic deformation, stiff constitutive models, numerical integration 0-96208  
 ingots, cooling regime in conditions of minimal thermal stress, modelling (*Russian*) 0-65194  
 inner planets orbits, numerical integration rel. to motions of perihelia 0-67531  
 interactive teaching package 0-86058  
 interstellar clouds fragmentation, three-dimensional hydrodynamical calcs. 0-62236  
 interstellar contracting CO clouds, fragmentation 0-67838  
 interstellar nonrotating magnetic gas clouds collapse, numerical calcs. 0-105299  
 isothermal horizontal circular cylinder, laminar free convection, thick boundary layer 0-64566  
 Keplerian systems, numerical simulations of collisional evolution 0-109342  
 magnetic flexible disc/head interface interaction analysis 0-92093  
 materials testing, strip with semicircular notches, tensile load conditions at end, interf. effects obs. 0-64455  
 mechanical contact, cylindrical shell, liquid and gas, breakaway from solid lodgement (*Russian*) 0-87744  
 mechanical system, randomly loaded, crossing probabilities, numerical anal. (*German*) 0-96186  
 MHD, unsteady thermal boundary layer problem, numerical treatment 0-92227  
 mHD flow past a semi-infinite flat plate with heat transfer, exact numerical solns. of boundary layer similarity eqns. 0-83861  
 molecules resonant states, wavefunctions of complex coord. method 0-106282  
 MOS capacitor formed over p-on-n semiconductor structure, G-V characts. 0-100532  
 multimode optical fibres, impulse response calculations 0-74486  
 multiply-charged plasma, temp. kinetics and population levels (*Russian*) 0-106952  
 non-Newtonian flow of a liquid with an anisotropic viscosity tensor: internal analysis 0-83820  
 objective analysis technique, for three-dimensional urban-scale wind fields construction 0-101407  
 ocean, wind driven, new class of steady solns. to wind-driven ocean problem 0-85667  
 ocean deep-water channel flow, rotating hydraulics theory 0-94539  
 ocean solitary Rossby waves over variable relief, numerical expts. rel. to stability 0-101372  
 oceanic circulation around New Zealand, numerical model 0-72538  
 parabolic free boundary problem, numerical soln. via Newton's method 0-69632  
 particle size distribution of particles obtained by suspension polymerisation, eval. using Coulter Counter data 0-76564  
 PB-HTGR, control-rod induced flux perturbations, numerical anal. using out-of-object instrumentation (*German*) 0-83179  
 periodic object single sideband Fresnel diffr. pattern studies 0-106440  
 pipe, asymmetrically heated, turbulent transport and thermal diffusivities 0-64636  
 pollution modelling, numerical estimation of unknown parameters (*Japanese*) 0-89702  
 quantum three particle system, action-angle variables 0-95708  
 radiation transfer eqn. in spherical geometry, numerical soln. 0-90329  
 Reynolds equation at very low spacing, compressible, numerical soln., factored implicit scheme, mag. recording appl. 0-92183  
 SAW interdigital transducers, quasi-static anal. using Green's function method 0-69621  
 semi-infinite crack tips, practical evaluation of stress intensity factors 0-99962  
 solar central receiver system, flux density integral for reflected sunlight, numerical anal. 0-93863  
 solar heating of buildings, numerical simulation of thermal performance 0-66942  
 solar model, constant mass, differentially rotating gaseous polytropes configurations 0-82338  
 solid-state diffusion from a limited source 0-70444  
 soliton interaction dynamics and nontopological stability in nonlinear model of complex scalar field 0-101719  
 spent nuclear fuel storage, supercriticality through optimum moderation 0-57896  
 spiral galaxies, non-linear corrugation waves numerical computations 0-67859  
 steel, welded-joints,  $\text{H}_2$  induced cracking, S content effect 0-97562  
 steel welds, bead-on-plate,  $\text{H}_2$  diffusion and trapping 0-96697  
 superradiance, spatial variation with time, numerical anal. (*Russian*) 0-78821  
 synchrotron radiation, angular and spectral distrib., modified Bessel functions of fractional order 0-91738  
 T-junction laminar flow, partially elliptic flow numerical calcs., recirculation 0-64632  
 thermal convection in closed gas centrifuge, eigenvector soln. of linearised eqns. 0-83797  
 thermal imaging scanners, mirror rotation axis optimisation 0-86426  
 tridimensional numerical calc. of magnetic fields using summation method (*German*) 0-106414  
 tsunami, island of Hawaii, 1979 November 25, numerical anal. by finite-element method 0-72449



**numerical analysis continued**

- two-phase flow, semi-implicit two-fluid calculational methods 0-103066  
viscoplastic medium, flow between two noncoaxial circular cylinders under pure shear 0-99938  
VLF signals, numerical study of satellite reception using waveguide concepts 0-90282  
volume phase holograms, non-sinusoidal high order modes 0-102665  
wave propagation in inhomogeneous media, determ. of structure from plane wave reflection response, numerical approx. 0-73183  
wave propagation in inhomogeneous media, determ. of structure from plane wave reflection response, direct problem 0-77628  
waveguides, two parallel thin-film 0-106626  
weather forecasting, short-range, effect of subjectively enhancing initial vorticity field 0-82008  
CO<sub>2</sub> vibrational transitions dipole matrix elements, numerical calc. 0-95594  
H embrittlement, trap theory 0-89325  
He-Xe 3.51  $\mu$  laser mode competition in axial mag. field 0-63974  
N glow discharge, volt-ampere charact. in gas flow (*Russian*) 0-106991  
NaCl gas-droplet counterflow heat exchanger, numerical model (*French*) 0-61396

**numerical control**

see also digital control; machine tools

- Nd:glass laser with numerical programmed control (*Russian*) 0-91811

**numerical methods**

see also convergence of numerical methods; predictor-corrector methods  
acoustic radiation problem, Schenck numerical method (*French*) 0-69589  
acoustics, evaluation of singular integrals in interface separation, new quadrature formulae 0-74559

- aerodynamics, transonic axisymmetric flow past slender body of revolution, integral equation method 0-74910  
algorithm for calc. of impurity concentration from sheet resistivity and sheet Hall coefficient data 0-70246  
annular plates, nonsymmetric postbuckling behaviour, numerical analysis 0-102968  
Atmospheric Cloud Physics Laboratory simulation, vorticity transport eqn. solns. 0-94690  
beam structures, thermally induced vibrations and heat conduction problem, numerical method 0-64427  
blood flow through deforming tube, numerical soln. 0-104614  
conformal transformations combined with numerical techniques, with applications to coupled-bar problems 0-83538  
cracks, plane elasticity, curvilinear crack edges concentrated forces and edge dislocations, numerical soln. 0-58970  
cylindrical plasma filament under axisymmetric perturbation 0-106853  
dielectrics containing impurities, carrier distrib. and currents, numerical simulation (*French*) 0-70718  
differential equations, second order, without first derivatives, fourth-order numerical method 0-86107  
earthquake, theory of fault rupture propagation 0-104910  
effective implicit time integration in analysis of fluid-structure problems 0-92040  
elastic cylinder with inserts and holes, torsion problem, integral eqn. soln. method 0-106717  
elastic shells, thin, doubly curved, numerical integration of triangular finite element 0-92044  
elastic-plastic problems, supplementary strain method, appl. 0-96205  
EM field problems having irregular boundaries, direct noniterative numerical soln. using network analogues 0-95766  
EM waves diffraction at surfaces with inhomogeneous admittance 0-69296  
Eulerian method for numerical anal. of LMFBR HCDA fuel-coolant interaction 0-68733  
fins, nonlinear problems, 1-D conduction, initial value problem 0-83726  
fission reactor digital simulator software development, kinetic equations integration, numerical solution method 0-68901  
flow in curved tube, finite difference anal. method 0-106846  
fluid dynamics, 2-D two-phase flows of nucleating and wet steam, time-marching method 0-69906  
fluid dynamics, drop coagulation in cross-over pipe flows of wet steam 0-74982  
fluid dynamics, Navier-Stokes equations, finite element soln., applied to blood flow 0-94269  
fluid dynamics, viscous flows with no-slip walls, incompressible Navier-Stokes eqn., pseudospectral method 0-69924  
geometrical optics teaching to engineers, matrix algebra methods 0-62415  
heat transfer, fast nonstationary processes, characteristic method calcs. 0-83796  
heat transfer and evaporation from cooled surfaces, nonlinear eqns. numerical soln. (*German*) 0-58893  
hyperbolic systems, high-order methods, dynamic problems 0-68033  
impact of cylindrical shell on surface of compressible fluid (*Russian*) 0-87746  
impact of spherical shell on surface of compressible fluid (*Russian*) 0-87747  
jet flow, under gravity integral equation method of soln. 0-59093  
lakes, unsteady flow, numerical model validation 0-72559  
light beam focusing optimisation, in moving nonlinear media, using gradient method 0-106578  
matrix function approximate factorisation algorithm 0-68022  
MHD equations, nonzero div B, effect on numerical soln. 0-69939  
MHD laminar flow, longitudinal dynamic effects determination, appl. (*Rumanian*) 0-64792  
MOS structure concentration profile numerical evaluation (*Slovak*) 0-65690  
multilayer cylindrical parts, residual stresses determ. 0-96206  
Navier-Stokes eqns., rotational flow avoidance, solns. (*German*) 0-59057  
Navier-Stokes equations, two dimensional, numerical soln. methods (*Russian*) 0-101718  
nondissipative medium, boundary problem soln. with surface discontinuity (*Russian*) 0-101716  
nuclear reactor dynamics, numerical integration using real integrating factors 0-68730  
perturbative numerical methods, local and accumulated truncation methods 0-62536  
plasma MHD, toroidal axisymmetric config., vacuum potential energy change, spectral codes 0-87869  
Poiseuille flow, compound matrix method 0-57096  
sensitivity theory for general systems of nonlinear equations 0-86954

**numerical methods continued**

- single-step, anal. by approx. of exponential function 0-94950  
solid particle systems, high Reynolds numbers, mass transfer, Karman-Pohlhausen method 0-79378  
static field problems, numerical soln. algorithms 0-95757  
steady-state laminar flow in turbulence amplifier, integration (*Bulgarian*) 0-106779  
Stefan problem, one-dimens., modified variable time step method 0-102960  
stellarator, MHD equilibrium and stability of plasma in toroidal geometry, 3-D computer code 0-70041  
Stokes problem, second-order difference scheme 0-90678  
stress-strain state of rotating shell for random loading, net-point and orthogonal die methods (*Russian*) 0-90676  
subsonic flow, diverging, stability aspects, time-dependent method 0-74906  
summed progressing wave formalism for initial value problem calcs. 0-92039  
thermal conduction, nonstationary, in composite bodies, numerical simulation (*Russian*) 0-92016  
thermal problems, nonhomogeneous, and Stefan single-phase problem in arbitrary domains 0-79102  
turbulent friction factor, calc. by TI-57, binary-search method 0-83788  
weather forecasting, atmospheric prediction models, computing and numerical methods 0-77095  
Al billet, hot extrusion, nonsteady state temp. distrib., numerical method 0-60886

**numerical methods, convergence** see convergence of numerical methods**Nyquist noise** see thermal noise**occultations**

- SAO 158687 by Uranus ring system struct. from photoelec. obs. 0-77348  
Abell cluster, lunar occultation obs. at 327 MHz, survey 0-73052  
AGK +19°0599 65 Cybele, 1979 October 18, obs. using photoelectric photometer (*Chinese*) 0-105172  
Charon (1978 P 1), occultation on 1980 April 6 probable 0-67651  
Charon (1978 P 1), probable stellar occultation, 1980 April 6, min. dia. 0-62071  
Crab Nebula, lunar occultation obs. at decametre wavelengths 0-62248  
532 Herculina, satellite detect from occultation obs. 0-67629  
lunar, appl. of deconvolution method 0-105174  
lunar occultation of Venus 0-67605  
lunar occultations from University of Illinois Prairie Observatory (1977-1978) 0-105148  
lunar occultations of Hyades, photoelec. obs. 0-72921  
lunar occultations of OTL radio sources at 327 MHz, position and struct. determ. 0-73060  
lunar occultations of OTL radio sources at 327 MHz, position and struct. 0-73061  
lunar occultations of OTL radiosources, position and struct. determ. from 327 MHz obs. 0-73062  
lunar occultations of stars, diameter meas., photoelec. obs. 0-72920  
lunar occultations scans, object shape retrieval from new algorithm 0-105149  
Moon, marginal zone, absolute elevations from stellar occultations 0-62047  
Neptune, stellar occultation obs. (1980 August 21) 0-109395  
Neptune by Jupiter, 1613 January 4, prediction rel. to obs. by Galileo 0-105485  
Pioneer 10 and 11 by Jupiter and Saturn, radio signals spectral broadening by planetary ionospheres 0-109391  
Pioneer Venus occultation experiment, radio science data generation 0-67492  
TX Piscium, disc brightness distrib. and envelope obs. from lunar occultation meas. 0-67725  
planetary atmospheres, turbulence detect. from spacecraft radio signal occultation 0-94734  
Pluto, appulse on 1980 April 6, no occultation from S. England 0-67650  
Pluto, no occultation of star on 1980 April, 6 ephemeris 0-62070  
SAO 75392 by 78 Diana, 1980 September 4, predicted central path revision 0-101547  
satellite solar occultation experiment, appl. to remote sensing of middle atmospheric aerosol 0-109269  
Saturn, upper neutral atm. and ionosphere, vertical struct., Pioneer 11 radius occultation obs. 0-82293  
stellar occultation by Charon (1978 P 1) light curve obs. and implications 0-94754  
stellar occultation by minor planet satellites 0-94741  
stellar occultations by 216 Kleopatra, 1980 October 10 and November 21, implications of photometric meas. of dia. and shape 0-94743  
 $\gamma$  Tauri, ang. diameter determ. from lunar occultation obs. 0-62119  
Uranus and rings, obs. of stellar occultation, (1980 August 15 to 16) 0-98610  
Uranus occultation of SAO 158687, planetary radius and ellipticity determ. 0-67648  
Uranus stellar occultation, 1980 August 15 to 16, reality of additional occultations questioned 0-109396  
Venera 9 and 10 satellites by Venus, atmosphere sounding during radio occultation 0-101543  
Viking orbiters, radio occultation meas. of Mars atmosphere and topography and atmosphere 0-72836  
Voyager 2 occultation of Jupiter, ionosphere struct. from radio obs. 0-77337  
X-ray sources occultations by Moon, first and last dates (1980 to 1985) 0-77513

**ocean water** see seawater**ocean waves**

- acoustic propagation through internal waves, refractive index modulation, parabolic moment eqns. 0-83698  
Agulhas Current, long-wave disturbances due to topographically induced changes in coastal inertial jet 0-72545  
W. Bay of Bengal, wave characts. during southwest monsoon of 1978 0-109152  
boundary current flow along continental margin, lee waves assoc. with topographic irregularity 0-72539  
boundary-forced planetary waves, model mid-ocean response to strong current variability 0-72541  
breaking wave effects on power plant intakes (*Italian*) 0-109148  
buoy for measurement ocean waves 0-85772  
S. California, wave parameterisations rel. to beach changes statistical prediction 0-98305

## ocean waves continued

- coastal trapped waves at low latitudes in a stratified ocean 0-90097
- coastal-trapped waves in upwelling frontal zone 0-104975
- continental shelf waves, scattering by longshore bottom topography vars. 0-67376
- continental shelf waves (trapped), recent advances 0-98348
- equatorial waves, evidence for continuous wave spectrum in Indian Ocean 0-98331
- frequency spectra and wavenumbers meas. method by recorder array (*Russian*) 0-109266
- geostrophic fronts, bores, breaking and blocking waves 0-104967
- growth and decay of 80 m waves, radar obs. 0-98344
- Gulf Stream surface waves, radar obs. program 0-85679
- harbour water levels, wave setup 0-67377
- height and spectrum remote obs. by HF skywave radar technique 0-90241
- height distrib. of waves, nonlinearity and finite band width 0-76993
- HF radar Doppler spectrum, anal. for ocean surface currents mapping 0-94626
- high-amplitude waves, representation by stream function (*French*) 0-76986
- high-frequency internal waves, obs. at ocean station P (Oregon coast) 0-98330
- internal solitons in Andaman Sea, and interaction with surface waves 0-104994
- internal waves, with horiz. varying Brunt-Vaisala freq. (*Russian*) 0-104965
- island and harbour diff. of waves, integral formulation of Helmholtz eqn. 0-81919
- Kelvin waves in equatorial region, affecting currents 0-98337
- Knight Inlet, British Columbia, lee wave prod. from stratified flow interaction with sill 0-101368
- Laccadive Sea (Lakshadweep), wave characts. 0-109151
- long barotropic waves and storm surges, model of W. coast of Norway 0-81907
- long internal Rossby waves, nonlinear propag. 0-81896
- long-period gravity waves in ice-covered sea 0-67372
- measurement of short gravity waves from platform, using TV camera 0-98335
- meter for inshore wavemetering, with radiotransmission of data 0-101460
- model of ocean-atmos. interaction, in hamiltonian formalism (*Russian*) 0-104964
- near-surface inertial oscillations in current records 0-109157
- non-rigid bed, water wave attenuation 0-69851
- nonlinear baroclinic waves, exptl. study of instability and mode selection in large basin 0-85669
- nonlinear deep water gravity waves, random inhomogeneous field evolution 0-69857
- nonlinear internal wave interactions, Langevin techniques appl. 0-67371
- nonlinear waves, probabilistic description 0-76997
- nonlinearity of waves in presence of light wind (*Russian*) 0-109165
- North sea wave ht. during gale, prediction formulae 0-98346
- oil on sea surface, thermal radioemission spectral characts. 0-85686
- Onslow Bay, eastern USA, existence of continental shelf waves 0-72529
- Oregon continental shelf and slope, internal waves rel. to barotropic and baroclinic tides 0-72543
- Pacific Ocean, equatorial, propagating forced wave rel. to 14°C isotherm slope annual var. 0-72537
- NW-Pacific ocean continental shelf waves rel. to sea level low-freq. vars. 0-101415
- power spectrum obs. in open ocean with cloverleaf buoy 0-104976
- pressure on vertical walls (*Chinese*) 0-79342
- radar and Doppler effect, meas. of wave height, length and velocity, OREME project (*French*) 0-94625
- radar imaging of ocean surface, SAR method 0-77173
- radar monitoring, ground wave and sky wave sensing techniques 0-109256
- radar profilometry for wave height, airborne method 0-85771
- reflection of radar signal from sea surface, spatial intensity fluctuations 0-109170
- ripples on carrier waves, distrib. and steepness 0-72548
- Rosby wave form. from disturbances in non stationary barotropic flow (*Russian*) 0-104963
- Rosby wave interaction with zonal flow (*Russian*) 0-104982
- Rosby wave propagation, effect of bottom relief random inhomogeneity 0-85676
- Rosby waves, rel. to nonlinear energy and enstrophy transfers in realistically stratified ocean 0-101370
- rotating fluids, Rosby and Kelvin waves, open boundary conditions 0-61810
- sand transport due to near-bottom orbital motion 0-98306
- sea surface roughness, rel. to mean wind speeds and turbulence at coastal site and offshore location 0-98406
- sea surface slope distrib. function determ. from Sun glitter, accuracy (*Russian*) 0-94611
- self-focusing of waves on deep water surface (*Russian*) 0-94536
- shallow water wave, refr. in presence of current 0-85680
- shallow water waves in rot. basin, integral formulation 0-81920
- shoaling region, obs. of press. and vel. in 10 m-l m depth region 0-76994
- short gravity waves, phase speeds of upwind and downwind travelling waves 0-98332
- short gravity waves in finite depth waters, wave packet instability 0-81908
- short gravity-capillary waves modulation by longer-scale periodic flows 0-57106
- short-fetch wind waves, near-surface Lagrangian wind and current vectors 0-72553
- solitary Rossby waves over variable relief, stability, analytical theory 0-101371
- solitary Rossby waves over variable relief, stability, numerical expts. 0-101372
- solitary wave, diffraction by circular island in ocean, shallow-water theory (*French*) 0-83803
- sound scattering by large sea surface inhomogeneities, phase function shape in shadowing conditions (*Russian*) 0-94530
- stable baroclinic Rossby wave propag. through mean shear flow 0-81895
- steady rotating flow over topography, steady  $\beta$ -plane channel, quasi-linear theory 0-92159
- sunlight fluctuations spatial and temporal correlation 0-94533
- surface drift induced by wind and waves 0-81914

## ocean waves continued

- surface film temp. fluctuations due to waves thinning viscous layer 0-109158
  - surface waves, remote sensing using one and two freq. microwave techniques 0-94622
  - tidal-period internal waves in Indian Ocean equatorial zone 0-85677
  - tide waves in channel, bottom friction in perturbation method 0-98354
  - transient development of waves created against a vertical cliff 0-72530
  - trench waves theory of propag. and obs. off Japan and Chile 0-72547
  - tsunami, island of Hawaii, 1979 November 25, numerical anal. by finite-element method 0-72449
  - tsunami accompanying Tonankai earthquake of 1944, source model (*Japanese*) 0-67344
  - tsunami at Oshima (W.Hokkaido), 1741 August 29, religious monuments (*Japanese*) 0-67345
  - tsunami height rel. to earthquake mag., empirical relation 0-94461
  - tsunami prediction and magnitude, coastal radar system appl. 0-82101
  - tsunami wave generation by finite bottom displacement (*Russian*) 0-109113
  - tsunamis in Kanto, 1677 and 1703, behaviour along Kujukuri-hama coast from old monuments (*Japanese*) 0-67339
  - uniform depth ocean, energy transmission by surface waves through an opening 0-61811
  - wave crest height, distrib. of max. values 0-76999
  - whitecaps and sea state rel. to wind vel. and atmospheric surface layer stability 0-72554
  - wind generated capillary waves, spectral characts. 0-59059
  - wind wave phase velocity, laboratory expts. 0-98350
  - wind waves data, appl. to climatic comparisons of estimated and measured winds from ships 0-105020
  - wind-generated water waves, spatial correl. rel. to freq. independent phase vels. 0-98333
- oceanic crust**
- Adak Canyon region, central Aleutians, seismicity and tectonics 0-61772
  - SWAlaska, episodic accretion and plutonism 0-101346
  - central Aleutians, ocean bottom seismograph meas. 0-89978
  - Arabian Sea, acoustic vel. of sedimentary rock beneath fan 0-72488
  - Arctic Ocean Basin, form. by circum-Arctic plate accretion and Pacific plate fragments isolation 0-98294
  - NE Atlantic, upper crustal struct., seismic study 0-61784
  - equatorial Atlantic (7 to 10°N), fracture zones lithospheric struct. (*Russian*) 0-104932
  - Atlantic fracture zones in equator region, gravimetric model 0-72483
  - Atlantis II Deep, geothermal brine system 0-94526
  - back-arc basins, asymmetric spreading 0-85636
  - basins, Arctic and N.Atlantic, devel. connection with N.E. Asia plate tectonics 0-85637
  - bathymetry profiles, flattening by radiogenic heating in convecting mantle 0-85642
  - Bering Island, tectonic struct. of mountainous region 0-90045
  - Bering Sea, crustal heat flow and tectonic explanation 0-109123
  - Canary Islands, age and crustal struct. 0-67355
  - Caribbean seismic network, preliminary results 0-61771
  - Cretaceous mid-ocean ridge basalt (MORB), Nd and Sr isotopic comps. and rare earth element abundances 0-94520
  - Dellwood knolls, role in triple junction tectonics off northern Vancouver Island 0-90067
  - Djibouti Republic, magnetic anomaly map and tectonic interpretation 0-61753
  - Galapagos Islands, t. spreading centre jumps 0-104877
  - Galapagos Rift hydrothermal fields, struct. and morphology of seafloor 0-72489
  - Galapagos spreading centre, volcanic rock differentiation trends 0-104937
  - geomagnetic anomaly of spreading centre, modelling of reversal boundary 0-109098
  - Guaymas Basin spreading axis, high-temp. hydrothermal deposit 0-101355
  - Gulf of Kutch, geomorphology, sediment and tectonic instability origin 0-76960
  - Gulf of Papua, crustal struct. from seismic data 0-72459
  - heat flow through floor of Scotia, S.Atlantic and Weddell Seas 0-94491
  - Hess Rise, W.Pacific, volcanic rocks petrology 0-90026
  - Iceland, sea floor morphology and mag. anomalies N of Iceland 0-89953
  - Iceland area, obs. of sea floor morphology and struct. south and west of Iceland 0-90068
  - Iceland-Faeroe Ridge, crustal struct. 0-90016
  - Indian Ocean, seafloor spreading history 0-61790
  - SE Indian Ridge, seafloor mag. anomalies rel. to chem. of mid-ocean ridge basalt 0-109102
  - Indo-Australian plate, deformed oceanic crust rel. to plate internal deform. 0-109134
  - induced electrical currents below ocean bottom with vertical water flow 0-104863
  - Japan-Bonin trench, crustal and upper mantle changes 0-72466
  - Juan de Fuca ridge system, heat flow meas., water circulation 0-72468
  - Kane Fracture Zone of Atlantic, seismic study of crust struct. 0-104936
  - Kuril-Kamchatka trench, seismic study of crust 0-89982
  - Kurile trench-Hokkaido rise system, flexure profile by plate model 0-72482
  - lithosphere stress, from calcs. on Icelandic thermal area rock stress 0-90012
  - Lomonosov Ridge Experiment (Lorex 79) in Arctic Ocean 0-77120
  - magnetic polarity record questioned by Arizona reversal chronology 0-72419
  - marine magnetic anomalies origin, implications of palaeomagnetism of Thetford Mines ophiolites, Quebec 0-61757
  - Mid-Atlantic Ridge, geology of submarine hydrothermal field at 26°N latit. 0-85641
  - Mid-Atlantic Ridge, median valley model from gravity obs. 0-90071
  - Mid-Atlantic Ridge basalts, geochem. variation along length of ridge 0-90027
  - Mid-Cayman Rise spreading centre, basalt glasses geochemical var. and petrogenesis 0-101364
  - mid-ocean ridge basalt, composition restrictions, fluid dynamical model 0-90025
  - mid-ocean ridge spreading rate, petrological evidence 0-109135
  - mid-ocean ridge, existence of mantle double partial melt zone 0-104940
  - mid-ocean ridge basalts, source evolution from Bay of Islands ophiolite complex Nd and Sr isotopic study 0-85651
  - Nauru Basin, trace element abundances in basalts 0-94499



**oceanic crust continued**

- New Hebrides arc, tidal tilt from localized ocean loading 0-98211  
 New Hebrides arc-trench system, structure 0-72465  
 Okhotsk Sea deep basin, seismic study of crust 0-89982  
 ophiolite complex of Point Sal, California, seismic vel. struct. 0-109110  
 ophiolite complexes, evidence for past magnetism 0-109092  
 ophiolite petrogenesis in oceanic crust, Nd and Sr isotope study 0-61782  
 origin by gross modification of continental crust, seismic evidence 0-89997  
 orogenic lherzolite petrogenesis in oceanic crust, Nd and Sr isotope study 0-61782  
 Owen fracture zone, NW Indian Ocean, ultramafics petrology rel. to nature of oceanic upper mantle 0-94519  
 Pacific Ocean, box cores from Ontong-Java Plateau, radiometric obs. 0-61793  
 E.Pacific Rise, hot springs and geophysical expts. 0-101360  
 E.Pacific Rise, hydrothermal heat flux of black smoker vents 0-94488  
 E.Pacific Rise, sulphide deposits obs., near 21°N 0-101361  
 E.Pacific Rise geothermal system, physical limits on geothermal fluid temp. and role of adiabatic expansion 0-101362  
 Pacific sea-floor topography and isostatic compensation mechanism (Hawaii region) 0-104945  
 Reykjanes Ridge, crustal struct. from seismic refr. 0-90020  
 Reykjanes Ridge, new heat flow obs. 0-90011  
 Reykjanes Ridge, Profile I on E. flank, seismic struct., RRISP 0-90019  
 Reykjanes Ridge, SE.flank, lithosphere evolution, seismic surface wave study 0-90022  
 Reykjanes Ridge crest, morphology near 62°N 0-90070  
 Reykjanes Ridge crest studied by surface waves with an earthquake-pair technique 0-90021  
 Reykjanes Ridge Iceland Seismic Experiment (RRISP 77), for crust struct. 0-90017  
 Reykjanes Ridge south of 60°N, evolution between 40 and 12 Myr before present 0-90069  
 ridge crest hot springs, obs. and implications 0-98304  
 E.Sootia Sea, back-arc basin, volatiles in submarine volcanic rock 0-67353  
 sea-floor topography, tectonic model using vol. expansion coeff. 0-90072  
 sea-mount loads affecting crust, isostatic compensation and geoid anomalies 0-109132  
 seismic shear velocity struct., porosity and petrology 0-72473  
 seismic sounding of ocean crust, suppression of sea-floor multiples 0-90231  
 seismograph records, computer processing method 0-85605  
 silicic lithology of spreading ridge, late-magma vap. transport of K 0-81877  
 Sunda trench and forearc basin, seismic study 0-72470  
 tectonic plate subduction zone seismicity, Makran coast, Iran 0-85635  
 topographically driven subcritical hydrothermal convection 0-101345  
 Troodos ophiolite metamorphism, implications for marine mag. anomalies 0-81812  
 Walvis Ridge, compensation mechanism 0-94448  
 Watkins seamount, Pacific Ocean, Cretaceous origin, palaeomagnetic obs. 0-104874  
 Weddell Sea, geomagnetic, bathymetric and seismic obs. of crust 0-104929

**oceanographic equipment**

- see also oceanographic techniques; water pollution detection and control*  
 acoustic current meter for measuring mean current or flow (German) 0-77163  
 advanced instrumentation system, St. Croix, USVI 0-67427  
 air-dropped expendable bathythermographs, mesoscale oceanographic mapping 0-101457  
 amperometric membrane probes, modified, for free and total residual Cl determ. in saline cooling waters 0-82112  
 APODAS ocean profiling automatic data acquisition system (Japanese) 0-85769  
 buoy for data acquisition, using Meteostat data transmission (German) 0-90224  
 diver-operable multiwavelength spectroradiometer 0-90251  
 drift buoys, deployed by aircraft and satellite tracked, operational test 0-90242  
 HF radar system, for ocean surface currents mapping 0-94626  
 lift bag, salvage device for deep ocean 0-82107  
 magnetometer for ULF-ELF geomag. fluctuations 0-77152  
 microprocessor-based instrument for seawater characts. meas. 0-67440  
 microwave radars, one and two freq., appl. to sea surface remote sensing 0-94622  
 microwave remote sensing instruments, Seasat, history 0-94678  
 multichannel electrooptical turbidity meter 0-67423  
 photometer for deep-sea work, using acoustic telemetering 0-98460  
 radiocommunication buoy, antennas and operating freqs. (Russian) 0-109253  
 remote sensing of sea surface, instrument characts. in presence of basic noise (Russian) 0-109267  
 satellite remote sensing system, USA proposal (NOSS) for 1986 launch 0-105088  
 scatterometer, satellite- and aircraft-borne, optimization of characts. for investigating underlying surfaces 0-67436  
 Seasat radar altimeter, initial performance assessment 0-94679  
 SEASAT radar altimeter, resolution capability preliminary estimates 0-72645  
 Seasat radioaltimeter, sensor file algorithms 0-94680  
 Seasat scanning multichannel microwave radiometer, antenna pattern corrections 0-94683  
 Seasat scanning multichannel microwave radiometer, calibration algorithm development 0-94682  
 Seasat scanning multichannel microwave radiometer, description and performance 0-94681  
 Seasat scatterometer, evaluation 0-94684  
 Seasat scatterometer, scattering coeff. algorithm 0-94685  
 Seasat synthetic aperture radar system 0-94686  
 Seasat visible and IR radiometer 0-94687  
 seismograph observation system for ocean-bottom investigations (Japanese) 0-94615  
 submarine quantum irradiance and photoperiod meter, with digital recording 0-98474  
 submersibles for research work, remotely operated vehicles 0-82105  
 submersibles for underwater research, commercially available vessels 0-82104

**oceanographic equipment continued**

- thermistors, glass rod type dynamic response 0-90243  
 turbid water, instrument of meas. light absorpt. coeff. 0-82076  
 wavemeter for inshore zone, with radiotransmission of data 0-101460  
 γ-ray field of seawater, meas. method (Russian) 0-109268
- oceanographic techniques**  
*see also oceanographic equipment; water pollution detection and control*  
 acoustic sounding of ocean-bottom subsurface layered media, spatial parameter estimation 0-77134  
 chlorophyll a analysis, using aircraft multispectral scanners 0-77164  
 climatology, hydrology, atmospheric research and meteorology from space, conference, Ajaccio, Corsica (1979 November 12 to 16) 0-62397  
 coastal radar system appl. to tsunami prediction and magnitude 0-82101  
 crustal seismograph records, computer processing method 0-85605  
 current determination by beta spiral method, vertical mixing effect 0-98459  
 current determination by obs. of induced EM fields, theory 0-61805  
 current pattern determination by aerial photography of markers 0-98483  
 data processing and analysis, in oceanographic research 0-94605  
 depth measurement using airborne pulsed Ne laser system 0-61908  
 diving physiology research facility 0-82106  
 drift buoys, deployed by aircraft and satellite tracked, operational test 0-90242  
 fluctuating current meas. by acoustic current meter (German) 0-77163  
 Gulf Stream surface waves, radar obs. program 0-85679  
 ice, dielectric relax. meas. by blocking layer method 0-103914  
 information collection, processing and anal., automation on small-computer base 0-101439  
 irradiance attenuation coefficient in a stratified ocean, meas. technique 0-98325  
 Langevin techniques for describing nonlinear internal wave interactions 0-67371  
 microwave remote sensing technology for marine oil pollution surveillance (Japanese) 0-76685  
 phytoplankton remote sensing from satellite, atm. optical props. 0-77105  
 radiocarbon dating of sediments by benzene variant method aboard ships 0-85770  
 remote sensing, appls. to oceanography and sea ice 0-77176  
 salinity in-situ measurement, Practical Salinity Scale 1978 0-67419  
 salinity measurement, elec. cond. obs., temp. and conc. depend. 0-67421  
 salinity of standard seawater, elec. cond. compared to KCl soln. 0-67420  
 salinity of standard seawater, elec. cond. obs. 0-72647  
 salinity of standard seawater, elec.cond./salinity/temp. relations 0-67422  
 sea ice age category differentiation through location and temp. observations using microwaves 0-67380  
 sea state radar monitoring, ground wave and sky wave sensing techniques 0-109256  
 sea surface inhomogeneities sensing via sound scatt., phase function shape in shadowing conditions (Russian) 0-94530  
 sea surface slope distrib. function determ. from Sun glitter, accuracy (Russian) 0-94611  
 sea surface waves, remote sensing using one and two freq. microwave techniques 0-94622  
 seawater, elec. cond. and salinity, temp. and press. depend. obs. 0-67368  
 seawater electrical conductivity compared to KCl standard solution, salinity scales 0-72646  
 sediment, <sup>230</sup>Th age, α-scintillation counting method 0-72636  
 statistical prediction, appl. to beach changes in S.California 0-98305  
 submarine sediments, automatic recognition by sonoprobe survey, acoustic reflection pattern model (Japanese) 0-85776  
 sulphate determ. in seawater, indirect anal. by atomic absorpt. 0-89556  
 surface currents mapping, HF radar system appl. 0-94626  
 surface parameters, retrieval from scanning multichannel microwave radiometer obs. 0-90261  
 surface temperature measurements, derivation from Meteostat image data 0-76985  
 surface UV reflectance meas. from airborne platform, techniques and instrumentation 0-98453  
 thermoanemometry, appl. to currents meas. on Baltic Sea coast (German) 0-101373  
 tidal currents, meas. by two-site HF Doppler radar system by using two-site HF 0-72533  
 turbulence meas. near seabed, digitisation and record length selection 0-104971  
 vertical eddy viscosity coeff. determ. method comparison 0-98326  
 water waves, wind-generated, spatial correls. rel. to freq. independent phase vels. 0-98333  
 wave frequency spectra and wavenumbers meas. method by recorder array (Russian) 0-109266  
 wave height measurement by radar, airborne method 0-85771  
 wave measurement with spar buoy 0-85772  
 wave phase velocity measurement method, TV meas. of refl. sky radiance 0-98335  
 wave structure, radar imaging method using SAR 0-77173  
 waves, HF skywave radar technique for height and spectrum 0-90241  
 C<sub>2</sub> determination method for marine sediments 0-104543  
<sup>137</sup>Cs/<sup>134</sup>Cs radioisotopes in seawater, Cs-selective resin determ. 0-94137  
 Se (-II,0), -(IV) and -(VI) composition of water, by gas chromatography method 0-81928

**oceanography**

- see also ocean waves; seawater; sediments; tides*  
 abyssal fan sediment in Arabian Sea, acoustic velocity 0-72488  
 accelerating flow horizontal divergence, turning vorticity eqn. anal. 0-77013  
 acoustic reflectivity of sea-floor 0-98302  
 acoustic subbottom data analysis through simulation, theoretical vertical and lateral model 0-74571  
 acoustics, two-point coherence function models with inhomogeneous background and anisotropy 0-81922  
 Agulhas Current, topographically induced changes in struct. of inertial coastal jet 0-72545  
 air-sea exchange of heat and water, model 0-61809  
 air-sea interaction, mean wind speeds and turbulence at coastal site and offshore location 0-98406  
 air-sea sensible and latent heat transfer coeffs., meas. 200 km from land 0-72552  
 ancient ocean composition, <sup>87</sup>Sr/<sup>86</sup>Sr, Jurassic to Pleistocene, Israel groundwater obs. 0-61804  
 Arabian Sea cooling, heat budget, feedback with atm. circulation 0-104979

## oceanography continued

- Arabian Sea near Persian Gulf inlet, vert. thermohaline struct. fluctuation 0-76991
- Arctic Alaska coast, fast ice, crystal c-axis alignment 0-67375
- Arctic ice cover, attenuation of 8 and 20 cm EM waves 0-67379
- Arctic Ocean, sea ice decay following CO<sub>2</sub>-induced atmospheric temp. rise 0-61802
- Arctic seas, surge level oscills. in shelf zones 0-77012
- Atlantic, <sup>14</sup>C pollution from nucl. weapons tests 0-89683
- NW Atlantic, acoustic transmission over long distance 0-90091
- N Atlantic, active layer thermal struct., synoptical variability (*Russian*) 0-109169
- N Atlantic, conditions in Jasin observation area (*Russian*) 0-109167
- N Atlantic, current heat transport across 25°N latitude 0-94537
- N Atlantic, deep water formation during last ice age 0-94535
- Atlantic, equatorial undercurrent at 30°W, seasonal variation 0-90090
- S Atlantic, glacial and interglacial oceanographic conditions from CaCO<sub>3</sub> and radiolarian distrib. 0-72556
- NW Atlantic, main pycnocline potential energy, dynamic height and salinity 0-85672
- N Atlantic, Mesozoic and Cainozoic, calcareous sediments depth distrib. 0-81866
- N Atlantic, midocean geostrophic vorticity balance 0-90096
- N Atlantic, mixing in Bermuda, Sargasso and Gulf Stream regions 0-98343
- NW Atlantic, Mn micronodule morphology and chemistry 0-81869
- N Atlantic, sea surface temp. year to year changes, (1948 to 1974) 0-67367
- Atlantic, temp. microstruct. obs. in equator region 0-98340
- N Atlantic, wind stress affecting large scale density struct. (*Russian*) 0-76989
- S. Mid-Atlantic Bight, LF current var. 0-81909
- Atlantic coastline, behaviour in Landes and Basque regions (*French*) 0-76987
- N Atlantic mid-depth circulation, Mediterranean contrib. to Norwegian-Greenland Sea 0-81899
- Atlantic nuclear waste disposal site, radionuclide redistrib. 0-85309
- N Atlantic Ocean, deep western boundary current core, <sup>3</sup>H conc. obs. 0-101380
- N Atlantic Ocean, tropical, atmospheric aerosols water-soluble K, Ca and Mg contents 0-72598
- N Atlantic rel. to Antarctic glaciation and eutrophication 0-61812
- E. equatorial Atlantic sediments, pore water metal concs. 0-101358
- E. equatorial Atlantic sediments, pore water metals concs. 0-101358
- N Atlantic subtropical gyre, beta spiral 0-101367
- Atlantis II Deep, geothermal brine system 0-94526
- atmosphere-ocean system models, max. attainable forecasting accuracy 0-82036
- E. Australian Current, evidence for flow separation 0-109160
- SE Baltic coast transit section, suspended load composition in calm and storm (*Russian*) 0-67360
- Baltic Sea, estuary region, suspension distrib. under river drifts influence (*Russian*) 0-98345
- Baltic Sea coast, currents meas. via thermoanemometry (*German*) 0-101373
- Baltic Sea coast sedimentary material differentiation (*Russian*) 0-104951
- Baltimore Canyon, submarine mass-wasting of sediments 0-101354
- Barents Sea, EM field of electrical currents in sea bottom and shore 0-104864
- baroclinic ocean dynamics, asymptotic state (*Russian*) 0-94531
- barotropic vorticity equation, new class of steady solns. 0-85667
- Bay of Bengal, tropical cyclone generated surges, numerical model 0-81923
- W. Bay of Bengal, wave characts. during southwest monsoon of 1978 0-109152
- beach changes in S. California, statistical prediction 0-98305
- Beaufort Sea, August ice cover vars. rel. to mesoscale weather conditions 0-101366
- Bellingham Bay, Washington, Hg loss rate from contaminated estuarine sediments 0-85310
- S. Benguela Current, upwelling site, wind effects and biology 0-104987
- Benguela upwelling system off N. Namibia, late Miocene origin, sediment evidence 0-104993
- benthic fauna Ca CO<sub>3</sub> shells in hydrothermal area, O isotope study 0-109173
- benthic ocean, flow structs. 0-72532
- Blake-Bahama Outer Ridge, bottom boundary layer, speed and temp. obs. 0-101374
- blast wave propagation in stratified ocean, theory (*Russian*) 0-81904
- Bombay coast region, water pollution physicochemical studies 0-104522
- bottom relief, random inhomogeneities, effect on Rossby wave propag. 0-85676
- boundary current flow along continental margin, effect of localised topographic irregularity 0-72539
- boundary-forced planetary waves, model mid-ocean response to strong current variability 0-72541
- Bristol Channel, tidal regime by numerical model 0-85670
- Bristol Channel tides, analytical wedge model 0-85671
- S California Bight, inshore circulation (1974-1977) 0-98327
- California coast, warm water patches rel. to marine fog and fog-stratus systems form. 0-77060
- California Current, nutrient upwelling, satellite thermal imagery and chem. anal. 0-101379
- California Current System 0-72555
- E. Canadian Arctic, sea ice meltwater, isotope study 0-77002
- Cariaco Trench, seawater temp. salinity and chemistry 0-98359
- NW Caribbean, methane content of deep water indicating seepage 0-81924
- E. Caribbean, deep water silicate content distrib. 0-76984
- chemical composition of surface microlayer (*Russian*) 0-104998
- chemistry, role of ridge crest hot springs 0-98304
- Chesapeake Bay sediment, time depend. transport, temp. and chloride obs. 0-81863
- chlorophyll gradient maps from U-2 aircraft platform over Pacific and Atlantic 0-101385
- circulation due to zonal wind stress, spin-up of stratified ocean 0-81900
- cliff waves, transient development of waves created against a vertical cliff 0-72530
- climatic effects of oceans, feedback effects rel. to quasi-cycles in meteorology 0-109239

## oceanography continued

- coastal circulation and wind-induced currents, review, book contrib. 0-98357
- Cochin backwaters, industrial pollution, impact on water quality and hydrographic features 0-76668
- cold skin layer, heat transfer through surface (*Russian*) 0-104985
- computer model for generating World ocean sound velocity profile 0-87624
- conference, on climatology, hydrology, atmospheric research and meteorology from space, Ajaccio, Corsica (1979 November 12 to 16) 0-62397
- connected basin natural oscillation, theory 0-61806
- continental shelf circulation, effects of buoyancy flux 0-72540
- continental shelf currents of Pacific NW, use of spin-up model 0-98338
- continental shelf wave on boundary current, model 0-77072
- coral reef epifauna, susceptibility to UV irradi. 0-98037
- Cretaceous plankton species extinction due to comet impact 0-76977
- Cretaceous-Tertiary boundary, plankton extinction and geochem. indicating extraterrestrial event 0-76976
- current determination by beta spiral method, vertical mixing effect 0-98459
- current flow theory, three-dimens. case 0-104990
- current flow theory, three-dimens. case 0-104991
- current flowing over continental shelf edge, shear layers 0-81903
- current large scale stability, deep layer and bottom topography influence 0-77004
- current pattern determination by aerial photography of markers 0-98483
- current tracer float trajectories, kinematic model 0-85682
- currents, idealised, mixed instability parameter obs. 0-98329
- currents, wind driven in deep water inshore region 0-81925
- deep sea disturbance due to surface storm, persistent nature (*Russian*) 0-81921
- deep sea mixing models, vertical and isopycnal mixing 0-76992
- deep-water channel flow, rotating hydraulics theory 0-94539
- Denmark Strait, temp. gradient microstruct., 1973 obs. 0-77003
- Denmark Strait overflow, contrib. to deep N. Atlantic 0-85665
- Drake Passage, temp. and flow spatial scales 0-101376
- drift buoys, deployed by aircraft and satellite tracked, operational test 0-90242
- dynamics of upper ocean, equilib. Langmuir circulation model 0-101381
- earthquake wave propag. along seafloor, theory 0-81843
- East Australian Current, surface jet, undercurrents and low Richardson number obs. 0-104978
- Ekman layer, exchange of momentum, estimation methods 0-98326
- El Nino 1976, sea surface topography response 0-81913
- EM fields induced by synoptic currents, theory 0-61805
- EM induction in ocean, Sq-induced current around land mass 0-72413
- EM induction of oceans affecting Sq field variations in IGY 0-72428
- energy sources and their exploitation 0-89588
- equatorial current generation 0-67374
- equatorial current system, non-linear theory 0-104988
- equatorial current system, non-linear theory 0-104989
- equatorial undercurrent, dynamics 0-72558
- equatorial undercurrent of Atlantic, near-surface layer changes 0-81901
- estuaries, hydrodynamic model using smooth elements, accuracy 0-98356
- estuaries of variable breadth and depth tidally induced residual currents 0-72544
- estuarine environment, natural suspended matter flocculation and electrokinetic pot. (*French*) 0-61817
- estuary, spread of river jet, models 0-98353
- estuary, well mixed, buoyancy effects on longitudinal dispersion 0-85681
- estuary circulation (partially mixed), two-dimens. model 0-109161
- estuary sediment containing lead pollution, rel. to flood control measures, California 0-76670
- explosive acoustic waves, empirical and theoretical laws comparison (*Russian*) 0-109150
- flood basalt isotopic abundances of Nd and Sr, Earth struct. models 0-72475
- E. Florida coast, Gulf Stream boundary eddies 0-85673
- Florida Current transport, fluctuations at periods between tidal and two weeks 0-72551
- formaldehyde, in marine air and rainwater, wet season obs. 0-85703
- fresh water and heat flux determ. from atm. obs. 0-104986
- frontogenesis of upper ocean, scalar redistribution 0-104992
- Galapagos Rift hydrothermal fields, struct. and morphology of seafloor 0-72489
- geomagnetic coast effect, review 0-94458
- geomagnetic variations causing water motion, theory 0-104962
- geostrophic flow over shallow topography 0-90120
- German Bight, airborne and ground data, Geoscientific Airborne Remote Sensing Programme (*German*) 0-67412
- E. Greenland Polar Front, submarine transects 0-85662
- Guaymas Basin, <sup>3</sup>He meas. rel. to mantle volatiles injections in Gulf of California 0-85640
- Gulf of Cadiz, Mediterranean outflow, vel. shear in deep steps 0-85663
- Gulf of California, upwelling rel. to <sup>32</sup>Si supply and radioactive half life determ. 0-91153
- Gulf of Mexico, Loop Current, laboratory simulation expts. 0-77006
- Gulf of St. Lawrence, buoyancy driven current system, mixing and circulation 0-90095
- Gulf Stream, anticyclonic eddy obs. in slope water aboard CGC Evergreen 0-72546
- Gulf Stream, propag. and evolution of cyclonic rings 0-81911
- Gulf Stream and the north east Atlantic temperature anomaly (*German*) 0-85684
- Gulf Stream anticyclonic eddy, energy in eddy 0-85683
- Gulf Stream branching region, current obs. 0-98339
- Gulf stream frontal zone thermohaline struct., comparison with Kuroshio 0-85678
- Gulf Stream position changes rel. to atmos. press. fields 0-98352
- Gulf Stream ring trajectories, obs. in 1976-8 period 0-98342
- N. hemisphere, sea surface temps. assoc. with poor summers in British Isles 0-109241
- hydrodynamic sea model, 3-D, variable vertical eddy viscosity, finite element anal. 0-85661
- Iceland-Faroe Ridge, eddies and meanders rel. to polar front 0-81898
- W Indian Ocean, 1975-1976 equatorial current obs. 0-104974
- N. Indian Ocean, dissolved petroleum content 0-98361
- Indian Ocean, evidence for continuous spectrum of equatorial waves 0-98331
- Indian Ocean, modern and ice-age surface water zonal temp. anomaly maps 0-77007



oceanography continued

Indian Ocean, MUSSON-77 expt. results 0-81926  
Indian Ocean, surface temp. rel. to Indian summer monsoon intensity 0-90121  
Indonesia, palaeobathymetry from sedimentology of Nias Island Neogene trench-slope deposits 0-104950  
internal solitary waves in stratified flows, cubic and quadratic nonlinearity 0-69856  
internal waves, high-frequency, obs. at ocean station P (Oregon coast) 0-98330  
irradiance attenuation coefficient in a stratified ocean, meas. technique 0-98325  
Kuroshio current, anomalous cyclonic meander (winter of 1978) 0-109171  
Kuroshio current, Izu Ridge bottom effect on current dynamics 0-90099  
Kuroshio current frontal zone thermohaline struct., comparison with Gulf Stream 0-85678  
Labrador Current, direct vel. obs. 0-101378  
Laccadive Sea, chemical oceanography 0-104995  
Laccadive Sea, trace metals concs. 0-104997  
Laccadive Sea (Lakshadweep), physical characts. 0-104966  
Laccadive Sea (Lakshadweep), wave characts. 0-109151  
Laccadive Sea waters, total Hg concs. 0-104996  
Lagrangian current vectors very close to short-fetch windswept sea surface 0-72553  
S.Lesser Antilles, mesoscale circulation 0-90094  
Ligurian continental shelf, and current autumnal data series anal. 0-85675  
Lomonosov Ridge Experiment (Lorex 79) in Arctic Ocean 0-77120  
longshore currents in Gulf of Mexico, due to hurricanes Anita and Babe 0-76998  
longshore movement of water, Texas gulf coast 0-76995  
longshore pressure gradients caused by offshore wind 0-67370  
longshore sediment transport by tidal current, outside surf zone 0-76961  
Marion Island, former sea levels in S.Atlantic 0-77008  
Marshall Island, nucl. test site <sup>137</sup>Cd, in marine organisms and sediment 0-109174  
Mediterranean circulation, var. due to river diversion 0-77014  
Mediterranean circulation in Sicily and Sardinian straits region 0-72527  
Mediterranean outflow, vel. shear in deep steps 0-85663  
E.Mediterranean sediments, heavy metal content, off Lebanon coast 0-769830  
Messina Strait, tidal currents 0-81917  
Messina Strait, tidal currents 0-81918  
meteorological tide, energy transfer from atmos. to ocean (Russian) 0-76988  
microwave brightness temp. distrib. over Bay of Bengal using SAMIR Satellite Microwave Radiometer data at 19 and 22 GHz 0-104980  
mixed layer, temp. gradient struct. and Batchelor spectrum 0-77000  
mixed layer evolution, laboratory investigation in homogeneous fluid (Russian) 0-94529  
mixing at oceanic front interface, interleaving process accompanying density difference 0-72525  
mixing mechanism in upper ocean, Langmuir circulation instability 0-104970  
Narara Bet, Gulf of Kutch, coastal currents, temp. and salinity 0-76990  
near-surface inertial oscillations in current records 0-109157  
New Zealand region, oceanic circulation numerical model 0-72538  
North Sea, circulation driven by wind, Norwegian Trench influence 0-98355  
North Sea, M<sub>2</sub> tidal elevations and currents, hydrodynamic model 0-104973  
North Sea, sea surface temp. year to year changes, (1948 to 1974) 0-67367  
North Sea surface topography, SeaSat-1 expt. geodetic aspects (German) 0-81805  
W.Norway coast, long barotropic waves and storm surges, model 0-81907  
Norwegian Current low freq. fluctuations, horizontal wavelength and energy interaction terms 0-101375  
oil film pollution, retardation of O<sub>2</sub> exchange with atmos. 0-109175  
old Mangalore port, India, channel siltation study 0-77005  
optical fields, constructed using probability theory (Russian) 0-109164  
origin of the oceans (Russian) 0-81857  
equatorial Pacific, 1976 El Nino, sea surface topography response 0-81913  
Pacific, bottom boundary layer currents, E. tropical region 0-109154  
N.Pacific, dissolved Ca and alkalinity distribs 0-90100  
NE.Pacific, Mn distrib. 0-101384  
NE.Pacific, ocean surface heat loss in cyclone regions 0-77009  
N.Pacific, sea surface temp. anomaly gradient rel. to mid-tropospheric circulation 0-85674  
NW.Pacific, surface temp. fronts variability, satellite obs. 0-90092  
N.Pacific, trace metal vertical profiles 0-67381  
N.Pacific Central environment at 35°N, phys. chem., biological characts. 0-76983  
Pacific N. Equatorial Countercurrent, Sverdrup transports 0-67369  
Pacific Ocean, annual var. in slope of 14°C isotherm along equator 0-72537  
Pacific Ocean, barotropic and baroclinic tides over continental slope and shelf off Oregon 0-72543  
Pacific Ocean, December sea surface temps. correl. with spring rains in California 0-77064  
Pacific Ocean, equatorial, temp. fine struct. obs. 0-98336  
NW.Pacific Ocean, relation between atmospheric press. and sea level 0-101415  
E.Pacific Ocean, tropical, N<sub>2</sub>O meas. in sea water and marine air 0-94542  
E.Pacific Rise, hydrothermal heat flux of black smoker vents 0-94488  
Pacific sea-floor topography and isostatic compensation mechanism (Hawaii region) 0-104945  
E. equatorial Pacific sediments, pore water nutrients and carbonate 0-101357  
Par River estuary, India, pollution transport and abatement methods 0-104521  
Persian Gulf and approaches, oil pollution, 1978 obs. 0-105000  
Peru-Chile undercurrent, southernmost extension 0-85664  
Peruvian upwelling system near 15°S, circulation 0-101377  
plastic debris floating in Mediterranean 0-104999  
poleward heat flux, by ocean gyre 0-85668

oceanography continued

pollutant dispersal and deposition, Th isotope analogue expts. to simulate coast region 0-81927  
quasi-isothermic layer and thermocline, model of active ocean layer (Russian) 0-109163  
Ross Ice Shelf (Antarctica), basal freezing, confirmed by core drilling 0-101393  
Rossby wave interaction with zonal flow (Russian) 0-104982  
rotating stratified fluid, parallel shear flow, baroclinic and barotropic instability 0-98328  
Sargasso Sea, optical props. of seawater (Russian) 0-94532  
Sargasso Sea, POLYMODE area, O<sub>2</sub> conc. rel. to eddy dynamics 0-85685  
Sargasso Sea, surface height vars. from Geos-3 altimetry obs. 0-104969  
Sargasso Sea, surface mixing layers 0-81906  
Scotian shelf (N.Atlantic Ocean), wind-induced, sea level changes 0-72531  
sea ice, Danish studies using Landsat and airborne sensor data 0-94527  
sea ice and glacial development in Late Cainozoic N.Hemisphere 0-90098  
sea ice underside, geometrical roughness props. 0-98334  
sea level, Pleistocene, record in S.Australian beach ridges rel. to Milankovitch theory of ice ages 0-98307  
sea level changes of N.Sea (1780-1980), German Bight 0-90089  
sea level transients, obs. by Geos 3 coincident orbits 0-72535  
sea level variations around British Isles, (1960-1975), multiple regression anal. 0-109149  
sea model, 3-D numerical, Galerkin method with polynomial basis set 0-72524  
Sea of Marmara sediment evidence for Late Quaternary water exchange 0-81916  
sea salt aerosol, atmospheric temp. sensors contamination 0-82095  
sea-floor topography, tectonic model using vol. expansion coeff. 0-90072  
sea-level lowering during Illinoian glaciation, Bahama 'blue hole' 0-72557  
sediment <sup>230</sup>Th dating technique, by  $\alpha$ -scintillation counting 0-72636  
sediment climate record, diatomaceous sediments of Gulf of California 0-98351  
sediment heat flow, equatorial Indian Ocean 0-76958  
sediment mixing and accumulation, near-shore, fallout radionuclide tracer obs. 0-81864  
sediment O<sub>2</sub> penetration at coastal site 0-104952  
sediment of continental shelf, anomalous declination due to slumping 0-76964  
sediment-water chem. exchange traced by <sup>222</sup>Rn obs. 0-101386  
sediments of deep-sea, <sup>14</sup>C age and vertical mixing 0-81865  
seismic T waves from Tonga earthquake (June 1977), human perception on Tahiti 0-61769  
Severn estuary, seasonal and spring neap tidal depend. of axial dispersion coeffs. 0-94534  
shallow sea, drift-gradient current vertical structure, model 0-77010  
solitary Rossby waves over variable relief, stability, analytical theory 0-101371  
solitary Rossby waves over variable relief, stability, numerical expts. 0-101372  
sound, spatial noise spectrum meas. in ocean for small observation baseline 0-102902  
sound refraction by sediments, for sonar studies 0-81902  
sound scattering by large sea surface inhomogeneities, phase function shape in shadowing conditions (Russian) 0-94530  
Southern Ocean, meso-scale dynamics 0-94525  
St Kilda shelf, tidal regime, press. gradient obs. 0-85666  
St. Lawrence estuary, tidally-generated residual motion 0-94541  
stratified ocean, nonlinear energy and enstrophy transfers 0-101370  
stratified ocean under stationary tropical cyclone, energetics (Russian) 0-61808  
stratified turbulent upper mixed layer, struct. determ. 0-104972  
submarine quantum irradiance and photoperiod, digital recording using self-contained instrument 0-98474  
subtropical front zone N. of Hawaii, wintertime circulation 0-109155  
sunlight fluctuations spatial and temporal correlation 0-94533  
surface, turbulent Ekman layer evolution 0-76996  
surface buoyancy flux anomalies, geostrophic eddy generation 0-81912  
surface currents due to atmos. disturbances of large-scale 0-109159  
surface currents mapping, HF radar system appl. 0-94626  
surface drift induced by wind and waves 0-81914  
surface film temp. fluctuations due to waves thinning viscous layer 0-109158  
surface heat loss in cyclone regions 0-77009  
surface mixed layer, calc. of temp. discontinuity layer bedding (Russian) 0-109166  
surface mixed layer, turbulent energy budget 0-72526  
surface seasonal temp. var. and mixed layer thickness 0-77011  
surface temp. relation to thermocline structure 0-98347  
surface temperature, isotope selective CO<sub>2</sub> interchange affecting trees rings 0-61814  
surface temperature measurements, derivation from Meteosat image data 0-76985  
surface temperature var., effect on atm. general circulation model 0-90122  
surface UV reflectance, meas. from airborne platform 0-98453  
surfactants affecting temp. of skin-layer, for oil slick studies (Russian) 0-109172  
symmetric instability of stratified geostrophic flow 0-98425  
synoptic eddies, numerical model (Russian) 0-81905  
synoptic variation of current and density fields, non-linear model (Russian) 0-104984  
synoptical disturbance in baroclinic ocean, two-layer model (Russian) 0-109162  
synoptical eddies, of the POLYMODE program (Russian) 0-104981  
Tasman Sea, biological productivity of warm-core eddy 0-61816  
temperature fluctuations, small-scale, in upper ocean layer, statistical regularities (Russian) 0-94528  
temperature gradient spectra in vertical direction, scaling theory 0-77001  
temperature-salinity curve, relation to global heat transport and atmospheric water transports 0-72534  
thermocline, small-scale turbulence (Russian) 0-61807  
thermocline disturbance evolution, theory (Russian) 0-104983  
thermocline response to transient atmos. forcing, N.Pacific (1976-8) 0-109156  
thermocline structure, non-stationary two-parameter model 0-101382



**oceanography continued**

- tide-generating currents, oscillating, three-dimensional structure 0-72542  
 trench waves theory of propag. and obs. off Japan and Chile 0-72547  
 tropical ocean and atmosphere, heat budget estimate 0-104968  
 turbulence meas. near seabed, digitisation and record length selection 0-104971  
 turbulent diffusion in vertical direction, estimation from dissipation obs. 0-98341  
 turbulent Ekman bottom boundary layer, effect of diurnal tidal currents 0-104977  
 underwater irradiances on horizontal surfaces, effects of clouds on diurnal var. 0-72549  
 underwater light in NE.Atlantic, obs. using new photometer in deep sea 0-98460  
 underwater sound, calcs. of acoustic transmission through eddies 0-64264  
 underwater sound, compressional wave attenuation in deep ocean sediments 0-79033  
 underwater sound, correlation measurement of reflection coeff. from bottom and surface of ocean 0-58848  
 underwater sound, correlation of bottom-reflected pseudonoise signals with transmitted signal 0-58846  
 underwater sound, correlation of pseudonoise signals in reflection from layered ocean bottom 0-87626  
 underwater sound, effects of class of random currents on transmission in channel with linear sound speed 0-87621  
 underwater sound, horizontal acoustic refraction through ocean mesoscale eddies and fronts 0-96085  
 underwater sound, LF propag. off Mission Beach, California 0-79035  
 underwater sound, multipath anal. of explosive source signals 0-79034  
 underwater sound, sediment rigidity effect on ocean bottom reflection loss in typical deep sea sediment 0-96083  
 underwater sound, shallow-water propag. over low-velocity bottom 0-74579  
 underwater sound, simplified calculation of ray-phase perturbations due to ocean-environmental variations 0-64266  
 underwater sound, stability and identification of acoustic multipaths 0-83697  
 underwater sound, stochastic internal-wave model for deep moving ocean 0-64267  
 underwater sound, viscous attenuation in high-porosity marine sediments 0-74577  
 underwater sound propag. in wedge-shaped ocean with penetrable bottom 0-74578  
 underwater sound scattering by marine organisms, review 0-64269  
 upper ocean temperature and salinity structure, obs. during POLE exp. 0-72536  
 upwelling in stratified ocean due to melting of glacier ice 0-81897  
 upwelling over shelf break, theory 0-72550  
 Vancouver Island region, terrestrial EM induction 0-104879  
 Vellar estuary, Fe precipitation, conc. determ. 0-77015  
 vertical natural laminar convection flows in cold water, buoyancy force reversals 0-59034  
 Virgin Islands, vertical current profiles and Richardson no. meas. 0-67378  
 Visakhapatnam coast, Bay of Bengal, clay sediments derived from inland sediments 0-76959  
 vortices, evolution of isolated nonlinear examples 0-81910  
 Wanganella Bank area, ocean dynamical conditions off E.Australia (*Russian*) 0-109168  
 warm front, oceanic, propagation, theory with appl. to Sagami Bay Kyu-cho phenomenon 0-94538  
 water movement and induced electrical currents in ocean bottom 0-104863  
 Weddell gyre 0-81894  
 Weddell Sea, bottom water origin, chem. tracer considerations 0-76982  
 Weddell Sea, bottom water variability 0-67366  
 Weddell Sea, fine structure meas. in temp.-compensated halocline 0-67373  
 whitecaps and sea state rel. to wind vel. and atmospheric surface layer stability 0-72554  
 wind stress coefficient over water surfaces, new evaluation 0-72603  
 wind waves data, appl. to climatic comparisons of estimated and measured winds from ships 0-105020  
 wind-driven currents on the continental shelf, review, book contrib. 0-98358  
 Winyah Bay estuary, S.Carolina, <sup>226</sup>Ra behaviour meas. 0-98360  
 Al content controlled by inorganic processes 0-61815  
<sup>24</sup>Al, concs. in sediments from coastal basins off California and Mexico 0-98303  
 CO<sub>2</sub> gas seep from seabed, Norton Sound, Alaska 0-67361  
 CO<sub>2</sub> in atmospheric, <sup>13</sup>C/<sup>12</sup>C vars. in last 22 yrs. role of ocean 0-104530  
 H<sub>2</sub> dissolved in N.Atlantic surface water, interchange with air 0-77057  
 Mn nodule origin (*Russian*) 0-81868  
 Mn nodules, maintenance at surface by bioturbation of fauna 0-101359  
<sup>24</sup>Pu, concs. in sediments from coastal basins off California and Mexico 0-98303

**OCR see optical character recognition****octet theory see SU<sub>3</sub> theory****ODMR see microwave-optical double resonance****oecology see ecology****OH<sup>-</sup>-centres**

KBr(Cl):OH<sup>-</sup>, cc U<sub>2</sub> to H<sub>2</sub>O<sup>-</sup> defects conversion after UV photodecomp. 0-107230

LiF:Mg, X-irrad., colour centres, ESR and UV absorpt. meas. 0-108069

**ohmic contacts**

- n-GaAs-Ge laser alloying to from ohmic contacts 0-58546  
 laser CVD, film physical props. and applications 0-93493  
 metal-semiconductor ohmic contact props., factors affecting contact resistance of semiconductors, theoretical model 0-60076  
 n-n homojunction, calc. of free carrier density profile in a semicond. near ohmic contact 0-70810  
 n-p junctions, determ. of transport parameters of minority carriers using electron microscope 0-65665  
 n<sup>+</sup>-Si-Al ohmic contacts, metallisation struts. for very shallow n<sup>+</sup>/p junctions 0-60084  
 thin film technology, appls. in energy, optics, and electronics, review 0-78932  
 transition metal silicides, refractory for ICs, review 0-100820  
 transmission line model, meas. of specific contact resistance of ohmic contacts 0-70826

**ohmic contacts continued**

- Ag-In<sub>3</sub>S<sub>2</sub>-Si layered struct., Hall effect, I-V characts., surface states (*Russian*) 0-97001  
 Al-In<sub>3</sub>S<sub>2</sub>-Si layered struct., Hall effect, I-V characts., surface states (*Russian*) 0-97001  
 Al-Si(Ge) eutectic alloys in screened ohmic contacts for solar cells 0-94090  
 Al<sub>3</sub>Ga<sub>1-x</sub>Sb-Pd contacts, struct., preparation elec. props. 0-65684  
 Al<sub>3</sub>Ga<sub>1-x</sub>Sb-Pd contacts, band gap depend. of barrier height 0-65685  
 Au-Ge contacts on GaAs, SEM and TEM obs. of struct. 0-100522  
 Au-polyacetylene, electrical properties of polyacetylene films (*Japanese*) 0-96888  
 n-BaTiO<sub>3</sub>, ohmic contact form. 0-92969  
 BaTiO<sub>3</sub>Nb, elec. props., contact material influence 0-70848  
 C-polyacetylene, electrical properties of polyacetylene films (*Japanese*) 0-96888  
 GaAs, alloying with Au and Au alloy ohmic contact metallisations, SEM and optical study 0-70820  
 n-GaAs, study of ohmic contacts 0-60083  
 GaAs:Se ohmic contacts, pulsed electron beam annealing donor density, mobility 0-65678  
 GaAs/metal contacts, recent developments in investigations of preparation and props. (*French*) 0-107909  
 GaAs-metal contacts, use of Ga to eliminate large As loss peaks 0-80370  
 GaInAsP, rectifying and ohmic contacts 0-80376  
 p-Ga<sub>1-x</sub>In<sub>x</sub>As<sub>1-y</sub>PyAs<sub>y</sub>/Au-Zn, specific contact resist. 0-84509  
 GaP, comparison of contact resistances of Au-Zn, Au-Zn-Sb, Au-Ge-Ni and Au-Ge-Ni-Sb alloyed contacts 0-70825  
 GaP-Pd contact system, low temp. alloyed contact formation 0-100519  
 p-InP, ohmic contact using Be-Au metallisation, low contact resist. 0-65677  
 p-InP-Cd(Zn), ohmic contact formation on InP by laser photochemical doping 0-80369  
 InP-Cu contact system, low temp. alloyed contact formation 0-100519  
 InSb-Au contact system, low temp. alloyed contact formation 0-100519  
 Mo-Si sputtered contacts, contact resistance 0-92970  
 Ni-Ge-Au evaporated contacts on GaAs, TEM obs. 0-75449  
 Pt-Si:As, silicide form. during laser irrad., p-n junctions and ohmic contacts 0-84397  
 PtSi film formation by ion sputtering and annealing, form. and exam. problems 0-100782  
 n-Si, bipolar ohmic contact with macroscopic recomb. centres. 0-80379  
 Si solar cells, all-plate low cost contact system 0-93992  
 Si solar cells with fire through contacts printed on anti-reflection coating 0-93993  
 p-Si-Al, ohmic contacts, Si dissoln. and recrystn. effects, computer calc. 0-103749  
 Si<sub>3</sub>N<sub>4</sub> antireflection coating for solar cells, reactive plasma process for forming metal grid patterns 0-93990  
 ZnSe, low resistance ohmic contacts using In-Ga liquid alloy, LED fabrication appl. 0-70823  
 ZnTe single crystal, Schottky-barrier diodes and ohmic contacts props. 0-96987

**ohmmeters****see also electric resistance measurement**

- high electrical resistance measurement, review of accuracy and sensitivity of various instruments and techniques 0-57331  
 new checking method for instruments having both uniform and non-uniform scales 0-62654  
 semi-precision linear ohmmeter, four decade ranges, 2% full scale accuracy 0-95109  
 three-terminal ohmmeter 0-57333

**oil technology**

- oil shales of Green River, USA, thermal decomposition rel. to elec. cond. obs. 0-104495  
 sea and beach persistent oil spill identification methods 0-90101  
 shale extraction in situ retort utilising fusion reactor 0-108780

**oiling (lubrication) see lubrication****oils, insulating see insulating oils****omega mesons**

- Dalitz arrays from K<sup>-</sup>p→π<sup>+</sup>π<sup>-</sup>π<sup>0</sup>A 0-105924  
 e<sup>+</sup>e<sup>-</sup>→ω-π<sup>+</sup>π<sup>-</sup>π<sup>0</sup>, 1.55 GeV 0-82984  
 e<sup>+</sup>e<sup>-</sup>→π<sup>+</sup>π<sup>-</sup>π<sup>0</sup>, 750-1100 MeV, ω and φ meson interference 0-105910  
 NN→(π, ρ, ω, f), statistical model 0-102028  
 ω→ωππ, current algebra techniques, pole plus remainder model, chiral symmetry breaking and QCD 0-62972

**omegatrons see cyclotrons****one-dimensional conductivity**

- coupled incommensurate charge density waves, 3D ordering, mean field theory calcs. 0-107719  
 DEM(TCNQ)<sub>2</sub>, ESR study 0-97127  
 disordered one-dimensional conductors, resistance fluctuations. 0-80256  
 distorted one-dimensional electron system, dynamical elec. cond. calc. 0-59962  
 hollandites, cryst. growth and structural props. 0-89129  
 hopping conductivity, one-dimensional bond percolation model 0-103655  
 intra-site vibration effects on elec. cond. in disordered Hubbard model 0-107775  
 inverse localisation length, numerical studies 0-80257  
 Landauer generalised formula 0-103680  
 lattice stability, phonon dispersion, Kohn anomaly 0-96603  
 libron effects on electron spectrum, theory 0-96854  
 linear conductor, CDWs and impurity effects 0-59967  
 NMP-TCNQ, partial charge transfer effect, one dimensional disordered Hubbard model study 0-70687  
 organic conductors, quasi one-dimensional, low temp. mag. susceptibility 0-93069  
 organic materials, electron-electron scatt. 0-107776  
 Peierls instability, lattice distortion, Kolmogorov Arnold Moser theorems, appl. to struct. problems in condensed matter 0-59878  
 Peierls instability, with arbitrary bandfilling 0-59968  
 Peierls transition, Frohlich model, one-dimens., CDW stability, electron-phonon coupling 0-65452  
 polyacetylene conductivity mechanism, Peierls phase one dimensional cond. (*Russian*) 0-88546  
 quasi one-dimensional conductor, CDW onset and pinning 0-70690  
 quasi-one-dimensional CDW systems, commensurability pinning of fluctuation cond. 0-75555  
 quasi-one-dimensional conductors, alloys, Peierls distortion 0-59965



**one-dimensional conductivity continued**

- quasi-one-dimensional electron-phonon system, electron jump effect on phase transition (*Russian*) 0-92673  
 quasi-one-dimensional model with long range interaction, coupled Tomonaga chain, exact soln. 0-96856  
 quinolinium (TCNQ)<sub>2</sub>, charge transport, proton spin-lattice relaxation 0-88545  
 superionic conductor, correls. among mobile ions role, microscopic model 0-107534  
 TCNQ complexes, elec. resist. and thermoelec. power meas. 0-107777  
 TCNQ salt, Ag.TCNQ, cryst. struct. 0-70186  
 TCNQ salt, dibenzo-TTF-TCNQCl<sub>2</sub>, one-dimens. mag. semicond., mag. and elec. props. 0-88601  
 TCNQ salt, MeDABCO(TCNQ)<sub>2</sub>, optical, elec., and mag. props. 0-65539  
 TCNQ salt, MEM(TCNQ)<sub>2</sub>, dielec. const. obs., DC and microwave cond. obs. 0-59963  
 TCNQ salt, TSeF-TCNQ, short-range ordering investigated by XDE 0-59652  
 TCNQ salts, crystallisation versus electrical conductivity 0-92885  
 TCNQ salts, elec. cond. spectrum fine struct. 0-96884  
 TCNQ salts, ETPP (TCNQ)<sub>2</sub> and DEPE (TCNQ)<sub>4</sub>, thermoelec. power 0-59966  
 TCNQ salts, TSF-TCNQ, and HMTSF-TCNQ, low temp. fast neutron irradiation, elec. cond. meas. 0-59964  
 tetracyanoplatinate, quasi 1d anion deficient, elec. and struct. props. 0-103683  
 tetraselenotetracene iodides, struct. and physical props., DC electrical cond. and EPR linewidth meas. 0-103312  
 (TMTSF)<sub>2</sub>PF<sub>6</sub>, ESR g-factor, linewidth, spin susceptibility, metal-insulator transition 0-103887  
 (TMTSF)<sub>2</sub>PF<sub>6</sub>, quasi-dimens. cond., diamagnetic AC susceptibility 0-103781  
 (TMTSF)<sub>2</sub>PF<sub>6</sub> (AsF<sub>6</sub>), linear-chain conductor, semicond.-metal transition in small elec. field 0-103730  
 (TMTSF)<sub>2</sub>X, (X=PF<sub>6</sub><sup>-</sup>, AsF<sub>6</sub><sup>-</sup>, SbF<sub>6</sub><sup>-</sup>, BF<sub>4</sub><sup>-</sup>, NO<sub>3</sub><sup>-</sup>) highly conducting salts, props. 0-59969  
 trapping behaviour, theoretical study 0-80258  
 TTF<sub>0.4</sub>TSeF<sub>0.6</sub>TCNQ, 2k<sub>F</sub> and 4k<sub>F</sub> CDWs, X-ray study 0-65474  
 (TTF)Cl<sub>2</sub>, disorder transition, cond. decrease and commensurate charge density waves 0-70153  
 TTF-TCNQ, anisotropic cond., X-ray effects 0-96855  
 TTF-TCNQ, elec. cond., SEM technique 0-86507  
 TTF-TCNQ, elec. resist., electron-phonon scatt. 0-92884  
 TTF-TCNQ, enthalpy of sublimation and vapour press. meas. 0-92661  
 TTF-TCNQ, implications of amplitude solitons in incommensurate Peierls systems 0-92841  
 TTF-TCNQ, Landau theory of phase transitions 0-92666  
 TTF-TCNQ, low temp. fast neutron irradiation, elec. cond. meas. 0-59964  
 TTF-TCNQ, metallic cond., nonlinear amplitude-phase interaction 0-88490  
 TTF-TCNQ, nonbonding intermolecular forces 0-83443  
 TTF-TCNQ, quasi one-dimensional low temp. mag. susceptibility 0-93069  
 TTF-TCNQ complex, trans-diethyl-dimethyl TTF-TCNQ, one-dimens. cond. 0-96853  
 TTF-TCNQ crystals, X-ray topographic study of cryst. perfection 0-96525  
 TTF-TCNQ low temp. mag. susceptibility, neutron irradiation effects 0-60311  
 TTF, donor-acceptor system, physico-chemical studies (*Hungarian*) 0-75554  
 two level commensurability in one-dimensional Peierls system (*Russian*) 0-70688  
 K<sub>1.54</sub>Mg<sub>0.77</sub>Ti<sub>7.25</sub>O<sub>16</sub>, hollandite, one-dimens. superionic cond., transport model 0-107529  
 K<sub>2</sub>[Pt(CN)<sub>4</sub>]Br<sub>0.3</sub>·3H<sub>2</sub>O, high press. structs. and phase transitions 0-107423  
 LiAlSiO<sub>4</sub>, β-eucryptite one-dimens. fast ion cond., temp. depend. of cryst. struct. 0-107191  
 β-Na<sub>0.33</sub>V<sub>2</sub>O<sub>5</sub>, quasi-one-dimensional conductor, NMR studies 0-93204  
 NbSe<sub>3</sub>, CDW noise, temp. and freq. depend. 0-103681  
 NbSe<sub>3</sub>, depinning props. of lower CDW, weak pinning model (*French*) 0-70630  
 NbSe<sub>3</sub>, interference effects of CDW motions 0-88544  
 (SN)<sub>2</sub>Br, ion implantation effect on elec. props. 0-65026  
 TCNQ salts, Qn(TCNQ)<sub>2</sub> and N-propyl-Qn(TCNO)<sub>2</sub>, low temp. mag. susceptibility, neutron irradiation effects 0-60311  
 (TSeT)<sub>2</sub>Cl complex, phase transform. under press., cond. (*Russian*) 0-92674  
 TTF-TCNQ, const. volume resistivity anomalous behaviour 0-103682  
 ZrS<sub>3</sub>, quasi one-dimens. semicond., elec. transport props. 0-107790

**one-dimensional conductors see one-dimensional conductivity****online operation**

- used for systems software in online and real-time systems but for hardware aspects see real-time systems  
 see also interactive systems; real-time systems  
 electrochemical system, LF impedance meas. technique using on-line computer 0-57339  
 particle size distribution meas., online stroboscopic microscope apparatus 0-101783  
 spectroscopic data base system status 0-104475

**Onsager relations see thermodynamics****Onsager theory of dielectrics see dielectric properties of substances****opacimeters see turbidimetry****opalescence**

- see also critical opalescence  
 No entries

**OPDAR see optical radar****operating amplifiers see operational amplifiers****operating systems (computers)**

- nerve fibre counting by pipeline multiminicomputer image processing 0-109013

**operational amplifiers**

- photoconduction decays, fast, measurement, DC-10 MHz low noise amplifier system 0-57326  
 review, operational amplifier behaviour 0-67959

**operational amplifiers continued**

- vented box loudspeaker analogue model 0-92015  
 Wheatstone bridge fed from a bilateral constant current source using electronic amplifier 0-57338

**operator training see training****optic mode of crystals see lattice dynamics****optical aberrations see aberrations****optical activity see optical rotation****optical auroras see aurora****optical character recognition**

- Korean alphabets holographic pattern recognition, discrimination enhancement using phase modulated matched filters 0-95854  
 optimised filter 0-95837  
 reading machine, multifont adaptable automatic, for blind people 0-104814

**optical coherent transients**

- see also photon echo  
 atomic systems, coherent transients theorem 0-99808  
 atoms, two photon excitation, time depend. emitted light spectra, perturbation theory 0-63605  
 free electron laser, coherent dynamics with arbitrary magnet geometry 0-83581  
 gaussian beam resonator, optical nutation 0-99807  
 generation by electro-optical laser modulator 0-102776  
 laser saturation spectroscopy, time-resolved, free induction decay of two-level resonances 0-102775  
 methyl iodide mol. nonlinear resonant interaction with pulsed subMM radiation (*Russian*) 0-99523  
 millimetric/submillimetric coherent transient spectroscopy 0-58651  
 quantum systems, at or spin two level, reson. EM wave excitation, free induction decay oscils. 0-63562  
 semiconductor, nonlinear coherence phenomena in exciton region 0-99806  
 semiconductors, two-photon nutation of coherent biexcitons 0-80191  
 spatial gratings, transient light-induced, by successive optical coherent pulses 0-64115  
 tetramethyl pyrazine in durene, phosphorescent mols., quantum beats in triplet states 0-58312  
 two-level system, backward photon echo and free induction decay generation 0-99805  
 KCl:KReO<sub>4</sub> free induction decay generation of ultrashort CO<sub>2</sub> pulses 0-74444  
 LaCl<sub>3</sub>:Pr<sup>3+</sup>, coherent transients by optical phase switching 0-95962  
 LaF<sub>3</sub>:Pr<sup>3+</sup>, ultraslow optical dephasing 0-58648  
 LaF<sub>3</sub>:Pr<sup>3+</sup>, ultraslow opt. dephasing at 2K 0-91864  
 NH<sub>3</sub>, transverse relax. time, T<sub>2</sub>, of inversion doublets from free induction decay 0-58281  
 Na vapour, Zeeman coherence, transient and stationary, polarisation spectroscopy 0-58212  
 Sml, Zeeman coherence, transient and stationary, polarisation spectroscopy 0-58212

**optical collimators**

- asymmetric fiber power splitter 0-83661  
 autocollimation instrument for checking angles and pyramidity of AR-90° prisms during manufacturing process 0-87570  
 automatic collimator used in X-ray comparator for meas. cutoff angle of piezoelec. quartz wafers 0-105755  
 automodulation collimator, for X-ray astronomy (*Russian*) 0-62018  
 frustrated total internal reflection element, adjustable as a function of the incidence angle of highly collimated light beams 0-96022  
 laser tracking system testing by 1 m unobscured IR collimator 0-78991  
 meniscus collimator viewfinder, optimisation of mirror light transmission coeffs. 0-74469  
 moving atmosphere simulation by rotating phase plate 0-79021  
 roof and other prisms, MTF tests 0-69571  
 Space Telescope pointing control fine guidance subsystem design 0-82201  
 telescopic collimating system, laser radiation directivity pattern axis spatial location 0-102748  
 H<sub>2</sub> maser frequency standard, stabilised using multitube collimator 0-91769

**optical communication**

- see also optical links  
 analogue video transmission feasibility using laser diode, over 30 km at 1.3 μm 0-58737  
 fibre communication advances, materials and techniques 0-102853  
 fibre optic systems, analytical review including survey of commercial systems 0-74489  
 fibre transmission, applications and cable techniques (*Japanese*) 0-87493  
 fibre transmission expts. at 34 Mb/s with HDB3 line code 0-64198  
 fibre-optic appls., techniques and predictions 0-87472  
 fibre-optic communication system performance at 1.55 μm with single-longitudinal-mode laser 0-87556  
 fibre-optic communication systems, book 0-73117  
 fibre-optic systems, future developments, impact on 'next generation' of electronic equipment, data ring concept 0-102808  
 fibre-optic transmission by laser diode analogue baseband modulation 0-58738  
 glass fibres for, colloquium, London, England (Jan. 1979) 0-67930  
 heterodyne receivers for atmospheric optical communications 0-58663  
 high-speed optical systems at 0.85 μm, modal noise and optical feedback 0-87323  
 historical and technical features review, future prospects (*Japanese*) 0-99863  
 integrated optics, colloquium, London, England (May 1980) 0-79008  
 integrated optics in fibre communication systems, introduction 0-79009  
 laser and electro-optical systems, conf., San Diego, CA, USA (Feb. 1980) 0-62392  
 light guide data transmission, review (*German*) 0-95996  
 light-wave propagation communication, glass fibres, attenuation characts. (*German*) 0-95997  
 lightguide theory and its implications in manufacturing 0-64186  
 long wavelengths beyond 2 microns (*Japanese*) 0-106469  
 multimode digital system wavelength multiplexing constraints in 850 nm region 0-63942  
 parallel plane diff. grating with periodic structure, diff. of plane wave 0-102620  
 perceptual coding in the cosing transform domain 0-102635  
 single mode fibres, optical communication techniques (*German*) 0-102811  
 step index fibre including gap, impulse response 0-83675



**optical communication continued**

- sub-optimal graded index optical fibre analysis using perturbation calculus 0-87480
- supervisory/service channel for fibre optic transmission systems 0-95803
- training, educational course status and effectiveness 0-62413
- transmission system planning (*French*) 0-87551
- white light, information processing and transmission 0-95833

**optical communication equipment**

- see also optical waveguides
- 1X2 optical switch using new type of pentagonal prism switch, for optical fibres 0-64148
- access couplers for single strand systems 0-58766
- acousto-optics, guided-wave, with appls. to wideband communications and signal processing, progress review 0-58801
- binary phase gratings for fibre-optic communications 0-64201
- bistable optical device development from integrated two-arm interferometer, appls. (*French*) 0-69555
- bypass switch for fibre-optic data bus systems 0-99826
- cable design considering structural imperfection 0-64184
- cables, connections and optical transmitters for optical fibre transmission systems (*German*) 0-99839
- coated optical fibre cable unit, internal stress due to compressive loads, optimum design 0-58717
- components for optical communication systems, review 0-87539
- DH photodiodes, diffusion limited transient response 0-70809
- diode lasers as transmitter source in optical communication, modulation, power consumption, optical links 0-102807
- directional coupler, interference filter all-fibre for wavelength division multiplexing 0-91900
- directional filter structure and characteristics for bidirectional transmission 0-58734
- fibre, single-mode systems, instability due to interference and polarization effects 0-58774
- fibre cable reliability, deterioration factors, splice point reliability, coating materials, static fatigue life (*Japanese*) 0-99848
- fibre cable testing, for lightwave communications systems 0-102865
- fibre cables, design, manufacture, laying and jointing (*Italian*) 0-99838
- fibre communication development trends, review 0-69521
- fibre communication system components, state-of-the-art survey (*German*) 0-69538
- fibre endface preparation by AC discharge heating and stretching 0-64232
- fibre optic communications, prospects for 1 to 1.6  $\mu\text{m}$  spectral range use 0-102848
- fibre optic signal transmission appls. (*German*) 0-69517
- fibre optic telecommunications systems, book 0-86049
- fibre preform manufacture using modified CVD process 0-64228
- fibre switch, single-mode, optimised design 0-106607
- fibre systems for telecommunications 0-91906
- fibre-optic communication in industry, appls., glass fibre props., connectors 0-87550
- fibre-optic communication systems, book 0-73117
- fibre-optic transmission system, semiconductor device reliability tests 0-58573
- frequency-channel multiplexer and four-channel integrated-optics coupler 0-91936
- glass and plastic fibre characts. and interconnection requirements 0-69513
- glass fibre long wavelength optical communication, materials and devices, review 0-99854
- glass fibres used for optical transmission systems (*German*) 0-69516
- integrated optical communication components in III-V semiconductor technology, overview 0-79012
- IR emitting diodes and injection lasers, optical communication appls. 0-58563
- laser diode module description and performance 0-64069
- laser diodes for fibre communications, characteristics and state of art (*Italian*) 0-58569
- lens, gradient-index rod, appl. in optical fibre communication systems 0-69488
- lens guide, low-loss image transmission 0-91872
- lightguide fibre, prototype drawing facility 0-64229
- lightguide fibre testing 0-64230
- lightwave sources and detectors 0-64068
- log-normal device optimal burn-in time 0-58743
- long-wavelength single-mode fibre transmission systems 0-58773
- matrix switching network for fibre-optic communication 0-58735
- monomode optical fibre bandwidth limitations and bend losses 0-87553
- multimode 3X2 fibre optical matrix switch 0-58764
- multimode fibre systems, low loss 4X4 switching network 0-58718
- multiplexer/demultiplexer, low-loss, using interf. filters 0-58728
- near IR (1 to 2  $\mu\text{m}$ ) optical communications, colloquium, London, England (May 1980) 0-86040
- nonblocking 8X8 optical matrix switch for fibre-optic communication 0-74485
- nonlinear distortions and noise in optical communication systems due to fibre connectors 0-96001
- optical fibre sources and detectors (*Italian*) 0-69390
- optical fibres, progress and components, review (*French*) 0-69524
- optoelectronic devices development 0-91902
- passive couplers for appl. in fibre optic systems 0-91903
- photodetectors, for optical fibre communication (*Japanese*) 0-78977
- rod lens analysis and application to optical fibre communications 0-87549
- self-imaging multiplexer and branching couplers 0-106629
- semiconductor laser diodes, present status and technology (*German*) 0-58561
- semiconductor laser intrinsic noise in optical communication systems 0-69394
- semiconductor laser modulation, non-linear distortion, communication systems appl. (*German*) 0-69395
- semiconductor laser sources for coherent optical-fibre systems 0-64159
- semiconductor light source for fibre optical communication 0-58653
- single fibre connectors and cable splice hardware, optical coupling theory 0-64187
- single mode fibre optical data bus with star couplers 0-64199
- submarine cable using glass fibre, expt. cable (*German*) 0-58711
- wavelength division multiplexer using optical fibre pieces 0-91917
- wavelength division multiplexing technology status and prospects 0-64203
- wavelength division multiplexing transmission technology 0-58727

**optical communication equipment continued**

- wavelength multiplexer, single-mode-fibre 0-102816
- GaAlAs laser diode, for heterodyne communication systems, high frequency stability 0-99727
- (GaAl)As-GaAs narrow stripe laser, improved optical communication system performance 0-102733
- GaAs double and narrow stripe laser structures 0-64062
- GaAs-Ga<sub>1-x</sub>Al<sub>x</sub>As DH LED, for optical fibre communication (*Japanese*) 0-78976
- Ga<sub>0.47</sub>In<sub>0.53</sub>As, photodetector applications 0-95140
- GaInAsP LEDs, 1.3-1.6  $\mu\text{m}$ , appl. in long haul high data rate fibre optic communication systems 0-102854
- In<sub>0.53</sub>Ga<sub>0.47</sub>As p-i-n photodiode-FET photoreceiver for 1.0 to 1.7  $\mu\text{m}$  wavelength optical fibre communications systems 0-58794
- InGaAsP photodetector, improved two wavelength demultiplexing 0-58795
- InGaAsP/InP injection lasers for long wavelength (1.1 to 1.6  $\mu\text{m}$ ) optical communication 0-58582
- In<sub>1-x</sub>Ga<sub>x</sub>As<sub>y</sub>P<sub>1-y</sub> DH lasers for 1.3 and 1.5  $\mu\text{m}$  optical fibre communications 0-91817
- LiNbO<sub>3</sub>-Ge acoustooptic modulator (*Japanese*) 0-69542
- PLZT ceramic, modulator for optical communication 0-78964
- SiO<sub>2</sub>-GeO<sub>2</sub>/SiO<sub>2</sub> load bearing optical cable, geophys. appls. 0-91923
- Xe short-arc lamp, current modulated, arc forms and instability 0-96399

**optical constants**

- see also light absorption; reflectivity; refractive index
- absorbing materials, optical consts. determ. using Fresnel formulae approximations 0-88946
- absorption coefficient, optical, absolute meas., photoacoustic spectroscopy 0-82828
- absorption measurement, optical materials, real time holographic interferometry 0-83569
- achromatic antireflection coatings, thin-layer, layer thickness calcs. 0-87468
- actinides and their fluorides, interband, collective and atomic (p,d) excitations, Z-160 eV, fast EELS 0-93443
- alloys, substitutionally disordered, optical cond., intraband transitions 0-103933
- canted magnetic structured materials, exciton spectra, optical props. 0-70622
- cermet film granular media, dielectric function theory, permittivity, percolation transport props. 0-88498
- chalcogenide glasses, O-free, cooling rate influence on optical consts. 0-88952
- composite material, complex dielectric const., bounds 0-108170
- electrode surface, anisotropy of optical props. 0-60534
- ferromagnetic semiconductors, free carrier absorpt. of radiation 0-97227
- films, optical constants, reflection spectra by Kramers Kronig method 0-76099
- glasses, gradient composition, optical props. 0-88947
- Green's function of optically anisotropic media (*German*) 0-93255
- Kramers-Kronig analysis (*Russian*) 0-80740
- LED, using Si, photovoltaic cell, absolute spectral sensitivity calibration, radiometry, photometry (*Chinese*) 0-86367
- measurement at two incidence angle values 0-101831
- measurement method using polarised light refl. coeffs., accuracy 0-73423
- measurement of magneto-optic rotation and ellipticity, spinning analyser ellipsometer (*Japanese*) 0-73419
- metals, IR optical consts., meas. by self-radiation method 0-84710
- multilayers, ultrathin, optical characts. 0-104005
- optical fibre parameter measurement using optical time domain reflectometer 0-58755
- photothermal deflection technique for absorpt. meas. in optically thin media, thermal lens effect comparison 0-105717
- plane parallel slab, optical const. determ. methods 0-60531
- quartz high-transmittance antiref. film, vacuum-etched 0-74449
- rare earths and their oxides and fluorides, interband, collective and atomic (p,d) excitations, Z-160 eV, fast EELS 0-93443
- semiconductor, optical absorpt. coeff. and minority-carrier diffusion length, differential photocurrent method of meas. 0-96896
- semiconductor films, polycryst., grain boundary effects 0-80890
- soil-derived atmospheric dusts, particle absorption contributions to mass extinction coefficients 0-61896
- sphericity standards, interferometric meas. (*German*) 0-87569
- transition metals, BCC, films, vac. evaporated, optical cond. 0-76100
- twisted nematic display with cholesteric dopant, transmission characteristic temp. depend. compensation 0-103934
- Ag film, ellipsometric response to CO adsorption 0-103571
- Ag foil, interface with liq., oxide props., refl. and scatt. light spectroscopy 0-60702
- Al<sub>2</sub>O<sub>3</sub>, transparent hot-pressed, transparent and translucent properties 0-60533
- An, optical constant meas., 100 to 1000 eV using transmission gratings 0-93258
- Au film, evap., temp. change and gas adsorpt. effect on opt. consts., ellipsometric obs. (*German*) 0-89081
- B:H amorphous films, optical band gap, thermal treatment effect 0-93415
- Ba film, semitransparent, opt. props. in 2-5.6 eV range, electronic transitions, thickness depend. (*French*) 0-108289
- C, amorphous grains, extinction coeffs., 0.21-340  $\mu\text{m}$ , lab. meas. rel. to interstellar grains 0-73020
- CO<sub>2</sub>-He-N<sub>2</sub>, absorpt. coeff. for 10.6  $\mu\text{m}$  CO<sub>2</sub> laser radiation, 295 to 650 K 0-92252
- CdGeAs<sub>2</sub> crystals, Bridgman grown, optical props. rel. to O<sub>2</sub> content of starting materials 0-81213
- Co, thin films, optical and magneto-optical permittivities 0-66163
- Cu film, optical consts. deduced from surface EM wave propag. 0-60697
- Cu-Sn(Al)(Ga) reflecting surface absorpt. coeffs. at 10.6  $\mu\text{m}$  0-95984
- CuCl vapour laser, output power limiting processes 0-91776
- Cu<sub>2</sub>S-CdS solar cells, optical absorption coefficient changes in Cu<sub>2</sub>S 0-93980
- D<sub>3</sub> Rydberg states, spectroscopic B<sub>0</sub> consts. 0-74109
- Fe, passive film form. in phosphate soln., intensity-following ellipsometry study 0-104345
- Fe-Cr alloys, in acid and neutral solns., thickness and optical constants of passive and transpassive films 0-66698
- Fe<sub>3</sub>O<sub>4</sub>B<sub>2</sub>O, metallic glass, optical and magneto-optical props. 0-84728
- Fe<sub>2</sub>O<sub>4</sub>, magnetite, optical props. in IR 0-97271
- GeSe<sub>2</sub> amorphous film, laser induced oscillatory phenomena 0-84711



**optical constants continued**

- p-GeTe, reflectance, and thermoref. spectra 0-80814  
 H<sub>1</sub>, Rydberg states, spectroscopic B<sub>0</sub> consts. 0-74109  
 In<sub>2</sub>SnO<sub>3</sub> film, effect of ambient atmosphere during annealing, elec. props. 0-97510  
 K smoke particles, optical props. 480 to 620 nm, rel. light scatt. cross sections meas. 0-97293  
 NH<sub>3</sub> solid film, absorpt. coeffs. determ. 50 to 7000 cm<sup>-1</sup> 0-97356  
 Na, IR and optical props., surface-plasmon-mediated absorpt. mechanism 0-93308  
 Ni, corrosion and passivation in phosphate soln., pH depend., ellipsometric study 0-104448  
 Ni film, evaporated, chemisorpt. of CO, ellipsometric investig. (*German*) 0-61156  
 β'-NiAl, electronic struct. and optical props. 0-97228  
 Ni<sub>2</sub>Ge<sub>3</sub>, amorphous and cryst. films, opt. props. in interband absorpt. region 0-66315  
 SbBr glass, IR reflectivity spectra 0-71403  
 Sc, interband, collective and atomic (p,d) excitations, Z-160 eV, fast EELS 0-93443  
 Sc<sub>2</sub>O<sub>3</sub>, interband, collective and atomic (p,d) excitations, Z-160 eV, fast EELS 0-93443  
 Se films, optical constants in visible region 0-97360  
 Se, threads in natural mordenite channels, optical absorpt., cond. (*Russian*) 0-89022  
 SeOCl<sub>2</sub>:Pr<sup>3+</sup>(Nd<sup>3+</sup>)(Er<sup>3+</sup>), SbCl<sub>3</sub>, acidified, Racah and Judd-Ofelt parameters in laser ligs. 0-106516  
 SiO<sub>2</sub> deposited on Ge, optical constants, reflection spectra by Kramers Kronig method 0-76099  
 SiO<sub>2</sub> film on Cu substrate, surface EM wave absorpt., optical consts. (*Russian*) 0-108216  
 SiO<sub>2</sub> films on Si, ellipsometric spectra, thickness determ. (*Chinese*) 0-86379  
 SiO<sub>2</sub> thin thermally grown oxide layers etching in HCl, ellipsometric control of Si surface form. (*Russian*) 0-104315  
 Sn, liq., optical props., 0.62-3.7 eV 0-75996  
 Ti, electropolished, optical props. from 1.8 to 3 eV 0-85088  
 TiO<sub>2</sub> layers, activated reative evaporation and absorpt. indices 0-97363  
 TiGaTe<sub>2</sub>, TiInTe<sub>2</sub>, and TiInSe<sub>2</sub>, IR refl. spectra 0-60605  
 UO<sub>2</sub>, 5f-magnetic semiconductor, spectroscopic data, review 0-97299  
 Y, interband, collective and atomic (p,d) excitations, Z-160 eV, fast EELS 0-93443  
 Y<sub>2</sub>O<sub>3</sub>, interband, collective and atomic (p,d) excitations, Z-160 eV, fast EELS 0-93443  
 ZnS, linear electrooptic coeff. dispersion 0-71380

**optical couplers**

- 4 port and 8 port kaleidoscope micro-optic star coupler for optical fibres 0-58681  
 access couplers for single strand systems 0-58766  
 asymmetric T-couplers for fibre optic data buses 0-102809  
 bidirectional optical systems, Rayleigh backscatt. freq. depend. 0-69511  
 binary phase gratings for fibre-optic communications 0-64201  
 blazed dielectric gratings with high beam coupling efficiencies 0-64211  
 channel waveguides, single-mode, prism coupling efficiency meas. 0-99878  
 components for optical communication systems, review 0-87539  
 contradiirectional frequency-selective couplers for guided-wave optics 0-102803  
 diode laser output stabilization by bevelled-end fibre coupling 0-91806  
 diode-laser-fibre coupling, effects of fibre propagation loss 0-74484  
 directional coupler, interference filter all-fibre for wavelength division multiplexing 0-91900  
 directional coupler as waveguide tap with infinitesimal insertion loss 0-99883  
 directional coupler for fibre transmission system (*Japanese*) 0-58693  
 directional coupler with lapped multimode fibres, characts. 0-91892  
 directional couplers with graded index profile, variational analysis 0-96037  
 fabrication using splicing technique, characteristics (*Japanese*) 0-87508  
 fact directional coupler switch/modulators, novel ps optical pulse sampling method 0-58784  
 far IR laser hybrid output couplers, metal mesh dielectric mirror design and fabrication 0-58554  
 fibre, double-core single-mode, as directional coupler 0-106597  
 fibre, graded-index, high index hemispherical microlens tip melt fabrication for coupling to GaAlAs laser 0-69506  
 fibre, single mode, hemispherical microlens tip fabrication for high efficiency coupling to InGaAsP laser 0-69505  
 fibre cables, connections and optical transmitters (*German*) 0-99839  
 fibre cables connections, in-the-field 0-69545  
 fibre connector loss evaluation by backscattering 0-58721  
 fibre connector technology, multimode, single-mode 0-87511  
 fibre connectors, nonlinear distortions and noise in optical communication systems 0-96001  
 fibre connectors, splices and couplers, design principles 0-58765  
 fibre coupling using graded-index rod lenses 0-91891  
 fibre joining techniques and connections to communication equipment (*Norwegian*) 0-64179  
 fibre lightguide cable connectors, Si chips manufacture for fibre alignment 0-64188  
 fibre multimode access coupler, fabrication method 0-87478  
 fibre optic connectors, precision and stability developments 0-69523  
 fibre optic interconnection, using compound-lens devices, telephone links appl. 0-74493  
 fibre optic rotation sensor, all-waveguide configuration, key element tests 0-58796  
 fibre optic system design and component selection 0-58767  
 fibre optics technology and connector systems, marketing 0-69522  
 fibre splice, elastic-tube 0-87527  
 fibre splice insertion loss meas., backscattering method 0-58720  
 fibre splicing, connecting and sheath joining (*Japanese*) 0-87497  
 fibre-optic communication in industry, appls., glass fibre props., connectors 0-87550  
 fibre-optic crossbar switch 0-74497  
 fibre-optic male connector with friction insert, ferrule and retainer 0-78968  
 fibre-optic planar multimode coupling structure fabrication by ion exchange 0-64233  
 fluoromethane TEM<sub>00</sub> far IR laser with integrated pump laser, metal mesh output coupler 0-58578

**optical couplers continued**

- four-channel integrated-optics coupler and frequency-channel multiplexer 0-91936  
 GaAs homojunction rib waveguide directional coupler switch 0-69554  
 graded-index waveguide coupling and matched joining, coherent states and light propag. 0-102625  
 grating coupler, chirped and curved, for focusing beam 0-78979  
 high efficiency single mode fibre/channel waveguide flip-chip coupling 0-58799  
 integrated and guided-wave optics, conference, Incline Village, NV, USA, January 1980 0-58772  
 integrated optics endfire coupler efficiency calc. and expt. 0-102863  
 integrated optics high quantum efficiency waveguide coupled photodetectors on Si substrate 0-58805  
 interconnecting fibre optics 0-69514  
 laser light source for spectroscopy, far-IR, using set of mirrors and lenses 0-73481  
 low loss, for coupling LED to fibre-optic system 0-91907  
 Michelson output coupler with one-dimensional grid, for optically pumped near MM laser 0-58555  
 moulded multifibre connectors using rectangular multirod arrangement 0-58685  
 nonlinear coherent coupler, new optical logic device 0-58630  
 passive devices for appl. in fibre optic systems 0-91903  
 planar optical waveguide interconnection method 0-58671  
 planar star coupler design for fibre optic systems 0-74474  
 planar star coupler for multimode fibres 0-99828  
 planar waveguide blazed dielectric diffraction gratings, anal. and design 0-58779  
 polarisation-independent optical switch using weighted directional coupler 0-58798  
 prism coupler fabrication technique 0-83685  
 prism coupling into clad uniform optical waveguides 0-96003  
 prism coupling into optical waveguide second harmonic generation 0-102763  
 quasilinearly tapered couplers, weighted coupling strength 0-83674  
 rotation-splice tapered fibre star coupler directivity and mode dependence 0-58748  
 self-centring technique for mounting microsphere coupling lens on fibre 0-74517  
 self-imaging multiplexer and branching couplers 0-106629  
 semiconductor laser efficient coupling into tapered hemispherical end single-mode fibre 0-99827  
 semiconductor source matching to thin-film planar and stripe waveguides 0-64174  
 single fibre connectors and cable splice hardware, optical coupling theory 0-64187  
 single mode fibre optical data bus with star couplers 0-64199  
 single-mode fibre optic directional coupler, fabrication and characts. 0-58683  
 slab waveguide star coupler for multimode optical fibres 0-87491  
 slab-type directional coupler with activated rhodamine 6G top layer, amplified oscill. 0-99718  
 snap connector for monofibre opt. cable 0-106609  
 subpicosecond gate, velocity-matched directional coupler 0-74512  
 tapered gap prism coupling to diffused LiNbO<sub>3</sub> waveguides 0-78967  
 thin film slab-type directional coupler covered with high-index absorbing material, damped oscill. 0-91908  
 three-waveguide system, interference effects on couplings 0-78969  
 twisted elliptical optical fibre, polarisation coupling 0-99831  
 welded optical fibre signal splitter 0-102814  
 GaAs p-n-i-n<sup>+</sup> semi-insulating struct. as integrated optical coupler 0-64212  
 GaAs-(GaAl)As DH injection laser with pillbox resonator, coupling with straight waveguide 0-58581  
 LiNbO<sub>3</sub>, channel waveguide to single-mode fibre high-efficiency flip-chip coupling 0-99833  
 LiNbO<sub>3</sub>, Ti-diffused optical waveguide coupled to GaAlAs DH laser, anal. 0-58706  
 LiNbO<sub>3</sub> waveguide modulators and switches, Ti-diffused, fabrication on directional coupler principle 0-83678  
 LiNbO<sub>3</sub>:Ti, coupled waveguide TE/TM mode splitter 0-64142  
 LiNbO<sub>3</sub>:Ti optical waveguide electrooptic devices, polarisation independ. directional coupler switch 0-58783  
 LiNbO<sub>3</sub>:Ti planar waveguide, edge coupling to GaAlAs DH laser diode 0-87559  
 Si connector parameters characts. 0-69544  
 Si Fabry-Perot couplers for optically pumped far IR lasers 0-69404  
 SrTiO<sub>3</sub> prism coupler for LiNbO<sub>3</sub> integrated optics very high throughput damage resistant waveguide modulator 0-58788
- optical design techniques**  
*see also optical instruments*  
 airport control tower cab, optical design 0-58661  
 antireflection coating, two-layer, error considerations in design 0-74477  
 aplanatic two mirror telescope from near-normal to grazing incidence, comparative performance anal. 0-58654  
 aplanatic waxicon insensitive to tilt errors, for high power laser beam transport 0-74460  
 binocular models, characts. and design features, review 0-74468  
 Cassegrain telescope design and tolerancing optimisation 0-82199  
 catadioptric objective, development (*German*) 0-102796  
 caustic point displacement due to generalised bending, third-order approx. 0-83656  
 chromatic aberrations of real rays, role of each lens in optical system 0-102655  
 COCHISE: laboratory spectroscopic studies of atmospheric phenomena with high sensitivity cryogenic instrumentation 0-95166  
 computer-aided, optimisation and interactive graphics improvements 0-78933  
 coronagraph diffraction limit problems and design approaches 0-82200  
 dichroic beam splitters, high-performance, for DF chem. lasers 0-95932  
 diffuse reflectors, light collection and dissemination 0-83658  
 digital image processing, architectural breakthroughs 0-63939  
 EKTRAMAX camera lens design and performance 0-77894  
 eyepeaks, imaginary front focal planes, negative collection lens, design considerations 0-64139  
 fibre, single mode, dispersion characts., correlation between numerical prediction and meas. 0-91890  
 fibre, single-mode, ultra-low-loss, optimised structure for fabrication 0-99843



**optical design techniques continued**

- fibre optic rotation sensor, all-waveguide configuration, key element tests 0-58796
- fibre optic system design and component selection 0-58767
- flat-field spectrograph design, holographic grating appl. 0-68264
- flexible fibre light-guides, viewing instrum. appls. 0-87545
- flexible high-resolution film recording system design 0-102828
- four-element lens systems of Cooke-triplet family design considerations 0-57404
- Fresnel lens optical design and utilisation, advantages and limitations 0-78936
- Gaussian optics parameters, HP-67 calculator program 0-106439
- general optical concentrator, max. radiant power density at receiver 0-102794
- generalised ray tracing, caustic surfaces, bending and merit function for optical design 0-102612
- gradient index optical elements and system design 0-106594
- gradient-index imaging, theory 0-69331
- gradient-index optics: a review 0-69478
- high performance system development and design at Carl Zeiss Jena works (*German*) 0-58660
- holographic elements, axisymmetrical, third order aberrations 0-69341
- holographic optical elements, third-order aberration theory and generalised aplanatic condition 0-74314
- hyperboloid lens manufacturing technique 0-96039
- hyperchromatic lens, expressions for first order chromatic aberrations 0-91879
- illumination system, optical design 0-64135
- image, disector tubes, echelle spectrographs, design considerations 0-91918
- instrument design, partial coherence effects 0-78767
- integrated grating circuit for guided-beam multiple division fabricated by electron-beam direct writing 0-91934
- interference spectrometer, high resolution, appl. to study of laser modal configuration (*Spanish*) 0-86458
- interferometer design for high vibration environment 0-95131
- interferometer spectrometers, field-widened 0-95146
- IR coating nonuniformity effect on precision optical systems, compensation by auxiliary laser 0-78926
- IR scanning system modular design, assembly and alignment 0-78989
- laser beam expander design corrected for Petzval curvature 0-74461
- laser beam refraction at spherical surface, distortion, geometrical optics calc. 0-95929
- laser integration into optical systems, Nd:YAG laser 0-78887
- laser pump system, analytical theory 0-106540
- lens, double Gaussian objective, design (*German*) 0-64134
- lens, gradient-index spherical, design for optical pickup systems 0-69483
- lens, photographic gradient singlet, design techniques based on total aberrations 0-69479
- lens design, least squares fitting of Zernike's polynomials to wave aberration function 0-83660
- lens design with simultaneous image spot, optical path difference, diffraction MTF and Seidel aberration minimisation 0-74459
- lens paraxial eqn. dimensional analysis 0-74462
- lensless scanning telescope, MTF 0-58655
- less design, applied optics conf., Oakland, CA, USA (May-June 1980) 0-101661
- linear Fresnel lens with grooves of finite size, solar radiation concentration 0-106592
- low-loss graded-index fibre, 3 km and 10 km preform design and modified CVD method 0-58746
- machine shop operations 0-96045
- meniscus collimator viewfinder, optimisation of mirror light transmission coeffs. 0-74469
- microdensitometry, linear, sensor optics design 0-62710
- mirror, asymmetric, with thin absorbing film, design 0-69493
- mirrors, dielectric multilayer, reflectance under slight absorpt. conditions 0-83655
- MTF tolerancing computer program 0-78934
- multilayer coating design achieving a broadband 90° phase shift 0-102801
- multilayer highly reflective coating design for wideband 90° phase shift 0-74464
- multimode graded index fibre parameter optimisation, design considerations 0-102804
- multispectral scanner, high resolution, for Earth obs., optical design 0-82174
- Nanjing lightweight 4 m telescope design and construction 0-105162
- night vision goggles, military low-cost, design and development 0-78990
- optical diode to enforce one-direction travelling wave operation 0-69427
- optical glass, refr. index tables and calcs. for optical designer 0-83650
- pancratic objectives, aberration stabilisation during focusing 0-102799
- photographic lens design, new developments and trends at Zeiss 0-62746
- planar star coupler design for fibre optic systems 0-74474
- plastic lenses, aspherical-surface, for large screen TV, optical design and evaluation 0-78937
- prism dimensional design, rhombic (*Czech*) 0-74494
- recording refractometer for optical glasses, 300 to 2600 nm range 0-57363
- reflex cameras, lens-array focusing system tests 0-86479
- schlieren 0-87544
- schlieren system, refractive index gradient, chromatic variation meas. technique 0-74471
- spectrophotometer, UV-visible, high throughput, optical and optomechanical design 0-95155
- submarine periscope optical design for laser rangefinding compatibility 0-78987
- superachromatic triplets, design method 0-64133
- system planning and design, w.r.t. primary aberrations (*Italian*) 0-69490
- system tolerancing, encircled energy performance prediction 0-78935
- systems engineering, seminar, San Diego, CA, USA (Aug. 1979) 0-77541
- systems engineering approach to optical design, fabrication and operation 0-95986
- table telescope, 10 m segmented-mirror 0-105163
- telescope, altazimuth mounted, primary mirror deflection and stress anal. 0-58659
- telescope, two-mirror objective systems, field lens group corrector 0-78945
- telescopes, 25 m equivalent aperture, optical and IR, design concepts 0-82203

**optical design techniques continued**

- thermal blooming cell design for use in evaluating adaptive optics 0-102780
- three-lens cemented component calcs., reduced secondary spectrum 0-102800
- two-mirror pancratic system, extraneous image plane highlights elimination 0-87467
- UV high-resolution optical telescope design 0-90335
- wavefront aberration polynomial, calc. 0-102614
- wavelength division multiplexing technology status and prospects 0-64203
- well-baffled axially symmetric system design program GOSBOP 0-78940
- Wolter lens component replication 0-95972
- zoom lens system design and manufacture 0-68288
- AlGaAs DH laser epilayer struct. optimization for integrated optical circuits 0-99879
- CO<sub>2</sub> laser fusion system optical design and analysis 0-74391
- He-Ne laser model LG-10, design (*Rumanian*) 0-87407
- LiNbO<sub>3</sub>:Ti branching optical waveguide, mode coupling 0-69518
- Nd-glass laser system, multichannel, for fusion experiments, model 0-58557

**optical detection of ENDOR** *see* ENDOR; *optical double resonance***optical detection of magnetic resonance (EPR)** *see* microwave-optical double resonance**optical detection of magnetic resonance (radiofrequency)** *see* magnetic double resonance; *optical double resonance***optical dispersion***see also* optical constants

- acrylic moulding formulations, optical and mech. props. 0-106582
- aerosols, multiple scatt. theory for spherical particles (*Russian*) 0-94599
- amplitude-phase holograms, optical parameter dispersion 0-58481
- anharmonic oscillator model for dispersive optical bistability 0-58623
- anomalous dispersion meas. using 4-beam Rozhdestvenskii interferometer 0-68245
- atmosphere, multiple scatt. theory for dispersive media with spherical particles (*Russian*) 0-94599
- bistability, absorptive and dispersive, in Fabry-Perot and ring-cavity geometries 0-95942
- dielectric thin film stack, control by stationary ratio method, refractive index dispersion influence (*French*) 0-60693
- dielectric waveguide hybrid and transverse mode dispersion calc. (*Russian*) 0-99857
- Doppler-free two-photon dispersion problem 0-106562
- Fabry-Perot cavity, dispersive optical bistability 0-78889
- fibre, basic terms, properties, uses (*Dutch*) 0-64166
- fibre, modal dispersion of power-law profiles with tails 0-95991
- fibre, PCVD, dispersion measurement by mode-locked synchronously-pumped dye laser 0-64191
- fibre, single mode, dispersion characts., correlation between numerical prediction and meas. 0-91890
- fibre, step-index, pulse dispersion, neutron irradiation effects 0-91897
- fibre attenuation and pulse dispersion due to neutron irradiation 0-58730
- fibre dispersion meas. with Nd:YAG laser at 1.06 to 1.6  $\mu\text{m}$  0-87555
- fibre loss, dispersion and polarisation meas. by acousto-optical tunable filter 0-102855
- fibre optic acoustical detector probe 0-91916
- fibre second generation systems, 1300 to 1600 nm 0-64163
- fibre waveguide mode properties, computation by propagating beam method 0-69502
- fibre-optic communication system performance at 1.55  $\mu\text{m}$  with single-longitudinal-mode laser 0-87556
- fibre with arbitrary index profile, pulse propagation and dispersion 0-78984
- FM mode locked laser, dispersion effect 0-74406
- gas DFB laser waveguide precision calc. and pulse energy obs. 0-58577
- gas lasers, mode interactions in longitud. mag. field, active medium dispersion effects 0-63967
- gases, stimulated Raman scatt. second Stokes component, dispersion effects 0-91857
- glass, high GeO<sub>2</sub>, zero material dispersion wavelength and waveguide props. 0-58733
- graded-index optical fibre intermodal dispersion, frequency-domain meas. 0-58729
- grating monochromator, Cary principle for determining dynamic dispersion 0-58666
- grazing light ray refraction in dispersion zone above optically homogeneous media interface 0-74297
- homogeneously broadened medium, absorption spectra of optical bistability with dispersion 0-102757
- homogeneously broadened medium with dispersion, optical bistability 0-83630
- image processing in incoherent light 0-87339
- IR and FIR tunable coherent sources utilising modulational instability 0-95967
- lightguide theory and its implications in manufacturing 0-64186
- low-loss multimode optical fibre characterisation for nuclear diagnostics 0-78501
- microscopical and Ewald dynamical diffraction theories, refl. and transmission, spatial dispersive dielec. slab 0-83548
- molecular lasers, laser pumping, dispersion 0-87375
- monomode fibre dispersion and bandwidth meas. by mode-locked Q-switched Nd:YAG laser 0-91933
- monomode fibre total dispersion and loss minima 0-91929
- monomode optical fibre bandwidth limitations and bend losses 0-87553
- monomode optical fibre design and fabrication for submerged cable applications 0-91932
- multimode fibres of arbitrary refr. index profile, pulse dispersion 0-74475
- optical fibre, soliton pulse propagation 0-58759
- optical fibre, vapour-oxidation fabricated, refractive index modulation, pulse dispersion 0-58756
- particle size distribution, spectral transparency method, improvements 0-86254
- plane-parallel plate, with spatial dispersion, light refl. and transmission coeffs. 0-88951
- predisperser for large plane-grating spectrograph 0-73477
- quasioptics in anisotropic and dispersive media 0-91943
- radiation fluctuations from light source 0-95857
- rectangular core fibre optic waveguide, dispersive props. 0-64172
- refractive index calcs. of optical materials, 0.365-2.6  $\mu\text{m}$  spectral region 0-87444
- self pulsing in dispersive optical bistability in ring cavity 0-78890



# optical dispersion continued

- semiconductor, carrier relaxation time anisotropy effect on free carrier dispersion studies 0-84474  
shadow methods for studying turbulence using reflection from a mirror in the medium 0-95801  
single mode fibre 1.1-1.3  $\mu\text{m}$  dispersion meas. by pulse synchronisation 0-64192  
single-mode fibres, axial refr. index dip effect on zero total dispersion wavelength 0-78962  
single-mode fibres, pulse distortion, Gaussian pulse propag. theory 0-78956  
slab waveguide, TE Mode dispersion rel. to DH semiconductor lasers 0-91886  
spatially dispersive crystal, reflectivity and transmittivity 0-99604  
stimulated Raman emission in single-mode fibres by Nd:YAG laser pumping in low-dispersion region at 1.3  $\mu\text{m}$  0-64100  
stripline waveguides, dispersion characts. and radiation fields 0-64155  
three-level molecular laser pumping and dispersion eqns. 0-69384  
two dimensional dispersion relations, phase problem appl. 0-102631  
waveguide, wavelength dispersion 0-91887  
waveguides, optical, nonlinear pulse propag. theory 0-83669  
Al(PO<sub>3</sub>)<sub>3</sub>-BaF<sub>2</sub>-Al<sub>2</sub>O<sub>3</sub> glasses, opt. props., group I-III fluorides effect 0-66143  
As<sub>2</sub>S<sub>3</sub>, two photon light absorpt. dispersion, induced linear light absorpt. (Russian) 0-66231  
CdGeP<sub>2</sub>, thermo-optic coefficient, dispersion 0-71396  
CdS thermo-optic coefficient, dispersion 0-71396  
CdSe thermo-optic coefficient, dispersion 0-71396  
CuGaS<sub>2</sub>, thermo-optic coefficient, dispersion 0-71396  
GaAs lasers, comments on host dispersion in ultra-short pulse generation 0-64024  
GaS, infrared optical props., polarisation depend., vibr. modes 0-100658  
GaSe, Faraday rot. near absorpt. edge, optical dispersion meas. 0-80757  
Ge-As-Se IR transmitting glass composition, prep. and props. 0-69474  
GeO<sub>2</sub> doped gradient optical fibres, pulse dispersion (German) 0-74496  
HF in absorption, anomalous dispersion meas. 0-95881  
Kr-Ar, phase matched, generation of Lyman- $\alpha$  radiation 0-91845  
Kr-Xe, phase matched, generation of Lyman- $\alpha$  radiation 0-91845  
K-LiAl, optical dispersion, room temp. reflectance spectra 0-66195  
PbSnTe, optical dielectric const. variation with carrier conc. 0-84709  
 $\beta$ -Pdn, electrical resistance, mag. susceptibility and IR freq. dispersion (Russian) 0-107759  
Rb vapour, Doppler-free two-photon dispersion and optical bistability 0-95940  
p-Si, heavily doped contact layers on IR detectors, IR transmissivity 0-108190  
ZnGeP<sub>2</sub>, thermo-optic coefficient, dispersion 0-71396  
ZnS, linear electrooptic coeff. dispersion 0-71380

# optical double resonance

- see also microwave-optical double resonance  
p-bromochlorobenzene, T<sub>1</sub> states, zero-field ODMR, MIDP and phosphorescence excitation spectra 0-74191  
p-dibromobenzene, T<sub>1</sub> states, zero-field ODMR, MIDP and phosphorescence excitation spectra 0-74191  
Doppler-free optical double reson. spectroscopy using single-freq. laser and modulation sidebands 0-68274  
fluoromethane, <sup>13</sup>C (<sup>13</sup>C), Doppler-free optical double reson. spectroscopy using single-freq. laser and modulation sidebands 0-68274  
formaldehyde-d<sub>2</sub> (d<sub>2</sub>) submillimetre lasers, optically pumped, assignment of laser lines 0-58513  
hexafluorobenzene, IR multiphoton excitation, vibr. energy redistrib. and hot band spectrum 0-95656  
ion, electromagnetically confined, laser cooled, double resonance and optical pumping 0-87155  
laser-RF double reson. spectroscopy of nucl. quadrupole moments, <sup>55</sup>Mn and <sup>50</sup>V appls. 0-57682  
methane-d, Doppler-free optical double reson. spectroscopy using single-freq. laser and modulation sidebands 0-68274  
methyl alcohol submm wave laser, optically pumped, intracavity double resonance obs. 0-58522  
non-Lorentzian laser lineshape and reversed peak asymmetry in double optical reson. 0-69443  
optical multistability, light self-modulation in double resonance (Russian) 0-106560  
propynal, IR-microwave double reson. and two-photon expts. 0-83396  
subnatural linewidth spectra by optical double reson. with two-photon pumping 0-74200  
BaO+Ar(CO<sub>2</sub>), in Ar flame, rot. and translational relax. by sub-Doppler optical-optical double reson. 0-95583  
CaF<sub>2</sub>,  $\Sigma$  ground state, laser-RF double reson. spectrosc. 0-69171  
GaAlAs, luminescence circular polarisation, electron optical orientation resonant variation (Russian) 0-84782  
GeH<sub>4</sub>, Doppler-free optical double reson. spectroscopy using single-freq. laser and modulation sidebands 0-68274  
HCl, liq., vibr. relax., IR double reson. 0-95712  
HNO A" excited state dipole moment, optical-optical double reson. Stark spectrosc. obs. 0-106337  
N<sub>2</sub><sup>+</sup>+He, N<sub>2</sub><sup>+</sup> selectively excited, collisional deactivation 0-83338  
NO, selectively excited rovibrational states, multiphoton ionisation spectra 0-69202  
NO, X<sup>2</sup>I<sup>+</sup> state, vibr. relax., IR-UV double reson. obs. 0-106338  
<sup>15</sup>NH<sub>3</sub>, Doppler-free optical double reson. spectroscopy using single-freq. laser and modulation sidebands 0-68274  
PH<sub>3</sub>, Doppler-free optical double reson. spectroscopy using single-freq. laser and modulation sidebands 0-68274  
Pr, metastable, F=7 $\rightarrow$ 6 Hfs, laser-RF double reson. spectroscopy 0-58170  
SiH<sub>4</sub>, Doppler-free optical double reson. spectroscopy using single-freq. laser and modulation sidebands 0-68274  
Sm, and isotopes, hfs, laser-RF double reson. spectroscopy 0-58170  
<sup>235</sup>U, ground and 1st excited states, hfs, laser fluoresc. and laser-RF double reson. spectroscopy 0-58170  
Yb, 4f<sup>14</sup>6s6p <sup>3</sup>P<sub>1</sub> and <sup>1</sup>P<sub>1</sub> levels, Stark effect, tensor polarisabilities 0-87080  
ZnS:In, recombination emission by optically detected magnetic resonance 0-66272

# optical elements

see also diffraction gratings; fibre optics; mirrors; monochromators; optical collimators; optical fibres; optical films; optical filters; optical isolators; optical modulation; optical prisms; optical waveguides; optical zone plates

# optical elements continued

- aspheric, testing in reflected light using blazed synthetic holograms 0-91881  
attenuator, variable, for use in single-mode fibre transmission systems 0-99821  
attenuator, wedged-plate, computer-controllable 0-99819  
attenuator metrological certification methods 0-91941  
autocollimators, instrum. for checking 0-77832  
beam splitting device for use with smoke chamber ray optics demonstrations 0-67990  
birefringent element, analogue, built from polarising wide field Michelson interferometer 0-91895  
bistable optical devices: an overview 0-58625  
bistable optical devices, overshoot switching 0-58776  
camera lens shutters, friction coefficient nonreproducibility evaluation 0-62765  
component polishing process modelling (German) 0-87565  
contact problems in optical surface shaping 0-74540  
dichroic beam splitters, high-performance, for DF chem. lasers 0-95932  
diffraction correlators invariant to optical element shifts 0-106471  
diffuser, weak, speckle pattern, spherical aberration effect 0-87476  
electro-optic reflector, controlled, temp. fields, thermal distortions 0-96021  
electrostatic protection technique for optical components in dusty environments 0-58657  
fibre optic rotation sensor, all-waveguide configuration, key element tests 0-58796  
fibre-optic polariser, in-line, formation and props. 0-106603  
flatness, interferometric examination techniques 0-69498  
frustrated total internal reflection element, adjustable as a function of the incidence angle of highly collimated light beams 0-96022  
giant pulse ruby laser, spring-loaded partial kinematic mount, precise alignment of optical components 0-74518  
gradient index optical elements and system design 0-106594  
gradient-index imaging, theory 0-69331  
grid polarisers for IR Fourier spectrometers 0-105724  
guided-beam splitter, refl. meas., fabrication method 0-74473  
high speed rot. mech. shutter design for pre-pulse protection 0-96032  
holographic, third-order aberration theory and generalised aplanatic condition 0-74314  
holographic elements, axisymmetrical, third order aberrations 0-69341  
holographic optical elements for incoherent polychromatic imaging 0-69349  
IR segmented composite window design 0-106621  
lens guide, low-loss image transmission 0-91872  
light shutter array, large area electronically controllable, using polyvinylidene fluoride bimorph vanes 0-58696  
multilayer beamsplitter coatings, accelerated fabrication method 0-102873  
nonlinear coherent coupler, new optical logic device 0-58630  
optomechanical converter, small-holes dia. meas. 0-77750  
passive shutters for ruby laser, use of KS glasses for generating subnanosec. pulses 0-102728  
phase anisotropy, temp. depend., intracavity method, meas. 0-78931  
polishing simulation calc. and results (German) 0-87566  
precision optical element testing by phase meas. interferometry 0-74520  
production quality trends and limits 0-69566  
production technology advances, seminar, London, England (April 1979) 0-67938  
rod, tapered gradient-index, geometrical optics 0-69322  
shaded circular apertures, encircled energy in diff. pattern, super-resolving and apodising props. 0-95787  
surface contact interaction zone, thickness calc. and distance meas. methodology (Russian) 0-99889  
tools for quick precision alignment of interferometric equipment 0-73429  
two coord. deflector, anisotropic diffraction and wide band scatt. 0-91920  
visual instruments, optical component contamination, effect on visibility of extended objects 0-64137  
volume reflecting grating parameters determ. for freq. selective optical elements (Russian) 0-74492  
welded optical fibre signal splitter 0-102814  
CO<sub>2</sub> laser Gemini fusion system optical performance 0-74392  
CaCO<sub>3</sub>, calcite linear polarizer, role in laser technology 0-64165  
NaCl 46 cm window optical evaluation facility 0-74526  
NaCl Czochralski crystal growth for large CO<sub>2</sub> laser windows 0-74525  
NaCl large window continuous polishing 0-74527  
NaCl window production for Antares CO<sub>2</sub> laser system 0-74524  
TeO<sub>2</sub>, two coord. deflector, anisotropic diffraction and wide band scatt. 0-91920  
ZnS CVD IR window, optical and physical characteristics 0-106620  
ZnSe laser windows, AR coated, photoacoustic chopping freq. studies using CO<sub>2</sub> laser 0-83629  
ZnSe laser windows, photoacoustic signal var. with chopping freq. 0-75309  
ZnSe/water, interface, laser-induced damage in ZnSe 0-102746

# optical fibres

- 4 port and 8 port kaleidoscope micro-optic star coupler for optical fibres 0-58681  
30.4 km graded index vapour-phase axial deposited fibre, props. 0-64149  
100 Gbit/s transmission rate, ext., review (French) 0-69525  
800 Mbit/s optical transmission experiments with dispersion-free fibres at 1.5  $\mu\text{m}$  0-58680  
access couplers for single strand systems 0-58766  
acoustical detector probe 0-91916  
alkali borosilicate system, self-focusing fibres with aperture of 0.18 0-87548  
alkali halides, polycrystalline, use as IR optical waveguide fibres 0-58750  
alkali lime germanosilicate GRIN fibre prep., losses and geometrical props. 0-69560  
analogue video transmission feasibility using laser diode, over 30 km at 1.3  $\mu\text{m}$  0-58737  
analysis using scalar approximation technique, accuracy 0-58703  
applications outside data transmission and communication, review 0-74482  
asymmetric fiber power splitter 0-83661  
asymmetric T-couplers for fibre optic data buses 0-102809  
attenuation, bandwidth, and refractive index meas. methods compared 0-64190

## optical fibres continued

attenuation and pulse dispersion due to neutron irradiation 0-58730  
 attenuation charact. meas. by backscatter technique (*Italian*) 0-106600  
 attenuation measurement by backscattering method, effect of noise 0-102824  
 attenuation measurement comparison among USA manufacturers 0-58747  
 attenuation measurements performed by backscattering technique 0-64152  
 attenuator, variable, for use in single-mode fibre transmission systems 0-99821  
 backscatter meas. theory (*German*) 0-91921  
 backscattering method for attenuation and connection insertion loss meas., anal. 0-58675  
 bandwidth determination in time domain, OTF meas., laser diode source evaluation 0-79002  
 beam to fibre coupling with low standing wave ratio 0-99822  
 benzil core fibres, void-free cryst. growth, X-ray diffr. and optical microscopy study 0-71586  
 bidirectional optical systems, Rayleigh backscatt. freq. depend. 0-69511  
 binary phase gratings for fibre-optic communications 0-64201  
 birefringence in slightly elliptical fibres 0-106602  
 birefringent, Faraday rotation 0-58672  
 bistable optical fibre switch, construction and performance 0-95994  
 borosilicate glass single-polarisation single-mode fibres 0-64205  
 borosilicate optical waveguide glass, B content determ. using nuclear track counting 0-95969  
 bundles and single fibres, appls. (*Japanese*) 0-78998  
 cable connectors, Si chips manufacture for fibre alignment 0-64188  
 cable design considering structural imperfection 0-64184  
 cable reliability, deterioration factors, splice point reliability, coating materials, static fatigue life (*Japanese*) 0-99848  
 cable vibration characteristics, fibre strain and optical loss meas. 0-99870  
 cables, design, manufacture, laying and jointing (*Italian*) 0-99838  
 cables, historical development (*Japanese*) 0-87494  
 cables connections, in-the-field 0-69545  
 cables design and testing, w.r.t. stress-strain behaviour 0-69551  
 capillary tubing delay lines for operation at 20 MHz 0-74654  
 characterisation techniques compared 0-64202  
 characteristics measurement using optical bench equipment 0-58695  
 clad-glass fibres, thermal stresses 0-107360  
 coated optical fibre cable unit, internal stress due to compressive loads, optimum design 0-58717  
 coating, secondary, rel. to transmission loss 0-58704  
 coating technology, overview 0-58828  
 coating with conical shape applicator 0-58820  
 coatings centering by monitoring forward scattering patterns 0-64146  
 communication, historical and technical features review, future prospects (*Japanese*) 0-99863  
 communication advances, materials and techniques 0-102853  
 communication development trends, review 0-69521  
 communication fibre endface preparation by AC discharge heating and stretching 0-64232  
 communication line with spectral multiplexing in 1.3  $\mu\text{m}$  region 0-74504  
 communication system components, state-of-the-art survey (*German*) 0-69538  
 communication system performance at 1.55  $\mu\text{m}$  with single-longitudinal-mode laser 0-87556  
 communication systems, analytical review including survey of commercial systems 0-74489  
 communication systems, book 0-73117  
 communications, prospects for 1 to 1.6  $\mu\text{m}$  spectral range use 0-102848  
 communications appls., techniques and predictions 0-87472  
 communications in industry, appls., glass fibre props., connectors 0-87550  
 components for optical communication systems, review 0-87539  
 compound glass, manufacturing process and fundamental charact. (*Japanese*) 0-99865  
 compound glass, nylon-covered, reliability and verification tests and results (*Japanese*) 0-99866  
 compound glass, total and scatt. loss coefficient meas. 0-69536  
 compound glass rod absorption coeff. calorimetry 0-106631  
 concatenated fibre-optic cable, cumulative baseband frequency response models 0-78983  
 conference, basic optical props. of materials, Gaithersburg, MD, USA (May 1980) 0-101668  
 connector loss evaluation by backscattering 0-58721  
 connectors, nonlinear distortions and noise in optical communication systems 0-96001  
 connectors, single- and multi-fibre, basic construction (*Japanese*) 0-87509  
 connectors, splices and couplers, design principles 0-58765  
 controlled fusion expt. shielding and earth loop elimination 0-74007  
 convertors, O/E and E/O, connected to both ends of optical fibre giving low-loss, broad band, non-inductive line (*Japanese*) 0-87510  
 coupled diode lasers, LF noise meas. 0-58542  
 coupler, fabrication using splicing technique, characteristics (*Japanese*) 0-87508  
 coupler, low loss, for coupling LED to fibre-optic system 0-91907  
 coupling using graded-index rod lenses 0-91891  
 current measurement appl. 0-96015  
 cutting tool and automatic splicing machine 0-87575  
 CVD fibre, long length strength 0-58752  
 data transmission systems for plasma diagnostics 0-79571  
 design, mech. props. and performance tests and practical applications (*Japanese*) 0-99867  
 diameter measurement using fast Fourier transform 0-91894  
 dielectric waveguide hybrid and transverse mode dispersion calc. (*Russian*) 0-99857  
 differential delay time relationship with propagation mode number study by effecting selective mode excitation (*Japanese*) 0-87504  
 differential mode delay rel. to refr. index profile, geometrical optics treatment 0-69529  
 m-dinitrobenzene core fibres, void-free cryst. growth, X-ray diffr. and optical microscopy study 0-71586  
 diode-laser-fibre coupling, effects of fibre propagation loss 0-74484  
 direction coupler, interference filter all-fibre for wavelength division multiplexing 0-91900  
 directional coupler with lapped multimode fibres, characts. 0-91892  
 directional filter structure and characteristics for bidirectional transmission 0-58734  
 dispersion meas. with Nd:YAG laser at 1.06 to 1.6  $\mu\text{m}$  0-87555

## optical fibres continued

dispersion measurement by mode-locked synchronously-pumped dye laser 0-64191  
 double-core single-mode, as directional coupler 0-106597  
 double-mode, propag. characts. 0-99834  
 drawing, by different heating methods, cooling rates 0-66538  
 drawing facility for lightguide fibres 0-64229  
 drawing out from blanks, high temperature resistance oven 0-74491  
 dual-mode fibre, spatial technique for modal delay difference meas. 0-78950  
 dynamic fatigue and strength degradation 0-58719  
 elliptical fibres, near-field correction factor 0-87490  
 elliptical multimode fibres, leaky ray correction factors 0-87487  
 elliptical step-index, tunnelling-radiating effect 0-58714  
 end face cut prep. and inspection techniques, review 0-74483  
 end face quality check 0-64164  
 excess loss increase mechanism of jacketed fibers at low temperature 0-83682  
 fabrication and construction of secondary coating for optimised design (*Japanese*) 0-87567  
 fabrication processes and transmission characts. (*Japanese*) 0-87496  
 fabrication study for long wavelength region (*Japanese*) 0-87499  
 fabrication using phase separation and leaching method (*French*) 0-106623  
 fatigue characts. improvement, using surface compression cladding 0-69549  
 fault location and backscattering meas. 0-64183  
 fibre-optic measurements, using standards and instruments 0-74488  
 fibre optic connectors, precision and stability developments 0-69523  
 filament waveguides for signal transmission in far IR region (*Czech*) 0-96017  
 filter, single mode fibre birefringent 0-58713  
 finite difference methods for propag. parameters calc. (*Russian*) 0-64189  
 floating zone crystal growth for IR optical waveguides 0-79019  
 FM analogue signal transmission system, advantages (*German*) 0-58679  
 fracture surface anal. 0-58754  
 furnace drawn, tensile strength 0-58751  
 fusion splicing machine for optical fibres 0-74516  
 future developments, impact on 'next generation' of electronic equipment, data ring concept 0-102808  
 gamma-irradiated, differential interferometric meas. of refr. index changes 0-78952  
 gas-dielectric fibre, wave conversion in irregular portion 0-74500  
 glass, for communications colloquium, London, England (Jan. 1979) 0-67930  
 glass and plastic fibre characts. and interconnection requirements 0-69513  
 glass core/polymer cladding, high numerical aperture 0-96024  
 glass fibre, forming process, characts., anal. techniques 0-58827  
 glass fibre, strengthening by molecular stuffing 0-58830  
 glass fibre, vapour phase materials and processes, review 0-58825  
 glass fibre attenuation characts., light-wave propag. communication (*German*) 0-95997  
 glass fibre drawing process, characterization and control 0-58826  
 glass fibre drawing process, extensional instabilities 0-89258  
 glass fibre long wavelength optical communication, materials and devices, review 0-99854  
 glass fibre refractive index profile meas. using interf. microscope with freq. shift 0-64175  
 glass fibres, flaw generation by indentation fracture technique 0-81156  
 glass fibres used for optical transmission systems (*German*) 0-69516  
 graded fibres, mode propag. time calc. using multimode theory (*German*) 0-58710  
 graded index, high index hemispherical microlens tip melt fabrication for coupling to GaAlAs laser 0-69506  
 graded index, impulse response based on mode coupling coefficient 0-58705  
 graded index, low temp. dependence of loss increase due to nylon jacket shrinkage, optimum cable unit 0-64182  
 graded index, mode coupling due to perturbation of index profile 0-106598  
 graded index, wave eqn. for propag. fields 0-58757  
 graded index fibre, error estimates for first order WKB calc. method 0-87488  
 graded-index, cables, transmission expts., 1.2-1.6  $\mu\text{m}$  wavelength range 0-102813  
 graded-index, manufacture, double-crucible method 0-83688  
 graded-index, mode eigenfunction computation propagating beam method 0-95988  
 graded-index, multimode, differential mode delay and attenuation meas., optimal excitation calc. 0-99842  
 graded-index, optical loss meas. in the field 0-102851  
 graded-index, semiconductor laser sources for coherent optical-fibre systems 0-64159  
 graded-index curved media, generalised Fresnel power transmission coefficients 0-102815  
 graded-index fibre excited by step-index fibre, baseband freq. response 0-99829  
 graded-index fibre vapour-phase axial deposition method, fibre characteristics 0-58824  
 graded-index fibres, mode analysis using scalar wave eqn. and direct numerical integration 0-78971  
 graded-index fibres for optical transmission system, investigation of MCVD and VAD methods (*Japanese*) 0-58692  
 graded-index multimode fibres, bandwidth characts., appl. on long-haul transmission systems 0-64180  
 graded-index optical fibre intermodal dispersion, frequency-domain meas. 0-58729  
 graded-index single-mode, expt. characterisation using far-field radiation pattern meas. 0-64150  
 graded-index VAD fibres, transmission loss meas. using laser diodes 0-87486  
 graded-index waveguide coupling and matched joining, coherent states and light propag. 0-102625  
 gradient-index fibre array, appl. in copying machine 0-69500  
 gradient-index fibre array, unevenness of illuminance 0-69482  
 gradient-index fibre lens, radiometric props. 0-69481  
 gradient-index light-focusing, image enhancement 0-69501  
 high density, parallel transmission system for data transmission (*Japanese*) 0-87507  
 High Density Connector Interface, fibre optic link 0-91901



## optical fibres continued

high numerical aperture multicomponent glass fibres 0-78949  
 high-speed optical systems at 0.85  $\mu\text{m}$ , modal noise and optical feedback 0-87323  
 high-strength fibre production and proof-testing 0-64204  
 hydrophones, comments on mechanism of transduction 0-58882  
 illuminating fibre bundles, improved characts. due to glasses type VS 1637 and VO 720 0-102844  
 index profile measurements of fibres and their evaluation 0-87538  
 index-matching fluids for long wavelength (1.2-1.6 micron) fibre-optic appls. 0-99841  
 inhomogeneous dielectric fibres transversely incident beam wave scatt. 0-96004  
 instrumentation appl. survey 0-83665  
 integrated and guided-wave optics, conference, Incline Village, NV, USA, January 1980 0-58772  
 interconnecting fibre optics 0-69514  
 interconnection using compound-lens devices, telephone links appl. 0-74493  
 intermode phase scanning for recovering phase-modulated signals on multimode optical fibres 0-58682  
 introduction to theory and applications, book 0-90617  
 IR and FIR tunable coherent sources utilising modulational instability 0-95967  
 IR coating nonuniformity effect on precision optical systems, compensation by auxiliary laser 0-78926  
 jacketed and cabled optical fibre low-temp. attenuation increase 0-58732  
 jacketed fibres, thermal characts. of phase shift 0-58670  
 jointing techniques and connections to communication equipment (*Norwegian*) 0-64179  
 laser diodes for fibre communications, characteristics and state of art (*Italian*) 0-58569  
 laser triggering through fiber optics of a low jitter spark gap 0-107000  
 launching and propagation of light in optical fibres 0-69504  
 lenslike fibres, density-matrix method applied to mode coupling 0-78970  
 light guide data transmission, review (*German*) 0-95996  
 light propagation, basic terms, properties, uses (*Dutch*) 0-64166  
 light sources and detectors (*Italian*) 0-69390  
 light velocity fibre optic wink-around expt. 0-90628  
 lightguide theory and its implications in manufacturing 0-64186  
 line image transmission through single fibre using spectral instrums. 0-102820  
 liquid crystal electro-optic switch, four-port, for unpolarized fibre light 0-58715  
 liquid-crystal optical fibre temp. probe rel. to thermometry and dosimetry of heat 0-98204  
 long-distance graded-index fibre bandwidth estimation 0-58742  
 long-haul communications optical fibre fault location method 0-64193  
 long-span single-mode fibre transmission characts. in long wavelength regions 0-99850  
 long-wavelength single-mode fibre transmission systems 0-58773  
 loss, dispersion and polarisation meas. by acousto-optical tunable filter 0-102855  
 loss estimation using backscatter technique, time domain reflectometry theoretical assumptions 0-74508  
 loss meas. of multi-mode fibres, non-destructive method 0-69550  
 low-loss graded-index fibre, 3 km and 10 km preform design and modified CVD method 0-58746  
 low-loss multimode optical fibre characterisation for nuclear diagnostics 0-78501  
 low-loss optical fibre evolution 0-69532  
 luminescence meas. in inaccessible or hazardous locations using bifurcated fibre luminometer 0-62712  
 male connector with friction insert, ferrule and retainer 0-78968  
 market trends, applications, performance characts. and prices 0-91904  
 market trends, worldwide 0-58699  
 matching of semiconductor sources to thin-film planar and stripe waveguides 0-64174  
 material selection criteria for  $\lambda > 1.8 \mu\text{m}$  0-87554  
 matrix switching network for fibre-optic communication 0-58735  
 measurement techniques for optical fibre specification 0-95998  
 measurement techniques for transmission loss and refractive index distribution (*Japanese*) 0-87498  
 mechanical and optical props. reproducibility, modified CVD prep. 0-69535  
 mechanical reliability, brittle failure 0-79001  
 mechanical reliability 0-91909  
 mechanical strength reinforcing and reliability improvement methods of fabrication (*Japanese*) 0-87568  
 microbend charact. and mech. prop. for design, applicational examples (*Japanese*) 0-87500  
 microbending eqns., exact time-dependent, solns. 0-87530  
 microbending losses in fibre waveguides and cables, depend. on numerical aperture 0-96025  
 modal dispersion of power-law profiles with tails 0-95991  
 mode properties, computation by propagating-beam method 0-69502  
 mode-coupled multimode W-fibre, analytical anal., scattering matrix method 0-99872  
 monofibre cable, snap connector 0-106609  
 monomode fibre dispersion and bandwidth meas. by mode-locked Q-switched Nd:YAG laser 0-91933  
 monomode fibre refractive index profile meas., near-field technique 0-91931  
 monomode fibre total dispersion and loss minima 0-91929  
 monomode fibres, novel method for transmitting images 0-69512  
 monomode optical fibre bandwidth limitations and bend losses 0-87553  
 monomode optical fibre design and fabrication for submerged cable applications 0-91932  
 moulded multifibre connectors using rectangular multirod arrangement 0-58685  
 multicore, high density, design and manufacture, characts. (*Japanese*) 0-87501  
 multifibre splicing and butting developments (*Japanese*) 0-87502  
 multilayer multimode optical fibre, ray theory, optimal distrib. of refractive index 0-87489  
 multilayered, fibres, pulse broadening 0-83676  
 multimode, freq. depend. of modal noise, speckle theory 0-102817  
 multimode, frequency characts. 0-58669  
 multimode, graded index, mode conversion coeff. meas. method 0-99820  
 multimode, impulse response calculation 0-74486  
 multimode, slab waveguide star coupler 0-87491

## optical fibres continued

multimode, splice loss and mode conversion 0-99830  
 multimode, transmission props. and theory (*Japanese*) 0-87495  
 multimode  $3 \times 2$  fibre optical matrix switch 0-58764  
 multimode access coupler, fabrication method 0-87478  
 multimode and single-mode connector technology 0-87511  
 multimode fibre bandwidth computation from measured index profiles 0-58740  
 multimode fibre communication systems, low loss  $4 \times 4$  switching network 0-58718  
 multimode fibre data bus systems, optical bypass switch 0-99826  
 multimode fibre lightguide, coherent light modulation 0-91926  
 multimode fibre link, modal noise 0-87536  
 multimode fibre optic interferometry, applications 0-86387  
 multimode fibres of arbitrary refr. index profile, pulse dispersion 0-74475  
 multimode fibres with index profiles varying along length, pulse propag. 0-87534  
 multimode graded index fibre parameter optimisation, design considerations 0-102804  
 multimode graded-index, near field intensity and modal power distribution 0-102810  
 multimode graded-index, observation of tubular modes 0-99840  
 multimode irregular focusing with random ellipticity, light propag. 0-74501  
 multimode optical fibre wavelength-filtering effects 0-58731  
 multimode optical fibres, fusion splicing using gas flame heat source, development of splicing machine 0-102866  
 multimode step-index, forward and backward stimulated Raman scatt. 0-58639  
 multimode W-type fibres, power flow numerical soln. 0-78955  
 multiplex transmission, wavelength-division, over multimode optical fibres, edge interference filters design 0-83677  
 multiplexer/demultiplexer, low-loss, using interf. filters 0-58728  
 near IR ( $1$  to  $2 \mu\text{m}$ ) optical communications, colloquium, London, England (May 1980) 0-86040  
 neutron and gamma induced transient absorpt. and luminesc. 0-58763  
 neutron irradiated, optical absorpt. spectra 0.7 to  $1.1 \mu\text{m}$  0-58762  
 nonblocking  $8 \times 8$  optical matrix switch for fibre-optic communication 0-74485  
 nonlinear effects, appl. to active and passive device fabrication 0-58638  
 optical communication system 0-91906  
 optical time domain reflectometry by photon counting 0-95122  
 optoelectronic devices development 0-91902  
 parabolic index, selective excitation by Gaussian beams 0-95992  
 parabolic index, with periodic bends, attenuation 0-74481  
 parabolic index fibres, LP<sub>mn</sub> mode excitation by Gaussian TEM<sub>00</sub>-beams, power coupling coeff. 0-78958  
 parabolic-index, vector wave asymptotic eigenvalues in inhomogeneous circular waveguide 0-96010  
 parabolic-index fibre modes, propag. characts., linearly polarised approx. 0-78972  
 parameter characterisation techniques, comparison 0-64147  
 parameter measurement using optical time domain reflectometer 0-58755  
 parameter specifications for optical waveguides, manufacturing processes 0-96041  
 passive couplers for appl. in fibre optic systems 0-91903  
 picture direct transmission via single optical fibre 0-106628  
 piezo-optical effects due to thermal stresses 0-87519  
 planar multimode coupling structure, fabrication by ion exchange 0-64233  
 planar star coupler design for fibre optic systems 0-74474  
 planar star coupler for multimode fibres 0-99828  
 plasma augmented vapour deposition 0-69561  
 polarisation optical time domain reflectometry, optical fibre technique 0-78959  
 polarisation-conversion wavelength-selective fibre switches 0-58736  
 polymer clad, for communication use, improvement and appl. 0-69546  
 polymer lightguide, light propag., nonlinearity, quasi-optical approx. 0-99837  
 preform, refractive index profile and cross-sectional geometry meas. method 0-91893  
 preform core diameter and Ge doping profile meas., X-ray nondestructive method 0-64231  
 preform manufacture using modified CVD process 0-64228  
 preform rod, refractive index profile meas. by transverse differential interferogram 0-64141  
 preforms, axially nonsymmetric refr. index distrib., nondestructive meas. 0-106601  
 preforms, refractive index distribution measurement using X-ray absorption measurements (*Japanese*) 0-87506  
 preparation methods and performance factors 0-69557  
 principle parameters for communication systems (*Italian*) 0-58694  
 progress and components, review (*French*) 0-69524  
 pulse propagation and dispersion in fibres with arbitrary index profile 0-78984  
 quartz, stimulated Raman scatt., Stokes components recording opposite to pump wave 0-106569  
 quartz glass, Ge and B dopants, OH impurities, preform material and fibre optic waveguide struct. 0-64173  
 radially inhomogeneous waveguide modes, vector wave characts. 0-78960  
 Raman scatt., guiding structs. effects on spontaneous and stimulated emission 0-58636  
 random-bend loss in single-mode and parabolic-index multimode fibre cables 0-78951  
 randomly distorted multimode, propag. theory, step index fibres (*French*) 0-74470  
 rectangular core fibre optic waveguide, dispersive props. 0-64172  
 rectangular cored multilayer fibre 0-83667  
 refracted near-field scanning, calibration technique 0-99823  
 refractive index matching fluids for long wavelength fibre-optic appl. 0-69470  
 refractive index profile distortion, stress-induced 0-91889  
 refractive index profile distortion due to thermal stresses 0-58726  
 refractive index profile microdensitometry 0-106632  
 refractive-index profile meas., scanning optical microscope 0-87535  
 remote control system for 1.5 MeV heavy-ion fusion preaccelerator 0-73993  
 research and development, advances, conf., Kingston, RI, USA (June 1978) 0-57005  
 resin protective coating performance evaluation, UV cured 0-69547



**optical fibres continued**

rod lens analysis and application to optical fibre communications 0-87549  
 rod-in-tube fabricated optical fibre characteristics 0-87574  
 rotation-splice tapered fibre star coupler directivity and mode dependence 0-58748  
 sandwich ribbon fibres for hybrid integration in high-index materials 0-79013  
 scattering, ray theory 0-69528  
 second generation systems, 1300 to 1600 nm 0-64163  
 selection criteria, practical approach to purchasing 0-91912  
 self-centring technique for mounting microsphere coupling lens on fibre 0-74517  
 Selfoc-type, Fourier hologram recording appl. 0-95850  
 signal polarisation statistical meas. 0-99877  
 signal transmission appls. (*German*) 0-69517  
 silica based optical fibre dopants for 1 to 1.8  $\mu\text{m}$  communications 0-91930  
 silicone and glass clad compound glass optical fibre comparison 0-69533  
 single fibre connectors and cable splice hardware, optical coupling theory 0-64187  
 single mode, bending induced birefringence 0-87537  
 single mode, dispersion characts., correlation between numerical prediction and meas. 0-91890  
 single mode, homogeneous CVD fabrication and characterisation 0-69562  
 single mode, pulse fluctuations, propagation 0-87475  
 single mode and graded-index multimode fibre cable random bend losses 0-58741  
 single mode CVD fibre, bend-induced birefringence obs. 0-58723  
 single mode fibre 1.1-1.3  $\mu\text{m}$  dispersion meas. by pulse synchronisation 0-64192  
 single mode fibre analysis and fabrication for low polarisation birefringence 0-58722  
 single mode fibre for current meas. system, birefr. induced by bends and twists 0-99832  
 single mode fibre near- and far-field characteristics, profile-independent representation 0-58739  
 single mode fibre optical data bus with star couplers 0-64199  
 single mode fibre polarisation stabilisation 0-58724  
 single mode fibres, optical communication techniques (*German*) 0-102811  
 single mode optical fibre, polarisation modulation 0-64176  
 single-mode, backscattering method analysis 0-106610  
 single-mode, cutoff wavelength meas., using refracted power technique 0-99844  
 single-mode, electro-optical polarisation control 0-91899  
 single-mode, fabrication by VAD 0-83687  
 single-mode, fabrication for 1.5 wavelength region 0-106627  
 single-mode, fractional wave devices and polarisation controllers 0-106606  
 single-mode, fusion splice loss anal. 0-64181  
 single-mode, hemispherical microlens tip fabrication for high efficiency coupling to InGaAsP laser 0-69505  
 single-mode, large-freq.-shifted three-way mixing in low dispersion wavelength region 0-99792  
 single-mode, numerical aperture effects on optical and mechanical props. 0-69548  
 single-mode, pressure sensitivity meas. and limitation 0-106605  
 single-mode, pulse distortion, Gaussian pulse propag. theory 0-78956  
 single-mode, simplified parameter based anal. 0-69507  
 single-mode, single-polarisation, with refractive-index pits on both sides of core 0-99846  
 single-mode, ultra-low-loss, optimised structure for fabrication 0-99843  
 single-mode, VAD, long-length, polarisation characts. 0-106604  
 single-mode fibre, wavefront distortion compensation in thick inhomogeneous medium 0-102762  
 single-mode fibre optic directional coupler 0-58683  
 single-mode fibre to LiNbO<sub>3</sub> channel waveguide high-efficiency flip-chip coupling 0-99833  
 single-mode fibre/channel waveguide flip-chip coupling, high efficiency 0-58799  
 single-mode fibres, axial refr. index dip effect on zero total dispersion wavelength 0-78962  
 single-mode optical fibres, backscattering signal anal. utilising wave optics approach 0-64151  
 single-mode systems, instability due to interference and polarization effects 0-58774  
 single-polarisation single-mode, exposed cladding fabrication 0-58725  
 SiO<sub>2</sub>, manufacture using modified CVD method (*Japanese*) 0-99864  
 soliton pulse propag. 0-58759  
 solitons in the theory of guided lightwaves 0-58760  
 spatial coherence and modal struct. 0-87531  
 splice, elastic-tube 0-87527  
 splice insertion loss meas., backscattering method 0-58720  
 splice methods for cables (*Japanese*) 0-58690  
 splicing, arc fusion, protection and reliability 0-69565  
 splicing, connecting and sheath jointing (*Japanese*) 0-87497  
 splicing techniques for compound glass and silica optical fibres (*Japanese*) 0-99890  
 splicing tools for field applications (*Japanese*) 0-87503  
 step index fibre including gap, impulse response 0-83675  
 step-index, modal-noise probability distrib. meas. and anal. 0-99859  
 step-index, nearly elliptical, with high eccentricity, fabrication for studying modes 0-95989  
 step-index, pulse dispersion, neutron irradi. effects 0-91897  
 step-index fibre, scattering from arbitrarily located off-axis inhomogeneity 0-58702  
 step-index fibres, pulse responses investig. using WKB approx. 0-91898  
 step-index optical fibre, scattering and guided mode conversion due to spherical object, theoretical anal. 0-64153  
 stimulated Raman emission in single-mode fibres by Nd:YAG laser pumping in low-dispersion region at 1.3  $\mu\text{m}$  0-64100  
 stimulated Raman scatt., backscatter in an optical fibre 0-64109  
 stimulated Raman scatt. dynamics, Stokes components recording opposite to pump wave 0-106569  
 stimulated Raman scattering, three-wave, rel. to fibre characts. (*French*) 0-78902  
 stress corrosion susceptibility constant, meas. 0-66680  
 sub-optimal graded index optical fibre analysis using perturbation calculus 0-87480  
 submarine cable using glass fibre, expt. cable (*German*) 0-58711  
 subpicosecond response meas. 0-78961

**optical fibres continued**

supervisory/service channel for fibre optic transmission systems 0-95803  
 switch, for single-mode fibre, optimised design 0-106607  
 switching, 1x2 optical switch using new type of pentagonal prism 0-64148  
 system design and component selection 0-58767  
 systems and field trials, review 0-58700  
 tapered hemispherical end single-mode fibre, efficient coupling from semi-cond. laser 0-99827  
 technology and connector systems, marketing 0-69522  
 telecommunication cable comprising 48 fibres, design and characts. (*Japanese*) 0-58688  
 telecommunication cable comprising 8 fibres, design and characts. (*Japanese*) 0-58689  
 telecommunication system developments 0-58678  
 telecommunications appl. 0-87482  
 telecommunications systems, book 0-86049  
 temporal frequency dependence of modal noise in fibres [optical] 0-58687  
 tensile strength and static fatigue, analysis using Weibull distribution for optimum design 0-85011  
 tension-coiled single-mode fibres, high birefr. 0-99858  
 testing of fibre cable for lightweight communications systems 0-102865  
 testing of lightweight cable 0-64230  
 total loss spectra, precise meas., automatic meas. system 0-64169  
 training, educational course status and effectiveness 0-62413  
 transmission, applications and cable techniques (*Japanese*) 0-87493  
 transmission cables, history and basic principles 0-69543  
 transmission characts. of optical waveguides with periodic external force 0-99873  
 transmission expts. at 34 Mb/s with HDB3 line code 0-64198  
 transmission loss characteristics of optical fibres under hydrostatic pressure 0-99869  
 transmission system, investigation of active and passive devices (*Japanese*) 0-58693  
 transmission system planning (*French*) 0-87551  
 transmission systems, 1.2-1.5  $\mu\text{m}$ , economic evaluations and forecasts 0-87533  
 transmission systems using optical fibres, cables and connections (*German*) 0-99839  
 twisted elliptical optical fibre, polarisation coupling 0-99831  
 two-layer elliptical fibre waveguides, first higher-mode cutoff 0-58684  
 two-mode fibre with near optimum index-profile, transmission characts. meas. 0-96000  
 ultra wide bandwidth, fabrication by vapour axial deposition method 0-69508  
 ultratrace impurities determ., and behaviour during production by CVD process (*Japanese*) 0-87505  
 unordered fibre bundles, parallel image transmission, multicomponent hologram arranger 0-78957  
 UV cured epoxy acrylate coated, zero stress ageing effect on strength 0-58753  
 UV radiation-induced losses during prepolymer coating crosslinking 0-87517  
 VAD, OH-free 0-99887  
 VAD, ultimately low OH content achievement, by optimised dehydration 0-99845  
 vapour phase axial deposited cable characts. (*Japanese*) 0-58691  
 vapour-oxidation fabricated, refractive index modulation, pulse dispersion 0-58756  
 video signal, fibre-optic transmission by laser diode analogue baseband modulation 0-58738  
 wavelength division multiplexer using optical fibre pieces 0-91917  
 wavelength division multiplexing transmission technology 0-58727  
 wavelength multiplexer, single-mode-fibre 0-102816  
 weakly guiding, modes calc. by integral representation technique 0-58758  
 weakly guiding fibres, Maxwell eqn. reformulation of EM propag. 0-78974  
 Ag halide optical fibres, extrusion, visible and IR transmission 0-58829  
 Ag halide polycrystalline fibre, 10.6  $\mu\text{m}$  transmission loss obs. 0-64197  
 BaF<sub>2</sub>, ultralow loss optical fibre material, loss mechanism 0-78920  
 BaO-GeO<sub>2</sub>-Na<sub>2</sub>O borosilicate core glasses for high numerical aperture fibres 0-69534  
 CsI, ultralow loss optical fibre material, loss mechanism 0-78920  
 GaAlAs DH laser coherent light, propagating in multimode optical fibre, speckle contrast 0-78978  
 (GaAl)As injection lasers operating with optical fibre external resonator, characts. 0-58544  
 (GaAl)As injection lasers operating with optical fibre resonators 0-91812  
 GdF<sub>3</sub>-BaF<sub>2</sub>-ZrF<sub>4</sub> glass fibres, IR transmission, losses, fabrication 0-87516  
 GeO<sub>2</sub> doped gradient optical fibres, pulse dispersion (*German*) 0-74496  
 GeO<sub>2</sub>-Al<sub>2</sub>O<sub>3</sub>-SiO<sub>2</sub> fibres, ageing effects of moisture on fatigue and tensile strength 0-66539  
 GeO<sub>2</sub>-Na<sub>2</sub>O borosilicate glass fibre prod. by phase separation and leaching 0-69558  
 GeO<sub>2</sub>-P<sub>2</sub>O<sub>5</sub>-SiO<sub>2</sub> graded-index fibres, effect of deposition rate on spectral loss 0-87485  
 GeO<sub>2</sub>-P<sub>2</sub>O<sub>5</sub>-SiO<sub>2</sub> graded index optical fibres optimised for 1.3  $\mu\text{m}$  wavelength region, fabrication techniques (*Japanese*) 0-99888  
 KCl, ultralow loss optical fibre material, loss mechanism 0-78920  
 LiF, ultralow loss optical fibre material, loss mechanism 0-78920  
 Na<sub>2</sub>O-B<sub>2</sub>O<sub>3</sub>-SiO<sub>2</sub> glass fibre, plastic coating influence on strength 0-58697  
 Na<sub>2</sub>O-B<sub>2</sub>O<sub>3</sub>-SiO<sub>2</sub> glass fibre, plastic-coated, liq. N<sub>2</sub> strength 0-58707  
 Na<sub>2</sub>O-B<sub>2</sub>O<sub>3</sub>-SiO<sub>2</sub> glass, low-loss GRIN fibres, double-crucible prod., loss and bandwidth meas. 0-69559  
 P<sub>2</sub>O<sub>5</sub>-SiO<sub>2</sub>-GeO<sub>2</sub> graded-index optical fibre, UV induced losses 0-87518  
 Si, advances in fabrication using MCVD process 0-99875  
 Si-O fibres, parametric excitation of anti-Stokes coherent stimulated scatt. (*Russian*) 0-58637  
 SiCl<sub>4</sub>-GeCl<sub>4</sub>-BCl<sub>3</sub> particulate layers consolidation, in fabrication of optical fibre preforms 0-60787  
 SiO<sub>2</sub> fibre lightguides, fused, zero stress strength reduction and transitions in static fatigue 0-87523  
 SiO<sub>2</sub> fibres, fused, drawn from rods, oxy-H<sub>2</sub> flame, prep., strength, dia. var. 0-102868  
 SiO<sub>2</sub>, fused silica fibre lightguide, static fatigue transitions 0-58744  
 SiO<sub>2</sub> glass, high rate MCVD of optical fibres 0-83671  
 SiO<sub>2</sub> glass, low loss optical fibre, radiation-induced IR absorpt. 0-87521  
 SiO<sub>2</sub> glass fibre, plastic-coated, liq. N<sub>2</sub> strength 0-58707  
 SiO<sub>2</sub>, three-wave stimulated Raman scatt. obs. (*French*) 0-78902



**optical fibres continued**

- SiO<sub>2</sub>, ultralow loss optical fibre material, loss mechanism 0-78920  
 SiO<sub>2</sub>:P<sub>2</sub>O<sub>5</sub>-GeO<sub>2</sub> core graded index fibre with SiO<sub>2</sub>:B<sub>2</sub>O<sub>3</sub>, P<sub>2</sub>O<sub>5</sub> cladding, low loss at 1.3 µm 0-99874  
 SiO<sub>2</sub>-GeO<sub>2</sub> core single mode fibre with SiO<sub>2</sub>:P<sub>2</sub>O<sub>5</sub> cladding, 1.6 µm, low loss 0-99874  
 SiO<sub>2</sub>-GeO<sub>2</sub>/SiO<sub>2</sub> load bearing optical cable, geophys. appls. 0-91923  
 SiO<sub>2</sub>:P<sub>2</sub>O<sub>5</sub>-GeO<sub>2</sub> optical fibres, CVD, losses, reactant impurity effects 0-87522  
 SiO<sub>2</sub>:Ge, B, P, radiation induced optical absorpt. spectra, 0.4 to 1.7 µm region 0-58761  
 TiCl<sub>3</sub>-TiBr<sub>3</sub>, KRS-6, ultralow loss optical fibre material, loss mechanism 0-78920

**optical films**

- see also *antireflection coatings*  
 absorptive coatings, at normal incidence, program for TI-59 calculator 0-84793  
 cholesteric liquid crystal coatings, superimposed left- and right-handed, peak refl. and colour gamut 0-74472  
 circular membrane reflector made by surface bending due to electrostatic tension 0-91876  
 coating removal by Al<sub>2</sub>O<sub>3</sub> powder and NH<sub>4</sub>HF<sub>2</sub> soln. 0-74521  
 cold light mirror multilayer coating deposition 0-87464  
 deposition automated control system, design principles 0-64220  
 dielectric coatings, optical characts., effect of electric field during film condensation 0-69539  
 dielectric refractive index and thickness meas. by optical method 0-82806  
 directional coupler covered with high-index absorbing material, damped oscill. 0-91908  
 dye laser, thin film waveguide evanescent type, gain meas. 0-95908  
 evaporator, tubular-type radiation-heated, ZnS film deposition 0-76191  
 fluorescent capping layers, powdered, solar cells wavelength shifting 0-85286  
 graded-thickness, vacuum-deposited, filters for solar corona obs. appl. 0-76164  
 interface total reflection and surface wave obs. 0-108292  
 interference coatings, applied optics conf., Oakland, CA, USA (May-June 1980) 0-101661  
 IR multilayer optical medium produced by negative photoresist spin-coating 0-74451  
 IR thin film plasma deposition processes 0-87466  
 laser damage, photoacoustic study 0-80098  
 metal oxide/fluoride mirror coatings, light scatt. and optical strength in UV range 0-106595  
 metallic thin film apodising and attenuating filters, phase shifts and aberrations 0-87552  
 microscopic interference obs. by reflection contrast 0-68248  
 mirror, asymmetric, with thin absorbing film, design 0-69493  
 monochromatic Maximeter control system for thin multielectric films, stopping criterion (French) 0-60694  
 multi-layer optical system, reflection and transmission coeffs. calcs., computer program 0-66316  
 multilayer, electric field distrib. and laser damage reduction 0-87420  
 multilayer beamsplitter coatings, accelerated fabrication method 0-102873  
 multilayer coating design achieving a broadband 90° phase shift 0-102801  
 multilayer coatings, high-refl. or antirefl., vol., interface absorpt. and scatt. losses 0-63915  
 multilayer dielectric mirrors, reflectance under slight absorpt. conditions 0-83655  
 multilayer highly reflective coating design for wideband 90° phase shift 0-74464  
 multilayers, ultrathin, optical characts. 0-104005  
 photoacoustic spectroscopy study 0-64124  
 porcelain-on-aluminium, low-absorptance 0-76393  
 quarter-wave mirrors, oblique incidence reflection coefficient, small absorption of layers effect 0-64140  
 reflection coefficient partial derivatives, matrix calc. (French) 0-89080  
 refractive index meas. method 0-68242  
 scintillators for extended UV response Si detectors 0-86412  
 specular reflectance standards for visible and infrared region using thin Al film vacuum deposited on optical flats (Japanese) 0-102789  
 stack, control by stationary ray method, refractive index dispersion influence (French) 0-60693  
 TTF-chloranil visual pressure or temperature indicator 0-87443  
 waveguide fibre coating technology, overview 0-58828  
 Ag halide thin-film optical recording medium 0-102786  
 Al coating reflectivity in vacuum UV, heating effect 0-95981  
 Cd<sub>2</sub>SnO<sub>4</sub> heat mirror on plastic sheet for radiation insulation of visible windows 0-95985  
 Cu-Sn(Al)(Ga) reflecting surface absorpt. coeffs. at 10.6 µm 0-95984  
 Er<sub>2</sub>O<sub>3</sub>·Ga<sub>2</sub>O<sub>3</sub>, LPE, spectroscopic props. 0-93419  
 In<sub>2</sub>O<sub>3</sub> thin film, sputter deposition form., optical and elec. props. 0-60123  
 In<sub>2</sub>SiO<sub>3</sub> thin film, sputter deposition form., optical and elec. props. 0-60123  
 MgF<sub>2</sub>-Na<sub>3</sub>AlF<sub>6</sub> thin film deposits, quenched ageing by chopping 0-97364  
 MgO-MgF<sub>2</sub> multilayer stack selective mirror with high reflectivity (French) 0-64131  
 Na<sub>3</sub>AlF<sub>6</sub> film on Si, fused quartz substrates, H<sub>2</sub>O absorpt., IR anal. 0-75446  
 Ni-P coating, electroless, ultra-black surface production by chemical treatment 0-76647  
 Si:B ion implanted layers, light refl. and transmission coeffs., computer program 0-66316  
 Si-Ag-Si heat mirror on plastic sheet for radiation insulation of visible windows 0-95985  
 Si-Si<sub>3</sub>N<sub>4</sub>-SiO<sub>2</sub> non absorbing double layers, optical parameters reflectivity by liquid immersion method 0-71503  
 SiO<sub>2</sub> films, vac. thermal evaporation, parameter stabilisation 0-87571  
 TiO<sub>2</sub> layers, activated reactive evaporation and absorpt. indices 0-97363  
 TiO<sub>2</sub>-Ag-TiO<sub>2</sub> heat mirror on plastic sheet for radiation insulation of visible windows 0-95985  
 Y<sub>2</sub>O<sub>3</sub> coated Ag mirror for the 0.5 to 14 µm region 0-87456  
 ZnS evaporated film, refl. loss on UV irr., ZnO form. 0-99813  
 ZnS, film on Si, fused quartz substrates, H<sub>2</sub>O absorpt., IR anal. 0-75446  
 ZnO, thin film, optical props. rel. to cryst. struct. 0-97357

**optical filters**

- see also *light absorption; optical films; optical isolators; spatial filters*  
 absorption measurement, optical materials, real time holographic interferometry 0-83569  
 acousto-optic tunable filter, programmable 0-74511  
 acousto-optical noncollinear UV tunable filter 0-102832  
 acousto-optical tunable filter spectrometer development 0-101848  
 acoustooptic guided-wave tunable, using collinear TE-TM mode conversion 0-102852  
 active optical devices, seminar, San Diego, CA, USA (August 1979) 0-101664  
 anisotropic frustrated-total-internal-refl. filter, space limited 0-102821  
 apodising filters, numerical exam., second moment of the point spread function 0-106611  
 aspheric testing, in-line and carrier freq. holograms, comparison 0-87349  
 birefringent element, analogue, built from polarising wide field Michelson interferometer 0-91895  
 birefringent filter mechanical tuning techniques 0-102834  
 birefringent single mode fibre filter 0-58713  
 character recognition, optimised filter 0-95837  
 cholesteric liquid crystal coatings, superimposed left- and right-handed, peak refl. and colour gamut 0-74472  
 cinefilm copying equipment using interference light filters, additive printing appl. (Russian) 0-62774  
 coating, reflection coefficient partial derivatives, matrix calc. (French) 0-89080  
 corrugated-waveguide optical demultiplexer mode couplings 0-64194  
 Dacron, multilayer, for CO<sub>2</sub> laser attenuation 0-58616  
 dielectric coatings, optical characts., effect of electric field during film condensation 0-69539  
 directional filter structure and characteristics for bidirectional transmission 0-58734  
 edge interference filters for WDM transmission over multimode opt. fibres 0-83677  
 electro-optic interference polarisation filter, Q-switching ruby laser with high-frequency control of lasing conditions 0-74363  
 electro-optical polarisation conversion and interference tunable filters 0-102829  
 electro-optical tunable filters, programmable 0-102830  
 fibre loss, dispersion and polarisation meas. by acousto-optical tunable filter 0-102855  
 gas concentration meas. using Raman intensity depend. on giant pulse laser polarization 0-98986  
 glass fibre attenuation characts., light-wave propag. communication (German) 0-95997  
 glass UV filter, stray radiation level reduction in SF-26 spectrophotometer 0-101852  
 helically ruled optical filter, spherical refl. characts. 0-64171  
 high-throughput filter for altering spectrum of multiple-frequency lasers 0-58553  
 integrated optical channel waveguide-CCD transversal filter 0-58797  
 interferometric, illum. with convergent beam, spectral response optimisation (French) 0-99868  
 laser Doppler velocimeter with direct spectral anal., for instantaneous vel. meas. 0-99782  
 laser ultrashort pulse form., filter clarification and amplification saturation coincidence 0-64085  
 matched filter correlator memory techniques and storage capacity 0-102643  
 metal-clad optical strip-line as cutoff mode filter 0-83680  
 metal-dielectric interference filters in transmitted light 0-96013  
 metallic thin film apodising and attenuating filters, phase shifts and aberrations 0-87552  
 microscope combined with TV equipment for teaching and quality control 0-82817  
 monochromatic light source with electronically variable wavelength 0-102791  
 multicavity IR electro-optical tunable filter 0-102831  
 multilayer filters, non normal incidence, optical monitoring, allowable tolerances (French) 0-87526  
 multilayer frustrated-total-internal-reflection filter, spatially limited 0-96014  
 multimode optical fibre wavelength-filtering effects 0-58731  
 multireflection interference-filter optical multiplexer/demultiplexer 0-58728  
 multistage interference-polarization filter for wavelength selection in dye lasers 0-64091  
 neutral density, for solar corona obs. using vacuum deposited graded-thickness films 0-76164  
 photographic colour printing, correcting light filter selection 0-62764  
 polarisation-conversion wavelength-selective fibre switches 0-58736  
 schlieren optical filtering for sound-intensity measurements 0-87672  
 solar receiver radiative loss and eye hazard evaluation by Net-Radiometer 0-89673  
 spectral, optimisation for arbitrary criterion by method of basic extremals 0-96011  
 spectral adaptation for receivers and light sources (German) 0-77837  
 strip-guides, polarisation filtering 0-102861  
 TEM images of dislocation core, optical filtering for noise removal 0-107254  
 thin film technology, appls. in energy, optics, and electronics, review 0-78932  
 three-stage birefringent filter, tuning over visible region 0-58667  
 waveguide mode filter on anisotropic thin film, anal. of two coupled modes with losses 0-79000  
 wavelength division multiplexing transmission technology 0-58727  
 LiNbO<sub>3</sub>:Ti optical waveguide electrooptic devices, polarisation independ. wavelength filters 0-58783  
 LiNbO<sub>3</sub>:Ti phase-matched waveguide electro-optic TE=TM mode converter 0-58749  
 LiNbO<sub>3</sub>:Ti waveguide electro-optic TE=TM mode converter-wavelength filter 0-64210  
 Si guided-wave acousto-optical devices 0-102864  
 SiO<sub>2</sub>, fused, filter in wide field-of-view SW radiometer for Earth radiation meas. 0-87473  
 TeO<sub>2</sub> acousto-optical tunable filter with microcomputer control 0-102833  
 ZnO thin film opt. waveguide, collinear acousto-optic interaction and appl. to tunable opt. filter 0-74509



optical free induction decay *see* optical coherent transients

### optical frequency conversion

*see also* optical harmonic generation; optical parametric devices  
acousto-optic diffraction degenerate regime, second harmonic, sum and difference freq. beams 0-74300  
alkali metal vapour, IR image upconversion using two-photon resonant optical four-wave mixing 0-58632  
coherence lengths and phase conjugation by degenerate four-wave mixing 0-64101  
difference frequency generation, Gaussian intensity profile effect 0-78906  
difference frequency generation by stimulated Raman scatt. using inhomogeneous electrostatic field 0-95954  
dye laser, tunable, 545-680 nm radiation efficient conversion to 360-415 nm UV range 0-74439  
fibre, single-mode, large-freq.-shifted three-way mixing in low dispersion wavelength region 0-99792  
fibre-optic parametric oscillator, sequence freq. generation 0-83636  
IR radiation, parametric up-conversion to visible range, review 0-64104  
IR-to-visible image conversion with a thick-layer hologram 0-87355  
liquid, nonlinear, high intensity light diff. by ultrasound 0-64270  
nonlinear crystal, broad-band light conversion 0-64103  
picosecond pulse sum frequency generation 0-91854  
picosecond signal processing with nonlinear integrated optics 0-99882  
pyroelectric ionisation upconverter for IR detection 0-77860  
spectroscopy, time-resolved, IR, using freq. upconversion, methyl isocyanide isomerisation obs. 0-57400  
sum frequency wave, conversion coeff. depend. on exciting spectrum width 0-99800  
two-photon resonant up-conversion with ultrashort pulses, nonsynchronous generation 0-83637  
ultrashort light pulse parametric freq. conversion 0-106570  
AgAsS<sub>3</sub>, proustite, parametric upconverter, temp. effects on tangential phase-matching condition 0-99804  
CO<sub>2</sub>, CW laser radiation, freq. conversion in Ti-Cs vapour mixture 0-74438  
CdSe down-conversion of LiNbO<sub>3</sub> broadly tunable picosecond IR source 0-74435  
CdSe, temp. depend. phase-matched nonlinear optical devices 0-99794  
Co:MgF<sub>2</sub>, tunable transition-metal-doped solid state lasers 0-58549  
Hg<sub>0.7</sub>Cd<sub>0.3</sub>Te nonlinear optical IR generation 0-58642  
KH<sub>2</sub>PO<sub>4</sub>, high-power picosecond pulse generation 218 to 316 nm 0-64106  
LiIO<sub>3</sub>, CW intracavity upconverter using Ar laser, noise props. 0-64099  
LiNbO<sub>3</sub>, intracavity upconverter for IR detect., limits to low noise equivalent power operation 0-74430  
LiNbO<sub>3</sub>:Ti diffused channel waveguide, optical parametric amplification 0-106564  
NH<sub>4</sub>H<sub>2</sub>PO<sub>4</sub>, blue tunable picosecond pulse generation by synchronous mixing of Nd:glass laser with sideband radiation 0-87431  
Ni:MgF<sub>2</sub>, tunable transition-metal-doped solid state lasers 0-58549  
Sr, CW VUV radiation generation by four-wave mixing 0-58640  
Ti vapour, He-Ne laser radiation freq. conversion 1.15  $\mu$ m to 377.6 nm 0-95948  
Ti vapour, Nd:glass laser output conversion from 1.06 micron to 388.1 nm 0-91850  
ZnGeP<sub>2</sub>, temp. depend. phase-matched nonlinear optical devices 0-99794

### optical glass

alkali borosiluminosilicate system, self-focusing fibres with aperture of 0.18 0-87548  
athermal glasses, chemically stable 0-102783  
birefringent element, analogue, built from polarising wide field Michelson interferometer 0-91895  
borosilicate optical waveguide glass, B content determ. using nuclear track counting 0-95969  
chalcofenide glasses, O-free, cooling rate influence on optical consts. 0-88952  
characteristics, electromagnetic, mechanical and thermal props. 0-106587  
chemical durability, pragmatic view 0-78921  
coloured, type K8, laser damage threshold, optical absorpt. influence 0-91830  
compound glass rod absorption coeff. calorimetry 0-106631  
cracked layer thickness determ. by chemical method, K8 and TFI glasses 0-64226  
diamond grinding of optical glass, kinetics 0-64224  
diffused channel waveguides, direct index meas. 0-87562  
fibre communication advances, materials and techniques 0-102853  
fibre preparation methods and performance factors 0-69557  
fibre waveguide, glass core/polymer cladding, high numerical aperture 0-96024  
filament waveguides for signal transmission in far IR region (Czech) 0-96017  
fluorophosphate glasses, containing rare earth ions, magneto-opt. characts. 0-64126  
fluorophosphate laser glasses, Nd doped, piezooptic coeffs. meas. 0-99815  
fluorophosphate optical glass development 0-106588  
graded-index antireflection coatings, high laser damage threshold 0-83628  
gradient index optical elements and system design 0-106594  
high volume low cost, as solar reflectors, compositions and weathering effects 0-106589  
hyperchromatic lens, expressions for first order chromatic aberrations 0-91879  
illuminating fibre bundles, improved characts. due to glasses type VS 1637 and VO 720 0-102844  
lens, double Gaussian objective, design (German) 0-64134  
light sensitive, review of types 0-91870  
local structure exam. by EXAFS 0-108301  
melting, fining, surface tension, diffusion, nucleation in microgravity 0-81016  
metallic and glass components compared 0-69473  
neutral absorbers of NS glass, meas. of transmission when irradiated with laser radiation 0-105692  
objectives, tolerancing of refr. index heterogeneity 0-78948  
opal glasses, phosphate opacified, phase comp. and struct. 0-64919  
phosphate, containing halogens glass formation 0-103254  
phosphate glasses, optical breakdown rel. to microscopic inhomogeneous struct. 0-102784  
phosphate laser glass, Nd doped, piezooptic coeffs. meas. 0-99815  
photochromic, thermochemical effects 0-87448

### optical glass continued

photochromic glasses, parameter standardisation 0-69476  
photographic colour printing, correcting light filter selection 0-62764  
physical props., seminar, San Diego, CA, USA (Aug. 79) 0-105423  
polished glass surface, reflected light phase rotation 0-66147  
quartz glass, Ge and B dopants, OH impurities, preform material and fibre optic waveguide struct. 0-64173  
recording refractometer for optical glasses, 300 to 2600 nm range 0-57363  
reflective glass colour standards 0-90878  
refractive index gradient, chromatic variation 0-74471  
refractive index gradients, form. using ion exchange diffusion 0-64227  
refractive index tables and calcs. for optical designer 0-83650  
refractometry, precision automatic vee block, for glass refr. index meas. 0-68243  
Selfoc lens, aberration improvement by glass composition and ion exchange process parameter choice 0-69486  
silicate glass surface, photodichroic for laser recording 0-102785  
silicone-glass hybrid Fresnel lens for solar energy concentration 0-61303  
solar energy absorbers, thermokinetics of glass and semi-transparent materials (French) 0-61410  
space charged particle environment effect 0-69472  
superchromatic triplets, design method 0-64133  
surface treatment by the low-energy ions of plasma accelerators 0-97608  
thermally tempered, surface stress meas. by crit. ray method 0-106766  
thin film glass lightguide boundary refraction expts. 0-106639  
third order susceptibility meas. by degenerate four wave mixing (Chinese) 0-84708  
three-lens cemented component calcs., reduced secondary spectrum 0-102800  
transparent dielectric, laser induced plasma at surface 0-79531  
UV high-power laser material, refractive props. and optical constants 0-106555  
waveguide, graded-index surface or buried, realized by ion exchange in glass 0-69499  
waveguide fabrication by low-temperature diffusion process 0-102867  
Ag halide, kinetics of photochromic processes 0-103930  
Ag halide photochromic glasses, colour centres struct. 0-66254  
Ag halide photochromic glasses, darkening mech., temp. depend. 0-87449  
Ag halide photochromic glasses, optical absorp. of Ag, optically induced dichroism 0-108177  
Al(PO<sub>3</sub>)<sub>2</sub>-BaF<sub>2</sub>-Al<sub>2</sub>O<sub>3</sub> glasses, opt. props., group I-III fluorides effect 0-66143  
As<sub>2</sub>S<sub>3</sub>, amorphous, struct., vibr. and electronic spectra 0-64908  
BaO-GeO<sub>2</sub>-Na<sub>2</sub>O borosilicate core glasses for high numerical aperture fibres, double crucible prep. 0-69534  
BeF<sub>2</sub>, glass, IR and UV transmission spectra 0-89019  
GdF<sub>3</sub>-BaF<sub>2</sub>-ZrF<sub>4</sub> glass fibres, IR transmission, losses, fabrication 0-87516  
Ge-As-Se IR transmitting glass composition, prep. and props. 0-69474  
Ge-As-Se-Te glasses for 8-12  $\mu$ m IR optics 0-69475  
Ge<sub>30</sub>As<sub>17</sub>Te<sub>53</sub>Se<sub>22</sub>-As<sub>2</sub>S<sub>3</sub>, two-layer antirefl. coating, error considerations in design 0-74477  
Na vapour resistant, CaF<sub>2</sub> coating apparatus 0-90874  
Na<sub>2</sub>O-Al<sub>2</sub>O<sub>3</sub>-B<sub>2</sub>O<sub>3</sub>-SiO<sub>2</sub>-AgCl(Br), photochromic glass, kinetics of thermal decolorisation 0-103931  
Na<sub>2</sub>O-B<sub>2</sub>O<sub>3</sub>-SiO<sub>2</sub>, containing halogens glass formation 0-103254  
Na<sub>2</sub>O-SiO<sub>2</sub> glass containing halogens glass formation 0-103254  
Nd:glass, comparative lasing characts. of silicate and phosphate laser glasses 0-74364  
P<sub>2</sub>O<sub>5</sub>-SiO<sub>2</sub> glass, flow for integrated optical cct. fabrication 0-79005  
SiO<sub>2</sub> glass, high rate MCDV of optical fibres 0-83671  
72SiO<sub>2</sub> window glass, thermal cond., temp. depend. at low temps. 0-65322  
SiO<sub>2</sub>-Al<sub>2</sub>O<sub>3</sub>-B<sub>2</sub>O<sub>3</sub> glass mech. strength increased by etching 0-97609  
SiO<sub>2</sub>-GeO<sub>2</sub>-B<sub>2</sub>O<sub>3</sub>-P<sub>2</sub>O<sub>5</sub>, optical waveguide glass, comp. determ., plasma emission spectra 0-87446

### optical harmonic generation

*see also* lasers

acousto-optic diffraction degenerate regime, second harmonic, sum and difference freq. beams 0-74300  
AM of second harmonic 0-78908  
atomic fluorescence detection, harmonic saturated spectroscopy method 0-104472  
biomolecule, non-centrosymmetry, optical second harmonic generation 0-72133  
bistable optical devices, overshoot and alternate switching, subharmonic generation 0-99790  
dielectric breakdown with picosecond laser pulses, SHG sharp increase 0-102769  
dye laser, second harmonic pulse structure and cavity length determ. 0-95935  
gaseous system, third harmonic generation, quantum theory 0-99795  
inhomogeneous crystal optimal length for SHG, parametric amplifier and oscillator 0-106568  
injection laser harmonic distortion analysis 0-58537  
ionic crystals, centrosymmetric, stimulated excitation of second harmonic, microscopic theory 0-91849  
IR tunable laser for semiconductor multiphoton spectroscopy (French) 0-82836  
laser plasma, convective parametric decay instability 0-64722  
laser resonator fourth harmonic generation cascade process (Russian) 0-99797  
liquid, nonlinear, high intensity light diff. by ultrasound 0-64270  
lithium formate cryst., 90° phase matching 0-88634  
metal surface, SHG, hydrodynamic theory of electron gas 0-87437  
metal surfaces, SHG, non-linear response to optical fields 0-83645  
MIM point-contact diode harmonic generators and mixers 0-60105  
nonlinear crystals, interference of optical harmonics 0-64102  
optimum focusing conditions for twelfth optical harmonic generation (German) 0-64098  
photon antibunching in parametric three-wave interaction 0-83638  
plasma diagnostics, laser, combination scattering method 0-79569  
prism coupling into optical waveguide second harmonic generation 0-102763  
pulsed coherent radiation source, 118 nm, for use in plasma diagnostics 0-106572  
ruby, phase modulated conjugate wave generation, hologram model 0-83643  
second-harmonic interferometers 0-101833



optical harmonic generation continued

semiconductor, elec. field induced optical SHG theory, Brillouin zone integral 0-69457  
semiconductors with direct band gaps, exciton-polariton interactions, Green's function approach 0-92831  
SHG, computer controlled intracavity, in CW ring dye laser 0-91841  
SHG by guided radiation mode coupling in thin film optical waveguide 0-106567  
sub-SHG, nonequilibrium transitions, semiclassical theory 0-83639  
temperature phase-matching curve hysteresis, SHG 0-91852  
tendon, rat-tail, coherent optical SHG 0-89796  
two-pass optical second-harmonic generation 0-74433  
two-photon interaction between coherent optical pulses and resonant media, third harmonic generation 0-91851  
two-photon resonant third-harmonic generation, pump depletion and saturation 0-69454  
uniaxial crystals, local field influence on electron contribution to linear electro-optical effect (*Russian*) 0-88968  
urea, fifth harmonic generation, high-efficiency high-power UV generation at 2128 Å 0-99793  
VUV radiation, narrowband tunable, at Lyman- $\alpha$  wavelength 0-78907  
Ca<sub>2</sub>Mg(Co)(Zn)(Mn)(Cd)(Ca)TeO<sub>6</sub>, optical SHG study of acentricity, ferroelec. of low temp. phases 0-71324  
Cd<sub>2</sub>Mg(Co)(Zn)(Mn)(Cd)(Ca)TeO<sub>6</sub>, optical SHG study of acentricity, ferroelec. of low temp. phases 0-71324  
Cr<sub>2</sub>B<sub>2</sub>O<sub>7</sub>Cl, cubic, approx. nonlinear optical susceptibility 0-78904  
CsD<sub>3</sub>AsO<sub>4</sub> crystals, SHG, temperature phase-matching curve hysteresis 0-91852  
Cu<sub>2</sub>B<sub>2</sub>O<sub>7</sub>Cl, cubic, approx. nonlinear optical susceptibility 0-78904  
Fe<sub>2</sub>B<sub>2</sub>O<sub>7</sub>l, cubic, approx. nonlinear optical susceptibility 0-78904  
GaAlAs laser nonlinearities, harmonic distortion 0-74357  
H detection by reson. fluoresc., coherent tunable VUV generation near Ly- $\beta$  transition 0-99798  
H, optical harmonic coefficients, third order, at low freqs. 0-78905  
I laser radiation, 2nd, 3rd and 4th harmonic generation 0-91844  
KH<sub>2</sub>PO<sub>4</sub> crystal, laser freq. conversion to produce UV coherent pulse, 45 GW, for laser fusion 0-69450  
KNbO<sub>3</sub>, SHG with Ga<sub>1-x</sub>Al<sub>x</sub>As laser 0-74431  
Kr gas, nonlinear susceptibility meas. via third harmonic generation, Lyman- $\alpha$  1216 Å source 0-95947  
Kr-Ar, phase matched, generation of Lyman- $\alpha$  radiation 0-91845  
Kr-Xe, phase matched, generation of Lyman- $\alpha$  radiation 0-91845  
KrF\* laser, generation of high-spectral-brightness tunable XUV radiation at 83 nm 0-91846  
LiH<sub>2</sub>PO<sub>3</sub>, P-H bond dipole direction, nonlinear optical coeffs. meas. 0-69253  
LiIO<sub>3</sub> crystal, SHG, thermoelastic stresses and nonlinear refract. effect 0-74437  
LiIO<sub>3</sub>, intracavity freq. doubling of Nd:YAG laser long pulse emission 0-102736  
LiNH<sub>2</sub>SO<sub>4</sub> and LiND<sub>2</sub>SO<sub>4</sub>, dielec. pyroelec., and thermal props. 0-60509  
LiNbO<sub>3</sub> crystals, SHG, temperature phase-matching curve hysteresis 0-91852  
LiNbO<sub>3</sub> layers, Li out-diffused, SHG phase matching temp. variation 0-69455  
LiNbO<sub>3</sub>:Fe(Nb), SHG, phase-matching temp., impurity influence 0-69463  
LiNbO<sub>3</sub>:Ti strip waveguide, SHG 0-102773  
(NH<sub>4</sub>)<sub>2</sub>BeF<sub>4</sub>, linear and nonlinear optical props. in incommensurate phase 0-69452  
NH<sub>4</sub>H<sub>2</sub>PO<sub>4</sub>, SHG method pulse width meas. of Nd:YAG laser (*Chinese*) 0-74732  
NH<sub>4</sub>H<sub>2</sub>PO<sub>4</sub> thin crystal, intracavity SHG of synchronously mode-locked CW dye laser 0-95945  
(NH<sub>4</sub>)<sub>2-x</sub>Rb<sub>x</sub>SO<sub>4</sub>, isomorphic impurity effect on dielec. and nonlinear optical props. 0-88911  
NO nonlinear laser spectroscopy, VUV harmonic generation 0-74175  
NaNO<sub>2</sub>, optical harmonic generation near ferroelec. transition 0-91858  
Nd:glass laser radiation, spatial coherence of fundamental and second harmonic 0-69442  
Nd:YAG laser, CW mode-locked and intracavity freq. doubled, anal. 0-58548  
Ni<sub>3</sub>B<sub>2</sub>O<sub>7</sub>Br, cubic, approx. nonlinear optical susceptibility 0-78904  
Sr<sub>2</sub>Mg(Co)(Zn)(Mn)(Cd)(Ca)(Sr)TeO<sub>6</sub>, optical SHG study of acentricity, ferroelec. of low temp. phases 0-71324  
SrTiO<sub>3</sub>, optical SHG near phase transition 0-71348  
SrTiO<sub>3</sub>, dispersive nonlinear dielectric, third harmonic generation (*Russian*) 0-95955  
Te crystal, SHG, 60% efficiency, 12.8  $\mu$ m NH<sub>3</sub> laser pumping 0-83640  
Te, SHG under two-photon reson. conditions 0-99803  
Te, strained and unstrained, SHG and propag. of CO<sub>2</sub> laser radiation 0-58641  
Xe, recently enhanced multiphoton ionisation and third harmonic generation 0-91526  
ZnGeP<sub>2</sub>, temp. depend. phase-matched nonlinear optical devices 0-99794

optical images

see also aberrations  
aberrational diffraction images, computation accuracy 0-87328  
analyser, semiautomatic, use in investigation of muscle biopsies 0-85466  
analysis system, math. morphology and algorithms 0-82799  
annular aperture, arbitrary point spread functions 0-87325  
aperture synthesis by object rotation in coherent imaging 0-69336  
apertures with triangular and assoc. filters, variable apodisation 0-63914  
apodising filters, numerical exam., second moment of the point spread function 0-106611  
apodization, optimal, by means of coupled calc. of pupil function and shape 0-95788  
apodization and image contrast: author's reply to comment 0-58466  
atmosphere, phase correlation scale effects rel. to atmospheric imaging chars. 0-94604  
beam, image-bearing, nonuniformly polarized, generation of time-reversed replica 0-69459  
bilaterally distorted image linear restoration using Wiener filters 0-83557  
catadioptric objective, development (*German*) 0-102796  
coded aperture imaging: the modulation transfer function for uniformly redundant arrays 0-99019  
coded aperture imaging, review 0-101914  
coherent imagery of extended objects 0-106465  
colour image evaluation from tristimulus values transfer functions measurements 0-87333

optical images continued

colour photography, image stability and dye fading mechanisms 0-62754  
computer-generated polarisation holography system and reconstructed image quality 0-102677  
computerized image reconstruction, computerized, fragment size choice 0-78785  
confocal scanning light microscopy, imaging modes 0-86401  
confocal scanning light microscopy with high aperture optics 0-86400  
confocal scanning microscope, image form. 0-68249  
contrast loss in presence of chromatic magnification difference, numerical estimate 0-95823  
correction of optical systems, automatic, with large tolerances (*German*) 0-95977  
diffraction and aberration effects, wave optical calc. 0-83549  
diffraction image intensity fluctuations in turbulent atm. after refl., Huygens-Kirchhoff principle calcs. 0-63926  
diffraction patterns for optical systems with pupils of non-uniform transmittance 0-87470  
diffuse object imaging in randomly inhomogenous medium with amplitude distortions 0-63928  
dispersion relations, two dimens., phase problem appl. 0-102631  
double exposure interferometry through speckle photography (*French*) 0-83568  
edge enhancement, real-time, using photorefr. effect 0-99642  
electrophotographic image information content and noise analysis 0-101861  
exponential transformation using film nonlinearity for optical homomorphic filtering 0-58467  
eye, aerial image modulation lowering, contribs. of retina and eye optical system 0-81584  
Fabry-Perot-interferometer imaging system for thermospheric temp. and wind meas. 0-101441  
flat image focussing spherical lens, used for Si light detector 0-91880  
formation, propag. problems connected with special source structs. 0-87272  
Fourier spectrometry, optimal apodisation 0-99641  
gradient-index imaging, theory 0-69331  
high-resolution astronomical imaging, results 0-82225  
high-resolution imaging by degenerate four-wave mixing 0-69458  
hologram image reconstruction without using reference beam, brightness chars. (*Russian*) 0-69348  
holograms, Fresnel amplitude and phase, reconstructed second-order image props. 0-63952  
holographic image contrast degradation with partially coherent light reconstruction 0-102678  
holographic image magnification, new methodology 0-95851  
holographic lensless Fourier transform, spherical wave illum. 0-74312  
holography, image contrast changes during recording in nonlinear media with local response 0-69346  
image, dissector tubes, echelle spectrographs, design considerations 0-91918  
imaging system point spread function determ. by scatt. of two monochromatic beams 0-87316  
interference transfer function with quadratic detect., coherent illum. 0-78782  
IR crystals, optical imaging of growth defects 0-64988  
irradiance moments optical calc., wave optical accuracy limitations 0-74302  
large-aperture optical system, energy distrib. calc. in diff. image of point 0-74305  
laser pulse autocorrelation by optical processing of Fabry-Perot spectrograms 0-58465  
lens, gradient-index rod, aberrations in multimode optical fibre devices 0-69487  
lens, gradient-index rod, evaluation by imaging 0-69485  
lens guide, low-loss image transmission 0-91872  
lens-array photographic system, depth of sharp focusing, resolution 0-62763  
level slicing performance using film nonlinearity (*Chinese*) 0-102628  
light field reconstruction accuracy after stimulated scatt. 0-78911  
line image transmission through single fibre using spectral instrums. 0-102820  
linearly degraded images, iterative image restoration 0-95807  
linearly degraded images, iterative restoration, reblurring procedure 0-99640  
liquid-crystal devices, variable-grating-mode, optical logic operations on binary images 0-106613  
Luneberg apodization problem 0-87302  
metallic thin film apodising and attenuating filters, phase shifts and aberrations 0-87552  
microscope, focusing technique for digital image anal. system 0-68250  
microscope, polarizing, with crossed polarizers, incoherent diff. imagery 0-101838  
microscope, scanning, multiple traversing of the object 0-90890  
microscope, scanning and conventional, Fourier imaging of phase information 0-73444  
microscope photometer/semiautomatic image anal. instrument system for morphometric and photometric wave meas. 0-82815  
monochromator using concave holographic grating and plane mirror, imaging props. 0-99856  
multi-image regeneration by white light processing 0-95814  
multiplex image coding, astronomical IR speckle interferometry appl. (*French*) 0-67580  
nonwhite noise, S/N ratio and detail detection 0-102648  
optoacoustic effect imaging 0-106473  
optoacoustic material probing and imaging, far IR 0-83559  
orientation angle calc. using image matrix transformation (*Russian*) 0-73314  
partially coherent image form. in two dimens., computer simulation 0-106434  
perceptual coding in the cosing transform domain 0-102635  
periodic structure with coherent illum., resolution depend. on number of elements, wavelength and focal length 0-63941  
phase problem in image formation: the determination of coherent transfer functions 0-87329  
phase recording using sensitised photooxidation reactions 0-87350  
photographic film grain noise in partially coherent imaging 0-101860  
photographic layer, homogeneous solid, diffusion, one-dimensional case (*German*) 0-73495  
photographic papers, polarised light refl. 0-64127

**optical images continued**

- phthalocyanine-alkane interface, charge transfer, rel. to photoelectro-  
phoretic image form. 0-65616
- pseudocolour density encoding, white-light, using contrast reversal  
0-83560
- real-time optical processing using the liquid crystal light valve 0-63936
- reconstruction, iterative computer method 0-102634
- restoration for invariant pointspread functions 0-69332
- satellite-generated radar images of the Earth 0-90249
- scanning microscope image formation 0-86399
- self-imaging, light-optical experiments (*German*) 0-63938
- Selfoc lens as imaging system, chromatic aberration 0-69480
- shaded circular apertures, encircled energy in diff. pattern, super-  
resolving and apodising props. 0-95787
- single projector for abutting images of two light valves 0-87458
- slit image seen in total internal reflection (*French*) 0-95810
- smectic A liquid crystals, thermooptical recording, echo images 0-91928
- speckle pattern interferometry, electronic, using digital image processing  
techniques 0-87322
- speckle patterns, image plane, statistical props. 0-63940
- star image at telescope focus, quality, rel. to photoelectric obs. efficiency  
0-62034
- statistical filter for image feature extraction 0-99636
- stereo-pair images, correlation error prediction 0-102636
- storage, photoferroelectric image storage in antiferroelectric-phase PLZT  
ceramics 0-71353
- strain measurement by speckle photography, hybrid optical and electronic  
image processing 0-99976
- subtraction through speckle modulated by Young fringes 0-95813
- surface profile from horizontal light source reflection, calc. from observed  
image 0-101777
- surface profile from horizontal light source reflection, image calc.  
0-101776
- systems performance quality evaluation (*German*) 0-95804
- telescope, image vergence variation with object distance change, general  
case 0-63934
- temporal coherence rel. to optical noise, partially coherent imaging  
0-102611
- texture pseudocolouring, single pass by spatial filtering 0-95809
- three-dimensional, no. of degrees of freedom 0-78794
- two-dimensional sampled imagery, aliasing and blurring effects 0-99635
- uneven interface of media with different refractive indices, statistical char-  
acts. of images 0-87331
- unordered fibre bundles, parallel image transmission, multicomponent  
hologram arranger 0-78957
- virtual image position determ., demonstration using TV camera 0-67992
- volume holograms for image restoration 0-83566
- volume-phase reflection hologram, recording medium thickness effect on  
image luminance 0-58479
- white light image speckle statistical props. 0-106461
- Zernike moment invariants, image analysis via general theory of moments  
0-102629
- LiNbO<sub>3</sub>:Fe, white-light image processing 0-87321
- LiNbO<sub>3</sub>-gap coupled Schottky diode memory correlator, grating coupled  
optical imaging 0-64143
- LiNbO<sub>3</sub>-pn-diode airgap convolver struct. optical scanner using single  
SAW pulse 0-64144

**optical information processing**

see also *spatial filters*

- acousto-optical correlator, with two-dimensional reference transparency,  
testing 0-106485
- acousto-optical signal processing system architectures and applications  
0-102652
- acousto-optical wideband programmable filter 0-102842
- active optical devices, seminar, San Diego, CA, USA (August 1979)  
0-101664
- algae sample analysis using coherent optical processing 0-98205
- ambiguity processing by joint Fourier transform holography 0-58468
- ambiguity-function generation using passive optical  $\tau$ -shift technique  
0-102647
- analogue data processing systems, polarised modulation of light (*Russian*)  
0-91884
- analogue processing systems, multichannel processing, spectral analyser,  
antenna system design appl. (*Spanish*) 0-95822
- annular aperture, arbitrary point spread functions 0-87325
- aperture synthesis by object rotation in coherent imaging 0-69336
- astronomical plates deconvolution by maximum entropy, appl. to M87 jet  
0-62032
- astronomy, thermal background subtraction in photodiode detectors  
0-90342
- band-limited function approx. realisation by low-pass filtering sequence of  
width-modulated pulses 0-95836
- bilinearly distorted image linear restoration using Wiener filters 0-83557
- biological shape pattern recognition, average similarities of Fourier spectra  
0-104818
- bipolar spatial filtering in incoherent optical systems, review of techniques  
0-95821
- blind deconvolution, zero phase blurring function estimation 0-106482
- charge-coupling photodetector for optical information processing 0-91753
- chromosome metaphase spread, automatic finding, prep. and eval. of  
object spectra 0-98168
- circularly symmetric positive filter function realisation by transparent  
rings 0-87343
- coded aperture imaging, review 0-101914
- coherence properties modification of light beam, optical processing appls.  
0-78769
- coherent codes, iterative improvement algorithm 0-87330
- coherent correlator operation in image segment identification, aerial photo-  
graph anal. 0-102654
- coherent feedback, flexible filter operations 0-87337
- coherent information processing by a pair of lenses in spherical wave  
illumination 0-95816
- coherent light valve processor, two-dimens. optical modulator 0-102840
- coherent optical implementation of generalized two-dimensional transforms  
0-95835
- coherent optical iterative extrapolation of 2-D band-limited signals  
0-78780
- coherent processing system, modification to achieve some redundancy  
0-106468
- colour film archival storage, white light processing technique 0-99637
- colour spatial filtering for image enhancement 0-87341
- computerised tomography, analogue optical method of information  
processing (*French*) 0-94349
- confocal feedback system for partial differential eqn. analogue soln.  
0-102630
- contactless thermal expansion meas. by double Michelson interferometer  
0-73317
- convolution of ps optical signals 0-58629
- correlation detection, optimization by prewhitening 0-95802
- correlation filtering for increasing diff. efficiency 0-96028
- correlation reduction, spatial filtering and variation of resolution  
0-102850
- correlative data processing system using semiconductor injection laser  
0-74307
- correlator, nonlinear t-E curve effects for matched spatial filter material  
0-95812
- correlometer (*Russian*) 0-63935
- cytological cell feature extraction using optical moments 0-98206
- diatom recognition and counting, matched-filter and statistical method  
0-101304
- diffraction correlators invariant to optical element shifts 0-106471
- diffusing surface optical autocorrelation 0-99646
- digital correlator signal preprocessing 0-83556
- digital image processing, architectural breakthroughs 0-63939
- dynamic spatial filtration of coded optical image signals from noise  
0-95826
- edge enhancement, real-time, using photorefr. effect 0-99642
- electron micrographs of layered silicates, optical filtering of faulted areas  
0-84035
- electronic image data processing using incoherent light 0-78793
- exponential transformation using film nonlinearity for optical homomor-  
phic filtering 0-58467
- Fabry-Perot spectrometer parameter evaluation, deconvolution methods  
0-105705
- Fabry-Perot-interferometer imaging system for thermospheric temp. and  
wind meas. 0-101441
- feature enhancement using noncoherent optical processing 0-99651
- feedback in incoherently illuminated systems 0-87336
- feedback processing by TV-optical method 0-87335
- feedback systems for analogue and digital optical image processing  
0-102650
- fibre laser plate for digital image processing, all-optical parallel logic  
operation 0-106463
- fibre optic signal processing devices 0-58768
- Fourier spectroscopy and multichannel long integration time techniques  
0-91751
- general multi-dimensional formulation of optical signal processing archi-  
tectures 0-78789
- generalised matched filters for coherent optical pattern recognition  
0-99654
- geophysical mapping and remote sensing by optical filtering 0-101458
- high-speed image information preprocessor using channel plate image  
intensifier 0-78982
- holography, autocorrelation of diatoms as a function of depth of focus  
[holography in biology] 0-67324
- holography and coherent optics, information theory, book 0-98764
- hybrid field-effect liquid-crystal light valve, optical data processing per-  
formance 0-99860
- image analyser, semiautomatic, use in investigation of muscle biopsies  
0-85466
- image analysis system, math. morphology and algorithms 0-82799
- image analysis via general theory of moments, Zernike polynomials  
0-102629
- image intensifier tube for optical image processing 0-99825
- image irradiance moments optical calc., wave optical accuracy limitations  
0-74302
- image processing applications at IBM Madrid Scientific Center 0-102657
- image processing in incoherent light 0-87339
- image restoration for invariant pointspread functions 0-69332
- image subtraction through speckle modulated by Young fringes 0-95813
- image understanding systems, seminar, San Diego, CA, USA (Aug. 79)  
0-94918
- imagery, 2-D sampled, aliasing and blurring effects 0-99635
- implicit sampling for noncoherent optical data processing 0-99652
- incoherent complex spatial filtering 0-95834
- incoherent feedback using TV 0-87334
- incoherent imagery system, introduction of partial coherence by holo-  
graphic components 0-95853
- incoherent optical correlation operations 0-99650
- incoherent optical discrete Fourier transform processing system 0-74303
- incoherent optical processor to make a 'spectrogram' of a 1-D function  
0-87528
- interferometer design, construction and interferogram processing, optical  
testing appl. 0-79020
- interferometric wavelength meas. with post-detection signal processing  
0-105699
- IR sensor noise reduction algorithms, Monte Carlo evaluation 0-95824
- IR surveillance, continuous-time signal processors 0-78781
- joint transform correlator performance rel. to wavefront modulator charac-  
teristics 0-102651
- laser and electro-optical systems, conf., San Diego, CA, USA (Feb. 1980)  
0-62392
- laser diode lensless MSF holographic optical element correlator, optical  
pattern recognition 0-102663
- laser pulse autocorrelation by optical processing of Fabry-Perot spectro-  
grams 0-58465
- line image transmission through single fibre using spectral instrums.  
0-102820
- linearly degraded images, iterative image restoration 0-95807
- linearly degraded images, iterative restoration, reblurring procedure  
0-99640
- liquid-crystal devices, variable-grating-mode, optical logic operations on  
binary images 0-106613
- liquid-crystal image transducer, normal incidence, on-state optical perfor-  
mance 0-99852
- losslessness of optical systems in a vectorial treatment 0-83558
- matched filter, multicapacity, for correlator appl., using birefr. object film  
0-74478
- matched filter visibility effects on the correlation function 0-96031



**optical information processing continued**

matched filtering improvements for coherent optical pattern recognition 0-78786  
 microchannel spatial light modulator 0-91913  
 microprocessor-based interferometric data reduction system versatility 0-73439  
 microscope, focusing technique for digital image anal. system 0-68250  
 microscope photometer/semiautomatic image anal. instrument system for morphometric and photometric value meas. 0-82815  
 multi-aperture system imaging props. 0-87332  
 multi-image regeneration by white light processing 0-95814  
 multiplexing, using phase modulation 0-95830  
 multisensor image pattern recognition, statistical and deterministic aspects 0-96647  
 narrowband optical signal, spectral width estimation 0-102627  
 nonlinear optical processing in real time 0-87338  
 nonwhite noise, S/N ratio and detail detection 0-102648  
 numerical calculation using optics 0-95832  
 object restoration beyond Rayleigh limit in presence of noise 0-102661  
 optical preprocessor, use in Earth-resources satellites 0-67430  
 optical reconstructions from projections via deconvolution 0-63962  
 optoacoustic effect imaging 0-106473  
 partial spatial coherence blur correction by postdetection image processing 0-78792  
 pattern recognition, discriminant hypersurface prod. by average filters 0-99649  
 pattern recognition, hybrid optical-digital processor for invariant moment computation 0-102646  
 pattern recognition, hybrid parallel optical and serial digital processing systems 0-99657  
 pattern recognition, seminar, San Diego, CA, USA (Aug. 1979) 0-98759  
 pattern recognition by diffraction pattern sampling 0-99643  
 pattern recognition by thermoplastic complex filter 0-99656  
 periodic structure defect detect. using optical processing 0-95829  
 photodichroic spatial light modulator for joint Fourier transform correlation 0-106617  
 photodiode array integration with optical power spectral analysis 0-99645  
 pick-up tube aperture distortion correction, optical method 0-95827  
 picosecond signal processing with nonlinear integrated optics 0-99882  
 precision optical evaluation by phase meas. interferometry 0-74533  
 pseudocolour density encoding, white-light, using contrast reversal 0-83560  
 quasi-staring IR sensor clutter rejection processor design 0-86417  
 radiography, flashing tomosynthesis 0-67243  
 radiography, holographic 3-D synthesis of X-ray pictures 0-67245  
 radiography, holographic methods of 3-D representation from no. of plane images 0-67244  
 random digital scene generation with specified statistics 0-99666  
 real-time incoherent subtraction of irradiance 0-74301  
 real-time optical processing using the liquid crystal light valve 0-63936  
 reconstruction, three-dimensional, from planar projections 0-99639  
 redundancy and parallel processing 0-95831  
 regularized object restoration, resolution beyond the diff. limit 0-87324  
 remote sensing multichannel data sets, integrated optical comparator 0-64213  
 SAW spectrum analyser in photon-counting mode, statistical props. 0-105712  
 scale and rotation invariant optical pattern recognition and classification 0-99655  
 scene content measurement from aerial images, appl. to building complex scene 0-78788  
 sequential coherent optical reconstruction from projections using a ROACH filter 0-63961  
 signal and image processing, US Air Force research programme 0-78791  
 solar spectra, line profiles, rough reconstruction from series of narrow-band filtergrams (Italian) 0-98564  
 space-time optics, speckle phenomena and white light correlations 0-106460  
 space-time random speckle pattern optical analysis 0-102682  
 space-to-temporal freq. conversion for image processing 0-87340  
 space-variant coherent optical processing 0-102638  
 space-variant processing with polychromatic light 0-87342  
 spatial frequency analysis with incoherent optical approach, using LED light panel 0-78779  
 spatial frequency plane filtering by dynamic coherent illumination 0-95825  
 spatial pattern recognition by spectral feature classification and coherent optical correlation 0-99644  
 speckle pattern interferometry, electronic, using digital image processing techniques 0-87322  
 spectrogram, elimination of bright continuous spectral background (Chinese) 0-106464  
 spread spectrum time- and space-integrating optical processor 0-78777  
 statistical filter for image feature extraction 0-99636  
 stellar spectroscopy, appl. of linear filtering theory to line profiles (Italian) 0-90340  
 strain meas. speckle photography with hybrid optical/electronic image processing 0-106768  
 strain measurement by speckle photography, hybrid optical and electronic image processing 0-99976  
 Sun glitter on sea, correl. function appl. to sea surface slope distrib. function determ. (Russian) 0-94611  
 surface-wave acousto-optic signal processors 0-102640  
 target discrimination methodology in remote sensing 0-58470  
 TEM images of dislocation core, optical filtering for noise removal 0-107254  
 textural pattern recognition, comparison of optical-digital and all-digital techniques 0-99638  
 texture analysis by hybrid optical/digital system 0-78787  
 texture pseudocolouring, single pass by spatial filtering 0-95809  
 thin phase structure detection method spatial filtering props., under partially coherent illum. 0-95828  
 three-dimensional display limits 0-83561  
 time integrating optical signal processing, acousto-optic 0-102641  
 time-integrating acousto-optical correlator design and performance 0-106618  
 tomography, transaxial scanners for reconstructing objects from their X-ray projections, review 0-102632  
 truth-table look-up optical processing utilizing binary and residue arithmetic 0-69334  
 two-beam interference pattern monitoring by phase modulation 0-77844

**optical information processing continued**

uneven interface of media with different refractive indices, statistical characts. of images 0-87331  
 unordered fibre bundles, parallel image transmission, multicomponent hologram arranger 0-78957  
 US-optical correlator for spatial freq. meas. 0-95995  
 vectorcardiography, 3-dimens. 0-94405  
 video interferogram analysis by TV camera-microprocessor system 0-73440  
 volume holograms for image restoration 0-83566  
 wavefront estimation from wavefront slope meas., least-squares curve fitting model 0-106467  
 wavefront reconstruction, linear filtering influence 0-99670  
 wavefront sensing by phase retrieval 0-106478  
 white light, information processing and transmission 0-95833  
 white light processing using diff. grating method 0-106470  
 X-ray tomogram reconstruction by holographic methods 0-67246  
 $\text{Bi}_{12}\text{SiO}_{20}$ , electrooptic photorefractive crystals, for optical information processing 0-74313  
 $\text{Bi}_{12}\text{SiO}_{20}$  PROM device, image recording and erasure mechanism 0-74490  
 $\text{Bi}_{12}\text{SiO}_{20}$ , photorefractive medium, real-time image processing via four-wave mixing 0-95944  
 $\text{CO}_2$  IR laser velocimetry, processing techniques and applications 0-87831  
 $\text{KDPO}_4$  photo-spatial light modulator, optical data processing 0-102839  
 $\text{LiNbO}_3$ , electrooptic photorefractive crystals, for optical information processing 0-74313  
 $\text{LiNbO}_3/\text{Fe}$ , white-light image processing 0-87321  
 $\text{LiNbO}_3/\text{Ti}$  waveguide, ps signal processing with planar, nonlinear integrated optics 0-64208  
 $\text{TeO}_2$  time-integrating acousto-optical correlator for chirp spectrum analyses 0-106474

**optical instrument testing**  
*see also aberrations*  
 control life test design 0-87572  
 double beam interferometer, meas. of background suppression and spectral detection 0-95130  
 Fourier transform spectrometer performance, instrumentation for assessment 0-95165  
 high-pressure gas equation-of-state meas. interferometry 0-77810  
 projectors, multispectral, MSP-4 objectives, photoelectric distortion meas. (German) 0-95976  
 reflex cameras, lens-array focusing system tests 0-86479  
 refractometer, IRF-454, specification, testing method and facilities 0-73424  
 ruby ring laser with forced mode locking 0-95915  
 single-particle-size spectrometer calibration and testing, monofilament fibres as substitute particles 0-58819  
 submarine periscope optical test equipment 0-78943

**optical instruments**  
*see also colorimeters; coronagraphs; ellipsometers; holographic instruments; light interferometers; optical microscopes; optical prisms; photometers; polarimeters; refractometers*  
 automatic optical length meas., defocusing effects (Japanese) 0-68174  
 backscatter/absorption chamber optical device, for water backscatt. absorpt. coeffs. determ. 0-82074  
 binocular models, characts. and design features, review 0-74468  
 binocular summation, fusion and tolerances 0-104588  
 coherence applications, seminar, San Diego, CA, USA (Aug. 1979) 0-77542  
 design, partial coherence effects 0-78767  
 diffractometer analogue of electron microscope 0-69494  
 electric dichroism measurement instrument with digital processing 0-82800  
 emissivity determination, metals and alloys, using low-inertia opt. dilatometry 0-59684  
 flexible fibre light-guides, viewing instrum. appls. 0-87545  
 focal reducer using Fresnel lens, appl. to stellar photometry 0-67568  
 focometer, F-1, for lens focal length meas. 0-64138  
 focusing to take account of eye accommodation 0-101811  
 glass thickness automatic measurement by laser beam 0-82744  
 hazemeter for window pollution assessment 0-67995  
 image analyser, semiautomatic, use in investigation of muscle biopsies 0-85466  
 image analysis system, math. morphology and algorithms 0-82799  
 instrument for checking autocollimators 0-77832  
 interactive image scanner, high resolution 0-94423  
 microscope photometer/semiautomatic image anal. instrument system for morphometric and photometric value meas. 0-82815  
 monochromatic Maximeter control system for thin multielectric films, stopping criterion (French) 0-60694  
 multiple-mirror telescope systems, astronomical appls. 0-94713  
 nodal slide, experimental and theoretical thick lens parameters comparison 0-67998  
 optometer, IR, highly sensitive, for accommodation microfluctuation dynamics study 0-81580  
 photodetector relative spectral sensitivity meas. method using two tandem monochromators (Japanese) 0-101840  
 photometric studies of low-absorption optical media, apparatus (Russian) 0-98965  
 precision, microcomputer-aided manufacture (German) 0-95116  
 precision instrum. production developments at Carl Zeiss Jena works (German) 0-57357  
 preprocessor, use in Earth-resources satellites 0-67430  
 production technology advances, seminar, London, England (April 1979) 0-67938  
 radial scale and grating production using radial metrological pattern generating engine 0-57282  
 reflection coupling device with LED, colour masters evaluation appl. (German) 0-95123  
 refractometer for eye refr. error meas. 0-81583  
 retroreflectometer, NBS reference 0-73410  
 rheometer, analytical, optical sliding contact, for flow visualisation at articular surface 0-104847  
 spectral image analysis device, Chromotron 0-83683  
 stereoscope for viewing aerial photographs, interpretoskop optics, modifications 0-105081  
 submicron particulates size determ. by sideway light scattering method 0-98883

**optical instruments continued**

- survey for Japan (*Japanese*) 0-73406
- target position meas., statistical model 0-101778
- thermal blooming cell design for use in evaluating adaptive optics 0-102780
- UV and IR instrument material mech. and thermal props. 0-106584
- visual instruments, optical component contamination, effect on visibility of extended objects 0-64137

**optical interferometers** *see light interferometers***optical isolators**

- gas mixture, absorbing, for isolation between amplifiers in TEA CO<sub>2</sub> laser 0-95911
- glass fibre long wavelength optical communication, materials and devices, review 0-99854
- GaAs-Al<sub>x</sub>Ga<sub>1-x</sub>As MOS rib waveguide polariser, modulator and isolator 0-64217
- InGaAsP/InP DH stabilised 1.3  $\mu$ m laser diode-isolator module for hybrid optical integrated ckt. 0-58583
- YIG thin film gyromag. waveguide, on GGG substrate, optical propag. props. Faraday effect 0-74513

**optical Kerr effect**

- alkyl-cyanobiphenyl homologues, isotropic-nematic phase, optical Kerr effect 0-91866
- cavity filled with Kerr dielectric, nonlinear effect of powerful laser radiation field 0-99787
- Cherenkov type parametric optical oscillator, optical saturation 0-102771
- forward degenerate four-wave mixing, propag. anal. 0-69468
- IR and FIR tunable coherent sources utilising modulational instability 0-95967
- p-methoxy-benzoate-p-n-pentylbenzene, isotropic phase nematogen optical Kerr const. 0-78919
- molecular polarizability, anisotropic, optical study (*Rumanian*) 0-74256
- neat liquids, broadened and oscill. optically induced Kerr kinetics 0-78901
- organic compounds, nonsaturated, Kerr effect kinetics induced by picosecond laser pulses 0-102779
- surface wave at a nonlinear interface 0-91867
- Kr-Ar, phase matched, generation of Lyman- $\alpha$  radiation 0-91845
- Kr-Xe, phase matched, generation of Lyman- $\alpha$  radiation 0-91845

**optical links**

- see also optical communication equipment*
- controlled fusion expt. shielding and earth loop elimination using fibre optics 0-74007
- convertors, O/E and E/O, connected to both ends of optical fibre giving low-loss, broad band, non-inductive line (*Japanese*) 0-87510
- diode-laser-fibre coupling, effects of fibre propagation loss 0-74484
- fibre cable composed of 8 fibres made by vapour phase axial deposition, characts. (*Japanese*) 0-58691
- fibre cable comprising 48 fibres, design and characts. (*Japanese*) 0-58688
- fibre cable comprising 8 fibres, design and characts. (*Japanese*) 0-58689
- fibre cable splice methods (*Japanese*) 0-58690
- fibre cables, historical development (*Japanese*) 0-87494
- fibre communication line with spectral multiplexing in 1.3  $\mu$ m region 0-74504
- fibre communications and devices, present and future developments, review 0-69521
- fibre connectors, single- and multi-fibre, basic construction (*Japanese*) 0-87509
- fibre fabrication study for long wavelength region (*Japanese*) 0-87499
- fibre jointing techniques and connections to communication equipment (*Norwegian*) 0-64179
- fibre optic interconnection, using compound-lens devices, telephone links appl. 0-74493
- fibre optic long-haul transmission systems, bandwidth characts. of graded-index multimode fibres 0-64180
- fibre optic systems and field trials, review 0-58700
- fibre optics use in telecommunications 0-87482
- fibre remote control system for 1.5 MeV heavy-ion fusion preaccelerator 0-73993
- fibre splicing tools for field applications (*Japanese*) 0-87503
- fibre systems for telecommunications 0-91906
- fibre telecommunication developments 0-58678
- fibre transmission, applications and cable techniques (*Japanese*) 0-87493
- fibre transmission system, investigation of active and passive devices (*Japanese*) 0-58693
- fibre transmission system using graded-index fibres manufactured by MCVD and VAD (*Japanese*) 0-58692
- fibre transmission systems, 1.2-1.5  $\mu$ m, economic evaluations and forecasts 0-87533
- fibre-optic communication in industry, appls., glass fibre props., connectors 0-87550
- fibre-optic communication systems, book 0-73117
- fibres, design, mech. props. and performance tests and practical applications (*Japanese*) 0-99867
- fibres, fabrication and construction of secondary coating for optimised design (*Japanese*) 0-87567
- fibres, fabrication processes and transmission characts. (*Japanese*) 0-87496
- fibres, high density, parallel transmission system for data transmission (*Japanese*) 0-87507
- fibres, measurement techniques for transmission loss and refractive index distribution (*Japanese*) 0-87498
- fibres, mechanical strength reinforcing and reliability improvement methods of fabrication (*Japanese*) 0-87568
- fibres, multicore, high density, design and manufacture, characts. (*Japanese*) 0-87501
- fibres, multimode, transmission props. and theory (*Japanese*) 0-87495
- fibres, splicing, connecting and sheath jointing (*Japanese*) 0-87497
- fibres differential delay time relationship with propagation mode number study by effecting selective mode excitation (*Japanese*) 0-87504
- fibres microbend charact. and mech. prop. for design, applicational examples (*Japanese*) 0-87500
- fibres system testing, optical time domain reflectometry by photon counting 0-95122
- FM optical fibre analogue signal transmission system (*German*) 0-58679
- heterodyne systems, using GaAlAs laser diode, high frequency stability 0-99727
- High Density Connector Interface, fibre optic link 0-91901
- historical and technical features review, future prospects (*Japanese*) 0-99863

**optical links continued**

- lens, gradient-index rod, appl. in optical fibre communication systems 0-69488
- light velocity fibre optic wink-around expt. 0-90628
- long-distance graded-index fibre bandwidth estimation 0-58742
- long-haul communications optical fibre fault location method 0-64193
- long-span single-mode fibre transmission characts. in long wavelength regions 0-99850
- monomode optical fibre design and fabrication for submerged cable applications 0-91932
- multifibre splicing and butting developments (*Japanese*) 0-87502
- multimode fibre data link, freq. depend. of modal noise, speckle theory 0-102817
- multimode fibre link, modal noise 0-87536
- polymer clad fibre appl. 0-69546
- silicone and glass clad compound glass optical fibre comparison 0-69533
- single mode fibres, optical communication techniques (*German*) 0-102811
- SiO<sub>2</sub>, manufacture using modified CVD method (*Japanese*) 0-99864
- X-ray wavelength and optical transmission waveguides (*German*) 0-99847

**optical mark reading** *see mark scanning equipment***optical masers** *see lasers***optical materials**

- see also glass; optical films; optical glass*
- absorption measurement, optical materials, real time holographic interferometry 0-83569
- acrylic moulding formulations, optical and mech. props. 0-106582
- alkali halide crystals, activated, physical phenomena and optical data processing appl. (*Russian*) 0-80819
- alkali halides, polycrystalline, use as IR optical waveguide fibres 0-58750
- benzil cored fibres, void-free cryst. growth, X-ray diffr. and optical microscopy study 0-71586
- birefringent plates, cracks, stress intensity factors, refl. caustics method 0-93718
- ceramic, KOI, homogeneity in terms of refr. index 0-64125
- ceramics, dispersion, double refraction and storage effects, material appls. (*German*) 0-69471
- ceramics, transparent ferroelectric, composition selection for appl. in light modulators (*Russian*) 0-91869
- chalcopyrite crystals, refractive index, temp. depend., appl. to nonlinear devices 0-60555
- conference, basic optical props. of materials, Gaithersburg, MD, USA (May 1980) 0-101668
- corundum, single crystal, dispersion medium for polishing 0-102870
- crystalline material optical absorption meas. 0-105718
- crystalline optical material props., symmetries and tensorial relationships 0-108174
- diffracting periodic structure generation by coherent beam interference 0-69570
- m-dinitrobenzene cored fibres, void-free cryst. growth, X-ray diffr. and optical microscopy study 0-71586
- electro-optical and nonlinear-optical materials, review 0-74450
- fibre material selection criteria for  $\lambda > 1.8 \mu$ m 0-87554
- fulgimide planar photochromic structures for optical waveguide components 0-64196
- halocarbon index matching fluids for long wavelength fibre-optic appl. 0-69470
- index-matching fluids for long wavelength (1.2-1.6 micron) fibre-optic appls. 0-99841
- IR multilayer optical medium produced by negative photoresist spin-coating 0-74451
- laser damage in transparent polymers of various atomic composition and viscoelastic props. 0-104017
- lens array characts. on illuminated intensity distribution (*Russian*) 0-106591
- metallic and glass components compared 0-69473
- military optical system temperature effects and counter-measures 0-78938
- one-component optical cement 0-87445
- optical recording techniques appl. (*Japanese*) 0-105730
- photoacoustic spectroscopy study 0-64124
- physical props., seminar, San Diego, CA, USA (Aug. 79) 0-105423
- plastic films, IR reflectance of aluminised thermal screens for energy conservation in greenhouses 0-64351
- PMMA, glassy, optical absorpt., visible region, determ. by laser calorimetry 0-66218
- PMMA, laser damage threshold, freq. and size depend. 0-104018
- polycarbonate, bisphenol A, birefringent plates, cracks, stress intensity factors, refl. caustics method 0-93718
- polymer structure and optical behaviour 0-106583
- polystyrene, glassy, optical absorpt., visible region, determ. by laser calorimetry 0-66218
- production technology advances, seminar, London, England (April 1979) 0-67938
- rare earth ion containing inorg. materials, 3 $\mu$ m band stimulated radiation 0-97306
- refractive index calcs. of optical materials, 0.365-2.6 $\mu$ m spectral region 0-87444
- refractive index variation from field-assisted ion exchange 0-74447
- retroreflector photometric and goniometric accuracy 0-86375
- silica based optical fibre dopants for 1 to 1.8  $\mu$ m communications 0-91930
- solar energy absorbers, thermokinetics of glass and semi-transparent materials (*French*) 0-61410
- space charged particle environment effect 0-69472
- transparent solid optical materials, laser damage statistics rel. to structural defect statistics 0-91829
- trivalent metal phosphates, condensed, synthesis in polyphosphoric acid melts, physicochem. equil. considerations 0-97419
- ultra low loss materials (*Japanese*) 0-106581
- UV and IR instrument material mech. and thermal props. 0-106584
- UV high-power laser material, refractive props. and optical constants 0-106555
- N-vinylcarbazole containing polymers, sensitization to Ar laser for single laser photothermoplastic devices 0-83651
- viologens electrochromic solutions, for display appl., oxidant impurities elimination 0-78922
- Ag halide polycrystalline fibre, 10.6  $\mu$ m transmission loss obs. 0-64197
- CaCO<sub>3</sub> calcite linear polarizer, role in laser technology 0-64165
- CdGeAs<sub>2</sub> crystals, Bridgman grown, optical props. rel. to O<sub>2</sub> content of starting materials 0-81213



# optical materials continued

- $\alpha$ -CsNd(PO<sub>3</sub>)<sub>4</sub>, single cryst. struct. and spectral-luminescent props. 0-96490
- Ge, polycrystalline thermal-imaging lens, optical requirements 0-69495
- KCl:OH, absorpt. in high-transparency region 0-89037
- LiNbO<sub>3</sub>:Fe spatial holograms, ageing mechanism and thermal fixing (*Russian*) 0-74311
- NaCl 46 cm window optical evaluation facility 0-74526
- NaCl Czochralski crystal growth for large CO<sub>2</sub> laser windows 0-74525
- NaCl large window continuous polishing 0-74527
- NaCl window production for Antares CO<sub>2</sub> laser system 0-74524
- NDP<sub>3</sub>O<sub>4</sub>, fluoresc. lifetime meas., IR and photoacoustic spectroscopy 0-60652
- Si single cryst., chem.-mech. polishing of low-scatt. optical surface 0-96040
- Sr<sub>1-x</sub>Ba<sub>x</sub>Nb<sub>2</sub>O<sub>6</sub> crystals, defect-free growth 0-108346
- SrTiO<sub>3</sub>, fabrication damage characterisation by internal and external meas. 0-102782
- TiBr<sub>3</sub>-TiH(Cl) crystals, photoelastic moduli 0-97230
- ZnS CVD IR window, optical and physical characteristics 0-106620

# optical microscopes

- see also optical microscopy*
- accommodation focusing control 0-82814
- automatic focusing servo mechanisms, piezoelec. and electrodynamic, for microscope objective 0-73445
- chromatic-aberration-free microscope optics 0-86395
- confocal scanning microscope, image form. 0-68249
- contact microscope for medical laboratory use 0-85540
- focusing technique for digital image anal. system 0-68250
- grainless focusing screen for light scatter reduction 0-101836
- high-temperature laser microscope, design details 0-90891
- interference microscope with freq. shift, for glass fibre refr. index profile meas. 0-64175
- large field, for use in semiconductor manufacture 0-82812
- laser Doppler microscope, vel. measuring device 0-68251
- laser projection microscope, transmitted light, Cu vapour laser as image amplifier 0-73446
- laser projection microscope, with brightness amplifier for biology and medicine 0-76875
- laser projection microscope with image-brightness amplifier using Pb and Mn vapour 0-106541
- Leitz Laborlux 11 and Leitz Laborlux 12, two new microscopes for the investigation of transparent objects 0-82813
- medical microscopy, advent of intelligent microscopes 0-81678
- microdensitometer performance, effective incoherence and flare tradeoff 0-77851
- phase contrast microscope attachment for weak phase object visibility 0-86396
- photomicrography, high resolution, zoom instrument with automatic exposure 0-62756
- photometer/semiautomatic image anal. instrument system for morphometric and photometric value meas. 0-82815
- photomicroscopes with automatic exposure control 0-86475
- polarizing microscope, with crossed polarizers, incoherent diff. imagery 0-101838
- polarizing microscope components and applications 0-98973
- projection, optical test equipment appls. in electronics industry (*German*) 0-77849
- quality control and industrial production, new microscopes 0-82816
- rotatable microscope stage, used for hybrid microcircuits inspection 0-90889
- scanning, imaging props. and appls. review 0-82811
- scanning, multiple traversing of the object 0-90890
- scanning and conventional, Fourier imaging of phase information 0-73444
- scanning for semicond. materials and devices 0-95136
- scanning microscope image formation 0-86399
- scanning mirror, with optical sectioning characs., ophthalmology appls. 0-85461
- scanning optical microscope as new metallographic tool 0-71852
- teaching microscope for investigation of transparent biological objects 0-82622
- TV microscopy system for teaching and quality control 0-82817
- UIM-21 and UIM-23 (USSR), fitting of length meas. heads 0-57257
- wide-angle concentric dome and shell production, double-pass null test 0-79022
- Au vapour brightness amplifier at 627.8 nm, for projection microscope 0-83616

# optical microscopy

- see also optical microscopes*
- F-actin, struct. changes in living muscle fibres, polarised UV fluoresc. microscopy 0-67037
- asbestos fibre counting by automatic image analysis 0-73538
- automatic fluorescence microscope photometry data processing and display (*German*) 0-86369
- automatic image analyzer appls., densitometric and geometric studies 0-98974
- baryta crystal gas-liquid inclusion meas. with microscope heating stage 0-76967
- benzil cored fibres, void-free cryst. growth, X-ray diff. and optical microscopy study 0-71586
- biological cell deposition system for deposition at predefined locations on microscopic slide 0-76876
- biological image processing (*Japanese*) 0-81784
- biological research, computer-assisted mapping with the light microscope 0-67308
- bituminous coal, identification of constituents for petrographic anal. 0-81888
- camera system for automatic photomicrography 0-82841
- camphor, rhombohedral, polycryst., compressive deform. and dynamic recrystn. 0-71698
- cartilage proteoglycan simultaneous localisation by light and electron microscopy 0-85571
- cell element observations in same sections by light microscopy, TEM and/or SEM 0-85556
- coke, metallurgical, microstruct., using refl. light microscopy and image anal. 0-66732
- coke, metallurgical, strength and struct. relationship 0-84997
- confocal scanning light microscopy, imaging modes 0-86401
- confocal scanning light microscopy with high aperture optics 0-86400

# optical microscopy continued

- contaminant particle microanalytical methods 0-86397
- correlative light microscopy, SEM and TEM of argentaffin cells 0-85557
- crystal optical orientation, large optical axis angles (*Chinese*) 0-68246
- cytofluorometric measurements by fluorescence extinction through a diaphragmed objective 0-67319
- diatom recognition and counting, matched-filter and statistical method 0-101304
- m-dinitrobenzene cored fibres, void-free cryst. growth, X-ray diff. and optical microscopy study 0-71586
- epidural neurostimulation, percutaneous, histological reaction, short and long term study results 0-67285
- failure analysis tools comparison and selection 0-71865
- fluorescence microscopy, incident light, specimen prep. method 0-82755
- fluorescence microscopy of living cells, low level, appls. of image intensification 0-94432
- fluorite crystal gas-liquid inclusion meas. with microscope heating stage 0-76967
- glass, float, low-Fe, weathered, surface, characterisation 0-93666
- glass micropipettes, comparative calibration by optical microscopy and SEM (*German*) 0-98201
- histological and cytological reflection contrast microscopy 0-72389
- holography, autocorrelation of diatoms as a function of depth of focus [holography in biology] 0-67324
- IC photomask and wafer linewidth meas. using optical spatial coherence 0-77850
- image formation, partially coherent, two dims., computer simulation 0-106434
- image formation, propag. problems connected with special source structs. 0-87272
- Incoloy 800, steam oxidised, oxide coating anal. 0-89399
- incubator, improved air stream, for use in high resolution time lapse cinematography 0-98196
- interference microscopy, for colour development and phase separation 0-100976
- interference obs. by reflection contrast 0-68248
- Interphako interference microscopy, refr. index profile determ. of light focusing rod 0-101832
- IR microscopy coupled with scanning photoluminescence spectrophotometry 0-73447
- Kevlar aramid fibre, regular fine bands obs. by polarization microscopy 0-107064
- Kohler illumination 0-90887
- laser-Raman microprobe studies of mineralizing tissues 0-76884
- low magnification phase contrast system, Olympus IMT microscope 0-68247
- magnetic micro-rheometer evolution and theory 0-92099
- metallisation corrosion, IR microscopy failure anal. 0-98976
- metallographic sample preparation, procedures 0-57272
- microphotography, exposure control, manual 0-98975
- myosin, struct. changes in living muscle fibres, polarised UV fluoresc. microscopy 0-67037
- neurons, section embedding technique for sequential light and electron microscopic exam. 0-67317
- particle size distribution meas., online stroboscopic microscope apparatus 0-101783
- petrographic anal. of bituminous coal, identification of constituents 0-81888
- petroleum feedstocks and cokes, graphitizability 0-93580
- photomicrography, exposure control 0-90888
- photomicrography of submicrometer birefringent contaminants in C black dispersions in polymer particles 0-62757
- placental villi, human, average diameter estimation by stereologic method 0-67318
- polarised light, evaluation of asbestos insulations 0-95134
- polarizing microscope components and applications 0-98973
- polybutylene terephthalate, melt crystallised, solvent crystallised films and moulded bars, morphological obs. 0-84101
- polydioxolan, crystn. kinetics, dilatometric analysis and microscopy obs. 0-79706
- polyethylene melt, cryst. kinetics during cooling, nucleation density effect 0-100181
- polyisocyanates, rigid backbone, ternary phase relationships obs. 0-59371
- polymer liquid-crystalline solns., struct. 0-103235
- polyoxymethylene, nascent, morphology, optical and electron microscopic obs. 0-59403
- polystyrene, shear bands, morphology and annealing behaviour 0-100873
- porcelain, crack propag. data applicability to failure prediction 0-81154
- pore size measurement, comparison of methods 0-62622
- quartz, subgrain boundaries, theoret. predictions and microscopic obs. methods 0-84187
- refractive-index profile meas. of optical fibres, using scanning optical microscope 0-87535
- sapphire ribbon crystals, EFG growth and charact., voids, grain boundaries and dislocations 0-103283
- scanning, CRTs with semiconductor laser screens 0-86398
- scanning attachment to dual-prism monochromator, appl. to cytospectrofluorometric installation 0-101837
- slippage in crystals, photogrammetric obs. method 0-100975
- spatial frequency plane filtering by dynamic coherent illumination 0-95825
- stearic acid crystals grown from solution, spatial correlation between growth spirals and inclusions 0-96527
- steel, 0.7% C, welded zone, fatigue strength and microstruct. (*Japanese*) 0-89339
- steel, Fe-V-C (1, 0.2 wt.%), austenite formation 0-84927
- steel, ferritic stainless, embrittlement 0-85041
- steel, plain C having ferrite-martensite mixed structs., microstructural parameters effect on fatigue strength (*Japanese*) 0-71735
- steel, rolled, anisotropic, fatigue fracture surface obs. (*Japanese*) 0-108546
- steel, structural, supercooled austenite, structural characts. of decomposition 0-60870
- steel, tool and high-speed, high freq. induction melting and centrifugal casting in instrumental anal. 0-84886
- steel ball bearing, fatigued, phase changes, nomenclature 0-89198
- steels, low-C, aged after quenching, rel. between micro-cracks and coexisting effects (*Japanese*) 0-81159
- submicron magnetic objects, mag. struct. study using magneto-optic micro-magnetometer 0-57349
- superconductor Faraday effect obs. in polarising microscope 0-70892



**optical microscopy continued**

- surface anal. tools review 0-103540  
 surface topography quantitative determ. by Nomarski differential interference contrast microscopy 0-73318  
 TV recording and display equipment 0-98972  
 ultramicroscopy in scanning microscopes 0-95137  
 vital microscopy, electronic thermostatic system 0-85537  
 Zircaloy, annealed, neutron irradiated, inhomogeneous deform. behaviour 0-85014  
 Zircaloy-4, resistance-welded, microstruct. of weld region 0-66549  
 Al-Si eutectic alloy, banded struct., SEM and optical microscopy 0-104144  
 Al<sub>2</sub>O<sub>3</sub> (96 wt.%), fractographic criteria for subcritical crack growth boundaries 0-81155  
 Al<sub>2</sub>O<sub>3</sub>, sintering temperature effect of titanate additions 0-60808  
 BaMoO<sub>4</sub> crystals, growth in SiO<sub>2</sub> gel under influence of elec. field 0-93469  
 BaO.6Fe<sub>2</sub>O<sub>3</sub>, solubility of CaO 0-100333  
 Be, irradiated with He<sup>+</sup> at 20 keV, surface damage and gas trapping profile meas. (*French*) 0-84218  
 CaSO<sub>4</sub>.2H<sub>2</sub>O, gypsum, cryst. growth rates and nucleation (*French*) 0-80959  
 CdI<sub>2</sub> polytypes, vapour growth mechanism 0-84124  
 Co-Ti-C, secondary precipitation and allotropic transform., TEM obs. 0-108453  
 Cu, irradiated with 20 keV He<sup>+</sup>, surface damage and gas trapping profile meas. (*French*) 0-84219  
 Cu, polycrystn., strain localisation during hot deform. 0-104195  
 Cu-Al thin film multistructure, Xe<sup>+</sup> ion beam cratering 0-66708  
 Cu-Ni-Ti system, reactions with melt in Cu-rich region (*Japanese*) 0-89202  
 Cu-Zn-Al,  $\beta_1'$  martensite crystal crossing rel. to reversible shape memory effect (*Japanese*) 0-108499  
 Cu<sub>3</sub>Al, disordered [001]-orientated single crysts., plastic deform., TEM and slip line studies 0-97541  
 Fe zone refined crystals, cryst. orientation and distrib. of stray grains 0-70509  
 Fe-Cr-Al (7, 5 wt.%), expt. stainless alloys, phys. and mech. props. 0-97637  
 Fe-Cu (4.54 wt.%) alloy, scaling behaviour, 700-1000°C, 1 atm. O<sub>2</sub> 0-93679  
 Fe-Ni, interference microscopy, for colour development and phase separation 0-100976  
 Fe-Ni-Cr alloy, carbide form. by C diffusion, precip. distrib. and morphology 0-104164  
 Fe-Ni-Cr-Al-Y, oxidation mechanism, Y addition effect on kinetics and oxide adherence 0-97623  
 Ga<sub>1-x</sub>Al<sub>x</sub>As based layer structures, optimum growth conditions, comp. and struct. perfection 0-104069  
 GaAs, alloying with Au and Au alloy ohmic contact metalisations, SEM and optical study 0-70820  
 GaAs, semi-insulating, optical and electron microscopy exam., line dislocation precipitates 0-70205  
 $\alpha(\beta)$ -Ga<sub>2</sub>Se<sub>3</sub>, cryst. growth, optical, X-ray diffr. and SEM study 0-71587  
 In-Tl, single crystal containing Li, X-ray study of FCC $\rightleftharpoons$ FCT transform. (*Japanese*) 0-108435  
 Li<sub>1+x</sub>P<sub>2</sub>O<sub>3+x</sub>, polyphosphate, melting and crystallisation 0-70376  
 MgO-Ni, heavily doped, defect characterisation, rel. to use as laser material 0-65000  
 Mo-W (30 wt.%), wrought, fracture, characteristic features 0-104278  
 Mo-Zr (0.15 wt.%), wrought, fracture, characteristic features 0-104278  
 Na<sub>2</sub>O-CaO-Al<sub>2</sub>O<sub>3</sub>-SiO<sub>2</sub> glass, crystn. for the purpose of obtaining vitreoceramics (*French*) 0-75163  
 Ni alloys, cast, interference microscopy, for colour development and phase separation 0-100976  
 Ni-Fe-Cr superalloy type 718, heat treatment effect on room temp. and elevated temp. fracture toughness response 0-100922  
 Pb<sub>1-x</sub>Te-Pb<sub>1-x</sub>Sn<sub>x</sub>Te (x,y $\leq$ 0.3), double heterostruct., LPE growth, heterointerface morphology 0-70550  
 SiC-ceramic, nondestructive evaluation, scanning photoacoustic microscopy 0-85115  
 Si<sub>3</sub>N<sub>4</sub>-ceramic, nondestructive evaluation, scanning photoacoustic microscopy 0-85115  
 (U,Pu)C, sintering, role of Ni as sintering additive 0-84892  
 $\alpha$ -U, strain rate effect on flow and fracture 0-100887  
 U-Y-C FBR nuclear fuels, phase anal., 1400°C 0-66485  
 UC, sintering, role of Ni as sintering additive 0-84892  
 Zr-H formation, of  $\delta$ - $\gamma$  transformation 0-84929  
 Zr-H formation, the  $\delta$ - $\epsilon$  transformation 0-84930

**optical model (nuclear) see nuclear optical model****optical modulation**

- acoustic sensor, fibre-optic, modulation processes 0-58771  
 acousto-optic modulator efficiency optimisation, sound diffraction profile model and expt. 0-106615  
 acousto-optic modulator for CO<sub>2</sub> laser rangefinder using heterodyne detect. 0-102825  
 acousto-optical modulator for mode-locked CW Nd:YAG laser 0-87419  
 acousto-optical modulator using coupled plane waveguides 0-69527  
 acousto-optical wideband programmable filter 0-102842  
 active optical devices, seminar, San Diego, CA, USA (August 1979) 0-101664  
 amplitude-phase holograms, optical parameter dispersion 0-58481  
 analogue data processing systems, polarised modulation of light (*Russian*) 0-91884  
 biqwartz modulator, light interf. effect on photoelec. polarimeter accuracy 0-62713  
 bistable optical devices, overshoot and alternate switching, subharmonic generation 0-99790  
 ceramics, transparent ferroelectric, composition selection for appl. in light modulators (*Russian*) 0-91869  
 channel waveguide interferometric modulator for EM field detection 0-74498  
 coherence modulation by US waves, partial coherence depend. on US parameters 0-58453  
 coherent birefringent optical pulse compression 0-106437  
 coherent light valve processor, two-dimens. optical modulator 0-102840  
 complex spatial coherence meas. by sinusoidal phase modulation 0-106446  
 continuum self-phase modulation and stimulated Raman scatt., combined effects 0-69460

**optical modulation continued**

- cooperative Raman scattering, effect of phase self-modulation of light 0-91855  
 coupled laser oscillators, injection modulation 0-99773  
 cyanobiphenyl liquid crystal IR modulator expts. 0-102837  
 diode laser, mode locking to external resonator, theory 0-106550  
 diode laser in external cavity, linearized theory 0-69391  
 dye DFB laser, N<sub>2</sub> laser pumped, self Q-switched, tunable picosecond pulse generation 0-69432  
 dye laser, tunable ultrashort pulse generation 0-95931  
 electro-optic bistable devices, optical regenerative oscill. and monostable pulse generation 0-106612  
 electro-optical laser modulator for optical coherent transient generation 0-102776  
 electro-optical light modulator with small nonactive losses 0-78981  
 electro-optical linear interferometric modulator for electromagnitic field detection 0-58782  
 electro-optical modulator, asymmetrical, electric field config. anal. (*Russian*) 0-91885  
 electro-optical multivibrator operation, in optical bistable device 0-58674  
 electro-optical space-time light modulator 0-69526  
 electro-optical spatial light modulator resolution, stored point charge effects 0-106616  
 electrooptic bistable devices, optical regenerative oscill., monostable pulse generation 0-96002  
 electrooptic four-modulator photopolarimeter, for Mueller matrix meas. 0-73417  
 electrooptic polarization modulated injection laser 0-58591  
 electrooptic prepulse suppression for fusion laser systems, using optically timed Pockels cells 0-102743  
 electrooptic radiation modulators utilizing semiconductor ridged waveguides 0-91925  
 electrostatic field distribution calc. (*Russian*) 0-87514  
 energy expenditure minimum for light wave modulation 0-58611  
 fact directional coupler switch/modulators, novel ps optical pulse sampling method 0-58784  
 far IR laser intracavity polarisation modulation by CdTe AC Faraday rotation 0-58613  
 ferroelectrics, photoelectric states in real time spatial light modulators, photorefractive effect 0-80676  
 ferromagnet, microwave modulation of light using magnetodynamic resonance 0-71393  
 fibre laser plate for digital image processing, all-optical parallel logic operation 0-106463  
 fibre optic rotation sensor, all-waveguide configuration, key element tests 0-58796  
 fibre optic system design and component selection 0-58767  
 fibre-optic transmission by laser diode analogue baseband modulation 0-58738  
 FIR lasers stabilizations, fast modulation technique 0-99777  
 GaAs homojunction rib waveguide directional coupler switch 0-69554  
 gas-lasers, single-mode, fluctuations of laser beam diameter, lens effect 0-64090  
 gel rods, elastic dilatational mode, light beam positional modulation 0-64167  
 Hartmann modified wavefront sensor performance 0-74522  
 heterostructure planar waveguides, guided-to-radiation mode conversion and appl. to light modulation 0-87557  
 hologram electronic heterodyne recording and self-interference term rejection 0-91756  
 holographic interferometry, linearised subfringe, modulation errors effect 0-78803  
 holographix correlometer with phase modulation, viscous, superviscous light scatt. media study 0-74321  
 hybrid field-effect liquid-crystal light valve, optical data processing performance 0-99860  
 image subtraction through speckle modulated by Young fringes 0-95813  
 image weak modulation detection in film grain noise with partially coherent illumination 0-77897  
 integrated and guided-wave optics, conference, Incline Village, NV, USA, January 1980 0-58772  
 integrated optical switching system with input modulator 0-99884  
 integrated optics for optical fibres, progress and components, review (*French*) 0-69524  
 integrated optics sub-ps gate 0-58809  
 interference pattern electronic heterodyne recording 0-74316  
 interferometer, modulated fibre ring, laser appl. 0-74506  
 IR and FIR tunable coherent sources utilising modulational instability 0-95967  
 joint transform correlator performance rel. to wavefront modulator characteristics 0-102651  
 laser beam expander for short cavity dye laser 0-87532  
 laser beam refraction at spherical surface, distortion, geometrical optics calc. 0-95929  
 laser beam resonant chopper performance characteristics and limitations 0-64084  
 laser interferometers, AM and FM operation and applications (*German*) 0-86389  
 laser pulse shaping on multiple rot. lines, using electro-optical cryst. modulator 0-78879  
 laser speckle reduction in image plane by US modulation of spatial coherence 0-106459  
 laser ultrashort pulse form., filter clarification and amplification saturation coincidence 0-64085  
 laser wavefront correlation transformations (*Russian*) 0-99778  
 light diffraction by real stationary US field in liquid 0-83551  
 liquid crystal cells exhibiting dynamic scatt. for light flux attenuation 0-102845  
 liquid crystals, piezoelectric effect use as light modulator 0-83679  
 liquid-crystal light modulator, time depend. of conductivity under dynamic scatt. conditions 0-64178  
 Mach-Zehnder type modulator, RF modulation characts. meas. method 0-74480  
 microcantilever electrostatic deflection system for transmission optical modulator array 0-87512  
 microchannel spatial light modulator 0-91913  
 MIS photosensitive high resolution struct., spatial light modulation with liq. cryst. 0-96026  
 modulated-Mueller-matrix photopolarimetry [MMMP]: a technique for the study of elastic light scattering by depolarizing temporally modulated media and surfaces 0-90882



**optical modulation continued**

movie camera, laser based, operation and applications 0-57405  
 multimode fibre coupler-type acoustic sensor, optical intensity modulation 0-102945  
 multimode fibre lightguide, coherent light modulation 0-91926  
 multiplexing, using phase modulation 0-95830  
 nematic liquid cryst., isotropic phase, pulse acoustic-optic modulator 0-95993  
 numerical calculation using optics 0-95832  
 oil layer, deformable, spatial light modulator as incoherent to coherent image transformer 0-96008  
 optical fibre, vapour-oxidation fabricated, refractive index modulation, pulse dispersion 0-58756  
 phase contrast microscope attachment for weak phase object visibility 0-86396  
 photodichroic spatial light modulator for joint Fourier transform correlation 0-106617  
 photoelastic modulator for direct-reading linear dichroism apparatus 0-98962  
 photoelastic radiation polarisation modulators, review 0-102846  
 picosecond optical sampling, cascade of waveguide interferometers driven by microwaves 0-99849  
 Pockels cell modulator, max. depth of light modulation 0-102819  
 Raman-Nath standing-wave mode-locking switch, modulation index 0-78980  
 randomly modulated pump, stimulated Raman scatt., method of successive approxs. 0-95951  
 RF target simulator using acousto-optical device 0-102843  
 ruby laser, ultrashort pulse generation by internal phase and amplitude modulation 0-106551  
 ruby ring laser with forced mode locking 0-95915  
 semiconductor etalon, optical bistability and ns modulation 0-64096  
 semiconductor Fabry-Perot interferometer retuning by optical excitation (*Russian*) 0-98970  
 semiconductor laser intensity modulation in GHz region, image tube streak camera obs. 0-87417  
 semiconductor laser modulation, non-linear distortion, communication systems appl. (*German*) 0-69395  
 semiconductor laser radiation, frequency self-modulation interpretation 0-64028  
 semiconductor lasers, picosecond pulse generation using reson. oscill. 0-87391  
 SHF light rangefinder, optical elements, orientation errors effects (*Russian*) 0-64158  
 signal and image processing, US Air Force research programme 0-78791  
 single mode optical fibre, polarisation modulation 0-64176  
 solid laser, multimode, with modulated resonator losses, radiation intensity fluctuations 0-74367  
 strip-guides, polarisation filtering 0-102861  
 sub-SHG, nonequilibrium transitions, semiclassical theory 0-83639  
 subpicosecond gate, velocity-matched directional coupler 0-74512  
 thermoplastic spatial light modulator 0-102841  
 travelling wave optical modulator using a directional coupler LiNbO<sub>3</sub> waveguide 0-96035  
 tunable single-sideband generation in IR 0-78876  
 US-optical, spatial freq. meas. 0-95995  
 wavefront reversal of beam with incomplete spatial modulation, small-scale distortions 0-95953  
 Al-In multicomponent binding layers, acoustic light modulator 0-87546  
 Al<sub>0.42</sub>Ga<sub>0.58</sub>As-GaAs-Al<sub>0.42</sub>Ga<sub>0.58</sub>As, etalon, optical bistability and modulation 0-58628  
 Bi<sub>2</sub>SiO<sub>20</sub> PROM device, image recording and erasure mechanism 0-74490  
 CO<sub>2</sub> laser, detuning effects of FM mode-locking 0-69434  
 CO<sub>2</sub> laser modulation, plasma injection into cavity 0-83626  
 CO<sub>2</sub> laser radiation, intracavity modulation of polarization direction 0-102744  
 CO<sub>2</sub> TEA Laser pulse, PCM with CdTe crystal Pockels modulator 0-102742  
 CdTe linear electro-optic translation of IR laser wavelengths 0-78878  
 DF-CO<sub>2</sub> chemical laser, amplification of long and short pulses 0-95883  
 GaAlAs DH laser diodes, small signal modulation, junction capacitance effect 0-83625  
 GaAlAs injection DH laser and GaAs Schottky-gate FET, monolithic integration 0-58593  
 GaAlAs laser nonlinearities, harmonic distortion 0-74357  
 GaAlAs light intensity modulators using p-n junctions 0-99871  
 Ga<sub>1-x</sub>Al<sub>x</sub>As DH injection laser, FM at microwave freq. rates 0-58610  
 GaAs 400 MHz TW laser modulator 0-87541  
 GaAs, Franz-Keldysh effect modulator parameters for integrated optics systems 0-106624  
 GaAs injection lasers, direct modulation enhancement effect of HF noise 0-83608  
 GaAs-Al<sub>0.1</sub>Ga<sub>0.9</sub>As electro-optic frequency- and polarisation-modulated injection laser 0-91810  
 GaAs-Al<sub>0.1</sub>Ga<sub>0.9</sub>As MOS rib waveguide polariser, modulator and isolator 0-64217  
 GaAs-GaAlAs injection lasers, narrow-stripe proton-implanted, high bit-rate modulation 0-91824  
 GaP-GaAsP planar heterostructure strip ridged waveguide under mech. load, polarisation modulation 0-96038  
 GaSb, piezoresistive vibrating circular membrane, reflectance light modulation 0-97232  
 p-Ge modulation of 3.39  $\mu$ m abs. by CO<sub>2</sub> laser irradi. (*Japanese*) 0-74410  
 Ge, piezoresistive vibrating circular membrane, reflectance light modulation 0-97232  
 H<sub>2</sub> Raman laser, multiple-pass-cell, controllable pulse compression 0-91825  
 He-Ne laser, beat freq., high displacement sensitivity meas. 0-95926  
 He-Ne laser, operating on 0.63, 3.39  $\mu$ m coupled transitions, intensity modulation 0-69365  
 InO<sub>3</sub>:Sn transparent conducting films, homeotropic orientation of liquid crystals (*Russian*) 0-108181  
 KCl:ReO<sub>4</sub> nonlinear absorption for CO<sub>2</sub> laser pulse compression and mode locking 0-74443  
 KD<sub>2</sub>PO<sub>4</sub> crystal electron-beam spatial light modulator, resolution 0-74503  
 KD<sub>2</sub>PO<sub>4</sub> photo-spatial light modulator, optical data processing 0-102839  
 KH<sub>2</sub>PO<sub>4</sub> electro-optic modulator crystals, piezoelec. induced acoustic transients 0-70316  
 LaF<sub>3</sub>:Pr<sup>3+</sup>, ultraslow opt. dephasing at 2K 0-91864

**optical modulation continued**

LiNbO<sub>3</sub> very high throughput damage resistant waveguide modulator 0-58788  
 LiNbO<sub>3</sub> waveguide modulators and switches, Ti-diffused, fabrication on directional coupler principle 0-83678  
 LiNbO<sub>3</sub>:Ti channel waveguide high-speed cutoff modulator 0-64195  
 LiNbO<sub>3</sub>:Ti digitally driven integrated optics amplitude modulator 0-58808  
 LiNbO<sub>3</sub>:Ti optical waveguide electrooptic devices, polarisation indep. directional coupler switch 0-58783  
 LiNbO<sub>3</sub>:Ti optical waveguide, surface wave mode conversion, static strain-optic effect 0-87561  
 LiNbO<sub>3</sub>:Ti single mode electrooptic waveguide modulator, high-speed operation 0-91915  
 LiNbO<sub>3</sub>-Ge acousto-optic modulator for 10.6  $\mu$ m CO<sub>2</sub> laser 0-99776  
 LiNbO<sub>3</sub>-Ge acoustooptic modulator (*Japanese*) 0-69542  
 NaCl, amplitude phase hologram recording on colloid type centres (*Russian*) 0-69347  
 Nd laser, stable passive switch using phthalocyanine dye, bleaching and relaxation 0-74368  
 Nd:glass laser, blue tunable picosecond pulse generation by synchronous mixing with sideband radiation in NH<sub>4</sub>H<sub>2</sub>PO<sub>4</sub> 0-87431  
 Nd:glass laser system, beam spatial profile optimization in amplifier channel 0-74407  
 Nd:YAG CW mode-locked laser, negative feedback power stabilization 0-69435  
 Nd:YAG laser, subnanosecond pulse generation at 100K 0-74397  
 Nd<sup>3+</sup>:YAG multimode laser radiation noise 0-74366  
 PLZT ceramic, modulator for optical communication 0-78964  
 Rb vapour, Gaussian pulse propag. under two-photon near reson. conditions 0-87441  
 SiO<sub>2</sub> thin film grating for LiNbO<sub>3</sub>:Ti waveguide mode convertor and reflector 0-64216  
 TeO<sub>2</sub> acousto-optic laser beam deflector using shear wave propag. slightly off (110) crystal axis (*Japanese*) 0-102818  
 VO<sub>2</sub> thin films, light modulation appls., optical props. at metal-insulator transition 0-87547  
 XeCl, high-energy subnanosecond pulse amplification 0-99770  
 Xef laser, output control by injection locking 0-74405  
 YIG thin film gyromag. waveguide, on GGG substrate, optical propag. props. Faraday effect 0-74513  
 ZnS, linear electrooptic coeff. dispersion 0-71380

**optical modulators** *see* modulators; *optical modulation*

**optical noise measurement**  
 electrophotographic image information content and noise analysis 0-101861  
 fibre coupled diode lasers, LF noise meas. 0-58542  
 nematic liquid crystal, orientational fluctuations causing light intensity fluctuations, spectral anal. 0-60618  
 nonwhite noise, S/N ratio and detail detection 0-102648  
 signal-dependent film-grain noise, optimal image estimation 0-102659

**optical parametric amplifiers**  
 inhomogeneous crystal optimal length for SHG, parametric amplifier and oscillator 0-106568  
 light flux brightness meas., EM vacuum fluctuations, quantum noise 0-57361  
 photon parametric creation in model cosmological problems, nonlinear optics equivalence 0-73085  
 pump statistics conversion by parametric amplification of picosecond light pulses 0-99802  
 CdSe 16  $\mu$ m parametric amplification with HF laser pumping 0-78910  
 LiNbO<sub>3</sub> grating-tuned picosecond IR source with CdSe down-conversion 0-74435  
 LiNbO<sub>3</sub>:Ti diffused channel waveguide, optical parametric amplification 0-106564

**optical parametric devices**  
*see also optical parametric amplifiers; optical parametric oscillators*  
 brightness determination of thermal source, use of optical parametric converter 0-98979  
 IR radiation, parametric up-conversion to visible range, review 0-64104  
 photon statistics of fields generated by correlated mode interf. 0-106500  
 ultrashort light pulse parametric freq. conversion 0-106570  
 AgAs<sub>3</sub>, proustite, parametric upconverter, temp. effects on tangential phase-matching condition 0-99804  
 KH<sub>2</sub>PO<sub>4</sub>, ultrashort light pulse parametric transform. under optimum interaction conditions 0-99791  
 LiI<sub>2</sub> CW intracavity upconverter using Ar laser, noise props. 0-64099

**optical parametric oscillators**  
*see also lasers*  
 Cherenkov type parametric optical oscillator, optical saturation 0-102771  
 fibre-optic parametric oscillator, sequence/freq. generation 0-83636  
 inhomogeneous crystal optimal length for SHG, parametric amplifier and oscillator 0-106568  
 IR tunable laser for semiconductor multiphoton spectroscopy (*French*) 0-82836  
 tunable IR solid-state laser characteristics and principles 0-87406  
 CdSe, temp. depend. phase-matched nonlinear optical devices 0-99794  
 LiNbO<sub>3</sub> grating-tuned picosecond IR source with CdSe down-conversion 0-74435  
 ZnGeP<sub>2</sub>, temp. depend. phase-matched nonlinear optical devices 0-99794

**optical phase conjugation**  
 beam, image-bearing, nonuniformly polarized, generation of time-reversed replica 0-69459  
 CARS, three-dimensional phase matching in four-wave mixing 0-83635  
 chlorophyll solution, degenerate four wave mixing, phase conjugated backward wave generation (*Chinese*) 0-87429  
 coherence lengths and phase conjugation by degenerate four-wave mixing 0-64101  
 degenerate four-wave mixing, hysteresis and optical bistability 0-69446  
 degenerate four-wave phase conjugation, signal-pump detuning effects 0-78895  
 DODCI, saturable absorber, picosecond phase-conjugate refl. 0-95960  
 dye saturable absorbers, picosecond phase-conjugate refl. 0-95960  
 dye solutions, degenerate four-wave mixing and phase conjugation (*Chinese*) 0-102765  
 forward degenerate four-wave mixing, propag. anal. 0-69468  
 four counterpropagating wave interaction in medium with cubic nonlinearity, dynamic holography concepts 0-91839  
 four wave interaction, light induced crit. behaviour in nonlinear system 0-95941



**optical phase conjugation continued**

- four-wave mixing spectroscopy, coherent cancellation of background 0-91842  
 imaging, high-resolution by degenerate four-wave mixing 0-69458  
 mirror component for optical cavity, Gaussian transverse modes 0-58595  
 mirror forming optical cavity, Hermite-Gaussian higher-order reson. modes 0-58594  
 photon echo and nonlinear mixing methods for phase conjugate wavefront generation 0-58650  
 plasma jet form. by focusing laser beam on plane target, investigation using wavefront method 0-75103  
 pulse time-reversal by four-wave mixing 0-91848  
 rhodamine 6G solution in alcohol, degenerate four wave mixing, phase conjugation (*Chinese*) 0-102765  
 ruby, phase modulated conjugate wave generation, hologram model 0-83643  
 ruby laser, with stimulated Brillouin scatt. complex conjugate mirror 0-87438  
 stimulated light scatt., wavefront reconstruction 0-64107  
 thermal defocusing of light beams, phase conjugation compensation method 0-64123  
 wavefront distortion compensation in thick inhomogeneous medium 0-102762  
 wavefront reversal in four-photon process, two-quantum reson. conditions (*Russian*) 0-106574  
 wavefront reversal with freq. shift, based on anti-Stokes stimulated Raman scatt. 0-74440  
 wavefront sensing by phase retrieval 0-106478  
 Al film, wave front reversal, holography applications (*Russian*) 0-58483  
 BaTiO<sub>3</sub>, photorefractive effects and light-induced charge migration 0-69447  
 Bi<sub>2</sub>SiO<sub>20</sub>, photorefractive, vibr. struct. mode pattern visualisation, phase conjugation and dynamic holography 0-95938  
 CO<sub>2</sub>, inverted, wavefront reversal, high efficiency 0-74436  
 CO<sub>2</sub> laser cavity and Ge phase-conjugate 10  $\mu$ m reflection expts. 0-78894  
 CO<sub>2</sub> laser fusion system 0-74429  
 Ge, high refl. phase conjugation at 10  $\mu$ m, intracavity CO<sub>2</sub> laser techniques 0-78894  
 Ge in TEA CO<sub>2</sub> laser cavity, wavefront reversal, high efficiency 0-74436  
 Ge, phase conjugation of 4  $\mu$ m for single line and multiline radiation 0-83641  
 Hg<sub>0.7</sub>Cd<sub>0.3</sub>Te nonlinear optical IR generation 0-58642  
 Hg<sub>1-x</sub>Cd<sub>x</sub>Te, degenerate four-wave mixing of 10.6  $\mu$ m radiation 0-95943  
 n-Hg<sub>1-x</sub>Cd<sub>x</sub>Te, optical phase conjugation 0-83644  
 KCl:ReO<sub>4</sub>, resonantly enhanced phase conjugation through degenerate four-wave mixing 0-58635  
 NH<sub>3</sub>, phase conjugation in an inhomogeneously broadened medium 0-83642  
 NH<sub>3</sub>, phase conjugation via degenerate four-wave mixing 0-106566  
 Na vapour thin cell forward phase conjugation obs. 0-78917  
 SF<sub>6</sub>, multiwavelength phase conjugation using multiline CO<sub>2</sub> TEA laser 0-91847  
 ZnSe crystals, degenerate four-wave interaction, nonlinear optics effects 0-91856

**optical prisms**

- 1X2 optical switch using new type of pentagonal prism switch, for optical fibres 0-64148  
 anamorphic, apochromatic connection (*Russian*) 0-87513  
 anisotropic, ray refr., appl. to atm. optics haloes 0-63916  
 autocollimation instrument for checking angles and pyramidity of AR-90° prisms during manufacturing process 0-87570  
 axicon axial intensity distrib., influence of laser beam divergence 0-95934  
 beam expander, single prism, for tunable dye laser (*Chinese*) 0-74389  
 binocular models, characts. and design features, review 0-74468  
 channel waveguides, single-mode, prism coupling efficiency meas. 0-99878  
 coupler fabrication technique 0-83685  
 coupling into clad uniform optical waveguides 0-96003  
 coupling into optical waveguide, second harmonic generation 0-102763  
 diamond, light coupling prism, Raman spectra for thin film props. study 0-88978  
 electrooptic surface prism laser deflector, for field destructive interference 0-87492  
 filter, multilayer frustrated-total-internal-refl., spatially limited 0-96014  
 gemstones, light coupling prism, Raman spectra for thin film props. study 0-88978  
 grating-prism, prism-prism and grating-grating compounds for deflection angle compensation 0-95990  
 image processing in incoherent light 0-87339  
 large high-precision prism grinding, use of 3G-71 lathe 0-102872  
 matching of semiconductor sources to thin-film planar and stripe waveguides 0-64174  
 nonblocking 8X8 optical matrix switch using 64 pentagonal prisms 0-74485  
 rhombic, dimensional design (*Czech*) 0-74494  
 ring laser, perturbed cavity calcs. 0-102739  
 roof and other prisms, MTF tests 0-69571  
 slit image seen in total internal reflection (*French*) 0-95810  
 tapered gap prism coupling to diffused LiNbO<sub>3</sub> waveguides 0-78967  
 testing of prism optics for laser interferometer, interf. meas. 0-105698  
 thin film electrooptic deflector using induced grating with variable blaze angle 0-99862  
 two-prism system, position and magnification chromatism calc. (*Russian*) 0-87515  
 waveguide, loss measurement, nondestructive, using three prisms 0-106596  
 LiNbO<sub>3</sub> waveguide, planar electro-optic prism array beam splitter 0-64209  
 Nd:glass laser, short pulse mode-locked, using prisms 0-83617  
 SrTiO<sub>3</sub> prism coupler for LiNbO<sub>3</sub> integrated optics very high throughput damage resistant waveguide modulator 0-58788

**optical projectors**

- cinema, 35 mm, new projection lenses 0-87469  
 deflection contour generation by white light projection speckle method 0-98881  
 dual slide fader control cct., using a triac dimmer 0-69489  
 holographic movie camera and projection system 0-78808

**optical projectors continued**

- illumination control of cine projectors, foreign equipment (*Russian*) 0-105741  
 lantern slide projector remote control using IR-60 infrared system (*German*) 0-95169  
 large-screen colour projection TV system, using electron-beam-scanned semiconductor laser quantoscope 0-99783  
 laser projection microscope, transmitted light, Cu vapour laser as image amplifier 0-73446  
 measuring, development and use of special mirror, examination of recording heads 0-83657  
 mirror system use in light-valve projectors (*Russian*) 0-78930  
 motion picture projection equipment for 16 mm films, perspectives (*Russian*) 0-77903  
 multispectral, MSP-4 objectives, photoelectric distortion meas. (*German*) 0-95976  
 operator's eye and projector having a thermoplastic target, characts 0-96023  
 reflective light valve projector efficiency and image uniformity improvement 0-87459  
 rotating lens system for cine projection with continuous film transport 0-62766  
 schlieren 0-87544  
 single projector for abutting images of two light valves 0-87458  
 slide projector, dissolve control unit provides cross-fading and operational sequence recording 0-77833  
 slide projector, electronic control apparatus (*Dutch*) 0-105731  
 wavelength and coherence effects 0-64136

**optical properties of substances**

- see also acousto-optical effects; birefringence; brightness; cathodochromism; colour; dichroism; dielectric function; electro-optical effects; electrochromism; magneto-optical effects; optical constants; optical Kerr effect; optical rotation; optical saturation; optical susceptibility; photochromism; piezo-optical effects; pleochroism; reflectivity; thermo-optical effects  
 cholesteric liquid crystals optical properties, diffraction nature, review 0-70123  
 conference, basic optical props. of materials, Gaithersburg, MD, USA (May 1980) 0-101668  
 DOBAMBC, ferroelec. liq. crystals, elec. and optical props., appls. (*Japanese*) 0-88943  
 filament waveguides for signal transmission in far IR region (*Czech*) 0-96017  
 glass fibre reinforced plastic, fatigue fracture kinetics studied by diffusion scatt. of luminous fluxes 0-76446  
 insulating crystal, many-photon transitions 0-103932  
 magnetic semiconductors, conference, Montpellier, France (Sept. 79) 0-94916  
 metallic thin films (*French*) 0-60692  
 metallic ultrathin filaments, dielectric and superconducting fluctuations, Peierls transition (*Russian*) 0-65742  
 metals, solid and liq., optical props. by spectroscopic ellipsometry, review 0-103929  
 phosphate system, containing halogens glass formation 0-103254  
 rough surfaces, discontinuous films, heterogeneous materials, review 0-103935  
 semiconductors, book 0-77554  
 spatial dispersion exponential model, boundary conditions (*Russian*) 0-75994  
 Hg, optical props. by spectroscopic ellipsometry, review 0-103929  
 Li, optical props. by spectroscopic ellipsometry, review 0-103929  
 Na optical properties by spectroscopic ellipsometry, review 0-103929  
 Na<sub>2</sub>O-B<sub>2</sub>O<sub>3</sub>-SiO<sub>2</sub>, containing halogens glass formation 0-103254  
 Na<sub>2</sub>O-SiO<sub>2</sub> glass containing halogens glass formation 0-103254  
 Sn, liq., optical props. by spectroscopic ellipsometry, review 0-103929

**optical pumping**

- see also lasers; multiphoton spectra  
<sup>32</sup>S<sub>1/2</sub>-<sup>32</sup>P<sub>3/2</sub>, spectral distrib. and collisional depolarisation of laser light, D<sub>2</sub>-fluorescence 0-58209  
 acetylene-d<sub>2</sub>, 17 to 21  $\mu$ m laser lines generated using CO<sub>2</sub> laser pump 0-69375  
 active particles, Lorenz-Mie scatt. theory paradox 0-74324  
 alkali halides, F-centres, ESR in different states of relaxed configuration 0-108067  
 anthracene, cryst., exciton aggregate possible form. under intense optical pumping, fluoresc. spectra 0-84772  
 atom, many-photon excitation by multimode radiation 0-74154  
 atom, resonance light scattering, intensity effects 0-91511  
 atomic metastability exchange collisions, Pauli principle effects 0-99536  
 atoms, laser excited, reactive collisions 0-66793  
 atoms, multiphoton rate equations, generalised 0-91525  
 carbon tetrafluoride <sup>12</sup>CF<sub>4</sub> laser, Doppler-limited absorption spectroscopy 0-74347  
 carbon tetrafluoride <sup>12</sup>CF<sub>4</sub> optically pumped laser efficiency 0-74348  
 carbon tetrafluoride laser, CF<sub>4</sub> molecule  $\nu_3 + \nu_4$  band optical pumping 0-74349  
 carbon tetrafluoride laser with optical pumping, freq. tuning and stabilisation 0-99706  
 carbon tetrafluoride pulsed laser characts., optically pumped by CO<sub>2</sub> laser 0-91778  
 Cd + molecules collisions 0-58338  
 chlorodifluoromethane subMM wave laser, optically pumped 0-87376  
 coaxial cable pulse forming network as rare gas halide laser pump 0-69424  
 colour centre laser pumped by flashlamp-pumped dye laser 0-102737  
 CW optically pumped far IR laser performance, determinative molecular parameters 0-69377  
 degenerate four-wave phase conjugation, signal-pump detuning effects 0-78895  
 cis-1,2-difluoroethene, CO<sub>2</sub> laser pumped, CW far IR laser lines 0-69372  
 cis-1,2-difluoroethylene laser, far IR CW optically pumped 0-69368  
 1,1-difluoroethylene submillimetric wave emission assignments 0-102708  
 difluoromethane, optically pumped, CW far IR laser line frequencies 0-102706  
 difluoromethane far IR laser gas, CW laser pumped, gain 0-69367  
 dimethyl sulphoxide, high efficiency stimulated Raman scatt. source (*Chinese*) 0-87433  
 dressed atom system, energy levels and reson. phenomena, universal algorithm 0-69111



**optical pumping continued**

dressed atom system, phase represent. applic. to reson. fluoresc., universal algorithm 0-69112  
 dye DFB laser, N<sub>2</sub> laser pumped, self Q-switched, tunable picosecond pulse generation 0-69432  
 dye laser, CW, pumped, stable multifreq. picosecond pulse emission, phase-locked radiation pumping 0-91789  
 dye laser, cylindrical active element with sheath, radiation intensity distrib. calc. 0-58531  
 dye laser, double mode-locked CW, pulse cross-correlation studies 0-69389  
 dye laser, flash lamp pumped, tuning by grazing incidence grating technique 0-95914  
 dye laser, N<sub>2</sub>-pumped subnanosecond pulse generation, design 0-87403  
 dye laser, tunable, N<sub>2</sub>-laser pumped, using single prism beam expander (Chinese) 0-74389  
 dye laser, tunable ultrashort pulse generation 0-95931  
 dye laser picosecond pulse generation, excitation by passively mode locked Ar laser 0-95930  
 energy level transitions, excitation by monochromatic laser radiation, Doppler-broadened transitions 0-78582  
 ethyl iodide submillimeter wave laser, optically pumped 0-87376  
 far IR CW optically pumped lasers, simple accurate method for wavelength meas. 0-106554  
 far IR laser gases, CW laser pumped, saturated and small-signal gain calc. 0-58521  
 far IR oscillator, optically pumped, parametric study 0-95862  
 fast atomic beam, optical reson. detect. by at. fluoresc. 0-102479  
 flashlamps, coaxial and preionised linear, comparison as pumping sources for high power dye lasers 0-102730  
 fluoromethane, <sup>12</sup>CH<sub>3</sub>F, far IR Raman laser line obs., CO<sub>2</sub> laser pumping 0-69381  
 fluoromethane, near-MM-wave laser synchronous pumping, ultrashort pulse generation at 496, 193 μm 0-102705  
 fluoromethane, optical pumping of far-IR molecular lasers by CW CO<sub>2</sub> waveguide laser 0-83615  
 fluoromethane+SF<sub>6</sub>(CS<sub>2</sub>), fluoromethane laser, buffer gases collisional narrowing 0-99710  
 fluoromethane high-power laser, tuning behaviour 0-63994  
 fluoromethane laser, optically pumped far-IR waveguide, output, temp. depend. 0-58512  
 fluoromethane optically pumped molecular laser, relax. oscils. 0-95875  
 fluoromethane TEM<sub>00</sub> far IR laser with integrated pump laser 0-58578  
 fluoromethane-<sup>13</sup>C, pulsed far IR emission 0-69370  
 fluoromethane-<sup>13</sup>C optically pumped molecular laser, relax. oscils. 0-95875  
 fluoromethane-SF<sub>6</sub>, 496-μm optically pumped laser, energy-transfer mechanisms 0-99712  
 formaldehyde-d (d<sub>2</sub>) submillimetre lasers, optically pumped, assignment of laser lines 0-58513  
 formic acid laser far IR pulse generation by Q-switched CO<sub>2</sub> laser pump source 0-69383  
 gas, resonance four-photon shift, optimal focusing of high-power pumping 0-95574  
 ground state alkali molecules, mag. shielding and spin-rot. interaction 0-87186  
 hole burning, photophysical and photochemical theories 0-58322  
 iodotrifluoromethane, high vibr. state excitation in high-power laser field, spectral characts. 0-91562  
 ion, electromagnetically confined, laser cooled, double resonance and optical pumping 0-87155  
 laser, double-current-confinement channelled-substrate struct., near-field and beam-waist position 0-106553  
 laser, far IR, injection phase locking 0-69431  
 laser, far IR optically pumped, monitoring by piezoelec. transducers 0-102729  
 laser far IR pulse generation by Q-switched CO<sub>2</sub> laser pump source 0-69383  
 laser pulses, double, generation, gradual cutting-off resonator losses 0-69433  
 laser pump sources, efficiency of Xe and Kr arc discharges 0-64812  
 laser pump system, analytical theory 0-106540  
 laser pumping system, thermodynamic calc. method 0-58551  
 laser three-photon transition theory 0-102690  
 methane backward Raman amplifier, KrF laser driven, high-efficiency energy extraction 0-106533  
 methanol, optical pumping of far-IR molecular lasers by CW CO<sub>2</sub> waveguide laser 0-83615  
 methanol, optically pumped CW subMM emission lines 0-95876  
 methanol 70 and 118 μm laser line diagnostic expts. 0-69387  
 methanol far IR laser, twin optically pumped, for plasma diagnostics 0-59306  
 methanol far IR laser gas, CW laser pumped, gain 0-69367  
 methanol far IR laser line Stark splitting obs. 0-58313  
 methanol far IR Stark spectroscopy and 9-P(34) CO<sub>2</sub> laser line 0-69145  
 methanol laser, CW, optically pumped, 170-μm emission, press. shift 0-106510  
 methanol laser, optically pumped, use of crystalline reflector in cavity 0-64080  
 methanol optically pumped 118.8 μm laser line, Stark splitting obs. 0-102710  
 methanol subMM laser line obs. 0-58523  
 methanol twin optically pumped far IR laser for plasma diagnostics 0-103189  
 methanol-d<sub>1</sub>, CH<sub>3</sub>DOH optically pumped CW far IR laser lines and frequencies 0-102707  
 methanol-d, optically pumped CW subMM emission lines 0-95876  
 methyl alcohol submm wave laser, optically pumped, intracavity double resonance obs. 0-58522  
 methyl cyanide, far IR laser line assignments 0-69380  
 methyl fluoride, <sup>13</sup>CH<sub>3</sub>F, high-power pulsed laser 0-69386  
 methyl fluoride, deuterated, optically pumped near-MM laser 0-69379  
 methyl fluoride laser far IR pulse generation by Q-switched CO<sub>2</sub> laser pump source 0-69383  
 methyl iodide, and deuterated, pulsed subMM lasers pumped by CO<sub>2</sub> laser 0-106511  
 methyl mercaptan, CW subMM emission lines, optical pumping 0-87381  
 methyl nitrile CW far IR mol. laser, optical pumping with <sup>16</sup>CO<sub>2</sub> and <sup>18</sup>CO<sub>2</sub> lasers 0-74343  
 methylfluoride, CW far IR mol. laser, optical pumping with <sup>16</sup>CO<sub>2</sub> and <sup>18</sup>CO<sub>2</sub> lasers 0-74343

**optical pumping continued**

Michelson output coupler with one-dimensional grid, for optically pumped near MM laser 0-58555  
 molecular energy level transitions, excitation by monochromatic laser radiation, Doppler-broadened transitions 0-78582  
 molecular laser, optical pumping in damped photodissoc. wave propag. in dense gas 0-99714  
 molecular laser, optically pumped, review 0-58519  
 molecular lasers, IR-FIR transferred Lamb-dip, standing wave saturation effects 0-58520  
 molecular lasers, laser pumping, dispersion 0-87375  
 molecular lasers, optically pumped, polarisation phenomena appl. 0-87384  
 molecular nonsteady-state luminesc. behaviour under narrowband laser excitation 0-87159  
 molecules excited by laser IR radiation, excited fraction determ. 0-78661  
 multiphoton cross-section determination by means of luminescence experiments 0-93377  
 near MM wave laser synchronous pumping, ultrashort pulse generation 0-69385  
 organic solutions, lasing, excitation by excimer laser radiation 0-64007  
 Orion methanol masers, evidence for IR pumping from interferometric and multitransitional study 0-67891  
 phenylloxazoly pyridinium salt dye lasers, flashlamp pumped, blue-greenlasing 0-95886  
 photon detector for subMM wavelengths using Rydberg atoms 0-77867  
 polyatomic molecules, multiple photon excitation, Bloch eqn. to rate eqn. transition 0-83437  
 POPOP solution dye lasers, multiplate reflectors 0-83606  
 propynal, CW far IR mol. laser, optical pumping with <sup>16</sup>CO<sub>2</sub> and <sup>18</sup>CO<sub>2</sub> lasers 0-74343  
 pulse time-reversal by four-wave mixing 0-91848  
 pump statistics conversion by parametric amplification of picosecond light pulses 0-99802  
 quantum magnetometer, alternating polarity modulating pulses, meas. errors (Russian) 0-90871  
 Raman spin-flip laser, multiply pumped, coherence effects 0-87398  
 randomly modulated pump, stimulated Raman scatt., method of successive approxs. 0-95951  
 resonance atom, spontaneous diffr. of light 0-91512  
 resonance light scattering, spectral props. and photon correls. 0-91510  
 rhodamine 6G dye in ethylene glycol, broadband optical diode, one directional traveling wave operation of ring laser 0-58606  
 rhodamine 6G-safranin-T mixed dye laser energy transfer, N<sub>2</sub> laser pumping source 0-58532  
 rhodamine G solutions, LiCl and NaClO<sub>4</sub> electrolyte influence on its lasing props. 0-91788  
 Rydberg atom maser emission, heterodyne detection 0-78822  
 semiconductor junction lasers, transport phenomena, junction effects and devices, book 0-98766  
 semiconductor laser, electron beam pumping efficiency, coating effect 0-91795  
 semiconductor laser, III-V book contrib. 0-99732  
 semiconductors, free carrier optical props., book contrib. 0-80738  
 spin oscillators, optically pumped, orientation depends. of oscill. freq. 0-78896  
 spin wave parametric excitation, stochastic auto-oscills., Kolmogorov entropy (Russian) 0-75749  
 stimulated hyper-Raman scattering in a molecular gas via a three-photon process to obtain IR and far IR radiation 0-58633  
 stimulated Raman scatt. excitation by wideband pump in optical waveguide 0-64108  
 superradiance waveguide laser, stimulated emission spectrum, leaky modes (Russian) 0-87400  
 tetrafluoromethane laser, pulsed, high repetition rate, average power limitations at 10.6 and 16 μm 0-58503  
 tetrafluoromethane molecule, laser spectrosc. and optical pumping from CO<sub>2</sub> laser 0-74202  
 three level system, coherently pumped, cooperative relax. 0-78816  
 three-level molecular laser pumping and dispersion eqns. 0-69384  
 three-level Mossbauer gamma-ray lasers, two-stage pumping 0-78857  
 TOPOT vapour dye lasers with multiplate reflectors 0-83606  
 tricarboyanine, laser dyes, flashlamp-pumped, photochemical stability 0-83604  
 unstable-resonator laser performance at near MM wavelengths 0-58607  
 wavefront reversal, transverse enhancement of coherence of scatt. field 0-95952  
 wavefront reversal of beam with incomplete spatial modulation, small-scale distortions 0-95953  
 Al<sub>2</sub>O<sub>3</sub>:Cr<sup>3+</sup>, ruby, reson. scatt. and trapping of 29 cm<sup>-1</sup> acoustic phonons 0-93403  
 Ba atom, laser excited, ionisation studies 0-83330  
 Ba, saturation spectroscopy with laser optical pumping 0-83324  
 Ba vapour, level populations, laser pumping effects 0-91507  
 Ba-Tl laser optically pumped by pair-absorption transitions, 1.5 μm emission obs. 0-58517  
 C<sub>2</sub>, interstellar, rot. fine-struct. levels radiative pumping rel. to obs. towards ζ Persei 0-67811  
 CO<sub>2</sub> high-power pump laser, direct narrow-line tuning 0-58579  
 CO<sub>2</sub> lasers, optically pumped, use of crystalline reflector in cavity 0-64080  
 CO<sub>2</sub> multiatmosphere laser tuning for methyl fluoride laser pumping 0-69421  
 CO<sub>2</sub> self-pumping on pulsed periodic energy input (Russian) 0-106506  
<sup>13</sup>C<sup>16</sup>O<sub>2</sub> laser, isotopically enriched, appl. in optically pumping far IR laser 0-58507  
 CO<sub>2</sub>-Br<sub>2</sub>-He mixture, possible gas lasers with solar excitation 0-99695  
 CO<sub>2</sub>\*+SO<sub>2</sub>, near-reson. energy transfer, fluoresc. obs. 0-106348  
 Ca atom, laser excited, ionisation studies 0-83330  
 CdS crystals, one-photon pumping, active layer structure, light amplification 0-78858  
 CdS, highly excited, stimulated emission process at 80K 0-97307  
 CdS monocrystal petal lasers, single-photon excitation (Russian) 0-99736  
 CdS platelet lasers, optically pumped, spatial and spectral distribution of laser emission 0-64032  
 CdS<sub>1-x</sub>Se<sub>x</sub> monocrystal petal lasers, single-photon excitation (Russian) 0-99736  
 CdSe 16 μm parametric amplification with HF laser pumping 0-78910  
 CdSe, fundamental absorpt. edge, influence of laser radiation intensity (Russian) 0-71445  
 Ce:LaF<sub>3</sub>, 286 nm laser, optically pumped 0-99738

## optical pumping continued

- ClF UV laser system 0-83597  
 ClO<sub>2</sub>, CW for IR mol. laser, optical pumping with <sup>16</sup>CO<sub>2</sub> and <sup>18</sup>CO<sub>2</sub> lasers 0-74343  
 Co:MgF<sub>2</sub>, tunable transition-metal-doped solid state lasers 0-58549  
 Cs atomic clock using laser optical pumping of Cs beam 0-101785  
 Cs cell, laser beam excitation, multipass, optical pumping and weak neutral current parity violation 0-58207  
<sup>133</sup>Cs, freq. standard, optimum conditions for population inversion for 0-0 transition 0-78824  
 DF-HBr CW optical resonance transfer laser 0-64003  
 D<sub>2</sub>O vapour high-power 385  $\mu$ m laser oscillator 0-69422  
 D<sub>2</sub>O, near-MM-wave laser synchronous pumping, ultrashort pulse generation at 385, 66  $\mu$ m 0-102705  
 Dy atom isotope separation, laser excitation, charge exchange with Cs<sup>+</sup> ions 0-83512  
 F<sub>2</sub> UV laser system 0-83597  
 GaAs:Zn optically pumped ribbon-whisker laser, picosecond pulses 0-99771  
 GaAs/GaInP DH, MBE grown, optically pumped laser action at 77K 0-95890  
 GaInPAs/InP heterostructure DFB laser under optical pumping, lasing chars. 0-87396  
 HCCF, CW for IR mol. laser, optical pumping with <sup>16</sup>CO<sub>2</sub> and <sup>18</sup>CO<sub>2</sub> lasers 0-74343  
 He, 3<sup>1</sup>P level, excitation and decay study up to high press. pumped by intense relativistic electron beam 0-74250  
 He Mz magnetometer, improving accuracy by reducing intensity of optical pumping 0-62700  
 He quantum magnetometer with optical pumping, sensitivity in 40-3000 Hz range (Russian) 0-90870  
 He<sup>+</sup>-He<sup>+</sup> mixture, relax. of 2<sup>3</sup>S, metastable atoms 0-102469  
 He<sub>2</sub>, laser-driven transitions to high Rydberg states 0-106360  
<sup>3</sup>He-<sup>4</sup>He mixture, optical pumping, transients theory 0-91509  
<sup>4</sup>He<sup>+</sup>, g-factor determ., optical pumping method 0-87085  
 Hg ions, relaxation two constants meas. of optically pumped stored Hg ions 0-106287  
 HgTl excimer laser, kinetics, optical excitation obs. 0-58527  
 Ho<sup>3+</sup>:BaYbF<sub>6</sub> 0-95902  
 Ho<sup>3+</sup>:LiYbF<sub>4</sub>, active medium for Nd laser freq. convertor, cascade stimulated emission 0-102727  
 I<sub>2</sub>, efficient laser action on 342 nm dye, ArF laser pumping 0-99703  
 I<sub>2</sub> laser, three-level, pumped by CW dye laser 0-63993  
 I<sub>2</sub> molecule B-X electron transition during Cu vapour laser optical pumping (Russian) 0-78845  
 In<sub>1-x</sub>Ga<sub>x</sub>P<sub>1-y</sub>As<sub>y</sub>-In<sub>1-x</sub>Ga<sub>x</sub>P<sub>1-z</sub>As<sub>z</sub>, visible spectrum multiple-quantum-well heterostruct. lasers 0-106537  
 K atomic Rydberg state tunable subMM laser 0-69378  
 K<sup>+</sup>K<sup>+</sup> collisions, charge exchange cross section 0-58374  
 K<sub>2</sub>, absorpt. and relax. const. determ. by optical laser pumping method 0-102550  
 LiF, picosecond generation on F<sub>2</sub><sup>+</sup> colour centres, induced mode synchronisation (Russian) 0-64033  
 LiNdP<sub>6</sub>O<sub>12</sub> laser, relaxation oscillations and mode spectra, high density pumping effect 0-69396  
 NH<sub>3</sub> 81.5  $\mu$ m subMM laser, optically pumped by N<sub>2</sub>O laser, freq. meas. 0-74415  
 NH<sub>3</sub> CW far IR laser lines, CO<sub>2</sub> laser pumping and Stark tuning 0-69382  
 NH<sub>3</sub> CW far IR laser lines, CO<sub>2</sub> laser pumping and Stark tuning 0-106508  
 NH<sub>3</sub>, far IR CW Raman lasing 0-83595  
 NH<sub>3</sub>, far IR emissions by IR pumping using N<sub>2</sub>O laser 0-74345  
 NH<sub>3</sub> laser, high-power efficient optically pumped, tunable over 770 to 890 cm<sup>-1</sup> range 0-91780  
 NH<sub>3</sub> laser transitions, CW, two-photon pumped 0-99702  
 NH<sub>3</sub> laser using a continuously tunable CO<sub>2</sub> laser, 11-13  $\mu$ m region 0-83596  
 NH<sub>3</sub>, near-MM-wave laser synchronous pumping, ultrashort pulse generation at 151  $\mu$ m 0-102705  
 NH<sub>3</sub>, stimulated hyper-Raman scatt. via 3-photon process to obtain IR and far IR radiation 0-58633  
<sup>15</sup>NH<sub>3</sub> far IR laser emission at 153, 375  $\mu$ m, optically pumped by <sup>13</sup>C<sup>16</sup>O<sub>2</sub> laser 0-58507  
<sup>15</sup>NH<sub>3</sub> far IR CW laser, optically pumped with <sup>13</sup>C<sup>16</sup>O<sub>2</sub> laser 0-78866  
 Na atom, cyclic interaction with circularly polarised laser radiation 0-78581  
 Na beam, laser beam irradi., reson. fluoresc. intensity, Bloch model calcs. 0-58206  
 Na, saturation spectra, crossover signals, effect of atomic alignment, optical pumping 0-58202  
 Na<sub>2</sub>, absorpt. and relax. const. determ. by optical laser pumping method 0-102550  
 NaF, F<sub>2</sub><sup>+</sup>-like colour centre, room temp. stable, CW laser, 0.99-1.22  $\mu$ m tunable 0-69399  
 Nd laser Mikron system, ultimate Xe pump lamp module operating conditions 0-91815  
 Nd:glass laser rod, pumped, thermal relaxation 0-69397  
 Nd:YAG pumped tunable sources, appl. to spectroscopy 0-58576  
 Nd:YAG laser reflection resonator with hole coupling 0-58597  
 Nd<sup>3+</sup>:Gd<sub>2</sub>Ga<sub>2</sub>O<sub>12</sub> pulse-pumped laser action at 1.054  $\mu$ m 0-64030  
 Nd<sup>3+</sup>:YAG laser, high repetition rate electrooptic Q-switching, birefringence 0-69430  
 Nd<sup>3+</sup>:YAG laser, pumping by alkali metal vapour arc discharge 0-78924  
 Nd<sup>3+</sup>:YAG laser, stable periodic-pulse, with CW pump 0-74400  
 Nd<sup>3+</sup>:YAG multimode laser radiation noise 0-74366  
 Ni:MgF<sub>2</sub>, tunable transition-metal-doped solid state lasers 0-58549  
 OCS, optically pumped CW subMM emission lines 0-95876  
 OH in flames, laser excitation dynamics 0-74201  
 Pb, superconducting film, spatially inhomogeneous state appearance under laser pumping conditions 0-93053  
 Rb, radiative lifetimes up to n=12 excited states, pulsed dye laser and superadiance excitation 0-83322  
 S I emission lines in late-type stars EUV spectra, optical pumping by O I lines 0-82359  
 S<sub>2</sub>, optically pumped superfluorescence molecular laser 0-63990  
 SF<sub>6</sub>, laser pumping in collisional region of nozzle beam, internal excitation, time-of-flight anal. 0-95719  
 SF<sub>6</sub>, multiphoton-excited,  $\nu_2 + \nu_4$  absorption and emission 0-63626  
 SF<sub>6</sub> + H<sub>2</sub> chemical laser, electron beam pumping 0-91784

## optical pumping continued

- SO<sub>2</sub>-<sup>18</sup>O<sub>2</sub> mixtures, IR laser pumped, intermol. vibr. energy transfer dynamics obs. 0-87207  
 Te crystal, SHG, 60% efficiency, 12.8  $\mu$ m NH<sub>3</sub> laser pumping 0-83640  
 Ti I, photodissociative pumping effect 0-58182  
 UF<sub>6</sub>, laser chemistry 0-69198  
 Yb I, high Rydberg levels of 4f<sup>14</sup> 6snd configs., very high resolution obs. 0-106300  
 Zn,Cd<sub>1-x</sub>S monocrystal petal lasers, single-photon excitation (Russian) 0-99736
- optical quantum generators** *see lasers*
- optical radar**  
*see also remote sensing by laser beam*  
 acousto-optic modulator for CO<sub>2</sub> laser rangefinder using heterodyne detect. 0-102825  
 airborne lidar system for geophysical and atmospheric expts. (Italian) 0-109277  
 atmospheric environmental research, appl. of lasers (German) 0-97849  
 atmospheric lidar scattering and relative humidity 0-77113  
 cloud extinction coefficient, estimation from multiwavelength lidar backscatter meas. 0-98446  
 coherent lidar target calibration, backscatter refl. for circularly polarised radiation 0-102750  
 differential absorption lidar, complementarity of UV and IR systems for atmospheric species meas. 0-72634  
 digital beam switch for 10.6  $\mu$ m laser radar 0-102836  
 digital beam switch for agile beam laser radar 0-58620  
 dusty IR Test-1 lidar obs., transmission meas. 0-99625  
 gas laser rangefinder and profilometer, high-resolution 0-102754  
 heterodyne optical radar S/N ratio in atmospheric turbulence 0-106558  
 laser and electro-optical systems, conf., San Diego, CA, USA (Feb. 1980) 0-62392  
 laser rangefinder and 3D object recognition algorithm 0-96016  
 laser tracking system testing by 1 m unobscured IR collimator 0-78991  
 lidar, cirrostratus clouds remote sounding and IR emissivity 0-82061  
 lidar measurements of high ice clouds, visible and IR optical props. calc. 0-82060  
 pollution plume transport and diffusion studies using fluorescence lidar 0-101139  
 Raman spectroscopy, remote spontaneous, new trends in recording of signals 0-73485  
 reference range for differential absorption lidars 0-89700  
 SHF light rangefinder, optical elements, orientation errors effects (Russian) 0-64158  
 submarine periscope optical design for laser rangefinding compatibility 0-78987  
 water depth measurement using airborne pulsed Ne laser system 0-61908  
 water vapour, Raman lidar meas., daytime atmosphere 0-85718  
 CO<sub>2</sub> laser radar used to measure average atmospheric temp. 0-90225  
 Nd:YAG laser as source for airborne lidar system for atmospheric expts. (Italian) 0-109278
- optical resolving power**  
*see also optical instrument testing*  
 air at Ti surface, optical breakdown, interferometric investigation 0-100064  
 alkali metal vapour, IR image upconversion using two-photon resonant optical four-wave mixing 0-58632  
 amplitude filtering for superresolution, maximum central irradiance under energy constraint 0-91914  
 apertures, multiple circular, located on circle, resolution 0-102615  
 calligraphic projection display resolution and contrast photometer and X-Y plotter 0-86373  
 centrally obstructed objective, resolution limit (German) 0-95811  
 channel waveguide array coupled to integrated C-CD, appl. 0-102860  
 COCHISE: laboratory spectroscopic studies of atmospheric phenomena with high sensitivity cryogenic instrumentation 0-95166  
 coded aperture imaging: the modulation transfer function for uniformly redundant arrays 0-99019  
 computerised tomography scanners, survey of noise, dose and contrast detectability and resolution 0-104750  
 confocal scanning microscope, image form. 0-68249  
 correlation reduction, spatial filtering and variation of resolution 0-102850  
 double beam interferometer, meas. of background suppression and spectral detection 0-95130  
 electro-optical spatial light modulator resolution, stored point charge effects 0-106616  
 endoscopic miniature camera with fibre-optic faceplate 0-77896  
 etalon-spectrograph system, improved resolution over wide spectral range 0-101843  
 exponential transformation using film nonlinearity for optical homomorphic filtering 0-58467  
 Fabry-Perot scanning interferometer, far IR performance 0-86388  
 far IR modular Fourier interferometer construction, very high resolution 0-57401  
 field meas. Fourier transform spectrometer 0-86470  
 flexible high-resolution film recorder system 0-102827  
 Fourier transform spectrometer, high resolution ruggedized 0-95152  
 high-resolution spectroscopy using tunable lasers 0-101849  
 holographic image magnification, new methodology 0-95851  
 holographic recorders, high resolution, using transparent electrophotographic film 0-102671  
 holographic scanner imaging systems, active and passive, 8 to 13  $\mu$ m, chars. 0-91755  
 holography, white light refl., developer compositions compared 0-102669  
 holography advantages for physical structure meas. and recording 0-95843  
 image reconstruction, computerized, fragment size choice 0-78785  
 imaging, high-resolution by degenerate four-wave mixing 0-69458  
 interferometer spectrometers, field-widened 0-95146  
 IR sky survey telescope, wide field photography 0-105167  
 IR spectrum deconvolution beyond the Doppler limit 0-86467  
 laser recording and information handling, seminar, San Diego, CA, USA (Aug. 1979) 0-101663  
 lens-array photographic system, depth of sharp focusing, resolution 0-62763  
 line image transmission through single fibre using spectral instrums. 0-102820  
 long-wave imaging with super-resolution by wavelength diversity 0-102675



**optical resolving power continued**

- machine part, rotating, surface finish, laser method for determ. 0-89454  
 MIS photosensitive high resolution struct., spatial light modulation with liq. cryst. 0-96026  
 monochromator using concave holographic grating and plane mirror, imaging props. 0-99856  
 object restoration beyond Rayleigh limit in presence of noise 0-102661  
 optical fibre, multimode, graded index, mode conversion coeff. meas. method 0-99820  
 periodic structure with coherent illum., resolution depend. on number of elements, wavelength and focal length 0-63941  
 point source pair, resolution, S/N ratio and meas. precision, revised numerical results 0-95806  
 predisperser for large plane-grating spectrograph 0-73477  
 pseudocolour density encoding, white-light, using contrast reversal 0-83560  
 regularized object restoration, resolution beyond the diff. limit 0-87324  
 resonator, Gardner-Fresnel-Kirchhoff propag. algorithm 0-83621  
 scanning microscope, imaging props. and appls., super-resolution, review 0-82811  
 scanning optical microscope for semicond. materials and devices 0-95136  
 shaded circular apertures, encircled energy in diff. pattern, super-resolving and apodising props. 0-95787  
 spectrophotometer for measuring small sharp absorption bands in solids at low temps. 0-86456  
 telescope-spectrometer combination, optical props. 0-87455  
 tetrafluoromethane molecule, laser spectrosc. and optical pumping from CO<sub>2</sub> laser 0-74202  
 tomography, computerized, NDT appls. (German) 0-76439  
 UV high-resolution optical telescope design 0-90335  
 KD<sub>2</sub>PO<sub>4</sub> crystal electron-beam spatial light modulator, resolution 0-74503

**optical rotation**

see also Faraday effect; Kerr magneto-optical effect; rotational isomerism

- absorbing anisotropic and gyrotropic slab between crossed polarisers, transmitted intensity patterns 0-78762  
 para-alkylanilines having optically active modes, vibr. relax. studied by absorpt. and fluoresc. spectra 0-83340  
 chemical reactions, prochiral, gravitational field effects 0-71899  
 chiral substances, electro-optical responses, Jones matrix, meas. system for rot. anisotropy 0-84723  
 cholesteryl decanoate, optical activity in blue phase 0-100641  
 cholesteryl esters, blue phase, model 0-88030  
 classical crystal optics, lattice dynamical background, review 0-97221  
 crystal gyrotropy, meas. in IR region 0-88957  
 cubic crystals, electro-optical effect rel. to spatial dispersion of permittivity 0-66151  
 cubic crystals, paramagnetic nonlinear Faraday effect, EM wave propagation (Russian) 0-80761  
 1,6-diazaspiro[4,4]nonane-2,7-dione, optical rot. strength calcs. 0-95793  
 dicalcium strontium propionate, ferroelec. domains, direct optical visibility 0-84704  
 ethylenediamine sulfate, cryst., induced gyrotropy of CrO<sub>4</sub><sup>2-</sup> ion 0-108175  
 free particle on helix, light circular dichroism and optical rotation, theoretical anal. 0-66146  
 gyrotropic absorbing crystals, nonorthogonal eigenwave refl. 0-99624  
 gyrotropic medium, Green's function and field of moving charges 0-58445  
 inhomogeneously magnetised media, Faraday effect, polarisation plane rotation (Russian) 0-66154  
 isotropic medium, moments of optical rotary power and circular dichroism 0-88956  
 lattice dynamical background of optical activity 0-93267  
 liquid crystal thin layer, polarised light ellipticity after passage 0-88036  
 methyl ethyl ether, charact. vibrs., isomer and isotope effects, rel. to reverse spectral problem 0-63613  
 molecular crystal, optical rotation induced by ultrasonic wave (Russian) 0-93270  
 molecules, optically active, coherent Raman scatt., quantum theory 0-69150  
 molecules, optically active and inactive, electric and mag. dispersion forces interaction 0-99533  
 molecules, Rayleigh and Raman optical activity, scatt. angle anal. 0-69151  
 nematic liquid crystals, induced cholesteric order by chiral 2,2'-spirobiindane derivatives (German) 0-64884  
 nonracemic mixtures, theory of chirality functions, concept of qualitative completeness 0-69255  
 parity non-conservation effect in atoms and molecules 0-68395  
 polarimetry, noise suppression by polarization-plane rotation-angle amplification 0-68241  
 polished glass surface, reflected light phase rotation 0-66147  
 poly-γ-benzyl-L(D)-glutamate, soln., liq. cryst. and pretransitional regions, optical rot. 0-66145  
 quartz, electron irradiation effects on optical, dielec., elastic props. 0-59521  
 Raman spectroscopy of chiral molecules in mag. fields 0-102532  
 reverse spectral problem, charact. vibrs. effects calcs. 0-63613  
 ring interferometers, optically active samples, polarisation props. (German) 0-77846  
 rotatory strength, gradient matrix eqn. of motion calcs. 0-95793  
 semiconductors polarised light nonlinear rotation 0-93268  
 2,2'-spirobiindane derivatives, chiral, cholesteric order induction in nematic systems (German) 0-64884  
 CaWO<sub>4</sub>, centrosymmetric cryst., linear electrogyration study 0-60540  
 CdP<sub>2</sub>, 442 class gyrotropic crystals, self-induced rot. of light polarisation plane 0-99810  
 GaAs-Al<sub>x</sub>Ga<sub>1-x</sub>As electro-optic frequency- and polarisation-modulated injection laser 0-91810  
 Gd<sub>2</sub>(MoO<sub>4</sub>)<sub>3</sub>, spontaneous rot. of plane of polarisation of light in external field 0-93282  
 H<sub>2</sub>O<sub>2</sub>, twisted mol., optical rot. strength calcs. 0-95793  
 KD<sub>2</sub>PO<sub>4</sub>, optical activity in paraelec. phase 0-60539  
 KH<sub>2</sub>PO<sub>4</sub> crystal, optical activity 0-71373  
 MBBA+optically active substance, pretransition optical rotation in isotropic phase (Russian) 0-92657  
 Na<sub>2</sub>O.SiO<sub>2</sub>-Tb<sub>2</sub>O<sub>3</sub> glass magnetooptical study 0-88976

**optical rotation continued**

- xPb<sub>5</sub>GeO<sub>4</sub>(VO<sub>4</sub>)<sub>2</sub>, (1-x)Pb<sub>5</sub>SiO<sub>4</sub>(VO<sub>4</sub>)<sub>2</sub>, solid solution of centrosymmetric crystals, electrically induced optical activity 0-108180  
 Pb<sub>5</sub>(Ge<sub>1-x</sub>Si<sub>x</sub>)O<sub>11</sub>, electrogyration, phase transition and dielectric props. 0-93269  
 PbMoO<sub>4</sub>, centrosymmetric cryst., linear electrogyration study 0-60540  
 SrMoO<sub>4</sub>, centrosymmetric cryst., linear electrogyration study 0-60540  
 YIG:Tb garnet, Faraday effect in strong mag. field (Russian) 0-100651  
 ZnP<sub>2</sub>, 442 class gyrotropic crystals, self-induced rot. of light polarisation plane 0-99810
- optical saturable absorption**  
 aerosol medium bleached zone, probe radiation propag., intensity and phase fluctuations 0-67411  
 benzene derivatives, monohalogenated, saturable absorpt. of CO<sub>2</sub> laser 0-69465  
 difference frequency generation by stimulated Raman scatt. using inhomogeneous electrostatic field 0-95954  
 DODCI, saturable absorber, picosecond phase-conjugate refl. 0-95960  
 dye, saturable, regenerative compression of mode-locked laser pulses 0-95925  
 dye compositions bleachable by I laser, for passive Q-switching 0-91826  
 dye saturable absorber, double mode locking of ruby laser 0-99763  
 dye saturable absorbers, picosecond phase-conjugate refl. 0-95960  
 dye solutions for laser beam modulation, population relaxation lifetime meas. (Russian) 0-95964  
 Fabry-Perot cavity, absorptive bistability, mean-field approx., truncated Bloch hierarchy 0-83631  
 hole burning, photophysical and photochemical theories 0-58322  
 laser, multimode, containing saturable absorbers, bistable operation 0-91862  
 laser amplifier pair mode locked by fast saturable absorber, periodic pulse soln. 0-83623  
 laser with saturable absorber, analogy with convective instability in two-component liquid layer heated from below 0-79319  
 laser with saturable absorber, stability of semiclassical solns. 0-78828  
 laser with unstable saturable absorber, fluctuations influence 0-83587  
 methane, saturated absorpt. meas. at 3.39 μm using multipath cell 0-74442  
 methane E-component stabilisation of He-Ne laser, freq. reproducibility 0-106507  
 methane locked freq. stabilisation of 3.39 μm He-Ne laser in dual feedback control 0-99772  
 molecular beam Ramsey reson. obs. by linear laser spectroscopy 0-99514  
 molecular laser, optical excitation by photodissoc. wave propag. in dense gas 0-74352  
 multicomponent gaseous saturable absorber for CO<sub>2</sub> laser Helios system, optimisation 0-74393  
 multiple-frequency excitation to increase signal strength in saturation spectroscopy 0-102774  
 nonlinear spectroscopy, recoil effects on Doppler-free lineshapes 0-82829  
 organic compounds usable as solvents in laser saturable absorber, nonlinear refr. index meas. 0-102758  
 organic laser dyes, nonlinear transmission including stimulated emission influence 0-99720  
 polymethine dye solutions, photochem. transformations and short-wavelength luminesc. 0-100686  
 polymethine saturable absorbing dyes, dual component fluoresc. lifetime meas. 0-106359  
 semiconductor laser, self-sustained pulsations 0-106522  
 SF<sub>6</sub>, buffered, 10.6 μm transmission props. for nanosecond pulses 0-58644  
 three-level system, narrow nonlinear resonances (Russian) 0-78898  
 three-state atom, saturated two-photon absorption in perturber gas 0-106310  
 time averaging for spectroscopy sensitivity improvement, using dye laser spectrometer 0-101850  
 two level system, homogeneously broadened, saturable absorpt., coherence effects 0-95958  
 two-level Doppler-broadened medium in Fabry-Perot, optical bistability 0-102759  
 velocity-changing collisions, study by time resolved saturated absorption 0-82832  
 (Al,Ga)As DH lasers, superlinear emission characts., negative resist. obs. 0-95895  
 p-AlAs, saturation characts. over CO<sub>2</sub> laser spectrum 0-83646  
 AlGaAs semiconductor lasers, single-mode stabilisation by traps 0-95893  
 p-AlSb, saturation characts. over CO<sub>2</sub> laser spectrum 0-83646  
 Ar<sup>+</sup> laser 582 THz stabilisation by I<sub>2</sub> cell, improvements 0-102741  
 CO<sub>2</sub> laser Antares fusion system power amplifier optics 0-74394  
 CO<sub>2</sub> laser pulse, nonlinear propagation, computer simulation (Japanese) 0-95963  
 Ca 657.3 nm line saturated absorption spectroscopy, photon-recoil component resolution 0-86457  
 CaF<sub>2</sub>:Sm<sup>2+</sup>, coherent population oscils. and hole burning observed using polarization spectroscopy 0-71457  
 GaAlAs DH lasers, self-sustained pulsation suppression, effect of SiO<sub>2</sub> facet coating films 0-95894  
 p-GaSb, saturation characts. over CO<sub>2</sub> laser spectrum 0-83646  
 p-Ge, saturable absorption of picosecond CO<sub>2</sub> laser pulses 0-95956  
 Ge, saturation of transmitted intensity of CO<sub>2</sub> laser pulses 0-64111  
 He-Ne laser stabilisation, I<sub>2</sub> absorption cell power densities 0-99767  
 He-Ne laser stabilisation by I<sub>2</sub> 612 nm saturated absorption 0-99765  
 He-Ne laser stabilisation by I<sub>2</sub> 611.8 nm saturated absorption 0-99766  
 I<sub>2</sub>, high-resolution saturated absorpt. spectroscopy with short light pulse coherent trains 0-64110  
 I<sub>2</sub>, molecular vapour, saturable absorpt., self-focusing and nonlinear susceptibility 0-83647  
 I<sub>2</sub>, RF optically heterodyned saturation spectroscopy, reson. degenerate four-wave mixing 0-74211  
<sup>127</sup>I<sub>2</sub>, rovibronic absorpt. lines, hyperfine struct. 0-78596  
<sup>127</sup>I<sub>2</sub> saturated absorption for He-Ne laser stabilisation, wavelength international comparisons 0-95872  
<sup>127</sup>I<sub>2</sub> stabilised ion laser, beat freq. intercomparisons at 514.5 nm 0-74338  
<sup>129</sup>I<sub>2</sub>, <sup>127</sup>I<sub>2</sub>, high resolution saturated absorption spectra at 633 nm using He-Ne laser 0-95637  
<sup>129</sup>I<sub>2</sub> rovibronic absorpt. lines, hyperfine struct. 0-78596  
 p-InAs, saturation characts. over CO<sub>2</sub> laser spectrum 0-83646  
 InSb, intensity depend. interband Faraday rot. obs., saturation and reson. enhancement effects 0-108186

**optical saturable absorption continued**

- KCl:ReO<sub>3</sub> nonlinear absorption for CO<sub>2</sub> laser pulse compression and mode locking 0-74443  
 LiNbO<sub>3</sub>:Fe, photoinduced scatt. and bleaching effect 0-95959  
 MnSb<sub>1-x</sub>Sn<sub>x</sub> films, Faraday rotation, optical absorpt. coeffs. 0-97242  
 Na<sub>2</sub>Al<sub>2</sub>Si<sub>2</sub>O<sub>7</sub>·nH<sub>2</sub>O (X=Cl, Br, I), X-ray irradi., thermal-erase cathodochromism and dihalide mol. centres (*Russian*) 0-66236  
 Nd laser, stable passive switch using phthalocyanine dye, bleaching and relaxation 0-74368  
 Ne\* 5882 Å line, Doppler free spectra, press. broadening and shifts, saturation spectroscopy 0-78565  
 SF<sub>6</sub> gaseous saturable absorber effects on eight-beam CO<sub>2</sub> laser fusion system performance 0-106577  
 SF<sub>6</sub>, nonlinear absorpt. of CO<sub>2</sub> laser pulse, computer simulation 0-106575  
 SF<sub>6</sub>, partial saturation of ν<sub>3</sub> ladder in IR absorpt., rate process model 0-58645

**optical saturation**

- see also optical saturable absorption*  
 atomic fluorescence detection, harmonic saturated spectroscopy method 0-104472  
 Cherenkov type parametric optical oscillator, optical saturation 0-102771  
 degenerate four-wave phase conjugation, signal-pump detuning effects 0-78895  
 free electron laser, saturation effects, classical theory 0-95864  
 free electron lasers, classical theory, saturation, perturbation calcs. 0-83580  
 free electron lasers, nonlinear saturation, thermal effects using EM pump 0-87364  
 gas, resonance four-photon shift, optimal focusing of high-power pumping 0-95574  
 Goldstone mode in stationary state of non-equilibrium dissipative system (*Chinese*) 0-87365  
 high-resolution spectroscopy using tunable lasers 0-101849  
 laser saturation spectroscopy, time-resolved, free induction decay of two-level resonances 0-102775  
 laser ultrashort pulse form., filter clarification and amplification saturation coincidence 0-64085  
 molecular lasers, IR-FIR transferred Lamb-dip, standing wave saturation effects 0-58520  
 molecular nonsteady-state luminesc. behaviour under narrowband laser excitation 0-87159  
 nonlinear optical amplifier, coherent radiation statistical props. 0-99691  
 nonlinear spectroscopy, coherent background noise elimination from saturation spectrosc. signals using freq. offset pump 0-62733  
 polarised light absorpt. spectra, forbidden transitions and discrete saturation 0-71464  
 saturable optical amplifier, quantum theory 0-78916  
 semiconductors, optical saturation for high carrier recomb. freq. (*Russian*) 0-88585  
 two-photon resonant third-harmonic generation, pump depletion and saturation 0-69454  
 CO<sub>2</sub> high-power pulsed laser, wave-optical resonator modelling, gain saturation law 0-99693  
 CO<sub>2</sub>, inverted, wavefront reversal, high efficiency 0-74436  
 CO<sub>2</sub> laser Antares fusion system optical diffraction computation 0-74424  
 CO<sub>2</sub> waveguide laser, saturation parameter meas. method 0-87372  
 Ca, stable and radioisotopes, hfs, isotope shifts, dye laser saturation spectroscopy, beam expt. 0-58169  
 Cu vapour pulsed laser, spectral comp. of superradiance, stimulated and spontaneous radiation 0-102713  
 DF-CO<sub>2</sub> chemical laser, amplification of long and short pulses 0-95883  
 InGaAsP-InP DH lasers, spatial hole burning, spontaneous emission saturation, direct obs. 0-95892  
 Xe 3.51 μm laser amplifiers, spectral narrowing and saturation induced rebroadening optical heterodyne obs. 0-63976  
 Xe-He, 3.51 μm laser amplifiers, spectral narrowing and saturation induced rebroadening optical heterodyne obs. 0-63976

**optical self-focusing**

- see also electrostriction; Kerr electro-optical effect; self-trapping*  
 active medium, EM field self-focusing, laser transverse struct. form. 0-87442  
 alkali borosiluminosilicate system, self-focusing fibres with aperture of 0.18 0-87548  
 convex analysis and variational inequalities (*Japanese*) 0-77606  
 empirical relationship for a nonlinear index coefficient 0-74445  
 Gaussian laser beam, transverse self-focusing and self-trapping investig., moment method 0-58652  
 Gaussian laser beams, Gaussian instability growth 0-69469  
 laser amplifier system, small-scale self-focusing 0-106580  
 laser beam self-focused in turbulent plasma, average field 0-79505  
 liquid crystal, isotropic phase, self-focusing stability of laser beam 0-99812  
 magnetoplasma, laser beam self-focusing 0-102778  
 molecular lasers, laser pumping, dispersion 0-87375  
 moving media, thermal self-focusing of laser beams 0-64122  
 nematic liquid crystal, gigantic optical nonlinearity, self focusing in oriented mesophase (*Russian*) 0-64120  
 optimisation of light beam focusing, in moving nonlinear media, using gradient method 0-106578  
 phosphate glasses, optical breakdown rel. to microscopic inhomogeneous struct. 0-102784  
 plasma, collisional, mixed mode operation, cross-focusing 0-83945  
 sapphire, damage by UV laser radiation, self-focusing mechanisms 0-76110  
 semiconductors, mixed and binary, nonlinear polarisability, self-action effects 0-99786  
 stimulated Brillouin scatt., three dimensional, for focused Gaussian beam 0-69456  
 CdS, nonlinear self-action effect and absolute two-photon absorption coeff. 0-83649  
 GaAs-AlGaAs DH injection laser with stripe contacts, radiation pulse shaped shape 0-91799  
 I atomic vapour, self-induced transparency and reson. self focusing 0-64114  
 I<sub>2</sub>, molecular vapour, saturable absorpt., self-focusing and nonlinear susceptibility 0-83647  
 Nd:glass laser system, beam spatial profile optimization in amplifier channel 0-74407

**optical storage devices**

- see also holographic storage*  
 polyvinylacetate film, dissolved polyester yellow, ablative optical recording 0-83555

**optical stores**

- see also holographic storage*  
 ablative optical recording, computer modelling 0-91752  
 alkali halide crystals, appl., activated (*Russian*) 0-80819  
 colour film archival storage, white light processing technique 0-99637  
 ferroelectric semiconductors appl. (*Russian*) 0-80749  
 focus error detection, skew beam and Foucault knife-edge techniques 0-102649  
 laser and electro-optical systems, conf., San Diego, CA, USA (Feb. 1980) 0-62392  
 laser image storage mass memory 0-102752  
 laser recording and information handling, seminar, San Diego, CA, USA (Aug. 1979) 0-101663  
 mass storage systems, digital optical data storage and retrieval 0-78790  
 metal thin film, preheating as aid to laser recording 0-102753  
 optoelectronic memory, bit-organised, method for information capacity increase 0-102656  
 PCM encoding and decoding for optical memories 0-102658  
 photoinduced surface storage of SAW patterns in LiNbO<sub>3</sub> 0-74309  
 wideband optical disc data recorder systems 0-102751  
 EuO film threshold characteristics in holographic and bit recording (*Russian*) 0-63944  
 PLZT ceramics photosensitivity enhancement by H- and He-ion implantation 0-96934  
 Te film, stability in moist air, rel. to information storage capability, atmospheric corrosion model 0-71774

**optical susceptibility**

- see also nonlinear optical susceptibility*  
 anharmonically coupled oscil., time depend. Hartree theory, susceptibility, absorpt. and Raman spectrum 0-58241  
 canted magnetic structured materials, exciton spectra, optical props. 0-70622  
 condensed matter, low frequency responses (*Chinese*) 0-80669  
 dielectric behaviour of materials undergoing dipole alignment transitions 0-88922  
 ferroelectric and other structural phase transitions at low temps. 0-75990  
 ferroelectric crystals, polariton light scatt. freq.-angle spectra, nonlinear susceptibility interference (*Russian*) 0-92834  
 ferrofluid, dielec. behaviour in uniform mag. field 0-60390  
 glass, third order susceptibility meas. by degenerate four wave mixing (*Chinese*) 0-84708  
 Jahn-Teller crysts., ferroelec. transitions, elastic and dielec. anomalies, microscopic model 0-71332  
 LF fluctuation, dissipation and relaxation properties, universality 0-84687  
 metallic ultrathin filaments, dielectric and superconducting fluctuations, Peierls transition (*Russian*) 0-65742  
 pyroelectric detector materials, thermal noise and dielec. response 0-75952  
 semiconductor thin films, ferroelectric properties, quantum size effect 0-97201  
 structural phase transitions, Landau theory 0-92639  
 TGS, L-α-alanine disordered regions, dielec. prop. changes in transition region 0-108159  
 thin island films, statistical theory for dielectric props. 0-80699  
 CaF<sub>2</sub>:Er, near-Debye dielectric responses 0-71291  
 DyVO<sub>4</sub> Jahn-Teller crystal, deform. induced transitions, elastic and dielectric characts. (*Russian*) 0-80726  
 KH<sub>2</sub>PO<sub>4</sub>, critical and tricritical phenomena, susceptibility, exponents 0-75976  
 K<sub>1-x</sub>Na<sub>x</sub>TaO<sub>3</sub> quantum ferroelectric, dielec. susceptibility 0-103922  
 KTa<sub>1-x</sub>Nb<sub>x</sub>O<sub>3</sub> quantum ferroelectric, dielec. susceptibility 0-103922  
 xPbTiO<sub>3</sub> + (1-x)PbCd<sub>1/3</sub>Nb<sub>2/3</sub>O<sub>3</sub>, phase transition spread, polarisation relaxation, dielectric susceptibility (*Russian*) 0-75922  
 RbH<sub>2</sub>PO<sub>4</sub>, critical and tricritical phenomena, susceptibility, exponents 0-75976  
 Si:P, dielec. susceptibility meas., polarisation catastrophe at metal-insulator transition 0-59873

**optical systems**

- see also adaptive optics*  
 aberrations, automatic correction routine 0-58464  
 acceptance testing with interferometer 0-95987  
 airborne multispectral scanner design 0-74458  
 amplitude filtering for superresolution, maximum central irradiance under energy constraint 0-91914  
 apodization, optimal, by means of coupled calc. of pupil function and shape 0-95788  
 bipolar spatial filtering, incoherent, review 0-102822  
 camera system for automatic photomicrography 0-82841  
 chromatic aberrations of real rays, role of each lens in optical system 0-102655  
 compensated levels, high-precision, geodetic appl. 0-101813  
 concentrator, compound parabolic, phase space conservation for incoherent prop. 0-69491  
 correction, automatic, with large tolerances (*German*) 0-95977  
 correlation filtering for increasing diff. efficiency 0-96028  
 design, w.r.t primary aberrations (*Italian*) 0-69490  
 diffraction and aberration effects, wave optical calc. 0-83549  
 diffraction patterns for optical systems with pupils of non-uniform transmittance 0-87470  
 diffuse reflectors, light collection and dissemination 0-83658  
 double exposure interferometry through speckle photography (*French*) 0-83568  
 driven member rotation uniformity test installation 0-92094  
 electro-optical system manufacture, test and process control changes 0-96044  
 electro-optics, systems aspects, seminar, Huntsville, AL, USA (May 1979) 0-94921  
 engineering, seminar, San Diego, CA, USA (Aug. 1979) 0-77541  
 eyepieces, imaginary front focal planes, negative collection lens, design considerations 0-64139  
 fast Fourier transform, two dimens., for optical systems analysis 0-78986  
 fibre, gradient-index light-focusing, image enhancement 0-69501  
 fibre array, gradient-index, appl. in copying machine 0-69500  
 fibre array, gradient-index, unevenness of illuminance 0-69482  
 fibre optic system design and component selection 0-58767  
 fibre optic systems and field trials, review 0-58700



**optical systems continued**

- fibre second generation systems, 1300 to 1600 nm 0-64163
- flow visualisation by foreign particle or energy optical tracing 0-96329
- Fourier hologram recording in optical system with synthetic aperture 0-95852
- gradient index optical elements and system design 0-106594
- Herschel's condition as wave optics theorem 0-87301
- high performance system development and design at Carl Zeiss Jena works (*German*) 0-58660
- holography, twin-image, chromatic lens system, astron. appls. 0-87346
- illumination system, optical design 0-64135
- image contrast loss in presence of chromatic magnification difference, numerical estimate 0-95823
- image quality evaluation (*German*) 0-95804
- imaging system point spread function determ. by scatt. of two monochromatic beams 0-87316
- imaging system requirements interacting with copier architecture 0-77895
- impact machines, pendulum, energy meas. using optical system 0-69746
- large-aperture optical system, energy distrib. calc. in diff. image of point 0-74305
- laser beam expander for short cavity dye laser 0-87532
- laser integration into optical systems, Nd:YAG laser 0-78887
- laser pump system, analytical theory 0-106540
- laser system, interferometric optical anal. 0-87401
- lens, gradient-index spherical, design for optical pickup systems 0-69483
- lens system, distortion by means of numerical transformation (*German*) 0-64132
- line image transmission through single fibre using spectral instrums. 0-102820
- long focal length aerial reconnaissance system response to thermal shock 0-78939
- longitudinal aberration calc. by stereo-self-collimation method (*Russian*) 0-91878
- losslessness of optical systems in a vectorial treatment 0-83558
- low-temperature chamber with fixed pressure, use of liquefied gases 0-57358
- machine shop operations 0-96045
- memory, bit-organised, method for information capacity increase 0-102656
- microscope photometer/semiautomatic image anal. instrument system for morphometric and photometric value meas. 0-82815
- military optical system temperature effects and counter-measures 0-78938
- moire system, for counting winding turns 0-73428
- MTF, two-dimensional, meas. by second order speckle statistics calc. 0-63937
- multidither hillclimbing adaptive optical system, secondary intensity maxima correction 0-106593
- multimode fibre link, modal noise 0-87536
- nonsymmetrical optical system, matrix representation 0-64130
- OTF measurement using autocorrelation method 0-58469
- periodic-pattern-defects omnidirectional-spatial-filter optical detection system 0-69333
- photographic materials, MTF automatic evaluation 0-95170
- photometer conversion to scanning microphotometer 0-86374
- processor, incoherent, for making 'spectrogram' of 1-D function 0-87528
- production quality trends and limits 0-69566
- production technology advances, seminar, London, England (April 1979) 0-67938
- ray differentials calc. algorithm (*Russian*) 0-87462
- reflection system, diffraction image intensity in turbulent atm., Huygens-Kirchhoff principle calcs. 0-63926
- remote sensing techniques, book 0-101675
- sensor system simulation and evaluation 0-96030
- shaded circular apertures, encircled energy in diff. pattern, super-resolving and apodising props. 0-95787
- shadow device, characts., scattering medium effects, Monte Carlo calcs. 0-99630
- solar power plant, direct tracking using two-mirror unit with plane and hyperboloidal counter-reflectors 0-91875
- space optics, conference Huntsville, Alabama (1979 May 22 to 24) 0-62385
- space optics, imaging X-ray optics workshop, Huntsville, Alabama (1979 May 22 to 24) 0-62384
- spectral analysis incoherent optical system, smoothness parameters meas. of polished surfaces 0-86261
- spectrophotometer measurement system for Hewlett-Packard 8450A model 0-68269
- spherical-cylindrical lens combination, combined 1-D image-orthogonal Fourier transform processing 0-58658
- star pointing with coelostat, Meudon solar tower 0-90338
- step-stare spaceborne optical system image motion compensation 0-90322
- step-stare spaceborne optical system smear compensation by focal plane manipulation 0-82172
- superachromatic triplets, design method 0-64133
- systems engineering approach to optical design, fabrication and operation 0-95986
- Tokamak, far IR laser collective scatt. system 0-59300
- tolerancing, encircled energy performance prediction 0-78935
- topogram sensitivity, wavefront correl. effect 0-69345
- trihedron optical system, for linear displacement meas., accuracy estimation 0-101780
- two-dimensional optical system MTF meas. by second-order speckle statistics computation 0-74304
- two-mirror pancratic system, extraneous image plane highlights elimination 0-87467
- variable-scale single-lens optical transform systems 0-58656
- well-baffled axially symmetric system design program GOSBOP 0-78940
- CO<sub>2</sub> laser Antares fusion system power amplifier optics 0-74394
- CO<sub>2</sub> laser fusion system, optical design considerations 0-78868
- Nd:glass laser system, beam spatial profile optimization in amplifier channel 0-74407
- Nd:glass laser system, multichannel, for fusion experiments, model 0-58557

**optical telescopes** see *telescopes*

**optical testing**

- see also *optical instrument testing; optical workshop techniques*
- aplanatic two mirror telescope from near-normal to grazing incidence, comparative performance anal. 0-58654

**optical testing continued**

- applied optics, fabrication and testing, conf., Oakland, CA, USA (May-June 1980) 0-101661
- aspheric, testing in reflected light using blazed synthetic holograms 0-91881
- aspheric testing, in-line and carrier freq. holograms, comparison 0-87349
- astronomical optical surface shaping process automation 0-105169
- astronomical optics testing by Hartmann method, estimation of reliability of results 0-67564
- attenuator metrological certification methods 0-91941
- autocollimation instrument for checking angles and pyramidity of AR-90° prisms during manufacturing process 0-87570
- automatic correction of optical systems with large tolerances (*German*) 0-95977
- birefringent plates, cracks, stress intensity factors, refl. caustics method 0-93718
- coherent fibre optics testing techniques 0-78992
- colour image evaluation from tristimulus values transfer functions measurements 0-87333
- complex aspheric mirror testing by phase meas. interferometry 0-74467
- compound glass optical fibres, total and scatt. loss coefficient meas. 0-69536
- computer-controlled interferometry, in-process production tool 0-74531
- concave paraboloidal mirror, prod. method, interferogram tests 0-58823
- contactless laser interferometer sweep gauge for diamond-turned surfaces 0-73441
- coronagraph objective component surface scatt. angular distrib. obs. 0-74463
- CVD optical fibre, long length strength 0-58752
- cylindrical mirror and lens optical figure characterisation with conventional interferometer 0-78944
- dark-field surface inspection using total internal reflection 0-74519
- diamond turned surface production, interferometric test repeatability 0-74538
- electro-optical system manufacture, test and process control changes 0-96044
- electronic phase meas. techniques 0-106643
- fibre-optic measurements, using standards and instruments 0-74488
- fibre, furnace drawn, tensile strength 0-58751
- fibre attenuation measurement comparison among USA manufacturers 0-58747
- fibre cable testing, for lightwave communications systems 0-102865
- fibre cable testing 0-64230
- fibre characterisation techniques compared 0-64202
- fibre end face quality check 0-64164
- fibre measurements using optical-bench equipment 0-58695
- fibre preform core diameter and Ge doping profile meas., X-ray nondestructive method 0-64231
- fibre splice insertion loss meas., backscattering method 0-58720
- fibres, compound glass, nylon-covered, reliability and verification tests and results (*Japanese*) 0-99866
- Fizeau interferometer, spherical-wave, direct phase meas. 0-95126
- focometer, F-1, for lens focal length meas. 0-64138
- Foucault, phase edge and wire optical test 0-96046
- Fourier transform lens, spatial invariance test 0-69492
- Hartmann modified wavefront sensor performance 0-74522
- interferometer, lateral shear, using twin three-beam holograms, lens tests appl. 0-99673
- interferometer design, construction and interferogram processing, optical testing appl. 0-79020
- interferometers, IR lateral shearing, as optical testing tools 0-68244
- interferometric examination of lenses, mirrors and optical systems, 3D display 0-69497
- interferometric examination techniques for lenses and other components 0-69498
- interferometric instrumentation as a cost-effective production tool 0-74535
- interferometric optical testing status and prospects 0-74529
- interferometry seminar, San Diego, CA, USA (Aug. 1979) 0-73096
- IR laser interferometer operation and testing 0-73433
- IR optical components and aspherics, 10.6  $\mu$ m interferometric testing 0-74523
- IR scanning system modular design, assembly and alignment 0-78989
- laser equipment, pulsed, multichannel device structure and testing (*German*) 0-95933
- laser system, interferometric optical anal. 0-87401
- laser tracking system testing by 1 m unobscured IR collimator 0-78991
- laser unequal path interferometer with electro-optical camera and mini-computer, fabrication/test appl. 0-77847
- lens testing, MTF-based optical sensitivity and tolerancing computer programs 0-83686
- long-haul communications optical fibre fault location method 0-64193
- long-radius concave optical surface curvature meas., differential technique 0-74534
- matched filter visibility effects on the correlation function 0-96031
- micro-optics testing, width meas. of slit test objects 0-64223
- mirror, single-point diamond-turned, performance before and after polishing 0-74466
- mirror fiducial system compatible with computer-controlled polishing facility 0-74539
- mirror testing using autocollimation method with multiple pendulum mirrors 0-102792
- monomode fibre selective excitation for differential group delay meas. 0-99876
- null testing in modified scatterplate interferometer, test of 20 cm diam. f/3 parabola 0-79015
- objective lenses, two-channel device for meas. transmission coeff. 0-106642
- pancratic objectives, aberration stabilisation during focusing 0-102799
- parabolic mirror testing by vibration-insensitive laser unequal path interferometer 0-74537
- parabolic mirror testing during fabrication by long-wavelength interferometer 0-74536
- point-diffraction interferometer principles and applications 0-74530
- polycarbonate, bisphenol A, birefringent plates, cracks, stress intensity factors, refl. caustics method 0-93718
- precision optical element testing by phase meas. interferometry 0-74520
- precision optical evaluation by phase meas. interferometry 0-74533
- precision testing techniques, using laser interferometers, microprocessors and computers 0-69563
- prism optics testing for laser interferometer, interf. meas. 0-105698



**optical testing continued**

- production technology advances, seminar, London, England (April 1979) 0-67938
- random digital scene generation with specified statistics 0-99666
- roof and other prisms, MTF tests 0-69571
- scatterplate interferometer principles, limitations and tolerances 0-73436
- Schmidt camera, simple null test for aspheric corrector plate 0-91940
- Shack interferometer for optical shop use 0-73434
- single mode fibre homogeneous CVD fabrication and characterisation 0-69562
- solar energy concentrators, reflecting, performance evaluation 0-87457
- spherical surfaces shape deviation determ., using sphero-interferometer (Czech) 0-58821
- sphericity standards, interferometric meas. (German) 0-87569
- standard test method development by ASTM 0-74528
- surface contact interaction zone, thickness calc. and distance meas. methodology (Russian) 0-99889
- surface topography quantitative determ. by Nomarski differential interference contrast microscopy 0-73318
- system acceptance testing with interferometer 0-95987
- systems engineering, seminar, San Diego, CA, USA (Aug. 1979) 0-77541
- testplate testing interferometry in precision optical shop 0-74532
- wavefront interpretation with Zernike polynomials 0-78776
- wide-angle concentric dome and shell production, double-pass null test 0-79022
- Wolter lens component replication 0-95972
- X-ray mirror profile meas. machine 0-69496
- Zygo interferometer system 0-73437
- NaCl 46 cm window optical evaluation facility 0-74526

**optical transfer function**

- annular aperture, arbitrary point spread functions 0-87325
- apodising filters, numerical exam., second moment of the point spread function 0-106611
- apodization and image contrast: author's reply to comment 0-58466
- autocorrelation method for measuring the transfer function of optical systems 0-58469
- biomedical gamma camera systems, methods for MTF meas. 0-94324
- blind deconvolution, zero phase blurring function estimation 0-106482
- coded aperture imaging: the modulation transfer function for uniformly redundant arrays 0-99019
- coherent feedback, flexible filter operations 0-87337
- coherent fibre optics testing techniques 0-78992
- colour image evaluation from tristimulus values transfer functions measurements 0-87333
- confocal scanning microscope, image form. 0-68249
- diffraction patterns for optical systems with pupils of non-uniform transmittance 0-87470
- double beam interferometer, meas. of background suppression and spectral detection 0-95130
- double beam interferometer for background suppression and spectral detection 0-95129
- electron optical convertor, pulsed, dynamic spatial MTF estimate 0-74502
- electron phase microscopy using spherically corrected foil lens, contrast transfer function (German) 0-83546
- eye, aerial image modulation lowering, contribs. of retina and eye optical system 0-81584
- eye, human, MTF of defocused optical system for incoherent monochromatic light 0-67072
- Fabry-Perot interferometer instrumental function for short light pulses 0-105704
- feedback systems for analogue and digital optical image processing 0-102650
- fibre bandwidth determination in time domain, OTF meas., laser diode source evaluation 0-79002
- filter, single mode fibre birefringent 0-58713
- flexible high-resolution film recorder system 0-102827
- gamma camera visual outcome units comparison, use of MTF 0-94323
- hologram recording medium, photochromic, heuristic exponential model appl. 0-78796
- holographic optical elements for incoherent polychromatic imaging 0-69349
- image contrast loss in presence of chromatic magnification difference, numerical estimate 0-95823
- image processing, analogue and digital, feedback, review 0-102639
- interference transfer function with quadratic detect., coherent illum. 0-78782
- IR segmented composite window design 0-106621
- lens design with simultaneous image spot, optical path difference, diffraction MTF and Seidel aberration minimisation 0-74459
- lens testing, MTF-based optical sensitivity and tolerancing computer programs 0-83686
- lens wavefront aberration, interferometric examination techniques, OTF meas. standards 0-69498
- lensless scanning telescope, MTF 0-58655
- matched filter visibility effects on the correlation function 0-96031
- medical imaging systems, information capacity considerations 0-98090
- micro-optics testing, width meas. of slit test objects 0-64223
- mountain and desert atmospheric MTF comparison 0-82063
- MTF, two-dimensional, meas. by second order speckle statistics calc. 0-63937
- MTF tolerancing computer program 0-78934
- multi-aperture system imaging props. 0-87332
- phase problem in image formation: the determination of coherent transfer functions 0-87329
- photographic film, undeveloped, MTF meas., target base dimension influence 0-102653
- photographic layer, homogeneous solid, diffusion, one-dimensional case (German) 0-73495
- photographic materials, MTF automatic evaluation 0-95170
- precision optical element testing by phase meas. interferometry 0-74520
- projection system, wavelength and coherence effects 0-64136
- projector having a thermoplastic target and operator's eye, characts. 0-96023
- roof and other prisms, MTF tests 0-69571
- scanning telephotometer, spatial transfer characts. 0-73415
- scintillation camera collimator image form. 0-89844
- thermoplastic spatial light modulator 0-102841

**optical transfer function continued**

- thin phase structure detection method spatial filtering props., under partially coherent illum. 0-95828
- two-dimensional optical system MTF meas. by second-order speckle statistics computation 0-74304
- uneven interface of media with different refractive indices, statistical characts. of images 0-87331
- wavefront sensing by phase retrieval 0-106478
- X-ray film/intensifying screen system, MTF and Wiener spectrum, film and screen quality effect (German) 0-73560
- X-ray film/ZZ (German) 0-73559
- X-ray images, electronic recording 0-62815
- Bi<sub>2</sub>SiO<sub>20</sub> PROM device, image recording and erasure mechanism 0-74490
- KD<sub>2</sub>PO<sub>4</sub> photo-spatial light modulator, optical data processing 0-102839
- Nd<sup>3+</sup>:YAG multimode laser radiation noise 0-74366
- ZnS CVD IR window, optical and physical characteristics 0-106620

**optical variables control**

- Al<sub>0.42</sub>Ga<sub>0.58</sub>As-GaAs-Al<sub>0.42</sub>Ga<sub>0.58</sub>As, etalon, optical bistability and modulation 0-58628

**optical variables measurement**

- see also colorimetry; densitometry; light velocity measurement; optical noise measurement; photometry; polarimetry; Q-factor measurement; refractive index measurement; streak photography; turbidimetry
- backscatter in optical fibres, theory (German) 0-91921
- bench equipment for optical fibre characteristics measurement 0-58695
- birefringent crystal faces, meas. method of growth and dissoln. rates 0-79719
- chiral substances, electro-optical responses, Jones matrix, meas. system for rot. anisotropy 0-84723
- compound glass optical fibres, total and scatt. loss coefficient meas. 0-69536
- constants at two incidence angle values 0-101831
- diode laser wavelength monitoring using fibre interferometer 0-74413
- dual-mode optical fibre, spatial technique for modal delay difference meas. 0-78950
- electric dichroism measurement instrument with digital processing 0-82800
- electro-optical apparatus, conformation of change in polypeptides 0-85336
- Faraday effect and susceptibility of garnet films, meas. using magneto-optical apparatus 0-105680
- fibre-optic measurements, using standards and instruments 0-74488
- fibre attenuation meas. by backscattering method, effect of noise 0-102824
- fibre attenuation measurement comparison among USA manufacturers 0-58747
- fibre attenuation measurements performed by backscattering technique 0-64152
- fibre parameter characterisation techniques, comparison 0-64147
- fibres, measurement techniques for transmission loss and refractive index distribution (Japanese) 0-87498
- film optical parameters meas. method, reevaluation 0-104004
- graded-index fibre, optical loss meas. in the field 0-102851
- graded-index optical fibre intermodal dispersion, frequency-domain meas. 0-58729
- grating absolute efficiency meas. device 0-87540
- interferometric wavelength meas. with post-detection signal processing 0-105699
- laser radiation intensity distrib. meas. using Bragg diffraction of light 0-64092
- laser radiation spatial distribution determ., mode parameters 0-95055
- laser wavelength calibration using optogalvanic effect, atlas 0-62727
- light scattering technique, comparison of optico-optical scattering and birefringence, of Wyoming Na bentonite suspensions 0-85226
- light transmission loss measurement by hazemeter 0-67995
- linear dichroism apparatus for extended wavelength ranges, direct-reading 0-98962
- loss of multi-mode fibres, non-destructive method 0-69550
- nanosecond laser pulse stretch meas. in underwater propagation 0-87426
- optical constants meas. method using polarised light refl. coeffs., accuracy 0-73423
- optical fibre attenuation charact. meas. by backscatter technique (Italian) 0-106600
- optical fibre characterisation, measurement techniques 0-95998
- optical fibre parameter measurement using optical time domain reflectometer 0-58755
- photodetector relative spectral sensitivity meas. method using two tandem monochromators (Japanese) 0-101840
- photoelectric distortion on MSP-4 objectives (German) 0-95976
- reflectivity, total, using specular-reflectance and diffuse reflectance references 0-73421
- resolution, S/N ratio and meas. precision, revised numerical results 0-95806
- semiconductor, optical absorpt. coeff. and minority-carrier diffusion length, differential photocurrent method of meas. 0-96896
- specular reflectance standards for visible and infrared region using thin Al film vacuum deposited on optical flats (Japanese) 0-102789
- streak camera dynamic range measurements, picosecond time resolution 0-73490
- surfaces, concave and convex, radii of curvature meas. 0-83654
- suspension of absorbing particles, simultaneous meas. of dichroism and birefringence in elec. field, photocurrent signal obs. 0-82801
- terrestrial solar spectral irradiance distrib. variations, sensitivity of solar transmittance, reflectance and absorbance 0-82739
- transmission coeff. of objective lenses, meas. using two-channel device 0-106642
- transmittance and reflectance, double-beam single-detector wavelength-modulating spectrometer, AGC 0-86447
- wavelengths of CW far IR optically pumped lasers, simple accurate meas. method 0-106554
- CdS plane parallel slab, optical const. determ. methods 0-60531

**optical waveguide components**

- see also optical couplers; optical isolators
- 1X2 optical switch using new type of pentagonal prism switch, for optical fibres 0-64148
- attenuator, variable, for use in single-mode fibre transmission systems 0-99821
- bistable optical fibre switch, construction and performance 0-95994
- coupled-waveguide TE/TM mode sputter 0-99855



**optical waveguide components continued**

- cutoff mode filter with structure of metal-clad optical strip-line 0-83680  
directional coupler as waveguide tap with infinitesimal insertion loss 0-99883  
fact directional coupler switch/modulators, novel ps optical pulse sampling method 0-58784  
fibre Faraday rotators in fibre Raman lasers 0-58775  
fibre optical rotation sensor, all-waveguide configuration, key element tests 0-58796  
fulgimide planar photochromic structures 0-64196  
geodesic lenses, anal. by beam propag. method 0-58686  
integrated optics, electrooptical channel waveguide matrix switch using total internal reflection 0-58810  
integrated optics Bragg-effect polarizer/analyzers and lens-less waveguide beam expanders 0-58807  
integrated optics sub-ps gate 0-58809  
integrated programmable planar waveguide components formed by optically writing Bragg diffraction gratings into photochromic structs. 0-79011  
microfabrication for guided-wave optical devices 0-58812  
mode filter on anisotropic thin film, anal. of two coupled modes with losses 0-79000  
planar waveguide blazed dielectric diffraction gratings, anal. and design 0-58779  
thin-film spectrograph for guided waves 0-58778  
LiNbO<sub>3</sub> lenses, diamond-turned aspheric geodesic waveguide lenses 0-58804  
LiNbO<sub>3</sub> very high throughput damage resistant waveguide modulator 0-58788  
LiNbO<sub>3</sub> waveguide modulators and switches, Ti-diffused, fabrication on directional coupler principle 0-83678  
LiNbO<sub>3</sub>:Ti 3-dB optical waveguide mode convertor using chirped gratings, power transfer 0-79014  
LiNbO<sub>3</sub>:Ti digitally driven integrated optics amplitude modulator 0-58808  
LiNbO<sub>3</sub>:Ti electro-optic branching waveguide, characts. 0-83681  
LiNbO<sub>3</sub>:Ti optical waveguide electrooptic devices polarisation independ. directional coupler switch and wavelength filters 0-58783  
LiNbO<sub>3</sub>:Ti optical waveguide channel branches 0-58811

**optical waveguide theory**

- see also guided light propagation*  
anisotropic graded-index waveguide, optical mode propag. const. calc. 0-69540  
Bloch waves in periodic planar optical waveguides 0-58777  
branching optical waveguide, mode coupling 0-69518  
cable design considering structural imperfection 0-64184  
corrugated optical disc waveguides 0-58701  
corrugated waveguides, effective index approach to distrib. feedback, TE polarisation 0-102859  
cross-talk noise analysis, optical multichannel waveguides 0-91922  
dielectric waveguide, corrugated, light emission 0-96027  
dielectric waveguide hybrid and transverse mode dispersion calc. (*Russian*) 0-99857  
differential mode delay rel. to refr. index profile, geometrical optics treatment 0-69529  
diffused waveguide, generalised parameters describing acoustooptic interaction 0-91924  
elliptical multimode fibres, leaky ray correction factors 0-87487  
excess loss increase mechanism of jacketed fibers at low temperature 0-83682  
fibre, multimode irregular focusing with random ellipticity, light propag. 0-74501  
fibre, rectangular cored multilayer fibre 0-83667  
fibre, single-mode systems, instability due to interference and polarization effects 0-58774  
fibre cables, single-mode and parabolic-index multimode, random-bend loss 0-78951  
fibre mode properties, computation by propagating beam method 0-69502  
fibre scattering, ray theory 0-69528  
fibres, backscatter meas. theory (*German*) 0-91921  
fibres, scalar approximation technique, accuracy 0-58703  
fibres with arbitrary index profile, pulse propag. and dispersion 0-78984  
finite element anal. 0-87558  
gas-dielectric fibre, wave conversion in irregular portion 0-74500  
graded fibres, mode propag. time calc. using multimode theory (*German*) 0-58710  
graded index fibre, error estimates to first order WKB calc. method 0-87488  
graded index fibre, wave eqn. for propag. fields 0-58757  
graded index planar lightguide, electrooptical diffraction 0-78995  
graded-index curved media, generalised Fresnel power transmission coefficients 0-102815  
graded-index fibres, mode analysis using scalar wave eqn. and direct numerical integration 0-78971  
graded-index multimode fibres, bandwidth characts., appl. on long-haul transmission systems 0-64180  
graded-index optical fibres, mode eigenfunction computation propagating beam method 0-95988  
grating, diffraction efficiency, Brewster's law 0-91935  
holography with guided optical waves, diff. efficiencies, theory 0-83563  
inhomogeneous circular waveguide, asymptotic eigenvalues of vector waves 0-96010  
inhomogeneous dielectric filled uniform waveguides, EM wave propag. 0-83666  
injection laser harmonic distortion analysis 0-58537  
integrated optical multimode waveguides, Fourier domain propagation calc. 0-64219  
launching and propagation of light in optical fibres 0-69504  
leaky dielectric waveguide, planar hollow structure, eigenmode analysis 0-78973  
lenslike fibres, density-matrix method applied to mode coupling 0-78970  
locally deformed slab waveguide propagation and diffraction patterns 0-106630  
lossy waveguide, Brewster phenomena, cut-off thickness 0-87524  
low-loss dielectric tube leaky waveguide, transmission characts. 0-95999  
Maxwell's eqn., numerical soln., refractive indices 0-87520  
monomode fibre total dispersion and loss minima 0-91929  
multilayer multimode optical fibre, ray theory, optimal distrib. of refractive index 0-87489

**optical waveguide theory continued**

- multimode fibre, impulse response calc. 0-74486  
multimode fibre, splice loss and mode conversion 0-99830  
multimode fibres, freq. depend. of modal noise, speckle theory 0-102817  
multimode fibres of arbitrary refr. index profile, pulse dispersion 0-74475  
multimode fibres with index profiles varying along length, pulse propag. 0-87534  
multimode graded index lightguide, mode coupling 0-78999  
multimode graded-index fibre, near field intensity and modal power distrib. 0-102810  
multimode W-type fibres, power flow numerical soln. 0-78955  
parabolic index fibres, LP<sub>00</sub>-mode excitation by Gaussian TEM<sub>00</sub>-beams, power coupling coeff. 0-78958  
parabolic index with random dielectric constant gradient, Gaussian beam propag. 0-58698  
parabolic-index fibre modes, propag. characts., linearly polarised approx. 0-78972  
polymer lightguide, light propag., nonlinearity, quasi-optical approx. 0-99837  
prism coupling into clad uniform optical waveguides 0-96003  
pulse propag., nonlinear, homogeneous and inhomogeneous waveguides 0-83669  
quasilinearly tapered couplers, weighted coupling strength 0-83674  
rectangular core fibre optic waveguide, dispersive props. 0-64172  
rib waveguide with trapezoidal cross section, numerical analysis 0-96009  
semitransparent thin cylinder, radiation-conduction heat transfer, lightguide approx. 0-96179  
SHG by guided radiation mode coupling in thin film optical waveguide 0-106567  
single mode fibre near- and far-field characteristics, profile-independent representation 0-58739  
single-mode, simplified parameter based anal. 0-69507  
single-mode fibres, pulse distortion, Gaussian pulse propag. theory 0-78956  
slab waveguide, TE Mode dispersion rel. to DH semiconductor lasers 0-91886  
step-index fibre, scattering from arbitrarily located off-axis inhomogeneity 0-58702  
step-index fibres, pulse responses investig. using WKB approx. 0-91898  
step-index optical fibre, scattering and guided mode conversion due to spherical object, theoretical anal. 0-64153  
superluminal radiator theory (*Russian*) 0-64156  
tapered optical slab waveguides with hypothetical boundaries 0-64185  
temporal frequency dependence of modal noise in fibres [optical] 0-58687  
thin-film two parallel waveguides, numerical anal. 0-106626  
three-waveguide system, interference effects on couplings 0-78969  
transmission characts. of optical waveguides with periodic external force 0-9873  
two-layer elliptical fibre waveguides, first higher-mode cutoff 0-58684  
two-mode fibre with near optimum index-profile, transmission characts. 0-96000  
wavelength dispersion 0-91887  
weakly anisotropic rectangular dielec. optical waveguides, wave propag. anal. using coupled modes 0-64154  
weakly guiding fibre, modes calc. by integral representation technique 0-58758  
weakly guiding fibres, Maxwell eqn. reformulation of EM propag. 0-78974  
GeO<sub>2</sub> doped gradient optical fibres, pulse dispersion (*German*) 0-74496  
LiNbO<sub>3</sub> waveguide, diffusion fabricated, angular variation calcs. using mode propag. const. 0-69540  
LiNbO<sub>3</sub>:Ti optical waveguide channel branches 0-58811  
LiNbO<sub>3</sub>:Ti single-mode waveguides, losses due directional changes 0-58789
- optical waveguides**  
*see also optical fibres; optical waveguide components; optical waveguide theory*  
acousto-optical modulator using coupled plane waveguides 0-69527  
acoustooptic tunable filter, using collinear TE-TM mode conversion 0-102852  
anisotropic optical waveguides based on Langmuir organic films 0-64177  
Bragg deflector, using photorefract. effect in As<sub>40</sub>Se<sub>15</sub>S<sub>35</sub>Ge<sub>10</sub> film loaded on LiNbO<sub>3</sub> waveguide 0-58673  
channel waveguide array coupled to integrated C-CD, appl. 0-102860  
channel waveguide interferometric modulator for EM field detection 0-74498  
channel waveguides, single-mode, prism coupling efficiency meas. 0-99878  
circular strip type, fabrication by Ag ion migration 0-96042  
coherent and nonlinear optics, conf., Leningrad, USSR (Jun. 1978) 0-98753  
conference, basic optical props. of materials, Gaithersburg, MD, USA (May 1980) 0-101668  
corrugated, resonant wave conversion 0-74505  
corrugated-waveguide optical demultiplexer mode couplings 0-64194  
DH lasers, phase and group indices 0-64016  
DH stripe geometry lasers, three-dimensional anal. of mode props. 0-64020  
dielectric strip waveguide, losses due to radiation of E<sub>11</sub><sup>x</sup> and E<sub>11</sub><sup>y</sup> waves from imperfect joint calc. 0-102847  
diffractive logic elements for optical computers 0-78993  
diffused channel waveguides, direct index meas. 0-87562  
dye DFB laser with integrated Si and polyurethane channel waveguide 0-74373  
dye laser, thin film waveguide evanescent type, gain meas. 0-95908  
elastic rubber waveguide, multimode thinfilm optical component fabrication 0-102857  
electrooptic radiation modulators utilizing semiconductor ridged waveguides 0-91925  
electrooptic surface prism laser deflector, for field destructive interference 0-87492  
energy diffraction input induced power depend. on impact parameter 0-64170  
far IR IC, antennas and waveguides for integration, review 0-69553  
ferrite film lightguides for nonreciprocal optical systems 0-99880  
filter, multilayer frustrated-total-internal-refl., spatially limited 0-96014  
flexible fibre light-guides, viewing instrum. appls. 0-87545  
fluoromethane laser, optically pumped far-IR waveguide, output, temp. depend. 0-58512



## optical waveguides continued

- four-layer waveguide diffractive injection efficiency optimisation (*Russian*) 0-64206
- Fresnel lenses in BaO optical waveguides 0-96034
- gas DFB laser waveguide precision calc. and pulse energy obs. 0-58577
- geodesic lens formation in diffusion fabricated optical waveguides 0-91937
- glass, fabrication by low-temperature diffusion process 0-102867
- glass, high  $\text{GeO}_2$ , zero material dispersion wavelength and waveguide props. 0-58733
- glass waveguides, diffused channel, multimode and single mode, direct index meas. 0-87562
- graded-index surface or buried, realized by ion exchange in glass 0-69499
- guided-beam splitter, refl. meas., fabrication method 0-74473
- heterostructure planar, guided-to-radiation mode conversion and appl. to light modulation 0-87557
- high quantum efficiency waveguide coupled photodetectors for integrated optics 0-58805
- hologram recording with guided reference and readout waves 0-106492
- indiffused waveguides with thin metal buffer,  $\text{TE}_0\text{-TM}_0$  mode splitting device 0-106638
- integrated grating circuit for guided-beam multiple division fabricated by electron-beam direct writing 0-91934
- integrated optical channel waveguide-CCD transversal filter 0-58797
- Langmuir-Blodgett films, lightguiding 0-79006
- laser interferometer, 500-m base, Earth surface deform. detect. 0-105087
- lens guide, low-loss image transmission 0-91872
- long-term stress failure probability estimation 0-58745
- loss measurement, nondestructive, using three prisms 0-106596
- pico-second optical sampling, cascade of waveguide interferometers driven by microwaves 0-99849
- planar ion-exchanged, fabrication technique 0-79003
- planar optical waveguide interconnection method 0-58671
- planar waveguide structure for integrated optics, props. (*Czech*) 0-96018
- power decay evaluation, backscatter technique 0-106599
- prism coupler fabrication technique 0-83685
- prism coupling into optical waveguide second harmonic generation 0-102763
- quartz lightguide resonator for  $\text{Nd}^{3+}$ :YAG laser, Raman generation 0-99735
- rectilinear optical resonators for curved metallic waveguides 0-69425
- refractive index, profile determ. of light focusing rod, Interphako interf. microscopy method 0-101832
- refractive index profile calc. from measured coupling angles 0-78954
- scattering problem, comparison of two perturbation theories 0-83662
- semiconductor clad, attenuation and propagation coeffs. 0-79004
- slab-type directional coupler with activated rhodamine 6G top layer, amplified oscill. 0-99718
- stimulated Raman scatt. excitation by wideband pump 0-64108
- strip-guides, polarisation filtering 0-102861
- stripe,  $\text{Ag}^+/\text{Na}$  ion exchanged, propag. characts. 0-83664
- stripe waveguides, dispersion characts. and radiation fields 0-64155
- superradiance waveguide laser, stimulated emission spectrum, leaky modes (*Russian*) 0-87400
- thick planar films, transmission method for index meas., modal effects 0-102862
- thin dielectric film optical waveguides, ideal fabrication technology, comparison of four techniques 0-79025
- thin film glass lightguide boundary refraction expts. 0-106639
- thin-film, on Si substrate, optical power losses calc. and obs. 0-106640
- thin-film, TE and TM modes phase-matching dielectric constant relations (*Japanese*) 0-58677
- thin-film multimode waveguides, higher order mode amplification 0-96012
- thin-film waveguide laser amplifier with lossy cladding 0-64074
- travelling wave optical modulator using a directional coupler  $\text{LiNbO}_3$  waveguide 0-96035
- X-ray wavelength and optical transmission waveguides (*German*) 0-99847
- Ag doped glass fabricated by solid-state electro-thermal diffusion, low-loss characts. 0-58792
- (Al,Ga)As:Zn planar stripe lasers with deep Zn diffusion, guiding mechanisms controlled by impurity concs. 0-78853
- $\text{CO}_2$  TEA waveguide laser, high power 0-91814
- $\text{CO}_2$  waveguide laser, multimode, excited by AC discharge 0-99754
- $\text{CO}_2$  waveguide laser, saturation parameter meas. method 0-87372
- $\text{CO}_2$  waveguide laser, tunability calc. (*Rumanian*) 0-87371
- $\text{CO}_2$  waveguide laser amplifier with strong discharge tube 0-74398
- $\text{CO}_2$  waveguide laser with pulsed high-freq. discharge 0-99755
- DCN waveguide lasers, optimised 190/195  $\mu\text{m}$ , amplifying medium characts. 0-99709
- GaAlAs mode stabilised separated multilayer stripe geometry DH laser, optical waveguide 0-64051
- GaAs, electron-beam excited, efficient generation of electron-hole plasma 0-76051
- GaAs oxide confined optical waveguides formed by lateral epitaxial growth 0-58815
- GaAs waisted-rib optical waveguides 0-74487
- GaAs-Al<sub>0.3</sub>Ga<sub>0.7</sub>As MOS rib waveguide polarizers 0-64207
- GaAs-Al<sub>0.3</sub>Ga<sub>0.7</sub>As MOS rib waveguide polariser, modulator and isolator 0-64217
- GaP-GaAsP planar heterostructure strip ridged waveguide under mech. load, polarisation modulation 0-96038
- InP-In<sub>0.53</sub>Ga<sub>0.47</sub>As<sub>0.5</sub>P<sub>0.5</sub>InP 1.53  $\mu\text{m}$  single-mode CW ridge-waveguide laser 0-64072
- $\text{K}_2\text{Li}_2\text{Nb}_2\text{O}_7$  films for optical waveguides epitaxial growth and characterisation 0-79016
- $\text{Li}(\text{Nb,Ta})\text{O}_3/\text{LiTaO}_3$ , multi-layer optical waveguide fabrication by LPE 0-71605
- $\text{LiNbO}_3$ , Ag-Li and Ti-Li ion exchange effects 0-58791
- $\text{LiNbO}_3$  branching waveguide, optical TE-TM mode splitter 0-96033
- $\text{LiNbO}_3$  channel waveguide to single-mode fibre high-efficiency flip-chip coupling 0-99833
- $\text{LiNbO}_3$ , cleaved, crystallographic and electrooptic props. 0-59575
- $\text{LiNbO}_3$ , Fe diffused, single-mode waveguide, comparison of bending losses in integrated optical circuits 0-83684
- $\text{LiNbO}_3$  layers, Li out-diffused, SHG phase matching temp. variation 0-69455
- $\text{LiNbO}_3$  optical waveguide surface, acoustooptical interaction for TE modes, metallisation effect 0-69541
- $\text{LiNbO}_3$  optical waveguides by ion implantation 0-106622

## optical waveguides continued

- $\text{LiNbO}_3$ , planar lightguide, optical mode interaction with standing elastic surface waves 0-99836
- $\text{LiNbO}_3$ , Ti-diffused optical waveguide coupled to GaAlAs DH laser, anal. 0-58706
- $\text{LiNbO}_3$  waveguide, planar electro-optic prism array beam splitter 0-64209
- $\text{LiNbO}_3$  waveguides, diffused channel, multimode and single mode, direct index meas. 0-87562
- $\text{LiNbO}_3$  waveguides, optical scattering phenomena 0-58786
- $\text{LiNbO}_3$ :Ti, coupled waveguided TE/TM mode splitter 0-64142
- $\text{LiNbO}_3$ :Ti, planar and channel optical waveguides, anisotropic diffusion expts. 0-64200
- $\text{LiNbO}_3$ :Ti, planar optical waveguides, processing and props. 0-78965
- $\text{LiNbO}_3$ :Ti, Ti diffusion process and control, waveguide characts. 0-58790
- $\text{LiNbO}_3$ :Ti branching optical waveguide, mode coupling 0-69518
- $\text{LiNbO}_3$ :Ti channel waveguide high-speed cutoff modulator 0-64195
- $\text{LiNbO}_3$ :Ti diffused channel waveguide, optical parametric amplification 0-106564
- $\text{LiNbO}_3$ :Ti diffused optical waveguide, guided light scatt. sources 0-78966
- $\text{LiNbO}_3$ :Ti diffused optical waveguide, efficient tapered gap prism coupling 0-78967
- $\text{LiNbO}_3$ :Ti diffused strip waveguide, optical propag. losses and coupling losses 0-58664
- $\text{LiNbO}_3$ :Ti electro-optic TE-TM mode convertor structure 0-64215
- $\text{LiNbO}_3$ :Ti in-diffused waveguide, refractive index profile calc. from measured coupling angles 0-78954
- $\text{LiNbO}_3$ :Ti optical waveguide, surface wave mode conversion, static strain-optic effect 0-87561
- $\text{LiNbO}_3$ :Ti phase-matched waveguide electro-optic TE $\rightleftharpoons$ TM mode convertor 0-58749
- $\text{LiNbO}_3$ :Ti planar waveguide, edge coupling to GaAlAs DH laser diode 0-87559
- $\text{LiNbO}_3$ :Ti single mode electrooptic waveguide modulator, high-speed operation 0-91915
- $\text{LiNbO}_3$ :Ti single-mode waveguide, fabrication by sequential combination of Ti diffusion and masked ion-implantation 0-58785
- $\text{LiNbO}_3$ :Ti single-mode waveguides, losses due directional changes 0-58789
- $\text{LiNbO}_3$ :Ti strip waveguide, SHG 0-102773
- $\text{LiNbO}_3$ :Ti waveguide, ps signal processing with planar, nonlinear integrated optics 0-64208
- $\text{LiNbO}_3$ :Ti waveguide electro-optic TE $\rightleftharpoons$ TM mode converter-wavelength filter 0-64210
- $\text{LiNbO}_3$ :Ti waveguides, convolution of ps optical signals 0-58629
- $\text{LiNbO}_3$ :Ti waveguides, absorption loss and photorefractive index changes 0-58787
- $\text{LiTaO}_3$ , Ag-Li and Ti-Li ion exchange effects 0-58791
- $\text{LiTaO}_3$  optical waveguide, Ag-Li ion exchange 0-91888
- $\text{Na}_2\text{O-B}_2\text{O}_3\text{-SiO}_2$ , optical waveguide glass, molar absorptivity of water 0-80066
- Si guided-wave acousto-optical devices 0-102864
- Si, optical waveguides along both sides of groove 0-96006
- Si photodiode for optical channel waveguides 0-102805
- $\text{SiO}_2$  ion implanted, radiation defects and optical props. 0-107293
- $\text{SiO}_2$  thin film grating for  $\text{LiNbO}_3$ :Ti waveguide mode convertor and reflector 0-64216
- YIG thin film gyromag. waveguide, on GGG substrate, optical propag. props. Faraday effect 0-74513
- ZnO film on oxidized Si, optical measure of acoustic quality 0-80893
- ZnO low-loss optical waveguides on amorphous substrates 0-58793
- ZnO piezoelectric films, RF planar-magnetron sputtered, characterisation 0-96751
- ZnO thin film, collinear acousto-optic interaction and appl. to tunable opt. filter 0-74509

## optical workshop techniques

- active abrasive conc. determ. by static method based on etch figure stars count 0-74544
- alkali lime germanosilicate GRIN fibre prep., losses and geometrical props. 0-69560
- applied optics, fabrication and testing, conf., Oakland, CA, USA (May-June 1980) 0-101661
- aspherical lens, polishing technique with equal polishing rate distrib. 0-58818
- astronomical optical surface shaping process automation 0-105169
- autocollimation instrument for checking angles and pyramidity of AR-90° prisms during manufacturing process 0-87570
- automated apparatus for grinding large optical components 0-102869
- coating removal by  $\text{Al}_2\text{O}_3$  powder and  $\text{NH}_4\text{HF}_2$  soln. 0-74521
- component polishing process modelling (*German*) 0-87565
- computer-controlled interferometry, in-process production tool 0-74531
- concave paraboloidal mirror, prod. method, interferogram tests 0-58823
- contact problems in optical surface shaping 0-74540
- cylindrical lens surface generation, grinding and polishing machinery design 0-79023
- diamond grinding of optical glass, kinetics 0-64224
- diamond tool bit machining, comparison with conventional optical process 0-69569
- diamond turning precision machine tool system 0-69568
- diffracting periodic structure generation by coherent beam interference 0-69570
- dispersion medium for polishing single cryst. corundum 0-102870
- drawing facility for lightguide fibres 0-64229
- electro-optical system manufacture, test and process control changes 0-96044
- element polishing simulation calc. and results (*German*) 0-87566
- evaporator, tubular-type radiation-heated, ZnS film deposition 0-76191
- fibre, single-mode, ultra-low-loss, optimised structure for fabrication 0-99843
- fibre, step-index, nearly elliptical, with high eccentricity, fabrication for studying modes 0-95989
- fibre coating technology, overview 0-58828
- fibre communication advances, materials and techniques 0-102853
- fibre crystals floating zone growth, far IR optical waveguides 0-79019
- fibre cutting tool and automatic splicing machine 0-87575
- fibre end face quality check 0-64164
- fibre endface preparation by AC discharge heating and stretching 0-64232



optical workshop techniques continued

fibre fabrication, OH-free VAD 0-99887  
fibre manufacture by double-crucible method 0-83688  
fibre manufacturing processes, parameter specifications 0-96041  
fibre modified CVD prep., optical and mechanical props. reproducibility 0-69535  
fibre plasma augmented vapour deposition 0-69561  
fibre preform manufacture using modified CVD process 0-64228  
fibre preparation methods and performance factors 0-69557  
fibre splicing techniques for compound glass and silica optical fibres (Japanese) 0-99890  
fibre splicing using arc fusion method, protection and reliability 0-69565  
fibre strengthening by molecular stuffing 0-58830  
fibre-optic polariser, in-line, formation and props. 0-106603  
fibres, compound glass, manufacturing process and fundamental charact. (Japanese) 0-99865  
fibres, fabrication processes and transmission characts. (Japanese) 0-87496  
fibres, single-mode, fabrication by VAD 0-83687  
fibres, VAD, ultimately low OH content achievement, by optimised dehydration 0-99845  
fibrescopes using leached fibre image bundles, manufacture 0-83670  
Fresnel lenses in BaO optical waveguides 0-96034  
fusion splicing machine for optical fibres 0-74516  
geodesic lens formation in diffusion fabricated optical waveguides 0-91937  
glass, refractive index gradients, form. using ion exchange diffusion 0-64227  
glass fibre, forming process, characts., anal. techniques 0-58827  
glass fibre drawing process, characterization and control 0-58826  
glass fibres for optical communications, colloquium, London, England (Jan. 1979) 0-67930  
glass optical fibre, vapour phase materials and processes, review 0-58825  
glass surfaces, cracked layer thickness determ., chemical method 0-64226  
glass tubing dia. and wall thickness meas., P-329M instrum. 0-86262  
graded-index fibre vapour-phase axial deposition method, fibre characteristics 0-58824  
gradient-index optics: a review 0-69478  
grinding tool surface contact area determination 0-64221  
guided-beam splitter, refl. meas., fabrication method 0-74473  
hyperboloid lens manufacturing technique 0-96039  
inorganic lithography using metallo-organic photoresists 0-79024  
integrated grating circuit for guided-beam multiple division fabricated by electron-beam direct writing 0-91934  
integrated optical grating circuit fabrication by electron beam direct writing 0-64214  
integrated optics, functional components, fabrication of microstructures in micrometre/submicrometre range, microlithographic techniques (German) 0-106637  
interferometric instrumentation as a cost-effective production tool 0-74535  
interferometry seminar, San Diego, CA, USA (Aug. 1979) 0-73096  
ion exchange, field assisted, for production of graded-index optical materials 0-74447  
IR multilayer optical medium produced by negative photoresist spin-coating 0-74451  
large high-precision prism grinding, use of 3G-71 lathe 0-102872  
lens blank fabrication with reduced finishing allowances 0-74541  
lens mass production yield estimation by centering tolerance simulation 0-78941  
lenses surface grinding and polishing, spectacle type, using automatic and semi-automatic machines (French) 0-58822  
leucosapphire, unique polishing features of hard crystals 0-64225  
linear Fresnel lens, fabrication process, solar radiation concentration 0-106592  
low-loss graded-index fibre, 3 km and 10 km preform design and modified CVD method 0-58746  
low-loss optical fibre fabrication for long wavelength region 0-99874  
machine shop operations 0-96045  
microfabrication for guided-wave optical devices 0-58812  
microgratings for guided-beam deflection, electron-beam direct-writing fabrication 0-102856  
milling spherical surfaces 0-64222  
mirror, nonaxisymmetric, fabrication by stressed mirror polishing 0-99885  
mirror, paraboloid, off-axis section, fabrication by stressed mirror polishing 0-99886  
mirror, single-point diamond-turned, performance before and after polishing 0-74466  
mirror fiducial system compatible with computer-controlled polishing facility 0-74539  
mirror reflectors, large, facet surface approx. methods (Russian) 0-69564  
multilayer beamsplitter coatings, accelerated fabrication method 0-102873  
multimode optical fibres, fusion splicing using gas flame heat source, development of splicing machine 0-102866  
Nanjing Astronomical Instruments Factory, lightweight 4 m telescope design 0-105162  
one-component optical cement 0-87445  
optical fibre coating with conical shape applicator 0-58820  
optical fibre multimode access coupler, fabrication method 0-87478  
parabolic mirror testing during fabrication by long-wavelength interferometer 0-74536  
planar multimode coupling structure fabrication by ion exchange 0-64233  
Polirot suspension, factors reducing polishing ability 0-74543  
Polirot suspension for optical component polishing, chem. antifoaming agents 0-74542  
polisher, computer controlled, efficiency 0-91938  
Polytron polishing pad, method and applications 0-69567  
prism coupler fabrication technique 0-83685  
production quality trends and limits 0-69566  
production technology advances, seminar, London, England (April 1979) 0-67938  
pyroceramic lightweight mirror blank fabrication using standard metal-working equip. 0-102871  
rod-in-tube fabricated optical fibre characteristics 0-87574  
rotating optical components in vac. system, using linear asynchronous motor drive 0-102874  
ruby, unique polishing features of hard crystals 0-64225

optical workshop techniques continued

self-centring technique for mounting microsphere coupling lens, on fibre 0-74517  
Selfoc lens, aberration improvement by glass composition and ion exchange process parameter choice 0-69486  
silicone and glass clad compound glass optical fibre comparison 0-69533  
single mode fibre homogeneous CVD fabrication and characterisation 0-69562  
spectacle lenses, astigmatic, technological construction (Russian) 0-99817  
spherical cementing fixtures for holding lenses by rigid method 0-96043  
spring-loaded partial kinematic mount for alignment of components in giant pulse laser 0-74518  
synthetic diamond drills, improved durability 0-87573  
system aspects of electro-optics, seminar, Huntsville, AL, USA (May 1979) 0-94921  
telescope primary mirror manufacture, monitored null corrector 0-78946  
testplate testing interferometry in precision optical shop 0-74532  
thin dielectric film optical waveguides, ideal fabrication technology, comparison of four techniques 0-79025  
thin film coating manufacture, automated deposition control system, design principles 0-64220  
thin film optical circuit fabrication using CO<sub>2</sub> laser 0-99881  
waveguide, circular strip type, fabrication by Ag ion migration 0-96042  
waveguide, graded-index surface or buried, realized by ion exchange in glass 0-69499  
waveguide fabrication in glass, optical, by low-temperature diffusion process 0-102867  
Wolter lens component replication 0-95972  
X-ray lithography for fabrication of submicrometer period gratings with precisely defined profiles for integrated optics applications 0-58814  
Ag halide optical fibres, extrusion, visible and IR transmission 0-58829  
BaO-GeO<sub>2</sub>-Na<sub>2</sub>O borosilicate core glasses for high numerical aperture fibres, double crucible prep. 0-69534  
CaF<sub>2</sub> vapour deposition apparatus for Na-resistant glass cell 0-90874  
GdF<sub>3</sub>-BaF<sub>2</sub>-ZrF<sub>4</sub> glass fibres, IR transmission, losses, fabrication 0-87516  
Ge-As-Se IR transmitting glass composition, prep. and props. 0-69474  
GeO<sub>2</sub>-Na<sub>2</sub>O borosilicate glass fibre prod. by phase separation and leaching 0-69558  
GeO<sub>2</sub>-P<sub>2</sub>O<sub>5</sub>-SiO<sub>2</sub> graded index optical fibres optimised for 1.3 µm wavelength region, fabrication techniques (Japanese) 0-99888  
LiNbO<sub>3</sub>:Ti Z-cut crystals, Ti diffusion process parameters 0-102849  
NaCl 46 cm window optical evaluation facility 0-74526  
NaCl Czochralski crystal growth for large CO<sub>2</sub> laser windows 0-74525  
NaCl large window continuous polishing 0-74527  
NaCl window production for Antares CO<sub>2</sub> laser system 0-74524  
Na<sub>2</sub>O-B<sub>2</sub>O<sub>3</sub>-SiO<sub>2</sub> glass fibre, plastic coating influence on strength 0-58697  
Na<sub>2</sub>O-B<sub>2</sub>O<sub>3</sub>-SiO<sub>2</sub> glass, low-loss GRIN fibres, double-crucible prod., loss and bandwidth meas. 0-69559  
Si, optical waveguides along both sides of groove 0-96006  
Si single cryst., chem.-mech. polishing of low-scatt. optical surface 0-96040  
SiO<sub>2</sub> fibres, fused, drawn from rods, oxy-H<sub>2</sub> flame, prep., strength, dia. var. 0-102868  
SiO<sub>2</sub> films, vac. thermal evaporation, parameter stabilisation 0-87571  
SrTiO<sub>3</sub>, fabrication damage characterisation by internal and external meas. 0-102782

optical zone plates

binary Fresnel zone plate construction, computer-generated holography 0-78809  
elliptical and hyperbolic zone plates produced by wavefront coherent superposition 0-78953  
Fresnel zone plate, appl. to neutrons imaging and focusing 0-106433  
x-ray zone plates fabricated using electron-beam and X-ray lithography 0-68335

optics

see also aberrations; adaptive optics; atmospheric optics; fibre optics; Fourier transform optics; geometrical optics; holography; integrated optics; nonlinear optics; optical elements; physical optics; quantum optics  
conference, Los Alamos, NM, USA (May 79) 0-73095  
conference, Madrid, Spain (Sept. 1978) 0-77547  
education, graduate, at Air Force Inst. of Technology, programme 0-62417  
education at Georgia Tech, development and current status overview 0-62420  
education at Texas Tech. University, programme methods 0-62424  
education programmes in US, attacks and recommendations 0-62410  
educational course in modern optics and lasers at San Diego State University 0-62423  
educational programmes and opportunities in US 0-62412  
educational programmes in US, attacks and recommendations 0-62409  
graduate degree programme, on-site, case study 0-62416  
graduate education at Carnegie-Mellon University, programmes review 0-62419  
graduate training at Optical Sciences Centre, programmes 0-62418  
Modern Optics Project Laboratory course at MIT, programme 0-62421  
optical systems, entropy and neugentropy (French) 0-102608  
teaching by Inst. of Optics, profile 0-62422  
undergraduate laboratory in American universities, status 0-62411

optimal control

see also dynamic programming; game theory  
absorption chillers, solar-fired, capacity modulation 0-66952  
classical filtering model, optimal impulse control, separation theorem (French) 0-90659  
differential eqn., canonical, functional relation expressed by Volterra series (French) 0-73159  
evolution equations, impulse and distributed control (French) 0-68049  
evolution equations, unknown control data, periods and type, optimal control, existence theorem (French) 0-62478  
heat storage device, off-peak, ambient temp. observer/predictor control system 0-66950  
multicore fission reactor, optimal control determ. from energy release profile (Russian) 0-73974  
nuclear reactors, PWR core control, multistage mathematical programming 0-91227  
satellite-gyrostatt reorientation, optimal attitude control 0-61980  
solar energy systems, modern control theory appl. reviews 0-66949  
spacecraft, optimal aerodynamic attitude control 0-77250

**optimal control** continued

stochastic systems, partially observable, measurer containing unknown variable parameters (*Russian*) 0-86218  
 telemetry device, chronically implanted, controlled transcutaneous powering 0-98152  
 variable speed wind power generator, control strategy for 3-phase output (*French*) 0-76591

**optimal systems**

filter, Kalman, digital, synthesis with a priori uncertainty of data 0-98934  
 restoration filter for Poisson noise impaired and linearly blurred images 0-106481  
 thermophysical process ambiguous data gathering and processing optimisation (*Russian*) 0-73335

**optimisation**

see also *mathematical programming; minimax techniques; minimisation*  
 aberrations, in electron optical systems 0-87290  
 antagonistic muscles, functional elec. stimulation optimisation, math. modelling, joint motion 0-61730  
 apodization, optimal, by means of coupled calc. of pupil function and shape 0-95788  
 astronomical information transfer, appl. of multiple-mirror telescope systems 0-94713  
 body joints, centres and angles of rotation meas., errors and optimisation study 0-61604  
 CECG waveform, statistical algorithm and struct. anal. 0-72341  
 character recognition, optimised filter 0-95837  
 composite, slab, spatially reinforced, optimisation in stability problem 0-102978  
 composite rib stiffened constructions, design criteria 0-102977  
 composite ribbed multilayer cylindrical shells, stability and optimal design 0-58949  
 computational techniques for many-beam struct. images in electron microscopy 0-95203  
 computer-aided optical design, optimisation and interactive graphics improvements 0-78933  
 convective annular/circular fin of minimum mass 0-79109  
 cooled epoxy resin vacuum mould computational simulation of design (*German*) 0-81020  
 CORAVEL, Cassegrain spectrophotometer, mask optimisation 0-82210  
 energy system modelling, New Zealand appl. 0-76590  
 experiment planning, appl. to calibration of X-ray radiometric analyser 0-61186  
 experiment planning, optimum plans calc. on convex polyhedrals 0-57084  
 fission reactor core energy distribution, algorithm for extremal control 0-83209  
 flat-plate photovoltaic array design optimisation 0-94037  
 four-layer waveguide diffractive injection efficiency optimisation (*Russian*) 0-64206  
 fusion reactor, FTR, equil. field coils, electrical supply system, optimisation and computer aided performance anal. 0-91288  
 geothermal energy resources for electricity generation, discounted cash flow anal. 0-85263  
 hypersonic three-dimensional shapes, optimal surfaces and total drag coeffs. 0-59068  
 IR detector-preamplifier for cryogenic spectrometer, optimization 0-95164  
 isotopic microgenerator design and construction optimisation due to min. power 0-108813  
 laser heating of metals, in oxidising medium 0-69445  
 laser ultra-short light pulse formation 0-64085  
 light beam focusing, in moving nonlinear media, using gradient method 0-106578  
 light beams propagation algorithms, thermal self-action problems and their compensation 0-106579  
 myoelectric signal processing, expt. demonstration of optimal myoprocessor performance 0-89882  
 myoelectric signal processing, optimal myoprocessor derivation 0-89881  
 n<sup>+</sup>-p-p<sup>+</sup> bifacial back surface field solar cells, optimisation of p<sup>+</sup> doping level by ion implantation 0-97784  
 neutron inelastic scattering, optimisation of struct. studying conditions (*Russian*) 0-79641  
 nuclear power station with VVER, for semi-peak load generation, mathematical model 0-68936  
 optical correlation detection, optimization by prewhitening 0-95802  
 oxide-semiconductor/base-semiconductor solar cells 0-81440  
 photovoltaic receiver for parabolic trough concentrator, optimisation 0-93983  
 radionuclides, short-lived, meas., counting statistics 0-58098  
 radiotherapy treatment planning, FORTRAN program for optimisation using complication probability factor 0-81686  
 reflection seismograms, simultaneous spherical divergence correction and optimal deconvolution 0-98258  
 reinforced plastic cylindrical shells, optimal design under dynamic constraints 0-102996  
 SAW filter design using optimisation technique 0-74671  
 scatterometer, satellite- and aircraft-borne, optimization of characts. for investigating underlying surfaces 0-67436  
 self-reproducing macromolecules, selection, controlled energy fluxes constraint 0-67027  
 solar cell collection grid structure, optimisation of area, shape and spacing 0-72042  
 solar collector with flat specular mirror, optimal tilt angles with seasonal variations 0-72081  
 solar energy concentrators, optimisation for tubular evacuated receivers aligned north-south 0-72015  
 solar energy systems, modern control theory appl. reviews 0-66949  
 solar heating systems, optimisation formulation of collector area based on TRNSYS computer code 0-61414  
 solar photovoltaic arrays, optimisation of total annual energy output from constant/adjustable tilt systems 0-94059  
 spacecraft solar arrays, in-orbit performance, review 0-94054  
 spectral filter, optimisation for arbitrary criterion by method of basic extremals 0-96011  
 square-field scanned image construction time optimisation (*Russian*) 0-63933  
 SQUID gradiometer, DC, thin-film, design optimisation 0-98951  
 superconducting magnet for magnetic flux compression, compression generator, PULSAR, design optimisation 0-68957

**optimisation** continued

surface heat exchanger, using generalised geometric characteristic and mean vel. (*Russian*) 0-82760  
 TEM crystal atomic structure imaging technique and applications 0-105752  
 thermal imaging scanners, mirror rotation axis optimisation 0-86426  
 thermoelectric heat pumps, single-stage, simplified method for optimization 0-108811  
 trunk pipeline systems, oil and gas, investigation and optimisation of thermal regimes 0-107579  
 X-ray diffraction topographic patterns, spectral sensitivity of TV system for visualisation (*Russian*) 0-62814  
 AlGaAs DH laser epilayer struct. optimization for integrated optical circuits 0-99879  
 CO-<sup>2</sup>He nuclear pumped laser, optimisation with 2 MeV protons 0-64000  
 Co permanent magnet material savings (*German*) 0-103851  
 Fe-Cr-Mo, white cast, optimising fracture toughness and abrasion resist. 0-85042  
 Li/SOC<sub>2</sub>, D cells, optimisation with respect to energy density, storability and safety 0-97775  
 Nd:glass laser system, beam spatial profile optimization in amplifier channel 0-74407

**optimum control** see *optimal control***opto-isolators**

optoelectronic devices development 0-91902

**optoacoustic spectroscopy** see *photoacoustic spectroscopy***optoelectronic devices**

see also *opto-isolators; photoelectric devices*  
 aerial colour photograph interpretation (*Russian*) 0-61920  
 angular meas. devices, error anal. method (*Russian*) 0-95066  
 free damped mech. vibration logarithmic decrement, optoelectronic meas. 0-92095  
 gas discharge phenomena meas. 0-107007  
 memory, bit-organised, method for information capacity increase 0-102656  
 nematic liquid crystal in contact with photoconductor EHD instability, nematic liquid crystal in contact with photoconductor 0-79695  
 refractometers, design, construction and quantitative characteristics (*Russian*) 0-62716  
 tachometer, with contamination prevention 0-73344  
 GaAs semi-insulating substrates, monolithic integration of optical and electronic devices, review 0-58543

**optons** see *opto-isolators***OPW calculations**

electron gas, uniform, electronic props. of H and He impurities 0-96807  
 Al dilute alloys, elec. resist., impurity and temp. depend. 0-65526  
 CuCl, band struct., OPW calc. and X-ray spectra meas. 0-75506  
 Se, charge density, self-consistent OPW and pseudopot. calcs. 0-92813  
 Se, trigonal, behaviour of optical gap under press. 0-80171  
 Sn, white, band masses and deformation pots., OPW pseudopotential model 0-100430  
 Sn, white, Fermi surface, dilational strain depend., OPW calcs. 0-84418  
 TiS<sub>2</sub>(Se<sub>2</sub>), valence density of states, Gilat-Raubenheimer method 0-88465  
 ZrS<sub>2</sub>(Se<sub>2</sub>), valence density of states, Gilat-Raubenheimer method 0-88465

**orbital calculation methods**

see also *APW calculations; atomic orbitals calculations; EHT calculations; GO calculations; GTO calculations; HMO calculations; KKR calculations; LCAO calculations; molecular orbitals calculations; NDO calculations; OPW calculations; PNO calculations; PPP calculations; STO calculations*  
 Brillouin theorem, proof 0-91415  
 CI, high-order replacements inclusion, appl. to H<sub>3</sub>O<sup>+</sup> inversion barrier 0-63504  
 floating orbital geometry optimisation with floating outer-shell basis functions 0-95517  
 inner charge defect method, appl. to bound and free excited atomic states 0-78511  
 positive orbital energies and the instabilities of orbital-optimized wave functions 0-58109  
 relativistic pseudopotential theories and corrections to Hartree-Fock method 0-63523  
 self consistent electron pair theory, perfect pairing valence bond generalisation 0-63532  
 spin-coupled particle-hole excitation, general matrix element formulas 0-69086

**orbitals, atomic** see *atomic structure***orbitals, molecular** see *molecular energy levels***order, long-range** see *long-range order***order, short-range** see *short-range order***order-disorder changes** see *order-disorder transformations***order-disorder transformations**

see also *polymorphic transformations*

adsorbed layers, order-disorder transition, effect on work function 0-59791  
 adsorbed overlayer, order-disorder transition, Ising model, LEED superlattice beam intensity distrib. 0-65371  
 alkylammonium metal tetrachlorides, struct. phase transitions 0-75348  
 alkylendiammonium metal tetrachlorides, struct. phase transitions 0-75348  
 alloy, binary, order-disorder transition kinetics, computer simulation 0-92643  
 alloy, binary, with arbitrary mole fraction, order disorder transition in case of FCC lattice 0-88295  
 alloys, binary, ferromagnetism and spatial long-range order 0-60159  
 amorphisation due to ion bombardment, SRO struct. 0-79844  
 aniline hydrobromide, ferroelastic, acoustic softening near transition temp. 0-96617  
 anthracene:tetracyanobenzene charge transfer complex, cryst. struct., temp. effects 0-96508  
 binary alloys, acoustic modes in random and correlated alloys, order-disorder transform. 0-65189  
 binary alloys, nonstoichiometric, mean field theory, improved approx. 0-79910  
 $\beta$ -brass, vacancy form., ordering effect, positron annihilation obs. 0-93427



order-disorder transformations continued

degenerate semiconductors, heterogeneous state, first-order phase transition, Ginzburg-Landau method analogue 0-70372  
dialkylammonium zinc dichlorobromides, long chain cpds., phase transitions, calorimetric study 0-70390  
distortive phase transitions, order-disorder and displacive regimes, mol. dynamics study 0-75324  
ferroelectrics, order-disorder, displacive transformations, tunnelling, phonons 0-75975  
graphite-K intercalation compounds, electronic props., resistivity, Hall effect and magnetoresistance 0-75585  
group theory end of ordering type phase transforms (*Russian*) 0-103287  
ice VII-ice VIII phase transition, second-order, Haus-Tanaka model 0-70385  
 $\alpha$ -In<sub>2</sub>Te<sub>3</sub>, I phase, order-disorder transform. for DO<sub>22</sub> struct., thermodynamic study 0-70155  
irradiation induced crystalline to amorphous transition, Gibbs energy 0-70371  
Landau theory of structural phase transitions 0-92639  
molecular solids, melting curves, Lennard-Jones Devonshire theory 0-65201  
multistate order-disorder model 0-70366  
perovskite structure, phase transitions due to octahedra rots. 0-70151  
polystyrene monodisperse latex, anomalous viscosity in disordered state 0-74822  
Potts model, three-state, first order phase transitions 0-60333  
pyridinium iodide, order-disorder phase transition and reorientation fluctuations studied by Raman spectra 0-80764  
spinel compounds, 1:3 octahedral order, review 0-88079  
static critical behaviour, structural phase transitions 0-92640  
superionic fluorites, structure and transport 0-84318  
TCNQ salt, TSeF-TCNQ, short-range ordering investigated by XDE 0-59652  
transition metal hydrides, H ordering, review 0-60850  
trimethylammonium cadmium trichloride, struct. phase transitions, low-freq. Raman scatt. obs. 0-80783  
(TTF)Cl<sub>4</sub>, disorder transition, cond. decrease and commensurate charge density waves 0-70153  
two dimensional system, ordering 0-107407  
vanadocene, order-disorder phase transition, sp. ht. and crystallographic study (*French*) 0-84131  
Ag-Mg (18.5 wt.%), rheological study of crystallographic order on creep (*French*) 0-97548  
AgNa(NO<sub>2</sub>)<sub>2</sub>, ferroelec., Raman scatt. and phase transitions 0-71349  
 $\beta$ -Al<sub>2</sub>Si, anharmonic thermal vibr. of cations 0-65214  
 $\tau$ -Al-Mn-C, permanent magnetism and microstruct. 0-75811  
 $\beta$ -Al<sub>2</sub>O<sub>3</sub>-Ag<sub>2</sub>O, stoichiometric and nonstoichiometric, structure comparison, phase transitions in stoichiometric compound (*French*) 0-60856  
CdHg alloy,  $\omega$  phase, mag. susceptibility anisotropy w.r.t. uniform compression (*Russian*) 0-71143  
Co-Pt, mag. annealing, form. of ordered phase, study using X-ray scatt. (*Russian*) 0-81052  
Co<sub>50</sub>Mn<sub>50</sub>Ga<sub>50- $x$</sub> , ordering and disordering phenomena, mag. study 0-70154  
Cu-Zn, rheological study of crystallographic order on creep (*French*) 0-97548  
Cu<sub>2</sub>Al thin films, fine-grained and disordered, low temp. ordering 0-97433  
CuI, ionic motions nature, mol. dynamics calcs., sp. ht. anomaly due to order-disorder transform. 0-107533  
CuIn<sub>2</sub>S<sub>4</sub>, sulphospinel electron diff. and electron microscopy study, order-disorder transform obs. 0-88080  
Cu<sub>1-x</sub>Mn<sub>x</sub>Al, and Cu<sub>2</sub>Mn<sub>2-y</sub>Al<sub>y</sub>, Heusler alloys, order-disorder transitions 0-59619  
Cu<sub>2</sub>VSe<sub>4</sub>, out of equil. mixed cond., off-centre positions and order-disorder transition, ultrafast nucl. relax. obs. 0-108103  
Dy, domain effects near order-disorder and order-order ferromagnetic transitions 0-65886  
Fe-Co-Ti(V)(Cr)(Mn), sp. ht. in ordered and disordered phases 0-71061  
Fe<sub>3</sub>Al, solid soln., rheological study of crystallographic order on creep (*French*) 0-97548  
Fe<sub>3</sub>Pd<sub>50</sub>, order-disorder transition, Mossbauer study 0-71268  
Fe<sub>3</sub>Pt austenite, long range order parameter, temp. depend. discussion 0-97481  
Fe<sub>3</sub>Pt austenites, ordering kinetics 0-104155  
Fe<sub>2</sub>VS<sub>2</sub> (0.20 < x < 1.00), phase diagram and order-disorder transition of vacancies 0-81039  
Ga-Se system, phase diagram and cryst. struct. of phases (*French*) 0-93544  
Gd, domain effects near order-disorder and order-order ferromagnetic transitions 0-65886  
Gd<sub>2</sub>Zr<sub>1-x</sub>O<sub>2-x/2</sub>, elec. cond. of ceramic solid solutions 0-107554  
He monolayer, phase diagram, order-disorder transition 0-107604  
HfV<sub>2</sub>D<sub>3</sub>, disordered solid solution, order-disorder transition 0-88321  
InSb, morphological and structural changes due to ion bombardment 0-79843  
KAg<sub>2</sub>I<sub>4</sub>, superionic phase transition, dynamical and crit. pt. props. 0-107535  
KD<sub>2</sub>PO<sub>4</sub>, coexistence states during first order transition, optical obs. 0-75350  
KH<sub>2</sub>(SeO<sub>3</sub>)<sub>2</sub> and KD<sub>2</sub>(SeO<sub>3</sub>)<sub>2</sub>, ferroelastic phase transition, mech. stress effect 0-70394  
KNiCl<sub>2</sub>, disorder as observed by electron diff. 0-75213  
La-D, phase transition, NMR meas. 0-66508  
La-H, ordered struct. near LaH<sub>2.65</sub> at 250K, NMR 0-66508  
LiAlSiO<sub>4</sub>,  $\beta$ -eucryptite one-dimens. fast ion cond., temp. depend. of cryst. struct. 0-107191  
LiRbSO<sub>4</sub>, order-disorder phase transitions with many-minimum potential, thermodynamic props. 0-96623  
Li<sub>2</sub>SO<sub>4</sub>.H<sub>2</sub>O, far IR spectra, H<sub>2</sub>O flipping motion, lattice modes 0-84258  
MgCd wire, elongation during disorder-order transform. (*Russian*) 0-104148  
NH<sub>4</sub>Ag<sub>2</sub>I<sub>4</sub>, superionic phase transition, dynamical and crit. pt. props. 0-107535  
NH<sub>4</sub>Br, heat capacity meas. near order-disorder transition 0-88332  
NH<sub>4</sub>Br:Cu<sup>2+</sup>, luminesc., orientation phase transition 0-100687  
NH<sub>4</sub>Br:Cl<sub>1-x</sub>, heat capacity meas. near order-disorder transition 0-88332  
NH<sub>4</sub>Cl, coexistence states during first order transition, optical obs. 0-75350  
NH<sub>4</sub>Cl, crit. behaviour near tricritical point, phenomenological interpretation 0-70389

order-disorder transformations continued

NH<sub>4</sub>Cl Raman spectra, pressure effects 0-97268  
NH<sub>4</sub>Cl(Br), effect of NH<sub>4</sub><sup>+</sup> internal motion on elec. and optical props. 0-100454  
(NH<sub>4</sub>)<sub>2</sub>SO<sub>4</sub>(BeF<sub>4</sub>), order-disorder phase transitions with many-minimum potential, thermodynamic props. 0-96623  
(NH<sub>4</sub>)<sub>2</sub>SnBr<sub>6</sub>, structural phase transitions study by Raman scatt. 0-93318  
NaClO<sub>3</sub>, lattice vibrations and sp. ht., neutron spectroscopic study 0-107388  
NaNO<sub>3</sub>, lattice vibration neutron diffusion study (*French*) 0-103429  
NaNO<sub>3</sub>, lattice vibrs., order-disorder transform., IR spectra study 0-65176  
Na<sub>3</sub>Pr(Cr<sub>2</sub>H<sub>2</sub>O<sub>3</sub>)<sub>2</sub>.2NaClO<sub>4</sub>.6H<sub>2</sub>O, absorpt., circular dichroism, and mag. circular dichroism spectra 0-97243  
Na<sub>6</sub>[Ti<sub>10</sub>(Nb<sub>10</sub>)<sub>12</sub>(Si<sub>6</sub>O<sub>17</sub>)<sub>2</sub>(OH)<sub>3</sub>].11H<sub>2</sub>O, zorite, X-ray cryst. struct. determ. 0-92513  
Nb-H(D), H ordering, review 0-60850  
NbD<sub>0.85</sub>, localised D vibrs., temp. depend., neutron inelastic scatt. study 0-107395  
NbH<sub>0.82</sub>, localised H vibrs., temp. depend., neutron inelastic scatt. study 0-107395  
NbH<sub>3</sub>, structural transform. rel. to order-disorder transform. 0-60858  
Nd<sub>2</sub>Zr<sub>1-x</sub>O<sub>2-x/2</sub>, elec. cond. of ceramic solid solutions 0-107554  
Ni-Al, rheological study of crystallographic order on creep (*French*) 0-97548  
Ni-Mn, ordered and disordered, press. effect on Curie temp. 0-71148  
Ni<sub>2</sub>Fe, change of H<sub>2</sub> diffusivity with order-disorder transformation 0-59729  
Ni<sub>3</sub>Mn, change of H<sub>2</sub> diffusivity with order-disorder transformation 0-59729  
Ni<sub>3</sub>Mn thin films, transmission spectra, structural order depend. 0-66318  
NiPt, quenched, ordering kinetics and domain struct. form. during isothermal tempering (*Russian*) 0-66502  
Ni<sub>3</sub>Pt, change of H<sub>2</sub> diffusivity with order-disorder transformation 0-59729  
Pd-D, crystallite size effects, simultaneous sorption and X-ray study 0-65237  
Pd-Si, amorphous thin films, laser irradi., metastable phases 0-96622  
Pt-Cr, disordered, atomic order-disorder transform. effect on resist. min. 0-65911  
Pt-Si, amorphous thin films, laser irradi., metastable phases 0-96622  
RbAg<sub>4</sub>I<sub>4</sub>, superionic phase transition, dynamical and crit. pt. props. 0-107535  
Rh (111), chemisorption of acetylene and ethylene, EELS, LEED and thermal desorption mass spectrometry 0-80057  
Sc<sub>0.5</sub>S, order-disorder transition, ionic model appl. 0-107096  
Si ion implanted, amorphous to crystalline transition due to laser irradi. 0-103451  
SrTiO<sub>3</sub>, ceramic, electrocaloric effects for refrigeration at cryogenic temp. 0-77789  
Ta-H, physical properties, plastic deformation, H ordering (*Ukrainian*) 0-71689  
Ta-H(D), H ordering, review 0-60850  
V-H(D), hydrogen ordering, review 0-60850  
V-Pt, sp. ht. and mag. meas. in ordered and disordered phases 0-70422  
VO<sub>2</sub>, metal-insulator transition and electronic struct., ion bombard. effects 0-92948  
ZrO<sub>2</sub>-Sc<sub>2</sub>O<sub>3</sub>-Yb<sub>2</sub>O<sub>3</sub> system, order-disorder phenomena, Raman spectra study 0-97254

ores see minerals

organic acids see organic compounds

organic compounds  
see also DNA; free radicals; macromolecules; organic semiconductors; organometallic compounds; plastics; polymers; proteins; Rochelle salt; waxes  
1,1-dimethyl-1-silacyclopentane, IR and Raman spectra 0-60577  
 $\alpha,\beta$ - $\beta$ -trifluoroacetone, liq.-liq. transition rel. to mol. motion, NMR study 0-70383  
abietic acid, transverse US wave propag., glass and liquid transition region 0-79883  
acenaphthylene pyrolysis, carbonaceous mesophase and disc-like liquid crystals 0-79687  
acetaldehyde, carbonyl addition, model transition states, vibr. anal. 0-71898  
acetaldehyde, dichroic effects, computational expts. 0-83424  
acetaldehyde, lowest Rydberg state, multiphoton ionisation spectra 0-83435  
acetaldehyde, multiphoton ionisation mass spectra 0-83436  
acetaldehyde, T<sub>2</sub>-relax. meas. press. depend. for rot. transitions, pulse spectrometer 0-78612  
acetaldehyde, UV photolysis, transient species IR spectra 0-86464  
acetaldehyde+CO<sub>2</sub> (00<sup>0</sup>1) mode deactivation, laser induced fluoresc. obs. 0-83453  
acetaldehyde-propane binary mixtures flowing through activated C, adsorpt. interference 0-107635  
acetate, deuterated, dimeric, single crystals., inelastic neutron scatt. 0-92867  
acetate, photo-oxidation at n-TiO<sub>2</sub> electrode 0-81331  
acetate ions adsorbed on Ag particles in aqueous soln. Raman spectra 0-69148  
acetate trihydrate:Mn<sup>2+</sup>, ESR, elec. cond. 0-93165  
acetate-ferrileghemoglobin, X-ray struct. anal., 3D refinement at resoln. of 2.0 Å 0-104554  
acetic acid, <sup>18</sup>F-labelled, carrier-free, production via a recoil labelling method 0-104756  
acetic acid, adsorbed on Cu (100), interaction with formic acid, EELS study 0-76120  
acetic acid, adsorption on Ag (111) and Pt (111), LEED obs. 0-80073  
acetic acid, adsorption on Fe and Ni, XPS study 0-76132  
acetic acid, and derivatives, vibr. spectra in soln. 0-63633  
acetic acid, liq., diamagnetism, mass mag. suscept. meas., temp. depend. 0-97054  
acetic acid, monomer and dimer, photoelectron spectrosc. 0-87172  
acetic acid, relative Raman scatt. cross section 0-10061  
acetic acid, vapour, chem. reaction effect on speed of sound 0-103100  
acetic acid+CO<sub>2</sub> (00<sup>0</sup>1) mode deactivation, laser induced fluoresc. obs. 0-83453  
acetic acid dimer, soln., vibr., IR spectra 0-63633

## organic compounds continued

- acetic acid odorant, nose stimulation, olfactory evoked brain pot., correl. anal. of recorded waveforms from human scalp (*Japanese*) 0-97946
- acetic acid vapours, clustering, effect of supersonic mol. beam sampling, mass spectrometric study 0-104481
- acetic acid- $^{13}\text{C}_1$ , in nematic phase soln., dipole-dipole couplings, selective spin population transfer investig. 0-60427
- acetic acid- $\text{d}_0$ (- $\text{d}_1$ ), Fermi reson., IR spectra band profiles 0-60569
- acetone,  $^{17}\text{O}$  chemical shift and NMR linewidth meas., self-association equilib. const. determ., mol. reorientations obs. 0-87148
- acetone, absorption bands, vibrational intensification obs., floating-orbital method 0-63619
- acetone, adsorbed on ZnO, decomp., IR and kinetic obs. 0-59780
- acetone, heat emission in crit. region, press. and heating surface temp. effects (*Russian*) 0-69634
- acetone, liq., diamagnetism, mass mag. suscept. meas., temp. depend. 0-97054
- acetone, macroscopic model for solvated ion dynamics, cation conductance calcs. 0-65261
- acetone, relative Raman scatt. cross section 0-100061
- acetone, vibr. dephasing theories, test using selective coherent ps. Stokes scatt. 0-59609
- acetone  $\text{A}^2\text{X-X}^2\text{II}$ , dissociative excitation, form. environment and parent mol. effects 0-78682
- acetone-chloroform-methyl isobutyl ketone, ternary phase diagrams, interactive computer program 0-71629
- acetone-methyl iodide liquid mixture, excess energy of vaporisation, US study 0-65209
- acetone-toluene-tetrachloromethane, mol. interaction and thermodynamic props. 0-71935
- acetonitrile- $\text{d}_3$ ,  $^2\text{H}$  NMR spectra, vibr. and asymmetry corrections to quadrupole coupling consts. 0-74184
- acetonitrile,  $^{13}\text{C}$  relaxation times anal. using J-diffusion model of mol. reorientation 0-87149
- acetonitrile, adsorpt. on Ag colloids, surface enhanced Raman spectra obs. 0-97251
- acetonitrile, adsorption on MgO, IR and TPD study 0-70528
- acetonitrile, dissolved in nematic EBBA, oriented  $\text{CH}_3$  group relax., multiple quantum NMR 0-66057
- acetonitrile, IR and Raman spectra, vibr. and reorientational and energy transfer width separation, rot. const. determ. 0-87131
- acetonitrile, macroscopic model for solvated ion dynamics, cation conductance calcs. 0-65261
- acetonitrile-HCl complex in liq. Xe, IR spectral study 0-95626
- acetonitrile-toluene-benzene, mol. interaction and thermodynamic props. 0-71935
- acetophenone,  $\text{T}_1$ - $\text{S}_0$  intersystem crossing, nonradiative decay rate, excitation energy depend. 0-63609
- acetophenone dispersed in benzene polycryst. host, active  $\text{N}_2$  induced chemilum. 0-60691
- acetophenones, di- and trisubstituted,  $\pi^*\pi$  systems, UV electronic absorpt. spectra 0-74132
- acetophenones, mono substituted, semi empirical  $\pi$ -electron calcs. 0-74131
- acetophenones, spectrosc. characs. using PPP SCF CI calcs. 0-102448
- 5-acetyl-5H-benzo[b]carbazole-5H-benz[b]carbazole, singlet-singlet energy transfer (*German*) 0-93402
- acetylcholine, diffusion in synaptic cleft of normal and myasthenia gravis human endplates 0-94198
- acetylcholine neurotransmitter, PCIO-INDO calcs. 0-58153
- acetylene,  $\text{A}^2\text{X-X}^2\text{II}$ , dissociative excitation, form. environment and parent mol. effects 0-78682
- acetylene, absorpt. coeffs. meas. in Nd laser emission band 0-78620
- acetylene, cryst., semiempirical atom-atom pots. appls. 0-100200
- acetylene, excited state, photochem. and spectrosc. investig. 0-95553
- acetylene, He-Ne laser line, high temp. absorpt., anal. by high resolution IR spectra 0-91554
- acetylene, higher excited states, electron energy loss spectra 0-91664
- acetylene, photoionisation cross section at distance from threshold, chemical bond influence 0-69196
- acetylene, reaction with Ni (100) and (110), room temp., UPS expts. 0-61151
- acetylene, relationships between higher-transition frequencies 0-69119
- acetylene, rot. vibr. anal., Raman spectra obs. 0-69146
- acetylene, synthesis in HF plasma torch 0-61099
- acetylene, triplet state quenching by foreign gases 0-91596
- acetylene, vibr. relax. study using laser-induced fluoresc. 0-74219
- acetylene +  $\text{C}_2$ ,  $\text{C}_2$  Swan band transition probabilities, collisional energy transfer effects 0-87214
- acetylene +  $\text{I}_2$ , laser-induced 1,2-diiodoethylene form., isomerisation 0-85157
- acetylene + inert gas, vibr. relax. study using laser-induced fluoresc. 0-74219
- acetylene(-d), Raman and vibr. spectra and force const. calcs. 0-108747
- acetylene adsorbed on Fe containing segregated C, hydrogenation, C-1s XPS spectra obs. 0-84366
- acetylene chemisorption on Rh (111), EELS, LEED and thermal desorption mass spectrometry 0-80057
- acetylene smoke aerosols, optical absorption to extinction ratio, photoacoustic determ. 0-58459
- acetylene-air flame, Li(Na)(K)(Mg)(Ca) damping consts., Lorentz collisions, mag. field effect 0-66805
- acetylene-air flame, multichannel apparatus detect. limits using atomic absorpt. spectra 0-76586
- acetylene-Ar van der Waals molecule, radiofreq. spectroscopy and Stark effect meas., equilib. struct. and props. 0-91543
- acetylene-cumulene dehydro annulenes, anomalous polarisation in resonance Raman spectra 0-60574
- acetylene- $\text{d}_0$ (- $\text{d}_1$ )(- $\text{d}_2$ ) metastable state, mol. beam elec. deflection obs. 0-74137
- acetylene- $\text{d}_2$ , 17 to 21  $\mu\text{m}$  laser lines generated using  $\text{CO}_2$  laser pump 0-69375
- acetylene- $\text{d}_2$ ( $\text{d}_1$ ), rot.-vibr. Raman spectra 0-83372
- acetylene-ethane, binary mixtures flowing through activated C, adsorpt. interference 0-107635
- acetylene-LiH, struct. and props., SCF ab initio calcs. 0-106250
- N-acetylglycine, X-irrad., stable radical electronic and mol. struct., ENDOR and ESR 0-80637
- acetylperoxy radicals, absorpt. spectrum and reaction kinetics 0-91571
- acid oxalate ion in aq. soln., vibr. studies, IR and Raman spectra 0-95589

## organic compounds continued

- acid phthalate curved crystal spectrograph, diffraction efficiency calc. method 0-79630
- acridine, temp. depend. of fluoresc. decay meas. using picosecond techniques 0-99518
- acridine orange, fluoresc. decay meas. by high repetition rate gated photon counting 0-86402
- acrolein, s-trans and s-cis, trapping from thermal mol. beams and UV-induced isomerisation in Ar matrices, enthalpy determ. 0-97688
- acrylamide aqueous solution, ultrasonic investigation (*Chinese*) 0-107371
- acrylonitrile, IR multiphoton dissociation, prod. of  $\text{CN}(\text{X}^2\Sigma^+)$  and  $\text{C}_2(\text{a}^3\Pi_u)$  radicals 0-63723
- acrylonitrile, NMR and relax. props., liq.-liq. transition rel. to mol. motion 0-70382
- actomyosin, X-irradiated ENDOR and ELDOR obs. 0-63689
- adamantane,  $\gamma$ -irrad., free radicals EPR and ENDOR 0-69170
- adamantane, cryst., vacancy formation energy, positron annihilation study 0-60706
- adamantane, derivatives in solution, mol. motion and methyl group rot. barriers from  $^{13}\text{C}$  NMR relax. times 0-74179
- adamantane, plastic and solid-solid transitions, Raman study 0-60590
- adamantane, plastic phase,  $\text{C}_4$  rot. jumps, existence and uniqueness 0-88067
- adamantane, thermal cond. and heat capacity under press. 0-80008
- adamantane powder, dipolar relaxation, short time behaviour, pulse method meas. 0-84667
- adamantane-adamantane interactions, expansion of intermol. energy in set of symmetry-adapted functions 0-106371
- 2-adamantanone, cryst. struct. in plastic phase 0-88065
- adenine, hydroxy and methoxy derivatives, absorption UV spectroscopy and electronic struct. of ionic and tautomeric forms 0-74177
- adenine, nucleic acid component, selective action by ps light pulses 0-72213
- adenine film, polycryst., energy conversion processes, quantum yields, 4 to 10 eV 0-88589
- adsorbent mesopores, capillary evaporation and struct. 0-107614
- aerosol OT-n-heptane-water, reversed micellar solution; addition of electrolyte, neutron small angle scattering 0-104468
- agarose gels, bubble prod., stabilisation by nonionic surfactants 0-76562
- L-alanine,  $^{17}\text{O}$  NMR chemical shifts and linewidths, pH dependence 0-80625
- L-alanine and DL-alanine, cryst., Raman band intensities of local group modes 0-93298
- L- $\alpha$ -alanine disordered regions in TGS crystals, dielec. props. 0-108159
- L-alanine powder, short dipolar relaxation time meas. by saturation method 0-60441
- aluminium copper tetrahalides, exchange, mag. anisotropy, and spin diffusion contribs. to EPR linewidth 0-80597
- alarm phonones, activity rel. to mol. similarity, electron density function meas. 0-91413
- 4-alcanyloxybenzoyloxy-4'-cyanoazobenzene series, influence of substituent on reentrant mesophases 0-88027
- 4-alcanyloxybenzoyloxy-4'-cyanobiphenyl series, influence of substituent on reentrant mesophases 0-88027
- 4-alcanyloxybenzoyloxy-4'-cyanostilbene series, influence of substituent on reentrant mesophases 0-88027
- alcohol H-complexes interactions, H-bond vibr. freq., anharmonic calcs. 0-99453
- alcohol-water mixtures, US attenuation meas., method of streaming 0-88272
- alcohols, vapour-liq. equilib. and heats of mixing, simplified group method anal. 0-96637
- alcohols in organic solvents,  $\text{H}_2\text{O}$  absorption 0-66788
- alicyclic compounds, nucl. spin-spin coupling via nonbonded interactions,  $\gamma$ -substituent effects 0-69078
- aliphatic amines, tertiary, fluoresc. decay 0-91590
- aliphatic compounds, nucl. spin-spin coupling via nonbonded interactions,  $\gamma$ -substituent effects 0-69078
- aliphatic ketones, freq.-topology-milieu relation, IR study, struct. and solvent effect (*French*) 0-95623
- alkali metal acid oxalates, neutron inelastic scatt. spectra in 2200-200  $\text{cm}^{-1}$  range 0-70327
- n-alkane, polymer, liq., mol. arrangement, computer model 0-92446
- n-alkanes, adsorption into bimolecular lipid layers 0-88435
- n-alkanes, anisotropic London dispersion forces, surface effects 0-74214
- n-alkanes, conduction band struct., LEED, secondary electron emission and UPS study 0-70601
- alkanes,  $\text{H}^+$  chemical shifts, extended Huckel calcs. with gauge in variant atomic orbitals 0-102449
- alkanes, light, solubility in liq.  $\text{N}_2$ , IR spectroscopy obs. 0-59654
- alkanes, liq., mol. struct., selective deuteration and IR vibr. spectra 0-96432
- n-alkanes, liq., Raman spectra, longit. acoustic modes and gauche-trans energy difference 0-93295
- n-alkanes, mol. Rydberg S $\rightarrow$ S and S $\rightarrow$ T transitions, semi-empirical SCF MO calc. 0-91453
- alkanes, nucl. spin-spin coupling via nonbonded interactions, conformational and substituent effects 0-69077
- n-alkanes, purification and single cryst. growth 0-71589
- alkanes, vapour-liq. equilib. and heats of mixing, simplified group method anal. 0-96637
- alkenes, 1,1-, 1,2-disubstituted, fragmentation modes in perturbational MO anal. 0-58138
- alkenes, IR multiphoton dissociation, IR detection of H atoms 0-83356
- 1-alkenyl-2-pyridones, photocyclisation rel. to energy storage 0-89680
- 4-n-alkoxybenzoyloxybenzylidene 4'-cyanoaniline series, nematic reentrant mesophases, phase diagrams 0-103467
- p-n-alkoxybenzoates of p-n-alkoxyphenyl, smectic A phases mol. struct. and elastic behaviour 0-59382
- p-alkoxybenzylidene-p-n-butylanilines, IR absorpt. spectra, elec. field effects, orientational order parameter determ. by IR dichroism 0-80778
- p-alkoxybenzylidene-p-aminocyananilines, IR absorpt. spectra, elec. field effect, orientational order parameter determ. by IR dichroism 0-80777
- 4,4'-n-alkoxybenzylidenamino-biphenyls, central Schiff's base linkage reversal effect on liq. cryst. props. 0-79683
- 4-alkoxyphenyl-4'-alkylbenzoates, mesomorphic props., terminal alkyl chain length effect 0-88024
- alkoxysilanes, mol. alignment of nematic liq. crystals, rel. to surface energy 0-100164
- alkyl benzenes, jet-cooled, vibr. relax., nanosecond time evolution 0-95584



## organic compounds continued

alkyl chains,  $^{13}\text{C}$  longitudinal relax. times and nuclear Overhauser enhancement anal. 0-83390  
 alkyl halide, amorphous, depolarisation thermocurrents and dielectric relaxation time distrib. (French) 0-60490  
 alkyl halide+K potentially reactive collisions, electronic excitation 0-74239  
 alkyl halide and  $\sigma^*$  anion radicals, stability 0-89468  
 alkyl halides, conform. energy calcs., polar bonds and polarisability, polaris. model appl. 0-58188  
 alkyl metal carbonyls, phosphine monosubstituted, LF vibrs., IR and Raman spectra 0-95585  
 5-alkyl-2-(4'-cyanophenyl)-1,3-dioxanes, nematic liq. cryst., synthesis and electro-optical characts. 0-88029  
 4-n-alkyl-4'-cyanobiphenyls, synthesis method from biphenyl 0-79684  
 alkyl-cyanobiphenyl homologues, isotropic-nematic phase, optical Kerr effect 0-91866  
 alkylammonium compounds, synthesis, exchange ion props. 0-64985  
 alkylammonium metal tetrachlorides, struct. phase transitions 0-75348  
 para-alkylanilines having optically active modes, vibr. relax. studied by absorpt. and fluoresc. spectra 0-83340  
 alkylbenzenes, jet-cooled, vibr. relax., absorpt. spectra 0-74236  
 alkylbenzenes, jet-cooled, vibr. relax., fluoresc. spectra 0-78694  
 1-4-n-alkylbenzoyloxyphenyl 2-(4'-cyanophenyl) ethane series, nematic reentrant mesophases, phase diagrams 0-103467  
 alkylene di-ammonium cadmium tetrachlorides, sp. ht. anomalies at phase transitions 0-70421  
 alkylenediammonium metal tetrachlorides, struct. phase transitions 0-75348  
 4-4-n-alkoxybenzoyloxy-benzylidene-4'-cyanoanilines, reentrant nematic and smectic phases 0-88308  
 N-4-n-alkoxybenzylidene-4-n-alkylanilines, smectic polymorphism, calorimetric study 0-88307  
 2-4-n-alkylphenyl-5-(4-n-alkoxyphenyl)-pyrimidines, smectic polymorphism, calorimetric study 0-88307  
 alkynoyl cations, struct., charge distrib., ab initio population anal. calcs. 0-58407  
 allene, IR multiphoton photolytic  $\text{C}_3$  prod.,  $\text{C}_3$  vibr. relax., chem. kinetics 0-66820  
 allene- $\text{d}_4$ , high resolution IR spectra 0-83365  
 1H-alloxazine, and derivatives electronic struct., photoelectron spectrosc. and ab initio study 0-106261  
 allyl radical, restricted SCF and MC SCF calc. of  $\text{C}_{2v}$  and  $\text{C}_s$  structs. 0-83289  
 allylamine, laser-microwave double and triple reson. 0-83397  
 allylamine, N-cis lone electron pair trans isomer, total dipole moment, rel. orientation 0-69259  
 amide+ $\text{Li}^+$ , pair pots., ab initio LCAO SCF MO calcs. 0-58184  
 amidinium salts,  $^{15}\text{N}$  NQR spectra,  $\text{H}^+$  relax. times 0-60448  
 amino acid residues, form. of mixed micelles and relative compatibility at interface 0-71951  
 amino acid transport in lymphoid cell lines, differences in ionising irradiation effects 0-72264  
 amino acids in C2 Antarctic carbonaceous chondrite, meteoric origin 0-67674  
 4-amino-2,2,6,6-tetramethylpiperidine-N-oxyl and deuterated derivatives, mag. resonance study 0-63686  
 2-amino-4-chlorophenol in solutions, IR absorpt. spectra 0-69135  
 4-amino-N-methylphthalimide in n-propanol, nanosecond laser fluorometry 0-102721  
 2-amino-p-cresol in solutions, IR absorpt. spectra 0-69135  
 aminoacetaldehyde, conformation calcs. rel. to protein struct. and bonding 0-74273  
 aminoboropolyynes, intermolecular interaction through triple bonds, internal rot. 0-106370  
 N(2-aminoethylcarbonyl)-5(6)-aminofluorescein, fluorescent labelling of polyspartamides 0-58426  
 4-aminomethyl-7-hydroxycoumarin, fluorescent labelling of polyspartamides 0-58426  
 aminopolyynes, intermolecular interaction through triple bonds, internal rot. 0-106370  
 2-aminopurine, in viscous soln., fluoresc. quenching, emission, intensity and reson. transfer (German) 0-91599  
 aminopyrazine, far IR spectra, barrier to planarity, pot. function and energy levels 0-69137  
 ammonia Rochelle salt, temp. depend. of optical axis angle, phase transitions (Russian) 0-97216  
 ammonium acetate, methyl groups, spin symmetry species, neutron scatt. transitions 0-92470  
 ammonium oxalate monohydrate: $\text{Mn}^{2+}$ , model for defect formation, EPR 0-103880  
 ammonium alginate, aq. solns., laminar flow heat transfer in helical coils 0-59030  
 amyl-acetate odorant, nose stimulation, olfactory evoked brain pot., correl. anal. of recorded waveforms from human scalp (Japanese) 0-97946  
 amylopectin, glycerin impregnated, dynamic viscoelasticity (Japanese) 0-104203  
 amylose, glycerin impregnated, dynamic viscoelasticity (Japanese) 0-104203  
 aniline, in p-xylene host cryst., phosphoresc. triplet state, ESR and MIDP obs. 0-66077  
 aniline, liq., depolarised light scatt. from shear waves 0-97288  
 aniline, liq., far IR absorpt. spectra, electric field effects 0-95625  
 aniline, liq., viscosity parameters, RF cond. meas. 0-96677  
 aniline having optically active modes, vibr. relax. studied by absorpt. and fluoresc. spectra 0-83340  
 aniline hydrobromide, ferroelastic, acoustic softening near transition temp. 0-96617  
 aniline hydrobromide, ferroelastic phase transition, Raman scatt. study 0-108195  
 aniline surfactants effectiveness, H absorpt. of steel, HCl conc. effect 0-108638  
 aniline-chlorophenol complexes,  $^{35}\text{Cl}$  NQR, inter- and intramol. interactions 0-63666  
 aniline-cyclohexane, hypersound velocity, absorption temp. depend. (Russian) 0-75303  
 aniline-cyclohexane solution, depolarised mol. light scatt. near critical exfoliation temp. (Russian) 0-108222  
 aniline- $\text{PbI}_2$ , intercalation cpd., heat capacity of low temp., intercalation effect (Russian) 0-92682  
 annulenes, graph theoretical polynomials 0-69048

## organic compounds continued

anthanthrene, mol. cryst. images in electron diffr. patterns 0-103315  
 anthracene:tetracene, electronic absorpt. spectrum, host-cryst. field effect 0-100669  
 anthracene:tetracyanobenzene charge transfer complex, cryst. struct., temp. effects 0-96508  
 anthracene, attachment energy as habit controlling factor 0-59421  
 anthracene, cryst., exciton aggregate possible form. under intense optical pumping, fluoresc. spectra 0-84772  
 anthracene, cryst., heat pulse propag., exciton condensation, time-resolved fluoresc. spectra 0-84771  
 anthracene, cryst., polariton luminesc. 0-84775  
 anthracene, electronic vibr. spectra, stochastic description, numerical modeling, comparison with expt. 0-63620  
 anthracene, in atmosphere, photooxidation on particulate matter 0-61487  
 anthracene, metastable triclinic phase 0-59452  
 anthracene, mol. crystal, meas. of US attenuation coeff. by optoacoustical methods (French) 0-70317  
 anthracene, nonequilibrium phonon propag. with freq. down-conversion 0-84260  
 anthracene, orientationally disordered cryst., lattice relax. effect 0-107278  
 anthracene, pulsed electron excitation, triplet excitons, spectral and electrical investigations 0-92828  
 anthracene, single cryst., CARS and CSRS, two-photon reson. effect 0-95946  
 anthracene, singlet exciton transitions, energies and oscillator strengths, boson theory with PPP wavefunctions 0-92820  
 anthracene, thick crystals, excitation spectrum of fluorescence 0-76068  
 anthracene, ultrathin films on fused quartz and sapphire 0-59812  
 anthracene, vap. phase dye laser media, photophysical parameters 0-95884  
 anthracene crystal, dynamical matrix eigenvectors from Raman scatt. 0-100315  
 anthracene crystals, pre-reson. Raman scatt., 4.2-30K 0-60571  
 anthracene derivatives in solution, polarisability and dipole moments, emission and absorpt. spectra obs. 0-69256  
 anthracene dianions in dimethyl ether, rotational diffusion meas. 0-65262  
 anthracene films, optical props., comparison between free and optical contact mounting 0-89079  
 anthracene in naphthalene crystal, second-order Stark shifts in optical spectrum 0-88966  
 anthracene in polychlorinated alkanes photochemical study by rapid scanning fluoresc. spectroscopy 0-86440  
 anthracene ion in liqs., photoelectron emission and photocond. 0-75600  
 anthracene Langmuir films, lightly substituted, AC and DC cond. 0-80425  
 anthracene microcrystals suspended in vapour-gas stream, naphthalene crystal nucleation 0-76165  
 anthracene single crystals, hole trapping by photo-oxidation products, injection currents (Russian) 0-92904  
 anthracene surface, Ar impact, Penning ionisation electron spectra and photoelectron spectra 0-66352  
 anthracene surface UV light irradiation effect on organic layer nucleation during crystallisation 0-75478  
 anthracene-amine cation radicals, electron transfer with heterocyclic and carbonyl anion radicals, triplet state electrogeneration 0-63803  
 anthracene-phenanthrene-tetracyanobenzene, CT-cryst., mini-excitons and lattice dynamics, ESR, optical and Raman spectra 0-60406  
 anthracene-pyrometallitic dianhydride cryst., refl. and absorpt. spectra of singlet charge transfer excitons 0-71442  
 anthracenes, exciplex form. with amines, form. kinetics and luminesc. props. 0-66792  
 anthracenes, substituted, disordered crystals, optical transforms 0-78783  
 9-anthraldehyde, struct. by TEM 0-79771  
 9,10-anthraquinone, lower triplet states, interactions and position, matrix isolation spectra 0-63634  
 anthraquinone, UV light effect on nucleation during crystallisation on anthracene surface 0-75478  
 anthraquinone in pentane solvent, sublevel phosphorescence spectra, molecular distortion 0-74190  
 anthraquinone pleochroic dyes in liq. cryst. soln., photostability, appl. to liq. cryst. displays 0-88961  
 anthraquinone-xanthone liq. soln., upper excited singlet state, delayed fluorescence 0-106345  
 anthrone, UV light effect on nucleation during crystallisation on anthracene surface 0-75478  
 9-anthranitrile, struct. by TEM 0-79771  
 antimalarial drugs, lifetime meas. via iterative convolution using fluorescence decay curves 0-57380  
 antipyrine, radiiodinated, prep. and stability for use in local blood flow determs. 0-94366  
 aromatic butadienes, dipole moment and dielectric relax. meas. 0-83516  
 aromatic compounds, out-of-plane mol. vibrs., force field approx. calcs. 0-91538  
 aromatic compounds in benzene polycrystalline host, active  $\text{N}_2$  induced chemilum., 77K 0-60691  
 aromatic ethylenes, dipole moment and dielectric relax. meas. 0-83516  
 aromatic hydrocarbons, molecular crystals, intermolecular interactions, spectroscopic studies, review 0-103958  
 aromatic hydrocarbons, sequential coupling 0-58297  
 aromatic hydrocarbons, vibronic calcs. 0-58238  
 aromatic systems, alternant, sign-alternation rule for triplet state 0-102420  
 aromatics, halogen substituted, as positronium inhibitor 0-93783  
 aryl cations, triplet state, multiple site splitting, ESR obs. 0-97126  
 arylbenzoxazols, lasing, excitation by excimer laser radiation 0-64007  
 3-arylcholesterol-2-enes and 3-arylcholesterol-3,5-dienes, synthesis and liq. cryst. props. 0-79689  
 aryloxazols, lasing, excitation by excimer laser radiation 0-64007  
 ascorbic acid adduct model systems, SCF calc., rel. to protein internal charge transfer 0-69072  
 ascorbic acid developer, lith development mechanism 0-77889  
 atmosphere organic compounds photooxidation, rates, reactivity and mechanism for reaction with OH radicals 0-72104  
 azaromatics, neutral and protonated, excited singlet and triplet states, charge densities, INDO calcs. 0-58152  
 azacyclobutadienes, conjugated mols. electronic struct. and geometry, Hartree-Fock instability 0-69055  
 azaphenanthrenes, lowest triplet state zero field splitting parameters calcs. 0-83391



## organic compounds continued

- azides, in polymer matrices, photooxidation, rel. to crosslinking 0-66832  
 azo dyes, UV-visible spectrophotometric 0-61207  
 p-azoxyanisole, directed crystn. in elec. and mag. fields 0-107052  
 p-azoxyphenetole, single cryst., deuterated, phonon dispersion curves, inelastic neutron scatt. obs. 0-84261  
 azulene, multiphoton ionisation, mass spectra 0-63717  
 azulene, ring currents hypersusceptibilities calcs. 0-102588  
 azulene vapour, IR and CO<sub>2</sub>-laser absorpt. spectra 0-87120  
 (2,2) (2,6) azulenophanes, mag. circular dichroism and anomalous fluorescence spectra 0-83398  
 barium methylsulphonate, X-ray powder cryst. data 0-59451  
 barium stearate film, low energy electron range meas. using radioisotope Auger electrons 0-70257  
 barium stearate single-layer Langmuir films, elastic and inelastic tunnelling 0-80403  
 Bengal pink-anthracene, mixed annihilation delayed fluorescence 0-74193  
 bent molecular organic crystals, electron diff. intensities 0-100132  
 benzaldehyde, and isomeric phthalaldehydes, dipole moments meas., conf. fig., ab initio MO calc. 0-58410  
 benzaldehyde, photoionisation mass spectra formation by UV laser radiation (*Russian*) 0-93781  
 benzaldehyde gas, nonradiative electronic transition 0-83413  
 benzaldehyde in methylcyclohexane,  $n\pi^*$  spectra 0-63627  
 benzaldehyde molecules, photoionisation mass-spectrometry with excimer KrF laser 0-95691  
 1,2-benzanthracene, secondary reson. radiation and hot energy transfer, soln. luminesc. 0-87167  
 benzene, absolute Raman scatt. cross-sections for totally symm. modes 0-102510  
 benzene, adsorbed on Al<sub>2</sub>O<sub>3</sub>, Raman spectroscopy study 0-65358  
 benzene, chemisorbed on Ni catalyst, Raman and vibr. spectra 0-108747  
 benzene, chemisorbed on W(100), decomp., UPS and thermal desorpt. obs. 0-59782  
 benzene, corrected valence force field, force constants calc. 0-63868  
 benzene, density meas. using flexible capillary 0-98886  
 benzene, deuterated and chemisorbed on glass, vibr. bands, Raman scatt. study 0-84737  
 benzene, diffusion coeff. meas., Fourier transform NMR, pulsed field gradient system 0-57353  
 benzene, dipole polarisability, finite-field SCF MO calcs. 0-83255  
 benzene, dynamic polarisabilities, calcs., superposition method of excited config., nonstationary perturbation theory eqns. 0-69257  
 benzene, equation of state studied using statistical theory results 0-84276  
 benzene, excitation spectra, cluster configuration method appl. 0-78546  
 benzene, first-ionisation Rydberg spectrum assignment via John-Teller splitting 0-69155  
 benzene, gaseous, critical and liquid, electron transport 0-64673  
 benzene, H<sup>+</sup> chemical shifts, extended Huckel calcs. with gauge in variant atomic orbitals 0-102449  
 benzene, IR spectra, fine struct. of rot.-vibr. bands 0-102504  
 benzene, IR spectrum deconvolution beyond the Doppler limit 0-86467  
 benzene, isotope-mass effects in self-diffusion 0-92695  
 benzene, liq., laser pulsation kinetics, optical damage effects 0-58614  
 benzene, liq., mol. motion at high press. 0-103509  
 benzene, liq., visible region absorpt. spectra, overtones meas. 0-78625  
 benzene, liquid, polarised light two photon thermal blooming near UV spectra 0-66216  
 benzene, mass spectra following reson. enhanced multiphoton ionisation 0-106362  
 benzene, mean free path meas., US relax. 0-59585  
 benzene, microwave line width and quadrupole moments, perturbation theory 0-69190  
 benzene, mol. cryst., reson. four-wave mixing, third order susceptibilities 0-100654  
 benzene, multiphoton ionisation fragmentation patterns, statistical theory 0-95693  
 benzene, multiphoton ionisation mass spectra 0-57420  
 benzene, nanosecond laser photolysis 0-66825  
 benzene, out-of-plane mol. vibrs., force field approx. calcs. 0-91538  
 benzene, phase transform. process, energy-dispersive X-ray diffractometry 0-96631  
 benzene, photoionisation mass spectra formation by UV laser radiation (*Russian*) 0-93781  
 benzene, quadrupole moments, elec. field-gradient birefringence method 0-95746  
 benzene, ring currents hypersusceptibilities calcs. 0-102588  
 benzene, S<sub>0</sub>-S<sub>1</sub> transitions, two-photon absorpt. spectra by nozzle beam-multiphoton ionisation method 0-63728  
 benzene, saturable absorpt. of CO<sub>2</sub> laser 0-69465  
 benzene, self-diffusion coefficients determ. by gel sectioning technique 0-92694  
 benzene, solid, double-quantum cross-polarization in solids 0-100623  
 benzene, soln., fluoresc., quenching in pulsed proton and alpha particle irradi., radiation quality effects 0-66259  
 benzene, static polarisability, ab initio SCF wave functions 0-74106  
 benzene, two photon absorptivity, ion cyclotron reson. photodissoc. spectra, CNDO/S-CI-perturbation theory 0-74123  
 benzene, vapour, solubility in polystyrene (*Japanese*) 0-59667  
 benzene, visible and UV photoionisation and fragmentation 0-69195  
 benzene+bromomethane, microwave line width and quadrupole moments, perturbation theory 0-69190  
 benzene+Hg, electronically excited, mol. fluoresc., vibr. relax. cross sections and equilibration rates determ. 0-87205  
 benzene+O(<sup>3</sup>P), phenol radical prod., crossed mol. beam investig. 0-71902  
 benzene (deutero)benzene, adsorpt. on Ag colloids, surface enhanced Raman spectra obs. 0-97251  
 benzene adsorbed on graphite, melting and orientation, NMR study 0-100403  
 benzene cation+benzene, trapped ion mass spectra 0-89470  
 benzene chemisorbed on Raney Ni, struct., neutron inelastic spectroscopy study 0-101038  
 benzene cryst., electron irradi., phenylcyclohexadienyl radical form., absorpt. and fluoresc. spectra study 0-89035  
 benzene derivatives, mol. electrostatic pot., approx. evaluation 0-58337  
 benzene excimer, nanosecond laser photolysis 0-66825  
 benzene liqs., refractive index, pressure effect 0-71375  
 benzene molecules, photoionisation mass-spectrometry with excimer KrF laser 0-95691  
 benzene radical cation in solid Ar, fluorescence spectra obs. 0-83382

## organic compounds continued

- benzene-d<sub>0</sub>-(d<sub>6</sub>), radiationless triplet decay, non-Condon effects 0-83405  
 benzene-d<sub>1</sub>, <sup>2</sup>H NMR spectra, vibr. and asymmetry corrections to quadrupole coupling consts. 0-74184  
 benzene-d<sub>6</sub>+N<sub>2</sub>+CO<sub>2</sub>, electronically excited, mol. fluoresc., vibr. relax. cross sections and equilibration rates determ. 0-87205  
 benzene-d+O(<sup>3</sup>P), phenol radical prod., crossed mol. beam investig. 0-71902  
 benzene-Dewar benzene, lower excited states pot. energy surfaces for isomerisation 0-104429  
 benzene-hexa-n-hexanoate, phase transitions and mesophase form., sp. ht. and IR spectra, 13 to 393K 0-79955  
 benzene-I<sub>2</sub>,  $\pi$ - $\sigma$  charge-transfer complex, frozen soln., Mossbauer spectra obs. 0-91655  
 benzene-p-xylene (p-dioxan) liq. mixture, excess energy of vaporisation, US study 0-65209  
 benzene-S systems, liq.-liq. phase separation 0-96658  
 benzene-TCNE, charge transfer theory, Mulliken population, ab initio calc., multiconfiguration scheme 0-106392  
 benzene/cyclohexane reversible chemical reaction systems for thermal energy transport 0-67009  
 benzenes, monosubstituted, NMR, high resolution, automated anal. by computer program DAVINS appl. 0-63669  
 benzenes, substituted, electronic struct., ab initio calcs., photoelectron spectra 0-58314  
 benzenoid aromatics, triplet zero field splitting parameters, ODMR obs., struct. effects 0-78636  
 benzil, cryst., excited triplet state spin-lattice relax. probabilities, temp. depend. (*Russian*) 0-88860  
 benzil, phase transition, far IR spectroscopy meas. 0-71407  
 benzil core fibres, void-free cryst. growth, X-ray diff. and optical microscopy study 0-71586  
 benzo(a)phenazine diaza derivatives, excited singlet and triplet states, charge density, INDO calcs. 0-58152  
 benzo(a)pyrene, pollution of lake sediment, western USA 0-61476  
 benzoic acid, dissolution, mass transfer at vibr. spheres 0-57220  
 benzoic acid, struct. refinement at room temp. 0-96502  
 benzonitrile, IR absorpt. and Raman bands, half-band width conc.-depend. 0-74171  
 benzonitrile-isooctane mixture, dielec. const. near consolute point, temp. and freq. depend. meas. 0-71292  
 benzophenone, cryst., charge carrier generation by exciton-exciton collisions 0-88568  
 benzophenone, laser spectroscopy by cascade photoionisation method in mass spectrometer 0-99496  
 benzophenone, migration of triplet excitons, EPR profiles and phosphoresc. decay data 0-84641  
 benzophenone, molecular nonsteady-state luminesc. behaviour under narrowband laser excitation 0-87159  
 benzophenone ketyl radical, in micelle, decay rate in mag. field, photolysis meas. 0-85154  
 benzophenone vapour, fluoresc. and phosphoresc., nonradiative transitions between triplet and singlet state obs. 0-99516  
 benzotriazole developer additives, effect on photographic development mechanism 0-77891  
 benzoxazole, aromatic derivatives, spectral luminesc. and lasing props. rel. to electronic struct. 0-99519  
 benzoyl ions, collisional activation mass spectra, energy depend. 0-104482  
 benzyl alcohol, dielectric time-domain spectrosc., short and refl. method 0-101805  
 benzyl alcohol, liq., viscosity parameters, RF cond. meas. 0-96677  
 benzyl bromide, photolysis, free radical form., investig. 0-102523  
 benzyl chloride, liq., viscosity parameters, RF cond. meas. 0-96677  
 benzyl chloride, photolysis, free radical form., investig. 0-102523  
 benzyl chloride+Cs<sup>+</sup>, beam reactions for 5.8 eV collision energy, mechanism 0-66777  
 benzyl chloride+SbF<sub>5</sub>, chemi-ionis. reaction, temp. depend., flow tube investig. 0-108701  
 benzyl mercury chloride, cryst. struct. and absorpt. calcs. 0-84166  
 benzyl radical, 1<sup>3</sup>B<sub>2</sub>-3<sup>2</sup>B<sub>2</sub> transition in absorpt. spectrum, extinction coeffs. 0-102523  
 benzyl radical, in solid Ar, absorption and photodissociation spectra 0-69156  
 benzyl radicals, monomethyl- and dimethyl-substituted, electronic spectra and electron affinity 0-63618  
 2-benzyl-5-benzylidenecyclopentanone, and substituted form, topochem. single-cryst.-to-single-cryst. photodimerisation 0-66819  
 biacetyl, quencher for triplet excitons in poly-N-vinylcarbazole 0-66267  
 biacetyl, triplet  $n\pi^*$  and  $\pi\pi^*$  transitions studied by low-energy electron diff. 0-83502  
 bicyclic ring compounds, Raman circular intensity differential spectra obs., mol. struct. 0-87130  
 $\Delta^5$ -bicyclo(3,2,0)heptane, conformational mobility 0-99587  
 bicyclobutyl+methylene, products decomposition, competitive channels and vibr. relax. 0-83336  
 bis-solicylato-diaquo calcium (II), cryst. struct. 0-100222  
 bile acids-absorption, effect of pelvic irradi. in gynaecological malignancy 0-67160  
 bio-organic materials, bioelectrochemical sensor using immobilised enzyme electrodes (*Japanese*) 0-109071  
 biphenyl:tetracene, electronic absorpt. spectrum, host-cryst. field effect 0-100669  
 1,1'-biphenyl, heat capacity anomalies due to successive phase transitions 0-96664  
 biphenyl, mol. cryst., reson. four-wave mixing, third order susceptibilities 0-100654  
 biphenyl, solid/melt interfacial tension and contact angles of small particles, determ. from crit. vel. of engulfing 0-79915  
 biphenyl, two photon absorptivities, CNDO/S-CI calc. with second order time depend. perturbation eqns. 0-74122  
 biphenyl mixtures with cholesteryl chloride, static and dynamic electro-optical props., cholesteric-nematic transition 0-100646  
 biphenyl polyenes, vibronic states, quasi-linear spectra (*Russian*) 0-95598  
 biphenyl-d<sub>0</sub>, Brillouin scatt. at room temp. 0-71433  
 biphenyls, cholesteric blue phases, struct. and props. 0-103243  
 2,2'-bipyridyl, two photon absorptivities, CNDO/S-CI calc. with second order time depend. perturbation eqns. 0-74122  
 1,6-bis(2,4-dinitrophenoxy)-2,4-hexadiyne, obs. of apparent ferroelec. transition 0-66121



## organic compounds continued

$\alpha$ -bis (N-methylsalicylaldiminato) copper II, one-dimens. spin- $1/2$  Heisenberg antiferromag., high-field spin dynamics 0-71224  
 bis-(p-toluene-sulphonate) of 2,4 hexadiyne 1,6 diol, X-ray scattering obs. of polymerisation mechanism and phase transition (*French*) 0-70399  
 bis-methylidgermyl chalcogenide,  $^1\text{H}$  and  $^{13}\text{C}$  NMR study, chemical shifts 0-71201  
 bis-methyldisilyl chalcogenide,  $^1\text{H}$  and  $^{13}\text{C}$  NMR study, chemical shifts 0-71201  
 bis-p-toluene sulphate of 2,4-hexadiyne-1,6-diol, X-ray scatt., incommensurable modulated struct. obs. 0-70185  
 borneol, methyl groups internal rotation,  $^{13}\text{C}$  spin lattice relaxation times and force field calcs. 0-74255  
 Brillouin scatt. and refr. index measurements 0-76035  
 bromobenzene, in potassium laurate mesophase, NMR, proton distance ratios and order tensor elements calcs. 0-63672  
 bromobenzene, liquid, vibr. relaxation, Brillouin spectra 0-108219  
 bromobenzene, saturable absorpt. of  $\text{CO}_2$  laser 0-69465  
 bromobenzene - $\text{d}_0$ (- $\text{d}_2$ ) radical cation, electron impact dissoci., secondary isotope effect 0-63836  
 bromobenzene ion fragmentation, photoelectron-photoion coincidence spectra 0-95682  
 4-bromobenzoyloxymethyl-trifluorosilane, cryst. struct., X-ray study 0-70187  
 p-bromochlorobenzene,  $T_1$  states, zero-field ODMR, MIDP and phosphorescence excitation spectra 0-74191  
 bromocyclotriphosphazatrienes,  $^{81}\text{Br}$  NQR, conformation investig. 0-63665  
 $\alpha$ -bromofluoro alkyl pi-radical, signs of hyperfine and quadrupole couplings, ESR determ. 0-97141  
 p-bromofluorobenzene, UV electronic absorption spectrum, band shape and molecular geometry 0-87147  
 bromofluorobenzenes,  $\text{He(I}\alpha)$  and  $\text{He(II}\alpha)$  photoelectron spectra, assignments, ionis. energies 0-78651  
 bromofluoromethylene radical, laser-induced fluoresc.,  $^1\text{A}''$ - $^1\text{A}'$  transition 0-91589  
 bromoform, highly excited vibr. states, thermal lensing spectrosc. and local mode model 0-87140  
 bromogermane radical anion, ESR spectra and struct. 0-87153  
 bromomethane, IR multiphotonic excitation, depend. on cell geometry, mol. fluoresc. and decomp. obs. 0-83430  
 bromomethane derivatives, NQR frequency of Br, substituent group effects 0-95648  
 N-bromosuccinimide, X-irrad., ESR study of Br and  $\sigma^*$  radical 0-66037  
 bromotrichloromethane, vac. UV absorpt. cross section 0-91574  
 bromotrifluoromethane, IR multiphoton selective dissoci., effect of acceptor radicals 0-66854  
 bromotrifluoromethane, vac. UV absorpt. cross section 0-91574  
 bromotrifluoromethane 823 laser line, simple accurate method for wavelength meas. 0-106554  
 bromotrifluoromethane cation, photodissoc. by quasi-continuum single IR photon absorption 0-61124  
 bromotrifluoromethyl cation, IR photodissoc. 0-87188  
 bumetanide- $^{14}\text{C}$ , whole body autoradiography in dogs by round saw method 0-72399  
 1-1-d $_2$ -but-1-ene skew form, microwave spectra, rot. const. and centrifugal distortion coefficients determ. 0-83351  
 trans-butadiene,  $\text{B}_{1u}$ -state dynamics in cooled supersonic expansion, electronic absorpt. spectra obs. 0-78629  
 butadiene, excitation spectra, cluster configuration method appl. 0-78546  
 trans-butadiene, polarisability, nonlinear elec. susceptibility, SCF calcs. 0-95547  
 butadiene, twisted zwitterionic excited states, SCF calcs. 0-58179  
 butane, dissociative excitation, form., environment and parent mol. effects 0-78682  
 butane, flexible chain molecules, momentum space diffusion eqns. 0-75142  
 butane, liq., enthalpy difference between rot. isomers, IR spectrosc. obs. 0-106404  
 n-butane, trans or gauche, solute mol., solvent mol. distrib. 0-96433  
 butanol, mean sojourn time of molecules on surfaces, meas. in practical vacuum system (*Japanese*) 0-57315  
 n-t-butanol in alkanes, molecular relaxation processes studied by  $^{13}\text{C}$  NMR 0-63654  
 1-butene, adsorbed on  $\delta\text{-Al}_2\text{O}_3$ , isomerisation, IR study 0-76554  
 butene, isomers, ion-mol. reactions, photoionisation mass spectra 0-81298  
 trans-2-butene+OH, reaction products,  $\text{O}_2$  and  $\text{NO}_2$  effects obs. 0-85156  
 1-butene adsorption on delta alumina, microgravimetric-IR study 0-75432  
 2-butene ion, fragmentation, angular momentum in ion-mol. reacts., RRKM calc. 0-66773  
 t-butyl acetate, rot. isomerism, dielect. and Raman spectra 0-106328  
 t-butyl alcohol, aq. soln. 0-88237  
 t-butyl alcohol, mixtures, assoc., thermodynamic study using 2-constant model 0-66789  
 t-butyl alcohol, self-assoc., linear and nonlinear dielec. effects obs. 0-60484  
 t-butyl bromide, vibr. relax. in pure liq. and soln., Raman spectra 0-66167  
 t-butyl bromide+Na, anisotropic interactions from double rainbow struct., interaction pot. meas. 0-99540  
 butyl cation, H-elimination, energy partitioning, transition state geometry calc. using MINDO/3 0-104430  
 t-butyl chloride, vibr. relax. in pure liq. and soln., Raman spectra 0-66167  
 t-butyl chloride+Na, anisotropic interactions from double rainbow struct., interaction pot. meas. 0-99540  
 t-butyl formate, rot. isomerism, dielect. and Raman spectra 0-106328  
 t-butyl iodide+Na 0-99540  
 tri-n-butyl phosphate, quantitative IR absorpt. meas. 0-87106  
 p-n-butyl-p'-heptanoyloxazobenzene oriented on NaCl  $\text{MgF}_2$  coated NaCl, surface phenomena and IR spectra 0-79678  
 n-butylamine-n-propanol, isothermal vapour-liquid equilib. 0-59639  
 p-n-butylaniline having optically active modes, vibr. relax. studied by absorpt. and fluoresc. spectra 0-83340  
 t-butylbenzene, two photon absorptivity, ion cyclotron reson. photodissoc. spectra, CNDO/S-CI-perturbation theory 0-74123  
 butyloxybenzylidene octylaniline, liq. cryst., phase transitions, calorimetric obs. 0-103466  
 butyloxybenzylidene octylaniline, liq. cryst. film, smectic B-A transition, mech. meas. 0-79918

## organic compounds continued

butyloxybenzylidene octylaniline, two- and three-dimensional smectic B liq. cryst. film, long range order 0-96442  
 butyloxybenzylidene octylaniline film, freely suspended, smectic A layer spacing, optical determ. 0-64883  
 3-butyn-1-ol, vibr. spectra, assignments, rot. isomerism 0-58257  
 cadmium arachidate mixed with cyanine dyes, mol. layers, photoelec. props. 0-80401  
 cadmium formate, anhydrous, cryst. struct. 0-107195  
 cadmium stearate based Langmuir films, deposition on p-CdTe, characts. and MIS struct. 0-92998  
 calcium behenate monomolecular layers between Al electrodes, nonlinear dielec. props. 0-80405  
 calcium dipicolinate trihydrate, IR and Raman spectra, isotopic frequency shift, mol. vibr. obs., point groups determ. 0-89001  
 calcium oxalate hydrates, crystn. kinetics, comparison for mono-, di-, and trihydrates 0-81528  
 calcium oxalate monohydrate, IR and Raman spectra, vibrational studies 0-69139  
 camphor, orientational disordering, thermodynamic props., stat. mech. model 0-96453  
 camphor, rhombohedral, polycryst., compressive deform. and dynamic recrystn. 0-71698  
 camphor methyl groups internal rotation,  $^{13}\text{C}$  spin lattice relaxation times and force field calcs. 0-74255  
 camphor odorant, nose stimulation, olfactory evoked brain pot., correl. anal. of recorded waveforms from human scalp (*Japanese*) 0-97946  
 capronate, proton spin-lattice relaxation in various phases (*Russian*) 0-97163  
 carbazine 720, single freq. CW dye laser operation in 690-700 nm gap 0-99719  
 carbazole:tetracene, electronic absorpt. spectrum, host-cryst. field effect 0-100669  
 carbazole, two photon absorptivities, CNDO/S-CI calc. with second order time depend. perturbation eqns. 0-74122  
 carbazole dispersed in benzene polycryst. host, active  $\text{N}_2$  induced chemilum. 0-60691  
 carbenes, heterosubstituted, singlet-triplet splitting depend. on heteroatom electronegativity and conform. 0-63553  
 carbohydrate compounds, X-irrad., trapped electrons, ESR and ENDOR obs. 0-93161  
 carbon tetrabromide, disordered phase, neutron, diffuse scatt. 0-79717  
 carbon tetrabromide, disordered phase, neutron diffuse scattering 0-79716  
 carbon tetrachloride, dual melting curves and metastability 0-92647  
 carbon tetrachloride, equation of state studied using statistical theory results 0-84276  
 carbon tetrachloride, liq., diamagnetism, mass mag. suscept. meas., temp. depend. 0-97054  
 carbon tetrachloride, phase transform. process, energy-dispersive X-ray diffractometry 0-96631  
 carbon tetrachloride, polarized light scatt., relaxation processes 0-60615  
 carbon tetrachloride, Stokes wave phase fluctuations in stimulated light scatt. (*Russian*) 0-87436  
 carbon tetrachloride, surface study, ellipticity coeff., ellipsometric method 0-84343  
 carbon tetrachloride, vac. UV absorpt. cross section 0-91574  
 carbon tetrachloride drops falling through  $\text{H}_2\text{O}$ , surfactants rel. to deform., oscill. (*French*) 0-66880  
 carbon tetrachloride-o-cresol-acetophenone (ethylmethylketone) (ethylacetate) mixtures, intermolecular interaction, US vel. meas. 0-79879  
 carbon tetrafluoride, atmospheric content, sources and residence time 0-61879  
 carbon tetrafluoride, liquid, comparison on interaction induced light scatt. and IR absorption 0-60561  
 carbon tetrafluoride  $^{12}\text{CF}_4$  laser, Doppler-limited absorption spectroscopy 0-74347  
 carbon tetrafluoride  $^{12}\text{CF}_4$  optically pumped laser efficiency 0-74348  
 carbon tetrafluoride laser,  $\text{CF}_4$  molecule  $\nu_3+\nu_4$  band optical pumping 0-74349  
 carbon tetrafluoride laser with optical pumping, freq. tuning and stabilisation 0-99706  
 carbon tetrafluoride pulsed laser characts., optically pumped by  $\text{CO}_2$  laser 0-91778  
 carbonyl anion radicals, electron transfer with anthracene-amine cation radicals, triplet state electrogeneration 0-63803  
 carbonyl groups, spin-lattice relax. mechanism, mathematical relaxation model (*German*) 0-80633  
 carborane, ortho- and para-, phase transition and mol. reorientation, isomer effects, PMR obs. 0-80628  
 carboxylic acid systems, H(D) complexes and dimers,  $\nu_{\text{CO}}$  IR band intensities 0-63715  
 $\beta$ -carotene, excitation profile of  $\nu_2$  line in resonance Raman spectrum, solvent effects 0-74173  
 CBNA, nematic-isotropic transition at high press., turbidity meas. 0-92655  
 CBOOA, smectic-A reentrant nematic transition under press., X-ray obs. 0-59637  
 CBOOA film, freely suspended, smectic A layer spacing, optical determ. 0-64883  
 cellulose complexes with pyrene and its derivatives, photosensitivity (*Russian*) 0-73506  
 cellulose nitrate, nonlinear viscoelastic deform., hydrostatic press. and third invariant of deviatoric stress tensor 0-93587  
 cellulose nitrate film ion data, dark-field illum. image recording photographic method 0-70031  
 cellulose nitrate thin foil manufacture for  $\alpha$  particle track detector (*Spanish*) 0-74091  
 cellulose triacetate, for electrochem. etching of fast neutron induced recoil tracks 0-91406  
 central rigid cores, mesogenic power, depolarised Rayleigh scatt. study 0-89012  
 cephalosporins, radiation-sterilisation by  $\gamma$ -irrad. 0-66822  
 cerebrin, thermotropic and lyotropic mesomorphism 0-76703  
 cetyltrimethylammonium bromide-1-butanol system, micellar conc. meas. using fluoresc. probe study 0-85217  
 chain mols., conformational transition kinetics 0-83339  
 chloranil pellets, thermally stimulated discharge current and dielectric studies 0-93236  
 4-chloro, 3-nitrotoluene, partially aligned in elec. field,  $^{13}\text{C}$  NMR, dipole moment determ. 0-78633



## organic compounds continued

- chloro(ethyl)silanes and its C derivatives, Raman spectra, mol. vibr. and rot. isomerism 0-87134  
 1-chloro-2,2-dimethylpropane, IR and Raman spectra, vibr. assignment 0-74169  
 1-chloro-2-methylpropane, IR and Raman spectra, vibr. assignment 0-74169  
 $\alpha$ -chloroacetamide, alkoxy radical form., effect, of  $\alpha$ -hydroxyacetamide, ESR study 0-80610  
 chloroacetic acid, soln., vibr., IR spectra 0-63633  
 chloroalkanes, vapour-liq. equilib. and heats of mixing, simplified group method anal. 0-96637  
 chloroanisoles,  $^{35}\text{Cl}$  NQR, inter- and intramol. interactions 0-63666  
 chlorobenzaldehyde,  $\text{a}^{\text{A}^*}\text{--X}^{\text{A}^*}$  phosphoresc., conformations and ground state fundamentals 0-78642  
 chlorobenzene, dielectric time-domain spectrosc., short and refl. method 0-101805  
 chlorobenzene, gas phase electron diff. struct. determ. 0-69251  
 chlorobenzene, in potassium laurate mesophase, NMR, proton distance ratios and order tensor elements calcs. 0-63672  
 chlorobenzene, liquid, vibr. relaxation, Brillouin spectra 0-108219  
 chlorobenzene,  $\text{S}_0\text{--S}_1$  transitions, two-photon absorpt. spectra by nozzle beam-multiphoton ionisation method 0-63728  
 chlorobenzene, saturable absorpt. of  $\text{CO}_2$  laser 0-69465  
 chlorobenzene drops falling freely through water, breakup 0-69899  
 chlorobenzene-cis-decalin, mixtures, dielec. const. and loss tangent in liq. and solid phases 0-100628  
 $\alpha$ -chlorobenzoic acid:  $\text{Nd}^{3+}(\text{Pr}^{3+})$  solid, vibrational spectra 0-84758  
 trans-1,4-chlorobromocyclohexane, liquid, crystalline and amorphous state, conformation and vibr. spectra, IR obs. 0-60568  
 chlorodifluoromethane, IR multiphoton dissoci., mag. field effect 0-93772  
 chlorodifluoromethane, unimol. reaction by IR radiation, rate consts. and prod. yield, fluence and intensity depend. 0-97713  
 chlorodifluoromethane subMM wave laser, optically pumped 0-87376  
 2-chloroethyl radical, struct., ab initio calcs. 0-83252  
 chlorofluorobenzene cations in gaseous phase, emission spectra and lifetimes in  $\text{B}(0^+)$  states 0-63711  
 chlorofluorobenzenes,  $\text{He(I}\alpha)$  and  $\text{He(II}\alpha)$  photoelectron spectra, assignments, ionis. energies 0-78651  
 chlorofluorocarbons in stratosphere,  $\text{O}_3$  layer depletion calc. using two-dimensional model 0-109221  
 chlorofluoromethane, computer based policy analysis to reduce human health impacts 0-89698  
 chlorofluoromethane induced IR cooling of atm., effect on general circulation model 0-90122  
 chlorofluoromethane photolysis in stratosphere, effect on  $\text{O}_3$  conc. 0-109197  
 chlorofluoromethanes, electron attachment, electron swarm method 0-69245  
 chloroform, highly excited vibr. states, thermal lensing spectrosc. and local mode model 0-87140  
 chloroform, liq., diamagnetism, mass mag. suscept. meas., temp. depend. 0-97054  
 D-chloroform, soln., Raman scattering tensor components 0-99508  
 chloroform sorption effect on cross-linked polyester film struct. (Russian) 0-59405  
 chloroform-d, in soln., vibr. and reorientational relax., Raman study 0-63636  
 D-chloroform-dimethylsulphoxide, soln., Raman scattering tensor components 0-99508  
 trans-1,4-chlorodicyclohexane, liquid, crystalline and amorphous state, conformation and vibr. spectra, IR obs. 0-60568  
 chloromethane +  $\text{Cl}^+$ , reactions at room temp. 0-93749  
 chloromethane gas, linear electro-optical effect 0-87843  
 chloromethyl formate, conformation potential energy surfaces, ab initio calcs. 0-69065  
 p-chloronitrobenzene, struct. determ. by electron diff., influence of  $\text{NO}_2$  group on C-Cl bond 0-69251  
 chloronitrotoluenes,  $^{35}\text{Cl}$  NQR temp. depend. 0-106334  
 chloroparaffins, lubrication of Ti alloys, friction and wear (Russian) 0-93657  
 chloropentafluoroethane, isotopically selective multiphoton dissoci.,  $\text{CO}_2$ -laser wavelength, pressure and additives effects 0-78666  
 chloropentafluoroethane-(He)(Xe)( $\text{O}_2$ )( $\text{H}_2$ )( $\text{NO}$ ), multiphoton dissoci.,  $^{13}\text{C}$  enrichment factor,  $\text{CO}_2$ -laser wavelength and fluence depend. 0-58331  
 o-chlorophenol-acetone (ethyl methyl ketone), thermodynamic and transport props. 0-92686  
 chlorophenols,  $^{35}\text{Cl}$  NQR, inter- and intramol. interactions 0-63666  
 chlorophyll, and related mol., in solid solns., fine-structured vibronic spectra under tunable dye laser excitation (Russian) 0-74164  
 chlorophyll, colloidal solns., elec. charge of particles 0-94438  
 chlorophyll a, absorpt. and fluoresc. spectra, observance of Stepanov relation 0-81554  
 chlorophyll a, cation radical formation by pulse radiolysis, oxidation and demetallation rate consts. 0-61505  
 chlorophyll a, Langmuir-Blodgett films, deposition onto  $\text{SnO}_2$  optically transparent electrode 0-80093  
 chlorophyll a dihydrate photoelectrochemical cell 0-61387  
 chlorophyll black lipid membranes photoelectric response, appl. to solar energy conversion 0-81482  
 chlorophyll in Pacific and Atlantic oceans, gradient maps from U-2 aircraft platform 0-101385  
 chlorophyll solution, degenerate four wave mixing, phase conjugated backward wave generation (Chinese) 0-87429  
 chlorophyll-a, fluoresc. at low concs., noise reduction by low pass filter for DC signal 0-87249  
 chlorophyll-a, hydration, field desorpt. mass spectral obs. 0-71936  
 chlorophyll-a radical cation lifetime in water-acetonitrile soln. 0-72136  
 chlorophyllide fluorescence quantum yield during photochlorophyllide reduction in etiolated leaves 0-81542  
 chlorophylls, mag. reson., site selected fluoresc. detection 0-69164  
 chloroplast discs, photoelectric response, appl. to solar energy conversion 0-81482  
 1-chloropropyne cation, internal energy decay studied by photoelectron-photoion coincidence spectroscopy 0-69185  
 chloroquinolines, photophys. behaviour, substituent and solvent effects 0-106342  
 chlorotrifluoromethane, multiphoton dissoci.,  $^{13}\text{C}$  enrichment (French) 0-91615  
 chlorotrifluoromethyl cation, IR photodissoc. 0-87188

## organic compounds continued

- cholesteric systems, with nonmesogenic additives, Keating-Bottcher theory 0-84057  
 cholesterol, solid-solid phase transitions, positron annihilation study 0-84289  
 cholesterol derivatives, mol. packing coeffs. and thermal stabilities 0-100201  
 cholesterol esters, molecular-optical, and structural anisotropy 0-84056  
 cholesterol decanoate, optical activity in blue phase 0-100641  
 cholesterol esters, blue phase, model 0-88030  
 cholesterol ethyl carbonate, long periods in sol. state, X-ray diff. study 0-96503  
 cholesterol ethyl carbonate, unit-cell dimensions and space group 0-84165  
 cholesterol laurate-cholesterol caprylate (75 wt.%), polymorphic behaviour, optical, elec. and dielec. meas. 0-65208  
 cholesterol myristate, cholesterologenic, blue phase, D NMR obs. 0-97151  
 cholesterol myristate, smectic A-cholesteric transition, tricritical behaviour, DTA and DSC study 0-65206  
 cholesterol nonanoate, cholesterologenic, blue phase, D NMR obs. 0-97151  
 cholesterol nonanoate, cyclohexanone admixture effect on mesophase order parameter, refr. index meas. 0-100165  
 cholesterol nonanoate-MBBA, liq. cryst. mixture, two colour display device 0-70116  
 cholesterol oleate, solid-solid phase transitions, positron annihilation study 0-84289  
 cholinesterase-acetylcholine soln., anion-cation site interactions, solvent effects on aggregate stability 0-61070  
 cis-1-cholobutadiene-1,3, microwave spectrum, struct., nuclear quadrupole coupling, distortion const., thermodynamic functions calc. 0-99500  
 chromatin, factors affecting the heat-induced increase in protein content 0-97882  
 chromatin, low-angle X-ray and neutron diff., interparticle effects 0-72134  
 chromatography and mass spectrometry, conference, Carlsbad, Czechoslovakia (April 79) 0-73097  
 chromophore phospholipid Langmuir films, photoeffects 0-80409  
 chrysene, excited singlet and triplet state, CARS obs. 0-83374  
 cinnoline, excited state absorpt. spectra and intersystem crossing kinetics 0-74176  
 cinnoline, prereson. Raman spectra, vibr. band intensities obs. 0-102515  
 clathrate hydrates, longitudinal acoustic vel. 0-88275  
 cobalt dimethyl glyoximate, molecular struct., cryst. structure 0-79769  
 cobalt stearate, monomolecular multilayers, XPS escape length depend. on emission angle, elastic scatt. role (Japanese) 0-84833  
 COC, cholesteric liq. cryst., positron lifetimes and phase transitions 0-59383  
 colloidal coating on Fe, corrosion protection, qualitative ellipsometric-electrochem. approach 0-104344  
 conjugated compounds, ring currents static octopole hyperpolarisabilities calcs. 0-102588  
 contact charge transfer complexes of organic molecules with  $\text{O}_2$ , CNDO/S calcs., absorpt. spectra obs. 0-69076  
 COOB film, freely suspended, smectic A layer spacing, optical determ. 0-64883  
 COOB-cholesteric liq. cryst. mixtures, helix pitch, temp. depend. 0-64895  
 copper, benzoate, one-dimens. antiferromag., heat capacity, field-induced crossover of spin-dimensionality 0-97099  
 copper (II) complex, bis(dithiocarbamate), HF-Slater-LCAO calcs., mag. coupling parameters and optical spectrum 0-99447  
 copper benzoate, low-dimensional Heisenberg antiferromag., high field magnetisation 0-80558  
 copper formate tetrahydrate, antiferromag. phase, neutron diff. study 0-93085  
 copper formate tetrahydrate, ice rule ferroelectric, polarisation correlations 0-97190  
 copper phthalocyanine, chlorinated, radiation damage mechanism 0-88000  
 copper phthalocyanine, simulated mol. images, point models and kinematical struct. amplitudes 0-103223  
 copper phthalocyanine, size distrib., transient elec. birefr. 0-85223  
 $\alpha$  copper phthalocyanine and chlorinated derivative mol. crystals, radiation damage in electron microscope 0-107328  
 copper phthalocyanine film, electron acceptor surface states due to  $\text{O}_2$  adsorption 0-88586  
 copper porphyrins, mag. susceptibility and EPR, sample grinding effects 0-60420  
 copper tetraamine sulphate, two-dimensional Heisenberg antiferromag., high field magnetisation 0-80558  
 cordycepin, X-ray cryst. struct. determ. 0-107198  
 coronene, minimal exposure high resolution electron microscopy 0-79653  
 coronene, triplet state, photomagnetism 0-97125  
 coryol, crystal structure determ. using NQUEST(x) function 0-64986  
 coumarin 102, excited state interaction dynamics, picosec. time-resolved spectral shift obs. 0-78624  
 coumarin 1, multiphoton cross-section determination by means of luminescence experiments 0-93377  
 coumarin dye molecules, CH stretching modes, population lifetime meas. 0-58185  
 coumarin laser dyes, solvent effects on photophysical parameters 0-91598  
 Creutz-Taube complex, mixed valence, reson. Raman calcs. using vibronic coupling model 0-79249  
 18-crown-6 complexed sodium-2, 6-di-n-butyl-p-benzoquinone ion pairs, soln. ESR spectra, temp. and conc. depend. 0-63675  
 18-crown-6 complexed sodium-duroquinone ion pairs, soln. ESR spectra, temp. and conc. depend. 0-63675  
 cyanine dye in lipid bilayer, photosensitization of semicond. electrode 0-75639  
 cyanine dye monolayer assemblies with Al and Ba electrodes, photovolt., dark cond. and photocond. 0-80400  
 cyanine dyes, excited electronic states, CNDO/S CI calc., visual pigment spectra appl. 0-85333  
 cyano compounds, liq. cryst. phases, incommensurate coexistent density fluctuations 0-79691  
 1-cyano-2-methyl-3-(cis-propenyl) cyclopropanes, rotational propensities and bond rupture identity 0-104437  
 4-cyano-4'-n-pentylbiphenyl, refr. index meas. and isotropic-nematic phase transition study, surface plasmon technique 0-84282  
 4-cyano-4'-octylbiphenyl, dielectric relax. anal. in nematic and smectic phases 0-108153



# organic compounds continued

cyano-biphenyl LC alignment on obliquely evaporated SiO<sub>2</sub> films 0-79677  
cyano-biphenyl series, nematogens and smectogens, props. characterised by even-odd effect 0-107046  
p-cyano-N,N-dimethylaniline in polar solvents, double fluorescence, theoretical model 0-58296  
cyanoacetylene,  $\nu_3$  vibr.-rot. band, diode laser spectrum 0-91563  
cyanoacetylene (HC<sub>3</sub>N), interstellar, in  $\Sigma$  state, collisional excitation by H<sub>2</sub> 0-109508  
cyanoacetylene in L 183 (L 134 N) dust cloud high density core, SHF obs. 0-105307  
cyanoacetylenes form. in atm. of C stars and W Hydrae 0-67708  
 $\alpha$ -cyanoacrylate adhesive in monolayer on bulk Al surface, IR spectra, H-bond form., stretching vibr. 0-87119  
2-cyanoaziridine, microwave rot. spectrum, assignments 0-91546  
4-cyanobenzoyloxy-4'-pentylstilbene, nematic, smectic A, and orthogonal smectic B phases 0-64890  
6-cyanobenzquinuclidine, intramol. electron-transfer excited state 0-58295  
4-cyanobiphenyl and 4'-alkyl- or 4'-alkoxy-substituted liq. cryst. derivatives, soln., absorpt. and fluoresc. spectra 0-87164  
cyanobiphenyl liquid crystal IR modulator expts. 0-102837  
4-cyanobiphenyl/4-cyano-p-terphenyl liq. cryst. mixture, order parameters of dissolved dyes 0-100167  
cyanobiphenyls molecular conformational mobility study by optical probing method (Russian) 0-92459  
t-cyanobutane, dielectric relaxation study, complex permittivity 0-80688  
cyanocyclopentane, microwave spectral study of axial and equatorial conformers 0-95604  
cyanodiacetylene cation, gas phase, UV emission spectra of A( $\pi^-$ ) $\rightarrow$ X( $\pi^-$ ) band system 0-95636  
cyanodiacetylene in mol. clouds Sagittarius B2 and Cloud 2, SHF obs. 0-101627  
cyanohexatriene, in mol. clouds Sagittarius B2 and Cloud 2, SHF obs. 0-101627  
cyanomethane-d<sub>0</sub>-d<sub>3</sub>, soln., for IR spectra, band shape and moment anal. 0-58252  
cyanooctylbiphenyl, smectic A phase, X-ray diffr. study 0-79690  
p-cyanophenyl p-n-alkyloxybenzoates, nematic, birefringence, polarisability and order parameter 0-100642  
3-cyanothiophene-<sup>35</sup>S(<sup>15</sup>N), partial r<sub>0</sub>-struct., microwave spectra 0-91552  
cyclic hydrocarbons, chemisorpt. on W(100) surface, decomp., UPS and thermal desorpt. obs. 0-59782  
cyclic ketones, electrochromism and electric dichroism for studying transitions to second excited singlet 0-63692  
cyclic mol. struct., topological characterisation 0-74254  
cyclic molecules, localised electronic vacancies lifetimes 0-106264  
cyclo-hexyl-ammonium-copper-trichloride, specific heat, ferromagnetic chain system 0-103491  
cycloalkanes, carbonyl charact. freqs., kinematic and pot. energy effects 0-95578  
cyclobutane(-d<sub>8</sub>), centrifugal distortion const. calc., rel. to struct. and mol. wt. 0-95580  
cyclobutane decomposition, vibr. excitation transients using variable encounter method 0-61072  
cyclobutanone, <sup>1</sup>H NMR anal., deconvolution technique 0-58289  
cyclobutanone, absorpt. of pulsed IR radiation and decomp., joulemeter and opto-acoustic obs. 0-58328  
cyclobutanone, electrochromism and electric dichroism for studying transitions to second excited singlet 0-63692  
 $\alpha$ -cyclodextrin and  $\alpha$ , $\beta$ -D-xylose, absorption mode spin-echo spectra appl. 0-78634  
cycloheptanone, electrochromism and electric dichroism for studying transitions to second excited singlet 0-63692  
cyclohexadienes, chemisorbed on W(100), decomp., UPS and thermal desorpt. obs. 0-59782  
cyclohexane, chemisorbed on W(100), decomp., UPS and thermal desorpt. obs. 0-59782  
cyclohexane, in benzene soln., mol. motion, correl. functions 0-96431  
cyclohexane, isotope-mass effects in self-diffusion 0-92695  
cyclohexane, liquid, density effect on transport properties 0-65264  
cyclohexane, rapid anal. by mass spectrometry/mass spectrometry 0-61173  
cyclohexane, self-diffusion coefficients determ. by gel sectioning technique 0-92694  
cyclohexane-aniline critical mixture, shear and critical fluctuations, instantaneous mapping of velocity gradients 0-79420  
cyclohexane-d<sub>12</sub>, Raman linewidth and molecular diameter meas. 0-69153  
cyclohexane-polystyrene mixture, Rayleigh and Brillouin scatt. and struct. relaxation 0-63640  
cyclohexanol, glassy cryst., diffuse X-ray scatt. study 0-100171  
cyclohexanol, orientationally disordered phase, Brillouin scatt. study 0-93351  
cyclohexanone, electrochromism and electric dichroism for studying transitions to second excited singlet 0-63692  
cyclohexene, chemisorbed on W(100), decomp., UPS and thermal desorpt. obs. 0-59782  
cyclohexene vapour, IR spectra anal. 0-63628  
cyclohexyl ammonium copper chloride, one dimensional spin  $\frac{1}{2}$  ferromag., mag. props. 0-71000  
1,2,6-cyclononatriene, mol. struct. and conformation, gas phase electron diff. 0-106400  
1,2-cyclooctadiene, conformational energy surface, Boyd's iterative force field investig. 0-95737  
cyclopentanone, electrochromism and electric dichroism for studying transitions to second excited singlet 0-63692  
cyclopentanone, n- $\pi^*$  transition, vibr. band intensities 0-74116  
cyclopentylamine, vibr. spectra and struct. 0-102516  
cyclophosphazene-DNA complex, spectrofluorometric and spectrophotometric investig. 0-95643  
cyclopropane, IR spectra studied by tunable laser,  $\nu_{10}+\nu_{11}$  band anal. 0-95615  
cyclopropane, liq., mol. dynamics, Raman and NMR studies of orientational motion 0-93296  
cyclopropane(-d<sub>8</sub>), centrifugal distortion const. and thermodynamic functions calc. 0-95582  
cyclopropane-d<sub>8</sub>, high resolution IR spectra, vibr. rot. band anal. 0-95621  
cyclopropyl cyanide, high-resolution microwave spectra, quadrupole hyperfine struct. of rot. transitions anal. 0-95601

# organic compounds continued

$\gamma$ -cyclopropyl-bis (1,3,3-trimethylindolenine-2-yl)pentamethinium fluoro-borate, exciton surface polaritons, reflecting faces obs. 0-65645  
cytosine, hydroxy and methoxy derivatives, absorption UV spectroscopy and electronic struct. of ionic and tautomeric forms 0-74177  
D-leucine, exchange diffusion in mouse Ehrlich ascites tumour cells, temp. reduction effect 0-67053  
DBTTF halogen complexes, IR, UV spectra, EPR study 0-108215  
decacyclene anion, photoexcited quartet state, transient EPR 0-78635  
trans-decaline-cyclohexane liq. mixtures, hole mobility, percolation model 0-65551  
n-decane, liq., thermal cond., meas. by transient hot-wire technique 0-103522  
decane-water-Na p-octylbenzene sulphonate-1-pentanol-NaCl, microemulsion system, existence of bicontinuous zone 0-104466  
decanoic acid, associated vapours, homogeneous nucleation 0-96638  
decylammonium chloride micelles, <sup>13</sup>C longitudinal relax. times and nuclear Overhauser enhancement anal. 0-83390  
DEM(TCNQ)<sub>2</sub>, ESR study 0-97127  
2-deoxyadenosine in aq. deaerated soln., new radiolysis mechanism 0-81350  
deoxyhaemoglobin, porphyrin-Fe-imidazole system, SCF-LCAO-ASMO and CI calcs. of low-lying multiplets and excited states 0-94155  
deoxyribonuclease I in aq. soln., inactivation by thermal neutrons 0-104664  
deuteromethane, crystalline, X-ray powder diff. study 0-96500  
dextran T-10 and  $\alpha$ -cyclodextrin, absorption mode spin-echo spectra appl. 0-78634  
di(alkylammonium)CdCl<sub>2</sub>Br<sub>2</sub>, solid-solid phase transitions 0-84290  
di(tert. butylperoxy)triphenylantimony, X-ray cryst. struct. determ. 0-92517  
1,6-di-p-methoxybenzene sulphonyloxy-2,4-hexadiyne, thermal polymerization, Raman spectra 0-103952  
diacetyl vapour, fluoresc. and phosphoresc., nonradiative transitions between triplet and singlet state obs. 0-99516  
diacetylene (TSHD), low temp. photopolymerisation, short chain intermediates obs. 0-93754  
diacetylene derivatives, solid-state polymerisation, isotope effects 0-66799  
diacetylene mixed crystals, co-crystallisation, influence of crystal composition on struct., reactivity in solid state 0-81324  
diacetylene monocarboxylic acids, multilayers, struct. phase transitions and polymerisability 0-80129  
diacetylene-d<sub>2</sub>, excited quintet states during photopolymerisation, ESR obs. 0-84635  
diacetylenes, photopolymerisation, solid-state reaction, photoacoustic calorimetric obs. 0-61089  
diacetylenes, solid state photopolymerisation, reaction products, electron spin resonance anal. 0-81338  
diacetylhydrazine, <sup>14</sup>N NQR lines fine structure 0-63667  
dialkyl tartrates, Raman circular intensity differential spectra obs., mol. struct. 0-87130  
dialkylammonium iron tetrachloride, antiferromag., mag. susceptibility meas. 0-60220  
dialkylammonium zinc dichlorobromides, long chain cpds., phase transitions, calorimetric study 0-70390  
diamantane, plastic and solid-solid transitions, Raman study 0-60590  
3,6-diaminophthalimide vapour, mol. electronic excitation energy degradation path depend. on pentane 0-74195  
diazanaphthalenes, excited state absorpt. spectra and intersystem crossing kinetics 0-74176  
diazaphenanthrenes, lowest triplet state zero field splitting parameters calcs. 0-83391  
1,6-diazaspiro[4.4]nonane-2,7-dione, optical rot. strength calcs. 0-95793  
p-diazines, polycyclic, T<sub>1</sub>( $\pi\pi^*$ ) $\rightarrow$ S<sub>0</sub> intersystem crossing, isotope effects, ODMR and phosphoresc. obs. 0-91586  
o-diazonaphthoquinones, thermal decomposition of light sensitive materials (Russian) 0-73504  
diazonium salts in aqueous solns. and polymer matrices, IR absorpt. spectra 0-76030  
dibenzofuran:anthracene, cryst., prompt fluoresc., temp. depend., trap effects (German) 0-93400  
dibenzoquinoxaline, T<sub>1</sub>( $\pi\pi^*$ ) $\rightarrow$ S<sub>0</sub> intersystem crossing, isotope effects, ODMR and phosphoresc. obs. 0-91586  
dibenzylketone, photolysis in micellar soln., quantum yield and <sup>13</sup>C enrichment 0-97711  
dibenzofuran, two photon absorptivities, CNDO/S-CI calc. with second order time depend. perturbation eqns. 0-74122  
p-dibromo-tetrafluorobenzene mol. cryst., in commensurate phase, quasi-elastic neutron scatt. 0-107386  
dibromoalkanes, energy partitioning in mass spectrometric displacement reactions 0-89471  
p-dibromobenzene, T<sub>1</sub> states, zero-field ODMR, MIDP and phosphorescence excitation spectra 0-74191  
dibromomethane, highly excited vibr. states, thermal lensing spectrosc. and local mode model 0-87140  
dibromonaphthalene, quasilinear chain excitons, Stark effects 0-97239  
1,3- and 1,4-dibromotetrafluorobenzene cations in gaseous state, emission spectra 0-63648  
dicalcium lead propionate, improper ferroelectric, dielectric props., IR radiation pyroelectric detection 0-80711  
dicalcium strontium propionate, ferroelec. domains, direct optical visibility 0-84704  
1-10-dicarba-closo-decaborane (10), mol. struct., vibr. and shrinkage corrections calc. from force field 0-95739  
dicarboxylic acids, IR spectra Davydov splitting, methylene chain pendular vibrations. (Russian) 0-89008  
dichloroacetic acid, soln., vibr., IR spectra 0-63633  
9,10-dichloroanthracene with iso-amyl acetate or esters as solvents, dye laser material 0-74354  
2,6-dichlorobenzamide, IR spectrum, vibr. assignment 0-95608  
p-dichlorobenzene, <sup>35</sup>Cl NQR line narrowing by nonreson. RF photon dressing 0-63662  
p-dichlorobenzene-naphthalene alloys, solid solns., NQR study 0-66063  
p-dichlorobenzene-p-dibromobenzene mixed crystals, triplet exciton migration, time resolved emission spectroscopy 0-89052  
4,4'-dichlorobenzophenone single crystals, mutual annihilation of triplet excitons, 1,5 and 4.2K, phosphoresc. obs. 0-80850  
2,2-dichlorobutane, liquid and solid, vibr. spectra, IR and Raman obs. 0-60567  
dichlorodifluoromethane, absorpt. meas., laser power density depend. 0-92251

## organic compounds continued

- dichlorodifluoromethane in stratosphere, height profile meas. at several latits. 0-72601  
 dichlorodifluoromethane, concentration in stratosphere, simultaneous inference using inversion algorithm 0-82000  
 dichloroethane drops falling freely through water, breakup 0-69899  
 $\beta,\beta'$ -dichloroethyl ether-iso-octane, critical indices, allowance for light double scatt. (*Russian*) 0-60624  
 dichlorofluoromethane pollution, conc. obs. in background troposphere air 0-97843  
 dichlorofluoromethyl peroxyhydrate, UV absorpt., spectra, photodissoc. lifetime meas. 0-83386  
 dichloromethane, highly excited vibr. states, thermal lensing spectrosc. and local mode model 0-87140  
 dichloromethane, mean free path meas., US relax. 0-59585  
 dichloromethane + F reaction products, modulated mol. beam mass spectrosc. obs. 0-97742  
 dichloromethane-cyclohexane, liq. mixture, intermol. vibrational energy transfer, US study 0-70313  
 dichloromethane- $d_0$ - $d_2$ , soln., far IR spectra, band shapes and moment anal. 0-58252  
 dichloromethane- $d_2$ , spectral densities determ. from spin-lattice relax. and spin-echo decay rates 0-75877  
 dichloromethane- $d_2$ , vibr.-vibr. energy transfer, laser-induced fluoresc. obs. 0-78689  
 dichloronaphthalenes, heavy atom effects on substrates of lowest triplet states, MIDP obs. 0-91594  
 1,8-dichlorooctane, quadrupolar relax. centres, limited spin diffusion 0-100649  
 2,2-dichloropropane, normal coordinate calcs. 0-60567  
 dicumyl peroxide, crosslinking of natural rubber rel. to modulus, swelling 0-59551  
 dicyanoketene, and isomeric forms, heat of form., ab initio STO-3G calcs. 0-58190  
 dicyclopentadiene, liq., CO<sub>2</sub> laser pulse induced chem. reactions 0-66821  
 diethyl ether, field ionisation, thermal energy distribution and energy deposition 0-95732  
 diethyl malonate-polystyrene, strongly opalescent critical isochore, scattered light intensity 0-71436  
 3,3-diethyl thiadiazocyanine iodide dye, stimulated fluoresc. and stimulated reson. Raman scatt. relationship 0-91853  
 diethylammonium cadmium tetrachloride, dielec. props., phase transition 0-80675  
 diethylammonium copper tetrabromide, mag. struct., NMR meas. 0-71192  
 diethylammonium manganese chloride, Heisenberg magnet, spin diffusion, EPR study 0-66019  
 5,5'-diethylbarbituric acid, EPR and INDO-MO study of radical formation after irradiation 0-93774  
 diethylcyanine, vibrational Raman bands, excitation profiles (*French*) 0-83380  
 3,3'-diethylthiadiazocyanine iodine-rhodamine 6G, energy transfer with increased local conc., Forster mechanism 0-69220  
 1,4-difluoro-2-butyne, sum of states, isometric group, symmetry no., thermodynamic functions 0-58186  
 difluoroacetic acid, soln., polarisable H bonds, IR spectrosc. obs. 0-58408  
 S,p-difluorobenzene, time resolved fluoresc. spectra, direct view of intramolecular vibr. redistribution 0-83341  
 2,2'-difluorobiphenyl, two photon absorptivities, CNDO/S-CI calc. with second order time depend. perturbation eqns. 0-74122  
 1,1-difluoroethane, mol. struct., gas phase electron diff. obs. 0-58385  
 1,1-difluoroethane, nucl. recoil <sup>18</sup>F chemistry at high press. 0-89510  
 difluoroethene, cis- and trans-, photoelectron-photoion coincidence study, fluoresc. obs. 0-95678  
 cis-1,2-difluoroethene, CO<sub>2</sub> laser pumped, CW far IR laser lines 0-69372  
 cis-1,2-difluoroethylene laser, far IR CW optically pumped 0-69368  
 1,1-difluoroethylene near-MM-wave emission assignments 0-58260  
 1,1-difluoroethylene submillimetric wave emission assignments 0-102708  
 difluoroiodomethane, vacuum UV photolysis, IF in solid Ar visible spectra 0-87137  
 difluoromethane, optically pumped, CW far IR laser line frequencies 0-102706  
 difluoromethane far IR laser gas, CW laser pumped, gain 0-69367  
 difluoromethylborane, nonrigid, symmetry group calcs. 0-106254  
 diformylhydrazine, <sup>14</sup>N NQR lines fine structure 0-63667  
 p,p'-dihexyloxytolan, flexoelec. coeff. in nematic phase, thermal depend. 0-79685  
 2,3-dihydropyran vapour, IR spectra anal. 0-63628  
 dihydroquinaxalinediones, conjugated mols. electronic struct. and geometry, Hartree-Fock instability 0-69055  
 dihydroxy benzenes in ethyl alcohol, dielec. dispersion charact. 0-75932  
 dihydroxy toluene in ethyl alcohol, dielec. dispersion charact. 0-75932  
 dihydroxyanthraquinone, light-induced proton transfer, photochem. hole-burning obs. 0-76535  
 4,6-dihydroxypyrimidine, aq. soln., reaction with OH, short-lived radicals, ESR 0-101031  
 1,2-diiodoethylene, form. from I<sub>2</sub> + acetylene, isomerisation 0-85157  
 diisopropylammonium copper chloride, mag. interactions, susceptibility, 2-230K 0-60237  
 dimethoxyethane and propylene carbonate mixed electrolyte solns., for high energy density batteries 0-76627  
 5,7-dimethoxyindane-1-one, cryst. and mol. struct. 0-100223  
 dimethoxymethane, vibr. spectra and rot. isomerism 0-106325  
 dimethyl ammonium manganese chloride, quasi one-dimensional mag. systems, impurity effects 0-71015  
 9,10-dimethyl anthracene, vap. phase dye laser media, photophysical parameters 0-95884  
 dimethyl disulphide + O(<sup>3</sup>P), absolute reaction rate const. determ. 0-89472  
 dimethyl ethyl amine, mol. struct. determ. by gas phase electron diff. 0-95743  
 dimethyl POPOP, multiphoton cross-section determination by means of luminescence experiments 0-93377  
 dimethyl sulphide + O(<sup>3</sup>P), fast flow reson. fluoresc. obs. of absolute rate const. 0-61077  
 dimethyl sulphoxide, high efficiency stimulated Raman scatt. source (*Chinese*) 0-87433  
 3,3'-dimethyl-1'-phenyl-6-nitro-spiro [(3H-7,8-benzochromen)-3,2'-indoline] (II), photochromic transform., temp. depend. 0-104456  
 3,3'-dimethyl-1'-phenylspiro [(3H-7,8-benzochromen)-3,2'-indoline] (I), photochromic transform., temp. depend. 0-104456

## organic compounds continued

- 1,5-dimethyl-2,4-hexadiene-Cu<sub>2</sub><sup>2+</sup> fluoresc. quenching method for determ. binding const. 0-89530  
 dimethyl-s-tetrazine, vapour, mol. fluoresc., photodissoc. product 0-81352  
 N,N-dimethylacetamide in tetrachloromethane, dielectric relax. and complex permittivity 0-108149  
 dimethylamine iron tetrachloride, antiferromag., mag. susceptibility meas. 0-60220  
 dimethylamine-HCl systems, H-bonded complexes studied by ab initio MO method, dipole moments determ. 0-83253  
 dimethylammonium cadmium tetrachloride, far IR refractive index, extinction coeff. and dichroism obs. 0-66144  
 dimethylammonium copper manganese chloride, two-dimens. mixed magnet, EPR 0-66030  
 dimethylammonium copper tetrabromide, quasi two-dimensional antiferromag., mag. behaviour 0-97098  
 dimethylammonium copper tetrachloride, crit. slowing down and anomalous relax. near Curie temp. 0-71053  
 dimethylammonium copper tetrachloride, ferromag., quasi two-dimensional, ordering temp., press. depend. 0-84601  
 dimethylammonium copper tetrachloride, two-dimens. ferromag., saturation of parallel-pumped magnons 0-97147  
 dimethylammonium copper tetrachloride-tetrabromide mixed cryst., mag. transition 0-65874  
 dimethylammonium copper tetrahalide, layer compound (CH<sub>3</sub>NH<sub>3</sub>)<sub>2</sub>Cu(Cl,Br)<sub>4</sub>, antiferro- to ferro- transition 0-108005  
 dimethylammonium manganese tetrachloride, antiferromag. and spin-flop resonance obs., 70 to 100 GHz 0-71190  
 dimethylammonium manganese trichloride: Cd(Cu), impurities in quasi-one-dimens. Heisenberg systems, anisotropy effect 0-80502  
 dimethylaniline, exciplex with anthracene, form. kinetics and luminesc. props. 0-66792  
 dimethylbenzaldehydes, in durene single cryst., zero-field splitting, guest and host isotope effects 0-107752  
 dimethyldichlorosilane, microwave spectrum, rot., centrifugal distortion and quadrupole coupling consts. 0-91547  
 dimethylformamide, intramolecular exchange rate determ. from <sup>13</sup>C spin-lattice relax. times 0-69169  
 dimethylhydrazine-oxyhaemoglobin interaction,  $\gamma$ -reson. spectroscopy 0-81525  
 dimethylketone, streaming current and cross-coeff. meas. in electrokinetic processes 0-76531  
 dimethylphosphines, IR spectra, coupling between methyl rocking, PH bending, and PC stretching, force field interpretation 0-69141  
 2,2-dimethylpropane-CO<sub>2</sub>, liq. vapour equil., 220 to 300K and 6.7 MPa 0-62821  
 dimethylsulphide, liq., solvated electrons, optical absorpt. spectrum obs. 0-97250  
 m-dinitrobenzene, oriented film, intermol. vibr. coupling, polarised IR spectra 0-97264  
 m-dinitrobenzene cored fibres, void-free cryst. growth, X-ray diff. and optical microscopy study 0-71586  
 4-(2',4'-dinitrobenzyl)-pyridine, photochromism, nanosec. laser absorpt. spectrosc. obs. 0-85193  
 dioctadecyl hydrogen maleate crystals, X-ray spectroscopic true 2d<sub>h</sub> value, 'effective' 2d value concept of Bragg spectrometer crystals 0-70081  
 dioctyl phthalate polydisperse, aerosol number and mass conc. meas. by elect. aerosol anal. 0-108753  
 p-dioxan-benzene liq. mixture, excess energy of vaporisation, US study 0-65209  
 p-dioxane-H<sub>2</sub>O at 11 and 25°C, US absorption 0-65171  
 dipalmitoyl lecithin bilayer, mol. tilt, X-ray diffraction obs. in gel phase 0-84059  
 dipalmitoylphosphatidylcholine, changes in vol. mag. susceptibility at the phase transition 0-76770  
 diphenyl anion salts, sublimed layer, electronic and IR absorpt. spectra 0-66189  
 9,10-diphenyl anthracene, vap. phase dye laser media, photophysical parameters 0-95884  
 2,5-diphenyl-1,3,4-oxadiazole, fluoresc. quantum efficiency, one-photon dissociation, temp. depends. 0-69180  
 2,5-diphenyl-1,3,4-oxadiazole, vapour, spectral, fluoresc., photochem. and laser props. 0-106344  
 2,5-diphenyl-1,3-oxazole vapour, spectral, fluoresc., photochem. and laser props. 0-106344  
 9,10-diphenylanthracene, refr. index meas. of frozen gas matrices, fluoresc. method 0-90884  
 diphenylanthracene in 2,2,4-trimethylpentane, light scatt. and fluoresc. standard by monochromator 0-57247  
 diphenylanthracene in benzene soln., extrinsic photocond. kinetics 0-92691  
 2,5-diphenylfuran vapour, spectral, fluoresc., photochem. and laser props. 0-106344  
 1,6-diphenylhexatriene, radiationless transitions and natural lifetimes, solvent effects 0-63622  
 diphenylpolyene molecules, excited electronic states, vibronic mixing, wave functions, method of fragments anal. 0-63615  
 dipicolinic acid, IR and Raman spectra, isotopic frequency shift, mol. vibr. obs., point groups determ. 0-89001  
 diplosporin derived from (1,2-<sup>13</sup>C)acetate, <sup>13</sup>C-<sup>13</sup>C coupling assignment using DANTE excitation 0-80617  
 dipotassium glucose-1-phosphate, X-irrad., ESR-ENDOR obs 0-60419  
 dipropylammonium manganese tetrachloride, two-dimens. weak ferromagnet, AC susceptibility 0-65823  
 diquinolyl cyanomethane, fluoresc. quantum yields, viscosity effects 0-60646  
 1,4-disilabutane, rot. isomerism, Raman and IR spectra 0-74168  
 dihiocarbamate complexes of Cr, Mn, Sn and Pb IR, electronic and mass spectra, mag. susceptibility, cond. meas. 0-97270  
 DOBAMBC, chiral smectic, ferroelec., press. and solute effects 0-103920  
 DOBAMBC, ferroelec. liq. crystals, elec. and optical props., appls. (*Japanese*) 0-88943  
 DOBAMBC, smectic A and ferroelec. smectic phases, <sup>13</sup>C NMR study 0-75153  
 docosane, purification and single cryst. growth 0-71589  
 DODCI, saturable absorber, picosecond phase-conjugate refl. 0-95960  
 DODCI in ethanol, DQOCI added, electronic energy transfer, real-time ps meas. 0-58311  
 DODCI in ethanol, malachite green added, electronic energy transfer, real-time ps meas. 0-58311



## organic compounds continued

dodecahexenes, sudden polarisation effect, ab initio and CI calcs. 0-58160  
 dodecane/dodecyltrimethylammonium micelles, type II mesophase, bilayer struct., NMR spectra study 0-75149  
 n-dodecane liqs., refractive index, pressure effect 0-71375  
 p-nodocylxy benzyldiene p-azophenyl aniline, smectic phases, mol. order, EPR study 0-79693  
 doublet radicals in nematic and smectic liq. crystals, ENDOR obs. 0-91585  
 DPPH, dil., saturated spin system, spin decoupling effect and variation of dipolar energy reservoir temp. 0-88877  
 duren crystalline complexes with octafluoronaphthalene, triplet exciton emissions 0-84760  
 dye in polymer matrices, electrochromic props. and use as probe of matrix softening around  $T_g$  0-84724  
 dye molecules adsorbed on Ag, Au and Cu films, absorpt. and luminesc. study 0-103981  
 dye monomolecular layers, energy transfer between sensitizers and acceptors 0-80861  
 dye proflavine bound to synthetic polynucleotides, selective laser photo-damage 0-99525  
 dye solutions for laser beam modulation, population relaxation lifetime meas. (Russian) 0-95964  
 dyes, fluoresc. spectra calcs.,  $\beta$ -variation method (German) 0-69182  
 EABAC, smectic A, nematic, and isotropic phases, NMR and quasilelastic neutron scatt. obs. 0-88022  
 EBBA, IR absorpt. spectra, elec. field effects, orientational order parameter determ. by IR dichroism, bend elastic consts. 0-80778  
 EBBA, nematic, orientational order, effect of hexa-n-alkoxy-triphenylene disc-like solutes 0-79682  
 EBBA, mol. and cryst. struct., X-ray diffr. study 0-88134  
 EBBA, nematic-isotropic transition at high press., turbidity meas. 0-92655  
 EBBA, NMR and Raman scatt. studies in nematic phase 0-100619  
 EBBA, orientational order in glassy and nematic phases, IR dichroism meas. 0-64891  
 EBBA, Tsvetkov parameter, temp. depend. 0-88035  
 EBBA, nematic, EPR investig. 0-108077  
 eicosane, purification and single cryst. growth 0-71589  
 n-eicosane, triclinic phase, self-diffusion, 295 to 309K 0-88359  
 electrochemiluminescence as possible source of coherent radiation, and role in biological processes (Russian) 0-76093  
 electron microscope imaging with superconducting lenses 0-73553  
 enolate anion from acetone, gas phase, negative ion chemistry 0-87060  
 eosin-Y, in n-alkohols (ethylene glycol)(glycerol), rot. relax., time-resolved fluoresc. depolaris., obs. 0-58300  
 epifluorohydrin, IR and Raman spectra and conformations 0-60576  
 erbium triethyl sulphate, single cryst.,  $H^+$  coords., NMR 0-97152  
 esters, long-chain, X- and Y-type multilayers, form. conditions and struct. characterisation 0-80127  
 esters, SLC, ferroelectric behaviour, specific heat, spontaneous polarisation 0-75958  
 estradiol,  $^{125}I$  labelled a  $\gamma$ -emitting estradiol analogue that binds to the estrogen receptor 0-61697  
 ethane, CH bond orbitals, internal rot. barriers, antisymmetrization effects 0-63529  
 ethane, diode laser spectra, baseline variations, elimination by ultra-low freq. filtering 0-90901  
 ethane, flow continuity in arterial capillary systems in cryogenic heat pipes 0-64536  
 ethane, gas, liq., and crit., electron mobility, density and temp. effects 0-92246  
 ethane, inclusion of nonbonded interactions in vibr. freq. calcs. 0-95590  
 ethane, internal rot. splittings, vibr.-rot.-torsion energy levels perturbations 0-91531  
 ethane, photoionisation cross section at distance from threshold, chemical bond influence 0-69196  
 ethane, photoionisation spectra, cond. hole model 0-58326  
 ethane, pure gas, enthalpy, Carlson-Thodos van der Waals eqn. calcs. 0-83878  
 ethane, rot. barriers, MS-SCF- $X_n$  calcs. 0-106267  
 ethane, solid, mol. reorientational motions, incoherent neutron scatt. studies 0-107070  
 ethane, supercritical, electron mobility as function of density and temp. 0-59163  
 ethane, unimol. decomp., energy transfer processes, Monte Carlo simulation 0-99555  
 ethane+ $He^+$ , 0.7-2 MeV, charge-changing collisions, electron capture 0-58372  
 ethane cation, relative stability of  $^2A_{1g}$ ,  $^2E_g$  states 0-58140  
 ethane gas, local mode overtone bands 0-83444  
 ethane-1,1,1-d<sub>3</sub>, gas-phase IR spectra, rot. fine struct. obs. 0-83359  
 ethanol, boiling at subatmospheric press., heat transfer rate, heating surface effects 0-69630  
 ethanol, electron solvation, ps laser study 0-101032  
 ethanol, H-bonding investigated with supersonic mol. beam using photoionisation quadrupole mass spectrometer 0-102543  
 ethanol, industrial, production from municipal cellulose waste 0-61502  
 ethanol, mean sojourn time of molecules on surfaces, meas. in practical vacuum system (Japanese) 0-57315  
 ethanol, multiphoton absorpt. and dissociation 0-99530  
 ethanol, polymorphic forms, mol. motion, NMR obs. 0-88885  
 ethanol, pulsed adsorption on Ge heteroepitaxial films, effect on elec. cond. 0-93014  
 ethanol fuel, substitution of large proportion of diesel fuel in diesel engines 0-61230  
 ethanol fuel for vehicles, gas turbines, and boilers, Brazil 0-61229  
 ethanol solution in benzene, dielec. relax. time by RF cond. meas. 0-71302  
 ethanol-d<sub>1</sub>(d<sub>2</sub>)(d<sub>3</sub>), glassy state, solvated electron geometry, electron spin echo modulation obs. 0-66009  
 ethanolic dye solution laser, cylindrical active element with sheath, radiation intensity distrib. calc. 0-58531  
 ethene, dipole polarisability, finite-field SCF MO calcs. 0-83255  
 ether+ $Li^+$ , pair pots., ab initio LCAO SCF MO calcs. 0-58184  
 ethidium bromide E-DNA, intercalated birefringent fibres, microspectrophotometric investig. (German) 0-57392  
 p-(p'-ethoxybenzylidene)amino-benzonitrile, cryst. struct. rel. to liq. crystallinity 0-100225  
 ethyl alcohol, liq., viscosity parameters, RF cond. meas. 0-96677

## organic compounds continued

ethyl alcohol, turbulent absorbing liq. medium, laser radiation thermal self-interaction 0-91868  
 ethyl alcohol-d<sub>2</sub>(-d<sub>1</sub>)(-d<sub>1</sub>)(-d<sub>2</sub>), internal rot. and microwave rot. spectra 0-69128  
 ethyl cation+alkane reaction, temp. and kinetic energy relative rate consts. determ. 0-81299  
 ethyl iodide, microwave spectra and internal rot. anal. 0-69130  
 ethyl iodide submillimeter wave laser, optically pumped 0-87376  
 ethyl radical, C-C bond barrier rot., IR spectra 0-76536  
 ethyl-furan-2-carboxylate, skeletal vibr. of IR spectra, conformational props., solvent polarity effect 0-87118  
 ethyl-p-azoxybenzoate, far IR and Raman spectra, smectic polymorphism 0-76022  
 ethylammoniumtetrachlorochromate, optical absorption intensity, short-range spin correlation 0-108185  
 ethylbenzene, vapour, conform. and struct. obs. 0-69247  
 ethylcyanodiacetylene cation, gas phase, UV emission spectra of  $A(\pi^-) \rightarrow \bar{X}(\pi^-)$  band system 0-95636  
 ethylcyclopropane, solid, liquid, vapour phase, IR and Raman vibr. spectra 0-84740  
 ethylene, absorpt. cross sections at CO<sub>2</sub> laser wavelengths, temp. and press. depend. 0-78613  
 ethylene, adsorption and decomposition on Ni films, coverage depend. meas. 0-96743  
 ethylene, adsorption on Ag (111) surface, XPS and UPS investigation 0-103573  
 ethylene, air pollution monitoring, computer controlled CO<sub>2</sub> laser absorpt. system 0-89699  
 ethylene, chemisorption of Pt, vibr. anal. of C<sub>2</sub>H<sub>3</sub> species 0-61150  
 ethylene, diatomics-in-mols., semiempirical valence bond  $\pi$ -electron theory 0-99461  
 ethylene, He-Ne laser line, high temp. absorpt., anal. by high resolution IR spectra 0-91554  
 ethylene, high density behaviour, extrapolated P<sub>0</sub>T surfaces and critical density 0-87834  
 ethylene, interaction with O<sub>2</sub> on Ag (110), LEED and AES obs. 0-89520  
 ethylene, IR absorpt. spectra of  $\nu_1$ ,  $\nu_{10}$  and  $\nu_4$  interacting band 0-83369  
 ethylene, molecular geometry optimisation, variable metric method, internal geometry 0-95744  
 ethylene, narrow resonances of multiple-photon IR absorpt. 0-99529  
 ethylene, photoionisation cross section at distance from threshold, chemical bond influence 0-69196  
 ethylene, polarisability, nonlinear elec. susceptibility, SCF calcs. 0-95547  
 ethylene, pot. energy and dipole moment surfaces, polarisation effect, ab initio CI calcs. 0-106272  
 ethylene, quadrupole moment tensor determ. by collision-induced absorpt. spectrum 0-91555  
 ethylene, rot. around double bond, four orbital-four-electron model 0-95592  
 ethylene, static polarisability, ab initio SCF wave functions 0-74106  
 ethylene, twisted, intervalence charge transfer and reson., sudden polarisation effect 0-69230  
 ethylene, vacuum ultraviolet absorption spectra 0-63653  
 ethylene, valence states, effective Hamiltonian from canonical transformation 0-74130  
 ethylene+C(2<sup>2</sup>S<sub>0</sub>) 0-74241  
 ethylene+Cl<sup>+</sup>, reactions at room temp. 0-93749  
 ethylene+CO<sub>2</sub><sup>+</sup>, rate coeffs. and product distribution determ. 0-97693  
 ethylene+CO<sub>2</sub>CO<sub>2</sub><sup>+</sup>, rate coeffs. and product distribution determ., dissociation energy and heat of form. 0-97693  
 ethylene+H<sub>2</sub>O<sup>+</sup>, rate constants determ. as function of relative kinetic energy 0-81292  
 ethylene+HBr, low temp. chain hydrobromination, kinetics and mechanism 0-93735  
 ethylene+Hg(2<sup>3</sup>P<sub>1</sub>), quenching rate consts. determ. with nanosecond light pulser with Hg vapour 0-100111  
 ethylene(-d<sub>4</sub>) clusters, IR photodissoc. 0-89506  
 ethylene(-d<sub>4</sub>), chemisorbed on Ni catalyst, Raman and vibr. spectra 0-108747  
 ethylene and propylene adsorbed on Ag, enhanced Raman spectra obs. 0-95607  
 ethylene as singlet methylene dimer, nonempirical double zeta calculations, zwitterionic singlet excited states 0-83258  
 ethylene chemisorption on Rh (111), EELS, LEED and thermal desorption mass spectrometry 0-80057  
 ethylene glycol adsorption on Al<sub>2</sub>O<sub>3</sub>, inelastic electron tunnelling spectroscopic study rel. to lubrication 0-70302  
 ethylene oxide, rot. relax., double reson. and Stark switching obs. 0-106340  
 ethylene oxide+CO<sub>2</sub>, (00<sup>0</sup>1) mode deactivation, laser induced fluoresc. obs. 0-83453  
 ethylene ozonide, ab initio gradient and MC SCF calc., conformational anal. 0-83290  
 ethylene-LiH, struct. and props., SCF ab initio calcs. 0-106250  
 ethylene-O<sub>2</sub>-N<sub>2</sub>-Al particle mixture, two-phase detonation and combustion (French) 0-61097  
 ethylenediamine, adsorption on Fe and Ni, XPS study 0-76132  
 ethylenediamine sulfate, cryst., induced gyrotropy of CrO<sub>4</sub><sup>2-</sup> ion 0-108175  
 ethylenic compounds, H<sup>+</sup> chemical shifts, extended Huckel calcs. with gauge in variant atomic orbitals 0-102449  
 ethylidene, rearrangement to ethylene, barriers, ab initio MO calcs. 0-104424  
 ethylenimine, pyrolysis product, microwave spectra, rot. distortion and electric quadrupole const. and rot. barriers determ. 0-78608  
 ethyloxirane, solid, liquid, vapour phase, IR and Raman vibr. spectra 0-84740  
 N-ethylphthalimide+olefins, photochemical reaction, absorpt., fluoresc., phosphoresc. and triplet-triplet absorpt. spectra 0-85197  
 ethynyl cation, dissociative recomb. cross section determ., merged beam obs. 0-78715  
 ethynyl radical, mm wave emission obs. of interstellar clouds 0-90503  
 exciplexes and excited aromatic molecules, donor-acceptor props., comparison of fluorescence quenching 0-69174  
 excitation energies, CNDO/S-CI method calc. appls. (German) 0-106275  
 F 0-92515  
 ferrous formate dihydrate, paramagnetic specific heat, decoration iteration transformation anal. 0-70938  
 film, thin, prep. methods in ultrahigh vacuum (Japanese) 0-84851

## organic compounds continued

flavins, meas. of sub ns fluoresc. decay by time-correl. photon counting and Ar laser 0-94429  
 fluorene:pyrene- $d_{10}$ , single cryst., host-guest triplet pairs, mag. field effect 0-60649  
 fluorene, molecular nonsteady-state luminesc. behaviour under narrowband laser excitation 0-87159  
 fluorene, two photon absorptivities, CNDO/S-CI calc. with second order time depend. perturbation eqns. 0-74122  
 fluorene+o-terphenyl, supercooled, liquid systems, dielectric and dynamic Kerr-effect studies 0-60496  
 fluorene crystal, doped, photochemical hydrogen abstraction, proton hyperfine structure via optical nuclear polarisation 0-63659  
 fluorescein, in n-alcohols (ethylene glycol)(glycerol), rot. relax., time-resolved fluoresc. depolaris. obs. 0-58300  
 fluorescein dye, halogen substituted, in dimethyl sulphoxide, spectral evidence for anion-counterion association 0-71909  
 1-fluoro, 2,4-dinitrobenzene, partially aligned in elec. field,  $^{13}\text{C}$  NMR, dipole moment determ. 0-78633  
 2-fluoro ethanol, Ar matrix, induced conformational isomerisation by IR irradi. 0-101010  
 fluoroacetylene, He(II) photoelectron spectra 0-91601  
 fluoroacetylene-d, Stark and microwave double reson. laser spectra 0-63690  
 fluoroanthene in micelles soln., fluoresc., halide ion induced quenching and enhancement 0-95672  
 fluorobenzene, liquid, vibr. relaxation, Brillouin spectra 0-108219  
 fluorobenzene, mol. reorientation and weak mol. interaction influence,  $^2\text{D}$  spin-lattice relax. obs. 0-106333  
 fluorobenzene, multiphoton ionisation spectrum in one-photon wavelength region 0-63727  
 fluorobenzene,  $S_0$ - $S_1$  transitions, two-photon absorpt. spectra by nozzle beam-multiphoton ionisation method 0-63728  
 fluorobenzene radical cations in solid Ne, laser-induced fluoresc. spectra, vibr. struct. of excited and ground states 0-95671  
 fluorobenzenes in Ne matrices, molecular cation electronic absorption spectra, new photolytic technique 0-58415  
 fluorocarbon solutions, dye-sensitized, spectroscopic obs. of 1.27  $\mu\text{m}$  and 1.58  $\mu\text{m}$  emission of single ( $\Delta_2$ ) mol.  $\text{O}_2$  0-85178  
 5-fluorocytosine, electron beam damage assessed by EELS 0-89809  
 fluoriadacetylene, He(II) photoelectron spectra 0-91601  
 fluoriiodomethane, vacuum UV photolysis, IF in solid Ar visible spectra 0-87137  
 fluoroformaldehyde, pot. energy surface characts., substitution effect 0-89505  
 fluoroiodomethane, vibr. excited, dissociation, trajectory calcs. using pot. energy surface parameters 0-76508  
 fluoromethane,  $^{12}\text{CH}_3\text{F}$ , far IR Raman laser line obs.,  $\text{CO}_2$  laser pumping 0-69381  
 fluoromethane,  $^{12}\text{C}$  ( $^{13}\text{C}$ ), Doppler-free optical double reson. spectroscopy using single-freq. laser and modulation sidebands 0-68274  
 fluoromethane, deuterium separation at high press. by ns  $\text{CO}_2$  laser multiple-photon dissoc. 0-91616  
 fluoromethane, near-MM-wave laser synchronous pumping, ultrashort pulse generation at 496, 193  $\mu\text{m}$  0-102705  
 fluoromethane, optical pumping of far-IR molecular lasers by CW  $\text{CO}_2$  waveguide laser 0-83615  
 fluoromethane, vibrational-translational transfer rate, optoacoustic meas. using short pulse  $\text{CO}_2$  laser 0-74258  
 fluoromethane+Cl( $^2\text{P}_{3/2}$ ,  $1/2$ ), photochlorination electron and oscill. energy 0-81320  
 fluoromethane+fluoromethane, collision induced mode selective energy transfer, fluoresc. obs. 0-69177  
 fluoromethane+HCN, HCN excited vibr. state,  $T_2$  meas. 0-102498  
 fluoromethane+ $\text{SF}_6(\text{CS}_2)$ , fluoromethane laser, buffer gases collisional narrowing 0-99710  
 fluoromethane laser, optically pumped far-IR waveguide, output, temp. depend. 0-58512  
 fluoromethane optically pumped molecular laser, relax. oscills. 0-95875  
 fluoromethane TEM $_{00}$  far IR laser with integrated pump laser 0-58578  
 fluoromethane- $^{13}\text{C}$ , pulsed far IR emission 0-69370  
 fluoromethane- $^{13}\text{C}$  optically pumped molecular laser, relax. oscills. 0-95875  
 fluoromethane- $\text{SF}_6$ , 496- $\mu\text{m}$  optically pumped laser, energy-transfer mechanisms 0-99712  
 fluoromethyl formate, conformation potential energy surfaces, ab initio calcs. 0-69065  
 fluoronitrobenzene, equilib. config. and barriers, microwave spectra 0-95606  
 fluorophenol cations, emission and photoelectron spectra in gaseous phase 0-58316  
 fluorostyrene, UV Raman spectra, reson. effect in photoreactive states 0-106326  
 fluoresceinisothiocyanate, fluorescent labelling of polyaspartamides 0-58426  
 formaldehyde, interstellar 5 GHz survey of southern dark clouds 0-73028  
 formaldehyde,  $^3\text{A}''$  state, zero-field splitting param., ab initio CI calcs. 0-99454  
 formaldehyde, electronic struct., dipole moments, mol. polarisability, force fields, ab initio calcs. 0-78531  
 formaldehyde, excited state vibr. freq. calcs. by method based on scaled ab initio force fields 0-87092  
 formaldehyde, force field calcs., damped least-squares method 0-91533  
 formaldehyde, in marine air and rainwater, wet season obs. 0-85703  
 formaldehyde, intermolecular interaction energies calcs. using minimal basis sets 0-78681  
 formaldehyde, interstellar absorption line in galactic radio sources, SHF obs. 0-77472  
 formaldehyde, isolated Voigt line, off-peak spectral absorpt. coeff. 0-106355  
 formaldehyde, mol., UV absorpt. cross-section, and stratosphere chem. 0-109209  
 formaldehyde, mol. Rydberg S-S and S-T transitions, semi-empirical SCF MO calc. 0-91453  
 formaldehyde, molecular beam rotation temp. meas. (French) 0-78724  
 formaldehyde, relative Raman scatt. cross section 0-100061  
 formaldehyde, relativistic Dirac-Fock multiconfig. SCF calcs. 0-99456  
 formaldehyde, selective laser photolysis for  $^{14}\text{C}$  enrichment 0-108720  
 formaldehyde, sequential coupling 0-58297  
 formaldehyde+Ar( $\text{N}_2\text{O}$ ), mol. isolated Voigt line, off-peak spectral absorpt. coeff. 0-106355

## organic compounds continued

formaldehyde+Br(F) reactions, rate consts. by EPR 0-93736  
 formaldehyde+Cl, photolysis, Fourier transform IR studies, metastable species detection 0-81293  
 formaldehyde+ClO radical, expt. showing no reactivity, stratospheric implications 0-90119  
 formaldehyde absorption in Lynds 134 dust cloud, turbulence determ., 6 cm obs. 0-94845  
 formaldehyde and its isotopic species, rot. spectra of ground vibr. state, rot. const. determ. 0-83350  
 formaldehyde anion radical, hyperfine coupling consts., vibr. depend., ab initio calcs. 0-87150  
 formaldehyde as probe to investigate dark cloud struct. EHF and SHF obs. 0-105317  
 formaldehyde dimers, matrix isolated, struct., IR spectra 0-99504  
 formaldehyde in galactic centre region 0-94852  
 formaldehyde in HD 97048 circumstellar shell, visible and IR obs. 0-85943  
 formaldehyde maser in IRS 1 in NGC 7358, SHF band obs. 0-67822  
 formaldehyde  $S_1$  levels, collisionless single rot. level lifetimes, elec. field depend. 0-63566  
 formaldehyde substituted with  $^{17}\text{O}$  and  $^{18}\text{O}$ , microwave spectra of ground vibr. states, rot. and distortion const. determ. 0-83349  
 formaldehyde- $d_0$  ( $-d_2$ ),  $S_1$  single rot. level lifetimes, isotope, elec. field and vibr. state depend. 0-78655  
 formaldehyde- $d_0$  ( $-d_1$  ( $-d_2$ ), matrix isolated, IR spectra, monomer absorpt. 0-99503  
 formaldehyde-d ( $d_2$ ) submillimetre lasers, optically pumped, assignment of laser lines 0-58513  
 formamide, force consts. and dipole moment derivatives, ab initio MO calcs. 0-95521  
 formamide-glyoxal, charge transfer theory, Mulliken population, ab initio calc., multiconfiguration scheme 0-106392  
 formate ions adsorbed on Ag particles in aqueous soln. Raman spectra 0-69148  
 formate, proton spin-lattice relaxation in various phases (Russian) 0-97163  
 formic acid,  $^{13}\text{C}$ , NMR spectra, transition intensities, off-resonance proton spin decoupling influence 0-74183  
 formic acid,  $^{16}\text{O}$ ,  $^{18}\text{O}$ , microwave spectra and centrifugal distortion consts. 0-83352  
 formic acid, adsorbed on Cu (100), interaction with acetic acid, EELS study 0-76120  
 formic acid, cryst., H bonded, IR spectrum computer simulation 0-97253  
 formic acid, fragmentation, fragment structs. and energies calcs. 0-74124  
 formic acid, on Ni surface, decomp., dipole interactions effects 0-61143  
 formic acid, soln., polarisable H bonds, IR spectrosc. obs. 0-58408  
 formic acid+ $\text{CO}_2$ , (00 $^0$ 1) mode deactivation, laser induced fluoresc. obs. 0-83453  
 formic acid (-d), microwave spectra and rot. consts., astrophysical appl. 0-91550  
 formic acid dimer, vibr. spectra, CNDO/2 interpretation (French) 0-58155  
 cis-formic acid geometry, force fields and fundamental vibr. freq., ab initio study 0-87040  
 formic acid ions, fragmentation, energy selected, photoelectron-photoion spectra 0-95676  
 formic acid laser far IR pulse generation by Q-switched  $\text{CO}_2$  laser pump source 0-69383  
 formic acid- $d_0$  ( $-d_1$  ( $-d_2$ ), vibr. spectra, CNDO/2 interpretation (French) 0-58155  
 formyl ion, electron impact rot. excitation, Glauber approx. with Coulomb effect 0-63840  
 formyl ion ( $\text{HCO}^+$ ), interstellar, shock enhancement of abundance in supernova remnant (IC 443) 0-82464  
 formyl radical ion, mm wave emission obs. of interstellar clouds 0-90503  
 free radicals, selective pulse NMR expts. 0-60452  
 free-base porphyrin, Zeeman shift meas. by photochem. hole-burning 0-83416  
 Freon 123, deuterium separation at high press. by ns  $\text{CO}_2$  laser multiple-photon dissoc. 0-91616  
 Freon electrohydrodynamic flow, jet dynamic pressure obs. (Russian) 0-59117  
 Freon-113, boiling and heat transfer on horizontal pipes with annular fins 0-74855  
 Freon-113, correlation properties near phase-separation boundary, gravitational field effect 0-107410  
 Freon-12, annular mist flow in tube, wall film mass flow rate 0-69905  
 fulvene, ring currents hypersusceptibilities calcs. 0-102588  
 furan, liq., US phase vel. decay in space and time 0-99891  
 furan, mean free path meas., US relax. 0-59585  
 furan, Penning election spectra and photoelectron spectra, rel. intensities 0-95725  
 furan, resonantly enhanced multiphoton ionisation 0-106362  
 furan-cyclohexane, liq. mixture, intermol. vibrational energy transfer, US study 0-70313  
 furane, cryst., low freq. vibr. spectrum, temp. depend., 12 to 253K 0-84743  
 gases, IR fluoresc. by  $\text{CO}_2$  laser 0-78619  
 gasoline-air flame, laser induced fluorescence spectra obs. 0-91587  
 germanium phthalocyanine, elec. cond. temp. depend. 0-80271  
 germiacylene- $d_0$  ( $-d_2$ ), centrifugal distortion const. and thermodynamic functions calcs. 0-95581  
 glasses, low temp. mol. mobility, NMR  $T_1$  meas. 0-60439  
 glucose, glucose oxidase determ., continuous flow anal. 0-61736  
 glutaric acid,  $\gamma$ -irrad. single crystals, free radical EPR obs. at 77K 0-81340  
 glycerin-water, solns., visualization of standing vortices behind cylinder 0-59151  
 glycerol, highly viscous state, static and dynamic Kerr effect obs. 0-60545  
 glycine,  $^{17}\text{O}$  NMR chemical shifts and linewidths, pH dependence 0-80625  
 X-glycine, cryst., Raman band intensities of local group modes 0-93298  
 glycine sulphate:L-alanine, unirradiated, optical spectroscopy of scintillations 0-80863  
 glycol, alq., in swelling equilib. with polyvinyl alcohol, interactions 0-104201  
 glyoxal, electron affinity at centrosymm. trans geometry 0-87225  
 glyoxal,  $S_0$ - $S_1$  band, opto-acoustic phase angle meas. 0-68256  
 glyoxal, singlet-triplet radiationless processes in mag. field 0-106347



## organic compounds continued

glyoxal, sum of states; isometric group, symmetry no., thermodynamic functions 0-58186  
 glyoxal, triplet  $n \rightarrow \pi^*$  and  $\pi \rightarrow \pi^*$  transitions studied by low-energy electron diff. 0-83502  
 glyoxal, vapour, predissoc. in  $S_1$  zero-point level states 0-102544  
 glyoxal-formamide, charge transfer theory, Mulliken population, ab initio calc., multiconfiguration scheme 0-106392  
 guanidine aluminium sulphate, lattice charge contribution to coordination polyhedron cryst. potential 0-103651  
 guanidine aluminium sulphate hexahydrate:  $Cr^{3+}$ , ESR spectra fine struct. 0-93169  
 guanidine aluminium sulphate hexahydrate, SEM obs. of ferroelec. domain struct. in single crystals. 0-97219  
 guanidinium aluminium sulphate hexahydrate, surface obs., SEM and AES expts. 0-71362  
 guanidinium aluminium sulphate hydrate, ferroelec., decoration patterns on cleavage surface, domain obs. 0-97218  
 guanidinium uranyl sulphate hydrate, ferroelec., decoration patterns on cleavage surface, domain obs. 0-97218  
 guanine nucleotides, purinic 8-CH exchange kinetic isotope effect, Raman spectral study 0-83381  
 haematoporphyrin, complexed with chloranil and tryptophan, energy spectra, transition moments and intermolecular distances 0-72127  
 haloalkane-aromatic complexes, ground and excited states, CNDO calcs. 0-69082  
 halobenzene cations, in solid. Ne matrix, slow vibr. relax., fluoresc. obs. 0-74194  
 halobenzene type ions, high resolution spectrosc. with new emission source (*French*) 0-57383  
 halocarbon index matching fluids for long wavelength fibre-optic appl. 0-69470  
 2-haloethanols, torsional interaction, IR spectra, ab initio calcs., 2-dimens. model 0-74160  
 halogermane radical anions, ESR spectra and struct. 0-87153  
 halomethanes, absorpt. coeffs. meas. in Nd laser emission band 0-78620  
 halomethanes, surface tension temp. dependence from triple point to critical point (*German*) 0-100376  
 5-halouracils, solid, radiation damage, free radicals in 5-fluorouracil single crystals. 0-71926  
 s-halouracils, solid, radiation damage obs., deoxyribose ring opening in single crystals. 0-71929  
 heavy-ion induced desorption of organic cpds. from solid surfaces 0-100739  
 n-heptane liqs., refractive index, pressure effect 0-71375  
 n-heptane/3-pentanone mixture, vap. press. meas., thermodynamic functions calcs. 0-75345  
 heptanoic acid, associated vapours, homogeneous nucleation 0-96638  
 n-heptyl-4-cyanobiphenyl, nematic phase, dielec. loss, diffusion equations 0-71305  
 p-p'-n-heptyl-cyanobiphenyl-isotropic solute systems, nematic-isotropic phase transformation, volumetric study 0-92653  
 4-n-heptyl-d<sub>5</sub>-oxybenzoic acid-d<sub>1</sub>, nematic and smectic phases, mol. and relative segmental order 0-96439  
 heptyloxyazobenzene, filamentary structures 0-107051  
 4-n-heptyloxybenzylidene-4'-n-hexylaniline, nematic and smectic phases, long mol. axis reorientation, LF dielec. dispersion 0-70124  
 4-n-heptyloxybenzylideneamino-4'-cyanobiphenyl, reentrant nematic phase and low temp. smectic phases 0-88031  
 heterocyclic anion radicals, electron transfer with anthracene-amine cation radicals, triplet state electrogeneration 0-63803  
 heterocyclic aromatic molecules, Penning electron spectra and photoelectron spectra, rel. intensities 0-95725  
 heterocyclic compounds, bond lengths, fifth overtone of C-H stretching vibrs. obs. 0-91528  
 heteroexcimers, intramolecular, picosecond time-resolved fluorescence studies 0-83401  
 hexa-n-alkoxy-triphenylene disc-like solute effect on orientational order of nematic EBBA 0-79682  
 hexachloroparaxylene, crystn. from heptane, optimising purification 0-100774  
 hexadecachlorophthalocyanato-copper discrimination of individual atoms in mol. images 0-100226  
 1,2 hexadecanediol, inelastic electron tunnelling spectroscopic study of lubrication props. 0-70302  
 hexadecanoic acid, inelastic electron tunnelling spectroscopic study of lubrication props. 0-70302  
 hexadecanol, inelastic electron tunnelling spectroscopic study of lubrication props. 0-70302  
 1,5-hexadiyne, time-depend. mass spectra, ionisation efficiency and breakdown curves 0-95747  
 1-Shexadiyne ion+neutral 1,5-hexadiyne, trapped-ion mass spectrometry 0-97694  
 hexafluorobenzene, IR multiphoton excitation, vibr. energy redistrib. and hot band spectrum 0-95656  
 hexafluorobenzene, liq., self-diffusion and density as functions of press. and temp. 0-92696  
 hexafluorobenzene anion-radicals in squalene, ESR spectrum optical detection 0-95655  
 hexafluorobenzene liq., electron mobility, percolation model 0-65551  
 hexafluorobenzene radical anion, <sup>13</sup>C hyperfine interaction, EPR obs. 0-83392  
 hexafluorobenzene-benzene liq. mixture, electron mobility, percolation model 0-65551  
 hexafluorobenzene-n-paraffins, binary liquid solns., self diffusion, spin echo meas. 0-65263  
 hexafluorocyclopropane, centrifugal distortion const. and thermodynamic functions calc. 0-95582  
 hexafluoroethane, chemical conversion and uniformity of etching SiO<sub>2</sub> in radial flow plasma reactor 0-76391  
 hexafluoroethane, photochem. prod., <sup>13</sup>C enrichment (*French*) 0-91615  
 hexafluoroethane, RF discharge chem., added acetylene effect, mechanistic model for fluorocarbon plasmas 0-84017  
 hexafluoroethane, rot. barriers, MS-SCF-X<sub>n</sub> calcs. 0-106267  
 bis(1,1,1,5,5,5-hexafluoropentane-2,4-dionato)dioxouranium (VI), isotope selective IR laser induced unimol. dissoc. 0-69197  
 hexafluoropropylene-<sup>18</sup>F nonequilibrium effects in moderated nuclear recoil experiments 0-89509  
 hexamethylbenzene in tetrachloromethane soln., local mode overtone bands 0-83444

## organic compounds continued

hexamethyldisiloxane plasma polymerised thin film, charge trapping characteristics. 0-96895  
 hexamethylenetetramine, mol. ultraslow rot. obs. using D probe spin alignment tech. 0-88890  
 hexamethylenetetramine, thermal cond. and heat capacity under press. 0-80008  
 hexamethylenetetramine, ultraslow tetrahedral jumps, deuteron NMR spin alignment obs. 0-66046  
 hexamethylethane, <sup>13</sup>C-<sup>13</sup>C dipolar interaction, NMR longit. cross relax. 0-93196  
 n-hexane, superheated, thermodynamic props. from ultrasound speed 0-92036  
 n-hexane liqs., refractive index, pressure effect 0-71375  
 n-hexane-cyclohexane mixture, viscosity and density, 25 to 100 C, up to 500 MPa 0-103510  
 n-hexane-ethanol liq. mixtures, electron mobility, percolation model 0-65551  
 n-hexane-perfluoro-n-hexane mixtures, US vel. and absorpt. mixtures 0-88281  
 n-hexane/3-pentanone(acetone) mixtures, vap. press. meas., thermodynamic functions calcs. 0-75345  
 hexanes, isomeric, 0-95732  
 hexanes, isomeric, unimol. decomp. processes following field ionisation, temp. depend. 0-95733  
 hexatriene, excitation spectra, cluster configuration method appl. 0-78546  
 hexatriene, polarisability, nonlinear elec. susceptibility, SCF calcs. 0-95547  
 1,3,5-hexatriene radical cation, in Ne matrix, laser induced fluoresc. and emission spectra 0-87163  
 hexose monophosphate, effects of X-irrad. on shunt pathway in human lymphocytes 0-76798  
 4-n-hexyloxybenzylidene-4'-n-hexylaniline, nematic and smectic phases, long mol. axis reorientation, LF dielec. dispersion 0-70124  
 hippuric acid, solid, second moment meas. by wide-line NMR 0-108081  
 hippuric acid, X-irrad. single cryst., <sup>14</sup>N and <sup>1</sup>H ENDOR study; 0-71240  
 hydrazone-oxyhaemoglobin interaction,  $\gamma$ -reson. spectroscopy 0-81525  
 hydrazine, decomp. on Ir(111) surface, N<sub>2</sub> emission, ang. depend. 0-97731  
 hydrazine, rocket fuel in ambient air, CO<sub>2</sub> laser absorption spectra and photoacoustic detection 0-104540  
 hydrazine adsorbed on Al, decomp., XPS obs. 0-92783  
 hydrocarbon formation on interstellar graphite grain surfaces 0-82458  
 hydrocarbon ions, mass spectra, H atom scrambling, delocalisation 0-58135  
 hydrocarbon molecules adsorbed on specimen surface, contamination by surface diffusion 0-99013  
 hydrocarbons, 30.4 nm He(II) photoelectron spectra 0-82589  
 hydrocarbons, <sup>13</sup>C chem. shifts, simplex optimised INDO calcs. 0-83284  
 hydrocarbons, alternate conjugated, topological props. of HOMO-LUMO separations 0-69049  
 hydrocarbons, aromatic, ultrasensitive detection by two-photon photoionisation 0-104473  
 hydrocarbons, atmospheric, potential contrib. to photochemical air pollution form. in United Kingdom 0-76682  
 hydrocarbons, average elec. polarisabilities and mag. susceptibilities, ab initio valence electron calcs. 0-87033  
 hydrocarbons, cyclic, non alternant, nonsingle instabilities of HF solns. 0-58164  
 hydrocarbons, liq., Compton profiles, bond additivity 0-93423  
 hydrocarbons, non-alternant, reson. energies 0-106278  
 hydrocarbons, thermal conductivity, corresponding states model 0-69964  
 hydrocarbons in Jupiter atmosphere, photochemistry rel. to Lyman alpha albedo 0-105194  
 1-hydronaphthyl radical, 4.2K absorpt. spectrum (*French*) 0-80809  
 hydronaphthyl radicals embedded in naphthalene cryst., optical transition energies and ionisation energies 0-78595  
 hydrophobic compounds, effect on luminesc. of spectrally sensitised AgBr microcrysts. 0-97331  
 hydroquinone developer, lith development mechanism 0-77889  
 $\beta$ -hydroxy acrolein, lower excited states, electronic struct. and H-bonding, ab initio SCF and CI calcs., photochemical mechanism 0-83278  
 4-hydroxy-2,2,6,6-tetramethylpiperidine, radiation-induced oxidation to paramag. nitroxide free radicals 0-81341  
 p-hydroxy-trans-cinnamic acid, cryst. struct. basis for absence of thermal mesomorphism 0-96509  
 para-hydroxyaniline, mol. complex., electronic struct., basis set and correlation effects 0-91436  
 hydroxymethyl radical +O<sub>2</sub>, rate coefficient meas. by laser magnetic resonance flow tube method 0-66767  
 8-hydroxyquinoline+Ti<sub>2</sub>CO<sub>3</sub>, solid state reaction 0-108708  
 hydrocarbons, on activated C, rel. between adsorption and polarizabilities 0-76558  
 imidazole, quadrupole coupling consts. interpretation, ab initio field gradient calcs. 0-58282  
 1-indanone, T<sub>1</sub>-S<sub>0</sub> intersystem crossing, nonradiative decay rate, excitation energy depend. 0-63609  
 indigo derivatives, fluorescence decay times, meas. by synchroscan streak camera 0-84759  
 industrial gaseous environment characterisation, Brinkley method 0-93817  
 interstellar grains, organic composition, IR obs. 0-77460  
 interstellar grains comprised of organic cpds., 3.4 microns absorpt. obs. 0-109514  
 interstellar organic compounds, gas phase chemistry model in diffuse and dense clouds 0-105298  
 inversion geometry, ab initio SCF calcs., basis set effects 0-78532  
 2-iodoacetamide, mol. struct., electron diff. obs. 0-63819  
 iodobenzene, liquid, vibr. relaxation, Brillouin spectra 0-108219  
 iodobenzene, soln., non-linear dielec. effect, comparison with fluoro, chloro and bromobenzene 0-60478  
 iodobenzenes, in potassium laurate mesophase, NMR, proton distance ratios and order tensor elements calcs. 0-63672  
 iodogermane radical anion, ESR spectra and struct. 0-87153  
 iodomethane, P-line and  $\nu_6$  band spectra using CO<sub>2</sub> laser absorpt. 0-69142  
 iodomethane, Raman band shapes, mol. oscill. bands (*German*) 0-69154  
 iodomethyl radical, vibr. excited, photofragmentation IR emission obs. 0-87162  
 3-iodopropene, rot. spectra, quadrupole hyperfine struct. 0-91545



## organic compounds continued

iodotrifluoromethane, high vibr. state excitation in high-power laser field, spectral charact. 0-91562  
 iodotrifluoromethane, IR multiphoton selective dissoc., effect of acceptor radicals 0-66854  
 ionisation potential and electron affinities of molecule containing C, N, O, and H atoms, semiempirical calcs. 0-78535  
 IR photoacoustic spectroscopy of solids and surface species 0-90909  
 (iron, chromium) carboxylates, heteronuclear trimer exchange clusters, ESR spectra 0-80603  
 iron formate dihydrate, mag. sp. ht.,  $S_z$ -term 0-60289  
 iron phthalocyanine, annealed, elec. cond., daylight exposure and thickness effect (*French*) 0-84484  
 10H-isalloxazine, and derivatives electronic struct., photoelectron spectrosc., and ab initio study 0-106261  
 isobacteriochlorins,  $\pi$  cation radicals, implications for  $\text{NO}_2^-$ ,  $\text{SO}_2^-$  reductases 0-63684  
 isobutene +  $\text{C}_2\text{O}$ , absolute reaction rate consts. meas. by laser induced fluorescence 0-93738  
 isobutylene, liq., vibr. phase relax. and freq. shifts, density and temp. effects 0-74235  
 isobutyric acid- $\text{H}_2\text{O}$ , liquid-vapour surface tension near liquid-liquid consolute point 0-107613  
 isobutyric acid-water critical mixtures, US and hypersonic study 0-88268  
 isobutyric acid-water near-critical liquid mixture, nucleation 0-92664  
 isocitrate dehydrogenase from *Azotobacter vinelandii*, essential amino-acid residues identification 0-76538  
 4-isocyanate-trans-stilbenes, donor substituted, anisotropic fluoresc. in low viscosity solvents (*German*) 0-93401  
 isooctane-benzonitrile mixture, dielec. const. near consolute point, temp. and freq. depend. meas. 0-71292  
 isopinocampheol, methyl groups internal rot.  $^{13}\text{C}$  spin lattice relaxation times and force field calcs. 0-74255  
 isopropanol-n-propanol aq. mixtures, US relax., US absorpt. and vel. meas. (*French*) 0-103426  
 isopropyl alcohol, adsorbed on ZnO, decomp., IR and kinetic obs. 0-59780  
 isopropyl benzene, mol. solid, temp. depend. UPS linewidths 0-89115  
 isopropyl radical, Ar matrix isolated, IR spectra and UV photolysis 0-66827  
 isopropyl radical, pot. energy surfaces, ab initio UHF calcs. 0-106258  
 isopropylaniline having optically active modes, vibr. relax. studied by absorpt. and fluoresc. spectra 0-83340  
 isopropylcyclopropane, solid, liquid, vapour phase, IR and Raman vibr. spectra 0-84740  
 isoquinoline, adsorbed on Ag, surface enhanced Raman spectrum 0-100400  
 isothiazole, rot. Zeeman effect, localised susceptibilities 0-91600  
 isovaline radiolacemization, cosmochemical implications 0-62087  
 kerosene-air flame laser induced fluorescence spectra obs. 0-91587  
 $\beta$ -lactam antibiotics, ab initio SCF-MO-LCAO calcs., amidic bond breaking, methoxy substitution effect 0-78533  
 lactams, N-methylated, cis-trans isomerism,  $^1\text{H}$  and  $^{13}\text{C}$  NMR obs. 0-106335  
 l-lactic acid,  $^{11}\text{C}$ -labelled, enzymatic synthesis 0-61695  
 lanthanide complex, struct. and equilib. by time resolved Eu(III) spectrosc. 0-78736  
 lanthanide ion bound to macromol., struct. and equilib. by time resolved Eu(III) spectrosc. 0-78736  
 lanthanide-porphyrin complexes, upper  $\pi\pi^*$  electronic states, fluoresc. 0-83410  
 lanthanum ethyl sulphate:Pr, phase transition under pressure, absorpt. spectra (*Russian*) 0-92667  
 lanthanum ethylsulphate: $\text{Gd}^{3+}$ , zero-field splitting, contributory mechanism 0-80231  
 lanthanum nicotinate dihydrate, cryst., nucl. quadrupole interactions, D atom coords., ENDOR obs. 0-97161  
 laser far IR pulse generation by Q-switched  $\text{CO}_2$  laser pump source 0-69383  
 lasing, excitation by excimer laser radiation 0-64007  
 lead phthalocyanine: $\text{O}_2(\text{I})$ , Schottky barrier effect on AC current response 0-75623  
 lead stearate, Langmuir-Blodgett multilayers, comp. and transfer mechanism 0-80125  
 lipid hydrocarbon chain, biomembrane, rot. motion and fluidity 0-76714  
 lipid peroxide formation in irradiated synthetic diets, storage effects 0-101025  
 lipids, struct. order in membranes, fluoresc. anisotropy data eval. 0-97873  
 liquefied petroleum gas, burning velocity, gas comp. and air/fuel ratio effects 0-66804  
 liquid, Moelwyn-Hughes parameter calc. from US data 0-59375  
 liquid, thermal cond., comparison of predicted values with experimental results at different temps. 0-103523  
 liquid binary mixtures, evaluation of excess internal pressure, Van der Waals' constant and ultrasonic velocity from Flory's theory 0-70310  
 liquid chromatography effluents on line anal., micro liq. chromatography-interfaced Fourier transform IR spectrophotometer 0-73483  
 liquid organic compound ionisation under atm. press. 0-86488  
 liquid phase elution chromatography for determining solubilities of organic liq. in  $\text{H}_2\text{O}$  0-71958  
 liquids, diamagnetism, mass mag. suscept. meas., temp. depend. 0-97054  
 lithium acetate, methyl groups, spin symmetry species, neutron scatt. transitions 0-92470  
 lithium ammonium tartrate dihydrate, ferroelectric-elastic phase transition, theoretical model and expt. (*Russian*) 0-75961  
 lithium formate, optical phonons, small oscillator strength meas. from frequency-angular polariton spectra 0-92629  
 lithium formate cryst.,  $90^\circ$  phase matching 0-58634  
 lithium oligopentadienyl and complexes, IR spectra (*Russian*) 0-71424  
 lithium osalate, neutron inelastic scatt. spectra in 2200-200  $\text{cm}^{-1}$  range 0-70327  
 lithium thallium tartrate, sp. ht., 0.3 to 25K, second-order ferroelec. transition 0-59674  
 long-chain organic molecules diffusion through polymer matrix, hydrostatic press. effect on diffusion coeff. 0-92697  
 lutetium diphthalocyanine, solid-state anion migration in anodic oxidation 0-60994  
 2,6-lutidine-water, anomalous supercooling near critical point 0-70384  
 2,6-lutidine-water critical mixture, spinodal decomposition, Rayleigh scatt. 0-70416

## organic compounds continued

2,6-lutidine-water thick films, interferometric obs. of crit. behaviour 0-93266  
 lysine, aq. solns.,  $\text{H}^+(\text{D}^+)$  exchange rates,  $^{17}\text{O}$  NMR linewidths, pH depend. 0-91661  
 magnesium hexahydrate  $\text{H}_2\text{EDTA}:\text{VO}^{2+}$ , single cryst., ESR spectra and spin Hamiltonian parameters 0-75845  
 malonic acid, and  $\alpha$ -alkyl derivatives, photoelectron spectra, lone-pair interactions 0-58315  
 malononitrile, cryst., phase transitions, Raman and IR obs. 0-88980  
 manganese acetate tetrahydrate, paramag. susceptibility, spin trimer model 0-97055  
 manganese adipate dihydrate, cryst. struct., H-bonding and O atom coordination 0-96506  
 manganese carboxylate, dodecanuclear mixed-valence, prep., struct., and mag. props. 0-107196  
 manganese formate dihydrate, Zn- and Mg-substituted, anomalous crit. phenomena 0-60316  
 manganese stearate: cadmium stearate, dil. quasi two-dimensional, ESR line width 0-71155  
 manganese stearate, Langmuir-Blodgett layers, high resolution X-ray diff. 0-80126  
 manganese stearate, two-dimensional mag. struct. 0-108040  
 MBBA, dielec. relax. in metastable modification of solid phase 0-84689  
 MBBA, flexoelec. coeff. in nematic phase, thermal depend. 0-79685  
 MBBA, fluorinated analogues, mesomorphic props. 0-70118  
 MBBA, frozen nematic glass, EPR spectra of copper and cobalt triazene-1-oxide complexes 0-88871  
 MBBA, IR absorpt. spectra, elec. field effects, orientational order parameter determ. by IR dichroism, bend elastic consts. 0-80778  
 MBBA, isotropic, surface-induced ordering 0-108176  
 MBBA, nematic, flexibility gradient of fatty acid spin labels, EPR study 0-71181  
 MBBA, nematic, mol. alignment on  $\text{SiO}$  film, film thickness effects 0-59384  
 MBBA, nematic liq. cryst., nonlinear optical amplification above Frederiks transition 0-95937  
 MBBA, nematic-isotropic transition at high press., turbidity meas. 0-92655  
 MBBA, NMR and Raman scatt. studies in nematic phase 0-100619  
 MBBA, orientational order in glassy and nematic phases, IR dichroism meas. 0-64891  
 MBBA, proton spin-lattice relax. in crit. regime 0-80631  
 MBBA, Raman spectra in cryst., frozen glassy, and liq. cryst. states 0-60601  
 MBBA, Tsvetkov parameter, temp. depend. 0-88035  
 MBBA nematic liquid crystals excited by 20 MHz US surface waves, acousto-hydrodynamic effects 0-76003  
 MBBA-cholesteryl nonanoate, liq. cryst. mixture, two colour display device 0-70116  
 MBBA- $\text{d}_{13}$ ,  $^1\text{H}$  spin-lattice relaxation, intermol. and intramol. contribs. 0-75873  
 MBBA- $\text{d}_{13}$ , nematic phase, rot. frame spin-lattice relax. 0-84668  
 MBBA-EBBA, controllable liq. cryst. transparency, electrooptical charact. 0-78996  
 MBBA-n-heptane, nematic soln., lattice model, thermodynamic functions (*Russian*) 0-64896  
 menthane ring compounds, Raman circular intensity differential spectra obs., mol. struct. 0-87130  
 mercuric trifluoroacetate, staining of polymer blends for TEM obs. of morphology 0-84103  
 metalloporphyrin, cation radical formation by pulse radiolysis, oxidation and demetalation rate consts. 0-61505  
 metalloporphyrin, low symmetry environment, Raman excitation spectra and absorpt. spectrum 0-74172  
 metalloporphyrins, two quantum fluoresc. excitation from higher excited electronic states 0-106350  
 methane, 25 to 40 eV electron dissoc. ionisation, proton formation 0-91690  
 methane,  $2\nu_3$  band,  $R_1$  line, spectrum reconstruction using test response 0-77884  
 methane,  $^{12}\text{C}$  and  $^{14}\text{C}$ , line parameters for  $\nu_2$  and  $\nu_4$  bands, isotope shifts, appl. to planetary atmospheres 0-95622  
 methane,  $^{13}\text{C}$  and  $^{12}\text{C}$ , line strength ratios of  $2\nu_3$  singlet 0-78616  
 methane, absolute line strengths meas. using dual-beam diode laser spectrometer 0-101853  
 methane, appl. of band-model parameters to Uranus visible and near IR spectrum 0-98609  
 methane, bond bending, bond orbitals rel. to nucl. motion 0-95513  
 methane, coord. bond calcs. 0-58129  
 methane, core 1s shakeup study, XPS and Xalpha calcs. 0-69064  
 methane, crystalline, struct. and compression at high press., room temp. 0-107199  
 methane, dilute gas, transport props., simple pair pot. model 0-87835  
 methane, energy quantities from localised charge densities, dependence on geometry and basis set 0-63525  
 methane, enrichment of D using vibrationally sensitized reaction 0-76532  
 methane, force consts. by modified Redington and Aljibury method 0-69261  
 methane,  $\text{H}_2$  production by steam reforming of natural gas, chemical kinetics 0-97815  
 methane, harmonic and anharmonic matrix elements comparison, appl. to vibrational energy transfer 0-63760  
 methane, intermolecular interaction energies calcs. using minimal basis sets 0-78681  
 methane, IR anal. of  $\nu_2$  and  $\nu_4$  bands (*French*) 0-87113  
 methane, Jovian line profiles near  $1.1 \mu$  as probe of cloud struct. and C/H ratio 0-62067  
 methane, liq., pure vibr. Raman spectra 0-97262  
 methane, liquid, comparison on interaction induced light scatt. and IR absorption 0-60561  
 methane, liquid, opto-acoustic study of weak optical absorpt. 0-93278  
 methane, longitudinal variability in Jupiter atm. visible spectra 0-82270  
 methane, mantle related thermodynamic props. and reactions at high press. and temp. 0-81874  
 methane, melting transitions, thermodynamic props., positional disordering energies 0-96452  
 methane, mol. cations, struct., Jahn-Teller effect, MINDO/3 calcs. 0-74135  
 methane, nucl. elec. shielding tensor calcs. 0-83296



## organic compounds continued

- methane, optical Ramsey resonance, in three separated fields produced by corner reflector, theory 0-74166  
 methane, orbital relax. energy for single and double ionis. from valence shells 0-106253  
 methane, outgassing from Ti sublimation pump 0-77796  
 methane, phase II, nuclear spin-lattice relax. and site symm. 0-97155  
 methane, photoacoustic Raman spectroscopy under pulsed laser excitation 0-82825  
 methane, pot. energy curves, Monte Carlo and SCF LCAO MO calcs. 0-63526  
 methane, quantum mech. rot. partition function 0-102501  
 methane, rotational state, avoided-crossing molecular beam spectroscopy 0-63730  
 methane, saturated absorpt. meas. at 3.39  $\mu\text{m}$  using multipath cell 0-74442  
 methane, SCF calcs. including polaris. functions 0-87034  
 methane, solid, melting curves, Lennard-Jones Devonshire theory 0-65201  
 methane, solid, phase II, Raman spectrum, vol. and temp. depend. 0-97260  
 methane, solid, plastic phase, mol. dynamics simulation 0-79715  
 methane, total scatt. cross sections for intermediate-energy positrons 0-91692  
 methane, troposphere vertical profile, eastern USA in winter 0-77035  
 methane, V-V energy transfer 0-83469  
 methane+ $^{18}\text{F}$ , nonequilibrium effects in moderated nuclear recoil experiments 0-89509  
 methane+Br $^+$ , total electron detachment cross sections for energies around threshold 0-99550  
 methane+Cl $^+$ , reactions at room temp. 0-93749  
 methane+H $_2\text{O}^+$ , rate constants determ. as function of relative kinetic energy 0-81292  
 methane+H $^+$ +H $_2^+$ +methyl radical, quantum calcs. 0-71911  
 methane+H, abstraction and exchange reaction, barrier height calc. using POL-CI wave functions 0-81304  
 methane+He $^+$ , 0.7-2 MeV, charge-changing collisions, electron capture 0-58372  
 methane+Kr $^{2+}$ , charge transfer reactions, rate coeffs. and product-ion distributions meas. 0-104431  
 methane+N $_2$ , N $_2$  fixation, catalytic processes in non-equilibrium plasma chemical reactors (*French*) 0-89483  
 methane+N $_2^+$ , deactivation, from laser-induced CO $_2$  fluoresce. obs. 0-63776  
 methane+Ne $^{2+}$ , charge transfer reactions, rate coeffs. and product-ion distributions meas. 0-104431  
 methane+O-methyl radical+OH reaction, photolytically initiated, high temp. kinetics meas. technique 0-61085  
 methane+O( $^1\text{P}$ ), barrier height and transition state geometry, POL-CI calc., H abstraction reaction 0-66782  
 methane+Rb,  $5^2\text{P}_{1/2} \rightarrow 5^2\text{P}_{3/2}$  excitation transfer cross section temp. depend. 0-91630  
 methane+SF $_6$ , vibr.-vibr. relax 0-99537  
 methane-(d $_4$ )+HF, collision relaxation rate constants and rot. equilibration time meas. 0-69213  
 methane 7300  $\text{\AA}$  band in Neptune atm., limb brightening, photometry obs. 0-82297  
 methane adsorbed submonolayer on graphite, structural transitions between epitaxially ordered phases 0-96740  
 methane backward Raman amplifier, KrF laser driven, high-efficiency energy extraction 0-106533  
 methane cation, photodissoc., ab initio RHF and MRD CI calcs. 0-95695  
 methane E-component stabilisation of He-Ne laser, freq. reproducibility 0-106507  
 methane He-Ne FM eliminated laser, freq. stability meas. 0-87423  
 methane locked freq. stabilisation of 3.39  $\mu\text{m}$  He-Ne laser in dual feed-back control 0-99772  
 methane locked He-Ne laser, freq. stability meas. 0-87422  
 methane production from cellulose by sewage bacteria 0-72005  
 methane stabilised He-Ne ring laser, nonlinear resonance freq. shift due to back scatt. (*Russian*) 0-78874  
 methane triple point sealed cells using stainless steel envelope 0-95099  
 methane-Ar proportional counter, light emission obs. 0-78488  
 methane-CO $_2$  reforming-methanation cycle for Solchem thermochemical solar energy transport 0-94096  
 methane-d $_0$ -(d $_4$ ), binary collision-induced light scatt., rot. Raman scatt. 0-78660  
 methane-d $_0$ -(d $_4$ ), binary collisions induced light scatt. 0-83428  
 methane-d $_0$ -(d $_4$ ), unimol. decomp., energy transfer processes, Monte Carlo simulation 0-99555  
 methane-d $_0$ -(d $_4$ ) vibrational state rotational struct., CARS spectra (*Russian*) 0-99513  
 methane-d $_1$ , high resolution spectra, line intensities, ground-state rot. const. determ. 0-83517  
 $\alpha$ -methane-d $_4$ , crystalline, X-ray powder diff. study 0-96500  
 methane-d $_4$ , solid, rot. tunnelling, neutron scatt. obs., isotope effect 0-92468  
 methane-d $_4$ , solid, tunnel splittings, heat capacity meas. 0-96451  
 methane-d $_4$ , vibr.-translational relax. 0-99537  
 methane-d $_4$ +Ar, vibr.-translational relax. 0-99537  
 methane-d $_4$ +methane, vibr. relaxation 0-99537  
 methane-d $_4$  (*Russian*) 0-91540  
 methane-d $_4$  monolayer films on graphite, neutron diffr. studies of phases 0-96739  
 methane-d, 4.5  $\mu\text{m}$  absorpt.,  $2\nu_6$  overtone band anal. 0-91557  
 methane-d, Doppler-free optical double reson. spectroscopy using single-freq. laser and modulation sidebands 0-68274  
 methane-methane interactions, expansion of intermol. energy in set of symmetry-adapted functions 0-106371  
 methane-N $_2$ , liq., N $_2$  Raman scatt. parameters, high resolution coherent active spectroscopy 0-66207  
 methane-N $_2$ , rapidly developing discharge, streak camera records interpretation 0-59280  
 methane-N $_2$ -isobutane gas mixture composition by Raman spectra 0-87124  
 methanes,  $^{12}\text{CH}_4$  and  $^{13}\text{CH}_4$ , IR spectra obs., anal. of  $\nu_2+\nu_3$  band 0-95614  
 methanol,  $\beta$ -irrad., radical truck struct., electron spin-echo obs. 0-93776  
 methanol, adsorption and decomp. on Ni (100) 0-66876

## organic compounds continued

- methanol, aqueous, damped coupled oscillator model used to study Fermi resonance 0-69152  
 methanol, coord. bond calcs. 0-58129  
 methanol, dissoc. ionisation mechanism, correlation diagram approach, mass spectra obs., metastable processes 0-95728  
 methanol, electron solvation, ps laser study 0-101032  
 methanol, far IR laser, intracavity pumped by TE CO $_2$  laser 0-87382  
 methanol, intermolecular interaction energies calcs. using minimal basis sets 0-78681  
 methanol, interstellar, 84.5 GHz and 96.7 GHz lines obs. in Sagittarius B2 and Orion A 0-62245  
 methanol, ionic dissoc., photoelectron-photoion coincidence spectroscopy 0-66774  
 methanol, liq., diamagnetism, mass mag. suscept. meas., temp. depend. 0-97054  
 methanol, molecular geometry optimisation, variable metric method, internal geometry 0-95744  
 methanol, multiphoton absorpt. and dissoc. 0-99530  
 methanol, optical pumping of far-IR molecular lasers by CW CO $_2$  waveguide laser 0-83615  
 methanol, optically pumped CW for IR laser lines, freq. meas. 0-58514  
 methanol, optically pumped CW subMM emission lines 0-95876  
 methanol, processes of photoionisation studied using ion-electron coincidence method 0-74204  
 methanol, trace detection using phase fluctuation optical heterodyne spectroscopy 0-68266  
 methanol, vibr. dephasing theories, test using selective coherent ps. Stokes scatt. 0-59609  
 methanol+Ar(Kr), methoxy radical prod., UV emission spectra 0-91572  
 methanol+H $_2^+$ , dissoc. charge transfer reaction studied at rel. translational energies from 600 eV to 5000 eV 0-104432  
 methanol+He $^+$ , dissoc. charge transfer reaction studied at rel. translational energies from 600 eV to 5000 eV 0-104432  
 methanol 118  $\mu\text{m}$  laser line, simple accurate method for wavelength meas. 0-106554  
 methanol (-d), H-bonding investigated with supersonic mol. beam using photoionisation quadrupole mass spectrometer 0-102543  
 methanol adsorption on Cu(110), XPS, UPS and thermal desorpt. study 0-84388  
 methanol derivation from lignite, fuel appl. 0-61223  
 methanol far IR laser, CW laser pumped, saturated and small signal gain calc. 0-58521  
 methanol far IR laser, twin optically pumped, for plasma diagnostics 0-59306  
 methanol far IR laser emission spectroscopy 0-58524  
 methanol far IR laser gas, CW laser pumped, gain 0-69367  
 methanol far IR laser line Stark splitting obs. 0-58313  
 methanol far IR Stark spectroscopy and 9-P(34) CO $_2$  laser line 0-69145  
 methanol fuel, substitution of large proportion of diesel fuel in diesel engines 0-61230  
 methanol fuel for vehicles, gas turbines, and boilers, Brazil 0-61229  
 methanol laser, 118  $\mu\text{m}$ , diagnostic experiments and modelling 0-58515  
 methanol laser, CW, optically pumped, 170- $\mu\text{m}$  emission, press. shift 0-106510  
 methanol laser, optically pumped, use of crystalline reflector in cavity 0-64080  
 methanol masers in Orion, interferometric and multitransitional study 0-67891  
 methanol optically pumped 118.8  $\mu\text{m}$  laser line, Stark splitting obs. 0-102710  
 methanol solution in benzene, dielec. relax. time by RF cond. meas. 0-71302  
 methanol solvation of Ag, geometrical model, electron spin-echo modulation obs. 0-63682  
 methanol sorption effect on cross-linked polyester film struct. (*Russian*) 0-59405  
 methanol subMM laser line obs. 0-58523  
 methanol-CO-H $_2$ O-NH $_3$ , solid mixture vibr. modes, IR spectra 0-90504  
 methanol-d $_1$ , (CH $_3$ DOH), microwave torsional-rot. spectrum, rel. to interstellar search 0-99498  
 methanol-d $_1$ , CH $_3$ DOH optically pumped CW far IR laser lines and frequencies 0-102707  
 methanol-d $_1$ , laboratory freqs. of J=2-1, a-type transitions 0-63624  
 methanol-d $_3$ , multiphoton absorpt. and dissoc. 0-99530  
 methanol-d, optically pumped CW subMM emission lines 0-95876  
 methanol-ethanol (n-propanol)(n-butanol) binary systems, excess vol. of mixing, dilatometric meas. 0-59656  
 methine dyes, spectral props., solvent effects 0-69181  
 methotrexate-dihydrofolate reductase complex form., conform., laser Raman obs. 0-104553  
 methoxide surface complexes on Li, He(I) photoelectron spectra, MO calcs. 0-83417  
 methoxy, Jahn-Teller induced rovibronic effect, nuclear spin-electron spin hyperfine Hamiltonian 0-83298  
 methoxy+NO, reaction rate upper limit, laser induced fluoresc. 0-85200  
 p-methoxy benzonitrile, IR absorpt. spectra, vibr. assignments 0-95609  
 methoxy prod. from methyl nitrite photolysis 0-85200  
 methoxy radical, LMR spectra anal. 0-63677  
 methoxy radical+NO, reaction rate meas. 0-76534  
 methoxy radical and deuterate, vibronic level fluoresc. spectrum 0-58305  
 methoxy radical prod. from 266 nm photolysis of methyl nitrite 0-76534  
 methoxy species on Ni (111), photoelectron spectra, electronic struct. and orientation 0-83420  
 p-methoxy-benzoate-p-n-pentylbenzene, isotropic phase nematogen optical Kerr const. 0-78919  
 p-methoxybenzoate-p-n-pentyl benzene, slow non-critical mol. reorientation in isotropic phase 0-84062  
 p-(p'-methoxybenzylidene)amino-phenyl acetate, cryst. struct. rel. to liq. crystallinity 0-100225  
 p-methoxybenzylidene-cyanoaniline, mol. and cryst. struct., X-ray diffr. study 0-88134  
 methoxydifluorophosphines-d $_0$  and -d $_3$ , IR and Raman spectra, mol. vibr. and struct. obs. 0-87103  
 2-methoxyethanol, methyl torsional barriers to internal rotation calc. 0-95603  
 2-methoxyethylamine, microwave spectra, H-bond, torsional motion and mol. vibr. obs., rot. isomerism, mol. moments determ. 0-95603  
 methyl(-d $_3$ ) ions, association reactions, isotopic exchanges, SIFT study, review 0-58435  
 methyl acetate, microwave spectra and internal rot. 0-87100



## organic compounds continued

methyl alcohol, dielec. relaxation spectroscopy in microwave region, double-beam interferometry (*German*) 0-71309  
 methyl alcohol, liq., viscosity parameters, RF cond. meas. 0-96677  
 methyl alcohol laser, freq. meas. at 4.25 THz using Josephson harmonic mixer and phase lock techniques 0-95078  
 methyl alcohol submm wave laser, optically pumped, intracavity double resonance obs. 0-58522  
 methyl alcohol-d<sub>3</sub>, Fermi resonance due to large amplitude vibr. 0-83519  
 methyl allenyl sulphide, UV absorpt. spectra, role of 3d valence-shell and 4s Rydberg-type atomic orbitals 0-83384  
 methyl ammonium aluminium sulphate, ferroelec., proton spin-lattice relax. time anomaly 0-60440  
 methyl azidoformate, microwave rot. spectrum, satellite transitions 0-69127  
 methyl bromide, <sup>13</sup>C relaxation times anal. using J-diffusion model of mol. reorientation 0-87149  
 methyl bromide, mol. force field at SCF ab initio levels, quantum-mechanical calc., LCAO-MO method 0-106319  
 methyl bromide, NQR and A<sub>1</sub>-A<sub>2</sub> splitting, RF spectrosc. inside laser cavity 0-91579  
 methyl cation + NH<sub>3</sub>, reaction kinetics, 0.04-1 eV (*French*) 0-66768  
 methyl chloride, mol. force field at SCF ab initio levels, quantum-mechanical calc., LCAO-MO method 0-106319  
 methyl chloride, rot. anal. of IR absorpt. spectra, mol. vibr., rot. const. determ. 0-99505  
 methyl chloroform, vap., multiphoton dissociation by CO<sub>2</sub> laser beam 0-61123  
 methyl cyanide, CH<sub>3</sub>CN and CH<sub>3</sub>NC, <sup>15</sup>N quadrupole coupling consts., ab initio calcs. 0-58283  
 methyl cyanide, far IR laser line assignments 0-69380  
 methyl cyanide + Cs(K), collisional ionisation obs. 0-95716  
 methyl cyanide-Ar mixture, thermal compd. in mag. field 0-100058  
 methyl cyanide-water (methanol), Ag<sup>+</sup> ion solvation, γ-irrad., ESR obs. 0-97726  
 methyl ethyl ether, charact. vibr., isomer and isotope effects, rel. to reverse spectral problem 0-63613  
 methyl ethyl ketone, processes of photoionisation studied using ion-electron coincidence method 0-74204  
 methyl fluoride, <sup>13</sup>CH<sub>3</sub>F, high-power pulsed laser 0-69386  
 methyl fluoride, coord. bond calcs. 0-58129  
 methyl fluoride, deuterated, optically pumped near-MM laser 0-69379  
 methyl fluoride, harmonic force field calcs. and exptl. configs. 0-63865  
 methyl fluoride, laser collision-induced energy absorpt. and vibr. excitation 0-74233  
 methyl fluoride, mol. force field at SCF ab initio levels, quantum-mechanical calc., LCAO-MO method 0-106319  
 methyl fluoride laser far IR pulse generation by Q-switched CO<sub>2</sub> laser pump source 0-69383  
 methyl fluoride laser pumped with continuously tunable multiatm. CO<sub>2</sub> laser 0-69421  
 methyl fluoroformate, isomer conformation, CNDO and ab initio STO calcs. 0-58151  
 methyl furan-2-carboxylate, skeletal vibr. of IR spectra, conformational props., solvent polarity effect 0-87118  
 methyl furan-2-thiolcarboxylate, skeletal vibr. of IR spectra, conformational props., solvent polarity effect 0-87118  
 methyl glyoxal, electron affinity at centrosymm. trans geometry 0-87225  
 methyl group, <sup>13</sup>C chemical shifts, H/H, H/Me and Me/Me interactions 0-95652  
 methyl group, proton tunneling reson. at low temp. 0-108087  
 methyl halides, mol. force field at SCF ab initio levels, quantum-mechanical calc., LCAO-MO method 0-106319  
 methyl halides, semiclassical theory for collision induced vibr.-rot. transitions 0-63767  
 methyl halides, vibr. energy relax., opto-acoustic obs. 0-95711  
 methyl iodide, <sup>13</sup>C, NMR spectra, transition intensities, off-resonance proton spin decoupling influence 0-74183  
 methyl iodide, <sup>13</sup>C relaxation times anal. using J-diffusion model of mol. reorientation 0-87149  
 methyl iodide, and deuterated, pulsed subMM lasers pumped by CO<sub>2</sub> laser 0-106511  
 methyl iodide, liq., mol. reorientation, dielec. and viscosity meas. 0-100157  
 methyl iodide, mol. force field at SCF ab initio levels, quantum-mechanical calc., LCAO-MO method 0-106319  
 methyl iodide, van der Waals mol., electron self-scavenging 0-95727  
 methyl iodide + Na, anisotropic interactions from double rainbow struct., interaction pot. meas. 0-99540  
 methyl iodide mol. nonlinear resonant interaction with pulsed subMM radiation (*Russian*) 0-99523  
 methyl iodide photodissoc. laser, kinetic model, cross-section calcs. 0-58530  
 methyl iodide-acetone liq. mixture, excess energy of vaporisation, US study 0-65209  
 methyl ion + H<sub>2</sub>O(He) ternary association reaction in energy range 0.04-0.1 eV 0-71896  
 methyl ion + HD(D<sub>2</sub>), isotopic exchange, interstellar implications 0-61087  
 methyl isocyanide, laser induced thermal isomerisation, obs. by new time resolved IR photographic technique 0-57400  
 methyl isocyanide photoisomerisation, laser isotope separation, C-isotope enrichment by one-photon vibr. photochemistry 0-81336  
 3-methyl lumiflavin, in soln., absorpt. spectrum 0-58277  
 N-methyl m-fluoroaniline, conformational anal., microwave spectra obs. 0-58247  
 methyl mercaptan, CW subMM emission lines, optical pumping 0-87381  
 methyl nitrile CW for IR mol. laser, optical pumping with <sup>16</sup>CO<sub>2</sub> and <sup>18</sup>CO<sub>2</sub> lasers 0-74343  
 s-methyl nitrite, methyl group rot. barriers in cis and trans forms, ab initio calcs. 0-74111  
 methyl orange, aq. soln., reson. Raman spectra of D and <sup>14</sup>N isotopes 0-91566  
 methyl peroxynitrate, UV absorpt., spectra, photodissoc. lifetime meas. 0-83386  
 N-methyl pyrrole, resonantly enhanced multiphoton ionisation 0-106362  
 methyl radical, hyperfine coupling consts., vibr. depend., ab initio calcs. 0-87150  
 methyl radical, vibr. excited, photofragmentation IR emission obs. 0-87162  
 methyl radical + O(F), infrared chemiluminescence obs. 0-61080

## organic compounds continued

5-methyl-1-thia-5-azacyclooctane-1-oxide perchlorate, single cryst. transform., evidence for intermediate state 0-88078  
 4-methyl-2,6-ditertiarybutylphenol, methyl group reorientation, classical dynamics, NMR relax. and inelastic neutron scatt. 0-88066  
 methyl-d<sub>3</sub> ion + HD(H<sub>2</sub>), isotopic exchange, interstellar implications 0-61087  
 methyl-d groups, reorienting or tunnelling spin-lattice relax. 0-97156  
 N-methyl-N-nitrosourea, electronic interactions with DNA, ESR obs. and INDO calcs. 0-94154  
 N-methyl-p-fluoroaniline, struct. of HNCH<sub>3</sub> group 0-95741  
 N-methylacetamide, solid, Fermi resons. 0-97266  
 o-methylacetophenone, laser flash photolysis, temp. depend. 0-93770  
 methylacetylene, ν<sub>s</sub> band, microwave and IR laser Stark spectrosc. 0-91558  
 methylamine, affinities for H<sup>+</sup>(Li<sup>+</sup>)(K<sup>+</sup>)(CH<sub>3</sub><sup>+</sup>), ab initio SCF calculations 0-102443  
 methylamine, C-N and N-H bond nucl. mag. isoscreening line diagrams 0-78555  
 methylamine, coord. bond calcs. 0-58129  
 methylamine, photochemical conversion to HCN with ArF laser, mol. fluorescence, obs. 0-97710  
 methylamine intercalated with 2H-TaS<sub>2</sub>, supercond. layer cpd., crit. field enhancement and reduced dimensionality 0-60152  
 methylamine liquid, 293K, solvated, electron decay kinetics obs., IR spectra 0-71928  
 methylamine-HCl systems, H-bonded complexes studied by ab initio MO method, dipole moments determ. 0-83253  
 methylammonium aluminium sulphate dodecahydrate, single crystals, high-order EPR transitions of Cr<sup>3+</sup> 0-108052  
 methylammonium alums, dielec. relax. near transition point 0-71301  
 methylammonium bromide, solid, phase transitions, PMR, DTA study 0-107421  
 methylammoniumtetrachlorochromate, optical absorption intensity, short-range spin correlation 0-108185  
 9-methylanthracene, solubilisation in water by hypercoiled polymethacrylic acid 0-91591  
 methylated benzene-1<sub>2</sub>, σ-σ charge transfer complex, frozen soln., Mossbauer spectra obs. 0-91655  
 methylbenzenes, 3p Rydberg transitions, multiphoton ionis. spectrosc. obs. 0-95644  
 methylbicyclobutyl decomposition intramolecular vibr. relax., competitive channels 0-83336  
 methylcyanodiacetylene cation, gas phase, UV emission spectra of A(π<sup>-</sup>)-X(π<sup>-</sup>) band system 0-95636  
 methylcyclohexane-polystyrene, coexistence curve, comparison obs. and free energy calc. 0-88323  
 methylcyclohexane-polystyrene, coexistence curves, range of simple scaling and critical exponents 0-88322  
 (+)-(3R)-methylcyclohexanone, vibr. optical activity, Raman obs. 0-102499  
 methylene, B<sub>1</sub>-A<sub>1</sub> separation, ab initio 0-106251  
 methylene, singlet-triplet excitation energy, relativistic correction 0-69059  
 methylene bromide, <sup>13</sup>C, NMR spectra, transition intensities, off-resonance proton spin decoupling influence 0-74183  
 methylene chloride, in EBBA-d<sub>23</sub>, intermol. dipolar random field cross-relax. term obs. 0-60438  
 methylene glycol(-d<sub>4</sub>)=formaldehyde(-d<sub>2</sub>) + H<sub>2</sub>O(D<sub>2</sub>O) Raman spectra and normal vibr. 0-58271  
 methylene ion + HD(D<sub>2</sub>), isotopic exchange, interstellar implications 0-61087  
 methylene peroxide, struct., energy levels, ab initio UHF and MRUHF NO CI calcs. 0-83287  
 methylene-d<sub>2</sub> ion + HD(H<sub>2</sub>), isotopic exchange, interstellar implications 0-61087  
 4,4'-methylenebis(1,3,5-trimethyl-4-imidazolin-2-one), cryst. and mol. struct. 0-107201  
 methylfluoride, CW for IR mol. laser, optical pumping with <sup>16</sup>CO<sub>2</sub> and <sup>18</sup>CO<sub>2</sub> lasers 0-74343  
 methylglyoxal, fluoresc. mag. field effect 0-102535  
 methylhalosilanes + CCl(X)I<sub>2</sub>, reaction rate const. determ. by kinetic absorpt. spectroscopy 0-97683  
 methylhydroperoxide, UV absorpt. spectra of vap. 0-69159  
 1-methylindole-n-butanol (ethyl acetate), soln., ground state complex form., fluoresc. spectra, Stoke's shift origin 0-58299  
 1-methylnaphthalene, two photon absorptivity, ion cyclotron reson. photodissoc. spectra, CNDO/S-CI-perturbation theory 0-74123  
 methylnitrite VUV photodissoc., NO electronically excited photofragment identification and quantum yield 0-99527  
 3-methylpentane glassy matrix, localised electrons, cavity model 0-107743  
 3-methylpentane-nitroethane, dynamical scaling and crit. point universality 0-88297  
 3-methylpentane-nitroethane critical binary liquid mixture, US absorpt. 0-107376  
 methylpropylether, trans-trans isomer, microwave spectra, struct., dipole moment and rot. barriers calcs. 0-83348  
 methylpyridine adsorbed on Ag, surface enhanced Raman spectra 0-83376  
 β-methylumbelliferone in ethanol solns., spontaneous luminesc. kinetics 0-74192  
 methylviologen, photoreduction to H<sub>2</sub>, adsorbed on cellulose, hydrogen economy 0-81491  
 methylzinc methoxide, tetrameric, X-ray cryst. struct. determ. 0-107197  
 micellar systems, aqueous, thermochemistry 0-61133  
 mixture analysis by high-resolution mass spectrometry/mass spectrometry 0-104476  
 molecular crystal, doped, two-particle electronic excitation, optical cooperative excitation 0-93368  
 molecular systems, polarisabilities, susceptibilities, electron impact ionis. cross-sections calcs. 0-63835  
 molecules, small, harmonic force consts., vibr. freqs., integrated intensities, MINDO/3 method 0-58411  
 molecules in monolayers, reactivity 0-81367  
 molecules involving B and C atoms, self-consistent charge calcs. of core-electron binding energy shifts 0-69084  
 dimolybdenum tetraformate, metal-metal bond energy, SCF-Xα-SW calcs. 0-78538  
 monoadipate-tetraquo-cobalt (II), cryst. struct., H-bonding scheme 0-96504



## organic compounds continued

monobromomethane+CO<sub>2</sub> mixture, Raman laser optical excitation, electron photoionization theory (*Russian*) 0-99711  
 monochloroacetic acid, isolated molecules, internal rotation, CNDO/2 calcs., IR spectra 0-69254  
 monochloroacetic acid single crystal, Zeeman and <sup>35</sup>Cl NQR investig. 0-66066  
 2(4)-monooxypyrimidines, gaseous, matrix, soln., tautomeric equilib., IR and UV absorpt. spectra 0-58256  
 monostearine crystals, spiral growth from organic soln. 0-93467  
 myoglobin, atomic vibr. mean square displacement, Rayleigh scatt. of Mossbauer radiation meas. (*Russian*) 0-100665  
 myosin, X-irradiated ENDOR and ELDOR obs. 0-63689  
 myristic acid, associated vapours, homogeneous nucleation 0-96638  
 naphthalene: pentacene, intermol. interaction dynamics and optical dephasing 0-64112  
 naphthalene:anthracene, pure and doped, delayed fluoresc. (*French*) 0-80846  
 naphthalene:tetracene, electronic absorpt. spectrum, host-cryst. field effect 0-100669  
 naphthalene, charge carrier drift mobility, semi empirical anal. 0-65553  
 naphthalene, diaza derivatives, excited singlet and triplet states, charge densities, INDO calcs. 0-58152  
 naphthalene, dipole polarisability, finite-field SCF MO calcs. 0-83255  
 naphthalene, doped, role of nonequilibrium phonons in stimulated radiation emission 0-103971  
 naphthalene, electron and hole off-diagonal mobility component determ. 0-65552  
 naphthalene, electron trapping, one-carrier TSC and SCL currents 0-70715  
 naphthalene, external mode one-density states, low freq. Raman scatt. spectra (*French*) 0-76012  
 naphthalene, in naphthalene-d<sub>8</sub>, Anderson-Mott transition model for excitation transport 0-96812  
 naphthalene, in naphthalene-d<sub>8</sub>, energy trapping from localised states 0-100440  
 naphthalene, mol. cryst., reson. four-wave mixing, third order susceptibilities 0-100654  
 naphthalene, mol. crystal, meas. of US attenuation coeff. by optoacoustical methods (*French*) 0-70317  
 naphthalene, multiphoton ionisation, mass spectra 0-63717  
 naphthalene, out-of-plane mol. vibrs., force field approx. calcs. 0-91538  
 naphthalene, phosphorescence spectra in rare gas matrices, multiplet struct. and pot. energy functions 0-106341  
 naphthalene, prereson. Raman spectra, vibr. band intensities obs. 0-102515  
 naphthalene, pure and doped, exciton-phonon luminesc. 0-84773  
 naphthalene, ring currents hypersusceptibilities calcs. 0-102588  
 naphthalene, singlet and triplet excimer interactions, exciton resons. 0-95535  
 naphthalene, singlet and triplet exciton percolation, tunnelling and thermalisation 0-84432  
 naphthalene, singlet exciton transitions, energies and oscillator strengths, boson theory with PPP wavefunctions 0-92820  
 naphthalene, solid/melt interfacial tension and contact angles of small particles, determ. from crit. vel. of engulfing 0-79915  
 naphthalene, solution, structured UV spectrum obtained by ultrafast two-pulse excitation 0-78630  
 naphthalene, sublimation, mass transfer at vibr. spheres 0-57220  
 naphthalene, surface dynamics, calc. 0-92772  
 naphthalene, vibr. relax. studied by four wave mixing (CARS), spectral lineshapes obs. 0-80762  
 naphthalene anthracene, crystal second-order Stark shifts in optical spectrum of anthracene 0-88966  
 naphthalene crystal, dynamical matrix eigenvectors from Raman scatt. 0-100315  
 naphthalene crystal nucleation on anthracene microcrystals suspended in vapour-gas stream 0-76165  
 naphthalene crystalline complexes with octafluoronaphthalene, triplet exciton emissions 0-84760  
 naphthalene dispersed in benzene polycryst. host, active N<sub>2</sub> induced chemilum. 0-60691  
 naphthalene in Ar matrix, geometry changes and multiplet struct., mol. fluoresc. and phosphoresc. obs. 0-95663  
 naphthalene mixed crystals, dimer reson. self-energy 0-99459  
 naphthalene molecular ion, two and four photon absorpt., dissociation 0-74210  
 naphthalene molecule in durene and xylene crystals, vibronic interactions 0-84755  
 naphthalene single crystals, steady creep obs. 0-75296  
 naphthalene-β-naphthol, concentration effects in exciton absorption region 0-108241  
 naphthalene-β-naphthol mixture, exciton absorpt. depolarisation 0-103972  
 naphthalene-d<sub>8</sub>, cryst., phonon dispersion curves calcs., low temp. 0-96599  
 naphthalene-h<sub>8</sub> and d<sub>8</sub>, isotopic mixed crystals, exciton spectra in IR region 0-71400  
 naphthalene-naphthol solid soln. system, excess thermodynamic functions 0-107445  
 naphthalenes, methyl substituted radical cations, UHF spin densities, additivity model calcs. 0-58139  
 naphthalene complexes, H-bonded, form. of ion pairs in presence of crown ethers, proton-transfer photoreactions 0-85199  
 naphtho[1,8-cd:4,5-c'd']bis[1,2,6]thiadiazine, mol., electronic, cryst. struct. 0-64984  
 2-(1-naphthyl)-5-phenyloxazole, vap. phase dye laser media, photophysical parameters 0-95884  
 naphthyl group, excited singlet state, intramol. fluoresc. quenching by halogeno substituents 0-102537  
 1-β-naphthyl-2-N-piperidinoethane, intramol. exciplex form., ground state conform. control 0-102547  
 β-naphthylamine, fluoresc. quenching and spectra, excited state reaction, red edge effect obs. 0-83400  
 naphthylamines, abnormal fluorimetric titration behaviour, kinetic anal., fluoresc. quantum yields and lifetime meas. 0-89560  
 naphthalene-m nitroaniline eutectic, excess thermodynamic functions 0-107445  
 natural gas mixtures, simulated, enthalpy and phase equil., correl. with modified Starling eqn. 0-61127  
 nematic liquid crqn. mixture, ZLI-207, nonideally oriented layers, Fredericksz transition dynamics 0-100163

## organic compounds continued

neopentane, diamond force const., rel. to crystal elastic consts., Raman freq., bulk compressibility and freq. assignments 0-65183  
 neopentane adsorbed on graphite, quasi two-dimens. fluid, NMR 0-102525  
 neopentane liq., local mode overtone bands 0-83444  
 nickel phthalocyanine film, electron acceptor surface states due to O<sub>2</sub> adsorption 0-88586  
 nickel-octaethylporphyrin, in benzene soln., reson. CARS and CSRS line shapes 0-74432  
 p-nitroacetophenone, effect on size of DNA mol. under electron irradiation 0-89807  
 n-nitroaniline, UV light effect on nucleation during crystallisation on anthracene surface 0-75478  
 nitroaniline admixture in TGS crystals, effect on thermal parameters 0-107580  
 p-nitroanilines, intramol. charge transfer satellites, XPS 0-78650  
 nitrobenzene<sup>-</sup>, positive ion formation energetics by negative ion charge stripping 0-78700  
 nitrobenzene, IR absorpt. and Raman bands, half-band width conc. depend. 0-74171  
 nitrobenzene, liquid and CCl<sub>4</sub> soln. shear waves and translation-rotation coupling obs. by depolarised Rayleigh scattering 0-71432  
 nitrobenzene/n-hexane (n-heptane), critical exponent β, phase coexistence curve anal., viscosity coeff. meas. 0-100327  
 nitrobenzol-n-hexane, hypersonic velocity, absorption temp. depend (*Russian*) 0-75303  
 nitrocellulose fibres, polarised light study 0-80736  
 nitrocyclopropane, vibr. spectra struct. and bonding 0-102520  
 nitroethane-3-methylpentane, liquid-vapour surface tension near liquid-liquid consolute point 0-107613  
 nitromethane, DETA sensitized, steady state detonation vel., chemical inhomogeneity effect 0-89493  
 nitromethane, solid, tunnel states investig. 0-103274  
 nitromethane, variable angle electron-impact excitation, transitions in 7-12 eV energy-loss range 0-69244  
 4-nitrophenyl-4-octyloxybenzoate/cholesteric liq. cryst. mixtures, helix pitch, temp. depend. 0-64895  
 l-nitropropane, gaseous, photolysis, primary processes, study at 22°C and 100°C 0-89507  
 nitrosamine, air sampling sorbents testing 0-77026  
 nitrosobenzene, fluoresc. quantum yields, determ. from Raman scatt. 0-58294  
 nitrosofluorene-lipid adducts, mutagenicity, ESR spectra investig. 0-91583  
 nitrosourea compounds, 2, anal. of interaction with X-radiation in rat brain tumour cells 0-72230  
 p-nitrotoluene crystal film, exciton spectrum, IR absorpt. and Raman scatt. 0-80771  
 nitroxide free radicals in liquids, electron spin-echo obs. 0-63685  
 nitroxide groups in crystals, H bonds and short intermolecular contacts 0-63855  
 nitroxide radical, long range Y-P hyperfine coupling, ESR spectra obs. 0-75858  
 nitroxide radicals, q- and A-tensor components, rot. mobility 2 mm EPR spectrosc. determ. 0-102530  
 nitroxide spin probes, unresolved hyperfine broadening convection in EPR, linewidth and Heisenberg spin exchange freq. determ. 0-71180  
 nitroxyl radicals, cyclic, conform. flexibility, EPR obs. 0-91581  
 NMP-TCNQ, partial charge transfer effect, one dimensional disordered Hubbard model study 0-70687  
 nonadecane, purification and single cryst. growth 0-71589  
 nonafluoroisobutane, IR spectra, spectral bandshape and intensity of C-H chromophore 0-83355  
 p-nonyloxybenzoic acid, smectic C phase, electro-optical effect (*Russian*) 0-92458  
 nonyloxybenzoic acid/cholesteric liq. cryst. mixtures, helix pitch, temp. depend. 0-64895  
 norbornadiene-quadracycline photoisomeric interconversion for solar energy chemical conversion and storage 0-89664  
 norbornane, derivatives in solution, mol. motion and methyl group rot. barriers from <sup>13</sup>C NMR relax. times 0-74179  
 norbornane, microwave spectrum and dipole moments 0-78606  
 nucleic acids, bases and base pairs, water struct. in soln., Monte Carlo simulation 0-76709  
 nucleic acids and their aggregates, optical activity, review, book contrib. 0-108847  
 nucleic acids bases, excited state dipole moments and geometries 0-95738  
 3'-nucleotide, calcs. to assess rigidity 0-61506  
 nucleotide base stacking interactions in vacuum, field mass spectrometry 0-81526  
 nylon 6-Li halide mixtures, viscoelastic behaviour, stress relaxation 0-58995  
 octadecylacrylamide films, oriented ultrathin, radiation-induced solid state polymerisation 0-80128  
 octafluoronaphthalene crystalline complexes with naphthalene and durene, triplet exciton emissions 0-84760  
 n-octane, liq., thermal cond., meas. by transient hot-wire technique 0-103522  
 n-octane fluid, spontaneous cavitation 0-69886  
 n-octane liqs., refractive index, pressure effect 0-71375  
 trans, trans-1,3,5,7-octatetraene, high-resolution one and two photon excitation spectra 0-78669  
 4-n-octyl-4'-cyanobiphenyl/4-n-decyl-4'-cyanobiphenyl mixture, dynamic characts. of electrooptical field with memory 0-108183  
 octyl-cyano-biphenyl, influence of laser light wave field on nematic phase (*Russian*) 0-92456  
 4-n-octyl-d<sub>11</sub>-oxybenzoic acid-d<sub>4</sub>, nematic and smectic phases, mol. and relative segmental order 0-96439  
 octylcyanobiphenyl, crit. heat. capacity near nematic-smectic A transition 0-100323  
 p-n-octyloxy benzylidene-p-toluidine, mol. order, EPR VAAC probe 0-70114  
 trans-p-n-octyloxy-α-methyl-p'-cyanophenyl cinnamate, mag. and elec. birefr. in isotropic phase 0-80744  
 p,p'-octyloxycyanobiphenyl, flexoelec. coeff. in nematic phase, thermal depend. 0-79685  
 octyloxycyanobiphenyl, nematic-smectic A transition, heat capacity study 0-88033  
 4-n-octyloxyphenyl 4-n-pentyloxybenzoate, permittivity, microwave dielectric relaxation 0-80671



## organic compounds continued

oil layer, deformable, spatial light modulator as incoherent to coherent image transformer 0-96008  
olefin+thiirane+O<sub>2</sub>+SO<sub>2</sub>, excited neutral metastable SO<sub>2</sub> form. mass spectrometric study 0-83300  
olefins+N-ethylphthalimide, photochemical reaction, absorpt., fluoresc., phosphoresc. and triplet-triplet absorpt. spectra 0-85197  
one-dimensional conductors, electron-electron scatt. 0-107776  
optical Kerr effect kinetics induced by picosecond laser pulses 0-102779  
organic molecules, multiphoton ionisation mass spectra by ArF excimer laser 0-81381  
ovalene, minimal exposure high resolution electron microscopy 0-79653  
oxalacetic acid-Mn<sup>2+</sup>-H<sub>2</sub>SO<sub>4</sub>-KBrO<sub>3</sub>, chaos type reactions anal. 0-85165  
oxalate ion in aq. soln., vibr. study and Raman bands 0-95588  
 $\alpha$ -oxalic acid dihydrate, H<sub>2</sub>O proton shielding tensor, multiple pulse proton NMR obs. 0-63655  
oxalic acid in aq. soln., vibr. studies, IR and Raman spectra 0-95589  
oxazine 720, single freq. CW dye laser operation in 690-700 nm gap 0-99719  
oxidation, catalytic effects on electrode reactions, review 0-61110  
oxirane cation, struct. rearrangement following vertical ionisation, ab initio CI calc. 0-58191  
oxoniomethylene cation, rearrangement to hydroxymethyl cation, barriers, ab initio MO calcs. 0-104424  
 $\beta$ -oxy butyric acid ethyl ester, scaled spectra using three joined pulse sequences 0-73405  
2-oxypheylbenzoxazol, proton intramolecular transfer, light absorpt. and emission, dichroism, polarised fluoresc. 0-87166  
p-alkoxybenzylidene-p-amino-2-chloropropyl-cinnamate, chiral smectic, dielec. props. 0-96441  
PAA, fluctuations near Rayleigh-Bernard instability, real time obs. by neutron scatt. 0-59390  
PAA, nematic, NMR study of ordering, intramol. mobility 0-100162  
PAA, Tsvetkov parameter, temp. depend. 0-88035  
PAA-di, nematic liquid crystal, NMR data, appl. of Landau-de Gennes theory 0-64893  
paeonol and urinary metabolites labelled with <sup>13</sup>C and D, synthesis and physicochem. props. 0-67250  
palmitic acid-choleic acid complex, cryst. struct. and van der Waals energy 0-64983  
PAP, Tsvetkov parameter, temp. depend. 0-88035  
2,2 paracyclophane, dimer vibration influence on emission spectrum 0-69133  
paradichlorobenzene, NQR freq., intermol. force effect 0-66065  
paradichlorobenzene, NQR study of the lattice dynamics (Russian) 0-97160  
n-paraffin, longitudinal acoustic mode, perturbing forces 0-70348  
paraffin, single crystal, STEM versus CTEM beam damage 0-103393  
paraffin microcrystals, electron diff. intensities 0-100132  
paraterphenyl, fluoresc. quantum efficiency, one-photon dissociation, temp. depends. 0-69180  
PCB and DDT residues, atmos. dry aerial deposition rate, meas. techniques 0-81506  
PEBAB, nematic, EPR investig. 0-108077  
pentacene, disordered solid layer, absorpt. spectra 0-93417  
pentacene, first excited singlet state, butterfly motion studied by fluoresc. spectra 0-78615  
pentacene, singlet exciton transitions, energies and oscillator strengths, boson theory with PPP wavefunctions 0-92820  
pentacene dianions in dimethyl ether, rotational diffusion meas. 0-65262  
pentacene in naphthalene, triplet state, EPR study by electron spin-echo and laser flash excitation 0-58172  
pentacene in naphthalene (p-terphenyl), mol. mixed crystals, optical dephasing and vibronic relax. 0-95957  
pentacene in p-terphenyl, intermolecular interactions, laser induced phonon probe 0-78991  
pentachlorotoluenes, positional isomers, <sup>13</sup>C Fourier transform NMR spectrometry, struct. and compositional anal. 0-91576  
pentadecanoic acid, insoluble monolayer, phase transition, simple lattice model 0-70527  
pentafluoroacetone, IR laser induced decomp., free radical mechanism 0-71924  
pentane, effect on 3,6-diaminophthalimide vapour molecule electronic excitation energy degradation path 0-74195  
pentane, liq., enthalpy difference between rot. isomers, IR spectrosc. obs. 0-106404  
pentane-benzene solution, vapour-liquid equilibrium study, vaporisation critical state (Russian) 0-79931  
n-pentyl 4-(4-n-dodecyloxybenzylidene-amino)-cinnamate, X-ray studies in smectic I phase 0-70119  
pentyl cyanobiphenyl, laser and electric field induced Kerr effect 0-84061  
pentyl-cyano-biphenyl, nematic, hydrodynamic parameters meas. with and without applied elec. field 0-100297  
4-n-pentyl-phenylthiol-4'-n-octyloxybenzoate, smectic A-smectic C' phase transition, high-resolution X-ray study 0-79921  
4-n-pentylbenzenethio-4'-n-octyloxybenzoates, birefr., crit. behaviour near smectic A-C transition 0-80745  
4-n-pentyl-phenyl-4'-n-octyloxybenzoate, nematic, dielec. relax. and freq. depend. of threshold voltage 0-60497  
N-4-n-pentyl-phenyl-4'-n-hexylaniline (50.6), unclassified smectic phase 0-75157  
4-n-pentylphenyl (pentylbenzoyloxy)-3-chlorobenzoate, flexoelec. coeff. in nematic phase, thermal depend. 0-79685  
peptides, bradykinin-potentiating, spatial structs. 0-95736  
perfluorobenzene, electron attachment, radiative and dissoc., negative ion lifetimes, ion cyclotron reson. spectra 0-74251  
perfluorocarbon-SF<sub>6</sub> mixtures, sparking C inhibition, decomp. product investig. 0-89478  
perfluorocyclobutane, electron attachment, radiative and dissoc., negative ion lifetimes, ion cyclotron reson. spectra 0-74251  
perfluoroethane+CIF<sub>3</sub>, thermal and photochem. reactions investig. 0-61117  
perfluoromethylcyclohexane, electron attachment, radiative and dissoc., negative ion lifetimes, ion cyclotron reson. spectra 0-74251  
perfluoromethylcyclohexane-methylcyclohexane, near-critical liquid mixture, nucleation 0-92664  
perfluorotoluene, electron attachment, radiative and dissoc., negative ion lifetimes, ion cyclotron reson. spectra 0-74251  
perhalo-compounds, labelled, high yields from <sup>18</sup>F and <sup>38</sup>Cl reactions with CCl<sub>4</sub>-x and C<sub>2</sub>F<sub>6</sub> 0-109025

## organic compounds continued

peroxylamine disulphonate, EPR lineshape, dispersion vs. absorpt. plots, modulation broadening and instrumental distortion 0-58290  
perylene, intermolecular interactions, laser induced phonon probe 0-78991  
perylene crystals, molecular exciton system, resonance Raman and fluorescence studies, dynamical effects 0-66169  
perylene-tetracarboxylic dianhydride pyrolysis for synthesis of C films with high conductivity 0-80983  
pesticide pollution in Soviet rivers concs. 0-81495  
pesticides and heavy metals in Bavarian snow 0-61488  
petroleum spills on water, control using gellants 0-61496  
phenanthrene, diaza derivatives, excited singlet and triplet states, charge density, INDO calcs. 0-58152  
phenanthrene, lowest triplet state zero field splitting parameters calcs. 0-83391  
phenanthrene, two photon absorptivities, CNDO/S-CI calc. with second order time depend. perturbation eqns. 0-74122  
phenanthrene, two-photon excitation spectra, exciton-phonon and intramol. vibronic coupling 0-84774  
phenanthrene-solvated electrons, diffusion controlled reactions in polar solvents, reaction parameters 0-97687  
phenazine, prereson. Raman spectra, vibr. band intensities obs. 0-102515  
phenol, aq. soln., electron ejection, picosec. obs. 0-87187  
phenol-phenyl complex, electrostatic mol. pot. contour maps, MODPOT and VRDDO calcs. 0-102463  
phenolate, aq. soln., electron ejection, picosec. obs. 0-87187  
phenolic compounds, electrooxidation, polymeric surface film form. on Pt electrodes 0-104450  
phenolic Mannich bases, dielec. relax. study 0-97196  
phenothiazine derivatives, semicond. elec. props., optical spectra, and EPR 0-103693  
6-phenoxy-5,11-naphthacenequinones, photochromism, molar extinction coeffs. meas. 0-66220  
phenyl acetylene, liq., phase relax., vibr. dephasing, Raman spectra obs. 0-91567  
2,2'-p-phenyl bis (5-phenyloxazole), vap. phase dye laser media, photo-physical parameters 0-95884  
phenyl cation, struct., ion-molecule reactions studied by trapped ion mass spectroscopy 0-102586  
phenylalanine, hydrated electron impact dissoc., laser flash photolytic investig. 0-58396  
4-phenylbenzylidene-4'-n-alkoxyanilines, central Schiff's base linkage reversal effect on liq. cryst. props. 0-79683  
phenylcyclohexadienyl radical form in electron irradi. benzene cryst., absorpt. and fluoresc. spectra study 0-89035  
phenylene derivatives, effect of substitution on liq. crystalline props. 0-70113  
2-phenylindole, in viscous soln., fluoresc. quenching, emission, intensity and reson. transfer (German) 0-91599  
phenylnaphthalenes isomers, fluoresc. lifetime difference and mol. geometry 0-69176  
phenyloxazolyl pyridinium salt dye lasers, flashlamp pumped, blue-greening 0-95886  
p-phenylphenol in stretched polyvinyl alcohol film, phosphorescent triplet states, ESR spectra obs. 0-83393  
p-phenylphenolate ion in stretched polyvinyl alcohol film, phosphorescent triplet states, ESR spectra obs. 0-83393  
phenylphosphines, and derivatives, <sup>1</sup>H, <sup>13</sup>C and <sup>31</sup>P NMR studies 0-87152  
3-phenylpropanol-hexane, nonlinear dielectric effect, critical exponent 0-93227  
phosphatidyl choline, oxidised, free radical formation on UV irradi. 0-76790  
phosphatidylcholine bilayers, fluidity changes and phase transitions, intramol. excimer fluoresc. obs. 0-85342  
phosphine, IR spectrum,  $\nu_1$  and  $\nu_2$  band analysis 0-83366  
phospholipid bilayers, carbonyl groups dynamics, <sup>13</sup>C chem. shift anisotropy obs. 0-85326  
phosphoranyl radicals obs. in ESR spectra of triphenylphosphine sulphide in deuterated methanol 0-84651  
photoemission and photoionisation in three stage model 0-100744  
photosystem I, of green plants and algae, CIDEP obs. 0-63679  
phthalazine, excited state absorpt. spectra and intersystem crossing kinetics 0-74176  
phthalazine, prereson. Raman spectra, vibr. band intensities 0-102514  
phthalic acid derivatives, excitation energies, CNDO/S-CI method calc. appls. (German) 0-106275  
phthalocyanine, free base, fluoresc. excitation spectrum, cooling in super-sonic free jet 0-95670  
phthalocyanine, quasiline emission spectra using low temp. laser luminesc. spectrosc. (Czech) 0-86445  
phthalocyanine, surface, luminesc. accompanied by ion implantation 0-60683  
phthalocyanine compounds, XPS and charge transfer 0-95681  
phthalocyanine dye for stable passive Nd laser switch, bleaching and relaxation 0-74368  
phthalocyanine layers, metal-free, between Ag and Al electrodes, switching effects 0-65706  
phthalocyanine metal free films, TSC, ferroelectric-semiconductor transition 0-66105  
phthalocyanine-alkane interface, charge transfer, rel. to photoelectro-photoretic image form. 0-65616  
phthalocyanine-Cu, photoemission multielectron effects from quasi-atomic Cu 0-93458  
phthalocyanines, elec. cond., compensation effect 0-100455  
phthalocyanines, metal free, mol. cryst. images in electron diff. patterns 0-103315  
phthalocyanine, doped photovoltaic cell, photoconductivity, elec. field induced fluoresc. quenching, charge carrier photogeneration 0-84485  
 $\beta$ -picoline-water solution, light scatt. spectra, ultra- and hypersonic absorpt. (Russian) 0-93353  
pinacryanol in ethanol, electronic relax., analysing light ps spectroscopy 0-95917  
 $\alpha$ -pinene, methyl groups internal rot. <sup>31</sup>C spin lattice relaxation times and force field calcs. 0-74255  
piperidinyloxy 2,2,6,6-tetramethyl radical, recrystallised samples, EPR study 0-100615  
piperidine-PbI<sub>2</sub>, intercalation cpd., heat capacity of low temp., intercalation effect (Russian) 0-92682



## organic compounds continued

planar aromatic hydrocarbons in polymer films, polarisation data interpretation, photoelectron spectroscopy appl. 0-58302  
 planar cyclic radicals, C-H proton isotropic hyperfine consts., C hybridisation 0-95646  
 plasma chromatography and electron capture detector, comparison between two techniques 0-61176  
 polar liquids, binary mixtures, Sarma and Rao's rel. for dielectric relax. time 0-88914  
 polar liquids in double layer capacitors, RF conduction, ion diffusion effect 0-107883  
 poly-2,4-hexadiene-1,6-diol bis (p-toluene sulfonate), exciton surface polaritons, reflecting faces obs. 0-65645  
 polycetylene, metallic, mixed Peierls phase, Hartree-Fock calcs. 0-70689  
 polyamine iodide-AgI solid electrolytes, elec. cond. and cryst. struct. 0-107537  
 polychlorinated biphenyls waste disposal by pyrolysis, plasma torch appl. 0-76487  
 polycrystalline dipeptides, X-irradiated. ENDOR and ELDOR obs. 0-63689  
 polycyclic aromatic hydrocarbon impurity luminescence spectral anal. in calcite 0-71483  
 polycyclic aromatic hydrocarbons sorbed on fly ash, recovery for quantitative determ. 0-61177  
 polycyclic conjugated compounds, isomeric, Kruszewski's rule for stability 0-106249  
 polyene chromophores, electronic absorpt. spectra, charact. spectral band criteria 0-63651  
 polyenes, electronic absorpt. spectra, charact. spectral band criteria 0-63651  
 polyenes, photoisomerisation, triplet pot. energy surfaces and normal mode anal. 0-108700  
 polyethylene, cross-linked, appl. as freeze-tolerant material for solar water heaters 0-66944  
 polyhydroxy compounds, X-irrad., trapped electrons, ESR and ENDOR obs. 0-93161  
 polymethine dye lasers, optical absorpt. 0-64009  
 polymethine dye nonequilib. protolytic forms, lasing, fluoresc. and nonradiative transitions 0-102722  
 polymethine dye solutions, photochem. transformations and short-wavelength luminesc. 0-100686  
 polymethine saturable absorbing dyes, dual component fluoresc. lifetime meas. 0-106359  
 polynuclear aromatic hydrocarbons, analysis by X-ray excited optical luminescence technique 0-66891  
 polynuclear aromatic hydrocarbons, synchronous excitation spectrofluorimetry (*Japanese*) 0-86452  
 polynucleotide solution, elec. birefringence, stabilised induced dipole behaviour 0-85349  
 polynucleotide solution, elec. field induced orientation and effects 0-85348  
 polypeptides, ionic and non-ionic, electro-optical studies of conformation 0-71379  
 polyphenyl 1 laser dye for pulsed and CW operation in UV 0-78850  
 polyphenylenes, lasing, excitation by excimer laser radiation 0-64007  
 polypropylene, isotactic, uniaxially oriented, Raman spectra (*French*) 0-60557  
 polyribonucleotides, dye tagged, aqueous solns., elec. induced fluoresc. changes 0-85346  
 polyyenes, intermolecular interaction through triple bonds, internal rot. 0-106370  
 POPOP, fluoresc. quantum efficiency, one-photon dissociation, temp. depends. 0-69180  
 POPOP solution dye lasers, multiplate reflectors 0-83606  
 POPOP vapour, spectral, fluoresc., photochem. and laser props. 0-106344  
 POPOP vapour lasing, buffer gases influence, theory 0-91790  
 porphyrin, hypersurface of adiabatic pot. calc. by CNDO/2 method, vibr. freqs., absorpt. spectra calc. 0-95543  
 porphyrin free base, vibr. and normal mode anal. 0-69122  
 porphine-d<sub>4</sub>, vibronic transitions, polaris. determ. 0-63614  
 porphyrin films, methine bridge substituted, surface photovolt. depend. on fabrication method 0-60119  
 porphyrin in n-octane Shpol'skii matrix, defect props., Monte Carlo obs. 0-63533  
 porphyrins, metal-free, EPR, sample grinding effects 0-60420  
 porphyrins in liquid crystal, oriented photoexcited triplets, EPR study 0-84636  
 potassium acid phthalate, crystal as Bragg mode analyser, Bragg refl. integral obs. 0-95204  
 potassium antimonyl tartrate, neutral aq. soln., gamma radiolysis 0-101030  
 potassium formate, X-ray cryst. struct. determ. 0-107194  
 potassium hydrogen malonate, carboxylic proton chem. shift tensor 0-58280  
 potassium hydrogen malonate, room-temperature ENDOR spectra obs. 0-106339  
 potassium laurate-1-decanol-water mixtures, biaxial nematic phase obs. 0-107409  
 potassium n-alkanoates, thermal behaviour, differential scanning calorimetry obs. 0-92650  
 potassium oscallate, neutron inelastic scatt. spectra in 2200-200 cm<sup>-1</sup> range 0-70327  
 potassium palmitate-water solution, deuterated, NMR asymmetry parameter 0-88882  
 praseodymium ethyl sulphate, phase transition under pressure, absorpt. spectra (*Russian*) 0-92667  
 praseodymium ethylsulphate:Sm, one-dimens. X-Y system, spin dynamics, electron spin echo meas. 0-66031  
 praseodymium tricarbamide acetate hydrate, cryst. struct., Patterson function anal. 0-79770  
 L-proline, structure amplitude phases, statistical-thermodynamic determ. 0-84028  
 propanal, methyl torsional pot. functions, LF Raman and IR vibr. spectra 0-95612  
 propane+He<sup>+</sup>, 0.7-2 MeV, charge-changing collisions, electron capture 0-58372  
 1,2-propane diol-dipropylene glycol, dielec. dispersion charact. 0-75932  
 propane flame, wake stabilized, response to sudden accel. or deceleration of free stream 0-61096  
 propanoic acid, adsorption on Ag (111) and Pt (111), LEED obs. 0-80073

## organic compounds continued

n-propanol, preferred conformers, PCILo study 0-95542  
 n-propanol-isopropanol aq. mixtures, US relax., US absorpt. and vel. meas. (*French*) 0-103426  
 propargyl alcohol, film growth on steel surface, ellipsometric obs. of corrosion inhibition (*Rumanian*) 0-60996  
 propiyl chloride(-d), 357-333 nm absorpt. system 0-69161  
 propiyl fluoride(-d), 290 nm absorpt. system 0-87142  
 propionitrile-hydrocarbon systems, critical solns., Kerr electrooptical Kerr effect meas. 0-100645  
 propionitriles (-O, NH, S), conformational investig., NMR, IR and semiempirical MO methods 0-95650  
 N-p-propoxybenzylidene-p-pentylaniline, orientational order in glassy and nematic phases, IR dichroism meas. 0-64891  
 propyl acetate-propyl alcohol, dielec. dispersion charact. 0-75932  
 propylene, adsorption on MgO:Mo catalyst, oxidation reactions, surface structs., IR absorpt. spectra obs. 0-66868  
 propylene, He-Ne laser line, high temp. absorpt., anal. by high resolution IR spectra 0-91554  
 propylene, high density behaviour, extrapolated PpT surfaces and critical density 0-87834  
 propylene and ethylene adsorbed on Ag, enhanced Raman spectra obs. 0-95607  
 propylene carbonate and dimethoxyethane mixed electrolyte solns., for high energy density batteries 0-76627  
 propynal, CW for IR mol. laser, optical pumping with <sup>16</sup>CO<sub>2</sub> and <sup>18</sup>CO<sub>2</sub> lasers 0-74343  
 propynal, IR-microwave double reson. and two-photon expts. 0-83396  
 propynal, rovibronic populations, collisionless IR multiphoton spectra, energy deposition, photoacoustic determ. 0-83354  
 propynal-d, in ground vibrational state, IR microwave double resonance spectra, rot. and centrifugal distortion const. determ. 0-83358  
 propynal-d, IR microwave double reson. spectroscopy 0-69172  
 propyne-d<sub>0</sub>(-d<sub>1</sub>), absolute and integrated IR intensities of fundamental modes 0-87179  
 propynyl cation+propyne, reactant structure effects 0-89469  
 prostaglandins, <sup>125</sup>I labelled (*Hungarian*) 0-94368  
 prostatic acid phosphatase, human, development of determ. by radioimmunoassay (*Japanese*) 0-98110  
 proteoglycans, swelling pressures at the concs. found in cartilaginous tissues 0-67327  
 protochlorophyll, mag. reson., site selected fluoresc. detection 0-69164  
 protoporphyrin IX, triplet states, flash photolysis, obs. 0-95555  
 protoporphyrin IX dimethyl ester, triplet states, flash photolysis, obs. 0-95555  
 pseudoazulenes, anomalous fluoresc., radiationless transitions 0-91593  
 PVK/PVK-TNF/TNF:PMG system, electrophotographic characts. 0-62759  
 pyrazine, <sup>14</sup>N quadrupole coupling consts., ab initio calcs. 0-58283  
 pyrazine, electronic energy transfer to metal surface, classical image dipole theory 0-97318  
 pyrazine, on Ag, time-resolved molecular electronic energy transfer 0-92957  
 pyrazine, prereson. Raman spectra, vibr. band intensities obs. 0-102515  
 pyrazine, reson. to the S<sub>2</sub>( $\pi, \pi^*$ ) state, Raman spectra calcs. 0-69147  
 pyrazine, vapour, fluoresc. quantum yields, rot. effects 0-95661  
 pyrene, distinction of delayed fluorescences S<sub>1</sub>→S<sub>0</sub> and S<sub>2</sub>→S<sub>0</sub> by selective quenching of S<sub>1</sub>→S<sub>0</sub> 0-69175  
 pyrene, luminescence of free and self-trapped excitons 0-108250  
 pyrene, migration between lipid vesicles in aq. soln., fluoresc. stopped-flow obs. 0-85360  
 pyrene, mol. ionisation pot., two photon ionisation, micellar interface effects on ionisation threshold 0-91609  
 pyrene, triplet state, excitonic energy transfer, phosphoresc. and delayed fluoresc., 2 to 300K 0-84776  
 pyrene, use in fluoresc. probe study of cetyltrimethylammonium bromide-1-butanol system 0-85217  
 pyrene crystals, anomalous emission excited near absorption edge 0-100682  
 pyrene dodecanoic acid, lateral diffusion at air-water interface, monomer excimer dynamics 0-92693  
 pyrene excimer fluorescence, erythrocyte membrane fluidity changes after X-irrad. obs. 0-72262  
 pyrene in n-heptane solution, laser two-photon ionisation spectroscopy, photoionisation threshold determ. 0-78668  
 pyrene picrate, crystal struct. oscill. and Weissenberg photographs 0-107200  
 pyrene solutions, radical ion pairs, pulse radiolysis, time resolved EPR spectra meas. by ODMR of fluoresc. 0-83395  
 pyridazine, prereson. Raman spectra, vibr. band intensities 0-102514  
 pyridine, <sup>15</sup>N quadrupole coupling consts., ab initio calcs. 0-58283  
 pyridine, adsorbed on Ag, 210-243 cm<sup>-1</sup> mode in surface enhanced Raman scatt. 0-89003  
 pyridine, adsorbed on Ag, Raman active librational modes 0-65359  
 pyridine, adsorbed on Ag electrode with graphitic C overlayer, Raman spectra obs. 0-103954  
 pyridine, adsorbed on gold substrate with Ag monolayer, giant Raman effect 0-63637  
 pyridine, adsorpt. on Ag colloids, surface enhanced Raman spectra obs. 0-97251  
 pyridine, adsorpt. on Pt/Al<sub>2</sub>O<sub>3</sub>, electron accepting sites 0-71947  
 pyridine, adsorption on Ag, UPS, AES and flash desorption meas. 0-92776  
 pyridine, adsorption on CuO and MgO powders for surface area determ. 0-107636  
 pyridine, deuterium substituted, Raman and IR vibr. spectra 0-84739  
 pyridine, macroscopic model for solvated ion dynamics, cation conductance calcs. 0-65261  
 pyridine, mean free path meas., US relax. 0-59585  
 pyridine, on Ag surface, enhanced Raman scatt., ultrahigh vac. study 0-88993  
 pyridine, Penning election spectra and photoelection spectra, rel. intensities 0-95725  
 pyridine, sorption on Ag, surface enhanced Raman scatt., mol.-surface separation depend. 0-92775  
 pyridine(-d), force consts. and vibr. spectra-by CNDO/2 force method 0-95540  
 (pyridine)<sub>2</sub>-NbS<sub>2</sub> intercalation complex, superlattice struct., NMR meas. 0-70180  
 pyridine adsorbed on Cu (110) surface, photoemission selection rules 0-100751



## organic compounds continued

- 4-pyridine carbaldehyde, microwave spectrum, rot. assignments, quadrupole coupling consts. 0-91548  
 pyridine N-oxide, in benzene, dipolar assoc. investig. 0-107035  
 pyridine on Ni-Co-Cr/Al<sub>2</sub>O<sub>3</sub> catalyst, IR spectra of adsorption and interaction 0-71946  
 pyridine-2,3,5,6-d<sub>4</sub>, vibr. spectra, IR and Raman, assignment 0-102519  
 pyridine-3,4,5-d<sub>3</sub>, vibr. spectra, IR and Raman, H exchange rates meas. 0-102518  
 pyridine-3,5-d<sub>2</sub>, vibr. spectra, IR and Raman, H exchange rates meas. 0-102518  
 pyridine-d<sub>4</sub>, vibr. spectra, IR and Raman, assignment 0-102519  
 pyridine-H-bond donors, D spin-lattice relax. meas., mol. interactions anal. (French) 0-87151  
 pyridine-l<sub>2</sub>, n-σ charge-transfer complex, frozen soln., Mossbauer spectra obs. 0-91655  
 pyridine-l<sub>2</sub> complexes, stability const. determ. by spectrophotometric methods 0-87056  
 pyridine-N-oxide, electronic struct. assignment, He I/He II intensities (German) 0-83423  
 pyridine-PbI<sub>2</sub>, intercalation cpd., heat capacity of low temp., intercalation effect (Russian) 0-92682  
 pyridine-water soln., reorientational relax. and activation energy of pyridine, depolarised Rayleigh scattering 0-76037  
 4-pyridinecarboxaldehyde monolayer in inelastic electron tunnelling spectroscopy junctions, Raman scatt. 0-93344  
 pyridines, monosubst., H<sub>2</sub>O complexes, n-π\* transitions, H bonding, MO theory 0-95550  
 pyridines in n-heptane soln., heat of adsorpt. on outgassed η-Al<sub>2</sub>O<sub>3</sub> 0-61154  
 pyridinium iodide, order-disorder phase transition and reorientation fluctuations studied by Raman spectra 0-80764  
 pyridinium manganese chloride, anhydrous, quasi one-dimensional mag. behaviour, heat capacity meas. 0-80549  
 pyridinium nickel chloride, anhydrous, quasi one-dimensional mag. behaviour, heat capacity meas. 0-80549  
 pyridinium pentasilver hexaoidide, solid electrolyte, contrib. of non-Brownian motion to transport props. 0-70453  
 pyridinium silver iodide, fast ion conductor, phase transitions, thermoelec. power meas. 0-107540  
 pyrimidine, bi-exponential decay, methylation and vibr. excitation, proximity effects 0-78641  
 pyrimidine, vapour, fluoresc. quantum yields, rot. effects 0-95661  
 pyrimidine, vapour, phosphoresc. 0-83408  
 pyrimidine nucleotides, UV reson. Raman excitation profiles 0-58265  
 pyrimidines, substituted analogues, absorption UV spectroscopy and electronic struct. of ionic and tautomeric forms 0-74177  
 pyrrole, Penning electron spectra and photoelectron spectra, rel. intensities 0-95725  
 pyrrole, resonantly enhanced multiphoton ionisation 0-106362  
 pyrrole-acetonitrile, H-bonded complex, ab initio MO calcs. 0-102440  
 pyruvic acid, <sup>13</sup>C-labelled, enzymatic synthesis 0-61695  
 quaterylene, minimal exposure high resolution electron microscopy 0-79653  
 quinacrine mustard, 2-step laser-induced photodamage 0-85198  
 Quinacrine Mustard, time-resolved fluoresc. spectrum 0-87165  
 quinazoline, excited state absorpt. spectra and intersystem crossing kinetics 0-74176  
 quinazoline, prereson. Raman spectra, vibr. band intensities obs. 0-102515  
 quinazolines, enzyme inhibitory, structure-activity quantitative study 0-78540  
 quinoline, liq., depolarised light scatt. from shear waves 0-97288  
 quinoline-l<sub>2</sub> complexes, stability const. determ. by spectrophotometric methods 0-87056  
 quinolinium (TCNQ)<sub>2</sub>, charge transport, proton spin-lattice relaxation 0-88545  
 quinolinium (TCNQ)<sub>2</sub>, random exchange Neisenberg antiferromag. chain, intermediate field magnetisation meas. 0-103857  
 quinones, triplet quenching by organometal cpds., time resolved CIDEP and ESR obs. 0-95654  
 quinones-Zn porphyrin, quinones sensitised reduction in vesicle systems 0-71897  
 quinoxaline, excited state absorpt. spectra and intersystem crossing kinetics 0-74176  
 quinoxaline, prereson. Raman spectra, vibr. band intensities 0-102514  
 quinoxaline, T<sub>1</sub>(ππ\*)→S<sub>0</sub> intersystem crossing, isotope effects, ODMR and phosphoresc. obs. 0-91586  
 quinuclidine struct. determ. by gas phase electron diffr. 0-95742  
 quinzarin in alcohol glasses, electron-phonon coupling, photochemical hole burning 0-97265  
 radialenes, graph theoretical polynomials 0-69048  
 rare-earth ethylenediaminetetraacetates, formation constants (French) 0-104458  
 9-cis retinal, visual pigment chromophore, twisting mechanism 0-58333  
 11-cis retinal visual pigment chromophore, twisting mechanism 0-58333  
 rhodamine, activated 6G top layer in slab-type directional coupler, amplified oscill. 0-99718  
 rhodamine 6 ZH solution, radiant transport effect on luminesc. duration 0-103995  
 rhodamine 6G<sub>2</sub> molecules in solution, photoluminescence study, fluorescence decay time 0-80832  
 rhodamine 6G, in binary compensated cholesteric mixture, electro-optical colour effect 0-71378  
 rhodamine 6G, in ethanol, time-depend. fluoresc. spectrum, using synchrotron radiation 0-62736  
 rhodamine 6G, in n-alcohols (ethylene glycol)(glycerol), rot. relax., time-resolved fluoresc. depolaris. obs. 0-58300  
 rhodamine 6G, in rigid matrix, conc. effects in spectra 0-83347  
 rhodamine 6G, molecular nonsteady-state luminesc. behaviour under narrowband laser excitation 0-87159  
 rhodamine 6G, tunable lasing molecule (Chinese) 0-74389  
 rhodamine 6G dye in ethylene glycol, broadband optical diode, one directional traveling wave operation of ring laser 0-58606  
 rhodamine 6G dye in quartz glass microcomp. matrix, as tunable solid laser 0-99734  
 rhodamine 6G dye laser, induced radiation spectral characts., effect of vibr. relax. 0-64008  
 rhodamine 6G ethanol soln., absorpt. and luminesc. spectra using picosecond excitation 0-106351

## organic compounds continued

- rhodamine 6G in dimethylsulphoxide, concentrational red shift and luminesc. spectra 0-83426  
 rhodamine 6G solution, absolute fluoresc. quantum yield determ. by calorimetric method 0-78851  
 rhodamine 6G solution in alcohol, degenerate four wave mixing, phase conjugation (Chinese) 0-102765  
 Rhodamine 6G-3,3'-diethylthiacarbocyanine iodine, energy transfer with increased local conc., Forster mechanism 0-69220  
 rhodamine 6G-safranin-T mixed dye laser energy transfer, 31 nm tuning range 0-58532  
 rhodamine B, absorption on Ag electrode, anisotropy of optical props. 0-60534  
 rhodamine B in ethylene glycol, fluoresc. decay meas. via modulated gain spectroscopy 0-63699  
 rhodamine G solutions, LiCl and NaClO<sub>4</sub> electrolyte influence on its lasing props. 0-91788  
 rhodamine-6G mode locked dye laser pulse width monitoring by rapid scan autocorrelator 0-87421  
 rhodamines, 5G, 6G, B, 3B in ethanol soln., luminesc. quenching by photoirradiation 0-87168  
 ring current theory 0-87240  
 RNA, conformational fluctuations, internal motion correl. times, <sup>31</sup>P NMR obs. 0-72135  
 RNA, solid hydrated samples, hysteresis loops, nonlinear dielectric properties 0-71294  
 Rochelle salt, ferroelec. phase transition, Raman scatt. study 0-97211  
 rubrene, electrochemilum. by DC, highly organised EHD convection obs. 0-71499  
 rubrene, in benzene soln., extrinsic photocond. kinetics 0-92691  
 RX<sup>-</sup>, radical anion stability conditions, pot. energy diagrams 0-85161  
 salicidenanilines, SLC, ferroelectric behaviour, specific heat, spontaneous polarisation 0-75958  
 salol, solid/melt interfacial tension and contact angles of small particles, determ. from crit. vel. of engulfing 0-79915  
 tris-sarcosine calcium chloride, elastic props., US damping 0-84229  
 saturated hydrocarbon+O(<sup>3</sup>P), reaction dynamics, model pot. surfaces, quasiclassical trajectory calcs. 0-97696  
 saturated hydrocarbon+O(<sup>3</sup>P)—OH+alkyl radical 0-97695  
 saturated hydrocarbon +O(<sup>3</sup>D<sub>2</sub>), chem. reaction dynamics. OH prod. investig. 0-101016  
 Schiff base azo dyes in nematic liq. cryst. hosts, order parameters, optical density meas. 0-84055  
 semicarbazide hydrochloride, vibr. spectra, normal coord. anal. 0-58255  
 semicarbazide-d<sub>6</sub>, vibr. spectra, normal coord. anal. 0-58255  
 serum thyroxine, radioimmunoassay by the antibody-coated test tube method (Japanese) 0-67237  
 silicon phthalocyanine, elec. cond. temp. depend. 0-80271  
 silicone oil, ionic behaviour, carrier mobility and viscosity 0-107453  
 silicone oil, Newtonian, vel. meas. in die entry region of capillary rheometer 0-99988  
 silyl acetylene, microwave spectra in ground and ν<sub>10</sub> vibr. state 0-78610  
 sodium 10-decanoate, γ-ray induced polymerisation in aq. micelle solns. 0-61093  
 sodium dodecyl sulphate: Gd<sup>3+</sup>, micellar system, chain folding, <sup>13</sup>C NMR obs. 0-61158  
 sodium dodecyl sulphate micelles-ω-(α-naphthyl) dodecanoic acid soln. fluoresc. decay obs. 0-61158  
 sodium fluorescein-rhodamine B, energy transfer in luminescent mixed solutions 0-103976  
 sodium oxalate, neutron inelastic scatt. spectra in 2200-200 cm<sup>-1</sup> range 0-70327  
 sodium oxalate:Cu<sup>2+</sup>, anhydrous spin Hamiltonian and bonding parameters and orbital-reduction factors 0-60408  
 sodium stearate, Langmuir-Blodgett multilayers, comp. and transfer mechanism 0-80125  
 sodium undecanoate/water system, lyotropic liq. cryst. struct. change due to polymerisation of amphiphilic component 0-59386  
 solute rejection by reverse osmosis, regular soln. theory-appl. (Japanese) 0-101041  
 solvents in laser saturable absorber, nonlinear refr. index meas. at 1.32 μm 0-102758  
 spectral line narrowing of triplet state, in laser excited experiments 0-63703  
 2,2'-spirobiindane derivatives, chiral, cholesteric order induction in nematic systems (German) 0-64884  
 spirohydrocarbons, strained, bond angles, interatomic distances, semiempirical and ab initio calcs. 0-95533  
 spiropyrans, polymer matrix effect on photochromism, thermal decolouration kinetics 0-76537  
 spiropyron solutions, nitro-substituted, electronic state participation in photochromy 0-81347  
 squaric acid, antiferroelec., struct. phase transition mechanism 0-75969  
 squaric acid, layered, antiferroelec., phase transition mechanism 0-97210  
 squaric acid, two dimensional antiferroelec., Brillouin scatt. at structural phase transition 0-71430  
 squaric acid, two-dimens. phase transition, Raman scatt. study 0-71401  
 squarylium dye films, surface photovolt. 0-75594  
 starch, glycerin impregnated, dynamic viscoelasticity. (Japanese) 0-104203  
 stearate, proton spin-lattice relaxation in various phases (Russian) 0-97163  
 stearic acid, adsorption on CuO and MgO powders for surface area determ. 0-107636  
 stearic acid, vacuum evaporated film, for low-loss capacitors 0-71317  
 stearic acid crystals grown from solution, spatial correlation between growth spirals and inclusions 0-96527  
 stearic acid films, evaporated, vac. effects 0-97435  
 stearic acid homogeneous vapour phase nucleation, diffusion cloud chamber obs. 0-79923  
 stearic acid multilayers, dielec. props. 0-80404  
 stilbene, adsorbed rhodamine 6Z, mol. cryst., role of excitonic and radiative mechs. of energy transport 0-108276  
 stilbene, cis and trans, transient spectra, radiative lifetimes and quantum yields 0-78640  
 stilbene, pulsed electron excitation, triplet excitons, spectral and electrical investigations 0-92828  
 trans-stilbene, soln., lifetime and anisotropic fluoresc., viscosity effects (German) 0-106352  
 stilbene anion radicals, photoinduced isomerisation, 77K 0-66818  
 stilbene aza-analogues, lowest excited states, INDO/S calcs. 0-95545



## organic compounds continued

stilbenes, prolate molecules in solvents, anisotropic fluoresc. (*German*) 0-69183  
 stilbenes, substituted, donor-acceptor interaction effects on excited singlet state polarity (*German*) 0-91470  
 strontium maleate tetrahydrate, cryst. struct., H-bonding scheme 0-96505  
 structures, topological code, modified Morgan algorithm 0-58122  
 styrene, two photon absorptivity, ion cyclotron reson. photodissoc. spectra, CNDO/S-CI-perturbation theory 0-74123  
 styrene, UV Raman spectra, reson. effect in photoreactive states 0-106326  
 styrene monomer, polymerisation by glow discharge method, formation mech. (*Japanese*) 0-61094  
 styrenes, 4-substituted, NMR substituent parameters, pattern recognition interpretation 0-58284  
 substituted phenolic compounds, effect on dark charge exchange process in photoactive pigment electrophotographic imaging system 0-62758  
 sucrose, crystn. rate in impure solns., influence of non-sugar and colouring substance quantity 0-100767  
 sucrose, single cryst., absorption spectrum of electron traps, pulse radiolysis obs. 0-93369  
 sucrose crystal formation, and growth, effect of same metallic impurities 0-100768  
 sucrose polydisperse aerosol number and mass conc. meas. by elect. aerosol anal. 0-108753  
 sulpholan, molecular solid, laboratory frame and rotating frame spin-lattice relax., pulsed NMR meas., phase transitions obs. 0-93197  
 supercrist. hydrocarbons radiolysis, electron reaction rate const./diffusion coeff. ratio 0-101033  
 surface contaminants, anal. by plasma chromatography-mass spectroscopy, and Raman microprobe technique 0-108773  
 sym-triazine, Landau mean field description, second-order phase transition, soft modes 0-108434  
 sym-trioxane, phase transition, polarised Raman spectra obs. 0-84742  
 Tanane, ferroelec. mol. cryst., strong piezoelec. coupling 0-75942  
 tartrate,  $\text{Na}[\text{K}-(\text{NH}_4)_2\text{C}_4\text{H}_4\text{O}_6\cdot 4\text{H}_2\text{O}]$ , dielec. relaxation 0-108152  
 TBACA, chiral, smectic C\* and H\* phases, mol. orientational ordering,  $^{15}\text{N}$  NQR study 0-75152  
 TBBA, mesophase identification by X-ray diffr. review 0-100166  
 TBBA liquid crystal, monoclinic cell parameters of solid, smectic and metastable phases, temp. dependence 0-70122  
 TCNE, hole drift mobility, temp. depend. and anisotropy, photocond. meas. 0-80314  
 TCNE-benzene, charge transfer theory, Mulliken population, ab initio calc., multiconfiguration scheme 0-106392  
 TCNQ, enthalpy of sublimation and vapour press. meas. 0-92661  
 (TCNQ)<sub>2</sub>, dimeric interactions, MO calcs., applicability to crystal struct. 0-75215  
 TCNQ complex, 1,2-di (N-ethyl-4-pyridinium) ethylene (TCNQ)<sub>4</sub> elec. resist. and thermoelec. power meas. 0-107777  
 TCNQ complex, dibenzotetrathiofulvalinium (TCNQ)<sub>2</sub>, elec. resist. and thermoelec. power meas. 0-107777  
 TCNQ complex, ethyltriphenylphosphonium (TCNQ)<sub>2</sub>, elec. resist. and thermoelec. power meas. 0-107777  
 TCNQ complexes, disordered, thermodynamics of random exchange models 0-103826  
 TCNQ ion radical salt, DECA(TCNQ)<sub>2</sub>, IR absorpt. spectra obs. of first-order transition 0-71397  
 TCNQ salt, Ag.TCNQ, cryst. struct. 0-70186  
 TCNQ salt, decamethylferrocenium, monomeric and dimeric, optical and EELS study 0-100660  
 TCNQ salt, dibenzo-TTF-TCNQCl<sub>2</sub>, one-dimens. mag. semicond., mag. and elec. props. 0-88601  
 TCNQ salt, K.TCNQ, EPR linewidth, ang. and freq. depend. 0-80591  
 TCNQ salt, MeDABCO(TCNQ)<sub>2</sub>, optical, elec., and mag. props. 0-65539  
 TCNQ salt, MEM(TCNQ)<sub>2</sub>, dielec. const. obs., DC and microwave cond. obs. 0-59963  
 TCNQ salt, n-methyl-n-ethylmorpholinium, unpaired electron states, IR refl. study 0-75491  
 TCNQ salt, TSeF-TCNQ, short-range ordering investigated by XDE 0-59652  
 TCNQ salts, elec. cond. spectrum fine struct. 0-96884  
 TCNQ salts, ETPP (TCNQ)<sub>2</sub> and DEPE (TCNQ)<sub>4</sub>, thermoelec. power 0-59966  
 TCNQ salts, TSF-TCNQ, and HMTSF-TCNQ, low temp. fast neutron irradiation, elec. cond. meas. 0-59964  
 teflon gas injected into shock layer flow, hypersonic flow past blunt body 0-74998  
 terephthalylidene-bis-(4-n-alkylanilines), smectic polymorphism, calorimetric study 0-88307  
 terpenes, methyl groups internal rotation,  $^{13}\text{C}$  spin lattice relaxation times and force field calcs. 0-74255  
 p-terphenyl, cryst., double injection and electrolum. 0-97342  
 p-terphenyl, cryst., exciton phosphoresc. at 300K 0-108277  
 terphenyl, two photon absorptivities, CNDO/S-CI calc. with second order time depend. perturbation eqns. 0-74122  
 p-terphenyl(-d<sub>4</sub>), Brillouin scatt. at room temp. 0-71433  
 p-terphenyl cryst., low lying single state 0-97320  
 p-terphenyl vapour, spectral, fluoresc., photochem. and laser props. 0-106344  
 tetra-glycine, cyclic, mol. polaris. and diamag. suscept. calcs. 0-63858  
 tetra-isoamyl phosphonium bromide hydrate, clathrate, cryst. struct., X-ray study 0-64987  
 tetra-l-alanine, cyclic, mol. polaris. and diamag. suscept. calcs. 0-63858  
 tetra-n-butylammonium halides in benzene, chloroform, CCl<sub>4</sub>, far IR spectra, ion-ion, ion-mol. interactions 0-60562  
 2,3,4,5-tetracetoxymercuri thiophene, dark-field imaging, computer simulation 0-100151  
 tetraalkylammonium hydroxide intercalates with TaS<sub>2</sub>, NbS<sub>2</sub>, prep. and struct. 0-79752  
 tetrabenzol[a, cd, j, lm]perylene evaporated film, crystn., time depend. as function of purity 0-88449  
 tetrabiromethane, electronic struct., X $\alpha$  SW calcs. 0-102447  
 tetrabromomethane, monoclinic monocryst., polarised Raman spectra (*French*) 0-93302  
 tetrabutylammonium europium yttrium isothiocyanate, conc.-depend. electron-phonon coupling, and self-quenching 0-60657  
 tetrabutylammonium iodide, alcoholic soln., repulsion phenomena in thin layers 0-107619

## organic compounds continued

tetracene, disordered, vapour deposited on glass substrate, fluoresc. and energy transfer 0-84761  
 tetracene, disordered solid layer, absorpt. spectra 0-93417  
 tetracene, intrastate scrambling in large mol. bound level struct. 0-63696  
 tetracene, singlet exciton transitions, energies and oscillator strengths, boson theory with PPP wavefunctions 0-92820  
 tetracene, unrelaxed fluoresc., direct picosecond obs. 0-89046  
 tetracene dianions in dimethyl ether, rotational diffusion meas. 0-65262  
 tetracene molecules in Ar clusters, excited state intramol. dynamics, laser-induced fluoresc. spectra obs. 0-78674  
 1,2,4,5-tetrachlorobenzene, exciton states in crystals and dimers 0-70620  
 1,2,4,5-tetrachlorobenzene, mol. solid, heat pulses, phonon-induced delocalisation of trapped excited triplet states 0-89053  
 1,2,4,5-tetrachlorobenzene, triplet exciton, ESR and optical absorption lines 0-96791  
 1,2,4,5-tetrachlorobenzene, triplet excitons, zero field ODMR 0-88891  
 tetrachlorodibenzo-p-dioxin determ. by low resolution gas chromatography-mass spectrometry 0-66893  
 tetrachloromethane, fluid, collision induced light scatt. intensity 0-103955  
 tetrachloromethane, liq. struct. and dynamics 0-79669  
 tetrachloromethane, liqs., refractive index, pressure effect 0-71375  
 tetrachloromethane, UV laser photolysis 0-66826  
 tetrachloromethane + Xe, excitation functions and rotational polarisation, chemiluminesc., crossed beam study 0-76491  
 tetracyanoethylene anion in acetone-d<sub>6</sub>, anion solvation, electron spin echo modulation 0-63676  
 tetracyanoethylene anion in methanol-d<sub>3</sub>(d<sub>1</sub>), anion solvation, electron spin echo modulation 0-63676  
 tetracyanoethylene in dimethylsulphoxide-d<sub>6</sub>, anion solvation, electron spin echo modulation 0-63676  
 tetracyanoplatinate, quasi 1d anion deficient, elec. and struct. props. 0-103683  
 tetraethylammonium neptunium hexachloride, Mossbauer spectra and mag. susceptibility meas. 0-108140  
 tetrafluoro-p-benzoquinone, mol. struct., gas phase electron diff. obs. 0-58386  
 1,1,1,2-tetrafluoroethane, mol. struct. studied by gas-phase electron diff., vibr. amplitudes, bond angles and lengths calc. 0-95740  
 tetrafluoroethane, specific refractivity, interferometric meas. 0-95124  
 tetrafluoroethylene, photolysis, CF<sub>2</sub> form., excitation by Hg 253.7 nm line, reson. fluoresc. spectra 0-63694  
 tetrafluoromethane,  $\nu_3 + \nu_4$  band, high resolution diode laser spectra 0-69138  
 tetrafluoromethane, binary collision-induced light scatt., rot. Raman scatt. 0-78660  
 tetrafluoromethane, binary collisions induced light scatt. 0-83428  
 tetrafluoromethane, collision-induced scatt., many-body corrs. 0-87127  
 tetrafluoromethane, electronic struct., X $\alpha$  SW calcs. 0-102447  
 tetrafluoromethane, liq., mol. reorientation 0-106320  
 tetrafluoromethane, liq. pure vibr. Raman spectra 0-97262  
 tetrafluoromethane, mol. consts. and mean vibr. amplitudes calcs. 0-106318  
 tetrafluoromethane, plasma etching of Si<sub>3</sub>N<sub>4</sub>(SiO<sub>2</sub>) in dry processing, active etchant species 0-79581  
 tetrafluoromethane, specific refractivity, interferometric meas. 0-95124  
 tetrafluoromethane, valence electron binding energies, molecular symmetry restrictions effect 0-63528  
 tetrafluoromethane + He gas mixture, collision induced for IR translational spectra 0-83353  
 tetrafluoromethane laser, pulsed, high repetition rate, average power limitations at 10.6 and 16  $\mu\text{m}$  0-58503  
 tetrafluoromethane molecule, laser spectrosc. and optical pumping from CO<sub>2</sub> laser 0-74202  
 tetrahydrofuran-Rb solution, polarised photoelectron and loose ion pair (Rb<sup>+</sup>, e) obs., optical-ESR study 0-85196  
 tetramethyl ammonium silver iodide, superionic solid film, surface diffusion coeff. 0-92709  
 tetramethyl pyrazine in durene, phosphorescent mols., quantum beats in triplet states 0-58312  
 tetramethyl-1,3-cyclobutanedithione-h<sub>12</sub> and -d<sub>12</sub>, visible spectra,  $\pi\pi^*$  transitions obs., mol. vibr. 0-97297  
 2,2,5,5-tetramethyl-4-phenyl-3-imidazolin-3-oxide-l-oxyl, deform. electron density determ., X-ray diffr. 0-88135  
 tetramethyl-p-benzoquinone, mol. struct., gas phase electron diff. obs. 0-58386  
 N,N,N',N'-tetramethyl-p-phenylenediamine, alkane soln., charge carrier generation, elec. field depend. 0-107846  
 2,2,2,6-tetramethyl-piperidino-oxo, cryst. growth and polymorphism 0-96645  
 tetramethylaminelithium(0), Li(CH<sub>3</sub>NH<sub>2</sub>)<sub>4</sub>, existence, conduction- and localised-electron spin reson. 0-66035  
 tetramethylammonium cobalt tetrachloride, ferroelectricity, triple 60 Hz D-E hysteresis loops 0-71365  
 tetramethylammonium cobalt tetrachloride, Raman spectra near incommensurate phase transitions 0-76013  
 tetramethylammonium hexafluorophosphate, X-ray cryst. struct. determ., full-matrix least-squares refinement 0-92514  
 tetramethylammonium hydrogen bis-trichloracetate (-d<sub>n</sub>),  $^{35}\text{Cl}$  NQR study 0-66064  
 tetramethylammonium neptunium hexachloride, Mossbauer spectra and mag. susceptibility meas. 0-108140  
 tetramethylammonium octahydrotriborate, NMR study of proton and B dynamics 0-93200  
 tetramethylammonium perfluorooctanoate-water, lamellar lyotropic liq. cryst., neutron diff. struct. obs. 0-64888  
 tetramethylammonium silver iodide superionic film, electrocodeposition, electrochem. cells 0-107478  
 tetramethylammonium tetrachlorocobaltate, ferroelec., pressure-temp. phase diagrams 0-97205  
 tetramethylammonium tetrachlorocuprate, incommensurate phase, neutron diff. study 0-79935  
 tetramethylammonium tetrachlorocuprate crystal, incommensurate-ferroelastic (commensurate) phase transition obs. 0-75352  
 tetramethylammonium tetrachloroferrate, press. induced ferroelectricity, dielec. and DTA meas. 0-80722  
 tetramethylammonium tetrachlorozincate, ferroelec., pressure-temp. phase diagrams 0-97205  
 tetramethylammonium tetrachlorozincate, incommensurate phase study, ferroelectric-paraelectric phases (*French*) 0-88318



## organic compounds continued

- tetramethylammonium tetrachlorozincate, X-ray study of incommensurate phase 0-71351  
 tetramethylammonium zinc tetrachloride, ferroelectricity, triple 60 Hz D-E hysteresis loops 0-71365  
 tetramethylammonium zinc tetrachloride, incommensurate phase transitions,  $^{13}\text{C}$  NMR study 0-75968  
 tetramethylammonium zinc tetrachloride, Raman spectra near incommensurate phase transitions 0-76013  
 tetramethylbutane in hexachlorobutadiene soln., local mode overtone bands 0-83444  
 tetramethyldiaminodiphenyl ketone, binder layer, photoinduced polarisation and voltage 0-75923  
 tetramethyldiaminodiphenylmethane, exciplex form. with anthracenes, form. kinetics and luminesc. props. 0-66792  
 tetramethyldioxetane, multiphoton dissociation, collisional vibr. relax., rate eqns. model 0-63729  
 tetramethylsiloxane dicarboxylic acid Langmuir films on Cu surface, surface EM wave absorpt. study 0-97359  
 tetraphenylarsonium, Raman and IR spectra of the dicyaniodate (I) ion 0-60572  
 tetraphenylboron sodium aq. soln., dielec. relaxation spectroscopy in microwave region, double-beam interferometry (*German*) 0-71309  
 tetraphenyldiethylenetriamine mixed valence polyiodides, crystalline struct. and optical props. 0-92516  
 tetraphenylphosphonium, Raman and IR spectra of the dicyaniodate (I) ion 0-60572  
 meso-tetraphenylporphine,  $\text{NH H}^+$  tunnelling rate 0-97158  
 tetraphenylsilane, crystn. from chem. transport reaction 0-104439  
 tetraselenotetracene iodides, struct. and physical props., DC electrical cond. and EPR linewidth meas. 0-103312  
 s-tetrazine, UV and vis. photodissoc., three-body half-collision dynamics 0-78664  
 s-tetrazine, vapour, reson. CARS spectrosc., radiationless relax. rate 0-78614  
 tetrabromomethane, thermal resistivity, heat capacity and phase diagram under pressure 0-65316  
 TGS:  $\alpha$ -alanine, single crystals, dielec. spectrum in RF range (*Russian*) 0-6097  
 TGS: nitroaniline, dielec. and pyroelec. props. 0-75916  
 TGS: L-alanine, unirradiated, optical spectroscopy of scintillations 0-80863  
 TGS, autostabilised state, elec. second harmonic generation 0-103921  
 TGS, crit. behaviour of thermal expansion, neutron diff. study 0-75371  
 TGS, deuterated, ferroelec., dielec. nonlinearity 0-75959  
 TGS, effect of  $\text{Fe}^{3+}$  admixture on phys. props. 0-76052  
 TGS, electrostrictive and dielec. coeffs., neutron diff. study 0-75943  
 TGS, ferroelec., vacuum cleaved, charge compensation 0-60510  
 TGS, ferroelec. activation field change 0-71358  
 TGS, ferroelec. single crystal, low freq. nonlinear effects 0-84490  
 TGS, ferroelectric hysteresis, dielectric and pyroelectric props. (*Chinese*) 0-88938  
 TGS, internal bias field, hysteresis loops (*Chinese*) 0-84705  
 TGS, internal field prod. in layer periodical domain struct. by X-ray irradiation 0-71359  
 TGS, investigation of switching characts. using cct. containing bipolar square pulse generator 0-62687  
 TGS, kinetics of domain formation during phase transition 0-66130  
 TGS, L- $\alpha$ -alanine disordered regions, dielec. prop. changes in transition region 0-108159  
 TGS, nitroaniline admixture effect on thermal parameters 0-107580  
 TGS, perfect and imperfect, sp. ht. and sound vel., crit. anomalies 0-71331  
 TGS, spontaneous polarisation, low temp. meas. 0-75921  
 TGS, static crit. phenomena, lattice defect influence 0-71336  
 TGS ( $-\text{d}_1$ ), sp. ht. near ferroelec. phase transition 0-70420  
 TGS and deuterated cpd., ferroelec. US relax. time constant 0-84257  
 TGS crystals, effects of radiation induced defects on internal bias field 0-88941  
 TGS powders, dielec. dispersion 0-97180  
 TGS substrate, influence of polarisation reversal on elec. cond. of CdTe thin film 0-65720  
 TGSe, ferroelec., dielec. nonlinearity 0-75959  
 TGSe, autostabilised state, elec. second harmonic generation 0-103921  
 thallium hexanoate, soliton conduction, elec. cond. field and temp. depend. anomaly (*Russian*) 0-103703  
 thiamine (vitamin  $\text{B}_{12}$ ), aq. soln., radiation induced reactions 0-93779  
 thiazole, rot. Zeeman effect, localised susceptibilities 0-91600  
 thiirane +  $\text{O}_3$ , autocatalytic reaction, stopped-flow study, reaction rate meas. 0-85152  
 thiirane + olefin +  $\text{O}_3$  +  $\text{SO}_2$  0-83300  
 thiirene- $\text{d}_0$  ( $-\text{d}_1$ ) ( $-\text{d}_2$ ), IR spectra, normal coordinate anal. 0-87107  
 thio-carbonyl chlorofluoride, second excited singlet state emission spectroscopy, resonance fluorescence obs. 0-69158  
 thioether +  $\text{Li}^+$ , pair pots., ab initio LCAO SCF MO calcs. 0-58184  
 thioformaldehyde,  $\text{A}^1\text{A}_2$   $\rightarrow$   $\text{X}^1\text{A}_1$  IR absorpt. spectra 0-83362  
 thioformaldehyde, electronic struct., dipole moments, mol. polarisability, force fields, ab initio calcs. 0-78531  
 thioformaldehyde, interstellar, 3 GHz absorpt. transition obs. 0-67837  
 thioindigo adsorbed on  $\text{Al}_2\text{O}_3$ , photoisomerisation 0-89503  
 thiones, N-H-S weak and medium strength H bonds, IR spectra 0-69132  
 thionine in sodium lauryl sulphate micellar solns., absorpt. spectra and fluoresc. yield, local dye conc. depend. 0-106343  
 thionine-coated electrode for photogalvanic cells, electrochem. and XPS anal. 0-72071  
 thiophene, mean free path meas., US relax. 0-59585  
 thiophene, Penning electron spectra and photoelectron spectra, rel. intensities 0-95725  
 thiophosgene, second excited singlet state emission spectroscopy, Franck-Condon anal. 0-69157  
 thiophosgene, vibronic anal. of electronic transition, inversion doubling splittings obs. 0-83388  
 thiourea, ferroelectric, Raman and IR study 0-71406  
 thiourea, incommensurate phase transitions. thermodynamic pot. 0-79941  
 thiourea, incommensurate phase, soft modes, condensation of even-order harmonics 0-103313  
 thiourea, incommensurate phase transition, X-ray and neutron scatt. study 0-75963  
 thiourea, polycryst., mol. dynamics under hydrostatic press., NMR study 0-80619

## organic compounds continued

- thiourea, struct., hydration, ab initio SCF calcs. 0-58142  
 Thiourea- $^{35}\text{S}$ , appl. to autoradiographic image intensification, quantitative anal. 0-90343  
 thiourea- $\text{d}_4$ -ferrocene inclusion cpd. mol. motion, PMR spectrum 0-84656  
 thioureas, alkyl and phenyl groups trisubstituted, conformation, steric and stacking interaction 0-95587  
 thioxanthone, fluoresc. and internal conversion, rel. to proximity effects 0-91592  
 thorium phthalocyanine, phase contrast characteristics in STEM 0-100153  
 thulium phthalocyanine, mol. image in high resolution electron microscopy, radiation damage effect 0-107203  
 thymidine monophosphate, gamma irradiated, inorganic phosphate release, in presence and absence of  $\text{O}_2$  0-67168  
 thymidine monophosphate aqueous solution, gamma irradiation effect on base damage, phosphate release 0-89806  
 thymine base damage release, DNA of  $\gamma$ -irradiated *Tetrahymena pyriformis* 0-72268  
 thymine damage production and excision, mammalian cell DNA, high-LET irradiation obs. 0-72261  
 thymine film, polycryst., energy conversion processes, quantum yields, 4 to  $10\text{ eV}$  0-88589  
 thyroxine, free, radioimmunoassay for quantitative meas. of serum conc. 0-94344  
 TMMC, antiferromag., nuclear spin-lattice relax. by solitons 0-97159  
 TMMC, crossover transition, effects on susceptibility and EPR shift 0-71047  
 TMMC, Cu-substituted, spin dynamics, neutron scatt. cross section 0-60312  
 TMMC, linear antiferromag., mag. phase diagram, expt. and theoretical study 0-71038  
 TMMC, low-symmetry spin distrib. effect on EPR line 0-66018  
 TMMC, one-dimens. antiferromag., nonlinear dynamics 0-80521  
 TMMC, one-dimens. magnet, local magnon modes 0-65829  
 TMNC, quasi one dimensional planar ferromag., low temp. NMR study in mag. field 0-97157  
 (TMTSF) $_{\text{AsF}_6}$ , linear-chain conductor, semicond.-metal transition in small elec. field 0-103730  
 (TMTSF) $_{\text{PF}_6}$ , ESR g-factor, linewidth, spin susceptibility, metal-insulator transition 0-103887  
 (TMTSF) $_{\text{PF}_6}$ , linear-chain conductor, semicond.-metal transition in small elec. field 0-103730  
 (TMTSF) $_{\text{PF}_6}$ , quasi-dimens. cond., diamagnetic AC susceptibility 0-103781  
 (TMTSF) $_{\text{X}}$ , ( $\text{X} = \text{PF}_6^-$ ,  $\text{AsF}_6^-$ ,  $\text{SbF}_6^-$ ,  $\text{BF}_4^-$ ,  $\text{NO}_3^-$ ) highly conducting salts, props. 0-59969  
 TCNQ complex, methyltriphenylphosphonium (TCNQ) $_2$ , elec. resist. and thermoelec. power meas. 0-107777  
 tolanes, molecular conformational mobility study by optical probing method (*Russian*) 0-92459  
 toluene, gaseous, critical and liquid, electron transport 0-64673  
 toluene, in benzene soln., mol. motion, correl. functions 0-96431  
 toluene, mol. struct., ab initio calcs. 0-106262  
 toluene, thermal cond., high-precision meas. by obs. technique 0-101792  
 toluene + OH( $\text{D}$ ), vibrational and rotational energy effect 0-76497  
 toluene cation in solid Ar, absorption and photodissociation spectra 0-69156  
 toluene-sodium dodecyl sulphate-butanol 1-water mixture, interface light scatt., interface tension meas. 0-76039  
 TOPOT vapour dye lasers, multilayer reflectors 0-83606  
 2-(2-tosylaminophenyl)-4H-3,1-benzoxazine-4-one, cryst. and mol. struct. 0-84167  
 tri-n-butyl ammonium picrate + o-terphenyl, liquid systems, dielectric and dynamic Kerr-effect studies 0-60496  
 tri-n-propylamine, fluoresc. decay 0-91590  
 tri-n-propylamine doped  $\text{CO}_2$  TEA laser, parametric meas. 0-78830  
 trialkylammonium, iodides, absorpt. and luminesc. spectra of self-localized excitons 0-97340  
 trialkylthioureas, N-H stretching vibrs. and conformation 0-95586  
 triamantane, plastic and solid-solid transitions, Raman study 0-60590  
 triazastilbenes, photoelectron spectrosc. 0-106353  
 triazine dithiols, for thermal stabilisation of PVC (*Japanese*) 0-108386  
 bis-triazolopyridazines, conformation calcs. by mol. mechanics and CNDO/2 method 0-69079  
 bis-triazolyls, conformation calcs. by mol. mechanics and CNDO/2 method 0-69079  
 tribenzylmethylammonium sulphate, condensed adsorbed layer, effect on electrode reaction rate 0-93769  
 2,4,6-tribromophenol, Raman and IR spectra, hydrogen bonds 0-84735  
 1,3,5-tribromotrifluorobenzene in gaseous state, emission spectra 0-63648  
 tricarbocyanine, laser dyes, flashlamp-pumped, photochemical stability 0-83604  
 1,1,2-trichloro-2,2-difluoroethane, vac. UV photodecomp. 0-66828  
 trichloroacetic acid, soln., vibr., IR spectra 0-63633  
 trichloroanilines in solutions, IR absorpt. spectra 0-69136  
 trichlorobenzene cation, selectively excited wavelength resolved emission spectra 0-87136  
 1,2,4-trichlorobenzene liq., mol. reorientation, translation and vibr. relax., Rayleigh and Raman spectra 0-95632  
 1,1,1-trichloroethane, polymorphism under high pressure (*French*) 0-96644  
 trichlorofluoromethane, UV laser photolysis 0-66826  
 trichlorofluoromethane in stratosphere, height profile meas. at several latitudes 0-72601  
 trichloromethane, chemisorption on Cu low-index and stepped surfaces, LEED, AES and UPS obs. 0-84391  
 trichloromethane- $\text{d}_0$ - $\text{d}_1$  soln., far IR spectra, band shape and moment anal. 0-58252  
 trichloromethane-d, Raman band shapes, mol. oscill. bands (*German*) 0-69154  
 trichloromethyl peroxyhydrate, UV absorpt., spectra, photodissoc. lifetime meas. 0-83386  
 2,4,6-trichlorophenol, Raman and IR spectra, hydrogen bonds 0-84735  
 trichlorophosphazone compound,  $\text{Cl}_3\text{P}(\text{NCCl}(\text{CF}_3))_2$ , nuclear quadrupole spin-lattice relax. 0-66062  
 trichlorosilane liquid, Si-H stretching mode vibr. dephasing, Raman study 0-84736  
 tricresyl phosphate-polystyrene solns., viscoelastic props., conc. depend. 0-76299



# organic compounds continued

p-tricyanovinylphenyldicyanomethide ion, donor props., cyclic voltammetry and  $\pi$ -complex form. 0-88520  
triethylamine, fluoresc. decay 0-91590  
triethylamine, photoionisation for imaging Cherenkov detector using gas-filled MWPC 0-91400  
triethylamine- $I_2$ , n-charge-transfer complex, frozen soln., Mossbauer spectra obs. 0-91655  
triethylenediamine, Raman spectra study (*French*) 0-80768  
trifluoroacetic acid, monomer and dimer, photoelectron spectrosc. 0-87172  
trifluoroacetic acid, soln., polarisable H bonds, IR spectrosc. obs. 0-58408  
trifluoroacetophenone+dimethoxy benzene. in acetonitrile photoreaction, nuclear spin polarisation, criterion for triplet-Overhauser mechanism 0-69168  
trifluorobenzene, equilib. config. and barriers, microwave spectra 0-95606  
sym-trifluorobenzene cation, Jahn-Teller effects, intermode interactions and intensity anomalies 0-78553  
sym-trifluorobenzene cation, Jahn-Teller effects, quadrupole coupling 0-78554  
trifluorobenzene cation, selectively excited wavelength resolved emission spectra 0-87136  
trifluorobenzene cations, Jahn-Teller distortions, quadratic and mode mixing effects., distortion geometry determ. 0-91462  
trifluoroethanol, H-bonding investigated with supersonic mol. beam using photoionisation quadrupole mass spectrometer 0-102543  
2,2,2-trifluoroethanol, multiphoton absorpt. and dissoc. 0-99530  
trifluoroethene- $d_0, d_1$ , mol. struct., microwave and electron diff. obs. 0-58084  
trifluoriodomethane, highly excited, intermol. vibr. energy transfer, transient UV absorpt. spectra 0-106381  
trifluoriodomethane, IR multi-photon excited mols. 0-74207  
trifluoriodomethane, laser microwave double reson. spectroscopy with CO<sub>2</sub> laser lines 0-87156  
trifluoriodomethane, vac. UV absorpt. cross section 0-91574  
trifluoriodomethane cation, photodissoc. by quasi-continuum single IR photon absorption 0-61124  
trifluoriodomethane nuclear pumped lasers, electron impact cross section meas. 0-63985  
trifluoriodomethyl cation, IR photodissoc. 0-87188  
trifluoromethane, IR spectra, spectral bandshape and intensity of C-H chromophore 0-83355  
trifluoromethane plasma etching of SiO<sub>2</sub>, optical spectroscopy appl. 0-87940  
trifluoromethanesulphonic acid, and salts, electrochem. characts. in nonaqueous solvents 0-89499  
trifluoromethyl bromide, microwave spectra, mol. rot., isotopic variation in bond lengths, Stark meas., dipole moments determ. 0-74165  
trifluoromethyl hydroperoxide(-d), CF<sub>3</sub> torsional vibrs., low freq. Raman spectra 0-91565  
trifluoromethyl hypochlorite, vibr. spectra and normal coord. anal. 0-102517  
trifluoromethyl hypofluorite, vibr. spectra and normal coord. anal. 0-102517  
trifluoromethyl hypofluorite (hypochlorite), CF<sub>3</sub> torsional vibrs., low freq. Raman spectra 0-91565  
trifluoromethyl iodide, microwave spectra, mol. rot., isotopic variation in bond lengths, Stark meas., dipole moments determ. 0-74165  
trifluoromethyl peroxyfluoride (peroxychloride), CF<sub>3</sub> torsional vibrs., low freq. Raman spectra 0-91565  
5-trifluoromethyluracil, electron beam damage assessed by EELS 0-89809  
triglycine calcium bromide:Cu<sup>2+</sup>, ESR studies 0-97136  
triglycine fluoberyllate, deuterated, dislocation line defect X-ray topographic analysis 0-59465  
triglycine sulphate, deuterated, reticulated target for pyroelectric vidicon, IR imaging 0-77858  
triglycine sulphate, ferroelec., decoration patterns on cleavage surface, domain obs. 0-97218  
trimethyl-d<sub>9</sub>-vinylsilane, IR and Raman spectra, struct., vibr. assignment, barriers to internal rot. calc. 0-87102  
trimethylamine, collision induced fluoresc. enhancement and quenching, relax. processes 0-83412  
trimethylamine, electronically excited isolated mol., relax. and intramol. processes 0-83411  
trimethylamine, fluoresc. decay 0-91590  
trimethylamine, SCF calcs. including polaris. functions 0-87034  
trimethylamine+BCl<sub>3</sub>→BCl<sub>3</sub>N(CH<sub>3</sub>)<sub>3</sub>, complex formation, reaction product isotopic composition change (*Russian*) 0-81316  
trimethylaminegallane, microwave, IR and Raman spectra, struct., vibr. assignment 0-95600  
trimethylammonium cadmium trichloride, struct. phase transitions, low-freq. Raman scatt. obs. 0-80783  
trimethylammonium cobalt trichloride, metamagnet, AC susceptibility and exchange consts. 0-70961  
trimethylammonium manganese trichloride, Heisenberg antiferromag. chain, specific heat and EPR 0-65931  
1,3,5-trimethylbenzene, rotational and vibrational energy effect 0-76497  
trimethylbromosilane, microwave spectra, struct., chemical bonding 0-95602  
trimethylcarbinol complexes in soln., weakly H-bonded, IR bandshapes 0-106354  
trimethylvinylsilane, IR and Raman spectra, struct., vibr. assignment, barriers to internal rot. calc. 0-87102  
1,3,5-trinitro 1,3,5-triazacyclohexane, shock-induced intramol. bond breaking, XPS and EPR study 0-76512  
trinitromethane, microwave and rot. spectra, effect of twist of NO<sub>2</sub> groups, rot. and centrifugal distortion const. determ. 0-95605  
trinitrotoluene, shock-induced intramol. bond breaking, XPS and EPR study 0-76512  
triethylphosphine oxide chromatography for trans-Pu solvent extraction recovery and purification 0-93826  
trioxane,  $\nu_{19}(E)=\nu_{20}(E)=1$  state, rot. spectrum assignment, microwave obs. 0-58248  
trioxane, in nitrobenzene soln., polymerisation, polyoxymethylene morphology 0-59403  
trioxane <sup>13</sup>C(<sup>18</sup>O) substituted, mol. consts. and rot. spectra 0-87096  
triphenylcarbinol complexes in soln., weakly H-bonded, IR bandshapes 0-106354

# organic compounds continued

triphenylene derivatives, hexasubstituted, disc-like cpd., mol. conform. and arrangement, semiempirical calcs. 0-107048  
triphenylene hexaocylbenzoate, carbonaceous mesophase and disc-like liquid crystals 0-79687  
triphenylmethane dye soln., electronic relax., viscosity-depend., using picosec. flash photolysis 0-66258  
triphenylmethyl-triphenylamine mixed cryst., optical coherence storage in spin states 0-58649  
triphenylphosphite, acoustically induced birefringence 0-93274  
tripropylamine, in CO<sub>2</sub> laser gas mixture, photoionisation meas. 0-78829  
tritycene hydrogenation products, ACC and TCC, cryst. data 0-100224  
tris(bipyridine)ruthenium(II)dichloride, fluoresc. decay meas. by high repetition rate gated photon counting 0-86402  
tris(ethylenediamine)metal(III), H bonding (*French*) 0-87241  
tris(hydroxymethyl)aminomethane, crystalline and plastic structs. phase transforms. studied by X-ray diff. 0-84130  
tris(trimethylstannyl)amine, gas phase electron diffraction 0-106401  
tris (3-mercapto-1, 3-diphenyl-2-propen-1-onato) Co(III), multiple twinning 0-100250  
tris-sarcosine calcium chloride:Mn<sup>2+</sup> ferroelec. dynamics, EPR and ENDOR study 0-75972  
tris-sarcosine calcium chloride, ferroelec. transitions, soft modes, Raman scatt. spectra obs. 0-80763  
tris-sarcosine calcium chloride, phase transition, hydrostatic press. effect, dielec. const. meas. 0-71327  
trissarcosine calcium chloride, ferroelec. phase transition, Raman and Brillouin scatt. studies 0-71340  
trissarcosine calcium chloride, ferroelec. transition, press. effect 0-84681  
tRNA in soln., selected topics review, book contrib. 0-108839  
tropolone,  $\pi$ - $\pi^*$  singlet state, H<sup>+</sup> tunnelling dynamics and equilib. geometry 0-102539  
truxene derivatives, temp. inverted nematic-columnar sequence in disc-like mesogens 0-88032  
tryptophan, aqueous, one and two photon ionisation by Na laser harmonics 0-69193  
tryptophan residue in horse liver alcohol dehydrogenase, room-temp. phosphoresc., temp. and enzymic complex form. effects 0-61512  
TTF<sub>0.4</sub>TSeF<sub>0.6</sub>-TCNQ, 2k<sub>F</sub> and 4k<sub>F</sub> CDWs, X-ray study 0-65474  
TTF, enthalpy of sublimation and vapour press. meas. 0-92661  
(TTF)<sub>2</sub>, dimeric interactions, MO calcs., applicability to crystal struct. 0-75215  
(TTF)Cl<sub>2</sub>, disorder transition, cond. decrease and commensurate charge density waves 0-70153  
TTF dimer, nonbonding intermolecular forces 0-83443  
TTF salts, mixed valent, Raman spectra, formal charge rel. to Raman freq. 0-93317  
TTF-chloranil visual pressure or temperature indicator 0-87443  
TTF-CuBDT, inter- and intra-chain exchange couplings, proton spin-lattice relax. time meas. 0-71220  
TTF-TCNQ, anisotropic cond., X-ray effects 0-96855  
TTF-TCNQ, CDW transition with tripling of period along chains 0-96805  
TTF-TCNQ, dimeric interactions, MO calcs., applicability to crystal struct. 0-75215  
TTF-TCNQ, elec. cond., SEM technique 0-86507  
TTF-TCNQ, elec. resist., electron-phonon scatt. 0-92884  
TTF-TCNQ, enthalpy of sublimation and vapour press. meas. 0-92661  
TTF-TCNQ, implications of amplitude solitons in incommensurate Peierls systems 0-92841  
TTF-TCNQ, Landau theory of phase transitions 0-92666  
TTF-TCNQ, low temp. fast neutron irradiation, elec. cond. meas. 0-59964  
TTF-TCNQ, metallic cond., nonlinear amplitude-phase interaction 0-88490  
TTF-TCNQ, quasi one-dimensional low temp. mag. susceptibility 0-93069  
TTF-TCNQ, Raman spectra, formal charge rel. to Raman freq. 0-93317  
TTF-TCNQ complex, trans-diethyl-dimethyl TTF-TCNQ, one-dimens. cond. 0-96853  
TTF-TCNQ crystals, X-ray topographic study of cryst. perfection 0-96525  
TTF-TCNQ low temp. mag. susceptibility, neutron irradiation effects 0-60311  
TTT<sup>+</sup> Br<sup>-</sup>, cryst. and mol. struct., X-ray method 0-107202  
TTT, donor-acceptor system, physico-chemical studies (*Hungarian*) 0-75554  
N<sub>2</sub>-undecylmethylflavin, high resolution fluoresc. and excitation spectroscopy, vibronic transitions obs. 0-78639  
unsaturated hydrocarbons, dipole polarisabilities, STO-4G calcs. 0-83255  
uracil, nucleic acid component, selective action by ps light pulses 0-72213  
uranyl phenanthraquinone radical ion complex, longitudinal spin-lattice relax. time determ. 0-108076  
urea, electron density distrib., multipolar expansion 0-96501  
urea, fifth harmonic generation, high-efficiency high-power UV generation at 2128 Å 0-99793  
urea molecule, bond-length corrections for external and internal vibrs. 0-106402  
urea-malonic acid, room-temperature ENDOR spectra obs. 0-106339  
ureas, alkyl and phenyl groups trisubstituted, conformation, steric and stacking interaction 0-95587  
uric acid occurrence, growth morphology of C<sub>5</sub>H<sub>4</sub>N<sub>4</sub>O<sub>3</sub> anhydrous monoclinic modification 0-84123  
uridine-5'-phosphate.2Na<sup>+</sup> single crystals, radiation damage, ESR obs. 0-108964  
uro-porphyrin I octa-n-dodecyl ester, discotic phase 0-103240  
valine surface, heavy-ion induced desorption of organic cpds. 0-100739  
valyl-h-IRNA synthetase of chick embryo brain, <sup>60</sup>Co  $\gamma$ -irrad. obs. 0-72222  
vapours, lasing characteristics 0-99716  
vibrational relaxation and dephasing, Raman spectra, review 0-88987  
vinyl cation, dissociative recomb. cross section determ., merged beam obs. 0-78715  
vinyl chloride, air pollution monitoring, computer controlled CO<sub>2</sub> laser absorpt. system 0-89699  
vinyl cyanide, IR multiphoton dissoc., CN internal energy distrib., time depend. 0-78638  
vinylloxirane, Raman and IR vibr. spectra and conformations 0-83379  
viologen films, on transparent oxide electrodes, morphology, electro-optical obs. 0-100703



**organic compounds continued**

- viologens electrochromic solutions, for display appl., oxidant impurities elimination 0-78922  
 water-imidazole, H bond interrupted chain, cooperative effects, STO-3G ab initio calcs. 0-63535  
 Wolffram's red salt, mixed valence, reson. Raman calcs. using vibronic coupling model 0-97249  
 xanthene dyes in n-alcohols (ethylene glycol) (glycerol), rot. relax., time-resolved fluoresc. depolaris. obs. 0-58300  
 xanthione, large zero-field splitting of lowest triplet state 0-58171  
 xanthone, in n-pentane, heat pulse induced delayed phosphorescence 0-83404  
 XY<sub>2</sub> bent symmetrical molecules, Coriolis coupling consts., centrifugal distortion consts. 0-58236  
 p-xylene-benzene liq. mixture, excess energy of vaporisation, US study 0-65209  
 ytterbium ethyl sulphate, crystal field effects on mag. and hyperfine props. of Yb<sup>3+</sup> 0-97101  
 zinc dialkylthiophosphate surface film, prep. and nature 0-104300  
 zinc oxalate, isothermal crystallisation from soln. 0-108336  
 zinc phthalocyanine, resonant two hole bound state at 3p core threshold 0-60750  
 zinc pyrochlorophyllide in nematic liquid crystals, oriented photoexcited triplets, EPR study 0-84636  
 zinc stearate, additive to UO<sub>2</sub> green pellet fuel, effect on sintering 0-68908  
 acetaldehyde, multiphoton ionisation meas., two-photon polarisation ratio of n-3s transition 0-91610  
 Ag, adsorpt. of N,N-dimethyl aniline, adsorpt. on Ag colloids, surface enhanced Raman spectra obs. 0-97251  
 Al-stearic acid-Al, low-loss thin film capacitor 0-71317  
 anthracene, polycrystalline, optical props., 3.2-9.3 eV 0-76097  
 Au deposition at high rates from organic plating baths (*French*) 0-66441  
 BH<sub>3</sub>-ethylene complex, semiorthogonalised orbitals, integral approx. scheme 0-83262  
 C-H Raman stretching bands in soln., vibr. freqs. and linewidth 0-78622  
 CCO radical, heat of form. calc., geometries excitation energies and vibr. freq. calc. using POL-CI wave functions 0-89512  
 CD<sup>+</sup>, in RF ion trap, laser induced fluoresc. spectrum, 0,0 vibr. band and rot. consts. 0-74189  
 CF<sub>3</sub>S, mol. consts., kinetic consts. method calcs. 0-58235  
 CF<sub>3</sub>Se, mol. consts., kinetics consts. method calcs. 0-58235  
 CH, interstellar, obs. in three bright rimmed mol. clouds 0-62238  
 CH, one-centre integrals of semiempirical theories of valence, ab initio calcs. 0-102441  
 CH radical, SCF theory, multiconfig., direct orbital optimisation 0-87049  
 CH radical, sputtered, rotational and vibrational excitation 0-69224  
 CH<sup>+</sup>, a<sup>1</sup>Π-b<sup>2</sup>Σ<sup>+</sup> transition moment, ab initio calcs. 0-87047  
 CH<sup>+</sup>, excited states, pot. curves and transition moments determ. by ab initio CI methods 0-106286  
 CH<sup>+</sup>, interstellar, <sup>12</sup>CH<sup>+</sup>/<sup>13</sup>CH<sup>+</sup> abundance ratio meas. 0-67809  
 CH+O reaction, absolute rate const. 0-97690  
 CH<sub>2</sub>, CI calcs. using modified virtual orbitals 0-58163  
 CH<sub>2</sub><sup>+</sup>, Walsh's rules and small bond angle states 0-106255  
 CH<sub>3</sub>, CH<sub>2</sub> and CH deformation vibration group frequencies and MO electron densities, interaction force const. 0-87101  
 CH<sub>3</sub><sup>+</sup> affinities of methylamine, ab initio SCF calculations 0-102443  
 CH<sub>3</sub><sup>+</sup> affinities of NH<sub>3</sub>, ab initio SCF calculations 0-102443  
 C,H, interstellar, distrib. in vicinity of young B-type stars (*Russian*) 0-105321  
 C<sub>2</sub>H<sub>2</sub><sup>+</sup>, dissociative recomb. cross section determ., merged beam obs. 0-78715  
 C<sub>2</sub>H<sub>2</sub> species formed in chemisorption of ethylene on Pt, vibr. anal. 0-61150  
 C<sub>2</sub>H<sub>2</sub><sup>+</sup>+HF, interaction, struct. and stability, ab initio calcs. 0-58347  
 CH(A<sup>2</sup>Δ) radicals, electronically excited, lifetimes and quenching rate constants meas. 0-69188  
 CHF radical,  $\tilde{A}'^2\text{A}''-\tilde{X}'^2\text{A}'$  transition, laser induced fluoresc. 0-95660  
 CH<sub>2</sub>OH<sup>+</sup>, IR photodissoc., fluence depend., saturation effects 0-78663  
 CH<sub>2</sub>PF<sub>3</sub>, nonrigid mol., tunnelling mechanisms, spectrosc. theory 0-78605  
 CN<sup>-</sup>, electron propagator theory, mol. electron affinities calcs. 0-83521  
<sup>13</sup>C, CIDNP, obs. in reactions of organic and inorganic radicals during pulse radiolysis 0-63660  
 Cd complexes, Cd(II) mixed halide complex anions, Raman spectra 0-58270  
 ClH-dimethyl ether, vibr.-rot. IR spectra, quantum and classical mechanics 0-91561  
 Co(III) salen complexes, O binding, reson. Raman obs. 0-58267  
 Cr dithiocarbamate complexes, IR, electronic and mass spectra, mag. susceptibility, cond. meas. 0-97270  
 Cu complex, bis(triphenylphosphine) phenanthroline copper (I), luminesc. spectra, decay times 0-60648  
 Cu II complex, extended X-ray absorpt. fine struct. study 0-104011  
 Cu phthalocyanine thin film electrodes, near IR photoelectrochemical responses 0-93766  
 D+PTFE, DF\* prod., Fourier transform IR spectroscopy 0-87105  
 ethanol-water system, complex dielec. permitt. in UHF region and NMR spectra (*Japanese*) 0-10620  
 F+benzene derivatives, deuterated, IR chemiluminesc. 0-102506  
 F+ethylene derivatives, deuterated, IR chemiluminesc. 0-102506  
 fluoromethane 496-μm laser, CO<sub>2</sub> laser pumping dispersion 0-87375  
 HCP, force fields and force consts. of electronically excited states 0-69116  
 He-Ne-methane ring laser, power resonances 0-99761  
 He-Ne-methane ring laser, freq. synchronisation interval for oppositely directed waves 0-99762  
 IBr-benzene in n-decane soln., IR line broadening by chemical exchange 0-87111  
 Ir(III) complex, cis-dichlorobis(4,4'-dimethyl 2,2'-bipyridine) iridium chloride 0-97319  
 K<sup>+</sup>CF<sub>3</sub>SeO<sub>2</sub><sup>-</sup>, IR and Raman spectra, normal coordinate anal. for CF<sub>3</sub>SeO<sub>2</sub><sup>-</sup> anion 0-87122  
 Li salt of β-ketoaldehyde, configurations of anions in solutions studied by IR spectroscopy, H-bond form. 0-87117  
 MBBA+optically active substance, pretransition optical rotation in isotropic phase (*Russian*) 0-92657  
 methane 2ν<sub>3</sub>-ν<sub>4</sub> and ν<sub>3</sub>+ν<sub>4</sub>-ν<sub>2</sub> hot bands, difference bands 0-63632  
 methane+Cl<sup>-</sup>, total electron detachment cross sections for energies around threshold 0-99550

**organic compounds continued**

- methane+NO, NO γ(0,0) band, oscillator strength and line broadening 0-106356  
 methane+S, electronically excited atom, reson. fluoresc. 0-99476  
 Mn dithiocarbamate complexes, IR, electronic and mass spectra, mag. susceptibility, cond. meas. 0-97270  
 N<sub>2</sub>-methane, liquid, high resolution CW CARS spectra 0-63635  
 NH<sub>4</sub><sup>+</sup>CF<sub>3</sub>SeO<sub>2</sub><sup>-</sup>, IR and Raman spectra, normal coordinate anal. for CF<sub>3</sub>SeO<sub>2</sub><sup>-</sup> anion 0-87122  
 Na<sub>2</sub>S<sub>2</sub>O<sub>8</sub>-picric acid-ethanol-H<sub>2</sub>O etchant for high-strength dual-phase steel 0-100951  
 PMMA, resonance size effect in space charge relaxation 0-75937  
 Pb dithiocarbamate complexes, IR, electronic and mass spectra, mag. susceptibility, cond. meas. 0-97270  
 Pd and Pt mixed valence complex, [Pd(ethylenediamine)<sub>2</sub>][Pt(ethylenediamine)<sub>2</sub>Cl<sub>2</sub>](ClO<sub>4</sub>)<sub>4</sub>, Raman spectra 0-84734  
 Pt complex, [2, 2', 2''-terpyridine PtCl]<sup>+</sup>, motion of Pt atoms, electron microscopy obs. 0-103314  
 Pt porphyrin in n-alkane single cryst. <sup>3</sup>E<sub>g</sub>-<sup>1</sup>A<sub>1g</sub> transition, Zeeman expts. at 4.2K 0-78645  
 Rb<sup>+</sup>CF<sub>3</sub>SeO<sub>2</sub><sup>-</sup>, IR and Raman spectra, normal coordinate anal. for CF<sub>3</sub>SeO<sub>2</sub><sup>-</sup> anion 0-87122  
 SO<sub>2</sub>-tetrachloromethane, solns., near critical point, ultrasound absorpt. obs. 0-65160  
 Si substrate for PMMA electron sensitive layer, 400 Å linewidth electron beam lithography 0-65392  
 Sn dithiocarbamate complexes, IR, electronic and mass spectra, mag. susceptibility, cond. meas. 0-97270  
 SnO<sub>2</sub>-copper phthalocyanine-Ag systems, elec. and electroluminescent behaviour 0-80864  
 TBSe, crit. behaviour, electrostrictive coupling role 0-71329  
 TCNQ, ab initio SCF LCAO band struct. calc. 0-70608  
 TCNQ salts, Qn(TCNQ)<sub>2</sub> and N-propyl-Qn(TCNQ)<sub>2</sub>, low temp. mag. susceptibility, neutron irradi. effects 0-60311  
 TGS, crit. behaviour, electrostrictive coupling role 0-71329  
 TGS, ferroelectric phase transition, high resolution NMR study 0-97214  
 (TMCHDT)<sub>2</sub>ClO<sub>4</sub>, organic conductor, struct. study (*French*) 0-88133  
 TMMC, antiferromagnetic chain, 3-D ordering temp. controlled by solitons and defects, mag. field depend. 0-60275  
 (TSeT)<sub>2</sub>Cl complex, phase transform. under press., cond. (*Russian*) 0-92674  
 TTF, ab initio SCF LCAO band struct. calc. 0-70608  
 TTF salts, intermolecular energy and struct. from atom-atom potentials 0-79738  
 TTF-TCNQ, const. volume resistivity anomalous behaviour 0-103682  
 TTF-TCNQ, high press. structural transitions, neutron scatter. study 0-96647  
 (TTF)<sub>2</sub>I<sub>3-x</sub>, incommensurate crystal phases symmetry, incommensurate basic struct., superspace group approach 0-79727  
 TTTI<sub>3-x</sub> complex, influence of press. on metal-dielectric phase transition (*Russian*) 0-92818  
 TI complex of lasaloid (X-537A), <sup>205</sup>Tl NMR study 0-58288  
 Zn-nucleotide, triphosphate complexes, <sup>35</sup>Cl NMR obs. 0-63661

**organic insulating materials**

- see also insulating oils; paper; plastics; rubber; silicones; varnish; waxes  
 carrier traps in polymeric insulating materials, investigation by X-ray induced thermally stimulated current and thermoluminescence methods 0-93240  
 epoxy resin insulation of HV electrodes, effect on dielec. breakdown voltage of polymer sheets 0-60502  
 ethylene propylene/polyolefin blends, radiation cross linking 0-66801  
 fusion reactor, FTIR outer poloidal field coil insulation and mould design 0-91261  
 gases, replacement for SF<sub>6</sub> 0-59313  
 glass fibre reinforced epoxy resin composites, fatigue behaviour, influence of superposition of elec. mech. and environmental stresses 0-97590  
 hexafluoropropylene-tetrafluoroethylene copolymer, surface component of vac. absorpt. and resorpt. currents, source of dielec. loss 0-70792  
 high molecular weight polyethylene for HV cables, characterisation using size exclusion chromatography 0-66897  
 Large Coil Program, insulation system cryogenic elec. test 0-91263  
 liquid conductivity and bulk charge determ. cell (*Russian*) 0-57328  
 methacrylic polymers, multiple dielectric relaxations, investigation by thermally stimulated current and creep methods 0-93238  
 neutron irradiation effects on organic insulators at 5K for superconducting magnets 0-107336  
 polyester thermoplastic, for electrical insulators 0-103685  
 polyethylene terephthalate polymer insulator, conduction and breakdown mechanism (*German*) 0-10469  
 polyimide films, transient current in time range 10<sup>-4</sup> to 10 s at temps. 180 to 280°C 0-65729  
 polymeric, cable insulation, radiation modification using electron beams 0-66848  
 polymeric insulating materials, water treeing initiation and growth, effects on cable service life 0-84698  
 polymers, surface component of vacuum absorpt. and resorpt. currents, surface charge accumulation 0-60063  
 polymers, surface component of vacuum absorpt. and resorpt. currents, origin and magnitude 0-70791  
 polyolefin, cross-linked, insulation system for wire and cable for locomotives 0-66851  
 polyolefin, cross-linked, irradiation appl. to provide improved insulation props. to wires and cables 0-66850  
 polypropylene film, dielectric relaxation, β-mode investigation 0-93239  
 polypropyromellitimide film, elec. cond., 120-180°C 0-60124  
 PVC, cross-linked, irradiation appl. to provide improved insulation props. to wires and cables 0-66850  
 PVC materials, cross-linkable, for wires and cable insulation 0-66849  
 solid insulating materials, dielectric properties at cryogenic temps. 0-90867  
 Valox 752m thermoplastic, for electrical insulators 0-103685

**organic molecule configurations**

## see also isomerism

- acetate-ferrihemoglobin, X-ray struct. anal., 3D refinement at resoln. of 2.0 Å 0-104554  
 acetone-toluene-tetrachloromethane, mol. interaction and thermodynamic props. 0-71935  
 acetonitrile-d<sub>3</sub>, <sup>2</sup>H NMR spectra, vibr. and asymmetry corrections to quadrupole coupling consts. 0-74184



## organic molecule configurations continued

- acetonitrile-toluene-benzene, mol. interaction and thermodynamic props. 0-71935  
 N-acetyl-D-alloisoleucine,  $^{13}\text{C}$  NMR, soln. struct., dynamics, proton relaxation mechanisms 0-76708  
 acetylene, excited state, photochem. and spectrosc. investig. 0-95553  
 acetylene chemisorption on Rh (111), EELS, LEED and thermal desorption mass spectrometry 0-80057  
 acetylene- $\text{d}_0$ -( $\text{d}_1$ )-( $\text{d}_2$ ) metastable state, mol. beam elec. deflection obs. 0-74137  
 acetylene-LiH, struct. and props., SCF ab initio calcs. 0-106250  
 N-acetylglycine, X-irrad., stable radical electronic and mol. struct., ENDOR and ESR 0-80637  
 alarm pheromones, activity rel. to mol. similarity, electron density function meas. 0-91413  
 aliphatic ketones, freq.-topology-milieu relation, IR study, struct. and solvent effect (French) 0-95623  
 alkanes, liq., mol. struct., selective deuteration and IR vibr. spectra 0-96432  
 alkyl halides, conform. energy calcs., polar bonds and polarisability, polaris. model appl. 0-58188  
 alkylnyl cations, struct., charge distrib., ab initio population anal. calcs. 0-58407  
 allyl radical, restricted SCF and MC SCF calc. of  $\text{C}_{2v}$  and  $\text{C}_s$  structs. 0-83289  
 2-amino-4-chlorophenol in solutions, IR absorpt. spectra 0-69135  
 2-amino-p-resol in solutions, IR absorpt. spectra 0-69135  
 aminoacetaldehyde, conformation calcs. rel. to protein struct. and bonding 0-74273  
 aminopyrazine, far IR spectra, barrier to planarity, pot. function and energy levels 0-69137  
 aniline, in p-xylene host cryst., phosphoresc. triplet state, ESR and MIDP obs. 0-66077  
 annulenes, graph theoretical polynomials 0-69048  
 anthraquinone in pentane solvent, sublevel phosphorescence spectra, molecular distortion 0-74190  
 aromatic polyesters, with S atoms, configurational props. 0-74269  
 azacyclobutadienes, conjugated mols. electronic struct. and geometry, Hartree-Fock instability 0-69055  
 azulene, multiphoton ionisation, mass spectra 0-63717  
 benzaldehyde, and isomeric phthalaldehydes, dipole moments meas., config., ab initio MO calc. 0-58410  
 benzene- $\text{d}_1$ ,  $^2\text{H}$  NMR spectra, vibr. and asymmetry corrections to quadrupole coupling consts. 0-74184  
 benzenoid aromatics, triplet zero field splitting parameters, ODMR obs., struct. effects 0-78636  
 benzoic acid, struct. refinement at room temp. 0-96502  
 benzyl mercury chloride, cryst. struct. and absorpt. calcs. 0-84166  
 bicyclic ring compounds, Raman circular intensity differential spectra obs., mol. struct. 0-87130  
 $\Delta^4$ -bicyclo(3,2,0)heptane, conformational mobility 0-99587  
 biologically active compounds, design using MOLY computer system 0-63852  
 biomolecule, non-centrosymmetry, optical second harmonic generation 0-72133  
 bromocyclotriphosphazatrienes,  $^{81}\text{Br}$  NQR, conformation investig. 0-63665  
 butadiene, twisted zwitterionic excited states, SCF calcs. 0-58179  
 t-butyl acetate, rot. isomerism, dielect. and Raman spectra 0-106328  
 butyl cation, H-elimination, energy partitioning, transition state geometry calc. using MINDO/3 0-104430  
 t-butyl formate, rot. isomerism, dielect. and Raman spectra 0-106328  
 3-butyne-1-ol, vibr. spectra, assignments, rot. isomerism 0-58257  
 cadmium formate, anhydrous, cryst. struct. 0-107195  
 carbenes, heterosubstituted, singlet-triplet splitting depend. on heteroatom electronegativity and conform. 0-63553  
 ceruloplasmin, human, calc. of rotation function for tetragonal. cryst. at 10 Å resoln. 0-108843  
 chloro(ethyl)silanes and its C derivatives, Raman spectra, mol. vibr. and rot. isomerism 0-87134  
 chlorobenzene, gas phase electron diff. struct. determ. 0-69251  
 trans-1,4-chlorobromocyclohexane, liquid, crystalline and amorphous state, conformation and vibr. spectra, IR obs. 0-60568  
 2-chloroethyl radical, struct., ab initio calcs. 0-83252  
 trans-1,4-chloriodiocyclohexane, liquid, crystalline and amorphous state, conformation and vibr. spectra, IR obs. 0-60568  
 p-chloronitrobenzene, struct. determ. by electron diff., influence of  $\text{NO}_2$  group on C-Cl bond 0-69251  
 cholesterol ethyl carbonate, long periods in sol. state, X-ray diff. study 0-96503  
 cis-1-cholobutadiene-1,3, microwave spectrum, struct., nuclear quadrupole coupling, distortion const., thermodynamic functions calc. 0-99500  
 chrysene, excited singlet and triplet state, CARS obs. 0-83374  
 cobalt dimethyl glyoximate, molecular struct., cryst. structure 0-79769  
 conference, Crystal XII, Canberra, Australia (Jan-Feb. 1980) 0-62388  
 cordycepin, X-ray cryst. struct. determ. 0-107198  
 coumarin laser dyes, fluoresc. quantum yields and lifetimes, polar solvent effects 0-87054  
 p-cyano-N,N-dimethylaniline in polar solvents, double fluorescence, theoretical model 0-58296  
 6-cyanobenzquinuclidine, intramol. electron-transfer excited state 0-82895  
 cyanobiphenyls molecular conformational mobility study by optical probing method (Russian) 0-92459  
 cyclic 3- and 4-membered ring cpds., saturated, ab initio struct. anal. 0-58192  
 cyclic 4-ring rotation-puckering, use of spherical coords. 0-58193  
 cyclic mol. struct., topological characterisation 0-74254  
 cyclobutane-( $\text{d}_4$ ), centrifugal distortion const. calc., rel. to struct. and mol. wt. 0-95580  
 cyclohexane- $\text{d}_{12}$ , Raman linewidth and molecular diameter meas. 0-69153  
 cyclohexene vapour, IR spectra anal. 0-63628  
 1,2,6-cyclononatriene, mol. struct. and conformation, gas phase electron diff. 0-106400  
 1,2-cyclooctadiene, conformational energy surface, Boyd's iterative force field investig. 0-95737  
 cyclopentylamine, vibr. spectra and struct. 0-102516  
 cyclophosphazene-DNA complex, spectrofluorometric and spectrophotometrics investig. 0-95643

## organic molecule configurations continued

- cyclopropane-( $\text{d}_4$ ), centrifugal distortion const. and thermodynamic functions calc. 0-95582  
 cytochrome c, PMR, eight-ring current model heme ring, conformation depend. shifts 0-74185  
 deuteromethane, crystalline, X-ray powder diff. study 0-96500  
 di(tert. butylperoxy)triphenylantimony, X-ray cryst. struct. determ. 0-92517  
 dialkyl tartrates, Raman circular intensity differential spectra obs., mol. struct. 0-87130  
 dibromoalkanes, energy partitioning in mass spectrometric displacement reactions 0-89471  
 1-10-dicarba-closo-decarborane (10), mol. struct., vibr. and shrinkage corrections calc. from force field 0-95739  
 dicyanoketene, and isomeric forms, heat of form., ab initio STO-3G calcs. 0-58190  
 1,1-difluoroethane, mol. struct., gas phase electron diff. obs. 0-58385  
 difluoromethylborane, nonrigid, symmetry group calcs. 0-106254  
 2,3-dihydropyran vapour, IR spectra anal. 0-63628  
 dihydroquinoxalinediones, conjugated mols. electronic struct. and geometry, Hartree-Fock instability 0-69055  
 5,7-dimethoxyindane-1-one, cryst. and mol. struct. 0-100223  
 dimethyl ethyl amine, mol. struct. determ. by gas phase electron diff. 0-95743  
 dimethyldichlorosilane, microwave spectrum, rot., centrifugal distortion and quadrupole coupling consts. 0-91547  
 diphenylpolyene molecules, excited electronic states, vibronic mixing, wave functions, method of fragments anal. 0-63615  
 DNA, possible conformations calcs. 0-76705  
 DNA compact form, tertiary struct., small angle X-ray scatt. 0-72129  
 EBBA, mol. and cryst. struct., X-ray diff. study 0-88134  
 EBBA, NMR and Raman scatt. studies in nematic phase 0-100619  
 epifluorohydrin, IR and Raman spectra and conformations 0-60576  
 ethane gas, local mode overtone bands 0-83444  
 ethyl-furan-2-carboxylate, skeletal vibr. of IR spectra, conformational props., solvent polarity effect 0-87118  
 ethylbenzene, vapour, conform. and struct. obs. 0-69247  
 ethylcyclopropane, solid, liquid, vapour phase, IR and Raman vibr. spectra 0-84740  
 ethylene, chemisorbed on Rh (111), EELS, LEED and thermal desorption mass spectrometry 0-80057  
 ethylene, molecular geometry optimisation, variable metric method, internal geometry 0-95744  
 ethylene as singlet methylene dimer, nonempirical double zeta calculations, zwitterionic singlet excited states 0-83258  
 ethylene ozonide, ab initio gradient and MC SCF calc., conformational anal. 0-83290  
 ethylene-LiH, struct. and props., SCF ab initio calcs. 0-106250  
 ethyloxirane, solid, liquid, vapour phase, IR and Raman vibr. spectra 0-84740  
 Faraday effect measurement in pulsed mag. field 0-80758  
 fluoronitrobenzene, equilib. config. and barriers, microwave spectra 0-95606  
 formaldehyde dimers, matrix isolated, struct., IR spectra 0-99504  
 formamide, force consts. and dipole moment derivatives, ab initio MO calcs. 0-95521  
 formic acid,  $^{13}\text{C}$ ,  $^{18}\text{O}$ , microwave spectra and centrifugal distortion consts. 0-83352  
 formic acid, fragmentation, fragment structs. and energies calcs. 0-74124  
 cis-formic acid geometry, force fields and fundamental vibr. freq., ab initio study 0-87040  
 haematoporphyrine, complexed with chloranil and tryptophane, energy spectra, transition moments and intermolecular distances 0-72127  
 haemocyanin of Limulus polyphemus, quaternary struct. 0-85337  
 halogermane radical anions, ESR spectra and struct. 0-87153  
 hexafluorobenzene, quadrupole moments, elec. field-gradient birefringence method 0-95746  
 hexafluorobenzene radical anion,  $^{13}\text{C}$  hyperfine interaction, EPR obs. 0-83392  
 hexafluorocyclopropane, centrifugal distortion const. and thermodynamic functions calc. 0-95582  
 hexamethylbenzene, quadrupole moments, elec. field-gradient birefringence method 0-95746  
 hexamethylbenzene in tetrachloromethane soln., local mode overtone bands 0-83444  
 hydrocarbon ions, mass spectra, H atom scrambling, delocalisation 0-58135  
 hydrocarbons, alternate conjugated, topological props. of HOMO-LUMO separations 0-69049  
 2-iodoacetamide, mol. struct., electron diff. obs. 0-63819  
 isopropyl radical, pot. energy surfaces, ab initio UHF calcs. 0-106258  
 isopropylcyclopropane, solid, liquid, vapour phase, IR and Raman vibr. spectra 0-84740  
 Kruzewski's rule, for stability of isomeric polycyclic conjugated cpds., proof 0-106249  
 liquid crystals, mol. conformation and orientational order, NMR studies, review 0-75151  
 malonic acid, and  $\alpha$ -alkyl derivatives, photoelectron spectra, lone-pair interactions 0-58315  
 manganese carboxylate, dodecanuclear mixed-valence, prep., struct., and mag. props. 0-107196  
 MBBA, NMR and Raman scatt. studies in nematic phase 0-100619  
 membrane-active complexon fragments, nonrigidity effects calcs. 0-91704  
 methane ring compounds, Raman circular intensity differential spectra obs., mol. struct. 0-87130  
 mesophase pitch, magnetically-oriented, phys. props., mol. struct. 0-64885  
 methane, mol. cations, struct., Jahn-Teller effect, MINDO/3 calcs. 0-74135  
 methane+ $\text{O}^+(\text{P})$ , barrier height and transition state geometry, POL-CI calc., H abstraction reaction 0-66782  
 methane cation, photodissoc., ab initio RHF and MRD CI calcs. 0-95695  
 $\alpha$ -methane- $\text{d}_4$ , crystalline, X-ray powder diff. study 0-96500  
 methanol, molecular geometry optimisation, variable metric method, internal geometry 0-95744  
 methotrexate-dihydrofolate reductase complex form., conform., laser Raman obs. 0-104553  
 p-methoxybenzylidene-cyanoaniline, mol. and cryst. struct., X-ray diff. study 0-88134



**organic molecule configurations continued**  
 methoxydifluorophosphine- $d_0$  and - $d_3$ , IR and Raman spectra, mol. vibr. and struct. obs. 0-87103  
 methyl fluoroformate, isomer conformation, CNDO and ab initio STO calcs. 0-58151  
 methyl furan-2-carboxylate, skeletal vibr. of IR spectra, conformational props., solvent polarity effect 0-87118  
 methyl furan-2-thiolcarboxylate, skeletal vibr. of IR spectra, conformational props., solvent polarity effect 0-87118  
 methyl group,  $^{13}\text{C}$  chemical shifts, H/H, H/Me and Me/Me interactions 0-95652  
 N-methyl m-fluoroaniline, conformational anal., microwave spectra obs. 0-58247  
 s-methyl nitrite, methyl group rot. barriers in cis and trans forms, ab initio calcs. 0-74111  
 N-methyl-p-fluoroaniline, struct. of  $\text{HNCH}_3$  group 0-95741  
 methylene peroxide, struct., energy levels, ab. initio UHF and MRUHF NO CI calcs. 0-83287  
 4,4'-methylenecis[1,3,5-trimethyl-4-imidazolin-2-one], cryst. and mol. struct. 0-107201  
 methylpropylether, trans-trans isomer, microwave spectra, struct., dipole moment and rot. barriers calcs. 0-83348  
 methylzinc methoxide, tetrameric, X-ray cryst. struct. determ. 0-107197  
 molecular crystals, optical diffr. patterns, comparison with X-ray scattering photographs 0-78783  
 molecules  $D_{6h}$ ,  $D_{3h}$  and  $D_{3d}$  appln. of Aliev-Watson maxima-minima criteria for quartic centrifugal distortion const. 0-87132  
 naphthalene, multiphoton ionisation, mass spectra 0-63717  
 naphtho[1,8-cd:4,5-c'd']bis[1,2,6]thiadiazine, mol., electronic, cryst. struct. 0-64984  
 neopentane liq., local mode overtone bands 0-83444  
 nicotinamide adenine dinucleotide, and reduced form, pH induced modification, Raman spectra 0-85343  
 nitrocyclopropane, vibr. spectra struct. and bonding 0-102520  
 nitroxide groups in crystals, H bonds and short intermolecular contacts 0-63855  
 nitroxyl radicals, cyclic, conform. flexibility, EPR obs. 0-91581  
 nucleic acids bases, excited state dipole moments and geometries 0-95738  
 organic dyes, fluoresc. spectra calcs.,  $\beta$ -variation method (German) 0-69182  
 palmitic acid-choleic acid complex, cryst. struct. and van der Waals energy 0-64983  
 papain models, active site  $\alpha$ -helix and ion pair stability 0-74265  
 pentachlorotoluenes, positional isomers,  $^{13}\text{C}$  Fourier transform NMR spectrometry, struct. and compositional anal. 0-91576  
 peptides, bradykinin-potentiating, spatial structs. 0-95736  
 peroxy chain radicals, reactivity and struct., EPR spectra, trapped in PTFE 0-66783  
 phenyl cation, struct., ion-molecule reactions studied by trapped ion mass spectroscopy 0-102586  
 phenylphthalenes isomers, fluoresc. lifetime difference and mol. geometry 0-69176  
 polydimethylsiloxane end-linked chains, nonGaussian effects 0-65127  
 potassium formate, X-ray cryst. struct. determ. 0-107194  
 n-propanol, preferred conformers, PCICO study 0-95542  
 propioly chloride(-d), 357-333 nm absorpt. system 0-69161  
 propioly fluoride(-d), 290 nm absorpt. system 0-87142  
 propynyl cation+propyne, reactant structure effects 0-89469  
 pyrrole-acetonitrile, H-bonded complex, ab initio MO calcs. 0-102440  
 quinoxalines, enzyme inhibitory, structure-activity quantitative study 0-58340  
 quinuclidine struct. determ. by gas phase electron diffr. 0-95742  
 radicalenes, graph theoretical polynomials 0-69048  
 9-cis retinal, visual pigment chromophore, twisting mechanism 0-58333  
 11-cis retinal visual pigment chromophore, twisting mechanism 0-58333  
 ribonuclease A, bovine, cryst. struct. determ. by X-ray and neutron diffr. 0-108841  
 ring current theory 0-87240  
 Schiff base azo dyes in nematic liq. cryst. hosts, order parameters, optical density meas. 0-84055  
 six-membered rings, conformation, nomenclature 0-78721  
 sodium dodecyl sulphate:  $\text{Gd}^{3+}$ , micellar system, chain folding,  $^{13}\text{C}$  NMR obs. 0-61158  
 sodium dodecyl sulphate micelles- $\omega$ -( $\alpha$ -naphthyl) dodecanoic acid soln. fluoresc. decay obs. 0-61158  
 stereodiagrams, 3D coordinates of mol. structs. 0-64824  
 tetrafluoro-p-benzoquinone, mol. struct., gas phase electron diffr. obs. 0-83486  
 1,1,1,2-tetrafluoroethane, mol. struct. studied by gas-phase electron diffr., vibr. amplitudes, bond angles and lengths calc. 0-95740  
 2,2,5,5-tetramethyl-4-phenyl-3-imidazalin-3-oxide-1-oxyl, deform. electron density determ., X-ray diffr. 0-88135  
 tetramethylbutane in hexachlorobutadiene soln., local mode overtone bands 0-83444  
 2-thio alkyl (allyl, benzyl) pyrimidines, IR and Raman spectra anal., mol. vibr. and symmetry (French) 0-87123  
 thiones, N-H-S weak and medium strong H bonds, IR spectra 0-69132  
 thiourea, struct., hydration, ab initio SCF calcs. 0-58142  
 thioureas, alkyl and phenyl groups trisubstituted, conformation, steric and stacking interaction 0-95587  
 thympoietin active fragment in  $\text{H}_2\text{O}$ , soln. conformation by DNMR spectroscopy 0-89710  
 tolanes, molecular conformational mobility study by optical probing method (Russian) 0-92459  
 2-(2-tosylaminophenyl)-4H-3,1-benzoxazine-4-one, cryst. and mol. struct. 0-84167  
 trialkylthioureas, N-H stretching vibrs. and conformation 0-95586  
 bis-triazolopyridazines, conformation calcs. by mol. mechanics and CNDO/2 method 0-69079  
 bis-triazolyls, conformation calcs. by mol mechanics and CNDO/2 method 0-69079  
 trichloroanilines in solutions, IR absorpt. spectra 0-69136  
 trifluorobenzene, equilib. config. and barriers, microwave spectra 0-95606  
 1,3,5-trifluorobenzene, quadrupole moments, elec. field-gradient birefringence method 0-95746  
 trifluorobenzene cations, Jahn-Teller distortions, quadratic and mode mixing effects., distortion geometry determ. 0-91462  
 trifluorodimethylmercury, gas phase mol. struct., electron diffr. and microwave spectra obs. 0-78609  
 trifluoroethene- $d_0$ ,  $d_1$ , mol. struct., microwave and electron diffr. obs. 0-58384

**organic molecule configurations continued**  
 trimethyl-d<sub>3</sub>-vinylsilane, IR and Raman spectra, struct., vibr. assignment, barriers to internal rot. calc. 0-87102  
 trimethylaminegallane, microwave, IR and Raman spectra, struct., vibr. assignment 0-95600  
 1,3,5-trimethylbenzene, quadrupole moments, elec. field-gradient birefringence method 0-95746  
 trimethylbromosilane, microwave spectra, struct., chemical bonding 0-95602  
 trimethylvinylsilane, IR and Raman spectra, struct., vibr. assignment, barriers to internal rot. calc. 0-87102  
 trioxane  $^{13}\text{C}$ ( $^{18}\text{O}$ ) substituted, mol. consts. and rot. spectra 0-87096  
 triphenylene derivatives, hexasubstituted, disc-like cpd., mol. conform. and arrangement, semiempirical calcs. 0-107048  
 triphenylmethane dye soln., electronic relax., viscosity-depend., using picosec. flash photolysis 0-66258  
 triptycene hydrogenation products, ACC and TCC, cryst. data 0-100224  
 tris(trimethylstannyl)amine, gas phase electron diffraction 0-106401  
 $\text{TTT}^+\text{Br}^-$ , cryst. and mol. struct., X-ray method 0-107202  
 ureas, alkyl and phenyl groups trisubstituted, conformation, steric and stacking interaction 0-95587  
 vinylloxirane, Raman and IR vibr. spectra and conformations 0-83379  
 water-imidazole, H bond interrupted chain, cooperative effects, STO-3G ab initio calcs. 0-63535  
 xanthene dyes in n-alcohols (ethylene glycol) (glycerol), rot. relax., time-resolved fluoresc. depolaris. obs. 0-58300  
 $\text{C}_2\text{H}_5^+ + \text{HF}$ , interaction, struct. and stability, ab initio calcs. 0-58347  
 Co II complexes, with tetradentate Schiff bases, synthesis, struct. and ESR obs. 0-80598  
 CuH, UV absorpt. spectra 0-87143  
 K salt of  $\beta$ -ketoaldehyde, configurations of anions in solutions studied by IR spectroscopy, H-bond form. 0-87117  
 Li salt of  $\beta$ -ketoaldehyde, configurations of anions in solutions studied by IR spectroscopy, H-bond form. 0-87117  
 Na salt of  $\beta$ -ketoaldehydes, configurations of anions in solutions studied by IR spectroscopy, H-bond form. 0-87117  
 $(\text{TMCHDT})_2\text{ClO}_4$ , organic conductor, struct. study (French) 0-88133

**organic molecule electronic structure** see *molecular electronic states*

**organic semiconductor materials** see *organic semiconductors*

#### organic semiconductors

acceptor-donor-acceptor complex, Frenkel excitons and ionic excited states 0-92824  
 adenine film, polycryst., energy conversion processes, quantum yields, 4 to 10 eV 0-88589  
 anthracene, metastable triclinic phase 0-59452  
 anthracene crystals, orientationally disordered, exciton trap depths 0-88481  
 anthracene Langmuir films, lightly substituted, AC and DC cond. 0-80425  
 anthracene-phenanthrene-TCNB, exciton transport obs. 0-65461  
 chromophore phospholipid Langmuir films, photoeffects 0-80409  
 copper phthalocyanine film, electron acceptor surface states due to  $\text{O}_2$  adsorption 0-88586  
 copper phthalocyanine-iodine, amorphous cpd. prep. by  $\text{I}_2$  diffusion in polycryst., triplet EPR signals obs. (Russian) 0-66016  
 2,6-N,N-diacyetyldiaminopyridine elec. cond.,  $\gamma$  dose and temp: (303-363K) effects 0-103696  
 2,6-N,N-dibenzoyldiaminopyridine elec. cond.,  $\gamma$  dose and temp. (303-363K) effects 0-103696  
 film, Schrieffer effect 0-60118  
 germanium phthalocyanine, elec. cond. temp. depend. 0-80271  
 Kapton, pyrolysed, cond. polymer, transport and mag. props. 0-96887  
 lead phthalocyanine: $\text{O}_2$ (I), Schottky barrier effect on AC current response 0-75623  
 magnesium phthalocyanine, film, depletion layer studies, temp. depend. of LF capacitance 0-65617  
 naphthalene, charge carrier drift mobility, semi empirical anal. 0-65553  
 naphthalene, electron and hole off-diagonal mobility component determ. 0-65552  
 naphthalene, electron trapping, one-carrier TSC and SCL currents 0-70715  
 nickel phthalocyanine film, electron acceptor surface states due to  $\text{O}_2$  adsorption 0-88586  
 phenothiazine derivatives, semicond. elec. props., optical spectra, and EPR 0-103693  
 phthalocyanine layers, metal-free, between Ag and Al electrodes, switching effects 0-65706  
 phthalocyanine metal free films, TSC, ferroelectric-semiconductor transition 0-66105  
 poly(p-phenylene), electronic struct., one-electron band theory 0-65450  
 poly- $\alpha$ -naphthol, semicond., isothermal depolarisation currents, electron trap parameters 0-60492  
 poly-N-vinylcarbazole thin amorphous film, hole drift mobility, mol. mass. depend. 0-75663  
 cis-polyacetylene:AsF<sub>6</sub>, conductivity meas., non-Ohmic effects 0-96891  
 polyacetylene:AsF<sub>6</sub>, thermopower and transport props. 0-65611  
 polyacetylene:AsF<sub>6</sub>(I), pure and doped, electronic excitations, momentum depend., EELS study 0-76121  
 polyacetylene:Br(Pd), ion implantation effect on elec. props. 0-65026  
 polyacetylene:SbF<sub>6</sub>, elec. cond. meas. 0-60055  
 polyacetylene, and derivatives, thin polycryst. film, solar cell applic. 0-92899  
 polyacetylene, doped, fluctuation-induced tunnelling cond. in metallic regime 0-65516  
 polyacetylene, electronic struct., one-electron band theory 0-65450  
 polyacetylene films, AsF<sub>6</sub> doped, photocond. and junction props. 0-70770  
 polyacetylene films, doping effect on elec. cond., chem. and optical props. 0-65572  
 polyacetylene films, doping investigation, insulator-metal transition, optical transmission meas. 0-103729  
 polyacetylene films, electrical properties (Japanese) 0-96888  
 polyacetylene films, stretch-aligned, prep. and morphology 0-66471  
 polycarbonate: tri-p-tolylamine, chemical control of conductivity 0-59984  
 polydiacetylene-toluenesulphonate, photocond. meas., 0.62-3.1 eV 0-70757  
 polydifluoroacetylene, electronic struct., tight-binding LCAO-SCF-MO calcs., prep. 0-70591  
 polyfluoroacetylene, electronic struct., tight-binding LCAO-SCF-MO calcs., prep. 0-70591



# organic semiconductors continued

- polymeric conductors, struct. and phys. props., symposium, San Jose, USA (March 1979) 0-62379
- polymethine semiconducting films, surface photovoltage 0-70857
- polypyrrole, electronic struct., one-electron band theory 0-65450
- porphyrin films, methine bridge substituted, surface photovolt. depend. on fabrication method 0-60119
- silicon phthalocyanine, elec. cond. temp. depend. 0-80271
- squarylium dye films, surface photovolt. 0-75594
- TCNQ complexes, elec. resist. and thermoelec. power meas. 0-107777
- TCNQ salt, dibenzo-TTF-TCNQCl<sub>2</sub>, one-dimens. mag. semicond.; mag. and elec. props. 0-88601
- TCNQ salt, K-TCNQ, EPR linewidth, ang. and freq. depend. 0-80591
- TCNQ salt, n-methyl-n-ethylmorpholinium, unpaired electron states, IR refl. study 0-75491
- TCNQ salts, elec. cond. spectrum fine structure 0-96884
- p-terphenyl, hopping cond. among localised states 0-70861
- p-terphenyl film, polycryst., charge carrier transport and DC cond. 0-70858
- tetracene, film, depletion layer studies, temp. depend. of LF capacitance 0-65617
- tetracene, hopping cond. among localised states 0-70861
- tetracelenotetracene iodides, struct. and physical props., DC electrical cond. and EPR linewidth meas. 0-103312
- thymine film, polycryst., energy conversion processes, quantum yields, 4 to 10 eV 0-88589
- (TMTSF)<sub>2</sub>PF<sub>6</sub>(AsF<sub>6</sub>), linear-chain conductor, semicond.-metal transition in small elec. field 0-103730
- TTT film, Schrieffer effect 0-60118
- Co complex, 2,6-N,N-diacetyldiaminopyridine-Co(II) elec. cond.,  $\gamma$  dose and temp. (303-363K) effects 0-103696
- Co complex, 2,6-N,N-dibenzoyldiaminopyridine-Co(II) elec. cond.,  $\gamma$  dose and temp. (303-363K) effects 0-103696
- Cr-phthalocyanine-Cr sandwich, I-V and C-V charactrs. 0-60106
- Ni complex, 2,6-N,N-diacetyldiaminopyridine-Ni(II) elec. cond.,  $\gamma$  dose and temp. (303-363K) effects 0-103696
- Ni complex, 2,6-N,N-dibenzoyldiaminopyridine-Ni(II) elec. cond.,  $\gamma$  dose and temp. (303-363K) effects 0-103696
- PF<sub>5</sub> dopant for polyacetylene 0-88171

# organometallic compounds

- amines, Raman and IR spectra, band intensity and assignment, force const. determ., vibr. props. (German) 0-87133
- benchrotrene, EHT method calcs., parametrisation, population anal. (French) 0-58157
- bistrifluoromethylmercury, scalar coupling between rare spins 0-66047
- n-butyl-lithium, intercalation with transition metal chalcogenophosphates, possible appl. in Li batteries 0-71446
- cyclopentadienyl platinum (IV) complexes, ring rot. meas. using mech. spectroscopy 0-74259
- cyclopentadienylhafniumdichloride, gaseous, far IR and Raman spectra 0-95624
- cyclopentadienyltitanium trichloride 0-95624
- cyclopentadienyltitaniumdichloride, gaseous, far IR and Raman spectra 0-95624
- cyclopentadienylzirconiumdichloride, gaseous, far IR and Raman spectra 0-95624
- decomposition by reaction with photoelectron, appl. to metal film deposition 0-71599
- dibenzenechromium-dibenzenevanadium, proton HFS data, ENDOR obs. 0-66073
- dibenzenevanadium, substituted in Fe dicyclopentadiene and dibenzenechromium proton HFS data, ENDOR 0-66073
- dibenzylchromium, EHT method calcs., parametrisation, population anal. (French) 0-58157
- dicyclopentadienyl Ti<sup>3+</sup>-N<sub>2</sub> compound complexes, reson. Raman scatt. 0-99510
- EHT method calcs., parametrisation, population anal. (French) 0-58157
- ferrocene, EHT method calcs., parametrisation, population anal. (French) 0-58157
- ferrocene, multiphoton dissoc. and ionisation by tuneable dye lasers 0-99524
- ferrocene, multiphoton ions. spectra, at Fe transitions 0-106361
- ferrocene, orthorhombic low-temp. cryst. phase, characterisation 0-96507
- ferrocene films, plasma-polymerised, carrier trapping, elec. cond. meas., 300 to 525K 0-100543
- lead alkyls in polluted atmospheres, conc. obs. 0-85313
- metallocenes, photoelectron spectra, band assignment 0-91604
- metallomacrocycles, mixed valent, cofacial assembly, cond. polymeric material 0-70143
- methylmercury halides+N<sub>2</sub>, A<sup>3</sup> $\Sigma_u^+$ -state quenching obs. 0-108693
- nickelocene, multiphoton dissoc. and ionisation by tuneable dye lasers 0-99524
- organolead cpds., quenching of carbonyl triplets in quinones, CIDEF and ESR obs. 0-95654
- organotin cpds., quenching of carbonyl triplets in quinones, CIDEF and ESR obs. 0-95654
- tetramethylgermanium, Zeeman spin-lattice relaxation rate maxima 0-84666
- tetramethyltin, adsorbed on graphite, nature of 2 D diffusion, Mossbauer meas. 0-84372
- titanocene, alkyl-substituted <sup>13</sup>C and <sup>1</sup>H NMR, chemical shifts prediction 0-63671
- trifluorodimethylmercury, gas phase mol. struct., electron diffraction and micro-wave spectra obs. 0-78609
- trimethyl tin chloride adsorbed on grafoil, Mossbauer study 0-80643
- trimethylantimony, use in VPE growth of GaAs<sub>1-x</sub>Sb<sub>x</sub> 0-60788
- trimethylarsenic, use in VPE growth of Ga<sub>1-x</sub>In<sub>x</sub>As 0-60788
- triphenyl tin chloride adsorbed on grafoil, Mossbauer study 0-80643
- vanadocene, order-disorder phase transition, sp. ht. and crystallographic study (French) 0-84131
- zirconocene dichlorides, alkyl-substituted, <sup>13</sup>C and <sup>1</sup>H NMR, chemical shifts prediction 0-63671
- Cu phthalocyanine, grain boundary struct., crystallographic planes 0-103366
- Fe dicyclopentadienyl-dibenzenevanadium, coalescence temps., full proton HFS tensor, ENDOR obs. 0-66073
- Np(IV)-tetracyclopentadienide complex, H<sup>1</sup>-NMR studies, paramagnetic moments, temp. depend. 0-93186

# organs (artificial body) see artificial organs

# origin of elements see element origin

# origin of life see evolution (biological)

# orthicons see television camera tubes

# orthogonalised plane wave calculations see OPW calculations

# orthosis see orthotics

# orthotics

# see also prosthetics

- beacon guidance system for walking blind aid 0-81676
- biomechanics, foundations and appls. (French) 0-89778
- cardiopulmonary resuscitator, programmable, for evaluation of standards 0-72374
- circulation augmentation, end-diastolic air compression boot 0-101291
- conference, London, England (Mar. 1980) 0-94926
- femoral fracture brace, biomech. study of function during stance 0-97990
- fractured bone fixing pins, stainless steel, strength, ultrasound effect 0-71710
- microprocessor based 4 channel preprogrammable stimulator for paralysis treatment (Slovenian) 0-104809
- multichannel implantable stimulator (Slovenian) 0-81773
- orthodontic appliance, facial skeleton strain distrib. 0-67143
- paralysed upper extremities rehabilitation systems, control signals (Slovenian) 0-81772
- wheelchair locomotion, power output requirements for manual operation 0-94416

# oscillations

- see also circuit oscillations; electromagnetic oscillations; harmonic oscillators; harmonics; liquid oscillations; piezoelectric oscillations; plasma oscillations; resonance; stability; vibrations; waves
- accretion disks, optically thick, pulsational instability to axially symm. oscils. 0-82190
- atmosphere, theory of travelling planetary waves in stratosphere 0-105030
- black holes, rotating, reson. freqs. of free oscils. rel. to gravit. waves 0-105271
- BT Cancri (38 Cancri),  $\delta$  Scuti star, multiple periods rel. to radial and nonradial pulsation periods 0-85948
- Cepheid stars with He enriched inhomogeneous outer layers, three mode reson. 0-101600
- ZZ Ceti white dwarfs, non-radial oscils. theory 0-82356
- cylindrical shell, reinforced lamina, intrinsic oscil. 0-99957
- disc in electrically conducting fluid, hydromagnetic flow due to torsional oscillations about non-zero mean 0-74992
- dissipative and nonequilibrium media, pulse spreading 0-94961
- Earth deformation, mag. field effects 0-109085
- Earth free modes excited by Indonesia earthquake, Aug. 19<sup>th</sup> 1977 obs. 0-61767
- Earth normal mode oscillations, tensor spherical harmonics appl. to anisotropic Earth model 0-98296
- Earth tides, forced oscils. theory assuming Earth as viscoelastic body 0-67333
- forced oscillations, averaging and chaotic motions 0-73166
- forced oscillations, existence and numerical approx. 0-62466
- forced periodic oscillations of the simple pendulum 0-94951
- galaxies, global instability of polytropic gaseous discs with Toomre density distrib. 0-98725
- gas, in tube, pressurisation in liq. He storage vessel 0-57305
- gas bubble pulsations in viscoelastic polymeric liquids, assoc. dissipation effects 0-59079
- gas torus in liquid, natural modes of pulsation 0-58999
- H-shaped section cylinder in laminar and turbulent flows, aerodynamic charact. 0-106813
- Mandel'shtam and nonlinear oscillations and wave theory, review 0-105515
- mechanical oscillator, relativistic spin quadrupole gravitational effect (Russian) 0-68103
- membrane, stability of nonlinear oscillations from Liapunov method 0-96212
- near resonant oscillating systems, integration in slow-fluctuation approx. 0-62483
- neutron star torsional oscils., period determ. 0-90464
- non-linear, free vibration, numerical soln. 0-68034
- nonlinear oscillator systems, primary resonances do not overlap 0-59176
- nonlinear oscillators, turning point approx. and appl. 0-67952
- nonlinear planar oscillators, stability of modes 0-74790
- nonlinear system with slowly varying parameters, resonance 0-62463
- ocean basins (connected), theory of natural oscils. 0-61806
- parametric instability, demonstration and discussion 0-57032
- parametrically excited, combination resonance of coupled second order systems with nonlinear damping 0-86078
- plate, vertical, free convection boundary layers and heat transfer 0-59002
- pulsating stars, modal selection theory rel. to double-mode Cepheids 0-82372
- relativistic oscillatory motion, general, Einstein's field eqns. 0-73217
- ribbed cylindrical shell with solid body, free oscil. 0-99956
- solar, surface oscillations and pulsations, rotation speeds 0-67676
- solar five-minute oscillations, horizontal energy flows struct. 0-62103
- solar oscillation periods, correl. with cosmic ray short-term fluctuations periods 0-67483
- solution of a highly non-linear oscillation equation, single particle analogue of field equations of chiral Lagrangian theories of pion interactions 0-62470
- stars, adiabatic nonradial oscils., freq. splitting by slow differential rot. 0-105233
- stars, junction conditions across perturbed contact discontinuities 0-94787
- stars, magnetic, stability with respect to high-order oscil. modes and convection 0-94781
- stellar pulsations, nonlinear coupling 0-62115
- Sun, 160 minute period, evidence 0-82324
- Sun, active region McMath 15403, 5 minute oscils., SHF obs. 0-98639
- Sun, high-freq. oscils. rel. to upper photosphere spectral line shifts 0-85912
- Sun, oscils. period obs. rel. to internal struct. 0-105226
- Sun 5-minute oscillations, C I 5380 Å line response, effects of granular convection 0-85910
- Sun global oscillations, implications limb darkening function possible temporal vars. 0-67677
- thin walled elements, unbound quasistatic random thermoelastic fields, oscillations 0-69673
- torsion pendulum, with anelastic solids of discrete relaxation spectra, resonant system 0-69687



**oscillations continued**

- tropical middle atmosphere, observational evidence of semiannual oscillation 0-109216  
 two-level system, Rabi oscillations in partially coherent field 0-102688  
 viscoelastic rod, standard linear body, free torsional oscils. 0-99940  
 wind induced oscillations, domains of stability 0-64441  
 Al-Ag, type-II superconductor, torque oscillations in mag. field (*Russian*) 0-103800  
 Fe-Si (3 wt.%), internal friction, instantaneous, depend. on phase of torsional oscils. (*Russian*) 0-71142  
 Fe-Si (3 wt.%), magnetisation variation during bending oscils., rel. to  $\Delta E$  effect (*Russian*) 0-65983  
 Ni, internal friction, instantaneous, depend. on phase of torsional oscils. (*Russian*) 0-71142

**oscillator strengths**

- acentric crystals, optical phonons, small oscillator strength meas. from frequency-angular polariton spectra 0-92629  
 anthracene, singlet exciton transitions, energies and oscillator strengths, boson theory with PPP wavefunctions 0-92820  
 anthracene-pyrometallitic dihydride cryst., refl. and absorpt. spectra of singlet charge transfer excitons 0-71442  
 atom, force experienced in electrostatic field, Feynman-Hellmann theorem and oscillator strengths 0-65275  
 atoms, near threshold struct. in K-shell spectra, photoionisation or fast charged particle ionisation 0-87064  
 atoms, oscill. strength in presence of level crossings 0-99480  
 benzene, liq., visible region absorpt. spectra, overtones meas. 0-78625  
 dynamic multipole polarisability, dispersion forces and oscillator strengths, Coulomb approx. 0-63520  
 excited states, oscill. strengths calcs., influence of wave function determ. method 0-99478  
 homologous ions series, struct.-related trends in line strengths and Stark widths 0-105157  
 hook spectra, evaluation limitations 0-90905  
 ionic crystals, oscillator strengths of defects, Smakula eqn. generalisation 0-108232  
 lithium formate, optical phonons, small oscillator strength meas. from frequency-angular polariton spectra 0-92629  
 3-methyl lumiflavin, in soln., absorpt. spectrum 0-58277  
 molecular interactions, two-body van der Waals coeff., combination rules 0-78677  
 n- $\pi^*$  singlet-singlet transition probabilities 0-95689  
 naphthalene, singlet exciton transitions, energies and oscillator strengths, boson theory with PPP wavefunctions 0-92820  
 pentacene, singlet exciton transitions, energies and oscillator strengths, boson theory with PPP wavefunctions 0-92820  
 singlet-triplet energy difference and singlet generalised oscillator strength, Lassetter-Diillon relation 0-63508  
 tetracene, singlet exciton transitions, energies and oscillator strengths, boson theory with PPP wavefunctions 0-92820  
 tunable laser interferometry, oscillator strength meas. 0-105697  
 Ag film, granular, transmission and reflection spectra, validity of sum rule 0-97358  
 Ar,  $2p^6$  shell, oscillator strength, photoionisation cross sections, electron shell alterations determ. (*Russian*) 0-58144  
 Ar, absorpt. spectra, field induced autoionisation near ionisation threshold 0-106301  
 Au film, granular, transmission and reflection spectra, validity of sum rule 0-97358  
 Ba, atom, electron impact step-wise excitation (*Russian*) 0-83497  
 BaF<sub>2</sub>, strain induced splitting and oscillator strength anisotropy of IR transverse optic phonon 0-92625  
 Be isoelectronic series, excited states, oscill. strengths calcs., influence of wave function determ. method 0-99478  
 BeF<sub>3</sub>:Eu<sup>3+</sup> glass, luminesc. of Eu<sup>3+</sup> transition probabilities 0-80845  
 C, vapour, Swan bands, oscillator strength 0-63712  
 CaF<sub>2</sub>, strain induced splitting and oscillator strength anisotropy of IR transverse optic phonon 0-92625  
 CdCr<sub>2</sub>S<sub>4</sub>, ferromag. semicond., IR refl. spectra, phonon props. and dielec. function 0-66191  
 Cl<sub>2</sub>, inner shell excited states, X-ray absorpt. spectra, HF calcs. 0-78536  
 Cr(II) lines, oscill. strengths in 2413-2718 Å wavelength range 0-106294  
 Cs, hook spectra, evaluation limitations 0-90905  
 Cs+He, interaction pot. and oscill. strength 0-91645  
 CuBr(CI)(I), polariton Raman spectra, oscillator strengths, temp. depend. 0-66197  
 EuO(S), ferromagnetic electronic structure, absorption, thermoreflection and thermotransmission spectra (*French*) 0-97300  
 EuP<sub>2</sub>O<sub>14</sub>, luminesc. of Eu<sup>3+</sup> transition probabilities 0-80845  
 Fe I, a<sup>2</sup>F<sub>4</sub> levels, relative oscillator strengths 0-63572  
 Fe XXII, coupling energy levels, oscillator strengths, electron-collision energies 0-69068  
 FeVIII-XXVI energy level tables and Grotrian diagrams 0-74142  
 GaAs:Cr, 0.84 eV no-phonon luminesc., fine struct. and origin 0-103980  
 Ga, -Jn,As, IR reflectivity, cluster effect on optical phonons 0-97259  
 Ge:B(AI)(Ga), shallow acceptor spectral line intensities 0-88517  
 H plasma, thermal emission and Debye shielding 0-64692  
 H, Stark and photoabsorption spectrum, density of oscillator strengths, atom c.f. semiconductor spectra 0-83318  
 HCl, C<sup>12</sup>X<sup>2</sup> system, (0, 0) and (0, 1) bands, oscillator strength determ. and UV spectra 0-91570  
 He, isoelectronic sequence, E1 and E2 oscillator strengths, MCHF calcs. 0-106292  
 He like atoms, dipole transitions, transition integral cancellation 0-69052  
 He metastable state, two- and three-photon ionisation 0-91518  
 He, tight bounds on multipole dispersion coefficient calcs. for interaction of atoms 0-83320  
 Hf IV, 6s <sup>2</sup>S<sub>1/2</sub>-6p <sup>2</sup>P<sub>1/2,3/2</sub> transition, relativistic oscillator strengths, influence of core polarisation 0-58132  
 Hg II line oscillator strength determ. in Ap-type stars, diffusion model implications 0-72966  
 Ho I, Ho II, excited level lifetimes and oscillator strengths, visible spectra 0-63573  
 Ho(NO<sub>3</sub>), solns., f-f transitions, intensity anal., correl. with cond. and US absorpt. 0-97292  
 I II, reson. lines, oscill. strengths determ. by absorption method 0-58214  
 KCN, Cl<sub>1-x</sub>, finite field local field catastrophe phenomena in spectra 0-92830  
 KD<sub>2</sub>H<sub>2</sub>PO<sub>4</sub> crystals, 0<x<0.98, light scatt. by polaritons 0-96802  
 KI, oscillator strengths of defects, Smakula eqn. generalisation 0-108232

**oscillator strengths continued**

- Kr, absorpt. spectra, field induced autoionisation near ionisation threshold 0-106301  
 Li I laser, 207 Å, oscillator strengths 0-83598  
 Li, optical oscill. strengths calcs. 0-91495  
 Lu III, 6s <sup>2</sup>S<sub>1/2</sub>-6p <sup>2</sup>P<sub>1/2,3/2</sub> transition, relativistic oscillator strengths, influence of core polarisation 0-58132  
 N, far vac. UV spectra, oscillator strengths for 3s, 4s, 5s, 3d and 4d <sup>4</sup>P-2p <sup>2</sup>S<sub>1/2</sub> 0-74178  
 N II, electron impact excitation cross sections, rel. to solar corona abundance 0-58391  
 NH<sub>3</sub>, electron impact, 35 keV, Bethe surface and Compton profile 0-87235  
 NO,  $\gamma$  band lines, collisional broadening coeff. and optical collision diameter 0-63714  
 NO,  $\gamma(0,0)$  band, collisional broadening parameters 0-63713  
 NO+N<sub>2</sub>(CO)<sub>2</sub>(CO)(CH<sub>3</sub>)(Ar), NO  $\gamma(0,0)$  band, oscillator strength and line broadening 0-106356  
 NaCl:Eu, secondary Eu phase dissolution, EPR and optical absorpt. study 0-96655  
 NaPO<sub>3</sub>:Eu<sup>3+</sup> glass, luminesc. of Eu<sup>3+</sup> transition probabilities 0-80845  
 Ne, dipole dynamic polarisabilities and two-photon photoionisation cross section calc., R-matrix approach 0-102444  
 Ni I, UV lines, oscillator strengths from hook method and absorpt. meas. in furnace 0-83319  
 Ni I solar photosphere from oscillator strength obs. 0-98625  
 Ni XII, XIII, XIV, XV, 3s-3p and 3p-3d transitions, oscillator strength and energy levels calcs. 0-83251  
 O III, electron impact excitation cross sections, independent particle model calcs. 0-63823  
 O IV bound states, oscillator strengths and photoionisation cross sections 0-106293  
 O isoelectronic sequence, optical oscillator strengths 0-63589  
 O<sub>2</sub>, Schumann-Runge continuum, oscill. strength and electron impact excitation 0-69121  
 O<sub>2</sub>, spin-forbidden transition intensities, selective heavy atom effects 0-58240  
 OH, (0,0) UV transitions, band oscill. strength 0-69162  
 OH<sup>+</sup>, rot.-vibr. bands, line positions, oscill. strengths transition probabilities 0-67828  
 Pr<sup>3+</sup>, anomalous hypersensitive <sup>3</sup>H<sub>4</sub>-<sup>3</sup>P<sub>2</sub> transition 0-106296  
 Rb atom in Xe, collision-induced dipole transitions, absorpt. meas. 0-95718  
 Se I, oscill. strength calc. 0-78571  
 SeOCl<sub>2</sub>:Pr<sup>3+</sup>(Nd<sup>3+</sup>)(Er<sup>3+</sup>), SbCl<sub>3</sub> acidified, Racah and Judd-Ofelt parameters in laser liqs. 0-106516  
 Si (III), excitation thresholds and oscillator strength calc. using CI wavefunctions 0-91496  
 SiH<sup>+</sup>, oscillator strengths and dissociation energy determ. from time resolved precision spectroscopy 0-58272  
 SrF<sub>2</sub>, strain induced splitting and oscillator strength anisotropy of IR transverse optic phonon 0-92625  
 Ti II, oscillator strengths from combined hook and emission expts. 0-87081  
 TI, ionisation limit and oscill. strength in VUV absorpt. spectra 0-74152  
 TI, oscill. strengths, semiempirical relativistic one-electron central field, model pot. calcs. 0-78575  
 UI plasma, absolute emission coeff. 0-64693  
 V VII, VIII, IX, X, 3s-3p and 3p-3d transitions, oscillator strength and energy levels calcs. 0-83251  
 Xe, 5s<sup>2</sup> shell, oscillator strength determ. (*Russian*) 0-58144  
 Yb II, 6s <sup>2</sup>S<sub>1/2</sub>-6p <sup>2</sup>P<sub>1/2,3/2</sub> transition, relativistic oscillator strengths, influence of core polarisation 0-58132  
 Zn, isoelectronic sequence, oscill. strength and MCHF wavefunctions, outer correl. 0-91505  
 Zn, solar photosphere abundance, discrepancy with meteorite abundance 0-72897  
 ZrF<sub>4</sub>:Eu<sup>3+</sup> glass, luminesc. of Eu<sup>3+</sup> transition probabilities 0-80845

**oscillators**

- see also Gunn oscillators; microwave oscillators; relaxation oscillators; tunnel diode oscillators  
 anharmonic oscillator model for dispersive optical bistability 0-58623  
 doubly tuned oscillator configuration, nonlinear mode interactions, freq. jump effects 0-77824  
 forced damped harmonic, meas. separation and half-width of components of doublets, high-Q systems 0-74590  
 fundamental mode, SAW resonators at 1.43 GHz appl. 0-87687  
 low-level gated, ion cyclotron resonance 0-86492  
 nonlinear oscillator and reflectors, periodic vibr. and impact characteristics 0-92089  
 rotating anharmonic oscillators in resonator, stimulated emission power 0-99689  
 two-resonator CRM oscillator with external feedback 0-87362  
 H, four dimensional oscillator, rot. invariance of coordinate transform., appl. to Stark problem 0-99436

**oscillograms see oscillographs****oscillograph recorders see oscillographs****oscillographs**

- see also cathode-ray oscilloscopes  
 DFS-8 spectrograph, attachment for oscillographic recording of line shapes 0-105721  
 fast process recording, galvanometer construction 0-73346  
 steel 45G2, fracture resistance, from impact bending tests and oscillograms 0-61047

**oscilloscopes, cathode-ray see cathode-ray oscilloscopes****Oseen method see flow****osmium**

- see also nuclei with .....  
 electronic energy band struct. 0-107697  
 isotopic anomalies from different ore deposits, LAMMA determ. 0-61800  
 thermal EMF quantum oscils. (*Russian*) 0-88543  
 wear coefficients determ. using pin-on-disc apparatus 0-76366  
 Cs<sub>2</sub>ZrBr<sub>6</sub>:Os<sup>4+</sup>, intraconfig. absorpt. and MCD spectra 0-80776  
 Cs<sub>2</sub>ZrCl<sub>6</sub>:Os<sup>4+</sup>, intraconfig. absorpt. and MCD spectra 0-80776  
<sup>187</sup>Os/<sup>186</sup>Os in terrestrial samples, rel. to use of Os isotopes as petrogenetic and geological tracers 0-89989  
 n-Si-Os Schottky contact barrier height meas. 0-65675



oxidation continued

catalytic oxidation of  $H_2$  and  $D_2$ , matrix isolation and laser fluoresc. obs. of prods. 0-66865  
chlorophyll a, cation radical formation by pulse radiolysis, oxidation and demetallation rate consts. 0-61505  
chlorophyll-a radical cation lifetime in water-acetonitrile soln. 0-72136  
 $CO_2$  ferrite, crystal structure, X-ray absorpt. spectra, chemical shifts 0-88118  
cobalt phthalocyanine, electrochromism and oxidation 0-93768  
cyclopentadiene-butyl vinyl ether copolymer, oxidative. degradation (*Japanese*) 0-108714  
DBTTF halogen complexes, IR, UV spectra, EPR study 0-108215  
diamond, synthetic, oxidized in fused salts, etch features 0-97604  
dipotassium glucose-1-phosphate, X-irrad., ESR-ENDOR obs 0-60419  
electrolyte, ionic mass transfer in narrow rectangular conduits 0-61105  
ferromagnetic metals, thermal oxidation rate determ. using nanowebemeters 0-61045

0-104350 GCFR advanced alloy cladding, oxidation behaviour in the environment

glass fibre reinforced plastic greenhouse sheets, ageing behaviour, natural and artificial weathering (*German*) 0-81226  
graphite, Fe-catalysed gasification, electron, microscopy 0-104358  
graphite, from reactor, quantitative microanalysis by laser emission spectroscopy 0-81384  
graphite monolayer on Ni (110) surface, oxidation mechanism 0-101037  
Hastelloy-X, Ni-Cr-Fe-Mo, cyclic oxidation resist. improvement by high temp. etching treatment 0-97627  
4-hydroxy-2,2,6,6-tetramethylpiperidine, radiation-induced oxidation to paramag. nitroxide free radicals 0-81341  
Incoloy 800, clean and steam oxidised, T<sub>2</sub> permeation 0-88364  
Incoloy 800, steam oxidised, oxide coating anal. 0-89399  
Inconel 600, nuclear reactor boiler corrosion, XPS 0-66709  
Inconel 600, nuclear reactor boiler corrosion, XPS 0-71816  
Inconel 800, simulated, steam oxidation 0-76405  
ion implanted, F influence on oxidation-induced stacking faults 0-65011

Josephson junction, fabricated by RF plasma oxidation, IV characts.  
(Japanese) 0-84564

liquid film, falling, O<sub>2</sub> adsorpt. with zero order react. in entrance region  
0-64652

lutetium diphthalocyanine, solid-state anion migration in anodic oxidation  
0-60994

metal oxidation, secondary ion energy spectroscopy 0-71788  
metal oxide thick film growth, fund. theory 0-89391

metal oxides, nonstoichiometric, work function and near-surface chem. diffusion 0-80034

metal surface oxidation study, vacuum microbalance investigation  
0-76552

metalloporphyrin, cation radical formation by pulse radiolysis, oxidation and demetalation rate consts. 0-61505

molten carbonate fuel cell, electrolyte comp. effect on electrode kinetics  
0-101092

optical fibre preparation methods and performance factors 0-69557  
optical image phase recording using sensitised photooxidation reactions

organic molecules, catalytic effects on electrode reactions, review

plasma oxidation in microwave discharge 0-76382

polyacetylene films, doping investigation, insulator-metal transition, optical transmission meas 0-103729

polyethylene, elec. cond. of high and low density samples, oxidation effects  
0-107784

polypyrrole films, electrochemical prep., and phys. characterisation  
0-70708

propylene, oxidation on MgO:Mo catalyst, surface structs., IR absorpt spectra obs. 0-66868

PVC, thermooxidative degradation, crosslinking and chain scission  
0-71912

PVC surfaces, natural and stabilised, composition, ageing, oxidation and weathering. ESCA obs. (French) 0-61139

quartz, single crysts., Ar and O<sub>2</sub> interaction at high temp., surface struct. changes (*German*) 0-96725

resistant alloys, metastable microcrystalline, appl. 0-84887  
rubber for prep of diene oligomers with hydroxyl groups (German)

0-85175  
semiconductor, tetrahedrally coordinated, review of surface struct. chem.

Si-N-Ce-O-SiO<sub>2</sub> materials: phase relations and strength 0-97465

solid surfaces, surface processes, and solid/gas interactions 0-71463  
sputtered refractory carbides: adhesion to metal substrates improved

0-76481 stainless steel austenitic surface interaction with  $O_2$  and work function

obs. 0-65364  
steel, austenitic stainless Cr-Ni (20-25 wt%), Nb stabilized, oxidation

steel, austenitic stainless, Cr-Ni (20, 25 wt.%), Nb stabilized, oxidation behaviour in CO<sub>2</sub>, surface ion implantation effect 0-71791

steel, Cr-Mn high temp. oxidation, sub-cinder layer formation, protective

steel, Cr-Mn, high temp. oxidation, sub-surface layer formation, protective coating role (Russian) 0-93686

steel, Cr-Mo, and used, mechanism of crack decoration of oxides by electrodeposition 0-97560

steel. Cr-Mo 10-14, 2-8 wt.%, heat-resist., creep-rupture strengths  
0-104271  
steel. Cr-Mo-V low-alloy. mech. props. and stress relief cracking. effects

steel, Cr-Mn-V low-alloy, mech. props. and stress relax. cracking, effects of impurities and deoxidation practice 0-66599

steel, Cr-Si, oxidation resist. in high pressure  $\text{CO}_2$ , Si effect 0-66/04  
steel, high and low C, wires, electroheated, thermal cycling and corrosion  
behaviour 0-61/006

steel, low-alloy, hardened deoxidised, delayed failure, influence of internal  
adsorpt. of impurities 0-60974

steel, low-alloy, oxidation resist., N effect 0-66706

steel, pearlitic structural, austenite grains, growth rate during heating  
0-100860  
steel, railway, oxidation by Fe-Si-Ca-V complex alloy, nonmetallic inclu-

steel, railway, oxidation by Fe-Si-Cr-V complex alloy, nonmetallurgical  
steel, stainless, 316, oxidation behaviour in the environment, appl. to

steel, stainless, austenitic, oxidation in  $\text{CO}_2$ , charged-particle nuclear tech-

steel, stainless, corrosion behaviour of composite materials in  $N_2O_4$  oxidis-

ing atmospheres (Russian) 0-76421

## oxidation continued

- steel, stainless, emittance, oxidation and surface roughness effects 0-96673
- steel, stainless, Fe-Cr-Al (15, 4 wt.%) Ferralloy, oxidation behaviour, Al and Y surface ion implantation effect 0-71790
- steel, stainless, heat treated, oxide comp. and corrosion susceptibility of grades 410 and 430, AES study 0-66692
- steel, stainless, oxidation, localised pit development, 1073-1173K 0-89414
- steel, type AISI 316, thermal passivation in controlled vacuum 0-76276
- steels, tempered with different Ni contents, scaling behaviour obs. 0-71817
- Stellite-6, XPS obs. of aqueous oxidation, surface comp. and gaseous oxidation effect 0-81238
- sulphides (Fe, Co, Ni, Cu, Zn), oxidation, hardness and electromechanical polishing response 0-71776
- tetracyanoplatates, quasi 1d anion deficient, elec. and struct. props. 0-103683
- transition metal silicides, refractory for ICs, review 0-100820
- transition metal sulphides, ion bombardment damage, XPS obs. 0-97404
- TZM-Mo alloy, mech. props., effect of exposure to high temp. He containing O<sub>2</sub>, room temp. study 0-93639
- Venus, oxidation state of atmosphere and crust from Pioneer Venus results 0-98586
- zinc phthalocyanine, electrochromism and oxidation 0-93768
- zircaloy, nuclear microprobe methods for investigating oxidative corrosion 0-71787
- Zircaloy cladding, enhanced steam oxidation by deformation under LWR LOCA 0-73917
- Zircaloy sheaths, oxidation rate calc. method 0-78394
- Zircaloy-2, anodic oxidation kinetics, in 0.05M oxalic acid (aq. and alcoholic) 0-104331
- Zircaloy-2, hot-pressed, influence of diffused C on structure and oxidation 0-61016
- Zircaloy-2, mech. props. after exposure to I<sub>2</sub>-methanol solutions, SEM study 0-93689
- Ag foil, interface with liq., oxide props., refl. and scatt. light spectroscopy 0-60702
- Ag-Cd(Ni), internally oxidised, oxide particle size control (*Japanese*) 0-89480
- Ag-In-Sn, internal oxidation, precipitation behaviour of oxide (*Japanese*) 0-66515
- Ag-In-Sn, internal oxidation, solute element and O<sub>2</sub> behaviour (*Japanese*) 0-89479
- Ag-O-Cs surface, oxidation, role of Cs suboxides in low work function surface layers, XPS 0-76131
- Ag-Zn, internally oxidized, elec. contact characts., alloying additions effect (*Japanese*) 0-88619
- Ag-Zn-Te(Sn)-(In), internally oxidised, oxide particle size control (*Japanese*) 0-89480
- AgCdO, powder metallurgy production, for switchgear in power engineering 0-104094
- Al (111), bonding of O, electronic struct. calcs., rel. to UPS data 0-59801
- Al (111), oxidation, initial stages, LEED anal. 0-80082
- Al anodic oxidation, in H<sub>2</sub>SO<sub>4</sub>, pH-values effect (*German*) 0-76419
- Al, creep behaviour, at high temp., influence of oxidation 0-97538
- Al, film and polished bulk specimens, initial stages of oxidation obs. using SIMS 0-81239
- Al, foil, influence of O<sub>2</sub>-pressure on oxidation rate, TEM study 0-104355
- Al foil electrolytic perforation, surface film phase composition obs. (*Russian*) 0-61004
- Al, initial interaction of O with single cryst. faces, LEED, AES and work function study 0-84392
- Al, oxide films, metal and O<sub>2</sub> transport, AES and inert marker, techniques 0-97641
- Al, thermal desorption of oxide film, influence of grain boundaries and recrystn. 0-61023
- Al-Li-Mg-Be alloys, phase composition of surface films, oxidation protection mechanism (*Russian*) 0-65417
- Al-Mg, foil, oxidation in O<sub>2</sub> atm., TEM study 0-104356
- Al-Mg, oxidation control study, electron opt. techniques eval. 0-85089
- Al-Mg (2.5wt.%) sheet, surface oxide state and weldability 0-59769
- Al-SiO<sub>2</sub> interface in MOS capacitors, conductivity effects of oxidation temperatures 0-100518
- Al<sub>2</sub>O<sub>3</sub> supermicrogrid preparation and props. use in electron microscopy, noise reduction 0-99010
- Al<sub>2</sub>O<sub>3</sub>/Fe, pore form. during oxidative annealing, grain growth slowing 0-100856
- Al<sub>2</sub>O<sub>3</sub>-SiO<sub>2</sub> glass ceramic, surface streaks and blisters, UV fluoresc. study 0-84347
- Al<sub>2</sub>O<sub>3</sub>-TiO<sub>2</sub> powder, plasma-prepared, morphology and phase constitution 0-100833
- Al(100) oxidised surface structure anal., extended appearance potential fine struct. study. 0-75411
- Al(111), oxide layer amorphous to cryst. surface transition, slow positron obs. 0-75417
- As(III) and As(V), redox stability in aq. soln. 0-61068
- Au/Cu, double layer film (*Japanese*) 0-61010
- Au-GaAs Schottky barrier solar cells, effect of interfacial oxide layer on cell characts. 0-61365
- BaO-B<sub>2</sub>O<sub>3</sub>-V<sub>2</sub>O<sub>5</sub> glass, oxidation-reduction of V, thermodynamics 0-85169
- Be, slowly oxidised, secondary electron yield changes, and AES characterisation 0-71524
- Be-Si-Al-O-N ceramic, phase assemblages, relationships with props. 0-60848
- C, amorphous, catalytic oxidation by Pd particles, TEM obs. 0-76555
- CO, catalytic oxidation on ferrites, IR spectrosc. investig. 0-89524
- CO, electrochemical oxidation in fused alkali metal carbonates 0-72040
- CO, on CoO, catalytic oxidation 0-71945
- CO oscillatory oxidation over Pt, theory 0-85215
- CO oscillatory oxidation over Pt, theory 0-85216
- CO, oxidation on Ir films, IR absorpt. spectroscopy 0-71398
- CaCeAl<sub>2</sub>O<sub>7</sub>, melilite struct., prep. and props. 0-93524
- Cd, oxidation, chemisorption and oxide regimes, UPS and EELS study 0-81236
- CdTe surface, sputter cleaning and dry oxidation, XPS and LEED study 0-108618
- Ce, oxidation agent for Fe-Armco, grain size and strength depend. on nonmetallic inclusions (*Russian*) 0-100894

## oxidation continued

- Ce-Si-Al-O-N ceramic, phase assemblages, relationships with props. 0-60848
- CeCo<sub>3</sub>-Cu<sub>x</sub>, 0 ≤ x ≤ internal oxidation kinetics, oxide struct., X-ray study 0-104329
- Cl+formaldehyde, photolysis, Fourier transform IR studies, metastable species detection 0-81293
- Co, XPS obs. of epitaxial CoO form. 0-66396
- Co-(Cr,Co)<sub>2</sub>C<sub>3</sub> eutectic, oxidation effect on toughness and strength 0-89404
- Co-Gd-Mo films, sputtered, O effects on mag. props. during annealing 0-89374
- Cr carbides, catalytic oxidation of H<sub>2</sub> 0-104462
- Cr, corrosion in SO<sub>2</sub>, 700-1000°C 0-97642
- Cr film, Cr<sub>2</sub>O<sub>3</sub> percentage determ., film struct. and elec. props. 0-103607
- Cr film, pattern generation by laser-induced oxidation 0-61009
- Cr, rare earth impurities effect 0-66703
- Cr-(Cr,Co)<sub>2</sub>C<sub>3</sub> eutectic, oxidation effect on toughness and strength 0-89404
- Cr<sub>2</sub>C<sub>3</sub> fibre reinforced Ni-based composite, oxidation and creep, Y additions effect 0-66685
- Cu, anodic oxidation, photoelectrochemical effects (*French*) 0-93701
- Cu, corrosion/protection by ion implantation of Al and Cr 0-71789
- Cu, EXAFS investigation 0-71808
- Cu film, on Au substrate, oxidation and interfacial behaviour, ion scatt. spectroscopy study 0-66691
- Cu, film, partially oxidised, EXAFS studies on superficial regions 0-75474
- Cu, high purity, identification of imperfections by thermal resistivity meas. 0-59951
- Cu, liq., deoxidation rates by CO<sub>2</sub>-CO gas mixture (*Japanese*) 0-89394
- Cu, oxidation kinetics, influence of intermediate annealing treatment 0-89412
- Cu, oxide identification by AES, EELS and UPS 0-60747
- Cu polycrystals, oxidation, secondary ion energy spectra 0-71788
- Cu, thin film, RMEED/SEM studies 0-100968
- Cu-Be, dynode surface, SEM and Auger microanalysis 0-100384
- CuAl<sub>2</sub>O<sub>4</sub>, pure and NiO promoted catalysts, surface oxidation state and comp., XPS study 0-76134
- CuFeS<sub>2</sub>, superficial degradation in air and water, XPS obs. (*French*) 0-89110
- Cu(I) complex, oxidation, fast reactions meas. by pulsed-flow instrument 0-66890
- CuO-containing glass, Cu<sup>+</sup> diffusion and oxidation 0-79980
- Cu<sub>2</sub>S, Cu<sub>1.8</sub>S, α-β transition, thermographic investigation of heats, entropies and activation energies 0-88314
- Fe, adsorption of O<sub>2</sub>, oxidation 0-108730
- Fe, FIM obs. 0-89388
- Fe oxides, phase equilibrium and microstructure interpretation 0-60847
- Fe sheet, cyclic oxidation and reduction kinetics in O<sub>2</sub>-H<sub>2</sub> atmosphere (*Korean*) 0-71906
- Fe-Cr, high-temp. oxidation, borate inhibitors 0-66705
- Fe-Cr (9 wt.%), oxidation studied using C<sup>18</sup>O<sub>2</sub> and D<sub>2</sub>O tracers 0-71784
- Fe-Cr alloy, sputter etching oxide film, comp. profile, quantitative AES 0-81383
- Fe-Cr-Al, HOS 875, oxidation, cyclic, role of thermal shock 0-97640
- Fe-Cr-Al, scales, α-Al<sub>2</sub>O<sub>3</sub>, early stages development at high temp. 0-89413
- Fe-Cr-Al (7, 5 wt.%), expt. stainless alloys, phys. and mech. props. 0-97637
- Fe-Cr-Al-Y, oxidation resistance, heat treatment and Al<sup>+</sup> ion implantation 0-71785
- Fe-Cr-Al-Y, scales, α-Al<sub>2</sub>O<sub>3</sub>, early stages development at high temp. 0-89413
- Fe-Cr-Ni, foil, in situ oxidation in HVEM 0-104354
- Fe-Cr-Ni based alloys, surface oxides at high temps., backscattering Raman spectroscopy 0-93291
- Fe-Cr-Si, oxidation resist. in high pressure CO<sub>2</sub>, Si effect 0-66704
- Fe-Cr-Ti (18, 0.1-0.9 wt.%), high temp. oxidation (*Japanese*) 0-71806
- Fe-Cu (4.54 wt.%) alloy, scaling behaviour, 700-1000°C, 1 atm. O<sub>2</sub> 0-93679
- Fe-Ni (50 wt.%), surface comp. and oxide film thickness after various surface treatments, AES study 0-66693
- Fe-Ni-Cr (30.6, 21.3 wt.%), Alloy 800, high temp. oxidation at low O<sub>2</sub> press., SEM, AES and electron probe microanal. study 0-93688
- Fe-Ni-Cr (44, 17 wt.%), nuclear microprobe methods for investigating oxidative corrosion 0-71787
- Fe-Ni-Cr-Al-Y, oxidation mechanism, Y addition effect on kinetics and oxide adherence 0-97623
- Fe-Ni-Cr-Y, Y addition effect on selective oxidation/diffusion phenomena relationship (*French*) 0-108623
- Fe-Si-Al, surface oxide layer struct., AES study 0-89396
- Fe-Si-Al (2.8-3.4, 0.0-86 wt.%) oxidation, annealing 0-89395
- Fe<sub>2</sub>C, catalytic oxidation of H<sub>2</sub> 0-104462
- Fe(CN)<sub>6</sub><sup>4-</sup> - Fe(CN)<sub>6</sub><sup>3-</sup>, redox reactions, mass transfer at vibr. spheres 0-57220
- Fe(CO)<sub>5</sub> adsorbed on graphite, oxidation to Fe<sub>2</sub>O<sub>3</sub>, Mossbauer spectra 0-60474
- (FeNi)PB amorphous wires, surface oxidation and annealing influence on induced anisotropy 0-100957
- Fe<sub>2</sub>O<sub>3</sub> films, electron microscopy and energy-loss spectroscopy 0-80137
- FeS<sub>2</sub>, superficial degradation in air and water, XPS obs. (*French*) 0-89110
- FeSO<sub>4</sub> oxidation by SO<sub>2</sub>-O<sub>2</sub>-H<sub>2</sub>SO<sub>4</sub> soln. 0-61083
- Ga-As-O, equilib. phase diagram, GaAs oxidation 0-104130
- Ga<sub>1-x</sub>Al<sub>x</sub>Sb, surface oxidation, Raman spectra, residual Sb layers 0-71419
- GaAs (110), order-disorder interaction with O<sub>2</sub>, LEED anal. 0-75445
- GaAs anodic oxide films, optical studies using rot. light-pipe reflectometer 0-76096
- GaAs, anodisation in HF O<sub>2</sub> plasma, oxide film form. mechanism and kinetics (*Japanese*) 0-93667
- GaAs cleaved (110) face, interaction with O<sub>2</sub>, influence of cleavage defects, AES study 0-66684
- GaAs, dislocation-free, point defects and rad. damage 0-88141
- GaAs oxide film form., ion implantation effects 0-100266
- GaAs oxides, plasma-grown, in situ meas. and anal. with spectroscopic ellipsometry 0-76386
- GaAs, polycryst., wet and dry oxides, comparative study by AES, SIMS and XPS 0-80116
- GaAs, selective plasma oxidation, interface props. 0-100933



oxidation continued

GaAs solar cell, polycryst., grain boundary passivation by oxidation, AES, SIMS and XPS obs. 0-81467  
GaAs thin film polycrystalline Schottky barrier solar cells, grain boundary chemistry 0-94067  
GaP-Cs-O simultaneous adsorption, oxidation interface chemical struct. 0-103584  
Gd-Co, amorphous films, mag. props. ferromag. reson. meas., 20-520°C (*Russian*) 0-97144  
Ge-O, Cu, amorphous thin film, impurity effects on struct. 0-107054  
H<sub>2</sub> electrochemical oxidation in fused alkali metal carbonates 0-72040  
H<sub>2</sub>+N<sub>2</sub>O, HO radical form. on Pt surface, laser-induced fluoresc. obs. 0-108738  
Hf electrode, surface oxide film, impedance and pot. behaviour 0-61001  
Hg<sub>0.8</sub>Cd<sub>0.2</sub>Te surface, sputter cleaning and dry oxidation, XPS and LEED study 0-108618  
HgTe surface, sputter cleaning and dry oxidation, XPS and LEED study 0-108618  
In, chemisorption of O<sub>2</sub>, XPS and static SIM spectral study 0-80055  
InAs, thermal oxidation, growth rate and chem. comp., temp. depend. 0-108619  
InGaAsP, anodic oxidation, refractive indices 0-97601  
InSb, optical constants and oxidation with various surface treatment (*Russian*) 0-88955  
InSb, Raman scattering study of unoxidised Sb in anodic oxide films 0-88985  
InSb, single crystal, chem. and ion etching, surface changes (*French*) 0-108614  
In<sub>2</sub>SnO<sub>3</sub> film, effect of ambient atmosphere during annealing, elec. props. 0-97510  
In<sub>2-x</sub>Sn<sub>x</sub>O<sub>3-y</sub>-insulator-poly-Si solar cells, photovoltaic conversion parameters 0-101093  
IrO<sub>2</sub>, electrochromic, oxidation state changes and struct. 0-100950  
LaB<sub>6</sub> (210) surface, work function, struct. and chemisorpt. stability, XPS, UPS and LEED 0-65344  
Mg (0001) face, incipient oxidation, EELS and LEED studies 0-81237  
Mg-Si-Al-O-N ceramic, phase assemblages, relationships with props. 0-60848  
MnO<sub>2</sub>, oxidation under UV irradiation rel. to Viking gas exchange reaction on Mars 0-72831  
Mo foil electrolytic perforation, surface film phase composition obs. (*Russian*) 0-61004  
Mo, mech. props., effect of exposure to high temp. He containing O<sub>2</sub>, room temp. study 0-93639  
Mo oxides, low-grade, soda roasting study (*Korean*) 0-93508  
Mo-Zr, nucleation conditions, effect on formation of oxide phase during internal oxidation (*Russian*) 0-81064  
MoS<sub>2</sub> solid lubricant, antifriction and elec. props. depend. on oxidation temp., dopant influence 0-108584  
MoSi<sub>2</sub>, oxidation behaviour, Ge additions effect (*German*) 0-71782  
MoSi<sub>2</sub> oxide film, dielec. props. and growth kinetics 0-81215  
Na<sub>2</sub>O-CaO-SiO<sub>2</sub> glass, redox phenomena evaluation in melting-finishing process, SO<sub>2</sub> evolution 0-84900  
Na<sub>2</sub>O-SiO<sub>2</sub>-(CaO) glass, molten, metal ion diffusion and redox behaviour, electrochemical studies 0-81332  
NaRHY zeolite, Rh complexes with CO and methyl iodide ligands, spectrosc. obs. 0-85159  
Nb films, oxidation, XPS study 0-80944  
Nb, oxidation mechanism, 673 to 823K 0-108644  
Nb-Nb<sub>2</sub>O<sub>5</sub>-Pb(In) Josephson junctions, props. of Nb<sub>2</sub>O<sub>5</sub> thermally grown tunnel barriers 0-100568  
Nb-NbO<sub>2</sub>-Pb superconductive tunnel junctions, oxide tunnelling barriers, ESCA characterisation 0-65745  
4NbO<sub>7.76</sub> thin film, FCC cell struct. investigation 0-92796  
NbSe<sub>2</sub> solid lubricant, antifriction and elec. props. depend. on oxidation temp., dopant influence 0-108584  
Ni (001) surface, Ar ion bombarded, enhancement of oxidation, AES study 0-97644  
Ni, adsorption of O<sub>2</sub>, oxidation 0-108730  
Ni alloys, heat resistant E1437B and E1929, surface condition, air stream effect 0-76409  
Ni base alloys, IN-702, IN-601, TD-Ni-Cr-Al, B-1900+Hf, oxidation, cyclic, role of thermal shock 0-97640  
Ni film, interaction with O<sub>2</sub>, AES, EELS, work function, and gravimetric meas. 0-75433  
Ni foil electrolytic perforation, surface film phase composition obs. (*Russian*) 0-61004  
Ni, galvanic oxidation in borate buffer soln. 0-100948  
Ni, oxidation, high temp., effect of C on cavity form., SEM study 0-97638  
Ni, oxidation kinetics, influence of intermediate annealing treatment 0-89412  
Ni, oxide films, metal and O<sub>2</sub> transport, AES and inert marker, techniques 0-97641  
Ni, oxidised surface, oxidising conditions effect on thermally stimulated exoelectron emission (*Japanese*) 0-89127  
Ni surface, (110), O<sub>2</sub> adsorption, LEED and ion scatt. study 0-84386  
Ni-Al (2 and 6 wt%), oxidation,  $\alpha$ -Al<sub>2</sub>O<sub>3</sub> growth, microstruct., precip. 0-108626  
Ni-Al-Cr-Cr<sub>3</sub>, eutectic alloy, directionally solidified, oxidation resistance, influence of Y 0-89409  
Ni-Cr (70 wt%), oxidation behaviour, 1073-1473K 0-89416  
Ni-Cr austenitic alloy, oxidation mechanism, intergranular diffusion effect (*French*) 0-81229  
Ni-Cr/Alu films, interdiffusion processes and oxidation phenomena 0-59735  
Ni-Cr-Al (20, 4 wt%), tensile stress effect on high temp. oxidation (*Japanese*) 0-89393  
Ni-Cr-W, oxidation behaviour in air at 1000-1250°C 0-89407  
Ni-Fe, adsorption of O<sub>2</sub>, oxidation 0-108730  
Ni-ThO<sub>2</sub>, oxidation, cyclic, role of thermal shock 0-97640  
 $\beta$ -NiAl, oxidation,  $\alpha$ -Al<sub>2</sub>O<sub>3</sub> growth and microstruct. 0-108627  
 $\beta$ -NiAl, oxide films, metal and O<sub>2</sub> transport, AES and inert marker, techniques 0-97641  
NiO, nonstoichiometric, near-surface and bulk chem. diffusion 0-80035  
NiO, powder pressed disc, oxidising conditions effect on thermally stimulated exoelectron emission (*Japanese*) 0-89127  
NiO, single cryst. cleavage plane, oxidising conditions effect on thermally stimulated exoelectron emission (*Japanese*) 0-89127  
Ni(100) oxidised surface structure anal., extended appearance potential fine struct. study. 0-75411

oxidation continued

Pb-In-(Au) base electrode film Josephson junctions, tunnel barrier oxide struct. 0-65750  
PbS, superficial degradation in air and water, XPS obs. (*French*) 0-89110  
PrO<sub>1.714</sub>, oxidation, kinetic study 0-108707  
Pt anode, oxide film growth in H<sub>2</sub>SO<sub>4</sub> solns., temp. study 0-71802  
Pt electrodes, polymeric surface film form. by electrooxidation of phenolic cpds., ellipsometric study 0-104450  
Pt resistance thermometers, effect of Pt oxidation 0-101794  
Pt, surface, (111), O<sub>2</sub> interactions, UPS, EELS and thermal desorption study 0-100409  
Pu, oxidation, binding energies, Auger and X-ray photoelectron spectra study 0-76550  
Si (111), intermediate oxidation state, core photoelectron absorpt. vs. chemical shifts 0-81220  
Si, ambient effect of O precipitation, self interstitial mechanisms, IR spectra, TEM study 0-66510  
Si, anodic oxidation, high electronic current density 0-89386  
Si based MOS device irradiation with  $\gamma$ -rays, minority carrier generation, CV characts. 0-88637  
Si, defect struct. of vitreous SiO<sub>2</sub> films, role of defect struct. in growth 0-65403  
Si, dislocation generation in local oxidation 0-107245  
Si, F-enhanced plasma growth of native layers, Auger profiles 0-93662  
Si film, low press. CVD prep., struct., elec. and optical props. 0-70548  
Si, float zone, process-induced effects on carrier lifetime and defects 0-81216  
Si, in high press. O<sub>2</sub>, residual stress, chemical etch rate, refr. index and density meas. 0-71768  
Si, ion implanted, dopant depend. of oxidation rate 0-89384  
Si, ion implanted, interstitial generation and loop form. during annealing in oxidising medium 0-107225  
Si, laser annealing for improved stacked-struct. oxide quality 0-65386  
Si, lattice strains induced by localized oxidation, high temp. real-time X-ray topographic studies 0-108489  
Si, oxidation induced by ion or electron bombardment, AES-SIMS study 0-108606  
Si, oxidation stacking faults, shrinkage and growth, bulk O<sub>2</sub> effects 0-96546  
Si, oxidation-induced Frank sessile dislocation loops, struct. change 0-75228  
Si, oxidation-induced stacking faults, distinction between clean and decorated faults by etching 0-79818  
Si, oxide scale microstruct. of oxidised single cryst. 0-108613  
Si, polycryst., morphological aspects 0-76388  
Si, polycrystalline, electrode shape effects on oxide conduction 0-96890  
Si, polycrystalline, thermal oxide anomalous stress 0-93661  
Si, polycrystalline multilayer support struct., control of deform. in dielec. isolated substrates 0-107681  
Si selective anodic oxidation in O<sub>2</sub> plasma 0-108610  
Si, solubility and transport behaviour of water, dissolution 0-93801  
Si surface, thermal oxidation induced defects, origin and growth (*Chinese*) 0-66681  
Si surfaces etched in CF<sub>4</sub> or CF<sub>4</sub>-O<sub>2</sub> plasma, morphology 0-93671  
Si, TEM and EELS identification of oxide precipitates 0-100723  
Si, thermal growth mechanisms of vitreous oxide layers 0-93675  
Si, thermal oxidation, role and effects of Cl 0-108622  
Si, thermal oxidation kinetics, steady-state transport anal. 0-71773  
Si, thermal oxidation kinetics, theoretical perspective 0-76387  
Si wafer, stacking faults, preoxidation gettering by reverse side P diffusion-induced misfit dislocations 0-60988  
Si:As(B), heavy-doping effects and impurity segregation during high-press. oxidation 0-65014  
Si:B, ion implanted, structure defects formation and behaviour under annealing in various ambients 0-65033  
Si:N, ion implanted, oxidation characts. 0-89385  
Si:P, polycrystalline laser recrystallised film on Si substrate, cryst. struct., thermal oxidation 0-65391  
Si:Sb, ion implanted, Sb diffusion during oxidation, snow-plough effect 0-88366  
Si-SiC chemical interaction in rarefied O<sub>2</sub> under pulsed action of concentrated solar radiation 0-71930  
Si-SiO<sub>2</sub> interface, electronic struct. calc. 0-100531  
Si-SiO<sub>2</sub> interface, thermally grown, surface pot. inhomogeneities after stress ageing 0-92993  
Si-SiO<sub>2</sub> interface, thermally grown oxide, spectroscopic ellipsometric anal. 0-107659  
Si-SiO<sub>2</sub> interface in MOS solar cells, operational characts. and struct. 0-93901  
SiC, controlled nucleation thermochemical deposition, charact. and props. 0-108355  
SiC, oxide scale microstruct. of oxidised single cryst. 0-108613  
Si<sub>3</sub>N<sub>4</sub> layers produced by ion implantation, oxidation inhibition and etching 0-103374  
Si<sub>3</sub>N<sub>4</sub>/ZrO<sub>2</sub>, hot-pressed, compressive surface stresses developed by oxidation induced phase change 0-60992  
Si<sub>3</sub>N<sub>4</sub>-CeO<sub>2</sub> additive, hot-pressing and oxidation behaviour 0-71618  
SiO<sub>2</sub> films, DC plasma Si anodisation, dielectric const., O<sub>2</sub> pressure influence 0-70564  
SiO<sub>2</sub> films, vac. thermal evaporation, parameter stabilisation 0-87571  
SiO<sub>2</sub> layer used for MOSFETs, electron trapping behaviour 0-92981  
SiO<sub>2</sub>, thermally grown films, thicknesses 30-600 Å, defect density meas. 0-84412  
SiO<sub>2</sub>-MgO-CaO-Al<sub>2</sub>O<sub>3</sub>-Ce,Fe, redox equilib., expt. 0-85171  
SiO<sub>2</sub> ultrathin oxide on Si, struct. obs. by high-resolution electron microscopy 0-103592  
Si(111), ion-bombard., O<sub>2</sub> adsorption, SIMS study 0-70522  
Sn, (100) surface, clean and O<sub>2</sub> exposed, slow positron studies, positronium formation 0-93429  
Sn-SnO<sub>2</sub>-Sn tunnelling junctions, fabrication by modified RF plasma oxidation method 0-103787  
Sn<sub>1-x</sub>Pb<sub>x</sub>Se(Te) films, rel. to annealing temp. and time, Mossbauer spectra, X-ray and microstruct. obs. 0-104311  
SnTe, mechanochem. and thermal oxidation comparison, Mossbauer obs. 0-104310  
SrTiO<sub>3</sub> surface, oxidation and reduction by D<sub>2</sub>O, H<sub>2</sub><sup>18</sup>O, D<sub>2</sub>, isotope exchange study 0-104461  
Ta, nonstationary heating and oxidation in low temp. plasma flow, heat and charge transfer obs. (*Russian*) 0-104341  
Ta<sub>2</sub>N<sub>3</sub> and TaN<sub>x</sub> films, thermal oxidation and resist. 0-60125

## oxidation continued

- 2Ta<sub>2</sub>O<sub>3</sub> thin film, FCC cell struct. investigation 0-92796  
 TaSi<sub>2</sub> films, on polycrystalline Si, oxidation characts. 0-97602  
 Te film, stability in moist air, rel. to information storage capability, atmospheric corrosion model 0-71774  
 (Ti,Cr)B<sub>2</sub>, sintering kinetics and props. 0-100811  
 Ti foil electrolytic perforation, surface film phase composition obs. (*Russian*) 0-61004  
 Ti, oxidation, linear, O diffusion coeff. depend. on rutile layer struct. (*French*) 0-104328  
 Ti, oxidation behaviour under pure O<sub>2</sub> atmos., temp. range 600-800°C 0-89415  
 Ti-Al-Sn-Zr, Ti-680, O contamination under high temp. (*Chinese*) 0-66688  
 Ti-Nb (4.32 wt%), high temp. oxidation kinetics under 1 bar pressure, 1255-1471K 0-89410  
 Ti-Ta (4.37 wt%), oxidation kinetics, 1258-1473K, and at pressure of 0.013, 0.133 and 1.0 bar 0-89411  
 TiO<sub>2</sub> brookite synthesis from Ti in NaF or Ti compounds, form. mechanism (*Japanese*) 0-93529  
 n-TiO<sub>2</sub> electrode, photo-oxidation of acetate and iodide 0-81331  
 n-TiO<sub>2</sub> electrode in AlCl<sub>3</sub>-NaCl melt, electrochem. and photoelec. props. 0-81328  
 V, oxidation in low press. O<sub>2</sub> at high temp. (*Japanese*) 0-71807  
 V<sub>2</sub>O<sub>5</sub> and lower oxides, defect structures and related props., review 0-59454  
 V<sub>2</sub>O<sub>5</sub> and lower oxides, electronic, optical, structural and surface props., review 0-88120  
 W, oxidation, WO<sub>3</sub> amorphous anodic film growth in acidic soln. 0-81232  
 W, oxidation mechanism, 773 to 973K 0-108644  
 WS<sub>2</sub> solid lubricant, antifiction and elec. props. depend. on oxidation temp., dopant influence 0-108584  
 WSi<sub>2</sub>, sputtered, props. for MOS IC appl. 0-70831  
 WSi<sub>2</sub>, steam-oxidized, Auger sputter profiling studies 0-107663  
 Y-Si-Al-O-N ceramic, phase assemblages, relationships with props. 0-60848  
 YIG:Ca, oxidising effects of high temp. annealing in reducing atmosphere 0-66696  
 Zn, surface oxidation, Auger spectrosc. obs. 0-97388  
 ZnS evaporated film, refl. loss on UV irradi., ZnO form. 0-99813  
 ZnS, superficial degradation in air and water, XPS obs. (*French*) 0-89110  
 ZnTe clean and adsorbed O<sub>2</sub> (110) surfaces, UV photoemission spectra (*Japanese*) 0-93456  
 Zr, breakaway oxidation kinetics at 623K, SEM study 0-97633  
 Zr, ion-implanted polycryst., thermal oxidation 0-71786  
 α-Zr, oxidation in O<sub>2</sub>-N<sub>2</sub> atmospheres 0-104353  
 Zr-Hf (2.2 wt%), high temp. oxidation in flowing O<sub>2</sub>, 873-1173K 0-93687  
 Zr-Nb (2.5 wt%), high temp. oxidation in flowing O<sub>2</sub>, 873-1173K 0-93687  
 Zr-Nb-Sn (3.0, 1.0 wt%), high temp. oxidation in flowing O<sub>2</sub>, 873-1173K 0-93687  
 Zr<sub>3</sub>Al, ordered, oxidation, weight gain and metallography 0-89398

## oxide coated cathodes

- see also thermionic electron emission  
 joule heating in emitting sites on various nonrefractory arc cathodes 0-100106  
 steel, mild, phosphate pickled, behaviour during deep electrolytical water enrichment, T meas. 0-93764  
 Ni, Medicus matrix cathode, surface characts. 0-66378

## oxygen

- see also nuclei with .....  
 adsorbed layer on W, Ar<sup>+</sup>(Ar<sup>+</sup>m)(Ar<sup>2</sup>su+) impact, electron emission obs. 0-60740  
 abundance in B-type stars in associations and general field 0-67702  
 adlayer effect on CO and H<sub>2</sub> adsorption and desorption on Fe(100) 0-71573  
 adsorbed layer on Ni {100}, crystallographic effects in low energy ion scatt., local ion-atom neutralisation 0-84377  
 adsorbed layer on Si (111) surface, ion scatt. obs. 0-59810  
 adsorbed on Ag (110), interaction with ethylene, LEED and AES obs. 0-89520  
 adsorbed on Al (111) surface, surface struct., LEED and SEXAFS data 0-92782  
 adsorbed on CdS, EPR of O radicals, temp. depend. 0-80612  
 adsorbed on graphite, props. calc. 0-103568  
 adsorbed on Nb, effect on polarised Balmer radiation from scatt. H<sup>2</sup>+ 0-99569  
 adsorbed on Ni surface, location of adsorbed atoms, surface channelling meas. 0-84373  
 adsorbed on Pt (111), chemisorbed and oxide states, low energy ion scatt. obs. 0-65372  
 adsorbed on W, surface diffusion, secondary electron emission study 0-76117  
 adsorption, on Pt(110) surface, Ar<sup>+</sup> bombardment effects on reactivity 0-89099  
 adsorption and catalytic reactions with H<sub>2</sub> and CO on Pt 0-81362  
 adsorption of mol. O<sub>2</sub> species on Ag (110) surface 0-103578  
 adsorption on and interaction with Ni film, AES, EELS, work function, and gravimetric meas. 0-75433  
 adsorption on Cu (001) surface, effect on surface barrier, LEED study 0-84378  
 adsorption on Cu (100) surface, LEED study 0-100408  
 adsorption on Cu (100) surface, reaction with CO 0-103583  
 adsorption on Cu vicinal surfaces, LEED study 0-103575  
 adsorption on Fe, oxidation 0-108730  
 adsorption on Fe(100), adsorbate coverage determ. by LEED, AES and XPS 0-103566  
 adsorption on graphite, partially localised, partially mobile monolayer films, adsorption isotherms 0-107646  
 adsorption on Ni, oxidation 0-108730  
 adsorption on Ni(110) surface, LEED and ion scatt. study 0-84386  
 adsorption on Ni (100) and reduction of surface oxide by H<sub>2</sub> 0-108741  
 adsorption on Ni-Fe, oxidation 0-108730  
 adsorption on polar ZnO surfaces, cond., EELS study 0-71525  
 adsorption on Pt (111) and Pt(S-12(111)×(111) surfaces, thermal desorption, AES, XPS, and LEED study 0-70534

## oxygen continued

- adsorption on Pt (111) surface, UPS, EELS and thermal desorption study 0-100409  
 adsorption on Re(0001), XPS, UPS and temp. programmed desorption 0-71574  
 adsorption on Ru (1120), ellipsometry-LEED study 0-103570  
 adsorption on SrTiO<sub>3</sub> surface, electron energy-loss spectra obs. 0-89521  
 adsorption on Zr, dissociation, and diffusion 0-80085  
 adsorption rate, on Ge (111) clean surface 0-59779  
 alkali metal chloride crystal, F centre energy level shift and splitting in O<sup>-</sup> field 0-70640  
 alkali metals, liquid, O<sub>2</sub> pot. and O<sub>2</sub> distrib. coeffs. between alkali and struct. metals 0-65231  
 ambient effect of precipitation in Si, self interstitial mechanisms, IR spectra, TEM study 0-66510  
 atmosphere, O<sub>2</sub> level rel. to O<sub>3</sub> content evolution 0-98400  
 in atmosphere, photodissoc. in stratosphere and mesosphere through solar UV radiation absorpt. 0-109248  
 atom, (<sup>1</sup>D<sub>2</sub>) state, quenching, rel. to O<sub>2</sub> b'<sup>1</sup>Σ<sub>g</sub><sup>+</sup> prod. and deactivation 0-76493  
 atom, (<sup>3</sup>P<sub>2</sub>) state, direct obs. from O<sub>2</sub> photolysis at 248 nm 0-101028  
 atom, ab initio effective valence shell Hamiltonian for neutral and ionic valence states 0-74117  
 atom, associative ionisation, merging beams experiment 0-63789  
 atom, photoionisation cross sections and asymmetry parameters, SCF Xα scatt. wave calcs. 0-63542  
 atom, spectra in Ar inductively coupled plasma 0-91473  
 atom in molecule, K-shell fluoresc. yield, statistical scaling 0-78644  
 atom or ion, sputtered from SiO<sub>2</sub> and oxidised Al surfaces, light emission 0-58199  
 atomic O<sub>2</sub> supersonic nozzle beam source development 0-58016  
 atomic source with improved long term stability for chemiluminescence reaction, mol. dissociation and recombination 0-93758  
 attachment cooling, press. depend. 0-91663  
 aurora, O<sub>2</sub> (<sup>1</sup>Δ<sub>g</sub>) emission, vibr. excitation process 0-82125  
 binding to Fe, Co-substituted myoglobins, comparisons, thermodynamic invest. 0-67030  
 blood, shear-induced augmentation of O<sub>2</sub> transfer 0-94274  
 blood gas catheter, fast-responding, flow-independent, for O<sub>2</sub> meas. 0-101277  
 bonding to Tokamak walls, XPS studies 0-80942  
 broad beam ion source used for sputtering and etching 0-69002  
 chemisorbed on Ni, influence on surface vibrs. 0-84361  
 chemisorption, effects on LaB<sub>6</sub>-(210) surface, XPS, UPS and LEED 0-65344  
 chemisorption, on Cu(110), enhancement during Ne<sup>+</sup> bombard. 0-65070  
 chemisorption, on graphite, influence of Fe as impurity 0-96732  
 chemisorption, on transition metals, chemisorpt. energy trends 0-107631  
 chemisorption on Al (111), electronic struct. calcs. rel. to UPS data 0-59801  
 chemisorption on austenitic stainless steel surface, electron spectroscopy, Auger spectra and work function obs. 0-65364  
 chemisorption on GaAs(110), ab initio theory 0-75612  
 chemisorption on Mg (0001) face, incipient oxidation, EELS and LEED studies 0-81237  
 chemisorption on Ni (111), adlayer phases and binding sites 0-80069  
 chemisorption on Pt 6(111)×(100), UPS studies 0-76151  
 chemisorption on Pt (111), XPS, UPS, EELS, and work function meas. 0-76139  
 chemisorption on reduced and stoichiometric SrTiO<sub>3</sub>(111), UPS and XPS studies, illum. effects 0-71572  
 chemisorption on Ru (001), uptake meas., thermal desorpt. spectroscopy and AES 0-108739  
 chemisorption on SnO<sub>2</sub>, elec. cond. and EPR meas. correlation 0-84369  
 chemisorption on W(110) surface, effects on dielec. function, refl. spectra 0-75616  
 chemisorption with CO on Pt surfaces, SCF-Xα cluster calcs. 0-65365  
 chloropentafluoroethane-O<sub>2</sub>, multiphoton dissociation, <sup>13</sup>C enrichment factor, CO<sub>2</sub> laser wavelength and fluence depend. 0-58331  
 coadsorption with Cs on Mo (110), electron emission props. and thermal stability 0-66878  
 coadsorption with K on Fe (110), XPS, UPS, AES, and LEED study 0-80084  
 contaminated Ni surface, coadsorption of Sn, AES study 0-88437  
 crystal, α-phase, exciton, exciton-magnon, and biexciton absorpt. at 1.5K 0-84750  
 desorption, photon-stimulated, angle-resolved, of O<sup>+</sup> from W (111) 0-88434  
 desorption from stainless steel, during laser irradi., etching, AES study 0-66338  
 desorption from W(100), photon and electron stimulated 0-100397  
 determination, in flue gas of 200 MW plant, trial operation (*Czech*) 0-89562  
 determination by <sup>3</sup>He activation anal. in Si<sub>3</sub>N<sub>4</sub> films on Si wafers 0-71981  
 diffusion in group V refractory metals, statistical calculations on Arrhenius lines 0-59722  
 diffusion in liquid Sb, activity coeff. 0-65267  
 diffusion rate in Au thin layers 0-100359  
 diffusivity and solubility in liq. metals, electrochem. obs. using solid oxide electrolytes 0-59669  
 dissociation by field-accelerated electrons, macroscopic props., rel. to dry air 0-61118  
 dye solution, amplified spontaneous emission, effect of O<sub>2</sub> 0-95885  
 electron stimulated desorption from W (110) stepped surface, atomic steps and defects influence 0-80091  
 electrons, field-accelerated, in dry air and pure O<sub>2</sub>, macroscopic props. comparison (*French*) 0-59161  
 ethylene-O<sub>2</sub>-N<sub>2</sub>-Al particle mixture, two-phase detonation and combustion (*French*) 0-61097



## oxygen continued

- evolution, H<sub>2</sub>O electrolysis, nucleate boiling, vapour bubble behaviour, heat and mass diffusion 0-67013
- exosphere O atoms, polar corona atom distrib. 0-82120
- flow regulator, solid-state, high-temperature 0-57301
- free surface and grain boundary chemistry in Fe alloys 0-75410
- fuel cell electrodes, galvanostatic switching curve shapes 0-66965
- Galaxy, O enrichment determ. from planetary nebulae O/H ratios 0-105328
- gas, pure rotational CARS obs. 0-99511
- gas, weakly ionised, electron transport coeffs., Boltzmann eqn. anal. (Japanese) 0-59183
- haemoglobin-O<sub>2</sub> equilibrium curve, instrument for determ. based on membrane diffusion 0-81761
- haemorrhagic shock, effect of anemia on O<sub>2</sub> transport 0-67330
- haemorrhagic shock, effect of increased blood-O<sub>2</sub> affinity on O<sub>2</sub> transport 0-67331
- half-monolayer on W (100), surface reconstruction kinetics 0-65375
- impurities effect on epitaxial regrowth of amorphous Si 0-84401
- impurity at glass-metal seal interface, composition and conc. determ. by AES 0-76587
- impurity in Nb, distrib. determ. by neutron activation anal. (Russian) 0-70243
- impurity in Zr-Cu, Nb-Ni and Ti-Ni amorphous alloys, effect 0-75168
- initial interaction with Al single cryst. faces, LEED, AES and work function study 0-84392
- initial reaction probability with Ba getter film, AES obs. 0-61153
- ions, Li-like Auger contribs. to electron impact ionisation 0-87231
- ions in Earth's upper atmosphere, coupled time-dependent diffusion eqns. 0-109285
- ions in Jupiter magnetosphere, plasma cloud injection from IO 0-90358
- isoelectronic sequence, optical oscillator strengths 0-63589
- isoelectronic sequence, X-ray spectra 0-87071
- KERMA values, consistent set for H, C, N, and O for neutrons from 10 to 80 MeV 0-68967
- lactate dehydrogenase, O<sub>2</sub> effect in radiolysis obs. 0-72223
- lead phthalocyanine:O<sub>2</sub>(I), Schottky barrier effect on CAC current response 0-75623
- liquid, exchange interaction, EPR absorpt. line shape anal. 0-71158
- liquid, modified droplet model, mean droplet interaction below T<sub>c</sub> 0-70363
- liquid, pure vibr. Raman spectra 0-97262
- low energy electron drift velocity at 293K 0-103101
- man's transport system, functional state, math. model 0-104548
- marine oil pollution, retardation of O<sub>2</sub> exchange with atmos. 0-109175
- marine sediments in coastal area, depth penetration of O<sub>2</sub> 0-104952
- microwave absorpt. at 60 GHz, for atmos. remote sensing 0-77172
- molecular, A<sup>2</sup>Δ<sub>u</sub> state, inversion, presence in nightglow and discharges 0-63616
- molecule, <sup>1</sup>Δ<sub>g</sub> singlet state, spectrosc. obs. in dye-sensitised fluorocarbon solns. 0-85178
- molecule, <sup>3</sup>Π<sub>g</sub> diatomic Rydberg states, ab initio CI calcs. 0-95554
- molecule, electron attachment threshold photoelectron spectra, vibr. excitation 0-83422
- molecule, electron coincidence spectrosc., valence electron momentum distrib. and binding energies 0-102583
- molecule, I and I' resonance series, vibr. level populations in autoionisation, photoelectron spectra, bond length determ. 0-91612
- molecule, liq. and gas, induced absorpt. spectral moment, mol. calcs. 0-63737
- molecule, low energy elastic and inelastic electron scatt., rot. transitions, close coupling calc. 0-78706
- molecule, mag. dipole transitions, line positions and strengths from stratospheric emission spectra 0-78604
- molecule, photoelectron asymmetry parameters 0-95684
- molecule, photoionisation cross section and asymmetry parameters calc. in UV region using static pot. 0-95692
- molecule, quenching of afterglow, quenching var., activator penetration to region inaccessible to quencher 0-64813
- molecule, Rydberg states, <sup>2</sup>Σ<sub>g</sub><sup>+</sup>, <sup>3</sup>Σ<sub>u</sub><sup>+</sup>, <sup>3</sup>Π<sub>g</sub>, <sup>1</sup>Π<sub>g</sub>, <sup>3</sup>Σ<sub>g</sub><sup>+</sup> symm.; ab initio CI study 0-99460
- molecule, Schumann-Runge continuum, oscill. strength and electron impact excitation 0-69121
- molecule, Schumann-Runge system, electronic transition probabilities 0-78603
- molecule, spin-forbidden transition intensities, selective heavy atom effects 0-58240
- molecule, structural second virial coeff., intermol. pot. and mag. scatt. 0-78678
- molecule, symmetry adapted wave function generation using group theoretical projection operators 0-102428
- molecule 0-58165
- molecules, b<sup>2</sup>Σ<sub>g</sub><sup>+</sup> state prod. and deactivation following O(<sup>1</sup>D<sub>2</sub>) quenching 0-76493
- monolayers, on graphite, mag. α-phase and α-β-phase transition 0-70530
- OH masers, interstellar, obs. near Orion population stars 0-67716
- order-disorder interaction with GaAs (110), LEED anal. 0-75445
- photon and electron stimulated desorption energy and angular distributions from W {001} 0-96734
- pionic, Auger electron emission (Russian) 0-69271
- planetary nebulae in Magellanic Clouds, He, N and O abundances, effects of excitation class 0-109519
- plasma, electron energy distrib. function, electron sink and plasma resist. effect (Russian) 0-106987
- plasma impurity in N<sub>2</sub> RF capacitive discharge, effect on heating 0-59312
- potential in equilibrium with impure high temp. inert gases 0-104135
- precipitation in Si, 650°C, IR absorpt. and X-ray diff. 0-76258
- production from H<sub>2</sub>O using solar energy, eval. of a hybrid process 0-104519
- pulmonary contusion and flail chest, effects on perfusion and O<sub>2</sub> exchange 0-67119
- quenching of dye fluorescence for surface flow visualisation 0-79422
- seawater, conc. in POLYMODE area (Sargasso Sea) rel. to eddy dynamics 0-85685
- sensors, solid electrolyte, noncatalytic electrodes 0-76573
- simultaneous interactions with Cl<sub>2</sub> on Ta under low press. and high temp. 0-71938
- solar flares, O I 1355.6 Å and C I 1355.8 Å lines obs. 0-90381
- solid γ-phase and liq., mol.-dynamic study of struct., dynamics 0-96467
- solubility in Ti-Al-Kh18 steel, thermodynamical anal. (Russian) 0-92676

## oxygen continued

- steel, stainless, stress corrosion susceptibility in high purity water, O<sub>2</sub> and temp. effects 0-61002
- supersonic molecular beam source, simple calibration method 0-82845
- thermosphere O, composition seasonal-latitudinal tidal struct. and mass density 0-101467
- transition metal-O bond energy in O<sub>2</sub> glow discharge, mass spectrometry obs. 0-64808
- upper atmosphere atom density, rel. to airglow intensity (Chinese) 0-90269
- Venus spectrum, <sup>1</sup>Δ<sub>g</sub>-<sup>3</sup>Σ<sub>g</sub><sup>+</sup> band, prod. mechanisms 0-82251
- Zircaloy-4, elastic props., O additions effect 0-66565
- O<sub>2</sub>+hydroxymethyl radical, rate coefficient meas. by laser magnetic resonance flow tube method 0-66767
- Al-O supercond. film, RF complex impedance meas., dynamic pinning 0-84573
- Ar-O<sub>2</sub> (6%) cryst., vibr. Raman spectra 0-60558
- Au-O bond energy glow discharge, mass spectrometry obs. 0-64808
- C+O<sup>+</sup> ion-molecule reaction, 15 eV energy O<sup>+</sup> production system 0-84817
- C<sub>2</sub>+O<sub>2</sub>, C<sub>2</sub>(X<sup>3</sup>Σ<sub>g</sub><sup>+</sup>) and C<sub>2</sub>(a<sup>3</sup>Π<sub>u</sub>) intersystem crossing and free radical kinetics 0-95668
- CH+O reaction, absolute rate const. 0-97690
- CO<sub>2</sub>-N<sub>2</sub>-He-O<sub>2</sub> discharge mixture, three body electron attachment to O<sub>2</sub> 0-64779
- Ca+O<sub>2</sub> reaction, chemiluminesc. absolute cross sections, photon yields and CaO dissociation energy 0-97697
- CaF<sub>2</sub>:O<sup>2-</sup>, CaF<sub>2</sub>:Na<sup>+</sup>, O<sup>2-</sup> and CaF<sub>2</sub>:Y<sup>3+</sup>, O<sup>2-</sup>, thermal depolarisation obs. of defect clusters 0-71299
- CdS-O<sub>2</sub>, photoactivated O desorption 0-100391
- CdSe-O<sub>2</sub>, photoactivated O desorption 0-100391
- Ce-S-O equilibrium in molten Fe (Chinese) 0-104423
- Cs-O<sub>2</sub>, desorption from W, activation energy 0-103562
- Fe, single cryst., segregation behaviour of S, O and P at (100) surface 0-100841
- α-Fe:O, valency effect of interstitials 0-65502
- GaAs:O<sub>2</sub>, impurity levels charact. using dark capacitance and photocapacitance transient techniques 0-59920
- GaAs:Cr:O semi-insulating monocrystal development and four-level model 0-88191
- GaAs:O, deep level, Franck-Condon shift, photocond. and Hall effect study 0-70642
- GaAs:O, electrolum., photolum., negative differential resist. rel. to recomb. processes 0-66304
- GaAs:O, junction barrier depletion region, capture from free-carrier tails 0-70802
- GaAs:O, semi-insulating, excitation temp. effect on TSC 0-70717
- GaAs:O epitaxial film, impurity states, photocapacitance spectra 0-65625
- GaAs:O p-n strucls., injection current and negative photocond., saturation mechanism 0-92967
- GaP:Cs-O simultaneous adsorption, oxidation interface chemical struct. 0-103584
- GaP:Zn, O, influence of impurity-absorbed illumination on luminesc. 0-93395
- Ge:O, Cu, amorphous thin film, impurity effects on struct. 0-107054
- Ge:O, IR absorpt. at low temp. (Chinese) 0-108228
- Ge:O, slow thermal relax. of cond. rel. to donor complexes 0-70704
- H+B<sup>+</sup>(<sup>4</sup>C<sup>+</sup>)(N<sup>4</sup>)(O<sup>4</sup>), (2≤q≤4, 5), cross sections at keV energies 0-78705
- H+O<sub>2</sub>+Ar, HO<sub>2</sub> free radical prod., rate const. calc. 0-101026
- H<sub>2</sub>-O<sub>2</sub> seeded system for MHD generator, elec. cond. 0-76642
- H<sub>2</sub>+O<sub>2</sub>, combustion, kinetic modeling and sensitivity anal. 0-89490
- HF with interstitial O, quantitative TEM obs. of small agglomerates 0-107227
- He-O mixture, RF discharge, mass spectroscopy, floating double probe meas. 0-84016
- He-O<sub>2</sub> DC discharge, electron distrib. function 0-92407
- N-O mixtures, positive glow corona in quasi-uniform fields 0-100104
- N<sup>+</sup>+O<sub>2</sub>, branching ratio kinetic energy depend. 0-97703
- N<sub>2</sub>-O<sub>2</sub> liquid, high resolution CW CARS spectra 0-63635
- N<sub>2</sub>-O<sub>2</sub> gas mixture, weakly ionised, electron transport coeffs. anal. (Japanese) 0-59184
- N<sub>2</sub>-O<sub>2</sub> mixture transient discharges, RF techniques 0-70067
- O 2.53 mm line, Zeeman splitting rel. to geomagnetic field vars. 0-77124
- O atmosphere spectral emission at 557.7 nm, 100 km altitude 0-61933
- O I 6300 Å airglow, anal. of consistency of ground-based obs. with satellite results 0-98496
- O I 7774 Å multiplet obs. of nightglow over Arecibo during magnetic storm 0-72663
- O I 8446 Å emission excitation mechanism, visible and IR obs. of Seyfert 1 galaxies 0-85991
- O I dayglow red emission at 630 nm in Mars atmosphere 0-62063
- O II, relative intensities and lifetimes in nebulae, conventional radiation theory 0-109513
- O III, electron impact excitation cross sections, independent particle model calcs. 0-63823
- O III forbidden lines in Omega Nebula (W38, M17, NGC 6618), IR spectra obs. 0-90495
- O IV bound states, oscillator strengths and photoionisation cross sections 0-106293
- O I(<sup>3</sup>P) in lower thermosphere, nighttime conc. obs., using new rocket borne instrument 0-105066
- O in atmosphere, effects on abundance of nearby supernova 0-94584
- O ion+Au, L-shell X-ray production and subshell ionisation cross sections meas. 0-91637
- O, spectral line shape in upper atm. following dissociative excitation 0-105097
- O V, 2s<sup>2</sup>S<sub>1/2</sub>-2s2p<sup>2</sup>P<sup>o</sup> intercombination line wavelength determ. 0-102470
- O V, E1 transition probabilities, lifetimes, CI calc. 0-83321
- O VI, 2s<sup>2</sup>S-2p<sup>2</sup>P reson. lines, wavelength determ. 0-102470
- O VII, electron impact collision rates, reinterpretation of solar emission line ratios 0-98624
- O VII line ratio for solar flare, X-ray obs., electron density determ. 0-82326
- O<sup>+</sup>, absolute electron impact ionisation cross section 0-83496
- O<sup>+</sup> isolated GaAs-GaAlAs DH laser compared with SiO<sub>2</sub> isolation 0-74382
- <sup>18</sup>O<sup>+</sup> ion implantation in channelling directions in Al, Ni, Cu single crystals, expt. conditions and range profile obs. 0-65022
- <sup>18</sup>O<sup>+</sup> ion implantation in channelling directions of Al, Cu and Ni single crystals, stopping power determ. 0-65078



## oxygen continued

- $O_2^-$  ion transport in  $\alpha$ -phase  $Bi_2O_3$  thermoelectric cell 0-92713  
 $O_2^-$  low partial press., thermogalvanic meas. using  $O_2^-$  ion conductors 0-73389  
 $O_2^-$  polarisability rel. to ferroelec. phase transitions 0-71326  
 $O_2^{++}$  electron impact ionisation, close coupling calcs. 0-106293  
 $O_2^{++}$  resonant-scatt. contributions to excitation rates 0-58393  
 $O_2^{++}$  enriched plasma in driving piston of solar flare-generated shock wave 0-72740  
 $O_2^{n-}$  ( $n=0$  to 2), core binding energy shifts,  $\Delta SCF$  calcs. 0-95558  
 $O_2^{n+}$  ions, role in solar wind interactions with lunar surface grains 0-62050  
 $O_2^+$  electron density ratio in 140-200 km height range of atmosphere 0-105102  
 $O+Al(Sn)$ , inner-shell multiple ionisation systematics, X-ray obs. 0-63790  
 $O+Ar(Kr)(Xe)$ , magnetically selected  $O(^3P)$  state scatt. 0-99543  
 $O+benzene(-d)$ , phenol radical prod., crossed mol. beam investig. 0-71902  
 $O+CS_2$ ,  $CS+SO$ , vibrational distribution of  $CS$ , laser-induced fluorescence meas. 0-71895  
 $O+H_2$ , classical trajectory calcs., ab initio surface, singlet state, rate consts. 0-66786  
 $O+H_2$ , pot. energy surfaces and reaction rates, ab initio calcs. 0-63531  
 $O+H_2O$ ,  $OH+OH$ , energy partitioning 0-101009  
 $O+H_2SO_4$ , atmosphere chemistry, collisional reaction probabilities 0-90168  
 $O+H_2(HCl)$ , relax. and chem. reaction, time resolved IR fluoresc. and mass spectrometry obs. 0-69177  
 $O+methane$ ,  $OH+methyl$  reaction, photolytically initiated, high temp. kinetics meas. technique 0-61085  
 $O+methyl$  radical, infrared chemiluminescence obs. 0-61080  
 $O+NF_3$ , electronically-excited free radical reactions 0-97707  
 $O+NaO$ , nightglow, excitation and abundance of  $Na$  0-98497  
 $O+saturated$  hydrocarbon, chem. reaction dynamics.  $OH$  prod. investig. 0-101016  
 $O+saturated$  hydrocarbon, reaction dynamics, model pot. surfaces, quasi-classical trajectory calcs. 0-97696  
 $O+saturated$  hydrocarbon- $OH+alkyl$  radical, reaction dynamics, mol. beam-laser induced fluoresc. obs. 0-97695  
 $O^++O_2$ ,  $O_2^+$  cross section kinetic energy depend., rate consts. meas. and Monte Carlo calcs. 0-78701  
 $O^++H_2(N_2)$ , reactant ion electronic states, effect on charge transfer cross sections 0-63809  
 $O^++N_2$ , charge exchange collision, rate coeff. and ionosphere implications 0-87224  
 $O^++O_2$ , charge exchange collision, rate coeff. and ionosphere implications 0-87224  
 $O^++O_2$ , excited ion reactions, charge transfer coeffs. at thermal energy 0-95721  
 $^{17}O+^{16}O$ , fractionation by chemical equilib. 0-89513  
 $^{18}O+^{16}O$ , fractionation by chemical equilib. 0-89513  
 $O^{2+}$  inert gas, electron transfer meas., 60-200 keV 0-83480  
 $O^{n+}+H$ , charge transfer cross sections, oscillatory behaviour in low-energy collisions 0-63806  
 $O^{n+}+N$ , charge exchange contribution to K-vacancy production 0-102553  
 $O_2$  1.27  $\mu m$  airglow, middle latit. meas. rel. to mesospheric  $O_3$  concs. 0-72606  
 $O_2$  5 mm absorption bands, long distance meas. of cloudy atm. by radiometry 0-90196  
 $O_2$  ( $\Delta$ ), atmospheric, collisional emission rel. to new diffuse bands in twilight 0-72662  
 $\alpha-O_2$ , antiferromagnetic polycrystal, splitting of exciton absorpt. lines in mag. field (Russian) 0-103943  
 $O_2$  atmos. spectra at 100 km altitude, (0-1) band 0-61933  
 $O_2$  atmospheric band system in nightglow, rocket meas. (Japanese) 0-94631  
 $O_2$ , atmospheric electric quadrupole transitions detection in A band 0-85746  
 $O_2$  concentrations, effect on radiation survival of cell spheroids 0-76792  
 $\gamma-O_2$ , cryst., vibr. Raman spectra 0-60558  
 $\beta-O_2$  crystal, thermodynamics of mol. libration motion (Russian) 0-70328  
 $\alpha-O_2$  crystals, absorpt. line polarisation biexciton existence (Russian) 0-108242  
 $\alpha-O_2$  crystals, absorption line biexciton polarisation (Russian) 0-89028  
 $\alpha-O_2$  crystals, spin ordering effect on light absorpt. (Russian) 0-89029  
 $O_2$  density in thermosphere, solar flux var. 0-72659  
 $O_2$  diffusion distance and necrosis development in multicell spheroids 0-81570  
 $O_2$  electron capture rate from geminate ion recombination fluoresc. data 0-74245  
 $O_2$  in liquid Xe, electron capture 0-102402  
 $O_2$  in Venus atmos.,  $O_2$ , Ar, CO abundances, error of Pioneer Venus chromatography obs. 0-105189  
 $O_2$  laser excited, quenching by  $CO_2$ ,  $H_2O$  and  $I_2$  0-99515  
 $O_2$  molecular fluid, Rayleigh and Raman light scatt. props., orientational and collision induced effects 0-63644  
 $O_2$  nightglow spectral intensity changes correl. with NaD spectra 0-61932  
 $O_2$  rotational Raman intensities and polarisability anisotropy change meas. with internuclear distance 0-63641  
 $O_2$  singlet in solns., luminesc. duration following pulsed laser excitation 0-76070  
 $O_2$  total scatt. cross sections for intermediate-energy positrons 0-91692  
 $O_2^-$ ,  $A^{II}$  state pot. energy curve, MCSCF calcs. 0-63565  
 $O_2^-$  ion, form. by  $O_2$  adsorp. on  $CaO$  0-61155  
 $O_2^{n+}$ ,  $^{II}$  state, quasi-bound levels, predissociation, band rot. anal., photofragment kinetic energy anal. 0-63650  
 $O_2$ -Ar mixtures, positronium form. and quenching, orthopositronium quenching cross section determ. 0-74261  
 $O_2$ - $CO_2$  mixture, temp. dependence of molecular vibr. relaxation freq. from 300 to 675K 0-74238  
 $O_2$ - $H_2$  mixture, temp. dependence of molecular vibr. relaxation freq. from 300 to 675K 0-74238  
 $O_2$ - $H_2$  plasma, electrical conductivity tensor in mag. field (Russian) 0-87864  
 $O_2$ -He mixture, temp. dependence of molecular vibr. relaxation freq. from 300 to 675K 0-74238  
 $O_2$ - $N_2$  mixture, attachment cooling, press. depend. 0-91663

## oxygen continued

- $O_2$ -seeded Ar plasma supersonic free jet expansion flow, population density measurements (Japanese) 0-96351  
 $O_2+N_2^+$ , electron capture and ion loss cross-section, 2.4-24.3 keV 0-58373  
 $O_2+Ar$ , molecular fluid mixtures, equilibrium props. 0-64867  
 $O_2+Ar^*$ , ion pair form. explained by charge transfer model 0-99546  
 $O_2+Ba$  crossed beam kinetics, BaO recoil velocity spectra 0-76500  
 $O_2+Br^+$ , total electron detachment cross sections for energies around threshold 0-99550  
 $O_2+C_2$ , IR laser photolysis of polyat. mols. photochem. appls. 0-66835  
 $O_2+C_2O$ , absolute reaction rate consts. meas. by laser induced fluoresc. 0-93738  
 $O_2+C_2$ , reaction kinetics, laser induced fluoresc. obs. of allene photolysis 0-66820  
 $O_2+C(^3S_0)$  0-74241  
 $O_2+Cl^+$ , total electron detachment cross sections for energies around threshold 0-99550  
 $O_2+Cl^+$ , reactions at room temp. 0-93749  
 $O_2+Cs$ , collisional ionisation, energy spectra of forward and backward directed positive and negative ions 0-87200  
 $O_2+Cs(K)$ , mol. target internal motion 0-78697  
 $O_2+H$ , collisional coherent excitation, meas. of Lyman  $\alpha$ -photons 0-99552  
 $O_2+H_2O^+$ , rate constants determ. as function of relative kinetic energy 0-81292  
 $O_2+HBr$ , rate consts. for vibr. energy transfer meas. using laser induced fluorescence technique 0-87206  
 $O_2+HCl$ ,  $HCl$   $v_0-v_1$  band perturbations, linewidth and shifts calcs., IR spectra obs. (French) 0-58251  
 $O_2+HF$ ,  $HF(v=3)$  relax. and rate consts. 0-61069  
 $O_2+He^+$ , 0.7-2 MeV, charge-changing collisions, electron capture 0-58372  
 $O_2+He^+$ , charge transfer product state distrib., time of flight obs. 0-87223  
 $O_2+HgBr$ , vibr. relax., rate coeffs., fluoresc. obs. 0-63697  
 $O_2+K$ , collisional ionisation, energy spectra of forward and backward directed positive and negative ions 0-87200  
 $O_2+K^{2+}$ , charge transfer reactions, rate coeffs. and product-ion distributions meas. 0-104431  
 $O_2+N_2$ , molecular fluid mixtures, equilibrium props. 0-64867  
 $O_2+N_2$ ,  $N_2$  fixation, catalytic processes in non-equilibrium plasma chemical reactors (French) 0-89484  
 $O_2+N_2^+$ , collisional dissociation cross-section, 2.4-24.3 keV 0-58373  
 $O_2+N_2+NO$ , mixtures with nonthermal vibr. excitation of mol.  $N_2$ , formula for calc. equilb. const. 0-76545  
 $O_2+N^+$ , electron capture and ion-loss cross-section, 2.4-24.3 keV 0-58373  
 $O_2+Ne^{2+}$ , charge transfer reactions, rate coeffs. and product-ion distributions meas. 0-104431  
 $O_2+O^+$ , charge exchange collision, rate coeff. and ionosphere implications 0-87224  
 $O_2+OH$ ,  $OH(v=1)$  relax., time resolved spectra 0-74240  
 $O_2+S^{4+}$ , ( $q=6-16$ ), K X-ray prod., charge-state depend. 0-106391  
 $O_2+SO_2=SO+O_2$ , gas phase reaction, rate coeffs. meas. 0-97704  
 $O_2+U^+(UO^+)$ , reaction cross-sections, ion beam apparatus study 0-97691  
 $O_2$  molecule, equilb. struct., vibr. freqs., SCF closed shell calcs. 0-74101  
 $O_2$  molecule, SCF-Cl calcs. 0-78517  
 $O_2^+$ , produced by collisional dissociation method, mass spectrometric study, dissociation energies determ. 0-95707  
 $O_2^+$ , hypothetical, mol. self-consistent study, possible prep. method (French) 0-91717  
 $O_2^+$ , produced by collisional dissociation method, mass spectrometric study, dissociation energies determ. 0-95707  
 $O(^3D)$  in thermosphere, quenching by electrons 0-94630  
 $O(^3D)+N_2$ , thermal rate coeff., products and branching ratios in ionosphere 0-82117  
 $O(^3D)+N_2$ , charge exchange, rate coeff. temp. depend. 0-77179  
 $O(^3D)+NH_3$ ,  $OH(v,N)+NH_3$ , bimodal OH rot. distrib. obs. and energy disposal 0-76501  
 $OH+NO(NO_2)(O_2)$ ,  $OH(v=1)$  relax., time resolved spectra 0-74240  
 $O(O_2^-)$ , optimum pot. model used to generate numerical pot., energies and electron affinities determ. 0-99534  
 $O(^3P)$ , atmospheric, ionisation freq. vars. during solar cycle 21 from airglow meas. 0-77195  
 $O(^3P)$  prod. by  $O_3$  photolysis, quantum yield determ. 0-78568  
 $O(^3P)+dimethyl$  disulphide, absolute reaction rate const. determ. 0-89472  
 $O(^3P)+dimethyl$  sulphide, fast flow reson. fluoresc. obs. of absolute rate consts. 0-61077  
 $O(^3P)+methane$ , barrier height and transition state geometry, POL-CI calc., H abstraction reaction 0-66782  
 $O(^3S)$  yield from  $O_3$ , photodissoc. at 1700-2000 Å 0-97714  
 $O(^3S)+N_2(X^3\Sigma_g^-) \rightarrow NO(^2\Sigma^+)+N(^4S)$ , MCSCF potential energy surface for collinear  $\Sigma^+$  pathway 0-63540  
 $O(^3\Sigma_g^- \rightarrow \Sigma_g^-)$ , in  $O-COS-O(^3\Sigma_g^-)/O_2$  system, chemiluminescence 0-66806  
 $^{16}O$  ions, mag. hyperfine interactions, PAC meas. 0-95734  
 $^{17}O$ , naturally abundant, nuclear quadrupole resonance spectrum for fine struct. detection 0-75881  
 $^{17}O/^{18}O$  ratio in Allende meteorite inclusion HAL, possible member of FUN family 0-105211  
 $^{18}O$  concentration in Amazon Basin water, evidence for recycling 0-81955  
 $^{18}O$  isotope shift in  $^{13}C$  NMR, struct. depend. 0-69165  
 $^{18}O/^{16}O$  ratio in precipitation, correl. with temp. and altitude 0-77067  
 $^{18}O/^{16}O$  variations in deep sea carbonate shells from East Pacific Rise hydrothermal field 0-109173  
 $^{18}O/^{16}O$  in atmosphere, photodissociation as source of atmospheric  $O_3$  0-94559  
 $O^++O_2$ , metastable ion reactions, rate consts. and ion mobility at 300K 0-95722  
 $O_2(b^3\Sigma_g^-)$ , temp. dependent quenching, photochemical study by  $H_2$ -VUV laser 0-63702  
 $PbO$ , thin film, microstruct. and thermal stress, doping effects 0-88458  
 $Re-O-Cl$  system, gas-transition metal interaction, kinetic model (French) 0-108740  
 $SO_2$ ,  $^{18}O$  mixtures, IR laser pumped, intermol. vibr. energy transfer dynamics obs. 0-87207  
 $Si:Al(Ga)$ ,  $O_2$  diffusion, conc. profile meas. 0-79990



## oxygen continued

- Si: Au, O, film, amorphous, elec. cond. meas. 0-80423  
 Si: O, A centre, theoretical study 0-75521  
 Si: O, carrier lifetime depth distrib. due to Ar ion implantation 0-70232  
 Si: O, carrier recomb. processes, role of vacancy-O complexes 0-65592  
 Si: O, Czochralski crystal, oxygen striation and thermally induced microdefects 0-100275  
 Si: O, Czochralski grown crystal, O precip., nucleation behaviour and dislocation loop form. (*Japanese*) 0-59664  
 Si: O, heat treated, excess carrier recomb. rate, defect levels 0-75579  
 Si: O, IR absorpt. at low temp. (*Chinese*) 0-108228  
 Si: O, implant redistribution, annealing effects, SIMS meas. 0-96561  
 Si: O, incorporation of O during pulsed-laser irradi. 0-96557  
 Si: O, ion implanted, nature of defect reverse annealing 0-88875  
 Si: O, kinetics of donor formation, under heat treatment in 450-900°C range 0-75523  
 Si: O wafers, impurity meas. by Fourier transform IR spectra 0-89030  
 Si: O wafers, impurity meas. by Fourier transform IR spectra at low temp. 0-89031  
 Si: P(O) p<sup>+</sup>-n<sup>+</sup> solar cells, comparison rel. to resistance to 1.5 MeV electron irradi., majority carrier trapping 0-94087  
 ZnTe: Li, O, Hagemark theory, O modification isoelectronic trap 0-75517

## oxygen compounds

- ESCA shifts and effective charges 0-78648  
 interstellar cloud gas phase chemistry 0-105319  
 OH, interstellar, VLBI synthesis obs. and struct. of maser source W3(OH) 0-105368  
 oxide crystals, rutile-type, interionic pots., cohesive energy, bulk modulus, calc. 0-79741  
 oxides, ABO<sub>4</sub> type, high press. phase transforms. and struct. types, cryst. chem. aspects 0-79940  
 oxides, dislocation climb model 0-100230  
 $\beta$ -Al<sub>2</sub>O<sub>3</sub>-OH<sup>+</sup>, proton dynamics neutron scatt. study 0-59408  
 Ar: OCS, liq., dissoc. studies 0-78716  
 Ar: OCS, O(S) and S(S) photodissociative prod., photoluminesc. excitation spectra, exciton energy transfer 0-89508  
 COS, asymmetry parameter, angle resolved photoelectron spectra, multiple scatt. method 0-63708  
 COS, high resolution UV photoelectron spectra 0-91603  
 COS + Cl<sup>+</sup>, reactions at room temp. 0-93749  
 He + OCS, emission spectra in He afterglow 0-87139  
 KCl: OH, absorpt. in high-transparency region 0-89037  
 KTaO<sub>3</sub>: OH<sup>-</sup>(OD<sup>-</sup>)(OT<sup>-</sup>), IR spectra, spectrosc. consts. 0-100671  
 Kr: OCS, O(S) and S(S) photodissociative prod., photoluminesc. excitation spectra, exciton energy transfer 0-89508  
 O<sub>2</sub> Δ<sub>g</sub>, produced in HF low-press. plasma, use in organic compd. synthesis 0-61099  
 OBF, band strengths, shock tube IR spectrosc. meas. 0-106358  
 OCS, electron impact excitation and ionisation 0-63837  
 OCS, IR spectra, diode laser calibration 0-83363  
 OCS, interstellar, in Ξ state, collisional excitation by H<sub>2</sub> 0-109508  
 OCS laser, for 16 μm range, review (*Rumanian*) 0-87408  
 OCS, microwave spectra, Ku-band Fourier transform spectrometer appl. 0-68265  
 millimeter wave rot. spectra, isotope shifts, freqs. and mol. consts. 0-78611  
 OCS, optically pumped CW subMM emission lines 0-95876  
 OCS, T, relax. meas. using budge-type superhet. microwave spectrometer 0-91551  
 OCS, vibr. energy transfer map 0-99560  
<sup>16</sup>O<sup>13</sup>C<sup>34</sup>S and <sup>16</sup>O<sup>13</sup>C<sup>34</sup>S, IR spectra, ν<sub>3</sub> band anal. 0-95620  
 OCS + benzene, microwave line width and quadrupole moments, perturbation theory 0-69190  
 OCS + He, translational-vibrational energy transfer, quantum dynamical study 0-63746  
 OCS + He<sup>+</sup>, dissoc. charge-transfer, CS<sup>+</sup>(B<sup>2</sup>Σ<sup>+</sup>-A<sup>2</sup>Π<sub>g</sub>) emission prod., Morse pot. Franck-Condon factors calc., vibr. anal. 0-99539  
 OCS + OH, lower atmosphere chem. 0-61870  
 OCS + S, electronically excited atom, neon. fluoresc. 0-99476  
 OCS, quantum yields for Se, I<sub>2</sub>, D<sub>2</sub>, and <sup>3</sup>P<sub>0,1,2</sub> atoms determ. in photolysis, lifetime and quenching rate meas. 0-97741  
 OH, (0,0) UV transitions, band oscill. strength 0-69162  
 OH A<sup>2</sup>Σ<sup>+</sup> state, laser excited, vibr. energy transfer, flame thermometry appls. 0-58349  
 OH astronomical maser sources OH 231.8+4.2, CY Canis Majoris, M1-92, UHF obs. 0-90550  
 OH emission, photometric obs. to find mesosphere neutral temp. 0-82121  
 OH, fundamental vibr. band, mag. rot. spectrosc. obs. 0-86446  
 OH in flames, laser excitation dynamics 0-74201  
 OH in mol. cloud in NGC 2264 0-94847  
 OH, interstellar, rot. excitation by H<sub>2</sub>, rel. to maser emission 0-62232  
 OH, interstellar, search for 18 cm absorpt. lines in high latit. H I clouds 0-67841  
 OH, interstellar, type IIc radio emission sources in (W33) (*Russian*) 0-62247  
 OH, isotope effects, Zeeman effect, far IR laser mag-reson. spectra obs. 0-63674  
 OH, laser induced fluoresc. spectrosc. for flame temperature meas. 0-90839  
 OH main line maser in interstellar cloud, pumping mechanism 0-67824  
 OH maser in pulsating Mira type variables atm., IR line overlap pumping mechanism 0-72764  
 OH maser pumping efficiency of Mira variable stars 0-82379  
 OH Meinel bands in nightglow, rocket meas. (*Japanese*) 0-94631  
 OH, optimum mol. consts. and term values, X<sup>2</sup>Π and A<sup>2</sup>Σ<sup>+</sup> states, vibr.-rot. and microwave freqs. 0-95577  
 OH, Pt catalytic oxidation of H<sub>2</sub> and D<sub>2</sub>, matrix isolation and laser fluoresc. obs. of prods. 0-66865  
 OH<sup>+</sup> fragment obs. from H<sub>2</sub>O threshold PES 0-78647  
 OH<sup>+</sup>, rot.-vibr. bands, line positions, oscill. strengths transition probabilities 0-67828  
 OH + Br<sub>2</sub>, hydroxyl radicals reactive scatt. 0-85172  
 OH + gaseous S compounds, lower atmos. chem. 0-61870  
 OH + H<sub>2</sub>O, OH linewidth rot. depend. on UV transitions 0-91606  
 OH + H<sub>2</sub>SO<sub>4</sub>, collisional reaction probabilities atmospheric chem. 0-90168  
 OH + H<sub>2</sub> → H<sub>2</sub>O + H, reaction product vibr. distrib., quasiclassical trajectory, calcs. 0-85162  
 OH + H<sub>2</sub> → H<sub>2</sub>O + hv, radiative association reaction for mol. synthesis in interstellar clouds 0-90509

## oxygen compounds continued

- OH + OCS(CS<sub>2</sub>), lower atmosphere chem. 0-61870  
 OH + organic compounds photooxidation reactions in atmosphere, rates, reactivity and mechanism 0-72104  
 OH + RH → H<sub>2</sub>O + R, radical substitution reaction 0-81321  
 OH + toluene (1,3,5-trimethylbenzene), rotational and vibrational energy effect 0-76497  
 OH + trans-2-butene, reaction products, O<sub>2</sub> and NO<sub>2</sub> effects obs. 0-85156  
 OH<sub>3</sub><sup>+</sup>, bond polarisability and force constants 0-69260  
 OH(A<sup>2</sup>Σ<sup>+</sup> → X<sup>2</sup>Π<sub>g</sub>) yields from H<sub>2</sub>O photodissoc. 0-71927  
 O<sub>2</sub><sup>+</sup> H<sub>2</sub>O, produced by collisional dissoc. method, mass spectrometric study, dissoc. energies determ. 0-95707  
 OH(v,N) bimodal rot. distrib. from O(1D<sub>2</sub>) + NH<sub>3</sub> 0-76501  
 ONCl, vibr. freq.; anharmonic ab initio/empirical pot. energy functions 0-99457  
 ONF, J transitions, rot. Zeeman effect 0-63707  
 OPBr<sub>3</sub>, mol. struct., electron diff. and spectroscopic vibr. amplitude 0-58387  
 O<sub>2</sub>(SO<sub>2</sub>), photodestruction 0-63722  
 OSiF<sub>3</sub> prod. from SiO + F<sub>2</sub>, matrix reactions, IR spectra and force consts. calcs. (*German*) 0-97718  
 QCS, static polarisability, ab initio SCF wave functions 0-74106

## ozone

- air composition at Barrow, Alaska, wind direction depend. 0-85704  
 air pollution, Jerusalem and Tel-Aviv at night time 0-89689  
 aircraft ambient and cabin air O<sub>3</sub> conc. simultaneous determ. 0-90198  
 atmosphere, chemistry and O<sub>3</sub> vars., depletion 0-104534  
 atmosphere, effects of energetic particle precip. on O<sub>3</sub> catalytic removal 0-109213  
 atmosphere, maintenance of zonal mean O<sub>3</sub> distrib. in N.Hemisphere 0-109220  
 atmosphere, mechanisms for transport in lower atm., general circulation model 0-109196  
 atmosphere, O<sub>3</sub> content evolution 0-98400  
 atmosphere, O<sub>3</sub> depletion as result of nearby supernova 0-94584  
 in atmosphere, photodissoc. in stratosphere and mesosphere through solar UV radiation absorpt. 0-109248  
 atmosphere, prod. through <sup>18</sup>O photodissoc. 0-94559  
 atmosphere, review of O<sub>3</sub> concs. over Australia 0-109223  
 atmosphere composition at 95 km altitude from Na enhancement region obs. 0-101466  
 atmosphere O<sub>3</sub>, conc. determ. by Chappuis-band absorpt. 0-77063  
 atmosphere O<sub>3</sub>, obs. of flux by transient eddies in 0 to 30 km height range 0-109224  
 atmosphere O<sub>3</sub> conc. at ground-level, Oslo, Norway, summer 1977 obs. 0-81965  
 atmosphere O<sub>3</sub> layer and evolution of life 0-104883  
 atmosphere O<sub>3</sub> photodissoc., annual var. of effects of diffuse solar radiation 0-109210  
 atmosphere O<sub>3</sub> total content, determ. using satellite meas. 0-77027  
 atmosphere total content, Dobson spectrophotometer meas. errors 0-72644  
 atmosphere total content using Dobson spectrophotometer, pollution and absorb. mol. errors 0-72643  
 atmosphere total O<sub>3</sub> determination, large particle light scatt. coeffs. approximation 0-82091  
 gas, UV absorpt. spectrum, Hartley continuum, IR laser induced changes 0-95639  
 generation in pure O<sub>2</sub> or dry air by field-accel. electrons (*French*) 0-59161  
 jet stream and associated O<sub>3</sub> enhancement (*Russian*) 0-94568  
 line and band strengths in IR spectra, variational calcs. 0-87112  
 line parameter data, 10 μm and 4.8 μm regions 0-61895  
 line position and intensities of 2ν<sub>3</sub>, ν<sub>1</sub> + ν<sub>2</sub> bands 0-87181  
 lower stratosphere content, Nimbus 4 remote sensing method 0-77154  
 mesosphere, O<sub>3</sub> concs. meas. from 1.27 μm O<sub>2</sub> airglow at middle latit. 0-72606  
 molecule, ab initio UHF and UHF-natural orbital CI studies 0-102452  
 molecule, photodissoc. cross section, vibr. excitation effects obs. 0-95696  
 molecule, UV absorpt. spectra, IR laser induced changes 0-83385  
 molecule + O<sub>3</sub>, reaction rate const., rel. to atmospheric processes 0-85155  
 nighttime concentration (15-68 km), Nimbus 6 obs. comparison with OAO-3 obs. 0-105016  
 photochemical tropospheric O<sub>3</sub> transport, effect on pollution at rural site 0-61481  
 photodissoc., O(S) yield at 1700-2000 Å 0-97714  
 photolysis, O(<sup>3</sup>P) quantum yield at 266 nm 0-78568  
 photolysis by sunlight, rate constants at ground level 0-61836  
 production by dissoc. of O<sub>2</sub> or air 0-61118  
 quenching of orthopositronium by O<sub>3</sub>, meas. by two-photon coincidence rate difference technique 0-74262  
 stratosphere, calc. of O<sub>3</sub> layer depletion by chlorofluorocarbons using two-dimensional model 0-109221  
 stratosphere, CO<sub>2</sub>-O<sub>3</sub> coupling in Cl free atm., photochemical-radiative column model 0-85723  
 stratosphere, instantaneous global O<sub>3</sub> balance including observed NO<sub>2</sub> 0-109211  
 stratosphere, net vertical flux, implication for troposphere O<sub>3</sub> budget 0-101402  
 stratosphere, O<sub>3</sub> behaviour and thermal structure during S. Hemisphere spring 0-105014  
 stratosphere, temp. and O<sub>3</sub> vars. (1958 to 1977) 0-109222  
 stratosphere, vertical distrib., during polar front passage over Uccle 0-94582  
 stratosphere composition, effect of chlorofluoromethan photolysis 0-109197  
 stratosphere concentration var. during total solar eclipse 0-105017  
 stratosphere content at mid-latitude, simultaneous N and S hemisphere obs. 0-77052  
 stratosphere O<sub>3</sub>-CO<sub>2</sub> coupling, photochemical radiative column model with Cl chemistry 0-85724  
 troposphere, O<sub>3</sub> mixing ratio meas. rel. to stratospheric-tropospheric exchange at polar latits. in summer 0-72599  
 troposphere, stratospheric source for O<sub>3</sub> overabundances over Pacific Ocean during Gamet, August 1977 0-72600  
 troposphere, surface conc. rel. to general weather situation 0-101397  
 troposphere O<sub>3</sub>, evidence for significant in situ photochemical source 0-72619  
 UV emitting lamps, method for estimation of O<sub>3</sub> concs. in vicinity 0-81765



## ozone continued

- F+O<sub>3</sub> reaction, FO(X<sup>2</sup>P<sub>1</sub>) radical VUV photoelectron spectra 0-104455  
 H+O<sub>3</sub>→HO<sub>2</sub>+O(<sup>1</sup>P), yields 0-71900  
 O<sub>3</sub> photolysis at 248 nm, O(<sup>1</sup>P<sub>1</sub>) direct obs. 0-101028  
 O<sub>3</sub>+H, reaction mechanism studied using photoionisation mass spectrometer, form. of O<sub>2</sub>(a<sup>1</sup>Δg) 0-85168  
 O<sub>3</sub>+HO<sub>2</sub>, reaction kinetics, laser mag. reson. obs. 0-102528  
 O<sub>3</sub>+He(B<sub>2</sub>)(H<sub>2</sub>), vibr. relax. rate consts. 0-74231  
 O<sub>3</sub>+NO, fs-states and rot. states, effect on reactivity 0-89473  
 O<sub>3</sub>+thiirane, autocatalytic reaction, stopped-flow study, reaction rate meas. 0-85152  
 O<sub>3</sub>+thiirane+olefin+SO<sub>2</sub>, excited neutral metastable SO<sub>2</sub> form. mass spectrometric study 0-83300  
 O<sub>3</sub>+Zn(Cd), matrix reactions, IR, Raman and visible spectra in Ar and N<sub>2</sub> matrices 0-87110  
 O<sub>3</sub>H<sup>+</sup>, isomeric structs. ab initio MO calcs. 0-83270

## ozonosphere

- chemistry and O<sub>3</sub> vars. depletion 0-104534  
 chlorofluoromethane photolysis in stratosphere, effect on O<sub>3</sub> conc. 0-109197  
 formaldehyde, chem. of stratosphere, UV absorpt. spectra implications 0-109209  
 halocarbon depletion of O<sub>3</sub> layer, climate effects 0-98436  
 remote sensing of lower stratosphere from Nimbus 4, O<sub>3</sub> content 0-77154  
 remote sensing of O<sub>3</sub> and temp. by satellite IR limb scanning method 0-105086  
 seasonal composition variation at high-latitude 0-77051  
 solar eclipse effect on NO<sub>2</sub> and O<sub>3</sub> conc. and atm. temp. 0-105017  
 stratosphere and troposphere, vertical distrib. during polar front passage 0-94582  
 total content, Dobson spectrophotometer meas. errors 0-72644  
 total content measurement, using Dobson spectrophotometer 0-72643  
 Br chemistry of stratosphere and O<sub>3</sub> depletion 0-98391  
 CO<sub>2</sub>-O<sub>3</sub> coupling, photochem. radiative column model with Cl chem. 0-85724  
 CO<sub>2</sub>-O<sub>3</sub> coupling in Cl free atm., photochemical-radiative column model 0-85723  
 HO<sub>2</sub>+ClO, reaction product distrib. 0-72586  
 O<sub>3</sub>, nighttime concentration (15-68 km), Nimbus 6 obs. comparison with OA0-3 obs. 0-105016  
 O<sub>3</sub>, partial press. profile over Uccle, Belgium, April-June 1979 obs. (French, Flemish) 0-98385  
 O<sub>3</sub>, partial pressure profile over Uccle, Belgium, 1979 obs. (French, Flemish) 0-94571  
 O<sub>3</sub>, stratosphere content at mid-latitude, simultaneous N and S hemisphere obs. 0-77052  
<sup>18</sup>O/<sup>16</sup>O, photodissociation as source of atmospheric O<sub>3</sub> 0-94559

## P invariance

- atoms, Hiller-Sucher-Feinberg identity, generalisation, accuracy for approx. wavefunctions 0-63512  
 atoms, many-electron, relativistic theory of P violation 0-91042  
 charmed baryon decays, nonleptonic, parity-violating, single-quark and two-quark transitions 0-68453  
 charmed baryon decays, weak hadronic, SU(3) dynamical scheme 0-68454  
 cosmological  $\nu$  sea, EM wave propagation, torsion background 0-77283  
 electron anapole moment, static parity violating coupling to EM field, unified gauge theory 0-68390  
 flavour changing weak radiative decays, short and long distance effects 0-73712  
 forbidden M<sub>1</sub> transitions, parity violation, stray static elec. fields 0-87078  
 massive particles with any spin, consistent eqns., Klein-Gordon divisor, review 0-73577  
 optical isomer crystal, energy difference due to parity nonconservation (Russian) 0-106405  
 parity non-conservation effect in atoms and molecules 0-68395  
 parity nonconservation in heavy atoms and weak magnetism in neutral currents (Russian) 0-82932  
 parity violation effects in neutron scattering and capture 0-105808  
 quantum field theory, relativistic, discrete symmetries 0-68387  
 Reggeization of elementary fermions in arbitrary renormalizable gauge theories 0-68367  
 SU(2)<sub>c</sub>⊗SU(2)<sub>L</sub>⊗U(1) weak model,  $\nu$  mass and spontaneous P nonconservation 0-62884  
 two-level system, hyperfine struct. transitions, weak interaction meas. (Russian) 0-58196  
 unified theory of EM and weak interactions 0-82928  
 D meson parity violating nonleptonic decays, vector meson dominance model 0-78058  
 e<sup>+</sup>d→e<sup>+</sup>np, polarised, parity violating asymmetry 0-78080  
 e<sup>+</sup>e<sup>-</sup> inclusive hadron prod., polarisation and p nonconservation asymmetries,  $\pi$ , K<sup>±</sup>, D<sup>±</sup> prod. 0-78084  
 eN elastic scatt., pol. e, nucleon form factors, P violating symmetry, Weinberg-Salam calcs. 0-68461  
 eN elastic scatt. in nuclei, P violating asymmetry due to weak neutral currents 0-73713  
 e<sup>+</sup>N→e<sup>+</sup>Δ(3/2, 3/2), P-odd asymmetry, P nonconserving neutral current interaction 0-57611  
 F parity violating nonleptonic decays, vector meson dominance model 0-78058  
 $\gamma p$ → lepton pair, P violating asymmetry 0-105901  
 $\mu$  decay correlations and lifetime meas. 0-77996  
 NN $\bar{N}$  couplings, parity-violating, QCD and MIT bag model, 1/2<sup>-</sup> resonance contribs., SU(6)<sub>c</sub>, symmetry 0-57540  
 pp, 45 MeV, longitudinally pol. p, parity nonconservation in anal. powers 0-57266  
 pp scatt., <300 MeV P-odd asymmetry for pol. p (Russian) 0-102063  
 pp scattering, parity violation at 50 MeV (German) 0-68471  
 pp scattering, parity violation meas. at 45 MeV 0-78092  
 Z<sup>+</sup>→p $\gamma$ , 1/2<sup>-</sup> resonance poles to parity-violating amplitude, two-quark weak transitions 0-78062  
 Bi, atomic, parity nonconservation effect (Russian) 0-77985  
 Bi, parity non-conservation effect 0-68395  
 H<sup>+</sup> photofragments angular distribution, parity favoured electric dipole transitions 0-58330  
<sup>1</sup>H, A=1, 2, nuclear electric dipole moments from P nonconserving atomic transitions 0-57681  
 He parity-violating elec. dipole transitions 0-69094

## P invariance continued

- He photofragments angular distribution, parity favoured electric dipole transitions 0-58330  
 Pu<sup>239</sup>, product separation asymmetry in fission by slow polarised neutrons (Russian) 0-106088  
 Tl, parity non-conservation effect 0-68395  
 U<sup>235</sup>, product separation asymmetry in fission by slow polarised neutrons (Russian) 0-106088

## p-n heterojunctions

- Al<sub>1-x</sub>Ga<sub>x</sub>As-GaAs heterophotoconvertors, HV, investigations 0-101097  
 differential admittance theory in the presence of surface electron states 0-96981  
 forward-biased, charge accumulation 0-107902  
 multilayered structures, impact ionisation 0-88621  
 p<sup>+</sup>-n(n<sup>+</sup>-p) heterojunction, optical absorpt. coeff. and minority-carrier diffusion length, differential photocurrent method of meas. 0-96896  
 p-n heterojunction solar cell, general formulation of current-voltage characteristics 0-80361  
 solar cell model, design and evaluation 0-93964  
 solar cells, polycrystalline and tandem, for high efficiencies, using compound semiconductors 0-72052  
 thin film heterostructure, energy spectrum study 0-70787  
 thin film heterostructures, optical transition selection rules 0-66319  
 Al-amorphous Ge-nSi, photoelectric props. 0-70822  
 AlGaAs heterojunctions, nonradiative recomb. vel. estimate from edge luminesc. props. 0-65668  
 AlGaAs heterojunction photocell with luminesc. wavelength converter 0-108800  
 Al<sub>0.35</sub>Ga<sub>0.65</sub>As-GaAs N-p heterojunction diodes, current suppression by cond. band discontinuity 0-80362  
 Al<sub>1-x</sub>Ga<sub>x</sub>As epitaxial layers on GaAs, struct. study by scanning Auger electron microscopy 0-80110  
 Al<sub>1-x</sub>Ga<sub>x</sub>As, p-n junction solar cells, effect of interface recombination on photoluminescence and current 0-93893  
 Al<sub>1-x</sub>Ga<sub>x</sub>As-GaAs heterostructure, quantum-well, hot electrons and phonons 0-84505  
 Al<sub>1-x</sub>Ga<sub>x</sub>As-GaAs heterostruct., varizional, parameter determ. by photoluminescence method (Russian) 0-108291  
 Al<sub>1-x</sub>Ga<sub>x</sub>As-GaAs quantum-well heterostruct., exciton in recomb. 0-103990  
 AlGaAsSb LPE growth, lattice-matched to GaSb, characterisation 0-60794  
 Al<sub>1-x</sub>Ga<sub>x</sub>As-Zn-GaAs solar cells by LPE, open circuit voltage, fill factor 0-101108  
 As-Te-Ge/n-Si, film on cryst., heterojunction, elec. and photovolt. props. 0-100514  
 Au-Al<sub>0.5</sub>Ga<sub>0.5</sub>As-GaAs heterojunction Schottky-barrier solar cells, barrier height enhancement 0-85284  
 Au-AlGaAs-GaAs heterojunction Schottky barrier solar cells, barrier height enhancement 0-94071  
 CdS, for thin film and ceramic solar energy convertors 0-93870  
 CdS/Cu<sub>2</sub>S heterojunction solar cells diffusion length determ. using minority carrier SEM 0-61359  
 CdS/Cu<sub>2</sub>S thin film heterojunctions, photocapacitance meas. of solar cell parameters 0-93897  
 n-CdS/n-InP/p-InP heteroface solar cell with ultrathin window layer, computer anal. 0-97788  
 n-CdS/p-ZnInSe<sub>2</sub> thin film solar cell, photovoltaic props. 0-89628  
 CdS-CdTe p-n junction screen printed thin film solar cells 0-72055  
 CdS-Cu<sub>2</sub>S heterojunction, energy-band struct., capacitance-voltage characteristics, illumination effects 0-96982  
 CdS-Cu<sub>2</sub>S junctions, carrier trap density, deep level defects 0-107801  
 CdS-Cu<sub>2</sub>S solar cells, microstructural study of heterojunction materials 0-93978  
 CdS-Cu<sub>2</sub>S solar cell, prep. and characts. (Croatian) 0-93876  
 CdS-InP(CdTe)(GaAs)(Ge), solar cell heterojunctions, CVD fabrication, photovoltaic response 0-93878  
 CdSe, for thin film and ceramic solar energy convertors 0-93870  
 CdSe-Sb<sub>2</sub>Se<sub>3</sub> heterojunction, photoelec. props. 0-70816  
 CdSnAs<sub>2</sub>-InP, n-p heterojunction, elec. props., electroluminesc., band struct. 0-75632  
 CdTe/Hg<sub>1-x</sub>Cd<sub>x</sub>Te multilayers, LPE growth 0-80104  
 CdTe-CdS heterojunctions, growth by closed-tube chem. transport, elec. props. 0-60070  
 CdTe-CdS heterojunction, photocapacitance and photocond. 0-96978  
 CdTe-CdS thin film p-n solar cells, spectral response temp. depend. 0-93871  
 CuGa<sub>0.5</sub>In<sub>0.5</sub>Se<sub>2</sub>/Zn<sub>0.25</sub>Cd<sub>0.75</sub>S heterojunction solar cell, preparation and props. 0-101110  
 Cu<sub>2</sub>S-CdS, role of deep levels in controlling photovoltaic props. 0-92941  
 Cu<sub>2</sub>S-CdS heterojunction solar cells, carrier transport, nonmonotonic band profiles 0-61361  
 Cu<sub>2</sub>S-CdS heterojunction interface, depth distribution profiles, Auger spectra 0-88622  
 Cu<sub>2</sub>S-CdS heterophotocells based on CdS films of stoichiometric composition, elec. and photoelec. props. 0-93873  
 Cu<sub>2</sub>S-CdS solar cell fabrication by magnetron reactive sputtering deposition 0-61363  
 Cu<sub>2</sub>S-CdS solar cells, interface recombination phenomena and tunnel effect 0-66978  
 Cu<sub>2</sub>S-CdS thin film planar junction devices, quantitative photon loss anal. 0-61362  
 Cu<sub>2</sub>S-ZnCd<sub>1-x</sub>S heterojunction, improved model of electro-optic behaviour 0-94023  
 Cu<sub>2</sub>S-CdS, copper sulphide growth features during formation (Russian) 0-107898  
 Cu<sub>2</sub>S-CdS p-n heterojunction, optical energy converter, struct. and recomb. props. 0-72065  
 Cu<sub>2</sub>S-CdS solar cells, SCL current 0-76634  
 (Ga, Al, As) heterostructures and compounds, electronic props., empirical pseudopot. calc. 0-80366  
 (GaAl)As, LPE, GaAs dissolution kinetic in undersaturated isothermal solns. in Ga-Al-As system 0-80106  
 GaAlAs light intensity modulators using p-n junctions 0-99871  
 GaAlAs/GaAs solar cells, efficiency optimisation at high and low current levels (French) 0-61348  
 GaAlAs-GaAs heterojunction solar cells, high temp. props. 25 to 300°C 0-94035  
 Ga<sub>1-x</sub>Al<sub>x</sub>As based layer structures, optimum growth conditions, comp. and struct. perfection 0-104069



p-n heterojunctions continued

Ga<sub>1-x</sub>Al<sub>x</sub>As heterostructure, LPE prep., growth and dissolution kinetics, thermodynamic and kinetic models 0-75456  
Ga<sub>1-x</sub>Al<sub>x</sub>As-GaAs p-n and p-p-n heterojunction solar cells, high efficiency, prep., eval. and characters (*Japanese*) 0-61342  
Ga<sub>1-x</sub>Al<sub>x</sub>As<sub>1-y</sub>P<sub>y</sub> epitaxial layer heterojunction, nonradiative recombination at misfit dislocations 0-96901  
GaAlAsSb-GaSb p-n heterojunction CCD, charge transfer, charge exchange 0-65658  
GaAs-Al<sub>0.4</sub>Ga<sub>0.6</sub>As heterojunction interface, two-dimensional hole gas obs., Shubnikov-de Haas meas. 0-80357  
GaAs-Al<sub>0.4</sub>Ga<sub>0.6</sub>As heterostructures, real-space electron transfer by thermionic emission, analytical model 0-100512  
GaAs-Al<sub>0.4</sub>Ga<sub>0.6</sub>As-GaP photocathodes, minority carrier diffusion length determ. by photoluminesc. 0-103992  
GaAs-AlGaAs solar cells (*Rumanian*) 0-93877  
GaAs-AlGaAs superlattices, inelastic light scatt. by two-dimens. electron gas 0-93360  
GaAs-Ga<sub>1-x</sub>Al<sub>x</sub>As DH lasers, electron beam induced current microscopy 0-95899  
GaAs-Ga<sub>1-x</sub>Al<sub>x</sub>As:Be, LPE, diffusion of Be into GaAs substrate 0-103517  
GaAs-Ga<sub>1-x</sub>Al<sub>x</sub>As DH laser material crystal cathodoluminescence, SEM analysis 0-97349  
GaAs-Ga<sub>1-x</sub>In<sub>x</sub> heterostructure, elastic stresses and substrate/epitaxial film mismatch, X-ray diff. method 0-92794  
GaAs-GaAlAs multilayer struct., Hall mobility enhancement 0-100511  
GaAs-GaAlAs superlattices, metalorganic VPE growth, in sites ellipsometry monitoring 0-70547  
GaAs-GaAlAs wafers, defects and degradation, transmission cathodolum. evaluation 0-65395  
GaAs-GaInAs structure, dislocation struct., TEM anal., appl. as IR LED 0-70206  
GaAs-GaP heterostructure, radiative recomb. under influence of mech. stresses 0-66291  
GaAs-GaSe n-p heterojunction, elec. props., interface states 0-65670  
GaAs-Ge, heterostructure, zincblende-on-diamond type systems, MBE growth, (110) orientation as preferred orientation 0-80099  
GaAs-InP heterojunction laser output wavelength control 0-74384  
GaAs-n-Al<sub>0.4</sub>Ga<sub>0.6</sub>As heterojunctions, selectively doped, FET 0-80364  
GaAs-Si heterojunction, IR quenching of photocapacitance 0-92968  
GaAs<sub>1-x</sub>P<sub>x</sub> heterostructure, LPE prep., growth and dissolution kinetics, thermodynamic and kinetic models 0-75456  
Ga<sub>1-x</sub>In<sub>x</sub>As<sub>1-y</sub>P<sub>y</sub>/GaAs structure, LPE growth and lattice const. matching conditions 0-59822  
GaP-Si, heteroepitaxial growth, electronic and optical props. 0-104075  
GaP-Si, heterostructure, zincblende-on-diamond type systems, MBE growth, (110) orientation as preferred orientation 0-80099  
Ge/GaAs (110) heterojunction, valence band discontinuity in XPS spectra, precise determ. 0-84834  
Ge-GaAs heterojunction, elec. and recomb. props., interface defect effects 0-80365  
HgCdTe-CdTe photodiode, 1.33  $\mu$ m, grown by LPE, phys. props. 0-107892  
InAsSb/GaSb broad-spectral-band IR detector, backside-illum. heterostructure approach 0-73450  
p-In<sub>0.53</sub>Ga<sub>0.47</sub>As:Zn on InP, elec. and optical props. 0-75662  
InGaAsP DH, luminesc., quantum efficiency determ. 0-108273  
InGaAsP LPE heterostructs., interface grading, Auger depth profile 0-103585  
InGaAsP-InP DH lasers, temp. dependence of threshold and elect. characts. 0-99725  
InGaAsP-InP high-gain heterojunction phototransistor 0-103745  
In<sub>0.3</sub>O<sub>2</sub>-SnO<sub>2</sub>-InP solar cell junctions, efficiency, InP surface props. 0-85288  
InP/In<sub>0.4</sub>As<sub>0.6</sub>P<sub>0.4</sub> interfaces, sputter-profiled, depth resolution degradation by cone form. 0-80094  
InP/InGaAs heterojunction phototransistor, high-sensitivity 0-100505  
InP/InGaAsP avalanche photodiodes, with guard ring structure 0-100506  
InP-InGaAsP p-n junction avalanche photodiodes, surface passivation techniques 0-100508  
InSe solar cells, photovoltaic conversion efficiency 0-61356  
In<sub>2-x</sub>Sn<sub>x</sub>O<sub>3-y</sub>-Ga<sub>1-x</sub>In<sub>x</sub>P<sub>1-y</sub>(InP,As<sub>1-y</sub>) heterojunction solar cells, chemistry and prep. 0-94073  
Pb<sub>1-x</sub>Hg<sub>x</sub>S-Si heterojunctions, elect. props. 0-100513  
PbS-Si heterojunction, chem. struct., AES anal. 0-76115  
PbS-Si heterojunction, related optical and IR detector props. 0-77866  
PbS-Si heterojunction, space charge capacitance, PbSn film thickness depend. 0-88630  
PbS-Si p-n heterojunctions, AC admittance meas. 0-96979  
Pb<sub>1-x</sub>Sn<sub>x</sub>Te-PbTe heterostructures, MBE produced on mica and LiNbO<sub>3</sub>, elec. props. study 0-88629  
PbTe-CdTe fabrication and characterisation (*German*) 0-89151  
n-PbTe-p-Pb<sub>1-x</sub>Sn<sub>x</sub>Te, heterojunctions, heavily doped, current-flow mechanisms 0-96974  
PbTe-Pb<sub>1-x</sub>Sn<sub>x</sub>Te n-p<sup>+</sup> heterojunction photodetector, hot wall evaporation technique 0-65673  
n-Si epitaxial layers on oppositely conducting substrates, two layer Hall coeff. meas. technique 0-80297  
a-Si In<sub>0.4</sub>Sn<sub>0.6</sub>As<sub>0.4</sub>P<sub>0.6</sub>/ZZ 0-101113  
Si, n<sup>+</sup>-p<sup>+</sup> structure with two-sided photosensitivity for terrestrial applications, structure and fabrication technology requirements 0-101096  
Si-GaSe n-p heterojunction, elec. characts., interface states 0-70812  
p<sup>+</sup>-Si<sub>1-x</sub>Ge<sub>x</sub>nSi junction diodes, lattice misfit effects on I-V characts. 0-70804  
Si<sub>1-x</sub>Ge<sub>x</sub>-GaAs, heterojunction, elec. and recomb. props., interface defect effects 0-80365  
SnO<sub>2</sub>/n<sup>+</sup>-pSi heterojunction solar cells, fabrication by paint-on-diffusant method 0-94048  
SnO<sub>2</sub>-GaTe(GaSe)(InSe) heterojunctions, photoelec. props. 0-96945  
SnO<sub>2</sub>-InP heterojunctions, elec. and photovoltaic characts. 0-75628  
SnO<sub>2</sub>-polySi solar cells, fabrication, grain size effects on device parameters 0-94045  
Zn<sub>0.4</sub>Cd<sub>0.6</sub>S-Cu<sub>2</sub>S heterojunction solar cells, props., comp. meas. of interfacial region 0-81472  
ZnO-CdTe heterojunctions and ZnO films preparation using spray pyrolysis 0-96985  
ZnO-Cu<sub>2</sub>O heterojunction solar cells, prop. by RF sputtering 0-93945  
ZnSe-Si heterojunctions, IR quenching of photocapacitance 0-92968

p-n homojunctions

education, forbidden energy gap meas. in Si and Ge p-n junctions 0-57027  
highly doped, behaviour of buried O<sub>2</sub> implanted layers 0-59499  
photoelectric converters, p-n mesa structure for investigating optical and energy characts. of solar and radiant energy concentrators 0-97783  
reduction doping using zone recrystn. with temp. gradient, two-layer struct. with p-n junction creation 0-104062  
semiconductors, amorphous, doped, electronic props. 0-80283  
n<sup>+</sup>-Si-Al ohmic contacts, metallisation struct. for very shallow n<sup>+</sup>/p junctions 0-60084  
solar cell, direct gap, theoretical limit efficiency 0-97795  
solar cell, polycryst., grain boundary influence on recomb. 0-93913  
solar cell arrays, Si, fixed-base, flat panels, possible developments for more competitive power production 0-72050  
solar cell fabrication, laser-induced p-n junction formation 0-93880  
solar cells, Si<sub>1-x</sub>Ge<sub>x</sub>, diffused p-n junction, electric and photoelectric props. 0-101095  
solar homojunction photovoltaic cells, conversion efficiency, maximum theoretical efficiency as a function of temp. 0-81469  
AlGaAs p-n diodes, I-V characts., tunnelling 0-100510  
AlSb Schottky barrier solar cells, characteristics and efficiency of Czochralski-grown crystals 0-61366  
BN glass transfer process 0-107459  
Cd<sub>0.4</sub>Hg<sub>0.6</sub>Te, epitaxial layer p-n junction, current-voltage characteristics of photovoltaic detectors, 1 to 15  $\mu$ m 0-86407  
Cd<sub>0.4</sub>Hg<sub>0.6</sub>Te, tunnelling effect in p-n junctions 0-75630  
CdSb:Al, p-n junction formation by laser emission, photoelectric effects (*Russian*) 0-70815  
CdSb:Al(In)(Ga)(Te), p-n junction formation by laser radiation 0-96983  
GaAs, electron irradi. induced defect levels, hydrostatic press. effect 0-92858  
GaAs homojunction solar cells, large-grained, passivation method to improve open-circuit voltage 0-94070  
GaAs, low-field study of p<sup>+</sup>nn<sup>+</sup> or p<sup>+</sup>pn<sup>+</sup> struct. on forward direction 0-60072  
GaAs, n<sup>+</sup>-n<sup>+</sup> and n<sup>+</sup>-p<sup>+</sup>-n<sup>+</sup> struct., ballistic electron motion at room temp. 0-80360  
GaAs n<sup>+</sup>-p<sup>+</sup>-n<sup>+</sup> ballistic structure 0-80359  
GaAs shallow-homojunction solar cells on single crystal GaAs and Ge substrates, CVD fabrication and conversion efficiency 0-61364  
GaAs shallow-homojunction solar cells, electron radiation effects 0-97798  
GaAs solar cells, photoeaction of p-n junction diodes 0-81464  
GaAs:Fe, p<sup>+</sup>-n<sup>+</sup> struct., photoelec. props. 0-107862  
GaAs:Fe p<sup>+</sup>-n<sup>+</sup> junction minority carrier trap meas. by photo-excited DLTS 0-96816  
GaAs:Fe reverse biased p<sup>+</sup>-n<sup>+</sup> struct., switching effect 0-88628  
GaAs:O p<sup>+</sup>-n<sup>+</sup> struct., injection current and negative photocond., saturation mechanism 0-92967  
GaAs:Si defect density before and after Zn diffusion, SEM and TEM obs. 0-96529  
GaAs:Si p-n junction LED, electroluminesc. efficiency 0-71491  
Ga<sub>0.47</sub>In<sub>0.53</sub>As, band-to-band tunnelling current 0-107895  
Ga<sub>1-x</sub>In<sub>x</sub>As epitaxial layer growth by organometallic pyrolysis, homojunction LED prep. 0-76194  
GaSb:Sn, p-n junction, electroluminesc. and photoluminesc. 0-66306  
Ge, low-field study of p<sup>+</sup>nn<sup>+</sup> or p<sup>+</sup>pn<sup>+</sup> struct. on forward direction 0-60072  
Ge p<sup>+</sup>-n<sup>+</sup> structures, charge transport under impurity freezeout conditions 0-92965  
Ge p<sup>+</sup>-n<sup>+</sup> structures, large-scale trap characts. 0-92966  
Ge, photo-EMF generation in saturation region 0-75635  
Ge:Li, Cu p-n junctions, current stimulated LiCu complex formation, photocurrents 0-107897  
n-Ge:Ni p<sup>+</sup>-n<sup>+</sup> struct., double-injection current-voltage characts. 0-60074  
HgCdTe epitaxial material, ion implantation, junction form. 0-100260  
InAs:(Mg), ion implanted, photocond., photo-EMF, and optical absorpt. spectra 0-70763  
In<sub>0.53</sub>Ga<sub>0.47</sub>As p-n photodiode-FET photoreceiver for 1.0 to 1.7  $\mu$ m wavelength optical fibre communications systems 0-58794  
In<sub>0.4</sub>Ga<sub>0.6</sub>As:Si p-n struct., electrolum. spectra, 77 to 300K 0-93408  
InGaAsP avalanche photodiodes, breakdown mechanism, donor conc. effect 0-70710  
In<sub>0.3</sub>SnO<sub>2</sub>-CdTe:P, p-n homojunction solar cell, elec., photovoltaic props., photoluminescence 0-81463  
InP n<sup>+</sup>-p<sup>+</sup> homojunction solar cells, high efficiency, LPE layer growth, photolithographic fabrication 0-93929  
InP p<sup>+</sup>-n abrupt junctions, ionisation coeffs., photomultiplication meas. 0-65655  
InP p-n junction, grain boundary etching 0-96541  
InP photodiodes, dark current and breakdown characts. 0-70806  
InP:Cd, p<sup>+</sup>-p<sup>+</sup>-n<sup>+</sup> junction form. by diffusion doping 0-84504  
InP:Cd(In), avalanche photodiode characts., impurity diffusion effects 0-70709  
InSb n<sup>+</sup>-p junctions, photocurrent spectrum near long wavelength edge of fundamental absorption band 0-100483  
n<sup>+</sup>-n-pGe avalanche photodiode, noise factors, internal quantum efficiency 0-70803  
Pb<sub>0.99</sub>Hg<sub>0.01</sub>Te photovoltaic detector produced by Sb<sup>+</sup> ion implantation 0-82821  
Pb<sub>1-x</sub>Mn<sub>x</sub>Te, photovoltaic effect, p-n junction, energy gap determ. 0-92931  
PbS<sub>1-x</sub>Se<sub>x</sub> (X=0.18) homojunction injection lasers, near-field emission 0-95896  
Si, advanced material for space solar cell 0-94007  
Si, amorphous, elec. props., ion implantation effects 0-79828  
Si, amorphous, solar cells, barrier props. determ. by differential I-V characts. meas. 0-94053  
Si amorphous p-n junctions, high current, characts. 0-70807  
Si, as-grown Czochralski crystal, multiple p-n junction structure obtained by heat treatment, appl. to solar cells 0-101099  
Si diode, impurity profiles, scanning electron microprobe anal. 0-79832  
Si, electrolytic anodic oxidation method of decoration 0-60069  
Si, electron beam scan annealed, deep levels 0-65481  
Si ion-controlled diodes, acid-base exposure effects, Si-SiO<sub>2</sub> interface state density 0-96984  
Si junction diode, diffused, with deep level traps, negative capacitance 0-96976  
Si, n<sup>+</sup>-p diode,  $\gamma$ -radiation defects, annealing and recomb. props. 0-65045



**p-n homojunctions** continued

- Si  $n^+p$  junction solar cells, electron irradi., DLTS spectra and defect effects 0-93999
- Si  $n^+p$  solar cell, forward and reverse bias tunnelling 0-85274
- Si p-i-n structure, ESR of conduction electrons 0-93179
- Si, p-n junction, current-voltage characts., misfit dislocations, high press. effects 0-65671
- Si p-n junction, reverse bias high voltage, secondary surface breakdown 0-70813
- Si p-n junction depletion layer, electron beam damage inhibition 0-70817
- Si p-n junction diodes and solar cells, minority carrier diffusion length 0-107894
- Si p-n junctions, avalanche breakdown anisotropy 0-70811
- Si p-n junctions, electron emission from depletion layers 0-100509
- Si p-n junctions, spin depend. surface recomb., electron irradiation effect 0-88627
- Si, p-n junctions, voltage-current characts., fast neutron irradi. effects (Russian) 0-65659
- Si planar semiconductor junctions, disruptive voltage calc., ionisation coeff. (Rumanian) 0-103746
- Si, polycryst. p-n junction solar cells, grain-boundary and intragrain recombination currents 0-81442
- Si, small signal equivalent circuit, finite carrier multiplication 0-65664
- Si solar cells, junction formation techniques using spray-on polymer dopants, cost effective, high throughput 0-94014
- Si solar cells,  $n^+p$ , Li-counterdoped, radiation damage 0-94000
- Si solar cells, photoreaction of p-n junction diodes 0-81464
- Si solar cells, polycrystalline p-n junctions, recombination currents, physical models 0-93892
- Si solar cells, radiation damage annealing mechanisms and low temp. annealing 0-94003
- Si solar cells, realisation by laser induced diffusion of deposited Sb 0-93998
- Si solar cells, single-crystal, HV, multijunction, parameters and characteristics 0-89615
- Si solar cells, solid source diffusion process for fabrication 0-93994
- Si, subnanosec. current drops in delayed breakdown 0-75633
- Si, subnanosec. current drops in delayed breakdown 0-75634
- Si:As, shallow junctions by high-dose implants 0-96694
- Si:As ion implanted shallow junction 0-70228
- Si:As  $p^+n$  junction, small area, acceptor level conc., determ. from TSC curves 0-75631
- Si:H, amorphous, HV photovoltaic cells, design parameters 0-101105
- Si:H, amorphous, solar-cells, charge collection and spectral response 0-85275
- a-Si:H film, glow discharge deposited, H profiles, doping level 0-84202
- Si:Sb vacuum deposited coating, p-n junction, pulsed electron beam annealing doping, diffusion 0-75480
- Si:V p-n junctions, thermal emission rates and capture cross sections of majority carriers at V centres 0-96980
- SiC (6H), blue-emitting diodes by CVD 0-97439
- SiC p-n junction, electroluminesc. 0-97343
- SiC p-n junction, epitaxial, grown by sublimation, elec. and struct. props. (Chinese) 0-60067
- SiC p-n junctions, current-voltage characts. 0-60073
- SiC p-n junctions, electrolum. spectra and kinetics 0-66305
- ZnGeP<sub>2</sub> p-n homodiode, polarisation photosensitivity and photopleochroism spectra 0-107866

**p-n junctions**

see also *p-n heterojunctions*; *p-n homojunctions*

- bevelled shallow junctions, spreading resistance data correction 0-80358
- converters, photoelectric, optical methods for checking parameters of semiconductor doped layer 0-93869
- deep impurity levels, spectroscopic determination by compensation method 0-108229
- diffused, space-charge recombination current 0-88623
- diffused, transition capacitance calc. methods, comparison (Rumanian) 0-88625
- diodes, Schottky vs. p-n, for various appls., charge carrier speed (Dutch) 0-65662
- double injection p-i-n structures in magnetic field 0-107899
- electric field maximum formulation for abrupt p-n junction with one side heavily doped 0-75629
- heat pulse technique for bonding thermoelectric modules contacts 0-107904
- magnetic injection of minority carriers 0-107900
- minority carrier lifetime-meas. technique using SEM-electron beam induced current 0-59999
- minority carrier transport parameters determ. using electron microscope 0-65665
- MOS-structure, with adjoining reversed biased p-n junction, charge pumping current and reverse current (German) 0-88636
- $p^+n$ ,  $n^+p$  solar cell structures on polycrystalline material, performance 0-89640
- $p^+n$  junction diffusion capacitance calc., discrepancy problems 0-60068
- photodiode, switching process and plasma effects, theory 0-65667
- photodiode terminology 0-70800
- Schottky gate n-p structure, depletion layer, pot. fluctuations 0-88512
- SEM, EBIC mode, stroboscopic principle and resolution enhancement 0-100515
- semiconductor layers, thin, theory of lifetime meas. with SEM, transient anal. 0-88573
- semiconductors, deep level carrier trapping and emission, transient spectroscopy, book contribution 0-80216
- small signal equivalent circuit, finite carrier multiplication 0-65664
- solar cell, front surface field effect, spectral response, theory 0-76633
- solar cells, polycryst., recomb. at grain boundaries, effect on photoresponse 0-108796
- surface depletion and inversion, arbitrary doping profile, theory 0-107912
- tunnel junction, photoinduced transitions, theory 0-65669
- tunnel junctions, phototransitions accompanied by impurity scatt. 0-107901
- voltage-current characts., fast neutron irradi. effects (Russian) 0-65659
- Pb<sub>0.72</sub>Sn<sub>0.18</sub>Te, layers on mica substrate, Hall constant peculiarities 0-75588

**P-V-T relations** see *equations of state***pacemakers**

see also *patient treatment*

- ohmic electrode-tissue contact resistance and voltage applied to myocardium, meas. method 0-67284

**pacemakers** continued

- testing in vivo, computerised system 0-94412
- Li-I<sub>2</sub> batteries for cardiac pacemakers, capacity rating system 0-97773

**packaging**

see also *encapsulation*; *modules*

- multifuel fluidised bed combustion packaged boiler to supply 10000 lb/h saturated steam at 100 psig 0-108779
- radioactive materials, package design, construction and testing for safe transportation 0-63412
- radioactive materials, safe transportation, using type A, exempt and LSA packages 0-63401
- semiconductor packages, hermetically sealed, calibration and anal. of moisture by gas mass spectrometry 0-90928

**packing** see *packaging***pair algebra** see *algebra***pair annihilation, electron** see *electron-positron interactions***pair breaking, Cooper** see *Cooper pairs***pair production, electron** see *electron pair production***pairing, Cooper** see *Cooper pairs***pairs, electron** see *electron pairs***palaeomagnetism**

- Adelaide Geosyncline, Australia, Late Precambrian palaeomagnetism 0-101325
- S.Africa, kimberlites, palaeomagnetic obs. and tectonic implications 0-109093
- N.African shield palaeomagnetic situation at end of Pan-African Orogeny (French) 0-85579
- S.Alps, Late Mesozoic pelagic limestone, megatectonic obs. from palaeomagnetism obs. 0-109095
- S.Alps, western region, palaeomag. and rock magnetic props. of Permian volcanics 0-89948
- N.American pole wandering, evidence from Montana Early Eocene intrusions 0-104868
- archaeological ceramics, Peru, geomag. variations over last 2000 yrs. 0-94455
- central Arizona, reversal chronology from volcanic sequence rel. to ocean floor polarity record 0-72419
- ash-flow tuffs, microanalytical recognition of TRM components 0-72497
- N.Atlantic, geomag. field Late Tertiary secular var. 0-109094
- averaging out of secular variations, theory 0-61755
- beach ridges in S.Australia, palaeomag. chronology rel. to Milankovitch theory of ice ages 0-98307
- Bingham distrib. function in palaeomagnetic studies 0-72649
- Blue Mountains, Oregon, Jurassic plutons tectonic rot., palaeomagnetic obs. 0-109099
- British Columbia, north-central, northward displacement during late Cretaceous/early Tertiary 0-76955
- Butte mining district, Montana, palaeomagnetism, rock magnetism and aspects of structural deformation 0-101326
- Cambrian red beds, Cartaret, Normandy, palaeomagnetic obs. 0-109088
- Canary Islands, palaeomagnetism and early magmatic history 0-72431
- Chile, Camaraca Formation of Middle Jurassic, palaeomag. and plate rotation 0-85586
- continental shelf sediment core, anomalous declination due to slumping 0-76964
- Coronation Geosyncline and Middle Proterozoic continental arrangement 0-94456
- Cretaceous pelagic carbonate rocks, mag. stratigraphy obs. review 0-104876
- Cretaceous section of Chilean Andes, palaeomag. and K-Ar age 0-85585
- data analysis by least squares line and plane method 0-109259
- dike burial depth estimation by mag. palaeogeobarometric method 0-98220
- Duffer Formation, Pilbara craton, Australia, 3.5 Ga old mag. field 0-104872
- Early Palaeozoic rocks from Australia 0-89959
- Egypt, field strength in Egyptian adobe bricks (3000-0BC) 0-104862
- Elberton pluton, Georgia, USA, palaeomag. of granite 0-72423
- NW.France, Eocambrian-Cambrian palaeomag. of Armorican Massif 0-72414
- Gondwanaland, east-west fit from palaeomagnetic data 0-61792
- Grenville series of Ontario, palaeomag. rel. to Ar isotope dating 0-98232
- Holocene lake sediments, N.Poland, palaeomag. records anal. rel. to short period secular geomag. vars. 0-98221
- SW.Iceland, geomag. excursion in late-glacial basalt outcrop 0-85587
- N.Iceland, lava succession, K-Ar dating, geological and palaeomagnetic obs. 0-109096
- Iceland, palaeointensity meas. on postglacial lavas 0-89952
- SW Iceland, stratigraphy and palaeomagnetism of Esja, Eyrafjall and Akrafjall mountains 0-89950
- inclination data analysis by statistical method 0-109101
- intensity and direction from long grain deposition orientation method 0-77148
- intensity determination of rock sample, reliability test 0-61917
- Israel, Mesozoic palaeomag. results and inferences for microplate struct. in Lebanon 0-61760
- Jurassic field polarity from Colorado and Wyoming rock 0-104875
- Jurassic rock in N.Armenia, palaeomagnetic directions rel. to remanent magnetisation 0-104870
- La Tinta Formation, Argentina, Late Precambrian, palaeomagnetism obs. 0-104860
- Lower Ordovician rocks of NW.Argentina, palaeomag. and K-Ar age 0-89938
- Lower Silesia, Tertiary volcanic rocks 0-98219
- Maikop series in Crimean-Caucasus region, palaeomagnetic obs. 0-89941
- marine ophiolite complexes, evidence for past magnetism 0-109092
- Moenkopi formation, SE.Utah, USA, magnetostratigraphy 0-72422
- Munster Basin, NW.Germany, upper Cretaceous limestones palaeomagnetism 0-89949
- nondipole moments, long term, in last 130 my. 0-104873
- palaeocene pole for N.America from central Montana alkalic intrusions 0-104869
- Palaeozoic anorthosite of Arden Pluton, Appalachian Piedmont, Delaware, USA 0-61752
- Paleocene pole in N.America from Gringo Gulch volcanic rock obs. 0-109091
- NW Peninsular Malaysia, palaeomag. evidence from Ordovician and Silurian rocks 0-89936



**palaeomagnetism continued**

Pliensbachian limestones at Bakonycsérnye (Hungary), resonance and mag. reversal pattern 0-90074  
 pole positions and palaeomag. directions, pole numbers (16/1 to 16/296) 0-72415  
 Proterozoic Belt Supergroup in Montana and Idaho, palaeopoles and polarity zonation 0-72420  
 Pyramid Lake, Nevada clay record rel. to geomagnetic excursions 0-101321  
 Recent tidal-flat sediments, post-depositional remanent magnetization 0-101320  
 red beds, Moenkope Formation, Arizona magnetisation acquisition 0-72421  
 Red Sea Hills, Egypt, Late Precambrian and Early Palaeozoic rock, polar wander obs. 0-109100  
 Searles Valley, California, lacustrine sediment core chronology 0-89955  
 Sicily, Mesozoic continental margin, palaeomagnetism and deformation 0-61761  
 silicic volcanics, Jurassic, from Nevada, thermochemical remanent magnetisation age rel. to palaeomagnetism 0-98310  
 Silurian-Devonian rocks of NW Argentina, palaeomag. and K-Ar age 0-89938  
 Sulawesi (E Indonesia) western arc, palaeomag. studies and fission-track dating rel. to tectonic history 0-89957  
 tectonic rotation and structural tilt in palaeomagnetic studies 0-109097  
 thermoremanent magnetisation intensity, cooling rate effect in single domain magnetite 0-109139  
 Theford Mines ophiolites, Quebec, palaeomagnetism 0-61757  
 Triassic Hound Island Volcanics, Alaska, crustal movement from palaeomagnetic obs. 0-89945  
 Watkins seamount, Pacific Ocean, Cretaceous origin, palaeomagnetic obs. 0-104874  
 weak dipole field epochs, nondipole components effect on auroral zone config. 0-105098  
 Yoldia Clay sequence from Denmark, 14-40000 yr B.P., geomag. variations 0-94454

**palladium**

see also nuclei with .....  
 adsorbed layer on W (110) surface, growth, struct., stability, desorption 0-59794  
 adsorbed on W (110), long range interatomic interactions with coadsorbed Re, W 0-59789  
 adsorption, of CO(NO) on SiO<sub>2</sub>-supported surface, IR spectrosc. obs. 0-92780  
 adsorption of H<sub>2</sub> on ribbon, thermal desorption and work function meas. 0-70538  
 catalyst for oxidant impurities elimination, in viologens electrochromic solutions 0-78922  
 catalytic oxidation of amorphous C by Pd particles, TEM obs. 0-76555  
 chemisorption of Cl<sub>2</sub> on (111) face, LEED, AES, thermal desorption, and work function meas. 0-75444  
 clusters, adsorption/desorption of CO, AES and thermal desorption meas. 0-75436  
 coated Si wafers, interference effects on irradiation with laser beam 0-66333  
 concentration determ. by gamma-ray absorption from <sup>119</sup>Sn<sup>m</sup> 0-108123  
 core level binding energies 0-71544  
 diffusion of H(D), role of tunnelling, reson./nonreson. approaches 0-59718  
 diffusion of H and trapping 0-70447  
 electrical resistivity due to interstitial H (D) 0-96848  
 electrodeposition, on to Al<sub>2</sub>Ga<sub>1-x</sub>Sb solid soln. 0-93505  
 electronic band struct. and photoemission 0-97410  
 film, elec. resist. 0-93013  
 film, quantum size effect, field emission study 0-70849  
 film, work function changes due to adsorbed H<sub>2</sub>, surface and interface dipoles 0-96972  
 fission product, corrosion of SiC coating of HTGR coated particle fuels 0-102237  
 ion plated onto Nb and Ta, prep., H<sub>2</sub> absorption and desorption rate (Japanese) 0-108358  
 lattice dynamics, local frequency spectrum, mean thermal displacement of H 0-59604  
 membrane, H atom interaction, superpermeability 0-81365  
 membrane, sorption of H<sub>2</sub>, adhesion and penetration probabilities, extreme values 0-101040  
 membrane for diffusion-cell for separation H<sub>2</sub> containing mixtures, solar furnace appl. 0-92245  
 metallic, positive muon Knight shift 0-71280  
 particles on UHV-cleaved mica substrate, obs. using scanning Auger microscopy 0-80149  
 phonon density of states determ. from thermodynamic functions 0-96616  
 photoemission spectra, valence band and core level satellite due to excitation of d electron 0-97408  
 polyacetylene-Pd, ion implantation effect on elec. props. 0-65026  
 proton-induced L-shell ionisation cross-sections 0-100707  
 recovery and use of noble metals from radioactive waste 0-99242  
 sd hybridisation, paramagnetic Curie temp. and susceptibility (Russian) 0-103808  
 silicide formation due to laser and electron beam annealing 0-84849  
 solubility of H, lattice defects influence, extended core model 0-88326  
 spin fluctuation model interpretation of mag. susceptibility 0-80477  
 substrate, Ag film growth, interface cpd. form., AES study (French) 0-80131  
 substrate for Ag epitaxial growth, influence on film growth modes (French) 0-84408  
 surface, (110), adsorbed Xe, anomalous 5p photoemission 0-100750  
 surface, (110), adsorption of S, characterised by LEED (French) 0-88422  
 surface, (111), adsorbed CO, Penning ionisation by metastable He beam, theory 0-60735  
 surface, CO chemisorpt., mol. cluster calc. 0-100407  
 surface, CO chemisorption, SIMS, XPS study 0-84382  
 surface, fast D<sub>2</sub> desorpt. mechanism, time-of-flight spectra 0-84379  
 surface, segregated S state, AES, EELS, UPS and XPS study 0-93452  
 surface (111), clean and CO covered, metastable He impact, electron emission, energy and ang. distrib. 0-60744  
 surface phenomena, electron microscopy 0-103556  
 thermomodulation spectra of high-energy interband transitions 0-108226  
 thin film, temp. coeff. of resist. meas. 0-107930  
 thin film on Si substrate, epitaxial silicide growth, LEED and AES study 0-103590

**palladium continued**

UV irradiated electroless selective plating, improvement 0-84848  
 wear coefficients determ. using pin-on-disc apparatus 0-76366  
 X-ray emission L-spectra, influence of temp., liq. N<sub>2</sub> temps. (Russian) 0-80907  
 AgCl:Pd<sup>+</sup>, ESR spectrum, quasistatic Jahn-Teller effect 0-71170  
 Al<sub>2</sub>Ga<sub>1-x</sub>Sb-Pd contacts, struct., preparation elec. props. 0-65684  
 Al<sub>2</sub>Ga<sub>1-x</sub>Sb-Pd contacts, band gap depend. of barrier height 0-65685  
 Au-Pd-Au sandwich, obs. of strongly enhanced mag. susceptibility 0-93076  
 CaS:Pd phosphors, trap and luminescent centre location, photo-, thermo- and electroluminescence studies 0-71482  
 Ge:Pd and pure, photoelectric props., surface states (Russian) 0-60043  
 H phase hardened, recrystallisation study 0-60883  
 MgO-Pd metal-ceramic reaction, micro/macro obs. 0-66467  
 Pd/Al thin film couples, thermal reactions 0-59830  
 Pd/Al<sub>2</sub>O<sub>3</sub>, adsorption of CO, IR study 0-108193  
 Pd-D, crystallite size effects, simultaneous sorption and X-ray study 0-65237  
 Pd-H system,  $\alpha$  and  $\alpha+\beta$  phases, annealed and deformed, anelastic effects 0-66567  
 Pd-H system, energy and electron density of states, improvements to theory 0-70636  
 Pd-H system, phase diagram and thermodynamic properties calcs. 0-66480  
 Pd-H system, solvus hysteresis 0-71659  
 Pd-Si, interface modification by ion implantation 0-70475  
 Pd-SiO<sub>2</sub> interface, work function changes due to adsorbed H<sub>2</sub>, surface and interface dipoles 0-96972  
 Pd<sub>2</sub>, ab initio relativistic core pot. studies of metal-metal bonding 0-106257  
 PdO-Pd miniature pH electrode description and use 0-89886  
 Si/Pd system, solid phase epitaxial growth control by C ion implantation 0-75466  
 n-Si-Pd diodes, chemical reduction process for fabrication 0-60082  
 Si-Pd-Si structure, epitaxial growth, backscattering and transmission electron microscopy studies of layered structures 0-80123  
 Si-Pd-Ti, silicide form. in evaporated films 0-80006  
 Ti-Pd, ion implanted, corrosion behaviour and Rutherford backscatt. anal. 0-71792

**palladium alloys**  
 see also palladium compounds  
 Ag-Pd, dil., virtual bound states, transport props. obs. 0-70667  
 Ag-Pd alloys, inert gas ion bombardment, dynamic surface composition changes, AES obs. 0-60745  
 Al-Pd, rapid quenching, struct. and decomp. 0-76244  
 Au-Pd, bicryst. thin film couples, interphase interfaces, TEM 0-70540  
 Au-Pd, dil., virtual bound states, transport props. obs. 0-70667  
 Au-Pd (1:50 wt.%), quenched, vacancy annihilation and short-range order formation, elec. resist. 0-108487  
 Au-Pt-Pd-Ag-Cu, commercial dental alloy, age-hardening characts. 0-89235  
 Au<sub>50-x</sub>Pd<sub>50-x</sub>Zn<sub>50-x</sub> (0≤x≤15.02)  $\beta'$ -phase, Hall effect and elec. cond. 0-107768  
 BaPdSn<sub>3</sub>, prep. and crystal structure (German) 0-84138  
 CePd<sub>3</sub>, fluctuating-valence compound, anomalous far IR absorption 0-66210  
 CePd<sub>3</sub>, mixed-valence, 3d and 4d core levels, XPS study 0-89111  
 CePd<sub>3</sub>-Er, dil., low field mag. susceptibility, electro-nuclear effects 0-60189  
 CePd<sub>3</sub>-MPd<sub>3</sub> mixed valent systems, nonlinear conc. depend. of resist. 0-65528  
 CoPd, single crystals, domain struct., temp. and field depend. 0-71085  
 Co<sub>2</sub>Pd film, ordered, stacking fault obs. by TEM and interpret. using many-beam theory 0-107680  
 Co<sub>2</sub>Pd<sub>30-x</sub>Si<sub>20-x</sub> amorphous, structural and mag. heterogeneities 0-80484  
 Cu-Pd, dil., screening charge density round  $\Delta Z = -1$  impurities, vacancies, NQR study 0-103897  
 Cu-Pd (4 at.%), anneal hardening mechanism 0-60879  
 Cu<sub>2</sub>MnAl-Pd<sub>2</sub> MnAl mixed Heusler alloys, mag. props. 0-60269  
 CuPd, chemical shift effects and origin of Pd 3d core level satellite 0-104039  
 Cu<sub>3</sub>Pd, periodic antiphase boundaries, electron microscopy study (French) 0-59481  
 Cu<sub>1-x</sub>Pd<sub>x</sub>MnSb, mag. phase transition 0-60268  
 Fe-Pd, magnetic after-effect of H isotopes 0-75817  
 Fe-Pd (1-2 wt.%), solution of <sup>119</sup>Sn, study by Mossbauer spectroscopy 0-75888  
 Fe-Pd (31.2 wt.%), thermoelastic FCC-FCT martensitic transformation 0-104156  
 Fe-Pd Invar, low temp. FCT phase obs. 0-93538  
 Fe-Pd Invar alloy, Young's modulus, magnetostriction, Curie temp. 0-65988  
 Fe-Pd Invar alloys, elec. and mag. props. and thermal expansion 0-75732  
 Fe<sub>2</sub>Pd<sub>50</sub>, order-disorder transition, Mossbauer study 0-71268  
 Fe<sub>2</sub>Pd<sub>50-x</sub>Si<sub>50-x</sub> amorphous, structural and mag. heterogeneities 0-80484  
 Fe<sub>2</sub>Pd<sub>50-x</sub>Si<sub>50-x</sub>, metallic glass, long range interaction and spin wave interactions 0-65949  
 Fe<sub>2</sub>Pd<sub>50-x</sub>Si<sub>50-x</sub> metallic glass, mag. transitions, weak ferromagnetism 0-100583  
 Gd-Pd, amorphous, mag. and elec. props. 0-80499  
 Gd-Pd, amorphous, mag. props. and ferromag. reson. 0-75862  
 Nb-Pd constitution diagram, metallographic and X-ray diffraction 0-89204  
 Ni-Pd, high mag. field effects, mag. isotherms near Curie point, exchange splitting energies 0-60272  
 Ni-Pd, itinerant electron ferromagnet, magnetovolume effects 0-60397  
 Ni-Pd, mag. moment distrib., one-mag.-species model calc. 0-65788  
 Ni-Pd-Mn ternary alloys, mag. characts., use for thermocouple 0-107995  
 Ni-Pd-Pt, metallic glass, electronic structure, pulsed NMR study 0-75869  
 (Ni<sub>0.5</sub>Pd<sub>0.5</sub>)<sub>82</sub>Pt<sub>18</sub> amorphous alloy, liquid-quenched, crystn. kinetics, effect of thermal history 0-100175  
 (Ni<sub>0.5</sub>Pd<sub>0.5</sub>)<sub>82</sub>Pt<sub>18</sub> amorphous alloy, liquid-quenched, crystn. kinetics, nucleation 0-100176  
 Pd alloy-H system,  $\alpha$ - $\beta$  phase transformations, hysteresis of press., elec. resistance, review 0-60859  
 Pd-Ag electrical contacts in H<sub>2</sub>S atmospheres, formation of contaminating layers (German) 0-71811  
 Pd-Ag thin-walled tubes, for thermal diffusion apparatus H diffuser 0-100358

**palladium alloys continued**

- Pd-Ag-H(D), elastic energy dissipation peak 0-60905  
 Pd-Au-Si, influence of struct. on elec. resist. of glass forming alloys 0-65518  
 Pd-Co, dil., breakdown of ferromag. order, magnetoresist. obs. 0-71046  
 Pd-Co, normal Hall effect (*Russian*) 0-103676  
 Pd-Co (0.1-45.7 at.%), thermo EMF at 4.2-300K (*Russian*) 0-92881  
 Pd-Cr, dil., temp. dependent scatt. 0-59973  
 Pd-Cu compound, KKR electronic struct. 0-59864  
 Pd-Cu-Si, glass form., crit. cooling rate 0-75169  
 Pd-Cu(Ag)(Au) alloys-H solid solutions, superconducting transition temp. behaviour (*Russian*) 0-70879  
 Pd-Fe, magnetic anisotropy near Curie point, quasi domain struct. (*Russian*) 0-65867  
 Pd-Fe, normal Hall effect (*Russian*) 0-103676  
 Pd-Fe, very dil., Mossbauer emission spectra, relax. effects 0-66084  
 Pd-Fe (0.54-8.0 at.%), thermo EMF at 4.2-300K (*Russian*) 0-92881  
 Pd-Fe-Mn, ferromagnet-spin glass, thermal expansion forced, magnetostriiction and magnetisation under high press. 0-65255  
 Pd-Fe(Co)(Ni), dilute ferromagnets, press. effect on Curie temp. 0-65873  
 Pd-H, H phase hardened, recrystallisation study 0-60883  
 Pd-H, mech. props., influence of dissolved H<sub>2</sub> (*Russian*) 0-81109  
 Pd-H dilute alloy, impurity elec. struct. 0-103643  
 Pd-H system,  $\alpha$  and  $\alpha+\beta$  phases, annealed and deformed, anelastic effects 0-66567  
 Pd-H system,  $\alpha$ - $\beta$  phase transformations, hysteresis of press., elec. resistance, review 0-60859  
 Pd-H system, energy and electron density of states, improvements to theory 0-70636  
 Pd-H system containing d impurities, chem. binding energies of point defects 0-107214  
 Pd-Mn, ferromagnetism to spin glass behaviour transition 0-71062  
 Pd-Mn (1-10 wt.%), mag. ordering, influence on resistivity 0-75557  
 Pd-Ni, normal Hall effect (*Russian*) 0-103676  
 Pd-Ni, spin fluctuation alloy, thermopower peak diffusion origin 0-88542  
 Pd-Ni, thermal expansion and magnetostriction meas. near crit. conc. for ferromagnetism 0-65881  
 Pd-Ni (15-90 at.%), thermo EMF at 4.2-300K (*Russian*) 0-92881  
 Pd-Ni-H, hydride formation in high press. range 0-65235  
 Pd-Ni-Si amorphous alloys, crystn. process during isothermal ageing 0-89275  
 Pd-noble metal solid solns., with dissolved H, thermodynamic props. 0-108402  
 Pd-Pt, adsorption, of CO(NO), on SiO<sub>2</sub>-supported surface, IR spectrosc. obs. 0-92780  
 Pd-Pt-H(D), elastic energy dissipation peak 0-60905  
 Pd-refractory metal/Si interactions, phase separation 0-65303  
 Pd-Rh-H and Pd-Ni-H, hydride formation in high press. range 0-65235  
 Pd-Si, amorphous, compositional study on short-range struct. 0-84095  
 Pd-Si, amorphous, struct., crystn. and Hall effect meas. 0-75178  
 Pd-Si, amorphous metallic glass, with defined local coordination, struct. model 0-84092  
 Pd-Si amorphous alloy, heat treated, low temp. lattice sp. ht. 0-75368  
 Pd-Si metallic glass, high-resolution electron microscopy 0-84097  
 Pd-Si-(Cu), amorphous, Hall effect meas. and electronic struct. 0-75551  
 Pd-Si-(Cu) amorphous ribbons, low temp. sp. ht., density of states trends 0-79957  
 Pd-W, substrate temp. influence on shallow contact formation on Si 0-96963  
 PdAg (4.7 at.%), effect of alloying on activation energy of H<sub>2</sub> diffusion 0-107571  
 PdAu surface, CO chemisorption, SIMS, XPS study 0-84382  
 PdAu (4.7 at.%), effect of alloying on activation energy of H<sub>2</sub> diffusion 0-107571  
 (Pd<sub>80</sub>Au<sub>20</sub>Si<sub>13</sub>)/Fe<sub>30</sub>, compositionally modulated amorphous film, diffusion, struct. relax. 0-103518  
 Pd<sub>1-x</sub>Cr<sub>x</sub>H<sub>x</sub>, resistive Kondo behaviour as function of Cr and H conc. 0-59971  
 Pd<sub>77.5</sub>Cu<sub>16.5</sub>Si<sub>6.5</sub>, heat of crystn. and viscous behaviour 0-75166  
 Pd<sub>77.5</sub>Cu<sub>16.5</sub>Si<sub>6.5</sub> metallic glass, glass transition temp., cooling rate depend. 0-75181  
 PdD<sub>0.73</sub>, (1, 1/2, 0)-superlattice reflection splitting near 50K, neutron diff. studies 0-70168  
 PdFe (4.7 at.%), effect of alloying on activation energy of H<sub>2</sub> diffusion 0-107571  
 Pd<sub>0.98</sub>Fe<sub>0.01</sub> Gd<sub>0.01</sub>, Pd-Gd exchange const., neutron diffuse scatt. meas. 0-71002  
 (Pd<sub>0.995</sub>Fe<sub>0.005</sub>)<sub>1-x</sub>Mn<sub>x</sub>, mag. behaviour at Fe sites, Mossbauer effect meas. 0-66085  
 PdH<sub>0.003</sub>, Kondo system, local moments, hyperfine fields, Mossbauer study 0-80478  
 $\beta$ -PdIn, electrical resistance, mag. susceptibility and IR freq. dispersion (*Russian*) 0-107759  
 Pd<sub>1-x</sub>Mn<sub>x</sub>H<sub>x</sub> alloy, spin glass, transition temp., susceptibility and EPR meas. 0-65930  
 Pd<sub>2</sub>MnIn<sub>1-x</sub>Sn, and Pd<sub>2</sub>MnIn<sub>1-x</sub>Sb, Heusler alloys, mag. order, disorder effects 0-88723  
 Pd<sub>2-x</sub>MnSb, struct., appl. as improved neutron polariser 0-60199  
 Pd<sub>2</sub>MnV<sub>1-x</sub>Sn, Heusler alloy, structural disorder, Mossbauer study 0-80650  
 PdNb, dilute, NMR obs. of <sup>93</sup>Nb 0-71203  
 PdNi(4.7 at.%), effect of alloying on activation energy of H<sub>2</sub> diffusion 0-107571  
 Pd,Pb, Li<sub>2</sub> ordered alloy, positive temp. depend. on strength, phase destabilization 0-81203  
 PdPb, crystal structure (*German*) 0-96472  
 Pd<sub>13</sub>Pb<sub>9</sub>, cryst. struct., X-ray study 0-103293  
 (Pd<sub>2</sub>Rh<sub>3</sub>)<sub>2</sub>H<sub>2</sub>, elec. resistivity studies 0-59957  
 PdRu (4.7 at.%), effect of alloying on activation energy of H<sub>2</sub> diffusion 0-107571  
 PdSi films, on Si, stress obs. 0-80145  
 PdSi films, on Si, stress obs. 0-80145  
 PdSi films on Si, lattice imaging obs. of structural details 0-103604  
 PdSi, form. in Si-Pd-Ti evaporated films 0-80006  
 Pd-Si-Si, substrate ion implantation, channelled, through metal silicide film 0-70231  
 Pd<sub>80</sub>Si<sub>20</sub>, amorphous alloy, partial struct. functions, X-ray, electron and neutron diff. studies (*Japanese*) 0-88050  
 Pd<sub>80</sub>Si<sub>20</sub> amorphous alloy, skip deform. and crit. shear stress, using tensile testing machine 0-89321

**palladium alloys continued**

- Pd<sub>80</sub>Si<sub>20</sub>, glass, deform. localisation, plastic instabilities and fracture 0-89320  
 Pd<sub>80</sub>Si<sub>20</sub> metallic glass, inelastic deform., free energy spectra 0-71699  
 Pd<sub>80</sub>Si<sub>20</sub> metallic glass, tensile deform., shear band form., high-speed cinematographic obs. 0-89322  
 Pd<sub>80</sub>Si<sub>20</sub> vapour quenched amorphous alloy, atomic arrangements 0-100173  
 Pd<sub>82</sub>Si<sub>18</sub>, stress/strain rate depend. of homogeneous flow 0-71687  
 (Pd<sub>86</sub>Si<sub>15</sub>)<sub>61</sub>/(Fe<sub>8</sub>B<sub>15</sub>)<sub>39</sub>, compositionally modulated amorphous film, diffusion, struct. relax. 0-103518  
 PdSiCu, amorphous, US attenuation and vel. studies at low temps. 0-88278  
 Pd<sub>2</sub>Sn<sub>2</sub> (x=0.95, y=0.05; x=3, y=1), Mossbauer spectra, high press. effects, force consts. 0-84669  
 Pd<sub>2</sub>Ti, Li<sub>2</sub> ordered alloy, positive temp. depend. on strength, phase destabilization 0-81203  
 Pd<sub>1-x</sub>W<sub>x</sub>, calc. of short-range order parameters from X-ray scatt. data (*Russian*) 0-75367  
 PdZr, photoemission study 0-104046  
 Pd<sub>30</sub>Zr<sub>70</sub>, amorphous alloys, supercond. transition temp., press. depend. 0-84524  
 Pd<sub>35</sub>Zr<sub>65</sub>, mag. susceptibility meas. 0-75740  
 n-Si-Pd<sub>2</sub>Si contact, interface struct. and Schottky barrier height, correl. obs. using TEM 0-100504  
 Si-Pd<sub>80</sub>Si<sub>20</sub>, amorphous, Pd<sub>2</sub>Si layer form., shallow contact 0-103586  
 SrPdSn<sub>3</sub>, prep. and crystal structure (*German*) 0-84138  
 Y<sub>3</sub>Pd, cryst. struct. 0-96474  
 Y<sub>1-x</sub>Tb<sub>x</sub>Pd<sub>3</sub>, magnetisation, magnetostriction, and inelastic neutron spectra 0-65998  
 Zr<sub>70</sub>Pd<sub>30</sub> amorphous alloys, struct. factors and radial distrib. functions 0-84096

**palladium compounds**

see also palladium alloys

- Pd and Pt mixed valance complex, [Pd(ethylenediamine)<sub>2</sub>Pt(ethylenediamine)<sub>2</sub>Cl<sub>2</sub>](ClO<sub>4</sub>)<sub>4</sub>, Raman spectra 0-84734  
 Pd-D, crystallite size effects, simultaneous sorption and X-ray study 0-65237  
 Pd-D-H, equilib. H/D separation factors 0-59668  
 Pd-H, Mossbauer study of local environment of substitutional Co and Fe impurities 0-60475  
 Pd-H(D), elastic energy dissipation peak 0-60905  
 Pd-Si, amorphous thin films, laser irradi., metastable phases 0-96622  
 PdD<sub>0.73</sub>, (1, 1/2, 0)-superlattice reflection splitting near 50K, neutron diff. studies 0-70168  
 PdD<sub>2</sub>, supercond. transition temp., isotope effect (*Russian*) 0-88665  
 $\beta$ -PdDx (x=0.710, 0.742, 0.754, 0.780), structural changes in temp. region of 50K anomaly 0-100131  
 PdH, ab initio relativistic core pot. studies of metal-H bonding 0-106257  
 PdH, superconducting transition critical temperature, BCS theory, phonon spectra (*Spanish*) 0-84535  
 PdH<sub>2</sub>, inelastic neutron scattering meas. of optical vibr. freq. distrib. 0-59605  
 PdH<sub>2</sub>, local, soft modes, superconductivity thermal neutron inelastic scatt. (*Chinese*) 0-70331  
 $\beta$ -PdH<sub>2</sub>, Mossbauer fraction, diffusion induced reduction 0-108131  
 PdH<sub>2</sub>, supercond. transition temp., isotope effect (*Russian*) 0-88665  
 PdH<sub>2</sub>, superconducting transition temp., inverse isotope effect, Einstein model 0-65734  
 PdO, free energy of form. using impedance dispersion analysis 0-108728  
 PdO-Pd miniature pH electrode description and use 0-89886  
 Pd<sub>2</sub>P<sub>0.8</sub>, pure and deuterated, cryst. struct., neutron diff. study 0-84152  
 Pd<sub>2</sub>P<sub>1-x</sub>, nonstoichiometric, H<sub>2</sub>(D<sub>2</sub>) solubility 0-59662  
 Pd-Si epitaxial islands on Si (001) substrate 0-96748  
 Pd-Si formation on Si with Pd-W alloys, effect of substrate temp. 0-96963

p.a.m. see pulse amplitude modulation

**paper**

see also paper industry

- charge decay and resistance parameters correlation determ. 0-70795  
 laser inexpensive detector, use of yellow and white bond paper 0-78880  
 photographic paper, resin-coated and polyethylene 0-86474  
 rubber, friction against paper and polymer film surfaces, microroughness effect 0-71763  
 veiling reflections and reflected glare from glossy paper, lighting conditions for visual comfort 0-76733

**paper industry**

- wood chippings, neutron technique for moisture meas. (*German*) 0-105661

paraelectric materials see dielectric materials

**paraelectric resonance**

- induction and echo form. under strong inhomogeneous broadening conditions 0-108168  
 single-pulse excitation of paraelectric induction and echo signals 0-80732  
 KCl:Li<sup>+</sup>, single-pulse excitation of paraelectric induction and echo signals 0-80732

**parallel processing**

- algorithms and data structs. for array processing 0-83530  
 coherent optical pattern recognition using normalized invariant moments 0-99653  
 optical, importance of redundancy 0-95831  
 pattern recognition, hybrid parallel optical and serial digital processing systems 0-99657  
 reflected-beam laser anemometry using photon correlator 0-106861  
 remote sensing multichannel data sets; integrated optical comparator 0-64213

paralleled resonator filters see band-pass filters

**paramagnetic-antiferromagnetic transitions**

see also Neel temperature

- classical mag. moment system, antiferromag. phase transition, secular dipole interactions 0-80551  
 copper benzoate, low-dimensional Heisenberg antiferromag., high field magnetisation 0-80558  
 copper tetraamine sulphate, two-dimensional Heisenberg antiferromag., high field magnetisation 0-80558  
 press. or stress induced, neutron scatt. obs. 0-65880  
 rare-earth germanides, R<sub>2</sub>Ge<sub>3</sub>, thermal expansion, phase transition effects 0-70433



paramagnetic-antiferromagnetic transitions continued

steel, austenitic, quenched state, influence of austenite stability on impact strength (*Russian*) 0-81146  
trimethylammonium manganese trichloride, Heisenberg antiferromag. chain, specific heat and EPR 0-65931  
AuMn, mag. struct., phase transition, and magnon spectrum, random anisotropy effects 0-88722  
B<sub>2</sub>O<sub>3</sub>·Fe<sub>2</sub>O<sub>3</sub>·nMO, (n=2 or 4, M=Mg, Co, Ni, Cu), mag. props., transitions 0-75763  
BiFeO<sub>3</sub>, ferroelec., antiferromag., cryst. and mag. struct., neutron diff. study 0-65786  
CeSb, antiferromag., first-order transitions, mag. phase diagram 0-60252  
Co complex, Co(II)(1,2,4-triazole)<sub>2</sub>(NCS)<sub>2</sub> quasi two-dimens. canted S=1/2 antiferromag. 0-70976  
CoCl<sub>2</sub>, antiferromag., phase diagram, heat capacity meas. 0-93126  
CoCl<sub>2</sub>·2H<sub>2</sub>O, Ising antiferromag., high field transverse magnetisation meas. 0-93143  
CoF<sub>2</sub>, antiferromag. crit. props., neutron scatt. obs. 0-88749  
Co<sub>1-x</sub>Zn<sub>x</sub>F<sub>2</sub>, antiferromag. crit. props., neutron scatt. obs. 0-88749  
Co(urea)<sub>2</sub>Cl<sub>2</sub>·2H<sub>2</sub>O, two-dimens. mag. props., cryst. struct., specific heat 0-75777  
Cr, mag. struct., phase transition, and magnon spectrum, random anisotropy effects 0-88722  
Cr-Co, phase transformations and magnetostriction (*Russian*) 0-103869  
Cr-Re, phase transformations and magnetostriction (*Russian*) 0-103869  
Cr-Si-V, (2, 0.1 at.%), paramag. to commensurate spin density wave transition 0-65875  
CrAs, high press. paramag. antiferromag. transitions, elec. props., band model development (*Russian*) 0-60277  
CsMnF<sub>3</sub>, mag. struct., phase transition, and magnon spectrum, random anisotropy effects 0-88722  
Cu<sub>2</sub>NiSi<sub>2</sub>S<sub>8</sub>, X-ray cryst. struct. determ., mag. props. 0-107172  
Dy, magnetocaloric effect and mag. phase transitions, 80 to 300K 0-60279  
DyPO<sub>4</sub>, mag. transitions under hydrostatic press., neutron diff. study 0-71030  
Fe complex, Fe(1,2,4-triazole)<sub>2</sub>(NCS)<sub>2</sub>, quasi-2-dimens. S=1/2 antiferromag., mag. props., hidden canting 0-107986  
FeBr<sub>2</sub>, metamagnet, unusual phase diagram, theory 0-93119  
FeF<sub>3</sub>, dielectric properties, IR spectra, lattice dynamics (*French*) 0-76026  
HVO<sub>4</sub>, below 1K, nuclear orientation study of Van Vleck enhanced nuclear antiferromagnet 0-88899  
K<sub>2</sub>FeO<sub>4</sub>, crit. slowing down of spin fluctuations, Mossbauer spectra and relax. theory 0-65882  
KMn<sub>1-x</sub>Ni<sub>x</sub>F<sub>3</sub>, antiferromag. crit. props., neutron scatt. obs. 0-88749  
LaVO<sub>3</sub>, successive phase transitions, X-ray anal. 0-108437  
γ-MnAu, antiferromag., phase diagram, X-ray diff. and Young's modulus meas. 0-71024  
Mn<sub>2</sub>GaN, sp. ht., 6 to 350K, mag. and crystallographic phase transitions 0-71060  
MnS, thermal cond., temp. depend., paramag.-antiferromag. transition effects 0-65321  
MnSO<sub>4</sub>, mag. struct. and phase transitions, neutron diff. study 0-60208  
Mn<sub>2</sub>ZnN, sp. ht., 6 to 350K, mag. and crystallographic phase transitions 0-71060  
NiO, linear birefringence in S-domains near antiferromag. phase transition 0-60261  
PrSb, magnetic to nonmagnetic transition, press. or stress induced, neutron scatt. obs. 0-65880  
TbP (As)(Sb)(Bi), mag. transitions, quadrupolar interaction effects 0-80512  
U<sub>2</sub>C<sub>3</sub>, elec. resist., 4 to 1900K, mag. transition at 54K 0-59953  
UN, photoelectron spectra study, core and valence levels, antiferromag. transition effects 0-66394  
Vl<sub>2</sub>, MCD spectra, interpretation rel. to mag. struct. 0-66222

paramagnetic Curie temperature see Curie temperature

paramagnetic-ferromagnetic transitions see ferromagnetic-paramagnetic transitions

paramagnetic properties of substances

see also paramagnetic resonance; paramagnetism  
bubble garnet film, non-implanted, surface mag. struct. 0-84628  
coal, mag. susceptibility and Mossbauer meas. 0-60464  
copper formate anhydrate, cryst. struct. and mag. props. 0-79768  
copper quaternary thiospinels, mag. and elec. props. (*French*) 0-65771  
coronene, triplet state, photomagnetism 0-97125  
dibenzenechromium-dibenzenevanadium, proton HFS data, ENDOR obs. 0-66073  
ferrous formate dihydrate, paramagnetic specific heat, decoration iteration transformation anal. 0-70938  
ferrous nitrosylhaemoglobin, NO binding, spin distrib., orbital model and mag. props. 0-81534  
glass, magnetic susceptibility measurement, torsional reson. technique 0-82796  
iron(II)-A-zeolites, reduction, mag. and Mossbauer study 0-71115  
localised spin fluctuations, Knight shift obs.; for α-Mn 0-60181  
manganese acetate tetrahydrate, paramag. susceptibility, spin trimer model 0-97055  
MgAl<sub>1-x</sub>Fe<sub>x</sub>O<sub>4</sub> solid solution system, solid state properties study 0-93094  
narrow-band with strong Coulomb correlations, electron sp. ht. (*Russian*) 0-103487  
niobates, mixed metal, Eu oxidation state, mag. props., Mossbauer study 0-66080  
paramagnetic liquid, mag. field effect on depolarised light scatt. (*Russian*) 0-80221  
polyparaphenylene:SbF<sub>5</sub>, pure and doped, metallic, absence of Pauli paramagnetism, mag. susceptibility meas. and ESR obs. 0-97060  
rare earth alloys, amorphous, with random anisotropy axes, spin excitations in paramag. phase 0-80476  
rare earth binary insulating compounds, exchange interactions, paramag. susceptibility expts. 0-60177  
rare earth manganites, catalytic activity correlated with paramag. Weiss constant 0-71941  
rare earth sesquioxides, exchange interactions, paramag. susceptibility expts. 0-60177  
ruthenates, ACu<sub>2</sub>Ru<sub>2</sub>O<sub>12</sub>, A=Na,Ca,Sr,Cd,La,Pr,Nd, synthesis, 'cryst. struct., mag. and elec. props. (*French*) 0-107151  
substitutional alloys of intermediate valence systems, static mag. susceptibility con. and temp. depend. 0-84586  
tantalates, mixed metal, Eu oxidation state, mag. props., Mossbauer study 0-66080

paramagnetic properties of substances continued

tetraethylammonium neptunium hexachloride, Mossbauer spectra and mag. susceptibility meas. 0-108140  
2,2,5,5-tetramethyl-4-phenyl-3-imidazolin-3-oxide-1-oxyl, deform. electron density determ., X-ray diff. 0-88135  
tetramethylammonium neptunium hexachloride, Mossbauer spectra and mag. susceptibility meas. 0-108140  
3d-transition metal complexes, low spin-high spin paramag. transition, Ising model calc. 0-93073  
transition metal intermetallic cpds., H absorption and mag. props. 0-60224  
transition metals, paramagnetic state, itinerant electron model 0-65769  
transition metals, paramagnetic susceptibility, phonon instability, mixed localised-collective electron states 0-103811  
Be<sub>1-x</sub>Mn<sub>x</sub>, Be-rich, NMR and paramag. susceptibility 0-71206  
C chars, thermally activated paramagnetism, mag. susceptibility meas. 0-75709  
CdTe:Mn<sup>2+</sup>, exciton refl. spectra and mag. susceptibility 0-66253  
CeB<sub>6</sub>, mag. and electronic props. 0-71048  
CeB<sub>6</sub>, magnetostriction, US absorpt. and thermal expansion 0-66004  
CeB<sub>6</sub>, intermediate valence state, XPS, resist. and susceptibility study 0-71565  
CeCo<sub>3</sub>, and ternary hydride, mag. props. 0-108007  
Ce(In, Sn)<sub>3</sub>, mag. susceptibility, temp. depend., intermediate valence 0-65779  
(Ce,La<sub>1-x</sub>)<sub>2</sub>Mg<sub>3</sub>(NO<sub>3</sub>)<sub>12</sub>·24H<sub>2</sub>O, adiabatic demagnetisation temp., mag. entropy (*Russian*) 0-65892  
CeNi<sub>3</sub>, and ternary system, structural and mag. studies on valence behaviour of Ce 0-103809  
CeNi<sub>3</sub>, and ternary hydride, mag. props. 0-108007  
Co complexes, Co(III) mixed complexes, orbital angular momentum reduction, <sup>59</sup>Co NMR chemical shift 0-58137  
Co(C<sub>2</sub>H<sub>5</sub>NO)<sub>6</sub>(ClO<sub>4</sub>)<sub>2</sub>[(BF<sub>4</sub>)<sub>2</sub>], X-Y antiferromagnet, Neel temp., spin correlation functions 0-60345  
CoCO<sub>3</sub>, LF exciton and Raman spectra, one-magnon and two-magnon scatt. 0-93333  
CoGa<sub>1-x</sub>Fe<sub>x</sub>O<sub>4</sub>, x=0.1-0.4, mag. susceptibility temp. depend. (*Russian*) 0-70957  
CoTi<sub>1-x</sub>Al<sub>x</sub>, mag. and electronic props., ferromag. and paramag. state 0-65814  
Cr-Ge system, XPS, X-ray and neutron diff. and mag. meas. to study chem. bonding and electronic struct. 0-60749  
CsCdBr<sub>3</sub>:Cr<sup>3+</sup>(Cr<sup>3+</sup>), EPR of impurities, charge compensation, X-ray effects 0-60407  
CsMgCl<sub>3</sub>(Br<sub>3</sub>):Cr<sup>3+</sup>(Cr<sup>3+</sup>), EPR of impurities, charge compensation, X-ray effects 0-60407  
CsNiF<sub>3</sub>, longit. paramag. susceptibility, reaction field approx. 0-97059  
Cs<sub>2</sub>NpCl<sub>6</sub>, Mossbauer spectra and mag. susceptibility meas. 0-108140  
Cu-Al-Co liquid alloys, constant Co-content of 5 wt.%, mag. props. (*German*) 0-88720  
Cu<sub>2-x</sub>Se, nonstoichiometric, diamag. and paramag. props., susceptibility meas. 0-70936  
Eu<sub>2</sub>IrH<sub>5</sub>, prep., cryst. struct., mag. and elec. props. 0-88117  
Eu<sub>2</sub>Sr<sub>1-x</sub>S<sub>x</sub>, paramag. susceptibility, expt. and comparison with high temp. series expansion 0-60176  
Fe dicyclopentadienyl-dibenzenevanadium, coalescence temps., full proton HFS tensor, ENDOR obs. 0-66073  
Fe, magnetic moments, local short range order, high temp. effects 0-65902  
Fe-Pt, Invar alloy, paramag. susceptibility 0-70940  
Fe-Ti, magnetism and H<sub>2</sub> storage 0-70941  
FeCl<sub>2</sub>, reorientation of mag. moments under mech. stresses at 0K 0-93153  
Fe<sub>1-x</sub>Mn<sub>x</sub>Cl<sub>2</sub>, low-lying electronic excitations in antiferromag. and paramag. phases Raman scatt. study 0-71414  
FeSO<sub>4</sub>, α- and β-forms, magnetic interactions, neutron inelastic scatt. study 0-107980  
FeSO<sub>4</sub>·n H<sub>2</sub>O (n=1,4,5,7), Fe<sup>2+</sup> ion mag. interaction with crystallisation water protons, proton NMR obs. 0-60447  
Fe(Sb<sub>1-x</sub>Te<sub>x</sub>)<sub>2</sub>, system cpds., prep., cryst. struct., elec. and mag. characteristics. 0-108349  
θ-Fe<sub>2</sub>V<sub>2</sub>O<sub>7</sub>, spin glass and paramag. props., susceptibility, EPR and Mossbauer studies 0-75782  
Fe<sub>2</sub>V<sub>2</sub>O<sub>7</sub>, spin glass transition range, cluster blocking distrib. function 0-80548  
Ga, magnetic susceptibility near melting point 0-60186  
Gd<sub>1-x</sub>Ca<sub>x</sub>Al<sub>3</sub>, mag. props. and phase relations 0-107991  
H<sub>2</sub>MoO<sub>3</sub>, electronic props., mag. susceptibility and spectra 0-80266  
<sup>2</sup>H<sub>2</sub>, BCC solid, nucl. mag. order and paramag. susceptibility 0-59757  
HgCr<sub>2</sub>S<sub>4</sub>, cooling efficiency near 60Kas mag. refrigerant 0-71034  
HgTe,  $\Gamma_8$  symm. acceptor centre hole mag. props. (*Russian*) 0-88733  
Ho(Ir,Rh<sub>1-x</sub>)<sub>4</sub>B<sub>4</sub> pseudoternary system/ supercond. and mag. ordering 0-70876  
HoVO<sub>4</sub>, RF susceptibility below 1K, mag. sp. ht. 0-84585  
K<sub>2</sub>CuF<sub>4</sub>, spin relax., crit. behaviour, high freq. susceptibility meas. 0-65936  
KMn<sub>1-x</sub>Mg<sub>x</sub>1-xF<sub>3</sub>, randomly diluted Heisenberg paramag. nucl. relax. 0-60444  
KMgF<sub>3</sub>:Ni<sup>2+</sup>, acoustic Faraday and Cotton-Mouton effects; theory 0-65987  
KMg<sub>1-x</sub>Mn<sub>x</sub>F<sub>3</sub>, disordered paramagnet, <sup>19</sup>F NMR study 0-71216  
KMnF<sub>3</sub>, Faraday effect mechanism in paramag. phase 0-60552  
LaCo<sub>3</sub>, Mott isolator, paramag. props., calc. 0-93071  
LaMg, Pauli paramagnet, mag. susceptibility, nonlinear band behaviour 0-75706  
LaNi<sub>3</sub> hydrides, 4.2K paramag. susceptibility 0-70934  
LaNi<sub>3</sub>, magnetism and H<sub>2</sub> storage 0-70941  
La<sub>1-x</sub>Tb<sub>x</sub>Al<sub>2</sub>, competing paramag. anisotropy from cryst. field and indirect quadrupolar coupling 0-60180  
LiTmF<sub>4</sub>, van-Vleck paramagnet, giant magnetostriction (*Russian*) 0-103872  
Mg<sub>2</sub>Ni, magnetism and H<sub>2</sub> storage 0-70941  
δ-Mn, paramag., antiferromag. and ferromag., magnetic moment calcs. 0-60223  
α-MnSeO<sub>4</sub>, magnetic interactions, neutron inelastic scatt. study 0-107980  
MnSi, weak itinerant magnetic compound, paramagnetic response function, polarised neutron scattering 0-107982  
NaA neolyte, Hg cluster transition to paramagnetic state due to mag. field (*Russian*) 0-60183  
NbSe<sub>3</sub>, mag. susceptibility, CDW effect 0-88716  
NdAg<sub>2</sub>, low temp. mag. meas. 0-107989



**paramagnetic properties of substances continued**

- Nd<sub>2</sub>Ag<sub>7</sub>, amorphous, mag. props. 0-60182  
 Nd<sub>2</sub>Y<sub>1-x</sub>Zn<sub>x</sub> amorphous, mag. susceptibility, 77 to 600K (*Russian*) 0-65776  
 Ni, mag. form factors in Stoner-like model 0-97061  
 Ni, muon spin rot. Knight shift, 637 to 906K 0-75908  
 Ni, paramag. region, Fe and Co impurity effects on susceptibility, Faraday obs. (*Russian*) 0-88731  
 NiF<sub>2</sub>, thermal expansion and magnetostriction, 55K to room temp. 0-80586  
 NiSe<sub>2</sub>, paramag. props., NMR, mag. susceptibility 0-60175  
 Ni<sub>2</sub>Zr<sub>1-x</sub> metallic glass, crystallisation kinetics, elec. resist. and mag. susceptibility meas. 0-136359  
 Np(IV)-tetracyclopentadienide complex, H<sup>1</sup>-NMR studies, paramagnetic moments, temp. depend. 0-93186  
 PbTe:In, mag. susceptibility, temp. depend., 4.2 to 200K 0-65773  
 Pd, sd hybridisation, paramagnetic Curie temp. and susceptibility (*Russian*) 0-103808  
 Pd, spin fluctuation model interpretation of mag. susceptibility 0-80477  
 PdH<sub>0.003</sub>Fe<sub>0.003</sub>, Kondo system, local moments, hyperfine fields, Mossbauer study 0-80478  
 PrAg, low temp. mag. meas. 0-107989  
 Pr<sub>2</sub>Ag<sub>70</sub>, Pr<sub>50</sub>Ag<sub>50</sub>, and Pr<sub>10</sub>Lu<sub>40</sub>Ag<sub>50</sub>, amorphous, mag. props. 0-60182  
 Pr<sub>1-x</sub>Ca<sub>x</sub>Al<sub>3</sub>, mag. props. and phase relations 0-107991  
 PrCo<sub>2</sub>, strongly exchange-enhanced paramagnetism, susceptibility 0-60179  
 PrIn<sub>2</sub>/Gd, indirect nuclear exchange interactions, ESR-linewidth meas., sp. ht. determ. 0-103825  
 PrNi<sub>2</sub>, LF dynamics and <sup>141</sup>Pr thermal relax., coupling parameter and RKKY exchange mechanism 0-103812  
 Pt, spin fluctuation model interpretation of mag. susceptibility 0-80477  
 Rb<sub>2</sub>CuBr<sub>4</sub>·2H<sub>2</sub>O, dynamic props. in paramag. state, spin-lattice relax. time meas. 0-71214  
 RbMnF<sub>3</sub>, Faraday effect mechanism in paramag. phase 0-60552  
 Sm-Eu alloy, dil., mag. and elec. hyperfine interac., TDPAD obs., paramag. behaviour, exchange integral 0-103908  
 Sm<sub>2</sub>Mn<sub>23-x</sub>Fe<sub>x</sub>, magnetic behaviour, temp. and comp. depend. 0-93090  
 TbPO<sub>4</sub>, zircon struct., cryst. field analysis 0-80232  
 Tb-Dy, dil., type I superconductor, paramag. Dy moment relax., Mossbauer spectra study 0-65755  
 Th<sub>2</sub>Co<sub>3</sub>, effect of absorbed H<sub>2</sub> on mag. behaviour 0-60184  
 Th<sub>2</sub>Ni<sub>3</sub>, effect of absorbed H<sub>2</sub> on mag. behaviour 0-60184  
 Ti-Nb-Zr-Fe, supercond. and paramag. props., effect of Fe additions (*Russian*) 0-65730  
 (Ti<sub>1-x</sub>V<sub>x</sub>)<sub>2</sub>O<sub>3</sub>, O<x<0.1, magnetisation and mag. moments 0-65772  
 Tm-Zn, paramagnetism, mag. excitations, exchanges interactions 0-88718  
 TmSe, intermediate valence. cpd., susceptibility, single-ion approach 0-70935  
 TmZn<sub>2</sub>, Mossbauer effect meas. in antiferromag. and paramag. states 0-71265  
 V, dynamic susceptibility, model pot. theory 0-75710  
 V, small particles, crystal structure, magnetic and superconducting props. 0-97121  
 V-Pt, sp. ht. and mag. meas. in ordered and disordered phases 0-70422  
 V<sub>2</sub>O<sub>5</sub>-V<sub>2</sub>O<sub>4</sub>-BaZnO<sub>2</sub> glass, V ion states, mag. and elec. props. 0-88556  
 V<sub>2</sub>S<sub>4</sub> and V<sub>2</sub>S<sub>8</sub>, itinerant antiferromag. spin fluctuations, NMR studies 0-93198  
 VSe<sub>2-x</sub>S<sub>x</sub> (0<x<2) solid solutions, characterisation 0-88730  
 V<sub>2</sub>Si, magnetic susceptibility, density of states model for lattice transformation in A-15 compounds 0-65219  
 VTe, mag. and elec. transport props. 0-92897  
 YIG: Si single crystals, mag. props. 0-107981  
 YMG, Pauli paramagnet, mag. susceptibility, nonlinear band behaviour 0-75706  
 YVO<sub>4</sub>:Nd<sup>3+</sup>, zircon struct., cryst. field analysis 0-80232  
 ZrV<sub>2</sub>, Knight shift vs. susceptibility plot 0-75712

**paramagnetic resonance**

- see also *acoustic paramagnetic resonance; CESR; CIDEP; electron spin-lattice relaxation; ENDOR; EPR line breadth; paramagnetic resonance of colour centres; paramagnetic resonance of free radicals; paramagnetic resonance of ions and impurities; spin echo (EPR); spin-spin relaxation*  
 analytical chemistry appls., conf., Denver, CO, USA (Aug. 1979) 0-90598  
 anisotropic rotational diffusion studied by passage saturation transfer EPR 0-60403  
 anthracene-phenanthrene-tetracyanobenzene, CT-cryst., mini-excitons and lattice dynamics, ESR, optical and Raman spectra 0-60406  
 azaphenanthrenes, lowest triplet state zero field splitting parameters calcs. 0-83391  
 carbohydrate compounds, X-irrad., trapped electrons, ESR and ENDOR obs. 0-93161  
 chalcogenide glasses, optical versus transport processes. 0-84449  
 coaxial microwave cavity for improved EPR sensitivity with loss solvents 0-62705  
 cryostat for low temperature X-irradiation and electron paramagnetic resonance 0-86321  
 dating method with digital ESR 0-86542  
 diacetylene-d<sub>2</sub>, excited quintet states during photopolymerisation, ESR obs. 0-84635  
 digitised EPR system, appln. to saturation transfer 0-77825  
 p-nodocycloxy benzylidene p-azophenyl aniline, smectic phases, mol. order, EPR study 0-79693  
 electric field modulated, appl. to study of ferroelectrics 0-75841  
 formaldehyde+Br reactions, rate consts. by EPR 0-93736  
 formaldehyde+F reactions, rate consts. by EPR 0-93736  
 fossil dating by ESR technique 0-95209  
 glasses, elec., mag., and optical props., conference, Troy, NY, USA (Aug. 1979) 0-105417  
 glasses, ESR, review 0-108049  
 high-temperature studies using CO<sub>2</sub> laser-heated EPR spectrometer 0-68233  
 Kapton, pyrolysed, cond. polymer, transport and mag. props. 0-96887  
 lowest triplet state zero field splitting parameters calcs. 0-83391  
 magnetic field operator 0-108051  
 magneto-optical effects, magnetic resonance saturation in paramagnetic system with quadrupole splitting 0-60404  
 membrane surfaces, antibody association kinetics with spin-label haptens 0-66787  
 metals, ESR of localised moments 0-71153

**paramagnetic resonance continued**

- N-methyl-N-nitrosourea, electronic interactions with DNA, ESR obs. and INDO calcs. 0-94154  
 molecules, high temp., appl. of ESR isolation technique 0-57399  
 NMR-ESR spectroscopy, miniature magnetic assembly, teaching 0-105467  
 organic molecular crystals, intermolecular interactions, spectroscopic studies, review 0-103958  
 paramagnets, low-dimens., EPR spectra 0-71154  
 phenanthrene, lowest triplet state zero field splitting parameters calcs. 0-83391  
 p-phenylphenol in stretched polyvinyl alcohol film, phosphorescent triplet states, ESR spectra obs. 0-83393  
 cis-polyacetylene film, unpaired electrons, isomerisation, EPR obs. 0-60405  
 polyhydroxy compounds, X-irrad., trapped electrons, ESR and ENDOR obs. 0-93161  
 polyparaphenylene:SbF<sub>6</sub>, pure and doped, metallic, absence of Pauli paramagnetism, mag. susceptibility meas. and ESR obs. 0-97060  
 porphyrins in liquid crystal, oriented photoexcited triplets, EPR study 0-84636  
 quick access sample system for low temp. K-band ESR and ENDOR 0-57352  
 quinones, triplet quenching by organometal cpds., time resolved CIDEP and ESR obs. 0-95654  
 size-quantised films, sound amplification under ESR conditions 0-70322  
 slotted tube resonator pulsed ESR and ODMR expts. 0-86360  
 spin system saturation characts., acoustic wave excitation (*Russian*) 0-66013  
 trapped electrons, ESR and ENDOR obs. 0-93161  
 1,3,5-trinitro 1,3,5-triazacyclohexane, shock-induced intramol. bond breaking, XPS and EPR study 0-76512  
 trinitrotoluene, shock-induced intramol. bond breaking, XPS and EPR study 0-76512  
 triplet states in photosystem I of spinach chloroplasts and subchloroplast particles 0-85344  
 TTF-TCNQ complex, trans-diethyl-dimethyl TTF-TCNQ, one-dimens. cond. 0-96853  
 zinc pyrochrochryllide in nematic liquid crystals, oriented photoexcited triplets, EPR study 0-84636  
 AgBr emulsion grains, adsorbed dyes, light-induced ESR spectra 0-88862  
 As<sub>2</sub>S<sub>3</sub>, glassy, photoinduced defects, EPR and absorpt. spectra 0-59398  
 B-C, B-C-Ti, B-C-Cr, paramagnetic centre struct. and defect form. 0-66034  
 Br matrix isolation ESR 0-106336  
 C, amorphous film, spin resonance, IR spectra, microhardness 0-71157  
 Ge-P-S glass system, EPR of intrinsic and Mn<sup>2+</sup> impurity centres 0-88870  
 Ge-S glass, melt-quenched photoinduced ESR, annealing behaviour and glass comp. depend. 0-71156  
 Ge<sub>2</sub>S<sub>8</sub>, amorphous, bulk and film forms, elec. props. and ESR study 0-103691  
 KN<sub>3</sub>, ESR undergraduate expt. 0-105471  
 NH<sub>2</sub>NO<sub>2</sub>, shock-induced intramol. bond breaking, XPS and EPR study 0-76512  
 NO<sub>2</sub>, Stark effect investig., using two-way EPR cavity system 0-90872  
 Se, glassy, localised electronic states, photoluminesc. and ESR studies 0-65501  
 Si, amorphous, EPR and spin-dependent effects 0-80592  
 Si, amorphous, glow discharge produced, defect creation, high optical excitation 0-97327  
 Si, amorphous, UHV evaporated, annealing behaviour of spin density 0-93163  
 Si, amorphous film, RF plasma deposition from SiCl<sub>4</sub>-H<sub>2</sub>, characterisation 0-66435  
 Si, amorphous films, hopping conduction, dangling bond generation by high temp. annealing 0-60115  
 Si, amorphous films, RF sputtering prep. at high Ar press., props. obs. 0-80418  
 Si, annealed, neutron-irradiated, EPR centre (S=1), characts. 0-71177  
 Si:H amorphous films, ESR, optical gap and elec. cond. meas. 0-75842
- paramagnetic resonance of colour centres**  
 inc. other defects involving initial vacancy or interstitial formation  
 alkali halide, dynamics of nonrelaxed and self-trapped holes (*Russian*) 0-80607  
 alkali halides, F-centres, ESR in different states of relaxed configuration 0-108067  
 alkali metal halide crystals, g-tensor anal. of S<sup>-</sup> and Se<sup>-</sup> centres, ESR 0-84650  
 ionic crystal defects, mag. reson. studies 0-108066  
 metal colloids in ionic cryst., preparation, optical, mag. resonance, elec. props. 0-59459  
 α-quartz, CNDO/2 calcs., electronic props. of perfect cluster, EPR parameters of O<sup>-</sup> vacancy 0-107701  
 quartz, synthetic, Al centres conc. and anomalous pleochroism depend. on crystn. parameters 0-107311  
 quartz, synthetic, deuteration, EPR and IR absorpt. characterisation 0-92721  
 α-quartz, synthetic, growth, defects induced by seed orientation 0-96454  
 trialkylammonium, iodides, absorpt. and luminesc. spectra of self-localized excitons 0-97340  
 β-Al<sub>2</sub>O<sub>3</sub>-Na<sub>2</sub>O, colour centre ESR by localised tunnelling states 0-108073  
 β-Al<sub>2</sub>O<sub>3</sub>-Na<sub>2</sub>O, X-ray induced defects, EPR and ENDOR study 0-60456  
 AlPO<sub>4</sub>, synthetic berillite, electron irrad. effects, ESR, ENDOR, optical spectral study 0-80608  
 Ca fluorapatites, carbonated, B-type, EPR of F<sup>+</sup>-centre after X-irrad. (*French*) 0-108065  
 CaCO<sub>3</sub>:Li, synthetic calcite, (CO<sub>3</sub>)<sub>2</sub><sup>2-</sup>-Li<sup>+</sup> defect after X-irrad., EPR study 0-75852  
 CaF<sub>2</sub>:Ni, X-irradiated, optical and EPR meas. 0-108235  
 CaO, additively coloured powder, F<sup>+</sup> centre, 295K (*Russian*) 0-84649  
 CaS, additively coloured powder, F<sup>+</sup> centre, 295K (*Russian*) 0-84649  
 CdS, electron and hole trapped centres, EPR, photoluminescence, photoconductivity study 0-108071  
 CsI:Na, X-ray irradiated, optical and ESR studies in IR absorption band 0-80828  
 EuO nonstoichiometric film, ESR spectra and exchange interaction 0-93176  
 KBr, cation defects creation mechanism 0-75224



**paramagnetic resonance of colour centres continued**

- KCl,  $Zr^{2+}$  centres in triplet state, EPR study 0-108068  
 KCl:Br ( $I^-$ ), interstitial atomic H centres, formation kinetics and struct.  
 MO calc. and EPR studies 0-75854  
 KCl:H, ENDOR and ESR study of anion sites 0-108118  
 KMgF<sub>3</sub>, F-centre ENDOR study 0-108117  
 KMg<sub>2</sub>[AlSi<sub>2</sub>O<sub>7</sub>]<sub>2</sub>F<sub>2</sub>, with excess Al, synthetic fluorophlogopite, radiation-induced paramag. O<sup>-</sup> centres 0-60417  
 LiF:Mg, X-irrad., colour centres, ESR and UV absorpt. meas. 0-108069  
 LiF:OH, neutron irrad., interstitial H-centres, ESR obs. 0-93175  
 LiH, defect form. at low temp., EPR, thermolum. and TSC study 0-107222  
 LiH, formation and annihilation of Li colloids and H bubbles 0-107228  
 Li<sub>2</sub>O pellets, sintered, neutron irradiated, ESR study 0-92566  
 LiYF<sub>4</sub>, electron-irrad. induced defects, optical and EPR study, impurity effects 0-66238  
 NaCl, migration of nonrelaxed holes, self-trapping, ESR and luminesc. obs. (Russian) 0-66033  
 NaCl(Br), X-ray or UV irradiated, cation defects creation mechanism 0-75224  
 Na<sub>2</sub>O-SiO<sub>2</sub>-CuO glass, gamma-irradiated, EPR and optical spectra 0-103885  
 NaReO<sub>4</sub>, EPR spectra of paramag. centres and free radicals 0-108072  
 RbCl:Br ( $I^-$ ), interstitial atomic H centres, formation kinetics and struct.  
 MO calc. and EPR studies 0-75854  
 RbCl(Br), cation defects creation mechanism 0-75224  
<sup>85</sup>RbCl isotope enriched crystal, optical registration of EPR F-centres (Russian) 0-103886  
 Si, amorphous layer prod. by ion implantation, diffusion broadening, ESR study 0-92552  
 Si:Ar(Ne)(O)(N), ion-implanted, defect reverse annealing, 550-650°C 0-88875  
 Si:H, amorphous, defect states, luminesc. and ESR obs. 0-76075  
 Si:P, polycryst. films, elec. props., EPR, defect states, doping effects 0-75660  
 n-SiC, thermal defects, ESR study 0-88876  
 SiO<sub>2</sub>, vitreous, paramag. centres associated with bonding defects 0-80609  
 $\alpha$ -W<sub>2</sub>V<sub>2</sub>O<sub>7</sub>, paramag. defect study by ESR 0-103881  
 Y<sub>2</sub>O<sub>3</sub>:Zr<sup>4+</sup>, F-centre charge state, ESR and thermally stimulated luminesc. obs. 0-60418  
 ZnS:Pb, blue luminesc., photoexcited EPR spectrum 0-108070  
 ZrSiO<sub>4</sub>, natural, radiation defect centre, EPR obs. 0-75853  
 ZrSiO<sub>4</sub>, X-irrad., trapping and emission centres, OH<sup>-</sup> ion contribution 0-80876

**paramagnetic resonance of conduction electrons see CESR****paramagnetic resonance of free radicals**

- N-acetylglycine, X-irrad., stable radical electronic and mol. struct., ENDOR and ESR 0-80637  
 adamantane,  $\gamma$ -irrad., free radicals EPR and ENDOR 0-69170  
 4-amino-2,2,6,6-tetramethylpiperidine-N-oxyl- and deuterated derivatives, mag. resonance study 0-63686  
 ATPase, Ca<sup>2+</sup>-depend., struct. rearrangements during function 0-81527  
 bacteriochlorophyll radicals, role in primary charge separation of Rhodospirillum rubrum 0-63688  
 bacteriopheophytin b radicals, role in primary charge separation of Rhodospirillum rubrum 0-63688  
 $\alpha$ -bromofluoro alkyl pi-radical, signs of hyperfine and quadrupole couplings, ESR determ. 0-97141  
 N-bromosuccinimide, X-irrad., ESR study of Br and  $\sigma^*$  radical 0-66037  
 cells, <sup>125</sup>IudR-labelled and X-irrad., 4.2K and above 0-72211  
 $\alpha$ -chloroacetamide, alkoxy radical form., effect, of  $\alpha$ -hydroxyacetamide, ESR study 0-80610  
 copper porphyrins, mag. susceptibility and EPR, sample grinding effects 0-60420  
 18-crown-6 complexed sodium-2, 6-di-*n*-butyl-p-benzoquinone ion pairs, soln. ESR spectra, temp. and conc. depend. 0-63675  
 18-crown-6 complexed sodium-diquinone ion pairs, soln. ESR spectra, temp. and conc. depend. 0-63675  
 cytochrome c oxidase, struct. of cytochrome a<sub>3</sub>-Cu<sub>2</sub> couple, NO binding studies 0-67039  
 DBTTF halogen complexes, IR, UV spectra, EPR study 0-108215  
 diacetylene, low temp. photochemical polymerisation, decay kinetics, ESR spectra obs. 0-100616  
 diacetylenes, solid state photopolymerisation, reaction products, electron spin resonance anal. 0-81338  
 5,5'-diethylbarbituric acid, EPR and INDO-MO study of radical formation after irrad. 0-93774  
 4,6-dihydroxypyrimidine, aq. soln., reaction with OH, short-lived radicals, ESR 0-101031  
 dipotassium glucose-1-phosphate, X-irrad., ESR-ENDOR obs 0-60419  
 DPPH, dil., saturated spin system, spin decoupling effect and variation of dipolar energy reservoir temp. 0-88877  
 EBRA, nematic, EPR investig. 0-108077  
 glutaric acid,  $\gamma$ -irrad. single crystals, free radical EPR obs. at 77K 0-81340  
 halogermane radical anions, ESR spectra and struct. 0-87153  
 hexafluorobenzene anion-radicals in squalane, ESR spectrum optical detection 0-95655  
 hexafluorobenzene radical anion, <sup>13</sup>C hyperfine interaction, EPR obs. 0-83392  
 4-hydroxy-2,2,6,6-tetramethylpiperidine, radiation-induced oxidation to paramag. nitroxide free radicals 0-81341  
 hyperfine struct., EPR cepstra method determ. 0-102531  
 isobacteriochlorins,  $\pi$  cation radicals, implications for NO<sub>2</sub><sup>-</sup>, SO<sub>2</sub><sup>-</sup> reductases 0-63684  
 Krebs II ascites cells, subcellular localisation and paramag. props. of observed signals 0-108952  
 MBBA, nematic, flexibility gradient of fatty acid spin labels, EPR study 0-71181  
 mesophase pitch, magnetically-oriented, phys. props., mol. struct. 0-64885  
 muscle proteins, rot. motions, saturation transfer EPR obs. 0-94151  
 nitrofluorene-lipid adducts, mutagenicity, ESR spectra investig. 0-91583  
 nitrocyhaemoglobin, electron spin distrib. 0-83528  
 nitroxide radical, long range Y-P hyperfine coupling, ESR spectra obs. 0-75858  
 nitroxide radicals, q- and A-tensor components, rot. mobility 2 mm EPR spectrosc. determ. 0-102530

**paramagnetic resonance of free radicals continued**

- nitroxide spin probes, unresolved hyperfine broadening convection in EPR, linewidth and Heisenberg spin exchange freq. determ. 0-71180  
 nitroxyl radicals, cyclic, conform. flexibility, EPR obs. 0-91581  
 organic doublet radicals in nematic and smectic liq. crystals, ENDOR obs. 0-91585  
 PEBAB, nematic, EPR investig. 0-108077  
 peroxy chain radicals, reactivity and struct., EPR spectra, trapped in PTFE 0-66783  
 peroxyamine disulphonate, EPR lineshape, dispersion vs. absorpt. plots, modulation broadening and instrumental distortion 0-58290  
 phenothiazine derivatives, semicond. elec. props., optical spectra, and EPR 0-103693  
 phosphatidyl choline, oxidised, free radical formation on UV irrad. 0-76790  
 phosphoranyl radicals obs. in ESR spectra of triphenylphosphine sulphide in deuterated methanol 0-84651  
 photosynthetic reaction centre chromophore organisation, high-resolution magnetophotoselection 0-97880  
 piperidinoyloxy 2,2,6,6-tetramethyl radical, recrystallised samples, EPR study 0-100615  
 PMMA, radical form. in explosive loading, electron spin reson. obs. 0-63678  
 PMMA bone cement, feasibility study 0-94318  
 PMMA in benzene solution, ultrasonic irradiation, polymer chain scissions obs. by ESR spectra and spin-trapping techniques 0-84653  
 polymethacrylamide copolymer, soluble, mobility of spin label bonded to chain end 0-63873  
 polypropylene, oriented, microcracks diagnostics by paramag. probe method 0-66736  
 polystyrene, plasma polymerised, free radicals, O<sub>2</sub> effects, EPR study 0-71179  
 polystyrene, plasma polymerised, free radicals, transient elec. current, EPR, heat treatment 0-71178  
 polystyrene in benzene solution, ultrasonic irradiation, polymer chain scissions obs. by ESR spectra and spin-trapping techniques 0-84653  
 polyvinylacetate in benzene solution ultrasonic irradiation, polymer chain scissions obs. by ESR spectra and spin-trapping techniques 0-84653  
 porphyrins, metal-free, EPR, sample grinding effects 0-60420  
 protein-peroxide radicals, <sup>17</sup>O-labelled 0-85345  
 pyrene solutions, radical ion pairs, pulse radiolysis, time resolved EPR spectra meas. by ODMR of fluoresc. 0-83395  
 re-entrant nematic phase, orientational order, electron reson. study 0-103242  
 tetraselenotetracene iodides, struct. and physical props., DC electrical cond. and EPR linewidth meas. 0-103312  
 uranyl phenanthraquinone radical ion complex, longitudinal spin-lattice relax. time determ. 0-108076  
 uridine-5'-phosphate.2Na<sup>+</sup> single crystals, radiation damage 0-108964  
 CdO-Al<sub>2</sub>O<sub>3</sub>-P<sub>2</sub>O<sub>5</sub> glass,  $\gamma$ -irrad., EPR study 0-84639  
 CdS, EPR of adsorbed oxygen radicals, temp. depend. 0-80612  
 Co complex, triazine-1-oxide complexes, EPR spectra in frozen nematic liq. crystal glass 0-88871  
 Cu complex, triazine-1-oxide complexes, EPR spectra in frozen nematic liq. crystal glass 0-88871  
 KD<sub>2</sub>PO<sub>4</sub>, X-irradiated, hysteresis effects obs. by ESR 0-103928  
 KH<sub>2</sub>AsO<sub>4</sub>,  $\gamma$ -irradiated, free radicals, EPR and ENDOR study of consequences of ferroelec. transition (French) 0-93209  
 KH<sub>2</sub>PO<sub>4</sub>, X-irradiated, hysteresis effects obs. by ESR 0-103928  
 KPF<sub>6</sub>,  $\gamma$ -irrad., trapped free radicals EPR obs. 0-63683  
<sup>81</sup>KrF in polycrystalline KrF, ESR spectra, struct. and dynamic parameters of radical sites determ. 0-84652  
 Li<sub>2</sub>O-Al<sub>2</sub>O<sub>3</sub>-P<sub>2</sub>O<sub>5</sub>:Cd<sup>2+</sup> glass,  $\gamma$ -irrad., EPR study 0-84639  
 Li<sub>2</sub>O-P<sub>2</sub>O<sub>5</sub>:Cd<sup>2+</sup> glass,  $\gamma$ -irrad., EPR study 0-84639  
 Mg<sub>2</sub>TiO<sub>4</sub>:Cu(Ni), ESR of Cu<sup>2+</sup> and Ni<sup>2+</sup> 0-97131  
 NaReO<sub>4</sub>, EPR spectra of paramag. centres and free radicals 0-108072  
 RbH<sub>2</sub>PO<sub>4</sub>, X-irradiated, hysteresis effects obs. by ESR 0-103928  
 Si biradical, six-coordinate, mol. mobility two-spin probe investig. 0-102529  
 SiF<sub>4</sub>Cl<sub>4</sub>-n in  $\gamma$ -irradiated solid solution of tetramethylsilane, EPR spectra obs. 0-80611  
 SiF<sub>3</sub>Cl (Br<sup>-</sup>)(I<sup>-</sup>) in  $\gamma$ -irradiated solid solution of tetramethylsilane, EPR spectra obs. 0-80611  
 SiH<sub>3</sub> radical, in Ar(Kr)(N<sub>2</sub>) matrix, anisotropic ESR spectroscopic parameters 0-63687  
 V complexes, <sup>51</sup>V quadrupole coupling tensors form EPR meas. 0-88866  
<sup>136</sup>XeF in polycrystalline XeF<sub>2</sub> or XeF<sub>4</sub>, ESR spectra, struct. and dynamic parameters of radical sites determ. 0-84652

**paramagnetic resonance of ions and impurities**

- see also paramagnetic resonance of ion group ions and impurities; paramagnetic resonance of palladium and platinum group ions and impurities; paramagnetic resonance of rare earth ions and impurities  
 aniline, in p-xylene host cryst., phosphoresc. triplet state, ESR and MIDP obs. 0-66077  
 aryl cations, triplet state, multiple site splitting, ESR obs. 0-97126  
 decacyclene anion, photoexcited quartet state, transient EPR 0-78635  
 diamond:Sb, implanted, radiation damage and annealing study 0-100263  
 dielectric crystal, APR and phonon spectroscopy to study paramagnetic ions 0-84634  
 dynamic Jahn-Teller effect in ESR spectra, Green's functions calcs. 0-84643  
 fluorene:pyrene-d<sub>10</sub>, single cryst., host-guest triplet pairs, mag. field effect 0-60649  
 interdoublet EPR spectrum ang. depend. for ions with arbitrary electron and nuclear spins in strong axial cryst. field 0-93164  
 methyl cyanide-water (methanol), Ag<sup>+</sup> ion solvation,  $\gamma$ -irrad., ESR obs. 0-97726  
 p-phenylphenolate ion in stretched polyvinyl alcohol film, phosphorescent triplet states, ESR spectra obs. 0-83393  
 $\alpha$ -quartz, dynamic interchange among three states of P, EPR obs. 0-66010  
 symmetry, effects of low site symmetry, review 0-71159  
 CaF<sub>2</sub>:U<sup>3+</sup>, anomalous magnetooptic props., optical detection of ESR and cross-relax. resonances 0-93287  
 CaO, formation of surface O<sub>2</sub><sup>-</sup> ion by O<sub>2</sub> adsorpt., EPR 0-61155  
 CaS, atomic and mol. centres of O, ESR and luminesc. methods (Russian) 0-84764  
 CaSe:Sn<sup>2+</sup>, EPR study of octahedral Sn<sup>2+</sup> centres, 4 to 290K (Russian) 0-84637  
 CdO-Al<sub>2</sub>O<sub>3</sub>-P<sub>2</sub>O<sub>5</sub> glass,  $\gamma$ -irrad., EPR study 0-84639



## paramagnetic resonance of ions and impurities continued

- KD<sub>2</sub>PO<sub>4</sub>:Ti<sup>2+</sup>, EPR of ferroelec. and paraelec. phases 0-66012  
 KH<sub>2</sub>PO<sub>4</sub>:Ti<sup>2+</sup>, EPR of ferroelec. and paraelec. phases 0-66012  
 KH<sub>2</sub>(SeO<sub>4</sub>)<sub>2</sub>, ferroelastic transition under uniaxial press., EPR study 0-59562  
 LiH, effect of surface hydrolysis to LiOH on IR absorption, X-ray luminesc. and EPR spectra 0-60660  
 Li<sub>2</sub>O-Al<sub>2</sub>O<sub>3</sub>-SiO<sub>2</sub>:Cd<sup>2+</sup> glass, ESR study 0-103879  
 Li<sub>2</sub>O-Al<sub>2</sub>O<sub>3</sub>-SiO<sub>2</sub>(P<sub>2</sub>O<sub>5</sub>):Cd<sup>2+</sup> glasses,  $\gamma$ -irrad., EPR study 0-84639  
 Li<sub>2</sub>O-P<sub>2</sub>O<sub>5</sub>:Cd<sup>2+</sup> glass,  $\gamma$ -irrad., EPR study 0-84639  
 LuPO<sub>4</sub>:Pb<sup>2+</sup>, EPR, hyperfine interactions 0-108050  
 MgO:Al, and nominally pure single crystal, thermally stimulated luminesc. rel. to temp., and EPR (*Russian*) 0-84789  
 NO<sub>2</sub> on Cu, ultrahigh vacuum ESR studies 0-97729  
 Na<sub>2</sub>Se<sub>2</sub>P<sub>2</sub>O<sub>7</sub>, fast-ion conductor, struct. phase transition 0-88362  
 Rb-tetrahydrofuran solution, polarised photoelectron and loose ion pair (Rb<sup>+</sup>, e) obs., optical-ESR study 0-85196  
 Si:Ar(Ne)(O)(N), ion-implanted, defect reverse annealing, 550-650°C 0-88875  
 Si:N, laser-annealed, Jahn-Teller distorted donor, EPR meas. 0-84642  
 Si-SiO<sub>2</sub>, ion implantation through SiO<sub>2</sub> film, recoil implantation of O, EPR study 0-88180  
 SiO<sub>2</sub> film, on GaP substrate, N ion implantation, optical refl. and EPR meas. 0-84197  
 SnO<sub>2</sub>, O chemisorption, elec. cond. and EPR meas. correlation 0-84369  
 YPO<sub>4</sub>:Pb<sup>2+</sup>, EPR, hyperfine interactions 0-108050  
 ZnO powder, effect of dry grinding in EPR and catalytic activity (*Japanese*) 0-84640

## paramagnetic resonance of iron group ions and impurities

- aluminium copper tetrahalides, exchange, mag. anisotropy, and spin diffusion contribs. to EPR linewidth 0-80597  
 aluminoborate glass, Fe and Cr ion interaction, mag. and spectral props. 0-103883  
 ammonium oxalate monohydrate:Mn<sup>2+</sup>, model for defect formation, EPR 0-103880  
 boracite, single cryst. prep. and phys. props. 0-100763  
 borate glass, ESR study of effect of glass composition on symmetry of Cr complexes 0-88052  
 borosilicate glass, Fe and Cr ion interaction, mag. and spectral props. 0-103883  
 copper phthalocyanine-iodine, amorphous cpd. prep. by I<sub>2</sub> diffusion in polycryst., triplet EPR signals obs. (*Russian*) 0-66016  
 corundum, defect cryst. struct. study 0-103316  
 diethylammonium manganese chloride, Heisenberg magnet, spin diffusion, EPR study 0-66019  
 dimethylammonium copper manganese chloride, two-dimens. mixed magnet, EPR 0-66030  
 dimethylammonium manganese tetrachloride, antiferromag. and spin-flop resonance obs., 70 to 100 GHz 0-71190  
 glass formation by meteorite impact, EPR study 0-85659  
 guanidine aluminium sulphate hexahydrate:Cr<sup>3+</sup>, ESR spectra fine struct. 0-93169  
 human serum Cu, EPR spectrum obs. 0-91582  
 (iron, chromium) carboxylates, heteronuclear trimer exchange clusters, ESR spectra 0-80603  
 lead acetate trihydrate:Mn<sup>2+</sup>, ESR, elec. cond. 0-93165  
 magnesium hexahydrate H<sub>2</sub>EDTA:VO<sup>2+</sup>, single cryst., ESR spectra and spin Hamiltonian parameters 0-75845  
 manganese stearate, two-dimensional mag. struct. 0-108040  
 methylammonium aluminium sulphate dodecahydrate, single crystals, high-order EPR transitions of Cr<sup>3+</sup> 0-108052  
 nitroxide free radical spin label EPR spectra, determ. of rot. correl. time and HFS coupling 0-74260  
 p-n-octyloxy benzyldiene-p-toluidine, mol. order, EPR VAAC probe 0-70114  
 oxide glasses,  $\gamma$ -irrad., CuO effects on EPR 0-84645  
 phosphate glasses, ESR of VO<sup>2+</sup> ions 0-100610  
 polyvinyl alcohol film containing Cu<sup>2+</sup> complexes, photoconductivity 0-107849  
 $\alpha$ -quartz:<sup>57</sup>Fe, anomalous hyperfine splitting 0-103650  
 ruby:Cr, relaxation behaviour, EPR study, environmental effects 0-66021  
 ruby, distant nuclei ESR and ENDOR experiments, dipole-dipole reservoir importance 0-71241  
 ruby, elec. field induced double quantum transitions 0-80595  
 scheelites, zero-field splitting of Mn<sup>2+</sup> ions 0-75531  
 sodium oxalate:Cu<sup>2+</sup>, anhydrous spin Hamiltonian and bonding parameters and orbital-reduction factors 0-60408  
 TMMC, crossover transition, effects on susceptibility and EPR shift 0-71047  
 TMMC, low-symmetry spin distrib. effect on EPR line 0-66018  
 triglycine calcium bromide:Cu<sup>2+</sup>, ESR studies 0-97136  
 trimethylammonium manganese trichloride, Heisenberg antiferromag. chain, specific heat and EPR 0-65931  
 tris-sarcosine calcium chloride:Mn<sup>2+</sup> ferroelec. dynamics, EPR and ENDOR study 0-75972  
 3d<sup>5</sup>-ions, variation of hyperfine splitting consts. with interatomic distance 0-97133  
 Ag halide, photochromic glasses, optical properties, effect of Cu ions 0-93364  
 AgGaS<sub>2</sub>:Fe, EPR of Fe-associated defect 0-60412  
 Al<sub>2</sub>O<sub>3</sub>:Cr, electron irradi. induced cond., TSC and EPR study 0-80277  
 Al<sub>2</sub>O<sub>3</sub>:Cr<sup>3+</sup>, inhomogeneous spin system, time evolution towards saturated state 0-88869  
 Al<sub>2</sub>O<sub>3</sub>-SiO<sub>2</sub>-MO-Fe<sub>2</sub>O<sub>3</sub> glass, M=Ca, Mg, Ba, Sr, UV and EPR absorpt. spectra 0-89018  
 AlPO<sub>4</sub>, synthetic berlinite, electron irradi. effects, ESR, ENDOR, optical spectral study 0-80608  
 (As<sub>0.4</sub>S<sub>0.6</sub>)<sub>100-2</sub>:Cu<sub>2</sub>, glassy, struct. and elec. cond. study 0-59399  
 BaMgF<sub>4</sub>:Mn<sup>2+</sup> ferroelec., EPR and ENDOR study, cryst. field tensor 0-71162  
 BaO-B<sub>2</sub>O<sub>3</sub>-V<sub>2</sub>O<sub>5</sub> glass, oxidation-reduction of V, thermodynamics 0-85169  
 BaO-V<sub>2</sub>O<sub>5</sub>-CuO semiconducting glasses, impurity effects, elec. resist. and EPR study 0-103692  
 BaTiO<sub>3</sub>:Fe<sup>3+</sup>, local position determ. by EPR 0-108057  
 BaV<sub>2</sub>O<sub>7</sub>:Cr, EPR spectra temp. depend., paramagnetic ion point symm. 0-71166  
 CaF<sub>2</sub>:Ni crystals, X-irradiated, EPR study of Ni<sup>2+</sup> and Ni<sup>3+</sup> 0-75849  
 CaF<sub>2</sub>:Mn, EPR and optical absorpt. spectra 0-93171  
 CaF<sub>2</sub>:Ni, X-irradiated, optical and EPR meas. 0-108235

## paramagnetic resonance of iron group ions and impurities continued

- Ca<sub>3</sub>Fe<sub>2</sub>Ge<sub>2</sub>O<sub>12</sub>, garnet, light absorpt. spectral study 0-93322  
 Ca<sub>3</sub>(PO<sub>4</sub>)<sub>2</sub>:Cu<sup>2+</sup>, ESR, high press. struct. transition 0-97134  
 CaV<sub>2</sub>O<sub>7</sub>:Cr, EPR spectra temp. depend., paramagnetic ion point symm. 0-71166  
 Cd complexes, dithiocyanato(diethylenetriamine) Cd(II) and dithiocyanato(pentamethyldiethylenetriamine) Cd(II), Cu<sup>2+</sup> doped, ESR 0-108059  
 Cd(ClO<sub>4</sub>)<sub>2</sub>.6H<sub>2</sub>O and Cd(ClO<sub>4</sub>)<sub>2</sub>.6D<sub>2</sub>O, single crystals, EPR study of phase transitions 0-66025  
 CdCr<sub>2</sub>Se<sub>4</sub>, Crit. relax. processes, mag. reson. expts. 0-60425  
 CdCr<sub>2</sub>Se<sub>4</sub>:Cu(Ag), ferromag. reson. and ESR line widths 0-60413  
 CdS:Mn, vacuum deposited film, Mn migration, EPR and X-ray study 0-65411  
 Co complex, Co(II)(1,2,4-triazole)<sub>2</sub>(NCS)<sub>2</sub> quasi two-dimens. canted S=1/2 antiferromag. 0-70976  
 Co complexes, Co II tetraphenylporphyrins, constraint, ESR and optical detect. 0-83394  
 Co II complexes, with tetradentate Schiff bases, synthesis, struct. and ESR obs. 0-80598  
 CoO-ZnO-MgO ternary systems, solid solns., struct. charact. 0-60629  
 CoS<sub>2</sub>, itinerant ferromagnet, ferromag. reson. and EPR meas. 0-66044  
 Co<sub>2</sub>Zn<sub>1-x</sub>Rh<sub>x</sub>O<sub>4</sub>, mag. props., EPR spectra, antiferromag. order 0-75736  
 CrN, antiferromagnetic EPR spectra, binding energy, isotropic exchange and ordering (*German*) 0-80604  
 CsCaCl<sub>3</sub>:Co(Mn), EPR, 4.2 to 450K, ferroelec. transition 0-60414  
 CsCdBr<sub>3</sub>:Cr<sup>3+</sup>(Cr<sup>2+</sup>), EPR of impurities, charge compensation, X-ray effects 0-60407  
 CsMgCl<sub>3</sub>(Br<sub>2</sub>):Cr<sup>3+</sup>(Cr<sup>2+</sup>), EPR of impurities, charge compensation, X-ray effects 0-60407  
 Cu complex, copper (II) [2,5-diphenyloxazole]<sub>2</sub> (ClO<sub>4</sub>)<sub>2</sub>.4H<sub>2</sub>O, ESR studies 0-88867  
 Cu complex, polyvinylimidazole.Cu(II) complex, ESR studies on dimer form. between copper ions 0-100613  
 Cu<sup>2+</sup> ion, ground state wavefunctions and ESR parameters 0-88868  
 Cu-Mn, exchange-coupled localised moments, Korringa relaxation rate 0-75851  
 Cu-Mn, zero field ESR in spin glass state 0-66017  
 Cu-Mn spin glass, spin freezing and exchange narrowing of mag. reson. 0-60411  
 CuCl, pressure depend. of structural, chemical, elec. and mag. props. 0-96596  
 CuCr<sub>2</sub>Se<sub>4</sub>, Crit. relax. processes, mag. reson. expts. 0-60425  
 CuCr<sub>2</sub>Se<sub>4</sub>, mag. reson. and valence state of Cu and Cr ions 0-60413  
 Cu(II) complex, 2,2',2''-triiminotriethylamine, EPR and optical absorpt. obs. 0-108055  
 Cu(II) complex, hexamethyltriaminotriethylamine, EPR and optical absorpt. obs. 0-108055  
 Cu(II)-DL-proline complex, ESR, magnetic susceptibility and optical absorption 0-93167  
 Fe<sup>3+</sup>, zero-field splittings, correl. with axial site distortions, superposition model 0-93168  
 Fe<sub>0.8</sub>Cu<sub>0.2</sub>Cr<sub>2</sub>S<sub>4</sub>, ESR spectra, elec. and mag. props., Curie temp. 0-97137  
 Fe<sub>3</sub>Ni<sub>3</sub>Cr<sub>14</sub>P<sub>12</sub>B<sub>6</sub>, Metglas 2826A, EPR at 20 GHz 0-75848  
 Fe<sub>2</sub>O<sub>3</sub>, ultrafine particles in PTFE matrix, EPR and Mossbauer study 0-100625  
 $\theta$ -Fe<sub>2</sub>V<sub>2</sub>O<sub>7</sub>, spin glass and paramag. props., susceptibility, EPR and Mossbauer studies 0-75782  
 GaAs:<sup>57</sup>Fe(<sup>57</sup>Fe), paramag. centres, identification from ESR and ENDOR spectra 0-80600  
 GaAs:Cr, Cr<sup>2+</sup> and Cr<sup>3+</sup> centres, thermal treatment effects, EPR 0-65492  
 GaAs:Cr, hole traps, ESR studies 0-75843  
 GaAs:Cr, photoionisation transition Cr<sup>3+</sup>-Cr<sup>2+</sup>, EPR studies 0-60638  
 GaBO<sub>3</sub>:Fe<sup>3+</sup>, ESR spectra, lattice parameters 0-93170  
 GaP:<sup>57</sup>Fe(<sup>57</sup>Fe), paramag. centres, identification from ESR and ENDOR spectra 0-80600  
 p-GaP:Cr, hole traps, ESR studies 0-75843  
 GaP:Fe<sup>3+</sup>, ESR spectrum, elec. field, uniaxial compression influence 0-103882  
 GaP:Ni(Fe), multivalence impurities, EPR and optical absorpt. meas. 0-75844  
 GdNi<sub>x</sub> (x=3, 3.5, 8.5), ferrimag., mag. reson. above and below Curie temp. 0-97148  
 Ge-P-S glass system, EPR of intrinsic and Mn<sup>2+</sup> impurity centres 0-88870  
 Ge<sub>2</sub>S<sub>7</sub>:Mn, bond struct. and character in Ge-S system, EPR obs. 0-66014  
 Ge<sub>20</sub>S<sub>60</sub>:Mn (Ag)(Cu), bond struct. and character in Ge-S system, EPR obs. 0-66014  
 HgCr<sub>2-x</sub>Al<sub>x</sub>Se<sub>4</sub> and HgCr<sub>2-x</sub>Ga<sub>x</sub>Se<sub>4</sub>, temp. depend. of ESR linewidth, 105-300K 0-71161  
 HgSe:Mn<sup>2+</sup>, temp. depend. of EPR of <sup>6</sup>S state ions 0-80593  
 InBO<sub>3</sub>:Fe<sup>3+</sup>, ESR spectra, lattice parameters 0-93170  
 KCr alum, relaxation behaviour, EPR study, environmental effects 0-66021  
 KCrAl<sub>1-x</sub>(SO<sub>4</sub>)<sub>2</sub>.12H<sub>2</sub>O, EPR of single crystals, zero-field splitting of Cr<sup>3+</sup> 0-66015  
 KMgF<sub>3</sub>, spin Hamiltonian parameters for Fe<sup>3+</sup> ions, superposition model anal. 0-108053  
 KMgF<sub>3</sub>:Fe<sup>2+</sup>, anomalous acoustic relax. absorpt. and APR 0-88864  
 K<sub>2</sub>Mn<sub>2</sub>F<sub>7</sub>, crit. EPR line broadening near Neel temp. 0-71165  
 K<sub>2</sub>O-MgO-B<sub>2</sub>O<sub>3</sub>:Cu<sup>2+</sup>, micro-inhomogeneities, EPR and Raman study 0-84800  
 K<sub>6</sub>(V<sub>2</sub>Mo<sub>10</sub>)VO<sub>40</sub>.13H<sub>2</sub>O, X-ray cryst. struct., electron spin resonance spectrum 0-88096  
 KVO<sub>3</sub>:Cr<sup>3+</sup>, study of ESR spectra 0-80601  
 KZnF<sub>3</sub>, spin Hamiltonian parameters for Fe<sup>3+</sup> ions, superposition model anal. 0-108053  
 (La<sub>2</sub>O<sub>3</sub>)<sub>1-x</sub>(CeO<sub>2</sub>)<sub>x</sub>:Mn, valence state of Mn, effect of annealing in H<sub>2</sub> atm., ESR obs. (*French*) 0-71164  
 (La<sub>2</sub>O<sub>3</sub>)<sub>0.95</sub>(CeO<sub>2</sub>)<sub>0.05</sub>:Mn<sup>2+</sup>, X-band EPR study 0-60409  
 Li aluminosilicate glasses, containing Cu and halogen impurities, ESR spectra 0-66027  
 LiAlSiO<sub>4</sub>:Cu,  $\beta$ -cryptite solid electrolyte, Cu<sup>2+</sup> EPR obs. of ion exchange props. 0-108056  
 LiF:Mg,Ti, defect states, ESR and ionic cond. study 0-108058  
 Li<sub>2</sub>O-TiO<sub>2</sub>-Al<sub>2</sub>O<sub>3</sub>-SiO<sub>2</sub> glass,  $\gamma$ -irrad., struct. position of Ti, EPR study 0-84644  
 LiVO<sub>3</sub>:Cr<sup>3+</sup>, study of ESR spectra 0-80601  
 LuBO<sub>3</sub>:Fe<sup>3+</sup>, ESR spectra, lattice parameters 0-93170



**paramagnetic resonance of iron group ions and impurities continued**

- Mg(NH<sub>4</sub>)<sub>2</sub>(SeO<sub>4</sub>)<sub>2</sub>·6H<sub>2</sub>O:Mn<sup>2+</sup>, EPR spectra 0-100608  
 MgO:Co<sup>2+</sup>, ESR linewidths of Co<sup>2+</sup> 0-80596  
 MgO:Cr, high resolution far IR spectroscopy of lower energy levels of Cr<sup>3+</sup> 0-80822  
 MgO:Cr<sup>2+</sup>, APR under applied stress 0-88865  
 MgO:Cr<sup>3+</sup>, EPR spectra obtained at room temp. and 1200°C 0-68233  
 MgO:Fe<sup>3+</sup>, EPR spectra obtained at room temp. and 1200°C 0-68233  
 MgO:Fe<sup>3+</sup> single crystal, exchange energy 0-96834  
 MgO-TiO<sub>2</sub>-Al<sub>2</sub>O<sub>3</sub>-SiO<sub>2</sub> glass, γ-irrad., struct. position of Ti, EPR study 0-84644  
 MgRb<sub>2</sub>(SeO<sub>4</sub>)<sub>2</sub>·6H<sub>2</sub>O:Mn<sup>2+</sup>, EPR spectra 0-100608  
 Mn<sup>2+</sup>, zero-field splittings, correl. with axial site distortions, superposition model 0-93168  
 Mn<sub>2</sub>Al<sub>2</sub>Si<sub>2</sub>O<sub>12</sub>, amorphous, spin-glass, insulating, Mn<sup>2+</sup> mag. reson. 0-65918  
 xMnO<sub>2</sub>(100-x)[19TeO<sub>2</sub>.PbO] glasses, EPR studies of Mn<sup>2+</sup> ion distribution 0-71167  
 Nd<sub>2</sub>Br<sub>2</sub>:Cu<sup>2+</sup>, pseudo-Jahn-Teller effect manifestation in ESR spectrum 0-71168  
 NH<sub>4</sub>Cl:Ni<sup>2+</sup>, EPR spectrum, spin Hamiltonian, zero-field splitting effects 0-97135  
 NaCl:Mn<sup>2+</sup>, Mg<sup>2+</sup>, doubly doped, ionic thermocurrent study of linear dimer 0-79977  
 Na<sub>2</sub>O·3SiO<sub>2</sub>:Fe<sup>3+</sup>, Fe<sup>3+</sup> glasses, Mossbauer and ESR spectra and internal friction 0-100865  
 Na<sub>2</sub>O·B<sub>2</sub>O<sub>3</sub>:Cu<sup>2+</sup>, Mn<sup>2+</sup> glasses, Cu<sup>2+</sup>-Mn<sup>2+</sup> interaction studied by ESR 0-93166  
 Na<sub>2</sub>O·MgO·B<sub>2</sub>O<sub>3</sub>:Cu<sup>2+</sup>, micro-inhomogeneities, EPR and Raman study 0-84080  
 Na<sub>2</sub>O·SiO<sub>2</sub>:CuO glass, gamma-irradiated, EPR and optical spectra 0-103885  
 Na<sub>2</sub>O·TiO<sub>2</sub>-Al<sub>2</sub>O<sub>3</sub>-SiO<sub>2</sub> glass, γ-irrad., struct. position of Ti, EPR study 0-84644  
 5Na<sub>2</sub>O·Fe<sub>2</sub>O<sub>3</sub>·8SiO<sub>2</sub>, glass crystallisation study by Fe<sup>3+</sup> EPR and Mossbauer spectra 0-64904  
 Na<sub>2</sub>O·11Al<sub>2</sub>O<sub>3</sub>, Cr, impurity ion struct., ESR study 0-80605  
 NaVO<sub>3</sub>:Cr<sup>3+</sup>, study of ESR spectra 0-80601  
 Ni complexes hexamethylamine nickel halides, Ni<sup>2+</sup> EPR in high pulsed mag. field, zero field splitting parameters 0-71160  
 NiPiCl<sub>6</sub>·6H<sub>2</sub>O, singlet-ground-state magnets, ESR at low temps. 0-97132  
 NiSiF<sub>6</sub>, dilute, single-spin cross-relax. calcs. 0-97129  
 NiSiF<sub>6</sub>·6H<sub>2</sub>O, non-Kramers system, spin-lattice relaxation at strong fields 0-100612  
 NiSnCl<sub>6</sub>·6H<sub>2</sub>O, singlet-ground-state magnets, ESR at low temps. 0-97132  
 PbF<sub>2</sub>:Fe<sup>3+</sup>, F<sup>-</sup> motion, ESR study 0-66023  
 PbO-SiO<sub>2</sub> glasses, high temp. ESR of Fe(III) 0-60410  
 Pd<sub>1-x</sub>Mn<sub>x</sub>H<sub>2</sub> alloy, spin glass, transition temp., susceptibility and EPR meas. 0-65930  
 RbH<sub>2</sub>(SeO<sub>4</sub>)<sub>2</sub>:VO<sup>2+</sup>, EPR spectra, spin Hamiltonian parameters 0-100609  
 RbVO<sub>3</sub>:Cr<sup>3+</sup>, study of ESR spectra 0-80601  
 ScBO<sub>3</sub>:Fe<sup>3+</sup>, ESR spectra, lattice parameters 0-93170  
 Si:Cr<sup>3+</sup>(Mn<sup>2+</sup>), spin-lattice relax. of Jahn-Teller centres, coexistence of minima with different symmetries 0-80602  
 Si:Fe, solubility study by EPR and neutron activation anal. 0-75361  
 SrO:Co, noncentral and interstitial ion complexes, ESR obs. 0-71169  
 SrO:Ni<sup>2+</sup>, EPR line splitting rel. to Jahn-Teller coupling and soft localised mode 0-66022  
 SrTiO<sub>3</sub>:Fe<sup>3+</sup>, order-disorder and central peak behaviour, EPR study 0-75970  
 TiO<sub>2</sub>, Mn<sup>3+</sup> ion electron spin-lattice relaxation 0-108054  
 VO<sup>2+</sup> ion impurities, in hydrated crystals, EPR obs. 0-97130  
 V<sub>2</sub>O<sub>5</sub> and lower oxides, defect structures and related props. 0-59454  
 V<sub>2</sub>O<sub>5</sub> and lower oxides, electronic, optical, structural and surface props., review 0-88120  
 V<sub>2</sub>O<sub>5</sub>, reduction in butyllithium, ESR study 0-100611  
 V<sub>2</sub>O<sub>5</sub>:CuO-BaO glass, unpaired electron localisation, ESR study 0-66026  
 α-W<sub>2</sub>V<sub>2</sub>O<sub>8</sub>, paramag. defect study by ESR 0-103881  
 zinc formatedihydrate:Co, spin lattice relax. of Co<sup>2+</sup> ions 0-75847  
 Zn(BF<sub>4</sub>)<sub>2</sub>·6H<sub>2</sub>O:Ni, phase transition study, EPR of diluted Ni<sup>2+</sup>, 98-298K 0-75846  
 ZnGa<sub>2</sub>O<sub>4</sub>:Cr<sup>3+</sup>, weak exchange interaction determ., ESR study 0-93107  
 Zn(NH<sub>4</sub>)<sub>2</sub>(SeO<sub>4</sub>)<sub>2</sub>·6H<sub>2</sub>O:Mn<sup>2+</sup>, EPR spectra 0-100608  
 ZnRb<sub>2</sub>(SeO<sub>4</sub>)<sub>2</sub>·6H<sub>2</sub>O:Mn<sup>2+</sup>, EPR spectra 0-100608  
 ZnSe:Ti<sup>2+</sup>, EPR meas. 0-80594  
 (ZrO<sub>2</sub>)<sub>0.9</sub>(Y<sub>2</sub>O<sub>3</sub>)<sub>0.1</sub>:Cr, Mn, stabilised single crystal, EPR of Mn<sup>2+</sup> and Cr<sup>3+</sup> obs. 0-66024

**paramagnetic resonance of palladium and platinum group ions and impurities**

- AgCl:Pd<sup>2+</sup>, ESR spectrum, quasistatic Jahn-Teller effect 0-71170  
 BaO-P<sub>2</sub>O<sub>5</sub>:Mo<sup>3+</sup> glass, EPR spectra, computer simulation 0-88872  
 Ba(PO<sub>3</sub>)<sub>2</sub>-WO<sub>3</sub>, electron-absorpt. spectra and structure of W centres 0-88873  
 Ge<sub>40</sub>Si<sub>60</sub>:Mn (Ag)(Cu), bond struct. and character in Ge-S system, EPR obs. 0-66014  
 H<sub>2</sub>MoO<sub>3</sub>, electronic props., mag. susceptibility and spectra 0-80266  
 MoS<sub>2</sub>, prep. and mag. props. (French) 0-93072  
 Nb complexes, <sup>93</sup>Nb quadrupole coupling tensors form EPR meas. 0-88866  
 Si:Au, EPR spectrum, strong nuclear quadrupole effect 0-93172  
 SiO<sub>2</sub>:Ag, cryst. and glassy, X-ray induced EPR and luminesc. centre 0-65043  
 TiO<sub>2</sub>:Mo<sup>3+</sup>, interstitial EPR, g-tensor and hyperfine tensor 0-84647  
 TiO<sub>2</sub>:Ru<sup>4+</sup>, rutile, EPR and cryst. field const. 0-60415

**paramagnetic resonance of rare earth ions and impurities**

- exchange induced broadening in low lying crystalline field system 0-108062  
 praseodymium ethylsulphate:Sm, one-dimens. X-Y system, spin dynamics, electron spin echo meas. 0-66031  
 rare earth mag. conc. cubic Laves phase cpds., ESR 0-71174  
 rare earth pseudobinary intermetallic compounds, ESR studies 0-108064  
 Au-Er, dil., EPR at 100 mK to 1K 0-66028  
 Au-Yb, dil., EPR at 100 mK to 1K 0-66028  
 Au-Yb thin films, ESR spectra, strain effects 0-71172  
 BaF<sub>2</sub>:Gd<sup>3+</sup>, spin-lattice coeffs., EPR study 0-66032  
 CaF<sub>2</sub>:rare earth ion, elec. dipole-dipole interaction, ionic thermocurrent and EPR study 0-108060  
 CaF<sub>2</sub>:Tm<sup>2+</sup>, ultra-low nuclear spin temp., low field behaviour, EPR study 0-100614

**paramagnetic resonance of rare earth ions and impurities continued**

- CdF<sub>2</sub>:Eu<sup>2+</sup>, EPR spectra, hydrostatic press. and temp. effects 0-84648  
 Ce<sub>2</sub>(SO<sub>4</sub>)<sub>3</sub>·8H<sub>2</sub>O:Gd<sup>3+</sup>, single cryst., EPR study, spin Hamiltonians 0-80606  
 Ce<sub>2</sub>, Sm, Pd<sub>2</sub>, intermediate valence of Ce, susceptibility, lattice const., ESR meas. 0-103648  
 Er, La<sub>1-x</sub>Be<sub>3</sub>, mag. sp. ht. and ESR, cryst. field interactions 0-60290  
 EuAl<sub>2</sub>S<sub>4</sub>, mag. susceptibility and EPR meas. 0-71173  
 EuGa<sub>2</sub>S<sub>4</sub>(Se<sub>4</sub>), mag. susceptibility and EPR meas. 0-71173  
 Eu, La<sub>1-x</sub>Al<sub>2</sub>, cryst. fields and exchange parameters, ESR meas. 0-71175  
 Eu, La<sub>1-x</sub>Al<sub>2</sub>, dil. EPR, cryst. fields and effective exchange interaction 0-66029  
 Eu<sub>1-x</sub>Sm<sub>x</sub>S, ESR, exchange interaction, susceptibility, elec. cond., thermoelectric power 0-93174  
 Gd magnetically conc. cubic Laves phase cpds., ESR 0-71174  
 Gd<sup>3+</sup> impurity ions, EPR spectra, linewidth narrowing due to spin-lattice relax. of lanthanide Kramers host ions 0-108061  
 Gd, La<sub>1-x</sub>Al<sub>2</sub>, cryst. fields and exchange parameters, ESR meas. 0-71175  
 GdNi<sub>x</sub>, (x=3, 3.5, 8.5), ferrimag., mag. reson. above and below Curie temp. 0-97148  
 Gd<sub>2</sub>Ni<sub>17-x</sub>Al<sub>x</sub>, EPR of Gd<sup>3+</sup> ions 0-97139  
 La-Gd, exchange-coupled localised moments, Korringa relaxation rate 0-75851  
 LaBe<sub>3</sub>:Er, ESR, appl. of exchange induced broadening in low lying crystalline field system 0-108062  
 LaCl<sub>3</sub>:Pr<sup>3+</sup>, coherent transients by optical phase switching 0-95962  
 LaM<sub>2</sub>-Gd, M=transition metal, correl. between g-shift and stability, EPR study 0-88874  
 La<sub>2</sub>MoO<sub>6</sub>, paramag. resonance and struct. 0-84162  
 La<sub>2</sub>(SO<sub>4</sub>)<sub>3</sub>·9H<sub>2</sub>O:Gd<sup>3+</sup>, single cryst., EPR study, spin Hamiltonians 0-80606  
 LiTmF<sub>4</sub>:rare earth, EPR spectra, elec. field effects, cryst. field interactions 0-71176  
 LiYF<sub>4</sub>, ESR spectra of non Kramers ions, elec. field influence 0-103884  
 LiYF<sub>4</sub>:rare earth, EPR spectra, elec. field effects, cryst. field interactions 0-71176  
 LuPO<sub>4</sub>:Gd<sup>3+</sup>, zircon struct. EPR investig., rel. to radiation resistance 0-97138  
 NaCl:Eu, secondary Eu phase dissolution, EPR and optical absorpt. study 0-96655  
 Pb<sub>2</sub>Ge<sub>2</sub>O<sub>11</sub>:Gd<sup>3+</sup>, displacive phase transition, S ion spin Hamiltonian parameter dependence on order parameter 0-70356  
 Pb<sub>2</sub>Ge<sub>2</sub>O<sub>11</sub>:Gd<sup>3+</sup>, ferroelec. transition, temp. depend., EPR study 0-66127  
 PrIn<sub>3</sub>Gd, indirect nuclear exchange interactions, ESR-linewidth meas., sp. ht. determ. 0-103825  
 PrNi<sub>2</sub>-Gd, dil., single crystal, ESR study 0-75850  
 RbCaF<sub>3</sub>:Gd, shift of first order transition under hydrostatic press. EPR of Gd<sup>3+</sup> meas. 0-59649  
 RbCaF<sub>3</sub>:Gd<sup>3+</sup>, struct. phase transition, EPR study 0-71171  
 RbCdF<sub>3</sub>:Gd<sup>3+</sup>, struct. phase transition, EPR study 0-71171  
 SeCl<sub>2</sub>:Er, proton distrib. and site energies, ESR meas. 0-59509  
 SePO<sub>4</sub>:Gd<sup>3+</sup>, zircon struct. EPR investig., rel. to radiation resistance 0-97138  
 SrCl<sub>2</sub>·6H<sub>2</sub>O:Gd<sup>3+</sup>, evaporation technique prep. of SrCl<sub>2</sub>:Gd<sup>3+</sup>, H<sub>2</sub>O content, EPR powder spectrum obs. 0-60416  
 SrF<sub>2</sub>:rare earth ion, elec. dipole-dipole interaction, ionic thermocurrent and EPR study 0-108060  
 YH<sub>2</sub>:Er, proton distrib. and site energies, ESR meas. 0-59509  
 YM<sub>2</sub>-Gd, M=transition metal, correl. between g-shift and stability, EPR study 0-88874  
 YPO<sub>4</sub>:Gd<sup>3+</sup>, zircon struct. EPR investig., rel. to radiation resistance 0-97138  
 Y<sub>2</sub>SiO<sub>5</sub>:Ce<sup>3+</sup>(Nd<sup>3+</sup>)(Er<sup>3+</sup>)(Yb<sup>3+</sup>), EPR and spin-lattice relax. 0-108063  
 YbCl<sub>3</sub>·6H<sub>2</sub>O:Gd<sup>3+</sup>, EPR, temp. depend., spin-lattice relax. time 0-93173

**paramagnetism**

- see also paramagnetic properties of substances  
 anisotropic paramagnet, spin dynamics, exchange-bond dilution effects 0-88763  
 crystal, magnetisation change by light pulse 0-70932  
 dielectric crystal, APR and phonon spectroscopy to study paramagnetic ions 0-84634  
 diluted Ising and Heisenberg systems with competing interactions, mag. ordering, appl. to Eu, Sr<sub>1-x</sub>S 0-65914  
 insulator-to-metal transition for half-filled Hubbard band in paramagnetic state 0-92817  
 Ising model, constant-coupling approx., successive phase transitions 0-97108  
 Ising model with competing interactions, critical properties and exact results 0-93129  
 Ising spin glass, d-dimensional, frustration effect and dilution problems 0-108018  
 liquid, depolarized light scatt. in mag. field 0-80759  
 low-dimensional paramagnets, EPR spectra 0-71154  
 metals, electronic struct. and magnetism, review 0-70573  
 mixed-spin paramagnet, dynamics 0-60173  
 NMR linewidth, paramagnetic contrbs. calcs. 0-58286  
 polarisation and magnetisation of electronic matter 0-75929  
 random binary Ising system with transverse field, Curie temp., paramagnetic susceptibility 0-65938  
 singlet-triplet system in paramag. phase, low-freq. response 0-60172  
 sphere, strongly magnetised, interaction with weakly magnetised particles carried by fluid flow 0-69320  
 spin glasses, dilute, at zero temperature, low concentration series expansion 0-93131  
 spin system, paramagnetic, two-level open system, kinetic theory of resonance and relaxation 0-88859  
 Van Vleck compounds, LF dynamics, NMR linewidth, RKKY exchange mechanism role 0-103812  
 Cu complex, Cu(H<sub>2</sub>O)<sub>6</sub><sup>2+</sup>, ligand hyperfine interactions, orbital angular momentum contrib. 0-96833

**parameter estimation**

- biological membrane, electrically excited, nonlinear dynamic models for simulation 0-94178  
 coupled-core nuclear reactor, distributed parameters identification, pseudorandom perturbation and correlation anal. 0-86966  
 flood event real-time predictors, stochastic model 0-67383  
 forward-looking IR sensor image segmentation by maximum likelihood parameter estimation 0-99662



**parameter estimation continued**

- linear predictive coded speech digitizers, background noise spectral subtraction 0-96140
- maximum entropy spectral estimation of frequency and arrival angle 0-96129
- Monte Carlo computations, multi-parameter, adaptive estimation procedures 0-105572
- nonstatistical parameter estimation adaptive algorithms 0-91995
- ocean-bottom subsurface layered media, spatial parameter estimation 0-77134
- one dimensional distributed parameter system parameter and state estimation, heat conduction experimental result (*Japanese*) 0-83727
- pollution modelling, numerical estimation of unknown parameters (*Japanese*) 0-89702
- respiratory mechanical behaviour lumped parameter models evaluation using simplex algorithm 0-89783
- time series, conference, Nottingham, England (Mar. 1977) 0-82580

**parameter identification** *see* **parameter estimation****parametric amplifiers**

- see also* **acoustic parametric amplifiers**; **microwave parametric amplifiers**; **optical parametric amplifiers**
- energy relations for bandlimited signals in gyromagnetic media (*German*) 0-91725

**parametric varactor diodes** *see* **varactors****Pariser-Parr-Pople calculations** *see* **PPP calculations****parity**

- see also* **baryon spin and parity**; **lepton spin and parity**; **meson spin and parity**; **nuclear spin and parity**; **P invariance**
- gyroscope weight reduction in left turning due to spontaneous symmetry breaking (*Japanese*) 0-98798
- orbital angular momentum and parity 0-77564
- He, ( $2p^3$ )P state, electron impact excitation, parity unfavoured transition 0-91680

**parsers** *see* **grammars****partial differential equations**

- see also* **boundary value problems**; **wave equations**
- active parts electrodynamic equations general solutions using orthotropic modelling (*Russian*) 0-99601
- anisotropic media, natural oscils., partial differential eqn. system 0-57091
- atmospheric transport problems, contaminant movement, Galerkin finite element method 0-74902
- Backlund transformations in several variables, differential geometric anal. 0-86073
- Boussinesq equation, group theoretical approach 0-82914
- conference, Bethlehem, PA, USA (June 1979) 0-86039
- curved domains, geodesic finite-difference method, simulation of tidal motion on sphere 0-109153
- deflagration waves, heterogeneous, flame model for gas phase, partial differential eqn. 0-85177
- diffusion, two-way, separation of variables, decaying and growing eigenfunctions 0-62594
- diffusion equation, nonlinear, invariance props., Lie-Backlund groups 0-62596
- diffusion in media with double diffusivity, discrete random walk model 0-92702
- drift diffusion unipolar conduction between parallel plate electrodes, closed form steady state solutions 0-91720
- electric machine end zone magnetic field calc. using approx. analytic method 0-106416
- electrodynamics, nonlinear, energy density convexity and hyperbolicity of partial differential eqns. (*French*) 0-62491
- elliptic equations and systems, free-boundary problem solution method 0-69941
- evolution equations, connection to P-type differential eqns. 0-57078
- filtration theory problem soln. (*Russian*) 0-74970
- fluid discontinuities, subgrid resolution in tracking methods 0-105506
- Heisenberg spin chain, operator equation, nonlinear differential form, auxiliary constraint 0-65762
- hydrodynamic calculations for container pipeline systems with non-Newtonian liquids 0-106817
- hyperbolic systems, high-order methods, dynamic problems 0-68033
- integrable evolution eqn. struct. 0-105492
- inverse scattering method, commutator representation of Painleve type ordinary differential eqns. 0-68052
- KdV equation, perturbative expansion and initial value problem 0-62487
- liquefied natural gas, nonsteady-state flow calculations in horizontal pipeline systems 0-106838
- Maxwell equation integration in laminar media 0-68059
- Miura transformation of Kaup and Mikhailov eqns. 0-57103
- neutron dynamical diffraction, gravitational and mag. field effects 0-59345
- nonlinear, special multi-soliton solns. 0-105763
- nonlinear diffusion equation, stable profile evolution 0-82731
- numerical methods for flows through porous media. II 0-69914
- optical processor, confocal feedback system for partial differential eqn. analogue soln. 0-102630
- plasma decay under constant voltage (*Russian*) 0-106988
- Poisson, MOST structure modelling, using hybrid computer (*Slovak*) 0-75643
- prolongation structure for a nonlinear equation with explicit space dependence 0-82664
- relativistic string moving in uniform static external field, 2-D space-time surface 0-57087
- scattering theory, propagation of singularities for the transmission problem and application to the inverse problem of scattering (*French*) 0-94994
- shells of revolution, computer program for linear and geometrically nonlinear static analysis, ISTRAN/SR (*Japanese*) 0-64500
- sine-Gordon equation, intrinsic geometry 0-86553
- sine-Gordon equation, separability, variable transforms 0-57102
- smoke-motion, numerical anal. by finite-elements method (*Japanese*) 0-69910
- steady-state laminar flow in turbulence amplifier, numerical integration (*Bulgarian*) 0-106779
- stimulated electron radiation due to wiggled magnetic field 0-58451
- SU(2) gauge field theory, nonlinear scalar field eqn., spherical symmetric exact solns. (*Chinese*) 0-62886
- time dependent heat conduction solution 0-106707
- transformation group techniques appl. to nonlinear fluid and plasma eqns. (*French*) 0-77623

**partial differential equations continued**

- two-dimensional infiltration in unsaturated soils, nonlinear diffusion eqn. numerical soln. 0-69918
- viscoelastic circular membrane, nonlinear, large axisymmetric deform. under its own weight 0-64380
- wave propagation in randomly inhomogeneous media, quasi-optical parabolic approx., validity analysis 0-106422
- wind-driven lake circulation models, boundary conditions 0-85688

**partial discharges**

- bubbles behaviour in electrically stressed liquid obs. 0-71313
- current and voltage instrument transformers, MV, constructional principles and production technology (*Hungarian*) 0-100118
- liquid hydrocarbons, electric breakdown, light emission investigation 0-93241
- mechanisms, of single-avalanche, Townsend and channel discharges (*Polish*) 0-79609
- power transformers, electromagnetic testing of partial discharges for failure and breakdown prevention (*Russian*) 0-97743

**particle accelerator accessories***see also* **storage rings**

- autoresonant, computer system data acquisition and processing 0-99433
- beam scanner design for cyclotron facility 0-99365
- CRYEBIS ion sources for Saturne synchrotron (*French*) 0-63432
- eight-magnet spin precession snakes, survey for new configurations 0-91352
- electron gun system, pulsed, for use with superconducting accelerator and free-electron laser 0-68989
- large multiwire proportional chambers for experiment NA3 at the CERN SPS 0-102388
- linear accelerator, pulse amplifier with digital gain control 0-68977
- linear accelerator beam profile scanner 0-101267
- optical reflector for energy extraction for electron synchrotron 0-78467
- phase space cooling for pp colliders at CERN and Fermilab 0-99360
- photon position monitors for CHES synchrotron source, using split photoelectron detectors and ionisation chamber 0-91336
- Princeton Cyclotron data acquisition system 0-102415
- pulse transformer design for pulse forming transmission line charging appls. 0-63419
- synchrocyclotron, in-line mass spectrometer, electrostatic filter 0-86490
- tanked tube for open air accelerators 0-99356
- vibrating wire beam profile monitor for electrostatic accelerator with high stability 0-99368
- ZGS, 30" bubble chamber 0-91304
- ZGS, Effective Mass Spectrometer 0-91310
- ZGS, superconducting magnet bubble chambers, history 0-91368
- ZGS streamer chamber and kaon physics 0-91308

**particle accelerators**

- see also* **beam handling equipment**; **beam handling techniques**; **cyclotrons**; **electron accelerators**; **electron ring accelerators**; **electrostatic accelerators**; **linear accelerators**; **proton accelerators**; **synchrotrons**
- ANL HVEM-TANDEM accelerator facilities 0-101896
- CERN, 25 years of physics, review 0-82626
- charged particle motion in alternating elec. fields, scaling conditions 0-63903
- conference, general congress, Societe Francaise de Physique, Toulouse, France (June 1979) 0-77536
- diagnostics using laser beam 0-95497
- heavy-ion fusion preaccelerator, 1.5 MeV, fibre-optic remote control system 0-73993
- high-energy physics, particles and interactions 0-77944
- ISX-B neutral beam injector expt. on prototype beam line 0-74039
- klystron development, UHF, 600 kW, stability and durability improvement (*German*) 0-106211
- laser accelerator, phase-adjusted focusing 0-63434
- leakage measurements, medical appls. 0-89839
- Leningrad Institute of Nuclear Physics synchrocyclotron, neutron source 0-87003
- multipurpose (*Japanese*) 0-87000
- radioisotope direct detection using accelerators 0-63468
- shielding problems (*Japanese*) 0-99343
- superconducting magnet stability problem at accelerators under high-energy particle irradiation, review (*Russian*) 0-68972
- synchrotron radiation, spectroscopic applications, properties, characteristics as radiation source (*Norwegian*) 0-63420
- thermal particle motion effect on autoresonance acceleration process (*Russian*) 0-69007

**particle backscattering***see also* **electron energy loss spectra**

- AES, quantitative, backscatt. effects, review 0-81398
- AES, quantitative, Monte Carlo calc. 0-84813
- amorphous layer thickness meas. by electron back scattering method 0-100721
- atomic transport and conc. profiles 0-59723
- diamond-Sb, implanted, radiation damage and annealing study 0-100263
- electron, in field emission gun SEM 0-100142
- electron, transport equation theory, SEM and EPMA appl. 0-57439
- electron channeling pattern, large angle, generation and appl. 0-100296
- electron detector, multi-purpose 0-102404
- electron imaging, in scanning Auger microprobe, tailored modulation techniques appl. 0-68305
- electron probe penetration and energy loss characts. in solid target, diffusion model 0-96585
- electron scattering in solids, high energy, Monte Carlo calcs. 0-96422
- emerald, artificial single crystal, distrib. of  $\text{Cr}^{3+}$  impurity 0-59505
- energy reflection by backscatt. and sputtering, total yields and ang. distrib. 0-89101
- heavy ions, low energy total backscattering 0-71535
- ion backscattering and implantation, H and He ions, computer simulation, comparison of MARLOWE and TRIM codes 0-66350
- ion beam surface crystallography, channelling and blocking effects, double alignment backscattering 0-63550
- ion implantation, range parameters, nucl. stopping power, ion backscatt. determ. 0-88232
- metal, electron-impurity scattering, lattice distortion effects, phase shifts, calc. 0-96860
- metal target preparation for stopping power meas. of channelled ions in low energy region 0-63431
- metallic thin films, electron backscattering, empirical study 0-108310
- metallic thin films, Everhart theory extension of backscattered electron energy spectra 0-108309



**particle backscattering continued**

- metals, analysis of H ratios and profiling using nucl. techniques and Rutherford backscatt. 0-61202
- metals, Z dependence of thick target  $\beta$ -ray backscattering 0-76118
- phosphosilicate glasses, P content determ. by Rutherford backscatt., PIXE, and activation anal. (*Hungarian*) 0-85233
- photon, spectra of gamma rays backscattered by infinite air (skyshine) 0-101436
- polythene, Z dependence of thick target  $\beta$ -ray backscattering 0-76118
- rare earth metal silicide thin film formation on (100), (111)Si substrates, backscattering study 0-70542
- Rutherford backscattering meas. at MeV energies, screening corrections 0-88204
- Rutherford scattering cross section correction 0-66369
- scanning Auger electron microscope, calc. of effects of backscattered electrons on spatial resolution 0-81412
- scanning Auger microscopy, effects of backscattering on resolution 0-104021
- SEM specimen-electron interactions 0-68317
- solid surface, backscattering of H, D, and He, positive charge fractions 0-66375
- solid surface,  $H^-$  ion backscatt. due to proton bombardment 0-99554
- solids, backscattering coeff. meas. of 15 to 60 keV electrons at various angles of incidence 0-80919
- spatial electron beam-matter interaction, model calcs. for Cu (*German*) 0-84815
- steel, stainless, retention and re-emission of 0.125-1 keV  $D^+$  ions 0-66349
- thin film, thickness determ., by electron backscattering 0-101904
- Ag, electron backscatt. by bulk target, theoretical model (*French*) 0-60722
- Al, defect structures depend. on Ca and Ga implanted species 0-59494
- Al, electron backscatt. by bulk target, theoretical model (*French*) 0-60722
- Al, implanted Xe behaviour during anodic oxidation 0-71800
- Al surface,  $^4He$  backscatt., Rutherford scatt. cross section correction test 0-66369
- Al surface bombardment by fast  $H^+$  0-66376
- Al-Sb(Zn), ion implanted electron beam annealing, ion backscatt. and TEM meas. 0-59500
- Al-Ge (0.1 wt.%), channelling meas. of Al interstitial atom trapping by Ge atoms 0-59537
- Au, backscatt. of H and He ions, fraction reflected 0-60741
- Au film, integrated condensation coeff. on NaCl cleavage faces, Rutherford ion backscatt. obs. 0-59827
- Au, H and He atom backscattering, ang. and energy distrib. 0-76123
- Au surface,  $^4He$  backscatt., Rutherford scatt. cross section correction test 0-66369
- Au/Ni(Ni-P), interdiffusion, backscatt. study 0-79991
- Au-Cu-Al thin film bilayer system, phase formation, backscattering spectra 0-96728
- Be, blisters due to He irradi., proton backscatt. study 0-75273
- Cs, backscatt. of H and He ions, fraction reflected 0-60741
- Cu, blisters due to He irradi., proton backscatt. study 0-75273
- Cu, electron backscatt. by bulk target, theoretical model (*French*) 0-60722
- Cu single crystals Au ion implanted, pulsed electron beam irradi. 0-65019
- Cu surface,  $^4He$  backscatt., Rutherford scatt. cross section correction test 0-66369
- Cu, surface morphology influence on sputtered yield angular distribution 0-65338
- CuInS<sub>2</sub> films, RF sputtered, growth and props. 0-80124
- CuInSe<sub>2</sub> amorphous thin film, flash evaporation, struct., stoichiometry 0-89150
- GaAs, amorphous layers, ion-implanted, low-temp. epitaxial regrowth 0-92790
- GaAs, ion beam induced annealing effects 0-59530
- GaAs, ion implanted, laser annealing 0-107296
- GaAs:Sn thermal diffusion from spin-on  $SnO_2/SiO_2$  source 0-96691
- GaAs:Zn, implanted, furnace annealed, electrical, Rutherford backscattering and TEM meas. 0-100272
- GaAs:Zn, implanted, laser annealing, elect., Rutherford backscattering and SEM meas. 0-100273
- Ga<sub>1-x</sub>In<sub>x</sub>-P MBE layers, comp., Rutherford scatt. and X-ray diff. meas. 0-75457
- p-Ga<sub>1-x</sub>In<sub>x</sub>PyAs<sub>1-y</sub>/Au-Zn, specific contact resist. 0-84509
- Gd, stopping power and energy straggling of  $^4He^+$  ions in vacuum-evaporated films 0-88231
- Ge, energy loss spectra of  $C^{2+}$  ions 0-65114
- Ge epitaxial film, ion implantation and electron beam anneal effects on carrier conc. 0-75255
- H, backscatt. from Au, charge fraction ang. depend. 0-71540
- He, backscatt. from Au, charge fraction ang. depend. 0-71540
- $He^+$ , isotope effects in elastic surface scatt. on sol. and liq. Ga 0-71536
- $^4He$  stopping power, 0.15 to 1 MeV, backscatt. determ. 0-88233
- Hg surface,  $^4He$  backscatt., Rutherford scatt. cross section correction test 0-66369
- Hg<sub>1-x</sub>Cd<sub>x</sub>Te, implanted with Hg, Al, damage and lattice location study 0-103381
- InP film, electron-beam annealed, surface conduction 0-84500
- LiF, alkali ion implantation, migration, segregation, effect on optical props. 0-100269
- MgO coated detector for SEM backscatter to secondary electron conversion 0-68332
- Nb, blisters due to He irradi., proton backscatt. study 0-75273
- $Ne^+$ , isotope effects in elastic surface scatt. on sol. and liq. Ga 0-71536
- Ni, energy loss spectra of  $C^{2+}$  ions 0-65114
- Ni film, amorphous layer covered, target prep. for channelled ion stopping power meas. 0-63431
- Ni, ion-implanted and virgin, laser irradi. effect, Rutherford backscatt. and channelling obs. 0-108306
- Ni surface, (110), O<sub>2</sub> adsorption, LEED and ion scatt. study 0-84386
- Ni-Pt silicide Schottky diodes, current-voltage characs. and comp. profiles 0-84508
- NiF, film preparation and characterisation 0-59815
- NiO-Al<sub>2</sub>O<sub>3</sub> reaction at film-substrate interface, Rutherford backscatt. obs. 0-59733
- NiSi<sub>2</sub> epitaxial film on (111) Si substrate, interfacial order, backscatter, channelling study 0-65390
- Pd-Si, amorphous thin films, laser irradi., metastable phases 0-96622

**particle backscattering continued**

- Pt (100) (5×20) and (1×1) surfaces, stability and reactivity, adsorption of H 0-75434
- Pt (111) surface, backscattering, channelling spectra, H adsorption, surface relaxation 0-71552
- Pt-Si, amorphous thin films, laser irradi., metastable phases 0-96622
- PtSi surface, and interface with Si, impurity effects 0-80037
- Pt<sub>2</sub>Si, and PtSi, growth rate for form. by Pt film deposition under ultrahigh vac. and controlled impurity atm. 0-65388
- Si (100), H adsorption, MeV ion scatt. study 0-80071
- Si, (111) surface, proton dechannelling under channelling, blocking and double alignment conditions 0-88235
- Si, amorphous, substrate orientation effect on regrowth by laser pulses, channelling, backscatter 0-84409
- Si, EFG ribbon, characterisation by ion beam tech. 0-79833
- Si films, RF sputtered, Ar conc. as function of operation frequency and discharge pressure 0-65393
- Si, gettering by ion damage, minority carrier lifetime and backscatt. study 0-100286
- Si, heavy ion induced disorder in surface and at shallow depths 0-59535
- Si heavy ion surface barrier detector, plasma delay times, electron backscattered from fission fragment or alpha particle 0-58095
- Si, impurity solubility limit after laser induced melting, Rutherford backscatt. spectrum 0-107426
- Si, ion bombardment, anomalous surface damage from channelling-backscatt. meas. 0-84222
- Si, ion implantation, high dose, solid phase epitaxial regrowth 0-103380
- Si, ion implanted, damage profiles, Rutherford backscattering 0-100733
- Si, ion implanted, radiation defect production at different temps. 0-103398
- Si, ion-implanted layers, epitaxial regrowth by laser beam and flash annealing 0-100420
- Si layers amorphized by molecular ions, laser annealing 0-103379
- Si surface, ion bombardment enhanced mixing of Ag layers, Rutherford backscatt. meas. 0-65034
- Si surface electron beam deposited silicide formation using scanning CW laser beam 0-66862
- Si: As(Pb), high-dose ion implanted and annealed, implant redistribution 0-107309
- Si:B diffusion at Si-SiO<sub>2</sub> interface, Auger spectra, Rutherford backscattering 0-70471
- Si:B(P)(As)(Sb)(Cu)(Fe), ion implanted, doping profile, pulsed laser annealing effects 0-88197
- n-Si:Ga laser doped, segregation, Rutherford backscattering 0-103483
- Si:Ga(As), laser-doped, impurity distrib., Rutherford backscatt. and channelling anal. 0-59507
- Si:P, incoherent light flash annealing, elec. props., backscattering spectra 0-97504
- Si:P, ion implanted, subsurface damage, TEM and channelled Rutherford backscatt. study 0-107337
- Si:Sb, ion implanted, annealed, dislocation generation, channelling and Rutherford backscatt. meas. 0-88158
- Si:Sb, ion implanted, annealing, Sb behaviour above solid solubility, Rutherford backscatt. meas. 0-88200
- Si:Sb, ion implanted, Sb diffusion during oxidation, snow-plough effect 0-88366
- Si:Sb, laser doping, evaporation loss and diffusion of Sb, under pulsed laser irradi. 0-59508
- Si:Sb, low energy ion implantation, profile determ. 0-88176
- Si:Sb(Ga)(Bi)(In), dopant solubility limit, laser irradi. effects 0-84295
- Si/Pd system, solid phase epitaxial growth control by C ion implantation 0-75466
- Si-Au system, ion implanted induced giant gettering, annealing effects 0-88221
- Si-CoSi<sub>3</sub>Si<sub>2</sub> double heteroepitaxy, solid phase and MBE 0-104063
- Si-Cr interfaces, metallurgical and electrical props. 0-60081
- Si-epitaxial film, ionised-cluster-beam deposited, cryst. and elec. characs. 0-70553
- Si-metal interface, silicide formation, interface marker technique obs. 0-59734
- Si-Pd-Si structure, epitaxial growth, backscattering and transmission electron microscopy studies of layered structures 0-80123
- Si-Pd-Ti, silicide form. in evaporated films 0-80006
- Si<sub>3</sub>B<sub>1-x</sub> films, anal. of H ratios and profiling using nucl. techniques and Rutherford backscatt. 0-61202
- SiC:H amorphous reactively sputtered film, H content effect on film props. 0-75459
- Si<sub>3</sub>O<sub>1-x</sub> films, anal. of H ratios and profiling using nucl. techniques and Rutherford backscatt. 0-61202
- TeO<sub>2</sub> thin films, dielec. props. rel. to fabrication conditions 0-97199
- Ti, energy loss spectra of  $C^{2+}$  ions 0-65114
- Ti-W films, bias-sputtered, quantitative anal. 0-80114
- TiI laser window films, stoichiometry, Rutherford backscatt. study 0-59831

**particle beam diagnostics**

- accelerator diagnostics using laser beam 0-95497
- beam profiles in uniform elec. field, including space charge effects 0-106222
- beam scanner design for cyclotron facility 0-99365
- betatron, orbit expansion and beam extraction, simulation 0-91353
- bunched beam, coherent transverse instability induced by kicker magnet 0-58015
- charged particle motion in mag. quadrupole element, linear transform. coeff. 0-78470
- coherent radiation from electrons in transverse periodic fields 0-78748
- conductance for the gas flow of an accelerating tube 0-102359
- current density meas. method for electron acceleration 0-102366
- deuteron beam estimation of density distrib. 0-68992
- energy spectrum monitoring in low-energy electron accelerators 0-68994
- fusion reactor, DITE-II, neutral beam ion source particle beam identification 0-99397
- fusion reactor, neutral beam injection reionisation power losses in duct, model 0-99385
- fusion reactor, PLT, neutral beam duct reionisation losses, obs. and power loss model 0-99383
- ion beam deceleration across mag. fields, expt. 0-99384
- K X-ray fluorescent multi-strip probe for accelerator beam studies 0-102362
- linear accelerators, resonator sensor for the parameter of charged-particle beams 0-68991

**particle beam diagnostics continued**

- magnetic analysis of charged particles,  $\alpha$ -,  $\beta$ - and mass spectrometers (*Russian*) 0-87011
- magnetomodulation device for current meas. of charged particle beam, 100  $\mu$ A-300 mA 0-68993
- nanosecond beam dynamics in linear electron accelerator 0-86996
- neutron rich fission fragments, excited state spin assignment, various methods 0-78506
- pulsed electron beams, measurement of current density distrib. and energy spectrum 0-63426
- pulseline driven neutralised linear ion accelerators, longit. instabilities 0-78459
- relativistic electron trajectories in self consistent field (*Russian*) 0-63435
- resonant oscillations driven by a nonlinear forcing term 0-78473
- RF ion beam choppers, ion motion (*Chinese*) 0-99371
- self-focused, relativistic, filamentation instability 0-74289
- SIN,  $\pi$ E3 channel, cloud and surface muon studies 0-74055
- SIN  $\pi$ E3 channel, pion prod. meas. 0-74056
- Texas A&M polarised proton beam meas. 0-102360
- TRIUMF stopped  $\pi$ -K channel 0-102364
- variable pion energies from a moderated fixed energy pion beam 0-78476
- vibrating wire beam profile monitor for electrostatic accelerator with high stability 0-99368
- X-ray diagnostics on collective heavy ion electron ring accelerators 0-102358
- Cs, ground state spins, moments, charge radii by laser spectroscopy 0-78147
- Rb, ground state spins, moments, charge radii by laser spectroscopy 0-78147

**particle beams**

- see also atomic beams; beam handling techniques; electron beams; ion beams; molecular beams; particle beam diagnostics; particle optics
- charged sphere, particle emission into mag. field 0-69304
- coherent interaction between waves and particle streams 0-58452
- cylindrical beam of constant density, self-consistent description 0-78754
- dipole particles in axisymmetric electrostatic and magnetostatic fields, meridional trajectories 0-78750
- electrostatic energy analyzer with an approximately homogeneous field 0-78753
- extraction element design for long pulse multi-megawatt neutral beam 0-102373
- focused 24 keV filtered neutron beam 0-63436
- fusion, reactor, MFTF, neutral beam accel power supply protection 0-102380
- fusion, TFTR, neutral beam sources overcurrent protection during spark down 0-102331
- fusion reactor, Doublet III, neutral beam injector system, instrumentation and control 0-99322
- fusion reactor, Doublet III, neutral beam interlock system using IR detector 0-106228
- fusion reactor, field reversed mirror neutral beam startup, hybrid plasma code simulation 0-99313
- fusion reactor, Heliotron E, neutral beam injector ion source power supply 0-99333
- fusion reactor, ISX-B, neutral beam system 0-99388
- fusion reactor, JET neutral injector overvoltage injection system 0-99398
- fusion reactor, JIPP T-II, neutral beam injection system, design and expt. test 0-106226
- fusion reactor, JT-60, prototype neutral beam injector unit 0-106225
- fusion reactor, MFTF, neutral beam source development 0-102368
- fusion reactor, MFTF, sustaining neutral beam power supply, shunt pre-conditioner, IBM-ASTAP anal. 0-102332
- fusion reactor, neutral beam injector mag. cusp plasma source, design and fabrication 0-99377
- fusion reactor, PDX, 6 MW Neutral Beam Project, overview 0-106223
- fusion reactor, PDX, neutral beam elec. power system, ion source supply upgrade 0-102330
- fusion reactor, PDX neutral beam injector, ion accel. structural anal. 0-102375
- fusion reactor, PDX neutral beam injector development 0-99375
- fusion reactor, PLT, neutral beam injection, power input and plasma temp. reconciliation 0-106224
- fusion reactor, rectangular plasma generator, advanced ion source for ion injectors 0-99376
- fusion reactor, TFTR, neutral beam injector prototype, construction and performance 0-99390
- fusion reactor, TFTR, neutral beam injector test facility construction 0-102336
- fusion reactor, TMX, injector system mech. design and installation 0-99393
- fusion reactor, TMX, neutral beam control systems 0-99323
- fusion reactor, TMX, neutral beam system startup 0-99306
- fusion reactor, Wendelstein VII-A, neutral beam injectors, performance 0-99389
- fusion reactor neutral beam injection, 120 keV, ion source 0-91357
- fusion reactor neutral beam injection, 24 MW 400 keV H beam 0-91356
- fusion reactor neutral beam source, 40 kV for TMX, engineering design 0-91358
- fusion reactor PDX, ORNL prototype neutral beam injection system, ion source development 0-99391
- fusion reactors, TFTR neutral beam support system 0-102376
- fusion reactors, Wendelstein VII and ASDEX, neutral beam injectors, HV power supply system, thyristor control 0-99332
- hyperon beam physics, review, book contrib. 0-68503
- JXFR, neutral beam injection system, gas-beam interaction secondary particles 0-106227
- magnetomodulation device for current meas. of charged particle beam, 100  $\mu$ A-300 mA 0-68993
- metal neutral beams, low energy (0.1 to 10 eV) prod. by laser vaporisation of metals 0-77910
- neutral beam, continuously operating, convectively cooled ion accelerator, mech. design and fabrication 0-102374
- neutral beam injector, continuous operation, water cooled U-tube extraction grid 0-99392
- neutral beam module component design and development for fusion reactor 0-91270
- neutral beam source, cryopumping and mag. shielding, fabrication and operating cost 0-106229
- neutral beam source manufacturing at Lawrence Livermore Laboratory 0-102377

**particle beams continued**

- neutral injector modular cryopumping system 0-105656
- neutron beams of the Leningrad Institute of Nuclear Physics synchrotron 0-87003
- neutron production by neutral beam sources, shielding design criteria for fusion program 0-99387
- PDX neutral beam injector, multi-aperture ion accel. electrodes thermal anal. 0-102371
- periplasmatron ion source for intense neutral beam 0-99380
- slow positron form. in MgO-coated moderators 0-62796
- small spherical particles, focusing by axisymmetric mag. fields 0-78755
- sputtered particles, vel. meas. by Doppler-shift laser spectrometer 0-62638
- turbulent stream, charge density vol. distrib. (*Russian*) 0-74288

**particle counters** see counters**particle counting**

- counting of microscopic particles in disperse systems (aerosols, colloids etc.)
- aerosol particle size meas., optical particle counter calibration by Doppler shift spectrometry 0-68173
- aerosols, dispersity analysis, automatic photoelec. analyser for size range 0.3-40  $\mu$ m 0-57251

**particle detectors**

- see also bubble chambers; ionisation chambers; particle track visualisation; position sensitive particle detectors; streamer chambers
- backscattered electron detector, forensic appls. 0-68319
- cellulose acetate solid state track detectors, catalytic oxidation sensitization (*Chinese*) 0-102399
- cellulose acetate solid state track detectors, swelling sensitisation (*Chinese*) 0-99422
- cellulose nitrate SSNTD, energy resolution enhancement for alpha particle detection 0-91392
- conference, nuclear power systems, San Francisco, CA, USA (Oct. 1979) 0-56994
- converted backscattered electron detection 0-68318
- cosmic ray telescope, solid state, detection system for heavy ions, element and isotope separation 0-67563
- data processing, high speed, histogram and tape writing 0-58101
- dielectric particle detector under pulsed power supply 0-74086
- Faraday cup detector and digitizer for routine monitoring of ion emission from laser-driven implosions 0-57268
- ion detector (*Chinese*) 0-78496
- MARK J detector at DESY 0-95282
- microprocessor-controlled data acquisition system for temporal/angular correl. between  $\beta$ - and  $\gamma$ -ray emission (*Spanish*) 0-106238
- multi-needle detector with cathodic focusing (*French*) 0-102391
- natural quartz SSNTD, etching characts. 0-91401
- neutron radiography by solid state nuclear track detectors 0-97671
- ngutron detector for determ. of transuranic element comp. of nuclear fuel cladding hulls 0-63471
- nuclear accident dosimetry system, Czechoslovakia 0-57978
- passive personnel portal detectors for nuclear materials diversion protection using gamma-ray and neutron detectors 0-78389
- portal monitors for detecting and safeguarding special nuclear materials 0-63406
- review of methods of detection and appl. of electronics and computer technology 0-106235
- segmented calorimeter, high energy performance, Monte Carlo simulation 0-58029
- solid dielectric detectors with breakdown phenomena and their applications in radioprotection 0-91388
- solid state nuclear track detectors, reactor neutron fluence meas. using Au and In foils 0-69035
- solid state track detectors in solutions of actinides,  $\alpha$  track registration 0-63486
- solid-state track recorder applications in U.S. nuclear reactor energy programs 0-95506
- SSNTD, AA 0-95500
- SSNTD, alpha sensitive plastic detectors for Rn gas conc. meas. 0-94617
- SSNTD, alpha sensitive plastic films for Rn gas conc. meas. 0-94618
- SSNTD, appl. to meas. reaction parameters for Pu(n,f) reactions 0-91201
- SSNTD, appl. to the search for superheavy elements 0-91200
- SSNTD, automatic scanning techniques 0-91387
- SSNTD, cellulose nitrate, for high energy neutron spectrometry 0-91394
- SSNTD, development and appls., [conf. Nilore, Rawalpindi, Pakistan March 1979] 0-90608
- SSNTD, development of etched nuclear tracks 0-91384
- SSNTD, effect of etching conditions on energy resolution of phosphate glass and polycarbonate detectors 0-91390
- SSNTD, electrochemical etching studies of the CR-39 plastic 0-91391
- SSNTD, nuclear track research activities at GSI 0-95501
- SSNTD, review of appls. in fission physics 0-91396
- SSNTD, track registration and development efficiency 0-91385
- SSNTD, track registration and development efficiency 0-91386
- SSNTD, visualization of latent damage trails etching, decoration and observation techniques, review 0-91382
- SSNTD for detection of heavy cosmic rays aboard Cosmos-936 0-94663
- SSNTD for exam. of heavy ion reactions, multiprong events due to multiple sequential fission 0-91199
- SSNTD for fast neutron meas. 0-91393
- SSNTD to detect environmental  $\alpha$ -emitters from natural sources 0-91292
- SSNTD using mica muscovite for high neutron fluence meas. 0-91395
- superconducting double multivibrator used as near- and medium-infrared radiation detector (*German*) 0-90892
- superheated superconducting colloid shower detector, rel. electron detection 0.1 to 6.0 GeV 0-91398
- survey assay meter developments at BNL for nuclear materials safeguarding appls. 0-69038
- synchronization of time measurements at widely spaced locations, VLF radio signals and standard TV transmissions 0-63487
- Al granular superconducting bolometer as mol. beam detector 0-73524
- <sup>3</sup>H monitors, calibration technique (*Czech*) 0-74075
- ZnP glass heavy-ion track detectors 3 to 120 MeV 0-91389



particle focusing *see focusing; particle optics*

particle lenses, electrostatic *see electrostatic lenses*

particle lenses, magnetic *see magnetic lenses*

particle optics

*see also aberrations; beam handling techniques; electrodynamics; electron optics; ion optics; particle beam diagnostics*  
accelerator, laser focusing, phase-adjusted 0-63434  
charged particle motion in alternating elec. fields, scaling conditions 0-63903

electrostatic coaxial lens, soln. techniques 0-69307

image formation with ultracold-neutron waves 0-78752

neutrons, imaging and focusing by zone plate 0-106433

particle range *see energy loss of particles*

particle scattering *see collision processes; energy loss of particles; particle backscattering; potential scattering; radiation effects; transport processes*

particle separators

No entries

particle size

aerosol size distribution by inverting spectral turbidity data 0-95796

alloy, dispersion hardened, work hardening due to Orowan loops, temp. depend. (Japanese) 0-66534

bore-silicate glass, birefringent, X-ray small-angle scatt. study 0-103937

ceramic powder synthesis from laser-heated gas phase reactants 0-93525

coarsening, time depend. of average particle size 0-79994

colloids, rigid, size distributions, transient electric birefringence 0-85223

concrete, fresh, behaviour under a vibr. action, large particle segregation (Japanese) 0-88329

copper phthalocyanine, size distrib., transient elec. birefr. 0-85223

diamond, ultradisperse, ESR, particle size and lattice microdistortions 0-97140

diamond coatings, for increased wear resist. 0-76371

dickite, unusual crystal habit, structural disorder 0-59445

disperse system, spectral transparency approx. by Legendre polynomials, distrib. density of particle size 0-95800

dust grains, atmospheric, mean radius rel. to transparency meas. on Maidanak mountain (Russian) 0-72627

dusty IR Test-1 lidar obs., transmission meas. 0-99625

electrophotographic developer, size distrib., particle charge and toner-carrier force (German) 0-73493

epoxy resin/particle composites, particle size effect in thermal expansion, filler effects on  $T_g$  0-84305

fine particles aggregation, mechanism and rate at uniform shear field 0-101046

graphite, suspensions, particle shape influence on light absorpt. in mag. field 0-60549

interstellar dust, effects of grain collisions in turbulent gas on initial size distrib. 0-77470

interstellar porous graphite grains, radii rel. to 2200 Å extinction hump 0-62228

interstellar solid particles in contracting clouds, turbulence rel. to particles growth and size differentiation 0-62251

kaolin grog particles, shape and density 0-97450

CW Leonis (IRC+10216), IR C star, circumstellar dust size var. rel. to intrinsic polarisation 0-67730

liquid particles, aerosol and hydrosol, separation by size in thermal fields 0-101044

metal submicron particle heating in hot gas, plasma metallurgy 0-81092

molecule embedded in dielec. spheroid, Raman and fluoresc. scatt. 0-99507

mortar bars, aggregate particle size influence as expansion caused by alkali-SiO<sub>2</sub> reaction 0-66762

near IR diffuse reflectance analysis anomalies 0-86383

phosphate fertilizer, specific activity of U and Th rel. to particle size 0-106244

polydisperse, vapour-liquid mixtures, acoustic velocity, damping decrement 0-66881

polydisperse dilute suspensions, of rod-like particles, anisotropy of electric polarisability 0-85224

polydisperse-particle-size-distribution function determined from intensity profile of angularly scattered light: comments 0-87311

polyethylene/ethylene vinyl acetate copolymer mixture, rel. between hyper-mol. struct. and stability (German) 0-64929

polymer/metal powder compacts, cond. threshold, particle size ratio effect 0-80337

random packing of spheres, computer simulation 0-77705

river sediments, transport mode depend. on particle size rel. to Martian outflow channels erosion 0-98363

scattering particle dimension determination, by direct Fourier cosine transformation of expt. SAXS data 0-79624

sepiolite, electric polarisability, anisotropy, length depend. of ionic contrib. 0-85224

sepiolite, size distributions, transient electric birefringence 0-85223

steel, high-strength low alloy, Nb(CN) precipitation and coarsening during hot compression 0-97514

turbulent flocculation, mathematical model (Japanese) 0-79389

water drops in stratosphere, size distrib. rel. to sulphate aerosol growth by condensation (Russian) 0-94566

Ag powder, ultrafine, sintering, coalescence growth stage 0-89174

Ag-Cd-(Ni), internally oxidised, oxide particle size control (Japanese) 0-89480

Ag-Zn-Te-(Sn)-(In), internally oxidised, oxide particle size control (Japanese) 0-89480

Ag<sub>2</sub>CO<sub>3</sub>, powder metallurgy production, for switchgear in power engineering 0-104094

AgI aerosol, particle radius depend. of ice-forming activity, verification of theory 0-101406

AgI aerosol particle size, struct. rel. to ice forming activity 0-61164

Al-Si (1.2 wt.%), dispersion hardened, work hardening due to Orowan loops, temp. depend. (Japanese) 0-66534

Al<sub>2</sub>O<sub>3</sub> ultrafine gel particle form. from NH<sub>3</sub>-AlCl<sub>3</sub> solution 0-93807

Al<sub>2</sub>O<sub>3</sub>-TiO<sub>2</sub> powder, plasma-prepared, morphology and phase constitution 0-100833

Al<sub>2</sub>O<sub>3</sub>(H<sub>2</sub>O)<sub>n</sub>, uniform colloidal dispersion, prep. by chem. reactions in aerosols 0-97735

Au, fine particles, gas evaporation technique for prep., X-ray diffr. study 0-75327

Au, fine particles, gas evaporation technique of prep., X-ray diffr. study, charact. temp. 0-75328

Au powder, ultrafine, sintering, coalescence growth stage 0-89174

β-Ca<sub>2</sub>-SiO<sub>2</sub>, reaction kinetics with CO<sub>2</sub> and water vapour 0-76484

particle size continued

Ca<sub>2</sub>SiO<sub>2</sub>, reaction kinetics with CO<sub>2</sub> and water vapour 0-76484

Cd films, struct. and props., X-ray diffr. spectra anal. 0-80119

Co single domain particles, randomly oriented easy axes and particle size distrib., coercivity 0-71119

CoFe<sub>2</sub>O<sub>4</sub> ultrafine particles, prep. and mag. props. 0-71116

Cu crystals, two-phase, recrystn. retardation, particle size, spacing effects 0-89242

Cu wire, tough-pitch, cupping fracture, Cu<sub>2</sub>O particle size effect 0-66668

Cu-SiO<sub>2</sub>, low-temp. recovery creep, Orowan loop accumulation 0-81126

Fe-Si (3wt.%), grain-oriented, secondary recryst., grain growth inhibition 0-89245

α-Fe<sub>2</sub>O<sub>3</sub>H, asymmetric line shapes of Mossbauer spectra (Chinese) 0-103902

<sup>2</sup>H-<sup>1</sup>H fuel pellet electrostatic injection (Japanese) 0-78434

In<sub>2</sub>O<sub>3</sub> smoke particles prepared by gas evap., morphology and coalescence growth 0-97738

Mg films, struct. and props., X-ray diffr. spectra anal. 0-80119

MgF<sub>2</sub> polycryst., quartz particle impacts no. effect on erosion in elastic-plastic response regime 0-81209

MgO, smoke particles, size distrib. 0-104471

MnZn ferrite powder prep., wet method 0-89180

MoO<sub>3</sub> smoke particles prepared by gas evap., morphology and coalescence growth 0-97738

NH<sub>4</sub>Cl, submicron particles, density, morphology 0-61166

NaCl monodisperse aerosol, dry size depend. of critical supersaturation for droplets nucleation 0-82003

Ni-Co-Al alloys, continuous precip., SEM, TEM, X-ray diffr. study 0-89220

NiO samples, colour difference, X-ray line broadening study 0-100206

Se, amorphous, vac. deposited on polymeric substrates, with dynamic coating device 0-100792

Si<sub>3</sub>N<sub>4</sub>, reaction-bonded, theoretical model of manufacture, effect of ambient reaction temp. and compact size 0-108379

steel, Nb, deform., recrystn. and precip. interaction 0-97515

V, small particles, crystal structure, magnetic and superconducting props. 0-97121

WC, sinterability of ultrafine powders obtained by CVD method 0-108378

WO<sub>3</sub> smoke particles prepared by gas evap., morphology and coalescence growth 0-97738

ZnO powder, effect of dry grinding in EPR and catalytic activity (Japanese) 0-84640

particle size measurement

aerosol, single droplet, size and mass meas. using electrodynamic balance 0-89535

aerosol particle size measuring device, using spectral transparency and small angle scatt. methods 0-95069

aerosol spectrometer using two-pulse Fraunhofer holography, fibrous particle motion anal. 0-58476

aerosols, Aitken range size distrib. meas. in N.Atlantic 0-98404

aerosols, dispersity analysis, automatic photoelec. analyser for size range 0.3-40 μm 0-57251

aerosols, electronic cascade impaction method for particle size distribution meas. 0-72652

aerosols, optical particle counter calibration by Doppler shift spectrometry 0-68173

aerosols, parallel plate electrostatic classifier 0-95070

aggregates, solid, aerosols, dynamic shape factors meas. appls. 0-61165

apparatus for sizes down to 5 μm 0-77753

atmospheric aerosol size distribution determ., optical attenuation meas. (Chinese) 0-72570

atmospheric environmental research, appl. of lasers (German) 0-97849

biological cell size meas. by static light scatt. Fourier transform 0-81793

contaminant particle microanalytical methods 0-86397

diffusion battery, screen type, theory 0-95208

disperse particles, determ. of spectrum of diameters from scattering of light 0-61169

distribution, spectral transparency method, improvements 0-86254

distribution meas., online stroboscopic microscope apparatus 0-101783

droplet size and falling velocity meas. using laser Doppler velocimeter 0-68185

droplets produced by pneumatic nebulisers, size meas. method 0-71992

dust, airborne, Raman laser microprobe analysis appl. 0-57390

dust, destruction degree, determ. in mech. screening 0-66882

EPIQUANT, automatic structure analyser 0-85116

holographically recorded particle field meas., Fraunhofer plane analysis 0-73306

laser Doppler velocimeter for particle size and density simultaneous determ. 0-98880

laser light scattering spectroscopy method and apparatus, averaged size and polydispersity index meas. 0-77754

laser radiation effects on particle properties, radiation pressure effect on particle motion (German) 0-102755

mean size calculation simplification 0-90814

optical single-particle-size spectrometer calibration and testing, monofilament fibres as substitute particles 0-58819

photometer, differential light scatt., for rapid analysis of particles in flow, appl. to biological cells 0-77834

Pioneer Venus Sounder Probe Particle Size Spectrometer 0-67510

polydisperse particle size distrib. function determ. from angularly scatt. light intensity profile 0-98879

polyethylene-polypropylene blend, size distribution determ. of spherical occlusions from photomicrographs (Czech) 0-89539

polymeric particles obtained by suspension polymerisation, particle size distrib. eval. using Coulter Counter data 0-76564

rubber powders, finely dispersed, sedimentometric anal. 0-66883

Streptococcus mutans 10449, size determ. by laser light scatt. 0-109062

submicron particulates size determ. by sideway light scattering method 0-89883

technology, IR applications 0-86431

water-petroleum emulsions, mean particle diameter and conc. determ. by light scatt. 0-89538

CaS, monodisperse particles form. from soln., light scatt. theory use in size estimation 0-76560

Li particle size distrib. meas. by SEM 0-101775

PuO<sub>2</sub>, particle size meas. in UO<sub>2</sub>-PuO<sub>2</sub> tablets, image analysis by LEITZ-TAS with process computer 0-68773



**particle sources**

- see also *ion sources; neutron sources; radioactive sources*  
 electron gun system, pulsed, for use with superconducting accelerator and free-electron laser 0-68989  
 electron spectroscopy, target sources, centrifuge method of prep. 0-74060  
 electron-photon beams from proton accelerators, EM interaction investigation (Russian) 0-106214  
 field emission electron gun, off-axis electron holography 0-101905  
 field emission source, micro Auger anal. 0-104020  
 fusion reactor, TFTR, neutral beam source, arc current modulator design 0-102379  
 high-flux beam source of He, Ne and Ar metastable atoms 0-58416  
 molecular structure and dynamics by pulsed mol. beams 0-102563  
 plasma electron source with high brightness, emitter and beam parameters 0-106218  
 positron, Au moderator surface preparation for increased yield 0-61011  
 positron apparatus for surface studies 0-86500  
 pulsed proton source, Penning type, beam parameters 0-87001  
 radioisotopes, production, for medical use, at TRIUMF 0-72325  
 GaAs spin-polarized electron source 0-69000  
<sup>22</sup>Na, glass positron source, preparation 0-102367

**particle spectrometers**

- see also *alpha-particle spectrometers; beta-ray spectrometers; electron spectrometers; gamma-ray spectrometers; neutron spectrometers; X-ray spectrometers*  
 amplitude dependent count rate losses in pulsed optical feedback preamplifiers 0-91366  
 analyzing voltage instability in modulation method of measuring solar wind 0-67565  
 Brookhaven multiparticle spectrometer drift chamber system 0-58044  
 calibration by electron capture reactions 0-63445  
 calibration of optical particle counter 0-68173  
 data anal., off-line, 168/E microprocessor 0-58102  
 electrostatic analyser with parabolic electrodes, particle energy distribution after traversing spectrometer 0-99000  
 focusing properties of a broad-range sector spectrometer with a 1/r-magnetic field 0-102383  
 gamma-ray spectrometers; calc. of radioactivity induced during spaceflight 0-102382  
 ion analyser enhancement based on MI-1305 mass spectrometer 0-105745  
 ion scattering spectrometer for surface studies 0-98995  
 ionisation spectrometer with gas Cherenkov counter, appl. to cosmic ray studies 0-94662  
 large aperture, beam monitoring tech., MWPC construction, data acquisition system 0-102381  
 magnetic spectrographs, use in nucl. reaction studies, review (Rumanian) 0-87012  
 microchannel plate based detector for a heavy ion beam spectrometer 0-58018  
 multiparameter gas-scintillation counter for heavy charged particles 0-58051  
 Omega spectrometer, CERN, modular trigger basic techniques 0-58104  
 plastic ball multi-detector large angle spectrometer for Belavac 0-58028  
 Princeton Cyclotron data acquisition system 0-102415  
 scintillation spectrometer stabilisation using LED reference light source 0-91365  
 sequential/parallel track selector, 1  $\mu$ s hardware pre-analyser for CERN Omicron spectrometer 0-91364  
 solid state nuclear track detectors, cellulose nitrate, for high energy neutron spectrometry 0-91394  
 SPEAR Mark II shower counter system 0-58031  
 $\nu$  detector based on combined operation of streamer chamber and Converse hodoscopic tubes 0-63455  
<sup>90</sup>Sr bremsstrahlung radiation meas. for well logging using Ge spectrometer 0-94619

**particle track visualisation**

- see also *bubble chambers; cloud chambers; nuclear track emulsions; scintillation chambers; spark chambers; streamer chambers*  
 borosilicate optical waveguide glass, B content determ. using nuclear track counting 0-95969  
 cellulose nitrate, energy loss critical rate for charged particles 0-74082  
 cellulose proton track visualisation detectors (French) 0-74080  
 charged particle track analysis of sandstone-type U ore 0-91405  
 energy resolution enhancement for alpha particle detection 0-91392  
 etched, statistical distrib. using computer image anal. 0-83235  
 fission track spark counting method for neutron monitoring 0-58080  
 LR115 cellulose nitrate detector system for personal dosimetry near high energy accelerators 0-58081  
 LR-115 plastic track detector, etching behaviour 0-99423  
 neutron fluence meas. using mica muscovite as track detector 0-106237  
 nuclear emulsions, track struct. and particle identification 0-91383  
 reactor core gamma dosimetry, solid state nucl. track detector appl. 0-95466  
 short lived particles, detection efficiency evaluation method 0-102390  
 silica aerogel Cherenkov detector development 0-58037  
 solid dielectric detectors with breakdown phenomena and their applications in radioprotection 0-91388  
 solid state track detectors, glass and plastic laser diff. appl. to determ. of etched track parameters 0-95499  
 solid-state track detectors, electron microscopy of etch pits 0-99424  
 SSNTD, automatic scanning techniques 0-91387  
 SSNTD, development and appls., [conf. Nilore, Rawalpindi, Pakistan March 1979] 0-90608  
 SSNTD, development of etched nuclear tracks 0-91384  
 SSNTD, effect of etching conditions on energy resolution of phosphate glass and polycarbonate detectors 0-91390  
 SSNTD, electrochemical etching studies of the CR-39 plastic 0-91391  
 SSNTD, review of appls. in fission physics 0-91396  
 SSNTD, track registration and development efficiency 0-91385  
 SSNTD, track registration and development efficiency 0-91386  
 SSNTD, visualization of latent damage trails etching, decoration and observation techniques, review 0-91382  
 SSNTD for fast neutron meas. 0-91393  
 time expansion chamber, relativistic rise meas. by cluster counting method 0-58030  
 track chamber slide processing, calibration programming problems (Russian) 0-73305  
 track etch detectors, neutron energy depend. and threshold energy 0-61703

**particle track visualisation continued**

- track radiography of heavy-ion induced sputtering 0-91404  
<sup>235</sup>U-fission track micromapping, exam. of U mobilisation processes in Precambrian sediments 0-98477  
 ZnP glass heavy-ion track detectors 3 to 120 MeV 0-91389

**particle tracks**

- see also *energy loss of particles*  
 detection and measurement of very short flight paths in nuclear emulsions 0-102389  
 fission track annealing and dating of vermiculite 0-81885  
 fission track annealing of sphene, fission track age-temp. relationship 0-98316  
 solid state track detectors in solutions of actinides,  $\alpha$  track registration 0-63486  
 Track Etch techniques for Li determ. in brain tissue 0-98133  
 U prospecting using microdistrib. anal. of Siwalik vertebrate fossils by nuclear Track Etch tech. 0-98489

**particle velocity analysis**

- see also *energy loss of particles; ion mobility; mass spectrometers; particle spectrometers*  
 aerosol spectrometer using two-pulse Fraunhofer holography, fibrous particle motion anal. 0-58476  
 laser radiation effects on particle properties, radiation pressure effect on particle motion (German) 0-102755  
 CO flame rise vel. meas. by particle-track method 0-89489

**particles, elementary** see *elementary particles***parton model**

- baryons and mesons, parton distrib. consistent with naive quark model and QCD 0-62937  
 conference, lepton-hadron physics, Karlsruhe, Germany (Sep. 1978) 0-73098  
 cut vertex formalism, parton model interpretation 0-86566  
 dilepton charge production cross section for  $\nu$  and  $\bar{\nu}$ , parton model 0-62966  
 double-logarithmic quark and form factors and the evolution of parton jets 0-68421  
 Drell-Yan process higher order corrections, QCD and parton model sum rules 0-95251  
 Drell-Yan processes, intrinsic transverse momentum, nongauge theories 0-82950  
 forward hard scattering in hadron-hadron collisions in the energy region  $\sim 10^{14}$  eV 0-86773  
 hadron+hadron  $\rightarrow \gamma\gamma X$ , scaling and quark mass dependence, quark parton model 0-73749  
 hadron+hadron inclusive cross section of symmetric hadron pairs produced, hard scatt., parton model and QCD 0-63052  
 hadron calorimeter expts., asymptotic power laws, QCD and parton model predictions 0-57560  
 hadron inclusive prod. cross sections at large  $P_T$  A-depend., quark-parton model (Russian) 0-86771  
 hadron inelastic scatt., secondary hadron multiplicity distribution, Regge like parton model (Russian) 0-78100  
 hadron jets, rapid parton and hadron distribution 0-86693  
 hadronic events, inelastic, non-diffractive, charge correlations in jets, quantum number effects 0-86764  
 hard processes, large rapidity separation of baryonic number, partons, and dual topology 0-95255  
 heavy meson inclusive semileptonic decays, lifetime estimates, quark-parton model difficulties 0-86704  
 high energy collisions, cumulative particle prod., parton recombination and quark-parton models 0-82956  
 high energy low  $P_T$  hadronic reactions, Pomeron contrib., parton fragmentation framework 0-73688  
 jets of quarks and gluons, leading logarithmic approx., parton interpretation 0-68433  
 lepton+hadron, deep inelastic scatt., quark-parton model with logarithmic scaling violation 0-78071  
 lepton pair prod. struct. functions, QCD improved quark-parton model 0-73671  
 meson structure function in covariant parton model context 0-78020  
 multiperipheral parton model, deep inelastic processes 0-82961  
 naive model, concept and appl. 0-73675  
 nucleon charge radii 0-91064  
 parton distribution functions,  $Q^2$ -depend., QCD parameterisation 0-82937  
 Pati-Salam model, higher order parton transition effects in deep inelastic scatt. 0-78008  
 polarised deep inelastic scatt., parton transverse momenta role, struct. function, QCD evolution 0-78034  
 QCD, long range parton correlations at large  $Q^2$  (Russian) 0-68428  
 QCD, parton jet and shower model 0-86663  
 quark-parton cascades in nuclei and secondary hadron spectra from hadron-nucleus collisions (Russian) 0-57623  
 Regge formalism, quark fragmentation functions for inclusive hadron production 0-68462  
 relativistic hadron, parton distrib. and Regge field theory parameters (Russian) 0-62931  
 relativity, general, zitterbewegung, atoms with point particles 0-57147  
 soft gluon resummation formulae for hard parton processes in QCD 0-105842  
 soft hadron-nucleus collisions, two chain parton model description 0-82944  
 structure functions, nonsinglet, parton distributions, QCD parameterisation, leading and next-to-leading order corrections 0-68456  
 totally inclusive leptoprod., scaling anal., target mass corrections in QCD parton model 0-102052  
 twist selection rule, mass zero representation partons 0-78027  
 Yang-Mills theory without gauge fixing, perturbation Feynman rule 0-57462  
 d inelastic screening, form factor at  $t \neq 0$  0-91070  
 ed, deep inelastic scatt., quark-parton model with logarithmic scaling violation 0-78071  
 $e^+e^-$  0-63010  
 $e^+e^-$  annihilation, hadron multiplicity distribution, Regge like parton model (Russian) 0-78100  
 $e^+e^-$  annihilation, opposite side quantum number correlations 0-105863  
 $e^+e^- \rightarrow \Delta X$ , polarisation effects in nonperturbative parton model, scaling 0-105912  
 $e^+e^- \rightarrow$  hadrons, parton model and QCD 0-105860  
 $e^+e^- \rightarrow VX$ , parton model, polarisation effects (Russian) 0-63002



parton model continued

ep, deep inelastic scatt., quark-parton model with logarithmic scaling violation 0-78071  
 $\gamma$ +hadron—lepton pair, perturbative QCD, twist-2 photon operator, parton subprocesses 0-73716  
 $\gamma^*\gamma^*\rightarrow 2$  jets in  $e^+e^-$ , parton model QCD corrections for doubly deep processes 0-73758  
 $\gamma q\rightarrow\pi q$  inclusive pion production in  $\gamma N$  and  $e^-N$  collisions, quark-parton model (Russian) 0-78073  
 $\nu N$  or  $\bar{\nu} N$ , deep inelastic scatt., quark-parton model with logarithmic scaling violation 0-78071  
 $\bar{\nu} p$  charged current interactions, quark fragmentation, quark-parton model test 0-68444  
p, degenerate parton gas model, quark-lepton identification 0-68416  
p production, compared to  $\pi$ , large transverse momentum, rearrangement of hard scattered partons 0-62934  
pp, 62 GeV/c, multiparticle prod. mech.,  $e^+e^-$  comparison in parton model 0-78103  
pp, 70 GeV,  $\pi^+$ ,  $K^+$ , p,  $\bar{p}$  prod. cross sections, QCD-parton model anal. (Russian) 0-63044  
pp, massive lepton pair prod., pion exchange model anal., quark parton interpretation (Russian) 0-82993  
pp elastic, differential and total cross sections, proton model, gluon-gluon annihilation 0-91114  
pp soft annihilation, parton description in three chain model 0-83009  
 $\pi$  EM form factor asymptotics in QCD perturbation theory, partonic interpretation (Russian) 0-62984  
 $\pi^- N$ , 16, 22 GeV, dimuon prod. parton intrinsic transverse momentum, QCD perturbation 0-63037  
 $\pi p$ , massive lepton pair prod., pion exchange model anal., quark parton interpretation (Russian) 0-82993  
W searches with hadron beams, parton model anal. 0-91046

Paschen-Back effect see Zeeman effect

passivation

glass, molten, reactions with conducting materials 0-85186  
MOS structure with phosphosilicate glass layer, flat-band voltage, effect of growth conditions 0-107913  
oxide films, passivating, transient growth kinetics 0-93672  
solar cells, MIS, inversion layer 0-101098  
solar cells, polycryst., influence of grain boundaries electronic structure on diode characts. 0-94068  
steel, austenitic stainless, repassivation kinetics study in Cl media 0-97614  
steel, ferritic stainless, effect of Cl ions on passive layers 0-59766  
steel, galvanised strip, passivation treatment 0-61146  
steel, mild, anodic polarisation behaviour in hot alkaline sulphide solns. 0-100949  
steel, Ni-Cr, anodic dissoln. in NaCl solns. at high current densities (Russian) 0-76396  
steel, stainless type 304, anodically polarised,  $Cl^-$  ion effect on passive film 0-97621  
steel, type AISI 316, thermal passivation in controlled vacuum 0-76276  
steels, stainless, passive state, electron spectroscopy anal. 0-59765  
tinplate, passivation treatment 0-61146  
Al-brass tubes, passivation treatment for atmospheric corrosion protection during storage and transport 0-85079  
Al<sub>2</sub>O<sub>3</sub>, anodic, passified, inhibition of reaction with water 0-89390  
Cd, high purity, passivity breakdown 0-100947  
Ce, gettering of H, mass spectrometry and microgravimetry study, rel. to HTGR gas purification 0-73374  
Co, passivation films in neutral and alkaline borate soln., modulation spectroscopic anal. (Japanese) 0-108628  
Cu anode, passivating behaviour and illum. effects in alkaline soln. 0-104449  
Fe, anodic behaviour in 1M H<sub>2</sub>SO<sub>4</sub>, influence of straining 0-97612  
Fe, corrosion and passivation in LiCl soln., peripheral velocity effect 0-61000  
Fe, dissolution and passivation kinetics in solns. containing O 0-76547  
Fe dissolution kinetics, and passivation depend. on temp. and ionic strength 0-97626  
Fe, passivated, Fe<sub>3</sub>O<sub>4</sub>-Fe<sub>2</sub>O<sub>3</sub> thin film, electron diffr. study (German, English) 0-89418  
Fe, passive film form. in phosphate soln., intensity-following ellipsometry study 0-104345  
Fe-Cr alloys, in acid and neutral solns., thickness and optical constants of passive and transpassive films 0-66698  
Fe-Cr-Ni, corrosion behaviour in hot conc. NaOH soln. (Japanese) 0-85082  
GaAs anodisation, ellipsometric study (Japanese) 0-97610  
GaAs homojunction solar cells, large-grained, passivation method to improve open-circuit voltage 0-94070  
GaAs solar cell, polycryst., grain boundary passivation by oxidation, AES, SIMS and XPS obs. 0-81467  
GaAs, surface passivation using composite Al<sub>2</sub>O<sub>3</sub> and native oxide, MIS characts. 0-93004  
GaAs, surface passivation using Si<sub>3</sub>N<sub>4</sub>, interface characts. 0-93005  
GaAs, surface passivation using Ga<sub>2</sub>O<sub>3</sub>N<sub>3</sub> based multiple insulating layers 0-93006  
GaAs thin film polycrystalline solar cells, props. and prep. 0-81437  
GaAs thin film polycrystalline Schottky barrier solar cells, grain boundary chemistry 0-94067  
GaAs thin film polycrystalline solar cells, grain boundary edge passivated 0-94069  
InP, surface passivation using composite Al<sub>2</sub>O<sub>3</sub> and native oxide, MIS characts. 0-93004  
InP-InGaAsP p-n junction avalanche photodiodes, surface passivation techniques 0-100508  
In<sub>2</sub>-Sn<sub>2</sub>O<sub>3</sub>, poly Si SIS solar cells 0-97787  
Mo fine tip cathode, field emission stability, rel. to passivation 0-100760  
Ni, anodic passive film form. in NaOH soln., refl. and ellipsometric study 0-104447  
Ni, corrosion and passivation in phosphate soln., pH depend., ellipsometric study 0-104448  
Ni passivation, S influence study by Auger and electron spectroscopy 0-65347  
Ni-Cr, anodic dissoln. in NaCl solns. at high current densities (Russian) 0-76396  
P<sub>2</sub>O<sub>5</sub>-SiO<sub>2</sub> glass film, thickness and IR spectrum changes on heat treatment in H<sub>2</sub> 0-70549  
PbTe, electrochemical surface reactions 0-76389

passivation continued

Si, point defects, H passivation 0-75515  
Si solar cells, surface passivation by SnO<sub>2</sub> films, effect on cell transport props. and short circuit current 0-61360  
SiN<sub>x</sub> films, plasma enhanced CVD, props., meas. and interpretations 0-80987  
SiN<sub>x</sub> films plasma deposition, process and props. 0-80986  
Si<sub>3</sub>N<sub>4</sub> amorphous film deposition by high rate DC reactive sputtering, passivation appl. 0-100784  
Si<sub>3</sub>N<sub>4</sub> film, plasma-activated (Japanese) 0-85073  
Ti, gettering of H, mass spectrometry and microgravimetry study, rel. to HTGR gas purification 0-73374  
 $\alpha$ -Ti sheet, texture dependent stress corrosion cracking in Br<sub>2</sub>-methanol soln. 0-71803  
W fine tip cathode, field emission stability, rel. to passivation 0-100760  
Zr, gettering of H, mass spectrometry and microgravimetry study, rel. to HTGR gas purification 0-73374

passive attenuators see attenuators

passive filters

laser pulse autocorrelation by optical processing of Fabry-Perot spectrograms 0-58465  
plasma line filter bank and high-speed correlator appl. to plasma line meas. at Chatanika 0-98507  
SAW, L-band low loss filter 0-74673  
SAW, with three-transducer configuration 0-74610  
SAW, Y-Z LiNbO<sub>3</sub>, filamentary defects visualisation at wafer inspection stage 0-75315  
SAW, Y-Z LiNbO<sub>3</sub>, filamentary defects, acoustic effects 0-75314  
SAW bandpass filter design, use of charge distribution model 0-74678  
SAW chirp, spectrum analyser appl. (Japanese) 0-79065  
SAW compensated filter used in wide spread MSK waveform generator 0-74670  
SAW filter appls. in consumer electronics, review 0-74675  
SAW filter design, low-sideband cascaded 0-74679  
SAW filter design applied to group-delay equaliser in TV rebroadcast transmitters 0-74676  
SAW filter design using optimisation technique 0-74671  
SAW filter design with diffraction compensation 0-74672  
surface skimming bulk wave bandpass filters using Y-rotated quartz 0-74583

patient care

echolocating blind mobility aid, interpretation of stereophonic output 0-108989  
microwave and temperature effects on the murine ocular lens in-vitro 0-89798

patient diagnosis

see also biomedical ultrasonics; electrocardiography; electroencephalography; medical diagnostic computing; radiography; radioisotope scanning and imaging; scanning radiography  
2D images, 3D enhancement scheme 0-101255  
acoustic holographic in medicine and biology, state of art and future 0-67175  
adenocarcinoma cell clump feature extraction methods in automated uterine cancer cytology (Japanese) 0-72362  
amblyopia, speedy evoked pt. methods for vision assessment 0-61661  
audiological diagnosis, use of click-evoked elec. brainstem responses 0-104689  
bibliography of diagnostic uses of US in medicine and biology 0-62407  
bone diseases, pt. use of stimulated positron emission in detect. and monitoring 0-81712  
brain, human, neural generator localisation underlying auditory evoked mag. fields 0-104703  
cardiograms, image processing, cardiac function meas. (Japanese) 0-94354  
chromosome classification system, banding technique 0-67320  
computer-based instrument using SK.2 cylindrical coordinator (Russian) 0-76856  
coronary artery disease, preclinical, detect. in male subjects using the omnigram 0-81767  
Coulter electrical sizing principle, appl. to new multiparameter system 0-89911  
ECG signals, diagnostical functions, effect of random noise (Croatian) 0-98169  
echocardiogram, M-mode, automatic computer anal. (Japanese) 0-72274  
echocardiographic tracking system, microprocessor-controlled 0-67169  
EEG, focal slow waves localisation 0-94406  
EEG, simple computer-generated dot-density topogram 0-94407  
electrical conductivity distributions imaging, systems limitation 0-89901  
electro-optics appl., 1980 development trends 0-85464  
electron microscopic diagnosis using clinical pathology liver and kidney samples, computer assisted 0-85485  
electrooculographic system for detect. of oculomotor abnormalities in neurological disorders 0-108888  
EMG, single pots., anal. by means of multivariate methods 0-98170  
endoscopic miniature camera with fibre-optic faceplate 0-77896  
endoscopy, rel. to double-contrast radiography in upper gastrointestinal tract haemorrhage 0-98063  
epilepsy diagnostics, EEG trace coding (French) 0-67277  
evoked responses, peripheral versus foveal, multiple sclerosis early diagnosis appl. 0-67276  
haematopoietic malignancy diagnosis, significance of SEM 0-85529  
heart block computer detect. by correl. of surface and endocardiac ECG 0-94410  
heart diagnosis, using two dimensional real-time sector scanning facilities 0-81672  
hemianopia, new mirror design for detect. 0-108992  
image processing in diagnostic radiology 0-81690  
imaging overview 0-98082  
imaging system evaluation using contrast-detail-dose anal. 0-98108  
intravenous angiography, digital video subtraction system 0-98089  
ionization phenomena, appls. in medical diagnosis and treatment, review 0-67240  
left ventricular localised wall motion abnormality assessment, usefulness of quantitative parameters 0-89848  
liver metastases diagnosis, conf., Brussels, Belgium (Nov.-Dec. 78) 0-82568  
mandibular movements diagnosis, system for meas. and processing (Japanese) 0-101249  
microwave appls. in diagnosis and pulmonary disease monitoring 0-85460



**patient diagnosis continued**

- microwave system, dual mode, to enhance early detect. of cancer 0-89823
- microwave thermography, appl. in cancer diagnosis (*Spanish*) 0-67195
- NMR imaging, improvement by low temp. SQUID detect., towards mol. kinetic meas. 0-104723
- NMR imaging, multiple sensitive point method 0-81679
- NMR imaging, review (*Japanese*) 0-94312
- NMR zeugmatographic imaging, gradient control device using microprocessor 0-89822
- proton imaging for medical applications 0-98129
- pulmonary fibrosis disease diagnosis; histological section SEM and energy-dispersive X-ray microanalysis 0-72314
- pulmonary oedema diagnosis by a surgically noninvasive microwave technique 0-61659
- radiographic dose reduction 0-98087
- radiographic imaging, 3-dimens. 0-85486
- radiography, backscatter X-ray technique 0-98096
- radiography, computed, low-dose X-ray imaging system 0-98092
- radiography, flashing tomosynthesis 0-67243
- radiography, holographic 3-D synthesis of X-ray pictures 0-67245
- radiography, holographic methods of 3-D representation from no. of plane images 0-67244
- radiography, information storage requirements 0-98086
- radiography applications of holography 0-67242
- radiology, diagnostic, analytical stereo system 0-67231
- schizophrenia, event-related auditory evoked pots. 0-85405
- serial quantitative EEG 0-61728
- sinus rhythm, diagnosis by IBM ECG anal. program (*Japanese*) 0-67278
- somatosensory evoked potentials, review of acquisition and anal. 0-101281
- spin warp NMR imaging and appls. to human whole-body imaging 0-101250
- SQUID appl., iron overloaded liver non-invasive diagnosis 0-101244
- stereopsis clinical test 0-61566
- stereovision techniques (*Japanese*) 0-67279
- stethophenendoscopes, design and production 0-104686
- synchronised diagnostic and treatment techniques 0-61727
- synovial fluid analysis by ferrography 0-101242
- thyroid diseases, scope of different methods of exam. (*German*) 0-89840
- tissue structures characterisation, method of obtaining an acoustic impedance profile 0-67171
- urinary bladder interferometry, holography of bladder deforms. in vitro, rabbit expt. 0-67201
- urinary bladder interferometry, tumour and lesion detect. by holography 0-67202
- US applications in obstetrics and gynecology, safety and pot. hazards, review 0-67170
- US arrays for real-time diagnostics, image quality (*German*) 0-61656
- US damage of DNA in lymphocyte cells 0-67148
- US imaging, prospects and limitations 0-98040
- US real-time scanner with pulsed Doppler and T-M facilities, obstetrical appls. 0-67172
- US signals in diffuse liver disease, computer anal. 0-67173
- viral infections diagnosis, contrib. of electron microscopy (*Italian*) 0-109024
- visual concomitancy testing, new method 0-94305
- vocal diseases, spectrographic speech anal. (*Japanese*) 0-85455
- X-ray images, electronic recording 0-62815
- X-ray tomogram reconstruction by holographic methods 0-67246
- <sup>31</sup>P NMR of the perfused heart 0-77534

**patient monitoring**

- see also electrocardiography; electroencephalography*
- arrhythmia ambulatory anal. in real-time with minicomputer 0-85523
- arrhythmia detection, edit and recall system, microprocessor-based 0-89891
- arrhythmia detection with a multi-microprocessor system for distributed and parallel processing 0-85524
- arrhythmia identification and verification by 3-channel eval. of long-term ECG records 0-85518
- arrhythmia monitoring, single scan algorithm for QRS-detect. and feature extraction 0-85520
- arrhythmia quantification, template matching algorithm evaluation 0-85519
- blood pressure ambulatory recordings, minicomputer processing 0-89887
- blood pressure automatic monitoring, long-term, minicomputer system 0-101276
- blood temperature monitoring during extracorporeal circulation, noncontact transducer 0-85513
- bone diseases, pot. use of stimulated positron emission in detect. and monitoring 0-81712
- calibrator for ECG/respiration monitor 0-98159
- canopy ventilation monitor for quantitative meas. of ventilation during sleep 0-104792
- cerebral activity monitor, using biofeedback rhythms inducing cct. (*Spanish*) 0-72359
- computer-based instrument using SK.2 cylindrical coordinator (*Russian*) 0-76856
- coronary artery bypass graft patient recovery trajectory classification algorithm 0-94411
- ECG, 24 hr, automatic analysis on minicomputer-based system 0-89889
- ECG, ambulatory, computer processing system 0-89897
- ECG, Frank xyz signal interpretation by unmodified 12-lead computer system 0-94400
- ECG, Holter recordings, low cost arrhythmia analyser, GRETA 0-94403
- ECG, Holter tape high speed digital anal. with full editing capability 0-89896
- ECG, QRS detector/delineator devel. and eval. 0-89892
- ECG 24 hr recording, anal. using operator-controlled computer system 0-89888
- ECG automated monitoring, new electrode system 0-89898
- ECG frequency-domain analysis 0-85521
- electric admittance blood flow monitor, clinical evaluation 0-81759
- extrasystole monitor using FIFO 0-72360
- gait quality indication by temporal asymmetry 0-98164
- heart beat counter, versatile digital SAMI 0-85510
- human sleep EEG, spindle pattern recognition by real-time anal. (*Japanese*) 0-89903
- microwave appls. in diagnosis and pulmonary disease monitoring 0-85460

**patient monitoring continued**

- myocardial ischaemia and necrosis monitoring in acute myocardial infarction 0-85525
- neonate cardiorespiratory monitoring, automatic system with microprocessor 0-94399
- neurosurgical intensive care, non-invasive monitoring techniques 0-81757
- perinatal radio telemetry 0-104722
- respiratory gas monitoring instrument using microprocessor (*Japanese*) 0-72358
- rheocardiography, 4-electrode, in computer-aided cardiac output determ. 0-61718
- SOLO monitor, microcomputer bedside monitor 0-94404
- spinal cord, injured, monitoring of residual function with sensory evoked pots. 0-81747
- SQUID gradiometer, second-derivative, magnetocardiogram meas. 0-104696
- supraventricular arrhythmia rapid anal. from long-term oesophageal recordings, drug assessment 0-89904
- telemetry, conf., Sapporo, Japan (June 1980) 0-90604
- telemetry device, chronically implanted, controlled transcutaneous powering 0-98152
- thermometer, electronic digital, for long-term patient monitoring 0-90849
- ventricular arrhythmia model 0-89893
- ventricular function monitor, ambulatory, CdTe detector, cardiac ejection fraction meas. 0-61680
- <sup>131</sup>I treated patients, monitoring of I excretions and used materials 0-89873
- K<sup>+</sup>, in vivo continuous monitoring using ISFET probes 0-85512

**patient treatment**

- see also biomedical ultrasonics; radiation therapy; surgery*
- antagonistic muscles, functional elec. stimulation optimisation, math. modelling, joint motion 0-61730
- aortic valve replacement, computerised simultaneous press./vol. anal. before and after 0-85531
- biofeedback training device for speech therapy, portable, microprocessor-based 0-104808
- bone stimulation devices, anal. of sinusoidal EM fields 0-108990
- conference on cardiac defibrillation and cardiopulmonary resuscitation, Lafayette, USA (Sept. 1979) 0-67929
- defibrillating trapezoidal waveforms, haemodynamic responses 0-72370
- defibrillation, myocardial damage, induction by open-chest low energy countershock, rabbit expts. 0-72150
- education, human body, live, thermodynamics of cooling for treatment purposes 0-73128
- electrical stimulation of paralysed muscle, actuator of locomotor system (*Slovenian*) 0-81771
- electro-optics appl., 1980 development trends 0-85464
- electrocoagulation, monoactive, controlled destruction and temp. distrib. 0-94176
- EMG biofeedback in hemiplegic patient treatment, comparison of actual and simulated treatment 0-104806
- epidural neurostimulation, percutaneous, histological reaction, short and long term study results 0-67285
- exercise therapy, walking simulator 0-81770
- functional electrical stimulation for paraplegic patients (*Croatian*) 0-109058
- gait measuring system for treatment evaluation, microprocessor controlled 0-61731
- hyperthermia, local, theoretical and expt. study, nonperfused phantom (*French*) 0-104559
- hyperthermia, localised, in the patient, clinical requirements 0-98173
- hypothermia, local, Giospast-1, thermoelec. apparatus 0-104807
- ionization phenomena, appls. in medical diagnosis and treatment, review 0-67240
- microwave diathermy with surface cooling, elevated temps. induced in human leg 0-61638
- pacing, meas. of ohmic electrode-tissue contact resistance and voltage applied to myocardium 0-67284
- pain control in man, medial thalamic permanent electrodes, electrophysiological and clinical study 0-67282
- paralysis treatment, microprocessor based stimulator (*Slovenian*) 0-104809
- paraplegic patient muscles, provision of functional use by elec. stimulation, review 0-101289
- spinal cord electrical stimulation, 2D finite element anal. 0-98054
- stereodynamic<sup>1</sup> interferential current, new electrotherapeutic technique 0-85458
- stereodynamic<sup>2</sup> interferential current therapy, fundamentals and initial results 0-85459
- supraventricular arrhythmia rapid anal. from long-term oesophageal recordings, drug assessment 0-89904
- synchronised diagnostic and treatment techniques 0-61727
- ventricular defibrillation with myocardial electrodes in the dog, calf pony, and pig 0-72369
- ventricular fibrillation and defibrillation 0-81769
- vision, vertical fixation disparity, correction by horizontal prism 0-67281
- whole-body hyperthermia, core body temp. regulation by oesophageal temp. feedback 0-72371
- wound treatment by RF EM radiation, rabbit expts. 0-61639

**pattern classification** *see pattern recognition***pattern recognition**

- see also computerised pattern recognition; speech recognition*
- binary image statistical modelling, enhancement and recognition (*Russian*) 0-63929
- biological pattern recognition, rotational matched spatial filter 0-76866
- biological shape pattern recognition, average similarities of Fourier spectra 0-104818
- biomedical Doppler US diagnostic technique of carotid artery disease, objective feature extraction 0-72273
- brain electrical potentials, approaches 0-109051
- chromosome analysis, problems and progress in automation 0-94436
- chromosome classification system, banding technique 0-67320
- coherent optical pattern recognition using normalized invariant moments 0-99653
- context-dependent automatic image screening system 0-95820
- correlator with matched filtering using band-limited illumination 0-69531
- cytological cell feature extraction using optical moments 0-98206
- diatom recognition and counting, matched-filter and statistical method 0-101304



# pattern recognition continued

- dimensionality reduction by linear regression with preselected cluster centres 0-106479
- ECG prototype waveforms generation by piecewise correlational averaging 0-109053
- edge detection, numerical, optical and hybrid methods compared 0-102662
- EEG automatic classification, decision rules comparison 0-109054
- EEG patterns during cognitive tasks, methodology and complex behaviours anal. 0-61531
- EEG signals hierarchical modelling 0-109052
- epilepsy diagnostics, EEG trace coding (*French*) 0-67277
- fast image recognition by generalised harmonic analysis (*Russian*) 0-63930
- feature enhancement using noncoherent optical processing 0-99651
- feedback systems for analogue and digital optical image processing 0-102650
- forward-looking IR sensor image segmentation by maximum likelihood parameter estimation 0-99662
- gastric X-ray image using Ba, feature point extraction method 0-101259
- generalised matched filters for coherent optical pattern recognition 0-99654
- hybrid optical-digital processor for invariant moment computation 0-102646
- hybrid parallel optical and serial digital processing systems 0-99657
- image analysis via general theory of moments, Zernike polynomials 0-102629
- image intensifier tube for optical image processing 0-99825
- image registration and differencing by coherent optical pattern recognition 0-99648
- image understanding systems, seminar, San Diego, CA, USA (Aug. 79) 0-94918
- incoherent optical correlation operations 0-99650
- integrated optics coherent correlator for real-time signal processing 0-79007
- IR signature classification system 0-86430
- laser diode lensless MSF holographic optical element correlator, optical pattern recognition 0-102663
- laser rangefinder and 3D object recognition algorithm 0-96016
- layered relaxation network for object detection 0-99659
- matched filtering improvements for coherent optical pattern recognition 0-78786
- meteorological field analysis and forecasting pattern-recognition theory methods appl. 0-98421
- mosaic IR image differencing for track assembly 0-86420
- multiclass, multivariate technique 0-87320
- multisensor image pattern recognition, statistical and deterministic aspects 0-99647
- neocognitron, self-organising neural network model, pattern recognition mechanism unaffected by shift in position 0-76745
- NMR substituent parameters, pattern recognition interpretation 0-58284
- nuclear reactor surveillance, pattern recognition techniques appl. 0-63351
- optical, by diffraction pattern sampling 0-99643
- optical, by thermoplastic complex filter 0-99656
- optical, discriminant hypersurface prod. by average filters 0-99649
- optical, seminar, San Diego, CA, USA (Aug. 1979) 0-98759
- optical coherent correlator operation in image segment identification, aerial photograph anal. 0-102654
- periodic-pattern-defects omnidirectional-spatial-filter optical detection system 0-69333
- perpendicular line intersection, detection method 0-69330
- photodiode array integration with optical power spectral analysis 0-99645
- psychological aspects (*Japanese*) 0-97919
- robust feature matching through maximal cliques 0-99671
- scene content measurement from aerial images, appl. to building complex scene 0-78788
- spatial, by spectral feature classification and coherent optical correlation 0-99644
- styrenes, 4-substituted, NMR substituent parameters, pattern recognition interpretation 0-58284
- submarine sediments, automatic recognition by sonar probe survey, acoustic reflection pattern model (*Japanese*) 0-85776
- texture analysis by hybrid optical/digital system 0-78787
- tunable spatial filtering with a Fabry-Perot etalon 0-58668
- US-optical correlator for spatial freq. meas. 0-95995
- vision, functional mechanisms in humans 0-81609
- vision, human recognition system with thinking, model 0-76744
- visual pattern recognition, models (*Japanese*) 0-97920
- visual search complexity estimation, for objects against nonuniform backgrounds 0-67086
- KD<sub>2</sub>PO<sub>4</sub> photo-spatial light modulator, optical data processing 0-102839

**Pattern diagrams** see crystallography; X-ray crystallography calculation methods

**p.c.m.** see pulse-code modulation

# Peierls instability

- electron-electron interaction effect on Peierls struct. transition (*Russian*) 0-70629
- Frohlich model, one-dimens., CDW stability, electron-phonon coupling 0-65452
- Ising chain, with next-nearest neighbour interactions, mag. responses to spin-Peierls transition 0-71054
- linear conductor, CDWs and impurity effects 0-59967
- magnetic order coexistence with charge density waves 0-97096
- mean-field theory of Peierls and spin-Peierls instabilities—commensurability, harmonics and dimerized-state pinning 0-108014
- metallic ultrathin filaments, dielectric and superconducting fluctuations, Peierls transition (*Russian*) 0-65742
- one-dimensional conductivity, with arbitrary bandfilling, Peierls instability 0-59968
- one-dimensional conductor, lattice distortion, Kolmogorov Arnold Moser theorems, appl. to struct. problems in condensed matter 0-59878
- one-dimensional conductor, lattice stability, phonon dispersion, Kohn anomaly 0-96603
- one-dimensional conductors, libron effects on electron spectrum, theory 0-96854
- Peierls one dimensional model, exact solution, electron spectra, static lattice deformation (*Russian*) 0-70609
- Peierls-Frohlich condensate, attracting solitons and discontinuous lock-in transition 0-92840
- polyacetylene, metallic, mixed Peierls phase, Hartree-Fock calcs. 0-70689

# Peierls instability continued

- polyacetylene conductivity mechanism, Peierls phase one dimensional cond. (*Russian*) 0-88546
- polyenes, long chain, electronic struct. in Peierls-PPP model 0-84423
- quasi-one-dimensional conductors, alloys, Peierls distortion 0-59965
- quasi-one-dimensional systems, spin-lattice Peierls instabilities, static and dynamic aspects 0-71052
- spin-Peierls phase diagrams, obs. and models 0-60330
- TCNQ salt, dibenzo-TTF-TCNQCl<sub>2</sub>, one-dimens. mag. semicond., mag. and elec. props. 0-88601
- transition in quantizing mag. field, possibility 0-103441
- two level commensurability in one-dimensional Peierls system (*Russian*) 0-70688
- Ga ultrathin metallic filaments, appearance of dielec. instability, coexistence with supercond. 0-103784
- Hg ultrathin metallic filaments, appearance of dielec. instability, coexistence with supercond. 0-103784
- In ultrathin metallic filaments, appearance of dielec. instability, coexistence with supercond. 0-103784
- Sn ultrathin metallic filaments, appearance of dielec. instability, coexistence with supercond. 0-103784
- TaS<sub>3</sub>, monoclinic form, cryst. struct. determ., Peierls type transition obs. (*French*) 0-88109

# Peltier effect

- metal-semiconductor thermoelectric coolers, effects of contact resist. and dopant conc. 0-81481
- multicomponent systems, rel. to electroepitaxy, theoretical model 0-65396
- thermocouple, thermometers, voltage generation, calibration 0-57295
- thermoelectric energy conversion, heat losses compensation due to thermal cond. through Peltier heat 0-107773

**PEM effect** see photoelectromagnetic effects

**Pendellosung fringes** see X-ray crystallography

# pendulums

- see also time measurement
- ball and spring, elliptical motion 0-82613
- bipedal locomotion, inverted pendulums stabilisation algorithm (*Japanese*) 0-81630
- computer-aided laboratory exercise 0-67985
- forced periodic oscillations of the simple pendulum 0-94951
- Foucault pendulum, continuously operating 0-73151
- impact machines, energy meas. using optical system 0-69746
- inverted, design and stabilisation control (*Japanese*) 0-73167
- multiple pendulum mirrors for telescope mirror testing 0-102792
- physical pendula, reconstructed 19th century expt. 0-82612
- quantum pendulums, classical, semiclassical and quantum aspects, teaching 0-101679
- random interactions anal. using computer (*Russian*) 0-73313
- slightly perturbed, bounce resonance and Kolmogorov entropy 0-57199
- viscoelastic rod, standard linear body, free torsional axills. 0-99940

# penetration depth (superconductivity)

- collective oscillations and electric field penetration, review 0-88678
- granular superconductors, coherence transition, structural disorder effects 0-88657
- hard superconductor, flux trapping, penetration depth determ. 0-100572
- point contacts, three-dimens. assembly, crit. currents and penetration depth 0-84560
- superconducting thin hollow cylinder, mag. field penetration, Ginzburg-Landau calcs. (*Russian*) 0-75674
- superconductor resistive state, coherence length, penetration depth 0-97030
- Sn film, crit. mag. fields, temp. depend., penetration depth thickness depend. 0-70908
- Ta<sub>70</sub>Nb<sub>30</sub>, Abrikosov vortex formation kinetics (*Russian*) 0-93055

# Penning ionisation

- anthracene surface, Ar impact, Penning ionisation electron spectra and photoelectron spectra 0-66352
- atomic collisional ionisation, Penning ionisation, laser induced, two step optical collisional perturbation sequence 0-63778
- cathode sheath, RF impedance study 0-106935
- collisional ionisation, Penning and associative ionisation produced by laser field 0-63802
- electron spectroscopy investig. of Penning ionisation processes 0-58364
- electronic and at. collisions, conf., Kyoto, Japan (Aug.-Sept. 1979) 0-57011
- excited atom thermal energy collisions, electron spectrometric studies 0-63788
- excited atoms, merging-beams experiments 0-63789
- heterocyclic aromatic molecules, Penning electron spectra and photoelectron spectra, rel. intensities 0-95725
- plasma, low-temp., with nonequilibrium ionisation, review 0-96343
- polarization phenomena in electronic and atomic collisions, review 0-83501
- Ar<sup>+</sup>+Fe(CO)<sub>5</sub>, chemiionisation and chemiluminescence reactions, Penning ionisation and fluoresc. obs. 0-97689
- Au, Auger spectra, N<sub>4s</sub>N<sub>6s</sub>N<sub>6p</sub> and N<sub>4s</sub>N<sub>6p</sub>O<sub>4s</sub> 0-89094
- CO adsorbed on Pd (111), metastable He impact, electron emission, energy and ang. distrib. 0-60744
- CO+He\*, Penning ionisation of CO adsorbed on Pd, theory 0-60735
- Cd+He, Penning ionisation cross section of target atom, for He(2<sup>3</sup>S<sub>1</sub>) 0-63777
- H<sub>2</sub>, hot-iron plasma, ion temp. and electron density depend. studied by laser light scatt. and emission spectroscopy 0-96342
- He+CS<sub>2</sub>, metastable atoms, energy transfer processes 0-83466
- He+OCS, emission spectra in He afterglow 0-87139
- He<sup>+</sup>Ne\*, Penning ionisation of metastable He\* 0-83472
- Ir, Auger spectra, N<sub>4s</sub>N<sub>6p</sub>N<sub>6p</sub> and N<sub>4s</sub>N<sub>6p</sub>O<sub>4s</sub> 0-89094
- Na+Na, crossed-beam collision, laser-induced Penning and assoc. ionisation, struct. obs. 0-83476
- Ne+CS<sub>2</sub>, metastable atoms, energy transfer processes 0-83466
- Ne<sup>+</sup>+Ar\*, Penning ionisation studied by merging-beams technique 0-91646
- Ne<sup>+</sup>+Fe(CO)<sub>5</sub>, chemiionisation and chemiluminescence reactions, Penning ionisation and fluoresc. obs. 0-97689
- Ne<sup>+</sup>+H<sub>2</sub>O, pot. energy surfaces, MO and CI calcs., Penning ionisation electron spectra 0-106376
- Pt, Auger spectra, N<sub>4s</sub>N<sub>6p</sub>N<sub>6p</sub> and N<sub>4s</sub>N<sub>6p</sub>O<sub>4s</sub> 0-89094
- Zn+He, Penning ionisation cross section of target atom, for He(2<sup>3</sup>S<sub>1</sub>) 0-63777



**penny-shaped cracks**

- cylinder with oblate spheroidal cavity or internal penny shaped crack under tension, stresses 0-69736
- Dugdale crack, dynamic effects in propagation, Hankel and Laplace transform methods 0-87741
- elastic solid, deformed, incompressible, penny-shaped crack problem 0-92085
- infinite transversely isotropic solid, stress intensity factor 0-69738
- mirror/flow-size relations, residual contact stresses effect 0-107363
- thermal stresses, elastic sphere embedded in infinite elastic space 0-64460
- transverse tension, stresses, micropolar elasticity 0-64459
- transversely isotropic solid, penny shaped crack, stress anal. 0-92083
- two bonded elastic solids interface, penny shaped crack, torsional wave interaction 0-64484
- US flaw detection, diffraction of normal modes by a compliant disk 0-87603

**pentary algebra** *see algebra***perception (hearing)** *see hearing***periodic system of elements**

- see also elements (chemical)*
- rare earth compound properties, periodicity at atom props. 0-96586

**peripheral models**

- see also multiperipheral models*
- boson, Green function, rainbow approach of scalar model (Russian) 0-68436
- heavy meson exchange effect on  $^1D_2$  and  $^3F_3$  N-N partial waves, dibaryon resonances 0-105874
- pion exchange at high energies, review 0-95259
- s-channel resonance model based on peripheral resonances, exotic peaks 0-91069
- tachyon exchange in two-body interactions 0-82960
- DD, DD\*, D $\bar{D}$ \*, charm molecules, dynamical model, light meson exchange 0-57572
- ed-cd, nucleon forces, meson exchange current effects, impulse approx., review 0-57603
- NN and  $\pi$ NN,  $\pi\pi$ NN bound states from NN potentials 0-62951
- NN dynamics at medium energies, elastic and inelastic scatt., unitary model 0-63101
- NN dynamics at medium energies, phase parameters, one pion exchange model 0-63102
- NN forward scatt., two and three pion cut contribs., nucleon exchange model 0-63103
- pn, inelastic charge exchange, quark interchange 0-86759
- pp, inelastic charge exchange, quark interchange 0-86759
- pp, massive lepton pair prod., pion exchange model anal., quark parton interpretation (Russian) 0-82993
- pp scatt., <300 MeV P-odd asymmetry for pol.  $\rho$  (Russian) 0-102063
- $\pi^+d$ , 15 GeV, high-mass even-g states, broad dipion states beyond g(1680) 0-68487
- $\pi^-n \rightarrow pX^-$ , 21, 205 and 360 GeV/c, reggeised one-pion-exchange 0-57649
- $\pi p$ , massive lepton pair prod., pion exchange model anal., quark parton interpretation (Russian) 0-82993
- $^3He$ , nuclear charge form factor, two-boson exchange charge density  $\pi$ ,  $\rho$ ,  $\omega$  exchanges 0-63073

**peripheral speed** *see velocity***peristaltic flow**

- asymptotic method for peristaltic transport 0-87805
- bio-fluid peristaltic transport, peripheral layer viscosity effects 0-61600
- blood in vessel with actively deforming wall, numerical simulation of movement 0-72205
- non-Newtonian fluid, long wavelength peristaltic transport, stream function and pressure field solns. 0-74922

**Permalloy**

- film, mag. microstruct. obs. in nonlinear ripple magnetis. case (Russian) 0-65971
- film, two-layer, Permalloy-Cu(Al), mag. anisotropy, grain boundary diffusion (Russian) 0-71122
- film break-cross-tie wall energy 0-88842
- film strip, unidirectional domain wall propag. with in-plane magnetisation 0-71134
- films, RF sputtered on Au, coercivity 0-80575
- hysteresis loops, reference materials characts. obs., temperature effect 0-80563
- isopermalloy, permeability stability calc. rel. to texture (Chinese) 0-65959
- magnetic properties and structure, environment effect during annealing, 50NP and 79NM alloys 0-60366
- magnetoresistive magnetic, field sensor, performance calc. 0-57342
- Permalloy-Mn film, diffusion aftereffect causing mag. state change (Russian) 0-103860
- RF sputtered films, O effects in mag. and elec. props. 0-100603
- T bar, domain wall study employing ferrofluid, rel. to magneto-optical Kerr effect meas. 0-60360
- thermomagnetic recording, resolving power of films with band domain struct. (Russian) 0-75769
- thin-film head pole struct., domain configurations, SEM obs. 0-65975
- (Fe $_{0.2}$ Ni $_{0.8}$ ) $_y$ , (SiO) $_y$ , Permalloy material, magnetisation, temp. and impurity atom conc. depend., band model calcs. (Russian) 0-93088

**permanent magnet motors**

- plastic magnet appl., anisotropic, based on moulding ferromagnetic powder material with plastics (Japanese) 0-60829

**permanent magnets**

- Alnico 8, permanent magnetic alloy, topography of precipitate phase (Chinese) 0-66512
- Alnico type YuNDK25DA alloy permanent magnets, thermal mag. hysteresis 0-75818
- coil and permanent magnet combination for large dia. ion source 0-74066
- high-coercivity, magnetisation characteristic linearity determ. using flux controlling technique (Russian) 0-100597
- ion beam transport equipment for low energy divergent H $_2$  beam 0-69001
- magnetic soft and hard materials, garnets, magnetic properties and applications, structural props. 0-65760
- metallic magnets investigation, present state (Polish) 0-107987
- plastic, anisotropic, based on moulding ferromagnetic powder material with plastics (Japanese) 0-60829
- $\tau$ -Al-Mn-C, permanent magnetism and microstruct. 0-75811

**permanent magnets continued**

- Co permanent magnet material savings (German) 0-103851
- Co-mischmetall system, phase relations, microstruct., mag. props. 0-104118
- Co $_3$ Sm crystals, microstruct., homogeneous precip. and nucleation 0-104160
- Cu-Ni-Fe, magnetic properties, heat treatment and compressive stress effects 0-60367
- Fe-Co-Ti-Al alloy type YuNDK magnets, metallographic method of distinguishing cracks 0-85096
- Fe-Cr-Co alloys, (5-9 wt.% Co), obtained by slow cooling under mag. field, permanent magnet props. 0-75797
- Fe-Cr-Co system, miscibility gap, microstruct., and mag. props. obs. 0-76228
- Fe-Cr-Co-Mo high energy permanent magnets, mag. props. 0-97119
- Mn-Al-C (70, 29.5 wt.%) alloy, Almax anisotropic mag. props. (Japanese) 0-60371
- SmCo $_5$ , free suspension in const. mag. field with aid of pyrolytic graphite 0-101807
- SmCo $_5$ , nucleation of reversed domains at Co $_2$ Sm $_2$  precip. 0-75791
- SmCo $_5$  permanent magnets, crystal texture effects on props. 0-100600
- SmCo $_5$ , sintered, hard mag. material, magnetisation behaviour 0-75805
- SmCo $_5$ , sintered, mag. after-effect, expt. and model 0-75816
- SmCo $_5$  sintered magnets, eutectoid decomp. 0-89219
- Sm $_2$ O $_3$ , sintered, coercive force and constitution, annealing temp. depend. (Russian) 0-88786
- Sm $_{0.91}$ Zr $_{0.09}$ (Co $_{0.68}$ Cu $_{0.10}$ Fe $_{0.22}$ ) $_{6.7}$ , alloy permanent magnet, coercive force (Russian) 0-65966

**permeability**

- albumin flux, differential permeability of endothelial and epithelial barriers, sheep expts. 0-81553
- blood-brain barrier, reversal of microwave-induced permeability 0-61641
- capillary permeability evaluation from multiple indicator data, effects of red cell and tissue exchange 0-10193
- carrier-mediated extraction, development 0-66870
- cellulose acetate membrane, asymmetric, elec. and electroosmotic transport behaviour in dialysis-osmosis expts. 0-108745
- cellulose diacetate membrane, diffusive permeability 0-104460
- cellulose diacetate membranes, unilayer, transport phenomena, hydration and dialysis coeffs. 0-76556
- cerebrovascular permeability, quantitative method for meas. of alterations 0-61748
- ferrites, microwave, dielectric constants and permeability (Chinese) 0-66096
- gel, heterogeneous two-phase, permeability 0-76563
- gelatin layer, dry, aqueous soln. penetration 0-85221
- glomerular permeability in foetal rabbit 0-85372
- heated porous body, impregnation with viscous liquid 0-79392
- hydromagnetic squeeze film between porous circular disks with velocity slip 0-74997
- Incoloy 800, clean and steam oxidised, T $_2$  permeation 0-88364
- lipid bilayer membranes, steady-state permeability behaviours induced by cyanine dyes 0-85357
- lung vascular permeability after microemboli, effect of platelet depletion, sheep obs. 0-97972
- magnesite artifacts, roasted, props., filler porosity effect 0-104099
- metallic membrane interface, mass transfer 0-81366
- molecular sieves, adsorp. of atmospheric gases, comparison of 13X and 4A at low temp., press. (German) 0-88423
- nexus, evidence for fixed charge, permeability, obs. 0-94193
- Pd membrane, H $_2$ -D $_2$  isotope separation 0-68959
- percolation, universal critical amplitude ratios 0-101765
- photographic developer, permeation into a gelatin layer, potentiometric exam. (Russian) 0-73500
- Polimal 109, polymer resin laminate, density porosity, water vapour diffusion sorption and permeation (Polish) 0-59665
- polymer films, permeation, diffusional time lags determ. 0-65272
- pyrocarbon coating, isotropic, gas permeability, neutron irradiation effect (French) 0-63260
- pyrocarbon coating, isotropic, gas permeability meas. (French) 0-63259
- red cell, human, increased passive permeability below 12°C 0-94185
- rocks, of water, shear thinning and shear-thickening polymer additives 0-72100
- Sanicro 31, T $_2$  permeation 0-88364
- sarcolemmal permeability changes during early myocardial anoxia 0-85371
- steel, bimetal, alloy with austenitic stainless, H permeability 0-107572
- steel, SAE 1045, permeation meas. of H trapping, rel. to cryst. microstruct. 0-84328
- Al, reaction with H $_2$ , influence of surface reactions on rate (Russian) 0-66863
- Fe, effect of anion and organic corrosion inhibitors on H $_2$  penetration rate 0-100938
- Fe, H $_2$  permeation, rel. to embrittlement, organic inhibitors, surface treatment 0-108635
- H $_2$ , change of diffusivity with order-disorder transformations in Ni $_3$ Fe, Ni $_3$ Pt and Ni $_3$ Mn 0-59729
- H $_2$  permeation reduction using Pd foil in liquid metal (Japanese) 0-68770
- H $_2$ , through Pd membrane, diffusion-cell for separation H $_2$  containing mixtures, solar furnace appl. 0-92245
- Nb, membrane, H permeation (Japanese) 0-100363
- Ni-Mn, permeability, diffusion and solubility of H 0-107573
- Pd membrane, H atom interaction, superpermeability 0-81365
- SiO $_2$ , fused, He solubility and diffusion above transform. range 0-79965
- ThO $_2$  microspheres, coated, coating permeability meas. 0-95343
- Ti, through Croloy steel for LMFBR steam generator 0-68775
- UO $_2$ -UC microspheres, coated, coating permeability meas. 0-95343

**permeability (magnetic)** *see magnetic permeability***permeability measurement (magnetic)** *see magnetic permeability measurement***permittivity**

- see also electric strength*
- alkali metal compounds, AsbO $_3$  1/6AF, dielec. spectroscopy study, 100 Hz to 10 MHz, 238 to 417K (German) 0-108144
- ammonium Rochelle salt, thermodynamics of ferroelec. transition 0-84702
- anisotropic artificial dielectrics, dispersion props, investigation, electrodynamic method 0-88903
- anisotropic inhomogeneous medium, elastic light scatt., orientation characterization 0-83553



## permittivity continued

anisotropic medium, inhomogeneity, orientation characterization by elastic light scatt. 0-83552  
 anisotropic semiconductors, light reflection in interband transition freq. (*Russian*) 0-88945  
 benzonitrile-isooctane mixture, dielec. const. near consolute point, temp. and freq. depend. meas. 0-71292  
 biological substances, tabulation for freq. range 10 kHz to 10 GHz 0-108143  
 1,6-bis(2,4-dinitrophenoxy)-2,4-hexadiyne, obs. of apparent ferroelec. transition 0-66121  
 Born model, electrostriction rel. to dielec. and thermoelastic props. 0-71322  
 t-butyl acetate, rot. isomerism, dielec. and Raman spectra 0-106328  
 t-butyl alcohol, self-assoc., linear and nonlinear dielec. effects obs. 0-60484  
 t-butyl formate, rot. isomerism, dielec. and Raman spectra 0-106328  
 castor oil dielectric fluid, microwave propag., permittivity effect, demonstration 0-105468  
 ceramics, transparent ferroelectric, composition selection for appl. in light modulators (*Russian*) 0-91869  
 cermet film granular media, dielectric function theory, permittivity, percolation transport props. 0-88498  
 chloranil pellets, thermally stimulated discharge current and dielectric studies 0-93236  
 chlorobenzene-cis-decalin, mixtures, dielec. const. and loss tangent in liq. and solid phases 0-100628  
 cholesteryl laurate-cholesteryl caprylate (75 wt.%), polymorphic behaviour, optical, elec. and dielec. meas. 0-65208  
 coal dispersions, solvent refined, elec. props., surface characts. 0-80333  
 composite material, complex dielectric const., bounds 0-108170  
 composite material, two-component, complex dielectric constant, exactly solvable microscopic geometries and rigorous bounds 0-75918  
 conjugate interfaces: interfaces between transparent media of the same reflection coefficient for the parallel polarization at the same angle of incidence 0-87299  
 cooperative Raman scattering, effect of phase self-modulation of light 0-91855  
 cubic lattice of polarisable spheres, dielectric constant 0-60483  
 4-cyano-4'-octylphenyl, dielectric relax. anal. in nematic and smectic phases 0-108153  
 t-cyanobutane, dielectric relaxation study, complex permittivity 0-80688  
 defective dielectrics, EM heating with time depend. param., WKB calcs. 0-71367  
 dicalcium lead propionate, improper ferroelectric, dielectric props., IR radiation pyroelectric detection 0-80711  
 dielectrics, field induced thermally stimulated polarisation-depolarisation currents, relaxation, book contribution 0-80687  
 diethylammonium cadmium tetrachloride, dielec. props., phase transition 0-80675  
 dihydroxy benzenes in ethyl alcohol, dielec. dispersion charact. 0-75932  
 dihydroxy toluene in ethyl alcohol, dielec. dispersion charact. 0-75932  
 N,N-dimethylacetamide in tetrachloromethane, dielectric relax. and complex permittivity 0-108149  
 dipolar hard sphere solvent with charged hard spheres, hypernetted chain approx. 0-61130  
 dipolar liquid time-variation of dispersion and absorption of third-order electric polarisation, mol. relax. times 0-60487  
 disilicate, piezoelectric glass ceramic, recrystallisation, pyroelectric response, permittivity 0-80703  
 DNA, calf-thymus Na-DNA eq. solns., dielec. behaviour in 5 kHz to 100 MHz range 0-85330  
 DOBAMBC, chiral smectic, ferroelec., press. and solute effects 0-103920  
 dust dielectric constant at X-band, effect of moisture content 0-72578  
 Earth surface layer, EM wave refl. and transmission coeffs., linear ramp model 0-61759  
 effective medium theory: mathematical determination of the physical solution for the dielectric constant 0-93230  
 electron gas, interacting, local-field correction to dielectric constant, review 0-107731  
 EM wave penetration into plasma, permittivity sign changes (*Russian*) 0-100477  
 ethyl acrylate ionomers, stress relax., dielec. const. effect 0-104200  
 ethylene-CO copolymer, dielec. absorpt. meas.; permittivity (*French*) 0-103916  
 ferrites, microwave, dielectric constants and permeability (*Chinese*) 0-66096  
 ferroelectric ceramic, polycryst., elasticity props., neutron bombardment effects 0-79856  
 ferroelectric ceramic, rel. to mech. and elec. losses, correl., theory and expt. 0-66133  
 ferroelectric crystals, dielectric const. meas. using automatic system (*German*) 0-90864  
 ferroelectrics, dielectric spectroscopy, transitions, permittivity 0-75914  
 ferroelectrics, negative capacitances, comparison with negative viscosities 0-66118  
 ferroelectrics, quantum transition suppression, pyroelectric, electrocaloric effects, specific heat 0-75984  
 fluid mixtures, dil., spherical mols., struct. and permittivity 0-92433  
 fluid nonpolar polarisable, local field at large distances from charge or dipole rel. to dielec. constant 0-83534  
 glass fibre reinforced plastics, ageing by boiling in water, effect on physico-mech. props. 0-60892  
 gyrotropic absorbing crystals, nonorthogonal eigenwave refl. 0-99624  
 gyrotropic media, artificial, EM scattering 0-106423  
 heavy water, over temp. range 473K to 643K 0-103912  
 ice, reflectivity meas. at mm wavelengths 0-66098  
 ice orientational correlation parameter, water mol. dipole moment 0-59407  
 iodobenzene, soln., non-linear dielec. effect, comparison with fluoro, chloro and bromobenzene 0-60478  
 ionic salts, melting transition statistical model, dielectric const., surface tension 0-70378  
 Kirkwood correl. factor relationship 0-93228  
 liquid crystals, prep. and phys. props., book 0-105444  
 liquid dielectrics, local field, two-parameter mean field approach 0-93232  
 liquid-vapour interface, non-polar fluid, variation of local field 0-80734  
 methyl iodide, liq., mol. reorientation, dielec. and viscosity meas. 0-100157  
 mixed salt solution approximating seawater composition, dielec. and radiation characts. 0-97184

## permittivity continued

nematic liquid crystal mixtures, dielec. permittivity dispersion 0-88921  
 nonuniform systems, effective conductivity from percolation and conduction theory 0-62597  
 4-n-octyloxyphenyl 4-n-pentyloxybenzoate, permittivity, microwave dielectric relaxation 0-80671  
 opaque region, piezobirefringence anal. 0-60541  
 optical waveguide, parabolic index with random dielectric constant gradient, Gaussian beam propag. 0-58698  
 p-alkoxybenzylidene-p'-amino-2-chloropropyl-cinnamate, chiral smectic, dielec. props. 0-96441  
 partially ionised plasma, theory of dielectric constant 0-59173  
 patient electrical conductivity and permittivity imaging, computing tomography technique 0-98055  
 phenolic Mannich bases, dielec. relax. study 0-97196  
 3-phenylpropanol-hexane, nonlinear dielectric effect, critical exponent 0-93227  
 phospholipid bilayer, ion permeability rel. to dielec. const. 0-81364  
 photoelasticity, nonlinear, in impure crystals, theory 0-108179  
 planar double layers, Derjaguin force formula 0-107890  
 plasma, collisional, mixed mode operation, cross-focusing 0-83945  
 plasma, moving weakly nonsteady, plasma wave propag. 0-106918  
 polar fluid, molecular pair effects, Onsager dielec. theory breakdown 0-75917  
 polar fluids, rigid, dielectric relaxation theory 0-60495  
 polar liqs. permittivity, computer simulation with hard sphere point dipole pot. 0-103911  
 polar molecules with fluctuating polarisability, dielec. theory 0-97178  
 polar solvents, solvated electron absorpt. spectra, intrasolvent and intersolvent corrs. 0-93840  
 poly(1,3-dioxane), dipole moments, dielectric const. meas 0-66099  
 poly-4-chlorostyrene, undiluted, dielec. relax. spectrum above Tg 0-97194  
 poly- $\gamma$ -benzyl-L-glutamate, synthetic polypeptide, nonlinear dielectric effect in nonpolar medium 0-84682  
 polyacetylene:1, dc microwave cond., permittivity 0-107843  
 polyacetylene film, anisotropy of dielec. const. 0-108146  
 polycarbonate,  $\gamma$ -irradiated, dielec. behaviour and glass transition 0-97182  
 polyethylene, low-density natural, at elevated temps. 0-97185  
 polymer, generation mechanism and characts. (*Japanese*) 0-60488  
 polyvinylidene fluoride, thermodynamic model and appl. 0-75955  
 1,2-propane diol-dipropylene glycol, dielec. dispersion charact. 0-75932  
 propyl acetate-propyl alcohol, dielec. dispersion charact. 0-75932  
 PZT ceramics, ferroelec. energy conversion under shock loading 0-108163  
 quartz, electron irradiation effects on optical, dielec., elastic props. 0-59521  
 rare earth aluminate, scandate and zirconate film coatings, electrophys. props. w.r.t. prep. technology 0-60781  
 rare earth arsenates,  $\text{RAsO}_4$ , ferroelectricity, dielec. meas. 0-60515  
 rare earth oxides, dielec. const. and loss at low temp. 0-93229  
 relaxation time distrib. function, first order moments from permittivity data (*French*) 0-88918  
 (Rochelle salt) $_2$ -(ammonium Rochelle salt) $_2$ , phase transitions, hydrostatic press. effects 0-93246  
 semiconductor, n-type, donor-polarizability enhancement as the insulator-metal transition is approached from the insulating side 0-80184  
 semiconductor, p-type, infrared absorption and plasma reflection 0-97284  
 semiconductor plasma, longitudinal oscillations 0-88583  
 semiconductors, degenerate, acoustodielectric effect, permittivity modulation by acoustic wave in resonance conditions 0-92944  
 semiconductors, photoconductivity measurement at UHF and at high excitation levels 0-65627  
 serum albumin, bovine, hydrated, dielec. and elec. props. 0-97854  
 serum low density lipoprotein, human, anomalous permittivity behaviour 0-81540  
 shadow methods for studying turbulence using reflection from a mirror in the medium 0-95801  
 shear SAW in high permittivity three-layer system (*Russian*) 0-80048  
 smectic phases, long mol. axis reorientation, LF dielec. dispersion 0-70124  
 snow, permittivity and attenuation, 4-12 GHz 0-85692  
 spatial dispersion exponential model, boundary conditions (*Russian*) 0-75994  
 squaric acid, layered, antiferroelec., phase transition mechanism 0-97210  
 Stockmayer fluids, static dielec. props. 0-93231  
 Stockmayer fluids with dipoles and quadrupoles, spherical harmonic coeffs., dielec. const. and Kerr factor calcs. 0-84678  
 Stockmayer molecular fluid, 2-dimens., permittivity and dynamic props. 0-103910  
 TCNQ salt, MeDABCO(TCNQ) $_2$ , optical, elec., and mag. props. 0-65539  
 TCNQ salt, MEM(TCNQ) $_2$ , dielec. const. obs., DC and microwave cond. obs. 0-59963  
 tetramethylammonium hydrogen bis-trichloracetate ( $-\text{d}_n$ ),  $^{35}\text{Cl}$  NQR study 0-66064  
 tetramethylammonium tetrachlorocobaltate, ferroelec., pressure-temp. phase diagrams 0-97205  
 tetramethylammonium tetrachlorocuprate crystal, incommensurate-ferroelastic (commensurate) phase transition obs. 0-75352  
 tetramethylammonium tetrachloroferrate, press. induced ferroelectricity, dielec. and DTA meas. 0-80722  
 tetramethylammonium tetrachlorozincate, ferroelec., pressure-temp. phase diagrams 0-97205  
 TGS- $\alpha$ -alanine, single crystals, dielec. spectrum in RF range (*Russian*) 0-66097  
 TGS: nitroaniline, dielec. and pyroelec. props. 0-75916  
 TGS, effect of  $\text{Fe}^{3+}$  admixture on phys. props. 0-76052  
 TGS, L- $\alpha$ -alanine disordered regions, dielec. prop. changes in transition region 0-108159  
 TGS, static crit. phenomena, lattice defect influence 0-71336  
 TGS powders, dielec. dispersion 0-97180  
 tris-sarcosine calcium chloride, phase transition, hydrostatic press. effect, dielec. const. meas. 0-71327  
 trissarcosine calcium chloride, ferroelec. transition, press. effect 0-84681  
 unidirectional fibre composites, anisotropic constituents, effect elastic moduli and other props. 0-58911  
 vinylidene fluoride-trifluoroethylene film, cryst. phase transition 0-66120  
 water, complex permittivity meas. and microwave heating for specific purities and salt. soln. 0-60480  
 water, reflectivity meas. at mm wavelengths 0-66098



## permittivity continued

- water-oil microemulsions, optical matching 0-61157  
 X-zeolites, dielectric relax. anal. 0-108153  
 Ag halides, static dielec. constant, strain derivatives 0-100629  
 AgCl(Br), electronic dielec. const., vol. depend., Clausius-Mossotti model 0-100630  
 AgNO<sub>3</sub>, single crystal, dielec. const., low temp. meas. 0-71290  
 AgNa(NO<sub>2</sub>)<sub>2</sub>, crit. dynamics, hydrostatic press. effect, dielec. props. meas. 0-71328  
 AgNa(NO<sub>2</sub>)<sub>2</sub>, order-disorder ferroelec., influence of hydrostatic press. on polarisation dynamics 0-103913  
 Al-stearic acid-Al, low-loss thin film capacitor 0-71317  
 AlF<sub>3</sub> in Al-AlF<sub>3</sub>-Al MIM thin film structures, dielec. and elec. props. (Slovak) 0-100536  
 Ar, gas, liquid, solid, refractive index, density and dielectric const. 0-66138  
 Ar-H<sub>2</sub>(Ne) liquid solution, dielectric props., intermolecular interactions (Russian) 0-88904  
 As-Ge-Te, chalcogenide glass, elec. cond. and dielec. const. 0-75567  
 As<sub>10</sub>Ge<sub>15</sub>Te<sub>75</sub>Ag<sub>8</sub>, glass, elec. and dielec. props., Ag additions effect 0-65558  
 (Ba,Sr)TiO<sub>3</sub>, ferroelec. props., press. depend., anharmonic oscillator model 0-80716  
 BaFe<sub>2</sub>O<sub>19</sub>, ferrite, DC cond., dielec. props., lattice consts. 0-80272  
 BaMn<sub>99</sub>Co<sub>01</sub>F<sub>4</sub>, magnetoec. phenomena, dielec. behaviour near Neel temp. 0-71151  
 BaMnF<sub>4</sub>, pure and Co doped, ferroelec. antiferromag., dielec. anomalies 0-71288  
 BaO-Nd<sub>2</sub>O<sub>3</sub>-TiO<sub>2</sub>-Bi<sub>2</sub>O<sub>3</sub> system ceramics, high stability low loss dielectric preparation 0-81008  
 (Ba,Sb)<sub>1-x</sub>TiO<sub>3</sub> 0-60514  
 BaTiO<sub>3</sub> ceramic dielectric capacitor, processing prop. relations, hysteresis, permittivity 0-80730  
 BaTiO<sub>3</sub> film, dielectric props. depend. on sinusoidal elec. field 0-71318  
 BaTiO<sub>3</sub> film, struct. and dielec. props. 0-60514  
 BaTiO<sub>3</sub>, paraelectric crystal, nonlinear props. 0-84699  
 BaTiO<sub>3</sub> RF sputtered ferroelectric film on Si substrate, ferroelectric props. 0-80697  
 BaTiO<sub>3</sub>:BaTi<sub>2</sub>O<sub>7</sub>, dielec. props. and microstruct. 0-60481  
 BaTiO<sub>3</sub>:Nb, elec. props., contact material influence 0-70848  
 Ba(Ti<sub>1-x</sub>Sn<sub>x</sub>)O<sub>3</sub> film, struct. and dielec. props. 0-60514  
 Ba(Ti<sub>1-x</sub>Sn<sub>x</sub>)O<sub>3</sub> thick film, ferroelec., phase transitions and dielec. props. 0-97215  
 Bi<sub>2</sub> film, exciton-phonon interaction, optical consts., Faraday effect, permitt. 0-59884  
 Bi<sub>2</sub>SiO<sub>30</sub> crystal, piezoelec. and SAW props. 0-75949  
 Bi<sub>2</sub>WO<sub>6</sub>, ferroelectric, dielectric props., elec. cond. and relaxation phenomena obs. 0-80692  
 CH<sub>3</sub>NH<sub>2</sub>Ga(SeO<sub>4</sub>)<sub>2</sub>·12H<sub>2</sub>O, dielec. relax. near transition temp. 0-60493  
 CaF<sub>2</sub>:Er, near-Debye dielectric responses 0-71291  
 CaF<sub>2</sub>:Li(Na)(K)(Rb), dielec. relax., activation energy, rel. to vacancy pair reorientation 0-88917  
 Ca<sub>2</sub>Nb<sub>2</sub>O<sub>7</sub>, ferroelectric phase transitions, dielec. constant and thermal expansion rel. to temp. 0-88934  
 Ca<sub>1-x</sub>Sr<sub>x/2</sub>Ba<sub>x/2</sub>Zr<sub>1-x/2</sub>Ti<sub>x/2</sub>O<sub>3</sub>, ceramic system, dielectric props., microwave resonator application 0-80674  
 CdGa<sub>2</sub>S<sub>4</sub>, IR refl. spectra 0-60604  
 Cd(NO<sub>3</sub>)<sub>2</sub>, phase transition, SHG, optical and dielec. meas. 0-71334  
 CdS, elastic, piezoelec. and dielec. props. 0-108157  
 CdS, elastic, piezoelectric, and dielec. props., 4.2 to 300K 0-60508  
 CdTi<sub>2</sub>Se<sub>4</sub>(Te<sub>4</sub>):Au, elec. cond., density, dielectric const., changes on fusion 0-88553  
 Co<sub>2</sub>Zn<sub>1-x</sub>Fe<sub>x</sub>O<sub>4</sub>, ferrite, DC cond., dielec. props., lattice consts. 0-80272  
 Cr<sub>2</sub>O<sub>3</sub>, dielec. const. in mag. field, nonlinear magnetoec. effect in Neel pt. region 0-66006  
 CsH<sub>2</sub>AsO<sub>4</sub> crystals, dielectric radiation effects, γ-radiation 0-93234  
 Cs(H<sub>1-x</sub>D<sub>x</sub>)<sub>2</sub>PO<sub>4</sub>, dielec. props., temp. meas. 0-71335  
 Cs<sub>2</sub>(MoO<sub>4</sub>) R=Dy, Ho, Er, permittivity temp. depend., polymorphic transition 0-92670  
 CuCl(Br), electronic dielec. const., vol. depend., Clausius-Mossotti model 0-100630  
 CuWO<sub>4</sub>, elec. cond., thermoelectric power and dielectric constant temp. depend. 0-96886  
 D-T, liq., dielectric constant and elec. cond. 0-84680  
 ethanol-water system, complex dielec. permitt. in UHF region and NMR spectra (Japanese) 0-100620  
 EuO(Se), complex elec. cond. anomalies 0-107812  
 Fe<sub>2</sub>B<sub>2</sub>O<sub>7</sub>, improper ferroelectric, dielectric props., IR radiation pyroelectric detection 0-80711  
 FeF<sub>2</sub>, dielectric properties, IR spectra, lattice dynamics (French) 0-76026  
 FeI boracite single crystals, dielectric, pyroelectric props., vapour phase transport growth 0-80673  
 GaAs, semi-insulating 0-60479  
 Ga<sub>2</sub>O<sub>3</sub>, B-type monoclinic, DC(AC) elec. cond., thermoelectric power, dielectric const., temp. depends. 0-59980  
<sup>4</sup>He, P-ρ-T data near vaporisation crit. point (Russian) 0-88373  
 Hf, electronic excitations, charact. energy loss meas. up to 50 eV 0-60723  
 HfO<sub>2</sub>, electronic excitations, charact. energy loss meas. up to 50 eV 0-60723  
 InSb, current-voltage characteristics at room temperature and high hydrostatic pressure 0-88560  
 InSb lattice, static dielec. const. and carrier conc. meas. via gyrotropic sphere reson. 0-97143  
 n-InSb, microwave helicon resonances, carrier density, mobility, dielectric const. 0-96930  
 KCl<sub>2</sub>Br<sub>1-x</sub>, dielectric const. determ. 0-108145  
 K<sub>2</sub>Fe(CN)<sub>6</sub>·3H<sub>2</sub>O, ferroelec. and paraelec. phases, dielec. props. meas. 0-60494  
 KH<sub>2</sub>PO<sub>4</sub>, critical and tricritical phenomena, susceptibility, exponents 0-75976  
 KH<sub>2</sub>PO<sub>4</sub> family of crystals, proton modes, dielec. spectroscopy 0-75915  
 KH<sub>2</sub>PO<sub>4</sub>-KD<sub>2</sub>PO<sub>4</sub> mixed crystals, dielec. spectra, sub-mm wavelengths 0-80724  
 KH<sub>2</sub>PO<sub>4</sub>-type ferroelectrics, dielec. props., four-cluster approx. 0-97202  
 K<sub>2</sub>H(SO<sub>4</sub>)<sub>2</sub>, and K<sub>2</sub>D(SO<sub>4</sub>)<sub>2</sub>, dielec. props. and phase transitions 0-60482  
 K<sub>2</sub>Li<sub>2</sub>Nb<sub>2</sub>O<sub>5</sub> films for optical waveguides epitaxial growth and characterisation 0-79016  
 K<sub>2</sub>OSiCl<sub>6</sub>, single cryst. with H<sup>+</sup> interstitials, protonic cond. from dielec. meas. 0-107515

## permittivity continued

- K<sub>2</sub>SO<sub>4</sub>, phase transform., mech. of thermal hysteresis, DTA, dilatometry and dielec. meas. 0-75353  
 K<sub>2</sub>SeO<sub>4</sub>, dielec. dispersion, 5-900 MHz, near incommensurate-commensurate transition 0-60522  
 KTa<sub>1-x</sub>Nb<sub>x</sub>O<sub>3</sub>, holographic storage using photorefractive effect, dielectric const. 0-78800  
 Kr, gas, liquid, solid, refractive index, density and dielectric const. 0-66138  
 Li<sub>2</sub>B<sub>2</sub>O<sub>7</sub>, ferroelectric glass, phase transition, permittivity, electrochromism, photochromism 0-80719  
 Li<sub>2</sub>GeO<sub>3</sub>, piezoelectric glass ceramic, recrystallisation, pyroelectric response, permittivity 0-80703  
 α-LiIO<sub>3</sub>, depolarisation current, dielectric const. relaxation behaviour (Chinese) 0-88905  
 LiNH<sub>2</sub>SO<sub>4</sub> and LiND<sub>2</sub>SO<sub>4</sub>, dielec. pyroelec., and thermal props. 0-60509  
 LiNbO<sub>3</sub> single crystals, growth from melt, Czochralski method (Chinese) 0-76171  
 Li<sub>2</sub>SiO<sub>3</sub>·H<sub>2</sub>O, far IR spectra, H<sub>2</sub>O flipping motion, lattice modes 0-84258  
 Li<sub>2</sub>SiO<sub>3</sub>, piezoelectric glass ceramic, recrystallisation, pyroelectric response, permittivity 0-80703  
 Li<sub>1-x</sub>Ta<sub>x</sub>Ti<sub>0.5</sub>Ti<sub>0.5</sub>O<sub>3</sub> (0≤x≤0.028), non-stoichiometric phase, crystallographic and dielec. props. 0-75212  
 MnNbO<sub>3</sub>, tetragonal, electronic struct., optical anisotropy 0-70599  
 Mg<sub>2</sub>SiO<sub>3</sub>:SiO<sub>2</sub>, elec. and dielec. props. 400-900°C 0-104953  
 Mg<sub>0.25</sub>Zn<sub>0.75</sub>Fe<sub>2</sub>O<sub>4</sub>, ferrite, DC cond., dielec. props., lattice consts. 0-80272  
 MoSi<sub>3</sub> oxide film, dielec. props. and growth kinetics 0-81215  
 ND<sub>2</sub>D<sub>2</sub>PO<sub>4</sub>, cryst., transverse and longit. elec. susceptibilities, modified Ising model calcs. 0-97203  
 ND<sub>2</sub>DSeO<sub>4</sub>, crystals, struct., IR spectra, dielec. props. 0-75919  
 (NH<sub>4</sub>)<sub>2</sub>BeF<sub>4</sub>, far-infrared and submillimetre dielectric response 0-80782  
 NH<sub>4</sub>Cl(Br), effect of NH<sub>4</sub><sup>+</sup> internal motion on elec. and optical props. 0-100454  
 NH<sub>4</sub>H<sub>2</sub>PO<sub>4</sub>, cryst., transverse and longit. elec. susceptibilities, modified Ising model calcs. 0-97203  
 (NH<sub>4</sub>)<sub>2</sub>H(SO<sub>4</sub>)<sub>2</sub>, phase transitions, dielec. study at low temps. 0-88902  
 NH<sub>4</sub>HSeO<sub>4</sub>, cryst. struct., dielec. and ferroelec. props. 0-60528  
 NH<sub>4</sub>SeO<sub>4</sub>, ferroelec., phase transitions, permittivity and pyroelectricity meas. 0-71350  
 (NH<sub>4</sub>)<sub>2</sub>SO<sub>4</sub>, static and dynamic dielec. behaviour 0-71337  
 NaCl, monoelectrolyte, highly mineralised salt soln., dielec. and radiation characts. 0-97184  
 Na<sub>1-x</sub>Li<sub>x</sub>NbO<sub>3</sub> mixture, ferroelec.-paraelec. transitions, dielec. props. meas. 0-66125  
 NaNO<sub>2</sub>, ferroelec., dielec. and thermal behaviour 0-80680  
 NaNO<sub>2</sub>, optical harmonic generation near ferroelec. transition 0-91858  
 NaNO<sub>3</sub>, hydrostatic press. effect on permittivity, phase transition, hysteresis 0-80670  
 NbSe<sub>3</sub>, freq. depend. conductivity 0-107838  
 Ni-I single crystals, mag. and dielectric props. 0-93095  
 NiBr boracite single crystals, dielectric, pyroelectric props., vapour phase transport growth 0-80673  
 NiWO<sub>4</sub>, AC elec. conductivity, thermoelec. power and dielec. const. 0-70736  
 NiZn ferrite, dielec. props., Jahn-Teller ion effects 0-97181  
 PLZT ceramic, ageing, dielec. props. 0-88940  
 PLZT ceramics, modified by Ca<sup>2+</sup>(Sr<sup>2+</sup>)(Nd<sup>3+</sup>)(Y<sup>3+</sup>), dielec. behaviour 0-60519  
 PLZT modified high voltage dielectric, permittivity, Curie temp., loss meas. 0-80720  
 (Pb, Sr)<sub>2</sub>Ge<sub>2</sub>O<sub>7</sub>, single crystals, growth and X-ray and dielec. investigations 0-88127  
 (Pb,Sr)TiO<sub>3</sub>, ferroelec. props., press. depend., anharmonic oscillator model 0-80716  
 (Pb<sub>1-x</sub>Ba<sub>x</sub>)<sub>2</sub>Ge<sub>2</sub>O<sub>11</sub>, ferroelec. phase transition, dielec. const. and quasi-elastic light scatt. 0-71289  
 PbCo<sub>1/2</sub>Te<sub>1/2</sub>O<sub>3</sub>, antiferroelec., high-frequency permittivity, temp. depend. 0-71325  
 Pb<sub>3</sub>(Ge<sub>1-x</sub>Si<sub>x</sub>)<sub>3</sub>O<sub>11</sub>, electrogyration, phase transition and dielectric props. 0-93269  
 PbI<sub>2</sub>, dielectric props., elec. cond., space charge polarisation 0-100631  
 PbIn<sub>0.5</sub>Nb<sub>0.5</sub>O<sub>3</sub>, ferroelectric, dielectric props. 0-103923  
 Pb(Mg<sub>1-x</sub>Nb<sub>x</sub>)<sub>2</sub>O<sub>3</sub>, electrostrictive effect 0-66113  
 Pb<sub>3</sub>(PO<sub>4</sub>)<sub>2</sub>, ferroelastic, dielectric anomalies, phase transitions, permittivity, relaxation (Russian) 0-71293  
 PbS(Se)(Te), energy gap and dielec. props., 77 to 373K 0-66100  
 PbSe<sub>0.5</sub>Nb<sub>0.5</sub>O<sub>3</sub>, single cryst., dielec. props. 0-66126  
 PbSe<sub>2</sub>Te<sub>1/3</sub>O<sub>3</sub>, ferroelec., high-frequency permittivity, temp. depend. 0-71325  
 PbSc<sub>2/3</sub>Te<sub>1/3</sub>O<sub>3</sub>-PbSc<sub>2/3</sub>W<sub>1/3</sub>O<sub>3</sub>(PbFe<sub>2/3</sub>Te<sub>1/3</sub>O<sub>3</sub>) ferroelec. props. and lattice consts. 0-60520  
 n-PbTe, low temperature electrical transport, Hall effect 0-84478  
 xPbTiO<sub>3</sub>+(1-x)PbCd<sub>1/3</sub>Nb<sub>2/3</sub>O<sub>3</sub>, phase transition spread, polarisation relaxation, dielectric susceptibility (Russian) 0-75922  
 Pb(Zr,Ti,Mg,W)O<sub>3</sub>, low-Q ceramics, props. and transducer appl. 0-75944  
 Pb(Zr,Ti)O<sub>3</sub>:Ni-silicon rubber flexible composite pyroelectric, dielectric props. 0-80704  
 Pb(Zr,Ti)O<sub>3</sub> ceramics, low temp. sintering, elec. and mech. props. 0-71616  
 Pb(Zr,Ti)O<sub>3</sub> ceramics with ladder type struct., prep. and props. 0-75945  
 Pb(Zr,Ti)O<sub>3</sub> ceramics, DC field sintering preparation, piezoelectric props., ageing behaviour 0-81211  
 Pb(Zr,Ti)O<sub>3</sub> films, ferroelec., ion beam deposition sputtered from multi-component targets 0-80974  
 Pb(Zr,Ti)O<sub>3</sub> internally electrode multilayers, piezoelectric props., permittivity, transducers 0-80672  
 Pb(Zr,Ti)O<sub>3</sub> internally electrode with Pt, resonance behaviour 0-84701  
 Pb(Zr,Ti)O<sub>3</sub>, porosity-permittivity relations, depolarising factors determ. and pore effects (Japanese) 0-97189  
 Pb(Zr,Ti)O<sub>3</sub>:Fe(Nb) ceramic, elec. and electromechanical props., depend. on dopants 0-81212  
 PbZr<sub>2</sub>Ti<sub>1-x</sub>O<sub>3</sub> ceramics, morphotropic phase boundary 0-81035  
 RbH<sub>2</sub>PO<sub>4</sub>, critical and tricritical phenomena, susceptibility, exponents 0-75976  
 RbHSO<sub>4</sub>, ferroelec., dielec. dispersion 0-97179  
 Rb<sub>2</sub>H(SO<sub>4</sub>)<sub>2</sub>, and Rb<sub>2</sub>D(SO<sub>4</sub>)<sub>2</sub>, dielec. props. and phase transitions 0-60482  
 RbH<sub>2</sub>(SeO<sub>3</sub>)<sub>2</sub>, dielec. relax. near ferroelec. Curie temp. 0-97207  
 RbNbW<sub>2</sub>O<sub>9</sub> crystals, growth and props. 0-104054



**permittivity continued**

- Rb<sub>2</sub>ZnCl<sub>4</sub>, dielec. dispersion, 5-900 MHz, near incommensurate-commensurate transition 0-60522  
 SF<sub>6</sub>, critical isochore, dielectric const. critical anomaly upper bound 0-84679  
 Sc, electronic excitations, charact. energy loss meas. up to 50 eV 0-60723  
 Sc<sub>2</sub>O<sub>3</sub>, electronic excitations, charact. energy loss meas. up to 50 eV 0-60723  
 Se-Ge-Te, chalcogenide glass, elec. cond. and dielec. const. 0-75567  
 Si p-channel MOS structure, stress effects on elec. props., press. transducer props. 0-100526  
 SiO<sub>2</sub> films, DC plasma Si anodisation, dielectric const., O<sub>2</sub> pressure influence 0-70564  
 SiO<sub>2</sub>-B<sub>2</sub>O<sub>3</sub>-Li<sub>2</sub>O-Al<sub>2</sub>O<sub>3</sub> (28, 2, 1 wt.%) glass, dielec. const. at 3 GHz 0-93233  
 Sm<sub>2</sub>O<sub>3</sub>, B-type monoclinic, DC(AC) elec. cond., thermoelectric power, dielectric const., temp. depends. 0-59980  
 Sn, liq., optical props., 0.62-3.7 eV 0-75996  
 Sn<sub>2</sub>P<sub>2</sub>S<sub>6</sub>, investigation of p-T diagram near a singular point (*Russian*) 0-88937  
 Sr<sub>0.5</sub>Bi<sub>0.5</sub>Nb<sub>2</sub>O<sub>7</sub> piezoelectric transducer, SAW props. 0-79037  
 Sr<sub>0.7</sub>Bi<sub>0.3</sub>Nb<sub>2</sub>O<sub>7</sub>, ceramic ageing dielec. props. 0-88940  
 SrF<sub>2</sub>-La, type-I dipole reorientation, activation vol. determ. from dielec. const. 0-88916  
 Sr<sub>1-x</sub>Na<sub>x</sub>Nd<sub>1-x</sub>Ta<sub>2</sub>O<sub>7</sub>, solid soln., ferroelectric phase transitions, dielec. constant and thermal expansion rel. to temp. 0-88934  
 Sr<sub>2</sub>Nb<sub>2</sub>O<sub>7</sub>, ferroelectric phase transitions, dielec. constant and thermal expansion rel. to temp. 0-88934  
 Sr<sub>2</sub>Ta<sub>2</sub>O<sub>7</sub>, ferroelectric phase transitions, dielec. constant and thermal expansion rel. to temp. 0-88934  
 SrTiO<sub>3</sub>, undispersive nonlinear dielectric, third harmonic generation (*Russian*) 0-95955  
 Ta<sub>2</sub>O<sub>5</sub> film, reactively sputtered on Si, dielectric and optical props. obs. (*Bulgarian*) 0-89144  
 Tb<sub>2</sub>(MoO<sub>4</sub>)<sub>3</sub>, improper ferroelectric, dielectric props., IR radiation pyroelectric detection 0-80711  
 Tb<sub>2</sub>O<sub>3</sub>, B-type monoclinic, DC(AC) elec. cond., thermoelectric power, dielectric const., temp. depends. 0-59980  
 TeO<sub>2</sub>, ferroelectric glass, phase transition, permittivity, electrochromism, photochromism 0-80719  
 TeO<sub>2</sub> thin films, dielec. props. rel. to fabrication conditions 0-97199  
 Ti, electropolished, optical props. from 1.8 to 3 eV 0-85088  
 TiO<sub>2</sub>, porosity-permittivity relations, depolarising factors determ. and pore effects (*Japanese*) 0-97189  
 TI halides, static dielec. constant, strain derivatives 0-100629  
 TiD<sub>2</sub>PO<sub>4</sub>, antiferroelectricity, permittivity, electric field double hysteresis loops 0-60512  
 Tm<sub>2</sub>O<sub>3</sub> film, between Al electrodes, prep. and elec. props. 0-60103  
 Y<sub>2</sub>Si film, optical props. (*Russian*) 0-93418  
 YTe, mag. and elec. transport props. 0-92897  
 WO<sub>3</sub>, amorphous anodic film growth on W in acidic soln. 0-81232  
 WO<sub>3</sub>-P<sub>2</sub>O<sub>5</sub> glass, AC cond. and dielec. props. 0-92717  
 Xe, gas, liquid, solid, refractive index, density and dielectric const. 0-66138  
 Y, electronic excitations, charact. energy loss meas. up to 50 eV 0-60723  
 Y<sub>2</sub>O<sub>3</sub>, electronic excitations, charact. energy loss meas. up to 50 eV 0-60723  
 Y<sub>2</sub>O<sub>3</sub>-AlN-SiO<sub>2</sub> oxynitride glasses, elec. props. 0-80267  
 ZnO, elastic, piezoelec. and dielec. props. 0-108157  
 Zr, electronic excitations, charact. energy loss meas. up to 50 eV 0-60723  
 ZrO<sub>2</sub>, electronic excitations, charact. energy loss meas. up to 50 eV 0-60723

**permittivity measurement**

- allyl ether, dielectric relaxation obs. at millimetric wavelengths 0-71311  
 automatic system for meas. with high interference rejection (*German*) 0-90864  
 complex permittivity, accurate meas. for wide range of materials in H<sub>01n</sub> mode cylindrical resonator (*Polish*) 0-73383  
 complex permittivity determ. for wide range of materials in coaxial cavity resonator with lumped capacitance (*Polish*) 0-73382  
 complex permittivity meas. using cylindrical cavity resonator in H<sub>01n</sub> mode, approx. method (*Polish*) 0-73384  
 conductive materials, Sh<sub>2</sub>-3 dielectric constant meter (USSR) 0-62689  
 dielectric cylinders, microwave meas. of permittivity using retarded waves (*Czech*) 0-95111  
 dielectric props. of biological substances, physical meas. 0-94417  
 high-field meas. at VLF (*French*) 0-98933  
 microwave freqs., two coupler method modification 0-100632  
 polymer films, dielectric constant meas. parallel to film surface 0-97183  
 solution dielectric constant meas., cell, student, research laboratory apps. 0-62433  
 tubular dielectric, complex permittivity and loss angle meas. in X-band using H<sub>011</sub> cavity resonator method (*German*) 0-62690

**personal computing**

- see also microcomputers  
 microcomputer use at University of Michigan 0-62431

**personnel**

- see also education; management; teaching; training  
 coal workers, localised-field magnetopneumographic meas. 0-104714  
 fission reactors, BWR, Enrico Fermi-2, system turnover, test and startup program 0-63338  
 ionising radiation, personnel exposures, dose limits 0-99350  
 nuclear power plant, Virgil C., startup, conduct of operations, organisation and personnel 0-63340  
 nuclear power plants, startup, staffing program, scope, tasks, resources, constraints, anal., implementation 0-63341  
 Project Manager organisation in nuclear plant turnover and startup 0-63339

**perturbation techniques**

- see also control system analysis  
 e-expansion technique, appl. to integral evaluation in critical dynamics 0-57187  
 coupled-core nuclear reactor, distributed parameters identification, pseudorandom perturbation and correlation anal. 0-86966  
 homopolar crystals, imperfect, lattice dynamics 0-59601  
 inertial confinement pellet fusion, perturbation theory for sensitivity and uncertainty anal. 0-68946

**perturbation techniques continued**

- motor output response to applied torque perturbations in man, nonlinearities evaluation 0-76771  
 solution of a highly non-linear oscillation equation, single particle analogue of field equations of chiral Lagrangian theories of pion interactions 0-62470  
 stellar rapidly rotating models with radiation press., struct. parameters calc. 0-67697  
 sub-optimal graded index optical fibre analysis using perturbation calculus 0-87480

**perturbation theory**

- see also quantum theory  
 adsorbed atoms, surface band splitting, theory, with appl. to He/graphite 0-60058  
 alicyclic compounds, nucl. spin-spin coupling via nonbonded interactions,  $\gamma$ -substituent effects 0-69078  
 aliphatic compounds, nucl. spin-spin coupling via nonbonded interactions,  $\gamma$ -substituent effects 0-69078  
 alkali metals, phonon dispersion curves using second-order perturbation theory 0-79893  
 alkanes, nucl. spin-spin coupling via nonbonded interactions, conformational and substituent effects 0-69077  
 alkenes, 1,1-, 1,2-disubstituted, fragmentation modes in perturbational MO anal. 0-58138  
 anharmonic oscill., classical versus quantum case (*Spanish*) 0-73210  
 anharmonic oscillator, perturbation series 0-57137  
 anharmonic oscillator, perturbation theory, hypervirial theorems 0-105535  
 anharmonic oscillators, partition function, statistical variation perturbation method 0-77648  
 anisotropic superconductors, upper critical field theory, perturbation theory study 0-75692  
 asymmetric Anderson model, ground state, perturbation approach 0-65504  
 atom, spontaneous radiation, near field calcs. 0-99493  
 atomic binding energies, determ. from fund. theorems involving electron density,  $\langle r^{-1} \rangle$  and  $Z^{-1}$  perturbation expansion 0-63521  
 atomic collisional ionisation, Penning ionisation, laser induced, two step optical collisional perturbation sequence 0-63778  
 atomic interaction dipoles, perturbation theory 0-78680  
 atomic interactions, retarded energy shift and pair polarisability, field theoretical perturbation theory 0-102560  
 atomic many-body perturbation theory with radially restricted basis functions 0-78526  
 atomic photoionisation anal. using relativistic random phase approximation and multichannel quantum defect theory 0-63602  
 atomic quadrupole shielding factors calc. using elec. field variant orbitals 0-106276  
 atoms, identical, dispersion intermolecular pot. anomaly prod. by intense radiation field 0-58336  
 atoms, perturbation var. calc. with contact interaction, effect of approx. zero order wavefunctions 0-58107  
 atoms, relativistic energies, perturbation calcs. 0-102453  
 atoms, two photon excitation, time depend. emitted light spectra, perturbation theory 0-63605  
 benzene, dynamic polarisabilities, calcs., superposition method of excited config., nonstationary perturbation theory eqns. 0-69257  
 benzene+bromomethane, microwave line width and quadrupole moments, perturbation theory 0-69190  
 benzene+OCS, microwave line width and quadrupole moments, perturbation theory 0-69190  
 binary solutions of dense liquids and gases, isothermal eqn. of state calcs. (*Russian*) 0-88292  
 bound-state properties calcs., theoretical error estimates 0-102425  
 chemical reactions, symmetry correl. and perturbation calcs. methods 0-104427  
 closed-shell system, polarisability and mag. susceptibility calc. by SCF and CI method 0-99443  
 collapsing pre-galactic H gas cloud, local stability, linear perturbation anal. 0-82513  
 contracted orbital formulation of many-body perturbation theory 0-87026  
 Coulomb potentials, screened, energy approximants and perturbation theory 0-106368  
 Coulombic systems, charged hard sphere system, rel. to restricted primitive model 0-64854  
 coupled HF-perturbation theory of atomic and mol. props., correl. corrections 0-106269  
 cyclone development along weak thermal fronts, model soln. 0-81994  
 deformation potential polaron, perturbation theory breakdown 0-84440  
 degenerate discrete levels, periodical perturbation (*Russian*) 0-86152  
 desorption, relaxation time approach limitations 0-93795  
 diacetylhydrazine, <sup>14</sup>N NQR lines fine structure 0-63667  
 diagrammatic perturbation theory, appl. to N<sub>2</sub>, CO<sub>2</sub>, BF<sub>3</sub> 0-58131  
 diformylhydrazine, <sup>14</sup>N NQR lines fine structure 0-63667  
 dilute alloy, perturbation expansion for the asymmetric Anderson Hamiltonian 0-80202  
 dilute gas, kinetic perturbation theory 0-100051  
 dilute gas transport props., logarithmic term in softness expansion 0-83872  
 displacive phase transition, S ion spin Hamiltonian parameter dependence on order parameter 0-70356  
 dynamic multipole polarisability 0-74252  
 education, Na Rydberg states, anomalous fine struct., perturbation model 0-57035  
 electron-ion system, effective ion interaction and force consts. 0-65185  
 ethylidene, rearrangement to ethylene, barriers, ab initio MO calcs. 0-104424  
 exchange perturbation theory for electron scatt., appl. elastic scatt. from H 0-78709  
 excited states, perturbation and SCF calcs. 0-102455  
 fermions, quantum field theory, large order perturb. theory, more than one coupling constant 0-77940  
 fluids, perturbation theory and thermodynamic props., CRIS model 0-92430  
 fluids, perturbation theory and thermodynamic props., inverse power and 6-12 pots. 0-92431  
 fluids, perturbation theory and thermodynamic props. 0-92429  
 fourth order perturbation theory, triple substitutions to electron correl. energy 0-74133



## perturbation theory continued

- free electron lasers, classical theory, saturation, perturbation calcs. 0-83580
- free polaron spectrum and convergence radius 0-70626
- $gr^{2N}$  anharmonic oscillator, perturbation theory 0-90712
- hard dumbbell fluids, RAM and BLIP function theories 0-79658
- heavy ion collisions, perturbed stationary state method, low energy collision and mol. resons. 0-78320
- hydrocarbons, average elec. polarisabilities and mag. susceptibilities, ab initio valence electron calcs. 0-87033
- inert gas atom, first excited config., intermediate coupling coeff. 0-83450
- intensity fluctuations and fourth-order coherence function in random media 0-78774
- interactions, point, periodic, one particle theory, polymers, monomolecular layers and crystals 0-105576
- interdoublet EPR spectrum ang. depend. for ions with arbitrary electron and nuclear spins in strong axial cryst. field 0-93164
- intermediate valence system, local polaron model 0-107717
- Ising chain, random bond, low temp. behaviour 0-57211
- Kolmogorov Arnold Moser theorems, appl. to struct. problems in condensed matter 0-59878
- Lennard-Jones fluid, two-centre, perturbation theory appl. using spherically averaged reference potential 0-64860
- limit cycle, symmetric bifurcation to asymmetric limit cycle, simple model 0-57080
- liquid metal, electronic density of states, pseudopotential calcs. 0-70578
- liquid metal, extension to dense partially ionised plasmas 0-75500
- liquids, simple, thermodynamically self-consistent theories, radial distrib. function, functional derivative 0-92435
- liquids and mixtures, statistical thermodynamics, book 0-90616
- macromolecules, cluster expansion 0-106408
- metal, simple, non muffin-tin corrections to eqn. of state (French) 0-59906
- metals, localised dynamic perturbations 0-73262
- metals, X-ray photoemission spectroscopy, anomalous, frequency dependence of exponents 0-71563
- methane, nucl. elec. shielding tensor calcs. 0-83296
- MISIM struct. inversion layer, symmetrical, carrier conc. calc. 0-75651
- modified virtual orbitals, HF calcs. of second order perturbation energy 0-102437
- molecular isotope partition function ratios, perturbation calcs., convergence 0-87239
- molecular polarisabilities calcs., superposition method of excited config., nonstationary perturbation theory eqn. 0-69257
- molecular rotational spectra, doublet splittings caused by tunnelling, perturbation treatment 0-91541
- molecular static polarisability, ab initio SCF wave functions 0-74106
- molecules, direct CI calcs. with multiconfigurational reference state 0-63506
- molecules, identical, dispersion intermolecular pot. anomaly prod. by intense radiation field 0-58336
- molecules, monochromatic wave perturbation, time depend. HF calcs. (French) 0-63516
- molecules, pair energy, perturbative corrections, incomplete basis set problem 0-78507
- naphthalene, singlet and triplet excimer interactions, exciton resons. 0-95535
- nonrelativistic one-dimensional problems, perturbation theory algorithm 0-82671
- odd anharmonic oscillators, perturbation theory 0-86106
- open resonators, diffraction losses for symmetrically tilted plane reflectors 0-58598
- open-shell system, polarisability and mag. susceptibility calc. by SCF and CI method 0-99443
- optically pumped laser three-photon transition theory 0-102690
- organic molecular crystals, charge carrier generation by exciton-exciton collisions 0-88568
- oxoniomethylene cation, rearrangement to hydroxymethyl cation, barriers, ab initio MO calcs. 0-104424
- perturbative numerical methods, local and accumulated truncation methods 0-62536
- perturbed ladder operator method, wavefunctions, matrix elements, closed form expressions 0-73203
- phase separation kinetics, Boltzmann's transport eqn. calcs. 0-79952
- plasma wave propagation, nonlinear Schrodinger equation, modified Zakharov-Shabat inverse scatt. problem 0-59200
- pure Yang-Mills perturbation theory, instanton sector renormalisation, zeroth sector comparison 0-105775
- quantum mechanical perturbation problems, resolution using integral eqn. 0-58112
- radial Schrodinger eqn. global numerical soln. by second order perturbation theory 0-68079
- radiative mass generation in perturbation theory and the renormalization group 0-86611
- Raman scattered light, Hanle effect influence 0-83323
- rare gas clusters, small, structure, thermodynamic properties 0-88341
- renormalisation group eqns. and analytic renormalisation 0-82865
- renormalisation group eqns. and analytic renormalisation 0-82866
- renormalisation theory, perturbative, general features, quantum action principles, pure Yang-Mills theory 0-105794
- resolvent operator expansion, generalised method, Schrodinger eqn. soln. appl. 0-86126
- ring laser diffraction theory, perturbation method 0-95919
- scaling and Pade approximants 0-91429
- Schrodinger equation, rearranged perturbation theory, nonlinear transformation 0-105542
- Schrodinger equation, step sizes for perturbative methods of solution 0-86110
- Schrodinger equation, systems of coupled equations, piecewise constant reference potential 0-86111
- Schrodinger equation eigenvalues, perturbation theory calc. without complete set of eigenfunctions 0-105519
- screened Coulomb pots., perturbation theory approach 0-63524
- second order matrix element eval., trial function linear transformation 0-62529
- second-row hydrides, nucl. spin-spin coupling consts., ab initio calcs. 0-95647
- selfgravitating systems, strongly interacting, perturbation methods 0-73234
- semiconductor surface space charge layers, subband struct., perturbation theory 0-84497

## perturbation theory continued

- semiconductor wires, size-quantised, two-photon interband absorpt. 0-93256
- semiconductors, deep defects, contrib. to binding energy 0-70634
- semiconductors, degenerate, acoustodielectric effect, permittivity modulation by acoustic wave in resonance conditions 0-92944
- semiconductors, heavily doped, hopping cond. activation energy, percolation method 0-70703
- semiconductors with direct band gaps, exciton-polariton interactions, Green's function approach 0-92831
- short gravity-capillary waves modulation by longer-scale periodic flows 0-57106
- simple liqs. with repulsive forces, thermodynamically selfconsistent theory 0-75139
- soliton lattice stability in coupled linear chain system 0-73282
- stationary, commutator possible appl., nth order expectation values 0-86116
- stochastic action integral interpretation of quantum mechanical transformation function 0-77644
- Stockmayer fluids with dipoles and quadrupoles, spherical harmonic coeffs., dielec. const. and Kerr factor calcs. 0-84678
- super ( $\phi^3$ ) model, large order perturbation theory 0-82876
- superconductor, EM wave nonlinear absorpt. near one-photon threshold 0-60142
- ten-electron systems, correl. energy, fourth order diagrammatic, many body Rayleigh Schrodinger perturbation theory 0-63556
- three-photon coalescence at electron 0-91026
- Tokamak plasma, confinement time meas. 0-87945
- total electronic energy, atoms and mols., SCF binding energy,  $Z^{-1}$  perturbation theory 0-83268
- transition density matrices, spin variables separation by Fock coordinate function and spin Hamiltonian methods 0-63513
- transition metals, correlation effects, perturb. treatment within Hubbard model 0-70582
- transition metals, correlation effects, perturbation treatment 0-59897
- transparency, self-induced, perturbed soliton solns., finite relax. time 0-58643
- two electron atom, energy levels, classical first order perturbation theory 0-58118
- two photon absorptivities, CNDO/SC-Cl calc. with second order time depend. perturbation eqns. 0-74122
- two photon absorptivity, ion cyclotron reson. photodissoc. spectra, CNDO/SC-Cl-perturbation theory 0-74123
- two state two mode vibronic coupling model, Born-Oppenheimer and crude adiabatic perturbation methods 0-87036
- two-centre Lennard-Jones liquids, free energy, perturbation theory 0-79656
- UHF orbitals, ionisation energy calcs. appls. 0-58141
- valence correlation energies, contributions of triply- and quadruply excited states determ. using perturbation theory 0-78545
- waveguide scattering problem, comparison of two perturbation theories 0-83662
- weakly interacting particle system, quantum field divergence disappearance in modified quantum dynamics 0-62537
- $Z_1^2$  effect, asymptotic, particle ionisation losses, perturbation theory (Russian) 0-101735
- ( $\gamma,n$ ), preequilibrium exciton model with evaporative component, photon-neutron spectra, giant resonances 0-57762
- Ar+HCl, inelastic scatt. exponential perturbation theories 0-74217
- Ar+N<sub>2</sub>, inelastic scatt. exponential perturbation theories 0-74217
- Ar+N<sub>2</sub>(O, CO), molecular fluid mixtures, equilibrium props. 0-64867
- ArH<sup>+</sup>, transition moments, perturbation calcs. 0-102542
- BH, elec. polarisabilities and dipole moments, var. perturbation obs. 0-63527
- CO, energy levels for perturbed Morse oscillators 0-78676
- CO, nucl. elec. shielding tensor calcs. 0-83296
- CO, one-electron props., corrections, Moller-Plesset perturbation theory calc. 0-95519
- Ce, isostructural solid-solid phase transitions, core collapse, cell theory 0-59620
- Cl, photoionisation cross section and reson. theory, many body perturbation theory, 3p and 3s subshells 0-69114
- Cl<sup>-</sup>, atomic core states, antishielding effects calcs. 0-83299
- Cs<sub>2</sub>MX<sub>6</sub> (M=Se, Te, X=Cl, Br),  $\Gamma_4^- (^3T_{1g})$  state, Jahn-Teller effect, luminesc. obs. 0-60650
- Cu, electrical resistance of edge dislocations (German) 0-96859
- H atom, Stark effect, second order correction for energy (Rumanian) 0-74147
- H, degenerate 3s-3d levels, in mag. field, eigenvalues, Bender-Wu formulas 0-83275
- H, in static multipole field, logarithmic perturbation expansion 0-91431
- H, perturbation theory and Pade approx. in electric field 0-91493
- H, quasi-stationary states in field of strong monochromatic wave, perturbation theory calcs. (Russian) 0-58145
- H, Stark effect, high orders of perturbation theory for excited states 0-87079
- H<sup>+</sup>, many-body perturbation theory with radially restricted basis functions 0-78526
- H<sub>2</sub>, Bender-Wu formula, SO(4,2) dynamical group and Zeeman effect, perturbation coeffs. determ. 0-95674
- H<sub>2</sub><sup>+</sup>, dynamic polarisabilities, variation-perturbation calcs. 0-87243
- H<sub>2</sub><sup>+</sup>, exchange perturbation theory 0-63518
- HCl, one-electron props., corrections, Moller-Plesset perturbation theory calc. 0-95519
- HCl, second order mag. props., coupled Hartree-Fock perturbation theory 0-87042
- HCl-inert gas rot.-vibr. line pressure broadening and shift calc. 0-69124
- HCl+I<sub>2</sub> gas, weak collisions, HCl spectral line broadening of IR spectra 0-74161
- HD, spin-spin coupling constant convergence, comparative study 0-63536
- HD<sup>+</sup>, Hellmann-Feynman theorem anomaly 0-63510
- HNF<sup>+</sup>, vertical ionisation pot. calc. by perturbation corrections to Koopmans' theorem 0-83520
- HO, free radical, dipole moments and Stark effects from microwave spectra 0-63623
- H<sub>2</sub>O, nucl. elec. shielding tensor calcs. 0-83296
- H<sub>2</sub>O, polarisability and mag. susceptibility calc. by SCF and CI method 0-99443
- H<sub>2</sub>O, vertical valence ionis. pot. calc. by perturbation, CI and CPA techniques 0-69263



## perturbation theory continued

- H<sub>2</sub>S, second order mag. props., coupled Hartree-Fock perturbation theory 0-87042  
 He energy levels, classical first order perturbation theory 0-58118  
 He metastable state, two- and three-photon ionisation 0-91518  
 He+H<sub>2</sub>, inelastic scatt. exponential perturbation theories 0-74217  
 He<sub>2</sub>, ground state, interaction energy, many-body perturbation theory calcs. 0-69210  
<sup>3</sup>He, liq., interface with nonmag. solid, Kapitza resist., quantum perturbation treatment 0-88385  
<sup>3</sup>He, superfluid A-phase, longitudinal mag. relax. 0-59751  
<sup>4</sup>He, superfluid, roton-roton interaction for large and zero momentum 0-84336  
 Hg atoms, elastic electron scatt., relativistic effects 0-102568  
 In, lattice dynamics, pseudopot. computation (*Russian*) 0-92617  
 In pnictides, mixed, impurity induced Raman scatt. spectra 0-88983  
 Li, 2s<sup>2</sup>2p double Auger rate 0-99489  
 Li isoelectronic sequence of three electron atoms, pair correlation study 0-74096  
 Li<sup>+</sup>+CO<sub>2</sub>, collisional excitation, quasiclassical trajectory calcs. 0-83467  
 Mg<sup>2+</sup> atomic core states, antishielding effects calcs. 0-83299  
 N<sub>2</sub>, vertical valence ionis. pot. calc., by perturbation, CI and CPA techniques 0-69263  
 N<sub>2</sub>+O<sub>2</sub>, molecular fluid mixtures, equilibrium props. 0-64867  
 NH<sub>3</sub>, nucl. elec. shielding tensor calcs. 0-83296  
<sup>15</sup>N, spin-lattice relax. time, quantum effect of NH<sub>4</sub><sup>+</sup> ion rot. 0-75875  
 Na, equilibrium struct. and phys. props., pseudopot. method 0-96778  
 Na<sup>+</sup> atomic core states, antishielding effects calcs. 0-83299  
 Ne isoelectronic series, second order correl. energy, Z depend. of irreducible-pair energies 0-91417  
 Ne, vertical valence ionis. pot. calc. by perturbation, CI and CPA techniques 0-69263  
 Ne-H<sub>2</sub> liq. mixtures, phase equilb. effects, thermodynamic perturb. theory (*Russian*) 0-92663  
 Ni, correlation effects, perturbation treatment 0-59897  
 Ni, correlation effects, perturb. treatment within Hubbard model 0-70582  
 OH+H<sub>2</sub>→H<sub>2</sub>O+H, reaction product vibr. distrib., quasiclassical trajectory, calcs. 0-85162  
 PH<sub>3</sub>, second order mag. props., coupled Hartree-Fock perturbation theory 0-87042  
 Pr<sup>3+</sup>, elec. multiple polarisabilities, discrete basis set calcs. 0-91456  
 RbAl(SO<sub>4</sub>)<sub>2</sub>·12H<sub>2</sub>O, spin-Hamiltonian with trigonal S<sup>I</sup> terms for describing <sup>51</sup>Fe<sup>3+</sup> ENDOR spectra 0-75885  
 RbGa(SO<sub>4</sub>)<sub>2</sub>·12H<sub>2</sub>O, spin-Hamiltonian with trigonal S<sup>I</sup> terms for describing <sup>51</sup>Fe<sup>3+</sup> ENDOR spectra 0-75885  
 SiH<sub>4</sub>, second order mag. props., coupled Hartree-Fock perturbation theory 0-87042  
 V<sub>2</sub>O<sub>5</sub>, energy band structure, tight-binding method 0-70602  
 ZnF<sub>2</sub>·Co<sup>2+</sup>, Raman tensor calcs. of isolated impurity in diamagnetic matrix 0-76025

## petrol engines see internal combustion engines

## petroleum industry

- Alaska oil pipeline, induced elec. currents meas. by gradient fluxgate and SQUID magnetometers 0-98231  
 feedstocks and cokes, graphitizability 0-93580

## pH

- acid rain, Pittsburgh (Pennsylvania) area 0-94129  
 artificial membranes, transport regulation by environmental H<sup>+</sup> conc. 0-89725  
 basalt, cement reinforcing fibre, alkali resist. 0-89377  
 blood, gas valves, anal. in mice following pulmonary irradiat. 0-104673  
 catheter tip pH electrodes for continuous intravascular recording 0-81755  
 chloroplasts, isolated, effect of temp. on photo-induced pH gradient 0-81566  
 cutting fluid, hydrolysed polyacrylonitrile based, operational characteristics 0-89359  
 electrolyte, effect on Cu electrolytic coating, adsorption of surface-active additives 0-100963  
 Incoloy 800, stress corrosion cracking in NaOH solns., electrochem. aspects, peening treatment 0-97618  
 Inconel 600, stress corrosion cracking in NaOH solns., electrochem. aspects, peening treatment 0-97618  
 Inconel 600 alloys, stress corrosion cracking, prediction in 10% NaOH soln. at 315°C 0-97616  
 jute, cement reinforcing fibre, alkali resist. 0-89377  
 lysine, aq. solns., H<sup>+</sup>(D<sup>+</sup>) exchange rates, <sup>17</sup>O NMR linewidths, pH depend. 0-91661  
 phenylalanine, hydrated electron impact dissociat., laser flash photolytic investig. 0-58396  
 poly-L-ornithine solution, <sup>15</sup>N NMR, coil-helix transition, solvent effects and pH depend. 0-74275  
 polycarboxylic acids, electrophoretic and viscometric props. 0-66811  
 proton transport across charged membrane and pH oscillations 0-61516  
 rainfall acidity, natural variance of pH time dependence 0-61840  
 steel, austenitic type 304, sensitised, intergranular stress corrosion cracking inhibition study 0-100939  
 steel, martensitic stainless, in SO<sub>4</sub> solns., activation pH and susceptibility to H<sub>2</sub> assisted stress corrosion cracking 0-97619  
 Al anodic oxidation, in H<sub>2</sub>SO<sub>4</sub>, pH-values effect (*German*) 0-76419  
 γ-Al<sub>2</sub>O<sub>3</sub> outgassed at 400, 650°C, heat of adsorp. of pyridines from soln., surface acidity 0-61154  
 Cd, high purity, passivity breakdown pH effect on pitting potential 0-100947  
 Cu-Be(2 wt.%), tarnish surface films, formed in ammoniacal Cu(II) solns. 0-97624  
 D<sub>2</sub>O, H<sup>+</sup>(D<sup>+</sup>) exchange rates, <sup>17</sup>O NMR linewidths, pH depend. 0-91661  
 Fe, anodic behaviour in 1M H<sub>2</sub>SO<sub>4</sub>, influence of straining 0-97612  
 Fe, passive film form. in phosphate soln., intensity-following ellipsometry study 0-104345  
 H<sub>2</sub>O, H<sup>+</sup>(D<sup>+</sup>) exchange rates, <sup>17</sup>O NMR linewidths, pH depend. 0-91661  
 HS<sub>n</sub><sup>2-</sup>, n=1-4, electronic struct., ab initio Hartree-Fock-Slater calcs. 0-74107  
 HS<sub>n</sub><sup>2-</sup>, n=1-4, electronic struct., ab initio Hartree-Fock-Slater calcs. 0-74107  
 H<sub>2</sub>S<sub>n</sub>, n=1-4, electronic struct., ab initio Hartree-Fock-Slater calcs. 0-74107  
 NH<sub>4</sub>H<sub>2</sub>PO<sub>4</sub>, cryst. growth in presence of Mn ions 0-93468

## pH continued

- Na<sub>2</sub>O-(CaO)-SiO<sub>2</sub>, diffusion controlled attack by aq. solns. 0-81218  
 Ni, corrosion and passivation in phosphate soln., pH depend., ellipsometric study 0-104448  
 pH control  
 drum boilers, working at 11.0 to 15.5 MPa, pH control by addition of caustic soda (*Russian*) 0-89420  
 pH factor see pH  
 pH measurement  
 atmospheric precipitation acidity measurement, error anal. applied to indirect methods 0-72108  
 equipment for the measurement of ions in solution, review 0-71983  
 fibre optic pH sensor, miniature, for physiological use 0-109074  
 model for potential difference across membrane, pH measurements using polarizable electrodes 0-76514  
 PdO-Pd miniature pH electrode description and use 0-89886  
 Si ion-controlled diodes, acid-base exposure effects, Si-SiO<sub>2</sub> interface state density 0-96984  
 phase angle meters see phase meters  
 phase changing circuits  
 see also phase shifters  
 pulsed NMR spectrometer incorporating phase-splitting circuit 0-62704  
 phase conjugation (optical) see optical phase conjugation  
 phase-contrast microscopy see microscopy  
 phase control  
 quantum oscillator, phase automatic freq. control parameters, optimal values (*Russian*) 0-77814  
 He-Ne low-gain laser amplifier, phase control 0-64059  
 phase diagrams  
 see also phase equilibrium; phase transformations  
 acetone-chloroform-methyl isobutyl ketone, ternary phase diagrams, interactive computer program 0-71629  
 alloy, binary, with arbitrary mole fraction, order disorder transition in case of FCC lattice 0-88295  
 alloy colour and colour stability as alloy design criteria 0-101005  
 alloys, binary, constitution diagrams, computer calc. (*Russian*) 0-84909  
 bis-(p-toluene-sulphonate) of 2,4 hexadiene 1,6 diol, X-ray scattering obs. of polymerisation mechanism and phase transition (*French*) 0-70399  
 CaO-SiO<sub>2</sub>-CO<sub>2</sub>, subsolidus and liquidus phase relationships to 30 kbar 0-85643  
 cemented carbides, physical and chem. nature 0-76265  
 chemisorbed layers, surface defects and thermodynamics 0-80068  
 commensurate and incommensurate charge-density wave states, nearly half-filled Frohlich model 0-107723  
 commensurate-incommensurate transition and melting in two-dimensions 0-75339  
 crystal growth and phase diagrams 0-66407  
 cubic crystals, tensile deform. induced transitions 0-59653  
 double phase transitions, physical value anomalies (*Russian*) 0-59622  
 electron system, two-dimensional, melting curve, phase diagram 0-57179  
 electron-hole paired systems, ferromagnetic ordering phase diagram 0-97097  
 excess enthalpy and excess entropy functions derivation by direct method from TX phase diagram, heats of mixing calc. 0-75366  
 ferrofluids, phase diagrams and eqn. of state 0-60280  
 first-order transition close to second-order transition 0-59625  
 gas-liquid-solid phase diagram, modified lattice-gas model 0-62591  
 glass characteristics, electromagnetic, mechanical and thermal props. 0-106587  
 glass-forming multicomponent systems, phase behaviour, miscibility, tie lines 0-84294  
 p-p'-n-heptyl-cyanobiphenyl-isotropic solute systems, nematic-isotropic phase transformation, volumetric study 0-92653  
 interacting linear Ising spin chain, phase transitions (*Russian*) 0-70920  
 ionic mixtures, phase diagrams and phase separation 0-77279  
 Ising antiferromagnet, FCC, nearest neighbour interactions, Monte Carlo method 0-80544  
 Ising model, modulated phase with solitons, phasons and devil's staircase 0-95044  
 magnetic order coexistence with charge density waves 0-97096  
 metal-dielectric transition, two-band model, Coulomb interactions, self-consistent calcs. (*Russian*) 0-80185  
 metallic glasses, stability 0-75184  
 methane adsorbed submonolayer on graphite, structural transitions between epitaxially ordered phases 0-96740  
 monomer-dimer system with attractive interactions on square lattice, nematic ordering 0-79681  
 multi-component crystal growth, kinetic equation theory, binary system crystallisation 0-88071  
 multicomponent systems, phase diagrams and thermodynamic data, electrochem. determ. 0-71922  
 multicomponent systems, rel. to electrodeposits, theoretical model 0-65396  
 Neel ferrimagnets, phase transitions, field-induced spin-orientational 0-75767  
 nucleation theory and first order phase transition dynamics near critical points 0-84284  
 phase transitions with two order parameters, Landau theory, mag. reorientation 0-103456  
 phosphate glasses, non-alkaline, transition states, phys. effects of fluors, phase diagrams and optical effects (*German*) 0-88045  
 poly-γ-benzyl-L-glutamate, soln., liquid crystal transitions anal. 0-65207  
 polyisocyanates, rigid backbone, ternary phase relationships obs. 0-59371  
 polymeric macromolecule containing mesogroups, phase diagrams (*Russian*) 0-58433  
 PVC-vinylchloride system, glass transition, vinylchloride influence (*German*) 0-79917  
 rare earth germanates, R<sub>2</sub>O<sub>3</sub>-GeO<sub>2</sub> system cpds., physicochem. characts. 0-97469  
 rare earth oxide containing systems, highly refractive, phase equilb. and metastable phases 0-97467  
 (rare-earth)<sub>2</sub>O-H<sub>2</sub>O, hydrothermal phase equilibria studies 0-104132  
 (Rochelle salt)<sub>2</sub>-(ammonium Rochelle salt)<sub>2</sub>, phase transitions, hydrostatic press. effects 0-93246  
 staged intercalation compounds, phase diagrams 0-60849  
 steel, Cr (2%), austenite decomp., phase diagrams and struct. form. kinetics 0-76223  
 steel, high-strength, dynamic yield strengths, phase transition press. and Hugoniot parameters 0-75331



## phase diagrams continued

- steels 4Kh4VMFSSh and 45Kh3V3MFSSh, grain size, hot deform. and austenitising effects 0-76286
- substitutional solid solutions, new phase nucleation mechanism 0-61135
- ternary, interactive computer program 0-71629
- ternary BCC alloys, ordering process, effect of short-range order (*Russian*) 0-84908
- tetrebromomethane, thermal resistivity, heat capacity and phase diagram under pressure 0-65316
- thermoelectric alloys, phase diagrams, and imperfection chemistry 0-108422
- thermophysical property research, metallurgical applications 0-97457
- thin film alloys, surface magnetism props., Curie temp., Ising model 0-108339
- 1,1,1-trichloroethane, polymorphism under high pressure (*French*) 0-96644
- trivalent metal phosphates, condensed, synthesis in polyphosphoric acid melts, physicochem. equil. considerations 0-97419
- two dimensional system, melting and condensation theory 0-57231
- uniaxial antiferromagnetic, phase diagram, spin flop transition (*Russian*) 0-100587
- uniaxial ferromagnet, domain struct. in mag. field 0-103853
- uniaxial ferromagnet domain struct., phase transition (*Russian*) 0-108044
- valence transition, entropy and phase diagram 0-59877
- Ag-Bi-S ternary system, DTA and X-ray diff. study 0-84917
- Ag-Ge-Te system, chalcogenide, phase equilibria and diagrams (*German*) 0-108418
- Ag-Sm system, phase diagram, eutectic temps., microstruct. (*German*) 0-104119
- Ag-Sn, liquid alloys, thermodynamic props. (*Japanese*) 0-108396
- Ag<sub>3</sub>Au<sub>1-x</sub>Cu<sub>x</sub>, phase relations, X-ray diff. and differential thermal anal. 0-108395
- AgBr-NaBr, phase diagram, miscibility, binodal curve and demixing kinetics, X-ray meas. 0-96659
- AgGaS<sub>2</sub>-AgGaSe<sub>2</sub> system, phase diagram, lattice consts., and IR spectra 0-60841
- AgI, thermal expansion under press. 0-92690
- Ag-S system, phase diagram, 100-600°C (*German*) 0-97471
- Al-Al<sub>3</sub>Pt<sub>3</sub> eutectic alloys, unidirectionally solidified, struct. study 0-108394
- Al-Al<sub>3</sub>Ti, directionally solidified, thermal stability during annealing, 435-660°C 0-108393
- Al-Cu, superconducting amorphous films of high stability 0-70889
- Al-Cu (4 wt.%) alloy, reversion process of Guinier-Preston zones, <sup>63</sup>Cu NMR obs. 0-60871
- Al-Fe (49 at.%) quenched alloy, neutron diffuse scatt., diffuse  $\omega$  phase obs. 0-84141
- Al-Si-Y alloy, phase equilibria in Al rich region (*Russian*) 0-93537
- AlN-Si<sub>3</sub>N<sub>4</sub>-Be<sub>3</sub>N<sub>2</sub> system, phase equilibria 0-60844
- Al<sub>2</sub>O<sub>3</sub>-Y<sub>2</sub>O<sub>3</sub>, melting behaviour and metastability determ. by optical DTA 0-92648
- Au-Co, liquidus line determ. by mag. meas. 0-60250
- Au-Cu-Al thin film bilayer system, phase formation, backscattering spectra 0-96728
- Au<sub>3</sub>Cu<sub>1-x</sub>Ag<sub>x</sub>, phase relations, X-ray diff. and differential thermal anal. 0-108395
- B-Si, (0 to 14.3 at.%), phase charact., regions of existence (*French*) 0-104117
- Ba, phase transitions under high press. 0-96641
- Ba<sub>0.45</sub>Fe<sub>0.35</sub><sup>2+</sup>Fe<sub>0.3</sub><sup>3+</sup>O<sub>46</sub>, temp.-mag. field phase diagram, torque method 0-60276
- BaO-TiO<sub>2</sub>-Al<sub>2</sub>O<sub>3</sub> system, subsolidus equilibria, X-ray powder diff. 0-108413
- BaO.6Fe<sub>2</sub>O<sub>3</sub>, solubility of CaO 0-100333
- BaSi<sub>3</sub>, trimorphic, transform. of three-connected Si nets, press.-temp. phase diagram, 40 kbar and 1000°C 0-75198
- Bi-MnBi eutectic region, of Bi-Mn phase diagram 0-81034
- BiVO<sub>4</sub>, ferroelastic phase transition, birefringence meas. at simultaneous high pressure and temp. 0-80743
- Ca-Cu system, enthalpy of form. of  $\gamma$ -phase CaCu<sub>5</sub> calorimetric determ. (*French*) 0-84915
- Ca-Mn-S-Se system, multicomponent solubilities 0-108416
- CaF<sub>2</sub>-AlF<sub>3</sub>-Na<sub>3</sub>AlF<sub>6</sub>-(Al<sub>2</sub>O<sub>3</sub>), phase equilibria, X-ray diff. and DTA meas. 0-108409
- CaF<sub>2</sub>-CaO-Al<sub>2</sub>O<sub>3</sub>, phase diagram contribution (*German*) 0-100830
- CaO-MgO-Cr<sub>2</sub>O<sub>3</sub>-Al<sub>2</sub>O<sub>3</sub>-ZrO<sub>2</sub>-SiO<sub>2</sub> system, subsolidus region characts. 0-97466
- CaO-SrO-Fe<sub>2</sub>O<sub>3</sub> system, phase relations, Sr hexaferrite field occurrence 0-93545
- CaO-V<sub>2</sub>O<sub>5</sub>-SiO<sub>2</sub> system, compatibility triangles 0-81037
- Cd-P, p-T-x phase diagram, thermodynamic props. 0-88300
- Cd-Sn binary system, high press. study 0-93539
- Cd-Tl binary alloy system at high press. 0-97461
- Cd<sub>1-x</sub>M<sub>x</sub> (M=Mg, Ca, Sr), solid soln., phase equilb. diagrams 0-108412
- CdO-WO<sub>3</sub>, phase rels. and cryst. struct. 0-108410
- CdSnAs<sub>2</sub>-Sn system, liquidus curve 0-59658
- CdTe-In system, equilb. phase diagram and liq. phase epitaxial growth of CdTe from In soln. (*Japanese*) 0-71634
- Ce, isostructural solid-solid phase transitions, core collapse, cell theory 0-59620
- Ce-In, phase equilibrium and cryst. struct. 0-66483
- Ce-Tl, phase equilibrium and cryst. struct. 0-66483
- CeAl<sub>3</sub>, resistivity and volumetric meas., phase diagrams, comparison with CeS 0-107789
- CeS, resistivity and volumetric meas., phase diagrams, comparison with CeAl<sub>3</sub> 0-107789
- Co-Ge binary system, phase diagram rel. to that of Ni-Ge (*French*) 0-97463
- Co-Ni-Zn, diagram of state, crystalline lattice consts., microhardness (*Russian*) 0-66479
- Co-Zn, physical-chemical metallurgy (*German*) 0-108390
- Co-Zr, amorphous phase form. in Zr-poor region, hardness and fracture strength (*Japanese*) 0-84914
- Cr-Al-C, ternary system, phase relationships 0-76230
- Cr-Fe-Ni,  $\gamma$ -solid soln., thermodynamic activity determ. at 1500K 0-108397
- Cr-Fe-Ni-Si, ternary phase equilibria for Cr-Fe-Ni rich portion, lattice stabilities 0-71628
- Cr-Ge system, phase diagram, thermal anal., X-ray diff., microhardness, and electron probe anal. (*French*) 0-97462

## phase diagrams continued

- Cr-Nb-Mo alloy system, comp. and temp. depend. alterations in mech. props., phase diagram interpret. (*Russian*) 0-85045
- Cr-Ni-Fe, ternary phase diagrams, interactive computer program 0-71629
- Cr-W-O, phase relations, thermodynamic props. of CrWO<sub>4</sub> and Cr<sub>2</sub>WO<sub>6</sub> 0-104120
- Cr<sub>2</sub>Si structure, rel. between phase diagrams and superconductivity 0-88330
- CsD<sub>2</sub>PO<sub>4</sub>, pseudo-one-dimensional ferroelec. and antiferroelec. transitions, phase diagram obs., soft modes 0-93245
- CsSbF<sub>6</sub>, high press. phase relations, vibr. spectra, and cryst. chemistry 0-108200
- Cu-Ag-Au, coherent phase diagram, theoretical calc. 0-70373
- Cu-Co (1.5 and 4 wt.%) alloy, coherent Co-rich separations obs. by positron annihilation (*Russian*) 0-89082
- Cu-Ni-S, molten, thermodynamic props. 0-104122
- Cu-Ni-Ti system, reactions with melt in Cu-rich region (*Japanese*) 0-89202
- Cu-Ni-Zn-Mn fine grained precipitation-hardenable alloy, high strength and ductility 0-100805
- Cu-Pb (Fe), liq., thermodynamic props. (*Polish*) 0-89199
- Cu<sub>2</sub>Ag<sub>1-x</sub>Au<sub>x</sub>, phase relations, X-ray diff. and differential thermal anal. 0-108395
- Cu<sub>2</sub>La<sub>1-x</sub>, splat-cooled, phase diagram and supercond. props. 0-70881
- r-CuMn, annealing ordered phase study by neutron diff. 0-89265
- Cu<sub>3-x</sub>Mn<sub>x</sub>Al, and Cu<sub>2</sub>Mn<sub>2-x</sub>Al<sub>x</sub>, Heusler alloys, order-disorder transitions 0-59619
- Cu<sub>2</sub>MoS<sub>8</sub>, constitution diagram, 11-2000K 0-108407
- DyCo<sub>5</sub>, noncollinear mag. struct. appearance in mag. fields, magnetostriiction meas. (*Russian*) 0-100607
- DyF<sub>3</sub>-CsF, phase diagrams and ternary fluorides (*French*) 0-81040
- DyF<sub>3</sub>-RbF, phase diagrams and ternary fluorides (*French*) 0-81040
- Dy<sub>2</sub>O<sub>3</sub>-ZrO<sub>2</sub>, phase diagram and long range ordering 0-93542
- Eu-B-C ternary and binary boundary systems, preparation techniques, X-ray analysis 0-60840
- EuO, physical and physicochem. props., review 0-96875
- FE-Zn, prep. and phase diagrams (*French*) 0-76231
- Fe, cast, alloyed and unalloyed, microsegregation thermodynamics 0-76261
- Fe-B, amorphous, crystn., metal or metalloid exchange influence 0-75172
- FE-C phase diagram, thermodynamic anal. 0-60846
- Fe-Co-Mo, phase relations in system at 1100°C 0-108392
- Fe-Co-Ti-Al alloy type Y<sub>2</sub>UNDK magnets, metallographic method of distinguishing cracks 0-85096
- Fe-Cr-O system, phase relations at 1200°C using diffusion couple technique 0-89205
- Fe-Cu-Zn, high-temperature phase diagrams (*German*) 0-108390
- Fe-M, (M=Cr, W, Mo, V, Ti), morphology and growth kinetics of  $\delta$ -pearlite formed by carburisation 0-108485
- Fe-Mn-Zn, high-temperature phase diagram (*German*) 0-108390
- Fe-Mo (13-20 at.%) binary alloys, spinodal decomp. on ageing, TEM and X-ray diff. study 0-97503
- Fe-Mo system, thermomech. props. 0-89208
- Fe-MuS eutectics, unidirectional solidification (*German*) 0-100827
- Fe-N phase diagram, thermodynamic anal. 0-60846
- Fe-Ni-Mo, phase relations in system at 1100°C 0-108392
- Fe-Ni-(P), phase diagram determ., 700 to 300°C 0-108399
- Fe-O system, thermodynamics of viüstite-haematite alloy melt (*Russian*) 0-65249
- Fe-O-Ca-Al system, inclusion precipitation diagram 0-108415
- Fe-Pd Invar, low temp. FCT phase obs. 0-93538
- Fe-Si system, melting equilibria study (*German*) 0-66473
- Fe-W-Cr-Mo system, mag. and mech. props. rel. to production methods (*Japanese*) 0-71107
- Fe-X (X=Cr, Mo, W), quenched rapidly from melts, nonequilb. phases (*Japanese*) 0-71630
- Fe-Zn, physical-chemical metallurgy (*German*) 0-108390
- Fe-Zn phase diagram, galvanization study (*French*) 0-66447
- Fe-Zr, amorphous phase form. in Zr-poor region, hardness and fracture strength (*Japanese*) 0-84914
- Fe<sub>0.394</sub>Ti<sub>0.606</sub>-O-S subsystem, equil. phase data under reducing conditions rel. to ilmenite upgrading 0-76240
- FeGa<sub>2</sub>Se<sub>4</sub>, elec. cond., mag. susceptibility 0-88301
- FeO<sub>2</sub>, wüstite field, thermodynamic props. and subphases, thermogravimetry, 1100-1300°C 0-76239
- Fe<sub>2</sub>VS<sub>2</sub> (0.20<x<1.00), phase diagram and order-disorder transition of vacancies 0-81039
- Ga-As-O, equilb. phase diagram, GaAs oxidation 0-104130
- Ga-Ge-Zn ternary alloys, thermodynamic props., EMF meas. 0-81033
- Ga-In-Sb system, phase diagram calcs. in Ga+In rich region 0-60842
- Ga-Se system, phase diagram and cryst. struct. of phases (*French*) 0-93544
- Ga-Se<sub>3</sub>, solid solution, elec. cond. 0-88301
- Ga-Se<sub>2</sub>FeSe, elec. cond., mag. susceptibility 0-88301
- Gd-C-N system, isothermal section at 1200°C, X-ray investigation (*German*) 0-93543
- GdBr<sub>3</sub>, crystal preparation, elec. resistance, phase transitions 0-97427
- Gd<sub>2</sub>O<sub>3</sub>-Ga<sub>2</sub>O<sub>3</sub> system, phase diagram relationships of garnet-perovskite transform. 0-97460
- Ge-As-Se-Te glasses for 8-12  $\mu$ m IR optics 0-69475
- Ge-Si, phase diagrams near melting point, Helmholtz free energy, heat of solution 0-70379
- Ge-Si-S system, glass formation, transition temp., crystallisation and melting 0-100178
- H<sub>2</sub>, solid, metallic, high density, thermodynamic props. 0-88337
- He monolayer, phase diagram, order-disorder transition 0-107604
- <sup>3</sup>He fluid-superfluid transition phase diagram, thermodynamic stability, fluctuations (*Russian*) 0-80023
- <sup>3</sup>He-<sup>4</sup>He tricritical mixture, universality under press. 0-103533
- Hf-Al-C, phase diagram and lattice constants, X-ray diff. method 0-89207
- Hg-Tl, phase limits, determ. by enthalpy functions along liquidus (*French*) 0-84911
- Hg<sub>2</sub>Cl<sub>2</sub>, p-T phase diagram, pressure effect on phase transition 0-107370
- In-Ga-As-Zn, phase diagram, LPE growth conditions for lattice matching on InP 0-70541
- In-Ga-P ternary system, low temp. phase diagram rel. to epitaxial growth 0-84916
- InAs-CdTe quasi-binary system, temp.-comp. diagram, physicochem. and thermodynamic analysis 0-104127



phase diagrams continued

InBr<sub>3</sub>-In<sub>2</sub>Te<sub>3</sub> quasibinary system, phase relations 0-100834  
InSb<sub>1-x</sub>Bi<sub>x</sub>, metastable epitaxial film, phase diagram 0-76238  
InVO<sub>4</sub>, synthesis and thermal props. (French) 0-97443  
KCl-CaCl<sub>2</sub>-NaCl, ternary phase diagrams, interactive computer program 0-71629  
KF-ErF<sub>3</sub>, thermal and X-ray phase anal. 0-92645  
KHSO<sub>4</sub>, phase diagram of 3.2 GPa, 450°C 0-76237  
KOH-KO<sub>2</sub>, phase diagram (French) 0-107177  
La-H, phase equilibria 0-66492  
LaMnO<sub>3</sub>, phase diagram, mag. moments, neutron diffr. study 0-108414  
Li-Al-Cl system, thermodynamic props., phase equil. 0-89211  
Li-LiH system, H isotope solubility thermodynamic singularities 0-81356  
Li-Pt, phase diagram for comp. range 0-40 at.% Pt, mag. and elec. props. (German) 0-84912  
Li<sub>2</sub>GeO<sub>4</sub>-Zn<sub>2</sub>GeO<sub>4</sub>, solid electrolyte system, phase diagram 0-66489  
Li<sub>2</sub>O-Al<sub>2</sub>O<sub>3</sub>-Cr<sub>2</sub>O<sub>3</sub> system, subsolidus equilibria 0-60843  
Li<sub>2</sub>O-MgO-Al<sub>2</sub>O<sub>3</sub> system, subsolidus phase equilibria 0-81036  
Li<sub>2</sub>O-TiO<sub>2</sub>, pseudobinary phase rotations, DTA and X-ray anal. 0-108411  
Mg-MgNi<sub>2</sub>-Zn, diagram of state, Zn solubility, initial phase precipitation (Russian) 0-66478  
Mg<sub>2</sub>GeO<sub>4</sub>-Mg<sub>2</sub>SiO<sub>4</sub> system, struct. similar solid soln. obs. and characts. 0-108403  
MgO-CaO-FeO-Fe<sub>2</sub>O<sub>3</sub>-SiO<sub>2</sub>-Cr<sub>2</sub>O<sub>3</sub>-Al<sub>2</sub>O<sub>3</sub> spinel refractories, physicochem. prod. conditions 0-89185  
Mn-Al-C, ferromag. alloy, transform. kinetics 0-76229  
γ-MnAu, antiferromag., phase diagram, X-ray diffr. and Young's modulus meas. 0-71024  
Mn<sub>2</sub>Ge<sub>2</sub>-Mn<sub>2</sub>N<sub>2</sub>, perovskite struct., phase transformations (French) 0-81048  
Mn<sub>2</sub>Ga<sub>2</sub>N<sub>2</sub>-C<sub>2</sub>, perovskite struct., phase transformations (French) 0-81048  
Mo-(Zr+V+C) (1.1 wt.%) alloy, phase composition, carbide phase microhardness (Russian) 0-60834  
Mo-Al-Ge, X-ray phase and microstructural anal. 0-93536  
Na<sub>2</sub>O-Ga<sub>2</sub>O<sub>3</sub> system β and β' phases, fast ion cond., prep. and phase comp. 0-59716  
Na<sub>2</sub>PO<sub>4</sub>-Ni<sub>3</sub>(PO<sub>4</sub>)<sub>2</sub> system, phase equilibrium diagrams, crystallographic study, double orthophosphates (French) 0-93546  
Na<sub>2</sub>XO<sub>4</sub> (X=S, Cr, Mo, W), anal. and calc. of binary and ternary phase diagrams 0-88299  
Nb-Al-C, phase diagram and lattice constants, X-ray diffr. method 0-89207  
Nb-H system, phase diagram and transforms., struct. obs. of various phases 0-104125  
Nb-Ir(Rh) system glasses, form., crystn. and microhardness, resist. obs. 0-89178  
Nb-Pd constitution diagram, metallographic and X-ray diffr. anal. 0-89204  
Nb-Rh, σ-phase alloy, superconductivity and resistance behaviour 0-70882  
Nb-Ti-O, isothermal and polythermal cross sections 0-96624  
Nb<sub>2</sub>Ge<sub>2</sub>Al<sub>2</sub>, ternary supercond. alloys, comp. variations 0-97022  
Nb<sub>2</sub>Sn, powder metallurgically produced, microstruct. characts. 0-89233  
Nd<sub>2</sub>O<sub>3</sub>-P<sub>2</sub>O<sub>5</sub>-H<sub>2</sub>O, phase diagram 0-66412  
Ni-Al-Nb ternary system, electron microprobe analysis of nickel-rich region at 1473K 0-71631  
Ni-Al-Ta dendritic monocrysts., directionally solidified, coarsening kinetics 0-108425  
Ni-Co-Mo, phase relations in system at 1100°C 0-108392  
Ni-Cr-Ta system, phase equil. of Ni rich region at 1523 and 1273K 0-93541  
Ni-Ge binary system, phase diagram rel. to that of Co-Ge (French) 0-97463  
Ni-H system, phase diagram and thermodynamic properties calcs. 0-66480  
Ni-Mo-W, diagram of state, W solubility, dispersion hardening (Russian) 0-66477  
Ni-Pd-Mn ternary alloys, mag. characts., use for thermosed 0-107995  
Ni-S, phase diagram calc. and thermodynamic props. of liq. phase 0-108401  
Ni-S incongruently subliming system, SEM and TEM obs. of high temp. transitions, temp.-comp. diagrams 0-104136  
Ni-Zn, physical-chemical metallurgy (German) 0-108390  
Ni-Zr, amorphous phase form. in Zr-poor region, hardness and fracture strength (Japanese) 0-84914  
Ni<sub>2</sub>Ge-Fe<sub>2</sub>Ge solid soln., flow stress, transition from positive to negative temp. depend. 0-60906  
Pb-Fe(Cu), liq., thermodynamic props. (Polish) 0-89199  
Pb-Te system, homogeneity region of PbTe investig., equil. const. of quasic. chem. reactions 0-108405  
Pb<sub>1</sub> direct gap polar semicond., electron hole liquid phase diagram (Russian) 0-93314  
Pb<sub>1</sub>, high press. phase diagram to 3.5 GPa 0-104126  
Pb<sub>2</sub>-In<sub>2</sub>Se<sub>3</sub>, phase investigation 0-66488  
Pb<sub>1-x</sub>Sn<sub>x</sub>Te<sub>1-x</sub>Se<sub>x</sub> solid solutions with constant lattice parameter, phase comp. 0-108417  
PbTe-Ga<sub>2</sub>Te<sub>3</sub>, phase interaction, DTA, XPA and microstructural anal. 0-96625  
PbTe-InTe system, phase interactions and solid soln. form., physicochem. and elec. characteris. 0-104129  
Pb(Ti,Zr)O<sub>3</sub> solid solutions, phase coexistence discrepancies 0-96662  
xPbTiO<sub>3</sub>+(1-x)PbCd<sub>1/3</sub>Nb<sub>2/3</sub>O<sub>3</sub>, phase transition spread, polarisation relaxation, dielectric susceptibility (Russian) 0-75922  
PbZr<sub>1-x</sub>Ti<sub>x</sub>O<sub>3</sub> ceramics, morphotropic phase boundary 0-81035  
Pd-H system, phase diagram and thermodynamic properties calcs. 0-66480  
Pd-Si, amorphous thin films, laser irr., metastable phases 0-96622  
Pt-Si, amorphous thin films, laser irr., metastable phases 0-96622  
Sb<sub>2</sub>Te<sub>2</sub>MoO<sub>4</sub>, synthesis, struct. and oxidation state (French) 0-64971  
ScCl<sub>3</sub>-NaCl-CsCl ternary system, cpd. form., thermogravim. investig. (Russian) 0-66490  
Si inversion layers, phase diagram in strong mag. fields 0-88492  
Si-Al-Be-C-N system, phase equilibria 0-60839  
Si-Ge system, phase diagram, lattice const. var. effects 0-97470  
Si-Te system, phase diagrams 0-89209  
Si<sub>3</sub>N<sub>4</sub>, low pressure CVD, thermochemical calcs. 0-108356  
Si<sub>3</sub>N<sub>4</sub>-SiO<sub>2</sub>-Y<sub>2</sub>O<sub>3</sub>, subsolidus phase relations 0-60845  
SiO<sub>2</sub>, low pressure CVD, thermochemical calcs. 0-108356  
Sm-H, phase equilibria 0-66492

phase diagrams continued

Sm<sub>2</sub>O<sub>3</sub>-Ga<sub>2</sub>O<sub>3</sub> system, garnet-perovskite transform., phase diagram relationships 0-97460  
SmS, physical and physicochem. props., review 0-96875  
Sn-Cd-Pb system, contacting layer struct. and phase composition (Russian) 0-66475  
Sn-Te, molten, elec. cond. and phase diagram 0-84454  
SnTe, dispersive transform., interband electron-phonon interactions, phase diagram 0-93252  
SnTe, structural phase transition threshold instability in strong EM field 0-103477  
SrF<sub>2</sub>-LaF<sub>3</sub>, tentative phase diagram 0-71633  
Sr<sub>2</sub>(Na<sub>2</sub>Bi<sub>0.5</sub>)<sub>1-x</sub> solid solutions, piezoelec. and ferroelec. props. (French) 0-108158  
TiF<sub>4</sub>-TCNQ, high press. structural transitions, neutron scatt. study 0-96647  
Ta-Al-C, phase diagram and lattice constants, X-ray diffr. method 0-89207  
Ta-H system, phase diagram and transforms., struct. obs. of various phases 0-104125  
Ta-Ir(Rh) system glasses, form., crystn. and microhardness, resist. obs. 0-89178  
Ta-Rh, σ-phase alloy, superconductivity and resistance behaviour 0-70882  
Tb(NO<sub>3</sub>)<sub>3</sub>-Fe(NO<sub>3</sub>)<sub>3</sub>-(NH<sub>4</sub>)<sub>2</sub>CO<sub>3</sub>-H<sub>2</sub>O system, cpd. form., comp. and props. 0-100832  
Tb<sub>2</sub>O<sub>3</sub>-H<sub>3</sub>PO<sub>4</sub>-H<sub>2</sub>O system, cpd. form., comp. and props. 0-100832  
TbP (As)(Sb)(Bi), mag. transitions, quadrupolar interaction effects 0-80512  
TeO<sub>2</sub>-P<sub>2</sub>O<sub>5</sub> system, glass struct., neutron diffr. study 0-70128  
Th-based metal alloy fuels for FBRs, determ. of solidus temperature 0-104124  
ThN-rare earth nitride mixed system, quasibinary existence (German) 0-91221  
Ti-Al-C, ternary system, phase relationships 0-76230  
Ti-Al(Mo), phase relations 0-108398  
Ti-Fe-Al(Mn), homogeneity and lattice parameters, Mn and Al effect on hydriding compd. FeTi 0-108400  
Ti-Mo(V), metastable diffusionless equilibria, high press. conditions 0-71627  
Ti-Ni, multiplicity of structural transitions, phase diagrams, elec. cond. meas. 0-71649  
Ti-Ni-Co, constitution diagram, isothermal section, interdiffusion coeffs. (Russian) 0-89200  
Ti-Ni-Fe, multiplicity of structural transitions, phase diagrams, elec. cond. meas. 0-71649  
TiO<sub>2</sub>-Al<sub>2</sub>O<sub>3</sub>-SiO<sub>2</sub> system, ternary glass-forming region and phys. props. 0-84919  
TiO<sub>2</sub>-x reduced, crystallographic shear planes, dislocation struct. 0-107175  
Ti, phase diagram and high press. phase transforms., DTA study (Russian) 0-66474  
Ti-Sn-Te system equilibria, polythermal and isothermal cross sections obs., ternary cpd. form. 0-104128  
Ti<sub>2</sub>O<sub>3</sub>-GeO<sub>2</sub> system, structure of thallium I germanates (French) 0-79754  
Ti<sub>2</sub>Te<sub>2</sub>-Ti<sub>2</sub>SnTe<sub>2</sub>-Ti<sub>2</sub>PbTe<sub>2</sub>, phase equil., DTA, SPA and microhardness meas. 0-96628  
TmSe and its mixed crystals., valence instabilities, phase diagram 0-70651  
TmSe<sub>1-x</sub>Te<sub>x</sub>, semicond. with valence instabilities, cryst. chem. considerations 0-100213  
U-Ba-C FBR nuclear fuels, phase anal., 1400°C 0-66487  
U-Co(Fe)(Mn)(Ni)(V) metallic glasses, glass form. and thermal stability 0-75183  
U-Pr-C FBR nuclear fuels, phase anal., 1400°C 0-66486  
U-Sr-C FBR nuclear fuels, phase anal., 1400°C 0-66487  
U-Y-C FBR nuclear fuels, phase anal., 1400°C 0-66485  
UC, miscibility with rare earth nitrides (German) 0-96654  
UC<sub>1-x</sub>N<sub>x</sub>-U-N<sub>2</sub>, phase diagram 0-84918  
V-Al-C, ternary system, phase relationships 0-76230  
V-H(D), struct. studies, DTA and TEM 0-66491  
V-W-O system, phase diagram and thermodynamic props. at high temps., in region W-VO<sub>2</sub>-VO<sub>2</sub>-V<sub>2</sub>O<sub>5</sub> 0-104133  
V<sub>2</sub>O<sub>5</sub>-V<sub>2</sub>O<sub>3</sub>-BaZnO<sub>3</sub> glass, V ion states, mag. and elec. props. 0-88556  
Xe adsorbed on graphite (0001) surface, monolayer liquid and solid struct. 0-65400  
(YGDyBiBi<sub>3</sub>)(FeAl)<sub>2</sub>O<sub>12</sub> epitaxial garnet film, uniaxial ferromagnet domain struct., phase transition (Russian) 0-108044  
Zn-As system, homogeneity range of ZnAs<sub>2</sub> and electrophys. props. 0-60833  
Zn-Sn-Bi, ternary phase diagrams, interactive computer program 0-71629  
ZnO-WO<sub>3</sub>, phase rels. and cryst. struct. 0-108410  
Zr-Al-C, phase diagram and lattice constants, X-ray diffr. method 0-89207  
Zr-Nb (2.5 wt.%), cold-worked, pressure tubing, metallography and mech. props. 0-89269  
ZrF<sub>2</sub>-BaF<sub>2</sub>-MF<sub>n</sub> (M=Na, Ca, Ln, Th, n=1, 2, 3, 4), vitreous phases, network formers, modifiers and stabilisers (French) 0-64909  
ZrO<sub>2</sub>-SiO<sub>2</sub>, liquid immiscibility, microstruct. of plasma dissociated ZrSiO<sub>4</sub> 0-107429  
ZrO<sub>2</sub>-x(cubic)-ZrO<sub>2</sub>-x(cubic+tetragonal), phase boundary 0-81038

phase equilibrium

see also phase diagrams; phase transformations; solutions  
alcohols, vapour-liq. equil. and heats of mixing, simplified group method anal. 0-96637  
alcohols in organic solvents, H<sub>2</sub>O absorption 0-66788  
alkanes, vapour-liq. equil. and heats of mixing, simplified group method anal. 0-96637  
block copolymers, microphase separation, thermodynamic treatment (Chinese) 0-79947  
n-butylamine-n-propanol, isothermal vapour-liquid equil. 0-59639  
cell design for use below 300K and to 9 MPa pres. 0-62821  
chloroalkanes, vapour-liq. equil. and heats of mixing, simplified group method anal. 0-96637  
F 0-76235  
high pressure phase equilibria and other fluid-phase properties, computational methods 0-75329  
high-pressure phase equilibria in mixtures using partition functions, computational methods 0-75330



## phase equilibrium continued

- liquid mixtures, showing phase splitting, modified Wilson eqn., phase equilib. prediction 0-96636
- liquid-solid coexistence line, phase instability and direct correl. function integral eqn. 0-65196
- liquid-vapour coexistence and correlations in interface 0-65212
- L<sub>1</sub> ordered alloys, positive temp. depend. of strength, phase destabilization 0-81203
- metal-H system, hydride formation in high press. range 0-65235
- metal-H system, multiplateau absorpt. isotherms, theory 0-103564
- multicomponent systems, intensive parameters, thermodynamic props. depend., stability conditions (*Russian*) 0-65186
- natural gas mixtures, simulated, enthalpy and phase equil., correl. with modified Starling eqn. 0-61127
- opal glasses, phosphate opacified, phase comp. and struct. 0-64919
- pentane-benzene solution, vapour-liquid equilibrium study, vaporisation critical state (*Russian*) 0-79931
- phase boundaries in first-order phase transitions, dynamics stability 0-107403
- polyethylene-polystyrene blends, crystn. characts. 0-103261
- polymer, low conc., complex coacervation occurrence condition 0-79944
- polymer films, Brillouin scatt. at transitions 0-70312
- polystyrene-methylcyclohexane, coexistence curve, comparison obs. and free energy calc. 0-88323
- polystyrene-methylcyclohexane, coexistence curves, range of simple scaling and critical exponents 0-88322
- rare earth oxide containing systems, highly refractive, phase equil. and metastable phases 0-97467
- (rare-earth)<sub>2</sub>O<sub>3</sub>-H<sub>2</sub>O, hydrothermal phase equilibria studies 0-104132
- Si<sub>3</sub>N<sub>4</sub>-Ce<sub>2</sub>O<sub>3</sub>-SiO<sub>2</sub> materials: phase relations and strength 0-97465
- solid-phase cell for 40 kbar, 1500°C operation, pressure and temp. distrib. 0-105669
- steel, Al semiskilled, (Fe,Mn)<sub>23</sub>O<sub>4</sub> inclusions, deoxidation, thermodynamic conditions 0-60830
- steel, Al-Cr, FeO-(Al,Cr)<sub>2</sub>O<sub>3</sub> inclusions, thermodynamics 0-60831
- steel, austenitic, Cr-Mn-B-N, phase composition and struct. transformations 0-104171
- steel, low C, dual-phase, law of mixtures, applicability 0-89346
- steel, Mn-Si-Cr-Mo, dual phase, as-rolled, continuous cooling transformation diagram to optimize composition 0-100829
- steel, stainless, carbide and intermetallic phases, quantitative anal. by X-ray diff. 0-66514
- steel, stainless, Cr-Ni-Mo, phase anal. of carbide phases after isothermal annealing (*Czech*) 0-89224
- systems far from thermodynamic equil., dissipative structures, broken symm. equil. phase transition theory 0-65827
- ternary system compound formation, comp. and props. w.r.t. component electron struct., computer prediction 0-103444
- trine systems, surfaces, isotherms-isobars (*Russian*) 0-65191
- triplet phase invariants, formula for acentric case 0-84115
- trivalent metal phosphates, condensed, synthesis in polyphosphoric acid melts, physicochem. equil. considerations 0-97419
- US velocity in crit. region water 0-59582
- Ag-Ge-Te system, chalcogenide, phase equilibria and diagrams (*German*) 0-108418
- Al-Fe-X-Si (X=transition metal), struct. and comp. by electron microscopy 0-88093
- Al-Si-Y alloy, phase equilibria in Al rich region (*Russian*) 0-93537
- Al<sub>2</sub>C<sub>3</sub>-Be<sub>2</sub>C-SiC system, phase analysis and TEM struct. obs. 0-108420
- AlN-Si<sub>3</sub>N<sub>4</sub>-Be<sub>3</sub>N<sub>2</sub> system, phase equilibria 0-60844
- β-Al<sub>2</sub>O<sub>3</sub>-K<sub>2</sub>O-MgO, cryst. struct., nonstoichiometry, ion-ion correlations 0-88129
- Al<sub>2</sub>O<sub>3</sub>-TiO<sub>2</sub> powder, plasma-prepared, morphology and phase constitution 0-100833
- Au-Sn, zeta and AuSn phases, heats of form. and heat contents 0-60837
- B<sub>2</sub>O<sub>3</sub>-Nb<sub>2</sub>O<sub>5</sub> system, phase equil. and phase struct. obs. by high resolution TEM 0-108419
- B<sub>2</sub>O<sub>3</sub>-SiO<sub>2</sub> glass, crack growth, phase separation effects 0-89336
- Be-Si-Al-O-N ceramic, phase assemblages, relationships with props. 0-60848
- Be<sub>3</sub>N<sub>2</sub>-BeSiN<sub>2</sub> system, crystallography and phase relationships, TEM and electron diff. study 0-92502
- Bi-MnBi eutectic region, of Bi-Mn phase diagram 0-81034
- C, potential in equilibrium with impure high temp. inert gases 0-104135
- CO<sub>2</sub>-2,2-dimethylpropane, liquid, -vapour equil., 220 to 300K and 6.7 MPa 0-62821
- Cd-Sn alloy, superconductivity and microstructure 0-107949
- Cd<sub>1-x</sub>M<sub>x</sub> (M=Mg, Ca, Sr), solid soln., phase equilib. diagrams 0-108412
- CdTe-In system, equil. phase diagram and liq. phase epitaxial growth of CdTe from In soln. (*Japanese*) 0-71634
- Ce-In, phase equilibrium and cryst. struct. 0-66483
- Ce-Si-Al-O-N ceramic, phase assemblages, relationships with props. 0-60848
- Ce-Tl, phase equilibrium and cryst. struct. 0-66483
- Co-mischmetall system, phase relations, microstruct., mag. props. 0-104118
- Co-WC hard alloys, rapidly quenched struct. 0-76233
- Co<sub>2</sub>Z ferroxplana form. process peculiarities 0-89368
- Cu-Al-Sn system, coexistence of different and brass like phases 0-89206
- Cu-Ni-Ti system, phase equilibria in Cu rich region and Cu-T quasi-binary constitution (*Japanese*) 0-89203
- Fe oxides, phase equilibrium and microstructure interpretation 0-60847
- Fe-Co-Al-Cu-Ti (40, 14, 7.5, 4.5 wt.%), metastable equilibrium, high coercive state (*Russian*) 0-66476
- Fe-Cr-Ni (12, 15 wt.%) austenitic alloy, Ni<sup>6+</sup> irradiated, void swelling and phase stability, Si and Ti effects 0-65055
- Fe-Cu-C, phase equilibria, 950 to 1500°C 0-60836
- Fe-Mo-C (0 to 4, 1 wt.%), phase equilibria at 1143, 1198 and 1253K 0-60835
- Fe-Nb-V-C-N, equilibrium comp. and solubility in steels, model of ideal solns. (*Russian*) 0-60832
- Fe-Ni (25 to 50%), FCC, meteorites and thermodynamic equil., Mossbauer and X-ray diff. study 0-88087
- Fe-Si system, melting equilibria study (*German*) 0-66473
- Fe-Ti-V-C-N, equilibrium comp. and solubility in steels, model of ideal solns. (*Russian*) 0-60832
- Fe-X-C (X=Cr, Mo, W), quenched rapidly from melts, nonequilibrium phases (*Japanese*) 0-71630
- Fe-Zn, homogeneous phases, Gibbs free energies of form., Knudsen effusion method 0-66481

## phase equilibrium continued

- Fe<sub>3</sub>Si<sub>3</sub>Ti<sub>3</sub>O<sub>6</sub>-O-S subsystem, equil. phase data under reducing conditions rel. to ilmenite upgrading 0-76240
- Fe<sub>0.9</sub>K<sub>1.5</sub>O<sub>1.7</sub>, ferrite, cryst. struct., nonstoichiometry, ion-ion correlations 0-88130
- Ga-As-O, equil. phase diagram, GaAs oxidation 0-104130
- GaP(As), liquid interaction parameters determ., 580-670°C 0-65197
- Gd<sub>1-x</sub>Ca<sub>x</sub>Al<sub>2</sub>, mag. props. and phase relations 0-107991
- In, liquid O<sub>2</sub> activity from electrochemical meas. 0-104123
- InAs-CdTe quasi-binary system, temp.-comp. diagram, physicochem. and thermodynamic analysis 0-104127
- InP(As), liquid interaction parameters determ., 580-670°C 0-65197
- La-H, H equil. press. 0-66492
- LaCrO<sub>3</sub>-Cr ceramic, prep., phase comp. and elec. cond. (*Polish*) 0-71621
- Li-Al-Cl system, thermodynamic props., phase equil. 0-89211
- Li-LiH liq.-vap. equil., activity coeff. 0-103468
- Li-LiH system, H isotope solubility thermodynamic singularities 0-81356
- 7LiAl, cryst. growth, Stockbarger method, struct. and homogeneity 0-89137
- LiF-AlF<sub>3</sub>, mixture at 1293K, thermodynamic function 0-104134
- Li<sub>2</sub>O-Al<sub>2</sub>O<sub>3</sub>-Cr<sub>2</sub>O<sub>3</sub> system, subsolidus equilibria 0-60843
- Li<sub>2</sub>O-MgO-Al<sub>2</sub>O<sub>3</sub> system, subsolidus phase equilibria 0-81036
- Mg-Si-Al-O-N ceramic, phase assemblages, relationships with props. 0-60848
- Mn-H, hydride formation in high press. range 0-65235
- Mo-Al-Ge, X-ray phase and microstructural anal. 0-93536
- Mo-W-N system, nitrated annealed samples, W replacement of Mo 0-76227
- MoS<sub>3</sub>, homogeneity size estimation, stacking fault conc. effect 0-96661
- Na<sub>2</sub>O-B<sub>2</sub>O<sub>3</sub>-GeO<sub>2</sub> system, glass-forming melts, mass spectrometry obs. of thermodynamic props. 0-97468
- Na<sub>2</sub>O-B<sub>2</sub>O<sub>3</sub>-SiO<sub>2</sub> glasses, phase-separated, leaching rate 0-104131
- Na<sub>2</sub>O-CaO-SiO<sub>2</sub>-H<sub>2</sub>O system gels, metastable nature 0-71952
- Na<sub>2</sub>PO<sub>3</sub>-Ni<sub>2</sub>(PO<sub>4</sub>)<sub>2</sub> system, phase equilibrium diagrams, crystallographic study, double orthophosphates (*French*) 0-93546
- Na<sub>2</sub>SO<sub>4</sub>-CoSO<sub>4</sub>-H<sub>2</sub>O, phase equil., activities, Pitzer eqn. calcs. (*Russian*) 0-65190
- Na<sub>2</sub>XO<sub>4</sub> (X=S, Cr, Mo, W), anal. and calc. of binary and ternary phase diagrams 0-88299
- Nb-Al-Ge-Cu, rapidly quenched, comp. and phase equil. 0-76235
- Nb-Al(Ga, Si, Ge, Sn)-Cu, rapidly quenched, comp. and phase equil. 0-76235
- Nb-D-H, equil. H/D separation factors 0-59668
- Nb-Ti-O, isothermal and polythermal cross sections 0-96624
- Nb-V system, H<sub>2</sub> absorpt. 0-59808
- Ne-H<sub>2</sub> liq. mixtures, phase equil. effects, thermodynamic perturb. theory (*Russian*) 0-92663
- Ni-Cr-Mo-W-Al-Ti, heat-resist., phase comp. 0-76250
- Ni-Cr-Ta system, phase equil. of Ni rich region at 1523 and 1273K 0-93541
- Ni-Fe-H and Ni-Co-H, hydride formation in high press. range 0-65235
- Ni-Pd-Mn ternary alloys, mag. characts., use for thermocouple 0-107995
- O<sub>2</sub>, potential in equilibrium with impure high temp. inert gases 0-104135
- PbO-MoO<sub>3</sub>-MO and PbO-WO<sub>3</sub>-MO systems, M=Ca, Ba, Mg, Sr, perovskite type cpds, detection 0-108404
- PbTe homogeneity region invest. in Pb-Te system, equil. const. of quasi-chem. reactions 0-108405
- Pd-D-H, equil. H/D separation factors 0-59668
- Pd-Rh-H and Pd-Ni-H, hydride formation in high press. range 0-65235
- Pr<sub>1-x</sub>Ca<sub>x</sub>Al<sub>2</sub>, mag. props. and phase relations 0-107991
- S-benzene systems, liq.-liq. phase separation 0-96658
- Se, liq., heat capacity and chem. equil. 0-103486
- Si-Al-Be-C-N system, phase equilibria 0-60839
- Si-Al-O-N system, phase analysis and TEM struct. obs. 0-108420
- Si-Al-O-N system, stable phase cryst. struct. and microstruct. obs. using TEM 0-108421
- α/β-Si<sub>3</sub>N<sub>4</sub>, phase yields during form., influencing factors 0-108408
- Si<sub>3</sub>N<sub>4</sub>-SiO<sub>2</sub>-Y<sub>2</sub>O<sub>3</sub>, subsolidus phase relations 0-60845
- SiO<sub>2</sub>, phase equilibrium and microstructure interpretation 0-60847
- Si<sub>6</sub>O<sub>15</sub><sup>6-</sup> double chain anion containing anhydrous silicates, synthesis, cryst. chem. 0-59444
- Sm-H, H equil. press. 0-66492
- Sm<sub>2</sub>Co<sub>2</sub>, sintered magnets, coercive force and constitution, annealing temp. depend. (*Russian*) 0-88786
- SnSe<sub>2</sub>, sublimation, temp. depend. of equil. constants 0-88312
- Tl, liquid, O<sub>2</sub> activity from electrochemical meas. 0-104123
- Tl-Se, liquid mixtures, press. effect on two-phase region 0-75347
- Tl-Sn-Te system equilibria, polythermal and isothermal cross sections obs., ternary cpd. form. 0-104128
- Tl<sub>2</sub>Te<sub>2</sub>, Tl<sub>2</sub>SnTe<sub>2</sub>, Tl<sub>4</sub>PbTe<sub>3</sub>, DTA, XPA and microhardness meas. 0-96628
- Y-Si-Al-O-N ceramic, phase assemblages, relationships with props. 0-60848
- YIG crystals, bulk growth from high temp. solns., props. 0-66413
- Zn-Bi, liquid, inconsistent conjugated liquidus 0-76232
- Zr-Ti-Be metallic glass, phase separation 0-97464

## phase equilibrium diagrams see phase diagrams

## phase-locked loops

- EKG spindle detection system, human and automatic validation 0-98154
- RF SQUID magnetometer, synchronous demodulation, amplitude- and phase-sensitive detection 0-105679

## phase measurement

- complex aspheric mirror testing by phase meas. interferometry 0-74467
- damped and undamped systems, phase relationships (*German*) 0-106746
- electronic phase meas. techniques in optical testing 0-106643
- Fizeau interferometer, spherical-wave, direct phase meas. 0-95126
- Hartmann modified wavefront sensor performance 0-74522
- interferometer, single mode optical fibre, small phase shift meas. 0-57366
- Kalman filters appl., digital, optimal, synthesis with a priori uncertainty of data 0-98934
- optical complex spatial coherence meas. by sinusoidal phase modulation 0-106446
- photoconductor carrier lifetime, nonequilibrium, phase method for determ. 0-65629
- precision optical element testing by phase meas. interferometry 0-74520
- precision optical evaluation by phase meas. interferometry 0-74533
- transmission acoustic microscopy, meas. using AM carrier 0-74665



**phase measurement continued**

- Cs stocks, experiments to reduce cavity phase shift errors in the Cs beam tube 0-98893  
Ge:Zn<sup>11</sup> carrier lifetime, nonequilibrium, phase method for determ. 0-65629

**phase meters**

- digital, Dranetz model 314, comparison with analogue techniques and significant advantages (*Italian*) 0-68211  
heterodyne holographic interferometry, electronic instrumentation employing phase meter 0-87352  
Kalman filters appl., digital, optimal, synthesis with a priori uncertainty of data 0-98934  
phase automatic freq. control parameters, optimal values (*Russian*) 0-77814  
pulse-phase, torque-meter, magnetically coupled pulse transducer with electronic phase meter 0-74819

**phase modulation**

- see also phase shift keying*  
electrooptic radiation modulators utilizing semiconductor ridged waveguides 0-91925  
fibre optic rotation sensor with low drift 0-69530  
holographic pattern recognition of Korean alphabets, discrimination enhancement using phase modulated matched filters 0-95854  
interference pattern electronic heterodyne recording 0-74316  
optical complex spatial coherence meas. by sinusoidal phase modulation 0-106446  
ruby, phase modulated conjugate wave generation, hologram model 0-83643  
ruby laser, ultrashort pulse generation by internal phase and amplitude modulation 0-106551  
two-beam interference pattern monitoring 0-77844

**phase regulation** *see phase control***phase shift circuits** *see phase shifters***phase shift keying**

- intermode phase scanning for recovering phase-modulated signals on multimode optical fibres 0-58682

**phase shift microphones** *see microphones***phase shifters**

- see also phase changing circuits*  
94 GHz bulk crystal electro-optical phase shift calc. 0-71382  
electronic phase meas. techniques in optical testing 0-106643

**phase space methods**

- quadrupole ion store, spatial distribution of ions derived by phase space anal. 0-95185  
quantum state determinations and phase space distributions, simultaneous meas. 0-90774

**phase transfer function** *see optical transfer function***phase transformations**

- see also critical fluctuations; heat of transformation; isothermal transformations; liquid crystal phase transformations; liquid-vapour transformations; phase diagrams; phase equilibrium; solid-liquid transformations; solid-state phase transformations; solid-vapour transformations; spinodal decomposition; vaporisation*  
 $\alpha,\beta$ -trifluoroacetonitrile, liq.-liq. transition rel. to mol. motion, NMR study 0-70383  
acrylonitrile, NMR and relax. props., liq.-liq. transition rel. to mol. motion 0-70382  
adatoms, elastic interaction between, near distortive phase transition 0-80080  
adparticle on substrate, pseudopot. near second-order phase transition 0-80065  
adsorbed layer, commensurate-incommensurate transition and domain walls 0-107654  
adsorbed layers, one-dimensional incommensurate structures at finite temperatures 0-103567  
binodal decomposition near crit. point, scaling hypothesis 0-79912  
brass bicrystals, two-phase ( $\alpha/\beta$ ), interphase boundary sliding at high temperature 0-88164  
chain subduction criterion, continuous phase transform, Landau thermodynamic methods 0-62606  
chemical model, Schlögl's, critical fluctuations near non-equilib. critical point 0-85150  
chemisorbed phases, phase transitions 0-107656  
classical spin system with long range interaction, phase transition existence conditions 0-88298  
continuous phase transition, universal combination of critical amplitudes from field theory 0-95051  
critical exponents to order  $\epsilon^3$  for  $\phi^3$  models of critical phenomena in 6- $\epsilon$  dimensions 0-86547  
dense neutron matter transitions, pion condensation and quark percolation models 0-77277  
1,2-dimyristoyl-sn-glycero-3-phosphoserine multilayers, phase transitions, temp. depend., ellipsometric study 0-108846  
1,2-dipalmitoyl-sn-glycero-3-phosphocholine multilayers, phase transitions, temp. depend., ellipsometric study 0-108846  
dipalmitoylphosphatidylcholine, changes in vol. mag. susceptibility at the phase transition 0-76770  
dipole pseudo-spin glasses, collective excitations 0-59617  
divalent Sr, Ba, Ca, Zn, Cd iodates, complex salts, phase transitions, cryst. struct. (*Chinese*) 0-70171  
DNA, phase transitions in water-ethanol solns. (*Japanese*) 0-89709  
dynamical cluster properties in the quantum statistical mechanics of phase transitions 0-77693  
elastic bars, phase boundary propagation, dynamic elastic bar theory, sound wave interactions 0-69706  
elastically coupled systems at marginal dimensionalities, crit. dynamics and stability 0-101769  
first order phase transitions, droplet models, renormalisation, singularities 0-95050  
Fokker Planck equations, quasiadiabatic solutions, time-dependent drift, fluctuation coefficients 0-90785  
glasses, defect reactions, ionicity dependence, negative-U states 0-88510  
group theoretical methods rel. to problems of classical Landau theory 0-73292  
heat release on phase boundary motion, self consistent treatment 0-103449  
incommensurate systems, discrete lattice effects 0-107402  
incommensurate-commensurate transition in two-dimensional sine-Gordon system 0-90789  
interacting linear Ising spin chain, phase transitions (*Russian*) 0-70920

**phase transformations continued**

- interstellar contracting CO clouds, phase transition rel. to fragmentation 0-67838  
Kellen-Simanzik eqn., correlation function scaling behaviour in phase transitions (*Russian*) 0-57502  
Korteweg-de Vries equation, higher-order, Backlund transforms. 0-77631  
latent heat storage, physical and chemical processes at low temps. 0-72091  
lattice gases with linear clusters, phase transitions 0-90787  
lattice systems, phase transition and surface tension 0-77713  
lattice systems with short-range and Coulomb interactions, phase transitions and reflection positivity 0-82715  
layered two dimensional Ising lattice, phase transitions, spin glasses (*Russian*) 0-65945  
lipid bilayer phase transition, cholesterol effect 0-85361  
long-range site percolation, crossover from mean-field to crit. behaviour 0-82728  
low temperature critical phenomena, review 0-73297  
magnetic semiconductors, conference, Montpellier, France (Sept. 79) 0-94916  
metastable states close to instability, phase transition parameter eqn. of motion 0-57230  
monolayer, one-dimens., Frank-van der Merwe model, incommensurate-commensurate crossover, transfer integral method 0-88426  
nonequilibrium phase transformation theory homogeneous fluctuation effect 0-84277  
nonequilibrium transient behaviour 0-93732  
nonisothermal meas. evaluation, non-existence of dynamic correction term 0-107406  
nucleon matter, phase transitions and eqn. of state at subnuclear densities 0-77278  
oriented bond percolation, threshold probability and correlation length exponent calc. 0-68146  
Peierls-Fröhlich condensate, attracting solitons and discontinuous lock-in transition 0-92840  
pentadecanoic acid, insoluble monolayer, phase transition, simple lattice model 0-70527  
percolation theory, review 0-98868  
perfect gas/vapour in variable cross-section channel, quasi-one-dimensional flow, numerical investigation 0-79403  
phase transition in elec. discharge plasma between parallel plates, compression by recomb. press. 0-64799  
phospholipid bilayer, one- and two-component, main phase transition, Landau phenomenological theory 0-97872  
photosynthetic systems, discovery of phase transitions 0-81539  
plane rotator model, Monte Carlo simulation 0-73295  
polyacrylamide gel and single chain in soln., laser light scatt. obs. near phase transitions 0-93808  
polymer macromolecules, volume interactions, coil-globule transition, statistical physics, review 0-78737  
polymer solution, weakly correlated, radial distrib. function 0-84050  
polymeric chain with rigid side branches, intramol. phase transition of 1st kind (*Russian*) 0-58432  
Potts model, hierarchical, three-state, high temp. susceptibilities 0-77723  
Potts model, three-state, effects of symmetry-breaking perturbations 0-105579  
Potts model, two dimensional three state, critical exponents 0-105583  
rotational like degrees of freedom system, phase transitions, thermodynamic props. 0-77737  
roughness fluctuation in layer between two phases 0-85147  
second order, modulation struct. form., Lifshitz invariants 0-92644  
second order transitions, positive definiteness checkpoint, incompatible inequalities 0-105596  
second-order phase transitions in crystals, equilibrium configurations, thermoelasticity theory 0-70364  
semiconductors nonequilibrium phase transitions, stability and dissipation, teaching 0-105479  
siloxane, temp. transitions, linear dilatometry and X-ray diff. obs. (*Russian*) 0-59404  
sine-Gordon system, two component, phase transition in two-dimens. 0-73279  
sound attenuation in magnetic field at the 2<sup>1/2</sup>-order phase transition (*Russian*) 0-100487  
statistical mechanical theory of the kinetics of phase transitions, review, book contrib. 0-73270  
structural and mag. phase transforms., integral rational basis of invariants (*Russian*) 0-62602  
structural phase transition, first order, anharmonic oscillator model in (1+1) dimensions 0-86239  
subharmonic lasers, quantum theory, first order non-equilib. phase transition 0-83584  
surface film phase transitions, conf., Erice, Sicily, Italy (Jun. 1979) 0-105429  
surface polariton scattering by order, parameter fluctuations near crit. pts. 0-92835  
systems far from thermodynamic equilib., dissipative structures, broken symm. equilib. phase transition theory 0-65827  
thermophysical property research, metallurgical applications 0-97457  
thylakoid membranes of wheat chloroplasts, proton spin-lattice relax. time, -8°C phase transition 0-108853  
two-dimensional classical sine-Gordon system, commensurate-incommensurate transition 0-62605  
Wigner lattice, screened, solid like phase transitions, statics 0-70370  
CO adsorbed on graphite, fluid-registered solid transition 0-59796  
CuBr<sub>2</sub>(Cl<sub>2</sub>), aq. soln., structural transition, neutron diff. study 0-64872  
 $\alpha$ -Fe<sub>2</sub>O<sub>3</sub>, asymmetric line shapes of Mossbauer spectra (*Chinese*) 0-103902  
K adsorbed on W, field emission flicker noise power rel. to phase transition 0-59795  
Kr adsorbed on graphite, commensurate-incommensurate transitions, low temp. theory 0-103582  
NiCl<sub>2</sub>, aq. soln., structural transition, neutron diff. study 0-64872  
Xe adsorbed on Cu, NaCl, stepped and disordered surfaces, two-dimens. phase transformations 0-103580  
ZnCl<sub>2</sub>, aq. soln., structural transition, neutron diff. study 0-64872

**phase transitions** *see phase transformations***phased arrays (antenna)** *see antenna phased arrays***phi mesons**

- Dalitz arrays from  $K^-\rho^+\pi^-\pi^0$  0-105924



**phi mesons continued**

- decays, hadronic, asymptotic freedom, one-photon or three-gluon exchange 0-62971  
 $e^+e^- \rightarrow \pi^+\pi^-\pi^0$ , 750-1100 MeV,  $\omega$  and  $\phi$  meson interference 0-105910  
 $\gamma p$ , 30-180 GeV,  $\rho$  and  $\phi$  elastic photoprod. cross sections 0-95278  
 $\phi \rightarrow \eta\gamma$ , quark loop model, SU(3) splitting of quark masses 0-62990  
 $\phi \rightarrow \phi\pi\pi$ , current algebra techniques, pole plus remainder model, chiral symmetry breaking and QCD 0-62972

**philosophical aspects**

- cosmology, philosophical relevance (*German*) 0-90652  
 Faraday and the concept of force 0-57048  
 mathematical theories and philosophical insights in cosmology 0-90650  
 mechanical interpretation of nature, J.J. Thomson's work 0-57049  
 non-Euclidean geometry and structures prior to Einstein, speculations (*German*) 0-90651  
 physics and arms race, physicists participation explored for general education students 0-70233  
 quantum interference effects in psychology, Schrodinger's cat, review 0-73158  
 Taoism, physical phenomena, physics and irrational (*French*) 0-90649

**phonographs** see *gramophones***phonon bottleneck** see *phonons***phonon-defect interactions**see also *lattice localised modes*

- brass, lattice thermal cond. component, 30 to 300K, microscopic mechanisms 0-107758  
 brass, lattice thermal cond. component, 4.2 to 30K, microscopic mechanisms 0-107757  
 diamond, Jahn-Teller coupling at neutral vacancy 0-71453  
 dislocation-phonon interactions, drag of phonon gas by moving dislocations 0-70218  
 dislocation-soft mode interaction in displacive transitions (*Russian*) 0-84172  
 disordered crystal, biphonon spectra, light absorpt. coeff. and density of states, CPA calc. 0-84271  
 ferroelastic, dislocation-phonon interactions, phase transition effects 0-59600  
 insulator, lattice thermal cond., point defect scatt. relax. rate role 0-70478  
 GaAs, lattice thermal cond., point defect scatt. relax. rate role 0-70478  
 LiF,  $\gamma$ -irrad. pure and Mg-doped, phonon scatt. and interstitial clusters 0-70254  
 ZnSe crystals, doped and undoped, optical absorption edge 0-60626

**phonon dispersion relations**

- acoustic gyrotropic tensor, in crystals, activity rel. to cryst. class 0-107378  
 actinide compounds, neutron scatt. studies 0-75716  
 alkali halides, lattice dynamics using breathing shell model 0-88285  
 alkali metals, lattice excitation dispersion relations 0-100314  
 alkali metals, phonon dispersion binding energy, compressibility, elastic consts. electron screening and Ashcroft pot. calcs. 0-65174  
 alkali metals, phonon dispersion curves using second-order perturbation theory 0-79893  
 alloys, force-and-mass disordered, average local-information transfer approx. 0-88290  
 p-azoxyphenetole, single cryst., deuterated, phonon dispersion curves, inelastic neutron scatt. obs. 0-84261  
 BCC transition metals, tensor force model, lattice dynamics 0-103428  
 binary compound, Kohn anomaly in optical phonon branch 0-92626  
 disordered lattice, phonon modes, lattice Green function expansion method 0-79900  
 half space layered cryst., vibr. spectrum, Brillouin zone (*Russian*) 0-100313  
 naphthalene- $d_8$ , cryst., phonon dispersion curves calcs., low temp. 0-96599  
 one-dimensional conductor, lattice stability, phonon dispersion, Kohn anomaly 0-96603  
 quartz, acoustic activity, inelastic neutron scatt. obs. (*French*) 0-103431  
 semiconductors, narrow-gap, plasmon-phonon interaction effect on optical phonon dispersion 0-103435  
 semiconductors, van Hove critical point region, electron-phonon interactions, dispersion law 0-70344  
 transition metal dihalides, layer struct., lattice dynamics, calc. 0-65177  
 Ag (111) surface phonon dispersion, He atom scatt. meas. 0-75426  
 Ag, lattice dynamics on Kreh's model 0-59594  
 Al-Ag, force-and-mass disordered alloys, vibr., average local-information transfer approx. 0-88290  
 Au, lattice dynamics on Kreh's model 0-59594  
 CdTe, lattice dynamics and phonon parameters bond bending force model 0-59595  
 CeD<sub>2.72</sub>, phonon dispersion relations 0-88287  
 CeSn<sub>3</sub>, intermediate valence cpd., search for phonon anomalies, inelastic neutron scatt. 0-100317  
 Cr, lattice dynamics, improved Fiełek model 0-59598  
 CsCN, inelastic neutron scatt. by coupled rotational and translational modes 0-70333  
 Cu-Pt system, phonon dispersion relations, force constant disorder effect 0-84263  
 EuS(Se)(Te), spin-assisted phonon Raman scatt., mag. phase depend. 0-71413  
 $\alpha$ -Fe, vibrational states, phonon dispersion, phonon softening 0-88289  
 GaAs, lattice dynamics, phonon freq., bond bending force model calcs. 0-70335  
 GaP, lattice dynamics and phonon parameters bond bending force model 0-59595  
 GaSb, lattice dynamics, phonon freq., bond bending force model calcs. 0-70335  
 GaSe, lattice dynamics and elastic props., Born-von Karman model study 0-70337  
 Ge, lattice dynamics under press 0-92627  
<sup>3</sup>He superfluid, Bose spectrum nonphonon branches (*Russian*) 0-92750  
 Hf, lattice dynamics, phonon dispersion, mode softening 0-107390  
 HgTe, phonon dispersion relations, neutron study 0-70340  
 InP, lattice dynamics and phonon parameters bond bending force model 0-59595  
 InSn, eight-parameter bond-bending forces model 0-70334  
 Ir, phonon/wave vector dispersion relations, Debye temp., modified axial symmetric model 0-70339  
 KD<sub>2</sub>PO<sub>4</sub>, acoustic phonon dispersion, elastic stiffness, light scatt. obs. 0-103966  
 K<sub>2</sub>SnCl<sub>6</sub>, elastic consts., inelastic neutron scatt. and US meas. 0-59553

**phonon dispersion relations continued**

- LaAgIn<sub>1-x</sub>, phonon dispersion, elastic consts. and struct. instability, soft mode behaviour 0-103436  
 Li, phonon limited resistivity struct. depend., Umklapp scatt., elastic consts. 0-88532  
 LiD, long-range three centre potentials, influence on lattice dynamics 0-96605  
 Mo, lattice dynamics, improved Fiełek model 0-59598  
 NH<sub>4</sub>X, X=halogen, phonon dispersion, cohesive and dielec. props. in three body force shell model 0-79892  
 Na, phonon limited resistivity struct. depend., Umklapp scatt., elastic consts. 0-88532  
 NaClO<sub>3</sub>, acoustic activity, inelastic neutron scatt. obs. (*French*) 0-103431  
 NaClO<sub>3</sub>, lattice vibrations and sp. ht., neutron spectroscopic study 0-107388  
 Nb, phonon dispersion curves, extended screened-shell model 0-96601  
 Nb-Zr alloy, BCC- $\omega$  phase transition, electronically driven nature 0-103433  
 Ni<sub>0.89</sub>Cr<sub>0.11</sub>, phonons with disorder caused by force consts., neutron diff. obs. and CPA calc. 0-96602  
 PbI<sub>2</sub>, 2H polypoly, optical mode inversion near M-critical point, neutron scatt. mass 0-103432  
 Rb halides, role of quantum effects in lattice dynamics, Debye temp., shell model calcs. 0-70336  
 RbAg<sub>3</sub>I<sub>6</sub>, single particle excitations, inelastic neutron scatt. obs. 0-59599  
 RbCN, acoustic and optical phonon dispersion at 300K 0-84266  
 Rb<sub>2</sub>WO<sub>6</sub>, low lying phonon dispersion curves, neutron scatt. study 0-92622  
 Se, trigonal, normal mode calcs. 0-84259  
 Se, trigonal and vitreous, sp. ht. and thermal cond., 3 to 300K 0-59676  
 Si, lattice dynamics under press 0-92627  
 $\alpha$ -Sn, lattice dynamics 0-107389  
 SnTe, displacive transform., interband electron-phonon interactions, phase diagram 0-93252  
 SrTiO<sub>3</sub>, ceramic, electrocaloric effects for refrigeration at cryogenic temp. 0-77789  
 Th, phonon dispersion relations, non-central electron fluid model 0-100312  
 ThC<sub>0.063</sub>, cryst. struct. and lattice dynamics 0-88088  
 TI, phonon spectrum from Krasko-Gurskii pseudopot. calc. 0-96608  
 TI<sub>2</sub>PSe<sub>4</sub>, phonon dispersion temp. depend. 0-96600  
 TI<sub>2</sub>TaS<sub>4</sub> and TI<sub>2</sub>PSe<sub>4</sub>, optical phonons, Raman spectra study 0-80790  
 $\alpha$ -U, CDW at 43K 0-80198  
 ZnS, lattice dynamics, phonon freq., bond bending force model calcs. 0-70335  
 ZnS(Se)(Te), thermal expansion and lattice dynamics under press. 0-100316  
 ZnSe, eight-parameter bond-bending forces model 0-70334  
 ZnTe, lattice dynamics and phonon parameters, bond bending force model lattice dynamics and phonon parameters bond bending force model 0-59595  
 Zr, BCC, phonon dispersion relations, d-electron contrib. to Cauchy discrepancy 0-92628  
 $\beta$ -Zr, phonon dispersion, modified Sharma-Joshi model 0-100311

**phonon drag**

- acoustoelectric effect, electron drag by coherent Lamb phonons in quantising magnetic field 0-80330  
 dislocation-phonon interactions, drag of phonon gas by moving dislocations 0-70218  
 graphite, thermoelectric power, low temperature, anomaly rel. to phonon drag 0-65610  
 metals, phonon-phonon scatt. role in lattice thermal cond., phonon drag, elec. cond. 0-70483  
 As<sub>2</sub>Sb<sub>2</sub>, semimetal, thermopower, thermomagnetic power, 4.5 to 77K 0-107825  
 Bi bounded semimetals, phonon two-stage drag of electrons, thermoelectric power, scatt. mechanism 0-92919  
 n-Ge, thermoelec. power in quantising mag. field, phonon-phonon interactions 0-107832  
 Ge:P, phonon drag thermoelectric power at low temp. 0-107828  
 Mo-Nb (Re), thermoelec. power, 4.2 to 300K 0-70683  
 NaMoNb<sub>2</sub>, elect. cond. mech., resist., Hall coeff. and thermoelec. power meas. 0-65603  
 Nb-Zr, thermoelec. power, 4.2 to 300K 0-70683  
 Pd-Co (0.1-45.7 at %), thermo EMF at 4.2-300K (*Russian*) 0-92881  
 Pd-Fe (0.54-8.0 at %), thermo EMF at 4.2-300K (*Russian*) 0-92881  
 Pd-Ni (15-90 at %), thermo EMF at 4.2-300K (*Russian*) 0-92881  
 n-Si, piezoresist. rel. to piezothermoelec. power, electron-phonon drag region 0-70737  
 n-Si:P, piezothermoelec. power in electron-phonon drag region, anisotropy 0-70738  
 Ta-W, thermoelec. power, 4.2 to 300K 0-70684

**phonon-electron interactions** see *electron-phonon interactions***phonon-exciton interactions**

- anthracene, cryst., polariton luminesc. 0-84775  
 anthracene-phenanthrene-tetracyanobenzene, CT-cryst., mini-excitons and lattice dynamics, ESR, optical and Raman spectra 0-60406  
 anthracene-pyromellitic dianhydride cryst., refl. and absorpt. spectra of singlet charge transfer excitons 0-71442  
 benzophenone, migration of triplet excitons, EPR profiles and phosphoresc. decay data 0-84641  
 coupled-mode excitations in cryst., relax. rates, theory 0-59881  
 II-VI semiconductor, resonant secondary emission spectra, relax. of energy and polarisation 0-93331  
 ionic crystal, anharmonism effect on exciton peak broadening in absorpt. spectra (*Russian*) 0-97317  
 layer crystals, exciton absorption of light 0-70623  
 molecular crystals, electronic excitation energy transfer, external elec. field effect 0-84431  
 molecular crystals, exciton-phonon coupling and exciton transport 0-84430  
 molecular crystals, phononless exciton band lineshape, excitation transfer, stochastic models 0-107711  
 molecular crystals with several sublattices, exciton-phonon interaction and Bose-Einstein condensation of Frenkel excitons 0-107713  
 naphthalene, pure and doped, exciton-phonon luminesc. 0-84773  
 naphthalene- $d_8$  and  $d_6$ , isotopic mixed crystals, exciton spectra in IR region 0-71400  
 octafluoronaphthalene crystalline complexes with naphthalene and durenene, triplet exciton emissions 0-84760



phonon-exciton interactions continued

organic molecular crystals, inelastic neutron scatt., exciton creation 0-70084  
perylene crystal, molecular exciton system, resonance Raman and fluorescence studies, dynamical effects 0-66169  
phenanthrene, two-photon excitation spectra, exciton-phonon and intramol. vibronic coupling 0-84774  
polar crystal, Frenkel exciton effective mass temp. depend., lattice displacement interactions (*Chinese*) 0-84429  
polar semiconductor, hot exciton transitions to excited states, interaction with acoustic phonons 0-96799  
polar semiconductors, two-phonon resonance Raman scattering 0-108204  
resonance light scattering and hot luminesc. of self-trapping excitons 0-93336  
resonant Raman scattering via virtual exciton 0-71412  
semiconductor films, exciton light absorption coefficient (*Russian*) 0-71504  
trap effects on exciton bands, masking by exciton-phonon coupling 0-80186  
AgBr, photoluminesc. study of excitons in high mag. fields 0-80843  
BiI<sub>3</sub> film, exciton-phonon interaction, optical consts., Faraday effect., permitt. 0-59884  
EuS(Se)(Te), spin-assisted phonon Raman scatt., mag. phase depend. 0-71413  
GaSe, exciton-phonon quasibound states, photocond. and luminesc. study 0-96800  
GeS, Urbach's rule, absorption edges 0-97224  
InSe, exciton and polaron anisotropies, reson. Raman scatt. study 0-76033  
MnO, magnon-sideband lineshape, exciton-phonon interaction effects 0-65846  
N<sub>2</sub>, solid, exciton-phonon coupling in strong coupling limit, temp. depend. 0-92616  
Si, free excitons, drift and diffusion, luminesc. obs. 0-84434  
Si-Li, bound-exciton excited states, uniaxial anal. 0-71475  
SnO<sub>2</sub>, exciton luminescence spectra, absorpt. spectra 0-89064  
TiO<sub>2</sub>, exciton luminescence spectra, absorpt. spectra 0-89064  
ZnSe, exciton emission, halfwidths, thermal and optical activation energies obs. (*French*) 0-66268

phonon-impurity interactions

see also lattice localised modes  
disordered crystal, biphonon spectra, light absorpt. coeff. and density of states, CPA calc. 0-84271  
local vibrations, impurity interactions, effect on spectral distrib. 0-96613  
reson. relax. time for impurity electrons and localised phonons interaction, appl. to thermal cond. 0-59590  
semiconductors, localised transition metal impurities, lattice relaxation in optical transition (*Polish*) 0-70345  
TGS, nitroaniline admixture effect on thermal parameters 0-107580  
Al<sub>2</sub>O<sub>3</sub>:Mn<sup>3+</sup>, Jahn-Teller Mn<sup>3+</sup> ions, phonon spectroscopy and thermal cond. meas. 0-88282  
Al<sub>2</sub>O<sub>3</sub>:Mn<sup>3+</sup> under uniaxial stress, Jahn-Teller model 0-88521  
 $\beta$ -Al<sub>2</sub>O<sub>3</sub>:NH<sub>4</sub><sup>+</sup>(Nd<sup>4+</sup>), polarised Raman scatt. 0-103947  
CdS:Ni, nonradiative recomb., photocond. spectra 0-70764  
CdTe:Fe<sup>2+</sup>, reson. relax. time for impurity electrons and localised phonons interaction, appl. to thermal cond. 0-59590  
Ge:Ga, resonant scattering of phonons by bound holes in temp. range 1 to 5K 0-75393  
KBr:Au<sup>+</sup>, optical absorpt. bands and MCD, electron-lattice interaction 0-108236  
KBr:MnO<sub>4</sub><sup>-</sup>, many-phonon impurity reson. Raman scatt. 0-60603  
LaCl<sub>3</sub>:Np<sup>4+</sup>, phonon-induced relax. in excited optical states, linewidth temp. depend. meas. 0-100688  
NaCl:NaBr, elastic wave damping, 300 to 1500 MHz, impurity effects 0-92602  
RbCl:Al<sup>3+</sup>, optical absorpt. bands and MCD, electron-lattice interaction 0-108236  
Se, trigonal and vitreous, sp. ht. and thermal cond., 3 to 300K 0-59676  
Si:B, resonant scattering of phonons by bound holes in temp. range 1 to 5K 0-75393  
YAG:Er, elastic wave damping, 300 to 1500 MHz, impurity effects 0-92602  
Zn-Mn, Kondo-system, ion implantation as method for study 0-70241  
ZnS:Fe<sup>2+</sup>, reson. relax. time for impurity electrons and localised phonons interaction, appl. to thermal cond. 0-59590

phonon-magnon interactions

antiferromagnetic insulators, lattice thermal cond. 0-65319  
antiferromagnets, easy-plane, nucl. spin wave relax. 0-65850  
ferromagnet, magnon-phonon interactions, Heisenberg exchange red. 0-80494  
metal, ferromag., antiferromag., magnetoelastic coupling effect on magnetoel. reson. 0-75837  
semiconductors, magnetic, spin wave electron amplification theory 0-97083  
spontaneous symmetry breaking and magnon-phonon spectra 0-65991  
CsMnCl<sub>3</sub>, antiferromagnetic resonance, parametric spin wave excitation (*Russian*) 0-93183  
CsMnCl<sub>3</sub>.2H<sub>2</sub>O, thermal cond. in mag. field 0-70481  
Eu chalcogenides, spin-dependent Raman scatt. from phonons 0-97274  
FeCl<sub>3</sub>, antiferromag., magnon-phonon interactions in thermal cond. 0-65315  
FeF<sub>2</sub>, theory of Raman scattering and IR obs. 0-71426  
KCoF<sub>3</sub>, antiferromag., with residual orbital moment, nucl. mag. relax. 0-71215  
MnCl<sub>2</sub>.4H<sub>2</sub>O, antiferromag., low temp. thermal cond. 0-65320  
YIG, sound vel., temp. depend., phonon scatt. processes 0-96598

phonon-phonon interactions

see also Umklapp process  
brass, lattice thermal cond. component, 30 to 300K, microscopic mechanisms 0-107758  
desorption, multiphonon processes, quantum-statistical theory 0-107641  
diamond, two-phonon bound state, Raman freq. 0-65179  
disordered crystal, biphonon spectra, light absorpt. coeff. and density of states, CPA calc. 0-84271  
disordered crystals, biphonon spectra, CPA calc. 0-70341  
elastic wave generation comparable to Bain deform., role of multiphonon processes (*Russian*) 0-84246  
II-VI semiconductor, resonant secondary emission spectra, relax. of energy and polarisation 0-93331

phonon-phonon interactions continued

insulators, high-intensity US wave vel., phonon-phonon interaction effects 0-70323  
metals, FCC, H<sub>2</sub> diffusion, isotope depend. 0-59727  
metals, light interstitials diffusion, multiphonon transition modes classification 0-70448  
metals, phonon-phonon scatt. role in lattice thermal cond., phonon drag, elec. cond. 0-70483  
molecular crystals, dipolar coupling and phonon symm. (*Chinese*) 0-103437  
polar semiconductors, two-phonon resonance Raman scattering 0-108204  
quasi-two dimensional conductor, galvanomagnetic props., optical analogy (*Russian*) 0-60108  
quasielastic light scattering near phase transitions 0-93362  
semiconductors and insulators, phonon cond., three-phonon N- and U-processes 0-65313  
tetrahedral lattice sites, selection rules for multiphonon transitions 0-92632  
tetrabromomethane, thermal resistivity, heat capacity and phase diagram under pressure 0-65316  
 $\alpha$ -Al<sub>2</sub>O<sub>3</sub>, single crystal transmission and reflectance IR phonon spectra, polariton dispersion 0-66170  
As<sub>2</sub>Se<sub>3</sub>-GeSe<sub>2</sub> glass, bulk and impurity IR absorpt. 0-71455  
Bi, optical phonon anharmonicity and melting, light scatt. study 0-60621  
CdP<sub>2</sub>, cryst., tetragonal, 2-phonon IR absorpt. 0-66176  
CdS, acoustic wave attenuation, phonon viscosity and dislocation drag 0-70319  
Cu, H<sub>2</sub> diffusion, isotope depend. 0-59727  
Cu,  $\mu$ <sup>+</sup> diffusion data anal., theory of incoherent direct and indirect multiphonon transitions 0-70448  
GaS, infrared optical props., polarisation depend., vibr. modes 0-100658  
GaSb, acoustic wave attenuation, phonon viscosity and dislocation drag 0-70319  
n-Ge, thermoelec. power in quantising mag. field, phonon-phonon interactions 0-107832  
<sup>4</sup>He, solid, thermal cond., 0.4 to 1.8K (*Russian*) 0-103535  
<sup>4</sup>He, superfluid, elementary excitations,  $\mu$ eV resolution study by neutron spin echo 0-65327  
HgSe, two-phonon resonant effect, far-infrared reflectivity 0-108203  
n-InSb, anomalous three LO phonon assisted cyclotron resonance 0-108078  
KBr:MnO<sub>4</sub><sup>-</sup>, many-phonon impurity reson. Raman scatt. 0-60603  
KBr:MnO<sub>4</sub><sup>-</sup>, model system, reson. Raman spectra, general behaviour obs. 0-60592  
Mn, Cd<sub>1-x</sub>Te, lattice vibrs., Raman and IR spectra meas. 0-93311  
Sb, optical phonon anharmonicity and melting, light scatt. study 0-60621  
SbSi-SbSBr system, ferroelec., anharmonic effects in far IR reflectivity spectra 0-76014  
n-Si, phonon-phonon relaxation 0-96609  
Si, phonon-phonon relaxation investigation for conventional and neutron doped crystals 0-96927  
 $\alpha$ -Ti, plastic deform., anharmonicity, and Gruneisen parameter 0-88246  
TiO<sub>2</sub>, anatase, Raman spectrum, temp. depend. 0-76027  
TiCl<sub>3</sub>, phonon difference band absorpt., far IR laser spectroscopy 0-93325  
UO<sub>2</sub>, electronic transitions, crystal field effects and phonons, phase transition 0-97303  
YIG, sound vel., temp. depend., phonon scatt. processes 0-96598  
Zn, optical phonon anharmonicity and melting, light scatt. study 0-60621  
ZnP<sub>2</sub>, cryst., tetragonal, 2-phonon IR absorpt. 0-66176

phonon-plasmon interactions

polar semiconductor, highly excited, optical dielec. function of electron-hole plasma 0-92847  
semiconductor, degenerate, surface optical phonons 0-70520  
semiconductors, narrow-gap, plasmon-phonon interaction effect on optical phonon dispersion 0-103435  
surface plasmarons, effect of finite thickness of accumulation layer, theory 0-103636  
CdS crystals, radiative recombination, high excitation rates 0-108269  
Fe<sub>2</sub>O<sub>4</sub>, magnetite, optical props. in IR 0-97271  
GaAs base laminated epitaxial struct., surface plasmon phonon polaritons (*Russian*) 0-59905  
GaP, Raman scatt. from plasmon-phonon coupled modes 0-93337  
GaSb, accumulation layer localised carriers interaction with LO phonons, Raman interference lineshapes 0-93338  
InSb, accumulation layer localised carriers interaction with LO phonons, Raman interference lineshapes 0-93338  
InSb, depletion layer, plasma and vibr. plasma type guided polaritons (*Russian*) 0-96933  
Pb<sub>1-x</sub>Ge<sub>x</sub>Te magnetoplasma reflectivity and transmission spectra 0-71428  
Si, non thermal laser induced ordering, plasma life time, phonon interactions 0-84481

phonon softening see soft modes

phonons

see also crystal surface and interface vibrations; electron-phonon interactions; lattice phonons; phonon-defect interactions; phonon dispersion relations; phonon-exciton interactions; phonon-impurity interactions; phonon-magnon interactions; phonon-phonon interactions; phonon-plasmon interactions; spin-phonon interactions; tunnelling spectra; tunnelling spectroscopy; vibrational states in disordered systems  
acoustic wave spontaneous birth in early Universe (*Russian*) 0-90593  
coherent phonons and excitons in biological systems, Bose condensation 0-67042  
quadrupole-phonon states, fifth label generating operator, props. and eigenvalues 0-79887  
quartz-liquid <sup>4</sup>He interface, saturation effects in phonon reflection 0-92736  
rare gas clusters, small, structure, thermodynamic properties 0-88341  
He, liq., multiphonon boundary of excitation spectrum, neutron and inelastic light scatt. 0-92740  
He, liq., phonon coupling of two-dimens. Wigner cryst. with second surface sound (*Russian*) 0-92756  
<sup>4</sup>He superfluid, phonon-roton excitation 0-107586  
<sup>4</sup>He, liq., excited states, variational calcs. 0-80017  
<sup>4</sup>He, liquid, long-wavelength phonon excitation, series expansion 0-88372  
<sup>4</sup>He, superfluid, excitation spectrum, RPA calc. involving simple pseudopot. 0-92738  
<sup>4</sup>He, superfluid film, solitons at low temps., Korteweg-de Vries eqn. 0-96717



**phosphate glasses**

- for iron and vanadium phosphate semiconducting glasses see *amorphous semiconductors*
- alkali metaphosphate,  $M_2O \cdot R_2O_3 \cdot P_2O_5$  ( $R=Y$  or rare earth), glass transition temps. and coeffs. of linear thermal expansion 0-88343
- alkali-alumino-phosphate:  $U$ , rontgenoluminesc. and fluoresc., radiative transitions obs. 0-103977
- alkaline earth metaphosphate,  $MO \cdot R_2O_3 \cdot P_2O_5$  ( $R=Y$  or rare earth), glass transition temps. and coeffs. of linear thermal expansion 0-88343
- ESR of  $VO^{2+}$  ions 0-100610
- fluorophosphate, magneto-opt. characts. 0-64126
- fluorophosphate optical glass development 0-106588
- glass formation in phosphate system containing halogens 0-103254
- laser glasses, phosphate and fluorophosphate, Nd doped, piezooptic coeffs. meas. 0-99815
- lasers, highly repetitive, development 0-69415
- metaphosphate glass:  $Nd^{3+}$ ,  $Yb^{3+}$ , luminesc., energy transmission and migration between  $Nd^{3+}$  and  $Yb^{3+}$  0-66297
- non-alkaline, transition states, phys. effects of fluors, phase diagrams and optical effects (*German*) 0-88045
- opal glasses, phosphate opacified, phase comp. and struct. 0-64919
- optical breakdown rel. to microscopic inhomogeneous struct. 0-102784
- sealants to Al alloys, elec. and mech. props., glass transition 0-81018
- solid state nuclear track detectors, effect of etching conditions on energy resolution of phosphate glass and polycarbonate detectors 0-91390
- AgI-Ag<sub>2</sub>O-P<sub>2</sub>O<sub>5</sub> glassy electrolyte galvanic cells 0-104513
- AgPO<sub>3</sub>-AgX ( $X=I, Br$ ), glass-forming regions, struct. model (*French*) 0-100464
- Al<sub>2</sub>O<sub>3</sub>-P<sub>2</sub>O<sub>5</sub>-Cr<sup>3+</sup>, absorpt. spectra, Fano antireson. and vibronic Lamb shift 0-71458
- Al(PO<sub>3</sub>)<sub>3</sub>-BaF<sub>2</sub>-Al<sub>2</sub>O<sub>3</sub> glasses, opt. props., group I-III fluorides effect 0-66143
- B<sub>2</sub>O<sub>3</sub>-V<sub>2</sub>O<sub>5</sub>-P<sub>2</sub>O<sub>5</sub> glass, mech. and elec. props 0-84228
- BaO-P<sub>2</sub>O<sub>5</sub>, US velocity rel. to elastic props. 0-103425
- BaO-P<sub>2</sub>O<sub>5</sub>-Mo<sup>3+</sup> glass, EPR spectra, computer simulation 0-88872
- BaO-WO<sub>3</sub>-P<sub>2</sub>O<sub>5</sub> struct. and IR spectra 0-64914
- Ba(PO<sub>3</sub>)<sub>2</sub>-AlF<sub>3</sub>-CaF<sub>2</sub>, elec. cond. and IR spectra 0-89005
- Ba(PO<sub>3</sub>)<sub>2</sub>-AlF<sub>3</sub>-MgF<sub>2</sub>, elec. cond. and IR spectra 0-89005
- Ba(PO<sub>3</sub>)<sub>2</sub>-fluoride glass, elec. cond., struct. 0-88056
- Ba(PO<sub>3</sub>)<sub>2</sub>-WO<sub>3</sub>, electron-absorpt. spectra and structure of W centres 0-88873
- CaO-P<sub>2</sub>O<sub>5</sub>, US velocity rel. to elastic props. 0-103425
- CaO-P<sub>2</sub>O<sub>5</sub>-Cr<sup>3+</sup>, absorpt. spectra, Fano antireson. and vibronic Lamb shift 0-71458
- CdO-Al<sub>2</sub>O<sub>3</sub>-P<sub>2</sub>O<sub>5</sub> glass,  $\gamma$ -irrad., EPR study 0-84639
- CdO-P<sub>2</sub>O<sub>5</sub> glass, thin film, elec. cond., high and low fields 0-80427
- K<sub>2</sub>O-Al<sub>2</sub>O<sub>3</sub>-P<sub>2</sub>O<sub>5</sub>-TiO<sub>2</sub>, structural role of Ti, kinetic study of chem. destruction 0-88055
- Li-La phosphate glass, Nd, Cr activated, Nd luminesc. quantum efficiency meas., Nd-Cr nonradiative transfer 0-66296
- LiCl-Li<sub>2</sub>O-P<sub>2</sub>O<sub>5</sub> glass system, vitreous domain, struct., elec. cond. (*French*) 0-70135
- Li<sub>2</sub>O-Al<sub>2</sub>O<sub>3</sub>-P<sub>2</sub>O<sub>5</sub>-Cd<sup>2+</sup>,  $\gamma$ -irrad., EPR study 0-84639
- Li<sub>2</sub>O-B<sub>2</sub>O<sub>3</sub>-P<sub>2</sub>O<sub>5</sub> glass, mech. and elec. props 0-84228
- Li<sub>2</sub>O-P<sub>2</sub>O<sub>5</sub>-Cd<sup>2+</sup> glass,  $\gamma$ -irrad., EPR study 0-84639
- Li-S-P-S-LiI, ionic cond. meas. from room temp. to glass transition temp. (*French*) 0-88355
- MgO-Al<sub>2</sub>O<sub>3</sub>-P<sub>2</sub>O<sub>5</sub> system glass, heat treatment of aluminium metaphosphate influence on thermolum. 0-108285
- MgO-P<sub>2</sub>O<sub>5</sub>, US velocity rel. to elastic props. 0-103425
- $\alpha$ -Na<sub>2</sub>Fe<sub>2</sub>(PO<sub>4</sub>)<sub>3</sub> orthophosphate, cryst. and vitreous, Mossbauer spectroscopy and mag. susceptibility (*French*) 0-80657
- Na<sub>2</sub>O-B<sub>2</sub>O<sub>3</sub>-P<sub>2</sub>O<sub>5</sub> glass, mech. and elec. props 0-84228
- Na<sub>2</sub>O-P<sub>2</sub>O<sub>5</sub>-Cr<sup>3+</sup>, absorpt. spectra, Fano antireson. and vibronic Lamb shift 0-71458
- Na<sub>2</sub>O-P<sub>2</sub>O<sub>5</sub>-CuO,  $\gamma$ -irrad., CuO effects on EPR 0-84645
- Na<sub>2</sub>O-P<sub>2</sub>O<sub>5</sub>-Y<sub>2</sub>O<sub>3</sub>-Tb<sub>2</sub>O<sub>3</sub> glass, conc. quenching of luminesc. in disordered system with dipolar interaction 0-89059
- NaPO<sub>3</sub>:Eu<sup>2+</sup>, luminesc. of Eu<sup>2+</sup>, transition probabilities 0-80845
- Nb<sub>2</sub>O<sub>5</sub>-V<sub>2</sub>O<sub>5</sub>-P<sub>2</sub>O<sub>5</sub> glasses and glass ceramics, elec. cond., struct. 0-84466
- Nd:glass, comparative lasing characts. of silicate and phosphate laser glasses 0-74364
- P<sub>2</sub>O<sub>5</sub>-R<sub>2</sub>O<sub>3</sub>-M<sub>2</sub>O ( $M'O$ ), ( $M$ =alkali metal,  $M'$ =alkaline earth,  $R=Y$  or rare earth), metaphosphate glass phosphors, fluoresc. props., activation conc. effect 0-89058
- SiO<sub>2</sub>-Na<sub>2</sub>O-CaO-P<sub>2</sub>O<sub>5</sub>, BIOGLASS, surface, Ca<sub>3</sub>(PO<sub>4</sub>)<sub>2</sub> film form., bonding to bone 0-85212
- SrO-P<sub>2</sub>O<sub>5</sub>, US velocity rel. to elastic props. 0-103425
- Tb<sub>2</sub>O<sub>3</sub>-P<sub>2</sub>O<sub>5</sub>-MO system glasses, ( $M=Mg, Ca, Sr, Ba$  or  $Pb$ ), photoluminesc. under X-ray excitation 0-89060
- TeO<sub>2</sub>-P<sub>2</sub>O<sub>5</sub> system, glass struct., neutron diff. study 0-70128
- WO<sub>3</sub>-P<sub>2</sub>O<sub>5</sub> glass, AC cond. and dielec. props. 0-92717
- Yb<sup>3+</sup> doped, luminesc. band struct., chronoscopic study at 4.2K 0-60663
- ZnP glass heavy-ion track detectors 3 to 120 MeV 0-91389

**phosphorescence**

- see also *fluorescent screens*; *MIDP*; *phosphors*
- adenine film, polycryst., energy conversion processes, quantum yields, 4 to 10 eV 0-88589
- 9,10-anthraquinone, lower triplet states, interactions and position, matrix isolation spectra 0-63634
- anthraquinone in pentane solvent, sublevel phosphorescence spectra, molecular distortion 0-74190
- aromatic compounds in benzene polycrystalline host, active N<sub>2</sub> induced chemilum., 77K 0-60691
- benzaldehyde gas, nonradiative electronic transition 0-83413
- benzaldehyde in methylcyclohexane, n $\pi^*$  spectra 0-63627
- benzophenone, migration of triplet excitons, EPR profiles and phosphoresc. decay data 0-84641
- benzophenone vapour, fluoresc. and phosphoresc., nonradiative transitions between triplet and singlet state obs. 0-99516
- p-bromochlorobenzene, T<sub>1</sub> states, zero-field ODMR, MIDP and phosphorescence excitation spectra 0-74191
- cell surface component rotational diffusion, time-resolved phosphoresc. anisotropy 0-97885
- chlorobenzaldehyde, a<sup>3</sup>A'<sup>-</sup>X<sup>1</sup>A' phosphoresc., conformations and ground state fundamentals 0-78642
- chloroquinolines, photophys. behaviour, substituent and solvent effects 0-106342

**phosphorescence continued**

- diacetyl vapour, fluoresc. and phosphoresc., nonradiative transitions between triplet and singlet state obs. 0-99516
- p-diazines, polycyclic, T<sub>1</sub>( $\pi\pi^*$ ) $\rightarrow$ S<sub>0</sub> intersystem crossing, isotope effects, ODMR and phosphoresc. obs. 0-91586
- p-dibromobenzene, T<sub>1</sub> states, zero-field ODMR, MIDP and phosphorescence excitation spectra 0-74191
- p-dichlorobenzene-p-dibromobenzene mixed crystals, triplet exciton migration, time resolved emission spectroscopy 0-89052
- 4,4'-dichlorobenzophenone single crystals., mutual annihilation of triplet excitons, 1.5 and 4.2K, phosphoresc. obs. 0-80850
- N-ethylphthalimide+olefins, photochemical reaction, absorpt., fluoresc., phosphoresc. and triplet-triplet absorpt. spectra 0-85197
- gelatin layers with and without AgNO<sub>3</sub>, phosphorescence kinetics curves (*Russian*) 0-62776
- molecular nonsteady-state luminesc. behaviour under narrowband laser excitation 0-87159
- naphthalene, phosphorescence spectra in rare gas matrices, multiplet struct. and pot. energy functions 0-106341
- naphthalene in Ar matrix, geometry changes and multiplet struct., mol. fluoresc. and phosphoresc. obs. 0-95663
- octafluoronaphthalene crystalline complexes with naphthalene and duren, triplet exciton emissions 0-84760
- organic molecular crystals, intermolecular interactions, spectroscopic studies, review 0-103958
- 2,2 paracyclophane, dimer vibration influence on emission spectrum 0-69133
- phosphorimetry, low-temp., conduction cooling system for sample introduction 0-87158
- poly-N-vinylcarbazole-biacetyl, triplet exciton quenching, exciton trapping model 0-66267
- pyrazine, electronic energy transfer to metal surface, classical image dipole theory 0-97318
- pyrazine, on Ag surface, time-resolved molecular electronic energy transfer 0-92957
- pyrene, triplet state, excitonic energy transfer, phosphoresc. and delayed fluoresc., 2 to 300K 0-84776
- pyrimidine, vapour, phosphoresc. 0-83408
- quantum beats, in phosphorescence 0-63704
- spectral line narrowing of triplet state, in laser excited experiments 0-63703
- p-terphenyl, cryst., exciton phosphoresc. at 300K 0-108277
- 1,2,4,5-tetrachlorobenzene, mol. solid, heat pulses, phonon-induced delocalisation of trapped excited triplet states 0-89053
- tetramethyl pyrazine in duren, phosphorescent moles., quantum beats in triplet states 0-58312
- thionine in sodium lauryl sulphate micellar solns., absorpt. spectra and fluoresc. yield, local dye conc. depend. 0-106343
- thymine film, polycryst., energy conversion processes, quantum yields, 4 to 10 eV 0-88589
- tryptophan residue in horse liver alcohol dehydrogenase, room-temp. phosphoresc., temp. and enzymic complex form. effects 0-61512
- xanthone, large zero-field splitting of lowest triplet state 0-58171
- xanthone, in n-pentane, heat pulse induced delayed phosphorescence 0-83404
- BaCl<sub>2</sub>, Sn-activated, luminescence studies 0-108246
- CaO, photoionisation of F-centre, luminesc. and photocond. meas. 0-66270
- KCl:Eu<sup>2+</sup> crystals, photostimulated afterglow investigation at room temp. 0-108259
- La<sub>2</sub>O<sub>3</sub>:Eu, slow phosphoresc., high press. study 0-80839
- MgAl<sub>2</sub>O<sub>4</sub>,  $\gamma$ -irradiated crystal, TSC, thermoelec. power, thermolum. and afterglow 0-75583
- Na<sub>2</sub>O-SiO<sub>2</sub> glasses, elementary electronic excitations, refl., luminesc., and photoemission meas. 0-84778
- SrS:Nd, phosphorescence decay, trapping levels 0-104003
- ZnS:Tb, Cu(Ag) phosphors, luminesc. props. 0-100690

**phosphorescence microwave double resonance** see *PMDR***phosphorescence microwave photoexcitation spectroscopy** see *PMDR***phosphors**

- see also *fluorescent screens*; *luminescence*
- alkaline earth oxides, photon multiplication and secondary electron-hole pairs generation (*Russian*) 0-66262
- emission and absorption characts. for fluorescent lamps (*Japanese*) 0-89067
- light sources, <sup>147</sup>Pm sealed sources (*Hungarian*) 0-91348
- powdered, in host material, solar cells wavelength shifting 0-85286
- rare earth double orthophosphates with alkali metals, conc. depend. of luminesc. props. 0-100673
- rare earth double orthophosphates with alkali metals, spectroscopic obs., struct. and chem. nature 0-100674
- rare earth germanates, R<sub>2</sub>O<sub>3</sub>-GeO<sub>2</sub> system cpds., physicochem. characts. 0-97469
- temperature meas. appl. using fibre optics 0-73360
- 2-(2-tosylaminophenyl)-4H-3,1-benzoxazine-4-one, cryst. and mol. struct. 0-84167
- Al<sub>2</sub>O<sub>3</sub> and double oxides, photon multiplication and secondary electron-hole pairs generation (*Russian*) 0-66262
- Al<sub>2</sub>O<sub>3</sub>:Si(Ti), sensitised TLD phosphor, photon energy dependence 0-78498
- BaCl<sub>2</sub>, Sn-activated, luminescence studies 0-108246
- BaF<sub>2</sub>:Pb crystal phosphor, emission spectra 0-66298
- CaF<sub>2</sub>:Dy, TLD-200, thermolum. phosphor, photolum. and absorpt. spectra, thermolum. mechanisms 0-97321
- CaO:Ce<sup>3+</sup>, Gd<sup>3+</sup> sensitization of Ce<sup>3+</sup> luminesc. by Gd<sup>3+</sup> 0-97326
- CaO:Eu<sup>3+</sup>, influence of crystal field on luminesc. (*Russian*) 0-80834
- CaS, atomic and mol. centres of O, ESR and luminesc. methods (*Russian*) 0-84764
- CaS:Ce, Na phosphor, photoluminescence and excitation spectra 0-89049
- CaS:Cu, colour centres, optical and thermal depths determ. 0-66275
- CaS:Nd, X-ray powder diff. anal. 0-100204
- CaS:Pd phosphors, trap and luminescent centre location, photo., thermo- and electroluminescence studies 0-71482
- CaSO<sub>4</sub>:Dy TLD phosphor,  $\gamma$  radiation changes in glow curve 0-60688
- CaSO<sub>4</sub>:Dy(Tm), thermolum. thermolum. phosphor, photolum. and absorpt. spectra, thermolum. mechanisms 0-97321
- CaSO<sub>4</sub>:Sm phosphors, X-irrad., thermoluminesc., charge compensation effects 0-97351
- CaSO<sub>4</sub>:Tm, sensitised TLD phosphor, photon energy dependence 0-78498



## phosphors continued

- Eu double metaphosphates with alkali metals or H, luminesc. props. 0-100675  
 InTa<sub>1-x</sub>Nb<sub>x</sub>O<sub>4</sub> system, structural and luminescent props. 0-84769  
 KBr:Ti, 480K thermal glow peak, Ti<sup>3+</sup> centres 0-108284  
 LaGaS<sub>2</sub>:Ce<sup>3+</sup>, luminesc. props. 0-103979  
 La<sub>2</sub>O<sub>3</sub>:S:Eu, high press. effect on luminesc. efficiency and lifetime, charge transfer absorpt. 0-66266  
 La<sub>2</sub>O<sub>3</sub>:S:Eu, slow phosphoresc., high press. study 0-80839  
 LiF, sensitised TLD phosphor, photon energy dependence 0-78498  
 LiF:Mg, TLD-100, thermolum. phosphor, photolum. and absorpt. spectra, thermolum. mechanisms 0-97321  
 MgO doped powder phosphors, photo- and thermostimulated luminesc. obs. (Russian) 0-66263  
 MgS:Ce<sup>3+</sup>, emission and excitation spectra (French) 0-93380  
 Mg<sub>2</sub>SiO<sub>4</sub>:Tb, sensitised TLD phosphor, photon energy dependence 0-78498  
 Mg<sub>2</sub>SiO<sub>4</sub>:Tb, thermolum. phosphor, photolum. and absorpt. spectra, thermolum. mechanisms 0-97321  
 P<sub>2</sub>O<sub>5</sub>-R<sub>2</sub>O<sub>3</sub>-M<sub>2</sub>O(M'O), (M=alkali metal, M'=alkaline earth, R=Y or rare earth), metaphosphate glass phosphors, fluoresc. props., activation conc. effect 0-89058  
 Sc<sub>2</sub>O<sub>3</sub> and double oxides, photon multiplication and secondary electron-hole pairs generation (Russian) 0-66262  
 SrCl<sub>2</sub>, in-activated, luminescence studies at 77 and 300K 0-108247  
 Si<sub>3</sub>N<sub>4</sub>:Mn, Zr phosphor, photodiode effect 0-107848  
 Tb<sub>2</sub>O<sub>3</sub>-P<sub>2</sub>O<sub>5</sub>-MO system glasses, (M=Mg, Ca, Sr, Ba or Pb), photoluminesc. under X-ray excitation 0-89060  
 YAlO<sub>3</sub>:Ce, fast decay UV phosphor 0-71471  
 Y<sub>2</sub>O<sub>3</sub> and double oxides, photon multiplication and secondary electron-hole pairs generation (Russian) 0-66262  
 Y<sub>2</sub>O<sub>3</sub>:Eu, cathodoluminesc. investig., appl. to cathode ray tube screening 0-108282  
 Y<sub>2</sub>O<sub>3</sub>:S:Eu, high press. effect on luminesc. efficiency and lifetime, charge transfer absorpt. 0-66266  
 YVO<sub>4</sub>:Eu, cathodoluminesc. investig., appl. to cathode ray tube screening 0-108282  
 ZnO phosphor fired with Zn, luminesc. in green and red region 0-66265  
 ZnO:Ce(Tb), electrolum. brightness, voltage and freq. depend. 0-60681  
 ZnS powder phosphors electroluminescent cells, AC electrolum. characts. (Japanese) 0-71489  
 ZnS:Ag, ZnS:CdS:Ag(Cu), cathodoluminesc. investig., appl. to cathode ray tube screening 0-108282  
 ZnS:Cu, Mn Cd electroluminescent powder panels, bulk and junction effects 0-89068  
 ZnS:Cu, spectral distrib., rise and decay behaviour (German) 0-60625  
 ZnS:Tb, Cu(Ag) phosphors, luminesc. props. 0-100690  
 Zn<sub>2</sub>SiO<sub>4</sub>:Mn, energy storage effect and retrieval 0-100684  
 ZnWO<sub>4</sub>, scintillation characts. 0-66256

## phosphorus

- see also nuclei with .....  
 addition to Fe-Ni-B amorphous alloy, effect on crystn. and elec. cond. 0-75179  
 addition to high Mn austenitic steel, effect on creep rupture (Korean) 0-93646  
 amorphous, prepared by chem. transport in low-pressure H<sub>2</sub> plasma, radial distrib. function 0-64899  
 amorphous, struct. by electron microscopy 0-84065  
 atom, ab initio effective valence shell Hamiltonian for neutral and ionic valence states 0-74117  
 atom, neutral, IR spectra and HFS 0-91478  
 atom, neutral, spectra and term anal. 0-91481  
 bone, sheep, transportable system for neutron activation anal. determ. of P 0-109066  
 contaminated Ni surface, coadsorption of Sn, AES study 0-88437  
 determination by activation anal. ( $\alpha$ n), ( $\alpha$ p) reacts. investig. 0-61206  
 determination in optical waveguide glass by DC plasma emission spectroscopy 0-87446  
 diffusion in Si, elastic deform. relax. and dislocation generation 0-79997  
 diffusion mechanism in Si, migration channels along vacancies and interstices 0-79996  
 impurities in low alloy steels, effect on neutron irradiation embrittlement 0-85055  
 impurity in Cr-Mo-V low-alloy steel, effect on high-temp. ductility and crack growth 0-66652  
 impurity migration from doped Si sources in epitaxial layers (Russian) 0-107570  
 ion implantation in laminar Si-SiO<sub>2</sub> systems struct. change investig. by MSSI (Russian) 0-107918  
 ion implantation of Ni, amorphous Ni-P prod. 0-75257  
 in natural waters, automated procedure for P determ. 0-81517  
 $\alpha$ -quartz:P, dynamic interchange among 3 states of P<sup>4+</sup>, EPR obs. 0-66010  
 red, atmospheric aerosol absorption to extinction coeff. ratio meas. 0-90217  
 reduction in sewage effluent by electrochemical process 0-104445  
 steel, grain boundary segregation, effect on brittle fracture after quenching and tempering (Russian) 0-81145  
 steel, hardenability, role of B and P segregation 0-97486  
 water pollution, P conc. streams draining from agricultural watershed 0-61474  
 water pollution control, phosphorus removal system, automation 0-76669  
 C:H:P film, amorphous elec. props., chem. modifications by doping with P 0-84523  
 CaSO<sub>4</sub>:Dy, phototransferred TL studies 0-80875  
 CdTe:P, ion implanted, elec. props. 0-65021  
 Fe, single cryst., segregation behaviour of S, O and P at (100) surface 0-100841  
 (FeNi)PB amorphous wires, surface oxidation and annealing influence on induced anisotropy 0-100957  
 Fe<sub>100-x</sub>P<sub>x</sub>, structural analysis of models for amorphous metallic alloys 0-103249  
 GaAs:P<sup>+</sup>, implantation profiles, backscatt. meas. 0-70238  
 Ge:Be, P, absorption of radiation, 0.6-2.8 mm, 4.2 to 20K 0-66332  
 Ge:P, charact. temp. and lattice thermal cond. 0-59743  
 Ge:P,  $\gamma$ -irradi., carrier trapping and recomb. at point radiation defects 0-107810  
 Ge:P, phonon drag thermoelectric power at low temp. 0-107828  
 In<sub>0.9</sub>Sn<sub>0.1</sub>:CdTe:P, p-n homojunction solar cell, elec., photovoltaic props., photoluminescence 0-81463

## phosphorus continued

- Ni-P undercoat, effect on struct. form. in sintered electrophoretic Cr<sub>3</sub>C<sub>2</sub> alloy coatings 0-61027  
 P II homologous ions series, Stark broadening trends 0-105157  
 P<sup>+</sup>, contracted Gaussian basis sets for mol. calcs. 0-83264  
 P<sup>+</sup>, static dipole quadrupole polarisabilities and shielding factors calc. using HF scheme 0-99450  
 P<sup>+</sup>-ion penetration tails in SiO<sub>2</sub>-Si two-layer system, expt. and computer anal. 0-75249  
<sup>31</sup>P NMR of the perfused heart 0-77534  
<sup>31</sup>P, obs. of DNMR using RYA-2308 radiospectrometer with attachment 0-98957  
<sup>31</sup>P-NMR spectra of chicken erythrocyte nucleosomes, temp. dependence 0-94280  
<sup>32</sup>P and <sup>45</sup>Ca determination in biological samples by Cherenkov and liq. scintillation counting 0-98183  
<sup>33</sup>P transmutation lethal effect on bacteriophage A13 mech. of DNA double helix rupture (French) 0-98018  
 Si epitaxial layers, grown in vac. at low temps. P and Sb doping 0-88189  
 Si:Au, P-induced point defects influence on Au gettering mechanism 0-65030  
 Si:B, P, long range enhancement of B diffusivity by P diffusion 0-103386  
 Si:H:P amorphous film, elec. cond., thickness and temp. depend. 0-65559  
 Si:P, amorphous, negative magnetoresist., localised mag. states 0-70731  
 Si:P, annealing after ion implantation, ellipsometric study 0-65018  
 Si:P, carrier lifetime depth distrib. due to Ar ion implantation 0-70232  
 Si:P, dielec. susceptibility meas., polarisation catastrophe at metal-insulator transition 0-59873  
 Si:P, dislocation dissc. mode obs. by weak-beam TEM 0-107259  
 Si:P, dislocations under high stress, stacking fault energies, TEM study 0-70202  
 Si:P, donor-polarizability enhancement as the insulator-metal transition is approached from the insulating side 0-80184  
 Si:P, doping during growth from gas phase, thermodynamic analysis 0-59489  
 n-Si:P, elec. cond. oscills., electron instability effects due to dislocations 0-103704  
 Si:P, heavily doped semicond., scatt. mechanism, resist. and Hall coeff. maxima 0-75586  
 Si:P, homogeneous nuclear transmutation technique, thyristors appl. 0-70236  
 Si:P, implanted low temp. annealed, elec. activation, damage depend. 0-88182  
 Si:P, impurity content characterisation, exciton luminesc. 0-60653  
 Si:P, incoherent light flash annealing, elec. props., backscattering spectra 0-97504  
 Si:P, ion implantation, channelled, through metal silicide film 0-70231  
 Si:P, ion implanted, doping profile, pulsed laser annealing effects 0-88197  
 Si:P, ion implanted, IR transmission and rel. spectra study 0-108244  
 Si:P, ion implanted, regrowth of damage structs. by laser annealing 0-107289  
 Si:P, ion implanted, subsurface damage, TEM and channelled Rutherford backscatt. study 0-107337  
 Si:P, ion implanted, TEM study after laser and furnace annealing 0-70234  
 Si:P, ion implanted crystalline and amorphous, laser annealing 0-97509  
 Si:P, ion implanted with small doses, defect annealing by nanosecond laser pulses 0-107297  
 Si:P, luminescence circular polarisation, emission by many exciton complexes 0-93398  
 Si:P, measurement techniques for determining P densities 0-75262  
 Si:P, neutron transmutation doping, elec. props. rel. to neutron fluence 0-96555  
 Si:P, neutron transmutation doping, resist. homogeneity rel. to compensation ratio 0-96556  
 Si:P, nonequilibrium solid solutions obtained by heavy ion implantation and laser annealing 0-92544  
 n-Si:P, piezothermoelec. power in electron-phonon drag region, anisotropy 0-70738  
 Si:P, polycryst., channelling of implanted P during MOS device processing 0-65017  
 Si:P, polycryst. films, elec. props., EPR, defect states, doping effects 0-75660  
 Si:P, polycrystalline laser recrystallised film on Si substrate, cryst. struct., thermal oxidation 0-65391  
 Si:P, proton-irradi., impurity uphill diffusion, vacancy mechanism 0-92719  
 Si:P, thermal cond., electron-phonon interaction at low temps. 0-92730  
 Si:P bipolar transistors, interstitial supersaturation and misfit dislocation climb, TEM study 0-70203  
 Si:P film, polycryst., heavily doped, mobility and carrier conc., optical determ. 0-66314  
 Si:P implanted, multicasting electron beam annealing 0-75242  
 p-Si:P implanted films, piezoresist. stress tensors, ion dose depend., -80 to 120°C 0-100538  
 Si:P polycrystalline layer, role in lattice defect reduction assoc. with P predeposition 0-70229  
 Si:P wafer, stacking faults, preoxidation gettering by reverse side P diffusion-induced misfit dislocations 0-60988  
 Si:P(O) p<sup>+</sup>-n<sup>+</sup> solar cells, comparison rel. to resistance to 1.5 MeV electron irradi., majority carrier trapping 0-94087  
 p-Si:P(P<sup>+</sup>) photolytic props. in HF 0-89504  
 Si:Sb:P, double implants, residual defect reduction after damage anneal 0-88170  
 Si-F-H:P, film, dark cond., struct., Raman scatt. 0-88588  
 Si-H:P amorphous film, dark cond., struct., Raman scatt. 0-88588  
 SiO<sub>2</sub>, P-doped amorphous, porous and hydrophilic, water adsorpt. and IR spectra obs. 0-80061  
 SiO<sub>2</sub>:P optical fibre, single-polarisation single-mode, exposed cladding fabrication 0-58725  
 SiO<sub>2</sub>:Ge, B, P, optical fibre, radiation induced optical absorpt. spectra, 0.4 to 1.7  $\mu$ m region 0-58761  
 SnO<sub>2</sub>:P, CVD films, elec. props., cryst. to amorphous transition effects 0-107933  
 SnO<sub>2</sub>:P, CVD growth and etching characts., doping effects 0-107667  
 Te:P, impurity spectroscopy 0-65499  
 ZnTe:P, ion implanted, cathodoluminescence emission spectrum 0-108281  
 ZnTe:P, shallow-acceptor, donor, free-exciton, and bound-exciton states 0-60667



**phosphorus compounds**

- ESCA shifts and effective charges 0-78648  
 metabolites,  $^{31}\text{P}$  spectroscopic zeugmatography 0-76872  
 phosphate and alkaline phosphate activity determ. by dual microcomputer-controlled stopped-flow spectrometer 0-57379  
 phosphate binder based chamotte concretes, strength props. 0-89305  
 phosphate containing materials, technological prod. processes, review 0-97452  
 trivalent metal phosphates, condensed, synthesis in polyphosphoric acid melts, physicochem. equil. considerations 0-97419  
 $\text{AgX-Ag}_2\text{O-P}_2\text{O}_5$  ( $\text{X}=\text{I}, \text{Br}, \text{Cl}$ ), glass formation and ionic conductivity 0-65290  
 Co-P alloys, geometric struct. models and diffraction exam. techniques 0-79700  
 $\text{Fe}_3\text{P}_2\text{P}_2\text{O}_7$ , amorphous and crystalline, electrochemical and semicond. behaviour (Russian) 0-101021  
 Ge-P-S glass system, EPR of intrinsic and  $\text{Mn}^{2+}$  impurity centres 0-88870  
 $\text{GeO}_2\text{-P}_2\text{O}_5\text{-SiO}_2$  graded index optical fibres optimised for 1.3  $\mu\text{m}$  wavelength region, fabrication techniques (Japanese) 0-99888  
 HCP, force fields and force consts. of electronically excited states 0-69116  
 $\text{H}_2\text{PNH}_2$ , inversion-rot. mechanism, basis set and geometry optimisation effects 0-83273  
 $\text{N}_2\text{P}_2\text{Br}_6$ ,  $^{81}\text{Br}$  NQR, conformation investig. 0-63665  
 $\text{Na}_2\text{S-P}_2\text{S}_5$ , glass forming region, struct. and ionic cond. 0-88358  
 $\text{Na}_2\text{S-P}_2\text{S}_5$ , synthesis, structure and ionic conduction (French) 0-65291  
 $\text{PCl}_3$ , bond polarisability and force constants 0-69260  
 $\text{PCl}_3$ , structural study at 123K (French) 0-88111  
 $\text{PCl}_3$ , sublimed phase studied by  $^{31}\text{P}$  NMR, Raman spectra and X-ray diff. 0-100209  
 $\text{PD}^+$ , IR emission spectra, rot. anal. and mol. parameters 0-69134  
 $\text{PF}_3$ , nuclear resonance, effects of intermolecular interactions and intramolecular dynamics 0-63658  
 $\text{PF}_3$ , dopant for polyacetylene 0-88171  
 $\text{PF}_3$ , nuclear resonance, effects of intermolecular interactions and intramolecular dynamics 0-63658  
 $\text{PH}^+$ , IR emission spectra, rot. anal. and mol. parameters 0-69134  
 $\text{PH}_3$ , conc. meas. by vacuum UV absorpt. spectra 0-71972  
 $\text{PH}_3$ , Doppler-free optical double reson. spectroscopy using single-freq. laser and modulation sidebands 0-68274  
 $\text{PH}_3$ , nucl. spin-spin coupling consts., ab initio calcs. 0-95647  
 $\text{PH}_3$  on Saturn, abundance, IR obs. 0-82278  
 $\text{PH}_3$ , second order mag. props., coupled Hartree-Fock perturbation theory 0-87042  
 PN, absorpt. and emission spectra, electronic transition and vibr. obs. 0-91573  
 $\text{PO}_2$  in K halides, ODMR in zero and weak mag. fields 0-88894  
 $\text{PO}_3^{3-}$ , ionisation energies, SCF-X $\alpha$  transition state calcs. 0-74115  
 $\text{P}_2\text{O}_5$  gas, for glazing ceramics 0-108609  
 $\text{P}_2\text{O}_5$  type water vapour sensor 0-98907  
 $\text{POCl}_3\text{:Pr}^{3+}$  fluoresc. and lifetimes of excited states 0-71466  
 $\text{POF}_3$ , nuclear resonance, effects of intermolecular interactions and intramolecular dynamics 0-63658  
 $\text{SiO}_2\text{-Al}_2\text{O}_3\text{-CaO-BaO-SrO-ZnO-Na}_2\text{O-K}_2\text{O-B}_2\text{O}_3$ , glaze effect of  $\text{P}_2\text{O}_5$  additions 0-60824  
 $\text{Sn}_2\text{P}_2\text{S}_6$ , investigation of p-T diagram near a singular point (Russian) 0-88937  
 $\text{Sn}_2\text{P}_2\text{S}_6(\text{Se}_2\text{S}_2)_{x_6}$ , ferroelec. tricit. phase transform., light transmission study 0-71355  
 $\text{V}_2\text{O}_5\text{-P}_2\text{O}_5\text{-Nb}_2\text{O}_5$  glasses, switching 0-88604

**phosphosilicate glasses**

- bridge structure across V-groove formed by etching in Si 0-104312  
 CVD, flow for integrated optical cct. fabrication 0-79005  
 CVD coatings, P content meas. using SEM and energy-dispersive X-ray anal. 0-76588  
 film, CVD, P conc. profile by etch rate technique 0-96450  
 film, passivation of MOS struct., flat-band voltage, effect of growth conditions 0-107913  
 film, thickness and IR spectrum changes on heat treatment in  $\text{H}_2$  0-70549  
 selective etching, to Si by plasma reactive sputter etching 0-81221  
 $\text{GeO}_2\text{-P}_2\text{O}_5\text{-SiO}_2$  graded-index fibres, effect of deposition rate on spectral loss 0-87485  
 $\text{Li}_2\text{O-SiO}_2\text{-P}_2\text{O}_5$  glass ceramic fibres, heat treatment, crystn., tensile strength 0-84995  
 $\text{Na}_2\text{O-P}_2\text{O}_5\text{-SiO}_2$  glass, metastable liquid immiscibility 0-100331  
 $\text{Na}_2\text{O-P}_2\text{O}_5\text{-SiO}_2$  glass, substitution of  $\text{Li}^+$ ,  $\text{Mg}^{2+}$ ,  $\text{Sr}^{2+}$ ,  $\text{Ba}^{2+}$ ,  $\text{Zn}^{2+}$  for  $\text{Na}^+$  0-100332  
 P content determ. by Rutherford backscatt., PIXE, and activation anal. (Hungarian) 0-85233  
 $\text{P}_2\text{O}_5\text{-SiO}_2\text{-GeO}_2$  graded-index optical fibre, UV induced losses 0-87518  
 $\text{SiO}_2\text{-GeO}_2\text{-B}_2\text{O}_3\text{-P}_2\text{O}_5$ , optical waveguide glass, comp. determ., plasma emission spectra 0-87446  
 $\text{SiO}_2\text{-P}_2\text{O}_5\text{-GeO}_2$  optical fibres, UV radiation-induced losses 0-87517  
 $\text{SiO}_2\text{-P}_2\text{O}_5\text{-GeO}_2$  optical fibres, CVD, losses, reactant impurity effects 0-87522

**photoacoustic effect**

- ceramics, piezoelectric, photoacoustic effect 0-84252  
 Doppler thermo-optical source of US waves 0-58852  
 excitation of sound by a moving optoacoustic source which emits pulses of arbitrary shape 0-79041  
 far IR optoacoustic material probing and imaging 0-83559  
 first order phase transitions at increasing and decreasing temp. studied 0-70320  
 imaging with the optoacoustic effect 0-106473  
 laser thermo-optical sound source in liquid, anal. of wave zone 0-87631  
 liquid, absorbing intense IR radiation, behaviour of pressure 0-102749  
 liquids, photoacoustic and photorefractive detect. of small absorpts., electrostrictive limits 0-108171  
 methane, liquid, opto-acoustic study of weak optical absorpt. 0-93278  
 moving pulsed optoacoustic sources for sound generation 0-87634  
 one dimensional theory for solids 0-65168  
 SAW generation using CW laser, NDT appl. 0-87683  
 semiconductor surface, depth profiling, optoacoustic technique 0-65337  
 solid, photoacoustic effect, three-dimensional 0-107379  
 solid, photoacoustic signal, heat loss influence 0-100308  
 thermal wave microscopy, physical processes 0-74652  
 thermal-wave microscopy, high-resolution studies 0-74647  
 thermally thin solids, photoacoustic effect 0-75304

**photoacoustic effect continued**

- transonic gas flow, optical excitation of intense acoustic waves 0-74564  
 Al, subsurface flaw detection by photoacoustic microscopy 0-66725  
 $\text{BaTiO}_3\text{Fe}_2\text{O}_3$ , photoacoustic effect, first order phase transitions at increasing and decreasing temp. 0-70320  
 $\text{CdS}$  crystals, orientational depend. of photoacoustic effect (Russian) 0-65167  
 $\text{CuCl}$ , mech. vibrs. in piezoelec. solid, excitation by light pulses 0-75305  
 $\text{CuSO}_4$  solution, thermo-optical excitation of sound by ns. laser pulses 0-79884  
 Fe films, ferromagnetic reson., photoacoustic detection 0-80613  
 Ga, solid-liq. transition, photoacoustic effect study 0-70320  
 Ge crystals, orientational depend. of photoacoustic effect (Russian) 0-65167  
 $\text{N}_2$ , liq., photoacoustic and photorefractive detect. of small absorpts., electrostrictive limits 0-108171  
 Ni films, ferromagnetic reson., photoacoustic detection 0-80613  
 $\text{SiC}$ -ceramic, nondestructive evaluation, scanning photoacoustic microscopy 0-85115  
 $\text{Si}_3\text{N}_4$ -ceramic, nondestructive evaluation, scanning photoacoustic microscopy 0-85115  
 $\text{VO}_2$ , photoacoustic effect at first order phase transitions at increasing and decreasing temp. 0-70320
- photoacoustic spectroscopy**  
 absorption coefficient, optical, absolute meas., photoacoustic spectroscopy 0-82828  
 biological and medical appls., book contrib. 0-109078  
 cell for liquids and solids, one-dimens. model generalisation 0-82827  
 cell for mirror scan Michelson interferometer 0-68277  
 ceramics, piezoelectric, photoacoustic effect 0-84252  
 chain reactions, photochem., opto-acoustic detect. method 0-90913  
 coal, cleaved surface, photoacoustic IR spectra 0-87104  
 crystalline material optical absorption meas. 0-105718  
 diacetylenes, photopolymerisation, solid-state reaction, photoacoustic photoacoustic obs. 0-61089  
 dyes, spectra and quantum yields (French) 0-101845  
 fluoromethane, vibrational-translational transfer rate, optoacoustic meas. using short pulse  $\text{CO}_2$  laser 0-74258  
 Fourier transform IR spectroscopy of liquid and solid samples 0-90911  
 glass, transition metal and rare-earth doped, photoacoustic spectrosc. 0-92611  
 glyoxal,  $\text{S}_0\text{-S}_1$  band, opto-acoustic phase angle meas. 0-68256  
 haemoglobin 'macroporous' particle study, photoacoustic spectrometry 0-85543  
 high-resolution photoacoustic spectroscopy for dopant depth profiling 0-77883  
 hydrazine rocket fuel in ambient air,  $\text{CO}_2$  laser absorption spectra and photoacoustic detection 0-104540  
 imaging and image processing 0-95143  
 industrial application possibilities 0-106692  
 IR photoacoustic Fourier transformed spectroscopy of solids 0-86465  
 IR photoacoustic spectra of solids 0-73484  
 laser photoacoustic detector spectroscopy, calibration using HD 5-0 transitions 0-77877  
 laser radiation action on condensed medium, hydrodynamic effects 0-93439  
 light scattering effects, diffusion processes 0-95144  
 methane, liquid, opto-acoustic study of weak optical absorpt. 0-93278  
 methane, photoacoustic Raman spectroscopy under pulsed laser excitation 0-82825  
 methyl halide-inert gas mixtures, vibr. energy relax., opto-acoustic obs. 0-95711  
 methyl halides, vibr. energy relax., opto-acoustic obs. 0-95711  
 microscope development which gives map of thermal properties of sample surface 0-73479  
 molecular solid, intermolecular interactions, laser induced phonon probe 0-79891  
 molecular vibrational-translational transfer rate, optoacoustic meas. using short pulse  $\text{CO}_2$  laser 0-74258  
 optical coatings and materials, photoacoustic spectroscopy study 0-64124  
 optoacoustic detection of absorption, sensitivity to laser geometry 0-73473  
 organic liquids, pulsed opto-acoustic spectroscopy 0-62743  
 pentacene in p-terphenyl, intermolecular interactions, laser induced phonon probe 0-79891  
 perylene, intermolecular interactions, laser induced phonon probe 0-79891  
 piezoelectric photoacoustic detection, theory and expt. 0-90904  
 principles and applications, PAS market 0-68258  
 propynal, rovibronic populations, collisionless IR. multiphoton spectra, energy deposition, photoacoustic determ. 0-83354  
 reflection-absorpt. spectroscopy for IR anal. of surface species 0-105723  
 relaxation time measurements in frequency and time-domain photoacoustic spectroscopy in condensed phases 0-82826  
 ruby, quantum efficiency, photoacoustic meas. 0-73472  
 semiconductor powders, band-gap energies, photoacoustic meas. 0-70579  
 smoke aerosols, optical absorption to extinction ratio, photoacoustic determ. 0-58459  
 solar selective coatings, photoacoustic determination of absorbance and emittance 0-77876  
 solid, phase transitions 0-69615  
 solid-state reaction, photoacoustic photocalorimetric obs. 0-61089  
 solids and surface species, IR photoacoustic spectroscopy 0-90909  
 spectrophone resonant cavities, theoretical model 0-92001  
 subsurface imaging 0-74648  
 surface analysis techniques and appls., symposium, Dayton, USA (Jun. 1979) 0-62363  
 thermally thick samples, quantitative spectroscopy 0-68257  
 thin film, laser damage, photoacoustic study 0-80098  
 trace-gas remote analysis, optoacoustic radiometry limitations 0-108759  
 water vapour, attenuation of HF/ $\text{CO}_2$  laser beam 0-61905  
 water vapour submillimetric-wave absorption obs. 0-61901  
 $\text{CO}_2$ , photoacoustic Raman spectroscopy under pulsed laser excitation 0-82825  
 $\text{D}_2\text{O}$ , pulsed opto-acoustic spectroscopy 0-62743  
 HCl, overtone vibr.-rot. bands, intracavity dye laser techniques meas. 0-91532  
 HD, 5-0 transition, intracavity photoacoustic detector spectrosc. obs. 0-77877  
 $\text{H}_2\text{O}$ , pulsed opto-acoustic spectroscopy 0-62743



photoacoustic spectroscopy continued

<sup>127</sup>I<sup>+</sup> Doppler-free optoacoustic spectroscopy 0-57396  
Nd<sup>3+</sup> ions, in solids, radiationless decay processes, laser photoacoustic spectroscopy meas. 0-84766  
NdP<sub>3</sub>O<sub>4</sub>, fluoresc. lifetime meas., IR and photoacoustic spectroscopy 0-60652  
SF<sub>6</sub>, CW CO<sub>2</sub> laser spectroscopy 0-83367  
SO<sub>2</sub>, vibr. relax., phase spectrophone method obs. 0-87059  
UF<sub>6</sub>, CW CO<sub>2</sub> laser spectroscopy 0-83367  
VO<sub>2</sub>:Al, photoacoustic effect study of phase transitions 0-69615  
WF<sub>6</sub>, CW CO<sub>2</sub> laser spectroscopy 0-83367  
ZnSe laser windows, AR coated, photoacoustic chopping freq. studies using CO<sub>2</sub> laser 0-83629  
ZnSe laser windows, photoacoustic signal var. with chopping freq. 0-75309

photobleaching see optical saturable absorption

photocapacitance

see also photodielectric effect  
magnesium phthalocyanine, film, depletion layer studies, temp. depend. of LF capacitance 0-65617  
MOS interface states density, photoemission obs. using photocurrent and photocapacitance meas. 0-92990  
tetracene, film, depletion layer studies, temp. depend. of LF capacitance 0-65617  
CdS/Cu<sub>2</sub>S thin film heterojunctions, photocapacitance meas. of solar cell parameters 0-93897  
CdS-Cu-S heterojunction, energy-band struct., capacitance-voltage charact., illumination effects 0-96982  
CdTe-CdS heterojunction, photocapacitance and photocond. 0-96978  
GaAs, photocapacitive MIS IR detector, spectral response, noise charact. 0-75644  
GaAs:Cr, deep levels, wavelength-modulated photocapacitance spectroscopy 0-76055  
GaAs:O epitaxial film, impurity states, photocapacitance spectra 0-65625  
GaAs-Si heterojunction, IR quenching of photocapacitance 0-92968  
Si, photocapacitive MIS IR detector, spectral response, noise charact. 0-75644  
Si:Sc, photocapacitance and photoconductivity 0-107859  
Si:Y, photoelectric props. 0-107860  
ZnSe-Si heterojunctions, IR quenching of photocapacitance 0-92968

photocatalysis see catalysis

photocathodes

see also photoemission  
image, dissector tubes, echelle spectrographs, design considerations 0-91918  
semiconducting photocathodes, carrier transport simulation, Monte Carlo method 0-71575  
sensitivity uniformity over surface, distortion of zone charact. by interference in substrate 0-58709  
Ag/p-In<sub>0.77</sub>Ga<sub>0.23</sub>As photocathode, field assisted photoemission to 2.1 microns 0-76130  
Ag-Cs-O photocathode, operation mechanism involving Cs<sub>2</sub>O<sub>2</sub> 0-66384  
Ag-O-Cs surface, oxidation, role of Cs suboxides in low work function surface layers, XPS 0-76131  
Al<sub>0.1</sub>Ga<sub>0.9</sub>As semitransparent photocathode, LPE, quantum efficiency spectrum 0-76153  
CsI photocathodes, efficiency evaluation for soft X-ray diagnostics 0-57442  
CuI photocathodes, efficiency evaluation for soft X-ray diagnostics 0-57442  
Ga<sub>1-x</sub>Al<sub>x</sub>As based layer structures, optimum growth conditions, comp. and struct. perfection 0-104069  
GaAs epitaxial multilayer photocathode structures, TEM obs. of dislocations generated 0-100241  
GaAs-Al<sub>0.1</sub>Ga<sub>0.9</sub>As-GaP, minority carrier diffusion length determ. by photoluminesc. 0-103992  
p-GaP photocathode, charge transfer via surface states, water photoelectrolysis anal. 0-75636  
InGaP/InGaAs struct. for transferred electron photocathodes, VPE growth and characterisation 0-76193  
p-InP field-assisted photocathodes, quantum efficiency 0-84831  
InP-In<sub>0.1</sub>Ga<sub>0.9</sub>As alloys, semiconductor photoemitters, field-assisted, 1-2 µm range 0-97396  
Si field emission photocathodes, emission current noise charact. 0-100746  
Si multiple tip field emission photocathode, photokinetics 0-100480

photocells see photoelectric cells

photochemistry

see also photochromism; photodissociation; photoelectrochemical cells; photolysis; photosynthesis  
air pollution, photochemical, potential form. in United Kingdom, numerical estimation method. 0-76682  
anthracene, in atmosphere, photooxidation on particulate matter 0-61487  
anthracene in polychlorinated alkanes photochemical study by rapid scanning fluoresc. spectroscopy 0-86440  
bis(9-anthryloxy)polyoxaalkanes, intramolecular excimer form. and photodimerisation, kinetic anal., rate constants determ. 0-66800  
atmosphere, annual var. of effects of diffuse solar radiation on O<sub>3</sub> photodissoc. 0-109210  
atmosphere, O<sub>2</sub> and O<sub>3</sub> photodissoc. in stratosphere and mesosphere through solar UV radiation absorpt. 0-109248  
atmosphere, one-dimensional photochemical model rel. to instantaneous global O<sub>3</sub> balance 0-109211  
atmosphere, photochemical air pollution initiation by HONO (nitrous acid) in urban air 0-76677  
atmosphere photooxidation reactions, rates, reactivity and mechanism for organic compounds reaction with OH radicals 0-72104  
azides, in polymer matrices, photooxidation, rel. to crosslinking 0-66832  
bacteriorhodopsin chromophore, light-induced isomerisation 0-108956  
benzyl radical, in solid Ar, absorption and photodissociation spectra 0-69156  
2-benzyl-5-benzylidenecyclopentanone, and substituted form, topochem. single-cryst.-to-single-cryst. photodimerisation 0-66819  
chain reactions, opto-acoustic detect. method 0-90913  
chemical reaction wave, propag. of coherent probe light pulse 0-61190  
colloidal photochromic dyes, quasi-crystals produced in applied electric field 0-85225  
diacetylene, low temp. photochemical polymerisation, decay kinetics, ESR spectra obs. 0-100616

photochemistry continued

diacetylene, photopolymerisation, optical absorpt. spectra, time depend., reaction kinetics 0-85174  
diacetylene (TSHD), low temp. photopolymerisation, short chain intermediates obs. 0-93754  
diacetylene monocarboxylic acids, multilayers, struct. phase transitions and polymerisability 0-80129  
diacetylene-d<sub>2</sub>, excited quintet states during photopolymerisation, ESR obs. 0-84635  
diacetylenes, photopolymerisation, solid-state reaction, photoacoustic photocalorimetric obs. 0-61089  
diacetylenes, solid state photopolymerisation, reaction products, electron spin resonance anal. 0-81338  
dicyclopentadiene, liq., CO<sub>2</sub> laser pulse induced chem. reactions 0-66821  
dihydroxyanthraquinone, light-induced proton transfer, photochem. hole-burning obs. 0-76535  
3,3'-dimethyl-1'-phenyl-6-nitro-spiro [(3H-7,8-benzochromen)-3,2'-indoline] (II), photochromic transform., temp. depend. 0-104456  
3,3'-dimethyl-1'-phenylspiro [(3H-7,8-benzochromen)-3,2'-indoline] (I), photochromic transform., temp. depend. 0-104456  
dimethyl-s-tetrazine, vapour, mol. fluoresc., photodissoc. product 0-81352  
2,5-diphenyl-1,3,4-oxadiazole, vapour, spectral, fluoresc., photochem. and laser props. 0-106344  
2,5-diphenyl-1,3-oxazole vapour, spectral, fluoresc., photochem. and laser props. 0-106344  
2,5-diphenylfuran vapour, spectral, fluoresc., photochem. and laser props. 0-106344  
dye chemistry for new instant film 0-81342  
endothermic reaction rate enhancement in EM field 0-66852  
N-ethylphthalimide+olefins, photochemical reaction, absorpt., fluoresc., phosphoresc. and triplet-triplet absorpt. spectra 0-85197  
F-region, Atmosphere Explorer photochemistry rel. to airglow obs. 0-98496  
fluorene crystal, doped, photochemical hydrogen abstraction, proton hyperfine structure via optical nuclear polarisation 0-63659  
fluorocarbon solutions, dye-sensitized, spectroscopic obs. of 1.27 µm and 1.58 µm emission of single ( $\Delta_g$ ) mol. O<sub>2</sub> 0-85178  
n-GaAs, stabilisation against photodecomposition, surface damage influence 0-76390  
gas phase chemical reactions in atmosphere, evaluated kinetic and photochemical data 0-101671  
hexafluoroethane, photochem. prod., <sup>13</sup>C enrichment (French) 0-91615  
highly excited molecular systems, high energy photochem. 0-66831  
hole burning, photophysical and photochemical theories 0-58322  
β-hydroxy acrolein, lower excited states, electronic struct. and H-bonding, ab initio SCF and CI calcs., photochemical mechanism 0-83278  
ionsphere, lower, photodetachment as source of reflecting layer below classical D-region 0-98508  
Jupiter atmosphere, hydrocarbon and H I photochemistry rel. to Lyman alpha albedo 0-105194  
laser field interaction, Floquet theory, HF appl. 0-63716  
laser induced photochem. of vibr. excited mols., review 0-71925  
macromolecules, nonlinear laser photomodification, radiation damage 0-61120  
methane isotopic mixtures, enrichment of D using vibrationally sensitized reaction 0-76532  
methyl isocyanide photoisomerisation, laser isotope separation, C-isotope enrichment by one-photon vibr. photochemistry 0-81336  
molecule+ molecule, enhancement by collision induced absorpt. of IR laser radiation 0-66798  
multiphoton processes, chemisorbed species on solid surfaces, desorption dynamics, quantum-stochastic approach 0-66864  
multiple photon photochemistry in low temp. matrices 0-76533  
naphthol complexes, H-bonded, form. of ion pairs in presence of crown ethers, proton-transfer photoreactions 0-85199  
optical image phase recording using sensitised photooxidation reactions 0-87350  
ozonosphere, photochemical-dynamical model rel. to maintenance of zonal mean O<sub>3</sub> distrib. in N.Hemisphere 0-109220  
phenylloxazoly pyridinium salt dye lasers, flashlamp pumped, blue-greenlasing 0-95886  
photofragment distrib. in two-photon photochem., isotope separation appl. 0-81344  
photogalvanic solar energy conversion, photochem. determ. of efficiency 0-89654  
photoresists, photochemical reaction rates, intensity depend., kinetic model 0-104452  
polyenes, photoisomerisation, triplet pot. energy surfaces and normal mode anal. 0-108700  
polymer spectral sensitivity and photochem. stability using Xe high press. lamp (German) 0-61119  
POPOP vapour, spectral, fluoresc., photochem. and laser props. 0-106344  
porous Vycor glass, quenching by O<sub>2</sub> and NH<sub>3</sub>, photoluminescence obs. 0-93773  
purification of materials with overlapping absorpt. spectra 0-78452  
PVC surfaces, natural and stabilised, composition, ageing, oxidation and weathering, ESCA obs. (French) 0-61139  
quinizarin in alcohol glasses, electron-phonon coupling, photochemical hole burning 0-97265  
reaction kinetics measurement and control using laser technology, free electron laser appl. 0-81349  
solar energy chemical conversion and storage using norbornadiene-quadracyclene photoisomeric interconversion 0-89664  
solar energy chemical storage, effect of micellar phase on photo-induced reactions 0-89678  
solar energy chemical storage, photosensitization mechanisms for energy storing isomerizations 0-89679  
solar energy chemical storage using novel photocyclization reactions of 1-alkenyl-2-pyridones 0-89680  
solar energy conversion, photo-induced electron transfer reactions in solution, organised assemblies and at interfaces 0-89677  
solar energy conversion and storage using artificial photosynthetic systems 0-89662  
stilbene anion radicals, photoinduced isomerisation, 77K 0-66818  
stratosphere, NO and ClO at twilight rel. to interpretation of conc. meas. via solar occultation 0-85756  
synchrotron radiation obs. appls. 0-66830  
p-terphenyl vapour, spectral, fluoresc., photochem. and laser props. 0-106344  
thioindigo adsorbed on Al<sub>2</sub>O<sub>3</sub>, photoisomerisation 0-89503



**photochemistry continued**

- toluene cation in solid Ar, absorption and photodissociation spectra 0-69156  
 troposphere, evidence for significant in situ photochemical O<sub>3</sub> source 0-72619  
 unimolecular IR multiphoton decomp., energy gained master eqn., approx. model and exact soln. 0-66829  
 visual phosphores, X-ray induced, mech. of formation, photochem. investigations 0-108877  
 zinc octaethyl porphyrin, soln., photochem. ionogenesis 0-61116  
 AlH<sub>3</sub>, synchronous photochem. processes in lattice 0-101029  
 Cl atoms, photorecombination, rate constants determ., identification of spectral distribution of recombinative emission intensity 0-85195  
 Cl+fluoromethane, photochlorination electron and oscill. energy 0-81320  
 ClF+SF<sub>6</sub> (perfluoroethane)(Xe), thermal and photochem. reactions investigated 0-61117  
 Cs-H<sub>2</sub> vapour, resonant character of laser induced formation of particles 0-89481  
 CsSnI<sub>3</sub>, surface props., Auger study, elec. cond. meas., photochem. study 0-66339  
 Cu phthalocyanine thin film electrodes, near IR photoelectrochemical responses 0-93766  
 Cu(II) complexes, reversible excited-state electron transfer reactions for solar energy conversion 0-89655  
 Fe-I system, photochemical conversion efficiency 0-71923  
 α-Fe<sub>2</sub>O<sub>3</sub>, photochem. props. of sintered and doped samples for solar photoelectrochem. cell appls. 0-89651  
 p-GaAs/heptyl viologen system, photoreduction, appl. in photoelectrochemical cells and photoelectrochromic displays 0-76640  
 H<sub>2</sub> photocatalytic production by carbohydrate conversion using RuO<sub>2</sub>/TiO<sub>2</sub>/Pt photocatalyst powder 0-94120  
 I<sub>2</sub>+acetylene, laser-induced 1,2-diiodoethylene form., isomerisation 0-85157  
 Li(2<sup>2</sup>P<sub>1/2,3/2</sub>), laser induced flame chemistry, saturated mode fluoresc. meas. 0-89491  
 NH<sub>3</sub> synthesis, industrial, using N<sub>2</sub> reducing solar cells 0-89632  
 NO in Earth's thermosphere, solar activity depend. 0-77178  
 Na(3<sup>2</sup>P<sub>1/2,3/2</sub>), laser induced flame chemistry, saturated mode fluoresc. meas. 0-89491  
 O<sub>2</sub> saturated hydrocarbon, chem. reaction dynamics. OH prod. investig. 0-101016  
 O<sub>3</sub> layer, photochemistry rel. to possible O<sub>3</sub> reductions and Earth surface UV radiation 0-94577  
 OH+RH→H<sub>2</sub>O+R, radical substitution reaction 0-81321  
 PbI<sub>2</sub>-Ag(Au)(Cu), light sensitive, internal photoelectric emission 0-107910  
 Rb-tetrahydrofuran solution, polarised photoelectron and loose ion pair (Rb<sup>+</sup>, e) obs., optical-ESR study 0-85196  
 Ru complex, [Ru(bpy)<sub>3</sub>]<sup>2+</sup>-Ti (III), photochem. H<sub>2</sub> prod. from aq. soln. 0-85192  
 Ru complexes, [Ru(bipy)<sub>3</sub>], (pq)<sub>3</sub>-<sup>2+</sup> mixed-ligand, electronic absorpt. and emission spectra meas. 0-71441  
 SF<sub>6</sub>+Si(surface), IR laser induced reaction, mol. vibr. and mol. dissoc. obs. 0-93798  
 Se-Ge amorphous films, obliquely deposited, photoinduced chem. changes 0-76385  
 Si surface electron beam deposited silicid formation using scanning CW laser beam 0-66862  
 Si-SiC chemical interaction in rarefied O<sub>2</sub> under pulsed action of concentrated solar radiation 0-71930  
 Sr<sub>2</sub> dimer, photoassoc., photoluminesc., collisional dissoc. 0-58303  
 n-TiO<sub>2</sub> electrode, photo-oxidation of acetate and iodide 0-81331  
 TiO<sub>2</sub>, nonstoichiometric anodic films, O incorporation kinetics 0-97733  
 U enrichment by photochemical laser, two-phase flow with condensation, mathematical model (French) 0-74029  
 UF<sub>6</sub>, laser chemistry 0-69198

**photochromism**

- colloidal photochromic dyes, quasi-crystals produced in applied electric field 0-85225  
 diamond, electron irradiated, photochromism 0-71454  
 3,3'-dimethyl-1'-phenyl-6-nitro-spiro [(3H-7,8-benzochromen)-3,2'-indoline] (II), photochromic transform., temp. depend. 0-104456  
 3,3'-dimethyl-1'-phenyl-spiro [(3H-7,8-benzochromen)-3,2'-indoline] (I), photochromic transform., temp. depend. 0-104456  
 4-(2',4'-dinitrobenzyl)-pyridine, photochromism, nanosec. laser absorpt. spectrosc. obs. 0-85193  
 fulgimide planar photochromic structures for optical waveguide components 0-64196  
 glass, light sensitive, review of types 0-91870  
 glass, parameter standardisation 0-69476  
 glass, thermochemical effects on photochromic props. 0-87448  
 hologram recording medium, characteristic transfer curve description, using heuristic exponential model 0-78796  
 integrated programmable planar waveguide components formed by optically writing Bragg diffraction gratings into photochromic structs. 0-79011  
 6-phenoxy-5,11-naphthacenequinones, photochromism, molar extinction coeffs. meas. 0-66220  
 PVC, Cu evaporated film, electron-induced metallochromic reaction for metal image formation 0-86476  
 spiroprans, polymer matrix effect 0-76537  
 spiropryan solutions, nitro-substituted, electronic state participation in photochromy 0-81347  
 Ag halide, glass, kinetics of photochromic processes 0-103930  
 Ag halide, photochromic glasses, optical properties, effect of Cu ions 0-93364  
 Ag halide glasses, optical absorpt. of Ag, optically induced dichroism 0-108177  
 Ag halide photochromic glasses, colour centres struct. 0-66254  
 Ag halide photochromic glass, darkening mech., temp. depend. 0-87449  
 KCl, additively coloured photochromic crystals, spectral sensitivity (Russian) 0-91871  
 KCl, amplitude-phase holograms, optical parameter dispersion 0-58481  
 Li<sub>2</sub>B<sub>2</sub>O<sub>7</sub>, ferroelectric glass, phase transition, permittivity, electrochromism, photochromism 0-80719  
 Na<sub>2</sub>O-Al<sub>2</sub>O<sub>3</sub>-B<sub>2</sub>O<sub>3</sub>-SiO<sub>2</sub>-AgCl(Br), photochromic glass, kinetics of thermal decolourisation 0-103931  
 TeO<sub>2</sub>, ferroelectric glass, phase transition, permittivity, electrochromism, photochromism 0-80719  
 V<sub>2</sub>O<sub>5</sub> amorphous film, photochromism and thermochromism 0-93254

**photoconducting devices**

- see also photoconductive cells; photodiodes; phototransistors*  
 opto-acoustic transducer structs., recent investigations 0-74688  
 photothermoplastic devices, single layer, sensitization of N-vinylcarbazole containing polymers to Ar laser 0-83651  
 GaAs, extrinsic, DC- and microwave-biased, performance 0-70750  
 Si:H, amorphous, image pickup devices 0-100481
- photoconducting materials**  
*see also photoconductor*  
 carrier lifetime, nonequilibrium, phase method for determ. 0-65629  
 film for rapid access instrumentation recording 0-62755  
 image charge transfer to electrographic film 0-101864  
 PVK/PVK-TNF/TNF.PMG system, electrophotographic characts. 0-62759  
 semiconductors, exhibiting negative photocond., photovoltaic effects 0-96943  
 N-vinylcarbazole containing polymers, sensitization to Ar laser for single layer photothermoplastic devices 0-83651  
 AlH<sub>3</sub>, synchronous photochem. processes in lattice 0-101029  
 Cd,Hg<sub>1-x</sub>Te, carrier lifetime, effect of comp. fluctuations and second-phase inclusions 0-80294  
 n-Cd,Hg<sub>1-x</sub>Te crystals, carrier recomb. in extrinsic conduction range 0-70722  
 Cd,Hg<sub>1-x</sub>Te, long term stability at 300K, rel. to device appl. 0-59978  
 CdS, spatial homogeneities exam., using DC and microwave techniques 0-93895  
 CdS, spectral sensitisation, role of local centres (Russian) 0-90924  
 CdS, surface photovoltage, characterisation 0-60033  
 Ge:Zn<sup>1+</sup> carrier lifetime, nonequilibrium, phase method for determ. 0-65629  
 Hg<sub>0.6</sub>Cd<sub>0.4</sub>Te LPE layer growth from Te-, Hg-, and HgTe-rich solns., comparison 0-76199  
 HgI<sub>2</sub>:CdS binder layer photoreceptor, surface charge characts. thickness depend. 0-57409  
 PbO layer vapour deposition, structure, and props. 0-65408  
 PbO, reactively evaporated, photocond., H<sub>2</sub>O induced phase transform. 0-60122  
 PbS-base photodetectors, struct. invest. by proton irradi. 0-104388  
 Se, appl. to xerography 0-57415  
 Se-As alloys, appl. to xerography 0-57415  
 SeTe/Si multilayer photoreceptor, transient photoconductivity (Japanese) 0-75596  
 Si, amorphous, undoped, photocond., continuous illum. effect 0-84486  
 Si photoconducting films, amorphous, undoped, I-V characts. of vacuum deposited films 0-60049  
 ZnO, adsorbing p- and n-type dyes, surfaces pot., UV light illum. effect 0-75624  
 ZnS, spectral sensitisation, role of local centres (Russian) 0-90924
- photoconductive cells**  
 nephelometer, photoelectric; for liquids 0-101812  
 two-photon photoconductivity detector for measurement of picosecond light pulses from Nd-glass laser 0-77772
- photoconductivity**  
*see also photoconducting devices; photoconducting materials*  
 adenine film, polycryst., energy conversion processes, quantum yields, 4 to 10 eV 0-88589  
 alkali halide thin films, high-field electron injection, ionic cond., photocond. 0-75665  
 amorphous, photogeneration, thermalisation model calcs., band gap (French) 0-75595  
 amorphous semiconductor, cond. mechanism and localised states (Japanese) 0-84467  
 amorphous semiconductors, modulated photocurrent, trap limited case (Japanese) 0-60030  
 anthracene, pulsed electron excitation, triplet excitons, spectral and electrical investigations 0-92828  
 anthracene ion in liqs., photoelectron emission and photocond. 0-75600  
 cadmium arachidate mixed with cyanine dyes, mol. layers, photoelec. props. 0-80401  
 carrier lifetime measurements from transient elect. photoresponses in solar cells 0-61346  
 chalcogenide glasses, photoconductivity dependences applied elec. field 0-107857  
 cyanine dye monolayer assemblies with Al and Ba electrodes, photovolt., dark cond. and photocond. 0-80400  
 diphenylanthracene in benzene soln., extrinsic photocond. kinetics 0-92691  
 electrophotographic films, surface charge meter using electrostatic induction (Japanese) 0-77886  
 EuSe, photocond. and photodiffusive voltage spectra 0-96940  
 ferroelectrics, photogalvanic current 0-70748  
 III-V semiconductor based layered multielectronic systems, electronic process investig. survey (Russian) 0-107891  
 inert gases, solid, V<sub>0</sub>-values, photoelectric determ. 0-92938  
 iron phthalocyanine, annealed, elec. cond., daylight exposure and thickness effect (French) 0-84484  
 Langmuir films, dye-sensitized, anisotropic photocond. 0-80327  
 Langmuir multilayer films with and without dye-sensitisers, elec. props. 0-97006  
 metal-semiconductor contact, frequency relationships of photocurrent and photo-EMF (Russian) 0-107908  
 MOS interface states density, photoemission obs. using photocurrent and photocapacitance meas. 0-92990  
 multistable self-wave media 0-86094  
 narrow gap semiconductors, recombination mechanisms, review 0-96905  
 nonlinear interference of EM fields, contrib. to transport coeffs. 0-80324  
 p-n heterojunction solar cell, general formulation of current-voltage characts. 0-80361  
 p-n tunnel junctions, photoinduced transitions, theory 0-65669  
 photoconduction decays, fast, measurement, DC-10 MHz low noise amplifier system 0-57326  
 photoexcitation effects during laser trimming on thin film resistors on Si 0-64093  
 phthalocyanine-alkane interface, charge transfer, rel. to photoelectro-photoretic image form. 0-65616  
 phthalocyanine, doped photovoltaic cell, photoconductivity, elec. field induced fluoresc. quenching, charge carrier photogeneration 0-84485  
 plant leaves, microwave photoconduction effects obs. 0-104637  
 polar crystals, relaxation currents; point defects (Russian) 0-100486  
 polyacetylene films, AsF<sub>5</sub> doped, photocond. and junction props. 0-70770



## photoconductivity continued

- polycrystalline film, photocond. probe studies 0-80326  
 polydiacetylene-toluenesulphonate, photocond. meas., 0.62-3.1 eV 0-70757  
 polyethylene, intrinsic photocond. under vacuum UV irradi. 0-70759  
 polyhexamethylene adipamide, photocond. 0-103718  
 polyhexamethylene adipamide, photocond. and dielectric props. 0-84489  
 polystyrene atactic carrier transport and photogeneration 0-80318  
 polyvinyl alcohol film containing  $\text{Cu}^{2+}$  complexes, photoconductivity 0-107849  
 rubrene, in benzene soln., extrinsic photocond. kinetics 0-92691  
 semiconductor, complex energy band under optical excitation, high-frequency negative cond. and population inversion 0-107858  
 semiconductor, doped, metal-insulator transition, anal. 0-88478  
 semiconductor, energy relaxation of photoexcited hot electrons in near-surface region 0-92928  
 semiconductor, optical absorpt. coeff. and minority-carrier diffusion length, differential photocurrent method of meas. 0-96896  
 semiconductor, photothermal cond., low temp. depend. 0-70756  
 semiconductor, spin-dependent recomb. and scatt. in presence of optical orientation of electrons 0-96908  
 semiconductor thin film electrode, photosensitization by cyanine dye in lipid bilayer 0-75639  
 semiconductor with superlattice, optoelectronic effect, theory 0-70768  
 semiconductors, amorphous, doped, electronic props. 0-80283  
 semiconductors, amorphous, electronic transport mechanisms and coeffs. 0-80282  
 semiconductors, book contrib. 0-84488  
 semiconductors, optical saturation for high carrier recomb. freq. (Russian) 0-88585  
 semiconductors, photoconductivity measurement at UHF and at high excitation levels 0-65627  
 semiconductors, photosensitive area localisation, expt. apparatus 0-75599  
 semiconductors, weakly doped compensated, hopping photoconductivity in disordered systems (Russian) 0-65573  
 short-pulse, transit time effects 0-70754  
 Si, ion implanted by high energy C ions structural and optical props. 0-107292  
 stilbene, pulsed electron excitation, triplet excitons, spectral and electrical investigations 0-92828  
 surface recombination velocity and diffusion length, meas. method, solar cell appl. 0-93965  
 suspension of absorbing particles, simultaneous meas. of dichroism and birefringence in elec. field., photocurrent signal obs. 0-82801  
 TCNE, hole drift mobility, temp. depend. and anisotropy, photocond. meas. 0-80314  
 N,N,N',N'-tetramethyl-p-phenylenediamine, alkane soln., charge carrier generation, elec. field depend. 0-107846  
 thymine film, polycryst., energy conversion processes, quantum yields, 4 to 10 eV 0-88589  
 transition metals, BCC, films, vac. evaporated, optical cond. 0-76100  
 Ag halide microcrystal, photoconductivity meas. by microwave technique 0-103719  
 AgBr evaporated layer response in ionisation semiconductor photographic system (German) 0-101859  
 $\alpha\text{-AgSbS}_2$  crystals, photoelectric props. 0-107861  
 $\text{Al/SiO}_2/\text{pSi}$  MIS solar cells, stability 0-85287  
 $\text{Al-amorphous Ge-nSi}$ , photoelectric props. 0-70822  
 $\text{Al}_x\text{Ga}_{1-x}\text{As}$ , electron mobility illumination, compensation, space charge regions, carrier scatt. 0-70691  
 $\text{AlGa}_{1-x}\text{Sb-Pd}$  contacts, band gap depend. of barrier height 0-65685  
 As chalcogenides, deep levels, photoluminesc. and photocond. 0-70641  
 As-S amorphous chalcogenide thin film, transient photoinduced phenomena 0-80884  
 As-Se amorphous system, photocond. props. 0-88587  
 $\text{As}_2\text{Se}_3$ , modulated photocurrent, analysed for trap-limited case (Japanese) 0-60030  
 $\text{As}_2\text{Se}_3\text{-Ge}$  glassy thin films, flash photoresponse 0-107863  
 $\text{As}_2\text{Se}_3\text{-Ag}$ , glassy semicond. film, prep. by photodiffusion of Ag, negative photocond. 0-92934  
 Au-oxide/n-GaAs struct., photocurrent relax. 0-92978  
 Au-dye/amorphous  $\text{SiO}_2\text{-Au}$  struct., dye-sensitised steady-state photocond. 0-107924  
 Au-oxide-n-GaAs MIS structures, reverse bias influence on photocurrent 0-107921  
 $\text{Ba}_2\text{Sr}_{0.5}\text{Nb}_2\text{O}_6$ , electronic props. and photoresponses 0-92925  
 $\text{Ba}_2\text{Sr}_{1-x}\text{Nb}_2\text{O}_6\text{-Ce}$ , pure and doped, photoelec. props. and photorefractive 0-60538  
 $\text{BaTiO}_3$ , photorefractive effects and light-induced charge migration 0-69447  
 $\text{BiGeO}_{20}$ , photocurrent oscils. in pulsed illumination rel. to piezoelec. props. 0-80325  
 $\text{Bi}_{12}\text{GeO}_{20}$  crystals, principal carriers obs., in dark and under laser illumination (Russian) 0-80312  
 $\text{Bi}_{12}\text{SiO}_{20}$  film, RF-sputtered, UV illumination effects obs. (Russian) 0-80313  
 CaO, photoionisation of F-centre, luminesc. and photocond. meas. 0-66270  
 $\text{CdCr}_2\text{S}_4(\text{Se}_4)$ , thermoreflectance, photoconductance, Raman scatt. near mag. phase transition 0-97298  
 $\text{CdCr}_2\text{Se}_4\text{-Ga(In)}$ , photoconductivity, photomagnetoresistance near Curie point (Russian) 0-100485  
 $\text{CdF}_2$ , colour centres, IR absorpt. and photocond. after UV irradi. 0-79784  
 $\text{CdF}_2\text{:NaF(AgF)}$ , colour centres, IR absorpt. and photocond. after UV irradi. 0-79784  
 $\text{n-Cd}_3\text{H}_2\text{O}_7\text{-Te}$ , photoelec. props. at 78K, relax. time, minority carrier extraction 0-107864  
 $\text{n-Cd}_3\text{H}_2\text{O}_7\text{-Te}$ , recombination due to surface excitation, photoconductivity, impurity states (Russian) 0-60042  
 $\text{CdS}$ , charged impurity centres, drift during passage of photocurrent 0-70767  
 $\text{CdS}$ , electron and hole trapped centres, EPR, photoluminescence, photoconductivity study 0-108071  
 $\text{CdS}$  epitaxial layers on sapphire, exciton struct. of absorpt., photoluminesc. and photocond. spectra 0-89027  
 $\text{CdS}$ , photocond., spectral depend. at high excitation intensity, exciton effects 0-65619  
 $\text{CdS}$ , spectroscopic study of local centre interaction, change with external illumination 0-80323

## photoconductivity continued

- $\text{CdS}$  thin layers, recryst. from  $\text{CdS-Cr}_2\text{O}_3$  mixtures, phys. and photoelec. props. 0-96935  
 $\text{CdS-Cu}$ , Cl films, photocond. growth and decay time 0-60041  
 $\text{CdS-Cu}$ , photocurrent, elec. field effect on recombination processes (Russian) 0-100484  
 $\text{CdS-Cu}$ , photosensitivity degradation mechanism 0-107851  
 $\text{CdS-Cu}$  sintered layers, relaxation photocurrent kinetics (Russian) 0-107852  
 $\text{CdS-Cu(Cl)}$  thin films, surface and bulk photoconc. 0-88653  
 $\text{CdS-Li}$ , luminescence bands, photocurrent spectra (Russian) 0-60677  
 $\text{CdS-Ni}$ , nonradiative recomb., photocond. spectra 0-70764  
 $\text{CdS-Te}_{1-x}$ , recryst. from  $\text{CdS-Te}_{1-x}\text{-Cr}_2\text{O}_3$  mixtures, photocond. props. 0-96936  
 $\text{CdSb:Al}$ , p-n junction formation by laser emission, photoelectric effects (Russian) 0-70815  
 $\text{CdSe-Cu}$ , impurity photocurrent, kinetics and oscils. 0-65624  
 $\text{CdSe-Sb}_2\text{Se}_3$ , heterojunction, photoelec. props. 0-70816  
 $\text{CdTe}$ , elec. and photoelec. props. due to double injection, quenching spectra 0-70765  
 $\text{CdTe}$ , minority carrier diffusion length from photocurrent meas. in semicond.-electrolyte boundary 0-65584  
 $\text{p-CdTe}$ , photocond., photoluminesc., spectral studies 0-88593  
 $\text{CdTe:Cl}$ , semi-insulating, impurity photocond. spectra, local state distrib. in band gap 0-107865  
 $\text{CdTe-CdS}$  heterojunction, photocapacitance and photocond. 0-96978  
 $\text{Cd}_{1-x}\text{Zn}_x\text{S}$  films, thermal evaporation prep., phys. props. 0-84410  
 $\text{Cd}_2\text{Zn}_{1-x}\text{S}$  films, chem. sprayed, carrier density and mobility 0-60121  
 $\text{Cs-Sr(He)}$  mixtures, photocond. at atm. press. 0-87844  
 Cu anode, passivating behaviour and illum. effects in alkaline soln. 0-104449  
 Cu, anodic oxidation, photoelectrochemical effects (French) 0-93701  
 $\text{CuInSe}_2$ , influence of impurities and free carriers on optical props. 0-108225  
 $\text{Cu}_2\text{O}$  solar cells, electrical and optical props., photocurrent anal. 0-101116  
 $\text{Cu}_2\text{O:Mn}$ , photomemory mobility components, charged centre conc. 0-103725  
 $\text{Cu}_{2-x}\text{S-CdS}$  p-n heterojunction, optical energy convertor, struct. and recomb. props. 0-72065  
 $\text{CuSbS}_2$  crystals, growth and characterisation 0-60770  
 $\text{EuO-Gd}$ , pure and doped, elec., mag., and optical props. rel. to electronic conc. 0-96880  
 $\alpha\text{-Fe}_2\text{O}_3$  electrode, carrier density determ. by optical absorpt. and photoelectrolysis spectra 0-71462  
 $\alpha\text{-Fe}_2\text{O}_3$ , photochem. props. of sintered and doped samples for solar photoelectrochem. cell appls. 0-89651  
 $\text{FePS}_3$ , layered semiconductors, optical and electronic props. 0-70761  
 $\text{FeS}_2$ , natural pyrite, photocond. spectra 0-70758  
 $\text{GaAlAs/GaAs}$  solar cells, efficiency optimisation at high and low current levels (French) 0-61348  
 GaAs, electron mobility illumination, compensation, space charge regions, carrier scatt. 0-70691  
 GaAs, epitaxial, residual donor identification by far IR photocond. 0-60047  
 GaAs, epitaxial, residual donor identification by far IR photoconductivity meas. 0-103717  
 GaAs, epitaxial struct., nonuniform electroconductivity (Russian) 0-70753  
 GaAs, exciton effects in photocond., photoluminesc. 0-96797  
 GaAs, extrinsic, DC- and microwave-biased, performance 0-70750  
 GaAs,  $\gamma$ - and electron irradiation, influence on recomb. characts. 0-71478  
 n-GaAs, LPE, deep trapping centre characterisation by Hall and photo-Hall meas. 0-88578  
 GaAs MOS solar cells by anodisation in active region 0-101107  
 GaAs, photoconductivity, impurity induced, low energy edge spectral shift 0-65630  
 GaAs, photoemission modulation by IR illumination, saturation photocurrents 0-108318  
 GaAs, proton irradiated, low energy, deep level defects and hole diffusion length meas. 0-60000  
 GaAs, surface photogalvanic effect, polarisation depend. photocurrents (Russian) 0-80322  
 GaAs:B, deep levels, optically stimulated transient current method (French) 0-59919  
 $\text{GaAs:Cr}$ , photoluminescence in strong electric fields 0-108270  
 $\text{GaAs:Fe}$ , p- $\pi$ -n struct., photoelec. props. 0-107862  
 $\text{GaAs:Ge}$ , Se transmutation shallow donor transition obs. 0-59925  
 $\text{GaAs:O}$ , deep level, Franck-Condon shift, photocond. and Hall effect study 0-70642  
 $\text{GaAs:O}$  p-p-n structs., injection current and negative photocond., saturation mechanism 0-92967  
 GaP, anomalous photoeffect on connected excitons (Russian) 0-92929  
 n-GaP electrode, photoanodic dissolution rate, effect on surface electronic band energies 0-103748  
 n-GaP, Bridgman crystals, hole traps, photocond. and thermal quenching study 0-75580  
 GaSe, exciton-phonon quasibound states, photocond. and luminesc. study 0-96800  
 GaSe, impurity photocond., induced illumination corresponding to fundamental absorption region 0-92933  
 $\text{Gd}_2(\text{MoO}_4)_3$ , ferroelec.-ferroelastic, photolum. and photocond. meas. 0-84768  
 $\text{Gd}_2(\text{MoO}_4)_3$ , one-dimensional ferroelectric image sensor with polymer photoconductor 0-80729  
 Ge, amorphous film, persistent photoconductivity, dangling bonds 0-84487  
 Ge, compensated, impurity photocond. relax times 0-88592  
 n-Ge, D<sup>-</sup> state struct. rel. to photocond. expts. 0-59924  
 Ge, dislocation electron states, from press. depend. of photocond. 0-96819  
 Ge, electron-hole liquid, MHD effects 0-80190  
 Ge, photothermal cond., low temp. depend. 0-70756  
 Ge:Li, Cu p-n junctions, current stimulated LiCu complex formation, photocurrents 0-107897  
 Ge:Pd and pure, photoelectric props., surface states (Russian) 0-60043  
 Ge:Sb, Zn(Hg), photoelec. props., 70 to 300K 0-65621  
 Ge:Sb,Cu, high resist. compensated, impurity of photocond., pulsed unipolar injection carriers 0-92935  
 Ge:Sb,Cu, photoelec. props., fast electron irradi. effects 0-60036



**photoconductivity continued**

- Ge:Zn photoresistor, current responsivity rel. to nonequib. hole lifetime 0-60035  
 n-Ge-metal Schottky barrier contacts, IR optoelectronic props., quantum detector appls. 0-75640  
 Ge-Si<sub>3</sub>N<sub>4</sub> system, potential barriers determ. from photoinjection carriers trapping 0-103756  
 p-GeS, crystalline, photoelectric props. 0-70769  
 GeSe, amorphous layers, photoconductance meas. 0-65632  
 Hg<sub>1-x</sub>Cd<sub>x</sub>Te hot-electron photoconductive detection of near mm wave radiation 0-57377  
 Hg<sub>1-x</sub>Cd<sub>x</sub>Te, recombination processes using impact ionization capture cross sections 0-75577  
 HgCr<sub>2</sub>Se<sub>4</sub>, thermoreflectance, photoconductance, Raman scatt. near mag. phase transition 0-97298  
 α-HgS films, sputter-deposited in Hg vapour, growth and props. 0-75467  
 HgSe film, anomalous photocond., electron microscope study 0-65623  
 n-InAs, photoelectric props., inhomogeneous impurity distrib. 0-107867  
 InAsS(Mg), ion implanted, photocond., photo-EMF, and optical absorpt. spectra 0-70763  
 In<sub>2</sub>O<sub>3</sub>-SnO<sub>2</sub>-Si SIS solar cells, reverse current-voltage characts. under illumination 0-89622  
 InP:Fe shallow trap thermally stimulated cond. spectroscopy, photocond. spectrum under DC conditions 0-65585  
 InP-InGaAsP p-n junction avalanche photodiodes, surface passivation techniques 0-100508  
 InSb, high-resistivity p-type or crystals of n-type, recombination processes, photocond. and photomag. effect meas. (Russian) 0-88567  
 InSb MOS structs., energy spectrum of traps in oxide layer 0-107922  
 InSb n<sup>+</sup>-p junctions, photocurrent spectrum near long wavelength edge of fundamental absorption band 0-100483  
 n-InSb, phonon-assisted cyclotron reson. strongly depend. on surface condition 0-70755  
 n-InSb, photoconductivity mechanism, 4.2 to 77K 0-70766  
 n-InSb, recombination processes using impact ionization capture cross sections 0-75577  
 InSe films, residual photocond., field quenching 0-60037  
 InSe, photoconductivity anisotropy at high optical excitation levels (Russian) 0-103721  
 KH<sub>2</sub>PO<sub>4</sub>, KD<sub>2</sub>PO<sub>4</sub>, crystals, photoresponse under laser irradi., impurity photocond. 0-100479  
 KNbO<sub>3</sub>, reduced, phase hologram recording, energy transfer and sensitivity 0-69338  
 LiNbO<sub>3</sub> pure and Fe doped, IR induced acousto-photorefractive memory effect 0-80746  
 LiNbO<sub>3</sub>:Cu(Fe), light induced charge transport, photovoltaic effects, impurity states 0-80317  
 LiNbO<sub>3</sub>:Fe, electro-optic cryst., light induced charge transport, holographic obs. 0-70747  
 LiTaO<sub>3</sub>:Cu(Fe), light induced charge transport, photovoltaic effects, impurity states 0-80317  
 LiTaO<sub>3</sub>:Fe, electro-optic cryst., light induced charge transport, holographic obs. 0-70747  
 MOS capacitor, photoionisation cross section and interface state density 0-92974  
 NiPS<sub>3</sub>, layered semiconductors, optical and electronic props. 0-70761  
 PLZT ceramics photosensitivity enhancement by H- and He-ion implantation 0-96934  
 Pb<sub>2</sub>GeO<sub>11</sub>, pulsed polarisation switching process depend. on illumination 0-93253  
 PbI<sub>2</sub>-Ag(Au)(Cu), light sensitive, internal photoelectric emission 0-107910  
 PbS, chem. deposited thin film, effect of morphological struct. on photosensitivity 0-70760  
 PbS-base photodetectors, struct. invest. by proton irradi. 0-104388  
 PbS-PbO vacuum evaporated films, elec. cond. and photocond. 0-75656  
 PbS-Sb<sub>2</sub>S<sub>3</sub> semicond., optical and photoelec. behaviour 0-96938  
 Pb<sub>1-x</sub>Sn<sub>x</sub>Te:In, Hall effect and photoconductivity (Russian) 0-103720  
 Rb<sub>2</sub>ZnBr<sub>4</sub>, ferroelec., photovoltaic and photorefractive phenomena 0-75598  
 S, orthorhombic, photogeneration of charge carriers 0-107844  
 Si, polycryst., photoelectret state following X-irrad. 0-60485  
 Sb<sub>2</sub>S<sub>3</sub>, defect drift in elec. fields and bistable switching 0-92947  
 SbSI, ferroelectric, dark current and spontaneous polarisation, ferro-paraelectric transitions obs. 0-60521  
 (Sb<sub>2</sub>Se<sub>3</sub>)<sub>0.7</sub>(Bi<sub>2</sub>Se<sub>3</sub>)<sub>0.3</sub>, solid soln., prep. and elec. properties of layered crystals 0-70762  
 Se, amorphous film, influence of wavelength on optical quenching of photoconductivity 0-60046  
 Se, amorphous film, photocond., dark cond., rel. to crystn. 0-88596  
 Se, amorphous layer, localised states in band gap 0-59928  
 Se, modulated photocurrent, analysed for trap-limited case (Japanese) 0-60030  
 Se, photoelectronic behaviour, in glass transition region 0-60045  
 Se, photosensitive particle migration, electrophotographic film structure and process 0-101863  
 Se, polycryst., low-frequency coupled photocurrent and temp. oscillation 0-60044  
 Se, trigonal, transverse magnetoresistance meas., influence of illumination 0-65607  
 Se-As, photoelectronic behaviour, in glass transition region 0-60045  
 SeTe/Se multilayer photoreceptor, transient photoconductivity (Japanese) 0-75596  
 Si, amorphous, elec. props., ion implantation effects 0-79828  
 Si, amorphous, transport results, interpretation 0-80260  
 Si, amorphous, undoped, photocond., continuous illum. effect 0-84486  
 Si, amorphous co-sputtered doped, photovoltaic material appl. 0-93488  
 Si, amorphous evaporated, picosecond optoelectronic detect., sampling and correlation meas. 0-100478  
 Si, amorphous films, halogenated and hydrogenated, elec. and optical props. 0-97016  
 Si, amorphous hydrogenated solar cells, field depend. quantum efficiency, electron-hole recombination 0-66971  
 Si based alloys, amorphous, photovoltaic behaviour, solar cell appl. 0-94051  
 Si based MIS structure, photoelectric characts. carrier injection levels (Russian) 0-96946  
 P-Si, conductivity and carrier lifetime, high injection effects 0-70719  
 Si, hydrogenated amorphous, gap states, comparison of photoemission and photocond. results 0-103724

**photoconductivity continued**

- Si, neutron and electron bombard., radiation defect recomb., photoelec. props. meas. 0-60039  
 Si, polycrystalline, Hall mobility 0-60006  
 Si:B photodiode front region collection efficiency models 0-96899  
 Si:F,H, amorphous, elec. and optical props. 0-60031  
 Si:Gd(Pr), photoconductivity anomalies due to mag. impurities (Russian) 0-103722  
 Si:H, amorphous, band tail absorpt., photocurrent meas. for Schottky barrier solar cell 0-60032  
 Si:H, amorphous, discharge prod., optically induced cond. changes 0-96937  
 Si:H, amorphous, HV photovoltaic cells, design parameters 0-101105  
 n-Si:H, amorphous, photoelectromagnetic effect 0-107845  
 Si:H, amorphous, Schottky diodes, elec. props., light-induced effects 0-103741  
 Si:H, amorphous, sputtered on Gd<sub>2</sub>(MoO<sub>4</sub>)<sub>3</sub>, ferroelec. domain wall motion, image scanning 0-83663  
 Si:H, amorphous thin film solar cells 0-81478  
 Si:H amorphous, solar cell structure, optical absorption by gap states 0-94052  
 Si:In extrinsic IR detector material with high responsivity compensated by neutron transmutation, float-zone growth 0-75597  
 Si:O, heat treated, excess carrier recomb. rate, defect levels 0-75579  
 Si:P, polycryst. films, elec. props., EPR, defect states, doping effects 0-75660  
 Si:Se, photocapacitance and photoconductivity 0-107859  
 Si:Y, photoelectric props. 0-107860  
 Si-F-H amorphous solar cells, DC glow discharge fabrication 0-72041  
 Si-F:H,P, film, dark cond., struct., Raman scatt. 0-88588  
 Si-H:P amorphous film, dark cond., struct., Raman scatt. 0-88588  
 Si-SiO<sub>2</sub>-Al, interface barrier energies for tunnel oxides, internal photoemission meas. 0-84512  
 Si-SiO<sub>2</sub>-Al with thick dielec. layer, photoelec. props. 0-92979  
 SiH<sub>4</sub> amorphous films, internal photoemission, metal contacts 0-96964  
 SiO<sub>2</sub>, As-implanted, electron trapping and detrapping characts. 0-65692  
 SiO<sub>2</sub> CVD layer, high current injection from Si rich SiO<sub>2</sub> film 0-80430  
 SiO<sub>2</sub> layers on Si, ionis. thresholds of electron traps 0-92983  
 SiO<sub>2</sub> tunnelling barrier asymmetry to electrons and holes in MOS struct., photocurrent 0-75645  
 SiO<sub>2</sub>:As<sup>+</sup> implanted layers in MOS struct., electron trapping and detrapping characts. 0-92982  
 Sr<sub>2</sub>Nb<sub>2</sub>O<sub>7</sub>, electronic props. and photoresponses 0-92925  
 Te, impurity spectroscopy 0-65499  
 Te, negative photoconductivity, intraband absorpt. (Russian) 0-107854  
 Te, photoconductivity in strong mag. fields, doping effects, impurity levels 0-75602  
 TiO<sub>2</sub> electrode, carrier density determ. by optical absorpt. and photoelectrolysis spectra 0-71462  
 n-TiO<sub>2</sub> electrode in AlCl<sub>3</sub>-NaCl melt, electrochem. and photoelec. props. 0-81328  
 TiO<sub>2</sub> electrodes, chemically modified, nature of surface states 0-107905  
 TiGaSe<sub>2</sub>, monocrystal, processes of recombination and trapping levels, photocond. meas. (Russian) 0-70751  
 V<sub>2</sub>O<sub>5</sub>, ferroelec. semicond., dielec. and elec. meas. 0-60516  
 ZnO, single crystals., photocond. lifetimes, Zn<sup>+</sup> hole traps 0-75581  
 ZnP, tetragonal crystals, polarisation study of photocond. 0-96942  
 ZnS(Se):Ni, optical absorpt., impurity ionisation, optical phonon coupling 0-88505  
 ZnSe, residual cond., recomb. of photoexcited carriers, Hall coeff. 0-75605

**photoconductors** *see* **photoconducting materials****photocopying***see also* **electrophotography**

No entries

**photocurrent** *see* **photoconductivity**; **photoemission****photodetectors**

- aerosols examination, mixed phase 0-86404  
 charge-coupling photodetector for optical information processing 0-91753  
 dual-grating direct-reading spectrograph mirror system design and performance 0-81397  
 fibre optics, photoelectric detection improvements 0-91919  
 flat image focussing spherical lens, used for Si light detector 0-91880  
 GaAs photo-FET high speed photoconductive integrated optical receiver 0-58816  
 imaging photon detector for geophysical and astrophysical research 0-86405  
 InSb detector system in Fourier spectrometer, use of improved preamplifier circuit, with integrator in feedback loop 0-73474  
 integrated optics high quantum efficiency waveguide coupled photodetectors on Si substrate 0-58805  
 microwave thermophotodetectors, based on cholesteric liquid crystals, analysis of diffuse light spectra 0-73457  
 multianode microchannel array photon-counting detectors 0-77869  
 multichannel radiometer, programmable, for Earth remote sensing 0-77253  
 multidetector scanner image striping abatement 0-102660  
 multiphoton detectors of laser radiation, statistical characts. 0-86408  
 near IR (1 to 2 μm) optical communications, colloquium, London, England (May 1980) 0-86040  
 optical communications systems, components, review 0-87539  
 for optical fibre communication (Japanese) 0-78977  
 optical sensor system simulation and evaluation 0-96030  
 optical storage focus error detection, skew beam and Foucault knife-edge techniques 0-102649  
 partially coherent radiation, optical heterodyne detection 0-77871  
 photoamplifier circuit, dynamic compensation of photodetector DC component temp. drift 0-73460  
 photodiode detector calibration using synchrotron radiation 0-90810  
 photographic flash light meas. instruments development (Hungarian) 0-57411  
 photon correlator, near ideal, with SAW device 0-68252  
 photon count statistics, detector temp. and field effect 0-74325  
 photosensor spectral responsivity calibration microprocessor system 0-86409  
 quadrant detector for STEM, appls. 0-77914  
 refractometer laser detector for anal. of liquids 0-101830  
 relative spectral sensitivity meas. method using two tandem monochromators (Japanese) 0-101840



**photodetectors continued**

- SAW spectrum analysers in photon-counting mode, statistical props. 0-105712
- self-scanned photodiode array, image detect. from Fabry-Perot spectrograph (*French*) 0-73465
- self-scanned photodiode array as multichannel spectrometric detector 0-73466
- semiconductor IR photodetectors, comparison of extrinsic and intrinsic devices, temp. limitations 0-73456
- seminar, optical radiation meas., San Diego, CA, USA (Aug., 1979) 0-86036
- Si detector array for AlGaAs laser array 0-58817
- solar cells,  $\text{Si}_x\text{Ge}_{1-x}$  diffused p-n junction, electric and photoelectric props. 0-101095
- Space Telescope spectrograph Digicons 0-85558
- spectral slit width correction for precision energy measurements 0-96020
- spectrally selective, for broadband radiometry 0-68255
- spectrophotometer, Hewlett-Packard 8450A UV/Vis model 0-68270
- subnanosecond optical detector developments 0-77870
- subnanosecond source studies from UV to beyond 1  $\mu\text{m}$ , simple inexpensive design 0-86433
- surface-barrier semiconductor, registration of pulsed radiation 0-91373
- switching process and plasma effects in photodiode, theory 0-65667
- temperature dependence of dark current and quantum efficiency 0-90896
- threshold level adjustable photodetector, design considerations 0-62724
- time resolution meas. of photoreceivers using gas-discharge lamps 0-73461
- two-photon photoconductivity detector for measurement of picosecond light pulses from Nd-glass laser 0-77872
- wavelength specific photodetector for the VUV 0-91380
- $\text{Au-n-Ga}_{1-x}\text{Al}_x\text{As-n-GaP}$  narrow-band variable-gap surface-barrier photodetector 0-96944
- Bi film fast-response photodetector, employing charge carrier photon entrainment 0-73462
- $\text{Ga}_{0.47}\text{In}_{0.53}\text{As}$  photodetector diode on GaAs substrate dark currents, tunneling, energy gaps, effective masses 0-70805
- GaAs photoconductors, extrinsic, DC- and microwave-biased, performance 0-70750
- $\text{Ga}_{0.47}\text{In}_{0.53}\text{As}$  photodetector applications 0-95140
- $\text{Hg}_{0.74}\text{Cd}_{0.25}\text{Te}$  thin film deposition on Si substrates by RF triode-sputtering, large-area photodetector arrays 0-80965
- InAsSb/GaSb broad-spectral-band IR detector, backside-illum. heterostructure approach 0-73450
- InGaAs-InP punch-through type photodetector fabricated by VPE 0-68253
- $\text{In}_{0.53}\text{Ga}_{0.47}\text{As}$  p-i-n photodiode-FET photoreceiver for 1.0 to 1.7  $\mu\text{m}$  wavelength optical fibre communications systems 0-58794
- InGaAsP, improved two wavelength demultiplexing 0-58795
- InGaAsP/InP phototransistors, fabrication by LPE, photodetectors 0-95139
- InGaAsP-InP high-gain heterojunction phototransistor 0-103745
- $\text{InGa}_{1-x}\text{As}_x\text{P}_{1-y}$  photodetector diode on InP substrate dark currents, tunneling, energy gaps, effective masses 0-70805
- $\text{LaF}_3$  superionic conductor insulating layer, used for photocapacitive detectors 0-92976
- PbS-base photodetectors, struct. invest. by proton irradi. 0-104388
- $\text{PbTe-Pb}_{1-x}\text{Sn}_x\text{Te}$  p-n<sup>+</sup> heterojunction photodetector, hot wall evaporation technique 0-65673
- Se photocon optical vibration transducer 0-77768
- Si, amorphous evaporated, picosecond optoelectronic detect., sampling and correlation meas. 0-100478
- Si diffused junction photodiode performance characteristics 0-80367
- Si photodetectors with increased blue sensitivity (*Rumanian*) 0-62720
- Si photodiode absolute spectral response self-calibration 0-73448
- Si photodiode for optical channel waveguides 0-102805

**photoelectric effect**

- ferroelectrics, optically induced internal fields 0-107855
- photoferroelectric image storage in antiferroelectric-phase PLZT ceramics 0-71353
- polyhexamethylene adipamide, photocond. and dielectric props. 0-84489
- AgBr, photoelectric effect at low temp. (*Russian*) 0-96947
- PLZT ceramic, visible light scatt. depend. on photoferroelectric space charge fields 0-80806
- PLZT ceramics photosensitivity enhancement by H- and He-ion implantation 0-96934
- SrS:Mn, Zr phosphor, photoelectric effect 0-107848

**photodiffusion effects** *see* **Dember effect****photodiodes**

- see also avalanche photodiodes*
- array integration with optical power spectral analysis 0-99645
- calibration using synchrotron radiation 0-90810
- electron beam depth profiling, using carrier collection models 0-70723
- enlarger exposure meter, using photodiode and multimeter 0-101857
- EUV photodiodes for high accuracy location of orbital plane in storage ring 0-91335
- fast solid-state camera for high-speed event diagnostics 0-78985
- gas scintillation proportional counters, large vacuum photodiode imaging appl. 0-58050
- $\text{HgCdTe/CdTe}$ , limited diffusion volume photodiode, characterisation 0-75627
- III-V DH photodiodes, diffusion limited transient response 0-70809
- InSb detector system in Fourier spectrometer, use of improved preamplifier circuit, with integrator in feedback loop 0-73474
- integrating photodiode detectors, thermal background subtraction 0-90342
- laser low-level pulse meas. system at 1.064, transfer standards 0-86253
- lightwave pulse regenerator for triggerable semiconductor lasers 0-69408
- optical fibre sources and detectors (*Italian*) 0-69390
- p-i-n, for optical fibre communication (*Japanese*) 0-78977
- p-n junction photodiode terminology 0-70800
- photometric working standard establishment using photoreceptors (*Japanese*) 0-98964
- photosensor spectral responsivity calibration microprocessor system 0-86409
- radio antenna arrays, incoherent optical 1-bit cross-correlators, radioastron. appls. 0-98555
- self-scanned photodiode array, evaluation for integrated optics spectrum analyser 0-58806
- self-scanned photodiode array, image detect. from Fabry-Perot spectrograph (*French*) 0-73465

**photodiodes continued**

- self-scanned photodiode array as multichannel spectrometric detector 0-73466
- self-scanning photodiode array for fast ion detection 0-87018
- switching process and plasma effects in photodiode, theory 0-65667
- TEM image and electron energy loss spectrum display by self-scanned linear Si photodiode arrays 0-68330
- transmission system, semiconductor device reliability tests 0-58573
- X-ray generators, meas. of peak voltage with PIN-photodiodes 0-105754
- $\text{Cd,Hg}_{1-x}\text{Te}$ , tunnelling effect in p-n junctions 0-75630
- $\text{CdSb:Al}$ , p-n junction formation by laser emission, photoelectric effects (*Russian*) 0-70815
- $\text{Ga}_{0.47}\text{In}_{0.53}\text{As}$  photodetector diode on GaAs substrate dark currents, tunneling, energy gaps, effective masses 0-70805
- $\text{GaAs}_{1-x}\text{Sb}_x$  photodiode, speed and sensitivity meas. 0-92937
- $\text{Ga}_{0.47}\text{In}_{0.53}\text{As}$  photodetector applications 0-95140
- $\text{HgCdTe}$  photodiodes formed by double-layer LPE 0-104078
- $\text{HgCdTe}$  reverse-biased photodiodes for wideband appls., excess noise 0-107876
- $\text{HgCdTe}$  solid solution photodiode for  $\text{CO}_2$  laser active medium study 0-95868
- $\text{HgCdTe-CdTe}$  photodiode, 1.33  $\mu\text{m}$ , grown by LPE, phys. props. 0-107892
- $\text{Hg}_{1-x}\text{Cd}_x\text{Te}$  photodiodes, long cutoff wavelength, effect of trap tunnelling on IR detector performance 0-73451
- InGaAs-InP punch-through type photodetector fabricated by VPE 0-68253
- $\text{In}_{0.53}\text{Ga}_{0.47}\text{As}$  photodiodes with dark current limited by generation-recombination and tunneling 0-107893
- $\text{InGa}_{1-x}\text{As}_x\text{P}_{1-y}$  photodetector diode on InP substrate dark currents, tunneling, energy gaps, effective masses 0-70805
- InP photodiodes, dark current and breakdown characts. 0-70806
- $\text{PbS,Se}_{1-x}\text{Te}_x$  multispectral photovoltaic IR detectors 0-105710
- $\text{Pb,Sn}_{1-x}\text{Se}_x$  multispectral photovoltaic IR detectors 0-105710
- Si, amorphous vacuum deposited p/unbiased photodiode and diode-voltage variable resistor combination 0-61380
- Si diffused junction photodiode performance characteristics 0-80367
- Si p-n junction diodes and solar cells, minority carrier diffusion length 0-107894
- Si photodiode absolute spectral response self-calibration 0-73448
- Si photodiode array, position-sensitive photon detector for the UV or X-ray range 0-90970
- Si photodiode for optical channel waveguides 0-102805
- Si photodiode internal quantum efficiency basis for absolute radiometric standard 0-86410
- Si ring photodiode reflectometer for cavity reflectance 0-86376
- Si:B photodiode front region collection efficiency models 0-96899
- $\text{ZnGeP}_2$  p-n homodiode, polarisation photosensitivity and photopleochroism spectra 0-107866

**photodisintegration**

- see also deuteron photodisintegration; photofission*
- $\text{Be}(\gamma,p)\text{X}$ , 180-420 MeV, quasifree NN system photodisintegration, p spectrum 0-106049
- $^3\text{He}(\gamma,p,n)$ , 80-120 MeV, proton energy distrib., diff. cross sections, direct breakup 0-86897
- $^4\text{He}$  photodisintegration, pair correlation study (*Russian*) 0-86899
- $^4\text{He}$  photodisintegration, total, dipole, and quadrupole cross sections, sum rules (*Russian*) 0-83094
- $^4\text{He}(\gamma,X)$ ,  $X=p,n$ , 50-150 MeV, total cross sections, quasiparticle formalism calcs. 0-78277
- $^4\text{He}(\gamma,pn)^3\text{H}$ , three particle photodisintegration, pole mechanism contrib. (*Russian*) 0-91176

**photodissociation**

- see also molecular photodissociation*
- IR multiphoton dissociation, quantal and classical calcs. 0-83431
- multiphoton dissociation, collisionless, laser pulse shape effect on product yield 0-78667
- $\text{CO}$ -haemoprotein photolysis, transient Raman study, quantum yield origin 0-67155
- KBr, X-irrad. crystals, halogen aggregation, absorpt. spectra obs. (*Russian*) 0-66234
- KCl and  $\text{KCl:NO}_2$ , X-irrad. crystals,  $\text{Cl}_2^-$  centres photodissoc., optical anisotropy and creation mechanisms (*Russian*) 0-66235
- $\text{N}_2$  in high press. air plasma, photodissoc. 0-64691
- W, multiphoton ionisation and absorpt. 0-95575
- $\text{XeF}_2(\text{C})$  state lifetime, quenching rate consts., photolysis in inert gas atmospheres 0-66816

**photodissociation of molecules** *see* **molecular photodissociation****photoelasticity**

- see also mechanical birefringence*
- 0-89016
- alkali halides, photoelastic consts., short range polarisability effect 0-80748
- birefringent material stress determ. in single hologram exposure 0-106770
- crack propag. angle prediction under tensile stress 0-87748
- crystalline optical material props., symmetries and tensorial relationships 0-108174
- cylindrical punch, three-dimensional stress field, photoelastic studies 0-93272
- elastic wave excitation by laser beam, through thermoelastic effect 0-103503
- elastoplastic medium with cylindrical cavity, stress distrib., photoelastic investigations, successive elastic solns. (*Polish*) 0-64391
- epoxy resin, stresses arising during high-speed droplet impact 0-71764
- glass, photoelastic const. for chem. strengthening, circular plate compression method (*Japanese*) 0-93279
- Homalite-100 plates, modified compact-tension specimens, dynamic anal. 0-97561
- isoclinic and isochromatic lines, simultaneous determ. by holographic recording using CW TEM laser 0-63946
- joints, stress concentrations, Modeltech method, full scale models and photoelastic coatings (*Polish*) 0-64369
- non-destructive photoelasticity, whole field method, visualisation of isochromatics and isoclinics (*French*) 0-64502
- nonlinear photoelasticity in impure crystals, theory 0-108179
- optical glass, thermally tempered, surface stress meas. by crit. ray method 0-106766
- orthotropic composite model materials, photoelastic calibration 0-87715



**photoelasticity continued**

- photothermoelastic technique, appraisal for transient 2D thermal stress analysis 0-79244  
 plate, photoelastic test evaluation (*German*) 0-92098  
 polycarbonate plates, modified compact-tension specimens, dynamic anal. 0-97561  
 polymethacrylic acid, swollen networks, viscoelastic photoelastic behaviour 0-59366  
 polyvinylidene fluoride, thermodynamic model and appl. 0-75955  
 quartz, fused, photoelastic light scatt. from surface Rayleigh waves 0-97235  
 sandwich composite beams, stress distrib. meas. under four-point bonding, multilayer buildup theory 0-96190  
 semiconductors, population inverted, resonant Brillouin scatt., photoelastic consts. 0-89015  
 stimulated acoustooptical effects due to nonlinear photoelasticity 0-103941  
 stress obs. in thin webs, under partial edge loading, influence of longitudinal stiffening determ. 0-79857  
 US propagation in solids, visualisation using Schlieren photoelastic apparatus (*Italian*) 0-88274  
 UV high-power laser material, refractive props. and optical constants 0-106555  
 BaF<sub>2</sub>, strain induced splitting and oscillator strength anisotropy of IR transverse optic phonon 0-92625  
 CaF<sub>2</sub>, strain induced splitting and oscillator strength anisotropy of IR transverse optic phonon 0-92625  
 CdIn<sub>2</sub>S<sub>4</sub>, Brillouin scatt., elastic and photoelastic consts. determ. 0-60619  
 CdS, population-inverted, resonant Brillouin scattering and photoelastic consts. 0-76042  
 CdS, resonant Brillouin scatt., photoelastic const., imag. part contrib. 0-108218  
 GaAs, population-inverted, resonant Brillouin scattering and photoelastic consts. 0-76042  
 Rb halides, photo-elastic constants and pressure derivatives of shear moduli 0-75284  
 SrF<sub>2</sub>, strain induced splitting and oscillator strength anisotropy of IR transverse optic phonon 0-92625  
 TiBr-TiI(Cl) crystals, photoelastic moduli 0-97230  
 ZnP<sub>2</sub>, Brillouin scattering and optical props. meas. 0-76041

**photoelectrets**

- ferroelectric semiconductors, props., book 0-82590  
 ferroelectrics, photoelectric states in real time spatial light modulators, photorefractive effect 0-80676  
 photoresist, KTRF, thermally stimulated discharge current studies 0-75924  
 tetramethyldiaminodiphenyl ketone, binder layer, photoinduced polarisation and voltage 0-75923  
 GeSe, amorphous layers, photoconductance meas. 0-65632  
 S, polycryst., photoelectret state following X-irrad. 0-60485  
 Si, high dislocation density crystals, photoelectret state investigation 0-79191

**photoelectric cells**

- see also *photoconductive cells; photovoltaic cells*  
 photoelectric converters, p-n mesa structure for investigating optical and energy characts. of solar and radiant energy concentrators 0-97783  
 review, Russian devices 0-57371

**photoelectric devices**

- see also *image sensors; photocathodes; photoconducting devices; phototubes*  
 aerosol counters, calibration by sedimentation method 0-99031  
 automatic photoelectric analyser of aerosol dispersity, 0.3-40  $\mu$ m size range 0-57251  
 correlative data processing system using semiconductor injection laser 0-74307  
 logarithmic photoelectric receiver for spectral ratio pyrometers (*Russian*) 0-57302  
 polarimeter, effect on accuracy of light interference in biquartz modulator 0-62713  
 shadow methods for studying turbulence using reflection from a mirror in the medium 0-95801  
 synchrotron radiation instrumentation utilising surface photoelect. effect 0-92927  
 vibrometers, analogue, systematic errors determ. 0-79246

**photoelectric effects** see *photoelectricity***photoelectric electron emission** see *photoemission***photoelectric emission** see *photoemission***photoelectric tubes** see *phototubes***photoelectricity**

- see also *Dember effect; photocapacitance; photoconductivity; photodielectric effect; photoelectrets; photoelectromagnetic effects; photoemission; photoionisation; photorefractive effect; photovoltaic effects*  
 bacteriorhodopsin, elec. response of a back photoreaction 0-98008  
 bacteriorhodopsin, photoelec. conversion in charged synthetic membranes 0-108954  
 ferromagnet, photoelectric effect rel. to saturation magnetisation 0-65618  
 interstellar dust grains, photoelectric effect rel. to gas heating by galactic UV radiation 0-67839  
 Langmuir-Blodgett films, elec. and photoelec. transport props., device appl. 0-80431  
 metal-semiconductor interface, photoelectron injection, quantum mech. transmission and optical phonon scatt. 0-84511  
 orofacial posture and movement, photo-elec. recording method 0-108995  
 photoelectron spectra, Auger electron spectra of atomic Fano resonances 0-93454  
 photogalvanic effect under electron-hole interaction conditions 0-88591  
 PMMA, large deforms. at tip of running crack, opt. interference obs. 0-85062  
 semiconductor, graded-gap, internal photo-effects, excess carrier distribts. 0-107847  
 semiconductor, n-type, nonequilibrium photoelectron distribts. and absolute negative cond. in quantising mag. fields 0-65622  
 semiconductor-photosensitive etching for hologram recording, attainable spatial freqs. 0-69343  
 solar energy conversion, photoelectric response of photosensitive liquid membranes and chloroplast discs 0-81482  
 synchrotron radiation instrumentation utilising surface photoelect. effect 0-92927

**photoelectricity continued**

- Vespa orientalis, photoelec. props. of 'yellow strips' on cuticle, math. model 0-104638  
 AgBr, photoexcited electrons and holes in latest image form., review 0-73496  
 $\alpha$ -AgSbS<sub>3</sub> crystals, photoelectric props. 0-107861  
 BaTiO<sub>3</sub>, electron exoemission unipolarity associated with phase transitions 0-97415  
 CdS:Li(Cu), pure and doped, electrodiffusion of shallow donors, photocurrent, TSC, and exciton luminesc. meas. 0-79992  
 p-CdTe, barrier heights of metals on etched surface 0-80378  
 GaAs based MOS capacitors, scanning photovoltage investigation 0-80396  
 GaAs:Cu, Te, photoelec. props. 0-92936  
 n-GaAs-metal Schottky barrier, ultrathin native oxide, thickness determ. from C-V and photoresponse meas. 0-70821  
 Ge (111), electron struct., photoelec. props. 0-100493  
 Ge, far IR photon drag and radiation pressure in refractive media 0-60048  
 Ge single crystals, photopiezoelectric effect under elastic deform. 0-107856  
 InP p<sup>+</sup>-n abrupt junctions, ionisation coeffs., photomultiplication meas. 0-65655  
 n-InSb, cond. electron cooling induced by CO laser and non-ohmic DC field 0-96941  
 KH<sub>2</sub>PO<sub>4</sub>, KD<sub>2</sub>PO<sub>4</sub> crystals, photoresponse under laser irrad. 0-100479  
 PLZT ceramic, proton implanted, photoferroelectric effect for image storage and display devices 0-80315  
 Pb<sub>1-x</sub>Sn<sub>x</sub>Te, x=0.2, monocrystal, photoelectric props. of p-n structures (*Russian*) 0-70808  
 Si based MOS capacitors, scanning photovoltage investigation 0-80396  
 Si, far IR photon drag and radiation pressure in refractive media 0-60048  
 Si MIS phototransistors, photoelec. props. at high illum. intensities 0-60101  
 n-Si-Re(Os) Schottky contact barrier height meas. 0-65675  
 SnO<sub>2</sub>-GaTe(GaSe)(InSe) heterojunctions, photoelec. props. 0-96945  
 TiInSe<sub>2</sub>, monocrystal, photoelec. props. (*Russian*) 0-70752
- photoelectrochemical cells**  
 see also *solar cells*  
 biological solar cells, photosynthetic bacterial reaction centres on sputtered C and SnO<sub>2</sub> electrodes 0-66981  
 chlorophyll a dihydrate photoelectrochemical cell 0-61387  
 electrochemistry, power sources and energy science 0-101023  
 energy conversion system, principles and appl. 0-89652  
 photogalvanic cell based on photolysis of Rb anions in THF 0-85294  
 photogalvanic solar energy conversion, photochem. determ. of efficiency 0-89654  
 photogalvanovoltaic cells and photovoltaic cells using glassy carbon electrodes 0-89630  
 photosynthetic reaction centre from bacteria working on SnO<sub>2</sub> electrode 0-94092  
 semiconductor, quantum efficiency and energy efficiency determ. by photo-thermal spectroscopy 0-72072  
 solar cell (*Dutch*) 0-85295  
 solar cells review of cell types and electrode props. 0-61385  
 solar energy conversion, photoelectrochem. processes 0-72068  
 solar energy conversion, use of oxide semiconductors as anodes 0-101120  
 solar energy conversion and storage using PEC regenerative and storage cells (*French*) 0-61386  
 solar H<sub>2</sub>O photoelectrolysis, H<sub>2</sub>/hydrocarbon fuel prod. via biomass conversion wastes 0-89653  
 thionine-coated electrode for photogalvanic cells, electrochem. and XPS anal. 0-72071  
 AgI-Ag<sub>2</sub>O-P<sub>2</sub>O<sub>5</sub>(MoO<sub>3</sub>) glassy electrolyte galvanic cells 0-104513  
 CdS film, chemical bath deposited, solar energy conversion by photoelectrochem. cells 0-108804  
 CdS:Te-based photoelectrochem. cell, luminesc., thermal manipulation of deactivation processes 0-81479  
 CdSe, chemically sprayed thin films as photoanode in photoelectrochem. cells, power charact. meas. 0-85293  
 CdSe film, electrodeposited, for photoelectrochemical cell for solar energy conversion 0-94093  
 CdSe film photoanodes for electrochem. photovoltaic cells, fabrication and evaluation 0-76641  
 CdSe photoanode improved efficiency by photoelectrochem. etching 0-104512  
 CdSe<sub>0.65</sub>Te<sub>0.35</sub>, polysulphide photoelectrochem. solar cell 0-72073  
 Cu(II) complexes, reversible excited-state electron transfer reactions for solar energy conversion 0-89655  
 $\alpha$ -Fe<sub>2</sub>O<sub>3</sub> electrode, carrier density determ. by optical absorpt. and photoelectrolysis spectra 0-71462  
 $\alpha$ -Fe<sub>2</sub>O<sub>3</sub>, photochem. props. of sintered and doped samples for solar photoelectrochem. cell appls. 0-89651  
 n-GaAs, metal filmed photoelectrochemical cell, energy conversion characts. 0-101118  
 p-GaAs/heptyl viologen system, appl. in photoelectrochemical cells and photoelectrochromic displays 0-76640  
 n-Ga<sub>1-x</sub>In<sub>x</sub>P photoelectrochemical cells, bandgap energy, electronic transition mode, and diffusion length 0-72070  
 p-GaP semiconducting photoelectrode 0-101119  
 H<sub>2</sub> prod., semiconductor-liquid junction systems, review 0-61453  
 LuRhO<sub>3</sub>, elec., mag. and photoelectrochemical props. 0-96925  
 n-Si, Fe<sub>2</sub>O<sub>3</sub>-coated, heterostruct. photoanode for photoelectrolysis of water 0-61384  
 Si:H, amorphous, photoelectrochem. behaviour 0-81480  
 n-SnO<sub>2</sub> pigmented solar cell for electrolysis of water, two-photon process 0-93932  
 TiO<sub>2</sub>, doping processes, influence on photoelectrochem. behaviour 0-79822  
 TiO<sub>2</sub> electrode, carrier density determ. by optical absorpt. and photoelectrolysis spectra 0-71462  
 n-TiO<sub>2</sub> photoelectrochemical electrodes, effect of Nb doping on quantum efficiency 0-101121  
 TiO<sub>2</sub>, sputtering defects, associated surface electron states; UPS, XPS and AES obs. 0-60755  
 n-WSe<sub>2</sub> electrode in aq. iodide medium, high efficiency photoelectrochemical solar cell 0-72069  
 ZrSe<sub>2</sub>, photo-intercalation: possible application in solar energy devices 0-108803



**photoelectromagnetic effects**

- semiconductor, photomagnetolectric effect, injection-level dependent lifetime 0-80319  
 semiconductors, photocarrier distrib. and photomagnetolectric effect near stimulated emission threshold 0-80320  
 CdHgTe photoelectromagnetic detector for 10.6  $\mu\text{m}$  radiation, non-cooled, performance 0-82818  
 Cd<sub>0.9</sub>Hg<sub>0.1</sub>Te, graded gap epitaxial layers, spectral characts. of photoelectromagnetic effect 0-60022  
 CdTe film, photogenerated carrier transport props. 0-88590  
 GaAs, photomag. effect anomalies and state of surface layer 0-100482  
 p-GaAs:Cr, semi-insulating, mobilities and carrier concentrations, temp. depend. 0-70702  
 InSb, high-resistivity p-type or crystals of n-type, recombination processes, photocond. and photomag. effect meas. (Russian) 0-88567  
 n-Si:H, amorphous, photoelectromagnetic effect 0-107845

**photoelectron multipliers** *see photomultipliers***photoelectron spectra**

- see also Auger effect; photoemission; X-ray photoelectron spectra*  
 acetic acid, monomer and dimer, photoelectron spectrosc. 0-87172  
 adsorbed layers, photoelectron diff. aximuthal patterns, struct. sensitivity 0-107644  
 alkali metal atoms, near-resonant two-photon ionis., non-Coulomb phase shifts of photoelectron partial waves 0-106302  
 alkali metals, outer p shells multiplet and satellite struct., photoelectron spectra 0-87039  
 n-alkanes, conduction band struct., LEED, secondary electron emission and UPS study 0-70601  
 1H-alloxazine, and derivatives electronic struct., photoelectron spectrosc. and ab initio study 0-106261  
 anthracene surface, Ar impact, Penning ionisation electron spectra and photoelectron spectra 0-66352  
 atom-ion core level shifts, ASCF calcs. 0-87176  
 atoms, power broadened two-photon ionisation, reson. lineshape and photoelectron spectra 0-58229  
 Auger electron spectra of atomic Fano resonances 0-93454  
 benzenes, substituted, electronic struct., ab initio calcs., photoelectron spectra 0-58314  
 bromobenzene ion fragmentation, photoelectron-photoion coincidence spectra 0-95682  
 bromofluorobenzenes, He(I $\alpha$ ) and He(II $\alpha$ ) photoelectron spectra, assignments, ionis. energies 0-78651  
 chlorofluorobenzene cations in gaseous phase, emission spectra and lifetimes in B(0<sup>+</sup>) states 0-63711  
 chlorofluorobenzenes, He(I $\alpha$ ) and He(II $\alpha$ ) photoelectron spectra, assignments, ionis. energies 0-78651  
 closed shell atoms, photoelectron ang. distrib. and spin polarisation, theory 0-91618  
 condensed phase photoelectron asymmetry 0-80930  
 cyanodiacyetylene cation, gas phase, UV emission spectra of  $A(\pi^{-1}) \rightarrow X(\pi^{-1})$  band system 0-95636  
 cyclic hydrocarbons, chemisorpt. on W(100) surface, decomp., UPS and thermal desorpt. obs. 0-59782  
 difluoroethene, cis- and trans-, photoelectron-photoion coincidence study, fluoresc. obs. 0-95678  
 ethylnanodiacyetylene cation, gas phase, UV emission spectra of  $A(\pi^{-1}) \rightarrow X(\pi^{-1})$  band system 0-95636  
 fluoroacetylene, He(II) photoelectron spectra 0-91601  
 fluorodiacyetylene, He(II) photoelectron spectra 0-91601  
 fluorophenol cations, emission and photoelectron spectra in gaseous phase 0-58316  
 formic acid ions, fragmentation, energy selected, photoelectron-photoion spectra 0-95676  
 heavily doped semicond., photoemission lineshapes of impurity levels, p-wave resonance 0-76154  
 heterocyclic aromatic molecules, Penning ejection spectra and photoelectron spectra, rel. intensities 0-95725  
 high-Z elements subshells, photoelectron angular distribution 0-99487  
 hydrocarbons, 30.4 nm He(II) photoelectron spectra 0-82589  
 III-V semiconductor-oxide interface states, photoemission obs. of energy levels induced by adsorpt. 0-93000  
 inert gas, atomic photoionisation, Dirac-Fock calcs., branching ratios and angular distrib. in p shells 0-63601  
 10H-isoalloxazine, and derivatives electronic struct., photoelectron spectrosc. and ab initio study 0-106261  
 isopropyl benzene, mol. solid, temp. depend. UPS linewidths 0-89115  
 localised and delocalised calcs. 0-63709  
 malonic acid, and  $\alpha$ -alkyl derivatives, photoelectron spectra, lone-pair interactions 0-58315  
 metal molecular clusters, UPS 0-80940  
 metal oxide, molecular adsorption, UPS studies, review 0-84374  
 metal oxides, ESCA, Madelung pot. effects 0-104036  
 metallocenes, photoelectron spectra, band assignment 0-91604  
 methanol, ionic dissoc., photoelectron-photoion coincidence spectroscopy 0-66774  
 methanol, processes of photoionisation studied using ion-electron coincidence method 0-74204  
 methoxide surface complexes on Li, He(I) photoelectron spectra, MO calcs. 0-83417  
 methoxy species on Ni (111), photoelectron spectra, electronic struct. and orientation 0-83420  
 methyl ethyl ketone, processes of photoionisation studied using ion-electron coincidence method 0-74204  
 methylnanodiacyetylene cation, gas phase, UV emission spectra of  $A(\pi^{-1}) \rightarrow X(\pi^{-1})$  band system 0-95636  
 molecule core 1s and 1b, photoelectron bands, vibr. excitations, ab initio calc. 0-63543  
 negative ions, sputtered, characteristic electronic and vibrational temp., laser photoelectron spectral meas. 0-66346  
 perovskites, d-band, concepts of surface states and chemisorption, book contrib. 0-107651  
 photoelectron ang. distrib. and spin polarisation, theory 0-91618  
 polyacetylene:AsF<sub>5</sub>, AES, XPS, UPS, and X-ray induced 0-66400  
 polyacetylene:I, electronic structure, XPS and UPS meas. 0-66385  
 polyethylene, conduction band struct., LEED, secondary electron emission and UPS study 0-70601  
 pyridine adsorbed on Cu (110) surface, photoemission selection rules 0-100751  
 pyridine-N-oxide, electronic struct. assignment, He I/He II intensities (German) 0-83423

**photoelectron spectra continued**

- rare earths cpds., Fano-resonances, surface and bulk effects in photoemission 0-97405  
 semiconductors, optical props. above band edge, book contrib. 0-84425  
 solid-state, with synchrotron radiation, review 0-71570  
 spin polarisation of photoelectrons, ang. depend. 0-78652  
 thermal light with orthogonally polarised multiple-peak spectrum, intensity fluctuations 0-87303  
 threshold photoion-photoelectron coincidences method for ion state selection 0-63718  
 triatomic molis., Renner-Teller effect, orbital angular momentum 0-78513  
 triazastilbenes, photoelectron spectrosc. 0-106353  
 trifluoroacetic acid, monomer and dimer, photoelectron spectrosc. 0-87172  
 water irradiated by photons up to 2 MeV, initial energies of Compton electrons and photoelectrons 0-108320  
 zinc phthalocyanine, resonant two hole bound state at 3p core threshold 0-60750  
 Ag (111) surface, ethylene adsorption, XPS and UPS investigation 0-103573  
 Ag clusters, chemisorption of I, UPS obs. 0-84830  
 Ag, photoionisation, photoelectron spectra 0-87086  
 Ag, polarised photoelectron yields in VUV region 0-106307  
 AgBr, vapour, photoelectron spectrosc., interpretation 0-95679  
 AgCl, vapour, photoelectron spectrosc., interpretation 0-95679  
 AgI, vapour, photoelectron spectrosc., interpretation 0-95679  
 Al (001), enhanced photoexcitation 0-80937  
 Al (111), angle-resolved UPS obs. of 2-dimens. band structs. of S, Se and Te 0-60059  
 Al (111), bonding of O, electronic struct. calcs., rel. to UPS data 0-59801  
 Ar, spin-polarised photoelectrons by circularly polarised synchrotron radiation 0-91516  
 As<sub>2</sub>S<sub>3</sub> and As<sub>2</sub>S<sub>4</sub> vapour-deposited films, valence states, thermal and photo-induced changes UPS study 0-93459  
 As<sub>2</sub>S<sub>3</sub>, amorphous, struct., vibr. and electronic spectra 0-64908  
 Au film, photoelectron emission, intershell interaction influence on 3d and 5d branching ratio 0-104038  
 Au subshell photoelectron branching ratio meas. using synchrotron radiation 0-66397  
 Au-3d transition metal alloys, UPS study, localised states 0-93449  
 Au(111), A-line valence bands, angle-resolved photoemission determ. 0-108323  
 BaTiO<sub>3</sub> (001), LEED and UPS studies 0-100747  
 BaTiO<sub>3</sub>, band struct. calc., interpretation of XPS and UPS spectra 0-70597  
 BaTiO<sub>3</sub>, photoelectron and optical spectra derived from self-consistent charge MO and band calcs. 0-96785  
 BaTiO<sub>3</sub>, valence band UPS and partial p and d density of states 0-71560  
 BaTiO<sub>3</sub>, XPS and UPS from surface defects 0-76136  
 BrF<sub>3</sub>, electronic struct. and ionisation pot., SCF DV Xalpha method 0-69057  
 BrF<sub>3</sub>, electronic struct. and ionisation pot., SCF DV Xalpha method 0-69057  
 C foil, extreme UV induced forward photoemission 0-76137  
 CO adsorbed on Ni, valence band photoemission, SCF MO CNDO calc. 0-100754  
 CO adsorbed on W, electron-stimulated desorption, photoemission, relax. energy 0-100401  
 CO asymmetry parameter, angle resolved photoelectron spectra, multiple scatt. method 0-63708  
 CO molecular adsorbed on Mo (110) surface, electronic states, photoemission spectra 0-65363  
 CO, oriented molecule, photoelectron ang. distrib., energy depend. 0-76152  
 CO, photoelectron ang. distributions, wavelength and vibr. state depend., reson. effects, asymmetry parameters 0-91602  
 CO, X<sub>2</sub>S<sup>+</sup>, vibr. levels, UPS electron attachment obs. 0-95683  
 CO<sub>2</sub>, asymmetry parameter, angle resolved photoelectron spectra, multiple scatt. method 0-63708  
 CO<sub>2</sub>, high resolution UV photoelectron spectra 0-91603  
 COS, asymmetry parameter, angle resolved photoelectron spectra, multiple scatt. method 0-63708  
 COS, high resolution UV photoelectron spectra 0-91603  
 CS<sub>2</sub>, asymmetry parameter, angle resolved photoelectron spectra, multiple scatt. method 0-63708  
 CS<sub>2</sub>, electronic autoionisation branching 0-91614  
 CS<sub>2</sub>, high resolution UV photoelectron spectra 0-91603  
 Cd, oxidation, chemisorption and oxide regimes, UPS and EELS study 0-81236  
 CdF<sub>2</sub>, UPS and XPS spectra, rel. to optical props. 0-66386  
 CdS-Au contacts, electronic states, vacuum UV photoelectron spectra 0-70827  
 CdSe-Au contacts, electronic states, vacuum UV photoelectron spectra 0-70827  
 CdTe-Au contacts, electronic states, vacuum UV photoelectron spectra 0-70827  
 Co, energy band dispersion and mag. exchange splitting, angle-resolved photoemission meas. 0-71567  
 Co, energy band dispersions and mag. exchange splitting 0-76146  
 CoS<sub>2</sub>(Se<sub>2</sub>), electronic struct., UPS and XPS study 0-80935  
 Cr film, 3p-3d intershell interaction, photoemission 0-80934  
 Cr<sup>3+</sup> compounds, 3p photoelectron spectra, light-induced changed in multiplet satellites 0-80946  
 CrOCl<sub>3</sub>, electronic structure and valence ionisation energies, obs. by ab initio and SW-X $\alpha$  methods 0-69073  
 Cs and CsCl, comparison of photoelectron spectra of Cs 5p levels 0-83419  
 Cu (001), M-point surface state, high-resolution angle resolved photoemission study 0-108322  
 Cu (001), O<sub>2</sub>, chemisorption, Cu3d-O2p interaction study by angular-resolved photoemission using synchrotron radiation 0-84836  
 Cu (100), ordered Cl overlayer, adatom bonding effects, photoemission study 0-104044  
 Cu (100) and (111) surfaces, high resolution normal and near-normal UPS 0-80933  
 Cu (111) surface, PES and band struct. calcs. 0-89118  
 Cu (111)/Na interface, UPS study of surface electronic struct. 0-80350  
 Cu, bulk and (001) film, extended tight-binding calcs. 0-70592  
 Cu, chemisorption on low-index and stepped surfaces, LEED, AES and UPS obs. 0-84391



## photoelectron spectra continued

- Cu film, photoelectron emission, intershell interaction influence on 3d and 5d branching ratio 0-104038  
 Cu surface, (100), O chemisorption, angle-resolved UPS study 0-84384  
 Cu surface, (110), methanol adsorption, XPS, UPS and thermal desorption study 0-84388  
 Cu, surface states, (100) and (111), polarisation depend. photoemission 0-100495  
 Cu-Ni, adsorption of  $H_2$ +CO on (110) surface, TDS and UPS obs. 0-80052  
 Cu-Ni, evaporation limited segregation 0-70513  
 Cu-Ni (110), adsorption of CO and  $H_2$ , UPS, thermal desorption, AES, and LEED study 0-80087  
 Cu-phthalocyanine, photoemission multielectron effects from quasi atomic Cu 0-93458  
 CuCl (100), obs. of p- and d-like surface states, angle resolved UPS study 0-104045  
 CuO, on Cu, identification by electron spectroscopic methods 0-60747  
 Cu<sub>2</sub>O, on Cu, identification by electron spectroscopic methods 0-60747  
 CuPd, chemical shift effects and origin of Pd 3d core level satellite 0-104039  
 CuS<sub>2</sub>(Se<sub>2</sub>), electronic struct., UPS and XPS study 0-80935  
 EuO:Gd, surface mag. props. 0-71566  
 FO(X<sup>2</sup>-I<sub>2</sub>) radical from F+O<sub>3</sub> reaction, VUV photoelectron spectra 0-104455  
 Fe (110), coadsorption of K and O<sub>2</sub>, XPS, UPS, AES, and LEED study 0-80084  
 Fe, energy band dispersion and mag. exchange splitting, angle-resolved photoemission meas. 0-71567  
 Fe<sub>2</sub>B<sub>16</sub>, metallic glass, ion implanted, UPS meas. 0-97411  
 FeBr<sub>3</sub>, transient species, He(I) photoelectron spectrosc. calcs., relativistic corrections 0-95677  
 Fe<sub>1-x</sub>(P,B), amorphous and crystalline, photoemission and band structure 0-60754  
 Ga, reson. photoemission shake-up and Auger processes at 3p photothreshold 0-100748  
 Ga<sub>1-x</sub>Al<sub>x</sub>As, varizone layer photoelectron yield depth estimation 0-100745  
 GaAs (110), surface core-level binding-energy shifts 0-103737  
 GaAs (110), with Al or Ga overlayers, interfacial electron states, UPS and LEED obs. 0-80377  
 GaAs epitaxial thin films with neg. electron affinity, photoelectron energy distrib. 0-100755  
 GaAs, valence-band dispersions, electron and hole lifetimes, angle-resolved photoemission 0-80947  
 GaP, reson. photoemission shake-up and Auger processes at 3p photothreshold 0-100748  
 GaS, Ge<sub>1-x</sub>, valence band states, composition depend., photoemission spectra study 0-100434  
 GaSb (110), surface core-level binding-energy shifts 0-103737  
 Gd, resonance recomb. lines in AES and photoelectron spectra 0-97390  
 Ge (100), dimer reconstruction, photoemission obs. 0-80939  
 GeSe, amorphous, film, thermally induced effects, UPS study 0-104042  
 GeSe<sub>2</sub>, amorphous, film, thermally induced effects, UPS study 0-104042  
 H, photoelectron spectra, rot. intensity distrib. 0-91605  
 HBr, photoelectron angular distrib. 0-58318  
 HI, photoelectron angular distrib. 0-58318  
 HNF<sub>2</sub> and DNF<sub>2</sub>, photoelectron spectra, vibr. struct. obs, ionisation pot. determ., ab initio calcs. of ionic geometry 0-83418  
 H<sub>2</sub>O threshold PES, OH<sup>+</sup> fragment obs. 0-78647  
 H<sub>2</sub>O<sup>+</sup>, vibr. and rot. struct., intensity factors and orbital angular momentum 0-83246  
 Hg, 5d level open shell interactions, 304 Å photoelectron spectrum 0-87087  
 α-HgS, gas-phase and solid-state Hg 5d photoionisation processes, direct comparison 0-76149  
 I, He (I) photoelectron spectrum by I<sub>2</sub> photodissoc. 0-83325  
 In, VUV photoelectron spectra, pseudo-atomic beam technique 0-58225  
 Ir (111), chemisorbed NH<sub>3</sub>, mol. adsorbate structs. from angular-resolved photoemission 0-76141  
 Ir, (111) surface states, surface Umklapp effects, photoelectron spectra 0-93457  
 Ir, chemisorption of H<sub>2</sub>, adsorption and desorption kinetics, struct. of overlayer 0-84367  
 K adsorbed on Fe(110), UPS and XPS meas. 0-95675  
 K adsorbed on Pt(111), UPS and XPS meas. 0-95675  
 Kr, spin-polarised photoelectrons by circularly polarised synchrotron radiation 0-91516  
 LaB<sub>6</sub> (100), (110), and (111), surface structs. and work functions 0-70512  
 LaB<sub>6</sub> (210) surface, work function, struct. and chemisorpt. stability, XPS, UPS and LEED 0-65344  
 LaB<sub>6</sub>, direct recomb. and Auger deexcitation channels of La 4d to 4f reson. excitations, photoemission spectra 0-66395  
 LaB<sub>6</sub> surfaces, (100), (110) and (111), electron states, UPS study 0-100752  
 LiNbO<sub>3</sub>, valence band UPS and partial p and d density of states 0-71560  
 LiNbO<sub>3</sub>, XPS and UPS from surface defects 0-76136  
 Mo (100), CO chemisorbed, surface kinetics, photoemission study method 0-80941  
 Mo, N<sub>2</sub>N<sub>2</sub>N<sub>4</sub>, super Coster Kronig processes 0-106303  
 N<sub>2</sub> adsorbed on Ni, valence band photoemission, SCF MO CNDO calc. 0-100754  
 N<sub>2</sub> asymmetry parameter, angle resolved photoelectron spectra, multiple scatt. method 0-63708  
 N<sub>2</sub><sup>+</sup>, partial photoionisation cross section and photoelectron angular distribution for X<sup>2</sup>Σ<sub>g</sub><sup>+</sup> state determ. 0-83429  
 N<sub>2</sub><sup>+</sup> X<sup>2</sup>Σ<sub>g</sub><sup>+</sup> state, vibr. states asymmetry parameter and photoelectron spectrum 0-95591  
 N<sub>2</sub>O, electronic autoionisation branching 0-91614  
 N<sub>2</sub>O<sup>+</sup>, dissoci., threshold photoelectron-photoion coincidence obs. 0-87189  
 Na adsorbed on Ni, photoemission, directional memory effects 0-100753  
 Nb, H chemisorption, photoemission studies 0-76145  
 Nb, N<sub>2</sub>N<sub>2</sub>N<sub>4</sub>, super Coster Kronig processes 0-106303  
 NbC, electronic structure, PES study 0-70594  
 Ni (001), chemisorption of CO, back donation in chemisorption bond, UPS study 0-107642  
 Ni (001) surface, electronic struct. of ordered S overlayers 0-84835  
 Ni (100), reson. behaviour of interband excitations in photoelectron spectra 0-104043

## photoelectron spectra continued

- Ni (100) and (110), reaction of acetylene, room temp., UPS expts. 0-61151  
 Ni (110) and (111), two-photon photoemission 0-76150  
 Ni (111), chemisorption and reaction of NH<sub>3</sub>, LEED, desorption and photoemission expts. 0-59799  
 Ni (111) and (110), laser-induced charge transfer to adsorbed CO, photoemission expts. 0-59798  
 Ni, adsorption of N<sub>2</sub>, photoemission and electronic struct., cluster calcs. 0-97403  
 Ni, band struct., angle-resolved photoemission meas. 0-71569  
 Ni, band struct. and multielectron excitations, angle-resolved photoemission determ. 0-76147  
 Ni, electronic structure, photoelectron spectra, theory 0-80168  
 Ni, energy band dispersion and mag. exchange splitting, angle-resolved photoemission meas. 0-71567  
 Ni, exchange splitting of 3d bands, angle-resolved photoemission meas. 0-71568  
 Ni, photoemission spectra, valence band and core level satellite due to excitation of d electron 0-97408  
 Ni surface, adsorbed CO, N<sub>2</sub>, valence band photoemission, SCF MO CNDO calc. 0-100754  
 Ni surface, clean and with adsorbed Na, photoemission, directional memory effects 0-100753  
 Ni<sup>2+</sup> compounds, 3p photoelectron spectra, light-induced changes in multiple satellites 0-80946  
 NiO, bulk props., initial state MO Ni<sub>4</sub>O<sub>4</sub> and Ni<sub>13</sub>O<sub>14</sub>, cluster model, lattice and force consts., photoemission and CT absorpt. spectra 0-84828  
 NiS<sub>2</sub>(Se<sub>2</sub>), electronic struct., UPS and XPS study 0-80935  
 O<sub>2</sub>, electron attachment threshold photoelectron spectra, vibr. excitation 0-83422  
 O<sub>2</sub>, I and I' resonance series, vibr. level populations in autoionisation, photoelectron spectra, bond length determ. 0-91612  
 Pb, 5d level open shell interactions, 304 Å photoelectron spectrum 0-87087  
 Pb, photoelectron spectra, electron correlations and spin-orbit interaction influence 0-102495  
 Pb subshell photoelectron branching ratio meas., using synchrotron radiation 0-66397  
 Pd, electronic band struct. and photoemission 0-97410  
 Pd, photoemission spectra, valence band and core level satellite due to excitation of d electron 0-97408  
 Pd surface, segregated S state, AES, EELS, UPS and XPS study 0-93452  
 Pd<sub>2</sub>, ab initio relativistic core pot. studies of metal-metal bonding 0-106257  
 PdH, ab initio relativistic core pot. studies of metal-H bonding 0-106257  
 Pt 6(111)×(100), clean and O<sub>2</sub>-covered, UPS studies 0-76151  
 Pt (111), chemisorption of mol. O<sub>2</sub>, XPS, UPS, EELS, and work function meas. 0-76139  
 Pt (111), interaction with water, thermal desorption, UPS, and XPS study 0-80088  
 Pt band-structure determ., angle-resolved photoemission 0-66398  
 Pt subshell photoelectron branching ratio meas. using synchrotron radiation 0-66397  
 Pt, surface, (111), O<sub>2</sub> interactions, UPS, EELS and thermal desorption study 0-100409  
 Pt<sub>2</sub>, ab initio relativistic core pot. studies of metal-metal bonding 0-106257  
 PtH, ab initio relativistic core pot. studies of metal-H bonding 0-106257  
 PtO<sub>x</sub> films, electronic struct., reduction processes, photoemission, optical absorpt. and resist. meas. 0-80931  
 Pt(111), A-line valence bands, angle-resolved photoemission determ. 0-108323  
 RbCl, electron bombard., colour centre photoemission, surface contamination and escape depth 0-66392  
 Re, electronic struct. and CO adsorption characts., XPS, UPS, and thermal desorption study 0-71571  
 Re<sub>2</sub>Br<sub>9</sub>, atomic clusters, electronic struct. and photoelectron spectra 0-69287  
 (Re<sub>2</sub>Cl<sub>9</sub>)<sup>3-</sup>, atomic clusters, electronic struct. and photoelectron spectra 0-69287  
 Re<sub>2</sub>Cl<sub>9</sub>, atomic cluster, electronic struct. and photoelectron spectra 0-69287  
 Re(0001), adsorption of O<sub>2</sub>, CO, NO, and H<sub>2</sub>O, XPS, UPS and temp. programmed desorption 0-71574  
 Rh, N<sub>2</sub>N<sub>2</sub>N<sub>4</sub>, super Coster Kronig processes 0-106303  
 Ru, N<sub>2</sub>N<sub>2</sub>N<sub>4</sub>, super Coster Kronig processes 0-106303  
 S-N system, inorganic, electronic struct. obs. by photoemission XPS and UPS, CNDO calcs. 0-78653  
 S<sub>2</sub>N<sub>2</sub>, photoelectron spectrum, interpretation, Green's function calcs. 0-87175  
 Se, amorphous film, highly disordered, UPS study 0-76148  
 SeCl<sub>2</sub>, photoelectron spectra 0-69186  
 Se<sub>2</sub>Cl<sub>2</sub>, photoelectron spectra 0-69186  
 Si, (001) and (111), geometrical and electronic struct., review 0-80039  
 Si (100), dimer reconstruction, photoemission obs. 0-80939  
 Si (111) surfaces, cleaved, electronic structure following Al adsorption 0-75610  
 Si, amorphous and crystalline, ion implanted, UPS meas. 0-97411  
 Si, hydrogenated amorphous, gap states, comparison of photoemission and photocond. results 0-103724  
 Si p-n junctions, electron emission from depletion layers 0-100509  
 Si-SiO<sub>2</sub> interface, barrier height in MOS tunnelling structures 0-88644  
 SiH<sub>x</sub> amorphous films, internal photoemission, metal-contacts 0-96964  
 SiO<sub>2</sub>, semi-insulating polycryst. films, AES and PES studies 0-107939  
 Si(111)-(7×7), and impurity stabilised Si(111)-(1×1) surface, photoemission studies 0-104041  
 SmS<sub>1-x</sub>P<sub>x</sub>, valence changes, XPS and UPS study 0-97402  
 Sn(S<sub>2</sub>Se<sub>1-x</sub>), valence band states, composition depend., photoemission spectra study 0-100434  
 SrF<sub>2</sub>, UPS and XPS spectra, rel. to optical props. 0-66386  
 SrTiO<sub>3</sub>, (100), LEED and UPS studies 0-100747  
 SrTiO<sub>3</sub> (111), O<sub>2</sub>, H<sub>2</sub> and H<sub>2</sub>O chemisorption, UPS and XPS studies, illum. effects 0-71572  
 SrTiO<sub>3</sub>, valence band UPS and partial p and d density of states 0-71560  
 TeCl<sub>2</sub>, transient species, He(I) photoelectron spectrosc. calcs., relativistic corrections 0-95677  
 Th, photoelectron spectra study, core and valence levels 0-66394



**photoelectron spectra continued**

- ThF<sub>4</sub>(Cl<sub>4</sub>), electronic struct., MS-SCF-X $\alpha$  calcs. and VUV photoelectron spectra 0-63710  
 ThN, photoelectron spectra study, core and valence levels 0-66394  
 TiC, electronic structure, PES study 0-70594  
 TiO<sub>2</sub>, sputtering defects, associated surface electron states, UPS, XPS and AES obs. 0-60755  
 TiO<sub>2</sub>-Ni (100) interface, electronic props., struct., comp., chemical bonding 0-84499  
 TiS<sub>2</sub>, band struct., angle-resolved photoemission studies 0-70610  
 TiSe<sub>2</sub>, band struct., angle-resolved photoemission studies 0-70610  
 Tl, 5d level open shell interactions, 304 Å photoelectron spectrum 0-87087  
 Tl, core level binding energies, UPS obs. 0-66388  
 Tl, VUV photoelectron spectra, pseudo-atomic beam technique 0-58225  
 U, photoelectron spectra study, core and valence levels 0-66394  
 UAl<sub>2</sub>(Co<sub>2</sub>), surface comp. and electronic struct., photoemission: study 0-66382  
 UC, electronic struct., comparison with photoemission spectra 0-91450  
 UF<sub>4</sub>(Cl<sub>4</sub>), electronic struct., MS-SCF-X $\alpha$  calcs. and VUV photoelectron spectra 0-63710  
 UN, electronic struct., comparison with photoemission spectra 0-91450  
 UN, photoelectron spectra study, core and valence levels 0-66394  
 UO<sub>2</sub>, photoelectron spectra study, core and valence levels 0-66394  
 Xe, photoionisation, spin-polarised photoelectrons angular distrib. 0-106306  
 Xe, resonantly enhanced multiphoton ionis., photoelectron energy anal. 0-63597  
 Xe subshell photoionisation, multichannel k-matrix calc., spin orbit interactions 0-63600  
 Zn, resonant two hole bound state at 3p core threshold 0-60750  
 ZnTe clean and adsorbed O<sub>2</sub> (110) surfaces, UV photoemission spectra (Japanese) 0-93456

**photoelectron spectroscopy**

- angle resolved photoelectron spectrometer for atoms and molecules using synchrotron radiation 0-90932  
 angle-resolved spectroscopy with cylindrical mirror analyzer, use of position-sensitive detector system 0-57426  
 1-chloropropyne cation, internal energy decay studied by photoelectron-photoion coincidence spectroscopy 0-69185  
 ellipsoidal mirror display analyzer system for electron energy and angular measurements 0-90908  
 ferrocyclochromes c<sub>3</sub>, anhydrous, ionisation pot., UV photoelectron spectrosc. obs. 0-85328  
 fixed energy photoelectron spectroscopy, technique 0-62797  
 magnetic order and spin depend. of electron scatt. meas technique using photoemission 0-60748  
 metallurgical applications of XPS, AES, and SIMS (French) 0-81253  
 phase-sensitive vidicon detector for angle-resolved electron spectroscopy 0-90933  
 photoionisation, absolute cross-sections, expt. meas. techniques 0-63598  
 semiconductor surface, instrument for angle-resolved UV photoemission spectroscopy (Japanese) 0-93455  
 semiconductor-metal contact investigation by photoelectron spectroscopy 0-100517  
 soft X-ray spectra, meas. by photoelectron anal. 0-73557  
 spectrometer, calibration using binding energy scale 0-90930  
 surface analysis techniques and appls., symposium, Dayton, USA (Jun. 1979) 0-62363  
 surface atomic and electronic struct. studied with synchrotron radiation 0-80945  
 synchrotron radiation, application to EXAFS and angle resolved photoemission spectrosc. (Korean) 0-74453  
 XPS azimuthal angular-depend. studies, using electron spectrometer 0-57428  
 Ag, adsorption of pyridine, UPS, AES and flash desorption meas. 0-92776  
 ZrS<sub>3</sub>, paired-anion ligand effects in valence band, photoemission spectrosc. obs. 0-87173  
 ZrSe<sub>3</sub>, paired-anion ligand effects in valence band, photoemission spectrosc. obs. 0-87173

**photoemission**

- see also photoelectron spectra; photoemissive devices  
 alkali halide, photo- and thermostimulated electron emission under ultrahigh vac. conditions (Russian) 0-66383  
 alkali halides, photoemission, energies and lineshapes 0-89119  
 electron microscopy, principles and appls. 0-89424  
 ferromagnet, itinerant electron, temp. depend. of angle-resolved photoemission 0-76142  
 lattices, FCC and BCC, optical transitions, dipole selection rules 0-97409  
 magnetic semiconductors, conference, Montpellier, France (Sept. 79) 0-94916  
 metal-semiconductor surface barrier structures, two-photon photoelec. effect 0-88594  
 MOS interface states density, photoemission obs. using photocurrent and photocapacitance meas. 0-92990  
 organic solids, photoemission and photoionisation in three stage model 0-100744  
 oriented orbitals, photoemission cross-sections, surface Green function formalism 0-93453  
 photostimulated field emission, triangular barrier pot. model 0-100759  
 quantum absorber theory, direct-action, photoelectron antibunching effect 0-57535  
 sample manipulation and rotation using ultra high vacuum angle resolving photoemission chamber 0-57317  
 semiconductor surface, instrument for angle-resolved UV photoemission spectroscopy (Japanese) 0-93455  
 ultrahigh vacuum setup for photo- and thermostimulated electron emission and luminesc. obs. (Russian) 0-66383  
 Al, autoionisation reson. determ. from photoelectron polarisation meas. 0-58221  
 Al, photoemission cross-sections for 2s and 2p levels 0-93453  
 Ar<sup>2+</sup> + H<sub>2</sub> collisions, ionisation and excitation resulting from electron capture 0-78683  
 Ba, resonant photoemission, time-depend. density-functional technique 0-89114  
 CO<sub>2</sub>, TEA laser, UV preionised, characts. 0-69414  
 CdCr<sub>2</sub>S<sub>4</sub>, photothreshold changes below mag. ordering temp. 0-97406  
 CdS:Cu sintered layers, relaxation photocurrent kinetics (Russian) 0-107852

**photoemission continued**

- Ce, resonant photoemission, time-depend. density-functional technique 0-89114  
 CsI photocathodes, efficiency evaluation for soft X-ray diagnostics 0-57442  
 Cs<sub>2</sub>Sb vacuum deposited photoemitter, XPS study 0-89122  
 Cu, single cryst., two-photon photoemission near single-photon photoelec. effect threshold 0-89121  
 CuI photocathodes, efficiency evaluation for soft X-ray diagnostics 0-57442  
 EuO:La(Gd), phototreshold changes below mag. ordering temp. 0-97406  
 Fe<sub>0.9</sub>O, photothreshold changes below mag. ordering temp. 0-97406  
 GaAs, modulation by IR illumination, saturation photocurrents 0-108318  
 GaP, adsorption and desorption of Cs, LEED, AES, and photoemission meas. 0-70532  
 GaSb, adsorption and desorption of Cs, LEED, AES, and photoemission meas. 0-70532  
 Ge-metal interface, internal photoemission mechanisms 0-60077  
 He+OCS, emission spectra in He afterglow 0-87139  
 p-InP field-assisted photocathodes, quantum efficiency 0-84831  
 InP-In<sub>0.5</sub>Ga<sub>0.5</sub>As alloy photocathodes, semiconductor photoemitters, field-assisted, 1-2  $\mu$ m range 0-97396  
 KCl, photoelectric emission in photon energy region 1.0 to 6.0 eV 0-108321  
 LiF, cryst., laser irradi., electron emission 0-80948  
 NaCl, cryst., laser irradi., electron emission 0-80948  
 Na<sub>2</sub>O-SiO<sub>2</sub> glasses, elementary electronic excitations, refl., luminesc., and photoemission meas. 0-84778  
 Si field emission photocathodes, emission current noise characts. 0-100746  
 Si-SiO<sub>2</sub>-Al, internal photoemission, pot. barrier height determ. 0-65699  
 Tl, autoionisation reson. determ. from photoelectron polarisation meas. 0-58221  
 Xe adsorbed on Pd (110), anomalous 5p photoemission, electron binding energies 0-100750  
 ZnAs<sub>2</sub>, Schottky diodes, elec. and photoelec. props., excitons 0-65653  
 ZnP<sub>2</sub>, Schottky diodes, elec. and photoelec. props., excitons 0-65653

**photoemission spectra see photoelectron spectra****photoemissive devices**

see also photocathodes; photoemission

No entries

**photoemissivity see photoemission****photofission**

- detector assembly for photofission and photoneutron studies using BF<sub>3</sub> detector 0-63484  
 fissionability, target mass depend. for  $\pi$ ,  $\gamma$ ,  $\alpha$ , p, cascade-evaporation and liquid drop calcs. (Russian) 0-106089  
<sup>209</sup>Bi( $\gamma$ ,f), 40-65 MeV, absolute total photofission cross section, compound nucleus form. 0-86934  
<sup>239</sup>Pu( $\gamma$ ,f), 15-55 MeV, photofission symmetric and asymmetric yields 0-83135  
<sup>232</sup>Th( $\gamma$ ,X) 5-18.3 MeV, photoneutron and photofission cross sections, giant resonance and deformations 0-68712  
<sup>238</sup>U( $\gamma$ ,f), 15-55 MeV, photofission symmetric and asymmetric yields 0-83135  
<sup>232</sup>Th( $\gamma$ ,f), BF<sub>3</sub> detector assembly for photofission and photoneutron studies 0-63484  
<sup>238</sup>U( $\gamma$ ,X), A=235, 236, 238, 5-18.3 MeV, photoneutron and photofission cross sections, giant resonance and deformations 0-68712  
<sup>238</sup>U( $\gamma$ ,f), A=235,238, 15-55 MeV, photofission symmetric and asymmetric yields 0-83135  
<sup>234</sup>U under barrier photofission, 4-5.7 MeV, fragment ang. distrib. (Russian) 0-106090  
<sup>238</sup>U subbarrier photofission, cross section and half-life, double hump model 0-102217  
<sup>238</sup>U( $\gamma$ ,f), <sup>135</sup>Xe, direct meas. of absolute and fractional indep. yields 0-78341  
<sup>238</sup>U( $\gamma$ ,f), BF<sub>3</sub> detector assembly for photofission and photoneutron studies 0-63484  
<sup>238</sup>U( $\gamma$ ,f), neutron capture  $\gamma$ -rays,  $\Gamma_{3,4}/\Gamma_1$  meas. 0-57813  
<sup>238</sup>U( $\gamma$ ,f), neutron capture  $\gamma$ -rays,  $\Gamma_{3,4}/\Gamma_1$  fractional indep. yield 0-57814  
<sup>238</sup>U( $\gamma$ ,f) 20 MeV, computer program for yield determ. of short-lived products 0-102215

**photoflash lamps see flash lamps****photoglow tubes see phototubes****photogrammetry**

- analytical bridging, solving problems encountered 0-105080  
 cameras, multi-, planar control in photogrammetric calibration for 3-D gait studies 0-67194  
 coastal mapping, problems due to water effects 0-104960  
 coherent correlator operation in image segment identification, aerial photograph anal. 0-102654  
 colour maps produced from B & W negatives exposed to visible and IR 0-109270  
 data analysis by collocation method 0-77130  
 image scanner technology for digital mapping systems 0-85773  
 Mars, topography, photogrammetric portrayal 0-67609  
 slippage in crystals, photogrammetric obs. method 0-100975  
 stereophotogrammetry, meas. of deform. in human body (Croatian) 0-108997  
 stereoscope for viewing aerial photographs, interpretoskop optics, modifications 0-105081

**photographic applications**

- see also photogrammetry; photolithography; remote sensing  
 astrometry, sky photography programme with wide-angle astrographs (Russian) 0-72747  
 atomisation units for powder metallurgy, gasdynamic and acoustic props. 0-66451  
 cellulose nitrate film ion data, dark-field illum. image recording photographic method 0-70031  
 Earth's atmosphere, optical parameters determ. by aerial photography at sunset 0-90219  
 environmental change detection in digitally registered aerial photographs 0-106477  
 fluid section flow pattern speckle photography 0-103096  
 fluorescein angiography of the ocular fundus 0-67185  
 fundus photography in optometric practice 0-67183



**photographic applications continued**

- general object deformation decomposition by speckle displacement 0-106486
- goniophotography in optometry 0-67182
- holographic interferometry and speckle photography, scatt. geometry, topology vector fields theory 0-87347
- maps extraction from satellite images 0-76899
- metal granules, form. mechanism study during centrifugal atomisation of rotating blank 0-100798
- neural unit activity rel. to movement, photographic technique for anal. 0-67310
- ocular cinema photography 0-67186
- ocular photodocumentation, conf., Birmingham, USA (Dec. 1977) 0-62362
- ocular photography, new instrumentation and techniques 0-67187
- ophthalmic photography, external 0-67180
- ophthalmic photography instrumentation, survey of clinical impressions 0-67188
- pin bowing in AGR fuel elements, meas. by camera device 0-106146
- pinched electron beam prod. expanding gas bubbles, fast photography obs. 0-79564
- pipe-exit flow visualisation using high-speed photography 0-106863
- pyrometry, optical, accuracy improvement using photography 0-62673
- Rayleigh-Benard flow, equal velocity fringes by speckle photography 0-75005
- scanning laser beam direct picture printers on photographic paper, appl. in life sciences (French) 0-72119
- slit lamp photodocumentation of ocular structure 0-67181
- sound triggered electronic photo flash unit, using variable time delay 0-57407
- speckle interferometric analysis of transient phenomena 0-105701
- spectral reflectance photography of the ocular fundus 0-67184
- spectroscopy, time-resolved, IR, using freq. upconversion, methyl isocyanide isomerisation obs. 0-57400
- square-field scanned image construction time optimisation (Russian) 0-63933
- strain meas. speckle photography with hybrid optical/electronic image processing 0-106768
- strain measurement by speckle photography, hybrid optical and electronic image processing 0-99976
- topographical mapping of the human face by Moire photography 0-85462
- US intensity pattern characterisation, thermographic-photographic technique 0-106689
- welded joint inspection by X-ray TV intrascope, photographic recording of images 0-86485
- As<sub>2</sub>S<sub>3</sub> chalcogenide glass films, photographic Ag photodoping to produce negative relief image 0-59490
- Fe-B amorphous ribbons formation, high-speed photography investigation 0-76216
- (YLuSmCa)<sub>3</sub>(GeFe)<sub>2</sub>O<sub>12</sub> garnet films, bubble expansion saturation vel., sampling optical photography 0-75820

**photographic developers** *see photographic materials***photographic development** *see photographic process***photographic emulsions**

- characteristic curve, projective approximation (Russian) 0-95180
- coated on birefringent substrate, construction of multipacuity matched filters 0-74478
- coating evenness in raw films, test results (Hungarian) 0-57410
- colour negative film Gevacolour type 682, 35 mm, 16 mm professional film making appl. 0-82838
- developed photographic emulsion, relation between exposure and optical density and charact. curve parameters (German) 0-105742
- diaz salt sensitised gelatin for holographic recording, grating form. 0-78798
- EM, electron exposure-dependent contrast transfer 0-104837
- evanescent wave holography using Gaussian beam, recording geometry and colour sensitivity 0-58473
- fine-grained bleached emulsion scatt. model and expt. 0-102670
- gelatin, effect of air humidity on photolayer thickness, holographic characteristics (Russian) 0-105736
- gradation characteristics, effect of absorbing layer on photosensitivity (Russian) 0-62778
- hologram recording, effects of photographic emulsion speed and contrast nonlinearity 0-106497
- holographic emulsion monobath and reversal processing techniques 0-102668
- image weak modulation detection in film grain noise with partially coherent illumination 0-77897
- instant film development, interdisciplinary and international approach 0-81342
- IR emulsions, sensitisation and use in vacuum-cold camera 0-90341
- latent image distrib., etching and recrystn. effects of solns. 0-77890
- luminescence rel. to latent image 0-73498
- nonoptimally exposed holograms, reprocessing techniques 0-58474
- partially coherent perpendicularly polarized vibrs., anisotropic photographic recording, interferograms 0-57364
- photolysis of ultra-fine grained emulsions, nature of produced colour centres (Russian) 0-73517
- photosensitivity, H<sub>2</sub> hypersensitisation with Au sensitizer (Russian) 0-73511
- removal from cinefilm waste using Protosubtylin 13x-I (Russian) 0-105734
- signal-dependent film-grain noise, optimal image estimation 0-102659
- sulphide sensitisation of cubic and octahedral emulsion microcrystals, effect on photographic ageing (Russian) 0-95181
- sulphide sensitisation of negative emulsions, quality composition of photosensitivity and fogging centres (Russian) 0-62781
- undeveloped photographic film, MTF meas., target base dimension influence 0-102653
- volume-phase reflection hologram, recording medium thickness effect on image luminance 0-58479
- Ag halide, visible luminescence obs. at or below 77K 0-108263
- Ag halide crystals, relative dissolution rates meas. by flow calorimetry 0-85220
- Ag halide emulsions, primitive and AgNO<sub>3</sub>-digested, IR luminescence obs. at 77K 0-103983
- Ag halide film physical props., effect of gelatin structure 0-97715
- Ag halide microcrystal, photoconductivity meas. by microwave technique 0-103719

**photographic emulsions continued**

- AgBr emulsion grains, adsorbed dyes, light-induced ESR spectra 0-88862
- AgBr emulsion grains, edge length dependence of ionic conductivity, space charge characteristics 0-88360
- AgBr emulsion layer with gelatin, IR absorpt. spectra before and after laser exposure (Russian) 0-62776
- AgBr evaporated layer response in ionisation semiconductor photographic system (German) 0-101859
- AgBr, Herschel effect, latent image centre struct. changes under laser irradi. 0-77900
- AgBr, luminescence of photographic emulsions sensitised by 1,1'-diethyl-2,2'-cyanine with Ag<sub>2</sub>S clusters (Russian) 0-73513
- AgBr microcrystals, spectrally sensitised, luminesc., effect of hydrophobic organic compounds 0-97331
- AgBr, very fine grained emulsions, effect of hole and electron acceptors on photosensitivity (Russian) 0-73515
- AgBr-AgI emulsion sensitivity improved by AgCl shell crystallisation (German) 0-104453
- Na<sub>2</sub>S<sub>2</sub>O<sub>8</sub> digested AgX emulsions, red-IR photoluminescence obs. at 77K 0-103982
- PbI<sub>2</sub> suspension, chem. sensitization 0-73492

**photographic filters** *see optical filters***photographic lenses***see also aberrations*

- Arriflex 35BP-II motion picture camera mounted with 350PF-1A zoom lens for wide-screen filming (Russian) 0-95176
- design, new developments and trends at Zeiss 0-62746
- development and trends at Zeiss 0-62745
- EKTRAMAX camera lens design and performance 0-77894
- four-element lens systems of Cooke-triplet family design considerations 0-57404
- gradient singlet, design techniques based on total aberrations 0-69479
- lens-array photographic system, depth of sharp focusing, resolution 0-62763
- long focal length aerial reconnaissance system response to thermal shock 0-78939
- long focal length reconnaissance lenses, response to thermal shock 0-77892
- PRAKTICAR, for B 35 mm reflex cameras 0-82839
- reflex cameras, lens-array focusing system tests 0-86479
- rotating lens system for cine projection with continuous film transport 0-62766
- wide angle correcting lens for underwater colour TV 0-91883
- zoom lens system design and manufacture 0-68288

**photographic light sources** *see light sources; photography***photographic material sensitivity**

- cellulose complexes with pyrene and its derivatives, photosensitivity (Russian) 0-73506
- colour sensimetry characteristic curves corresponding to visual impression 0-82803
- colour sensimetry system based on spectral densitometer 0-82804
- cyclorubber with bisazides, effect of photoresist layer thickness on photosensitivity (Russian) 0-73510
- developed photographic emulsion, relation between exposure and optical density and charact. curve parameters (German) 0-105742
- electrophotographic molecular recording media, photosensitivity during nanosecond exposure (Russian) 0-73516
- electrophotography, deterioration of coloured images due to illum. in diaprojector (Russian) 0-62782
- emulsions, H<sub>2</sub> hypersensitisation with Au sensitizer (Russian) 0-73511
- fogging effect of an electric field on a photographic film (Russian) 0-62783
- limiting sensitivity of photographic materials in process of direct blackening (Russian) 0-90920
- optical density, depend. on exposure for photographic action by high energy electrons, 250 to 1000 kV (Russian) 0-90923
- photographic development, nucleation and growth phenomena 0-101858
- programming of sensimetric problems on microcalculator Electronica B3-21 (Russian) 0-77901
- Ag halide crystals, effect of redox potential on photosensitivity (Russian) 0-73507
- Ag halides, latent image centres, determ. of stability and dims. (Russian) 0-90922
- Ag halides, theory of supersensitisation, review (Russian) 0-62786
- AgBr emulsion grains, adsorbed dyes, light-induced ESR spectra 0-88866
- AgBr evaporated layer response in ionisation semiconductor photographic system (German) 0-101859
- AgBr, luminescence of photographic emulsions sensitised by 1,1'-diethyl-2,2'-cyanine with Ag<sub>2</sub>S clusters (Russian) 0-73513
- AgBr, very fine grained emulsions, effect of hole and electron acceptors on photosensitivity (Russian) 0-73515
- AgBr-AgI emulsion sensitivity improved by AgCl shell crystallisation (German) 0-104453
- AlH<sub>3</sub>, synchronous photochem. processes in lattice 0-101029
- BiI<sub>3</sub> photosensitive layers, optical and thermal development (Russian) 0-73512
- KCl, additively coloured photochromic crystals, spectral sensitivity (Russian) 0-91871
- Ni(N<sub>2</sub>H<sub>4</sub>)<sub>2</sub>B<sub>2</sub>H<sub>7</sub> development, effect on photosensitivity of paper (Russian) 0-73509
- PbI<sub>2</sub> suspension, chem. sensitization 0-73492
- TiO<sub>2</sub> photographic layers, sensitivity enhancement by addition of Ag<sup>+</sup> during cuprous development (Russian) 0-62780

**photographic materials***see also photographic emulsions*

- ambiguity processing by joint Fourier transform holography 0-58468
- ascorbic acid developer, lith development mechanism 0-77889
- benzotriazole developer additives, effect on photographic development mechanism 0-77891
- colour component triads, colorimetric determ. for positive materials (Russian) 0-95178
- colour film archival storage, white light processing technique 0-99637
- colour positive developer consumption, bromine ion extraction from overflow using ion exchange resins (Russian) 0-105733
- connection between the topography of luminescence centres and the latent image (Russian) 0-62785
- daguerreotypes, plates and process obs., by electron microprobe analysis 0-68286
- o-dianzaphthoquinones, thermal decomposition of light sensitive materials (Russian) 0-73504



**photographic materials continued**

- electrographic toner, recycled in xerographic development system, cycle distrib. 0-62760  
 electrophotographic developer, size distrib., particle charge and toner-carrier force (*German*) 0-73493  
 exponential transformation using film nonlinearity for optical homomorphic filtering 0-58467  
 film, for SEM, electron beam photographic recording system 0-101903  
 film cleaning by ultrasonic liquid cavitation and acceptable solvents 0-62769  
 film grain noise in partially coherent imaging 0-101860  
 film movement nonuniformity study in film-advance channel 0-68285  
 films, 16 mm Fujicolor reversal film RT 500 and RT125 0-106585  
 films, new Gevacolor negative film type 682 0-106586  
 frequency contrast charact., effect of Ag content and Ni image intensification processing (*Russian*) 0-95183  
 frequency-contrast characteristics, determ. by interference-diffraction method (*Russian*) 0-73501  
 gelatin layers with and without  $\text{AgNO}_3$ , phosphorescence kinetics curves (*Russian*) 0-62776  
 holographic transmission charact., determ. from amplitude coeff. for hologram recording (*Russian*) 0-91760  
 homogeneous solid layer, diffusion, one-dimensional case (*German*) 0-73495  
 hydroquinone developer, lith development mechanism 0-77889  
 liquid photopolymer materials, mathematical modelling of hardening, layer thickness and exposure parameters (*Russian*) 0-62784  
 MTF automatic evaluation 0-95170  
 optical density measurement accuracy by means of optical wedge 0-73416  
 optical image phase recording using sensitised photooxidation reactions 0-87350  
 optical recording materials (*Japanese*) 0-105730  
 paper, resin-coated and polyethylene 0-86474  
 papers, polarised light refl. 0-64127  
 photoconducting film for rapid access instrumentation recording 0-62755  
 photoflash units, chemical and electronic, temporal spectral charact., meas. method 0-95171  
 photometric calibrator appl., inverse fourth power, NBS development 0-73412  
 positive film density, depend. on conc. of stabilizers and antifoggants added to developer (*German*) 0-73497  
 PVC, Cu evaporated film, electron-induced metallochromic reaction for metal image formation 0-86476  
 quality improvement, colour spots detection using laser-operated device (*German*) 0-57412  
 short time exposure, expt. technique 0-86477  
 video disc master recording, high density, replication by contact printing 0-62761  
 X-ray film/intensifying screen system, MTF and Wiener spectrum, film and screen quality effect (*German*) 0-73560  
 Ag halides, fundamental absorpt., nature and function of A-centres determ. the extra band at the long wave edge (*Russian*) 0-76060  
 Ag latent image particles, electronic effects 0-82840  
 Ag-complexes, stability increase during simultaneous photographic development and fixing (*Russian*) 0-95179  
 AgBr, connection between the topography of luminescence centres and the latent image (*Russian*) 0-62785  
 AgBr crystal produced by action of free radicals, developability 0-66838  
 AgBr layer, sensitised, topography of developed centres 0-73491  
 AgBr, photo-EMF relaxation, temp. depend. 230 to 316K (*Russian*) 0-73508  
 AgBr, photodielectric effect at low temp. (*Russian*) 0-96947  
 AgBr, photoexcited electrons and holes in latest image form., review 0-73496  
 AgCl crystal growth in gelatin soln. 0-64942  
 As<sub>2</sub>Se<sub>3</sub>-Ag photosensitive semiconductor-metal systems, effect of As<sub>2</sub>S<sub>3</sub> barrier layer (*Russian*) 0-62777  
 CdS, spectral sensitisation, role of local centres (*Russian*) 0-90924  
 MnBi, problems for holographic recording (*Russian*) 0-91761  
 $\text{Ni}(\text{NH}_3)_6^{++}$ , photographic developer, potentiodynamic polarisation curves for Ag-less development (*Russian*) 0-90921  
 $\text{NiSO}_4$ , photographic developer, potentiodynamic polarisation curves for Ag-less development (*Russian*) 0-90921  
 $\text{PbI}_2$ -Ag, photolysis, effect of  $\text{PbI}_2$  photo-EMF effect (*Russian*) 0-92939  
 Se, appl. to xerography 0-57415  
 Se, electrophotographic charact., of films rel. to viscosity of bulk specimens (*Russian*) 0-73505  
 Se-As alloys, appl. to xerography 0-57415  
 ZnS, spectral sensitisation, role of local centres (*Russian*) 0-90924

**photographic process**

- see also photochemistry  
 accuracy for chemical photographic processing of colour positive motion picture films (*Russian*) 0-93780  
 benzotriazole developer additives, effect on photographic development mechanism 0-77891  
 cinefilm copying equipment using interference light filters, additive printing appl. (*Russian*) 0-62774  
 continuous film copying equipment (*German*) 0-68281  
 contrast reversal, appl. to reversal of photographic transparencies 0-57406  
 daguerreotypes, plates and process obs., by electron microprobe analysis 0-68286  
 developed photographic emulsion, relation between exposure and optical density and charact. curve parameters (*German*) 0-105742  
 development, nucleation and growth phenomena 0-101858  
 diazo salt sensitised gelatin for holographic recording, grating form. 0-78798  
 dye chemistry for new instant film 0-81342  
 exponential transformation using film nonlinearity for optical homomorphic filtering 0-58467  
 holographic emulsion monobath and reversal processing techniques 0-102668  
 holography, white light refl., developer compositions compared 0-102669  
 Hough-Powell digitizer for processing film from bubble chamber Mirabelle in  $\text{K}^+$  expt. at 32 GeV/c 0-69040  
 image intensification processing, effect on paper freq. contrast charact., for varying Ag content (*Russian*) 0-95183  
 latent image distrib., etching and recrystn. effects of solns. 0-77890  
 lith development mechanism, developing agents 0-77889

**photographic process continued**

- luminescence rel. to latent image 0-73498  
 mass spectrometric photoplate processing, microcomputer based system 0-62787  
 monochrome photographic print exposure control cct. (*Danish*) 0-62748  
 non-Ag process based on polyvinyl spirit-transition metal halide system (*Russian*) 0-73502  
 optical density, depend. on exposure for photographic action by high energy electrons, 250 to 1000 kV (*Russian*) 0-90923  
 permeation of photographic developer into a gelatin layer, potentiometric exam. (*Russian*) 0-73500  
 photoactive pigment electrophotographic imaging system, dark charge exchange process 0-62758  
 photoconducting film for rapid access instrumentation recording 0-62755  
 positive film density, depend. on conc. of stabilizers and antifoggants added to developer (*German*) 0-73497  
 positive photoresist film exposure, formal kinetics (*German*) 0-104454  
 print timer, using ring of LEDs 0-77899  
 PVC, Cu evaporated film, electron-induced metallochromic reaction for metal image formation 0-86476  
 reversal cinefilm development, effect of temperature, concentration factors on speed of process (*Russian*) 0-105735  
 sulphide sensitisation of negative emulsions, quality composition of photosensitivity and fogging centres (*Russian*) 0-62781  
 thermostatic control device for developing bath (*Spanish*) 0-77898  
 toner deposition by cascade development with developing electrode (*German*) 0-73494  
 volume holograms, mode theory allowing for photographic process nonlinearity 0-102673  
 xerographic process, role of photoreceptors (*Japanese*) 0-82842  
 Ag halide sensitised gelatin processing, phase volume hologram form. 0-78797  
 Ag latent image particles, electronic effects 0-82840  
 Ag speck nucleation and phase formation in latent image 0-97716  
 Ag-complexes, stability increase during simultaneous photographic development and fixing (*Russian*) 0-95179  
 AgBr, connection between the topography of luminescence centres and the latent image (*Russian*) 0-62785  
 AgBr crystal produced by action of free radicals, developability 0-66838  
 AgBr dispersion in gelatin, adsorbed S and Au, transient absorpt. spectra, latent image form. and decay 0-66837  
 AgBr layer, sensitised, topography of developed centres 0-73491  
 AgBr, photoexcited electrons and holes in latest image form., review 0-73496  
 AgBr(Cl) vapour-deposited epitaxial film, surface structure 0-59814  
 AgCl, luminescence fatigue, adsorbed Ag atoms 0-66281  
 AgI, connection between the topography of luminescence centres and the latent image (*Russian*) 0-62785  
 BiI, photosensitive layers, optical and thermal development (*Russian*) 0-73512  
 $\text{Ni}(\text{N}_2\text{H}_4)_6\text{B}_2\text{H}_7$ , development, effect on photosensitivity of paper (*Russian*) 0-73509  
 $\text{Ni}(\text{NH}_3)_6^{++}$ , photographic developer, potentiodynamic polarisation curves for Ag-less development (*Russian*) 0-90921  
 $\text{NiSO}_4$ , photographic developer, potentiodynamic polarisation curves for Ag-less development (*Russian*) 0-90921  
 Se, appl. to xerography 0-57415  
 Se-As alloys, appl. to xerography 0-57415  
 $\text{TiO}_2$  photographic layers, sensitivity enhancement by addition of  $\text{Ag}^+$  during cuprous development (*Russian*) 0-62780

**photographic recording media** see *photographic materials***photographic techniques** see *photography***photography**

- see also cinematography; colour photography; electrophotography; microphotography; photographic applications; photographic lenses; photographic materials; photographic process; radiography; streak photography  
 additive photographic film printers, programmed control of light metering valves (*Russian*) 0-95174  
 astronomy, near IR photography with vacuum-cold camera 0-90341  
 camera, 35 mm compact, with fully automatic exposure control 0-90916  
 deformation measurement, out-of-plane, using holographic interferometry and speckle photography, comparative accuracy 0-78804  
 densitometer measurement transformation into spectral density distrib. and colour coordinates (*Russian*) 0-77902  
 EM, external photographic system 0-101902  
 enlarger digital timer, 0.1 second steps or 0.1 minute steps 0-77893  
 enlarger exposure meter, using photodiode and multimeter 0-101857  
 exposure meter and development timer, used for photographic enlarger 0-101856  
 exposure meter for electronic flash 0-77835  
 exposure prediction techniques, still, motion-picture photography appl. 0-66817  
 film movement nonuniformity study in film-advance channel 0-68285  
 flash light meas. instruments development (*Hungarian*) 0-57411  
 flash sequencer, using thyristor control 0-62749  
 flash unit triggered by acoustic shock wave, cct. details objections in rapid motion photography appl. 0-101862  
 flashlamp trigger circuit 0-62750  
 grainless focusing screen for light scatter reduction 0-101836  
 high speed raster cameras, image dissection and mech. scanning for photographic recording (*Russian*) 0-95182  
 illumination timer for hobby photography (*German*) 0-98992  
 images autoradiographic intensification using  $\text{Thiouracil-}^{35}\text{S}$ , quantitative anal. 0-90343  
 instant, lab. appl. 0-90915  
 integral photography method, limiting achievable parameter values of various subjects 0-101866  
 IR sky survey telescope, wide field photography 0-105167  
 laser gas breakdown, shock and ionisation waves, photographic absorpt. obs. 0-87967  
 level slicing performance using film nonlinearity (*Chinese*) 0-102628  
 light sources, guide number formulae for pulsed illumination systems (*Russian*) 0-73503  
 metal cluster growth and props., appl. to photographic processes, conf., Villeurbanne, France (Sep. '79) 0-105431  
 multicolour frames, method for checking quality 0-105728  
 phasometric method of measuring the thicknesses of transparent recording carriers and substrates (*Russian*) 0-73514



**photography continued**

- photomicrography, high resolution, zoom instrument with automatic exposure 0-62756
- photomicrography, exposure control 0-90888
- photomicrography of submicrometer birefringent contaminants in C black dispersions in polymer particles 0-62757
- pseudocolour density encoding, white-light, using contrast reversal 0-83560
- recording of fast processes, extension of meas. parameter ranges 0-57413
- SEM, photographic recording system 0-101903
- slave triggers for photographic flash 0-95168
- sound triggered flash cct., using variable time delay 0-57414
- speckle, double-exposure, analysis using electro-optical readout system 0-62708
- speckle photography, double exposure, anal. technique 0-62718
- stereo image digitiser for automatic feature extraction 0-106614
- stereoscope for viewing aerial photographs, interpretoskop optics, modifications 0-105081
- system for recording the activation times of pulsed light sources 0-73488
- temperature control using electronic thermostat, with 0.1°C accuracy and economical operation 0-77774
- thermography of fast processes, appl. to photographic recording of combustion processes (*Russian*) 0-62779
- timer, touch controlled, photography appls. (*Spanish*) 0-86478
- triggered light pulse generator for recording fast processes 0-105727
- Ag<sup>+</sup> ion automatic sensor-analyser for photographic fixing bath regeneration systems (*Russian*) 0-95172

**photoionisation**

- absolute cross-sections, exptl. meas. techniques 0-63598
- acetaldehyde, lowest Rydberg state, multiphoton ionisation spectra 0-83435
- acetaldehyde, multiphoton ionisation mass spectra 0-83436
- acetic acid vapours, clustering, effect of supersonic mol. beam sampling, mass spectrometric study 0-104481
- acetylene, photoionisation cross section at distance from threshold, chemical bond influence 0-69196
- alkali atoms, excited state, laser photoionisation theory, hyperfine coupling effect 0-102493
- alkali metal atom, near-resonant two-photon ionis., non-Coulomb phase shifts of photoelectron partial waves 0-106302
- alkali metal atoms, spin-polarised, near-reson. two-photon ionis., light polarisation effects 0-106308
- anthracene ion in liqs., photoelectron emission and photocond. 0-75600
- atom, multiphoton ionisation, effects of self-induced reson. 0-91519
- atom, two step reson. photoionisation, multimode and level degeneracy effects 0-78583
- atom+atom, two photon ionisation, radiative collision effect 0-106388
- atom ionisation, polarisation of photoelectrons, review 0-78584
- atomic, photoionisation, fluoresc. radiation polarisation 0-87076
- atomic and molecular processes, developments in ab initio methods 0-63550
- atomic photoionisation, selective, use in laser isotope separation and spectrosc., review 0-83332
- atomic photoionisation anal. using relativistic random phase approximation and multichannel quantum defect theory 0-63602
- atoms, multiphoton ionisation, reson. effects, light coherence effects 0-58232
- atoms, multiphoton ionisation dynamics 0-91517
- atoms, near threshold struct. in K-shell spectra, photoionisation or fast charged particle ionisation 0-87064
- atoms, polarisation of electrons and nuclei in resonant multiphoton ionisation 0-99486
- atoms, power broadened two-photon ionisation, reson. lineshape and photoelectron spectra 0-58229
- azulene, multiphoton ionisation, mass spectra 0-63717
- benzaldehyde molecules, photoionisation mass-spectrometry with excimer KrF laser 0-95691
- benzene, multiphoton ionisation fragmentation patterns, statistical theory 0-95693
- benzene, multiphoton ionisation mass spectra 0-57420
- benzene, S<sub>0</sub>-S<sub>1</sub> transitions, two-photon absorpt. spectra by nozzle beam-multiphoton ionisation method 0-63728
- benzene, visible and UV photoionisation and fragmentation 0-69195
- benzene molecules, photoionisation mass-spectrometry with excimer KrF laser 0-95691
- benzophenone, laser spectroscopy by cascade photoionisation method in mass spectrometer 0-99496
- bromobenzene ion fragmentation, photoelectron-photoion coincidence spectra 0-95682
- butene, isomers, ion-mol. reactions, photoionisation mass spectra 0-81298
- 2-butene ion, fragmentation, angular momentum in ion-mol. reacts., RRKM calc. 0-66773
- chlorobenzene, S<sub>0</sub>-S<sub>1</sub> transitions, two-photon absorpt. spectra by nozzle beam-multiphoton ionisation method 0-63728
- 1-chloropropylene cation, internal energy decay studied by photoelectron-photoion coincidence spectroscopy 0-69185
- closed shell atoms, photoelectron ang. distrib. and spin polarisation, theory 0-91618
- computer controlled photoionisation mass spectrometer 0-77905
- cosmic dust, photoelectric yield of insulating dust grains 0-90507
- detector, gas chromatograph, appl. 0-71963
- dye proflavine bound to synthetic polynucleotides, selective laser photodamage 0-99525
- electronic and at. collisions, conf., Kyoto, Japan (Aug.-Sept. 1979) 0-57011
- electronic and at. collisions, conference, Kyoto, Japan (Aug.-Sept. 1979) 0-62394
- ethane, photoionisation cross section at distance from threshold, chemical bond influence 0-69196
- ethane, photoionisation spectra, cond. hole model 0-58326
- ethanol, H-bonding investigated with supersonic mol. beam using photoionisation quadrupole mass spectrometer 0-102543
- ethylene, photoionisation cross section at distance from threshold, chemical bond influence 0-69196
- excimer laser characts. 0-102712
- ferrocene, multiphoton dissociation and ionisation by tuneable dye lasers 0-99524
- ferrocene, multiphoton ionis. spectra, at. Fe transitions 0-106361
- fluorobenzene, multiphoton ionisation spectrum in one-photon wavelength region 0-63727

**photoionisation continued**

- fluorobenzene, S<sub>0</sub>-S<sub>1</sub> transitions, two-photon absorpt. spectra by nozzle beam-multiphoton ionisation method 0-63728
- formic acid ions, fragmentation, energy selected, photoelectron-photoion spectra 0-95676
- furan, resonantly enhanced multiphoton ionisation 0-106362
- gas mixture, self sustained volume photoionisation discharge existence conditions 0-79610
- 1,3,5-hexatriene radical cation, in Ne matrix, laser induced fluoresc. and emission spectra 0-87163
- high energy electron spectroscopy techniques 0-62740
- hydrocarbons, aromatic, ultrasensitive detection by two-photon photoionisation 0-104473
- inert gas, atomic photoionisation, Dirac-Fock calcs., branching ratios and angular distrib. in p shells 0-63601
- inert gas mixture, electrophotoionization discharge, laser pumping 0-91781
- inert gases, self-sustained discharge possibility with bulk photoionisation impurities 0-75113
- ionospheres, ionic reactions in lab. and planetary atmospheres 0-59168
- laser-induced selective multiphoton processes: impact on nuclear physics, chemistry and biology 0-61122
- metastable atomic or molecular species, multiphoton transition detection 0-58231
- methanol, processes of photoionisation studied using ion-electron coincidence method 0-74204
- methanol (-d), H-bonding investigated with supersonic mol. beam using photoionisation quadrupole mass spectrometer 0-102543
- methyl ethyl ketone, processes of photoionisation studied using ion-electron coincidence method 0-74204
- N-methyl pyrrole, resonantly enhanced multiphoton ionisation 0-106362
- methylbenzenes, 3p Rydberg transitions, multiphoton ionis. spectrosc. obs. 0-95644
- molecular electron scatt. and photoionisation shape-resonance enhanced nuclear motion effects 0-63603
- molecule, cross section by complex basis function calcs. of solvent matrix elements 0-78662
- multiphoton absorption above ionisation threshold 0-58224
- multiple, infrared laser 0-69194
- Na, fluoresc. study, reson. radiation illum. 0-83314
- naphthalene, multiphoton ionisation, mass spectra 0-63717
- NGC 7662, planetary nebula, photoionisation model with charge transfer reactions rel. to emission-line spectrum 0-62233
- nickelocene, multiphoton dissociation and ionisation by tuneable dye lasers 0-99524
- nonresonant multiphoton atomic ionisation in stochastic EM field (*Russian*) 0-99490
- organic molecules, multiphoton ionisation mass spectra by ArF excimer laser 0-81381
- organic solids, photoemission and photoionisation in three stage model 0-100744
- organic vapours, air pollution detection by variable selectivity photoionisation analyser 0-81511
- phenol, aq. soln., electron ejection, picosec. obs. 0-87187
- phenolate, aq. soln., electron ejection, picosec. obs. 0-87187
- photoelectron ang. distrib. and spin polarisation, theory 0-91618
- planetary nebulae, photoionisation models for He I 584 Å transfer problem 0-67550
- planetary nebulae, photoionisation models for permitted lines excitation 0-109527
- planetary nebulae of galactic halo, photoionisation models and chemical abundances of K 648, 49+88.1° and (108-76.1°) 0-109507
- polyatomic molecules, photoionisation cross section and efficiency, double ion chamber meas. 0-91613
- polyatomic molecules, visible and UV photoionisation and fragmentation 0-69195
- propynyl cation+propyne, reactant structure effects 0-89469
- pyrene, mol. ionisation pot., two photon ionisation, micellar interface effects on ionisation threshold 0-91609
- pyrene in n-heptane solution, laser two-photon ionisation spectroscopy, photoionisation threshold determ. 0-78668
- pyrrole, resonantly enhanced multiphoton ionisation 0-106362
- QSO emission-line region clouds, photoionisation model for absorpt. spectrum 0-62308
- quasar clouds, photoionisation models for He I 584 Å transfer problem 0-67550
- quasars photoionised clouds model, Mg II and Fe II lines excitation 0-67896
- resonant ionisation spectroscopy, chem.-physics appls. 0-68259
- resonant multiphoton ionisation, pulse area effects 0-91514
- resonant phenomena, complex stabilisation method 0-78515
- rotated-coordinate method, rel. to stabilisation method 0-74097
- semiconductors, deep level impurity photoionisation cross-section 0-65485
- semiconductors, impurity photoionisation, quantum-defect, billiard-ball model comparison 0-65486
- Seyfert galaxies photoionised clouds model, Mg II and Fe II lines excitation 0-67896
- surface layers, photon induced ion desorption, surface atom core ionisation, Auger decay 0-59809
- synchrotron radiation techniques for studying atomic physics 0-63583
- threshold photoion-photoelectron coincidences method for ion state selection 0-63718
- triethylamine, for imaging Cherenkov detector using gas-filled MWPC 0-91400
- trifluoroethanol, H-bonding investigated with supersonic mol. beam using photoionisation quadrupole mass spectrometer 0-102543
- tryptophan, aqueous, one and two photon ionisation by Na laser harmonics 0-69193
- unimolecular decomposition, photon catalysed, first-order rate constant 0-99528
- XPS, quantitative, rel. to subshell photoionis. cross-sections and electron mean free path 0-81389
- zinc octaethyl porphyrin, soln., photochem. ionogenesis 0-61116
- acetaldehyde, multiphoton ionisation meas., two-photon polarisation ratio of n-3s transition 0-91610
- Ag, photoionisation, photoelectron spectra 0-87086
- Ag, photoionisation cross sections, electron-impact inverse mean free paths, and stopping powers for each subshell 0-69113
- Ag, polarised photoelectron yields in VUV region 0-106307
- Ar, 2p<sup>2</sup> shell, oscillator strength, photoionisation cross sections, electron shell alterations determ. (*Russian*) 0-58144



## photoionisation continued

- Ar, optical gas breakdown, reduced threshold in two-freq. field 0-64819  
 Ar, outer  $p_{1/2}$  subshell photoionisation, polarised electrons, relativistic RPA calcs. 0-83331  
 Au subshell photoelectron branching ratio meas. using synchrotron radiation 0-66397  
 Ba,  $4d^{10}$  shell, photoionisation cross sections, electron shell alterations determ. (*Russian*) 0-58144  
 Ba atom, laser excited, ionisation studies 0-83330  
 Ba, double ionisation, 20-25 eV photoionisation cross sections 0-83328  
 C I photoionisation by sunlight, C II line excitation 0-58223  
 CO, photoelectric cross section and angular distribution calcs. 0-58323  
 CO, photoelectron ang. distributions, wavelength and vibr. state depend., reson. effects, asymmetry parameters 0-91602  
 CO,  $X^2\Sigma^+$ , vibr. levels, UPS electron attachment obs. 0-95683  
 CO $^+$ +D $_2$ , state selected reaction cross-sections, coincidence technique obs. 0-66797  
 CO $_2$  laser, atmospheric pulsed photoionisation, active medium optical homogeneity 0-58508  
 CO $_2$  laser gas mixture, vol. photo-preionisation by VUV radiation 0-87966  
 CO $_2$  laser gas mixture seeded with tripropylamine, photoionisation meas. 0-78829  
 CO $_2$ , photoionisation, nuclear motion effects 0-58324  
 CO $_2$  TEA laser, UV preionisation, parametric studies 0-64040  
 CS $_2$ +CS $_2$ -CS $_2^+$ +CS+e $^-$ , chemionisation, mol. beam photoionisation 0-76495  
 Ca atom, laser excited, ionisation studies 0-83330  
 CaO, photoionisation of F-centre, luminesc. and photocond. meas. 0-66270  
 Cl, photoionisation cross section and reson. theory, many body perturbation theory, 3p and 3s subshells 0-69114  
 Cr, multiphoton ionisation and absorpt. 0-95575  
 Cs, 2-photon and 4-photon ionisation cross-sections, absolute determ. 0-83326  
 Cs,  $4d^{10}$  shell, photoionisation cross sections, electron shell alterations determ. (*Russian*) 0-58144  
 Cs, 6s-electron photoionisation, ab initio calcs. 0-91523  
 Cs, excited state, laser photoionisation theory, hyperfine coupling effect 0-102493  
 Cs, photoionisation cross sections determ. in vacuum UV using Xe excimer laser 0-102494  
 Cs, two photon ionisation, destructive interference effect 0-74153  
 Cs two-photon ionisation, effective order nonlinearity var. 0-106304  
 Cs $^+$  ion source, CW monoenergetic, by photoionisation 0-63910  
 Cs-Sr(He) mixtures, photocond. at atm. press. 0-87844  
 Cs $_2$ ,  $\tilde{a}^1A_g$ -state detect. by reson. enhanced multiphoton ionis. spectrosc. 0-95551  
 $^{151}\text{Eu}$  ( $^{153}\text{Eu}$ ) excitation transfer, effect on selective photoionisation 0-99538  
 Fe, inner-shell vacancies, cascade decay, multiple ionisation and X-ray emission calcs. 0-87072  
 Fe(CO) $_5$ , multiphoton ionis. spectra, at Fe transitions 0-106361  
 GaAs, photoionisation of impurities with deep levels 0-65484  
 GaAs-Cr, photoionisation transition Cr $^{3+}$ -Cr $^{2+}$ , EPR studies 0-60638  
 H like atoms, multiphoton ionisation Pade-Sturmian approach 0-87089  
 H like atoms, photoionisation in homogeneous elec. field (*Russian*) 0-106309  
 H, three-photon reson. photoionis. in plasma 0-58640  
 H, two photon ionisation in presence of one photon ionisation, cross section calc. 0-83327  
 H $^-$ , two-electron photodetachment threshold, blackbody radiation effects 0-91524  
 H $_2^+$ +H $_2$ , state selected reaction cross sections, coincidence technique obs. 0-66797  
 He, 2S metastable states, singlet and triplet; two and three photon ionisation cross section, absolute determ. 0-83329  
 He, laser-induced breakdown 0-96339  
 He, metastable, multiphoton transition detection,  $n^3S$ - $n^3D$  splitting meas. 0-58231  
 He metastable state, two- and three-photon ionisation 0-91518  
 He, photoionis. cross-section, hyperspherical coord. method calcs. 0-102496  
 He, photoionisation above  $n=2$  photoionis. threshold 0-102497  
 He, photoionisation cross sections up to  $n=2$  excited state, evidence of autoionisation 0-91520  
 He+NO, multiphoton ionisation spectra in supersonic expansion, laser enhanced collisional effects 0-83459  
 He(I), XPS relative intensity and photoionisation cross-section 0-63599  
 He(II), 0-63599  
 $\alpha$ -HgS, gas-phase and solid-state Hg 5d photoionisation processes, direct comparison 0-76149  
 K $_2$ , supersonic mol. beam, isotope selective two-step photoionisation study 0-74203  
 Kr, 6p levels, two-photon excitation, time resolved fluoresc., quenching, lifetimes and photoionisation cross section 0-78587  
 Kr, outer  $p_{1/2}$  subshell photoionisation, polarised electrons, relativistic RPA calcs. 0-83331  
 Li, two photon ionisation in presence of one photon ionisation, cross section calc. 0-83327  
 N $_2^+$ , partial photoionisation cross section and photoelectron angular distribution for  $X^2\Sigma_g^+$  state determ. 0-83429  
 NH $_3$ , expansion cooled, mol. photoionisation, rot. struct., rot. predissoc. of excited states 0-91611  
 NO, selectively excited rovibrational states, multiphoton ionisation spectra 0-69202  
 NO $_2$ , laser spectroscopy by cascade photoionisation method in mass spectrometer 0-99496  
 N $_2O^+$ , dissoci., threshold photoelectron-photoion coincidence obs. 0-87189  
 Na arc lamp, light-induced ignition method 0-77599  
 Na, excited 4D and 5S state, absolute photoionisation cross-section 0-99488  
 Ni, M $_{II,III}$  spectrum, ab initio calculation 0-83276  
 $^{23}\text{Np}$  electron transition excitation following K-shell photoionisation, deexcitation  $\gamma$ -rays 0-78196  
 O IV bound states, oscillator strengths and photoionisation cross sections 0-106293  
 O $_2$ , photoionisation cross section and asymmetry parameters calc. in UV region using static pot. 0-95692  
 Pb, photoelectron spectra, electron correlations and spin-orbit interaction influence 0-102495

## photoionisation continued

- Pb subshell photoelectron branching ratio meas., using synchrotron radiation 0-66397  
 photoionisation cross section and asymmetry parameters calc. in UV region using static pot. 0-95692  
 Pt subshell photoelectron branching ratio meas. using synchrotron radiation 0-66397  
 SiO $_2$  layers on Si, ionis. thresholds of electron traps 0-92983  
 Sr-Cs mixture, laser induced collisional two-photon ionisation, fluoresc. monitoring 0-91515  
 Tl, ionisation limit and oscill. strength in VUV absorpt. spectra 0-74152  
 Xe,  $4d^{10}$  and  $3d^{10}$  shell, photoionisation cross sections, electron shell alterations determ. (*Russian*) 0-58144  
 Xe, outer  $p_{1/2}$  subshell photoionisation, polarised electrons, relativistic RPA calcs. 0-83331  
 Xe photoionisation, spin-polarised photoelectrons angular distrib. 0-106306  
 Xe, recently enhanced multiphoton ionisation and third harmonic generation 0-91526  
 Xe subshell photoionisation, multichannel k-matrix calc., spin orbit interactions 0-63600  
 Y, XPS relative intensity and photoionisation cross-section 0-63599  
 Yb I, high Rydberg levels of  $4f^{14}$   $gsnd$  configs., very high resolution obs. 0-106300  
 Zr, XPS relative intensity and photoionisation cross-section 0-63599

## photolithography

- see also masks; photoresists  
 conference on electron, ion and proton beam technology, conf., Boston, MA, USA (29 May-1 June, 1979) 0-67927  
 integrated optics, functional components, fabrication of microstructs. in micrometre/submicrometre range, microlithographic techniques (*German*) 0-106637  
 Josephson junctions fabrication, tunnelling through edge-grown barriers 0-100567  
 spatial period division, submicrometre linewidth grating prod. 0-69556  
 thin-film waveguide, on Si substrated, optical power losses calc. and obs. 0-106640  
 UV irradiated electroless selective plating, improvement 0-84848  
 wafer exposure camera, optical, step-and-repeat, with dark field automatic alignment 0-68283  
 waterless planographic plate development 0-105729  
 X-ray, fabrication of submicrometre period gratings with precisely defined profiles for integrated optics applications 0-58814  
 X-ray lithography using synchrotron radiation, resist sensitivity 0-62820  
 X-ray microfabrication for guided-wave optical devices 0-58812  
 x-ray zone plates fabricated using electron-beam and X-ray lithography 0-68335  
 GaAs wafer, double-etching technique for submicron channel fabrication, laser fabrication appl. 0-74387  
 Si chip manufacture for fibre alignment in lightguide cable connectors 0-64188  
 Si, optical waveguides along both sides of groove 0-96006

## photoluminescence

- see also fluorescence; phosphorescence  
 alkali cyanides, mol. excitons, X-ray excited emission spectra obs. 0-66287  
 alkali halide crystals, activated, physical phenomena and optical data processing appl. (*Russian*) 0-80819  
 anthracene, cryst., polariton luminesc. 0-84775  
 antibunching phenomena on single-scatterer fluorescence in weak-field limit 0-63580  
 1,2-benzanthracene, secondary reson. radiation and hot energy transfer, soln. luminesc. 0-87167  
 calcite, luminescence spectral anal. of polycyclic aromatic hydrocarbon impurities 0-71483  
 CdS, green edge luminescence spectrum, temp. depend. 0-108274  
 chalcogenide glasses, Luminescence, temp. depend. rel. to nonradiative transitions 0-71485  
 chalcogenide glasses, optical versus transport processes. 0-84449  
 coumarin 1, multiphoton cross-section determination by means of luminescence experiments 0-93377  
 diamond, Jahn-Teller coupling at neutral vacancy 0-71453  
 dimethyl POPOP, multiphoton cross-section determination by means of luminescence experiments 0-93377  
 disordered systems, electronic energy transfer, generalized master eqn. 0-57221  
 dosimeter glass, radiophotoluminescence intensity change by intense laser light 0-89050  
 glass, electron migration and spectral relax., random-walk model 0-80280  
 glasses, non-radiative recombination at valence-alternation pairs 0-89048  
 highly anisotropic scatt. medium, luminesc. of layer 0-100685  
 III-V semiconductor epitaxial structures as wide-gap substrates, minority carrier diffusion length determ. by photoluminesc. 0-103992  
 III-V semiconductors, optical transitions, effect of perturbed k-selection and gap shrinkage 0-66257  
 III-V semiconductors, radiative recomb., optical evaluation review 0-60647  
 intermolecular energy transfer and high energy excitations, in condensed phase 0-66269  
 ionic crystal, fundamental luminescence at high ionisation levels (*Russian*) 0-103985  
 liquid, migration mechanism of approaching particles, energy transfer, luminesc. quenching study 0-100343  
 metaphosphate glass: Nd $^{3+}$ , Yb $^{3+}$ , luminesc., energy transmission and migration between Nd $^{3+}$  and Yb $^{3+}$  0-66297  
 methylcyclohexane glasses,  $\gamma$ -irradiated in presence of naphthalene, isothermal luminesc. 0-93388  
 3-methylpentane glasses,  $\gamma$ -irradiated in presence of naphthalene, isothermal luminesc. 0-93388  
 microspecimens obs., with size  $\geq 0.8$  mm, installation for 300 to 1100 mm range 0-57381  
 naphthalene, pure and doped, exciton-phonon luminesc. 0-84773  
 optical fibre, neutron and gamma induced transient absorpt. and luminesc. 0-58763  
 partially oriented molecules, uniaxial, two-photon processes, polarised spectrosc. 0-74209  
 phosphate glass: Yb $^{3+}$ , luminesc. band struct., chronoscopic study at 4.2K 0-60663  
 photographic emulsion, luminescence rel. to latent image 0-73498



**photoluminescence continued**

- poly-N-vinyl carbazole, pulsed laser excitation, time resolved fluoresc., 0-89041
- polymer chains with rigid bonds, local relax. times, mol. dynamics study (*Russian*) 0-59373
- polymethine dye solutions, photochem. transformations and short-wavelength luminesc. 0-100686
- polynuclear aromatic hydrocarbons, analysis by X-ray excited optical luminescence technique 0-66891
- porous Vycor glass, quenching by  $O_2$  and  $NH_3$ , photoluminescence obs. 0-93773
- pyrene, luminescence of free and self-trapped excitons 0-108250
- quartz, luminescence centres at 396 and 280 nm 0-103996
- rare earth double orthophosphates with alkali metals, conc. depend. of luminesc. props. 0-100673
- rare earth double orthophosphates with alkali metals, spectroscopic obs., struct. and chem. nature 0-100674
- rare earth germanates,  $R_2O_3 \cdot GeO_2$  system cpds., physicochem. characts. 0-97469
- recombination kinetics, subject to allowance for correl. between particles 0-80858
- resonant optical excitation, luminesc. rel. to light scattering (*Japanese*) 0-84781
- rhodamine 6 Z solution, radiant transport effect on luminesc. duration 0-103995
- rhodamine 6G, molecules in solution, photoluminescence study, fluorescence decay time 0-80832
- rhodamine G solutions, LiCl and  $NaClO_4$  electrolyte influence on its lasing props. 0-91788
- sapphire, neutron bombard., F-centre fluorescence, photoluminescence 0-100676
- semiconductor, biexcitons, one-photon radiative recomb. 0-70621
- semiconductor epitaxial layers, varizational, parameter determ. by photoluminescence method (*Russian*) 0-108291
- semiconductors, amorphous, luminescence 0-80862
- semiconductors, exciton and domain luminesc., book 0-82588
- semiconductors, intervalley electron-electron scattering effect on optical transitions 0-108267
- semiconductors, quasi-equilib. approx. 0-84779
- semiconductors, radiative recomb., book contrib. 0-84784
- solutions, photoluminesc. decay time, donor conc. effect 0-66299
- steel, trace element UV emission, spectrochem. anal. (*French*) 0-71997
- trialkylammonium, iodides, absorpt. and luminesc. spectra of self-localized excitons 0-97340
- ultrahigh vacuum setup for photo- and thermostimulated electron emission and luminesc. obs. (*Russian*) 0-66383
- uniaxially compressed crystal, exciton molecule radiation (*Russian*) 0-108264
- Ag halide, visible luminescence obs. at or below 77K 0-108263
- Ag halide emulsions, primitive and  $AgNO_3$ -digested, IR luminescence obs. at 77K 0-103983
- AgBr, luminescence of photographic emulsions sensitised by 1,1'-diethyl-2,2'-cyanine with  $Ag_2S$  clusters (*Russian*) 0-73513
- AgBr microcrystals, spectrally sensitised, luminesc., effect of hydrophobic organic compounds 0-97331
- AgBr, photoluminesc. study of excitons in high mag. fields 0-80843
- $AgGaSe_2$ , two-photon absorpt. and short pulse stimulated recombination 0-89054
- Ag,HgI<sub>4</sub>, preparation, optical and luminescence spectra 0-104064
- $AgNO_3$ , soln., visible luminescence obs. at or below 77K 0-108263
- $AgNO_3$ - $Ag_2S$  system, visible luminescence obs. at or below 77K 0-108263
- $Ag_2O$ , exciton luminesc. spectra, mag. field influence 0-80860
- Ag<sub>2</sub>S sols, red-IR photoluminescence obs. at 77K 0-103982
- AlGaAs heterojunctions, nonradiative recomb. vel. estimate from edge luminesc. props. 0-65668
- n-Al<sub>1-x</sub>Ga<sub>x</sub>As, ion implanted films, optical and luminesc. props. 0-60699
- Al<sub>1-x</sub>Ga<sub>x</sub>As, p-n junction solar cells, effect of interface recombination on photoluminescence and current 0-93893
- Al<sub>1-x</sub>Ga<sub>x</sub>As, pure and Ge doped, shallow acceptor photoluminescence 0-76064
- Al<sub>1-x</sub>Ga<sub>x</sub>As:Cu, variable-gap semicond., impurity props., carrier recomb. 0-96907
- Al<sub>1-x</sub>Ga<sub>x</sub>As-GaAs quantum-well heterostruct., exciton in recomb. 0-103990
- Al<sub>1-x</sub>Ga<sub>x</sub>Sb, soln.-grown, photolum. 0-71476
- AlN, luminesc. excitation spectrum and band struct. 0-84783
- $\alpha-Al_2O_3$ , polarised luminescence in neutron- and proton-irradiated single crystals 0-66271
- $\alpha-Al_2O_3$ , recombination luminescence mechanism 0-71477
- Al<sub>2</sub>(WO<sub>4</sub>)<sub>3</sub>:Cr(Eu), and undoped crystals, luminesc. obs. 0-89047
- Ar:N<sub>2</sub>O, O(<sup>1</sup>S) photodissociative prod., photoluminesc. excitation spectra, exciton energy transfer 0-89508
- Ar:OCS, O(<sup>1</sup>S) and S(<sup>1</sup>S) photodissociative prod., photoluminesc. excitation spectra, exciton energy transfer 0-89508
- As chalcogenides, deep levels, photoluminesc. and photocond. 0-70641
- As<sub>2</sub>S<sub>3</sub>, amorphous, time resolved luminesc. 0-66288
- a-As<sub>2</sub>S<sub>3</sub>, time-resolved photoluminescence study 0-89057
- As<sub>2</sub>Se<sub>3</sub>, amorphous radiative interband recombination 0-66286
- As<sub>2</sub>Se<sub>3</sub> and As<sub>2</sub>Se<sub>3</sub> semicond. glasses, densified, photoluminesc., inelastic deform. effect 0-66293
- BaCl<sub>2</sub>:Pb crystal phosphor, emission spectra 0-66298
- BaCd<sub>2</sub>Si<sub>2</sub>O<sub>7</sub>, cell const., luminesc. of various rare-earth activators 0-93376
- Ba<sub>2</sub>SiO<sub>4</sub>Br<sub>2</sub>:Eu, blue emitting X-ray luminescent material for intensifying screens (*French*) 0-66260
- BaTiO<sub>3</sub>, intrinsic luminesc. 0-71467
- BaY<sub>2</sub>Si<sub>2</sub>O<sub>7</sub>, cell const., luminesc. of various rare-earth activators 0-93376
- BeF<sub>2</sub>:Eu<sup>3+</sup> glass, luminesc. of Eu<sup>3+</sup>, transition probabilities 0-80845
- Bi<sub>1-x</sub>GeO<sub>3</sub>:Dy(Ho)(Er), luminesc., emission and excitation spectra 0-103975
- CaF<sub>2</sub>:Dy, TLD-200, thermolum. phosphor, photolum. and absorpt. spectra, thermolum. mechanisms 0-97321
- CaF<sub>2</sub>:Eu<sup>2+</sup>, photoluminesc. mag. circ. polaris. 0-89056
- CaF<sub>2</sub>:Mn, low temp. X-irrad., Mn centres, optical absorpt. and emission props. 0-60635
- CaS:Ce, Na phosphor, photoluminescence and excitation spectra 0-89049
- CaS:Cu, colour centres, optical and thermal depths determ. 0-66275
- CaS:Pd phosphors, trap and luminescent centre location, photo-, thermo- and electroluminescence studies 0-71482

**photoluminescence continued**

- CaSO<sub>4</sub>:Dy(Tm), thermolum. thermolum. phosphor, photolum. and absorpt. spectra, thermolum. mechanisms 0-97321
- CdIn<sub>2</sub>S<sub>4</sub> single crystals, recombination process and localised levels 0-93383
- Cd<sub>1-x</sub>Mn<sub>x</sub>Te, exchange induced ionization of bound excitons, luminesc. meas. 0-97328
- Cd<sub>2</sub>Nb<sub>2</sub>O<sub>7</sub>, photolum. and carrier drift mobility at ferroelec. transition 0-71469
- CdS crystals, electron-hole plasma, carrier optical orientation 0-100689
- CdS crystals, radiative recombination, high excitation rates 0-108269
- CdS, electron and hole trapped centres, EPR, photoluminescence, photoconductivity study 0-108071
- CdS epitaxial layers on sapphire, exciton struct. of absorpt., photoluminesc. and photocond. spectra 0-89027
- CdS, multiphoton cross-section determination by means of luminescence experiments 0-93377
- CdS, spectroscopic study of local centre interaction, change with external illumination 0-80323
- CdS thin films, growth and evaluation for fabrication of high performance photovoltaic solar cells 0-93501
- CdS:Cu, photocurrent, elec. field effect on recombination processes (*Russian*) 0-100484
- CdS:In(Cl) concentration quenching mechanism of luminescence 0-97336
- CdS:Li, complex luminescence centres, recombination-stimulated conversion 0-108268
- CdS:Li, luminescence bands, photocurrent spectra (*Russian*) 0-60677
- CdS:Li, pure and doped, green edge luminesc., complex nature of centres 0-60671
- CdS:Li(Cu), pure and doped, electrodiffusion of shallow donors, photocurrent, TSC, and exciton luminesc. meas. 0-79992
- CdS:Na, Hagemark theory, green edge emission line intensity 0-75517
- CdS:Te-based photoelectrochem. cell, luminesc., thermal manipulation of deactivation processes 0-81479
- CdSi<sub>1-x</sub>Se<sub>x</sub>, chem. comp. and luminescence obs. 0-80869
- CdSi<sub>1-x</sub>Se<sub>x</sub>, mixed crystals, deformation effects on free excitons 0-76073
- CdSe, recombination mechanism at dislocations, photoluminescence 0-103993
- CdSe, single crystals, luminesc. of electron-hole plasma 0-60675
- CdTe crystals, exciton luminescence spectra rel. to shallow impurity conc. 0-97335
- p-CdTe, nondoped, heat treatment in vacuum, dissoc. obs. effects on struct. and props. (*Japanese*) 0-60662
- p-CdTe, photocond., photoluminesc., spectral studies 0-88593
- CdTe, recombination radiation due to high-density excitons 0-93392
- CdTe:Li(Cl), acceptor states study by donor acceptor pair excitation luminesc. 0-100683
- CdTe:Mn<sup>2+</sup>, luminesc. and magneto-optic reson., mag. field effect 0-93390
- CdTe(Se):Co, impurity luminescence no phonon line depend. on temp., Debye temp. 0-66273
- CdZnS thin films, growth and evaluation for fabrication of high performance photovoltaic solar cells 0-93501
- Cd<sub>1-x</sub>Zn<sub>x</sub>S heteroepitaxial single-cryst. layers, photoluminesc. props. 0-100692
- CsBr:Cu<sup>+</sup>, excitation and absorpt. spectra 0-108255
- CsCl, luminesc. in vac. UV range above and below phase transition temp. 0-93399
- CsI:Na<sup>+</sup>(K<sup>+</sup>), luminesc. processes 0-103989
- Cs<sub>2</sub>MX<sub>6</sub>(M=Se, Te, X=Cl, Br),  $\Gamma_4$ (<sup>2</sup>T<sub>1g</sub>) state, Jahn-Teller effect, luminesc. obs. 0-60650
- CsMnF<sub>3</sub>, exciton migration, excitation and luminesc. study (*Russian*) 0-66264
- Cs<sub>2</sub>NaYCl<sub>6</sub>:Bi<sup>3+</sup>, luminescence props., emission and excitation spectra 0-108262
- $\alpha$ -CsNd<sub>2</sub>(PO<sub>4</sub>)<sub>3</sub>, single cryst. struct. and spectral luminescent props. 0-96490
- CsPbCl<sub>3</sub>, electronic struct. and optical props. in fundamental absorpt. region 0-93367
- CuI, single crystals, growth and optical props. 0-93470
- Cu<sub>2</sub>O, exciton luminesc. spectra, mag. field influence 0-80860
- Eu double metaphosphates with alkali metals or H, luminesc. props. 0-100675
- Eu<sup>2+</sup> impurities in cubic crystals, 5d-4f radiative transition probability calc. 0-71474
- Eu<sub>1-x</sub>La<sub>x</sub>Ta<sub>2</sub>O<sub>10</sub>, polycryst., luminesc. and excitation spectra 0-60659
- EuNa<sub>2</sub>Mg<sub>2</sub>(VO<sub>4</sub>)<sub>3</sub>, disordered, thermal quenching of luminesc. 0-71472
- EuP<sub>2</sub>O<sub>14</sub>, luminesc. of Eu<sup>3+</sup>, transition probabilities 0-80845
- Eu<sub>2</sub>Sr<sub>1-x</sub>S, magneto-optical redshift in absorpt. and photoluminesc., mag. short-range order 0-71388
- n-GaAs epitaxial film, radiative recomb. under influence of mech. stresses 0-66291
- (GaAl)As DH laser wafer, photoluminesc. improvement with buffer layer 0-64014
- GaAlAs, luminescence circular polarisation, electron optical orientation resonant variation (*Russian*) 0-84782
- Ga<sub>1-x</sub>Al<sub>x</sub>As, epitaxial, radiative deep states 0-76061
- Ga<sub>1-x</sub>Al<sub>x</sub>N heteroepitaxial films, photoluminesc., cathodoluminesc. 0-66292
- Ga(As,P):N, isoelectronic impurity states, long-range, short-range model 0-75524
- GaAs, electron gas coding influence in ion-bombarded layers 0-108272
- GaAs, electron-spin relaxation and recomb. kinetics, time-resolved luminesc. study 0-108074
- GaAs, excited luminescence, influence of IR illumination 0-76072
- GaAs, exciton effects in photocond., photoluminesc. 0-96797
- GaAs,  $\gamma$ - and electron irradiation, influence on recomb. characts. near surface 0-71478
- GaAs, hot photoluminescence spectrum on pumping across the L-valley (*Russian*) 0-103984
- n-GaAs, ion implanted films, optical and luminesc. props. 0-60699
- GaAs, luminescence emitted from deep centres, plastic deform. effect on internal quantum efficiency 0-60672
- p-GaAs, MBE grown, As<sub>2</sub> and As<sub>4</sub> effects on photolum. 0-103974
- GaAs, spin-dependent recomb., photoluminesc. obs. 0-60666
- GaAs:Cr, 0.84 eV no-phonon luminesc., fine struct. and origin 0-103980
- GaAs:Cr, photoluminescence, YAG laser or krypton laser 0-60668
- GaAs:Cr, photoluminescence in strong electric fields 0-108270
- GaAs:Cr, semi-insulating, Zeeman studies of 0.839 eV emission 0-103987



## photoluminescence continued

- GaAs:Cr semi-insulating wafer, heat treatment technique for no thermal conversion 0-100857  
 n-GaAs:Ge, film, substrate temp. depend. of Ge incorporation during MBE 0-76196  
 GaAs:O, electrolum., photolum., negative differential resist. rel. to recomb. processes 0-66304  
 GaAs:Si, accelerated growth rate effect on MBE, Hall mobility and photolum. meas. 0-104067  
 GaAs:Si, influence of stoichiometry on recomb. processes 0-93396  
 GaAs:V, ion implanted, luminesc., level splitting 0-97338  
 GaAs:W<sup>2+</sup>, radiative transitions, photoluminesc. obs. 0-108271  
 GaAs-GaAlAs DH lasers, strain-enhanced luminesc. degradation, photoluminesc. obs. 0-69392  
 GaAs-GaP heterostructure, radiative recomb. under influence of mech. stresses 0-66291  
 GaAs<sub>1-x</sub>P<sub>x</sub>, indirect-gap, evidence for exciton localization by alloy fluctuations, photolum. 0-66276  
 GaAs<sub>1-x</sub>P<sub>x</sub>N, photolum. and electrolum. study of N isoelectronic traps 0-89061  
 GaAs<sub>1-x</sub>P<sub>x</sub>(Te), bound exciton stress depend., piezoluminescence, photoluminescence 0-80206  
 GaAs<sub>1-x</sub>Sb<sub>x</sub>, (x≤0.05), band gap, temp. depend., from edge photolum. meas. 0-71486  
 GaInAs-InP, growth by low-pressure metalorganic CVD 0-71595  
 GaN, photoluminesc. spectra, energy distrib. 0-97339  
 GaN:Zn, n-i struct., anomalous luminesc. 0-80865  
 n-GaP, ion implanted films, optical and luminesc. props. 0-60699  
 GaP:Bi,N, photoluminesc., electroluminesc., 4.2 to 300K, excitons and hole traps 0-108275  
 GaP-Ce(Dy)(Pr) epitaxial films, photoluminesc. spectra 0-66294  
 GaP-Co, optical spectra and Zeeman anal. of Co 3d<sup>7</sup> state 0-66247  
 GaP-Co(Ni), photolum. excitation spectroscopy 0-80841  
 GaP-S(Se), donor bound exciton excited states 0-66284  
 GaP:Zn, O, influence of impurity-absorbed illumination on luminesc. 0-93395  
 p-GaP:Zn,S, spin polarisation of donors and acceptors in mag. field, optical and microwave study 0-93393  
 GaP,As<sub>1-x</sub>N, luminesc. of N bound state excitons, local-environment effects 0-100691  
 GaSb:Sn, p-n junction, electroluminesc. and photoluminesc. 0-66306  
 GaSe, deep free and constrained excitons and biexcitons, collective interactions (Russian) 0-66282  
 GaSe, exciton luminesc. kinetics, intermediate electron-hole states 0-93389  
 Gd<sub>2</sub>(MoO<sub>4</sub>)<sub>3</sub>, ferroelec.-ferroelastic, photolum. and photocond. meas. 0-84768  
 Ge, exciton condensation, light scatt. by electron-hole drops 0-84435  
 Ge, mag. field luminesc. lifetime, quantum oscills., phonon wind effects 0-93385  
 Ge, nonequilibrium charge carrier-mag. field interaction electron-hole drops, recombination (Russian) 0-75511  
 Ge:B(Al)(Ga), shallow acceptor spectral line intensities 0-88517  
 Ge:In (Sb) and pure cryst., kinetics of strain-confined large electron-hole drop and its clinging exciton system 0-75508  
 GeSe<sub>2</sub>, glassy, powdered and bulk, fatigue of photolum. 0-80855  
 GeSe<sub>2</sub>, powdered crystalline, photoluminescence intensity under continuous excitation 0-71480  
 Hg<sub>1-x</sub>Cd<sub>x</sub>Te, near band-gap photoluminesc., bound exciton luminesc. obs. 0-103973  
 InAs and solid solutions, recombination mechanisms of excess carriers, luminesc. obs. 0-97337  
 p-In<sub>0.53</sub>Ga<sub>0.47</sub>As:Zn on InP, elec. and optical props. 0-75662  
 InGaAsP, bandgap energy by electroreflectance and photoluminesc. spectra 0-107700  
 InGaAsP DH, luminesc., quantum efficiency determ. 0-108273  
 InGaAsP-InP DH lasers, perturbed InP growth, photoluminesc. study 0-106518  
 In<sub>0.3</sub>Ga<sub>0.7</sub>P, N free and implanted, photoluminescence study 0-97322  
 InGaPAs LPE layers, compositional inhomogeneity, photoluminesc. obs. 0-75451  
 In<sub>1-x</sub>Ga<sub>x</sub>P<sub>1-y</sub>As<sub>y</sub>, lattice-matched epitaxial layers, LPE growth on GaAs(100), characterisation 0-75465  
 In<sub>2</sub>O<sub>3</sub>-SnO<sub>2</sub>-CdTe:P, p-n homojunction solar cell, elec., photovoltaic props., photoluminescence 0-81463  
 In<sub>2</sub>O<sub>3</sub>-SnO<sub>2</sub>-InP solar cell junctions, efficiency, InP surface props. 0-85288  
 InP films, organometallic VPE grown, props. 0-96753  
 InP, luminescence, hot electron effects 0-66277  
 InP, model for ~1.10 eV emission band 0-66289  
 InP, photoluminescence meas. using diamond-anvil press. cell 0-108256  
 InP, VPE growth for MESFET's 0-103602  
 InSb, reabsorbed radiative recomb. and photon recycling 0-76076  
 Ir(III) complex, cis-dichlorobis(1,10-phenanthroline) iridium chloride, luminesc. excited states, solvent effects 0-97319  
 KBr, F-centre lifetime, perturbation effects, luminesc. meas. 0-108252  
 KBr:Ti, luminesc., decay model for A<sub>1</sub> and A<sub>2</sub> emissions 0-93379  
 KBr(I), photostimulated recomb., electron spin polarisation 0-60673  
 KCl:Cu<sup>+</sup> excitation and absorpt. spectra 0-108255  
 KCl:Eu<sup>2+</sup> crystals, photostimulated afterglow investigation at room temp. 0-108259  
 KCl:SnCl<sub>2</sub>, photostimulated hole recombination luminesc. (Russian) 0-80833  
 KCl:Sr crystal, Z<sub>1</sub> colour centre, luminesc. study 0-64993  
 KCl(Br), F-centre emission, mag. circular polarisation 0-108251  
 KCl(Br)(I):Ga<sup>+</sup>, polarisation of Ga<sup>+</sup> centre A<sub>T</sub> emission, temp. depend. 0-80842  
 KI, growth time of π emission in picosecond range 0-76067  
 KI:Ti, polarised luminesc. of (Ti<sup>3+</sup>)<sub>2</sub> centres 0-71473  
 Kr:OCS, O('S) and S('S) photodissociative prod., photoluminesc. excitation spectra, exciton energy transfer 0-89508  
 La<sub>2</sub>BeO<sub>4</sub>:Nd<sup>3+</sup>(Pr<sup>3+</sup>), cryst. growth, spectral and laser properties in <sup>4</sup>F<sub>3/2</sub>-<sup>4</sup>I<sub>11/2</sub> and <sup>4</sup>F<sub>3/2</sub>-<sup>4</sup>I<sub>13/2</sub> transitions 0-80853  
 LaGaO<sub>3</sub>:Ce<sup>3+</sup>, phosphor, luminesc. props. 0-103979  
 LaO<sub>2</sub>S:Eu, high press. effect on luminesc. efficiency and lifetime, charge transfer absorpt. 0-66266  
 Li-La phosphate glass, Nd, Cr activated, Nd luminesc. quantum efficiency meas., Nd-Cr nonradiative transfer 0-66296  
 LiCl, radiation effects on decay time of F-centre emission 0-93381  
 LiF:Mg, TLD-100, thermolum. phosphor, photolum. and absorpt. spectra, thermolum. mechanisms 0-97321

## photoluminescence continued

- LiH, effect of surface hydrolysis to LiOH on IR absorption, X-ray luminesc. and EPR spectra 0-60660  
 LiInS<sub>2</sub>, blue-band emission 0-76062  
 LiSi<sub>4</sub>O<sub>10</sub>, energy transfer, cryst. struct. and chemical composition effect 0-108248  
 Lu<sub>2</sub>(WO<sub>4</sub>)<sub>3</sub>:Cr(Eu), and undoped crystals, luminesc. obs. 0-89047  
 MgO doped powder phosphors, photo- and thermostimulated luminesc. obs. (Russian) 0-66263  
 MgO, photoluminesc. during mechanical deform. 0-60665  
 MgO:Cr<sup>3+</sup>, emission and excitation spectra 0-93387  
 MgO:Cr<sup>3+</sup>, optical excitation transfer 0-97325  
 MgO:Ni<sup>2+</sup>, near IR luminesc. from isolated and exchange-coupled Ni<sup>2+</sup> ion pairs, temp. depend. 0-93382  
 MgS:Ce<sup>3+</sup> phosphors, emission and excitation spectra (French) 0-93380  
 Mg<sub>2</sub>SiO<sub>4</sub>:Tb, thermolum. phosphor, photolum. and absorpt. spectra, thermolum. mechanisms 0-97321  
 MgUO<sub>4</sub>, energy transfer, cryst. struct. and chemical composition effect 0-108248  
 Mn complex, with 4-benzylpyridine hydrochloride, photoluminesc. props. 0-89044  
 Mn,Cd<sub>1-x</sub>Se single crystals, photoluminesc., composition depend. 0-80854  
 NH<sub>4</sub>Br:Cu<sup>+</sup>, luminesc., orientation phase transition 0-100687  
 Na<sub>8</sub>Al<sub>2</sub>Si<sub>6</sub>O<sub>24</sub>.Cl(Br)(I), cathodochromic sodalites, coloured crystals, tunnel and recomb. luminesc., temp. depend. (Russian) 0-66261  
 NaCl, migration of nonrelaxed holes, self-trapping, ESR and luminesc. obs. (Russian) 0-66033  
 NaCl:Ga<sup>+</sup>, polarisation of Ga<sup>+</sup> centre A<sub>T</sub> emission, temp. depend. 0-80842  
 NaF:U, luminesc. spectra, Vibr. struct. 0-80840  
 Na<sub>2</sub>MgF<sub>6</sub>, defects induced by X- and vacuum UV irradi., optical and elec. study 0-107319  
 Na<sub>2</sub>O-P<sub>2</sub>O<sub>5</sub>-Y<sub>2</sub>O<sub>3</sub>-Tb<sub>2</sub>O<sub>3</sub> glass, conc. quenching of luminesc. in disordered system with dipolar interaction 0-89059  
 Na<sub>2</sub>O-SiO<sub>2</sub> glasses, elementary electronic excitations, refl., luminesc., and photoemission meas. 0-84778  
 NaPO<sub>3</sub>:Eu<sup>3+</sup> glass, luminesc. of Eu<sup>3+</sup>, transition probabilities 0-80845  
 Na<sub>2</sub>S<sub>2</sub>O<sub>3</sub> digested AgX emulsions, red-IR photoluminescence obs. at 77K 0-103982  
 NaY<sub>1-x</sub>Sm<sub>x</sub>F<sub>4</sub>, luminesc. expt. suggesting Sm<sup>3+</sup> ion pairing 0-76065  
 Nd:silicate glass, resonance laser excitation, inhomogeneously broadened emission spectra 0-66295  
 Nd<sup>3+</sup> glass luminesc. band profile deform. under free-oscillation conditions 0-71487  
 Ne:H, exciton states and L<sub>α</sub>L<sub>β</sub> emission 0-93372  
 PbI<sub>2</sub>, first-order 2H-4H polytype transition, exciton spectroscopic study 0-59647  
 PbI<sub>2</sub>, multiphoton cross-section determination by means of luminescence experiments 0-93377  
 PbI<sub>2</sub>, photoexciton interaction, luminescence spectra, polariton dispersion diagram 0-93397  
 PbMg<sub>1/2</sub>Nb<sub>1/2</sub>O<sub>3</sub>, photolum. and carrier drift mobility at ferroelec. transition 0-71469  
 PbMoO<sub>4</sub>, doped and undoped single crystals, polarisation of luminesc. and assignments 0-76069  
 PbO, laser excitation IR spectra, photoluminescence obs., rot. anal., rot. const. determ. 0-95619  
 PbO, single crystals, exciton and impurity luminesc. 0-60674  
 PbS<sub>1-x</sub>Se<sub>x</sub>, thin film, stimulated emission, temp. depend. 0-66232  
 Pb<sub>1-x</sub>Sn<sub>x</sub>Se epitaxial layers, radiative and nonradiative recomb. processes 0-60670  
 Pb<sub>1-x</sub>Sn<sub>x</sub>Se solid solns., photoluminesc. spectra, energy band parameter determ. 0-71484  
 Pb<sub>0.78</sub>Sn<sub>0.22</sub>Te, Pb<sub>0.91</sub>Sn<sub>0.09</sub>Se, radiative and nonradiative recombination 0-80849  
 Pb<sub>1-x</sub>Sn<sub>x</sub>Te:Ce(In), solid solutions, impurity states in photoluminescence spectra (Russian) 0-97333  
 Pb<sub>1-x</sub>Sn<sub>x</sub>Te:In, impurity influence on photoluminescence at large excitation levels (Russian) 0-93384  
 PbTiO<sub>3</sub>, photolum. and carrier drift mobility at ferroelec. transition 0-71469  
 PbWO<sub>4</sub>, doped and undoped single crystals, polarisation of luminesc. and assignments 0-76069  
 RbCl(Br), F-centre emission, mag. circular polarisation 0-108251  
 RbI, luminesc. spectra induced by pulsed Ne<sup>+</sup> and electron beams and X-rays 0-80851  
 RbI, photostimulated recomb., electron spin polarisation 0-60673  
 RbMnF<sub>3</sub>:Er<sup>3+</sup>, absorption, emission, excitation and lifetime meas. 0-71460  
 RbMnF<sub>3</sub>:Fr, pure and doped, unirradiated and electron irradi., energy transfer 0-108254  
 SbSI, photolum. spectra in ferroelec. phase, 600-800 nm., 14-100K 0-71468  
 Sc<sub>2</sub>(WO<sub>4</sub>)<sub>3</sub>:Cr(Eu), and undoped crystals, luminesc. obs. 0-89047  
 Se, glassy, localised electronic states, photoluminesc. and ESR studies 0-65501  
 Si, amorphous, glow discharge produced, defect creation, high optical excitation 0-97327  
 Si, annealed, photoluminesc. anal. of defects 0-80836  
 n-Si, bound excitons and bound multiexciton complexes, excitation spectra 0-96792  
 Si, free excitons, drift and diffusion, luminesc. obs. 0-84434  
 Si, hydrogenated amorphous, laser annealing, photolum. spectra 0-100713  
 Si, impurity content characterisation, exciton luminesc. 0-60653  
 Si, ion implanted films, optical and luminesc. props. 0-60699  
 Si, radiative recomb. centre accumulation due to high temp. electron irradi. 0-93394  
 Si, uniaxially stressed, excitonic molecule emission spectra, electron valley degeneracy effects 0-60669  
 Si:Al, localised exciton bound to isoelectronic trap 0-66283  
 Si:B, bound many-exciton complexes, luminescence spectra, mag. props. 0-103994  
 Si:H, amorphous, defect photoluminesc. meas. 0-97334  
 Si:H, amorphous, defect states, luminesc. and ESR obs. 0-76075  
 Si:H, amorphous, geminate recombination model for photoluminescence decay 0-71481  
 Si:H, amorphous, temp. depend. of photolum. 0-89063  
 Si:H,Li, amorphous, photoluminescence obs. 0-66280  
 Si:K, bound exciton luminescence in mag. field (Russian) 0-108278  
 Si:Li, bound-exciton excited states, uniaxial anal. 0-71475



**photoluminescence continued**

- Si:Li, photolum. of bound exciton and bound multiexciton complex, Zeeman effect 0-108265  
 Si:O:H amorphous, time resolved luminesc. 0-66288  
 Si:P, luminescence circular polarisation, emission by many exciton complexes 0-93398  
 Si-H, amorphous, sputtered, photolum. obs. 0-80856  
 $\alpha$ -SiC, afterglow stimulated by IR radiation (*Russian*) 0-89066  
 SiC LED, defect luminesc. 0-89069  
 SiC, laser Raman spin-flip scatt. from excitons, luminesc. 0-80786  
 SiC polytypes, free exciton luminesc. meas., phonon energies 0-80852  
 SiC, spin-flip scatt. of laser light from photoexcited excitons 0-93330  
 SiO<sub>2</sub>, exciton study, luminescent centres as exciton detectors 0-66278  
 SiO<sub>2</sub>, vitreous, pure and Ge doped, luminescence centres at 396 and 280 nm 0-103996  
 SiO<sub>2</sub>:Ag, cryst. and glassy, X-ray induced EPR and luminesc. centre 0-65043  
 SiO<sub>2</sub>:LiO<sub>2</sub>:Al<sub>2</sub>O<sub>3</sub> glass, luminesc., polarisation degree distrib. 0-108257  
 SnO<sub>2</sub>, exciton luminescence spectra, absorpt. spectra 0-89064  
 Sr, dimer, photoassoc., photoluminesc., collisional dissociation 0-58303  
 SrB<sub>2</sub>O<sub>4</sub>:Eu<sup>2+</sup>, luminesc. of high-pressure phases 0-100680  
 Sr<sub>2</sub>Gd<sub>1-x</sub>Tb<sub>x</sub>GaO<sub>3</sub>, Gd<sup>3+</sup>→Tb<sup>3+</sup> energy transfer, emission and excitation spectra (*French*) 0-84770  
 SrTiO<sub>3</sub>, photolum. and carrier drift mobility at ferroelec. transition 0-71469  
 TbF<sub>3</sub>:Sm<sup>3+</sup>, induced visible emission of Sm<sup>3+</sup> 0-97330  
 TbO<sub>2</sub>:P<sub>2</sub>O<sub>5</sub>:MO system glasses, (M=Ge, Ca, Sr, Ba or Pb), photoluminesc. under X-ray excitation 0-89060  
 TiO<sub>2</sub>, exciton luminescence spectra, absorpt. spectra 0-89064  
 UO<sub>6</sub><sup>4-</sup>, octahedral uranate group, charge transfer transition and luminesc. 0-97324  
 YAG:Cr, optical detection of phonons 0-92630  
 YAG:Ho<sup>3+</sup>, spectroscopy, stimulated emission 0-93374  
 Y<sub>2</sub>O<sub>3</sub>:Eu, high press. effect on luminesc. efficiency and lifetime, charge transfer absorpt. 0-66266  
 Y<sub>2</sub>UO<sub>12</sub>, energy transfer, cryst. struct. and chemical composition effect 0-108248  
 ZnCr<sub>2</sub>O<sub>4</sub>, antiferromag. spinel, absorpt. and luminesc. spectra 0-66225  
 ZnO, exciton luminesc., 16 to 77 K 0-97329  
 ZnO, single cryst., photo- and thermoluminescence 0-66311  
 ZnS ion beam etching, topographic changes, amorphisation, luminescence study 0-76078  
 ZnS, ion implantation effects on luminesc., thermo-EMF 0-88178  
 ZnS:Cu crystal, powder, epitaxial film, luminescence anomalous thermal 0-76077  
 ZnS:In, recombination emission by optically detected magnetic resonance 0-66272  
 ZnS:Ni, IR luminesc. and absorpt. spectroscopy 0-108261  
 ZnS:Tb, Cu(Ag) phosphors, luminesc. props. 0-100690  
 ZnS(Se)(Te):Co, impurity luminescence no phonon line depend. on temp., Debye temp. 0-66273  
 ZnSe, band-edge photoluminesc., far-below band-gap excitation 0-76063  
 ZnSe, blue photoluminesc. excited with strong laser radiation 0-93391  
 ZnSe, donor-acceptor pair emissions characts. (*French*) 0-108249  
 ZnSe, exciton emission, halfwidths, thermal and optical activation energies obs. (*French*) 0-66268  
 ZnSe, luminesc., hot electron effects 0-66277  
 ZnSe, MBE growth, elec. and optical props. 0-75462  
 ZnSe, near band edge photoluminescence, electron-hole recombination 0-80835  
 ZnSe, resonance Raman scatt., exciton-polariton luminescence (*Russian*) 0-97287  
 ZnSe, thermally treated crystals 0-60661  
 ZnSe:Te, photolum. excitation spectroscopy 0-80841  
 ZnSe(Te), photolum. excitation spectra of tightly bound holes, valence band contrib. 0-60658  
 Zn<sub>2</sub>SiO<sub>4</sub>:Mn, energy storage effect and retrieval 0-100684  
 p-ZnSnAs, LPE, electronic struct. obs. by laser excited photolum. 0-60654  
 ZnTe, MBE growth, elec. and optical props. 0-75462  
 ZnTe crystals, polariton effects in luminesc. 0-103988  
 ZnTe, irradiation induced radiative centers obs. 0-66290  
 ZnTe, low voltage green LED, struct. double diffusion procedure 0-100697  
 ZnTe, pure and P(As) doped, shallow-acceptor, donor, free-exciton, and bound-exciton states 0-60667  
 ZnTe, secondary emission, transient behaviour under band-to-band excitation 0-108266  
 ZnTe:As, impurity identification and characterisation, capacitance, luminescence and IR absorption 0-60639  
 ZnTe:Li, Zeeman splitting of ground and excited acceptor states, selective pair luminesc. 0-84780  
 ZnWO<sub>4</sub>, scintillation characts. 0-66256  
 ZrF<sub>4</sub>:Eu<sup>3+</sup> glass, luminesc. of Eu<sup>3+</sup>, transition probabilities 0-80845  
 ZrS<sub>3</sub>, photolum. from excitons 0-66274

**photolysis**

see also photodissociation

- acetaldehyde, UV photolysis, transient species IR spectra 0-86464  
 acetylene, excited state, photochem. and spectrosc. investig. 0-95553  
 allene, IR multiphoton photolytic C<sub>3</sub> prod., C<sub>3</sub> vibr. relax., chem. kinetics 0-66820  
 anthracene single crystals, hole trapping by photo-oxidation products, injection currents (*Russian*) 0-92904  
 Bengal pink-anthracene, mixed annihilation delayed fluoresc. 0-74193  
 benzene, nanosecond laser photolysis 0-66825  
 benzene excimer, nanosecond laser photolysis 0-66825  
 benzophenone ketyl radical, in micelle, decay rate in mag. field, photolysis meas. 0-85154  
 benzyl radicals, monomethyl- and dimethyl-substituted, electronic spectra and electron affinity 0-63618  
 chlorofluoromethane in stratosphere, effect on O<sub>3</sub> conc. 0-109197  
 dibenzylketone, photolysis in micellar soln., quantum yield and <sup>13</sup>C enrichment 0-97711  
 difluoriodomethane, vacuum UV photolysis, IF in solid Ar visible spectra 0-87137  
 4-(2',4'-dinitrobenzyl)-pyridine, photochromism, nanosec. laser absorpt. spectrosc. obs. 0-85193  
 fluorobenzenes in Ne matrices, molecular cation electronic absorption spectra, new photolytic technique 0-58415

**photolysis continued**

- fluoriodiomethane, vacuum UV photolysis, IF in solid Ar visible spectra 0-87137  
 formaldehyde, selective laser photolysis for <sup>13</sup>C enrichment 0-108720  
 free radical reactions, photolytically initiated, high temp. kinetics meas. technique 0-61085  
 iodomethyl radical, vibr. excited, photofragmentation IR emission obs. 0-87162  
 IR laser photolysis of polyat. mols. photochem. appls. 0-66835  
 isopropyl radical, Ar matrix isolated, IR spectra and UV photolysis 0-66827  
 kinetic IR spectroscopy IR, appl. to biochem. systems 0-98178  
 methoxy prod. from methyl nitrite photolysis 0-85200  
 methyl radical, vibr. excited, photofragmentation IR emission obs. 0-87162  
 3-methyl-3-buten-2-one copolymers with styrene and methyl methacrylate, photodegradation (*Japanese*) 0-108725  
 o-methylacetophenone, laser flash photolysis, temp. depend. 0-93770  
 methylamine, photochemical conversion to HCN with ArF laser, mol. fluoresc. obs. 0-97710  
 methylviologen, photoreduction to H<sub>2</sub>, adsorbed on cellulose, hydrogen economy 0-81491  
 1-nitropropane, gaseous, primary processes, study at 22°C and 100°C 0-89507  
 pentafluoroacetone, IR laser induced decomp., free radical mechanism 0-71924  
 photographic emulsions, ultra-fine grained, nature of produced colour centres (*Russian*) 0-73517  
 polymethine dye solutions, photochem. transformations and short-wavelength luminesc. 0-100686  
 protoporphyrin IX, triplet states, flash photolysis, obs. 0-95555  
 protoporphyrin IX dimethyl ester, triplet states, flash photolysis, obs. 0-95555  
 quinaquine mustard, 2-step laser-induced photodamage 0-85198  
 quinones, triplet quenching by organometal cpds., time resolved CIDEP and ESR obs. 0-95654  
 quinones-Zn porphyrin, quinones sensitised reduction in vesicle systems 0-71897  
 tetrachloromethane, UV laser photolysis 0-66826  
 tetrafluoroethylene, photolysis, CF<sub>2</sub> form., excitation by Hg 253.7 nm line, reson. fluoresc. spectra 0-63694  
 trichlorofluoromethane, UV laser photolysis 0-66826  
 triphenylmethane dye soln., electronic relax., viscosity-depend., using picosec. flash photolysis 0-66258  
 water, biophotolysis, living electrode of algae as long-lived photoconverter 0-104510  
 water, CW and flash photoelectrolysis using ferroelectric photoanodes 0-81339  
 water, photoelectrolysis, using Fe<sub>2</sub>O<sub>3</sub>-coated n-Si heterostruct. photoanode 0-61384  
 water, photoelectrolysis with TiO<sub>2</sub> catalyst 0-60755  
 water photoelectrolysis, rel. to charge transfer via surface states of semiconductor 0-75636  
 AgBr dispersion in gelatin, adsorbed S and Au, transient absorpt. spectra latent image form. and decay 0-66837  
 AgCl, luminescence fatigue, adsorbed Ag atoms 0-66281  
 BiI<sub>3</sub> photographic film, photochem. decomposition kinetics (*Russian*) 0-93782  
 C<sub>2</sub> radical kinetics prod. by IR photolysis of acrylonitrile 0-95668  
 C<sub>2</sub>+NO, laser-induced chemilum. reaction 0-61101  
 C<sub>2</sub>S<sub>2</sub> photolysis, S(3D<sub>2</sub>) electronically excited state prod. 0-99476  
 Cd<sub>2</sub>GeO<sub>4</sub> anode for H<sub>2</sub>O photoelectrolysis 0-108716  
 CdIn<sub>2</sub>O<sub>4</sub> anode for H<sub>2</sub>O photoelectrolysis 0-108716  
 Cd<sub>2</sub>SnO<sub>4</sub> anode for H<sub>2</sub>O photoelectrolysis 0-108716  
 Cl+formaldehyde, photolysis, Fourier transform IR studies, metastable species detection 0-81293  
 H<sub>2</sub> photochemical dissociation utilising solar energy for H<sub>2</sub> prod., review 0-61452  
 H<sub>2</sub>, production of exciton states and L<sub>m</sub>L<sub>g</sub> emission of H atoms in Ne matrix 0-93372  
 HN<sub>3</sub>, UV photolysis 0-101027  
 HO<sub>2</sub>, detection by laser excited fluoresc., press. depend. of fluoresc. and photolytic interferences 0-95666  
 H<sub>2</sub>O, biophotolysis for H prod. using solar energy 0-61457  
 H<sub>2</sub>O for H<sub>2</sub> prod. using chlorophyll photocatalysts 0-61458  
 H<sub>2</sub>O photoelectrolysis, H<sub>2</sub>/hydrocarbon fuel prod. via biomass conversion wastes 0-89653  
 H<sub>2</sub>O photolysis using biological and artificial catalysts for H prod. 0-61444  
 H<sub>2</sub>O photolysis using Pt/(chlorophyll a.2H<sub>2</sub>O) reaction for H<sub>2</sub> production 0-89663  
 H<sub>2</sub>O, using solar energy for H<sub>2</sub> prod., feasibility of large scale generation 0-72095  
 I<sub>2</sub>, photolytic cage effect in gas phase 0-81345  
 ICN, A-state photolysis, I(<sup>2</sup>P<sub>1/2,3/2</sub>) branching ratio wavelength depend. 0-81335  
 p-InP-Cd(Zn), ohmic contact formation on InP by laser photochemical doping 0-80369  
 K<sub>2</sub>Zr<sub>2</sub>(O<sub>2</sub>)<sub>7</sub>:F<sub>2</sub>:2H<sub>2</sub>O, photodecomp. 0-108724  
 methyl nitrite, 266 nm photolysis, methoxy radical prod. 0-76534  
 MoF<sub>6</sub>, in Ar matrix, photolysis, MoF<sub>3</sub> form., IR spectrum 0-87115  
 NH<sub>3</sub>+O<sub>2</sub>, reaction mechanism, flash photolysis obs. 0-104425  
 O+methane→OH+ethyl radical, photolytically initiated, high temp. kinetics meas. technique 0-61085  
 O<sub>2</sub> photolysis, O(<sup>1</sup>P) quantum yield at 266 nm 0-78568  
 O<sub>2</sub> photolysis at 248 nm, O(<sup>3</sup>P) direct obs. 0-101028  
 O<sub>2</sub> photolysis by sunlight, rate constants at ground level 0-61836  
 OCSe, quantum yields for Se, <sup>1</sup>S<sub>0</sub>, <sup>1</sup>D<sub>2</sub>, and <sup>3</sup>P<sub>0,1,2</sub> atoms determ. in photolysis, lifetime and quenching rate meas. 0-97741  
 O(<sup>1</sup>D<sub>2</sub>)+NH<sub>3</sub>→OH(v,N)+NH<sub>2</sub>, bimodal OH rot. distrib. obs. and energy disposal 0-76501  
 O<sub>2</sub>(b<sup>3</sup>Σ<sub>g</sub><sup>-</sup>), temp. dependent quenching, photochemical study by H<sub>2</sub>-VUV laser 0-63702  
 PbI<sub>2</sub>-Ag, photographic mat., photolysis, effect of PbI<sub>2</sub> photo-EMF effect (*Russian*) 0-92939  
 Rb anions, THF soln., photolysis, appl. to photogalvanic cell 0-85294  
 Se, isotope effects, Rydberg levels-ground state transitions, rot. const., VUV spectra obs. 0-58279  
 p-Si(P<sup>+</sup>) photolytic props. in HF 0-89504  
 SiO+F<sub>2</sub>, matrix reaction, OSiF<sub>2</sub> prod., IR spectra and force consts. calcs. (*German*) 0-97718



**photomagnetic effect**

- coronene, triplet state, photomagnetism 0-97125
- paramagnetic crystal, magnetisation change by light pulse 0-70932
- SQUID magnetometer, photomagnetic meas. appl. 0-98950
- CdCr<sub>2</sub>Se<sub>4</sub>, magnetic semiconductor, photoinduced centre kinetics 0-71110
- CdCr<sub>2</sub>Se<sub>4</sub>, magnetisation, study of photoinduced charges 0-80567
- Cd<sub>0.1</sub>Hg<sub>0.9</sub>Te, photothermoelectric effect in mm range 0-92932
- Fe garnet, optical radiation interaction with magnetostatic waves 0-76009
- Ge, photomagnetic effect, space inhomogeneous nonequilibrium carrier lifetimes (*Russian*) 0-71152
- n-Ge, proton and  $\gamma$  irradi., minority carrier recombination 0-65591
- InSb-NiSb, photovolt. effects rel. to theory of semicond. with internal elec. short circuits 0-65620
- K vapour, mag. props. changes under laser irradi., induced EMF obs. 0-100059
- Mn ferrite, magnetic permeability, photoinduced reduction (*Rumanian*) 0-75794
- Rb vapour, mag. props. changes under laser irradi., induced EMF obs. 0-100059
- Si, photovoltaic and photomagnetic effects, rel. to intervalley electron transfer 0-60034
- YIG, electron and  $\gamma$ -irrad., photomagnetic effect 0-103877

**photometers**

- see also photometry; spectrophotometers*
- additive photographic film printers, programmed control of light metering valves (*Russian*) 0-95174
- astronomical photoelectric photometer, appl. to occultations obs. (*Chinese*) 0-105172
- conversion to scanning microphotometer 0-86374
- cytrophotometer, automatic 2-wave, with a calculator 0-104820
- differential light scattering photometer, for rapid analysis of particles in flow, appl. to biological cells 0-77834
- double-beam, for meas. small changes in optical absorption 0-62709
- enlarger exposure meter, using photodiode and multimeter 0-101857
- enlarger exposure meter, with digital display (*Dutch*) 0-101865
- exposure meter and development timer, used for photographic enlarger 0-101856
- exposure meter errors during colour photographic printing 0-101818
- focal grating photometer for magnitude difference determ. of double stars 0-67567
- illumination control of cine projectors, foreign equipment (*Russian*) 0-105741
- integrating wide-field IR photometer for globular clusters study 0-62029
- microphotometry, compensation for fluctuations in illumination 0-73413
- microscope photometer/semiautomatic image anal. instrument system for morphometric and photometric value meas. 0-82815
- nondispersive IR photometer selectivity improvement (*German*) 0-90880
- oceanographic photometer for deep-sea work, using acoustic telemetering 0-98460
- photographic colour printing, correcting light filter selection 0-62764
- photographic exposure meter for electronic flash 0-77835
- repetitive filter cycle photometer, with sky background compensation 0-62025
- retroreflectometer, NBS reference 0-73410
- scanning telephotometer, spatial transfer characts. 0-73415
- SEC Vidicon photometer, appl. to photometry of  $\omega$  Centauri main sequence 0-90491
- spherical integrating photometers, luminous flux meas. accuracy, expt. anal. of group discharge lamps (*Polish*) 0-73407
- stellar chopping photometer to eliminate auroral sky background 0-72776
- stellar photometry of rapid fluctuations, microprocessor controlled instrument (*Spanish*) 0-82222
- submarine quantum irradiance and photoperiod meter, with digital recording 0-98474
- telephotometer for aerosol scattering function determ. 0-105055
- NO photometric process analyser using resonance absorption method 0-57360

**photometric light sources**

- integrating photometer screen error minimisation using linear numerical model 0-95117
- optical-null spectrophotometers, photometric scale nonlinearity 0-101816
- spherical integrating photometers, luminous flux meas. accuracy, expt. anal. of group discharge lamps (*Polish*) 0-73407
- working standard establishment using photoreceptors (*Japanese*) 0-98964

**photometry**

- see also brightness; colorimetry; densitometry; spectrophotometry; stellar photometry*
- 0957+561A, B, double quasar, IR obs. of quasar and intervening galaxy 0-73065
- aerosol, solar radiation absorpt., visual photometric meas. technique 0-85750
- antimalarial drugs, lifetime meas. via reiterative convolution using fluorescence decay curves 0-57380
- asteroid 216 Kleopatra, photometry rel. to comp., diameter, elongated shape and possible stellar occultations 0-94743
- asteroids, photographic photometry with Schmidt telescope during 1977 and 1978 0-72844
- astronomical occultations photometry, photoelectric photometer appl. (*Chinese*) 0-105172
- astronomical photoelectric photometry, data recording system for KSC 60 cm reflecting telescope (*Japanese*) 0-94717
- astronomical photometry, investigation of double astrograph system (*Russian*) 0-72771
- astronomy, thermal background subtraction in photodiode detectors 0-90342
- 3C 273, UVB obs., (1975 to 1979) 0-62309
- C-CD camera description performance and calibration 0-73499
- calibrator, inverse fourth power, NBS optical density standards development and appl. 0-73412
- calligraphic projection display resolution and contrast photometer and X-Y plotter 0-86373
- Charon (1978 P 1), stellar occultation obs., 1980 April 6, rel. to satellite dia. and struct. 0-94754
- clusters of E and S0 galaxies, colour distribution rel. to redshift 0-105361
- comets, isophotometric atlas, pt. II 0-109377
- Deimos, photometry from Viking orbiter images 0-72838
- electrical instruments in photometric laboratory, selection, care, and use 0-86283

**photometry continued**

- 45 Eugenia, rot. period and photoelec. light curve determ. 0-72846
- force-flow chromatography, alkaline earth ions detected by photometric method 0-71965
- Fourier transform spectrometer performance, instrumentation for assessment 0-95165
- galaxies, photometry of remote clusters 0-105364
- galaxies, spectroscopy and photometry rel. to evolution of faint objects 0-105353
- galaxies, UVB photoelectric photometry and photometric parameters 0-67855
- galaxies, V-K colours and IR Hubble diagram for giant ellipticals 0-105359
- galaxies near late-type spiral NGC 4945, radial vels. and BV photometry 0-109547
- Galilean satellites, photometry of Io, Europa and Callisto, 1976 to 1979, possible solar variability detect. 0-98623
- glass fibre reinforced plastic, fatigue fracture kinetics studied by diffusion scatt. of luminous fluxes 0-76446
- globular clusters, UV energy distrib. from Orbiting Astronomical Observatory photometry 0-73009
- globular clusters near galactic centre, IR studies 0-82434
- grazing incidence spectrometry, photometric calibration of 1.0 m spectrometer 0-92386
- integrating photometer screen error minimisation using linear numerical model 0-95117
- integrating sphere window, illum. distrib. uniformity (*Chinese*) 0-86368
- light flux brightness meas., EM vacuum fluctuations, quantum noise 0-57361
- micro-optics testing, width meas. of slit test objects 0-64223
- Moon, photometric function and new three-dimensional scatt. indicatrix 0-101538
- NDIR, partially layered detector, function and properties 0-105696
- NGC 253, barred spiral galaxy, detailed surface photometric study 0-105327
- NGC 3227, Seyfert galaxy, photoelectric and spectroscopic study and comparison with galaxy chain (VV 150) 0-98724
- NGC 3686 galaxy quartet, surface photometry, mass distrib. and group stability 0-62297
- NGC 4314, barred spiral galaxy, UVB surface photometry of central region 0-77482
- NGC 604, H II region in M 33, H $\beta$  photometry and Fabry-Perot interferometry rel. to core-halo struct. 0-85984
- NGC 6440, globular cluster, surface photometry of cluster core 0-82436
- opaque surface, roughness determ., photometric method 0-95072
- optical radiation composition and effects and usage in plant experiments (*Hungarian*) 0-109076
- panoramic, background subtraction problem (*Italian*) 0-98570
- Phobos, photometry from Viking orbiter images 0-72838
- photometric studies of low-absorption optical media, apparatus (*Russian*) 0-98965
- PKS 2126-15, QSO ( $z=3.27$ ), JHK photometric obs. 0-94888
- planetary photometry, theory 0-67601
- Q 0420-388, QSO ( $z=3.13$ ), JHK photometric obs. 0-94888
- quartz in metamorphic rocks, photometric method for c-axis fabrics anal. 0-101456
- retroreflectance measurements, unified coordinate system 0-73408
- retroreflecting material metrology, errors in luminous refl., chromaticity meas. 0-68235
- retroreflector photometric and goniometric accuracy 0-86375
- retroreflector photometry, meas. error rel. to aperture size 0-73409
- Rhea, planetary, 1976 to 1979, rel. to possible solar variability detect. 0-98623
- rough surface reflection, empirical representation of goniophotometric data 0-87314
- seminar, optical radiation meas., San Diego, CA, USA (Aug. 1979) 0-86036
- sky background estimation on starfield plate 0-67577
- spectral adaptation for receivers and light sources (*German*) 0-77837
- spiral galaxies, early-type, multiaperture UVB photometric props. 0-98706
- stellar colour photometry through clouds, appl. of single repetitive filter cycle photometer 0-62025
- stellar photoelectric photometry, efficiency as function of image quality 0-62034
- stellar photometry, appl. of focal reducer using Fresnel lens 0-67568
- stopped-flow apparatus for rapid mixing and study of two fluids under high hydrostatic pressures 0-98929
- thickness measurement of Al coating on polyethylene terephthalate 0-62626
- visibility measurement, photometric contrast (*German*) 0-95118
- VV 150, galaxy chain, photoelectric and spectroscopic study 0-98724
- X-ray astronomy, spectroscopic and photometric facilities of 80 cm X-ray telescope (*German*) 0-109358
- X-ray source fields from Einstein Observatory, RI photometry with CCD camera 0-62315
- Ba, forced-flow chromatography, detection by photometric method 0-71965
- Ca, forced-flow chromatography, detection by photometric method 0-71965
- Mg, forced-flow chromatography, detection by photometric method 0-71965
- Si multielement photoelectric convertors, p-n mesa structure for investigating optical and energy characts. of solar and radiant energy concentrators 0-97783
- Si:P, measurement techniques for determining P densities 0-75262
- Sr, forced-flow chromatography, detection by photometric method 0-71965

**photomultiplier tubes *see photomultipliers*****photomultipliers**

- bias effects in photomultiplier used in laser Doppler anemometry 0-59140
- dissector pickup tube operating as a counter 0-95153
- gain stabilisation with high counting rate, feedback resistor series effect appl. 0-106232
- gain-changing protection circuit, scintillation neutron detector 0-74074
- gas concentration meas. using Raman intensity depend. on giant pulse laser polarization 0-98986
- neutron counter, scintillation, photomultiplier noise characteristics 0-74077



**photomultipliers continued**

- peak detection of current pulses, recording of  $10^{-12}$  lm fluxes 0-73471  
 photocathode sensitivity uniformity over surface, distortion of zone char-  
 act. by interference in substrate 0-58709  
 photon counter design for low light detection systems, spectroscopy, catho-  
 dolum. materials appl. 0-105711  
 rate dependent photomultiplier gain, time depend. 0-87020  
 review, Russian devices 0-57371  
 scintillation counters, time-of-flight, electronics system for Mark II Detec-  
 tor 0-58093  
 scintillator, sampling grid, calibrated intensity monitor for intense high  
 energy charged particle beams 0-69034  
 subnanosecond optical detector developments 0-77870  
 time resolution studies of fast photomultipliers 0-99415  
 ultra-fast detectors for laser fusion diagnostics, quenched plastic scintilla-  
 tor with microchannel plate photomultiplier 0-74084  
 wavelength specific photon detector for the VUV 0-91380  
 Pb-glass total absorption counters, photomultiplier size at high energy  
 0-74085  
 Si intensified target image detector for inductively coupled plasma emis-  
 sion spectrometer 0-86439

**photon counting**

- acridine orange, fluoresc. decay meas. by high repetition rate gated photon  
 counting 0-86402  
 antibunching in resonance fluorescence in presence of atomic number fluc-  
 tuations 0-91764  
 atomic vapour quantum counter for upconversion of narrowband IR radia-  
 tion in 1.5-20  $\mu$ m region, expt. results 0-73455  
 Charlier approximation in photocount statistics 0-74328  
 correlator for meas. transient waveforms of very weak fluorescence  
 0-87250  
 cross-beam rate correlation, advances 0-58621  
 design for low light detection systems, spectroscopy, cathodoluminescent  
 materials appl. 0-105711  
 detector for subMM wavelengths using Rydberg atoms 0-77867  
 electric field light scattering by photon counting and signal averaging  
 0-95794  
 Gaussian-Lorentzian light, photon counting distrib. factorial moment, spat-  
 ial coherence 0-83571  
 Geiger coordinate counters for UV and X-ray photons 0-69026  
 inversion problem in photon counting with dead time 0-99682  
 laser anemometry and other photon correlation data, stabilized model-  
 fitting approach 0-58622  
 level crossing detection through photon counting distrib. second factorial  
 moment meas. 0-99485  
 multinode microchannel array photon-counting detectors 0-77869  
 non-classical effects in the statistical properties of light, review 0-99686  
 non-gaussian field, clipped time autocorrelation function of intensity fluc-  
 tuations 0-106472  
 nonlinear optical amplifier, coherent radiation statistical props. 0-99691  
 optical time domain reflectometry by photon counting 0-95122  
 parametric processes, photon statistics of fields generated by correlated  
 mode interf. 0-106500  
 proportional response photon counter, meas. of energy albedo of backscat-  
 tered photons 0-99408  
 proportional response photon counter 0-87021  
 reflected-beam laser anemometry using photon correlator 0-106861  
 resonance light scattering, spectral props. and photon correl. 0-91510  
 ring dye laser, optical bistability and first order phase transition 0-95918  
 SEM, cathodoluminescence, detector system 0-101898  
 statistics of photon count, detector temp. and field effect 0-74325  
 superposed coherent and chaotic radiation, computer simulation 0-58485  
 thermal light with orthogonally polarised multiple-peak spectrum, intensity  
 fluctuations 0-87303  
 thermal particles, multimode laser light scatt., photon statistics 0-99631  
 time-resolved fluorescence spectroscopy using pulsed lasers 0-57393  
 tris(bipyridine)ruthenium(II)dichloride, fluoresc. decay meas. by high  
 repetition rate gated photon counting 0-86402  
 unclipped digital correlator constr. for photon correlation spectroscopy  
 0-57387  
 weak light signal detection by single photon counting (Chinese) 0-77873

**photon-deuteron interactions**

- see also *photon-deuteron scattering*  
 $\bar{d}d \rightarrow \pi^0$ , multiple scatt. contrib. to threshold photoprod. 0-73718  
 $\gamma d \rightarrow np$ , 300 MeV, dibaryon resonance manifestation, pseudo-independent  
 amplitude elimination (Russian) 0-57612  
 $\gamma d \rightarrow np$ , 400-700 MeV, p polarisation (Russian) 0-106046  
 $\gamma d \rightarrow pn$ , 250 to 800 MeV, differential cross-section and proton polarisa-  
 tion, theoretical models 0-78081  
 $\gamma d \rightarrow pn$ , proton polarisation energy depend., 400-700 MeV (Russian)  
 0-63000

**photon-deuteron scattering**

see also *photon-deuteron interactions*

No entries

**photon echo**

- gas, photon echo in a magnetic field at small areas of the exciting pulses  
 0-95961  
 irreversible relaxation time contribution to photon echo decay 0-58646  
 localised electron-phonon system, strongly coupled, photon echo phenome-  
 non 0-64118  
 naphthalene: pentacene, intermol. interaction dynamics and optical dephas-  
 ing 0-64112  
 Optical nutation and phonon echo by phase shift of a light wave 0-78914  
 optical spectroscopy of crystals, review 0-83648  
 paraelectric induction theory, strong inhomogeneous broadening  
 0-108168  
 pentacene in naphthalene (p-terphenyl), mol. mixed crystals, optical dephas-  
 ing and vibronic relax. 0-95957  
 phase-conjugate wave front generation using photon echoes 0-58650  
 polyethylene, microwave photon echo 0-66330  
 resonant gaseous media, photon echo meas. of population, orientation,  
 alignment relaxation times (Russian) 0-91863  
 RF superradiance generated to optical pulses under photon-echo conditions  
 0-95858  
 ruby, light echo signal correlation with exciting pulse shape (Russian)  
 0-106576  
 ruby, optical nutation echoes, Stark switching obs. 0-69467  
 ruby, reversed light echo due to two pulse laser resonance excitation (Rus-  
 sian) 0-87439  
 ruby crystal, photon echo generation, control method 0-87440

**photon echo continued**

- smectic A liquid crystals, thermo-optical recording, echo images 0-91928  
 stimulated optically induced nucl. spin polaris., optical coherence storage  
 0-58649  
 transitions, identification by photon-echo technique 0-78915  
 two-level system, backward photon echo and free induction decay genera-  
 tion 0-99805  
 two-level system, optical echo signal form. in single-pulse and stimulated  
 excitation regimes 0-58647  
 Na, D-lines, inert gas broadening, photon echo meas. 0-91475  
 Na vapour, laser induced population grating 0-69466  
 Na vapour thin cell forward phase conjugation obs. 0-78917

**photon-hadron interactions**

- see also *photon-hadron scattering*; *photon-nucleon interactions*  
 charm photoprod. with linearly pol. photons, QCD calcs., gluons 0-68464  
 lepton pair production, perturbative QCD, twist-2 photon operator, parton  
 subprocesses 0-73716  
 multiperipheral parton model, deep inelastic processes 0-82961  
 $\gamma\gamma$ , Higgs boson photoproduction 0-78068

**photon-hadron scattering**

see also *photon-hadron interactions*

No entries

**photon interactions** see *photon-deuteron interactions*; *photon-hadron interac-*  
*tions*; *photon-lepton interactions*; *photon-nucleus reactions*; *photon-photon*  
*interactions*

**photon-lepton interactions**

- see also *photon-lepton scattering*  
 three-photon coalescence at electron 0-91026

**photon-lepton scattering**

see also *photon-lepton interactions*

No entries

**photon-nucleon interactions**

- see also *photon-nucleon scattering*; *photon-proton interactions*  
 two gluon mechanisms, quarkonia, glueballs and Higgs scalars 0-78077  
 $\gamma\gamma \rightarrow \pi\pi$ , threshold-450 MeV, energy dependent multipole anal. 0-78082  
 $\gamma N$ , exclusive photoprod. reactions, Okubo-Zweig-Iizuka rule 0-95277  
 $\gamma N$ , inclusive pion production due to  $\gamma q \rightarrow \pi q$  process, quark-parton model  
 (Russian) 0-78073  
 $\gamma n$ , n electric polarisability, from photoabsorption cross-section 0-57597  
 $\gamma N \rightarrow \Delta\pi$ , mag. dipole photoexcitation, singular integral eqns., polynomial  
 ambiguity 0-57608  
 $\gamma N \rightarrow \text{jet} + X$ , QCD cross sections 0-73715  
 $\gamma N \rightarrow \mu\mu X$ , QCD cross sections 0-73715  
 $\gamma n \rightarrow \pi^+ p$ , 0.9-1.65 GeV, pol.  $\gamma$ , cross section asymmetry (Russian)  
 0-86728  
 $\gamma n \rightarrow \pi^+ p$ , 700 to 1200 MeV, recoil proton polarisation 0-78075  
 $\gamma N \rightarrow \pi^+ X$ , QCD cross sections 0-73715  
 $\pi^+ \pi^-$  photoprod., low energy, emission ang. depend. (Russian) 0-57769

**photon-nucleon scattering**

see also *photon-nucleon interactions*; *photon-proton scattering*

No entries

**photon-nucleus reactions**

- for inelastic photon-nucleus scattering, see "photon-nucleus scattering"  
 see also *photodisintegration*; *photon-deuteron interactions*; *photon-*  
*nucleon interactions*  
 baryonic inclusive spectra in hadron-, photon- and H1-nucleus collisions,  
 fireball model 0-86892  
 cascade model, space-time model, tests and predictions 0-68633  
 [CC]  $^{12}\text{C}(\gamma, \pi^+)^{12}\text{B}$ , nuclear critical opalescence study 0-105988  
 differential polarisation coefficients for  $(\gamma, X)$  reactions 0-73838  
 electric dipole sum rule in correlated nuclear matter 0-83056  
 electron pair production, 1-10 GeV, total cross section meas. 0-78280  
 giant dipole resonance intermediate struct. using  $(n, \gamma)$  and  $(\gamma, n)$ , Brink  
 hypothesis test 0-63150  
 neutrino pair photoprod. in strong mag. field, pulsar neutrino luminosity  
 (Russian) 0-68648  
 neutron dosimetry, photointerference corrections for reactor pressure vessel  
 lifetime studies 0-99345  
 semileptonic weak and EM interactions, multipole operators, HO single  
 particle matrix elements 0-73840  
 spallation,  $A=23$  to 127 targets, mass yield distrib. 0-73835  
 $(\gamma, d)$ , odd-Z light nuclei, from  $(e, d)$ , cross section, E2 transistors giant  
 resonance and clusters 0-63169  
 $(\gamma, n)$ , 45-160 MeV, cross sections in quasi-deuteron model for direct reac-  
 tions 0-63170  
 $(\gamma, n)$ , preequilibrium exciton model with evaporative component, pho-  
 toneutron spectra, giant resonances 0-57762  
 $(\gamma, \pi)$ , photopion reaction sensitivity to optical pot. 0-78278  
 $(\gamma, \pi^+)$ , low energy photoprod., emission ang. depend. (Russian) 0-57769  
 $(\gamma, X)$ ,  $A=154-209$ , 7-20 MeV, total photoabsorption cross section  
 0-57766  
 $^{18}\text{O}(\gamma, \sigma_0)$ , 19-32 MeV, E1 and E2 cross section, E1-E2 phase difference  
 0-63172  
 $^{16}(\gamma, X)$ , bremsstrahlung weighted cross section, two-body correlations  
 effects, linked cluster expansion 0-106047  
 $\text{Ag}(\gamma, X)$ ,  $X = p, d, ^1\text{H}, ^4\text{He}$ , cascade-evaporation 0-57770  
 $^{27}\text{Al}(\gamma, X)$ , 3-30 MeV, photoabsorption cross section, giant dipole reso-  
 nances 0-78254  
 $\text{Al}(\gamma, X)$  photoabsorption cross-section, Levinger's factor, mass number  
 dependence 0-63165  
 $\text{Au}(\gamma, X)$ ,  $X = p, d, ^1\text{H}, ^4\text{He}$ , cascade-evaporation 0-57770  
 $\text{Be}(\gamma, X)$  photoabsorption cross-section, Levinger's factor, mass number  
 dependence 0-63165  
 $\text{Be}(\gamma, p)X$ , 180-420 MeV, quasifree NN system photodisintegration, p  
 spectrum 0-106049  
 $^{209}\text{Bi}(\gamma, X)$ , 3-30 MeV, photoabsorption cross section, giant dipole reso-  
 nances 0-78254  
 $^{12}\text{C}(\gamma, \pi^0 p)$ , 0.7-1.65 GeV, cross section asymmetry of  $\pi^0$  photoprod.  
 (Russian) 0-63164  
 $^{12}\text{C}(\gamma, n\alpha)^{10}\text{Be}$ , electric quadrupole transition cross-sections, behind giant  
 resonance (Russian) 0-78281  
 $^{12}\text{C}(\gamma, p)^{11}\text{B}$ , electric quadrupole transition cross-sections, behind giant  
 resonance (Russian) 0-78281  
 $^{12}\text{C}(\gamma, p\alpha)^{10}\text{Li}$ , electric quadrupole transition cross-sections, behind giant  
 resonance (Russian) 0-78281  
 $^{12}\text{C}(\gamma, \pi^+)^{12}\text{N}$ , total cross section calc.,  $\Delta(1232)$  contrib. 0-91175  
 $^{12}\text{C}(\gamma, \pi^+ p)$ , final state interaction, distorted and plane wave momentum  
 distbs. 0-78275  
 $^{12}\text{C}(\gamma, \pi^0)$ , pionic and EM  $A^*$  resonance excitation 0-91160



## photon-nucleus reactions continued

- <sup>13</sup>C( $\gamma, n$ ), 6.5-9.3 MeV, ang. distrib., E1, M1 and E2 excitations, resonance radiative widths 0-68581
- <sup>14</sup>Ca, photoneutron cross-section above giant dipole resonance region, quasi-monochromatic photon beam (French) 0-78276
- Ca( $\gamma, X$ ), photoabsorption cross-section, Levinger's factor, mass number dependence 0-63165
- Ce, photoneutron cross-section above giant dipole resonance region, quasi-monochromatic photon beam (French) 0-78276
- C( $\gamma, X$ ) photoabsorption cross-section, Levinger's factor, mass number dependence 0-63165
- Ce( $\gamma, X$ ), X=p,d,t, He, He, cascade-evaporation 0-57770
- Ge( $\gamma, e^-$ ), cross section near threshold, atomic electron screening effects 0-78279
- H( $\gamma, \pi^-$ ), 3.4-18 GeV,  $\pi$ NN form factor and differential cross sections, one pion exchange 0-68526
- H( $\gamma, \pi^-$ ), multiple scatt. contrib. to threshold photoprod. 0-73718
- H( $\gamma, \pi^-$ )<sub>ann</sub>, n-n final state interaction effects 0-102181
- H( $\gamma, \pi^-$ ), 210-700 MeV, total and differential cross sections from impulse approx. 0-68647
- H( $\gamma, \pi^-$ ), A=1, 2, 1-10 MeV, photoprod. yields, DWIA anal., dipole photoprod. amplitudes 0-68645
- He( $\gamma, \pi^-$ )<sup>3</sup>H cross section near threshold 0-83093
- He( $\gamma, \pi^-$ ), A=3, 4, 1-10 MeV, photoprod. yields, DWIA anal., dipole photoprod. amplitudes 0-68645
- Li( $\gamma, X$ ), X=p, 10.2-15.4 MeV bremsstrahlung, photoreaction mechanisms 0-68644
- Li, pseudointegration, cluster model wave function, bremsstrahlung weighted cross-section 0-63163
- Li-X, photoabsorption cross-section, Levinger's factor, mass number dependence 0-63165
- <sup>14</sup>N,  $\gamma$ -p, C, cross-section and <sup>12</sup>C distrib., quasi-deuteron, mechanism 0-63166
- <sup>14</sup>N( $\gamma, \pi^-$ ), DWIA anal., wave function and  $\pi$  optical pot. effects on cross section 0-63168
- <sup>14</sup>N( $\gamma, \pi^-$ ), anomalous <sup>14</sup>N<sub>g</sub>-<sup>14</sup>C<sub>g</sub> transition, Kroll Ruderman terms 0-63167
- <sup>20</sup>O, photoneutron cross-section above giant dipole resonance region, quasi-monochromatic photon beam (French) 0-78276
- O( $\gamma, n_0$ ), 21.6-25.7 MeV, ground state photoneutron polarisation ang. distrib. 0-57745
- O( $\gamma, p$ ), N, electric quadrupole transition cross-sections, behind giant resonance (Russian) 0-78281
- O( $\gamma, \pi^-$ ), 200-350 MeV, cross sections, DWIA anal. 0-106048
- O( $\gamma, \pi^-$ ), total cross section,  $\Delta$ -hole states damping,  $\pi^0$  exchange,  $\Delta$  isobar hole model 0-91174
- O( $\gamma, X$ ) photoabsorption cross-section, Levinger's factor, mass number dependence 0-63165
- Pb, photoneutron cross-section above giant dipole resonance region, quasi-monochromatic photon beam (French) 0-78276
- <sup>3</sup>S, photoneutron cross-section above giant dipole resonance region, quasi-monochromatic photon beam (French) 0-78276
- <sup>28</sup>Si( $\gamma, p$ ), 18.1-29 MeV, photoproton energy spectra, contribs. to giant dipole resonance 0-78245
- Sn, photoneutron cross-section above giant dipole resonance region, quasi-monochromatic photon beam (French) 0-78276
- Ta, photoneutron cross-section above giant dipole resonance region, quasi-monochromatic photon beam (French) 0-78276
- Ta( $\gamma, X$ ), 3-50 MeV, photoabsorption cross section, giant dipole resonances 0-78254
- Ti( $\gamma, X$ ), 5-18.3 MeV, photoneutron and photofission cross sections, giant resonance and deformations 0-68712
- Ti( $\gamma, n$ ), 15-27.5 MeV, giant dipole resonance splitting, dynamic collective model 0-57755
- U, photoneutron cross-section above giant dipole resonance region, quasi-monochromatic photon beam (French) 0-78276
- U( $\gamma, X$ ), A=235, 236, 238, 5-18.3 MeV, photoneutron and photofission cross sections, giant resonance and deformations 0-68712
- Zn( $\gamma, n$ ), above GDR region, cross sections, DWBA anal. 0-63173
- Zn, statistical and pre-equilibrium cross sections and multiplicities from data 0-68646

## photon-nucleus scattering

- see also photon-deuteron scattering, photon-nucleon scattering
- geophysical prospecting, allowance for scattered gamma radiation Russian 0-105067
- ( $\gamma, \gamma$ ), 2.5-3.5 MeV, level photoexcitation 0-78193
- ( $\gamma, \gamma$ ), 412, 468, 662 keV, elastic scatt. cross sections, Rayleigh scattering anal. 0-86898
- ( $\gamma, \gamma$ ), low energy computing of photon scattering amplitude 0-68643
- (B $\gamma, \gamma$ ), resonance scatt., molecular orientation effects 0-78252
- <sup>14</sup>N( $\gamma, \gamma$ ), 32 MeV, energy spectra, d prod. process (Russian) 0-91177
- <sup>14</sup>C( $\gamma, \gamma$ ), 28.5-39 MeV, cross sections and giant resonances, E2 strength 0-63122
- <sup>14</sup>C( $\gamma, \gamma$ ), total photoabsorption and elastic cross sections, spectroscopic information (Russian) 0-83095
- <sup>16</sup>Er( $\gamma, \gamma$ ), 14.4-16.6 MeV,  $\gamma$ -vibr. band head transitions, dynamic collective model 0-57662
- <sup>16</sup>Li( $\gamma, \gamma$ ), 32 MeV, energy spectra, d prod. process (Russian) 0-91177
- <sup>16</sup>N( $\gamma, \gamma$ ), 6.324 MeV, resonance scatt. cross section temp. depend. in BN, NH<sub>4</sub>Cl 0-57767
- <sup>16</sup>N( $\gamma, \gamma$ ), zero point vibr. energy in BN and NH<sub>4</sub>Cl 0-59593
- <sup>16</sup>O( $\gamma, \gamma$ ), total photoabsorption and elastic cross sections, spectroscopic information (Russian) 0-83095
- Pb( $\gamma, \gamma$ ), 344-1408 keV, <sup>192</sup>Pu  $\gamma$  rays, differential cross sections 0-99170
- <sup>192</sup>Pu( $\gamma, \gamma$ ), 14 MeV, highly excited spin-1 resonances, spin and radiative widths 0-86876
- U( $\gamma, \gamma$ ), 0.1-1.5 MeV, Delbruck and Rayleigh scatt., differential cross sections 0-102180

## photon-photon excitations see polaritons

## photon-photon interactions

- see also photon-photon scattering
- e<sup>+</sup>e<sup>-</sup> collisions, jet prod. and two-photon annihilation, hadron spectra 0-81121
- e<sup>+</sup>e<sup>-</sup>  $\rightarrow$  e<sup>+</sup>e<sup>-</sup> X, virtual 2 photon processes, luminosity functions, rapidity distrib., QED factors 0-86734
- e<sup>+</sup>e<sup>-</sup>  $\rightarrow$  e<sup>+</sup>e<sup>-</sup>  $\gamma$   $\gamma$ , jets,  $\gamma$  $\gamma$   $\rightarrow$  q $\bar{q}$  contrib. to cross section, QCD corrections 0-78106
- e<sup>+</sup>e<sup>-</sup>  $\rightarrow$  e<sup>+</sup>e<sup>-</sup> q $\bar{q}$ (q) + jet,  $\gamma$  $\gamma$  initiated 3 jet events in QCD 0-102057
- e<sup>+</sup>e<sup>-</sup> initiated  $\gamma$  $\gamma$  processes, charged pair prod.,  $\ell^+ \rightarrow \gamma \gamma$  width 0-91123

## photon-photon interactions continued

- $\gamma^* \gamma^* \rightarrow 2$  jets in e<sup>+</sup>e<sup>-</sup>, parton model QCD corrections for doubly deep processes 0-73758
- $\gamma$  $\gamma$  in electron storage rings, Dalitz-Yennie type equivalent photon spectrum 0-86774
- $\gamma$  $\gamma$   $\rightarrow$  K<sup>+</sup>K<sup>-</sup>, 20-36 GeV,  $\Phi$ (1019) prod., cross sections 0-105907
- $\gamma$  $\gamma$   $\rightarrow$   $\pi^+ \pi^- \pi^+ \pi^-$ ,  $\rho$ (1.2) production 0-102056
- photon-photon scattering see also photon-photon interactions
- QED tests of electron propagator, vacuum polarisation 0-77994
- photon polarisation neutral current effect in bremsstrahlung and pair production 0-73655
- positronium, triplet, asymmetrical decay, two- and threefold polarisation correlation of photons 0-57536
- photon-proton interactions see also photon-proton scattering
- $\gamma$  $\pi$   $\rightarrow$   $\pi^+ \pi^- \pi^+ \pi^-$ , K<sup>+</sup>K<sup>-</sup>, K<sup>0</sup>K<sup>0</sup> final state comparisons above resonance region 0-105906
- $\gamma$  $\pi$ , 30-180 GeV,  $\rho$  and  $\phi$  elastic photoprod. cross sections 0-95278
- $\gamma$  $\pi$ , 40-70 GeV, inclusive D<sup>0</sup> photoprod. cross sections, pair and associated prod. 0-91097
- $\gamma$  $\pi$ , heavy quark particle photoprod., QCD model, vector dominance implications 0-86730
- $\gamma$  $\pi$   $\rightarrow$  lepton pair, P violating asymmetry 0-105901
- $\gamma$  $\pi$   $\rightarrow$  (pp) $\pi$ , inclusive and exclusive pp photoprod. S(1936) prod. 0-86729
- $\gamma$  $\pi$   $\rightarrow$  K<sup>+</sup>K<sup>-</sup>  $\pi^+ \pi^-$ , 20-70 GeV, K<sup>+</sup>K<sup>-</sup> threshold enhancement 0-78076
- $\gamma$  $\pi$   $\rightarrow$   $\pi^+ \pi^-$ , 340 MeV, pol. p, first resonance region,  $\pi^+$  photoprod., T-asymmetry (Russian) 0-62997
- $\gamma$  $\pi$   $\rightarrow$   $\pi^+ \pi^-$ , photoproduction, in low-energy region, complex multipole amplitudes 0-68463
- $\gamma$  $\pi$   $\rightarrow$   $\pi^+ \pi^-$ , 0.6 to 1.8 GeV, backward angles,  $\eta$ -cusp 0-57609
- $\gamma$  $\pi$   $\rightarrow$   $\pi^+ \pi^-$ , 390-975 MeV, differential cross section 0-86725
- $\gamma$  $\pi$   $\rightarrow$   $\pi^+ \pi^-$ , 400 to 1142 MeV, recoil proton polarisation 0-82981
- $\gamma$  $\pi$   $\rightarrow$   $\pi^+ \pi^-$ , 450 to 800 MeV, proton polarisation, Walker-type anal., P<sub>11</sub>(1470), D<sub>13</sub>(1470), S<sub>11</sub>(1535) resonances 0-73721
- $\gamma$  $\pi$   $\rightarrow$   $\pi^+ \pi^-$ , high energies, semiempirical amplitude anal. dispersion relations and Regge poles 0-86726
- $\gamma$  $\pi$   $\rightarrow$   $\pi^+ \pi^-$ , low energies, complex amplitudes in s- and p-wave approx. 0-102053
- $\gamma$  $\pi$   $\rightarrow$   $\pi^+ \pi^-$ , 1.35-1.65 GeV, pol.  $\gamma$ , resonance energy region, cross section asymmetry (Russian) 0-86727
- $\gamma$  $\pi$   $\rightarrow$   $\pi^+ \pi^-$ , 600-1875 MeV, pol. p and  $\gamma$ , G and H polarisation parameters 0-99105
- $\gamma$  $\pi$   $\rightarrow$   $\pi^+ \pi^-$ ,  $\pi^+ \pi^-$ , K<sup>+</sup>K<sup>-</sup>, K<sup>0</sup>K<sup>0</sup> final state comparisons above resonance region 0-105906
- $\gamma$  $\pi$   $\rightarrow$   $\pi^+ \pi^- \pi^+ \pi^-$ , 20-70 GeV,  $\omega$ <sup>0</sup> state enhancement at 1.25 GeV 0-86708
- $\gamma$  $\pi$   $\rightarrow$   $\pi^+ \pi^- \pi^+ \pi^-$ ,  $\rho$ (1.6) production 0-102056
- $\gamma$  $\pi$   $\rightarrow$   $\pi^+ \pi^- \pi^+ \pi^-$ ,  $\pi^+ \pi^-$ , diffractive production, jet-like structure 0-57606
- $\gamma$  $\pi$   $\rightarrow$   $\pi^+ \pi^-$ , large p<sub>T</sub>, perturbative QCD 0-86723
- $\gamma$  $\pi$   $\rightarrow$  q $\bar{q}$ , quark-antiquark jet diffractive photoprod. in perturbative QCD 0-86714
- $\gamma$  $\pi$   $\rightarrow$   $\rho^+ \rho^-$ , 2.8 to 4.8 GeV, cross-sections,  $\rho$  spin density matrices 0-62999
- $\gamma$  $\pi$   $\rightarrow$   $\rho^+ \rho^-$ , 2.8 to 4.8 GeV, cross-sections,  $\rho$  spin density matrices 0-62999
- $\gamma$  $\pi$   $\rightarrow$  W<sup>+</sup>W<sup>-</sup>, current algebra and sum rules high energy W<sup>+</sup> prod. 0-102039
- $\gamma$  $\pi$   $\rightarrow$   $\pi^+ \pi^-$ , 20-70 GeV, dipion enhancement,  $\rho$ (1600) observation 0-78079
- $\gamma$  electric polarisability, from photoabsorption cross-section 0-57597
- $\gamma$   $\rightarrow$  K<sup>+</sup>K<sup>-</sup>( $\Sigma^0$ ),  $\pi^+ \pi^-$ ,  $\pi^+ \pi^-$ , K<sup>+</sup>K<sup>-</sup>, K<sup>0</sup>K<sup>0</sup> final state comparisons above resonance region 0-105906
- photon-proton scattering see also photon-proton interactions
- Compton scattering, 375 to 1150 MeV, differential cross section 0-57604
- photon scattering see photon-deuteron scattering; photon-hadron scattering; photon-lepton scattering; photon-nucleus scattering; photon-photon scattering
- photon transport theory fusion reactors, TFTR test cell, calc. dose rates from induced activity, Monte Carlo methods 0-57967
- nonlinear radiation transport, soln. by renormalisation group method 0-67555
- radiative transfer calculations, appln. of multiband method 0-95333
- terrestrial  $\gamma$  radiation transport in plane semi-infinite geometry 0-73284
- Pb/H<sub>2</sub>O stratified radiation shields, calc. of gamma-ray buildup factors using BIGGI 4T code 0-86994
- photons see also cosmic ray photons; gamma-rays; light; photon transport theory; X-rays
- distribution functions, QCD predictions using Altarelli-Parisi eqns. 0-78019
- emission from blackbody, thermodynamic laws, teaching 0-105451
- fine-structure constant, coupled Maxwell and Dirac eqns., QED 0-62894
- heavy guided photon in gravit. field 0-67949
- production, hadronic, AB- $\gamma$ X, scaling and quark mass dependence, quark parton model 0-73749
- quantum absorber theory, direct-action, photoelectron antibunching effect 0-57835
- spin dependent photon structure functions from Drell-Yan and e<sup>+</sup>e<sup>-</sup> reactions 0-82973
- splitting into 3, cosmological limits, spectral broadening, frequency-dependent and multiple red-shifts 0-77284
- unpolarised lepton-lepton collisions, photon 3rd struct. function, QCD implications 0-73708
- pp, 31-63 GeV, direct photon prod. at large p<sub>T</sub>,  $\pi^0/\gamma$  prod. ratio 0-63038
- pp, 62.4 GeV/c, direct single photon prod. at large p<sub>T</sub> 0-91113
- pp, ISR energies, high p<sub>T</sub>  $\pi^0$  and single photon events, associated charged particle multiplicity 0-63039
- photomuclear reactions see photon-nucleus reactions
- photothoresis
- phthalocyanine-alkane interface, charge transfer, rel. to photoelectro-phoretic image form. 0-65616
- spectrometer for spectral dependence meas. of radiometric force on micron sized particle 0-105719
- spectroscopy, broadband photophoretic 0-86469
- photoelasticity discs, doubly-connected, noncircular, full yielding at collapse, photoplastic verification 0-74756



**photoplasticity** continued

- CdS(Se)(Te), charged dislocations, flow of charge with plastic deform. 0-85010
- CdTe, crystal size depend. of photoplastic effect 0-92592
- ZnO(S)(Se)(Te), charged dislocations, flow of charge with plastic deform. 0-85010

**photorefractive effect**

- Bragg deflector, using photorefract. effect in  $As_{40}Se_{15}S_{35}Ge_{10}$  film loaded on  $LiNbO_3$  waveguide 0-58673
- edge enhancement, real-time, using photorefr. effect 0-99642
- electro-optic crystals, hologram formation arbitrary transport length anal., photovoltaic effects 0-78802
- ferroelectrics, photoelectric states in real time spatial light modulators, photorefractive effect 0-80676
- liquids, photoacoustic and photorefractive detect. of small absorpts., electrostrictive limits 0-108171
- optical fibre, nonlinear effects, appl. to active and passive device fabrication 0-58638
- $Ba_2NaNb_2O_{15}:Fe,Mo$ , photorefractive mechanism and photoelec. props. 0-71381
- $Ba_2Sr_{1-x}Nb_2O_{15}:Ce$ , pure and doped, photoelec. props. and photorefractive 0-60538
- $BaTiO_3$ , holographic storage props. 0-87354
- $BaTiO_3$ , photorefractive effects and light-induced charge migration 0-69447
- $Bi_{12}SiO_{20}$ , electrooptic photorefractive crystals for optical information processing 0-74313
- $Bi_{12}SiO_{20}$ , photorefractive, vibr. struct. mode pattern visualisation, phase conjugation and dynamic holography 0-95938
- $Bi_{12}SiO_{20}$ , photorefractive medium, real-time image processing via four-wave mixing 0-95944
- $KNbO_3$  crystals, reduced, hologram recording and erasure sensitivity (Russian) 0-78795
- $KNbO_3$ , reduced, phase hologram recording, energy transfer and sensitivity 0-69338
- $KTa_{1-x}Nb_xO_3$ , holographic storage using photorefractive effect, dielectric const. 0-78800
- $LiNbO_3$ , electrooptic photorefractive crystals for optical information processing 0-74313
- $LiNbO_3$ , hologram storage depend. on envelope field, space charge field 0-78801
- $LiNbO_3$ , photoinduced surface storage of SAW patterns 0-74309
- $LiNbO_3$  photorefractive crystals for computer interfaced optical memory system, hologram characterisation 0-58475
- $LiNbO_3$  pure and Fe doped, IR induced acousto-photorefractive memory effect 0-80746
- $LiNbO_3$ , pure and Fe doped, two-photon photorefractivity 0-80753
- $LiNbO_3:Fe$ , holographic recording and thermal fixing, invest. of mechanisms 0-78810
- $LiNbO_3:Fe$ , photoinduced refractive index discontinuities at surface 0-75999
- $LiNbO_3:Fe$ , white-light image processing 0-87321
- $N_2$  liq., photoacoustic and photorefractive detect. of small absorpts., electrostrictive limits 0-108171
- $Rb_2ZnBr_4$ , ferroelec., photovoltaic and photorefractive phenomena 0-75598
- $Sr_{1-x}Ba_xNb_2O_6$ , photorefractive in space charge field, phase transitions 0-97229

**photoresistors**

- 3-channel far IR detector based on coded Si:B, Ge:B, n-GaAs photoresistors 0-101839
- dilatometer appl., with high stability and sensitivity, for polymers testing 0-81251
- temperature profile recorder using InSb photoresistor 0-105642
- Ge:Zn photoresistor, current responsivity rel. to nonequilibrium hole lifetime 0-60035
- PbSe base, infrared detector with thermal stability over range 0°C to 60°C 0-73458

**photoresists**

- see also *electron resists*
- conference on electron, ion and proton beam technology, conf., Boston, MA, USA (29 May-1 June, 1979) 0-67927
- cyclorubber with bisazides, effect of photoresist layer thickness on photosensitivity (Russian) 0-73510
- o-diazonaphthoquinones, thermal decomposition during drying and storing of photoresist layers (Russian) 0-73504
- metallo-organic photoresists for inorganic lithography 0-79024
- negative, spin-coating technique for producing multilayer IR optical medium 0-74451
- photochemical reaction rates, intensity depend., kinetic model 0-104452
- polymer photoresist, KTRF, thermally stimulated discharge current studies 0-75924
- polymethyl methacrylate, use of synchrotron radiation in X-ray lithography 0-62820
- positive photoresist film exposure, formal kinetics (German) 0-104454
- positive photoresists, FP-383, prod. of holograms (Russian) 0-74323
- positive resist, plasma etching durability, additive effects 0-66683
- SAW devices, standing waves and other interference elimination 0-69614
- Cr films, photoresist film on reverse gas plasma etching 0-97634
- Se-Ge amorphous films, obliquely deposited, photoinduced chem. changes 0-76385
- $SiO_2$ , etching characts. in trifluoromethane gas plasma 0-76392

**photosphere**

- absorption lines formation in inhomogeneous medium, rel. to waves and convective motions (Russian) 0-72901
- active region, mag. field correl. with circularly polarised 6 cm emission 0-62096
- active region oscills., standing Alfvén wave driven by photospheric vel. field 0-98639
- active regions, elec. currents as solar wind energy source 0-94768
- boundary magnetic field effects on cylindrical prominences 0-90396
- convective motion scales, ensemble-averaged eqns. 0-67698
- damping constant and microturbulent velocities determ., study of errors (Russian) 0-72899
- down-draught development at sunspot origin, hydrodynamic anal. 0-72908
- faculae, inhomogeneous model 0-109415
- faculae rel. to sunspot cycle 0-90390
- flare model based upon photospheric dynamo action 0-62102
- granular convection, effects in response of C I 5380 Å response to solar luminosity vars. 0-85910

**photosphere** continued

- granulation, 2-dimens. power spectrum analysis, data processing 0-101570
- granulation, mean vertical vel. 0-62094
- granulation scales, penetrative instabilities theory for convective modes in solar atmosphere 0-109406
- granulation structure, vertical motion models 0-90375
- granulation structure, vertical motions spatial and temporal behaviour obs. 0-85912
- limb darkening function at 5012 Å, possible vars. 0-67677
- magnetic field, importance for coronal energy storage, solar flare model 0-72906
- magnetic fields, possible explanation for fine struct. 0-98646
- McMath region 13043, opposite polarity sunspots collision rel. to centimetre-wave sources rapid var. 0-67688
- models and rotational temps. of  $C_2$  and  $MgH$  0-62099
- network properties, link with sunspot plage fragment characts. 0-98634
- oscillations of 160-min. period, no terrestrial atmospheric extinction effects 0-105216
- oscillations producing, coronal arcades mag. instability, two ribbon flares origin 0-72911
- oscillations with 160 min. period, terrestrial origin refuted (Russian) 0-98629
- solar rotation from Doppler obs. 0-105219
- supergranulation cells, equatorial rotation rate 0-90388
- surface oscillations and pulsations, rotation speeds 0-67676
- temperature minimum, absolute brightness temp. meas. in far IR with balloon-borne interferometer 0-62095
- velocity gradients retrieval from photospheric line asymmetries, linearised approach 0-62093
- Fe I lines, damping const. determ. preliminary results (Russian) 0-72900
- Fe I lines, line broadening, Smirnov Roueff pot. calcs. 0-98632
- Mg I and II, line profiles calc., comparison with expt. results 0-82320
- Ni I abundance from oscillator strength obs. 0-98625
- Zn abundance, discrepancy with meteorite abundance 0-72897

**photosynthesis**

- bacterial photosynthetic reaction centres, light induced electron spin polarisation 0-63681
- bioenergetics 0-61521
- biomass, review of possible energy conversion processes (French) 0-93843
- biomass energy production and the photosynthetic pathway 0-61393
- biomembranes, electron and proton transport 0-67052
- blue-green algae, absorpt. spectrum, struct. resolution 0-76715
- Chlamydomonas mutants, chlorophyll spectral forms and chloroplast struct. 0-81556
- Chlamydomonas mutants with inactive photosystem 2, electron transport chain disturbance 0-94179
- Chlorella biomass growth, efficiency rel. to solar energy utilisation 0-67049
- chlorophyll a, absorpt. and fluoresc. spectra, observance of Stepanov relation 0-81554
- chlorophyll-a, hydration, field desorpt. mass spectral obs. 0-71936
- chlorophyll-a radical cation lifetime in water-acetonitrile soln. 0-72136
- chlorophyllide fluorescence quantum yield during photochlorophyllide reduction in etiolated leaves 0-81542
- chloroplast fluorescence, investigated using laser spectrofluorimetry 0-81558
- chloroplasts, isolated, effect of temp. on photo-induced pH gradient 0-81566
- chromatophores of *R. rubrum*, induction of elec. pot. diff. by laser flash 0-81560
- early reactions in green-plant photosystem. I 0-104567
- electron conformation interactions in fast photosynthetic processes 0-94183
- electron transfer reactions in carrier mol. complexes, kinetics and thermodynamics 0-108859
- electron tunnelling, thermal and photoassisted, theory, fast charge separation in photosynthesis 0-89730
- energy and electron transfer speed, time resolution meas. (Russian) 0-94161
- enhancement and chromatic transitions, modelling 0-104565
- entropy of radiation and its role during photosynthesis 0-108858
- gastropod photosynthesis with incorporated algal chloroplast, Placobranchus sp. 0-61522
- hydrocarbons production for chemical feedstock 0-89661
- membranes, functional processes, polarisation effects 0-67045
- phase transitions discovery in photosynthetic systems 0-81539
- photoelectrochemical conversion, using bacteria reaction centre working on  $SnO_2$  electrode 0-94092
- photosystem I, of green plants and algae, CIDEP obs. 0-63679
- photosystem I of Chlorella, electron phototransfer in reaction centres, hole-burning spectroscopy 0-81561
- primary step, analogue reaction in a porphyrin-quinone linked mol. 0-89720
- R. sphaeroides, polarisation of photosynthetic membranes and reaction centres in elec. field 0-94277
- reaction centre chromophore organisation, high-resolution magnetophotoselection 0-97880
- reaction centre functional reconstitution in planar lipid bilayers 0-97881
- reaction centre spectroscopy by tunable picosec. parametric oscillators 0-61513
- reaction centres, triplet population, mag. field and g-factor differences effect 0-97879
- repression b 2-deoxy-D-glucose, low-temp. fluoresc. spectra of intact Chlorella cells 0-81559
- Rhodospirillum rubrum, chromatophores electron transport chain, functional organisation 0-81555
- solar energy conversion, microbial production of energy sources from biomass 0-61392
- solar energy conversion, photoelectric response of photosensitive liquid membranes and chloroplast discs 0-81482
- solar energy conversion and storage using artificial photosynthetic systems 0-89662
- solar energy conversion utilising biomass 0-61391
- spinach chloroplasts, laser photoinduced changes in high freq. dielectric constant 0-85449
- triplet states in photosystem I of spinach chloroplasts and subchloroplast particles, EPR obs. 0-85344
- vegetation canopies, solar radiation absorpt. simulation 0-104635



**photosynthesis continued**

- H<sub>2</sub> photobiological prod., key enzymes and biochem. systems, tech. problems of H<sub>2</sub> prod., review 0-61446  
 H<sub>2</sub> production by biological and biochemical solar energy conversion, review 0-61454

**phototelegraphy see facsimile****photothermal conversion**

see also solar absorber-convertors

- hot water supply systems using solar collectors, technical problems (*German*) 0-94106  
 passive solar heating systems, calc. of heat-transport-medium flow rate in heat receivers 0-99913  
 R and D by US DOE 0-89674  
 solar desalination unit with evaporation chamber, test results 0-96178  
 solar energy collector design for low capital costs and least steady-state heat losses 0-104517  
 solar energy cooling, operating systems and current developments, review 0-85265  
 solar energy storage area design coefficients for consumer demand and solar radiation (*Rumanian*) 0-89670  
 solar heating system for dwellings, temp. regime investigations 0-97802  
 solar house heating system, possibilities of integrating heat pump (*Rumanian*) 0-97804  
 solar installation for refrigeration and water heating, energy characts. 0-101124  
 solar power generation, system developments and research aims (*German*) 0-108799  
 solar systems installation for domestic heating (*German*) 0-94103  
 solar thermoelectric generators, metallic thermo-electric materials utilisation, economic characts. 0-101122  
 solar water heating systems, economic assessment based on measured performance 0-97807  
 space heating, solar installations for utilisation of solar radiation and heat from outside air (*German*) 0-94104  
 space heating, water heating system using solar collectors (*German*) 0-94105  
 spectrally selective surfaces for photothermal conversion of solar energy 0-101125  
 sun-mill, version of dunking-bird, solar-powered, gravity-assisted heat engine 0-89672  
 thin film technology, appls. in energy, optics, and electronics, review 0-78932

**phototransistors**

- GaAs photo-FET high speed photoconductive integrated optical receiver 0-58816  
 InGaAsP/InP phototransistors, fabrication by LPE, photodetectors 0-95139  
 InGaAsP-InP high-gain heterojunction phototransistor 0-103745  
 InP/InGaAs heterojunction phototransistor, high-sensitivity 0-100505  
 Si MIS phototransistors, photoelec. props. at high illum. intensities 0-60101  
 Si phototransistors, slow contamination and fast surface state effects, SEM study 0-107896

**phototubes**

see also photocathodes; photomultipliers

- streak camera tubes with picosecond time resolution, dynamic range measurements 0-73490

**photovoltaic cells**

see also solar cells

- aggregating cells in series and parallel, technique 0-93954  
 Al<sub>1-x</sub>Ga<sub>x</sub>As-GaAs heterophotoconvertors, HV, investigations 0-101097  
 array modules and systems, circuit design considerations 0-93955  
 comparative evaluation (*Italian*) 0-60023  
 concentrator array technology, status report 0-94024  
 conductor-insulator-semicond. (CIS) solar cells, noncrystalline (poly and amorphous), interface importance 0-81466  
 diffusion, chemical reactions, contamination, AES and SIMS 0-72066  
 distributed series resistance effects in photovoltaic devices 0-93968  
 electric power sources, applications overview (*Italian*) 0-72044  
 electrical load feeding prospects (*Italian*) 0-60028  
 encapsulation of photovoltaic cells using silicone materials 0-94019  
 flat plate module design evolution, influence of module requirements 0-94065  
 front surface field solar cell, spectral response, theory 0-76633  
 G. Donegani Institute activity (*Italian*) 0-60027  
 GaAs, polycrystalline, grain boundary resistance meas. effect on solar cell performance 0-93891  
 Galileo works activities (*Italian*) 0-60029  
 glassy C electrodes for photogalvanovoltaic and photovoltaic cells 0-89630  
 homojunction solar cells, conversion efficiency, maximum theoretical efficiency as a function of temp. 0-81469  
 LAMEL activities (*Italian*) 0-60026  
 lifecycle cost minimisation, sizing anal. 0-94039  
 line-focus parabolic-trough photovoltaic arrays, active and passive cooling 0-93988  
 MIS solar cells with diffused back surface field (BSF), and diffused junction solar cells with MIS BSF 0-94074  
 p-n junction photodiode terminology 0-70800  
 parabolic concentrator arrays, collector end shadowing effects minimisation 0-93987  
 photovoltaic technology, conf., San Diego, CA, USA (Jan, 1980) 0-86041  
 phthalocyanine, doped photovoltaic cell, photoconductivity, elec. field induced fluoresc. quenching, charge carrier photogeneration 0-84485  
 point-focus Fresnel lens photovoltaic arrays, active and passive cooling 0-93988  
 power system elements, efficiency and terminology summary 0-97790  
 power system reliability assurance methods 0-61315  
 Schottky barrier solar cells, back-illuminated, theoretical performance 0-61345  
 semiconductor-electrolyte junction photovoltaic cells, interface charge transfer, recombination rate, C-V characts. 0-70818  
 solar cell electricity, cost reduction possibilities 0-97793  
 solar cell panels and systems, US DOE photovoltaic program 0-93879  
 solar cells, polycryst., influence of grain boundaries electronic structure on diode characts. 0-94068  
 solar cells, polycryst., recomb. at grain boundaries, effect on photoresponse 0-108796  
 solar cells in undersea environment, performance 0-93900

**photovoltaic cells continued**

- solar devices, modular system (*German*) 0-89629  
 solar energy plant electricity storage, battery appls. potential 0-72067  
 solar flat panel procurement, qualification test results 0-94064  
 solar photovoltaic cells for remote islands telecommunication repeater stations power supply 0-61382  
 solar photovoltaic system feeding unusual length radio link, characteristics and design data 0-61383  
 Solarex two-axis tracking linear concentrating collector system, design and operation 0-93989  
 technological and economic barriers to be overcome for competitive power production 0-72049  
 thermal/photovoltaic system powers Texas house, performance data and power conditioning equipment 0-94036  
 thin film prep. for solar energy utilisation 0-84847  
 tunnelling MIS structures photovoltaic energy conversion, band struct. 0-92995  
 Al/magnesium phthalocyanine/Nesatron, depletion layer studies, temp. depend. of LF capacitance 0-65617  
 Al/tetracene/Nesatron, depletion layer studies, temp. depend. of LF capacitance 0-65617  
 AlGaAs heterojunction photocell with luminesc. wavelength converter 0-108800  
 AlGaAs-GaAs proton irradiated solar cells, deep level defects and recombination parameters 0-94032  
 Al<sub>2</sub>O<sub>3</sub> MIS Schottky structures, photovoltaic response 0-101115  
 CdO, aqueous-deposited films, struct. and electronic props. for solar cell appls. 0-100797  
 CdS, aqueous-deposited films, struct. and electronic props. for solar cell appls. 0-100797  
 CdS solar cells, construction, solar photovoltaic systems for remote communications power supply 0-66980  
 CdS:Cu(Cl) thin films, surface and bulk photoconc. 0-88653  
 n-CdS/p-ZnIn<sub>2</sub>Se<sub>4</sub> thin film solar cell, photovoltaic props. 0-89628  
 CdS-CdTe p-n junction screen printed thin film solar cells 0-72055  
 CdTe thin film polycrystalline solar cells prepared by electrodeposition 0-93948  
 CdTe thin films, oriented, VPE growth, infrared transmission, photovoltaic cells 0-59825  
 Cu(In<sub>1-x</sub>Ga<sub>x</sub>Se<sub>2</sub>)<sub>1-x</sub>Te<sub>2</sub> pentenary alloy compounds for photovoltaic solar energy conversion 0-93971  
 Cu<sub>2</sub>S-CdS solar cells with interdigitated grid, current-voltage analysis 0-93981  
 Cu<sub>2</sub>S-CdS collection coefficient theoretical anal. at conjunction 0-101094  
 GaAs antireflecting MOS solar cells, epitaxial and polycryst. using OM-CVD techniques 0-94072  
 GaAs polycryst. solar cell diagnostics using IR electroluminesc. 0-93885  
 GaAs prospects (*Italian*) 0-60025  
 GaAs solar cells, photoreaction of p-n junction diodes 0-81464  
 GaAs thin film polycrystalline Schottky barrier solar cells, grain boundary chemistry 0-94067  
 In<sub>2</sub>O<sub>3</sub>-SnO<sub>2</sub>-InP solar cell junctions, efficiency, InP surface props. 0-85288  
 InP homojunction solar cell, antirefl. coated, high-efficiency 0-104505  
 n-InP, MOS solar cells, electrical and photovoltaic characteristics 0-85276  
 InP thin films for photovoltaic devices 0-93972  
 Si, as-grown Czochralski crystal, multiple p-n junction structure obtained by heat treatment, appl. to solar cells 0-101099  
 Si concentrator solar cells, effects of nonuniform illumination 0-93942  
 Si, fixed-base, flat panels, possible developments for more competitive power production 0-72050  
 Si, grain boundary defects in thin semicrystalline material 0-93889  
 a-Si ITO/ZZ 0-101113  
 Si, low series resistance photovoltaic concentrator 0-93940  
 Si n<sup>+</sup>-p solar cell, forward and reverse bias tunnelling 0-85274  
 Si p<sup>+</sup>-n<sup>+</sup> back surface field concentrator solar cells 0-93939  
 Si, polycrystalline, solar cells, grain-boundary hydrogenation technique for improvement 0-85273  
 Si, polycrystalline Czochralski-grown, MIS solar cell characterisation using scanned laser response exam. 0-93884  
 Si polycrystalline film, effect of defects/grain boundaries on photovoltaic mech. 0-93883  
 Si, prospects (*Italian*) 0-60024  
 Si ribbon growth by laser zone melting 0-93482  
 Si solar cell parameters, grain size dependence 0-94049  
 Si solar cells, photoreaction of p-n junction diodes 0-81464  
 Si solar cells, review of physics underlying recent improvements 0-93974  
 Si solar concentrator cell, effects of nonuniform illumination and temp. profiles under concentrated sunlight 0-93941  
 Si<sub>3</sub>F<sub>8</sub>, amorphous efficient carrier generation for solar photovoltaic energy conversion 0-92906  
 Si<sub>3</sub>H, amorphous, HV photovoltaic cells, design parameters 0-101105  
 Si<sub>3</sub>H, amorphous, horizontal cascade type integrated photovoltaic cell module 0-94091  
 Si<sub>3</sub>H, amorphous, solar-cells, charge collection and spectral response 0-85275  
 Si<sub>3</sub>H, amorphous thin film solar cells 0-81478  
 Si-ion-ceramic, short-circuit current density meas. using light-beam-induced-current tech. 0-93887  
 Si-SiO<sub>2</sub>-CdS solar cell, I-V characteristics 0-89621  
 Si<sub>3</sub>Ge<sub>2</sub>, diffused p-n junction, electric and photoelectric props. 0-101095  
 SiH<sub>4</sub>, amorphous, solar cells, short circuit-currents and collection efficiencies 0-94028  
 ZnO, aqueous-deposited films, struct. and electronic props. for solar cell appls. 0-100797  
 Zn<sub>3</sub>P<sub>2</sub> thin polycrystalline films for solar photovoltaic cells 0-97797

**photovoltaic effects**

see also Dember effect

- anomalous photovoltaic effect of ferroelectrics, review 0-65628  
 chromophore phospholipid Langmuir films, photoeffects 0-80409  
 copper phthalocyanine film, electron acceptor surface states due to O<sub>2</sub> adsorption 0-88586  
 cyanine dye monolayer assemblies with Al and Ba electrodes, photovolt., dark cond. and photocond. 0-80400  
 electro-optic crystals, hologram formation arbitrary transport length anal., photovoltaic effects 0-78802



**photovoltaic effects continued**

- electrooptic crystals, holographic recording, photogalvanic effect mechanism of nonlinear wave interaction 0-102672  
 EuSe, photocond. and photodiffusive voltage spectra 0-96940  
 ferroelectric, large-gap type, vibronic theory and opt. props., anomalous bulk photovoltaic effect 0-103939  
 ferroelectric semiconductors, props., book 0-82590  
 ferroelectrics, bulk photovoltaic effect response coeff. 0-65631  
 ferroelectrics, optically induced internal fields 0-107855  
 MIS structure, fast surface states density, photoelectric methods of determ. 0-70835  
 MIS structure, surface state density, determ. from surface saturation photo-EMF meas. 0-75652  
 nickel phthalocyanine film, electron acceptor surface states due to O<sub>2</sub> adsorption 0-88586  
 piezoelectric ceramics, photovoltaic effect application to information storage 0-80316  
 polyacetylene films, AsF<sub>5</sub> doped, photocond. and junction props. 0-70770  
 polymer films, photovoltaic props., solar cell appls. 0-60040  
 polymethine semiconducting films, surface photovoltaic effect 0-70857  
 porphyrin films, methine bridge substituted, surface photovolt. depend. on fabrication method 0-60119  
 semiconductor, diffusion length, meas. by surface photovoltage method effects of optical beam size 0-60002  
 semiconductor with internal elec. short circuits, bulk photovolt. effects, calc. 0-65620  
 semiconductors, exhibiting negative photocond., photovoltaic effects 0-96943  
 semiconductors, photocond., photoelec. effects, book contrib. 0-84488  
 solar cell, diffusion equation, surface boundary condition 0-66975  
 solar cell fabrication, photovoltaic process based on thick film technique 0-94016  
 squarylium dye films, surface photovolt. 0-75594  
 thin film solar cells, unified anal. of potential 0-81436  
 water, CW and flash photoelectrolysis using ferroelectric photoanodes 0-81339  
 AgBr, photo-EMF relaxation, temp. depend. 230 to 316K (*Russian*) 0-73508  
 p-Al<sub>0.9</sub>Ga<sub>0.1</sub>As film, variable-gap photo-EMF 0-65626  
 Al<sub>0.9</sub>Sb Schottky structures, photovoltaic response 0-10115  
 AlSb Schottky barrier solar cells, characteristics and efficiency of Czochralski-grown crystals 0-61366  
 AlSb solar cell material, epitaxy, ionicity and bond struct. 0-61367  
 Ba<sub>2</sub>NaNb<sub>2</sub>O<sub>7</sub>:Fe,Mo, photorefraction mechanism and photoelec. props. 0-71381  
 Bi film fast-response photodetector, employing charge carrier photon entrainment 0-73462  
 Bi<sub>2</sub>WO<sub>6</sub> layered ferroelectric, anomalous photovoltaic effect, photovoltaic current 0-75603  
 Cd<sub>0.17</sub>Hg<sub>0.83</sub>Te-Au(In) contacts, photo-effect in the 77-300K range, barrier height estimation 0-107850  
 Cd,Hg<sub>1-x</sub>Te, epitaxial layer p-n junction, current-voltage characteristics of photovoltaic detectors, 1 to 15 μm 0-86407  
 CdS, surface photovoltage, characterisation 0-60033  
 CdS, XPS, secondary illumination effects, band bending, level shifts 0-108324  
 CdS/Cu<sub>2</sub>S, polycryst. thin film photovoltaic materials, photon loss anal., expt. determ. 0-93888  
 CdS-InP(CdTe)(GaAs)(Ge), solar cell heterojunctions, CVD fabrication, photovoltaic response 0-93878  
 CdSb:Al, p-n junction formation by laser emission, photoelectric effects (*Russian*) 0-70815  
 CdSb:Al(In)(Ga)(Te), p-n junction formation by laser radiation 0-96983  
 CdTe-Au(In) contacts, photo-effect in the 77-300K range, barrier height estimation 0-107850  
 Cr-SiO<sub>2</sub>-Si MIS solar cells, photovoltaic performance and interface states, nucl. radiation effects 0-94004  
 CuGa<sub>0.5</sub>In<sub>0.5</sub>Se<sub>2</sub>/Zn<sub>0.3</sub>Cd<sub>0.7</sub>S heterojunction solar cell, preparation and props. 0-101110  
 CuGaSe<sub>2</sub> single crystals, electrical and photovoltaic props. 0-92940  
 Cu<sub>2</sub>O-Cu diode junction, Schottky barrier, electronic structure and minority carrier diffusion length (*French*) 0-65682  
 Cu<sub>2</sub>S-CdS heterojunctions, role of deep levels in controlling photovoltaic props. 0-92941  
 GaAlAs/GaAs solar cells, efficiency optimisation at high and low current levels (*French*) 0-61348  
 GaAs epitaxial film, photo-EMF echo at 4.2K 0-60038  
 GaAs, primary radiation defect separation by elec. field 0-92522  
 GaAs, XPS, secondary illumination effects, band bending, level shifts 0-108324  
 GaAs:Zn, sign inversion of the linear photogalvanic effect (*Russian*) 0-80321  
 GaP-Si, heteroepitaxial growth, electronic and optical props. 0-104075  
 p-GaSe, back wall Schottky barrier cells, diffusion length, RT spectral response meas. 0-107806  
 p-Ge, laser radiation excited, gradient EMF anisotropy 0-75604  
 Ge p-n junction, photo-EMF generation in saturation region 0-75635  
 p-GeS, crystalline, photoelectric props. 0-70769  
 GeSe, amorphous layers, photoconductance meas. 0-65632  
 InAs:S(Mg), ion implanted, photocond., photo-EMF, and optical absorpt. spectra 0-70763  
 In<sub>1-x</sub>Ga<sub>x</sub>Sb, energy gap, temp. depend. and photovoltaic effect 0-70746  
 In<sub>2</sub>O<sub>3</sub>-SnO<sub>2</sub>-CdTe:P, p-n homojunction solar cell, elec., photovoltaic props., photoluminescence 0-81463  
 n-InSb, MIS diode, time-dependent photovoltaic effect 0-75601  
 InSb-NiSb, photovolt. effects rel. to theory of semicond. with internal elec. short circuits 0-65620  
 InSe solar cells, photovoltaic conversion efficiency 0-61356  
 In<sub>2</sub>Se<sub>3</sub>-SnO<sub>2</sub> amorphous film-SnO<sub>2</sub> system, photovoltaic spectra, annealing effect (*Japanese*) 0-92926  
 In<sub>2</sub>-<sub>3</sub>Sn<sub>3</sub>-<sub>4</sub>insulator-poly-Si solar cells, photovoltaic conversion parameters 0-101093  
 KNbO<sub>3</sub> reduced, phase hologram recording sensitivity, energy transfer, photovoltaic effects 0-78799  
 La<sub>2</sub>Ti<sub>2</sub>O<sub>7</sub> layered ferroelectric anomalous photovoltaic effect, photovoltaic current 0-75603  
 LiNbO<sub>3</sub>, anomalous photovoltaic effect obs., Anderson method 0-88595  
 LiNbO<sub>3</sub>:Cu(Fe), light induced charge transport, photovoltaic effects, impurity states 0-80317  
 LiNbO<sub>3</sub>:Fe, holographic recording and thermal fixing, invest. of mechanisms 0-78810

**photovoltaic effects continued**

- LiTaO<sub>3</sub>:Cu(Fe), light induced charge transport, photovoltaic effects, impurity states 0-80317  
 Nd<sub>2</sub>Ti<sub>2</sub>O<sub>7</sub>, layered ferroelectric, anomalous photovoltaic effect, photovoltaic current 0-75603  
 Pb<sub>0.97</sub>Hg<sub>0.03</sub>Te photovoltaic detector produced by Sb<sup>+</sup> ion implantation 0-82821  
 PbI<sub>2</sub>, photo-EMF, effect on photolysis of PbI<sub>2</sub>-Ag (*Russian*) 0-92939  
 Pb<sub>1-x</sub>Mn<sub>x</sub>Te, photovoltaic effect, p-n junction, energy gap determ. 0-92931  
 PbTe photovoltaic detector, detectivity limits 0-105709  
 Pr<sub>2</sub>Ti<sub>2</sub>O<sub>7</sub> layered ferroelectric, anomalous photovoltaic effect, photovoltaic current 0-75603  
 Rb<sub>2</sub>ZnBr<sub>4</sub>, ferroelec., photovoltaic and photorefractive phenomena 0-75598  
 SbSI, anomalous photovoltaic effect 0-70749  
 SbSi<sub>0.3</sub>Br<sub>0.7</sub>, anomalous photovoltaic effect 0-70749  
 Se<sub>1-x</sub>Te<sub>x</sub>-Se<sub>1-x</sub>Te<sub>x</sub> junctions, photovoltaic effects and rectification phenomena 0-84506  
 Si based alloys, amorphous, photovoltaic behaviour, solar cell appl. 0-94051  
 Si, cast, growth structure and photovolt. props. of solar cells 0-94008  
 Si, float zone, meas. of deep levels by photovoltage spectroscopy 0-103723  
 Si phototransistors, slow contamination and fast surface state effects, SEM study 0-107896  
 Si, photovoltaic and photomagnetic effects, rel. to intervalley electron transfer 0-60034  
 Si polycrystalline-metal Schottky barrier solar cells, elec. and photovoltaic contact props. 0-93936  
 Si wafers, Czochralski grown, minority carrier transport props., laser beam scan for homogeneity anal., photovoltaic cell appls. 0-92905  
 Si:F,H, amorphous, elec. and optical props. 0-60031  
 SnO<sub>2</sub>-InP heterojunctions, elec. and photovoltaic characs. 0-75628  
 Sr<sub>2</sub>Nb<sub>2</sub>O<sub>7</sub>, layered ferroelectric, anomalous photovoltaic effect, photovoltaic current 0-75603  
 T-metal, thin film contact, time evolution of photovoltaic effect 0-65687  
 Zn<sub>3</sub>P<sub>2</sub>, polycryst. thin film photovoltaic materials, photon loss anal., expt. determ. 0-93888  
 Zn<sub>3</sub>P<sub>2</sub>-metal contacts, photoelectric props. 0-92930  
 ZnSe, minority carriers diffusion length by surface photovoltage method 0-60003

**photovoltaic generators, solar** *see photovoltaic cells; solar cells***phthalocyanines** *see organic compounds***physical chemistry**

- see also chemical analysis; chemical equilibrium; chemical reactions; chemical structure; crystal chemistry; electrochemistry; nuclear chemistry; pH; photochemistry; radiation chemistry; radiochemistry; solvated electrons; surface chemistry; thermochemistry*  
 No entries

**physical data, collections of** *see collections of physical data***physical instrumentation control**

- Auger microprobe, scanning, computerised image processing 0-68304  
 bubble chamber film analysis, semiautomatic measuring system 0-58105  
 calorimeter, low temperature investigations, simple off-line arrangement 0-90850  
 Dewar flask, self-opening valve for N<sub>2</sub>, decanting siphon 0-57310  
 flowmeters and level meters, commercial instruments survey (*French*) 0-83871  
 gas chromatography-mass spectrometry, computerised, data-blocking cross-correlation peak detection 0-62725  
 Joyce-Loebl microdensitometer, computer control for objective-prism spectra meas. 0-105173  
 microcomputer interfaced spectrophotometer for kinetic studies 0-62726  
 microprocessor controlled long lived alpha emitter monitor 0-58069  
 microprocessor controlled multipoint recorder with graphical video output for reactor core temperatures 0-57873  
 monochromator, programmable, for ICP emission spectrometry, intensity meas. 0-62728  
 monochromator scanning control system using microprocessor, spectral line shift correction (*Japanese*) 0-57384  
 NMR magnetometer, large-scale automation 0-57343  
 phosphate and alkaline phosphate activity determ. by dual microcomputer-controlled stopped-flow spectrometer 0-57379  
 portable microprocessor controlled neutron spectrometer, NE213 organic scintillator 0-58022  
 radiotelescope control system, 8 cm instrument at Toyokawa, Japan 0-98549  
 radiotelescope RT-22, automatic obs. by computer 0-109359  
 ring specimens, computer controlled mag. meas. system 0-86346  
 Space Telescope pointing control fine guidance subsystem design 0-82201  
 thermal desorption mass spectroscopy, computer control, data acquisition, appls. 0-61181  
 thyristor temp. regulator for pulsed NMR spectrometer 0-105687  
 vacuumuems, ionisation, with cold or hot cathodes (*Czech*) 0-73376  
 voltammetric analysis, automatic controller, design 0-71968  
 H masers, with automatically tuned resonators 0-95859  
 H<sub>2</sub>SO<sub>4</sub> mist monitor, semicontinuous 0-61495

**physical metallurgy** *see metallurgy***physical optics**

- education, lateral-angular magnification relationship for simple magnifier 0-57031  
 Herschel's condition as wave optics theorem 0-87301  
 holography and coherent optics, information theory, book 0-98764  
 wave and particle descriptions of light, equivalence, rel. to radar freq. shift 0-101692

**physics**

- see also physics computing*  
 computer-aided teaching, hinted finding scheme, simulation appls. (*French*) 0-98777  
 contemporary needs, conf., Nathiagali, Pakistan (June 1978) 0-62387  
 current developments review (book) 0-77600  
 nature, unity of, as an incentive to research (*German*) 0-77533

**physics computing**

- see also computerised instrumentation; spectroscopy computing*  
 3-D computer program for nonlinear EM fields, TOSCA 0-95765  
 acetone-chloroform-methyl isobutyl ketone, ternary phase diagrams, interactive computer program 0-71629



**physics computing continued**

achromatic antireflection coatings, thin-layer, layer thickness calcs. 0-87468  
 n-alkane, polymer, liq., mol. arrangement, computer model 0-92446  
 alloys, binary, constitution diagrams, computer calc. (*Russian*) 0-84909  
 alloys, ion-implanted, integral Gaussian profile determ. method 0-107313  
 alloys, segregating phases identification, single crystals, radiographs computer calc. 0-84934  
 amorphous Ising system, computer simulation 0-60299  
 amorphous materials, dispersive transport, computer simulation, time of flight signals 0-70696  
 amorphous solid, structural defects, computer simulation study 0-88040  
 antireflection coating, multilayer achromatic, extended region of low reflection coeff. values 0-95982  
 atmospheric sound absorpt., personal computer program 0-96065  
 atom-atom collision cascades localisation, impurity and thermal vibr. influence, computer simulation method 0-88227  
 axisymmetric transducers, with various boundary conditions, single integral computer method for Green's function 0-87591  
 BWR in-core neutron detector sensitivity to control rod vibr. using neutron noise anal. 0-57910  
 calorimeter, low temperature investigations, simple off-line arrangement 0-90850  
 calorimeter for temp. range 4-380K 0-98915  
 cathode lens having a quasispherical field 0-95782  
 CEPADAS, real-time computer program for off-site radiological impact assessment of nuclear facilities 0-95475  
 chromatography, nonlinear, nonideal, computer simulation models 0-62639  
 cluster systems, program for calc. electronic struct. with double self-consistency-Bersuker's method 0-69289  
 collinear asymmetric model reaction probabilities quantum and quasiclassical calcs. 0-85145  
 confined plasma column, soft X-ray lasing action conditions 0-74346  
 COREF-1 nuclear fuel behaviour code, appl. to LMFBF during overpower transient 0-57853  
 crack propagation, computer simulation 0-59573  
 crystal growth, dynamic computer models 0-103284  
 crystal setting, and data reduction, on a PW 1100 diffractometer, program using simple method based on real space 0-59342  
 crystal structural fragment, automatic construction, taking account of attainable chem. bond lengths 0-92419  
 crystallographic orientations distribution function, computer calc. for cubic metals 0-64827  
 dark-field imaging, computer simulation 0-100151  
 data handling and standard practices 0-58009  
 dense fluids, relative motion of atomic pairs investigated in short-time regime 0-96426  
 dislocation motion, lattice resist., effect of impurity interstitials 0-84170  
 disordered structures, two-dimensional, computer program for modelling (*French*) 0-59337  
 dose-rate conversion factors for external exposure to photons and electrons, modifications to DOSFACTOR code 0-104775  
 DOSFACTOR code, dose-rate conversion factors for external exposure to photons and electrons 0-104775  
 elastomeric bearings, high-capacity, laminated, finite-element anal. 0-96197  
 electron diffraction patterns, point, computer indexing 0-100136  
 electron micrograph, 500 kV, atomic resolution, computer image processing 0-100149  
 electron microscopy, bright field images, signal-to-noise enhancement in incoherent superposition 0-101906  
 electron microscopy, many-beam structure images, optimal comput. techniques 0-95203  
 electron microscopy, phase contrast simulation, of Au cluster atoms on W support film 0-100150  
 electron trajectories in multi-element electrostatic cylinder lenses, program for calculation 0-87283  
 equation of state variables calculation using TI-59 0-77738  
 ERATO code, plasma MHD stability, convergence of solns. 0-83906  
 experiment planning, optimum plans calc. on convex polyhedrals 0-57084  
 experimental data processing method based on piecewise-linear dependences 0-62640  
 fatigue limit, in bi-freq. loading 0-104289  
 FBR analysis, general multigroup nodal procedure based on response matrix principles (for FBR analysis) 0-57827  
 feed through eddy current transducer, numerical anal. or operating mode during ferromagnetic rod inspection 0-108670  
 fibre reinforced composites, fracture processes modelling, digital computer appl. 0-65147  
 fission reactor materials, ion penetration distance calculations with multi-group transport computer codes 0-102246  
 fission reactor materials damage by heavy ion bombardment, comparison of analytical and Monte Carlo computer codes 0-102245  
 fluid dynamics, Navier-Stokes equations, finite element soln., applied to blood flow 0-94269  
 fluid flow problems, incompressible, free surfaces 0-106774  
 fluid structure and dynamical props., computer simulation, using Monte Carlo and mol. dynamic methods (*German*) 0-69757  
 Fourier transform IR spectrometer software package for phase correction 0-95162  
 fracture analysis, 2D linear, elastic, finite element anal. vs. the edge function method 0-99963  
 fragile lattice packings of spheres in 4D space 0-100194  
 free electron lasers, energy transfer, computer simulation 0-83578  
 Frevel ZRD-SEARCH-MATCH program, for powder diff. anal., generalisation 0-59341  
 frontal method for structural mechanics, algorithm for excluding unknowns 0-79157  
 fusion driven symbiotic energy systems, neutronic and economic anal. of CTR blanket using XSDRNPM code 0-57955  
 fusion reactor, MFTF, end loss region high energy plasma gettering 0-102343  
 fusion reactor, mFTF plasma diagnostics Data Acquisition System 0-99319  
 fusion reactor, TEXTOR, mag. diagnostics and monitoring systems data acquisition 0-99320  
 fusion reactors, PLT and PDX data acquisition systems, networking and distrib. processing improvements 0-99318  
 G1M/HYBRID quasi-equilib. MHD code for plasma simulation 0-64689  
 gas-filled microballoons, radiation effects MEDUSA code calcs. 0-83220

**physics computing continued**

Gaussian optics parameters, HP-67 calculator program 0-106439  
 GROCS, underground heat flow model for solar source heat pump system 0-66987  
 high pressure phase equilibria and other fluid-phase properties, computational methods 0-75329  
 high-pressure phase equilibria in mixtures using partition functions, computational methods 0-75330  
 hopping conduction, random one-dimens. system, Monte Carlo computer simulation 0-80278  
 image contrast loss in presence of chromatic magnification difference, numerical estimate 0-95823  
 image reconstruction, iterative computer method 0-102634  
 interference fringes, algorithm for fast digital analysis 0-73426  
 ion backscattering and implantation, H and He ions, computer simulation, comparison of MARLOWE and TRIM codes 0-66350  
 ion beam trajectory focusing effects on toral reflection coeff., computer studies 0-89102  
 ionic crystals, defects, computer modelling, review 0-107205  
 isopermalloy, permeability stability calc. rel. to texture (*Chinese*) 0-65959  
 laboratory experiments, graphic computer simulations 0-105470  
 laminates analysis, desktop calculator library module appl. 0-77764  
 laser anemometry and other photon correlation data, stabilized model-fitting approach 0-58622  
 laser pump system, analytical theory 0-106540  
 laser system, interferometric optical anal. 0-87401  
 lattice images of crystal defects, computer simulation 0-107208  
 Laue photograph indexing and monocystal orientation determination by computer, new approach (*Chinese*) 0-79636  
 LEED, surface potential barrier, reflection and transmission coeffs., Schrodinger eqn. 0-87998  
 lens testing, MTF-based optical sensitivity and tolerancing computer programs 0-83686  
 light wave diff. by complex spectral composition US 0-95939  
 linear magnetic solenoid reactor plasmas, dynamic behaviour 0-64751  
 LMFBF fuel, fission gas behaviour during overpower transient, calcs. using COREF-1 code 0-57853  
 low field magnet, computer controlled, for optical and magnetic resonance studies 0-95113  
 magnetic field and force eqns., solns. using programmable calculator 0-91721  
 magnetic first order instability in finite model system 0-65932  
 magnetic materials search, appl. of cybernetic prediction systems 0-108048  
 magnetic model systems 0-65924  
 metal, BCC, twin boundary and stacking fault structs., computer simulation 0-59485  
 metals, FCC, twist boundaries, struct. invest. using computer simulation technique 0-84185  
 metals, interstitial loop growth, pulsed irradiation effects 0-88210  
 mirror, dielectric, Rayleigh scatt. at 441.6 nm 0-97367  
 moire, computer generated, for profile testing 0-105689  
 molecules containing heavy atoms, program for calc. electronic struct. by quasirelativistic method 0-69088  
 multi-layer optical system, reflection and transmission coeffs. calcs., computer program 0-66316  
 nonperiodic objects, reconstruction from electron micrographs using correlation methods 0-86527  
 nuclear decay scheme construction from gamma transitions and coincidences, SMUDLA 0-83063  
 nuclear energy level lifetime measurement using on-line computer and registration time shift compensation 0-68577  
 nuclear facilities, off-site radiological impact assessment real-time computer program CEPADAS 0-95475  
 nuclear materials safeguarding, statistical anal. of materials accountability, computer simulation 0-73933  
 numerical analysis and computational methods in physics, computer appls. 0-62456  
 optical coatings, absorptive, at normal incidence, program for TI-59 calculator 0-84793  
 optical fibre preform, refractive index profile and cross-sectional geometry meas. method 0-91893  
 optical multilayer filters, non normal incidence, optical monitoring, allowable tolerances (*French*) 0-87526  
 optical recording, ablative 0-91752  
 optical resonator, annular, adaptive mirror effects on performance 0-58596  
 ORIGIN2 point-depletion and decay computer code 0-99248  
 PEST, plasma instability, axisymmetric, in non-circular Tokamak 0-87877  
 photographic materials, MTF automatic evaluation 0-95170  
 photoionisation TEA CO<sub>2</sub> laser (*Russian*) 0-83589  
 physical optics farfield inverse scatt., mathematical inversion technique for nondestructive eval. 0-69580  
 plane coalescence, at grain boundaries 0-70221  
 plasma, simulation anomalous transport processes, G1M/HYBRID quasi-equilib. MHD code 0-64689  
 plasma instability, axisymmetric, in non-circular Tokamak 0-87877  
 plasma MHD, nonlinear time-dependent hydromagnetic model, spatial and temporal finite-difference techniques 0-59192  
 plasma MHD, stability code, ERATO, convergence of solns. 0-83906  
 plasma MHD, toroidal axisymmetric config., vacuum potential energy change, spectral codes 0-87869  
 plasma transport, anomalous, electron temp. gradient instability 0-75034  
 polymers, breaking down of anharmonic chain, computer calc. 0-106410  
 polymers, glassy, craze surface displacements, model 0-93651  
 polynuclear clusters, programs for calc. electronic struct. by Mulliken-Wolfsberg-Helmholtz method 0-69288  
 proton channelling simulation, for diamond 0-79849  
 prototype autoresonant, accelerator, computer system, data acquisition and processing 0-99433  
 pyrometry, photoelec., radiance temp. direct calc. 0-73367  
 radioactive waste disposal safety criteria, ORIGIN2 point-depletion and decay computer code 0-99248  
 radioactivity, decay product radioactive accumulation, FORTRAN program 0-68611  
 radioisotope transport in terrestrial food chains, dynamic modelling using RAGTIME code 0-104776  
 radionuclide decay, computer simulation, levels, transitions, internal conversion 0-63136



## physics computing continued

RAGTIME code for dynamic modelling of radioisotope transport in terrestrial food chains 0-104776  
 random packing of spheres, computer simulation 0-77705  
 reactor analysis, 3-D integral transport code SHETAN 0-63238  
 reactor analysis neutron thermalisation, THERMOS spectrum code, accurate reduced mesh model 0-57829  
 rectangular laminated plate, free vibr., freq. and shape determ., complex boundary conditions 0-79203  
 refractories, strength and thermal properties, automated test system 0-100986  
 rotating disc problem, Taylor coefficients, computational methods 0-106802  
 segmented calorimeter, high energy performance, Monte Carlo simulation 0-58029  
 semiconductor, deep levels, review 0-103640  
 SHETAN—a three-dimensional integral transport code for reactor analysis 0-63238  
 SIMULATE, general multigroup nodal procedure based on response matrix principles [for FBR analysis] for FBR anal. 0-57827  
 single crystals, growth simulation 0-88069  
 SMUDLA, nuclear decay scheme construction from gamma transitions and coincidences 0-83063  
 SNM safeguards, LASL DYMAC accountability system, software development 0-99212  
 solar buildings, climatological design assessment interactive CAD techniques 0-61289  
 solar energy concentrators, segmented parabolic mirrors, optical performance anal. by THEK computer code (French) 0-61294  
 solar ground coupled heat transfer, expt. and GROCS computer model of heat pump system 0-66987  
 solar heating of buildings, numerical simulation of thermal performance 0-66942  
 solar ponds, salt gradient, computer simulation of thermal behaviour 0-101126  
 solidifying melt, two phase zone formation, convection (Russian) 0-93547  
 spin glass, computer simulation 0-60299  
 square duct, developing turbulent flow and heat transfer, computational procedure 0-69926  
 steel, mild, corrosion rate meas. in  $H_2SO_4$  using microprocessor controlled potentiostat 0-71798  
 STEM, image formation, 2-D computer simulation of heavy atom model compounds 0-75135  
 superposed coherent and chaotic radiation, computer simulation 0-58485  
 teaching using SWTP 6800 system in BASIC 0-98776  
 TEM, high resolution, surface struct. of (001) Au film 0-100383  
 ternary phase diagrams, interactive computer program 0-71629  
 ternary solution phases, empirical methods of predicting and representing thermodynamic props. 0-70423  
 ternary system compound formation, comp. and props. w.r.t. component electron struct., computer prediction 0-103444  
 texture of materials, data acquisition and processing 0-64828  
 THEK analysis of optical perform. of segmented parabolic mirrors (French) 0-61294  
 THERMOS spectrum code, accurate reduced mesh model for neutron thermalisation 0-57829  
 thin film condensates coalescence, influence on morphological changes, modelling 0-107676  
 thin film deposition process, line-edge profile simulation appl. 0-104068  
 three-dimensional topographic mensuration, laser electro-optic system 0-99784  
 Tokamak data processing, no. of computers required 0-59252  
 toroidal pinch discharge, preionisation phase, numerical computation 0-64696  
 track chamber slide processing, calibration programming problems (Russian) 0-73305  
 TRANSPORT, design program for charged particle beam transport systems 0-106220  
 TRNSYS optimization formulation for solar heating systems 0-61414  
 two-phase anisotropic medium, interfacial dislocation, stresses, displacements and energy calc. 0-79786  
 two-phase cryst. structures, orientational electron microdiff. anal. with aid of OMEGA program 0-103218  
 two-phase flow, horizontal stratified, 1-D two-fluid eqns. for LWR LOCA 0-91226  
 unified field theories, relativistic, computer field interaction simulation system 0-68412  
 US propagation in solids, visualisation using Schlieren photoelastic apparatus (Italian) 0-88274  
 X-ray diffraction energy dispersive diagrams, eval. using small computer on-line techniques 0-92423  
 X-ray equivalent reflections averaging, using small computers 0-79634  
 X-ray integration method, extension of  $\sin^2\psi$  method (German) 0-92420  
 X-ray powder diffraction, research and quality assurance appl. 0-73556  
 X-ray stress meas., computer-aided system (Japanese) 0-104366  
 Al alloys, fatigue crack initiation, computer simulation 0-100893  
 Al, tilt boundary,  $\Sigma=5$ , struct. and atomic vibr., computer simulation 0-70223  
 Au, atomic struct. of large angle [001] twist boundary, determ. by computer modelling and X-ray diff. study 0-70162  
 Au, polycrystn., deformed, computer simulation of vacancy annihilation to dislocations (Japanese) 0-88205  
 $CO_2$  laser pulse, nonlinear propag. characts., computer simulation 0-106575  
 $CaF_2$ , mol. dynamics studies of superionic conductors 0-107547  
 Cr-Fe-Ni-Si, ternary phase equilibria for Cr-Fe-Ni rich portion, lattice stabilities 0-71628  
 Cr-Ni-Fe, ternary phase diagrams, interactive computer program 0-71629  
 Cu, point and planar defects, computer simulation 0-59455  
 Cu vapour laser, rate processes, computer simulation 0-69371  
 $Cu_{50}Zr_{50}$ , amorphous alloy, computer simulation of atomic structure 0-70125  
 Fe polycrystals, grain misalignment, electron microscope determ. (Russian) 0-103358  
 Fe-Si, grain oriented steel, grain struct. by computer mapping 0-88168  
 Fe-Si-C, austenitic, C diffusivity (German) 0-92705  
 $FeF_3$ , amorphous, struct. and mag. props., computer model 0-96446  
 $Fe_{2.25}P_{0.75}$  amorphous alloy, atomic struct., computer simulation 0-88043  
 HCl liq., time correlation function, computer simulation 0-79670

## physics computing continued

KCl-CaCl<sub>2</sub>-NaCl, ternary phase diagrams, interactive computer program 0-71629  
 Mg, HCP, vacancy clusters and interstitials, computer simulation study 0-64992  
 Mo polycrystals, grain misalignment, electron microscope determ. (Russian) 0-103358  
 Na-K liquid alloys, struct., X-ray and neutron diff. meas. 0-107041  
 NaI(Tl) detectors, response functions to terrestrial  $\gamma$ -radiation, computer program 0-83233  
 $Na_2XO_4$  (X=S, Cr, Mo, W), anal. and calc. of binary and ternary phase diagrams 0-88299  
 Si, ion penetration, computer program 0-88185  
 Si surface, (111), energy states, computer renormalisation-group calc. 0-75617  
 p-Si-Al, ohmic contacts, Si dissoln. and recrystn. effects, computer calc. 0-103749  
 Si-SiO<sub>2</sub>, two layer system, P<sup>+</sup>-ion penetration tails, expt. and computer anal. 0-75249  
 Ti-Mo(V), metastable diffusionless equilibria, high press. conditions 0-71627  
 $^{238}U(\gamma,f)$  20 MeV, computer program for yield determ. of short-lived products 0-102215  
 YIG, vitreous electric-field-gradient distrib., Mossbauer quadrupole splitting meas. 0-75901  
 Zn-Sn-Bi, ternary phase diagrams, interactive computer program 0-71629  
 Zr(Ca,Y)O<sub>2-x</sub>, local ionic arrangement, X-ray diff. study 0-100203

## physics fundamentals

see also classical field theory; complementarity; cosmology; elementary particles; fundamental law tests; mechanics; quantum field theory; quantum theory; relativity; thermodynamics; units (measurement)  
 causal paradoxes implied by hypothetical coexistence of positive- and negative-mass matter 0-82685  
 causality, localisation and spreading of wave packets 0-90715  
 Diracs hypothesis on time depend. of fundamental consts. 0-90772  
 large-scale uniformity of physical laws, evidence from QSO absorpt. redshifts 0-73079  
 laws, physicist's role 0-105523  
 thermoelasticity, dynamic theory, based on causality principle 0-69657

## physiological models

see also brain models; neurophysiology; physiology  
 alpha-rhythm, neural vet model 0-76719  
 antagonistic muscles, functional elec. stimulation optimisation, math. modelling, joint motion 0-61730  
 arm posture control, spring model and equivalent neural network 0-101196  
 arterial stenosis, math. model 0-72202  
 arterial system model validity, quantitative evaluation 0-61599  
 articular cartilage single layer model, flow fields created by a sliding load 0-104630  
 atrial contraction, model anal. of contrib. to ventricular filling 0-85424  
 audition coordinating cerebral activity model 0-85404  
 auditory detection of intensity increments of narrowband noise signals, amplitude model 0-61591  
 auditory models and signal processing, conf., Munster, Germany (Sep. 1978) 0-90610  
 auditory nerve fibre model 0-94227  
 auditory perception nonlinear model with autocorrel. feedback 0-81615  
 autoregressive model order selection applied to physiological signals 0-104780  
 ballistic walking, math. model of swing phase 0-67131  
 bipedal locomotion, inverted pendulums stabilisation algorithm (Japanese) 0-81630  
 blood, rheological behaviour, viscoelastic model (French) 0-76779  
 blood in vessel with actively deforming wall, numerical simulation of movement 0-72205  
 brightness perception and retinal rivalry in binocular vision, integrated model 0-101180  
 capillary tracer exchange, 4-phase model 0-101152  
 cartilage, model for surface flow 0-85431  
 cell survival curves, biological variability model 0-108978  
 cells, volumetric changes during freezing and thawing, thermodynamic model 0-108863  
 cochlea, one-dimensional model illustrating resonance 0-61581  
 cochlear models—1978 0-94221  
 colonic electrical control activity, human, computer model 0-61537  
 colour vision, line elements 0-97910  
 colour vision models, vector magnitude operation, derivation from signal detect. theory 0-101174  
 compartment tracer flow modelling and digital imaging 0-101257  
 cone, computer-driven hardware model, response obs. 0-72402  
 cortical evoked potentials, math. model for source localisation, somatosensory stimulation 0-89774  
 cranial structure exposed to RF radiation, thermal response model 0-94285  
 cytoplasm spherical drop with effective surface tension influenced by oscillating enzymatic reactions 0-108862  
 distributed type associative memory model with quantised Hadamard transform 0-108867  
 drug elimination interactions, physiological flow model in rat 0-81628  
 duodenal slow waves, human, anal. and modelling. 0-72146  
 egg cell membranes, starfish, inward rectification blocking model 0-61523  
 electromechanical model for human articular cartilage 0-104631  
 ERG, oscillatory pots., analogue circuit model and frog obs. 0-89750  
 erythrocyte tank-treading motion in a shear flow 0-104568  
 excitation properties of the squid axon membrane and model systems with current stimulation 0-67054  
 exhalation in lung model, effect of ventilation and diffusion nonuniformity 0-104603  
 extracellular potentials generated by curved fibres in a vol. conductor, modelling 0-97889  
 eye, accommodation and vergence static behaviour, computer simulation of interactive dual-feedback system 0-94205  
 fetal head moulding, finite element model investigation 0-67129  
 finger tapping by both hands, coordinated, two coupled oscillators as model 0-101163  
 haemodynamic model for phasic press. and flow in large arteries 0-94254



**physiological models continued**

- heart, ellipsoidal model, appl. to left ventricular contractions study 0-104608
- heart contraction mechanism, modelling 0-72204
- Hodgkin-Huxley standard model, squid axons in reduced external  $\text{Ca}^{2+}$  0-94188
- human retinal image processing, two-channel model 0-94215
- intestinal myoelectrical models, pulse synchronisation expts. 0-67061
- intestinal tissue, electronic modelling of slow-waves and spike-activity 0-89737
- intravascular radioactive tracers, calc. of residence time distribns. in fields of external registration 0-72291
- kidney, six-tube vasa recta model as test problem 0-104610
- kidney model, numerical soln. by multiple shooting 0-104609
- Korotkoff sounds, model expt. on generation 0-98207
- Leaky-Integrator Neuron Model, input-output relationship 0-72152
- left ventricle, math. model of mechs. 0-101195
- left ventricle, model study of isovolumic and non-isovolumic contracts 0-85428
- locomotion dynamics, human, math. model 0-97981
- lumbar spine, human, dynamic 3D modelling, computer code 0-108948
- lung, deposition of inhaled particles, airway generations of normal subjects 0-67125
- lung, deposition of particles in model airways 0-72192
- lung, finite element model for macroscopic deform. 0-108945
- lung, macroscopic deformation, finite element model 0-89781
- lung mathematical models, effect of common dead space on inert gas exchange 0-67126
- lung parenchyma, math. model 0-108940
- mechanism of production of summing potential, hair cell functional differences, elec. cct. model 0-72176
- membrane, electrogenic ion transport along oligomer channels capable of conformational transitions 0-108854
- membrane bilayers, quasitwo dimens., theoretical models 0-76713
- mesomorphic monolayers, quasitwo dimens., theoretical models 0-76713
- micropolar fluid model for blood flow through narrow tubes 0-67109
- mucociliary flow mechanics, channel model obs. 0-97957
- multipath neural systems, statistical anal. 0-101162
- muscle, anatomical model, internal pressure effects 0-67103
- muscle, multifibre preparation, intercellular clefts influence on pot. and current distrib. 0-72145
- muscle actions, model for semi-quantitative studies 0-61605
- muscle stretch reflex system, math. model (*Japanese*) 0-67067
- nerve fibre membrane analogue-code conversion, ionic mechanisms 0-81575
- nerve impulse conduction along a myelinated fibre, math. model 0-94195
- neural encoder, adaptive model 0-97897
- neuromuscular unit discharge during muscle fatigue, structural model anal. 0-67066
- neuron electronic model (*Spanish*) 0-104580
- neuron model, two-terminal electronic circuit 0-61526
- neuron model as component of neural network, hardware realisation 0-61534
- neuron soma model with high reliability and low power consumption 0-72392
- orientation sensitivity of visual movement detection system activating landing response of blowflies 0-101176
- oscillatory neural networks in the rabbit hippocampus 0-89743
- Paramecium excitation, model anal. 0-61524
- patellofemoral joint, anal. model 0-104625
- photosynthesis, modelling of enhancement and chromatic transitions 0-104565
- prolate spheroidal models of humans in near field of short electric dipole, irradi. 0-104639
- proton transport across charged membrane and pH oscillations 0-61516
- pupillary light reflex system, modelling and identification 0-61554
- radiation science, role of models 0-67144
- radioisotope imaging, digital images, math. models and physiological parameters 0-98107
- radioisotope uptake of bone-seeking radioisotopes in normal bone rel. to blood flow 0-94320
- radiolysis of heterogeneous inanimate systems, radiobiology appl. 0-66824
- respiratory mechanical behaviour lumped parameter models evaluation using simplex algorithm 0-89783
- respiratory period prediction, men exercising while wearing masks, comparative model study 0-94253
- respiratory resistance, central and peripheral, estimation using elec. analogue model 0-81636
- running, influence of track compliance 0-61602
- skeletal blood flow, implications for bone-scan interpretation 0-72199
- skeletal muscle, lumped and population stochastic models, implications and predictions 0-76724
- skeletal muscles, contracting, simulation studies of mech. stretch 0-94263
- soft tissues, elastic stress/strain relation based on a struct. model 0-101205
- spectral sensitivity of human eye, colour coordinates number triple (*Russian*) 0-76741
- spectral sensitivity of human eye, deductive derivation of mathematical model (*Russian*) 0-76740
- sperm, human, flagellar propulsion in cervical mucus, interaction hydrodynamics model 0-97878
- spinal cord electrical stimulation, 2D finite element anal. 0-98054
- spine, human, finite element model for in vivo freq. response anal. 0-104623
- striate cortex functional architecture quantitative model 0-89747
- stuttering model, movement disorder 0-94241
- substance diffusion in tissue with nonlinear consumption, math. model 0-67326
- substrate exchange between vascular and extravascular compartments, saturation kinetics 0-104571
- temperature measurement, human body-temp. sensor-environment system, analogue model of interaction 0-104783
- thermoregulation, math. model 0-94173
- tooth support, model of periodontal vasculature 0-85434
- torso surface isopotential simulation using simple conduction-elec. field model with Neumann boundary 0-89706
- ventricular arrhythmia model 0-89893
- vertebrate retina modelling and simulation, extended networks 0-108884
- vertebrate retina neuronal activities modelling and simulation 0-85386

**physiological models continued**

- Vespa orientalis, photoelec. props. of 'yellow strips' on cuticle, math. model 0-104638
- vision, associative learning model, voltage-dependent  $\text{Ca}^{2+}$  and  $\text{K}^{+}$  conductances 0-72166
- vision, gloss perception, model using binocular cells in lateral geniculate body 0-72167
- vision, inductive colour contrast, expt. investigation of model (*Russian*) 0-76739
- visual difference thresholds modelling, appl. of ordered topological vector spaces 0-104587
- visual pattern recognition (*Japanese*) 0-97920
- visual processing, nonlinear, in cat's retina 0-85385
- visual system simulator, human (*Russian*) 0-76877
- vocal cord vibration, continuous model 0-85418
- walking, connections between different legs, quantitative model 0-101161
- walking, individual leg control, model 0-101160
- work-effort ratio of a large muscle group, theoretical model 0-108949
- $\text{Na}^{+}$  saturation kinetics in frog skin, compartmental aspects 0-67050
- $\text{O}_2$  transport system, functional state, math. model 0-104548

**physiological optics** see vision**physiology**

- see also blood; haemodynamics; hearing; neurophysiology; physiological models; speech; vision
- blood, US Doppler-shift waveforms, physiological interpretation 0-89814
- corneal sensitivity and thickness after wearing PMMA and gas-permeable contact lenses 0-61544
- diving physiology research facility 0-82106
- dolphin, lung collapse and intramuscular circulation during diving 0-81643
- eye, jerk nystagmus, some new findings 0-67074
- eye, saccadic latency predictability in a novel voluntary oculomotor task 0-72157
- flow problem, one tube 0-89703
- hearing loss, ageing, statistical study of urban population not subjected to occupational noise (*French*) 0-81623
- industrial noise onset effects on physiological and psychological functions 0-91959
- ionising radiation induced behavioural and physiological changes in rats, hormonal radioprotection 0-98026
- microwave chronic exposure, physiological and behavioural effects, rat obs. 0-6152
- saccadic eye movements, small, perceptual function 0-61577
- telemetry system, implantable, multichannel, for physiological research 0-67292
- telemetry system, totally implantable, for dimensions meas., animal physiological research 0-67294
- thermoregulatory behaviour of rats subjected to microwave irradi. 0-81547
- tissue surrounding single capillaries, substrate concs. 0-97853
- visual accommodation, reaction and response times obs. 0-67073
- visual patterns having the same coordinates pre- and post-saccades, interaction 0-61551
- visual saccades, small, lack of useful purpose considerations 0-61553
- Ag-Sn alloys and amalgams, electrochem. considerations, corrosion in physiological soln. 0-93760

**pi mesons** see pions**pick-up reactions**

- heavy ion stripping and pickup reactions on closed shell nuclei, level shifts, DWBA 0-91168
- ( $\alpha$ , $^3\text{C}$ ), 90.3 MeV, multi- $\alpha$ -cluster transfer and direct pickup cross sections 0-57760
- (d, $^6\text{Li}$ ), A=144-238, alpha-cluster transfer from alpha-decaying nuclei 0-91166
- (N, $\alpha$ ), microscopic finite-range anal. 0-63181
- (p,d), pol. p. 65 MeV, A=12-94, differential cross sections and anal. powers, pickup 0-91172
- (p,X), 400 GeV/c, deuteron prod. mechanism, pick up reactions 0-83096
- $^{13}\text{C}$ (d,  $^3\text{He}$ ), isospin violating direct reaction, Coulomb interaction role 0-102170
- $^{13}\text{C}$ (d, t), isospin violating direct reaction, Coulomb interaction role 0-102170
- $^{40}\text{Ca}$ ( $^1\text{B}$ , $^{12}\text{C}$ ), 32, 68 MeV, single proton pickup, DWBA anal., optical pot. 0-106037
- $^{40}\text{Ca}$ ( $^1\text{B}$ , $^{12}\text{C}$ ), 51.5 MeV, p pickup, DWBA anal. with Woods-Saxon and double folding optical pots. 0-102171
- $^{40}\text{Ca}$ ( $^{13}\text{C}$ , $^{14}\text{N}$ ), 40, 68 MeV, single proton pickup, DWBA anal., optical pot. 0-106037
- $^{42}\text{Ca}$ (p,t) form factor, hole and continuum contribs. for pick-up reactions 0-78256
- Cd(p,t), 11-15 MeV,  $^{104}\text{Cd}$ , A=104-116, low lying level scheme, mass excess 0-73807
- Cr( $^{14}\text{C}$ , $^{16}\text{O}$ ), 51 MeV, pickup reaction,  $^{48,50}\text{Ti}$  excited states and transition ang. distribns. 0-95308
- $^{151}\text{Eu}$  narrow band and pickup strength, shape coexistence from (d,t) 0-86799
- $^{56}\text{Fe}$ ( $^4\text{He}$ , $\alpha$ ), 18 MeV,  $^{55}\text{Fe}$  levels,  $J^\pi$ , spectroscopic factors, DWBA anal. 0-99127
- Gd(p, $\alpha$ ), 17 MeV,  $^{153,155}\text{Eu}$  single proton hole states in pickup reactions 0-78128
- Mo( $^6\text{Li}$ , $^3\text{B}$ ), 90 MeV,  $^{92,96}\text{Zr}$  first excited  $0^+$  state transition strength 0-78260
- Nd( $^3\text{He}$ , $\alpha$ ), 24 MeV,  $^{145, 147, 149}\text{Nd}$ , single neutron hole states spectroscopic factors, DWBA anal. 0-78109
- Nd(d,t), 17 MeV,  $^{145, 147, 149}\text{Nd}$ , single neutron hole states spectroscopic factors, DWBA anal. 0-78109
- Nd(t, $\alpha$ ),  $^{147}\text{Pm}$ , A=143-153, odd-A, spectroscopic factors, shell model anal. 0-78137
- $^{58}\text{Ni}$ ( $^3\text{He}$ , $\alpha$ ), 130 MeV, selected transition, DWBA anal., cross sections 0-83086
- Sm(p, $\alpha$ ), 17 MeV  $^{147,149,151}\text{Pm}$  single proton hole states in pickup reactions 0-78128
- $^{111}\text{Sn}$ ( $^3\text{He}$ , $\alpha$ ), 39 MeV,  $^{115}\text{Sn}$  weak coupling neutron hole states 0-73786
- Ti( $^{14}\text{C}$ , $^{16}\text{O}$ ), 51 MeV, pickup reaction,  $^{44,46}\text{Ca}$  excited states and transition ang. distribns. 0-95308



**pick-up tubes, television** *see television camera tubes*

# **pick-ups**

acceleration pick-ups, miniature vibrator for mechanical calibration (*German*) 0-95095  
read head for magnetic tape recorders using magneto-resistance principle 0-87688

**pickups** *see pick-ups*

**pictorial bandwidth compression** *see bandwidth compression*

# **picture processing**

*see also computerised picture processing; pattern recognition*

analogue and digital optical image processing, feedback, review 0-102639  
bandpass filters, multiple, appl. 0-109002  
bilinearly distorted image linear restoration using Wiener filters 0-83557  
binary image statistical modelling, enhancement and recognition (*Russian*) 0-63929  
bipolar spatial filtering, incoherent, review 0-102822  
blind deconvolution, zero phase blurring function estimation 0-106482  
blurring due to object movement, image reconstruction from projections 0-78784  
C-CD imager, edge enhancement using 3×3 pixel neighbourhood operator functions 0-102644  
chromosome analysis, problems and progress in automation 0-94436  
context-dependent automatic image screening system 0-95820  
digital filtering for image processing (*Italian*) 0-98573  
digital image change detection 0-102637  
digitizer and image analyzer, microcomputer-controlled 0-86270  
direct transmission via single optical fibre 0-106628  
edge detection, numerical, optical and hybrid methods compared 0-102662  
edge point linking by thresholding 0-99665  
electron microscopy, image processing system for micrographs based on minicomputer 0-73549  
electronic image data processing using incoherent light 0-78793  
feedback systems for analogue and digital optical image processing 0-102650  
geological IR multispectral aircraft scanner data, image processing 0-98454  
human retinal image processing, two-channel model 0-94215  
image alignment errors due to aliasing 0-106480  
image bandwidth compression, scene analysis algorithms and rule-based controller 0-95819  
image correlation based on extracted edges 0-99658  
image formation using fan-beam scanning and noncircular source motion 0-101913  
image registration and differencing by coherent optical pattern recognition 0-99648  
image registration using material information 0-99664  
image restoration using a norm of maximum information 0-102633  
image restoration using maximum information norm 0-106476  
image segmentation and texture unit cell size determ. 0-95817  
image segmentation based on second-order grey level statistics 0-99663  
image transmission through monomode fibres, restoration using grating 0-69512  
Image Understanding Program philosophy and results 0-95818  
image understanding systems, seminar, San Diego, CA, USA (Aug. 79) 0-94918  
laser image storage mass memory 0-102752  
M87 jet, optical photograph deconvolution by maximum entropy 0-62032  
maps extraction from satellite images 0-76899  
matched filter correlator memory techniques and storage capacity 0-102643  
medical 2D images, 3D enhancement scheme 0-101255  
medical image processing, introduction (*Japanese*) 0-81699  
medical X-ray video images, enhancement 0-94353  
microwave holography, 3D image-construction technique and appl. to microwave diagnostics 0-83565  
mosaic IR image differencing for track assembly 0-86420  
multi-image regeneration by white light processing 0-95814  
multidetector scanner image stripping abatement 0-102660  
multisensor image pattern recognition, statistical and deterministic aspects 0-99647  
natural terrain scenes, segmentation-based boundary-modelling processor 0-99661  
nuclear medicine, image processing review 0-81694  
octagonal distance transformation of digitised binary pictures appl. to rib image recognition in chest radiographs 0-89842  
optical fibre laser plate for digital image processing, all-optical parallel logic operation 0-106463  
optimal restoration filter for Poisson noise impaired and linearly blurred images 0-106481  
orthogonal transforms program for medical scintigrams 0-72365  
partial spatial coherence blur correction by postdetection image processing 0-78792  
photographic images, quantitative anal. of autoradiographic image intensification using Thiourea-<sup>35</sup>S 0-90343  
polychromatic processing technique for colour image transparencies 0-86473  
protein supramolecular structure, ordered, electron micrographs, image processing 0-89923  
radioastronomy, Clean and Restore technique appl. to WSRT and Northern Cross radiotelescope obs. (*Italian*) 0-98563  
radiographic inspection algorithm speedup by array processor 0-108659  
radiographs, industrial, discontinuous registration using profile analysis and piecewise correlation techniques 0-102645  
radiography, contour extraction (*Japanese*) 0-81702  
real-time incoherent subtraction of irradiance 0-74301  
reconstruction, three-dimensional, from planar projections 0-99639  
robust feature matching through maximal cliques 0-99671  
segmentation and texture anal. 0-98167  
segmentation using material information 0-102642  
serum-electrophoresis, quantitative, by digital picture processing (*German*) 0-94306  
stereo-pair images, correlation error prediction 0-102636  
thermal imager pictures delining, using digital processing technique 0-106466  
time-varying images, object displacement estimation adaptive algorithm 0-99668  
tunable spatial filtering with a Fabry-Perot etalon 0-58668  
two-tone image analysis using one-dimensional autocorrelation function (*Russian*) 0-63931

# **picture processing continued**

Venera 9 televised pictures of Venus cloud layer, geometrical correl. methods 0-67604  
vibration measuring system using interf. fringes TV detect. and electronic image processing 0-103004  
video-electronic hologram interferometry for in-plane displacement measurement 0-106488  
volume holograms for image restoration 0-83566  
weak modulation detection in film grain noise with partially coherent illumination 0-77897  
weather satellite picture processor for TIROS-N series, visible and IR pictures 0-67439  
X-ray computerised tomography, system resolution recovery by motion blur recovery technique 0-105756  
X-ray images, electronic recording 0-62815  
KD<sub>2</sub>PO<sub>4</sub> photo-spatial light modulator, optical data processing 0-102839

**picture transmission** *see facsimile*

**picture tubes, television** *see television picture tubes*

**piezo-magneto-optical effects** *see magneto-optical effects; piezo-optical effects*

# **piezo-optical effects**

*see also piezoreflectance*

benzene liqs., refractive index, pressure effect 0-71375  
diamond, Jahn-Teller coupling at neutral vacancy 0-71453  
diamond, uniaxial stress splitting of E to E transitions at trigonal centres in cubic crystals 0-97312  
n-dodecane liqs., refractive index, pressure effect 0-71375  
ferroelectric semiconductors, appl. to optical storage (*Russian*) 0-80749  
fibre pressure sensitivity meas. and limitation 0-106605  
fluorophosphate laser glasses, Nd doped, piezooptic coeffs. meas. 0-99815  
gel rods, elastic dilatational mode, light beam positional modulation 0-64167  
n-heptane liqs., refractive index, pressure effect 0-71375  
n-hexane liqs., refractive index, pressure effect 0-71375  
hologram interference fringe bending analysis and expt. 0-106494  
mixed crystals, of equimol. conc. with NaCl struct., piezo-optic birefringence theory 0-100643  
modulators, photoelastic radiation polarisation, review 0-102846  
n-octane liqs., refractive index, pressure effect 0-71375  
optical fibre, refractive index profile distortion, stress-induced 0-91889  
optical fibre refractive index profile distortion due to thermal stresses 0-58726  
optical fibres, piezo-optical effects due to thermal stresses 0-87519  
PET films, one-way drawn, constant strain effects, IR meas. 0-60584  
phosphate laser glass, Nd doped, piezooptic coeffs. meas. 0-99815  
polyvinylidene fluoride, electro-optic and elasto-optic effects 0-80754  
semiconductors, optical props. under press., book contrib. 0-84715  
tetrachloromethane liqs., refractive index, pressure effect 0-71375  
TTF-chloranil visual pressure or temperature indicator 0-87443  
BaF<sub>2</sub>, strain induced splitting and oscillator strength anisotropy of IR transverse optic phonon 0-92625  
Ba<sub>2</sub>NaNb<sub>2</sub>O<sub>15</sub>, high press. phase transitions, Raman scatt. studies 0-71402  
BaTiO<sub>3</sub>, elasto-optic effect near ferroelec. transition, temp. depend. 0-97233  
CaF<sub>2</sub>, strain induced splitting and oscillator strength anisotropy of IR transverse optic phonon 0-92625  
CdS, mixed crystals, deformation effects on free excitons 0-76073  
CdTe film, exciton spectra, press. and temp. depend. 0-80886  
CsBr, F-centre absorpt., uniaxial stress effects 0-60634  
Cu<sub>2</sub>O, reson. Raman scatt. from stress-split forbidden excitons 0-93332  
Cu<sub>2</sub>O, uniaxial stress effects on excitons 0-60589  
Cu<sub>2</sub>VS<sub>4</sub>, Raman linewidth of A<sub>1</sub> mode under high press., reson. effects 0-108210  
EuO, ferromagnetic piezotransmission behaviour in magnetic field 0-97272  
EuO, transmission and resistivity, stress modulation effect near Curie temperature 0-96874  
n-GaAs epitaxial film, radiative recomb. under influence of mech. stresses 0-66291  
GaAs, conduction band effective mass, influence of high uniaxial stress 0-80162  
GaAs, luminescence emitted from deep centres, plastic deform. effect on internal quantum efficiency 0-60672  
GaAs p-n junctions, electron irradi. induced defect levels, hydrostatic press. effect 0-92858  
GaAs-GaP heterostructure, radiative recomb. under influence of mech. stresses 0-66291  
GaAs<sub>1-x</sub>P<sub>x</sub>(Te), bound exciton stress depend., piezoluminescence, photoluminescence 0-80206  
GaP:S, ground and excited states of bound exciton complex, stress effects 0-65463  
GaP-GaAsP planar heterostructure strip ridged waveguide under mech. load, polarisation modulation 0-96038  
α-GaSe, Raman scatt., hydrostatic press. effect 0-84745  
Ge, polycrystalline thermal-imaging lens, optical requirements 0-69495  
Ge:Zn, G and D lines, stress induced components 0-71447  
Hg(CN)<sub>2</sub>, phonon freq. anomalous press. depend., mol. struct. distortion 0-88981  
InP, depend. of phonon spectrum on hydrostatic press., Raman spectra 0-93315  
InP, photolum. meas. using diamond-anvil press. cell 0-108256  
InP, press. depend. of direct absorption edge 0-93365  
KCl-KBr, with equimol. conc., piezo-optic birefringence theory 0-100643  
K<sub>2</sub>SeO<sub>4</sub>, Raman spectra, effects of temp., substitutional cations, and stress 0-71405  
La<sub>2</sub>O<sub>3</sub>:Eu, high press. effect on luminesc. efficiency and lifetime, charge transfer absorpt. 0-66266  
La<sub>2</sub>O<sub>3</sub>:Eu, slow phosphoresc., high press. study 0-80839  
LiNbO<sub>3</sub>, planar lightguide, optical mode interaction with standing elastic surface waves 0-99836  
LiNbO<sub>3</sub>:Ti optical waveguide, surface wave mode conversion, static strain-optic effect 0-78561  
MgO, photoluminesc. during mechanical deform. 0-60665  
ND<sub>4</sub>I, Raman spectrum, press. effects 0-97261  
NH<sub>4</sub>Cl Raman spectra, pressure effects 0-97268  
NH<sub>4</sub>I, Raman spectrum, press. effects 0-97261  
NDP<sub>14</sub>, fluoresc. lifetime meas., IR and photoacoustic spectroscopy 0-60652



**piezo-optical effects continued**

- PLZT ceramics, elastooptic effect, stress induced birefr. 0-60543  
 Pb<sub>2</sub>Ge<sub>2</sub>O<sub>11</sub>, ferroelec. transition, US and elasto-optic props. 0-60527  
 Se, trigonal, behaviour of optical gap under press. 0-80171  
 Se, trigonal, Raman scatt. at very high press. 0-60566  
 Si, elasto-optic constants, real and imaginary, direct absorpt. and Raman scatt. meas. 0-97234  
 p-Si, heavily doped, intra- and interband Raman scatt. by free carriers 0-108208  
 Si, stretched, lattice vibr. anharmonicity, influence of stress on elastic moduli, Raman spectra 0-80791  
 Si-Li, bound-exciton excited states, uniaxial anal. 0-71475  
 SiO<sub>2</sub>, thin film grating for LiNbO<sub>3</sub>:Ti waveguide mode converter and reflector 0-64216  
 SiO<sub>2</sub>-LiO<sub>2</sub>-Al<sub>2</sub>O<sub>3</sub> glass, luminesc., polarisation degree distrib. 0-108257  
 Sr<sub>2</sub>Ba<sub>1-x</sub>Nb<sub>2</sub>O<sub>6</sub>, high press. phase transitions, Raman scatt. studies 0-71402  
 SrF<sub>2</sub>, strain induced splitting and oscillator strength anisotropy of IR transverse optic phonon 0-92625  
 Sr<sub>2</sub>Nb<sub>2</sub>O<sub>7</sub>, high press. phase transitions, Raman scatt. studies 0-71402  
 Te, trigonal, Raman scatt. at very high press. 0-60566  
 TiO<sub>2</sub>, rutile, first order Raman spectrum, uniaxial stress effects 0-66196  
 TiO<sub>2</sub>, rutile, first-order Raman spectrum, uniaxial-stress depend. 0-60586  
 TiBr-TiI(Cl) crystals, photoelastic moduli 0-97230  
 Y<sub>2</sub>O<sub>3</sub>:Eu, high press. effect on luminesc. efficiency and lifetime, charge transfer absorpt. 0-66266  
 ZnIn<sub>2</sub>S<sub>4</sub>, Raman scatt., hydrostatic press. effect 0-84745  
 ZnS, reson. Brillouin scatt. and piezobirefringence 0-93348  
 ZnTe film, exciton spectra, press. and temp. depend. 0-80886

**piezoelectric devices**

- see also crystal filters; crystal resonators; piezoelectric transducers*  
 acceleration sensors, lower limiting frequency and indication threshold (German) 0-95093  
 accelerometers, effect of strain sensitivity on accel. meas. of flexural vibrations 0-58991  
 acoustical holographic piezoelectric integrated acoustic array, system anal. 0-79067  
 ceramics, photovoltaic effect application to information storage 0-80316  
 deformable mirrors for wavefront error correction, piezoelectric material requirements 0-78928  
 earphones, usefulness in recording brain stem auditory evoked pots. 0-94389  
 electrostatic voltage sensor (Japanese) 0-105632  
 laser pump shaping on multiple rot. lines, using piezoelec. length tuner 0-78879  
 light shutter array, large area electronically controllable, using polyvinylidene fluoride bimorph vanes 0-58696  
 microscope objective, piezoelec. and electrodynamic automatic focusing servo mechanisms 0-73445  
 photoacoustic thermal-wave microscopy, high resolution studies 0-74647  
 polyvinylidene fluoride piezoelec. film for adaptive deformable mirror system 0-74455  
 quartz crystal microbalance for sorption studies under dynamic conditions 0-73323  
 RF sputtering systems, discharge suppression within piezoelectric gas admission valves 0-100110  
 C piezoresistive gauges, shock loading and unloading behaviour up to 5 GPa 0-87750  
 Pb(Zn,Ti)O<sub>3</sub>, piezoelectric electrically deformable diffraction grating 0-78963

**piezoelectric effects** *see piezoelectricity***piezoelectric filters** *see crystal filters***piezoelectric materials**

- see also piezoelectric semiconductors; piezoelectric thin films; piezoelectro-activity*  
 ceramic, piezoelectric, US instrument for determ. characts. 0-66752  
 ceramic, reflection and transmission of elastic waves at boundary with water 0-87588  
 ceramics, photovoltaic effect application to information storage 0-80316  
 crystals, elastic surface waves 0-103558  
 deformable mirrors for wavefront error correction, piezoelectric material requirements 0-78928  
 disilicate, piezoelectric glass ceramic, recrystallisation, pyroelectric response, permittivity 0-80703  
 electro-optical and nonlinear-optical materials, review 0-74450  
 electrostatic voltage sensor (Japanese) 0-105632  
 piezoelectric-semiconductor struct., nonlinear acoustoelectric effects for large amplitude SAW 0-92942  
 plasmon transformation into SAW in piezoelec. cryst. 0-59903  
 polar materials, appl. to SAW and other devices 0-66114  
 polydomain ferroelec. crystals, phys. const., self consistent calcs. 0-88942  
 polyvinylidene fluoride, bimorph vanes, use in large area electronically controllable light shutter array 0-58696  
 polyvinylidene fluoride, corona-charged, surface effects 0-66102  
 polyvinylidene fluoride, hysteresis phenomena under high elec. field 0-66134  
 polyvinylidene fluoride, poling process, kink propag. model 0-80679  
 polyvinylidene fluoride, props., polarisation and appls. 0-75947  
 polyvinylidene fluoride acoustic transducer arrays, fabrication on Si wafer 0-74683  
 polyvinylidene fluoride film, biaxially oriented, charact. for transducer appl. 0-88931  
 polyvinylidene fluoride film polymer transducer, with US appl., durable lead attachment techniques 0-79094  
 polyvinylidene fluoride films, SH and Lamb waves propag. 0-75948  
 α-quartz, doubly-rotated-cut, numerical anal. of props. of SAWs 0-74616  
 quartz, effects of the He ion implantation on SAW propag. 0-75421  
 quartz, elastic constants and piezoelec. props. 0-92590  
 quartz, with metallic overlay films for temp. compensation, SAW device appls. 0-79043  
 quartz crystals, oscillating, surface patterns obs., energy trapping appl. 0-71323  
 quartz crystals with TTC-cut (Danish) 0-60504  
 quartz substrate covered with metal or quartz powder, dynamic SAW reflecting struct. 0-74565  
 quartz with zero temp. coeff. of delay, SAW propag. characts. 0-75420  
 SAW devices and temperature compensation techniques 0-74614  
 shape-dependent damping 0-93242  
 specific directions of plane elastic waves in thin quartz crystal plates 0-92601

**piezoelectric materials continued**

- Tanane, ferroelec. mol. cryst., strong piezoelec. coupling 0-75942  
 transmitters and receivers for medical ultrasonics 0-76819  
 vinylidene-fluoride-trifluoroethylene copolymer, piezoelectricity 0-88930  
 Ag<sub>3</sub>SbS<sub>3</sub>(As<sub>2</sub>S<sub>3</sub>), electroacoustic echo, ultrasonic wave attenuation (*Russian*) 0-88280  
 α-AlPO<sub>4</sub> as SAW substrate material, piezoelec. props. 0-80710  
 α-AlPO<sub>4</sub>, berlinite, H<sub>2</sub>O conc. determ. by Raman scatt. 0-76572  
 Ba<sub>2-x</sub>Sr<sub>x</sub>TiSi<sub>2</sub>O<sub>8</sub>, piezoelec. crystals, SAW characts. 0-84354  
 BaTiO<sub>3</sub>, polycrystalline ferroelectric, grain-size dependent props. 0-71352  
 BaTiO<sub>3</sub>, polydomain ferroelec. crystals., phys. const., self consistent calcs. 0-88942  
 BeO, wurtzite-type crystals, lattice dynamics including the effect of electronic extension 0-59586  
 Bi<sub>2</sub>FeO<sub>20</sub>, longitudinally vibrated bars, reson. freq., DC elec. field effects, elastic coupling polarising correction terms 0-60503  
 BiGeO<sub>20</sub>, photocurrent oscils. in pulsed illumination rel. to piezoelec. props. 0-80325  
 Bi<sub>2</sub>SiO<sub>20</sub> crystal, piezoelec. and SAW props. 0-75949  
 Cs<sub>2</sub>SO<sub>4</sub>, piezoelectric, crystal struct. studied by X-ray diffr. 0-100208  
 CuCl, mech. vibrs. in piezoelec. solid, excitation by light pulses 0-75305  
 KD<sub>2</sub>PO<sub>4</sub>, neutron scattering from coupled polar-elastic waves 0-92623  
 KH<sub>2</sub>PO<sub>4</sub>, electro-optic modulator crystals., piezoelec. induced acoustic transients 0-70316  
 Li<sub>2</sub>GeO<sub>3</sub> piezoelectric glass ceramic, recrystallisation, pyroelectric response, permittivity 0-80703  
 LiIO<sub>3</sub>, transverse gap elastic waves, expt. 0-59576  
 LiNbO<sub>3</sub>, effects of He ion implantation on SAW propag. 0-75421  
 LiNbO<sub>3</sub>, finite difference anal. of SAW 0-75423  
 LiNbO<sub>3</sub>, parametric phonon echo obs. 0-59588  
 LiNbO<sub>3</sub>, piezoelec., SAW interaction with secondary electrons 0-80708  
 LiNbO<sub>3</sub>, SAW, suppression of harmonic generation by ZnO thin-film loading 0-84355  
 LiNbO<sub>3</sub> substrate, covered with metal or quartz powder, dynamic SAW reflecting struct. 0-74565  
 LiNbO<sub>3</sub>, temp. coeff. of freq. determ. 0-75316  
 LiNbO<sub>3</sub>-Si, acoustoelectronic memory, effect of band-bending 0-70771  
 Li<sub>2</sub>SiO<sub>4</sub>, piezoelectric glass ceramic, recrystallisation, pyroelectric response, permittivity 0-80703  
 NH<sub>4</sub>Cl, piezoelec. effect near nonferroelastic phase transition 0-66116  
 PVF<sub>2</sub>, thin film SAW transducers for 8 MHz delay line 0-58876  
 Pb(Mg<sub>1/3</sub>Nb<sub>2/3</sub>)O<sub>3</sub>-PbTiO<sub>3</sub>-PbZrO<sub>3</sub> ceramics, HF filters appl. additives effect obs. (Japanese) 0-60507  
 PbScO<sub>3</sub>NbO<sub>3</sub>, single cryst., dielec. props. 0-66126  
 Pb<sub>0.94</sub>Sn<sub>0.06</sub>Ti<sub>0.47</sub>Zr<sub>0.53</sub>O<sub>3</sub>, piezoelectric ceramic, stress relax., time depend. deformation 0-60899  
 Pb,Sr<sub>1-x</sub>(Zr,Ti,Nb)O<sub>3</sub>, hydrophone ceramic, effect of one-dimensional uniaxial stress 0-80705  
 Pb(Ti,Zr)O<sub>3</sub> solid solutions, phase coexistence discrepancies 0-96662  
 xPbTiO<sub>3</sub> + (1-x)PbCd<sub>1/3</sub>Nb<sub>2/3</sub>O<sub>3</sub>, phase transition spread, polarisation relaxation, dielectric susceptibility (*Russian*) 0-75922  
 Pb(Zr,Ti,Mg,W)O<sub>3</sub>, low-Q ceramics, props. and transducer appl. 0-75944  
 Pb(Zn,Ti)O<sub>3</sub> piezoelectric electrically deformable diffraction grating 0-78963  
 Pb(Zn<sub>1/3</sub>Nb<sub>2/3</sub>)O<sub>3</sub>-PbTiO<sub>3</sub>-PbZrO<sub>3</sub> ceramics, HF filters appl. additives effect obs. (Japanese) 0-60507  
 Pb(Zr,Ri)O<sub>3</sub>:Ni-silicon rubber flexible composite pyroelectric, dielectric props. 0-80704  
 Pb(Zr,Ti)O<sub>2</sub> ceramic, surface barrier electroreflectance, hysteresis, ageing 0-80752  
 Pb(Zr,Ti)O<sub>3</sub> ceramics, low temp. sintering, elec. and mech. props. 0-71616  
 Pb(Zr,Ti)O<sub>3</sub> ceramics with ladder type struct., prep. and props. 0-75945  
 Pb(Zr,Ti)O<sub>3</sub> ceramics, DC field sintering preparation, piezoelectric props., ageing behaviour 0-81211  
 Pb(Zr,Ti)O<sub>3</sub> fibre arrays in epoxy cement, ferroelectric ceramic-plastic composites 0-81015  
 Pb(Zr,Ti)O<sub>3</sub>, fracture and deform. 0-79870  
 Pb(Zr,Ti)O<sub>3</sub> internally electrode multilayers, piezoelectric props., permittivity, transducers 0-80672  
 Pb(Zr,Ti)O<sub>3</sub>, PCD ceramic, pyroelectric props. 0-100635  
 Pb(Zr,Ti)O<sub>3</sub>, piezoelectric ceramics, low fluence neutron irradi. effects 0-92564  
 Pb(Zr,Ti)O<sub>3</sub>, research grade, hydrophone ceramic, effect of one-dimensional uniaxial stress 0-80705  
 Pb(Zr,Ti)O<sub>3</sub> type 1 ceramic, appl. in Langevin type sonar transducer, performance characts. 0-79095  
 Pb(Zr<sub>0.5</sub>Ti<sub>0.48</sub>)O<sub>3</sub>, polycrystalline ferroelectric, grain-size dependent props. 0-71352  
 Pb(Zr<sub>1-x</sub>Ti<sub>x</sub>)O<sub>3</sub> solid solution, piezoelectric ceramic, prop. improvement by multiple substitution 0-80702  
 Sr Nb<sub>2</sub>O<sub>6</sub>, crystallography, polymorphism and isomerism, X-ray diffr. and DTA study 0-100216  
 Sr<sub>0.8</sub>Ba<sub>0.2</sub>Nb<sub>2</sub>O<sub>6</sub> piezoelectric transducer, SAW props. 0-79037  
 Sr<sub>x</sub>(Na<sub>0.5</sub>B<sub>0.5</sub>)<sub>1-x</sub> solid solutions, piezoelec. and ferroelec. props. (French) 0-108158

**piezoelectric oscillations**

- cylindrical shell, inhomogeneous, torsional wave motion 0-60506  
 external friction reduction by forced piezoelec. oscillation 0-92096  
 powder, memory echo, dipolar field contrib. 0-84700  
 transducers of tall, narrow elements of acoustic imaging array, vibration mode 0-74690  
 PLZT pyroelectric detectors, delayed onset of piezoelec. oscils. 0-75953

**piezoelectric resonators** *see crystal resonators***piezoelectric semiconductor materials** *see piezoelectric semiconductors***piezoelectric semiconductors**

- acoustoelectric current, second harmonics 0-80329  
 acoustoelectric effect, effect of diffusion of charge carriers (*Russian*) 0-65633  
 degenerate, transverse magnetoresist. in strong field, quantum effect 0-80299  
 electro-optical and nonlinear-optical materials, review 0-74450  
 α-LiIO<sub>3</sub> powders, temp. depend. of electro-acoustic echo 0-66115  
 magnetised semiconductor plasma, EM wave amplitude modulation and demodulation 0-84482  
 n-type, magnetoactive, Brillouin instability in magnetostatic field 0-78909  
 piezoelectric nondegenerate semicond., magnetoacoustic effects of nonparabolic band struct. 0-96948  
 plasma, parametric excitation of helicon and acoustic waves 0-107837  
 polar materials, appl. to SAW and other devices 0-66114



**piezoelectric semiconductors continued**

- n-AlSb, acoustoelectric effect due to piezoelectrically active wave 0-80331  
 CdS, elastic, piezoelec. and dielec. props. 0-108157  
 CdS, elastic, piezoelectric, and dielec. props., 4.2 to 300K 0-60508  
 CdS, single crystals, US luminesc. obs. 0-76092  
 CdS, stimulated Mandelstam-Brillouin scatt. on acoustic phonon amplification (*Russian*) 0-71437  
 CdS, thin plates, piezosemiconductors, second harmonic acoustoelectric current obs. 0-80329  
 CdS(Se), piezoelec. semicond., sound absorption 0-60051  
 n-GaP, acoustoelectric effect due to piezoelectrically active wave 0-80331  
 GaSb, piezoresistive vibrating circular membrane, reflectance light modulation 0-97232  
 Ge, piezoresistive vibrating circular membrane, reflectance light modulation 0-97232  
 Ge single crystals, photopiezoelectric effect under elastic deform. 0-107856  
 n-InSb, Brillouin instability in magnetostatic field 0-78909  
 Se, SAW propag. on Y-cut plate and X-axis 0-75313  
 Se, SAW vel. and electromech. coupling factor 0-75422  
 Se, trigonal, acoustoelectric current saturation 0-60053  
 Se,  $Te_{1-x}$ , acoustoelectric current saturation 0-60053  
 SiC, acoustic props. study at 9.43 GHz 0-65169  
 Te, acousto-optical props. at wavelength of  $10.6 \mu\text{m}$  0-76001  
 ZnO, elastic, piezoelec. and dielec. props. 0-108157  
 ZnO film on Corning 7059 glass and Si, SAW transducer appl. 0-80138  
 ZnO film on glass substrate, high-rate deposition using DC reactive magnetron sputtering 0-80978  
 ZnO film on oxidized Si, optical measure of acoustic quality 0-80893  
 ZnO, influence on frequency-temp. coeff. of SAW devices 0-79066  
 ZnO/quartz for SAW device materials, expt. study of props. 0-80050  
 ZnO/Si acoustoelectric devices, magnetron discharge sputtering prep. 0-80332  
 ZnS film on Corning 7059 glass and Si, SAW transducer appl. 0-80138

**piezoelectric thin films**

- polyvinylidene fluoride, piezoelec., nonlinear dynamic response 0-75946  
 polyvinylidene fluoride, plasma poling, piezoelec. and pyroelec. responses 0-71296  
 polyvinylidene fluoride, poled, short duration unipolar stress pulse detection, generation 0-106695  
 polyvinylidene fluoride films, HF US absorpt. meas., 300 to 1500 MHz 0-74667  
 polyvinylidene fluoride films for SAW transducers on Si substrates 0-74618  
 polyvinylidene fluoride piezoelectric film, Lamb and SH wave attenuation (*French*) 0-79196  
 vinylidene fluoride-trifluoroethylene film, cryst. phase transition 0-66120  
 AlN, piezoelectric film, low temp. growth by RF reactive planar magnetron sputtering method 0-76175  
 ZnO film, RF sputtered, characterization for SAW transducers 0-80138  
 ZnO film on glass substrate, high-rate deposition using DC reactive magnetron sputtering 0-80978  
 ZnO, optical measure of acoustic quality 0-80893  
 ZnO, RF planar-magnetron sputtered, characterisation 0-96751  
 ZnO thin-film loading of  $\text{LiNbO}_3$ , suppression of SAW harmonic generation 0-84355  
 ZnO/quartz for SAW device appls., expt. study of props. 0-80050  
 ZnO/Si using magnetron discharge sputtering, acoustoelectric device appls. 0-80332  
 ZnS film, RF sputtered, characterization for SAW transducers 0-80138

**piezoelectric transducers**

- acoustic defectoscopes, low freq., elec. simulation of compound piezoelec. transducers 0-102956  
 acoustic Lamb wave focusing devices 0-79093  
 acoustic signal distortion, piezoelec. transducers 0-87637  
 amplitude-frequency response determ. for acoustic emission 0-87699  
 arbitrarily electrode piezoelec. plate acoustic spatial response determ. 0-99910  
 automatic setup for continuous meas. of internal friction and elastic moduli of solids 0-108652  
 broadband, production 0-61044  
 ceramic, LF characts., consequences for Fabry-Perot interferometry 0-86390  
 ceramic buzzers for high sound levels 0-92005  
 ceramic piezoelectric transducer, anomalous radiation pattern due to parasitic Lamb wave generation 0-96170  
 composite, of low freq. acoustic flaw detector, natural freq. calc. 0-89450  
 composite piezotransducer for LF acoustic inspection using electrical models 0-104393  
 contactive, spectrum of natural freqs. 0-69623  
 cylindrical, influence on spectrum of natural freqs. 0-87694  
 depolarised, by heat treatment, for improved resoln. 0-104196  
 electret applications, book contrib. 0-80709  
 electric field, nonuniform, expt. study 0-102955  
 electromechanical polygonal ring, analysis of influence of oscillatory modes on transducer characts. 0-87697  
 flexural-extensional behavior of composite piezoelectric circular plates 0-58879  
 force transducers, calibration by absolute impulsive method 0-105627  
 grating-array acoustic-surface-wave transducers and reflectors 0-58884  
 included scanner for corner reflector acoustic channel 0-106705  
 inspection using piezoelect. 0-104392  
 interdigital transducer on piezoelectric half space, spectrum of emanating acoustic waves 0-79044  
 layered, generalized orthogonality of normal modes 0-58885  
 medical ultrasonics, transmitters and receivers from piezoelectric materials 0-76819  
 microphones with rigidly supported piezopolymer membranes 0-64330  
 mosaic transducers for GHz bandwidth bulk acoustic delay line 0-74657  
 optically-controlled acoustic transducers, piezoelect. and electrostrictive 0-74638  
 opto-acoustic transducer structs., recent investigations 0-74688  
 opto-acoustic transducers, improved equivalent ckt. 0-74658  
 optoacoustic monitor for optically pumped far IR laser 0-102729  
 photoacoustic effect in piezoelectric ceramics 0-84252  
 piezoceramic, blind reading aid using conversion of optical images into vibrotactile 0-85533  
 piezoceramic aperiodic transducer, mech. load study 0-87700  
 piezoceramic transducers, transient charact. 0-106704

**piezoelectric transducers continued**

- piezoceramic transducers for generation of acoustic pulses having prescribed shape 0-87691  
 polarised polyvinylidene fluoride film, piezoelectric transducer 0-75993  
 polyvinylidene fluoride as transducer material 0-75947  
 polyvinylidene fluoride film, biaxially oriented, charact. for transducer appl. 0-88931  
 polyvinylidene fluoride film appl., poled, short duration unipolar stress pulse detection, generation 0-106695  
 polyvinylidene fluoride film polymer transducer, with US appl., durable lead attachment techniques 0-79094  
 polyvinylidene fluoride films, HF US absorpt. meas., 300 to 1500 MHz 0-74667  
 pressure sensor using  $\text{TiSb-19}$  piezoelectric ceramic 0-105670  
 probe, conversion ratios 0-69624  
 pulsed opto-acoustic spectroscopy 0-62743  
 PVF<sub>2</sub> transducers for NDT 0-76476  
 radiation and reception field investigations; piezoelectric probe, pulse mode, Kirchhoff approx. 0-87636  
 radiator of longitudinal acoustic waves with an inhomogeneous elec. field 0-87693  
 SAW, characterization of RF sputtered ZnO and ZnS films by X-ray diffraction anal. 0-80138  
 SAW phase shifter with 3 interdigital transducers 0-79062  
 SAW transducers based on layered systems, calc. of electromech. coupling coeff. squared 0-87690  
 shear-mode acoustic wave receiving, transfer characts. 0-87696  
 shock wave propagation in shock tubes, investigations on suitability of piezoelectric and magnetoelastic detectors (*Polish*) 0-79351  
 sonar transducer, Langevin type, made from  $\text{Pb}(\text{Zr,Ti})\text{O}_3$  type 1 ceramic; performance characts. 0-79095  
 surface excited, thick, acoustic fields 0-102957  
 surface excited, thick, transient, pulse and amplitude-frequency charact. 0-102958  
 surface excited, US field 0-64331  
 thickness-extensional trapped energy mode transducer array, increased bandwidths and mode shapes 0-74633  
 Tonpilz, design using nonlinear gatt programming 0-106696  
 transducer, performance calc. 0-77771  
 UD-24 instrument, piezoelec. US transducers 0-108664  
 ultrasonic pulsed measuring instrum., signal shape anal. 0-87678  
 unidirectional SAW transducers, 3-phase equivalent ckt. model 0-74627  
 US, discs attached to metal rods and metal plates 0-96166  
 US imaging biomedical micro-array technology for improved image quality (*German*) 0-98052  
 US meas. with piezoelectric transducers, absolute calibration 0-79099  
 US receiving array having power response 0-74653  
 US surface excited thick piezoelectric transducer, output current form 0-87701  
 US transducer element tuning 0-87684  
 vibration mode in tall, narrow elements of acoustic imaging array 0-74690  
 vibrocontact, performance calc. 0-77771  
 AlN, piezoelectric film, low temp. growth by RF reactive planar magnetron sputtering method 0-76175  
 $\text{KH}_2\text{PO}_4$  electro-optic modulator crystals, piezoelec. induced acoustic transients 0-70316  
 $\text{LiIO}_3$  and quartz, acoustic field distrib., Bragg diff. method 0-97231  
 $\text{Pb}(\text{Zr,Ti})\text{O}_3$  internally electrode multilayers, piezoelectric props., permittivity, transducers 0-80672  
 $\text{Pb}(\text{Zr,Ti})\text{O}_3$  ceramic transducer for generation and detection of unipolar stress pulses 0-64328  
 $\text{Sr}_{0.5}\text{Ba}_{0.5}\text{Nb}_2\text{O}_7$  piezoelectric transducer, SAW props. 0-79037
- piezoelectricity**  
 see also electrostriction; piezoelectric devices; piezoelectric materials; piezoelectric oscillations  
 acoustic wave propagation, group vel. characts. 0-92613  
 acoustic waves, parametric excitation in presence of electron currents (*Russian*) 0-80328  
 backward waves and acoustic scanning, nonlinear interaction of vol. and surface waves 0-79040  
 Bleustein-Gulyaev surface waves behaviour in periodically corrugated piezoelectric medium 0-87616  
 bone, role of stress-gradient effects 0-67113  
 capacitance type AC dilatometer for piezoelectric and electrostriction const. meas. 0-77747  
 ceramic, nonlinear charge release under uniaxial press. 0-80706  
 ceramic plates, bending strains, electromechanical transformation, energetic method of calc. (*Ukrainian*) 0-71320  
 constant deformable dielectrics, coupled mechanoelectric fields, piezoelectricity and Lamb problem 0-58899  
 dielectrics, piezoelectricity, mechano-electric coupled fields, polarisation gradient 0-75940  
 electrets, piezo- and pyroelectric props. 0-80685  
 electroelasticity for piezoelectric medium with cuts, 2-D boundary value problems 0-71319  
 electroelasticity problems, numerical soln. 0-80707  
 ferroelectric ceramics, materials and dielec. props., review 0-75957  
 inhomogeneous piezoelectrics, electromechanical props. prediction 0-103919  
 liquid crystals, piezoelectric effect use as light modulator 0-83679  
 macroscopic quadrupole effects as method of obs. of struct. transforms in crystals 0-71321  
 phonon echoes and long-time storage in piezoelectric powders (*Japanese*) 0-70330  
 photoacoustic detection, theory and expt. 0-90904  
 piezoceramics, converters of shock wave mech. energy into elec. power 0-61429  
 polyvinylidene fluoride, piezoelec. const. calc. 0-103918  
 polyvinylidene fluoride film, hysteresis and dipolar orientation 0-97217  
 semiconductor-piezoelectric structure, vol. acoustic wave excitation in nonlinear interaction with surface waves 0-69582  
 shear surface waves, generalised 0-92770  
 superlattices, plasmons, two-dimens., due to piezoelec. effect 0-92845  
 surface polaron states, polaron-phonon interactions in piezoelectric crystal 0-70790  
 torsional wave propag. in infinite piezoelec. cylinder (622) cryst. class 0-87642  
 vibrations, waves, flexure, fracture, fundamental equations 0-60505  
 vinylidene-fluoride-trifluoroethylene copolymer, piezoelectricity 0-88930



**piezoelectricity** continued

- wurtzite-type crystals, lattice dynamics including the effect of electronic extension 0-59586  
 zincblende-type crystals, electromodulation, piezomodulation, theory 0-93281  
 CdS, elastic, piezoelec. and dielec. props. 0-108157  
 CdS polycrystalline films, high strain sensitivity 0-93017  
 CuCl, interface supercond., piezoelec. hypothesis 0-60128  
 p-Ge, piezo Hall effect meas. 0-96883  
 $\text{KD}_2\text{PO}_4$ , neutron scattering from coupled polar-elastic waves 0-92623  
 $\text{NH}_4\text{Cl}$ , piezoelec. effect near nonferroelastic phase transition 0-66116  
 $\text{Pb}(\text{Zr,Ti})\text{O}_3$  ceramics with ladder type struct., prep. and props. 0-75945  
 $\text{Pb}(\text{Zr,Ti})\text{O}_3$ , internally electrode with Pt, resonance behaviour 0-84701  
 SbSI, absorption edge, elec. field effect rel. to ferroelec. props. 0-97240  
 ZnO, elastic, piezoelec. and dielec. props. 0-108157

**piezoreflectance**

- zincblende-type crystals, electromodulation, piezomodulation, theory 0-93281  
 $\text{CdCr}_2\text{Se}_4$ , modulated piezoreflection spectra 0-97237  
 GaAs Schottky-barrier, linear and quadratic electroreflectance, minicomputer-controlled meas. 0-97241  
 GaSb, piezoresistive vibrating circular membrane, reflectance light modulation 0-97232  
 Ge, piezoresistive vibrating circular membrane, reflectance light modulation 0-97232  
 ZnTe films, internal stress effect on fund. refl. spectra 0-60701

**piezoresistance**

- n-InSb, anomalous Hall effect, stress depend. 0-65598  
 metallic glasses, elec. resist., press. depend. 0-96841  
 plastically deformed compound semiconductors, electronic transport and opt. props. of dislocations 0-80212  
 polyacetylene, pristine and doped, press. effects on resist. 0-103698  
 thermal strains, effect of support, theory 0-88647  
 $\text{CoS}_2$ , narrow-band ferromag., high press. effect on anomalous elec. resist. 0-70698  
 Cu-Mn alloy, manganin, hysteresis-corrected calibration under shock loading 0-74818  
 CuCl powder compacts, DC voltage depend. resist. under press. 0-80334  
 $\text{Cu}_{40}\text{Zr}_{60}$ , amorphous alloys, supercond. transition temp., press. depend. 0-84524  
 $\text{EuB}_6$ , resist., Hall effect, and magnetoresist. under hydrostatic press., 4.2 to 300K 0-96879  
 EuO, transmission and resistivity, stress modulation effect near Curie temperature 0-96874  
 EuO:Gd, elec. cond. under hydrostatic press., Curie temp. 0-96881  
 $\text{Fe}_0\text{Co}_{1-x}\text{S}_2$ , narrow-band ferromag., high press. effect on anomalous elec. resist. 0-70698  
 $\alpha\text{-Fe}_2\text{O}_3$ , elec. resist. and phase transition under shock compression 0-72496  
 $\text{FeSiO}_4$ , fayalite, elec. cond. obs. under shock compression 0-81873  
 GaAs, electron irradi. induced defect levels, hydrostatic press. effect 0-92858  
 GaSb, piezoresistive vibrating circular membrane, reflectance light modulation 0-97232  
 GaTe, transport properties under hydrostatic pressure 0-75589  
 Ge, piezoresistive vibrating circular membrane, reflectance light modulation 0-97232  
 Ge, plastically deformed under high temp. creep conditions, elec. props. 0-92915  
 I, metallic, mol. and monatomic phase, elec. resist. at high press. and low temp. 0-65638  
 $\text{In}_{1-x}\text{Ga}_x\text{As}$ ,  $P_{1-x}$ , evidence for alloy scatt. from press. induced changes of electron mobility 0-88548  
 n-InP:Cr, press. depend. of elec. resist. and Cr ionisation energy 0-80281  
 InSb, current-voltage characteristics at room temperature and high hydrostatic pressure 0-88560  
 $\text{KTA}_{0.9}\text{Nb}_{0.1}\text{O}_3$ , pressure-induced resistance and colour change obs. 0-75608  
 Ni-Y, amorphous, elec. resist., press. depend. 0-96841  
 $\text{Pb}_{0.82}\text{Sn}_{0.18}\text{Te}$ , film, effect of hydrostatic pressure on props. 0-70862  
 $\text{Pd}_{1-x}\text{Zr}_x$ , amorphous alloys, supercond. transition temp., press. depend. 0-84524  
 n-Si, piezoresist. rel. to piezothermoelec. power, electron-phonon drag region 0-70737  
 n-Si:P, piezothermoelec. power in electron-phonon drag region, anisotropy 0-70738  
 p-Si:P implanted films, piezoresist. stress tensors, ion dose depend., -80 to 120°C 0-100538  
 SmS, semiconducting, piezoresistance at 80K 0-59990  
 Te, two types of carriers 0-60013  
 Ti, polycrystal, discontinuous electrical resistivity, low temp. active strain-  
*(Russian)* 0-103666  
 TmSe, elec. resist. under press. at very low temp. 0-96878  
 $\text{U}_2\text{P}_3$ , press. effects on elec. resist. and Curie temp. 0-75559  
 Yb foil gauge, lateral compressive stresses meas. in shock-loaded PMMA 0-103007

**piezoresistive devices** see *piezoelectric devices***piles (nuclear fission)** see *fission reactors***pinch effect**

- anomalous transport processes in radially compressed reversed-field configurations, numerical simulation 0-64689  
 collisionless flow and end loss from a high-energy theta-pinch plasma 0-92365  
 Columbia Torus-1 belt pinch high beta toroidal device, preionisation, optimisation 0-92368  
 compact reverse-field pinch for small demonstration fusion reactor 0-95413  
 dense pinch, electron-positron pair production in EM field *(Russian)* 0-100092  
 diffuse linear pinch, dispersion differential eqn. in MHD, approx. 0-64694  
 diffuse theta-pinch, ion temp. meas. *(Japanese)* 0-87951  
 energy spectra of accelerated deuterons in a plasma focus 0-103110  
 ETA-BETA II, reverse field pinch, expt. tests and performance 0-102312  
 ETA-BETA II RFP, diffuse pinch, temp. and confinement results 0-74028  
 ETA-BETA II RFP, vacuum system design and operation 0-95450  
 field reversed pinches, microinstability effect on MHD stability 0-79460  
 focus plasma, pinch column form. and stability 0-96380

**pinch effect** continued

- Garching Belt-Pinch IIa, effect of q on confinement and stability 0-96384  
 high current RFP devices and the pulsed RFP reactor 0-79556  
 high velocity plasma fluxes 0-87860  
 high-density Z-pinch experiment pulse power supply, design and operation 0-70028  
 ion energy distribution in plasma focus during second pinch compression 0-75070  
 linear pinch plasma, extreme UV spectra of light impurity ions, appl. of grazing incidence spectrometer 0-59276  
 microinstabilities in field reversed Z pinches, persistence of MHD stability 0-87872  
 micropinch in a high-current diode, review 0-103183  
 multicharged ion heating in Z-pinch, column compression, temp. and density *(Russian)* 0-64754  
 neo-Z-pinch, mag. fusion appls. 0-103180  
 paramagnetic spheromak formation in a combined zee and theta pinch 0-92372  
 PIACE-R1, design fabrication and testing 0-92378  
 plasma, infinitely conducting, pinch effect, dynamical accumulation towards neutral line of magnetic field 0-83977  
 plasma shell, cylindrical, apparatus for production 0-106948  
 reversed field configuration, equilibrium and stability and confinement props. 0-87932  
 reversed field pinch, numerical studies 0-87931  
 reversed field pinch, RFX constructional details 0-91277  
 reversed field pinch expt. in small compact torus STP-1 0-75043  
 reversed-field pinch plasma model 0-87935  
 REXIMPLIO expt., quasi-spherical plasma compression 0-79546  
 screw-pinch, equilibrium and stability 0-87934  
 spheromak formation by theta pinch 0-106962  
 theta pinch, Fe impurity effective dielectronic recombination rates meas. 0-79570  
 theta pinch, H plasma, mag. piston study *(Russian)* 0-83971  
 theta pinch, low density, step-like mag. piston 0-103182  
 theta pinch, low density plasma, microinstabilities 0-79496  
 theta pinch, spark channel quasi-spherical compression, electron temp. 0-87920  
 theta pinch discharge, radial EM energy flow and plasma heating power 0-64747  
 theta pinch plasma density radial profile measurements using quasiquadrature interferometer 0-70038  
 theta-pinch fusion system with liner exploded by thermonuclear neutrons 0-79547  
 theta-pinch Ti ion injection by  $\text{CO}_2$  laser, spectroscopic anal. 0-79577  
 thin-skin pinch, stability, influence of thick conducting liner and superconducting wall, dispersion relation 0-64766  
 toroidal pinch discharge, preionisation phase, numerical computation 0-64696  
 Vlasov equilibria, local Maxwellian velocity distribution 0-87928  
 Z discharge relaxation between electrodes 0-75089  
 Z-pinch, optimum, stability calcs. *(Russian)* 0-106956  
 Z-pinch, stabilised, reversed current effect 0-79539  
 Z-pinch turbulence spectroscopic detection and anal. *(Russian)* 0-100098  
 Z-pinches of intense energy-density driven by high voltage storage lines 0-87952  
 ZT-40, modelling in G2M diffusion code 0-79557  
 ZT-40, reverse field pinch engineering prototype 0-102316  
 ZT-40, toroidal pinch, power supply crowbar transformer, low leakage and high current 0-102322  
 ZT-S expt., pitch programming 0-87933  
 ZT-S reversed field pinch simulations 0-83993  
 Al laser plasma, high-Z, temp. meas. from bremsstrahlung emission 0-87914  
 $\text{CO}_2$  laser system, pulsed, for fusion research 0-58556  
 InSb, pinch effect at room temp. 0-65615

**pin cushion-induction** see *aberrations***Piobert lines** see *Luder's bands***pion-baryon interactions**

- see also *pion-baryon scattering*; *pion-hyperon interactions*; *pion-nucleon interactions*  
 $N\pi\pi$  system, s-wave final state interactions 0-57638

**pion-baryon scattering**

- see also *pion-baryon interactions*; *pion-hyperon scattering*; *pion-nucleon scattering*  
 No entries

**pion decay**

- $\pi^- \rightarrow e^- \gamma$ , isospin-breaking, chiral limit, conserved-vector-current violation,  $\sigma$  model 0-62988  
 $\pi^- \rightarrow e^- \gamma$ , modified quark loop model, form factors, struct. functions, radiative decay 0-91088  
 $\pi^- \rightarrow e^- \gamma$  and  $\text{SU}(3) \times \text{SU}(3)$   $\sigma$ -model 0-78054  
 $\pi^0 \rightarrow 2\gamma$ , decay width as signal for nuclear matter phase transition, Primakoff effect 0-86842  
 $\pi^0 \rightarrow 2\gamma$ , tensor-trace and triangle anomalies 0-73709  
 $\pi^0 \rightarrow \gamma\gamma$  ( $\pi^+ \pi^- \gamma$ ), chiral quark model anal. *(Russian)* 0-105900  
 $\pi^0$  decay in supernova shell, gamma-ray emission 0-101602

**pion-hyperon interactions**

- see also *pion-hyperon scattering*  
 No entries

**pion-hyperon scattering**

- see also *pion-baryon interactions*  
 No entries

- pion interactions** see *lepton-hadron interactions*; *meson-meson interactions*; *photon-hadron interactions*; *pion-baryon interactions*; *pion-nucleus reactions*; *pion-pion interactions*

**pion-nucleon interactions**

- see also *pion-nucleon scattering*; *pion-proton interactions*  
 $\sigma$  term in hybrid chiral bag model, PCAC and  $\text{SU}(3) \times \text{SU}(3)$  symmetry violation 0-78096  
 hadron interactions, effective radius quantum number depend., quark sum rules *(Russian)* 0-102062  
 higher-twist effects in QCD, deep inelastic scattering and the Drell-Yan process 0-102020  
 s-channel resonance prod. in  $\pi N$  scatt., amplitude zeros in Mandelstam plane 0-73686  
 $N(1360) \Gamma < 67$  resonance,  $\pi N$  channel, dibaryon pp resonance systematics 0-68481



## pion-nucleon interactions continued

- N $\rightarrow\Delta(1232)$  electromagnetic transition form factor and pion-nucleon dynamics at moderate energies 0-57598  
 N form factor, isovector, meson field theory, pseudoscalar  $\pi$ N interaction 0-62986  
 $\pi$ N, 50-200 GeV/c, multiparticle production, multiplicities, cross sections and ang. distrib. 0-86768  
 $\pi$ N charge exchange scatt., Regge pole, model calcs. 0-102071  
 $\pi$ N collisions, N $\rightarrow\pi$ N $\pi$  diffractive dissociation, Deck mechanism (*Russian*) 0-86699  
 $\pi$ N in nucleus, diffraction dissociation, dip and kink structs., differential cross sections 0-95284  
 $\pi$ N $\rightarrow\pi$ N, kinematic singularity free helicity amplitudes, crossing matrix anal. props. 0-95285  
 $\pi$ N, 16, 22 GeV, dimuon prod. parton intrinsic transverse momentum, QCD perturbation 0-63037  
 $\pi$ n, 40 GeV/c, many pion systems in inclusive reactions, transverse momentum effects (*Russian*) 0-57654  
 $\pi$ N, 40 GeV/c in  $^{12}\text{C}$ , multinuclear inclusive process correlation functions (*Russian*) 0-68500  
 $\pi$ N, in  $^{12}\text{C}$ , 40 GeV/c, one- and multi-nucleon interactions, secondary charged particle multiplicity (*Russian*) 0-83013  
 $\pi$ N, in C, 5 GeV/c,  $\pi^0$  and n inclusive spectra, cascade model (*Russian*) 0-68490  
 $\pi$ N $\rightarrow\gamma$ X, 50 GeV, gamma prod. characteristics in emulsion reactions 0-68492  
 $\pi$ N in Ne, 25, 50 GeV/c, secondary particle multiplicity and multiple scatt. model anal. (*Russian*) 0-83014  
 $\pi$ N $\rightarrow\mu^+\mu^-$ X, K $^-/\pi^-$  structure function ratio using Drell-Yan process 0-86718  
 $\pi$ n $\rightarrow pX^-$ , 21, 205 and 360 GeV/c, reggeised one-pion-exchange 0-57649  
 $\pi$ N $\rightarrow\psi$ X, 225 GeV, bottom meson pair production limit 0-73750

## pion-nucleon scattering

- see also pion-nucleon interactions; pion-proton scattering  
 amplitudes, singularities of zero trajectories, dual model predictions 0-63021  
 partial wave analysis, S- and P-wave scatt. lengths 0-63019  
 sigma term from threshold data 0-57633  
 sigma term related to scatt. length, Altarelli-Cabibbo-Maiani relation derivation 0-57632  
 sum rules, finite-energy, three component duality 0-82996  
 zero trajectories of invariant  $\pi$ N amplitudes 0-102067  
 $\pi$ N, 6-200 GeV, amplitude anal. in impact parameter representation, non-zero polarisation, shell struct. (*Russian*) 0-86752  
 $\pi$ N elastic scatt., nonstatic model for nuclear reactions 0-102125  
 $\pi$ N low energy scatt. from N,  $\Delta$  poles, low energy theorems 0-86751  
 $\pi$ N, 2-15 GeV/c, in Ge, Si, influence of channelling on scattering 0-73729  
 $\pi$ NN vertex function and off-mass-shell  $\pi$ N scatt. 0-73739

## pion-nucleus reactions

- for inelastic pion-nucleus scattering, see "pion-nucleus scattering"  
 see also pion-nucleon interactions  
 deformed nuclei, absorption of slow  $\pi^-$ , mesic atoms 0-78321  
 fissionability, target mass depend. for  $\pi$ ,  $\gamma$ ,  $\alpha$ , p, cascade-evaporation and liquid drop calcs. (*Russian*) 0-106089  
 radiological imaging, use of inelastic high energy particle interactions 0-61675  
 single charge exchange and inelastic scatt. cross sections relationship 0-102204  
 total pion absorption cross section, A depend., proton yields 0-106081  
 truncated pion-nucleon amplitudes and pion-nucleus interactions 0-68708  
 ( $\pi, 2\pi$ ), possible probe for pion condensation precursor phenomena 0-78330  
 ( $\pi^-$ ,  $\gamma$ ), lp shell nuclei, response function comparison with ( $e, e'$ ) 0-63143  
 ( $\pi^-$ , NN), low energy pion absorption,  $\sigma + \omega$  model, optical pots., real  $\rho^2(r)$  pot. 0-83125  
 ( $\pi, p$ ), A=12-181, proton yields, number of nucleons involved in pion absorption 0-63209  
 ( $\pi, \pi$ ) single and double charge exchange in resonance region, geometrical limit 0-86930  
 ( $\pi^+, \pi^-$ ) A=9-32, 180 MeV 0-105960  
 ( $\pi^+, \pi^0$ ), isobaric analogue state obs. in  $\text{CH}_2$ ,  $^7\text{Li}$ ,  $^{13}\text{C}$ ,  $^{27}\text{Al}$ ,  $^{58}\text{Ni}$ ,  $^{90}\text{Zr}$ ,  $^{208}\text{Sn}$ ,  $^{208}\text{Pb}$  0-106078  
 ( $\pi^-$ ,  $\nu$  CC),  $\psi \rightarrow \mu^+\mu^-$ , CC $\rightarrow\mu^+\nu$ X, 225 GeV/c, search for extra  $\mu$  0-82967  
 ( $\pi^-$ ,  $\psi$ X), 225 GeV, bottom meson pair production limit 0-73750  
 ( $\pi, X$ ), effective S-wave  $\pi$ NN interaction, effects in nuclear matter 0-105985  
 ( $\pi^-$ , X), n and charged particle emission following  $\pi^-$  capture 0-73867  
 ( $\pi^-$ , X), z=6, 7, 8, 35, 47, charged heavy particle emission after pion capture (*Russian*) 0-69271  
 ( $\pi^+$ , X), 85 to 245 MeV, capture cross sections for Li, C, Al, Fe, Nb, Bi 0-73869  
 ( $\pi^+$ , X), absorption cross section in range 20 to 280 MeV for Al, Ti, Cu, Sn, Au nuclei 0-78327  
 $\pi$ -atomic states in A=12-52, nuclear structure influence, doorway processes 0-99588  
 $\pi^-$  absorption at rest, high spin state excitation,  $\pi$ -condensation and  $\Delta^{++}$  (*Russian*) 0-86927  
 $\pi$ N in nucleus, diffraction dissociation, dip and kink structs., differential cross sections 0-95284  
 $^{27}\text{Al}(\pi^+, \pi^+ \text{N})$ , 180-255 MeV, quasielastic pion scatt. coincidence expt. interpretation, impulse approx. 0-68704  
 $^9\text{Be}(\pi^-, \pi \text{N})$ , 1 GeV/c, heavy fragment knockout process,  $^8\text{Li}$  ang. distrib. 0-106036  
 C ( $\pi^-$ , p) 1.5-5 GeV/c, cumulative proton polarisation (*Russian*) 0-86896  
 $^{12}\text{C}$ ,  $\pi^+$  absorption in flight, cross section, 91-143 MeV 0-63212  
 $^{12}\text{C}(\pi, X)$ , Kalinkin-Shmonin model, expt. data 0-86931  
 $^{12}\text{C}(\pi^-, X)$ , 40 GeV/c, cumulative pions and nucleus total disintegration probability (*Russian*) 0-57807  
 $^{12}\text{C}(\pi^-, \pi^+ p)$ , 100, 180 MeV, knock out reaction, cross section and pion distortion in DWIA 0-91167  
 $^{12}\text{C}(\pi^-, X)$ , 85-245 MeV, true absorption and scatt. in (3,3) resonance region 0-102207  
 $^{12}\text{C}(\pi^+, \pi^+ p)$ , 100, 130 MeV, quasi-elastic scatt. cross section 0-102208  
 $^{12}\text{C}(\pi^+, \pi^+ \text{N})$ , 291 MeV, quasielastic scatt., differential cross sections, Monte-Carlo data fit 0-68703  
 $^{12}\text{C}(\pi^+, \pi^+ \text{N})$ , 180-255 MeV, quasielastic pion scatt. coincidence expt. interpretation, impulse approx. 0-68704

## pion-nucleus reactions continued

- $^{12}\text{C}(\pi^+, \pi^+ p)$ , 180 MeV,  $\pi^+$  to  $\pi^-$  cross-section ratio 0-73868  
 $^{12}\text{C}(\pi^+, \pi^+ p)$ , 120-226 MeV, inelastic scatt. and charge exchange coupled channels calcs. 0-57804  
 $^{12}\text{C}(\pi^+, \pi^+)$ , 0-300 MeV, cross sections, pion-nucleus optical pot. including nuclear Hamiltonian 0-68706  
 $^A\text{Ca}(\pi^+, \pi^+ \text{N})$ , A=40, 44, 48, 291 MeV, quasielastic scatt., differential cross sections, Monte-Carlo data fit 0-68703  
 C( $\pi^+$ ,  $\pi^+$ X), X=He or d, 170 MeV, cross sections and ang. distrib. direct knock-out mechanism (*Russian*) 0-86887  
 C( $\pi, p$ ), 170 MeV, two stage and knock out contribs.,  $\pi^+$ ,  $\pi^-$  spallation differences (*Russian*) 0-68632  
 $^{133}\text{Cs}(\pi, p)$ , stopped  $\pi^-$ ,  $^{132}\text{I}$  yield and  $\gamma$ -ray spectra 0-86857  
 $^{133}\text{Cs}(\pi, p)$  stopped  $\pi^-$ ,  $^{132}\text{I}$  isomer and gamma-ray spectrum 0-78199  
 Cu( $\pi^-$ , X), stopped pions, radioactive product yields 0-83126  
 Cu( $\pi^-$ , p) 1.5-5 GeV/c, cumulative proton polarisation (*Russian*) 0-86896  
 Cu( $\pi^-$ ,  $\psi$  (3700)), 50 GeV, formation cross-sections (*Russian*) 0-106082  
 $^2\text{H}(\pi, p)$ , cross sections, Faddeev like eqns., absorption effects for scatt. 0-86928  
 $^2\text{H}(\pi, p)$  in resonance region, theoretical models 0-83123  
 $^2\text{H}(\pi^-, n)$ , multiple scatt. corrections, off-shell rescatt. effects, effective range 0-83127  
 $^2\text{H}(\pi^-, p)$ , p exchange current effects on pion absorption, cross section enhancement 0-57803  
 $^2\text{H}(\pi^-, p)$  H, total cross section, ang. distrib. and asymmetry parameter 0-63182  
 $^2\text{H}(\pi^+, p)$ , pionic disintegration, absorptive  $\pi$ -nucleus optical pot., microscopic model 0-99191  
 $^3\text{H}(\pi^-, \gamma)$  3n, rest  $\pi$ , resonance branching ratio, bound state upper limit 0-99162  
 $^3\text{He}$ , liquid, pionic K X-ray transition energies and Lorentzian widths 0-78727  
 $^3\text{He}(\pi^+, \pi^0)$ , form factor sensitivity in Glauber multiple scatt. formalism 0-105964  
 $^3\text{He}(\pi^+, \pi^0)$  H, optical potential in momentum representation 0-78324  
 $^4\text{He}(\pi^-, \pi^+ p)$ , 5 GeV/c, quasielastic scatt., cross section, form factor final state interactions 0-99190  
 $^4\text{He}(X, X)$ , 120, 145, 165 MeV, total and differential cross sections 0-78326  
 $^6\text{Li}(e, e')$ , 76-141 MeV, form factors, appl. to ( $\pi^-, \gamma$ ), phenomenological model 0-83068  
 $^A\text{Li}(\pi, p)$ , A=6, 7, 75, 175 MeV, differential cross sections, reaction mechanisms 0-78332  
 $^9\text{Nb}(\pi^-, X)$ , stopped  $\pi^-$ ,  $^{86,87}\text{Ym.s}$  isomeric yield ratios and  $\gamma$ -spectra 0-86857  
 N( $\pi, \pi$ ), 170 MeV, two stage and knock out contribs.,  $\pi^+$ ,  $\pi^-$  spallation differences (*Russian*) 0-68632  
 N( $\pi^+$ ,  $\pi^+$ X), X=He or d, 170 MeV, cross sections and ang. distrib. direct knock-out mechanism (*Russian*) 0-86887  
 $^A\text{O}(\pi^+, \pi^+)$ , A=16, 18, cross section and ang. distrib., Glauber and coherent fluctuation models (*Chinese*) 0-102211  
 $^{16}\text{O}(\pi, \pi p)$ , 163 MeV, coincidence expt. 0-78334  
 $^{16}\text{O}(\pi^-, 2n)$ , stopped  $\pi^-$ ,  $^{14}\text{N}$  levels and excitation energies, kinematically complete investigation 0-99128  
 $^{16}\text{O}(\pi^+, \pi^+)$ , 240 MeV, integrated and doubly differential cross sections 0-68702  
 O( $\pi^+$ ,  $\pi^+$ X), X=He or d, 170 MeV, cross sections and ang. distrib. direct knock-out mechanism (*Russian*) 0-86887  
 O( $\pi, p$ ), 170 MeV, two stage and knock out contribs.,  $\pi^+$ ,  $\pi^-$  spallation differences (*Russian*) 0-68632  
 $^{208}\text{Pb}(\pi^+, \pi^+ \text{N})$ , 180-255 MeV, quasielastic pion scatt. coincidence expt. interpretation, impulse approx. 0-68704  
 Pb( $\pi^-$ , p) 1.5-5 GeV/c, cumulative proton polarisation (*Russian*) 0-86896  
 $^{24}\text{Sc}(\pi^-, X)$ , stopped  $\pi^-$ , yields and  $\gamma$ -rays 0-86857  
 Ta( $\pi^-$ , X), stopped pions, radioactive product yields 0-83126

## pion-nucleus scattering

- see also pion-nucleon scattering  
 A=1, 2, 3, 4, 12, 16 nuclei, intermediate energies, collective isobaric resonance 0-63208  
 Feshbach-Villars formalism and pion-nucleon scattering, relativistic scatt. theory, T-matrix 0-63211  
 finite nuclei,  $\Delta$ -resonance self energy, Fermi broadening,  $\pi$ -nucleus optical pot. 0-68707  
 Israel Physical Society 1980 annual meeting, Rehovot, Israel (April 1980) 0-94909  
 Lee model use in pion-nucleus scatt. theory testing 0-78325  
 lowest order optical pot. containing  $\pi$  emission and absorption effects 0-73865  
 single charge exchange and inelastic scatt. cross sections relationship 0-102204  
 ( $\pi, \pi$ ), elastic scatt. relativistic kinematics, differential cross sections 0-63210  
 ( $\pi, \pi$ ), Weinberg chiral Lagrangian nonlinear terms, nuclear binding, optical pot. 0-78329  
 ( $\pi, \pi$ ), (3,3) resonance region, Brown-Rho bag model descript. 0-57806  
 ( $\pi^-, \pi^+$ ) from Be, C, Al, Cu, Sn, Pb, 70, 125, 175 GeV/c 0-83128  
 ( $\pi^-, \pi^+$ ),  $\pi^-$  nuclear response enhancement, continuum effects, stretched state isospin mixing 0-86929  
 $\pi^+ p$ , 2-9.5 GeV/c, wide angle elastic scatt., differential cross section 0-73730  
 $^{12}\text{C}(\pi^+, A^*)$ , A\* excitation, A\* model unified description 0-102205  
 $^{12}\text{C}(\pi^+, \pi^+)$ , 260 MeV, short range correlations from Glauber multiple diffraction theory (*Chinese*) 0-102210  
 $^{12}\text{C}(\pi^+, \pi^+)$ , nonlinear meson dynamics and binding corrections, optical pots. 0-106080  
 $^{12}\text{C}(\pi^-, \pi^+)$ , 40 GeV, semi-coherent elastic scatt., angular distrib. 0-68701  
 $^{12}\text{C}(\pi^+, X)$ , 85-245 MeV, true absorption and scatt. in (3,3) resonance region 0-102207  
 $^{12}\text{C}(\pi^+, \pi^+)$ , 0-300 MeV, cross sections, pion-nucleus optical pot. including nuclear Hamiltonian 0-68706  
 $^{12}\text{C}(\pi, \pi)$ , elastic and inelastic near  $\pi\text{N}(3,3)$  reson. 0-73870  
 $^{12}\text{C}(\pi^+, \pi^+ p)$ , 120-226 MeV, inelastic scatt. and charge exchange, coupled channels calcs. 0-57804  
 $^A\text{Ca}(\pi, \pi)$ , A=40, 48, 40-241 MeV, first and second order optical pots., resonance behaviour 0-68624  
 $^2\text{H}(\pi^+, \pi^+ \gamma)$ , 269, 298, 324 MeV, radiative scatt. cross section, internal emission and recoil corrections 0-57805  
 $^2\text{H}(\pi^+, \pi^+)$ , low energies, Coulomb interaction (*Russian*) 0-83129



## on-nucleus scattering continued

- $^2\text{H}(\pi, \pi)$ , pole terms and absorption in p-wave  $\pi\text{d}$  interaction 0-86932  
 $^2\text{H}(\pi, \pi)$ , 140-260 MeV, (3,3) region, tensor force, cross sections, pol. parameters 0-68641  
 $^2\text{H}(\pi, \pi)$ , 142, 256 MeV, form factor-backward scatt. correlation, tensor polarisation 0-99189  
 $^2\text{H}(\pi, \pi)$ , high energies, total cross sections from refined Glauber model 0-78322  
 $^2\text{H}(\pi, \pi)$ , low energy scatt. absorption effects, cross sections, Faddeev like equations 0-86928  
 $^2\text{H}(\pi, \pi)$ , pion absorption effect from threshold to resonance 0-99193  
 $^2\text{H}(\pi, \pi)$ , relativistic Faddeev calc. 0-102066  
 $^2\text{H}(\pi, \pi)$ , scatt. length, exchange current contrib. 0-78328  
 $^2\text{H}(\pi^+, \pi^+)$ , 49 MeV, P-wave dispersive contrib.  $\pi$  and  $\rho$  rescatt. 0-78331  
 $^2\text{H}(\pi^+, \pi^+)$ , 130 to 350 MeV,  $180^\circ$  scatt. 0-78335  
 $^2\text{H}(\pi^-, \pi^-)$ , 140-260 MeV, backward scatt., differential cross sections 0-99194  
 $^4\text{He}(\pi^+, \pi^+)$ ,  $A=1,2$ , 130-280 MeV,  $180^\circ$  excitation function, dibaryon resonance signals 0-68619  
 $^4\text{He}(\pi, \pi)$ , 1 GeV, backward scatt., nonstable meson-nucleon interaction cross section, resonance (Russian) 0-68559  
 $^4\text{He}(\pi, \pi)$ , 68-154 MeV, single and double collision differential cross section calcs. (Russian) 0-106083  
 $^4\text{He}(\pi, \pi)$ , elastic interactions in JINR high press. streamer chamber, triggering system 0-102400  
 $^4\text{He}(\pi, \pi)$ , elastic interactions in JINR high press. streamer chamber, selection criteria 0-102401  
 $^4\text{He}(\pi, \pi)$ , optical potential in momentum representation 0-78324  
 $^4\text{He}(\pi, \pi)$ , 145, 180 and 195 MeV, relationship to  $^3\text{He}(e, e)$  0-78323  
 $^4\text{He}(\pi, \pi)$ , elastic data inconsistencies and dispersion relations above 33 resonance 0-68700  
 $^4\text{He}(\pi, \pi)$ , elastic interactions in JINR high press. streamer chamber, selection criteria 0-102401  
 $^4\text{He}(\pi, \pi)$ , single scatt. optical pot., Pauli principle and binding effects on cross section 0-86933  
 $^4\text{He}(\pi^+, \pi^+)$ ,  $A=3,4$ , 260 to 310 MeV, differential cross sections 0-99192  
 $^{24}\text{Mg}(\pi^+, \pi^+)$ , pion spectra, absolute cross section 0-78333  
 $^{40}\text{Ar}(\pi^+, \pi^+)$ ,  $A=16, 18$ , resonance region, proton and neutron distrib. 0-91195  
 $^{16}\text{O}(\pi, \pi)$ , nonlinear meson dynamics and binding corrections, optical pots. 0-106080  
 $^{16}\text{O}(\pi, \pi)$  optical pot., local field correction 0-68705  
 $^{89}\text{Y}(\pi, \pi)$ , giant reson. excitation 0-73834  
 $^{90}\text{Zr}(\pi, \pi)$ , 226 MeV, giant reson. examination 0-73871

## pion-pion interactions

- see also pion-pion scattering  
 resonances, dominant, pole positions, partial waves 0-63020  
 $\pi^- \text{p} \rightarrow \text{n} + \text{K}^0$  ( $k=1$  to 5), 1.3 to 3.8 GeV/c, differential and total cross-sections 0-83000  
 $\pi^- \text{p} \rightarrow \text{n} \pi^0$ , 1.3 to 3.8 GeV/c, differential and total cross-sections 0-83000  
 $\pi\pi \rightarrow \text{NN}$ , helicity amplitude, extrapolation of  $S^1=0$ -wave 0-91112  
 $\pi^+ \pi^- \rightarrow \text{mesons}$ , multimeson inclusive spectra and recombination model, multi-quark structure functions, predictions 0-73751

## pion-pion scattering

- see also pion-pion interactions  
 amplitude, unitarity, analyticity, crossing symmetry props., partial waves 0-57641  
 cross-section from  $\pi^+ \text{n} \rightarrow \text{p} \pi^+$ , reggeised one-pion-exchange 0-57649  
 self-interactions, nonperturbative, scatt. amplitudes containing only convergent integrals 0-68480  
 p-resonance production, quasipotential approach, linear  $\sigma$ -model 0-86755  
 $\pi\pi$ ,  $\rho$ -meson contrib. in broken chiral symmetry model, phase shifts and lengths (Russian) 0-86756  
 $\pi\pi$  scatt. lengths, rigorous phenomenological anal. 0-102070  
 $\pi\pi\pi$  amplitude construction, approx. scheme from analyticity, crossing symmetry and unitarity (German) 0-91111  
 $\pi^+ \pi^-$ , QCD, one-gluon-exchange, resonating group method, soft-core approx. 0-63025

## pion production

- accelerators, linear and cyclic, production, uses and properties of  $\pi$  (French) 0-63417  
 [CC]  $^{12}\text{C}(\gamma, \pi^+)^{11}\text{B}$ , nuclear critical opalescence study 0-105988  
 coherent pion prod. in high energy heavy ion collisions, pion laser 0-73856  
 diffractive hadronic reactions, statistical description of multipion prod. 0-95260  
 hadron + nucleus, spatial temporal development, nuclear hadronic cascades 0-63040  
 (HI,  $\pi\text{X}$ ), 125-400 MeV/N, low energy  $0^\circ$  pion prod., charge ratio 0-95324  
 meson dipion cascade decays, current algebra techniques, pole plus remainder model, chiral symmetry breaking and QCD 0-62972  
 neutron stars, pion condensate form. rel. to cooling 0-77443  
 nuclear collisions, central, standard deviation of  $\pi$  multiplicity (Russian) 0-73864  
 nuclear collisions, coherent  $\pi$  production (French) 0-78311  
 photoproduction amplitudes, Padé approximants and dispersion relation solns. 0-91096  
 pion electroproduction from the nucleon near threshold 0-68651  
 SIN E3 channel, pion prod. meas. 0-74056  
 superdense celestial bodies, pionisation effect rel. to eqn. of state 0-67773  
 D- $\text{K}^0$ , charm-changing weak hadronic current, models 0-57585  
 D $^0 \rightarrow \text{K}^- \pi^+$ , quark total number conservation, D $^+$  lifetime longer than D $^0$  0-57590  
 D $^0 \rightarrow \text{K}^0 \pi^0$ ,  $\Delta T=1$  constraints and final state interactions 0-95267  
 D $^0 \rightarrow \text{K}^0 \pi^0$ , quark total number conservation, D $^+$  lifetime longer than D $^0$  0-57590  
 D $^+ \rightarrow \text{K}^0 \pi^+$ , quark total number conservation, D $^+$  lifetime longer than D $^0$  0-57590  
 dd $\rightarrow \pi^+$ , multiple scatt. contrib. to threshold photoprod. 0-73718  
 e $^+ \text{e}^- \rightarrow \gamma^* \rightarrow \gamma + \text{hadrons}$ , QCD predictions 0-63009  
 e $^+ \text{e}^- \rightarrow \text{hadrons}$ , 12, 30 GeV,  $\pi, \text{k}, \text{p}$  production 0-105916  
 e $^+ \text{e}^-$  inclusive hadron prod., polarisation and p nonconservation asymmetries,  $\text{K}^0$ , D $^0$  prod. 0-78084  
 e $^+ \text{e}^- \rightarrow \pi^+ \pi^-$  ( $\text{K}^+ \text{K}^-$ ),  $\sqrt{s}=1.5$  GeV, EM timelike form factors for  $\pi$  and K 0-91089  
 e $^+ \text{e}^- \rightarrow \pi^+ \pi^- \pi^0$ , 1.45-1.875 GeV,  $\omega$  behaviour at 1.55 GeV 0-82984  
 e $^+ \text{e}^- \rightarrow \pi^+ \pi^- \pi^0$ , 750-1100 MeV,  $\omega$  and  $\phi$  meson interference 0-105910

## pion production continued

- $\pi^+ \text{e}^- \rightarrow \pi^+ \pi^- \pi^0$ , 1.45-1.875 GeV,  $\rho$  behaviour at 1.55 GeV 0-82984  
 en-en $\pi$ , pol. e, P-odd asymmetry and cross sections, SU(2) $\times$ U(1), SU(3) $\times$ U(1) calcs. (Russian) 0-62998  
 e $^- \text{N}$ , inclusive pion production due to  $\gamma\text{q} \rightarrow \pi\text{q}'$  process, quark-parton model (Russian) 0-78073  
 $\eta \rightarrow \pi\pi\gamma$ , quark loop model, SU(3) splitting of quark masses 0-62990  
 ( $\gamma, \pi$ ), photopion reaction sensitivity to optical pot. 0-78278  
 ( $\gamma, \pi^+$ ), low energy photoprod., emission ang. depend. (Russian) 0-57769  
 $\gamma \rightarrow \pi\text{n}$ , threshold-450 MeV, energy dependent multipole anal. 0-78082  
 $\gamma \text{N}$ , exclusive photoprod. reactions, Okubo-Zweig-Iizuka rule 0-95277  
 $\gamma \text{N}$ , inclusive pion production due to  $\gamma\text{q} \rightarrow \pi\text{q}'$  process, quark-parton model (Russian) 0-78073  
 $\gamma \text{N}$ ,  $\pi^+$  photoprod., low energy, emission ang. depend. (Russian) 0-57769  
 $\gamma \text{N} \rightarrow \Delta\pi$ , mag. dipole photoexcitation, singular integral eqns., polynomial ambiguity 0-57608  
 $\gamma \text{n} \rightarrow \pi^+ \text{p}$ , 0.9-1.65 GeV, pol.  $\gamma$ , cross section asymmetry (Russian) 0-86728  
 $\gamma \text{n} \rightarrow \pi^+ \text{p}$ , 700 to 1200 MeV, recoil proton polarisation 0-78075  
 $\gamma \text{N} \rightarrow \pi^+ \text{X}$ , QCD cross sections 0-73715  
 $\gamma \text{n} \rightarrow \pi^+ \text{p}$ ,  $\pi^+ \text{n}$ ,  $\pi^- \text{p}$ ,  $\text{K}^+ \Lambda$ ,  $\text{K}^+ \Sigma^0$  final state comparisons above resonance region 0-105906  
 $\gamma \text{p} \rightarrow \text{K}^+ \text{K}^- \pi^+ \pi^- \text{p}$ , 20-70 GeV,  $\text{K}^+ \text{K}^-$  threshold enhancement 0-78076  
 $\gamma \text{p} \rightarrow \pi\pi^*$ , 340 MeV, pol. p, first resonance region,  $\pi^+$  photoprod., T-asymmetry (Russian) 0-62997  
 $\gamma \text{p} \rightarrow \pi\pi^0$ , photoproduction, in low-energy region, complex multipole amplitudes 0-68463  
 $\gamma \text{p} \rightarrow \pi^0 \text{p}$ , 0.6 to 1.8 GeV, backward angles,  $\eta$ -cusp 0-57609  
 $\gamma \text{p} \rightarrow \pi^0 \text{p}$ , 390-975 MeV, differential cross section 0-86725  
 $\gamma \text{p} \rightarrow \pi^0 \text{p}$ , 400 to 1142 MeV, recoil proton polarisation 0-82981  
 $\gamma \text{p} \rightarrow \pi^0 \text{p}$ , 450 to 800 MeV, proton polarisation, Walker-type anal.,  $\text{P}_{11}(1470)$ ,  $\text{D}_{13}(1470)$ ,  $\text{S}_{11}(1535)$  resonances 0-73721  
 $\gamma \text{p} \rightarrow \pi^0 \text{p}$ , high energies, semiempirical amplitude anal. dispersion relations and Regge poles 0-86726  
 $\gamma \text{p} \rightarrow \pi^+$ , low energies, complex amplitudes in s- and p-wave approx. 0-102053  
 $\gamma \text{p} \rightarrow \pi^+ \text{n}$ , 1.35-1.65 GeV, pol.  $\gamma$ , resonance energy region, cross section asymmetry (Russian) 0-86727  
 $\gamma \text{p} \rightarrow \pi^+ \text{n}$ , 600-1875 MeV, pol. p and  $\gamma$ , G and H polarisation parameters 0-99105  
 $\gamma \text{p} \rightarrow \pi^+ \text{n}$ ,  $\pi^+ \text{n}$ ,  $\pi^- \text{p}$ ,  $\text{K}^+ \Lambda$ ,  $\text{K}^+ \Sigma^0$  final state comparisons above resonance region 0-105906  
 $\gamma \text{p} \rightarrow \pi^+ \pi^- \pi^+ \pi^- \text{p}$ , 20-70 GeV,  $\omega \pi^0$  state enhancement at 1.25 GeV 0-78078  
 $\gamma \text{p} \rightarrow \pi^+ \pi^- \pi^+ \pi^- \pi^+ \pi^- \text{p}$ , diffractive production, jet-like structure 0-57606  
 $\gamma \text{p} \rightarrow \pi \text{X}$ , large  $p_T$ , perturbative QCD 0-86723  
 $\gamma \text{p} \rightarrow \pi^+ \pi^- \text{p}$ , 20-70 GeV, dipion enhancement,  $\rho'(1600)$  observation 0-78079  
 $\text{K}^0 \rightarrow \text{K} \pi$ ,  $k=2$  or 3, Racah time reversal, a C,P,T scheme 0-78056  
 $\text{K}^0 \rightarrow \pi^+ \mu^- \nu_\mu$ , transverse polarisation of  $\mu$ , violation of time-reversal invariance 0-68448  
 $\text{K}^- \text{d} \rightarrow \pi^- \Delta$ , pole in  $^3\text{S}_1$  hyperon-nucleon scattering amplitudes 0-102068  
 $\text{Kp}$ , 70 GeV/c, total and differential cross-sections for  $\pi$  and K production 0-63050  
 $\text{kp}$ , large  $p_T$  pion $^0$  prod., meson structure functions, quark distrib. functions 0-86714  
 $\text{K}^- \text{p}$ , 32 GeV/c, exclusive reactions, diffractive dissociation processes,  $\pi^- \text{p}$  and  $\text{K}^+ \text{K}^-$  prod. 0-86760  
 $\text{K}^- \text{p} \rightarrow \text{K}^0 \pi^+ \text{n}$ , 6 GeV/c,  $\text{K}^+$  and  $\text{Q}_2$  signals, partial wave anal. 0-86754  
 $\text{K}^- \text{p} \rightarrow \text{K}^0 \pi^+ \text{p}$ , 4.2 GeV/c, multichannel anal. 0-73736  
 $\text{K}^- \text{p} \rightarrow \Delta \pi^0$ , 6 GeV/c, baryon exchange reactions,  $\eta\text{NN}$  coupling constant, A polarisation, nucleon-Regge exchange 0-78098  
 $\text{K}^- \text{p} \rightarrow \Delta \pi^0$ , baryon Regge exchange, FESR anal. 0-63022  
 $\text{K}^- \text{p} \rightarrow \pi^+ \Sigma^0$  and  $\pi^+ \text{p} \rightarrow \text{K}^- \Sigma^+$ , exchange degeneracy 0-57634  
 $\text{K}^- \text{p} \rightarrow \pi^+ \text{Y}^*$ ,  $\text{Y}^* = \Sigma^*$  or  $\text{Y}^* = (1385)$ , 7 GeV/c, hypercharge exchange in line-reversed  $\pi^+ \text{p}$  and  $\text{K}^- \text{p}$  0-82998  
 $\text{K}^- \text{p} \rightarrow \pi^+ \Sigma^+$ , box diagram calcs. unitarity corrections in strong interactions 0-91110  
 $\text{K}^- \text{p} \rightarrow \Sigma^- \pi^+$ , backward differential cross section 0-63024  
 $\text{K}^- \text{p} \rightarrow \Sigma^- \pi^+ \pi^+$ , 4.15 GeV/c, nondiffractive  $\text{A}_1$  production, double-Regge model 0-78097  
 $\text{K}^+ \text{p} \rightarrow \text{K}^+ \pi^+ \pi^+$ , 2.7 to 32 GeV/c, impact parameter bounds, energy and effective mass dependence 0-57640  
 $\text{K}^+ \text{p} \rightarrow \pi^- \pi^- \text{X}$ , 32 GeV/c, two-pion correlations, Monte Carlo model 0-83008  
 $\text{NN} \rightarrow (\pi, \rho, \omega, \text{f})$ , statistical model 0-102028  
 $\text{NN}$  dynamics at medium energies, elastic and inelastic scatt., unitary model 0-63101  
 $\text{NN} \rightarrow \text{NN}\pi$ , polarization analysis of reactions with four spin-1/2 particles 0-86745  
 $\text{NN} \rightarrow \pi\pi\pi$ , kinematic singularity free helicity amplitudes, crossing matrix anal. props. 0-95285  
 $\text{np} \rightarrow \text{d} \pi^+ \pi^-$ , 1.73 GeV/c effective mass spectrum ( $\pi^+ \pi^-$ ), narrow enhancements 0-86741  
 $\text{np} \rightarrow \pi^+ \text{d}$ , differential cross sections for 470-590 MeV, ang. distrib. 0-57628  
 $\text{pN}$ ,  $\text{K}^0$  and  $\pi^-$  prod. rates, SU(3) symmetry violation in quark jet 0-82966  
 $\nu \text{n} \rightarrow \mu^- \pi^+$ , neutral current process, excitation function, cross section ratio 0-78053  
 $\nu \text{n} \rightarrow \mu^- \pi^+$ , expt. results comparison to theory 0-102038  
 $\bar{\nu} \text{p} \rightarrow \mu^+ \pi^-$ , 5-70 GeV, cross section,  $1=1/2$  prod. amplitude 0-62962  
 ( $\text{p}, \pi$ ), hopes and realities, review, book contrib. 0-73849  
 ( $\text{p}, \pi^+$ ), 585 MeV,  $A=1-208$ , differential cross section and pol. parameter 0-106056  
 ( $\text{p}, \pi^+$ ), 585 MeV, cross sections, polarisation parameter for H, D, Be, C, O, Al, Ni, Cu, Mo, Pb targets 0-73848  
 ( $\text{p}, \text{X}$ ), 200 GeV/c in emulsion, fireball parameters and  $\pi$  emission 0-95317  
 ( $\text{P}, \text{X}$ ), 22.6 GeV/c, pion  $p_T$  distrib. in emulsion 0-95319  
 ( $\text{p}, \text{X}$ ), 400 GeV,  $A=6-180$ ,  $\text{p}, \pi^+$  and  $\text{K}^+$  backward prod., invariant cross sections 0-102188  
 pd, 70 GeV,  $\pi^+$ ,  $\text{K}^+$ , p, prod. with 0.5-2.2 GeV/c transverse momenta, yield ratio, QCD (Russian) 0-83012  
 pN, 22.6 GeV in emulsion, cluster size in pionisation region 0-78099  
 pN, 67 GeV/c, in Be, Al, Cu, inclusive  $\pi^+$ ,  $\text{K}^+$ , p prod. cross sections (Russian) 0-86769  
 pN, 67 GeV/c, nuclear targets,  $\pi^+$ ,  $\text{K}^+$ , p, p yields (Russian) 0-68501  
 pN, 70 GeV in emulsion, pion cluster obs. 0-86762



## pion production continued

- $\rho\pi$ - $\pi\pi$ , temperature parameter for thermal-like emission spectra, fluctuations 0-68482  
 $\rho\rho$ , 70 GeV,  $\pi^\pm$ ,  $K^\pm$ , p,  $\bar{p}$  prod. cross sections, QCD-parton model anal. (Russian) 0-63044  
 $\rho\rho$ , 8.8 GeV/c, exclusive annihilation processes, cross sections, quark model anal. 0-105920  
 $\rho\rho$ , ISR energies, high  $p_T$   $\pi^0$  and single photon events, associated charged particle multiplicity 0-63039  
 $\rho\rho$ , large  $P_T$  pion<sup>0</sup> prod., meson structure functions, quark distrib. functions 0-86714  
 $\rho\rho$  annihilations, multipion distrib., statistical bootstrap model 0-68472  
 $\rho\rho$ - $\pi\pi$ , 400 to 600 MeV, production cross sections 0-78091  
 $\rho\rho$ - $\pi\pi$  ( $\rho\pi\pi^+$ ) ( $\bar{\rho}\pi\pi^-$ ), 8.8 GeV/c, one pion prod. cross sections, Deck model anal. 0-105919  
 $\rho\rho$ - $\pi\pi\pi$ , 12 GeV/c, final state diffraction dissociation, cross section 0-99109  
 $\rho\rho$ - $\pi^0X$ , intermediate  $p_\perp$  distribution through a QCD resummation mechanism 0-83010  
 $\rho\rho$ - $\pi^0X$ , pol. p, 24 GeV/c, high  $p_T$   $\pi^0$  prod., spin. depend. 0-105935  
 $\rho\rho$ - $\pi^+$  d, 515 and 575 MeV, spin depend. parameter meas. 0-73734  
 $\rho\rho$ - $\pi X$ , large- $P_T$  reactions in broken color gauge theory 0-95292  
 $\rho\rho$ - $\pi X$ ,  $\pi^\pm$  average transverse momentum energy depend., scaling relation 0-91116  
 $\rho\rho$ - $\pi\pi$ , 1-2 GeV/c, Barrelet zero anal., resonant struct. 0-73735  
 $\rho\rho$ - $\pi\pi$ , 1-2 GeV/c, resonance region, partial waves, positivity constraints 0-99107  
 $\pi^0$  photoprod. in  $^{12}\text{C}(\gamma, \pi^0 p)$  at 0.7-1.65 GeV, cross section asymmetry meas. (Russian) 0-63164  
 $\pi^0$  high  $p_T$  prod. ang. depend., inclusive cross sections, scaling 0-91119  
 $\pi^0$  d, 15 GeV, neutral three pion resonance prod., pure  $I=1$  exchange 0-57644  
 $\pi N$ - $\pi\pi N$ , kinematic singularity free helicity amplitudes, crossing matrix anal. props. 0-95285  
 $\pi$  n, 40 GeV/c, many pion systems in inclusive reactions, transverse momentum effects (Russian) 0-57654  
 $\pi$  N, in C, 5 GeV/c,  $\pi^0$  and n inclusive spectra, cascade model (Russian) 0-68490  
 $\pi NN$  dynamics, Faddeev approach, 0-1200 MeV pp scatt. 0-57625  
 $\pi\rho$ , large  $P_T$  pion<sup>0</sup> prod., meson structure functions, quark distrib. functions 0-86714  
 $\pi\rho$ - $\pi X$ , high  $p_T$   $\pi^0$  prod., leading particle contrib., QCD calcs. 0-73746  
 $\pi$  p, 100, 200, 360 GeV/c, inclusive prod. of  $\pi^0$ ,  $K_S^0$ ,  $\Lambda^0$ ,  $\bar{\Lambda}^0$ , cross sections 0-73745  
 $\pi$  p, 40 GeV/c, many pion systems in inclusive reactions, transverse momentum effects (Russian) 0-57654  
 $\pi$  p- $K_S^0 K^\pm \pi^\mp$  n, 3.95 GeV/c, E(1420) quantum numbers and branching ratio 0-95286  
 $\pi$  p-n+ $k^0$  ( $k=1$  to 5), 1.3 to 3.8 GeV/c, differential and total cross-sections 0-83000  
 $\pi$  p, 32 GeV/c,  $\pi$  and  $\rho^0$  inclusive prod., f and  $\eta$  cross section estimates (Russian) 0-68498  
 $\pi$  p- $(\pi^+ \pi^- \pi^0) \Delta^{++}$ , 16 GeV/c, partial wave anal.,  $\omega^*$  and  $A_2^0$  0-63033  
 $\pi$  p- $\pi\pi N$ , 1.4-1.7 GeV, isobar model partial wave anal., baryon resonance decay 0-86750  
 $\tau \rightarrow \nu, n\pi$ , T-violation effects, neutrino mass (Russian) 0-95294  
 $\tau \rightarrow \rho\pi\nu$ , quark model, current algebra model, divergence of axial vector current 0-57655  
 $\tau \rightarrow \nu, \gamma$ ,  $\pi$  form factors, axial-vector and structure dependent, vector meson dominance model 0-62989  
 $\Delta^0 B(\pi^+)$ , A=10,11, 200 MeV, pion energy spectra for discrete final states, cross sections 0-106057  
 $^3\text{Be}(\epsilon, \pi^+)$ , 1848 MeV, virtual photon spectrum, virtual photon theory test 0-102183  
 $^A C(\pi^+)$ , A=12,13, 200 MeV, pion energy spectra for discrete final states, cross sections 0-106057  
 $^A C(\pi^+)$ , A=12,13, 200 MeV, analogue and nonanalogue state cross sections 0-99130  
 $^{12}\text{C}(^{12}\text{C}, X)$ , two fireball model, pp correlations and inclusive pion spectrum 0-68694  
 $^{12}\text{C}(a, X)$ ,  $a=p, d, ^4\text{He}$ ,  $^{12}\text{C}$ , 4.2 GeV/c, multitudes of secondary negative particles, momentum distrib. ratios (Russian) 0-63178  
 $^{12}\text{C}(\gamma, \pi^-)$  N, total cross section calc.,  $\Delta(1232)$  contrib. 0-91175  
 $^{12}\text{C}(\gamma, \pi^-)$  p, final state interaction, distorted and plane wave momentum distrib. 0-78275  
 $^{12}\text{C}(\gamma, \pi^0)$ , pionic and EM  $A^*$  resonance excitation 0-91160  
 $^{12}\text{C}(\pi^+, X)$ , 40 GeV/c, cumulative pions and nucleus total disintegration probability (Russian) 0-57807  
 $^{40}\text{Ca}(^{40}\text{Ca}, x)$ , relativistic, compression and pion distrib., Monte Carlo calc. 0-73853  
 $\text{Cl}(\text{Ar}, X)$ , 0.4-1.8 GeV/u, multipion prod. energy depend. 0-106065  
 $\text{C}(\pi^+)$  240 MeV inclusive pion production (Russian) 0-86908  
 $\text{Cu}(\pi^+)$  240 MeV inclusive pion production (Russian) 0-86908  
 $c^+c^-$  annihilation, quark jets, transverse momentum profile 0-57621  
 $(\text{Hl}, \pi)$ ,  $\pi$  radiation from relativistic heavy ion 0-73863  
 $^1\text{H}(\gamma, \pi^+)$ , 3.4-18 GeV,  $\pi NN$  form factor and differential cross sections, one pion exchange 0-68526  
 $^1\text{H}(n, \pi^0)^2\text{H}$ , differential cross sections for 470-590 MeV, ang. distrib. 0-57628  
 $^1\text{H}(\pi^+)^2\text{H}$ , pol. p, total cross section, ang. distrib. and asymmetry parameters 0-63182  
 $^2\text{H}(\delta, \pi^0)$ , multiple scatt. contrib. to threshold photoprod. 0-73718  
 $^2\text{H}(\gamma, \pi^-)nn$ , n-n final state interaction effects 0-102181  
 $^2\text{H}(n, \pi^-)$ , 400-580 MeV, differential cross sections and ang. distrib. 0-86906  
 $^2\text{H}(n, \pi^+)^3\text{He}$ , 400 to 580 MeV at backward pion angles 0-73847  
 $^2\text{H}(\pi^+)$ , 400-470 MeV, backward  $\pi$  differential cross sections and anal. power 0-86905  
 $^4\text{H}(\gamma, \pi^0)$ , A=1, 2, 1-10 MeV, photoprod. yields, DWIA anal., dipole photoprod. amplitudes 0-68645  
 $^4\text{He}(\gamma, \pi^+)^3\text{H}$  cross section near threshold 0-83093  
 $^3\text{He}(\pi^+)$ , A=3, 4, 1-10 MeV, photoprod. yields, DWIA anal., dipole photoprod. amplitudes 0-68645  
 $\text{K}(\text{Ar}, X)$ , 0.4-1.8 GeV/u, multipion prod. energy depend. 0-106065  
 $\text{K}^+ p \rightarrow \pi^+ X$ , 32 GeV, topological cross sections 0-102085  
 $^{14}\text{N}(\gamma, \pi^-)$ , DWIA anal., wave function and  $\pi$  optical pot. effects on cross section 0-63168  
 $^{14}\text{N}(\gamma, \pi^+)$ , anomalous  $^{14}\text{N}_{\text{gs}} \rightarrow ^{14}\text{C}_{\text{gs}}$  transition, Kroll Ruderman terms 0-63167  
 $^{16}\text{O}(\epsilon, \pi^+)$ , 180.4 MeV, virtual photon spectrum, virtual photon theory test 0-102183

## pion production continued

- $^{16}\text{O}(\gamma, \pi^+)$ , 200-350 MeV, cross sections, DWIA anal. 0-106048  
 $\text{Pb}(^{12}\text{C}, X)$ , 1-2 GeV/n, central collision threshold phenomena, pion prod. 0-95326  
 $^{181}\text{Ta}(a, X)$ ,  $a=p, d, ^4\text{He}$ ,  $^{12}\text{C}$ , 4.2 GeV/c, multitudes of secondary negative particles, momentum distrib. ratios (Russian) 0-63178
- pion-proton inclusive interactions**  
hadronic two-jet events, momentum unbalance, parton transverse momentum 0-57652  
neutral particle production in 4 to 2100 GeV interactions, review (Russian) 0-68489  
 $\pi\rho$ , large  $P_T$  pion<sup>0</sup> prod., meson structure functions, quark distrib. functions 0-86714  
 $\pi\rho \rightarrow \mu^+ \mu^- X$ , quark transverse momentum effect in bag model 0-86668  
 $\pi\rho \rightarrow \pi X$ , high  $p_T$   $\pi^0$  prod., leading particle contrib., QCD calcs. 0-73746  
 $\pi$  p, 100, 200, 360 GeV/c, inclusive prod. of  $\pi^0$ ,  $K_S^0$ ,  $\Lambda^0$ ,  $\bar{\Lambda}^0$ , cross sections 0-73745  
 $\pi$  p, 100 GeV/c, inclusive meson and strange particle prod., energy partition 0-95289  
 $\pi$  p, 340 GeV, associated charm prod. evidence,  $D^+$  prod. 0-86767  
 $\pi$  p, 40 GeV/c, many pion systems in inclusive reactions, transverse momentum effects (Russian) 0-57654  
 $\pi$  p, 70 GeV/c, direct electron prod. from charm particle pair decay,  $e/\pi$  ratio 0-105928  
 $\pi$  p, 70 GeV/c, directly produced electrons from charmed D particle decay, cross sections 0-73755  
 $\pi$  p, multiple production processes regularities, Monte Carlo model 0-102082  
 $\pi$  p- $(\rho\rho)X^0$ , narrow  $\rho\rho$  state search 0-78102  
 $\pi$  p- $\rho X$ , 12 GeV/c, absorbed Mueller-Regge model for backward inclusive p prod. 0-73752  
 $\pi$  p- $\pi^+ X$ , triple Pomeron coupling, Reggeon treatment 0-68488  
 $\pi$  p- $\rho^0 \pi^+ X$ , diffractive contrib. in multi-Regge factorisation 0-73753  
 $\pi^+$  p, 32 GeV/c,  $\pi$  and  $\rho^0$  inclusive prod., f and  $\eta$  cross section estimates (Russian) 0-68499  
 $\pi^+$  p, 32 GeV/c, slow proton and  $\Delta^{++}(1236)$  inclusive prod. (Russian) 0-63046  
 $\pi^+$  p- $K^+ K^+$  (892)X, 16 GeV/c 0-86765  
 $\pi^+$  p, 130, 200 GeV, jet prod. cross sections, QCD anal. and scale breaking 0-99111  
 $\pi^+$  p, 147 GeV/c, inclusive  $\Delta^{++}$  prod., cross section energy depend. 0-57651  
 $\pi^+$  p, fireball model, universal scaling function 0-57646  
 $\pi^+$  p,  $\pi^+/\pi^-$  inclusive ratio in quark recombination model 0-102022
- pion-proton scattering**  
see also pion-proton inclusive interactions; pion-proton scattering  
correlation between  $\pi$  and accompanying large transverse momentum particle (Russian) 0-86758  
 $\pi\rho$ -baryons by diquark-quark fusion model 0-102065  
 $\pi\rho$ , direct photon prod., Compton and annihilation process contrib. 0-105925  
 $\pi\rho$ , inelastic charge exchange scatt., diffraction approach, convergent polynomial expansion, scaling 0-78095  
 $\pi\rho$ , massive lepton pair prod., pion exchange model anal., quark parton interpretation (Russian) 0-82993  
 $\pi$  p, 150 GeV/c, leading particles and diffraction dissociation, 2-, 4- and 6-prong events 0-68486  
 $\pi$  p, 2-14 GeV/c, total cross section, narrow baryon search 0-105922  
 $\pi$  p- $\eta$  n, Regge pole model with phenomenological residue function 0-102077  
 $\pi$  p- $\eta(\eta')$  n, 8.45 GeV/c, differential cross section ratio,  $\eta'$  decay branching 0-78094  
 $\pi$  p- $K_S^0 K^\pm \pi^\mp$  n, 3.95 GeV/c, E(1420) quantum numbers and branching ratio 0-95286  
 $\pi$  p- $K^0 \Lambda$ , 3.5 GeV/c,  $\Lambda$  polarisation, high statistics meas. 0-57637  
 $\pi$  p- $K^0 \Sigma^+$ , 1395 to 2375 MeV/c, differential cross-section and polarisation 0-57635  
 $\pi$  p- $K^0 K^-$  n, 62 GeV, spin-5 boson resonance at 2300 MeV 0-102078  
 $\pi$  p- $K^0(890) \Lambda^0/\Sigma^0$ , 10 GeV/c,  $K^0$  polarisation meas. in hypercharge exchange reaction 0-63017  
 $\pi$  p- $\Lambda K$ , low energy, amplitude anal., Lagrangian model 0-82995  
 $\pi^+ p \rightarrow (\pi^+ \pi^- \pi^0) \Delta^{++}$ , 16 GeV/c, partial wave anal.,  $\omega^*$  and  $A_2^0$  0-63033  
 $\pi^+ p \rightarrow \Delta^{++} p$ , 9.8 GeV/c, narrow  $\rho\rho$  state search 0-57636  
 $\pi^+ p \rightarrow K^+ \Sigma^+$  and  $K^+ p \rightarrow \pi^+ \Sigma^+$ , exchange degeneracy 0-57634  
 $\pi^+ p \rightarrow K^+ \Sigma^+$  and line reversed reaction  $K^+ p \rightarrow \pi^+ \Sigma^+$ , simple Regge pole model 0-78093  
 $\pi^+ p \rightarrow K^+ Y^+$ ,  $Y^+ = \Sigma^+$  or  $Y^{*+}(1385)$ , 7 GeV/c, hypercharge exchange in line-reversed  $\pi^+ p$  and  $K^+ p$  0-82998  
 $\pi^+ p \rightarrow K^+(890) Y^+$ ,  $Y^+ = \Sigma^+$  or  $Y^{*+}(1385)$ , 7 and 11.5 GeV/c, hyperon polarisation, vector meson decay angular distrib. 0-82997  
 $\pi^+ p \rightarrow \pi^+ n$ , 1.4-1.7 GeV, isobar model partial wave anal., baryon resonance decay 0-86750
- pion-proton scattering**  
see also pion-proton interactions  
large momentum transfer, multiple-scattering model, three-quark proton 0-63031  
ZGS, strong interaction counter expts. 0-91305  
 $\pi$  p, 2-14 GeV/c, total cross section, narrow baryon search 0-105922  
 $\pi$  p elastic scatt., 2.22-3.5 GeV/c, backward polarisation 0-82999  
 $\pi$  p elastic scatt., 3.42-5.03 GeV/c, narrow baryon search in differential cross section 0-105921  
 $\pi$  p elastic scattering, 2 GeV/c region, high precision meas. 0-91109  
 $\pi^+$  p, nonrelativistic scatt., Coulomb corrections 0-82994  
 $\pi^+ p \rightarrow \pi^+ \gamma$ , 165 MeV, monotonically decreasing photon energy spectrum no  $\Delta^{++}(1232)$  bump 0-68476  
 $\pi^0$  p, 0 to 350 MeV, elastic and charge-exchange scatt., partial wave anal.,  $\Delta$  resonances, review 0-63018  
 $\pi^0$  p, 100 GeV/c, polarisation parameters and ang. distrib. for elastic scatt. 0-95287  
 $\pi^0$  p, elastic scatt., and diffractive dissociation, Regge model with  $\alpha_P(0) >$  (Russian) 0-57630  
 $\pi^0$  p large angle elastic scatt., 20, 30 GeV/c, dimension counting rule test 0-83003
- pion scattering** see lepton-hadron scattering; meson-meson scattering; photon-hadron scattering; pion-baryon scattering; pion-nucleus scattering; pion-pion scattering  
**pions**  
charge radius, coloured quark field theory 0-62945  
compositeness from wave function renormalisation constant 0-101997  
deep inelastic structure functions in massive quark model 0-86717



ions continued

EM form factor asymptotics in QCD perturbation theory, partonic interpretation (*Russian*) 0-62984

EM form factor factorisation and asymptotic behaviour in QCD 0-91090

EM mass shifts, asymptotic bounds and causality conditions 0-73704

hadron building blocks, pionic mass intervals in narrow and S-state resonances 0-105875

mammalian cells, lethally damaged, proliferation obs. after irradiation by various particles 0-108971

mass in improved static bag model 0-73667

microdosimetry of the pion beam at TRIUMF 0-109037

modified quark loop model, form factors, structure functions, radiative decay 0-91088

structure functions from inclusive production data, nonstrange quark distributions 0-86715

testes, mice, comparative effects of various radiations on weight loss and spermatogenic stem-cell survival 0-108976

 $e^-e^+ \rightarrow \pi^+\pi^-(K^+K^-)$ ,  $\sqrt{s}=1.5$  GeV, EM timelike form factors for  $\pi$  and  $K$  0-91089 $\pi$  form factors, axial-vector and structure dependent, vector meson dominance model 0-62989 $\pi^+$  radiation therapy, in vivo beam localisation by positron activation 0-72316 $\pi^+$  radiobiological evaluation of suitability for tumour therapy 0-67166 $\pi^+\pi^-$  EM polarisabilities, sum rules, coloured quark field theory 0-57561 $^4\text{H}$ , pionic, pion mass high accuracy meas. from transitions 0-106406 $\text{Ti}$ , pionic, pion mass high accuracy meas. from transitions 0-106406

pipe diffusion see diffusion in solids

pipeline processing

nerve fibre counting by pipeline multiminicomputer image processing 0-109013

pitch detection see acoustic variables measurement

PIXE see ion microprobe analysis

plages see Sun

planet Mercury see Mercury (planet)

planetary atmospheres

aerobraking for planetary orbit missions 0-109338

diffuse reflection problem, invariance principles and integral eqns. for radiation fields in plane atmosphere 0-67559

erosion of planetary and satellite atmospheres, by energetic atomic particles 0-72736

flow of rot. liq., western boundary currents and detached layers 0-81984

formation from  $\text{N}_2$  reservoir, solar nebula  $\text{NH}_3$  synthesis, kinetic model 0-62041

giant planets, detectability of liq. methane, laboratory optical absorption spectra meas. 0-93278

giant planets, radiowave refraction 0-98608

greenhouse effect for Earth, Venus and Jupiter 0-101544

inert gases in terrestrial planet atmospheres, accretion from protoplanetary nebula 0-109385

Io, form. of Na clouds and regolith by micrometeoroid impact 0-77330

Io, non-linear standing Alfvén wave current system 0-72869

Io, plasma torus, ion density spatial distrib. 0-72861

IO,  $\text{SO}_2$ , frost IR spectra and deposition processes 0-77331Io,  $\text{SO}_2$  model atmos. and ionosphere 0-72853

Io, volcanic activity model based on plasma obs. 0-72870

Io's torus, charged particle radial diffusion 0-72859

Io plasma disc, model of plasma injection 0-72860

Io plasma torus, effects on Jupiter kilometric radiation spatial and temporal distrib. 0-77328

ionospheres, ionic reactions in lab. and planetary atmospheres 0-59168

ionospheres of major planets, review of pre-Voyager knowledge 0-90351

Jupiter, atmosphere map at 2400 Å from Voyager 2 obs. 0-77336

Jupiter, atmospheric constitution, structure and dynamics 0-105186

Jupiter, aurora due to protons, nightside 0-85890

Jupiter, cloud distrib. between Voyager 1 and 2 missions, 5 micron obs. 0-77345

Jupiter, constituents, comparison with Saturn, visible obs. (*French*) 0-101550

Jupiter, current disc of magnetosphere, modeled using Pioneer 10 data 0-101551

Jupiter, decametric and hectometric radio emission obs. 0-67644

Jupiter, disturbances and dislocations, triggering factors 0-72867

Jupiter, dust in magnetosphere derived from Io volcanoes 0-85889

Jupiter, fast moving bright spot obs. in North Temperate Current C 0-67640

Jupiter, Great Red Spot, atmosphere baroclinic model, solitary waves on unsymmetric shear flow 0-82266

Jupiter, H I Lyman  $\alpha$  emission, Voyager 2 EUV obs. 0-77338Jupiter, H Lyman- $\alpha$  brightness, longit. asymm. 0-72852

Jupiter, hydrocarbon and H I photochemistry rel. to Lyman alpha albedo 0-105194

Jupiter, Io torus and magnetosphere Birkeland currents 0-105198

Jupiter, IR spatial scans 0-82268

Jupiter, Lyman  $\alpha$  albedo, Copernicus UV obs. 0-94747Jupiter, Lyman  $\alpha$  albedo rel. to solar activity 0-98601

Jupiter, magnetosheath sunward flow, depend. on solar wind pressure. 0-72857

Jupiter, magnetosphere, Io torus, latitudinal plasma oscills. 0-85892

Jupiter, magnetosphere, tailward directed ion beam 0-72854

Jupiter, magnetosphere and bow shock, Voyager 2 magnetometer obs. 0-77339

Jupiter, magnetosphere energetic ions and electrons Voyager 2 obs. 0-77342

Jupiter, magnetosphere low energy plasma, Voyager obs. 0-72855

Jupiter, magnetosphere shape and field, model 0-72868

Jupiter, magnetosphere trapped energetic particle spectrum 0-72711

Jupiter, magnetotail structure inferred from plasma obs. 0-72864

Jupiter, methane and  $\text{NH}_3$  bands, longitudinal variability, visible obs. 0-82270Jupiter,  $\text{NH}_3$  abundance from visible obs. 0-82269Jupiter,  $\text{NH}_3$  vertical density profiles from IR and radioelectric emissivity data 0-82267

Jupiter, radioemission at 100 kHz, from magnetosphere 0-85891

Jupiter, S II forbidden line emission round planet, distrib. and intensity 0-85885

Jupiter, S II torus, longitudinal asymmetry visible spectra 0-82271

Jupiter, thermal structure from Voyager 2 IR obs. 0-77335

Jupiter, Voyager low energy charged particle expt. results 0-98605

planetary atmospheres continued

Jupiter, whistler mode chorus obs. and Io torus implications 0-72862

Jupiter, whistler propagation in magnetosphere, theory 0-72863

Jupiter, wind vector, eddy momentum and energy conversion obs. 0-72851

Jupiter as source of electrons observed at Earth orbit 0-90357

Jupiter atmosphere, cloud structure and C/H ratio from methane line profiles near  $1.1 \mu$  0-62067

Jupiter ionosphere, electrons accelerated rel. to S-bursts frequency drift meas. at different frequencies 0-85888

Jupiter ionosphere, spectral broadening meas. by Pioneers 10 and (11) 0-109391

Jupiter ionosphere, Voyager 2 occultation, radio obs. 0-77337

Jupiter ionosphere and magnetosphere, Cotton-Mouton effect rel. to decametric radio emission modulation 0-67643

Jupiter magnetosphere, electrostatic waves obs. 0-72865

Jupiter magnetosphere, HF and LF events from Voyager 2 obs. 0-77344

Jupiter magnetosphere, Io interaction with plasma torus 0-98604

Jupiter magnetosphere, kilometric radiation ray tracing 0-72866

Jupiter magnetosphere, kilometric radiation spatial and temporal studies 0-77328

Jupiter magnetosphere, plasma cloud injection from Io, S and O ions discontinuities 0-90358

Jupiter magnetosphere, plasma corotation lag from Voyager 1 obs. 0-90361

Jupiter magnetosphere, plasma waves from Voyager 2, radio obs. 0-77343

Jupiter magnetosphere, Voyager 2 obs. of hot plasma environment 0-77341

Jupiter magnetosphere 0-72858

Jupiter magnetosphere and bow shock, plasma densities from Voyager 2 obs. 0-77340

Jupiter magnetosphere disturbed by Ganymede, Voyager-2 obs. 0-72856

Jupiter mid-magnetosphere, equatorial protons instability 0-67642

Jupiter radiation belt, erosion of Ganymede atmosphere by energetic atomic particles 0-72736

Jupiter radiation belts, particle fallout mechanism for Io local gas emission (*Russian*) 0-82275

light scattering, by optically thin spherically symmetric atmosphere rel. to brightness at zenith near terminator 0-109382

light scattering by optically thin inhomogeneous spherically symmetric atmosphere 0-67600

magnetospheres, effect on cosmic ray propagation 0-101517

Mars, atmosphere boundary layer, momentum and heat turbulent flux, Viking 1 obs. 0-72810

Mars, atmosphere dust content rel. to longit. var. of 2.8 cm brightness temp. 0-105191

Mars, climate oscills., latitude depend. and oscill. spectra 0-90355

Mars, cloud formations, reflectivity time var., visible photometry obs. 0-72840

Mars,  $\text{CO}_2$  atmosphere erosion by solar wind energetic atomic particles 0-72736Mars,  $\text{CO}_2$  ice clouds, brightness temp. and radiative props. 0-105192

Mars, crater generated lee waves 0-72824

Mars, diurnal props. of clouds over Tharsis volcanoes 0-94738

Mars, dust affecting surface and atmosphere heating 0-67625

Mars, dust storm of 1971, cloud form., multicolour TV photometry obs. 0-101546

Mars, dust storms, opacity from Viking IR thermal mapping 0-82253

Mars, general circulation model, including dust and topography 0-90354

Mars, ionosphere and magnetosphere interaction with solar wind 0-72835

Mars, magnetic minerals, obs. by Viking extended mission 0-72830

Mars, O I dayglow red emission at 630 nm 0-62063

Mars, radiative equilibrium temp. affected by  $\text{O}_3$  0-72827

Mars, relative humidity 0-72826

Mars, sand blown by wind, threshold windspeed 0-72811

Mars, significance for volatile storage and atmospheric history of  $\text{CO}_2$  adsorption and capillary condensation on clays 0-72833

Mars, spectral line shape of O following dissociative excitation 0-105097

Mars, sulphate aerosol formation from volcanoes, and deposition 0-72828

Mars, wind erosion, yardang evidence 0-67623

Mars, wind patterns rel. to sand sea (erg) in north polar region 0-67624

Mars, wind streaks, seasonal and secular var., Mariner 9 and Viking obs. 0-67622

Mars atmosphere pressure, annual cycle meas. by Viking landers 1 and 2 0-72812

Mars atmospheres, Viking orbiters radio occultation meas. during one Martian year 0-72836

Mercury exosphere simulation, Monte Carlo methods 0-67588

Mercury exosphere simulation, Monte Carlo methods 0-67589

methane,  $^{12}\text{C}$  and  $^{14}\text{C}$ , line parameters for  $\nu_2$  and  $\nu_4$  bands, isotope shifts, appln. to planetary atmospheres 0-95622

microwave absorption in atmosphere of giant planets induced by collisions of H molecules 0-90350

multiple scattering of light, Hovenier's exit function eqn., numerical props. 0-62054

Neptune, albedo and brightness temp.,  $5 \mu$  IR obs. 0-82300

Neptune, ammonia and water vapour contents 0-90366

Neptune, atmospheric structure from stellar occultation obs. (1980 August 21) 0-109395

Neptune, limb brightening in 7300 Å methane band, photometry obs. 0-82297

Neptune atmosphere, equatorial flow model rel. to rot. 0-67653

Neptune atmosphere, UV albedo meas. 0-82295

radiative transfer, key eqn. exact soln., Laplace transform and linear singular operators method 0-67536

radiative transfer, synthetic scattering phase function 0-98541

radiative transfer, time-dependent, exact soln. of integro-differential eqn. via Laplace transform 0-94703

radiative transfer, two stream approx. 0-109383

radiative transfer in finite atmosphere, exact soln. of basic eqn. via Laplace transform 0-94702

radiative transfer in planetary atmosphere,  $F_N$  method for polarisation studies 0-98540

radiometry in quasi-isotropic atmosphere 0-90345

Rayleigh-scattering dense atmosphere with true absorption, single-scatter. albedo determ. method 0-94704

response to heat sources and perturbations (*Chinese*) 0-85748

Saturn, ammonia and N mixing ratio in troposphere 0-94748

Saturn, constituents, comparison with Jupiter, visible spectra obs. (*French*) 0-101550



## planetary atmospheres continued

- Saturn, imaging, photometry and polarimetry obs. from Pioneer 11 probe 0-82289
- Saturn, limb darkening and brightness temp., 1.30 cm interferometry obs. 0-82279
- Saturn, magnetosphere, trapped radiation belts, particle absorpt., Pioneer 11 obs. 0-82287
- Saturn, magnetosphere interaction with solar wind, Pioneer 11 obs. 0-82282
- Saturn,  $\text{NH}_3$  abundance from visible obs. 0-82269
- Saturn,  $\text{NH}_3$  vertical density profiles from IR and radioelectric emissivity data 0-82267
- Saturn, Pioneer 11 IR radiometry obs. 0-82290
- Saturn, ring system-ionosphere interaction 0-94751
- Saturn, upper neutral atm. and ionosphere, vertical struct., Pioneer 11 radius occultation obs. 0-82293
- Saturn, UV photometry from Pioneer 11 probe 0-82288
- Saturn ionosphere, spectral broadening meas. by Pioneer (11) 0-109391
- Saturn magnetosphere, bowshock and magnetopause detect. by Pioneer 11, mag. field determ. 0-82283
- Saturn magnetosphere, cosmic ray cutoff rigidities 0-72873
- Saturn magnetosphere, energetic ions and electrons, Pioneer 11 obs. 0-82286
- Saturn magnetosphere, interactions with satellites and rings 0-82285
- Saturn magnetosphere, trapped radiation, absorpt. by satellites and ring, Pioneer 11 obs. 0-82284
- Saturn upper atmosphere, struct. from Titan eclipse light curve 0-90362
- spacecraft braking problem in Jupiter atmosphere, ballistic and navigation aspects 0-61981
- Titan, atmosphere organic chemistry, review 0-90364
- transfer equation, in semi-infinite atmosphere with albedo ( $\omega > 1$ ) 0-82184
- turbulence determ. from radio occultations of spacecraft 0-94734
- Uranus, albedo and brightness temp., 5  $\mu\text{m}$  IR obs. 0-82300
- Uranus, albedo and spectral features from IR obs. 0-82299
- Uranus, ammonia and water vapour contents 0-90366
- Uranus, appl. of methane band-model parameters to visible and near IR spectrum 0-98609
- Uranus, D/H ratio from visible spectra obs. 0-82296
- Uranus atmosphere, equatorial flow model rel. to rot. 0-67653
- Uranus atmosphere, UV albedo meas. 0-82295
- Venus, aerosol model 0-101545
- Venus, atmosphere structure instruments on Pioneer entry probes 0-67562
- Venus, atmospheric constitution, struct. and dynamics 0-105186
- Venus, cloud microstructure, optical props.,  $\text{H}_2\text{SO}_4$  atmosphere-aerosol study 0-72808
- Venus, clouds, IR absorption and scattering, particle size dispersion effect 0-109384
- Venus, dark face, atmospheric constitution, pictures from NASA Venus Pioneer space vehicle (*French*) 0-94735
- Venus, exosphere, hydrogen Lyman  $\alpha$  emission 0-105188
- Venus, flow of solar wind behind planet, model 0-98531
- Venus, IR brightness temp., daytime minima 0-77309
- Venus, magnetosphere press. balance, outside dayside ionopause 0-90353
- Venus, nephelometer on Pioneer Venus Sounder and small probes 0-67511
- Venus,  $\text{O}_2$ ,  $^{13}\text{C}$ ,  $^{18}\text{O}$  band, prod. mechanisms 0-82251
- Venus,  $\text{O}_2$ , Ar, CO abundances, error of Pioneer Venus chromatography obs. 0-105189
- Venus, oxidation state of atmosphere and crust from Pioneer Venus results 0-98586
- Venus, Pioneer Bus neutral gas mass spectrometer 0-67513
- Venus, Pioneer Differential Long Baseline Interferometry expt., wind meas. 0-67578
- Venus, Pioneer Orbiter radiometer (VORTEX) 0-67504
- Venus, Pioneer small probes net flux radiometer expt. 0-67512
- Venus, Pioneer Sounder Probe gas chromatograph 0-67507
- Venus, Pioneer Sounder Probe neutral gas mass spectrometer 0-67506
- Venus, Pioneer Sounder Probe Particle Size Spectrometer 0-67510
- Venus, Pioneer Sounder Probe Solar Flux Radiometer 0-67508
- Venus, Pioneer Venus Orbiter neutral gas mass spectrometer expt. 0-67502
- Venus, radiance meas. using Pioneer Venus Solar Flux Radiometer 0-82198
- Venus, review of Venera data 0-72804
- Venus, spectral line shape of O following dissociative excitation 0-105097
- Venus, surface reflections of Pioneer Venus descent vehicles radio emission, atm. data 0-105187
- Venus, upper atmosphere, aerosol layer obs. from polarimetry 0-90352
- Venus, UV cloud model from polarimetric obs. 0-82250
- Venus atmosphere, C and N species prod. by thunderstorms 0-98587
- Venus atmosphere, radio waves attenuation investigation by bistatic radar method 0-62061
- Venus atmosphere, scattered solar radiation fluxes spectral and altitude distrib. 0-62059
- Venus atmosphere, struct., and light, heat and wind regimes from space vehicles 0-62062
- Venus atmosphere and surface, investigation by radiosounding from Venera 9 and 10 satellites 0-101543
- Venus cloud layer, struct. according to Venera 9 televised pictures 0-67604
- Venus daylight spectrum, 1250 to 1430  $\text{\AA}$ , Pioneer Venus obs. 0-77311
- Venus environment, plasma wave investigation by Pioneer Venus Orbiter 0-67497
- Venus ionosphere, electron temp. probe on Pioneer Venus Orbiter 0-67500
- Venus ionosphere, mag. flux ropes nature (*Russian*) 0-77313
- Venus ionosphere, Pioneer Venus Orbiter planar retarding potential analyser plasma expt. 0-67501
- Venus ionosphere, thermal diffusion calcs. 0-72806
- Venus ionosphere composition, meas. by ion mass spectrometers on Pioneer Venus Bus and Orbiter 0-67499
- Venus magnetic tail, unipolar induction effects 0-62060
- Venus plasma environment, study via plasma analyser expt. on Pioneer Venus Orbiter 0-67498
- Venus upper atmosphere, N detect. 0-77310

## planetary nebulae

- 49+88.1°, halo planetary nebula, photoionisation models and chemical abundances 0-109507

## planetary nebulae continued

- 60-7°1, radial vel. meas. of central star FG Sagittae rel. to binary star model 0-98664
- 108-76.1°, halo planetary nebula, photoionisation models and chemical abundances 0-109507
- 158+17°1, new nearby object on POSS E-print 0-98701
- Abell 30, obs. of ejected material from central star 0-82474
- Abell 46, central star found to be eclipsing binary 0-73027
- Abell 46, IUE spectroscopic obs. of eclipsing binary nucleus 0-98693
- abundances of He, Ne, Ar, N, and Cl 0-109532
- atomic and molecular data for planetary nebulae, heavy particle processes 0-109528
- catalogue, of new and misclassified planetary nebulae 0-109378
- central star evolutionary scenario towards white dwarf stage, composition effect 0-109427
- central stars, spectra, temps., binaries and peculiar stars 0-109435
- central stars, temps. determ. rel. to nebulae evolution 0-67724
- central stars of solar mass, evolution 0-109428
- chemical abundance determ. from weak diagnostic spectral lines 0-109531
- classification according to abundance, chem. kinetic and spatial props. 0-109509
- classification according to chemical abundance 0-109530
- cosmic dust in planetary nebulae, theoretical data review 0-109536
- distance scale, new, rel. to galactic distrib. 0-67819
- distance scale of planetary nebulae, meas. methods 0-109521
- distances, determ. through nebular ionised mass/nebula radius relation 0-101625
- dust in planetary nebulae, observational review 0-109535
- dust temperature and mass, IR photometry obs. 0-94850
- element abundance and classification, implications for galaxy abundance 0-109530
- element abundances, He/H, N/O and  $^3\text{He}$ , implications for previous evolution 0-105237
- ESO 263-PN 02, spectroscopic obs. 0-101626
- evolution, implications of nuclei temps. and masses 0-82344
- evolution after central star ejection, review 0-109533
- extinction rel. to turbulent interstellar medium in Galaxy 0-62220
- far UV flux determ. from nebula ionisation state 0-72945
- Galaxy chemical evolution, role of planetary nebulae 0-109541
- He2-442, UVK photometry and spectroscopic obs. (*Russian*) 0-94817
- high-excitation, IUE satellite obs. 0-94860
- IC 418, C abundance from visible and IUE obs. 0-82451
- IC 418, UV spectra and C abundance 0-67832
- interstellar extinction, average model, from planetary nebulae obs. 0-62221
- interstellar medium, ionisation, heating and stirring, role of planetary nebulae, review 0-109540
- ionisation, influence of He shell flashes in nuclei 0-73021
- ionisation models rel. to spectra, theory 0-109529
- IR emission, advances in obs. and review of line and continuum radiation 0-109525
- K 648, halo planetary nebula, low Ar abundance meas. 0-82443
- K 648, halo planetary nebula, photoionisation models and chemical abundances 0-109507
- M1-2, possible eclipsing binary central star 0-105239
- in M31 (Andromeda Galaxy) and companions, planetary nebulae props. 0-109520
- M4-18, spectroscopic obs. of compact object 0-67829
- in M87, extended emission from large number of nebulae (*Russian*) 0-77492
- M 2-9, structural changes (1952-78) 0-82456
- in Magellanic Clouds, identification, luminosity function and numbers 0-67815
- in Magellanic Clouds, space distrib., excitation classes and comps. 0-109519
- major axes correl. with interstellar mag. field direction, hydromagnetic model 0-82473
- models, theoretical, low to medium excitation objects 0-67817
- morphology and struct. 0-109534
- nearby object in Lynx found on POSS E-print 0-98701
- NGC 3242, 7009, 6210, high excitation planetary nebulae, high dispersion EUV obs. 0-77466
- NGC 7027, H $\alpha$  emission spatial distrib. obs. 0-98698
- NGC 7027, He I 2.0  $\mu\text{m}$  line strength rel. to He I 584  $\text{\AA}$  transfer problem 0-67550
- NGC 7027, microns unidentified feature, high resolution spectra 0-82466
- NGC 7027, physical conditions and CNO elements abundances 0-82459
- NGC 7662, photoionisation model with charge transfer reactions rel. to emission-line spectrum 0-62233
- O/H ratios, meas. rel. to Galaxy O enrichment 0-105328
- observations and theory, IAU Symposium 76, Ithaca, New York, USA (1977 June 6 to 10) 0-105435
- optical studies, review of recent advances 0-109522
- origin from giant stars, internal struct. and evolution 0-109537
- physical processes, advances in theory 0-109527
- PK 108-76°1, 49+88°1, halo planetary nebulae, low Ar abundances meas. 0-82443
- planetary nebulae central stars, atmospheric models 0-109434
- planetary nebulae central stars, spectra, temps., binaries and peculiar stars 0-109435
- PN 173+3.1, near galactic anticentre, coords., radial vel. and orbit 0-105309
- proto-planetary nebulae, props. and comparison with planetary nebulae 0-109538
- radio emission, advances in obs. 0-109526
- refractory elements gas-phase abundances, hot stellar wind model 0-109516
- FG Sagittae, 1975-8 spectral obs. of peculiar variable 0-72959
- HM Sagittae, near-IR spectrographic obs. of young object 0-94810
- SchuWe-3, spectroscopic obs. 0-101626
- in southern hemisphere, IR and SHF obs. 0-90496
- statistics of spatial and velocity distrib., review 0-109518
- survey of Palomar Sky Survey E-prints 0-82460
- UV observations, accuracy and interpretation 0-109524
- UV observations, review 0-109523
- 19 W32 and 43, galactic centre planetary nebulae search 0-90506
- H II, region observational props. connected with planetary nebulae 0-109539
- He I 584  $\text{\AA}$  in quasars and gaseous nebulae, line transfer problem and line strength 0-67550



**lanetary nebulae** continued

- He II, Lyman  $\alpha$  photons absorpt. rel. to forbidden lines intensities 0-67833  
S abundances, determ. from IR line meas. 0-82444

**lanetary rings** *see planetary satellites***lanetary satellite atmospheres** *see extraterrestrial atmospheres; planetary atmospheres***lanetary satellites***see also Moon*

- 1966 S 2, positional obs., 1980 March 15 0-85893  
1966 S 2 and 1980 S 15-18, separations from Saturn 0-67645  
1978 P 1, speckle interferometric obs. (1980 June) 0-101553  
1978 P 1, speckle obs. rel. to orbital radius and system mass and density 0-109394  
1979 J 1 and 2, Voyager 1 imagery analysis 0-67639  
1979 J 1 discovery by Voyager 2 camera 0-77334  
1979 J 1-3, satellite periods from Voyager 1 and 2 data 0-105196  
1980 S 10, precise positions, 1980 March 15 to 16, and relation to Dione 0-85893  
1980 S 1, 3, 6, 25, new Saturnian satellites, positional obs., (1980 March 9 to 14) 0-94749  
1980 S 3, 13, positional obs. (1980 March 15 and 16) 0-85893  
1980 S 7 to 14, Saturnian satellites, obs. (1980 March 13 to April 8) 0-62068  
Amalthea, effect of proximity to Roche limit on dynamical behaviour of ejecta 0-98592  
Amalthea, coupled to Jovian ionosphere 0-72869  
analytical satellite theory in extended phase space 0-67524  
asteroids, satellite detect. from occultation obs. 0-67629  
Callisto, evolution from derived crustal description 0-82265  
Callisto, IR emission spectra 0-82264  
Charon, Pluto's satellite, discovery and review of data (book) 0-82591  
Charon (1978 P 1), occultation on 1980 April 6 probable 0-67651  
Charon (1978 P 1), probable stellar occultation, 1980 April 6, min. dia. 0-62071  
Charon (1978 P 1), satellite of Pluto, positions and dynamical parameters 0-62069  
Charon (1978 P 1), stellar occultation obs., 1980 April 6, rel. to satellite dia. and struct. 0-94754  
Charon (1978 P 1) probably no occultation of star on 1980 April 6, ephemeris 0-62070  
comets ejection hypothesis, celestial mechanical aspects 0-62080  
commensurabilities in solar system 0-109418  
Deimos, loose material downslope movement obs. 0-94737  
Deimos, photometry from Viking orbiter images 0-72838  
Earth, ring system form. assoc. with Eocene terminal event 0-76890  
Earth, search for natural or artificial objects located at Earth-Moon libration points 0-98647  
evolution of planetary and satellite systems, computer program 0-77308  
fluid drops as cosmological models, stellar evolution, solar system origin, planetary geology 0-73086  
Galilean satellites, astrometric position determ. (*French*) 0-77326  
Galilean satellites, astrometric position determ. 0-77327  
Galilean satellites, astrometry using image photometric anal. technique. (*French*) 0-85880  
Galilean satellites, improved ephemerides for Voyager mission 0-62066  
Galilean satellites, Jupiter Orbiter Mission CCD camera 0-85859  
Galilean satellites, position determ. in 1978 using Double Zeiss Astrograph (*French*) 0-72809  
Galilean satellites, surface features from Voyager 2 obs. 0-72871  
Galilean satellites, water ice existence, IR spectral reflectance obs. 0-82263  
Ganymede, atmosphere erosion by radiation belt energetic atomic particles 0-72736  
Ganymede, effect on Jupiter magnetosphere, Voyager 2 obs. 0-77341  
Ganymede, surface model and characts. from radar obs. 0-90359  
Ganymede disturbing Jovian magnetosphere 0-72856  
Iapetus, relative reflectance meas. at 1.6 and 2.2  $\mu$ m 0-98607  
Io, 'volcanic' outbursts, elec. current origin explanation 0-82276  
Io, effect on S II ring round Jupiter 0-90360  
Io, form. of Na clouds and regolith by micrometeoroid impact 0-77330  
Io, global SO<sub>2</sub> abundance upper limit 0-77332  
Io, indirect link with forbidden S II emission variability round Jupiter 0-85885  
Io, interaction with plasma torus 0-98604  
Io, local gas emission mechanism (*Russian*) 0-82275  
Io, non-linear standing Alfvén wave current system 0-72869  
Io, plasma cloud injection into Jupiter magnetosphere, S and O ions discontinuities 0-90358  
Io, plasma torus, ion density spatial distrib. 0-72861  
Io, plasma torus implications of whistler mode chorus obs. 0-72862  
Io, SO<sub>2</sub> frost IR spectra and deposition processes 0-77331  
Io, SO<sub>2</sub> model atmos. and ionosphere 0-72853  
Io, trapped electrons accel. rel. to S-bursts freq. drift meas. at different freqs. 0-85888  
Io, volcanic activity model based on plasma obs. 0-72870  
Io, volcanoes as source of magnetosphere dust 0-85889  
Io's torus, charged particle radial diffusion 0-72859  
Io interaction with environment, Jupiter Voyager imagery analysis 0-105197  
Io plasma disc, model of plasma injection 0-72860  
Io plasma torus, effects on Jupiter kilometric radiation ray tracing 0-72866  
Io plasma torus, radiative cooling and spectra 0-72850  
Io plasma torus model in whistler propagation study 0-72863  
Io plasma torus props. from Voyager EUV data 0-82262  
Io plasma-torus and Jupiter magnetosphere Birkeland currents 0-105198  
Io torus, latitudinal plasma oscils. 0-85892  
Io torus, plasma density from Voyager 1 occultation 0-77337  
Io torus, Voyager 2 EUV obs. 0-77338  
Io-related Jovian radio emission, S-bursts occurrence with L-bursts and freq. upper limit 0-85887  
Jupiter, micrometeorite impact, ion emission on satellite surfaces 0-77362  
Jupiter, photometry of Io, Europa and Callisto, 1976 to 1979, possible solar variability detect. 0-98623  
Jupiter, ring and Galilean satellites, Voyager 2 IR obs. 0-77335  
Jupiter, ring system, summary of recent research 0-72875  
Jupiter, rings, Voyager 1 obs. (*French*) 0-82281  
Jupiter, satellite orbits, three dimens. periodic orbit determ. 0-67526  
**planetary satellites** continued  
Jupiter, triple shadow phenomena caused by Galilean satellites (AD 1900-2100) ephemerides 0-67641  
Jupiter, Voyager 1 data summary (*Russian*) 0-82274  
Jupiter ring, dust EM scatt. lifetimes 0-82273  
Jupiter ring system, dust derived from Io volcanoes 0-85889  
Mars, crater density interpretation 0-82252  
Marian satellites, effect of proximity to Roche limit on dynamical behaviour of ejecta 0-98592  
Mimas, effect on Saturn's magnetic field (*Russian*) 0-94752  
Neptune, ring, observational evidence in 1846-7 from Lassell and Challis 0-67652  
orbits, third and fourth-order perturbations rel. to flattening of planet 0-67529  
Phobos, grooves distrib., morphology and possible origin 0-72837  
Phobos, orbital inclination evolution 0-67628  
Phobos, photometry from Viking orbiter images 0-72838  
polytropic satellite in central orbit, Roche problem and appl. to Saturn's rings 0-82179  
resonant orbits about Jupiter, Periodic Comet Boethin (1975 I) case 0-72883  
Rhea, planetary, 1976 to 1979, rel. to possible solar variability detect. 0-98623  
ring systems, review of physical studies 0-72874  
saturn, 1966 December and 1980 March positions for five satellites 0-94750  
Saturn, 1980 March Pic du Midi obs. 0-67646  
Saturn, 1980 S 24 and 1966 S 2, 1980 April obs. 0-82280  
Saturn, absorpt. of trapped radiation, Pioneer 11 obs. 0-82284  
Saturn, absorption of particles, ring and satellite discoveries, Pioneer 11 obs. 0-82287  
Saturn, astrometric obs. from McCormick Observatory (1977) 0-105200  
Saturn, interactions with magnetosphere 0-82285  
Saturn, particle flux, Pioneer 11 meteoroid detector obs. 0-82291  
Saturn, ring system, summary of recent research 0-72875  
Saturn, ring system-ionosphere interaction 0-94751  
Saturn, rings, history and perturbation anal. (*French*) 0-82281  
Saturn, satellite analyses and electromagnetic obs. (1980 March) 0-77346  
Saturn, satellite associated clouds, Pioneer UV photometry obs. 0-82288  
Saturn, satellites and rings, imaging, photometry and polarimetry obs. from Pioneer 11 probe 0-82289  
Saturn, satellites I-IX, astrometry obs. from McDonald Observatory (1975-1976) 0-105199  
Saturn A and B rings, surface brightness obs. (*Russian*) 0-72872  
Saturn E-ring, obs. during (March 1980) 0-67647  
Saturn E-ring rel. to Enceladus orbit, max. density from CCD obs. 0-94750  
Saturn F-ring, discussion based on Pioneer 11 obs. 0-105202  
Saturn ring disappearances (1600 to 2100) 0-72876  
Saturn ring system, brightness enhancements rel. to existence of supposed satellites (1980 S 7 and 23) 0-94749  
Saturn rings, brightness temp., 1.30 cm interferometry obs. 0-82279  
Saturn rings, IR brightness scans 0-90363  
Saturn rings, model constraints from radar obs. of polarisation and albedo 0-82277  
Saturn rings, new ring detection by focal coronagraph (*French*) 0-72772  
Saturn rings, unilluminated side, 20  $\mu$ m brightness temp. 0-109392  
Tethys, effect on Saturn's magnetic field (*Russian*) 0-94752  
Titan, atmosphere organic chemistry, review 0-90364  
Titan, detectability of liq. methane, laboratory optical absorpt. spectra meas. 0-93278  
Titan eclipse by Saturn, light curve obs. rel. to Saturn upper atmosphere struct. 0-90362  
Titan-Hyperion resonances and close approaches, restricted three-body problem anal. 0-77347  
Uranus, ring system, struct. from photoelec. obs. of 5AO 158687 occultation 0-77348  
Uranus, ring system, summary of recent research 0-72875  
Uranus, rings, occultation obs. (*French*) 0-82281  
Uranus, satellites and rings, albedo and spectral features from IR obs. 0-82299  
Uranus ring, form. and stability 0-82302  
Uranus ring system, reality of occultation events a to g, 1980 August 15 to 16 questioned 0-109396  
Uranus rings, obs. of stellar occultation, (1980 August 15 to 16) 0-98610  
Uranus satellites, astrometric obs. 0-67654  
**planetoids** *see asteroids*  
**planets**  
*see also asteroids; comets; Earth; Jupiter; Mars; Mercury (planet); Neptune; planetary satellites; Pluto; Saturn; Uranus; Venus*  
astrometry with Danjon astrolabe, review (*French*) 0-94715  
atmospheres, response to heat sources and perturbations (*Chinese*) 0-85748  
comets ejection hypothesis, celestial mechanical aspects 0-62080  
computer simulations of planetary system evolution 0-94733  
conference on planetary sciences, Rome, Italy (Apr. 1979) 0-77537  
crater morphology from impact spacecraft imagery 0-62052  
density structure, max. entropy inversion 0-67602  
dynamical control of interplanetary bodies, resonances and close encounters 0-82260  
dynamo theorems 0-81810  
evolution of planetary and satellite systems, computer program 0-77308  
exploration by spacecraft 0-105146  
extra-solar planetary systems, detection by Space Telescope 0-109356  
extrasolar planetary systems, direct imaging 0-82426  
extrasolar planetary systems, dynamical instability and detection 0-82429  
extrasolar systems, detection using space-borne interferometers 0-109357  
flattening, gravit. pot. expansion rel. to satellite orbits third and fourth-order perturbations 0-67529  
formation, primordial solar nebula struct. and evolution 0-62042  
formation models 0-62058  
formation of planetary system, Titius-Bode law 0-62057  
giant planets, detectability of liq. methane, laboratory optical absorpt. spectra meas. 0-93278  
giant planets, gravitational effects on comet orbits evolution 0-98613  
hydrostatic ellipticity calculation algorithm 0-62055  
inner planets, second order perturbation theory (*French*) 0-72801  
inner planets orbits, discrepancies in motions of perihelia 0-67531



**planets continued**

- interior differentiation processes, trace elements as probes 0-98584
- interiors, condensed matter physics 0-77307
- interiors, generalisation of Vaschenko Zubarev formula for Gruneisen parameter 0-90030
- Jovian planet interior heat production 0-98606
- magnetic field, spherical dynamo with anisotropic- $\alpha$  effect 0-81809
- magnetic field of rot. body, model 0-82249
- magnetism of planets, review 0-98585
- non-solar planets, cosmic ray Cherenkov photons effect on IR interferometric search 0-98523
- orbit stability in binary systems, Hill's method appl. 0-94834
- orbital elements from Munich meridian obs. (1941-61) (*German*) 0-77306
- orbits, computation using Chebyshev polynomials and appl. to minor planets (*French*) 0-61997
- origin, initial rotation periods and relative formation times (*Chinese*) 0-105182
- outer solar system, mass distrib. and planet form. 0-77349
- perturbations of cometary orbits, rel. to long-period comets inclination and perihelion latit. distrib. 0-101563
- perturbing planet coordinates, expression through perturbed planet eccentric anomaly 0-67530
- photometric properties, theory 0-67601
- planetesimals, collisional growth and relative vel. 0-82247
- positions, low-precision formulae 0-61990
- pyroxenes from planetary basalt, silicate mineralogy study 0-72802
- radio wave emission, obs. during JIKIKEN (EXOS-B) satellite initial phase (*Japanese*) 0-94675
- rectangular coordinates, approximation via Chebyshev polynomials (*Russian*) 0-62033
- regolith reprocessing by cratering, erosion of material layer which loses charact. props. 0-62053
- ring systems, review of physical studies 0-72874
- rotational alignment in nuclei and planets 0-90636
- solar wind sputtering rate 0-85835
- Space Shuttle, small planetary missions 0-109339
- surfaces, appl. of statistical methods 0-101540
- synodic periods rel. to climatic changes in China 0-85741
- terrestrial, basin and crater form., oscillating peak model 0-101539
- terrestrial, cratered surface entropy 0-101541
- thermal radiation intensity field modelling; principles 0-62056
- thermodynamics of black planet, surface Carnot interaction 0-85877
- tidal friction rel. to Solar System stability 0-82233
- wave tilt sounding of multilayered structures on planetary surfaces 0-61926

**planimeters** *see area measurement***planning**

- experiment, appl. to calibration of X-ray radiometric analyser 0-61186
- experiment, optimum plans calc. on convex polyhedrals 0-57084
- fusion reactor, TFTR, preoperational test plan, manpower loading and scheduling 0-102340
- materials testing by statistical methods (*German*) 0-93725
- nuclear power plant, Virgil C., startup, conduct of operations, organisation and personnel 0-63340
- nuclear power plants, capital cost considerations, optimum plant size 0-63416
- nuclear power plants, startup, staffing program, scope, tasks, resources, constraints, anal., implementation 0-63341
- Project Manager organisation in nuclear plant turnover and startup 0-63339
- radiotherapy treatment planning, FORTRAN program for optimisation using complication probability factor 0-81686
- standard sample homogeneity evaluation, optimal obs. planning 0-93721
- wind power exploitation on large scale, physical planning aspects in Holland 0-61241

**plants (industrial)** *see industrial plants***plants (power)** *see power plants***plasma**

*see also electromagnetic wave propagation in plasma; plasma-beam interactions; plasma impurities; plasmons; relativistic plasmas; solid-state plasma*

- astrophysical, charged particle accel. by MHD shock waves 0-101532
- astrophysical, high temp., thermal bremsstrahlung radiation 0-94697
- astrophysical, instability of self-gravitating isotropic pressure plasma 0-72763
- astrophysical, nonrelativistic electrons interaction with radiation in mag. field 0-109354
- astrophysical clouds, comptonisation of X-rays, radiation spectra 0-85850
- astrophysical dense plasmas, transport coeffs. 0-77280
- astrophysical dense plasmas nuclear reactions, simple classical fluids theory 0-75141
- astrophysical inhomogeneous medium, polarised radiation transfer 0-99607
- astrophysical plasma, phase transfer, optical spectral line emission bursts (*Russian*) 0-77286
- astrophysical plasma, rotating, effect of suspended particles on gravit. instability 0-109347
- astrophysical plasma, shock accel. of galactic cosmic rays 0-82155
- astrophysical plasma, shock accel. of particles, review 0-82192
- astrophysical plasma, turbulent bremsstrahlung of Langmuir waves 0-62009
- astrophysical plasmas, di-electronic recombination (*French*) 0-82188
- astrophysical plasmas, energy release, flares and particle acceleration in close binary system (*Russian*) 0-73005
- astrophysical plasmas, energy spectrum of particles accelerated near singular line of mag. field (*Russian*) 0-90332
- astrophysical plasmas, laboratory expts. on dense matter in laser driven fusion 0-75077
- astrophysical plasmas, mirror instability, mag. field first adiabatic invariant breaking 0-67546
- astrophysical plasmas, nonthermal processes in diffuse magnetised plasmas, wave physics, book 0-105446
- astrophysical plasmas in mag. and gravitational fields, MHD separation of high energy plasma 0-67547
- astrophysics, dense plasmas and nuclear reactions theory 0-77281
- astrophysics, relativistic modes of tearing instability in background plasma 0-62012
- auroral oval, dayside, plasma density rel. to neutral wind profiles between 115 and 175 km altitude 0-98494

**plasma continued**

- auroral zone, nighttime scintillation localised enhancements struct. 0-98506
- Cassiopeia A, electron kinetic instability rel. to radio spectrum secular flattening 0-101637
- collisionless gravitating systems, gravitational pot. nonlinear eqns. determ., astrophysical appl. 0-67560
- cometary, acceleration in solar wind, rel. to ion-acoustic turbulence (*Russian*) 0-106923
- cometary plasma tails, general morphology rel. to Swan Cloud, 1974 January 11 in Comet Kohoutek (1973 XII) 0-98612
- conference, general congress, Societe Francaise de Physique, Toulouse, France (June 1979) 0-77536
- Earth bow shock, conference, Strasbourg, France (1978 August 31 to September 1) 0-82573
- Earth bow shock, initial ISEE mag. field obs. 0-90307
- Earth bow shock, kinetic models of shocks in collisionless plasma 0-90330
- Earth bow shock plasma, possible generation mechanisms of low-freq. waves ( $\leq 50$  Hz) 0-90312
- Earth plasma sheet, magnetised plasma slow convection theory 0-109312
- electron flows stabilisation 0-109411
- F-region, interhemispheric ion transport induced by neutral zonal winds 0-98509
- F-region plasma cloud, intermediate wavelength E $\times$ B gradient drift instability 0-105114
- galactic corona, prod. and heating mechanism 0-82492
- interplanetary collisionless shock waves, thickness 0-90314
- interplanetary medium, first evidence and early studies of Earth bow shock 0-85816
- interplanetary medium, low-freq. waves obs. in vicinity of Earth bow shock 0-90311
- interplanetary medium, theory of magnetic shocks in collisionless plasma 0-85854
- interstellar plasmas, ion chemistry 0-62254
- Io plasma torus, effects on Jupiter kilometric radiation ray tracing 0-72866
- Io plasma torus, effects on Jupiter kilometric radiation spatial and temporal distrib. 0-77328
- Io torus, Voyager 2 EUV obs. 0-77338
- Io torus props. from Voyager EUV data 0-82262
- ionosphere, auroral convection over  $60^\circ \leq \lambda \leq 75^\circ$  from Millstone Hill incoherent scatter 0-67454
- ionosphere, auroral zone, irregularities, simultaneous rocket probe, scintillation and incoherent scatter radar obs. 0-94640
- ionosphere, effect of recomb. processes and plasma nonisothermability on thermal parametric instability 0-61967
- ionosphere, effect on obs. of solar type III radio bursts 0-72904
- ionosphere, elec. fields and plasma convection in dayside auroral oval 0-98501
- ionosphere, lower, plasma processes rel. to atmosphere mass distrib. by latitude 0-90115
- ionosphere, lower hybrid drift instabilities, electron collisional effects 0-101484
- ionosphere, nonlinear interaction with microwaves from solar power satellite, theoretical anal. (*Japanese*) 0-94634
- ionosphere, plasma bubbles spatial relationship with 1 m equatorial spread-F irregularities 0-67457
- ionosphere, plasma convection at high latitudes, model rel. to incoherent scatter obs. 0-72687
- ionosphere, role in time dispersion of EM pulses 0-94645
- ionosphere, simultaneous obs. of field-aligned currents and plasma drift vels. by Atmosphere Explorer C 0-72681
- ionosphere, wave meas. via satellite-borne cross-power spectrum analysers 0-94621
- ionospheric plasma props. around S. Atlantic geomagnetic anomaly region (*Japanese*) 0-72695
- Jupiter, magnetosphere energetic ions and electrons Voyager 2 obs. 0-77342
- Jupiter ionosphere and Io torus, Voyager 1 and 2 radio occultation obs. 0-77337
- Jupiter magnetosphere, electrostatic waves obs. 0-72865
- Jupiter magnetosphere, HF and LF events from Voyager 2 obs. 0-77344
- Jupiter magnetosphere, Io interaction with plasma torus 0-98604
- Jupiter magnetosphere, kilometric radiation ray tracing 0-72866
- Jupiter magnetosphere, kilometric radiation spatial and temporal studies 0-77328
- Jupiter magnetosphere, plasma cloud injection from Io, S and O ions discontinuities 0-90358
- Jupiter magnetosphere, plasma corotation lag from Voyager 1 obs. 0-90361
- Jupiter magnetosphere, plasma waves from Voyager 2, radio obs. 0-77343
- Jupiter magnetosphere, Voyager 2 obs. of hot plasma environment 0-77341
- Jupiter magnetosphere and bow shock, plasma densities from Voyager 2 obs. 0-77340
- Jupiter mid-magnetosphere, equatorial protons instability 0-67642
- laboratory, magnetosphere, and astrophysical plasma knowledge interaction 0-59166
- magnetosheath, Prognos 4 obs. of  $\leq 2$  MeV electrons and cold plasma 0-90296
- magnetosheath, turbulence rel. to solar wind ion injections in morning auroral oval 0-98502
- magnetosphere, beam-plasma interaction expt. using electron beam from JIKIKEN satellite (*Japanese*) 0-94655
- magnetosphere, cause of plasma sheet thinning during substorms 0-72705
- magnetosphere, elec. field in VLF to HF range, EXOS-B obs. 0-67478
- magnetosphere, hydromag. energy spectra depend. on solar wind vel. and interplanetary mag. field direction 0-67476
- magnetosphere, inverse loss cone electrons temp. anisotropy relaxation due to interaction with electrostatic waves (*Russian*) 0-109314
- magnetosphere, JIKIKEN (EXOS-B) satellite stimulated plasma wave expts. (*Japanese*) 0-94649
- magnetosphere, mode of propag. electrostatic plasma waves and radio waves determ. using stimulated plasma wave results (*Japanese*) 0-94650
- magnetosphere, open model plasma populations 0-90295
- magnetosphere, polar cap convection after interplanetary mag. field becomes northward 0-94658
- magnetosphere, polar cap plasma flow entry region longit. position 0-67472



- plasma continued
- magnetosphere, proton-cyclotron instabilities in non-uniform loss-cone plasma 0-90286
- magnetosphere, radio and plasma waves obs. during JIKIKEN (EXOS-B) satellite initial phase (*Japanese*) 0-94675
- magnetosphere, variability of plasma sheet dynamics assoc. with substorms 0-98518
- magnetosphere, VLF plasma waves obs. and comparison with high energy electron flux by EXOS-B satellite (*Japanese*) 0-94652
- magnetosphere boundary layer, field-aligned currents theory 0-67473
- magnetosphere longitudinal currents, dynamic processes in turbulence development 0-67469
- magnetosphere plasma sheet, plasma flows rel. to discrete auroras occurrence and lifetimes 0-67447
- meteors ionisation columns, initial radii meas. 0-94762
- multicharged ion thermal charge exchange reaction, rel. to astrophysics 0-63815
- neutron stars plasma accretion, interaction with mag. field and accretion flow hydrodynamics 0-109452
- planetary nebulae, hydromagnetic model for major axes correl. with interstellar mag. field 0-82473
- plasmopause, electron density profile meas. stimulated plasma wave results (*Japanese*) 0-94650
- plasmaphere, mid-latitude, nighttime electron content, geophysical disturbance effects, 1974 August to November 0-94642
- plasmaphere, wave-particle interactions, ELF-HF obs. from EXOS-B 0-67467
- pulsar, plasma coupling, boundary conditions 0-94823
- pulsar open magnetosphere, plasma instabilities as source of coherent radio emission 0-82403
- pulsars, finite force face cold plasma atm. models, plasma differential rot. 0-77378
- radio sources, beam and cloud stability 0-67893
- rockets, RF discharge produced plasma rel. to payload charge neutralisation during electron beam emission 0-77258
- Saturn, magnetosphere interaction with solar wind, Pioneer 11 obs. 0-82282
- Scorpius X-1, thermal bremsstrahlung from hot plasma 20-75 keV obs. 0-98741
- solar active regions magnetic fields, appl. of new approach to force-free field 0-62011
- solar atmosphere, acoustic waves interaction with mag. flux tubes 0-85911
- solar atmosphere, force-free mag. fields evolution, nonequilib. states and preflare stage 0-105213
- solar atmosphere, MHD fluctuations due to magnetosonic wave propag. in warm plasma 0-77275
- solar corona, electron beam injections rel. to type IV radio burst quasi-periodic struct. 0-62097
- solar corona, holes, temp. decrease, plasma density effect on wave absorpt. (*Russian*) 0-77374
- solar corona, intensity ratios of fine-struct. components of H like ions reson. lines 0-101581
- solar corona, Langmuir turbulence rel. to quasi-stable particle accel. and type I radio bursts (*Chinese*) 0-105220
- solar corona, plasma flow along sheared mag. arches 0-62092
- solar coronal plasma turbulent pulsations, efficiency of four-plasmon interactions in radar signal refl. 0-101582
- solar flare, electron density determ. from X-ray spectra obs. 0-82326
- solar flare, transient plasma X-ray spectra, electron density and temp. diagnostics 0-77368
- solar flare accelerated particles, nucl. composition and Coulomb losses 0-72913
- solar flare plasma, Langmuir turbulence spectrum estimate from X-ray obs. 0-82329
- solar flare plasma, new atomic data for Fe<sup>19+</sup> spectra 0-67545
- solar flares, transient plasma X-ray lines, rate coeff. determ. 0-72903
- solar flares, X-ray line spectra from transient plasma 0-98626
- solar flares experimental simulation, merging of two current carrying plasma columns (*Japanese*) 0-94775
- solar transition zone, nonresonant heating mechanism (*Chinese*) 0-85921
- solar wind, Alfvén waves, non-linear interaction with compressive fast magnetosonic waves 0-105142
- solar wind, anisotropic struct. of plasma irregularities obs. using interplanetary scintillations 0-67489
- solar wind, deceleration upstream from Earth bow shock rel. to diffuse upstream ions origin 0-98528
- solar wind, dynamic mag. struct. of large amplitude Alfvénic vars. 0-72734
- solar wind, energetic particle meas. upstream of Earth bow shock 0-90308
- solar wind, He<sup>+</sup> flux after interplanetary shock, Imp 7 obs. 0-101520
- solar wind, low freq. continuum from ISEE 3, thermal electrostatic noise, LF obs. 0-101519
- solar wind, MHD turbulence props. 0-61977
- solar wind, monochromatic non-WKB Alfvén waves, normals evolution 0-101521
- solar wind, obs. of backstreaming protons near Earth bow shock 0-90309
- solar wind, obs. of fully developed anisotropic MHD turbulence 0-94669
- solar wind, plasma fluid aspects 0-90313
- solar wind, plasmadynamical processes review (*German*) 0-109323
- solar wind, stream interaction regions, microscale instabilities 0-72739
- solar wind, upstream particle events close to bow shock and 200 R<sub>E</sub> upstream 0-77247
- solar wind corotating interaction regions, energetic particles shock accel. 0-82159
- solar wind interaction regions, N-S mag. field component solar cycle dependent configurations 0-98529
- solar wind turbulent plasma, radio wave propag. meas. using three satellites 0-101518
- stellar atmospheres, higher order fluid eqns. for multicomponent nonequilibrium plasma 0-105156
- stellar coronal plasma, EUV spectra and contribs. to diffuse EUV background 0-62324
- stellar evolved C cores, nuclear energy generation rates and energy dissipation 0-82339
- Sun, plasma hydrodynamic motion in convective element intrinsic mag. field 0-101583
- Sun, use of MHD pulses as diagnostic technique 0-109405
- tetrafluoromethane, plasma etching of Si<sub>3</sub>N<sub>4</sub>(SiO<sub>2</sub>) in dry processing, active etchant species 0-79581
- plasma continued
- thermodynamics of low-temp. plasma with nonequilibrium ionisation, review 0-96343
- Venus environment, plasma wave investigation by Pioneer Venus Orbiter 0-67497
- Venus environment, study via plasma analyser expt. on Pioneer Venus Orbiter 0-67498
- Venus ionosphere, electron temp. probe on Pioneer Venus Orbiter 0-67500
- Venus ionosphere, flute instability, mag. flux rope development (*Russian*) 0-77313
- Venus ionosphere, Pioneer Venus Orbiter planar retarding potential analyser plasma expt. 0-67501
- very-low-q discharges in DIVA confinement and MHD characts. 0-64765
- white dwarf degenerate cores, thermomagnetic instability conditions 0-77395
- X-ray sources, compact, plasma oscills. rel. to radio emission 0-62317
- He, hollow-cathode type discharge, spectroscopic obs., laser light source appl. 0-59335
- plasma accelerators *see collective accelerators*
- plasma applications
- see also plasma arc spraying; plasma deposition; plasma devices*
- accel. of projectiles to hypervelocities using series of imploded annular plasma discharges 0-74042
- DC plasma excitation source, interference effects 0-86434
- electron source with high brightness, emitter and beam parameters 0-106218
- fissioning plasma from gas phase nucl. reactor, appl. 0-64794
- flowing afterglow plasma ion source, appls. 0-87955
- ignition of constant-current vacuum arcs, plasma stream cathode spot excitation 0-75111
- industrial utilisation, synthesis, powder, metallurgical and surface treatments, review (*French*) 0-96398
- intraresonator absorption spectroscopy in plasma jet, laser stimulation optimisation 0-77881
- laser pulse detector, fast nondamagable, using gaseous plasma 0-95138
- laser-plasma ion source for ion implantation in solids 0-78474
- mass separation by weakly ionised plasma centrifuge 0-106985
- materials preparation, plasma chemistry of heterogeneous systems 0-61100
- metal oxide reduction by electron cyclotron reson. plasma of H, model study on discharge cleaning 0-76548
- metal surface, plasma cleaning and etching, removal of C 0-97645
- metal-vapour recombination lasers using segmented plasma excitation 0-74370
- nitriding in glow discharges, influence on phase comp. and plasticity of diffusion layer (*Russian*) 0-76400
- plasma chemistry, history, diagnostics, production, organic compd. synthesis 0-61099
- polymerisation by glow discharge method, formation mech. (*Japanese*) 0-61094
- thin oxide films, form. in microwave plasma 0-76382
- Al film, and native oxide film, etching in carbon tetrachloride plasmas 0-76407
- Al plasma etching, undercutting phenomena 0-97635
- CO<sub>2</sub> laser, mode locking obs. by intracavity plasma injection 0-83624
- CO<sub>2</sub> laser modulation, plasma injection into cavity 0-83626
- CO<sub>2</sub> laser power variation detection via plasma tube impedance changes 0-69437
- LaF<sub>3</sub>, VUV luminescence, conference, Moscow, USSR (Apr. 1978) 0-62378
- Si, amorphous, hydrogenation using DC and HF plasma treatment 0-59497
- Si compounds, plasma etching, gas flow-rate depend. 0-97603
- Si, etching in He-F<sub>2</sub> plasma, etch rates, mass spectra, direct ion sampling study 0-79510
- Si purification, plasma melting zone technique (*French*) 0-89141
- Si purification, plasma melting zone technique, optimisation (*French*) 0-89142
- Si selective anodic oxidation in O<sub>2</sub> plasma 0-108610
- Si<sub>3</sub>N<sub>4</sub> antireflection coating for solar cells, reactive plasma process for forming metal grid patterns 0-93990
- Si<sub>3</sub>N<sub>4</sub>(SiO<sub>2</sub>) plasma etching, plasma processes involved in dry processing using CF<sub>4</sub> active etchant species 0-79581
- SiO<sub>2</sub>, etching in He-F<sub>2</sub> plasma, etch rates, mass spectra, direct ion sampling study 0-79510
- SiO<sub>2</sub>, relief, plasma etching, tapered wall prod. 0-97606
- Sn-SnO<sub>2</sub>-Sn tunnelling junctions, fabrication by modified RF plasma oxidation method 0-103787
- TiCl<sub>4</sub>, reduction in steady beam-plasma discharge 0-100099
- U plasma fueled reactor, use as power supply for nuclear pumped laser system 0-63247
- plasma arc sprayed coatings
- consolidation by laser remelting 0-93697
- wear resistant coatings, operating principles and applications (*French*) 0-76418
- Sm-Co, amorphous, plasma-sprayed, role of Ar or H<sub>2</sub> atm. in mag. props. and crystn., rel. to H<sub>2</sub> storage 0-64898
- SmCo<sub>5</sub>, high coercivity isotropic plasma-sprayed magnet, eutectoid decomp. 0-80568
- SmCo<sub>5</sub>, isotropic plasma-sprayed high coercivity magnet, eutectoid decomp. 0-75810
- plasma arc spraying
- process parameters, dimensionless complex parameters appl. 0-66426
- projection plasma arc, transferred or not transferred, for anti-wear surfacing (*French*) 0-76418
- Ag, plasma arc spraying, chem. reaction with plasma gases 0-66427
- Cr-Al<sub>2</sub>O<sub>3</sub> powder targets for plasma-ion spray deposition of resistance films 0-84897
- Cu, plasma arc spraying, chem. reaction with plasma gases 0-66427
- Ni, plasma arc spraying, chem. reaction with plasma gases 0-66427
- Ni-Cr-Al<sub>2</sub>O<sub>3</sub> powder targets for plasma-ion spray deposition of resistance films 0-84897
- SiC fibre reinforced Al, plasma-formed semifinished products, props. 0-84890
- Ti, plasma arc spraying, chem. reaction with plasma gases 0-66427
- TiC, plasma arc spraying, chem. reaction with plasma gases 0-66427
- W, plasma arc spraying, chem. reaction with plasma gases 0-66427
- Zn, plasma arc spraying, chem. reaction with plasma gases 0-66427
- Zr, plasma arc spraying, chem. reaction with plasma gases 0-66427



**plasma-beam interactions**

- see also *electromagnetic wave propagation in plasma; plasma production and heating by laser beam*  
 alpha particle beam incident on fully ionised H plasma, energy loss and stopping power 0-64742  
 Brillouin and Raman scattering of an extraordinary mode in a magnetized plasma 0-92269  
 Buneman instability nonlinear saturation 0-79467  
 classical collisional theory of beam-driven plasma currents 0-87906  
 cold electron beam in pure runaway regime, collective drag and instabilities 0-83949  
 density profile near laser-plasma critical surface, flux limited thermal cond. effects 0-87857  
 discharge, electron kinetics, charge particle finite lifetime effect 0-92404  
 discharge, electron kinetics, deexcitation processes effect 0-92405  
 DITE Tokamak, beam driven current meas. 0-106940  
 electric double layer, electron velocity distrib. on high pot. side 0-70010  
 electron beam, collisional relax. on injection into plasma 0-64738  
 electron beam, energy coupling to expanding thick-shelled target 0-96365  
 electron beam, high-power, relax. oscillations 0-64744  
 electron beam, kinetic, quasilinear relax., self-similar solns. 0-64702  
 electron beam, relativistic, propag. in strong mag. field (*Japanese*) 0-91737  
 electron beam, three dimens. quasilinear relax. (*Russian*) 0-83947  
 electron beam driven Tokamaks, review 0-99317  
 electron beam emission from rockets, beam-plasma discharge ignition rel. to payload charge neutralisation 0-77258  
 electron beam heating and beam energy distrib. in E-region approximated plasma 0-103163  
 electron beam produced inert gas plasmas, UV to near IR laser lines 0-92334  
 electron beam relaxation in high density weakly ionised gas (*Russian*) 0-106943  
 electron beam stabilised mirror confined gas, hot electron population study 0-100089  
 electron beam stopping process in hydrodynamic stage of streaming instability, boundary value treatment 0-103164  
 electron beam-magnetoplasma, radiation at or near electron plasma frequency, transverse modes 0-106942  
 electron beam-plasma interaction in magnetosphere, JIKIKEN satellite expt. (*Japanese*) 0-94655  
 electron beam-plasma system, Simon short-circuit effect, freq. shift 0-96366  
 electron beams, relativistic, theoretical scheme for axial compression 0-96367  
 electron-beam-heating from foiless diode 0-103168  
 electron-beam-sustained discharge, plasma contraction by mag. field of current 0-100115  
 electrostatic ion cyclotron instability driven by a deflected ion beam 0-87879  
 EM soliton propagation in nonequilibrium dispersive media (*Russian*) 0-106933  
 energy lost by fast electrons in laser plasma 0-103165  
 fast ion beams, quasilinear relax. in non-circular cross-section Tokamak (*Russian*) 0-106938  
 focus plasma, pinch column form. and stability 0-96380  
 heavy ion beam-induced ion-acoustic turbulence (*Russian*) 0-106923  
 heavy-particle acceleration by charge-density waves in vacuum and in plasma 0-70044  
 HF electric field, nonlinear behaviour just before beam-plasma discharge initiation 0-87904  
 hybrid reactor blanket, secondary neutron streaming in plasma vacuum cavities 0-95416  
 impulsive electron beam, axial injection into SF<sub>6</sub>, discharge and oscill. 0-59316  
 inertial fusion appls. 0-59250  
 inhomogeneous beam-plasma system, continuous oscill. spectrum (*Russian*) 0-106937  
 instabilities in plasma media with absorption 0-64743  
 intense ion beam propag. in z-discharge plasma channels, straight and tapered 0-83948  
 intense relativistic electron beam-plasma system, coupled transverse oscillations, kinetic description 0-64741  
 ion acceleration by space charge waves in straight-line electron beam 0-103166  
 ion acoustic solitons in beam plasma system with nonisothermal electrons generated by ion-beam 0-103151  
 ion beam, explosively unstable waves, pump field method obs. 0-92333  
 ion beam, light, propag. in plasma channel 0-75064  
 ion beam production from interaction with Nd:YAG laser radiation bursts 0-106939  
 ion beam-plasma collective interactions, high current-density 0-75066  
 ion beam-plasma system, absolute and convective instabilities of electrostatic ion cyclotron waves 0-64740  
 ion beam-plasma system, higher-order modes of space charge waves 0-69992  
 ISX-B, neutral beam power system 0-91283  
 JXFR, neutral beam injection system, gas-beam interaction secondary particles 0-106227  
 Langmuir waves, large amplitude, nonlinear Landau damping and form. of standing nonlinear waves 0-92292  
 magnetic field instability of plasma in EM beam 0-64745  
 magnetically insulated coaxial line, ion beam effects 0-87297  
 magnetized inhomogeneous plasma, wave reson. and conversion 0-92313  
 MFTF, neutral beam module component design and development 0-91270  
 MFTF, start up neutral beam power supply system 0-91281  
 MFTF, sustaining neutral beam power supply, cct. anal. using ASTAP and EMTP codes 0-91284  
 MFTF, sustaining neutral beam power supply system, modelling with ASTAP code 0-91285  
 modulated electron beams, instability, spatially separated in plasma 0-70012  
 negative ion beam instability spatial development in rarefield gas (*Russian*) 0-92314  
 neutral beam heating in the Princeton Large Torus 0-106950  
 neutral beam injection for Doublet III, two-gap magnet design and performance 0-92379  
 neutral beam injection in electrostatic plasma-confinement experiments in a tandem mirror system 0-70025  
 neutral beam US development program and review 0-92348

**plasma-beam interactions continued**

- nonlinear mode coupling and saturation of decay instability in ion beam-plasma system 0-83931  
 oblique Langmuir solitons under free path conditions (*Russian*) 0-79477  
 ponderomotive laser-plasma effects subject to strong magnetic fields and collisions 0-87905  
 positive ions in plasma formed by dense beam of negative ions in gas, drift mechanism (*Russian*) 0-103160  
 Raman backscatter in high temperature, inhomogeneous plasmas 0-92268  
 relativistic electron beam, EM instability collisional effects 0-64725  
 relativistic electron beam, intense, coupled dipole oscills. 0-64739  
 relativistic electron beam in magnetised plasma, relax. processes, nonlinear theory, instability (*Russian*) 0-103162  
 relativistic electron beam in plasma, relaxation (*Russian*) 0-103161  
 relativistic electron beam with variable charge neutralisation degree, equilibrium 0-59249  
 relativistic electron beam-plasma instability, macro- and microscopic models 0-75065  
 relativistic electron beams, collective accel., beamfront velocity effects 0-75063  
 relativistic electron beams, EM instability and stopping power of plasma 0-92289  
 relativistic electron beams, plasma prod. from diatomic gases, mag. field diffusion 0-83955  
 resonance absorption, self-consistent density profiles for obliquely incident light 0-64758  
 resonant excitation of slow low-freq. waves by opposite moving electron beams (*Russian*) 0-92336  
 RF emission, plasma wave scatt. by ion-acoustic waves in nonequilibrium plasma 0-64733  
 rotating proton layer, transient magnetic field reversal 0-70027  
 stimulated Brillouin scattering from pre-ionised plasma 0-92267  
 stimulated ion Compton backscattering in laser plasma interaction 0-79511  
 strong turbulence effects on the kinetic beam-plasma instability 0-59207  
 strongly turbulent stabilization of electron beam-plasma interactions 0-92521  
 superbanana limiter as a possible edge cooling scheme 0-92362  
 superthermal electron beam, relax. due to Coulomb collisions in plasma 0-106941  
 TFR, neutral beam power system 0-91282  
 Tokamak plasmas, beam driven currents, trapped electrons effect 0-70011  
 toroidal plasmas, beam driven currents, trapped electrons effect 0-70011  
 toroidal plasmas, beam induced currents 0-92335  
 unshielded plasma waveguide excitation by modulated electron beam 0-79512  
 velocity angle scattering of a relativistic electron beam during transport through plasma 0-92337  
 velocity modulated neutralised ion beam, evolution in potential wells, ion density distrib. (*Russian*) 0-100082  
 Fe XXII, XXIV, XXV, charge exchange recomb. in Princeton large torus during beam heating 0-100067  
 H glow discharge, electron macroscopic props. (*Russian*) 0-92403  
 H plasma beam, electron macroscopic props. (*Russian*) 0-92403  
 H<sub>2</sub> beam discharge, electron kinetics in collisionless non-equilibrium plasma 0-92402  
 He cryogenic glow discharge, effect of laser radiation (10.6  $\mu$ m) 0-64803  
 Ti XX 0-100067
- plasma collision processes**  
 see also *plasma transport processes; plasma-wall interactions*  
 air plasma, radiowave interaction, electron velocity, collision cross-section depend. 0-103155  
 Alfvén mode, current driven, electron-ion collisions and full dispersion function, numerical anal. 0-64726  
 alkali metal atoms, charge exchange, exciplex or excimer form. in plasma 0-75026  
 alkali metal vapour-H plasma, charge exchange role in optical props. 0-59284  
 anomalous intensity ratios in H like L <sub>$\alpha$</sub>  doublet in optically thick laser prod. plasmas 0-103186  
 astrophysical plasmas, di-electronic recombination (*French*) 0-82188  
 atomic collision processes and X-ray and UV lasers 0-64787  
 Bernstein waves, propagation in inhomogeneous plasma, dispersion rel., quasi-linear equations, diffusion coeff. determ. 0-75044  
 charge exchange neutrals, emitted from rot. plasma, meas. 0-106979  
 colliding plasma evolution, EM computer simulations 0-87926  
 collisional drift modes, anomalous skin effect, enhanced particle penetration during fuelling, nonlinear theory 0-64703  
 collisional plasma, modulation instability, turbulence by const. wave pumping (*Russian*) 0-103139  
 conductance theory, quantum-statistical, of nonideal plasmas 0-79440  
 coupled mode equations, linearised, space time solns. 0-87884  
 current-driven collisional drift and Alfvén instabilities in sheared mag. field 0-92286  
 cusp fields, plasma confinement time investigation using Monte Carlo simulation, collision effects 0-64770  
 density fluctuation in collisional plasma 0-75053  
 deterministic description of atomic processes 0-59169  
 dielectronic satellite spectra, electron collisions, corona model theory 0-59188  
 dissociative recombination of H<sub>3</sub>O<sup>+</sup> and D<sub>3</sub>O<sup>+</sup> at elevated electron and gas temperatures, rate coeff. determ. 0-63747  
 draft waves driven by temperature gradients, ballooning limit 0-106917  
 drift mode, current driven, electron-ion collisions and full dispersion function, numerical anal. 0-64726  
 electric double layer, electron velocity distrib. on high pot. side, electron-electron interactions 0-70010  
 electric field compression near a plasma electrode 0-64736  
 electrical conductivity tensor for H<sub>2</sub>O<sub>2</sub> plasma in mag. field (*Russian*) 0-87864  
 electron beams, modulated, non-linear oscillation theory (*Russian*) 0-106898  
 electron collision effect on wave-breaking in cold plasma 0-96353  
 electron density fluctuation spectrum, very high collision freq. effects 0-87847  
 electron distribution function, steady state response to applied electric field, e<sup>-</sup>e<sup>+</sup> collisions 0-83883  
 electron gas, screening of ionic motions by electronic background 0-64678



**asma collision processes continued**

- electron-neutral collisions, calc. with respect to momentum transfer, new approach to Boltzmann collision integral 0-92255  
 electrostatic plasma probe, neuron membrane physical analogue 0-79573  
 EM instability of relativistic electron beam penetrating in infinite plasma, collisional effects 0-64725  
 EM wave resonance tuning of magnetoactive plasma (*Russian*) 0-83914  
 excited atoms, radial distrib., prod. by surface wave (*French*) 0-96349  
 excited gas, resonant optical discharge 0-92343  
 explosive instabilities, nonlinear perturbation 0-59199  
 fusion chain reactions, kinetics, high electron temps., interactions with D-T plasma 0-68945  
 glow discharge, cathode dark space ionisation avalanche with cold cathode (*Russian*) 0-84013  
 halide ions, recombination, exciplex or excimer form. in plasma 0-75026  
 harmonics generation in inhomogeneous plasma (*Russian*) 0-83916  
 HF discharge, ionisation overheat instability in EM wave field (*Russian*) 0-106990  
 high temperature plasma, physics, book 0-98767  
 high-Z emitters in ultradense plasmas, hydrogenic profiles, perturbing ion effects 0-79566  
 hot collisional plasma filled waveguide, wave propag. 0-92331  
 hydrogenic ion lines, red shift in plasma 0-103128  
 instability, electrostatic, parametric, due to thermal coupling 0-79465  
 ion distribution in collisional HF-discharge in RF range (*Russian*) 0-106986  
 ionospheres, ionic reactions in lab. and planetary atmospheres 0-59168  
 L-2 stellarator, ohmic heating discharges with gas puffing 0-79593  
 Langmuir wave interference, electron collisions (*Russian*) 0-69970  
 laser scatt. in plasma 0-83905  
 laser targets, dynamics, 2-D three-temperature MHD model 0-70014  
 line broadening in atomic and ionic emissions from plasmas (*French*) 0-79434  
 line broadening theory, screening process dynamics (*Russian*) 0-69988  
 lower-hybrid waves in collisional plasmas with field-aligned current, instability 0-75045  
 magnetic field instability of plasma in EM beam 0-64745  
 magnetic fields of hot dense plasmas, particle probes sensitivity 0-70037  
 mass renormalization in stochastic acceleration of particles (*Russian*) 0-100066  
 mirror, plasma confinement time investigation using Monte Carlo simulation, collision effects 0-64770  
 moving collisional plasma and moving plasma with intrinsic spatial dispersion, emission of longit. waves 0-87848  
 multicharged ion and nucleus electron capture during collisions (*Russian*) 0-87850  
 multicharged ion thermal charge exchange reaction, rel. to astrophysics 0-63815  
 multiply charged ion, electron capture into different excited states in plasma 0-64679  
 neutral beam heating in the Princeton Large Torus 0-106950  
 nonequilibrium plasma, kinetic theory of spectral line broadening 0-59187  
 nonisothermal plasma electron ensemble, nonstationary behaviour, kinetic description 0-59171  
 particle scattering by low freq. waves, effective scatt. freq., eval. method 0-83882  
 phase transition in elec. discharge plasma between parallel plates, compression by recomb. press. 0-64799  
 population inversion due to plasma expansion into ambient gas, electron cooling 0-96363  
 radiative emission rates for low- and medium-Z elements in high temp. plasmas 0-103125  
 rarefied electron gas, space depend. electron transport by integral approach 0-92257  
 recombination in laser-prod. plasma 0-106871  
 relativistic Boltzmann theory, reduction of collision integrals 0-79560  
 relativistic plasma collisions instability (*Russian*) 0-83913  
 Rydberg atom, electron collisions 0-63833  
 screening in one dimens. plasma 0-65478  
 self absorption of He like satellite lines in high density fusion plasmas 0-64776  
 Stark broadening of isolated Sn II lines in cool plasma, semi-empirical calcs. 0-59186  
 stopping power of a nonequilibrium plasma for incident alpha particles 0-64742  
 superthermal electron beam, relax. due to Coulomb collisions in plasma 0-106941  
 temperate multi-species plasma around ion cyclotron freq. range, plane wave propagation 0-75050  
 thermal parametric instability, effect of recomb. processes 0-61967  
 theta-pinch Ti ion injection by CO<sub>2</sub> laser, spectroscopic anal. 0-79577  
 thin foil layered targets, Rayleigh-Taylor instability in laser irradiation 0-87876  
 Tokamak, anomalous diffusion with light and heavy impurities, drift wave depend. 0-64677  
 Tokamaks, computer simulation of trapped electron modes 0-106874  
 turbulent plasma, magnetic charged particle, linear response theory 0-64727  
 vibrational kinetics and plasma characts. in CO-N<sub>2</sub> discharge 0-59331  
 Vlasov equilibria, local Maxwellian velocity distribution 0-87928  
 wave penetration into half-space collisional plasma 0-106928  
 weakly nonideal inert gas impulse plasma, Coulomb cross-section calcs. 0-103113  
 Al surface, multiply charged ion interactions, laser plasma 0-70007  
 Al, vacuum arc, excited state density theory 0-100107  
 Ar plasma, low density, shock-heated, effective collision freq. calcs., electron temp. meas. 0-75025  
 CO<sub>2</sub> dissociation in a nonequilibrium plasma 0-87851  
 CO<sub>2</sub>-N<sub>2</sub>-He-O<sub>2</sub> discharge mixture, three body electron attachment to O<sub>2</sub> 0-64779  
 Cu, laser light absorpt. by plasma with very steep density gradient 0-96348  
 D+PTFE, DF\* prod., Fourier transform IR spectroscopy 0-87105  
 Fe XXII, XXIV, XXV, charge exchange recomb. in Princeton large torus during beam heating 0-100067  
 H plasma, recombining, weakly ionised, population inversion 0-87849  
 H plasma, thermal emission and Debye shielding 0-64692  
 H, Stark broadening, model microfield methods calcs. 0-92274  
 H(S)+Ar(P<sub>0,2</sub>), energy transfer collisions, Lyman- $\alpha$  emission profile obs., in microwave discharge and reaction cell 0-58359

**plasma collision processes continued**

- He, collisional excitation transfer for 3<sup>1,3</sup>P and D states 0-106387  
 He II plasma, spectral line shifts, electron collision induced 0-106879  
 N<sub>2</sub> plasma heating in electrodeless RF capacitive discharge, mechanism, impurity effect 0-59312  
 N(D<sup>2</sup>,P) metastable production by electron collisions in DC glow discharge 0-59274  
 Ne plasma, electron collision ionisation, electron kinetic behaviour during elec. field perturbation (*German*) 0-64676  
 Ti XX 0-100067
- plasma confinement**  
*see also magnetic traps; pinch effect; plasma focus; plasma impurities; plasma-wall interactions*  
 absolute dissipative drift-wave instabilities in Tokamaks 0-92296  
 adiabatic equilibrium calculations of major-radius compression in a Tokamak 0-106964  
 adiabatic invariant J, finite- $\beta$  effect in axisymmetric tokamaks 0-79538  
 Alcator A Tokamak, soft X-ray imaging 0-73563  
 Alcator high density Tokamak, ion temp. profile reconstruction (*Russian*) 0-106959  
 anomalous drift wave transport in high temp. plasmas, thermodynamic stability 0-69980  
 antiparallel structure build-up and stability in systems with mag. barrier 0-92371  
 Asperator NP-3, nonplanar helical mag. axis system, line of force, toroidal effect 0-70020  
 Asperator NP-L stellarator, mag. field config. meas. 0-92367  
 atomic processes determining the plasma-wall interaction 0-59247  
 axisymmetric high-beta tandem-mirror reactor, MHD stability 0-75042  
 axisymmetric mirror machines, long thin approx., stability and field singularity 0-83933  
 axisymmetric plasma equilibrium, stability 0-106915  
 ballooning stable profiles in circular Tokamaks 0-92317  
 beam-induced tensor pressure Tokamak equilibria 0-106965  
 CLEO stellarator, low and zero current plasma confinement 0-83983  
 colliding plasma evolution, EM computer simulations 0-87926  
 collisionless plasma, polarisation by single-mode pot. drift wave 0-106920  
 Columbia Torus-I belt pinch high beta toroidal device, preionisation, optimisation 0-92368  
 column, HF field effect on diffusion and convection 0-103173  
 column, wave coupling in non-neutral plasma 0-75054  
 column-wall interactions in Tokamak, in-situ meas. on PDX 0-59248  
 compact reverse-field pinch for small demonstration fusion reactor 0-95413  
 compact toroidal ignition experiment, support struct. anal. by numerical code 0-106167  
 conference, controlled fusion and plasma physics, Oxford, England (Sept. 1979) 0-77545  
 convective amplification of drift waves and thermal fluctuation levels in a stable plasma 0-83932  
 convective cell nonlinear excitation and anomalous diffusion, in inhomogeneous plasma 0-79468  
 convex analysis and variational inequalities (*Japanese*) 0-77606  
 cryogenic rings, current induction and decay 0-106972  
 CT6B Tokamak, measurement of plasma column displacement 0-84001  
 Culham Levitron, drift island diffusion 0-59267  
 current density profile measurements in the Proto-Cleo torsatron 0-83995  
 current driven modes, cold mantle systems, stability props. 0-92287  
 cylindrical system with heavy inertial layer, neutron yield, explosion-induced D-T compression 0-68944  
 cylindrically confined cold plasma, overdense and steep density, plane EM wave scattering 0-70005  
 cylindrically symmetric mirror plasma, shear stabilisation 0-83978  
 dense plasma ionisation and cohesion, critical density and press., approx. formulas 0-59253  
 direct energy conversion and control of unstable burn by cyclic major radius compression and decompression 0-87936  
 dispersion relation for instability hindrance in a magnetically confined plasma with finite press. 0-59221  
 disruptions in Tokamaks and small scale turbulence 0-59266  
 DITE, low Q discharges 0-92374  
 DITE bundle convertor, density meas. 0-92373  
 DITE Tokamak, beam driven current meas. 0-106940  
 DIVA Tokamak, q=1 mag. surface noncircular cross-section, in low-q discharge 0-100090  
 draft waves driven by temperature gradients, ballooning limit 0-106917  
 drift wave, low freq., pseudoclassical diffusion in Tokamak (*Chinese*) 0-69990  
 EBT, ray tracing near electron cyclotron freq. 0-103178  
 EBT heating, electron-cyclotron absorption and microwave propagation 0-64749  
 electron cyclotron emission from Tokamak plasmas with mildly superthermal electrons 0-92270  
 electron cyclotron radiation from a high density Tokamak 0-92266  
 electron cyclotron resonance heating of Tokamak plasmas, fluctuations and instability 0-83956  
 electron-beam-sustained discharge, plasma contraction by mag. field of current 0-100115  
 electrostatic confinement in EM trap, ion current decay (*Russian*) 0-79543  
 electrostatic plasma-confinement experiments in a tandem mirror system 0-70025  
 electrostatic wave, stochastic ion motion, mag. field config. depend. 0-59229  
 electrostatically focused ions, spherical potential profile, meas. 0-64762  
 elliptical plasma source, radiation emission distrib. 0-103124  
 ELMO Bumpy Torus, ray tracing near electron cyclotron freq. 0-83975  
 EM wave in inhomogeneous magnetoactive plasma, total absorpt. effect (*Russian*) 0-106944  
 EM waves in plane inhomogeneous plasma in presence of mag. field shear, appl. to plasma diagnostics (*Russian*) 0-103140  
 end loss from a high-beta plasma column 0-79537  
 energy confinement comparison of ohmically heated stellarators to Tokamaks 0-92360  
 energy confinement scaling and poloidal beta in high density Tokamaks 0-96381  
 equilibrium and stability of high- $\beta$  toroidal multipoles 0-64769  
 equilibrium currents, effect on separatrix characts. in I=3 stellarator 0-64706  
 exact Vlasov equilibria for field-reversing rings 0-87925



**plasma confinement continued**

- exploding liner gas confinement, liner velocity effects 0-79541
- fast ion beams, quasilinear relax. in non-circular cross-section Tokamak (Russian) 0-106938
- filament ellipticity, energy lifetime in T-8 apparatus (Russian) 0-87930
- flux conserving Tokamak MHD equilibrium evolution 0-75088
- force-free analytical three dimensional toroidal MHD-equilibria of arbitrary cross section 0-106885
- free-boundary equilibrium of a high- $\beta$  Tokamak 0-92376
- FT Tokamak, scaling of energy confinement time for discharges with  $Z_{\text{eff}} = 1$  0-92363
- FT-1 Tokamak, discharges in low density plasma (Russian) 0-106958
- fusion products in Tokamak plasma, deposition and thermalisation 0-83895
- fusion reactor magnetic confinements, international collaboration 0-63390
- fusion reactor plasma heating and confinement, review 0-63388
- fusion tokamak reactors, status and prospects 0-102292
- fusion-fission magnetically confined reactors, review 0-74019
- Garching Belt-Pinch IIa, effect of  $q$  on confinement and stability 0-96384
- gyrokinetic modes, spatial struct. in toroidal geometry 0-79489
- heating by EM wave transmission in mag. field (Russian) 0-103167
- Heliotron E, helical coil design, mag. field perturbations 0-99300
- Heliotron E, neutral beam injector ion source power supply 0-99333
- Heliotron E, vacuum chamber construction using electron beam welding 0-106180
- hexapole Tokamak, axisymmetric jumps, interpretation 0-106966
- HF EM field, turbulent model of plasma column (Russian) 0-83915
- high beta plasma surrounded by cond. shell, dynamic stabilisation 0-96354
- high beta toroidal device, preionisation, optimisation 0-92368
- high density, in multiple mirror 0-92364
- high voltage opening switch using spoiled electrostatic confinement 0-103205
- high-beta flux conserving equilibrium, resistive magnetic flux diffusion 0-87873
- high-beta Tokamak plasma, stability to ballooning modes 0-75091
- high-beta toroidal plasma, stable confinement in levitated octupole 0-75090
- impinging plasmas, mag. field generation, Nernst refrigeration 0-79526
- inertial confinement, advanced engineering requirements, review 0-95421
- inertial confinement, ion-beam wet-wood-burners using limited mass targets 0-102301
- inertial confinement, USA research 0-78448
- inertial confinement fusion, appl. of intense charged particle beams overlap 0-91242
- inertial fusion reactors, feedback-controlled laser-guided pellets 0-73997
- initial confinement fusion, use of black-body radiation as fusion driver 0-91241
- ion temp. and parametric decay development in RF-generated stellarator plasma 0-79436
- laser inertial containment, principles and problems (French) 0-78437
- laser-driven fusion, validity of hydrodynamic approximation 0-75087
- linear magnetic solenoid reactor plasmas, dynamic behaviour 0-64751
- LINUS, impinging liq. liner system, engineering anal. 0-99315
- low- $\beta$  plasmas, turbulence, spectral struct., Bhom diffusion coeffs., determ. 0-106924
- lower hybrid wave turning point location, nonuniform magnetoplasma 0-79473
- lower hybrid waves, trajectories and damping in Tokamak plasma 0-83922
- magnetic confinement system, surface problems caused by dissolved  $H_2$  0-57946
- magnetic field analysis in complex geometry (French) 0-79535
- magnetic field line trajectory calc., Kolmogorov Arnold Moser surface 0-59263
- magnetic field penetration through slits in ideal shield 0-78745
- magnetic fields of hot dense plasmas, particle probes sensitivity 0-70037
- magnetic island,  $m=2$ , high-energy runaway orbits 0-64767
- magnetic island coalescence, 2-dimens. MHD eqns. 0-64695
- magnetically confined plasma, external conducting open sheet, stability effects 0-92302
- magnetically confined plasmas, expressions for nonclassical energy and particle flows 0-75031
- major disruptions in the TOSCA Tokamak 0-83979
- maser emission, by plasma produced electrons orbiting a positively charged wire 0-92272
- MHD equilibrium, with axisymmetry and noncircular cross section, free boundary soln. to eqn. (Chinese) 0-59260
- Microtor Tokamak, LF microturbulence, far IR laser scatt. 0-96362
- Mirror-Torus-System-1 with divertor mag. field, plasma density and depolarisation current 0-70022
- moving plasmoid reactors using advanced fuel, modularisation 0-99312
- multiple fusion confinement with 2 MA levitated superconducting coil 0-106191
- Nagoya Bumpy Torus, confinement studies 0-78445
- negative shear ferromak for stabilization of current disruptions in toroidal discharge 0-106971
- nonlinear phenomena by the Tokamak helical mode evolution 0-92398
- numerical simulation of disruptions and loss in Tokamak plasma 0-70026
- paramagnetic spheromak formation in a combined zee and theta pinch 0-92372
- particle confinement scaling experiments in the Culham Levitron 0-92361
- PIACE-R1, design fabrication and testing 0-92378
- plasma column, position control system, stability 0-106982
- plasma confinement in mirror and cusp fields, Monte Carlo simulation 0-96379
- polymer-coated laser fusion targets, compression to  $10 \times \text{liq. DT density}$  0-83964
- PRETEXT, poloidal field coil code, expt. verification 0-92377
- radiation emission spatial distrib. reconstruction in torus 0-103123
- reactor, Tokamak, fuel injection, dynamic burn control 1-D transport code 0-68948
- reactor, Tokamak, toroidal magnetic field ripple, burn control 0-63375
- reactor ignition, overheated underdense Tokamak plasma, two-zone model and 1-D transport code 0-63376
- reversed current effect in stabilised Z-pinch 0-79539
- reversed field configuration, equilibrium and stability and confinement props. 0-87932
- reversed field confinement by rotating relativistic electron beam 0-92370

**plasma confinement continued**

- reversed-field pinch plasma model 0-87935
- RF driven current generation by lower hybrid waves in Tokamak 0-103116
- RF plugging and heating, rel. to plasma impedance 0-96378
- rotamak, compact torus generated by rot. mag. field 0-83980
- rotating plasma reactors, longitudinal confinement, stability equilibrium and heating problems 0-74001
- rotating proton layer, transient magnetic field reversal 0-70027
- screw-pinch, equilibrium and stability 0-87934
- self-similar power-driven expansion into vac. problem, approximate solns. 0-79540
- space-charge double layers, anal. using fluid theory 0-75062
- spheromak formation by theta pinch 0-106962
- stationary MHD eqns. for rotating toroidal plasma 0-92278
- stellarator, plasma losses, quasi-neoclassical law 0-79544
- stellarators, magnetic hill effects on equilibrium 0-79558
- stochastic orbits in Tokamak, statistical description, low freq. fluctuations 0-59265
- superbanana limiter as a possible edge cooling scheme 0-92362
- Takamak plasma density profiles from electron cyclotron radiation spectra 0-103179
- TEXTOR, interferometric and polarimetric diagnostics 0-70039
- TFR Tokamak at ionisation equilibrium, heavy impurities 0-106970
- thermonuclear ignition, inertially confined fusion, high density effects 0-86981
- thin line cusp magnetoplasma sheath, RF feedback stabilisation 0-70009
- tokamak, horizontal plasma position control by feedforward-feedback system with digital computer 0-75093
- Tokamak, impurity transport (Russian) 0-106957
- Tokamak, JFT-2, particle and heat transport during lower hybrid heating 0-70021
- Tokamak, low-beta and high-beta regime stable to ballooning modes 0-75083
- Tokamak, metal impurity reduction by working gas injection 0-106963
- Tokamak, nonlinear perturbation, feedback effect (Russian) 0-83967
- Tokamak, plasma MHD equilib., var. method (Russian) 0-106960
- Tokamak, radiative and particle power losses, bolometric meas. 0-73996
- Tokamak, small aspect ratio, flat current noncircular, unstable MHD spectrum 0-69989
- Tokamak, stochastic particle orbits, statistical description 0-79466
- Tokamak, T-10, stainless steel limiter expts. in ohmic heating region (Russian) 0-83969
- Tokamak, T-4, corpuscular diagnostics by charge exchange of plasma ions at artificial target (Russian) 0-83968
- Tokamak and CTR reactors, mobile diaphragm operation mode (Russian) 0-83966
- Tokamak equilibrium, high- $\beta$ , second order effects 0-70024
- Tokamak equilibrium, inverse problem, iterative metric method 0-106883
- Tokamak fusion reactor, RF injection for refuelling and impurity control 0-87921
- Tokamak fusion reactors, refuelling pellets, self-propulsion force exerted by anisotropic ablation 0-106969
- Tokamak generated W radiation, Ag I isoelectronic sequence identification 0-83981
- Tokamak high beta stability 0-96383
- tokamak impurity-control techniques 0-75082
- Tokamak plasma model position control model 0-92383
- Tokamak plasmas, advanced-fuel, ignition and thermal stability 0-86970
- Tokamak studies in the USSR 0-74022
- Tokamak TO-1, feedback system effect on plasma parameters (Russian) 0-103174
- Tokamak with non-circular cross-section, ballooning modes, stability (Russian) 0-103141
- Tokamak-fusion reactors, He exhaust 0-75084
- Tokamaks, Alfvén nonlinear gravit. drift waves and  $\beta$  limitations 0-92369
- Tokamaks, computer simulation of trapped electron modes 0-106874
- Tokamaks, energy confinement scaling, Frascati Torus results 0-79536
- Tokamaks, injected ion loss due to spatial field ripple 0-92321
- Tokamaks, lower hybrid heating, simulation using BALDUR 1-D transport code 0-92339
- Tokamaks, position instability analysis, effective mode approx. 0-103145
- Tormac, Gaussian HeII 4686 Å spectral lines, Doppler and Stark broadening effect, turbulence 0-106980
- toroidal, overlapping and stochasticity, critical limits 0-59268
- toroidal mag. field, thermal cond. with stochastic inhomogeneity (Russian) 0-83973
- toroidal magnetic confinement, progress, rel. to fusion reactor requirements 0-59261
- toroidal pinch discharge, preionisation phase, numerical computation 0-64696
- toroidal plasma-containing system, EM oscil. spectrum 0-79471
- toroidal plasmas, equilib. energy principle with global invariants 0-92366
- toroidal solenoids, helically wound, form factor calcs. 0-100091
- toroidal trap, plasma rot. effect on neoclassical transport of impurities (Russian) 0-83972
- torsatron, superconducting mag. engineering design 0-99297
- torsatrons, mag. surfaces, particle orbits, neutral injection 0-79551
- torsatrons, toroidal vacuum fields, particle orbits 0-79445
- transition from Pastukhov to collisional confinement in a magnetic and electrostatic well 0-103181
- trapped particle anomalous transport in Tokamak, scaling laws 0-103115
- ultrahigh vacuum transfer system, 15 cm diameter, for remote plasma-wall interaction expts. 0-86327
- US magnetic fusion program, survey 0-91249
- Vlasov equilibria, local Maxwellian Velocity distribution 0-87928
- wall confined shock heated fusion reactor, design 0-99314
- wave trajectories and electron cyclotron heating in Tokamak plasmas 0-83923
- weakly-ionised plasma, magnetised, unstable oscillations, influence on radial electric field (Russian) 0-103175
- Z-pinch turbulence spectroscopic detection and anal. (Russian) 0-100098
- Zeta plasma, field line reconnection and density fluctuations 0-69975
- ZT-S reversed field pinch simulations 0-83993
- $Ar^{6,17+}$  filled glass shell, symmetric laser compression 0-64759
- CD laser produced plasma recombination laser, power output enhancement by plasma confinement 0-63989
- Fe XV, line intensity and linewidths at high electron density, generalised population ratio 0-99481



**asma confinement continued**

- H<sub>1</sub>, ACT-1 toroidal plasma, externally launched ion Bernstein wave 0-106967  
 Ti spongy metallic protective gettered coating for thermonuclear reactor walls (*Russian*) 0-106154  
 Ti Tokamak plasma, atomic struct., highly ionized states 0-75086  
 UF<sub>6</sub>, high temp. fissioning plasma core reactors, fluid mechanical confinement 0-63248

**asma containment see plasma confinement****asma density**

- Alcator high density Tokamak, ion temp. profile reconstruction (*Russian*) 0-106959  
 asymmetric electron density profile, interferometric meas., laser-created plasma 0-75085  
 breakdown, ionising wave propag. mechanisms 0-83941  
 caviton dynamics at crit. density 0-106909  
 classical plasma dynamics 0-83888  
 cold mantle, density scaling laws 0-83889  
 collisionless flow and end loss from a high-energy theta-pinch plasma 0-92365  
 collisionless plasma expansion and fast ion generation at plasma-vacuum boundary 0-59257  
 corona, laser induced microsphere, electron density profile, interaction and transport profile 0-107008  
 current sheet, near line of zero mag. field, numerical anal. (*Russian*) 0-83908  
 DC arc plasma, alterations in spectral line intensities due to external mag. fields 0-79621  
 deexcitation wave emission and thermal fluctuations of inhomogeneous plasma (*Russian*) 0-106892  
 dense plasma focus, ruby laser holographic diagnostics (*Japanese*) 0-100097  
 dense plasma ionisation and cohesion, critical density and press., approx. formulas 0-59253  
 DITE bundle convertor, density meas. 0-92373  
 DITE Tokamak, beam driven current meas. 0-106940  
 double layers from ion acoustic instability numerical simulation 0-59220  
 Doublet III, plasma density, shaping and characteristics 0-74018  
 electrode contact processes, microplasma diagnostics 0-59325  
 electrodynamic mechanisms of limitation of the electron concentration in a laser spark (*Russian*) 0-59333  
 electron, microwave p-i-n diode modulator, transient plasma instability meas. (*German*) 0-87942  
 electron beam stabilised mirror confined gas, hot electron population study 0-100089  
 electron density meas. by far IR laser beam deflection 0-59296  
 electron density meas. by two-freq. band microwave interferometer 0-83890  
 electron-beam-sustained discharge, plasma contraction by mag. field of current 0-100115  
 electrostatic confinement in EM trap, ion current decay (*Russian*) 0-79543  
 electrostatic plasma-confinement experiments in a tandem mirror system 0-70025  
 EM macroparticle acceleration, high press. gas temp. density 0-79583  
 EM oscill. spectrum, toroidal plasma-containing system 0-79471  
 EM pulse, conversion to Langmuir wave in plasma 0-92308  
 EM waves incident on warm plasma half-space dual propag. and absorpt., density and temp. depend. 0-75048  
 estimation method for electron temp. and density in <sup>3</sup>He plasma and <sup>3</sup>He-Ar plasma 0-64785  
 exploding liner gas confinement, liner velocity effects 0-79541  
 far IR laser scatt. meas. of nonthermal density fluctuations 0-59297  
 filament ellipticity, energy lifetime in T-8 apparatus (*Russian*) 0-87930  
 fission reactor, gas-discharge, fuel element component conc., plasma temp. profile instabilities 0-63253  
 fluctuation of density in collisional plasma 0-75053  
 fluctuations study by small angle CO<sub>2</sub> laser scatt. 0-59285  
 FT Tokamak, non-thermal electron distrib. function 0-83891  
 FT-1 Tokamak, discharges in low density plasma (*Russian*) 0-106958  
 gas discharge columns with electron prod. and loss rates linear and quadratic in electron density, electron density distrib. 0-96400  
 gas stream with dispersive impurity, initial region boundaries, impurity velocities (*Russian*) 0-100069  
 Hall current and gyroviscosity effect on conducting, rotating viscous plasma stability 0-75041  
 heating in lower hybrid freq. range, temp., ion diffusion 0-83954  
 HF discharge, ionisation overheat instability in EM wave field (*Russian*) 0-106990  
 high velocity jets generated by plasma focus and shock-wave expt., temp. and density meas. (*Russian*) 0-106882  
 impulse spark study using two-wavelength interferometry 0-86391  
 inert gas ion laser, high voltage-low press. discharges, stationary props. 0-92400  
 inert gas mixtures, high-press., collisional radiative recomb. 0-63595  
 ion-acoustic holes in a two-electron-temperature plasma 0-59205  
 ions in steady-state plasma, excited levels population probabilities, asymptotic behaviour 0-79438  
 L-2 stellarator, ohmic heating discharges with gas puffing 0-79593  
 laser fusion, progress at Lawrence Livermore Lab., USA 0-57945  
 linear magnetic solenoid reactor plasmas, dynamic behaviour 0-64751  
 low-density plasmons, electron temp. meas. by He spectrosc. 0-103192  
 lower hybrid wave turning point location, nonuniform magnetoplasma 0-79473  
 magnetic driving energy of the collisional tearing modes 0-92301  
 magnetically confined plasmas, expressions for nonclassical energy and particle flows 0-75031  
 magnetized inhomogeneous plasma, wave reson. and conversion 0-92313  
 magnetoplasma dynamic arcjet, density meas. by CO<sub>2</sub> laser interferometry 0-59277  
 measurement using AM active microwave method 0-87948  
 micropinch in a high-current diode, review 0-103183  
 microtearing modes and anomalous transport in Tokamaks, self consistent calc. 0-59222  
 Mirror-Torus-System-I with divertor mag. field, plasma density and depolarisation current 0-70022  
 multi-ion system, modulation instability of ion acoustic waves 0-69996  
 multi-region global transport model for Tokamaks 0-92264  
 multicharged ion heating in Z-pinch, column compression, temp. and density (*Russian*) 0-64754

**plasma density continued**

- narrow inhomogeneous layer, surface wave-incident radiation nonlinear interaction 0-100080  
 negative ion beam instability spatial development in rarefield gas (*Russian*) 0-92314  
 negative wave momentum density in plasma 0-79463  
 non-LTE plasma props. and at. processes, medium to high press. 0-59170  
 noncircular Tokamak, time evolution of elongation ratio and Mirnov oscill. 0-64763  
 nonlinear interaction, electron collision freq., self-consistent eqn. (*Russian*) 0-75055  
 nonlinear scattering of upper hybrid laser radiation by electron Bernstein modes in a plasma 0-64720  
 nonstationary plasma, anomalous radiation intensity 0-87898  
 oblique Langmuir solitons under free path conditions (*Russian*) 0-79477  
 overdense column, reson. microwave absorpt. 0-64732  
 p-polarised EM wave struct. near point of reflection (*Russian*) 0-103118  
 pellet refuelling of a divertor Tokamak 0-91247  
 phase transition in elec. discharge plasma between parallel plates, compression by recomb. press. 0-64799  
 pinched high velocity plasma fluxes 0-87860  
 plasma, emission and absorption coeff. at high electron density 0-103121  
 polarisation of picosecond excited continuous X-ray radiation (*Russian*) 0-59190  
 polymer-coated laser fusion targets, compression to 10×liq. DT density 0-83964  
 ponderomotive craters, in phased waveguide array plasma, form. by microwave irradiat. 0-83885  
 positive column, ionisation and temp. effect on charged particle profile and density 0-79596  
 positive column, subnormal, ion and electron radial distrib., theoretical description 0-79598  
 positive column of high-voltage diffuse discharge, nonstationary processes 0-64802  
 pressure, virial kinetic definition, spherical geometry calcs. (*French*) 0-69973  
 profile near laser-plasma critical surface, flux limited thermal cond. effects 0-87857  
 Pulsator Tokamak, electron density limitation 0-96385  
 Q-machine, single ended, collisionless, steady-state parameters and Buneman instability 0-59227  
 quadrupole ion store, spatial distribution of ions derived by phase space anal. 0-95185  
 radial stability of density profiles for obliquely incident light 0-92350  
 reactive plasma, optical emission spectroscopy, emission intensities and reactive density, correl. method 0-92385  
 resonance absorption, self-consistent density profiles for obliquely incident light 0-64758  
 resonant excitation of slow low-freq. waves by opposite moving electron beams (*Russian*) 0-92336  
 Schlieren measurements of plasma kinematics during current disruptions in Tokamaks 0-92395  
 self absorption of He like satellite lines in high density fusion plasmas 0-64776  
 shock generated turbulence, obs. in mag. plasma by CO<sub>2</sub> laser scatt. 0-84003  
 slow wave struct., nonlinear coupling with lower hybrid waves near plasma surface 0-92309  
 space charge ionising waves, high velocity propagation 0-87889  
 spectroscopic electron density meas., hot point low induction vacuum spark gas (*Russian*) 0-92390  
 SPICA, impurity radiation, density and temp. 0-87859  
 superspense glow discharge, effect of transverse magnetic field on ion concentration 0-87972  
 Takamak plasma density profiles from electron cyclotron radiation spectra 0-103179  
 thermal instability, mag. field generated, in laser heated plasma, hydrodynamic effects 0-96355  
 thermonuclear ignition, inertially confined fusion, high density effects 0-86981  
 theta pinch, low density, step-like mag. piston 0-103182  
 theta pinch plasma density radial profile measurements using quasiquadrature interferometer 0-70038  
 Thomson scattering meas. of heating process 0-59272  
 Tokamak, edge effects and impurities, influence on thermal stability 0-87892  
 Tokamak, large magnetic field ripples, electric probe meas. 0-83976  
 Tokamak, T-4, corpuscular diagnostics by charge exchange of plasma ions at artificial target (*Russian*) 0-83968  
 Tokamak discharge microwave preionisation at electron cyclotron resonance 0-83896  
 Tokamak electron temp. and density profiles from electron cyclotron radiation spectra 0-59293  
 Tokamak reactors, neutral beam injection, energy and power requirements 0-91243  
 Tokamak TO-1, feedback system effect on plasma parameters (*Russian*) 0-103174  
 toroidal plasmas, high temp., electron cyclotron emission meas. by mesh filter method 0-75101  
 UV photoplasma, electron density, microwave meas. 0-75097  
 X-ray diagnostics, hot lab. and astrophysical plasma 0-59282  
 X-ray line radiation from cylindrical Al plasma, calc. model 0-64777  
 X-ray monochromatic images for hot plasma ion and temp. distrib. 0-64772  
 Z-pinch turbulence spectroscopic detection and anal. (*Russian*) 0-100098  
 Zeta plasma, field line reconnection and density fluctuations 0-69975  
 Ar arc plasma, partial LTE for lower excited levels of Ar I 0-79565  
 Ar decaying pulsed discharge plasma, acoustic waves density modulation 0-103143  
 Ar discharge, ion density profile, reson. laser light meas. 0-92401  
 Ar, formation in crossed electric and magnetic fields, optical spectra 0-79452  
 Ar, plasma, jet, optical studies using Schlieren and shadow methods 0-59279  
 Ar plasma parameters, microwave scanning technique 0-64773  
 Ar<sup>16,17+</sup> filled glass shell, symmetric laser compression 0-64759  
 Au, thin foil, enhanced electron energy deposition heated, soft X-ray vacuum UV spectra 0-80901  
 C plasma, spectral and absorpt. coeffs. 0-69985  
 CO<sub>2</sub> laser beam scatt. by microscopic fluctuations in plasma density 0-79574



**plasma density continued**

- Cs, Knudsen arc, electron beam heating and ionisation 0-75114  
 cu, laser light absorpt. by plasma with very steep density gradient 0-96348  
 Fe XV, line intensity and linewidths at high electron density, generalised population ratio 0-99481  
 H dense thermal plasma, radiation emission 0-103120  
 H line broadening and shift due to plasma ions (*Russian*) 0-96350  
 H plasma, thermal emission and Debye shielding 0-64692  
 H plasma target investig. (*Russian*) 0-106981  
 H spark, laser-triggered, electron densities meas. 0-106975  
 H<sub>2</sub> hot-iron plasma, ion temp. and electron density depend. studied by laser light scatt. and emission spectroscopy 0-96342  
 He and H $\beta$ , Stark profiles, ion-motion effect 0-63592  
 He, hollow-cathode type discharge, spectroscopic obs., laser light source appl. 0-59335  
 He II 4686 Å line, Stark profile meas. in high density plasma 0-96390  
 He, positive column plasmas, metastable atom density meas. by improved self absorpt. method 0-87968  
 He-I<sup>+</sup> laser discharge, positive column, particle densities 0-103215  
 Hg-Tl-I discharges, 50 Hz, axial segregation effect on elec. field strength 0-59320  
 K<sub>2</sub>O-Al<sub>2</sub>O<sub>3</sub>-2SiO<sub>2</sub>-BaO plasma emitter 0-96368  
 Mg plasma, heated by ruby laser pulses, X-ray emission spectrum 0-64781  
 N<sub>2</sub>-He plasma, laser produced, high press. amplified stimulated emission 0-78843  
 N<sub>2</sub>-methane, rapidly developing discharge, streak camera records interpretation 0-59280  
 N(<sup>2</sup>D,<sup>2</sup>P) metastable production by electron collisions in DC glow discharge 0-59274  
 Ne, nuclear induced plasma, simulated 0-64786  
 Ne plasma, electron collision ionisation, electron kinetic behaviour during elec. field perturbation (*German*) 0-64676  
 Ne positive column plasmas, metastable atom density meas. by improved self absorpt. method 0-87968  
 Y<sub>2</sub>O<sub>3</sub> plasma, eqn. of state investig. 0-75027

**plasma deposited coatings**

- elastic properties, acoustic meas. (*Russian*) 0-97519  
 fluorocarbon polymer thin films for lubrication of Au contact surfaces 0-89157  
 rare-earth aluminate, scandate and zirconate films, film coatings, electrophys. props. w.r.t. prep. technology 0-60781  
 Al, film on Si(111) substrate, struct., props. depend. on vapour flow, ionisation (*Russian*) 0-75453  
 AlN films, RF glow discharge deposited, current-voltage characts. 0-84515  
 Al<sub>2</sub>O<sub>3</sub>-NiCr composite, plasma sputtering of electroheating coatings, elec props. (*Russian*) 0-108350  
 B-H amorphous films, optical band gap, thermal treatment effect 0-93415  
 C, amorphous film, spin resonance, IR spectra, microhardness 0-71157  
 C diamondlike layers, RF plasma deposited, frictional props. 0-71762  
 C films, diamond-like, on Si, colour chart 0-97366  
 Cu-Fe, explosive plasma sputtered coatings, struct. and props. (*Russian*) 0-100783  
 InO<sub>3</sub>:Sn transparent conducting films, homeotropic orientation of liquid crystals (*Russian*) 0-108181  
 Mn-Cr-Ti layers on low C steel, composite, residual stresses rel. to arcpaying parameters (*German*) 0-104077  
 S-based amorphous semicond. film, prep. by plasma decomp. of H<sub>2</sub>S-N<sub>2</sub>-NH<sub>3</sub>, and characterisation 0-80422  
 Si, amorphous, elec. props., ion implantation effects 0-79828  
 Si, amorphous, glow discharge deposited, mobility edge calc. 0-80220  
 Si, amorphous, glow discharge produced, defect creation, high optical excitation 0-97327  
 Si, amorphous film, RF plasma deposition from SiCl<sub>4</sub>-H<sub>2</sub>, characterisation 0-66435  
 Si, amorphous films, halogenated and hydrogenated, elec. and optical props. 0-97016  
 Si polycrystalline films, characts. 0-80988  
 Si:H amorphous films, conductivity and temp. dependence of optical gap 0-100462  
 Si:H amorphous films, IR spectrum and struct. 0-97277  
 a-Si:H film, glow discharge deposited, H profiles, doping level 0-84202  
 Si-F-H-P, film, dark cond., struct., Raman scatt. 0-88588  
 Si-H-P amorphous film, dark cond., struct., Raman scatt. 0-88588  
 Si<sub>3</sub>B<sub>1-x</sub> films, anal. of H ratios and profiling using nucl. techniques and Rutherford backscatt. 0-61202  
 Si<sub>1-x</sub>C<sub>x</sub>:H glow discharge films, local atomic struct., XPS and AES study 0-93448  
 Si<sub>3</sub>C<sub>1-x</sub>H<sub>2</sub> amorphous films, IR absorpt. bands 0-100705  
 SiN film, elastic stiffness and thermal expansion coeffs. 0-107451  
 SiN, films, plasma-deposited, radial wafer-to-wafer uniformity 0-104073  
 SiN, films, process and props. 0-80986  
 Si<sub>3</sub>N<sub>4</sub> and SiO<sub>2</sub> on InP, interface props., n-channel MOSFET action 0-93003  
 Si<sub>3</sub>N<sub>4</sub>, surface passivation of GaAs and interface props. 0-93005  
 SiO<sub>2</sub> thin films, deposition and characterisation study 0-80133  
 Si<sub>3</sub>O<sub>2-x</sub> films, anal. of H ratios and profiling using nucl. techniques and Rutherford backscatt. 0-61202  
 WC, explosive plasma sputtered coatings, struct. and props. (*Russian*) 0-100783

**plasma deposition**

- high energy beam deposition in CO/He and Ar/Kr/F<sub>2</sub> gas mixtures 0-63999  
 ion plating, evaporation sources, gaseous media, and transport modes 0-80984  
 IR thin film plasma deposition processes 0-87466  
 LPCVD-type plasma-enhanced deposition system [for semiconductor wafer processing] 0-60791  
 optical fibres, plasma augmented vapour deposition 0-69561  
 semiconductor film growth, multilayer systems, spectroscopic ellipsometry, review 0-103603  
 thin films, deposition techniques, review 0-80964  
 GaAs, selective plasma oxidation, interface props. 0-100933  
 GaAs thin films, reactively sputtered, ESCA/XPS study 0-97430  
 HfO<sub>2</sub> crystallite growth from oxide plasmas, growth morphology 0-59417  
 P, amorphous, prepared by chem. transport in low-press. H<sub>2</sub> plasma, radial distrib. function 0-64899

**plasma deposition continued**

- S-based amorphous semicond. film, prep. by plasma decomp. of H<sub>2</sub>S-N<sub>2</sub>-NH<sub>3</sub>, and characterisation 0-80422  
 Si, amorphous film, glow discharge deposition, rate enhancement by mag. field 0-65412  
 a-Si p-n and c-Si p-n junction solar cells, design concept difference 0-94031  
 Si polycrystalline films, characts. 0-80988  
 Si solar cells, polycrystalline, from recrystallized plasma deposited thin films 0-104509  
 SiN<sub>x</sub> films, plasma enhanced CVD, props., meas. and interpretations 0-80987  
 SiN<sub>x</sub> films, process and props. 0-80986  
 Si<sub>3</sub>N<sub>4</sub>, MIS struct. form. by reactive deposition on n-InSb substrates, C/V meas. 0-103752  
 SiO<sub>2</sub> liq. cryst. alignment films prod. by RF plasma beam technique 0-76198  
 SiO<sub>2</sub> thin films, deposition and characterisation study 0-80133  
 ThO<sub>2</sub> crystallite growth from oxide plasmas, growth morphology 0-59417  
 UO<sub>2</sub> crystallite growth from oxide plasmas, growth morphology 0-59417  
 ZrO<sub>2</sub> crystallite growth from oxide plasmas, growth morphology 0-59417

**plasma devices**

- see also magnetohydrodynamic converters; plasma diodes; plasma focus; plasma guns; stellarators; Tokamak devices  
 AA 0-99380  
 AC electrodeless narrow gap discharge, anal. and plasma display design 0-70063  
 ACT-1, current generation by unidirectional lower hybrid wave 0-92306  
 antenna, focusing hog-horn antenna for microwave diagnostics in plasma machines 0-96395  
 bragg effects in microwave transmission through stationary plasma structures 0-83944  
 centrifuge, crossed-field, ion wind effect on separation 0-79591  
 centrifuge, weakly ionised, for mass separation 0-106985  
 Culham Levitron, drift island diffusion 0-59267  
 electron beam switch, microwave energy compression 0-96396  
 electron emitter with constricted arc discharge, characts., anode spots effects 0-70040  
 electron gun with plasma cathode and built-in gas generator 0-106947  
 EM macroparticle acceleration, high press. gas temp. density 0-79583  
 fusion, international fusion technology program 0-95423  
 fusion reactor engineering, conf. San Francisco, USA (Nov. 1979) 0-91248  
 fusion reactor Zephyr experiment, toroidal chamber, ASDEX project (*German*) 0-73992  
 Hall accelerator, variations in performance when using He gas (*Russian*) 0-103195  
 heavy-particle acceleration by charge-density waves in vacuum and in plasma 0-70044  
 JET, control system, communications, diagnostics, data storage and anal., NORD computers 0-68943  
 JXFR, neutral beam injection system, gas-beam interaction secondary particles 0-106227  
 large volume magnetic multipole plasma source, operating characts. 0-100084  
 levitron, overlapping and stochasticity, critical limits 0-59268  
 magnetic confinement, structural anal., combined interactive/batch computer environment 0-91255  
 PLACE-R1, design fabrication and testing 0-92378  
 polychlorinated biphenyls waste disposal by pyrolysis, plasma torch appl. 0-76487  
 position control system for plasma column, stability 0-106982  
 puffatron, charge exchange neutrals, emitted from rot. plasma, meas. 0-106979  
 reflection triode, prod. of high current ion beams (*Russian*) 0-83230  
 review, laboratory plasma devices 0-79589  
 rotating plasma device, G-II device for plasma research (*Japanese*) 0-70042  
 shutter for multichannel Nd:glass laser 0-64088  
 spheromak devices, magnetohydrostatic equilibrium config. 0-83965  
 switches, high press. surface discharge, review 0-103208  
 thermonuclear fusion research, economic factors 0-73991  
 three-electrode DC Ar plasma source for optical emission spectrometry 0-62735  
 Tokamak gettering, Ti thin films, H absorption and desorption, Auger electron spectrosc. 0-75092  
 Tokamak plasma, line spectra of highly ionised heavy atoms 0-79567  
 Tokamak reactors, role of  $\alpha$ -particles review 0-86971  
 Tokamak Thor, discharge, electron distribution function, laser Thomson scatt. 0-59327  
 Tokamaks, PLT and PDX, X-ray diagnostics 0-75104  
 toroidal solenoids, helically wound, form factor calcs. 0-100091  
 tritium filling and monitoring apparatus for particle beam inertial confinement fusion targets 0-57949  
 waveguide containing relativistic electron beam, slow cyclotron waves 0-106983  
 H, ACT-1 toroidal plasma, externally launched ion Bernstein waves 0-106967  
 H plasma target investig. (*Russian*) 0-106981

**plasma diagnostic techniques**

- see also plasma probes  
 acid phthalate curved crystal spectrograph, diffraction efficiency calc. method 0-79630  
 air arc temp. meas. by N<sub>2</sub><sup>+</sup> integrated emission coeffs. 0-59314  
 AM active microwave method for density meas. 0-87948  
 calorimetric system for recording plasma blowoff and scattered light distributions from laser plasmas 0-59287  
 cellulose nitrate film ion data, dark-field illum. image recording photographic method 0-70031  
 DC plasma atomic emission spectroscopy system, characterisation of interelement enhancement effect 0-89549  
 DFS-8 spectrograph, attachment for oscillographic recording of line shapes 0-105721  
 diffraction radiation characts. of an open conducting periodic struct. temp. and elec. conc. determ. (*Ukrainian*) 0-70004  
 double-pass rapid-scanning Fourier transform spectrometer, appl. to Tokamak plasma 0-59299  
 Earth's neighbourhood, investigation of origins of plasma using OPEN program 0-109318  
 electron density meas. by far IR laser beam deflection 0-59296



**plasma diagnostic techniques continued**

- estimation method for electron temp. and density in  $^3\text{He}$  plasma and  $^3\text{He-Ar}$  plasma 0-64785  
 Fabry-Perot interferometer appls. 0-59302  
 far IR laser scatt. meas. of nonthermal density fluctuations 0-59297  
 Faraday rotation, mag. field determ. in hot plasma (*Rumanian*) 0-87950  
 Fourier transform spectrometer, double-pass rapid-scanning 0-103190  
 Frascati experiment, neutron yield determ. Ag-activated Geiger counter calibration 0-99409  
 grazing incidence spectrometry, photometric calibration of 1.0 m spectrometer 0-92386  
 IMPATT source, frequency-stabilised, 115 GHz 0-67573  
 intracresator absorption spectroscopy in plasma jet, laser stimulation optimisation 0-77881  
 ion energy and momentum spectrometer with high resolution, for investigating expanding laser blow-off plasmas 0-86495  
 IR and millimetric waves and applications, conf., Miami Beach, USA (Dec. 1979) 0-57009  
 IR holography at 10.6  $\mu\text{m}$  for laser diagnostics 0-84007  
 Josephson junctions, applications in plasma physics 0-103194  
 laser plasma, 5-20 keV X-ray emission spectrum investigation using nucl. emulsions 0-92392  
 magnetic tape method obs. of self generated mag. fields 0-64775  
 MFTF, plasma diagnostics system 0-95444  
 microwave p-i-n diode modulator, transient plasma instability meas. (*German*) 0-87942  
 opticalvalvic double-resonance spectroscopy 0-57385  
 plasma chemistry, history, diagnostics, production, organic compd. synthesis 0-61099  
 pressure sensor using TsTS-19 piezoelectric ceramic 0-105670  
 rapid-scan polarising Michelson interferometer and InSb detector calibration 0-59305  
 self absorption of He like satellite lines in high density fusion plasmas 0-64776  
 shearing interferometer for dense laser prod. inhomogeneous plasma (*Russian*) 0-83994  
 soft X-ray imaging instrument for the Alcator A Tokamak 0-73563  
 space potential measurements with particle beam probes 0-84006  
 Sun, use of MHD pulses as diagnostic technique 0-109405  
 superheterodyne tracking cct. for mm-wave measurements 0-59288  
 TFTR, general arrangement of diagnostics 0-95445  
 TFTR, neutron spectrometer mech. design 0-95498  
 theta pinch, emission line time histories, impurity ion dielectronic recombination rates 0-79570  
 theta pinch plasma density radial profile measurements using quasiquadrature interferometer 0-70038  
 time-gated optical imaging system meas. of laser target emitted light angular distrib. 0-79572  
 Tokamak, JET, far IR interferometer design 0-59295  
 Tokamak, PLT, electron cyclotron radiation Fourier transform diagnostics 0-59292  
 Tokamak electron temp. and density profiles from electron cyclotron radiation spectra 0-59293  
 Tokamak far IR Fourier transform spectroscopic Michelson interferometer 0-59294  
 Tokamak far IR Fourier transform spectroscopy resolution limits 0-59298  
 toroidal plasmas, high temp., electron cyclotron emission meas. by mesh filter method 0-75101  
 trifluoromethane plasma etching of  $\text{SiO}_2$ , optical spectroscopy appl. 0-87940  
 UV holographic microinterferometer and probe beam design for plasma probing 0-59270  
 wave diagnostics in Venus environment, by Pioneer Venus Orbiter instrument 0-67497  
 X-ray catoptrical crossed-mirror imaging at grazing incidence 0-77923  
 X-ray diagnostics, hot lab. and astrophysical plasmas 0-59282  
 X-ray diagnostics, plasmas in PLT and PDX Tokamaks 0-75104  
 X-ray emission in laser imploded targets, three-dimens. reconstruction 0-79563  
 X-ray emission spectrum of plasma focus meas., using Ross filters and Si detectors 0-59273  
 X-ray line shift for high density laser produced plasma diagnostics 0-64778  
 X-ray microradiographs of laser fusion targets, improved image analysis techniques 0-79562  
 X-ray spectrometer, high-speed, multichannel, bremsstrahlung of hot electron component obs. 0-57445  
 CsI photocathodes, efficiency evaluation for soft X-ray diagnostics 0-57442  
 Cu-like ions, 4s-4p reson. lines and transitions obs. by means of laser prod. plasma, appl. to Tokamaks 0-99468  
 CuI photocathodes, efficiency evaluation for soft X-ray diagnostics 0-57442  
 H atom analyser using Cs heat pipe, low energy appl. 0-70043  
 H $_{\alpha}$  plasma, diagnostics using reson. multiphoton ionis. 0-58640  
 LiF curved crystal spectrograph, diffraction efficiency calc. method 0-79630  
 UF $_6$ , high temp. fissioning plasma core reactors, fluid mechanical confinement 0-63248  
 Zn-like ions, 4s-4p reson. lines and transitions obs. by means of laser prod. plasma, appl. to Tokamaks 0-99468

**plasma diagnostics**

- see also plasma density; plasma diagnostic techniques; plasma diagnostics by laser beam; plasma temperature  
 air plasma, optical emission, localised oscill. mode obs. 0-83903  
 alkali metal vapour-H plasma, charge exchange role in optical props. 0-59284  
 anomalous intensity ratios in H like  $L_{\alpha}$  doublet in optically thick laser prod. plasmas 0-103186  
 arcs, helical form model 0-103199  
 Asperator NP-L stellarator, mag. field config. meas. 0-92367  
 Beta-II, magnetised coaxial plasma gun mechanical design and construction 0-91271  
 bremsstrahlung X-rays emitted from electron cyclotron reson. plasma, degree of polarisation 0-87944  
 BWO appl., 110 to 170 GHz, using Sm-Co ring magnets (*German*) 0-105684  
 charge exchange neutrals, emitted from rot. plasma, meas. 0-106979  
 coaxial plasma guns, breakdown phase, optical and elec. meas. 0-70036

**plasma diagnostics continued**

- coherent wave particle interaction in Q-machine plasma, electrostatic analyser diagnostics 0-59226  
 Columbia Torus-1 belt pinch high beta toroidal device, preionisation, optimisation 0-92368  
 computational model for spectral and radiative characts. in Kr and Xe arcs 0-64812  
 conference, New York, USA (Oct. 79) 0-73093  
 continuum absorpt. and emission spectra of nonideal plasmas, approx. calcs. 0-75035  
 corpuscular diagnostics by charge exchange of plasma ions at artificial target, in Tokamak T-4 (*Russian*) 0-83968  
 CT6B Tokamak, measurement of plasma column displacement 0-84001  
 D $_{\alpha}$  spectral profile measurements on TFR plasmas 0-92397  
 dense plasma focus, strong subnanosecond field variations 0-70035  
 dielectronic satellite spectra, electron collisions, corona model theory 0-59188  
 diffuse theta-pinch, ion temp. meas. (*Japanese*) 0-87951  
 dissociative recombination of  $\text{H}_3\text{O}^+$  and  $\text{D}_3\text{O}^+$  at elevated electron and gas temperatures, rate coeff. determ. 0-63747  
 double layers from ion acoustic instability numerical simulation 0-59220  
 drift wave instability, current-driven,  $\theta$ -probe obs. 0-59204  
 dynamic Stark effect in  $\text{H}_2$  and neutral He spectral lines for elec. field strength meas. in waveguide 0-69103  
 EBT, ray tracing near electron cyclotron freq. 0-103178  
 electric arc, horizontal, in inhomogeneous mag. field, mass spectrometric anal. 0-79620  
 electric arcs, temperature estimation from self-reversed spectral lines 0-75110  
 electric discharge with disc cathode in He flow, spectrosc. investig. 0-64809  
 electric field fluctuations spectrum, laser fluoresc. spectroscopy meas. 0-87946  
 electric field intensity meas. in stabilised arc, plate probe meas. 0-75095  
 electrode contact processes, microplasma diagnostics 0-59325  
 electrodynamic mechanisms of limitation of the electron concentration in a laser spark (*Russian*) 0-59333  
 electron beam heating and beam energy distrib. in E-region approximated plasma 0-103163  
 electron beam stabilised mirror confined gas, hot electron population study 0-100089  
 electron density meas. by two-freq. band microwave interferometer 0-83890  
 electron energy distribution function meas. using delay line differentiator (*Japanese*) 0-84002  
 electron energy distribution in a low-pressure RF discharge 0-87979  
 electron energy transport into layered targets irradiated by  $\text{CO}_2$ -laser light 0-69979  
 electron temperature in glow discharge in transverse mag. field, spectrosc. method meas. 0-87855  
 electrostatic ion analysers for laser prod. plasma detection, space charge effects 0-96392  
 electrostatic plasma-confinement experiments in a tandem mirror system 0-70025  
 elliptical plasma source, radiation emission distrib. 0-103124  
 EM waves in plane inhomogeneous plasma in presence of mag. field shear, appl. to plasma diagnostics (*Russian*) 0-103140  
 emission line shapes from a rotating ring radiator 0-83998  
 exploding-pusher-tamper areal density, neutron activation meas. 0-91237  
 extreme UV spectroscopy of the 2XIIIB neutral-beam-heated fusion mirror machine 0-74002  
 fibre-optic data transmission systems 0-79571  
 fine struct. of plasma satellites of He 492.2 nm line 0-59235  
 flute modes, similar freq., simultaneous feedback stabilisation 0-103146  
 focusing hog-horn antenna for microwave diagnostics in plasma machines 0-96395  
 Frascati 1 MJ plasma focus facility, deuteron energy distrib. 0-87957  
 FT Tokamak, non-thermal electron distrib. function 0-83891  
 fusion reactor, MFTF, supervisory control and diagnostics system, database management system 0-99326  
 fusion reactor, MFTF, supervisory control and diagnostics system, database management system, data structs. 0-99327  
 gas flow, nonequilibrium ionisation and Hall EMF 0-69981  
 graphite vapour cloud, laser-prod., temp. conditions investig. 0-59290  
 harmonic emission mechanisms, three-halves, from laser-produced plasma 0-59283  
 heat transfer rates to flat plate from normally-impinging N plasma jet 0-75061  
 HF electric field, nonlinear behaviour just before beam-plasma discharge initiation 0-87904  
 high beta toroidal device, preionisation, optimisation 0-92368  
 high-Z emitters in ultradense plasmas, hydrogenic profiles, perturbing ion effects 0-79566  
 hollow cathode discharge with variable voltage 0-59336  
 impulse spark study using two-wavelength interferometry 0-86391  
 inert gas ion laser, high voltage-low press. discharges, stationary props. 0-92400  
 inert gas plasma, electron-beam produced, laser action of ionized and neutral atomic lines 0-106929  
 interstellar medium, far IR fine structure line obs. 0-62253  
 ion emission from laser plasma, secondary electron emission effects on detect. efficiency 0-100096  
 ion energy distribution, electrostatic retarding field energy analyser 0-70032  
 ion spectra, high-energy, periodical modulations, emitted by 1 kJ plasma focus 0-59310  
 ion temperature determ., appl of secondary electron emission to energy anal. of energetic neutrals 0-59278  
 ions, multicharged, in plasma produced by laser, spectral line profiles (*French*) 0-79528  
 laboratory, magnetosphere, and astrophysical plasma knowledge interaction 0-59166  
 laser driven implosions, hydrodynamic instabilities 0-64756  
 laser plasma, 5-20 keV X-ray emission spectrum investigation using nucl. emulsions 0-92392  
 laser produced plasma, solid in high press. gas atm. in elec. field, spatial struct. (*Russian*) 0-83962  
 laser produced plasma parameters determ. from shape of single optically thick line profile 0-103191  
 laser spectroscopy in intense magnetic fields 0-62738  
 laser-produced high-Z plasma, X-ray diagnostics 0-75074



## plasma diagnostics continued

- laser-produced plasma, props. meas. (*Korean*) 0-96373  
 laser-produced plasma, X-ray spectra 0-75075  
 laser-produced plasma continua, for absorpt. spectroscopy in VUV and XUV 0-75094  
 line broadening in atomic and ionic emissions from plasmas (*French*) 0-79434  
 line radiation emission, from hot dense Al plasma 0-79456  
 linear pinch plasma, extreme UV spectra of light impurity ions, appl. of grazing incidence spectrometer 0-59276  
 linear turbulently heated plasma, secondary emission detector obs. 0-75100  
 low temperature inhomogeneous dense plasmas, optical diagnostics 0-75096  
 low-density plasmons, electron temp. meas. by He spectrosc. 0-103192  
 low-pass interference filters for Tokamak plasma diagnostics 0-64783  
 magnetic dipole transitions in TiXIV, TiXV, TiXVII ground state terms in Tokamak discharge 0-63575  
 MFTF, supervisory control and diagnostics system software 0-99324  
 mFTF plasma diagnostics Data Acquisition System 0-99319  
 microtearing modes and anomalous transport in Tokamaks, self consistent calc. 0-59222  
 Microtor Tokamak, LF microturbulence, far IR laser scatt. 0-96362  
 microwave discharge, fast wave emission diagnostics 0-92391  
 multiply charged ion interactions with Al surface, laser induced plasma 0-70007  
 neutral high power beams, optical diagnostics 0-92394  
 nonlinear phenomena by the Tokamak helical mode evolution 0-92398  
 nuclear generated plasmas,  $^3\text{He}$  and  $^{235}\text{Uf}_6$  excitation, spectra obs. 0-83997  
 optical detector correlation measurements of turbulent ionization and ion-acoustic waves 0-59329  
 particle and energy balance by corpuscular diagnostics 0-92399  
 pinched electron beam prod. expanding gas bubbles, fast photography obs. 0-79564  
 plasma, emission and absorption coeff. at high electron density 0-103121  
 plasma optical transparency evaluation, line broadening effect 0-79453  
 polarization and millisecond spectral measurements of electron cyclotron emission from DITE Tokamak 0-92396  
 polymer-coated laser fusion targets, compression to  $10\times$  liq. DT density 0-83964  
 probe cct. used in pulsed plasma diagnostics 0-87947  
 PULSATOR, impurities in high density regime 0-79579  
 radiation temperature of proton beam induced plasma 0-100094  
 reactive plasma, optical emission spectroscopy, emission intensities and reactive density, correl. method 0-92385  
 resonant Balmer line irradiation of H plasma, theory and laser spectrosc. meas. 0-75099  
 ring cusp, plasma width meas. 0-87927  
 Schlieren measurements of plasma kinematics during current disruptions in Tokamaks 0-92395  
 screening efficiency of the scrape off plasma in the shadow of a poloidal limiter 0-79576  
 soft X-ray population inversion in laser plasmas, reson. photoexcitation, photon-assisted processes 0-87378  
 solar coronal plasma density, determ. from reson. lines fine struct. components 0-101581  
 space potential determ. and storage in fast changing plasma 0-87949  
 space potential measurements with particle beam probes 0-84006  
 spatial emission profiles from inductively coupled plasma, matrix effects 0-75036  
 spectra, overlapping doublet, escape factor 0-96391  
 spectra from plasmas induced by  $^3\text{He}$  or  $^{235}\text{Uf}_6$  reactions 0-64784  
 spectroscopic electron density meas., hot point low induction vacuum spark gas (*Russian*) 0-92390  
 Stark broadening of isolated Sn II lines in cool plasma, semi-empirical calcs. 0-59186  
 Stark shift by inhomogeneous strong E field, X-ray Lyman profile 0-106977  
 stationary nonequilibrium distributions of ions produced in the interaction with an electron thermostat (*Russian*) 0-64684  
 stopping power of a nonequilibrium plasma for incident alpha particles 0-64742  
 superradiation from non-ideal plasmas in electric field 0-83904  
 sustained optical discharges in molecular gases 0-100085  
 Tokamak plasma density profiles from electron cyclotron radiation spectra 0-103179  
 TEXTOR, interferometric and polarimetric diagnostics 0-70039  
 TEXTOR, mag. diagnostics and monitoring systems data acquisition 0-99320  
 TFR, electron cyclotron frequency emission and transmission meas. 0-79575  
 TFR 600 Tokamak, soft X-ray meas., mag. topology near  $q=1$  surface 0-79580  
 thermal fluctuations and leaking radiation from laser-produced plasma 0-87953  
 theta-pinch Ti ion injection by  $\text{CO}_2$  laser, spectroscopic anal. 0-79577  
 Thomson scattering meas. of heating process 0-59272  
 time-resolved X-ray spectroscopy of laser-produced plasmas 0-84004  
 Tokamak, JFT-2, particle and heat transport during lower hybrid heating 0-70021  
 Tokamak, large magnetic field ripples, electric probe meas. 0-83976  
 Tokamak Alcator C far IR emission diagnostics of electron temp. 0-59291  
 Tokamak plasma, confinement time meas. 0-87945  
 Tokamak plasma, line spectra of highly ionised heavy atoms 0-79567  
 tokamak plasma, new atomic data for  $\text{Fe}^{19+}$  spectra 0-67545  
 Tokamak plasma, Thomson scatt. with repetitively Q-switched ruby laser 0-59271  
 Tormac, Gaussian HeII 4686 Å spectral lines, Doppler and Stark broadening effect, turbulence 0-106980  
 Townsend avalanche, vacuum UV spectra 0-64810  
 transport functions by precision arc expts., H Balmer spectrum 0-103187  
 transverse HF discharge, electron energy distrib. from spectra (*Russian*) 0-84012  
 turbulent plasma, magnetised, line shape of optical satellites 0-75098  
 two ion components, meas. by collective laser scatt. 0-92388  
 ultrahigh vacuum transfer system, 15 cm diameter, for remote plasma-wall interaction expts. 0-86327  
 unipolar pulsed LCD discharge, spectrum, time scanning 0-64774  
 UV photoplasma, electron density, microwave meas. 0-75097

## plasma diagnostics continued

- vacuum UV emission from low temp. air plasma, investig. 0-69982  
 Venus ionosphere, Pioneer Venus Orbiter planar retarding potential analyser plasma expt. 0-67501  
 Venus plasma environment, study via plasma analyser expt. on Pioneer Venus Orbiter 0-67498  
 vibrational kinetics and plasma characts. in  $\text{CO}-\text{N}_2$  discharge 0-59331  
 Voigt profile, Lorentz component true halfwidths and line intensities 0-87943  
 W VII-A stellerator, line emission, poloidal and toroidal asymmetry 0-79578  
 X-ray absorption lines, signature for preheat level in non-explosive laser implosions 0-106978  
 X-ray bremsstrahlung polarisation and anisotropy, evidence of suprathermal electron fluxes 0-103193  
 X-ray emission, electron temp. meas. 0-103127  
 X-ray line radiation from cylindrical Al plasma, calc. model 0-64777  
 X-ray monochromatic images for hot plasma ion and temp. distrib. 0-64772  
 X-ray production by laser plasma in strong elec. field 0-70034  
 X-ray shadowgraphy of laser driven implosions 0-92393  
 X-ray spectrometry of laser compressed microballoons 0-87954  
 Z-pinch turbulence spectroscopic detection and anal. (*Russian*) 0-100098  
 Z-pinch of intense energy-density driven by high voltage storage lines 0-87952  
 Ar arc plasma, partial LTE for lower excited levels of ArI 0-79565  
 Ar arc plasmas, steady-state and decaying, mol. gas impurities 0-103177  
 Ar decaying pulsed discharge plasma, acoustic waves density modulation 0-103143  
 Ar discharge, ion density profile, reson. laser light meas. 0-92401  
 Ar plasma parameters, microwave scanning technique 0-64773  
 $\text{Ar}^{16,17+}$  filled glass shell, symmetric laser compression 0-64759  
 Ar-air, transformer plasmatron, LF discharge, electrical and energy props. 0-103200  
 $\text{CO}_2$  laser beam scatt. by microscopic fluctuations in plasma density 0-79574  
 $\text{CO}_2$  laser prod. microballoon plasma, fast ion emission 0-103172  
 $\text{CO}_2-\text{N}_2-\text{He}-\text{O}_2$  discharge mixture, three body electron attachment to  $\text{O}_2$  0-64779  
 $\text{CO}_2+\text{N}_2+\text{He}$ , glow discharge positive ion species identification (*Russian*) 0-84014  
 Cl X-ray emission spectra, detect. from Alcator-A Tokamak 0-92389  
 Co, X-ray transitions in laser produced plasma 0-100093  
 Cr, X-ray transitions in laser produced plasma 0-100093  
 Cr(II) lines, oscil. strengths in 2413-2718 Å wavelength range 0-106294  
 Cs plasma, generation by adiabatic compression, elec. cond. and thermodynamic parameters meas. 0-59180  
 Fe IX, X, XI, effective dielectronic recombination rates in H plasma, emission time histories 0-79570  
 H dense thermal plasma, radiation emission 0-103120  
 H line broadening and shift due to plasma ions (*Russian*) 0-96350  
 H plasma, K impurities, optical props. 0-103119  
 H spark, laser-triggered, electron densities meas. 0-106975  
 $\text{H}_2-\text{SiH}_4$  glow discharge, emission spectroscopy of Si H 0-69984  
 $\text{H}_2$  and  $\text{H}_2^+$  spectral profiles from neutral beams and plasmas in high mag. fields 0-83999  
 $\text{H}\alpha$  and  $\text{H}\beta$ , Stark profiles, ion-motion effect 0-63592  
 He continuum radiation, 109 to 540 nm, meas. in arc plasma (*German*) 0-106932  
 He II 4686 Å line, Stark profile meas. in high density plasma 0-96390  
 He, low press. discharge, electron free streaming waves expansion 0-79595  
 He plasma, low-density, electron temp. determ. from He I 3889 Å and 5016 Å line intensities 0-96394  
 He, positive column plasmas, metastable atom density meas. by improved self absorpt. method 0-87968  
 He-Cd vapour excitation in hollow cathode discharge 0-64815  
 Mg plasma, heated by ruby laser pulses, X-ray emission spectrum 0-64781  
 Mo X-ray emission spectra, detect. from Alcator-A Tokamak 0-92389  
 Mo XIII-XVIII, spectrum 20 to 90 Å from laser-prod. plasma and low-inductance vac. spark 0-102473  
 N, nonequilibrium plasma, thermocouple diagnostics 0-103188  
 $\text{N}_2-\text{H}_2$  arc, bent and rot., flow mechanism 0-70047  
 $\text{N}_2$ -methane, rapidly developing discharge, streak camera records interpretation 0-59280  
 $\text{N}_2-\text{O}_2$  mixture transient discharges, RF techniques 0-70067  
 $\text{N}^{(D,P)}$  metastable production by electron collisions in DC glow discharge 0-59274  
 Ne, excited atoms concentration determ., in high-frequency and glow discharges (*Russian*) 0-70050  
 Ne, low press. discharge, electron free streaming waves expansion 0-79595  
 Ne, nuclear induced plasma, simulated 0-64786  
 Ne positive column plasmas, metastable atom density meas. by improved self absorpt. method 0-87968  
 Ne pulsed transverse discharge, spectrosc. absorpt. investig. with nanosec. time resolution (*Russian*) 0-64782  
 Ni, X-ray transitions in laser produced plasma 0-100093  
 S ( $\text{S-He}$ ) discharges, stability, emission spectra 0-107003  
 $\text{SF}_6$ , high-current discharge plasma column, radiation charact. and struct. (*Russian*) 0-106989  
 $\text{SF}_6$ -inert gas mixture, high power cylindrical spark discharge, dynamic and visible charact. 0-64816  
 Ti II, oscillator strengths from combined hook and emission expts. 0-87081  
 $\text{Y}_2\text{O}_3$  capillary discharge plasma, temp., radiation screening elimination 0-64682

## plasma diagnostics by laser beam

- air plasma, TEA  $\text{CO}_2$  laser-produced, using solid targets, induced shock waves 0-64729  
 asymmetric electron density profile, interferometric meas., laser-created plasma 0-75085  
 atomic collision processes and X-ray and UV lasers 0-64787  
 Balmer series transitions for laser plasma diagnostics 0-64780  
 combination scattering method 0-79569  
 CW far-infrared laser scattering from a laboratory plasma ion acoustic wave 0-106974  
 dense plasma focus, ruby laser holographic diagnostics (*Japanese*) 0-100097



**plasma diagnostics by laser beam continued**

- density fluctuations study by small angle CO<sub>2</sub> laser scatt. 0-59285  
 electron density in pulsed laser discharges, interferometric meas. 0-96393  
 electron density meas. by far IR laser beam deflection 0-59296  
 electron directed velocity meas., optimised method using laser scatt. incoherent regions 0-79561  
 EM field during metal evap. at laser focus, RF signal recording obs. 0-59281  
 far IR laser scatt. meas. of nonthermal density fluctuations 0-59297  
 ion-acoustic fluctuations, CO<sub>2</sub> laser study 0-83946  
 IR holography at 10.6  $\mu$ m for laser diagnostics 0-84007  
 jet form. by focusing laser beam on plane target, investigation using wave-front method 0-75103  
 laser-produced plasma motion and lateral energy flow meas. 0-75102  
 magnetoplasma dynamic arcjet, density meas. by CO<sub>2</sub> laser interferometry 0-59277  
 methanol far IR laser, twin optically pumped 0-59306  
 methanol twin optically pumped far IR laser 0-103189  
 pulsed coherent radiation source, 118 nm 0-106572  
 pulsed submillimeter laser with optical pumping appl., construction and expt. parameters 0-58565  
 shock generated turbulence, obs. in mag. plasma by CO<sub>2</sub> laser scatt. 0-84603  
 submillimetric-wave laser Thomson scatt. ion temp. diagnostic implementation in Tokamak 0-59301  
 Thompson scattering diagnostics of low density plasmas, Nd:glass laser system 0-96388  
 Tokamak, far IR laser collective scatt. system 0-59300  
 toroidal controlled fusion poloidal mag. field meas. by far IR Faraday rotation 0-59303  
 turbulence meas. by CO<sub>2</sub> laser light collective scatt. 0-84005  
 ultra-fast detectors for laser fusion diagnostics, quenched plastic scintillator with microchannel plate photomultiplier 0-74084  
 A) plasma, laser produced, reflectance meas. 0-79568  
 Ar arc, high current, interferometric and spectroscopic study 0-59275  
 Ar, plasma, jet, optical studies using Schlieren and shadow methods 0-59279  
 CO<sub>2</sub> laser beam-diagnostics techniques, laser beam parameter monitoring 0-64089  
 CO<sub>2</sub> laser system, pulsed, for fusion research 0-58556  
 CO<sub>2</sub> long-pulse 2 GW single longit. mode source for laser-matter expts. 0-78860  
 DCN waveguide lasers, optimised 190/195  $\mu$ m, radiation source for plasma diagnostics 0-99709  
 D<sub>2</sub>O vapour high-power 385  $\mu$ m laser oscillator 0-69422  
 H<sub>2</sub> plasma diagnostics by reson. multiphoton ionis. 0-58640  
 He-Ne laser and interferometer systems (Czech) 0-87941  
 Hg vapour discharges, high-press., e-beam initiated, laser absorpt. meas. 0-92412

**plasma diodes**

- coaxial plasmatron, characteristics (Russian) 0-59311  
 field emission medium energy diode, electron flow, HF oscills. 0-79582  
 flat, with cathode filament, theory 0-103197  
 magnetically insulated diode, hollow electron beam pot. 0-70046  
 micropinch in a high-current diode, review 0-103183  
 particle beam interactions with plasma, inertial fusion appls. 0-59250  
 plasmatron, discharge stabilised, by gas blown through porous wall 0-75105  
 Ar-air, transformer plasmatron, LF discharge, electrical and energy props. 0-103200

**plasma filled waveguides**

- cylindrical waveguide filled with uniaxial, collisional, hot and moving plasma, dispersion for TE and TM modes 0-106934  
 diffraction radiation characts. of an open conducting periodic struct., temp. and elect. conc. determ. (Ukrainian) 0-70004  
 electron nonlinear waves in strongly magnetised plasma 0-79472  
 EM wave resonance tuning of magnetoactive plasma (Russian) 0-83914  
 guided electron plasma waves, propag. along cylinder, dissipative processes effects 0-92332  
 lower-hybrid waves, focusing and channelling during HF-breakdown of gas (Russian) 0-106890  
 microwave discharge, fast wave emission diagnostics 0-92391  
 ponderomotive craters, in phased waveguide array plasma, form. by microwave irradi. 0-83885  
 power reflection, transmission and absorption coefficients for a moving plasma slab in a rectangular waveguide 0-106925  
 radiation from waveguide, rel. to plasma wave scatt. by ion-acoustic oscills. 0-87886  
 RF emission, plasma wave scatt. by ion-acoustic waves in nonequilib. plasma 0-64733  
 uniaxial anisotropic relativistic warm plasma, EM wave propag. and attenuation 0-59246  
 wave propag. in hot collisional plasma filled waveguide 0-92331  
 wave radiation by oscillating electric dipole in moving warm plasma 0-87868  
 H, ACT-1 toroidal plasma, externally launched ion Bernstein wave 0-106967

**plasma flow**

- see also *plasma focus; plasma magnetohydrodynamics*  
 arcs, wall-stabilised, free recovery with imposed laminar and turbulent flows 0-59321  
 bunch enlargement in vac. (Russian) 0-83907  
 collisionless flow and end loss from a high-energy theta-pinch plasma 0-92365  
 collisionless shocks, ions nonfluid behaviour at high Mach numbers 0-90330  
 electron directed velocity meas., optimised method using laser scatt. incoherent regions 0-79561  
 gas flow, nonequilib. ionisation and Hall EMF 0-69981  
 gas stream with dispersive impurity, initial region boundaries, impurity velocities (Russian) 0-100069  
 hollow electron beam pot. in magnetically insulated diode 0-70046  
 ion beam generation increase through moving plasma boundary 0-63439  
 laser produced plasma, transition from isentropic to isothermal expansion 0-92279  
 laser produced plasmas, self-consistent profile modification in underdense region 0-75038  
 laser-driven fusion, validity of hydrodynamic approximation 0-75087  
 laser-generated, ion beam production from interaction with Nd:YAG laser radiation bursts 0-106939

**plasma flow continued**

- layer expansion near barrier irradiated by laser in high density gas 0-70016  
 magnetised plasma interaction with neutral gas, threshold vel. 0-59241  
 MFTF, plasma streaming system, description 0-91280  
 moving cold magnetised plasma, wave propag., polarisation relations and dispersion eqns. 0-64723  
 nonequilibrium gas relaxation in supersonic nozzle, analysis method 0-74941  
 nonlinear interaction, electron collision freq., self-consistent eqn. (Russian) 0-75055  
 plasma dynamics, Soviet literature growth and duplication parameters (Russian) 0-59191  
 plasmatron, discharge stabilised, by gas blown through porous wall 0-75105  
 polarisation of picosecond excited continuous X-ray radiation (Russian) 0-59190  
 resistive hose instability in relativistic electron beam 0-67947  
 resonance absorption, self-consistent density profiles for obliquely incident light 0-64758  
 shear flow, electrostatic instability, theory and appl. to magnetopause and solar wind 0-96359  
 slow convection of magnetised plasma, appl. to Earth plasma sheet 0-109312  
 thermal instability, mag. field generated, in laser heated plasma, hydrodynamic effects 0-96355  
 toroidal trap, plasma rot. effect on neoclassical transport of impurities (Russian) 0-83972  
 vacuum arc plasma flow in plasma-optical system (Russian) 0-106992  
 waveguide, rectangular, filled with uniaxial anisotropic relativistic warm plasma, EM wave propag. and attenuation 0-59246  
 welding arc, EM forces effect on plasma flows, calc. 0-83912  
 welding arcs, gas velocity fields modelling 0-75039  
 H pellet in plasma, transonic flow in ablation cloud 0-64735  
 N glow discharge, volt-ampere charact. in gas flow (Russian) 0-106991  
 O<sub>2</sub>-seeded Ar plasma supersonic free jet expansion flow, population density measurements (Japanese) 0-96351  
 Si compounds, plasma etching, gas flow-rate depend. 0-97603  
 SiO<sub>2</sub>, plasma etching, gas flow-rate depend. 0-97603

**plasma focus**

- breakup-initiated shockfront development in 2-kJ plasma focus discharge 0-70001  
 closed poloidal heliotron, accelerated electron focusing (Russian) 0-106961  
 current carrying double layer production in focus device 0-83953  
 dense plasma focus, ruby laser holographic diagnostics (Japanese) 0-100097  
 dense plasma focus, strong subnanosecond field variations 0-70035  
 energy spectra of accelerated deuterons in a plasma focus 0-103110  
 fast high voltage plasma focus, current and neutron yield scaling 0-64752  
 Frascati 1 MJ plasma focus facility, deuteron energy distrib. 0-87957  
 Frascati experiment, neutron yield determ. Ag-activated Geiger counter calibration 0-99409  
 high velocity jets generated by plasma focus and shock-wave expt., temp. and density meas. (Russian) 0-106882  
 ion energy distribution in plasma focus during second pinch compression 0-75070  
 ion spectra, high-energy, periodical modulations, emitted by 1 kJ plasma focus 0-59310  
 Mather type PF devices, optimisation using 2D snow plow code 0-87956  
 pinch column form. and stability 0-96380

**plasma generation see plasma production****plasma guns**

- Beta-II, magnetised coaxial plasma gun mechanical design and construction 0-91271  
 coaxial plasma guns, breakdown phase 0-70036  
 compact 5 $\times$ 10<sup>-12</sup> A/s rail-gun pulser for laser plasma shutter 0-70017  
 gas injected washer plasma gun 0-100083  
 MFTF, plasma streaming system, description 0-91280  
 reversed field mirror reactors, startup using coaxial plasma guns, scaling laws 0-99279  
 vacuum arc plasma flow in plasma-optical system (Russian) 0-106992  
 Ba rail gun for plasma injection 0-59255

**plasma heating**

- see also *plasma focus; plasma production and heating by laser beam*  
 asymmetric plasma resistivity, creation using waves 0-103171  
 axial shock heating applied to compact toroid plasma formation 0-95402  
 beam-induced tensor pressure Tokamak equilibria 0-106965  
 beat heating by two Gaussian beams in extraordinary mode 0-64746  
 Bernstein dispersion relation for oblique propagation 0-75052  
 Bernstein waves, propagation in inhomogeneous plasma, dispersion rel., quasi-linear equations, diffusion coeff. determ. 0-75044  
 burn period plasma current maintenance, rectifying first wall, cct. anal. 0-102307  
 cluster ion mean specific size, effects of break-up ratios and distrib. functions of specific size 0-75068  
 collisional drift modes, anomalous skin effect, enhanced particle penetration during fuelling, nonlinear theory 0-64703  
 complex ray analysis for plasmas 0-83902  
 conference, controlled fusion and plasma physics, Oxford, England (Sept. 1979) 0-77545  
 convective plasma loss by ion-cyclotron RF field, elimination by mode control 0-83957  
 coupling to the fast wave at lower hybrid frequencies 0-75069  
 cylindrical system with heavy inertial layer, neutron yield, explosion-induced D-T compression 0-68944  
 dissociative recombination of H<sub>2</sub>O<sup>+</sup> and D<sub>2</sub>O<sup>+</sup> at elevated electron and gas temperatures, rate coeff. determ. 0-63747  
 distortion of the thermal-ion distribution during neutral-injection heating 0-103169  
 DITE, neutral injection heating 0-92347  
 Doublet III, ohmic heating E-coil vacuum breaker system, function and operation 0-102323  
 EBT, ray tracing near electron cyclotron freq. 0-103178  
 EBT heating, electron-cyclotron absorption and microwave propagation 0-64749  
 electric field heated nonisothermal plasma, nonstationary electron behaviour, kinetic description 0-59171



**plasma heating continued**

electron beam heating and beam energy distrib. in E-region approximated plasma 0-103163  
 electron cyclotron heating, superthermal electrons 0-64753  
 electron cyclotron resonance heating of Tokamak plasmas, fluctuations and instability 0-83956  
 electron heating, ion cyclotron influence in min-B mirror trap 0-79521  
 electron plasma cooling by cyclotron radiation 0-69986  
 electron-beam-heating from foilless diode 0-103168  
 electrons heating in lower ionosphere by horizontal lightning discharges 0-90283  
 electrostatic wave, magnetised plasma charged particle stochastic accel. 0-59230  
 ELMO Bumpy Torus, microwave coupling 0-99328  
 ELMO Bumpy Torus, ray tracing near electron cyclotron freq. 0-83975  
 EM wave in inhomogeneous magnetoactive plasma, total absorpt. effect (Russian) 0-106944  
 EM waves incident on warm plasma half-space dual propag. and absorpt., density and temp. depend. 0-75048  
 energy confinement comparison of ohmically heated stellarators to Tokamaks 0-92360  
 energy of a turbulent, current-carrying plasma in a strong electric field 0-79514  
 Engineering Test Facility/International Tokamak Reactor, plasma physics characts. 0-95420  
 ERA compression system, IPP-Japan 0-95490  
 excited gas, resonant optical discharge 0-92343  
 field reversed mirror neutral beam startup, hybrid plasma code simulation 0-99313  
 FT-1 Tokamak, electron cyclotron heating expt. 0-75071  
 FT-1 Tokamak, lower hybrid heating, energy balance 0-79523  
 fused metal foil operating switch for inductively driven plasma implosions generation 0-70018  
 fusion chain reactions, kinetics, high electron temps., interactions with D-T plasma 0-68945  
 fusion products in Tokamak plasma, deposition and thermalisation 0-83895  
 fusion reactor, BBC CQK 200-4 modulator tube for sustaining neutral beam power supply 0-99290  
 fusion reactor, High Voltage Switch Tube, for Neutral Beam Power System 0-99291  
 fusion reactor, MFTF, neutral beam source development 0-102368  
 fusion reactor, rectangular plasma generator, advanced ion source for ion injectors 0-99376  
 fusion reactor plasma heating and confinement, review 0-63388  
 heating in lower hybrid freq. range, temp., ion diffusion 0-83954  
 HF discharge, ionisation overheat instability in EM wave field (Russian) 0-106990  
 HF heating by MHD waves of finite press. plasma (Russian) 0-83950  
 high-frequency heating of inhomogeneous plasma in  $\omega \geq \omega_{hi}$  freq. range (Russian) 0-106946  
 hot-ion-mode ignition in a Tokamak reactor 0-73999  
 hybrid waves, lower, backscatter, effect of waveguide boundary conditions 0-64709  
 ICRF heating in TFR at the ion-ion hybrid resonance 0-74020  
 inertial confinement, black body radiation implosion in ablator, driver, gas, pellet system 0-73990  
 inertial confinement fusion, Angara 5 features and design principles, accel. module 0-63384  
 inertial confinement fusion, pulsed power aspects, overview 0-63382  
 inhomogeneous RF plasma, absorption and parametric decay of extraordinary waves 0-59206  
 instability, electrostatic, parametric, due to thermal coupling 0-79465  
 intense ion beam propag. in z-discharge plasma channels, straight and tapered 0-83948  
 ion beam-plasma collective interactions, high current-density 0-75066  
 ion heating by current-driven turbulence in inhomogeneous plasma 0-96370  
 ion heating due to collisionless drift-wave turbulence 0-106949  
 ion source, electron backstream to source plasma region 0-96369  
 ion temp. and parametric decay development in RF-generated stellarator plasma 0-79436  
 ion-ion hybrid resonance damping and heating in the ERASMUS Tokamak 0-92345  
 ionosphere, electron distrib. rel. to production rate and heating 0-105103  
 ionosphere, heating by powerful radio emission with random modulation of carrier freq. 0-109310  
 ISX-B, electron cyclotron microwave heating 0-99329  
 ISX-B, high power neutral beam injection studies 0-79545  
 ISX-B, neutral beam power system 0-91283  
 Japanese Tokamak research, impurity control, low-q discharge, scaling law, RF heating 0-74015  
 JIPP T-II, simultaneous neutral beam injection and lower hybrid heating 0-79516  
 JXFR, neutral beam injection system, gas-beam interaction secondary particles 0-106227  
 klystron development, UHF, 600 kW, stability and durability improvement (German) 0-106211  
 L-2 stellarator, ohmic heating discharges with gas puffing 0-79593  
 linear compression of plasma vortex 0-64755  
 linear magnetic solenoid reactor plasmas, dynamic behaviour 0-64751  
 linear turbulently heated plasma, secondary emission detector obs. 0-75100  
 lower hybrid wave heating, electron distrib. function (Russian) 0-83951  
 lower hybrid wave heating simulation in nonuniform plasma 0-64771  
 lower hybrid waves, propag. in toroidal plasma 0-83927  
 lower hybrid waves, trajectories and damping in Tokamak plasma 0-83922  
 magnetic mirror ion confinement increases, Joule heating 0-83985  
 magnetoacoustic heating by ion Landau damping 0-92341  
 MFTF, sustaining neutral beam power supply, oct. anal. using ASTAP and EMTP codes 0-91284  
 MFTF, sustaining neutral beam power supply system, modelling with ASTAP code 0-91285  
 multicharged ion heating in Z-pinch, column compression, temp. and density (Russian) 0-64754  
 multimewatt gyrotron design for controlled thermonuclear reactor heating 0-59256  
 neutral beam heating in the Princeton Large Torus 0-106950  
 neutral beam injection, 120 keV, ion source 0-91357  
 neutral beam injection, 24 MW 400 keV H beam 0-91356

**plasma heating continued**

neutral beam injection, energy and power requirements 0-91243  
 neutral beam module component design and development for MFTF 0-91270  
 neutral beam source, 40 kV for TMX, engineering design 0-91358  
 neutral beam US development program and review 0-92348  
 neutral high power beams, optical diagnostics 0-92394  
 noncircular Tokamak, heating by collisional slowing of fast ions 0-95403  
 nonlinear cross-field ion acoustic instability and plasma heating 0-83928  
 Ohmic heating in stellarator Uragan-2, MHD-instability and limiting currents (Russian) 0-106881  
 Ohmic heating of plasma in apparatus with spatial axis, MHD-instability (Russian) 0-106945  
 overdense column, reson. microwave absorpt. 0-64732  
 PDX neutral beam injector development 0-99375  
 PETULA Tokamak, lower hybrid heating expts. 0-83958  
 PLT, fusion neutron yield during D neutral beam injection 0-79522  
 PLT, ICRF heating for two-ion regime 0-83959  
 PLT, neutral beam injection, power input and plasma temp. reconciliation 0-106224  
 PLT, neutral beam injection and ICRF heating, charge exchange meas. 0-83892  
 pulsed power acceleration for fusion reactor ignition 0-63383  
 R-OM stellarator, MHD resonant HF heating 0-79518  
 reactor, Tokamak, fuel injection, dynamic burn control 1-D transport code 0-68948  
 reactor, Tokamak, toroidal magnetic field ripple, burn control 0-63375  
 reactor ignition, overheated underdense Tokamak plasma, two-zone model and 1-D transport code 0-63376  
 relativistic electron beam, energy transfer, axial variation 0-87909  
 relativistic electron beam diodes, wave shaping, numerical study 0-87911  
 RF anomalous penetration in collisionless plasma 0-64730  
 RF driven current generation by lower hybrid waves in Tokamak 0-103116  
 RF heating, mode conversion process, localised absorption 0-103170  
 RF heating of fusion plasma (Japanese) 0-92338  
 RF oscillation ponderomotive accel. of electrons in elec. double layer 0-70010  
 RF plasma heating, resonant surface accessibility, surface wave role 0-92346  
 RF plasma heating, surface wave role, resonant surface accessibility 0-75072  
 RF plugging and heating, rel. to plasma impedance 0-96378  
 RF-method for currentless plasma production and heating 0-79519  
 rotating plasma reactors, longitudinal confinement, stability equilibrium and heating problems 0-74001  
 second-harmonic generation of upper-hybrid radiation in a plasma 0-79506  
 self heating and saturation due to numerical instabilities 0-75067  
 shock-heated dense Ar, Kr and Xe plasmas, calc. of equilibrium props. (Japanese) 0-79513  
 solar corona, heating by fast electron streams 0-105228  
 spectroscopic electron density meas., hot point low induction vacuum spark gas (Russian) 0-92390  
 stellarator, current turbulent ion heating, modulation stability 0-79525  
 stellarator W VII-A, neutral injection 0-83960  
 stochastic heating, relativistic electron generation (Russian) 0-83952  
 stochastic heating of plasmas in inhomogeneous magnetic fields 0-59231  
 stochastic ion heating by an electrostatic wave in a sheared magnetic field 0-79520  
 Sun, coronal thermal stability during fast mode wave heating 0-90397  
 surface heating, density rippling, and propagation cones in high-power lower-hybrid heating 0-92342  
 temperate multi-species plasma around ion cyclotron freq. range, plane wave propagation 0-75050  
 TFR, electron cyclotron heating, computer simulation 0-79517  
 TFTR, neutral beam power system 0-91282  
 thermal enhancement of plasma by EM wave transmission in mag. field (Russian) 0-103167  
 thermal ion distribution distortion by neutral injection heating 0-92344  
 theta pinch, spark channel quasi-spherical compression, electron temp. 0-87920  
 theta pinch discharge, radial EM energy flow and plasma heating power 0-64747  
 Thomson scattering meas. of heating process 0-59272  
 TM-1-MH Tokamak, HF heating expts. 0-79527  
 TNS, electron cyclotron heating startup system, design 0-99330  
 Tokamak, JFT-2, parametric heating by RF near lower hybrid freq. 0-70023  
 Tokamak, JFT-2, particle and heat transport during lower hybrid heating 0-70021  
 Tokamak, low-beta and high-beta regime stable to ballooning modes 0-75083  
 Tokamak, relativistic electron beam injection 0-87910  
 Tokamak, second harmonic electron cyclotron resonance heating 0-64750  
 Tokamak, T-10, stainless steel limiter expts. in ohmic heating region (Russian) 0-83969  
 Tokamak and tandem mirror reactors, neutral beam injection and superconducting magnets 0-63391  
 Tokamak data processing, no. of computers required 0-59252  
 Tokamak discharge microwave preionisation at electron cyclotron resonance 0-83896  
 Tokamak fusion reactors, stable equilibria using supplemental heating 0-91244  
 Tokamak ignition equilibria and thermal stability 0-74005  
 tokamak induction heating coils, 50 kA prototype superconducting cable, critical current 0-106196  
 Tokamak plasma, lower hybrid wave propag. and damping, numerical study 0-64698  
 Tokamak plasma, quasi-mode parametric excitations in lower-hybrid heating 0-64748  
 Tokamak plasmas, advanced-fuel, ignition and thermal stability 0-86970  
 tokamak power reactor, electron cyclotron reson. heating by gyrotrons 0-99331  
 Tokamaks, lower hybrid heating, simulation using BALDUR 1-D transport code 0-92339  
 toroidal plasma, quasispherical liner compression 0-92381  
 toratrons, mag. surfaces, particle orbits, neutral injection 0-79551  
 turbulent plasma, impinged charged particle, linear response theory 0-64727



**plasma heating continued**

- W VII-A stellarator, neutral injection, heating efficiencies, deposition profiles 0-79524
- wall confined shock heated fusion reactor, design 0-99314
- wave trajectories and electron cyclotron heating in Tokamak plasmas 0-83923
- WEGA stellarator, lower hybrid heating 0-79515
- Wendelstein VII-A, neutral beam injectors, performance 0-99389
- $\alpha$ -particle heating of subignited plasma 0-92340
- Ar arc heating, high-pressure complex heat exchange expt. (*Russian*) 0-75112
- Cs, Knudsen arc, electron beam heating and ionisation 0-75114
- (D,T), reaction rate parameter, temp. dependence, fusion process in Maxwellian DT plasma 0-59254
- D ion source for high voltage neutral beams for fusion reactors 0-99379
- Fe XXII, XXIV, XXV, charge exchange recomb. in Princeton large torus during beam heating 0-100067
- H, ACT-1 toroidal plasma, externally launched ion Bernstein wave 0-106967
- H plasma, magnetic piston study in theta-pinch (*Russian*) 0-83971
- H<sub>2</sub> beam discharge, electron kinetics in collisionless non-equilibrium plasma 0-92402
- N glow discharge, volt-ampere charact. in gas flow (*Russian*) 0-106991
- N<sub>2</sub> plasma heating in electrodeless RF capacitive discharge, mechanism, impurity effect 0-59312
- Ti XX 0-100067
- UF<sub>6</sub>, high temp. fissioning plasma core reactors, fluid mechanical confinement 0-63248

**plasma impurities**

- see also *plasma-wall interactions*
- atomic processes determining the plasma-wall interaction 0-59247
- Columbia Torus-1 belt pinch high beta toroidal device, preionisation, optimisation 0-92368
- conductivity, electrical, classical, plasma impurities, Sonin polynomial distrib. function (*Russian*) 0-83894
- divertorless Tokamaks, limiter pumping system 0-95463
- DTHR, advanced bundle divertor design 0-99281
- flow reversal expt., result anal. 0-106875
- fusion reactor, STARFIRE project, impurity control system 0-102345
- gas stream with dispersive impurity, initial region boundaries, impurity velocities (*Russian*) 0-100069
- high beta toroidal device, preionisation, optimisation 0-92368
- high-Z emitters in ultradense plasmas, hydrogenic profiles, perturbing ion effects 0-79566
- ISX-B tokamak, design of bundle divertor expt. 0-102341
- JFT-2 Tokamak, impurity ion sputtering 0-79554
- magnetic confinement system, surface problems caused by dissolved H<sub>2</sub> 0-57946
- MFTF, plasma buildup, contaminant control 0-95461
- microarcing studies in low temp. RF-plasma 0-96407
- multiply charged, electron capture into different excited states in plasma 0-64679
- neo-Z-pinch, mag. fusion appls. 0-103180
- PDX Tokamak, surface analysis station 0-79586
- LiD, D<sub>2</sub> flux and energy incident on probe, power balance, impurity generation 0-79553
- PULSATOR, impurities in high density regime 0-79579
- reactor ignition, overheated underdense Tokamak plasma, two-zone model and 1-D transport code 0-63376
- rotating plasma reactors, longitudinal confinement, stability equilibrium and heating problems 0-74001
- superbanana limiter as a possible edge cooling scheme 0-92362
- TFR Tokamak at ionisation equilibrium, heavy impurities 0-106970
- TFR Flexibility Modification, in-torus surface pumping, Ti and Zr/Al gettering 0-95451
- theta-pinch Ti ion injection by CO<sub>2</sub> laser, spectroscopic anal. 0-79577
- Thor Tokamak, wall conditioning by cleaning H discharges 0-78440
- Tokamak, anomalous diffusion with light and heavy impurities, drift wave depend. 0-64677
- Tokamak, edge effects and impurities, influence on thermal stability 0-87892
- Tokamak, impurity transport (*Russian*) 0-106957
- Tokamak, metal impurity reduction by working gas injection 0-106963
- Tokamak fusion reactor, RF injection for refuelling and impurity control 0-87921
- tokamak impurity-control techniques 0-75082
- Tokamak plasma, line spectra of highly ionised heavy atoms 0-79567
- Tokamak TO-1, feedback system effect on plasma parameters (*Russian*) 0-103174
- Ar arc plasmas, steady-state and decaying, mol. gas impurities 0-103177
- Cs, trace identification in neutral-beam research 0-95401
- Fe IX, X, XI, effective dielectronic recombination rates in H plasma, emission time histories 0-79570
- H<sub>2</sub> contamination in He plasma, satellites of He 492.2 nm line, fine struct. interpretation 0-59235
- Mo impurity flux, time resolved, in DITE Tokamak 0-63373
- N<sub>2</sub> plasma heating in electrodeless RF capacitive discharge, mechanism, impurity effect 0-59312
- Na, trace identification in neutral-beam research 0-95401
- Ti impurity flux, time resolved, in DITE Tokamak 0-63373

**plasma in solids** see *solid-state plasma***plasma instability**

- see also *plasma oscillations*
- absolute dissipative drift-wave instabilities in Tokamaks 0-92296
- adiabatic invariant J, finite- $\beta$  effect in axisymmetric tokamaks 0-79538
- advanced fuel fusion reactor wall loading limitations and stability index beta 0-99311
- air, wall-stabilised arc, step and sinusoidal current change response 0-103209
- air plasma, optical emission, localised oscill. mode obs. 0-83903
- Alfvén ion cyclotron mode in diffuse high-beta plasmas, local stability 0-92294
- Alfvén mode, current driven, electron-ion collisions and full dispersion function, numerical anal. 0-64726
- Alfvén nonlinear gravit. drift waves and  $\beta$  limitations in Tokamaks 0-92369
- Alfvén-ion cyclotron instability, stabilisation in inhomogeneous media 0-59210

**plasma instability continued**

- anomalous drift wave transport in high temp. plasmas, thermodynamic stability 0-69980
- anomalous transport from plasma waves 0-59182
- anomalous transport processes in radially compressed reversed-field configurations, numerical simulation 0-64689
- anomalous viscosity due to EM instability in turbulent plasma 0-106901
- anomalous viscosity due to EM instability in turbulent plasma, nonlinear theory 0-106902
- antiparallel structure build-up and stability in systems with mag. barrier 0-92371
- axis encircling ion gyro-instability 0-79494
- axis encircling ion gyroinstability 0-64715
- axisymmetric high-beta tandem-mirror reactor, MHD stability 0-75042
- axisymmetric mirror machine, MHD stable confinement possibilities 0-83988
- axisymmetric mirror machines, long thin approx., stability and field singularity 0-83933
- ballooning effect in flute oscillations and plasma stability limits in ambipolar trap (*Russian*) 0-106955
- ballooning modes in low-beta and high-beta Tokamak 0-75083
- ballooning stable profiles in circular Tokamaks 0-92317
- beam-plasma instability singularities, anomalous Doppler effect 0-75040
- beta limits for Tokamak experiments 0-83937
- Buneman instability and steady-state parameters in collisionless single ended Q-machine 0-59227
- Buneman instability nonlinear saturation 0-79467
- cold electron beam in pure runaway regime, collective drag and instabilities 0-83949
- collapse instability nature in Tokamak, surface currents (*Russian*) 0-92310
- colliding relativistic plasma instabilities with relativistic temps. (*Russian*) 0-83913
- collisional drift modes, anomalous skin effect, enhanced particle penetration during fuelling, nonlinear theory 0-64703
- collisional plasma, modulation instability, turbulence by const. wave pumping (*Russian*) 0-103139
- collisionless contact discontinuity, stability, astrophys. appls. 0-62002
- collisionless drift instability, discrete unstable modes, transition to turbulence, theory and expt. 0-59240
- collisionless mirror instability, of equatorial protons in Jupiter mid-magnetosphere 0-67642
- collisionless plasma, polarisation by single-mode pot. drift wave 0-106920
- collisionless sheath stability 0-106936
- computerised analysis, collaboration collection report 0-73106
- conductors with MHD sausage instabilities, elec. resist. 0-100076
- coupled mode equations, linearised, space time solns. 0-87884
- coupled resistive g/ion temperature gradient instability 0-79481
- coupled three wave system, instability saturation, bifurcations and strange attractor 0-59233
- criterion for absolute instability of a wave in a nonuniform medium 0-106903
- current convective instability in auroral zone, rel. to localised nighttime scintillation enhancements 0-98506
- current driven modes, cold mantle systems, stability props. 0-92287
- current-driven collisional drift and Alfvén instabilities in sheared mag. field 0-92286
- current-driven HF drift wave, inhomogeneous plasma instability 0-59204
- cylindrically symmetric mirror plasma, shear stabilisation 0-83978
- destabilization of drift-universal eigenmodes by toroidal effects 0-103148
- diffuse linear pinch, dispersion differential eqn. in MHD, approx. 0-64694
- dispersion relation for instability hindrance in a magnetically confined plasma with finite press. 0-59221
- dissipative balloon non-threshold modes (*Russian*) 0-70000
- double layer formation in multiple plasma device 0-83897
- double layers, electric field collapse phenomena, Buneman instability (*Russian*) 0-79476
- double tearing mode, linear anal. 0-92277
- draft waves driven by temperature gradients, ballooning limit 0-106917
- drift cone mode instability simulation 0-83930
- drift cyclotron loss cone instability, nonlinear saturation 0-83929
- drift mode, current driven, electron-ion collisions and full dispersion function, numerical anal. 0-64726
- drift wave eigenmodes, effect of finite ion Larmor radius (*Chinese*) 0-103133
- drift waves, eigenmodes with arbitrary radial wavelengths, stability 0-64710
- drift-dissipative instability suppression in lower-hybrid pump wave field 0-106921
- drift-mode stability analysis for the Tandem Mirror 0-64704
- electric field compression near a plasma electrode 0-64736
- electron beam relaxation in high density weakly ionised gas (*Russian*) 0-106943
- electron beam stabilised mirror confined gas, hot electron population study 0-100089
- electron beam stopping process in hydrodynamic stage of streaming instability, boundary value treatment 0-103164
- electron beam-magnetoplasma, radiation at or near electron plasma frequency, transverse modes 0-106942
- electron beams, modulated, non-linear oscillation theory (*Russian*) 0-106898
- electron Bernstein modes, nonlinear scatt. of upper hybrid laser radiation 0-64720
- electron cyclotron instability suppression by selective cyclotron damping 0-83939
- electron cyclotron resonance heating of Tokamak plasmas, fluctuations and instability 0-83956
- electron kinetic instability in Cassiopeia A, rel. to radio spectrum secular flattening 0-101637
- electron magnetised plasma, stability in circularly polarised EM wave field 0-87897
- electron plasma cooling by cyclotron radiation 0-69986
- electron temperature gradient driven microtearing mode 0-96361
- electronegative gas discharge, spontaneous oscils. 0-87977
- electrostatic drift instability of Tokamak plasmas 0-96358
- electrostatic flow shear instability, theory and appl. to magnetopause and solar wind and appl. to 0-96359
- electrostatic instability, ion-cyclotron, current-driven, TFR Tokamak 0-64711



**plasma instability continued**

- electrostatic ion cyclotron instability driven by a deflected ion beam 0-87879
- electrostatic microinstabilities, transport theory 0-79443
- electrostatic parametric instability, due to thermal coupling 0-79465
- electrostatic waves in magnetosphere, rel. to inverse loss cone electrons temp. anisotropy relaxation (*Russian*) 0-109314
- EM instability of relativistic electron beam penetrating in infinite plasma, collisional effects 0-64725
- EM oscill. spectrum, toroidal plasma-containing system 0-79471
- EM wave dissipation and superstrong turbulence in inhomogeneous plasma (*Russian*) 0-83919
- equilibrium and stability of high- $\beta$  toroidal multipoles 0-64769
- equilibrium currents, effect on separatrix characts. in  $l=3$  stellarator 0-64706
- ERA compression system, IPP-Japan 0-95490
- explosive instabilities, nonlinear perturbation 0-59199
- explosively unstable waves, in ion beam-plasma system, pump field method obs. 0-92333
- field reversed pinches, microinstability effect on MHD stability 0-79460
- finite- $\beta$  plasma, crit. conditions for drift, drift-Alfvén and drift-tearing instabilities in sheared mag. field 0-64699
- fission reactor, gas-discharge, fuel element component conc., plasma temp. profile instabilities 0-63253
- flute modes, similar freq., simultaneous feedback stabilisation 0-103146
- forced oscills. generated by point antenna, drifting plasma (*French*) 0-79470
- FT-1 Tokamak, discharges in low density plasma (*Russian*) 0-106958
- fusion reactors, liquid metal linear implosion systems with blade lattice for rotational stabilisation 0-73994
- Garching Belt-Pinch IIa, effect of  $q$  on confinement and stability 0-96384
- gas discharge instability near electrode 0-70064
- gas flow, nonequib. ionisation and Hall EMF 0-69981
- glow discharge, superheating ionisation instability with rot. elec. field 0-79611
- gravitational instability of rot. plasma, effect of suspended particles 0-109347
- gravitational instability of self-gravitating isotropic press. plasma theory 0-72763
- gyrokinetic modes, spatial struct. in toroidal geometry 0-79489
- Hall current and gyroviscosity effect on conducting, rotating viscous plasma stability 0-75041
- heat flux limitation by ion-acoustic instability 0-92304
- heavy-particle acceleration by charge-density waves in vacuum and in plasma 0-70044
- helical equilibria, stability code ERATO 0-79493
- hexapole Tokamak, axisymmetric jumps, interpretation 0-106966
- HF discharge, ionisation overheat instability in EM wave field (*Russian*) 0-106990
- high beta plasma surrounded by cond. shell, dynamic stabilisation 0-96354
- high density plasma stability in multiple mirror 0-79483
- high temperature plasma, physics, book 0-98767
- high-beta flux conserving equilibrium, resistive magnetic flux diffusion 0-87873
- high-beta Tokamak plasma, stability to ballooning modes 0-75091
- high-beta toroidal plasma, stable confinement in levitated octupole 0-75090
- high-n ballooning theory, stability of axisymmetric tokamak equilib. 0-64705
- imploding plasma liners, MHD instability effects 0-75081
- instability of two dimensional waves, critical drift velocities, oscill. growth factor (*Russian*) 0-106922
- intense relativistic electron beam-plasma system, coupled transverse oscillations, kinetic description 0-64741
- interaction of plasma with strong EM wave, efficient transformation of radiation frequency 0-106931
- interchange stability of axisymmetric field reversed equilibria 0-59214
- internal kink mode in Tokamaks 0-92318
- ion acoustic instability in polar cap ionosphere, rel. to plasma flow entry region position 0-67472
- ion beam-plasma system, absolute and convective instabilities of electrostatic ion cyclotron waves 0-64740
- ion pressure gradient driven drift modes; 3-dimens. fluid simulation 0-103150
- ion temp. and parametric decay development in RF-generated stellarator plasma 0-79436
- ion-acoustic instability, double layer form., numerical simulation 0-59220
- ion-acoustic instability in solar wind, wave-particle interactions rel. to particle vel. distrib. (*German*) 0-109323
- ionosphere-plasma interaction with gravity waves, elec. field and current prod. 0-61957
- Kelvin-Helmholtz instability at magnetopause, rel. to magnetosphere hydromag. energy spectra 0-67476
- Kelvin-Helmholtz instability through porous medium of two superposed plasmas 0-106886
- kinetic ballooning modes, theory 0-79484
- kinetic equations for low frequency instabilities in inhomogeneous plasmas 0-83886
- kink instabilities of a plasma column with elliptical cross-section 0-79495
- Langmuir collapse, dimensionality and dissipation 0-87880
- Langmuir localised perturbation, spontaneous radiation emission 0-69987
- Langmuir turbulence, numerical modelling, solitons, nonlinear interactions 0-70030
- laser discharge, high-power, stabilisation with mag. field 0-99739
- laser driven implosions, hydrodynamic instabilities 0-64756
- laser light parametric absorpt., convective parametric instability 0-100073
- laser plasma, convective parametric decay instability 0-64722
- laser produced plasma, parametric instabilities in two electron temp. plasma (*Japanese*) 0-96377
- laser produced plasma, three halves harmonic spectra, time resolved obs. 0-79529
- linear stability of high-m drift-tearing modes 0-64716
- linearly unstable mode stabilisation by reson. nonlinear coupling to damped modes 0-59234
- local sufficient condition for MHD stability in closed line systems 0-83910
- lower hybrid wave turbulence effect on tearing mode instability 0-92322

**plasma instability continued**

- lower hybrid waves, current-driven electrostatic ion-cyclotron instability 0-103149
- lower-hybrid waves in collisional plasmas with field-aligned current instability 0-75045
- magnetic driving energy of the collisional tearing modes 0-92301
- magnetic field instability of plasma in EM beam 0-64745
- magnetically confined plasma, external conducting open sheet, stability effects 0-92302
- magnetised, parametric instabilities with well separated freq. (*Chinese*) 0-106887
- magnetised plasma stability in large amplitude circularly polarised wave dispersion relations 0-59223
- magneto-parametric instabilities, two-fluid model 0-85851
- magnetoactive plasma, modulational instability caused by Langmuir oscillations 0-92297
- major disruptions in the TOSCA Tokamak 0-83979
- medium beta plasma with velocity gradients, dispersion relation for drift waves 0-64719
- MHD, generalised Lorenz eqns., strange attractors 0-59232
- MHD, stability code, ERATO, convergence of solns. 0-83906
- MHD, toroidal axisymmetric config., vacuum potential energy change spectral codes 0-87869
- MHD devices, plasma ionization instability, dynamic suppression, switching modeling 0-59308
- MHD instability stabilisation by force free mag. fields 0-83911
- MHD stability analysis of axisymm. surface current model equilibria for  $N=0$  and  $\neq 0$  modes 0-92276
- MHD-instability and limiting currents during Ohmic heating in stellarator Uragan-2 (*Russian*) 0-106881
- MHD-ZZ (*Russian*) 0-106945
- microinstabilities in field reversed Z pinches, persistence of MHD stability 0-87872
- microinstabilities in inhomogeneous plasma with incident  $\alpha$ -particle beam effect on stopping power 0-64742
- microtearing modes and anomalous transport in Tokamaks, self consistent calc. 0-59222
- microtearing modes and anomalous transport in Tokamaks 0-92316
- microwave p-n diode modulator, transient plasma instability meas. (*German*) 0-87942
- mode converted lower hybrid solitons, stability in parametric region 0-92303
- modulated electron beams, instability, spatially separated in plasma 0-70012
- modulation instability and inhomogeneous Langmuir fields in plasma (*Russian*) 0-106894
- modulational instability of nonlinear wave propagation in relativistic plasmas 0-106911
- multi-ion system, modulation instability of ion acoustic waves 0-69996
- negative ion beam instability spatial development in rarefield gas (*Russian*) 0-92314
- negative shear ferromak for stabilization of current disruptions in toroidal discharge 0-106971
- nonlinear cross-field ion acoustic instability and plasma heating 0-83922
- nonlinear magnetostatic modes and twisting modes with magnetic islands 0-106900
- nonlinear mode coupling and saturation of decay instability in ion beam-plasma system 0-83931
- nonlinear mode coupling model equations, topological struct. 0-75056
- nonlinear theory of collisional drift-waves in toroidal geometry and anomalous skin effects in Tokamaks 0-92320
- nonlinear theory of unstable plane waves and solitons 0-87888
- nonlinear three wave mode coupling, instability saturation 0-87881
- nonlinear time-dependent hydromagnetic model, spatial and temporal finite-difference techniques 0-59192
- numerical simulation of disruptions and loss in Tokamak plasma 0-70026
- oblique Langmuir solitons under free path conditions (*Russian*) 0-79477
- origin of galaxies in expanding Universe, plasma cond. and instabilities, MHD soln. 0-62283
- oscillations spatial mode stabilisation algorithms 0-64721
- overdense column, reson. microwave absorpt. 0-64732
- overheat acoustic instability in pulsed laser discharge (*Russian*) 0-103142
- parametric, microwave p-n diode modulator, transient plasma instability meas. (*German*) 0-87942
- parametric instabilities, cascade saturation induced by monochromatic driver pump 0-79491
- parametric instabilities of inhomogeneous plasma in presence of long-wave low frequency oscillations (*Russian*) 0-103136
- parametric instabilities set up by EM radiation in non-uniform magnetoactive plasma (*Russian*) 0-106889
- parametric instability, exact soln. for non-uniform plasma and pumping field (*Russian*) 0-83920
- parametric instability, thermal fluctuation effect in inhomogeneous plasma (*Russian*) 0-106897
- parametric instability due to a low frequency whistler wave 0-83926
- particle beam instabilities in plasma media with absorption 0-64743
- peeling instability in toroidal MHD equilibrium configuration 0-79488
- pinch, thin-skin, stability, influence of thick conducting liner and superconducting wall, dispersion relation 0-64766
- plasma transport, anomalous, electron temp. gradient instability 0-75034
- position instability analysis, effective mode approx. in Tokamak 0-103145
- positional stability of a current-carrying plasma in an  $l=2$  stellarator field 0-106906
- positive column of high-voltage diffuse discharge, nonstationary processes 0-64802
- potential small-scale instabilities of inhomogeneous plasma in crossed electric and magnetic fields 0-79492
- pressure driven ballooning modes, numerical studies 0-92282
- proton-cyclotron instabilities, in non-uniform loss-cone magnetospheric plasma 0-90286
- Pulsator Tokamak discharges with AC modulation 0-96386
- QUISTOR, space charge and ion stability 0-86487
- radial stability of density profiles for obliquely incident light 0-92350
- reactor, Tokamak, toroidal magnetic field ripple, burn control 0-63375
- relativistic electron beam, intense, coupled dipole oscills. 0-64739
- relativistic electron beam in magnetised plasma, relax. processes, nonlinear theory, instability (*Russian*) 0-103162
- relativistic electron beam-plasma instability, macro- and microscopic models 0-75065
- relativistic electron beams, EM instability and stopping power of plasmas 0-92289



**plasma instability continued**

relativistic MHD growth and decay discontinuities 0-92280  
 relativistically covariant formulation in theory of plasma stability 0-75046  
 resistive g mode, parallel viscosity influence 0-79486  
 resistive hose instability in relativistic electron beam 0-67947  
 resistive-g and ion temp. gradient in sheared magnetic field 0-64708  
 reverse loss-cone instability in bipolar trap (*Russian*) 0-106893  
 reversed field configuration, equilibrium and stability and confinement props. 0-87932  
 reversed field pinch expt. in small compact torus STP-1 0-75043  
 reversed-field pinch plasma model 0-87935  
 RF emission, plasma wave scatt. by ion-acoustic waves in nonequilibrium plasma 0-64733  
 ripple loss of fast ions in a large Tokamak 0-92382  
 rotating plasma, MHD stability criterion 0-79487  
 rotating plasma reactors, longitudinal confinement, stability equilibrium and heating problems 0-74001  
 rotation instability on collisionless FLR plasma, nonlinear theory 0-79485  
 runaway electron induced microscopic instabilities (*Chinese*) 0-103134  
 screw instability of finite cond. gas (*Russian*) 0-92311  
 screw-pinch, equilibrium and stability 0-87934  
 self heating and saturation due to numerical instabilities 0-75067  
 shear flow stability and Alfvén waves in magnetised plasma 0-96360  
 sheared systems, low- $\beta$  plasma, MHD interchange instability 0-64717  
 solar flare plasma instability and turbulence, review 0-62100  
 solar wind, stream interaction regions, microscale instabilities 0-72739  
 spheromak devices, magnetohydrostatic equilibrium config. 0-83965  
 spheromak, ideal MHD stability 0-92281  
 Spheromak fusion reactors, MHD equil. and stability, numerical anal. 0-74000  
 stable route to the high  $\beta_p$  regime 0-92319  
 stellarator, MHD equilibrium and stability of plasma in toroidal geometry, 3-D computer code 0-70041  
 stellarator fields,  $m=2$  tearing mode, linear growth rate 0-75037  
 stellarators, equilibrium and stability calcs. 0-83982  
 stochastic instability control in tokamak by pulsed RF modulation 0-59245  
 stochastic mag. field fluctuations, self-consistent model 0-100074  
 strong turbulence effects on the kinetic beam-plasma instability 0-59207  
 strongly turbulent stabilization of electron beam-plasma interactions 0-59251  
 surface waves, HF, parametric excitation using slanted, incident EM waves (*Russian*) 0-87874  
 SW parametric instability of inhomogeneous plasma, semi-bounded by vac. (*Russian*) 0-83917  
 tearing instability in background plasma, relativistic modes 0-62012  
 tearing modes, ion dynamics effects, eigenmode eqns. 0-59212  
 thermal instability, mag. field generated, in laser heated plasma, hydrodynamic effects 0-96355  
 thermal parametric instability, effect of recomb. processes 0-61967  
 thermal-convective instability of partially ionized plasma, radiative transfer, medium porosity and collisional effects 0-67538  
 thermionic triode, oscils. in low press. inert gas discharge 0-79590  
 thermonuclear instability and fueling, cold plasma layer surface fueling source 0-59196  
 theta pinch, low density, step-like mag. piston 0-103182  
 thin foil layered targets, Rayleigh-Taylor instability in laser irradiation 0-87876  
 thin line cusp magnetoplasma sheath, RF feedback stabilisation 0-70009  
 Tokamak, anomalous diffusion with light and heavy impurities, drift wave depend. 0-64677  
 Tokamak, edge effects and impurities, influence on thermal stability 0-87892  
 tokamak, horizontal plasma position control by feedforward-feedback system with digital computer 0-75093  
 Tokamak, ideal MHD stability 0-59216  
 Tokamak, JFT-2, parametric heating by RF near low hybrid freq. 0-70023  
 Tokamak, large aspect ratio, two-dimens. drift-wave stability 0-79479  
 Tokamak, non circular, small-aspect-ratio, high mode number ballooning instabilities, max.  $\beta$ -value 0-73995  
 Tokamak, nonlinear perturbation, feedback effect (*Russian*) 0-83967  
 Tokamak, small aspect ratio, flat current noncircular, unstable MHD spectrum 0-69989  
 Tokamak, stochastic particle orbits, statistical description 0-79466  
 Tokamak, T-10, stainless steel limiter expts. in ohmic heating region (*Russian*) 0-83969  
 Tokamak and CTR reactors, mobile diaphragm operation mode (*Russian*) 0-83966  
 Tokamak fusion reactors, stable equilibria using supplemental heating 0-91244  
 Tokamak high beta stability 0-96383  
 Tokamak ignition equilibria and thermal stability 0-74005  
 Tokamak plasma, Thomson scatt. with repetitively Q-switched ruby laser 0-59271  
 Tokamak plasmas, advanced-fuel, ignition and thermal stability 0-86970  
 Tokamak TO-1, feedback system effect on plasma parameters (*Russian*) 0-103174  
 Tokamak trapped particles, interaction in amplitude moderated RF fields 0-79497  
 Tokamak with non-circular cross-section, ballooning modes, stability (*Russian*) 0-103141  
 Tokamaks, computer simulation of trapped electron modes 0-106874  
 Tokamaks, ideal MHD mode stabilisation and optimisation 0-79480  
 Tokamaks, injected ion loss due to spatial field ripple 0-92321  
 Tokapole II, non-circular Tokamak, axisymmetry instability 0-87877  
 toroidal axisymmetric plasma, ideal and resistive ballooning modes 0-83936  
 toroidal geometry, characterisation of the essential spectrum of an operator rel. to plasma stability (*French*) 0-92284  
 trapped ion eigenmodes, two dimens. anal. 0-83935  
 trapped particle anomalous transport in Tokamak, scaling laws 0-103115  
 turbulent plasma, parametric instabilities, anomalous energy absorpt., dispersion eqn. 0-92291  
 two Langmuir wave parametric decay instability, self-trapped EM pump wave effects 0-96357  
 two-stream instability, occurrence in collisionless shocks at high Mach numbers 0-87893

**plasma instability continued**

two-stream plasma, development of instability of dispersed waves (*Russian*) 0-103138  
 vibrational kinetics and plasma characs. in CO-N<sub>2</sub> discharge 0-59331  
 Vlasov equilibria, local Maxwellian velocity distribution 0-87928  
 W VII-A (2,1) tearing mode depend. on stellarator field 0-79550  
 wave-particle transport from electrostatic instabilities 0-83898  
 Weibel instabilities, temp. anisotropy driven, statistical thermodynamics 0-75047  
 Z discharge relaxation between electrodes 0-75089  
 Zeta plasma, field line reconnection and density fluctuations 0-69975  
 CO<sub>2</sub>-N<sub>2</sub> electroionisation laser mixture, ionisation instability of semi self maintaining discharge 0-63971

**plasma interactions** see *plasma collision processes***plasma jets**

heat transfer rates to flat plate from normally-impinging N plasma jet 0-75061  
 high velocity jets generated by plasma focus and shock-wave expt., temp. and density meas. (*Russian*) 0-106882  
 laser beam focused in plane target, jet form., investigation using wavefront method 0-75103  
 magnetoplasma dynamic arcjet, density meas. by CO<sub>2</sub> laser interferometry 0-59277  
 Ar, optical studies using Schlieren and shadow methods 0-59279  
 H $\alpha$  and H $\beta$ , Stark profiles, ion-motion effect 0-63592  
 He I 447.1 and 492.2 nm lines, ion motion effects on Stark profiles 0-69105  
 N, high intensity arcs, anode contraction region modeling 0-103210  
 Xe, radiating, bulk energy distrib. 0-75107  
 Y<sub>2</sub>O<sub>3</sub> capillary discharge plasma, temp., radiation screening elimination 0-64682

**plasma magnetohydrodynamics**

accelerators, electrodynamic characs. 0-64788  
 Alfvén waves, soln. for MHD equations, properties (*Russian*) 0-106891  
 anisotropic MHD turbulence in solar wind, obs. 0-94669  
 anisotropic plasma, relativistic MHD 0-92380  
 anisotropically conducting plasma in inhomogeneous elec. and mag. fields, current calc. (*Russian*) 0-74995  
 anomalous transport processes in radially compressed reversed-field configurations, GIM/HYBRID quasi-equilib. MHD code 0-64689  
 arcjet, density meas. by CO<sub>2</sub> laser interferometry 0-59277  
 cathode, sheaths in K<sub>2</sub>CO<sub>3</sub> seeded petroleum MHD combustion plasma 0-87870  
 collisionless plasma, Chew-Goldberger-Low theory with finite Larmor radius corrections 0-75024  
 conductors with MHD sausage instabilities, elec. resist. 0-100076  
 convection, two velocity hydrodynamic eqn. solution (*Russian*) 0-79459  
 current sheet, near line of zero mag. field, numerical anal. (*Russian*) 0-83908  
 current-driven collisional drift and Alfvén instabilities in sheared mag. field 0-92286  
 diffuse linear pinch, dispersion differential eqn. in MHD, approx. 0-64694  
 DITE, low Q discharges 0-92374  
 double tearing mode, linear anal. 0-92277  
 drift-mode stability analysis for the Tandem Mirror 0-64704  
 EBT, toroidal MHD equilibrium 0-87871  
 equilibrium, with axisymmetry and noncircular cross section, free boundary soln. to eqn. (*Chinese*) 0-59260  
 exploding wire burst phase, simulation by one-dimens. MHD code 0-75080  
 Faraday MHD generator-operating region 0-103132  
 field reversed pinches, microinstability effect on MHD stability 0-79460  
 finite- $\beta$  plasma, crit. conditions for drift, drift-Alfvén and drift-tearing instabilities in sheared mag. field 0-64699  
 flux conserving Tokamak MHD equilibrium evolution 0-75088  
 force-free analytical three dimensional toroidal MHD-equilibria of arbitrary cross section 0-106885  
 generalised Lorenz eqns., strange attractors 0-59232  
 gravitational instability of rot. plasma, effect of suspended particles 0-109347  
 Hall current and gyroviscosity effect on conducting, rotating viscous plasma stability 0-75041  
 HF heating by MHD waves of finite press. plasma (*Russian*) 0-83950  
 high temperature plasma, physics, book 0-98767  
 high-beta flux conserving equilibrium, resistive magnetic flux diffusion 0-87873  
 high-n ballooning theory, stability of axisymmetric tokamak equil. 0-64705  
 hydromagnetic eqns. for infinitely long plasma cylinder, unstable soln., pulsar mag. fields 0-96352  
 imploding plasma liners, MHD instability effects 0-75081  
 incompressible viscous fluid, MHD flow past accelerated plate, Hall effects 0-92275  
 instability and Ohmic heating of plasma in apparatus with spatial axis (*Russian*) 0-106945  
 interchange stability of axisymmetric field reversed equilibria 0-59214  
 ion beam, pulsed, incident on mag. barrier, virtual anode form. 0-103131  
 ion-acoustic waves, soln. for MHD equations, properties (*Russian*) 0-106891  
 ionization instability, dynamic suppression, switching modelling of MHD device 0-59308  
 laser targets, dynamics, 2-D three-temperature MHD model 0-70014  
 line sources, elec. and mag., interaction with moving magnetoplasma slab, EM radiation 0-67537  
 local sufficient condition for MHD stability in closed line systems 0-83910  
 magnetic island coalescence, 2-dimens. MHD eqns. 0-64695  
 magneto-acoustic waves, soln. for MHD equations, properties (*Russian*) 0-106891  
 merging of two current carrying plasma columns, solar flare exptl. simulation (*Japanese*) 0-94775  
 MHD instability stabilisation by force free mag. fields 0-83911  
 MHD-instability and limiting currents during Ohmic heating in stellarator Uragan-2 (*Russian*) 0-106881  
 microinstabilities in field reversed Z pinches, persistence of MHD stability 0-87872  
 nonequilibrium plasma MHD flow between parallel discs, tangential vel. effects 0-64697  
 nonlinear axisymmetric MHD equilibria, numerical soln. 0-79461



**plasma magnetohydrodynamics continued**

- nonlinear time-dependent hydromagnetic model, spatial and temporal finite-difference techniques 0-59192  
 nova outburst, equatorial belt formation, plasma current rings model, double adiabatic MHD 0-67757  
 origin of galaxies in expanding Universe, plasma cond. and instabilities, MHD soln. 0-62283  
 particle acceleration by MHD shock turbulence 0-87894  
 peeling instability in toroidal MHD equilibrium configuration 0-79488  
 pinch effect, dynamical accumulation towards neutral line of magnetic field 0-83977  
 plasma focus, fast high voltage, current and neutron yield scaling 0-64752  
 pressure driven ballooning modes, numerical studies 0-92282  
 relativistic MHD growth and decay discontinuities 0-92280  
 relativistic MHD symmetric flows eqn. of motion (*Russian*) 0-83992  
 reversed field pinch expt. in small compact torus STP-1 0-75043  
 rotating plasma, MHD stability criterion 0-79487  
 rotation of a classical toroidal plasma 0-59193  
 shear Alfvén waves, quasi-linear theory 0-64714  
 shear flow stability and Alfvén waves in magnetised plasma 0-96360  
 sheared systems, low- $\beta$  plasma, MHD interchange instability 0-64717  
 shock, MHD, superadiabatic excitation in collisionless plasma 0-79503  
 spheromak, ideal MHD stability 0-92281  
 Spheromak fusion reactors, MHD equilb. and stability, numerical anal. 0-74000  
 stability analysis of axisymm. surface current model equilibria for  $N=0$  and  $n=0$  modes 0-92276  
 stability code, ERATO, convergence of solns. 0-83906  
 stationary MHD eqns. for rotating toroidal plasma 0-92278  
 stellarator, MHD equilibrium and stability of plasma in toroidal geometry, 3-D computer code 0-70041  
 stellarator equations of motion calcs. 0-103198  
 stellarator fields,  $m=2$  tearing mode, linear growth rate 0-75037  
 stochastic mag. field fluctuations, self-consistent model 0-100074  
 strange attractor for MHD flow 0-59194  
 supersonic flow of combustion products, nonequilibrium physicochemical processes, open-cycle MHD generator 0-103196  
 thermal mode ray trajectory in inhomogeneous magnetoplasma 0-106884  
 thermal-convective instability of partially ionized plasma, radiative transfer, medium porosity and collisional effects 0-67538  
 Tokamak, ideal MHD stability 0-59216  
 Tokamak, plasma MHD equilb., var. method (*Russian*) 0-106960  
 Tokamak, small aspect ratio, flat current noncircular, unstable MHD spectrum 0-69989  
 Tokamak blanket, liq. Li module stresses due to changing poloidal mag. field 0-95435  
 Tokamak equilibrium, inverse problem, iterative metric method 0-106883  
 Tokamak plasma, control systems, construction and simulation study (*Japanese*) 0-100100  
 Tokamaks, ideal MHD mode stabilisation and optimisation 0-79480  
 Tokapole II, non-circular Tokamak, axisymmetry instability 0-87877  
 toroidal axisymmetric config., vacuum potential energy change, spectral codes 0-87869  
 toroidal pinch discharge, preionisation phase, numerical computation 0-64696  
 turbulence, 2-D, hydrodynamic and plasma applications, dynamical eqns., diffusion, MHD, superfluidity, review 0-69769  
 very-low-q discharges in DIVA confinement and MHD characts. 0-64765  
 vibrations in toroidal confinement with special parameter distrib. 0-83909  
 wave growth and decay in high temp. gas 0-79458  
 CO<sub>2</sub>-N<sub>2</sub> electroionisation laser mixture, ionisation instability of semi self maintaining discharge 0-63971  
 Cs-Xe solar-pumped MHD excimer laser, modelling 0-95873  
 H plasma, freely expanding, population inversion obs. 0-95877  
 N<sub>2</sub>-H<sub>2</sub> arc, bent and rot., flow mechanism 0-70047

**plasma measurement techniques** *see plasma diagnostic techniques***plasma oscillations**

- see also plasma waves*  
 axially-symmetric ambipolar trap, flute oscills. stability limits (*Russian*) 0-103176  
 axisymmetric plasma equilibrium, stability 0-106915  
 Chirikov-Taylor model, turbulent diffusion calc. 0-79469  
 collisional plasma, modulation instability, turbulence by const. wave pumping (*Russian*) 0-103139  
 distribution function for inhomogeneous plasma 0-59218  
 drift-dissipative instability suppression in lower-hybrid pump wave field 0-106921  
 echo in semi-bounded plasma, electrostatic sheath potential profiles for boundary 0-64712  
 electron beams, modulated, non-linear oscillation theory (*Russian*) 0-106898  
 electron nonlinear waves in strongly magnetised plasma 0-79472  
 EM oscill. spectrum, toroidal plasma-containing system 0-79471  
 EM wave in inhomogeneous magnetoactive plasma, total absorpt. effect (*Russian*) 0-106944  
 EM waves, nonlinear generation in electron-positron plasma (*Russian*) 0-106973  
 field emission medium energy diode, electron flow, HF oscills. 0-79582  
 flute oscillations and plasma stability limits in ambipolar trap, ballooning effect (*Russian*) 0-106955  
 forced oscills. generated by point antenna, drifting plasma (*French*) 0-79470  
 hemispherical monopole surrounded by plasma layer, Tonks-Dattner reson. and input admittance 0-87887  
 inhomogeneous beam-plasma system, continuous oscill. spectrum (*Russian*) 0-106937  
 instability of two dimensional waves, critical drift velocities, oscill. growth factor (*Russian*) 0-106922  
 intense relativistic electron beam-plasma system, coupled transverse oscillations, kinetic description 0-64741  
 ion-acoustic fluctuations, CO<sub>2</sub> laser study 0-83946  
 ionisation wave, obs. of phase modulation 0-69993  
 Langmuir oscills., 2-dimens. distrib., critical rate of collapse (*Russian*) 0-106896  
 Langmuir turbulence, numerical modelling, solitons, nonlinear interactions 0-70030  
 laser-target impact, HF oscill. excitation (*Russian*) 0-92353  
 low-freq. oscillation spectrum in weakly ionised plasma 0-87885

**plasma oscillations continued**

- lower hybrid waves, current-driven electrostatic ion-cyclotron instability 0-103149  
 magneto-acoustic oscillations, pressure and viscosity effects 0-79464  
 magnetoactive plasma, modulational instability caused by Langmuir oscillations 0-92297  
 microtearing modes and anomalous transport in Tokamaks, self consistent calc. 0-59222  
 negative ion beam instability spatial development in rarefield gas (*Russian*) 0-92314  
 noncircular Tokamak, time evolution of elongation ratio and Mirnov oscill. 0-64763  
 nonlinear theory of unstable plane waves and solitons 0-87888  
 nonlinear wave packet acceleration and slowing down 0-59203  
 oblique Langmuir solitons under free path conditions (*Russian*) 0-79477  
 parametric instabilities of inhomogeneous plasma in presence of long-wave low frequency oscillations (*Russian*) 0-103136  
 radiation from waveguide, rel. to plasma wave scatt. by ion-acoustic oscills. 0-87886  
 relativistic electron beam, intense, coupled dipole oscills. 0-64739  
 relaxation oscillations in high-power electron beam-plasma system 0-64744  
 resonant excitation of slow low-freq. waves by opposite moving electron beams (*Russian*) 0-92336  
 RF oscillation ponderomotive accel. of electrons in elec. double layer 0-70010  
 stabilisation of spatial mode, algorithm 0-64721  
 Tokamak, sawtooth oscillations, mag. islands and disruptions 0-83940  
 toroidal pinch discharge, preionisation phase, numerical computation 0-64696  
 unneutralized electron cloud injection and containment in bumpy toroidal mag. field 0-64761  
 very-low-q discharges in DIVA confinement and MHD characts. 0-64765  
 weakly-ionised plasma, magnetised, unstable oscillations, influence on radial electric field (*Russian*) 0-103175  
 whistler mode signals generation in presence of enhanced fluctuations in plasmas 0-92293  
 H line broadening and shift due to plasma ions (*Russian*) 0-96350  
 SF<sub>6</sub> discharge and oscill. due to axial injection of impulsive electron beam 0-59316  
 SF<sub>6</sub> gas, low press., excitation of nonlinear wave by repeated pulsed electron beam 0-87878  
 Si, non thermal laser induced ordering, plasma life time, phonon interactions 0-84481
- plasma probes**  
*see also Langmuir probes*  
 arc tracks in T-10 Tokamak, wall erosion by unipolar arcs 0-64811  
 arcs, wall-stabilised, free recovery with imposed laminar and turbulent flows 0-59321  
 Columbia Torus-1 belt pinch high beta toroidal device, preionisation, optimisation 0-92368  
 computer processing of probe measurements 0-62640  
 conducting bodies in dense multicomponent gas, electric effects, method of separation 0-96389  
 cooled electric probes in dense plasma, thermal diffusion effects 0-92384  
 current density profile measurements in the Proto-Cleo torsatron 0-83995  
 delay line differentiator for meas. of electron energy distrib. function (*Japanese*) 0-84002  
 electric field prod. in air near laser spark, probe obs. (*Russian*) 0-59334  
 electrostatic plasma probe, neuron membrane physical analogue 0-79573  
 Elmo Bumpy Torus heavy ion probe 0-59286  
 emissive probe, potential meas. in magnetised gas 0-100095  
 high beta toroidal device, preionisation, optimisation 0-92368  
 instantaneous triple-probe method for direct display of plasma parameters in low density continuum plasma 0-84000  
 ion extraction by small orifice probe, sheath effects 0-59307  
 ion temperature determ. in mag. field, gridded probe method 0-70033  
 Langmuir probe sweeping circuit 0-83996  
 low pressure gas discharge meas. 0-96412  
 magnetic fields of hot dense plasmas, particle probes sensitivity 0-70037  
 organic surface contaminants, anal. by plasma chromatography-mass spectroscopy, and Raman microprobe technique 0-108773  
 plasma-wall sheath, secondary electrons, Langmuir probe obs. 0-92387  
 pulsed plasma diagnostics, double probe cct. 0-87947  
 resonance probe applications in geophysics and in laboratory (*Chinese*) 0-90226  
 reversed current effect in stabilised Z-pinch 0-79539  
 sheath thickness to Debye length ratio for slightly ionised continuum plasma 0-70008  
 theta pinch discharge, radial EM energy flow and plasma heating power 0-64747  
 Tokamak current profile meas. by neutral beam probe (*Japanese*) 0-96397  
 water vapour, electron energy distrib. function, electron sink and plasma resist. effect (*Russian*) 0-106987  
 waves, lower hybrid, in octopole Tokamak, ray trajectories 0-64707  
 C electrodes, used in emission spectrography, isotopic labelling study (*Hungarian*) 0-106976  
 H<sub>2</sub> plasma ion temperature determ. in mag. field, gridded probe method 0-70033  
 He-O<sub>2</sub> DC discharge, electron distrib. function 0-92407  
 Mo impurity flux, time resolved, in DITE Tokamak 0-63373  
 Ne, nuclear induced plasma, simulated 0-64786  
 O<sub>2</sub>, electron energy distrib. function, electron sink and plasma resist. effect (*Russian*) 0-106987  
 Ti impurity flux, time resolved, in DITE Tokamak 0-63373
- plasma production**  
*see also exploding wires and foils; plasma production and heating by laser beam*  
 air, atmospheric, cylindrically converging blast waves 0-92180  
 air, plasma, optical absorpt. coeff. at 1000 atm, 13000K, N<sub>2</sub> photodissoc. 0-64691  
 crossed field plasma discharges characts. 0-100116  
 current carrying double layer production in focus device 0-83953  
 cylindrical plasma shell, apparatus for production 0-106948  
 dense plasma ionisation and cohesion, critical density and press., approx. formulas 0-59253  
 diatomic gases, plasma prod. by relativistic electron beams mag. field diffusion 0-83955  
 disc LaB<sub>6</sub> cathode for plasma production in magnetic field 0-106951



- plasma production continued  
electron beam produced inert gas plasmas, UV to near IR laser lines 0-92334  
electron beam produced plasma, IF emission spectrum and form. kinetics 0-102533  
electronic excitation and ionisation temp. meas. in ICP Ar source, H<sub>2</sub>O vapour effects 0-75028  
exploding wire burst phase, simulation by one-dimens. MHD code 0-75080  
field reversed mirror neutral beam startup, hybrid plasma code simulation 0-99313  
fusion reactor, neutral beam injector mag. cusp plasma source, design and fabrication 0-99377  
fusion reactor, rectangular plasma generator, advanced ion source for ion injectors 0-99376  
heating in lower hybrid freq. range, temp., ion diffusion 0-83954  
high current discharge from cold LaB<sub>6</sub> cathode 0-107011  
imploding plasma liners, MHD instability effects 0-75081  
inert gas plasma, electron-beam produced, laser action of ionized and neutral atomic lines 0-106929  
inertial confinement, black body radiation implosion in ablator, driver, gas, pellet system 0-73990  
ion source, electron backstream to source plasma region 0-96369  
large volume magnetic multipole plasma source, operating characts. 0-100084  
low-temperature plasma production by electron beam ionisation of gas mixture 0-87908  
MFTF, start up neutral beam power supply system 0-91281  
mirror-confined plasma, large-radius, high-beta 0-87907  
nuclear generated plasmas, <sup>3</sup>He and <sup>235</sup>UF<sub>6</sub> excitation, spectra obs. 0-83997  
nuclear induced plasmas and nuclear pumped lasers, conf., Orsay, France (May 1978) 0-62393  
periplasmatron ion source for intense neutral beam 0-99380  
pinched electron beam prod. expanding gas bubbles, fast photography obs. 0-79564  
plasma chemistry, history, diagnostics, production, organic compd. synthesis 0-61099  
Q-machine, single ended, collisionless, steady-state parameters and Buneman instability 0-59227  
Q-machine plasma, coherent wave particle interaction 0-59226  
radiation temperature of proton beam induced plasma 0-100094  
reflex discharge, plasma quiescence 0-64806  
reversed field mirror reactors, startup using coaxial plasma guns, scaling laws 0-99279  
solving transient process in electrical explosion of conductor in restricted volume of liquid (*Russian*) 0-100088  
spatial emission profiles from inductively coupled plasma, matrix effects 0-75036  
spectra from plasmas induced by <sup>3</sup>He or <sup>235</sup>UF<sub>6</sub> reactions 0-64784  
turbulent plasma, impinged charged particle, linear response theory 0-64727  
vacuum breakdown in elec. field in range (5-7)×10<sup>6</sup> V/cm 0-87973  
Ar-Kr(Xe)(N<sub>2</sub>), electron beam ionis., low temp. plasma prod. 0-87908  
Au, thin foil, enhanced electron energy deposition heated, soft X-ray vacuum UV spectra 0-80901  
Cs plasma, generation by adiabatic compression, elec. cond. and thermodynamic parameters meas. 0-59180  
K<sub>2</sub>O-Al<sub>2</sub>O<sub>3</sub>-2SiO<sub>2</sub>-BaO plasma emitter 0-96368  
Li plasma, elec. cond. at 12.5-50 MPa, (7-50)×10<sup>3</sup>K 0-64685  
SF<sub>6</sub> gas, low press., excitation of nonlinear wave by repeated pulsed electron beam 0-87878
- plasma production and heating by laser beam**  
ablative acceleration model for moderate laser intensities 0-92351  
ablative laser fusion implosion, scaling laws and spatial struct. 0-87915  
ablative mode compression experiments of spherical targets by glass laser GEKKO IV (*Japanese*) 0-100086  
acceleration of thin foil targets under intense laser irradiation 0-92356  
air, plasma, slow burning gasdynamics, due to Nd laser beam (*Russian*) 0-108715  
air at Ti surface, optical breakdown, interferometric investigation 0-100064  
air plasma, TEA CO<sub>2</sub> laser-produced, using solid targets, induced shock waves 0-64729  
amplifier module radiation heating at DELFIN 0-92359  
asymmetric electron density profile, interferometric meas., laser-created plasma 0-75085  
Balmer series transitions for laser plasma diagnostics 0-64780  
caviton dynamics at crit. density 0-106909  
cellulose nitrate film ion data, dark-field illum. image recording photographic method 0-70031  
collisional plasma, mixed mode operation, cross-focusing 0-83945  
collisionless plasma expansion and fast ion generation at plasma-vacuum boundary 0-59257  
confined plasma column, soft X-ray lasing action conditions 0-74346  
continuous X-ray radiation, picosecond ruby laser heating (*Russian*) 0-75079  
continuum source, laser-produced plasma, for absorpt. spectroscopy in VUV and XUV 0-75094  
convective parametric decay instability in a laser plasma 0-64722  
corona, laser induced microsphere, electron density profile, interaction and transport profile 0-107008  
deflagration waves supported by thermal radiation 0-64757  
dense matter, laser driven fusion, laboratory expts. 0-75077  
deuteron source, laser-plasma 0-78475  
diagnostics, X-ray line shift of seeded Ne 0-64778  
dielectric surface, photoinduced surface discharge 0-88929  
double layer spherical targets, implosion process under laser irradiation 0-92354  
electrodynamic mechanisms of limitation of the electron concentration in a laser spark (*Russian*) 0-59333  
electron energy transport into layered targets irradiated by CO<sub>2</sub>-laser light 0-69979  
electron transport, high energy, numerical modelling (*Japanese*) 0-96346  
erosion plasma burst, effect of dynamic stresses 0-79532  
expansion, ion energy distrib., charge transfer effects 0-106953  
exploding pusher target, computer simulation (*Japanese*) 0-96376  
exploding-pushertamper areal density, neutron activation meas. 0-91237  
fast electrons, resistive inhibition from laser prod. plasma in low density Au target 0-87916
- plasma production and heating by laser beam continued**  
filament ellipticity, energy lifetime in T-8 apparatus (*Russian*) 0-87930  
fusion, progress at Lawrence Livermore Lab., USA 0-57945  
gas, high pressure, near solid target, laser plasma evolution 0-96375  
gas breakdown, multiply-charged plasma, temp. kinetics and population levels (*Russian*) 0-106952  
graphite vapour cloud, laser-prod., temp. conditions investig. 0-59290  
harmonic emission mechanisms, three-halves, from laser-produced plasma 0-59283  
high-Z plasma, X-ray diagnostics 0-75074  
hot electron energy relaxation and transport (*Japanese*) 0-96347  
hydrodynamic instabilities in laser driven implosions 0-64756  
imaging space-time-density contours in gas, overlapping pulse technique 0-73320  
implosion studies, laser-matter interactions at Limeil 0-92357  
inertial confinement, advanced engineering requirements, review 0-95421  
inertial confinement fusion, pulsed power aspects, overview 0-63382  
inertial confinement fusion reactor, appl. PWR fuel rod reenriching 0-106174  
inertial confinement fusion target, formation of uniform solid fuel layers 0-95432  
inertial fusion reactors, feedback-controlled laser-guided pellets 0-73997  
inertial fusion results from Shiva 0-92358  
instabilities, parametric, in two electron temp. plasma (*Japanese*) 0-96377  
ion beam production from interaction with Nd:YAG laser radiation bursts 0-106939  
ion emission from laser plasma, secondary electron emission effects on detect. efficiency 0-100096  
ions, multicharged, in plasma produced by laser, spectral line profiles (*French*) 0-79528  
jet form, by focusing laser beam on plane target, investigation using wavefront method 0-75103  
lase fusion, wavelength scaling, benefits of lasers with wavelength less than one micron 0-75073  
laser driven inertial confinement fusion, pulse power technology 0-63385  
laser fusion cryogenic target characterisation by wavefront shearing interferometer 0-74008  
laser fusion experiments at KMSF 0-92355  
laser fusion physical processes, investigation 0-74024  
laser light parametric absorpt., convective parametric instability 0-100073  
laser plasma, 5-20 keV X-ray emission spectrum investigation using nucl. emulsions 0-92392  
laser produced plasma, three halves harmonic spectra, time resolved obs. 0-79529  
laser pulse irradiation of metallic targets, absorpt. studies 0-79455  
laser radiation, nonlinear scatt. by fast ion waves in plasma 0-106916  
laser spherical heating, combination scatt. diagnostics 0-79569  
laser target interaction in air, shock wave diff., reflection (*Chinese*) 0-83961  
laser-erosion plasma, kinetics in its later stage, i.e. after laser pulse 0-64760  
laser-irradiated target, electron accel. by reson. 0-75076  
laser-plasma interaction and ablative acceleration of thin foils at 10<sup>12</sup>-10<sup>15</sup> W/cm<sup>2</sup> 0-83963  
laser-target impact, HF oscill. excitation (*Russian*) 0-92353  
lateral energy transport from laser prod. plasma 0-59258  
layer expansion near barrier irradiated by laser in high density gas 0-70016  
light angular distrib. emitted from laser target, time-gated optical imaging system meas. 0-79572  
low Z plasma, 1.06 μm low pulse reson. absorption 0-87903  
magnetic field generation in laser-produced plasma 0-77818  
magnetic tape method obs. of self generated mag. fields 0-64775  
mechanical response to giant laser pulse, recoil impingement meas. 0-80910  
MHD model, 2-D three-temperature, for dynamics of laser target 0-70014  
multiple confinement of ion laser produced plasma 0-83974  
non-uniform laser plasma, stimulated Raman light scatt. spectrum (*Russian*) 0-106926  
nonlinear scattering of upper hybrid laser radiation by electron Bernstein modes in a plasma 0-64720  
NOVA, high speed rot. mech. shutter design for pre-pulse protection 0-96032  
Nova, mechanical design, overview 0-91279  
NOVA, pulsed power control system, fibre-optic multi-tapped computer bus 0-95443  
optical discharges by laser radiation, continuous equilib. plasma maintenance 0-59259  
optical measurements of plasma motion and lateral energy flow 0-75102  
polarisation of picosecond excited continuous X-ray radiation (*Russian*) 0-59190  
polymer-coated laser fusion targets, compression to 10×liq. DT density 0-83964  
population inversion due to plasma expansion into ambient gas, electron cooling 0-96363  
probe investigations of the electric fields produced in air near a laser spark (*Russian*) 0-59334  
properties meas. (*Korean*) 0-96373  
pulse detector, fast nondamageable, using gaseous plasma 0-95138  
pulsed heating profile width and total coupling changes with pulse length and press. 0-71520  
radial stability of density profiles for obliquely incident light 0-92350  
radiation absorption in magnetoplasma, rel. to laser fusion 0-92273  
reflectivity and temp., scaling laws of laser plasma 0-87913  
resonance absorption, self-consistent density profiles for obliquely incident light 0-64758  
resonance absorption in CO<sub>2</sub> laser-plasma targets interaction experiments 0-106954  
second harmonic emission spectrum, near threshold 0-87912  
second harmonic generation suppression effect (*Russian*) 0-87899  
shearing interferometer for dense laser prod. inhomogeneous plasma (*Russian*) 0-83994  
shocks, imploding, cylindrical and spherical, fusion yield estimation 0-79530  
short-pulse laser backscatter from gas target 0-79454  
short-wave emission, initial plasma parameters 0-99692  
soft X-ray population inversion in laser plasmas, reson. photoexcitation, photon-assisted processes 0-87378



**plasma production and heating by laser beam continued**

- solid in high press. gas atm. in elec. field, spatial struct. (Russian) 0-83962  
 spherical multipole magnetic trap, plasma containment 0-87937  
 staged laser heating of a magnetically confined plasma 0-83522  
 steel, mild, laser microspectral anal. 0-108769  
 superelastic laser energy conversion, efficient plasma heating 0-96372  
 sustained optical discharges in molecular gases 0-100085  
 target, cylindrical shell, thermal vibrs., general soln. 0-95433  
 thermal coupling of 2.8- $\mu$ m laser radiation to metal targets 0-76107  
 thermal instability, mag. field generated, in laser heated plasma, hydrodynamic effects 0-96355  
 theta-pinch Ti ion injection by CO<sub>2</sub> laser, spectroscopic anal. 0-79577  
 time-resolved X-ray spectroscopy of laser-produced plasmas 0-84004  
 transition from isentropic to isothermal expansion 0-92279  
 transition from isentropic to isothermal expansion in laser-produced plasmas 0-87918  
 transparent dielectric, laser induced plasma at surface 0-79531  
 two beam CO<sub>2</sub> laser Lekko II expts. (Japanese) 0-100087  
 wavelength dependence of energy absorption in laser-plasmas 0-87917  
 X-ray absorption lines, signature for preheat level in non-explosive laser implosions 0-106978  
 X-ray bremsstrahlung polarisation and anisotropy, evidence of suprathermal electron fluxes 0-103193  
 X-ray emission, electron temp. meas. 0-103127  
 X-ray emission in laser imploded targets, three-dimens. reconstruction 0-79563  
 X-ray microradiographs of laser fusion targets, improved image analysis techniques 0-79562  
 X-ray production by laser plasma in strong elec. field 0-70034  
 X-ray shadowgraphy of laser driven implosions 0-92393  
 X-ray spectra of laser-produced plasma 0-75075  
 X-ray spectrometry of laser compressed microballoons 0-87954  
 Al laser plasma, high-Z, temp. meas. from bremsstrahlung emission 0-87914  
 Al plasma, laser produced, reflectance meas. 0-79568  
 Al target, multiple-pulse thermal coupling at 3.8  $\mu$ m wavelength 0-96371  
 Al target in air, plasma form. due to CO<sub>2</sub> laser pulse interaction 0-96374  
 Ar, CW optical discharge in laser plasmatron mode 0-75078  
 Ar<sup>16+</sup> filled glass shell, symmetric laser compression 0-64759  
 B III plasma, efficient heating by superelastic laser energy conversion 0-96372  
 B<sub>2</sub>O<sub>3</sub> laser-produced plasmas, isotopic enhancement 0-92349  
 CO<sub>2</sub> laser prod. microballoon plasma, fast ion emission 0-103172  
 CO<sub>2</sub> laser system, pulsed, for fusion research 0-58556  
 CO<sub>2</sub> long-pulse 2 GW single longitud. mode source for laser-matter expts. 0-78860  
 Cd laser produced plasma recombination laser, power output enhancement by plasma confinement 0-63989  
 Cu, laser light absorpt. by plasma with very steep density gradient 0-96348  
 Cu-like ions, 4s-4p reson. lines and transitions obs. by means of laser prod. plasma, appl. to Tokamaks 0-99468  
 D pellets, ionisation by Nd laser radiation 0-70015  
 He-like ions of third sequence elements, blue satellite to resonance lines 0-70013  
 Mg plasma, heated by ruby laser pulses, X-ray emission spectrum 0-64781  
 Mo XIII-XVIII, spectrum 20 to 90 Å from laser-prod. plasma and low-inductance vac. spark 0-102473  
 N<sub>2</sub>-He plasma, laser produced, high press. amplified stimulated emission 0-78843  
 Zn-like ions, 4s-4p reson. lines and transitions obs. by means of laser prod. plasma, appl. to Tokamaks 0-99468

**plasma sheaths**

- see also plasma confinement  
 arc, high-intensity, anode boundary layer, one-dimens. anal. 0-96401  
 breakdown to glow transition in plasma filled gap 0-100105  
 breakup-initiated shockfront development in 2-kJ plasma focus discharge 0-70001  
 cathode, sheaths in K<sub>2</sub>CO<sub>3</sub> seeded petroleum MHD combustion plasma 0-87870  
 collisionless sheath stability 0-106936  
 electric sheath and presheath in a collisionless, finite ion temperature plasma 0-64737  
 glow discharge, laterally spreading, short, edge struct. 0-59328  
 Penning discharge, cathode sheath, RF impedance study 0-106935  
 probe, small orifice type, sheath effects on ion extraction 0-59307  
 probe investigations of the electric fields produced in air near a laser spark (Russian) 0-59334  
 secondary electrons in plasma-wall sheath, Langmuir probe obs. 0-92387  
 space-charge double layers, anal. using fluid theory 0-75062  
 thickness to Debye length ratio for slightly ionised continuum plasma 0-70008  
 thin line cusp magnetoplasma sheath, RF feedback stabilisation 0-70009

**plasma shock waves**

- air plasma, optical absorpt. coeff. at 1000 atm, 13000K, N<sub>2</sub><sup>+</sup> photodissoc. 0-64691  
 air plasma, TEA CO<sub>2</sub> laser-produced, using solid targets, induced shock waves 0-64729  
 breakdown, ionising wave propag. mechanisms 0-83941  
 breakup-initiated shockfront development in 2-kJ plasma focus discharge 0-70001  
 cold collisionless plasma with random inhomogeneous density distrib. 0-70002  
 collisionless shocks, kinetic models 0-90330  
 collisionless shocks, simulation and laboratory expts. 0-87893  
 current sheet, near line of zero mag. field, numerical anal. (Russian) 0-83908  
 erosion plasma burst, effect of dynamic stresses 0-79532  
 Faraday MHD generator-operating region 0-103132  
 heating dense Ar, Kr and Xe plasmas, calc. of equilibrium props. (Japanese) 0-79513  
 high velocity jets generated by plasma focus and shock-wave expt., temp. and density meas. (Russian) 0-106882  
 imploding shocks in plasma, approx. analytical solns. 0-83942  
 impulse spark study using two-wavelength interferometry 0-86391  
 laser gas breakdown, shock and ionisation waves, photographic absorpt. obs. 0-87967

**plasma shock waves continued**

- laser-erosion plasma, kinetics in its later stage, i.e. after laser pul. 0-64760  
 layer expansion near barrier irradiated by laser in high density gas 0-70016  
 magnetic shocks in collisionless plasma, theory 0-85854  
 MHD shock, superadiabatic excitation in collisionless plasma 0-79503  
 particle acceleration by MHD shock turbulence 0-87894  
 plasma, emission and absorption coeff. at high electron density 0-10312  
 theta pinch, spark channel quasi-spherical compression, electron temp. 0-87920  
 transverse ionising shock wave, soln. for problem of nonstationary evolution of magnetic struct. 0-70003  
 transverse magnetic field effects, review 0-103153  
 wall confined shock heated fusion reactor, design 0-99314  
 DT pellets, laser-driven fusion, imploding shocks 0-79530  
 H<sub>2</sub>, transverse ionising shock wave, soln. for problem of nonstationary evolution of magnetic struct. 0-70003  
 SF<sub>6</sub>-inert gas mixture, high power cylindrical spark discharge, dynamic and visible charact. 0-64816  
 Y<sub>2</sub>O<sub>3</sub> capillary discharge plasma, temp., radiation screening elimination 0-64682

**plasma simulation**

- auroral arcs formation and V-potential double layers 0-103185  
 Buneman instability nonlinear saturation 0-79467  
 colliding plasma evolution, EM computer simulations 0-87926  
 controlled Tokamak plasma 0-59269  
 cusp fields, plasma confinement time investigation using Monte Carlo simulation, collision effects 0-64770  
 double layer spherical targets, implosion process under laser irradiation 0-92354  
 double layers from ion acoustic instability numerical simulation 0-59220  
 drift cone mode instability simulation 0-83930  
 electric double layer, electron velocity distrib. on high pot. side 0-70010  
 EM waves, delay line simulation, wave propag. in dispersive and attenuating media 0-82606  
 fast electrons, resistive inhibition from laser prod. plasma in low density Au target 0-87916  
 field reversed mirror neutral beam startup, hybrid plasma code simulation 0-99313  
 fusion reactor, TEXT, poloidal field power systems, design and anal. 0-102328  
 ion beam extraction, computer simulation, finite element method 0-96387  
 ion pressure gradient driven drift modes; 3-dimens. fluid simulation 0-103150  
 Langmuir turbulence, numerical modelling, solitons, nonlinear interactions 0-70030  
 laser fusion, parameter study of exploding pusher target (Japanese) 0-96376  
 low power Tokamak experimental fusion power plant, scoping studies with empirical scaling, SISYFUS code 0-102309  
 lower hybrid wave heating simulation in nonuniform plasma 0-64771  
 Mather type PF devices, optimisation using 2D snow plow code 0-87956  
 mirror, plasma confinement time investigation using Monte Carlo simulation, collision effects 0-64770  
 numerical simulation of anomalous transport processes in radially compressed reversed-field configurations 0-64689  
 numerical simulation of disruptions and loss in Tokamak plasma 0-70026  
 plasma confinement in mirror and cusp fields, Monte Carlo simulation 0-96379  
 Raman backscatter in high temperature, inhomogeneous plasmas 0-92268  
 ripple loss of fast ions in a large Tokamak 0-92382  
 rotating proton layer, transient magnetic field reversal 0-70027  
 solar flares experimental simulation, merging of two current carrying plasma columns (Japanese) 0-94775  
 strong turbulence effects on the kinetic beam-plasma instability 0-59207  
 Tandem Mirror Reactor startup and shutdown, simulation and control 0-99277  
 Tandem Mirror Reactor steady state, simulation and control 0-99278  
 TFR, electron cyclotron heating, computer simulation 0-79517  
 theta pinch, low density, step-like mag. piston 0-103182  
 Tokamak plasma, control systems, construction and simulation study (Japanese) 0-100100  
 Tokamak plasma model position control model 0-92383  
 Tokamaks, computer simulation of trapped electron modes 0-106874  
 toroidal plasma, quasispherical liner compression 0-92381  
 turbulence, strong, Langmuir, review 0-59237  
 ZT-S reversed field pinch simulations 0-83993

**plasma temperature**

- air, wall-stabilised arc, step and sinusoidal current change response 0-103209  
 air arc temp. meas. by N<sub>2</sub><sup>+</sup> integrated emission coeffs. 0-59314  
 air plasma flow in channel inlet zone, local heat transfer 0-64687  
 Alcatraz high density Tokamak, ion temp. profile reconstruction (Russian) 0-106959  
 arc, high-intensity, anode boundary layer, one-dimens. anal. 0-96401  
 auroral arcs formation and V-potential double layers 0-103185  
 bremsstrahlung X-rays emitted from electron cyclotron reson. plasma, degree of polarisation 0-87944  
 bunch enlargement in vac. (Russian) 0-83907  
 charge exchange neutrals, emitted from rot. plasma, meas. 0-106979  
 collisionless flow and end loss from a high-energy theta-pinch plasma 0-92365  
 collisionless magnetoplasma, EM wave conversion to extraordinary wave 0-79451  
 continuous X-ray radiation, picosecond ruby laser heating (Russian) 0-75079  
 coupled resistive g/ion temperature gradient instability 0-79481  
 CT-6 Tokamak device, development, test operation (Chinese) 0-87919  
 DC arc plasma, alterations in spectral line intensities due to external mag. fields 0-79621  
 diffuse discharge, current constriction near anode in combustion product plasma 0-103201  
 diffuse theta-pinch, ion temp. meas. (Japanese) 0-87951  
 dissociative recombination of H<sub>2</sub>O<sup>+</sup> and D<sub>2</sub>O<sup>+</sup> at elevated electron and gas temperatures, rate coeff. determ. 0-63747  
 distortion of the thermal-ion distribution during neutral-injection heating 0-103169



plasma temperature continued  
 double-pass rapid-scanning Fourier transform spectrometer meas. in Tokamak plasma 0-59299  
 edge cooling using superbanana limiter 0-92362  
 electric arc, horizontal, in inhomogeneous mag. field, mass spectrometric anal. 0-79620  
 electric arcs, temperature estimation from self-reversed spectral lines 0-75110  
 electrical conductivity of high temp. imperfect gas (*Russian*) 0-100072  
 electrode contact processes, microplasma diagnostics 0-59325  
 electron, microwave p-i-n diode modulator, transient plasma instability meas. (*German*) 0-87942  
 electron cyclotron emission from Tokamak plasmas with mildly superthermal electrons 0-92270  
 electron directed velocity meas., optimised method using laser scatt. incoherent regions 0-79561  
 electron plasma relax. characts., 3-30 eV 0-79612  
 electron plasma waves in a two-temperature plasma 0-92285  
 electron temperature gradient driven microtearing mode 0-96361  
 electron temperature in glow discharge in transverse mag. field, spectrosc. method meas. 0-87855  
 electronic excitation and ionisation temp. meas. in ICP Ar source, H<sub>2</sub>O vapour effects 0-75028  
 electrostatic plasma-confinement experiments in a tandem mirror system 0-70025  
 EM macroparticle acceleration, high press. gas-space density 0-79583  
 EM waves incident on warm plasma half-space dual propag. and absorpt., density and temp. depend. 0-75048  
 emission line shapes from a rotating ring radiator 0-83998  
 estimation method for electron temp. and density in <sup>3</sup>He plasma and <sup>3</sup>He-Ar plasma 0-64785  
 exploding liner gas confinement, liner velocity effects 0-79541  
 Fabry-Perot interferometer meas. 0-59302  
 filament ellipticity, energy lifetime in T-8 apparatus (*Russian*) 0-87930  
 fission reactor, gas-discharge, fuel element component conc., plasma temp. profile instabilities 0-63253  
 Fourier transform spectrometer, double-pass rapid-scanning, for plasma diagnostics 0-103190  
 gas breakdown, multiply-charged plasma, temp. kinetics and population levels (*Russian*) 0-106952  
 glow discharge, superheating ionisation instability with rot. elec. field 0-79611  
 graphite arc, in Ar flow, meas. of anode voltage drop 0-84022  
 graphite vapour cloud, laser-prod., temp. conditions investig. 0-59290  
 heating in lower hybrid freq. range, temp., ion diffusion 0-83954  
 HF discharge, ionisation overheat instability in EM wave field (*Russian*) 0-106990  
 high velocity jets generated by plasma focus and shock-wave expt., temp. and density meas. (*Russian*) 0-106882  
 inert gas ion laser, high voltage-low press. discharges, stationary props. 0-92400  
 inert gas mixtures, high-press., collisional radiative recomb. 0-63595  
 ion temperature determ., appl. of secondary electron emission to energy anal. of energetic neutrals 0-59278  
 ion temperature determ. in mag. field, gridded probe method 0-70033  
 ion-acoustic waves freq. and damping from dispersion relations 0-69991  
 L-2 stellarator, ohmic heating discharges with gas puffing 0-79593  
 Langmuir system, kinetic theory of mag. field generation 0-69974  
 laser plasma, reflectivity and temp., scaling laws 0-87913  
 laser produced plasma, lateral energy transport 0-59258  
 laser-generated, ion beam production from interaction with Nd:YAG laser radiation bursts 0-106939  
 laser-irradiated target, electron accel. by reson. 0-75076  
 laser-produced high-Z plasma, X-ray diagnostics 0-75074  
 laser-produced plasma, X-ray spectra 0-75075  
 linear turbulently heated plasma, secondary emission detector obs. 0-75100  
 low-density plasmons, electron temp. meas. by He spectrosc. 0-103192  
 magnetically confined plasmas, expressions for nonclassical energy and particle flows 0-75031  
 MHD wave growth and decay in high temp. gas 0-79458  
 multi-ion system, modulation instability of ion acoustic waves 0-69996  
 multi-region global transport model for Tokamaks 0-92264  
 multicharged ion heating in Z-pinch, column compression, temp. and density (*Russian*) 0-64754  
 neutral beam heating in the Princeton Large Torus 0-106950  
 noncircular Tokamak, time evolution of elongation ratio and Mirnov oscill. 0-64763  
 nonlinear drift wave evolution, model eqn. 0-100075  
 nonlinear interaction, electron collision freq., self-consistent eqn. (*Russian*) 0-75055  
 parametric instability, thermal fluctuation effect in inhomogeneous plasma (*Russian*) 0-106897  
 PLT, neutral beam injection, power input and plasma temp. reconciliation 0-106224  
 PLT, neutral beam injection and ICRF heating, charge exchange meas. 0-83892  
 polarisation of picosecond excited continuous X-ray radiation (*Russian*) 0-59190  
 population inversion due to plasma expansion into ambient gas, electron cooling 0-96363  
 positive column, ionisation and temp. effect on charged particle profile and density 0-79596  
 radiation temperature of proton beam induced plasma 0-100094  
 radiative emission rates for low- and medium-Z elements in high temp. plasmas 0-103125  
 runaway electron critical velocity in magnetised gas (*Chinese*) 0-87845  
 space charge ionising waves, high velocity propagation 0-87889  
 SPICA, impurity radiation, density and temp. 0-87859  
 stationary nonequilibrium distributions of ions produced in the interaction with an electron thermostat (*Russian*) 0-64684  
 submillimetric-wave laser Thomson scatt. ion temp. diagnostic implementation in Tokamak 0-59301  
 sustained optical discharges in molecular gases 0-100085  
 T-10 Tokamak, electron cyclotron emission meas. 0-92375  
 thermonuclear fusion, breakeven condition on hot-ion mode 0-78439  
 theta pinch, spark channel quasi-spherical compression, electron temp. 0-87920  
 Thompson scattering diagnostics of low density plasmas, Nd:glass laser system 0-96388  
 Thompson scattering meas. of heating process 0-59272

# plasma temperature continued

Tokamak, edge effects and impurities, influence on thermal stability 0-87892  
 Tokamak, metal impurity reduction by working gas injection 0-106963  
 Tokamak, T-4, corpuscular diagnostics by charge exchange of plasma ions at artificial target (*Russian*) 0-83968  
 Tokamak, temp. fluctuations and heat transfer 0-74003  
 Tokamak Alcator C far IR emission diagnostics of electron temp. 0-59291  
 Tokamak discharge microwave preionisation at electron cyclotron resonance 0-83896  
 Tokamak electron temp. and density profiles from electron cyclotron radiation spectra 0-59293  
 Tokamak far IR Fourier transform spectroscopy resolution limits 0-59298  
 Tokamak ignition equilibria and thermal stability 0-74005  
 Tokamak TO-I, feedback system effect on plasma parameters (*Russian*) 0-103174  
 Tokamaks, PLT and PDX, X-ray diagnostics 0-75104  
 toroidal plasmas, high temp., electron cyclotron emission meas. by mesh filter method 0-75101  
 transition from isentropic to isothermal expansion in laser-produced plasmas 0-87918  
 transport functions by precision arc expts., H Balmer spectrum 0-103187  
 two-electron temp. plasma, ion acoustic holes 0-59205  
 two-temperature He plasma, transport props. 0-92260  
 X-ray diagnostics, hot lab. and astrophysical plasma 0-59282  
 X-ray emission, electron temp. meas. 0-103127  
 X-ray monochromatic images for hot plasma ion and temp. distrib. 0-64772  
 Z-pinch of intense energy-density driven by high voltage storage lines 0-87952  
 Al laser plasma, high-Z, temp. meas. from bremsstrahlung emission 0-87914  
 Al, vacuum arc, excited state density theory 0-100107  
 Ar arc plasma, partial LTE for lower excited levels of ArI 0-79565  
 Ar discharge, ion density profile, reson. laser light meas. 0-92401  
 Ar, formation in crossed electric and magnetic fields, optical spectra 0-79452  
 Ar plasma, low density, shock-heated, effective collision freq. calcs., electron temp. meas. 0-75025  
 Ar plasma arc, wall-confined, nonequilibrium effects 0-70058  
 Ar<sup>16,17+</sup> filled glass shell, symmetric laser compression 0-64759  
 C plasma, spectral and absorpt. coeffs. 0-69985  
 Cs(Ar-Cs) plasmas, electron momentum transfer cross section, cyclotron reson., temp., cond., and vel. meas. 0-106930  
 D+PTFE, DF\* prod., Fourier transform IR spectroscopy 0-87105  
 H atom analyser using Cs heat pipe, low energy appl. 0-70043  
 H dense thermal plasma, radiation emission 0-103120  
 H plasma, thermal emission and Debye shielding 0-64692  
 H<sub>2</sub> hot-iron plasma, ion temp. and electron density depend. studied by laser light scatt. and emission spectroscopy 0-96342  
 H<sub>2</sub> plasma ion temperature determ. in mag. field, gridded probe method 0-70033  
 H<sub>2</sub>-SiH<sub>4</sub>, glow discharge, emission spectroscopy of Si H 0-69984  
 H $\alpha$  and H $\beta$ , Stark profiles, ion-motion effect 0-63592  
 He II 4686 Å line, Stark profile meas. in high density plasma 0-96390  
 He plasma, low-density, electron temp. determ. from He I 3889 Å and 5016 Å line intensities 0-96394  
 He<sub>2</sub> high press. afterglows, reviews 0-64823  
 Hg-Tl-I discharges, 50 Hz, axial segregation effect on elec. field strength 0-59320  
 K<sub>2</sub>O-Al<sub>2</sub>O<sub>3</sub>-2SiO<sub>2</sub>-BaO plasma emitter 0-96368  
 Kr water-cooled arc lamp, anode, temp. distrib. along length, anode geometry effects 0-106994  
 Mg plasma, heated by ruby laser pulses, X-ray emission spectrum 0-64781  
 N, high intensity arcs, anode contraction region modeling 0-103210  
 N<sub>2</sub>-H<sub>2</sub> arc, bent and rot., flow mechanism 0-70047  
 Ne, nuclear induced plasma, simulated 0-64786  
 SF<sub>6</sub> plasma thermodynamic props. at arc extinction temp. and pressures 0-79435  
 SF<sub>6</sub>-inert gas mixture, high power cylindrical spark discharge, dynamic and visible charact. 0-64816  
 U1 plasma, absolute emission coeff. 0-64693  
 Y<sub>2</sub>O<sub>3</sub> capillary discharge plasma, temp., radiation screening elimination 0-64682  
 Y<sub>2</sub>O<sub>3</sub> plasma, eqn. of state investig. 0-75027

# plasma theory

see also Debye-Huckel theory  
 adiabatic invariant J, finite- $\beta$  effect in axisymmetric tokamaks 0-79538  
 adiabatic to stochastic motion transition, Kolmogorov Arnold Moser surface 0-59175  
 amplification of radiation near cyclotron frequency due to electron population inversion 0-92271  
 anomalous heat conductivity for a weakly ionized plasma in a strong magnetic field 0-100070  
 bremsstrahlung cross-sections, 1- and 2-photon, Debye shielding corrections 0-106157  
 bunch enlargement in vac. (*Russian*) 0-83907  
 coherent wave particle interaction in Q-machine plasma, electrostatic analyser diagnostics 0-59226  
 cold semi-infinite plasma, three wave interaction 0-79462  
 colliding relativistic plasma instabilities with relativistic temps. (*Russian*) 0-83913  
 collisional relax. of electron beam injected into plasma, Fokker-Planck eqn. anal. 0-64738  
 collisionless plasma, Chew-Goldberger-Low theory with finite Larmor radius corrections 0-75024  
 collisionless plasma expansion and fast ion generation at plasma-vacuum boundary 0-59257  
 complex nonlinear impedance of flat antenna 0-103130  
 computational model for spectral and radiative characts. in Kr and Xe arcs 0-64812  
 conducting bodies in ionised multicomponent gas, electric effects, method of separation 0-96389  
 conference on plasma intrinsic stochasticity, Cargese, France (June 1979) 0-59174  
 convective amplification of drift waves and thermal fluctuation levels in a stable plasma 0-83932



**plasma theory continued**

correlation function, long time asymptotic behaviour, influence of waves on relax. processes (*Chinese*) 0-59195  
 correlation measurements of turbulent ionization and ion-acoustic waves 0-59329  
 Coulomb systems, equilb. distrib. functions expansion in power of density 0-64681  
 coupled waves in stratified Chew-Goldberger-Low plasma 0-87875  
 critical transition to stochasticity 0-57202  
 current production by rotating mag. fields 0-79442  
 current sheet, near line of zero mag. field, numerical anal. (*Russian*) 0-83908  
 decaying plasma, nonequilb. props. during afterglow modulation by acoustic waves 0-103144  
 dense plasma ionisation and cohesion, critical density and press., approx. formulas 0-59253  
 diffusion of electrons through excited atomic or ionic states, role of collective interactions 0-79433  
 dispersion relation for instability hindrance in a magnetically confined plasma with finite press. 0-59221  
 dissipative non-Hamiltonian dynamical system, stochastic props. and strange attractors 0-57200  
 double layer formation in multiple plasma device 0-83897  
 double layers modelled by numerical integration of Vlasov-Poisson system 0-92290  
 drift cyclotron loss cone instability, nonlinear saturation 0-83929  
 eikonal expansion of the Vlasov-Maxwell equations valid near cyclotron resonance 0-92300  
 electric pot. distrib. in plasma 0-106876  
 electrodynamic mechanisms of limitation of the electron concentration in a laser spark (*Russian*) 0-59333  
 electron and plasma stream reflection at a nonadiabatic mirror 0-87929  
 electron autoreson. accel. at nonlinear ECR in growing mag. field 0-87867  
 electron beam-magnetoplasma, radiation at or near electron plasma frequency, transverse modes 0-106942  
 electron cloud in equilb., mag. field effect, pot. and space charge distrib. 0-92410  
 electron cyclotron emission from Tokamak plasmas with mildly superthermal electrons 0-92270  
 electron cyclotron radiation from a high density Tokamak 0-92266  
 electronic excitation and ionisation temp. meas. in ICP Ar source, H<sub>2</sub>O vapour effects 0-75028  
 EM waves in magneto-active plasma, group velocity direction 0-59201  
 energy lost by fast electrons in laser plasma 0-103165  
 equation of state, for classical 1-component plasma 0-83887  
 equilibrium in free boundary case, variational principle calcs., wall interaction (*Chinese*) 0-69972  
 excitation spectrum of relativistic quantum plasma, covariant Wigner function approach 0-87938  
 geometrical optics formalism 0-83925  
 gyrokinetic modes, spatial struct. in toroidal geometry 0-79489  
 harmonics generation in inhomogeneous plasma (*Russian*) 0-83916  
 helical stellarator, Asperator NP-3, toroidal discharge forbidden region 0-79592  
 high beta plasma surrounded by cond. shell, dynamic stabilisation 0-96354  
 high-n ballooning theory, stability of axisymmetric tokamak equilb. 0-64705  
 imploding plasmas, mag. field generation, Nernst refrigeration 0-79526  
 inert gas ion laser, high voltage-low press. discharges, stationary props. 0-92400  
 inhomogeneous plasma, generation of higher harmonics of resonant radiation 0-106880  
 ion acoustic wave, self excited, in hot plasma, dispersion theory 0-92283  
 ion temp. and parametric decay development in RF-generated stellarator plasma 0-79436  
 ion-acoustic pulse generation by 2 EM pulses at difference freqs. in collisionless plasma 0-79475  
 ion-acoustic waves freq. and damping from dispersion relations 0-69991  
 ions in steady-state plasma, excited levels population probabilities, asymptotic behaviour 0-79438  
 kinetic equation in the kinetic region of the dilute and nonuniform electron plasma 0-103109  
 kinetic equations for low frequency instabilities in inhomogeneous plasmas 0-83886  
 kinetic theory of neutrals in a bounded plasma slab with inhomogeneous ion temperature and density 0-87861  
 kinetic theory of the collisional scrape off layers 0-79439  
 Korteweg-de Vries eqn. and 2nd Painleve transcendent, boundary value problem in plasma theory 0-69971  
 Landau equation, non-Markovian terms 0-79432  
 laser-driven fusion, validity of hydrodynamic approximation 0-75087  
 liquid metal perturbation theory, extension to dense partially ionised plasmas 0-75500  
 local mean field theory, basis problems 0-92253  
 Lyapunov characteristic exponents and stochasticity 0-59177  
 Lyapunov characteristic numbers and Kolmogorov entropy, stochasticity of dynamical systems 0-59178  
 magnetic field distortion near an ablating H<sub>2</sub> pellet, effect on Tokamak reactor refuelling 0-64734  
 magnetic field line trajectory calc., Kolmogorov Arnold Moser surface 0-59263  
 magnetic island, m=2, high-energy runaway orbits 0-64767  
 magnetic properties in strong field for one-component plasma 0-100068  
 magnetised plasma interaction with neutral gas, threshold vel. 0-59241  
 magnetised plasma stability in large amplitude circularly polarised wave, dispersion relations 0-59223  
 many component plasmas with self consistent field, variational principles and canonical theory 0-87856  
 many-electron ion plasma, thermodynamic functions calcs. 0-103108  
 Maxwell-Klimontovich equations for turbulent plasma, renormalisation 0-75500  
 mean spherical model 0-87846  
 MHD, generalised Lorenz eqns., strange attractors 0-59232  
 MHD equilibrium, with axisymmetry and noncircular cross section, free boundary soln. to eqn. (*Chinese*) 0-59260  
 N particle Coulomb system, eqn. of state, virial theorem calcs. (*French*) 0-64680  
 negative wave momentum density in plasma 0-79463  
 non-LTE, props. and at. processes, medium to high press. 0-59170

**plasma theory continued**

nonequilibrium plasma, kinetic theory of spectral line broadening 0-59187  
 nonisothermal plasma electron ensemble, nonstationary behaviour, kinetic description 0-59171  
 nonlinear oscillator systems, primary resonances do not overlap 0-59176  
 nonlinear processes in magnetised plasma, nonstationary HF pressure (*Russian*) 0-106895  
 nonlinear theory of unstable plane waves and solitons 0-87888  
 one component plasma, charged hard sphere theory 0-106873  
 one-component plasma in two and three dimens., static props., semi-analytic theory 0-87853  
 optically thin plasmas, He II excited states, role of direct ionisation excitation 0-102579  
 partially ionised plasma, theory of dielectric constant 0-59173  
 particle motion, regular and stochastic, Hamiltonian formalism 0-59167  
 particle orbits in ion rings 0-92254  
 particle transport in HF heated magnetised plasma 0-87863  
 pendulum, bounce resonance and Kolmogorov entropy 0-57199  
 phase transition in elec. discharge plasma between parallel plates, compression by recomb. press. 0-64799  
 plasma dispersion for strong coupling 0-103111  
 positive column, ionisation and temp. effect on charged particle profile and density 0-79596  
 pressure, virial kinetic definition, spherical geometry calcs. (*French*) 0-69973  
 primordial lepton gas, elec. cond., Landau, Boltzmann eqn. calcs. (*French*) 0-75030  
 probe investigations of the electric fields produced in air near a laser spark (*Russian*) 0-59334  
 radiation emission spatial distrib. reconstruction in torus 0-103123  
 radiation from warm plasma column with open ended coaxial line 0-106878  
 radiative emission rates for low- and medium-Z elements in high temp. plasmas 0-103125  
 relativistically covariant formulation in theory of plasma stability 0-75046  
 resonance cone, in inhomogeneous magnetoplasma column, theoretical anal. 0-83884  
 reversed current effect in stabilised Z-pinch 0-79539  
 rotation instability on collisionless FLR plasma, nonlinear theory 0-79485  
 screening efficiency of the scrape off plasma in the shadow of a poloidal limiter 0-79576  
 screening in one dimens. plasma 0-65478  
 second harmonic emission spectrum from laser prod. plasma near threshold 0-87912  
 self-consistent kinetic theory of stochasticity 0-59179  
 space potential determ. and storage in fast changing plasma 0-87949  
 Stark broadening of isolated Sn II lines in cool plasma, semi-empirical calcs. 0-59186  
 stationary nonequilibrium distributions of ions produced in the interaction with an electron thermostat (*Russian*) 0-64684  
 strings in heavy-light gas mixture, self induced particle separation (*Russian*) 0-79441  
 superradiation from non-ideal plasmas in electric field 0-83904  
 test particle in mag. field, pot. 0-106872  
 thermal conductivity and thermal diffusion coefficient of high-temp. plasma in mag. field 0-92256  
 thermodynamics and structure of two-component classical plasma, mean spherical approx. 0-64683  
 time-dependent processes in collisionless plasma, anal. numerical calcs. 0-87858  
 Tokamaks, energy confinement scaling, Frascati Torus results 0-79536  
 transformation group techniques appl. to nonlinear fluid and plasma eqns. (*French*) 0-77623  
 transverse waves in magnetoplasma subjected to stochastic mag. field, normal mode approach 0-75049  
 turbulent plasma collective modes, sum-rule anal. 0-59238  
 two dimensional real matter, low density free energy in canonical thermodynamics plasmas 0-87852  
 two-component plasma, mean spherical model 0-87854  
 Vlasov theory for magnetised plasma, coherent state approach 0-64675  
 wave energy density and wave momentum density of species in collisionless plasma 0-79437  
 weakly nonideal inert gas impulse plasma, Coulomb cross-section calcs. 0-103113  
 Weibel instabilities, temp. anisotropy driven, statistical thermodynamics 0-75047  
 whistler-Alfvén turbulence interaction 0-75058  
 Ar arc plasma, partial LTE for lower excited levels of Ar I 0-79565  
 H plasma, recombining, weakly ionised, population inversion 0-87849  
 H, Stark broadening, model microfield methods calcs. 0-92274  
 H<sup>+</sup>-He<sup>2+</sup> mixture, fully ionised, two-component plasma, mean spherical model 0-87854  
 Li plasma, elec. cond. at 12.5-50 MPa, (7-50)×10<sup>3</sup>K 0-64685  
 Li-D equation of state under extreme conditions, solid state to plasma region 0-69976  
 Y<sub>2</sub>O<sub>3</sub> plasma, eqn. of state investig. 0-75027

**plasma thermocouples** see *plasma devices; thermocouples*  
**plasma torches** see *plasma devices*  
**plasma transport processes**  
 see also *Vlasov equation*  
 ablative laser fusion implosion, scaling laws and spatial struct. 0-87915  
 air, wall-stabilised arc, step and sinusoidal current change response 0-103209  
 air plasma, radiowave interaction, electron velocity, collision cross-section depend. 0-103155  
 air plasma flow in channel inlet zone, local heat transfer 0-64687  
 Alfvén mode, current driven, electron-ion collisions and full dispersion function, numerical anal. 0-64726  
 anisotropic resistivity across mag. field, effect of ion-acoustic turbulence 0-59236  
 anomalous, electron temp. gradient instability 0-75034  
 anomalous drift wave transport in high temp. plasmas, thermodynamic stability 0-69980  
 anomalous heat conductivity for a weakly ionized plasma in a strong magnetic field 0-100070  
 anomalous resistivity, effects on collisionless shocks structure 0-87893  
 anomalous transport from plasma waves 0-59182



**plasma transport processes continued**

anomalous transport-processes in radially compressed reversed-field configurations, numerical simulation 0-64689  
 anomalous viscosity due to EM instability in turbulent plasma 0-106901  
 anomalous viscosity due to EM instability in turbulent plasma, nonlinear theory 0-106902  
 arc discharge, dense plasma, radiative thermal cond. and elec. cond. coeffs. determ. 0-75033  
 astrophysical, magnetospheric, and lab. plasma knowledge interaction 0-59166  
 asymmetric plasma resistivity, creation using waves 0-103171  
 axial particle drift in the positive column of a discharge 0-100113  
 beam discharge, electron kinetics, charge particle finite lifetime effect 0-92404  
 beam discharge, electron kinetics, deexcitation processes effect 0-92405  
 beam-induced currents in toroidal plasmas 0-92265  
 Bernstein waves, propagation in inhomogeneous plasma, dispersion rel., quasi-linear equations, diffusion coeff. determ. 0-75044  
 breakdown wave propagation in ionised gas in nanosecond discharges 0-87890  
 bunch enlargement in vac. (*Russian*) 0-83907  
 Buneman instability nonlinear saturation 0-79467  
 burn period plasma current maintenance, rectifying first wall, cct. anal. 0-102307  
 caviton dynamics at crit. density 0-106909  
 charged particle transport, multigroup formalism to solve Fokker-Planck eqn. 0-68159  
 Chirikov-Taylor model, turbulent diffusion calc. 0-79469  
 classical diffusion equation soln. for fully ionised plasma 0-103114  
 closed poloidal heliotron, accelerated electron focusing (*Russian*) 0-106961  
 collapse instability nature in Tokamak, surface currents (*Russian*) 0-92310  
 collisional drift modes, anomalous skin effect, enhanced particle penetration during fuelling, nonlinear theory 0-64703  
 collisionless shocks, kinetic models 0-90330  
 column, HF field effect on diffusion and convection 0-103173  
 conductance theory, quantum-statistical, of nonideal plasmas 0-79440  
 conducting bodies in ionised multicomponent gas, electric effects, method of separation 0-96389  
 conductivity, electrical, classical, plasma impurities, Sonin polynomial distrib. function (*Russian*) 0-83894  
 confinement in multislit EM trap, model description (*Russian*) 0-96382  
 continuous X-ray radiation, picosecond ruby laser heating (*Russian*) 0-75079  
 convective amplification of universal drift modes 0-59208  
 convective cell nonlinear excitation and anomalous diffusion, in inhomogeneous plasma 0-79468  
 convective plasma loss by ion-cyclotron RF field, elimination by mode control 0-83957  
 cooled electric probes in dense plasma, thermal diffusion effects 0-92384  
 corona, laser induced microsphere, electron density profile, interaction and transport profile 0-107008  
 coupled resistive g/ion temperature gradient instability 0-79481  
 cross-field electron transport due to thermal electromagnetic fluctuations 0-92258  
 CT-6 Tokamak device, development, test operation (*Chinese*) 0-87919  
 Culham Levitron, drift island diffusion 0-59267  
 current carrying double layer production in focus device 0-83953  
 current density profile measurements in the Proto-Cleo torsatron 0-83995  
 current generated by alpha-particle loss in Tokamak reactors 0-106877  
 current generation by unidirectional lower hybrid wave in ACT-1 0-92306  
 current production by rotating mag. fields 0-79442  
 current sheet, near line of zero mag. field, numerical anal. (*Russian*) 0-83908  
 current-driven HF drift wave, inhomogeneous plasma instability 0-59204  
 dense pinch, electron-positron pair production in EM field (*Russian*) 0-100092  
 diffuse discharge, current constriction near anode in combustion product plasma 0-103201  
 diffusion across mag. field effect of ion-acoustic turbulence 0-59236  
 diffusion of electrons through excited atomic or ionic states, role of collective interactions 0-79433  
 discharge, two-temperature, transport eqns., transient phenomena 0-96402  
 distribution of particles in stochastic fields 0-79448  
 DITE Tokamak, beam driven current meas. 0-106940  
 double layer formation in multiple plasma device 0-83897  
 double layers, electric field collapse phenomena, Buneman instability (*Russian*) 0-79476  
 double layers from ion acoustic instability numerical simulation 0-59220  
 drift kinetic equation, num. soln. 0-59172  
 drift mode, current driven, electron-ion collisions and full dispersion function, numerical anal. 0-64726  
 drift of positive ions in plasma formed by dense beam of negative ions in gas (*Russian*) 0-103160  
 drift wave, low freq., pseudoclassical diffusion in Tokamak (*Chinese*) 0-69990  
 electric discharge with disc cathode in He flow, spectrosc. investig. 0-64809  
 electric field compression near a plasma electrode 0-64736  
 electrical and heat conductivity, H transport functions by precision arc expts. 0-103187  
 electrical conductivity of high temp. imperfect gas (*Russian*) 0-100072  
 electrical conductivity tensor for H<sub>2</sub>O<sub>2</sub> plasma in mag. field (*Russian*) 0-87864  
 electron autoreson. accel. at nonlinear ECR in growing mag. field 0-87867  
 electron beam stabilised mirror confined gas, hot electron population study 0-100089  
 electron beams, modulated, non-linear oscillation theory (*Russian*) 0-106898  
 electron cyclotron emission from Tokamak plasmas with mildly superthermal electrons 0-92270  
 electron energy transport into layered targets irradiated by CO<sub>2</sub>-laser light 0-69979  
 electron temperature gradient driven microtearing mode 0-96361  
 electron transport, high energy, numerical modelling (*Japanese*) 0-96346  
 electrostatic confinement in EM trap, ion current decay (*Russian*) 0-79543

**plasma transport processes continued**

electrostatic microinstabilities, transport theory 0-79443  
 ELMO Bumpy Torus, radial transport in collisionless regimes 0-79447  
 EM macroparticle acceleration, high press. gas temp. density 0-79583  
 energy confinement comparison of ohmically heated stellarators to Tokamaks 0-92360  
 energy confinement scaling and poloidal beta in high density Tokamaks 0-96381  
 energy deposition of fast  $\alpha$  particles in a fully ionized deuterium-tritium plasma 0-92259  
 energy of a turbulent, current-carrying plasma in a strong electric field 0-79514  
 energy transport from 1.06  $\mu$ m and 0.53  $\mu$ m laser plasmas interactions at 10<sup>15</sup> W cm<sup>-2</sup> 0-92261  
 excited gas, resonant optical discharge 0-92343  
 field emission medium energy diode, electron flow, HF oscils. 0-79582  
 field reversed mirror confinement, finite gyro-radius effects 0-83989  
 fission reactor, gas-discharge, fuel element component conc., plasma temp. profile instabilities 0-63253  
 fissioning plasma from gas phase nucl. reactor, appl. 0-64794  
 flame plasma with presence of current, EM radiation obs. (*Russian*) 0-103126  
 flux motion in curvilinear plasma-optical system (*Russian*) 0-83893  
 FT Tokamak, non-thermal electron distrib. function 0-83891  
 fueling and thermonuclear instability, cold plasma layer surface fueling source 0-59196  
 fusion products in Tokamak plasma, deposition and thermalisation 0-83895  
 fusion reactor pellet re-fuelling feasibility 0-91246  
 gas flow, nonequilib. ionisation and Hall EMF 0-69981  
 graphite arc, in Ar flow, meas. of anode voltage drop 0-84022  
 guiding center drift equations in mag. coordinate system 0-87865  
 Hall current and gyroviscosity effect on conducting, rotating viscous plasma stability 0-75041  
 heat flux limitation by ion-acoustic instability 0-92304  
 heat transfer rates to flat plate from normally-impinging N plasma jet 0-75061  
 heating in lower hybrid freq. range, temp., ion diffusion 0-83954  
 hollow electron beam pot. in magnetically insulated diode 0-70046  
 impurity flow reversal expt., result anal. 0-106875  
 inert gas ion laser, high voltage-low press. discharges, stationary props. 0-92400  
 inert gases, atomic alignment in positive column (*Russian*) 0-87981  
 ion acoustic wave, self excited, in hot plasma, dispersion theory 0-92283  
 ion acoustic waves method of plasma potential meas. 0-59289  
 ion heating by current-driven turbulence in inhomogeneous plasma 0-96370  
 ion wave effects in open cylindrical magnetoplasma device, turbulent thermal insulation 0-106914  
 ionosphere plasma interaction with gravity waves, elec. field and current prod. 0-61957  
 JET, transport calcs. for approach to ignition 0-92263  
 kinetic theory, for dense plasmas transport coeffs. 0-77280  
 Langmuir system, kinetic theory of mag. field generation 0-69974  
 laser plasmas, hot electron energy relaxation and transport (*Japanese*) 0-96347  
 laser targets, dynamics, 2-D three-temperature MHD model 0-70014  
 linear compression of plasma vortex 0-64755  
 longitudinal electrical resistivity in magnetic field, shielding effect (*Chinese*) 0-69977  
 low- $\beta$  plasmas, turbulence, spectral struct., Bhom diffusion coeffs., determ. 0-106924  
 magnetic island coalescence, 2-dimens. MHD eqns. 0-64695  
 magnetically confined plasmas, expressions for nonclassical energy and particle flows 0-75031  
 mass renormalization in stochastic acceleration of particles (*Russian*) 0-100066  
 MHD accelerators, electrodynamic characts. 0-64788  
 MHD channel, anisotropically conducting plasma in inhomogeneous elec. and mag. fields, current calc. (*Russian*) 0-74995  
 MHD devices, plasma ionization instability, dynamic suppression, switching modelling 0-59308  
 MHD generator, plasma turbulence in combustion channel 0-75057  
 microtearing modes and anomalous transport in Tokamaks, self consistent calc. 0-59222  
 microtearing modes and anomalous transport in Tokamaks 0-92316  
 mirror devices, axial particle transport, finite mean free path effects 0-83900  
 Mirror-Torus-System-1 with divertor mag. field, plasma density and depolarisation current 0-70022  
 multi-ion system, modulation instability of ion acoustic waves 0-69996  
 multi-region global transport model for Tokamaks 0-92264  
 multiphase medium plasma dynamics, Soviet literature growth and duplication parameters (*Russian*) 0-59191  
 nonideal plasma, electric conductivity up to 10<sup>6</sup>K 0-103112  
 nonlinear fluctuation-dissipation theorem, nonpotential perturbation fields (*Russian*) 0-59225  
 nonlinear interaction, electron collision freq., self-consistent eqn. (*Russian*) 0-75055  
 nonlinear magnetostatic modes and twisting modes with magnetic islands 0-106900  
 nonlinear scattering of upper hybrid laser radiation by electron Bernstein modes in a plasma 0-64720  
 numerical simulation of disruptions and loss in Tokamak plasma 0-70026  
 origin of galaxies in expanding Universe, plasma cond. and instabilities, MHD soln. 0-62283  
 parametric interaction of waves in plasma with random large-scale inhomogeneities (*Russian*) 0-103137  
 particle and energy balance by corpuscular diagnostics 0-92399  
 particle transport in HF heated magnetised plasma 0-87863  
 plasma decay under constant voltage (*Russian*) 0-106988  
 polarisation of picosecond excited continuous X-ray radiation (*Russian*) 0-59190  
 ponderomotive laser-plasma effects subject to strong magnetic fields and collisions 0-87905  
 position instability analysis, effective mode approx. in Tokamak 0-103145  
 positive column, ionisation and temp. effect on charged particle profile and density 0-79596  
 positive column, subnormal, ion and electron radial distrib., theoretical description 0-79598



## plasma transport processes continued

- positive column gas discharge with external ionisation, voltage-current charactrs. 0-96408  
 positive column of high-voltage diffuse discharge, nonstationary processes 0-64802  
 potential small-scale instabilities of inhomogeneous plasma in crossed electric and magnetic fields 0-79492  
 pressure, virial kinetic definition, spherical geometry calcs. (French) 0-69973  
 primordial lepton gas, elec. cond., Landau, Boltzmann eqn. calcs. (French) 0-75030  
 radiation temperature of proton beam induced plasma 0-100094  
 rarefied electron gas, space depend. electron transport by integral approach 0-92257  
 reactor, Tokamak, fuel injection, dynamic burn control 1-D transport code 0-68948  
 reactor ignition, overheated underdense Tokamak plasma, two-zone model and 1-D transport code 0-63376  
 reduction and inversion due to plasma rotation and ion-neutral friction 0-79444  
 relativistic Boltzmann theory, reduction of collision integrals 0-79560  
 relativistic charged particle motion in Tokamaks, electric field and slowing down effects 0-92262  
 relativistic electron beams, gradB transport, bunching and focusing 0-96345  
 relativistic electron beams, theoretical scheme for axial compression 0-96367  
 resistive hose instability in relativistic electron beam 0-67947  
 resonant excitation of slow low-freq. waves by opposite moving electron beams (Russian) 0-92336  
 reversed field pinch, numerical studies 0-87931  
 reversed-field pinch plasma model 0-87935  
 RF driven current generation by lower hybrid waves in Tokamak 0-103116  
 RF plugging and heating, rel. to plasma impedance 0-96378  
 RINGBOOG II, toroidal discharges with cold blankets 0-83901  
 runaway electron critical velocity in magnetised gas (Chinese) 0-87845  
 screw instability of finite cond. gas (Russian) 0-92311  
 slow convection of magnetised plasma, appl. to Earth plasma sheet 0-109312  
 spectroscopic electron density meas., hot point low induction vacuum spark gas (Russian) 0-92390  
 stellarator, current turbulent ion heating, modulation stability 0-79525  
 stellarators, particle orbits and toroidal vacuum fields 0-79450  
 stellarators, toroidal vacuum fields, particle orbits 0-79445  
 stochastic mag. field fluctuations, self-consistent model 0-100074  
 stochasticity due to mag. perturbations in axisymmetric geometries 0-87866  
 stopping power of a nonequilibrium plasma for incident alpha particles 0-64742  
 strings in heavy-light gas mixture, self induced particle separation (Russian) 0-79441  
 superthermal electron beam, relax. due to Coulomb collisions in plasma 0-106941  
 suprathermal electron fluxes, evidence from X-ray bremsstrahlung polarisation and anisotropy 0-103193  
 surface ion acoustic waves in non isothermal gas layer (Russian) 0-87891  
 tandem mirror plasmas, alpha particle dynamics 0-83986  
 TFR 600 Tokamak, electron heat transport anomaly 0-79449  
 thermal conductivities and coefficients of thermal diffusion of high temp. plasma 0-64690  
 thermal conductivity and thermal diffusion coefficient of high-temp. plasma in mag. field 0-92256  
 thermal ion distribution distortion by neutral injection heating 0-92344  
 thermal mode ray trajectory in inhomogeneous magnetoplasma 0-106884  
 thermal parametric instability, effect of recomb. processes 0-61967  
 thermionic triode, oscills. in low press. inert gas discharge 0-79590  
 Tokamak, energetic ion slowing and transport coeff. by Makokot code 0-83899  
 Tokamak, impurity transport (Russian) 0-106957  
 Tokamak, JFT-2, particle and heat transport during lower hybrid heating 0-70021  
 Tokamak, large magnetic field ripples, electric probe meas. 0-83976  
 Tokamak, T-4, corpuscular diagnostics by charge exchange of plasma ions at artificial target (Russian) 0-83968  
 Tokamak, temp. fluctuations and heat transfer 0-74003  
 Tokamak current profile meas. by neutral beam probe (Japanese) 0-96397  
 Tokamak discharge microwave preionisation at electron cyclotron resonance 0-83896  
 Tokamak fusion reactors, neutral beam injector penetrations, limiting neutron streaming, neutron flux calc. 0-95400  
 Tokamak plasma, beam driven currents, trapped electrons effect 0-70011  
 Tokamak plasma, runaway electrons and current drive 0-74004  
 Tokamak reactors, neutral beam injection, energy and power requirements 0-91243  
 Tokamak TO-1, feedback system effect on plasma parameters (Russian) 0-103174  
 Tokamak-fusion reactors, He exhaust 0-75084  
 Tokamaks, lower hybrid heating, simulation using BALDUR 1-D transport code 0-92339  
 toroidal mag. field, thermal cond. with stochastic inhomogeneity (Russian) 0-83973  
 toroidal plasmas, beam driven currents, trapped electrons effect 0-70011  
 toroidal plasmas, beam induced currents 0-92335  
 toroidal trap, plasma rot. effect on neoclassical transport of impurities (Russian) 0-83972  
 torsatron, stochastic elec. field effect on transport of low collision freq. plasma 0-79446  
 torsatrons, mag. surfaces, particle orbits, neutral injection 0-79551  
 torsatrons, particle orbits and toroidal vacuum fields 0-79450  
 torsatrons, toroidal vacuum fields, particle orbits 0-79445  
 transition from isentropic to isothermal expansion in laser-produced plasmas 0-87918  
 trapped particle anomalous transport in Tokamak, scaling laws 0-103115  
 turbulent plasma blanket, anomalous heat transport 0-83224  
 two-temperature He plasma, transport props. 0-92260  
 velocity angle scattering of a relativistic electron beam during transport through plasma 0-92337  
 velocity modulated neutralised ion beam, evolution in potential wells, ion density distrib. (Russian) 0-100082

## plasma transport processes continued

- velocity-space diffusion in perpendicularly propag. electrostatic wave 0-59228  
 Vlasov equilibria, local Maxwellian velocity distribution 0-87928  
 W VII-A stellarator, particle and energy transport 0-83222  
 water vapour, electron energy distrib. function, electron sink and plasma resist. effect (Russian) 0-106987  
 wave-particle transport from electrostatic instabilities 0-83898  
 weakly nonideal inert gas impulse plasma, Coulomb cross-section calcs. 0-103113  
 X-ray line radiation from cylindrical Al plasma, calc. model 0-64777  
 Z-pinch turbulence spectroscopic detection and anal. (Russian) 0-100098  
 ZT-40, modelling in G2M diffusion code 0-79557  
 ZT-S reversed field pinch simulations 0-83993  
 $\alpha$  particles slowing down diffusion in fusion reactor gas (Chinese) 0-87862  
 Al, plasma, transfer eqn. soln. using freq. and angle averaged photon escape probabilities 0-64688  
 Ar discharge, ion density profile, reson. laser light meas. 0-92401  
 Ar, formation in crossed electric and magnetic fields, optical spectra 0-79452  
 Ar, low-press. glow discharge, elec. charactrs. of positive column 0-100112  
 Cs, dense plasma, ionisation equilib. and cond., ion clusters effects 0-75032  
 Cs plasma, generation by adiabatic compression, elec. cond. and thermodynamic parameters meas. 0-59180  
 Cs vapour, electrical cond. near saturation point 0-69967  
 Cs(Ar-Cs) plasmas, electron momentum transfer cross section, cyclotron reson., temp., cond., and vel. meas. 0-106930  
 H glow discharge, electron macroscopic props. (Russian) 0-92403  
 H plasma, K impurities, optical props. 0-103119  
 H plasma, magnetic piston study in theta-pinch (Russian) 0-83971  
 H plasma beam, electron macroscopic props. (Russian) 0-92403  
 H plasma target investig. (Russian) 0-106981  
 H<sub>2</sub> beam discharge, electron kinetics in collisionless non-equilibrium plasma 0-92402  
 H<sub>2</sub> transport in toroidal plasma using multigroup discrete ordinates methodology 0-69978  
 H-He gas mixtures, 1000-25000K, transport property correlations 0-75029  
<sup>2</sup>H-<sup>3</sup>H ionised plasma, fast  $\alpha$  particle energy deposition, transport eqn. 0-100071  
 H $\alpha$  and H $\beta$ , Stark profiles; ion-motion effect 0-63592  
 He I 447.1 and 492.2 nm lines, ion motion effects on Stark profiles 0-69105  
 He, low press. discharge, electron free streaming waves expansion 0-79595  
 He-O<sub>2</sub> DC discharge, electron distrib. function 0-92407  
 Hg, plasma, dense weakly ionised, thermo EMF, calc. 0-64686  
 Kr, low-press. glow discharge, elec. charactrs. of positive column 0-100112  
 Kr, plasma, high-press. arc discharge, elec. cond. 0-59181  
 Li plasma, elec. cond. at 12.5-50 MPa, (7-50)  $\times 10^3$  K 0-64685  
 N glow discharge, volt-ampere charact. in gas flow (Russian) 0-106991  
 N<sub>2</sub>, high intensity arcs, anode contraction region modeling 0-103210  
 N<sub>2</sub>, weakly ionised, electron transport coeffs., Boltzmann eqn. anal. (Japanese) 0-59183  
 N<sub>2</sub>-Cu arc plasma, transport coeffs. 0-96344  
 N<sub>2</sub>-O<sub>2</sub> gas mixture, weakly ionised, electron transport coeffs. anal. (Japanese) 0-59184  
 Ne, low press. discharge, electron free streaming waves expansion 0-79595  
 Ne plasma, electron collision ionisation, electron kinetic behaviour during elec. field perturbation (German) 0-64676  
 O<sub>2</sub>, electron energy distrib. function, electron sink and plasma resist. effect (Russian) 0-106987  
 O<sub>2</sub>, weakly ionised, electron transport coeffs., Boltzmann eqn. anal. (Japanese) 0-59183  
 SF<sub>6</sub>-inert gas mixture, high power cylindrical spark discharge, dynamic and visible charact. 0-64816  
 Xe, plasma, high-press. arc discharge, elec. cond. 0-59181

## plasma turbulence

- Alfvén wave turbulence, interaction with whistler wave turbulence 0-64728  
 amplification of ion cyclotron waves via high frequency electron plasma wave turbulence 0-92305  
 anisotropic MHD turbulence in solar wind, obs. 0-94669  
 anomalous transport from plasma waves 0-59182  
 anomalous viscosity due to EM instability in turbulent plasma 0-106901  
 anomalous viscosity due to EM instability in turbulent plasma, nonlinear theory 0-106902  
 arcs, wall-stabilised, free recovery with imposed laminar and turbulent flows 0-59321  
 charged particle, impinged, linear response theory 0-64727  
 Chirikov-Taylor model, turbulent diffusion calc. 0-79469  
 circumsolar plasma, Venera 10 radio signal spectral meas. 0-109326  
 collective modes, sum-rule anal. 0-59238  
 collisional drift modes, anomalous skin effect, enhanced particle penetration during fuelling, nonlinear theory 0-64703  
 collisional plasma, modulation instability, turbulence by const. wave pumping (Russian) 0-103139  
 collisionless plasma, polarisation by single-mode pot. drift wave 0-106920  
 correlation measurements of turbulent ionization and ion-acoustic waves 0-59329  
 discrete unstable modes, transition to turbulence, theory and expt. 0-59240  
 disruptions in Tokamaks and small scale turbulence 0-59266  
 dissipative non-Hamiltonian dynamical system, stochastic props. and strange attractors 0-57200  
 drift wave turbulence, exact Gaussian soln. 0-92325  
 electric field compression near a plasma electrode 0-64736  
 EM wave depolarisation in plasma with MHD turbulence (Russian) 0-103154  
 EM wave dissipation and superstrong turbulence in inhomogeneous plasma (Russian) 0-83919  
 energy of a turbulent, current-carrying plasma in a strong electric field 0-79514  
 fine struct. of plasma satellites of He 492.2 nm line 0-59235  
 heavy ion beam-induced ion-acoustic turbulence (Russian) 0-106923



**plasma turbulence continued**

- HF EM field, turbulent model of plasma column (*Russian*) 0-83915  
 inhomogeneous RF plasma, absorption and parametric decay of extraordinary waves 0-59206  
 ion heating by current-driven turbulence in inhomogeneous plasma 0-96370  
 ion heating due to collisionless drift-wave turbulence 0-106949  
 ion sound soliton-Langmuir wave interactions (*Russian*) 0-100077  
 ion-acoustic, effect of turbulence on anisotropic resistivity and particle transport across mag. field 0-59236  
 ion-acoustic turbulence, quasilinear evolution excited by return current 0-79502  
 ion-acoustic turbulence in solar corona, four-plasmon interactions rel. to radar signal refl. 0-101582  
 Langmuir, strong, simulations review 0-59237  
 Langmuir and ion acoustic wave coupling, turbulence spectra, light absorption 0-87902  
 Langmuir plasma, self-magnetised collapse dynamics 0-92327  
 Langmuir turbulence, ion sound upconversion, comments 0-92324  
 Langmuir turbulence, numerical modelling, solitons, nonlinear interactions 0-70030  
 Langmuir turbulence in solar corona, four-plasmon interactions rel. to radar signal refl. 0-101582  
 Langmuir turbulence in solar corona, rel. to quasi-stable particle accel. and type I radio bursts (*Chinese*) 0-105220  
 Langmuir waves, numerical modelling of 1-D turbulence, acoustic oscillations effect (*Russian*) 0-103135  
 Langmuir waves, turbulent bremsstrahlung process 0-62009  
 laser beam self-focused in turbulent plasma, average field 0-79505  
 laser plasma, convective parametric decay instability 0-64722  
 linear turbulently heated plasma, secondary emission detector obs. 0-75100  
 low- $\beta$  plasmas, turbulence, spectral struct., Bhom diffusion coeffs., determ. 0-106924  
 lower hybrid wave turbulence effect on tearing mode instability 0-92322  
 magnetoactive plasma, modulational instability caused by Langmuir oscillations 0-92297  
 mass renormalization in stochastic acceleration of particles (*Russian*) 0-100066  
 Maxwell-Klimontovich equations for turbulent plasma, renormalisation 0-79500  
 MHD generator, plasma turbulence in combustion channel 0-75057  
 MHD turbulence, generalised Lorenz eqns., strange attractors 0-59232  
 MHD turbulence in solar wind, props. 0-61977  
 Microtor Tokamak, LF microturbulence, far IR laser scatt. 0-96362  
 multicharged ion heating in Z-pinch, column compression, temp. and density (*Russian*) 0-64754  
 overdense column, reson. microwave absorpt. 0-64732  
 parametric interaction of waves in plasma with random large-scale inhomogeneities (*Russian*) 0-103137  
 partially ionised plasma, strong turbulence 0-79499  
 particle acceleration by MHD shock turbulence 0-87894  
 plasma, turbulent, parametric instabilities, anomalous energy absorpt., dispersion eqn. 0-92291  
 quasilinear theory, mode coupling 0-79498  
 renormalized Compton scattering and nonlinear damping of collisionless drift waves 0-69998  
 Rossby wave turbulence, exact Gaussian soln. 0-92325  
 shock generated turbulence, obs. in mag. plasma by CO<sub>2</sub> laser scatt. 0-84003  
 solar flare plasma instability and turbulence, review 0-62100  
 solar wind upstream of Earth bow shock, nonlinear plasma processes 0-85833  
 stationary MHD eqns. for rotating toroidal plasma 0-92278  
 stellarator, current turbulent ion heating, modulation stability 0-79525  
 strong turbulence and anomalous diffusion in mag. field 0-59239  
 strong turbulence effects on the kinetic beam-plasma instability 0-59207  
 strongly turbulent stabilization of electron beam-plasma interactions 0-59251  
 Tokamak, far IR laser collective scatt. system 0-59300  
 Tormac, Gaussian HeII 4686 Å spectral lines, Doppler and Stark broadening effect, turbulence 0-106980  
 turbulence, 2-D, hydrodynamic and plasma applications, dynamical eqns., diffusion, MHD, superfluidity, review 0-69769  
 turbulent plasma, magnetised, line shape of optical satellites 0-75098  
 vortex-acoustic ion wave turbulence, statistical mechanics 0-92326  
 vortices in laser-produced plasmas 0-79501  
 whistler-Alfvén turbulence interaction 0-75058  
 Z-pinch turbulence spectroscopic detection and anal. (*Russian*) 0-100098  
 CO<sub>2</sub> laser light collective scatt. meas. 0-84005  
 H glow discharge, electron macroscopic props. (*Russian*) 0-92403  
 H plasma, magnetic piston study in theta-pinch (*Russian*) 0-83971  
 H plasma beam, electron macroscopic props. (*Russian*) 0-92403  
 H<sub>2</sub> beam discharge, electron kinetics in collisionless non-equilibrium plasma 0-92402

**plasma-wall interactions**

- see also *plasma impurities*  
 ablation stabilised arc theory 0-70072  
 advanced fuel fusion reactor wall loading limitations and stability index beta 0-99311  
 air, wall-stabilised arc, step and sinusoidal current change response 0-103209  
 air plasma flow in channel inlet zone, local heat transfer 0-64687  
 alumina confined arc, ablation-induced effects 0-70073  
 anomalous transport processes in radially compressed reversed-field configurations, numerical simulation 0-64689  
 arcs, wall-stabilised, free recovery with imposed laminar and turbulent flows 0-59321  
 atomic and surface physics, conf., Salzburg, Austria (Feb. 1980) 0-57010  
 atomic processes determining the plasma-wall interaction 0-59247  
 blanket, NOEL (No External Leak), thermal anal. and tests 0-95459  
 CT-6 Tokamak plasma props. (*Chinese*) 0-103159  
 DC glow discharge in tube with walls of different catalytic activity 0-100103  
 Doublet III, limiter performance, design and material selection 0-106162  
 electron cyclotron reson. ion source with permanent mags., plasma-wall interaction expts. 0-99378  
 equilibrium in free boundary case, variational principle calcs., wall interaction (*Chinese*) 0-69972

**plasma-wall interactions continued**

- heat transfer rates to flat plate from normally-impinging N plasma jet 0-75061  
 Kharkov stellarators, plasma-wall interactions 0-79552  
 magnetic confinement system, surface problems caused by dissolved H<sub>2</sub> 0-57946  
 MFTF, end loss region high energy plasma gettering 0-102343  
 narrow inhomogeneous layer, surface wave-incident radiation nonlinear interaction 0-100080  
 negative ion emission in electrode layer of low-temp. plasma 0-70006  
 nonexponential Debye shielding rel. to electrode-plasma pot. difference 0-100081  
 perspex confined arc, ablation-induced effects 0-70073  
 reactive plasma, optical emission spectroscopy, emission intensities and reactive density, correl. method 0-92385  
 secondary electrons in plasma-wall sheath, Langmuir probe obs. 0-92387  
 solid H pellet interaction with magnetised plasma 0-78451  
 Tokamak, blanket and first wall design concept, thermal and hydraulic anal. 0-95460  
 Tokamak, current transitions at plasma-wall interface 0-83984  
 Tokamak, electrically isolated target, formation of arcing, role of runaway electrons 0-64764  
 Tokamak fusion test reactor, thermal response of first wall limiters 0-79585  
 Tokamaks, column wall interactions, in-situ meas. on PDX 0-59248  
 ultrahigh vacuum transfer system, 15 cm diameter, for remote plasma-wall interaction expts. 0-86327  
 C bonding to Tokamak walls, XPS studies 0-80942  
 N, high intensity arcs, anode contraction region modeling 0-103210  
 O bonding to Tokamak walls, XPS studies 0-80942  
 SF<sub>6</sub> plasma interaction with solid polymer, emission-spectra 0-87960  
 UF<sub>6</sub>, high temp. fissioning plasma core reactors, fluid mechanical confinement 0-63248
- plasma waves**  
 see also *magnetohydrodynamic waves; plasma oscillations; plasma shock waves*  
 absolute dissipative drift-wave instabilities in Tokamaks 0-92296  
 Alfvén, current driven, electron-ion collisions and full dispersion function, numerical anal. 0-64726  
 Alfvén nonlinear gravit. drift waves and  $\beta$  limitations in Tokamaks 0-92369  
 Alfvén surface waves, propag. along cylindrical plasma columns 0-106913  
 Alfvén wave turbulence, interaction with whistler wave turbulence 0-64728  
 Alfvén waves, in stochastic mag. field, Khasminskii's theorem 0-59198  
 Alfvén waves, resonant absorption 0-92323  
 Alfvén waves, soln. for MHD equations, properties (*Russian*) 0-106891  
 amplification of ion cyclotron waves via high frequency electron plasma wave turbulence 0-92305  
 amplification of radiation near cyclotron frequency due to electron population inversion 0-92271  
 anomalous transport from plasma waves 0-59182  
 asymmetric plasma resistivity, creation using waves 0-103171  
 Bernstein dispersion relation for oblique propagation 0-75052  
 Bernstein waves, propagation in inhomogeneous plasma, dispersion rel., quasi-linear equations, diffusion coeff. determ. 0-75044  
 breakdown wave propagation in ionised gas in nanosecond discharges 0-87890  
 Brillouin and Raman scattering of an extraordinary mode in a magnetized plasma 0-92269  
 caviton, dissipative three-dimens. Langmuir soliton, formation (*Russian*) 0-83943  
 caviton dynamics at crit. density 0-106909  
 coherent wave particle interaction in Q-machine plasma, electrostatic analyser diagnostics 0-59226  
 collisionless plasma, polarisation by single-mode pot. drift wave 0-106920  
 convective amplification of drift waves and thermal fluctuation levels in a stable plasma 0-83932  
 convective amplification of universal drift modes 0-59208  
 convective cell nonlinear excitation and anomalous diffusion, in inhomogeneous plasma 0-79468  
 convective cells, nonlinear excitation by interchange modes and spectrum cascade processes 0-69997  
 converging ion acoustic soliton excitation in double plasma type device 0-106907  
 converging nonlinear resonance cone trajectories 0-92299  
 correlation function, long time asymptotic behaviour, influence of waves on relax. processes (*Chinese*) 0-59195  
 coupled mode equations, linearised, space time solns. 0-87884  
 coupled three wave system, instability saturation, bifurcations and strange attractor 0-59233  
 coupled waves in stratified Chew-Goldberger-Low plasma 0-87875  
 coupling to the fast wave at lower hybrid frequencies for plasma heating 0-75069  
 criterion for absolute instability of a wave in a nonuniform medium 0-106903  
 Culham Levitron, drift island diffusion 0-59267  
 Culham Levitron, electrostatic fluctuations 0-79482  
 decay of a lower-hybrid wave to two lower-hybrid waves 0-87883  
 decaying plasma, nonequib. props. during afterglow modulation by acoustic waves 0-103144  
 deexcitation wave emission and thermal fluctuations of inhomogeneous plasma (*Russian*) 0-106892  
 deflagration wave formed by ion waves, energy from fusion reaction effects 0-79478  
 delay line simulation, wave propag. in dispersive and attenuating media 0-82606  
 density fluctuation in collisional plasma 0-75053  
 destabilization of drift-universal eigenmodes by toroidal effects 0-103148  
 discrete unstable modes, transition to turbulence, theory and expt. 0-59240  
 dispersion equations in moving media, relativistic electrodynamics 0-57089  
 dissipative balloon non-threshold modes (*Russian*) 0-70000  
 double layers modelled by numerical integration of Vlasov-Poisson system 0-92290  
 draft waves driven by temperature gradients, ballooning limit 0-106917  
 drift, current driven, electron-ion collisions and full dispersion function, numerical anal. 0-64726



## plasma waves continued

- drift wave, HF, current-driven inhomogeneous plasma instability 0-59204  
 drift wave, low freq., pseudoclassical diffusion in Tokamak (*Chinese*) 0-69990  
 drift wave eigenmodes, effect of finite ion Larmor radius (*Chinese*) 0-103133  
 drift wave turbulence, exact Gaussian soln. 0-92325  
 drift waves, eigenmodes with arbitrary radial wavelengths, stability 0-64710  
 drift waves, magnitude of radial electric field determ. (*Russian*) 0-103175  
 drift waves in sheared mag. field, variational method calcs. 0-106910  
 EBT heating, electron-cyclotron absorption and microwave propagation 0-64749  
 echo, linear, in plasma with strongly inhomogeneous magnetic field 0-106919  
 eikonal expansion of the Vlasov-Maxwell equations valid near cyclotron resonance 0-92300  
 electron acoustic solitary wave propag. in magnetoplasma 0-75051  
 electron beam, kinetic, quasilinear relax., self-similar solns. 0-64702  
 electron beam-magnetoplasma, radiation at or near electron plasma frequency, transverse modes 0-106942  
 electron beam-plasma system, Simon short-circuit effect, freq. shift 0-96366  
 electron beams, modulated, non-linear oscillation theory (*Russian*) 0-106898  
 electron Bernstein modes, nonlinear scatt. of upper hybrid laser radiation 0-64720  
 electron collision effect on wave-breaking in cold plasma 0-96353  
 electron cyclotron emission from Tokamak plasmas with mildly superthermal electrons 0-92270  
 electron free streaming waves expansion in low press. discharges 0-79595  
 electron gas, screening of ionic motions by electronic background 0-64678  
 electron nonlinear waves in strongly magnetised plasma 0-79472  
 electron plasma waves, ionospheric, excitation by strong microwaves from solar power satellite, theoretical anal. (*Japanese*) 0-94634  
 electron plasma waves in a two-temperature plasma 0-92285  
 electrostatic, magnetised plasma charged particle stochastic accel. 0-59230  
 electrostatic, perpendicularly propag., vel.-space diffusion 0-59228  
 electrostatic, stochastic heating of plasmas in inhomogeneous magnetic fields 0-59231  
 electrostatic, stochastic ion motion, mag. field config. depend. 0-59229  
 electrostatic, three-wave interaction in oscillating elec. field 0-69995  
 electrostatic drift instability of Tokamak plasmas 0-96358  
 electrostatic drift mode coupling in torus 0-59213  
 electrostatic pulse generation by two electromagnetic pulses 0-92295  
 electrostatic wave excited by current pulse in warm magnetoplasma, theory 0-77240  
 electrostatic waves, nonlinear motion, particle trapping 0-64713  
 electrostatic waves in Jupiter magnetosphere, obs. 0-72865  
 electrostatic waves in magnetosphere, rel. to inverse loss cone electrons temp. anisotropy relaxation (*Russian*) 0-109314  
 EM drift waves, eigenvalues, coupled second-order differential eqns., numerical soln. method 0-94976  
 EM pulse, conversion to Langmuir wave in plasma 0-92308  
 EM soliton propagation in nonequilibrium dispersive media (*Russian*) 0-106933  
 EM wave dissipation and superstrong turbulence in inhomogeneous plasma (*Russian*) 0-83919  
 EM wave penetration into half-space collisional plasma 0-106928  
 EM wave resonance tuning of magnetoactive plasma (*Russian*) 0-83914  
 EM waves, nonlinear generation in electron-positron plasma (*Russian*) 0-106973  
 EM waves in magneto-active plasma, group velocity direction 0-59201  
 EM waves in plane inhomogeneous plasma in presence of mag. field shear, appl. to plasma diagnostics (*Russian*) 0-103140  
 EM waves propagating along mag. field in strongly anisotropic relativistic plasma, dispersion props. 0-67542  
 emission, absorption and transfer of waves in astrophysical diffuse magnetised plasmas, book 0-105446  
 excited atoms, radial distrib., prod. by surface wave (*French*) 0-96349  
 explosively unstable, in ion beam-plasma system, pump field method obs. 0-92333  
 geometrical optics formalism 0-83925  
 guided electron plasma waves, propag. along cylinder, dissipative processes effects 0-92332  
 guided solitary waves from Boussinesq eqns. 0-92298  
 harmonics generation in inhomogeneous plasma (*Russian*) 0-83916  
 HF EM field, turbulent model of plasma column (*Russian*) 0-83915  
 HF heating by MHD waves of finite press. plasma (*Russian*) 0-83950  
 high temperature plasma, physics, book 0-98767  
 hybrid waves, lower, backscatter, effect of waveguide boundary conditions 0-64709  
 inhomogeneous RF plasma, absorption and parametric decay of extraordinary waves 0-59206  
 instability, electrostatic, parametric, due to thermal coupling 0-79465  
 instability of two dimensional waves, critical drift velocities, oscill. growth factor (*Russian*) 0-106922  
 ion acceleration by space charge waves in straight-line electron beam 0-103166  
 ion acoustic soliton reflection and transmission at plasma interface 0-106899  
 ion acoustic solitons in beam plasma system with nonisothermal electrons generated by ion-beam 0-103151  
 ion acoustic wave, self excited, in hot plasma, dispersion theory 0-92283  
 ion acoustic waves, diverging cylindrical, recurrence investigation 0-79474  
 ion acoustic waves, ionospheric, excitation by strong microwaves from solar power satellite, theoretical anal. (*Japanese*) 0-94634  
 ion acoustic waves method of plasma potential meas. 0-59289  
 ion beam-plasma collective interactions, high current-density 0-75066  
 ion beam-plasma system, absolute and convective instabilities of electrostatic ion cyclotron waves 0-64740  
 ion beam-plasma system, higher-order modes of space charge waves 0-69992  
 ion heating by current-driven turbulence in inhomogeneous plasma 0-96370  
 ion heating due to collisionless drift-wave turbulence 0-106949

## plasma waves continued

- ion pressure gradient driven drift modes; 3-dimens. fluid simulation 0-103150  
 ion sound soliton-Langmuir wave interactions (*Russian*) 0-100077  
 ion wave, far IR laser scatt. diagnostics 0-59297  
 ion wave effects in open cylindrical magnetoplasma device, turbulent thermal insulation 0-106914  
 ion-acoustic, effect of turbulence on anisotropic resistivity and particle transport across mag. field 0-59236  
 ion-acoustic, from parametric instability, microwave p-i-n diode modulator, transient plasma instability meas. (*German*) 0-87942  
 ion-acoustic holes in a two-electron-temperature plasma 0-59205  
 ion-acoustic pulse generation by 2 EM pulses at difference freqs. in collisionless plasma 0-79475  
 ion-acoustic solitons, two-dimens. interaction 0-106908  
 ion-acoustic solitons with a temperature gradient 0-79490  
 ion-acoustic wave, phase velocity 0-103147  
 ion-acoustic waves, soln. for MHD equations, properties (*Russian*) 0-106891  
 ion-acoustic waves and turbulent ionis., correlation meas. 0-59329  
 ion-acoustic waves freq. and damping from dispersion relations 0-69991  
 ion-acoustic waves in solar wind, wave-particle interactions rel. to particle vel. distrib. (*German*) 0-109323  
 ion-cyclotron RF field, plasma convective loss, elimination by mode control 0-83957  
 ion-cyclotron waves in topside ionosphere, noise source 0-101470  
 ionisation wave, obs. of phase modulation 0-69993  
 ionisation waves, in positive column, wave packet propag. 0-96356  
 ionosphere plasma interaction with gravity waves, elec. field and current prod. 0-61957  
 kilometeric radiation in Jupiter magnetosphere, spatial and temporal studies 0-77328  
 Langmuir and ion acoustic wave coupling, turbulence spectra, light absorption 0-87902  
 Langmuir collapse, dimensionality and dissipation 0-87880  
 Langmuir wave interference, electron collisions (*Russian*) 0-69970  
 Langmuir wave production, ion sound upconversion, comments 0-92324  
 Langmuir waves, large amplitude, nonlinear Landau damping and form. of standing nonlinear waves 0-92292  
 Langmuir waves, numerical modelling of 1-D turbulence, acoustic oscillations effect (*Russian*) 0-103135  
 Langmuir waves, turbulent bremsstrahlung process 0-62009  
 Langmuir waves in Vlasov plasma, nonlinear theory, wave-particle interaction 0-64701  
 Langmuir waves in Vlasov plasma, nonlinear theory, wave-wave interaction 0-64700  
 laser gas breakdown, shock and ionisation waves, photographic absorpt. obs. 0-87967  
 longitudinal waves in an electron plasma in a weak magnetic field 0-92312  
 low-frequency waves, obs. in vicinity of Earth bow shock 0-90311  
 low-frequency waves ( $\leq 50$  Hz), possible generation mechanisms with appl. to Earth bow shock 0-90312  
 lower hybrid drift waves in magnetosphere boundary layer, excitation by field-aligned currents 0-67473  
 lower hybrid solitons, envelopes in magnetic fields 0-59224  
 lower hybrid wave, nonresonant parametric decay, quasi-modes 0-59197  
 lower hybrid wave, unidirection, current generation in ACT-I 0-92306  
 lower hybrid wave heating, electron distrib. function (*Russian*) 0-83951  
 lower hybrid wave heating simulation in nonuniform plasma 0-64771  
 lower hybrid wave turbulence effect on tearing mode instability 0-92322  
 lower hybrid wave turning point location, nonuniform magnetoplasma 0-79473  
 lower hybrid waves, current-driven electrostatic ion-cyclotron instability 0-103149  
 lower hybrid waves, in octopole Tokamak, ray trajectories 0-64707  
 lower hybrid waves, propag. in toroidal plasma 0-83927  
 lower hybrid waves, trajectories and damping in Tokamak plasma 0-83922  
 lower hybrid waves in nonuniform plasmas, geometric optics 0-83924  
 lower oblique whistler resonance cone, interference struct. in Maxwellian magnetoplasma 0-59219  
 lower-hybrid waves, focusing and channelling during HF-breakdown of gas (*Russian*) 0-106890  
 lower-hybrid waves in collisional plasmas with field-aligned current, instability 0-75045  
 lower-hybrid-drift instability in field reversed plasmas 0-59209  
 magnetised, parametric instabilities with well separated freq. (*Chinese*) 0-106887  
 magnetized inhomogeneous plasma, wave reson. and conversion 0-92313  
 magneto-acoustic waves, soln. for MHD equations, properties (*Russian*) 0-106891  
 magnetoacoustic heating by ion Landau damping 0-92341  
 magnetoacoustic resonance in strongly inhomogeneous He plasma 0-69994  
 magnetoactive collisional plasma, dielectric tensor, refl. index and attenuation 0-59202  
 magnetoactive plasma, low frequency waves excitation, relativistic effects (*Russian*) 0-103184  
 magnetosonic and Alfvén waves, transfer by solar wind 0-67490  
 magnetosonic cavity modes, complex plasma loading impedance meas. 0-59215  
 magnetosonic waves, rel. to fine struct. of magnetic shocks in collisionless plasma 0-85854  
 magnetosonic waves near Earth bow shock, propag. and transport from initial ISEE obs. 0-90307  
 maser emission, by plasma produced electrons orbiting a positively charged wire 0-92272  
 medium beta plasma with velocity gradients, dispersion relation for drift waves 0-64719  
 Microtor Tokamak, LF microturbulence, far IR laser scatt. 0-96362  
 mode conversion of lower-hybrid waves 0-87882  
 mode converted lower hybrid solitons, stability in parametric regions 0-92303  
 modulational instability of nonlinear wave propagation in relativistic plasmas 0-106911  
 moving collisional plasma and moving plasma with intrinsic spatial dispersion, emission of longit. waves 0-87848  
 moving weakly nonsteady plasma, propag. of plasma waves 0-106918  
 multi-ion system, modulation instability of ion acoustic waves 0-69996



**plasma waves continued**

narrow inhomogeneous layer, surface wave-incident radiation nonlinear interaction 0-100080  
 negative wave momentum density in plasma 0-79463  
 non-neutral column, wave coupling 0-75054  
 nonlinear Alfvén wave in an ultra-relativistic electron-positron plasma 0-106905  
 nonlinear drift wave evolution, model eqn. 0-100075  
 nonlinear equilibrium state of wave-beam, kinetic theory (*Russian*) 0-106888  
 nonlinear mode coupling model equations, topological struct. 0-75056  
 nonlinear processes in magnetised plasma, nonstationary HF pressure (*Russian*) 0-106895  
 nonlinear scattering of laser radiation by fast ion waves in plasma 0-106916  
 nonlinear Schrödinger equation, modified Zakharov-Shabat inverse scatt. problem 0-59200  
 nonlinear subharmonic wave generation in nonuniform plasmas 0-106912  
 nonlinear theory of collisional drift-waves in toroidal geometry and anomalous skin effects in Tokamaks 0-92320  
 nonlinear theory of unstable plane waves and solitons 0-87888  
 nonlinear three wave mode coupling, instability saturation 0-87881  
 nonlinear wave packet acceleration and slowing down 0-59203  
 nonlinear waves in cold plasma, classical Vlasov plasma description through quantum numerical methods 0-92288  
 nonresonant decay of lower hybrid waves 0-92315  
 oblique collision of ion-acoustic solitons 0-83934  
 oblique Langmuir solitons under free path conditions (*Russian*) 0-79477  
 parametric instabilities of inhomogeneous plasma in presence of long-wave low frequency oscillations (*Russian*) 0-103136  
 parametric instabilities set up by EM radiation in non-uniform magnetoactive plasma (*Russian*) 0-106889  
 parametric instability, thermal fluctuation effect in inhomogeneous plasma (*Russian*) 0-106897  
 parametric instability due to a low frequency whistler wave 0-83926  
 parametric interaction of waves in plasma with random large-scale inhomogeneities (*Russian*) 0-103137  
 particle scattering by low freq. waves, effective scatt. freq., eval. method 0-83882  
 propagation in moving cold magnetised plasma, polarisation relations and dispersion eqns. 0-64723  
 propagation in self-gravitating isotropic press. plasma theory 0-72763  
 proton-cyclotron frequency harmonic waves, rel. to instabilities in nonuniform loss-cone magnetospheric plasma 0-90286  
 radiation from waveguide, rel. to plasma wave scatt. by ion-acoustic oscils. 0-87886  
 relativistic plasma, nonlinear dispersion relation for transverse wave 0-87939  
 renormalized Compton scattering and nonlinear damping of collisionless drift waves 0-69998  
 resistive drift Alfvén waves in sheared mag. fields 0-64718  
 resonance cone, in inhomogeneous magnetoplasma column, theoretical anal. 0-83884  
 resonance cone in inhomogeneous magnetoplasma column, quasistatic approx. 0-64724  
 resonances in the ion cyclotron range in toroidal geometries 0-83938  
 resonant excitation of slow low-freq. waves by opposite moving electron beams (*Russian*) 0-92336  
 RF driven current generation by lower hybrid waves in Tokamak 0-103116  
 RF emission, plasma wave scatt. by ion-acoustic waves in nonequilibrium plasma 0-64733  
 RF plasma heating, resonant surface accessibility, surface wave role 0-92346  
 Rossby wave turbulence, exact Gaussian soln. 0-92325  
 second order harmonic surface wave generation by fundamental wave 0-92307  
 second-harmonic generation of upper-hybrid radiation in a plasma 0-79506  
 shear Alfvén waves, quasi-linear theory 0-64714  
 shear flow stability and Alfvén waves in magnetised plasma 0-96360  
 single Langmuir solitons, perturbation anal. 0-69999  
 slow wave struct., nonlinear coupling with lower hybrid waves near plasma surface 0-92309  
 solar corona, direct conversion of Langmuir waves into o-mode waves 0-72896  
 solar corona, electron flows stabilisation in inhomogeneous plasma 0-109411  
 soliton solutions in media with inverse dispersion 0-103152  
 solitons, numerical modelling of Langmuir turbulence 0-70030  
 solitons of flexural EM waves in magnetoactive plasma (*Russian*) 0-83918  
 space charge ionising waves, high velocity propagation 0-87889  
 spectrum of ionospheric waves, meas. via satellite-borne cross-power spectrum analysers 0-94621  
 spherical thermal waves in laser produced plasma 0-59217  
 stimulated Brillouin scattering initiated by ponderomotive force density fluctuations 0-103129  
 stimulated plasma waves in magnetosphere, appl. to plasmopause meas. and propag. waves mode determ. (*Japanese*) 0-94650  
 stimulated plasma waves in magnetosphere, JIKIKEN (EXOS-B) satellite expts. (*Japanese*) 0-94649  
 stimulated scattering processes, saturation by electrostatic daughter waves nonlinear decay 0-79509  
 stimulated waves in magnetosphere, prod. by JIKIKEN electron beam-plasma interaction expt. (*Japanese*) 0-94655  
 surface heating, density rippling, and propagation cones in high-power lower-hybrid heating 0-92342  
 surface ion acoustic waves in non isothermal gas layer (*Russian*) 0-87891  
 surface waves, HF, parametric excitation using slanted, incident EM waves (*Russian*) 0-87874  
 SW parametric instability of inhomogeneous plasma, semi-bounded by vac. (*Russian*) 0-83917  
 theta pinch, low density, step-like mag. piston 0-103182  
 three wave interaction in cold semi-infinite plasma 0-79462  
 Tokamak, large aspect ratio, two-dimens. drift-wave stability 0-79479  
 Tokamak plasma, lower hybrid wave propag. and damping, numerical study 0-64698  
 Tokamak plasma, quasi-mode parametric excitations in lower-hybrid heating 0-64748  
 trajectories and electron cyclotron heating in Tokamak plasmas 0-83923

**plasma waves continued**

transverse waves in magnetoplasma subjected to stochastic mag. field, normal mode approach 0-75049  
 trapped ion mode inhibition by drift wave fluctuation 0-59211  
 two Langmuir wave parametric decay instability, self-trapped EM pump wave effects 0-96357  
 two-stream plasma, development of instability of dispersed waves (*Russian*) 0-103138  
 ultra-relativistic electron-positron plasma, macroscopic wave behaviour 0-106904  
 unshielded plasma waveguide excitation by modulated electron beam 0-79512  
 upper hybrid mode emissions in magnetosphere, obs. during JIKIKEN (EXOS-B) satellite initial phase (*Japanese*) 0-94675  
 velocity modulated neutralised ion beam, evolution in potential wells, ion density distrib. (*Russian*) 0-100082  
 Venus environment, plasma wave investigation by Pioneer Venus Orbiter 0-67497  
 VLF waves, magnetospheric, obs. and comparison with high energy electron flux by EXOS-B satellite (*Japanese*) 0-94652  
 wave radiation by oscillating electric dipole in moving warm plasma 0-87868  
 wave-particle transport from electrostatic instabilities 0-83898  
 whistler mode signals generation in presence of enhanced fluctuations in plasmas 0-92293  
 whistler waves, rel. to fine struct. of magnetic shocks in collisionless plasma 0-85854  
 whistler-Alfvén turbulence interaction 0-75058  
 Ar decaying pulsed discharge plasma, acoustic waves density modulation 0-103143  
 CO<sub>2</sub> laser beam scatt. by microscopic fluctuations in plasma density 0-79574  
 H, ACT-I toroidal plasma, externally launched ion Bernstein wave 0-106967  
 Hg vapour line splitting on Tonks-Dattner reson. 0-59317  
 SF<sub>6</sub>, discharge and oscill. due to axial injection of impulsive electron beam 0-59316  
 SF<sub>6</sub> gas, low press., excitation of nonlinear wave by repeated pulsed electron beam 0-87878

**plasmotrons** see *plasma diodes*  
**plasmoids** see *plasma*  
**plasmons**  
 see also *phonon-plasmon interactions; solid-state plasma*  
 A-15 compounds, disordered, resist. and supercond. transition temp. 0-107944  
 adsorbate and clean surfaces, electronic props. (*French*) 0-80344  
 CDW distorted solid, quasi-one-dimens., charge density fluctuations and dielec. matrix 0-107726  
 chemisorption, image charge effects, surface plasmons 0-84381  
 chemisorption, image charge effects on adsorbate valence spectra, perturbational study 0-84380  
 4-cyano-4'-n-pentylbiphenyl, refr. index meas. and isotropic-nematic phase transition study, surface plasmon technique 0-84282  
 diamond, quasiparticle states, quantitative calc. 0-88499  
 dispersion for strong coupling 0-103111  
 electron excitation of plasmons and interband transitions, book 0-77555  
 electron gas, degenerate, in metal or semicond. slabs, surface plasmon damping 0-88501  
 electron gas, dielectric function, dynamical exchange decoupling, plasmon dispersion, SDW and CDW 0-59900  
 excitation during X-ray scatt. 0-108297  
 exciton energy levels, influence of exciton gas and electron-hole plasma 0-96795  
 inelastic positron scatt. in electron gas, plasmon excitation 0-92843  
 inert gas solids, collective excitations and EELS, calc. 0-92842  
 Josephson junction, ultrasmall, dynamic Stark splitting 0-103790  
 metal, plasmon satellite struct. in (e,2e) process 0-96809  
 metal surface, force on moving charge, spatial dispersion effects 0-65646  
 metal surface, mol. vibr. energy transfer, classical EM theory 0-96806  
 metal surface, rough, anomalous low-freq. Raman scatt. from localised acoustic vibrs. 0-93307  
 metal surface electrodynamics, optical refl. coeffs. and surface plasmon dispersion law 0-75619  
 metallic rough surface, reflection loss for s and p polarised waves near surface plasmon freq. (*French*) 0-97225  
 metallic surface energy, exchange and correl. contrib., wave-vector decomp. 0-75615  
 metallic thin films (*French*) 0-60692  
 metals, classical plasma frequency in long-wavelength limit, quantum correction 0-107728  
 metals, inelastic scatt. of fast electron, plasma oscillations effect 0-100439  
 metals, unidimensional, plasmon freq., effect of nonuniform electron density profile (*Russian*) 0-59896  
 narrow gap semiconductors, recombination mechanisms, review 0-96905  
 nonlinear surface-wave interaction, in plasmalike media, theory 0-107839  
 piezoelectric crystal, plasmon transformation into SAW 0-59903  
 polycrystalline:AsF<sub>3</sub>(I), pure and doped, electronic excitations, momentum depend., EELS study 0-76121  
 polystyrene coated Ag holographic grating, Raman spectra enhancement by plasmon surface polaritons 0-80885  
 semiconductor, MM wave guiding and control by surface plasmons 0-103713  
 semiconductor, non-equilibrium, acoustic plasma oscils. generation 0-96811  
 solar corona, efficiency of four-plasmon interactions in radar signal refl. from Sun 0-101582  
 soliton solution in the wake interaction due to virtual plasmon exchange 0-65108  
 spherical particle, surface enhanced Raman scatt. by molecules 0-95629  
 superconducting thin films Cooper pairs, photon scatt. on plasmons, Landau-Ginzburg theory 0-65738  
 superlattice, image pot. enhancement by static elec. field 0-92846  
 superlattices, plasmons, two-dimens., due to piezoelec. effect 0-92845  
 surface enhanced Raman scattering surface plasmon model 0-108211  
 surface magnetoplasmon type polaritons, LF, existence criterion in Faraday config. 0-96961  
 surface plasmon dispersion relation at short wavelengths 0-96962  
 surface plasmon dispersion relation in presence of surface roughness 0-65650



**plasmons continued**

- surface polariton dispersion curve, optical obs., demonstration 0-101690  
voids and particles, Van der Waals energy between them, from asymptotic to close contact 0-80351  
waveguide scattering problem, comparison of two perturbation theories 0-83662  
Ag foil, surface-plasmon resonance, roughness-induced wavelength corrections 0-108288  
Ag foils, surface plasma-wave reflectance and roughness-induced scatt. 0-66228  
Ag, surface plasmon dispersion relation in presence of surface roughness 0-65650  
Al, Auger spectra, KLL and KLV, screening effects and plasmon gains 0-80913  
Al, small spheres, bulk plasmons damping 0-75561  
Al-Mn(Ni)(Cu), dil., core and valence band spectra, XPS study 0-84837  
Au/Al thin film, Al diffusion studied by attenuated total reflection method 0-92722  
CO, adsorbed on jellium, surface plasmon relax. energies 0-70537  
Dy<sub>2</sub>S<sub>3</sub>, optical props. and electronic struct. in fund. absorpt. region 0-80817  
EuO (100), EELS, Eu valence in surface region and high energy giant reson. 0-84816  
FeCl<sub>3</sub> intercalated with graphite, stage 1, dielec. response and intraband plasmon dispersion 0-59902  
Ge, volume plasmon, cryst. orientation influence 0-80921  
La<sub>2</sub>S<sub>3</sub>, optical props. and electronic struct. in fund. absorpt. region 0-80817  
Li, plasmon satellite struct. in (e,2e) process 0-96809  
β-LiAl, optical dispersion, room temp. reflectance spectra 0-66195  
Mg, Auger spectra, KLL and KLV, screening effects and plasmon gains 0-80913  
Mg, XPS, plasmon gains as monitor of incomplete relax., interference effects and sudden to adiabatic limits transition 0-66390  
N<sub>2</sub> film, on metal or sapphire substrates, luminescence and nonradiative energy transfer to surfaces 0-97350  
Na, Auger spectra, KLL and KLV, screening effects and plasmon gains 0-80913  
Na, IR and optical props., surface-plasmon-mediated absorpt. mechanism 0-93308  
Na, plasmon satellite struct. in (e,2e) process 0-96809  
Na, XPS, plasmon gains as monitor of incomplete relax., interference effects and sudden to adiabatic limits transition 0-66390  
Nd<sub>2</sub>O<sub>3</sub>, EELS, low loss peak due to plasmon 0-79953  
Nd<sub>2</sub>S<sub>3</sub>, optical props. and electronic struct. in fund. absorpt. region 0-80817  
Pb<sub>1-x</sub>Sn<sub>x</sub>Se epitaxial layers, radiative and nonradiative recomb. processes 0-60670  
Pb<sub>0.75</sub>Sn<sub>0.25</sub>Te, Pb<sub>0.9</sub>Sn<sub>0.09</sub>Se, radiative and nonradiative recombination 0-80849  
Si, Auger spectra, KLL and KLV, screening effects and plasmon gains 0-80913  
Si, bulk plasmon dispersion, electron energy loss spectra meas. 0-59899  
Si, laser induced dense plasma, dynamics 0-65612  
Si, non thermal laser induced ordering, plasma life time, phonon interactions 0-84481  
TiH<sub>2</sub> and TiD<sub>0.9</sub>, surface charact., AES, EELS, SIMS, and XPS study 0-65343  
US(Se)(Te), electronic struct. and exchange band splitting, optical refl. meas. 0-66226

**plastic after-flow** *see recovery-creep***plastic afterflow** *see recovery-creep***plastic crystals**

- adamantane, cryst., vacancy formation energy, positron annihilation study 0-60706  
adamantane, plastic and solid-solid transitions, Raman study 0-60590  
adamantane, plastic phase, C<sub>4</sub> rot. jumps, existence and uniqueness 0-88067  
adamantane, thermal cond. and heat capacity under press. 0-80008  
2-adamantanone, cryst. struct. in plastic phase 0-88065  
camphor, orientational disordering, thermodynamic props., stat. mech. model 0-96453  
carbon tetrabromide, disordered phase, neutron, diffuse scatt. 0-79717  
carbon tetrabromide, disordered phase, neutron diffuse scattering 0-79716  
diamantane, plastic and solid-solid transitions, Raman study 0-60590  
dilatometer for PVT meas. of liquids and plastic crystals at low temperature 0-68208  
ethane, solid, mol. reorientational motions, incoherent neutron scatt. studies 0-107070  
ethanol, polymorphic forms, mol. motion, NMR obs. 0-88885  
methane, solid, plastic phase, mol. dynamics simulation 0-79715  
orientational disorder, group theory method 0-107091  
orientational disordering, melting transitions, thermodynamic props. 0-96452  
orientational disordering, thermodynamic props., stat. mech. model 0-96453  
orientational dynamics, neutron scatt. data interpret. using functions derived from group theory 0-107092  
sulpholan, molecular solid, laboratory frame and rotating frame spin-lattice relax., pulsed NMR meas., phase transitions obs. 0-93197  
tetrabromomethane, thermal resistivity, heat capacity and phase diagram under pressure 0-65316  
triadmantane, plastic and solid-solid transitions, Raman study 0-60590  
tris(hydroxymethyl)aminomethane, plastic struct., phase transform. studied by X-ray diff. 0-84130  
DCl, plastic cryst. phase, struct. and dynamics 0-92469  
Li<sub>2</sub>SO<sub>4</sub>, fast ion conductors, X-ray diff., neutron diff., and Brillouin scatt. study 0-107170  
γ-O<sub>2</sub>, mol.-dynamic study of struct., dynamics 0-96467  
O<sub>2</sub>, two-dimensional adsorbed layer on graphite, props. calc. 0-103568

**plastic deformation**

- see also Bauschinger effect; buckling; creep; ductility; elastoplasticity; kink bands; Luder's bands; necking; plastic flow; serrated yielding; shape memory effects; slip; superplasticity*  
acoustic emission appl. to materials testing plastic strain and growing cracks identification 0-81252  
alkali halides, dislocation dynamics studied by nucl. spin relax. meas. 0-108091  
alloys, high temperature, creep failure criteria 0-65150

**plastic deformation continued**

- alloys, machining damage, depth of surface layers determ. 0-85094  
alloys, statistical model in conditions of monotonous cyclic loading (*Bulgarian*) 0-70296  
angled elliptic notch problem under biaxial loading, strain failure criterion 0-79235  
BCC crystal, cyclic deformation, irreversible glide and shape changes 0-103356  
beams thin-walled, of open cross section, finite-element model 0-74767  
bending beam, slip line development 0-58928  
brass, Cu-Zn (39/40) wt.%, shape memory effect and martensitic transform. depend. on heating-cooling cycles (*Russian*) 0-97482  
α-brass, plane stress ductile fracture, prestrain effects 0-108532  
brass, plastic deformation, stress-strain relation of integral type 0-74754  
brass, soft 70/30, density changes, void growth in biaxial stress fields, plastic deformation 0-71692  
brass, spring alloys, microplastic deform. and endurance limit 0-81197  
brittle fracture, statistical theory, dislocation mechanism, crack propagation (*Chinese*) 0-106755  
camphor, rhombohedral, polycryst., compressive deform. and dynamic recrystn. 0-71698  
carbonate minerals, deform. twinning mechanisms 0-79814  
cellulose nitrate, nonlinear viscoelastic deform., hydrostatic press. and third invariant of deviatoric stress tensor 0-93587  
ceramic materials, fine-grained, cyclic plastic deform. as cause for thermal expansion hysteresis 0-89290  
ceramics and brittle solids, abrasive wear, role of plastic deform. and fracture 0-108594  
complex loading of materials, plastic deform. 0-99939  
composite materials, tension stability, deformation up to failure (*Russian*) 0-75289  
composite superconductor, flux jumps and training 0-70911  
composite three-layer cylindrical shells, initial stressed and deformed state 0-102974  
compression tests, uniaxial, for plastic deform. (*Hungarian*) 0-97658  
concrete, reinforced slabs, punching shear strength under in-plane biaxial tension 0-100876  
constructional materials, creep, viscosity, resist. to inelastic deform. 0-89309  
contact film absorption on plastic deform. of contacting bodies (*Russian*) 0-93596  
containment vessel, cylindrical, submerged, dynamic plastic response, design formulae 0-83759  
convexity condition in an elastic-plastic material (*German*) 0-106734  
cord-rubber laminates, two-ply balanced, interlaminar-shear strain study 0-97526  
coupling phenomena in thermoplasticity 0-87721  
crack edge tip, exact analytic soln. 0-69734  
crack growth stability anal. using catastrophe theory 0-74810  
crack tip, plastic deform., metallographic anal. by recrystn. 0-85029  
crack tips, blunt, elastic-plastic stress field, plane stress and plane strain (*Chinese*) 0-64469  
cracks, penny-shaped, ductile, dynamic effects in propagation, Hankel and Laplace transform methods 0-87741  
cracktip under incipient creep deform., stress field and modified J-integral (*Japanese*) 0-103411  
creep fracture, failure mechanism involving grain boundary sliding and brittle crack extension 0-97557  
creep test method for plastic deformation, high temp. tests (*Hungarian*) 0-97660  
crystal growth, creation of stress and dislocations (*Russian*) 0-103277  
crystal surface elastic props., surface tension tensor, volume stress (*Russian*) 0-100389  
crystalline bodies, plastic strain and microcrack propag. 0-81199  
crystalline materials, fracture, stress relaxation effect 0-88256  
crystals, quantum effects in plasticity 0-59561  
cubic crystals, compression test, double slip kinematics 0-65005  
cyclic strain diagrams recording under nonisothermal conditions, review 0-71830  
cylinders, discretely stiffened, buckling under axial compression 0-64408  
cylindrical beam, impact effect on rigid wall (*German*) 0-106763  
damage analysis under nonproportional cycling 0-97556  
defect dimension determination by acoustic emission 0-104381  
defect dynamics, field equations, four dimensional space-time setting 0-96521  
deformation resistance, depend. on hot press. working speed (*Russian*) 0-65126  
difficult-to-form metals, deformation broaching 0-108473  
disoidal agglomerate, stress pattern, distributed loading effect during diametral compression test 0-60934  
discrete obstacle model, dislocation and stress field distrib. 0-79794  
disks, doubly-connected, elastoplastic, full yielding at collapse, noncircular shapes 0-74755  
disks, doubly-connected, noncircular, full yielding at collapse, photoplastic verification 0-74756  
dislocation cell form. during plastic deform., TEM obs. 0-60935  
dislocation structure, high press. effects, plastic deform. (*Russian*) 0-88159  
dislocation velocity, thermal activation exam. of applied stress and temp. depend., expt. methods (*French*) 0-59474  
dislocations, collective behaviour, velocity of slip band and mobile dislocation densities, HVEM study (*French*) 0-65006  
dynamic crack-tip fields according to deformation theory 0-64481  
dynamic response of a slab of elastic-viscoplastic material that exhibits induced plastic anisotropy 0-83737  
edge superdislocations, resist. to motion, temp. depend. expressions (*Russian*) 0-79789  
elastic-plastic bodies, localisation of deformation, bifurcation modes 0-79167  
elastic-plastic problems, supplementary strain method, appl. 0-96205  
elastically vibrating single crystal, simultaneous diff. effect on rocking curve 0-107019  
elastoplastic relaxing media, shock waves struct., distribution model 0-58961  
elastoplasticity, shakedown problems for elastic plastic solids with piecewise linear yield surface 0-79173  
electron microscopy, HV, in situ obs. techniques and applics., review (*Japanese*) 0-59351  
epoxy resin, plastic deform. effect on crack propag. 0-97563  
epoxy resin, plastic deform. mechanism 0-97534  
explosive forming, computer numerical simulation 0-59560



# plastic deformation continued

extrusion, reverse cold impact, appl. of ultrasonic radial oscillations (*Russian*) 0-97441  
fatigue, hydrostatic stress-sensitive relationship for biaxial stress conditions 0-74805  
ferromagnetic solids, magnetomechanical effects, magnetostriction, hysteresis, stress, yielding, fatigue damage, crack growth (*Polish*) 0-71150  
fibre reinforced composites, deformability characteristics, reinforcement scheme effect 0-58930  
fibre reinforced composites, reinforcement scheme optimisation with respect to deformability at assigned stresses 0-69689  
fibre reinforced composites, stress redistribution dynamics during fibre rupture 0-64394  
fibre reinforced composites with high work of fracture 0-81029  
fine fragmented crystals, complex struct. analysis by electron microscopy 0-104416  
fission reactor materials, clad failure prediction during FBR overpower transiency, JANE code 0-78363  
fission reactor materials, thermomechanical transient anal., strain-rate dependent plasticity 0-79864  
flat sheets, tensile deformation analysis 0-96198  
fluorite, use of proton irradi. to reveal growth and deform. features 0-84216  
formulation of plasticity theory in tension and expansion space (*German*) 0-106733  
fracture toughness tests, J integral, work for failure and work for plastic deform. 0-61061  
fragmented structures, dislocation and disclination kinetics (*Russian*) 0-79788  
frame, plane, impulsively loaded, large deflections, mode approx. technique extension 0-83757  
fuel pins, fast breeder, fuel-cladding mech. interaction, obs. and anal. 0-86959  
Gauss principle, in rolling theory, deformed and kinematic eqns. (*Russian*) 0-65124  
glass, mechanical destruction role of relaxation processes 0-89282  
glass fibre reinforced plastic, fracture dynamics 0-100906  
glass fibre reinforced plastic laminates, strength and deformability, artificial ageing effect 0-60893  
grain boundaries, plasticity 0-65135  
graphite, ion bombarded, light gases, structural study using TEM 0-92570  
Griffith fracture tests, for plastic deform. (*Hungarian*) 0-97666  
grinding, role of elastic and plastic behaviours (*Japanese*) 0-100868  
Hastelloy-X, low cycle fatigue crack propagation at 25°C and 760°C 0-104270  
high strain rate behaviour, incremental elastic-viscoplastic constitutive eqns. integration 0-85138  
high strain rate material behaviour and testing techniques, J.D. Campbell memorial lecture 0-82627  
high strain rate processes, review 0-84864  
hollow cylinder sagging, optimum equation 0-99945  
hot metal, dynamic yield characts. during multistage deform., plastometer design 0-85135  
ice, plastic deformation, ultrasonic wave attenuation by dislocations (*French*) 0-59564  
II-VI compounds, charged dislocations and plastic deform. 0-107264  
impulsively loaded rigid plastic beam, max. residual deformations, approx. solns. (*Chinese*) 0-8916  
indentation hardness and microhardness test methods for plastic deform. (*Hungarian*) 0-97664  
indenters, rigid, rough, rotating, plane strain collapse theory 0-79172  
inhomogeneous, reference degree of deform. definition (*German*) 0-99936  
inorganic glass, effect of liq. medium on process of mechanical destruction 0-89283  
internal friction, and plastic strain rate, phenomenological rel. 0-75301  
internal friction test method, for plastic deform. (*Hungarian*) 0-97662  
internal stress, stochastic model for dip test in steady-state creep 0-58915  
ionic crystals, dislocations, review 0-107236  
load-deflection curve, post-buckling behaviour of Hutchinson's plastic buckling model 0-64411  
low C steel, explosive-thermal treatment, sulphide cracking decrease, hydrogen embrittlement (*Russian*) 0-108477  
machine tools, chip geometry and cutting forces 0-93629  
macroscopic quadrupole effects as method of obs. of struct. transforms in crystals. 0-71321  
metal, axisymmetric plastic deformation, method of characteristics (*Russian*) 0-69682  
metal, FCC, dislocation behaviour at high strain rates, US detection method, data analysis basis 0-85136  
metal, polycrystalline, strain hardening, dislocation link length model 0-84953  
metal, single crystal, dislocation loop formation, during deformation in quantising mag. fields (*Russian*) 0-103354  
metal, thin-walled cylinder, elongation upon torsion 0-64386  
metal fatigue tests for plastic deformation (*Hungarian*) 0-97665  
metal sheet, circular, impulsive press. by underwater wire explosions, dynamic plastic deform. 0-84866  
metal surfaces, abrasive wear theory based on shear effects 0-89363  
metal tube, dynamic lateral compression, strain rate effects 0-83758  
metal tubes, crushed between rigid plates, large deformation compression 0-66579  
metallic powder materials, deform., boundary conditions on sliding surfaces 0-60978  
metals, atomic mobility under pulsed loading conditions (*Russian*) 0-96684  
metals, BCC, plastic deform., review 0-104213  
metals, constitutive model at high strain-rate, shear modulus, yield strength 0-75292  
metals, cubic, heavily deform., development of lattice curvature 0-81136  
metals, failure model in conditions of monotonous cyclic loading (*Bulgarian*) 0-70296  
metals, fatigue resistance, processes leading to failure 0-94907  
metals, generalised constitutive eqns. 0-104219  
metals, inelastic cyclic strain under nonuniform stress state conditions, residual stresses effect 0-81132  
metals, longitudinal flow velocity distribution in rolling (*Russian*) 0-93575  
metals, microinhomogeneous plastic deformation, rules 0-89307  
metals, residual stress on drawing calcs. by stress state changes variational principle (*Russian*) 0-65125

# plastic deformation continued

metals, resist. against plastic deform. (*Bulgarian*) 0-88248  
metals, submicroscopic defects, influence on HVEM in-situ expts. 0-103392  
metals, time dependent plastic deformation, thermodynamic model 0-76309  
metals, wave movement, resonance phenomena in deformation zone during rolling (*Russian*) 0-65123  
metals and alloys, shock wave effect on martensitic transform. (*Russian*) 0-96595  
metals and alloys, strain rate history, endochronic theory of viscoplasticity 0-65122  
moire method of measurement (*Polish*) 0-69749  
non-associated plasticity and elastoplasticity, rate boundary value problems, variational principles 0-87726  
nonlinear stress-strain rate relations, effects on deformation and fracture of materials in creep range 0-58938  
nuclear reactor pressure vessels, strain measurements 0-79865  
para-polyamide based fibres, struct. deform. props. 0-60928  
PET films, one-way drawn, constant strain effects, IR meas. 0-60584  
piezoelectric transducer automatic setup, for continuous meas. of internal friction and elastic moduli of solids 0-108652  
plain strain contained plastic deformation, elastic-plastic laws, finite element anal. 0-92073  
plane-strain work hardening, meas. and anal. 0-81073  
plastic fracturing materials, work inequalities and stress-strain relations 0-103000  
plastic rate sensitivity with large deformations, simplified method for membrane action 0-64403  
plate, elastic-plastic, flexed in its plane, stress concentrations, method of small parameter (*Russian*) 0-74759  
plate, two-layered, with imperfect bonding, resting on fluid half-space, vibrations 0-74792  
plate weakened by equal-armed cross-shaped crack, plastic strain and fracture 0-69740  
PMMA, crazing, deform. kinetics 0-84990  
PMMA, glassy atactic, thermodynamic analysis of plastic deform. modes, 150 to 330K 0-84999  
PMMA, large deforms. at tip of running crack, opt. interference obs. 0-85062  
PMMA, plastic deform. by crazing (*Japanese*) 0-93619  
polycarbonate, amorphous, yield behaviour in oriented and unoriented condition, effect of temp. 0-97537  
polycarbonate, ductile, large strain cyclic deform. 0-85000  
polycarbonate, rigid plastic, yield behaviour (*Japanese*) 0-93620  
polycrystals elastic-plastic deformation, plane geometrical model and finite element calc. 0-79860  
polyethylene, high density, ductile, large strain cyclic deform. 0-85000  
polyethylene, linear, draw temp. and mol. wt. effect on draw ratio and Young's modulus 0-84998  
polyethylene, rheological behaviour at high shear strain rates (*French*) 0-66574  
polyethylene spherulites, thin melt-cast films, high density, deform. process in non-equatorial regions 0-81124  
polyethylenes, ultra-high modulus, manufacture by drawing through conical die 0-66583  
polymer spherulites, deformation mechanism, linear isothermal viscoelasticity theory 0-58924  
polypropylene, crystalline, yield behaviour in oriented and unoriented condition, effect of temp. 0-97537  
polypropylene, ductile, large strain cyclic deform. 0-85000  
polypropylene, ultrahigh modulus, tensile drawing, mol. wt. effect 0-104211  
polypropylene film, double-exposure speckle pattern obs. of tensile deform., displacement, Poisson's ratio and stress relax. 0-84795  
polystyrene, atactic, indentation recovery 0-84988  
polystyrene, shear bands, morphology and annealing behaviour 0-100873  
polystyrene-polyethylene block copolymer, deformation ratios, Poisson ratio and adhesion, dilatometric obs. 0-60937  
porous materials, deformation theory of plasticity (*Russian*) 0-75291  
porous materials, density variation during plastic shaping 0-84873  
porous metals, plasticity, stress-strain curves, yield stresses, strain vectors 0-83738  
pressure transient analysis in piping systems including the effects of plastic deformation and cavitation 0-74775  
PVC, crazing, deform. kinetics 0-84990  
PVC, rigid plastic, yield behaviour (*Japanese*) 0-93620  
quartz, subgrain boundaries, theoret. predictions and microscopic obs. methods 0-84187  
rate-independent plasticity, axiomatic model 0-87717  
rigid plastic solids under lateral pressure, uniqueness of plain strain deformation 0-64404  
rigid-plastic medium, ideal, surface force strength lower limit under plain strain 0-99937  
rod, cantilever, terminal moments, nonlinear anal. 0-74763  
rod, elastoplastic, dynamic bending and residual deformation (*Russian*) 0-75293  
rod of rate-sensitive material, elastic-plastic tension-torsion analysis 0-83741  
rods and plates, strain-rate-sensitive material, elastic-plastic wave propag. mech. 0-69724  
SEM, combined deformation/heating stage, acoustic emission rate meas. 0-101892  
semiconductor, dislocation struct. and elec. props. 0-70201  
semiconductors, electron-hole drop formation, phonon wind influence (*Russian*) 0-92825  
sheet material, method for strength meas. under biaxial tension 0-66717  
shell, rectangular flexible elastoplastic, yield theory and deformation theory appl. 0-74773  
shell of revolution, corrugated, thermoelastic plastic deform. at finite displacements 0-74772  
shells, complex profile, installation for deform. processes 0-81261  
shells, large inelastic deformations for arbitrary shape, TRUMP element appl. 0-92068  
shells, plastic, explosive forming, computer numerical simulation 0-59560  
silicone elastomers, dental impression materials, dimens. stability, holographic and interferometric study 0-67204  
single crystals, homogeneous plastic deform. by dislocation glide (*French*) 0-84232  
solid deformable body, residual stresses by creating holes, holographic interferometry appl. (*German*) 0-79243



**plastic deformation continued**

stability of multilayer composites under inelastic deformations 0-99944  
 stator windings, failure mechanisms under thermal cycling (*Japanese*) 0-104189  
 steel, low alloy, high strength, hot compression dynamic precip. and coarsening of Nb(CN) 0-97514  
 steel, Al killed, density changes, void growth in biaxial stress fields, plastic deformation 0-71692  
 steel, alloy, 15KhM1 and 20KhM1, plastic deform. with thermal cycling 0-89310  
 steel, alloy, deformation, rapid dynamic, at  $-196^{\circ}\text{C}$  0-104220  
 steel, alloy, sheet, crack-propag. resist. in heat-affected zone in presence of H, rolling direction and preliminary plastic tensile strain effects 0-60971  
 steel, alloy, tensile test, regulated, strength and deform. characteristic values, consistency (*German*) 0-93712  
 steel, alloy A533B1, neutron irradiat., flow growth characts. by acoustic monitoring 0-100918  
 steel, austenitic, ageing and plastic deform. effect on struct. and mech. props. of N15Kh5G3T3 (*Russian*) 0-71691  
 steel, austenitic, Cr-Mn-N, plastic deformation influence on internal friction, relaxation processes (*Russian*) 0-100870  
 steel, austenitic, explosive-thermal treatment, sulphide cracking decrease, hydrogen embrittlement (*Russian*) 0-108477  
 steel, austenitic stainless, stacking fault energy, effect of N 0-107279  
 steel, austenitic stainless, type 304, cyclic creep during unbalanced tension-compression loading at elevated temp. 0-97545  
 steel, austenitic stainless, type SUS 304, low cycle fatigue strength reduction factor (*Japanese*) 0-104259  
 steel, austenitic stainless SUS 301, stress corrosion cracking susceptibility, effect of strain-induced  $\alpha'$ -martensite (*Japanese*) 0-104335  
 steel, C, hot plastic deform., vac. colour etching investigation 0-61036  
 steel, C, low temperature strength, preliminary plastic deform. effect 0-81128  
 steel, C, recrystallization annealing, grain growth, effect of type of deform. 0-100847  
 steel, C, type SFVV1, low cycle fatigue strength reduction factor (*Japanese*) 0-104259  
 steel, cold strained, defects interaction with carbide strengthening phases, carbide decomp. degree (*Russian*) 0-84955  
 steel, cold worked, original struct. effect on softening during heating 0-60882  
 steel, Cr, post-hotforming recrystallisation condition, use of NEOPHOT 2 and EPIQUANT 0-84949  
 steel, Cr-Mn(Ni), Mn and Ni additions, effect on corrosion resistance and hardness 0-104342  
 steel, Cr-Mo-V pressure vessel, microstruct. parameters and yielding rel. to plastic deform. 0-89318  
 steel, Cr-Ni-Mo-V, austenite form. during heating, influence of recrystn. during tempering (*Russian*) 0-104188  
 steel, En 24, Cr, V, deform. effect on decomp. of austenite, carbide precipitation 0-84938  
 steel, fatigue crack tip plastic deform., X-ray diffr. investigation (*Russian*) 0-104251  
 steel, high C, type 7KhFNSh, plastic deform. influence of X-ray interference line breadth (*Russian*) 0-93599  
 steel, high-strength structural type StE47, specimen geometry and plastic deform. effect on fracture mechanics (*German*) 0-66613  
 steel, low alloy-high strength, deforms. during cold crack developments in welded joints 0-81142  
 steel, low and medium C, dynamic and static strength, strain rate and temp. depend. of flow stress 0-85139  
 steel, low C, fatigue life, variable strain ranges (*Czech*) 0-60956  
 steel, low C, initial stages of plastic deform. (*Japanese*) 0-93618  
 steel, low C, type En3, high strain deform., struct. and props. 0-89301  
 steel, low C type 08KP, plastic deform. depend. on grain size (*Russian*) 0-66580  
 steel, low-alloy, plastic deform. mechanisms under dynamic loading 0-100883  
 steel, low-C containing Ti, sheets, recrystn. texture effects on plastic strain ratio and deep-drawing (*Chinese*) 0-66527  
 steel, maraging, ageing kinetics and struct. of N12K7MSTYu, effect of high temp. deform. of austenite (*Russian*) 0-84960  
 steel, martensitic, fatigue life, low-cycle, temp. and strain rate effects 0-85056  
 steel, martensitic-aged, plastic deformation influence in type N17K12MST steel on mech. props. (*Russian*) 0-76305  
 steel, medium and high C, deformation ageing, entropy, free energy, dislocations (*Russian*) 0-66581  
 steel, medium C, microflow and strain hardening under cyclic loading 0-104182  
 steel, microalloyed, hot-rolled, Nb(C,N) precip. and austenite recrystn. 0-97513  
 steel, mild, 1019 AISI, acoustic emission generated during deform. 0-60921  
 steel, mild, cold rolled, texture and plastic anisotropy rel. to alloying and precipitation (*French*) 0-108475  
 steel, mild, cyclic strain enhanced dissolution in  $\text{NH}_4\text{NO}_3$ , corrosion fatigue props. 0-85083  
 steel, mild, fatigue crack propagation, stress ratio effect 0-71733  
 steel, Nb(V), (Al), hot-rolling, laboratory simulation, recrystn. of austenite 0-97512  
 steel, Ni (17 wt.%), martensitic deform. temp., cryst. struct. effect (*Russian*) 0-66576  
 steel, Ni-Cr-Mo-V, corrosion fatigue crack growth in NaOH soln., cathodic pot. effect 0-89403  
 steel, pearlite, deform. and fracture mechanisms, HV SEM obs. 0-104243  
 steel, pearlitic, struct. variations under plastic strain and subsequent heating, cementite decomp. (*Russian*) 0-84954  
 steel, plastic deform., density changes (*German*) 0-60908  
 steel, plastic loosening and deform. defect healing during recovery annealing of 12Kh18N10T (*Russian*) 0-66530  
 steel, spring alloys, microplastic deform. and endurance limit 0-81197  
 steel, stainless, deformation, rapid dynamic, at  $-196^{\circ}\text{C}$  0-104220  
 steel, stainless, fracture and crack tip plastic zones, in situ obs. 0-108686  
 steel, stainless, high temp., smoothing for plastic pre-straining of material cut by turning (*Russian*) 0-60911  
 steel, stainless, in-situ obs. of deform. in HVEM 0-103338  
 steel, stainless, stress corrosion testing, slow strain rate, elevated temp. and high press. study 0-97615

**plastic deformation continued**

steel, stainless, type 304, viscoplastic model, uniaxial, based on total strain and overstress 0-64387  
 steel, stainless, type 316, low cycle fatigue props. in vac., fracture mode 0-85021  
 steel, stainless 304, explosive loading technique for uniform plastic expansion at high strain rates 0-81273  
 steel, stainless type 316, in-situ HVEM studies under ion beam irradiation 0-103396  
 steel, structural, strained in tension after tempering, compression effects on struct. changes (*Russian*) 0-66577  
 steel, structural, wide plate tensile testing eval. (*German*) 0-100969  
 steel, tempered, notched, impact bending tests, cold brittleness curves 0-71758  
 steel, tempering effect on fatigue strength 0-60891  
 steel, TRIP, fatigue strength 0-108552  
 steel, type 10G2SAF, yield strength, influence of deform. rate (*Bulgarian*) 0-89315  
 steel, type 20Kh deformed, austenite grain size, inheritance effect with quenching and tempering 0-60881  
 steel, type VKV, deform. strengthening of bainite phase (*Russian*) 0-100851  
 steel (*German*) 0-100869  
 steel E1736, creep, viscosity, resist. to inelastic deform. 0-89309  
 steel SW7M, low-cycle fatigue at high hardness levels (*Polish*) 0-89323  
 steel welds, bead-on-plate, H<sub>2</sub> diffusion and trapping 0-96697  
 steels, alloy, stress relax. data anal. using total strain-time parametric method (*Japanese*) 0-104198  
 steels 4Kh4VMFSSh and 45Kh3V3MFSSh, grain size, hot deform. and austenitising effects 0-76286  
 steels 60, 18Kh2N4MA, 17GSND, and 12Kh21N5T structure after high-speed cold plastic deformation 0-76316  
 stiff constitutive models, numerical integration, inelastic deform. 0-96208  
 strain and damage electrical measurement method (*French*) 0-71854  
 strain state determination, automated method, dividing nets appl. 0-100982  
 straining experiments, in situ, strong frictional force, quantitative anal. 0-100244  
 stress relaxation theory, for plastic deform. (*Hungarian*) 0-97661  
 structural deformation under dynamic loading, state variable description of material behaviour 0-85137  
 structural member, dynamic loading and plastic response, review 0-83756  
 structure during cutting, investigation by TEM (*Japanese*) 0-70086  
 surface irregularities, deformation under static loads 0-58985  
 tensile test, uniaxial, for plastic deform. (*Hungarian*) 0-97657  
 thermal activation analysis, of plastic deformation and dislocation motion using stress and temp. jumps 0-74771  
 thermoplastic layers, isothermal smoothing of surface deformation (*Russian*) 0-76394  
 thermoviscoplasticity theory based on infinitesimal total strain 0-87719  
 torsional deformation testing for plastic deformation, fracture (*Hungarian*) 0-97659  
 tube, thick-walled, axisymmetric deformation in presence of upper yield point (*Russian*) 0-74758  
 uniaxially compressed crystal, exciton molecule radiation (*Russian*) 0-108264  
 viscoelastic-plastic tube, successive deformation under cyclic, temp. variation 0-92074  
 viscoplasticity theory based on infinitesimal total strain and nonlinear viscoelasticity 0-79164  
 wire reinforced Al, stress-deformed state, elastic, strength props. (*Russian*) 0-76303  
 wrought metals, plastic deform. testing, X-ray line profile anal. (*Hungarian*) 0-97663  
 X-ray scattering by deformed cryst., theory (*Russian*) 0-70077  
 zincblende-type crystals, sublattice displacement from elect. or mech. deform. 0-81123  
 Zircaloy PWR fuel cladding deformation tests under mainly convective cooling conditions 0-57862  
 Zircaloy-2 fuel tubes, low cycle fatigue studies at room temp., 300 and  $350^{\circ}\text{C}$  0-93637  
 Zircaloy-4, stress-relieved and cold-worked, stress relaxation in bending at  $673\text{K}$  0-93609  
 Zircaloy-4 cladding deformation under LOCA transient heating conditions, analytical modelling 0-104236  
 Ag FCC crystals, compressively activated slip, theoretical latent hardening 0-65128  
 Ag, microcrack propagation and plastic strain 0-81187  
 Ag, tensile deformed, dynamic recrystn. (*German*) 0-84959  
 Ag-Ni (10 wt.%) wire, plastically deformed, fracture struct. (*German*) 0-71744  
 Ag-Sn, splat-quenched, X-ray diffr. study 0-81094  
 Al alloy, type 7175 T 651 (*French*) 0-65145  
 Al alloy, types L73 and L88, fatigue crack propagation, stress ratio effect 0-71733  
 Al anodic films, acoustic and electron-emission during deform. 0-80143  
 Al bicrystal, plastically deformed, slip heterogeneities 0-79858  
 Al, commercial purity, density changes, void growth in biaxial stress fields, plastic deformation 0-71692  
 Al, commercially pure, stress-strain curves, cyclic loading initial stage (*Japanese*) 0-93617  
 Al, creep behaviour, at high temp., influence of oxidation 0-97538  
 Al, deformed in uniaxial and equibiaxial tension, dislocation arrangements 0-108516  
 Al FCC crystals, compressively activated slip, theoretical latent hardening 0-65128  
 Al foil,  $\alpha$ -particle irradiat. under fusion reactor conditions, He bubble alignment during deform. 0-107345  
 Al foil, deformation, laser optical scanning obs. 0-100995  
 Al foil, internal friction changes during low temp. plastic deform. (*Russian*) 0-100304  
 Al foil, laser irradiat., fracture props. (*Russian*) 0-108523  
 Al, initial stages of plastic deform. (*Japanese*) 0-93618  
 Al, microcrack propagation and plastic strain 0-81187  
 Al notched bars, deform. behaviour and strength having biaxial state of stress at notch root (*Japanese*) 0-81116  
 Al, plastic deformation thermal activation parameters from creep kinetics, and stress relaxation 0-71717  
 Al, polycrystalline, HVEM in-situ investigation of creep mechanism 0-104214



**plastic deformation continued**

- Al single crystals, (100) oriented, deform. temp. effect on stage IV deform. (*Japanese*) 0-66587
- Al single crystals, relation between axial orientation rotating and deform. banding 0-104206
- Al, strain rate sensitivity and ductility, trace element conc. effect 0-66597
- Al-(Mg)(Fe), pure (dilute), large wire drawing plastic deform. 0-108508
- Al-Cu, high strength, type 2024-T3, crack growth, fatigue induced surface deform., holographic detect. 0-85120
- Al-Cu, type 2036-T4, plane-strain work hardening, meas. and anal. 0-81073
- Al-Cu (4 wt.%), supersaturated and aged conditions, high strain deform. 0-60907
- Al-Cu (4 wt.%) alloy, high temp. cyclic deform.,  $\theta'$  particle dissolution obs. 0-108515
- Al-Cu-Mg, type RR55, high strength, creep behaviour, effect rel. to anodic coatings, SEM study 0-97542
- Al-Cu-Mg type 2036, thermomech. treatment, flow stress anal., effect in mech. props. 0-93584
- Al-Cu-Si-Mg, deform. simulation using torsional test, elastoplastic constitutive eqn. 0-93594
- Al-Cu(Mg), low freq. internal friction during plastic deform. (*Chinese*) 0-103420
- Al-Cu(Si)(Mg) binary and ternary alloys, dimensional changes in heat treatment 0-89271
- Al-Mg-Si alloy, Mg<sub>2</sub>Si dispersion hardened US waveguides, concentrators (*Polish*) 0-89237
- Al-Ni (6 wt.%), fine-grained, deform. in tension and torsion 0-85008
- Al-Si(9.3, 12) with graphite particles seizure resistance study using Hohen wear tester 0-89360
- Al-Zn-Mg (3.6, 1.95 wt.%), ageing and plastic deform., effect on structure, electron microsc. and X-ray diff. study (*Russian*) 0-81108
- Al-Zn-Mg-Cu (6, 2.5, 1.5 wt.%), deform. simulation using torsional test, elastoplastic constitutive eqn. 0-93594
- Al-Zn-Mg-Cu (6.2, xwt.%) type alloy, fatigue crack propag., Cu content and recryst. effect 0-60960
- Al<sub>2</sub>O<sub>3</sub>, fine grained, basal slip and nonaccommodated grain boundary sliding 0-60916
- Al<sub>2</sub>O<sub>3</sub>, fine grained, interface-controlled diffusional creep 0-60915
- Al<sub>2</sub>O<sub>3</sub>-SiO<sub>2</sub> refractory, creep, viscosity, resist. to inelastic deform. 0-89309
- Ar, solid, diffusion processes in plastic deform. (*Russian*) 0-92591
- Bi, deformation calculations, band struct. variation, electron phase transitions due to deform. (*Russian*) 0-65137
- Bi, strain hardening curve correlation with slip band nucleation stress spectra 0-70217
- Bi<sub>1-x</sub>Sb<sub>x</sub>, deformation calculations, band struct. variation, electron phase transitions due to deform. (*Russian*) 0-65137
- Cd crystals, X-ray topographic examination of basal dislocation glide, generation and locking 0-88156
- Cd, single crystals., plasticity study during deformation by twisting (*Russian*) 0-93597
- CdS, dislocation motion, TEM obs. 0-79799
- CdS(Se)(Te), charged dislocations, flow of charge with plastic deform. 0-85010
- CdSe, recombination mechanism at dislocations, photoluminescence 0-103993
- Co, particle formation by evap., electron microscopy obs. of interaction processes 0-104053
- Co, single crystal, cavitation erosion, role of twinning 0-107272
- Co-CoAl, two phase, interaction between deform., fracture initiation and propag. 0-85006
- Co-Ti-C, secondary precipitation and allotropic transform., TEM obs. 0-108453
- CoO single crystals, strain rate deform. characts., yield stresses and work hardening 77 to 1400K 0-60939
- Cr-Nb-Mo alloy system, comp. and temp. depend. alterations in mech. props., phase diagram interpret. (*Russian*) 0-85045
- Cr-Ni compressor disk, surface plastic deform., optimal method 0-60924
- CrO<sub>2</sub> semidry refractory, struct. and mech. props., surface-active agents effect 0-89304
- CsI crystals, relation of struct. and bond type to slip geometry 0-88165
- Cu, acoustic losses due to strong ultrasonic and static stress fields 0-79886
- Cu, annealed, plastic strain during non-proportional loading 0-89291
- Cu, fatigue crack propag., influence of specimen thickness (*German*) 0-66669
- Cu, high purity, creep cavitation topology, high temperature region (*Czech*) 0-65138
- Cu, high purity, identification of imperfections by thermal resistivity meas. 0-59951
- Cu, high-purity, grain size and strain rate influence on mech. behaviour, precursors existence 0-85016
- Cu, microcrack propagation and plastic strain 0-81187
- Cu, OFHC effect of cold drawing under combined stress 0-60912
- Cu, plastic deformation thermal activation parameters from creep kinetics and stress relaxation 0-71717
- Cu, plastically deformed, lattice strain distrib. (*German*) 0-85012
- Cu, polycryst., surface layer hardening by multiple impact 0-108469
- Cu, polycrystn., strain localisation during hot deform. 0-104195
- Cu, recrystallization annealing, grain growth, effect of type of deform. 0-100847
- Cu single crystals, neutron irradiated, secondary slip 0-88161
- Cu, single crystals, neutron irradiated, stresses and secondary slip between overlapping and dislocation arrays 0-88162
- Cu, single crystals., (110) oriented, tensile deformed, HVEM of recrystn., recrystallised state 0-89256
- Cu, single crystals., cyclically and unidirectionally deform. X-ray diff. study 0-89319
- Cu, single crystals., deformed in [001] and [111] axes, cell structs., TEM 0-70209
- Cu single crystals., deformed, HVEM study of recrystn. texture 0-104179
- Cu, tensile deformed (110) orientated single cryst., recrystn., high voltage electron microscopy study 0-84958
- Cu-Ag (3 at.%), plastically deformed, lattice strain distrib. (*German*) 0-85012
- Cu-Al, short range order and static distortion contribution to residual elec. resistivity (*Russian*) 0-70672
- Cu-Al (5 wt.%), subjected to tension-compression fatigue, deform. and fracture strength (*Japanese*) 0-93644
- plastic deformation continued**
- Cu-Al<sub>2</sub>O<sub>3</sub>(SiO<sub>2</sub>)(TiO<sub>2</sub>) alloys, internally oxidised, plastically deformed, influence of particle form on primary loop nature (*French*) 0-103344
- Cu-Be (2 at.%), plastic deform. and dislocation substruct. 0-76307
- Cu-Cd (1.0 wt.%), yield stress and flow stress 0-97524
- Cu-Cr (0.75 wt.%), deformation characts., fully reversed cyclic strain with fatigue cracks and dislocation struct. 0-81148
- Cu-Ni-Al (5, 2.5 at.%), precip. hardening (*Japanese*) 0-71663
- Cu-Ni-Sn (15, 8 wt.%), prior deform. effect on spinodal age hardening 0-108465
- Cu-Si (6.5 at.%), plastic deformation, HVEM study (*French*) 0-66605
- Cu-SiO<sub>2</sub>, in-situ deform. in HVEM 0-103338
- Cu-SiO<sub>2</sub>, low-temp. recovery creep, Orowan loop accumulation 0-81126
- Cu-Sn industrial bronzes, Sn diffusion in deform. zone influence on wear resistance, friction (*Russian*) 0-108582
- Cu-Sn-Al, deform at high temps. (*Polish*) 0-89284
- Cu-Zn, interface sliding of FCC and BCC boundaries 0-104240
- (Cu-Au)-Co, single crystals, solid soln. and particle strengthening, superposition 0-97495
- Cu<sub>3</sub>Au, disordered [001]-orientated single crystals., plastic deform., TEM and slip line studies 0-97541
- DyVO<sub>4</sub> Jahn-Teller crystal, deform. induced transitions, elastic and dielectric characts. (*Russian*) 0-80726
- Fe, anodic behaviour in 1M H<sub>2</sub>SO<sub>4</sub>, influence of straining 0-97612
- Fe, Armco, fatigue crack propag., influence of specimen thickness (*German*) 0-66669
- Fe, Armco, microflow and strain hardening under cyclic loading 0-104182
- Fe, Armco, plastic zone around fatigue crack, vac. effect 0-100914
- Fe, cast, contact deformation, reverse slipping effect (*Russian*) 0-97591
- Fe, cast, US study of sections undergoing deform. or thermal cycling 0-104285
- Fe cast with spheroidal graphite, fine cryst. struct. on tempering (*Russian*) 0-96476
- Fe, internal friction in plastic deformation process (*Chinese*) 0-88259
- Fe, particle formation by evap., electron microscopy obs. of interaction processes 0-104053
- Fe, pure, cathodic charging effect on creep and tensile deformation 0-76320
- Fe thin layers, vacuum coated on PMMA, mag. behaviour during mech. stress cycles (*German*) 0-80581
- Fe, volume changes and defect healing due to plastic deform. (*Russian*) 0-81139
- Fe-Ag (50 wt.%), plastic behaviour in compression, deform. rate effect (*French*) 0-71711
- Fe-Al, single crystals, deform. at high temps. 0-81125
- Fe-Cr-Al (12, 3 wt.%), internal friction and rigidity modulus, strain amplitude depend. (*Japanese*) 0-92606
- Fe-Cr-Ni (18, 14 wt.%),  $\gamma$  to  $\epsilon$  to  $\alpha$  martensitic transform., external stress effect, double tensile deform. exam. 0-108438
- Fe-Mn, mechanical twinning of close-packed hexagonal  $\epsilon$ -phase during plastic deform. (*Russian*) 0-60909
- Fe-N single crystals, plastic deform. in temp. range 4.2 to 300K 0-76321
- Fe-Ni-Al-Co-Cu-Ti YundK type, S effect on mech. props. 0-60927
- Fe-Ni-C (25, 0.2 wt.%), strain-induced martensite (*Korean*) 0-71646
- Fe-Ni-C austenitic alloy, banding struct. formed by deform. 0-71713
- Fe-Ni-Cr based alloy, KhN35VTYu, temp. depend. of energy of fracture, influence of  $\gamma'$  phase (*Russian*) 0-81147
- Fe-Si, fatigue fracture fractography in broad strain-amplitude range, in air and vacuum 0-81186
- Fe-Si, microflow and strain hardening under cyclic loading 0-104182
- Fe-Si (3 at.%), deformation and electron bombardment, influence on dislocation struct., 20-500°C (*Russian*) 0-92536
- Fe-Si (3 wt.%), electron irradiated, yield strength and elongation 0-76325
- Fe-Zn alloys, coercive force anisotropy after cold plastic deform. (*Bulgarian*) 0-75809
- Fe<sub>32</sub>Ni<sub>36</sub>Cr<sub>14</sub>P<sub>12</sub>B<sub>6</sub> Metglas, bending deform., shear band form., high-speed cinematographic obs. 0-89322
- Fe<sub>40</sub>Ni<sub>40</sub>P<sub>14</sub>B<sub>6</sub>, amorphous, mag. polarisation in approach to ferromag. saturation 0-80560
- GaAs, luminescence emitted from deep centres, plastic deform. effect on internal quantum efficiency 0-60672
- GaP/Si heterostruct., differential thermal contraction, plastic deform., fracture 0-108494
- Ge, nonequilibrium charge carrier-mag. field interaction electron-hole drops, recombination (*Russian*) 0-75511
- Ge, plastically deformed under high temp. creep conditions, elec. props. 0-92915
- Ge, stationary creep depend. on deform. stabilisation of material struct. (*Russian*) 0-100300
- GeTe, stoichiometry deviations influence on mech. props., 25-500°C 0-103410
- InBi single crystal, deform. mode under dynamic indentation 0-88163
- InP single crystals, uniaxial compression deform. characts. 0-84991
- p-InSb, influence of plastic deform. on elec. props. 0-103711
- InSb, X-ray topographic evidence of asymmetrical pre-yield behaviour 0-75229
- KCl, microcrack propagation and plastic strain 0-81187
- LiF bicrystal, high-angle tilt boundary and edge dislocation intersection effects 0-79836
- LiF crystal, contact damage obs. by cathodoluminesc. 0-71728
- LiF crystals, relation of struct. and bond type to slip geometry 0-88165
- LiF, dislocation structure, influence of variable deform. temp. 0-70211
- LiF, kinetics analysis of stress relaxation 0-65136
- LiF, microcrack propagation and plastic strain 0-81187
- LiF, strain hardening curve correlation with slip band nucleation stress spectra 0-70217
- LiF:Co, flow stress changes during precipitation 0-92594
- $\alpha$ -Li<sub>2</sub>O, surface defect layer struct. due to mechanical working (*Russian*) 0-100238
- MgO crystal, contact damage obs. by cathodoluminesc. 0-71728
- MgO crystals., plastic deform. activation parameters, rel. between macroscopic and in-situ HVEM expts. 0-103355
- MgO crystals., radiation damage influence on deform. in HVEM 0-103391
- MgO, deformed, cathodolum. obs. by STEM 0-76088
- MgO, fracture and crack tip plastic zones, in situ obs. 0-108686
- MgO, high temperature prestrain effect on plastic props., dislocation struct. 0-79866
- MgO, photoluminesc. during mechanical deform. 0-60665
- MgO single crystal., impact wear characts. 0-76374



## plastic deformation continued

- MgO:Li, mech. deformed crystals, imprinting of slip bands using Li impurities 0-59473
- MgO:Al<sub>2</sub>O<sub>3</sub> spinel, plastic deformation at T<1000°C, slip systems 0-108505
- MgO:Li<sub>2</sub>Al<sub>2</sub>O<sub>3</sub> spinel, high temp. deform., cryst. orientation effect 0-107263
- Mn<sub>2</sub>Si<sub>3</sub>, elastic moduli, phase transitions, ultrasonic velocity 0-92589
- Mo, dislocation structure of diffusional welding zone (*Russian*) 0-96531
- Mo, fatigue of single crystals, dislocation struct. and strain localisation (*Russian*) 0-71741
- Mo fibre reinforced Cu, rule of mixtures of deform. parameters in stage III 0-97532
- Mo fibre reinforced Cu with weak interfaces, stability of tensile deform. 0-97533
- Mo, fracture and crack tip plastic zones, in situ obs. 0-108686
- Mo, plastically deformed single cryst., mag. susceptibility (*Russian*) 0-93074
- Mo polycrystn., cyclically deformed, dislocation arrangements 0-108506
- Mo-Re(Os)(Ru), recovery after deform. and annealing, destrengthening mechanism (*Russian*) 0-97546
- Mo-TiC lamellar eutectic composite, deformation and strength, room temp. to 2073K (*Japanese*) 0-71702
- NaCl, dislocation density in monocrystal deformed under high hydrostatic press. 0-70216
- NaCl, microcrack propagation and plastic strain 0-81187
- NaCl:Cd<sup>2+</sup>, dielectric loss following plastic deform. 0-84690
- Na<sub>2</sub>O-CaO-SiO<sub>2</sub> glass foils, HVEM in-situ straining expts. 0-104216
- Nb, deformed polycryst.,  $\gamma$ -peak obs. and interpret. in internal friction, 300-500K 0-81098
- Nb-Zr-N biphas alloy, recrystallization annealing 0-104180
- Nb<sub>2</sub>Sn, hot isostatically pressed, plastic deform. 0-108510
- Ni alloy KhN56VMKYu, creep, viscosity, resist. to inelastic deform. 0-89309
- Ni alloys, creep transients, friction stress and recovery, dislocation substruct. 0-60933
- Ni, dislocation structure evolution after hydroextrusion (*Russian*) 0-96530
- Ni, microcrack propagation and plastic strain 0-81187
- Ni, oxidation, high temp., effect of C on cavity form., SEM study 0-97638
- Ni, particle formation by evap., electron microscopy obs. of interaction processes 0-104053
- Ni, plastically deformed, positron trapping rate, temp. depend. 0-71507
- Ni, single cryst., cyclically deformed, HVEM in-situ deform. study 0-103339
- Ni, slip character, H effect 0-89287
- Ni spring alloys, microplastic deform. and endurance limit 0-81197
- Ni, strain amplitude-depend. damping and modulus (*Japanese*) 0-92606
- Ni thin-walled cylinder, elongation upon torsion 0-64386
- Ni, volume changes and defect healing due to plastic deform. (*Russian*) 0-81139
- Ni-Cr, (30 wt.%), collective dislocation movements, in situ study 0-100243
- Ni-Cr (33 at.%), plastic deformation, HVEM study (*French*) 0-66605
- Ni-Cr-Co-Ti-Mo-W-Al (14, 9.8, 5, 4, 3.9, 3 wt.%), low cycle fatigue, prior heat treatment effect 0-60962
- Ni-H, thermally charged, serrated yielding 0-85007
- Ni-Ni<sub>3</sub>Mo system, deformation microstruct. 0-93591
- Ni-Ti/Cu composite, plastic deform. influence on internal friction (*Russian*) 0-100871
- Ni<sub>3</sub>Fe, domain struct. after tensile deform., dislocation effects 0-71083
- Ni<sub>3</sub>Fe, polycrystalline alloy evolution of slip-line pattern during straining 0-103362
- Pb, plastic properties over wide range of strain rates 0-71693
- PbS, crystals, relation of struct. and bond type to slip geometry 0-88165
- Pb<sub>1-x</sub>Sn<sub>x</sub>Te<sub>1-x</sub>In<sub>x</sub>, tunnelling impurity self-localisation, anomalous props. nature (*Russian*) 0-59915
- Pd-H(D), elastic energy dissipation peak 0-60905
- Pd<sub>3</sub>Si<sub>2</sub>, metallic glass, tensile deform., shear band form., high-speed cinematographic obs. 0-89322
- Pd<sub>1-x</sub>W<sub>x</sub>, calc. of short-range order parameters from X-ray scatt. data (*Russian*) 0-75367
- Pt, tension-strained, thermostimulated exoelectron emission, excitation mechanism (*Russian*) 0-71581
- 239PuO<sub>2</sub>, stoichiometric, high-temp. deformation 0-81111
- RbMnCl<sub>3</sub>, twinning struct., cryst. domains, orientation mag. transition (*Russian*) 0-107275
- Se, amorphous, US relaxation and retardation of deform. near T<sub>g</sub> point 0-84256
- Si, controlled dislocation formation, struct. density (*Russian*) 0-107244
- Si crystals, dynamic processes associated with stacking faults and deform. twins, HVEM in-situ obs. 0-103369
- Si crystals, in-situ HVEM obs. of dislocation processes during high temp. deform. 0-103342
- Si, deformed, annealed and recrystallized, struct., implications for solar cells 0-60922
- N-Si, deformed, thermal treatment effect on elec. cond. and dislocation mobility 0-107265
- Si, high dislocation density crystals, photoelectret state investigation 0-97191
- Si, plastically deformed, dislocation structure with different sample orientation 0-70207
- Si, stationary creep depend. on deform. stabilisation of material struct. (*Russian*) 0-100300
- SiC, effect of crystallographic anisotropy on Knoop microhardness 0-66626
- Si<sub>3</sub>N<sub>4</sub>, hot-pressed, creep and strain recovery 0-100874
- steel, Nb, deform., recrystn. and precip. interaction 0-97515
- Ta-H, physical properties, plastic deformation, H ordering (*Ukrainian*) 0-71689
- Ti, fast neutron irradi., twinning deform. at room temp. 0-65061
- Ti, fatigue damage, SEM, X-ray diffr. and surface trace anal. 0-85040
- Ti metal-metal interface, adhesion energy, surface treatment and ion implantation effects 0-107660
- $\alpha$ -Ti, plastic deform., anharmonicity, and Gruneisen parameter 0-88246
- Ti, polycrystal, discontinuous electrical resistivity, low temp. active straining (*Russian*) 0-103666
- Ti, twinning deformation, neutron irradiation effects 0-75236
- Ti, volume changes and defect healing due to plastic deformation. (*Russian*) 0-81139
- plastic deformation continued
- Ti-Al-Cr-Mo-V, VT22 alloy, metastable  $\beta$ -phase decay under continuous heating, plastic strain effect (*Russian*) 0-71656
- Ti-Al-Mo-Cr (4.5, 5, 1.5 wt.%), weld metal,  $\alpha/\beta$  interface sliding 0-108512
- Ti-Al-Mo-Zr, compressor disk, surface plastic deform., optimal method 0-60924
- Ti-Al-Sn, alloy 6242, dynamic effects of flow and fracture during isothermal forging 0-76343
- Ti-Er(Y), effects of Er and Y additives on deformation behaviour 0-81121
- Ti-Fe (1.4 wt.%), polymorphic transform. due to plastic deform., positron annihilation 0-79939
- Ti-Mo-Zr-Sn (11.5, 6.0, 4.5 wt.%) alloy, struct. as affected by processing history 0-84972
- $\beta$ -Ti-V metastable alloys, fatigue crack propag. 0-60964
- TiC, deform. at high temps. 0-104239
- TiC, frictional characts. and contact-zone deform. in homogeneity range 0-66673
- TiO<sub>2-x</sub>, reduced, crystallographic shear planes, dislocation struct. 0-107175
- $\alpha$ -U, mech. props. at very high strain rates, double-notch shear test use 0-85131
- $\alpha$ -U, strain rate effect on tensile flow and fracture 0-84992
- U<sub>3</sub>Si, reversible twinning, in-situ obs. 0-104241
- V<sub>2</sub>Si, supercond. structure and properties (*German*) 0-93631
- W, deformed, surface layer struct. effect on polygonisation and recryst., X-ray diffr. anal. and metallographic exam. (*Russian*) 0-84948
- W, plastically deformed single cryst., mag. susceptibility (*Russian*) 0-93074
- Y, polycrystn., plastic deform. at different deform. speeds, dislocation glide (*Russian*) 0-93598
- YIG, electron and  $\gamma$ -irrad., photomagnetic effect 0-103877
- Zircaloy-4, deformation behaviour between 77 and 900K 0-71686
- Zn alloys, rolled and press. die-cast, creep and deformation behaviour (*German*) 0-66611
- Zn crystal, {1122}{1123} slip system, deform. stress, dislocation density depend. (*Russian*) 0-103353
- Zn crystals X-ray topographic examination of basal dislocations 0-88156
- Zn, microcrack propagation and plastic strain 0-81187
- Zn, nitrided, yield strength, influence of deform. rate (*Bulgarian*) 0-89315
- Zn, single cryst., contribution of basal dislocations to residual elec. resist. (*Russian*) 0-75539
- Zn single cryst., dislocation velocity and plastic deform. 0-64998
- Zn, twinning, influence of dislocation drag, mag. field effects 0-59472
- ZnO(S)(Se)(Te), charged dislocations, flow of charge with plastic deform. 0-85010
- ZnS crystals, structural change under plastic deform., partial dislocation movement 0-79736
- ZnSe, electric charge transport by dislocations 0-103709
- Zr, mag. susceptibility, plastic deform. effect (*Russian*) 0-65984
- Zr<sub>3</sub>Al, deformed and irradi., lattice defects obs., superlattice dislocations and defect clusters 0-107261
- ZrO<sub>2</sub>, CaO stabilised, preferred slip system 0-66585
- plastic flow
- see also ductility; Luder's bands; necking; rheology
- abraded surfaces, topography rel. to contact area and abrasion mechanism 0-58986
- annealed OFHC Cu, plastic behaviour 0-59559
- Bragg bubble glass, struct. and plastic flow 0-84091
- brass, cold rolling, inhomogeneous texture 0-89251
- $\beta$ -brass, uniaxial tension and compression, cyclic stress-strain behaviour 0-75551
- $\beta$ -brass bicrystals, shear-incompatible, grain boundary contrib. to Bauschinger effect 0-97550
- consecutive energy barriers system, reaction kinetics theory 0-106730
- corner theories, time-independent incremental behaviour at corner of yield surface 0-64388
- creep, generalised variational principles, Lagrange multiplier method applied to flow theory (*Chinese*) 0-79171
- cropping and blanking, plastic flow, fracture, crack propagation 0-74761
- dislocation distrib., fracture relation, plastic flow at crack tip, slip line theory 0-64482
- disperse systems, plastic, laminar flow in circular tubes 0-87798
- ductile fracture, strain hardening and damage relationship 0-108564
- elastic-plastic plates and shells, flow rule for lowering buckling stresses (*Japanese*) 0-99949
- FCC material, irradiation induced creep, climb induced glide model 0-89292
- granular materials, shear deformation, entropy model 0-84233
- inelastic membrane shells of revolution, large deformations in plastic flow theory 0-58917
- isotropic body, finite element method for volume integration 0-74770
- lecithin-water system, lamellar phase, rheology 0-89779
- metals, longitudinal flow velocity distribution in rolling (*Russian*) 0-93575
- metals, porous, plastic flows, microscopic frictional effects, J<sub>2</sub>-flow potential and yield function 0-64384
- metals, rheological interpretation of planar deformed state in extremal friction regime (*Russian*) 0-64385
- orthorhombic symmetry, yield surface characts. 0-64405
- plastic wave theory, comparison of predictions with impact expts. 0-83742
- PMMA, craze zones at crack tips, validity of Dugdale model, comment 0-108535
- PMMA, craze zones at crack tips, validity of Dugdale model 0-108534
- polyethylene film, minimum running thickness, biaxial extensional flow study 0-100993
- pressure sintering, inhomogeneous flow and effective press. 0-93512
- reinforced material, thin layer, compression between plane parallel plates (*Russian*) 0-87725
- Rene 80, dislocation behaviour during plastic deform. (*Japanese*) 0-108504
- soil, plastic flows, microscopic frictional effects, J<sub>2</sub>-flow potential and yield function 0-64384
- steel, effect of H<sub>2</sub> on phys. and mech. props. 0-101657
- steel, mild, plastic flow localisation under dynamic torsional loading, crit. variables 0-85015



**plastic flow continued**

- steel 45-antifrictional alloys friction pairs, electrochem.-mech. investigation (*Russian*) 0-76367
- Stouffer-Bodner constitutive model 0-92071
- stress and configuration, elastic and plastic strain increments 0-87718
- stretch zone width and striation spacing. The comparison of theories and experiments 0-85051
- transition metal-metalloid glasses, struct. and plastic flow, review 0-84090
- viscoplastic material, mixing process, Bingham model, two-dimens. flow (*German*) 0-92076
- viscoplastic materials, dynamic convergence theorem for strain and work hardening 0-96199
- Zircaloy, annealed, neutron irradiated, inhomogeneous deform. behaviour 0-85014
- Ag, cold rolling, inhomogeneous texture 0-89251
- Al, 6061-T6, pressure shear impact in transverse displacement interferometer, plastic flow 0-81137
- Al, cold rolling, inhomogeneous texture 0-89251
- Al, cold rolling of 1100 plates, substruct. development 0-108476
- Be-Ni(Y)(Al), plastic deform., flow stresses, fracture (*Russian*) 0-108496
- Cd, single crystals., plasticity study during deformation by twisting (*Russian*) 0-93597
- CrO<sub>2</sub> semidry refractory, struct. and mech. props., surface-active agents effect 0-89304
- Cu, OFHC effect of cold drawing under combined stress 0-60912
- Cu, swaged, inhomogeneous work hardening (*German*) 0-76267
- Cu-Al(Au)(Ga)(Ni)(Pd)(Rh)(Zn) (4 at.%), anneal hardening mechanism 0-60879
- Fe<sub>40</sub>Ni<sub>40</sub>P<sub>14</sub>B<sub>6</sub>, Metglas 2826, hot forming 0-84980
- Mg-Mn-Ce (1.5, 0.3 wt%), superplasticity role of diffusional creep (*Russian*) 0-97528
- NaCl, high-temp. deformed, dislocation grain subboundaries (*Russian*) 0-96534
- Na<sub>2</sub>O-CaO glass, shear deform. under pyramidal indentations 0-84989
- Na<sub>2</sub>O-CaO-SiO<sub>2</sub> glass, hot erosion plastic flow and fracture 0-89354
- Ni<sub>2</sub>(Al, Nb) single crystal, yield stress, orientation and temp. depend. 0-108511
- Ni<sub>2</sub>Ge-Fe<sub>2</sub>Ge solid soln., flow stress, transition from positive to negative temp. depend. 0-60906
- NiO, stress relief and plastic flow in temp. range 1323-1473K 0-89302
- Pd<sub>80</sub>Si<sub>20</sub>, glass, deform. localisation, plastic instabilities and fracture 0-89320
- Pd<sub>3</sub>Si<sub>18</sub>, stress/strain rate depend. of homogeneous flow 0-71687
- $\alpha$ -Ti, determination of microflow parameters from compression tests 0-66584
- $\alpha$ - $\beta$  Ti Widmanstätten alloy interfaces, elastic interact. stresses, effect on plastic flow onset 0-104218
- $\alpha$ -U, strain rate effect on flow and fracture 0-100887
- Y, plastic deformation props., deformation ageing, plastic flow, dislocation-impurity interactions (*Russian*) 0-66582
- Y, polycrystn., plastic deform. at different deform. speeds, dislocation glide (*Russian*) 0-93598
- Zn, pure single cryst., fracture stress 0-104269

**plastic strain** *see plastic deformation***plastic theory** *see plasticity***plasticity**

- see also elastoplasticity; photoplasticity; superplasticity*
- bar, rectangular, necked, void growth, finite element anal. 0-64383
- beams thin-walled, of open cross section, finite-element model 0-74767
- binary, ternary oxides, dislocation motion and high temp. plasticity 0-59468
- boundary element method appl. to plasticity 0-69680
- brittle solid, atomically sharp cracks, TEM study 0-71729
- composite material, mechanical behaviour, book 0-94935
- composite with plate like inclusions, plastic props., sintered Al-Al<sub>2</sub>O<sub>3</sub> results (*Russian*) 0-58923
- coupling phenomena in thermoplasticity 0-87721
- crack edge tip deformation, exact analytic soln. 0-69734
- creep modelling incorporating initial strain and ageing 0-58939
- discrete structures under dynamic loading, work hardening adaptation 0-74726
- disperse systems, instrument for strength props. determ. 0-76426
- dynamic plasticity, linear eqns., pulse loading, lumped-mass model, mode approx. technique 0-74769
- existence-uniqueness result for some models of thermoplasticity 0-92077
- field theory, integral presentations of second-rank tensors 0-69690
- fission reactor materials, thermomechanical transient anal., strain-rate dependent plasticity 0-79864
- flat rolling theory with spread, cross-section warping (*German*) 0-92064
- formulation of plasticity theory in tension and expansion space (*German*) 0-106733
- grain boundaries 0-65135
- L-plasticity, boundary value problems for plane strain or stress 0-58926
- materials with memory, thermodynamics 0-64356
- metals, plastic yield criteria, interpolation scheme 0-64400
- metals, residual stress on drawing calcs. by stress state changes variational principle (*Russian*) 0-65125
- metals, rheological interpretation of planar deformed state in extremal friction regime (*Russian*) 0-64385
- metals, theory extension to three dimens. and appl. to geophysics 0-104955
- metals and alloys, strain rate history, endochronic theory of viscoplasticity 0-65122
- microcrystalline alloys, metastable, rapidly quenched particulates, props. appl. and production 0-84887
- nitriding in glow discharges, influence on phase comp. and plasticity of diffusion layer (*Russian*) 0-76400
- nonlinearity viscoplastic liquid, convective dissipative heat exchange 0-87772
- plate, hole enlargement under plane stress conditions, viscoplastic rate sensitive constitutive eqns. 0-79163
- plate, simply supported circular, transverse shear and rot. inertia, dynamic plastic response 0-79175
- porous materials, deformation theory of plasticity (*Russian*) 0-75291
- porous media, plasticity as function of porosity (*Russian*) 0-75290
- porous metals, plasticity, stress-strain curves, yield stresses, strain vectors 0-83738
- Prandtl punch problem, finite element model for plane-strain plasticity 0-58940

**plasticity continued**

- punch stretching, localised necking, finite element anal. 0-102971
- rate type constitutive eqns., free energy of viscoelastic and viscoplastic materials 0-79168
- rate-independent plasticity, axiomatic model 0-87717
- shell, viscous plastic layers, viscous elastic filler, variable loading (*Russian*) 0-69695
- spheroplastic, spherical shells, supporting capacity 0-87723
- statically admissible stress fields in plane plastic problems 0-58919
- steel, age hardened, dynamics of cyclic plasticity (*Czech*) 0-108464
- steel, austenite, carbide strain hardened, strength and plasticity, effect of Mn content (*Russian*) 0-97500
- steel, fatigue and cyclic plasticity rel. to struct. inhomogeneity 0-81184
- steel, high speed, props. after electroslog remelting 0-104139
- steel, high strength, dislocation sweeping model for hydrogen assisted subcritical crack growth 0-97577
- steel, high strength, subcritical crack growth, role of time delayed H<sub>2</sub> assisted plastic zone growth 0-97576
- steel, stainless, fracture micromechanism when kept isothermally in sulphur pulp 0-76355
- steel, stainless, porous sheet, mech. strength, bend and reverse bend tests (*Russian*) 0-93595
- steel, stainless, type 304, viscoplastic behaviour, strain rate sensitivity, creep, relaxation, tensile tests 0-66727
- steel, stainless, type 304, viscoplastic model, uniaxial, based on total strain and overstress 0-64387
- steel, type Kh13N9D2MT martensitic aged, struct. and mech. props. (*Russian*) 0-92600
- steel bearing rings, optimisation of thermomechanical working parameters (*Russian*) 0-93579
- strand with axial load, static plastic behaviour 0-69685
- subgrain imaging, in bulk specimens to study localised plasticity using SEM 0-66609
- thermoplasticity, time evolution under quasistatic conditions, existence theorems 0-74764
- thermoviscoplasticity theory based on infinitesimal total strain 0-87719
- torsion pendulum, with anelastic solids of discrete relaxation spectra, resonant system 0-69687
- uniaxial stress/strain relations, generalisation 0-83739
- unloading wave propagation in cylindrical, semi-infinite, elastic-plastic rod, asymptotic behaviour 0-69659
- viscoplastic and elastoplastic structures, partial shakedown under thermomechanical loading path (*French*) 0-74757
- viscoplastic kinematic hardening model, cyclic loading appl., yield surface 0-79162
- viscoplastic material, mixing process, Bingham model, two-dimens. flow (*German*) 0-92076
- viscoplastic materials, dynamic convergence theorem for strain and work hardening 0-96199
- viscoplastic medium, flow between two noncoaxial circular cylinders under pure shear 0-99938
- viscoplasticity theory based on infinitesimal total strain and nonlinear viscoelasticity 0-79164
- Al-Cu-Mn (1-5.2, 0-0.6 wt%), N alloying and comp. effect on mech. props. (*Bulgarian*) 0-71719
- Al-Mg sheet, artificial stress raiser effect on strength and local plasticity of weld joint 0-81130
- Al-Mn sheet, artificial stress raiser effect on strength and local plasticity of weld joint 0-81130
- C polymeric chains, reduced from poly(tetrafluoroethylene), plasticity of C skeleton 0-89488
- Cu, annealed, plastic strain during non-proportional loading 0-89291
- Cu-Cr(SiO<sub>2</sub>), single crystals., yield and pre-yield behaviour rel. to aging time 0-81103
- Fe-Ag (50 wt.%), plastic behaviour in compression, deform. rate effect (*French*) 0-71711
- Fe-Si (2.6 wt.%) single cryst., crack propag., controlled plastic crack tip opening rate 0-60943
- MgO, high temperature prestrain effect on plastic props., dislocation struct. 0-79866
- Mo single crystals, orientation and alloying effect on mech. props. (*Russian*) 0-71706
- Mo-Nb-C, mech. props., effect of alloying and Mo cryst. orientation (*Russian*) 0-71706
- Ni alloy, fatigue and cyclic plasticity rel. to struct. inhomogeneity 0-81184
- Ni alloys, plasticity, heat treatment effect 0-76277
- Ni, hardness after-effect studied by anelastic relaxation 0-66570
- Ni, sintered, pressed, plasticity as function of porosity (*Russian*) 0-75290
- $\beta$ -NiAl, ordered, hardness after-effect studied by anelastic relaxation 0-66570
- Pb, plastic properties over wide range of strain rates 0-71693
- SiC, reaction-bonded, impact erosion by ang. Al<sub>2</sub>O<sub>3</sub> particles 0-89362
- Ti-Al-Mo-V (8, 1, 1 wt.%), Widmanstätten colonies, fracture toughness 0-85031
- V<sub>2</sub>Si, supercond. structure and properties (*German*) 0-93631
- Y<sub>2</sub>O<sub>3</sub>, dislocation and plasticity dissociation 0-107247
- Zn, internal friction anomalies in temp. initiated brittle-plastic transition (*Russian*) 0-96648
- Zr, ion-implanted polycryst., thermal oxidation 0-71786

**plastics**

- see also glass fibre reinforced plastics; polymers*
- acrylic moulding formulations, optical and mech. props. 0-106582
- coated optical glass fibres, liq. N<sub>2</sub> strengths 0-58707
- CR-39 plastic, electrochem. etching, optimum conditions 0-95505
- crack growth stability anal. using catastroph theory 0-74810
- creep of metals and plastics under combined stresses. A review 0-59567
- electrochemical etching studies of the CR-39 plastic solid state nuclear track detectors 0-91391
- epoxy resin, plastic deform. mechanism 0-97534
- foam insulation, spray-on, crack inspection using dye solution or X-ray opaque solution 0-76440
- Homalite-100 plates, modified compact-tension specimens, dynamic anal. 0-97561
- lenses, aspherical-surface, for large screen TV, optical design and evaluation 0-78937
- LR-115 plastic track detector, etching behaviour 0-99423
- optical material physical props., seminar, San Diego, CA, USA (Aug. 79) 0-105423
- Perspex, positronium form. and decay, elec. field effect 0-97369



## plastics continued

- perspex confined arc, ablation-induced effects 0-70073  
 photothermoplastic material recorded information visualisation by schlieren projector 0-87544  
 plastic:Eu<sup>3+</sup>, Faraday rotation sign oscill. in very strong mag. fields (*Russian*) 0-88973  
 Plexiglas, fast cracks propag. and interaction 0-100905  
 Plexiglas 0-66592  
 plexiglass composite, long term strength and durability 0-75294  
 polycarbonate, glassy, fatigue crack initiation in high strain fatigue tests 0-97564  
 polycarbonate, yield behaviour (*Japanese*) 0-93620  
 polyester thermoplastic, for electrical insulators 0-103685  
 polyimide, directional O ion beam etching, compared with reactive ion etching 0-71781  
 polypropylene, (Moplen) influence of temp. and mol. wt. on high speed fracture mechanics 0-76341  
 projector having a thermoplastic target and operator's eye, characts. 0-96023  
 PVC, glassy, fatigue crack initiation in high strain fatigue tests 0-97564  
 PVC, yield behaviour (*Japanese*) 0-93620  
 reflectance, aluminised thermal screens for energy conservation in green-houses 0-64351  
 reinforced, load-bearing capacity, effect of one-sided heating 0-81135  
 resins, secondary coating of optical fibres, effect on transmission props. 0-58704  
 sheet blowing and extruding, process identification for automatic process control (*German*) 0-81023  
 shock compression at 30 kbar, expansion adiabats 0-66592  
 solid state nuclear track detectors, effect of etching conditions on energy resolution of phosphate glass and polycarbonate detectors 0-91390  
 testing, automation 0-76443  
 testing device, for prop. changes at high temps. (*German*) 0-66741  
 textolite glass, stress relax. calc. from creep curves 0-71709  
 thermoplastic, low-profile polyester moulding materials (*Polish*) 0-66523  
 thermoplastic complex filter for optical pattern recognition 0-99656  
 thermoplastic layers, isothermal smoothing of surface deformation (*Russian*) 0-76394  
 thermoplastic plates, strength meas. when supported by annular ring 0-81257  
 thermoplastic sheet, deep drawing (*German*) 0-104114  
 thermoplastic spatial light modulator 0-102841  
 thermosetting, characterisation by thermal anal. 0-61204  
 ultradrawing technique, solid state coextrusion 0-84979  
 urethane elastomer, thermoplastic, dilute soln., viscosity and sedimentation 0-103512  
 Valox 752m thermoplastic, for electrical insulators 0-103685  
 N-vinylcarbazole containing polymers, sensitization to Ar laser for single laser photothermoplastic devices 0-83651  
 viscoplastic material, mixing process, Bingham model, two-dimens. flow (*German*) 0-92076

## plastics industry

- adaptive control of molecular weight distribution in polymers 0-58434

plates (anodes) *see anodes*plating (electroplating) *see electroplating*

## platinum

- see also nuclei with .....*  
 (111) surface, backscattering, channelling spectra, H adsorption, surface relaxation 0-71552  
 adsorption, of CO, mol. internal optic modes, mol. dipole model 0-100395  
 adsorption and catalytic reactions of H<sub>2</sub>, CO, and O<sub>2</sub> 0-81362  
 adsorption of acetic and propanoic acids on (111), LEED obs. 0-80073  
 adsorption of K on Pt(111), UPS and XPS meas. 0-95675  
 adsorption of NO on (111) surface, EELS, thermal desorption, LEED, and AES study 0-80086  
 adsorption of O<sub>2</sub> on (110) surface, Ar<sup>+</sup> bombardment effects on reactivity 0-89099  
 adsorption of O on (111) and (S)-12 (111)X(111) surfaces, thermal desorption, AES, XPS, and LEED study 0-70534  
 adsorption of water on (111) surface, thermal desorption, UPS, and XPS study 0-80088  
 anode, oxide film growth in H<sub>2</sub>SO<sub>4</sub> solns., temp. study 0-71802  
 atom, L-shell internal excitation accompanying L-capture 0-95726  
 Auger spectra, N<sub>4s</sub>N<sub>6s</sub>N<sub>6s</sub> and N<sub>4s</sub>N<sub>6s</sub>O<sub>4s</sub> 0-89094  
 band-structure determ., angle-resolved photoemission 0-66398  
 catalyst, on C electrode, surface area loss in H<sub>2</sub>PO<sub>4</sub> 0-101091  
 catalytic oxidation of H<sub>2</sub> and D<sub>2</sub>, matrix isolation and laser fluoresc. obs. of prods. 0-66865  
 chemisorbed water on (111) surface, EELS spectra, vibr. freqs. 0-80920  
 desorption of Cl<sub>2</sub> on (111) face, LEED, AES, thermal desorption, and work function meas. 0-75444  
 chemisorption of CO and O<sub>2</sub>, SCF-X $\alpha$  cluster calcs. 0-65365  
 chemisorption of H<sub>2</sub> on Pt(111) plane and stepped surfaces, bond breaking, model pot. 0-108744  
 chemisorption of mol. O<sub>2</sub> on (111) surface, XPS, UPS, EELS, and work function meas. 0-76139  
 core-electron excitation edges 0-66345  
 crucibles, surface changes rel. to Fe anal. 0-61192  
 desorption of Ar, gas surface interactions, 3-D generalised Langevin model appl. 0-107637  
 desorption of Xe, gas surface interactions, 3-D generalised Langevin model appl. 0-107637  
 diffusion and saturation solubility in Pb, melting curve, conc. profiles 0-88365  
 electrocatalysts for methanol oxidation in acid electrolyte with improved steady state activity for fuel cell appls. 0-76629  
 electrode reactions with molten glass 0-85186  
 electrode surface, oxide layers, anisotropy of optical props. 0-60534  
 electrodes, polymeric surface film form. by electrooxidation of phenolic cpds., ellipsometric study 0-104450  
 electron irradiated, selfinterstitial atomic defect interaction radii, recovery expts. and error sources 0-65049  
 emissivity, integral, meas., modulation technique 0-62672  
 energy band structure, X-ray emission spectra, APW calc. 0-92811  
 EXAFS amplitudes, many-body effects 0-97379  
 film, growth on amorphous Si:H, AES and LEED study 0-88447  
 film, polycrystalline, trapping of <sup>3</sup>He and <sup>4</sup>He ions at room temp. 0-84221

## platinum continued

- film characterisation technique, APFIM, time-of-flight spectroscopy 0-75138  
 implantation on Cr-Ni Nb stabilized austenitic stainless steel surface, effect on oxidation behaviour 0-71791  
 ion irradiation damage, temp. depend., electron microscopy obs. of defect kinetics 0-107339  
 luminescence characteristics of pure surfaces acted on by flux of field emission electrons 0-100695  
 MOS structure Pt diffused, hysteresis and memory props. 0-96992  
 neutron damage, positron annihilation 0-65056  
 neutron irradiated, recovery spectrum, resist. obs., Au addition effect and defect conc. depend. 0-65057  
 phonon density of states determ. from thermodynamic functions 0-96616  
 photodecomposition over Pt/TiO<sub>2</sub> catalysts 0-81337  
 resistance thermometers, effect of Pt oxidation 0-101794  
 resistance thermometers, heat leaks effect anal. 0-57296  
 resistance thermometers, temp. range influence on error due to non-linearity (*Russian*) 0-90841  
 resistance thermometry, medium precision, A/D convertor appl. 0-86297  
 SEM exam., ultra-high vacuum, secondary electron emission dependence on electron beam dose, surface interactions from AES and ELS 0-61209  
 silicide formation due to laser and electron beam annealing 0-84849  
 single crystal spheres, electrolytic deposition of Zn 0-104080  
 spin fluctuation model interpretation of mag. susceptibility 0-80477  
 STEM, Pt on  $\gamma$ -Al<sub>2</sub>O<sub>3</sub>, atomic number contrast, supported catalyst particles 0-79651  
 subshell photoelectron branching ratio meas., synchrotron radiation 0-66397  
 surface, (100), reconstruction, superstruct., model 0-103551  
 surface, (111), O<sub>2</sub> interactions, UPS, EELS and thermal desorption study 0-100409  
 surface, chemisorbed CO, IR refl.-absorpt. spectra, adsorbate island struct. 0-84385  
 surface, chemisorption of ethylene, vibr. anal. of C<sub>2</sub>H<sub>4</sub> species 0-61150  
 surface, CO chemisorpt., mol. cluster calc. 0-100407  
 surface, CO oscillatory oxidation, theory 0-85215  
 surface, CO oscillatory oxidation, theory 0-85216  
 surface 6(111)X(100), clean and O<sub>2</sub>-covered, UPS studies 0-76151  
 surface (997), partial faceting, He beam scatt. and LEED study 0-103547  
 surface and subsurface adsorbed O, low energy ion scatt. obs. 0-65372  
 surface dipole moment calc. 0-60060  
 surfaces (100) (5X20) and (1X1), stability and reactivity, adsorption of H 0-75434  
 thermomodulation spectra of high-energy interband transitions 0-108226  
 thermostimulated exoelectron emission, excitation mechanism (*Russian*) 0-71581  
 valence bands, angle-resolved photoemission determ. 0-108323  
 wear coefficients determ. using pin-on-disc apparatus 0-76366  
 Al<sub>2</sub>O<sub>3</sub>-Pt metal-ceramic reaction, micro/macro obs. 0-66467  
 As<sub>2</sub>Se<sub>3</sub>-Pt, impurity effects on elec. props. 0-103699  
 C<sup>+</sup>O<sup>+</sup> ion-molecule reaction, 15-eV energy O<sup>+</sup> production system 0-84817  
 CdTe/SnCl<sub>2</sub>/Pt, solar cell photoelectric props. (*Spanish*) 0-85290  
 NaCl<sub>4</sub> on Pt and Ir surfaces, adsorption kinetics 0-84393  
 Ni/Pt/Si(111) Schottky diodes, current-voltage characts. and comp. profiles 0-84508  
 Pb(Zr,Ti)O<sub>3</sub>, internally electroded with Pt, resonance behaviour 0-84701  
 Pt alloys, influence of Rh, Au, Mo, W, Zr, Hf alloying elements on creep activation energy at high temp. (*Chinese*) 0-66573  
 Pt thin-film temp. sensor (*Japanese*) 0-105645  
 Pt/Al<sub>2</sub>O<sub>3</sub>, electron accepting sites by pyridine absorpt. 0-71947  
 Pt/ZrO<sub>2</sub>, porous electrode/solid electrolyte system, interface polarisation effects 0-61114  
 Pt-C replicas, for rapid aimed replica prep. 0-61037  
 Pt-Cr(Si) interface, low-temp. diffusion, ambient effects 0-100355  
 Pt-polymer-Au capacitor, electroforming, negative resist., electron emission 0-80406  
 Pt-Si Schottky barriers on Si, laser formation and characts. 0-60079  
 Pt-Si:As, silicide form. during laser irr., p-n junctions and ohmic contacts 0-84397  
 Pt-SiO<sub>2</sub>, cermet films, struct. and prop. 0-96956  
 Pt<sub>2</sub>, ab initio relativistic core pot. studies of metal-metal bonding 0-106257  
 Si:Pt, hole capture cross-section at E<sub>v</sub>+0.34 eV, capacitance meas. (*French*) 0-65493  
 Si:Pt, implanted and laser annealed, segregation and increased dopant solubility 0-65016

## platinum alloys

- see also platinum compounds*  
 Ni-Pt-Pt, metallic glass, electronic structure, pulsed NMR study 0-75869  
 rare earth alloys, R<sub>2</sub>Pt (R=Gd, Tb, Dy, Ho, Er), magnetic susceptibility meas., mag. transition obs. 0-60222  
 rare earth-Pt, RPt<sub>3</sub>, low temp. mag. susceptibility 0-93075  
 Ag-Pt, dil., virtual bound states, transport props. obs. 0-70667  
 Al-Al<sub>3</sub>Pt, eutectic alloys, unidirectionally solidified, struct. study 0-108394  
 Al-Ni(Pt)(Zn), rapidly solidified, twinned dendrites 0-70572  
 Al-Pt, rapid quenching, struct. and decomp. 0-76244  
 Au-Pt, dil., virtual bound states, transport props. obs. 0-70667  
 Au-Pt-Pd-Ag-Cu, commercial dental alloy, age-hardening characts. 0-89235  
 C/Pt-W (8 wt.%), desorption of K from C film surfaces 0-59784  
 CeNi<sub>2</sub>-CePt<sub>3</sub> system, structural and mag. studies on valence behaviour of Ce 0-103809  
 Co-Pt, mag. annealing, form. of ordered phase, study using X-ray scatt. (*Russian*) 0-81052  
 Co-Pt ferromagnetic alloy, 6 T ultrasonic study of magnetoelectric coupling 0-93154  
 Cr<sub>0.995</sub>Pt<sub>0.005</sub> alloy, mag. struct., neutron diff. study 0-60198  
 Cu-Mn-Pt spin glasses, anisotropic exchange interactions, effect of non-mag. impurities 0-80534  
 Cu-Pt, dil., screening charge density round  $\Delta Z = -1$  impurities, vacancies, NQR study 0-103897  
 Cu-Pt system, phonon dispersion relations, force constant disorder effect 0-84263  
 Cu-Pt-O alloys, dil., O-metal interactions, activity coeff. meas. at 1423K 0-93792



**platinum alloys continued**

- Cu<sub>3</sub>Pt, antiphase domains morphology 0-108460  
 EuPt<sub>3</sub> compounds, partial valence change, <sup>151</sup>Eu Mossbauer and magnetisation obs. 0-70167  
 Fe-Pt, Invar, magnetoelastic contribs. to US vel., elastic const., and susceptibility 0-75829  
 Fe-Pt, Invar alloy, paramag. susceptibility 0-70940  
 Fe-Pt, itinerant electron ferromagnet, magnetovolume effects 0-60397  
 Fe-Pt Invar, elastic and mag. props., magnetoelastic interaction effects (*Russian*) 0-84631  
 Fe-Pt Invar alloys, magnetocrystalline anisotropy const. determ. 0-65861  
 Fe<sub>2</sub>Pt, ordered ferromagnetic alloy, magnetic excitation obs. 0-70978  
 FePt<sub>3</sub>, metamagnetic transitions in external fields 0-60272  
 Fe<sub>3</sub>Pt, atomic thermal vibr. anisotropy, martensitic transform. model (*French*) 0-70355  
 Fe<sub>3</sub>Pt austenite, long range order parameter, temp. depend. discussion 0-97481  
 Fe<sub>3</sub>Pt austenites, ordering kinetics 0-104155  
 Fe<sub>3</sub>Pt austenitising conditions on M<sub>1</sub> temp. 0-81088  
 Fe<sub>3</sub>Pt Invar alloy, anomalous Curie const., susceptibility meas. 0-75731  
 Fe<sub>3</sub>Pt Invar alloy, thermal expansion and spontaneous magnetisation, Invar anomalies, low spin model 0-71001  
 Li-Pt, phase diagram for comp. range 0-40 at.% Pt, mag. and elec. props. (*German*) 0-84912  
 Ni-Pt alloys, magnetic-moment distrib. neutron study 0-97066  
 NiPt, quenched, ordering kinetics and domain struct. form. during isothermal tempering (*Russian*) 0-66502  
 Ni-Pt, change of H<sub>2</sub> diffusivity with order-disorder transformation 0-59729  
 P+Nb, dil. alloy, NMR obs. of <sup>93</sup>Nb 0-71203  
 Pd-Pt, adsorption, of CO(NO), on SiO<sub>2</sub>-supported surface, IR spectrosc. obs. 0-92780  
 Pd-Pt-H(D), elastic energy dissipation peak 0-60905  
 PrPt<sub>3</sub>, hyperfine sp. ht. and magnetisation meas. at 4.2K 0-75775  
 PrPt<sub>3</sub>, sp. ht., differential susceptibility and elec. resist. meas., 1.4-40K 0-71063  
 Pt-Au, dil., recovery spectrum after thermal neutron irradi., Au effect and defect conc. depend. 0-65057  
 Pt-Au, surface segregation, comp. depth profiles meas. using atom-probe field ion microscope 0-100380  
 Pt-Co, dil., skew scatt. Hall effect, magnetoresist. and mag. anisotropy, orbital magnetism of impurity 0-70678  
 Pt-Co system, low temp. susceptibility 0-65920  
 Pt-Cr, disordered, atomic order-disorder transform. effect on resist. min. 0-65911  
 Pt-Cr, shallow silicide contact 0-70819  
 Pt-Fe, dil., breakdown of ferromag. order, magnetoresist. obs. 0-71046  
 Pt-Fe, dil., skew scatt. Hall effect, magnetoresist. and mag. anisotropy, orbital magnetism of impurity 0-70678  
 Pt-Fe, very dil., Mossbauer emission spectra, relax. effects 0-66084  
 Pt-Fe alloy, ordered, T-c phase diagram, antiferro- and ferromagnetism (*Russian*) 0-65871  
 Pt-Fe ordered alloy, multiply mag. phase transitions 0-60264  
 Pt-Fe(Co), dilute ferromagnets, press. effect on Curie temp. 0-65873  
 Pt-Mn, dil., skew scatt. Hall effect, magnetoresist. and mag. anisotropy, orbital magnetism of impurity 0-70678  
 Pt-Ni vacuum condensates on Si and SiO<sub>2</sub>, thermally treated, X-ray anal. (*Russian*) 0-70559  
 Pt-refractory metal/Si interactions, phase separation 0-65303  
 Pt-Si thermally degenerated Schottky diodes, resonant tunnelling 0-100503  
 Pt-Si:As, silicide form. during laser irradi., p-n junctions and ohmic contacts 0-84397  
 Pt-transition metal, dil., impurity resist. 0-92875  
 Pt-W, substrate temp. influence on shallow contact formation on Si 0-96963  
 PtBi<sub>3</sub>-h<sub>3</sub>, cryst. struct. (*German*) 0-107113  
 Pt<sub>3</sub>Co, radiation damage profiles from low energy Ne<sup>+</sup>, bombard. 0-70268  
 PtCr, AC susceptibility near percolation limit, ordered and disordered alloy 0-65900  
 Pt<sub>3</sub>Cr, ferrimag., magnetisation density, polarised neutron diff. meas. 0-60204  
 Pt<sub>0.75</sub>(Cr<sub>1-x</sub>Mn<sub>x</sub>)<sub>0.25</sub>, pseudobinary, magnon energy derivation 0-107996  
 Pt<sub>3</sub>In(Sn)(Pb)(Ti)(Cr)(Al)(Ga), L<sub>1</sub><sub>2</sub> ordered alloy, positive temp. depend. on strength, phase destabilization 0-81203  
 PtMn, spin glass, nonlinear susceptibility and sp. ht. 0-60304  
 PtPb<sub>0.7</sub>Bi<sub>1.3</sub>, crystal structure (*German*) 0-84139  
 Pt<sub>3</sub>PbBi<sub>7</sub>, cryst. struct. (*German*) 0-107113  
 Pt<sub>3</sub>Sb, L<sub>1</sub><sub>2</sub> ordered alloy, positive temp. depend. on strength, phase destabilization 0-81203  
 PtSi film formation by ion sputtering and annealing, form. and exam. problems 0-100782  
 PtSi films, on Si, stress obs. 0-80145  
 PtSi, growth rate for form. by Pt film deposition under ultrahigh vac. and controlled impurity atm. 0-65388  
 PtSi Schottky-barrier monolithic IRCCD focal plane 0-86427  
 PtSi, substrate ion implantation, channelled, through metal silicide film 0-70231  
 PtSi surface, and interface with Si, impurity effects 0-80037  
 Pt<sub>3</sub>Si, growth rate for form. by Pt film deposition under ultrahigh vac. and controlled impurity atm. 0-65388  
 PtV, dil. alloys, NMR obs. of <sup>51</sup>V 0-71203  
 V-Pt, sp. ht. and mag. meas. in ordered and disordered phases 0-70422

**platinum compounds**

- see also platinum alloys*  
 complexes, INDO calcs. for predicting ground-state props., charge distributions and force const. determ. 0-83283  
 intercalation, electron microscopy 0-84164  
 phthalocyanine, reson. Raman excitation profiles, solvent effects 0-102512  
 Wolfram's red salt, mixed valence, reson. Raman calcs. using vibronic coupling model 0-97249  
 K<sub>2</sub>Pt(CN)<sub>4</sub>, muonic X-ray radiation anisotropy (*German*) 0-69267  
 K<sub>2</sub>Pt(CN)<sub>4</sub>Br<sub>0.3</sub>3H<sub>2</sub>O, anisotropic radiation damage in electron microscopy, diff. spot fading rate obs. 0-107329  
 Ni-Pt silicide Schottky diodes, current-voltage characts. and comp. profiles 0-84508  
 Pd and Pt mixed valence complex, [Pd(ethylenediamine)<sub>2</sub>Pt(ethylenediamine)<sub>2</sub>Cl<sub>2</sub>](ClO<sub>4</sub>)<sub>4</sub>, Raman spectra 0-84734

**platinum compounds continued**

- Pt complex, [2, 2', 2''-terpyridine PtCl]<sup>+</sup>, motion of Pt atoms, electron microscopy obs. 0-103314  
 Pt complex, bis [4-(n-butyl)-styryl dithiolato] Pt nematic complex with strong IR absorption 0-88305  
 Pt dithiene complexes, mesomorphic props. 0-88026  
 Pt-Si, amorphous thin films, laser irradi., metastable phases 0-96622  
 PtBr<sub>4</sub><sup>2-</sup>-PtBr<sub>6</sub><sup>2-</sup> doped in Cs<sub>2</sub>ZrBr<sub>6</sub>, mixed valence, absorpt. spectra, vibronic struct. 0-97308  
 PtH, ab initio relativistic core pot. studies of metal-H bonding 0-106257  
 PtO, films, electronic struct., reduction processes, photoemission, optical absorpt. and resist. meas. 0-80931  
 PtSb<sub>2</sub>, high field elec. props., impact ionisation 0-96892  
 PtSi formation on Si with Pt-W alloys, effect of substrate temp. 0-96963  
 PtSi, parallel contacts, Schottky barrier height meas. 0-96965
- pleochroism**  
*see also dichroism*  
 anthraquinone pleochroic dyes in liq. cryst. soln., photostability, appl. to liq. cryst. displays 0-88961  
 quartz, synthetic, Al centres conc. and anomalous pleochroism depend. on crystn. parameters 0-107311  
 ZnGeP<sub>2</sub> p-n homodiode, polarisation photosensitivity and photopleochroism spectra 0-107866
- plexiglas** *see plastics*
- plotters**  
 calligraphic projection display resolution and contrast photometer and X-Y plotter 0-86373  
 colour plotter system for computer graphics output, appls. in geoscience 0-98467  
 interface for serial computer terminals 0-98904  
 pictorial electrographic printing, tone reproduction and screen design 0-62752  
 x-y recorder sweep generator, sweep speed dependent on four terminal network transfer charact. 0-62649
- plugs (electric)** *see electric connectors*
- Pluto**  
 1978 P 1, speckle interferometric obs. (1980 June) 0-101553  
 1978 P 1, speckle obs. rel. to orbital radius and system mass and density 0-109394  
 appulse on 1980 April 6, no occultation from S.England 0-67650  
 astrometry (1973 to 1979) 0-85894  
 Charon (1978 P 1), occultation on 1980 April 6 probable 0-67651  
 Charon (1978 P 1), probable stellar occultation, 1980 April 6, min. dia. 0-62071  
 Charon (1978 P 1), satellite of Pluto, positions and dynamical parameters 0-62069  
 Charon (1978 P 1), stellar occultation obs., 1980 April 6, rel. to satellite dia. and struct. 0-94754  
 composition constraints and mass-radius relationships 0-82298  
 discovery and review of data (book) 0-82591  
 no occultation of star on 1980 April 6, ephemeris 0-62070  
 orbital motion, long term librational character 0-94753
- plutonium**  
*see also nuclei with .....*  
*see also fission of plutonium*  
 accountability, computerised gamma spectrometer system for meas. isotopic and total Pu conc. in solns. 0-63363  
 accountability, nondestructive assay using neutron counting, calorimetry and gamma spectrometry 0-63266  
 accountability and control, field nondestructive assay measurements as applied to process inventories 0-63265  
 assay and accountability using neutron correlation meas. tech. 0-69015  
 assay of large samples using portable neutron coincidence counter 0-69041  
 biologically important physicochemical props. and methods of human contamination (*French*) 0-98004  
 calorimetric nondestructive assay for in-field meas. 0-71874  
 determination, in irradi. fuel dissolver soln. by isotope dilution alpha spectrometry 0-78428  
 dose to lung and bone from contaminated soils, statistical uncertainties 0-109028  
 elastic constants at elevated temps., noncontact meas. tech. 0-104405  
 environmental contamination, review 0-101136  
 environmental impact of Pu-bearing materials, linear regression anal. 0-85308  
 fallout in alkaline, saline lakes 0-97826  
 fissile material accountability using controlled potential coulometry 0-63298  
 fuel reprocessing, spectrophotometric determ. of Pu 0-78433  
 isotope composition, determ. using gamma spectrometry 0-66915  
 isotopic analysis by resin-bead mass spectrometry for materials safeguards 0-78392  
 isotopic composition, determ. using precise absolute gamma spectroscopic meas. 0-66916  
 isotopic composition, determ. using thermal ionisation spectrometry with automatic data eval. 0-66913  
 isotopic composition, nondestructive anal. using gamma spectrometry 0-63392  
 isotopic safeguards analysis to determ. Pu content in nuclear fuels 0-99210  
 lung burdens in Austrian residents 0-109042  
 monitoring of PU holdup in glove-gox exhaust filter by gamma ray detection 0-78458  
 nondestructive assay meas. using NaI(Tl) detectors during fabrication plant decommissioning 0-63495  
 nondestructive analysis, calibration by calorimetric assay 0-71878  
 nondestructive assay of large samples 0-71871  
 nondestructive element and isotope assay 0-71870  
 nuclear materials safeguards, Pu accountability by ceric oxidation, ferrous reduction and dichromate titration 0-63364  
 oxidation, binding energies, Auger and X-ray photoelectron spectra study 0-76550  
 passive assay using Euratom variable dead-time neutron counter 0-69042  
 portal monitors for detecting and safeguarding special nuclear materials 0-63406  
 radioactive effluent, Pu and Am inventory of ecosystem near a nuclear facility 0-97820  
 radiological implications of Pu recycling in HTGR fuels 0-68777  
 reactor fuel, input accountability in reprocessing plants, tracer tech. using Mg and Pb 0-73919



**plutonium continued**

- reactor fuel, production and availability, uses, reprocessing, fast reactor fuel cycles 0-68767  
 reactor fuel extraction processing of nuclear fuel fluxes, effect of flux oscill. on Pu accumulation, math. simulation 0-63355  
 recovery by radioactive waste processing, volume reduction of organic alpha waste by pyrohydrolysis 0-95366  
 safeguarding, automated ion-exchange system for rapid Pu separation from impurities 0-78383  
 safeguarding, computer-assisted controlled potential coulometric determ. 0-78384  
 safeguarding, determ. of U and Pu content of fuels using isotope correl. tech. 0-68834  
 safeguarding, Pu content determ. in irradiated fuel assemblies 0-68806  
 safeguarding, tracer techniques for Pu input accountability in reprocessing plants 0-68827  
 safeguarding using resin bead mass spectroscopy 0-73984  
 safeguards, product soln. gamma-ray NDA using K-absorption edge densitometer 0-83162  
 safeguards accountability, NDA of crated waste by gamma-ray and neutron coincidence counting 0-83166  
 safeguards assay, isotopic meas. by gamma ray spectrometry using two-detector method 0-83161  
 safeguards verification methods for input-accountability meas. at reprocessing plant 0-95349  
 St. Severin chondrite, U and Pu distrib. 0-72889  
<sup>238,240</sup>Pu(V) in alkaline freshwater pond, determ. by coprecipitation technique 0-71988  
 Pu fallout detection using fission tracks prod. with neutron irradi. spectra 0-95479  
 Pu safeguards accountability, gamma-ray meas. of Pu and Am in molten salt residues 0-83165  
<sup>A</sup>Pu, A=239, 240, distrib. of fallout Pu in southern Finns 0-109045  
<sup>A</sup>Pu, A=239,242, muonic atom lifetimes from muon induced fission 0-69269  
<sup>237</sup>Pu, bioaccumulation in inland water and marine algae (German) 0-108820  
<sup>238</sup>Pu, alpha spectrometric determ. 0-81404  
<sup>239</sup>Pu, (U,Pu)<sub>2</sub>O<sub>3</sub> fuels 0-71873  
<sup>239</sup>Pu, distrib. and behaviour in Urazoko Bay sediment 0-97825  
<sup>239</sup>Pu, nanocurie amounts, lesions in CBA mice 0-81657  
<sup>239</sup>Pu, transuranic trace analysis using resonance ionisation spectroscopy of inert gases 0-93833  
<sup>241</sup>Pu, concs. in sediments from coastal basins off California and Mexico 0-98303  
<sup>244</sup>Pu standard reference material for nuclear materials safeguards appls. 0-78373  
 U-<sup>238</sup>Pu-<sup>237</sup>Np GCRF fuel cycle to produce isotopically denatured Pu for LWR 0-78427

**plutonium alloys**

- Pu-Ga (1 wt.%), alloy powder, hydriding kinetics 0-76503  
 PuRu<sub>2</sub>, intermetallic cpd., sublimation thermodynamics 0-96639  
 Th-Pu (20 wt.%) metal fuels, compatibility with cladding alloys for FBR appls. 0-102242  
 Th-Pu-U-Zr (20, 4, 8 wt.%) metal fuels, compatibility with cladding alloys for FBR appls. 0-102242  
 U-Pu-Zr(Th) LMFBR metal fuel elements, development and performance 0-78556

**plutonium compounds**

- see also plutonium alloys  
 thermal reactor fuel cycles, actinide wastes toxicity limitations (German) 0-99220  
 Pu(C<sub>2</sub>O<sub>4</sub>)<sub>2</sub> precipitator, dynamic process model for nuclear materials safeguards 0-83150  
<sup>239</sup>PuO<sub>2</sub>, stoichiometric, high-temp. deformation 0-81111  
<sup>239</sup>PuO<sub>2</sub>, inhaled by baboons and dogs, comparison of early mortality 0-108977  
<sup>239</sup>PuO<sub>2</sub> inhaled by rhesus monkeys, cytogenetic and other biological effects 0-108968  
 (U,Pu)C, nuclear fuel, irradiation induced creep meas. 0-93605  
 (U,Pu)(C,N) and (U,Pu)N, high burn-up simulated, Pu self diffusion 0-92712  
 (U,Pu)C FBR fuel pins, irradi. behaviour w.r.t. fission gas release, fuel/clad compatibility, Pu migration 0-57847  
 (U,Pu)C LMFBR fuel, Na-bonded, consequences of rapid Na loss on fuel behaviour 0-102238  
 (U,Pu)C, pellet and sphere-pac nuclear fuels, comparative irradi. tests 0-78367  
 (U,Pu)C, sintering, role of Ni as sintering additive 0-84892  
 (U,Pu)C<sub>1-x</sub>N<sub>x</sub> LMFBR MX-type fuels, fission gas release and microscopic swelling 0-73921  
 (U,Pu)O<sub>2</sub> 0-63252  
 (U,Pu)O<sub>2</sub>, fission gas release and retention in irradi. nuclear fuels 0-57841  
 (U,Pu)O<sub>2</sub> fuel pin behaviour during FFTF 3c/s reactivity insertion event, TREAT expt. anal. 0-102240  
 UO<sub>2</sub>-PuO<sub>2</sub> fuel pin, hyperstoichiometric, post irradiation examination 0-63258  
 U<sub>0.77</sub>Pu<sub>0.23</sub>O<sub>2+x</sub>, oxygen potential in temp. range 1523 to 1822K 0-106113

**PMDR**

- PO<sub>2</sub><sup>-</sup>, in K halides, ODMR in zero and weak mag. fields 0-88894

**PMPS see PMDR****p.m.r. see proton magnetic resonance****pneumodynamics**

- see also lung  
 airway, collapsible, fluid-dynamic flapping, sound generation and flow limitation 0-94258  
 airway changes induced by histamine or vagal stimulation, vol. history effects 0-67115  
 airway closure, importance in limiting max. expiration in normal man 0-104606  
 airway smooth muscle, contracted, hysteresis, dog expts. 0-81634  
 alveolar gas exchange, effect of altered gas diffusivity 0-97970  
 bronchial collapsibility of excised dog lungs, effect of lung surface tension 0-67118  
 canopy ventilation monitor for quantitative meas. of ventilation during sleep 0-104792  
 deformations of lung at minimal vol. 0-97977

**pneumodynamics continued**

- deposition of inhaled particles, airway generations of normal subjects 0-67125  
 deposition of particles in model airways 0-72192  
 diffusivity effects on pulmonary gas transport and mixing 0-108927  
 dynamic compliance, freq. dependence, anal. from 1 breathing cycle 0-97967  
 elastic recoil rel. to ageing healthy males and females 0-67117  
 electro-aerosols, precipitation in the airways, effect of electrostatic scatter 0-108929  
 exercise body plethysmograph, head-out, for extrathoracic airways investigation 0-81754  
 exhalation in lung model, effect of ventilation and diffusion nonuniformity 0-104603  
 expiratory end pressure, positive, shifting of left ventricular diastolic press.-area curves 0-104604  
 fibrous particle motion anal. by two-pulse Fraunhofer holography 0-58476  
 flowmeter, hot-wire, evaluation for clinical appls. 0-72346  
 fossorial mammal ventilation, obs. in hypoxic and hypercapnic conditions 0-72195  
 gas analyzer, response time, incorporation in gas exchange computations 0-72344  
 gas transport models, boundary conditions and geometry 0-85426  
 hyperthermia due to exercise, effects on breathing pattern 0-72196  
 inert gas exchange, mathematical lung models, effects of common dead space 0-67126  
 inhaled particle deposition appl. of human lung airways models 0-89776  
 inspiratory inhibition, sustained graded, phasic lung vol. changes, cat 0-101201  
 lobar atelectasis forces, intact dog obs. 0-97966  
 lung volume, online calc. by digital computer 0-72351  
 lung volume estimation method, constant inflation pressure 0-67306  
 magnetometers, use to vol.-reference flow-vol. curves 0-104694  
 mammalian lung airways, aerosol deposition in anatomical models, theoretical evaluation 0-81627  
 maximal flow in man, viscosity and density dependence 0-101202  
 maximum flow time dependence as index of nonuniform emptying 0-72197  
 MEV curves, smoothing by digital filtering 0-98157  
 nasal flowmeter for preterm infants, self-retaining 0-98158  
 neuromuscular blockade, effects on respiratory mechs. in conscious man 0-81632  
 occluded airway pressure, difference with generated muscle press. 0-67101  
 occlusive sleep apnea, respiratory mechs. and timing 0-97973  
 peribronchial fluid pressure rel. to vascular and airway press. and interstitial oedema 0-97971  
 physiological compartment tracer flow modelling and digital imaging 0-101257  
 plethysmograph, body, vol.-displacement using large flowmeter without press. compensation 0-72345  
 postural effects on lung vols. and asynchronous ventilation, anaesthetised horses 0-97968  
 pressure-volume curves inflection points, 3-balloon-catheter system obs. 0-72190  
 pulmonary contusion and flail chest, effects on perfusion and O<sub>2</sub> exchange 0-67119  
 radioisotope cinepneumography, flow-vol. imaging of the respiratory cycle 0-94343  
 respiratory apparatus effects on breathing pattern 0-104602  
 respiratory gas monitoring instrument using microprocessor (Japanese) 0-72358  
 respiratory mechanical behaviour lumped parameter models evaluation using simplex algorithm 0-89783  
 respiratory oscillations, altitude effects disclosed by identification methods 0-97979  
 respiratory period prediction, men exercising while wearing masks, comparative model study 0-94253  
 respiratory resistance, central and peripheral, estimation using elec. analogue model 0-81636  
 respirometric open systems, error anal. (German) 0-104782  
 switch valve, lightweight, remotely actuated, for rebreathing exercise studies 0-101278  
 upper airway patency in the human infant, influence of airway press. and posture 0-97978  
 ventilation by HF oscill., beagle expts. 0-104607  
 ventilation-perfusion relationship in young healthy awake and anaesthetised-paralysed man 0-67120  
 ventilators for animals, automatic sigh feature 0-98186  
 ventilatory responses to elastic loading at constant PaCO<sub>2</sub> in hypercapnic hyperpnea 0-67121  
 volume shifts with partial submersion of isolated lung lobes 0-81631  
 washout curves using N<sub>2</sub>, multiple-breath, new method for anal. 0-101199  
 CO<sub>2</sub> pressure, end-tidal and arterial diff. obs. 0-72193  
 CO<sub>2</sub> pressures in dogs during acute hypercapnia, arterial-expired differences 0-72198
- PNO calculations**  
 C<sub>2</sub>H<sub>3</sub><sup>+</sup> + HF, interaction, struct. and stability, ab initio calcs. 0-58347
- Pockels effect**  
 cell driver of fast rise time and high repetition rate using thyatron 0-69537  
 light modulation, max. depth, Pockels cell modulator 0-102819  
 light modulator with small nonactive losses 0-78981  
 shutter for laser pulse shaping, Pockels cell with programmable transmission control 0-64162  
 space-time light modulator 0-69526  
 CdTe crystal Pockels modulator, FCM of CO<sub>2</sub> TEA laser pulse 0-102742  
 GaAs, intracavity modulation of polarization direction of CO<sub>2</sub> radiation 0-102744  
 Nd:YAG laser, Q-switched, pulse stretching using Pockels cell 0-95927
- point contacts**  
 HF rectification at low temp. in point contacts between identical metals 0-105706  
 IR detector tunnelling and rectification characteristics, geometrical and multiple image interactions 0-57376  
 IR point-contact diode tunnelling and rectification rel. to electrode geometry 0-57378



**point contacts continued**

- Josephson contacts, three-dimens. assembly, crit. currents and penetration depth 0-84560  
 metal-barrier-metal diodes, I-V characts., nonlinear mechanism in low voltage region 0-88618  
 metal-vacuum-metal point contact junction characts., Green's function calc. 0-103744  
 metals, struct. of  $d^2J/dV^2$  characts. of point contacts 0-96975  
 MIM point-contact diode harmonic generators and mixers 0-60105  
 multiple flux quantum transitions, comparison with I-U characts. using Nb-point contacts 0-60149  
 Ag-Se, between metal electrodes, current-voltage characts. (*French*) 0-97005  
 Ag-Se thin film, switching and Ag movement, point contact technique 0-60107  
 Bi-Sb alloys, metal-semimetal point contacts, volt-ampere characteristics (*Russian*) 0-65683  
 Fe, electron-phonon coupling, point contact spectroscopy obs. (*Russian*) 0-70342  
 Ni, electron-phonon coupling, point contact spectroscopy obs. (*Russian*) 0-70342  
 W-Ni(Co) point-contact diodes as harmonic generators and mixers, DC bias dependence 0-75653

**point defect scattering**

*used for carrier scattering by point defects*

- BP film, high temp. thermolec. power, scattering processes 0-80305  
 FeCl<sub>3</sub>, antiferromag., magnon-phonon interactions in thermal cond. 0-65315

**point defects**

*see also colour centres; interstitials; point defect scattering; vacancies (crystal)*

- alkali halides, effect of ionisation of condensing flux on nucleation of metal films 0-107675  
 alkali halides, matter transport rel. to point defect parameters 0-107488  
 alkali metal halides, defect production in cation sublattice, mechanisms 0-96510  
 alloys, rapidly quenched crystalline, struct., and heat treatment effects 0-76292  
 bimolecular recombination controlled generation, theoret. approx. eval. (*Russian*) 0-103323  
 binary, ternary oxides, dislocation motion and high temp. plasticity 0-59468  
 Bragg reflections, ratio of integral intensities, determ. struct. perfection of single crystals 0-87987  
 creep, irradiation induced, correlation of theory with expt. evidence 0-88255  
 creep, irradiation induced, dislocation glide enabled by preferred absorption of point defects 0-88250  
 crystal surface elastic props., surface tension tensor, volume stress (*Russian*) 0-100389  
 diamond, effective ion interaction and force consts., model of Si point defect 0-65185  
 dislocation damping, unified theory, point defect dragging 0-88144  
 dislocation percolation through absolute obstacles in impurity crystals (*Russian*) 0-70196  
 elastic amorphous medium, relax. by defect diffusion 0-58925  
 elastic interaction with grain boundaries 0-59483  
 electron displacement damage simulation in HVEM irradi. 0-107325  
 GaAs, dislocation-free, radiation damage 0-88141  
 homopolar crystals, imperfect, lattice dynamics 0-59601  
 III-V semiconductors, point defects and deep traps, thermodynamic history, model 0-59908  
 insulator, lattice thermal cond., point defect scatt. relax. rate role 0-70478  
 interaction with edge dislocation near solid surface 0-79834  
 ion polarisation and point defect resistivity in metals 0-103672  
 ionic crystal defects, mag. reson. studies 0-108066  
 ionic crystals, statistical space charge waves 0-103321  
 lattice defects, characterisation 0-103320  
 magnetic domain boundary, interacting with localised defects, unidimensional flow of configs. (*Russian*) 0-65954  
 magnets, randomly distributed point defects, critical exponents, renormalisation theory 0-60346  
 metal, electron irradi., elastic point defect-dislocation interactions, defect dragging model extension 0-65050  
 metal colloids in ionic cryst., preparation, optical, mag. resonance, elec. props. 0-59459  
 metals, dynamical props. of point defects, book contrib. 0-103317  
 metals, point defect diffusion controlled reaction theory, book contrib. 0-103318  
 metals, point defect dynamic props. and diffusion controlled reactions, book 0-101674  
 near-surface impurities, adiabatic potential 0-70786  
 polar crystals, relaxation currents; point defects (*Russian*) 0-100486  
 $\alpha$ -quartz, electron irradi., defect struct. and radiolysis 0-107321  
 semiconductor defects, spectroscopic techniques to study of electronic props. 0-84446  
 steel, austenitic stainless, creep dependence on electron irradi., in type SS316 steel, dislocation motion (*Russian*) 0-108495  
 steel, microstructure of 0Kh16N15M3B after creep tests in BR-10 reactor, electron, microscope invest. (*Russian*) 0-92531  
 surfaces and interfaces, elastic energy of point defects and inclusions 0-73272  
 US absorpt. near displacive phase transitions, anomalous temp. depend. 0-92612  
 Ag halides, matter transport rel. to point defect parameters 0-107488  
 $\beta$ -Al<sub>2</sub>O<sub>3</sub>, defect props. and ionic transport 0-107486  
 Ar, solid, X-ray induced point defects 0-59514  
 CdI<sub>2</sub>, polytypic crystals, dielectric loss behaviour 0-66108  
 CdSe, recombination mechanism at dislocations, photoluminescence 0-103993  
 CdTe, low temp. themal cond., growth parameter influence 0-92725  
 Cu alloys, FCC, climb of extended dislocations due to irradiation in HVEM 0-103343  
 Cu, electron irradi., elastic point defect-dislocation interactions, defect dragging model extension 0-65050  
 Cu foils, electron-irradiated, point defect agglomerates, HVEM invest. during in-situ annealing 0-84213  
 Cu, high purity, identification of imperfections by thermal resistivity meas. 0-59951

**point defects continued**

- Cu-Al alloy, irradi. in HVEM, climb of dissociated dislocations and point defect absorpt. 0-107257  
 Fe-Al (40 at.%) and Fe-Al (50.5 at.%) ordered alloys, 20K neutron irradi. effects, stoichiometry depend., resist. obs. (*French*) 0-84215  
 GaAs, electroluminescent study of irradi. induced struct. damage, athermal annealing 0-108280  
 GaAs,  $\gamma$ - and electron irradiation, influence on recomb. characts. near surface 0-71478  
 GaAs, homogeneity region calc. 0-92681  
 GaAs, laser annealing of point defects 0-107224  
 GaAs, lattice thermal cond., point defect scatt. relax. rate role 0-70478  
 Ge:P(Sb)(Bi),  $\gamma$ -irrad., carrier trapping and recomb. at point radiation defects 0-107810  
 InAs:Sn, single crystals, defect formation 0-88606  
 n-InP,  $\gamma$ -ray and electron irradi., annealing of radiation point defects, elec. cond. and Hall coeff. meas. 0-65051  
 Li<sub>2</sub>N, defect props. and ionic transport 0-107486  
 MgF<sub>2</sub> obs. of radiation induced point defects, cross-relaxation processes, polarised  $\beta$ -active nuclei 0-60431  
 MgO crystals, geometrical-statistical parameters of dislocation interactions with point obstacles 0-103341  
 MgO:Fe<sup>2+</sup>, point defect complex-edge dislocation interaction energies, atomistic calc. 0-107314  
 Mo, electron irradi. in HVEM, anisotropy of damage prod. 0-107322  
 Nb<sub>2</sub>Ge, low temperature electron, neutron irradi. effects on critical temp. (*French*) 0-75669  
 Nb<sub>2</sub>Sn, supercond. props., effect of neutron irradi. 0-80463  
 Ni dilute alloys, implant profiles modification by radiation enhanced diffusion and segregation 0-88217  
 Ni-Cr-Fe alloys, radiation enhanced precip. and dissolution of precipitates, point defect kinetics and dislocation obs. 0-108467  
 Ni<sub>3</sub>Al(Ga), off-stoichiometric alloy, inverse mag. susceptibility rel. to defect conc. 0-60216  
 Sb, electron microscope irradiation effects, agglomeration of point defects, dislocation climb and loops (*French*) 0-59518  
 Se, glassy, localised electronic states, photoluminesc. and ESR studies 0-65501  
 Si, float zone crystal, dislocation creation and elimination 0-107072  
 Si, laser annealing of point defects 0-107224  
 Si, point defects, H passivation 0-75515  
 Si:Au, P-induced point defects influence on Au gettering mechanism 0-65030  
 Si:B ion implanted, strain profiles from X-ray rocking curves 0-107290  
 Si:P, ion implanted with small doses, defect annealing by nanosecond laser pulses 0-107297  
 Ti(Fe, Co), off-stoichiometric alloy, inverse mag. susceptibility rel. to defect conc. 0-60216  
 TiO<sub>2</sub>, sputtering defects, associated surface electron states, UPS, XPS and AES obs. 0-60755  
 V<sub>2</sub>O<sub>5</sub> and lower oxides, electronic, optical, structural and surface props., review 0-88120  
 V<sub>2</sub>Si, supercond. props., effect of neutron irradi. 0-80463  
 W, low-energy ion bombardment, depth of sputtering damage obs. by FIM 0-60734  
 Yb<sub>2</sub>O<sub>3</sub>, electronic cond. rel. to partial press. of O<sub>2</sub> of high temp. (*French*) 0-59979  
 ZnSe, multiphonon ionisation of deep point centres in a charged dislocation field (*Russian*) 0-100281
- point groups** *see crystal atomic structure*
- point to point radio links** *see radio links*
- Poiseuille flow**  
 bead-spring-type model in nonuniform vel. gradient, dil. soln. kinetic theory results 0-64628  
 boundary value problems, compound matrix method 0-57096  
 cholesteric liquid crystals, steady low shear rate flow normal to helical axis 0-96443  
 colloidal particles, Poiseuille flow, total particle conc. axial change 0-108752  
 complementary variational principles for Poiseuille flow 0-96310  
 flat plate streaming potential investigations: hydrodynamics and electrokinetic equivalency 0-106777  
 pentyl-cyano-biphenyl, nematic, hydrodynamic parameters meas. with and without applied elec. field 0-100297  
 periodic flow in a curved tube 0-69920  
 pipes, porous, complementary variational principles for steady and unsteady Poiseuille flow 0-92225  
 plane, nonlinear stability by high order amplitude expansions 0-74975  
 plane flow, direct optical meas. of vel. gradients 0-59132  
 plane parallel flow, free convection in Couette and Poiseuille flows, numerical simulation 0-99995  
 sphere between plane parallel boundaries, creeping parallel motion, strong interaction theory 0-103075  
 spherical particle in circular tube flows, lateral migration 0-92221  
 steady laminar flow through channel with symmetrical constriction in step form 0-100036  
 suspensions of charged particles, laminar tube flow, entrance deposition 0-59100  
 viscoelastic liquids, Poiseuille flow, hole-press. meas., computer model 0-59080
- Poisson ratio**  
 alkali halides, Poisson ratio and Gruneisen parameter, vol. depend. anal. 0-96614  
 anisotropic materials, Poisson coefficients, allowable values 0-64370  
 creep modelling incorporating initial strain and ageing 0-58939  
 eddy current determination 0-65116  
 infinite medium containing periodic ribbon-like inclusions, local intensification of thermal stresses (*Japanese*) 0-96195  
 plasma coatings, elastic properties, acoustic meas. (*Russian*) 0-97519  
 polycrystalline materials, effect of grain boundary sliding on anelasticity 0-96592  
 polypropylene film, double-exposure speckle pattern obs. of tensile deform., displacement, Poisson's ratio and stress relax. 0-84795  
 polystyrene-polyethylene block copolymer, deformation ratios, Poisson ratio and adhesion, dilatometric obs. 0-60937  
 slab, surface displacements for high speed rubs 0-83767  
 steel, austenitic stainless, N-alloyed 0-108490  
 steel, Cr-Mn (13, 19 wt.%), elastic const. behaviour, anomalous, low temp. 0-97521  
 Al<sub>2</sub>O<sub>3</sub> refractories, fracture, J-integral meas. 0-108537



**Poisson ratio continued**

- BaO-P<sub>2</sub>O<sub>5</sub>, glass, US velocity rel. to elastic props. 0-103425  
 CaO-P<sub>2</sub>O<sub>5</sub>, glass, US velocity rel. to elastic props. 0-103425  
 GaS, elastic prop. anisotropy, Debye temp. (Russian) 0-88244  
 MgO-P<sub>2</sub>O<sub>5</sub>, glass, US velocity rel. to elastic props. 0-103425  
 SrO-P<sub>2</sub>O<sub>5</sub>, glass, US velocity rel. to elastic props. 0-103425

**polar cap absorption** *see ionospheric electromagnetic wave propagation***polar cap flow** *see airglow***polar semiconductor materials** *see polar semiconductors***polar semiconductors**

- see also ferroelectric semiconductors; piezoelectric semiconductors*  
 ambipolar semiconductors, thermoelectric redistribution of carriers 0-107830  
 crystalline thin films, surface vibr. states, IR absorpt. spectra obs. (Russian) 0-60606  
 highly excited, optical dielec. function of electron-hole plasma 0-92847  
 hot exciton transitions to excited states, interaction with acoustic phonons 0-96799  
 piezoelectric polar materials, appl. to SAW and other devices 0-66114  
 polariton propagation between semiconductor-metallic screen interface (Spanish) 0-84510  
 quasi-monopolar semiconductors, I/V characts., effect of weak diffusion 0-70824  
 resonance electron-phonon Raman scatt., cross-section oscils. 0-60598  
 secondary cyclotron emission giant oscillations of intensity and line shape 0-66192  
 strongly anisotropic, electron-hole liq. in mag. field 0-59890  
 surface biection in polar semicond., binding energy calc. 0-96796  
 two-phonon resonance Raman scattering 0-108204  
 GaP, electron-hole drops, self-consistent surface calculation 0-65464  
 PbI<sub>2</sub> direct gap polar semicond., electron hole liquid phase diagram (Russian) 0-93314

**polarimeters**

- see also polarimetry*  
 automated polarimeter for determ. of ellipsometric characts. of optical surfaces 0-101822  
 Compton polarimeter, calc. of linear polarisation sensitivity 0-77839  
 electrooptic four-modulator photopolarimeter, for Mueller matrix meas. 0-73417  
 holographic platform, optical path stabilisation with magneto-optic periodic grating 0-99678  
 modulators, photoelastic radiation polarisation, review 0-102846  
 Mossbauer 14.4 keV gamma-ray source, design, calibration and polarimeter 0-86535  
 multichannel polarimeter, data acquisition and control system (Japanese) 0-77842  
 multichannel polarimeter, description (Japanese) 0-77841  
 photoelectric, effect on accuracy of light interference in biquartz modulator 0-62713  
 two-channel polarimeter, for ionospheric Faraday effect meas. at 140 MHz, first results 0-61912

**polarimetry**

- see also ellipsometry; polarimeters*  
 condensed gases, solid phase transition, optical meas. in diamond-anvil cells 0-73381  
 crystal gyrotropy, meas. in IR region 0-88957  
 Faraday effect measurement in pulsed mag. field 0-80758  
 modulated-Mueller-matrix photopolarimetry [MMMP]: a technique for the study of elastic light scattering by depolarizing temporally modulated media and surfaces 0-90882  
 noise suppression by polarization-plane rotation-angle amplification 0-68241  
 Norikura Observatory, use of coronagraph (Japanese) 0-82223  
 optical fibre signal polarisation statistical meas. 0-99877  
 orthorhombic crystal, birefr. and refr. index determ., refl. method 0-86380  
 single mode fibre polarisation stabilisation 0-58724  
 spectropolarimetry with an intensifier-dissector-scanner 0-109367  
 Ge, standard measures of magneto-optical rotation of plane of polarisation in IR region 0-60551  
 InSb, standards for magneto-optical rotation, charge carrier density determ. in semiconductors 0-60551

**polarisability**

- see also atomic polarisability; molecular polarisability*  
 alkali chalcogenides, electronic polarisabilities and ion sizes 0-59432  
 alkali halides, photoelastic const., short range polarisability effect 0-80748  
 alkaline earth chalcogenides, electronic polarisabilities and ionic radii of metal and chalcogenide ions in cryst. state 0-100198  
 alkaline earth halides, electronic polarisabilities and ion sizes 0-59432  
 bacteria, E.coli strains in aq. suspension, polarisability anisotropy and aminoglycoside antibiotic effects 0-85441  
 colloids, interfacial electric polarisability, and interactions 0-108751  
 electron gas, two-dimensional, in mag. field, polarisability 0-107888  
 liquid crystals, orientational order parameter, optical birefr. meas., polarisation field problems 0-79688  
 polaritons, LT mixed mode, dispersion relation 0-65470  
 polymer film, small-angle light scatt., Debye-Bueche theory treatment of multiple scatt. 0-84794  
 rutile-type compounds, crystal binding energies and electronic polarisabilities 0-75202  
 semiconductor, n-type, donor-polarizability enhancement as the insulator-metal transition is approached from the insulating side 0-80184  
 n, electric polarisability, from photoabsorption cross-section 0-57597  
 p, electric polarisability, from photoabsorption cross-section 0-57597  
 AgCl(Br), electronic dielec. const., vol. depend., Clausius-Mossotti model 0-100630  
 CaF<sub>2</sub>, fast ion transport, computer simulation 0-107485  
 CuCl(Br), electronic dielec. const., vol. depend., Clausius-Mossotti model 0-100630  
 Ge, donor polarizability, multivalley effective mass calc. 0-96817  
 In<sub>2</sub>Zn<sub>3</sub> and In<sub>2</sub>Cd<sub>3</sub>, solid electrolytes, ion transport mechanism and polarisability role, comparison with Cu<sup>+</sup> and Ag<sup>+</sup> cond. 0-107531  
 MoS<sub>3</sub>, molybdenite band structural props. rel. to supercond. and semicond. 0-96781  
 NaCl-type crystals, ionic polarisabilities, pseudopot. calc. 0-88913  
 O<sup>2-</sup> polarisability rel. to ferroelec. phase transitions 0-71326  
 Si, donor polarizability, multivalley effective mass calc. 0-96817  
 Tl<sub>2</sub>ZnBr<sub>4</sub>(I<sub>2</sub>), solid electrolytes, ion transport mechanism and polarisability role, comparison with Cu<sup>+</sup> and Ag<sup>+</sup> cond. 0-107531

**polarisation**

- see also beta-ray polarisation; deuteron polarisation; dielectric polarisation; electron spin polarisation; gamma-ray polarisation; light polarisation; neutron polarisation; nuclear polarisation; photon polarisation; polarisation in elementary particle interactions; polarisation in elementary particle scattering; polarisation in nuclear reactions and scattering; proton polarisation*  
 Abell 401, X-ray galaxy cluster, radio emission polarisation 0-98731  
 aerosol, thin flat, EM wave scatt. and absorpt. 0-91723  
 atmospheric precipitation properties using radar polarisation techniques 0-61925  
 atomic systems, dynamic multipole polarisability 0-74252  
 3C 219, double radio galaxy, high-resolution polarisation obs. at 1.48 and 4.89 GHz 0-77500  
 3C 31, radio jets linearly polarised brightness distrib. rel. to mag. field struct. 0-82526  
 trans-1,4-chlorobromocyclohexane, liquid, crystalline and amorphous state, conformation and vibr. spectra, IR obs. 0-60568  
 trans-1,4-chloriodocyclohexane, liquid, crystalline and amorphous state, conformation and vibr. spectra, IR obs. 0-60568  
 cosmic microwave background radiation, polarisation in anisotropic universe 0-82552  
 cosmological models with anisotropic curvature, polarisation effects 0-94903  
 Cygnus X-1 (X-2, X-3), X-ray polarisation obs. from OSO 8 0-90571  
 Earth, E-polarisation rel. to boundary conditions for EM field above two-dimensional inhomogeneous struct. 0-85595  
 Earth crust, resistivity and induced polarisation (IP) survey for delineating saline water and fresh water zones 0-104867  
 Earth induced polarisation (IP) sounding, effects of EM coupling in electrode arrays over uniform half-space 0-101324  
 electron band structure, optically induced in external plane wave field 0-106432  
 EM radiation, scattered, polarisation in presence of internal energy sources 0-67541  
 EM radiation in media with spatial dispersion, spatial coherence formation and polarisation increase 0-106442  
 field-induced molecular multipoles, local polarisation theory 0-74141  
 galaxies, nearby, radio continuum polarisation obs. rel. to mag. fields (German) 0-109544  
 GL 2591, protostellar source, 3  $\mu$ m ice absorpt. band, linear polarisation obs. 0-105303  
 gyrotopic medium, Green's function and field of moving charges 0-58445  
 AM Herculis (4U 1814+50), linear and circular polarisation modulation with orbital period 0-105403  
 ionosphere, Faraday effect meas. at 140 MHz using two-channel polarimeter first results 0-61912  
 Jupiter, linear polarisation study at 2.7 GHz with Cambridge 5 km telescope 0-82272  
 Jupiter radio emission, Stokes parameters obs. at 11 and 18 cm wavelength 0-67637  
 Kerr metric effect on EM wave plane of polarization 0-94827  
 M87 radio emission, Faraday rot. in radio/X-ray halo 0-67844  
 magnetically ordered crystals, absorbent, EM waves polarisation 0-108189  
 magnetisable and polarisable media with microstructure, models 0-88708  
 muonic atoms, X-ray emission polarisation (German) 0-69268  
 muonic X-rays, circular polarisation (German) 0-69266  
 NGC 315, radio jets linearly polarised brightness distrib. rel. to mag. field struct. 0-82526  
 nonlinear dissipative media, circularly polarised EM waves 0-63891  
 OH 205.1-14.1, unusual OH maser, left circularly polarised 1667 MHz line obs. during flare 0-98734  
 photosynthetic membranes, functional processes, polarisation effects 0-67045  
 plasma, moving cold magnetised, wave propag., polarisation relations and dispersion eqns. 0-64723  
 radiation transfer, polarised, in inhomogeneous medium 0-99607  
 relic radiation in anisotropic universe, polarisation and anisotropy 0-67917  
 role of polarisation in atomic and nuclear physics 0-63162  
 Scorpius X-1, mag. field determ. via linear polarisation spectrum (Russian) 0-90344  
 solar 6 cm radio emission, polarisation obs. of active region and burst sources 0-62096  
 solar flares, polarisation and directivity of hard X-ray bremsstrahlung from thermal source 0-90374  
 solar wind MHD turbulence, Alfvénic and slow magnetosonic modes polarisation 0-61977  
 vacuum polarisation by ambient mag. field, effects on Compton scatt. by unmagetised electrons 0-86631  
 vacuum polarisation by strong mag. field, effects of Thomson scatt. 0-86632  
 Virgo A (M87), linear polarisation distrib. at 610 MHz, Westerbork map 0-62302  
 wave packet polarisation, in X-ray monochromators, dynamic theory (Russian) 0-64826  
 X-radiation, cryst.-monochromated, polarisation factor, assessment of errors 0-100121  
 X-radiation, cryst.-monochromated, polarisation factor, weighted scheme for products 0-100122  
 X-ray crystal monochromators, determ. of polarisation ratio 0-99018  
 Al, autoionisation reson. determ. from photoelectron polarisation meas. 0-58221  
 Tl, autoionisation reson. determ. from photoelectron polarisation meas. 0-58221  
 ZrO<sub>2</sub>/Pt solid electrolyte/porous electrode system, interface polarisation effects 0-61114

**polarisation in elementary particle interactions**

- charm photoprod. with linearly pol. photons, QCD calcs., gluons 0-68464  
 deep inelastic scatt., parton transverse momenta role, struct. function, QCD evolution 0-78034  
 gluon fragmentation, polarised, in  $e^+e^-$ ,  $e^+q$  and hadron scattering 0-82988  
 high energy lepton pair prod. with pol. hadrons, P and C violations 0-99068  
 interfacing theory and experiment in polarization studies 0-73837  
 lepton pair production, QCD and hard-scatt. model, spin-spin asymmetries 0-63014  
 target mass effects in polarized electroproduction 0-78072



**polarisation in elementary particle interactions continued**

- $e^+d \rightarrow e^+n$ , polarised, parity violating asymmetry 0-78080  
 $e^+e^- \rightarrow$  jets, transversely polarised annihilation, charged gluon jets, Pati-Salam model 0-86739  
 $e^+e^- \rightarrow \Delta X$ , polarisation effects in nonperturbative parton model, scaling 0-105912  
 $e^+$  inclusive hadron prod., polarisation and p nonconservation asymmetries,  $\pi$ ,  $K^\pm$ ,  $D^\pm$  prod. 0-78084  
 $e^+e^- \rightarrow l^+l^-$ , neutral current effects around vector resonances, polarisation 0-105878  
 $e^+e^- \rightarrow q\bar{q}g$ , gluon bremsstrahlung, neutral current and beam polarisation effects 0-99106  
 $e^+e^- \rightarrow q\bar{q}g$ , gluon fragmentation, polarised 0-82988  
 $e^+e^- \rightarrow q\bar{q}g$ , long, polarised beams, beam-event asymmetry, massless QCD null result 0-91104  
 $e^+e^- \rightarrow$  three jets, acoplanar angle relative to beam polarisation, vector/scalar gluons 0-63005  
 $e^+e^- \rightarrow VX$ , parton model, polarisation effects (Russian) 0-63002  
 $e^+e^- \rightarrow VX$ , polarisation states and differential cross sections for  $\pi A_1$  and  $\rho^0$  (Russian) 0-102059  
 $e^+e^- \rightarrow \pi\pi$ , pol. e, P-odd asymmetry and cross sections,  $SU(2) \times U(1)$ ,  $SU(3) \times U(1)$  calcs. (Russian) 0-62998  
 $e^+e^- \rightarrow c\bar{q}g$ , gluon fragmentation, polarised 0-82988  
 $\gamma d \rightarrow np$ , 400-650 MeV, proton polarisation and possible dibaryon resonances 0-105908  
 $\gamma d \rightarrow np$ , 400-700 MeV, p polarisation (Russian) 0-106046  
 $\gamma d \rightarrow pn$ , 250 to 800 MeV, differential cross-section and proton polarisation, theoretical models 0-78081  
 $\gamma n$ , n electric polarisability, from photoabsorption cross-section 0-57597  
 $\gamma n \rightarrow \pi^+ p$ , 0.9-1.65 GeV, pol.  $\gamma$ , cross section asymmetry (Russian) 0-86728  
 $\gamma n \rightarrow \pi^- p$ , 700 to 1200 MeV, recoil proton polarisation 0-78075  
 $\gamma p$ , p electric polarisability, from photoabsorption cross-section 0-57597  
 $\gamma p \rightarrow$  lepton pair, P violating asymmetry 0-105901  
 $\gamma p \rightarrow \pi^+ \pi^0$ , 340 MeV, pol. p, first resonance region,  $\pi^+$  photoprod., T-asymmetry (Russian) 0-62997  
 $\gamma p \rightarrow \pi^0 p$ , 400 to 1142 MeV, recoil proton polarisation 0-82981  
 $\gamma p \rightarrow \pi^0 p$ , 450 to 800 MeV, proton polarisation, Walker-type anal.,  $P_{11}(1470)$ ,  $D_{13}(1470)$ ,  $S_{11}(1535)$  resonances 0-73721  
 $\gamma p \rightarrow \pi^- n$ , 1.35-1.65 GeV, pol.  $\gamma$ , resonance energy region, cross section asymmetry (Russian) 0-86727  
 $\gamma p \rightarrow \pi^- n$ , 600-1875 MeV, pol.p and  $\gamma$ , G and H polarisation parameters 0-99105  
 $h_1 h_2 \rightarrow l^+ l^- X$ , massive lepton pair prod., polarisation and spin effects 0-105929  
 $K_1^0 \rightarrow \pi^- \mu^+ \nu_\mu$ , transverse polarisation of  $\mu$ , violation of time-reversal invariance 0-68448  
 $K^+ p \rightarrow \Delta$ , 6 GeV/c, baryon exchange reactions,  $\eta NN$  coupling constant, A polarisation, nucleon-Regge exchange 0-78098  
 $K^+ p \rightarrow \Lambda^0$ , 6 GeV/c, baryon exchange reactions,  $\eta NN$  coupling constant, A polarisation, nucleon-Regge exchange 0-78098  
 $K^+ p \rightarrow \pi^+ \pi^0$  and  $\pi^+ p \rightarrow K^+ \pi^0$ , exchange degeneracy 0-57634  
 $K^+ p \rightarrow \pi^+ Y^+$ ,  $Y^+ = \Sigma^+$  or  $Y^* (1385)$ , 7 GeV/c, hypercharge exchange in line-reversed  $\pi^+ p$  and  $K^+ p$  0-82998  
 $K^+ p \rightarrow \pi^+ Y^+$ ,  $Y^+ = \Sigma^+$  or  $Y^* (1385)$ , 7 and 11.5 GeV/c, hyperon polarisation, vector meson decay angular distrib. 0-82997  
 $\Lambda$  hyperon polarisation, meas. by hybrid Monte Carlo tech. 0-99431  
 $N^+$  vector meson, polarised deep inelastic collisions in nuclei (Russian) 0-102209  
 $NN \rightarrow NN\pi$ , polarization analysis of reactions with four spin-1/2 particles 0-86745  
 $\nu(F)N$ , pol.N, deep inelastic processes from valence straton distrib. functions (Chinese) 0-99095  
 $\nu_e e \rightarrow \nu_e e$ , weak and EM radiative corrections, sensitivity test 0-105880  
 $\nu_n \rightarrow \mu^- p$ , Higgs boson exchange effects on second-class currents 0-91075  
 $\bar{\nu}_p \rightarrow \mu^- n$ , Higgs boson exchange effects on second-class currents 0-91075  
 $\bar{\nu}_p$ , 100, 200 GeV, elastic scatt., polarisation effects at large momentum transfer, quark model (Russian) 0-83005  
 $\bar{\nu}_p$ , pp, pol. and unpol. beams, hadronic jets, vector bosons, QCD and weak interference 0-57648  
 $pp$  inclusive scattering, 6 GeV/c, depolarisation parameter, dominance of natural parity exchange 0-78088  
 $pp \rightarrow \pi^+ X$ , pol.p, 24 GeV/c, high  $p_T$  prod., spin. depend. 0-105935  
 $pp \rightarrow \pi^+ d$ , 515 and 575 MeV, spin depend. parameter meas. 0-73734  
 $\pi^+ \pi^+$  EM polarisabilities, sum rules, coloured quark field theory 0-57561  
 $\pi^- p$  elastic scatt., 2.22-3.5 GeV/c, backward polarisation 0-82999  
 $\pi^- p \rightarrow K^0 \Lambda$ , 3.5 GeV/c, A polarisation, high statistics meas. 0-57637  
 $\pi^- p \rightarrow K^0 \Sigma^+$ , 1395 to 2375 MeV/c, differential cross-section and polarisation 0-57635  
 $\pi^- p \rightarrow K^0(890) \Lambda^0/\Sigma^0$ , 10 GeV/c,  $K^0$  polarisation meas. in hypercharge exchange reaction 0-63017  
 $\pi^+ p \rightarrow K^+ \Sigma^+$  and  $K^+ p \rightarrow \pi^+ \Sigma^+$ , exchange degeneracy 0-57634  
 $\pi^+ p \rightarrow K^+ Y^+$ ,  $Y^+ = \Sigma^+$  or  $Y^* (1385)$ , 7 GeV/c, hypercharge exchange in line-reversed  $\pi^+ p$  and  $K^+ p$  0-82998  
 $\pi^+ p \rightarrow K^*(890) Y^+$ ,  $Y^+ = \Sigma^+$  or  $Y^* (1385)$ , 7 and 11.5 GeV/c, hyperon polarisation, vector meson decay angular distrib. 0-82997

**polarisation in elementary particle scattering**

- hadron scatt. mediated by  $q\bar{q} \rightarrow q\bar{q}$  and  $g\bar{g} \rightarrow g\bar{g}$  0-82988  
 ZGS, polarised beam results, review 0-99361  
 e scattering, polarised on spin-zero and polarised spin-1/2 targets, covariant formulation 0-78069  
 eN elastic scatt., pol. e, nucleon form factors, P violating symmetry, Weinberg-Salam calcs. 0-68461  
 ep, polarised scattering, asymmetries, gauge models 0-62991  
 $K^+ n$  elastic scatt., 0.851-1.351 GeV/c, polarisation parameter 0-68478  
 $K^+ p$  elastic scatt., 0.955-1.272 GeV/c, polarisation parameter 0-86753  
 $\mu$  scattering, polarised, on spin-zero and polarised spin-1/2 targets, covariant formulation 0-78069  
 NN, 12 GeV, spin depend., quark exchange evidence 0-102074  
 $np \rightarrow np$ , polarisation phenomena in close-to-forward scatt., intermediate energy region 0-78086  
 $pp$ , 100, 300 GeV/c, polarisation parameters and ang. distrib. for elastic scatt. 0-95287  
 $pp$ , 45 MeV, longitudinally pol. p, parity nonconservation in anal. powers 0-57626  
 $pp$ , parity violation meas. at 45 MeV 0-78092  
 $pp$  elastic scatt., 1-3 GeV/c, pol. p, spin parameters A and  $A_{nn}$  0-95304  
 $pp \rightarrow pp$ , high-energy, polarisation and energy dependence 0-63030

**polarisation in elementary particle scattering continued**

- $pp \rightarrow pp$ , polarisation phenomena in close-to-forward scatt., intermediate energy region 0-78086  
 $pp \rightarrow pp$ , polarisation structure and Pomeron flip, Regge pole model 0-102073  
 $pp$  scatt., <300 MeV P-odd asymmetry for pol.  $\rho$  (Russian) 0-102063  
 $pp$  scatt. amplitude, phase anal. ambiguities, cross sections and polarisation parameter (Russian) 0-86749  
 $pp$  scattering, parity violation at 50 MeV (German) 0-68471  
 $pp$  small angle scatt., 312-575 MeV, pol. p, Wolfenstein and polarisation parameters 0-57629  
 $\pi N$ , 6-200 GeV, amplitude anal. in impact parameter representation, non-zero polarisation, shell struct. (Russian) 0-86752  
 $\pi^+ p$ , 100 GeV/c, polarisation parameters and ang. distrib. for elastic scatt. 0-95287

**polarisation in nuclear reactions and scattering**

- A=70, heavy-ion induced fission-evaporation reactions, magnetic substrate distrib., nuclear alignment 0-73857  
 cool compound nucleus formation with oriented heavy ions,  $^{258}104$  and  $^{260}106$  prod. 0-99179  
 deep inelastic electro-creation by polarised vector mesons (Russian) 0-102209  
 deep inelastic heavy ion reactions, fast light particles and heavy ejectile ang. correlation 0-57791  
 differential polarisation coefficients for  $(\gamma, X)$  reactions 0-73838  
 excited nuclear levels, polarisation induced by at. orientation 0-91144  
 gamma reactions initiated by polarised particles, Legendre polynomial coeffs. 0-73107  
 interfacing theory and experiment in polarization studies 0-73837  
 low energy polarised beam expts., review, book contrib. 0-68642  
 (n,n), polarised neutrons, 2.50 MeV, meas. of small angle scattering ( $<1^\circ$ ) 0-99432  
 role of polarisation in atomic and nuclear physics 0-63162  
 spin  $\pm 1/2$  polarised neutrons, differential scatt. by chiral systems, coupled oscill. model 0-102177  
 (d,d), pol. d, 56 MeV, A=16-208, cross sections, optical parameters, anal. powers 0-78270  
 (d,d), pol.d, 52 MeV, A=12-197, vector anal. power and optical parameters 0-57764  
 (d,d) medium heavy nuclei, optical model anal., cross sections, anal. powers 0-73839  
 (n, $\gamma$ ), polarized space parity nonconservation, optical pot. and GDR parameters (Russian) 0-86803  
 (p, 2p), pol. p, quasi-free scatt. on closed shell nuclei, effective polarisation 0-91173  
 (p,d), pol. p, 65 MeV, A=12-94, differential cross sections and anal. powers, pickup 0-91172  
 (p, $\pi^\pm$ ), 585 MeV, A=1-208, differential cross section and pol. parameter 0-106056  
 (p, $\pi^\pm$ ), 585 MeV, cross sections, polarisation parameter for H, D, Be, C, O, Al, Ni, Cu, Mo, Pb targets 0-73848  
 (p, X), A=12-209, pol.p, 65 MeV, continuum spectra anal. powers 0-102178  
 $^4H(d,d)$ , 5-45 MeV deuteron wave function asymptotic D- to S-state normalisation, anal. power 0-78304  
 $^{10}Ag(p,p')$ , pol.p, 6.06 MeV, anal. powers, large absorption pot., optical model 0-83092  
 $^{27}Al(n,\gamma)$ , pol. Al and n, 0.017 eV,  $^{28}Al$  levels, transitions and spin 0-78153  
 $^{38}Ar(\alpha,n\gamma)$ ,  $^{41}Ca$ , spin and parity from angular distrib. and linear polarisation of  $\gamma$  0-63079  
 $^{10}B(d,p)$ ,  $^{11}B$ , 2.5 to 21.0 MeV, angular distrib., DWBA analysis 0-68675  
 $^{209}Bi(p,p'(d)X)$ , pol. p, 65 MeV, anal. powers of continuum energy spectra 0-68637  
 $C(\pi^+ p)$ , 1.5-5 GeV/c, cumulative proton polarisation (Russian) 0-86896  
 $^{12}C(\mu^+, \nu)^{12}B$ , polarisation studies, muon capture, weak interaction aspects 0-68655  
 $^{12}C(n,n)$ , spin-flip probability to first  $2^+$  level 0-78288  
 $^{12}C(p,p')$ , pol. p, 800 MeV, unnatural parity states excitation, anal. powers and isospin 0-68538  
 $^{12}C(p,p')$ , 20-40 MeV, pol. p, anal. powers, imaginary spin-orbit pot., coupled channels anal. 0-102179  
 $^{12}C(p,p)$ , pol. p, 14.23 MeV resonance broadening, nuclear recoil, atomic excitation effects 0-102165  
 $^{40}Ca(p,p')$ , pol. p, A=40-48, 800 MeV, diff. cross sections, anal. powers, DWIA anal., high spin levels 0-83067  
 $Cu(\pi^+ p)$ , 1.5-5 GeV/c, cumulative proton polarisation (Russian) 0-86896  
 (d,d), A=24-54, pol.d, 20 MeV, quadrupole transition amplitudes 0-99148  
 $^{18}F$  1.04 MeV state lifetime and  $\gamma$ -transition polarisation from  $^{18}O(p,n)$  0-106016  
 $^{19}F$ , nuclear dealignment of multiply ionised 3 and 6 MeV atoms recoiling in gases 0-78267  
 $^{56}Fe(p,p')$ , pol. p, 800 MeV, diff. cross sections, anal. powers, DWIA anal. 0-83067  
 $^{58}Fe$  levels,  $J^\pi$ , anal. powers and cross sections from  $^{56}Fe(t,p)$  pol.t 0-68539  
 $^{40}Ge(t,p)$ , pol.t, A=70.72, octupole oscillations modes from anal. powers,  $3^-$  octupole transition 0-102142  
 $^{1}H(n,n)$ , 16.9 MeV, anal. power, F-wave contrib. 0-63158  
 $^{1}H(n,n)$ , pol. n, 13.5-16.9 MeV, anal. power and spin-orbit phase parameters 0-78269  
 $^{1}H(n,n)$ , pol. n, 50 MeV, anal. power 0-68639  
 $^{1}H(n,p,n)$ , pol. np, 50 MeV, spin correlation parameter  $A_{yy}(\theta)$ , phase shift anal. 0-68530  
 $^{1}H(p,p)$ , 1-3 GeV/c, pol. p, spin parameters A and  $A_{nn}$  0-95304  
 $^{1}H(p,p)$ , 6.141 MeV, anal. power, Paris pot. predictions 0-63156  
 $^{1}H(p,p)$ , pol.p, 9.57 MeV, spin correlation parameter, phase shift anal. 0-102112  
 $^{1}H(\pi^+ \pi^-)^2H$ , pol. p, total cross section, ang. distrib. and asymmetry parameters 0-63182  
 $^2H(d,n)$ , pol.d, anal. power and polarisations in R-matrix methodology, comparison with (d,p) 0-78273  
 $^2H(d,p)$ , pol.d, anal. power and polarisations in R-matrix methodology, comparison with (d,n) 0-78273  
 $^2H(e,e)$ , form factors, tensor pol., and two-nucleon force calcs. 0-106045  
 $^2H(\gamma,n)$ , 20.3 MeV, linearly pol.  $\gamma$ , neutron yield and cross section 0-91171  
 $^2H(\gamma,n)^1H$ , 400-700 MeV, p polarisation (Russian) 0-106046



**polarisation in nuclear reactions and scattering continued**

- <sup>3</sup>H( $\gamma$ ,n)p, 375-650 MeV, proton polarisation energy depend. at CMS angle 90° (*Russian*) 0-63159
- <sup>2</sup>H(p,p)n, 22.7 MeV, proton analysing power 0-78302
- <sup>2</sup>H(p,p), 800 MeV, differential cross sections and anal. powers 0-83091
- <sup>2</sup>H(p,p), pol.p, spin rot. and depolarisation, NN amplitude double spin flip part 0-78271
- <sup>2</sup>H(p, $\pi^+$ ), 400-470 MeV, backward  $\pi$  differential cross sections and anal. power 0-86905
- <sup>2</sup>H( $\pi$ , $\pi$ ), 140-260 MeV, (3,3) region, tensor force, cross sections, pol. parameters 0-68641
- <sup>2</sup>H( $\pi$ , $\pi$ ), 142, 256 MeV, form factor-backward scatt. correlation, tensor polarisation 0-99189
- <sup>4</sup>He(p,p), 1.05 GeV, cross sections and polarisations, correlation effects calcs. 0-57774
- <sup>4</sup>He(p,p), 200-500 MeV, differential cross section and anal. power 0-68640
- <sup>165</sup>Ho(<sup>165</sup>Ho,X), deep inelastic, spin and transferred ang. momentum alignment 0-106043
- <sup>46</sup>K levels, J $\pi$  and tensor anal. powers from <sup>46</sup>Ca(d, $\alpha$ ), pol.d 0-102113
- <sup>7</sup>Li(<sup>7</sup>Li), aligned Li ions, electric quadrupole moment of <sup>7</sup>Li 0-78141
- <sup>6</sup>Mg(p,p'), pol.p, 5.5-17.5 MeV, cross sections and anal. powers, autocorrelations 0-106042
- <sup>54</sup>Mn low lying 2p-4h states, J $\pi$  from tensor anal. powers of <sup>56</sup>Fe(d, $\alpha$ ), pol.d 0-99124
- <sup>55</sup>Mn(n, $\gamma$ ), pol. Mn and n, 0.017 eV, <sup>56</sup>Mn levels, transitions and spins 0-78154
- <sup>96</sup>Mo(t,p), pol.t, cross section and anal. powers, struct. depend., DWBA anal. 0-78272
- <sup>100</sup>Mo(<sup>14</sup>N,<sup>12</sup>B), 200 MeV, <sup>12</sup>B spin polarisation in deep inelastic collision 0-63160
- <sup>100</sup>Mo(<sup>14</sup>N,<sup>12</sup>B), 90 MeV, spin alignment of products, semi-classical model calcs. 0-73859
- Mo(t,p), pol.t, 17 MeV,  $\Lambda$ Mo, A=98,102, anal. powers, transitions, shape coexistence states, DWBA anal. 0-86895
- <sup>13</sup>N giant dipole resonance population amplitude and phase, E1 reaction amps. from <sup>12</sup>C(p, $\gamma$ ), pol. p 0-63145
- <sup>14</sup>N(d, $\alpha$ ), pol.d, 1.5-3 MeV, vector anal. capacity for two  $\alpha$ -particle groups 0-78266
- <sup>23</sup>Na $\mu$ , polarised,  $\beta$ -decay asymmetry and mag. moment from Na(n, $\gamma$ ) 0-91157
- <sup>20</sup>Ne 13482 keV level, parity violating effects in two resonance interference from <sup>19</sup>F(p, $\alpha$ ) pol. p 0-83033
- <sup>20</sup>Ne giant E1 resonance intermediate struct. from <sup>19</sup>F(p, $\gamma$ ), pol. and unpol. 0-78251
- <sup>20</sup>Ne(d<sub>pol</sub>,p), 10 MeV, <sup>21</sup>Ne deduced spectroscopic factors, levels and anal. powers 0-83087
- <sup>58</sup>Ni, A=60, 62, 66, levels, J $\pi$ , anal. powers and cross sections from Ni(t,p)pol.t 0-68539
- <sup>58</sup>Ni(<sup>3</sup>He, $\alpha$ ), A=58, 60, 62, 22 MeV, analysing power and cross sections, Co proton-hole states 0-68663
- <sup>58</sup>Ni(<sup>7</sup>Li,<sup>7</sup>Li), 14.22 MeV, alignment axis orientation depend. of cross section, mass quadrupole moment alignment 0-68638
- <sup>58</sup>Ni(p,p'(d)X), pol. p, 65 MeV, anal. powers of continuum energy spectra 0-68637
- <sup>59</sup>Ni levels, cross section and vector anal. power, ang. distrib. from <sup>59</sup>Ni(<sup>7</sup>Li,<sup>6</sup>Li), pol.<sup>7</sup>Li 0-106044
- <sup>60</sup>Ni high spin states, J $\pi$ , T<sub>1/2</sub>, ang. distrib. and polarisations from <sup>60</sup>Fe(<sup>7</sup>Li,p<sub>2n</sub> $\gamma$ ) 0-99116
- <sup>60</sup>Ni(p, $\alpha$ )<sup>37</sup>Co(3/2 $\pi^+$ ), anomalous analyzing power, DWBA calc. 0-86894
- <sup>16</sup>O(d,X), X=d or N, elastic scatt. and stripping, three body calc. 0-91165
- <sup>16</sup>O( $\gamma$ ,n<sub>0</sub>), 21.6-25.7 MeV, ground state photoneutron polarisation ang. distrib. 0-57765
- <sup>16</sup>O(p,p'), 20-40 MeV, pol. p, anal. powers, imaginary spin-orbit pot., coupled channels anal. 0-102179
- <sup>16</sup>O(p<sub>pol</sub>,2p), cross section, analysing power, energy sharing spectra, distorted wave impulse approx. 0-78291
- <sup>208</sup>Pb(<sup>208</sup>Pb,X), giant resonance polarisation pots. from nucleus-nucleus effective pot. 0-78248
- <sup>208</sup>Pb(d,p), tensor analyzing power, deuteron wave functions 0-99137
- Pb( $\pi^+$ ,p) 1.5-5 GeV/c, cumulative proton polarisation (*Russian*) 0-86896
- <sup>106</sup>Pd(t,p), pol.t, cross section and anal. powers, struct. depend., DWBA anal. 0-78272
- <sup>239</sup>Pu(n,f) slow polarised neutrons, product separation asymmetry (*Russian*) 0-106088
- <sup>32</sup>S(n,n), spin-flip probability to first 2 $\pi^+$  level 0-78288
- <sup>41</sup>Sc 2p-1h intermediate struct. resonances, anal. powers, J $\pi$  from <sup>40</sup>Ca(p,p' $\gamma$ ) 0-86883
- <sup>4</sup>Se(d<sub>pol</sub>,d), A=76,78,80,82, 12 MeV, two-step scatt. process via J $\pi$ =2 $\pi^+$ , excited states 0-57781
- <sup>28</sup>Si(d<sub>pol</sub>,p $\gamma$ ), <sup>29</sup>Si, low lying energy level structure, multi-step reaction calcs. 0-68537
- <sup>28</sup>Si(n,n), spin-flip probability to first 2 $\pi^+$  level 0-78288
- <sup>28</sup>Si(p,p'(d)X), pol. p, 65 MeV, anal. powers of continuum energy spectra 0-68637
- <sup>30</sup>Si(p, $\gamma$ ), pol.p, 6.4-15.0 MeV, cross section and anal. power ang. distrib. 0-99168
- Si(<sup>30</sup>Pu,<sup>30</sup>Pu), giant multipole resonance region, optical model anal. 0-57779
- <sup>124</sup>Sn(n,n), pol. thermal, parity violation near resonance, DWBA calcs. 0-68528
- Sn(p,p<sub>0</sub>), pol.p, 6.77-8.8 MeV, cross sections, optical parameters and nuclear radius A-depend. 0-57773
- <sup>126</sup>Ta(t,p), pol.t, cross section and anal. powers, struct. depend., DWBA anal. 0-78272
- <sup>212</sup>Th(<sup>14</sup>B,<sup>12</sup>B), 129 MeV, <sup>12</sup>B spin polarisation 0-63161
- <sup>4</sup>U(n,f), A=233,235, ejection fission products angular depend. on thermally polarised neutron capture (*Russian*) 0-86941
- <sup>233</sup>U(n,f), thermal polarised neutrons, neutron emission P-odd asymmetry (*Russian*) 0-78338
- <sup>233</sup>U(n,f) slow polarised neutrons, product separation asymmetry (*Russian*) 0-106088
- <sup>186</sup>W(t, $\alpha$ ), pol.t, 17 MeV, <sup>185</sup>Ta single proton states and rot. bands, J $\pi$  0-91130
- <sup>92</sup>Zr levels, J $\pi$ , cross sections, vector anal. power, optical parameters from <sup>91</sup>Zr+pol. d 0-78268

**polariscopes see polarimeters****polaritons**

- acentric crystals, optical phonons, small oscillator strength meas. from frequency-angular polariton spectra 0-92629
- anisotropic continuum, with anisotropic surface layer, coeff. of attenuated total reflection 0-60535
- anisotropic transition layer, surface polariton spectra in presence of resonance 0-88484
- anthracene, cryst., polariton luminesc. 0-84775
- anthracene films, optical props., comparison between free and optical contact mounting 0-89079
- classical and quantum mechanical aspects (*French*) 0-103634
- classical crystal optics, lattice dynamical background, review 0-97221
- coupled-mode excitations in cryst., relax. rates, theory 0-59881
- $\gamma$ -cyclopropyl-bis (1,3,3-trimethylindolenine-2-yl)pentamethinium fluoroborate, exciton surface polaritons, reflecting faces obs. 0-65645
- ferrimagnet, two sublattice, mag. polaritons 0-65845
- ferroelectric bodies, deformable, coupled acousto-optic modes 0-96093
- ferroelectric crystals, polariton light scatt. freq.-angle spectra, nonlinear susceptibility interference (*Russian*) 0-92834
- ferromagnetic slab, asymmetrical guided mag. polaritons 0-88738
- light hyper-Raman scatt. by polaritons, active spectroscopy (*Russian*) 0-60623
- lithium formate, optical phonons, small oscillator strength meas. from frequency-angular polariton spectra 0-92629
- LT mixed mode, dispersion relation 0-65470
- magneto-optic Raman scattering of Raman-inactive phonon polaritons 0-91843
- neutron scattering from equilibrium and non-equilibrium phonons, excitons and polaritons 0-84032
- plasmon surface polariton dispersion curve, optical obs., demonstration 0-101690
- poly-2,4-hexadiyne-1,6-diol bis (p-toluene sulfonate), exciton surface polaritons, reflecting faces obs. 0-65645
- polystyrene coated Ag holographic grating, Raman spectra enhancement by plasmon surface polaritons 0-80885
- semiconductor, direct band gap type, polariton theory of reson. electronic Raman scatt. on neutral donor levels 0-108194
- semiconductor, resonant Brillouin scattering of exciton polaritons 0-93357
- semiconductor surfaces, optical props., book contrib. 0-80737
- semiconductor-metallic screen interface, polariton propag. (*Spanish*) 0-84510
- semiconductors with direct band gaps, exciton-polariton interactions, Green's function approach 0-92831
- surface magnetoplasmon type polaritons, LF, existence criterion in Faraday config. 0-96961
- surface polariton motion in thin surface layer, nonstationary phenomenological theory (*German*) 0-88608
- surface polaritons, theory and spectroscopy uses 0-92835
- Ag:Al<sub>2</sub>O<sub>3</sub>:Al tunnel-junction struct., surface polariton mean free path, roughness 0-93008
- $\alpha$ -Al<sub>2</sub>O<sub>3</sub>, single crystal transmission and reflectance IR phonon spectra, polariton dispersion 0-66170
- CdS, additional waves and polariton dispersion, reflectivity, transmittivity spectra 0-71443
- CdS, three-branch exciton-polariton dispersion, direct meas. by reson. Brillouin scatt. 0-60620
- CdTe, exciton magnetoreflectance spectra, multicomponent polaritons, Zeeman splitting 0-88974
- CuBr, dielectric dispersion, two-photon absorpt. 0-76045
- CuBr(Cl)(I), polariton Raman spectra, oscillator strengths, temp. depend. 0-66197
- CuCl, dielectric function for semiconductors with high exciton conc. 0-84443
- CuCl, three-branch polariton dispersion curve, two-oscillator model 0-92832
- GaAs base laminated epitaxial struct., surface plasmon phonon polaritons (*Russian*) 0-59905
- GaSe films, optical props. at lattice vibr. freqs., IR and Raman spectra 0-60696
- e-GaSe films, optical props. in IR region, metal substrate effect 0-71502
- InP, surface phonon polariton dispersion and damping, frustrated total internal refl. meas. 0-80792
- InSb, depletion layer, plasma and vibr. plasma type guided polaritons (*Russian*) 0-96933
- KD<sub>2</sub>H<sub>21</sub>(-x)<sub>3</sub>PO<sub>4</sub> crystals, 0<x<0.98, light scatt. by polaritons 0-96802
- LiIO<sub>3</sub> crystal, noncollinear stimulated Raman scatt. using parallel pump beam 0-78912
- $\alpha$ -LiIO<sub>3</sub>, Fermi resonance in surface polariton spectra (*Russian*) 0-71423
- PbI<sub>2</sub>, photoexcitation interaction, luminescence spectra, polariton dispersion diagram 0-93397
- SiC, dielectric coating effect on surface polaritons, optical const. (*Russian*) 0-88489
- SiC with dielectric coating, surface polaritons, waveguide modes 0-80195
- SrTiO<sub>3</sub>, centrosymmetric crystal, phonon polariton hyper-Raman scatt. obs. 0-76028
- ZnS, Raman scatt. by phonon polaritons 0-103959
- ZnSe films, long wavelength IR polariton emission band thermal shift and broadening 0-92833
- ZnSe, resonance Raman scatt., exciton-polariton luminescence (*Russian*) 0-97287
- ZnTe crystals, polariton effects in luminesc. 0-103988
- ZnTe, secondary emission, transient behaviour under band-to-band excitation 0-108266

**polarization in elementary particle interactions see polarisation in elementary particle interactions****polarization in elementary particle scattering see polarisation in elementary particle scattering****polarographs see polarography****polarography**

see also voltammetry (chemical analysis)

- alternating current electrode processes, review 0-61107
- automatic controller for polarography, design, operational sequence 0-71968
- polarographic detection for high performance liquid chromatography, conference, Carlsbad, Czechoslovakia (April 79) 0-73097
- pulse polarography, microcomputer-controlled polarograph appls. 0-66895



**polarography** continued

- reverse pulsed polarography, reversibility characterisation, electrode reaction product determ. 0-66889
- ZnCl<sub>2</sub>-KCl-NaCl, molten system, containing Ni<sup>2+</sup> ions, appl. to electrorefining 0-66810

**polarons**

see also small polaron conduction

- acoustic deformation pot. polarons, linear energy-momentum relations 0-80196
- bound, non-perturbative variational method 0-88485
- deformation potential polaron, perturbation theory breakdown 0-84440
- electron radius of qyatron in polaron model 0-88486
- electron-phonon system, kinetic equation, chronological and antichronological T-products 0-70627
- electronic localised state at edge dislocations, parabolic dispersion law (Russian) 0-65479
- electrons in surface phonon field 0-107885
- energy bound to Coulomb potential 0-88487
- energy eigenvalue, systematic calculation procedure 0-84439
- ferromagnetic semiconductor, energy and mobility of spin polarons 0-70982
- ferromagnetic semiconductor, mag. polaron stability 0-96803
- free polaron spectrum and convergence radius in perturbation theory 0-70626
- free-particle and mag. masses, equivalence 0-107718
- generalised path integral formalism, ground state energy corrections 0-84438
- intermediate valence system, local polaron model 0-107717
- large radius polaron, bound-state spectrum 0-59894
- metal-semiconductor disordered interface, supercond. transition temp. enhancement by bipolaron interface centres 0-84528
- Mott insulators, excitonic spin polarons, appl. of Nagaoka's theorem for electron-hole pair 0-107978
- nonpolar fluid, excessive electrons near crit. points 0-92836
- periodic solutions of the classical polaron and bipolaron systems 0-100438
- piezoelectric crystal, surface polaron states, polaron-phonon interactions 0-70790
- polar crystal, polaron effective mass temp. depend., electron interaction (Chinese) 0-84436
- polyacetylene, intrinsic conformational defect states 0-65500
- polydiacetylene, intrinsic conformational defect states 0-65500
- semiconductor, ferromag., polaron solitary waves 0-70625
- semiconductor, ferromag., spin polaron props., effect on carrier scatt. 0-60233
- semiconductor, magnetophonon resonance oscills., peak shape, theory 0-107824
- semiconductor thin film, polaron near-threshold spectrum 0-65471
- semiconductors, temp. depend. electronic cond. 0-59975
- small polaron theory, translational symm. breaking transform. 0-92838
- surface exciton energies and radii 0-92829
- AgBr, cyclotron reson. of polarons at high density excitation 0-75859
- CdS, polaron cyclotron resonance freq. shifts, halfwidths, cumulant expansion method calcs. (Russian) 0-88880
- Eu chalcogenides, mag. polaron stability 0-96803
- EuO, transmission and resistivity, stress modulation effect near Curie temperature 0-96874
- EuO(Se), complex elec. cond. anomalies 0-107812
- Fe<sub>2</sub>O<sub>3</sub>, neutron diffuse scatt. due to molecular polarons 0-88488
- GaAs, surface exciton energy 0-92829
- Gd<sub>2</sub>O<sub>3</sub>, B-type monoclinic, DC(AC) elec. cond., thermoelectric power, dielectric const., temp. depends. 0-59980
- <sup>3</sup>He, FCC, vacancy induced spin polarons 0-59756
- <sup>3</sup>He, HCP, vacancy-induced transitions 0-88395
- He, solid, as mag. semicond., analogy to Mott insulator 0-96720
- InSe, exciton and polaron anisotropies, reson. Raman scatt. study 0-76033
- LiNbO<sub>3</sub>, optical absorption of hole centres, polaron model 0-97314
- NiO, dipole orientation from bound polaron hopping 0-84437
- PbMoO<sub>4</sub>, optical absorption of hole centres, polaron model 0-97314
- Sm<sub>2</sub>O<sub>3</sub>, B-type monoclinic, DC(AC) elec. cond., thermoelectric power, dielectric const., temp. depends. 0-59980
- Sm<sub>0.75</sub>Y<sub>0.25</sub>S, mixed-valence, electron-lattice correlations, EXAFS studies 0-76103
- Tb<sub>2</sub>O<sub>3</sub>, B-type monoclinic, DC(AC) elec. cond., thermoelectric power, dielectric const., temp. depends. 0-59980
- Te, photoconductivity in strong mag. fields, doping effects, impurity levels 0-75602
- TlBr, resonant polaron coupling and excitons under mag. field 0-71383
- YAG, optical absorption of hole centres, polaron model 0-97314

**poles and zeros**

- atomic eigenfunctions, nodal structure 0-57122
- event location by recursive least squares prediction 0-96131
- one dimensional function, resolution into sum of exponentials, roots of polynomial 0-77603
- polynomials, zeros, sum rules 0-57521
- polynomials, zeros, sum rules 0-62888
- zeta function of quartic oscillator 0-62532

**polishing**

see also electrolytic polishing

- arsenides (Ti, V, Cr, Mn, Fe, Co, Ni, Cu, Zn, Ga, Ge), oxidation, hardness and electromechanical polishing response 0-71776
- aspherical lens, polishing technique with equal polishing rate distrib. 0-58818
- borides (Ti, V, Cr, Mn, Fe, Co, Ni), oxidation, hardness and electromechanical polishing response 0-71776
- carbides (Ti, V, Cr, Mn, Fe), oxidation, hardness and electromechanical polishing response 0-71776
- corundum, single crystal, dispersion medium for polishing 0-102870
- cylindrical lens surface generation, grinding and polishing machinery design 0-79023
- diamond surface, polished, RHEED pattern 0-65345
- epoxy, mica filled, polishing by abrasive papers and lapping cpds. 0-108620
- glass, rare earth elements use as dopants (Polish) 0-97455
- glass surface, polished and laser-annealed, characterisation by ellipsometry 0-103544
- jet electropolishing, monitoring of transmission electron microscope foil thinning, PP-8 radiometer (USSR) 0-73525

**polishing** continued

- lenses surface, spectacle type, using automatic and semi-automatic machines (French) 0-58822
- leucosapphire, unique polishing features of hard crystals 0-64225
- metal surface electrochemical smoothing, roughness, diffusional pre-electrode layer (Russian) 0-76401
- mirror, nonaxisymmetric, fabrication by stressed mirror polishing 0-99885
- mirror, paraboloid, off-axis section, fabrication by stressed mirror polishing 0-99886
- mirror, single-point diamond-turned, performance before and after polishing 0-74466
- mirror fiducial system compatible with computer-controlled polishing facility 0-74539
- monocrystal surface layer damage depend. on abrasive working parameters (Russian) 0-76368
- optical element polishing simulation calc. and results (German) 0-87566
- optical coating removal by Al<sub>2</sub>O<sub>3</sub> powder and NH<sub>4</sub>HF<sub>2</sub> soln. 0-74521
- optical component polishing process modelling (German) 0-87565
- optical shop computer-controlled interferometry, in-process production tool 0-74531
- Polirit suspension, factors reducing polishing ability 0-74543
- polisher, computer controlled, efficiency 0-91938
- Polytron polishing pad, method and applications 0-69567
- porous materials, effects of different methods of prep. on reproducing surface 0-60995
- ruby, unique polishing features of hard crystals 0-64225
- semiconductor TEM 90° cross-section and 1° angle-lap specimen prep. 0-71881
- silicate glasses, polishing, surface characts. using grazing X-ray reflection (French) 0-65353
- smoothness parameters meas. of polished surfaces, using spectral analysis optical system 0-86261
- steel, stainless, smoothing for plastic pre-straining of material cut by turning (Russian) 0-60911
- steel, surface state influence on etching effect 0-81235
- sulphides (Fe, Co, Ni, Cu, Zn), oxidation, hardness and electromechanical polishing response 0-71776
- thin-wall cylinder cold rolling method 0-66535
- two-surface analysis, of polished sections in scanning electron microscope 0-77912
- Al-Cu-Mg, type D16T, thin-wall cylinder cold rolling method 0-66535
- Fe, sintered, influence of metallographic treatment on pore analysis 0-76417
- Fe-TiC pseudofused composite magnetoabrasive powders, props. 0-100926
- InP (110) surfaces, cleaved and polished-sputtered-annealed, LEED and AES study 0-103550
- InSb, optical constants and oxidation with various surface treatment (Russian) 0-88955
- n-InSb, phonon-assisted cyclotron reson. strongly depend. on surface condition 0-70755
- Mo alloys (MChVP and TsM10VD), erosion, effect of ion bombardment dose and previous surface treatment 0-89419
- Mo-Zr-Ti (0.5, 0.1%), adhesive wear polishing of 25 mm spheres 0-89397
- NaCl large window continuous polishing 0-74527
- Nb, mono- and polycrystn., crystallographic orientation, etching technique determ. 0-71814
- Nb-N(O)(C) system, specimen prep. for metallography (German, English) 0-89439
- PLZT ceramic, thin wafer production polishing process 0-81214
- Si single cryst., chem.-mech. polishing of low-scatt. optical surface 0-96040
- Si single crysts., mech. polishing with reagent, activation energy effects (Japanese) 0-89379
- Si wafers, floating-zone, etch struct. on microdefects as affected by dopants and surface treatment 0-79773
- StrTiO<sub>3</sub>, fabrication damage characterisation by internal and external meas. 0-102782
- Ta-N(O)(C) system, specimen prep. for metallography (German, English) 0-89439
- Ti-Al-Cr-Mo, type VTZ-1, machinability, using different abrasive materials (Russian) 0-97593
- Ti-Al-Mo, type VT14, machinability, using different abrasive materials (Russian) 0-97593
- V-N(O)(C) system, specimen prep. for metallography (German, English) 0-89439

**pollution**

- see also air pollution; pollution detection and control; water pollution; water treatment
- Birmingham, England, heat island synoptic climatology (1965-74) 0-85740
- city lights obs. by Defense Meteorological Satellite Program 0-104494
- conference, Osaka, Japan (Nov. 1979) 0-98756
- disposition assessments for decontamination and decommissioning of inactive nuclear sites, data requirements 0-95474
- dose-rate conversion factors for external exposure to photons and electrons, modifications to DOSFACTER code 0-104775
- dosimetry calculations due to radionuclides in aquatic food chains, NEP-TUN interactive code in FORTRAN 0-109039
- Earth albedo, anthropogenic changes and effects on climate 0-81893
- ecosystem analysis methods for the assessment of inactive nuclear sites 0-95476
- environmental radioactive pollution by U industry, monitoring using analytical chemistry 0-95488
- environmental radioactivity near a radioactive waste disposal site 0-98148
- geological medium interfered with by man, geophys. investigation methods 0-85323
- geopressed geothermal energy production plant, environmental effects 0-97764
- geothermal power developments and environmental pollution 0-61470
- heat release effect on general circulation and climate 0-89694
- magnetosphere, contamination by spacecraft at geosynchronous orbit 0-72701
- modelling, numerical estimation of unknown parameters (Japanese) 0-89702
- nuclear facilities, off-site radiological impact assessment real-time computer program CEPADAS 0-95475



**pollution continued**

- nuclear power, environmental impact 0-101143  
 nuclear site decontamination, radiochemical anal. of environmental samples 0-95477  
 radioactive actinides, man-made, health effects compared to natural radionuclides 0-61647  
 radioactive waste, biochemical and chemical processes leading to radionuclide transport from low-level waste burial sites 0-101275  
 radioactive waste, sorption of actinides in igneous rocks 0-95367  
 radioactive waste geologic disposal, geotoxicity hazard index 0-97822  
 radioactive waste underground disposal, solutes movement through aqueous fissures in porous rocks 0-94553  
 radioactivity in W.Cumbria, Pu and <sup>137</sup>Cs conc. in environmental samples and possible maritime effect 0-108817  
 radioisotope transport in terrestrial food chains, dynamic modelling using RAGTIME code 0-104776  
 radiological assessment of inactive nuclear sites, statistical design and anal. 0-95473  
 radiological assessment of inactive nuclear sites 0-95478  
 radiological survey of inactive nuclear sites, quality assurance 0-95472  
 safety and environmental pollution (*German*) 0-63370  
 Ural disaster questioned, possible fallout from atmospheric test 0-76666  
 urban heat island convergence in calm periods, St. Louis USA 0-90169  
<sup>241</sup>Am, concs. in sediments from coastal basins off California and Mexico 0-98303  
<sup>137</sup>Cs, intake by Bikini Island residents, model using bioassay data 0-109043  
 Pu-bearing materials, environmental impact of transportation, linear regression anal. 0-85308  
<sup>A</sup>Pu, A=239, 240, distrib. of fallout Pu in southern Finns 0-109045  
<sup>241</sup>Pu, concs. in sediments from coastal basins off California and Mexico 0-98303  
<sup>99m</sup>Tc contamination of laboratory personnel, its degree and routes 0-98147

**pollution detection and control**

- see also air pollution detection and control; noise abatement; remote sensing; waste disposal; water pollution detection and control; water treatment*  
 asbestos fibres concentration meas., in air and liquid, analytical methods review 0-72120  
 conference, Rochester, NY, USA (May 1979), polluted rain 0-82585  
 environment, global background pollution, ecological monitoring program 0-81518  
 environment monitoring ground radioactive burial site (*Japanese*) 0-67015  
 environmental control technology R and D, environmental impact of energy storage technology development 0-61471  
 environmental remote sensing, molecular absorpt. methods 0-72651  
 environmental science and engineering advances, book 0-105448  
 geological medium interfered with by man, geophys. investigation methods 0-85323  
 hair, human, PIXE analysis, correction factor, rel. to pollution monitoring 0-61743  
 nuclear power station, contamination monitoring station (*Polish*) 0-74033  
 radioactive waste storage, in situ instrumentation for meas. of radionuclide migration 0-95485  
 radioactive waste storage, long term subsurface migration of radionuclides 0-95483  
 radioactive waste storage, radionuclide migration determ., adsorption of Cs(I), Sr(II), Eu(III), Co(II), and Cd(II) by Al<sub>2</sub>O<sub>3</sub> 0-99240  
 radioactive waste storage, Sr, Cs, Co sorption meas. on soil sediment 0-95482  
 radionuclide migration from buried radioactive waste 0-95484  
 Raman laser microprobe analysis appl. 0-57390  
 Raman spectroscopy, remote spontaneous, new trends in recording of signals 0-73485  
 soil homogeneity evaluation by radionuclide tracer breakthrough curve interpretation for radwaste storage appls. 0-97821  
 space-borne remote sensing (*Italian*) 0-109333  
 trace element profile of a California Redwood tree for environmental monitoring 0-97850  
 tunable IR solid-state laser characteristics and principles 0-87406  
<sup>222</sup>Rn diffusion through U mill tailings covers, coeff. meas., lab. techniques 0-95387  
 SO<sub>2</sub>, ground-level conc. calcs. near a nuclear facility 0-97823  
<sup>90</sup>Sr bremsstrahlung radiation meas. for well logging using Ge spectrometer 0-94619

**polonium**

- see also nuclei with .....*  
<sup>210</sup>Po, nucl. alpha decay, electron inner shell vacancy creation, semi quantal approach 0-68607

**polonium compounds**

No entries

**polyelectrolytes** *see electrolytes; polymers***polymer films**

- see also dielectric thin films; insulating thin films*  
 acrylourethane coatings, radiation curable, tensile, elongation and modulus props. appl. techniques 0-66847  
 antistatic polymer film surfaces, microammeter meas. method for elec. conductivity 0-98932  
 Brillouin scattering at transitions 0-70312  
 bulk electric conduction parallel to film surface 0-92889  
 characterisation, by TEM 0-103270  
 copolymer thermoplastic layers, isothermal smoothing of surface deformation (*Russian*) 0-76394  
 defects obs., Raman microprobe-microscope appl. 0-62737  
 dielectric constant meas. parallel to film surface 0-97183  
 3,4-dimethyl-1,2,5-thiadiazol plasma polymerised film for holographic recording 0-106490  
 electrets, charge distribution determ. (*German*) 0-75920  
 electrification, frictional, temp. and friction speed dependence obs. 0-70798  
 electrochromic materials, polymer-modified electrode characts. 0-66149  
 ethylene-vinyl acetate copolymers, extrusion and heavy duty films, radiation crosslinking, struct. effect 0-66844  
 ferrocene films, plasma-polymerised, carrier trapping, elec. cond. meas., 300 to 525K 0-100543  
 fluorocarbon polymer, plasma-deposited thin films for lubrication of Au contact surfaces 0-89157

**polymer films continued**

- glassy and rubbery, isotope effect in H<sub>2</sub> and D<sub>2</sub> diffusion, T<sub>g</sub> region behaviour 0-84327  
 n-hexatriacontane, vacuum deposited on alkali halide crystals, structure and heat treatment 0-103600  
 latex film composite, glass transition temp. determ. using thermomech. curves 0-75342  
 light scattering, small-angle, Debye-Bueche theory treatment of multiple scatt. 0-84794  
 micropores, localisation prior to electron microscopy 0-103271  
 Nafion, densities and expansion coeffs. as function of various parameters 0-79711  
 Nylon 6, prior high-press. treatment effects, weight swelling, density, IR crystallinity, X-ray and viscosity obs. 0-81025  
 Nylon-12, casting conditions effect on polymorphism 0-84903  
 optical fibres development, polymer clad, for communication use 0-69546  
 optical polarisation data interpretation of aromatic hydrocarbons in stretched films, photoelectron spectroscopy appl. 0-58302  
 parylene (vacuum deposited polymeric coating), appl. to electronics 0-108607  
 permeation, diffusional time lags determ. 0-65272  
 PET, biaxial orientation, refr. index meas. by Raman and IR spectrosc. 0-60583  
 PET, charge effects at Al electrodes obs. 0-75625  
 PET, dyed, local mech. stresses, IR spectrosc. determ. 0-65418  
 PET films, one-way drawn, constant strain effects, IR meas. 0-60584  
 photon and electron absorbed-dose detector 0-91379  
 photoresist, KTRF, thermally stimulated discharge current studies 0-75924  
 photovoltaic properties, for solar cell appls. 0-60040  
 PMMA, electron beam scattering, Monte Carlo simulation 0-100148  
 PMMA film, doped, time resolved absorpt. spectra, decay kinetics of exciplex state 0-84098  
 PMMA film in small area lateral MIMS device, cond., switching 0-97003  
 polarised polyvinylidene fluoride film, piezoelectric transducer 0-75993  
 poly(ethyl vinyl ketone) film, reacted with phosphoryl chloride, elec. cond. 0-97599  
 poly(vinyl alcohol) porous film, polymerisation and porosity 0-107063  
 poly(N-vinylcarbazole): trinitrofluorenone films photovoltaic properties for solar cell appls. 0-60040  
 poly- $\alpha$ -naphthol, semicond., isothermal depolarisation currents, electron trap parameters 0-60492  
 poly-N-vinylcarbazole thin amorphous film, hole drift mobility, mol. mass. depend. 0-75663  
 poly-p-xylylene films, carrier traps, X-ray induced TSC, thermolum. and dielec. loss study 0-88570  
 cis-polyacetylene:AsF<sub>5</sub>, conductivity meas., non-Ohmic effects 0-96891  
 polyacetylene:AsF<sub>5</sub>, soliton doping mechanism, mag. susceptibility meas. 0-107979  
 polyacetylene:SbF<sub>5</sub>, elec. cond. meas. 0-60055  
 polyacetylene, halogen doped, mass spectrometric anal. 0-108771  
 cis-polyacetylene, unpaired electrons, isomerisation, EPR obs. 0-60405  
 polyacetylene, variable density, synthesis, elec. cond., thermopower 0-60016  
 polyacetylene film, anisotropy of dielec. const. 0-108146  
 polyacetylene films, AsF<sub>5</sub> doped, photocond. and junction props. 0-70770  
 polyacetylene films, doping effect on elec. cond., chem. and optical props. 0-65572  
 polyacetylene films, doping investigation, insulator-metal transition, optical transmission meas. 0-10379  
 polyacetylene films, electrical properties (*Japanese*) 0-96888  
 polyacetylene films, stretch-aligned, prep. and morphology 0-66471  
 polyacetylene films, tensile props. and partial alignment 0-104210  
 polyacetylene films, undoped, nonlinear current-voltage charcts. 0-75574  
 polyacrylic acid film, structuration and mech. props., EM obs. (*Russian*) 0-59406  
 polyamide-polyurethane copolymer dispersions, structuration and relax. props., coating from props. 0-76559  
 polybutylene terephthalate, melt crystallised, solvent crystallised films and moulded bars, morphological obs. 0-84101  
 polycarbonate: tri-p-tolylamine, chemical control of conductivity 0-59984  
 polycarbonate, and charge-transfer complex modifications, isothermal dark currents 0-88559  
 polycarbonate, and charge-transfer complex modifications, TSC 0-88572  
 polycarbonate films, high temp. relaxations 0-97187  
 polydimethyl siloxane-b-styrene-b-dimethyl siloxane block copolymer, morphology, mech. props. 0-64930  
 polyester film, cross-linked, low-mol. wt. substance sorption effect on struct. (*Russian*) 0-59405  
 polyester yellow in polyvinylacetate film, ablative optical recording 0-83555  
 polyester-hydrazide, aromatic, fibres and films, synthesis and props. (*Japanese*) 0-103887  
 polyethylene, injection times for charging obs., with aid of computer 0-70796  
 polyethylene film, minimum running thickness, biaxial extensional flow study 0-100993  
 polyethylene films, corona charged, charge trapping 0-88571  
 polyethylene spherulites, thin melt-cast films, high density, deform. process in non-equatorial regions 0-81124  
 polyethylene terephthalate, injection times for charging obs., with aid of computer 0-70796  
 polyethylene terephthalate, metallised coatings fracture under laser irradi. (*Russian*) 0-76333  
 polyethylene terephthalate films, current peaks obs. with linearly increasing voltage 0-88654  
 polyethylene-paraffin wax, blends, rapid cooling processing techniques 0-84905  
 polyethylene/polypropylene blends, surface growth of fibres and films 0-66470  
 polyethylenes, extrusion and heavy duty films struct. parameters influence on cross-linking by radiation 0-66844  
 polyhexamethylene adipamide, photocond. and dielectric props. 0-84489  
 polyimide films, transient current in time range 10<sup>-4</sup> to 10 s at temps. 180 to 280°C 0-65729  
 trans-1,4-polyisoprene crystals, press. effect on growth rate 0-88064  
 polymethyl methacrylate, use of synchrotron radiation in X-ray lithography 0-62820  
 polypropylene, double-exposure speckle pattern obs. of tensile deform., displacement, Poisson's ratio and stress relax. 0-84795



**polymer films continued**

- polypropylene film, dielectric relaxation,  $\beta$ -mode investigation 0-93239  
 polypyromellitimide, elec. cond., 120-180°C 0-60124  
 polypyrrole films, electrochemical prep., chem. and phys. characterisation 0-70708  
 polystyrene:1 films, thermally stimulated discharge, I conc. and polarisation temp. depend. 0-107937  
 polystyrene,  $\gamma$ -Fe<sub>2</sub>O<sub>3</sub> powder filled, mag. films, packing and particle orientation (*Japanese*) 0-104115  
 polystyrene, energy losses and straggling for H<sup>+</sup> and He<sup>+</sup> beams (*Russian*) 0-84226  
 polystyrene, isotactic gel film, Fourier transform IR spectrum 0-104465  
 polystyrene, uniaxially stretched atactic thin film, mol. orientation, polarized Raman study 0-103951  
 polystyrene coated Ag holographic grating, Raman spectra enhancement by plasmon surface polaritons 0-80885  
 polystyrene film, graft, positive-ion emission in thermal destruction 0-66381  
 polystyrene film, thermally stimulated discharge currents 0-71300  
 polystyrene films, soln. grown, elec. cond. meas. 0-97020  
 polystyrene thin films, TSC and surface charge meas. 0-103769  
 polyvinyl acetate,  $\gamma$ -Fe<sub>2</sub>O<sub>3</sub> powder filled, mag. films, packing and particle orientation (*Japanese*) 0-104115  
 polyvinyl alcohol film containing Cu<sup>2+</sup> complexes, photoconductivity 0-107849  
 polyvinyl butyral,  $\gamma$ -Fe<sub>2</sub>O<sub>3</sub> powder filled, mag. films, packing and particle orientation (*Japanese*) 0-104115  
 polyvinylacetate film, dissolved polyester yellow, ablative optical recording 0-83555  
 polyvinylbutyral, elec. and dielec. props., mol. wt. effect on charge storage 0-97192  
 polyvinylidene fluoride, acoustic transducer-receiver appl., flexible configuration, activated by laser 0-83724  
 polyvinylidene fluoride, corona-charged, surface effects 0-66102  
 polyvinylidene fluoride, electro-optic and elasto-optic effects 0-80754  
 polyvinylidene fluoride, plasma poling, piezoelec. and pyroelec. responses 0-71296  
 polyvinylidene fluoride, poled, short duration unipolar stress pulse detection, generation 0-106695  
 polyvinylidene fluoride, pyroelectric transient response 0-75956  
 polyvinylidene fluoride, thermodynamic model and appl. 0-75955  
 polyvinylidene fluoride, X-ray induced TSC 0-75578  
 polyvinylidene fluoride film, biaxially oriented, charact. for transducer appl. 0-88931  
 polyvinylidene fluoride film, hysteresis and dipolar orientation 0-97217  
 polyvinylidene fluoride film, pyroelec. camera tube for IR imaging, thermal diffusivity of Bi-Bi<sub>2</sub>O<sub>3</sub> black layer 0-57369  
 polyvinylidene fluoride film polymer transducer, with US appl., durable lead attachment techniques 0-79094  
 polyvinylidene fluoride films, HF US absorpt. meas., 300 to 1500 MHz 0-74667  
 polyvinylidene fluoride films, SH and Lamb waves propag. 0-75948  
 polyvinylidene fluoride films for SAW transducers on Si substrates 0-74618  
 polyvinylidene fluoride piezoelec. film for adaptive deformable mirror system 0-74455  
 polyvinylidene fluoride piezoelectric film, Lamb and SH wave attenuation (*French*) 0-79196  
 polyvinylidene fluoride SAW transducers, evaluation of performance 0-74617  
 PTFE grafted membranes, struct.-properties relationships, bifunctionality (*French*) 0-61137  
 PTFE grafted membranes, struct.-properties relationships (*French*) 0-61136  
 PTFE grafted membranes, struct.-properties relationships for poly-N-vinylpyrrolidone-containing membranes (*French*) 0-61138  
 PVC, frictional electrification, contrib. of mol. motion of polymer 0-70798  
 PVC film, testing device, for prop. changes at high temps. (*German*) 0-66741  
 PVC films, soln. grown, DC cond. mechanisms, field and temp. depend. 0-97021  
 PVC in metal sandwich struct., switching props., voltage- and current-controlled negative resist. 0-103767  
 PVDF pyroelectric IR detector (*Japanese*) 0-105714  
 PVF<sub>2</sub> transducers for NDT 0-76476  
 pyroelectric polymer IR detector (*Japanese*) 0-105713  
 resin protective coating, UV cured, for optical fibre/cable 0-69547  
 RF discharge prep. using monomer organic semicond., elec. props. obs. 0-80432  
 rubber, friction against paper and polymer film surfaces, microroughness effect 0-71763  
 stretched, impurity mol. orientation, proton intramolecular transfer, light absorpt. and emission, dichroism, polarised fluoresc. 0-87166  
 surface film form. on Pt electrodes by electrooxidation of phenolic cpds. 0-104450  
 thickness monitor, using differential electronic circuit 0-73315  
 trinitrofluorenone: poly (N-vinylcarbazole) films photovoltaic properties for solar cell appls. 0-60040  
 vinylidene fluoride-trifluoroethylene film, cryst. phase transition 0-66120  
 vinylidene fluoride-trifluoroethylene copolymer, piezoelectricity 0-88930

**polymer melts**

- annular flow, secondary normal stress difference 0-106816  
 Barus effect, and normal stress effect in steady shear flow case 0-64589  
 blended polymer melts, flow indices (*Japanese*) 0-79360  
 blends, fluctuation dynamics, spinodal decomp. 0-79943  
 Brillouin scattering at transitions 0-70312  
 crystallisation from melt 0-84107  
 dynamics, self-diffusion const., relax. time and viscosity 0-64874  
 entangled polymer liquid, phenomenological consequences of Doi-Edwards viscoelasticity theory 0-79250  
 equation of state analysis w.r.t. Ising fluid model 0-79907  
 fibre reinforced polymer, soaking, wetting and compounding of materials during production (*German*) 0-93535  
 flow birefringence meas., influence of parasitic birefringences 0-88963  
 flow-induced crystallisation, conference, Midland, MI, USA (Aug. 1977) 0-82576  
 gas bubble pulsations and assoc. dissipation effects 0-59079  
 generalised polymer problems, Flory exponents 0-107039  
 heat transfer to polymer melt flowing through duct 0-103049

**polymer melts continued**

- laminar and melt fracture flow through successive capillaries 0-59085  
 normal stress measurement, modification to Weissenberg rheogoniometer unit 0-69750  
 orientable polymer fluid, Ericksen's anisotropic fluids theory extension 0-79359  
 perfluorinated polymer, Krytox 143-AB, viscous, viscoelastic and dielectric properties 0-70440  
 PET, P-V-T relationships 0-107400  
 PMMA melt, stress relax. at large deformations 0-58994  
 poly(ethylene terephthalate), stress-induced crystn. from melt, optical studies 0-84113  
 poly(m-xylene adipamide), molten, gel form. kinetics (*Japanese*) 0-108757  
 poly(vinylcarbazole), stress-induced crystn. from melt, optical studies 0-84113  
 poly-4-chlorostyrene, undiluted, dielec. relax. spectrum above T<sub>g</sub> 0-97194  
 poly-4-methylpentene-1, P-V-T relationships 0-107400  
 polyalkylene isophthalates, surface tension meas. by sessile bubble method (*Japanese*) 0-75405  
 1,4-polybutadiene, stress-induced crystn. from melt, optical studies 0-84113  
 polybutene-1, P-V-T relationships 0-107400  
 polycaprom  $\alpha$ -polyethyleneterephthalate melts, two-phase blend, rheological props. (*Russian*) 0-58997  
 polycarbonate, secondary flow and stress birefringence patterns in pressure hole 0-64590  
 polydimethylsiloxanes, rubbery and liq., hypersonic sound vel., Brillouin spectra meas. 0-75308  
 polyethylene, branched, P-V-T relationships 0-107400  
 polyethylene, high and low density, secondary flow and stress birefringence patterns in pressure hole 0-64590  
 polyethylene, low and high density, normal stress and Barus effect 0-64589  
 polyethylene, solid liq., secondary electron emission spectroscopy 0-80916  
 polyethylene flow crystallisation, in extensional flow developed by convergent capillaries, props. 0-84111  
 polyethylene fractions, quasi-binary systems, solidification and crystn. 0-84108  
 polyethylene melt, cryst. kinetics during cooling, nucleation density effect 0-100181  
 polyethylene melt, high density, oscillating flow during extrusion, model anal. 0-100016  
 polyethylene melt, oscillatory flow through capillary 0-103046  
 polyethylene ribbons, flow-induced crystn. from melt, in dies fed by single screw extruder 0-84110  
 polyethylene terephthalate, solid and molten, press. effects on compressibility and crystn., thermodynamic interpret. 0-84102  
 polyethylene-paraffin wax, blends, rapid cooling processing techniques 0-84905  
 polyethyleneterephthalate-polycapromamide melts, two-phase blend, rheological props. (*Russian*) 0-58997  
 polymer additive effects on wall slip and viscosity in flow through capillaries (*German*) 0-59086  
 polymethylsiloxane-2, liq., thermodynamic props. at high press., US prop. meas. (*Russian*) 0-65157  
 polyolefine, liq., memory effect 0-103268  
 polypropylene, flow-induced crystn. from melt, in dies fed by single screw extruder 0-84110  
 polypropylene, normal stress and Barus effect 0-64589  
 polypropylene, P-V-T relationships 0-107400  
 polypropylene glycol melt, mol. motion, dielectric and Kerr effect relax. obs. 0-60498  
 polypropylene-polyethylene blends, capillary flow, rheology and morphology 0-59088  
 polypropylene-polyethylene blends, flow behaviour in capillaries 0-59087  
 polystyrene, isotactic, spherulite radial growth retardation by SiO<sub>2</sub> nucleation 0-107066  
 polystyrene, secondary flow and stress birefringence patterns in pressure hole 0-64590  
 polystyrene melts, flame-retardant high-impact, shear viscosity-temp.-shear rate relationships 0-59691  
 polysulphone, P-V-T relationships 0-107400  
 PTFE, P-V-T relationships 0-107400  
 relaxation oscillators using unstable flow of polymer melts (*French*) 0-79361  
 rheological properties at low shear stresses, meas. using sandwich type creep rheometer 0-59153  
 sol-gel transition, US attenuation meas. 0-101043  
 static bulk props., reptation Monte Carlo method, LJ pot. 0-64868  
 styrene-butadiene-styrene block copolymer, melt rheology 0-87751  
 styrene-butadiene-styrene block copolymer, stress relax. following steady-state flow, residual shear stress development 0-83772  
 styrene/acrylic terpolymers, viscoelastic props. 0-64509  
 suspension of interacting particles, cell model theory of shear viscosity 0-103048  
 trifluoropropylmethylsiloxane fluids, viscoelastic props., mechanical impedance, viscosity and density meas. 0-79249

**polymer solutions**

- $\theta$ -domain, tricrit. props. in poor solvent 0-103450  
 air bubbles, production, pulsation and damping 0-69879  
 bead suspension, time depend. viscoelastic behaviour polystyrene solution, glass 0-99982  
 biopolymers, N-acetyl-D-alloisoleucine, soln. struct., dynamics, proton relaxation mechanisms 0-76708  
 bubble behaviour in pulsating pressure, natural freqs. 0-64591  
 carboxymethyl cellulose, aqueous soln., diffusion and mass transfer from rotating disc 0-83827  
 cellulose, fibrous crystn., from flowing solns. 0-84106  
 cellulose acetate, solvent effect on lyotropic mesomorphism 0-70121  
 cellulose acetate butyrate, in soln., hydrodynamic behaviour 0-64876  
 chain statics and dynamics, Lennard-Jones interaction, calcs. 0-58425  
 chains, freely rotating, depolarised light scatt. spectrum calcs. 0-78731  
 chains, helical wormlike, statistical mechanics, anisotropic light scatt. near the rod limit 0-93346  
 chains with rigid bonds, local relax. times, mol. dynamics study (*Russian*) 0-59373  
 colloidal particles in polymer soln., depletion stabilisation and depletion flocculation, theory 0-89534  
 conformational mobility, fluorescence obs. 0-63877



## polymer solutions continued

constitutive eqn. with factorised memory function 0-70105  
 crown ether-containing polymers, in alkali salt solns., complexation, viscosity obs. 0-64877  
 crystallisation from solution 0-84105  
 crystallisation kinetic data, status of anal. 0-84104  
 dextran, aq. soln., conc., PMR (*Russian*) 0-71225  
 dextran fractions, production, characterisation and solution properties 0-59368  
 dextrans, branched, cross-section factor correction in small-angle X-ray scatt. data 0-84048  
 diffusion equation with hydrodynamic interaction, equiv. normal coord. 0-79966  
 diffusion of a chain, conc. effects 0-70103  
 diffusion of ionic species, meas. by diffusion controlled electrolysis 0-74920  
 dilute, coherent scattering law, continued fraction formalism 0-103234  
 dilute, extensional and sink flow in channel 0-74925  
 dilute, mod. wt. depend. of partial specific vol. 0-99594  
 dilute, regularly alternant, thermodynamic props. self avoiding random walk calcs. (*French*) 0-59369  
 dumbbells, nearly-Hookean, dilute soln., rheological equation of state 0-100321  
 dynamic scaling theories at nonzero concs., tagged chain translational diffusion coeffs. 0-75143  
 elastic, load bearing capacity of squeeze film flow 0-103051  
 elastic, vel. meas. in die entry region of capillary rheometer 0-99988  
 elastic fluids, shear-thinning, Carreau viscosity eqn., creeping motion of spheres 0-87753  
 electric field-induced optical rectification, rel. to electro-optic kerr effect 0-84726  
 epoxy/graphite composite and cured epoxy resin, thermal expansion and swelling 0-92450  
 excluded volume parameters, light scatt. obs., graphical calcs. 0-89009  
 flexible chain molecules, mutual interpenetration, fluorescence obs. 0-63877  
 flexible ring polymer, intrinsic viscosity 0-103511  
 flow birefringence, localized, induced behind obstacles in polymer soln. (*French*) 0-93275  
 flow through sand filters, flow resistance 0-79395  
 flow-induced crystallisation, conference, Midland, MI, USA (Aug. 1977) 0-82576  
 gel rods, elastic dilatational mode, light beam positional modulation 0-64167  
 generalised polymer problems, Flory exponents 0-107039  
 glassy soln., fluoresc. yield, polarisation and decay., temp. depend. 0-89043  
 HPAM dilute polymer solutions, elongational flow 0-103047  
 hydroxyethyl cellulose, polymer segments, fluoresc. depolarisation on conjugated spin labels 0-91711  
 hydroxypropyl cellulose/H<sub>2</sub>O, rheo-optics of shear and elongational flow, quiescent and flow birefringent characts. 0-83773  
 ionomer solutions, in water, gel form. and demixing transition 0-61172  
 latex spheres in H<sub>2</sub>O, photon correlation spectroscopy, diffusion coeffs. determ. 0-93802  
 light scattering, dynamic, by flexible macromols. in fluctuating elec. field 0-84722  
 liquid-crystalline solns., struct. 0-103235  
 long polymers in solution, props., direct renormalisation method for study 0-59370  
 low conc., complex coacervation occurrence condition 0-79944  
 macromolecule, charged, in external elec. field, spherical case 0-75145  
 macromolecules, volume interactions, coil-globule transition, statistical physics, review 0-78737  
 medical polymers, chem. problems, conf., Prague, Czechoslovakia (Aug. 1977) 0-56996  
 metal fraction contents and properties, meas. by eddy current method (*Russian*) 0-76571  
 mixed solvents, preferential adsorpt. coeff. rel. to mol. dimens. 0-103237  
 Monsanto X-500 aromatic polyamide hydrazide soln., light scatt. study 0-76038  
 Monte Carlo study, scaling props., excluded vol. expansion 0-96435  
 nonlinear response to uniaxial shear flow histories 0-59084  
 normal stress measurement, modification to Weissenberg rheogoniometer unit 0-69750  
 normal stress measurement of dilute polymer solutions 0-83776  
 nylon 6.6 in 100% H<sub>2</sub>SO<sub>4</sub>, primary normal-stress difference coeff., dependence on molecular wt. 0-87752  
 orientable polymer fluid, Erickson's anisotropic fluids theory extension 0-79359  
 oscillatory flow in U-tube manometers, effect of drag reducing polymer additives 0-64584  
 osmotic pressure, correlation functions, in grand canonical formalism 0-100159  
 PMMA, syndiotactic, solns. in toluene, NMR obs. of struct. and dynamics of associates 0-75867  
 PMMA in benzene solution, ultrasonic irradiation, polymer chain scissions obs. by ESR spectra and spin-trapping techniques 0-84653  
 poly(2-vinyl pyridine), dil. solns., translational diffusion, chain conformation influence 0-103508  
 poly(sodium 10-undecenoate), form. by  $\gamma$ -ray induced polymerisation in aq. micelle solns. 0-61093  
 poly-4-vinylpyridine, electro-optic study of conformational changes induced by heavy metal ions 0-84725  
 poly-4-vinylpyridine, intramol. mobility and local density in soln. spin mark method obs. (*Russian*) 0-70107  
 poly-4-vinylpyridine, mol. dynamics and local density in conc. soln., spin mark method obs. (*Russian*) 0-70108  
 poly- $\gamma$ -benzyl-L-(D)-glutamate, soln., liq. cryst. and pretransitional regions, optical rot. 0-66145  
 poly- $\gamma$ -benzyl-L-glutamate, soln., liquid crystal transitions anal. 0-65207  
 poly- $\gamma$ -benzyl-L-glutamate, synthetic polypeptide, nonlinear dielectric effect in nonpolar medium 0-84682  
 poly-L-glutamic acid-Na, cooperativity parameter determ. from viscometry 0-75147  
 poly-L-ornithine, <sup>15</sup>N NMR, coil-helix transition, solvent effects and pH depend. 0-74275  
 poly-m-phenylene-isophthalamide in dimethylacetamide, flow birefringence (*Russian*) 0-66148  
 poly-p-chlorophenyl glycidyl ether, struct., tacticity and addition isomerism, <sup>13</sup>C NMR 0-58427

## polymer solutions continued

poly-p-phenylene terephthalamide/H<sub>2</sub>SO<sub>4</sub> 0-83773  
 poly-p-tert-butylphenylmethacrylate, soln., viscometric behaviour 0-88016  
 polyacenaphthalene, glassy soln., fluoresc. yield, polarisation and decay., temp. depend. 0-89043  
 polyacrylamide, aq. soln., thermodynamic props., light scatt. obs. (*Russian*) 0-71439  
 polyacrylamide aqueous solution, ultrasonic investigation (*Chinese*) 0-107371  
 polyacrylamide gel and single chain in soln., laser light scatt. obs. near phase transitions 0-93808  
 polyacrylamide Separan MG200, aq. soln., rheological props. 0-64507  
 polyacrylonitrile, hydrolysed, cutting fluid, operational characteristics 0-89359  
 polyaspartamides, fluorescent labelling 0-58426  
 1,2-polybutadiene, crosslinked in states of strain, entanglement networks, swelling anisotropy obs. 0-79666  
 polybutadiene, dil. soln., viscosity, temp. depend., solvent effects 0-59686  
 polybutadiene and butadiene-styrene in tetrahydrofuran, second virial coeffs. 0-65188  
 polybutadiene-poly- $\alpha$ -methylstyrene copolymers, struct. obs., prep. (*French*) 0-59401  
 polycaprolactam, and copolymers, optical anisotropy and rigidity 0-88959  
 polycyclohexanamide, and copolymers, optical anisotropy and rigidity 0-88959  
 polydicarboxylic acids, electrophoretic and viscometric props. 0-66811  
 polydimethyl siloxane solns., US attenuation meas. 0-107372  
 polydimethylsiloxane chains, end-linked, swollen model networks, stress/strain isotherms and elastic modulus 0-79668  
 polydisperse systems, photon correlation spectroscopy, diffusion coeffs. determ. 0-93802  
 polyelectrolyte soln., counterion condensate around line charge as  $\delta$ -function, nonlinear Poisson-Boltzmann theory 0-85184  
 polyelectrolytes, saturation of induced dipole moment, orientation mechanism and electro-optical effects 0-84785  
 polyesterimides, solns., ultrasonic vel. and Rao formalism 0-103422  
 polyethylene, alcohol infused, loss peaks due to secondary groups 0-84688  
 polyethylene, flow-induced fibril form. from soln. 0-59402  
 polyethylene, molten, effect of hydrostatic press. on long-chain organic mol. diffusion 0-92697  
 polyethylene oxide, dilute aqueous solution, effect of chemical additives on flow 0-83823  
 polyethylene oxide, dilute solution, flow round circular cylinder 0-69882  
 polyethylene oxide, polymer segments, fluoresc. depolarisation on conjugated spin labels 0-91711  
 polyisobutylene in toluene solution, effect of capillary materials on drag reduction (*German*) 0-87785  
 polyisocyanates, rigid backbone, ternary phase relationships obs. 0-59371  
 polymer solns., not infinitely dilute, second-order fluid coeffs., conc. depend. 0-106771  
 polymers in liquid stream, Toms effect mechanism, turbulent drag decrease 0-79270  
 polymethacrylamide copolymers, mobility of spin label bonded to chain end 0-83873  
 polymethacrylic acid, swollen networks, viscoelastic photoelastic behaviour 0-59366  
 Polyoxy, drag reduction meas. in square duct, anomalous effects due to polymer degradation 0-83824  
 polypeptides, helical, conc. solns., rheological behaviour and liq. cryst. order 0-83771  
 polyribonucleotides, dye tagged, aqueous solns., elec. induced fluoresc. changes 0-85346  
 polystyrene, bridge method for meas. dielectric relaxation 0-82793  
 polystyrene, in solns., intrinsic viscosity rel. to mol. wt., unperturbed dimensions 0-65268  
 polystyrene, ordered monodisperse latexes, viscoelasticity and flow props. 0-58992  
 polystyrene, solns., diffusion coeffs. meas., Fourier transform NMR, pulsed field gradient system 0-57353  
 polystyrene, solns., sedimentation behaviour, branching effects determ. 0-66887  
 polystyrene and butadiene-styrene in tetrahydrofuran, second virial coeffs. 0-65188  
 polystyrene in benzene or cyclohexane, zero shear-rate intrinsic viscosities 0-75376  
 polystyrene in benzene solution, ultrasonic irradiation, polymer chain scissions obs. by ESR spectra and spin-trapping techniques 0-84653  
 polystyrene latex particles, swollen, aggregation studied by photon correlation spectrosc. 0-66886  
 polystyrene latex spheres, characterisation using light scattering spectrom. 0-95753  
 polystyrene networks swollen in cyclohexane, swelling equil. and light scatt. at theta conditions 0-107036  
 polystyrene solns., correlations of network model parameters 0-106772  
 polystyrene solution, constitutive models, exptl. tests based on birefringence data 0-100015  
 polystyrene solution, differential meas. of ultrasonic velocity (*French*) 0-75302  
 polystyrene-benzene, polymer excluded volume exponent, experimental verification of n vector model for n=O 0-70104  
 polystyrene-cyclohexane mixture, Rayleigh and Brillouin scatt. and struct. relaxation 0-63640  
 polystyrene-cyclohexane system, temp. depend. of hydrodynamic lengths 0-92449  
 polystyrene-methylcyclohexane, coexistence curve, comparison obs. and free energy calc. 0-88323  
 polystyrene-methylcyclohexane, coexistence curves, range of simple scaling and critical exponents 0-88322  
 polystyrene-polyethylene/propylene block copolymer, micelle form. in lubricating oil 0-61171  
 polystyrene-tricresyl phosphate solns., viscoelastic props., conc. depend. 0-76299  
 polystyrenesulphonates, in dioxane-water mixtures, heats of dilution meas. 0-59655  
 polystyrenesulphonic acid, in dioxane-water mixtures, heats of dilution meas. 0-59655  
 polystyrene, benzene soln., characterisation using light scattering spectrom. 0-95753  
 polyvinyl acetate, and conc. solns., viscosity meas. 0-65269



**polymer solutions continued**

- polyvinyl alcohol networks, swelling equil. with dil. salt solns., thermoelastic behaviour, hydroxyl group interact. 0-79667  
 polyvinylacetate in benzene solution ultrasonic irradiation, polymer chain scissions obs. by ESR spectra and spin-trapping techniques 0-84653  
 poor solvent, loop expansion of irreducible diagrams 0-100160  
 PPT in 100% H<sub>2</sub>SO<sub>4</sub>, primary normal-stress difference coeff., dependence on molecular wt. 0-87752  
 protonated and deuterated mixtures, partial miscibility 0-107037  
 PVA, aq. solns., US absorpt., acetate groups effects (*Russian*) 0-65162  
 PVC plastisol, flow behaviour at high shear rate (*German*) 0-92186  
 quasi-elastic light scatt., slow modes 0-74271  
 radiation scattering, quasielastic, Rouse-Zimm model 0-84047  
 Rayleigh scattering, intermolecular correlations effect 0-75146  
 renormalised field theory, polydispersity 0-74270  
 rheology based on a finitely extensible bead-spring chain model 0-83775  
 rigid, modified Oseen tensor, superposition approximation appl. 0-92447  
 rodlike particles, polydisperse soln., isotropic-nematic phase transition, Onsager theory 0-100324  
 scaling theories for general interaction potentials 0-99592  
 sedimentation field-flow fractionation in macromolecule characterization 0-66879  
 sedimentation rates for low mol. wt. materials in dilute region 0-108756  
 shear thinning and shear thickening additives in reservoir flooding for oil recovery 0-72100  
 short range correlation between elements of long polymer in good solvent 0-59367  
 small angle neutron scatt., single chain form factors 0-107038  
 sodium polystyrene sulphonate in aq. soln., quasi-elastic light scatt. 0-100661  
 spherical polymer, long time tail in diffusion 0-88018  
 static bulk props., reptation Monte Carlo method, LJ pot. 0-64868  
 submerged jets impinging on baffle, flow and mass transfer, polymer additive effects 0-92194  
 transport properties, conc. effects 0-64875  
 unsaturated polyester resins, gelation, viscosity meas. (*Polish*) 0-59690  
 urethane elastomer, thermoplastic, dilute soln., viscosity and sedimentation 0-103512  
 viscosity measurement method at high press. 0-69955  
 viscous drag of two-dimensional contours moving in a weak polymer solution 0-100014  
 weak polymer solutions, flow props. in narrow channel between rotating and stationary discs (*Russian*) 0-59089  
 weakly correlated, radial distrib. function 0-84050

**polymerisation**

- A-copolymerisation, on basis of oligodienedihydrazides and diepoxides, cross-linked polymer characts. (*Russian*) 0-58431  
 acetylene, polymerisation, variable density polyacetylene prop., elec. props. 0-60016  
 acetylene adsorbed on Fe containing segregated C, hydrogenation, C-1s XPS spectra obs. 0-84366  
 adaptive control of molecular weight distribution 0-58434  
 1,6-bis(2,4-dinitrophenoxy)-2,4-hexadiyne, effect on apparent ferroelec. transition 0-66121  
 bis-(p-toluene-sulphonate) of 2,4 hexadiyne 1,6 diol, X-ray scattering obs. of polymerisation mechanism and phase transition (*French*) 0-70399  
 1,6-di-p-methoxybenzene sulphonyloxy-2,4-hexadiyne, thermal polymerization, Raman spectra 0-103952  
 diacetylene, low temp. photochemical polymerisation, decay kinetics, ESR spectra obs. 0-100616  
 diacetylene, photopolymerisation, optical absorpt. spectra, time depend., reaction kinetics 0-85174  
 diacetylene (TSHD), low temp. photopolymerisation, short chain intermediates obs. 0-93754  
 diacetylene derivatives, solid-state polymerisation, isotope effects 0-66799  
 diacetylene mixed crystals, co-crystallisation, influence of crystal composition on struct., reactivity in solid state 0-81324  
 diacetylene monocarboxylic acids, multilayers, struct. phase transitions and polymerisability 0-80129  
 diacetylene-d<sub>2</sub>, excited quintet states during photopolymerisation, ESR obs. 0-84635  
 diacetylenes, photopolymerisation, solid-state reaction, photoacoustic calorimetric obs. 0-61089  
 diacetylenes, solid state photopolymerisation, reaction products, electron spin resonance anal. 0-81338  
 N,N-diethylacrylamide, cross-linked copolymer, improved mech. props. 0-61091  
 3,4-dimethyl-1,2,5-thiadiazol plasma polymerised film for holographic recording 0-106490  
 dynamic living polymers, thermodynamic enhancement of oligomers, end-group interactions 0-58423  
 esters, long-chain, X- and Y-type multilayers, form. conditions and struct. characterisation 0-80127  
 ethylene propylene/polyolefin blends, radiation cross linking 0-66801  
 fibre reinforced polymer, soaking, wetting and compounding of materials during production (*German*) 0-93535  
 fibrin, modification by synthetic polymers 0-61090  
 flow-through reactor, low-temp. polymerisation conditions 0-61092  
 hexamethyldisiloxane plasma polymerised thin film, charge trapping characts. 0-96895  
 N-hydroxyethyl acrylamide-styrene(methyl methacrylate) copolymers, synthesis, anion active membrane transport appl. 0-61142  
 IR thin film plasma deposition processes 0-87466  
 lithium polyisoprene, struct. regularity and crystn. 0-103269  
 medical polymers, chem. problems, conf., Prague, Czechoslovakia (Aug. 1977) 0-56996  
 methylmethacrylate soln., aqueous, polymerisation under pulse electronic accelerator irradiation 0-66802  
 octadecylacrylamide films, oriented ultrathin, radiation-induced solid state polymerisation 0-80128  
 plasma polymerisation by glow discharge method, formation mech. (*Japanese*) 0-61094  
 poly(m-xylene adipamide), molten, gel form. kinetics (*Japanese*) 0-108757  
 poly(vinyl alcohol) porous film, polymerisation and porosity 0-107063  
 poly-m-toluenylsilsesquioxane mesomorphic struct., form. during polymerisation (*Russian*) 0-61095  
 trans-polyacetylene obtained by polymerisation on TiO<sub>2</sub>, Raman spectrum (*Spanish*) 0-88988  
 polyacrylamide, high mol. wt., prep. by electron beam irradi. 0-76222

**polymerisation continued**

- 1,2-polybutadiene, dynamic viscoelastic props. in curing process 0-76298  
 polychlorotrifluoroethylene, crystalline and amorphous peaks, dielectric props. 0-93237  
 polydimethylsiloxanes, equilibrated, living oligomer distrib., end-group interactions 0-58423  
 polydiphenylgermylene, crystn. from chem. transport reaction 0-104439  
 polyisobutylene, SiO<sub>2</sub> grafted, synthesis and characterization 0-97456  
 polymer thin films formed in RF discharge using monomer organic semi-cond., elec. props. obs. 0-80432  
 polymethacrylic acid, stereoregular, synthesis, <sup>13</sup>C NMR obs. 0-58422  
 polyphenylene sulphide, high mol. wt. soluble resin, prep., mech. props. 0-60828  
 polypyrrole films, electrochemical prep., chem. and phys. characterisation 0-70708  
 polystyrene-b-isoprene-b-styrene, struct. regularity and crystn. 0-103269  
 PVC granule morphology during polymerisation, kinetic parameters influence (*German*) 0-85176  
 silicone elastomers, dental impression materials, dimens. stability, holographic and interferometric study 0-67204  
 sodium 10-undecanoate, γ-ray induced polymerisation in aq. micelle solns. 0-61093  
 sodium undecanoate/water system, lyotropic liq. cryst. struct. change due to polymerisation of amphiphilic component 0-59386  
 solidification front propagation, residual stress levels, polymerisation 0-59635  
 suspension polymerisation, particle size distrib. of obtained particles, eval. using Coulter Counter data 0-76564  
 synthetic polymer chemistry, developments 0-63875  
 toluene-sulphonate-diacetylene, thermal polymerisation, near IR absorpt. and low lying states obs. 0-71399  
 trioxane, in nitrobenzene soln., polymerisation, polyoxymethylene morphology 0-59403  
 UPS polymerization technique, production of special polymers (*German*) 0-93533  
 K<sub>2</sub>O-Al<sub>2</sub>O<sub>3</sub>-P<sub>2</sub>O<sub>5</sub>-TiO<sub>2</sub>, structural role of Ti, kinetic study of chem. destruction 0-88055  
 Si<sub>3</sub>-H<sub>3</sub>, noncrystalline film, struct., interatomic distances, SRO 0-107053  
 SiO<sub>2</sub> fibres, freeze formed from polysilicic acid aq. soln. 0-71609  
 TiO<sub>2</sub>-SiO<sub>2</sub> glass form. by low temp. chem. polymerisation 0-84899

**polymers**

- see also elastomers; filled polymers; glass fibre reinforced plastics; glass transition; plastics; polymer films; polymer melts; polymer solutions; rubber  
 A-150 plastic-equivalent gas for ionisation chambers, dosimetry appl. 0-81745  
 ABS substrate, Sn autocatalytic deposition 0-100965  
 ABS-rubber modified, two-phase struct. influence on fracture toughness (*German*) 0-66666  
 adaptive control of molecular weight distribution 0-58434  
 adhesion ability enhancement by block copolymer incorporation (*Russian*) 0-61065  
 adhesive bonds with metals, shear resist., polymer crystn. effect 0-89462  
 adsorbed polymer chains, surface restricted self avoiding walks span, mol. weight depend. 0-65360  
 adsorption, of molecules, Green matrix local impurity SCF calcs. 0-92778  
 adsorption in condensed phases, statistical mechanics 0-84365  
 n-alkane, polymer, liq. mol. arrangement, computer model 0-92446  
 amorphous, struct. rel. to mech. props. 0-79173  
 bis(9-anthryloxy)polyoxaalkanes, intramolecular excimer form. and photodimerisation, kinetic anal., rate constants determ. 0-66800  
 application of cross-polarisation <sup>13</sup>C NMR with magic angle spinning, solid material studies 0-77819  
 Araldite, high vacuum sealant at liq. N<sub>2</sub> temp. 0-57319  
 Araldite B specimens, dynamic fracture toughness, influence on dynamic crack propag. 0-99966  
 aromatic polyesters, with S atoms, configurational props. 0-74269  
 atmospheric resistance, distrib. function determ. and anal. (*German*) 0-81225  
 bioelectrets, electrets in biomaterials and biopolymers 0-80686  
 biological macromolecules, conformation studied by calorimetry, review 0-97870  
 biopolymer model compounds, calorimetric instrumentation used for studies 0-61746  
 biopolymers, chromophore aggregates in Frenkel exciton model, dynamic perturbation effects on circular dichroism intensity 0-93273  
 biopolymers, deform. under uniaxial stretching during UV irradi. 0-108935  
 biopolymers, electro-optical changes, chem. and rotational contribs. 0-85352  
 biopolymers, tautomeric forms protonation, ab initio HF Roothaan SCF calcs. 0-78534  
 bismaleimide resin, charact. by differential scanning calorimetry 0-71869  
 bisphenol A-phthalic anhydride epoxy resin, diglycidyl ether, Rayleigh scatt., Brillouin and IR spectra 0-66211  
 blends, selective staining method for TEM obs. of morphology 0-84103  
 block copolymer chain conformations 0-69282  
 block copolymers, microphase separation, thermodynamic treatment (*Chinese*) 0-79947  
 breaking down of anharmonic chain, computer calc. 0-106410  
 bubble rupture between two solid walls, effect of drag-reducing polymers on cavitation 0-106822  
 cable insulation, radiation modification using electron beams 0-66848  
 carrier traps in polymeric insulating materials, investigation by X-ray induced thermally stimulated current and thermoluminescence methods 0-93240  
 cast-epoxy resins, AC breakdown-voltage characts. (*Japanese*) 0-88927  
 cellulose, degradation by high voltage electrons 0-100283  
 cellulose, dielec. relax. studies, TSD meas. 0-88907  
 cellulose, mobility of adsorbed water, NMR pulse obs. 0-108835  
 cellulose acetate membrane, asymmetric, elec. and electroosmotic transport behaviour in dialysis-osmosis expts. 0-108745  
 cellulose acetate membrane, asymmetric, elec. and electroosmotic transport behaviour in hyperfiltration expts. 0-108746  
 cellulose char. O<sub>2</sub> chemisorpt. kinetics 0-96730  
 cellulose diacetate membrane, diffusive permeability 0-104460  
 cellulose diacetate membranes, unilayer, transport phenomena, hydration and dialysis coeffs. 0-76556



## polymers continued

- cellulose fibre, gamma-irrad., and storage effects on props. (Russian) 0-61121
- cellulose fibre formation in stirred dimethyl sulphoxide-paraformaldehyde soln. 0-104440
- cellulose fibres, elec. anisotropy 0-97220
- cellulose fibres, with planar crimp, tensile deformation 0-84235
- ceramic filled with polymer,  $ZrO_2$  stabilised, fracture mechanism (Russian) 0-100895
- chain, linked rigid body, Brownian dynamics 0-74267
- chain, zero component field (French) 0-69280
- chain mols., conformational transition kinetics 0-83339
- chain partition function, equivalence of quantum many-body problem 0-57181
- chain with rigid side branches, intramol. phase transition of 1st kind (Russian) 0-58432
- chitin (poly-N-acetyl-D-glucosamine), dynamic mech. behaviour, effect of water 0-97522
- chitosan (poly-D-glucosamine), dynamic mech. behaviour, effect of water 0-97522
- classification, fabrication techniques and appl., historical development, 1979 status and future trends 0-93532
- colloidal suspension, steady state shear flow coupled to conc. fluctuations 0-61170
- composite, wire-reinforced, dynamically loaded, crack propagation and arrest 0-97567
- composite matrix materials, spacecraft, space radiation effects evaluation 0-70263
- conducting materials, struct. and phys. props., symposium, San Jose, USA (March 1979) 0-62379
- conference, Mainz, Germany (Sept. 1979) 0-58429
- conformation, correlated walk model calc. 0-78733
- conjugated and saturated chain, electronic struct., review 0-59860
- contact electrification, meas. using computer-controlled apparatus 0-86341
- contact potential and charge exchange meas., at Hg-polymer interface 0-75642
- cooled epoxy resin vacuum mould computational simulation of design (German) 0-81020
- copolymer, semicryst. random, characterisation by small angle neutron and X-ray scatt. 0-75189
- copolymer globule model, orientationally-ordered liq. cryst. state (Russian) 0-59389
- crack extension micromechanisms, review 0-108561
- crack tip failure mechanism modelling 0-108565
- creep under plane stress, nonlinear viscoelasticity models appl. 0-89308
- cross-linked, with different degrees of hardening, bulk-creep prediction 0-104223
- crosslinking, rel. to azide photooxidation in polymer matrix 0-66832
- crystal orientation distributions, thermodynamically controlled 0-84112
- crystallisation, review 0-64925
- crystallisation, under mol. orientation, formation of stacked lamellar struts. 0-84109
- cyclopentadiene-butyl vinyl ether copolymer, oxidative degradation (Japanese) 0-108714
- degradation, reaction product volatility effect on thermogravimetric anal. 0-104316
- denture base materials, multi-station machine for fatigue testing 0-108648
- denture base polymers, fatigue test machine 0-66712
- diacetylene, low temp. photochemical polymerisation, decay kinetics, ESR spectra obs. 0-100616
- diacetylene, photopolymerisation, optical absorpt. spectra, time depend., reaction kinetics 0-85174
- dielectric breakdown, DC trees caused by space charge accumulation, carrier injection and trapping effects 0-84695
- dielectric breakdown theories, mol. and morphological features rel. to elec. strength, review (Japanese) 0-60501
- dielectric conduction and breakdown, conf., Gainesville, FL, USA (Oct.-Nov. 1979) 0-82564
- N,N-diethylacrylamide, cross-linked copolymer, improved mech. props. 0-61091
- direct renormalisation group procedure for polymer chain 0-91712
- DNA and other biopolymers, radiolysis 0-67163
- dynamic living polymers, thermodynamic enhancement of oligomers, end-group interactions 0-58423
- electrets, fundamental aspects of research, book 0-77552
- electrets, piezo- and pyroelectric props. 0-80685
- electrification by metals, contact time effect obs. 0-70829
- electrochemical mass transfer, drag-reducing polymers, effects, comparative study 0-76528
- electrolytes, solid polymer,  $H_2O$  electrolysis,  $H_2$  technology 0-67012
- entanglement, topological theory, chain centre friction coeffs. 0-91709
- epoxide resin, low temp. crack prop. 0-85020
- epoxides, dielectric relax. and deform props., cross-link density effect (Russian) 0-60942
- epoxy, elastomer-modified, loading rate depend. fracture prop. 0-76342
- epoxy cement for  $Pb(Zr,Ti)O_3$  fibre arrays, ferroelectric ceramic-plastic composites 0-81015
- epoxy EDT-10, rigid polymer, thermal stress isothermal relaxation 0-71683
- epoxy materials, crack blunting mechanisms 0-66624
- epoxy resin, arc resistance tests in various gas insulators (Japanese) 0-81250
- epoxy resin, interaction with  $SF_6$  plasma, in glow discharge, emission spectrum 0-87960
- epoxy resin, plastic deform. effect on crack prop. 0-97563
- epoxy resin, plastic deform. mechanism 0-97534
- epoxy resin, stresses arising during high-speed droplet impact 0-71764
- epoxy resin adhesives, capillary flow and bond strength 0-71883
- epoxy resin bond layer, prep. methods, ultimate thickness 0-71884
- epoxy resin microcircuitry elements, thermoelastic phenomena (Polish) 0-93724
- epoxy resin RDGE MPDA hardened with dispersed Al, light scatt., holographic correlometer study 0-74321
- epoxy resin subjected to extensional creep, dynamic props. 0-71697
- epoxy resins, charact. by differential scanning calorimetry 0-71869
- epoxy-rubber particulate composite, toughness and fracture mech. 0-71727
- ethyl acrylate ionomers, stress relax. 0-104200

## polymers continued

- ethylene propylene rubber, effect of electrode profile on dielec. breakdown voltage, epoxy resin insulation system 0-60502
- ethylene propylene/polyolefin blends, radiation cross linking 0-66801
- ethylene vinyl alcohol copolymer, prep., props. and appls. (German) 0-89194
- ethylene-CO copolymer, dielec. absorpt. meas., permittivity (French) 0-103916
- ethylene-Co copolymers and  $-SO_2$  copolymers prep. by catalysis and  $^{60}Co$   $\gamma$ -radiation, mech. props. 0-66841
- ethylene-methyl acrylate, random copolymer, review 0-108330
- ethylene-vinyl acetate copolymer, powdered, prep. by emulsion polymerisation (Japanese) 0-104110
- ethylene-vinyl acetate-vinyl chloride graft copolymers, rel. between morphology and toughness (German) 0-66665
- ethylene-vinyl alcohol copolymer, drawn samples, annealing effect around  $T_g$  temps. on shrinkage and mol. orientation 0-79712
- ethylene-vinyl alcohol copolymers, H bonding study by near-IR spectra (Japanese) 0-78734
- fibrin, modification by synthetic polymers 0-61090
- gel, heterogeneous two-phase, permeability 0-76563
- glasses, enthalpy relax., scanning calorimetry technique 0-90851
- glasses, mech. or elec. props, struct. recovery (French) 0-59393
- glassy, craze surface displacements, model 0-93651
- glassy, elec. resist., corresponding states relationship 0-59704
- glassy polymers, HVEM in-situ deform. 0-104215
- glassy polymers double NMR, appl. of cross relaxation dynamics in modulated systems 0-71242
- glassy state,  $^{13}C$  NMR (German) 0-93188
- graphite/epoxy laminate, T300/S208, proof testing under cyclic tension-tension fatigue 0-81249
- graphite/epoxy laminates, statistical fatigue, high load effect 0-93642
- hardening of liquid photopolymer materials, mathematical modelling (Russian) 0-62784
- hexafluoropropylene-tetrafluoroethylene copolymer, surface component of vacuum absorpt. and resorpt. currents, surface charge accumulation 0-60063
- hexafluoropropylene-tetrafluoroethylene copolymer, surface component of vac. absorpt. and resorpt. currents, source of dielec. loss 0-70792
- HF storage and loss moduli, determination using US immersion apparatus 0-74668
- high field conduction and breakdown in solid dielectrics, review 0-84691
- high molecular weight polyethylene for HV cables, characterisation using size exclusion chromatography 0-66897
- high-impact polymers, HVEM in-situ deform. 0-104215
- hydrophilic polymers, ESCA evaluation of surface layer water structuring and protein adsorpt. 0-108758
- N-hydroxyethyl acrylamide-styrene(methyl methacrylate) copolymers, synthesis, anion active membrane transport appl. 0-61142
- hydroxyethyl cellulose, microviscosity, mobility profile 0-91710
- ill-condensed matter, summer school, Les Houches, France (July-Aug. 1978) 0-82561
- infinite conjugated polymers,  $\pi$ -electron energy and energy gap, topological calcs. 0-91713
- insulating materials, water treeing initiation and growth, effects on cable service life 0-84698
- interrelations, raw materia 0-63876
- jute, cement reinforcing fibre, alkali resist. 0-89377
- Kapton, positron source, temp. depend. 0-93426
- Kapton, pyrolysed, cond. polymer, transport and mag. props. 0-96887
- Kevlar aramid fibre, regular fine bands obs. by polarization microscopy 0-107064
- latex solids, agglomerating and dewatering 0-104470
- lightguide, light propag., nonlinearity, quasi-optical approx. 0-99837
- long-term strength prediction, review 0-104226
- longitudinal acoustic mode, perturbing forces 0-70348
- loss-loss, dielectric loss meas., automatic, high resolution, at 100 MHz to 300 MHz and  $2^\circ C$  to  $40^\circ C$  0-68219
- macromolecule, microconformation by fast exchange NMR spectra 0-102593
- macromolecules, molecular structure, conformation and properties 0-63874
- magnet appl. based on moulding with ferromagnetic powder material (Japanese) 0-60829
- matrix effect on photochromism of spiropyran 0-76537
- melting, theoretical aspects 0-59633
- metal polymer contact, charge transfer and contact charge spectroscopy 0-65680
- metal polymer contact, charge transfer and contact charge spectroscopy 0-65681
- metal polyphosphinates, bulk compressibility meas. to 30 kbar 0-76306
- metal-polymer, ply-separation resist. polymer polarity effect (Russian) 0-61064
- metal-polymer sliding, wear eqn. in terms of fatigue and topography of sliding surfaces 0-108597
- methacrylic polymers, multiple dielectric relaxations, investigation by thermally stimulated current and creep methods 0-93238
- 3-methyl-3-buten-2-one copolymers with styrene and methyl methacrylate, photodegradation (Japanese) 0-108725
- methylundecanhydride hardened phenol formaldehyde resin, hardening kinetics and mech. losses 0-66520
- mixing, heats 0-61132
- model polymer, conformation theory, correlated walk model 0-74268
- molecular ultraslow rot. obs. using D probe spin alignment tech. 0-88890
- molecular weight distribution of multi-functional polymers 0-83531
- molecular weight ratio, number-average: weight-average, polydispersity 0-74274
- mylar, positron source, temp. depend. 0-93426
- mylar, substrate for  $^4He$  film growth, vap. press. meas. 0-70499
- mylar/adhesive/Al laminates, mech. interactions 0-81112
- Nafion, densities and expansion coeffs. as function of various parameters 0-79711
- Nafion per fluorosulphonic acid ion exchange membranes, Mossbauer spectroscopy 0-80659
- networks, stochastic cross-linked, modulus of elasticity, functionality effects (German) 0-59555
- NMR, review 0-88888
- novolac and novolac allyl ether electrets, thermal depolarisation, chem. struct. effect 0-71297
- nylon, positronium form. and decay, elec. field effect 0-97369



# polymers continued

- Nylon 6,6, sliding behaviour against Cu or Al spheres at cryogenic temps. 0-66671
- nylon 6, water effects on TSC 0-75925
- nylon 6 (polycapromide), salted, glass transition temp. and elastic modulus, moisture effect 0-103465
- Nylon 6 gut yarn, fine struct. change in twisting, annealing and untwisting, microbeam X-ray obs. 0-81026
- Nylon 6 gut yarn, fine struct. change in twisting, annealing and untwisting, X-ray and electron microscopy obs. 0-84904
- 1-nylon stress-strain curve 0-60938
- optical fibre waveguide, glass core/polymer cladding, high numerical aperture 0-96024
- para-polyamide based fibres, struct. deform. props. 0-60928
- particles, photomicrography of submicrometer birefringent contaminants in C black dispersions 0-62757
- PCA metal adhesive bonds, shear resist., polymer crystn. effect 0-89462
- perspex, electronic conduction and isothermal dielectric relax. 0-80285
- PET, amorphous, intrinsic birefringence calc. from wide angle X-ray scatt. 0-108178
- PET, crystallization, lamellar growth kinetics and thickness 0-103266
- PET, surface component of vacuum absorpt. and resorpt. currents, surface charge accumulation 0-60063
- PET, surface component of vacuum absorpt. and resorpt. currents, origin and magnitude 0-70791
- phthalocyanine polymer, dynamic mech. props. and fracture energy 0-100866
- plasticizer effect on polymer characts. (German) 0-92467
- PMMA, absorbing defect role in laser damage 0-108308
- PMMA, birefringence in elec. field 0-88962
- PMMA, C-H stretching and bending vibrs. in Raman spectra 0-93300
- PMMA, crack size and effective specific work for failure determ. 0-85108
- PMMA, craze zones at crack tips, validity of Dugdale model, comment 0-108535
- PMMA, craze zones at crack tips, validity of Dugdale model 0-108534
- PMMA, crazing, deform. kinetics 0-84990
- PMMA, creep compliance calc. from short-term creep expts. 0-89303
- PMMA, cross-linked positive electron resist, synthesis and props. 0-76221
- PMMA, ductile glassy, notch brittleness under plane strain 0-100900
- PMMA, estimation of activation parameters in sclerometric tests 0-66625
- PMMA, experimental separation of coherent component of X-ray scattering prior to RDF anal. 0-64838
- PMMA, fatigue life enhancement, prior crazing 0-89331
- PMMA, glass-rubber transition, time-temp. superposition, shear creep compliance meas. 0-88309
- PMMA, glassy, optical absorpt., visible region, determ. by laser calorimetry 0-66218
- PMMA, glassy atactic, thermodynamic analysis of plastic deform. modes, 150 to 330K 0-84999
- PMMA, Gruneisen const. and thermal props., temp. depend., 4-300K, Brillouin scatt. obs. 0-100662
- PMMA, hydrostatic extrusion 0-108479
- PMMA, instantaneous crack resist. during stable crack propag. 0-85058
- PMMA, Kerr electro-optical effect, relative phase retardation meas. in elec. stressed samples 0-84716
- PMMA, large deforms. at tip of running crack, opt. interference obs. 0-85062
- PMMA, laser damage threshold, freq. and size depend. 0-104018
- PMMA, neutron and gamma irradiation effects 0-66839
- PMMA, optical damage threshold, alteration methods 0-99814
- PMMA, plastic deform. by crazing (Japanese) 0-93619
- PMMA, radical form. in explosive loading, electron spin reson. obs. 0-63678
- PMMA, reactor irradi., growth of macroscopic radiolytic gas bubbles, diffusion model 0-65058
- PMMA, rigid polymer, thermal stress isothermal relaxation 0-71683
- PMMA, shock loaded, lateral compressive stresses meas. using Yb piezoresist. gauges 0-103007
- PMMA, space radiation effects evaluation 0-70263
- PMMA based plastics, specific fracture energy depend. on crack growth rate, mol. struct. effect 0-66639
- PMMA bone cement, free radical EPR, feasibility study 0-94318
- PMMA moist surface mech. strength reduced by electric charge (Russian) 0-60486
- PMMA organic glass, stress relax. calc. from creep curves 0-71709
- PMMA plates with flawed fastener holes, static fracture testing 0-97651
- Polaroid K, oriented analogue of polyacetylene, reson. Raman spectroscopy 0-66208
- polyethylene-polypropylene blend, extruded, thermal swelling and mech. characterisation 0-81110
- Polimal 109 based H<sub>2</sub>O emulsion, laminate prep. open pore density and content (Polish) 0-59665
- poly(1,3,4-thiadiazole amide), from thermal cyclodehydration of polydiacylthiosemicarbazides (Japanese) 0-108388
- poly(1,3-dioxane), dipole moments, dielectric const. meas 0-66099
- poly(3,3-dimethyl oxetane), conform. energies and random-coil config. meas. 0-99590
- poly(di-n-heptyl itaconate), alkyl side chain independent relax., double glass transition 0-59636
- poly(dihydroxypropyl methacrylate), surface charact., by contact angle methods 0-61140
- poly(hydroxyethyl methacrylate), surface charact., by contact angle methods 0-61140
- poly(methoxyethyl methacrylate), surface charact., by contact angle methods 0-61140
- poly(octadecyl ethylene), temp. depend. of 720 cm<sup>-1</sup> IR band 0-97281
- poly(octadecyl ethylene oxide), temp. depend. of 720 cm<sup>-1</sup> IR band 0-97281
- poly(p-phenylene), AsF<sub>6</sub> doped, highly cond. charge transfer complexes, elec. and optical props. 0-70778
- poly(p-phenylene), electronic struct., one-electron band theory 0-65450
- poly(spiro[2,4]hepta-4,6-diene) molecular characterisation, glassy state props. 0-64928
- poly(vinyl cinnamate), excited state, low-energy EELS and INDO/S calcs. 0-106407
- poly(vinylidene fluoride) phase II, field induced phase transitions 0-96640

# polymers continued

- poly methylene oxide bulk sample, spherulite primary nucleation, determ. from spherulite shapes 0-70359
- poly-4,4-diphenylphthalateinterphthalamide, mol. mass distrib., sedimentation and fractionation method meas. (Russian) 0-71957
- poly-arylate-dimethyl siloxane, polyblock copolymers, struct., thermodynamic stability (Russian) 0-64931
- poly-m-toluenylsilsequioxane mesomorphic struct., form. during polymerisation (Russian) 0-61095
- poly-N-vinyl carbazole, hole hopping mobility, transit pulse dispersion 0-65565
- poly-N-vinyl carbazole, pulsed laser excitation, time resolved fluoresc., 0-89041
- poly-N-vinyl carbazole, trap-free lifetime, neutral traps, hopping systems 0-65566
- poly-N-vinylcarbazole-biacetyl, triplet exciton quenching, exciton trapping model 0-66267
- poly-N-vinylpyrrolidone-containing nonionisable membranes, equilib. props. struct. (French) 0-61138
- polyacetonitrile in MIM capacitor, electroforming, negative resist., electron emission 0-80406
- polyacetylene:AsF<sub>6</sub>, AES, XPS, UPS, and X-ray induced 0-66400
- polyacetylene:AsF<sub>6</sub>, thermopower and transport props. 0-65611
- polyacetylene:AsF<sub>6</sub>(I), pure and doped, electronic excitations, momentum depend., EELS study 0-76121
- polyacetylene:Br(Pd), ion implantation effect on elec. props. 0-65026
- polyacetylene:I, dc microwave cond., permittivity 0-107843
- polyacetylene:I, electronic structure, XPS and UPS meas. 0-66385
- polyacetylene:I, NMR struct. investigation 0-108082
- polyacetylene:I, pure and doped, reson. Raman spectroscopy 0-66208
- polyacetylene, AsF<sub>6</sub> doped, X-ray absorpt. meas., 5K to room temp. 0-71516
- trans-polyacetylene, bulk crystallinity, small-angle X-ray diffr. study 0-103263
- polyacetylene, continuum model for solitons 0-65472
- polyacetylene, doped, elec. cond. and thermopower 0-96951
- polyacetylene, doped, fluctuation-induced tunnelling cond. in metallic regime 0-65516
- polyacetylene, electronic struct., one-electron band theory 0-65450
- polyacetylene, intrinsic conformational defect states 0-65500
- polyacetylene, lightly doped, phenomenological theory of soliton formation 0-103644
- polyacetylene, mag. soliton defect ESR study 0-80590
- polyacetylene, pristine and doped, press. effects on resist. 0-103698
- polyacetylene, soliton formation and cis trans isomerization 0-76505
- polyacetylene, variable density, synthesis, elec. cond., thermopower 0-60016
- polyacetylene, vibr. excitations of charged solitons 0-108201
- polyacetylene conductivity mechanism, Peierls phase one dimensional cond. (Russian) 0-88546
- trans-polyacetylene obtained by polymerisation on TiO<sub>2</sub>, Raman spectrum (Spanish) 0-88988
- polyalkane imides, crystallisability, supermol. and crystalline structures 0-84100
- polyamide, aromatic, fibre, high modulus, mol. and supramol. struct. 0-79710
- polyamide, viscoelastic, linearity conservation 0-108492
- polyamide fibres, differently matted, meas. of diffuse reflectance spectra, using SPEKOL spectrophotometer 0-77836
- polyamides, extended chain aromatic, fibres, tensile strength and moduli 0-81021
- polyamides containing 1,3-cyclohexane rings, cryst. struct. 0-103262
- polyaryloxyphosphazene copolymers, thermal, morphological and rheological props. 0-103265
- polybutadiene, dihydroxy-terminated, with unattached styrene-butadiene copolymer, stress relax. 0-104202
- 1,2-polybutadiene, dynamic viscoelastic props. in curing process 0-76298
- polybutadiene, hexafluoro acetone substituted, H-NMR and <sup>19</sup>F-NMR spectroscopy (German) 0-103893
- 1,2-polybutadiene crosslinked in strain states; entanglement networks, stress-birefr. relations 0-66590
- polybutadiene-poly- $\alpha$ -methylstyrene copolymers, struct. obs., prep. (French) 0-59401
- polybutadienes, radiation chemically cross-linked, charact. by pyrolysis gas chromatography (German) 0-81348
- polybutylene terephthalate, melt crystallised, solvent crystallised films and moulded bars, morphological obs. 0-84101
- polycapromide, addition to high-activity carburiser 0-76412
- polycapromide, metal adhesive bonds, shear resist., polymer crystn. effect 0-89462
- polycapromide, oriented filaments, mech. props. 0-66550
- polycarbonate,  $\gamma$ -irradiated, dielec. behaviour and glass transition 0-97182
- polycarbonate, amorphous, yield behaviour in oriented and unoriented condition, effect of temp. 0-97537
- polycarbonate, bisphenol A, birefringent plates, cracks, stress intensity factors, refl. caustics method 0-93718
- polycarbonate, bisphenol A, WAXS pattern, temp. effect and thermal history 0-93583
- polycarbonate, bisphenol-A, mol. wt. determ. using gel permeation chromatography 0-58424
- polycarbonate, ductile, large strain cyclic deform. 0-85000
- polycarbonate, ductile glassy, notch brittleness under plane strain 0-100900
- polycarbonate, glassy, fatigue crack initiation in high strain fatigue tests 0-97564
- polycarbonate, glassy state, enthalpy relax., thermal density fluctuations 0-95678
- polycarbonate, neck propag., rel. to dry craze growth mechanism 0-95563
- polycarbonate, yield behaviour (Japanese) 0-93620
- polycarbonate fast neutron dosimeter, development and comparison with conventional emission dosimeter 0-86990
- polycarbonate plates, modified compact-tension specimens, dynamic anal. 0-97561
- polycarbonate styrene-acrylonitrile copolymer mixture, determ. of phase structure, electron microscopy 0-103272
- polycarbonate-polyethylmethacrylate blends, kneading characts. (Japanese) 0-104112
- polychlorotrifluoroethylene, crystalline and amorphous peaks, dielectric props. 0-93237



## polymers continued

- polydiacetylene, crystalline and amorphous,  $\gamma$ -ray effects, gel form. and crosslinking 0-93777
- polydiacetylene, intrinsic conformational defect states 0-65500
- polydiacetylene-toluenesulphonate, photocond. meas., 0.62-3.1 eV 0-70757
- polydiacetylenes, visual conformational transitions, absorpt. and fluoresec. spectra, pH and electrolyte effect 0-102590
- polydiacylthiosemicarbazides, synthesis and thermal cyclodehydration (*Japanese*) 0-108388
- polydiethylsiloxane, mol. motion, NMR spin relax. data re-interpret. 0-84664
- polydifluoroacetylene, electronic struct., tight-binding LCAO-SCF-MO calcs., prep. 0-70591
- polydimethylsiloxane, crosslinked, stress/strain relations from large compression to high elongation 0-66589
- polydimethylsiloxane end-linked chains, nonGaussian effects 0-65127
- polydimethylsiloxanes, equilibrated, living oligomer distrib., end-group interactions 0-58423
- polydimethylsiloxanes, rubbery and liq., hypersonic sound vel., Brillouin spectra meas. 0-75308
- polydioxolan, crystn. kinetics, dilatometric analysis and microscopy obs. 0-79706
- polydiphenylgermylene, crystn. from chem. transport reaction 0-104439
- polydiphenylsiloxane, thermodynamics of fusion 0-84280
- polydisperse, mol. wt. distrib. correl. with props. (*Russian*) 0-69286
- polydisperse homopolymers, glass transition temp., mol. mass depend. 0-92656
- polyenes, long chain, electronic struct. in Peierls-PPP model 0-84423
- polyester, temp. index, rapid determ. by dynamic thermogravimetry 0-85101
- polyester copolymer, modified with polypropylene glycol, addition to pro-oxylated bisphenol A, effect on mech. props. (*Polish*) 0-60902
- polyester moulding materials (*Polish*) 0-66523
- polyester resin, arc resistance tests in various gas insulators (*Japanese*) 0-81250
- polyester resin, cross-linked unsaturated, synthesis and fracture toughness 0-93634
- polyester resin concrete, effects of styrene-unsaturated polyester ratio on props. (*Japanese*) 0-89299
- polyester resins unsaturated, enhanced elasticity, chem. resist. tests (*Polish*) 0-60901
- polyester-hydrazide, aromatic, fibres and films, synthesis and props. (*Japanese*) 0-108387
- polyether-alkali metal salt adducts, cond. investigation rel. to use as solid electrolytes 0-59708
- polyethylene-Br<sub>2</sub>(I.), films, electron-beam induced carrier mobility and elec. breakdown 0-80429
- polyethylene, <sup>60</sup>Co gamma rays effects obs., on loss tangent variation (*German*) 0-75266
- polyethylene,  $\gamma$ -irrad., asymmetric 002 X-ray line profiles, analysis 0-96567
- polyethylene, chlorinated, semicryst. random, characterisation by small angle neutron and X-ray scatt. 0-75189
- polyethylene, conduction band struct., LEED, secondary electron emission and UPS study 0-70601
- polyethylene, creep during shear deform. with applied hydrostatic press. 0-76324
- polyethylene, dielectric props., investigation for morphology changes created by mechanical drawing and annealing 0-84697
- polyethylene, elec. cond. of high and low density samples, oxidation effects 0-107784
- polyethylene, electron beam crosslinking process for high voltage power cable 0-66846
- polyethylene, electronic energy states and charge density contours studied muffin tin orbitals technique 0-80164
- polyethylene, environmental stress cracking correl. with liq. sorption for low-swelling liqs. 0-81165
- polyethylene, equation of state for semicrystalline, crystalline polymers 0-65187
- polyethylene, extruded semicryst., thermal cond. and specific heat, <1K 0-59742
- polyethylene, for dry insulation in power cables (*Spanish*) 0-81024
- polyethylene, halogen-doped, carrier transport and breakdown characteristics (*Japanese*) 0-96889
- polyethylene, high density, ductile, large strain cyclic deform. 0-85000
- polyethylene, high density, solid state coextrusion, geometric factors effect 0-71704
- polyethylene, high density, solid state coextrusion, technique for ultradrawing thermoplastics 0-84979
- polyethylene, high mol. wt., porous, hot drawing 0-60894
- polyethylene, high press. phase, US, DTA, and X-ray diff. study 0-75188
- polyethylene, high-density, impact fracture behaviour, adiabatic heating at crack tip 0-85142
- polyethylene, high-density, solid-state coextrusion, mol. wt. distrib. effect 0-104212
- polyethylene, high-density unoriented, damage buildup kinetics under creep conditions, during prolonged loading 0-60932
- polyethylene, interaction with SF<sub>6</sub> plasma, in glow discharge, emission spectrum 0-87960
- polyethylene, intrinsic photocond. under vacuum UV irrad. 0-70759
- polyethylene, irradiation, crystallinity and crosslinking efficiency 0-66843
- polyethylene, Kerr electro-optical effect, relative phase retardation meas. in elec. stressed samples 0-84716
- polyethylene, linear, draw temp. and mol. wt. effect on draw ratio and Young's modulus 0-84998
- polyethylene, linear, melt-crystallised sharp fraction, lamellar morphology, electron microscopy obs. 0-84099
- polyethylene, low density, melting and crystallisation, DSC characterisation 0-64927
- polyethylene, low density, morphology and props. 0-64926
- polyethylene, low-density, environmental stress cracking, surfactant soln. effect 0-89376
- polyethylene, low-density natural, permittivity and loss factor meas. at elevated temps. 0-97185
- polyethylene, melt-crystallised fractions, surface and full-strand melting, small-angle X-ray scatt. obs. 0-84279
- polyethylene, microwave photon echo 0-66330
- polyethylene, mol. ultraslow rot. obs. using D probe spin alignment tech. 0-88890

## polymers continued

- polyethylene, nonoriented partially cryst., kinetic damage accumulation cure 0-71753
- polyethylene, phase characterisation, Raman spectra study (*French*) 0-93303
- polyethylene, phase orientation by stretching, Raman study (*French*) 0-93304
- polyethylene, photodegradation mechanism, from yield strength, elongation and mol. wt. studies (*Japanese*) 0-76311
- polyethylene, positronium form. and decay, elec. field effect 0-97369
- polyethylene, resist. to stress corrosion cracking, ionising radiation effect (*German*) 0-81224
- polyethylene, rheological behaviour at high shear strain rates (*French*) 0-66574
- polyethylene, single crystal, electron microscopy study 0-103273
- polyethylene, single crystal, fold domain boundaries, TEM 0-107065
- polyethylene, solid liq., secondary electron emission spectroscopy 0-80916
- polyethylene, space radiation effects evaluation 0-70263
- polyethylene, space-charge storage under high DC voltage condition, TSC meas. (*German*) 0-75576
- polyethylene, stretched, birefringence rel. to struct. changes 0-84714
- polyethylene, surface component of vacuum absorpt. and resorpt. currents, surface charge accumulation 0-60063
- polyethylene, surface component of vacuum absorpt. and resorpt. currents, origin and magnitude 0-70791
- polyethylene, ultra high mol. wt.; sliding behaviour against Cu or Al spheres at cryogenic temps. 0-66671
- polyethylene, vinyl group reactions during  $\gamma$ -irrad., crystallinity effect, absorbance obs. 0-81346
- polyethylene and resin-coated photographic papers 0-86474
- polyethylene cable grade crosslinked, effect of electrode profile on dielec. breakdown voltage, epoxy resin insulation system 0-60502
- polyethylene fibre, high-strength high-modulus, morphology and tensile prop. relations 0-103264
- polyethylene fibre prod. by surface growth method, mech. props. 0-104108
- polyethylene films electrical conductivity under various conditions (*French*) 0-70869
- polyethylene lattice, inclusion of chain defects, stat. approach 0-75190
- polyethylene oxide, nascent and annealed, X-ray study of crystal structure 0-64922
- polyethylene oxide-polystyrene-polyethylene oxide triblock copolymer, surface and full-strand melting, small-angle X-ray scatt. obs. 0-84279
- polyethylene phthalate-metal adhesive bonds, shear resist., polymer crystn. effect 0-89462
- polyethylene surface-growth fibres, hot drawing 0-97517
- polyethylene terephthalate, low temp. sp. ht., effect of cooling rate 0-100336
- polyethylene terephthalate, mean mol. orientation factors, from IR spectra and acoustic method 0-70142
- polyethylene terephthalate, oriented, amorphous, stress-induced crystn., shrinkage meas. 0-92466
- polyethylene terephthalate, shear compliances meas. of oriented sheet 0-104363
- polyethylene terephthalate, solid and molten, press. effects on compressibility and crystn., thermodynamic interpret. 0-84102
- polyethylene terephthalate, TSC and thermolum. due to electron detrapping by local mol. motions 0-96898
- polyethylene terephthalate polymer insulator, conduction and breakdown mechanism (*German*) 0-100469
- polyethylene terephthalate-metal adhesive bonds, shear resist., polymer crystn. effect 0-89462
- polyethylene terephthalate substrate, thickness determ. of Al coating using photometry 0-62626
- polyethylene-polypropylene blend, size distribution determ. of spherical occlusions from photomicrographs (*Czech*) 0-89539
- polyethylene-polystyrene blends, crystn. characts. 0-103261
- polyethylene/ethylene vinyl acetate copolymer mixture, rel. between hypermol. struct. and stability (*German*) 0-64929
- polyethylene/polypropylene blends, surface growth of fibres and films 0-66470
- polyethylenepolyamine hardened epoxy resin, hardening kinetics and mech. losses 0-66520
- polyethylenes, ultra-high modulus, manufacture by drawing through conical die 0-66583
- polyfluoroacetylene, electronic struct., tight-binding LCAO-SCF-MO calcs., prep. 0-70591
- polyfurfuryl alcohol charcoal, adsorpt. isotherms of organic vapours 0-96731
- polyheteroarylenes, linear, conform. and struct., statistical calcs. (*Russian*) 0-69284
- polyhexamethylene adipamide, photocond. 0-103718
- polyimide resin, charact. by differential scanning calorimetry 0-71869
- polyimides, temp. index, rapid determ. by dynamic thermogravimetry 0-85101
- polyisobutylene, SiO<sub>2</sub> grafted, synthesis and characterization 0-97456
- polyisoprene, small angle neutron scatt., single chain form factors 0-107038
- trans-1,4-polyisoprene crystals, press. effect on melting temp. and lamellar thickness, press. crystn. 0-88302
- polymer between planes, crossover between dimensionalities, Monte-Carlo study 0-74272
- polymer chain dynamic critical index calcs. by renormalisation method 0-87256
- polymeric macromolecule containing mesogroups, phase diagrams (*Russian*) 0-58433
- polymetaphenylene isophthalamide, mean mol. orientation factors, from IR spectra and acoustic method 0-70142
- polymethacrylic acid, stereoregular, synthesis, <sup>13</sup>C NMR obs. 0-58422
- polymethyl methacrylate, subthreshold luminesc. 0-93414
- polymethylene, short chains, rot. isomeric representation 0-87254
- polymethylene crystals, lattice vibrations 0-59607
- polymethylene-polystyrene-(polymethylmethacrylate) blends, kneading characts. (*Japanese*) 0-104112
- polymethylmethacrylate, numerical description of treeing for dielectric breakdown 0-100633
- polymethylmethacrylate-polycarbonate blends, kneading characts. (*Japanese*) 0-104112
- polymethylmethacrylate-polystyrene-polyethylene blends, kneading characts. (*Japanese*) 0-104112



# polymers continued

polyolefin, cross-linked, insulation system for wire and cable for locomotives 0-66851  
polyolefin, cross-linked, irradiation appl. to provide improved insulation props. to wires and cables 0-66850  
polyolefins, ultra-high modulus, production by tensile drawing and hydrostatic extrusion 0-81022  
polyoxadiazoles, cyclochain, conform. parameters calc. 0-78732  
polyoxymethylene, nascent, morphology, optical and electron microscopic obs. 0-59403  
polyoxymethylene, transitions and relaxation spectrograph 0-65204  
polyoxymethylenes, dielectric property relaxation, unidentical relaxator system activation model (*Russian*) 0-80694  
polyoxymethylenes, dielectric relaxation, molecular mechanism (*Russian*) 0-88923  
polyparabenzamide, mean mol. orientation factors, from IR spectra and acoustic method 0-70142  
polyparaphenylene: SbF<sub>6</sub>, pure and doped, metallic, absence of Pauli paramagnetism, mag. susceptibility meas. and ESR obs. 0-97060  
polyparaphenylene terephthalamide, mean mol. orientation factors, from IR spectra and acoustic method 0-70142  
polyphenylacetylene cis-trans isomers, rel. mol. wt. distrib., heating effect 0-106409  
polyphenylene oxide thin films, electrochem. prep., impurity effects on cond., electroforming 0-88655  
polyphenylene sulphide, high mol. wt. soluble resin, prep., mech. props. 0-60828  
polypropylene, crystalline, yield behaviour in oriented and unoriented condition, effect of temp. 0-97537  
polypropylene, ductile, large strain cyclic deform. 0-85000  
polypropylene, isomeric, microconformation from slow exchange <sup>13</sup>C-NMR spectra of low mol. wt. compds. 0-102592  
polypropylene, isotactic, equation of state for semicrystalline, crystalline polymers 0-65187  
polypropylene, isotactic, low temp. annealing, differential scanning calorimetry obs. 0-60895  
polypropylene, isothermal crystn., effect of contact with fibrous substrates 0-79708  
polypropylene, microstruct. changes during large strain cyclic deform. 0-66627  
polypropylene, oriented, microcracks diagnostics by paramag. probe method 0-66736  
polypropylene, ultrahigh modulus, tensile drawing, mol. wt. effect 0-104211  
polypropylene fibrillated film reinforced cement matrix for low cost sheeting 0-80996  
polypropylene films, dielec. props., impurity effects 0-71304  
polypropylene sheet, deep drawing (*German*) 0-104114  
polypropylene substrate, Sn autocatalytic deposition 0-100965  
polypropylenes, iso- and syndio-tactic, Raman tacticity bands, vibr. spectrum 0-66193  
polypyromellitimide, mean mol. orientation factors, from IR spectra and acoustic method 0-70142  
polypyrrrole, electronic struct., one-electron band theory 0-65450  
polyquinazolones containing pendant imide groups, prep. and props. (*Japanese*) 0-104111  
polysiloxene, irradiat., linear, IR and solubility obs. 0-93775  
polystyrene: Br<sub>2</sub>(I<sub>2</sub>), films, electron-beam induced carrier mobility and elec. breakdown 0-80429  
polystyrene, atactic, indentation recovery 0-84988  
polystyrene, atactic, structure elucidation, model construction and X-ray methods (*German*) 0-103267  
polystyrene, bimodal mol. wt. blends, recoverable compliance 0-66568  
polystyrene, conform. and near all-trans extended-chain model relevant in gels, X-ray diff. patterns interpret. 0-79707  
polystyrene, cyclically deformed under shear, energy dissipation, static tensile-compressive stress effect 0-104225  
polystyrene, epimerised isotactic, methylene C mag. resonance spectra 0-63878  
polystyrene, glass-rubber transition, time-temp. superposition, shear creep compliance meas. 0-88309  
polystyrene, glassy, crazing and brittle fracture on flat die indentation 0-60970  
polystyrene, glassy, optical absorpt., visible region, determ. by laser calorimetry 0-66218  
polystyrene, halogen-doped, carrier transport and breakdown characteristics (*Japanese*) 0-96889  
polystyrene, high impact, etching in CrO<sub>3</sub>-H<sub>2</sub>SO<sub>4</sub> soln. (*Russian*) 0-81223  
polystyrene, mean mol. orientation factors, from IR spectra and acoustic method 0-70142  
polystyrene, photon penetration, photon backscatt. incidence angle depend. 0-104008  
polystyrene, plasma polymerised, free radicals, O<sub>2</sub> effects, EPR study 0-71179  
polystyrene, plasma polymerised, free radicals, transient elec. current, EPR, heat treatment 0-71178  
polystyrene, polymer chain, internal friction range, HF viscosity theory (*French*) 0-79968  
polystyrene, polymerisation by glow discharge method, formation mech. (*Japanese*) 0-61094  
polystyrene, positronium form. and decay, elec. field effect 0-97369  
polystyrene, rubber modified, two-phase struct. influence on fracture toughness (*German*) 0-66666  
polystyrene, shear bands, morphology and annealing behaviour 0-100873  
polystyrene, solubility of benzene vapour (*Japanese*) 0-59667  
polystyrene, sulphonated, polyelectrolyte solution, correlations and dynamics 0-104446  
polystyrene, surface component of vacuum absorpt. and resorpt. currents, surface charge accumulation 0-60063  
polystyrene, surface component of vacuum absorpt. and resorpt. currents, origin and magnitude 0-70791  
polystyrene, total reflection Raman spectroscopy study 0-80784  
polystyrene, viscoelastic, linearity conservation 0-108492  
polystyrene atactic carrier transport and photogeneration 0-80318  
polystyrene interfacial colloidal crysts., microscopic obs. 0-97737  
polystyrene latexes, monodisperse, model colloid systems 0-89545  
polystyrene melts, flame-retardant high-impact, shear viscosity-temp.-shear rate relationships 0-59691  
polystyrene monodisperse latex, anomalous viscosity in disordered state 0-74822

# polymers continued

polystyrene particles, monodisperse, dil. and conc. aqueous dispersions, elec. cond., surface cond. and double-layer polarisation 0-89533  
polystyrene-diethylmalonate, strongly opalescent critical isochore, scattered light intensity 0-71436  
polystyrene-polyethylene blends, crystn. characts. 0-103261  
polystyrene-polyethylene block copolymer, deformation ratios, Poisson ratio and adhesion, dilatometric obs. 0-60937  
polystyrene-polyethylene-(polymethylmethacrylate) blends, kneading characts. (*Japanese*) 0-104112  
polystyrenes, anionic, TSC obs. of T<sub>g</sub> and T<sub>h</sub> transitions 0-84686  
polysulfonamide, optically active, synthesised by interfacial polycondensation, mol. wt. determ. 0-99595  
polystyrene, neutron and gamma-irradiation effects 0-66839  
polytetrahydrofuran in MIM capacitor, electroforming, negative resist., electron emission 0-80406  
polythene, Z dependence of thick target  $\beta$ -ray backscattering 0-76118  
polythioethers, bis(methylthio)alkane model compds. vibr. spectra 0-58430  
polyurethane, foaming parameters determ. from US wave vel. 0-71885  
polyurethane, segmented, domain struct., deform. effect 0-93623  
polyurethane cement, viscosity and shear strength, components influence (*German*) 0-93729  
polyurethane foams, elastic, stability against organic solvents (*German*) 0-85074  
polyurethane solid foams, creep laws (*German*) 0-65139  
polyvinyl acetal, temp. index, rapid determ. by dynamic thermogravimetry 0-85101  
polyvinyl alcohol, mean mol. orientation factors, from IR spectra and acoustic method 0-70142  
polyvinyl alcohol swollen in aqueous glycol, network thermoelasticity, interactions 0-104201  
polyvinylidene chloride, crystalline, preferred chain conform., mol. models 0-79709  
polyvinylidene chloride, normal vibr. analysis using conform. model 0-83529  
polyvinylidene chloride charcoal, adsorpt. isotherms of organic vapours 0-96731  
polyvinylidene fluoride, bimorph vanes, use in large area electronically controllable light shutter array 0-58696  
polyvinylidene fluoride, cryst., struct. phase transition theory, free energy, uniaxial stress 0-64924  
polyvinylidene fluoride, cryst. form II, anisotropy of dielec. relax. 0-103915  
polyvinylidene fluoride, dielec. breakdown and elec. cond., room temp. to 150°C 0-60500  
polyvinylidene fluoride, hysteresis phenomena under high elec. field 0-66134  
polyvinylidene fluoride, melt-solidified, crystn. and morphology 0-103461  
polyvinylidene fluoride, piezoelec., nonlinear dynamic response 0-75946  
polyvinylidene fluoride, piezoelec. const. calc. 0-103918  
polyvinylidene fluoride, piezoelec. props., polarisation and appls. 0-75947  
polyvinylidene fluoride, poled, dielec. relax. spectra 0-80690  
polyvinylidene fluoride, poling process, kink propag. model 0-80679  
polyvinylidene fluoride, pyroelectricity, low temp. behaviour, due to origin 0-88932  
polyvinylimidazole: Cu(II) complex, ESR studies on dimer form. between copper ions 0-100613  
polyvinylquinazoline-I<sub>2</sub> complexes, absorpt. spectra and elect. cond. 0-92891  
POM, creep compliance calc. from short-term creep expts. 0-89303  
powder compact with metal, cond. threshold, particle size ratio effect 0-80337  
prepolymers, H-NMR and <sup>19</sup>F-NMR spectroscopy (*German*) 0-103893  
propylene-butene copolymers, PB centred tetrad <sup>13</sup>C NMR spectra assignment 0-58428  
PTFE,  $\gamma$ -ray effects on 19 and 30°C phase transitions, Fourier transform IR spectroscopy 0-103387  
PTFE, creep and recovery under hydrostatic compression in programmed loading 0-100881  
PTFE, electronic energy states and charge density contours studied muffin tin orbitals technique 0-80164  
PTFE, interaction with SF<sub>6</sub> plasma, in glow discharge, emission spectrum 0-87960  
PTFE, matrix for ultrafine Fe<sub>2</sub>O<sub>3</sub> particles, EPR and Mossbauer study 0-100625  
PTFE, nonlinear creep, compression bulk modulus 0-66593  
PTFE, stress-time analogy under shear and hydrostatic pressure in creep regime 0-104227  
PTFE, surface component of vacuum absorpt. and resorpt. currents, surface charge accumulation 0-60063  
PTFE, surface component of vacuum absorpt. and resorpt. currents, origin and magnitude 0-70791  
PTFE, trapped peroxy chain radicals, reactivity and struct., EPR spectra 0-66783  
PTFE, wear, sliding speed, contact press. and rubbing surface temp. 0-76372  
pulsed NMR technique for meas. radiation effects in polymer 0-66051  
PVC, crazing, deform. kinetics 0-84990  
PVC, cross-linked, irradiation appl. to provide improved insulation props. to wires and cables 0-66850  
PVC, Cu evaporated film, electron-induced metallochromic reaction for metal image formation 0-86476  
PVC, ductile glassy, notch brittleness under plane strain 0-100900  
PVC, fatigue life, influence of cyclic loading conditions 0-76350  
PVC, for dry insulation in power cables (*Spanish*) 0-81024  
PVC, glass-rubber transition, time-temp. superposition, shear creep compliance meas. 0-88309  
PVC, glassy, fatigue crack initiation in high strain fatigue tests 0-97564  
PVC, mean mol. orientation factors, from IR spectra and acoustic method 0-70142  
PVC, oriented mouldings, struct. order 0-60896  
PVC, rigid, internal struct. of diamond shaped cavities 0-66628  
PVC, rigid plate, notching method effect on Charpy impact values, fractographic considerations (*Japanese*) 0-108541  
PVC, rigid resin, TEM studies of morphology, processing effects 0-108385  
PVC, surface component of vacuum absorpt. and resorpt. currents, surface charge accumulation 0-60063  
PVC, surface component of vacuum absorpt. and resorpt. currents, origin and magnitude 0-70791



## polymers continued

- PVC, thermal stabilisation by triazine dithiols (*Japanese*) 0-108386  
 PVC, thermooxidative degradation, crosslinking and chain scission 0-71912  
 PVC, yield behaviour (*Japanese*) 0-93620  
 PVC charcoal, adsorpt. isotherms of organic vapours 0-96731  
 PVC surfaces, natural and stabilised, composition, ageing, oxidation and weathering, ESCA obs. (*French*) 0-61139  
 PVC thermal degradation, reinitiation mechanism of HCl catalysis 0-71944  
 PVC-Cu composites with chemically deposited ultrafine copper particles 0-93534  
 PVC-vinylchloride system, glass transition, vinylchloride influence (*German*) 0-79917  
 PVK/PVK-TNF/TNF.PMG system, electrophotographic characts. 0-62759  
 pyrolysis, high-temp., heat transfer processes at gas/solid surface (*Russian*) 0-61152  
 quantitative analysis by pyrolysis gas chromatography 0-61180  
 radiation curing of selected structural adhesives, lap shear strength props. 0-66842  
 Raman active longitudinal-acoustical mode spectra interpretation 0-103950  
 resins, preregs and composites, charact. by differential scanning calorimetry 0-71869  
 rigid, modified Oseen tensor, superposition approximation appl. 0-92447  
 scanning-transmission electron microscopy for polymer research 0-76460  
 self-avoiding walks with span limitations, cubic lattice, mean square end-to-end distance 0-62568  
 short polymer chains, end-to-end vector, distrib. function 0-87254  
 silane coupling agent deposited on E-glass fibre, hydrolysis and drying effect on siloxane bonds 0-85072  
 siloxane, temp. transitions, linear dilatometry and X-ray diff. obs. (*Russian*) 0-59404  
 solid insulating materials, dielectric properties at cryogenic temps. 0-90867  
 solid polymer electrolyte  $H_2O$  electrolysis, appl. to  $H_2$  prod. 0-61442  
 solidification, as dissipative process 0-65205  
 solidification front propagation, residual stress levels, polymerisation 0-59635  
 solute orientation in stretched polymer matrix, dichroism anal. 0-75998  
 solutes in stretched polymers, linear dichroism methods for analysis 0-63693  
 spacecraft materials, electron and proton irradi. effects 0-70262  
 specific fracture surface energy, meas., review (*French*) 0-104275  
 spectral sensitivity and photochem. stability using Xe high press. lamp (*German*) 0-61119  
 spherulite, cryst. lattice strains, mech. behaviour, X-ray diff. detect. 0-59558  
 spherulites, deformation mechanism, linear isothermal viscoelasticity theory 0-58924  
 spray-on dopants, junction formation technique, cost effective, high throughput 0-94014  
 steel, sheets bonded with low density polyethylene, static fatigue (*French*) 0-108522  
 stochastic model, Edwards' model 0-68140  
 structure and optical behaviour 0-106583  
 structure determination from elastooptometric parameters 0-64923  
 styrene-acrylonitrile copolymer, crazing and brittle fracture on flat die indentation 0-60970  
 styrene-divinylbenzene copolymers, porosity variation and swelling 0-97493  
 styrene-sodium methacrylate copolymers, Raman spectra, ion clustering 0-71416  
 substrates, amorphous Se vac. deposited, with dynamic coating device 0-100792  
 surface, supramol. struct. characterisation, use of C X-radiation 0-79705  
 surface component of vacuum absorpt. and resorpt. currents, origin and magnitude 0-70791  
 surface component of vacuum absorpt. and resorpt. currents, surface charge accumulation 0-60063  
 surface free energy determination (*Polish*) 0-84362  
 synthetic polymer chemistry, developments 0-63875  
 Teflon, gamma irradiated, free four-term analysis of positron lifetime spectra 0-76101  
 teflon, sliding behaviour against Cu or Al spheres at cryogenic temps. 0-66671  
 Teflon FEP, N implanted, TSC spectra 0-88912  
 telechelic, chain extension, qualitative aspects 0-95752  
 testing, photoresistor dilatometer design, with high stability and sensitivity 0-81251  
 tetrafluoroethylene hexafluoropropylene copolymer, surface component of vacuum absorpt. and resorpt. currents, origin and magnitude 0-70791  
 thermotropic polymers, cholesteric with mesogenic moieties and flexible spacers in main chain, synthesis and light reflection 0-88028  
 thin film, micrometeroid penetration expts. performed in laboratory 0-77292  
 thin-wall tubes, rupture time determ. 0-64473  
 toluene-sulphonate-diacetylene, thermal polymerisation, near IR absorpt. and low lying states obs. 0-71399  
 topological entanglements, gauge description 0-99593  
 trans-polyacetylene, intrinsic, electron-phonon coupling 0-79901  
 transparent, absorbing defect role in laser damage 0-108308  
 transparent polymers with various atomic composition and viscoelastic props., laser damage 0-104017  
 1,3,5-trioxane-1, 3-dioxolane copolymer, semicryst. random, characterisation by small angle neutron and X-ray scatt. 0-75189  
 TSC, generation mechanism and characts. (*Japanese*) 0-60488  
 urea-formaldehyde charcoal, adsorpt. isotherms of organic vapours 0-96731  
 urea-formaldehyde resins, book 0-73114  
 vinyl copolymers, containing fluorescent groups, optically active 0-102594  
 vinyl polymers, precip. from solns., temp. determ. (*German*) 0-85208  
 N-vinylcarbazole containing polymers, sensitization to Ar laser for single laser photothermoplastic devices 0-83651  
 viscoelastic droplet break-up, in nonuniform shear flow 0-64588  
 water absorption, osmotic effects 0-65366  
 X-ray scattering, expt. separation of coherent component prior to RDF anal. 0-64838  
 C polymeric chains, reduced from poly(tetrafluoroethylene), reactivity 0-89488

## polymers continued

- PMMA, polymer chain, internal friction range, HF viscosity theory (*French*) 0-79968  
 PVF<sub>2</sub> polymer probe for mapping pressure field from arrays 0-74669  
 PVF<sub>2</sub>, thin film SAW transducers for 8 MHz delay line 0-58876  
 Ti corrosion, by hot perfluoropolyether type Krytox MLO-71-6 0-93684
- polymorphic transformations**  
*see also displacive transformations; order-disorder transformations*  
 alkali hydrides, structural transition from NaCl to CsCl type under high press. 0-96458  
 brass,  $\alpha$ - $\beta$  phase transformation caused by friction 0-76378  
 carbon tetrachloride, dual melting curves and metastability 0-92647  
 ice VI, shock compression expts. for Hugoniot function 0-84248  
 ice VII-ice VIII phase transition, second-order, Haus-Tanaka model 0-70385  
 kinetics model, computer modelling (*Russian*) 0-97478  
 mechanical hysteresis in polymorphic transition region 0-79942  
 metal-insulator transition, chemical mechanism, thermodynamics, vacancies 0-103626  
 polyvinylidene fluoride, cryst., struct. phase transition theory, free energy, uniaxial stress 0-64924  
 quartz, coexistence states during first order transition, optical obs. 0-75350  
 quartz, electro-optical props. near phase transition 0-80756  
 quartz, Fourier transform IR spectroscopy of vibr. states at high temp. 0-97256  
 quartz, thermal expansion near  $\alpha$ - $\beta$  transition under uniaxial stresses 0-70429  
 quasi binary eutectic systems, with inclusive phases, hardness, transform., decomposition (*Russian*) 0-97572  
 rare-earth intermetallics,  $R_2Co_2$ , polymorphism of Ce subgroup alloys, eutectic decomposition (*Russian*) 0-66504  
 steel, alloy, high-speed, struct. changes investigation by hot hardness and quench dilatometry (*French*) 0-76249  
 steel, Cr with metastable austenite, wear resist., temp. effect 0-76370  
 steel, Cr-Ni-(Mo), cast, intercritical heat treatment (*Czech*) 0-89268  
 steel, ferrite-austenite transition, diffusion const. of C and carburisation rate const., thermopower meas. 0-89216  
 steel, low impurity, peritectic transformations, influence on initial struct., solidification, grain boundaries (*Russian*) 0-66621  
 steel, maraging, ageing kinetics and struct. of N12K7M5TYu, effect of high temp. deform. of austenite (*Russian*) 0-84960  
 steel, Mn-Sn-(Nb), extra low C, shear transformation struct. (*German*) 0-60873  
 2,2,6,6-tetramethyl-piperidino-oxy, cryst. growth and polymorphism 0-96645  
 thiourea, polycryst., mol. dynamics under hydrostatic press., NMR study 0-80619  
 tris(hydroxymethyl)aminomethane, crystalline and plastic structs. phase transforms. studied by X-ray diff. 0-84130  
 Van der Waals film adsorbed on graphite, two-dimensional phase transitions 0-107653  
 XX Ce,  $\gamma$ - $\alpha$  phase transition, study by Compton scattering 0-59650  
 AgZn,  $\beta'$ - $\beta$  transformation, effect of additional elements 0-66507  
 $Al_2O_3$ , derived from boehmite, phase transformations and microstruct. 0-60857  
 $Al_2O_3$ , sintering as function of phase comp. 0-66464  
 Au, vacancy size effect, surface energy in small particles and bulk specimens 0-75223  
 BN, conversion of wurtzite into cubic form, stress state effect 0-64943  
 BN cutter contact plates, struct. and phase changes on working steel (*Russian*) 0-108433  
 $BaSi_2$ , trimorphic, transform. of three-connected Si nets, press.-temp. phase diagram, 40 kbar and 1000°C 0-75198  
 $BaTiO_3$ , periodic domain struct. and opalescence at tetragonal to orthorhombic transition 0-66131  
 $BaTiO_3$ , powders, Bragg reflection integral intensities due to structural anomalies 0-107098  
 $Bi_2O_3$ , polymorphic transformation and elec. resistivity (*Japanese*) 0-93555  
 C, hard, heat-treated under pressure, characterisation of carbon phase by electron microscope 0-60855  
 $C_2S$ , influence of polymorphic transform. on sinter stability (*Russian*) 0-66503  
 $CaCr_2O_4$ ,  $\beta$ -to- $\alpha$  transform. temp., effect of partial  $O_2$  press. 0-84292  
 $Ca_2Mg(Co)(Zn)(Mn)(Cd)(Ca)TeO_6$ , optical SHG study of acentricity ferroelec. of low temp. phases 0-71324  
 $\gamma$ - $Ca_2SiO_4$ , polymorphic transformation scheme 0-71642  
 $Ca_2SiO_4$ , structurally related phases, high-temp. X-ray powder diff. 0-81050  
 $Cd_2Mg(Co)(Zn)(Mn)(Cd)(Ca)TeO_6$ , optical SHG study of acentricity, ferroelec. of low temp. phases 0-71324  
 $Cd(NO_3)_2$ , phase transition, SHG, optical and dielec. meas. 0-71334  
 Ce, surface and volume props., flow props., surface layer thickness (*Russian*) 0-59760  
 Ce,  $\gamma$ -La, dil.,  $\gamma$ - $\alpha$  transition temp. and press., elec. resist. meas. up to 10 kbar 0-59643  
 Co-Ti-C, secondary precipitation and allotropic transform., TEM obs. 0-108453  
 Cr-Ge system, phase diagram, thermal anal., X-ray diff., microhardness, and electron probe anal. (*French*) 0-97462  
 $CsCrCl_3$ ,  $\alpha$ - $\beta$  phase transition, dynamical aspects and thermodynamic theory 0-70404  
 $CsCrCl_3$ , Jahn-Teller induced phase transitions 0-70391  
 $CsLiSO_4$ , crystal structures of I and III phases, twins 0-70181  
 $CsR(MoO_4)$   $R= Dy, Ho, Er$ , permittivity temp. depend., polymorphic transition 0-92670  
 Cu-Zn-Al, reversible shape memory effect (*Japanese*) 0-108500  
 Cu, Ag, I crystals, layer structs., X-ray diff. studies 0-96457  
 $CuFe_2O_4$ , Jahn-Teller type crystal distortions 0-103904  
 $Cu_2S$ ,  $Cu_3S$ ,  $\alpha$ - $\beta$  transition, thermographic investigation of heats, entropies and activation energies 0-88314  
 $Cu_2S$ , digenite, X-ray determ. of structural transitions 0-92474  
 $Cu_2Se$ , kinetics of polymorphic  $\alpha$ - $\beta$  transformation (*Russian*) 0-70152  
 Fe, polycryst., influence of  $\alpha$ - $\gamma$  transform. on creep (*Russian*) 0-89289  
 Fe-C-Mn-V, austenite microstruct. memory (*German*) 0-84977  
 $\alpha$ -Fe-Ni (3-12 wt.%), structure and  $\gamma$ - $\alpha$  polymorphic transform. kinetics 0-71645  
 Fe-Ni (32 wt.%), EMF appearance during  $\gamma$ - $\alpha$  transform. (*Russian*) 0-89215



# polymorphic transformations continued

- Fe-Ni alloy, reverse martensitic transform., shape deform. reversibility 0-66506
- Fe-Ni-C alloy with single-component martensite texture,  $\alpha \rightarrow \gamma$  transform., changes in shape (*Russian*) 0-104152
- Fe-Ni-Co-Ti, coherent particles effect inherited by martensite on  $\alpha \rightarrow \gamma$  transformation (*Russian*) 0-108443
- GaNbO<sub>4</sub>, polymorphic transition under high press. 0-100835
- Hf, polymorphic transition, emission images obs. in temp. range 1800-2100°K 0-100836
- In, vacancy size effect, surface energy in small particles and bulk specimens 0-75223
- In-Sb, cryst. struct. after appl. of high press., supercond. transition temp. 0-70169
- In-Sn alloy crystals, phase changes and shape memory effect (*Japanese*) 0-108502
- In-Tl, single crystal containing Li, X-ray study of FCC $\rightleftharpoons$ FCT transform. (*Japanese*) 0-108435
- In<sub>2</sub>Se<sub>3</sub>, transitions of high temp.  $\alpha$  form (*French*) 0-92473
- La, surface and volume props., flow props., surface layer thickness (*Russian*) 0-59760
- La<sub>2</sub>S<sub>3</sub>,  $\alpha \rightarrow \beta$  transition, temp. and thermodynamic characts., role in thermal dissoc. 0-104457
- NH<sub>4</sub>Br, supercooled, polymorphic transform., struct. correspondences and mechanisms 0-107097
- NH<sub>4</sub>Br-Tl, and pure crystals, luminesc., VUV irradiated at 80K (*Russian*) 0-84763
- NH<sub>4</sub>ClO<sub>4</sub>, polymorphous phase transition mechanism 0-79737
- NH<sub>4</sub>LiSO<sub>4</sub>, point group symm. at high press. phase 0-70150
- Na<sub>2</sub>CO<sub>3</sub>, phys. props. related to phase transitions 0-96643
- Na<sub>2</sub>Cr<sub>2</sub>(PO<sub>4</sub>)<sub>3</sub>, crystallographic data, ionic conductivity (*French*) 0-88077
- Na<sub>2</sub>Fe<sub>2</sub>(PO<sub>4</sub>)<sub>3</sub>, crystallographic data, ionic conductivity (*French*) 0-88077
- Nd, surface and volume props., flow props., surface layer thickness (*Russian*) 0-59760
- NiS inclusions in glass, microcracking, fracture mech. description 0-89333
- NiS, thermodynamic study of  $\alpha \rightarrow \beta$  transition (*French*) 0-60854
- PbI<sub>2</sub>, first-order 2H-4H polytype transition, exciton spectroscopic study 0-59647
- PbO, reactively evaporated, photocond., H<sub>2</sub>O induced phase transform. 0-60122
- PbSnF<sub>4</sub>, allotropic transformations 0-84926
- Pd alloy-H system,  $\alpha \rightarrow \beta$  phase transformations, hysteresis of press., elec. resistance, review 0-60859
- Pd-H system,  $\alpha \rightarrow \beta$  phase transformations, hysteresis of press., elec. resistance, review 0-60859
- Pr, surface and volume props., flow props., surface layer thickness (*Russian*) 0-59760
- RbCrCl<sub>3</sub>,  $\alpha \rightarrow \beta$  phase transition, dynamical aspects and thermodynamic theory 0-70404
- RbCrCl<sub>3</sub> crystals,  $\beta \rightarrow \gamma$  structural phase transition, lattice dynamical anal. 0-84291
- RbCrCl<sub>3</sub>, Jahn-Teller induced phase transitions 0-70391
- RbNbWO<sub>6</sub>, pyrochlore struct., tetragonal to cubic phase transition 0-75355
- SiC, HVEM obs. of various polytypes 0-76248
- SiC, polycryst., high resolution TEM study of  $\beta \rightarrow \alpha$  transform. 0-84928
- SnF<sub>2</sub>, second order  $\beta \rightarrow \gamma$  transition, neutron diffr. and NMR obs. 0-107095
- Sr<sub>2</sub>Mg(Co)(Zn)(Mn)(Cd)(Ca)(Sr)TeO<sub>6</sub>, optical SHG study of acentricity, ferroelec. of low temp. phases 0-71324
- SrMnO<sub>3-x</sub>, O-deficiency induced polymorphs and elec. cond. 0-71643
- Ti alloys, reversibility of martensitic transformations (*Russian*) 0-108442
- Ti-Fe (1.4 wt.%), polymorphic transform. due to plastic deform., positron annihilation 0-79939
- Ti-Mo, structure associated with BCC to omega transform. (*Russian*) 0-108432
- Ti-V (10 at.%),  $\alpha \rightarrow \omega$  transformation, electron diffr. evidence of intermediate BCC phase 0-81051
- Ti<sub>2</sub>Al<sub>3</sub>, thermal diffusivity, near FCC to BCC transition 0-59740
- TiO<sub>2</sub>, rutile, Raman study at high press. 0-89002
- Tl, phase diagram and high press. phase transforms., DTA study (*Russian*) 0-66474
- U-Nb (14 at.%), martensitic and polymorphic transformations 0-60861
- U<sub>3</sub>O<sub>8-x</sub>, phase transition to U<sub>3</sub>O<sub>21+x</sub>, study by elec. cond. meas. 0-100489
- WO<sub>3</sub>, electronically induced lattice distortion, screening effect on vibrs. 0-75356
- $\alpha$ -Zn<sub>3</sub>P<sub>2</sub>, rel. to lattice parameters and thermal expansion, 80-320K, X-ray obs. 0-75373
- ZnS crystals, structural change under plastic deform., partial dislocation movement 0-79736
- Zr-Nb, structure associated with BCC to omega transform. (*Russian*) 0-108432
- Zr-Ru, alloy Zr rich, Ru solubility, eutectic, decay,  $\alpha \rightarrow \beta$  transform., struct. (*Russian*) 0-65227
- ZrO<sub>2</sub>, enthalpy and heat capacity at 1100-2500K 0-103472

# polymorphism

- see also crystal structure; isomorphism; polymorphic transformations
- 4-4-n-alkyloxybenzoyloxy-benzylidene-4'-cyanoanilines, reentrant nematic and smectic phases 0-88308
- N-4-n-alkyloxybenzylidene-4-n-alkylanilines, smectic polymorphism, calorimetric study 0-88307
- 2-4-n-alkylphenyl-5-(4-n-alkyloxyphenyl)-pyrimidines, smectic polymorphism, calorimetric study 0-88307
- chloritoid intergrown polytype identification by electron multiple scatt. 0-70184
- convergent beam electron microscopy for materials science 0-107028
- ethanol, polymorphic forms, mol. motion, NMR obs. 0-88885
- ethyl-p-azobenzoate, far IR and Raman spectra, smectic polymorphism 0-76022
- Nylon-12 film, casting conditions effect on polymorphism 0-84903
- organic molecular crystals, use of atom-atom pots. in interpreting behavior, book contrib. 0-84136
- polytype relative stabilities, entropy contribs. 0-100197
- polytypes, computer simulation 0-79734
- polytypes, one-dimens. Kronig-Penney model and calcs. 0-75494
- rare earth oxyorthotitanates, crystallochem. classification 0-107142
- rare-earth intermetallics, R<sub>2</sub>Co<sub>2</sub>, polymorphism of Ce subgroup alloys, eutectic decomposition (*Russian*) 0-66504

# polymorphism continued

- terephthalylidene-bis-(4-n-alkylanilines), smectic polymorphism, calorimetric study 0-88307
- transition metal chalcogenide layer compounds, convergent beam electron microscopy obs. 0-108689
- 1,1,1-trichloroethane, polymorphism under high pressure (*French*) 0-96644
- water, random network model, liq. and ice polymorphs enthalpy and heat content 0-64869
- BaCrO<sub>3</sub>, 27 layer polytype, struct. determ. 0-107162
- BaTiO<sub>3</sub> polymorph, hexagonal, low temp. and surface CO<sub>2</sub> adsorption and desorption 0-80713
- Be<sub>3</sub>N<sub>2</sub>-BeSiN<sub>3</sub> system, crystallography and phase relationships, TEM and electron diffr. study 0-92502
- Ca<sub>2</sub>Si<sub>2</sub>O<sub>7</sub>(OH)<sub>2</sub>, xonotlite, polytype identification from electron diffr. patterns 0-72519
- CdI<sub>2</sub> polytypes, vapour growth mechanism 0-84124
- CdI<sub>2</sub> polytypic crystals, dielectric loss behaviour 0-66108
- CdIn<sub>2</sub>Se<sub>4</sub>, high resolution electron microscopic study of polytypism 0-88119
- CdS films, chem. deposited, growth kinetics and polymorphism 0-75463
- CdS, polytype relative stabilities, entropy contribs. 0-100197
- Co-Al alloy, multilayer martensite phases, illustration of polytype structures 0-84932
- Co<sub>2</sub>(AsO<sub>4</sub>)<sub>2</sub>, polymorph, cryst. struct., closest packing 0-70174
- CuF<sub>2</sub>, high temp. polymorphism and thermal props. 0-75199
- CuFe<sub>2</sub>S<sub>3</sub>, cubanite polymorph, synthesis above 200°C and 1 GPa, lattice constants 0-108367
- Cu<sub>2</sub>-S, digenite, X-ray determ. of structural transitions 0-92474
- $\alpha$ -FeGa<sub>2</sub>S<sub>4</sub>, 1T polytype, cryst. struct. refinement (*French*) 0-103304
- FeS polymorph formation, Fe corrosion in aq. H<sub>2</sub>S 0-81231
- Ge-Se system, phase diagram and cryst. struct. of phases (*French*) 0-93544
- HBO<sub>3</sub>, cubic, monoclinic and orthorhombic forms, H bonding, IR and Raman spectra 0-76029
- HfO<sub>2</sub>, high pressure polymorphism 0-59429
- $\chi_{1-x}$  mixtures, high-temp. solids and melts, struct., thermodynamic props., Raman spectra obs. 0-66174
- MgF<sub>2</sub>, high temp. polymorphism and thermal props. 0-75199
- MnF<sub>2</sub>, high temp. polymorphism and thermal props. 0-75199
- NiF<sub>2</sub>, high temp. polymorphism and thermal props. 0-75199
- PbSnF<sub>4</sub>, anionic conductor, thin films and ceramics 0-107556
- S, irradi., allotropic modifications and activity distrib. 0-70255
- SiC, HVEM obs. of various polytypes 0-76248
- SiC, polytype relative stabilities, entropy contribs. 0-100197
- SiC polytypes, free exciton luminesc. meas., phonon energies 0-80852
- SiC polytypes, lattice imaging studies on intergrowth structs. 0-107025
- Sr Nb<sub>2</sub>O<sub>6</sub>, crystallography, polymorphism and isomerism, X-ray diffr. and DTA study 0-100216
- Ta-Ga, crystal struct. at high press. 0-88112
- TiBr<sub>3</sub>, polymorphism, XPS obs. 0-97398
- TiCl<sub>3</sub>, polymorphism, XPS obs. 0-97398
- WO<sub>3</sub> polymorph, hexagonal, cryst. struct. imaging by high-resolution electron microscopy 0-103309
- YSeF, orthorhombic polytype 140, struct. study (*French*) 0-88102
- ZnF<sub>2</sub>, high temp. polymorphism and thermal props. 0-75199
- ZnS, polytype relative stabilities, entropy contribs. 0-100197
- ZnS:TM<sup>2+</sup>, charge compensation and polytypism influences on fluorescence 0-89051
- ZrO<sub>2</sub>, high pressure polymorphism 0-59429

# polynomials

- see also splines (mathematics)
- failure analysis of damage zone in laminates 0-85059
- geomagnetic secular variation in Europe, analytical representation on basis of observatory data 0-101323
- Hermite polynomials and one-dimensional restoration in radio astronomy 0-82217
- Lie groups, nilpotent, smooth functions Fourier transforms 0-99067
- one dimensional function, resolution into sum of exponentials, roots of polynomial 0-77603
- spectra differentiation, filtering props. of polynomial methods 0-66900
- visual information processing, multi-input system representation, polynomial algorithm properties 0-101445
- Zernike moment invariants, image analysis via general theory of moments 0-102629
- Zernike polynomial generalisation, optimum balanced wavefront aberrations for annular apertures 0-95805
- Zernike polynomials for optical wavefront interpretation 0-78776
- zeros, sum rules 0-57521
- zeros, sum rules 0-62888

# polytypism see polymorphism

# Pomeranchuk poles and trajectories

- cylindrical mixing phenomena in dual topological unitarisation, pomerons, reggeons and gluonic states 0-86696
- dual topological expansion, Reggeon and Pomeron slopes 0-102032
- Glauber approach and the triple-pomeron coupling 0-68435
- glueball pomeron singularity cancellation 0-73687
- high energy low P<sub>t</sub> hadronic reactions, Pomeron contrib., parton fragmentation framework 0-73688
- P+f diffraction model, two component duality and flavouring, Regge fits and pomerons 0-95261
- P+f model, flavour and baryon number renormalisation 0-78050
- particle multiple prod. cross section in model with pomeron intercept  $\alpha_p > 1$  (*Russian*) 0-82959
- pion exchange at high energies, review 0-95259
- Pomeranchuk-Okun hypothesis, Pomeranchuk theorem and modifications (*German*) 0-91067
- two component pomeron, ratio of real to imaginary parts 0-91068
- K<sup>+</sup>p-K<sup>+</sup>X, triple Pomeron coupling, Reggeon treatment 0-68488
- p scattering, dipole pomeron model, 70 to 400 GeV/c 0-105927
- pp-cX, pX exotic, triple-Regge formalism, Pomeron exchanges 0-63041

# Poole-Frenkel effect

- amorphous chalcogenides, Poole-Frenkel effect, charged dangling bonds model 0-59994
- glass, high-field ionic and polaronic cond., dielec. relax., Poole-Frenkel theory 0-100351
- polyacetylene films, undoped, nonlinear current-voltage charcts. 0-75574
- polystyrene films, soln. grown, elec. cond. meas. 0-97020
- p-terphenyl film, polycryst., charge carrier transport and DC cond. 0-70858



**Poole-Frenkel effect continued**

- Al-Al<sub>2</sub>O<sub>3</sub>-Dy thin junctions, Poole-Frenkel effect obs. and cause 0-80398  
 n-GaAs surface barrier diodes for nuclear radiation detection, deep trapping centres 0-92849  
 Mo-chalcogenide glass-Mo-Al struct., strong elec. field effects 0-97004  
 Ru<sub>3</sub>Ti<sub>1-x</sub>O<sub>3</sub> films, percolation elec. cond. in strong electric fields (*Russian*) 0-84471  
 TiO<sub>2</sub> film, ion plated, DC cond. study 0-100457  
 Tm<sub>2</sub>O<sub>3</sub> film, between Al electrodes, prep. and elec. props. 0-60103  
 ZnTe, elec. field and impurity conc. effects on ionisation energy of impurities, appl. to acceptors 0-88514  
 ZnTe films, simple and modified Poole-Frenkel cond. 0-97017

**popcorn noise** *see random noise*

**population inversion**

- see also laser theory; lasers; stimulated emission*  
 active particles, Lorenz-Mie scatt. theory paradox 0-74324  
 atomic collision processes and X-ray and UV lasers 0-64787  
 atomic collisional gas-discharge laser feasibility 0-91779  
 chemically reacting flow heterogeneous mixing, energy level population inversion 0-78848  
 collective atomic system population inversion driven by classical field 0-63964  
 collective processes in slightly inverted and absorbing media 0-87367  
 confined plasma column, soft X-ray lasing action conditions 0-74346  
 diatomic molecules, N<sub>2</sub> and CO nuclear pumped lasers, electron impact cross section meas. 0-63985  
 dye laser spectral props., hole-burning effects 0-102718  
 fluoromethane, <sup>13</sup>C, pulsed far IR emission 0-69370  
 Fresnel formulas and law of stimulated emission 0-58489  
 gas laser three-level gain medium, semiclassical theory, population pulsations and interf. effects 0-95863  
 homonuclear selective population inversion in AB system 0-75865  
 inert gas nuclear pumped lasers, electron impact cross section meas. 0-63985  
 ion kinetics in high-pressure laser plasmas 0-64002  
 methanol far IR laser emission spectroscopy 0-58524  
 molecular laser, optical excitation by photodissoc. wave propag. in dense gas 0-74352  
 moving striations, conditions for self-excitation 0-69358  
 photodissociation, switched, for inversion of atomic and molecular species 0-74206  
 plasma expansion into ambient gas, electron cooling 0-96363  
 radiofrequency pulse sequences which compensate their own imperfections, appln. to population inversion 0-77827  
 semiconductor, complex energy band under optical excitation, high-frequency negative cond. and population inversion 0-107858  
 semiconductors, population inverted, resonant Brillouin scatt., photoelastic consts. 0-89015  
 semiconductors with Zn blende struct., resonant Brillouin scattering 0-76042  
 soft X-ray population inversion in laser plasmas, reson. photoexcitation, photon-assisted processes 0-87378  
 superfluorescence, two-level atoms system, quantum theory, incl. propag. effects 0-58491  
 three-level laser, rate equations 0-69356  
 trifluoriodomethane nuclear pumped lasers, electron impact cross section meas. 0-63985  
 two level atom, coherent and Raman scatt. spectra, secondary emissions 0-69449  
 two level system, homogeneously broadened, saturable absorpt., coherence effects 0-95958  
 two-level system, crossing of optical resonances by chirped pulses 0-87084  
 CO, solid, CO laser excited, strong vibr. population inversion 0-58547  
 CO<sub>2</sub> gasdynamic laser, population inversion, press. effect 0-102692  
 CO<sub>2</sub> gasdynamic laser with partial inversion at 16  $\mu$ m, gain calcs. 0-78833  
 CO<sub>2</sub>, inverted, wavefront reversal, high efficiency 0-74436  
 CO<sub>2</sub> laser cavity and Ge phase-conjugate 10  $\mu$ m reflection expts. 0-78894  
 CO<sub>2</sub>-Br<sub>2</sub>-He mixture, possible gas lasers with solar excitation 0-99695  
 CO\* prod. from Ar\*+CO<sub>2</sub>, use in laser systems 0-63824  
 Cd+N<sub>2</sub>, vap., creation of inverse population of atomic Cd 6<sup>3</sup>S and 5<sup>3</sup>P<sub>2</sub> levels 0-58219  
 GAs, population inverted semicond., resonant Brillouin scatt., photoelastic consts. 0-89016  
 H, inverted, optical gain at Lyman- $\alpha$  spectral line 0-95880  
 H plasma, freely expanding, population inversion obs. 0-95877  
 H plasma, recombining, weakly ionised, population inversion 0-87849  
 He+Ne, 2<sup>1</sup>S<sub>0</sub>-level excitation, rate const., temp. depend. 0-87218  
<sup>3</sup>He-Ar(Xe)(Kr)(Cl), nucl. lasing, population inversion mechanism 0-63980  
 N<sub>2</sub> pulsed laser, construction and theoretical explanation (*Slovak*) 0-95874  
 N<sub>2</sub>-He plasma, laser produced, high press. amplified stimulated emission 0-78843  
 Nd:YAG giant pulse lasers, energy characts., superradiance effects 0-64031  
 TI, inverted atomic populations, obs. of stimulated level shifting 0-58218  
 UF<sub>6</sub> nuclear pumped lasers, electron impact cross section meas. 0-63985

**porosity**

*see also porous materials*

- anodic film, behaviour of emulsion particles during electrodeposition 0-104357  
 benzene adsorbent mesopores, capillary evaporation and struct. 0-107614  
 borosilicate glass, powder, sintering, foaming by chemical reactions 0-81017  
 ceramic, creep, porosity depend. 0-97530  
 ceramics, crack extension micromechanisms, review 0-108567  
 coatings, porosity determination by hydrostatic weighing 0-66714  
 coke, metallurgical, strength and struct. relationship 0-84997  
 cokes, metallurgical, struct. and strength 0-93610  
 continuous ingots, two phase zone critical parameters during casting (*Russian*) 0-93549  
 crystal growth, cylindrical pores growth, numerical calcs. 0-92471  
 diamond, synthetic powder, thermal cond. 0-96702  
 dielectric coatings, optical characts., effect of electric field during film condensation 0-69539  
 electrodes, effect of porosity 0-66815

**porosity continued**

- electrographic porosity test, reclassification as nondestructive method (*German*) 0-97652  
 FBR fuel pin failure, fuel porosity and crack effects on transient over-pressure analysis 0-71760  
 graphite, polygranular, flexural strength after heat treatment porosity correl. 0-84996  
 graphite, thermal conductivity, effect of porosity 0-65314  
 haematite, degree of reduction, potential relaxation due to cracks (*Russian*) 0-66770  
 haematite reduction to magnetite, stress development mechanism (*Russian*) 0-93553  
 magnesite artifacts, roasted, props., filler porosity effect 0-104099  
 magnesite refractories, unfired, by resin phosphate binding 0-104101  
 measurement of plate porosity, by measuring pneumatic conductivity (*Polish*) 0-92097  
 metallic fibre knitted gauze permeable materials, mech. props. 0-66607  
 nuclear fuel, gas release and swelling, operational model, grain boundary gas 0-95346  
 plasticity as function of porosity (*Russian*) 0-75290  
 Polimal 109, polymer resin laminate, density porosity, water vapour diffusion sorption and permeation (*Polish*) 0-59665  
 poly(vinyl alcohol) porous film, polymerisation and porosity 0-107063  
 pore size measurement, comparison of methods 0-62622  
 porosimeter, continuous scan mercury type, pore pot. contrib. to hysteresis 0-77928  
 porous glass:In, effect of press. on transition temp. 0-97027  
 powder metallurgy, fatigue strength significance (*German*) 0-60946  
 pressure sintering, inhomogeneous flow and effective press. 0-93512  
 steel, powder forged, fatigue, surface treatment effect 0-85048  
 steel, stainless, porous sheet, pore dimensions, filtration and permeability (*Russian*) 0-76480  
 styrene-divinylbenzene copolymers, porosity variation and swelling 0-97493  
 Al, constitutive equation for porous materials with strength, press. effects 0-79875  
 Al foils, high strength, vapour deposited on curved surfaces, quantitative characterisation 0-80144  
 Al-Li-Mg-Be alloys, phase composition of surface films, oxidation protection mechanism (*Russian*) 0-65417  
 Al-Mg(Cu)(Si), (5.0(4.5)(11.8) wt.%), ingots, vibr. effect during solidification on porosity formation 0-108426  
 Al<sub>2</sub>O<sub>3</sub> bioceramic synthesis, for orthopedic purposes, props. (*Polish*) 0-66465  
 Al<sub>2</sub>O<sub>3</sub>, transparent hot-pressed, transparent and translucent properties 0-60533  
 C, polygranular, flexural strength after heat treatment porosity correl. 0-84996  
 CaHPO<sub>4</sub>, powder and granules with starch mucilage binder, surface topography variation under compression 0-80998  
 Fe, sintered, influence of metallographic treatment on pore analysis 0-76417  
 $\beta$ -FeOOH, lattice imaging and pore struct., high resolution electron microscopy obs. 0-103310  
 Ge-Si alloys, hot-pressed, fine-grained, boundary scatt. of phonons, lattice thermal cond. 0-107583  
 HfO<sub>2</sub>, stabilised comps., elastic props. rel. to porosity and temp. 0-81096  
 KCl, cryst. isolated pore healing under press., dislocation struct. evolution (*Russian*) 0-100245  
 Li<sub>2</sub>O, porosity, dependence on thermal diffusivity and thermal conductivity, 200-900°C 0-92726  
 Mo crystals, joined by compression during heating, structural changes (*Russian*) 0-108513  
 N<sub>2</sub> adsorbent mesopores, capillary evaporation and struct. 0-107614  
 NH<sub>4</sub>Cl, submicron particles, density, morphology 0-61166  
 Nb<sub>3</sub>Sn, powder metallurgically produced, microstruct. characts. 0-89233  
 Ni alloy ZrSi<sub>2</sub>U, US method of porosity detection 0-71828  
 Ni-Cd sealed battery electrode performance meas. 0-66962  
 NiO, prepared by thermal decomp. of Ni(OH)<sub>2</sub>, microporosity and irreversible water vapour adsorption 0-80060  
 Ni<sub>2</sub>Zn ferrite, ZrO<sub>2</sub> additions influence on sintering and physicochem. props. 0-108369  
 PbS films, polycryst. and epitaxial, small-angle X-ray scatt. and electron density inhomogeneities 0-96758  
 Pb(Zr,Ti)O<sub>3</sub>, porosity-permittivity relations, depolarising factors determ. and pore effects (*Japanese*) 0-97189  
 SiO<sub>2</sub> films, vac. thermal evaporation, parameter stabilisation 0-87571  
 (Ti,Cr)B<sub>2</sub>, sintering kinetics and props. 0-100811  
 TiO<sub>2</sub>, porosity-permittivity relations, depolarising factors determ. and pore effects (*Japanese*) 0-97189  
 UO<sub>2</sub>-PuO<sub>2</sub>, fuel pellets, porosity meas. methods (*German*) 0-73915  
 WC-Ni hard alloy composite, sintered, void healing 0-60821  
 ZrO<sub>2</sub>, partially stabilized, processing defects 0-97558  
 ZrO<sub>2</sub>-CaO(Y<sub>2</sub>O<sub>3</sub>) ceramics with grainy structure, props., effect of heating to 2000°C 0-104194

**porous materials**

*see also flow through porous media*

- anisotropic magnets, approach to mag. saturation 0-93146  
 coke, chamber and formed (*German*) 0-100356  
 coke, metallurgical, microstruct., using refl. light microscopy and image anal. 0-66732  
 density variation during plastic shaping 0-84873  
 diffusion of gases in porous solids, Monte Carlo simulation 0-65299  
 generalised  $\alpha$ -model, eqn. of state, sound vel. 0-65154  
 hydromagnetic squeeze film between porous circular disks with velocity slip 0-74997  
 interstellar porous grains, free-space equil. temps. calc., rel. to optical props. 0-62223  
 interstellar porous graphite grains, rel. to 2200 Å extinction hump 0-62228  
 laser reflectors, cooling, prospects for use of porous materials 0-91809  
 leaching from model porous bodies by reflection spectroscopy 0-100031  
 metallurgical coke, mech. behaviour charact. (*French*) 0-104371  
 metals, plasticity, stress-strain curves, yield stresses, strain vectors 0-83738  
 mixture theory, formulation of incompressible porous media models 0-96184  
 nuclear fuels, fission gas precipitation into intra- and intergranular porosity, theory 0-57849  
 outgassing, area/vol. config. influence 0-84371



# porous materials continued

oxide, porous transparent films as antirefl. coatings for glass surfaces, low refr. index 0-74448  
plasticity, deformation theory (*Russian*) 0-75291  
plasticity as function of porosity (*Russian*) 0-75290  
poly(vinyl alcohol) porous film, polymerisation and porosity 0-107063  
polymer charcoal, adsorpt. isotherms of organic vapours 0-96731  
polymer filled ceramic, ZrO<sub>2</sub> stabilised, fracture mechanism (*Russian*) 0-100895  
polymer films. micropore localisation, electron microscopy 0-103271  
sintering, behaviour of pore filled with const. amount of gas 0-66450  
sintering, gases influence, behaviour of assembly of pores filled with gas 0-84877  
steel, chemicothermal treatment, diffusional basis 0-104343  
steel, sintered, fracture of residual pores 0-76352  
steel, stainless, porous sheet, mech. strength, bend and reverse bend tests (*Russian*) 0-93595  
steel, stainless, porous sheet, pore dimensions, filtration and permeability (*Russian*) 0-76480  
surface preparation, effect of different methods on porosity 0-60995  
US bulk compressional wave obs. 0-64235  
water-saturated struct. of sintered glass beads, elastic wave speeds, Biot's theory confirmation 0-103418  
X-zeolites, dielectric relax. anal. 0-108153  
Al anodising, porous films formed in chromic acid 0-100966  
Al, constitutive equation for porous materials with strength, press. effects 0-79875  
Al-SiC cermet elasticity, porosity meas. by US means 0-81101  
Al<sub>2</sub>O<sub>3</sub> porous transparent films as antirefl. coatings for glass surfaces, low refr. index 0-74448  
Al<sub>2</sub>O<sub>3</sub>:Fe, pore form. during oxidative annealing, grain growth slowing 0-100856  
D-D fusion reactor, neutronics aspects of a porous blanket 0-83217  
Fe powder based sintered porous permeable materials, diffusion chromising 0-100958  
Fe-Cu-C sintered porous materials, machinability 0-66457  
Fe-Ni, sintered, porosity determ. by US attenuation and sound vel. meas. (*German*) 0-76437  
Li ferrites, porous, porosity effect on saturation of magnetisation 0-108036  
MgCr<sub>2</sub>O<sub>4</sub>-TiO<sub>2</sub>, porous ceramics, humidity-sensitive electrical conduction 0-107782  
MgCr<sub>2</sub>O<sub>4</sub>-TiO<sub>2</sub> porous ceramic humidity sensors 0-86325  
Na<sub>2</sub>O-CaO glass phlogopite mica powders, composite fabrication, cellular struct. 0-84902  
Na<sub>2</sub>O-P<sub>2</sub>O<sub>5</sub>-SiO<sub>2</sub> glass, substitution of Li<sup>+</sup>, Mg<sup>2+</sup>, Sr<sup>2+</sup>, Ba<sup>2+</sup>, Zn<sup>2+</sup> for Na<sup>+</sup> 0-100332  
Ni sintered permeable materials with bidisperse structure, pore-forming additions effect 0-84885  
Pb(Zr,Ti)O<sub>3</sub> ceramics with ladder type struct., prep. and props. 0-75945  
Pb(Zr,Ti)O<sub>3</sub>, porosity-permittivity relations, depolarising factors determ. and pore effects (*Japanese*) 0-97189  
Pt/ZrO<sub>2</sub> porous electrode/solid electrolyte system, interface polarisation effects 0-61114  
SiO<sub>2</sub>, P-doped amorphous, porous and hydrophilic, water adsorpt. and IR spectra obs. 0-80061  
SiO<sub>2</sub>-Al<sub>2</sub>O<sub>3</sub> porous catalysts, EPMA quantitative anal., new correction calc. method, modified ZAF method (*Japanese*) 0-93822  
SiO<sub>2</sub>-MgO porous catalysts, EPMA quantitative anal., new correction calc. method, modified ZAF method (*Japanese*) 0-93822  
TiO<sub>2</sub>, porosity-permittivity relations, depolarising factors determ. and pore effects (*Japanese*) 0-97189  
W, chromising 0-100959  
W-Cu pseudoalloy, porous, chromising 0-100959  
ZrO<sub>2</sub>, porous, sintered stabilised microspheres, strength and fracture studies 0-85019

**porous media** *see* porous materials

**porphyrins** *see* organic compounds

**Portevin-Le Chatelier effect** *see* serrated yielding

# posistors

No entries

# position control

*see also attitude control*  
microscopic cell deposition system for deposition at predefined locations on microscopic slide 0-76876  
differential games, stable position control 0-68024  
Fourier transform spectrometer, high resolution ruggedized 0-95152  
lens, optical axis designation method 0-102798  
mirrors, plane, spatially separated, adjustment to coplanarity, interferometric technique 0-95974  
plasma column, position control system, stability 0-106982  
plasma control by feedforward-feedback system with digital computer 0-75093  
precision measuring table with hollow rotor asynchronous motor, digital control system 0-105607  
translation motors for position with micron precision (*German*) 0-86271  
CO<sub>2</sub> laser Helios fusion target positioning with orthogonal telescopes 0-74421

**position finding** *see* navigation

# position measurement

*see also astrometry*  
capacitive indicators, linear and angular (*German*) 0-57256  
computerised tomographic scan edge position uncertainty reduction by density derivative processing 0-109017  
coordinate meas. uncertainty computation program (*German*) 0-86256  
eye position measurement, method for implantation of mag. search coils 0-85548  
identifiable sound source location from time differences of arrival 0-91951  
machine tool position feedback by laser interferometer 0-73438  
optical instrument, target position meas., statistical model 0-101778  
PWR control rod digital position indicating system (*Japanese*) 0-63314  
scintistor, luminous line coord. meas. 0-96019  
vidicon appl. to low intensities meas., with Si-intensified target (*German*) 0-98545

# position sensitive particle detectors

alpha, position-sensitive, use of the SnO<sub>2</sub>-Si heterotransition 0-91375  
amplifier-shaper for drift chambers 0-69033

# position sensitive particle detectors continued

angle-resolved photoelectron spectroscopy with cylindrical mirror analyzer, detection of azimuthal angles 0-57426  
astronomy, Lixiscope, X-ray and gamma-ray telescope system 0-62020  
atomic physics applications and possible detector constructions based on microchannel plates 0-63472  
backscattered electron detector, multi-purpose 0-102404  
Brookhaven multiparticle spectrometer drift chamber system 0-58044  
centroid of charge determ. 0-58064  
cylindrical wire proportional chambers, electrostatic field formulae, distrib. and asymmetry 0-78493  
discrete struct. influence on accuracy of coordinates determination 0-58076  
drift chamber based detector for X-ray scatt. expts. 0-58045  
drift chamber data acquisition, microprocessor based system 0-58066  
drift chamber with printed-board cathodes and flat solevoidal delay lines 0-74088  
electron spectrometer using new multidetector based on charge-coupled imaging device 0-86502  
electronics for proportional drift tubes 0-106241  
fast X-ray diffractometer based on a spherical drift multiwire proportional chamber with digital position encoder 0-90969  
fission detector, avalanche, parallel plate, particle induced fission coincidence measurements 0-63485  
flash chambers for neutrino detection, construction and performance 0-58026  
gamma ray detection system, 3-D, fabrication and efficiency 0-63483  
gas scintillation proportional counter for X-ray astronomy 0-58053  
gaseous detectors, evolutionary steps 0-58041  
graded-density cathode method for position determ. in multiwire proportional counters 0-87017  
high density projection chamber 0-58027  
imaging Cherenkov detector using gas-filled MWPC, photoionisation of triethylamine 0-91400  
imaging gas scintillation counter for X-ray astronomy 0-98551  
induction wire proportional counter with sub-mm positron resolution 0-91399  
large drift chamber system for use in an iron spectrometer 0-58046  
molecular biology, contracting muscle, dynamic structure, X-ray scatt., time resolved, rapid data collection systems 0-61740  
multiparameter focal plane detector, development of capacitively coupled distributed parameter delay lines 0-78491  
MWPC, flat area detector data acquisition system for X-ray crystallography 0-91381  
MWPC, gas amplification factors and detection efficiencies 0-74079  
MWPC, gas ionisation by double photon absorption using pulsed lasers 0-99414  
MWPC, position determ. method using graded density cathodes 0-102396  
MWPC, position sensitive, pulse shape from cathode RC Lines, zero-cross time meas. 0-58038  
MWPC construction for large aperture spectrometer 0-102381  
MWPC with wire plane cathodes, extension of standard formulae for elec. fields 0-99413  
neutron counter, position sensitive, high precision position readout 0-58063  
neutron time of flight single crystal diffractometer using a position sensitive detector 0-99404  
parallel grid imaging proportional counter optimized for detection of low brightness stellar XUV-sources 0-58049  
photon position monitors for CHESS synchrotron source, using split photoelectron detectors and ionisation chamber 0-91336  
positron imaging, Anger-type bar cameras, positron imaging 0-61687  
proportional counter, direct position and time digitizer 0-58090  
proportional counter, resistive wire, multi-anode, focal plane detector 0-63464  
proportional counter for neutrons 0-63459  
scintillation counter, light signal propag. speed. for spatial resolution determ. 0-69028  
self-scanning photodiode array for fast ion detection 0-87018  
SF5 lead glass Cherenkov counter, high energy photon position determ. 0-58032  
superconducting detector of ionizing particles 0-63460  
time detector, channel plate, for heavy ions 0-63466  
X-ray spectrometer for low-intensity imaging 0-86539  
zero-degree tagging system used for photon-photon experiments at DCI 0-102394  
Ar-ethane gas mixture, XX 0-63467  
Ge detectors, high purity, event timing, compared to Ge(Li) detectors 0-69018  
Ge(Li) detectors, coaxial, zero cross-over timing 0-69017  
Si detectors and Pb absorber plate, telescope structure, high energy muon flux measurement 0-58061  
Si photodiode array, position-sensitive photon detector for the UV or X-ray range 0-90970  
Si(Li)-emulsion shower counter for cosmic ray electron obs. 0-58033  
Xe-ethane gas mixture, electron drift velocity and other transport coeffs. 0-63467  
Xe-filled MWPC for hard X-ray imaging with sub-mm spatial resolution 0-99418

**positioning** *see* position control

# positive column

*see also glow discharges*  
alkali metal vapour discharge, low-press., energy balance eqns. 0-87969  
axial particle drift in the positive column of a discharge 0-100113  
correlation measurements of turbulent ionization and ion-acoustic waves 0-59329  
electronegative gas discharge, spontaneous oscills. 0-87977  
gas discharge with external ionisation, voltage-current characs. 0-96408  
gas-discharge column with allowance for metastable atom effect, excitation of strata 0-96410  
inert gases, atomic alignment (*Russian*) 0-87981  
ionisation waves, in positive column, wave packet propag. 0-96356  
moving striations, conditions for self-excitation 0-69358  
neutral gas, ionisation and temp. effect on charged particle profile and density 0-79596  
plasma, in high voltage diffuse discharge, nonstationary processes 0-64802  
space-charge double layers, anal. using fluid theory 0-75062



**positive column continued**

- subnormal column, ion and electron radial distrib., theoretical description 0-79598
- two-step ionisation, var. calcs. 0-70056
- water vapour, electron energy distrib. function, electron sink and plasma resist. effect (*Russian*) 0-106987
- Ar, low-press. glow discharge, elec. characts. of positive column 0-100112
- Ar-CO glow discharges, positive ion spectra, ion clusters obs. 0-64807
- He positive column discharge, IR optogalvanic spectrosc. using F-centre laser 0-78563
- He, positive column plasmas, metastable atom density meas. by improved self absorpt. method 0-87968
- He-CO glow discharges, positive ion spectra, ion clusters obs. 0-64807
- He-Cd vapour excitation in hollow cathode discharge 0-64815
- He-I<sup>+</sup> laser discharge, particle densities 0-103215
- Hg positive column, electron energy distrib., numerical soln. of Boltzmann eqn. 0-87982
- Kr, low-press. glow discharge, elec. characts. of positive column 0-100112
- N-O mixtures, positive glow corona in quasi-uniform fields 0-100104
- Na-Xe, excimer lasers, high-power discharges, models 0-69373
- Ne discharge in high press. narrow tube, Kadomtsev-Nedospasov instability 0-107004
- Ne positive column plasmas, metastable atom density meas. by improved self absorpt. method 0-87968
- O<sub>2</sub>, electron energy distrib. function, electron sink and plasma resist. effect (*Russian*) 0-106987

**positive feedback** *see feedback***positive ray sources** *see ion sources***positive rays** *see ion beams***positive temperature coefficient thermistors** *see thermistors***positons** *see positrons***positron annihilation** *see electron positron interactions***positron annihilation in liquids and solids**

- adamantane, cryst., vacancy formation energy, positron annihilation study 0-60706
- alkali chlorides, positron-trapping colour centre dynamics, positron annihilation study 0-108294
- alkali silicate glasses, struct. and thermal props. 0-84075
- applications (*Chinese*) 0-66322
- aromatics, halogen substituted, as positronium inhibitor 0-93783
- $\beta$ -brass, vacancy form., ordering effect, positron annihilation obs. 0-93427
- brass, vacancy formation energies in mixed  $\alpha + \beta'$  phase 0-59456
- cholesterol, solid-solid phase transitions, positron annihilation study 0-84289
- cholesteryl oleate, solid-solid phase transitions, positron annihilation study 0-84289
- COC, cholesteric liq. cryst., positron lifetimes and phase transitions 0-59383
- diffusion of positrons to surfaces 0-71506
- iterative unfolding method for positron annihilation radiation spectra measured with Ge(Li) detectors 0-93733
- kapton, temperature dependence of positron source 0-93426
- line shape Doppler broadening, lifetime spectroscopy, formation inhibition by solvated electron precursor scavenging 0-93784
- liquid, positronium pick-off annihilation, improved bubble model 0-93424
- liquid alloys, positron annihilation due to vacancy trapping, simplified model (*Russian*) 0-71511
- metals, positron response to thermal expansion 0-84306
- metals, positron trapping by defects influence of positron-phonon and electron-phonon interactions (*Russian*) 0-93425
- Mossbauer effect and positron annihilation, review of appls. (*French*) 0-80899
- mylar, temperature dependence of positron source 0-93426
- nonpolar liquids, enhancement of positronium form. caused by scavenging of highly mobile positive holes 0-69265
- polymers, positronium form. and decay, elec. field effect 0-97369
- quartz, fused, positronium form. and decay, elec. field effect 0-97369
- steel, positron meas., for trapping mechanism detection 0-84798
- Teflon, gamma irradiated, free four-term analysis of positron lifetime spectra 0-76101
- transition metals, itinerant and localised d-electrons, positron annihilation data 0-93428
- Ag, positron annihilation spectra, Doppler-broadened, temp. depend., 9 to 1098K 0-71510
- Ag surface, positronium emission 0-80897
- Al, neutron damage, positron annihilation 0-65056
- Al, positron annihilation and vacancy formation, Doppler broadening study 0-60708
- Al surface, positronium emission 0-80897
- Al-Mg, dil., ang. correlation of annihilation radiation from impurity trapped positrons 0-104010
- Al-Mg (0.1 at. %), neutron damage, positron annihilation 0-65056
- Al-Zn-Mg, age-hardenable, precipitation and dissolution processes, positron annihilation and X-ray small-angle scattering comparison 0-89238
- Al(111), oxide layer amorphous to cryst. surface transition, slow positron obs. 0-75417
- Bi solid and liquid, positron annihilation temp. depend. 0-108296
- CaCO<sub>3</sub> single crystals, positron annihilation, two photon angular correlation 0-108295
- Cd, positron trapping at low temp. lifetime spectra 0-84799
- CdS(Se)(Te), positron annihilation study 0-60713
- Cu, prevacancy temperature depend. of positron annihilation, Doppler broadening lineshape parameters 0-60709
- Cu surface, positronium emission 0-80897
- Cu, vacancy form. enthalpy, positron annihilation meas. 0-97371
- Cu-Co (1.5 and 4 wt. %) alloy, coherent Co-rich separations obs. by positron annihilation (*Russian*) 0-89082
- Fe, electron-irradiated, positron lifetime meas. 0-93431
- Fe, pure and doped, electron irradiat., mag. aftereffect 0-88838
- $\alpha$ -Fe-C, electron irradiat., vacancy-C interaction, positron lifetime meas. 0-75264
- Fe-C, electron-irradiated, positron lifetime meas. 0-93431
- Fe<sub>80</sub>B<sub>20</sub>, metallic glass, Doppler broadening of positron annihilation  $\gamma$ -radiation and elec. resist. 0-66321
- Fe<sub>78</sub>Mo<sub>2</sub>B<sub>20</sub>, metallic glass, Doppler broadening of positron annihilation  $\gamma$ -radiation and elec. resist. 0-66321

**positron annihilation in liquids and solids continued**

- Fe<sub>32</sub>Ni<sub>36</sub>Cr<sub>14</sub>P<sub>12</sub>B<sub>6</sub>, metallic glass, Doppler broadening of positron annihilation  $\gamma$ -radiation and elec. resist. 0-66321
- Ga solid and liquid, positron annihilation temp. depend. 0-108296
- GaAs, positron annihilation depend. on doping 0-60710
- GaP:Ti(Co)(Ni), positron annihilation meas. rel. to deep levels study 0-60712
- Ge, neutron-irradiated, positron lifetime 0-97374
- H<sub>2</sub>O(D<sub>2</sub>O), positronium formation, isotope effects 0-93432
- He, positron decay rate nonlinear density depend. 0-71509
- KCl:Ag positron annihilation and impurity states 0-97375
- KCl:Sr, positron annihilation and trapping in A-centres 0-84802
- LiF,  $\gamma$ -irrad. induced defects, positron capture and annealing obs. 0-60707
- Mo, gamma irradiated defects, interaction with positrons (*Russian*) 0-97372
- Mo, void containing, positron annihilation characts. 0-80898
- NaCl, temperature dependence of positron source 0-93426
- NaCl:Ag, positron annihilation and impurity states 0-97375
- NaCl:Sr, positron annihilation and trapping in A-centres 0-84802
- Nb, neutron-irradiated, positron annihilation ang. correl. meas. 0-93430
- Nb-Zr (3 wt. %), neutron-irradiated, positron annihilation ang. correl. meas. 0-93430
- NbSe<sub>2</sub>, pure and intercalated with ethylenediamine, positron annihilation study 0-84801
- Ni, plastically deformed, positron trapping rate, temp. depend. 0-71507
- Ni, positron lifetime meas., 4.2 to 1700K, monovacancy form. enthalpy 0-97370
- Ni surface, positronium emission 0-80897
- Pt, neutron damage, positron annihilation 0-65056
- SF<sub>6</sub>, liq., positronium bubble states, temp. depend. 0-108293
- Se, trigonal and amorphous, positron lifetimes, positronium form. 0-60711
- Si, electron-irradiated crystals, positron trapping, temp. depend. 0-104009
- Si epitaxial film, containing struct. defects formed during growth, positron annihilation 0-93433
- Sn, (100) surface, clean and O<sub>2</sub> exposed, slow positron studies, positronium formation 0-93429
- Sn, positron annihilation in fine particles, surface trapped states 0-84800
- Sn, thermally induced vacancies, positron trapping 0-89083
- Ti-Fe (1.4 wt. %), polymorphic transform. due to plastic deform., positron annihilation 0-79939
- V, electron-irradiated, positron annihilation study 0-70259
- Zn, electron momentum distrib., neutron-induced defects, positron annihilation study, for single cryst. 0-71508
- ZnSe, positron annihilation study 0-60713

**positron scattering** *see electron impact***positron states**

- inelastic positron scatt. in electron gas, plasmon excitation 0-92843
- semiconductors, defective surface layer, surface positron states 0-75526
- Ag (100) and (111) surfaces, positronium form. due to slow positron trapping 0-107748
- Cu (111) surface, positronium form. due to slow positron trapping 0-107748
- KCl:Ag positron annihilation and impurity states 0-97375
- NaCl:Ag, positron annihilation and impurity states 0-97375
- Se, trigonal and amorphous, positron lifetimes, positronium form. 0-60711
- Sn, (100) surface, clean and O<sub>2</sub> exposed, slow positron studies, positronium formation 0-93429

**positronium***see also electron pairs*

- annihilation line shape Doppler broadening, lifetime spectroscopy, formation inhibition by solvated electron precursor scavenging 0-93784
- decay, asymmetrical, two- and threefold polarisation correlation of photons 0-57536
- electrons and positrons in dense gases, review 0-103106
- energy interval measurement by obs. Zeeman transition in microwave spectra 0-69274
- exotic atoms, conf., Erice, Sicily, (1979) 0-67939
- formation and quenching in Ar-O<sub>2</sub> mixtures, orthopositronium quenching cross section determ. 0-74261
- formation in positron+alkali metal atom collisions, first Born approx. 0-83525
- formation in positron+alkali metal atom collisions, pseudopot. calcs. 0-83524
- formation inhibition by Br substituted benzenes 0-93783
- inhibition processes of positronium formation, role of solvation properties of solvents 0-93786
- liquid, positronium pick-off annihilation, improved bubble model 0-93424
- metals, surface positronium formation, stopping distance, positron-phonon interactions 0-96582
- nonpolar liquids, enhancement of positronium form. caused by scavenging of highly mobile positive holes 0-69265
- nylon, positronium form. and decay, elec. field effect 0-97369
- orthopositronium decay ray meas. by Michigan apparatus 0-69274
- orthopositronium quenching by O<sub>3</sub>, meas. by two-photon coincidence rate difference technique 0-74262
- Perspex, positronium form. and decay, elec. field effect 0-97369
- polarisation effects in tripositronium decay into electron and photon (*Russian*) 0-58421
- polyethylene, positronium form. and decay, elec. field effect 0-97369
- polystyrene, positronium form. and decay, elec. field effect 0-97369
- positronium nitrate, [NO<sub>3</sub><sup>-</sup>;e<sup>+</sup>], existence, Hartree-Fock-Roothaan calcs. 0-83254
- positronium nitrite, [NO<sub>2</sub><sup>-</sup>;e<sup>+</sup>], existence, Hartree-Fock-Roothaan calcs. 0-83254
- quartz, fused, positronium form. and decay, elec. field effect 0-97369
- relativistic two-fermion equations with instantaneous potential 0-101918
- (e<sup>+</sup>e<sup>-</sup>) atom, Coulomb disintegration, cross sections and energy spectra (*Chinese*) 0-102589
- Ag (100) and (111) surfaces, positronium form. due to slow positron trapping 0-107748
- Cu (111) surface, positronium form. due to slow positron trapping 0-107748
- H, positron elastic scattering, S-wave phase shifts calc., least squares method 0-106374
- H<sub>2</sub>O(D<sub>2</sub>O), positronium formation, isotope effects 0-93432



**positronium continued**

- He, fluid, positronium and electron bubbles, density-functional theory 0-80016  
 Li+positron, positronium formation in highly excited states, first Born approx. 0-58420  
 SF<sub>6</sub>, liq., positronium bubble states, temp. depend. 0-108293  
 Se, trigonal and amorphous, positron lifetimes, positronium form. 0-60711  
 Sn, (100) surface, clean and O<sub>2</sub> exposed, slow positron studies, positronium formation 0-93429

**positrons**

- see also electron pairs; electrons*  
 Bragg reflection from Al and Cu surfaces obs. 0-103221  
 cosmic ray positrons, galactic, primary source, prod. rate, and escape probability 0-109319  
 gases, molecular, total scatt. cross sections for intermediate-energy positrons 0-91692  
 mobility edge in gaseous He 0-83880  
 radiation therapy using  $\pi^+$ , in vivo beam localisation by positron activation 0-72316  
 slow, time bunching for annihilation lifetime and pulsed laser photon absorpt. expts. 0-95492  
 slow positron form. in MgO-coated moderators 0-62796  
 slow positrons, narrow beam emission from negative electron affinity surfaces 0-89091  
 source, Au moderator surface preparation for increased yield 0-61011  
 superheavy collision system, radiative processes, search for positron emission 0-63752  
 superheavy ion-atom collisions, quasiats., K-vacancy form., positron emission 0-63753  
 $\mu^-e^+$  pair production in  $\nu_e N$  interaction (*Russian*) 0-91076  
 Ag, electron (positron), impact, K- and L-shell ionisation,  $K\alpha$  and L X-rays meas. 0-99575

**potassium**

- see also nuclei with .....*  
 adlayer effect on CO and H<sub>2</sub> adsorption and desorption on Fe(100) 0-71573  
 adsorbed on Pt(111), UPS and XPS meas. 0-95675  
 adsorbed on W, field emission flicker noise power 0-59795  
 adsorption of K on Fe(110), UPS and XPS meas. 0-95675  
 adsorption on Fe(100), adsorbate coverage determ. by LEED, AES and XPS 0-103566  
 atmosphere aerosols over tropica N Atlantic Ocean, water-soluble K, Ca and Mg contents 0-72598  
 atom, damping const. in acetylene-air flame, Lorentz collisions, mag. field effects 0-66805  
 atom, first excited D-level, hyperfine struct. meas. by cascade, fluoresc. spectrosc. 0-69101  
 atom, isotope shifts of individual nS and nD levels 0-102489  
 atom, Rydberg state optical excitation, collision ionisation processes 0-102561  
 atomic vapour, resonant interaction with laser, Vavilov-Cherenkov effect (*Russian*) 0-106573  
 axonal membrane of mammals (myelinated fibres), K channel conduction 0-61538  
 axons, giant, squid, interaction of Ba<sup>2+</sup> with K<sup>+</sup> channels 0-85379  
 channel flow, incipient boiling superheats 0-74709  
 coadsorption with O<sub>2</sub> on Fe (110), XPS, UPS, AES, and LEED study 0-80084  
 crystal struct., van der Waals and repulsive interaction 0-84137  
 de Haas-van Alphen freq. and Fermi surface anisotropy, press. depend. 0-59856  
 determination in minerals, electron probe analysis with low temperature sample holder (*French*) 0-85248  
 Earth mantle content, inferred from heat loss argument 0-76943  
 elastic constants, appl. of model pseudopot. to elastic const. 0-59845  
 ground state alkali molecules, mag. shielding and spin-rot. interaction 0-87186  
 ground state of solids, spin density functional method, binding energy, compressibility 0-65477  
 Grüneisen parameter, press. depend. 0-65184  
 intercalation compounds with graphite, <sup>13</sup>C NMR spectra 0-66048  
 ion implantation in LiF, migration, segregation, effect on optical props. 0-100269  
 isotope separation in solution by thermal diffusion 0-87236  
 laser, tunable subMM, using atomic K Rydberg states 0-69378  
 liquid, density, at near critical temp. 0-103407  
 liquid, interionic interaction theory, pseudopotential calcs. (*Russian*) 0-79675  
 liquid, mean spherical approx. and effective pair pots. 0-70099  
 liquid, O<sub>2</sub> pot. and O<sub>2</sub> distrib. coeffs. between alkali and struct. metals 0-65231  
 magnetic property volume depend., Knight shifts, electron spin response 0-88729  
 magnetoresistivities, longitudinal elec. and thermal, meas. 0-88541  
 metal impurity effect on residual elec. resistance (*Russian*) 0-84457  
 molecular beam, isotope selective two-step photoionisation study 0-74203  
 molecular ground state thermalisation speed, collision cross-sections meas. (*Russian*) 0-78723  
 molecular laser, optically pumped, review 0-58519  
 molecule, absorpt. and relax. const. determ. by optical laser pumping method 0-102550  
 phasons, transverse, freq. dispersion relation in CDW state 0-96804  
 positronium, formation in positron+alkali metal atom collisions, first Born approx. 0-83525  
 positronium formation in positron+alkali metal atom collisions, pseudopot. calcs. 0-83524  
 resistivity and thermoelec. ratio, electron-electron scatt. contrib. 0-70670  
 self-diffusion, high temp. bulk modulus determ. 0-79976  
 smoke particles, optical props. 480 to 620 nm, rel. light scatt. cross sections meas. 0-97293  
 soft X-ray emission edge, temp. depend. 0-89090  
 spallogenic isotopes in Fe meteorites, radial distrib. 0-67488  
 thermopower and elec. cond., relationship at low temps. (*Russian*) 0-92882  
 ultrasonic attenuation at low temp., spherical Fermi surface model 0-84255  
 vapour, mag. props. changes under laser irr., induced EMF obs. 0-100059  
 C/Pt-W (8 wt.%), desorption of K from C film surfaces 0-59784

**potassium continued**

- Cs:K<sup>+</sup>, luminesc. processes 0-103989  
 H plasma, K impurities, optical props. 0-103119  
 K I isoelectronic sequence, transition probabilities, cancellations 0-91503  
 K<sup>+</sup>, photodetachment and at. polarisability 0-91522  
 K<sup>+</sup>, activity-dependent extracellular fluctuations in canine Purkinje fibres 0-89733  
 K<sup>+</sup> conductance absence in central myelinated axons 0-108871  
 K<sup>+</sup> currents in squid axons, single channel recordings 0-76721  
 K<sup>+</sup> external conc., starfish egg cell membranes, inward rectification blocking model 0-61523  
 K<sup>+</sup>, H<sub>2</sub>O affinity, ab initio SCF calcs. 0-58125  
 K<sup>+</sup>, in vivo continuous monitoring using ISFET probes 0-85512  
 K-rich globules in Luna 20 soil, SEM obs. 0-67591  
 K<sup>+</sup> affinities of methylamine, ab initio SCF calculations 0-102443  
 K+alkyl halide potentially reactive collisions, electronic excitation 0-74239  
 K+CO, rotational inelastic scatt., uniform semiclassical sudden approx. 0-99544  
 K+H<sub>2</sub>S(DS), collisional ionisation, positive and negative ion energy spectra obs. 0-63775  
 K+H<sup>+</sup> (H), single-electron capture total cross sections 0-91656  
 K+He, 4<sup>2</sup>P state j<sub>1</sub>m<sub>1</sub>-j<sub>2</sub>m<sub>2</sub> Zeeman transition, total cross section energy depend. 0-83475  
 K+K<sup>+</sup> collisions, charge exchange cross section 0-58374  
 K+methyl cyanide, collisional ionisation obs. 0-95716  
 K+NaK reactive collisions studied using circularly polarised laser fluorescence 0-69215  
 K+O<sub>2</sub>, collisional ionisation, energy spectra of forward and backward directed positive and negative ions 0-87200  
 K+O<sub>2</sub>, mol. target internal motion 0-78697  
 K+UF<sub>6</sub>, ionisation reactions, absolute cross sections 0-99565  
 K<sub>2</sub>+halogens(SnCl<sub>4</sub>)(MoF<sub>6</sub>)(UF<sub>6</sub>), ionisation reactions, absolute cross sections 0-99565  
 K<sup>+</sup> affinities of NH<sub>3</sub>, ab initio SCF calculations 0-102443  
 Si:K, bound exciton luminescence in mag. field (*Russian*) 0-108278  
 Si-SiO<sub>2</sub>:K<sup>+</sup>, physics, electron and ion motion (*Dutch*) 0-60093  
 SiO<sub>2</sub>:K, ion trapping and mobility, energy levels 0-92985
- potassium alloys**  
 FePC molten and amorphous alloys, struct. factors 0-79674  
 K-Cs, extreme UV absorpt. spectra 0-97294  
 K-Cs, thermal conductivity determ. 0-107760  
 K-Rb, extreme UV absorpt. spectra 0-97294  
 K-Rb, internal energy, heat of mixing, entropy, dielectric function 0-88340  
 K<sub>2</sub>Ga<sub>13</sub>, X-ray cryst. struct. determ. 0-92479  
 Na-K, internal energy, heat of mixing, entropy, dielectric function 0-88340  
 Na-K, surface tension theory for liquid mixtures 0-88404  
 Na-K liq. alloy, Moelwyn-Hughes parameter calc. from US data 0-59375  
 Na-K liquid alloys, struct., X-ray and neutron diff. meas. 0-107041  
 Na-K liquid alloys, triplet correlation functions and thermodynamics, solute partial structure factor 0-64881
- potassium compounds**  
*see also potassium alloys; Rochelle salt*  
 acid oscilator, neutron inelastic scatt. spectra in 2200-200 cm<sup>-1</sup> range 0-70327  
 acid phthalate curved crystal spectrograph, diffraction efficiency calc. method 0-79630  
 antimonyl tartrate, neutral aq. soln., gamma radiolysis 0-101030  
 germanate crystals and glasses, struct. and stability, IR spectra meas. 0-64911  
 graphite-K intercalation compound, effect of H addition on superconducting transition temp. 0-70872  
 halides, elastic constants, temp. derivatives at constant volume 0-59549  
 halides, lattice dynamics in five parameter model 0-107382  
 halides, spin lattice relaxation meas. of O<sub>2</sub> centres 0-88863  
 intercalation compounds with graphite, electronic props., de Haas-van Alphen effects and Fermi surfaces 0-75498  
 intercalation compounds with graphite, electronic props., resistivity, Hall effect and magnetoresistance 0-75585  
 KAlF<sub>4</sub>, single cryst., prep. and struct. (*French*) 0-79762  
 laurate-1-decanol-water mixtures, biaxial nematic phase obs. 0-107409  
 porcelain, crack propag. data applicability to failure prediction 0-81154  
 potassium formate, X-ray cryst. struct. determ. 0-107194  
 potassium hydrogen malonate, room-temperature ENDOR spectra obs. 0-106339  
 TCNQ salt, K-TCNQ, EPR linewidth, ang. and freq. depend. 0-80591  
 $\beta$ -Al<sub>2</sub>O<sub>3</sub>-(K,Li)<sub>2</sub>O and  $\beta$ -Al<sub>2</sub>O<sub>3</sub>-(K,Sn)<sub>2</sub>O, ionic cond. and Raman spectra 0-107509  
 $\beta$ -Al<sub>2</sub>O<sub>3</sub>-(Na,K)<sub>2</sub>O, equil. distrib. of ionic species 0-107511  
 $\beta$ -Al<sub>2</sub>O<sub>3</sub>-(Na,K)<sub>2</sub>O, model calcs. of cond. anomalies, pot. energies of cation arrangements 0-107510  
 $\beta^*$ -Al<sub>2</sub>O<sub>3</sub>-K<sub>2</sub>O, ionic cond. at room temp. 0-107513  
 $\beta$ -Al<sub>2</sub>O<sub>3</sub>-K<sub>2</sub>O, low-energy excitation spectra, localised modes 0-59606  
 $\beta^*$ -Al<sub>2</sub>O<sub>3</sub>-K<sub>2</sub>O, single cryst. Raman scatt., cond. mechanism and cryst. struct. 0-66209  
 $\beta$ -Al<sub>2</sub>O<sub>3</sub>-K<sub>2</sub>O-MgO, cryst. struct., nonstoichiometry, ion-ion correlations 0-88129  
 Au condensation kinetics, on KCl 0-88453  
 BeF<sub>2</sub>-KF-CaF<sub>2</sub>-AlF<sub>3</sub>-EuF<sub>3</sub> fluoroberyllate glass, Eu<sup>3+</sup> fluoresc. linewidth 0-66285  
 Fe<sub>10/92</sub>K<sub>1/8</sub>O<sub>17</sub>, ferrite, cryst. struct., nonstoichiometry, ion-ion correlations 0-88130  
 GeO<sub>2</sub>-K<sub>2</sub>O, glass, Raman spectra, struct. and crystn. 0-92463  
 K salt of  $\beta$ -ketoaldehyde, configurations of anions in solutions studied by IR spectroscopy, H-bond form. 0-87117  
 $\beta$ -K-Al<sub>2</sub>O<sub>3</sub>, far IR absorpt., Bevers-Ross sites, interstitials 0-66240  
 KAlF<sub>4</sub>, dissoc. enthalpies, mass spectrometric determ., heat of form. 0-97720  
 KAg<sub>14</sub>, superionic cond., pressure effect on phase transitions 0-70405  
 KAg<sub>16</sub>, superionic phase transition, dynamical and crit. pt. props. 0-107535  
 K<sub>2</sub>As<sub>2</sub>O<sub>6</sub>, X-ray single-cryst. struct. determ., Patterson method 0-96484  
 KB<sub>2</sub>H<sub>6</sub>, NMR study of proton and boron dynamics 0-71210  
 KBO<sub>2</sub>, vapour over heated solid, XPS, obs. 0-87171  
 K<sub>2</sub>Ba(NO<sub>3</sub>)<sub>2</sub>, elastic props. 0-96588  
 K<sub>2</sub>BiNb<sub>2</sub>O<sub>15</sub> substrate for K<sub>3</sub>LiNb<sub>2</sub>O<sub>15</sub> film for optical waveguide, cryst. struct., dielectric props. 0-79016



**potassium compounds continued**

- ( $K_{1/4}Bi_{1/4}$ )( $Zn_{1/6}Nb_{5/6}$ ) $O_3$ , cation disordered perovskite, elastic consts. and thermal expansion 0-96587  
 KBr, activation coefficients and solvation numbers in mixed methanol solvents 0-81334  
 KBr, colour centre form. under polarised UV irradi., dichroism in absorption spectra 0-107232  
 KBr crystals, binding forces and eqns. of state, inner electron contrib., calc. 0-64950  
 KBr, decay and time resolved emission spectra from  $\sigma$ -excitons produced by heavy-ion irradiation 0-89071  
 KBr, defect accumulation under electron irradi. at 4K 0-107233  
 KBr, defect modes due to H<sup>-</sup>-D<sup>-</sup> pair impurities 0-59602  
 KBr, defect modes due to substitutional anion-pair and cation-pair impurities in ionic crystals 0-92540  
 KBr, F-centre emission, mag. circular polarisation 0-108251  
 KBr, F-centre lifetime, perturbation effects, luminesc. meas. 0-108252  
 KBr, gamma and additively coloured, dissolving in pure water, lyoluminesc. mechanism 0-100693  
 KBr, gamma-irrad., hologram recording by F-centre bleaching 0-78814  
 KBr, heavy metal ion implantation, mol. unit form. 0-100267  
 KBr, intra impurity local oscill. composition tone absorpt. band anharmonic temp. broadening (*Russian*) 0-60642  
 KBr, irradiated at room temp., stored energy 0-79839  
 KBr, molten, solutions of K, conc. fluctuations, small angle neutron scat. study 0-92448  
 KBr, photostimulated recomb., electron spin polarisation 0-60673  
 KBr, prep. of crystals containing impurities of specified amounts (*Russian*) 0-66424  
 KBr, quenched single cryst., hardness var. with load 0-76337  
 KBr, recomb. in ionic crystals, defect interaction 0-84206  
 KBr, recomb. in ionic crystals, defect interactions 0-84207  
 KBr, self-trapped exciton form. via thermally induced defect reactions 0-60687  
 KBr, transverse optic mode self-energy at 100 and 300K, expt. determ. 0-84265  
 KBr, X-irrad. crystals, halogen aggregation, absorpt. spectra obs. (*Russian*) 0-66234  
 KBr:Au<sup>+</sup>, optical absorpt. bands and MCD, electron-lattice interaction 0-108236  
 KBr:CN<sup>-</sup>, neutron scat. studies of (CN)<sup>-</sup> defects 0-92620  
 KBr:CN<sup>-</sup>, tunnelling motion of dipolar impurities, absorption spectra 0-66239  
 KBr:Ga<sup>3+</sup>, polarisation of Ga<sup>3+</sup> centre A<sub>T</sub> emission, temp. depend. 0-80842  
 KBr:I<sup>-</sup>, OH<sup>-</sup>, luminesc. of interstitial atomic H 0-89062  
 KBr:Mg<sup>2+</sup>, dopant aggregation and precipitation 0-107306  
 KBr:Mg<sup>2+</sup>(Ca<sup>2+</sup>)(Sr<sup>2+</sup>)(Ba<sup>2+</sup>), defect struct., Mott-Littleton technique study 0-59487  
 KBr:MnO<sub>4</sub><sup>-</sup>, many-phonon impurity reson. Raman scat. 0-60603  
 KBr:MnO<sub>4</sub><sup>-</sup>, model system, reson. Raman spectra, general behaviour obs. 0-60592  
 KBr:OH<sup>-</sup>, cc U<sub>2</sub> to H<sub>2</sub>O<sup>-</sup> defects conversion after UV photodecomp. 0-107230  
 KBr:PO<sub>4</sub><sup>3-</sup>, ODMR in zero and weak mag. fields 0-88894  
 KBr:Sr<sup>2+</sup>, Cu<sup>+</sup>, thermolum. response, extension of two-step reaction model 0-89075  
 KBr:Ti, 480K thermal glow peak, Ti<sup>3+</sup> centres 0-108284  
 KBr:Ti, electroluminescence, spectra and quantum yield activator conc. depend., cond. changes 0-89070  
 KBr:Ti, luminesc., decay model for A<sub>T</sub> and A<sub>X</sub> emissions 0-93379  
 KBr:Zn<sup>2+</sup>, optical absorpt. bands rel. to charge transfer 0-66245  
 KBr:Kl, mixed crystals, microhardness, theory 0-75298  
 KBr:<sub>x</sub>(CN)<sub>x</sub>, mixed mol. cryst., coupled rot. and translational modes 0-84267  
 KBrO<sub>3</sub>-H<sub>2</sub>SO<sub>4</sub>-Mn<sup>2+</sup>-oxalacetic acid, chaos type reactions anal. 0-85165  
 KC<sub>24</sub>, press. induced staging transition 0-79938  
 KCN, dynamics of CN<sup>-</sup> ions near phase transitions at 83K 0-80717  
 KCN, inelastic neutron scat. by coupled rot. and translational modes 0-79895  
 KCN, multidomain birefr. solid, light scat. and IR transmission spike 0-60587  
 KCN, Raman diffusion spectra, IR absorpt. in phases II and III (*French*) 0-84741  
 KCN:Cl<sub>2</sub>, finite field local field catastrophe phenomena in spectra 0-92830  
 K<sup>+</sup>:CN<sup>-</sup>, Cl<sub>2</sub>, influence of structural disorder on exciton spectra 0-108224  
 KCaF<sub>3</sub>, IR refl. spectra, vibr. modes, optical vibr. freq., Kramers Kronig anal. 0-66190  
 KCaF<sub>3</sub>, struct. phase transitions, DSC, birefr., and neutron powder diff. obs. 0-70149  
 K<sub>2</sub>Ca[B<sub>2</sub>O<sub>6</sub>(OH)<sub>4</sub>]<sub>2</sub>·8H<sub>2</sub>O, synthetic, X-ray cryst. struct. study, H bond geometry 0-92509  
 KCdF<sub>3</sub>, IR refl. spectra, vibr. modes, optical vibr. freq., Kramers Kronig anal. 0-66190  
 KCl (Br) aqueous solutions, IR absorpt.  $\mu_1$  (CN) band parameter temp., conc. study (*Russian*) 0-80801  
 KCl, activation coefficients and solvation numbers in mixed methanol solvents 0-81334  
 KCl, additively coloured photochromic crystals, spectral sensitivity (*Russian*) 0-91871  
 KCl, adsorption-desorption behaviour on W (110) and W (111) surfaces 0-75442  
 KCl, amplitude-phase holograms, optical parameter dispersion 0-58481  
 KCl and KCl:NO<sub>2</sub>, X-irrad. crystals, Cl<sub>2</sub><sup>-</sup> centres photodissoc., optical anisotropy and creation mechanisms (*Russian*) 0-66235  
 KCl, Born-Mayer parameters of He and Ar, interstitial interaction with neighbouring ions 0-100228  
 KCl, cation defects creation mechanism 0-75224  
 KCl cryst., Sr and Na impurities radial distrib., influence of form of cryst. front 0-107312  
 KCl, cryst. isolated pore healing under press., dislocation struct. evolution (*Russian*) 0-100245  
 KCl crystal active element for colour-centre laser, thermal strain anal. 0-91804  
 KCl crystals, Eu<sup>2+</sup> concentration effect on lattice parameter and density of crystals 0-88169  
 KCl, defect modes due to H<sup>-</sup>-D<sup>-</sup> pair impurities 0-59602  
 KCl, defect modes due to substitutional anion-pair and cation-pair impurities in ionic crystals 0-92540

**potassium compounds continued**

- KCl, dilute metal solutions in molten salts, optical absorption, F-centre model for bound state 0-89023  
 KCl, electron range-energy relation, thermally created lattice vacancies effect 0-92574  
 KCl, F-centre emission, mag. circular polarisation 0-108251  
 KCl, F-centre formation at highly excited triplet states of self-trapped excitons 0-76066  
 KCl, F-centre relaxation kinetics, temp. depend. following electron irradi. 0-92527  
 KCl, fine structure of X-ray absorption spectra 0-71514  
 KCl, gamma and additively coloured, dissolving in pure water, lyoluminesc. mechanism 0-100693  
 KCl,  $\gamma$ -irrad., F-centre absorpt., flash-stimulated changes 0-92524  
 KCl, heavy metal ion implantation, mol. unit form. 0-100267  
 KCl, ionic cond., defect parameters, diffusion coeffs. 0-79978  
 KCl, irradiated at room temp., stored energy 0-79839  
 KCl, microcrack propagation and plastic strain 0-81187  
 KCl, photoelectric emission in photon energy region 1.0 to 6.0 eV 0-108321  
 KCl, photofragment spectra, bond energies and excited state symmetries 0-87190  
 KCl, positron-trapping colour centre dynamics, positron annihilation study 0-108294  
 KCl, prep. of crystals containing impurities of specified amounts (*Russian*) 0-66424  
 KCl, pure and Ba doped, symm. of elastic fields due to defect displacements, diffuse X-ray scat. 0-70256  
 KCl single cryst., stress birefr. 0-60542  
 KCl solution, elec. cond. obs. for seawater salinity scale 0-72646  
 KCl solution, streaming current and cross-coeff. meas. in electrokinetic processes 0-76531  
 KCl surface, sublimation kinetics, elec. field influence, terrace-ledge-kink model 0-84287  
 KCl surface, VUV irradi., colour centre layer, angle-of-incidence derivative ellipsometry and reflectometry 0-73420  
 KCl, thermoluminesc., halogen and alkali impurity effects 0-97352  
 KCl, two-dimens. nucleation and hole nucleation, mol. beam method (*German*) 0-93499  
 KCl, two-dimens. nucleation rate on the (100) surfaces, mol. beam method, 289-343°C (*German*) 0-93500  
 KCl, ultralow loss optical fibre material, loss mechanism 0-78920  
 KCl, X-ray irradiated, first-stage F-centre prod. 0-107231  
 KCl, X-ray irradiated, vacancy conc. determ., thermal expansion meas. 0-79782  
 KCl, Z<sub>2</sub> centres in triplet state, EPR study 0-108068  
 KCl:Ag, X-irrad., thermoluminesc. study of Ag centres 0-80874  
 KCl:Ag positron annihilation and impurity states 0-97375  
 KCl:Ba<sup>2+</sup>, localised stress relaxation in excess vacancy system, prismatic loops (*Russian*) 0-88160  
 KCl:Br (I<sup>-</sup>), interstitial atomic H centres, formation kinetics and struct. MO calc. and EPR studies 0-75854  
 KCl:Br<sup>2+</sup>, solid solution periodic precipitation in inhomogeneous conc. field 0-103485  
 KCl:Ca<sup>2+</sup>, Z<sub>2</sub> centre thermolum. 0-80879  
 KCl:Ca(Yb), Z<sub>2</sub> and Z<sub>2</sub><sup>+</sup> centres, excited state, magneto-optical spectra 0-108233  
 KCl:CdCl<sub>2</sub>, elec. cond., role of electrode material, surface precipitation effects 0-59985  
 KCl:Cs<sup>+</sup>(I<sup>-</sup>), low-temp. heat capacity enhancement due to impurities 0-107442  
 KCl:Cu<sup>+</sup>, excitation and absorpt. spectra 0-108255  
 KCl:Cu<sup>+</sup>, exciton bands, optical absorpt. and MCD spectra 0-80821  
 KCl:Eu<sup>2+</sup> crystals, photostimulated afterglow investigation at room temp. 0-108259  
 KCl:Ga<sup>3+</sup>, polarisation of Ga<sup>3+</sup> centre A<sub>T</sub> emission, temp. depend. 0-80842  
 KCl:He, ENDOR and ESR study of anion sites 0-108118  
 KCl:KReO<sub>4</sub> free induction decay generation of ultrashort CO<sub>2</sub> pulses 0-74444  
 KCl:Li, (F<sub>2</sub><sup>+</sup>)<sub>A</sub> centres, optical props. 0-89026  
 KCl:Li, X-irrad., F<sub>A</sub> centres, thermolum. studies 0-80878  
 KCl:Li (F<sub>2</sub><sup>+</sup>)<sub>A</sub> centres, tunable CW laser action 0-87399  
 KCl:Li F<sub>2</sub>(II) centre laser, pumped by flashlamp-pumped dye laser 0-102737  
 KCl:Li<sup>+</sup>, single-pulse excitation of paraelectric induction and echo signals 0-80732  
 KCl:Mg<sup>2+</sup>, dopant aggregation and precipitation 0-107306  
 KCl:Mg<sup>2+</sup>(Ca<sup>2+</sup>)(Sr<sup>2+</sup>)(Ba<sup>2+</sup>), defect struct., Mott-Littleton technique study 0-59487  
 KCl:Na, F<sub>B</sub> centre energy levels 0-107738  
 KCl:OH, absorpt. in high-transparency region 0-89037  
 KCl:OH, cc U<sub>2</sub> to H<sub>2</sub>O<sup>-</sup> defects conversion after UV photodecomp. 0-107230  
 KCl:PO<sub>4</sub><sup>3-</sup>, ODMR in zero and weak mag. fields 0-88894  
 KCl:Pb, impurity distrib., light scat. and microhardness study, heat treatment 0-96562  
 KCl:Pb<sup>2+</sup>, ion energetic parameters comparison with alkaline earth fluoride crystals 0-66243  
 KCl:Pb<sup>2+</sup>, pure and doped, electrolytically coloured, elec. cond. and optical absorpt. meas. 0-100668  
 KCl:Pb<sup>2+</sup>, X-ray irradi., electron-trapped centres, Pb<sup>+</sup> and Pb<sup>0</sup>, optical absorpt. spectra 0-71461  
 KCl:ReO<sub>4</sub>, resonantly enhanced phase conjugation through degenerate four-wave mixing 0-58635  
 KCl:ReO<sub>4</sub><sup>-</sup> nonlinear absorption for CO<sub>2</sub> laser pulse compression and mode locking 0-74443  
 KCl:SO<sub>4</sub><sup>2-</sup>, ionic cond., defect parameters, diffusion coeffs. 0-79978  
 KCl:SnCl<sub>3</sub>, photostimulated hole recombination luminesc. (*Russian*) 0-80833  
 KCl:Sr, positron annihilation and trapping in A-centres 0-84802  
 KCl:Sr crystal, Z<sub>4</sub> colour centre, luminesc. study 0-64993  
 KCl:Sr<sup>2+</sup>, ionic cond., defect parameters, diffusion coeffs. 0-79978  
 KCl:Sr<sup>2+</sup>, Cu<sup>+</sup>, thermolum. response, extension of two-step reaction model 0-89075  
 KCl:Sr<sup>2+</sup>(SO<sub>4</sub><sup>2-</sup>), defect parameters, self-consistent set, ionic cond. meas. 0-107487  
 KCl:Ti, electroluminescence, spectra and quantum yield activator conc. depend., cond. changes 0-89070  
 KCl:Ti, temp. depend. of cathodolum. (*Russian*) 0-80868  
 KCl:Ti (0.003 to 0.27 mol.%), electrolum. 0-71490



# potassium compounds continued

- KCl:Zn<sup>2+</sup>, optical absorpt. bands rel. to charge transfer 0-66245  
KCl-CaCl<sub>2</sub>-NaCl, ternary phase diagrams, interactive computer program 0-71629  
KCl-CuCl eutectic fused salt, potential as intermediate temp. solar heat transfer and storage medium 0-101135  
KCl-KBr, mixed crystals, microhardness, theory 0-75298  
KCl-KBr, solution hardening and softening at low temp. 0-108462  
KCl-KBr, with equimol. conc., piezo-optic birefringence theory 0-100643  
KCl-NaCl mixed crystals, contact angles and free energies at solid/melt interface 0-64937  
KCl-ZnCl<sub>2</sub>, molten, US velocity, thermodynamic quantities and struct. (Japanese) 0-88270  
KCl-ZnCl<sub>2</sub>, molten, US absorption coeffs. and bulk viscosity coeffs. (Japanese) 0-88271  
KCl<sub>1-x</sub>Br<sub>x</sub>, impurity centre local vibrs., comp. depend. of spectral parameters 0-79898  
KCl<sub>1-x</sub>Br<sub>x</sub>, bulk modulus, room temp. to 400°C 0-92588  
KCl<sub>1-x</sub>Br<sub>x</sub>, dielectric const. determ. 0-108145  
KCl<sub>1-x</sub>Br<sub>x</sub>, mixed crystals, thermolum. and optical absorption studies 0-104000  
KClO<sub>3</sub>, <sup>35</sup>Cl NQR appl. in thermometry below 77K 0-66067  
KClO<sub>3</sub>, AC electrical conductivity meas. between temp. range 25-325°C, automated technique 0-59699  
KClO<sub>3</sub>, electrical conductivity, frequency dependence 0-65288  
KCoCr<sub>2</sub>(VO<sub>4</sub>)<sub>3</sub>, synthesis and cryst. struct. 0-88114  
KCoF<sub>3</sub>, antiferromag., with residual orbital moment, nucl. mag. relax. 0-71215  
KCoF<sub>3</sub>, antiferromag. domain wall motion under external stress 0-80583  
KCoF<sub>3</sub>, IR refl. spectra, vibr. modes, optical vibr. freq., Kramers Kronig anal. 0-66190  
K<sub>2</sub>CoF<sub>4</sub>, 2-dimens. Ising antiferromag., mag. excitons, Raman scatt. obs. 0-66181  
K<sub>2</sub>CoF<sub>4</sub>, two-dimens. Ising antiferromag., nearest neighbour correl. function, birefr. expts. 0-71386  
KCr alum, relaxation behaviour, EPR study, environmental effects 0-66021  
K<sub>2</sub>Cr<sub>2</sub>O<sub>7</sub>, Cr <sup>7</sup>p<sub>0</sub> state, radiative lifetime in matrices, meas. using laser ablation and selective excitation 0-71959  
KCr<sub>2</sub>Al<sub>2</sub>(SO<sub>4</sub>)<sub>2</sub>·12H<sub>2</sub>O, EPR of single crystals, zero-field splitting of Cr<sup>3+</sup> 0-66015  
KCrO<sub>2</sub>, two-dimens. mag. props. rel. to cryst. struct. 0-75776  
K<sub>2</sub>CuCl<sub>4</sub>·2H<sub>2</sub>O, hyperfine and super-exchange interactions 0-103654  
KCuCr<sub>2</sub>(VO<sub>4</sub>)<sub>3</sub>, synthesis and cryst. struct. 0-88114  
KCuF<sub>3</sub>, linear chain Heisenberg antiferromag., nearest neighbour correl. function, birefr. expts. 0-71386  
KCuF<sub>3</sub>, one-dimens. antiferromag., spin waves, neutron scatt. study 0-65848  
K<sub>2</sub>CuF<sub>4</sub>, layered spin system, planar rotator symmetry, phase transition 0-65951  
K<sub>2</sub>CuF<sub>4</sub>, magnon condensation obs. in quasi-2D planar ferromag. phase 0-60232  
K<sub>2</sub>CuF<sub>4</sub>, spin relax., crit. behaviour, high freq. susceptibility meas. 0-65936  
K<sub>2</sub>CuF<sub>4</sub>, two-dimens. ferromag., saturation of parallel-pumped magnons 0-97147  
K<sub>2</sub>Cu<sub>1-x</sub>Zn<sub>x</sub>F<sub>4</sub>, Curie temp., Cu conc. depend. 0-60255  
KD<sub>2</sub>AsO<sub>4</sub>, ferroelec., high temp. phase transition, Raman spectra 0-71338  
KD<sub>2</sub>AsO<sub>4</sub>, ferroelectric, high temp. phase transitions, proton dynamics 0-76023  
KD<sub>2</sub>H<sub>2</sub>(<sub>1-x</sub>)PO<sub>4</sub> crystals, 0 < x < 0.98, light scatt. by polaritons 0-96802  
K(D<sub>2</sub>H<sub>1-x</sub>)<sub>2</sub>PO<sub>4</sub> ferroelec., dielec. props., four-cluster approx. 0-97202  
K(D<sub>2</sub>H<sub>1-x</sub>)<sub>2</sub>(SeO<sub>3</sub>)<sub>2</sub>, ferroelastic, anelastic and elastic infra-low freq. props. 0-70304  
KD<sub>2</sub>PO<sub>4</sub>, acoustic phonon dispersion, elastic stiffness, light scatt. obs. 0-103966  
KD<sub>2</sub>PO<sub>4</sub>, coexistence states during first order transition, optical obs. 0-75350  
KD<sub>2</sub>PO<sub>4</sub> crystal, electro-optical extraction of Nd:YAG laser pulses (German) 0-87416  
KD<sub>2</sub>PO<sub>4</sub> crystal, photoresponse under laser irradi. 0-100479  
KD<sub>2</sub>PO<sub>4</sub> crystal electron-beam spatial light modulator, resolution 0-74503  
KD<sub>2</sub>PO<sub>4</sub>, neutron scattering from coupled polar-elastic waves 0-92623  
KD<sub>2</sub>PO<sub>4</sub>, optical activity in paraelec. phase 0-60539  
KD<sub>2</sub>PO<sub>4</sub>, phase transitions study, role of cryst. struct. determ. 0-75197  
KD<sub>2</sub>PO<sub>4</sub>, photo-spatial light modulator, optical data processing 0-102839  
KD<sub>2</sub>PO<sub>4</sub>, polarisation fluctuations, wavevector depend. 0-71295  
KD<sub>2</sub>PO<sub>4</sub>, transparent dielec., thermal analysis of laser-induced damage 0-66336  
KD<sub>2</sub>PO<sub>4</sub>, X-irradiated, hysteresis effects obs. by ESR 0-103928  
KD<sub>2</sub>PO<sub>4</sub>:Ti<sup>2+</sup>, EPR of ferroelec. and paraelec. phases 0-66012  
KD<sub>2</sub>PO<sub>4</sub>-type ferroelectrics, parametric tunnelling-like reson. 0-66119  
K<sub>2</sub>D(SO<sub>4</sub>)<sub>2</sub>, dielec. props. and phase transitions 0-60482  
KD<sub>2</sub>(SeO<sub>3</sub>)<sub>2</sub>, ferroelastic phase transition, mech. stress effect 0-70394  
KD<sub>2</sub>(SeO<sub>3</sub>)<sub>2</sub>, phase transition, neutron scatt. study 0-73351  
KdY(MoO<sub>4</sub>)<sub>2</sub>, polarised IR and Raman struct., <sup>92</sup>Mo/<sup>100</sup>Mo isotope effect 0-108198  
β-K<sub>2</sub>Er<sub>2</sub>F<sub>7</sub>, crystal struct. (French) 0-107164  
KF, one electron props., SCF-Alpha scattered wave method 0-83279  
KF:LiF photodichroic spatial light modulator for joint Fourier transform correlation 0-106617  
KF-AlF<sub>3</sub>, ion-molecule equilibria studied by mass spectrometric method, heats of dissoc. and form. calc. 0-104479  
KF-ErF<sub>3</sub>, phase diagram 0-92645  
KF-UF<sub>4</sub>, ion-molecule equilibria, heat of form. and dissoc. and electron affinities determ. 0-104480  
KF-UF<sub>4</sub>, molten binary mixtures, viscosity meas. 0-65270  
KF(Cl)(Br)(I), emission band of F-centre 0-76071  
K<sub>2</sub>Fe(CN)<sub>6</sub>, pressure induced reduction, Raman spectra 0-66776  
K<sub>2</sub>Fe(CN)<sub>6</sub>-KCl, press. induced reduction, IR spectra after pressurization 0-66776  
K<sub>2</sub>Fe(CN)<sub>6</sub>·3H<sub>2</sub>O, ferroelec. and paraelec. phases, dielec. props. meas. 0-60494  
K<sub>2</sub>FeCl<sub>4</sub>(H<sub>2</sub>O), antiferromag., press. depend. on spin-flop transition 0-80505  
KFeF<sub>4</sub>, amorphous, mag. props. and Mossbauer spectra, speromagnetism and micromagnetism 0-75778  
K<sub>2</sub>FeF<sub>4</sub>, antiferromagnet, two-dimensional, mag. excitations 0-80492  
K<sub>2</sub>FeF<sub>4</sub>, charge transport and polarisation 0-80681

# potassium compounds continued

- K<sub>2</sub>FeF<sub>4</sub>, two dimensional easy plane antiferromag., neutron scatt. expts. 0-65838  
K<sub>2</sub>FeF<sub>4</sub>, two-dimensional antiferromag., with easy-plane anisotropy, mag. excitations and two-magnon Raman scatt. 0-65839  
K<sub>2</sub>FeF<sub>4</sub>, two-dimensional antiferromag., cryst. field effects, Mossbauer spectroscopy 0-71254  
K<sub>2</sub>FeF<sub>5</sub>, mag. struct. and one-dimens. antiferromagnetism 0-60209  
K<sub>2</sub>FeF<sub>5</sub>, one-dimensional antiferromag. systems, Mossbauer studies 0-71266  
K<sub>2</sub>Fe<sub>2</sub>F<sub>7</sub>, two-dimensional antiferromag., cryst. field effects, Mossbauer spectroscopy 0-71254  
KFe(MoO<sub>4</sub>)<sub>2</sub>, phase transitions at 312 and 139K 0-70396  
K<sub>2</sub>FeO<sub>4</sub>, crit. slowing down of spin fluctuations, Mossbauer spectra and relax. theory 0-65882  
KGd(WO<sub>4</sub>)<sub>2</sub>:Ho<sup>3+</sup>, stimulated emission at low temps. 0-106526  
KH, structural transition from NaCl to CsCl type under high press. 0-96458  
KH<sub>2</sub>AsO<sub>4</sub>, ferroelec. phase, <sup>75</sup>As NQR, press. and temp. depend. 0-71227  
KH<sub>2</sub>AsO<sub>4</sub>, ferroelec., high temp. phase transition, Raman spectra 0-71338  
KH<sub>2</sub>AsO<sub>4</sub>, ferroelec., dielec. props., four-cluster approx. 0-97202  
KH<sub>2</sub>AsO<sub>4</sub>, ferroelectric phase transition under high hydrostatic press., mol. dynamics, NQR study 0-75880  
KH<sub>2</sub>AsO<sub>4</sub>, ferroelectric, high temp. phase transitions, proton dynamics 0-76023  
KH<sub>2</sub>AsO<sub>4</sub>, γ-irradiated, free radicals, EPR and ENDOR study of consequences of ferroelec. transition (French) 0-93209  
KH<sub>2</sub>AsO<sub>4</sub>, proton modes, dielec. spectroscopy 0-75915  
KH<sub>2</sub>AsO<sub>4</sub>, thermal cond., anomalous temp. behaviour near structural phase transition (Russian) 0-75394  
K(H<sub>1-x</sub>D<sub>x</sub>)<sub>2</sub>P<sub>4</sub>, polarised impurity cluster effects in light scatt. expts. 0-71431  
K(H<sub>1-x</sub>D<sub>x</sub>)<sub>2</sub>PO<sub>4</sub>, polarisation relaxation time and Landau kinetic coeff. rel. to degree of deuteration 0-84251  
KH<sub>2</sub>(<sub>1-x</sub>)<sub>2</sub>P<sub>2</sub>O<sub>7</sub>, proton modes, dielec. spectroscopy 0-75915  
KH<sub>2</sub>PO<sub>4</sub> and KD<sub>2</sub>PO<sub>4</sub>, thermal cond., anomalous temp. behaviour near structural phase transition (Russian) 0-75394  
KH<sub>2</sub>PO<sub>4</sub>, Brillouin-Rayleigh scatt. studies near ferroelec. transition temp. 0-76036  
KH<sub>2</sub>PO<sub>4</sub>, Burgers vector sign determ. for nearly screw dislocations, X-ray obs. 0-59467  
KH<sub>2</sub>PO<sub>4</sub>, crit. behaviour near tricritical point, phenomenological interpretation 0-70389  
KH<sub>2</sub>PO<sub>4</sub>, crit. behaviour, dilatometric study 0-92689  
KH<sub>2</sub>PO<sub>4</sub>, critical and tricritical phenomena, susceptibility, exponents 0-75976  
KH<sub>2</sub>PO<sub>4</sub> crystal, laser freq. conversion to produce UV coherent pulse, 45 GW, for laser fusion 0-69450  
KH<sub>2</sub>PO<sub>4</sub> crystal, optical activity 0-71373  
KH<sub>2</sub>PO<sub>4</sub> crystal, photoresponse under laser irradi. 0-100479  
KH<sub>2</sub>PO<sub>4</sub> electro-optic modulator crystals, piezoelec. induced acoustic transients 0-70316  
KH<sub>2</sub>PO<sub>4</sub> family of crystals, proton modes, dielec. spectroscopy 0-75915  
KH<sub>2</sub>PO<sub>4</sub>, ferroelectric-elastic phase transition, theoretical model and expt. (Russian) 0-75961  
KH<sub>2</sub>PO<sub>4</sub>, ferroelectric transition, order-disorder character of hydrogen bond 0-93251  
KH<sub>2</sub>PO<sub>4</sub>, filiform crystals at low temp., tensile strength determ. 0-100877  
KH<sub>2</sub>PO<sub>4</sub>, growth and dissolution kinetics, temp. and pH effect 0-88070  
KH<sub>2</sub>PO<sub>4</sub>, high-power picosecond pulse generation 218 to 316 nm 0-64106  
KH<sub>2</sub>PO<sub>4</sub>, NMR spin echoes, indirectly induced 0-71239  
KH<sub>2</sub>PO<sub>4</sub>, nonlinear crystals, interference of optical harmonics 0-64102  
KH<sub>2</sub>PO<sub>4</sub>, phase transitions study, role of cryst. struct. determ. 0-75197  
KH<sub>2</sub>PO<sub>4</sub> single crystal evidence for spiral growth on pyramidal faces 0-84120  
KH<sub>2</sub>PO<sub>4</sub>, single crystal neutron diffraction study at high pressure 0-92497  
KH<sub>2</sub>PO<sub>4</sub>, spontaneous polarisation, low temp. meas. 0-75921  
KH<sub>2</sub>PO<sub>4</sub> type ferroelectrics, Green's function theory of phase transitions with pseudo-spin-lattice coupled mode model 0-71354  
KH<sub>2</sub>PO<sub>4</sub>, ultrashort light pulse parametric transform. under optimum interaction conditions 0-99791  
KH<sub>2</sub>PO<sub>4</sub>, X-irradiated, hysteresis effects obs. by ESR 0-103928  
KH<sub>2</sub>PO<sub>4</sub>:Ti<sup>2+</sup>, EPR of ferroelec. and paraelec. phases 0-66012  
KH<sub>2</sub>PO<sub>4</sub>-type ferroelectrics, tunnelling integral 0-70156  
KH<sub>2</sub>PO<sub>4</sub>-type ferroelectrics, dielec. props., four-cluster approx. 0-97202  
KHSO<sub>4</sub>, phase diagram of 3.2 GPa, 450°C 0-76237  
KHSO<sub>4</sub>:Fe<sup>3+</sup>, DC cond. meas., mechanism 0-65285  
K<sub>2</sub>H(SO<sub>4</sub>)<sub>2</sub>, dielec. props. and phase transitions 0-60482  
KHSO<sub>4</sub>·KH<sub>2</sub>PO<sub>4</sub>, cryst. struct. 0-75211  
KH<sub>2</sub>(SeO<sub>3</sub>)<sub>2</sub>, ferroelastic transition under uniaxial press., EPR study 0-59562  
KH<sub>2</sub>(SeO<sub>3</sub>)<sub>2</sub>, ferroelastic phase transition, mech. stress effect 0-70394  
K<sub>2</sub>Hg(CN)<sub>4</sub>, third order elastic consts. 0-84231  
K<sub>2</sub>, defect modes due to substitutional anion-pair and cation-pair impurities in ionic crystals 0-92540  
K<sub>2</sub>, electron range-energy relation, thermally created lattice vacancies effect 0-92574  
K<sub>2</sub>, growth time of π emission in picosecond range 0-76067  
K<sub>2</sub>, inelastic light scattering of localised vibration of interstitial H atom in alkali halides 0-88998  
K<sub>2</sub>, irradiated at room temp., stored energy 0-79839  
K<sub>2</sub> microcrystals, UV spectra by diffuse reflectance technique, surface electronic transitions obs. 0-75614  
K<sub>2</sub>, oscillator strengths of defects, Smakula eqn. generalisation 0-108232  
K<sub>2</sub>, perturbed by Jahn-Teller centers, lattice dynamics 0-107394  
K<sub>2</sub>, photostimulated recomb. electron spin polarisation 0-60673  
K<sub>2</sub>, self trapped exciton form. time at <sup>1</sup>S<sub>0</sub><sup>+</sup> state under pulsed electron beam in ps range 0-97347  
K<sub>2</sub>, self-trapped exciton form. via thermally induced defect reactions 0-60687  
K<sub>2</sub>:Cu<sup>2+</sup>, exciton bands, optical absorpt. and MCD spectra 0-80821  
K<sub>2</sub>:Ga<sup>3+</sup>, polarisation of Ga<sup>3+</sup> centre A<sub>T</sub> emission, temp. depend. 0-80842  
K<sub>2</sub>:PO<sub>2</sub>, ODMR in zero and weak mag. fields 0-88894  
K<sub>2</sub>:Pb, absorpt. spectra of Pb<sup>2+</sup> centres 0-76058  
K<sub>2</sub>:Ti, decay of fast component of impurity luminesc. excitation in A-absorption band (Russian) 0-84767



## potassium compounds continued

- KI:Ti, polarised luminesc. of  $(Ti^{3+})_2$  centres 0-71473  
 KI:Zn<sup>2+</sup>, optical absorpt. bands rel. to charge transfer 0-66245  
 KI(Br)(Cl), fundamental luminescence at high ionisation levels (*Russian*) 0-103985  
 K<sub>2</sub>InCl<sub>3</sub>·H<sub>2</sub>O, crystal structure and H-bonding 0-64978  
 KLa(MoO<sub>4</sub>)<sub>3</sub>, solubility in aq. K<sub>2</sub>MoO<sub>4</sub> solns., hydrothermal conditions 0-96651  
 K<sub>2</sub>Li<sub>2</sub>Nb<sub>2</sub>O<sub>7</sub> films for optical waveguides epitaxial growth and characterisation 0-79016  
 KLu(WO<sub>4</sub>)<sub>3</sub>:Er<sup>3+</sup>, room temp. stimulated emission obs. 0-106527  
 KM<sub>2</sub>F<sub>3</sub>, bond energy, equilib. distances and compressibility calcs. 0-70159  
 KM<sub>2</sub>Mg<sub>1-x</sub>F<sub>3</sub>, randomly diluted Heisenberg paramag. nucl. relax. 0-60444  
 K<sub>2</sub>(M<sub>1</sub>Ti<sub>1-x</sub>)<sub>2</sub>O<sub>7</sub> (M = Mg, Zn, Ni, Cu, Fe<sup>III</sup>, Mn<sup>III</sup>), (0.7 ≤ x ≤ 0.9), new layer struct. (*French*) 0-84149  
 K<sub>2</sub>MX<sub>6</sub> (M = Sn, Re, Os, Ir, Pt; X = Cl, Br), heavy metal ion implantation, mol. unit form. 0-100267  
 KMg<sub>2</sub>AlSi<sub>2</sub>O<sub>10</sub>F<sub>2</sub>, dislocations, subgrain boundaries, X-ray diffr. topography study (*Chinese*) 0-88149  
 KMgCr<sub>2</sub>(VO<sub>4</sub>)<sub>3</sub>, synthesis and cryst. struct. 0-88114  
 KMgF<sub>3</sub>, F-centre ENDOR study 0-108117  
 KMgF<sub>3</sub>, spin Hamiltonian parameters for Fe<sup>3+</sup> ions, superposition model anal. 0-108053  
 KMgF<sub>3</sub>:Co<sup>2+</sup>, <sup>4</sup>T<sub>1</sub>-<sup>4</sup>T<sub>2</sub> transition, zero-phonon lines intensities 0-75529  
 KMgF<sub>3</sub>:Cr<sup>2+</sup>, HF phonon spectroscopy using supercond. tunnel junctions 0-65178  
 KMgF<sub>3</sub>:Fe<sup>2+</sup>, anomalous acoustic relax. absorpt. and APR 0-88864  
 KMgF<sub>3</sub>:Ni<sup>2+</sup>, acoustic Faraday and Cotton-Mouton effects, theory 0-65987  
 KMgF<sub>3</sub>:Yb<sup>3+</sup>, perovskite type cryst., ENDOR meas. 0-80638  
 K<sub>2</sub>Mg<sub>2</sub>LiSi<sub>2</sub>O<sub>30</sub>, cryst. struct., X-ray diffr. and IR spectra (*French*) 0-107158  
 KMg<sub>2</sub>LiSi<sub>2</sub>O<sub>10</sub>F<sub>2</sub>·NaMg<sub>2</sub>LiSi<sub>2</sub>O<sub>10</sub>F<sub>2</sub>, solid soln., solid solubility and swelling characs. 0-59660  
 K<sub>2</sub>Mg<sub>2</sub>M<sub>2</sub>Si<sub>2</sub>O<sub>30</sub> (M = Cu, Fe, Zn, Mg), cryst. struct., X-ray diffr. and IR spectra (*French*) 0-107158  
 KMg<sub>1-x</sub>Mn<sub>x</sub>F<sub>3</sub>, disordered paramagnet, <sup>19</sup>F NMR study 0-71216  
 K<sub>1-x</sub>Mg<sub>0.77</sub>Ti<sub>0.23</sub>O<sub>16</sub>, hollandite, one-dimens. superionic cond., transport model 0-107529  
 K<sub>2</sub>Mg<sub>2</sub>Ti<sub>8-x</sub>O<sub>16</sub>, stochastic Langevin dynamics study of correlated ionic motion in 1-D solid electrolytes 0-65279  
 KMg<sub>2</sub>[AlSi<sub>2</sub>O<sub>10</sub>]F<sub>2</sub> with excess Al, synthetic fluorophlogopite, radiation-induced paramag. O centres 0-60417  
 KMnF<sub>3</sub>, 185K structural transition, wavevector reversed ultrasound study 0-75306  
 KMnF<sub>3</sub>, critical dynamics of sound 0-103424  
 KMnF<sub>3</sub>, Faraday effect mechanism in paramag. phase 0-60552  
 KMnF<sub>3</sub>, IR refl. spectra, vibr. modes, optical vibr. freq., Kramers Kronig anal. 0-66190  
 KMnF<sub>3</sub>, Mossbauer gamma quanta scattering near 186K transition 0-108126  
 KMnF<sub>3</sub>, second-order displacive transition region, static and dynamic characs. determ. 0-70409  
 KMnF<sub>3</sub>, specific heat near Neel temp. (*Russian*) 0-100340  
 KMnF<sub>3</sub>:Rb, phase transition and atomic motions, NMR study 0-75872  
 K<sub>2</sub>MnF<sub>4</sub>, ordered quadratic-layer Heisenberg antiferromag., nucl. spin-magnon relax. 0-71217  
 K<sub>2</sub>MnF<sub>4</sub>:Zn(Mg)(Ni), mag. effects of impurities 0-65869  
 K<sub>2</sub>MnF<sub>4</sub>:Zn(Mg)(Ni), local magnetisation, NMR and Green's function study 0-65870  
 K<sub>2</sub>Mn<sub>2</sub>F<sub>7</sub>, crit. EPR line broadening near Neel temp. 0-71165  
 K<sub>2</sub>Mn<sub>2</sub>F<sub>7</sub>, quadratic double layer antiferromag., two-magnon Raman scatt. 0-66183  
 KMn<sub>1-x</sub>Me<sub>x</sub>F<sub>3</sub> (Me = Mg<sup>2+</sup>, Fe<sup>2+</sup>, Co<sup>2+</sup> and Ni<sup>2+</sup>) Bridgman growth, 0-60764  
 K<sub>2</sub>Mn<sub>2</sub>Mg<sub>1-x</sub>F<sub>4</sub>, impure two-dimensional system, ESR line reson. shift due to low symmetric spin distrib. 0-93162  
 KMn<sub>1-x</sub>Ni<sub>x</sub>F<sub>3</sub>, antiferromag. crit. props., neutron scatt. obs. 0-88749  
 K<sub>2</sub>MoO<sub>4</sub>, aq. soln., solubility of KLa(MoO<sub>4</sub>)<sub>3</sub> 0-96651  
 K<sub>2</sub>Mo<sub>2</sub>O<sub>10</sub> melt volatility, solubility of YAl<sub>3</sub>(BO<sub>3</sub>)<sub>4</sub> 0-65211  
 K<sub>2</sub>MoO<sub>4</sub>F<sub>3</sub>, ferroelec. transition obs. 0-75989  
 K<sub>2</sub>Mo<sub>15</sub>S<sub>10</sub>, superconducting chalcogenides containing Mo<sub>6</sub> and Mo<sub>9</sub> clusters 0-103804  
 K<sub>2</sub>Mo<sub>2</sub>S<sub>11</sub>, prep. and struct., Mo<sub>12</sub> cluster in Mo<sub>12</sub>S<sub>14</sub> unit 0-107168  
 K<sub>2</sub>Mo<sub>15</sub>Se<sub>10</sub>, superconducting chalcogenides containing Mo<sub>6</sub> and Mo<sub>9</sub> clusters 0-103804  
 K<sub>2</sub>Mo<sub>2</sub>V<sub>2</sub>O<sub>10</sub>·8H<sub>2</sub>O, containing structurally new K-coordinated octamolybdo-pentavanadate anion, cryst. struct. 0-96479  
 KN<sub>2</sub>, ESR undergraduate expt. 0-105471  
 KNO<sub>3</sub>, activation coefficients and solvation numbers in mixed methanol solvents 0-81334  
 KNO<sub>3</sub>, calcite-type crystals, topotaxial decomp. TEM obs. 0-108710  
 KNO<sub>3</sub> in alkali halides tablets, phase transition and ion exchange, IR spectra 0-79937  
 KNO<sub>3</sub>, Raman and IR spectra and lattice vibrs. 0-60565  
 3KN<sub>3</sub>·2Ca(NO<sub>3</sub>)<sub>2</sub>, glass form. from liq., struct. transform., Raman spectrum obs. 0-64916  
 3KN<sub>3</sub>·2ZnCl<sub>2</sub>, glass form. from liq., struct. transform., Raman spectrum obs. 0-64916  
 K<sub>1-x</sub>Na<sub>x</sub>Cl, impurity centre local vibrs., comp. depend. of spectral parameters 0-79898  
 K<sub>2</sub>Na(Fe,Cu,Ni)<sub>24</sub>S<sub>26</sub>Cl<sub>2</sub>, jersherite, X-ray cryst. struct. determ. 0-92512  
 K<sub>2</sub>NaGaF<sub>6</sub>:Cr<sup>3+</sup>, magneto-optical study of <sup>2</sup>T<sub>1g</sub>, <sup>4</sup>T<sub>2g</sub>, <sup>2</sup>E<sub>g</sub>-<sup>4</sup>A<sub>2g</sub> transitions 0-71384  
 KNaSO<sub>4</sub>, X-ray cryst. struct. determ. 0-64963  
 K<sub>2</sub>Na(SO<sub>4</sub>)<sub>2</sub>, X-ray cryst. struct. determ. 0-64963  
 K<sub>1-x</sub>Na<sub>x</sub>TaO<sub>3</sub>, quantum ferroelectric, dielec. susceptibility 0-103922  
 KNbO<sub>3</sub>, crystals, reduced, hologram recording and erasure sensitivity (*Russian*) 0-78795  
 KNbO<sub>3</sub>, cubic, temp. depend. of intensity of X-ray interference 0-59613  
 KNbO<sub>3</sub>, displacive ferroelectric, effective charge determ. 0-97212  
 KNbO<sub>3</sub>, domain struct. at transitions from twinned phase, appl. to tetragonal-orthorhombic transition 0-71360  
 KNbO<sub>3</sub>, ferroelec. cryst., IR and Raman spectra, mode coupling 0-66194  
 KNbO<sub>3</sub>, reduced, phase hologram recording, energy transfer and sensitivity 0-69338  
 KNbO<sub>3</sub>, reduced, phase hologram recording sensitivity, energy transfer, photovoltaic effects 0-78799

## potassium compounds continued

- KNbO<sub>3</sub>, SHG with Ga<sub>1-x</sub>Al<sub>x</sub>As laser 0-74431  
 K<sub>2</sub>Nb<sub>15</sub>O<sub>35</sub>:F<sub>18</sub>, cryst. struct. determ. (*French*) 0-96489  
 K<sub>2</sub>Nb<sub>6</sub>O<sub>14</sub>:F<sub>9</sub>, cryst. struct. determ. (*French*) 0-96489  
 KNiCl<sub>3</sub>, disorder as observed by electron diffr. 0-75213  
 KNiCr<sub>2</sub>(VO<sub>4</sub>)<sub>3</sub>, synthesis and cryst. struct. 0-88114  
 KNiF<sub>3</sub>, <sup>19</sup>F spin-lattice relaxation 0-93211  
 KNiF<sub>3</sub>, magnetostriction, X-ray diffraction and strain gauge meas. 0-65997  
 K<sub>2</sub>NiF<sub>4</sub>, ordered quadratic-layer Heisenberg antiferromag., nucl. spin-magnon relax. 0-71217  
 K<sub>2</sub>Ni<sub>2</sub>F<sub>7</sub>, quadratic double layer antiferromag., two-magnon Raman scatt. 0-66183  
 K<sub>2</sub>O·Al<sub>2</sub>O<sub>3</sub>·P<sub>2</sub>O<sub>5</sub>·TiO<sub>2</sub>, structural role of Ti, kinetic study of chem. destruction 0-88055  
 K<sub>2</sub>O·Al<sub>2</sub>O<sub>3</sub>·2SiO<sub>2</sub>·BaO plasma emitter 0-96368  
 K<sub>2</sub>O·B<sub>2</sub>O<sub>3</sub>·Fe<sub>2</sub>O<sub>3</sub>, γ-irrad., Mossbauer spectroscopic study 0-108132  
 K<sub>2</sub>O·CaO·BaO·B<sub>2</sub>O<sub>3</sub>, glass, refraction, refractive index from 0.365 to 2.50 μm 0-88953  
 K<sub>2</sub>O·CaO·SiO<sub>2</sub> glasses, Auger analysis, alkali signal decrease 0-61189  
 K<sub>2</sub>O·MgO·Al<sub>2</sub>O<sub>3</sub>, ionic cond. 0-107480  
 K<sub>2</sub>O·MgO·B<sub>2</sub>O<sub>3</sub>:Cu<sup>2+</sup>, micro-inhomogeneities, EPR and Raman study 0-84080  
 K<sub>2</sub>O·Na<sub>2</sub>O·Al<sub>2</sub>O<sub>3</sub>·SiO<sub>2</sub> glass, ion exchange kinetics and interdiffusion mechanisms 0-80003  
 K<sub>2</sub>O·PbO·SiO<sub>2</sub>, glass, effect of DC on corrosion of SnO<sub>2</sub> electrodes 0-85075  
 K<sub>2</sub>O·SiO<sub>2</sub> glasses, Auger analysis, alkali signal decrease 0-61189  
 KOH gas-cryostat system, isotopic equilibrium near phase transition points (*Russian*) 0-91697  
 KOH·KO<sub>2</sub>, phase diagram (*French*) 0-107177  
 K<sub>2</sub>O·Na<sub>2</sub>O·B<sub>2</sub>O<sub>3</sub>·SiO<sub>2</sub>, glass character of elec. cond. 0-103516  
 (K<sub>2</sub>O)<sub>x</sub>(SiO<sub>2</sub>)<sub>1-x</sub> glass, pure and with As<sub>2</sub>O<sub>3</sub>, Raman study of As 0-84733  
 2K<sub>2</sub>O·11TiO<sub>2</sub>·3H<sub>2</sub>O fibre+Ba(OH)<sub>2</sub> hydrothermal reaction to form BaTiO<sub>3</sub> fibres (*Japanese*) 0-93527  
 K<sub>2</sub>OSiCl<sub>6</sub>, Cl NQR spectra by Fourier transform methods 0-75879  
 K<sub>2</sub>OSiCl<sub>6</sub>, impurity H<sup>+</sup> ion motion, <sup>35</sup>Cl NQR obs., 77 and 298K 0-60451  
 K<sub>2</sub>OSiCl<sub>6</sub>, single cryst. with H<sup>+</sup> interstitials, protonic cond. from dielec. meas. 0-107515  
 KPFe<sub>4</sub>, γ-irrad., trapped free radicals EPR obs. 0-63683  
 K<sub>2</sub>PbCu(NO<sub>3</sub>)<sub>6</sub>, incommensurate Jahn-Teller transition, Huang scatt. 0-70401  
 K<sub>2</sub>PbCu(NO<sub>3</sub>)<sub>6</sub>, phase transition obs., commensurate and incommensurate structural phase transitions in Jahn-Teller system 0-70403  
 KPb<sub>13</sub>·2H<sub>2</sub>O, X-ray cryst. struct. determ. 0-64958  
 K<sub>2</sub>Pb[Co(NO<sub>3</sub>)<sub>6</sub>], X-ray cryst. struct. determ. 0-88106  
 K<sub>2</sub>Pt(CN)<sub>4</sub>Br<sub>0.3</sub>·3H<sub>2</sub>O, CDW system, nonlinear amplitude-phase interaction 0-88490  
 K<sub>2</sub>Pt(CN)<sub>4</sub>Br<sub>0.3</sub>·3H<sub>2</sub>O, anisotropic radiation damage in electron microscopy, diff. spot fading rate obs. 0-107329  
 K<sub>1-x</sub>Rb<sub>x</sub>Cl, impurity centre local vibrs., comp. depend. of spectral parameters 0-79898  
 K<sub>2</sub>ReCl<sub>6</sub>, elastic constants, softening of acoustic modes, obs. by Brillouin scattering 0-71440  
 KReO<sub>4</sub>, heat capacity and thermodynamic props., 8 to 304K 0-100335  
 KReO<sub>4</sub>, nuclear electric hexadecapole interactions 0-65513  
 KReO<sub>4</sub>, quadrupole spin echo with two-frequency action, amplification and modulation 0-108116  
 K<sub>2</sub>SO<sub>4</sub>·Ag<sub>2</sub>SO<sub>4</sub> mixtures, surface comp., AES and XPS obs. 0-81386  
 K<sub>2</sub>SO<sub>4</sub>, anhydrous, struct. relationships w.r.t. fast ion cond. 0-107188  
 K<sub>2</sub>SO<sub>4</sub>, longitudinal-acoustic soft mode in phase transition 0-75326  
 K<sub>2</sub>SO<sub>4</sub>, phase transform., mech. of thermal hysteresis, DTA, dilatometry and dielec. meas. 0-75533  
 β-K<sub>2</sub>SO<sub>4</sub> type crystals, structural transitions 0-75349  
 K<sub>2</sub>SO<sub>4</sub>·Ag<sub>2</sub>SO<sub>4</sub> mixtures, surface comp., AES and XPS obs. 0-81386  
 K<sub>2</sub>S<sub>2</sub>O<sub>8</sub> as flux material for transition metal oxide cryst. growth 0-71582  
 K<sub>2</sub>Sb<sub>2</sub>O<sub>7</sub>, solid state synthesis (*French*) 0-104438  
 K<sub>2</sub>SbO<sub>3</sub>·1/6KF<sub>3</sub>, dielec. spectroscopy study, 100 Hz to 10 MHz, 238 to 417K (*German*) 0-108144  
 K<sub>2</sub>Se<sub>2</sub>(OH)<sub>2</sub>Si<sub>2</sub>O<sub>12</sub>, crystal struct., X-ray diffr. study 0-79763  
 K<sub>2</sub>SeBr<sub>6</sub>, rotational phase transitions, cryst. struct., X-ray diffr. study 0-70400  
 K<sub>2</sub>SeO<sub>4</sub>, 1D displacive modulation, struct. using superspace-group concept 0-79726  
 K<sub>2</sub>SeO<sub>4</sub>, dielec. dispersion, 5-900 MHz, near incommensurate-commensurate transition 0-60522  
 K<sub>2</sub>SeO<sub>4</sub>, elastic props. at commensurate-incommensurate transition, Brillouin scatt. and US study 0-93248  
 K<sub>2</sub>SeO<sub>4</sub>, ferroelectricity, triple 60 Hz D-E hysteresis loops 0-71364  
 K<sub>2</sub>SeO<sub>4</sub>, hexagonal-orthorhombic transition, Brillouin scatt. study 0-97208  
 K<sub>2</sub>SeO<sub>4</sub>, incommensurate to ferroelec. transition, hydrostatic press. effects, neutron scatt. study 0-108166  
 K<sub>2</sub>SeO<sub>4</sub>, phase mode in incommensurate phase, Raman scatt. obs. 0-80766  
 K<sub>2</sub>SeO<sub>4</sub>, Raman spectra, effects of temp., substitutional cations, and stress 0-71405  
 K<sub>2</sub>SeO<sub>4</sub>, structural transition, polarised Raman spectra 0-75349  
 K<sub>2</sub>SeO<sub>4</sub>, ultrasonic study in temp. range of incommensurate phase transform. 0-88276  
 K<sub>2</sub>SnCl<sub>6</sub>, elastic const., inelastic neutron scatt. and US meas. 0-59553  
 K<sub>2</sub>SnCl<sub>6</sub>, elastic constants, softening of acoustic modes, obs. by Brillouin scattering 0-71440  
 K<sub>2</sub>SnCl<sub>6</sub>, phase-transition-induced dipolar relax. 0-66107  
 K<sub>2</sub>Ta<sub>2</sub>Nb<sub>2</sub>O<sub>3</sub>, pressure-induced resistance and colour change obs. 0-75608  
 KTa<sub>1-x</sub>Nb<sub>x</sub>O<sub>3</sub>, holographic storage using photorefractive effect, dielectric const. 0-78800  
 KTa<sub>1-x</sub>Nb<sub>x</sub>O<sub>3</sub> quantum ferroelectric, dielec. susceptibility 0-103922  
 KTaO<sub>3</sub>, electrocaloric effect for refrigeration at cryogenic temp. 0-77789  
 KTaO<sub>3</sub>·Li, ferroelec. transition and atomic motions, <sup>7</sup>Li NMR study 0-75872  
 KTaO<sub>3</sub>:OH (OD) (OT) (OT), IR spectra, spectrosc. const. 0-100671  
 K<sub>1+x</sub>Ta<sub>1-x</sub>W<sub>1-x</sub>O<sub>6</sub> pyrochlore system, comp. depend. of ionic cond. 0-107517  
 K<sub>2</sub>TeCl<sub>6</sub>, cryst. data from Guinier powder diagrams (*German*) 0-79751  
 K<sub>2</sub>Te<sup>IV</sup>Te<sup>VI</sup>O<sub>12</sub>, mixed tellurate, cryst. chem. and elec. cond. (*French*) 0-107150



**potassium compounds continued**

- $K_{1-x}(Ti_{1-x}M_{1+x})O_3$ ,  $M=Nb$ , Ta, layer compound, cryst. struct., nonstoichiometry 0-64972  
 $KTi_3SbO_9$ , X-ray cryst. struct. determ. (French) 0-107178  
 $KTi_3Ta_3O_{17}$ , chemically twinned rutile struct., X-ray study 0-107149  
 $K_{1.64}Ti_{1.32}Fe_3O(SO_4)_6 \cdot 5H_2O$ , X-ray cryst. struct. determ. 0-92483  
 $KTi(SeO_4)_2$ ,  $K_3Ti(SeO_4)_3$ , and  $K_5Ti(SeO_4)_4$ , cryst. struct. (French) 0-84148  
 $K_2UO_2Cl_4$  melts and mixtures, thermogravimetric determ. of uranyl cation state 0-101050  
 $K_8(V_2Mo_{10})VO_{40} \cdot 13H_2O$ , X-ray cryst. struct., electron spin resonance spectrum 0-88096  
 $KVO_3 \cdot Cr^{2+}$ , study of ESR spectra 0-80601  
 $\beta-K_{0.7}V_2O_5$ , heat of form. and sp. ht., 450 to 900 K 0-61129  
 $K_2WO_4F_3$ , ferroelec., transition obs. 0-75989  
 $KY_3F_{10}Eu^{2+}$ , cryst. field parameters and intensity parameters, J-mixing effects 0-59932  
 $KY(WO_3)_2 \cdot HO^+$ , stimulated emission at low temps. 0-106526  
 $KYbHP_2O_8$ , thermal decomp., thermogravimetric and X-ray obs. 0-101013  
 $K_2ZnBe_2(SiO_4)(Si_2O_7)$ , cryst. struct. determ. 0-88121  
 $K_2Zn(CN)_6$ , third order elastic consts. 0-84231  
 $K_2ZnCl_4$ ,  $^{35}Cl$  NQR study of incommensurate phase transition 0-60450  
 $K_2ZnCl_4$ , ferroelectricity, triple 60 Hz D-E hysteresis loops 0-71365  
 $K_2ZnCl_4$ , incommensurate phase transitions,  $^{35}Cl$  NQR study 0-75968  
 $K_2ZnCl_4$ , modulated struct. in ferroelec. phase, X-ray obs. 0-64970  
 $K_2ZnF_6$ , exchange interactions of transition metal ions in orbitally degenerated excited states 0-65512  
 $K_2ZnF_6$  single crystal growth, Czochralski method 0-97421  
 $K_2ZnF_6$  spin Hamiltonian parameters for  $Fe^{3+}$  ions, superposition model anal. 0-108053  
 $K_2ZnF_6 \cdot Yb^{3+}$ , perovskite type cryst., ENDOR meas. 0-80638  
 $K_2ZnF_6$ , charge transport and polarisation 0-80681  
 $K_2Zr_2(O_3)_2F_2 \cdot 2H_2O$ , photodecomp. 0-108724  
 $K[(OH)_{0.42}(O_2)_{0.58}]$ , cubic solid soln., structural and mag. study (French) 0-107177  
 $K_3[Pt(CN)_4]Br_{0.3} \cdot 3H_2O$ , high press. structs. and phase transitions 0-107423  
 $KBr$ , inelastic light scattering of localised vibration of interstitial H atom in alkali halides 0-88998  
 $LiCl-KCl$ , molten mixture, struct., diffusion, cond., mol. dynamics calc. 0-64871  
 $MnNbO_3$ , orthorhombic, electronic struct., SCF-MS-X $\alpha$  calc. 0-70600  
 $MnNbO_3$ , tetragonal, electronic struct., optical anisotropy 0-70599  
 $Mg(NO_3)_2 \cdot RNO_3$  ( $R=Li, Na, K$ ), thermogravimetric anal. of dehydration processes (Japanese) 0-66791  
 $NaBr$ , cation defects creation mechanism 0-75224  
 $NaCl-KCl$ , molten, alkaline earth oxides solubility products, potentiometric determ. 0-76488  
 $NaCl-KCl$  novel encapsulant for LEC growth of GaSb single crystals 0-93475  
 $NaCl-KCl$  system, interdiffusion, miscibility, Kirkendall effect 0-107568  
 $Na_2O-K_2O-Al_2O_3-SiO_2$ , structure of modified surface layer, internal friction method 0-103258  
 $PbLi-Kl$  alloys, fundamental abs. edge, potential as solar convertor 0-101128  
 $SiO_2-Al_2O_3-CaO-BaO-SrO-ZnO-Na_2O-K_2O-B_2O_3$ , glaze effect of  $P_2O_5$  additions 0-60824  
 $SiO_2-Al_2O_3-K_2O$  glass ceramic interaction with Pb borosilicate glaze 0-84398  
 $SiO_2-PbO-B_2O_3-Al_2O_3-CaO-Na_2O-K_2O$  glaze, interaction with aluminosilicate glass-ceramics 0-84398  
 $Sn-KCl$  granular superconductors, far IR absorpt. 0-84548  
 $ZnCl_2-KCl-NaCl$ , molten system, containing  $Ni^{2+}$  ions, appl. to electrorefining, polarographic study 0-66810

**potential energy curves and surfaces of molecules**

- for Morse curves see Morse potential  
 see also molecular vibration  
 chloromethyl formate, conformation potential energy surfaces, ab initio calcs. 0-69065  
 classical harmonic oscillators, microcanonical ensemble, Monte Carlo sampling 0-102459  
 classical many-body collision model incorporating Heisenberg and Pauli principles 0-63511  
 cyanocyclopentane, microwave spectral study of axial and equatorial conformers 0-95604  
 cycloalkanes, carbonyl charact. freqs., kinematic and pot. energy effects 0-95578  
 1,2-cyclooctadiene, conformational energy surface, Boyd's iterative force field investig. 0-95737  
 diatomic molecule, Franck Condon factors, vibr. rot. interaction effect 0-74198  
 diatomic molecules, bound, hybrid potential function 0-69209  
 diatomic mols., pot. energy curves representation 0-87061  
 diatomic mols., spurious avoided crossing detection 0-87057  
 difference electrostatic mol. pot. contour maps, basis set superposition effect 0-102462  
 electronic degrees of freedom, classical models 0-63507  
 electronic spin orbit interaction, molecular Aharonov-Bohm effect 0-83303  
 ethylene, pot. energy and dipole moment surfaces, polarisation effect, ab initio CI calcs. 0-106272  
 ethylene as singlet methylene dimer, nonempirical double zeta calculations, zwitterionic singlet excited states 0-83258  
 exchange reactions, light atom, quantum dynamics 0-101011  
 fluoroformaldehyde, pot. energy surface characts., substitution effect 0-89505  
 fluoromethyl formate, conformation potential energy surfaces, ab initio calcs. 0-69065  
 2-haloethanols, torsional interaction, IR spectra, ab initio calcs., 2-dimens. model 0-74160  
 harmonic and Morse oscillator freq. change influence on Franck-Condon factors 0-106312  
 isopropyl radical, pot. energy surfaces, ab initio UHF calcs. 0-106258  
 large internuclear separations, discrete mol. energies calcs. 0-91472  
 methane, pot. energy curves, Monte Carlo and SCF LCAO MO calcs. 0-63526  
 minimum energy reaction paths, reactive domains of energy hypersurfaces and stability 0-71893

**potential energy curves and surfaces of molecules continued**

- molecule-ion collision system pot. curves at low collision energies, beam studies 0-61088  
 oxirane cation, struct. rearrangement following vertical ionisation, ab initio CI calc. 0-58191  
 phenol-phenyl complex, electrostatic mol. pot. contour maps, MODPOT and VRDDO calcs. 0-102463  
 polyatomic molecules, small, analytical functions for pot. energy surfaces 0-102457  
 porphyrin, hypersurface of adiabatic pot. calc. by CNDO/2 method, vibr. freqs., absorpt. spectra calc. 0-95543  
 potentials, anisotropic, from rotationally inelastic and elastic cross sections, direct inversion method 0-69090  
 resonant states, potential surfaces, complex coord. calcs. in adiabatic approx. 0-102464  
 resonant states, potential surfaces, complex coord. calcs. using stationarity condition 0-102465  
 scattering amplitude calculations, role of radiative crossings between potentials of dressed mol. 0-63642  
 strongly coupled systems, one dimens. barriers, transfer rate 0-63735  
 symmetrical molecules 0-102458  
 triatomic mols., bound state, mol. Aharonov-Bohm effect 0-83302  
 1,2,4-trichlorobenzene liq., mol. reorientation, translation and vibr. relax., Rayleigh and Raman spectra 0-95632  
 vibrational predissociation in hydrogen bonded complexes 0-61078  
 $Ag_2$ , Harris-Pohl selected valence electron split-shell MO calcs. 0-91439  
 $Ar-HBr$ , intermol. pot. energy surfaces calcs. 0-91625  
 $Ar_2$ , van der Waals dimer, intermol. pot., SCF CI ab initio calcs. 0-106274  
 $ArH$ , excited states, theoretical pot. curves 0-95548  
 $ArH^+$ , transition moments, perturbation calcs. 0-102542  
 $ArHCl$ , Van der Waals mols., SCF energies and dispersion forces 0-74279  
 $Ar.HF$ , Van der Waals mols., SCF energies and dispersion forces 0-74279  
 $Ar.H_2O$ , Van der Waals mols., SCF energies and dispersion forces 0-74279  
 $Au_3$ , Harris-Pohl selected valence electron split-shell MO calcs. 0-91439  
 $BH_4^+$ , pot. energy surfaces and mol. deform. induced by external cation 0-106285  
 $Ba_2^{2+}$ , very long lived vibr. states, lifetimes, WKB calc. 0-78560  
 $Be_2(^3\Sigma_g^-)$ , binding energy, ab initio pot. curves, interacting correlated fragments method 0-63557  
 $Br_2$ ,  $B^2\Pi(O_2^+)$  predissoc. rates, analytical interpretation 0-91617  
 $C_3$ , ground state pot. surfaces, analytical functions 0-83304  
 $C_3(C_2^-)$ , pot. energy curves calc. using SCF, MCSCF and CI methods, dissociation energies, bond lengths, electron affinity 0-95523  
 $CH^+$ , a  $^1\Pi-b^3\Sigma^-$  transition moment, ab initio calcs. 0-87047  
 $CH^+$ , excited states, pot. curves and transition moments determ. by ab initio CI methods 0-106286  
 $CO_2$ , stretch-stretch interaction force const., electron correlation influence, ab initio CI study 0-58161  
 $Ca_3$ ,  $A^2\Sigma_u^+-X_2\Sigma_u^+$  system, laser induced fluoresc., pot. energy curve and mol. consts. 0-58307  
 $Ca_3$ , ground state, multiple scatt. X $\alpha$  calcs. 0-58149  
 $CaCl$ ,  $B^2\Sigma^+-X^2\Sigma^+$  transitions, rot. anal. by laser spectroscopy 0-91536  
 $CaCl$ ,  $X^2\Sigma$  pot. energy curves, polarisability and dissociation 0-91629  
 $CeO$ , dissociation energy, rel. band strengths of  $a_2-X_2$  and  $b_2-X_2$  systems 0-99495  
 $Cl_2$ +muonium ( $H$ )(D), pot. energy surfaces, inversion calcs. 0-93734  
 $Cs_2^{2+}$ , low-lying states, MC SCF+CI 0-69053  
 $Cs_2MX_4$  ( $M=Se, Te, X=Cl, Br$ ),  $\Gamma_4^- (^1T_{1g})$  state, Jahn-Teller effect, luminesc. obs. 0-60650  
 $Cu_3$ , Harris-Pohl selected valence electron split-shell MO calcs. 0-91439  
 $D+H_2$  reaction, transition state theory calculations, kinetic isotope effect explanation 0-66784  
 $H+D_2$  reaction, transition state theory calculations, kinetic isotope effect explanation 0-66784  
 $H+HCl$ , semi-empirical pot. energy surfaces calc. by diatomics-in-molecules method 0-95556  
 $H_2$ , lowest singlet and triplet states, interactions, electronic force calcs. 0-63742  
 $H_2^+$ , ground state, pot. energy curves, 1/R expansion coeff. calcs. 0-91472  
 $H_2-H_2$ , intermol. pair pot., ab initio SCF-CI surface 0-91457  
 $H_2+He$ , vibr. relax. cross section 0-99494  
 $H_3$ , diatomic state mixing parameter 0-74139  
 $H_4$ , pot. energy surfaces, valence bond calcs. 0-74129  
 $HCN$ , ground state pot. surfaces, analytical functions 0-83304  
 $HF-HCl$ , SCF energy hypersurface, stationary points, thermodynamics of form. 0-102436  
 $HNO$ , low-lying states, pot. energy surfaces calcs. 0-102460  
 $(H_2O)_2$ , difference electrostatic mol. pot. contour maps, basis set superposition effect 0-102462  
 $H.PNH_2$ , inversion-rot. mechanism, basis set and geometry optimisation effects 0-83273  
 $H_2S^+$ ,  $^2B_1$ ,  $^4A_1$  and  $^2B_2$  electronic states, pot. energy curves, CI calcs. 0-87048  
 $He_2$ , 600 Å emission continuum struct., in 700-900 Å region in glow discharge 0-95641  
 $He_2$ , ground state, interaction energy, many-body perturbation theory calcs. 0-69210  
 $He$ , high press. afterglows, reviews 0-64823  
 $I_2(I_2^+)(I_2^-)$ , HF and SCF calcs., pot. curves, electron affinity and quadrupole moment determ. 0-95527  
 $Kr-HCl$ , intermol. pot. energy surfaces calcs. 0-91625  
 $LiBF_3$ , nonrigid mol. struct. and stability, ab initio calcs. 0-83259  
 $LiBeF_3$ , pot. energy surface, struct., stability and internuclear distances, ab initio calc. 0-58147  
 $LiCa$ , laser chemiluminesc. 0-93759  
 $(LiH)_3$  complex, SCF interaction energy nonadditivity 0-91437  
 $LiH_2(LiD_2)(LiT_2)$ , pot. surfaces, fundamental freqs. and thermodynamic functions 0-69205  
 $LiH(LiD)(LiT)$ , pot. surfaces, fundamental freqs. and thermodynamic functions 0-69205  
 $LiI$  UV photodissoc. cross section, reson. ionis. Li detection 0-63719  
 $Mg_2$ , ground state, multiple scatt. X $\alpha$  calcs. 0-58149  
 $N_2$ , electron impact dissociation, EELS,  $N_2^+$  autoionisation 0-106397  
 $N_2$ , multi-config. SCF super-CI calc., density matrix formulation 0-78547  
 $^{14,15}N_2$ , Fourier spectrometry and IR emission spectra 0-83368



**potential energy curves and surfaces of molecules continued**

- $N_2^{2+}$ , low-lying electronic states, pot. energy curves calcs. by SCF technique, vibr. and ionisation consts. 0-69091  
 $N_2^{2+}$ , recomb. energy determ. from pot. curves 0-58335  
 $NH_3^{1+}$ , pot. energy curves, model pot. method, orbiting and reson. effects 0-63815  
 $NH_2$ , pot. energy curves of  $X^2B_1$ ,  $A^2A_1$ ,  $^2B_2$  valence-shell and  $\pi_2^*3s$ -type Rydberg states calc. by CI 0-74138  
 $NO_2$ , ground state pot. surface, ab initio LCAO MO SCF calcs. 0-102461  
 $O^n$  ( $n=0$  to 2), core binding energy shifts,  $\Delta$ SCF calcs. 0-95558  
 $O_2$ ,  $^3\Pi_u$  diabatic Rydberg states, ab initio CI calcs. 0-95554  
 $O_2$ ,  $^3\Sigma_g^-$  ground state, pot. energy curve, direct CI method appl. 0-58165  
 $O_2$ ,  $A^1\Pi_u$  state pot. energy curve, MCSCF calcs. 0-63565  
 $ONCl$ , vibr. freq., anharmonic ab initio/empirical pot. energy functions 0-99457  
 $S$  (S-He) discharges, stability, emission spectra 0-107003  
 $ScO$ , pot. energy curves and dissoc. energy of  $X^2\Sigma$  state 0-69203  
 $SiH^+$ , mol. consts., pot. curves and dissoc. energy determ. from time resolved precision spectroscopy 0-58272  
 $Se_2$ , dispersion damping functions and interaction energy calcs. 0-78673  
 $XeF_3$ , pseudopotential SCF-MO studies, equilb. struct., stretch-stretch interaction force const. 0-95525  
 $XeF_4$ , pseudopotential SCF-MO studies, equilb. struct., stretch-stretch interaction force const. 0-95525  
 $XeF_5^+$ , pseudopot. SCF MO studies, steric aspects of struct. and force fields, Jahn-Teller effect 0-99444  
 $XeF_6$ , pseudopot. SCF MO studies, steric aspects of struct. and force fields, Jahn-Teller effect 0-99444

**potential energy functions**

see also Lennard-Jones potential; molecular vibration; Morse potential; muffin-tin potential

- alkali halide mols., electronic polarisability, ionic radii and repulsive pot. parameters, mol. consts. 0-87242  
 alkali hydride molecules, pot. energy function, rot. const., vibr. const., and binding energy 0-99532  
 alkali hydrides, lattice props. from interaction pot. energy function 0-100199  
 alloys, ordered, thermal and static displacements effect on axial shadow pattern width and shape (Russian) 0-107024  
 aminopyrazine, far IR spectra, barrier to planarity, pot. function and energy levels 0-69137  
 atomic, optimum pot. model used to generate numerical pot., energies and electron affinities determ. 0-99534  
 atomic Rydberg states, Coulomb and Yukawa pot., wave functions and quantum defects, Schwinger's var. principle 0-63549  
 atomic vapours, three-level system, collisional effects in saturation spectroscopy, appl. to Na 0-78579  
 atoms, electron densities and electrostatic pot. calc. 0-102430  
 atoms, electrostatic pot. at nuclei, mathematical formulations 0-106369  
 benzene derivatives, mol. electrostatic pot., approx. evaluation 0-58337  
 chloro(ethyl)silanes and its C derivatives, Raman spectra, mol. vibr. and rot. isomerism 0-87134  
 composite interatomic potential, validity over large atomic separation 0-84225  
 Coulomb potentials, screened, energy approximants and perturbation theory 0-106368  
 dense gases, vel. autocorrelation function, memory function 0-59154  
 diatomic molecule, vibr.-rot. states, high accuracy wave functions and energies 0-74159  
 diatomic molecules, bound, hybrid potential function 0-69209  
 diatomic molecules, dissoc. energy determ., Simmons-Parr-Finlan pot. calcs. 0-58128  
 differential scattering cross-section, Brinkman pot. calcs. 0-106373  
 distorted wave matrix elements for inverse power pots., approx. analytic evaluation 0-83442  
 ethyl alcohol- $d_0$ (- $d_1$ )(- $d_1$ )(- $d_2$ ), internal rot. and microwave rot. spectra 0-69128  
 exponential cosine screened Coulomb pot., s-states, Ecker-Weizel approx. calcs. 0-101732  
 gas, thermophysical props. inversion, anisotropic pot. energy function generation 0-99531  
 hard-sphere liquid, pair pot. softness effect on liq., struct. factor 0-88012  
 HCP lattice, Ewald potential calc. 0-64948  
 hydrides, first row, bending pot. calc. using MINDO approx., force const., equilb. geometry 0-95544  
 interatomic potentials, Regge poles positions and residues, inverse power pots. 0-83439  
 interionic force pot. in ideal dipolar gas 0-96330  
 ionic crystals, defects, computer modelling, review 0-107205  
 isolated molecules, vibration relax. theory, adiabatic approx. 0-58237  
 JWKB phase integrals, higher order, evaluation 0-87195  
 light atoms (up to Ni), contact term, use of local spin density functional method 0-58158  
 lipid hydrocarbon chain, biomembrane, rot. motion and fluidity 0-76714  
 liquid crystal ordering and theory of mol. dispersion forces and pair pots. 0-64886  
 local scaled Schrodinger relations and the virial theorem, kinetic energy operator 0-78527  
 molecules, electron densities and electrostatic pot. calc. 0-102430  
 molecules, electrostatic pot. at nuclei, mathematical formulations 0-106369  
 molecules containing 1st row atoms, K-shell binding energy shifts, NDDO MO calcs. 0-58413  
 naphthalene, phosphorescence spectra in rare gas matrices, multiplet struct. and pot. energy functions 0-106341  
 naphthalene in Ar matrix, geometry changes and multiplet struct., mol. fluoresc. and phosphoresc. obs. 0-95663  
 nonpolar molecules, intermol. interactions in intense radiation field 0-78679  
 palmitic acid-choleic acid complex, cryst. struct. and van der Waals energy 0-64983  
 poly(spiro[2,4]hepta-4,6-diene) molecular characterisation, glassy state props. 0-64928  
 polyatomic mol. force consts. and heat of atomisation, approx. separable pot. function 0-78675  
 polyatomic molecule, intramolecular coord. relax., generalised classical theory 0-78589  
 polyatomic mols. in liqs., vibr. energy relax. 0-63611

**potential energy functions continued**

- polymers, computer simulation 0-79734  
 porphyrin in n-octane Shpol'skii matrix, defect props., Monte Carlo obs. 0-63533  
 real fluids, short range repulsions and long range attractions, simple pair pot. model 0-64850  
 $RX^+$ , radical anion stability conditions, pot. energy diagrams 0-85161  
 second virial coefficient data, complete iterative inversion method calcs. 0-83448  
 symmetric double-well potential, semiclassical inversion 0-83447  
 two body T matrices derived from strong potentials 0-63732  
 Ag, thin film deposited on Si, work function (French) 0-80353  
 Al, thin film deposited on Si, work function (French) 0-80353  
 $\beta$ - $Al_2O_3$ -(Na,K) $_2O$ , model calcs. of cond. anomalies, pot. energies of cation arrangements 0-107510  
 Ar, liquid, diffusion coefficient for model potentials through means square displacement 0-70098  
 $BCl_3$ , NCO, soln., force fields and normal modes, vibr. spectra, IR and Raman obs. (French) 0-58266  
 $BX_3$ , NCS (X=Cl, Br, I), soln., force fields and normal modes, vibr. spectra, IR and Raman obs. (French) 0-58266  
 $Br_2$  in liq. Ar, effective intramol. pot. 0-69208  
 $Br_2$ , model potential SCF calcs. 0-95528  
 $CO_2$ , VV processes, estimation of almost resonant molecular energy transfer due to multipolar pot. 0-91642  
 $CO_2+H_2$ , collinear atom-triatom transition probabilities for anharmonic triatom pots., quantum mech. calcs. 0-83455  
 $CO_2+Kr$ , collinear atom-triatom transition probabilities for anharmonic triatom pots., quantum mech. calcs. 0-83455  
 $C_2O_2$ , semirigid bender, rot.-vibr. energy level separations obs., struct. and pot. functions determ. 0-83446  
 $Ca_2$ , vibr.-rot. states, high accuracy wave functions and energies 0-74159  
 Ce, isostructural solid-solid phase transitions, core collapse, cell theory 0-59620  
 $Cl_2$ , model potential SCF calcs. 0-95528  
 $D_2$ , compressed fluid, vibrational population relaxation time obs. 0-69219  
 Ga trihalides, vibr. anal., pot. const. determ., mol. compliance and Coriolis coupling const. calc. 0-95579  
 $H_2$ , diatomic transition operators,  $L^2$  basis expansions,  $^1\Sigma$  and  $^3\Sigma$  state pots. 0-63519  
 $H_2$ , electronic chemical pot., natural orbitals occupation numbers and electronegativity 0-63509  
 $H_2O$ , ST2, discrepancy between Monte Carlo and mol. dynamics calc. using truncated pot.-anal., internal energy determ. 0-95702  
 $H_2O+H_2O$ , pair pot. near H bonded equilb. config., amorphous and crystalline solid and liq. 0-64946  
 He-He, energy and interaction potential of two ground-state atoms 0-63740  
 $HgBr_2$ , electronic struct. and photodissoc., effective core pots. and POL(1) CI wave function 0-63560  
 $HgCl_2$ , electronic struct. and photodissoc., effective core pots. and POL(1) CI wave function 0-63560  
 $I_2$ , model potential SCF calcs. 0-95528  
 In trihalides, vibr. anal., pot. const. determ., mol. compliance and Coriolis coupling const. calc. 0-95579  
 LiBr, pair pot., dipole moment, polarisability tensor, bond length depend., finite field SCF calcs. 0-58127  
 Mo surface, clean and gas covered, He\* impact, deexcitation, pot. energy transfer mechanism 0-60743  
 $^{14}N_2+CO$ , vibr.-vibr. energy transfer, long and short range pot. effect 0-99556  
 $^{15}N_2+CO$ , vibr.-vibr. energy transfer, long and short range pot. effect 0-99556  
 $^{14}N^{15}N+CO$ , vibr.-vibr. energy transfer, long and short range pot. effect 0-99556  
 $NO_2$ , hydrate clusters, ground-state HF pot., Monte Carlo simulation, energy surfaces and rot. barriers 0-106412  
 Na, equilibrium struct. and phys. props., pseudopot. method 0-96778  
 Na, liquid, diffusion coefficient for model potentials through mean square displacement 0-70098  
 Na+methyl iodide, anisotropic interactions from double rainbow struct., interaction pot. meas. 0-99540  
 Na+t-butyl bromide, anisotropic interactions from double rainbow struct., interaction pot. meas. 0-99540  
 Na+t-butyl chloride, anisotropic interactions from double rainbow struct., interaction pot. meas. 0-99540  
 Na+t-butyl iodide, anisotropic interactions from double rainbow struct., interaction pot. meas. 0-99540  
 $Na_2$ , molecular electronic struct. for lowest  $^3\Sigma_u^+$ ,  $^1\Sigma_u^+$ ,  $^3\Sigma_g^+$ ,  $^1\Pi_u$ ,  $^1\Pi_g$ ,  $^3\Pi_u$  and  $^3\Pi_g$  states 0-63738  
 $Ne+D_2$ , anisotropic inversion pot., rot. inelastic cross sections 0-78696  
 $O_2$ , photoionisation cross section and asymmetry parameters calc. in UV region using static pot. 0-95692  
 $OH+H_2$ , interaction pot. energy rel. to OH rot. excitation at interstellar temps. 0-62232  
 $O^-(O_2^-)$ , optimum pot. model used to generate numerical pot., energies and electron affinities determ. 0-99534  
 Pd adsorbed on W (110), long range interatomic interactions with coadsorbed Re, W 0-59789  
 $Pd_2$ , ab initio relativistic core pot. studies of metal-metal bonding 0-106257  
 $PdH$ , ab initio relativistic core pot. studies of metal-H bonding 0-106257  
 photoionisation cross section and asymmetry parameters calc. in UV region using static pot. 0-95692  
 $Pt_2$ , ab initio relativistic core pot. studies of metal-metal bonding 0-106257  
 $PtH$ , ab initio relativistic core pot. studies of metal-H bonding 0-106257  
 Re adsorbed on W (110), long range interatomic interactions with coadsorbed Pd 0-59789  
 TTF stacks, intermolecular energy and struct. from atom-atom potentials 0-79738  
 W adsorbed on W (110), long range interatomic interactions with coadsorbed Pd 0-59789

**potential energy surfaces for collision processes**

- alkali atom (ion)+inert gas, collision studies of quasi-one-electron systems 0-63750  
 atom+ion collision system pot. curves at low collision energies, beam studies 0-61088



potential energy surfaces for collision processes continued

atom+molecule, rotational rainbow maxima: a time dependent study 0-58353  
atom+molecule reaction dynamics, translational energy effect, review 0-76489  
atoms, chemical ionisation, classical description, complex interaction pot., exponential representation 0-99570  
benzene-Dewar benzene, lower excited states pot. energy surfaces for isomerisation 0-104429  
chemical reactions, quantum chemical methods appls. 0-93752  
diatomic isovalent systems, pot. curves, ab initio MRD-CI method 0-83293  
fluoriodomethane, vibr. excited, dissociation, trajectory calcs. using pot. energy surface parameters 0-76508  
gas phase chemical reactions in IR laser field, collision-induced absorpt. spectra 0-76499  
minimum energy reaction paths, reactive domains of energy hypersurfaces and stability 0-71893  
minimum energy reaction paths, virial theory implications 0-97686  
mol. target internal motion 0-78697  
molecule+ion collision system pot. curves at low collision energies, beam studies 0-61088  
molecules, chemical ionisation, classical description, complex interaction pot., exponential representation 0-99570  
multicharged ion thermal charge exchange reaction, rel. to astrophysics 0-63815  
multiply charged ion+atom, autoionisation, electron and photon emission 0-63813  
non-adiabatic transitions induced by rotational coupling 0-106385  
nonadiabatic cage reactions, relaxation hindrance 0-93740  
polyenes, photoisomerisation, triplet pot. energy surfaces and normal mode anal. 0-108700  
XH-Y complexes, IR absorpt. spectra, intramol. coupling influence, pot. energy surfaces derivation 0-91624  
Ar+HCl, differential cross section, quasiclassical close coupling approx. 0-63743  
Ar+HHe<sup>+</sup>, ab initio pot. energy data, SCF-LCAO calcs. 0-63530  
Be<sup>+</sup>+He(Ne)(Ar), Be II 2<sup>2</sup>P excitation, alignment and orientation 0-91647  
CO<sub>2</sub>+H<sub>2</sub>, rot. transfer, ab initio intermol. pot. energy surface 0-58354  
CO<sub>2</sub>+He, rot. inelastic collision, ab initio SCF, electron gas and pot. energy surfaces 0-83468  
C(2 S<sub>0</sub>)+H<sub>2</sub>(O<sub>2</sub>)(ethylene) 0-74241  
Cs<sup>+</sup>+benzyl chloride, beam reactions for 5.8 eV collision energy, mechanism 0-66777  
D+FD(FH), low barrier quantum models vibrational deactivation 0-69216  
D+H<sub>2</sub> reaction, transition state theory calculations, kinetic isotope effect explanation 0-66784  
D+H<sub>2</sub>, rearrangement collision, vibr. excitation effects 0-71910  
D<sub>2</sub>+HD(Ne)(Ar), state-resolved Δj=2 rot. transitions 0-63772  
H<sup>-</sup>-H<sub>2</sub> system, pot. energy surfaces 0-74215  
H+alkali metal atom, interaction potentials 0-63736  
H+D<sub>2</sub> reaction, transition state theory calculations, kinetic isotope effect explanation 0-66784  
H+FH(FD), low barrier quantum model, vibrational deactivation 0-69216  
H+H<sub>2</sub>, collinear reaction, Delves radial coord. S-matrix propag. calcs. 0-108695  
H+H<sub>2</sub>, reaction probability, max. entropy derivation, statistical theories 0-66781  
H+H<sub>2</sub>, reactions and collisions in IR laser field, collision-induced absorpt. spectra 0-76499  
H+H<sub>2</sub>, sudden rot. reactive scatt., 3-dimens., approx. quantum mech. calcs. 0-76498  
H+H<sub>2</sub>(D<sub>2</sub>)(T<sub>2</sub>) reactions, accurate pot. energy surface, isotope effects, quasiclassical trajectory study 0-97698  
H+HCO→H<sub>2</sub>+CO, classical trajectory study 0-93750  
H+methane, abstraction and exchange reaction, barrier height calc. using POL-CI wave functions 0-81304  
H+O<sub>2</sub>+Ar, HO<sub>2</sub> free radical prod., rate const. calc. 0-101026  
H+O<sup>+</sup>(N<sup>n+</sup>)(C<sup>n+</sup>)(B<sup>n+</sup>), charge transfer cross sections, oscillatory behaviour in low-energy collisions 0-63806  
H<sup>+</sup>+CO (Σ), ground state pot. energy surface, ab initio SCF calc., protonated equilb. geometry 0-83301  
H<sup>+</sup>+CO(Σ), vibr. excitation calc., close coupling and sudden approx. 0-78561  
H<sup>+</sup>+D<sub>2</sub>, collisional complex form. 0-58339  
H<sup>+</sup>+H<sub>2</sub>, rot. and vibr. excitation, energy loss obs. 0-63773  
H<sup>+</sup>+H<sub>2</sub>, vibr. excitation, ab initio CI pot. energy surface calcs. 0-74228  
H<sup>+</sup>+H<sub>2</sub>, vibr.-rot excitation, ab initio CI pot. energy surface calcs. 0-74229  
H<sup>+</sup>+H<sub>2</sub>(CO<sub>2</sub>), vibr. excitation, 10-30 meV 0-58358  
H<sub>2</sub>+Cl(Br)(I)(F), gas phase H-atom transfer reactions, struct.-reactivity correl., pot. energy surfaces 0-104433  
H<sub>2</sub>+D<sub>2</sub>, reactive and inelastic scatt., semiempirical pot. energy surfaces calcs. 0-74140  
H<sub>2</sub>+H(D)(T) reactions, accurate pot. energy surface, isotope effects, quasiclassical trajectory study 0-97698  
H<sub>2</sub>+Pt(111) surfaces, interactions, bond breaking activity, model pot. 0-108744  
HF+Li→LiF+H, pot. energy surface, SCF and CI calcs. 0-71904  
H<sub>2</sub>O<sup>+</sup>, ab initio potential energy surface study by CI techniques, equilibrium conform. determ., mol. dissociation pathways 0-78550  
H<sub>2</sub>O<sup>+</sup>, spin and rot. fine struct., orbital angular momentum 0-83247  
H<sub>2</sub>O<sup>+</sup>, vibr. and rot. struct., intensity factors and orbital angular momentum 0-83246  
He-LiH, rot. inelastic collisions, ab initio pot. energy surface calcs. 0-87208  
He+ArH<sup>+</sup>, ab initio pot. energy data, SCF-LCAO calcs. 0-63530  
He+CO<sub>2</sub>, translational-vibrational energy transfer, quantum dynamical study 0-63746  
He+H<sub>2</sub>, pot. energy surface, ab initio calcs., van der Waals const. determ. 0-106372  
He+H<sup>+</sup>, differential scatt., 1-12 eV, high resolution beam meas. 0-58348  
He+HCN, translational-vibrational energy transfer, quantum dynamical study 0-63746  
He+LiH, rot. inelastic collisions, dynamics 0-87209  
He+LiH, rot. inelastic collisions, state-to-state cross sections determ. 0-87210

potential energy surfaces for collision processes continued

He+OCS, translational-vibrational energy transfer, quantum dynamical study 0-63746  
He(2 S, 2<sup>2</sup>S)+Ne(e<sup>-</sup>), transition probs., pots. 0-58371  
K+O<sub>2</sub>, mol. target internal motion 0-78697  
Li<sup>+</sup>+CO<sub>2</sub>, collisional excitation, quasiclassical trajectory calcs. 0-83467  
Li<sup>+</sup>+ether(thioether)(amide), pair pots., ab initio LCAO SCF MO calcs. 0-58184  
LiH+He, rot. inelastic collisions, rigid shell models 0-99545  
Li\*(2<sup>2</sup>P<sub>1</sub>)+H<sub>2</sub>(D<sub>2</sub>), collision induced quenching and fine struct. transition rate coefficients meas. 0-74221  
Li(2p)+H<sub>2</sub>(N<sub>2</sub>), Li(2p) excitation, alignment and orientation obs. 0-63794  
NH<sub>3</sub>, spin and rot. fine struct., orbital angular momentum 0-83247  
NH<sub>3</sub>, vibr. and rot. struct., intensity factors and orbital angular momentum 0-83246  
Na+Na, electronic-field pot. curves determ. for large interatomic distances, excitation cross sections calc. 0-95704  
Na+Ne, potential curves from a model potential (French) 0-78685  
Na\*H<sub>2</sub>, potential energy surfaces 0-74215  
Ne<sup>+</sup>+H<sub>2</sub>O, pot. energy surfaces, MO and CI calcs., Penning ionisation electron spectra 0-106376  
O+H<sub>2</sub>, classical trajectory calcs., ab initio surface, singlet state, rate consts. 0-66786  
O+H<sub>2</sub>, pot. energy surfaces and reaction rates, ab initio calcs. 0-63531  
O+saturated hydrocarbon, reaction dynamics, model pot. surfaces, quasiclassical trajectory calcs. 0-97696  
O+saturated hydrocarbon→OH+alkyl radical, reaction dynamics, mol. beam-laser induced fluoresc. obs. 0-97695  
OH+H<sub>2</sub>→H<sub>2</sub>O+H, reaction product vibr. distrib., quasiclassical trajectory calcs. 0-85162  
O<sup>+</sup>(<sup>4</sup>S)+N<sub>2</sub>(X<sup>1</sup>Σ<sub>g</sub><sup>+</sup>)→NO<sup>+</sup>(X<sup>1</sup>Σ<sup>+</sup>)+N(<sup>4</sup>S), MCSCF potential energy surface for collinear <sup>4</sup>Σ pathway 0-63540

**potential scattering**  
anisotropic potential scattering in classical mechanics (Russian) 0-62541  
attractive potential, r<sup>-(s+2)</sup> type, SL(2,R) acting on quaternions 0-57125  
black hole, Reissner-Nordstrom, coupled gravitational and EM perturb., scatt. matrix, energy conversion, quasi-normal modes 0-67775  
bound states, sufficient condition for existence, potential without spherical symmetry 0-68070  
charged particle pot. scatt. in laser field, eikonal theory, quasi-static approx. 0-77647  
construction of L<sup>2</sup> dependent potentials 0-86129  
Coulomb scattering, N-particle, cluster props. 0-73192  
Coulomb scattering as the limit of scattering off smoothly screened Coulomb potentials 0-94986  
cross-sections, total, boundedness 0-77639  
degenerate electron gas, with elastic scatt., form of memory function 0-101753  
Dirac distributions, perturb. of self-adjoint Hamiltonians, Green's functions and wavefunctions, scattering theories 0-62514  
education, Rutherford's scattering formula via the Runge-Lenz vector 0-73141  
education, Schrodinger eqn. solns. using approximate nucleon-nucleon and A-nucleon pots. 0-62429  
Fermi problem for rigid rotor, 2-dimens. case (Russian) 0-86153  
few-body quantum mechanical system, sum of two-body potential operators 0-62516  
functional integral for scatt. amplitude in presence of long range interaction 0-101734  
hadronic matter, string junction model and spectrum energy density of string 0-57556  
Heisenberg-Ising spin chain quantum inverse scatt. method, Jordan-Wigner transformation 0-93068  
high-momentum transfers and completeness of the Mandelstam program in potential scattering 0-82668  
inverse problem for radial Schrodinger eqn., incorrect nature 0-86139  
inverse scatt., Newton's method modification at fixed energy 0-73207  
inverse scattering, one-dimens. Schrodinger eqn. pot. from S-matrix 0-57127  
inverse scattering in three dims. 0-86130  
inverse scattering problem in the eikonal approximation (Russian) 0-57522  
ion+electron collision, resonant electron bremsstrahlung (Russian) 0-102580  
linear scattering problem for finite depth eqn., Miura maps 0-105534  
many-body problem, vertex function and crossing symmetry 0-62515  
metal foils, low energy heavy ion multiple scatt. in finite range potential 0-70283  
modified Coulomb potentials, bounds for phase-shifts 0-57112  
multichannel scatt. theory for temp. depend. Hamiltonians, charge transfer problem 0-90695  
non-local potential problems, Perey effect, WKB method 0-68077  
nonlinear evolution eqns., inverse scatt. method, conservation laws (Russian) 0-105804  
nonrelativistic bound s-states in linear central potential 0-82936  
oscillating potentials, scatt. matrix 0-57126  
path integral formulation, central scattering potentials 0-82906  
peratisation technique, iteration approach 0-86100  
phase shifts, high energy behaviour for Coulomb-like potentials 0-98814  
phase space packets, time depend., differential cross sections obtained by superoperator methods 0-105544  
propagation properties, bound and scatt. states 0-73204  
pseudo Coulomb problem, group O(2,1), irreducible representation 0-73209  
scattering by singular potentials of the general type at high energies 0-63141  
Schrodinger eqn., 1-D, oscillatory integral approach, semiclassical, linear and parabolic potentials 0-57124  
Schrodinger operator, scattering theory and continuous spectra for class of strongly oscillating potentials 0-77638  
semiclassical scattering theory, spurious excitation 0-73142  
semiconductors, electron-electron collision effect on current voltage characts. in quantising mag. field 0-103705  
separable potentials 0-90708  
spectral and scatt. theory, Schrodinger operator with singular attractive potential 0-86151  
spin-orbit potentials, quantum scattering theory inverse problem, fixed energy Jost functions (Russian) 0-68082  
square well potential, separable representation 0-82922



**potential scattering continued**

- T-matrix eikonal expansion, higher order terms 0-86149
- transit time measures in scattering theory, time depend. Schrodinger eqn. 0-73194
- transmission coeff. for 1-D potential barrier, discretisation of Schrodinger eqn. 0-57123
- two-body, off-shell wave matrix 0-82681
- $\pi\pi \rightarrow \pi\pi$ , p-resonance production, quasipotential approach, linear  $\sigma$ -model 0-86755
- $^4\text{He}(\alpha, \alpha)$ , nuclear separable plus Coulomb interaction 0-83106
- $^4\text{He}(\alpha, \alpha)$ , size change of  $\alpha$  effect on phase shift, generator coordinate and variational methods (Chinese) 0-68683

**potential transformers**

- MV, constructional principles and production technology (Hungarian) 0-100118
- oil immersed transformers, dissolved gas causes and phenomena, anal. (German) 0-76570

**potentials (bioelectric) see bioelectric potentials****potentials (electric) see electric potential****potentiometers**

- see also voltage measurement
- potentiostat, P-04, for electrochem. meas. 0-61185
- unit power standard for 53.57 to 78.33 GHz 0-90808

**powder diffraction cameras see cameras; X-ray crystallography apparatus****powder metallurgy**

- agglomerate structure parameters of powders in the incoherent zone in rolling 0-84876
- applications, history and development 0-68014
- atomisation units, gasdynamic and acoustic props. 0-66451
- boronising, physicochem. characts. 0-61024
- bronze powders, electric-pressure sintering onto cylindrical parts in fluidised bed 0-100960
- compaction, stereoscopic SEM micrographs, quantitative anal. 0-57433
- deformation, boundary conditions on sliding surfaces 0-60978
- densification, electrohydraulic effect appl. 0-60798
- densification during isostatic compression 0-66449
- dynamic hot pressing, process parameters for parts of varying complexity 0-100799
- fatigue strength significance (German) 0-60946
- granular materials, hot isostatic pressing in sheaths, process parameters calc. 0-84874
- granular materials, rolling, granule kinematics 0-84875
- granules, form. mechanism study during centrifugal atomisation of rotating blank 0-100798
- hard metal powders, electric-pressure sintering onto cylindrical parts in fluidised bed 0-100960
- high strain rate processes, review 0-84864
- Inconel 718, grain growth during sintering 0-97449
- manufacture by CaH method,  $\text{Ca}(\text{OH})_2$  separation 0-84878
- metal submicron particle heating in hot gas, plasma metallurgy 0-81092
- microcrystalline alloys, metastable, rapidly quenched particulates, props. appl. and production 0-84887
- plasma industrial utilisation, synthesis, powder, metallurgical and surface treatments, review (French) 0-96398
- preforming using high-voltage electrical discharge 0-84872
- recent developments, Sweden 0-93514
- steel, 10R6M5 and 10R6MSK5, atomised powders (Russian) 0-97446
- steel, Cr-W-Mo-Co, high-speed, from atomised powders, mech. and cutting props. 0-66556
- steel, Cu-Ni-Mo (2, 2, 0.25 wt.%), sintering, kinetic characts. 0-60805
- steel, high-speed tool, properties, powder metallurgy prep. method (Czech) 0-60800
- steel, high-speed tool, sput quenching, props. and struct. 0-76294
- steel, Mn, sintered, production, effect of initial Fe powder struct. on mech. props. 0-104095
- steel, Ni-Mo-C (2.0, 0.2, 0.4 wt.%) sintered, struct. transforms. and mech. props. after quenching 0-66557
- steel, Ni-Mo-C (5, 0.5, 0.5 wt.%), sintered, effects of powder and sintering variables on props. 0-104093
- steel, powder forged, fatigue, surface treatment effect 0-85048
- steel, sintered, fracture of residual pores 0-76352
- steel, stainless, 20Kh13, prep. by diffusion impregnation 0-60803
- steel (alloy)-TiC (70, 30 wt.%) composite, sintered, wear resist. 0-100815
- steel powder, high speed, S and O reduction in a  $\text{H}_2$  gas stream 0-61015
- Ag powder, ultrafine, sintering, coalescence growth stage 0-89174
- AgCdO, powder metallurgy production, for switchgear in power engineering 0-104094
- Al powders, electric-pressure sintering onto cylindrical parts in fluidised bed 0-100960
- Al-Cu(0-10 wt.%) sintered compacts, mech. props. rel. to sintering 0-76210
- Al-steel mixture, wear resistant, produced by compaction by discrete shock waves 0-84882
- Au powder, ultrafine, sintering, coalescence growth stage 0-89174
- Be, sintered, physicochem. props. anisotropy, BeO inclusions effect 0-60804
- Cu-BN composite electrode machining tools, dynamic hot pressing 0-84889
- Cu-Ni, sintering, Kirkendall effect 0-93518
- Fe, air-atomised, manufacture with predetermined characts. 0-100808
- Fe based sintered porous permeable materials, diffusion chromising 0-100958
- Fe, cold-pressed, props., effect of air 0-100810
- Fe, ore, wet sieving in fine grain range (German) 0-93515
- Fe powder, electroless Ni plating 0-61026
- Fe powder, final reduction annealing in vibrating bed 0-84883
- Fe powder, reduction annealing, comminution of sintered cakes 0-66456
- Fe, powder-forged, elastic consts., density depend. 0-84987
- Fe, recryst. annealing effect on struct. and technological props. (Czech) 0-89250
- Fe reduced powder manufacture, collision speed effect 0-84884
- Fe, sintered, austenitic nitriding and bainitic hardening 0-85084
- Fe-B, for infiltration of Fe compacts 0-60806
- Fe-Si (3 to 5 wt.%) sinters, mag. props., Si and Fe-Si additions effect 0-71104
- Fe-Si-C mixed powder, cast Fe powder sintering study (Japanese) 0-108373
- Mo electronics industry applications, prep. processing and props. 0-89171
- Mo powder, influence of powder reduction processes on props. 0-89175
- Mo, sintered, gas evolution and degassing 0-100814

**powder metallurgy continued**

- Nb<sub>3</sub>Al, prep. by reduction of Nb<sub>2</sub>O<sub>5</sub> and Al<sub>2</sub>O<sub>3</sub> by CaH<sub>2</sub>, thermodynamic calc. 0-100809
  - Nb<sub>3</sub>Sn, multifilamentary superconductor preparation by 'in situ' and cold powder methods, review 0-93522
  - Nb<sub>3</sub>Sn, powder metallurgically produced, microstruct. characts. 0-89233
  - Ni alloy ZHS6U, US method of porosity detection 0-71828
  - Ni base superalloys, rapid solidification, use in gas turbine engines 0-84888
  - Ni, carbonyl powder, dislocation density sintering 0-108372
  - Ni coatings, detonation powder spray deposition 0-61028
  - Ni sintered permeable materials with bidisperse structure, pore-forming additions effect 0-84885
  - Ni, sintering kinetics, metallographic study 0-93519
  - Ni-base superalloys, powder metallurgical, creep-rupture at intermediate temps. 0-97568
  - Ni-Cr-Al sintered alloy, hot vac. pressure, fracture and mech. charact. 0-66667
  - Ni-Cr-Ti rapidly solidified superalloys, surface segregation 0-76263
  - Ni-Cr-W-Co granules type ZHS6U, EP741, hot hydrostatic pressing 0-60796
  - Ni-ferrite powders, form. in presence of Li<sub>2</sub>SO<sub>4</sub>-Na<sub>2</sub>SO<sub>4</sub> molten salts, prep. and characts. 0-84869
  - SiC fibre reinforced Al, plasma-formed semifinished products, props. 0-84890
  - (Ti,Cr)B<sub>2</sub>, sintering kinetics and props. 0-100811
  - Ti base composite sintered bearing materials, metallic solid lubricant infiltrated, antifriction props. 0-60981
  - Ti powder metallurgy, developments 0-100801
  - TiC-(Mo-Cr-Ni-Mn) steel alloy, optimum comp. and manufacture conditions, Mn effect 0-84896
  - W-Ni-Fe system, reduction kinetics and alloy form. 0-60801
  - WC-Ni hard alloy composite, sintered, void healing 0-60821
  - W<sub>50</sub>Fe<sub>50</sub> glassy alloy, refractory, triode sputtered 0-75185
  - Zn, fine powder, electrodeposition 0-60802
  - ZrB<sub>2</sub>-Nb, reactions between components 0-100812
- powder sprayed coatings**
- Fe-Si gas-flame spray deposited protective coating, for C steel heat exchanger 0-61025
  - Ni coatings, detonation powder spray deposition 0-61028
- powder spraying**
- detonation deposition of coatings, monitoring method 0-60780
  - enamelling by electrostatic frit powder spraying 0-97428
  - Cr-Al<sub>2</sub>O<sub>3</sub> powder targets for plasma-ion spray deposition of resistance films 0-84897
  - Cr<sub>2</sub>O<sub>3</sub>-ZrO<sub>2</sub> granules, from spray drying of suspensions 0-104100
  - Ni-Cr-Al<sub>2</sub>O<sub>3</sub> powder targets for plasma-ion spray deposition of resistance films 0-84897
  - SiC fibre reinforced Al, plasma-formed semifinished products, props. 0-84890
- powder techniques see powder technology**
- powder technology**
- see also densification; hot pressing; powder metallurgy; powder spraying; sintering
  - ceramic compounds, lyophilisation parameters, freeze-drying synthesis 0-97453
  - ceramic powder synthesis from laser-heated gas phase reactants 0-93525
  - coatings, in metal finishing, review 0-104330
  - deforming powders, self-diffusion coeffs. in failure zones and percolation 0-76209
  - diamond powder, consolidation by thermal decomposition of methane and benzene 0-66448
  - diamond powders, Mo coated, X-ray diffr. study 0-100936
  - dolomite, powders sintering, decarbonisation cycle effect 0-104102
  - dry ball milling, breakage parameters variation with ball and powder loading 0-80999
  - ethylene-vinyl acetate copolymer, powdered, prep. by emulsion polymerisation (Japanese) 0-104110
  - ferrites, soft, spray firing for presintered powder prep. 0-89181
  - fine particle mixtures, morphological anal. 0-104087
  - hot pressing powder layer on steel backing plate, joint form. kinetics 0-100961
  - laser applications in materials processing, seminar, San Diego, CA, USA (Aug. 79) 0-90609
  - magnetite, powders sintering, decarbonisation cycle effect 0-104102
  - NASICON solid electrolyte, processing and phys. props. 0-60820
  - nonisothermal periodic current meas. using standard DC shunt with magnetic powder monitoring, frequency errors 0-104398
  - ordered mixtures production, humidity effect 0-76208
  - particles in dilute suspension in general flow, mass flow and density meas. 0-101784
  - pressure sintering, inhomogeneous flow and effective press. 0-93512
  - PVC-Cu composites with chemically deposited ultrafine copper particles 0-93534
  - quartz sand, high-conc. suspension, prod. principles 0-66463
  - semiconducting  $\alpha\text{-Fe}_2\text{O}_3$  ceramics preparation, gas sensor for city gas appl. (Japanese) 0-61498
  - Si<sub>3</sub>N<sub>4</sub>-Ce<sub>2</sub>O<sub>3</sub>-SiO<sub>2</sub> materials: phase relations and strength 0-97465
  - single crystals under large loads, theoretical elastic behaviour, review and appl. 0-71681
  - sintering, surface redistribution by grain boundary diffusion 0-84871
  - Al-Cu(0-10 wt.%) sintered compacts, mech. props. rel. to sintering 0-76210
  - Al-Si-N-O system, comps. corresponding to  $\beta'$ -sialon phase reaction hot-pressing 0-84891
  - $\beta'$ -Al<sub>2</sub>O<sub>3</sub>-Na<sub>2</sub>O solid electrolyte, tube fabrication from cast ceramic tape 0-60819
  - $\beta'$ -Al<sub>2</sub>O<sub>3</sub>-Na<sub>2</sub>O solid electrolyte, processing and phys. props. 0-60820
  - Al<sub>2</sub>O<sub>3</sub>-ZrSiO<sub>4</sub> granular corundum-zircon refractory, development 0-66462
  - BN, contact reactions with Ti and WC-Co at high pressures 0-61029
  - BaFe<sub>2</sub>O<sub>7</sub> powders, fast reaction presintering 0-97445
  - Ba(V<sub>1-x</sub>Ti<sub>x</sub>)S<sub>2</sub> synthesis and struct. phase transitions 0-107415
  - Cr<sub>2</sub>O<sub>3</sub>-Al<sub>2</sub>O<sub>3</sub> solid soln., Vickers micro-hardness 0-66629
  - Fe ore super-concentrate, deep drawing props. by integrated powder technology route 0-100806
  - Fe-C (graphite, 0.3 wt.%), powder-forged, elastic consts., density depend. 0-84987
  - Fe-Cu: graphite-BaSO<sub>4</sub>-CuSO<sub>4</sub>, friction material, solid state sintering kinetics 0-104096



**powder technology continued**

Ge powder electrodeposition, from molten fluoride mixtures 0-60797  
MgO-NaCl refractory clinkers, Cr containing, densification, thermal treatment and phase composition effect (*French*) 0-76219  
MnZn ferrite, microstructure and initial permeability, presintering process effect 0-89367  
MnZn ferrite powder prep., wet method 0-89180  
MnZn ferrite powders, reactive, mag. materials obtained by compaction 0-89182  
MnZn ferrites, post sinter-cooling rates effects 0-89369  
Na<sub>2</sub>O-Ca glass powders, mixed with CO<sub>3</sub> compounds, cellular-struct. glass fabrication 0-108382  
Nb<sub>40</sub>Fe<sub>40</sub>P<sub>14</sub>B<sub>6</sub>, metallic glass, explosive compaction, mech. props. 0-89176  
Ni-Zn-Co ferrites, synthesis from solid solns. of schoenite-type salts 0-93511  
PLTZ powder preparation, hydrolysis ball mixing 0-81006  
PbMo<sub>3</sub>S<sub>7</sub> wire, powder processed, crit. current density and field 0-80466  
Si-SiO<sub>2</sub>-Mg-Cu powder compact, nitridation to form Si<sub>3</sub>ON<sub>2</sub> whiskers (*Japanese*) 0-93674  
SiAlON, prepared from siliceous sand and Al powder, hot pressing, steatite contamination effects (*Japanese*) 0-93528  
SiC, pressureless-sintered, high temp. strength (*Japanese*) 0-104299  
SiC-AlB<sub>2</sub> (0.61 to 1.2 wt.%), hot pressed, microstruct. 0-93563  
Si<sub>3</sub>N<sub>4</sub>, high-speed rolling bearings, fatigue strength 0-93655  
Si<sub>3</sub>N<sub>4</sub>-CeO<sub>2</sub> additive, hot-pressing and oxidation behaviour 0-71618  
Sr<sub>2</sub>(Na<sub>2</sub>BiO<sub>3</sub>)<sub>1-x</sub>TiO<sub>3</sub> ferroelec. ceramic, hot pressing, numerical simulation (*French*) 0-76220  
TaC and Ta<sub>2</sub>C, self-propag. high-temp. synthesis 0-60815  
Ti-Al-V (6.4 wt.%), porous compacts, determ. of effective stress in hot pressing 0-100807  
UO<sub>2</sub> powder compaction, force transmission and friction 0-71620  
YIG, open die hot pressing, spin wave and FMR line width 0-89170  
ZrO<sub>2</sub> ceramic, dense nonstabilized, fabrication by hydrothermal reaction sintering 0-97451  
ZrO<sub>2</sub>, partially stabilised ceramics, strengthening, post-sintering heat treatment 0-97518  
ZrO<sub>2</sub>, partially stabilized, processing defects 0-97558

**powders**

see also densification; granular structure; particle size; powder sprayed coatings; powder spraying; sintering  
borosilicate glass, powder, sintering, foaming by chemical reactions 0-81017  
brittle, shock wave disintegration test method 0-66744  
density measurement by pycnometry 0-69903  
diamond, synthetic, thermal cond. 0-96702  
diamond, ultradisperse, ESR, particle size and lattice microdistortions 0-97140  
discoidal agglomerate, stress pattern, distributed loading effect during diametral compression test 0-60934  
divalent Sr, Ba, Ca, Zn, Cd iodates, complex salts, phase transitions, cryst. struct. (*Chinese*) 0-70171  
electrostatic spark hazard identification and control, during collection in container 0-69291  
high speed rot., spin diffusion, NMR spin lattice relax. obs. of D 0-66056  
metal, on piezoelec. substrate, dynamic SAW reflecting struct. 0-74565  
metal powder, method for TEM study 0-84038  
mixtures, diffuse reflectance, quantitative anal. 0-87308  
monolithic materials for creating high pressures, anvil device with tungsten 0-73377  
near IR diffuse reflectance analysis anomalies 0-86383  
nonisothermal devitrification kinetics 0-92465  
phonon electroacoustic echoes, storage mechanisms 0-75606  
piezoelectric, phonon echoes and long-time storage (*Japanese*) 0-70330  
polymer filled ceramic, ZrO<sub>2</sub> stabilised, fracture mechanism (*Russian*) 0-100895  
quartz, on piezoelec. substrate, dynamic SAW reflecting struct. 0-74565  
random packing of spheres, computer simulation 0-77705  
rubber, finely dispersed, sedimentometric anal. 0-66883  
semiconducting powders, band-gap energies, photoacoustic meas. 0-70579  
wet particulate systems, pendular band strength between unequal-sized spherical particles 0-104418  
Ag<sub>2</sub>S+Ln<sub>2</sub>S<sub>3</sub>, reaction rate, production of ionic semiconductors 0-93741  
Ag<sub>2</sub>SbS<sub>3</sub>(AsS<sub>3</sub>), electroacoustic echo, ultrasonic wave attenuation (*Russian*) 0-88280  
Al, annealed and powder sintered (SAP 895), sputtering under D<sup>+</sup> and <sup>3</sup>He<sup>+</sup> bombardment, microstruct. effects study 0-84821  
Al<sub>2</sub>O<sub>3</sub>, support for MnO<sub>2</sub> catalyst, N adsorption obs. of dispersion modes 0-81363  
Al<sub>2</sub>O<sub>3</sub>-TiO<sub>2</sub> powder, plasma-prepared, morphology and phase constitution 0-100833  
BaFe<sub>2</sub>O<sub>9</sub>, powder, milled and annealed, phase composition, lattice conts. and crystallite size 0-71677  
BaFe<sub>2</sub>O<sub>9</sub> powders, fast reaction presintering 0-97445  
Ba<sub>2</sub>NaNb<sub>5</sub>O<sub>15</sub>, X-ray powder diffraction data determ. (*Chinese*) 0-70170  
BaTiO<sub>3</sub>, powders, Bragg reflection integral intensities due to structural anomalies 0-107098  
BaTiO<sub>3</sub>:BaTiO<sub>3</sub>, dielec. props. and microstruct. 0-60481  
CaHPO<sub>4</sub>, powder and granules with starch mucilage binder, surface topography variation under compression 0-80998  
Co, ferromagnetic micropowder, cryst. struct., coercivity, remanence, saturation 0-65967  
Cr-Fe-C (28.4, 9.1 wt.%) prep. from FeCr<sub>2</sub>O<sub>4</sub> chromite 0-100804  
CrO<sub>2</sub> and CrO(OH), fine particle obs. of cryst. morphology and topotaxy 0-65969  
Cu, compressed powder, thermal cond. meas. (*German*) 0-70669  
Cu powder compacts, yield curve comparison, different loading paths (*Japanese*) 0-93621  
CuCl powder compacts, DC voltage depend. resist. under press. 0-80334  
CuO powder, surface area determ. by adsorpt. of stearic acid and pyridine 0-107636  
Cu<sub>2</sub>S+Ln<sub>2</sub>S<sub>3</sub>, reaction rate, production of ionic semiconductors 0-93741  
Fe, carbonyl powder, specific elec. conductivity, 5 to 200 MPa (*German*) 0-70664  
Fe, ferromagnetic micropowder, cryst. struct., coercivity, remanence, saturation 0-65967  
Fe small, particle motion effect on Mossbauer spectra 0-84671  
Fe-Co, ferromagnetic micropowder, cryst. struct., coercivity, remanence, saturation 0-65967

**powders continued**

Fe-TiC pseudofused composite magnetoabrasive powders, props. 0-100926  
Fe<sub>1-x</sub>O, wustite, AES study, ion and electron bombard. effects 0-76114  
α-Fe<sub>2</sub>O<sub>3</sub>, hematite, AES study, ion and electron bombard. effects 0-76114  
Fe<sub>2</sub>O<sub>4</sub>, magnetite, AES study, ion and electron bombard. effects 0-76114  
GeO<sub>2</sub> glass, nonisothermal devitrification kinetics 0-92465  
GeSe<sub>2</sub>, glassy, powdered and bulk, fatigue of photolum. 0-80855  
GeSe<sub>2</sub>, powdered crystalline, photoluminescence intensity under continuous excitation 0-71480  
MgO powder, surface area determ. by adsorpt. of stearic acid and pyridine 0-107636  
MnO<sub>2</sub> porous powders, Al<sub>2</sub>O<sub>3</sub> and SiO<sub>2</sub> coated, changes in surface free energy for N adsorption 0-84363  
Mo powder, influence of powder reduction processes on props. 0-89175  
Na<sub>6</sub>Al<sub>6</sub>(Si<sub>0.95</sub>Ge<sub>0.05</sub>)<sub>6</sub>O<sub>24</sub>.2NaBr, Ge-doped sodalite powders, UV absorpt. band 0-71452  
Na<sub>2</sub>O-B<sub>2</sub>O<sub>3</sub>-SiO<sub>2</sub> glass-Ni compact, indented, strength and fracture toughness 0-93636  
Na<sub>2</sub>O-Ca glass powders, mixed with CO<sub>3</sub> compounds, cellular-struct. glass fabrication 0-108382  
NaReO<sub>4</sub>, EPR spectra of paramag. centres and free radicals 0-108072  
Ni-Fe<sub>2</sub>O<sub>3</sub> powders, obtained in presence of fused salts prep. and characts. 0-84869  
Ni-Zn-Co ferrites, synthesis from solid solns. of schoenite-type salts 0-93511  
Se powder compacts, sintered, electrical cond. 0-70693  
SiN powder formation, in high-temp. N flow (*Russian*) 0-100818  
SiO<sub>2</sub>, support for MnO<sub>2</sub> catalyst, N adsorption obs. of dispersion modes 0-81363  
Sn, positron annihilation in fine particles, surface trapped states 0-84800  
SrBaNaNb<sub>5</sub>O<sub>12</sub>, X-ray powder diffraction data determ. (*Chinese*) 0-70170  
Sr<sub>2</sub>(Co<sub>1-x</sub>M<sub>x</sub>)<sub>12</sub>, M=Mn, Ti, Zr, powders, influence of substitutes on mag. props. 0-100601  
Sr<sub>2.05</sub>Na<sub>0.95</sub>Nb<sub>5</sub>O<sub>15</sub>, X-ray powder diffraction data determ. (*Chinese*) 0-70170  
TiC<sub>x</sub>N<sub>y</sub>, powder preparation, physical, chemical props. (*Russian*) 0-76212  
UO<sub>2</sub> pellets, sinterability, particle size effect 0-104098  
UO<sub>2</sub> powder compaction, friction between particles and die walls 0-71620  
W, powder, gas adsorption and desorption (*Russian*) 0-75429  
W, powder preparation by WO<sub>3</sub> reduction in H plasma jet (*Russian*) 0-76211  
ZnO powder, effect of dry grinding in EPR and catalytic activity (*Japanese*) 0-84640  
ZnS:Cu crystal, powder, epitaxial film, luminescence anomalous thermal 0-76077

**power amplifiers**  
Antares CO<sub>2</sub> laser power amplifier, design 0-69423  
stochastic beam cooling expts., low-noise wide-band power amplifier system 0-58011

**power cables**  
see also power overhead lines; superconducting cables; underground cables  
dry insulation, materials used and characteristics (*Spanish*) 0-81024  
fusion reactor, TFTR, power line, variable freq. AC harmonic content 0-99293  
HV, high molecular weight polyethylene insulation characterisation using size exclusion chromatography 0-66897  
HV cable, PE-insulated, electron beam crosslinking process development 0-66846  
nuclear reactor power and control cable tests to IEEE standards 0-57884

**power control**  
see also load regulation  
CW laser radiation power stabilisation by external control element 0-91832  
telemetry, totally implantable, integrated power controllers and RF data transmitters 0-67295

**power conversion**  
see also direct energy conversion  
superconducting magnet for magnetic flux compression, compression generator, PULSAR, design optimisation 0-68957  
CO<sub>2</sub> fundamental condensation cycles in steam and nucl. power plants, performance characts. 0-63368

**power converters**  
amorphous magnetic alloys, review, engineering magnetic props. and potential applications 0-71078  
switched-mode mains supplies for charging, NiCd accumulators (*German*) 0-66961  
variable speed wind power generator, control strategy for 3-phase output (*French*) 0-76591

**power distribution networks** see distribution networks

**power factor**  
see also reactive power  
Na MHD generators, optimisation for maximum power factor (*Rumanian*) 0-64793

**power factor measurement**  
No entries

**power factor meters** see power factor measurement

**power factor Q** see Q-factor

**power generation, electric** see electric power generation

**power generators, electric** see electric generators

**power lines** see power cables

**power measurement**  
see also wattmeters  
far IR and near MM wave power energy meter calibration 0-57373  
laser, far IR optically pumped, monitoring by piezoelec. transducers 0-102729  
laser energy meter (*French*) 0-102790  
laser energy meters for calibrations at most principal laser wavelengths 0-99741  
laser pulse energy, picosecond order meas. (*French*) 0-74412  
loudspeakers, monitor for meas. of acoustic power response 0-87674  
reactive, three-phase two wattmeters, meas. errors (*Croatian*) 0-105677  
reactive power meter for periodical signals in range 50 Hz to 5 kHz (*Spanish*) 0-86339  
SI units fundamentals (*French*) 0-95059



**power measurement continued**

- unit power standard for 53.57 to 78.33 GHz 0-90808
- VHF power measurements using Hall effect (*Polish*) 0-95112
- wheelchair locomotion, power output requirements for manual operation 0-94416

**power overhead lines**

- see also *overhead line conductors; power cables; power transmission*
- cooling by corona wind of heated cylinder in still air, expt. 0-84023
- EM field, rel. to suicide 0-94287

**power overhead transmission lines** see *power overhead lines***power packs** see *power supplies to apparatus***power plants**

- see also *solar power; space vehicle power plants; wind power plants*
- brine solns. as energy resource, reverse electrodialysis cells 0-85271
- coastal, breaking wave effects on power plant intakes (*Italian*) 0-109148
- emissions detection, microscopic samples molecular analysis, using Raman microprobe 0-57391
- fuel cell power plants for utility applications 0-66967
- large-scale elec. energy storage, review 0-89676
- molten carbonate fuel cell power plant, eng. development 0-66969
- osmotic power plants, closed-cycle 0-67000
- total energy systems, energy cascading principles (*French*) 0-76621
- H<sub>2</sub>PO<sub>3</sub> fuel cells, commercial prototype plant for dispersed electric power generation 0-66968

**power station computer control**

- nuclear control guidelines 0-106119
- nuclear power stations, computerised monitoring and control system at Trawsfynydd 0-86965
- nuclear reactor protection systems, reliability anal. using Markov methods 0-91229
- He cooled reactor turbine control experiences Fort St. Vrain HTGR (*German*) 0-57927

**power station load**

- nuclear power stations, load factors and availability achieved with light water and heavy water reactors (*Slovenian*) 0-68843

**power stations**

- see also *energy resources; geothermal power stations; hydroelectric power stations; nuclear power stations; power plants; solar power stations; steam power stations; tidal power stations*
- coal conversion technologies, health and environmental effects 0-81493
- coal-fired MHD flow facility, development and operation 0-66982
- environmental noise, coal-fired power stations 0-76683
- flue gas analysis, in 200 MW plant, trial operation with Westinghouse O<sub>2</sub> probe (*Czech*) 0-89562
- fossil fuels for use in MHD power stations 0-72074
- fuel cell, 4.8 MW DC 0-89608
- heat treatment, post weld, during construction and maintenance 0-93574
- industrial utilisation of energy, book 0-61222
- MHD power systems, coal-fired, retrofitting to existing non-coal power stations 0-66983
- power plant dynamics and control, conf. Hyderabad, India (Feb. 1979) 0-91215
- steam-gas combined, based on natural gas resources from North Sea, economics and possibilities (*Norwegian*) 0-101073
- thermal energy storage in industry and power stations 0-67002
- waste heat utilisation for fish farming and agriculture (*German*) 0-101080
- wood-waste fired power plants, economic feasibility anal. 0-66923

**power supplies to apparatus**

- see also *cells (electric); constant current sources; power plants; power supply circuits; prosthetic power supplies*
- artificial heart blood heat exchangers with radioisotopic power supplies 0-85532
- batteries development, Li-MnO<sub>2</sub>, Sanyo with high energy densities 0-85272
- flash X-ray machine, distributed pulse power system anal. using SCEP-TRE circuit code techniques 0-68336
- fusion, reactor, MFTF, neutral beam accel power supply protection 0-102380
- fusion reactor, Doublet III, plasma shape control, 1.5 Megawatt DC chopper power supply 0-102333
- fusion reactor, Doublet-III, frequency generator-rectifier system performance 0-102326
- fusion reactor, FTR, equilib. field coils, electrical supply system, optimisation and computer aided performance anal. 0-91288
- fusion reactor, Heliotron E, neutral beam injector ion source power supply 0-99333
- fusion reactor, ISX-B, neutral beam power system 0-91283
- fusion reactor, MFTF, power supply system, digital simulation using EMTF code 0-91286
- fusion reactor, MFTF, start up neutral beam power supply system 0-91281
- fusion reactor, MFTF, sustaining neutral beam power supply, cct. anal. using ASTAP and EMTF codes 0-91284
- fusion reactor, MFTF, sustaining neutral beam power supply, shunt preconditioner, IBM-ASTAP anal. 0-102332
- fusion reactor, neutral beam ion source, core snubber network design, fabrication and testing 0-102378
- fusion reactor, PDX, neutral beam elec. power system, ion source supply upgrade 0-102330
- fusion reactor, PHIBEX, poloidal field power supply for ignition, computer based cct. anal. 0-102329
- fusion reactor, TEXT, motor-generator power supply system 0-99292
- fusion reactor, TEXT, poloidal field power systems, design and anal. 0-102328
- fusion reactor, TEXT, toroidal field coil power supply, thyristor controlled 0-91289
- fusion reactor, TEXTOR, poloidal coil system power distrib. system 0-102327
- fusion reactor, TFTR, neutral beam power system 0-91282
- fusion reactor, TFTR, power line, variable freq. AC harmonic content 0-99293
- fusion reactor, TMX, mag. control system 0-95442
- fusion reactors, JT-60, poloidal field power supply system, AC voltage behaviour, simulation 0-91287
- fusion reactors, MFTF, sustaining neutral beam power supply system, modelling with ASTAP code 0-91285
- fusion reactors, PDX, shaping field-equilib. field power supply rectifier upgrade study 0-91290

**power supplies to apparatus continued**

- fusion reactors, Wendelstein VII and ASDEX, neutral beam injectors, HV power supply system, thyristor control 0-99332
- fusion reactors 0-102325
- gamma spectrometer protection and operation simplification, by relay device attachment 0-57447
- high-density Z-pinch experiment pulse power supply, design and operation 0-70028
- ion source for fusion reactor, 1000-kVa arc power supply 0-99396
- Pockels cell driver of fast rise time and high repetition rate using thyristor 0-69537
- spark chamber, multigap, HV supply cct. for parallel feeding 0-63456
- X-ray pulse generator giving bell-shaped pulses with thyristor based power supply 0-57446

**power supply, emergency** see *emergency power supply***power supply circuits**

- see also *constant current sources; power supplies to apparatus*
- electronics for the physicist with applications, book 0-62403
- GaAs laser diode power supply control cct. (*German*) 0-78852

**power supply industry** see *electricity supply industry***power supply systems** see *power systems***power system analysis computing**

- see also *power system computer control*
- fission reactor safety, fault tree anal. using Monte Carlo and anal. methods (*Spanish*) 0-57870
- fusion reactor, FTR, equilib. field coils, electrical supply system, optimisation and computer aided performance anal. 0-91288
- fusion reactors, MFTF, sustaining neutral beam power supply system, modelling with ASTAP code 0-91285
- photovoltaic system analysis computer program; SOLCEL-II 0-94058

**power system CAD**

- see also *power system computer control*
- fusion reactor, MFTF, sustaining neutral beam power supply, cct. anal. using ASTAP and EMTF codes 0-91284
- fusion reactor, MFTF, sustaining neutral beam power supply, shunt preconditioner, IBM-ASTAP anal. 0-102332

**power system computer aided analysis** see *power system analysis computing***power system computer aided design** see *power system CAD***power system computer control**

- see also *power station computer control; power system analysis computing; power system CAD*
- fusion reactor, MFTF, electrical systems, overview 0-91278
- fusion reactor, TMX, mag. control system 0-95442

**power system control**

- see also *load regulation; power system computer control*
- fusion reactor, Tandem Mirror Reactor startup and shutdown, simulation and control 0-99277
- fusion reactor, Tandem Mirror Reactor steady state, simulation and control 0-99278
- photovoltaic transient analysis program for electrical and thermal anal. 0-94061
- power system that includes wind energy generators, model based regulation 0-61256
- variable speed wind power generator, control strategy for 3-phase output (*French*) 0-76591

**power system protection**

- see also *lightning protection; overcurrent protection; overvoltage protection; relay protection*
- AC, protective relaying, TFTR pulsed loads 0-63387
- fusion, reactor, MFTF, neutral beam accel power supply protection 0-102380
- photovoltaic terrestrial systems, protection from lightning effects 0-89648

**power systems**

- see also *distribution networks; total energy systems*
- 25 kW solar photovoltaic flat panel power supply for electrodialysis water desalination unit 0-89643
- fusion reactor, TFTR, electrical power blanket module, conceptual design 0-102339
- large-scale elec. energy storage, review 0-89676
- photovoltaic power conditioning system for professional services office building 0-89646
- photovoltaic powered 20-hp DC/AC irrigation system and 3-kW N generator 0-89645
- power plant dynamics and control, conf. Hyderabad, India (Feb. 1979) 0-91215
- solar photovoltaic power system, design and performance charact. 0-89644
- wind power plants, integration into existing power systems, implications 0-61258

**power transformers**

- crowbar transformer, low leakage and high current for ZT-40 toroidal pinch power supply 0-102322
- electromagnetic testing of partial discharges for failure and breakdown prevention (*Russian*) 0-97743
- oil immersed transformers, dissolved gas causes and phenomena, anal. (*German*) 0-76570
- Co<sub>7</sub>Fe<sub>2</sub>Ni<sub>10</sub>(Si<sub>2</sub>B)<sub>28</sub>, amorphous, soft mag. props., switched-mode power supply appls. 0-88850
- Fe-B-C amorphous alloys for use in power transformers 0-88808
- Fe<sub>40</sub>Ni<sub>40</sub>(Mo<sub>5</sub>Si<sub>2</sub>B)<sub>10</sub>, amorphous, soft mag. props., switched-mode power supply appls. 0-88850

**power transmission**

- see also *distribution networks*
- solar power satellites microwave power transmission system rectennas, Yagi-Uda receiving elements design, characteristics and economics 0-66938

**power transmission lines**

- AC, electromagnetic fields, health effects regulation 0-94286
- biological effects of ELF electric fields: some US research results 0-94278
- cap-and-pin-type insulators, resistance to high current arcing for 110 and 400 kV power transmission lines (*Polish*) 0-70049
- health risks of high-Blu gas pipeline and electric power transmission systems 0-104520
- high electric field biological effects on human nervous systems 0-89739
- high-voltage transmission lines, depend. of instantaneous rainfall rate 0-98471



power transmission lines continued

HV lines to 800 kV, elec. and mag. field effects on human beings (*French, English*) 0-72209  
power line equipment, field work investigating corrosive effects (*Norwegian*) 0-97631  
pulse transformer design for pulse forming transmission line charging appls. 0-63419

power utilisation

see also domestic appliances; drives; environmental engineering; heating; metering; refrigeration; transportation  
KS-7F solar kitchen, economic effects on economy 0-89590  
oil shale extraction in situ retort utilising fusion reactor 0-108780  
space heating using solar heating installation, technical and operational details (*Dutch*) 0-72013

PPP calculations

acetophenones, spectrosc. characts. using PPP SCF CI calcs. 0-102448  
anthracene, singlet exciton transitions, energies and oscillator strengths, boson theory with PPP wavefunctions 0-92820  
trans-butadiene, polarisability, nonlinear elec. susceptibility, SCF calcs. 0-95547  
ethylene, polarisability, nonlinear elec. susceptibility, SCF calcs. 0-95547  
hexatriene, polarisability, nonlinear elec. susceptibility, SCF calcs. 0-95547  
naphthalene, singlet exciton transitions, energies and oscillator strengths, boson theory with PPP wavefunctions 0-92820  
nucleic acids bases, excited state dipole moments and geometries 0-95738  
organic dyes, fluoresc. spectra calcs.,  $\beta$ -variation method (*German*) 0-69182  
pentacene, singlet exciton transitions, energies and oscillator strengths, boson theory with PPP wavefunctions 0-92820  
tetracene, singlet exciton transitions, energies and oscillator strengths, boson theory with PPP wavefunctions 0-92820

praseodymium

see also nuclei with .....  
addition to Ni-Cr austenitic stainless steel, effect on heat resist. and comp. of non-metallic inclusions 0-76315  
atom, metastable,  $F=7\pi/6$  hfs, laser-RF double reson. spectroscopy 0-58170  
o-chlorobenzoic acid:Pr<sup>3+</sup>, solid, vibrational spectra 0-84758  
impurity in metallic host, exchange interaction, electrical resistivity 0-84453  
lanthanum ethyl sulphate:Pr, phase transition under pressure, absorpt. spectra (*Russian*) 0-92667  
localised 4f shell breakdown under press. 0-70411  
surface and volume props., flow props., surface layer thickness (*Russian*) 0-59760  
transport properties, low temp., effect of mag. field 0-70679  
BaY<sub>2</sub>Si<sub>2</sub>O<sub>17</sub>:Pr<sup>3+</sup>, luminesc. props. 0-93376  
GaP:Pr epitaxial films, photoluminesc. spectra 0-66294  
La-Pr/AlO<sub>3</sub>/Al tunnel junctions, cond. meas., cryst. field effects 0-88694  
La<sub>2</sub>BeO<sub>4</sub>:Pr<sup>3+</sup> crystal, absorption and luminescence spectra studies, crystal-field splitting scheme of Pr<sup>3+</sup> ion manifolds determ. 0-80853  
LaCl<sub>3</sub>:Pr<sup>3+</sup>, coherent transients by optical phase switching 0-95962  
LaF<sub>3</sub>:Pr<sup>3+</sup>, optical coherence storage in spin states, echo lifetime 0-58649  
LaF<sub>3</sub>:Pr<sup>3+</sup>, optical meas. of spin-lattice relaxation of dilute nuclei 0-93212  
LaF<sub>3</sub>:Pr<sup>3+</sup>, ultraslow optical dephasing 0-58648  
LaF<sub>3</sub>:Pr<sup>3+</sup>, ultraslow opt. dephasing at 2K 0-91864  
LiYF<sub>4</sub>:Pr<sup>3+</sup>, NMR meas. of hyperfine const. of Pr<sup>3+</sup> excited state 0-88895  
LiYF<sub>4</sub>:Pr<sup>3+</sup>, electron-irrad. induced defects, optical and EPR study 0-66238  
POCl<sub>3</sub>:Pr<sup>3+</sup>, fluoresc. and lifetimes of excited states 0-71466  
Pr IV, 3d and 4f energy level parametrisation, Slater parameters and correl. corrections 0-87041  
Pr<sup>3+</sup>, anomalous hypersensitive <sup>3</sup>H<sub>4</sub>→<sup>3</sup>P<sub>2</sub> transition 0-106296  
Pr<sup>3+</sup>, elec. multipole polarisabilities, discrete basis set calcs. 0-91456  
SeOCl<sub>2</sub>:Pr<sup>3+</sup>, SbCl<sub>5</sub> acidified, Racah and Judd-Ofelt parameters in laser liqs. 0-106516  
Si:Pr, photoconductivity anomalies due to mag. impurities (*Russian*) 0-103722  
ZnO:Pr, electrolum. brightness, field strength and freq. depend. 0-100696

praseodymium alloys

mischmetal-Co system, phase relations, microstruct., mag. props. 0-104118  
La alloys, supercond., Pr-doped, crystal field effects, tunnelling within mK range 0-70907  
La<sub>0.8-x</sub>Pr<sub>0.2</sub>Au<sub>20</sub>, amorphous, mag. and supercond. props. 0-75713  
Pr-Ni, amorphous, thermal stability, crystn., DSC and elec. resist. study 0-107060  
PrAg<sub>11</sub>, low temp. mag. meas. 0-107989  
Pr<sub>21</sub>Ag<sub>79</sub>, amorphous, sp. ht. at low temp. 0-75780  
Pr<sub>21</sub>Ag<sub>79</sub>, Pr<sub>50</sub>Ag<sub>50</sub>, and Pr<sub>10</sub>Lu<sub>40</sub>Ag<sub>50</sub>, amorphous, mag. props. 0-60182  
PrAl<sub>2</sub>Ga<sub>3</sub>, synthesis, NMR and X-ray absorpt. studies 0-108083  
Pr<sub>1-x</sub>Ca<sub>x</sub>Al<sub>2</sub>, mag. props. and phase relations 0-107991  
PrCo<sub>5</sub>, strongly exchange-enhanced paramagnetism, susceptibility 0-60179  
PrCo<sub>5-x</sub>Si<sub>x</sub>, high field first order transitions, role of K<sub>3</sub> anisotropy const. 0-65879  
PrCo<sub>5</sub>, sorption at press. up to 1500 atm. 0-97819  
PrCo<sub>7</sub>, polymorphism of Ce subgroup alloys, eutectic decomposition (*Russian*) 0-66504  
PrFe<sub>2</sub>, high field Mossbauer study 0-75893  
PrFe<sub>2</sub>, Laves phase, mag. props., Mossbauer spectra, crystalline field mag. anisotropy 0-65851  
PrIn<sub>3</sub>, nucl. orientation of <sup>144</sup>Pm in singlet ground state, exchange interaction and cryst. field splitting obs. 0-71275  
PrIr<sub>2</sub>, sp. ht., differential susceptibility and elec. resist. meas., 1.4-40K 0-71063  
PrIr<sub>2</sub>, cryst. struct. 0-96473  
PrIr<sub>2</sub>(Pt<sub>2</sub>)(Rh<sub>2</sub>)(Ru<sub>2</sub>), hyperfine sp. ht. and magnetisation meas. at 4.2K 0-75775  
Pr<sub>1-x</sub>La<sub>x</sub>Al<sub>2</sub>, amorphous, low temp. excitations, specific heat 0-100337  
(Pr<sub>1-x</sub>La<sub>x</sub>)<sub>2</sub>In, mag. props. 0-108009  
PrMg<sub>2</sub>, cryst. field study, inelastic neutron scatt. and sp. ht. meas. 0-59939  
PrNi<sub>5</sub>, LF dynamics and <sup>141</sup>Pr thermal relax., coupling parameter and RKKY exchange mechanism 0-103812  
PrNi<sub>5</sub>-Gd, dil., single crystal, ESR study 0-75850

praseodymium alloys continued

PrNi<sub>11</sub>, sorption at press. up to 1500 atm. 0-97819  
Pr<sub>60</sub>Ni<sub>31</sub>, amorphous, Curie temp., mag. susceptibility and coercive force, 4.2 to 300K 0-93092  
Pr<sub>3</sub>Os, cryst. struct. 0-96474  
PrPt<sub>2</sub>, sp. ht., differential susceptibility and elec. resist. meas., 1.4-40K 0-71063  
PrPt<sub>3</sub>, low temp. mag. susceptibility 0-93075  
PrRh<sub>2</sub>, sp. ht., differential susceptibility and elec. resist. meas., 1.4-40K 0-71063  
PrRh<sub>3</sub>, Sny. crystallography X-ray powder diffr. study 0-100217  
PrRu<sub>2</sub>, sp. ht., differential susceptibility and elec. resist. meas., 1.4-40K 0-71063  
PrSn<sub>3</sub>, thermal expansion and transverse elastic const. near mag. phase transition 0-60394  
Pr<sub>3</sub>Tl, thermal expansion and transverse elastic const. near mag. phase transition 0-60394

praseodymium compounds

see also praseodymium alloys  
ethylsulphate:Sm, one-dimens. X-Y system, spin dynamics, electron spin echo meas. 0-66031  
praseodymium ethyl sulphate, phase transition under pressure, absorpt. spectra (*Russian*) 0-92667  
Na<sub>3</sub>Pr(C<sub>4</sub>H<sub>9</sub>O<sub>2</sub>), 2NaClO<sub>4</sub>.6H<sub>2</sub>O, absorpt., circular dichroism, and mag. circular dichroism spectra 0-97243  
Pr H<sub>2</sub>, optical vibr. spectra of H, inelastic neutron scatt. study 0-107391  
Pr tinted glasses, transparency, dichroism and colour effects (*Polish*) 0-71371  
Pr-H(D), lattice parameters 0-64982  
PrAsO<sub>4</sub>, ferroelectricity, dielec. meas. 0-60515  
Pr<sub>1-x</sub>Ca<sub>x</sub>MnO<sub>3</sub>, struct. and magnetisation study 0-65804  
PrCl<sub>3</sub>, anhydrous, Nd<sup>3+</sup> absorption spectra and quantum states (*Chinese*) 0-89032  
PrCo<sub>2</sub>Ge<sub>2</sub>, crystal and magnetic structure obs. 0-64976  
Pr<sub>2</sub>Cu<sub>2</sub>O<sub>4</sub>, magnetic properties obs. 0-70937  
PrCu<sub>3</sub>Ru<sub>4</sub>O<sub>12</sub>, synthesis, cryst. struct., mag. and elec. props. (*French*) 0-107151  
PrF<sub>3</sub>, laser action of Pr<sup>3+</sup> 0-95901  
PrFe<sub>2</sub>As<sub>12</sub>, synthesis and cryst. struct. 0-84154  
PrFe<sub>2</sub>Sb<sub>12</sub>, prep. and cryst. struct. 0-100211  
PrIn<sub>3</sub>Gd, indirect nuclear exchange interactions, ESR-linewidth meas., sp. ht. determ. 0-103825  
PrN, miscibility with UC (*German*) 0-96654  
Pr<sub>2</sub>NiO<sub>4</sub>, magnetic properties obs. 0-70937  
PrO<sub>1.714</sub>, oxidation, kinetic study 0-108707  
Pr(OH)<sub>3</sub>, electronic heat capacity, 0.45 to 4.2K, phase transition at 1.21K 0-59673  
PrOs<sub>4</sub>As<sub>12</sub>, synthesis and cryst. struct. 0-84154  
PrOs<sub>4</sub>Sb<sub>12</sub>, prep. and cryst. struct. 0-100211  
PrRu<sub>4</sub>As<sub>12</sub>, synthesis and cryst. struct. 0-84154  
PrRu<sub>4</sub>Sb<sub>12</sub>, prep. and cryst. struct. 0-100211  
PrSb, magnetic to nonmagnetic transition, press. or stress induced, neutron scatt. obs. 0-65880  
Pr<sub>2</sub>Se<sub>2</sub>(S<sub>4</sub>), induced ferromagnet, mag. props. under hydrostatic press. 0-60395  
Pr<sub>2</sub>Sn<sub>2</sub>Mo<sub>2</sub>S<sub>8</sub>, supercond. props. 0-97023  
Pr<sub>2</sub>Ti<sub>2</sub>O<sub>7</sub>, ferroelec. layer type struct., cryst. growth 0-108348  
Pr<sub>2</sub>Ti<sub>2</sub>O<sub>7</sub>, layered ferroelectric, anomalous photovoltaic effect, photovoltaic current 0-75603  
U-Pr-C FBR nuclear fuels, phase anal., 1400°C 0-66486  
U<sub>1-x</sub>Pr<sub>x</sub>S, mag. phase diagram 0-71027  
ZrF<sub>4</sub>-BaF<sub>2</sub>-PrF<sub>3</sub> F<sup>-</sup> ion cond. glasses, cond. process 0-107477

preamplifiers

charge sensitive preamplifier, fast low power, loop phase shift and delays 0-58089  
integrating preamplifier, for InSb IR detectors 0-90337  
IR detector-preamplifier for cryogenic spectrometer, optimization 0-95164  
low-temperature UHF detector, with low noise preamplifier based on n-type InSb 0-68230  
multiwire proportional counter, linear read out electronics, hybrid preamplifier realisation 0-58091  
muscle spindle afferents identification during in vivo recordings in man 0-98155  
photoconduction decays, fast, measurement, DC-10 MHz low noise amplifier system 0-57326  
InSb photodiode, in Fourier spectrometer, noise compensation using integrator in feedback loop 0-73474

precipitation

microstructural process and features only  
see also Guinier-Preston zones; segregation; Widmanstätten structure  
Al-Zn-Mg (5.1 wt.%), decomp. process, TEM study 0-71660  
alloys, creep cavitation control, intergranular precipitates role 0-66664  
alloys, phase transition premonitory phenomena, exam. by electron diffr. and microscopy (*French*) 0-59651  
alloys, substitutional, electrical resist., long and short range orders effect 0-107761  
Alnico 8, permanent magnetic alloy, topography of precipitate phase (*Chinese*) 0-66512  
convergent beam electron microscopy for materials science 0-107028  
creep and growth, irradiation induced, solute effects on defect precip. rate 0-88252  
Dispersalloy, Sn-Hg amalgam,  $\gamma_2$  precip. suppression and gettering kinetics 0-71651  
ferrite, transform. kinetics, grain size, alloying element effect, carbide precip. 0-93560  
Incoloy 901, foil prep. for TEM exam. 0-88001  
Inconel 600, thermal treatment, grain boundary microstruct. and SCC resistance 0-71675  
Inconel 617, creep, morphological changes of carbides, affect on creep props. 0-108509  
ordered alloys with periodic struct., decomp. invest. (*Russian*) 0-93558  
pigeonite, inverted, from SW Norway, precipitation temp. estimation 0-72500  
precipitate and dislocation loop strain and stress field calcs. using affine transformations 0-106722  
re-solution in low dose irradiations 0-93559  
solid solution, binary, radiation-induced instability, contrib. of dissipative processes 0-65039



## precipitation continued

- solid solution, supersaturated, cellular precip. features, review (*Russian*) 0-84937
- spherical precipitate isotropic diffusion controlled growth 0-100344
- steel; low alloy; high strength, hot compression dynamic precip. and coarsening of Nb(CN) 0-97514
- steel, 12% W, eutectic carbides struct. and comp. during heating 0-76283
- steel, alloy type, photoemission electron microscope obs. of high temp. precip. behaviour 0-108456
- steel, austenite, carbide strain hardened, strength and plasticity, effect of Mn content (*Russian*) 0-97500
- steel, austenitic, friction in vacuum of type U8 steel under microshock loading (*Russian*) 0-108583
- steel, austenitic Fe-Mn-V-C, ageing characts., discontinuous precip. nature 0-84940
- steel, austenitic stainless, MC precipitate comp., APFIM study 0-104161
- steel, austenitic stainless, phosphide analysis using nonaqueous electrolyte potentiostatic etching method (*Japanese*) 0-89221
- steel, austenitic type EI-69, carbide transformations on precipitation of C from austenite (*Russian*) 0-97487
- steel, C, phosphide analysis using nonaqueous electrolyte potentiostatic etching method (*Japanese*) 0-89221
- steel, Cr, lower bainite transform., significance of carbide precip. 0-97476
- steel, Cr-Mo, Mn and Si effect on temper embrittlement, comp. and carbide precip. effects 0-85037
- steel, Cr-Mo (2.25, 1.0 wt.%), temper embrittlement, effect of P, Sn, comp. and carbide precip. 0-85036
- steel, Cr-Mo-Ni-WV (6, 4, 3, 2 wt.%), tempering and secondary hardening, TEM obs. (*Chinese*) 0-104245
- steel, Cr-Mu-W, carbide form., W effect 0-76259
- steel, Cr-Ni-C (3, 1, 0.6 wt.%), grain boundary sulphide precip. and hot ductility (*Japanese*) 0-71654
- steel, En 24, Cr, V, deform. effect on decomp. of austenite, carbide precipitation 0-84938
- steel, eutectoid, Si partitioning during pearlite transform., analytical electron microscopy applic. 0-108458
- steel, ferritic Cr-Mo type, microanalysis of precipitates using TEM 0-108688
- steel, ferritic stainless, phosphide analysis using nonaqueous electrolyte potentiostatic etching method (*Japanese*) 0-89221
- steel, heating effect on phase composition, microstruct. and mech. props. 0-100859
- steel, high C, investigation of transformations during tempering by nuclear gamma resonance method (*Russian*) 0-76256
- steel, high speed, props. after electroslog remelting 0-104139
- steel, high strength weld metal, fractography, microstructure and reheated zone toughness effects (*Japanese*) 0-108543
- steel, HSLA, V and N effect on recovery and recrystn. during and after hot working 0-84973
- steel, low C, cold rolled, graphite precip. and S segregation, AES investigation (*Japanese*) 0-89222
- steel, maraging, intermetallic phases precip. study by electron microscopy (*Polish*) 0-89217
- steel, medium C, 40MnB, dissoln. and precipitation of  $M_{23}(C,B)_6$  (*Chinese*) 0-66511
- steel, microalloyed, hot-rolled, Nb(C,N) precip. and austenite recrystn. 0-97513
- steel, microalloyed, types V1599, V1600, V1286, NbCN precipitation in undeformed austenite 0-89230
- steel, mild, cold rolled, texture and plastic anisotropy rel. to alloying and precipitation (*French*) 0-108475
- steel, Nb(V), (Al), hot-rolling, laboratory simulation, recrystn. of austenite 0-97512
- steel, Si, grain-oriented, high permeability, dissoln. and precip. of AlN and MnS 0-89223
- steel, stainless, carbide and intermetallic phases, quantitative anal. by X-ray diffr. 0-66514
- steel, stainless, Cr-Cu (17, 0.6 to 1.1 wt.%), texture 0-84957
- steel, stainless, Cr-Ni-Mo, phase anal. of carbide phases after isothermal annealing (*Czech*) 0-89224
- steel, stainless, precip. obs using convergent beam electron microscopy 0-108689
- steel, stainless 316, soln. annealed, cavity alignment and precipitation during dual ion bombardment 0-70273
- steel, stainless type 304,  $M_{23}C_6$  precipitation for various cooling cycles 0-60887
- steel, structural, second phase particle effects on impact strength 0-108581
- steel, W-Co-Mo-Cr-V-C (8.5, 8.1, 4.5, 3.5, 2.2, 1.02 wt.%), phase composition, struct. and props. 0-104163
- steel foil, microanalysis by energy dispersive X-ray spectrometry (*French*) 0-85250
- thermally induced structural changes, specimen surface influence 0-103559
- thin films, precipitation and nuclei form. in presence of condensation centres, thermodynamic model 0-103594
- Zircaloy-2, hydride precipitation and growth at crack tips, electron optical obs. 0-108449
- Ag-Cd peritectic system, separate crystallisation of phases (*Russian*) 0-66497
- Ag-In-Sn, internal oxidation, precipitation behaviour of oxide (*Japanese*) 0-66515
- Al alloy, FIM and microanalysis, developments 0-100155
- Al, fracture mechanism 0-100903
- Al-Sb(Zn), ion implanted electron beam annealing, ion backscatt. and TEM meas. 0-59500
- Al-Cu (2-5 wt.%), precipitation total surface influence on resistivity (*French*) 0-71650
- Al-Cu (4 wt.%) alloy, neutron irradi., weak-beam dark-field obs. of dislocations near  $\theta'$  precipitates 0-107333
- Al-Li-Mn (2.8, 0.3 wt.%), recrystallised sheet, fracture behaviour, SEM and TEM study 0-97566
- Al-Mg, Si alloy, void form. under different precip. conditions, after Al ion irradi. 0-59529
- Al-Mg (2 wt.%), hardening and fracture characts.,  $\beta$ -phase dissolution role 0-81178
- Al-Mg-Si, ageing sequence study by electron microdiff. 0-81068
- Al-Mg-Si alloy, STEM microdiff. obs. of precip. struct. 0-104167

## precipitation continued

- Al-Mg-Si alloys, ductile intergranular fracture mechanisms, void formation and nucleation 0-108578
- Al-Mn (1 wt.%), single crystals, rolled to {123}[412], recrystn. textures 0-104183
- Al-Ni (6 wt.%) alloy, misorientation between subgrains, second-phase particles role, STEM microdiff. obs. 0-104415
- Al-Si (0.57 at.%), Si precipitate dissolution kinetics 0-84935
- Al-Zn, grain boundary reaction sites, determ. of struct. aspects, by electron microscopy 0-103359
- Al-Zn (38 at.%), TEM study of precipitation processes or different microstructures during ageing 0-93561
- Al-Zn (70, 30 wt.%), decomp. study, 25-160°C (*Czech*) 0-89225
- Al-Zn-Mg, oriented growth of precipitates on dislocations, model 0-108448
- Al-Zn-Mg (3.6, 1.95 wt.%), ageing and plastic deform., effect on structure, electron microsc. and X-ray diffr. study (*Russian*) 0-81108
- Al-Zn-Mg (3.87, 1.79 wt.%), oriented growth of precipitates on dislocations, TEM obs. 0-108447
- Al-Zn-Mg alloy, TEM characteris. of precipitates 0-104166
- $Al_2O_3$ /Fe, pore form. during oxidative annealing, grain growth slowing 0-100856
- Au, Co-hardened, characterisation by Mossbauer spectroscopy, Co precip. formation 0-80108
- Au-Ge contacts on GaAs, SEM and TEM obs. of struct. 0-100522
- Be ingot, high-purity, TEM obs. of BeO dispersion 0-104165
- $Ca_2(Al,Fe,Cr)O_4$  solid soln., planar interfaces, TEM obs. 0-65008
- CdTe, low temp. thermal cond., growth parameter influence 0-92725
- CdTe:Cu films, impurity behaviour, Hall mobility and hole density meas. 0-80420
- CdTe:In precipitation and out-diffusion of solute during cooling 0-100840
- $CeCo_{5-x}Cu_x$ ,  $0 \leq x \leq$  internal oxidation kinetics, oxide struct., X-ray study 0-104329
- Co-Ti-C, secondary precipitation and allotropic transform., TEM obs. 0-108453
- Co-W alloy electrolytic coatings, heat treatment effects on coercivity, hysteresis and structure (*Russian*) 0-60381
- $Co_3Sm$  crystals, microstruct., homogeneous precip. and nucleation 0-104160
- Cr condensates, lattice const., internal stresses (*Russian*) 0-107141
- CsI:Ti, precipitation of Ti solid solns. 0-70419
- Cu, cementation, electrochem. nucleation and growth on Fe and Al, TEM 0-104451
- Cu, cementation, on Fe, deposit struct., reaction rates, SEM 0-104421
- Cu:Co precipitates, mag. anisotropy, precipitate shape, coercive force 0-80500
- Cu-Au-Fe, ferromag. ordering in FCC  $\gamma$ -Fe precipitates, Mossbauer study 0-71267
- Cu-Be (1.8 wt.%) alloy, discontinuous precip. form. and growth, TEM obs. 0-104169
- Cu-Be (2 at.%), plastic deform. and dislocation substruct. 0-76307
- Cu-Be-Co, discontinuous reaction, analytical TEM 0-100842
- Cu-Fe (1.5 wt.%), precipitation-effect on void formation during electron irradiation 0-84211
- Cu-Fe system, ageing and reversion phenomena study 0-89274
- Fe, cast, pearlitic, nodular graphite type, struct. evolution (*French*) 0-93551
- $\alpha$ -Fe, nitrided, aging at room temp. 0-71679
- Fe, pure, hydrogen-charged, initial cracking obs. 0-108580
- Fe, reaction with methane at 750 C micro Auger anal. 0-104020
- Fe-B amorphous alloy, annealed, microstruct. and mag. domain changes 0-75790
- Fe-Co-V-(Ni), annealing effect on microstruct. rel. to mag. and mech. props. 0-89267
- Fe-Cr-Al (7, 5 wt.%), expt. stainless alloys, phys. and mech. props. 0-97637
- Fe-Mn (1 at.%), strain age hardening 0-108472
- Fe-Mn-Ni-V-C (0.5, 3.0, 1.0, 0.2 wt.%), austenite decomp., isothermal transform. characts. 0-97477
- Fe-Mn-V-C (0.5, 1.0, 0.2 wt.%), austenite decomp., isothermal transform. characts. 0-97477
- $\alpha$ -Fe-N, supersaturated solid solns., N atom precip. kinetics, resist. meas. 0-60864
- Fe-N alloys, secondary ion emission, phase transforms. effect (*Russian*) 0-66347
- Fe-Ni-C, quenched martensite, annealing during cathodic hydrogenation, 200°C (*French*) 0-93573
- Fe-Ni-Cr alloy, carbide form. by C diffusion, precip. distrib. and morphology 0-104164
- Fe-O-Ca-Al system, inclusion precipitation diagram 0-108415
- Fe-Si (3wt.%), grain-oriented, secondary recryst., grain growth inhibition 0-89245
- $\alpha$ -Fe-Ti, ion implanted, microstruct., ion beam anal. and TEM study 0-107294
- $\alpha$ -Fe-Ti, ion implanted, with C impurity, microstruct. of TiC precip. 0-66513
- Fe-Ti-C, rapidly quenched by splat-cooling 0-84923
- Fe-Zn, physical-chemical metallurgy (*German*) 0-108390
- GaAs:Si defect density before and after Zn diffusion, SEM and TEM obs. 0-96529
- GaAs:Zn(Cr), As precipitation at dislocations, TEM study 0-79820
- GaP:Si, defect struct. and tetrahedral precipitates, TEM study 0-107246
- Ge-Si alloys, n-type, phosphorus doped, precipitation effects due to heat treatment 0-107833
- Hg<sub>1-x</sub>Fe<sub>x</sub>Te, struct. invest. using X-ray diffr. and electron microscopy 0-75365
- KBr(Cl):Mg<sup>2+</sup>, dopant aggregation and precipitation 0-107306
- KCl:Ba<sup>2+</sup>, localised stress relaxation in excess vacancy system, prismatic loops (*Russian*) 0-88160
- KCl:Br<sup>+</sup>, solid solution periodic precipitation in inhomogeneous conc. field 0-103485
- KCl:CdCl<sub>2</sub>, elec. cond., role of electrode material, surface precipitation effects 0-59985
- KCl:Pb, impurity distrib., light scatt. and microhardness study, heat treatment 0-96562
- LiF:Co, flow stress changes during precipitation 0-92594
- Li<sub>2</sub>GeO<sub>4</sub>-Zn<sub>2</sub>GeO<sub>4</sub>, solid electrolyte system, phase diagram 0-66489
- Mg-Al-Zn (94.3, 3.9, 1.8 wt.%), precip. on dislocations, weak-beam TEM 0-76264



precipitation continued

Mg-MgNi<sub>2</sub>-Zn, diagram of state, Zn solubility, initial phase precipitation (*Russian*) 0-66478  
 Mg-Mn-Ce (1.5, 0.3 wt%), superplasticity role of diffusional creep (*Russian*) 0-97528  
 Mg-Nd-Zn dilute alloy, metallography and precip. kinetics 0-71655  
 Mg-Zn (5 wt%), age hardening, X-ray diff. anal. (*Chinese*) 0-104173  
 Mg-Zn alloy, aged, one dimensional transition phase  $\beta_2$ , crystallographic obs. (*Chinese*) 0-60865  
 MgO:Ni, heavily doped, defect characterisation, rel. to use as laser material 0-65000  
 MnSi-Si system, striations and cryst. struct. of matrix 0-103292  
 MnSi<sub>1-1.73</sub> crystal growth and characterisation 0-93474  
 Mo:C (110) surface, segregation, precip. and desorpt. of C, AES and LEED study (*French*) 0-103480  
 Mo-Zr, nucleation conditions, effect on formation of oxide phase during internal oxidation (*Russian*) 0-81064  
 (Mo<sub>0.4</sub>Ru<sub>0.4</sub>)<sub>80</sub>Si<sub>10</sub>B<sub>10</sub>, amorphous supercond. matrix, flux pinning by MoRu precip. 0-65756  
 NaCl, impurity precipitation and grain boundary diffusion 0-107567  
 NaCl:Ca crystals, surface recrystn., moisture effect 0-84950  
 NaCl:Mg<sup>2+</sup>(Ba<sup>2+</sup>), dopant aggregation and precipitation 0-107306  
 NaNO<sub>3(2)</sub>, precipitation from mixed aq. solns. 0-100191  
 Nb, single cryst., fluxoid pinning by small nitride precip. 0-70913  
 Nb-Ge, compounds with A15 structure, films, TEM study (*French*) 0-80135  
 Nb-Ge-Si, compounds with A15 structure, films, TEM study (*French*) 0-80135  
 Nb-H system, accommodation effects during hydride precipitation, TEM 0-89218  
 Nb-Si, compounds with A15 structure, films, TEM study (*French*) 0-80135  
 Nb<sub>2</sub>Sn film formation, solubility, precipitating processes (*Russian*) 0-92792  
 Ni, NMR study of metal precipitated onto a cathode (*Russian*) 0-93185  
 Ni precipitates, isothermal annealing influence on structural state, X-ray diff. anal. (*Russian*) 0-100849  
 Ni superalloy, STEM microanal. of precipitates and their nuclei 0-81067  
 Ni-Al (2 and 6 wt%), oxidation,  $\alpha$ -Al<sub>2</sub>O<sub>3</sub> growth, microstruct., precip. 0-108626  
 Ni-Al-Mo (12.7, 21.6 wt%), directionally solidified eutectic composite, precipitation 0-108454  
 Ni-Al(Si) foils, ion irradi., surface effects on precip. morphology 0-104168  
 Ni-base superalloy, STEM microanalysis of precipitates 0-104492  
 Ni-Co-Al alloys, continuous precip., SEM, TEM, X-ray diff. study 0-89220  
 Ni-Co-C solid solution, C precipitation, Ni<sub>3</sub>Co ordering, Ni-Co lattice parameter meas. (*Czech*) 0-60867  
 Ni-Cr-Co based alloy, IN-738 turbine blades, hot isostatically pressed investment castings, effect of heat treatment on grain boundary struct. 0-89270  
 Ni-Cr-Co superalloy, combined TEM, FIM, atom probe microanalysis of precipitates and carbide phase comp. 0-100844  
 Ni-Cr-Fe alloys, radiation enhanced precip. and dissolution of precipitates, point defect kinetics and dislocation obs. 0-108467  
 Ni-Cr-W, oxidation behaviour in air at 1000-1250°C 0-89407  
 Ni-Zn, physical-chemical metallurgy (*German*) 0-108390  
 NiO, undoped and Al doped, Ni self-diffusion, vacancy-impurity complex effects 0-107493  
 Pb-Ag (0.068 wt%), Ag precipitation kinetics and activation energy 0-66517  
 Pb-As (~0.01 wt%), enhanced precip. phenomena, invest. of mechanism by elec. resist. meas. 0-104162  
 Pb-Au, interstitial and substitutional distrib. 0-84204  
 Pb-Bi, temp. regime of crystn. on rapid cooling (*Russian*) 0-66495  
 Pb-Sb-As (1.1-1.8, ~0.01 wt%), enhanced precip. phenomena, invest. of mechanism by elec. resist. meas. 0-104162  
 RbCl:CoCl<sub>2</sub> system, precipitate form., ionic cond. meas. 0-96653  
 Si, ambient effect of O precipitation, self interstitial mechanisms, IR spectra, TEM study 0-66510  
 Si, crucible grown, virgin and implanted, laser irradiation effects on surface structure 0-92768  
 Si crystal, Czochralski grown, enhanced Borrmann effect 0-70191  
 Si, crystal defects and impurities interaction obs. by electron microscopic methods 0-65003  
 Si crystals, annealed, oxide precipitates identification, TEM, EELS 0-100723  
 Si, Czochralski grown, oxide precip. homogeneous nucleation 0-65221  
 Si, Czochralski grown, oxide precipitates, diffusion-limited growth 0-97484  
 Si, Czochralski grown crystal, O precip., nucleation behaviour and dislocation loop form. (*Japanese*) 0-59664  
 Si n<sup>+</sup>-p solar cells, degradation mechanisms associated with Ti impurities 0-81465  
 Si, precipitation of O, 650°C, IR absorpt. and X-ray diff. 0-76258  
 Si:Al, precipitation of solid soln., effect of gamma irradiation 0-59515  
 Si:Bi, ion-implanted, solid phase epitaxial growth during annealing, super-saturated solid soln. form. 0-103384  
 Si:Cu, precipitate morphology, IR microscopy study (*Chinese*) 0-103539  
 Si:Fe, ion implanted, laser annealing studies using Mossbauer spectroscopy 0-79827  
 Si:In, clustering and precipitation, time-dependent perturbed ang. correlation meas. 0-65234  
 Si:P polycrystalline layer, role in lattice defect reduction assoc. with P predeposition 0-70229  
 Si:P(As)(B), nonequilibrium solid solutions obtained by heavy ion implantation and laser annealing 0-92544  
 Si(111):Pb ion implanted amorphous layers, recrystallisation, impurity out-diffusion model (*Chinese*) 0-88363  
 SmCo<sub>5</sub>, nucleation of reversed domains at Co<sub>2</sub>Sm<sub>2</sub> precip. 0-75791  
 SmCo<sub>5</sub>, sintered magnets, eutectoid decomp. 0-89219  
 Sn-Bi(Pb)(Ga), temp. regime of crystn. on rapid cooling (*Russian*) 0-66495  
 steel, Nb, deform., recrystn. and precip. interaction 0-97515  
 Ta, acoustic emission induced by hydride formation 0-76257  
 Ta-H, physical properties, plastic deformation, H ordering (*Ukrainian*) 0-71689  
 Ti-Al-Cr-Mo-V, VT22 alloy, metastable  $\beta$ -phase decay under continuous heating, plastic strain effect (*Russian*) 0-71656

precipitation continued

Ti-Al-V (6.4 wt.%), ion irradiated, microstruct. study using TEM 0-96572  
 Ti-Fe, H storage material, Mossbauer surface studies, Fe clusters 0-97167  
 Ti-Mo-Zr-Sn (11.5, 6, 4.5 wt.%),  $\beta$  III, mech. props. rel. to heat treatment 0-84961  
 Ti-Mo-Zr-Sn (11.5, 6.0, 4.5 wt.%) alloy, struct. as affected by processing history 0-84972  
 Ti-Mo-Zr-(Al) (15, 5 (3) wt.%), quenched and aged metastable  $\beta$ -phase, crystallography, morphology and decomposition 0-76262  
 Ti-N<sub>2</sub>, condensate formed by plasma flow precipitation in vacuum, cryst. and surface props. (*Russian*) 0-100788  
 Ti-Nb-Si, amorphous alloy, supercond. props. and crystn. behaviour, TEM and DTA study (*Japanese*) 0-84536  
 Ti-Nb-Zr-Ta, superconducting props. comp. depend., stress effects and precipitation behaviour, X-ray scatt. 0-93059  
 Ti-Si amorphous alloy, melt-quenched, transform. studies and mech. props. 0-100838  
 Ti<sub>70</sub>Co<sub>20</sub>B<sub>10</sub>, amorphous alloys, crystn. behaviour, TEM study (*Japanese*) 0-84087  
 TiD<sub>2</sub>, nucleation and growth in D<sub>3</sub><sup>+</sup> implanted Ti, TEM study 0-97717  
 Ti<sub>70</sub>Fe<sub>20</sub>B<sub>10</sub>, amorphous alloys, crystn. behaviour, TEM study (*Japanese*) 0-84087  
 Ti<sub>70</sub>Ni<sub>20</sub>B<sub>10</sub>, amorphous alloys, crystn. behaviour, TEM study (*Japanese*) 0-84087  
 V, dehydrogenation by annealing with Zr foils, internal friction meas. 0-96736  
 V wire, deformed in torsion, internal friction, H effect 0-76300  
 V/Cu-Ga, composite superconductor, V<sub>3</sub>Ga phase form., TEM obs. (*Russian*) 0-84933  
 V-Ti-C, high temp. carbide form., electron microscopy study 0-89228  
 V<sub>3</sub>Ga, supercond. A15 phase, prep. by controlled precip. 0-81000  
 W wire, AKS-doped, second phase particle obs. by TEM, SEM and atom probe microanalysis 0-108457  
 Zn single cryst., dislocation velocity and plastic deform. 0-64998  
 Zn-Ga, temp. regime of crystn. on rapid cooling (*Russian*) 0-66495  
 Zr, hydride precipitation and growth at crack tips, electron optical obs. 0-108449  
 Zr-H alloy, precip. of  $\gamma$ -ZrH, shear mechanism 0-104170  
 Zr-N<sub>2</sub>, condensate formed by plasma flow precipitation in vacuum, cryst. and surface props. (*Russian*) 0-100788  
 Zr-Nb (2.5 wt.%), hydride precipitation and growth at crack tips, electron optical obs. 0-108449  
 ZrO<sub>2</sub>, partially stabilised ceramics, strengthening, post-sintering heat treatment 0-97518  
 ZrO<sub>2</sub>-CaO (15 mol.%), precipitation and ordering 0-100837  
 ZrO<sub>2</sub>-Y<sub>2</sub>O<sub>3</sub> (9 mol.%), precipitation and ordering 0-100837  
 precipitation, electrostatic see electrostatic precipitators; precipitation (physical chemistry)  
 precipitation (atmospheric) see atmospheric precipitation  
 precipitation (meteorology) see atmospheric precipitation  
 precipitation (physical chemistry)  
 for precipitation within solid systems (microstructural changes) see precipitation  
 see also coagulation; crystal growth from solution; flocculation  
 cellulose acetate butyrate, in soln., hydrodynamic behaviour 0-64876  
 cellulose fibre formation in stirred dimethyl sulphoxide-paraformaldehyde soln. 0-104440  
 oxalate precipitation for separation of Am, Cm, and trivalent lanthanides 0-83202  
 rubber, blooming by waxes 0-104109  
 silicate gardens, growth morphology, mechanisms 0-100765  
 vinyl polymers, precip. from solns., temp. determ. (*German*) 0-85208  
 Pu(V) in alkaline freshwater pond, determ. by coprecipitation technique 0-71988  
 Al chalcogenate and chalcogenite double salts, form. laws and acid-base props. 0-101070  
 Al(OH)<sub>3</sub>, precip. from solns. containing Li ions, X-ray diff. patterns and comp. determ. 0-76502  
 Ga chalcogenate and chalcogenite double salts, form. laws and acid-base props. 0-101070  
 Ge<sub>2</sub>Si<sub>3</sub>, glass form. and characterisation (*German*) 0-64913  
 Ge<sub>2</sub>Se<sub>3</sub>, glass form. and characterisation (*German*) 0-64913  
 In chalcogenate and chalcogenite double salts, form. laws and acid-base props. 0-101070  
 Tb(NO<sub>3</sub>)<sub>3</sub>-Fe(NO<sub>3</sub>)<sub>3</sub>-(NH<sub>4</sub>)<sub>2</sub>CO<sub>3</sub>-H<sub>2</sub>O system, cpd. form., comp. and props. 0-100832  
 Tb<sub>2</sub>O<sub>3</sub>-H<sub>3</sub>PO<sub>4</sub>-H<sub>2</sub>O system, cpd. form., comp. and props. 0-100832  
 precipitation ageing see precipitation hardening  
 precipitation annealing see precipitation hardening  
 precipitation hardening  
 dislocation physics research of F.R.N. Nabarro 0-62441  
 Nimonic 80A, order hardening, comparison between revised theory and expt. 0-93565  
 steel, age hardened, dynamics of cyclic plasticity (*Czech*) 0-108464  
 steel, Al-Ti-(Mo), Al-Ti-V-(Mo), Al-Ti-Nb-(Mo) and Al-V-(Mo) low-alloy, toughness improvement through Ti additions 0-66525  
 steel, austenitic Fe-Mn-V-C, ageing characts., discontinuous precip. nature 0-84940  
 steel, austenitic stainless, ageing at high temp., effect on creep props. SEM 0-97516  
 steel, austenitic stainless, precipitation of M<sub>23</sub>C<sub>6</sub> type carbide on twin boundaries 0-89226  
 steel, C-Mn-V-Cb-N, high strength low alloy, controlled-rolled 0-100803  
 steel, cold strained, defects interaction with carbide strengthening phases, carbide decomp. degree (*Russian*) 0-84955  
 steel, Cr-Mn(Ni), Mn and Ni additions, effect on corrosion resistance and hardness 0-104342  
 steel, Cr-Mo-Mn-Si-W (3, 1.95, 1.55, 1.45, 0.95 wt.%), struct. and props. 0-104175  
 steel, maraging, Fe-Cr-Co-Mo, phase transforms. during high temp. austenitisation and solid soln. decomp. (*Russian*) 0-66524  
 steel, Mn-V reinforcing type, strain ageing characts. rel. to mech. props. 0-84969  
 steel, Si (3 wt.%), textured, secondary recrystn., precip. annealing effect (*Japanese*) 0-71662  
 steel, stainless 304 sol. of annealed and thermally-aged, high-cycle fatigue behaviour 0-100923



**precipitation hardening continued**

- steels, low alloy, particle coarsening reactions, effect of cold deform. 0-71664  
 thermophysical property research, metallurgical applications 0-97457  
 Al age-hardenable alloys, dissolution processes, positron annihilation and X-ray small-angle scattering comparison 0-89238  
 Al-Cu (4 wt.%) alloy, high temp. cyclic deform.,  $\theta'$  particle dissolution obs. 0-108515  
 Al-Li-Mn (2.8, 0.3 wt.%), recrystallised sheet, fracture behaviour, SEM and TEM study 0-97566  
 Al-Mg<sub>2</sub>Si alloy, STEM microdiff. obs. of precip. struct. 0-104167  
 Al-Mg-Si alloys, cast, precip.-rich zones on grain boundaries, soln. heat treatment conditions effect on mech. props. 0-104176  
 Al-Zn-Mg (2.2, 4.7 at.%), precipitate free zones, X-ray microanal. 0-108768  
 Al-Zn-Mg alloy, TEM characteris. of precipitates 0-104166  
 Al-Zr (1-13 wt.%), rapidly quenched, extended solid solubility, grain refinement and age-hardening 0-76266  
 AlCu-NiCo (5 at.%),  $\theta'$  hardened, creep mechanism 0-85013  
 Co-Ni-Cr-Nb (40, 18, 1.8 wt.%), precipitation behaviour of NbC, effect of ageing temp. on morphology 0-89227  
 Cu alloy, precipitation strengthened compositions with oxide particles, condensed, struct. criteria and thin layer possibilities (*Russian*) 0-89236  
 Cu-Be (1.8 wt.%) alloy, discontinuous precip. form. and growth, TEM obs. 0-104169  
 Cu-Co single cryst., precip. hardening (*German*) 0-84946  
 Cu-Cr-SiO<sub>2</sub> system, age and dispersion strengthened, dislocation struct. around SiO<sub>2</sub> particles 0-108468  
 Cu-Cr(SiO<sub>2</sub>), single crystals, yield and pre-yield behaviour rel. to aging time 0-81103  
 Cu-Fe (1.5 wt.%) alloy, void form. during irradi. in HVEM, reactor irradi. simulation and ageing effects 0-107327  
 Cu-Ni-Al (5, 2.5 at.%), precip. hardening (*Japanese*) 0-71663  
 Cu-Ni-Nb (30, 0.9 at.%), precipitate free zones, X-ray microanal. 0-108768  
 Cu-Ni-Sn (15, 8 wt.%), prior deform. effect on spinodal age hardening 0-108465  
 Cu-Ni-Ti, ordering within precipitates, TEM obs. 0-108461  
 Cu-Ni-Zn-Mn fine grained precipitation-hardenable alloy, high strength and ductility 0-100805  
 Cu-Ti, strengthened by modulated structs., anomalous age hardening effects 0-97497  
 (Cu-Au)-Co, single crystals, solid soln. and particle strengthening, superposition 0-97495  
 Cu-Au-Co single cryst., precip. hardening (*German*) 0-84946  
 Fe-Mo (13-20 at.%) binary alloys, spinodal decomp. on ageing, TEM and X-ray diff. study 0-97503  
 Fe-Mo-CaF<sub>2</sub> sintered composite, struct. and mech. props., heat treatment effect 0-66526  
 Fe-Mo-Ta, ternary Laves phase strengthening 0-108466  
 Fe-Ni-Al(Cu) (12, 0.5, 0.5 to 3 wt.%), Cu addition strengthening at 77K, mech. props. 0-60875  
 Fe-Ni-Co-W(Mo) (18.65, 8.99, 4.87 wt.%), ageing charact., 380-530°C 0-60876  
 Fe-Ni-Cr alloy, carbide form. by C diffusion, precip. distrib. and morphology 0-104164  
 Fe-Ni-Ti-(Cu) (12, 0.25, 2 wt.%), Cu addition strengthening at 77K, mech. props. 0-60875  
 Fe-Ni-V-(Cu) (12, 2, 2 wt.%), Cu addition strengthening at 77K, mech. props. 0-60875  
 Fe-Ni-(Cu) (12, 0.5 to 3 wt.%), Cu addition strengthening at 77K, mech. props. 0-60875  
 Mg-Zn (5 wt.%), age hardening, X-ray diff. anal. (*Chinese*) 0-104173  
 Ni alloy, precipitation strengthened compositions with oxide particles, condensed, struct. criteria and thin layer possibilities (*Russian*) 0-89236  
 Ni-Al, order hardening, comparison between revised theory and expt. 0-93565  
 Ni-base wrought superalloy, creep and stress rupture behaviour in air and vacuum 0-60918  
 Ni-Cr-Co superalloy, combined TEM, FIM, atom probe microanalysis of precipitates and carbide phase comp. 0-100844  
 Ni-Cr-Fe alloys, radiation enhanced precip. and dissolution of precipitates, point defect kinetics and dislocation obs. 0-108467  
 Ni-Fe-Cr superalloy 718, heat treatment effect on room temp. and elevated temp. fracture toughness response 0-100922  
 Ti-Al-Mo-Cr alloy weldment containing orthorhombic martensite, auto-tempering behaviour and alpha precip. strengthening 0-84976  
 $\beta$ -Ti-Mo-Zr-Sn(11.5, 6, 4.5 wt.%), metastable phase III, microstruct. and age hardening response 0-84945

**prediction theory** *see filtering and prediction theory***predictor-corrector methods**

- see also Runge-Kutta methods*  
 supersonic two-phase flow, nonequilibrium, condensation, boundary condition numerical anal. 0-64565

**predissociation of molecules** *see molecular predissociation***prerotation** *see rotation***presentation, technical** *see technical presentation***presintering** *see sintering***pressing, hot** *see hot pressing***pressure**

- see also atmospheric pressure and density; high-pressure phenomena and effects; radiation pressure; vapour pressure*  
 dew point temp. change with pressure, calc., nomogram 0-77607  
 Freon electrohydrodynamic flow, jet dynamic pressure obs. (*Russian*) 0-59117  
 Mars atmosphere pressure, annual cycle meas. by Viking landers 1 and 2 0-72812  
 matter under very high pressure (*French*) 0-90811  
 proteoglycans, swelling pressures at the concs. found in cartilaginous tissues 0-67327  
 sintering, inhomogeneous flow and effective press. 0-93512  
 solar atmosphere, gas pressure rel. to nonequilibrium, mag. field states and preflare stage 0-105213  
 transformer oil electrohydrodynamic flow, jet dynamic pressure obs. (*Russian*) 0-59117  
 triple correlation of the pressure in subsonic circular jets and nonlinear interaction of instability waves 0-69893  
 turbulent flow noise generation, role of tornado-like vortices 0-69811

**pressure continued**

- wall-pressure spectrum in turbulent boundary layer, rel. to noise generation by boundary layer-surface interactions 0-69810  
 wave generation and propagation by spark discharges in liquids (*Japanese*) 0-70060  
**pressure, atmospheric** *see atmospheric pressure and density*  
**pressure control**  
*see also vacuum control*  
 evaporator design for gas phase electron diffraction 0-57424  
 multidimensional gas chromatography, pressure balancing techniques 0-89576  
 self-contained regulators, selecting and sizing 0-82759  
**pressure measurement**  
*see also vacuum measurement; vapour pressure measurement*  
 atmosphere remote sensing from satellite using MM wave radar system 0-67443  
 automated electromanometer, appl. for nuclear materials safeguarding 0-99211  
 balance, improved floating-element spinning mechanism 0-86331  
 balances, effective area at low press. 0-86332  
 blood, partial pressure of gases meas., in vitro electrochemical sensors 0-67303  
 blood pressure, human, noninvasive meas. (*Japanese*) 0-94395  
 blood pressure, indirect meas., meaning of max. oscills. point in cuff press. 0-94396  
 blood pressure, indirect meas. method, review 0-94383  
 blood pressure automatic monitoring, long-term, minicomputer system 0-101276  
 blood pressure measurement with portable systems using Korotkov sounds, meas. accuracy 0-76855  
 blood pressure recording, simple method for fidelity improvement, Korotkov sounds 0-76811  
 calibration system improvement using ruby R<sub>1</sub> fluorescence 0-98928  
 carotid back pressures in conjunction with cerebral angiography 0-98119  
 catheter, multi-transducer, for intraluminal press. recording in vivo 0-89879  
 catheter pressure meas., transducer smearing correction using microprocessor based discrete deconvolution 0-67275  
 constant pressure manometer with frequency read out, electrocapillary element appl. 0-73380  
 critical light reflection at a plastic/glass interface and appl. to foot press. meas. 0-81681  
 dilatometer for PVT meas. of liquids and plastic crystals at low temperature 0-68208  
 elastomagnetic pressductor, design, theoretical and operating charact. (*Czech*) 0-68205  
 electrical sensors, seven types (*German*) 0-77772  
 fibre optical interferometers for length, temp., pressure and force meas. 0-98971  
 foot pressure distributions, technique for display 0-85508  
 fuel rod gas pressure meas. during LOFT, sensor description 0-57876  
 intracranial pressure measurement system 0-109084  
 intracranial pressure and its epidural meas. 0-101282  
 Langmuir film balance meas. system 0-62659  
 low and differential pressure meas. by pressure divider 0-90862  
 McLeod gauge, capillary depression phenomena, Hg vapour drag effect 0-98923  
 membrane hydrophone for 0.5 to 15 MHz range, press. meas. in US fields 0-108987  
 membrane pressure converters, errors arising due to differential heating 0-62680  
 microcomputer-based blood-pressure recorder (*Japanese*) 0-67139  
 oesophageal manometry by liquid-filled catheters 0-85514  
 pipeline, pressure-switch for multipoint meas., computer data acquisition system 0-62679  
 pressure balance standards, international comparison over 1 to 10 MPa range 0-105671  
 pressure changes in interconnected chambers, mathematical model 0-108678  
 pulse-pressure generator, quasistatic method for stepped pressure, transducer testing 0-62678  
 resistance bridge with linear charact., appl. to press. meas. using electroresistive gauges or extensometric transducers (*Polish*) 0-73385  
 SI units fundamentals (*French*) 0-95059  
 soil, using capacitive sensor with polyurethane foam dielectrics (*Slovak*) 0-86281  
 Speer carbon resistors as pressure gauges 0-95108  
 standards for oil-operated pressure balances, intercomparison between NPL and LNE 0-98877  
 strain gauges for industrial pressure measurement (*Hungarian*) 0-86278  
 surface friction in turbulent boundary layer, meas. using plane Pitot tube 0-79284  
 transducers, freq. charact. meas., review of meas. apparatuses 0-62650  
 TTF-chloranil visual pressure or temperature indicator 0-87443  
 units for pressure, definitions and areas of use 0-77745  
 unsteady pressure coefficients digital measuring unit for wind tunnel tests (*French*) 0-68169  
 US system for blood press. anal. during treadmill stress testing 0-81674  
 variable pressure manometer, electrocapillary element appls. and properties 0-73379  
 Ar, compressed gas, PVT meas. at high press. 0-98927  
 Ge:Au film strain gauges (*Japanese*) 0-105631  
 O<sup>2-</sup> low partial press., thermogalvanic meas. using O<sup>2-</sup> ion conductors 0-73389  
 O<sub>2</sub> partial pressure, absolute meas. using impedance dispersion analysis on PdO form. 0-108728  
 T gas nuclear bombardment targets, pressure monitoring system 0-99370  
**pressure sintering** *see sintering*  
**pressure transducers**  
 biomedical semiconductor pressure transducer (*Japanese*) 0-94394  
 catheter pressure meas., transducer smearing correction using microprocessor based discrete deconvolution 0-67275  
 constant pressure manometer with frequency read out, electrocapillary element appl. 0-73380  
 intracranial pressure meas. in newborns, new non-invasive technique 0-67272  
 measurement of frequency characteristics, review of meas. apparatuses 0-62650  
 miniature implantable, biomedical appl. IC fabrication techniques 0-76849

**pressure transducers continued**  
monolithic capacitive press. transducers for deep-body biomedical appls., pulse-period output 0-67274  
monolithic capacitive pressure sensor with pulse-period output electronics on same chip 0-81752  
optomechanical pressure transducers, designing and testing 0-105662  
piezoelectric pressure sensor 0-105670  
pressure measurement, elastomagnetic pressductor, design, theoretical and operating charact. (*Czech*) 0-68205  
protection, parylene (vacuum deposited polymeric coating) appl. 0-108607  
semiconductor strain gauge, method to improve temp. stability 0-87826  
testing, pulse-pressure generator, quasistatic method for stepped pressure 0-62678  
thick-film strain gauges and pressure transducers 0-57285  
variable pressure manometer, electrocapillary element appls. and properties 0-73379  
Bi foil element, determ. normal stress components in solid state high pressure test cell 0-73378  
Cu-Ni/Au-Ni multilayer films deposited on membrane, use as strain gauge 0-65713  
 $Pb_{0.82}Sn_{0.18}Te$  film, effect of hydrostatic pressure on props. 0-70862  
Si diaphragm pressure sensor, integrated signal conditioning 0-76859  
Si p-channel MOS structure, direct parametric press. transducer props. 0-100526

**pressure vessels**  
AE during fatigue crack expansion 0-108675  
conference, Berlin, Germany (Aug. 1979) 0-77539  
crack detection by magnetic crack detection and dye-penetrant inspection 0-100994  
electrophysiological measurement, high-press. chamber 0-98185  
HTGR prestressed concrete pressure vessels, design of removable closures for large cavities 0-78356  
IR investigations of gases, pressure cell 0-83522  
neutron noise analysis in PWR and BWR power reactors 0-86964  
nuclear reactor containment structure design and service loads 0-106138  
nuclear reactor pressure vessels, strain measurements 0-79865  
PWR containment vessel optimisation 0-106137  
PWR LOCA reflow, effect of low containment press. on peak cladding temp. 0-57897  
reactor pressure vessels, thick steel sections, inspection by US nondestructive examination 0-102258  
stability of thin-walled pressure vessels of elastic-plastic linear hardening material 0-92075  
steel, A533B alloy, fatigue crack growth of irradiated pressure vessel steels in simulated, reactor-grade water environment 0-97582  
steel, alloy A533B1, neutron irradiation, flow growth characts. by acoustic monitoring 0-100918  
steel, fracture toughness of nuclear pressure vessels 0-81172  
steel, Mn-Mo-Ni (A533 B), ductile-brittle transition, material fracture temp. depend., Gauss distrib. function 0-97574  
steel, testing by pendulum impact machines, energy meas. using optical system 0-69746  
steels, irradiated pressure vessel, reference fracture toughness curves 0-100921  
steels, nuclear reactor pressure vessel steels, optimum chem. comp. rel. to props. 0-93517  
weld metal, submerged arc irradiated, reference fracture toughness curves 0-100921  
Cr-Mo steel types JIS SCM V 2, SCM V 3 and SCM V 4, high-temp. high-cycle fatigue props., press. vessel appls. (*Japanese*) 0-93650

**primary cells**  
developments in electrochemical energy sources (*German*) 0-97770  
graphite fluorides,  $(CF)_n$  and  $(C_2F)_n$ , prep., struct., discharge characts., electrode props. 0-89502  
Leclanche cell, impedance spectrum of an undischarged cell 0-89604  
small-sized batteries development, Japanese industry and market trends 0-81429  
tetramethylammonium silver iodide superionic film, electrocodeposition, electrochem. cells 0-107478  
thermal battery cells using molten nitrates as electrolyte and oxidiser 0-76624  
transition metal chalcogenides, reversible electrodes appls. 0-61112  
volt dissemination method and standard cell enclosure design 0-98876  
Ag-Zn batteries, miniature, fabrication and characts. (*Polish*) 0-93866  
Au/solid electrolyte/Au, charge storage with various electrolytes 0-89605  
Li batteries with voltage compatibility with conventional systems 0-97777  
Li battery, button type, using CuO as cathode 0-97779  
Li metal for battery industry, sources and preparation 0-97781  
Li nonaqueous battery iron sulphides preparation, characts. and appls. 0-97778  
Li primary batteries, development trends. 0-101083  
Li/SO<sub>2</sub> battery, characts. and appls. 0-97774  
Li/SO<sub>2</sub> cells, DTA, safety studies 0-81428  
Li/SOCl<sub>2</sub> cells, abuse tests 0-97776  
Li/SOCl<sub>2</sub> cells, high rate discharge characts. 0-72021  
Li/SOCl<sub>2</sub> D cells, optimisation with respect to energy density, storability and safety 0-97775  
Li/SOCl<sub>2</sub> primary cells, SOCl<sub>2</sub> reduction mech. in supporting electrolyte 0-108792  
Li/TiS<sub>2</sub> cell with solvate melt, discharge characts. and lack of rechargeability 0-72022  
Li-(CF)<sub>n</sub> high energy density battery, cathode materials evaluation 0-97780  
Li-I<sub>2</sub> batteries for cardiac pacemakers, capacity rating system 0-97773  
Li-I<sub>2</sub> battery, construction, performance and reliability 0-97771  
Li-I<sub>2</sub> cell for commercial and medical appls. 0-97772  
Li-MnO<sub>2</sub> batteries development, Sanyo, with high energy densities 0-85272  
Mg-AgCl seawater battery, performance and EMF at great ocean depths 0-76623  
MnO<sub>2</sub>, doped, dry cell depolariser, hydrazine reduction kinetics 0-89603  
MnO<sub>2</sub>, preparation and characterisation of doped samples for appl. as dry battery depolarisers 0-89602  
Zn electrode development, dispersed, electric vehicles appl. (*French*) 0-70223  
ZnCl<sub>2</sub> energy systems for public utility and automotive appls. 0-101082

**primary cosmic radiation** see *primary cosmic rays*

**primary cosmic rays**  
antiparticles and collisions in interstellar medium 0-77241

**primary cosmic rays continued**  
electron component in galactic disc, estimate from gamma-ray emission obs. 0-82540  
galactic cosmic ray electrons, 30-1000 GeV, emulsion chamber obs. 0-85827  
origin, appl. of galactic models with halo to proton nucleon component 0-61971  
Ne to Fe nuclei, 200 to 650 MeV/nucleon, relative abundances 0-77246  
**printed circuits**  
fabrication, detrimental effect of aged Sn-Pb surfaces 0-108625  
PCB contacts, additive-free hard Au appls. 0-108718  
protection, parylene (vacuum deposited polymeric coating) appl. 0-108607  
solar cells automated production, with wraparound contacts 0-76635

**printers**  
electronic ink system protection, parylene (vacuum deposited polymeric coating) appl. 0-108607  
laser beam printer scanning system with f- $\theta$  lens 0-78942  
pictorial electrographic printing, tone reproduction and screen design 0-62752

**printing**  
additive photographic film printers, programmed control of light metering valves (*Russian*) 0-95174  
images, scanning laser beam direct picture printers on photographic paper, appl. in life sciences (*French*) 0-72119  
photographic print timer, using ring of LEDs 0-77899  
waterless planographic plate development 0-105729

**prismatic dislocations**  
KCl:Ba<sup>2+</sup>, localised stress relaxation in excess vacancy system, prismatic loops (*Russian*) 0-88160  
ZnO, irradiation in high voltage electron microscope dislocation loops study 0-88157

**prisms (optical)** see *optical prisms*

**probability**  
see also *game theory; Monte Carlo methods; queueing theory; random processes; statistics*  
accidents at nuclear power stations (*Portuguese*) 0-68844  
accidents during work, mapping of reasons using error beams by function sensed computations of admission probabilities (*German*) 0-68027  
comets, discovery probability and reality of concentration of perihelia of concentration of perihelia 0-67660  
complete computer program in FORTRAN, for analysis of variance and means 0-98792  
deterministic dynamics to probabilistic descriptions 0-68029  
entropy, information and statistical, and law of large numbers, opacity of statistics (*French*) 0-73288  
exponential distribution MTBF confidence limits determ. using Epstein and Harters methods 0-98790  
failure, high temp., life fraction rule and probabilistic approach 0-93608  
fission reactor Pu fuel facility damage from high winds, risk anal. 0-63356  
fission reactors, BWR decay heat removal systems, probabilistic risk assessment, fault and event tree anal. 0-63333  
fission reactors, failure probability distrib. from observed failure data, beta distrib. 0-63335  
fission reactors, operator reliability, Weibull distrib. model 0-63336  
Fokker-Planck equation with spatial coordinate-dependent moments, path integral soln. 0-77688  
master equations, discrete, continued fraction solns. not obeying detailed balance 0-101758  
measurement errors, distribution function determ. feasibility for various sample sizes 0-90806  
metallic structures initial fatigue quality characterisation using equivalent-initial-flaw-size distribution 0-58978  
multiple comparisons for Poisson rates 0-98789  
nonlinear statistical theories, fluctuation effects, truncation schemes of cumulant hierarchies 0-68133  
nuclear power stations, probabilistic methods, safety assessment, Fed. Rep. Germany 0-106124  
nuclear power stations, probabilistic methods in safety analysis and regulations in France 0-106123  
nuclear power stations, structural reliability, conference, Berlin, Germany (Aug. 1979) 0-105422  
nuclear safety analysis, methodology and appls. of probabilistic risk assessment 0-63352  
photon counting with dead time, inversion problem 0-99682  
polymer, long, short range correlations in solution 0-59367  
PWR vessel and primary circuits estimation of reliability, probabilities and adaptive models 0-106125  
quantum theory, probabilistic formulation, hidden variables theory 0-62508  
radiotherapy treatment planning, FORTRAN program for optimisation using complication probability factor 0-81686  
sample sizes for comparing two proportions 0-98791  
severe local storms, automated 12 to 36 hour probability forecasts 0-77062  
stochastic cellular systems, model (*German*) 0-90661  
stochastic point process with continuous probability measure, non-parametric test (*French*) 0-57184  
thunderstorms, automated 12 to 36 hour probability forecasts 0-77062  
weather prediction, normalised variance anal. for meteorological time series, F-distribution (*Chinese*) 0-67388  
H II regions density and ionisation, joint probability density function 0-77468

**probes**

see also *electron probes; muon probes; plasma probes*  
brain cell, parylene (vacuum deposited polymeric coating) appl. 0-108607  
conductivity probe design for use with bridge instrument, wide range of test solns. 0-95110  
eddy current imaging flaw detection system 0-89426  
fibre optic acoustical detector probe 0-91916  
five-hole, for complex flow field meas. calibration and appl. 0-69951  
flow direction probes for turbomachine technology 0-87824  
flow meas., two-dimensional nonsteady, X-hot wire probe method (*Japanese*) 0-59134  
gaseous insulating materials, elec. pot. meas. by corona probe 0-82790  
Hall effect, linearity improvement of type TLMK Hall probes (*Slovak*) 0-82795  
impedance probe calibration, for vacuum meas. in single component two-phase mixture (*Italian*) 0-62677



**probes continued**

- in vivo probe measurement technique for determining dielectric properties at VHF through microwave frequencies 0-85542
  - ion temperature, for ionosphere sounding by rockets, system designs (*Japanese*) 0-85838
  - Microprobe Mole/plasma chromatograph system, for anal. of compounds on micron scale 0-101049
  - near-surface defects, US detection and analysis (*German*) 0-93728
  - neurological, parylene (vacuum deposited polymeric coating) appl. 0-108607
  - NMR probe using single IC for HF head for magnetic field meas. 0-62697
  - nuclear power station heat exchangers, eddy current probe for nondestructive testing of transfer tubes (*Japanese*) 0-81246
  - optical fibre, use in remote inelastic light scatt. probe 0-58769
  - optoacoustic material probing and imaging, far IR 0-83559
  - phase distribution in two-phase steam flows, effects of probe position 0-87799
  - piezoelectric probe, conversion ratios 0-69624
  - single-coil triple-tuned NMR probe for simultaneous stimulation of  $^1\text{H}$ ,  $^2\text{H}$  and  $^{13}\text{C}$  resonances 0-86364
  - spherical Pitot, for flow meas., construction and calibration (*Italian*) 0-69957
  - surface geometry meas., signal processing and analysing device, Herbert-Sigma (*French*) 0-57254
  - thermal, for gas high stationary temperature meas. 0-95101
  - thermal cond. meas. cylindrical probe improvement 0-92033
  - triple-sensor, for turbulent flow-field investigations 0-100043
  - US flaw detection, focusing probes 0-104383
  - US materials testing, imperfect coupling between probe and test piece, effects (*German*) 0-85122
  - US transmission line of probe for hot metal inspection, spurious signals 0-66754
  - VHF waveguide dielectric scatt. model for pulse-probe data interpretation (*Russian*) 0-62682
  - water-wave height probe with calibration stabilized for changes in water conductivity 0-57280
  - PVF<sub>2</sub> polymer probe for mapping pressure field from arrays 0-74669
- process computer control**
- image analysis by LEITZ-TAS with process computer 0-68773
  - mirror fiducial system compatible with computer-controlled polishing facility 0-74539
  - nuclear materials safeguards, microscopic process monitoring [for nuclear materials safeguards] of fuel reprocessing facilities to prevent material diversion 0-83153
  - nuclear materials safeguards in Th-U fuel reprocessing facility, computerised analytical process control system 0-78429
  - plasma control by feedforward-feedback system with digital computer 0-75093
  - TLD reader, microcomputer controlled 0-69044

**process computers**

- multiaxis neutron diffractometer automation 0-102417

**process control**

- see also process computer control*
- automatic measurement systems, meas. of characts., compound and element-by-element methods 0-62612
- electro-optical system manufacture, test and process control changes 0-96044
- on-line wet chemical colorimetric analysis 0-81378
- ore dressing X-ray spectrometric analysis centre 0-86541
- plastics sheet blowing and extruding, process identification for automatic process control (*German*) 0-81023
- polyurethane foam, processing machines and systems, motor car components appl. (*German*) 0-71955
- pumping, automatic ionisation vacuumeters, with cold or hot cathodes (*Czech*) 0-73376

**processors (program) *see* program processors****Procopiu effect**

- No entries

**product control *see* quality control****production**

- this heading is restricted to industrial production*
- see also assembling; manufacture; quality control; reliability*
- Ag-Zn batteries, miniature, fabrication and characts. (*Polish*) 0-93866
- C fibres, engineering applications, production requirements and mech. props. 0-89168
- Li metal for battery industry, sources and preparation 0-97781

**production control**

- see also process control; quality control*
- optical instrument, precision, microcomputer-aided manufacture (*German*) 0-95116
- optical projectors, MSP-4 objectives, photoelectric distortion meas. (*German*) 0-95976
- pipes, hot-rolled, automatic mag. quality control on prod. line 0-108661

**production schedules *see* production control****production testing**

- diamond turned surface production, interferometric test repeatability 0-74538
- Lovisa Nuclear Power Station, in Finland, guarantee testing for output and efficiency (*Russian*) 0-102291
- US, automatic noise-blanking, pulse-timing discriminator 0-76472
- vibration, multiple shaker considerations 0-79047

**program compilers**

- AKAIHOSHI flexible real time software system for radio astronomy obs. 0-82214

**program processors**

- see also program compilers*
- hierarchical computer networks for processing data base generated by X-ray CT scanner 0-81732
- pre- and post-processing techniques for complex analysis 0-94965

**production control**

- see also process control; production control*
- additive photographic film printers, programmed control of light metering valves (*Russian*) 0-95174
- diamond turning precision machine tool system 0-69568
- Nd:glass laser with numerical programmed control (*Russian*) 0-91811

**programmer training *see* training****programming, mathematical *see* mathematical programming****programs (computer listings) *see* complete computer programs****projectiles**

- see also ballistics; missiles; rockets; weapons*
- artillery shells, radiographic inspection algorithm speedup by array processor 0-108659
- continuous-wave transmitting, passive array tracking 0-94955

**projectors (optical) *see* optical projectors****promethium**

- see also nuclei with .....*
- nuclear battery, characts. of luminophores and photoelements (*Bulgarian*) 0-72084
- $\text{Pm}^{3+} + \text{UO}_2^{3+}$  solution, nuclear pumped liq. lasers, LASL program 0-64011
- $^{144}\text{Pm}$ , in  $\text{PrIn}_3$ , impurity beh. viour obs. using oriented nuclei  $\gamma$ -ray anisotropy meas. 0-71275
- $^{147}\text{Pm}$ , sealed sources for phosphor light sources (*Hungarian*) 0-91348

**promethium alloys**

- No entries

**promethium compounds**

- see also promethium alloys*
- No entries

**prominences (solar) *see* solar prominences****propagation, wave *see* wave propagation****proportional counters**

- see also position sensitive particle detectors*
- background determ. by hard cosmic radiation 0-69027
- cosmic ray air shower observation, counter prod. characts. and lifetime determ. 0-98526
- cylindrical wire proportional chambers, electrostatic field formulae, distrib. and asymmetry 0-78493
- design principles and characts. of  $3 \times 1.5$  m proportional chamber 0-69024
- diamond-anvil press, cell for X-ray diffr. obs. with solid-state or proportional counter 0-75119
- digitisers of time and pulse height, monolithic flash A/D convertor 0-63475
- dual proportional counter for recording transition radiation 0-63458
- electronic device for registering signals, K405KhP1 IC (USSR) 0-91376
- electronics for proportional drift tubes 0-106241
- fast X-ray diffractometer based on a spherical drift multiwire proportional chamber with digital position encoder 0-90969
- gas proportional scintillation detectors with uniform electric fields, secondary scintillation model 0-74087
- gas scintillation proportional counter, gas fillings, preliminary studies 0-58054
- gas scintillation proportional counters, large vacuum photodiode imaging appl. 0-58050
- graded-density cathode method for position determ. in multiwire proportional counters 0-87017
- high resolution gas scintillation proportional counter for studying low energy cosmic X-ray sources 0-58052
- imaging Cherenkov detector using gas-filled MWPC, photoionisation of triethylamine 0-91400
- imaging gas scintillation counter for X-ray astronomy 0-98551
- induction wire proportional counter with sub-mm positron resolution 0-91399
- large load characts. of  $3 \times 1.5$  m proportional chamber 0-69025
- large multiwire proportional chambers for experiment NA3 at the CERN SPS 0-102388
- large-area gas-scintillation proportional counters for in-vivo measurement of plutonium and americium 0-58086
- magnetosphere proportional counter, with thin mica windows, for low-energy particles 0-109260
- Mossbauer spectroscopy, conversion electron, cryogenic proportional He counter 0-69010
- MWPC, appl. of large-scale electronics 0-106235
- MWPC, beta-ray imaging device for radiochromatography 0-102387
- MWPC, CERN Omega Spectrometer, modular trigger basic techniques 0-58104
- MWPC, clinical, low energy radionuclide distrib. 0-61679
- MWPC, cylindrical, event triggers, correlation of wire addresses 0-58092
- MWPC, flat area detector data acquisition system for X-ray crystallography 0-91381
- MWPC, gas amplification factors and detection efficiencies 0-74079
- MWPC, gas ionisation by double photon absorption using pulsed lasers 0-99414
- MWPC, linear read out electronics, hybrid preamplifier realisation 0-58091
- MWPC, position determ. method using graded density cathodes 0-102396
- MWPC, position sensitive, pulse shape from cathode RC Lines, zero-cross time meas. 0-58038
- MWPC, very low press. operational props. 0-58043
- MWPC construction for large aperture spectrometer 0-102381
- MWPC wire tension control system 0-102397
- MWPC wire tension meas. by non-contact method 0-74081
- MWPC with wire plane cathodes, extension of standard formulae for elec. fields 0-99413
- neutron detector, position sensitive, high precision position readout 0-58063
- neutron dose and quality factor meas. by tissue equivalent proportional counters 0-58079
- parallel grid imaging proportional counter optimized for detection of low brightness stellar XUV-sources 0-58049
- photon counter, meas. of energy albedo of backscattered photons 0-99408
- photon counter with proportional response 0-87021
- position sensitive gas scintillation proportional counter for X-ray astronomy 0-58053
- position sensitive proportional counter, resistive wire, multi-anode, focal plane detector 0-63464
- position-sensitive counter for neutrons 0-63459
- position-sensitive proportional counter, direct position and time digitizer 0-58090
- proton recoil proportional counter tests at TREAT 0-58072
- relativistic electron energy loss distrib. in thin gas layers of proportional counters 0-99429

# proportional counters continued

- Rossi counter equivalent dose meas. in high-energy radiation fields 0-94376  
 SPEAR Mark II shower counter system 0-58031  
 Ar-CH<sub>4</sub> proportional counter, light emission obs. 0-78488  
<sup>14</sup>C counters, for small samples dating 0-82102  
<sup>3</sup>He proportional counters, thermal neutron detection performance, temp. depend. 0-58071  
 Kr photo-ionization proportional scintillation chamber 0-58056  
 Xe high pressure proportional, scintillation camera for X-and  $\gamma$ -ray imaging 0-99412  
 Xe proportional scintillation detector, energies and angles of emission of <sup>252</sup>Cf fission fragments 0-63488  
 Xe-filled MWPC for hard X-ray imaging with sub-mm spatial resolution 0-99418

# prospecting (geophysical) see geophysical prospecting

# prosthetic power supplies

- long-term implantable devices energy sources 0-98175

# prosthesis

- see also artificial limbs; artificial organs; orthotics; sensory aids  
 aortic valve prostheses, hydrodynamic losses eval. 0-72378  
 biomechanics, foundations and appls. (French) 0-89778  
 bone cement used to grout hip prosthesis, stress distrib. obs. 0-104816  
 bone fracture callus mech. props., intramedullary nailing rel. to plating 0-85438  
 breast, silicone, dose obs. 0-98144  
 ceramic bone implants, material science of Ca<sub>3</sub>(PO<sub>4</sub>)<sub>2</sub>, Ca<sub>4</sub>P<sub>2</sub>O<sub>9</sub>, Ca<sub>3</sub>(PO<sub>4</sub>)<sub>2</sub>H<sub>2</sub>O 0-93523  
 conference, London, England (Mar. 1980) 0-94926  
 dental porcelains, determ. of U content and dose to oral mucosa 0-89830  
 dentistry, methods and appls. for holographic interferometry 0-67203  
 denture base materials, multi-station machine for fatigue testing 0-108648  
 dentures, EM vibrator 0-104716  
 disk valves, max. opening rel. to aortic blood flow characts. 0-108941  
 dowl-retained prostheses cementation, new hydrostatic pressure change recording apparatus 0-67287  
 electronic eye for blind people, implementation through the optical nerve (Croatian) 0-109060  
 glass-ceramic implants, loaded, expt. studies on anchoring in the femur (German) 0-81624  
 haemofol mitral valve, results of flow visualisation expts. 0-104632  
 heart valve, trileaflet, design, fabrication and evaluation 0-94415  
 heart valves, appraisal of power loads on elements 0-104811  
 heart valves, dynamics 0-72379  
 heart valves, mechanical haemolysis fluid dynamics 0-97999  
 hip, total prosthesis, 3D stress anal. of femoral stem 0-98176  
 hip prosthesis stem loosening in human femur, biomechanical causes investigation 0-85435  
 hydroxylapatite, biological implant material, fatigue and fracture strength from diametral tests, after various treatments 0-60953  
 implantable prostheses, review 0-101292  
 implanted prosthesis failure analysis techniques and results 0-89906  
 materials for orthopaedic implants, review 0-76862  
 Muller screws, fractured femoral necks fixation, mech. investigation 0-72377  
 myoelectrically controlled systems, five-state, error rate obs. 0-72376  
 orthopaedics, exptl., quantitative eval. of holographic deform. investigations 0-67197  
 paralysed upper extremities rehabilitation systems, control signals (Slovenian) 0-81772  
 PMMA bone cement, free radical EPR, feasibility study 0-94318  
 prosthetic, heart valves, load cell for meas. of dynamic forces 0-104815  
 sensory and neural, development (French) 0-89905  
 sensory feedback system for above knee prosthesis (Japanese) 0-72372  
 speech and language prostheses evaluation 0-76864  
 steel, austenitic stainless, fretting corrosion of orthopaedic implant materials by bone cement 0-104813  
 steel, stainless, orthopaedic, type En58J, Mo ion-plating, corrosion fatigue 0-66694  
 synovial joints, appl. of generalised Reynolds eqn. for porous boundaries 0-87803  
 wear, holographic studies using optical contouring 0-67288  
 Ag-Sn alloys and amalgams, electrochem. considerations, corrosion in physiological soln. 0-93760  
 Al<sub>2</sub>O<sub>3</sub> bioceramic synthesis, for orthopedic purposes, props. (Polish) 0-66465  
 Ti-Al-V (6, 4 wt%), fretting corrosion of orthopaedic implant materials by bone cement 0-104813

# protactinium

- see also nuclei with .....

No entries

# protactinium compounds

No entries

# protection

- see also alarm systems; corrosion protection; power system protection; protective coatings; radiation protection; safety  
 fibre splicing, arc fusion 0-69565  
 fusion reactor, Doublet III, neutral beam interlock system using IR detector 0-106228  
 magneto-inductive flowmeters, installation, earthing, isolation, protection against explosion (German) 0-64662  
 photomultiplier gain-changing protection circuit, scintillation neutron detector 0-74074  
 vacuum systems, 0-105666  
 X-ray tubes, rotary anode, HV insulation, discharges due to back scattered electrons elimination (German) 0-105758

# protective coatings

- see also corrosion protective coatings; wear resistant coatings  
 boride coatings on C and alloy steel, spectroscopic thickness determ. 0-85099  
 ceramics, glazing with gaseous P<sub>2</sub>O<sub>5</sub> 0-108609  
 chromising porous W and W-Cu pseudoalloys 0-100959  
 fibre pressure sensitivity meas. and limitation, using silicon rubber coating 0-106605  
 graphite fibre epoxy composites, eutectic coating moisture barriers 0-81228  
 IR thin film plasma deposition processes 0-87466  
 laser CVD, film physical props. and applications 0-93493

# protective coatings continued

- metal and metal oxide spacecraft thermal control materials, low-energy proton effects 0-70288  
 optical fibre coatings centering by monitoring forward scattering patterns 0-64146  
 optical waveguide fibre coating technology, overview 0-58828  
 parylene (vacuum deposited polymeric coating), appl. to electronics 0-108607  
 plastic coated optical glass fibres, liq. N<sub>2</sub> strengths 0-58707  
 plastic coating of Na<sub>2</sub>O-B<sub>2</sub>O<sub>3</sub>-SiO<sub>2</sub> glass fibres, influence on strength 0-58697  
 plastic resin coated optical fibres, effect of secondary coating technique on transmission loss 0-58704  
 polyamide-polyurethane copolymer dispersions, structuration and relax. props., coating from props. 0-76559  
 porcelain-on-aluminium, low-absorptance 0-76393  
 refractory ceramic coatings, for high temp. use, current status (Japanese) 0-71619  
 resin, UV cured, for optical fibre/cable 0-69547  
 solar cells, degradation processes of electrophysical characts. during long-term operation 0-89617  
 spacecraft thermal control coatings, electron and proton irradi. effects 0-70262  
 steel, Cr-Mn, high temp. oxidation, sub-cinder layer formation, protective coating role (Russian) 0-93686  
 steel, stainless, highly protective film development by surface treatment 0-66699  
 tinplate surfaces, Auger depth profiling and anal. 0-59768  
 Al rich surface layer, barrier to chemical attack of float glass by water (French) 0-89378  
 Cr, diffusion coating, an Fe powder based sintered porous permeable materials 0-100958  
 Cu, electrodeposited, Ni alloy protection against hydrogen embrittlement, aerospace engine appl. 0-76416  
 Fe-Cr alloys, in acid and neutral solns., thickness and optical constants of passive and transpassive films 0-66698  
 Fe-Si gas-flame spray deposited protective coating, for C steel heat exchanger 0-61025  
 FePO<sub>4</sub> coating on Armco Fe, Fourier transform IR absorpt.-reflection spectra 0-71500  
 Ge, on Sn superconducting thin films, effect on excess elec. cond. 0-65741  
 NiF<sub>2</sub> film preparation and characterisation 0-59815  
 Si<sub>3</sub>N<sub>4</sub> films on Si wafers, O determ. by <sup>3</sup>He activation anal. 0-71981  
 Ti spongy metallic protective gettered coating for thermonuclear reactor walls (Russian) 0-106154  
 TiB<sub>2</sub> thick film on low C steel substrate, CVD in US field, crystallite size 0-84854  
 TiC coatings, on cemented carbides, struct. and hardness 0-59771  
 TiC coatings on steels and hard alloys 0-76414  
 TiO<sub>2</sub> layers, activated reactive evaporation and absorpt. indices 0-97363  
 Y<sub>2</sub>O<sub>3</sub> coated Ag mirror for the 0.5 to 14  $\mu$ m region 0-87456  
 Zn hot galvanisation coatings, production components, installation and power supply (French) 0-66686  
 ZnO, spacecraft thermal control material, low-energy proton effects 0-70288

# protective relays see relay protection

# proteins

- see also gelatin

- $\alpha$ -helical, possible role in membrane charge transfer processes 0-81524  
 acetylcholine receptor protein structure 0-85339  
 acid phosphatase of glial smooth endoplasmic reticulum, transport into damaged axons, role of microtubules 0-85381  
 actin, mol. basis for chemomechanical energy transduction in muscle 0-72143  
 F-actin, struct. changes in living muscle fibres, polarised UV fluoresc. microscopy 0-67037  
 actin in the inner ear, struct. of the stereocilium 0-108918  
 actomyosin from a non-muscle system, tension generation 0-76781  
 adsorbed layers on field-emitted tips, removal by UV radiation 0-104836  
 adsorbed on polymer surfaces, structural changes 0-89712  
 adsorption on surface of hydrophilic polymers, water structuring, ESCA evaluation 0-108758  
 albumin, adsorbed layers on polystyrene, contact angle meas. 0-61508  
 albumin flux, differential permeability of endothelial and epithelial barriers, sheep expts. 0-81553  
 alcohol dehydrogenase, horse liver, tryptophan residue room-temp. phosphoresc., temp. and enzymic complex form. effects 0-61512  
 amino acid neighbourhood relationships, breakdown into overlapping doublets, triplets, and quadruplets 0-67035  
 apomyoglobin reconstituted with <sup>111</sup>In(III)mesoporphyrin IX, rot. correl. time determ. 0-76698  
 ATPase, Ca<sup>2+</sup>-activated, of sarcoplasmic reticulum, rot. motion and evidence for oligomeric structs. 0-72124  
 ATPase, Ca<sup>2+</sup>-depend., struct. rearrangements during function 0-81527  
 bacterio-opsin, changes in protonation state during reconstitution of bacteriorhodopsin 0-89707  
 bacteriorhodopsin radicals, role in primary charge separation of Rhodospseudomonas viridis 0-63688  
 bacteriorhodopsin radicals, role in primary charge separation of Rhodospseudomonas viridis 0-63688  
 bacteriorhodopsin, effect of high press. on absorpt. spectrum and isomeric composition 0-67041  
 bacteriorhodopsin, elec. response of a back photoreaction 0-98008  
 bacteriorhodopsin, photoelec. conversion in charged synthetic membranes 0-108954  
 bacteriorhodopsin chromophore, light-induced isomerisation 0-108956  
 bacteriorhodopsin in purple membrane, orthorhombic 2D crystal form 0-85362  
 bacteriorhodopsin membrane preps. associated with lipid-water interface, form. of elec. pot. diff. 0-81551  
 beta sheet structures, anal. and prediction by combinatorial approach 0-76710  
 biological macromolecules, conformation studied by calorimetry, review 0-97870  
 biomolecules+chloranil, charge transfer interaction, equilib. const., enthalpy and entropy determ., mol. polarisability 0-89708  
 Clq of human complement, neutron scatt. obs., conformational calcs. 0-81537  
 carboxyhaemoglobin, carp, variability of mag. moment 0-94159



## proteins continued

- catalase, glucose embedded, measurement and reduction of radiation damage in frozen hydrated crystalline specimens 0-89810  
 ceruloplasmin, human, calc. of rotation function for tetragonal. cryst. at 10 Å resoln. 0-108843  
 chemical analysis using PIXE 0-61691  
 chemical reactions, rate coeffs., viscosity effects 0-71890  
 chromatin from cultured mammalian cells, radiolysis, DNA-protein cross-links formation 0-81655  
 collagen, 3-dimens. struct., rel. to props. of connective tissue 0-67038  
 collagen, polarisation, contribution of permanent and induced dipole moments, elec. birefringence 0-85351  
 collagen fibril,  $^2\text{H}$  NMR of mol. motion 0-67034  
 collagen molecular organisation and connective tissues props. 0-97858  
 collagen type supramolecular structs., 2 possible mechs. of formation 0-76702  
 conformational analysis, algorithms and data structs. for array processing 0-83530  
 crystal structural analysis by electron diffr., single scatt. approx., domains of validity 0-101150  
 cytochrome, 3-D coordinates from stereodiagrams 0-64824  
 cytochrome  $b_5$ , cryst. struct., analysis by electron diffr., single scatt. approx., domains of validity 0-101150  
 cytochrome  $c_1$ , anhydrous film, elec. cond., temp. and ambient press. depend. 0-85327  
 cytochrome  $c_1$ , haeme-haeme mag. interaction, Mossbauer obs. 0-108836  
 cytochrome  $c_1$ -hydrogenase, reduction kinetics, Mossbauer spectra 0-67031  
 cytochrome  $c$ , effects of UV and temp. on optical props. and enzymatic activity 0-81648  
 cytochrome  $c$ , low freq. modes and excitation profiles, reson. Raman spectra 0-94428  
 cytochrome  $c$ , PMR, eight-ring current model heme ring, conformation depend. shifts 0-74185  
 cytochrome  $c$ , protein influence on haeme, Raman difference spectroscopy 0-72125  
 cytochrome  $c$  oxidase, Cu ENDOR 0-94170  
 cytochrome  $c$  oxidase, macromolecular struct., electron microscopy and image anal. 0-89716  
 cytochrome  $c$  oxidase, struct. of cytochrome  $a_3$ -Cu $_2$  couple, NO binding studies 0-67039  
 deoxyhaemoglobin, Fe(II)-N $_4$ (His-F8) stretching freq. rel. to quaternary struct. 0-94160  
 deoxyhaemoglobin, ferrous heme of high-spin type, MCD spectra in Soret, visible and near IR regions 0-94156  
 dispersions, viscoelastic effects, shear viscosity and primary normal stress difference 0-87754  
 DNA, molecular motions, investigated by  $^3\text{P}$  and  $^{13}\text{C}$  NMR relaxation 0-63657  
 DNA helix destabilising protein cryst., electron microscopy 0-85338  
 dopamine, thermal blooming spectroscopy 0-86441  
 edestin, protein-peroxide radicals,  $^{17}\text{O}$ -labelled, EPR obs. 0-85345  
 electron diffraction, low dose, of wet protein cryst. 0-85550  
 electron microscopy of nucleic acids, basic protein film method 0-104844  
 electron radiation damage on primary and secondary struct. level 0-89808  
 electrophoresis of proteins in intercellular bridges 0-89734  
 enzyme-linked immunosorbent assay, apparatus for meas. light absorbance of small vols. of liquids 0-72387  
 enzyme-mediated multidimensional inflection points in nonequilib. linear behaviour 0-72122  
 enzymes, molecular struct. reconstruction from electron microscopy images 0-89715  
 factor VIII, native and modified, surface adsorption and mol. interactions, ellipsometric obs. 0-104555  
 ferredoxin, Fe atoms at active centre, exchange integral of antiferromag. interaction 0-76697  
 ferredoxin, *S. platensis* [2Fe-2S], struct. and evolution of chloroplast-type ferredoxins 0-94165  
 ferrocyclochrome  $c_1$ , anhydrous, ionisation pot., UV photoelectron spectrosc. obs. 0-85328  
 ferrocyclochrome  $c$ , mol. dynamics simulation 0-87255  
 ferrous nitrosylhaemoglobin, NO binding, spin distrib., orbital model and mag. props. 0-81534  
 fibrinogen, adsorbed layers on polystyrene, contact angle meas. 0-61508  
 fibrinogen, bovine, high energy-induced aggregation, time resolved spectra 0-61655  
 fibrinogen, native and modified, surface adsorption and mol. interactions, ellipsometric obs. 0-104555  
 film, at liq. interfaces, dilatational props. 0-94255  
 film, at liq. interfaces, shear rheological props. 0-94256  
 globular, in water, proton NMR spin echo decay comparative investigation 0-81541  
 glutamine synthetase, neg. stained, image reconstruction of low and high dose micrographs 0-85551  
 glutamine synthetase macromolecular struct., electron microscopy and image anal. 0-89716  
 glycoproteins, fast axonal transport in guinea pig auditory neurons 0-104573  
 haemoglobin, human, maleimide spin labeled, proton ENDOR spectra obs. 0-89719  
 haemoglobin, Jahn-Teller pseudo effect rel. to Fe release and conformational changes 0-76701  
 haemoglobin, low freq. modes and excitation profiles, reson. Raman spectra 0-94428  
 haemoglobin, mutual and tracer diffusion coeffs., photon correl. obs. 0-72123  
 haemoglobin, nanosec. probe of dynamics using time resolved reson. Raman scatt. 0-94162  
 haemoglobin, quaternary struct., hydration and self-association,  $^1\text{H}$  NMR obs. 0-67040  
 haemoglobin, suspending medium, dielec. props., human erythrocyte obs. 0-76716  
 haemoglobin equilibria in soln., surface free energy model 0-81535  
 haemoglobin haem structure after photo-deligation, Raman spectra 0-61510  
 haemoglobin macroporous particle study, photoacoustic spectrometry 0-85543  
 haemoglobin- $\text{O}_2$  equilibrium curve, instrument for determ. based on membrane diffusion 0-81761

## proteins continued

- high density lipoprotein-3 macromolecule observation using CTEM and STEM with negative staining 0-85561  
 high performance liquid chromatography 0-61174  
 immunoglobulin, human, high energy-induced aggregation, time resolved spectra 0-61655  
 internal charge transfer, ascorbic acid adduct model systems, SCF calc. 0-69072  
 o-iodotyrosine, intramol. effects of  $^{125}\text{I}$  decay 0-108973  
 kinases, cAMP-depend., membrane-localised, and regulation, of slow inward current, frog heart 0-81567  
 lactate dehydrogenase, H-forms, radioimmunoassay 0-67219  
 lactate dehydrogenase,  $\text{O}_2$  effect in radiolysis obs. 0-72223  
 leghaemoglobin, thermal denaturing in cryst. and soln. 0-108849  
 liver alcohol dehydrogenase, proton relay system, SCRF PCE theory, CNDO/2 calcs. 0-85325  
 lumirhodopsin, photoconversion at 77K, quantum efficiency estimation 0-67081  
 lysosomal enzymes, pigeon tissue, effects of sub-lethal  $\gamma$ -ray dose 0-98022  
 lysozyme, absorption mode spin-echo spectra appl. 0-78634  
 lysozyme, search for superconducting regions 0-101149  
 lysozyme hydration, correl. of diverse types of meas. 0-61507  
 membrane integral proteins, mobility increase in spherocytic erythrocytes obs. 0-81569  
 membrane multilayers, thickness depend. of props. 0-89726  
 membranes, structural order of lipids and proteins, fluoresc. anisotropy data eval. 0-97873  
 metalloenzymes, model for biological active sites, ab initio calcs. 0-104551  
 metalloproteins, metal nuclei, biophysical appls. of NMR, review, book contrib. 0-109081  
 metarhodopsin transition, triggering of light-induced change in Ca binding, rod disk membranes 0-94211  
 methaemoglobin, struct. change on addition of inositol hexaphosphate 0-72130  
 molecular weight and ultrastruct. determ. in STEM 0-85562  
 molecular weight determ. by monolayer surface press. meas. technique 0-89526  
 multi-enzyme complex carrying out electron transfer, asymptotic anal. of functioning 0-81523  
 muscle proteins, rot. motions, saturation transfer EPR obs. 0-94151  
 myoglobin, refolding kinetics by diffusion-collision-adhesion model 0-94157  
 myoglobins, Fe-, Co-substituted,  $\text{O}_2$  binding, comparisons, thermodynamic investig. 0-67030  
 myosin, muscle contraction process, 10 ms time resolution X-ray diffr. 0-61741  
 myosin, muscle cross bridge rotation during contraction, fluctuations in polarised fluoresc. 0-97856  
 myosin, struct. changes in living muscle fibres, polarised UV fluoresc. microscopy 0-67037  
 myosin S-1, mol. basis for chemomechanical energy transduction in muscle 0-72143  
 nicotinamide adenine dinucleotide, and reduced form, pH induced modification, Raman spectra 0-85343  
 nitrosylhaemoglobin, electron spin distrib. 0-83528  
 oxyhaemoglobin-hydrazine (dimethylhydrazine) interaction,  $\gamma$ -reson. spectroscopy 0-81525  
 oxymyoglobin, evidence for conformational and diffusional mean square displacements 0-89713  
 pancreatic trypsin inhibitor, bovine, macromol. dynamics, high resolution NMR investig. 0-91708  
 papain models, active site  $\alpha$ -helix and ion pair stability 0-74265  
 phenylalanine+chloranil, charge transfer interaction, equilib. const., enthalpy and entropy determ., mol. polarisability 0-89708  
 phosphoryl transfer enzymes, biophysical appls. of NMR, review, book contrib. 0-109081  
 phosphorylase A crystals, automated struct. determ., from micrographs 0-92425  
 $\beta$ -phycoerythrin crystals, twinned by merohedry, diffr. data treatment 0-108845  
 polypeptide chains, struct. of conduction and valence band 0-76700  
 polypeptides, electronic struct., side-chain disorder effect 0-76706  
 purple membrane fragment suspensions, elec. dichroism obs., trimer model interpret. 0-89728  
 pyrophosphatase, inorganic, of yeast, cryst. growth, derivatives formation, heavy atoms positions 0-108842  
 radioactive tracers, improved labelling with  $^{99\text{m}}\text{Tc}$  by stannous tartrate reduction of pertechnetate 0-72324  
 relaxation times in solid-state theory and one-dimensional molecular systems (Russian) 0-100640  
 representation, unique method 0-67036  
 Rhacopholus embryo yolk platelets, freeze fracture study of crystalline struct. 0-104552  
 rhodopsin,  $\alpha$ -helix orientation, spectroscopic study 0-89711  
 rhodopsin and thermal intermediates, fast struct. fluctuations in protein component 0-72137  
 rhodopsin chromophore, and desmethyl analogues, theory 0-94169  
 ribonuclease A, bovine, cryst. struct. determ. by X-ray and neutron diffr. 0-108841  
 ribonuclease A, microviscosity, mobility profile 0-91710  
 RNA, molecular motions investigated by  $^3\text{P}$  and  $^{13}\text{C}$  NMR relaxation 0-63657  
 SCF-LCAO-ASMO and CI calcs. of low-lying multiplets and excited states 0-94155  
 serum albumin, bovine, high energy-induced aggregation, time resolved spectra 0-61655  
 serum albumin, bovine, hydrated, dielec. and elec. props. 0-97854  
 serum albumin, bovine, labelling with  $^{57}\text{Co}$ , expts. 0-85495  
 serum albumin, bovine, mutual and tracer diffusion coeffs., photon correl. obs. 0-72123  
 serum albumin, human,  $^{125}\text{I}$  labelled, geometrical dilution (French) 0-104742  
 serum low density lipoprotein, human, anomalous permittivity behaviour 0-81540  
 structure and bonding, quantum theory, ab initio calcs. 0-61509  
 structure of proteins involved in active membrane transport, review, book contrib. 0-108844  
 supramolecular structure, ordered, electron micrographs, image processing 0-89923

proteins continued

Tanford-Kirkwood theory of protein titration, proposed extensions 0-101147  
thymopietin active fragment in H<sub>2</sub>O, soln. conformation by DNMR spectroscopy 0-89710  
tomato bushy stunt virus, 3-D coordinates from stereodiagrams 0-64824  
tryptophan+chloranil, charge transfer interaction, equilib. const., enthalpy and entropy determ., mol. polarisability 0-89708  
tubulin antigens, agarose gel electrophoretic determ. of mol. weights 0-67313  
tyrosin+chloranil, charge transfer interaction, equilib. const., enthalpy and entropy determ., mol. polarisability 0-89708  
US absorpt. and vel. in mammalian tissue, dependence on constituent proteins 0-61621  
zein, protein-peroxide radicals, <sup>17</sup>O-labelled, EPR obs. 0-85345  
CO-haemoprotein photolysis, transient Raman study, quantum yield origin 0-67155  
CO-myoglobin, mol. tunnelling, isotope effect, time resolved IR Fourier transform obs. 0-72126

proton absorption

No entries

proton accelerators

see also cosmotrons

CERN, 25 years history and equipment (French) 0-98778  
cooling channel for injection into linear accelerator 0-68973  
future technologies in high-energy physics, collective accelerators, laser accelerators, single-pass collectors 0-78466  
ISABELLE full cell, ultrahigh vacuum system 0-77798  
ISABELLE ultrahigh vacuum system, self-modulating ion gauge 0-82786  
KEK synchrotron, proton attenuation lengths in paraffin, concrete and iron around targets 0-102412  
pulsed source, Penning type, beam parameters 0-87001  
Texas A&M polarised proton beam meas. 0-102360  
TRIUMF, 500 MeV, 100  $\mu$ A isotope production facility 0-68985  
ZGS, external proton beams 0-91307

proton affinity

O<sub>3</sub>H<sup>+</sup>, isomeric structs. ab initio MO calcs. 0-83270

proton angular distribution

see also proton spectra

Al(Ne,X), proton inclusive spectra, direct plus thermal model 0-57799  
Cl(Ar,X), proton inclusive spectra, direct plus thermal model 0-57799  
K(Ar,X), proton inclusive spectra, direct plus thermal model 0-57799  
U(Ne,X), proton inclusive spectra, direct plus thermal model 0-57799

proton beam effects see proton effects

proton belt see radiation belts

proton detection and measurement

cellulose acetate solid state track detectors, catalytic oxidation sensitization (Chinese) 0-102399  
cellulose proton track visualisation detectors (French) 0-74080  
position sensitive proportional counter, resistive wire, multi-anode, focal plane detector 0-63464  
proportional counter tests at TREAT 0-58072  
surface barrier detector, peak changes under particle irradi. 0-58077  
A hyperon polarisation, meas. by hybrid Monte Carlo tech. 0-99431

proton-deuteron interactions

see also proton-deuteron scattering

pd, 355-1066 MeV/c, total and annihilation cross sections, S meson search 0-68473  
pd, 70 GeV,  $\pi^+$ , K<sup>+</sup>, p,  $\bar{p}$  prod. with 0.5-2.2 GeV/c transverse momenta, yield ratio, QCD (Russian) 0-83012  
pd annihilation,  $\bar{p}$ n mass spectrum enhancement, double scatt. effect 0-78090  
pd $\rightarrow$ NX, <500 MeV/c, narrow  $\bar{N}$ N state search 0-57627

proton-deuteron scattering

see also proton-deuteron interactions

phase shifts near deuteron break-up threshold (French) 0-73728

proton effects

benzene, soln., fluoresc., quenching in pulsed proton and alpha particle irradi., radiation quality effects 0-66259  
cells, human, multinucleate and micronucleus formation obs. 0-72219  
channelling of relativistic protons in bent crystals., theory 0-96581  
fluorite, use of proton irradi. to reveal growth and deform. features 0-84216  
metal and metal oxide spacecraft thermal control materials, low-energy proton effects 0-70288  
metallic bar, 30 MeV proton excitation of reson. oscils. 0-64431  
polymer spacecraft materials, electron and proton irradi. effects 0-70262  
spacecraft thermal control coatings, electron and proton irradi. effects 0-70262  
surface barrier detector, peak changes under particle irradi. 0-58077  
Al, proton irradiation, Al atomic displacement position study 0-103401  
(AlGa)As DH lasers, comparison of 'normal' lasers and lasers exhibiting light jumps 0-106519  
(AlGa)As stripe geometry, proton-bombardment delineated DH laser, lifetime 0-106520  
AlGaAs-GaAs proton irradiated solar cells, deep-level defects, recombination mechanisms, performance characts. 0-81459  
AlGaAs-GaAs proton irradiated solar cells, deep level defects and recombination parameters 0-94032  
Al<sub>0.5</sub>Ga<sub>0.5</sub>As triggerable semiconductor lasers made by deep proton bombardment 0-69408  
 $\alpha$ -Al<sub>2</sub>O<sub>3</sub>, polarised luminescence in neutron- and proton-irradiated single crystals 0-66271  
BaTiO<sub>3</sub>:Co, voltaic current appearance on proton irradi. 0-104032  
Cr-SiO<sub>2</sub>-Si MIS solar cells, photovoltaic performance and interface states, nucl. radiation effects 0-94004  
Cu, proton-irradiated, H<sub>2</sub> gas-bubble struct., study at 300K 0-92569  
D re-emission from C target, proton induced 0-70270  
GaAs, H ion bombard., carrier removal effects 0-92542  
GaAs, H<sup>+</sup> irradiation, effect on electrical props. 0-65567  
GaAs, proton irradiated, low energy, deep level defects and hole diffusion length meas. 0-60000  
GaAs, radiation damage caused by proton bombardment, observation using TEM 0-75276  
GaAs Schottky barrier structure, defects from proton irradiation, thermal transients and optical capacity (French) 0-59534  
GaAs solar cells, electron and proton radiation damage 0-94034  
n-Ge, proton and  $\gamma$  irradi., minority carrier recombination 0-65591

proton effects continued

n-InSb, proton irradi. defects energy level scheme, transport props. meas. 0-96576  
p-InSb:Ge, proton irradi. defects energy level scheme, transport props. meas. 0-96576  
PLZT ceramics photosensitivity enhancement by H- and He-ion implantation 0-96934  
PbS-base photodetectors, struct. invest. by proton irradi. 0-104388  
Si solar cells, proton irradiated, processing influence on elec. performance 0-94001  
Si solar cells, ultrathin, electron and proton effects 0-94002  
Si:Al(Ga), O<sub>2</sub> diffusion, conc. profile meas. 0-79990  
Si:B(P), proton-irrad., impurity uphill diffusion, vacancy mechanism 0-92719  
U, irradiation growth during fission fragment and proton bombard. 0-92568  
ZnO, spacecraft thermal control material, low-energy proton effects 0-70288

proton excited X-ray emission see ion microprobe analysis

proton interactions see electron-proton interactions; kaon-proton interactions; lepton-nucleon interactions; photon-proton interactions; pion-proton interactions; proton-deuteron interactions; proton-nucleus reactions; proton-proton interactions

proton magnetic moment

No entries

proton magnetic resonance

N-acetyl-D-alloisoleucine, soln. struct., dynamics, proton relaxation mechanisms 0-76708  
l-alanine powder, short dipolar relaxation time meas. by saturation method 0-60441  
biomembrane, water transport determ. methods (Rumanian) 0-94435  
 $\alpha$ -bis (N-methylsilylaldiminato) copper II, one-dimens. spin-1/2 Heisenberg antiferromag., high-field spin dynamics 0-71224  
bis-methyldigermyl chalcogenide, <sup>1</sup>H and <sup>13</sup>C NMR study, chemical shifts 0-71201  
bis-methyldisilyl chalcogenide, <sup>1</sup>H and <sup>13</sup>C NMR study, chemical shifts 0-71201  
blood, normal and pathologic, NMR T<sub>2</sub> relax. time studies 0-81682  
blood flow measurements by NMR of the intact body 0-81680  
carborane, ortho- and para-, phase transition and mol. reorientation, isomer effects, PMR obs. 0-80628  
cellulose, mobility of adsorbed water, NMR pulse obs. 0-108835  
cyclobutanone, <sup>1</sup>H NMR anal., deconvolution technique 0-58289  
cytochrome c, PMR, eight-ring current model heme ring, conformation depend. shifts 0-74185  
delayed Fourier transformation technique for resolution enhancement 0-74181  
deoxyhaemoglobin, proton NMR, modified DEFT technique for obs. hyperfine shifted line, T<sub>1</sub> values meas. 0-76871  
dextran, aq. soln., conc., PMR (Russian) 0-71225  
DNA internal motions, <sup>31</sup>P NMR and PMR 0-97855  
erbium triethyl sulphate, single cryst., H<sup>+</sup> coords., NMR 0-97152  
haemoglobin, quaternary struct., hydration and self-association obs. 0-67040  
halobenzenes in potassium laurate mesophase, proton distance ratios and order tensor elements calcs. 0-63672  
hexafluorobenzene-n-paraffins, binary liquid solns., self diffusion, spin echo meas. 0-65263  
MBBA, proton spin-lattice relax. in crit. regime 0-80631  
MBBA-d<sub>13</sub>, <sup>1</sup>H spin-lattice relaxation, intermol. and intramol. contribs. 0-75873  
medical imaging, H tomography and pot. for imaging other body constituents 0-98062  
medical imaging, multiple sensitive point method 0-81679  
methyl ammonium aluminium sulphate, ferroelec., proton spin-lattice relax. time anomaly 0-60440  
methyl group, proton tunneling reson. at low temp. 0-108087  
methylammonium bromide, solid, phase transitions, PMR, DTA study 0-107421  
methylene chloride, in EBBA-d<sub>3</sub>, intermol. dipolar random field cross-relax. term obs. 0-60438  
muscle, skeletal, water protons NMR relax. times anisotropy obs. 0-85341  
organic free radicals, solid, selective pulse NMR expts. 0-60452  
 $\alpha$ -oxalic acid dihydrate, H<sub>2</sub>O proton shielding tensor, multiple pulse proton NMR obs. 0-63655  
phase-sensitive displays for proton 2D J spectra 0-77830  
phenylphosphines, and derivatives, <sup>1</sup>H, <sup>13</sup>C and <sup>31</sup>P NMR studies 0-87152  
PMMA, syndiotactic, solns. in toluene, NMR obs. of struct. and dynamics of associates 0-75867  
polyisocyanates, rigid backbone, ternary phase relationships obs. 0-59371  
Portland cement, absorbed H<sub>2</sub>O, pulsed NMR study 0-84665  
potassium hydrogen malonate, carboxylic proton chem. shift tensor 0-58280  
proteins, globular, in water, proton NMR spin echo decay comparative investigation 0-81541  
silicate glass, hydrated, proton and <sup>23</sup>Na wide-line NMR study 0-84659  
spin warp NMR imaging and appls. to human whole-body imaging 0-101250  
spin-lattice relaxation times prolongation, regionally ischemic dog heart tissue 0-101216  
tetramethylammonium octahydrotriborate, NMR study of proton and B dynamics 0-93200  
tetramethylgermanium, Zeeman spin-lattice relaxation rate maxima 0-84666  
thylakoid membranes of wheat chloroplasts, proton spin-lattice relax. time, -8°C phase transition 0-108853  
thymopietin active fragment in H<sub>2</sub>O, soln. conformation by DNMR spectroscopy 0-89710  
tissue, rabbit, comparison of NMR water proton T<sub>1</sub> relax. times 0-101221  
tissues, normal and malignant, pulsed NMR obs. 0-94171  
TTF-CuBDT, inter- and intra-chain exchange couplings, proton spin-lattice relax. time meas. 0-71220  
water, liq., proton spin-lattice relax. by slow proton exchange 0-60437  
water mobility in blood plasma, NMR determ., viscosity correl. to 1/T<sub>2</sub> 0-67176  
zirconocene dichlorides, alkyl-substituted, <sup>13</sup>C and <sup>1</sup>H NMR, chemical shifts prediction 0-63671



## proton magnetic resonance continued

- $\beta$ -Al<sub>2</sub>O<sub>3</sub>·NH<sub>4</sub><sup>+</sup>, PMR relax. time obs. of ionic motion 0-71213  
 $\beta$ -Al<sub>2</sub>O<sub>3</sub>·NH<sub>4</sub><sup>+</sup>, and  $\beta'$ -Al<sub>2</sub>O<sub>3</sub>·NH<sub>4</sub><sup>+</sup>·H<sub>2</sub>O, single cryst. PMR and proton motion 0-108101  
 $\gamma$ -AlOOH, boehmite, proton pair obs. from NMR absorpt. spectra 0-75866  
 Ca<sub>2</sub>[B<sub>2</sub>O<sub>3</sub>]Cl<sub>2</sub>H<sub>2</sub>O, hilgardite, PMR of water mol. 0-84655  
 (Cu,Zn)Cs<sub>2</sub>(SO<sub>4</sub>)<sub>2</sub>·6(H<sub>2</sub>D)<sub>2</sub>O Tutton salt, proton spin-lattice relax. time, proton conc. depend. and spin diffusion role 0-71221  
 CuSO<sub>4</sub>·5H<sub>2</sub>O, low freq. spin dynamics, proton relax. study 0-71218  
 ErCl<sub>3</sub>·6H<sub>2</sub>O, single cryst., H<sup>+</sup> coords., NMR 0-97152  
 FeSO<sub>4</sub>·n H<sub>2</sub>O (n=1,4,5,7), Fe<sup>2+</sup> ion mag. interaction with crystallisation water protons, proton NMR obs. 0-60447  
 HIO<sub>3</sub>, PMR spectra, homonuclear and heteronuclear broadening separation 0-77828  
 H<sub>10</sub>MoO<sub>3</sub> and H<sub>17</sub>MoO<sub>3</sub> bronzes, NMR relax. obs. at 77<T<450K, H diffusion 0-108089  
 H<sub>16</sub>MoO<sub>3</sub> bronze, proton shift tensors PMR meas. 0-71202  
 H<sub>2</sub>O in biological samples, PMR, fast-exchange model interpretation via differential kinetics clarified 0-67033  
 HfV<sub>2</sub>H<sub>21</sub>, proton NMR relax. time and Knight shifts, diffusional activation energies meas., sorption props. 0-75871  
 KB<sub>3</sub>H<sub>8</sub>, NMR study of proton and boron dynamics 0-71210  
 LaH<sub>2.69</sub> two-phase behaviour 0-93189  
 Np(IV)-tetracyclopentadienide complex, H<sup>1</sup>-NMR studies, paramagnetic moments, temp. depend. 0-93186  
 Rb<sub>2</sub>CuBr<sub>4</sub>·2H<sub>2</sub>O, dynamic props. in paramag. state, spin-lattice relax. time meas. 0-71214  
 Sb<sub>2</sub>O<sub>3</sub>·H<sub>2</sub>O, crystalline, <sup>1</sup>H NMR study of proton transport 0-60446  
 SiH<sub>4</sub> film, amorphous, H-associated disorder modes, PMR spin-lattice relax. time meas. 0-93202  
 YH<sub>3</sub>, location of H, PMR rigid-lattice second moment meas. 0-71198  
 ZrMn<sub>2</sub>H<sub>x</sub>, proton NMR relax. time and Knight shifts, diffusional activation energies meas., sorption props. 0-75871

## proton-nucleus reactions

- for inelastic proton-nucleus scattering, see "proton-nucleus scattering"  
 see also neutron-proton interactions; proton-proton interactions; proton radiative capture  
 A=54-82, ground state transition strengths from (p,t) reactions 0-95305  
 correlation strength at 400 GeV, dependence on target size, multiplicity and cluster size 0-78287  
 emulsion reaction, 300 GeV/c, new stars containing only black tracks 0-78285  
 fissionability, target mass depend. for  $\pi$ ,  $\gamma$ ,  $\alpha$ , p, cascade-evaporation and liquid drop calcs. (Russian) 0-106089  
 hydrodynamic model 0-68671  
 light relativistic ion-target interactions, particle emission 0-102193  
 relativistic nuclear collisions, p, d, and t inclusive energy spectra 0-63199  
 (p,p), backward inclusive prod. mech. probing, differential cross section 0-68668  
 (p, 2p), pol. p, quasi-free scatt. on closed shell nuclei, effective polarisation 0-91173  
 (p, $\alpha$ ), 72 MeV, <sup>27</sup>Al, <sup>59</sup>Co, <sup>90</sup>Zr, <sup>197</sup>Au, <sup>208</sup>Pb, <sup>232</sup>Th targets, spectra and angular distrib. 0-68660  
 (p,d), 51.9 MeV, forbidden transition ang. distrib., CCBA and DWBA anal. 0-86848  
 (p,d), (p,t), deep hole states observed in particle transfer reactions 0-68511  
 (p,d), pol. p, 65 MeV, A=12-94, differential cross sections and anal. powers, pickup 0-91172  
 (p,d), inclusive cross section, constituent-constituent multiple scatt. model for dependence on atomic number 0-83101  
 (p,n), 1 GeV, A=7-212, charge exchange scatt., Glauber diffractive theory anal. (Russian) 0-83103  
 (p,n), 120 MeV,  $\sigma^0$  cross sections, Gamow-Teller matrix elements for A=7-90 0-86860  
 (p,n), A=12, 24, 28, isovector M1 excitations, current and spin contribs. 0-68582  
 (p,n), A=89-130, anomalous optical pot. for sub-Coulomb protons 0-102190  
 (p,n), A=89-130, sub-Coulomb protons, anomalous optical pot. 0-102191  
 (p,n), A=90 region, reaction cross section, statistical model calcs. 0-68674  
 (p,n), anomalous optical potential for sub-Coulomb barrier protons, 2 particle 1 hole states 0-105948  
 (p,n), pion exchange at intermediate energy 0-63179  
 (p,d), quasifree scatt., break-up cross section at high energies 0-99174  
 (p, $\pi$ ), hopes and realities, review, book contrib. 0-73849  
 (p, $\pi^+$ ), 585 MeV, A=1-208, differential cross section and pol. parameter 0-106056  
 (p, $\pi^+$ ), 585 MeV, cross sections, polarisation parameter for H, D, Be, C, O, Al, Ni, Cu, Mo, Pb targets 0-73848  
 (p, spallation), 480 MeV, medium to heavy mass targets, deep spallation products 0-83085  
 (p, $\tau$ ), 72 MeV, <sup>27</sup>Al, <sup>59</sup>Co, <sup>90</sup>Zr, <sup>197</sup>Au, <sup>208</sup>Pb, <sup>232</sup>Th targets, spectra and angular distrib. 0-68660  
 (p,X), 200 GeV/c in emulsion, fireball parameters and  $\pi$  emission 0-95317  
 (P,X), 22.6 GeV/c, pion p<sub>T</sub> distrib. in emulsion 0-95319  
 (p,X), 400 GeV, A=6-180,  $\bar{p}$ ,  $\pi^+$  and K<sup>+</sup> backward prod., invariant cross sections 0-102188  
 (p,X), 400 GeV, in emulsion, two-particle rapidity correlation 0-63054  
 (p,X), 400 GeV/c, deuteron prod. mechanism, pickup reactions 0-83096  
 (p,X), 640 MeV, fast proton emission, two particle differential cross sections (Russian) 0-106058  
 (p,X), 70 GeV/c in emulsion, forward-backward rapidity correl. and asymmetry 0-95320  
 (p,X), A=10-152, thermonuclear reaction rates, thick target meas. 0-73108  
 (p, X), A=12-209, pol.p, 65 MeV, continuum spectra anal. powers 0-102178  
 (p,X), complete fusion barrier and evaporation from <sup>194</sup>Hg 0-68715  
 (p,X), high energy, Glauber anal., produced particle-A relation (Chinese) 0-102192  
 (p,X), multi-chain model, charged particle distrib. 0-83098  
 (p,X), neutron excess isotope prod. in fragmentation reactions <sup>6,8</sup>He, <sup>7,8,9,11</sup>Li (Russian) 0-86888  
 (p,X), relativistic collisions, slow and fast fragment correlations, multiplicity association 0-86886  
 (p,X), p annihilation on heavy nuclei, nuclear matter props. 0-63185

## proton-nucleus reactions continued

- Ag(p,f), 1 GeV, binary fission, possible mass instability of correlated fragments 0-83133  
<sup>27</sup>Al(p,X), X=p,n, $\alpha$ , 6.44 MeV, <sup>28</sup>Si resonance wave functions from differential cross sections 0-78239  
<sup>27</sup>Al(p, $\alpha$ ), <sup>28</sup>Si 4<sup>+</sup> state lifetime by blocking effect method (Russian) 0-91152  
<sup>27</sup>Al(p, $\alpha$ ), 0.731 MeV, <sup>28</sup>Si 12.291 MeV level width, axial blocking meas. 0-63086  
<sup>27</sup>Al(p,n)<sup>27</sup>Si, cross sections and thermonuclear reaction rates 0-73852  
<sup>197</sup>Au(p,X), 72 MeV, pre-equilibrium emission (German) 0-68657  
<sup>197</sup>Au(p,X), 0.2-6.0 GeV, product cross sections, mass yields, spallation products 0-83088  
<sup>197</sup>Au(p, $\alpha$ ), 72 MeV, pre-equilibrium emission (German) 0-68657  
<sup>197</sup>Au(p, $\pi^+$ ), A=10,11, 200 MeV, pion energy spectra for discrete final states, cross sections 0-106057  
<sup>11</sup>B(p, n)<sup>11</sup>C, steel B depth distrib. meas. using time of flight method 0-71986  
<sup>11</sup>B(p,<sup>6</sup>Li)<sup>6</sup>Li, 51.9 MeV, five nucleon transfer mechanisms, DWBA calcs. 0-73845  
 Ba(p, t), 52 MeV, <sup>132</sup>Ba, A=132, 134, 136, negative parity states, J<sup>+</sup>, transitions, DWBA anal. 0-86810  
<sup>209</sup>Bi(p,p'(d)X), pol. p, 65 MeV, anal. powers of continuum energy spectra 0-68637  
<sup>79</sup>Br(p,n)<sup>79</sup>Kr, low lying levels 0-105972  
<sup>1</sup>C(p, $\pi^+$ ), A=12,13, 200 MeV, pion energy spectra for discrete final states, cross sections 0-106057  
<sup>1</sup>C(p, $\pi^+$ ), A=12,13, 200 MeV, analogue and nonanalogue state cross sections 0-99130  
<sup>12</sup>C(p,X), 4.2 GeV/c, multitudes of secondary negative particles, momentum distrib. ratios (Russian) 0-63178  
<sup>12</sup>C(p,X), 50 MeV, effective cross sections 0-78284  
<sup>12</sup>C(p,X), reaction and scatt. dynamics, optical and coupled channel anal. 0-78297  
<sup>12</sup>C(p,2p), asymmetric energy-sharing mode, half distorted-wave formalism, intermediate giant resonance 0-68656  
<sup>12</sup>C(p, $\alpha$ ), 45.2 MeV, cross sections, finite range DWBA anal., cluster form factors 0-68666  
<sup>12</sup>C(p,n), 144 MeV, charge exchange, one pion exchange and PCAC tests 0-78299  
<sup>42</sup>Ca(p,t) form factor, hole and continuum contribs. for pickup reactions 0-78256  
<sup>44</sup>Ca(p,n)<sup>44</sup>Sc, reaction rates in stars 0-82183  
<sup>44</sup>Ca(p,n), 18-45 MeV, <sup>44</sup>K excited levels, J<sup>+</sup>, transitions and lifetimes 0-68544  
<sup>48</sup>Ca(p,n), 160 MeV, <sup>48</sup>Sc spin-flip isovector giant resonance, T<sub>1/2</sub>, Gamow-Teller strength 0-106019  
<sup>48</sup>Ca(p,n), nucleon optical potential from Lane model 0-83097  
<sup>48</sup>Ca(p,t)<sup>46</sup>Ca(0<sup>+</sup>g.s.), 20 and 40 MeV, two step process, deuteron break-up effect 0-73844  
<sup>112</sup>Cd(p,n)<sup>112</sup>In low lying levels, transitions, T<sub>1/2</sub>, multiplicities and mixing ratios 0-68545  
 Cd(p,t), 11-15 MeV, <sup>112</sup>Cd, A=104-116, low lying level scheme, mass excess 0-73807  
<sup>140</sup>Ce(p,2n), <sup>138</sup>Pr medium spin states, J<sup>+</sup>, transitions and shape 0-86779  
<sup>140</sup>Ce(p,n), <sup>140</sup>Pr isobaric analogue resonances, de-excitation cascade, K-shell ionisation, spin depend. 0-78202  
 Co(p,<sup>3</sup>He X), 72 MeV, pre-equilibrium emission (German) 0-68657  
 Co(p, $\alpha$ ), 72 MeV, pre-equilibrium emission (German) 0-68657  
 C(p, $\pi^+$ ) 240 MeV inclusive pion production (Russian) 0-86908  
<sup>50</sup>Cr(p,d), 55 MeV, <sup>49</sup>Cr ground analogue state fine struct., l=3 states differential cross section 0-63152  
 Cu(p, $\pi^+$ ) 240 MeV inclusive pion production (Russian) 0-86908  
<sup>19</sup>F(p, $\alpha$ ) pol. p, <sup>20</sup>Ne 13482 keV level, parity violating effects in two resonance interference 0-83033  
<sup>19</sup>F(p, $\alpha$ )<sup>16</sup>O, <sup>20</sup>Ne quartet states 0-105973  
 Gd(p, $\alpha$ ), 17 MeV, <sup>153,155</sup>Eu single proton hole states in pickup reactions 0-78128  
<sup>76</sup>Ge(p,n)<sup>76</sup>As, 1.8-2.7 MeV, <sup>76</sup>As excited states, excitation functions and decays ang. distrib., cross sections (Russian) 0-63089  
 Ge(p,n)<sup>76</sup>As, 25 MeV, <sup>76</sup>As, A=71, 73, levels, J<sup>+</sup>, transitions, T<sub>1/2</sub> 0-57684  
<sup>1</sup>H(p, $\pi^+$ )<sup>2</sup>H, pol. p, total cross section, ang. distrib. and asymmetry parameters 0-63182  
<sup>2</sup>H(p,2p), 22.7 MeV, proton analysing power 0-78302  
<sup>2</sup>H(p,p,X), 19 GeV/c, Thomas Reiche Kuhn sum rule appl., mean energy losses 0-91192  
<sup>2</sup>H(p, $\pi^+$ ), 400-470 MeV, backward  $\pi$  differential cross sections and anal. power 0-86905  
<sup>3</sup>H(p,n), <sup>4</sup>He continuum microscopic calcs. cross sections and levels 0-57702  
<sup>3</sup>H(p,n), 1.24, 1.8 GeV, differential cross section, spin independ. Glauber model interpretation 0-63183  
<sup>3</sup>H(p,n)<sup>3</sup>He charge exchange reaction, multifold diffr. scatt. theory (Russian) 0-78303  
<sup>3</sup>He(p, $\pi^+$ )<sup>4</sup>He, 415 MeV, angular distrib., microscopic description, generalisation of ( $\pi$ , $\pi$ ) (Chinese) 0-63188  
<sup>123</sup>I production from <sup>123</sup>Xe formed in spallation reactions by 660 MeV protons, medical apps. 0-85494  
<sup>123</sup>I(p,n)<sup>123</sup>Xe, <sup>123</sup>I prod. from <sup>123</sup>Xe—<sup>123</sup>I, at 58 MeV 0-94369  
 Kr(p,n)<sup>81,82m</sup>Rb, <sup>81,82m</sup>Rb prod. for positron emission tomography 0-98068  
<sup>6</sup>Li(p,n), 144 MeV, charge exchange, one pion exchange and PCAC tests 0-78299  
<sup>6</sup>Li(p,p,d), 670 MeV, large angle quasifree scatt., spectroscopic factor, momentum distrib., cluster model 0-63184  
<sup>7</sup>Li(p, $\alpha$ ), 45 MeV, <sup>7</sup>Li— $\alpha$  virtual decay vertex constant 0-78231  
<sup>7</sup>Li(p, $\alpha$ ), 4.5-12 MeV, <sup>7</sup>Be high spatial symmetry excited states, resonances, rot. band 0-86780  
<sup>7</sup>Li(p,n), 24.8-45 MeV, <sup>7</sup>Be effective for charge exchange analogues of Gamow-Teller transitions 0-57726  
<sup>25</sup>Mg(p,n)<sup>25</sup>Al, cross sections and thermonuclear reaction rates 0-73852  
<sup>26</sup>Mg(p,n), 24.6-45 MeV, <sup>26</sup>Al 1<sup>+</sup>T=0 states, isobaric analogue state, spin-isospin effective interaction 0-68553  
<sup>26</sup>Mg(p,n)<sup>26</sup>Al<sup>18</sup>, 5.2-6.9 MeV, cross section via accelerator mass spectrometry 0-99175  
<sup>26</sup>Mg(p,t), <sup>24</sup>Mg ground and  $\gamma$ -bands, direct and multistep processes 0-102094  
 Mg(p,n), 35 MeV, <sup>24</sup>Al, A=24,25,26, giant M1 strength, comparison with cross sections 0-86878  
<sup>92</sup>Mo(p,p<sup>3</sup>n), 60 MeV, <sup>89</sup>Mo<sup>0</sup> levels, transitions and half life 0-86858

## proton-nucleus reactions continued

- <sup>98</sup>Mo(p,n), 3-6.3 MeV, <sup>98</sup>Tc 14  $\mu$ s isomer, low lying levels and transitions 0-73802
- <sup>100</sup>Mo(p,n), 3-5.2 MeV, <sup>100</sup>Tc  $\mu$ s isomers, isomeric transitions and mean lives 0-73803
- <sup>14</sup>N(p,X), 50 MeV, effective cross sections 0-78284
- <sup>14</sup>N(p,n), 144 MeV, charge exchange, one pion exchange and PCAC tests 0-78299
- <sup>142</sup>Nd(p,2n), <sup>141</sup>Pm medium spin states, J $\pi$ , transitions and shape 0-86779
- <sup>142</sup>Nd(p,2n), 14.9-20.2 MeV, <sup>145</sup>Pm level struct., J $\pi$  and lifetimes, cluster-vibr. model anal. 0-91125
- <sup>150</sup>Nd(p,2n $\gamma$ ), <sup>149</sup>Pm levels, bands, transitions, in-beam spectroscopy, particle-rotor anal. 0-78125
- <sup>4</sup>Ni(p,X), A=58, 64, 7.6 10 GeV/C, isotopic cross section ratios, He, Li fragments isotopic effects (*Russian*) 0-63154
- <sup>4</sup>Ni(p,x $\gamma$ ), 80-164 MeV, A=58, 60, 62, 64, prod. cross sections, pre-equilibrium phase 0-78301
- <sup>4</sup>Ni(p $\alpha$ ,  $\alpha$ ), A=58, 60, 62, 22 MeV, analysing power and cross sections, Co proton-hole states 0-68663
- <sup>58</sup>Ni(p,p'(d)X), pol. p, 65 MeV, anal. powers of continuum energy spectra 0-68637
- <sup>60</sup>Ni(p, $\alpha$ )<sup>57</sup>Co(3/2<sup>+</sup>), anomalous analyzing power, DWBA calc. 0-86894
- <sup>23</sup>Np(p,f), 11-26 MeV, product yield 0-91197
- <sup>23</sup>Np(p,Li)<sup>11</sup>C, 51.9 MeV, five nucleon transfer mechanisms, DWBA calcs. 0-73845
- <sup>16</sup>O(p,X), 50 MeV, effective cross sections 0-78284
- <sup>16</sup>O(p $\alpha$ ,2p), cross section, analysing power, energy sharing spectra, distorted wave impulse approximation 0-78291
- <sup>18</sup>O(p,n), 3.75 MeV, <sup>18</sup>F 1.04 MeV state lifetime and  $\gamma$ -transition polarisation 0-106016
- <sup>18</sup>O(p,t), exact finite range DWBA calcs., realistic triton and nuclear wave functions 0-63191
- <sup>18</sup>O(p,t), finite range DWBA anal. with realistic triton wave function 0-78300
- <sup>208</sup>Pb(p,n), 120,160 MeV, <sup>208</sup>Bi M1 isobaric analogue resonances and giant spinflip resonances 0-106030
- <sup>208</sup>Pb(p,n), nucleon optical potential from Lane model 0-83097
- <sup>208</sup>Pb(p,t), finite range DWBA anal. with realistic triton wave function 0-78300
- Pb(p,d), 9 GeV, nuclear emulsion expt. 0-78292
- Pb(p,t), pairing vibr. band, microscopic struct. and wave functions 0-91126
- <sup>193</sup>Pt(p,t), 25 MeV, <sup>193</sup>Pt low lying negative parity states and shape 0-68540
- <sup>81</sup>Rb-<sup>81</sup>Kr generators, aspects of production, elution and automation, medical appls. 0-61696
- <sup>85</sup>Rb, excitation functions, medical appls. 0-78286
- <sup>28</sup>Si(p,(d)X), pol. p, 65 MeV, anal. powers of continuum energy spectra 0-68637
- <sup>28</sup>Si(p, $\pi^+$ ), <sup>28</sup>Si 3/2<sup>+</sup> and 5/2<sup>+</sup> states population, (d,p) comparison 0-95307
- <sup>29</sup>Si(p, $\alpha$ ), 13.5-15.5 MeV, <sup>30</sup>P level width isospin depend., excitation functions, statistical anal. 0-78152
- <sup>147</sup>Sm(p,2n) 19 MeV, <sup>146</sup>Eu 9<sup>+</sup> isomer,  $\gamma$ -decay, high spin particle-hole multiplet population 0-63066
- <sup>152</sup>Sm(p,t), <sup>152</sup>Sm ground and  $\gamma$ -bands, direct and multistep processes 0-102094
- Sm(p,t), 17 MeV <sup>147,149,151</sup>Pm single proton hole states in pickup reactions 0-78128
- Sm(p,t), even isotopes, high energy neutron pairing strength, two neutron holes, resonances 0-78116
- <sup>4</sup>Sn(p,X), A=112, 124, 7.6, 10 GeV/C, isotopic cross section ratios, He, Li fragments isotopic effects (*Russian*) 0-63154
- <sup>125</sup>Sn(p,n), statistical multistep direct emission, p-h and DWBA calcs. 0-106035
- Sn(p,n), even isotopes, 4-10 MeV, cross sections, optical parameters and nuclear radius A-depend. 0-57773
- Sn(p,t), 89 MeV, <sup>118,120,122</sup>Sn deep hole states, excitation energies and ang. distrib. 0-86792
- <sup>87</sup>Sr(p,2n $\gamma$ ), 22.8 MeV, <sup>87</sup>Y level struct.,  $\gamma$ -spectroscopy and J $\pi$  0-83040
- <sup>181</sup>Ta(p,X), 4.2 GeV/c, multitudes of secondary negative particles, momentum distrib. ratios (*Russian*) 0-63178
- <sup>181</sup>Ta(p,n), 5.76-9.83 MeV, <sup>181</sup>W level density, n spectra and ang. correl., direct and nonequilibrium processes (*Russian*) 0-68631
- <sup>181</sup>Ta(p,n)<sup>181</sup>W, multi-step compound and direct reactions, statistical theory 0-57761
- <sup>126</sup>Te(p,n), 2<sup>+</sup> $\rightarrow$ 2<sup>+</sup> transition multipole mixing ratio 0-78198
- <sup>232</sup>Th(p,f), 29-97 MeV, Rb, In and Cs relative independ. yields, charge division 0-102218
- <sup>232</sup>Th(p,f), 52.5 MeV, fission probability 0-99195
- <sup>49</sup>Ti(p,n), 0.74-3.25 MeV, cross section and thermonuclear reaction rates, nucleosynthesis 0-102187
- <sup>205</sup>Tl(p,5n)<sup>201</sup>Pb-<sup>201</sup>Tl, yields and excitation functions for Pb radioactivities, medical appls. 0-67249
- <sup>205</sup>Tl(p,d), 26.1 MeV, <sup>204</sup>Tl neutron hole states, J $\pi$  and spectroscopic factors 0-86783
- <sup>238</sup>U(p,X), 0.8-400 GeV 0-83099
- <sup>238</sup>U(p,X), 400 GeV, <sup>4</sup>Sc, A=44m,46,47,48, fragment emission, two-step model applicability 0-99177
- <sup>238</sup>U(p,n), 11-29 GeV, three dims. charge dispersion curves, isobaric yields 0-102111
- <sup>51</sup>V(p,X), X= $\gamma$  or n, 0.93-4.47 MeV, cross sections, competition effects, Hauser-Feshbach calcs. 0-91184
- <sup>183</sup>W(p,t), 21 MeV, <sup>181</sup>W levels (neutron and collective) and J $\pi$ , ang. distrib. 0-78160
- W(p,t), 21 MeV, <sup>183</sup>W, A=178, 180, 182, 184, levels and J $\pi$ , ang. distrib. 0-78159
- <sup>176</sup>Yb(p,3n), 22.7 MeV, <sup>174</sup>Lu isomeric levels,  $\gamma$ -spectra, T 1/2 and decay modes 0-99151
- <sup>90</sup>Zr(p,n), nucleon optical potential from Lane model 0-83097
- <sup>90</sup>Zr(p,n), 120 MeV, <sup>90</sup>Nb giant particle hole resonances, Gamow-Teller strength 0-86877
- <sup>92</sup>Zr(p, $\alpha$ ), <sup>89</sup>Y gamma transitions, microscopic finite-range anal. 0-63181

## proton-nucleus scattering

see also neutron-proton scattering; proton-proton scattering

stable isotope tracer analysis by proton scattering 0-104487

(p,p), 0.1-1 GeV, optical pot., vol. integrals and root mean square radii 0-106054

## proton-nucleus scattering continued

- (p,p), 1 GeV elastic and inelastic scatt., diff. minima filling mechanism (*Russian*) 0-86907
- (p,p), <100 MeV, Coulomb corrections to NN coupled states, nonrelativistic scatt. theory 0-78114
- (p,p), small distances, new electrodynamics approach 0-63180
- (p,p), statistical significance of spreading widths for doorway states, reply to comments 0-63147
- (p,p) and (p,p), from Be, C, Al, Cu, Sn, Pb, 70, 125, 175 GeV/c 0-83128
- (p,p'), 800 MeV, cross sections, quasifree knockout mechanisms, PWIA calcs. 0-78294
- (p,p'), compound nucleus lifetimes from X-ray method, statistical properties 0-78295
- (p,p'), single neutron states, two step process and effective interaction 0-78290
- (p,p'), unnatural parity states excitation,  $\pi$ -condensate instability effects, DWBA anal. 0-78168
- (p,p') inelastic spectra in high energy continuum, single and multiple scatt. mechanisms 0-57777
- <sup>107</sup>Ag(p,p'), pol.p, 6.06 MeV, anal. powers, large absorption pot., optical model 0-83092
- <sup>21</sup>Al(p,X), X=p,n, $\alpha$ , 6.44 MeV, <sup>28</sup>Si resonance wave functions from differential cross sections 0-78239
- <sup>12</sup>C(p,X), reaction and scatt. dynamics, optical and coupled channel anal. 0-78297
- <sup>12</sup>C(p,p'), 1<sup>+</sup> (T=1, 15.1 MeV) state excitational pionic modes, M1 form factor 0-78195
- <sup>12</sup>C(p,p'), 122 MeV, level excitation, cross sections, effective NN interaction, DWIA anal. 0-78197
- <sup>12</sup>C(p,p'), 122 MeV, precritical phenomena 0-83089
- <sup>12</sup>C(p,p'), 22-27 MeV, 1<sup>+</sup> state de-excitation  $\gamma$ -ray ang. distrib., tensor force effects, DWBA anal. 0-68580
- <sup>12</sup>C(p,p'), 800 MeV, 15.11 MeV state diff. cross section, nuclear critical opalescence search 0-105984
- <sup>12</sup>C(p,p'), pol. p, 800 MeV, unnatural parity states excitation, anal. powers and isospin 0-68538
- <sup>12</sup>C(p,p' $\gamma$ ), 23.5-27 MeV, 1<sup>+</sup> state spin flip meas. DWBA anal., cross sections 0-68529
- <sup>12</sup>C(p,p'), 20-40 MeV, pol. p, anal. powers, imaginary spin-orbit pot., coupled channels anal. 0-102179
- <sup>12</sup>C(p,p), 14-45 MeV, differential cross section and spin-flip probabilities, giant resonances 0-73850
- <sup>12</sup>C(p,p), bremsstrahlung near 1.7 MeV resonance 0-68670
- <sup>12</sup>C(p,p), pol. p, 14.23 MeV resonance broadening, nuclear recoil, atomic excitation effects 0-102165
- <sup>12</sup>C(p,p), radial sensitivity of optical pot. 0-86869
- <sup>12</sup>C(p,p), spin-flip probability to first 2<sup>+</sup> level 0-78288
- <sup>40</sup>Ca(p,p'), pol. p, A=40,48, 800 MeV, diff. cross sections, anal. powers, DWIA anal., high spin levels 0-83067
- <sup>40</sup>Ca(p,p'), isovector dipole strength excitation in giant resonance region 0-83066
- <sup>40</sup>Ca(p,p'), 800 MeV, high energy octupole giant resonance, ang. distrib. 0-86879
- <sup>40</sup>Ca(p,p' $\gamma$ ), 6.02-6.48 MeV, <sup>41</sup>Sc 2p-1h intermediate struct. resonances, anal. powers, J $\pi$  0-86883
- <sup>40</sup>Ca(p,p' $\gamma$ ), 6.25 MeV, triple  $\alpha$ , correlation, 3<sup>-</sup> exit channel, resonances, single particle states 0-68626
- <sup>40</sup>Ca(p,p), 30 MeV, optical pot. imaginary part calcs. 0-86868
- <sup>40</sup>Ca(p,p), absorbing optical pot., Coulomb correction term 0-73831
- <sup>40</sup>Ca(p,p'), DWIA test in Glauber theory, transition density 0-99173
- <sup>106</sup>Cd(p,p')<sup>106</sup>Cd, simultaneous nucl. and K-shell excitation, <sup>107</sup>In lifetime meas. 0-63130
- <sup>55</sup>Co(p,p'), 6 MeV, level energies, branching ratios lifetimes and spins 0-63093
- <sup>4</sup>Cr(p,p), A=50, 52, 6 MeV, elastic and inelastic differential cross sections, spin flip probability (*Russian*) 0-91187
- <sup>6</sup>Cu(p,p') negative parity level excitation, gamma ray obs., test for core excitation model 0-68534
- <sup>1</sup>F(p,p' $\gamma$ ), 1459 $\rightarrow$ 110 keV transition, E2/M1 mixing ratio 0-106013
- <sup>56</sup>Fe(p,p'), A=54, 56, 6 MeV, resonances, spin flip and cross section depends. Hauser Feshbach anal. (*Russian*) 0-83084
- <sup>56</sup>Fe(p,p'), pol. p, 800 MeV, diff. cross sections, anal. powers, DWIA anal. 0-83067
- <sup>56</sup>Fe(p,p), 6 MeV, elastic and inelastic, quadrupole deformation, IAR excitation, optical pots. (*Russian*) 0-63149
- <sup>1</sup>H(p,X), elastic, inelastic and charge exchange cross sections in optical model 0-68665
- <sup>1</sup>H(p,p), 1-3 GeV/c, pol. p, spin parameters A and A<sub>nn</sub> 0-95304
- <sup>1</sup>H(p,p), 6.141 MeV, anal. power, Paris pot. predictions 0-63156
- <sup>1</sup>H(p,p), pol.p, 9.57 MeV, spin correlation parameter, phase shift anal. 0-102112
- <sup>2</sup>H(p,p), 800 MeV, differential cross sections and anal. powers 0-83091
- <sup>2</sup>H(p,p), back angle elastic cross sections in Kerman-Kissinger model, inelasticity corrections 0-106060
- <sup>2</sup>H(p,p), pol.p, spin rot. and depolarisation, NN amplitude double spin flip part 0-78271
- <sup>2</sup>H(p,p), tensor asymmetries, deuteron D-wave and non-eikonal effects, Glauber model 0-78296
- <sup>2</sup>H(p,p) large angle elastic scatt., d form factor at large q<sup>2</sup> 0-102189
- <sup>2</sup>H(p,p $\gamma$ ), elastic cross sections, bremsstrahlung, threshold and Coulomb effects 0-91186
- <sup>3</sup>H(p,p), <sup>4</sup>He continuum microscopic calcs. cross sections and levels 0-57702
- <sup>3</sup>H(p,p), 1.24 GeV, differential cross section, spin independ. Glauber model interpretation 0-63183
- <sup>4</sup>He(p,p), 1.05 GeV, cross sections and polarisations, correlation effects calcs. 0-57774
- <sup>4</sup>He(p,p), 200-500 MeV, differential cross section and anal. power 0-68640
- <sup>4</sup>He(p,p), 788 MeV, back angle diffraction struct., Dirac, eqn. optical model 0-68667
- <sup>4</sup>He(p,p), differential cross-section, multifold diff. scatt. theory (*Russian*) 0-78303
- H(p,x), direct and charge transfer scattering processes, second quantisation 0-78289
- <sup>4</sup>K(p,p $\gamma$ ), 1.58 MeV, parity doublet gamma lifetimes, 3/2 levels, parity mixing 0-78209
- <sup>4</sup>Mg(p,p'), A=24, 26, isovector dipole strength excitation in giant resonance region 0-83066



**proton-nucleus scattering continued**

- <sup>24</sup>Mg(p,p), 14-45 MeV, differential cross section and spin-flip probabilities, giant resonances 0-73850  
<sup>26</sup>Mg(p,p'), pol.p, 5.5-17.5 MeV, cross sections and anal. powers, autocorrelations 0-106042  
<sup>27</sup>Mg(p,p), 1.9-4.0 MeV, <sup>27</sup>Al isobaric analogue resonances, spectroscopic factors and  $\gamma$ -rays 0-86873  
Mo(p,p $\gamma$ ), odd isotopes, excited d-states from analogue resonances and p- $\gamma$  correlations 0-68546  
<sup>14</sup>N(p,p'), 122 MeV, level excitation, cross sections, effective NN interaction, DWIA anal. 0-78197  
<sup>14</sup>N(p,p'), 25-40 MeV, level cross sections, optical parameters, DWBA anal., tensor effective interaction 0-68555  
<sup>58</sup>Ni(p,p), 800 MeV, elastic and inelastic, cross section, deformation lengths, optical and DWBA anal. 0-68664  
<sup>16</sup>O(p,p'), 20-40 MeV, pol. p, anal. powers, imaginary spin-orbit pot., coupled channels anal. 0-102179  
<sup>208</sup>Pb(p,p'), 135 MeV, normal parity level excitation, J $\pi$ , differential cross sections 0-57690  
<sup>208</sup>Pb(p,p'), 800 MeV, high energy octupole giant resonance, ang. distrib. 0-86879  
<sup>208</sup>Pb(p,p), 0.8 GeV, cross sections, optical anal. np RMS radius difference,  $\Delta r_{np}$  0-63187  
<sup>208</sup>Pb(p,p), 30 MeV, optical pot. imaginary part calcs. 0-86868  
<sup>102</sup>Pd(p,p $\gamma$ ), long lived  $E^0$  state,  $E^0$  transitions 0-73804  
<sup>32</sup>S(p,p), 14-45 MeV, differential cross section and spin-flip probabilities, giant resonances 0-73850  
<sup>32</sup>S(p,p), spin-flip probability to first 2 $^+$  level 0-78288  
<sup>45</sup>Sc(p,p'), levels, J $\pi$ , transitions and lifetimes 0-63091  
<sup>28</sup>Si(p,p), 14-45 MeV, differential cross section and spin-flip probabilities, giant resonances 0-73850  
<sup>28</sup>Si(p,p'), isovector dipole strength excitation in giant resonance region 0-83066  
<sup>28</sup>Si(p,p), spin-flip probability to first 2 $^+$  level 0-78288  
Si( $p_{pol}$ ,  $p_{pol}$ ), giant multipole resonance region, optical model anal. 0-57779  
<sup>154</sup>Sm(p,p'), 0.8 GeV, ang. distrib. and multipole moments, DWBA and coupled channel anal. 0-105969  
<sup>116</sup>Sn(p,p'), 800 MeV, high energy octupole giant resonance, ang. distrib. 0-86879  
Sn(p,p), pol.p, 6.77-8.8 MeV, cross sections, optical parameters and nuclear radius A-depend. 0-57773  
<sup>51</sup>V(p,p'), 6 MeV, levels, spins and EM props., shell model anal. 0-63092  
<sup>176</sup>Yb(p,p'), 0.8 GeV, ang. distrib. and multipole moments, DWBA and coupled channel anal. 0-105969  
Zr(p,p $\gamma$ ), odd isotopes, excited d-states from analogue resonances and p- $\gamma$  correlations 0-68546

**proton polarisation**

- $\gamma$ d $\rightarrow$ pn, proton polarisation energy depend., 400-700 MeV (Russian) 0-63000

**proton production**

- central high energy heavy ion collisions, possible finite particle number effects, p spectra 0-99181  
hard scattering process, parton model, p to  $\pi$  ratio at large transverse momentum 0-62934  
pulsed source, Penning type, beam parameters 0-87001  
relativistic heavy ion collisions, central and peripheral, p emission patterns 0-73860  
relativistic nuclear collisions, p, d, and t inclusive energy spectra 0-63199  
total pion absorption cross section, A depend., proton yields 0-106081  
 $e^+e^- \rightarrow np$ , polarised, parity violating asymmetry 0-78080  
 $e^+e^- \rightarrow$  hadrons, 12, 30 GeV,  $\kappa$ ,  $\pi$ ,  $\rho$  production 0-105916  
 $\gamma$ d $\rightarrow$ np, 300 MeV, dibaryon resonance manifestation, pseudoindependent amplitude elimination (Russian) 0-57612  
 $\gamma$ d $\rightarrow$ pn, 250 to 800 MeV, differential cross-section and proton polarisation, theoretical models 0-78081  
 $\gamma$ d $\rightarrow$ pn, proton polarisation energy depend., 400-700 MeV (Russian) 0-63000  
 $\gamma$ n $\rightarrow$  $\pi^-$ p, 700 to 1200 MeV, recoil proton polarisation 0-78075  
 $\gamma$ p $\rightarrow$  $\pi$ p, 450 to 800 MeV, proton polarisation, Walker-type anal.,  $P_{11}(1470)$ ,  $D_{13}(1470)$ ,  $S_{11}(1535)$  resonances 0-73721  
K $d \rightarrow \bar{K}^0$ p, 1.45, 1.65 GeV/c,  $\bar{K}^0$  p invariant mass enhancement 0-57639  
(N,N' $X$ ), shower proton and meson transverse momenta, intranuclear cascade model 0-102185  
np $\rightarrow$ px, baryonium exchange, triple-Regge couplings 0-86763  
 $\nu n \rightarrow \nu$ pn, neutral current process, excitation function, cross section ratio 0-78053  
(p,2p), backward inclusive prod. mech. probing, differential cross section 0-68668  
(p,X), 400 GeV, A=6-180,  $\pi^+$ ,  $\pi^-$  and K $^+$  backward prod., invariant cross sections 0-102188  
(p,X), 640 MeV, fast proton emission, two particle differential cross sections (Russian) 0-106058  
pd, 70 GeV,  $\pi^+$ , K $^+$ , p,  $\bar{p}$  prod. with 0.5-2.2 GeV/c transverse momenta, yield ratio, QCD (Russian) 0-83012  
pN, 67 GeV/c, in Be, Al, Cu, inclusive  $\pi^+$ , K $^+$ , p,  $\bar{p}$  prod. cross sections (Russian) 0-86769  
pN, 67 GeV/c, nuclear targets,  $\pi^+$ , K $^+$ , p,  $\bar{p}$  yields (Russian) 0-68501  
pp, 70 GeV,  $\pi^+$ , K $^+$ , p,  $\bar{p}$  prod. cross sections, QCD-parton model anal. (Russian) 0-63044  
( $\pi$ ,p), A=12-181, proton yields, number of nucleons involved in pion absorption 0-63209  
 $\pi^- n \rightarrow pX^-$ , 21, 205 and 360 GeV/c, reggeised one-pion-exchange 0-57649  
 $\pi^- p \rightarrow pX$ , 12 GeV/c, absorbed Mueller-Regge model for backward inclusive p prod. 0-73752  
 $\pi^- p$ , 32 GeV/c, slow proton and  $\Delta^{++}(1236)$  inclusive prod. (Russian) 0-63046  
<sup>197</sup>Au(<sup>16</sup>O,p)X, 315 MeV, high energy p emission, fireball and preequilibrium anal. 0-91194  
<sup>12</sup>C( $\gamma$ , $\pi$ ), final state interaction, distorted and plane wave momentum distrib. 0-78275  
<sup>4</sup>He ( $\pi^-$ ,  $\pi$ ), 5GeV/c, quasielastic scatt., cross section, form factor, final state interactions 0-99190  
<sup>4</sup>Li( $\pi$ p), A=6, 7, 75, 175 MeV, diffential cross sections, reaction mechanisms 0-78332  
<sup>4</sup>Ni(<sup>3</sup>He, p), 8, 10 MeV, A=58, 60, 62, p spectra compound nucleus contrib., odd-even effect 0-106061

**proton production continued**

- <sup>58</sup>Ni(<sup>40</sup>Ar,X), 280 MeV, deep inelastic, light fragments, thermal equilib., ang. momentum transfer 0-63203  
<sup>28</sup>Si( $\gamma$ ,p), 18.1-29 MeV, photoproton energy spectra, contribs. to giant dipole resonance 0-78242
- proton-proton inclusive interactions**  
depolarisation parameter, dominance of natural parity exchange 0-78088  
fireball model three component, appl. to pp interactions above 9 GeV 0-62946  
hadron production, phase transition in Feynman-Wilson analogue fluid, multiplicities, plateaux, cross-sections 0-73744  
hadronic two-jet events, momentum unbalance, parton transverse momentum 0-57652  
meson production, multimeson inclusive spectra and recombination model, multi-quark structure functions 0-73751  
neutral particle production in 4 to 2100 GeV interactions, review (Russian) 0-68489  
pp collisions, high energy, fireball mass, rapidity, spin distrib. 0-57645  
probabilistic quark-model approach to p fragmentation 0-63049  
scaling-in-the-mean hypothesis 0-68497  
K $^{*+}(892)$  production at 12 and 24 GeV/c 0-86765  
pp, 100 GeV/c, inclusive meson and strange particle prod., energy partition 0-95289  
pp, 147 GeV/c, inclusive  $\Delta^{++}$  prod., cross section energy depend. 0-57651  
pp, 22.4 GeV/c, charged particle average energy, mass independ. calc., multiplicity depend. (Russian) 0-63045  
pp, 300 GeV/c, inclusive prod. of K $^0$ ,  $\Lambda^0$  K $^{*+}(890)$  and  $\Sigma^+(1385)$  0-95290  
pp, 31-63 GeV, direct photon prod. at large  $p_T$ ,  $\pi^0/\gamma$  prod. ratio 0-63038  
pp, 405 GeV/c,  $\rho^0$ , f,  $\bar{f}$ , h meson prod., cross sections 0-105930  
pp, 53, 63 GeV, massive electron pair prod., T ang. decay, scaling function 0-68495  
pp, 53, 63 GeV,  $\Upsilon$  and  $\psi$  prod., dielectron decay angles 0-68496  
pp, 5.7 GeV/c, single particle inclusive spectra, Mueller-Regge approach 0-73727  
pp, 62 GeV/c, multiparticle prod. mech.,  $e^+e^-$  comparison in parton model 0-78103  
pp, 70 GeV,  $\pi^+$ , K $^+$ , p,  $\bar{p}$  prod. cross sections, QCD-parton model anal. (Russian) 0-63044  
pp, high energies,  $\Sigma^+(1385)$  inclusive prod., minimised wave function model calcs. (Russian) 0-63047  
pp, ISR energies, high  $p_T$   $\pi^0$  and single photon events, associated charged particle multiplicity 0-63039  
pp, ISR energies, p fragmentation, D $^+$  prod. from  $\Lambda_c^*$  and  $\Lambda_b$  decay 0-102080  
pp, large  $p_T$  pion $^0$  prod., meson structure functions, quark distrib. functions 0-86714  
pp, pp, 12-405 GeV, low  $p_T$  meson prod., quark-antiquark formation model 0-63056  
pp, pp, 130, 200 GeV, jet prod. cross sections, QCD anal. and scale breaking 0-99111  
pp, pp, multiple production processes regularities, Monte Carlo model 0-102082  
pp, pp, pol. and unpol. beams, hadronic jets, vector bosons, QCD and weak interference 0-57648  
pp, secondary hadron absolute yield, L=1 meson prod., quark model (Chinese) 0-99113  
pp $\rightarrow$ annihilations, multipion distrib., statistical bootstrap model 0-68472  
pp $\rightarrow$  $\Delta^+(1232)X$ , 32 GeV, cross sections 0-105937  
pp $\rightarrow$  $\gamma X$ , perturbative QCD anal. 0-63042  
pp high energy annihilation in nuclei, multiple scattering models 0-102079  
pp $\rightarrow$ K $^+$ X,  $p\bar{K}^-$  exotic, triple-Regge formalism, Pomeron exchanges 0-63041  
pp $\rightarrow$ K $^{*+}(892)X$ , 3.6 GeV, factorisation hypothesis test 0-102055  
pp multiplicities, viscosity effect in Landau hydrodynamical model 0-63055  
pp $\rightarrow$  $\mu^+\mu^-X$ , 62 GeV,  $\psi$  and  $\gamma$  cross sections, scaling function 0-105932  
pp $\rightarrow$ nX, baryonium exchange, triple-Regge couplings 0-86763  
pp $\rightarrow$ pX, 205 GeV/c, leading p spectrum, random walk hypothesis, geometric bremsstrahlung model 0-68493  
pp $\rightarrow$ pX, pp exotic, triple-Regge formalism, Pomeron exchanges 0-63041  
pp $\rightarrow$  $\pi^+X$ , intermediate  $p_\perp$  distribution through a QCD resummation mechanism 0-83010  
pp $\rightarrow$  $\pi^0X$ , pol.p, 24 GeV/c, high  $p_T$   $\pi^0$  prod., spin. depend. 0-105935  
pp $\rightarrow$  $\pi^0\pi^0X$ , high transverse momentum, correlations 0-105933  
pp $\rightarrow$  $\pi^+X$ , large- $p_T$  reactions in broken color gauge theory 0-95292  
pp $\rightarrow$  $\pi^+X$ ,  $\pi^+$  average transverse momentum energy depend., scaling relation 0-91116  
pp $\rightarrow$  $\psi X$ ,  $p\bar{\psi}$  exotic, triple-Regge formalism, Pomeron exchanges 0-63041  
pp soft annihilation, parton description in three chain model 0-83009  
pp $\rightarrow$  $\Sigma(1385)X$ , 3.6 GeV, factorisation hypothesis test 0-102055  
pp annihilations, studied using topological cross-section differences between pp and pp at 48.9 GeV/c 0-83011

**proton-proton interactions**

- see also proton-proton inclusive interactions; proton-proton scattering  
dibaryon resonant states, narrow peaks in cross-section 0-63016  
inelastic charge exchange, quark interchange 0-86759  
multiperipheral process, interference terms in transition, amplitudes, correlation expansions 0-62953  
SU $_1(2) \times$ U(1) and SU $_1(2) \times$ SU $_R(2) \times$ U(1) predictions at high Q $^2$ , neutral currents, Z-bosons 0-63029  
pp, 355-1066 MeV/c, total and annihilation cross sections, S meson search 0-68473  
pp, 62.4 GeV/c, direct single photon prod. at large  $p_T$  0-91113  
pp, 8.8 GeV/c, exclusive annihilation processes, cross sections, quark model anal. 0-105920  
pp, D, B, K prod., QCD model for heavy flavour prod., two gluon annihilation 0-86744  
pp, diffraction dissociation, dip and kink structs., differential cross sections 0-95284  
pp, heavy lepton prod. and decay, supersymmetrical model of weak and EM interactions (Russian) 0-86748  
pp, massive lepton pair prod., pion exchange model anal., quark parton interpretation (Russian) 0-82993  
pp annihilation cross sections, corrected differences, fireball model, diffraction cross sections 0-91108  
pp $\rightarrow$ baryons by diquark-quark fusion model 0-102065

**proton-proton interactions continued**

- pp bremsstrahlung, 730 MeV,  $\gamma$ -energies of  $<300$  MeV, differential cross section 0-99108  
 pp-d $\pi$ , 400 to 600 MeV, production cross sections 0-78091  
 pp-e $^+$ e $^-$ , magnetic nucleon form factor, p-meson type contribs. 0-57596  
 pp-e $^+$ e $^-$  annihilation, weak neutral current effects (*Russian*) 0-105837  
 pp interactions, 48.9 GeV, elastic and topological cross-sections 0-83007  
 pp- $\bar{n}$ n, 0.119-1.046 GeV/c, charge exchange cross section 0-63015  
 pp-pppp, 11.75 GeV/c, baryonium states, cross section and branching ratio 0-95288  
 pp-pp $\pi^0$ (pp $\pi^+$ )( $\bar{n}$ p $\pi^-$ ), 8.8 GeV/c, one pion prod. cross sections, Deck model anal. 0-105919  
 pp-pp $\pi\pi$ , 12 GeV/c, final state diffraction dissociation, cross section 0-99109  
 pp- $\pi^+$ d, 515 and 575 MeV, spin depend. parameter meas. 0-73734  
 pp- $\pi\pi$ , 1-2 GeV/c, Barrelet zero anal., resonant struct. 0-73735  
 pp- $\pi\pi$ , 1-2 GeV/c, resonance region, partial waves, positivity constraints 0-99107  
 pp resonant annihilation,  $\eta_c$  charmonium state prod. cross section 0-82991  
 pp-S- $\pi$ -pp, S meson as baryonium state 0-62938  
 S(1936), evidence against existence from pp interaction 0-78089  
 pp- $\pi^+\pi^-$  ( $K^+K^-$ ), T, U and V resonances 0-68485

**proton-proton scattering**

- see also proton-proton interactions*  
 bell's inequalities from the field concept in general relativity 0-105771  
 depolarisation parameter, dominance of natural parity exchange 0-78088  
 Drell-Yan process, quark-quark contrib. 0-73731  
 Faddeev approach, 0-1200 MeV pp scatt.,  $\pi$ NN dynamics 0-57625  
 gluon distribution in proton from result anal. 0-82939  
 impact parameter distribution of pp inelastic overlap integral from pp elastic scatt. and total cross-sections 0-83001  
 large angle elastic scatt., unitarity condition and partial cross sections 0-82990  
 large momentum transfer, multiple-scattering model, three-quark proton 0-63031  
 parity violation at 50 MeV (*German*) 0-68471  
 parity violation meas. at 45 MeV 0-78092  
 polarisation and energy dependence 0-63030  
 polarisation phenomena in close-to-forward scatt., intermediate energy region 0-78086  
 polarisation structure and Pomeron flip, Regge pole model 0-102073  
 preasymptotic effects in large angle elastic scatt. amplitudes, quasipot. scatt. (*Russian*) 0-57631  
 SIN expts., 400 to 600 MeV 0-73733  
 smooth interpolation between Orear- and fixed angle scaling behaviour of the scattering amplitude 0-105873  
 Van der Waals type model for high energy large momentum transfer pp scattering 0-73740  
 pp, 1 GeV, elastic scatt. amplitude, phase shift anal. (*Russian*) 0-86746  
 pp, 1-3 GeV/c, total cross section differences, singlet and triplet contribs. anal. 0-68474  
 pp, 100, 200 GeV, elastic scatt., polarisation effects at large momentum transfer, quark model (*Russian*) 0-83005  
 pp, 100, 300 GeV/c, polarisation parameters and ang. distrib. for elastic scatt. 0-95287  
 pp, 2-9.5 GeV/c, wide angle elastic scatt., differential cross section 0-73730  
 pp, 23.4-62 GeV, scatt. amp., differential cross section from eikonal model (*Russian*) 0-57642  
 pp, 45 MeV, longitudinally pol. p, parity nonconservation in anal. powers 0-57626  
 pp, 970 MeV, Wolfenstein polarisation rotation, coeff., phase shift anal. (*Russian*) 0-86747  
 pp, elastic scatt. amplitude in quark diquark model 0-102075  
 pp, pp, elastic scatt. and diffractive dissociation, Regge model with  $\alpha_p(0) > 1$  (*Russian*) 0-57630  
 pp, simple Coulomb correction for phase shifts, on-shell approx. 0-82989  
 pp elastic, differential and total cross sections, proton model, gluon-gluon annihilation 0-91114  
 pp elastic scatt., 1-3 GeV/c, pol. p, spin parameters A and  $A_{nn}$  0-95304  
 pp elastic scatt. at high energies and large momentum transfer, review (*Russian*) 0-105926  
 pp interactions, 48.9 GeV, elastic and topological cross-sections 0-83007  
 pp large angle elastic scatt., cross section beyond 2nd maximum, unitarity condition (*Russian*) 0-83004  
 pp scatt.,  $<300$  MeV P-odd asymmetry for pol. p (*Russian*) 0-102063  
 pp scatt. amplitude, phase anal. ambiguities, cross sections and polarisation parameter (*Russian*) 0-86749  
 pp scatt. at higher energies, differential cross section ratio scaling 0-73741  
 pp scatt. cross section at high momentum transfer, geometrical scaling, energy depend. (*Russian*) 0-102064  
 pp small angle scatt., 312-575 MeV, pol. p, Wolfenstein and polarisation parameters 0-57629  
 $^{208}\text{Pb}(p,p')$ , 135 MeV, normal parity excitations, microscopic description, NN interaction shape 0-57691

**proton radiative capture**

- radiative nucleon capture, pure resonance model, direct-semidirect model, pure semidirect model 0-78257  
 $\pi^-p \rightarrow n\gamma$ , test of pion range monitor, medical appls. 0-72317  
 $^{26}\text{Al}(p,\gamma)^{27}\text{Si}$ , reaction rate in explosive H burning 0-85929  
 $^7\text{Be}(p,\gamma)$ , low energy cross section from direct, capture potential model 0-102184  
 $^{12}\text{C}(p,\gamma)$ , pol. p,  $^{13}\text{N}$  giant dipole resonance population amplitude and phase, E1 reaction amps. 0-63145  
 $^{42}\text{Ca}(p,\gamma)^{43}\text{Sc}$ , reaction rates in stars 0-82183  
 $^{52}\text{Cr}(p,\gamma)$ ,  $^{53}\text{Mn}$  fragmented  $g_{9/2}$  isobaric analogue resonance,  $\gamma$ -spectra and excitation functions 0-68627  
 $\text{Cu}(p,\gamma)$ , 1.7-7.2 MeV,  $^{64}\text{Zn}$ , A=64, 66 levels and primary E1 transition strength functions 0-91149  
 $^{19}\text{F}(p,\gamma)$ , pol. and unpol., 3.5-10 MeV  $^{20}\text{Ne}$  giant E1 resonance intermediate struct. 0-78251  
 $^A\text{Fe}(p,\gamma)^A\text{Co}$ , A=54,56, giant dipole resonance splitting, direct-semidirect capture model anal. 0-106055  
 $^{56}\text{Fe}(p,\gamma)$ , 2-4 MeV,  $^{57}\text{Co}$  state alignment,  $\gamma$ -transitions and ang. distrib. 0-73797  
 $^2\text{H}(p,\gamma)^3\text{He}$ , 450, 550 MeV, differential cross sections, inverse reaction comparison 0-86904

**proton radiative capture continued**

- $^3\text{H}(p,\gamma)$ , 17-31 MeV,  $^4\text{He}$   $2^+$  resonance evidence at 40 MeV 0-86880  
 $\text{Li}(p,\gamma)$ , cross section and spectroscopic factors from direct capture pot. model 0-99171  
 $^7\text{Li}(p,\gamma)$ ,  $^8\text{Be}$   $1^+$  and  $1^-$  levels, expt. and shell model calcs. 0-63095  
 $^{23}\text{Mg}(p,\gamma)$ , 0.3-0.4 MeV,  $^{24}\text{Al}$  T=1 states, resonances,  $J^\pi$  and transitions 0-99131  
 $^{25}\text{Mg}(p,\gamma)^{26}\text{Al}$ , reaction rate in explosive H burning 0-85929  
 $^{26}\text{Mg}(p,\gamma)$ , 1.6-3.95 MeV,  $^{27}\text{Al}$  isobaric analogue resonances, spectroscopic factors and  $\gamma$ -rays 0-86873  
 $^{28}\text{Mg}(p,\gamma)$ , 80-355 keV,  $^{27}\text{Al}$  levels, resonances,  $J^\pi$ , branching and mixing ratios 0-99132  
 $\text{Mg}(p,\gamma)$ , 0.3-2.1 MeV,  $^A\text{Al}$ , A=25,26,27 levels, resonances,  $\gamma$ -ray branching ratios 0-86875  
 $\text{Mg}(p,\gamma)$ , 0.3-2.1 MeV, stellar H burning in explosive C burning 0-86875  
 $^{53}\text{Mn}(p,\gamma)$ ,  $^{56}\text{Fe}$  isobaric analogue resonance levels, branching ratios 0-68617  
 $^{64}\text{Ni}(p,\gamma)$ , 2-4 MeV,  $^{63}\text{Cu}$  state alignment,  $\gamma$ -transitions and ang. distrib. 0-73797  
 $\text{Ni}(p,\gamma)$ ,  $^{64}\text{Cu}$  A=29,63, Doppler shift attenuation factors, level lifetimes, resonances 0-57741  
 $^{23}\text{Si}(p,\gamma)$ , 0.73, 1.75 MeV,  $^{30}\text{P}$  T=1 state decay, lifetimes and branching ratios, analogue E2 transitions 0-68598  
 $^{38}\text{Si}(p,\gamma)$ , pol.p, 6.4-15.0 MeV, cross section and anal. power ang. distrib. 0-99168  
 $^{49}\text{Ti}(p,\gamma)$ , 0.74-3.25 MeV, cross section and thermonuclear reaction rates, nucleosynthesis, IAR effects 0-102187  
 $^{51}\text{V}(p,X)$ , X= $\gamma$  or n, 0.93-4.47 MeV, cross sections, competition effects, Hauser-Feshbach calcs. 0-91184  
 $^{62}\text{Zn}(p,\gamma)$ , 2-4 MeV  $^{69}\text{Ga}$  state alignment,  $\gamma$ -transitions and ang. distrib. 0-73797

**proton scattering** *see electron-proton scattering; kaon-proton scattering; lepton-nucleon scattering; photon-proton scattering; pion-proton scattering; proton-deuteron scattering; proton-nucleus scattering; proton-proton scattering*

**proton spectra**

- magnetosphere inner radiation belt proton spectra from Kosmos 721 satellite 0-72699  
 inner radiation belt protons, energy and pitch angle distrib. analytic study 0-67471  
 $\text{Al}(\text{Ne,X})$ , proton inclusive spectra, direct plus thermal model 0-57799  
 $^{27}\text{Al}(d,pX)$  80 MeV, inclusive proton spectra, d break-up, DWBA anal. 0-91190  
 $^{197}\text{Au}(d,pX)$ , 80 MeV, inclusive proton spectra, d break-up, DWBA anal. 0-91190  
 $\text{Cl}(\text{Ar,X})$ , proton inclusive spectra, direct plus thermal model 0-57799  
 $\text{K}(\text{Ar,X})$ , proton inclusive spectra, direct plus thermal model 0-57799  
 $^{93}\text{Nb}(d,pX)$ , 80 MeV, inclusive proton spectra, d break-up, DWBA anal. 0-91190  
 $\text{U}(\text{Ne,X})$ , proton inclusive spectra, direct plus thermal model 0-57799

**proton-surface impact** *see ion-surface impact*

**protonium** *see protons*

**protonosphere** *see upper atmosphere*

**protons**

- see also cosmic ray protons; delayed protons*  
 asymptotically free SU(5) grand unification, proton stability, renormalisation group 0-82929  
 decay, baryon number nonconservation, expt. status 0-57594  
 decay, unified theory of elementary-particle forces 0-105827  
 disintegration, concepts of leptons and quarks, unified field theory (*French*) 0-91038  
 Earth bow shock energetic protons meas. in upstream solar wind 0-90308  
 electric polarisability, from photoabsorption cross-section 0-57597  
 gluon distribution from elastic pp scatt. 0-82939  
 inner structure, observation in collisions producing jet of debris 0-57569  
 interplanetary medium, proton number density and flux energy rel. to shock waves thickness 0-90314  
 intrinsic charm from non-negligible uuddc Fock component 0-86691  
 Jupiter mid-magnetosphere, equatorial protons instability 0-67642  
 O(10), SU(4) colour subgroup, fractional charged gauge boson, proton half-life 0-73644  
 parton gas model, degenerate, quark-lepton identification 0-68416  
 inner radiation belt protons, energy and pitch angle distrib. analytic study 0-67471  
 radiation therapy, high-energy proton beam, physical meas. using tissue substitutes 0-81720  
 solar wind, obs. of backstreaming protons near Earth bow shock 0-90309  
 structure function, higher order asymptotic freedom corrections, from deep inelastic scatt. 0-105905  
 structure function nonsinglet moments from deep inelastic lepton scatt., QCD 0-62980  
 SU(5) and SO(10) grand unification, flavour mixing and proton instability (*Russian*) 0-68413  
 SU(5) grand unification, p lifetime and branching ratio, bag model wavefunctions 0-78004  
 SU(5) grand unification, superheavy fermions and proton lifetime (*Russian*) 0-91036  
 SU(5) grand unified theory, proton lifetime estimate accuracy 0-101967  
 subcomponent models of quarks and leptons in SU(3) subcolour, proton decay 0-78035  
 transport across charged membrane and pH oscils. 0-61516  
 universe ultimate fate, effect of finite proton lifetime 0-82560  
 pp, ISR energies, p fragmentation,  $D^+$  prod. from  $\Lambda_c^*$  and  $\Lambda_b$  decay 0-102080

**proximity effect**

- DC Josephson effect, proximity systems with magnetic impurities 0-100554  
 DC Josephson effect for superconducting proximity Kondo alloys 0-88690  
 elastic scattering, appl. of Anderson theorem 0-84568  
 energy gap anisotropy, normal layer proximity effect 0-84558  
 inhomogeneous superconductivity, Ginzburg-Landau theory 0-88672  
 N-S boundary resistivity, tunnelling contact resistance (*Russian*) 0-93048  
 parametrically coupled Josephson bridges, resistive state, proximity effect (*Russian*) 0-100550  
 S-wave and P-wave superconductors, absence of proximity effect 0-93033  
 superconductors, magnetic impurity low temp. behaviour, transition temp., specific heat, free energy 0-88691  
 weak links, steady-state and RF props. 0-84563  
 Au/In proximity effect bridges, square arrays, transition temps. 0-84557  
 In film, Josephson arrays, proximity effect junctions 0-84553



**proximity effect continued**

- Nb, proximity electron tunnelling spectroscopy 0-107964  
 Nb-Al, tunnelling expts. on normal metal backed by Al 0-65751  
 Nb-NbO<sub>2</sub>-Pb tunnel junction, temp. depend. of effective Nb energy gap 0-80454  
 Nb-Pb supercond. tunnel junction proximity effect, theory 0-65752  
 Nb-Pb tunnel junction, crit. Josephson current, proximity effect model 0-93047  
 Pb-Cu(Ag) double layers, intermetallic boundary effects, tunnelling 0-88692

**pseudobinary semiconductors** *see* II-VI semiconductors; III-V semiconductors; III-VI semiconductors; IV-VI semiconductors; semiconductor materials

**pseudopotential methods**

- adparticle on substrate, pseudopot. near second-order phase transition 0-80065  
 alkali halides, elastic constants, temp. depend., pseudopot. calc. 0-65120  
 alkali metals, bulk modulus and eqns. of state under press. 0-88293  
 alkali metals, effective ion-ion potential, compressibility and force consts. 0-70158  
 alkali metals, Fermi surface topological changes due to uniaxial stresses 0-92810  
 alkali metals, Grüneisen parameters, influence of press. on lattice anharmonicity and temp. depend. 0-79905  
 alkali metals, liq., Fermi energy, density of states, electronic props., exchange and correl. effects 0-96774  
 alkali metals, partial pressure contributions to equation of state 0-107401  
 alkali metals, phonon dispersion binding energy, compressibility, elastic consts. electron screening and Ashcroft pot. calcs. 0-65174  
 alloys, nearly free electron like, indeterminacy of a priori pseudopot., effects on form factors 0-103608  
 cohesive energy calcs., frozen core approx. and pseudopotential theory validity 0-64949  
 covalent semiconductors, electronic interface states in intrinsic stacking-faults 0-75522  
 electrical conductivity of high temp. imperfect gas (Russian) 0-100072  
 electronic structure and solid props., rel. to chemical bonding, book 0-86044  
 form factors of free ion pseudopot., calc. 0-59849  
 liquid metal, electronic density of states, pseudopotential calcs. 0-70578  
 liquid metals of groups IIB, IIIB, and IV, thermoelectric power, pseudopotential calc. 0-59959  
 metal, electron-impurity scattering, lattice distortion effects, phase shifts, calc. 0-96860  
 metal, work function, pseudopot. calc. 0-96970  
 metals, compressibility local pseudopot. approach 0-65129  
 metals, simple, elastic moduli, chem. trends, pseudopot. method 0-107355  
 metals, simple, static props., Thomas-Fermi-pseudopotential approach 0-75514  
 nontransition metals, electron density, bulk and surface props. relation 0-103609  
 one-dimensional periodic system, energy spectrum of defects, pseudopot. approach (Russian) 0-59909  
 positronium, formation in positron+alkali metal atom collisions, first Born approx. 0-83525  
 positronium formation in positron+alkali metal atom collisions, pseudopot. calcs. 0-83524  
 relativistic norm-conserving pseudopotential 0-70584  
 relativistic pseudopotential theories and corrections to Hartree-Fock method 0-63523  
 self-consistent atomic pseudopotential, appl. to band struct. determ. 0-59846  
 semiconductors, optical props. above band edge, book contrib. 0-84425  
 semilocal technique, testing of arbitrariness and limits 0-91446  
 simple metals, model pseudopot. appl. to various props. 0-59845  
 spin-dependent correlated atomic pseudopotentials 0-107686  
 X $\alpha$  method with pseudopotentials 0-83282  
 Ag (110), electroreflectance, surface state contrib. 0-80755  
 Ag, mag. susceptibility, Animalu model pot. calc. 0-75711  
 Al, dynamic susceptibility, model pot. theory 0-75710  
 Al, energy and elastic constants 0-59435  
 Al, K X-ray absorption, K-emission spectrum, band struct. using APW method 0-97380  
 Al, liquid, dynamical struct. factor calc. 0-64880  
 AlCl<sub>3</sub>, pseudopot. calcs. 0-91446  
 AlF<sub>3</sub>, pseudopot. calcs. 0-91446  
 AlH<sub>3</sub>, pseudopot. calcs. 0-91446  
 Al, Mg<sub>1-x</sub> liquid alloys, vols. and entropies of mixing, calc. 0-75363  
 Au (110), electroreflectance, surface state contrib. 0-80755  
 Au, mag. susceptibility, Animalu model pot. calc. 0-75711  
 Cd<sub>3</sub>As<sub>2</sub>, energy band structure calc. 0-75504  
 Cd<sub>3</sub>(As<sub>2</sub>P<sub>1-x</sub>)<sub>2</sub>, 0 $\leq$ x $\leq$ 1.0, band struct. calc. near Brillouin zone centre 0-107703  
 CdGa<sub>2</sub>(S<sub>1-x</sub>Se<sub>x</sub>)<sub>4</sub> solid solns., band struct. behaviour w.r.t. comp. (French) 0-107699  
 CdGa<sub>2</sub>S<sub>4</sub>(Se<sub>2</sub>)<sub>4</sub>, band struct., pseudopot. method 0-92816  
 Cd<sub>1-x</sub>Hg<sub>x</sub>Ga<sub>2</sub>S<sub>4</sub> solid solns., band struct. behaviour w.r.t. comp. (French) 0-107699  
 Cd<sub>1-x</sub>Mg<sub>x</sub>, energy spectrum pseudopotential calcs., mag. props., impurity scatt. (Russian) 0-65430  
 Cl<sub>2</sub>, pseudopot. calcs. 0-91446  
 Cs halides, F-centre energy levels, ion-size effects, calc. 0-96519  
 Cs<sub>2</sub><sup>2+</sup>, interaction potential determ., comparison between all-electron frozen core and pseudo-potential results 0-69054  
 Cu (110), electroreflectance, surface state contrib. 0-80755  
 Cu, dynamic susceptibility, model pot. theory 0-75710  
 Cu, mag. susceptibility, Animalu model pot. calc. 0-75711  
 Cu-Al, short range order and static distortion contribution to residual elec. resistivity (Russian) 0-70672  
 F<sub>2</sub>, pseudopot. calcs. 0-91446  
 (Ga, Al, As) heterostructures and compounds, electronic props., empirical pseudopot. calc. 0-80366  
 GaAs-AlAs mixed crystals, valence charge distrib. and elec. field gradients 0-80239  
 Ge-Si, phase diagrams near melting point, Helmholtz free energy, heat of solution 0-70379  
 HCl, pseudopot. calcs. 0-91446  
 HF, pseudopot. calcs. 0-91446  
<sup>4</sup>He, superfluid, excitation spectrum, RPA calc. involving simple pseudopot. 0-92738  
 In, lattice dynamics, pseudopot. computation (Russian) 0-92617

**pseudopotential methods continued**

- In<sub>0.69</sub>Tl<sub>0.31</sub>, supercond. transition temp., specific heat, pseudopotential form factor 0-97026  
 K, liquid, interionic interaction theory, pseudopotential calcs. (Russian) 0-79677  
 K+He, <sup>4</sup>P state j<sub>1</sub>m<sub>1</sub>-j<sub>2</sub>m<sub>2</sub> Zeeman transition, total cross section energy depend. 0-83475  
 KCl:Na, F<sub>2</sub> centre energy levels 0-107738  
 Li, energy and elastic constants 0-59435  
 Li, phonon limited resistivity struct. depend., Umklapp scatt., elastic consts. 0-88532  
 Na, equilibrium struct. and phys. props., pseudopot. method 0-96778  
 Na liquid, interionic interaction theory, pseudopotential calcs. (Russian) 0-79675  
 Na, phonon limited resistivity struct. depend., Umklapp scatt., elastic consts. 0-88532  
 NaCl-type crystals, ionic polarisabilities, pseudopot. calc. 0-88913  
 Ni complex, nickel-bis-dithiolene, pseudopot. MCSCF and limited CI calcs. 0-83292  
 Pb, liq., elec. resist. calcs., pseudopot. depend. 0-96840  
 Sb, electronic struct., depend. on hydrostatic pressure 0-80158  
 Se, amorphous, electronic struct. and optical props., pseudopot. calc. 0-65428  
 Se, bonding coordination defects 0-59927  
 Se, charge density, self-consistent OPW and pseudopot. calcs. 0-92813  
 Se, electronic struct. of cryst. phases and hydrostatic press. effects 0-59865  
 Se, glassy, structural excitation energies of defects, pseudopot. approach 0-107061  
 Si, (001) (2 $\times$ 1) reconstructed surface, dimer model self consistent calcs. 0-88613  
 Si (111)-1 $\times$ 1, electronic struct. of surface, model pseudopot. calc. 0-65651  
 Si, ground state props. in density-functional pseudopot. approach 0-92803  
 Si, local pseudopotential, Gaussian band charge model 0-88477  
 Si, total energy calcs. by r-space method, Wannier functions 0-88503  
 Sn, white, band masses and deformation pots., OPW pseudopotential model 0-100430  
<sup>119</sup>Sn temp. depend. isomer shift, pseudopot. approach 0-84675  
 Te, amorphous, electronic struct. and optical props., pseudopot. calc. 0-65428  
 Te, electronic struct. of cryst. phases and hydrostatic press. effects 0-59865  
 Te<sub>2</sub><sup>2+</sup>, pseudopot. SCF-MO calcs., spectrum assignments 0-83269  
 V, dynamic susceptibility, model pot. theory 0-75710  
 ZnGa<sub>2</sub>S<sub>4</sub>, band struct., pseudopot. method 0-92816
- pseudoternary semiconductors** *see* ternary semiconductors
- psi mesons**  
 decays, hadronic, asymptotic freedom, one-photon or three-gluon exchange 0-62971  
 hadron-hadron inclusive interactions, charmed particle production,  $\eta_c$ ,  $\psi$  and other  $c\bar{c}$  bound states 0-63036  
 heavy quarkonium states, hadronic transitions, QCD anomalies for T<sup>+</sup> and  $\psi'$  0-105888  
 M<sub>2</sub>-M<sub>0(e)</sub> and M<sub>T</sub>-M<sub>0(b)</sub> lower bounds, concave and convex pots. 0-91057  
 production, gluon-gluon fusion model, gluon distrib. x-depend. 0-62922  
 QCD low energy tests, gluon non-zero effective mass,  $\psi$  decays 0-91054  
 quarkonium spectroscopy in a potential model with vacuum-polarization corrections 0-78038  
 radiative decay width from glueball model 0-62941  
 $\chi$ - $\psi\gamma$ , charmonium EI radiative transitions and quark mag. moments 0-86721  
 e<sup>+</sup>e<sup>-</sup>  $\rightarrow\psi(3770)$ , cross section,  $\psi$  mass, total width and e<sup>+</sup>e<sup>-</sup> partial width 0-73696  
 $\mu$ N, 209 GeV,  $\psi$  diffractive prod. cross section,  $\psi\rightarrow\mu^+\mu^-$  decays 0-102054  
 $\mu$ N- $\nu\psi$ X, neutral current  $\psi$  prod., Z<sup>0</sup>-gluon fusion model 0-78015  
 pN in Fe, 400 GeV/c,  $\psi(3100)$  prod. 0-57650  
 pp, 53, 63 GeV, T and  $\psi$  prod., dielectron decay angles 0-68496  
 pp  $\rightarrow\mu^+\mu^-$  X, 62 GeV,  $\psi$  and  $\gamma$  cross sections, scaling function 0-105932  
 $\psi\rightarrow 3\gamma$ , heavy narrow state search,  $\eta'$  and  $\eta_c$  branching ratios 0-57600  
 $\psi(4.03)\rightarrow DD(D^*D, DD^*, D^*D^*)$ , vector state strong decay 0-78057  
 $\psi(4.03)$ , isospin and G-parity, model independent prediction 0-86689  
 $\psi$  associated with gluon, hadronic prod. 0-105846  
 $\psi\rightarrow DD$  radial excitations of charmonium 0-102046  
 $\psi\rightarrow\eta\gamma\psi$ , charmonium, hyperfine interaction, nonperturbative treatment 0-62944  
 $\psi\rightarrow\eta'\gamma$ , QCD, width, exclusive OZI violating radiative decay 0-68458  
 $\psi\rightarrow\eta\gamma$ , conflict with single parameter scheme for radiative decays of vector mesons 0-86720  
 $\psi\rightarrow\mu^+\mu^-$ , search for extra  $\mu$  in ( $\pi^-$ ,  $\psi$  CC), 225 GeV/c 0-82967  
 $\psi'$ ,  $\psi$  decay branching ratios, isospin and flavour symmetry breaking 0-95264  
 $\psi'$  and  $\psi$  decay ratios, composite particle matrix elements 0-95266  
 $\psi\rightarrow\chi\gamma$ , charmonium EI radiative transitions and quark mag. moments 0-86721  
 $\psi\rightarrow\pi^+\psi$ , isospin isolating decay, branching ratio 0-57601  
 $\psi\rightarrow\psi\eta(\pi^0)$ , decay branching ratios 0-105889  
 $\psi\rightarrow\psi\pi\pi$ , current algebra techniques, pole plus remainder model, chiral symmetry breaking and QCD 0-62972  
 $\psi''(3770)$ , mass width from quark model 0-73723  
 $\psi''(3.772)$ , ground state admixture in potential model 0-102033  
 Cu( $\pi^-$ ,  $\psi$  (3700)), 50 GeV, formation cross-sections (Russian) 0-106082
- PSK** *see* phase shift keying
- psychological optics** *see* vision
- psychology**  
 acoustical research into life sciences, review 0-97925  
 astigmatism and orientation preference in human infants 0-61542  
 attentional processes study, contrib. of EEG spectral band anal. (French) 0-61721  
 auditory sensations evoked by pulsed microwave fields, some peculiarities 0-61636  
 behaviour patterns in cod released by elec. stimulation of olfactory tract bundles 0-97951  
 behavioural sensitivity of a domestic bird to 60-Hz AC and to DC mag. fields 0-61622  
 classical conditioning of microwave-induced hyperthermia, rat obs. 0-61629

# psychology continued

- conditioning, auditory stimuli and the cutaneous eyeblink reflex, human obs. 0-67090
- decision making, split-second, electrophysiological signs, auditory stimuli 0-89771
- EEG patterns during cognitive tasks, controlled tasks anal. 0-67059
- EEG patterns during cognitive tasks, methodology and complex behaviours anal. 0-61531
- eye and hand motor systems, optimal response in pointing at a visual target 0-61567
- hearing, combination tones and relation with suppression, psychophysical meas. 0-108910
- hearing, contralateral cueing effects in backward masking 0-61587
- hearing, difference tone perception at low freqs. 0-67087
- hearing, forward masking, mechanism and freq. distrib. of two-tone suppression 0-108909
- hearing, frequency discrimination for masked tones 0-76754
- hearing, precedence effect, possible role in avoidance of interaural ambiguities 0-61588
- hearing, psychophysical 2-tone suppression, stimulus component level effects 0-61584
- hypnotic suggestion, meas. of effects in elec. induced muscle contract (*Slovenian*) 0-81571
- industrial noise onset effects on physiological and psychological functions 0-91959
- intellectual activity, classification of normal and anomalous forms, quantised-wave theory of coherent brain appl. (*Russian*) 0-76722
- intellectual activity, psychoheuristic relationship of psychotom strcuts. and giftedness strcuts. introduction, quantised wave theory of coherent brain appl. (*Russian*) 0-76723
- ionising radiation induced behavioural and physiological changes in rats, hormonal radioprotection 0-98026
- magnetophosphenes, quantitative determ. of thresholds 0-61620
- manic depression, abnormal red cell membrane Li transport 0-61525
- mental activity evoking pupil dilation, link with intelligence 0-61532
- microwave chronic exposure, physiological and behavioural effects, rat obs. 0-67152
- microwave exposed rats and mice, behavioural obs. 0-61631
- microwave irradiation and ambient temp. interaction, rat behavioural alterations 0-67153
- microwave radiation and dextroamphetamine, combined effects on rat behaviour, expt. obs. 0-61635
- moment of inertia, human sensitivity, psychophysical study 0-72180
- neocognitron, self-organising neural network model, pattern recognition mechanism unaffected by shift in position 0-76745
- operant behaviour and rectal temp. during 2.45-GHz microwave irradi., squirrel monkey obs. 0-61630
- operant behaviour induced by microwave radiation, effect of psychoactive drugs 0-61632
- physics teaching and personality development assessment (*German*) 0-67966
- psychoacoustic experiments using freq. and amplitude modulated stimuli 0-94236
- psychophysical 2-tone suppression as function of input level for  $f_2/f_1 > 1.0$  0-76756
- psychophysical tuning curves for combination tones  $2f_1-f_2$  and  $f_2-f_1$  0-76755
- quantum interference effects in psychology, Schrodinger's cat, review 0-73158
- radiation exposure, perception of harm 0-85450
- reaction time, N1-P2 corrls. at the single-trial level 0-85389
- reading without a fovea 0-76748
- RF radiation exposed chicks, behavioural obs. 0-61633
- sensorineural hearing loss, freq. selectivity and speech discrimination 0-61593
- spatial frequency tuning studies, psychometric curves description by probability summation 0-61576
- speech reception threshold, reliability in the determ., psychometric function 0-61657
- vision, apparent contrast matching, narrow-band spatial mechanism 0-61571
- vision, associative learning model, voltage-dependent  $Ca^{2+}$  and  $K^+$  conductances 0-72166
- vision, Bezold-Brucke hue shifts, short-flash obs. 0-72170
- vision, colour-contingent movement aftereffect, interocular transfer obs. 0-61578
- vision, cone spectral mechanisms, ERG and psychophysical obs. 0-61565
- vision, grating induction, a new type of aftereffect 0-72175
- vision, gratings moving in opposite directions, summation and discrimination 0-72169
- vision, human recognition system with thinking, model 0-76744
- vision, saturation enhancement in coloured Hermann grids varying only in chroma 0-72168
- vision, simultaneous and successive contrast obs. 0-76742
- visual psychometric discrimination of spatial freqs. in different orientations 0-81590

# PTC thermistors see thermistors

# publishing

- astronomy, cost effectiveness in terms of publications and citations of Kitt Peak National Observatory telescopes 0-90334
- Indian scientific and technical Journals critical evaluation 0-94906

# pulp industry see paper industry

# pulsars

- see also neutron stars; radiofrequency cosmic radiation
- atom motion in very strong mag. fields, mass anisotropy effect (*Russian*) 0-67557
- classification method from period change and radio luminosity (*Chinese*) 0-85963
- coherent radio emission, source 0-82403
- composition of outer crust, influence of mag. field 0-101610
- crust, infinitely magnetised H atom theory 0-77282
- decametric radio emission, similarity with Jovian emission (*Russian*) 0-77333
- dispersion data anal., scale height determ. 0-85965
- distribution, birthrate and flux density distrib. 0-98681
- emission mechanism, AC Josephson effect hypothesis 0-82404
- energy emission 0-82450
- evolution rel. to torques, magnetic moment and pair production 0-62169
- finite force face cold plasma atm. models, plasma differential rot. 0-77378

# pulsars continued

- formation, from evolution of mass-accreting white dwarfs 0-77281
- gamma-ray obs. of galactic small-scale structure 0-98743
- gamma-ray production mechanism 0-77433
- gravitational radiation, collapsed objects and exact solns., Einstein Centenary Summer School, Perth, Australia, 1979 January 0-105434
- hydromagnetic eqns. for infinitely long plasma cylinder, unstable soln., pulsar mag. fields 0-96352
- magnetosphere, plasma waves propag. along mag. field in strongly anisotropic relativistic plasma 0-67542
- magnetosphere, relativistic particle curvature radiation 0-77434
- magnetospheres, axisymmetric, method of soln. of self-consistent description 0-94825
- micropulses, drifting subpulses and nonradial oscills. 0-67766
- microstructure, radiowave propag. in turbulent shearing plasma 0-94822
- new discoveries, 102.5 MHz obs. of three objects (*Russian*) 0-67764
- NP 0532, Crab pulsar, Compton emission model using gamma-ray data 0-67902
- NP 0532, Crab pulsar, lunar occultation obs. at decametre wavelengths 0-62248
- NP 0532, Crab pulsar, magnetized cracks in crust rel. to matter flow, radio, X-ray and optical emissions 0-72990
- NP 0532, Crab pulsar, random walk timing noise anal. 0-77432
- NP 0532, Crab pulsar, relativistic material ejection rel. to Crab Nebula model 0-62230
- NP 0532, rotation parameters, temporal var. 0-62170
- nuclear neutrino pair photoprod. in strong mag. field, pulsar neutrino luminosity (*Russian*) 0-68648
- observational data 0-77435
- observational properties, rel. to use as cosmic laboratories for study of neutron stars and hadron matter 0-77442
- oscillation period, increase with time, gravit. mechanism 0-67765
- $P_3$  period, corrl. with mag. field and age 0-90461
- periods, positions and proper motions determ. from pulse arrival times, UHF, obs. 0-77431
- plasma coupling, boundary conditions 0-94823
- polarised radiation at 430 MHz, statistical summary 0-67760
- PSR 0031-07, drifting subpulses obs. and implications for pulsar models 0-67763
- PSR 0355+54, pulse shape change, 11 cm obs. 0-67761
- PSR 0531+21, Crab pulsar,  $\gamma$ -ray obs. with COS-B (*Danish*) 0-82544
- PSR 0611+22, short time scale integrated pulse shape vars. 0-105267
- PSR 0833-45, Vela pulsar,  $\gamma$ -ray obs. with COS-B (*Danish*) 0-82544
- PSR 0833-45, Vela pulsar, age determ. 0-77436
- PSR 0833-45, Vela pulsar, Compton emission model using gamma-ray data 0-67902
- PSR 0833-45, X- and gamma-ray emission from Vela SNR (*Russian*) 0-94861
- PSR 0833-45, Vela pulsar, pulsed soft X-ray flux, upper limits 0-105268
- PSR 1822-09, balloon-borne gamma-ray obs. 0-105269
- PSR 1913+16, binary pulsar, nature from observational data 0-77435
- PSR 1913+16, binary pulsar, relativistic observable effects 0-77438
- PSR 1913+16, binary system, test of relativistic effects (*Dutch*) 0-62172
- PSR 1913+16, optical candidate, astrometry and high-speed photometry 0-101609
- PSR 1913+16, X-ray and timing meas. correlations, grav. radiation, gas cloud friction 0-62171
- radiation, subpulse and micropulse emissions rel. to neutron star crusts torsional oscills. 0-90464
- radiation source form, mechanism, mag. annihilation (*Chinese*) 0-77440
- radio emission, effects of superfluidity in neutron star 0-77441
- radio emission, millisecond intensity var. 0-98682
- radio emission rapid variation, mechanism (*Russian*) 0-77437
- radio emission scintillation, decorrelation bandwidth rel. to dispersion measure 0-85964
- radio pulsar, model involving neutron star elec. field 0-109453
- rotation measures, determ. of galactic mag. field components 0-85966
- rotational behaviour rel. to superfluidity 0-98683
- rotational energy loss, slowing down index and time derivs. 0-67762
- scintillation, freq.-time struct., means for detecting interstellar electron density irregularities 0-101608
- in southern hemisphere, polarisation obs. at 1612 MHz 0-90462
- spectra, charact. feature interpretation 0-109451
- SS 433, massive black hole and pulsar models rel. to precessional motion origin of 164 $\mu$  period 0-62138
- superfluid phase transition for neutron star matter 0-101607
- surface structure, props. of condensed matter in huge mag. fields 0-82187
- Vela pulsar (PSR 0833-45), radiation model 0-94824
- H I absorpt., meas. in seven low-latit. pulsars 0-101606

# pulsatile flow

- see also peristaltic flow
- air flow over rearward facing step, flow separation meas. 0-69885
- arterial stenosis, math. model 0-72202
- blood, studies in model of human aortic arch 0-104633
- blood flow in artery, pulsatile flow 0-106845
- channels, constricted or dilated, pulsatile flow at high Reynolds number 0-74985
- horizontal gas-liquid stream, flow vel. meas. 0-96301
- MHD pulsating viscous flow superposed on steady laminar motion 0-92228
- placenta, human, detect. of pulsatile flow in situ by impedance meas. 0-104799
- pulsating turbulent pipe flow, velocity field and press. gradients 0-64641
- quantitative representation of nonrepetitive temporal behavior 0-92101
- resonant hydraulic circuit pulsatile water flow meas. using laser Doppler velocimeter 0-103091
- suture line stress in end-to-side anastomosis, math. assess. in pulsatile flow 0-97986
- viscoelastic tube, pulsatile flow, non-Newtonian effects (*French*) 0-59113
- Ar, supersonic pulsed flow from conical nozzle 0-103056

# pulse amplifiers

- DC couple linear pulse amplifier, fast, gain and phase response design 0-58088
- linear accelerator, pulse amplifier with digital gain control 0-68977
- photoconduction decays, fast, measurement, DC-10 MHz low noise amplifier system 0-57326



**pulse amplitude analysers** *see pulse height analysers*

**pulse amplitude modulation**

optical fibre transmission expts. at 34 Mb/s with HDB3 line code 0-64198

**pulse circuits**

*see also demodulators; digital circuits; modulators; pulse generators*  
oscilloscope low repetition trigger cct., for high speed pulse observation (Spanish) 0-62657

**pulse-code modulation**

*see also delta modulation*

digital speech interpolation system called adaptive DPCM with time assignment speech interpolation 0-99903  
encoding and decoding for optical memories 0-102658  
speech transmission, forward and backward prediction in adaptive differential PCM over nonideal channels 0-99902  
speech waveform coders, objective quality meas. equipment and method 0-91981  
CO<sub>2</sub> TEA Laser pulse, PCM with CdTe crystal Pockels modulator 0-102742

**pulse generators**

*see also multivibrators; square-wave generators; time bases*

bipolar square, for investigation of ferroelec. switching characts. 0-62687  
computer programmable digital pulse generator for Fourier NMR spectroscopy 0-98959  
digital signal generator for rapid scan differential pulse voltammetry 0-61182  
functional generator of controlling voltage of energy modulator for synchrotron injector 0-68975  
fusion reactor, TEXT, motor-generator power supply system 0-99292  
linear accelerator with S-band subharmonic prebuncher for picosecond single electron pulse (Japanese) 0-78460  
NMR appl. of pulse programmer 0-57347  
picosecond pulse generation scheme for injection lasers 0-87418  
Q-switched Nd:YAG oscillator for stable time-tunable operation in nanosec. regime 0-99759  
random tail pulse generator for simulation of nuclear radiation detector signals 0-74093  
triggered light pulse generator for recording fast processes 0-105727  
ultrashort current pulse generation and meas. using Josephson devices 0-90827  
X-ray, with thyristor based power supply, bell shape pulses generation 0-57446

**pulse height analysers**

biomedical rectilinear scanner, multichannel analyser interface 0-101254  
digital events analyser of low-cost construction 0-57267  
megachannel pulse height analyser for gamma-ray coincidence analysis 0-99430  
microprocessor multichannel analyzer laboratory project 0-101685  
microprocessor-controlled, transfer of blood pressures and neural activities for computer anal. 0-72356  
Mossbauer effect work, function generator using IC 0-68334  
multichannel analysers for X-ray spectroscopy (Hungarian) 0-95205  
MWPC, position sensitive, pulse shape from cathode RC Lines, zero-cross time meas. 0-58038  
radiation monitoring, multi-channel analyser, portable microprocessor controlled, accessories, data acquisition 0-63474  
time to pulse height converters, theoretical and experimental spectra comparison 0-102406  
Ge intrinsic detector and multichannel analyzer in 5.1 cm borehole probe 0-63451  
NaI(Tl) scintillation detectors, microprocessor-based multichannel analyzer 0-91378

**pulse modulation**

*see also demodulators; modulators; pulse amplitude modulation; pulse-code modulation*  
PbS mosaic array pulse-bias modulation 0-86414

**pulse motors** *see stepping motors*

**pulse oscillators** *see pulse generators*

**pulse transformers**

air core shielded spiral transformers, pulse forming transmission line charging appls. 0-63419  
automatic resistance thermometer bridge 0-98913

**pulse width modulation**

magnetic tape recording, time reference signal, IRIG and NASA code formats 0-57262  
optical fibre transmission expts. at 34 Mb/s with HDB3 line code 0-64198  
optics, band-limited function approx. realisation by low-pass filtering sequence of width-modulated pulses 0-95836

**pulverised coal** *see pulverised fuels*

**pulverised fuels**

*see also coal*

coal dust mass flow meas. methods (German) 0-92242  
CO concentration meas. in coal pulverising plant, IR gas analysers 0-89572

**pumped-storage power stations**

underground pumped hydroelectric storage plants, high-head turbomachinery, cost anal. 0-61432

**pumping** *see pumps*

**pumping (optical)** *see optical pumping*

**pumping plants**

horizontal-axis wind-turbine system for pumping duties in Third World agriculture, design 0-61259

**pumping stations** *see pumping plants*

**pumps**

*see also vacuum pumps*

biomedical pumps for pulsed insulin delivery, modification 0-101290  
incompressible fluid flow, one dimensional, calc. 0-79402  
jet, circulation of the two-phase mixture 0-82771  
microinjector, characts. calc. 0-77809  
peristaltic, lab. appls. 0-98905

**purification, crystal** *see crystal purification*

**Purkinje effect** *see vision*

**push pull microphones** *see microphones*

**p.w.m.** *see pulse width modulation*

**pyroelectric devices**

conference, Minneapolis, MN, USA (June 1979) 0-77535

**pyroelectric devices continued**

detector, background noise limited 0-82820

detector, direct meas. of IR laser radiation multiphoton mol. absorp. 0-102545

detector, performance evaluation method 0-82819

detector, thin film, temp. fluctuation noise 0-77861

detector for subnanosecond CO<sub>2</sub> laser pulse meas. 0-78884

detectors, sub-100 ps, 10.6  $\mu$ m damage threshold meas. 0-77859

dicalcium lead propionate, improper ferroelectric, dielectric props., IR radiation pyroelectric detection 0-80711

electret applications, book contrib. 0-80709

ferroelectric materials for dielectric power conversion, dielectric prop. anal. 0-80712

homodyne detection at 100 GHz with a pyroelectric detector 0-105650

imaging tube, sensitivity and geometrical resolution improvement (German) 0-105715

ionisation upconverter for IR detection 0-77860

IR detectors, effect of substrate on current responsivity 0-73454

IR signature classification system 0-86430

laser spatial profile meas. by pyroelectric vidicon camera 0-87425

polymer IR detector (Japanese) 0-105713

polyvinylidene fluoride film, pyroelec. camera tube for IR imaging, thermal diffusivity of Bi-Bi<sub>2</sub>O<sub>3</sub> black layer 0-57369

PVDF IR detector (Japanese) 0-105714

pyroelectric high power density heat engine, dielectric losses, polarisation 0-80689

pyroelectric vidicons, figures of merit, material parameters 0-77855

thermal imaging with pyroelectric vidicon camera 0-86288

three-dimensional thin pyroelectric IR detector simulation 0-57375

triglycine sulphate, deuterated, reticulated target for pyroelectric vidicon IR imaging 0-77858

Fe<sub>3</sub>B<sub>2</sub>O<sub>7</sub>, improper ferroelectric, dielectric props., IR radiation pyroelectric detection 0-80711

LiTaO<sub>3</sub> monolithic pyroelectric array, IR detectors 0-77857

LiTaO<sub>3</sub>/CCD hybrid focal plane, IR imaging and detection, crosstalk 0-77856

SrTiO<sub>3</sub> ceramic, electrocaloric effects for refrigeration at cryogenic temp. 0-77789

Tb<sub>2</sub>(MoO<sub>4</sub>)<sub>3</sub>, improper ferroelectric, dielectric props., IR radiation pyroelectric detection 0-80711

**pyroelectricity**

automated simultaneous meas. of electrical properties 0-57335

1,6-bis(2,4-dinitrophenoxy)-2,4-hexadiyne, obs. of apparent ferroelectric transition 0-66121

detector, background noise limited 0-82820

detector materials, thermal noise and dielec. response 0-75952

disilicate, piezoelectric glass ceramic, recrystallisation, pyroelectric response, permittivity 0-80703

electrets, piezo- and pyroelectric props. 0-80685

ferroelectric, tetragonal, irradiated by laser pulses, spatial temp. and bound-charge distrib. 0-103927

ferroelectric materials for dielectric power conversion, dielectric prop. anal. 0-80712

ferroelectrics, quantum transition suppression, pyroelectric, electrocaloric effects, specific heat 0-75984

literature guide, 1979 0-57019

literature guide, (1978-9) 0-62404

phthalocyanine metal free films, TSC, ferroelectric-semiconductor transition 0-66105

polyvinylidene fluoride, plasma poling, piezoelec. and pyroelec. responses 0-71296

polyvinylidene fluoride, poling process, kink propag. model 0-80679

polyvinylidene fluoride, pyroelectric transient response 0-75956

polyvinylidene fluoride, pyroelectricity, low temp. behaviour, due to origin 0-88932

polyvinylidene fluoride, thermodynamic model and appl. 0-75955

primary and secondary, review 0-93243

pyroelectric high power density heat engine, dielectric losses, polarisation 0-80689

TGS: nitroaniline, dielec. and pyroelec. props. 0-75916

TGS, ferroelectric hysteresis, dielectric and pyroelectric props. (Chinese) 0-88938

Al-SiO<sub>2</sub>-Si, pyroelectricity 0-100524

Ba(NO<sub>3</sub>)<sub>2</sub>·H<sub>2</sub>O, pyroelec., room temp. cryst. struct. 0-96491

(Ba,Sb)<sub>2</sub>TiO<sub>3</sub> 0-60514

BaTiO<sub>3</sub> film, struct. and dielec. props. 0-60514

Ba(Ti<sub>0.9</sub>Sn<sub>0.1</sub>)<sub>2</sub>O<sub>7</sub> film, struct. and dielec. props. 0-60514

CsCuCl<sub>3</sub>, phase transition, refr. index, electrooptic coeff., pyroelec. signal, and NQR meas. 0-70386

Cu-Cl boracite, pyroelec. coeff. meas. 0-75951

Fe-I boracite, pyroelec. coeff. meas. 0-75951

Fe<sub>3</sub>B<sub>2</sub>O<sub>7</sub>, boracite single cryst., nucleation control density growth 0-80955

FeI boracite single crystals, dielectric, pyroelectric props., vapour phase transport growth 0-80673

Fe<sub>2</sub>O<sub>3</sub>, lattice parameters, NMR freqs., and magnetoelec. pots. near 12K 0-71146

K(H<sub>1-x</sub>D<sub>x</sub>)<sub>2</sub>P<sub>4</sub>, polarised impurity cluster effects in light scatt. expts. 0-71431

Li<sub>2</sub>GeO<sub>3</sub> piezoelectric glass ceramic, recrystallisation, pyroelectric response, permittivity 0-80703

LiNH<sub>2</sub>SO<sub>4</sub> and LiND<sub>2</sub>SO<sub>4</sub>, dielec. pyroelec., and thermal props. 0-60509

LiNbO<sub>3</sub>:Fe, exoelectron emission in pyroelectric regime 0-76158

Li<sub>2</sub>SiO<sub>3</sub> piezoelectric glass ceramic, recrystallisation, pyroelectric response, permittivity 0-80703

Li<sub>2</sub>SiO<sub>3</sub>, pyroelectric glass-ceramics 0-75950

Li<sub>1-x</sub>Ta<sub>1.5x</sub>Ti<sub>0.5x</sub>O<sub>3</sub> (0 ≤ x ≤ 0.028), non-stoichiometric phase, crystallographic and dielec. props. 0-75212

NH<sub>4</sub>HSeO<sub>4</sub>, ferroelec. phase transition, pyroelec. props. 0-60513

NH<sub>4</sub>HSeO<sub>4</sub>, ferroelec., phase transitions, permittivity and pyroelectricity meas. 0-71350

Ni<sub>3</sub>B<sub>2</sub>O<sub>7</sub>, Br, boracite single cryst., nucleation control density growth 0-80955

NiBr boracite single crystals, dielectric, pyroelectric props., vapour phase transport growth 0-80673

PLZT pyroelectric detectors, delayed onset of piezoelec. oscills. 0-75953

PLZT, thin, elec. cond. and pyroelectric behaviour 0-75954

Pb<sub>3-x</sub>(Cs, Bi)<sub>x</sub>Ge<sub>2</sub>O<sub>11</sub> 0-75960

Pb<sub>3-x</sub>Nd<sub>x</sub>Ge<sub>2</sub>O<sub>11</sub>, ferroelec. props. 0-75960

**pyroelectricity continued**

- Pb(Zn<sub>1/3</sub>Nb<sub>2/3</sub>)O<sub>3</sub> single cryst., pyroelec. props., meas. under laser beam illum. 0-66117  
 Pb(Zr,Ri)O<sub>3</sub>/Ni-silicon rubber flexible composite pyroelectric, dielectric props. 0-80704  
 Pb(Zr,Ti)O<sub>3</sub>, PCD ceramic, pyroelectric props. 0-100635  
 SbSI, ferroelectric, dark current and spontaneous polarisation, ferro-piezoelectric transitions obs. 0-60521  
 SrTiO<sub>3</sub> ceramic, electrocaloric effects for refrigeration at cryogenic temp. 0-77789

**pyrolysis**

- acenaphthylene pyrolysis, carbonaceous mesophase and disc-like liquid crystals 0-79687  
 ammoniates, appl. to solar energy storage 0-76656  
 benzene, liq., laser pulsation kinetics, optical damage effects 0-58614  
 cellulose char, O<sub>2</sub> chemisorpt. kinetics 0-96730  
 complex systems, pyrolysis and combustion charact., Fourier transform IR spectroscopy 0-86462  
 diamond powder, consolidation by thermal decomposition of methane and benzene 0-66448  
 o-dianaphthoquinones, thermal decomposition of light sensitive materials (Russian) 0-73504  
 dolomite, powders sintering, decarbonisation cycle effect 0-104102  
 Earth mantle elements compounds and modifications, high press. and temp. thermodynamics 0-81874  
 ethylenimine, pyrolysis product, microwave spectra, rot. distortion and electric quadrupole const. and rot. barriers determ. 0-78608  
 Kapton, pyrolysed, cond. polymer, transport and mag. props. 0-96887  
 magnesite, powders sintering, decarbonisation cycle effect 0-104102  
 methanol, adsorption and decomp. on Ni (100) 0-66876  
 mica, natural, high  $\gamma$ - and electron-irrad. doses effect on annealing behaviour, thermal decomp. resist. 0-60897  
 perylenetetracarboxylic dianhydride pyrolysis for synthesis of C films with high conductivity 0-80983  
 petroleum feedstocks and cokes, graphitisability 0-93580  
 polybutadienes, radiation chemically cross-linked, charact. by pyrolysis gas chromatography (German) 0-81348  
 polychlorinated biphenyls waste disposal by pyrolysis, plasma torch appl. 0-76487  
 polydiacylthiosemicarbazides, synthesis and thermal cyclodehydration (Japanese) 0-108388  
 polymers, high-temp. pyrolysis, heat transfer processes at gas/solid surface (Russian) 0-61152  
 polyquinazolones containing pendant imide groups, prep. and props. (Japanese) 0-104111  
 radioactive waste processing, volume reduction of organic alpha waste by pyrohydrolysis 0-95366  
 very low pressure pyrolysis, gas-gas and gas-wall average energy transfer 0-93739  
 wood energy in W. Virginia 0-72006  
 wood sawdust, flash pyrolysis, cyclone, solar gas-solid chemical reactor (French) 0-61296  
 wood wastes, gasification, using flash pyrolysis and concentrated solar energy (French) 0-61226  
 Al, coating prod. by thermal decomp. of Al alkyls 0-104076  
 Al<sub>2</sub>O<sub>3</sub>-NH<sub>4</sub><sup>+</sup>, single cryst. characts. and AC cond. obs. 0-107514  
 3.5Al<sub>2</sub>O<sub>3</sub>-2SiO<sub>2</sub>, mullite, decomposition by SiO<sub>2</sub> volatilisation 0-61082  
 CaO-6Al<sub>2</sub>O<sub>3</sub>, thermodynamic stability, reaction with Ti, Cr and Zr oxides 0-92687  
 CuSO<sub>4</sub>·5H<sub>2</sub>O, dehydration into trihydrate obs. using monocryst. platelets, product domains shape 0-71905  
 $\delta$ -FeO(OH), study of thermal decomp. by X-ray diffr., electron diffr. and TEM 0-66790  
 GaAlAs-GaAs lasers, channelled substrate, prepared by combination of organometallic pyrolysis and LPE 0-99745  
 Ga<sub>1-x</sub>In<sub>x</sub>As epitaxial layer growth by organometallic pyrolysis, homojunction LED prep. 0-76194  
 H<sub>2</sub>O direct thermal decomposition utilising solar energy for H<sub>2</sub> prod., thermodynamics, review 0-61450  
 H<sub>2</sub>O pyrolysis, solar-H<sub>2</sub> energy systems, theory 0-61448  
 H<sub>2</sub>O pyrolysis using Fe-Cl thermochem. cycle for H<sub>2</sub> prod., chem. engineering anal. 0-97811  
 KYbHP<sub>2</sub>O<sub>7</sub>, thermal decomp., thermogravimetric and X-ray obs. 0-101013  
 La<sub>2</sub>S<sub>3</sub>, unsaturated and saturated vapour press., 673-1173K, thermal dissociation pattern 0-104457  
 MgCa(CO<sub>3</sub>)<sub>2</sub>, dolomite, partial thermal decomp. into MgO and CaCO<sub>3</sub>, product cryst. growth 0-108706  
 MoS<sub>3</sub>, prep. and mag. props. (French) 0-93072  
 Ni-Zn-Co ferrites, synthesis from solid solns. of schoenite-type salts 0-93511  
 Si<sub>3</sub>N<sub>4</sub>O, thermal decomp. 0-81311  
 SiO<sub>2</sub>, appl. to solar energy storage 0-76656  
 TeO<sub>2</sub>/Cl<sub>2</sub> thermal decomposition, matrix isolation IR and mass spectra 0-81306  
 ZnCl<sub>2</sub>(NCR)<sub>2</sub>, R=CH<sub>3</sub> or C<sub>2</sub>H<sub>5</sub>, thermal decomp., thermogravimetric and differential thermal anal. (Chinese) 0-81291

**pyromagnetic effects** *see magnetocaloric effects***pyrometers**

- see also temperature measurement*  
 band radiation pyrometry for error reduction in transmission coeff. calc. of IR radiation energy depend. on atmospheric props. (German) 0-105649  
 bench for metrological certification and testing of radiant-flux sensors (RFS) 0-98977  
 blackbody for energy calibration of infrared equipment 0-86377  
 chopping pyrometer for remote meas. below 200°C (German) 0-86313  
 contactless temperature meas., IR techniques and detectors (German) 0-86314  
 fast-response pyrometer, calibration 0-90852  
 industrial IR detector markets and device limitations 0-86432  
 industrial IR instrumentation sources and optical components 0-87453  
 IR, performance parameters and applications (German) 0-86315  
 logarithmic photoelectric receiver for spectral ratio pyrometers (Russian) 0-57302  
 modular form, for white- and band-limited radiation (Russian) 0-90853  
 optical, accuracy improvement using photography 0-62673  
 photoelectric pyrometry, radiance temp. direct calc. 0-73367  
 PPT and PChD pyrometers (Russian) 0-68203  
 radiation pyrometer, for molten cast Fe, design and field test (Japanese) 0-98917

**pyrometers continued**

- spectral ratio pyrometers of Spektropir 7 and 8 types (Russian) 0-90854  
 standard temperature lamps, with W ribbon filaments 0-95102  
 temp. meas. of bodies heated in solar furnaces 0-86312

**Q** *see Q-factor***Q-factor**

- acoustic resonance, definition and errors arising 0-69572  
 charged particle recoils rel. to neutron energy 0-63397  
 Earth interior, Q-factor freq. depend. rel. to seismic pulse propag. 0-72438  
 piezoceramic aperiodic transducer, mech. load study 0-87700  
 quartz, IR radiation extinction coeff. rel. to mechanical Q 0-100653  
 quartz crystals with TTC-cut (Danish) 0-60504

**Q-factor measurement**

- microwave cavity, analytic method using reflection coeff. vs. freq. 0-98937  
 neutron measurements of Oak Ridge National Labs. Dosimetry Appls. Research Facility 0-83237

**Q power factor** *see Q-factor***Q-switching***see also lasers*

- dye DFB laser, N<sub>2</sub> laser pumped, self Q-switched, tunable picosecond pulse generation 0-69432  
 dye laser, ultrashort pulse generation, self Q-switching mechanism 0-58612  
 electrooptic polarization modulated injection laser 0-58591  
 fluoromethane TEM<sub>00</sub> far IR laser with integrated pump laser 0-58578  
 introductory concepts and results, Q-switching and mode-locking, book contrib. 0-106504  
 laser microspectral analysis, forensic appl. 0-81385  
 laser resonator fourth harmonic generation cascade process (Russian) 0-99797  
 Nd:glass multichannel laser with plasma shutter 0-64088  
 POPOP solution dye lasers, multilayer reflectors 0-83606  
 ruby laser with electrooptical shutter, emission spectrum narrowing and single freq. giant pulse lasing 0-78877  
 ruby laser with high-frequency control of lasing conditions 0-74363  
 ruby pulsed laser real-time holographic interferometry 0-74319  
 solid laser characts. control, using optical delay lines, free-generation, Q-switching and mode-locking regimes 0-99758  
 stimulated Brillouin scatt. mechanism of laser resonator Q-switching 0-106552  
 TOPOT vapour dye lasers with multilayer reflectors 0-83606  
 CO<sub>2</sub> laser, mode locking obs. by intracavity plasma injection 0-83624  
 CO<sub>2</sub> laser modulation, plasma injection into cavity 0-83626  
 CO<sub>2</sub> lasers, IR saturable absorpt. in benzene, chlorobenzene and bromobenzene 0-69465  
 CO<sub>2</sub> Q-switched laser pump source for CH<sub>3</sub>OH/D, CHOOH and CH<sub>3</sub>F lasers 0-69383  
 CO<sub>2</sub> rotating-mirror Q-switched TEA laser, mode sweeping effects 0-99769  
 CoCl<sub>2</sub>·6H<sub>2</sub>O solution in ethanol, thin absorbing film, nonlinear optical props., Q-switch appl. 0-91836  
 HF laser with flow-through chem. active medium, pulsed-periodic regime realisation 0-106513  
 Ho:LiYF<sub>4</sub> laser, TEM<sub>00</sub> mode and Q-switched operation 0-74395  
 I photodissociation laser, characts. of new dye comps. for passive switches 0-91826  
 Nd:glass, subnanosecond pulse oscillator, investigation by high-speed oscillography 0-74411  
 Nd:glass laser with US Q-switch 0-64034  
 Nd:YAG laser, Q-switched, pulse stretching using Pockels cell 0-95927  
 Nd<sup>3+</sup>:YAG, Q-switching mechanism by intracavity stimulated Brillouin scatt. 0-106552  
 Nd<sup>3+</sup>:YAG laser, high repetition rate electrooptic Q-switching, birefringence 0-69430  
 Nd<sup>3+</sup>:YAG multimode laser radiation noise 0-74366  
 Ni:MgF<sub>2</sub>, tunable transition-metal-doped solid state lasers 0-58549

**QC** *see quality control***quadrupole crystal field interactions** *see crystal hyperfine field interactions***quadrupole lenses** *see electron lenses; electrostatic lenses; magnetic lenses***quadrupole mass analysers and filters** *see mass spectrometer components and accessories***quadrupole moments**

- see also atomic electric moment; molecular moments; nuclear electric moment; nuclear quadrupole resonance*  
 crystals, NMR quadrupolar effects, RF energy absorpt., relaxation times (Russian) 0-71235  
 finite ligand size and the Sternheimer antishielding factor  $\gamma_{\infty}$  0-103653  
 (rare-earth)Al<sub>2</sub>Ga<sub>2</sub>, synthesis, NMR and X-ray absorpt. studies 0-108083  
 sigma phase alloys, NMR and electric-field gradients 0-108109  
 trinuclear exchange clusters, Dzyaloshinsky coupling effects in Mossbauer spectra (Russian) 0-108142  
 CuFe<sub>2</sub>O<sub>4</sub>, Jahn-Teller type crystal distortions 0-103904  
 Dy, visible spectra obs., hyperfine struct., mag. dipole and electric quadrupole interaction const. anal. 0-91698  
<sup>7</sup>Li electric quadrupole moment, from Coulomb scatt. of aligned <sup>7</sup>Li ions 0-78141  
 Nb complexes, <sup>93</sup>Nb quadrupole coupling tensors form EPR meas. 0-88866  
 RbH<sub>2</sub>(SeO<sub>3</sub>)<sub>2</sub> crystal, incommensurable phase, quadrupole moment study 0-97213  
 TbP (As)(Sb)(Bi), mag. transitions, quadrupolar interaction effects 0-80512  
 V complexes, <sup>51</sup>V quadrupole coupling tensors form EPR meas. 0-88866  
 V-Ni sigma phase alloys, NMR and electric-field gradients 0-108109

**quality control***see also reliability*

- airframe material defectometry, quantitative test specifications (German) 0-89427  
 BWR containment vessels of prestressed concrete, pressure tests 0-81254  
 colour control of ultramarine pigments 0-62711  
 complete computer program in FORTRAN, for analysis of variance and means 0-98792  
 consumer product quality assurance, colorimetric theory and equipment (German) 0-86372  
 destructive examination of materials with data processing, microprocessor application (German) 0-93714



**quality control continued**

- diamond turned surface production, interferometric test repeatability 0-74538
- dielectric loss of polymers meas., automatic, at 100 MHz to 300 MHz and 2°C to 40°C 0-68219
- heat treatment, electromagnetic quality inspection with specified intensity of internal field 0-108677
- hierarchical systems, calibration errors influence on end item performance 0-98788
- holography, industrial, principles, applications (*German*) 0-95841
- HTGR fuel rod fabrication, estimation and control 0-83215
- large monocrystal X-ray reflection/scanning and transmission topographic methods 0-96415
- materials testing, planning and evaluation by statistical methods (*German*) 0-93725
- natural and industrial objects, chem. anal., future programme, computer appls. 0-104484
- nuclear reactor pressure vessels, strain measurements 0-79865
- optical instrument control life test design 0-87572
- optical microscopes for quality control and industrial production 0-82816
- optical shop interferometric instrumentation as a cost-effective production tool 0-74535
- photographic paper, using laser-operated device (*German*) 0-57412
- pipes, hot-rolled, automatic mag. quality control on prod. line 0-108661
- product appearance, CIE Standard Observer colour specification 0-61539
- production testing, multiple shaker considerations 0-79047
- radiographic equipment, computer-assisted quality assurance 0-89838
- raw material acceptance testing for dielectric applications 0-97646
- retail equity, NBS Standard Reference Materials 0-86249
- sapphire and Si surfaces, using IR and UV specular reflectance meas. 0-108684
- sphalerite, hydrothermal single crystals, feasibility of optical methods for quality control 0-89065
- stators, using thermovision flaw detector 'Stator-1', meas. channel 0-76449
- steel 40 G, coercimeters with attached electromagnets used for quality control 0-108672
- steels, heat treatment of 30KhN2MFA and 40Kh, nondestructive mag. quality control method 0-108662
- structural material analysis by computerized tomography 0-101001
- surface metrology using peak counting, quality control 0-95065
- testing of measuring instruments, determ. of valid interval between tests values 0-57284
- thyroid function radioimmunoassay, computer program (*French*) 0-94348
- TV microscopy system for teaching and quality control 0-82817
- US nondestructive inspection system, microprocessor utilization 0-71845
- wind power plant development, low cost approach 0-61268
- Fe nodular parts, comparison of sonic-resonance and US velocity techniques for quality control 0-97654
- Ga<sub>2</sub>Al<sub>3</sub>-As-GaAs heteroepitaxial layer distortion characterisation by X-ray multiple diff. 0-96754
- Li-I, battery, construction, performance and reliability 0-97771
- Nb-Ti, multifilamentary, Mirror Fusion Test Facility, superconductor core manufacturing and quality 0-93521
- Si wafers layers, multilayer ellipsometry, layer thickness and refr. index determination of layers 0-95121

**quality factor** *see Q-factor***quanticle theory of chemical binding** *see bonds (chemical)***quantisation**

- Bohr-Sommerfeld quantization of pseudospin Hamiltonians 0-105537
- constrained dynamical systems, quantisation by Weyl correspondence 0-77650
- constrained Hamiltonian systems, generators of symmetry transformations 0-57138
- constrained systems, quantization in paths integral formalism 0-94966
- cosmology, particle pair creation, canonical quantisation for Chitre-Hartle model 0-62342
- Dirac propagator from path integral quantization of the pseudoclassical spinning particle 0-86577
- droplet model and neutral currents, operator form 0-91043
- equation of motion, commutation relations for quantum mechanics and QFT, quantisation 0-105541
- fermion field with broken SU<sub>2</sub> symm., two-dimensional isotopic model (*Russian*) 0-73616
- Fock quantisation for indefinite metric gauge fields 0-77942
- friction, stochastic quantisation, nonlinear wave eqn. 0-98825
- functorial geometric quantization and Van Hove's theorem 0-86108
- gauge fields, canonical quantisation in axial gauge with indefinite metric, perturbation calc. 0-101928
- gauge theories, quantisation, without fixing gauge, functional technique 0-57471
- geometric quantization and gravitational collapse 0-90752
- geometric quantization and quantum mechanics, book 0-94908
- geometry of the quantization of angular momenta (I<sub>s,j</sub>) in fields of central symmetry 0-105530
- gravity, sum over paths quantisation, 2-submanifold boundary value problem 0-105566
- Hamiltonian with ergodic behaviour, classical quantisation 0-86148
- integral transform related to quantization 0-94978
- Lagrangian-Hamiltonian systems, partial quantisation (*Portuguese*) 0-77653
- many-body problem, dissipative system wave eqn. 0-86104
- massive spin-1 particles in external symmetrical tensor field, quantisation and noncausality 0-105790
- matter quantisation without quantising related fields 0-105525
- momentum observables, quantisation and measurement 0-98815
- Nelson's stochastic field, tensor field quantisation 0-105574
- Noether's theorem and exact invariants for time-dependent systems 0-86114
- nonrelativistic quantum mechanics, fibre bundles (*German*) 0-90699
- para-Fermi quantization in the representation of SO(n) 0-86554
- path integral quantisation in curved space, independent of form of Hamiltonian 0-68071
- photon field quantisation and dipole ghosts (*Chinese*) 0-101929
- photons, antibunching effect, and direct-action quantum absorber theory 0-57535
- quadratic friction quantisation, point object in viscous field 0-68076
- relativistic particles, with isotopic spin, kinematics, geometric quantisation 0-62871

**quantisation continued**

- Schrodinger's variational quantisation method in stochastic framework 0-105532
- second quantization for composite particles, reactive collisions, and unstable particles 0-57116
- soliton, extended particle, quantisation, degeneracy of eigenstates 0-73594
- stochastic quantisation processes, review, Markov processes, Martingales, quantum dynamics 0-94969
- Weyl quantisation, bounded operators 0-90697
- quantisation (communications)** *see analogue-digital conversion*
- quantitative analysis** *see chemical analysis*
- quantum beat spectra**
  - atom, quantum beats in two-photon resonance fluorescence 0-91488
  - quantum beats, in phosphorescence 0-63704
  - tetramethyl pyrazine in durene, phosphorescent mols., quantum beats in triplet states 0-58312
  - three level atom at high photon densities, reson. fluoresc. interference effects 0-87073
  - <sup>2</sup>H nuclei, spin-1 particle, eight-dimensional spin space determ. by NMR 0-60428
  - He, depolarising collision cross sections, quantum beat obs. 0-87203
  - He<sup>+</sup> impact on C foil, quantum beat pattern depend. on foil thickness 0-58343
  - HeH<sup>+</sup> impact on C foil, quantum beat pattern depend. on foil thickness 0-58343
  - <sup>14</sup>N II, 2p<sup>3</sup> P<sub>1</sub>, hyperfine struct. after ion beam surface impact at grazing incidence 0-58403
  - Na vapour, superradiance, quantum beat spectra 0-106311
- quantum beat spectroscopy**
  - atomic transitions, 0 and 2π rotations distinguished by quantum interference 0-91485
  - delayed quantum beat subnatural linewidth spectroscopy 0-77879
  - superfluorescence beats, theory incl. quantum fluctuations and finite sample size 0-102686
  - superhigh-resolution spectroscopy based on interference of states 0-102687
  - Na vapour, Zeeman coherence, transient and stationary, polarisation spectroscopy 0-58212
  - Sml, Zeeman coherence, transient and stationary, polarisation spectroscopy 0-58212
- quantum chemistry**
  - see also chemical reactions; orbital calculation methods; perturbation theory; potential energy surfaces for collision processes; pseudopotential methods; quantum statistical mechanics; quantum theory; reaction kinetics; wave functions*
  - No entries
- quantum counters** *see photon counting*
- quantum electrodynamics**
  - see also electromagnetism*
  - (2+1) dimensional compact QED, combined WKB-variational method, vacuum tunnelling 0-101960
  - θ-vacua and confinement in two-dimensional models 0-77990
  - n-bubble diagram contrib. to electron g-2, zeta function coeffs. 0-62897
  - Abraham force, comment and observation 0-73626
  - anomalous dimension and infrared behavior for high energy QED 0-101958
  - arbitrary plane wave EM field, electron motion, radiational corrections, mass operator (*Russian*) 0-57534
  - Aspect experiment, objective reality, causality in QED 0-99076
  - bagged complex scalar field, EM interaction, fine struct. const., possible dynamic origin 0-86635
  - Bernard Gregory 1979 lectures 0-77992
  - charge confinement, Schwinger model compared with (QED)<sub>4</sub> 0-62902
  - charge-field formulation of quantum electrodynamics (QEMED) 0-95232
  - charged particle interaction, mag. field energy, spatial distrib. of interaction contrib. 0-73625
  - charges, magnetic, self-dual Lorentz covariant Lagrangian 0-57525
  - Compton scattering by nonmagnetised electrons in ambient mag. field, vacuum polarisation effects 0-86631
  - confining gauge theories, quark correlation functions in massive QED<sub>2</sub> 0-105845
  - conformed invariance 0-99074
  - construction of two-dimensional quantum electrodynamics 0-86627
  - dimensional renormalisation, trace and axial anomalies, Zimmermann like identities, massive QED 0-101959
  - electron model, semiclassical, Casimir self-stress in dielectric and conducting balls 0-86625
  - electron nonrelativistic scatt. in quantised EM field 0-77993
  - electron-muon symmetry of Callan-Symanzik function: two-lepton case 0-73627
  - EM field in space with torsion, semi-minimal coupling principle 0-77675
  - EM fields, generalised, second quantisation 0-99072
  - EM wave propagation, nonlinear, in strong mag. fields, second harmonic generation 0-77988
  - energy-momentum tensor anomalies in spherical space-time for massless QED 0-73628
  - Euclidean QED, on lattice, continuum limit, Schwinger functions, vacuum expectation values 0-73624
  - evolution operator, quark struct. of states, two dimensional massless electrodynamics (*Russian*) 0-73630
  - experimental tests (*Chinese*) 0-77997
  - fine-structure constant, coupled Maxwell and Dirac eqns., lepton and quark-like solutions 0-62894
  - free charged particle interacting with intense laser pulse, energy momentum gain 0-101963
  - free EM field quantisation, gauge invariant fields 0-105817
  - free tensor potential equivalence in QED 0-73579
  - gauge invariant wave mechanics and the Power-Zienau-Woolley transformation 0-99073
  - Goppert-Mayer gauges for intense-field electrodynamics 0-99075
  - gravitational trace anomaly renormalisation in QED 0-57532
  - Green's function in external elec. field and combination with mag. field and plane-wave field 0-101964
  - hadron polarization operator in superrenormalizable model, rainbow approx. of (λ/2)φ model 0-105821
  - heavy particle effects, factorised local operators, renormalisation group 0-62898
  - heavy particle effects, factorised local operators, renormalisation group 0-62899

# quantum electrodynamics continued

Higgs boson decay, QED and QCD radiative corrections 0-95275  
infrared attractive fixed points, gauge symmetries, QED and anti-grandunification 0-95213  
infrared structure, derivation from first principles 0-101962  
intense field, perturbation theory expansion parameter 0-62900  
intermediate vector boson decay, QED and QCD radiative corrections, hadronic jets 0-73759  
isotropic cosmological models, vacuum stress energy tensor and particle creation (*German*) 0-94901  
isotropic universe, particle creation and vacuum polarisation, cosmological models 0-90582  
Josephson-junction capacitor, QED theory 0-93049  
light-magnetic field interactions (*Russian*) 0-73632  
magnetic fields, flux string and monopole, geometric configuration, compared to  $O(3)$  nonlinear  $\sigma$ -model 0-75527  
many-electron atoms, foundations of relativistic theory, Hamiltonian  $H_+$  and  $h_-$ , and related relativistic HF eqn. derivation 0-99458  
minimally nonlocal quantum electrodynamics without potentials for bound electrons 0-86626  
multiparticle production in chromoelectric flux tube model in 1+1 dims. field theory 0-73666  
non Abelian gauge theories in external electromagnetic fields (*Russian*) 0-57533  
non-relativistic fermions, Ward identity 0-86633  
nonlinear approach, conformal invariance and fine-structure constant 0-91023  
one scalar charged particle QED 0-99071  
path-dependent quantum formulation of electromagnetism with magnetic charges 0-86628  
PETRA QED tests, implications for weak neutral current struct. 0-86657  
photon-intensive EM wave interaction in uniform mag. field (*Russian*) 0-86636  
photons, antibunching effect, and direct-action quantum absorber theory 0-57535  
polarisation operator in ladder approx., renormalisation group 0-73629  
positronium, triplet, asymmetrical decay, two- and threefold polarisation correlation of photons 0-75536  
QCD contributions to vacuum polarization 0-91059  
QCD contributions to vacuum polarization 0-105834  
(QED), functional determinant absolute bound 0-68402  
quantum theory, stochastic electrodynamics formulation (*Spanish*) 0-82925  
radiation theory, multipolar Hamiltonian QED and quantum optics 0-86634  
relativistic two particle bound state energy levels, gauge invariance 0-77989  
renormalisation, dimensional, coupling constants and masses 0-57523  
renormalisation group equations, invariant charge function 0-57529  
renormalised transition amplitudes, gauge independence, Green functions 0-57530  
scalar electrodynamics in nonsimply connected space-time, topological mass generation 0-82924  
scale-covariant gravity theory, electrodynamics involvement 0-109350  
Schwarzschild space-time, vacuum polarisation induced by gravitation 0-82410  
Schwinger model, equivalent boson theory, anomaly-free Ward-Takahashi identities 0-82873  
Schwinger model, Ward identity, fermion axial vector current divergence, chiral invariant regulator field 0-57524  
solids, EM field quantum field theoretical treatment (*German*) 0-91022  
space-time structure of jet hadronization 0-91024  
spacelike features and asymptotic behaviour of  $e^+e^-$  annihilation 0-86630  
spinning charge, torsion contrib. to magnetic field 0-77676  
static EM angular momentum, in vacuo obs. 0-73631  
stochastic nonlinear electrodynamics, partial in central field of force 0-86629  
superconducting ring with weak links, critical voltage for flux tunnelling 0-75685  
supersymmetric, renormalised supercurrents and scale anomaly 0-105818  
supersymmetric, supercurrent gauge invariance,  $\alpha$ -independ. 0-95233  
synchrotron radiation transition rates in intense-field regime 0-77991  
tests of electron propagator, vacuum polarisation 0-77994  
Thomson scattering in strong mag. field, vacuum polarisation effects 0-86632  
three photon vertex in QED, renormalisation group anal., Callan-Symanzik eqn. 0-105822  
three-photon coalescence at electron 0-91026  
two-potential formulation of electrodynamics with magnetic monopoles (*Russian*) 0-62893  
two-quantum radiation of a particle travelling uniformly in a refracting medium (*Russian*) 0-62901  
U(1) lattice gauge model, phase transition in four-dimensional compact QED 0-105820  
unified theory of elementary-particle forces 0-105827  
Universe, isotropy, vacuum polarisation contrib. to energy content of Universe 0-73083  
vacuum, empty, fields and quanta, strong gravity, particle-antiparticle annihilations 0-68400  
vacuum behavior in two-dimensional scalar electrodynamics 0-105819  
vacuum polarisation in background grav. field, effect on photon vel. 0-91025  
vacuum polarization and a non-Newtonian gravitation 0-62896  
vacuum polarization in a nonsimply connected spacetime 0-57531  
Ward identity, axial vector current divergence, chiral invariant regulator field 0-57526  
Ward identity of dilation current 0-68401  
Yang-Mills theory, covariant canonical formalism, quark confinement, absence of localised coloured/charged physical states 0-57573  
zero-energy eigenstates for the Dirac boundary problem 0-101961  
 $e^-$ , anomalous magnetic moment, QED test 0-77996  
 $e^+e^- \rightarrow \mu^+\mu^-$ , 9.4 to 31.6 GeV, QED test 0-101965  
 $e^+e^- \rightarrow \mu^+\mu^- X$ , virtual 2 photon processes, luminosity functions, rapidity distrib., QED factors 0-86734  
 $e^+e^- \rightarrow \mu^+\mu^- (\gamma\gamma)$ , 27.7-31.6 GeV, QED test, Weinberg angle 0-77995  
 $e^+e^- \rightarrow \mu^+\mu^- (\mu^+\mu^-)(\gamma\gamma)$ , 12-31.6 GeV, QED test and Weinberg angle 0-91027  
 $e^+$  final states,  $q\bar{q}$  decay, semiclassical model, vacuum polarisation by colour field 0-63011

# quantum electrodynamics continued

$e^+e^- \rightarrow$  hadrons, R problem, QED and QCD corrections, quarks and leptons 0-95281  
 $e^+e^- \rightarrow \mu^+\mu^-$ , 9.4 GeV, QED test 0-101965  
 $\mu^-$ , anomalous magnetic moment, QED test 0-77996  
 $\mu^-$  g-factor, ( $g-2$ ) expts., review, book contrib. 0-68403  
 $q\bar{q}$ , fine-hyperfine splittings and Lorentz structure of confining potential with vacuum polarisation corrections 0-78041  
quantum electronics see quantum optics  
quantum field theory  
see also axiomatic field theory; Bethe-Salpeter equation; dispersion relations; gauge field theory; meson field theory; nonlinear field theory; quantisation; quantum field theory of elastic scattering; quantum field theory of interactions; Reggeon field theory; relativistic quantum field theory; renormalisation; scaling phenomena; Schwinger source theory; unified field theories  
aesthetic field equations, sinusoidal solns. 0-77937  
asymptotic behaviour in quantum field theory, renormalisation group analysis 0-68378  
baryons with arbitrary spin, generalisation of Dirac eqn., group scheme 0-73615  
collective coordinate method in the canonical formalism: Bogolubov's transformation 0-105776  
completely positive mapping families in  $\ast$ -algebra 0-94971  
composite quantised field theory and bound states (*Chinese*) 0-86543  
conference, fundamentals in quantum theory and field theory, Flagler Beach, FL, USA (Feb.-Mar. 79) 0-57114  
d'Alambert's equation, canonical formulation of field solns., Dirac's field 0-68343  
dimensional reduction and axial anomalies 0-86561  
dimensional regularization of composite operators in scalar field theory 0-73573  
effective action, quantum mechanical definition using time depend. variational principle 0-57457  
equation of motion, commutation relations for quantum mechanics and QFT, quantisation 0-105541  
fermion field with broken  $SU_2$  symm., two-dimensional isotopic model (*Russian*) 0-73616  
field operator for unstable particle and complex mass description in local QFT (*German*) 0-90981  
Fierz-Pauli field theories, smooth massless limit 0-73590  
finite integration range for zero modes 0-86150  
free scalar charge field, local nets of algebra of observables 0-99039  
generalised Feynman-Nelson model for free scalar field theory 0-105769  
higher-order Hamiltonian formalism in field theory 0-105766  
lagrange multiplier formalism for spin-2 fields 0-90982  
Liouville equation, Goursat problem regular solns. 0-105795  
Markovian homogeneous multicomponent Gaussian fields 0-77933  
massive particles with any spin. consistent eqns., Klein-Gordon divisor, review 0-73577  
multilocal quantum field theory, Fock-space technique, particle creation effects 0-77945  
 $O(10)$  spontaneous symmetry breaking for Higgs fields 0-105812  
 $O(N)$  model,  $1/N$  expansion summability 0-73582  
photon field quantisation and dipole ghosts (*Chinese*) 0-101929  
quantum many-particle systems in curved spacetime 0-98751  
spin-1 fields, supersymmetric non-polynomial vector multiplets and causal propagation 0-91012  
spinor and scalar fields in 4-D non-Euclidean momentum space, eqns. of motion, vacuum momentum 0-68379  
strong EM field, quantum theory, c-number semiclassical description 0-105540  
superalgebra in  $(0,1)$  integration of supersymmetrical Liouville eqn. (*Russian*) 0-101947  
superconducting systems, electrodynamics and quantum theory 0-60134  
von Neumann theorem, generalisation to irreproducible meas. 0-62862  
von Neumanns theorem for irreducible measurement 0-91007  
quantum field theory of elastic scattering  
see also elementary particle scattering; relativistic scattering theory  
't Hooft electromagnetic tensor for Higgs fields of arbitrary isospin 0-68364  
classical and prequantised field theories, analyticity of scattering operator 0-73611  
electron+monopole, scatt. through small angles, Dirac-Schwinger monopole 0-68398  
EM and gravitational two-particle potentials, fourth order, from scattering operator 0-73598  
geometrical unification of gauge and Higgs fields 0-99077  
Ginzburg-Landau equations, N-vortex solutions, Higgs field 0-82863  
Higgs and gauge fields, group actions on principle bundles and dimensional reduction 0-105770  
left-right symmetric model from general horizontal symmetry, Cabibbo angle, CP violation 0-101972  
neutron matter-quark matter phase transition, QCD and extended Higgs model, instantons 0-91062  
space-dispersion approach to the explanation of the Higgs-mechanism 0-90975  
supergravity, super Higgs effect, gravitino masses and couplings 0-62562  
Yang-Mills fields, finite-diagram theory, sixth-order scatt. amplitudes 0-73585  
 $Z_2$  lattice gauge Higgs theories, Monte-Carlo calcs. 0-86593  
ed elastic scatt. at high momentum transfer 0-82977  
 $\bar{\nu}_e \rightarrow \mu^+\mu^-$ , exotic lepton number violation and neutrino Majorana masses, Higgs sector 0-86615  
quantum field theory of gravitation  
see also elementary particle gravitational interactions; gravitons; supergravity  
 $\sigma$ -model, nonlinear, supersymmetric, Ricci-flat Kahler manifolds and supersymmetry 0-90994  
antisymmetric tensor fields coupled to gravity, renormalisability 0-90765  
asymptotically flat quantum grav. field, spin  $1/2$  0-68121  
Birkhoff theorems for  $R+R'$  gravity theories with torsion 0-82705  
black-hole, Kerr-Newman, quantised massless field, instability 0-82409  
boson field, equal-time commutator, general relativity, indefinite-metric 0-68119  
conformally flat space, strong gravity field coupled to  $SO(3)$  gauge field 0-62563  
 $CP^2$  vierbien singularities in half integral spin fields with EM background 0-73572



**quantum field theory of gravitation continued**

differential geometry methods in gauge and gravitational theories 0-90768  
 dimensionally reduced quantum gravity, one-loop counterterms 0-86193  
 dualism of field and matter in the general theory of relativity (*German*) 0-90748  
 early Universe, gauge theories, grav. constant time depend. and antigravity 0-90591  
 Einstein's impact on theoretical physics 0-77677  
 Einstein vacuum and Einstein-Maxwell space-times, infinitesimal holonomy group structure and geometrization 0-73252  
 Einstein-Cartan theory in the spin coefficient formalism 0-101742  
 EM and gravitational two-particle potentials, fourth order, from scattering operator 0-73598  
 EM fields in space-times with local rotational symmetry 0-82694  
 EM phenomena induced by weak grav. fields, possible gravitational wave detector 0-82692  
 extended inertial frames, de Sitter space, projective relativity, quantisation on curved manifold 0-90764  
 Finsler spaces, physical aspects underlying the field theory 0-101745  
 free gravitational field quantisation 0-90767  
 gauge fields resulting from compact internal symmetry groups 0-95022  
 gauge theory with alternative to black holes 0-57168  
 gauge theory with no black holes 0-82702  
 Gauss-Bonnet and Bianchi identities in Riemann-Cartan type gravitational theories 0-86190  
 general relativity, quantum mechanical one-particle state, interfering neutron beam expt. 0-95025  
 Goto-Imamura difficulty, resolution without Schwinger term 0-86191  
 gravitation as gauge theory of Poincaré group 0-86189  
 gravitational bubbles, radiative corrections to covariant massless quartically self-interacting meson theory 0-62826  
 gravitational field gauge theories, review 0-98848  
 gravitational instantons and their interactions 0-90766  
 gravitational monopoles, path depend. approach for Einstein's eqn. 0-77682  
 gravitational radiative corrections as the origin of spontaneous symmetry breaking 0-86192  
 gravitational trace anomaly renormalisation in QED 0-57532  
 gravitationally induced CP effects, quantum gravodynamics, QCD quark sector 0-86616  
 gravitino, axial current anomaly, Faddeev-Popov ghosts 0-68120  
 graviton, impossibility of non-zero rest mass 0-95023  
 graviton scatt. amplitude, gauge invariance 0-82700  
 hidden ghosts in antisymmetric tensor gauge fields coupled to gravity 0-82889  
 high-energy gravity and the very early universe 0-98847  
 instantons, gravitational, flavour currents of QCD, Green's functions, foam-like structure of space-time 0-62825  
 instantons, gravitational, self-dual soln. to Euclidean gravity 0-68118  
 isotropic universe, particle creation and vacuum polarisation, cosmological models 0-90582  
 isotropic Universe, quantum gravitational effects, spontaneous particle production (*Russian*) 0-94711  
 Lagrangian formulation, conservation laws, relativistic gravitation (*Russian*) 0-68337  
 lattice massive dual fields for gravity 0-105779  
 Lorentzian manifold, Kähler-metrics 0-73251  
 Minkowski space, conformal geometry, hyperbolic world lines 0-57167  
 mutually interacting Bose fields, external potential problems, geometrical approach 0-101744  
 non-distinguishable field and space variables in QFT, supergravity appl. 0-98845  
 nonlinearity, Newton constant's role 0-90761  
 nonlocalisation, connection with geometrical theory of gauge fields 0-82696  
 Planck energy nonconserving fluctuations and strong forces 0-57551  
 Poincaré group gauge theory, geometric meaning, equivalence to Einstein-Cartan gravitation 0-62845  
 quadratic lagrangians in a space with torsion and the theory of the spinor gauge field 0-91006  
 quantum gravity, choral of symmetries in general relativity 0-105565  
 quantum stress energy in nearly conformally flat spacetimes 0-57170  
 recursive calculation of axially symmetric stationary Einstein fields 0-77661  
 right translation invariant metrics and variational principles on principal bundle, gauge theories (*Chinese*) 0-101743  
 Robertson-Walker metric, pair prod., propagator method appl. 0-105564  
 semiclassical relativity, weak field limit 0-57169  
 solitary-wave motion for gravitating particles 0-62565  
 soliton solutions of stationary axi-symmetric gravitational fields 0-73253  
 space-time, foam-like structure, Bjorken scaling violation due to gravitational field 0-77939  
 spin-2 gluon-graviton model with baryon-number nonconservation 0-57565  
 spin-2-gravity coupling, consistency problems 0-77681  
 spinning particle in grav. field with torsion, eqns. of motion (*Chinese*) 0-62546  
 spinor field theory, generalized spin structures on 4-D space-times 0-62564  
 spinor formalism 0-90762  
 stimulated emission processes in gravitational fields, regions of constant shift 0-82703  
 strong gravity, field equations, strong interactions, de Sitter microsphere idea of hadrons 0-68111  
 strong gravity, short range pots., type II solns. 0-77683  
 SU(2) gauge fields coupled to strong gravity, Coulomb like solutions 0-82701  
 sum over paths quantisation, 2-submanifold boundary value problem 0-105566  
 time reversibility 0-82704  
 U<sub>4</sub> theory of gravity, unique spherically symmetric soln. in tetraparallelism limit 0-90763  
 unified gauge theory of gravitational and strong interactions 0-95016  
 unified scalar-free theory, order-R vacuum functional, with spontaneous scale breaking 0-78003  
 vacuum, empty, fields and quanta, strong gravity, particle-antiparticle annihilations 0-68400  
 vacuum decay, quantum and semiclassical gravitational effects 0-86194  
 vacuum polarization and non-Newtonian gravitation 0-62896

**quantum field theory of gravitation continued**

Wheeler's 'rule of unanimity' in quantum cosmology 0-98846  
 Yang-Mills theory, broken symmetry soln., Higgs fields and Einstein gravity action 0-101746

**quantum field theory of interactions**  
 see also elementary particle coupling constants; elementary particle interactions; Feynman diagrams; quantum electrodynamics; quantum field theory of gravitation; quantum field theory of strong interactions; quantum field theory of weak interactions; vertex functions  
 Einstein's impact on theoretical physics 0-77677  
 factorised completely X symmetric S-matrix characterisation, multicomponent field theories 0-105800  
 fermions, quantum field theory, large order perturb. theory, more than one coupling constant 0-77940  
 identical particle indistinguishability, field quantisation Lie algebraic approach 0-77984  
 parton model interpretation of cut vertex formalism 0-86566

**quantum field theory of strong interactions**  
 see also elementary particle strong interactions; Lee model  
 energy momentum tensor of quantised fields, vacuum averages, bag model of hadrons 0-91005  
 massive CP<sup>n</sup> sigma models, topological struct., finite action configurations 0-57476  
 mean spherical model in 1+1 dimens., strong and weak coupling connection 0-82888  
 Planck energy nonconserving fluctuations and strong forces 0-57551  
 quark confinement, bag models, field theoretic, renormalisation and translation invariance 0-62932  
 vacuum spontaneously broken symmetry of Higgs field and Bose condensation 0-82912

**quantum field theory of weak interactions**  
 see also elementary particle weak interactions; Weinberg model  
 SU(2|1) electroweak interactions, implications for 6 extra time dimensions 0-77998

**quantum fluids**  
 see also boson systems; fermion systems; liquid helium  
 polymer expansion for quantum many-body problem 0-57181

**quantum generators (optical)** see lasers

**quantum mechanics** see quantum theory

**quantum numbers** see quantum theory

**quantum optics**  
 see also photon counting  
 absorptive optical-bistability, transmitted light spectrum and dynamic response function 0-99789  
 absorptive optical bistability transient, local relax., quantum statistical treatment 0-91838  
 active and passive particles, extinction 0-102684  
 active particles, Lorenz-Mie scatt. theory paradox 0-74324  
 active particles, Lorenz-Mie scatt. theory paradox 0-102683  
 anharmonic oscillator model for dispersive optical bistability 0-58623  
 atom, resonance light scattering, intensity effects 0-91511  
 atom, spontaneous radiation, near field calcs. 0-99493  
 atom-photon interaction quantum fluctuations, at. beam focusing by radiation press. 0-58217  
 atomic state, superradiant, excitation by pulse of quantum field 0-87359  
 atomic systems, coherent transients theorem 0-99808  
 atoms, motion in optical freq. radiation trap 0-78818  
 bistability, absorptive and dispersive, in Fabry-Perot and ring-cavity geometries 0-95942  
 bistability, exact semiclassical treatment of ring cavity 0-58627  
 bistability in bad cavity limit, Fokker-Planck eqn. approach 0-64116  
 cavity, optical bistability, long-time behaviour 0-78892  
 collective atomic system population inversion driven by classical field 0-63964  
 conference, New York, USA (Jun. 1980) 0-90614  
 cooperative cascade emission, linear stochastic theory 0-74326  
 cooperative cascade emission theory, nonlinear evolution 0-74327  
 cooperative resonance fluorescence, multiple sidebands, semiclassical calcs. 0-99685  
 Dicke maser model-van der Waals spin system thermodynamic equivalence 0-83572  
 Dicke model for a multicomponent system 0-74329  
 Dicke state N two level atom assembly, radiation emission theory 0-69350  
 double radiooptical resonance, signal propag. and shape 0-87360  
 dressed atom system, energy levels and reson. phenomena, universal algorithm 0-69111  
 dynamic self-diffraction of coherent light beams, review 0-102777  
 Fabry-Perot cavity, dispersive optical bistability 0-78889  
 Fabry-Perot cavity, optical bistability, standing wave effects 0-91837  
 Fabry-Perot interferometer, optical bistability, inhomogeneous broadening, mean field approx. 0-90885  
 free electron laser, multiphoton analysis 0-78826  
 free electron laser, quantum theory for strong fields 0-83583  
 free electron lasers, quantum mechanical and classical theories 0-83579  
 gamma-Lorentzian intensity fluctuations, integrated, statistics 0-102685  
 gaseous dipolar media, semiclassical theory, appl. to gas laser 0-83586  
 gaseous medium, two-photon-absorbing, polarised light propag., quantum effects 0-103107  
 gaseous system, third harmonic generation, quantum theory 0-99795  
 gaussian beam resonator, optical nutation 0-99807  
 generalised P-representations in quantum optics 0-87356  
 Goldstone mode in stationary state of non-equilibrium dissipative system (*Chinese*) 0-87365  
 laser, multimode, containing saturable absorbers, bistable operation 0-91862  
 laser field interaction, Floquet theory 0-63716  
 laser saturation spectroscopy, time-resolved, free induction decay of two-level resonances 0-102775  
 light generation at impurity atoms in ferroelectrics and LC, fluctuation effects (*Russian*) 0-91767  
 many-particle systems, reson. weak light field scatt., intensity correl. function 0-95855  
 multilevel system, group theoretical method for coherent effects calc. 0-106502  
 multiphoton absorption and emission processes, photon statistics calcs. 0-78819  
 N two-level atom system, single-mode reson. radiation field interaction 0-78817

**quantum optics** continued  
n-photon resonance phenomena, finite laser bandwidth effect 0-58230  
negative light absorption by medium with selective freq. modulation of quantum oscillators 0-106501  
non-centresymmetric media, phase transitions into spontaneous coherent state (*Russian*) 0-69353  
nonlinear wave rectification, quantum limit 0-83634  
optical bistability with dispersion 0-78893  
photon emission from mol. and electronic transitions, quantum dynamics, semiclassical description 0-105466  
photon position observable, Ludwig axiomatic quantum mechanical formulation, quantum optics 0-73206  
quantum electronics and Einstein's theory of radiation 0-98782  
radiation fluctuations from light source 0-95857  
radiation theory, multipolar Hamiltonian QED and quantum optics 0-86634  
Ramsey resonance, of two-level mols., in three separated fields produced by corner reflector, theory 0-74166  
reflection of light, from spatially nonuniform amplifying medium 0-106444  
resonance atom, spontaneous diffr. of light 0-91512  
resonance fluorescence, photon correlation laser linewidth effects 0-83316  
resonance fluorescence in Markovian stochastic fields 0-83573  
resonance phase transition in two-level lattice system, thermodynamics 0-69351  
resonant media, pulse counterpropagation and nonlinear interaction, transverse effect computation 0-106563  
saturable optical amplifier, quantum theory 0-78916  
self pulsing in absorptive optical bistability, analytical description 0-78891  
self pulsing in dispersive optical bistability in ring cavity 0-78890  
simple quantum model, periodic spontaneous collapse and revival 0-73208  
spherically symmetric molecules, many-photon excitation in IR laser field 0-95596  
sub-poissonian statistics of an anharmonic oscillator in thermal equilibrium 0-82669  
subharmonic lasers, quantum theory, first order non-equilib. phase transition 0-83584  
superfluorescence, two-level atoms system, quantum theory, incl. propag. effects 0-58491  
three level atoms, coherent nonlinear mechanism for optical bistability 0-102756  
three level system, coherently pumped, cooperative relax. 0-78816  
three level system, interference between one and two photon processes, occupation probabilities 0-63965  
transition probability in two level systems, damping of states, crossing terms (*Russian*) 0-78820  
two level atom system, coherently driven, cooperative fluoresc. 0-87357  
two-level atom, driven by reson. multimode laser, light scatt., statistical props. 0-91489  
two-level atom, reson. fluoresc., atomic operators 0-63579  
two-level atom system, absorptive optical bistability, photon antibunching 0-58486  
two-level atoms, multiphoton cooperative radiation, SCF approx. calcs. 0-95856  
two-level atoms in solids, resonant interaction model for long-wavelength photons 0-91765  
two-level Doppler-broadened medium in Fabry-Perot, optical bistability 0-102759  
two-level system, in strong reson. field, saturation, temp. and spectrum characts. 0-99690  
two-level system, optimal control of resonance radiation processes 0-106498  
two-level system, Rabi oscillations in partially coherent field 0-102688  
two-level system, spontaneous emission, non-Markovian effects 0-58487  
two-level system in resonant multifrequency field with structureless noise (*Russian*) 0-91766  
VUV radiation, narrowband tunable, at Lyman- $\alpha$  wavelength 0-78907  
wavefront reversal in four-photon process, two-quantum reson. conditions (*Russian*) 0-106574  
Ba I, light shift induced zero-field level crossing 0-58220

**quantum solids**  
*see also solid helium*  
superharmonic approximation for quantum crystal 0-92615

**quantum statistical mechanics**  
*see also jellium; many-body problems; quantum fluids; quantum solids; quantum theories of fluid structure*  
 $\lambda_0\Phi^4$  field theory, 3 space-time dimensions, renormalisation, analytical continuation to imaginary time 0-86563  
anharmonic oscillator, trial Hamiltonians for quantum statistical treatment 0-77652  
anharmonic oscillators, partition function, statistical variation perturbation method 0-77648  
anharmonic quartic oscillators, statistical mechanics 0-98817  
Bose gas, impenetrable, one particle reduced density matrix, Painleve-type eqn. 0-62576  
Bose statistics, para-, Lie superalgebra, osp(1,2n), creation and annihilation operators 0-62572  
chemical reaction diffusion systems, quantum statistical theory, multi-channel reactive scatt. 0-81284  
class of sum rules for system of identical particles 0-91019  
desorption, multiphonon processes, quantum-statistical theory 0-107641  
disorder variables and para-fermions in two-dimensional statistical mechanics 0-98853  
dynamical cluster properties in the quantum statistical mechanics of phase transitions 0-77693  
energy levels, statistical mechanics method, perturbative variational approach 0-62513  
ensembles for random matrices of Hamiltonians with small time reversal noninvariant part 0-77694  
Euclidean Yukawa<sub>2</sub> quantum field theory, FKG correlation inequality 0-68357  
extended objects, correl. functions in one-dimens. kink-bearing systems 0-86204  
fermion-boson isotopic mixture, ground state configuration, theory 0-107601  
fermions, quantum mechanics of ground state 0-82713  
Feynman postulates, modified set, superposition principle 0-82657

**quantum statistical mechanics** continued  
Grassman number systems, Hamiltonian formalism, canonical quantisation by Feynman path-integral 0-77697  
Hawking effect, temp. relativity, axiomatic field theory 0-109456  
invertibility, decay, and asymptotic dynamics 0-57172  
Ising magnet, kinetic processes, 1-D chain, magnetic relaxation, quantum stat. mechs. 0-80471  
Ising magnet, kinetic processes, reduction of statistical description of system during evolution 0-80470  
lattice systems with short-range and Coulomb interactions 0-82715  
Liouville problem, quasi-particle dynamics from a given kinetic eqn., inverse 0-101749  
macroobservables, reconstruction in embedding method 0-77691  
many-fermion systems, partial level density for widely varying values of the range of interaction 0-58120  
matrix order and W\*-algebras in operational approach 0-77690  
motion of quantum particle in medium with dynamical disorder 0-68125  
neutrino systems, relativistic kinetic theory of transport processes 0-73283  
nonlinear oscillators, 1-D, intramolecular vibr. energy transfer, quantal, classical and statistical behaviour 0-91641  
nonlinear response of a system in connection with entropy maximum 0-95047  
nonlinear waves in cold plasma, classical Vlasov plasma description through quantum numerical methods 0-92288  
nonrelativistic electron in const. parallel elec. and mag. fields, thermodynamic characteristics 0-90777  
one component classical charged particle gas, thermodynamic grand function using collective coordinates 0-73289  
one-dimensional solitary-wave-bearing scalar fields, statistical mechanics, ideal-gas phenomenology 0-105792  
open quasi-free systems, time evolution 0-95030  
open system, current-carrying states in quantum statistics 0-90802  
operator formalism of statistical mechanics of gauge theory in covariant gauges 0-86591  
partition functions, coherent states and upper bounds in Hilbert space 0-57173  
phase space distributions and quantum state determinations, simultaneous meas. 0-90774  
planar spin system with annealed bond disorder 0-57212  
plasmas, nonideal, quantum-statistical conductance theory, force-force correlation function method 0-79440  
polymer expansion for quantum many-body problem 0-57181  
quantum friction and statistical mechanics 0-77649  
quantum harmonic oscill. chain, relaxation dynamics (*Russian*) 0-94992  
quantum partition functions, explicit classical bounds 0-90775  
single eigenvalue distrib. for non-zero mean matrix ensembles, correct form 0-73198  
Slater determinants, energy functional, extremum problem, Hartree-Fock equations, gradient method 0-62573  
SO(2N+1) algebra, time-dependent Hartree-Bogoliubov theory, quantisation 0-62575  
space density functions, positive phase, position and momentum joint distrib. 0-62509  
spectral properties of products of projections in quantum probability theory 0-98807  
supernovae, thermodynamic of nucleon, lepton, photon mixture, quantum mechanical calcs. 0-77273  
velocity of light Markov process, Klein-Gordan quantum statistic, quantum mechanics 0-98808  
Wigner distribution and quantum ergodicity 0-82711  
wigner function and normal ordering 0-57176

**quantum statistics** *see quantum statistical mechanics*

**quantum statistics of many-particle systems** *see quantum statistical mechanics*

**quantum theories of fluid structure**  
*see also liquid theory; quantum fluids*  
cavity-biased (T,V, $\mu$ ) Monte Carlo method, computer simulation 0-92434  
hard spheres, quantum mechanical virial coeff., two point Pade approx. 0-79657  
Percus-Yevick pair correlation function for hard sphere fluid, series representation 0-103232

**quantum theory**  
*see also Clebsch-Gordan coefficients; complementarity; correspondence principle; indeterminacy; perturbation theory; quantisation; quantum field theory; spin hamiltonians; wave mechanics*  
4-atomism, theory 0-94967  
Aharonov-Bohm effect, commutation relations, irreducible representations 0-57132  
algebra of physical magnitudes 0-82658  
angle-angular momentum variables in quantum mechanics, commutation relations 0-86112  
anharmonic oscill., classical versus quantum case (*Spanish*) 0-73210  
anharmonic oscillator, Feynman-Dyson series asymptotic expansion 0-62503  
anharmonic oscillators, nonseparable problem with exchange, classical limit 0-57120  
asymptotic series by  $H^0$  strictly singular perturbations 0-62498  
atomic interactions, retarded energy shift and pair polarisability, field theoretical perturbation theory 0-102560  
axiomatic operational quantum mechanics 0-57139  
Backlund transformations, canonical struct. 0-86141  
Bells inequality, quantum generalisations for different space-time regions 0-101728  
Bloch electrons in magnetic field, quantum numbers 0-96768  
bonding of particles of quantum systems 0-101724  
Born summation appl. to quantum mechanical models 0-90718  
Born's discovery of the quantum-mechanical matrix calculus 0-82615  
Bose-like oscillator, uncertainty relation for canonical variables 0-62539  
Brownian motion, connection with quantum theory 0-90786  
canonical transformations, nonlinear and nonbijective to action and angle variables 0-105517  
causality, localisation and spreading of wave packets 0-90715  
causality, macroscopic, Einstein correlation, CPT symmetry, decreasing probabilities, advanced waves, antiparticles 0-68073  
chemical reactivity, reliability of quantum mechanical predictions, config. of reaction prod., H-bonded species 0-108691  
coherent hyper-Raman scattering from isotropic material, quantum theory 0-106327



## quantum theory continued

coherent states and projective representation of the linear canonical transformations 0-82662  
 coherent states for general potentials; three dimensional systems 0-90716  
 coherent states for general potentials, time evolution 0-90717  
 completely positive mapping families in \*-algebra 0-94971  
 complex diffusion processes, transforms., and nonrelativistic quantum mechanics 0-82670  
 complex diffusion processes and nonrelativistic quantum mechanics 0-90707  
 conference, fundamentals in quantum theory and field theory, Flagler Beach, FL, USA (Feb.-Mar. 79) 0-57114  
 connected partially ordered set of events in time measurement 0-77640  
 CPT invariance, quantum mechanical interpretation 0-105805  
 currents and local currents in Galilean quantum mechanics 0-77641  
 curvilinear coordinate and momentum operators in configuration representation 0-105521  
 damped harmonic oscillator, quantum friction in c-number picture 0-94980  
 Davidson's generalization of the Feynman-Nelson stochastic model of quantum mechanics 0-62531  
 de Broglie waves, dispersion relation 0-67949  
 decaying states in rigged Hilbert space formulation 0-62521  
 degenerate discrete levels, periodical perturbation (*Russian*) 0-86152  
 density matrix formulation, physical interpretation 0-57115  
 diamagnetic band structure, first principles calc. 0-88470  
 differential equations, second order, without first derivatives, fourth-order numerical method 0-86107  
 Dirac distributions, perturb. of self-adjoint Hamiltonians, Green's functions and wavefunctions, scattering theories 0-62514  
 disjointness of  $\beta$ -KMS states with different chemical potential 0-62530  
 education, nonspreading wave packets, physical interpretation of Berry Balazs wave function 0-57040  
 Einstein's part in the development of quantum concepts 0-98781  
 Einstein's work and effect on atomic physics at the turn of the century (*German*) 0-90648  
 Einstein and the quantum problem (*German*) 0-90725  
 Einstein-Podolsky-Rosen experiment, Bell inequality for spin  $s$  0-90713  
 Einstein-Bohr debate, who was right 0-90724  
 electron gas, inhomogeneous, virial and Hellmann-Feynman theorems 0-88494  
 electron penetration, single-barrier transmission, phase-integral. approx. 0-86140  
 EM potentials, arguments against Aharonov-Bohm effect, Marton expt. 0-73205  
 equation of motion, commutation relations for quantum mechanics and QFT, quantisation 0-105541  
 equivalence principle, evolution to general relativity 0-98779  
 equivalent electrons, J allowed values in jj coupling, teaching 0-90624  
 Ermakov systems, nonlinear superposition, and solutions of nonlinear equations of motion 0-86125  
 extremum sufficient condition in classical action integral, eigenvalue problem, education 0-105462  
 fermion systems, operator ordering, functional integrals 0-62574  
 Feynman path integral and gauge invariance 0-82601  
 Feynman path integrals with Gaussian measure, Laplace transform method 0-62522  
 finite integration range for zero modes 0-86150  
 force on nucleus in non-stationary state, definition and anal. 0-105526  
 formulae derivation for  $y_m(r, x_r)$  0-98811  
 formulae for  $y_m(r, x_r)$  0-98810  
 Fourier transform, fractional order, appl. to quantum mechanics and electron motion in magnetic field 0-82665  
 frictional quantum mechanical system, one-dimens. scatt. model for coherence in stopping power problem 0-101736  
 Galilei covariant theory, minimal EM coupling 0-77634  
 Gelfand-Levitan method for operator fields 0-57136  
 generalised Feynman-Nelson model for free scalar field theory 0-105769  
 generalized absorber theory and the Einstein-Podolsky-Rosen paradox 0-90714  
 generalized Hamiltonian theory: central coordinates 0-105538  
 geometric quantization and quantum mechanics, book 0-94908  
 geometry, physical, group manifold 0-105522  
 gravitation, neutron interference fringes due to gravitational potential, role of gravity in quantum mechanics 0-62495  
 gravity role, neutron interferometer expt. 0-86176  
 hadronic matter, string junction model and spectrum energy density of string 0-57556  
 Hamiltonian model of computers 0-101727  
 Hanle effect, level-crossings effect on He I D<sub>3</sub>-line polarization in solar prominences 0-94772  
 harmonic oscillators, position and momentum eigenstates, superposed coherent states 0-57135  
 Hartree equations, time-dependent, global solutions, and nonlinear Schrodinger eqn. 0-73193  
 Heisenberg/Lie/symplectic formulations, problematic aspects 0-62497  
 Helmholtz equation, 1-D three-body problem, Sommerfeld Maluzhinetz transformation 0-62524  
 hidden variables model, proposed test 0-86109  
 hidden variables theory, probability measure in Hilbert space 0-62508  
 Hilbert space, commutativity of two projections 0-68083  
 hypervirial theorems and co-ordinate transformation in quantum mechanics 0-86137  
 integrating factors for single systems, general nonconservative systems 0-90706  
 interference and phase shift due to Earth's rotation 0-82679  
 inverse scatt., Newton's method modification at fixed energy 0-73207  
 involution and differentiation generalised functions, 3-D, associative algebra 0-68080  
 Jordan algebra state space characterisation in quantum mechanics 0-86105  
 Klein-Gordon particles, charged, quantum kinetic theory, linear kinetic eqn. 0-57178  
 Lie-admissible symmetry, representation theory 0-62870  
 Lie-Backlund operators, exam. of isomorphic correspondence between classical and quantum-mech. invariants 0-90700  
 liquid-gas critical point, quantum mechanical effects, theory 0-103452  
 local theories, probabilistic and deterministic, inequalities of Einstein locality 0-82656  
 logarithmic Schrodinger equation, soliton dynamics 0-57130  
 Lyapunov variable, entropy and meas. in quantum mechs. 0-77739

## quantum theory continued

macroobservables, reconstruction in embedding method 0-77691  
 many particle systems, time inversion and mobility 0-101722  
 many-body problem, vertex function and crossing symmetry 0-62515  
 many-fermion quantum mechanics, coherent-state representation 0-94988  
 Markov classical processes, nonequivalence to quantum mechanics 0-62583  
 maser with beam of inflying atoms, spectral line broadening mechanism 0-106503  
 matrix order and W\*-algebras in operational approach 0-77690  
 measurement perturbations, repeated, quantum system decay and reduction laws 0-62496  
 measurement process, interpretation problems 0-57117  
 measurement theory, mechanism of reduction of wave packet 0-86146  
 measurement theory, wave packet reduction 0-105536  
 metal particles, small, dielectric function and IR absorption 0-60607  
 microrealistic explanation of quantum phenomena 0-82659  
 molecular quantum systems, time dependent Born-Oppenheimer approximation 0-105518  
 molecular structure, quantum theory, interpretation problems 0-106248  
 molecular structure and shapes, quantum mechanical view 0-102422  
 molecular structure hypothesis, quantum mechanical aspects 0-102421  
 molecular structure theory, quantum topology 0-106247  
 narrow resonances, high energy mag. resonances, exactly soluble model 0-86134  
 neutron interference, gravity and inertial effects, principle of equivalence at quantum level 0-77669  
 new gauge transformation for a generalized quantum representation 0-86136  
 Newton-Wigner position operator derivation 0-98821  
 nodeless wave function quantum theory 0-57119  
 non-completeness argument, EPR anal. 0-105533  
 non-Gaussian wave packet time evolution 0-57133  
 nonergodic classical statistical theory 0-77646  
 nonintegrable quantum system, irregular part of discrete energy spectrum, statistical theory 0-82667  
 nonlinear spin relaxation theory 0-90701  
 nonlocality detection, rel. to game of quandle 0-86143  
 nonrelativistic quantum mechanics, fibre bundles (*German*) 0-90699  
 nontunnelling particle penetration through potential barriers, Lee model calcs. 0-73213  
 nuclear decay,  $\gamma$ -decay of coherent rotational states, random quantum meas. 0-73855  
 observables, relative compatibility and joint distributions 0-105524  
 operator symbols in the description of observable-state systems 0-57140  
 oscillator, quartic, zeta function 0-62532  
 overlapping avoided crossings, rel. to quantum stochasticity 0-90694  
 partial inner product spaces, topological considerations 0-94977  
 particle statistics from induced representations of a local current group 0-57129  
 particle wave behaviour, experimental observation system 0-62535  
 photon position observable, Ludwig axiomatic quantum mechanical formulation, quantum optics 0-73206  
 Planck, Max Karl Ernst Ludwig (1858-1947), quantum and relativity theories 0-68008  
 Poincare group representations, momentum and position variables, complete decomposition theory 0-62511  
 potential well particle escape, time-depend. Schrodinger eqn. soln. 0-86118  
 power series soln. of coupled eqns. and three-body problem 0-86145  
 protein, structure and bonding, quantum theory, ab initio calcs. 0-61509  
 pseudo Nilsson quantum numbers, goodness in asymptotic limit 0-99138  
 psychology, quantum interference effects, Schrodinger's cat, review 0-73158  
 quanta from a diachronical aspect 0-90723  
 quantum tunneling through a rectangular barrier using  $|\psi|^2$  and flux, education 0-105457  
 quantum mechanical perturbation problems, resolution using integral eqn. 0-58112  
 quantum mechanical two centre problem, noncomplete integral algebra (*Russian*) 0-86154  
 quantum mechanics, logical foundation 0-94975  
 quantum numbers as hidden parameters, in causal interpretation of wave mechanics (*French*) 0-68062  
 quantum oscillators, matrix element diagrams 0-105455  
 quantum-mechanical kinetic energy as measure of information in distribution 0-101725  
 quasiclassical estimates on moments of the energy levels 0-98806  
 relativistic electron wave equation 0-101702  
 relativistic isolated unstable system, extended variables 0-62525  
 relativistic quantum theory with correct conservation laws 0-82677  
 resolvent operator on dense set of quantum states, spatial localisation, second-sheet singularities 0-77645  
 resonances, scattering theory and rigged Hilbert spaces 0-94987  
 role of mathematics in a physical theory (*German*) 0-90726  
 rotation operators, time-depend. aspects, teaching 0-90634  
 scattering operator of few-body quantum mechanical system, sum of two-body potential operators 0-62516  
 scattering resonances, tunnelling decay, absorbing boundary layer 0-57121  
 scattering theory, variable interval variable step method for soln. of linear second order coupled differential eqn. 0-105527  
 Schnurs, combinatorial hierarchy, spin dichotomy and conservation of quantum numbers 0-68383  
 Schrodinger equation, Brownian motion interpretation challenged 0-94974  
 Schrodinger equation eigenvalues, perturbation theory calc. without complete set of eigenfunctions 0-105519  
 second order matrix element eval., trial function linear transformation 0-62529  
 semiclassical Green's function, energy-representation 0-90692  
 semiclassical scattering theory, spurious excitation 0-73142  
 semigroups and the density matrix formulation of quantum mechanics 0-57118  
 sequential events and objectivistic probabilities, quantum logic 0-94973  
 simple quantum model, periodic spontaneous collapse and revival 0-73208  
 singular state problems, monopole pair energy levels, charged monopole-electron system (*Chinese*) 0-101733  
 solid state physics, historical aspects, symposium, London, England (Apr.-May 1979) 0-56999

**quantum theory continued**  
space density functions, positive phase, position and momentum joint distribs. 0—62509  
spectral properties of products of projections in quantum probability theory 0—98807  
spin-orbit potentials, quantum scattering theory inverse problem, fixed energy Jost functions (*Russian*) 0—68082  
spins, arbitrary no., quantum mech. vector addition 0—57134  
stationary perturbation theory, commutator possible appl., nth order expectation values 0—86116  
stimulated Raman scatt. quantum theory 0—106565  
stochastic electrodynamics formulation (*Spanish*) 0—82925  
stochastic quantum mechanics, dissipative forces, operator algebra 0—98826  
strong EM field, quantum theory, c-number semiclassical description 0—105540  
SU(2) coherent state representation, path integrals 0—62502  
SU(N) symmetric quantum dynamical systems,  $N \rightarrow \infty$ , energy spectrum for singlet and adjoint states 0—62880  
subsystems, bilinear maps between generalised Hilbert spaces 0—62507  
superposition principle and sectors in quantum logics 0—94970  
superselection rules, quantum measurement, and the Schrodinger's cat 0—86103  
symmetric groups, generation algorithms 0—98813  
thin film heterostructures, optical transition selection rules 0—66319  
time evolution operator in quantum mechanics 0—82610  
time-dependent invariants with applications in physics 0—57131  
topological shifts in the Aharonov-Bohm effect 0—82674  
transition probability between not necessarily stationary states 0—73212  
transition to classical theory 0—105523  
tunnelling, reaction coord. method 0—62500  
unbounded Hermitian operators, low-lying eigenstates, method 0—98812  
unitary group formulation of many-electron theory and quantum organic chemistry 0—106270  
unitary-antiunitary group representations 0—98809  
vacuum bubble evaporation and thermodynamics, surface oscill. consideration 0—62608  
velocity of light Markov process, Klein-Gordon quantum statistic, quantum mechanics 0—98808  
virial inequalities, quantum and relativistic 0—62609  
von Neumann's measurement theory, phase relationship observation 0—105539  
wave-corpucle. duality, Planck's, Einstein's, de Broglie's, Schrodinger's contributions to development (*German*) 0—68016  
wave-particle duality and quantum theory, attitudes, 1900-1920 0—57061  
weakly interacting particle system, quantum field divergence disappearance in modified quantum dynamics 0—62537  
Weyl's association, Wigner's function and affine geometry 0—98823  
Wigner distribution functions, canonical transformation representation in quantum mechanics 0—90702  
wigner function and normal ordering 0—57176  
Zeeman effect, linear, relativistic correction, Coulomb field 0—102484  
CO<sub>2</sub> energy levels for perturbed Morse oscillators 0—78676  
H, Kepler problem regularisation on quotient of conformally flat manifold 0—82663  
H, perturbation theory and Pade approx. in electric field 0—91493  
H<sub>2</sub>, Bender-Wu formula, SO(4,2) dynamical group and Zeeman effect, perturbation coeffs. determ. 0—95674  
H<sub>2</sub>, ortho-para conversion, magneto-catalytic reaction, quantum formulation 0—108750  
<sup>3</sup>He, liq., interface with nonmag. solid, Kapitza resist., quantum perturbation treatment 0—88385

**quantum theory of light** *see quantum electrodynamics*  
**quantum theory of many-body problems** *see many-body problems*  
**quark confinement**

$\theta$ -vacua and confinement in two-dimensional models 0—77990  
 $\nu$ -dimensional Yang-Mills and  $(\nu-1)$ -dims. nonlinear  $\sigma$ -model connection, quark confinement, dual strings 0—90978  
 $\sigma$ -model supersymmetric dynamics on pre-QCD level with elementary quarks and composite gluons 0—82886  
't Hooft's disorder parameter, meson like configurations contribution, confinement phase 0—86574  
anomalous muon capture and lepton number conservation 0—86654  
asymptotic freedom infrared instability 0—73678  
bag model, isobaric ensemble and multiplicity distrib. (*Russian*) 0—82952  
bag model, primordial transverse momentum,  $\sigma_L/\sigma_T$  ratio 0—82938  
bag model with toroidal glueballs 0—102009  
bag models, field theoretic, renormalisation and translation invariance 0—62932  
bagged hadronic matter 0—73664  
baryon spectrum, s-wave, phenomenological quark-quark interaction 0—101984  
baryon spectrum and the forces between quarks 0—102004  
baryon synthesis from unconfined primordial quarks 0—57566  
baryonium, nuclear and quark confinement forces 0—68431  
baryons, binding energy and rest mass of constituents, total symmetry effects (*French*) 0—63068  
bottomium, potential models, non-relativistic description 0—68426  
Breit equation, Klein paradox 0—57506  
charge confinement, Schwinger model compared with (QED)<sub>4</sub> 0—62902  
charge invariance, QCD, renormalisation group, confining and asymptotically free soln. 0—62881  
charm, elementary particle theories, properties (*Spanish*) 0—73681  
charm photoprod. with linearly pol. photons, QCD calcs., gluons 0—68464  
charmonium, mass in QCD 0—105867  
charmonium, potential models, non-relativistic description 0—68426  
chiral symmetry breaking in gauge theories 0—95244  
colour confining forces and effects saturation 0—73672  
colour geometrodynamics, eightfold way, review 0—95243  
composite particle EM form factors, asymptotic behaviour 0—62927  
confining gauge theories, quark correlation functions in massive QED<sub>2</sub> 0—105845  
cosmological f-g fields relevant to quark confinement 0—86659  
coupling constant inverse, energy perturbation expansion and eigenvalue 0—86658  
CP<sup>n-2</sup> models in more than 2-dimens., confinement props. 0—86570  
CP invariance, QCD confinement of colour, modification of axion scheme 0—73663  
cylindrical mixing phenomena in dual topological unitarisation, pomerons, reggeons and gluonic states 0—86696

**quark confinement continued**  
deep inelastic scatt., inclusive observables and hard gluon emission 0—99094  
dense neutron matter, quark percolation theory of phase transitions 0—77277  
division of matter, confinement of quarks and gluons (*Polish*) 0—68417  
double-logarithmic quark and form factors and the evolution of parton jets 0—68421  
dynamical preon model from primordial QCD 0—105840  
effective Lagrangian with two color-singlet gluon fields 0—86680  
energy momentum tensor of quantised fields, vacuum averages, bag model of hadrons 0—91005  
exotic atoms, conf., Erice, Sicily, (1979) 0—67939  
exotic quark states 0—73679  
extended hadrons, creation and annihilation thermodynamics 0—62925  
fermion field, nonlinear, origin of four quark flavours, quantum numbers, isosymmetry breaking 0—62920  
finite quark mass effects on supdense quarkion configurations 0—105852  
forces between leptons and quarks, a gauge field phenomena 0—91008  
four quark mesons, recoupled wave functions, phase inconsistency 0—68425  
gauge invariant gluons, Hamiltonian operator 0—105843  
geometrical approach to elementary particles 0—105865  
giant MIT bag, hot quark matter, from relativistic ideal Fermi gas 0—99083  
glueball pomeron singularity cancellation 0—73687  
glueball spectra, prod. and decay for QCD and SU(n) gauge theories 0—62941  
glueballs, production and properties of gluonium 0—73674  
gluon and quark jets in a recursive model motivated by quantum chromodynamics,  $\Upsilon$  decay 0—62936  
gluon and quark population evolution in QCD jets, numerical estimates 0—101987  
gluon condensation and QCD 0—102007  
gluon exchange in meson spectroscopy 0—102013  
gluon-gluon interactions, hadron prod. and  $\sigma$ (total) growth at high energies 0—91049  
gluonic boundary conditions, quark mass depend. and quark condensation 0—86671  
hadron beam jets structure at small  $P_T$  0—102014  
hadron properties from quark models and confinement schemes 0—105864  
hadron-hadron 3-jet collisions, charge conjugation asymmetries and tri-linear gluon coupling 0—105934  
Hamilton-Jacobi formalism for strings, string-gauge theory link 0—78048  
harmonically confined q  $\bar{q}$  system, relativistic wave eqn. 0—95247  
heavy baryon spectroscopy in the QCD bag model 0—105866  
heavy meson weak decays, heavy quark decay, QCD corrections, real gluon role 0—57586  
heavy quark bound states, production and decay 0—102008  
heavy quark bound states of top quark and antiquark pairs, QCD test 0—68430  
heavy quark infrared safe weak decay, dimensional regularisation techniques, gluonic corrections 0—102087  
heavy quark prod., nonperturbative gluoprod. versus perturbative QCD fusion models, B and  $\psi$  0—91058  
heavy quarkonium states, decay rate to lepton pairs, gluonic corrections 0—102043  
heavy quarks and new particles 0—73661  
heavy quarks in QCD (*French*) 0—78017  
heavy vector meson annihilation to lepton pairs, hadronic corrections 0—68424  
hidden colour and the isobar content of the deuteron 0—102024  
Higgs boson decay, gluon final states, differential sphericity and thrust distrib. 0—86655  
inclusive vector meson production in fragmentation regions of meson at small  $P_T$  0—105931  
instanton system weakly interacting with anti-instanton system, external electric fields, structure and stability 0—77956  
large  $p_T$  photoproduction, gluon fragmentation function extraction, scaling 0—105853  
large  $p_T$  hadronic collisions, QCD sensitive test, quark and gluon jets 0—57647  
lattice SU(N) gauge theory, vacuum structure, large-scale 0—57470  
light meson radiative decay, Zweig law (*Russian*) 0—102051  
link operator formulation and string breaking for confinement without van der Waals forces 0—101994  
M<sub>2</sub>-M<sub>g(c)</sub> and M<sub>2</sub>-M<sub>g(b)</sub> lower bounds, concave and convex pots. 0—91057  
manifestly gauge invariant gluon eqns. from Yang-Mills fields 0—86681  
massless 't Hooft model, tachyonic modes, vanishing of scalar density 0—77949  
meson photocoupling in quark model 0—82954  
meson scattering, quark model asymptotic completeness 0—73738  
MIT bag, 1-dimens., structure function L<sub>0</sub> approx. correction 0—101985  
MIT bag model, charmed and b-flavoured hadron mag. moments 0—95271  
mixing matrix and CP violation for n quark generations 0—101986  
Nambu Goldstone realisation for vector gluon-quark theories, gluon vertices 0—68415  
Nambu string model, scatt. amplitude (*Russian*) 0—86695  
non-Abelian Block-Nordsieck conjecture, counter-example 0—78021  
nonperturbative gluon jet model, gluon fragments, meson prod. 0—68420  
nonperturbative QCD, large N<sub>c</sub>, QCD bag model, instantons and  $\eta'$  mass 0—57559  
nonrelativistic bound s-states in linear central potential 0—82936  
OZI rule, justification in QCD 0—62924  
PETRA results for fluons, nuclear forces, t-quarks and quark-lepton symmetry 0—86731  
pre-quarks and fractional charges 0—91048  
Q<sup>2</sup> dependence for quark and gluon fragmentation functions, QCD predictions, Altarelli-Parisi eqns. 0—78018  
QCD, 2-dimens. multiflavour, local colour symmetry breakdown, massive gluons and quarks 0—82942  
QCD, colour ferromag. vacuum states, two loop energy densities, MIT bag constant 0—99085  
QCD, confinement and long range gauge fields 0—73668  
QCD, gauge independ. approach to hard processes, structure functions, gluons 0—86665  
QCD, ghost gluon bound state and pseudoscalar mixing 0—86685  
QCD, hadron masses, behaviour of constituent quarks 0—57557  
QCD, stagnant gauge for gluon propagator 0—57554



## quark confinement continued

- QCD and superdense matter, quark and gluon plasma, hadronic structure, neutron stars, hadron collisions, review 0-73683  
 QCD low energy tests, gluon non-zero effective mass,  $\psi$  decays 0-91054  
 QCD polarisation operator at finite temps. and densities, one loop approx., gluons (*Russian*) 0-68427  
 QCD processes, large IR corrections, soft gluon emission 0-78028  
 qCD scattering processes with hard gluon emission, jet prod. 0-62939  
 QCD vacuum, asymptotic freedom, quark confinement, Yang-Mills theory for strong interactions 0-73638  
 QCD vacuum in strong external gauge fields, spontaneously, broken chiral symmetries 0-57555  
 QCD vacuum of background SU(2) gauge field, colour mag. permeability 0-78023  
 quantum relativistic strings and the multiplicative dual model (*Russian*) 0-82958  
 quark electric dipole moment in Kobayashi-Maskawa theory with gluonic corrections (*Russian*) 0-86688  
 quark-gluon field coupling const., meson mass differences (*Russian*) 0-105898  
 quark-nucleon phase diagram and quantum chromodynamics 0-105855  
 quarkonium systems, sum rules 0-68423  
 quasiconfinement in colour gauge symmetry, unconfined quarks and gluons 0-86686  
 Regge-pole approach to charmonium and bottomium 0-86697  
 relativistic membrane, quantum dynamics 0-57552  
 relativistic wave equation and mass spectrum of gluonium 0-73596  
 resonance-saturation picture, scaling violation patterns 0-82940  
 semi-classical models for gluon jets and leptonproduction based on the massless relativistic string 0-105861  
 six- and eight-quark models, weak interactions 0-99086  
 soft gluon resummation formulae for hard parton processes in QCD 0-105842  
 space-time structure of jet hadronization 0-91024  
 spin-2 gluon-graviton model with baryon-number nonconservation 0-57565  
 structure functions, bounds for the ratio of anomalous dimensions, scalar gluon theories 0-57595  
 SU(2) $\times$ U(1) with four flavours, relation between Cabibbo angle and quark masses 0-105872  
 SU(5) electroweak-strong interaction model, broken colour symmetry and gluon mass 0-73650  
 SU(5) grand unification, p lifetime and branching ratio, bag model wavefunctions 0-78004  
 SU(N) lattice gauge theories, Wilson and 't Hooft loop behaviour 0-57493  
 sufficient condition, model-independent 0-91050  
 thermodynamics of confined quarks 0-95249  
 triple gluon vertex meas. from gluon jet spread 0-82946  
 unconfined quarks and gluons, quasiconfinement model, confining and nonconfining phase transition 0-86687  
 universal Regge slope  $\alpha'$  from the QCD gluon propagator 0-78026  
 Yang-Mills theory, covariant canonical formalism, quark confinement, absence of localised coloured/charged physical states 0-57573  
 Yang-Mills theory, equations of motion finite range classical solns., confinement 0-57474  
 d, gluon distrib. from elastic dd scatt. 0-82939  
 D<sup>0</sup>, D<sup>+</sup> decays, gluon enhancements in charmed-meson decays 0-95265  
 D<sup>+</sup>, weak decay constant from bag model extension 0-62967  
 $\Delta_{D^*}(1925)$  baryonic degrees of freedom, nonrelativistic, harmonic oscillator quark model mass formula 0-91066  
 e<sup>+</sup>e<sup>-</sup>  $\rightarrow$  jets, transversely polarised annihilation, charged gluon jets, Pati-Salam model 0-86739  
 e<sup>+</sup>e<sup>-</sup>  $\rightarrow$  3 jets, integer charge quark model, gluon jets 0-91101  
 e<sup>+</sup>e<sup>-</sup>  $\rightarrow$  3 jets, three gluon coupling in perturbative QCD 0-105913  
 e<sup>+</sup>e<sup>-</sup> annihilation, charge current asymmetry as QCD test, neutral gluons 0-57616  
 e<sup>+</sup>e<sup>-</sup> annihilation, gluon jets, multiplicity and ang. distrib. asymmetries 0-91105  
 e<sup>+</sup>e<sup>-</sup> annihilation, QCD and jet acollinearity, quark-gluon coupling 0-105914  
 e<sup>+</sup>e<sup>-</sup> annihilation at high energies and search for the t-quark continuum contribution 0-102012  
 e<sup>+</sup>e<sup>-</sup>  $\rightarrow$  charmed hadrons, quark mass effect on fragmentation functions 0-91098  
 e<sup>+</sup>e<sup>-</sup>  $\rightarrow$  gluon and quark jets 0-91100  
 e<sup>+</sup>e<sup>-</sup>  $\rightarrow$   $\gamma^*$ -hadrons, hadron calorimetric meas., QCD predictions, gluon emission 0-91102  
 e<sup>+</sup>e<sup>-</sup>  $\rightarrow$  hadrons, 12, 30 GeV, jets, quark fragmentation and coupling constant, QCD comparison 0-105915  
 e<sup>+</sup>e<sup>-</sup>  $\rightarrow$  multihadrons, planar three jet events, gluon bremsstrahlung, strong coupling constant 0-57617  
 e<sup>+</sup>e<sup>-</sup>  $\rightarrow$  QQ, heavy quark study approach 0-105859  
 e<sup>+</sup>e<sup>-</sup>  $\rightarrow$  q $\bar{q}$ g, cross sections and ang. distrib. 0-102061  
 e<sup>+</sup>e<sup>-</sup>  $\rightarrow$  q $\bar{q}$ g, gluon bremsstrahlung, neutral current and beam polarisation effects 0-99106  
 e<sup>+</sup>e<sup>-</sup>  $\rightarrow$  three jets, acoplanar angle relative to beam polarisation, vector/scalar gluons 0-63005  
 eN, deep inelastic scatt., quark model, field-theoretic, quark indistinguishability, nucleon structure function 0-62993  
 ep, deep inelastic scatt.,  $\sigma_L/\sigma_T$  ratio from quark model 0-82979  
 $\eta_c$  associated with gluon, hadronic prod. 0-105846  
 F<sup>+</sup>  $\rightarrow$   $\tau^+ \nu$ , gluon enhancements in charmed-meson decays 0-95265  
 F<sup>+</sup>, weak decay constant from bag model extension 0-62967  
 $\gamma p$ , heavy quark particle photoprod., QCD model, vector dominance implications 0-86730  
 K $\rightarrow$ 3 $\pi$ , relativistic quark model anal. 0-99096  
 K charge radius, coloured quark field theory 0-62945  
 K $\rightarrow$  $\pi e(\mu)\gamma$ , quark mass ratios 0-105884  
 $\mu N$  deep inelastic scattering, gluon jets 0-105862  
 NN, 12 GeV, spin depend., quark exchange evidence 0-102074  
 NNp couplings, parity-violating, QCD and MIT bag model, 1/2<sup>-</sup> resonance contribs., SU(6), symmetry 0-57540  
 $\nu N$ , two gluon mechanisms, quarkonia, glueballs and Higgs scalars 0-78077  
 $\nu N \rightarrow \nu X$ , neutral current  $\psi$  prod., Z<sup>0</sup>-gluon fusion model 0-78015  
 $\bar{p}p$   $\rightarrow$  charm quarks 0-102040  
 p, degenerate parton gas model, quark-lepton identification 0-68416  
 p, gluon distrib. from elastic pp scatt. 0-82939  
 pp, D, B, K prod., QCD model for heavy flavour prod., two gluon annihilation 0-86744

## quark confinement continued

- pp elastic, differential and total cross sections, proton model, gluon-gluon annihilation 0-91114  
 $\pi$  charge radius, coloured quark field theory 0-62945  
 $\pi^- N \rightarrow \psi X$ , 225 GeV, bottom meson pair production limit 0-73750  
 $\psi$  associated with gluon, hadronic prod. 0-105846  
 $\psi$  production, gluon-gluon fusion model, gluon distrib. x-depend. 0-62922  
 QQ, bound system, dynamics 0-73676  
 qq, fine-hyperfine splittings and Lorentz structure of confining potential with vacuum polarisation corrections 0-78041  
 QQ, potential energy, gluon distrib. 0-62929  
 qq(q $\bar{q}$ )<sup>2</sup> mesons, mass formula 0-62958  
 qq spectra, heavy systems, equaltime relativistic wave eqn. with confining potential 0-77977  
 QQ systems, two gluon decay widths, short range quark gluon effective vertex 0-86669  
 $\Sigma^+ \rightarrow p\gamma$ , 1/2<sup>-</sup> resonance poles to parity-violating amplitude, two-quark weak transitions 0-78062  
 t-quarkonium decay props. (*Russian*) 0-105856  
 T, production and decay in quark fusion model 0-102018  
 T(9.46) orthoquarkonium decay, jet profiles, three gluon structure 0-73698  
 T(9.46)  $\rightarrow$  hadrons, gluon spin and colour, QCD nontrivial test 0-82971  
 T(9.4)  $\rightarrow$  charmonium, quarkonium prod. via one gluon mechanism 0-95263  
 T production, photon-gluon fusion model, gluon distrib. x-depend. 0-62922  
 V  $\rightarrow \rho \mu^+ \mu^-$ , vector meson decay EM form factors in bag model (*Russian*) 0-62982  
<sup>2</sup>H nuclei, spin-1 particle, eight-dimensional spin space determ. by NMR 0-60428
- quark models**  
 see also colour model  
 additive quark model and multiparticle production off emulsion nuclei at 50 GeV 0-68491  
 asymptotically free gauge theories, higher twist effects, four quark operator anomalous dimensions 0-105848  
 bag model, meson and massive photon production 0-105850  
 bag model, primordial transverse momentum,  $\sigma_L/\sigma_T$  ratio 0-82938  
 bagged hadronic matter 0-73664  
 baryon electric dipole moments in CP noninvariant Kobayashi-Maskawa theory (*Russian*) 0-105897  
 baryon magnetic moments, ground-state, SU(6) symmetry 0-78064  
 baryon mass relations in internal SU(6) symmetry 0-82962  
 baryon resonances, EM transitions, multipole moments in single quark transition model 0-62985  
 baryon spectroscopy and photoproduction couplings using new baryon wavefunctions 0-102016  
 baryonium, geometrical approach 0-91065  
 baryonium, ground state hyperfine splitting, harmonic oscillator potential anal. 0-68422  
 baryonium, nuclear and quark confinement forces 0-68431  
 baryons, b-quark, magnetic moments, broken SU(5) symmetry 0-95257  
 baryons, leptonic decays and mag. moments in nonlocal quark model (*Russian*) 0-86711  
 baryons and mesons, parton distrib. consistent with naive quark model and QCD 0-62937  
 Bjorken scaling violation, QCD and models of quarks with substructure 0-105851  
 bootstrap topological approach to quarks and leptons 0-95253  
 bottom hadrons, masses and allowed decays, SU(5) quark model 0-62954  
 bottom mesons, weak decays, strong correction meas. 0-82970  
 bottomium, potential models, non-relativistic description 0-68426  
 Cabibbo angle calcs., mass matrices in Weinberg-Salam model 0-86674  
 charm particle spectroscopy 0-73680  
 charmed baryon decays, nonelectronic, parity-violating, single-quark and two-quark transitions 0-68453  
 charmed baryons, weak decays, quark model framework 0-62976  
 charmonium, potential models, non-relativistic description 0-68426  
 charmonium decay, effective strong coupling constant for timelike Q<sup>2</sup> 0-99091  
 charmonium electromagnetic decay, relativistic eval. 0-68459  
 charmonium resonances above open charm threshold, nonrelativistic quark model 0-78039  
 composite leptons and quarks, anomalous mag. moment, flavour as dynamical quantum number 0-105854  
 composite leptons and quarks, mag. moment 0-105896  
 conference, lepton-hadron physics, Karlsruhe, Germany (Sep. 1978) 0-73098  
 Coulombic qq bound states, short range behaviour, quark mass 0-78033  
 deep inelastic leptonproduction, meson bound state contrib. to  $\sigma_L/\sigma_T$  0-78029  
 deformed shell model for quarks 0-62919  
 diffractive dissociation processes and quark-antiquark jets 0-95246  
 distribution of masses of leptons and hadrons 0-99093  
 division of matter, confinement of quarks and gluons (*Polish*) 0-68417  
 Drell-Yan processes, A-depend. of valence and sea quark contribs. 0-86684  
 E<sub>0</sub> model of unified interactions, asymptotically free, mass relations and interactions 0-73642  
 eight-lepton and eight-quark unification based on Grassmann algebra 0-105824  
 electroweak and strong interactions without the t quark 0-73640  
 evolution operator, quark struct. of states, two dimensional massless electrodynamics (*Russian*) 0-73630  
 fast mesons as dressed quark fragmentation products, Kuti-Weisskopf model 0-91061  
 flavor-changing effective neutral-current couplings in the Weinberg-Salam model 0-86649  
 flavour changing neutral currents with b quarks and/or  $\tau$  leptons 0-73656  
 forward hard scattering in hadron-hadron collisions in the energy region  $\sim 10^{14}$  eV 0-86773  
 four-quark static bag model in two dimensions 0-78037  
 gluon fragmentation, polarised, in e<sup>+</sup>e<sup>-</sup>, e<sup>-</sup>q and hadron scattering 0-82988  
 gluon mass, lower bound in integer-quark-charge model 0-78042  
 hadron collisions, lepton pair production, qq annihilation within same hadron, structure function anal. validity 0-57622

# quark models continued

hadron inclusive prod. cross sections at large  $P_T$  A-depend., quark-parton model (*Russian*) 0-86771  
hadron interactions, effective radius quantum number depend., quark sum rules (*Russian*) 0-102062  
hadron interactions, inclusive processes, multiplicity and scaling, resonance production, additive quark model, SU(6) theory, review 0-63043  
hadron isospin classification, same finite group for mesons and baryons (*Chinese*) 0-62887  
hadron magnetic dipole transition, quark anomalous mag. moments (*Russian*) 0-82975  
hadron production, inclusive, quark fragmentation and triple Regge models, quark decay functions 0-62921  
hadron properties from quark models and confinement schemes 0-105864  
hadron-induced and  $e^+e^-$  annihilation, multiplicity ratio 0-105877  
hadron-nucleus (nucleon), relativistic secondary multiplicities, constituent quark rescatt. 0-63034  
hadronic collisions, jet structure, two-jet events, glueball-Pomeron identity, dual field theory 0-63051  
hadronic fragmentation processes, valence quarks 0-101982  
hadronic interiors, meas. and charge distrib., hadronic diffraction scatt. 0-73817  
hadrons and baryonium, geometrical approach 0-91065  
heavy meson inclusive semileptonic decays, lifetime estimates, quark-parton model difficulties 0-86704  
heavy quark infrared safe weak decay, dimensional regularisation techniques, gluonic corrections 0-102087  
heavy quark mesons, inclusive hadronic prod. (*Russian*) 0-86770  
heavy quarkonium decays, renormalisation group approach, exclusive two meson and inclusive decays 0-82972  
heavy quarks, mass power law 0-62955  
heavy quarks and new particles 0-73661  
hierarchical fermion masses from grand unification 0-105832  
high energy collisions, cumulative particle prod., parton recombination and quark-parton models 0-82956  
high energy lepton pair prod. with pol. hadrons, P and C violations 0-99068  
high-energy physics, particles and interactions, accelerators 0-77944  
inelastic diffraction cross section, quark model and three reggeon limit 0-102035  
inelastic processes, cluster model with repulsion and correlation anal. (*Russian*) 0-102026  
integer-charged quarks in the SU(5) grand unified theory 0-68410  
internal quantum numbers for quarks and leptons in bootstrap approach 0-95254  
 $K^0 \rightarrow K^0$  transition in the standard SU(3)⊗SU(2)⊗U(1) scheme (*Russian*) 0-82951  
left-right symmetric model from general horizontal symmetry, Cabibbo angle, CP violation 0-101972  
left-right symmetry breaking and fermion masses 0-105810  
light hadronic spectroscopy, expt. and quark model interpretations, review, book contrib. 0-68438  
massless  $t$  Hooft model, tachyonic modes, vanishing of scalar density 0-77949  
meson electroproduction in correlating quark rearrangement model 0-86666  
meson leptonic decay, quark spinors in bound quark system, small component effects 0-73694  
meson scattering, quark model asymptotic completeness 0-73738  
meson-baryon large angle elastic scatt. calcs. 0-83002  
MIT bag model, static electroweak props., PCAC 0-73645  
mixing matrix and CP violation for  $n$  quark generations 0-101986  
multi-channel baryonium and some peculiarities of its decays (*Russian*) 0-105857  
multiple hadron production and struct. from 10 GeV to 10 TeV interactions 0-57653  
naive quark model predictions for meson mass and baryon mass and mag. moment 0-78036  
Nambu Goldstone realisation for vector gluon-quark theories, gluon vertices 0-68415  
neutral pseudoscalar meson radiative decays,  $K_{14}$  decay in chiral quark model (*Russian*) 0-105900  
new elementary particles, quark and composite models (*German*) 0-57570  
nonleptonic decays, Weinberg-Salam and harmonic oscillator quark model 0-102048  
nonrelativistic bound s-states in linear central potential 0-82936  
penguins in  $\Delta S=1$  nonleptonic weak decays 0-91086  
pre-quarks and fractional charges 0-91048  
properties in relativistic quark model with strong binding 0-102023  
proton, inner structure, observation in collisions producing jet of debris 0-57569  
 $Q^0$  dibaryon resonances, orbitally excited mass spectrum, decays 0-73670  
quark and hadron jets, charge and energy flow in cascade models 0-102017  
quark diagrams as spectral representations of quark masses (*Russian*) 0-82953  
quark-lepton unification in SU( $N>5$ ) 0-73646  
quarkonium spectroscopy in a potential model with vacuum-polarization corrections for  $\psi$ ,  $T$  0-78038  
quaternionic chromodynamics as a theory of composite quarks and leptons 0-82948  
radially excited states in baryon resonance pionic decays, relativistic quark model 0-95268  
recombination model,  $\pi^+/\pi^-$  ratio in meson-proton inclusive interactions 0-102022  
Regge formalism, quark fragmentation functions for inclusive hadron production 0-68462  
relativistic nuclear collisions, pulsating blobs of quark matter in hydrodynamical model 0-83122  
rishon model of quarks and leptons with double SU(2) symmetry and Dirac magnetic moments 0-82943  
semi-classical models for gluon jets and leptonproduction based on the massless relativistic string 0-105861  
singlet quark form factor exponentiation in leading logarithm approx. 0-91091  
six- and eight-quark models, weak interactions 0-99086  
string junction model and spectrum energy density of string 0-57556  
structure of hadrons containing heavy quark, MIT bag model 0-86672  
SU<sub>c</sub> grand unification model, two ( $V-A$ ) and one ( $V+A$ ) generations of quarks and leptons 0-57538  
SU(2)<sub>c</sub>×U(1) gauge model, mixing angles and CP violation 0-73648

# quark models continued

SU(2)<sub>c</sub>×U(1) gauge theory, four flavours, Cabibbo angle natural relations and bounds 0-57550  
SU(2)<sub>c</sub>×U(1) gauge model, chiral SU(2)×SU(2) symmetry and electron mass 0-57542  
SU(2)<sub>c</sub>×U(1) model, fermion and Higgs multiplet structure, universality 0-62909  
SU(3) wave eqns. for quarks 0-57571  
SU(5)×SU(2) unification, horizontal symmetry due to quantised motion along internal axes 0-62905  
SU(5) and SO(10) grand unification, flavour mixing and proton instability (*Russian*) 0-68413  
subquark model of leptons and quarks, unification, currents and exotic states 0-86683  
superconductivity phase transition in meson states, quark quasiparticle model (*Chinese*) 0-102021  
T-baryonium system, four-body potential in multi-quark states 0-101996  
tensor meson radiative decay in SU(6)×O(3) broken symmetry quark model 0-73710  
top mesons, weak decays, strong correction meas. 0-82970  
U(1)×SU<sub>c</sub>(2)×SU(3) theory, integer charge quarks, lepton hadronic processes (*Russian*) 0-86653  
unitary symmetry in baryon-antibaryon systems (*Chinese*) 0-102000  
valence quark clusters in nucleon structure functions from neutrino scatt. 0-95252  
weak and EM radiative corrections to low-energy processes 0-95274  
Weinberg-Salam model, D<sub>s</sub> group, 2 values of Cabibbo angle, 4 quark flavours 0-68405  
Weinberg-Salam model, extended, Higgs-induced neutral processes, natural-flavour conservation, K-symmetries 0-57539  
Wilson loop critical point behaviour in gauge and lattice gauge theories 0-90993  
Zweig forbidden processes, intermediate vector particle model, neutral vector mesons (*Chinese*) 0-62918  
b-quark mesons, mass, quark model predictions 0-95256  
BB annihilation process, simple geometrical picture 0-95291  
bb meson state lifetimes, R predictions above bottom threshold, quark model 0-99097  
cc qq states, decay, hadronic and photo-prod.,  $e^+e^-$  annihilation prod. 0-99092  
D→Kπ(Kππ), nonleptonic decay rates, quark diagrams and pole approx. 0-86707  
D→Kπν, charm-changing weak hadronic current, models 0-57585  
D-meson decay, hadronic, role of free-quark pairs 0-78059  
D<sup>0</sup> Cabibbo suppressed hadronic decays, Cabibbo universality fake violation, RH currents 0-73699  
D<sup>0</sup> decay enhancement mechanism, quark diagram with gluon prod. 0-105891  
D<sup>0</sup>→K<sup>0</sup>π<sup>+</sup>, quark total number conservation, D<sup>+</sup> lifetime longer than D<sup>0</sup> 0-57590  
D<sup>0</sup>→K<sup>0</sup>π<sup>0</sup>, ΔT=1 constraints and final state interactions 0-95267  
D<sup>0</sup>→K<sup>0</sup>π<sup>0</sup>, quark total number conservation, D<sup>+</sup> lifetime longer than D<sup>0</sup> 0-57590  
D<sup>0</sup> nonleptonic decay, quark annihilation hypothesis test 0-102044  
D<sup>0</sup>→D<sup>0</sup> mixing, flavour-changing Higgs bosons 0-62915  
D<sup>+</sup>→K<sup>0</sup>π<sup>+</sup>, quark total number conservation, D<sup>+</sup> lifetime longer than D<sup>0</sup> 0-57590  
DD molecular charmonium from dual diagram and Schrodinger eqn. 0-86660  
Δ-Δ resonance in nonrelativistic quark model 0-86692  
δ-meson four quark nature (*Russian*) 0-101999  
Δ<sub>35</sub>(1925) baryonic degrees of freedom, nonrelativistic, harmonic oscillator quark model mass formula 0-91066  
 $e^+e^- \rightarrow 3$  jets, integer charge quark model, gluon jets 0-91101  
 $e^+e^-$  annihilation, Q<sup>2</sup> duality test with nonrelativistic potentials 0-102011  
 $e^+e^-$  annihilation, quark jet fragmentation into mesons and baryons, chain decay model 0-63001  
 $e^+e^-$  annihilation, superheavy flavour prod., weak current effects, Z<sup>0</sup> effects 0-57614  
 $e^+e^-$  annihilation and hadron-induced events, multiplicity ratio 0-105877  
 $e^+e^- \rightarrow$  jets, particle ratios from quark statistical model 0-73724  
 $e^+e^- \rightarrow$  jets, t-quark pair prod. effects in annihilation, Kobayashi-Maskawa model 0-86733  
 $e^+e^- \rightarrow$  O particle, decay, mass, prod. from Zweig rule intermediate vector particle model (*Chinese*) 0-73697  
eN, deep inelastic scatt., quark model, field-theoretic, quark indistinguishability, nucleon structure function 0-62993  
ep, deep inelastic scatt.,  $\sigma_1/\sigma_T$  ratio from quark model 0-82979  
 $\eta(\eta') \rightarrow \gamma\gamma$ , quark model tests 0-78067  
 $\eta \rightarrow \pi\pi\gamma$ , quark loop model, SU(3) splitting of quark masses 0-62990  
 $\eta(957)$  meson, quark model description for prod. and decay 0-62970  
 $\eta'$  EM decay,  $\eta$ - $\eta'$  mixing and gluons 0-62981  
 $\eta' \rightarrow \pi\pi\pi$ , amplitude satisfying Adler conditions, relativistic quark pair creation model 0-95262  
 $\eta' \rightarrow \pi\pi\pi$ ,  $\delta\eta'\pi$  and  $\delta\eta\pi$  coupling constant ratio,  $\delta(980)$  quark content 0-82955  
F-meson decay, hadronic, role of free-quark pairs 0-78059  
F<sup>+</sup> nonleptonic decay, quark annihilation hypothesis test 0-102044  
γN, exclusive photoprod. reactions, Okubo-Zweig-Iizuka rule 0-95277  
γq→πq' inclusive pion production in γN and e<sup>-</sup>N collisions, quark-parton model (*Russian*) 0-78073  
K, deep inelastic structure functions in massive quark model 0-86717  
K→3π, relativistic quark model anal. 0-99096  
K structure functions from inclusive prod. data, nonstrange quark distrib. 0-86715  
K<sub>1</sub>→π<sup>+</sup>π<sup>-</sup>(π<sup>0</sup>π<sup>0</sup>), CP violation parameters in six quark model (*Russian*) 0-62974  
K\*→Kγ, quark loop model, SU(3) splitting of quark masses 0-62990  
K<sup>0</sup>→K<sup>0</sup>, weak neutral current diagonalization, mixing amplitude, multi-quark gauge model (*Russian*) 0-68414  
kp, large P<sub>T</sub> pion<sup>0</sup> prod., meson structure functions, quark distrib. functions 0-86714  
Λ(1405) and kaonic H atom, KN interaction model 0-68479  
μ<sup>+</sup>N→hadron shower, charm-pair production effects 0-73748  
n electric dipole moment, CP violation in gauge theories 0-91041  
N form factor, isovector, meson field theory, pseudoscalar πN interaction 0-62986  
N structure function model from hard consistent quark interactions, scaling violations 0-86719



## quark models continued

- NN large angle elastic scatt., spin-spin asymmetries and flavour depend., quark interchange 0-86743  
 NN scattering in the nonrelativistic quark model, total elastic cross section (*Russian*) 0-68475  
 $\nu$ , charmonium and strangeonium, linear+Coulomb pot. study, high  $\alpha_s$  regime 0-62935  
 $\nu(\bar{\nu})N$ , pol.N, deep inelastic processes from valence straton distrib. functions (*Chinese*) 0-99095  
 $\nu(\bar{\nu})N \rightarrow \mu^+ \mu^- X$ , dimuon rate and strange quark sea 0-62961  
 $\bar{\nu}N$  deep inelastic scatt., net charge in current fragmentation region, quark fragmentation 0-62964  
 $\nu N$ —hadron shower, charm-pair production effects 0-73748  
 $\bar{\nu}p$  charged current interactions, quark fragmentation, quark-parton model test 0-68444  
 $\Omega \rightarrow \Theta e(\mu)\bar{\nu}$  or  $\Theta^* e(\mu)\bar{\nu}$ , branching ratios and lepton energy spectra 0-73701  
 $P \rightarrow \gamma^* 1^1$ , EM characts. for pseudoscalar meson decay in nonlocal quark model (*Russian*) 0-102050  
 $pn$ , inelastic charge exchange, quark interchange 0-86759  
 $pN$ —hadron shower, charm-pair production effects 0-73748  
 $pp$ , 100, 200 GeV, elastic scatt., polarisation effects at large momentum transfer, quark model (*Russian*) 0-83005  
 $pp$ , 8.8 GeV/c, exclusive annihilation processes, cross sections, quark model anal. 0-105920  
 $pp$ , elastic scatt., amplitude in quark diquark model 0-102075  
 $pp$ , ISR energies,  $p$  fragmentation,  $D^+$  prod. from  $\Lambda_c^*$  and  $\Lambda_b$  decay 0-102080  
 $pp$ , inelastic charge exchange, quark interchange 0-86759  
 $pp$ , large  $P_T$  pion<sup>0</sup> prod., meson structure functions, quark distrib. functions 0-86714  
 $\bar{p}p$ ,  $pp$ , 12-405 GeV, low  $P_T$  meson prod., quark-antiquark formation model 0-63056  
 $pp$ , probabilistic quark-model approach to  $p$  fragmentation 0-63049  
 $pp$ , secondary hadron absolute yield,  $L=1$  meson prod., quark model (*Chinese*) 0-99113  
 $pp$ —baryons by diquark-quark fusion model 0-102065  
 $pp$ —mesons, multimeson inclusive spectra and recombination model, multi-quark structure functions 0-73751  
 $pp$ — $pp\bar{p}p$ , 11.75 GeV/c, baryonium states, cross section and branching ratio 0-95288  
 $\bar{p}p$ — $S$ — $\bar{p}p$ ,  $S$  meson as baryonium state 0-62938  
 $pp$  scatt., Drell-Yan process, quark-quark contrib. 0-73731  
 $\bar{p}p$ —baryons by diquark-quark fusion model 0-102065  
 $\phi$  decays, hadronic, asymptotic freedom, one-photon or three-gluon exchange 0-62971  
 $\phi \rightarrow \eta\gamma$ , quark loop model, SU(3) splitting of quark masses 0-62990  
 $\pi$ , deep inelastic structure functions in massive quark model 0-86717  
 $\pi$ , modified quark loop model, form factors, struct. functions, radiative decay 0-91088  
 $\pi$ , structure functions from inclusive prod. data, nonstrange quark distrib. 0-86715  
 $\pi \rightarrow e\nu\gamma$ , isospin-breaking, chiral limit, conserved-vector-current violation,  $\sigma$  model 0-62988  
 $\pi \rightarrow e\nu\gamma$  and SU(3) $\times$ SU(3)  $\sigma$ -model 0-78054  
 $\pi$  mass in improved static bag model 0-73667  
 $\pi N$   $\sigma$  term in hybrid chiral bag model, PCAC and SU(3) $\times$ SU(3) symmetry violation 0-78096  
 $\pi^- N$  in Ne, 25, 50 GeV/c, secondary particle multiplicity and multiple scatt. model anal. (*Russian*) 0-83014  
 $\bar{p}p$ , direct photon prod., Compton and annihilation process contrib. 0-105925  
 $\bar{p}p$ , large  $P_T$  pion<sup>0</sup> prod., meson structure functions, quark distrib. functions 0-86714  
 $\bar{p}p \rightarrow \mu^+ \mu^- X$ , quark transverse momentum effect in bag model 0-86668  
 $\psi$  (4.03), isospin and G-parity, model independent prediction 0-86689  
 $\psi$  decays, hadronic, asymptotic freedom, one-photon or three-gluon exchange 0-62971  
 $\psi$ ,  $\psi$  decay branching ratios, isospin and flavour symmetry breaking 0-95264  
 $\psi'$  and  $\psi$  decay ratios, composite particle matrix elements 0-95266  
 $\psi''$  (3770), mass width from quark model 0-73723  
 $qq$ , fine-hyperfine splittings and Lorentz structure of confining potential with vacuum polarisation corrections 0-78041  
 $qq$  interactions and nonrelativistic quark model 0-73682  
 $qq(q\bar{q})$  mesons, mass formula 0-62958  
 $QQ$  systems, inequalities 0-78022  
 $qq\bar{q}q$  diquonium states, production in  $e^+e^-$  processes 0-57615  
 $S^*$  scalar meson, four-quark nature (*Russian*) 0-68432  
 $s\bar{s}$  vector mesons, hadronic decays and props., nonrelativistic quark model 0-105892  
 $t$ -quark mass predictions from Glashow determinant condition 0-86677  
 $t$ -quark mesons, mass, quark model predictions 0-95256  
 $t\bar{t}$  states,  $t$  threshold, potential model predictions 0-86682  
 $t\bar{t}$  vector meson, proposed 40 GeV mass 0-62942  
 $\tau \rightarrow \nu\mu\gamma$ , quark model, current algebra model, divergence of axial vector current 0-57655  
 $T$ , production and decay in quark fusion model 0-102018  
 $T(9.46)$  orthoquarkonium decay, jet profiles, three gluon structure 0-73698  
 $T$  and charmonium spectra, common pot. fit,  $T''-T$  mass difference 0-86712  
 $u$  decays, hadronic, asymptotic freedom, one-photon or three-gluon exchange 0-62971  
 $D^0 \rightarrow \bar{D}^0$ , weak neutral current diagonality, mixing amplitude, multi-quark gauge model (*Russian*) 0-68414  
 $K \rightarrow \pi e^+ e^-$ , six-quark model, CP violation 0-78055

## quarks

- see also quark confinement; quark models  
 composite leptons and quarks, mag. moment 0-105896  
 composite quarks and leptons, mag. moments 0-91056  
 division of matter, confinement of quarks and gluons (*Polish*) 0-68417  
 $E_8$  model of unified interactions, asymptotically free, mass relations and interactions 0-73642  
 electric dipole moment in Kobayashi-Maskawa theory with gluonic corrections (*Russian*) 0-86688  
 electric neutrality of matter at milligram level, quark search 0-105939  
 electroweak symmetry group, B-L U(1) generator and quark-lepton symmetry 0-57549

## quarks continued

- EM fine struct., Fermi weak coupling, Newtonian grav. constants, unified relation 0-101974  
 EM form factors 0-99102  
 evolution operator, quark struct. of states, two dimensional massless electrodynamics (*Russian*) 0-73630  
 exotic atoms, conf., Erice, Sicily, (1979) 0-67939  
 fermion masses and hierarchy of symmetry breaking,  $u$  and  $d$  quarks 0-86618  
 fine-structure constant, coupled Maxwell and Dirac eqns., QED 0-62894  
 fourth generation of quarks and leptons, mass formula 0-105876  
 fragmentation in field-theoretic model of composite hadrons and  $e^+e^-$  annihilation 0-82986  
 fundamental constituents of matter and unification of weak and electromagnetic interactions 0-62940  
 grand unification with exceptional group  $E_6$ , symmetry breaking, SU(5) relations, quark masses 0-68407  
 grand unified wave function for quarks and leptons 0-91034  
 hadron leptonproduction, nuclear targets, quark-nucleon inclusive cross section, heavy lepton pairs 0-57607  
 hadron magnetic dipole transition, quark anomalous mag. moments (*Russian*) 0-82975  
 hadronic two-jet events, momentum unbalance, parton transverse momentum in  $pp$ ,  $\pi p$  0-57652  
 horizontal cosmic ray penetrating particles identification, fractional charge search (*Chinese*) 0-101514  
 LEP, design, tests of unified field theories and quark properties, search for new quarks and leptons 0-74048  
 mass, electroweak contrib. 0-101990  
 mass differences of up and down quarks, grand unification 0-62978  
 masses in scalar dynamics, gluon theories compared with QCD 0-57553  
 momentum subtraction scheme, quark mass depend. cancellation in anomalous dims. 0-77965  
 neutron matter-quark matter phase transition, QCD and extended Higgs model, instantons 0-91062  
 neutron stars, quark beta decay and cooling 0-82406  
 PETRA results for fluons, nuclear forces,  $t$ -quarks and quark-lepton symmetry 0-86731  
 QDD, quantum dath dynamics, SU(3) model for composite quarks and leptons 0-91055  
 relativistic cosmology, interactions with leptons 0-90590  
 rishon model for quarks and leptons, topological bootstrap approach 0-78047  
 rishon model of quarks and leptons with double SU(2) symmetry and Dirac magnetic moments 0-82943  
 search for quarks in matter, mag. levitation electrometer results 0-102088  
 singlet quark form factor exponentiation in leading logarithm approx. 0-91091  
 SO(10) unification, composite structs., quark and lepton composite models 0-57547  
 stars, beta decay 0-82398  
 SU(3) wave eqns. for quarks 0-57571  
 SU(5), unification of weak, EM and strong interactions, review 0-105814  
 SU(5) gauge model, masses, mixing angles, CP violation and b-quark decay 0-78006  
 SU(5) grand unification, heavy coloured Higgs scalars, b-quark mass 0-57543  
 SU(5) without symmetry constraints, unified model of quarks and leptons, conservation laws 0-101968  
 subcomponent models of quarks and leptons in SU(3) subcolour, proton decay 0-78035  
 subquark model of leptons and quarks, unification, currents and exotic states 0-86683  
 supergrand exceptional unification and quark-lepton constituents 0-91030  
 supergrand unification in  $E_8$ , quark-lepton assignments, symmetry breaking scheme 0-68408  
 tumbling gauge theories with chiral fermion fields, symmetry breaking 0-99042  
 unification of EM, weak and strong interactions, quark and lepton mass, quark fractional charge, baryon asymmetry 0-73637  
 unified field theories, proton and neutron disintegration, concepts of leptons and quarks (*French*) 0-91038  
 unified models of quarks and leptons, B-L conservation and B nonconservation 0-95229  
 b-quark production from  $\nu N$ , SU(2) $\times$ SU(2) $\times$ U(1) gauge group mixing angles 0-68445  
 C-quark, mass difference to be quark 0-78022  
 $\chi \rightarrow \psi\gamma$ , charmonium E1 radiative transitions and quark mag. moments 0-86721  
 $e^+e^- \rightarrow$  jets, on-shell QCD quark form factor from two particle correlations 0-86740  
 $e^+e^-$  annihilation, hadron and lepton prod.,  $\tau$ -lepton decay,  $K^*$ ,  $p$ ,  $\bar{p}$  yields, quark flavours 0-73725  
 $e^+e^- \rightarrow b\bar{b}$ , heavy quark masses and C- and P-odd asymmetries, Weinberg-Salam model (*Russian*) 0-102060  
 $e^+e^-$ —hadrons, 33-35.8 GeV, new quark flavour search, cross sections and thrust 0-86736  
 $e^+e^-$ —hadrons, R problem, QED and QCD corrections, quarks and leptons 0-95281  
 $K \rightarrow \pi e(\mu)\gamma$ , quark mass ratios 0-105884  
 $\bar{e}e$  annihilation in Weinberg-Salam model, number of quarks and leptons (*Russian*) 0-102041  
 $\nu N$ , heavy-quark production,  $t$  and  $b$ -quarks, SU(2) $\times$ SU(2) $\times$ U(1) gauge group mixing angles 0-68445  
 $\bar{\nu}N$ ,  $K^0$  and  $\pi^-$  prod. rates, SU(3) symmetry violation in quark jet 0-82966  
 $\bar{p}p$ —charm quarks 0-102040  
 $\psi \rightarrow \chi\gamma$ , charmonium E1 radiative transitions and quark mag. moments 0-86721  
 $t$ -quark mass predictions from Glashow determinant condition 0-86677  
 $t$ -quark production from  $\nu N$ , SU(2) $\times$ SU(2) $\times$ U(1) gauge group mixing angles 0-68445

## quartz

- acoustic activity, inelastic neutron scatt. obs. (*French*) 0-103431  
 antireflection film, vacuum-etched high-transmittance 0-74449  
 c-axis fabrics in metamorphic rocks, anal. via photometric method 0-101456  
 cell parameter variations between 94 and 298 K 0-96497  
 crystal growth, defects induced by seed orientation 0-96454

## quartz continued

- crystal structure rearrangement due to neutron irradiation 0-64981  
 crystalline, birefringence, temp. depend., intracavity method meas. 0-78931  
 crystals with TTC-cut (*Danish*) 0-60504  
 dental composites, acrylic acid grafted on particles by gamma-radiation 0-66840  
 dislocation fine structure under electron irradiation 0-70213  
 dislocations, electron irradiation, induced vitrification 0-107252  
 dissolution in liq. Si, effect of C, rel. to melt growth of Si 0-70414  
 doubly-rotated-cut, numerical anal. of props. of SAWs 0-74616  
 dynamic wetting angle of dry lyophilic surface 0-88405  
 elastic constants and piezoelec. props. 0-92590  
 elastic plates, rotated-Y-cuts, high frequency vibrations 0-96216  
 electro-optical props. near phase transition 0-80756  
 electron irradiation, defect struct. and radiolysis 0-107321  
 electron irradiation effects on optical, dielec., elastic props. 0-59521  
 electronic structure of  $\alpha$ -quartz, local disorder influence 0-59870  
 etching characteristics of a natural quartz track detector 0-91401  
 first order transition, coexistence states, optical obs. 0-75350  
 Fourier transform spectroscopy of obs. states at high temps. 0-97256  
 fused, damage by UV laser radiation, avalanche ionization mechanism 0-76110  
 fused, photoelastic light scatt. from surface Rayleigh waves 0-97235  
 fused, positronium form. and decay, elec. field effect 0-97369  
 fused, substrate for ZnS, Na<sub>3</sub>AlF<sub>6</sub> films, H<sub>2</sub>O absorpt., IR anal. 0-75446  
 fused, thermal cond., temp. depend. at low temps. 0-65322  
 glass struct. study using small-angle X-ray scatt. 0-84071  
 heat transfer at low temps., lattice thermal cond. 0-92729  
 high-frequency phonon lifetimes 0-70338  
 inclusion obs., solid-liquid-gas, Raman microprobe-microscope appl. 0-62737  
 interdigital transducer on piezoelectric half space, spectrum of emanating acoustic waves 0-79044  
 interface with liq. <sup>4</sup>He, saturation effects in phonon reflection 0-92736  
 ion implanted, radiation defects and optical props. 0-107293  
 IR radiation extinction coeff. rel. to mechanical Q 0-100653  
 light scattering polarisation props. at  $\alpha$ - $\beta$  phase transition 0-108220  
 lightguide resonator for Nd<sup>3+</sup>:YAG laser, Raman generation 0-99735  
 low, CC Si-O bond characteristics 0-84132  
 low, ionicity of Si-O bond 0-84133  
 luminescence centres at 396 and 280 nm 0-103996  
 metallic overlay films for temp. compensation SAW device appls. 0-79043  
 muonium spin precession quadrupole effects 0-75910  
 naturally deformed, dynamic recrystn. during creep, dislocation substruct., Mg alloy comparison 0-109142  
 nonlinear crystals, interference of optical harmonics 0-64102  
 optical fibre, stimulated Raman scatt., Stokes components recording opposite to pump wave 0-106569  
 orientation of industrially cut alpha quartz AT plates 0-92008  
 piezoelectric crystal microbalance for sorption studies: under dynamic conditions 0-73323  
 piezoelectric material for electrostatic voltage sensor (*Japanese*) 0-105632  
 piezoelectric transducer, acoustic field distrib., Bragg diffraction method 0-97231  
 PMMA, quartz- and glass-particle reinforced, abrasive wear 0-97594  
 powder, dry ball milling, breakage parameters variation with ball and powder loading 0-80999  
 powder on piezoelec. substrate, dynamic SAW reflecting struct. 0-74565  
 $\alpha$ -quartz:<sup>57</sup>Fe, anomalous hyperfine splitting 0-103650  
 $\alpha$ -quartz:P, dynamic interchange among 3 states of P<sup>4+</sup>, EPR obs. 0-66010  
 $\alpha$ -quartz, CNDO/2 calcs., electronic props. of perfect cluster, EPR parameters of O<sup>-</sup> vacancy 0-107701  
 $\alpha$ -quartz, Renninger effect, forbidden X-ray reflections 0-64980  
 quartz, single crystals, Ar and O<sub>2</sub> interaction at high temp., surface struct. changes (*German*) 0-96725  
 $\alpha$ -quartz, temp. in high-pressure shock state 0-72490  
 quartzite, vitrified, and quartzite based refractory concretes, prep. and props. 0-89188  
 reflective dot array for high-performance signal processing, development 0-74623  
 reflector-array-compressor devices, use of Y-cut quartz 0-74625  
 sand, high-conc. suspension, prod. principles 0-66463  
 SAW and SBAW on doubly-rotated cuts 0-74584  
 SAW propagation, effects of He ion implantation 0-75421  
 SAW propagation, characts. on quartz with zero temp. coeff. of delay 0-75420  
 SAW propagation, acoustoelectric methods 0-84359  
 smoky, gamma-irradiated, short-time-scale spht. meas. 0-59672  
 space group C<sub>3</sub>2-C<sub>3</sub>2, habit variation 0-107090  
 specific directions of plane elastic waves in thin quartz crystal plates 0-92601  
 subgrain boundaries, theoret. predictions and microscopic obs. methods 0-84187  
 substrate, anthracene ultrathin film deposition 0-59812  
 surface, XPS study 0-93451  
 surface damage by X-rays,  $\gamma$ -rays, neutrons, SEM study 0-79837  
 surface irregularities in quartz plates due to mechanical, chemical treatment, piezoelectric resonators appl. (*Polish*) 0-9380  
 surface skimming bulk wave propagation in Y-rotated cuts 0-74583  
 synthetic, Al centres conc. and anomalous pleochroism depend. on crystn. parameters 0-107311  
 synthetic, deuteration, EPR and IR absorpt. characterisation 0-92721  
 thermal expansion near  $\alpha$ - $\beta$  transition under uniaxial stresses 0-70429  
 torsional vibration frequency temp. depend. 0-70294  
 wafers, surface contaminant estimation methods, cleaning process appl. (*Polish*) 0-89381  
 MgF<sub>2</sub> polycryst., quartz particle impacts no. effect on erosion in elastic-plastic response regime 0-81209  
 SiO<sub>2</sub>:Ag, X-ray induced EPR and luminesc. centre 0-65043  
 Sn film-quartz substrate interface, anomalous transmittance for thermally radiated phonons of thin metal films (*Russian*) 0-103664  
 ZnO/quartz for SAW device materials, expt. study of props. 0-80050

## quartz resonators see crystal resonators

## quasars

- see also BL Lacertae-type objects; cosmology; galaxies; radiofrequency cosmic radiation; stars  
 0957+561, radioastron. obs. of assumed double quasars 0-105381

## quasars continued

- 0957+561A, B, double quasar, IR obs. of quasar and intervening galaxy 0-73065  
 1610-771, radio QSO with steep optical spectrum, obs. 0-94887  
 2A 2251-179, X-ray quasar, UV photometry 0-82349  
 absorption line redshifts, distrib. 0-90563  
 absorption lines and intergalactic clouds 0-62311  
 absorption redshifts, evidence for large-scale uniformity of physical laws 0-73079  
 anisotropic radio emission model 0-62304  
 Arp QSO-galaxy associations, nature 0-90564  
 black hole model, supercritical accretion on disc theory 0-105272  
 brightness, cyclic depend. on parameter  $\ln(1+z)$  0-105382  
 brightness rapid variability, search in eight quasars and BL Lacertae objects 0-90567  
 broad line regions, luminosity and radio emission in active nuclei and quasars 0-105340  
 3C 119, 286, 345, 454.3, 5 milliarcsecond resolution maps at 1.67 GHz 0-82531  
 3C 147, 3C 286, VLBI obs. at 329 MHz 0-67898  
 3C 147, hybrid mapping on Very Large Array, SHF obs. 0-82534  
 3C 273, detailed UV obs. with IUE 0-94886  
 3C 273, interplanetary scintillation spectra obs. 0-72741  
 3C 273, search for 1-20 MeV gamma rays, balloon-borne obs. 0-67912  
 3C 273, UV obs., (1975 to 1979) 0-62309  
 4C 32.69, quasar with radio jet, high resolution radio obs. 0-105375  
 3C 345, VLBI obs. at 1.67 GHz 0-94885  
 3C 345 and 454.3, 102 MHz obs. of interplanetary scintillations (*Russian*) 0-94889  
 3C 351, VLA maps and outer lobe optical emission search 0-105376  
 4 C 39.25, compact radio source, search for time-depend. radio fine struct. 0-90552  
 3C 446, 1980 June outburst, UV photometry 0-86010  
 3C catalogue faint red QSO candidates, spectrophotometry and red shifts 0-67897  
 CG 135+1, search for 1-20 MeV gamma rays, balloon-borne obs. 0-67912  
 Cherenkov line radiation, QSO emission-like spectra (*Chinese*) 0-105378  
 chronometric cosmology, tests using galaxy and quasar samples 0-86022  
 GQ Comae Berenices, QSO or N galaxy, spectrophotometry obs. 0-77488  
 compact synchrotron sources variability, model of knots spontaneous form. in relativistic flows 0-105369  
 Compton scattering in sources with synchrotron reabsorption 0-72761  
 Comptonised spectrum, Monte Carlo simulation 0-90566  
 conference on high redshift objects, IAU Symposium 92, Los Angeles (August 1979) 0-101669  
 CTA 102, 5 milliarcsecond resolution maps at 1.67 GHz 0-82531  
 CTIO 4 m survey, visible and UV spectrophotometry 0-86009  
 CTIO Curtis Schmidt survey -40° zone, discoveries and spectrophotometry 0-73064  
 D2 radio structure sources, 11 cm obs. 0-67895  
 distribution in depth 0-105383  
 emission-line regions clouds, absorpt. spectrum synthesis 0-62308  
 evolutionary constraints from galaxy star counts 0-82507  
 faint blue objects, nature and distrib. 0-82476  
 faint components, VHF and SHF obs. 0-90547  
 fast spectral line variability interpretation (*Russian*) 0-77286  
 giant black holes, mass-density diagram (*French*) 0-94828  
 gravitational lens effect, focusing by slowly rotating relativistic spherical mass 0-105155  
 gravitational mirage (*French*) 0-94710  
 IR sources, optical identification problems 0-105392  
 IR spectra, H I line ratios 0-105391  
 luminosity, X-ray to optical ratio, determ. ratio 0-94719  
 massive black holes binary systems, model for quasars and active galactic nuclei 0-109546  
 MCS 141, 232, 275, spectra interpretation, visible obs. 0-90562  
 MCS QSOs, radio obs. of 70 optically selected objects 0-105377  
 millimetre wave emission, rapid variability obs. (*Russian*) 0-90559  
 Molonglo Deep Survey QSOs, optical spectra and redshifts 0-94884  
 MR 2251-178, nearby QSO in cluster of galaxies 0-67900  
 narrow line absorption systems, form. model 0-82535  
 nuclei, VLBI hybrid mapping 0-105356  
 number-magnitude relation rel. to luminosity function and cosmological evolution 0-77507  
 optical counterparts of radio sources, galaxies and quasars, astrometry 0-90551  
 optical identifications of extragalactic radio sources 0-105373  
 optically discovered, search for radio emission 0-90561  
 optically selected QSOs, radio study 0-82536  
 OTL source positions and struct. form 327 MHz obs. of lunar occultations 0-73061  
 PG 1115+08, triple QSO, probable gravitational lens 0-86012  
 PHL 1092, narrow line quasar, discovery of extreme Fe II emission 0-77508  
 photon splitting into 3, cosmological limits, spectral broadening, frequency-dependent and multiple red-shifts 0-77284  
 PKS 2126-15 ( $z=3.27$ ), JHK photometric obs. 0-94888  
 Q0353-383, QSO abundance anomalies, UV and visible spectral obs. 0-82532  
 Q0957+561, double quasar, components brightness ratio var. 0-77509  
 Q 0420-338 ( $z=3.13$ ), JHK photometric obs. 0-94888  
 Q 0957+561 A,B, UV spectra and gravit. lens interpretation 0-82537  
 QSO 0957+561, double quasar, 6 cm wavelength obs. 0-62312  
 QSO 0957+561, double quasar, visible spectrophotometry, gravitational lens interpretation 0-82533  
 QSO 0957+561, double quasar as gravitational lens, 6 cm VLA obs. 0-101647  
 QSO 0957+561 AB, double quasar, IR spectrum confirms gravitational lens 0-77510  
 QSO absorption spectra origin 0-105387  
 QSO redshifted 21 cm absorption line clouds 0-62310  
 QSO resonance lines as luminosity calibrators 0-105388  
 QSO revised optical catalogue 0-105177  
 QSO spectral indices and cut off energy determ. from photoionisation of cold dense universes 0-77526  
 QSO-galaxy group assoc., 3C 273 field obs. 0-105385  
 QSOs, linear polarisation meas., SHF obs. 0-73058  
 QSOs, luminosity and emission line intensity ratios 0-86011  
 QSOs near bright galaxies, non-cosmological redshifts 0-105386  
 QSOs with assoc. galaxies, spectroscopic search 0-105355



**quasars continued**

- radial distribution, uniformity in chronometric cosmology rel. to X-ray background 0-105409
- radiatively driven winds for different power law spectra 0-90565
- radio emission, variable, temporal characts. (*Russian*) 0-62307
- radio quasars, compact, apparent magnitude-redshift relations for resolved and unresolved sources (*Chinese*) 0-105380
- redshift distribution, implications for evolution of galaxies 0-90527
- redshifted clouds, 21 in line studies 0-105389
- redshifts, teaching consideration 0-90621
- redshifts distributions, periodicity 0-62313
- relativistic plasmon ejection as activity indicator (*Russian*) 0-67870
- rotation measures and data processing 0-86006
- spectra, absorpt. effects due to intergalactic pyrolytic graphite whiskers 0-94866
- spectra, Mg II and Fe II lines excitation 0-67896
- spectra of large red shift quasars, implications of neutrino rest mass for H I obs. problem (*Russian*) 0-105414
- superfine radiostructure determ. using interstellar scintillations (*Russian*) 0-77297
- systematic surveys with slitless spectrum technique 0-105384
- Tololo quasar candidates, comparison with positions of bright galaxies 0-77506
- transverse motions, determ. from relativistic Doppler formula for redshift (*Chinese*) 0-105379
- UV continuum source in list of galaxies with UV continua, identification as probable QSO 0-67585
- UV obs., implications 0-105390
- X-ray background contrib. 0-105405
- X-ray background source possibility 0-94898
- X-ray detection of cosmological objects 0-62323
- X-ray observations of objects at cosmological distances from the 'Einstein' observatory 0-105171
- X-ray quasars, evolution rel. to contrib. to X-ray background 0-82551
- X-ray sources, low redshift, visible spectra and UBVR photometry 0-105397
- Fe II lines, permitted, form. and relative intensities rel. to low excitation region parameters 0-62278
- Fe II UV lines, spectrophotometry obs. of 11 QSOs 0-73063
- H I Lyman  $\alpha$  absorpt. line distrib., intergalactic origin 0-67899
- He I 584 Å in quasars and gaseous nebulae, line transfer problem and line strength 0-67550

**quasi-particles**

- see also excitons; helicons; magnons; phonons; plasmons; polaritons; polarons; ripples; rotors; solitons
- clean superconductor, effect of impurity scatt. on thermally induced charge imbalance 0-60135
- covalent crystal, dynamical correlation effects on quasiparticle Bloch states 0-88499
- dynamics, inverse Liouville problem, quasi-particle dynamics from a given kinetic eqn. 0-101749
- Enskog quasiparticle, non-Hamiltonian dynamics 0-101750
- ferromagnetic semiconductor, doped, electron spin polarisation and conduction band struct. 0-65449
- gas-metal interactions, scatt. dynamics 0-92787
- granular metal, supercond. transition, increased resistance rel. to quasiparticle tunnelling 0-88689
- Hubbard model, narrow-band region, quasiparticles, electron relax. and transport props. 0-80151
- Hubbard model, split-band solution and energy gap, narrow-band region 0-75484
- metals, simple, quasiparticle props., density functional approx., electron gas calc. 0-96808
- metals, superconductivity studied by electron-phonon and Coulombian e-e coupling strength and quasi particle mass 0-88666
- metals and alloys, electrons at Fermi surface, book 0-105445
- molecular crystals with several sublattices, exciton-phonon interaction and Bose-Einstein condensation of Frenkel excitons 0-107713
- multiband system, electron pairing, radiation effect 0-88679
- nonequilibrium superconductors, ferromag. ordering of quasi-particles and rise of domains 0-107958
- nuclear collective model, two-phonon states, effect of Pauli principle 0-68565
- semiconductor, electron excitation spectra in field of two travelling waves 0-65514
- superconducting weak links, quasiparticle-injected, simple-heating-induced Josephson effects 0-70904
- superconductor, nonequilib., with wideband source of quasiparticles, kinetic theory 0-80442
- superconductor-insulator-superconductor quasiparticle mixers, conversion gain prediction 0-70901
- superconductor-insulator-superconductor quasiparticle tunnel junctions, as microwave detectors 0-65744
- superconductors, nonequilibrium states, narrow nonequilibrium sources (*Russian*) 0-88687
- thin optical irradiated superconductors, phonon spectrum and phonon temp. definition 0-93037
- Al particles, small supercond. nuclear spin-lattice relax. meas. 0-88681
- Al-Mn(Cr)(V), dil., supercond., nucl. spin relax. and quasiparticle excitations 0-88680
- Al-PbBi superconducting tunnel junctions, optically illuminated, quasiparticle energy distribution 0-75688
- Cs, Fermi surface and quasiparticle props., density functional approx. 0-96771
- CsNiF<sub>6</sub>, nonlinear excitations, 1D-ferromag., neutron scatt. 0-70949
- EuO magnetic semiconductor, quasiparticle lifetimes, CPA study 0-65443
- <sup>3</sup>He, liq., interface with nonmag. solid, Kapitza resist., quantum perturbation treatment 0-88385
- <sup>3</sup>He, liquid, polarisation potentials, viscosity, thermal cond., spin diffusion 0-88389
- <sup>3</sup>He, normal liquid, elementary excitations, density and spin density, zero sound mode, press. depend. RPA model calcs. 0-59749
- <sup>3</sup>He, superfluid A-phase, ion mobility tensor, ion-quasiparticle scatt. 0-59753
- In whiskers from Sn-In alloys, current carrying, superconductivity breakdown 0-60133
- Li, Fermi surface and quasiparticle props., density functional approx. 0-96771
- Ni, quasi-particle energies, two-hole XPS satellite 0-66399

**quasi-particles continued**

- Pb-PbO<sub>2</sub>-Pb small supercond. tunnel junctions, effect of capacitance in I-V characts., high-freq. obs. 0-80448
  - Rb, Fermi surface and quasiparticle props., density functional approx. 0-96771
  - Si MOSFET, surface quantum states, two-dimensionality of many-body effects 0-103740
  - Sn, supercond. tunnel junction, quasiparticle excitation by  $\alpha$ -particles 0-103791
  - W-Re amorphous alloys, phase-slip and localisation diffusion lengths 0-107747
- quasi-stellar objects** see *quasars*
- quasi-stellar sources** see *quasars*
- quasimolecules**
- alkali atom (ion)+inert gas, collision studies of quasi-one-electron systems 0-63750
  - atmosphere Van der Waals mol. comp., 5-90 km altitude 0-85699
  - collision systems  $\alpha(Z_1+Z_2)\geq 1$ , quasimolecular 1  $\sigma$  orbital, excitation and spectroscopy 0-87199
  - heavy ion collisions, electron EM field interaction, quantised field formalism 0-83478
  - superheavy and intermediate atomic collision systems, UNILAC expts. 0-63751
  - superheavy collision system, radiative processes, search for positron emission 0-63752
  - superheavy ion-atom collisions, quasiats., K-vacancy form., positron emission 0-63753
  - triatomic van der Waals mols., rot. predissoc. 0-63721
  - van der Waals mol. rot. predissociation study, complex coord. method 0-74205
  - Ar<sub>2</sub> van der Waals dimer, intermol. pot., SCF CI ab initio calcs. 0-106274
  - Ar.HCl, Van der Waals mols., SCF energies and dispersion forces 0-74279
  - Ar.HF, Van der Waals mols., SCF energies and dispersion forces 0-74279
  - Ar.H<sub>2</sub>O, Van der Waals mols., SCF energies and dispersion forces 0-74279
  - I<sub>2</sub>Ar<sup>+</sup>, product state distrib. and binding energy 0-63857
  - I<sub>2</sub>He, van der Waals mol., photodissoc. 0-63765
  - I<sub>2</sub>He<sup>+</sup>, product state distrib. and binding energy 0-63857
  - I<sub>2</sub>Ne<sup>+</sup>, product state distrib. and binding energy 0-63857
  - Kr<sub>2</sub><sup>+</sup>, formed in 50 keV Kr<sup>2+</sup>+Kr collisions, Auger transitions obs. by electron-scattered-ion coincidence method 0-74243
- quench hardening**
- steel case depth after quench hardening, inspection using coercimeters 0-104377
  - Cr-Ni-Mo 40KhN2MA, magnetostriction used in inspection after heat treatment 0-108673
  - steels, Cr-C-Mn(Ni), struct. prop. rel., design of struct. steels for high strength and toughness 0-97491
  - Ti-Mo-Zr-Sn (11.5, 6, 4.5 wt.%),  $\beta$  III, mech. props. rel. to heat treatment 0-84961
  - Ti-Ni (48 to 53 at.%), heat treatment and deviation from stoichiometry 0-104192
- quenching (optical)** see *radiation quenching*
- quenching (thermal)**
- see also quench hardening
  - Al-Zn-Mg (5.1 wt.%), decomp. process, TEM study 0-71660
  - alkali glasses, rapidly quenched, alkali ion cond. 0-107559
  - alloys, rapidly quenched crystalline, struct., and heat treatment effects 0-76292
  - amorphism, techniques for determ. very short room temp. lifetimes 0-84981
  - binary alloys, quenched, vacancy concs. 0-107212
  - brittle ceramics, effect of data scatter on apparent thermal stress failure mode 0-60949
  - ceramics, brittle, heat-transfer variables effect as thermal stress resist., meas. by quenching expts. 0-79871
  - disordered metal ribbon production by ultrarapid quenching 0-71612
  - energy spike development and quenching depend. on thermal diffusion 0-88367
  - F 0-76235
  - Ising model, quenched-bond disorder, cluster extension of effective-interaction approximation 0-93130
  - low temperature techniques and devices 0-76291
  - melt extraction technology, advances 0-76207
  - metallic coatings, electric field atomisation from melt 0-76174
  - metallic glass, current exptl. data on struct., review 0-88058
  - metallic glass, prep. and phys. props. development 0-81003
  - metallic glass, splat cooled, mag. props. 0-80491
  - metallic glasses, formation and rapid quenching techniques 0-76214
  - metallic glasses, stability 0-75184
  - metals, quenched, vacancy cluster form. process 0-92706
  - metals, rapidly quenched, conf., Brighton, England (July 1978) 0-67934
  - microcrystalline alloys, metastable, produced by rapid particulate quenching, props. and appls. 0-84887
  - nonisothermal devitrification kinetics 0-92465
  - plasma industrial utilisation, synthesis, powder, metallurgical and surface treatments, review (*French*) 0-96398
  - polyethylene, irradiation, crystallinity and crosslinking efficiency 0-66843
  - polyethylene-paraffin wax, blends, rapid cooling processing techniques 0-84905
  - rare earth oxide containing systems, highly refractive, phase equilb. and metastable phases 0-97467
  - roller-plate technique, for thin film prep. from melt 0-71607
  - sapphire, neutron bombard., F-centre fluorescence, photoluminescence 0-100676
  - steel, alloy, high-speed, struct. changes investigation by hot hardness and quench dilatometry (*French*) 0-76249
  - steel, alloy, quenched carbonitrided, multicycle fatigue failure 0-104283
  - steel, austenitic, quenched state, influence of austenite stability on impact strength (*Russian*) 0-81146
  - steel, austenitic, strength, ductility and fracture toughness, N and Cr effects 0-100878
  - steel, C, massive martensitic transformation kinetics 0-81060
  - steel, C, quenched, restoration of austenite grains during rapid heating (*Russian*) 0-76272
  - steel, C-Cr (1.0, 1.5 wt.%), 52100 bearing steel, control of surface residual stress by heat treatment 0-97501

**quenching (thermal)** continued

steel, carburized and quenched, residual stresses (*Japanese*) 0-89262  
 steel, Cr-Mn type, martensite struct. after quenching and HTMT, X-ray diff. obs. 0-84975  
 steel, Cr-Mo-V pressure vessel, microstruct. parameters and yielding rel. to plastic deform. 0-89318  
 steel, Cr-Ni, pendant drop melt extracted, struct. and props. 0-76242  
 steel, Cr-Ni-Mo-V, austenite form. during heating, influence of recrystn. during tempering (*Russian*) 0-104188  
 steel, Cr-Si-Mn-Ni-Mo-C, resist. to deform. and fracture, C effect 0-71757  
 steel, Cr-W(Mo), quenched, carbide reactions during tempering 0-89229  
 steel, ferritic stainless, embrittlement 0-85041  
 steel, high alloy Cr-Mo-W, splat quenched, formation of metastable austenite 0-84974  
 steel, high strength, treatment effect on ductility and strength 0-60880  
 steel, high-speed tool, splat quenching, props. and struct. 0-76294  
 steel, high-strength low alloy, Nb(CN) precipitation and coarsening during hot compression 0-97514  
 steel, low-alloy structural 16G2 and 16GFR, struct. and props. after quenching and tempering 0-76280  
 steel, maraging stainless, phase transformation and mech. props. rel. to heat treatment (*Chinese*) 0-66501  
 steel, martensitic, sp. ht. and magnetisation meas. 1.2 to 10K 0-71059  
 steel, martensitic-aged, plastic deformation influence in type N17K12M5T steel on mech. props. (*Russian*) 0-76305  
 steel, Mn-B-V, low alloy, transform. singularities (*Russian*) 0-104116  
 steel, Mn-C-Si-Cu (0.95, 0.85, 0.25, 0.16 wt.%), fibrous-banded fracture mechanism 0-104280  
 steel, Ni, 11.6%, quenched cylinder residual stresses, boring/turning and X-ray diff. obs. (*German*) 0-93586  
 steel, Ni, high-strength, impact fatigue strength, heat treatment conditions effect 0-76285  
 steel, Ni-Co-Cr, high-strength medium C, Cr effect on props. 0-76339  
 steel, Ni-Mo-C (2.0, 0.2, 0.4 wt.%) sintered, struct. transforms. and mech. props. after quenching 0-66557  
 steel, Ni-Mo-C (5, 0.5, 0.5 wt.%), sintered, effects of powder and sintering variables on props. 0-104093  
 steel, pearlitic, heat treatment effect on fracture resistance, microstruct. and mech. props. 0-104191  
 steel, platelike parts, quenching, temp. field calc. 0-60889  
 steel, structural, 34KhN3M, heat treatment effect on magnetostriction 0-104306  
 steel, type 20Kh deformed, austenite grain size, inheritance effect with quenching and tempering 0-60881  
 steel, W alloy, microstruct. and hardness, splat quenching effect 0-76293  
 steel, W-Co-Mo-Cr-V-C (8.5, 8.1, 4.5, 3.5, 2.2, 1.02 wt.%), phase composition, struct. and props. 0-104163  
 steel (*French*) 0-66670  
 steel fine structure after heat treatment, X-ray diff. exam. 0-60890  
 steels, induction hardened bearing, rolling contact strength (*Japanese*) 0-93568  
 steels, low-C, aged after quenching, rel. between micro-cracks and coxing effect (*Japanese*) 0-81159  
 steels, tempered with different Ni contents, scaling behaviour obs. 0-71817  
 superconducting metastable alloys, review of current work 0-81002  
 Ag-Cu surface alloyed films, laser melt quenched, microstruct. 0-76423  
 Ag-Sn, splat-quenched, X-ray diff. study 0-81094  
 AgI/Ag oxy salt system, vitreous solid electrolytes, conductance mechanism 0-107560  
 Al alloy RR58, low cycle fatigue at 423K, prior treatment effect 0-104254  
 Al alloys, metastable microcrystn., appl. 0-84887  
 Al binary alloys, rapid quenching, struct. and decomp. 0-76244  
 Al-Ag, type-II superconductor, torque oscillations in mag. field (*Russian*) 0-103800  
 Al-Ag (7.27 wt.%), peculiarities exhibited during fatigue loading (*Chinese*) 0-71723  
 Al-Cu (3 wt.%) single cryst., stress aging, oriented precipitation (*Japanese*) 0-71652  
 Al-Cu-Mg type 2036, thermomech. treatment, flow stress anal., effect in mech. props. 0-93584  
 Al-Cu(Si)(Mg) binary and ternary alloys, dimensional changes in heat treatment. 0-89271  
 Al-Cu(0-10 wt.%) sintered compacts, mech. props. rel. to sintering 0-76210  
 Al-Mg (4 wt.%), struct. and strengthening in hot working 0-84968  
 Al-Mg-Si, type 6010, microstruct. characs. influence on formability, heat treatment 0-81090  
 Al-Ni (3-18wt.%), gun-quenched from melt, struct. 0-76225  
 Al-Si (0.57 at.%), Si precipitate dissolution kinetics 0-84935  
 Al-Si melt, microheterogeneity (*Russian*) 0-103238  
 Al-Zn alloys, interfacial stability of planar solid-liq. interface during solidification 0-104145  
 Al-Zn-Mg, TEM and calorimetric study 0-76290  
 Al-Zn-Mg alloy, Ag addition and pre-precipitation treatment, influence on GP zone growth 0-71658  
 Al-Zn-Mg granules and bands rolled from them, heat treatment 0-100862  
 Al-Zn-Mg-Cu alloys, heat treatment optimisation 0-60888  
 Al-Zr (1-13 wt.%), rapidly quenched, extended solid solubility, grain refinement and age-hardening 0-76266  
 $\alpha$ -Al<sub>2</sub>O<sub>3</sub>:V<sup>3+</sup>(V<sup>4+</sup>)(Co<sup>3+</sup>)(Co<sup>2+</sup>), optically and thermally stimulated reactions, absorpt. spectra 0-80825  
 Au, quenched polycryst., vacancy loss at grain boundaries 0-59477  
 Au-Co, electron scatt., spin-orbit effects 0-65533  
 Au-Fe alloys, magnetism and atomic clustering 0-103810  
 Au-Fe ion implanted alloy, Mossbauer conversion electron scatt. 0-88898  
 Au-Pd (150 wt.%), quenched, vacancy annihilation and short-range order formation, elec. resist. 0-108487  
 Au<sub>1</sub>Mn<sub>4</sub> ordered phase formation, electron diff. and microscopy study 0-107418  
 Au<sub>3</sub>1Ni<sub>16</sub>, vapour quenched amorphous alloy, atomic arrangements 0-100173  
 Au<sub>3</sub>Si<sub>16</sub>, amorphous vacuum-deposited and liquid-quenched films, diffusion and crystn. 0-84094  
 Au<sub>2</sub>Si<sub>3</sub>m, metastable phase, substruct. unit cell (*German*) 0-88091  
 BaO-Fe<sub>2</sub>O<sub>3</sub>-(Na<sub>2</sub>O) glass, rapidly quenched, mag. and ferrimag. props. 0-75744

**quenching (thermal)** continued

Ba<sub>2</sub>RF<sub>7</sub> (R=Dy, Ho, Er, Tm, Yb, Lu, Y), superstructure phases, prep., thermal characterisation and X-ray powder diff. 0-96494  
 Bi<sub>2</sub>O<sub>3</sub>, polymorphic transformation and elec. resistivity (*Japanese*) 0-93555  
 CaF<sub>2</sub>:Er, defect structure, quenching effect, dielec. relax. and optical absorption 0-65031  
 CaF<sub>2</sub>-xH<sub>2</sub>, ionic cond. determ. from admittance and dielec. loss meas. (*French*) 0-107479  
 Cd<sub>1-x</sub>M<sub>x</sub> (M=Mg, Ca, Sr), solid soln., phase equilb. diagrams 0-108412  
 Co-B-Si amorphous alloy, liq. quenched, elec. resist. and cyclic deform. 0-59949  
 Co-Nb-C, obtained by liq. quenching, superconductivity 0-75699  
 Co-Sn system, phase Co<sub>5</sub>Sn obtained by splat cooling (*German*) 0-104147  
 Co-Ti-C, secondary precipitation and allotropic transform., TEM obs. 0-108453  
 Co-WC hard alloys, rapidly quenched struct. 0-76233  
 Co<sub>50</sub>Ga<sub>50</sub>, frequency depend. magnetisation, superparamagnetic behaviour 0-84624  
 Cu, quenched, Hall coefficient, relaxation times, Fermi surface 0-84460  
 $\alpha$ -Cu-Al (6 to 17 at.%), short-range order investigated by diffuse X-ray scatt. (*Russian*) 0-104187  
 Cu-Al-Ni Marmon alloys, rapid solidification and ageing 0-76245  
 Cu-Au alloys, vacancy and divacancy migration activation energies, elec. cond. meas. 0-88140  
 Cu-Be, SCC in NH<sub>3</sub> 0-104326  
 Cu-Cr (0.75 wt.%), deformation characs., fully reversed cyclic strain with fatigue cracks and dislocation struct. 0-81148  
 Cu-Fe system, ageing and reversion phenomena study 0-89274  
 Cu-Ni-Fe, magnetic properties, heat treatment and compressive stress effects 0-60367  
 Cu-Zr amorphous alloy, splat cooled, local order and amorphous struct. 0-88061  
 Cu<sub>2</sub>MnIn<sub>1-x</sub>Sn<sub>x</sub> alloy, compositional SRO, hyperfine interactions 0-71065  
 Cu<sub>40</sub>Nb<sub>30</sub>X<sub>30</sub> (X=Ti, Zr, Hf), superconductors with metastable ordered structs. 0-108484  
 Cu<sub>2</sub>O, Cu inclusions and annealing, optical and IR absorpt. obs. 0-60630  
 Cu<sub>0.57</sub>Zr<sub>0.43</sub> amorphous alloy, neutron diff. obs. of struct. 0-88060  
 (Fe,Cu,Ni)-Si(B), amorphous mag. alloy, magnetostriction rel. to soft mag. props. 0-84633  
 Fe based alloy, amorphous, liq. quenched, struct., thermal stability and mech. props. 0-88059  
 Fe, cast, white, high Cr, phase composition, B effect 0-104172  
 Fe, splat-quenched, microhardness and martensite 0-76359  
 Fe-B, amorphous alloy, mag. props. 0-84618  
 Fe-B, rapidly quenched, metastable phases 0-76234  
 Fe-B amorphous ribbons formation, high-speed photography investigation 0-76216  
 Fe-B metallic ribbons, correl. between quenching temp. and mech. and mag. props. 0-89373  
 Fe-B ribbon, microhardness, and static coercive force, melt overheating effect 0-84978  
 Fe-B-Si amorphous alloy, liq. quenched, elec. resist. and cyclic deform. 0-59949  
 Fe-C-X, glasses and metastable cryst. phases, third element effect 0-75171  
 Fe-Cr-Co (28, 10.5 wt.%) ductile magnet alloy, humidity-induced H<sub>2</sub> embrittlement 0-89406  
 Fe-Mo-CaF<sub>2</sub> sintered composite, struct. and mech. props., heat treatment effect 0-66526  
 Fe-Ni Invar alloys, splat quenched, mag. props. 0-75799  
 Fe-Ni-B glassy ribbons melt spinning, gas boundary layer effects 0-76217  
 Fe-Ni-C austenitic alloy, banded struct. formed by deform. 0-71713  
 Fe-Ni-P-B amorphous ribbons, form. by melt spin technique 0-76215  
 Fe-Pd Invar alloy, Young's modulus, magnetostriction, Curie temp. 0-65988  
 Fe-Si (3 wt.%) high-permeability grain-oriented steel, quenching effect on primary recrystn. texture development 0-84956  
 Fe-Si-Al, Sendust, ribbon-form, prep. by rapid quenching, mech. and mag. props. 0-71611  
 Fe-Si-Al ribbon-form Sendust alloy made by rapid roll quenching, mag. props., recording head appls. 0-81001  
 Fe-Ti-C, rapidly quenched by splat-cooling 0-84923  
 Fe-X-C (X=Cr, Mo, W), quenched rapidly from melts, nonequilib. phases (*Japanese*) 0-71630  
 Fe-Zn, quenched, martensite struct. and hardness, electron microscope exam. (*Russian*) 0-66619  
 Fe<sub>60</sub>B<sub>20</sub>, amorphous, crystn. 0-75187  
 Fe<sub>80</sub>B<sub>20</sub> metallic glass, crystn. kinetics 0-84083  
 Fe<sub>83.4</sub>B<sub>16.6</sub>, amorphous, mag. props. and microstruct., cooling rate and melt overheating effects 0-65965  
 Fe<sub>83.4</sub>B<sub>16.6</sub>, amorphous, mag. props., melt overheating and cooling rate effects 0-89371  
 Fe<sub>80</sub>(C<sub>1-x</sub>B<sub>x</sub>)<sub>20</sub> amorphous alloy,  $\alpha$ -Fe crystn., morphology 0-70129  
 (Fe<sub>60</sub>Ni<sub>40</sub>)<sub>100-x</sub>B<sub>x</sub> and (Fe<sub>100-x</sub>Ni<sub>x</sub>)<sub>80</sub>B<sub>20</sub> amorphous alloys, X-ray diff. struct. determ. 0-64906  
 Fe<sub>80-x</sub>Ni<sub>20</sub>B<sub>20</sub> and Fe<sub>80-x</sub>Ni<sub>20</sub>P<sub>10</sub>B<sub>6</sub> amorphous alloys, microhardness correl. with mag. props. 0-88826  
 Fe<sub>40</sub>Ni<sub>40</sub>B<sub>20-x</sub>P<sub>x</sub> metallic glasses, local struct. and dynamic disorder of Fe and Ni, EXAFS obs. 0-89088  
 Fe<sub>40</sub>Ni<sub>40</sub>P<sub>10</sub>B<sub>6</sub>, amorphous, resistometric study of short-range ordering rel. to heat treatment 0-70140  
 (Fe<sub>1-x</sub>Ni<sub>x</sub>)<sub>75</sub>Si<sub>10</sub>B<sub>15</sub> amorphous alloys, cold rolled and as-quenched, mag. anisotropy 0-97089  
 Fe<sub>80</sub>P<sub>10</sub>C<sub>7</sub>, amorphous and crystalline, electrochemical and semicond. behaviour (*Russian*) 0-101021  
 Fe<sub>2</sub>Pd<sub>82-x</sub>Si<sub>18</sub> metallic glass, mag. transitions, weak ferromagnetism 0-100583  
 Fe<sub>0.545</sub>Sb, temperature effect on lattice const., Mossbauer spectra and density 0-88124  
 n-GaAs, Bridgman crystals, hole traps, photocond. and thermal quenching study 0-75580  
 Ge, acceptor complex spectra, tunnelling H systems 0-89036  
 Ge-S glass, melt-quenched photoinduced ESR, annealing behaviour and glass comp. depend. 0-71156  
 Ge-S-Se, glass formation 0-103251  
 GeO<sub>2</sub> glass, nonisothermal devitrification kinetics 0-92465



**quenching (thermal)** continued

- In-Sb, crystal. struct. after appl. of high press., supercond. transition temp. 0-70169  
 KBr, quenched single cryst., hardness var. with load 0-76337  
 KCl:Ca<sup>2+</sup>, Z.-centre thermolum. 0-80879  
 La-Al amorphous alloys, internal friction, relaxation process 0-92607  
 La-Au, splat-quenched, Mossbauer effect and elec. resist., amorphous struct. 0-84676  
 Li<sub>2</sub>B<sub>2</sub>O<sub>4</sub>-LiFe<sub>2</sub>O<sub>4</sub>, borate glass, mag. props. of Fe<sup>3+</sup> cations 0-100599  
 Li<sub>2</sub>B<sub>2</sub>O<sub>4</sub>-LiFe<sub>2</sub>O<sub>4</sub> glass, rapidly quenched, mag. and ferrimag. props. 0-75744  
 LiF:Co, flow stress changes during precipitation 0-92594  
 Li<sub>2</sub>O-Al<sub>2</sub>O<sub>3</sub>, rapidly quenched glasses, Li ion cond., elec. cond. 0-100346  
 Li<sub>2</sub>O-Bi<sub>2</sub>O<sub>3</sub>, rapidly quenched glasses, Li ion cond., elec. cond. 0-100346  
 Li<sub>2</sub>O-Ga<sub>2</sub>O<sub>3</sub>, rapidly quenched glasses, Li ion cond., elec. cond. 0-100346  
 MgCd wire, elongation during disorder-order transform. (Russian) 0-104148  
 MgF<sub>2</sub>-Na<sub>2</sub>AlF<sub>6</sub>, thin film deposits, quenched ageing by chopping 0-97364  
 Mn-Al-C, ferromag. alloy, transform. kinetics 0-76229  
 MnZn ferrite, microstructure and initial permeability, presintering process effect 0-89367  
 MnZn ferrites, post sinter-cooling rates effects 0-89369  
 Mo-based metallic glass development 0-89172  
 Mo-Ru-(Si), amorphous superconductors, prep. by electron beam evaporation and liq. quenching, crit. temp. 0-103776  
 Mo<sub>70</sub>Si<sub>30</sub>B<sub>10</sub>, amorphous alloys obtained by liq. quenching, superconductivity 0-75670  
 Na<sub>2</sub>O-SiO<sub>2</sub>, glass drops, quenched from liq. state, thermally treated, density profile 0-81085  
 Nb-Al-Ge-Cu, rapidly quenched, comp. and phase equilib. 0-76235  
 Nb-Al(Ga, Si, Ge, Sn)-Cu, rapidly quenched, comp. and phase equilib. 0-76235  
 Nb-Ir(Rh) system glasses, form., crystn. and microhardness, resist. obs. 0-89178  
 Nb<sub>2</sub>(Al,Ge) and Nb<sub>2</sub>(Al,Si), liq. quenched, supercond. props. 0-84580  
 Nb<sub>2</sub>Si Al<sub>5</sub> phase from amorphous Nb-Si alloys, high-press. synthesis 0-93516  
 Nb<sub>2</sub>Si, substituted, splat cooling influence on supercond. T<sub>c</sub> and stoichiometry 0-80439  
 Ni base superalloys, rapid solidification, use in gas turbine engines 0-84888  
 Ni based alloy, amorphous, liq. quenched, struct., thermal stability and mech. props. 0-88059  
 Ni ferrite, quenched, Neel temp. and initial susceptibility 0-75762  
 Ni-Al-Mo (12.7, 21.6 wt.%), directionally solidified eutectic composite, precipitation 0-108454  
 Ni-Cr-Ti rapidly solidified superalloys, surface segregation 0-76263  
 Ni-Nb-C, obtained by liq. quenching, superconductivity 0-75699  
 Ni-P amorphous alloys, electrodeposited and melt-quenched atomic and electronic structures 0-88062  
 Ni-Ti-Al superalloy, pendant drop melt extracted, struct. and props. 0-76242  
 (Ni<sub>0.5</sub>Pd<sub>0.5</sub>)<sub>82</sub>P<sub>18</sub> amorphous alloy, liquid-quenched, crystn. kinetics, effect of thermal history 0-100175  
 (Ni<sub>0.5</sub>Pd<sub>0.5</sub>)<sub>82</sub>P<sub>18</sub> amorphous alloy, liquid-quenched, crystn. kinetics, nucleation 0-100176  
 NiPt, quenched, ordering kinetics and domain struct. form. during isothermal tempering (Russian) 0-66502  
 Ni<sub>1</sub>Sb, temperature effect on lattice consts., Mossbauer spectra and density 0-88124  
 Pb-Ag (0.068 wt.%), Ag precipitation kinetics and activation energy 0-66517  
 Pd-Cu-Si, glass form., crit. cooling rate 0-75169  
 Pd-Si, amorphous thin films, laser irradi., metastable phases 0-96622  
 Pd<sub>77</sub>Cu<sub>80</sub>Si<sub>16.5</sub> metallic glass, glass transition temp., cooling rate depend. 0-75181  
 Pd<sub>80</sub>Si<sub>20</sub>, vapour quenched amorphous alloy, atomic arrangements 0-100173  
 Pt-Si, amorphous thin films, laser irradi., metastable phases 0-96622  
 n-Si, fast electron irradiated, annealing of defects 0-89259  
 Si ribbons for solar cells, ultra high speed growth, elec. props. 0-89162  
 Si-Fe, solubility study by EPR and neutron activation anal. 0-75361  
 n-SiC, thermal defects, ESR study 0-88876  
 Si<sub>2</sub>Fe<sub>100-x</sub> polycryst. ribbon, prep. by rapid quenching, and props. 0-75803  
 Sn-Ni electrodeposited equatonic alloy, cryst. struct., X-ray, electron diff. anal. 0-79748  
 Ta-Ir(Rh) system glasses, form., crystn. and microhardness, resist. obs. 0-89178  
 Te<sub>80</sub>Ge<sub>20-x</sub>A<sub>x</sub> glasses, rapid melt cooled, glass transition and stability range 0-75170  
 Ti base alloys, melt-extracted polycryst., mech. props. 0-76360  
 Ti-Al-Cr-Mo-V, VT22 alloy, metastable  $\beta$ -phase decay under continuous heating, plastic strain effect (Russian) 0-71656  
 Ti-Mo-V-Al-Cr-Fe (4.8, 4.7, 5.2, 1.1, 1.0 wt.%), structural changes during heating up to 1000°C, DTA study (Russian) 0-93552  
 Ti-Mo-Zr-Sn (11.5, 6, 4.5 wt.%),  $\beta$  III, mech. props. rel. to heat treatment 0-84961  
 Ti-Mo-Zr-(Al) (15, 5 (3) wt.%), quenched and aged metastable  $\beta$ -phase, crystallography, morphology and decomposition 0-76262  
 Ti-Mo(V), metastable diffusionless equilibria, high press. conditions 0-71627  
 Ti-Ni (48 to 53 at.%), heat treatment and deviation from stoichiometry 0-104192  
 Ti-Si amorphous alloy, melt-quenched, transform. studies and mech. props. 0-100838  
 TiO<sub>2-x</sub> reduced, crystallographic shear planes, dislocation struct. 0-107175  
 Ti<sub>2</sub>Te<sub>3</sub>-Ti<sub>2</sub>SnTe<sub>3</sub>-Ti<sub>2</sub>PbTe<sub>3</sub>, phase equilib., DTA, SPA and microhardness meas. 0-96628  
 U-Mo (2 wt.%), depleted, effect of microstruct. on mech. props. 0-108497  
 U-Nb (14 at.%), martensitic and polymorphic transformations 0-60861  
 UC, quenched-in defects, formation, migration and resistivity 0-64990  
 UCN, quenched-in defects, formation, migration and resistivity 0-64990  
 V-O alloys, quenched, local ordering of O, electron microscopy and diff. 0-59453  
 V<sub>2</sub>Ga, supercond. Al<sub>5</sub> phase, prep. by controlled precip. 0-81000  
 V<sub>2</sub>O<sub>5</sub>, amorphous semicond., solubility and fibrous texture 0-75162  
 WC-Co hard alloys, hot-pressed, wear resist. under abrasive friction, heat treatment effect 0-66555

**quenching (thermal)** continued

- W<sub>50</sub>Si<sub>20</sub>B<sub>10</sub>, amorphous alloys obtained by liq. quenching, superconductivity 0-75670  
 Zn-As system, homogeneity range of ZnAs<sub>2</sub> and electrophys. props. 0-60833  
 ZnS:Cu crystal, powder, epitaxial film, luminescence anomalous thermal 0-76077  
 ZnSe, near band edge photoluminescence, electron-hole recombination 0-80835  
 Zr-Ru, alloy Zr rich, Ru solubility, eutectic decay,  $\alpha \rightleftharpoons \beta$  transform., struct. (Russian) 0-65227
- queueing theory**  
 cyclic queue models of semiconductor noise and vehicle fleet operations 0-80336  
 waiting time in stationary state for queue with server of walking type (autonomous service) 0-90657
- queueing theory** see *queueing theory*
- R and D management** see *research and development management*
- R-centres**  
 alkali metal halides, analysis of spin-Hamiltonian parameters of heteronuclear XY defects 0-88509  
 CdS:Cu, photosensitivity degradation mechanism 0-107851  
 CdS:In(Cl) concentration quenching mechanism of luminescence 0-97336
- R waves** see *Rayleigh waves*
- Racah coefficients** see *angular momentum theory*
- radar**  
 see also *Doppler effect; optical radar*  
 reflectivity profile, Z-factor, classification by rain types 0-101420  
 wave and particle descriptions of light, equivalence, rel. to radar freq. shift 0-101692
- radar altimeters** see *radioaltimeters*
- radar antennas**  
 Fresnel zone and diffraction fields anal. near boresight of acoustic radar antennas 0-64318  
 HF radar system for ocean surface currents mapping, new antenna concept 0-94626
- radar applications**  
 atmosphere radar technique, for dynamic struct. of middle atmos. 0-105078  
 atmosphere study, MST radar at Poker Flat, Alaska 0-90254  
 coastal radar system appl. to tsunami prediction and magnitude 0-82101  
 digital data composition for satellite and radar imagery 0-67413  
 electrojet, equatorial, plasma instability and electron density irregularities, HF radar obs. 0-105112  
 equatorial anomaly, counter electrojet assoc. changes, upward drift reversal obs. 0-109297  
 equatorial counter-electrojet, electron drift vel., radar obs. 0-82126  
 equatorial electrojet, three metre irregularities depend. on Zenith angle, radar obs. 0-105109  
 geodesy, SEASAT radar altimeter resolution capability 0-72645  
 ground imaging from satellite by synthetic-aperture, digital processing techniques 0-61914  
 Gulf Stream surface waves, radar obs. program 0-85679  
 hurricane detection by Doppler radar for coast of U.S.A. 0-67414  
 lava flow terrain, radar imaged by satellite 0-98285  
 meteorology, airborne pulse Doppler radar 0-85757  
 meteorology radar, echoes from distributed targets, averaging of time, angle and range 0-109264  
 middle atmosphere struct. and dynamics from VHF radar obs. 0-105032  
 modelling of influx of meteoric matter with radar observations (Russian) 0-67664  
 Moon, radar contact in 1946 0-85866  
 ocean surface currents mapping, HF radar system appl. 0-94626  
 ocean surface waves, radar imaging method using SAR 0-77173  
 ocean wave radar monitoring, ground wave and sky wave sensing techniques 0-109256  
 ocean waves, growth decay of 80 m waves, radar obs. 0-98344  
 ocean waves, remote obs. using HF skywave radar technique 0-90241  
 rain measurement and forecasting in UK using radar as part of integrated system, progress and plans 0-98490  
 rain measurement by dual-polarisation radar, drop size and fall rate 0-72650  
 rainfall, convective, meas. over small areas using high-density raingauges and radar 0-77157  
 rainfall measurement, combined usage of radar and radiometry techniques (Chinese) 0-109272  
 rainfall measurement by radar, methods and interpretation of data 0-81969  
 rainfall on convective days, analysed with respect to radar obs. atmos. parameters 0-109205  
 satellite radiosounding, appl. to Venus atmosphere and surface investigation by (Venera 9 and 10) 0-101543  
 sea surface waves, remote sensing using one and two freq. microwave techniques 0-94622  
 sea waves, height, length and velocity, radar and Doppler effect, OREME project (French) 0-94625  
 space station, scheme for automatic rendezvous with unmanned (or manned vehicle) 0-77249  
 stratosphere and mesosphere radar studies, UHF and VHF, review 0-90180  
 stratosphere turbulence near tropopause, review of radar obs. 0-90179  
 subsurface radar using video pulse for deep probing in Earth, pulse propagation in lossy media using LF window 0-74282  
 subsurface sounding of ground water in deserts and glaciers 0-67437  
 tidal currents, meas. by two-site HF Doppler radar system by using two-site HF 0-72533  
 troposphere, radar obs. during clear air conditions, review 0-90178  
 upper atmosphere studies 0-72661  
 Venus, distance from Earth determ. using radar, appl. to space craft navigation 0-109386  
 Venus radar mapping, Pioneer Venus Orbiter mapper design and operation 0-67495  
 weather forecasting processing of radar and satellite imagery data 0-109252  
 wind measurement (absynoptic scale) using dual Doppler radar and vel. azimuth display 0-109263  
 wind vertical component in lower atmos., clear air Doppler methods 0-72642

**radar cross-sections**

scatterometer on satellites and aircraft for investigating underlying surface, optimization of characts. 0-67436

**radar echo areas** *see radar cross-sections***radar equipment**

Altair incoherent scatter radar for equatorial spread-F meas. 0-61927  
 Chatanika incoherent scatter radar, use of high-speed correlator and filter bank for plasma line meas. 0-98507  
 HF radar system, for ocean surface currents mapping 0-94626  
 meteorological radar equipment, pulse-wise interpretation of echo-signals (*Russian*) 0-67432  
 Pioneer Venus Orbiter, radar mapper design and operation 0-67495  
 scatterometer on satellites and aircraft for investigating underlying surface, optimization of characts. 0-67436  
 Seasat synthetic aperture radar system 0-94686

**radar measurement**

atmosphere study, MST radar at Poker Flat, Alaska 0-90254  
 atmospheric precipitation properties using radar polarisation techniques 0-61925  
 clouds, radar reflectivity rel. to cloud dynamics and microphysics 0-61877  
 cross-section measurements from satellites and aircraft for underlying surfaces, scatterometer 0-67436  
 Dynasonde virtual height meas. methods, comparisons, accuracy and interpretation 0-94643  
 glacier thickness and water content, radar measurement technique 0-98369  
 ionosphere, auroral zone, irregularities, simultaneous rocket probe, scintillation and incoherent scatter radar obs. 0-94640  
 ionosphere, equatorial radar backscatter plumes spatial relationship with plasma bubbles 0-67457  
 ionosphere, lower, wind obs. by Kyoto meteor radar 0-67444  
 ionosphere plasma line, meas. at Chatanika with high-speed correlator and filter bank 0-98507  
 Kelvin-Helmholtz instability, jet stream generated, radar obs. and model 0-90165  
 lake ice, microwave radar and radiometric remote sensing meas. 0-85691  
 Mars, radar altimetry of S.Tharsis 0-98591  
 Mars, radar characts. of rough planar surfaces 0-98589  
 meteors, simultaneous visible and radar obs. technique 0-77354  
 meteors ionisation columns, initial radii meas. 0-94762  
 Moon, 3 cm radar obs. from Luna 16 to 24 spacecraft 0-77302  
 ocean wave height measurement by radar, airborne method 0-85771  
 ocean waves, remote obs. using HF skywave radar technique 0-90241  
 rainfall, convective, meas. over small areas using high-density raingauges and radar 0-77157  
 sporadic meteors, ionisation height meas., VHF obs. 0-82312  
 thermosphere, middle, incoherent scatter radar studies 0-72654  
 thermosphere, winter motions radar in S.hemisphere meteor region 0-109287  
 tidal currents, meas. by two-site HF Doppler radar system by using two-site HF 0-72533  
 Venus atmosphere, radio waves attenuation investigation by bistatic radar method 0-62061  
 Venus surface, bistatic radar meas. by Venera 9 and 10 satellites 0-101543  
 VHF radar aurora and strong HF backscatt. comparison 0-61960  
 warm frontal region, wind and precipitation struct., Doppler radar study 0-81995

**radar systems**

acoustic radar systems, microcomputer appl. 0-106685  
 HF radar system, for ocean surface currents mapping 0-94626  
 MM wave, conf., London (Apr. 1980) 0-67441  
 MM wave, for remotely sensing atmospheric pressure from satellite 0-67443  
 Venus Orbital Imaging Radar, aerobraking appl. 0-109338  
 Zephyr, meteorological meas. appls. 0-90228

**radar telescopes** *see radiotelescopes***radar theory**

backscattered pulse shape, small-angle multiple scatt. in random media 0-77079  
 dual-Doppler radar, meteorological, coverage area as function of meas. accuracy and spatial resolution 0-82093  
 signal reflection from sea surface, spatial intensity fluctuations 0-109170  
 solar corona reflection of radar signal, efficiency of four-plasmon interactions 0-101582

**radiance** *see brightness***radiation**

*see also atmospheric radiation; beta-rays; cathode rays; electromagnetic waves; heat radiation; radiation effects; radiative transfer; stellar radiation*

acoustic radiation by instability waves in turbulent shear layer 0-79341  
 energy standards (*Japanese*) 0-62620  
 radiating particles of finite size, Dirac's subtraction formalism (*German*) 0-91740

**radiation belts**

*see also atmospheric electron precipitation; atmospheric proton precipitation*  
 charged particle fluxes, obs. by JIKIKEN scientific satellite (*Japanese*) 0-94654  
 electron beams, counterstreaming, at altitudes of 1  $R_E$  over auroral zone 0-67474  
 electron flux, high energy, obs. and comparison with VLF emissions by EXOS-B satellite (*Japanese*) 0-94652  
 electron flux variations, in inner radiation belt 0-67470  
 electron intensity fluctuations meas. from Cosmos 484 satellite 0-72698  
 electrons, evidence for trapped flux limit from pulsating aurorae 0-72666  
 injection location affecting energetic particle spectra 0-72711  
 inner, proton spectra from Kosmos 721 satellite 0-72699  
 inner zone electron precipitation, meas. 0-67452  
 inner-zone protons, energy and pitch angle distrib. analytic study 0-67471  
 inverse loss cone electrons, temp. anisotropy quasi-linear relaxation due to interaction with electrostatic waves (*Russian*) 0-109314  
 outer, electron intensity increase, link with magnetosphere disturbance 0-77225  
 outer radiation belt, maximum fluxes of electrons with  $E > 1$  MeV (1958-1971) 0-61668

**radiation belts continued**

permanent trapping in phase space 0-72709  
 ring current of magnetic storm, origin by inward displacement of trapped particles 0-72708

**radiation biology** *see biological effects of radiation***radiation chemistry**

*see also chemical effects of nuclear reactions and scattering; photolysis; radiochemistry; radiolysis*  
 acrylourethane coatings, radiation curable, tensile, elongation and modulus props. appl. techniques 0-66847  
 adamantane,  $\gamma$ -irrad., free radicals EPR and ENDOR 0-69170  
 air, dissoc. by field-accelerated electrons, macroscopic props., rel. to pure  $O_2$  0-61118  
 benzene cryst., electron irrad., phenylcyclohexadienyl radical form., absorpt. and fluoresc. spectra study 0-89035  
 N-bromosuccinimide, X-irrad., ESR study of Br and  $\sigma^*$  radical 0-66037  
 cephalosporins, radiation-sterilisation by  $\gamma$ -irrad. 0-66822  
 ceric/thallous dosimetry at less than 1000 rad 0-63400  
 $\alpha$ -chloroacetamide, alkoxy radical form., effect, of  $\alpha$ -hydroxyacetamide, ESR study 0-80610  
 5,5'-diethylbarbituric acid, EPR and INDO-MO study of radical formation after irrad. 0-93774  
 dimethylsulphide, liq., solvated electrons, optical absorpt. spectrum obs. 0-97250  
 dipotassium glucose-1-phosphate, X-irrad., ESR-ENDOR obs 0-60419  
 ethylene propylene/polyolefin blends, radiation cross linking 0-66801  
 ethylene-Co copolymers and - $SO_2$  copolymers prep. by catalysis and  $^{60}Co$   $\gamma$ -radiation, mech. props. 0-66841  
 ethylene-vinyl acetate copolymers, extrusion and heavy duty films, radiation crosslinking, struct. effect 0-66844  
 fibre reinforced polymer, soaking, wetting and compounding of materials during production (*German*) 0-93535  
 glasses, electron scavenging, hopping controlled time-depend. reaction rates 0-108723  
 glutaric acid,  $\gamma$ -irrad. single crystals, free radical EPR obs. at 77K 0-81340  
 halogermane radical anions, ESR spectra and struct. 0-87153  
 5-halouracils, solid, radiation damage, free radicals in 5-fluorouracil single crystals. 0-71926  
 s-halouracils, solid, radiation damage obs., deoxyribose ring opening in single crystals. 0-71929  
 hippuric acid, X-irrad. single cryst.,  $^{14}N$  and  $^1H$  ENDOR study; 0-71240  
 4-hydroxy-2,2,6,6-tetramethylpiperidine, radiation-induced oxidation to paramag. nitroxide free radicals 0-81341  
 insulating and sheath materials for wire and cable, crosslinking by irradiation 0-66845  
 isocitrate dehydrogenase from Azotobacter vinelandii, essential amino-acid residues identification 0-76538  
 lipid peroxide formation in irrad. synthetic diets, storage effects 0-101025  
 methanol,  $\beta$ -irrad., radical truck struct., electron spin-echo obs. 0-93776  
 methyl cyanide-water (methanol),  $Ag^+$  ion solvation,  $\gamma$ -irrad., ESR obs. 0-97726  
 methylamine liquid, 293K, solvated electron decay kinetics obs., IR spectra 0-71928  
 methylmethacrylate soln., aqueous, polymerisation under pulse electronic accelerator irradiation 0-66802  
 3-methylpentane glassy matrix, localised electrons, cavity model 0-107743  
 molecules in degenerate electronic state, IR laser radiation effects 0-81351  
 nitrosourea compounds, 2, anal. of interaction with X-radiation in rat brain tumour cells 0-72230  
 octadecylacrylamide films, oriented ultrathin, radiation-induced solid state polymerisation 0-80128  
 photoabsorption data appls. 0-93778  
 PMMA, neutron and gamma irradiation effects 0-66839  
 polyacrylamide, high mol. wt., prep. by electron beam irrad. 0-76222  
 1,2-polybutadiene crosslinked in strain states; entanglement networks, stress-birefr. relations 0-66590  
 polybutadienes, radiation chemically cross-linked, charact. by pyrolysis gas chromatography (*German*) 0-81348  
 polydiacetylene, crystalline and amorphous,  $\gamma$ -ray effects, gel form. and crosslinking 0-93777  
 polyethylene, electron beam crosslinking process for high voltage power cable 0-66846  
 polyethylene, irradiation, crystallinity and crosslinking efficiency 0-66843  
 polyethylene, vinyl group reactions during  $\gamma$ -irrad., crystallinity effect, absorbance obs. 0-81346  
 polyethylene-glass fibre composites, gamma-irradiated filler 0-66840  
 polyethylenes, extrusion and heavy duty films struct. parameters influence on cross-linking by radiation 0-66844  
 polymer systems for adhesive applications, radiation curing, lap shear strength props. 0-66842  
 polymeric cable insulation, radiation modification using electron beams 0-66848  
 polymethacrylic acid, stereoregular, synthesis,  $^{13}C$  NMR obs. 0-58422  
 polyolefin, cross-linked, irradiation appl. to provide improved insulation props. to wires and cables 0-66850  
 polysiloxene, irrad., linear, IR and solubility obs. 0-93775  
 polysytene, neutron and gamma-irradiation effects 0-66839  
 pulsed NMR technique for meas. radiation effects in polymer 0-66051  
 PVC, cross-linked, irradiation appl. to provide improved insulation props. to wires and cables 0-66850  
 PVC, Cu evaporated film, electron-induced metallochromic reaction for metal image formation 0-86476  
 PVC materials, cross-linkable, for wires and cable insulation 0-66849  
 quartz dental composites, acrylic acid grafted on particles by gamma-radiation 0-66840  
 radical radiation formation in solid organic compounds 0-85201  
 sodium 10-undecanoate,  $\gamma$ -ray induced polymerisation in aq. micelle solns. 0-61093  
 thiamine (vitamin  $B_{12}$ ), aq. soln., radiation induced reactions 0-93779  
 thymidine monophosphate, gamma irradiated, inorganic phosphate release, in presence and absence of  $O_2$  0-67168  
 thymidine monophosphate aqueous solution, gamma irrad. effect on base damage, phosphate release 0-89806  
 transition metal sulphides, ion bombardment damage, XPS obs. 0-97404  
 Ar, energetic electron degradation spectra and initial yields 0-95724



**radiation chemistry continued**

- Ar, gas, electron thermalization time and position distribution meas. 0-93771  
 CdO-Al<sub>2</sub>O<sub>3</sub>-P<sub>2</sub>O<sub>5</sub> glass,  $\gamma$ -irrad., EPR study 0-84639  
 CuClO<sub>4</sub>, neutron activated, radiation annealing 0-93569  
 H<sub>2</sub>O, crystalline ice, localised excess electrons yield studied as function of dose rate 0-97712  
 KPF<sub>6</sub>,  $\gamma$ -irrad., trapped free radicals EPR obs. 0-63683  
 Kr, gas, electron thermalization time and position distribution meas. 0-93771  
 Li<sub>2</sub>O-Al<sub>2</sub>O<sub>3</sub>-SiO<sub>2</sub>(P<sub>2</sub>O<sub>5</sub>):Cd<sup>+</sup> glasses,  $\gamma$ -irrad., EPR study 0-84639  
 Li<sub>2</sub>O-P<sub>2</sub>O<sub>5</sub>:Cd<sup>+</sup> glass,  $\gamma$ -irrad., EPR study 0-84639  
 MnO<sub>2</sub>, oxidation under UV irradiation rel. to Viking gas exchange reaction on Mars 0-72831  
 Ne, gas, electron thermalization time and position distribution meas. 0-93771  
 NiClO<sub>4</sub>, neutron activated, radiation annealing 0-93569  
 O<sub>2</sub>, dissoci. by field-accelerated electrons, macroscopic props., rel. to dry air 0-61118  
 SiF<sub>4</sub>Cl<sub>4</sub>-n in  $\gamma$ -irradiated solid solution of tetramethylsilane, EPR spectra obs. 0-80611  
 SiF<sub>3</sub>Cl<sup>-</sup>(Br<sup>-</sup>)(I<sup>-</sup>) in  $\gamma$ -irradiated solid solution of tetramethylsilane, EPR spectra obs. 0-80611  
 TiD<sub>2</sub>, nucleation and growth in D<sub>3</sub><sup>+</sup> implanted Ti, TEM study 0-97717  
 V<sub>2</sub>O<sub>5</sub>, electron beam induced decomposition, appearance pot. spectroscopy 0-85203  
 Xe, gas, electron thermalization time and position distribution meas. 0-93771

**radiation counters** *see counters*

**radiation damage** *see radiation effects*

**radiation detection and measurement**

- see also alpha-particle detection and measurement; beta-ray detection and measurement; electron detection and measurement; gamma-ray detection and measurement; hyperon detection and measurement; meson detection and measurement; muon detection and measurement; neutrino detection and measurement; neutron detection and measurement; particle detectors; proton detection and measurement; radioactivity measurement*  
 acoustic noise production in polar medium, possible radiation detection method 0-63493  
 bibliography (1972-76) (*German*) 0-95510  
 cosmic rays, studies using gas Cherenkov counter with ionisation spectrometer 0-94662  
 degree meter for radiation meas. 0-87024  
 double filter system for Rn/Th measurements in environment and exhaled breath 0-57988  
 effects meas., units selection 0-98870  
 electrostatic sparks detection and characts., by radio methods 0-68217  
 environmental radioactivity, determ. for dose assess. 0-85321  
 glass dosimeter reader, design improvements (*French*) 0-57970  
 human internal radiation counting, Los Alamos multiple simultaneous system 0-61709  
 internal contamination monitoring in GDR 0-67259  
 ionisation chamber dose meter unit for emergency operations (*French*) 0-57977  
 ionising radiation, detection device, electret based (*French*) 0-57971  
 large-area gas-scintillation proportional counters for in-vivo measurement of plutonium and americium 0-58086  
 Lexan spectrometry, relativistic projectile fragments, imaging and identification 0-63442  
 liquid scintillation techniques, appl. in low level activity assessment 0-58082  
 mixed radiations, device for dose-equivalent index determ. (*Russian*) 0-57976  
 radioisotope direct detection using accelerators 0-63468  
 radioisotope transport in terrestrial food chains, dynamic modelling using RAGTIME code 0-104776  
 ratemeters, with variable time const., error determ. 0-95507  
 superconducting double multivibrator used as near- and medium-infrared radiation detector (*German*) 0-90892  
 thermal defect in materials determ., using total-absorption calorimeters 0-99427  
 thermally stimulated luminescence application, radiation dosimetry, book contribution 0-80882  
 whole body counters, international intercomparison 0-78504  
 wrist watch dosimeter for ionising radiations, practicality tests 0-57972  
 Ge detector system for inhaled radionuclide detection and meas. 0-57990  
<sup>32</sup>P-Cherenkov radiation, counting efficiency improvement, wavelength-shifting compounds investigation 0-90893  
 Pu accountability, nondestructive assay using neutron counting, calorimetry and gamma spectrometry 0-63266  
 Pu, accountability and control, field nondestructive assay measurements as applied to process inventories 0-63265  
 Pu nondestructive assay meas. using NaI(Tl) detectors during fabrication plant decommissioning 0-63495  
 Rn and daughters meas. methods in underground and free atmosphere air 0-57987  
 Rn, long term average level meas. instrument 0-58085  
<sup>222</sup>Rn, atmospheric, two-filter continuous monitor 0-58097  
<sup>222</sup>Rn, conc. in air, absolute determ. using cellulose nitrate track detector 0-63492

**radiation detectors** *see particle detectors*

**radiation dosimetry** *see dosimetry*

**radiation effects**

- see also acoustic wave effects; alpha-particle effects; beta-ray effects; biological effects of radiation; deuteron effects; electron beam effects; gamma-ray effects; hyperon effects; ion beam effects; laser beam effects; meson effects; neutron effects; proton effects; radiation chemistry; radiation hardening; voids (solid); X-ray effects*  
 Al<sub>5</sub> compounds, disordered, reordering kinetics 0-96678  
 alkali halide, crystal, irradiation-induced defects 0-107316  
 alkali halides, divalent cation doped, irradiated, first-stage F-centre prod. 0-107231  
 alkali halides, F-centre accumulation, radiation induced, temp. depend. 0-59460  
 atom-atom collision cascades localisation, impurity and thermal vibr. influence, computer simulation method 0-88227  
 ATS-6 solar cell flight expt., radiation damage, summary results 0-94005  
 cables, mineral insulated, radiation induced currents 0-65037

**radiation effects continued**

- conference, atomic collisions in solids, Hamilton, Canada (Aug. 1979) 0-62375  
 creep testing, extensometric method, for inside nuclear reactor channels 0-100998  
 defect production, exact solns. of models for continuous and pulsed irradiation, implications for stability and fluctuations 0-65041  
 deformation due to stress induced preferred adsorption induced dislocation anisotropy 0-75265  
 dislocation climb, in modulated struts. under irradiation conditions 0-70195  
 displacement damage, analytical calc. 0-70250  
 dose rate dependent effects of total ionising dose irradiation, annealing 0-70249  
 elastomeric materials, selection for vacuum seals 0-77797  
 electrets, radiation-induced charge storage and polarisation effects 0-80684  
 electronic components, space radiation environment effects, laboratory simulation 0-94689  
 elemental semiconductors, group IV, Mossbauer spectroscopy of defects, radiation damage and deep levels 0-59533  
 fast negatively charged particles, resonance scatt. phenomena in single cryst. 0-65047  
 fission reactor materials, ion penetration distance calculations with multi-group transport computer codes 0-102246  
 fusion reactor first wall, radiation damage simulation using fission reactor test facilities 0-57950  
 fusion reactor first-wall performance under ion bombardment and cyclic stresses, in-reactor materials testing 0-104407  
 fusion reactor structural materials, accident-related dose rate calc. 0-95411  
 fusion reactors, inertial confinement, first walls, void growth, analytical model 0-63377  
 fusion reactors, inertial confinement, interstitial loop formation, point defect clustering 0-63378  
 gas-filled microballoons, radiation effects MEDUSA code calcs. 0-83220  
 graphite, irradi., lattice expansion, vacancies and interstitials contrib., bond order role 0-65042  
 H<sup>+</sup> colour centre, radiation-tunnel decay 0-103327  
 ionic crystals, defects, computer modelling, review 0-107205  
 ionic crystals, influence of defect interaction upon their recomb. 0-84206  
 ionic crystals, lattice defects, conference, Canterbury, England (Sept. 1979) 0-105420  
 irradiation growth, contrib. of grain shape to anisotropy 0-92556  
 irradiation induced crystalline to amorphous transition, Gibbs energy 0-70371  
 LMFBR materials, interstitial loop nucleation and growth during irradiation, Fokker-Planck equation, numerical soln. 0-57857  
 LMFBR materials, interstitial loop nucleation and growth during irradiation, Fokker-Planck equation, numerical soln. 0-68796  
 macromolecules, nonlinear laser photomodification, radiation damage 0-61120  
 magnon-photon interaction in ferromagnets, construct. and radiation effects 0-71188  
 mass flux, irradiation enhanced, dislocation interactions 0-88206  
 measurement units selection 0-98870  
 metal, irradi., containing pre-existing dislocations, interstitial loop form. kinetics 0-65040  
 metal colloids in ionic cryst., preparation, optical, mag. resonance, elec. props. 0-59459  
 metals, radiation defect treatment at annealing stages V and VI (*Russian*) 0-71676  
 metals, radiation induced vaporisation, press. behaviour 0-84288  
 metals, void growth and time-lag, statistical theory 0-88208  
 Moliere potential, ion transport theory, differential cross sections 0-88209  
 MOS structures, radiation-induced positive charge, thermal annealing 0-75648  
 narrow-band semiconductor, growth of epitaxial layers, activation by UV and IR radiation 0-71598  
 Nimonic, irradiated, void nucleation, numerical evaluation 0-70252  
 non-metallic crystals, electric field influence on defect creation mechanism 0-70251  
 optical fibres, UV radiation-induced losses rel. to colour centre form. 0-87517  
 optical materials and components, space charged particle environment effect 0-69472  
 PMMA, space radiation effects evaluation 0-70263  
 point-defect clustering during irradiation 0-92521  
 polyethylene, photodegradation mechanism, from yield strength, elongation and mol. wt. studies (*Japanese*) 0-76311  
 polyethylene, resist. to stress corrosion cracking, ionising radiation effect (*German*) 0-81224  
 polyethylene, space radiation effects evaluation 0-70263  
 polymer composite matrix materials, spacecraft, space radiation effects evaluation 0-70263  
 precipitate re-solution in low dose irradiations 0-93559  
 primary knocked-on atoms effect, computing method 0-107318  
 radiation damage, meas. of loss of gaseous elements from thin samples 0-96568  
 research on radiation damage, (1950-60) 0-62446  
 satellite solar cell power plant, operating experience 0-94055  
 semiconductor, kinetics of defect cluster annealing 0-84209  
 semiconductors, doped and amorphous, ionised centre diffusion accel. by electrostatic fields 0-70473  
 semiconductors, glassy, diamm., photostructural changes, mechanism 0-92557  
 semiconductors and insulators, radiation damage, mechanisms, review 0-107315  
 sink strengths for thin film surfaces and grain boundaries 0-88207  
 solid solution, binary, radiation-induced instability, contrib. of dissipative processes 0-65039  
 steel, heat resistant, tensile strain and endurance, normal and radiation conditions, linear load variation 0-81189  
 steel, stainless, irradiated, void nucleation, numerical evaluation 0-70252  
 strain measurement, extensometric method, for inside nuclear reactor channels 0-100998  
 superconductor, crit. temp., micropower-induced enhancement (*Russian*) 0-93023  
 thermal defect in materials determ., using total-absorption calorimeters 0-99427

**radiation effects continued**

- undersaturated alloys, irradiated, solute segregation kinetics, via drift and defect-solute complexes 0-60872
- vacancies and interstitials, irradiated, induced, recombination rate 0-96516
- void swelling, nucleation theory 0-65038
- AgI aerosol, ice forming activity, UV irradiated effect 0-71950
- Al foil, solar wind ion bombardment, lunar surface modification 0-109325
- Al, narrow superconducting bridges, microwave radiation stimulated  $T_c$  enhancement 0-84537
- Al-Si<sub>3</sub>N<sub>4</sub>-SiO<sub>2</sub>-Si, MNOS structures degradation under UV irradiation effect 0-107923
- CdF<sub>2</sub>, colour centres, IR absorpt. and photocond. after UV irradiation 0-79784
- CdF<sub>2</sub>:NaF(AgF), colour centres, IR absorpt. and photocond. after UV irradiation 0-79784
- Hg-polymer interface, UV exposed, contact potential and charge exchange meas. 0-75642
- KBr(CI):OH<sup>-</sup>, cc U<sub>2</sub> to H<sub>2</sub>O<sup>-</sup> defects conversion after UV photodecomp. 0-107230
- KCl,  $\gamma$ -irradiated, F-centre absorpt., flash-stimulated changes 0-92524
- NaMgF<sub>2</sub>, defects induced by X- and vacuum UV irradiation, optical and elec. study 0-107319
- Na<sub>2</sub>O-CaO-SiO<sub>2</sub>, glass, formation of colour centres, linear absorption of UV radiation 0-103328
- P<sub>2</sub>O<sub>5</sub>-SiO<sub>2</sub>-GeO<sub>2</sub> graded-index optical fibre, UV induced losses 0-87518
- Si solar cells, capacitance transient spectra of processing- and radiation-induced defects 0-61340
- Si:H, amorphous, Schottky diodes, elec. props., light-induced effects 0-103741
- SiO<sub>2</sub> (6H), IR absorpt., UV illumination effects, defect levels 0-66251
- SiO<sub>2</sub>, thin films, radiation-induced trapping centres, rel. to MOS transistor technology 0-107804
- SiO<sub>2</sub>-Ge, B, P, optical fibre, radiation induced optical absorpt. spectra, 0.4 to 1.7  $\mu$ m region 0-58761
- Ti-70A superalloy, fusion reactor blanket structures, radiation resistance 0-63379
- Ti-Al-V, fusion reactor blanket structures, radiation resistance 0-63379
- ZnS evaporated film, refl. loss on UV irradiation, ZnO form. 0-99813
- ZrSiO<sub>4</sub>, natural, radiation defect centre, EPR obs. 0-75853

**radiation hardening**

- mica, natural, high  $\gamma$ - and electron-irradiated, doses effect on annealing behaviour, thermal decomp. resist. 0-60897
- steel, stainless, Type 316, neutron irradiated, effects on tensile props. and microstruct. 0-65059
- steel, US strengthening treatment effect on fatigue resistance 0-81193
- Fe-Ni, dilute, irradiation softening effect on yield stress 0-76319
- Fe-Si, dilute, irradiation softening effect on yield stress 0-76319
- Fe-V, dilute, irradiation softening effect on yield stress 0-76319
- MgO crystals, radiation damage influence on deform. in HVEM 0-103391
- Mo, neutron irradiated, radiation anneal hardening mechanism 0-71678
- Nb, neutron irradiated, radiation anneal hardening (*Japanese*) 0-89243
- Ni-Cr-Fe alloys, radiation enhanced precip. and dissolution of precipitates, point defect kinetics and dislocation obs. 0-108467

**radiation hardening (electronics)**

- X-ray source, industrial, use for electronic component radiation effects work, calibration 0-63402

**radiation injuries** *see biological effects of radiation***radiation monitoring***see also dosimetry*

- <sup>222</sup>Rn flux through multilayered covers cover U mill tailings 0-95487
- ACEL commercial products, contrib. to nuclear medicine and radiation processing 0-81736
- aerosol surveillance system evaluation 0-57984
- air ionisation probe for  $\alpha$ ,  $\beta$ ,  $\gamma$  hand and shoe monitor 0-58084
- air monitoring system for  $\alpha$ -activity and nuclide specific noble gas meas. 0-63408
- air monitoring systems for radioiodine and inert gases, evaluation 0-95480
- centralized TLD service and record keeping in Canada 0-58003
- conference, radiation protection monitoring advances, Vienna, Austria (June 1978) 0-57007
- disposition assessments for decontamination and decommissioning of inactive nuclear sites, data requirements 0-95474
- dose-rate conversion factors for external exposure to photons and electrons, modifications to DOSFACTER code 0-104775
- double filter system for Rn/Th measurements in environment and exhaled breath 0-57988
- ecosystem analysis methods for the assessment of inactive nuclear sites 0-95476
- environment monitoring ground radioactive burial site (*Japanese*) 0-67015
- environmental radioactive pollution by U industry, monitoring using analytical chemistry 0-95488
- environmental radioactivity, radiation dosimetry control, exposure rate monitoring of natural radiation reference field 0-67017
- fast neutron criticality monitor, response to prompt critical bursts 0-63398
- field measurements, relationship to calibration values 0-58002
- gamma and X-ray, phys. quantities used 0-99344
- geotoxicity hazard index for radioactive waste storage 0-97822
- human internal radiation counting, Los Alamos multiple simultaneous system 0-61709
- imaging alpha detector, radioactive contamination monitoring appl. 0-102384
- integrated radiochemical laboratory for radiological environmental anal., design 0-57994
- internal contamination monitoring in GDR 0-67259
- ionising radiation, personnel exposures, dose limits 0-99350
- JOYO experimental fast reactor, radiation protection monitoring programme 0-57992
- laser, far IR optically pumped, monitoring by piezoelec. transducers 0-102729
- laser light, dosimeter for health physics evaluation of operating conditions at laser installations 0-76835
- liquid effluents, aquatic radiological impact anal., radiocaesium transport in sediment 0-95486
- low-level transuranic storage, radwaste Sr, Cs, Co sorption meas. on soil sediment 0-95482
- radiation monitoring continued**
- LWPR, radiological emergency monitoring and instrumentation, Federal guidance 0-57961
- microprocessor controlled long lived alpha emitter monitor 0-58069
- multi-channel analyser, portable microprocessor controlled, accessories, data acquisition 0-63474
- multiple element  $\alpha$ -spectrometry for individuals and environment monitoring 0-58024
- neutron monitor calibration, standard fields at Physikalisch-Technische Bundesanstalt 0-57999
- nuclear facilities, off-site radiological impact assessment real-time computer program CEPADAS 0-95475
- nuclear power station, Zarnowice, contamination monitoring station (*Polish*) 0-74033
- nuclear site decontamination, radiochemical anal. of environmental samples 0-95477
- on-line radiation monitoring at a nuclear fuel reprocessing plant 0-95469
- particulate contamination monitoring, recent developments 0-57985
- personal, effect of environmental radiation, thermoluminescent dosimeter (*Japanese*) 0-61707
- personal dosimetry instrument for airborne radon daughter meas. (*French*) 0-57989
- personal sampling devices for atmospheric contamination monitoring (*French*) 0-57986
- personnel dosimetry methods introduced in the Czechoslovak national laboratories 0-57969
- photon radiation meas. in nuclear power stations 0-63403
- pion range monitor, test using the radiative capture  $\pi^+p \rightarrow \pi^0 n \gamma$  0-72317
- portable body monitoring system, NRPB experience 0-104773
- protection monitoring in tropical developing countries 0-57997
- purpose and aims 0-57968
- PWR containment air monitoring system 0-57965
- PWR radioactive gaseous effluents, release trends in US 1977 0-95481
- radiation units in SI system, conversion problems 0-57244
- radioactive effluent, Pu and Am inventory of ecosystem near a nuclear facility 0-97820
- radioactive waste storage, in situ instrumentation for meas. of radionuclide migration 0-95485
- radioactive waste storage, long term subsurface migration of radionuclides 0-95483
- radioactive waste storage, radionuclide migration determ., adsorption of Cs(I), Sr(II), Eu(III), Co(II), and Cd(II) by Al<sub>2</sub>O<sub>3</sub> 0-99240
- radioisotope transport in terrestrial food chains, dynamic modelling using RAGTIME code 0-104776
- radiological assessment of inactive nuclear sites, statistical design and anal. 0-95473
- radiological assessment of inactive nuclear sites 0-95478
- radiological survey of inactive nuclear sites, quality assurance 0-95472
- radionuclide migration from buried radioactive waste 0-95484
- radiowaste storage, soil homogeneity evaluation by radionuclide tracer breakthrough curve interpretation 0-97821
- reference radiations for radiation protection dose meter calibration (*French*) 0-57998
- shadow-shield background reduction method 0-108999
- sky-shine computational procedure (*German*) 0-74036
- spent nuclear fuel inventory confirmation technique using Cherenkov light intensity meas. 0-78419
- statistical methodology for radiological surveying 0-57993
- Thailand's first nuclear power plant, radiation monitoring programme 0-57996
- Three Mile Island malfunction, monitoring, radiation exposure 0-57960
- TLD system, automated, for gamma radiation monitoring 0-57964
- TLDs, use in personal monitoring, judgement of abnormal value by glow curve (*Japanese*) 0-106208
- track-etch monitor for reactor power anal., evaluation 0-78418
- transuranic aerosol measurement system and its field results 0-58068
- transuranic elements in air at nuclear reprocessing plant, monitoring system 0-63409
- university hot laboratory, radiation monitoring programme 0-57991
- whole body counters, international intercomparison 0-78504
- wrist watch dosimeter for ionising radiations, practicality tests 0-57972
- $\alpha$ -emitting effluents from nuclear processing plant, detection and meas. 0-95468
- CO<sub>2</sub> laser Helios fusion system beam diagnostics 0-78882
- CaSO<sub>4</sub>:Dy Teflon TL dosimeters, thin, development for  $\beta$ -dosimetry in personnel monitoring 0-63399
- Ge detector system for inhaled radionuclide detection and meas. 0-57990
- <sup>3</sup>H monitors, calibration technique (*Czech*) 0-74075
- I, radioactive, air sampling system, separation into gaseous and particulate fractions 0-57962
- Pu fallout detection using fission tracks prod. with neutron irradiated spectra 0-95479
- Pu holdup in glove-box exhaust filter, in-line monitoring by gamma ray detection 0-78458
- <sup>239</sup>Pu, evaluation of portal monitors for the detection of nuclear materials 0-63406
- Rn and daughters meas. methods in underground and free atmosphere air 0-57987
- Rn, long term average level meas. instrument 0-58085
- Rn monitoring, TLD, passive detector, U mill field 0-57963
- Rn monitoring instrumentation 0-106204
- <sup>222</sup>Rn, conc. in air, absolute determ. using cellulose nitrate track detector 0-63492
- <sup>222</sup>Rn concentration meas. by plastic detectors to determ. environmental  $\alpha$ -emitters from natural sources 0-91292
- <sup>222</sup>Rn diffusion through U mill tailings covers, coeff. meas., lab. techniques 0-95387
- <sup>222</sup>Rn gas detection using Track Etch system for U exploration 0-98488
- Si diffused junction detector for alpha air monitoring instrumentation 0-58083
- <sup>90</sup>Sr bremsstrahlung radiation meas. for well logging using Ge spectrometer 0-94619
- radiation monitors** *see radiation monitoring*
- radiation patterns, antenna** *see antenna radiation patterns*
- radiation pressure**
- see also acoustic streaming*
- atom-photon interaction quantum fluctuations, at. beam focusing by radiation press. 0-58217
- atomic beam deceleration and monochromatisation laser radiation press. 0-102491



**radiation pressure continued**

- atomic velocity distrib. hole-burning by EM radiation 0-64674  
 atoms, motion in optical freq. radiation trap 0-78818  
 atoms, reson. radiation force, quantum mech. fluctuations, influence on at. motion 0-58233  
 comets, radiation pressure accel. effect on neutral species brightness profiles, average random walk model 0-77351  
 dielectric cylinder, infinite, randomly oriented, radiation press. 0-58454  
 Earth, IR radiation press. on Castor satellite meas. from Cactus accelerometer results 0-77251  
 gas translational nonequilibrium in reson. EM field 0-96340  
 gravitational wave interferometer, quantum mechanical radiation press. fluctuations 0-90770  
 HZ Herculis, light curve, radiation pressure effects in X-ray binary 0-105280  
 interstellar dust, grain growth by radiation pressure induced coagulation 0-94851  
 laser pulse amplification through energy exchange with electron beam via nonlinear radiation press. effects 0-95776  
 laser radiation effects on particle properties, radiation pressure effect on particle motion (*German*) 0-102755  
 liquid, absorbing intense IR radiation, behaviour of pressure 0-102749  
 neutral atoms, stimulated Coulomb interaction in external resonance field 0-83449  
 nonspherical particle, optical levitation for light scattering obs. 0-58455  
 optical levitation of single particle to study quasi-elastic light scatt. theory 0-99620  
 particle properties, particle heating by radiation absorption, effect of radiation press. (*German*) 0-106556  
 plasma interaction with laser radiation, light press. nonlinear force, polarisation influence 0-100078  
 quasar winds, radiative acceleration for different power law spectra 0-90565  
 radiation pressure, appl. to satellites inertially fixed pitch stabilisation 0-101523  
 resonance ponderomotive effects in EM wave scatt. and emission 0-69301  
 resonant impurity gas, translational nonequilibrium in resonance optical field (*Russian*) 0-106865  
 solar, effect on anomalistic period of artificial satellites 0-77255  
 stellar rapidly rotating models with radiation press., struct. parameters calc. 0-67697  
 three-body problem, restricted classical case, generalisation for radiation press. 0-85843  
 universe, Friedmann model, effect of decoupled radiation field press. on density perturbations growth 0-109567  
 Ge, far IR photon drag and radiation pressure in refractive media 0-60048  
 Mg<sup>+</sup> laser cooled ions bound in Penning trap, high-resolution optical spectra 0-102487  
 SF<sub>6</sub> molecule drift mobility due to IR laser radiation (*Russian*) 0-69192  
 Si, far IR photon drag and radiation pressure in refractive media 0-60048

**radiation protection**

- see also radiation monitoring  
 absorbed dose distrib. in thin layers rel. to electron beam incidence 0-83226  
 accelerator shielding problems (*Japanese*) 0-99343  
 achievement, standards and value judgements 0-101273  
 acoustic radiation, performance of custom-moulded earplugs 0-104774  
 actinide radioactive waste, biological hazards, consequences for LMFBR fuel recycling 0-86960  
 Babcock & Wilcox hot cell facility 0-68910  
 conference, Bologna, Italy (Oct. 1977) 0-62367  
 conference, radiation protection monitoring advances, Vienna, Austria (June 1978) 0-57007  
 dose meter calibration for radiation protection in European Community 0-58000  
 ear protection systems, attenuation produced at each normal freq., Noise Reduction Rating calc. (*Spanish*) 0-109041  
 ear protectors, use of sound levels for assessing adequacy 0-104771  
 eye shields, individualised, for electron beam therapy and low-energy photon irradi. 0-109040  
 FBR fuel handling, radiation safety 0-73985  
 field measurements, relationship to calibration values 0-58002  
 fusion reactor, MFTF, intense neutron environment, test cell side wall design, shielding materials 0-102318  
 gamma rays, 6 MeV, penetrating shielding materials, energy and ang. flux density spectra 0-63393  
 gamma-ray buildup factors for Pb/H<sub>2</sub>O stratified radiation shields 0-86994  
 glass dosimeter reader, design improvements (*French*) 0-57970  
 hot cell, rigid hoist articulated grapple system development for enhanced remote maintenance 0-68968  
 hot cell complex, Japan, users comments (*Japanese*) 0-91296  
 hot cell complex in Japan, University use (*Japanese*) 0-91295  
 hot cell for synthesis of labeled organic compounds 0-68970  
 hot cell oil filled Pb glass shielding windows, maintenance and refurbishment 0-68969  
 improved radiation shielding using packed mixed size Pb particles, nuclear plant maint. appls. (*Japanese*) 0-106207  
 impulsive and continuous noise, combined dose meas. 0-102929  
 ionising radiation, detection device, electret based (*French*) 0-57971  
 laboratory-scale shielded cell for <sup>252</sup>Cf 0-63405  
 laboratory-scale shielded cell for <sup>252</sup>Cf 0-74035  
 linear accelerator, local absorber in accelerating section to reduce radiation level 0-83229  
 man-made EM fields and georadiations, effects on man (*Polish*) 0-67258  
 mixed  $\beta$ - $\gamma$  dosimetry, ionisation and scintillation counters 0-57975  
 mixed radiations, device for dose-equivalent index determ. (*Russian*) 0-57976  
 MPD reduction suggestion to meet requirements of higher safety 0-85499  
 nuclear fuel reprocessing plant, radiation exposure due to exhaust air (*German*) 0-57940  
 nuclear medicine laboratory, radiation safety 0-104772  
 nuclear power plant safety, West German policy (*German*) 0-57865  
 penicillamine-treated mice, survival following whole-body irradi. 0-98030  
 personnel dosimetry methods introduced in the Czechoslovak national laboratories 0-57969

**radiation protection continued**

- plutonium, biologically important physicochemical props. and methods of human contamination (*French*) 0-98004  
 purpose and aims 0-57968  
 radioactive materials, IAEA transport information collection system, influence on improved safety measures 0-63413  
 radioactive materials, IAEA transport regulations, underlying radiation protection principles 0-63414  
 radioactive materials, safe transportation, using type A, exempt and LSA packages 0-63401  
 radioisotopes used in Hungary, development of protection (*Hungarian*) 0-90644  
 radiological implications of Pu recycling in HTGR fuels 0-68777  
 remote maintenance to comply with new legislation limiting occupational radiation exposure, in United States 0-106210  
 RF EM fields (300 KHz-100 GHz), human exposure safety level 0-89869  
 safety standards for X-rays and ionising radiation 0-98146  
 solid dielectric detectors with breakdown phenomena and their applications in radioprotection 0-91388  
 space flights, prolonged, radiation danger to man 0-61711  
 standards, quantitative risk 0-61708  
 therapeutic <sup>131</sup>I solutions, precaution for minimising exposure due to vaporisation 0-101274  
 thermal flash protective goggles, PLZT ceramic bonded lens assembly manufacture 0-79018  
 thermal flash protective goggles, PLZT ceramic thin wafer electrode slotting process 0-79017  
 ultra-thin dosimeter for skin dose assessment, development 0-57974  
 university hot laboratory, radiation monitoring programme 0-57991  
 VVER type nuclear reactors, in Soviet Union, biological shielding problems 0-106127  
 X-ray attenuation measurements on Y tung shielding material (*German*) 0-98145  
 B<sub>2</sub>C reflector-shield concept for fusion reactor designs 0-102293  
 B<sub>2</sub>C-304 stainless steel cermet for nuclear shielding appls. 0-102352  
 B<sub>2</sub>C-Cu cermet fabrication for neutron shielding appls. 0-102354  
 B<sub>2</sub>C-phenolic fibre reinforced composite for nuclear shielding appls. 0-102353  
<sup>125</sup>I, shielding of (*Japanese*) 0-63404  
 PLZT thermal, flash, ferroelectric protective goggles 0-81746  
 PLZT/TFPD thermal/flash protective lens assembly, polarised delamination investigation 0-78929
- radiation quenching**  
 acetylene, triplet state quenching by foreign gases 0-91596  
 2-aminopurine, in viscous soln., fluoresc. quenching, emission, intensity and reson. transfer (*German*) 0-91599  
 benzene, soln., fluoresc., quenching in pulsed proton and alpha particle irradi., radiation quality effects 0-66259  
 Cd + molecules collisions 0-58338  
 chalcogenide glasses, Luminescence, temp. depend. rel. to nonradiative transitions 0-71485  
 3,6-diaminophthalimide vapour, mol. electronic excitation energy degradation path depend. on pentane 0-74195  
 N-ethylphthalimide + olefins, photochemical reaction, absorpt., fluoresc., phosphoresc. and triplet-triplet absorpt. spectra 0-85197  
 exciplexes and excited aromatic molecules, donor-acceptor props., comparison of fluorescence quenching 0-69174  
 glyoxal, S<sub>0</sub>→S<sub>1</sub> band, opto-acoustic phase angle meas. 0-68256  
 inert gas atom + halogen mol., halide form., relax. and quenching 0-81314  
 liquid, migration mechanism of approaching particles, energy transfer, luminesc. quenching study 0-100343  
 molecule, photodissociation recomb. afterglow, quenching var., activator penetration to region inaccessible to quencher 0-64813  
 molybdates, alkaline earth, U activated, scheelite struct. luminesc. props. vibr. modes and quenching temp. 0-60651  
 naphthyl group, excited singlet state, intramol. fluoresc. quenching by halogeno substituents 0-102537  
 $\beta$ -naphthylamine, fluoresc. quenching and spectra, excited state reaction, red edge effect obs. 0-83400  
 naphthylamines, abnormal fluorimetric titration behaviour, kinetic anal., fluoresc. quantum yields and lifetime meas. 0-89560  
 nonlinear luminescence quenching at high pumping levels, microscopic theory 0-89040  
 organic scintillators, vap. phase dye laser media, photophysical parameters 0-95884  
 orthopositronium quenching by O<sub>3</sub>, meas. by two-photon coincidence rate difference technique 0-74262  
 2-phenylindole, in viscous soln., fluoresc. quenching, emission, intensity and reson. transfer (*German*) 0-91599  
 phthalocyanine, doped photovoltaic cell, photoconductivity, elec. field induced fluoresc. quenching, charge carrier photogeneration 0-84485  
 poly-N-vinylcarbazole-biacetyl, triplet exciton quenching, exciton trapping model 0-66267  
 porous Vycor glass, quenching by O<sub>2</sub> and NH<sub>3</sub>, photoluminescence obs. 0-93773  
 positronium formation and quenching in Ar-O<sub>2</sub> mixtures, orthopositronium quenching cross section determ. 0-74261  
 pyrene, distinction of delayed fluorescence S<sub>1</sub>→S<sub>0</sub> and S<sub>2</sub>→S<sub>0</sub> by selective quenching of S<sub>1</sub>→S<sub>0</sub> 0-69175  
 quinones, triplet quenching by organometal cpds., time resolved CIDEP and ESR obs. 0-95654  
 rhodamine 6 Zh solution, radiant transport effect on luminesc. duration 0-103995  
 rhodamines, 5G, 6G, B, 3B in ethanol soln., luminesc. quenching by photoirradiation 0-87168  
 ruthenium tris-bipyridyl, excited state electron transfer quenching, H<sub>2</sub>O photoreduction mediators effects 0-102536  
 tetrabutylammonium europium yttrium isothiocyanate, conc.-depend. electron-phonon coupling, and self-quenching 0-60657  
 thiocarbonyl chlorofluoride, second excited singlet state emission spectroscopy, resonance fluorescence obs. 0-69158  
 tungstates, alkaline earth, U activated, scheelite struct. luminesc. props. vibr. modes and quenching temp. 0-60651  
 tungstates, U-doped, perovskite struct., luminesc. quenching, QMSCC calcs. 0-71470  
 Ar saturated solutions, NO<sub>2</sub><sup>-</sup> effects on spectral distribution and intensity of sonoluminescence 0-76091



**radiation quenching continued**

- Bi<sub>2</sub>, radiative lifetime and self-quenching cross sections meas. from laser induced fluorescence expt. 0-69189  
 Br<sub>2</sub>, kinetics of excited states using laser excitation, radiative lifetimes and collisional deactivation 0-74237  
 Br<sub>2</sub>, single rot. states, lifetimes and collisional quenching cross sections determ. by obs. fluoresc. decay 0-91595  
 CH(A<sup>1</sup>Δ) radicals, electronically excited, lifetimes and quenching rate constants meas. 0-69188  
 CN\*, B<sup>2</sup>Σ<sup>+</sup> state, fluoresc. decay dynamics, collisional quenching and radiative lifetimes 0-58306  
 CO, dΔ state, low energy electron impact excitation and radiative decay 0-91691  
 Ca+Ca(Mg)(inert gas), metastable <sup>2</sup>P-state, quenching reactions, fluoresc. meas. 0-102477  
 CdO:Ce<sup>3+</sup>, Gd<sup>3+</sup>, sensitization of Ce<sup>3+</sup> luminesc. by Gd<sup>3+</sup> 0-97326  
 Cd(P<sub>2</sub>O<sub>7</sub>) + CO(CO<sub>2</sub>)(NO), absolute quenching cross section, phase-shift method 0-58340  
 CdS:In(Cl) concentration quenching mechanism of luminescence 0-97336  
 CdTe, elec. and photoelec. props. due to double injection, quenching spectra 0-70765  
 (Co,Cr,Fe)<sub>2</sub>O<sub>4</sub>, (Co,Rh,Fe)<sub>2</sub>O<sub>4</sub> film magneto-optical switches, for laser beam synchronisation 0-58615  
 Cu<sup>2+</sup>-1,5-dimethyl-2,4-hexadiene, fluoresc. quenching method for determ. binding const. 0-89530  
 EuNa<sub>2</sub>Mg<sub>2</sub>(VO<sub>4</sub>)<sub>3</sub>, disordered, thermal quenching of luminesc. 0-71472  
 GaAs:Cr, photoluminescence in strong electric fields 0-108270  
 Ge:Se, electron-hole pair lifetime, quenching temp. influence 0-59889  
 H<sub>2</sub>, E,F<sup>2</sup>Σ<sup>+</sup> state, collisional and radiative props. 0-58357  
 HCl, overtone vibr.-rot. bands, intracavity dye laser techniques meas. 0-91532  
 He, 3<sup>1</sup>P level, excitation and decay study up to high press. pumped by intense relativistic electron beam 0-74250  
 He<sup>+</sup> + inert gas, collisional quenching cross sections, two-state theory calcs. 0-69217  
 Hg+H<sub>2</sub>(CO)(NH<sub>3</sub>)(ethylene), quenching rate constants determ. with nanosecond light pulser with Hg vapour 0-100111  
 K+NaK reactive collisions studied using circularly polarised laser fluorescence 0-69215  
 KBr(I), photostimulated recomb., electron spin polarisation 0-60673  
 Kr, 6p levels, two-photon excitation, time resolved fluoresc., quenching, lifetimes and photoionisation cross section 0-78587  
 Kr+F<sub>2</sub>, KrF form., relax. and quenching 0-81314  
 Li\*(<sup>2</sup>P<sub>1/2</sub>)+H<sub>2</sub>(D<sub>2</sub>), collision induced quenching and fine struct. transition rate coefficients meas. 0-74221  
 N<sub>2</sub>+HgX<sub>2</sub> (X=halide), A<sup>2</sup>Σ<sup>+</sup> state quenching obs. 0-108693  
 N<sub>2</sub>+methylmercury halides, A<sup>2</sup>Σ<sup>+</sup> state quenching obs. 0-108693  
 N<sub>2</sub>\*+H<sub>2</sub>O(H<sub>2</sub>S)(methane), deactivation, from laser-induced CO<sub>2</sub> fluoresc. obs. 0-63776  
 Na, high Rydberg states, quenching in strong 1.06 μm laser field 0-95559  
 Na<sub>2</sub>Al<sub>2</sub>Si<sub>2</sub>O<sub>7</sub>Cl(Br)(I), cathodochromic sodalites, coloured crystals, tunnel and recomb. luminesc., temp. depend. (Russian) 0-66261  
 Na<sub>2</sub>O-P<sub>2</sub>O<sub>5</sub>-Y<sub>2</sub>O<sub>3</sub>-Tb<sub>2</sub>O<sub>3</sub> glass, conc. quenching of luminesc. in disordered system with dipolar interaction 0-89059  
 NdP<sub>2</sub>O<sub>7</sub>, fluoresc. lifetime meas., IR and photoacoustic spectroscopy 0-60652  
 O, (<sup>1</sup>D<sub>2</sub>) state, quenching, rel. to O<sub>2</sub> b<sup>1</sup>Σ<sub>g</sub><sup>+</sup> prod. and deactivation 0-76493  
 O<sub>2</sub> b<sup>1</sup>Σ<sub>g</sub><sup>+</sup> state prod. and deactivation following O(<sup>1</sup>D<sub>2</sub>) quenching 0-76493  
 O<sub>2</sub>, laser excited, quenching by CO<sub>2</sub>, H<sub>2</sub>O and I<sub>2</sub> 0-99515  
 OCSe, quantum yields for Se, <sup>1</sup>S<sub>0</sub>, <sup>3</sup>D<sub>2</sub>, and <sup>3</sup>P<sub>0,1,2</sub> atoms determ. in photolysis, lifetime and quenching rate meas. 0-97741  
 O<sub>2</sub>(b<sup>1</sup>Σ<sub>g</sub><sup>+</sup>), temp. dependent quenching, photochemical study by H<sub>2</sub>-VUV laser 0-63702  
 RbI, photostimulated recomb., electron spin polarisation 0-60673  
 Se, amorphous film, influence of wavelength on optical quenching of photoconductivity 0-60046  
 SeO<sub>2</sub>+Ar(N<sub>2</sub>)(CO<sub>2</sub>), radiative lifetime and quenching rates 0-95685  
 Xe+Cl<sub>2</sub>(F<sub>2</sub>), XeCl(XeF) form., relax. and quenching 0-81314  
 Xe+Ne, quenching of excited Xe\*(<sup>3</sup>P<sub>2</sub>, <sup>3</sup>P<sub>1</sub>, <sup>1</sup>P<sub>1</sub>) states 0-63578  
 XeCl laser, B-X, form. and quenching kinetics 0-74341  
 XeF<sub>2</sub>(C) state lifetime, quenching rate constants, photolysis in inert gas atmospheres 0-66816  
 XeF\*, B<sup>2</sup>Σ<sup>+</sup> and C<sup>2</sup>I<sub>3/2</sub> states, fluoresc. decay dynamics, collisional quenching and radiative lifetimes 0-58306  
 XeF\*, electron impact excitation, temp. depend. quenching rate consts. 0-63701  
 XeF\*+F<sub>2</sub>+Xe, temp. dependent quenching rate constants 0-63701  
 XeF\*, production via laser absorpt. processes at 193 nm, quenching kinetics 0-91466  
 ZnS:Tb, Cu(Ag) phosphors, luminesc. props. 0-100690

**radiation therapy**

- accelerator leakage measurements 0-89839  
 brachytherapy program used with the Philips Treatment Planning System 0-81738  
 brain low dose elective, in small cell lung carcinoma 0-67253  
 breast treatment, modified 3-field technique 0-104737  
 bronchogenic cancer, small cell, undifferentiated, role of radiation therapy in treatment 0-67226  
 build-up curves of scanned high energy electron beams, Sagittaire linear accelerator 0-89864  
 cancer, by controlled local heating, 915 MHz or 2450 MHz 0-76860  
 cancer treatment, survival times and response rates 0-72315  
 cancer treatment appl. of microwave arrays for localised tumour heating 0-94308  
 carcinoma of anterior tonsillar pillar and soft palate-uvula, treatment methods comparison 0-98121  
 Cathetron, high intensity CO, gynaecological cancer therapy 0-72300  
 cervical carcinoma, para-aortic irradi. 0-72307  
 cervical carcinoma, radiotherapeutic approaches 0-67227  
 cervix, IB carcinoma, role of radiation therapy 0-67228  
 cervix carcinoma, extended field technique complications, correl. of radiation and surgical parameters 0-67225  
 chest wall irradiation, technique to improve electron dose distrib. homogeneity 0-72332  
 computed tomography for radiotherapy planning 0-94334  
 computerised tomography utility, estimate of outcome 0-67229

**radiation therapy continued**

- computerized tomography, use in therapy program development (French) 0-85472  
 conference, Philadelphia, USA (Apr.-May 1980) 0-94913  
 current field heating, localised, as an adjunct to radiation therapy 0-98056  
 depth dose and off-axis characts. of TLD in therapeutic pion beams 0-101271  
 dosage calculation and compensation, basic data 0-104765  
 dose planning, revision of tissue-max. ratio and scatter-max ratio concepts 0-76840  
 dose response curves, methods of extraction 0-94374  
 dosimetric considerations of very large <sup>60</sup>Co fields 0-104766  
 dosimetry, <sup>60</sup>Co total body irradi. at 220 cm source axis distance 0-104768  
 dosimetry, algorithm for calc. of central ray TAR and TMR values 0-76844  
 dosimetry, procedures with electron and photon beams 0-101266  
 electron beam applicator, variable field, dosimetry evaluation 0-76839  
 electron therapy, up to 20 MeV, phys. aspects 0-85474  
 emitted radiation, clarification of concept, brachytherapy dosimetry appl. 0-76843  
 epithermal neutron field for <sup>10</sup>B neutron capture therapy, prod. using FBR 0-61692  
 external beam, planning using the Edinburgh algorithm 0-94316  
 fast electrons, computerised treatment planning, dose distrib. calc. 0-81740  
 fast neutron beam for medical use, production and definition (French) 0-69003  
 fast neutron beams, linear regression anal. of γ-dose 0-89866  
 fast neutron therapy using <sup>252</sup>Cf (Japanese) 0-98112  
 film dosimetry of multiple electron beam ports with wedges 0-98138  
 gliomas, malignant, anal. of dose-effect relationship 0-72331  
 gliomas, malignant, high dose radiation therapy 0-67254  
 gliotic cancer, T3, anal. of close time-vol. factors 0-104764  
 hard X-ray machine, RT 305, phys. aspects and appl. 0-81709  
 head and neck cancer, advanced and recurrent, short course high fractional dose irradi. 0-72297  
 head and neck squamous-cell carcinoma, advanced, fractionation schedules 0-98123  
 head and neck tumours, treatment in air rel. to treatment in hyperbaric O<sub>2</sub> 0-72298  
 head holder for treatment of head and neck cancers 0-94333  
 heavy ion therapy, treatment planning programme 0-72295  
 hyperthermia, deep local, induction by US and EM fields, problems and choices 0-94283  
 hyperthermia, localised, comparison of EM and US diathermy 0-104725  
 hyperthermia by magnetically induced currents, freq.-depth-penetration, comments and reply 0-108991  
 implantation device, preloaded custom-designed, for T1-T2 carcinoma of the floor of the mouth 0-94335  
 interstitial dosimetry, utilisation of the computerised tomography scanner 0-104770  
 intracavity implant therapy, appl. of linear programming to dose optimisation 0-72329  
 intracavity therapy using remote afterloading technique (Japanese) 0-81730  
 lasers, therapeutic appl. (French) 0-108996  
 light-ion flux mixed with collimated fast-neutron beams 0-81723  
 linear accelerator, 4 MV, use for whole-body irradi. 0-109001  
 linear accelerator, SL 75-200, neutron and gamma doses in entrance mazes of treatment rooms 0-85500  
 linear accelerator beam profile scanner 0-101267  
 linear accelerator dosimetry control system, solid state 0-94371  
 linear accelerator X-ray beams, off-axis beam quality change 0-78461  
 Lipowitz metal shielding thickness for dose reduction of 6-20 MeV electrons 0-76842  
 Luer lock afterloading device for <sup>192</sup>Ir brachytherapy 0-104735  
 lung cancer, interstitial brachytherapy, 20 year experience 0-72302  
 lung carcinoma, extended fractionation study 0-72305  
 lung dose in half body radiotherapy, determ. by computerised tomography 0-104763  
 lymphocytes, peripheral, population changes following radiation therapy to limited and extended fields 0-72236  
 malignant melanoma, dosimetric consideration 0-94372  
 mammary carcinoma, primary radiotherapy, review (German) 0-61693  
 mammary carcinoma stage II, postoperative therapy programme 0-72285  
 mandible, radiation necrosis, dental factors, radiotherapy complication 0-98021  
 mandible, radiation necrosis, factors influencing onset, radiotherapy complication 0-98020  
 maxillary antrum, squamous cell carcinoma, cervical lymph node metastases 0-72304  
 microdosimetry of the pion beam at TRIUMF 0-109037  
 microstrip antenna for biomedical applications 0-89826  
 microstrip slot radiator for medical appls. 0-108994  
 microwave antenna, invasive, for locally-induced hyperthermia for cancer therapy 0-67193  
 microwave applicators, comparison of stray radiation patterns 0-61660  
 microwave applicators for localised hyperthermia treatment of malignant tumours 0-89824  
 microwave diathermy applicator with choke, 2450 MHz, slab-loaded, direct contact 0-89825  
 microwave diathermy direct-contact circular aperture applicator with corrugated flange, design 0-67190  
 microwave effects research, medical appls. and hazards, 1940-60 0-86066  
 microwave heating combined with radiation therapy, skin and tumor thermal enhancement ratios 0-67192  
 microwave hyperthermia, localised, biomedical devices 0-104724  
 microwave hyperthermia, microwave leakage during treatment 0-76820  
 microwave hyperthermia to cancer treatment (Spanish) 0-89795  
 microwave hyperthermia treatment and thermometry system 0-72280  
 monocyte function rel. to irradi. in breast cancer patients 0-72238  
 mycosis fungoides, electron beam therapy 0-72286  
 neck node metastases, effectiveness of microwave hyperthermia combined with ionising radiation 0-94307  
 oncology, historical developments 0-81708  
 optimal treatment schedules for fractionated irradi. of tumours, math. derivation 0-98078  
 organ shielding and localisation in a diverging treatment beam, simple method 0-94317



**radiation therapy continued**

- oropharynx, advanced carcinomas, fast neutron teletherapy, efficacy obs. 0-72296
- oropharynx, squamous cell carcinomas 0-67925
- ovarian cancer, whole abdominal irradiat. by moving-strip technique 0-72301
- parasternal lymphoscintigraphy, radiation treatment planning implications, breast cancer 0-72299
- patient's surface contour measuring device 0-104717
- photoluminescent thermometer probes, temp. meas. in microwave fields 0-104721
- pion<sup>-</sup>, radiobiological evaluation of suitability for tumour therapy 0-67166
- pion<sup>-</sup> end, in vivo beam localisation by positron activation 0-72316
- prostatic cancer, preoperative extended field radiation using <sup>125</sup>I seed implants 0-72303
- proton beam, high-energy, physical meas. using tissue substitutes 0-81720
- radioactive seed implants, computation of dose distrib. 0-101265
- RF heating for solid tumour destruction, animal expts. 0-61637
- risk due to unwanted neutrons, estimation by dose calcs. 0-81714
- scanning electron beam, semi-empirical model for dose distrib. generation 0-94373
- secondary sections for radiotherapy plane section (German) 0-89841
- source motion, calc. in intracavity moving-beam and multipositional irradiat. 0-104759
- spot scanning system for proton radiotherapy 0-89836
- squamous cell carcinoma of head and neck, time-dose factors anal. 0-72333
- tethered float radiometer for US therapy equipment output power meas. 0-104691
- thyroid cancer, radiotherapy technique 0-94337
- tissue compensators, use in improving dose uniformity in total body irradiat. 0-104767
- tissue-equivalent compensators for 4-MV X-rays, basic data 0-98069
- total body irradiation, radiobiological bases 0-104667
- total body techniques for bone marrow transplantation, review 0-104738
- transverse axial film tomography with a therapy simulator 0-81716
- treatment planning, computerised, accuracy 0-72328
- treatment planning, FORTAN program for optimisation using complication probability factor 0-81686
- treatment planning, inhomogeneity correction methods compared with Monte Carlo data 0-61698
- treatment planning, value of computerised tomography scanning 0-72294
- treatment planning and the distortion of computerised tomography images 0-76830
- treatment planning for irregular fields 0-81739
- tumour registration system 0-81710
- US hyperthermia, localised, design of heating protocols 0-104693
- US probes, power meas. by use of semiconductor strain gauges 0-87679
- Vena cava, superior, optimum radiation schedule in obstruction treatment, importance of <sup>99m</sup>Tc scintangiograms 0-72334
- <sup>60</sup>Co sources for total body irradiat., uniformity and standardisation 0-94338
- <sup>137</sup>Cs gynecologic insertions, expt. derived algorithm for computer calc. dose rates 0-101264
- Pb sheets, thin, as tissue compensators for larger field irradiat. 0-104736
- radiationless transitions** see *nonradiative transitions*
- radiative corrections**
- "radiative corrections" is distinguished in use from "electromagnetic corrections" by application to atomic and molecular spectra see also *electromagnetic corrections*; *radiative shifts*
- inner-shell vacancy creation, ionised fragments probability distrib. 0-83274

**radiative lifetimes**

- acridine, temp. depend. of fluoresc. decay meas. using picosecond techniques 0-99518
- alkaline earth halides:Eu<sup>2+</sup>, fluorescence lifetime and quantum efficiency for 5d-4f transitions 0-100681
- antimalarial drugs, lifetime meas. via reiterative convolution using fluorescence decay curves 0-57380
- atom+diamon, energy correction of infinite order sudden approx., improved phase shift approach 0-95710
- atom and ion, radiative lifetime laws 0-74150
- atoms, monovalent, transition probabilities calcs. (Russian) 0-63594
- benzene cryst., electron irradiat., phenylcyclohexadienyl radical form., absorpt. and fluoresc. spectra study 0-89035
- bromofluoromethylene radical, laser-induced fluoresc., <sup>1</sup>A'-<sup>1</sup>A' transition 0-91589
- chain with light emitting ends, radiative lifetime, recombination kinetics 0-108260
- chlorofluorobenzene cations in gaseous phase, emission spectra and lifetimes in B(0<sup>+</sup>) states 0-63711
- chloroquinolines, photophys. behaviour, substituent and solvent effects 0-106342
- coumarin laser dyes, fluoresc. quantum yields and lifetimes, polar solvent effects 0-87054
- coumarin laser dyes, solvent effects on photophysical parameters 0-91598
- diamonic mols., electronic transition probabilities, isoelectronic, isovalent corrls. for transition strength and vibr. consts. 0-87182
- dilute systems, donor fluorescence at high trap concentration 0-71479
- 1,6-diphenylhexatriene, radiationless transitions and natural lifetimes, solvent effects 0-63622
- DODCI in ethanol, DQOCI added, electronic energy transfer, real-time ps meas. 0-58311
- DODCI in ethanol, malachite green added, electronic energy transfer, real-time ps meas. 0-58311
- dyes, fast mode-locking, IR fluoresc. and laser action obs. 0-102717
- fluorobenzenes in Ne matrices, molecular cation electronic absorption spectra, new photolytic technique 0-58415
- formaldehyde S<sub>1</sub> levels, collisionless single rot. level lifetimes, elec. field depend. 0-63566
- formaldehyde-d<sub>6</sub>-(d<sub>2</sub>), S<sub>1</sub> single rot. level lifetimes, isotope, elec. field and vibr. state depend. 0-78655
- inert gas atom, first excited config., intermediate coupling coeff. 0-83450
- inert gas crystal, lattice vibrs. and radiative transitions of implanted ions (Russian) 0-69098
- inert gas mixtures, high-press., collisional radiative recomb. 0-63595
- methine dyes, spectral props., solvent effects 0-69181
- molecular interaction with EM fields, classical theory 0-95686

**radiative lifetimes continued**

- molecules, transition probability evaluation in double asymmetric pot. well 0-69120
- multicharged ions, transitions between energy levels in strong external field, relativistic calcs. (Russian) 0-63547
- n- $\pi^*$  singlet-singlet transition probabilities 0-95689
- optical collisions, solvable model 0-91638
- perfluorobenzene, electron attachment, radiative and dissoc., negative ion lifetimes, ion cyclotron reson. spectra 0-74251
- perfluorocyclobutane, electron attachment, radiative and dissoc., negative ion lifetimes, ion cyclotron reson. spectra 0-74251
- perfluoromethylcyclohexane, electron attachment, radiative and dissoc., negative ion lifetimes, ion cyclotron reson. spectra 0-74251
- perfluorotoluene, electron attachment, radiative and dissoc., negative ion lifetimes, ion cyclotron reson. spectra 0-74251
- poly-N-vinylcarbazole-biacetyl, triplet exciton quenching, exciton trapping model 0-66267
- polymethine saturable absorbing dyes, dual component fluoresc. lifetime meas. 0-106359
- positronium formation and quenching in Ar-O<sub>2</sub> mixtures, orthopositronium quenching cross section determ. 0-74261
- quantum oscillators, matrix element diagrams 0-105455
- radiative collisions, solvable model 0-91638
- sputtered excited states, secondary photon emission, role of transition probability 0-102483
- stilbene, cis and trans, transient spectra, radiative lifetimes and quantum yields 0-78640
- trans-stilbene, soln., lifetime and anisotropic fluoresc., viscosity effects (German) 0-106352
- three-electron systems, transition probabilities calcs. 0-99479
- two-state collision problems, distorted-wave formula for transition probabilities 0-69212
- Al XIII, 1s2p<sup>3</sup>P<sub>2</sub> and 1s2p<sup>3</sup>P<sub>0</sub> levels, radiative lifetimes and hyperfine induced decay 0-74149
- (AlGa)As stripe geometry, proton-bombardment delineated DH laser, lifetime 0-106520
- Ar atoms in Ne matrix, radiative and nonradiative lifetimes in excited states 0-69106
- Ar II arcs, transition probabilities, statistical inference 0-106357
- Ar+Kr, (4p<sup>5</sup>5p) and (4p<sup>5</sup>5p) states, radiative lifetimes and two-body collisional deactivation rate consts. 0-95572
- Ba (5d6p)<sup>3</sup>D<sub>3</sub> state, lifetime meas. by dye laser spectrosc. 0-78577
- Ba<sup>+</sup> ions confined in cylindrical RF trap, lifetime meas., laser probing 0-95573
- Ba<sub>2</sub><sup>2+</sup>, very long lived vibr. states, lifetimes, WKB calc. 0-78560
- BaO, excited electronic states, lifetimes and transition moments 0-87177
- BeF<sub>2</sub>:Eu<sup>3+</sup> glass, luminesc. of Eu<sup>3+</sup>, transition probabilities 0-80845
- Bi<sub>2</sub>, lifetime and self-quenching cross sections meas. from laser induced fluorescence expt. 0-69189
- Br<sub>2</sub>, kinetics of excited states using laser excitation, radiative lifetimes and collisional deactivation 0-74237
- Br<sub>2</sub>, single rot. states, lifetimes and collisional quenching cross sections determ. by obs. fluoresc. decay 0-91595
- C IV (C V), UV line identifications and lifetime meas. 0-106288
- C<sub>2</sub> vapour, Swan bands, oscillator strength 0-63712
- C<sub>2</sub>+acetylene, C<sub>2</sub> Swan band transition probabilities, collisional energy transfer effects 0-87214
- CH(A<sup>2</sup>) radicals, electronically excited, lifetimes and quenching rate constants meas. 0-69188
- CHF radical, <sup>1</sup>A'-<sup>1</sup>A' transition, laser induced fluoresc. 0-95660
- CN, B<sup>2</sup> $\Sigma^+$ , A<sup>2</sup> $\Pi$  0-0 and 1-0 bands, laser excitation spectra 0-91588
- CN\*, B<sup>2</sup> $\Sigma^+$  state, fluoresc. decay dynamics, collisional quenching and radiative lifetimes 0-58306
- CO, d<sup>3</sup> $\Delta$  state, low energy electron impact excitation and radiative decay 0-91691
- C<sup>II</sup>, effective lifetime in N and air 0-102704
- Ca, 4p<sup>1</sup> <sup>1</sup>S<sub>0</sub>-4s4p <sup>1</sup>P<sub>1</sub>-4s<sup>2</sup> <sup>1</sup>S<sub>0</sub> cascade rate, two photon coincidence meas. technique 0-95576
- Ca, 4s4p <sup>1</sup>p<sub>1</sub> level Hanle effect density depend., lifetime 0-91494
- Ca, forbidden transitions, radiative lifetimes, MCSCF and CI calcs., time of flight spectra for metastable state 0-91498
- CaO, photoionisation of F-centre, luminesc. and photocond. meas. 0-66270
- Cd, transition probabilities, 5<sup>1</sup>P<sub>2</sub> level lifetime meas. 0-91500
- Cd(<sup>3</sup>P<sub>1</sub>) radiation imprisonment lifetime, inert gas effect, phase-shift method 0-58213
- Ce<sup>3+</sup> impurities in cubic crystals, 5d-4f radiative transition probability calc. 0-71474
- Ci<sup>14+</sup>+Cu, K X-ray production and radiative electron capture, fluoresc. yield determ. 0-99553
- Cr <sup>3</sup>P<sub>0</sub> state, radiative lifetime in matrices, meas. using laser ablation and selective excitation 0-71959
- Cs<sup>+</sup> excited levels, hyperfine struct. and lifetimes 0-63590
- Cu IV, wavelength region 700-1200 Å, extended analysis 0-99473
- Eu<sup>2+</sup> impurities in cubic crystals, 5d-4f radiative transition probability calc. 0-71474
- EuP<sub>2</sub>O<sub>7</sub>, luminesc. of Eu<sup>3+</sup>, transition probabilities 0-80845
- F, spin-orbit splitting and <sup>2</sup>P<sub>1/2</sub> radiative lifetime, absorpt. spectrosc. meas. 0-87063
- <sup>155</sup>Gd L<sub>2,3</sub> subshell X-ray fluorescence and Coster-Kronig yields from <sup>155</sup>Er decay 0-69102
- H<sub>2</sub>, E,F $\Sigma_g^+$  state, collisional and radiative props. 0-58357
- H<sub>2</sub>, electron impact, H<sub>2</sub> and H<sub>2</sub><sup>+</sup> lines emission, intensity decay curves meas. 0-83505
- HB rot. relaxation, diffusion theory 0-106313
- HCl, rot. relaxation, diffusion theory 0-106313
- He(2<sup>1</sup>S, 2<sup>3</sup>S)+Ne(e<sup>-</sup>), transition probs., pots. 0-58371
- He II, 6p<sup>2</sup>P and 6p<sup>2</sup>D levels, radiative lifetimes meas. 0-78576
- Ho I, Ho II, excited level lifetimes and oscillator strengths, visible spectra 0-63573
- <sup>155</sup>Ho L<sub>2,3</sub> subshell X-ray fluorescence and Coster-Kronig yields from <sup>165</sup>Er decay 0-69102
- IF emission spectrum and form. kinetics in electron-beam-produced plasma 0-102533
- InP, luminescence, hot electron effects 0-66277
- K I isoelectronic sequence, transition probabilities, cancellations 0-91503
- KBr:Ti, luminesc., decay model for A<sub>2</sub> and A<sub>1</sub> emissions 0-93379
- Kr, 6p levels, two-photon excitation, time resolved fluoresc., quenching, lifetimes and photoionisation cross section 0-78587
- Kr atoms in Ne matrix, radiative and nonradiative lifetimes in excited states 0-69106

**radiative lifetimes continued**

- Kr VII, beam-foil excitation,  $4s4p^1P^o$  level decay simulation 0-78578  
 $\text{LaF}_3\text{R}^{3+}$ , R=rare earths, crystal field anal., intensity calcs. 0-100670  
 $\text{La}_2\text{O}_3\text{S:Eu}$ , high press. effect on luminesc. efficiency and lifetime, charge transfer absorpt. 0-66266  
 $\text{LiCl}$ , radiation effects on decay time of F-centre emission 0-93381  
 $\text{Mg}(\text{Mg}^{2+})$ , lifetime meas., beam foil spectra, comparison with numerical coulomb approx. calc. 0-58367  
 $\text{N}_2$ , electron excitation of Birge-Hopfield bands ( $b^1\pi_u-X^1\Sigma_g^+$ ) 0-95731  
 $\text{N}_2^+-\text{He}$  ion nuclear pumped lasers feasibility study and quenching 0-64001  
Na II, spectrum, config. superposition and transition probabilities calcs. 0-87082  
 $\text{NaPO}_3\text{:Eu}^{3+}$  glass, luminesc. of  $\text{Eu}^{3+}$ , transition probabilities 0-80845  
 $\text{NdP}_2\text{O}_{12}$ , fluoresc. lifetime meas., IR and photoacoustic spectroscopy 0-60652  
Ne ( $2p^3p$ ) states, radiative lifetimes, collisional deactivation rate consts. 0-69107  
Ni I, UV lines, oscillator strengths from hook method and absorpt. meas. in furnace 0-83319  
O II, relative intensities and lifetimes in nebulae, conventional radiation theory 0-109513  
O IV bound states, oscillator strengths and photoionisation cross sections 0-106293  
O V, EI transition probabilities, lifetimes, CI calc. 0-83321  
OCSe, quantum yields for Se,  $^{15}\text{O}$ ,  $^{13}\text{O}$ , and  $^{31}\text{P}_{1/2}$  atoms determ. in photolysis, lifetime and quenching rate meas. 0-97741  
 $\text{POCl}_3\text{Pr}^{3+}$ , fluoresc. and lifetimes of excited states 0-71466  
 $\text{PbS}_{1-x}\text{Se}_x$  thin film, stimulated emission, temp. depend. 0-66232  
Rb II, lifetimes in  $4p^55p$  config., precision meas. and calc. 0-102488  
Rb, radiative lifetimes up to  $n=12$  excited states, pulsed dye laser and superradiance excitation 0-83322  
 $\text{RbMnF}_3\text{:Fr}$ , pure and doped, unirradiated and electron irradi., energy transfer 0-108254  
S IV,  $3s^23p^2P-3s3p^2^4P$  multiplet, energy levels and transitions, appl. to solar atm. 0-87028  
 $\text{SF}_6+\text{Li}^+(\text{H}^+)$ , mode selective vibr. excitation 0-58351  
SbI, decay branching ratios meas., transition probabilities derivation 0-95642  
 $\text{SeO}_2+\text{Ar}(\text{N}_2)(\text{CO}_2)$ , radiative lifetime and quenching rates 0-95685  
Si, excited states lifetimes, fluoresc. decay curves 0-58175  
 $\text{Si}(\text{Si}^+)(\text{Si}^{2+})(\text{Si}^{3+})$ , excited levels, radiative lifetimes, beam foil spectra 0-58368  
TbAG, reson. electronic Raman effect, interferences, lifetime meas. 0-93294  
Ti atoms sputtered from Ti, Ti oxides, photon emission, nonradiative transition effects 0-58208  
Ti II, oscillator strengths from combined hook and emission expts. 0-87081  
Ti III, IV, V, radiative lifetime meas. using beam-foil technique, 700 to 1900 Å 0-78574  
Xe atoms in Ne matrix, radiative and nonradiative lifetimes in excited states 0-69106  
 $\text{XeF}_2(\text{C})$  state lifetime, quenching rate consts., photolysis in inert gas atmospheres 0-66816  
 $\text{XeF}^+$ ,  $\text{B}^2\Sigma^+$  and  $\text{C}^2\Pi_{3/2}$  states, fluoresc. decay dynamics, collisional quenching and radiative lifetimes 0-58306  
XeI, visible lines, absolute transition probabilities 0-69108  
 $\text{Xe}^*$ , synchrotron radiation excited, time resolved spectroscopy 0-69092  
 $\text{Y}_2\text{O}_3\text{S:Eu}$ , high press. effect on luminesc. efficiency and lifetime, charge transfer absorpt. 0-66266  
 $\text{ZrF}_4\text{:Eu}^{3+}$  glass, luminesc. of  $\text{Eu}^{3+}$ , transition probabilities 0-80845

**radiative shifts**

No entries

**radiative transfer**

- atmosphere, aerosol particles effects on  $\text{CO}_2$   $15\mu\text{m}$  radiance rel. to error in satellite retrieved temp. profiles 0-98449  
atmosphere, comparison of theoretical and experimental long-wave IR fluxes (*Russian*) 0-94598  
atmosphere, multiple scatt. effect on radiometric determ. of rain attenuation at millimetre wavelengths 0-90260  
atmosphere, radiative transfer model rel. to anomalous gray shades in DMSP visible imagery 0-71111  
atmosphere, urban, radiative effects of elevated pollutant layers on temp. struct. and pollutant dispersion 0-97841  
atmosphere effects on radiative transfer, conference, San Diego, California (1979 August 29 to 30) 0-62376  
atmosphere radiative transfer eqn., soln. using Elsasser scheme 0-77112  
atmospheric, fixed cloud-top temp. and fixed cloud-top altitude approximations for temp. profile 0-72616  
atmospheric optical props., appl. to satellite remote sensing of phytoplankton 0-77105  
blackbody function efficient computation, two-series approach 0-79128  
Chandrasekhar H-equation, soln. by Newtons method 0-87710  
clear atmosphere, radiative transport and thermal turbulence (*French*) 0-82018  
cloud shape and mutual shading effects 0-101430  
clouds, mathematical model of radiative transfer 0-90215  
comoving-frame eqn. of transfer in spherically symmetric flows, soln. for relativistic flows 0-82181  
evolved stars expanding envelopes, coupled radiative transfer eqns. for CO thermal and maser emission 0-82334  
expanding envelopes, Lyman  $\alpha$  quanta scattering (*Russian*) 0-67556  
 $F_N$ -method for problems with reflective boundary conditions 0-79124  
F, G, K-type stars, giants and dwarfs chromospheres, wave dissipation of mechanical energy 0-82340  
fibreglass insulating materials, radiative heat transfer rel. to optical props. 0-100367  
finite atmosphere, exact soln. of basic eqn. via Laplace transform 0-94702  
gas dynamics equation soln. (*Russian*) 0-64653  
heat transfer, with isotropic scatt. and gaseous absorpt., optical path length calcs. 0-79125  
Hercules X-1, line photons transfer rel. to cyclotron features in X-ray spectrum 0-86015  
integral equation spectrum, calc. for semi-infinite medium 0-67540  
to plasma torus, radiative cooling and spectra 0-72850  
laser beam off-axis propag. in low visibility weather conditions, non-small-angle scatt. 0-102621

**radiative transfer continued**

- line wings, polarized radiative transfer, excited state interference 0-105158  
low-temperature blackbody source 0-73355  
mantle radiative cond. from shock compressed  $\text{Fe}^{2+}$  bearing MgO absorpt. spectrum 0-90039  
microwave remote sensing, thermal emission from terrain, theory 0-77151  
multidimensional media, physical effects of radiative transfer 0-72758  
neutron star X-ray emission models 0-62175  
neutron stars, Eddington luminosity limit and supercritical accretion, time-indep. calcs. 0-67768  
neutron stars, magnetic, surface layers, radiative heat transfer theory 0-94826  
non-LTE transfer, asymptotics of partial redistrib. 0-62008  
nonlinear radiation transport, soln. by renormalisation group method 0-67555  
plane atmosphere, invariance principles and integral eqns. for radiation fields 0-67559  
plane parallel atmospheres, radiative transfer eqn. soln. 0-67409  
plane-parallel atmosphere with polynomial emission source distrib. 0-94700  
planetary atmosphere,  $F_N$  method for polarisation studies 0-98540  
planetary atmosphere, light scatt. by optically thin atmosphere rel. to brightness at zenith near terminator 0-109382  
planetary atmosphere, single-scatt. albedo determ. for Rayleigh-scatt. atmosphere with true absorpt. 0-94704  
planetary atmospheres, two stream approx. 0-109383  
planetary finite atmospheres, key eqn. exact soln., Laplace transform and linear singular operators method 0-67536  
polarisation effects on surface due to radiative transfer (*French*) 0-79127  
polarisation of scattered radiation, in medium with internal energy sources 0-67541  
polarised light transfer problem in presence of absorpt., soln. 0-67561  
polarised radiation transfer in inhomogeneous media 0-99607  
polarized radiation transfer in X-ray pulsars, analytical solns. 0-94894  
polydisperse media, optical characts., approx. representation 0-63922  
protostellar envelope evolution, radiative transfer and spectrum 0-77384  
relativistic electron beam relaxation in dense gas, radiative energy transfer 0-69968  
relict radiation in anisotropic universe, transfer eqn. soln. rel. to polarisation and anisotropy 0-67917  
resonance line scattering in absorbing medium, scaling laws 0-98538  
semi-infinite atmosphere with albedo  $\omega>1$ , transfer eqn. 0-82184  
semitransparent thin cylinder, radiation-conduction heat transfer, light-guide approx. 0-96179  
solar corona, radiation heat flux rel. to expansion 0-90377  
solar prominences, H line radiation diffusion 0-67694  
spectral line formation depth in mag. field, theory (*Chinese*) 0-105159  
spectral lines formation in inhomogeneous medium, appl. to solar photosphere (*Russian*) 0-72901  
spherical dust shell around central star, two-shell moment method for radiative transfer 0-62001  
spherical geometry, numerical soln. of radiation transfer eqn. 0-90329  
spherically symmetric flows with nonmonotonic vel. fields, radiative transfer 0-94699  
starlight interstellar polarisation, fluctuation theory 0-82442  
stellar finite atmosphere, key eqn. exact soln., Laplace transform and linear singular operators method 0-72762  
stellar atmospheres, spherical transonic flow, reson. line radiative transfer 0-94698  
stellar weak interaction rates for sd-shell nuclei, appl. to supernovae 0-82336  
stellar winds, steady state transonic wind model, radiative cooling effects 0-77391  
Stokes parameters and mag. field vector profiles (*Chinese*) 0-77386  
stratified turbid medium, small-angle approx. soln. (*Russian*) 0-82057  
stratosphere,  $\text{CO}_2\text{-O}_3$  coupling in CI free atm., photochemical-radiative column model 0-85723  
stratosphere aerosol, radiation transport model rel. to climatic effects of aerosol layer modification 0-98408  
stratosphere  $\text{O}_3\text{-CO}_2$  coupling, photochemical radiative column model with Cl chemistry 0-85724  
supernova remnant optical emission spectra, effect of shock wave intermediate zone radiative cooling 0-109517  
supernovae, type I, conservative scatt. theory for effects of line overlapping on spectra (*Russian*) 0-105266  
surrounding variable source of heating radiation, IR flux development 0-105324  
synthetic scattering phase function for radiation transfer 0-98541  
T Tauri nebula, Lyman continuum transfer rel. to ionisation and emission line spectrum 0-67820  
thermal-convective instability of partially ionized plasma, radiative transfer, medium porosity and collisional effects 0-67538  
three-term radiative transfer, inverse soln. by  $F_N$  and Monte Carlo methods 0-109352  
time-dependent radiative transfer, exact soln. of integro-differential eqn. via Laplace transform 0-94703  
transport or diffusion calculations, appln. of multiband method 0-95333  
troposphere, IR radiative exchange from six-layer general circulation model 0-101432  
troposphere, radiative cooling rate and flux, theory 0-85711  
Venus atmosphere, scattered solar radiation fluxes spectral and altitude distrib. 0-62059  
X-ray sources, time-dependent Comptonisation and X-ray reverberations rel. to rapid time variability 0-86013  
Zeeman line profile, mag. field determ., appl. of radiative transfer problem soln. 0-82221  
Al, plasma, transfer eqn. soln. using freq. and angle averaged photon escape probabilities 0-64688  
C, paint type coating layer with spherical pigment, radiative transfer theory 0-61405  
 $\text{CO}_2$  ice spheres, IR scatt. and absorpt. props. 0-97269  
 $\text{FeO}_3$ , paint type coating layer with spherical pigment, radiative transfer theory 0-61405  
He I 584 Å in quasars and gaseous nebulae, line transfer problem and line strength 0-67550  
Hg discharge, high-pressure, NaI and TlI additives, line broadening and radiative transport 0-74199



**radiative transfer continued**

- Ta surface, nonstationary heating and oxidation in low temp. plasma flow, heat and charge transfer obs. (*Russian*) 0-104341  
 TiO<sub>2</sub>, paint type coating layer with spherical pigment, radiative transfer theory 0-61405

**radicals, free** *see free radicals***radio applications**

- see also radioastronomy; radiocommunication; radionavigation*  
 geological prospecting using VLF surface mode, wave tilt meas. 0-77139  
 perinatal radio telemetry 0-104722  
 time correlation of seismic events 0-90253

**radio broadcasting**

- studio architectural acoustics, 'Deutsche Welle' building construction and meas. (*German*) 0-106668  
 time and freq. meas., users' manual 0-94934

**radio links**

- see also microwave links; radiocommunication*  
 rain attenuation above 11 GHz 0-98410  
 solar photovoltaic system feeding unusual length radio link, characteristics and design data 0-61383  
 tropospheric effects on radio communication, book 0-62400

**radio receivers**

- see also superheterodyne receivers*  
 ceramic filters appl., using Pb(Zn<sub>1/3</sub>Nb<sub>2/3</sub>)O<sub>3</sub>-PbTiO<sub>3</sub>-PbZrO<sub>3</sub> and Pb(Mg<sub>1/3</sub>Nb<sub>2/3</sub>)O<sub>3</sub>-PbTiO<sub>3</sub>-PbZrO<sub>3</sub> (*Japanese*) 0-60507  
 heterodyne freq. analyzer, detection of 200 to 400 GHz weak microwave signals 0-94716

**radio reception**

- see also atmospherics*  
 ionospheric layers E, F, and D, effect on SW reception 0-67451  
 VLF signals, numerical study of satellite reception using waveguide concepts 0-90282

**radio reception quality** *see radio reception***radio relay systems** *see radio links***radio studios**

- architectural acoustics, 'Deutsche Welle' building construction and meas. (*German*) 0-106668

**radio systems**

- see also mobile radio systems*  
 large-aperture radio system for meteor studies 0-85870

**radio transceivers** *see transceivers***radioactive age determination** *see radioactive dating***radioactive chemical analysis**

- see also radiochemistry*  
 biological sample <sup>32</sup>P and <sup>45</sup>Ca determ. by Cherenkov and liq. scintillation counting 0-98183  
 biological samples, neutron-activated, determ. of short-lived radionuclides 0-109067  
 counting techniques for analytical appls. in biology and medicine 0-81794  
 distribution in extended medium, qualitative and quantitative anal., mathematical modelling 0-71985  
 fissile material assay by neutron coincidence process 0-76578  
 geophysical samples, <sup>10</sup>Be distrib. meas. using tandem van de Graaff accelerator 0-61924  
 isotope detection in terrestrial and extraterrestrial samples, tandem accelerator appl. 0-61923  
 lactate dehydrogenase, H-forms, radioimmunoassay 0-67219  
 nuclear site decontamination, radiochemical anal. of environmental samples 0-95477  
 prostatic acid phosphatase, human, development of determ. by radioimmunoassay (*Japanese*) 0-98110  
 radiochromatography, beta-ray imaging using a multiwire proportional counter 0-102387  
 radioimmunoassay, fitting of general form of fundamental physical model 0-94150  
 radioimmunoassay, review, book contrib. 0-109021  
 serum thyroxine, radioimmunoassay by the antibody-coated test tube method (*Japanese*) 0-67237  
 thyroid function radioimmunoassay, quality control, computer program (*French*) 0-94348  
 thyroxine, free, radioimmunoassay for quantitative meas. of serum conc. 0-94344  
<sup>239,240</sup>Pu(V) in alkaline freshwater pond, determ. by coprecipitation technique 0-71988  
 GaP:Cr epitaxial layers, Cr conc. profile determ. 0-65029  
 MnO<sub>2</sub>:Li(Mo)(V), of Zn<sup>2+</sup> ions, kinetics, <sup>65</sup>Zn γ-ray scintillation investig. 0-70529  
<sup>210</sup>Pb determination in sediment core from ocean floor off Californian coast 0-72101

**radioactive dating**

- see also geochronology*  
 Allende meteorite, <sup>40</sup>Ar-<sup>39</sup>Ar ages 0-98621  
 Bruderheim, L6 chondrite, U-Pb age and 500 Ma shock event in L-group meteorites parent body 0-98616  
 digital ESR dating method 0-86542  
 Donegal granite, Ireland, emplacement age by isotope chronology 0-67356  
 education, radioactive dating and population growth by dice game 0-57030  
 fission track dating using U glasses, error analysis 0-95503  
 groundwater <sup>14</sup>C dating, possible subsurface prod. of <sup>14</sup>C 0-85690  
 isotope detection in terrestrial and extraterrestrial samples, tandem accelerator appl. 0-61923  
 lava succession in N.Iceland, K-Ar dating, geological and palaeomagnetic obs. 0-109096  
 marine sediment, α-scintillation counting of <sup>230</sup>Th 0-72636  
 Murray (C-2) carbonaceous chondrite, I-Xe age and trapped Xe components 0-98618  
 ocean sediments, radiocarbon dating by benzene variant method aboard ship 0-85770  
 rinneite, Rb-Sr dating of potash salt deposits 0-67429  
 sediments of deep-sea, <sup>14</sup>C age and vertical mixing 0-81865  
 TLD evaluation of internal beta-dose rate for archaeological dating 0-98478  
<sup>40</sup>Ar-<sup>39</sup>Ar age and irradiation history of Luna 24 basalts 0-82245  
 C<sup>13</sup> ion source for radiocarbon dating using tandem accelerators 0-94620  
<sup>14</sup>C dating, high energy mass spectrometer appls. 0-101917

**radioactive dating continued**

- <sup>14</sup>C dating, meas. of <sup>14</sup>C abundance vars. in wines with 11-year solar cycle, (1909 to 1952) 0-109249  
<sup>14</sup>C dating of coastal marine sediments, fossil C effect 0-98308  
<sup>14</sup>C dating of small samples via proportional counting 0-82102  
<sup>14</sup>C measurement in known age specimens, cosmic ray intensity determ. 0-101516  
 K-Ar dating, evolution of excess <sup>40</sup>Ar in Alpine biotites from <sup>40</sup>Ar-<sup>39</sup>Ar anal. 0-94521  
 U-Pb ages of pegmatites in Enderby Land, Antarctic 0-76946

**radioactive decay periods**

- <sup>294</sup>110, naturally occurring superheavy element search, alpha emission half-life 0-63139  
<sup>258</sup>114, high spin pot. energy surfaces, fission barrier, α-, γ-decay half lives, yrast spectrum 0-73764  
 beta strength function, half life and delays, nuclear- and astro-physics consequences 0-102149  
 beta strength function structures, nuclear- and astro-physics consequences 0-99152  
 calibration materials for X and γ-ray spectrometers, decay data 0-106221  
 neutron rich nuclei, beta decay half lives, expt. techniques 0-78224  
 quantum radiation, data handbook 0-94933  
 radionuclides, short-lived, meas., counting statistics 0-58098  
 Z=37-43, neutron rich fission products, mass energy surface, decay props. 0-78228  
<sup>100</sup>Ag<sup>8m</sup> decay, <sup>100</sup>Pd levels and γ-transitions 0-83077  
<sup>110</sup>Ag, decay period, least square fitting, pocket calculator program with variable precision 0-67976  
<sup>243</sup>Am half life and α-activity 0-102159  
<sup>139</sup>Ba, γ-ray emission probabilities and half-life obs. 0-57723  
<sup>188</sup>Bi alpha decay half lives 0-57749  
<sup>Δ</sup>Br, A=89-91, delayed neutron emission probabilities, β-decay half-lives 0-83078  
<sup>Δ</sup>Fr, A=201-203, alpha decay, branching ratios, mass excess and half life 0-99154  
<sup>Δ</sup>I, A=139-141, delayed neutron emission probabilities, β-decay half-lives 0-83078  
<sup>35</sup>K decay, <sup>35</sup>Ar levels, transitions and β-delayed protons 0-91156  
<sup>Δ</sup>Lu, A=160-163, decay and T<sub>1/2</sub>, <sup>160,163</sup>Yb transitions 0-102146  
<sup>24</sup>Na half-life determ., T<sub>1/2</sub>=(14.964±0.015) h 0-95311  
<sup>Δ</sup>Pb, A=183,184, alpha decay half lives 0-57749  
<sup>241</sup>Pu half life from α-spectrometry and <sup>241</sup>Am ingrowth 0-68609  
<sup>241</sup>Pu half-life determ. by mass spectrometry 0-78232  
<sup>32</sup>Si, half life determined from varved Gulf of California sediment core 0-91153  
<sup>32</sup>Si half life from tandem accelerator mass spectrometry 0-95313  
<sup>32</sup>Si half life via accelerator mass spectrometry 0-95314  
<sup>180m</sup>Tm, β- and EC branching ratios, K-internal conversion coeff., γ-intensities, T<sub>1/2</sub> 0-68601  
<sup>146</sup>Tb decay and T<sub>1/2</sub>, <sup>146</sup>Gd lowest 2<sup>+</sup> state, J<sup>π</sup> and transitions 0-105979  
<sup>99m</sup>Tc, in hexahalogen complexes, decay const. determ. 0-106020  
<sup>230</sup>Th alpha-decay half life from specific activity method 0-102157  
<sup>233</sup>U, half-life determ. 0-57750  
<sup>Δ</sup>W(<sup>12</sup>C,f), A=182, 183, 184, 186, 80 to 115 MeV, lifetime meas. by crystal-blocking tech. 0-91198  
<sup>Δ</sup>W(<sup>16</sup>O,f), A=182, 183, 184, 186, 80 to 115 MeV, lifetime meas. by crystal-blocking tech. 0-91198  
<sup>Δ</sup>W(<sup>19</sup>F,f), A=182, 183, 184, 186, 80 to 115 MeV, lifetime meas. by crystal-blocking tech. 0-91198

**radioactive decay schemes**

- see also nuclear energy levels*  
 characteristic function eqn. of Markov process, Langevin process applications 0-57192  
 Gardner analysis of decay components with strong fluctuations 0-102161  
 nuclei far from line of beta stability, mass spectroscopic anal. techniques, book contrib. 0-69014  
 quantum radiation, data handbook 0-94933  
 radionuclide decay, computer simulation, levels, transitions, internal conversion 0-63136  
<sup>222</sup>Rn, props. and behaviour of short lived daughter nuclides in the atmos. (*Japanese*) 0-72339  
<sup>235</sup>U, decay product radioactive accumulation, FORTRAN program 0-68611  
<sup>235</sup>U, radioactive series decay, computer simulation 0-102160  
<sup>238</sup>U, decay product radioactive accumulation, FORTRAN program 0-68611  
<sup>238</sup>U, radioactive series decay, computer simulation 0-102160

**radioactive lifetimes** *see radioactive decay periods***radioactive sources**

- see also radioisotopes*  
 IAEA regulations for safe transportation 0-63410  
 IAEA transport information collection system, influence on improved safety measures 0-63413  
 IAEA transport regulations, underlying radiation protection principles 0-63414  
 international regulatory control for safe transportation 0-63411  
 package design, construction and testing for safe transportation 0-63412  
 safe transportation, using type A, exempt and LSA packages 0-63401  
<sup>241</sup>Am-Be, C content in coal determ., by neutron inelastic scattering (*Czech*) 0-101048  
<sup>252</sup>Cf, H content in coal determ., by neutron inelastic scattering (*Czech*) 0-101048  
<sup>60</sup>Co sources for total body irradiation, uniformity and standardisation 0-94338  
<sup>137</sup>Cs, parametric definition 0-91346  
<sup>147</sup>Pm, sealed sources for phosphor light sources (*Hungarian*) 0-91348  
<sup>147</sup>Pm small-size nuclear battery, characts. of luminophores and photoelements (*Bulgarian*) 0-72084  
<sup>238</sup>Pu-Be, C content in coal determ., by neutron inelastic scattering (*Czech*) 0-101048  
<sup>239</sup>Pu-Be, C content in coal determ., by neutron inelastic scattering (*Czech*) 0-101048

**radioactive tracers**

- <sup>99m</sup>Tc labelled heparin for imaging of acute myocardial infarcts, dog expts. 0-81733  
 adsorption and electrocatalytic phenomena, radiotracer method investig. appls. radiotracer 0-70525

**radioactive tracers continued**

- antipyrine, radioiodinated, prep. and stability for use in local blood flow determs. 0-94366
- bleomycin, effect of dose loading and double labelling with  $^{57}\text{Co}$  and  $^{125}\text{I}$  on animal tissue distrib. 0-67220
- cyclosporin A labelled with  $^{123}\text{I}$  or  $^{125}\text{I}$ , prep. and biodistrib. 0-85496
- drug radioreceptor analysis applications 0-94315
- haemoglobin, mutual and tracer diffusion coeffs., photon correl. obs. 0-72123
- intravascular radioactive tracers, calc. of residence time distrib. in fields of external registration 0-72291
- leucocytes, radioactive-labelled, appl. for proof of inflammations 0-67218
- liquid flow rates through pipes, applicability of experimental meas. methods 0-100044
- medicine, nuclear, production of useful radioisotopes, Los Alamos Meson Physics Facility 0-67251
- paenonol and urinary metabolites labelled with  $^{13}\text{C}$  and D, synthesis and physicochem. props. 0-67250
- perhalo-compounds, labelled, high yields from  $^{18}\text{F}$  and  $^{38}\text{Cl}$  reactions with  $\text{CCl}_4$ ,  $\text{C}_2\text{F}_6$  0-109025
- physiological compartment tracer flow modelling and digital imaging 0-101257
- proteins, improved labelling with  $^{99m}\text{Tc}$  by stannous tartrate reduction of pertechnetate 0-72324
- serum albumin, bovine, mutual and tracer diffusion coeffs., photon correl. obs. 0-72123
- $^{11}\text{C}$ -l-lactic acid, enzymatic synthesis 0-61695
- $^{11}\text{C}$ -pyruvic acid, enzymatic synthesis 0-61695
- $^{14}\text{C}$ -labelled bumetanide, whole body autoradiography in dogs by round saw method 0-72399
- $^{57}\text{Co}$  labelling of bovine serum albumin, expts. 0-85495
- $^{18}\text{F}$ -5-fluorouracil studies in humans and animals 0-109000
- $^{18}\text{F}$ -labelled acetic acid, carrier-free, production via a recoil labelling method 0-104756
- $^{67}\text{Ga}$ -citrate, comparative evaluation of pulmonary lesions 0-94327
- $^{197}\text{HgCl}_2$ , renal uptake meas., single tracer method for background subtraction 0-67217
- $^{125}\text{I}$  labelled estradiol, a  $\gamma$ -emitting estradiol analogue that binds to the estrogen receptor 0-61697
- $^{125}\text{I}$  labelled estrogen derivatives 0-81734
- $^{125}\text{I}$  labelled human serum albumin, geometrical dilution (French) 0-104742
- $^{125}\text{I}$  labelled prostaglandins (Hungarian) 0-94368
- $^{125}\text{I}$ -fibrinogen, multiwire proportional chamber, low energy radionuclide distrib. 0-61679
- $^{131}\text{I}$ -ortho-iodohippurate absorbed kidney dose calc., literature review 0-76841
- $^{111}\text{In}$  labelled human platelets, dose obs. 0-94370
- $^{111}\text{In}$  oxinate, comparative study as abscess scanning agent 0-94328
- $^{111}\text{In}$  oxinate labelled autologous granulocytes, comparative study as abscess scanning agent 0-94328
- $^{111}\text{In}$ -bleomycin, comparative evaluation of pulmonary lesions 0-94327
- $^{111}\text{InCl}_3$ , comparative study as abscess scanning agent 0-94328
- $^{113m}\text{In}$ -tripolyphosphate, new radiopharmaceutical for bone scanning 0-67247
- Mg tracer techniques for Pu nuclear fuel input accountability in reprocessing plants 0-73919
- $^{15}\text{NH}_3$  intravenous injection, absorbed radiation dose calcs. 0-94375
- $^{92}\text{Nb}^{60}$ , production and impregnation in polystyrene microspheres for X-ray detector calibration 0-74065
- Pb tracer techniques for Pu nuclear fuel input accountability in reprocessing plants 0-73919
- $^{81}\text{Rb}$ ,  $^{81}\text{Kr}$  generators, aspects of production, elution and automation, medical appls. 0-61696
- T balance in surface water reservoir, molecular exchange 0-72565
- $^{99m}\text{Tc}$ , assay of radioactive impurity in pertechnetate eluted from  $^{99}\text{Mo}$ - $^{99m}\text{Tc}$  generator (Japanese) 0-81735
- $^{99m}\text{Tc}$  labelled (Sn)DTPA, comparison of 4 commercial preps. in glomerular filtration rate meas. 0-81704
- $^{99m}\text{Tc}$  labelled DTPA and MDP, compensative value on brain lesion (Japanese) 0-67235
- $^{99m}\text{Tc}$  labelled EHPD, uptake quantification in sacroiliac scintigraphy, comparative study 0-94326
- $^{99m}\text{Tc}$  methylene diphosphonate, immediate renal imaging and renography, clinical evaluation 0-98126
- $^{99m}\text{Tc}$ , pyrophosphate and hydroxymethylene diphosphonate carriers, comparison in acute myocardial infarction 0-94342
- $^{99m}\text{Tc}$ -HIDA, synthesis of 5 new isomers and comparison with  $^{99m}\text{Tc}$ - (2,6-dimethyl)HIDA 0-72323
- $^{99m}\text{Tc}$ -MDP, lymphography appl. (Japanese) 0-94352
- $^{99m}\text{Tc}$ - (p-butyl) iminodiacetic acid, clinical evaluation in hepatobiliary imaging (Japanese) 0-67236
- $^{99m}\text{Tc}$ -citrate, comparative evaluation of pulmonary lesions 0-94327
- $^{99m}\text{Tc}$ -hepatobiliary agents, absorbed dose estimation 0-72330
- $^{99m}\text{Tc}$ -labelled erythrocytes, spleen scanning in humans 0-67230
- $^{99m}\text{Tc}$ -microspheres, bladder wall dose after administration 0-109030
- $^{123m}\text{Tc}$ -labelled adrenal-imaging agents, radiation dosimetry 0-101268
- $^{201}\text{TlCl}$ , tumour scintigraphy by intraarterial injection (Japanese) 0-98111
- $^{62}\text{Zn}/^{62}\text{Cu}$  generator, source of  $^{62}\text{Cu}$  for radiopharmaceuticals 0-67248
- $^{65}\text{Zn}$ , in zinc oxalate, isothermal crystallisation from soln. 0-108336

**radioactive waste**

- see also fission reactor materials; fusion reactor materials; materials handling; radioactivity; waste disposal
- $^{222}\text{Rn}$  flux through multilayered covers cover U mill tailings 0-95487
- actinides, biological hazards, consequences for LMFBR fuel recycling 0-86960
- actinides, decay heat estimation, summation calcs. and Standard eqns., review 0-63317
- actinides, man-made, health effects compared to natural radionuclides 0-61647
- air pollution, laser-Raman microprobe anal. of suspended particulates 0-76687
- air pollution, X-ray absorption spectra for chem. characterisation of atmospheric aerosols 0-61501
- air pollution, X-ray absorption spectra for chem. characterisation of atmospheric aerosols 0-72121
- air pollution over N. Atlantic obs. of fission products and  $^{222}\text{Rn}$  0-77074
- alpha waste production and proliferation hazard of different fuel cycles 0-83214

**radioactive waste continued**

- American Nuclear Society proceedings (conf. Las Vegas, NV, June 1980) 0-94920
- atmospheric pollution by radionuclides, diffusion calcs. (German) 0-61484
- Biblis nuclear power station, waste production, storage and disposal 0-68903
- biochemical and chemical processes leading to radionuclide transport from low-level waste burial sites 0-101275
- biological effects, cancers and mutations 0-76791
- buildings, indoor airborne radioactivity calcs. 0-63305
- BWR spent fuel element storage, neutron physical aspects 0-68841
- BWR spent fuel safeguarding, nondestructive assay using gamma spectrometry 0-68802
- canister materials for radwaste containment 0-102279
- cemented radioactive wastes, stability improvement method 0-57869
- combustion in Julich Incinerator (German) 0-73976
- conference, Osaka, Japan (Nov. 1979) 0-98756
- confinement device for determ. of whole-body radionuclide concs. in live ducks 0-67299
- containment, Ti-alloy canister materials, corrosion in saline radioactive waste isolation environments 0-104349
- containment materials, EPR investig. 0-97138
- W. Cumbria, Pu and  $^{137}\text{Cs}$  concs. in environmental samples and possible maritime effect 0-108817
- decay heat estimation, summation calcs. and Standard eqns., review 0-63317
- decommissioning of Pu fuel fabrication plant, nondestructive assay meas. using NaI(Tl) detectors 0-63495
- density measuring meter, digital, remotely operated 0-68927
- disposal, Czechoslovak Research Institute activities (Slovak) 0-83188
- disposal, popular assumptions, critical examination 0-106141
- disposal by solidification and burial, geological aspects 0-63316
- disposal in geologic formations, site selection criteria 0-106142
- disposal of low- and intermediate-level radwaste, Canadian R and D program 0-99255
- disposal safety criteria, choosing risk assessment methods 0-99247
- disposal safety criteria, ORIGEN2 point-depletion and decay computer code 0-99248
- disposal safety criteria, radionuclide chain transport through heterogeneous media 0-99250
- disposal under seabed 0-89588
- doses to public from nuclear industry, health risks from various power sources 0-57899
- dosimetric data tables 0-105438
- dosimetry calculations due to radionuclides in aquatic food chains, NEP-TUN interactive code in FORTRAN 0-109039
- ecological search for radiation effects in Hanford nuclear waste ponds and streams 0-89804
- environment monitoring ground radioactive burial site (Japanese) 0-67015
- environmental protection, reactor safety and waste handling (Hungarian) 0-91224
- environmental radioactivity, determ. for dose assess. 0-85321
- environmental radioactivity near a radioactive waste disposal site 0-98148
- FBR fuel handling, radiation safety 0-73985
- FBR safety and economics, leak detection, cooling, waste disposal 0-63303
- fission gas release from high burn-up oxide fuel, predictions in ELESIM code 0-57864
- fission products, decay heat estimation, summation calcs. and Standard eqns., review 0-63317
- fuel elements recycling and thermal re-irradiation, technical, economic and safety problems (German) 0-99269
- fusion reactor blanket material impurity hazardous activity and dose rates, biological hazard pot. 0-102315
- gas-chromatography, beta radio effluents, window flow counter 0-93824
- geologic depositories, safety criteria for high-level waste storage 0-95379
- geologic disposal, geotoxicity hazard index 0-97822
- geologic disposal, modelling of radionuclide transport and decay products 0-78415
- geologic disposal, safety anal., functional relations of risk to input data uncertainties 0-83189
- geologic repositories, NRC waste disposal safety criteria 0-99246
- geologic repositories, operation of the Waste Isolation Pilot Plant 0-99264
- geologic repositories, risk assessment 0-95359
- geologic repositories, US DOE program for terminal storage 0-95381
- geologic repositories, waste disposal safety criteria 0-99245
- geologic repository, methodology for repository siting in different geologic media 0-102268
- geologic repository, US DOE site identification criteria for waste isolation 0-102267
- geologic storage, effect of adsorption of Tc and I radioisotopes by minerals 0-83203
- geological disposal, sorption of actinides in igneous rocks 0-95367
- getter development for radioaesium, obs. of Cs-SiO<sub>2</sub>-Al<sub>2</sub>O<sub>3</sub> system interactions 0-83208
- high level, solidified in borosilicate glass,  $\gamma$ -scanning as integrity test (German) 0-78426
- high level waste containing granules coated and embedded in metal as an alternative to HLW glasses (German) 0-83186
- high level waste repositories, siting criteria, implications of policy/regulation changes 0-102269
- high level wastes, oxalate precipitation for separation of Am, Cm, and trivalent lanthanides 0-83202
- HLW fixation in SYNROC-B sintered ceramics, comp. and phase charact. 0-106126
- IAEA regulations for safe transportation 0-63410
- IAEA transport information collection system, influence on improved safety measures 0-63413
- IAEA transport regulations, underlying radiation protection principles 0-63414
- immobilisation, review of waste forms, and waste processing 0-102280
- incineration studies at Los Alamos 0-73963
- incinerator for alpha solid waste, prototype operation 0-73964
- international regulatory control for safe transportation 0-63411
- irradiated fuel elements recycling plant design modifications and safety of used nuclear fuel during storage and disposal (German) 0-99219
- irradiated nuclear reactor fuel rod components, EM separation, feasibility 0-99224



## radioactive waste continued

- Lac du Bonnet batholith, Canada, geological reconnaissance for nuclear waste disposal 0-73977  
 leach test methods for solidified radwaste 0-102277  
 liquid effluents, aquatic radiological impact anal., radiocaesium transport in sediment 0-95486  
 liquid scintillation wastings, combustion system (*Japanese*) 0-63503  
 liquid scintillation wastings, vaporisation apparatus (*Japanese*) 0-63502  
 low level, transport regulations, proposed changes 0-68896  
 low level waste disposal technology, US DOE R and D program 0-99254  
 low-level radioactive wastes: public fears and political strategies 0-102272  
 low-level radwaste treatment, volume reduction systems, progress report 0-99260  
 low-level transuranic storage, radwaste Sr, Cs, Co sorption meas. on soil sediment 0-95482  
 low-level waste disposal guidelines using the RWDCS methodology 0-99262  
 low-level waste management, US DOE strategy, public acceptance 0-102270  
 low-level waste management and safety, public acceptance 0-102271  
 low-level waste siting needs—an overview 0-99261  
 LWR fuel waste disposal using linear accelerator fission product transmutor 0-63365  
 LWR spent fuel, alpha spectrometric meas. for SNM verification 0-78424  
 LWR spent fuel, non-destructive anal. using inherent and induced neutron radiation (*Russian*) 0-68805  
 LWR spent fuel, nondestructive meas. and verification for materials safeguards 0-78420  
 LWR spent fuel elements, disposal in geologic isolation, feasibility study report 0-106140  
 LWR spent fuel elements, gamma spectrometric meas. of burnup U/Pu ratio and cooling time for materials safeguards 0-78423  
 management, EEC policy 0-95376  
 management, industry experience in low-level waste siting—regulatory, political, and business considerations 0-99257  
 management, shallow burial ground disposal for low- and intermediate level waste, French experience 0-95380  
 management, storage and transportation in Sweden 0-95378  
 management, technological progress, EEC conclusions and recommendations 0-106133  
 management, technological progress, EEC R&D programme 0-106132  
 management, US DOE organization for waste materials characterization 0-102273  
 management, US DOE program, role of Materials Characterisation Centre 0-102275  
 management, US DOE program, role of the Materials Review Board 0-102274  
 management, US DOE waste management program 0-95375  
 management, US NBS proposals for measurement standards 0-102276  
 management alternatives for low-level waste using decision tree analysis 0-99259  
 management of high-level waste, French research program for solidification and disposal in borosilicate glass 0-95377  
 management of low-level radioactive wastes in Illinois 0-99256  
 management technology, present European situation 0-106131  
 marine cephalopods, radioactive trace elements obs. 0-94379  
 materials accountability, U and P NDA of crated waste by gamma-ray and neutron coincidence counting 0-83166  
 medical electron linear accelerator, radioactive and toxic gas production 0-94378  
 natural salt repositories, thermomigration of brine inclusions in NaCl single crystals 0-99251  
 neutron source intensity in random absorption medium (*French*) 0-74057  
 nonstationary heat processes in spent nuclear fuel element containers (*Bulgarian*) 0-69637  
 nuclear fuel burnup determination using Aragonite  $\gamma$  detector 0-63262  
 nuclear fusion reactor materials, social aspects (*Dutch*) 0-106153  
 nuclear generating station, waste disposal and licensing (*German*) 0-99222  
 nuclear materials, nondestructive neutron assay for accountability and criticality control 0-66759  
 nuclear materials safeguards and materials control, meas. tech. conf. Charleston, SC, USA (November 1979) 0-77544  
 nuclear power stations, licensing procedure, public participation under Atomic Energy Act (*German*) 0-102256  
 nuclear power stations, waste management principles modifications (*German*) 0-102255  
 Port Granby radioactive waste storage site leakage into Lake Ontario, water quality obs. 0-97829  
 processing, volume reduction of organic alpha waste by pyrohydrolysis 0-95366  
 public acceptance of a low-level waste burial facility 0-95382  
 radiological implications of Pu recycling in HTGR fuels 0-68777  
 radionuclide migration from buried radioactive waste 0-95484  
 radwaste evaporator improvement 0-91232  
 remote handling, history at Los Alamos 0-78417  
 reprocessing nuclear fuels, waste storage, nuclear burning and types of reactor (*French*) 0-91235  
 reprocessing plants, Purex-type, schematic flowsheet comparison (*German*) 0-57936  
 resuspended radioisotopes, possible importance of short-term exposure 0-85501  
 safe transportation, using type A, exempt and LSA packages 0-63401  
 shallow earth burial stabilisation, natural loose rock as biobarrier to prevent waste transportation 0-95385  
 site selection and equipment planning for radioactive waste disposal at Gorleben (*German*) 0-68855  
 sludge removal demonstration from Savannah River storage tank 0-73958  
 sludge sample collection system at Savannah River 0-73959  
 sol-gel technology for waste fixation 0-83207  
 solid high-level waste, evaluation of radiation stability 0-102278  
 solidification facility for high heat SRP waste 0-73960  
 solidification of high-level radwaste, production facility 0-83201  
 solidification process using vinyl ester resin with improved free-water and leachability characts. 0-99265  
 spectrum in stellar spectra, means of detecting extraterrestrial civilisations 0-82230

## radioactive waste continued

- spent fuel bundle counters for CANDU reactors, appl. of safeguards design principles 0-63347  
 spent fuel heatup following loss of water during storage 0-83205  
 spent fuel storage, supercriticality through optimum moderation 0-57896  
 spent fuel storage and disposal and plant building and operating legislation (*German*) 0-99223  
 spent fuel subassemblies, nondestructive assay, comparison of calcs. and meas. 0-78421  
 spent fuel transportation, commercial experience in US 0-63310  
 spent fuel verification by gamma-ray spectroscopy for materials safeguards 0-78422  
 spent fuel waste products, delayed neutron nondestructive assay instrumentation, Monte Carlo calculational design 0-81271  
 spent nuclear fuel elements, intermediary storage, stationary temp. level determ. calc. method 0-91223  
 spent nuclear fuel inventory confirmation technique using Cherenkov light intensity meas. 0-78419  
 spent nuclear fuel stored in basalt, chances of reintroduction into biosphere, analysis 0-106144  
 storage, in situ instrumentation for meas. of radionuclide migration 0-95485  
 storage, long term subsurface migration of radionuclides 0-95483  
 storage, radionuclide migration determ., adsorption of Cs(I), Sr(II), Eu(III), Co(II), and Cd(II) by  $\text{Al}_2\text{O}_3$  0-99240  
 storage, soil homogeneity evaluation by radionuclide tracer breakthrough curve interpretation 0-97821  
 storage and shipment of spent fuel elements INFCE Working Group 6 (*German*) 0-102257  
 storage in salt domes, conceptual design 0-106143  
 storage of spent fuel elements in steel canisters, air cooling (*German*) 0-57867  
 storage on open-air bed at CAMEN in concrete containers (*Italian*) 0-78401  
 storage study, groundwater vel. estimation 0-82111  
 SYNROC-B ceramic for radwaste disposal, feasibility of subsolidus sintering 0-83198  
 thermal reactor fuel cycles, actinide wastes toxicity limitations (*German*) 0-99220  
 time-tested underground structures suitable for isolating low-level waste 0-95383  
 toxicity reduction in Auegan fusion reactor 0-106175  
 trace radionuclides in soil— $\text{X}$ -ray meas. using  $\text{Si}(\text{Li})$ -NaI spectrometer 0-58020  
 transceramic, from nuclear power plants, storage vessels and methods (*Dutch*) 0-68845  
 transmutation of by-product actinides to reduce high-level radwaste storage times 0-95384  
 transportation of commercial low-level radwaste 0-99258  
 treatment and disposal (*French*) 0-99221  
 treatment and disposal methods (*German*) 0-57868  
 underground disposal, solutes movement through aqueous fissures in porous rocks 0-94553  
 underground nuclear waste repositories, risk assessment using reliability models 0-57898  
 underground repository of high-level radwaste, water intrusion scenario studies, anal. and re-eval. 0-73950  
 underwater solution to nuclear fuel storage problem 0-86963  
 Urazoko Bay,  $^{239}\text{Pu}$ ,  $^{137}\text{Cs}$  and  $^{60}\text{Co}$  distrib. and behaviour 0-97825  
 utilisation, fertility value of gamma-irradiated sewage sludge 0-99243  
 utilisation, recovery of noble metals 0-99242  
 utilisation, sewage sludge treatment with gamma irradiation 0-102284  
 utilisation, sewage solids as supplemental feed for ruminants grazing rangeland forage 0-99244  
 utilisation of defence nuclear wastes as conservable resources 0-99241  
 vitrification for high level waste from LWR fuel 0-73961  
 vitrification for waste immobilisation 0-83199  
 vitrification of fission product soln. from spent fuel reprocessing (*German*) 0-73975  
 vitrification using in-can melting process 0-83204  
 volume reduction options, total cost sensitivity to fixed charge rate and inflation 0-99263  
 Waste Isolation Pilot Plant, retrieval methods and equipment 0-73962  
 Wylfa air-cooled dry store, design, operation, safety 0-57900  
 $^{239}\text{Pu}$  in alkaline freshwater pond, determ. by coprecipitation technique 0-71988  
 $^{129}\text{I}$  in bovine thyroid glands, activation anal. obs. 0-94380  
 $^{129}\text{I}$  radioisotope, fixation with Portland cement, radiation stability tests 0-83200  
 Pb encapsulation of radioactive waste, risk assessment 0-99249  
 Pu and Am inventory of ecosystem near a nuclear facility 0-97820  
 Pu dose to lung and bone from contaminated soils, statistical uncertainties 0-109028  
 Pu environmental contamination, review 0-101136  
 Pu, lung 0-109042  
 Pu-bearing materials, environmental impact of transportation, linear regression anal. 0-85308  
 $^{239}\text{PuO}_2$ , inhaled by baboons and dogs, comparison of early mortality 0-108977  
 Rn emanation from  $\alpha$ -emitting waste, expts. 0-98314  
 $^{222}\text{Rn}$  diffusion through U mill tailings covers, coeff. meas., lab. techniques 0-95387  
 $^{90}\text{Sr}$  concentrations in pronghorn antelope bones near a nuclear fuel reprocessing plant 0-89875  
 $\text{UO}_2$  low enriched fuel rods, storage and transportation, critical separation in water with fixed neutron poisons 0-73918  
 $^{137}\text{Cs}$ , A=133,135, interference with low-energy meas. systems 0-89872

## radioactivity

- see also alpha decay; atmospheric radioactivity; beta-decay; radioactive decay periods; radioactive decay schemes; radioactive sources; radioactive tracers; radioactivity measurement; radiochemistry; spontaneous fission  
 aggregate recoil theory 0-57062  
 beta decay Rumanian standard (*Rumanian*) 0-68603  
 comets, primordial, interiors radiogenic melting 0-67659  
 decay analysis method, comparison to least squares 0-102162  
 depositions, shallow, on body surfaces, meas. using M X-rays 0-67223  
 drinking water, Finland, internal radiation doses due to radioactivity 0-109029  
 drinking water, Finland, natural radioactivity 0-108819

radioactivity continued

Earth crust radiogenic heat production, model 0-85619  
Earth mantle, radiogenic heating in convecting mantle rel. to oceanic bathymetry flattening 0-85642  
environmental radioactivity in W.Cumbria, Pu and <sup>137</sup>Cs concs. and possible maritime effect 0-108817  
granites of E.United States, radioactive elements concs. rel. to low-temp. geothermal resources 0-85264  
history, Frederick Soddy and the practical significance of radioactive matter 0-86068  
incidents, national arrangements, review 0-102355  
lunar soil samples from Luna-24, radioactivity and cosmic ray dose rate, thermolum. obs. 0-67596  
Mare Crisium, regolithic radioactivity 0-62045  
medicine, residual activity in syringes after radiopharmaceutical injection (*Japanese*) 0-98113  
metal surfaces, radioactive contamination 0-68771  
meteorites, appl. to galactic cosmic ray solar modulation (*Bulgarian*) 0-72728  
rock U isotope disequilibrium due to  $\alpha$ -recoil and soln. effects 0-98314  
standards for medical use 0-67232  
statistical density functions for radioactive decay and counting 0-73828  
supernovae, Type I, radioactive excitation source model for late time spectra 0-105264  
Wyoming, heat flow and radioactivity 0-72469  
<sup>112</sup>Cd<sup>m</sup>, in marine organisms and sediment around Marshall Island ncl. test site 0-109174  
U prospecting, geochemistry of inclosure radioactivity 0-85766

radioactivity measurement

see also *radioactivity measuring apparatus*  
air monitoring systems for radioiodine and inert gases, evaluation 0-95480  
borehole  $\gamma$ -ray logging, exact inverse filters 0-94609  
distribution in extended medium, qualitative and quantitative anal., mathematical modelling 0-71985  
environmental radioactivity near a radioactive waste disposal site 0-98148  
phosphate fertilizer, specific activity of U and Th rel. to particle size 0-106244  
radionuclides, short-lived, meas., counting statistics 0-58098  
rocks and soils, Ge(Li) detectors for  $\gamma$ -radioactivity meas. 0-67418  
shadow-shield background reduction method 0-108999  
shielded syringes, radioactivity checking instrument 0-94325  
tackishade sampling to measure airborne radioactivity (*Hungarian*) 0-94136  
 $\gamma$ -emitting radioelements, meas. of weak doses (*French*) 0-91410  
Ce in marine sediments, determination method 0-104543  
Rn mapping in U exploration, exclusion of <sup>220</sup>Rn signal 0-61916  
U<sup>235</sup> in pegmatites, homogenised fission track anal. using solid state track detector 0-97719

radioactivity measuring apparatus

Rn emanation rate measuring apparatus consisting of sealed chamber and scintillation cell, rock samples apl. 0-63494  
scintillation detector, gain stabilising scheme, gated radioactive source and broad digital window 0-63453  
seawater  $\gamma$ -ray field, meas. system (*Russian*) 0-109268

radioactivity protection see radiation protection

radioaltimeters

see also *aircraft instrumentation; radionavigation*  
Seasat, altimeter sensor file algorithms 0-94680  
Seasat, initial performance assessment 0-94679  
SEASAT radar altimeter, resolution capability preliminary estimates 0-72645

radioastronomical observations

see also *radiosources (astronomical)*  
0816+526, cD galaxy, classical double radiosource, 4885 MHz obs. 0-109545  
2033+59, appl. of Clean and Restore technique to Northern Cross radiotelescope obs. (*Italian*) 0-98563  
Abell 2029 galaxy cluster, radio and SAS 3 X-ray obs. 0-82519  
Abell 2197 and 2199, Westerbork survey at 610 MHz, 18W catalogue 0-67883  
Abell 401, X-ray cluster of galaxies, radio emission distrib. 0-98731  
Abell cluster, lunar occultation obs. at 327 MHz, survey 0-73052  
Abell cluster radio sources, spectra and optical identification, SHF obs. 0-98729  
AO 0235, mapping with uncalibrated visibility data, 5011 MHz obs. 0-77295  
R Aquarii, symbiotic star, radio mol. maser line obs. 0-72960  
AS 501, compact H II region, OH main-line maser emission obs. 0-67716  
B335, mol. cloud, continuum emission mapping at 89.6 GHz 0-94842  
B 35, bright rimmed molecular cloud, CH obs. 0-62238  
binary galaxies, dynamics and masses from 21 cm obs. 0-105332  
bright galaxy nuclei, optical and radio survey, sample selection and obs. 0-73039  
3C 111, radio galaxy, obs. at 1.38 cm wavelength with resolutions up to 8" (*Russian*) 0-109558  
3C 119, 286, 345, 454.3, quasars, 5 milliarsecond resolution maps at 1.67 GHz 0-82531  
4C 13.17A, B, in X-ray cluster of galaxies Abell 401, radio emission distrib. 0-98731  
3C 147, 3C 286, quasars, VLBI obs. at 329 MHz 0-67898  
3C 147, hybrid mapping on Very Large Array, SHF obs. 0-82534  
3C 219, double radio galaxy, high-resolution 0-77500  
3C 225.0, UHF and EHF obs. of foreground cold diffuse cloud 0-105311  
3C 236, radio galaxy, 6-49 cm obs. of double source 0-82528  
3C 279, interplanetary scintillations and solar wind vel., SHF obs. (*Russian*) 0-77248  
3C 31, radio galaxy, mag. field struct. in radio jets 0-82526  
4C 32.69, quasar with radio jet, high resolution radio obs. 0-105375  
3C 345, quasar, VLBI obs. at 1.67 GHz 0-94885  
3C 345 and 454.3, quasars, 102 MHz obs. of interplanetary scintillations (*Russian*) 0-94889  
3C 351, quasar, VLA maps and outer lobe optical emission search 0-105376  
3C 388, galaxy in Abell 643, classical double radiosource, 4885 MHz obs. 0-109545

radioastronomical observations continued

4C 39.25, compact radio source, search for time-depend. radio fine struct. 0-90552  
4C 39-08, appl. of Clean and Restore technique to WSRT obs. (*Italian*) 0-98563  
3C 405 (Cygnus A), radio galaxy, obs. at 1.38 cm wavelength with resolutions up to 8" (*Russian*) 0-109558  
3C 465, extended radio galaxy, multifrequency UHF and SHF obs. 0-105338  
4C 47.51, complex radiogalaxy, aperture synthesis obs. 0-94883  
4C 53.37 (1638+538), tailed radiogalaxy, dual curved jets 0-62265  
3C 84 (Perseus A, NGC 1275), Seyfert galaxy, 5' halo SHF obs. 0-105372  
3C sources, possible giant radio structure discovery at 11 cm 0-67895  
calibration radio sources, flux density at 8420 MHz rel. to Virgo A 0-86004  
Cancer cluster, Westerbork survey at 610 MHz 0-67884  
Cassiopeia A, secular decrease in 927 MHz flux, radio flux density obs. 0-67840  
cD and related galaxies in poor clusters, pencil beam obs. of radio emission at 6 cm 0-62293  
cD galaxies and related objects in poor clusters, 1400 MHz pencil beam obs. 0-62263  
Centaurus A (NGC 5128), radio galaxy, obs. at 1.38 cm wavelength with resolutions up to 8" (*Russian*) 0-109558  
CG195.5+4.5, upper limit to 59.35 s periodic radio emission at 18 cm 0-86018  
Circinus X-1, binary model, orbital eccentricity from X-ray and radio obs. 0-98735  
circumsolar plasma, Venera 10 radio signal spectral meas. 0-109326  
Cloud 2, mol. cloud, detect. of HC<sub>3</sub>N (cyanodiacetylene) and HC<sub>3</sub>N (cyanohexatriyne), SHF obs. 0-101627  
clusters of galaxies, microwave search for ionised gas 0-82477  
clusters of galaxies, rich X-ray emitting clusters, VHF obs. 0-62294  
compact extragalactic radio sources, interpretation of spectra 0-62299  
Crab Nebula, compact source flux density meas. by interferometer 0-62252  
Crab Nebula, lunar occultation obs. at decametre wavelengths 0-62248  
CTA 102, quasar, 5 milliarsecond resolution maps at 1.67 GHz 0-82531  
CTB 1, UHF emission and radio shell of SNR 0-77461  
V645 Cygni (GL 2789), IR and EHF spectroscopy 0-72956  
V1500 Cygni (Nova 1975), radio obs. and analysis 0-67726  
Cygnus A, radiogalaxy structure at 150 MHz 0-101646  
Cygnus Loop, UHF emission and filamentary structure of SNR 0-77461  
Cygnus X-1, X-ray binary, variable star, SHF obs. 0-73071  
dark clouds, <sup>13</sup>C<sup>18</sup>O/<sup>12</sup>C<sup>18</sup>O double ratio, isotopic fractionation evidence 0-73017  
dark clouds, formaldehyde obs., 5 GHz survey 0-73028  
decametric storm burst source positions, UTR-2 obs. at 25 MHz 0-90403  
double radio sources, hot spots behaviour 0-94882  
DR15, galactic H II region, obs. at 408, 1407 and 2695 MHz 0-94881  
DR 21, HF calibration source, flux density obs. at 8420 MHz 0-86004  
early-type stars, mass loss from radio obs. at 6 cm 0-82347  
Effelsburg 100 m radiotelescope, first obs. at 7 mm wavelength, props. and performance 0-62013  
40 Eridani, multiple star system undetected at 4885 MHz 0-105282  
extragalactic compact sources with faint components, VHF and SHF obs. 0-90547  
extragalactic flat spectrum sources, VLBI UHF and SHF obs. 0-90549  
extragalactic radio sources, confusion-limited survey at 4.755 GHz, source list and areal distrib. 0-98577  
extragalactic radio sources, search for compact sources at low freqs. (81.5 MHz) 0-90553  
extragalactic radio sources, variable radio emission temporal characts. (*Russian*) 0-62307  
extragalactic radio sources study of emission variability in millimeter wave range (*Russian*) 0-90559  
extragalactic radiosources, variable with flat spectra, 90 GHz flux density 0-73056  
extragalactic sources, deep survey of selected regions at 4.85 GHz 0-77502  
extragalactic sources, QSOs and galaxies, linear polarisation meas., SHF obs. 0-73058  
extragalactic sources, rot. measure, linear polarisation obs. at 7.2 cm 0-82530  
extragalactic sources with strong mm components, simultaneous radio obs. 0-73055  
formaldehyde as probe to investigate dark cloud struct. EHF and SHF obs. 0-105317  
G74.9+1.2, continuum obs. at 2695 MHz of SNR 0-67830  
G 261.9+5.5, H I 21 cm obs., H I clouds in SNR 0-62229  
G 84.2-0.8, high resolution 1415 and 2695 MHz obs. of SNR 0-98702  
galactic anticentre, 21 cm obs. of H I stream 0-90524  
galactic centre, H radio recombination line obs. of arc-like source 0-82498  
galactic H I, combined northern and southern survey, photographic presentation 0-62241  
galactic H I 21 cm line obs. for southern hemisphere 0-85987  
galactic sources, H110 $\alpha$  line and formaldehyde absorption line obs., SHF obs. 0-77472  
galaxies, 3 cm obs. of 141 optically bright objects 0-73040  
galaxies, 408 MHz obs. of 91 spirals 0-98720  
galaxies, bright, 1415 MHz continuum survey 0-94869  
galaxies, distance scale from IR magnitude/H I vel.-width relation 0-82480  
galaxies, elliptical, extended radio sources, partial synthesis maps at 2.7 and 8.1 GHz 0-105330  
galaxies, H I vel. widths and IR magnitudes rel. to distance scale and expansion rate outside Local Supercluster 0-105325  
galaxies, isolated, continuum survey at 5 GHz 0-105333  
galaxies, large, H I mapping survey obs. 0-94870  
galaxies, nearby, radio continuum obs. (*German*) 0-109544  
galaxies, radio continuum obs. at 11 cm 0-94872  
Galaxy central region, improved H I data rel. to barlike model of inner Galaxy gas distrib. 0-67845  
galaxy clusters, central regions, 3.5 and 4.0 mm obs. (*Russian*) 0-82525  
galaxy clusters, scattering of microwave background, 9 mm obs. 0-105366  
galaxy clusters, scattering of microwave background radiation 0-105367



## radioastronomical observations continued

- Ganymede, surface model and characts. from radar obs. 0-90359  
 Geminid meteor stream, struct. from radar obs. 0-82310  
 globular cluster fields, radio continuum obs. at 2.7, 4.8 and 10.7 GHz 0-101619  
 globular clusters, high sensitivity search for main-line OH emission 0-62207  
 HD 192163, Wolf-Rayet star in ring nebula HGC 6888, SHF obs. 0-82386  
 Herbig-Haro objects 7-11, compact H II region and H<sub>2</sub>O maser sources 0-73019  
 Herbig-Haro objects and surrounding dark clouds, NH<sub>3</sub> 23 GHz obs. 0-72934  
 HR 1099, 10 GHz radio emission from RS Canum Venaticorum binary 0-82427  
 IC 1396, H II region three dimens. model from 2695 MHz high resolution map 0-105316  
 IC 1396 (Sharpless 131), 2695 MHz continuum map of H II region 0-105310  
 IC 342, Scd galaxy, central regions IR and radio emission rel. to star form. 0-62256  
 IC 342, Scd galaxy, H I large-scale struct. obs. 0-67857  
 IC 342, Scd galaxy, struct. from H I obs. 0-73045  
 interplanetary scintillation, obs. rel. to solar wind plasma irregularities anisotropic struct. 0-67489  
 interplanetary scintillation spectra, radio spectrograph obs. 0-72741  
 interstellar dark clouds, radio continuum interferometric search for newly formed H II regions 0-98699  
 interstellar dark clouds, radio continuum interferometry rel. to newly formed H II regions physical props. 0-105301  
 interstellar H<sub>2</sub>O maser emission, new sources detect. 0-62298  
 interstellar H<sub>2</sub>O masers in NGC 6334, positions and spectra rel. to star form. 0-73025  
 interstellar HCN, absorpt. lines obs. towards Cassiopeia A 0-101624  
 interstellar HCO<sup>+</sup>, shock enhancement of abundance in supernova remnant (IC 443) 0-82464  
 interstellar methanol, 84.5 GHz and 96.7 GHz lines obs. in Sagittarius B2 and Orion A 0-62245  
 interstellar thioformaldehyde (H<sub>2</sub>CS), 3 GHz absorpt. transition obs. 0-67837  
 IRC+10374, IRC+10523, IR stars, H<sub>2</sub>O maser emission detect. 0-62298  
 Jupiter, decametric and hectometer radio emission obs. 0-67644  
 Jupiter, magnetosphere HF and LF events from Voyager 2 obs. 0-77344  
 Jupiter, non-lo decametric radiation obs. at freqs. above 30 MHz 0-85886  
 Jupiter, radiation belts, 21 cm maps from all rot. aspects 0-105195  
 Jupiter, radioemission at 100 kHz, from magnetosphere 0-85891  
 Jupiter, study at 2.7 GHz with Cambridge 5 m telescope 0-82272  
 Jupiter, whistler mode chorus obs. and Io torus implications 0-72862  
 Jupiter ionosphere, spectral broadening meas. by Pioneers 10 and (11) 0-109391  
 Jupiter ionosphere, Voyager 2 occultation, radio obs. 0-77337  
 Jupiter magnetosphere, plasma waves from Voyager 2, radio obs. 0-77343  
 Jupiter radio emission, Stokes parameters obs. at 11 and 18 cm wavelength 0-67637  
 Jupiter S-bursts, freq. drift meas. at different freqs. throughout several storms 0-85888  
 Jupiter S-bursts, occurrence with L-bursts and freq. upper limit 0-85887  
 Kleinmann-Low nebula, NH<sub>3</sub> obs. and hot core source 0-73016  
 L 183 (L 134 N) dust cloud, NH<sub>3</sub> and cyanoacetylene mapping at 23 GHz 0-105307  
 BL Lacertae, major radio outburst, (1980 April 17 to May 6) 0-73043  
 LSI+61°303, supergiant Be star, radio emission and radial vel. periodic vars. 0-62149  
 Lynds 134 dust cloud turbulence, formaldehyde obs. at 6 cm. 0-94845  
 Lynds 1551, CO obs. of dark cloud and stellar wind driven shocks 0-105318  
 inner M101 galaxy group, H I obs. 0-67885  
 M31, H I emission in NE region, 21cm obs. 0-90537  
 M31, line intensity distrib., contour maps, vel. profiles, 21 cm HI line survey 0-73038  
 M33 direction, H I 21 cm emission/absorpt. obs. 0-62262  
 M82, H125α recomb. line, SHF obs. 0-82486  
 M87, 2 and 6 cm VLA obs. of jet 0-105345  
 M87, millisecond radio bursts discovery 0-73034  
 Magellanic Stream H I regions, fine struct., 21 cm obs. 0-90523  
 Markarian 348, Seyfert galaxy, H I envelope, 21 cm obs. 0-82504  
 Markarian 3, Seyfert galaxy radio maps, SHF obs. 0-82501  
 Markarian 668 (=OQ 208), Seyfert, H83α and H99α radio recomb. lines detect. 0-94864  
 Mars, dynamics obs. from Viking lander tracking data anal. 0-77314  
 Mars, orbit determination on basis of radar and visible observations 0-90323  
 Mars, radar altimetry of S.Tharsis 0-98591  
 Mars, radar characts. of rough planar surfaces 0-98589  
 Mars atmosphere and topography, Viking orbiters radio occultation meas. during one Martian year 0-72836  
 MC2 1210+121 and 1620+103, radio-quiet BL Lacertae-type objects 0-101641  
 MCS 1307+121, BL Lacertae object, radio spectrum shape, VHF and SHF obs. 0-67866  
 meteor rate depend. on geomag. activity and coronal activity 0-67662  
 meteors, optical brightness rel. to ionised trail props. 0-77354  
 meteors ionisation columns, initial radii meas. 0-94762  
 microwave background anisotropy, galactic dust emission 0-77524  
 millimetre region cosmic background radiation, large scale anisotropy meas. 0-82553  
 molecular cloud in NGC 2264, NH<sub>3</sub> and OH line emission mapping, SHF and UHF 0-94847  
 molecular clouds as galaxy spiral struct. tracer, 2.6 mm CO survey 0-105346  
 molecular clouds associated with refl. nebulae, CO emission, EHF obs. 0-82447  
 Moon, 3 cm radar obs. from Luna 16 to 24 spacecraft 0-77302  
 MWC 349, Be star, spectral EHF obs. 0-105262  
 MXB 1730-335 (Rapid Burster), microwave bursts obs. 0-62320  
 NGC 1023 galaxy group, H I obs. and possible intergalactic H I cloud discovery 0-67886

## radioastronomical observations continued

- NGC 1023 galaxy group, H I radial vels. rel. to group membership and mass/light ratio 0-82521  
 NGC 1052, elliptical galaxy, field, H I emission mapping and line profiles 0-98719  
 NGC 1275, Seyfert galaxy, nucleus struct. (Russian) 0-62288  
 NGC 1275 (Perseus A), correl. between optical and radio variability (Russian) 0-77505  
 NGC 1569, dwarf irregular galaxy, H I obs. 0-90538  
 NGC 2264, H II region, classification of optical, IR and radio obs. data 0-67818  
 NGC 2264, mol. cloud, continuum emission mapping at 89.6 GHz 0-94842  
 NGC 2366 H II region visible and radio obs. 0-77475  
 NGC 315, radio galaxy, mag. field struct. in radio jets 0-82526  
 NGC 4485/90 interacting galaxies, radio continuum and H I obs. 0-62274  
 NGC 4565, warped Sb galaxy, H I distrib. 21 cm obs. 0-109542  
 NGC 672 and IC 1727, interacting galaxies, H I obs. and computer modeling 2 km line obs. 0-67853  
 NGC 7538, IRS 1, formaldehyde maser, SHF band obs. 0-67822  
 NGC 7538 and Sharpless 159, H II region/mol. cloud complex, H I aperture synthesis obs. 0-90510  
 NGC 7822, NGC 281, bright rimmed mol. clouds, CH obs. 0-62238  
 NGC 925, barred spiral galaxy, high-resolution H I obs. 0-105329  
 NP 0532, Crab pulsar, lunar occultation obs. at decametre wavelengths 0-62248  
 NRAO 150, compact radio source, search for time-depend. radio fine struct. 0-90552  
 OH 205.1-14.1, unusual OH maser, new flare report and 1667 MHz line obs. 0-98734  
 OH 351.78-0.54, UHF obs. of brightest OH maser (1980 August) 0-101644  
 OH masers, interstellar, obs. near Orion population stars 0-67716  
 Ooty occultation extragalactic sources radio spectrum obs. in SHF 0-105371  
 ρ Ophiuchi dark cloud, <sup>13</sup>CO self absorpt., EHF obs. 0-90500  
 ρ Ophiuchi mol. cloud, continuum emission mapping at 89.6 GHz 0-94842  
 Orion methanol masers, interferometric and multitransitional study 0-67891  
 Orion Nebula, radio obs. of nearby H I distrib. and vels. 0-105322  
 Orion population stars, OH emission survey 0-67716  
 OTL radio sources, position and struct. determ. from 327 MHz lunar occultation obs. 0-73061  
 OTL radio sources, position and struct. determ. from 327 MHz obs. 0-73060  
 OTL radiosources, position and struct. determ. from 327 MHz lunar occultation obs. 0-73062  
 Parkes 2700 MHz survey sources, 408 MHz obs. 0-86008  
 periodicity investigation in special objects at 21 cm 0-82529  
 Pioneer 11 at Saturn, trajectory var., carrier freq. Doppler shift, Saturn mass determ. 0-82294  
 Pioneer Venus occultation experiment, radio science data generation 0-67492  
 PKS 0735+178, flat radio spectrum, 0.3-90 GHz obs. 0-94880  
 planetary nebulae, advances in radio obs. 0-109526  
 planetary nebulae in southern hemisphere, IR and SHF obs. 0-90496  
 PSR 0031-07, drifting subpulses obs. and implications for pulsar models 0-67763  
 PSR 0355+54, pulse shape change, 11 cm obs. 0-67761  
 PSR 0611+22, short time scale integrated pulse shape vars. 0-105267  
 pulsars, 102.5 MHz obs. of three new pulsars (Russian) 0-67764  
 pulsars, low-latit., H I absorpt. spectra meas. 0-101606  
 pulsars, periods, positions and proper motion determ. from pulse arrival times, UHF, obs. 0-77431  
 pulsars, polarised radiation at 430 MHz, statistical summary 0-67760  
 pulsars, radio emission, millisecond intensity var. 0-98682  
 pulsars in southern hemisphere, polarisation obs. at 1612 MHz 0-90462  
 QSO 0957+561, double quasar, 6 cm wavelength obs. 0-62312  
 QSO 0957+561, double quasar as gravitational lens, 6 cm VLA obs. 0-101647  
 QSO redshifted 21 cm absorption line clouds 0-62310  
 QSOs, optically selected, radio study 0-82536  
 QSOs, radio obs. of 70 optically selected MCS objects 0-105377  
 QSOs, redshifted clouds, 21 cm line studies 0-105389  
 quasars 0957+561, radioastron. obs. of assumed double quasars 0-105381  
 quasars, optically discovered, search for radio emission 0-90561  
 radio galaxies components, fly away velocities upper limits (Russian) 0-62306  
 radiogalaxies from B2 Catalogue, optical identification, radio positions and redshifts 0-86005  
 radiosources, positions and optical identifications, 966 MHz survey 0-73059  
 radiosources of intermediate strength, statistical props. 0-62303  
 ring galaxies, radio continuum emission 0-67846  
 S140, mol. cloud, continuum emission mapping at 89.6 GHz 0-94842  
 Sa spiral galaxies, H I study 0-98714  
 Sa type spiral galaxies, redshifted 21 cm line profiles, radio obs. 0-73041  
 Sagittarius B2, mol. cloud, detect. of HC<sub>3</sub>N (cyanodiacetylene) and HC<sub>3</sub>N (cyanohexatriene), SHF obs. 0-101627  
 Saturn, ionosphere electron density from Pioneer II radio occultations 0-94751  
 Saturn, limb darkening and brightness temp., 1.30 cm interferometry obs. 0-82279  
 Saturn, upper neutral atm. and ionosphere, vertical struct., Pioneer 11 radius occultation obs. 0-82293  
 Saturn ionosphere, spectral broadening meas. by Pioneer (11) 0-109391  
 Saturn rings, model constraints from radar obs. of polarisation and albedo 0-82277  
 Scorpius X-1, high energy X-ray and SHF radio obs. 0-73067  
 SETI at 18 cm, high sensitivity search 0-82229  
 Sharpless 115, evolved H II region, struct. from UHF obs. 0-105313  
 Sharpless 159 and NGC 7538, H II region/mol. cloud complex, H I aperture synthesis obs. 0-90510  
 SN 1572 (Tycho's supernova), small dia. radio source discovery and precise position 0-98680  
 SN 1979c in NGC 4321 (M100), detect. at 60 nm wavelength 0-82402  
 soil, surface refl. characts. for radar, obs. from Luna spacecraft 0-72798  
 solar active region and bursts, 6 cm obs. with 6" resolution 0-62096

radioastronomical observations continued

solar filament, synthesized map at 6 cm with about 15" resolution 0-90380  
solar flares, radio brightness distrib. processing in one-dimensional synthesis (*Italian*) 0-98628  
solar noise storm, drifting pulsations obs. 0-62105  
solar type IV radio burst quasisperiodic struct., anal. and interpretation 0-62097  
solar wind, electron density fluctuations obs. by radioscintillation 0-61978  
solar wind, low freq. continuum from ISEE 3, thermal electrostatic noise, LF obs. 0-101519  
solar wind turbulent plasma, radio wave propag. meas. using three satellites 0-101518  
spiral galaxies, redshifted 21 cm absorption line clouds 0-62310  
sporadic meteors, ionisation height meas., VHF obs. 0-82312  
SS 433, 180 mm interferometric obs. of triple structure 0-105259  
SS 433, change in radio struct., 1980 January to June, from VLBI obs. 0-109557  
SS 433, search for radio spectral lines in UHF 0-109556  
Stephan's Quintet, redshifted H I associations 0-67882  
Stephen's Quintet, broadband 21 cm H I emission 0-109554  
Sun, active region McMath 15403, 5 minute oscills., SHF obs. 0-98639  
Sun, active regions, 3 cm radio emission spectral slope, flare-associated variations 0-98630  
Sun, anal. of solar radio obs. at 3.2 and 10 cm at Purple Mountain Observatory (*Chinese*) 0-105223  
Sun, drift pair bursts, polarisation obs., position and freq. characts. 0-85925  
Sun, impulsive mm-wave bursts, quasi-quantization 0-94770  
Sun, quiet spatial structure during 1977 October eclipse, VLA 6 cm obs. 0-72895  
Sun, rapid var. of centimetre-wave sources above McMath region 13043 rel. to optical phenomena 0-67688  
Sun, relation between type I (metre wave) radio sources and proton events (*Chinese*) 0-105222  
Sun, S-component source spectra, correl. with flare occurrence, EHF obs. 0-101579  
Sun, two dimens. maps at 408 MHz 0-85922  
Sun, type III bursts, assoc. with flaring X-ray bright points 0-67681  
Sun, type III bursts, position and polarisation, VHF and HF obs. 0-105214  
Sun, type III bursts, radio spectra obs., effect of interactions in ionospheric plasma 0-72904  
Sun, type III bursts during decametric storm 0-90399  
Sun, type IIb bursts, 25 MHz obs. and theoretical model 0-90400  
Sun, type V radio bursts, position and polarisation, HF and VHF obs. 0-105215  
Sun under quiet conditions, SHF brightness temp. distrib., RATAN-600 obs. (*Russian*) 0-94776  
supernova remnants in LMC, SHF obs. 0-67864  
supernova remnants in young objects NGC 6946, search for radio emission from four young objects 0-77473  
Taurus A, secular decrease in 927 MHz flux, radio flux density obs. 0-67840  
Tycho's SNR (3C 10), distance, Westerbork H I obs. 0-101633  
variable extragalactic sources with steep spectrum, VHF and SHF obs. 0-90548  
Venus, microrelief irregularities mean height, determination from radio transillumination data 0-72807  
Venus, Pioneer radar data, planet's topography (*German*) 0-105190  
Venus, spin vector determ. by radar obs. 0-105185  
Venus, surface reflections of Pioneer Venus descent vehicles radio emission, atm. data 0-105187  
Venus atmosphere, radio waves attenuation investigation by bistatic radar method 0-62061  
Venus atmosphere and surface, investigation by radiosounding from Venera 9 and 10 satellites 0-101543  
Virgo A (M87), Westerbork map at 610 MHz 0-62302  
Virgo cluster galaxies, 1.4 GHz continuum survey 0-98721  
Virgo cluster spiral galaxies, H I deficiency from 21 cm obs. 0-62277  
14W12, in X-ray cluster of galaxies Abell 401, radio emission distrib. 0-98731  
19 W32, 43 and 109, galactic centre planetary nebulae search 0-90506  
W33, OH radio emission sources obs. (*Russian*) 0-62247  
W3(OH), interstellar OH maser, struct. from VLBI synthesis obs. 0-105368  
W3 H II region, CO, CS and HCN obs. LF obs. 0-82446  
W3/W4/W5 region, heavy optical obscuration obs. 0-62301  
W49A, W51A, compact H II regions, H10 $\alpha$  recomb. line, aperture synthesis obs. 0-105314  
W50, continuum obs. at 2695 MHz of SNR 0-67830  
W58, galactic star-forming region, CO obs. 0-67810  
W80 (Pelican Nebula), CO obs. of expanding mol. shell surrounding H II region 0-105296  
28 W sources and catalogue in NGC 7000 IC 5070 H II region complex 0-105308  
X-ray sources, extragalactic, positional and spectral data, HF obs. 0-86019  
X-ray sources in galactic bulge, radio continuum obs. at 2.7, 4.8, and 10.7 GHz 0-101619  
CO in nearby galaxies, survey 0-62276  
H I envelopes round spiral galaxies, 21 cm obs. 0-90520  
H I regions, high-latit., obs. in OH 18 cm lines 0-67841  
H I regions towards extragalactic radio sources, 21 cm emission, and absorpt. obs. 0-94854  
H I survey, contour maps, 21 cm obs. 0-85986  
H II regions, <sup>12</sup>C<sup>18</sup>O and <sup>13</sup>C<sup>18</sup>O J=2-1 transitions obs. 0-73022  
H II regions, H16 $\alpha$  recomb. line obs. at 1425 MHz 0-90512  
H II regions, He abundance from 15 and 22 GHz recombination line obs. 0-98703  
H II regions, small, with exciting stars, radio maps 0-62224  
H<sub>2</sub>O maser source in Orion A, obs. of outburst (*Russian*) 0-105320  
H<sub>2</sub>O maser sources in galactic plane, southern hemisphere survey 0-73054  
H<sub>2</sub>O masers, 22 GHz galactic plane survey, 14 new sources 0-77464  
OH astronomical maser sources OH 231.8+4.2, CY Canis Majoris, M1-92, UHF obs. 0-90550

radioastronomical techniques

astrometry, influence of troposphere on radio-interferometric meas. of coordinates 0-67581  
background radiation spectrum meas. in near-mm region 0-62327  
clean and restore technique, appl. to WSRT and Northern Cross radiotelescope obs. (*Italian*) 0-98563  
cross-correlators, incoherent optical 1-bit for radio antenna arrays 0-98555  
data processing of radiosource rotation measures 0-86006  
extragalactic radio sources modelling, appl. to complex source (3C 288) 0-90558  
gravitational background radiation, possible detection by Doppler tracking interplanetary spacecraft 0-67914  
gravitational radiation stochastic background detection using Doppler tracking of spacecraft 0-67913  
image synthesis from projections 0-67579  
interferometric meas. of Haystack-Westford base line vector 0-89929  
linear restoration using Hermite polynomials 0-82217  
meteor modelling with radar observations, adaptation techniques (*Russian*) 0-67664  
meteor trail studies using large-aperture radio system 0-85870  
meteors, simultaneous visible and radar obs. technique 0-77354  
Pioneer Venus occultation experiment, radio science data generation 0-67492  
plasma wave instrument on Pioneer Venus Orbiter, design and performance 0-67497  
radar signal reflection from Sun, efficiency of four-plasmon interactions 0-101582  
satellite radiosounding, appl. to Venus atmosphere and surface investigation by (Venera 9 and 10) 0-101543  
solar flares rich in <sup>3</sup>He, 8666 MHz superfine structure line detection 0-109417  
source, mapping with uncalibrated visibility data 0-77295  
source parametric determ. method from spinning satellite obs. 0-85871  
spectral index determ. of radio emission of individual solar regions 0-94723  
three dimensional spatial autocorrelation function meas. reduction 0-67576  
Venus microrelief irregularities mean height, determination from radio transillumination data 0-72807  
Venus radar mapping, Pioneer Venus Orbiter mapper design and operation 0-67495  
VLBI hybrid mapping of nuclei of radio galaxies and quasars 0-105356

**radioastronomy**  
*see also pulsars; quasars; radiofrequency cosmic radiation; radiosources (astronomical); radiotelescopes; solar radiofrequency radiation*  
AKAIHOSHI flexible real time software system 0-82214  
bandpass interference filters for 1-3 mm window 0-109368  
calibration sources, flux density at 8420 MHz rel. to Virgo A 0-86004  
Cosmic Background Explorer, satellite instrumentation 0-61988  
EM spectrum, overcrowding and use by radio astronomy 0-85874  
formaldehyde substituted with <sup>17</sup>O and <sup>18</sup>O, microwave spectra of ground vibr. states, rot. and distortion const. determ. 0-83349  
formic acid (-D), microwave spectra and rot. consts., astrophysical appl. 0-91550  
IMPATT source, frequency-stabilised, 115 GHz 0-67573  
interstellar molecular transitions, rest freqs. 0-62218  
ionospheric daytime effect on radioastronomical intensity meas. and interferometry 0-67450  
meteor recording freq., influence of form and orientation of antenna directivity diagram (*Russian*) 0-67665  
Moon, radar contact in 1946 0-85866  
Pioneer Venus Differential Long Baseline Interferometry expt. 0-67578  
planetary atmosphere, occulting spacecraft signal, turbulence determin. 0-94734  
solar power satellites, effect of transmissions on radio-astronomical research 0-61291  
spectroscopy (*Japanese*) 0-62031  
WARC 1979 regulations, impact on space appl. and research 0-105147

**radiocarbon dating** *see radioactive dating*

**radiochemistry**  
*see also radioactive chemical analysis; radioactive tracers*  
actinide solutions, differential alpha radiography using solid state track detectors 0-71932  
anodic electrolysis of radioactive isotopes (*Hungarian*) 0-93765  
aromatics, halogen substituted, as positronium inhibitor 0-93783  
1,1-difluoroethane, nucl. recoil <sup>18</sup>F chemistry at high press. 0-89510  
fission, discovery, research of 1930's, '40's, Otto Hahn 0-57063  
history, early research 0-86067  
hot atom+mol. reaction, steady state vel. distrib., Boltzmann eqn. with BGK elastic collision model 0-66856  
hot cell for synthesis of labeled organic compounds 0-68970  
improved labelling with <sup>99m</sup>Tc by stannous tartrate reduction of pecth-nate 0-72324  
isovaline radiocaramization, cosmochemical implications 0-62087  
multicurie radiochemical separations, remote system 0-71933  
perhalo-compounds, labelled, high yields from <sup>18</sup>F and <sup>38</sup>Cl reactions with CCl<sub>4</sub>, F<sub>4</sub>-x and C<sub>2</sub>F<sub>6</sub> 0-109025  
positronium formation inhibition by solvated electron precursor scavenging, line shape Doppler broadening, lifetime spectroscopy 0-93784  
rapid automated nuclear chemistry, short lived fission products, reactor safety 0-81353  
Au, <sup>18</sup>F recoil ranges by irradiation of O<sub>2</sub> with <sup>3</sup>He and <sup>4</sup>He particles 0-71931  
<sup>11</sup>C-l-lactic acid, enzymatic synthesis 0-61695  
<sup>11</sup>C-pyruvic acid, enzymatic synthesis 0-61695  
<sup>123</sup>I, production in LASL radiochemistry hot cells 0-72326  
Na<sup>224</sup>mTcO<sub>4</sub> solution, special chambers for production (*Hungarian*) 0-93785  
Ra, annual rate of release to atmosphere as result of coal combustion in UK 0-93787  
U<sup>235</sup> in pegmatites, homogenised fission track anal. using solid state track detector 0-97719

**radiocommunication**  
*see also mobile radio systems; radio links; radio reception*  
interstellar link using Sun as gravitational lens antenna 0-62040  
interstellar travel and communication, bibliography 0-101677  
microwave Earth-space link, rain cell attenuation 0-94586



**radiocommunication continued**

- propagation problems connected with special source structs., review 0-87272  
VHF noise field strength at 95 MHz over India, meas. techniques and obs. 0-109294

**radiocrystallography** *see X-ray crystallography***radiofrequency and microwave spectra of diatomic inorganic molecules**

- see also nuclear magnetic resonance; paramagnetic resonance*  
diatomic mols., RF excited inductively coupled Ar plasma spectroscopy 0-86358  
interstellar molecular transitions, rest freqs. 0-62218  
 $^{12}\text{C}^{16}\text{O}$  and  $^{13}\text{C}^{18}\text{O}$  J=2-1 transitions obs. towards galactic H II regions 0-73022  
GaBr, rot. analysis of  $^3\text{I}_{0,1}-\text{X}^1\Sigma^+$  transition 0-69129  
Gal, rot. spectrum, EHF spectra obs. 0-58245  
 $\text{I}_2$ , B-X transitions, rot.-vibr. hyperfine coupling consts., extension to other levels 0-63625  
 $\text{O}_2$ , 60 GHz absorpt. spectra for atmos. remote sensing 0-77172

**radiofrequency and microwave spectra of organic molecules and substances**

- see also nuclear magnetic resonance; paramagnetic resonance*  
acetaldehyde,  $\text{T}_2$ -relax. meas. press. depend. for rot. transitions, pulse spectrometer 0-78612  
benzene-bromomethane, microwave line width and quadrupole moments, perturbation theory 0-69190  
benzene-OCS, microwave line width and quadrupole moments, perturbation theory 0-69190  
1-1-d<sub>3</sub>-but-1-ene skew form, microwave spectra, rot. const. and centrifugal distortion coefficients determ. 0-83351  
caesium perfluoro-octanoate/ $\text{D}_2\text{O}$  system,  $^2\text{H}$  NMR quantum orders, RF pulses 0-103892  
cis-1-cholobutadiene-1,3, microwave spectrum, struct., nuclear quadrupole coupling, distortion const., thermodynamic functions calc. 0-99500  
2-cyanoaziridine, microwave rot. spectrum, assignments 0-91546  
cyanocyclopentane, microwave spectral study of axial and equatorial conformers 0-95604  
3-cyanothiophene- $^{34}\text{S}$  ( $^{15}\text{N}$ ), partial  $r_0$ -struct., microwave spectra 0-91552  
cyclopropyl cyanide, high-resolution microwave spectra, quadrupole hyperfine struct. of rot. transitions anal. 0-95601  
dimethyldichlorosilane, microwave spectrum, rot., centrifugal distortion and quadrupole coupling consts. 0-91547  
ethyl alcohol-d<sub>6</sub>-(d<sub>1</sub>)-(d<sub>2</sub>)-(d<sub>3</sub>), internal rot. and microwave rot. spectra 0-69128  
ethyl iodide, microwave spectra and internal rot. anal. 0-69130  
ethylidenimine, pyrolysis product, microwave spectra, rot. distortion and electric quadrupole const. and rot. barriers determ. 0-78608  
ethynyl radical, mm wave emission obs. of interstellar clouds 0-90503  
fluorene crystal, doped, photochemical hydrogen abstraction, proton hyperfine structure via optical nuclear polarisation 0-63659  
fluoronitrobenzene, equilib. config. and barriers, microwave spectra 0-95606  
formaldehyde substituted with  $^{17}\text{O}$  and  $^{18}\text{O}$ , microwave spectra of ground vibr. states, rot. and distortion const. determ. 0-83349  
formic acid,  $^{16}\text{C}$ ,  $^{18}\text{O}$ , microwave spectra and centrifugal distortion consts. 0-83352  
formic acid (-d), microwave spectra and rot. consts., astrophysical appl. 0-91550  
formyl radical ion, mm wave emission obs. of interstellar clouds 0-90503  
interstellar molecular transitions, rest freqs. 0-62218  
methanol-d<sub>1</sub>, ( $\text{CH}_2\text{DOH}$ ), microwave torsional-rot. spectrum, rel. to interstellar search 0-99498  
methanol-d<sub>1</sub>, laboratory freqs. of J=2-1, a-type transitions 0-63624  
2-methoxyethylamine, microwave spectra, H-bond, torsional motion and mol. vibr. obs., rot. isomerism, mol. moments determ. 0-95603  
methyl acetate, microwave spectra and internal rot. 0-87100  
methyl azidoformate, microwave rot. spectrum, satellite transitions 0-69127  
methyl bromide, NQR and  $\text{A}_1\text{-A}_2$  splitting, RF spectrosc. inside laser cavity 0-91579  
methyl iodide mol. nonlinear resonant interaction with pulsed subMM radiation (*Russian*) 0-99523  
N-methyl m-fluoroaniline, conformational anal., microwave spectra obs. 0-58247  
methylacetylene,  $\nu_5$  band, microwave and IR laser Stark spectrosc. 0-91558  
methylpropylether, trans-trans isomer, microwave spectra, struct., dipole moment and rot. barriers calcs. 0-83348  
norbornane, microwave spectrum and dipole moments 0-78606  
propynal-d, IR microwave double reson. spectroscopy 0-69172  
4-pyridine carbaldehyde, microwave spectrum, rot. assignments, quadrupole coupling consts. 0-91548  
silyl acetylene, microwave spectra in ground and  $\nu_{10}$  vibr. state 0-78610  
thioformaldehyde, interstellar,  $2_{1,1}-2_{1,2}$  transition obs. and rest freq. 0-67837  
trifluorobenzene, equilib. config. and barriers, microwave spectra 0-95606  
trifluorodimethylmercury, gas phase mol. struct., electron diff. and microwave spectra obs. 0-78609  
trifluoriodomethane, laser microwave double reson. spectroscopy with  $\text{CO}_2$  laser lines 0-87156  
trifluoromethyl bromide, mol. rot. and isotopic variation in bond lengths, Stark meas., dipole moment determ. 0-74165  
trifluoromethyl iodide, microwave spectra, mol. rot., isotopic variation in bond lengths, Stark meas., dipole moments determ. 0-74165  
trimethylaminegallane, microwave, IR and Raman spectra, struct., vibr. assignment 0-95600  
trimethylbromosilane, microwave spectra, struct., chemical bonding 0-95602  
trinitromethane, microwave and rot. spectra, effect of twist of  $\text{NO}_2$  groups, rot. and centrifugal distortion const. determ. 0-95605  
trioxane,  $\nu_{19}(\text{E})=\nu_{20}(\text{E})=1$  state, rot. spectrum assignment, microwave obs. 0-58248

**radiofrequency and microwave spectra of polyatomic inorganic molecules**

- see also nuclear magnetic resonance; paramagnetic resonance*  
interstellar molecular transitions, rest freqs. 0-62218  
ArHBr, ArHCl, and isotopic forms, rot. spectra, mol. struct., mol. consts. 0-58246  
CO-HBr, weakly bound, rot. spectra 0-91544  
CO-HCl, weakly bound, rot. spectra 0-91544  
CO-HF, weakly bound, rot. spectra 0-91544  
FCP, microwave spectrum, struct., dipole moment and vibr.-rot. props. obs. 0-91549

**radiofrequency and microwave spectra of polyatomic inorganic molecules continued**

- HCN and HNC, mm wave emission obs. of interstellar clouds 0-90503  
 $\text{HO}_2$  free radical, dipole moments and Stark effects from microwave spectra 0-63623  
 $\text{H}_2\text{O}$  dimer, partially deuterated, microwave spectra and struct. 0-74212  
 $\text{H}_2\text{O}$ -HF heterodimer, H bonding, microwave rot. spectrum, mol. geometry and moment 0-99501  
KrHBr, KrCHl, and isotopic forms, rot. spectra, mol. struct., mol. consts. 0-58246  
 $\text{NH}_3$  inversion lines from nonmetastable rotational levels, SHF obs. of Kleinmann-Low nebula 0-73016  
 $\text{NH}_3+\text{H}_2$ ,  $\text{NH}_3$  inversion transition, linewidths and  $\text{T}_1/\text{T}_2$  ratio 0-99499  
NHD, rotational transitions, microwave optical double resonance obs. 0-58293  
OCS, microwave spectra, Ku-band Fourier transform spectrometer appl. 0-68265  
OCS, millimeter wave rot. spectra, isotope shifts, freqs. and mol. consts. 0-78611  
OCS,  $\text{T}_2$  relax. meas. using budge-type superhet. microwave spectrometer 0-91551  
 $\text{SO}_2$ , microwave spectra, Ku-band Fourier transform spectrometer appl. 0-68265  
 $\text{SO}_2$ ,  $\text{T}_2$  relax. meas. using budge-type superhet. microwave spectrometer 0-91551

**radiofrequency cosmic radiation**

- see also pulsars; quasars; radioastronomy*  
anisotropy on large angular scale 0-105407  
background anisotropy, galactic dust emission 0-77524  
background meas. with Cosmic Background Explorer, satellite instrumentation 0-61988  
background radiation fluctuations produced by evolving hierarchical cosmologies 0-101655  
background spectrum meas. in near-mm region 0-62327  
cosmic microwave background radiation, polarisation in anisotropic universe 0-82552  
cosmological microwave black body radiation spectrum, implications for Population III stars 0-67915  
discovery of microwave background, history 0-57074  
galactic H I 21 cm line obs. for southern hemisphere 0-85987  
galactic nonthermal radio spectrum, rel. to cosmic ray electrons spectrum and gamma-rays prod. 0-62257  
galactic radio spectrum, influence of primordial black holes 0-62179  
homogeneous cosmologies, dipole and quadrupole anisotropies 0-109572  
ionosphere radionoise absorpt., impulsive quasi-periodic variations 0-105116  
magnetosphere cosmic noise absorption during substorms 0-72727  
microwave background, anisotropy rel. to early universe density-temp. fluctuations observability 0-82554  
microwave background, generation by intergalactic pyrolytic graphite whiskers 0-94866  
3K microwave background, in Universe expansion model 0-98746  
microwave background, rel. to cosmology and element origin 0-62359  
microwave background, residual fluctuations, gravitational effects 0-62332  
microwave background, review 0-62336  
microwave background, search for temp. change produced by ionised gas in clusters of galaxies 0-82477  
microwave background, temp. dips due to X-ray clusters of galaxies from sources large-scale struct. 0-82524  
microwave background, upper limit to temp. fluctuations at 4.755 GHz 0-98577  
microwave background angular distrib., large scale fluctuations 0-62328  
microwave background angular distrib., small scale fluctuations 0-62329  
microwave background dipole anisotropy, dynamical inferences 0-62330  
microwave background fluctuations, recombination epoch effects 0-62333  
microwave background in Bianchi type V universe 0-98744  
microwave background in direction of clusters of galaxies (*Russian*) 0-94899  
microwave background small-scale fluctuations, consequences of neutrino rest mass (*Russian*) 0-109576  
microwave background spectrum, distortion by pregalactic dust 0-67916  
microwave background spectrum 0-105406  
microwave background spectrum and G-varying cosmology 0-86020  
microwave background spectrum and isotropy rel. to cosmic turbulence 0-98747  
microwave background temp. fluctuation, constraints on primordial evolution in hot Universe 0-105411  
millimetre region cosmic background radiation, large scale anisotropy meas. 0-82553  
QCD black body radiation, big bang universe hadron era 0-62341  
relict radiation in anisotropic universe, polarisation and anisotropy 0-67917  
relict radiation temp. fluctuations rel. to universal structure evolution 0-105360  
scattering of microwave background in clusters of galaxies, 9 mm obs. 0-105366  
scattering of microwave background radiation in clusters of galaxies 0-105367  
spectral distortions in microwave background longward of 3 mm 0-62326  
spectrum distortions in background 0-62334

**radiofrequency heaters** *see radiofrequency heating***radiofrequency heating**

- biological effects and dosimetric data useful for RF safety standards development, review 0-67154  
biological effects of radiowaves and microwaves 0-98011  
biomedical microwave hyperthermia treatment and thermometry system 0-72280  
cancer treatment appl. of microwave arrays for localised tumour heating 0-94308  
combined microwave heating and radiometry methods 0-85465  
cranial structure exposed to RF radiation, thermal response model 0-94285  
defective dielectrics, EM heating with time depend. param., WKB calcs. 0-71367  
diathermy applicator for irradi. of rat brain 0-94425  
dosimetric measurements of far-fields in full-scale man model 0-67255  
fusion plasma (*Japanese*) 0-92338  
fusion reactor, ELMO Bumpy Torus, microwave coupling 0-99328  
fusion reactor, ISX-B, electron cyclotron microwave heating 0-99329



# radiofrequency heating continued

fusion reactor, TNS, electron cyclotron heating startup system, design 0-99330  
hyperthermia, deep local, induction by US and EM fields, problems and choices 0-94283  
hyperthermia, localised, comparison of EM and US diathermy 0-104725  
hyperthermia in tissue-like substances, EM and US induction 0-98012  
ionsphere, heating by powerful radio emission with random modulation of carrier freq. 0-109310  
labelled microspheres, localised embedding by microwave heating of tissues of hypothermic dogs 0-61640  
microstrip antenna for biomedical applications 0-89826  
microstrip slot radiator for medical appls. 0-108994  
microwave antenna, invasive, for locally-induced hyperthermia for cancer therapy 0-67193  
microwave diathermy direct-contact circular aperture applicator with corrugated flange, design 0-67190  
microwave heating combined with radiation therapy, skin and tumor thermal enhancement ratios 0-67192  
microwave heating with mass transfer using Luikov's system equations 0-106715  
microwave hyperthermia, localised, biomedical devices 0-104724  
microwave power absorption differences between normal and malignant tissue 0-104640  
neck node metastases, effectiveness of microwave hyperthermia combined with ionising radiation 0-94307  
skin, pig, combined effects of X-irrad. and microwave heating 0-94290  
skin, pig, response to combined X-irrad. and microwave heating 0-61653  
steel, C, hardened by HF current, mech. testing method 0-61053  
tissue-equivalent medium, heating patterns produced by 434 MHz Erbrotherm UHF<sup>99</sup> 0-98013  
tumours, solid, destruction by RF heating 0-61637  
vasodilation, peripheral, induced in squirrel monkeys by microwaves 0-104682  
water, complex permittivity meas. and microwave heating for specific purities and salt. soln. 0-60480  
Fe-Ni-Mn, Invar, collapse and thermal effects, Mossbauer study 0-100624  
Si monocystal peripheral fusion channelling under HF heating (*Russian*) 0-59627  
Si solar cells, junction formation techniques using spray-on polymer dopants, cost effective, high throughput 0-94014

# radiofrequency interference

*see also atmospheric; whistlers*  
atmospheric noise data for tropical regions 0-61875  
ground wave atmospherics generated by lightning return strokes, initial peaks, model 0-61876  
isotropic RF electric/magnetic field strength meter, design 0-82751  
nuclear power plant equipment electromagnetic interference and RFI effects 0-57880  
thermal noise, zero point energy noise term presence 0-68213  
tropospheric effects on radio communication, book 0-62400

# radiofrequency spectra of diatomic inorganic molecules *see radiofrequency and microwave spectra of diatomic inorganic molecules*

# radiofrequency spectra of inorganic solids

*see also nuclear magnetic resonance; paramagnetic resonance*  
crystals, NMR quadrupolar effects, RF energy absorpt., relaxation times (*Russian*) 0-71235  
CrBr<sub>3</sub>, HF spectra, susceptibility, spin waves in domain walls (*Russian*) 0-80909

# radiofrequency spectra of organic molecules and substances *see radiofrequency and microwave spectra of organic molecules and substances*

# radiofrequency spectra of polyatomic inorganic molecules *see radiofrequency and microwave spectra of polyatomic inorganic molecules*

# radiofrequency spectrometers

*see also magnetic resonance spectrometers*  
NMR radio spectrometers, meas. of field uniformities in gap of precision magnets 0-105683  
NMR radiospectrometers, calc. of optimal configuration of shims 0-73398  
NMR spectrometers, SQUID-based, sensitivity limit 0-98961  
RE-1306 radiospectrometer for crystals obs., using LF modulation of magnetic field 0-57350  
RYa-2308 radiospectrometer, attachment for obs. of DNMR in <sup>31</sup>P 0-98957

# radiofrequency spectroscopy

*see also magnetic resonance spectroscopy; nuclear magnetic resonance; radiofrequency spectrometers*  
double-quantum saturation spectroscopy, laser and RF, appl. to H 0-77880  
inductively coupled Ar plasma spectroscopy, RF excited, for diatomic mol. spectra 0-86358  
time domain spectroscopy of dielectrics, survey 0-68212  
Ar-acetylene van der Waals molecule, radiofreq. spectroscopy and Stark effect meas., equilb. struct. and props. 0-91543  
Hg ions, relaxation two constants meas. of optically pumped stored Hg ions 0-106287

# radiofrequency sputtering

CuInSe<sub>2</sub> thin film fabrication for solar cell apps. 0-100786  
high-rate vapour quenching techniques and use in amorphous phase prep. 0-80977  
Josephson junction, fabricated by RF plasma oxidation, IV characts. (*Japanese*) 0-84564  
Langmuir probe technique, plasma characts. in sputtering 0-80929  
magnetic bubble materials, props. and preparation models, review (*Rumanian*) 0-93149  
permalloy films, O effects on mag. and elec. props. 0-100603  
piezoelectric gas admission valves, discharge suppression 0-100110  
thin film optical circuit fabrication using CO<sub>2</sub> laser 0-99881  
Al, magnetron sputtering in Ar and Ar/O<sub>2</sub> mixtures, discharge characts. 0-89145  
Al metallisation for VLSI 0-66429  
Al, planar magnetron sputtering, H<sub>2</sub> effect on Ar discharge 0-80970  
Al-Cu alloy metallisation sputter deposition for VLSI 0-66429  
Al-Si alloy metallisation sputter deposition for VLSI 0-66429  
Al-Si-Cu alloy metallisation sputter deposition for VLSI 0-66429  
Al-Si-Mg alloy metallisation sputter deposition for VLSI 0-66429  
AlN, piezoelectric film, low temp. growth by RF reactive planar magnetron sputtering method 0-76175

# radiofrequency sputtering continued

Au-Ti<sub>0.3</sub>W<sub>0.7</sub>, thermal annealing study of metallisation on Si 0-80134  
BaFe<sub>2</sub>O<sub>4</sub> amorphous film, prep. by RF sputtering, crystallisation 0-76183  
BaPb<sub>1-x</sub>Bi<sub>x</sub>O<sub>3</sub>, superconducting thin films, RF sputtering prep. 0-76181  
Ba,Sr<sub>1-x</sub>Ti<sub>x</sub>O<sub>3</sub>, ferroelec. film, heteroepitaxial growth in cathode sputtering 0-93486  
CuInSe<sub>2</sub> thin films for solar cells, radiofrequency sputtering technique, elec. props. 0-93487  
Gd-Co based amorphous sputtered films, microstruct. variability and mag. anisotropy, implanted ion effects 0-88459  
Ge, black, solar selective absorber characterisation 0-80112  
Hg<sub>0.74</sub>Cd<sub>0.25</sub>Te thin film deposition on Si substrates by RF triode-sputtering, large-area photodetector arrays 0-80965  
In<sub>2</sub>O<sub>3</sub>:Sn, RF magnetron sputtered film, elec. and optical props. 0-104065  
InSb<sub>1-x</sub>Bi<sub>x</sub>, multitarget RF sputtering, metastable phase, conductivity transition 0-76178  
Nb,Ge(Si), RF sputtered films, amorphous atomic scale struct. 0-84064  
Si, amorphous, prep. by reactive RF sputtering in Ar-silane mixtures, undoped, n-type and p-type targets 0-76182  
Si, amorphous co-sputtered doped, photovoltaic material appl. 0-93488  
Si, amorphous films, RF sputtering prep. at high Ar press., props. obs. 0-80418  
Si, amorphous layers, RF-sputtered on sapphire, crystallisation by CW ion laser annealing 0-80109  
Si films, RF sputtered, Ar conc. as function of operation frequency and discharge pressure 0-65393  
Si:F, amorphous alloys, RF sputtering prep. in SiF<sub>4</sub>-Ar gas mixture, spectra 0-80772  
Si:H, amorphous, sputtered Schottky barrier solar cells, conduction mechanism 0-104506  
SiO<sub>2</sub> films sputtered in H-Ar mixed gas, enhanced step coverage 0-75470  
ZnO sputtered films, undoped and Ga doped, props. rel. to deposition conditions 0-107935  
ZnO/Si using magnetron discharge sputtering, acoustoelectric device apps. 0-80332  
ZnO-Cu<sub>2</sub>O heterojunction solar cells, prop. by RF sputtering 0-93945

# radiogalaxies *see galaxies; radiosources (astronomical)*

# radiogoniometers *see goniometers*

# radiographs (x-ray photography) *see radiography*

# radiography

*see also electrophotography; neutron radiography; nondestructive testing; radioisotope scanning and imaging; scanning radiography*  
alloys, segregating phases identification, single crystals, radiographs computer calc. 0-84934  
angiocardiology, digital multiprocessor system 0-94362  
backscatter X-ray technique, medical apps. 0-98096  
bone, mineral content, coherent scatt. of photons 0-67238  
bone structure, anal. by X-ray pictures (*German*) 0-89828  
chest photofluorograms, computer anal. and appl. to automated screening 0-72282  
chest radiograms, rib image recognition using octagonal distance transformation of digitised binary pictures 0-89842  
chest X-ray automated anal. 0-98098  
cineangiocardiology, accuracy of ventricular models and localisation of contraction anomalies 0-89845  
cineangiograms, computerised anal. system 0-72284  
cineangiography, automatic detect. of apex of heart 0-89847  
cineangiography, left ventricular contour segmentation from anatomical landmark trajectories and its application to wall motion analysis 0-94363  
cineangiocardiology of left ventricle, automatic processing and cardiac function display techniques (*Japanese*) 0-72311  
coded aperture imaging: the modulation transfer function for uniformly redundant arrays 0-99019  
coded aperture imaging, review 0-101914  
collimators, semi-automatic and automatic, manufactured by Medisor Works 0-85475  
computed, low-dose X-ray imaging system 0-98092  
computerised image smoothing and edge enhancement 0-109015  
contour extraction (*Japanese*) 0-81702  
couch-cover, heatable, use in X-ray exams. (*German*) 0-104751  
dental patients, X-ray exposure obs. 0-104761  
diagnostic, analytical stereo system 0-67231  
diamond, synthetic monocrystals, inclusions phase comp., radiographic method 0-100978  
dose distribution calculation method for bone- and lung-equivalent material (*German*) 0-61704  
dose reduction in medical diagnosis 0-98087  
doses from X-ray units used outside radiology 0-89856  
double-contrast, rel. to endoscopy in upper gastrointestinal tract haemorrhage 0-98063  
double-contrast technique for individual small intestine sections (*German*) 0-61694  
electron microscope autoradiography of isolated mols. 0-85564  
electronic recording of X-ray images 0-62815  
endocardium motion during contraction, anal. method 0-109072  
equipment, computer-assisted quality assurance 0-89838  
equipment, state of the art 0-81688  
femoral neck fractures, meas. of fissure, X-ray picture anal. (*Croatian*) 0-109023  
film development by machine, risk of faults (*German*) 0-90972  
film/intensifying screen system, MTF and Wiener spectrum, film and screen quality effect (*German*) 0-73560  
film/ZZ (*German*) 0-73559  
films, selected, response to <sup>14</sup>C-β-radiation 0-90937  
finger doses received by radiologists during Chiba needle percutaneous cholangiography 0-81737  
flashing tomosynthesis 0-67243  
flaw detection, correction of shadow images 0-89456  
flaw dimensions in direction of irradiation determ. from radiographs with aid of defectometer 0-71863  
fluoroscopic examinations, multi-image camera for spot radiography 0-109020  
free-focus, using conventional films, exposures in a simulated clinical study 0-89835  
gamma ray source, choice for welded joint monitoring 0-104396  
gastric X-ray image using Ba, feature point extraction method 0-101259



**radiography continued**

- granularity of screen-film systems, assessment by entropy method 0-98070  
 Hiroshima mass radiologic gastric surveys, examinees' doses 0-89858  
 history, X-ray engineering, development in the operating theatre 0-101703  
 holographic 3-D synthesis of X-ray pictures 0-67245  
 holographic methods of 3-D representation from no. of plane images 0-67244  
 holography applications 0-67242  
 image analysis by LEITZ-TAS with process computer 0-68773  
 image computer-controlled subtraction procedures 0-109014  
 image intensifier noise evaluation, digital method 0-98097  
 image quality, effect of inadequate screen-film contact (*German*) 0-61057  
 image quality in photon imaging 0-81687  
 image quantitative analysis by TV image analyser 0-109008  
 image receptor, large area, with electrophoretic display 0-98091  
 image segmentation and texture unit cell size determ. 0-95817  
 image storing equipment of Medisor Works 0-85476  
 image understanding systems, seminar, San Diego, CA, USA (Aug. 79) 0-94918  
 industrial, discontinuous registration using profile analysis and piecewise correlation techniques 0-102645  
 inspection algorithm speedup by array processor 0-108659  
 intensifying screen, role of reflective layer 0-62816  
 intervertebral joints, painful, meas. of movement by biplanar radiography 0-98079  
 intravenous angiography, digital video subtraction system 0-98089  
 intravenous angiography using computerised fluoroscopy 0-81689  
 ionography, sensitivity and edge enhancement determ., theory and expt. 0-89833  
 laser fusion targets, X-ray microradiographs, improved image analysis techniques 0-79562  
 left ventricle dynamic geometry in intact unanaesthetised man, midwall motion 0-85491  
 left ventricular localised wall motion abnormality assessment, usefulness of quantitative parameters 0-89848  
 left ventricular wall motion anal., externally referenced polar coord. system 0-89846  
 lung structure visibility and sharpness at 90, 140 and 350 kV 0-98124  
 lung volume measurement from supine portable chest radiographs 0-81703  
 magnification angiography, usefulness in the field of pneumology 0-89829  
 mammography, absorbed dose evaluation, Monte Carlo simulation studies 0-98143  
 mammography, model to analyse radiographic factors 0-76828  
 mammography, simulation of X-ray spectra 0-76826  
 medical diagnosis, information storage requirements 0-98086  
 medical imaging, conference, San Diego, USA (Aug. 1979) 0-94919  
 medical imaging overview 0-98082  
 medical imaging system evaluation by contrast-detail-dose analysis 0-98140  
 medical imaging system evaluation using contrast-detail-dose anal. 0-98108  
 metal fatigue crack detection using nondestructive evaluation (NDE) methods 0-71826  
 microfocus projection, scattering effect on contrast 0-100973  
 microphotodensitometry in traumatology and orthopaedic surgery (*Croatian*) 0-109022  
 motor-tilted diagnostic examination device Model UV-5B 0-85479  
 mucociliary tracheal clearance vel., radiological method for determ. 0-104727  
 multispectral X-ray imaging, nonlinear techniques 0-72293  
 optical fibre preform core diameter and Ge doping profile meas., X-ray nondestructive method 0-64231  
 pancreas, scintigraphy rel. to endoscopic retrograde parenchymography (*Japanese*) 0-81725  
 penetrometer cassette, multiple exposure, for meas. of effective kilovoltage of diagnostic X-ray beams 0-61662  
 percutaneous cricothyroid bronchography (*Dutch*) 0-85471  
 photographic images, quantitative anal. of autoradiographic image intensification using Thioarea-<sup>35</sup>S 0-90343  
 productivity of radiographic inspection method 0-71861  
 projection radiography in medicine, future trends 0-98083  
 receiver operating characteristics curves and their use in diagnostics (*German*) 0-98109  
 regional left ventricular wall motion in coronary heart disease 0-85490  
 RMS focal spot, validity considerations 0-81691  
 rotating disk device for slit radiography of the chest 0-98116  
 scatter to primary radiation ratio variation obs. 0-81722  
 scattered radiation grids, method for testing 0-81717  
 scoliotic spine, anal. of changes using 3D technique 0-94346  
 Shroud of Turin, scientific investigation 0-87576  
 signals and relationship 0-95808  
 skeletal diagnostics, direct magnification, exposure technique and timing 0-104747  
 skull, struct. changes due to Recklinghausen's disease, X-ray and nuclear medicine diagnosis (*German*) 0-76831  
 small intestine, babies, X-ray exam. technique 0-104739  
 spot-camera of Medisor Works 0-85477  
 steel, austenitic stainless, butt welds, US exam., comparison with radiographic techniques 0-93710  
 steel, N determ. by track autoradiography 0-100979  
 steel, radiography with the 25000 R/min Linac 0-97656  
 steel, tempered martensitic, type AISI 4140, role of C in embrittlement phenomena 0-93652  
 stereoscopic image evaluating device, Medisor Model SZRK 0-85478  
 stereoscopic X-ray unit for medical diagnostic sets 0-85467  
 stomach examination, quality improvement by use of fine-focus tubes 0-85468  
 Super Rotalix Ceramic, new type of X-ray tube 0-104749  
 testing equipment, device characts. (*German*) 0-76438  
 texture, multicomponent axial, quantitative evaluation 0-85100  
 three-dimensional imaging 0-85486  
 tibia, human, simplified method of radiographic anal. of its cross-section, anthropometric correls. 0-89827  
 tomogram reconstruction by holographic methods 0-67246  
 video images, enhancement 0-94353  
 video subtraction procedures, computer-controlled 0-98102  
 videodensitometry in angiography 0-104745

**radiography continued**

- welded joint, radiographic inspection, standardization of sensitivity and flaw size 0-89455  
 welded joint inspection by X-ray TV intrascopy, photographic recording of images 0-86485  
 welded joints, radiographic inspection, real flaws detectability evaluation 0-81266  
 welds and castings, differential method of balancing out thickness-variation effects in radiography 0-66748  
 Wisconsin mammographic kVp cassettes, evaluation of spectral response 0-81715  
 X-ray camera attachment for aimed investigation of fractures 0-85102  
 X-ray tubes, meas. of focal spot size 0-89831  
 xeromammography, image quality 0-89834  
 xeroradiography, sensitivity and edge enhancement determ., theory and expt. 0-89833  
 Al-Cu, type 1100, synchrotron radiation microradiography 0-85121  
 Al-Cu-Mn, type 2219, synchrotron radiation microradiography 0-85121  
 Ba<sub>2</sub>SiO<sub>4</sub>Br<sub>2</sub>·Eu, blue emitting X-ray luminescent material for intensifying screens (*French*) 0-66260  
 Cu-Al (14.3 wt.%), <sup>110</sup>Ag diffusion in  $\beta/\gamma_2$  interphase boundary 0-79989  
 N determination by track autoradiography 0-100979  
 PbS-base photodetectors, proton radiography 0-104388

**radioisotope scanning and imaging**

- see also computerised tomography; scanning radiography*  
 abscess scanning, comparison of <sup>111</sup>In-labelled agents 0-94328  
 adrenal scintigraphy with <sup>131</sup>I-19-iodocholesterol, Cushing's syndrome diagnosis 0-72289  
 Anger camera/computer system using seven pinhole collimator for myocardial perfusion tomography 0-61663  
 angiocardigrams, image enhancement and left ventricular contour extraction techniques appl. 0-72283  
 angiography, gated, use of computer-generated functional images to define ventricular boundaries 0-85487  
 angiography of the left ventricle using the first-pass technique (*German*) 0-109019  
 angiography technique for assessment of regional wall motion abnormalities 0-85488  
 autoradiograms of serial sections, preparation for electron microscopy 0-67312  
 biofoal diverging collimator for equilibrium radionuclide ventriculography 0-72310  
 blood flow, regional, assessment by intravenous injection of <sup>99m</sup>Tc pertechnetate 0-104732  
 bone, diffuse alterations, quantitative assessment of <sup>99m</sup>Tc-MDP scans 0-72287  
 bone, healing fracture, blood flow rel. to <sup>85</sup>Sr uptake 0-72187  
 bone, normal, uptake of bone-seeking radioisotopes rel. to blood flow 0-94320  
 bone, X-irradiated, changes in <sup>99m</sup>Tc pyrophosphate imaging 0-72239  
 bone blood flow, meas. with a <sup>133</sup>Xe washout method 0-72288  
 bone fracture healing, significance of scintigraphy (*German*) 0-76833  
 bone revascularisation processes study method, local blood flow dynamic anal. using <sup>85</sup>Sr 0-81684  
 bone-scan interpretation, implications of skeletal blood flow 0-72199  
 brain, imaging, comparative study with  $\gamma$ -camera, single-photon emission CT, and transmission CT 0-109004  
 brain angioscintigraphy in posterior view, clinical value 0-72290  
 brain diagnosis, comparative study of radionuclides and computerised tomography 0-72320  
 brain lesions, compensative value of <sup>99m</sup>Tc labelled DTPA and MDP (*Japanese*) 0-67235  
 bronchoscopic tumour localisation, small radiation detector probes, scintillation and semiconductor detectors 0-61676  
 camera aperture for data collection optimisation 0-67221  
 cardiac blood pool, ECG-gated emission computerised tomography 0-98117  
 cardiac function and anatomy evaluation, complementary role of echocardiography and radionuclide imaging, book contrib. 0-101241  
 cardiac imaging, ECG-gated, motion phantom for computerised tomography 0-98115  
 cardiac nuclear medicine for clinicians, book 0-98765  
 cardiac nuclear medicine instrumentation, review, book contrib. 0-101260  
 cardiac scintigrams, time gated, analysis by digital boundary detect. techniques 0-98081  
 cardiac scintigraphic image handling using microprocessor system 0-85489  
 cardiac shunt detection with the short-lived radioactive gases 0-94357  
 cardiac trauma evaluation 0-94361  
 cardiac US and nuclear medicine, complementary roles 0-98051  
 cardiology, beat-by-beat validation of ECG gating [nuclear medicine] 0-98071  
 cardiology, nuclear, automated chest parsing algorithm 0-61678  
 cardiology, performance characts. of a commercial ECG gate 0-98073  
 cardiology, sequential meas. of ventricular vols. and cardiac output 0-94319  
 cardiovascular nuclear medicine, an overview 0-85480  
 cardiovascular nuclear medicine, instrumentation and data processing, ventricular function evaluation 0-85481  
 cardiovascular shunts, detection and quantitation with commonly available radioisotopes 0-94356  
 cinepneumography, flow-vol. imaging of the respiratory cycle 0-94343  
 clinical realisation and engineering pot. 0-98084  
 coded-aperture imaging of the heart, improved aperture 0-98072  
 computerised tomographic section, synthesis and enhancement 0-109003  
 computer software package for internal dose calc. 0-98139  
 computerised axial tomography from multiple  $\gamma$ -camera views using freq. filtering 0-94321  
 computerised tomography, double-tracer, multiple-organ, transaxial, radiotracer distrib. localisation and characterisation 0-98128  
 computerised tomography, positron emission, crystal size optimisation 0-61681  
 computerised tomography, positron emission, data acquisition and processing electronics 0-61690  
 computerised tomography, positron emission CT device with continuously rotating detector ring 0-81697  
 computerised tomography, single photon emission, review 0-81698  
 computerised tomography, single-photon, physical attributes 0-109007  
 computerised tomography, single-photon emission, imaging capabilities of Ge camera 0-61668

# radioisotope scanning and imaging continued

conference, Detroit, USA (June 1980) 0-105418  
data collection station, based on autonomous CAMAC crate 0-61689  
diagnostic techniques in nuclear medicine, review, book contrib. 0-72322  
digital image change detection 0-102637  
digital images, math. models and physiological parameters 0-98107  
dynamic scintigraphy with high temporal resolution 0-94322  
ear middle, and sinuses, ventilation and clearance using  $^{133}\text{Xe}$  0-98075  
elementary particle interactions, radiological imaging appls. 0-61675  
embryo, radiation absorbed dose estimates from some nuclear medicine procedures 0-104760  
European nuclear medicine, present status and future trends 0-94331  
Ewing's sarcoma, place of bone scanning 0-72308  
films for nuclear medicine, sensitometry 0-72292  
focal-plane tomography, image reconstruction using digital computer 0-61674  
gamma camera visual outcome units comparison, use of MTF 0-94323  
gamma emitting organs, 2 and 3-dimens. digital Fourier reconstruction 0-101705  
gated blood pool scan, radioisotope evaluation of ventricular performance 0-85483  
gated cardiac scintigram anal., digital boundary detect. techniques 0-98106  
graphic code generation for black and white scintigrams (French) 0-104743  
heart, equilibrium left ventricular ejection fraction determ., background noise estimation 0-94365  
hepatic metastases,  $\gamma$ -scan accuracy for detect., comparative study with grey scale ultrasonography (French) 0-104741  
hepatobiliary scintigraphy, characts. of  $^{99\text{m}}\text{Tc}$ -E-HIDA (Japanese) 0-81729  
image processing in nuclear medicine, review 0-81694  
image understanding systems, seminar, San Diego, CA, USA (Aug. 79) 0-94918  
instrumentation, recent developments 0-81692  
intracranial radiolabelled particulate imaging 0-94360  
intrahepatic lithiasis detection, sequential scintiphotography with  $^{99\text{m}}\text{Tc}$  pyridoxylidene-glutamate 0-72309  
intravascular radioactive tracers, calc. of residence time distrib. in fields of external registration 0-72291  
kidney,  $^{99\text{m}}\text{Tc}$  methylene diphosphonate, immediate renal imaging and renography, clinical evaluation 0-98126  
Laguerre functions, appl. to washout curves 0-81521  
left ventricle, 3D image expression 0-104731  
left ventricular edges detect. methods 0-98132  
left ventricular function, radioisotope evaluation with nonimaging probes 0-85484  
left ventricular function assessment using radionuclide techniques, technical considerations, review, book contrib. 0-101261  
left ventricular function evaluation by myocardial scintigraphy and radionuclide angiocardiology (Japanese) 0-81724  
leucocytes, radioactive-labelled, appl. for proof of inflammations 0-67218  
liquid-scintillation vial system, biphasic, for radiometry, modifications 0-101253  
liver, gamma-camera image improvement using physiological gating mechanism 0-98065  
lung, Bayer map evaluation in  $^{57}\text{Co}$ -bleomycin scintigraphy (Japanese) 0-72319  
lung, estimates of radiation absorbed doses from radionuclides 0-101269  
lymphography using  $^{99\text{m}}\text{Tc}$ -MDP (Japanese) 0-94352  
medical imaging, conference, San Diego, USA (Aug. 1979) 0-94919  
medical imaging overview 0-98082  
microprocessor systems for data acquisition, image processing, RIA anal., patient data retrieval 0-61670  
mobile nuclear medical instrumentation, review 0-101262  
multidimensional space and time signal processing in biology and medicine 0-85493  
myocardial  $^{201}\text{Tl}$  scintigram anal., nonredundant coded aperture tomographic method 0-94364  
myocardial imaging with  $^{201}\text{Tl}$ , subtraction imaging using  $^{201}\text{TlCl}$  and  $^{99\text{m}}\text{TcO}_4^-$  0-72318  
myocardial infarction, acute, comparison of  $^{99\text{m}}\text{Tc}$  pyrophosphate with  $^{99\text{m}}\text{Tc}$  hydroxymethylene diphosphonate 0-94342  
myocardial infarcts, acute modified  $^{99\text{m}}\text{Tc}$  heparin for imaging, dog expts. 0-81733  
myocardial perfusion imaging, quantitative aspects, review 0-94358  
myocardial perfusion imaging with  $^{201}\text{Tl}$ , single photon emission computerised tomography (Japanese) 0-98114  
myocardial uptake of  $^{201}\text{Tl}$ , correl. with local perfusion, dog expts. (French) 0-104740  
myocardium, transverse computerised axial tomography with  $^{201}\text{Tl}$  0-67222  
neoplasm localisation with radionuclides, review 0-67215  
organ blood flow measurements, effect of instantaneous partition coeff. of  $\text{Xe}$  0-101256  
osteomyelitis, suspected, in children, value of radioisotope bone scanning 0-67216  
pancreas, multiplane tomographic imaging 0-98076  
pancreas, scintigraphy rel. to endoscopic retrograde parenchymography (Japanese) 0-81725  
parasternal lymphoscintigraphy, radiation treatment planning implications, breast cancer 0-72299  
parathyroid, possible imaging with  $^{67}\text{Ga}$  and other Al analogues 0-101252  
phlebography, appl. to lower extremity venous thrombosis 0-94330  
physiologic tomography, noninvasive meas. of myocardial metabolism, blood flow and function 0-104730  
physiological compartment tracer flow modelling and digital imaging 0-101257  
pinhole and continuous projections, limited angle 3-D reconstruction 0-61667  
positron computerised tomography (Japanese) 0-94347  
positron emission computed tomograph, POSITOLGICA 0-104753  
positron emission computerised tomography, 3-D image reconstruction, Fourier deconvolution method 0-61669  
positron emission-computed tomography, multi-slice, design criteria, shielding 0-61673  
positron imaging, positron sensitive detectors 0-61687  
positron ring camera scanning and an exact subdivision of the Radon transform 0-81721

# radioisotope scanning and imaging continued

positron tomograph, Donner 280-crystal, data acquisition, image reconstruct. and display 0-61671  
precision computer display techniques 0-98100  
precision computer display techniques in nuclear medicine 0-109011  
proportional chamber, multiwire, low energy radionuclide distrib. 0-61679  
pulmonary lesions evaluation, comparison of  $^{67}\text{Ga}$ -citrate,  $^{111}\text{In}$ -bleomycin and  $^{99\text{m}}\text{Tc}$ -citrate 0-94327  
pyrophosphate myocardial imaging, review 0-94359  
quantitation of infarct size using radionuclides 0-85492  
rectilinear scanner, multichannel analyser interface 0-101254  
renal uptake measurements using  $^{197}\text{HgCl}_2$ , single tracer method for background subtraction 0-67217  
renography, comparative study in hydration and dehydration (Japanese) 0-81726  
sacroiliac scintigraphy,  $^{99\text{m}}\text{Tc}$ -EHDP uptake quantification, comparative study 0-94326  
scintillation camera collimator image form. 0-89844  
scintillation camera field uniformity, global and local, statistical features 0-61677  
semiconductor gamma-cameras in nuclear medicine 0-81693  
skin, perfusion, quantitative meas. with  $^{133}\text{Xe}$  0-81707  
skull, struct. changes due to Recklinghausen's disease, X-ray and nuclear medicine diagnosis (German) 0-76831  
spleen scanning in humans using  $^{99\text{m}}\text{Tc}$ -labelled erythrocytes 0-67230  
stress  $^{201}\text{Tl}$  scintigram anal. methods comparison 0-89851  
subtraction scintigraphy with  $^{67}\text{Ga}$ -citrate and  $^{99\text{m}}\text{Tc}$ -colloid in the diagnosis of intrahepatic masses 0-104752  
thyroid, accumulation curve of radioiodine and its role in diagnostics (Hungarian) 0-94341  
thyroid  $^{131}\text{I}$  uptake determination (Hungarian) 0-94339  
thyroid scintigraphy, clinical comparative study of  $^{99\text{m}}\text{TcO}_4^-$  and  $^{123}\text{I}$ -Na (Japanese) 0-81728  
tomograph, positron emission, ring detector, attenuation, scatt. radiation and random coincidences 0-61684  
tomography, computerised, longitudinal, bilateral collimator, gamma camera and minicomputer 0-61666  
tomography, emission computed, Compton scatter correction, integral transport method 0-61683  
tomography, Fourier multi-aperture 0-61685  
tomography, positron emission, CSF detector 0-61688  
tomography, single photon emission, camera configs., performance anal. 0-61686  
tomography, single photon emission, nuclear medicine computer interfaced to Anger multiplane scanner 0-61665  
tomography, X-ray fluorescence techniques, I distrib. in thyroid gland 0-61664  
tomography simulator, emission computed, design 0-61672  
tumour and organ affinity of  $^{201}\text{Tl}$  0-67234  
tumour concentrating properties studies using  $^{18}\text{F}$ -5-fluorouracil 0-109000  
tumour detection status of  $^{67}\text{Ga}$  0-98074  
tumour scintigraphy by intraarterial injection of  $^{201}\text{TlCl}$  (Japanese) 0-98111  
TV displays, 4 standard types, comparative study 0-109005  
Vena cava, superior, optimum radiation schedule in obstruction treatment, importance of  $^{99\text{m}}\text{Tc}$  scintigrams 0-72334  
venography, lower extremity, recognition of systemic portal shunts 0-94329  
ventricular function monitor, ambulatory, CdTe detector, cardiac ejection fraction meas. 0-61680  
ventricular performance, 1st pass radioisotope assess. 0-85482  
ventriculography, computerised, assessment of LV wall motion and regional kinetics 0-89850  
vertebrae, abnormal accumulations found in the bone scintigram of cancer patients 0-67233  
whole body autoradiography of bumetanide- $^{14}\text{C}$  in dogs by round saw method 0-72399  
NaI(Tl) scintillation cameras, image artifacts and counting losses 0-94345  
 $^{81,82\text{m}}\text{Rb}$  production for positron emission tomography 0-98068

**radioisotope separation** see isotope separation

**radioisotopes**  
see also radioisotope scanning and imaging  
 $^{222}\text{Rn}$  flux through multilayered covers cover U mill tailings 0-95487  
AECL commercial products, contrib. to nuclear medicine and radiation processing 0-81736  
air monitoring systems for radioiodine and inert gases, evaluation 0-95480  
alkali metal radioisotopes, hyperfine spectroscopy, nucl. props. 0-57677  
anodic electrolysis of radioactive isotopes (Hungarian) 0-93765  
artificial, 25 years of use and production in Hungary (Hungarian) 0-94340  
artificial, initial stages of use in Hungary (Hungarian) 0-90643  
biological effects of inhaled radionuclides 0-94288  
biological samples, neutron-activated, radiochem. determ. of short-lived radionuclides 0-109067  
blood-organ transfer kinetics of radioisotopes 0-109044  
bone-seeking, dosimetry, comparative study in man, rhesus monkey, beagle and miniature pig 0-72338  
committed effective dose equivalent conversion factors for intake of selected radionuclides 0-67256  
depositions, shallow, on body surfaces, meas. using M X-rays 0-67223  
detection using accelerators 0-63468  
dosimetric data tables 0-105438  
half-lives measurements for 35 radionuclides 0-83070  
Hungarian development in the use of radioisotopes (Hungarian) 0-90646  
lunar soil samples from Luna 24 and Apollo 16, natural radioactivity meas. 0-67595  
medical application of a compact cyclotron, isotope production (Japanese) 0-104757  
medicine, nuclear, production of useful radioisotopes, Los Alamos Meson Physics Facility 0-67251  
nuclear radwaste geologic disposal, modelling of radionuclide transport and decay products 0-78415  
Pecs University Biophysics Unit, Hungary, 25 years of radioisotope appls. (Hungarian) 0-90647  
production, bremsstrahlung beams rel. to proton beams 0-63424  
production, for medical use, at TRIUMF 0-72325



## radioisotopes continued

- production, remote flow system, connecting target and purification systems 0-69004  
 production using electron accelerators, terms used 0-91347  
 quantum radiation, data handbook 0-94933  
 radiation protection, development in use of radioisotopes in Hungary (Hungarian) 0-90644  
 radioactive transport in the aquatic ecosystem, foodweb model 0-104777  
 resuspended, possible importance of short-term exposure 0-85501  
 review of the development in the use of radioisotopes (Hungarian) 0-90645  
 short-lived, meas., counting statistics 0-58098  
 spectral unfolding method to determine source depth distribution 0-81719  
 ultrasonographers, pot. hazard from previously administered radionuclides 0-98120  
 X-ray characteristics in neutron activation anal. at 14 MeV 0-93827  
<sup>99</sup>Tc emitting radioelements, meas. of weak doses (French) 0-91410  
<sup>26</sup>Al in primordial comet interiors, contrib. to radiogenic melting 0-67659  
 Ba, radioisotopes, at. beam laser spectroscopy, hyperfine struct., nucl. moments and radii 0-57678  
<sup>7</sup>Be production in atm. and transport from Sun, tracer for terrestrial-solar relationship 0-98525  
<sup>10</sup>Be, distrib. in geophysical samples meas. using tandem van de Graaff accelerator 0-61924  
<sup>75</sup>Br, excitation functions for production, pot. nuclear medicine appls. 0-98135  
<sup>14</sup>C β-rays, biological hazards, cell killing effects, E. coli expts. 0-89805  
<sup>14</sup>C dating of coastal marine sediments, fossil C effect 0-98308  
<sup>14</sup>C released to atmosphere, dynamic model for estimating radiation dose to world population 0-89852  
 Ca, stable and radioisotopes, hfs, isotope shifts, dye laser saturation spectroscopy, beam expt. 0-58169  
<sup>45</sup>Ca and <sup>32</sup>P determination in biological samples by Cherenkov and liq. scintillation counting 0-98183  
<sup>144</sup>Ce, effects of repeated inhalation exposure of mice to <sup>144</sup>CeO<sub>2</sub> 0-104676  
<sup>144</sup>Ce, inhalation exposed mice, toxicity, dosimetry and <sup>144</sup>Ce retention 0-89874  
<sup>144</sup>Ce repeated inhalation exposure of <sup>144</sup>CeO<sub>2</sub>, retention and dosimetry 0-109034  
<sup>252</sup>Cf, medical appl., fast neutron therapy (Japanese) 0-98112  
<sup>60</sup>Co, distrib. and behaviour in Urazoko Bay sediment 0-97825  
 Cs, liquid effluents, aquatic radiological impact anal., radiocaesium transport in sediment 0-95486  
<sup>134</sup>Cs and <sup>137</sup>Cs at Atlantic nuclear waste disposal site, radionuclide redistribution 0-85309  
<sup>137</sup>Cs, distrib. and behaviour in Urazoko Bay sediment 0-97825  
<sup>137</sup>Cs gynecologic insertions, expt. derived algorithm for computer calc. dose rates 0-101264  
<sup>137</sup>Cs, intake by Bikini Island residents, model using bioassay data 0-109043  
<sup>137</sup>Cs/<sup>134</sup>Cs radioisotopes in seawater, Cs-selective resin determ. 0-94137  
<sup>137</sup>Cs-irradiation, response of pig skin, various schedules of irradiation 0-72237  
<sup>18</sup>F, prep. with an electron linear accelerator, medical and biological appls. 0-98136  
<sup>59</sup>Fe, self-diffusion in Fe-V (Czech) 0-88352  
<sup>68</sup>Ga, new generator, medical appls. 0-76834  
 I, radioactive, air sampling system, separation into gaseous and particulate fractions 0-57962  
<sup>121</sup>I, A=131-2, comparative effects in rat thyroid glands 0-104670  
<sup>121</sup>I, prep. from gaseous TeF<sub>6</sub>, nuclear medicine appl. (French) 0-98137  
<sup>121</sup>I prod. from <sup>121</sup>(p,n)<sup>121</sup>Xe, <sup>121</sup>I, at 58 MeV 0-94369  
<sup>121</sup>I production from <sup>121</sup>Xe formed in spallation reactions by 660 MeV protons, medical appls. 0-85494  
<sup>121</sup>I, production in LASL radiochemistry hot cells 0-72326  
<sup>121</sup>I, determ. of exposure rate constant using a scintillation detector 0-89863  
<sup>121</sup>I in the thyroid, 2-probe meas. method 0-81718  
<sup>121</sup>I, intramol. effects of decay in o-iodotyrosine 0-108973  
<sup>121</sup>I, intranuclear atoms not bound to DNA, radiotoxicity 0-104655  
<sup>121</sup>I photons, absorbed fractions in the thyroid 0-109032  
<sup>121</sup>I, release in autoclave sterilization of radioimmunoassay kit (Japanese) 0-81727  
<sup>121</sup>I seed implants in prostatic cancer, preoperative extended field radiation 0-72303  
<sup>121</sup>I, shielding of (Japanese) 0-63404  
<sup>121</sup>I, variation of γ-counting efficiency with sample composition 0-83238  
<sup>121</sup>I photons, absorbed fractions in the thyroid 0-109032  
<sup>121</sup>I radioactive waste, fixation with Portland cement, radiation stability tests 0-83200  
<sup>129</sup>I, tandem accelerator mass spectrometry 0-86494  
<sup>131</sup>I, adsorption by minerals 0-83203  
<sup>131</sup>I, age-related radiosensitivity obs. of guinea pig thyroid glands 0-104671  
<sup>131</sup>I, behaviour during rinsing in in-pile loop after fission product release expt. 0-73879  
<sup>131</sup>I concentrations in air, milk and antelope thyroids in southeastern Idaho 0-89871  
<sup>131</sup>I, estimation of γ dose to gastric wall after administration of isotope (Japanese) 0-98141  
<sup>131</sup>I manipulated in syringes, radiation exposure obs. 0-67252  
<sup>131</sup>I produced radiation, low-dose, somatic mutations induction in Tradescantia 0-72266  
<sup>131</sup>I treated patients, monitoring of I excretions and used materials 0-89873  
<sup>85</sup>Kr atmospheric concentration in North and South Hemisphere 0-93756  
<sup>52m</sup>Mn, new short-lived, generator-produced radionuclide, positron tomography appl. 0-109006  
<sup>15</sup>N labelled NH<sub>3</sub> production for medical appl. 0-72327  
<sup>22</sup>Na injection, testis mass loss obs., mouse 0-67156  
<sup>22</sup>Na injection or X-irrad. of mice, sperm count reduction and abnormal sperm increase 0-108961  
<sup>32</sup>P and <sup>45</sup>Ca determination in biological samples by Cherenkov and liq. scintillation counting 0-98183  
 Pu dose to lung and bone from contaminated soils, statistical uncertainties 0-109028  
<sup>239</sup>Pu, A=239, 240, distrib. of fallout Pu in southern Finns 0-109045  
<sup>239</sup>Pu, bioaccumulation in inland water and marine algae (German) 0-108820

## radioisotopes continued

- <sup>239</sup>Pu, comparison of early mortality in baboons and dogs after inhalation of <sup>239</sup>PuO<sub>2</sub> 0-108977  
<sup>239</sup>Pu, distrib. and behaviour in Urazoko Bay sediment 0-97825  
<sup>239</sup>Pu, inhalation of <sup>239</sup>PuO<sub>2</sub>, by rhesus monkeys, cytogenetic and other biological effects 0-108968  
<sup>239</sup>Pu, nanocurie amounts, lesions in CBA mice 0-81657  
<sup>226</sup>Ra, A=226, 228, content in groundwater of Fall Line aquifers 0-89682  
<sup>226</sup>Ra short lived daughter disequilibrium in a mixed maritime and continental atmosphere 0-108822  
<sup>226</sup>Ra in public water supplies, conc. determ. (German) 0-94138  
<sup>81,82m</sup>Rb production for positron emission tomography 0-98068  
<sup>81</sup>Rb, excitation functions of proton induced nuclear reactions on <sup>85</sup>Rb, medical appls. 0-78286  
<sup>220,223</sup>Rn daughters, 2-count filter method for meas. in air 0-63480  
 Rn and Rn daughters, background concs. in Canadian homes 0-104546  
 Rn and Rn daughters in Howe Caverns, USA, doses to employees and public 0-89859  
 Rn, atmospheric, accumulation in calcite caves 0-104531  
 Rn concentration in dwellings and influencing factors 0-108832  
 Rn daughter concentrations in different atmospheres 0-85316  
 Rn daughters in atmospheric air, efficiency of HV-70 filters for sampling 0-108827  
 Rn monitoring instrumentation 0-106204  
<sup>211</sup>Rn production by <sup>209</sup>Bi(<sup>7</sup>Li,5n), excitation function 0-95323  
<sup>222</sup>Rn, conc. in air, absolute determ. using cellulose nitrate track detector 0-63492  
<sup>222</sup>Rn, conc. in free air (Hungarian) 0-94128  
<sup>222</sup>Rn concentration in tunnel air, atmospheric press. and precipitation effects (Japanese) 0-97845  
<sup>222</sup>Rn emanation from building materials, plastic α-track detectors study 0-101144  
<sup>222</sup>Rn, props. and behaviour of short lived daughter nuclides in the atmos. (Japanese) 0-72339  
<sup>222</sup>Rn, theoretical, evaluation of emanation under a variety of conditions 0-104545  
<sup>90</sup>Sr concentrations in pronghorn antelope bones near a nuclear fuel reprocessing plant 0-89875  
<sup>95m</sup>Tc, adsorption by minerals 0-83203  
<sup>99m</sup>Tc, beta-decay and dose calcs. 0-91154  
<sup>99m</sup>Tc contamination of laboratory personnel, its degree and routes 0-98147  
<sup>99m</sup>Tc generators, operational assessment by performance indices 0-94332  
<sup>99m</sup>Tc manipulated in syringes, radiation exposure obs. 0-67252  
<sup>201</sup>Tl, transverse computerised axial tomography of the myocardium 0-67222  
<sup>201</sup>Tl, tumour and organ affinity 0-67234  
<sup>203</sup>Tl(p,n)<sup>203</sup>Pb, <sup>201</sup>Tl, yields and excitation functions for Pb radioactivities, medical appls. 0-67249  
 U, determ. of content in dental porcelains and dose to oral mucosa 0-89830  
 U, determ. of content in some Indian coal and flyash samples 0-104547  
<sup>133</sup>X calibration of environmental and personal dosimeters 0-86992  
 Xe whole-body counting and dose determs. 0-89853  
<sup>127</sup>Xe, A=133,135, interference with low-energy meas. systems 0-89872  
<sup>127</sup>Xe, health physics, dose calcs. 0-98142  
<sup>127</sup>Xe charcoal traps, simple leak tests, nuclear medicine appl. 0-104734  
<sup>133</sup>Xe in a plastic catheter, diffusion dynamics obs. 0-79973
- radiology**  
 see also patient diagnosis; patient treatment; radiation therapy; radioisotope scanning and imaging  
 digital image change detection 0-102637  
 elementary particle interactions, radiological imaging appls. 0-61675  
 Gevamat 240 developing machine, constancy testing by test film strips in a radiological practice (German) 0-95206  
 image processing in diagnostic radiology 0-81690  
 liver metastases diagnosis, conf., Brussels, Belgium (Nov.-Dec. 78) 0-82568  
 optical reconstructions from projections via deconvolution 0-63962  
 proton imaging for medical applications 0-98129  
 sequential coherent optical reconstruction from projections using a ROACH filter 0-63961  
 tumour blood flow, meas. by photon activation, <sup>15</sup>O decay technique 0-104755
- radiolysis**  
 cellulose fibre, gamma-irrad., and storage effects on props. (Russian) 0-61121  
 chemical processes induced radiolytically in well defined aqueous systems 0-66823  
 chlorophyll a, cation radical formation by pulse radiolysis, oxidation and demetallation rate consts. 0-61505  
 cholesteric liquid crystals, gamma-ray irrad. effects, dosimetry, thermography appls. (Spanish) 0-92457  
 chromatin from cultured mammalian cells, DNA-protein cross-links formation 0-81655  
 2'-deoxyadenosine in aq. deaerated soln., new radiolysis mechanism 0-81350  
 4,6-dihydroxypyrimidine, aq. soln., reaction with OH, short-lived radicals, ESR 0-101031  
 DNA and other biopolymers 0-67163  
 ethanol, electron solvation, ps laser study 0-101032  
 heterogeneous inanimate systems, radiobiology appl. 0-66824  
 lactate dehydrogenase, O<sub>2</sub> effect in radiolysis obs. 0-72223  
 metalloporphyrin, cation radical formation by pulse radiolysis, oxidation and demetallation rate consts. 0-61505  
 methanol, electron solvation, ps laser study 0-101032  
 PMMA, reactor irrad., growth of macroscopic radiolytic gas bubbles, diffusion model 0-65058  
 potassium antimonyl tartrate, neutral aq. soln., gamma radiolysis 0-101030  
 pulse, fast chemical reactions obs. (Czech) 0-81325  
 pulsed radiolysis, nonlinear radiation-acoustic phenomena 0-79029  
 pyrene solutions, radical ion pairs, pulse radiolysis, time resolved EPR spectra meas. by ODMR of fluoresce. 0-83395  
 α-quartz, electron irrad., defect struct. and radiolysis 0-107321  
 radiation sensitivity, conf., Rome, Italy (Sept. 1978) 0-62368  
 sucrose, single cryst., absorption spectrum of electron traps, pulse radiolysis obs. 0-93369  
 supercrit. hydrocarbons radiolysis, electron reaction rate const./diffusion coeff. ratio 0-101033

# radiolysis continued

- synthetic fuel prod. by direct radiolysis using fusion radiation sources 0-61227
- CO III-EDTA solution, radiolysis by charged particles through  ${}^6\text{Li}(\text{n},\alpha){}^3\text{H}$  reaction 0-93788
- ${}^{13}\text{C}$ , CIDNP, obs. in reactions of organic and inorganic radicals during pulse radiolysis 0-63660
- $\text{H}_2\text{O}$  vapour,  $\text{H}_2$  production by thermoradiation dehydrogenation using nuclear power, kinetic anal. 0-67010
- $(\text{NH}_4)_2\text{SO}_4\cdot\text{MnO}_4\cdot\text{X}$ , X-ray irradiat. damage, optical absorpt. spectra study 0-66246
- $\text{NaOH}:\text{CrO}_2^{2-}(\text{NO}_2^-)$ , electron tunnelling, pulse radiolysis 0-108722
- $\text{NaOH}:\text{Fe}(\text{CN})_6^{3-}$ , electron tunnelling, pulse radiolysis 0-108722
- $\text{Tb}^{3+}$ , aqueous soln., radioluminescence intensity conc. depend. 0-87055

# radiometers

- see also infrared detectors; microwave detectors*
- blackbody for energy calibration of infrared equipment 0-86377
- calibration blackbody, radiation methods, CHT-2R oven (USSR) 0-62722
- cm-wave radiometer, with enhanced long-term stability, for solar radio emission obs. 0-109361
- Fourier transform spectrometer performance, instrumentation for assessment 0-95165
- IR radiometer with pyroelectric radiation receptor 0-101842
- liquid-scintillation vial system, biphasic, for radiometry, modifications 0-101253
- microwave, atmospheric water vapour studies at 22.235 GHz 0-72610
- microwave, microprocessor-based signal processing unit 0-77874
- microwave, rain attenuation measurement at X, K bands appl. 0-68254
- multiband radiometer for field research 0-90250
- multichannel radiometer, programmable, for Earth remote sensing 0-77253
- multipurpose, history of development for thermal-vacuum testing at Johnson Space Center 0-90894
- narrow-field radiometer response in quasi-isotropic atmosphere 0-90345
- neutron, testing techniques standardisation, in Soviet Union 0-99405
- nuclear multichannel, automatic channel separating system (*Russian*) 0-58094
- optical sensor system simulation and evaluation 0-96030
- Pioneer Venus Orbiter radiometer (VORTEX) 0-67504
- Pioneer Venus small probes net flux radiometer experiment 0-67512
- Pioneer Venus Sounder Probe IR radiometer 0-67509
- Pioneer Venus Sounder Probe Solar Flux Radiometer 0-67508
- PP-8 (USSR), monitoring of transmission electron microscope foil thinning by jet electropolishing 0-73525
- satellite IR radiometer, calibration 0-101440
- Seasat scanning multichannel microwave, calibration algorithm development 0-94682
- Seasat scanning multichannel microwave, description and performance 0-94681
- Seasat scanning multichannel microwave antenna pattern corrections 0-94683
- Seasat visible and IR radiometer 0-94687
- spectral radiometer for determ. of solar radiation spectral distrib. for solar cell appls. 0-61369
- spherical radiometer, theoretical anal. 0-62721
- standard apparatus to measure the radiant thermal flux density 0-62674
- tethered float radiometer for US therapy equipment output power meas. 0-104691
- TIROS-N microwave sounder unit for global temp. distribution meas. 0-90265
- UV, Spectroline DM series, UV appl. 0-77854
- X-ray radiometric analyser, appl. of expt. planning 0-61186
- Si radiometer for meas. of synchrotron flux from SURF II storage ring 0-90895
- Si radiometer for storage ring synchrotron radiation 0-86411
- Si ring photodiode reflectometer for cavity reflectance 0-86376
- $\text{SiO}_2$ , fused, filter in wide field-of-view SW radiometer for Earth radiation meas. 0-87473

# radiometry

- see also radiometers*
- atmosphere boundary layer temp. profile determ. from ground-based 60 GHz radiometry (*German*) 0-82097
- atmosphere parameters, retrieval from scanning multichannel microwave radiometer obs. 0-90261
- atmosphere radiances meas. from TIROS-N processing for temp. sounding 0-77133
- atmosphere temperature, impact of satellite sounding data on weather forecasts 0-77028
- broadband, using spectrally selective detectors 0-68255
- cirrostratus clouds, IR emissivity meas. by remote sounding 0-82061
- cloudy atm., long distance meas. by radiometry 0-90196
- combined microwave heating and radiometry methods 0-85465
- Earth's surface in presence of vegetation cover, microwave radiation spectra 0-68239
- fibre lens, gradient index, radiometric props. 0-69481
- fundamental quantities and partial coherence effects 0-77838
- incandescent lamp calibration for spectral irradiance by absolute radiometers 0-102788
- irradiance scales intercomparison, 90 to 250 nm wavelength range 0-98963
- lake ice, microwave radar and radiometric remote sensing meas. 0-85691
- microwave, for determination of cloud atmospheric parameters 0-67435
- microwave brightness temp. distrib. over Bay of Bengal using SAMIR Satellite Microwave Radiometer data at 19 and 22 GHz 0-104980
- MM wave radiometry conducted at Appleton Laboratory 0-67442
- MM wave sensors, conf., London (Apr. 1980) 0-67441
- neutron absorption radiometric testing of materials, review 0-71860
- nuclear materials, safeguards applications of far infrared radiometric techniques for the detection of contraband 0-83156
- nuclear materials safeguards applications of far infrared radiometric techniques for the detection of contraband 0-73925
- ocean surface parameters, retrieval from scanning multichannel microwave radiometer obs. 0-90261
- optical coherence applications, seminar, San Diego, CA, USA (Aug. 1979) 0-77542
- Pacific Ocean, box cores from Ontong-Java Plateau, radiometric obs. 0-61793
- photodiode detector calibration using synchrotron radiation 0-90810
- photophoretic spectroscopy, broadband 0-86469

# radiometry continued

- radiation temperature, reflectivity, emissivity meas. of room temp. materials (*Chinese*) 0-101814
- rain attenuation, radiometric determ. at millimetre wavelengths, multiple-scatt. effects metric determ. at millimetre wavelengths, multiple-scatt. effect 0-90260
- rain attenuation at 10 and 11 GHz, radiometric measurements 0-67397
- rainfall rate detect over ocean and land by spaceborne microwave radiometry 0-101423
- Raman spectra, radiometric correction 0-90899
- remote sounding of high clouds, visible and LR optical props. from lidar and radiometer meas. 0-82060
- sea ice age category differentiation through location and temp. observations using microwaves 0-67380
- seminar, optical radiation meas., San Diego, CA, USA (Aug. 1979) 0-86036
- snow, parameters investigation by radiometry in 3 to 60 mm wavelength region 0-72561
- solar receiver radiative loss and eye hazard evaluation by Net-Radiometer 0-89673
- specular reflection, use for radiation thermometry (*Japanese*) 0-101795
- stratosphere observations with balloons 0-85763
- synchrotron radiation as an absolute standard source 0-90879
- terrestrial surface temperature sensing, emissivity correction for thermal radiation interpretation 0-82092
- Si photodiode internal quantum efficiency basis for absolute radiometric standard 0-86410
- Si, photovoltaic cell, absolute spectral sensitivity calibration, radiometry, photometry (*Chinese*) 0-86367
- p-Si:P semiconductor detector in radiometric inspection problems 0-62819
- U, National Uranium Resource Evaluation (NURE) aerial radiometric survey data interpretation via principal components anal. 0-101438

# radiometry, ultraviolet *see photometry*

# radionavigation

- Loran-C signal, ground wave propag. theory 0-94580
- radio methods, quasi-single freq. Doppler-Faraday technique 0-77128
- satellite solar cell power plant, operating experience 0-94055

# radios *see radio receivers*

# radiosondes

# *see also meteorological instruments*

No entries

# radiosources (astronomical)

- see also BL Lacertae-type objects; pulsars; quasars*
- 0816+526, CD galaxy, classical double source, 4885 MHz obs. 0-109545
- 1308+32, BL Lacertae object, rapid optical outburst, 1980 June to July 0-98733
- 1610-771, radio QSO with steep optical spectrum, obs. 0-94887
- 2033+59, appl. of Clean and Restore technique to Northern Cross radio telescope obs. (*Italian*) 0-98563
- HR 1099, RS Canum Venaticorum type binary, light and colour curve meas. 0-73004
- Abell 2029 galaxy cluster, radio and SAS 3 X-ray obs. 0-82519
- Abell 401, X-ray cluster of galaxies, radio emission distrib. 0-98731
- Abell cluster, lunar occultation obs. at 327 MHz, survey 0-73052
- in Abell clusters of galaxies, spectra and optical identification, SHF obs. 0-98729
- accretion disk model, gas flow above alpha disk 0-62161
- AO 0235, mapping with uncalibrated visibility data, 5011 MHz obs. 0-77295
- R Aquarii, UV, visible and 85 GHz continuum obs. 0-85946
- arc-like source, H radio recombination line obs. of galactic centre 0-82498
- AS 501, compact H II region, OH main-line maser emission obs. 0-67716
- astrometric catalogues 0-105180
- B2 source counts and isotropy of faint sources 0-105374
- B2 sources assoc. with elliptical galaxies, orientation 0-77501
- B 35, bright rimmed molecular cloud, CH obs. 0-62238
- bright galaxy nuclei, optical and radio survey, sample selection and obs. 0-73039
- 5C1 sources, optical identification by photographic photometry and spectra 0-77503
- 3C 10 (Tycho's SNR), distance, Westerborg H I obs. 0-101633
- 3C 111, radio galaxy, obs. at 1.38 cm wavelength with resolutions up to 8" (*Russian*) 0-109558
- 3C 120, radio galaxy, vars. in optical spectrum (*Russian*) 0-90540
- 3C 120, Seyfert galaxy, spectrophotometric obs. of assoc. nebulosity 0-67890
- 3C 120, Seyfert galaxy nuclei, optical variability, UVB obs. 0-73049
- 4C 13.17A, B, in X-ray cluster of galaxies Abell 401, radio emission distrib. 0-98731
- 3C 219, double radio galaxy, high-resolution 0-77500
- 3C 225.0, UHF and EHF obs. of foreground cold diffuse cloud 0-105311
- 3C 236, radio galaxy, 6-49 cm obs. of double source 0-82528
- 3C 273, field, QSO-galaxy group assoc. 0-105385
- 3C 279, interplanetary scintillations and solar wind vel., SHF obs. (*Russian*) 0-77248
- 3C 288, complex extragalactic radio source, radio brightness distrib. model 0-90558
- 4C 29.03, towards M33, H I 21 cm emission/absorpt. obs. 0-62262
- 3C 31, radio galaxy, mag. field struct. in radio jets 0-82526
- 4C 32.69, quasar with radio jet, high resolution radio obs. 0-105375
- 3C 345, quasar, VLBI obs. at 1.67 GHz 0-94885
- 3C 388, galaxy in Abell 643, classical double source, 4885 MHz obs. 0-109545
- 4 C 39.25, compact radio source, search for time-depend. radio fine struct. 0-90552
- 4C 39-08, appl. of Clean and Restore technique to WSRT obs. (*Italian*) 0-98563
- 3C 405 (Cygnus A), radio galaxy, obs. at 1.38 cm wavelength with resolutions up to 8" (*Russian*) 0-109558
- 3C 465, extended radio galaxy, multifrequency UHF and SHF obs. 0-105338
- 4C 47.51, complex radiogalaxy, aperture synthesis obs. 0-94883
- 3C 48, interplanetary scintillations obs. rel. to solar wind plasma irregularities anisotropic struct. 0-67489
- 4C 53.37 (1638+538), tailed radiogalaxy, dual curved jets 0-62265



## radiosources (astronomical) continued

- 3C 58, Crab-type supernova remnant, comparison of optical and radio emission 0-73023  
 3C 84 (Perseus A, NGC 1275), Seyfert galaxy, 5' halo SHF obs. 0-105372  
 3C catalogue faint red QSO candidates, spectrophotometry and red shifts 0-67897  
 3C sources, possible giant radio structure discovery at 11 cm 0-67895  
 4C sources between declinations 20° and 40°, samples 0-73057  
 calibration sources, flux density at 8420 MHz rel. to Virgo A 0-86004  
 Cancer cluster, Westerbork survey at 610 MHz 0-67884  
 RS Canum Venaticorum binary stars, mag. starspot model for photometric and spectroscopic behaviour 0-109488  
 RS Canum Venaticorum stars, H $\alpha$  line variability, visible spectra obs. 0-105277  
 Cassiopeia A, foreground interstellar HCN absorpt. obs. 0-101624  
 Cassiopeia A, secular decrease in 927 MHz flux, radio flux density obs. 0-67840  
 Cassiopeia A, supernova remnant, explanation of secular flattening of radio spectrum 0-101637  
 Cassiopeia A historical records 0-77430  
 Cassiopeiae A, supernova remnant, historical records 0-72792  
 Cassiopeiae A, supernova remnant, mag. field origin 0-85989  
 catalogue of positions, reference sources 0-105176  
 cD and related galaxies in poor clusters, pencil beam obs. of radio emission at 6 cm 0-62293  
 cD galaxies and related objects in poor clusters, 1400 MHz pencil beam obs. 0-62263  
 Centaurus A (NGC 5128), nucleus, radio and X-ray variability model 0-90522  
 Centaurus A (NGC 5128), radio galaxy, obs. at 1.38 cm wavelength with resolutions up to 8" (Russian) 0-109558  
 Cepheus IV star formation region, continuum and recomb. lines, SHF obs. 0-90501  
 Circinus X-1, changes in optical, IR and radio emission 0-67910  
 compact extragalactic radio sources, apparent superluminal motion, models, review 0-77504  
 compact extragalactic sources, anisotropic radio emission model 0-62304  
 compact extragalactic sources, radio spectra interpretation 0-62299  
 compact radio quasars, apparent magnitude-redshift relations for resolved and unresolved sources (Chinese) 0-105380  
 compact synchrotron sources variability, model of knots spontaneous form. in relativistic flows 0-105369  
 3CR sources, quasars and galaxies, optical identification 0-90555  
 Crab Nebula, compact source flux density meas. by interferometer 0-62252  
 Crab Nebula, lunar occultation obs. at decimetre wavelengths 0-62248  
 CTB 1, UHF emission and radio shell of SNR 0-77461  
 CUL sources in ZA catalogue, positional and spectral data, HF obs. 0-86019  
 Cygnus A, radiogalaxy structure at 150 MHz 0-101646  
 Cygnus X, connection with Cygnus X-ray superbubble 0-90575  
 Cygnus X region, far IR survey 0-82538  
 Cygnus X-1, X-ray binary, variable star, SHF obs. 0-73071  
 Cygnus-X region, embedded IR source GL 2636, visible and IR obs. 0-105302  
 double radio sources, hot spots behaviour 0-94882  
 double sources, beam and cloud stability, shear layers, two dims. computations 0-67893  
 double sources, galaxies, evolutionary characts. (Chinese) 0-86007  
 double sources statistical props., asymmetry and components flux ratio 0-67892  
 DR15, galactic H II region, obs. at 408, 1407 and 2695 MHz 0-94881  
 DR 21, HF calibration source, flux density obs. at 8420 MHz 0-86004  
 elliptical galaxies, extended sources, partial synthesis maps at 2.7 and 8.1 GHz 0-105330  
 elliptical galaxies, radio sources orientation rel. to galaxies minor axes 0-82527  
 evolved stars expanding envelopes, CO thermal and maser emission 0-82334  
 extended double sources and central radio cores, symm. 0-86003  
 extended extragalactic double radio sources, expansion speeds from ang. struct. 0-67894  
 extragalactic, 408 MHz obs. of Parkes 2700 MHz survey sources 0-86008  
 extragalactic, method for distance determ. 0-109559  
 extragalactic compact sources with faint components, VHF and SHF obs. 0-90547  
 extragalactic flat spectrum sources, VLBI UHF and SHF obs. 0-90549  
 extragalactic high-latitude sources, search for OH 18 cm absorpt. lines in projected H I clouds 0-67841  
 extragalactic radio sources, search for compact sources at low freqs. (81.5 MHz) 0-90553  
 extragalactic radio sources, variable radio emission temporal characts. (Russian) 0-62307  
 extragalactic radio sources study of emission variability in millimeter wave range (Russian) 0-90559  
 extragalactic source based positional reference frame, finding charts and optical identification 0-101645  
 extragalactic sources, confusion-limited survey at 4.755 GHz, source list and areal distrib. 0-98577  
 extragalactic sources, deep survey of selected regions at 4.85 GHz 0-77502  
 extragalactic sources, line of sight galactic H I emission and absorpt. obs. 0-94854  
 extragalactic sources, QSOs and galaxies, linear polarisation meas., SHF obs. 0-73058  
 extragalactic sources, rot. measure, linear polarisation obs. at 7.2 cm 0-82530  
 extragalactic sources with strong mm components, simultaneous radio obs. 0-73055  
 extragalactic variable sources with flat spectra, 90 GHz flux density 0-73056  
 faint radio sources statistics, interpretation of interplanetary scintillation meas. at 81.5 MHz 0-90554  
 Fornax A (NGC 1316), optical study of giant radiogalaxy 0-77479  
 FXP 0520-66, flaring X-ray pulsar, nature and optical identification (Russian) 0-77521  
 G74.9+1.2, continuum obs. at 2695 MHz of SNR 0-67830  
 G 84.2-0.8, high resolution 1415 and 2695 MHz obs. of SNR 0-98702

## radiosources (astronomical) continued

- galactic, anticorrelation with soft X-ray sources, plasma cloud interpretation 0-82514  
 galactic central region, sources and obscuration 0-77487  
 galactic nonthermal radio spectrum, rel. to cosmic ray electrons spectrum and gamma-rays prod. 0-62257  
 galactic sources, H10 $\alpha$  line and formaldehyde absorption line obs., SHF obs. 0-77472  
 galaxies, 3 cm obs. of 141 optically bright objects 0-73040  
 galaxies, bright, 1415 MHz continuum survey 0-94869  
 galaxies, distance scale from IR magnitude/H I vel.-width relation 0-82480  
 galaxies, elliptical, extended radio sources, optical positions 0-105331  
 galaxies, nearby, interstellar CO survey 0-62276  
 galaxies, nearby, radio continuum obs. (German) 0-109544  
 galaxies, optical counterparts, astrometry 0-90551  
 galaxies, radio components fly away velocities (Russian) 0-62306  
 galaxies, radio continuum obs. at 11 cm 0-94872  
 galaxies, red shift dependence of proper densities and colours 0-62286  
 galaxies, relativistic fluids flow through channels, self-similar solns. and stability 0-62006  
 galaxies active nuclei, massive black hole binaries model rel. to radio jets struct. 0-109546  
 galaxies and quasars, VLBI hybrid mapping of nuclei 0-105356  
 galaxies from B2 Catalogue, optical identification, radio positions and redshifts 0-86005  
 Galaxy central region, improved H I data rel. to barlike model of inner Galaxy gas distrib. 0-67845  
 galaxy clusters, central regions, 3.5 and 4.0 mm obs. (Russian) 0-82525  
 GB2 1400 MHz survey sources, spectral index depend. counts 0-98732  
 globular cluster fields, radio continuum obs. at 2.7, 4.8 and 10.7 GHz 0-101619  
 HR 1099, 10 GHz radio emission from RS Canum Venaticorum binary 0-82427  
 HR 1099 (V711 Tauri), RS Canum Venaticorum star, H $\alpha$  line variability, visible spectra obs. 0-105277  
 HR 5110, Algol type RS Canum Venaticorum star, H $\alpha$ , yu photometry obs. 0-105276  
 HR 5110, RS Canum Venaticorum binary, V photometry near radio outburst time 0-90469  
 IC 342, Scl galaxy, central regions IR and radio emission rel. to star form. 0-62256  
 intermediate strength sources, statistical props. 0-62303  
 interstellar H<sub>2</sub>O maser emission, new sources detect. 0-62298  
 interstellar H<sub>2</sub>O masers in NGC 6334, positions and spectra rel. to star form. 0-73025  
 interstellar HCO<sup>+</sup>, shock enhancement of abundance in supernova remnant (IC 443) 0-82464  
 interstellar OH and H<sub>2</sub>O masers, form. by thermal instability of radiative shock 0-67821  
 IRC+10374, IRC+10523, IR stars, H<sub>2</sub>O maser emission detect. 0-62298  
 BL Lacertae, major radio outburst, (1980 April 17 to May 6) 0-73043  
 LS I+61°303, variable binary radio star (BI Ib), X-ray emission detect. 0-105400  
 LSI+61°303, supergiant Be star, radio emission and radial vel. periodic vars. 0-62149  
 M87, 2 and 6 cm VLA obs. of jet 0-105345  
 M87, Faraday rot. in radio/X-ray halo 0-67844  
 M87, millisecond radio bursts discovery 0-73034  
 M87, spectroscopic evidence for large central mass 0-94873  
 M87, UV spectrum, IUE obs. 0-82502  
 magnetized spheroids, anisotropic explosions 0-67532  
 mapping with uncalibrated visibility data 0-77295  
 Markarian 3, Seyfert galaxy radio maps, SHF obs. 0-82501  
 masers, collision-collisional pumping model collisions (Russian) 0-90560  
 MCS 1307+121, BL Lacertae object, radio spectrum shape, VHF and SHF obs. 0-67866  
 MSH 11-54 (H1122-59), supernova remnant, X-ray obs. 0-82463  
 MWC 349, Be star, spectral EHF obs. 0-105262  
 MXB 1730-335 (Rapid Burster), microwave bursts obs. 0-62320  
 NGC 1275, Seyfert galaxy, nucleus struct. (Russian) 0-62288  
 NGC 315, radio galaxy, mag. field struct. in radio jets 0-82526  
 NGC 741, 1316, 7626, radio galaxies, dynamics 0-94871  
 NGC 7538, IRS 1, formaldehyde maser, SHF band obs. 0-67822  
 NGC 7538 and Shershell 159, H II region/mol. cloud complex, H I aperture synthesis obs. 0-90510  
 NGC 7822, NGC 281, bright rimmed mol. clouds, CH obs. 0-62238  
 NGC 925, barred spiral galaxy, high-resolution H I obs. 0-105329  
 North Polar Spur (Radio Loop 1), X-ray obs. 0-105370  
 NRAO 150, compact radio source, search for time-depend. radio fine struct. 0-90552  
 OC, 253, towards M33, H I 21 cm emission/absorpt. obs. 0-62262  
 OH 205.1-14.1, unusual OH maser, new flare report and 1667 MHz line obs. 0-98734  
 OH 205.1-14.1 in Lynds 1630 dark cloud, coincident IR source obs. 0-101630  
 OH 231.8+4.2, OH maser source, UHF spectra obs. 0-90550  
 OH 351.78-0.54, UHF obs. of brightest OH maser (1980 August) 0-101644  
 OH masers, interstellar, obs. near Orion population stars 0-67716  
 Ooty occultation extragalactic sources radio spectrum obs. in SHF 0-105371  
 optical identifications of extragalactic radio sources 0-105373  
 OQ 208 (=Markarian 668), Seyfert galaxy, H83 $\alpha$  and H99 $\alpha$  radio recomb. lines detect. 0-94864  
 Orion A, H<sub>2</sub>O maser source outburst obs. (Russian) 0-105320  
 Orion A, methanol 84.5 GHz and 96.7 GHz lines obs. 0-62245  
 Orion methanol masers, interferometric and multitranstional study 0-67891  
 Orion Nebula, radio obs. of nearby H I distrib. and vels. 0-105322  
 OTL sources, position and struct. determ. from 327 MHz lunar occultation obs. 0-73061  
 OTL sources, position and struct. determ. from 327 MHz lunar occultations obs. 0-73062  
 OTL sources, position and struct. determ. from 327 MHz obs. 0-73060  
 parameter determ. method from differing satellite obs. 0-85871  
 periodicity investigation at 21 cm 0-82529  
 Perseus A (NGC 1275), correl. between optical and radio variability (Russian) 0-77505

**radiosources (astronomical) continued**

UV Piscium, RS Canum Venaticorum star, identification with X-ray source H0118+067, X-ray obs. 0-101654  
 PKS 2126-15, QSO ( $z=3.27$ ), JHK photometric obs. 0-94888  
 planetary nebulae, advances in radio obs. 0-109526  
 planetary nebulae, radio fluxes rel. to distances determined from ionised mass/radius relation 0-101625  
 planetary nebulae, southern, SHF obs. 0-90496  
 Puppis A supernova remnant, X-ray spectra var. with position 0-82472  
 Q 0420-388, QSO ( $z=3.13$ ), JHK photometric obs. 0-94888  
 QSOs, detection of ten MCS objects in SHF 0-105377  
 QSOs, optically selected, radio study 0-82536  
 QSOs from Molongui Deep Survey, optical spectra 0-94884  
 quasar 0957+561, radioastron. obs. of assumed double quasars 0-105381  
 recombination lines, high-n, Zeeman splitting 0-58210  
 relativistic blast waves that accelerate 0-67534  
 ring galaxies, radio continuum emission 0-67846  
 Roberts 22, bipolar nebula with OH emission, visual, radio and IR obs. 0-94859  
 rotation measures and data processing 0-86006  
 Sa spiral galaxies, H I study 0-98714  
 Sa type spiral galaxies, redshifted 21 cm line profiles, radio obs. 0-73041  
 Sagittarius B2, He recombination line obs. interpretation 0-62300  
 Sagittarius B2, methanol 84.5 GHz and 96.7 GHz lines obs. 0-62245  
 Seyfert 1 galaxies, H I Balmer lines correl. with disk struct. 0-82503  
 Sharpless 159 and NGC 7538, H II region/mol. cloud complex, H I aperture synthesis obs. 0-90510  
 SN 1572 (Tycho's supernova), small dia. radio source discovery and precise position 0-98680  
 SN 1979c in NGC 4321 (M100), detect. at 60 nm wavelength 0-82402  
 SNR radio shells, spectral index distrib. 0-77462  
 space distrib. from short wavelength surveys 0-62305  
 spectroscopy (*Japanese*) 0-62031  
 SS 433, 164<sup>th</sup> period as precessional motion, massive black hole and pulsar models 0-62138  
 SS 433, 180 mm interferometric obs. of triple structure 0-105259  
 SS 433, accreting black hole model 0-85958  
 SS 433, accretion disc viscosity determ. using slaved disc model 0-62110  
 SS 433, beam acceleration, radiation and precession theory 0-72971  
 SS 433, beam models, energetics anal., possible triple system 0-90433  
 SS 433, change in radio struct., 1980 January to June, from VLBI obs. 0-109557  
 SS 433, deviations from standard model 0-98669  
 SS 433, disk-driven precession 0-94803  
 SS 433, dissipative infall model 0-67749  
 SS 433, emission regions and black hole accretion disk 0-67746  
 SS 433, general spectral features 0-77421  
 SS 433, IR variability obs. 0-98676  
 SS 433, light curves, double peak and binary-like period, photometry 0-94804  
 SS 433, magnetic X-ray binary model 0-109447  
 SS 433, models of supercritical accretion discs around black holes 0-105272  
 SS 433, nearby faint, highly-contorted nebular filament discovery 0-94855  
 SS 433, no 6-day periodicity in 1978 June-1980 Feb. obs. period 0-62150  
 SS 433, radial vel. curve low amplitude section, visible spectra anal. 0-67737  
 SS 433, reality of 6-day periodicity in spectral lines wavelengths var. 0-67743  
 SS 433, relativistic beam interaction with interstellar matter, mass loss rate, visible obs. 0-101629  
 SS 433, review of obs. and theories 0-72987  
 SS 433, search for radio spectral lines in UHF 0-109556  
 SS 433, spectral features interpreted a precessing neutron star with jets, possible binary 0-90447  
 SS 433, V band photometry and broad min. prediction (1980 April-May) 0-82390  
 SS 433 inside SNR, unique spectrum 0-82381  
 supernova remnants, electron acceleration mechanism 0-85988  
 supernova remnants, radio evolution, generalized theoretical approach 0-85990  
 supernova remnants, source counts rel. to galactic supernova outbursts frequency 0-62168  
 supernova remnants in LMC, SHF OBS. 0-67864  
 synchrotron sources, form. of universal and diffusion regions of relativistic electrons non-linear spectra 0-109555  
 V711 Tauri (HR 1099), RS Canum Venaticorum star, BV light curve during (1978-79) 0-105279  
 transparent synchrotron astronomical sources, internal Faraday rot. effect 0-72760  
 Tycho's supernova (SN 1572), unsuccessful search for optical stellar remnant 0-101603  
 UHF survey, positions and optical identifications, for sources selected at 966 MHz 0-73059  
 variable extragalactic sources with steep spectrum, VHF and SHF obs. 0-90548  
 Virgo A, core object, comparison of 5 and 23 GHz maps 0-82488  
 Virgo A (M87), Westerbork map at 610 MHz 0-62302  
 Virgo cluster galaxies, 1.4 GHz continuum survey 0-98721  
 Virgo cluster spiral galaxies, H I deficiency from 21 cm obs. 0-62277  
 14W12, in X-ray cluster of galaxies Abell 401, radio emission distrib. 0-98731  
 W1 (S171), optical supernova remnant radial vel. field 0-62250  
 W32, 43 and 109, galactic centre planetary nebulae search 0-90506  
 W33, OH radio emission sources obs. (*Russian*) 0-62247  
 W3(OH), interstellar OH maser, struct. from VLBI synthesis obs. 0-105368  
 W3 H II region, CO, CS and HCN obs. LF obs. 0-82446  
 W3/W4/W5 region, heavy optical obscuration obs. 0-62301  
 W49A, W51A, compact H II regions, H10 $\alpha$  recomb. line, aperture synthesis obs. 0-105314  
 W50, conditions for assoc. with SS 433, models 0-67737  
 W50, continuum obs. at 2695 MHz of SNR 0-67830  
 W50, probable supernova remnant, relation to (SS 433) 0-72987  
 W50, supernova remnant, optical spectrum 0-90557  
 W58, galactic star-forming region, CO obs. 0-67810  
 W80 (Pelican Nebula), CO obs. of expanding mol. shell surrounding H II region 0-105296

**radiosources (astronomical) continued**

18W catalogue of radiosources in Abell 2197 and 2199, Westerbork survey at 610 MHz 0-67883  
 29, 30 and 31W catalogues, Virgo cluster galaxies 0-98721  
 28 W sources and catalogue in NGC 7000 IC 5070 H II region complex 0-105308  
 X-ray sources, compact, radio emission origin 0-62317  
 H I in field of elliptical galaxy NGC 1052, 21 cm emission mapping and line profiles 0-98719  
 H II blisters, dusty, appearance at radio and IR wavelengths 0-85979  
 H II regions, compact, in interstellar dark clouds, radio continuum interferometry 0-98699  
 H II regions, newly formed, in interstellar dark clouds, physical props. from radio continuum interferometry 0-105301  
 H II regions, origin from supernovae explosions 0-67877  
 H<sub>2</sub>O maser sources in galactic plane, southern hemisphere survey 0-73054  
 H<sub>2</sub>O masers, 22 GHz galactic plane survey, 14 new sources 0-77464  
 OH astronomical sources OH 231.8+4.2, CY Canis Majoris, M1-92, UHF obs. 0-90550  
 OH maser emission, rot. excitation by H<sub>2</sub> at interstellar temps. 0-62232  
 OH radio emission sources, type IIc, in W33, obs. (*Russian*) 0-62247  
 OH type I maser sources, model 0-90556

**radiostars see radiosources (astronomical)****radiotelescopes**

see also *radioastronomy*  
 antenna arrays, incoherent optical 1-bit cross-correlators for digital signal processing 0-98555  
 cm-wave radiometer, with enhanced long-term stability, for solar radio emission obs. 0-109361  
 Culgoora, correlator back-end, advantages and disadvantages 0-85865  
 Effelsburg 100 m radiotelescope, first obs. at 7 mm wavelength, props. and performance 0-62013  
 global radio solar telescope network, solar activity monitoring appl. 0-82202  
 heterodyne freq. analyzer, detection of 200 to 400 GHz weak microwave signals 0-94716  
 interferometer, tropospheric influence in differential meas. of astrometric coordinates 0-67581  
 large-aperture radio system for meteor studies 0-85870  
 NIRFI reflector of light construction with prestressed guyed rod 0-91360  
 Northern Cross radiotelescope, appl. of Clean and Restore technique to obs. of 2033+59 (*Italian*) 0-98563  
 radioheliograph control system, 8 cm instrument at Toyokawa, Japan 0-98549  
 RT-22, automatic obs. by computer 0-109359  
 Salyut 6 submm. telescope with InSb receiver 0-67566  
 super. synthesis telescope, Japan, 10-m $\phi$  5-element array performance 0-98548  
 UTR-2 based heliograph, 25 MHz obs. of solar storm burst source positions 0-90403  
 WSRT, appl. of Clean and Restore technique to obs. of (4C 39-08) (*Italian*) 0-98563

**radiotherapy see radiation therapy****radiowave propagation**

see also *electromagnetic wave propagation*  
 angular scattering of water drops and ice particles [electromagnetic interference], freq. above 10 GHz appl. 0-109183  
 antennas, horizontal, above infinite plane Earth, input impedance and current distrib. 0-90259  
 Arctic ice cover, attenuation of 8 and 20 cm EM waves 0-67379  
 atmosphere, propag. of microwaves, refr. and absorpt. coeffs., optimal orthogonal expansion props. 0-98414  
 atmospheric noise data for tropical regions 0-61875  
 atmospheric refractive effect, ducting phenomena 0-94557  
 attenuation due to water vapour, microwave radiometer study at 22.235 GHz 0-72610  
 attenuation in atmosphere of Venus by bistatic radar method 0-62061  
 auroral zone activity coupled to mid-latitude radiowave absorpt. 0-61945  
 backscattered pulse shape, small-angle multiple scatt. in random media 0-77079  
 circumsolar plasma, radio signal spectral lines formation 0-92330  
 circumsolar plasma, Venera 10 radio signal spectral meas. 0-109326  
 classical propagation criteria and effect of atmospheric anomalies 0-67390  
 cloud liquid H<sub>2</sub>O obs. from 28 GHz satellite signal absorpt. 0-94623  
 in critical coupling media, comparison of generalised WKB and Kat-senelbaum's methods 0-91728  
 D-region, radiowave heating at HF, consequent MF absorpt. effects 0-94646  
 decametric wave propagation, ionosphere conditions forecasting by CNET, in France (*French*) 0-85790  
 dispersion by plasma ejected from BL Lacertae objects 0-82516  
 Earth-ionosphere waveguide, program to compute EM fields in irreg. spheroidal model 0-94638  
 ELF propag. in nonstratified Earth-ionosphere waveguide, integral eqn. method 0-61959  
 ELF waves in Earth-ionosphere cavity, field eqn. for inhomogeneous ionosphere 0-61950  
 extended path with single obstacle, attenuation factor calc. 0-95775  
 extinction cross section for single particles at 100 GHz 0-82116  
 F-region, generalized magnetoionic formulae 0-61963  
 fading from spaced receiver obs. at Thumba 0-109296  
 FM-CW radar signal propag. in lower atoms. 0-90186  
 giant planets, atmospheric radiowave refraction 0-98608  
 ground wave atmospherics generated by lightning return strokes, initial peaks, model 0-61876  
 ground wave attenuation function for a spherical Earth with arbitrary surface impedance 0-94585  
 ionosphere, A1 absorption measurements at 2.4 and 5.6 MHz 0-82132  
 ionosphere, decametric freq. shift of magnetoionic component 0-105104  
 ionosphere, global MF absorpt. variations, empirical formula 0-77204  
 ionosphere, ionisation irregularity drift motion from spaced fading and scintillation obs. 0-82133  
 ionosphere, metallic ions of meteor origin effect in VHF forward scattering, contribution to sporadic-E formation 0-67461  
 ionosphere, model computations of scintillation caused by equatorial bubbles 0-94641



**radiowave propagation continued**

- ionosphere, morphological features of winter absorpt. anomaly at middle latitudes. 0-67459
- ionosphere, radio pulse dispersion and virtual height determ. 0-61954
- ionosphere, radio window theory, transmission coeff. 0-61953
- ionosphere, scintillation, power law phase screen model, strong scatt. 0-61962
- ionosphere, scintillation, power law phase screen model, weak scatt. 0-61961
- ionosphere, self-focusing instability in oblique ionosonde meas. 0-105101
- ionosphere, short wave radio absorpt. in winter, rel. to O<sup>+</sup> airglow 0-77184
- ionosphere, time dispersion of EM pulses 0-94645
- ionosphere, VHF scintillation, assoc. with reversal of horiz. elec. field 0-101489
- ionosphere, VLF and LF propagation and eigenmode scatt. relations 0-61944
- ionosphere, VLF focusing during solar eclipse 0-61965
- ionosphere LF radiowave absorpt., variation during solar cycle 0-77193
- long-delay echoes, 28 MHz amateur band obs. 0-90277
- Loran-C signal, ground wave propag. theory 0-94580
- low latitude whistlers, lower and upper freq. cut-off explanation 0-82131
- magnetoplasma, refr. index profiles in layered media, extraordinary mode 0-77223
- magnetosphere, radio window theory, transmission coeff. 0-61953
- magnetosphere, side-band mutual interaction of whistler-mode waves 0-82148
- mesosphere VHF radar signal scattering, tropical latitude 0-90193
- meteor rate seasonal var., atmos. ionisation effect on LF radio navigational signals 0-82309
- microwave absorption in atmosphere of giant planets induced by collisions of H molecules 0-90350
- microwave attenuation due to precip. of water vapour in atmosphere, meteorological data, raindrop spectral distrib. (German) 0-90176
- microwave Earth-space link rain cell attenuation 0-94586
- microwave radiation from solar power satellite, theoretical anal. of non-linear interaction with ionosphere (Japanese) 0-94634
- microwave radiometer for rain attenuation measurement at X, K bands 0-68254
- middle atmosphere, 50 MHz radiowave depolarisation on backscattering 0-85729
- MM wave systems, atmospheric attenuation factors 0-67405
- MM waves, conf., London (Apr. 1980) 0-67441
- modulation in turbulent shearing plasma, pulsar microstructure 0-94822
- NWC VLF signal in magnetosphere, Doppler shift meas. by JIKIKEN (EXOS-B) satellite (Japanese) 0-94651
- planetary atmosphere, occulting spacecraft signal, turbulence determin. 0-94734
- plasma with layered struct., use of Fuchsian differential eqns. 0-75060
- propagation problems connected with infinitesimal point source, review 0-90194
- radar echoes from clear air, mechanisms 0-90181
- radar reflectivity profile classified by rain types 0-101420
- radar signal scatt. from turbulent air, VHF and UHF 0-85728
- rain attenuation above 10 GHz, regression curves for tropical areas 0-90111
- rain attenuation above 11 GHz, radio links appl. 0-98410
- rain attenuation at 10 and 11 GHz, radiometric measurements 0-67397
- rain attenuation prediction methods comparative analysis, radiowave propagation appl. 0-109182
- ray trajectories in ionospheric waveguide, influence of inhomogeneities 0-61966
- ray trajectory props. in irregular ionospheric waveguide 0-90284
- refraction corrections for exponential atmosphere, real-time computational method 0-98432
- scalar microwaves propagation in medium with severe random nonuniformities, Green's function 0-69297
- scattering by 1-D power law phase screen 0-77220
- scattering in presence of background slab, algorithm for profile reconstruction 0-94644
- scattering of microwave background in clusters of galaxies, 9 mm obs. 0-105366
- scattering of microwave background radiation in clusters of galaxies 0-105367
- scintillation by ionosphere, statistical study 0-109306
- scintillation of VHF, UHF and SHF in equatorial ionosphere, theory 0-61946
- sinusoidal surfaces, scatt. patterns 0-58448
- solar wind turbulent plasma, radio wave propag. meas. using three satellites 0-101518
- sporadic-E affecting ELF wave propag. at nighttime 0-77202
- stratosphere and troposphere, VHF radar scatt. and refl. 0-90182
- surface geology sensed by ground mode radiowave propag., glaciated area of USA 0-76979
- thermosphere, lower, echo from ionospheric sublayers 0-61956
- thunderstorm location by single station techniques, improved method, radiowave propag. effects 0-67438
- trans-horizon propagation path over sea, transmission loss due to ducting at 1.8 GHz 0-105041
- trans-equatorial radiowave propag. in freq. range 28 to 432 MHz, amateur bands, obs. and expts. 0-101491
- trans-equatorial radiowave propag. over 21 year period, VHF/UHF signals, theories 0-109311
- trans-ionospheric radio wave scintillation, time struct. 0-90281
- troposphere, nonuniform wave guide, coupled mode anal. 0-94587
- troposphere waveguide, effect of elevated M-inversion 0-90195
- tropospheric effects on radio communication, book 0-62400
- tropospheric long-distance propag., multiple scatt. effect 0-109229
- VHF radar aurora and strong HF backscatt. comparison 0-61960
- VHF scintillation at high-latitude, analytical formulas 0-77224
- VHF scintillation at high-latitude near 70°W 0-77221
- VHF signal scintillation, from ETS-2 satellite, obs. of Waltair and Calcutta 0-109295
- VLF emission modulation freq. shift relative to geomagnetic pulsation freq. 0-77229
- VLF signals, numerical study of satellite reception using waveguide concepts 0-90282
- whistler mode, obs. of plasma drift and ionosphere-magnetosphere coupling 0-77239
- X-band, dielectric constant of dust, effect of moisture content 0-72578

**radium**

- see also nuclei with .....
- <sup>226</sup>Ra, A=226, 228, content in groundwater of Fall Line aquifers 0-89682
- <sup>222</sup>Ra short lived daughter disequilibrium in a mixed maritime and continental atmosphere 0-108822
- <sup>226</sup>Ra, behaviour in Pee Dee River-Winyah Bay estuary, S.Carolina 0-98360
- <sup>226</sup>Ra in public water supplies, conc. determ. (German) 0-94138

**radium compounds**

No entries

**radium emanation** see radon**radius measurement** see diameter measurement**radius of curvature measurement** see curvature measurement**radon**

see also nuclei with .....

- <sup>222</sup>Rn flux through multilayered covers cover U mill tailings 0-95487
- atmosphere, <sup>222</sup>Rn daughter products, measurement using diffusion sampler 0-81510
- atmosphere boundary layer, diurnal var. for USA Gulf Coast 0-101404
- atmospheric, accumulation in calcite caves 0-104531
- background concentrations of Rn and Rn daughters in Canadian homes 0-104546
- concentration in dwellings and influencing factors 0-108832
- daughter concentrations in different atmospheres 0-85316
- daughters in atmospheric air, efficiency of HV-70 filters for sampling 0-108827
- detection methods in underground and free atmosphere air 0-57987
- doses to employees and public from Rn and Rn daughters in Howe Caverns, USA 0-89859
- earthquake, precursory soil Rn changes, San Jacinto, California 0-94468
- earthquake precursory changes of groundwater Rn content 0-94467
- earthquake precursory Rn changes, California active faults 0-94465
- earthquake precursory Rn changes, in shallow subsurface of New York State 0-94463
- earthquake precursory Rn changes, Izu-Oshima-kinkai earthquake (1978) 0-94472
- earthquake precursory Rn changes in California Transverse Ranges 0-94464
- emanation from rock specimens and powders, apparatus for measurement of rates 0-63494
- gas concentration meas. using alpha sensitive plastic detectors 0-94617
- gas concentration measurement using alpha sensitive plastic films for U exploration 0-94618
- geophysical exploration by Rn mapping in U exploration, exclusion of <sup>220</sup>Rn signal 0-61916
- Hawaii, ground Rn survey of Puna geothermal area 0-85657
- liquid, calc. of critical density 0-59547
- lung cancer rel. to Rn in dwellings 0-89870
- monitoring instrumentation 0-106204
- seismicity near Lake Jocassee, S.Carolina, precursory changes of groundwater Rn 0-94466
- Ra, annual rate of release to atmosphere as result of coal combustion in UK 0-93787
- <sup>220,222</sup>Rn daughters, 2-count filter method for meas. in air 0-63480
- <sup>222</sup>Rn, atmospheric, two-filter continuous monitor 0-58097
- <sup>211</sup>Rn production by <sup>209</sup>Bi (Li,Sn), excitation function 0-95323
- <sup>220</sup>Rn decay products attachment to flowing aerosols using centrifuge 0-61167
- <sup>222</sup>Rn integrated meas. of long-distance transport for U ore detection 0-98476
- <sup>222</sup>Rn as tracer for sediment-water chem. exchange in coastal zone 0-101386
- <sup>222</sup>Rn, conc. in free air (Hungarian) 0-94128
- <sup>222</sup>Rn concentration in tunnel air, atmospheric press. and precipitation effects (Japanese) 0-97845
- <sup>222</sup>Rn concentration meas. by plastic detectors to determ. environmental  $\alpha$ -emitters from natural sources 0-91292
- <sup>222</sup>Rn diffusion through U mill tailings covers, coeff. meas., lab. techniques 0-95387
- <sup>222</sup>Rn emanation from building materials, plastic  $\alpha$ -track detectors study 0-101144
- <sup>222</sup>Rn gas detection using Track Etch system for U exploration 0-98488
- <sup>222</sup>Rn, props. and behaviour of short lived daughter nuclides in the atmos. (Japanese) 0-72339
- <sup>222</sup>Rn, theoretical, evaluation of emanation under a variety of conditions 0-104545

**radon compounds**

No entries

**rail traffic**

see also railways

- noise, diesel electric locomotives, SD40-2 noise under various operating conditions 0-102924

**railroads** see railways**railways**

see also locomotives; traction

- high speed ground transportation vehicles gas-flow-controlled arcs for power collection 0-70054
- noise protection screens, meas. (German) 0-102916
- passenger coaches, structure-borne noise suppression (German) 0-91957
- underground, natural rubber for vibration insulation 0-96099

**rain**

- acid rain, Pittsburgh (Pennsylvania) area 0-94129
- acidity, natural variance of pH time dependence 0-61840
- aerosol, scavenging of particles by cloud drops and small rain drops, elec. field effect 0-82001
- Amazon Basin, water recycling, <sup>18</sup>O conc. study 0-81955
- annual rainfall, stochastic anal. rel. to effects of urbanisation 0-98407
- attenuation in radiowave propagation above 11 GHz, radio links appl. 0-98410
- attenuation of radiowaves at X, K bands, microwave radiometer design 0-68254
- W.Australia, rainfall rate meas. during tropical cyclone by satellite microwave sensing 0-98485
- banded rainfall distrib. over S.England, wintertime 0-82023
- Bedford Ouse River, rainfall-runoff behaviour rel. to stream flow and water quality models 0-81956
- Belgium, monthly rainfall maps (French, Flemish) 0-94583
- Brazil, precipitable water, distrib. maps 0-77075
- British spring weather, survey (1950 to 1979) 0-98427

- rain** continued  
 British winters (1659 to 1979), study of temp. correl. with precipitation 0-98444  
 California, spring rains correl. with Pacific Ocean December sea surface temps. 0-77064  
 cold front, obs. of 3-D circulation, precipitation and wave motions 0-90142  
 cold front of midlatitude cyclone, cloud and precipitation struct. 0-109192  
 conference, Rochester, NY, USA (May 1979), polluted rain 0-82585  
 convective day precipitation, correl. with atmos. parameters observed by radar 0-109205  
 convective mean rainfall, meas. over small areas using high-density rain-gauges and radar 0-77157  
 cooling towers affecting rainfall, statistical study 0-109202  
 cumulus clouds, warm rain and salt seeding, numerical simulation 0-90201  
 Darling River system floods, chronological evolution, Nimbus-5 radiometry obs. 0-94543  
 drop formation at cloud top, effect on charge separation 0-81999  
 droplet size and falling velocity. meas. using laser Doppler velocimeter 0-68185  
 drought in streamflow series, statistical characts. 0-105009  
 earthquake precursory rainfall, S. California 0-85615  
 flood event real-time predictors, stochastic model 0-67383  
 flood forecasting model from rainfall catchment and evaporation data, retention hysteresis 0-81951  
 S. Florida, description and field testing of digital recording system for tipping bucket raingauges 0-77161  
 Florida Area Cumulus Experiment (FACE) rainfall results, seeding effect or natural variability 0-82002  
 formaldehyde, in marine air and rainwater, wet season obs. 0-85703  
 GATE mean rainfall patterns, isohyet maps from radar maps 0-90172  
 SW. Germany, heavy rainfall from May 22 to 24 (1978) (*German*) 0-61869  
 Hunan and Zhejiang Provinces, rainy season, long range forecasting 0-90204  
 instantaneous rainfall rate, technique and influence on high-voltage transmission lines 0-98471  
 intensity characts. of rainfall, possibility of using monthly averages in calcs. 0-105040  
 IR broadband transmission rel. to meteorological events 0-85744  
 Jerusalem, seasonal precip. temporal fluctuations 0-72618  
 large scale rain systems, vertical vels. and precipitation patterns, model 0-85727  
 laser-radiation-intensity fluctuations in rainfall, statistical characts. 0-101433  
 London area rainstorm of 16-17th Aug. 1977 0-77093  
 Mahanadi basin, India, climatic study of river regime 0-81941  
 measurement by dual-polarisation radar, drop size and fall rate 0-72650  
 mesoscale rainbands in extratropical cyclones, assoc. cloud microphysics and dynamics 0-82030  
 microwave absorption, rel. to pollutant gases monitoring from space using passive sensing techniques 0-76690  
 microwave attenuation at 10, 11 GHz, radiometric measurements 0-67397  
 microwave attenuation due to precip. of water vapour in atmosphere, meteorological data, raindrop spectral distrib. (*German*) 0-90176  
 microwave signal attenuation by rain cell, Earth-satellite link 0-94586  
 monsoon, West Coast of India, rainfall features 0-61874  
 monsoon breaks, effects of surface press. 10 to 20-day westward propag. mode 0-94592  
 monsoon over Calcutta, rel. to VLF atmospheric anomalies 0-82127  
 monsoon over Indian region, energy anal. by baroclinic model 0-77073  
 Montreal, rain estimation using geostationary satellite data 0-90244  
 passive microwave obs. from Nimbus satellites 0-101422  
 plum rains in Shanghai, mid-range forecasting (*Chinese*) 0-109232  
 Port Moresby, Papua New Guinea, rainfall trend, (1945 to 1976) 0-98430  
 radar and radiometry techniques combined use for rainfall meas. (*Chinese*) 0-109272  
 radar measurement of rainfall, methods and interpretation of data 0-81969  
 radar observations of rainfall, appl. to hydrology 0-90263  
 radar polarisation techniques for precip. props. determ. 0-61925  
 radar reflectivity profile classified by rain types 0-101420  
 radiowave attenuation, radiometric determ. at millimetre wavelengths, multiple-scatt. effects 0-90260  
 rain attenuation prediction methods comparative analysis, radiowave propagation appl. 0-109182  
 rain-gauges, dual-gauge and Wyoming shield systems 0-61928  
 rainbow, anomalous arc due to refl. image of Sun from water surface 0-77114  
 rainfall prediction for short response time hydrological basins 0-98491  
 rate detect over ocean and land by spaceborne microwave radiometry 0-101423  
 regression curves for tropical rain attenuation above 10 GHz, terrestrial and satellite telecommunication, broadcasting systems appl. 0-90111  
 remote sensing techniques from satellite borne microwave radiometry 0-105085  
 Sahel drought, Africa, 1967 to 1974, Earth surface albedo vars. investigation 0-76981  
 seeding studies application of lidar remote sensing 0-109203  
 sequential sampler, design, construction and operation 0-105090  
 short-duration rainfall, runoff calc. method (*French*) 0-77143  
 Southern Hemisphere, moisture conditions and precipitation efficiency 0-98424  
 Spalding, Lincolnshire, rainfall series discontinuities 0-105026  
 St. Louis, Missouri, pollutant source strength-rainfall relationships investigation 0-77059  
 thunderstorm, precipitation obs. immediately after lightning stroke 0-77055  
 thunderstorms near Langmuir Laboratory, airborne and ground based studies 0-85725  
 trace constituents in Indian west coast SW monsoon rainwater 0-81967  
 Trinidad, conc. determ. 0-82045  
 United Kingdom, use of radar as part of integrated system for rain meas. and forecasting 0-98490  
 United States west coast, rainfall rel. to Nimbus 6 liq. water data over NE. Pacific Ocean 0-82005  
 S. Wales floods of late December 1979, meteorological anal. 0-98429
- rain** continued  
 warm frontal clouds in midlatitude cyclones, air motion and precipitation 0-109193  
 weather forecasting processing of radar and satellite imagery data 0-109252  
 Zambia, weather during rainy system rel. to upper westerly waves interaction with intertropical convergence zone 0-90175  
 S pollutant removal from atmosphere by rain, modeling method 0-85318
- rainfall** *see rain*
- Raman effect** *see Raman spectra*
- Raman lasers**  
 backward Raman amplifier for excimer laser pulse compression, parasitic superfluoresc. suppression 0-69453  
 coherence effects in multiply pumped spin-flip Raman laser 0-87398  
 double resonance Raman amplifier, theory 0-87434  
 Faraday rotators in fibre Raman lasers 0-58775  
 fibre Raman lasers 0-102767  
 fluoromethane,  $^{12}\text{CH}_3\text{F}$ , far IR Raman laser line obs.,  $\text{CO}_2$  laser pumping 0-69381  
 fluoromethane high-power laser, tuning behaviour 0-63994  
 frequency conversion, via stimulated Raman scattering 0-69451  
 gas concentration meas. using Raman intensity depend. on giant pulse laser polarization 0-98986  
 IR, for 16  $\mu\text{m}$  range, review (*Rumanian*) 0-87408  
 methane backward Raman amplifier, KrF laser driven, high-efficiency energy extraction 0-106533  
 narrow-linewidth high-efficiency Raman amplification and spectral compression 0-102770  
 optical fibres, Raman scatt., guiding structs. effects on spontaneous and stimulated emission 0-58636  
 quartz multimode lightguide in pulsed  $\text{Nd}^{3+}$ :YAG laser resonator, intense Raman generation 0-99735  
 tunable IR solid-state laser characteristics and principles 0-87406  
 $\text{Br}_2 + \text{CO}_2$  mixture, Raman laser optical excitation, electron phototransition theory (*Russian*) 0-99711  
 $\text{CO}_2 + \text{COS}$  mixture, Raman laser optical excitation, electron phototransition theory (*Russian*) 0-99711  
 $\text{CO}_2 + \text{monobromomethane}$  mixture, Raman laser optical excitation, electron phototransition theory (*Russian*) 0-99711  
 $\text{Cl}_2 + \text{N}_2$  mixture, Raman laser optical excitation, electron phototransition theory (*Russian*) 0-99711  
 GaP semiconductor Raman laser 0-78864  
 $\text{H}_2$  laser, stimulated Raman scatt., appl. to holography 0-91782  
 $\text{H}_2$  Raman laser, multiple-pass-cell, controllable pulse compression 0-91825  
 $\text{H}_2$ , stimulated Raman scatt. gain of Nd laser radiation by rot. levels 0-69464  
 $\text{Hg}_{0.77}\text{Cd}_{0.23}\text{Te}$  nonlinear optical IR generation 0-58642  
 $\text{NH}_3$ , far IR CW Raman lasing 0-83595  
 $\text{NH}_3$ , stimulated hyper-Raman scatt. via 3-photon process to obtain IR and far IR radiation 0-58633  
 n- $\text{Pb}_{0.88}\text{Sn}_{0.12}\text{Te}$  spin flip Raman laser pumped by TE  $\text{CO}_2$  laser, characts. 0-87397  
 $\text{S}_2 + \text{N}_2$  (*Russian*) 0-99711
- Raman scattering** *see Raman spectra*
- Raman spectra**  
*see also molecular rotation; molecular vibration; Raman spectra of diatomic inorganic molecules; Raman spectra of inorganic liquids and solutions; Raman spectra of inorganic solids; Raman spectra of organic molecules and substances; Raman spectra of polyatomic inorganic molecules; Raman spectroscopy; stimulated Raman scattering*  
 adsorbates, on metals, enhanced Raman scatt., including nonlocal metal response, nonradiative modes excitation 0-88994  
 adsorbed molecule, in electrochem. systems, Raman scattering 0-60563  
 adsorbed molecules, Raman and fluoresc. enhancement by surface roughness 0-102511  
 adsorbed molecules on metal surfaces, giant Raman effect 0-65374  
 adsorbed mols., effective reson. Raman spectra 0-97730  
 amorphous solids, Raman intensities, connection with EXAFS Debye-Waller factors 0-108214  
 anharmonically coupled oscills., time depend. Hartree theory, susceptibility, absorpt. and Raman spectrum 0-58241  
 antiferromagnet, two-dimensional, with easy-plane anisotropy, mag. excitations and two-magnon Raman scatt. 0-65839  
 atomic level field splitting, resonant cooperative light scatt. (*Russian*) 0-74148  
 atoms, two photon excitation, time depend. emitted light spectra, perturbation theory 0-63605  
 carotenoid molecules in living cells of chlorella, vibrational state population 0-97861  
 coherent hyper-Raman scattering from isotropic material, quantum theory 0-106327  
 condensed media, vibrational relaxation studied by picosecond or Raman spectrosc., review 0-80797  
 conference, Moscow, USSR (Mar. 1978) 0-62377  
 cooperative Raman scattering, effect of phase self-modulation of light 0-91855  
 diatom+diatom, effect on depolarised light scatt. linewidths 0-58321  
 disordered systems, phononless Raman scattering 0-76031  
 forbidden rotational and vibr.-rot. transitions in strong optical field, spontaneous and stimulated Raman scatt. 0-74174  
 Hanle effect, influence on Raman scattered light 0-83323  
 incommensurate crystals, first order Raman scatt. from unbounded phonons 0-88990  
 inhomogeneous high temperature plasmas, Raman scatt. simulations 0-92268  
 intermolecular spectroscopy and dynamical properties of dense systems, conf., Varenna, Italy (1978) 0-82581  
 kramers-Kronig relations and resonance Raman scattering 0-97267  
 light hyper-Raman scatt. by polaritons, active spectroscopy (*Russian*) 0-60623  
 liquid, Raman band profile, vibr. dephasing and intermolecular interactions 0-60556  
 liquid drop, Raman scattering by forced surface oscills. 0-92763  
 liquids, vibrational relaxation studied by picosecond or Raman spectrosc. 0-80797  
 magnetised plasma, Brillouin and Raman scatt. by extraordinary mode 0-92269  
 methane backward Raman amplifier, KrF laser driven, high-efficiency energy extraction 0-106533



**Raman spectra** continued

- methane- $N_2$ -isobutane gas mixture composition by Raman spectra 0-87124  
 methyl iodide, vibrational dephasing by translational collision 0-87202  
 microprobe analysis, laser, principles and appl. 0-57390  
 molecular liqs., anisometric, Raman spectra components, vibr. reson. coupling and noncoincidence effect 0-69149  
 molecular scattering of light, spatial dispersion, distributed dipole and local multipole approx. 0-80796  
 molecule, pre-reson. Raman scatt. by t-type mode near A-T electronic transition 0-58261  
 molecule embedded in dielec. spheroid, Raman and fluoresc. scatt. 0-99507  
 molecules, optically active, coherent Raman scatt., quantum theory 0-69150  
 molecules, Rayleigh and Raman optical activity, scatt. angle anal. 0-69151  
 molecules adsorbed on rough surfaces, Rayleigh, Mie and Raman scatt. 0-83378  
 monolayer in inelastic electron tunnelling spectroscopy junctions, surface enhanced Raman scatt. 0-93344  
 monolayer on metal surface, giant Raman scatt., review 0-93343  
 monolayer on metal surface, giant Raman scatt. theory 0-93345  
 nonlocality effects on optical phenomena in bounded solids, developments 0-93328  
 optically isotropic molecules, collision-induced scatt., many-body correls. 0-87127  
 organic surface contaminants, anal. by plasma chromatography-mass spectroscopy, and Raman microprobe technique 0-108773  
 oriented atoms, electronic Raman reson. scatt., statistical theory 0-102467  
 paramagnetic crystal, magnetisation change by light pulse 0-70932  
 partially oriented molecules, uniaxial, two-photon processes, polarised spectrosc. 0-74209  
 photosynthetic systems, discovery of phase transitions, Stokes Raman scatt. 0-81539  
 polar semiconductors, secondary cyclotron emission giant oscillations of intensity and line shape 0-66192  
 polar semiconductors, two-phonon resonance Raman scattering 0-108204  
 pyridine, adsorbed on Ag surface, Raman active librational modes 0-65359  
 quasiequilibrium sample, light scatt. and thermal radiation, phenomenological approach 0-91840  
 relative Raman line intensities, extended Huckel valence basis sets 0-106329  
 resonance light scattering, spectral props. and photon correls. 0-91510  
 resonance light scattering and hot luminesc. of self-trapping excitons 0-93336  
 resonance Raman lineshapes and fluorescence in strong radiation fields 0-87074  
 resonant coherent Raman scatt. spectra of excited molecules 0-87129  
 resonant light scattering from magnetic excitations, review 0-97290  
 resonant Raman spectra, overtone intensity distrib., effect of excited electronic state 0-87128  
 resonant secondary emission components classification, theory applic. to expt. 0-93339  
 resonant secondary emissions by impurities in crystals 0-93335  
 semiconductor, deep impurity centres, elastic light scattering 0-97315  
 semiconductor, direct band gap, electronic Raman scatt. of polarised light on donor levels 0-93309  
 semiconductors, degenerate, resonance Raman scatt., Green's function approach 0-80781  
 semiconductors, free carrier optical props., book contrib. 0-80738  
 simple solid, scatt. cross sections determ. 0-93334  
 solutions, resonance Raman lineshape studies of vibrational and rotational relaxation 0-60560  
 spherical particle, surface enhanced Raman scatt. by molecules 0-95629  
 stimulated Raman scatt. Dewar cell for biomedical appls. 0-99799  
 surface enhanced Raman scattering surface plasmon model 0-108211  
 surface enhanced Raman spectra, image dipole description, critical review 0-87125  
 surface roughness effect on surface enhanced Raman scatt. 0-83377  
 tetrahedral mol. fluids, collision induced light scatt. intensity 0-103955  
 two level atom, coherent and Raman scatt. spectra, secondary emissions 0-69449  
 vibrational dephasing by translational collision 0-87202  
 Ag, adsorbed pyridine, 210-243  $\text{cm}^{-1}$  mode in surface enhanced Raman scatt. 0-89003  
 $\text{CN}^-$  on Ag surface, Raman active librational modes 0-65359  
 $\text{H}_2\text{O}$ , resonance Raman spectra for detection bacteria and algae 0-94418  
 Pd and Pt mixed valence complex,  $[\text{Pd}(\text{ethylenediamine})_2]\text{Pt}(\text{ethylenediamine})_2\text{Cl}_2(\text{ClO}_4)_4$ , Raman spectra 0-84734

**Raman spectra of diatomic inorganic molecules**

- air pollutant gases and vapours, relative Raman scatt. cross section 0-100061  
 Lennard-Jones fluids, orientational and collision induced light scatt. 0-63644  
 rotational Raman intensities and polarisability anisotropy change meas. with internuclear distance 0-63641  
 scattering amplitude calculations, role of radiative crossings between potentials of dressed mol. 0-63642  
 $\text{Br}_2$ , chemisorbed on zeolites, Raman spectra 0-93301  
 $\text{Br}_2$  in Ar matrix, reson. Raman scattering amplitude damping in discrete reson. limit 0-58262  
 $\text{Br}_2$ , Q branches of  $\Delta n=1$  profiles, calcs., rotation effect on scatt. amplitudes 0-63643  
 CN, monolayer on Ag surface, vibr. spectra, picosec. Raman gain technique 0-91859  
 CO adsorbed on Ag, Au films, enhanced Raman scatt. mechanism in ultrahigh vacuum 0-107645  
 CO, chemisorbed on  $\text{Al}_2\text{O}_3$ -supported Rh-Cu catalysts, IR spectra (French) 0-60559  
 CdO, formed by matrix reactions, IR, Raman and visible spectra 0-87110  
 DT, vibr. rot. Raman anal. 0-87126  
 $\text{H}_2$ , fluid, Raman meas., 0.2-630 kbar, at room temp. 0-58269  
 $\text{I}_2$ , chemisorbed on zeolites, Raman spectra 0-93301  
 $\text{N}_2$ , fluid, light scatt. orientational memory function at moderate density 0-102521

**Raman spectra of diatomic inorganic molecules** continued

- $\text{N}_2$  in nonequilibrium gas-dynamic current, vibr.-level populations determ. by Raman scatt. 0-99509  
 $\text{N}_2$ , pure rot. CARS obs. 0-99511  
 $\text{N}_2$ , stimulated scattering investigation, 1-4 atm press. range 0-91568  
 $\text{NO}_2(\text{N}_2\text{O}_4)$  surface decomposition, resonance and spontaneous Raman spectra 0-61144  
 $\text{Ne}_2$ , collision induced Raman spectra and diatom polarisability 0-63647  
 $\text{O}_2$ , pure rot. CARS obs. 0-99511  
 $\text{SO}_2$  surface reaction and decomposition on zeolites, resonance Raman study 0-61145  
 ZnO, formed by matrix reactions, IR, Raman and visible spectra 0-87110

**Raman spectra of inorganic liquids and solutions**

- electrolyte, soln. and cryst. (German) 0-80804  
 water, coherent Raman ellipsometry, vibr. stretching region and liq. struct. obs. 0-93341  
 water, Raman and IR spectrum in overtone OH stretching region 0-58263  
 CO, liq., pure vibr. Raman spectra 0-97262  
 $\text{CS}_2$  liquid, Rayleigh and Raman bands, intensities of interaction induced components 0-63645  
 Cr complex, tris(2,2'-bipyridine)Cr(III), excited states, Raman spectra 0-97263  
 $\text{H}_2$ , fluid, Raman meas., 0.2-630 kbar, at room temp. 0-58269  
 $\text{I}_{1-2}$  mixtures, high-temp. solids and melts, struct., thermodynamic props., Raman spectra obs. 0-66174  
 $3\text{KNO}_3-2\text{Ca}(\text{NO}_3)_2$ , glass form. from liq., struct. transform., Raman spectrum obs. 0-64916  
 $3\text{KNO}_3-2\text{ZnCl}_2$ , glass form. from liq., struct. transform., Raman spectrum obs. 0-64916  
 $\text{MgCl}_2$ -alkali metal chloride system, solid and molten states, struct. props., Raman spectra 0-76011  
 $\text{N}_2$ , liq., pure vibr. Raman spectra 0-97262  
 $\text{N}_2$  liquid, in Kr, methane, and CO, Raman scatt. parameters, high-resolution coherent active spectroscopy 0-66207  
 $\text{N}_2$  liquid, vibrational dephasing, computer simulation, pair potential effect 0-63863  
 $\text{N}_2\text{-Ar}(\text{Kr})(\text{O}_2)(\text{CO})(\text{CH}_4)$ , liquid, high resolution CW CARS spectra 0-63635  
 $\text{O}_2$ , liq., pure vibr. Raman spectra 0-97262  
 $3\text{RbNO}_3-2\text{Ca}(\text{NO}_3)_2$ , glass form. from liq., struct. transform., Raman spectrum obs. 0-64916  
 $\text{SbCl}_3/\text{AlCl}_3$  molten mixtures, Raman spectra 0-93305  
 Se, Raman spectra, crystn. processes 0-60608  
 $\text{SeCl}_4\text{-SbCl}_5$  systems, Raman spectra (German) 0-93324  
 Te, Raman spectra, crystn. processes 0-60608  
 $\text{ZnCl}_2(\text{Br}_2)(\text{I}_2)$  glassy aqueous solutions, Raman spectral study 0-84738

**Raman spectra of inorganic solids**

- alkali halides, localised vibration of interstitial H atom 0-88998  
 $\text{B}_2\text{O}_3\text{-Li}_2\text{O-LiCl}$ , ionic conductor, IR refl. Raman study 0-66173  
 diamond, light coupling prism, Raman spectra for thin film props. study 0-88978  
 diamond, two-phonon bound state, Raman freq. 0-65179  
 electrolyte, soln. and cryst. (German) 0-80804  
 four-wave mixing spectroscopy in crystals., nonlinear spectroscopy developments 0-91861  
 gemstones, light coupling prism, Raman spectra for thin film props. study 0-88978  
 glass structure, vibr. spectroscopy studies 0-84732  
 glasses, elec., mag., and optical props., conference, Troy, NY, USA (Aug. 1979) 0-105417  
 graphite intercalation with Li, Raman scatt. study 0-88999  
 graphite- $\text{Br}_2$  stage 2 intercalation cpds., Raman spectra 0-80787  
 graphite- $\text{H}_2\text{SO}_4\text{F}$  intercalation compound, Raman spectral study (French) 0-60581  
 ice, O-H and O-D bond stretching vibrs., Raman spectra at atmospheric press. 0-66166  
 II-VI semiconductor, resonant secondary emission spectra, relax. of energy and polarisation 0-93331  
 metal surface, rough, anomalous low-freq. Raman scatt. from localised acoustic vibrs. 0-93307  
 metal surface molecule enhanced Raman scatt., rough surface spheroidal model 0-84744  
 molecular optical laser examiner appl. 0-62737  
 optical fibres, Raman scatt., guiding structs. effects on spontaneous and stimulated emission 0-58636  
 perovskites, ordered cubic, cationic effect on intramolecular forces, stretching force const. 0-88979  
 phosphate glasses, non-alkaline, transition states, phys. effects of fluors, phase diagrams and optical effects (German) 0-88045  
 polar semiconductor crystalline thin films, surface vibr. states, IR absorpt. spectra obs. (Russian) 0-60606  
 Raman spectra, vibr. anal. 0-93312  
 rare earth double orthophosphates with alkali metals, spectroscopic obs., struct. and chem. nature 0-100674  
 rare earth orthoferrites, Raman scatt. from magnons, anisotropy consts. determ. 0-66178  
 rare earth oxyphosphates, IR and Raman spectra, vibr. assignments, cryst. struct. characts. 0-97258  
 resonance Raman scatt. singularities (Russian) 0-89007  
 resonant Raman scattering via virtual exciton 0-71412  
 Rochelle salt, ferroelectric, Raman and IR study 0-71406  
 $\beta\text{-Sb}_2\text{O}_3$ , Raman spectra, vibr. anal. 0-93312  
 semiconductor, direct band gap type, polarization theory of reson. electronic Raman scatt. on neutral donor levels 0-108194  
 semiconductors, exciton effect in interband electronic Raman scattering 0-103946  
 semiconductors, light induced electron drift, two-photon transitions (Russian) 0-107853  
 semiconductors, optical props. due to phonons, book contrib. 0-80805  
 semiconductors, polar, resonance electron-phonon Raman scatt., cross-section oscils. 0-60598  
 semiconductors with direct band gaps, exciton-polariton interactions, Green's function approach 0-92831  
 superconductors, phonon Raman scatt. 0-100657  
 talc, vibr. mode assignments, Raman microprobe spectra 0-88977  
 thiourea, ferroelectric, Raman and IR study 0-71406  
 trissarcosine calcium chloride, ferroelec. phase transition, Raman and Brillouin scatt. studies 0-71340

**Raman spectra of inorganic solids continued**

- Ag, sorption of pyridine, surface enhanced Raman scatt., mol.-surface separation depend. 0-92775  
 $\text{Ag}_3\text{AsS}_3$ , and  $\text{Ag}_3\text{SbS}_3$ , Raman spectra obs. of low-temp. phases 0-93327  
 $\text{Ag}_3\text{AsS}_3$ , proustite, phonons and soft modes at ferroelec. transition 0-60524  
 $\text{Ag}_2\text{HgI}_4$ , Raman line shape and ionic cond., coupled mode model 0-66171  
 $\text{AgNa}(\text{NO}_2)_2$ , ferroelec., Raman scatt. and phase transitions 0-71349  
 $\text{AgNa}(\text{NO}_2)_2$ , ferroelec. cryst., Raman spectrum, phase transition, comparative anal. with  $\text{NaNO}_2$  0-88935  
 $\text{AlF}_3$  based glasses, chem., thermal and optical props. (*French*) 0-70139  
 $\text{AlF}_3\text{-M}_2\text{F}$  glasses, M=alkaline earth, density-of-states and structural forms, Raman spectra study 0-97255  
 $\beta\text{-Al}_2\text{O}_3\text{-(Na,Li)}_2\text{O}$ , NMR, Raman and IR spectra, and X-ray diff., heat treatment induced changes 0-107508  
 $\text{Al}_2\text{O}_3$ , Raman spectroscopy study of adsorbed molecules 0-65358  
 $\beta\text{-Al}_2\text{O}_3\text{:NH}_4^+\text{(Nd}^{3+}\text{)}$ , polarised Raman scatt. 0-103947  
 $\beta\text{-Al}_2\text{O}_3\text{-(Na,Li)}_2\text{O}$ ,  $\beta\text{-Al}_2\text{O}_3\text{-(K,Li)}_2\text{O}$  and  $\beta\text{-Al}_2\text{O}_3\text{-(K,Sn)}_2\text{O}$ , ionic cond. and Raman spectra 0-107509  
 $\beta^+\text{-Al}_2\text{O}_3\text{-Ag}_2\text{O(K}_2\text{O)(Li}_2\text{O)(Na}_2\text{O)(Rb}_2\text{O)}$ , single cryst. Raman scatt., cond. mechanism and cryst. struct. 0-66209  
 $\gamma\text{-AlOOH}$  and  $\gamma\text{-AlOOD}$ , struct. and  $\text{D}_{2h}^{17}$  space group anal. 0-89000  
 $\alpha\text{-AlPO}_4$ , berlinite,  $\text{H}_2\text{O}$  conc. determ. by Raman scatt. 0-76572  
 $\alpha\text{-AlPO}_4$  crystal, totally symm. high-freq. fund. vibrs., identification refinement 0-100656  
 $\text{Ar}_2\text{O}_2$  (6%) cryst., vibr. Raman spectra 0-60558  
As-Se amorphous system, Raman scatt. 0-88984  
 $\text{As}_2\text{S}_5$ , amorphous, struct., vibr. and electronic spectra 0-64908  
 $\text{As}_{50}\text{S}_{100-x}$  glasses, Raman spectrum and structure 0-60593  
 $\text{As}_{20}\text{Sb}_{80}\text{Si}$  cryst., ferroelec., soft mode Raman and IR spectroscopy 0-76016  
 $\text{As,Sb}_{1-x}\text{Si}$  mixed crystals, phonon coupling, ferroelectric phase transition, Raman study 0-108165  
 $\text{B}_2\text{O}_3$  and alkali borate glasses, Raman study at high temps. 0-93306  
 $\text{B}_2\text{O}_3\text{-V}_2\text{O}_5\text{-P}_2\text{O}_5$ , glass, mech. and elec. props 0-84228  
 $\text{BaMnF}_4$ , spectroscopy near ferroelec. transition, dielec. anomalies near mag. ordering temp. 0-75965  
 $\text{Ba}_2\text{NaNb}_2\text{O}_{15}$ , high press. phase transitions, Raman scatt. studies 0-71402  
 $\text{BaTa}_2\text{O}_8$ , structural study X-ray diff., IR absorpt. and Raman spectra (*French*) 0-107173  
 $\text{BaTiO}_3$ , ferroelec. cryst., IR and Raman spectra, mode coupling 0-66194  
 $\text{BaTiO}_3$ , polymorph, hexagonal, low temp. and surface  $\text{CO}_2$  adsorption and desorption, Raman spectra obs. 0-80713  
 $\text{Bi}_{2-x}\text{La}_x\text{WO}_6$ , synthesis and crystallography 0-66459  
 $\text{Bi}_2\text{SiO}_5\text{:Sn(Mo)}$ , Raman scatt. spectra, impurity effect 0-80795  
 $\text{CO}_2$ , solid, Fermi reson. press. tuning, Raman spectra 0-93293  
 $\text{CS}_2$ , second order Raman spectrum in condensed phase 0-93299  
 $\text{CaCl}_2\text{(Br)}_2\text{(I)}_2$ , glassy aqueous soln., LF region Raman spectra 0-84729  
 $\text{CaO-Al}_2\text{O}_3\text{-SiO}_2$  glasses, density-of-states and structural forms, Raman spectra study 0-97255  
 $\text{CdCr}_2\text{S}_4\text{(Se}_4\text{)}$ , thermoreflectance, photoconductance, Raman scatt. near mag. phase transition 0-97298  
 $\text{CdInGaS}_4$ , crystal, Raman scattering spectra, polarisation meas. (*Russian*) 0-71410  
 $\text{Cd}_{1-x}\text{Mn}_x\text{Te}$  mixed crystals, Raman spectra 0-103961  
 $\text{CdS}$ , doped, amorphous antiferromagnet model, susceptibility and spin-flip Raman scatt. meas. 0-97057  
 $\text{CdS}$  electronic two- and one-photon Raman scatt. via biexcitons, stimulated config. obs. mag. field shift 0-103963  
 $\text{CdS}$ , pure spin diffusion without charge transport, spin flip Raman scatt. obs. 0-93329  
 $\text{CdS}$ , two-photon absorpt. effect on hyper-Raman scatt. 0-74441  
 $\text{CdSe:Li}$ , pure and doped, reson. Raman and Brillouin scatt., elastic exciton-defect scatt. 0-80788  
 $\text{CeH}_3$ , phonon features in IR and Raman spectra 0-93310  
 $\text{Ce}_2(\text{SO}_4)_3\cdot 9\text{H}_2\text{O(D}_2\text{O)}$ , polarised Raman spectra, vibr. props. and role of lattice  $\text{H}_2\text{O}$  0-66201  
 $\text{CoCO}_3$ , LF exciton and Raman spectra, one-magnon and two-magnon scatt. 0-93333  
Cs salts, Raman and IR spectra of the dicyaniodate (I) ion 0-60572  
 $\text{CsCoBr}_3$ , ID Ising antiferromagnet, spin dependent Raman scattering from phonons and electronic excitations 0-103948  
 $\text{CsCoBr}_3$ , quasi ID Ising antiferromag., polarised Raman scatt. from mag. excitations 0-66182  
 $\text{CSHg(CN)}_3$ , CN and HgC stretching vibrations and HgCN bending vibration assignments 0-69140  
 $\text{Cs}_2\text{NaErCl}_6$ , mag. susceptibility and IR and Raman spectra meas., crystal field splitting determ. 0-100652  
 $\text{CSbF}_6$ , high press. phase relations, vibr. spectra, and cryst. chemistry 0-108200  
 $\text{CuBr(CI)(I)}$ , LF light scatt. spectra in superjonic cond. phases, ion motion obs. 0-108217  
 $\text{CuBr(CI)(I)}$ , polariton Raman spectra, oscillator strengths, temp. depend. 0-66197  
 $\text{CuCl}$  crystal resonant Raman scatt. and luminescence competition (*Japanese*) 0-80770  
 $\text{CuCl}$ , exciton spatial dispersion determ., two-photon Raman scatt. via excitonic mol. state 0-60595  
 $\text{Cu}_2\text{O}$ , reson. Raman scatt. from stress-split forbidden excitons 0-93332  
 $\text{Cu}_2\text{O}$ , uniaxial stress effects on excitons 0-60589  
 $\text{Cu}_2\text{VS}_4$ , Raman linewidth of  $\text{A}_1$  mode under high press., reson. effects 0-108210  
 $\text{Dy}_2\text{S}_3$ , vibr. spectra, factor-group anal. 0-80793  
Eu chalcogenides, resonant Raman scattering model via magnetic exciton in ferromagnetic phase 0-93326  
Eu chalcogenides, spin-dependent Raman scatt. from phonons 0-97274  
 $\text{EuO(S)(Te)}$ , spin order and fluctuations, Raman scatt. study 0-97273  
 $\text{EuS-Ga}_2\text{S}_3\text{-GeS}_3$ , chalcogenide glasses, conditions of form. of glassy prod. (*French*) 0-100325  
 $\text{EuS(Se)(Te)}$ , spin-assisted phonon Raman scatt., mag. phase depend. 0-71413  
 $\text{EuTe}$ , antiferromag. semicond., Raman scatt., spin-phonon interactions 0-66185  
 $\text{EuTe}$ , mag. 'Bragg' scatt. obs. through Raman scatt. 0-66179  
Fe-Cr-Ni based alloys, surface oxides at high temps., backscattering Raman spectroscopy 0-93291

**Raman spectra of inorganic solids continued**

- $\text{FeF}_2$  antiferromag., anomalous anti-Stokes/Stokes Raman scatt. intensity ratio 0-66177  
 $\text{FeF}_2$ , interacting phonon-magnon states, theory of Raman scattering and IR obs. 0-71426  
 $\text{Fe}_{1-x}\text{Mn}_x\text{Cl}_2$ , disordered, Raman scatt. from  $\text{Fe}^{2+}$  and Neel temp. 0-60579  
 $\text{Fe}_{1-x}\text{Mn}_x\text{Cl}_2$ , low-lying electronic excitations in antiferromag. and paramag. phases Raman scatt. study 0-71414  
 $\text{Fe}_{1-x}\text{Zn}_x\text{F}_2$ , dil. antiferromag., electronic and mag. props., Raman scatt. and optical absorpt. study 0-108207  
 $\text{Fe}_{1-x}\text{Zn}_x\text{F}_2$ , electronic Raman scatt., mag. anisotropy 0-66184  
 $\text{Ga}_{1-x}\text{Al}_x\text{Sb}$ , surface oxidation, Raman spectra, residual Sb layers 0-71419  
GaAs, electronic Raman scatt. of polarised light on donor levels 0-93309  
GaAs, Raman scattering from nonequilibrium LO phonons with picosecond resolution 0-80779  
GaAs-AlAs superlattice, folded acoustic phonons obs., Raman scatt. 0-88996  
GaP, light scatt. by LO phonons, high-resolution study 0-80798  
GaP, Raman scatt. from plasmon-phonon coupled modes 0-93337  
p-GaP, spin-flip Raman scattering, review 0-108209  
GaSb, accumulation layer localised carriers interaction with LO phonons, Raman interference lineshapes 0-93338  
p-GaSb, heavily doped, LO phonon-carrier interaction, Raman interf. lineshapes 0-93319  
GaSe films, optical props. at lattice vibr. freqs., IR and Raman spectra 0-60696  
e-GaSe, Raman scatt., hydrostatic press. effect 0-84745  
 $\text{GaSe}_{1-x}\text{Te}_x$ , Raman scatt., optical phonons and phase transition 0-66202  
 $\text{GaSe}_{1-x}\text{Te}_x$ , Raman spectra, phonon freq. 0-97286  
 $\alpha\text{-GaTe}$ , single cryst., Raman scatt. 0-60599  
B-GdO<sub>3</sub>, monoclinic single cryst., Raman spectrum 0-103953  
 $\text{Gd(OH)}_3$ , dynamical effects of interaction between 4f electrons and optical phonons 0-108196  
 $\text{GeO}_2\text{-K}_2\text{O(Na}_2\text{O)(Li}_2\text{O)}$ , glass, Raman spectra, struct. and crystn. 0-92463  
p-H<sub>2</sub>, solid, time-resolved CARS, disorder effects on coherent vibr. states 0-93342  
HBO<sub>3</sub>, cubic, monoclinic and orthorhombic forms, H bonding, IR and Raman spectra 0-76029  
 $\text{Hg(CN)}_2$ , phonon freq. anomalous press. depend., mol. struct. distortion 0-88981  
 $\text{Hg}_2\text{Cl}_2$ , neutron and Raman scatt. studies, ferroelastic transitions 0-76015  
 $\text{HgCr}_2\text{Se}_4$ , thermoreflectance, photoconductance, Raman scatt. near mag. phase transition 0-97298  
 $x_{1-x}$  mixtures, high-temp. solids and melts, struct., thermodynamic props., Raman spectra obs. 0-66174  
In pnictides, mixed, impurity induced Raman scatt. spectra 0-88983  
InP, depend. of phonon spectrum on hydrostatic press., Raman spectra 0-93315  
InSb, accumulation layer localised carriers interaction with LO phonons, Raman interference lineshapes 0-93338  
p-InSb, heavily doped, LO phonon-carrier interaction, Raman interf. lineshapes 0-93319  
InSb, Raman scattering study of unoxidised Sb in anodic oxide films 0-88985  
p-InSb, spin-flip Raman scattering, review 0-108209  
InSe, exciton and polaron anisotropies, reson. Raman scatt. study 0-76033  
 $\text{KBr:MnO}_4^-$ , many-phonon impurity reson. Raman scatt. 0-60603  
 $\text{KBr:MnO}_4^-$ , model system, reson. Raman spectra, general behaviour obs. 0-60592  
KCN, dynamics of  $\text{CN}^-$  ions near phase transitions at 83K 0-80717  
KCN, Raman diffusion spectra, IR absorpt. in phases II and III (*French*) 0-84741  
 $\text{K}_2\text{CoF}_4$ , 2-dimens. Ising antiferromag., mag. excitons, Raman scatt. obs. 0-66181  
 $\text{KD}_2\text{AsO}_4$ , ferroelec., high temp. phase transition, Raman spectra 0-71338  
 $\text{KD}_2\text{AsO}_4$ , ferroelectric, high temp. phase transitions, proton dynamics 0-76023  
 $\text{KDy(MoO}_4\text{)}_2$ , polarised IR and Raman struct.,  $^{92}\text{Mo}/^{100}\text{Mo}$  isotope effect 0-108198  
 $\text{K}_3\text{Fe(CN)}_6$ , pressure induced reduction, Raman spectra 0-66776  
 $\text{K}_2\text{FeF}_4$ , two-dimensional antiferromag., with easy-plane anisotropy, mag. excitations and two-magnon Raman scatt. 0-65839  
 $\text{KF(FeO}_4\text{)}_2$ , phase transitions at 312 and 139K 0-70396  
 $\text{KH}_2\text{AsO}_4$ , ferroelec., high temp. phase transition, Raman spectra 0-71338  
 $\text{KH}_2\text{AsO}_4$ , ferroelectric, high temp. phase transitions, proton dynamics 0-76023  
 $\text{K}_2\text{InCl}_4\cdot\text{H}_2\text{O}$ , crystal structure and H-bonding 0-64978  
 $\text{K}_3\text{MnF}_3$ , quadratic double layer antiferromag., two-magnon Raman scatt. 0-66183  
 $\text{KNO}_3$ , Raman and IR spectra and lattice vibrs. 0-60565  
 $\text{K}_2\text{NaGaF}_6\text{:Cr}^{3+}$ , magneto-optical study of  $^2\text{T}_{1g}$ ,  $^4\text{T}_{2g}$ ,  $^2\text{E}_g\text{-}^4\text{A}_{2g}$  transitions 0-71384  
 $\text{KNbO}_3$ , ferroelec. cryst., IR and Raman spectra, mode coupling 0-66194  
 $\text{K}_3\text{NiF}_3$ , quadratic double layer antiferromag., two-magnon Raman scatt. 0-66183  
 $\text{K}_2\text{O-MgO-B}_2\text{O}_3\text{:Cu}^{2+}$ , micro-inhomogeneities, EPR and Raman study 0-84080  
 $(\text{K}_2\text{O})_x(\text{SiO}_2)_{1-x}$  glass, pure and with  $\text{As}_2\text{O}_3$ , Raman study of As 0-84733  
 $\text{K}_2\text{SeO}_4$ , phase mode in incommensurate phase, Raman scatt. obs. 0-80766  
 $\text{K}_2\text{SeO}_4$ , Raman spectra, effects of temp., substitutional cations, and stress 0-71405  
 $\text{K}_2\text{SeO}_4$ , structural transition, polarised Raman spectra 0-75349  
La-B, amorphous, B-rich, low freq. modes, Raman scatt. obs. 0-108202  
 $\text{La}_2\text{S}_3$ , vibr. spectra, factor-group anal. 0-80793  
 $\text{LiCl-Li}_2\text{O-P}_2\text{O}_5$  glass system, vitreous domain, struct., elec. cond. (*French*) 0-70135  
 $\text{LiCl(Br)(I)}$ , glassy aqueous soln., LF region Raman spectra 0-84729  
 $\text{LiH}_2\text{PO}_4$ , Raman and IR spectra of transverse and longitudinal modes (*French*) 0-60573  
 $\text{LiIO}_3$  crystal, noncollinear stimulated Raman scatt. using parallel pump beam 0-78912



## Raman spectra of inorganic solids continued

- Li<sub>2</sub>O-Al<sub>2</sub>O<sub>3</sub>-SiO<sub>2</sub>-TiO<sub>2</sub> system glasses, Raman spectra obs. of glass-ceramics form. 0-60825  
 Li<sub>2</sub>O-B<sub>2</sub>O<sub>3</sub>-P<sub>2</sub>O<sub>5</sub>, glass, mech. and elec. props 0-84228  
 Li<sub>2</sub>O-LiX-B<sub>2</sub>O<sub>3</sub> glass, X=halogen, high anionic cond. of new solid electrolytes 0-107546  
 Li<sub>2</sub>S-GeS<sub>2</sub>, glass forming region, struct. and ionic cond. 0-88358  
 Lu<sub>2</sub>O<sub>3</sub>-Si<sub>2</sub>O<sub>7</sub>-Eu<sub>2</sub>O<sub>3</sub>, synthesis and spectroscopic study 0-84846  
 MgCl<sub>2</sub>-alkali metal chloride system, solid and molten states, struct. props., Raman spectra 0-76011  
 MgO:Co<sup>2+</sup>, electronic and impurity-induced Raman scatt. 0-100659  
 Mn(CO), Br-Re(CO)<sub>5</sub>Br, polycryst.,  $\nu$ (CO) vibr. intermol. Raman intensity transfer 0-60564  
 Mn,Cd<sub>1-x</sub>Te, lattice vibr., Raman and IR spectra meas. 0-93311  
 Mn,Cd<sub>1-x</sub>Te, phonons, Raman scatt. and IR absorpt. meas. (French) 0-97275  
 $\beta$ -N<sub>2</sub> cryst., vibr. Raman spectra 0-60558  
 $\alpha$ -N<sub>2</sub> solid, time-resolved CARS, disorder effects on coherent vibr. states 0-93342  
 ND<sub>4</sub>I, Raman spectrum, press. effects 0-97261  
 ND<sub>4</sub>IO<sub>4</sub>, Raman spectra, libration lattice modes 0-60575  
 NH<sub>4</sub>Cl Raman spectra, pressure effects 0-97268  
 NH<sub>4</sub>I, Raman spectrum, press. effects 0-97261  
 NH<sub>4</sub>IO<sub>4</sub>, Raman spectra, libration lattice modes 0-60575  
 NH<sub>4</sub>NO<sub>3</sub> crystals, NH<sub>4</sub><sup>+</sup> ion symmetry in phases II-V, Raman spectra obs. 0-66200  
 (NH<sub>4</sub>)<sub>2</sub>SnBr<sub>6</sub>, structural phase transitions study by Raman scatt. 0-93318  
 NaAlCl<sub>4</sub>, Raman spectra, cryst. struct. (French) 0-60578  
 NaCN, Raman diffusion spectra, IR absorpt. in phases II and III (French) 0-84741  
 NaH<sub>2</sub>(SeO<sub>3</sub>)<sub>2</sub>,  $\beta$  to  $\delta$  ferroelec. transition under press. Raman spectra study 0-80725  
 NaI:F, electron-lattice coupling of F-centres, optical props. 0-60641  
 Na<sup>15</sup>N, <sup>14</sup>N<sub>2</sub>-O<sub>3</sub> mixed crystal, Raman spectra determ. of phonon density of states (Russian) 0-93313  
 Na<sub>2</sub>O-B<sub>2</sub>O<sub>3</sub>-P<sub>2</sub>O<sub>5</sub>, glass, mech. and elec. props 0-84228  
 Na<sub>2</sub>O-Li<sub>2</sub>O-Al<sub>2</sub>O<sub>3</sub>-H<sub>2</sub>O, water mol. vibr., IR and Raman spectra 0-89006  
 Na<sub>2</sub>O-MgO-B<sub>2</sub>O<sub>3</sub>:Cu<sup>2+</sup>, micro-inhomogeneities, EPR and Raman study 0-84080  
 Na<sub>2</sub>S-P<sub>2</sub>S<sub>5</sub>, glass forming region, struct. and ionic cond. 0-88358  
 Na<sub>2</sub>S-XS<sub>2</sub>, X=Si, Ge, glass forming region, struct. and ionic cond. 0-88358  
 Na<sub>2</sub>SbS<sub>4</sub>, vibrational spectra, internal SbS<sub>4</sub> vibr. assignments 0-66199  
 Na<sub>2</sub>SbS<sub>4</sub>·9H<sub>2</sub>O(D<sub>2</sub>O), vibrational spectra, internal SbS<sub>4</sub> and H<sub>2</sub>O(D<sub>2</sub>O) vibr. assignments 0-66199  
 NbSe<sub>2</sub> (2H), Raman scatt. from supercond. gap excitations 0-93340  
 NbSe<sub>2</sub> (2H), Raman scatt. by supercond. gap excitations, coupling to CDWs 0-103956  
 Nd(OH)<sub>3</sub>, dynamical effects of interaction between 4f electrons and optical phonons 0-108196  
 Nd<sub>2</sub>S<sub>3</sub>, vibr. spectra, factor-group anal. 0-80793  
 Ni<sup>2+</sup> + MoO<sub>3</sub> catalyst on Al<sub>2</sub>O<sub>3</sub>, Raman spectrum 0-108742  
 NiO-Cr<sub>2</sub>O<sub>3</sub>-MgSiO<sub>3</sub> methanation catalyst, S-resistant, IR and Raman spectra 0-93290  
 NiS<sub>2</sub>,  $\gamma$ -Se<sub>2</sub>, first-order Raman scattering 0-108206  
 $\gamma$ -O<sub>2</sub> cryst., vibr. Raman spectra 0-60558  
 PCl<sub>3</sub>, sublimed phase studied by <sup>31</sup>P NMR, Raman spectra and X-ray diff. 0-100209  
 Pb electrode, in situ surface phase study by laser Raman spectroscopy 0-103542  
 (Pb<sub>1-x</sub>Bi<sub>x</sub>)<sub>2</sub>Ge<sub>2</sub>O<sub>11</sub>, ferroelec. phase transition, dielec. const. and quasi-elastic light scatt. 0-71289  
 PbI<sub>2</sub> direct gap polar semicond., electron hole liquid phase diagram (Russian) 0-93314  
 PbNb<sub>2</sub>O<sub>6</sub>, IR absorpt. spectra and diffuse Raman scatt., normal coord. anal. (French) 0-66198  
 PbO-SiO<sub>2</sub> glasses, density-of-states and structural forms, Raman spectra study 0-97255  
 12PbO·6SiO<sub>2</sub>·PbSO<sub>4</sub>, crystn. from 2PbO-SiO<sub>2</sub>-xSO<sub>3</sub> melts, struct. and vibr. spectra 0-59400  
 PbTa<sub>2</sub>O<sub>6</sub>, IR absorpt. spectra and diffuse Raman scatt., normal coord. anal. (French) 0-66198  
 PbTiO<sub>3</sub>, amorphous, crystallisation process, DTA and Raman spectroscopy meas. 0-75161  
 Rb halides, role of quantum effects in lattice dynamics, Debye temp., shell model calcs. 0-70336  
 RbCaCl<sub>3</sub>, Raman scatt. study of phase transitions 0-71411  
 RbClO<sub>3</sub>/RbBrO<sub>3</sub> mixed crystals, internal optic modes obs., Raman and IR reflectance spectra 0-76024  
 RbCoF<sub>4</sub>, 2-dimens. Ising antiferromag., mag. excitons, Raman scatt. obs. 0-66181  
 Rb<sub>2</sub>FeF<sub>4</sub>, two-dimensional antiferromag., with easy plane anisotropy, mag. excitations and two-magnon Raman scatt. 0-65839  
 Rb<sub>2</sub>ZnBr<sub>4</sub>, soft modes obs. by Raman scatt. 0-97283  
 Rb<sub>2</sub>ZnBr<sub>4</sub>(Cl<sub>4</sub>), Raman spectra near incommensurate phase transitions 0-76013  
 (SNI<sub>4</sub>)<sub>x</sub> crystals, reson. Raman scatt. meas. 0-66203  
 Se, amorphous, bulk, Raman scatt. near T<sub>g</sub> 0-60596  
 Se, amorphous, bulk, reson. Raman scatt. 0-60597  
 Se, amorphous, Raman spectra, crystn. processes 0-60608  
 Se, trigonal, Raman scatt. at very high press. 0-60566  
 SeCl<sub>4</sub>-SbCl<sub>3</sub> systems, Raman spectra (German) 0-93324  
 Si, amorphous layers, RF-sputtered on sapphire, crystallisation by CW ion laser annealing 0-80109  
 Si, elasto-optic constants, real and imaginary, direct absorpt. and Raman scatt. meas. 0-97234  
 p-Si, heavily doped, intra- and interband Raman scatt. by free carriers 0-108208  
 Si, laser pulsed heating, lattice temp., Raman meas. 0-80780  
 Si, stretched, lattice vibr. anharmonicity, influence of stress on elastic moduli, Raman spectra 0-80791  
 Si, temperature during CW laser heating, Raman scatt. meas. 0-76109  
 Si, thin slabs, vibr. freq. calcs., dimens. effect 0-60585  
 Si-F-H-P, film, dark cond., struct., Raman scatt. 0-88588  
 Si-H-P amorphous film, dark cond., struct., Raman scatt. 0-88588  
 SiC, laser Raman spin-flip scatt. from excitons, luminesc. 0-80786  
 p-SiC, spin-flip Raman scattering, review 0-108209  
 SiC, spin-flip scatt. of laser light from photoexcited excitons 0-93330  
 SiO<sub>2</sub> fibres, LF optical phonons, Raman spectra 0-80789

## Raman spectra of inorganic solids continued

- SiO<sub>2</sub> films, Si-rich, amorphous Si region obs. 0-84400  
 SiO<sub>2</sub>-Li<sub>2</sub>O-Li<sub>2</sub>SO<sub>4</sub>, glass-forming region, struct. and ionic cond. 0-84320  
 Sn<sub>2</sub>P<sub>2</sub>S<sub>6</sub>, ferroelec. semicond., phase transition and lattice dynamics 0-60526  
 Sn<sub>2</sub>P<sub>2</sub>S<sub>6</sub>, soft mode props., Raman scatt. study 0-60525  
 SnS<sub>2</sub>(1-x)S<sub>2x</sub> solid soln. system, long-wavelength optical phonons, Raman scatt. study 0-80794  
 SnS<sub>2</sub>-Se<sub>2</sub>, layer cryst., Raman active modes 0-80767  
 Sr<sub>2</sub>Ba<sub>1-x</sub>Nb<sub>2</sub>O<sub>6</sub>, high press. phase transitions, Raman scatt. studies 0-71402  
 Sr<sub>2</sub>Nb<sub>2</sub>O<sub>6</sub>, high press. phase transitions, Raman scatt. studies 0-71402  
 SrTa<sub>2</sub>O<sub>6</sub>, structural study X-ray diff., IR absorpt. and Raman spectra (French) 0-107173  
 SrTa<sub>2</sub>O<sub>6</sub>, soft optic phonon responsible for structural phase transition, Raman scatt. meas. 0-96618  
 SrTiO<sub>3</sub>, centrosymmetric crystal, phonon polariton hyper-Raman scatt. obs. 0-76028  
 SrTiO<sub>3</sub>, disorder manifestation, light scatt. spectra, high temp. 0-76017  
 SrTiO<sub>3</sub>, ferroelectric modes, Raman spectra, neutron scatt. meas. 0-80727  
 SrTiO<sub>3</sub>, heavily reduced, soft mode behaviour 0-71409  
 TaSe<sub>2</sub> (2H), Raman scatt. from CDW 0-93340  
 TbAg, reson. electronic Raman effect, interferences, lifetime meas. 0-93294  
 Tb(OH)<sub>3</sub>, dynamical effects of interaction between 4f electrons and optical phonons 0-108196  
 Te, amorphous, Raman spectra, crystn. processes 0-60608  
 Te, trigonal, Raman scatt. at very high press. 0-60566  
 TiO<sub>2</sub>, anatase, Raman spectrum, temp. depend. 0-76027  
 TiO<sub>2</sub>, rutile, first order Raman spectrum, uniaxial stress effects 0-66196  
 TiO<sub>2</sub>, rutile, first-order Raman spectrum, uniaxial-stress depend. 0-60586  
 TiO<sub>2</sub>, rutile, Raman study at high press. 0-89002  
 TiO<sub>2</sub>-SiO<sub>2</sub> glass system, Raman and hyper-Raman light scatt. spectra 0-66187  
 TiS<sub>3</sub>, linear chain compound, lattice props., Raman spectral study 0-71421  
 TiSe<sub>2</sub> (1T), Raman studies of lattice dynamics 0-103962  
 Tl<sub>4</sub>(M<sub>2</sub>/2)<sup>2+</sup>(I<sub>4</sub>)<sup>2-</sup>, (M=Pb, Ag, Au, (Bi<sub>0.5</sub>Tl<sub>0.5</sub>)), struct., rel. to phonon spectra 0-71425  
 Tl<sub>2</sub>SeO<sub>4</sub>, structural transition, polarised Raman spectra 0-75349  
 Ti<sub>2</sub>Ta<sub>2</sub>S<sub>4</sub> and Ti<sub>2</sub>PS<sub>4</sub>, optical phonons, Raman spectra study 0-80790  
 (V<sub>1-x</sub>Cr<sub>x</sub>)<sub>2</sub>O<sub>3</sub>, Raman scatt. and phase transitions 0-71420  
 V<sub>1</sub>, mag. Bragg' scatt. obs. through Raman scatt. 0-66179  
 V<sub>1</sub>, spin-dependent Raman scatt. from phonons 0-97274  
 V<sub>2</sub>O<sub>3</sub>, Raman scatt. and phase transitions 0-71420  
 W, chemisorbed H<sub>2</sub>, vibr. spectra characs., adsorption sites 0-70535  
 WS<sub>2</sub> (2H), layered cpd., Raman scatt. 0-103960  
 Xe, two-phonon difference scatt. 0-60588  
 Y-B, amorphous, B-rich, low freq. modes, Raman scatt. obs. 0-108202  
 YIG, one-magnon Raman scatt., Faraday rot. 0-66156  
 Y(OH)<sub>3</sub>, dynamical effects of interaction between 4f electrons and optical phonons 0-108196  
 Zn<sub>1-x</sub>Cd<sub>x</sub>Se, mixed crystals, antireson. in phonon spectrum, Raman spectroscopy 0-88992  
 ZnCl<sub>2</sub>(Br<sub>2</sub>)(I<sub>2</sub>) glassy aqueous solutions, Raman spectral study 0-84738  
 ZnF<sub>2</sub>:Co<sup>2+</sup>, Raman tensor calcs. of isolated impurity in diamagnetic matrix 0-76025  
 ZnIn<sub>2</sub>S<sub>4</sub>, Raman scatt., hydrostatic press. effect 0-84745  
 ZnIn<sub>2</sub>S<sub>4</sub>, vibr. spectrum, Raman study 0-97278  
 ZnP<sub>2</sub>, resonance Raman scatt. singularities (Russian) 0-89007  
 ZnS, Raman scatt. by phonon polaritons 0-103959  
 ZnSe films, reson. Raman spectra 0-80888  
 ZnSe, resonance Raman scatt., exciton-polariton luminescence (Russian) 0-97287  
 p-ZnTe, spin-flip Raman scattering, review 0-108209  
 ZnTe:Li, electron-phonon interactions in Raman scatt. 0-60594  
 ZrO<sub>2</sub>-Sc<sub>2</sub>O<sub>3</sub>-Yb<sub>2</sub>O<sub>3</sub> system, order-disorder phenomena, Raman spectra study 0-97254  
 ZrS<sub>2</sub>, excitonic transition, reson. Raman spectra, Franck-Condon factors 0-97252

## Raman spectra of organic molecules and substances

- 1,1-dimethyl-1-silylcyclopentane, IR and Raman spectra 0-60577  
 acetate ions adsorbed on Ag particles in aqueous soln. Raman spectra 0-69148  
 acetonitrile, adsorp. on Ag colloids, surface enhanced Raman spectra obs. 0-97251  
 acetonitrile, Raman spectra, vibr. and reorientational and energy transfer width separation, rot. const. determ. 0-87131  
 acetylene, rot. vibr. anal., Raman spectra obs. 0-69146  
 acetylene-cumulene dehydro annulenes, anomalous polarisation in resonance Raman spectra 0-60574  
 acetylene-d<sub>2</sub>(d<sub>1</sub>), rot.-vibr. Raman spectra 0-83372  
 acid oxalate ion in aq. soln., vibr. studies, IR and Raman spectra 0-95589  
 adamantane, plastic and solid-solid transitions, Raman study 0-60590  
 air pollutant gases and vapours, relative Raman scatt. cross section 0-100061  
 L-alanine and DL-alanine, cryst., Raman band intensities of local group modes 0-93298  
 n-alkanes, liq., Raman spectra, longit. acoustic modes and gauche-trans energy difference 0-93295  
 alkyl metal carbonyls, phosphine monosubstituted, LF vibr., IR and Raman spectra 0-95585  
 aniline hydrobromide, ferroelastic phase transition, Raman scatt. study 0-108195  
 anthracene, single cryst., CARS and CSRS, two-photon reson. effect 0-95946  
 anthracene crystal, dynamical matrix eigenvectors from Raman scatt. 0-100315  
 anthracene crystals, pre-reson. Raman scatt., 4,2-30K 0-60571  
 anthracene-phenanthrene-tetracyanobenzene, CT-cryst., mini-excitons and lattice dynamics, ESR, optical and Raman spectra 0-60406  
 1,2-benzanthracene, secondary reson. radiation and hot energy transfer, soln. luminesc. 0-87167  
 benzene, absolute Raman scatt. cross-sections for totally symm. modes 0-102510  
 benzene, deuterated and chemisorbed on glass, vibr. bands, Raman scatt. study 0-84737  
 benzene, mol. cryst., reson. four-wave mixing, third order susceptibilities 0-100654

**Raman spectra of organic molecules and substances continued**

benzene (deuterobenzene) adsorpt. on Ag colloids, surface enhanced Raman spectra obs. 0-97251  
 benzonitrile, IR absorpt. and Raman bands, half-band-width conc.-depend. 0-74171  
 bicyclic ring compounds, Raman circular intensity differential spectra obs., mol. struct. 0-87130  
 biphenyl, mol. cryst., reson. four-wave mixing, third order susceptibilities 0-100654  
 bis(methylthio)alkanes, model compounds of polythioethers, vibr. spectra 0-58430  
 t-butyl acetate, rot. isomerism, dielect. and Raman spectra 0-106328  
 t-butyl bromide, vibr. relax. in pure liq. and soln., Raman spectra 0-66167  
 t-butyl chloride, vibr. relax. in pure liq. and soln., Raman spectra 0-66167  
 t-butyl formate, rot. isomerism, dielect. and Raman spectra 0-106328  
 3-butyne-1-ol, vibr. spectra, assignments, rot. isomerism 0-58257  
 calcium dipicolinate trihydrate, IR and Raman spectra, isotopic frequency shift, mol. vibr. obs., point groups determ. 0-89001  
 calcium oxalate, anhydrous, IR and Raman spectra, vibrational studies 0-69139  
 calcium oxalate monohydrate, IR and Raman spectra, vibrational studies 0-69139  
 $\beta$ -carotene, excitation profile of  $\nu_2$  line in resonance Raman spectrum, solvent effects 0-74173  
 chloro(ethyl)silanes and its C derivatives, Raman spectra, mol. vibr. and rot. isomerism 0-87134  
 1-chloro-2,2-dimethylpropane, IR and Raman spectra, vibr. assignment 0-74169  
 1-chloro-2-methylpropane, IR and Raman spectra, vibr. assignment 0-74169  
 trans-1,4-chlorobromocyclohexane, liquid, crystalline and amorphous state, conformation and vibr. spectra, IR obs. 0-60568  
 D-chloroform, soln., Raman scattering tensor components 0-99508  
 chloroform-d in soln., vibr. and reorientational relax., Raman study 0-63636  
 D-chloroform-dimethylsulphoxide, soln., Raman scattering tensor components 0-99508  
 cinnoline, prereson. Raman spectra, vibr. band intensities obs. 0-102515  
 Creutz-Taube complex, mixed valence, reson. Raman calcs. using vibronic coupling model 0-97249  
 cyclohexane-d<sub>12</sub>, Raman linewidth and molecular diameter meas. 0-69153  
 cyclopentadienylhafniumdichloride, gaseous, far IR and Raman spectra 0-95624  
 cyclopentadienyltitanium dichloride, gaseous, far IR and Raman spectra 0-95624  
 cyclopentadienyltitaniumtrichloride, gaseous, far IR and Raman spectra 0-95624  
 cyclopentadienylzirconiumdichloride, gaseous, far IR and Raman spectra 0-95624  
 cyclopentylamine, vibr. spectra and struct. 0-102516  
 cyclopropane, liq., mol. dynamics, Raman and NMR studies of orientational motion 0-93296  
 cytochrome c, low freq. modes and excitation profiles, reson. Raman spectra 0-94428  
 cytochrome c, protein influence on haeme, Raman difference spectroscopy 0-72125  
 deoxyhaemoglobin, Fe(II)-N<sub>2</sub>(His-F8) stretching freq. rel. to quaternary struct. 0-94160  
 1,6-di-p-methoxybenzene sulphonyloxy-2,4-hexadiyne, thermal polymerization, Raman spectra 0-103952  
 dialkyl tartrates, Raman circular intensity differential spectra obs., mol. struct. 0-87130  
 diamantane, plastic and solid-solid transitions, Raman study 0-60590  
 2,2-dichlorobutane, liquid and solid., vibr. spectra, IR and Raman obs. 0-60567  
 dicyclopentadienyl Ti<sup>3+</sup>-N<sub>2</sub> compound complexes, reson. Raman scatt. 0-99510  
 diethylethanamine, vibrational Raman bands, excitation profiles (French) 0-83380  
 dimethoxymethane, vibr. spectra and rot. isomerism 0-106325  
 N,N-dimethyl aniline, adsorpt. on Ag colloids, surface enhanced Raman spectra obs. 0-97251  
 dipicolinic acid, IR and Raman spectra, isotopic frequency shift, mol. vibr. obs., point groups determ. 0-89001  
 1,4-disilabutane, rot. isomerism, Raman and IR spectra 0-74168  
 EBBA, NMR and Raman scatt. studies in nematic phase 0-100619  
 epifluorohydrin, IR and Raman spectra and conformations 0-60576  
 ethyl iodide, microwave spectra and internal rot. anal. 0-69130  
 ethyl-p-azoxybenzoate, far IR and Raman spectra, smectic polymorphism 0-76022  
 ethylcyclopropane, solid, liquid, vapour phase, IR and Raman vibr. spectra 0-84740  
 ethyloxirane, solid, liquid, vapour phase, IR and Raman vibr. spectra 0-84740  
 fluorostyrene, UV Raman spectra, reson. effect in photoreactive states 0-106326  
 formate ions adsorbed on Ag particles in aqueous soln. Raman spectra 0-69148  
 furane, cryst., low freq. vibr. spectrum, temp. depend., 12 to 253K 0-84743  
 X-glycine, cryst., Raman band intensities of local group modes 0-93298  
 guanine nucleotides, purinic 8-CH exchange kinetic isotope effect, Raman spectral study 0-83381  
 haemoglobin, low freq. modes and excitation profiles, reson. Raman spectra 0-94428  
 haemoglobin, nanosec. probe of dynamics using time resolved reson. Raman scatt. 0-94162  
 haemoglobin haem structure after photo-deligation, Raman spectra 0-61510  
 iodomethane, Raman band shapes, mol. oscill. bands (German) 0-69154  
 isobutylene, liq., vibr. phase relax. and freq. shifts, density and temp. effects 0-74235  
 isopropylcyclopropane, solid, liquid, vapour phase, IR and Raman vibr. spectra 0-84740  
 isouquinoline, adsorbed on Ag, surface enhanced Raman spectrum 0-100400  
 lithium formate, optical phonons, small oscillator strength meas. from frequency-angular polariton spectra 0-92629

**Raman spectra of organic molecules and substances continued**

malononitrile, cryst., phase transitions, Raman and IR obs. 0-88980  
 MBBA, NMR and Raman scatt. studies in nematic phase 0-100619  
 MBBA, Raman spectra in cryst., frozen glassy, and liq. cryst. states 0-60601  
 menthane ring compounds, Raman circular intensity differential spectra obs., mol. struct. 0-87130  
 metallomacrocycles, mixed valent, cofacial assembly, cond. polymeric material 0-70143  
 metalloporphyrin, low symmetry environment, Raman excitation spectra and absorpt. spectrum 0-74172  
 methaemoglobin, struct. change on addition of inositol hexaphosphate 0-72130  
 methane, liq., pure vibr. Raman spectra 0-97262  
 methane, solid, phase II, Raman spectrum, vol. and temp. depend. 0-97260  
 methanol, aqueous, damped coupled oscillator model used to study Fermi resonance 0-69152  
 methotrexate-dihydrofolate reductase complex form., conform., laser Raman obs. 0-104553  
 methoxydifluorophosphine-d<sub>0</sub> and -d<sub>3</sub>, IR and Raman spectra, mol. vibr. and struct. obs. 0-87103  
 methyl orange, aq. soln., reson. Raman spectra of D and <sup>14</sup>N isotopes 0-91566  
 (+)-(3R)-methylcyclohexanone, vibr. optical activity, Raman obs. 0-102499  
 methylene glycol(-d<sub>4</sub>)=formaldehyde(-d<sub>2</sub>)+H<sub>2</sub>O(D<sub>2</sub>O) Raman spectra and normal vibr. 0-58271  
 methylpyridine adsorbed on Ag, surface enhanced Raman spectra 0-83376  
 molecular crystals, intermolecular interactions, spectroscopic studies, review 0-103958  
 molecular crystals, mol. orientation defects, effect on polarised IR and Raman spectra 0-88989  
 molecules D<sub>6h</sub>, D<sub>3h</sub> and D<sub>3d</sub>, appl. of Aliev-Watson maxima-minima criteria for quartic centrifugal distortion const. 0-87132  
 naphthalene, external mode one-density states, low freq. Raman scatt. spectra (French) 0-76012  
 naphthalene, mol. cryst., reson. four-wave mixing, third order susceptibilities 0-100654  
 naphthalene, prereson. Raman spectra, vibr. band intensities obs. 0-102515  
 naphthalene, vibr. relax. studied by four wave mixing (CARS), spectral lineshapes obs. 0-80762  
 naphthalene crystal, dynamical matrix eigenvectors from Raman scatt. 0-100315  
 neopentane, diamond force const., rel. to crystal elastic consts., Raman freq., bulk compressibility and freq. assignments 0-65183  
 nicotinamide adenine dinucleotide, and reduced form, pH induced modification, Raman spectra 0-85343  
 nitrobenzene, IR absorpt. and Raman bands, half-band width conc.-depend. 0-74171  
 nitrocyclopropane, vibr. spectra struct. and bonding 0-102520  
 nitrosobenzene, fluoresc. quantum yields, determ. from Raman scatt. 0-58294  
 p-nitrotoluene crystal film, exciton spectrum, IR absorpt. and Raman scatt. 0-80771  
 organic molecules, C-H Raman stretching bands in soln., vibr. freqs. and linewidth 0-78622  
 organic mols., relative Raman intensities, CNDO/2 INDO param. effect 0-95633  
 organic solids, vibr. relax. and dephasing Raman spectra, review 0-88987  
 organometallic amines, Raman spectra, band intensity and assignment, force const. determ., vibr. props. (German) 0-87133  
 oxalate ion in aq. soln., vibr. study and Raman bands 0-95588  
 oxalic acid in aq. soln., vibr. studies, IR and Raman spectra 0-95589  
 2,2-paracyclophane, dimer vibration influence on emission spectrum 0-69133  
 n-paraffin, longitudinal acoustic mode, perturbing forces 0-70348  
 perylene crystal, molecular exciton system, resonance Raman and fluorescence studies, dynamical effects 0-66169  
 PET, biaxial orientation, refr. index meas. by Raman and IR spectrosc. 0-60583  
 phenazine, prereson. Raman spectra, vibr. band intensities obs. 0-102515  
 phenyl acetylene, liq., phase relax., vibr. dephasing, Raman spectra obs. 0-91567  
 phthalazine, prereson. Raman spectra, vibr. band intensities 0-102514  
 PMMA, C-H stretching and bending vibrs. in Raman spectra 0-93300  
 Polymid K, oriented analogue of polyacetylene, reson. Raman spectroscopy 0-66208  
 polyacetylene:I, pure and doped, reson. Raman spectroscopy 0-66208  
 trans-polyacetylene obtained by polymerisation on TiO<sub>2</sub>, Raman spectrum (Spanish) 0-88988  
 polyethylene, phase characterisation, Raman spectra study (French) 0-93303  
 polyethylene, phase orientation by stretching, Raman study (French) 0-93304  
 polymer, longitudinal acoustic mode, perturbing forces 0-70348  
 polymers, Raman active longitudinal-acoustical mode spectra interpretation 0-103950  
 polynuclear aromatic hydrocarbons, synchronous excitation spectrofluorimetry (Japanese) 0-86452  
 polypropylene, isotactic, uniaxially oriented, Raman spectra (French) 0-60557  
 polypropylenes, iso- and syndio-tactic, Raman tacticity bands, vibr. spectrum 0-66193  
 polystyrene, total reflection Raman spectroscopy study 0-80784  
 polystyrene, uniaxially stretched atactic thin film, mol. orientation, polarized Raman study 0-103951  
 polystyrene coated Ag holographic grating, Raman spectra enhancement by plasmon surface polaritons 0-80885  
 propanal, methyl torsional pot. functions, LF Raman and IR vibr. spectra 0-95612  
 propyl chloride(-d), 357-333 nm absorpt. system 0-69161  
 pyrazine, prereson. Raman spectra, vibr. band intensities obs. 0-102515  
 pyrazine, reson. to the S<sub>2</sub>( $\pi,\pi^*$ ) state, Raman spectra calcs. 0-69147  
 pyridazine, prereson. Raman spectra, vibr. band intensities 0-102514  
 pyridine, adsorbed on Ag electrode with graphitic C overlayer, Raman spectra obs. 0-103954  
 pyridine, adsorbed on Ag surface, enhanced Raman scatt., ultrahigh vac. study 0-88993



**Raman spectra of organic molecules and substances continued**

- pyridine, adsorpt. on Ag colloids, surface enhanced Raman spectra obs. 0-97251
- pyridine, deuterium substituted, Raman and IR vibr. spectra 0-84739
- pyridine, on Au substrate with Ag monolayer, giant Raman effect 0-63637
- pyridine, sorbed on Ag, surface enhanced Raman scatt., mol.-surface separation dep. 0-92775
- pyridine-2,3,5,6-d<sub>4</sub>, vibr. spectra, IR and Raman, assignment 0-102519
- pyridine-3,4,5-d<sub>3</sub>, vibr. spectra, IR and Raman, H exchange rates meas. 0-102518
- pyridine-3,5-d<sub>2</sub>, vibr. spectra, IR and Raman, H exchange rates meas. 0-102518
- pyridine-d<sub>5</sub>, vibr. spectra, IR and Raman, assignment 0-102519
- 4-pyridinecarboxaldehyde monolayer in inelastic electron tunnelling spectroscopy junctions 0-93344
- pyridinium iodide, order-disorder phase transition and reorientation fluctuations studied by Raman spectra 0-80764
- pyrimidine nucleotides, UV reson. Raman excitation profiles 0-58265
- quinazoline, prereson. Raman spectra, vibr. band intensities obs. 0-102515
- quinoxaline, prereson. Raman spectra, vibr. band intensities 0-102514
- retinal chromophore, reson. Raman spectra obs. of struct. 0-94168
- Rochelle salt, ferroelec. phase transition, Raman scatt. study 0-97211
- squaric acid, two-dimens. phase transition, Raman scatt. study 0-71401
- styrene, UV Raman spectra, reson. effect in photoreactive states 0-106326
- styrene-sodium methacrylate copolymers, Raman spectra, ion clustering 0-71416
- sym-trioxane, phase transition, polarised Raman spectra obs. 0-84742
- tetrabromomethane, monoclinic monocryst., polarised Raman spectra (French) 0-93302
- tetrachloromethane, fluid, collision induced light scatt. intensity 0-103955
- tetrafluoromethane, collision-induced scatt., many-body correls. 0-87127
- tetrafluoromethane, liq., pure vibr. Raman spectra 0-97262
- tetramethylammonium cobalt tetrachloride, Raman spectra near incommensurate phase transitions 0-76013
- tetramethylammonium zinc tetrachloride, Raman spectra near incommensurate phase transitions 0-76013
- tetraphenylarsonium, Raman and IR spectra of the dicyanoiodate (I) ion 0-60572
- tetraphenyldithiopyranilidene mixed valence polyiodides, crystalline struct. and optical props. 0-92516
- tetraphenylphosphonium, Raman and IR spectra of the dicyanoiodate (I) ion 0-60572
- 2-thio alkyl (allyl, benzyl) pyrimidines, IR and Raman spectra anal., mol. vibr. and symmetry (French) 0-87123
- trans-polyacetylene, intrinsic, electron-phonon coupling 0-79901
- triamentane, plastic and solid-solid transitions, Raman study 0-60590
- 2,4,6-trichlorophenol, Raman and IR spectra, hydrogen bonds 0-84735
- 1,2,4-trichlorobenzene liq., mol. reorientation, translation and vibr. relax., Rayleigh and Raman spectra 0-95632
- trichloromethane-d, Raman band shapes, mol. oscill. bands (German) 0-69154
- 2,4,6-trichlorophenol, Raman and IR spectra, hydrogen bonds 0-84735
- trichlorosilane liquid, Si-H stretching mode vibr. dephasing, Raman study 0-84736
- triethylenediamine, Raman spectra study (French) 0-80768
- trifluoromethyl hydroperoxide(-d), CF<sub>3</sub> torsional vibrs., low freq. Raman spectra 0-91565
- trifluoromethyl hypochlorite, vibr. spectra and normal coord. anal. 0-102517
- trifluoromethyl hypofluorite, vibr. spectra and normal coord. anal. 0-102517
- trifluoromethyl hypofluorite (hypochlorite), CF<sub>3</sub> torsional vibrs., low freq. Raman spectra 0-91565
- trifluoromethyl peroxyfluoride (peroxychloride), CF<sub>3</sub> torsional vibrs., low freq. Raman spectra 0-91565
- trimethyl-d<sub>3</sub>-vinylsilane, IR spectra, struct., vibr. assignment, barriers to internal rot. calc. 0-87102
- trimethyl-d<sub>3</sub>-vinylsilane, Raman spectra, struct., vibr. assignment, barriers to internal rot. calc. 0-87102
- trimethylaminegallane, microwave, IR and Raman spectra, struct., vibr. assignment 0-95600
- trimethylvinylsilane, Raman spectra, struct., vibr. assignment, barriers to internal rot. calc. 0-87102
- tris-sarcosine calcium chloride, ferroelec. transitions, soft modes, Raman scatt. spectra obs. 0-80763
- TTF salts, mixed valent, Raman spectra, formal charge rel. to Raman freq. 0-93317
- TTF-TCNQ, Raman spectra, formal charge rel. to Raman freq. 0-93317
- vinylloxirane, Raman and IR vibr. spectra and conformations 0-83379
- Wolffram's red salt, mixed valence, reson. Raman calcs. using vibronic coupling model 0-97249
- BCl<sub>3</sub>·NCO, soln., force fields and normal modes, vibr. spectra, IR and Raman obs. (French) 0-58266
- BX<sub>3</sub><sup>+</sup>/NCS<sup>-</sup> (X=Cl, Br, I), soln., force fields and normal modes, vibr. spectra, IR and Raman obs. (French) 0-58266
- CO-haemoprotein photolysis, transient Raman study, quantum yield origin 0-67155
- Cd complexes, Cd(II) mixed halide complex anions, Raman spectra 0-58270
- Co(II) salen complexes, O binding, reson. Raman obs. 0-58267
- K<sup>+</sup>CF<sub>3</sub>SeO<sub>2</sub><sup>-</sup>, IR and Raman spectra, normal coordinate anal. for CF<sub>3</sub>SeO<sub>2</sub><sup>-</sup> anion 0-87122
- NH<sub>4</sub><sup>+</sup>CF<sub>3</sub>SeO<sub>2</sub><sup>-</sup>, IR and Raman spectra, normal coordinate anal. for CF<sub>3</sub>SeO<sub>2</sub><sup>-</sup> anion 0-87122
- Ni catalyst, chemisorption of ethylene(-d), Raman and vibr. spectra 0-108747
- Pt phthalocyanine, reson. Raman excitation profiles, solvent effects 0-102512
- Rb<sup>+</sup>CF<sub>3</sub>SeO<sub>2</sub><sup>-</sup>, IR and Raman spectra, normal coordinate anal. for CF<sub>3</sub>SeO<sub>2</sub><sup>-</sup> anion 0-87122

**Raman spectra of polyatomic inorganic molecules**

- air pollutant gases and vapours, relative Raman scatt. cross section 0-100061
- IR multiple-photon excited molecules 0-74207
- methane, photoacoustic Raman spectroscopy under pulsed laser excitation 0-82825
- trifluoriodomethane, IR multi-photon excited mols. 0-74207

**Raman spectra of polyatomic inorganic molecules continued**

- water vapour, Raman lidar meas., daytime atmosphere 0-85718
- Al<sub>2</sub>Cl<sub>6</sub>, matrix isolated, vibr. spectra, isotopic fine struct. and valence force field calcs. 0-58258
- C<sub>2</sub>N<sub>2</sub>, 2ν<sub>4</sub> band overtones, Raman intensities, bond polarisability theory 0-63639
- CO<sub>2</sub>, collision-induced Raman spectrum, theoretical studies 0-63646
- CO<sub>2</sub>, near critical point Rayleigh and Raman scatt., Fermi diad 0-80765
- CO<sub>2</sub>, photoacoustic Raman spectroscopy under pulsed laser excitation 0-82825
- CS<sub>2</sub>, liquid, Rayleigh and Raman bands, intensities of interaction induced components 0-63645
- CdF<sub>2</sub>(FCI)(FBr), matrix isolated IR and Raman spectra, assignments, force consts., isotope effects and thermodynamic props. 0-63631
- CdO<sub>2</sub>, formed by matrix reactions, IR, Raman and visible spectra 0-87110
- CsBrCN, Raman and IR vibr. spectra, struct. 0-102513
- CsClCN, Raman and IR vibr. spectra, struct. 0-102513
- CsI<sub>2</sub>CN, Raman and IR vibr. spectra, struct. 0-102513
- D<sub>2</sub>O, pulsed opto-acoustic spectroscopy 0-62743
- H<sup>14</sup>N<sub>2</sub>, rotational-vibrational Raman spectrum of ν<sub>2</sub> band 0-91564
- H<sub>2</sub>O, pulsed opto-acoustic spectroscopy 0-62743
- H<sub>2</sub>O, Raman and IR spectrum in overtone OH stretching region 0-58263
- Hg complex, methylethynylmercury(II)(-d<sub>1</sub>-d<sub>3</sub>-d<sub>4</sub>), vibr. spectra and normal coord. calcs. 0-58259
- Hg(CN)<sub>2</sub><sup>-</sup> ion, CN and HgC stretching vibrations and HgCN bending vibration assignments 0-69140
- HgF<sub>2</sub>(FCI)(FBr), matrix isolated IR and Raman spectra, assignments, force consts., isotope effects and thermodynamic props. 0-63631
- NH<sub>3</sub>, stimulated hyper-Raman scatt. via 3-photon process to obtain IR and far IR radiation 0-58633
- NO<sub>2</sub>(N<sub>2</sub>O<sub>4</sub>) surface decomposition, resonance and spontaneous Raman spectra 0-61144
- Ni<sub>3</sub>, in solid Ar, reson. Raman spectra 0-63638
- SF<sub>6</sub>, IR multi-photon excited mols. 0-74207
- SF<sub>6</sub>, vibr. coupling in collision-induced Raman scatt. 0-83373
- Tl<sub>2</sub>F<sub>2</sub>(Cl<sub>2</sub>), assignment of vibr. Raman and IR spectra bands 0-58268
- ZnF<sub>2</sub>(FCI)(FBr), matrix isolated IR and Raman spectra, assignments, force consts., isotope effects and thermodynamic props. 0-63631
- ZnO<sub>2</sub>, formed by matrix reactions, IR, Raman and visible spectra 0-87110

**Raman spectroscopy**

- see also Raman lasers; Raman spectra
- air pollution, laser-Raman microprobe anal. of suspended particulates 0-76687
- catalysts, laser Raman spectroscopy in controlled atm. rot. cell 0-86437
- chemical species anal. in conjunction with liq. phase chromatography (French) 0-93823
- chiral molecules in mag. fields 0-102532
- coherent Raman loss spectroscopy, appl. to conc. meas. and fundamental spectrosc. 0-89580
- coloured solids, line focus method for recording laser Raman spectra 0-90897
- double resonance Raman amplifier, theory 0-87434
- frequency shifts, determ. by Raman difference spectrosc. 0-78654
- frequency-modulated shot noise limited stimulated Raman gain laser system for monolayer vibr. spectroscopy 0-62744
- gas concentration meas. using Raman intensity depend. on giant pulse laser polarization 0-98986
- interface total reflection and surface wave obs. 0-108292
- inverse Raman AC coupled spectroscopy, detection limits 0-86454
- laser microprobe analysis principles and appl. 0-57390
- laser microprobe appl. to molecular analysis, particle characts. determ. 0-57391
- light hyper-Raman scatt. by polaritons, active spectroscopy (Russian) 0-60623
- matrix isolation Raman spectroscopy, water pollution detect. appl. 0-108829
- Microprobe Mole/plasma chromatograph system, for anal. of compounds on micron scale 0-101049
- microprobe studies of mineralizing tissues 0-76884
- mole (molecular optical laser examiner) appl. 0-62737
- monomode fibre dispersion and bandwidth meas. by mode-locked Q-switched Nd:YAG laser 0-91933
- multipass-systems for Raman spectroscopic gas analysis (German) 0-81393
- optical fibre, use in remote inelastic light scatt. probe 0-58769
- organic surface contaminants, anal. by plasma chromatography-mass spectroscopy, and Raman microprobe technique 0-108773
- polyethylene melt, cryst. kinetics during cooling, nucleation density effect 0-100181
- radiometric correction of spectra 0-90899
- remote spontaneous, new trends in recording of signals 0-73485
- rotational Raman studies, folded BOXCARs 0-101846
- spectrometer calibration using Kr<sup>+</sup> laser plasma lines 0-57394
- stimulated Raman scattering under resonance illumination conditions 0-64105
- surface analysis techniques and appls., symposium, Dayton, USA (Jun. 1979) 0-62363
- synchronous excitation spectrofluorometry (Japanese) 0-86452
- triple monochromator a spectrometer in Raman scatt. (French) 0-96007
- vidicon Raman spectrometer, appl. to heme protein study 0-94428
- Nd:YAG pumped tunable sources, appl. to spectroscopy 0-58576

**Ramsauer effect see collision processes****random functions**

- see also random processes
- randomly-inhomogeneous conducting media, generalised charac. computation using random function theory (Russian) 0-75535

**random noise**

- see also thermal noise
- 1/f noise, nonlinear mechanism 0-96955
- 1/f noise, quantum theory 0-100491
- 1/f noise in electrical conductors, survey 0-107878
- atomic collisions and radiation trapping, analysis using charact. noise of strong EM wave 0-99492
- disordered systems, spontaneous echoes, spectral diffusion decay 0-84270
- ECG signals, diagnostic functions, effect of random noise (Croatian) 0-98169

random noise continued

education, Poisson statistics demonstration using X-ray tube, electronic 'shot noise' 0-73129  
fibre-optic interferometer gyro, thermally induced nonreciprocity 0-58665  
Hall effect, 1/f noise, mobility fluctuations 0-92950  
homogeneous electron irradiation (*German*) 0-102603  
III-V semiconductors, noise calc. using Monte-Carlo method 0-75575  
inhomogeneous Boltzmann gas, lumped phase space, non-linear diffusion approx., stochastic hydrodynamic theory 0-64666  
n-InSb Corbino disc, acoustic noise effect on I-V characts. (*Russian*) 0-100492  
interaction of determinate packet with random noise, in Burgers' equation 0-106650  
LF fluctuation, dissipation and relaxation properties, universality 0-84687  
linear system, mean square response to nonstationary random excitation 0-57085  
Mandelstam-Brillouin stimulated scatt., amplitude and phase time oscills. noise (*Russian*) 0-87435  
medical US imaging, stochastic noise influence on perceived image 0-98053  
MIM cathodes, LF noise sources and reduction 0-108328  
multimode fibre link, modal noise 0-87536  
period analysis at high noise level 0-73263  
Photographic Zenith Tube at Tokyo Astron. Observatory, observational errors anal. 0-98547  
point reactor kinetic eqn. with Gaussian reactivity fluctuation, exact soln. 0-68735  
relaxation spectra, superposition, 1/f noise 0-105575  
semiconductor, homogeneous, nondegenerate, single-level Schockley-Read-Hall recomb. centres, flicker noise 0-70779  
semiconductors, mobility-fluctuation description of 1/f noise 0-84496  
SQUID, RF, LF noise expt. exam. 0-98947  
SQUID, thermodynamic equilibrium fluctuations generation by Josephson junction, Werthamer theory 0-100564  
SQUID magnetometer, AC-biased 0-98948  
stochastic characteristics of the burst noise 0-98855  
superfluorescence-initiating noise source, average strength meas. 0-58492  
symmetry principles and 1/f noise 0-68136  
two-level system in resonant multifrequency field with structureless noise (*Russian*) 0-91766  
visual detection, effect of photon noise 0-61559  
Al granular films, vortex noise at supercond. transition 0-84530  
Al thin conducting film, electromigration under superimposed DC and noise powers 0-107879  
Al thin films 1/f noise, depend. on internal mech. stresses 0-65711  
Al<sub>2</sub>O<sub>3</sub> supermicrogrid preparation and props. use in electron microscopy, noise reduction 0-99010  
Bi whiskers, excess 1/f noise, 50 to 350K 0-92951  
GaAs injection lasers, direct modulation enhancement effect of HF noise 0-83608  
GaAs, photocapacitive MIS IR detector, spectral response, noise characts. 0-75644  
Gd, coil noise due to permeability fluctuations at phase transition temp. 0-84598  
He-Ne laser, 6328 Å power fluctuations due to striation noise 0-78834  
InGaAs avalanche photodiode, 1.3 µm, noise performance, -190°C 0-57370  
n<sup>+</sup>-n-pGe avalanche photodiode, noise factors, internal quantum efficiency 0-70803  
Nb superconducting point contact, singularities of I-V curve and voltage fluctuations 0-93044  
NbSe<sub>3</sub>, CDW noise, temp. and freq. depend. 0-103681  
NbSe<sub>3</sub> interference effects of CDW motions 0-88544  
Si, photocapacitive MIS IR detector, spectral response, noise characts. 0-75644  
n<sup>+</sup>nn<sup>+</sup> Si planar device, hot electron flicker noise at 78K 0-103732  
W surface, adsorbed K, field emission flicker noise power 0-59795

random number generation

digital scene generation with specified statistics 0-99666

random phase approximation *see* RPA calculations

random processes

*see also* Brownian motion; fluctuations; Markov processes; probability; queueing theory; stochastic processes  
absorption time by a random trap distribution 0-86209  
acceleration through random classical radiation, thermal effects 0-73191  
background ensembles, nonlinear modeling 0-95037  
binary galaxies, random optical pairs in Turner's (1976) sample 0-67849  
chaos, external noise and Fredholm theory 0-86216  
chaotic turbulent flows, scaling behaviour, Lyapunov characteristic exponent 0-86217  
coaxial electron and atomic beams sequential multiple scatterings, random walk approach 0-99574  
column with nonlinear restraints and random initial displacement, buckling 0-79192  
comets neutral atmospheres, average random walk model for mol. phot. dissociation 0-77351  
correlated particle migration in cryst. struct. (*Russian*) 0-96683  
cosmic ray muons, time distribution, random and nonrandom components of arrival times 0-72732  
coupled random walk process theory, Fokker-Planck eqn. calcs. 0-77710  
crystal lattice sites, many-particle random motion 0-92703  
diffusion in random networks near percolation threshold, ant in labyrinth problem 0-77732  
disordered systems, random walks and AC cond. 0-70661  
EM wave propagation, in one-dimensional, randomly inhomogeneous medium, with specularly reflecting walls 0-105514  
ensembles for random matrices of Hamiltonians with small time reversal noninvariant part 0-77694  
errors of meas. instrument analysis, under transient conditions, based on instantaneous frequency response 0-77741  
evolution systems, meas., rel. to master eqn., Bayesian anal. 0-90782  
excitons, coherent and incoherent motion in continuous time random walk framework 0-59882  
fluctuations, random, moment behaviour of soln. processes for nonlinear stochastic differential eqns. (*Japanese*) 0-95039  
functional equations, random, stochastic approx. in Banach space (*Japanese*) 0-95038  
Gaussian Markov random fields, discrete parameter, generalised potential theory 0-57185  
general matrix approach to residual spectra 0-94947

random processes continued

generalised random walks, transform. of recursion relations 0-101757  
geophysical data, detrending and smoothing techniques 0-67425  
glass, electron migration and spectral relax., random-walk model 0-80280  
Henon mapping, topological horseshoe, chaotic behaviour 0-73257  
hopping conduction in disordered insulator, continuous-time random walk model 0-96863  
hopping conductivity, one-dimensional bond percolation model 0-103655  
hysteretic systems under random excitation, equivalent linearisation 0-79210  
intersection characteristics (*Russian*) 0-90660  
interstellar dust, grains random vels. and collisions in turbulent gas 0-77470  
limit cycle, symmetric bifurcation to asymmetric limit cycle, simple model 0-57080  
linear systems acted upon by Poisson processes 0-57196  
marginal local instability of quasi-periodic motion, separation distance effects 0-82633  
molecular crystals, disordered, incoherent, electronic energy transfer in impurity band 0-75525  
multivariate response relationships, appl. matrices to treatment of residual spectra 0-68132  
NGC 4151, Seyfert galaxy, shot noise model for repeated X-ray flaring 0-90534  
nonlinear differential equations, random behaviour 0-77706  
nonparametric forecasting method for stationary processes, appl. to random meas. (*French*) 0-90780  
nonstationary random vibrations of multiple-mass systems 0-69728  
nuclear decay, γ-decay of coherent rotational states, random quantum meas. 0-73855  
Nyquist formula, quadratic generalisations 0-57198  
one-body approx., disordered system spectral props., Schrodinger eqn., random fields 0-90696  
packing of spheres, computer simulation 0-77705  
parking problem, asymptotic estimates, jammed state density 0-86206  
percolation theory, review 0-98868  
period analysis at high noise level 0-73263  
phase statistics in coherently superposed Gaussian speckle patterns 0-102626  
quantification of stochastic process, principles of quantification noise (*Spanish*) 0-57190  
quantum system, nonintegrable, irregular part of discrete energy spectrum, statistical theory 0-82667  
quasi-maximum likelihood method appl., to systems with complete connections (*Rumanian*) 0-57183  
quasistationary processes and universal codes 0-91994  
random binary Ising system with transverse field, Curie temp., paramagnetic susceptibility 0-65938  
Schrodinger equation, randomly fluctuating interaction term, uncertainty in nature 0-62499  
self avoiding walk and supersymmetry 0-101756  
self-avoiding lattice walks with high coordination and small excluded volume 0-77718  
self-avoiding walks with nearest- and next-nearest-neighbour steps 0-86222  
selfavoiding random walk problem, direct renormalisation method 0-77703  
single mass vibroimpact system, response to white noise random excitation 0-64454  
space-time random speckle pattern optical analysis 0-102682  
span-constrained random walks, on cubic lattice, internal configs. 0-68148  
spectral analysis, method of moments 0-68137  
spectral density relationships, harmonic response characts. effect, random excitations 0-62582  
spins, block, defined by random field, convergence 0-101759  
stellar turbulent convection equations, ensemble averaging 0-67698  
strong coupling expansion for classical statistical dynamics, randomly driven system 0-105568  
thermometer errors analysis, thermoelectric, Pt-Rh 0-77783  
thin walled elements, unbound quasistatic random thermelastic fields, oscillations 0-69673  
turbulence in systems with small parameters 0-105571  
two dimensional walks 0-95034  
underwater ambient acoustic noise, compound random process 0-83699  
vibrations, statistical data digital processing method (*Japanese*) 0-64430  
wave propagation in randomly inhomogeneous media, quasi-optical parabolic approx., validity analysis 0-106422  
wave reflected from randomly inhomogeneous layer description, by series satisfying causality condition 0-106420  
Weiner-Einstein processes, Markov, maxima and first-passage-time statistics 0-68134

**range finding** *see* distance measurement  
**range of particles** *see* energy loss of particles  
**ranging (sonar)** *see* sonar  
**rare earth alloys**  
*see also* cerium alloys; dysprosium alloys; erbium alloys; europium alloys; gadolinium alloys; holmium alloys; lanthanum alloys; lutetium alloys; neodymium alloys; praseodymium alloys; promethium alloys; rare earth compounds; samarium alloys; terbium alloys; thulium alloys; ytterbium alloys  
amorphous, exhibiting Mossbauer spectra, mean mag. props. (*French*) 0-80489  
amorphous, ferromag. state, non-axial elec. field gradient effect 0-75728  
amorphous, with random anisotropy axes, spin excitations in paramag. phase 0-80476  
amorphous alloys, random anisotropy magnetism 0-65853  
crystal field effects rel. to mag. props. 0-59933  
ferromagnetic properties, book contrib. 0-75725  
indirect magnetic interactions, NMR anal. 0-71193  
intermediate valence, models for anomalous alloys 0-96827  
intermetallic compounds, ferromagnetic properties, book contrib. 0-75726  
Kondo singularity, Anderson-Smith model 0-80479  
magnetic excitations, review of neutron scatt. data 0-60227  
magnetically concentrated cubic Laves phase cpds., ESR 0-71174  
mischmetal-Co system, thermomagnetic analysis of intermediate phases 0-93115  
mischmetal-Mg, appl. to H<sub>2</sub> storage 0-72093  
phase structure, dimens. anal. 0-96470  
phonons in systems with valence transitions 0-96611



## rare earth alloys continued

- quadrupole interactions, parastriction 0-60400  
stacking faults and magnetism, transform. effects 0-75840  
transition metal alloys, amorphous, electronic and mag. props. 0-93093  
transition metal alloys,  $\text{RM}_2\text{Si}_2\text{-Ge}$ , and  $\text{RM}_{1-x}\text{Al}_x\text{-x}$ , magnetism and hyperfine interactions, magnetisation and Mossbauer effect studies 0-75892  
transition metal-rare earth alloys, amorphous, ferrimag., spin arrangements in large fields 0-75718  
transition metal-rare earth alloys, disordered, magnetisation behaviour 0-71099  
Fe, magnetoelasticity and moment rot., US vel. calc. and neutron scatt. meas. 0-65992  
R-Al alloys amorphous, model calcs. of mag. props. 0-84616  
R-Co, plastic magnet appl., anisotropic, based on moulding ferromagnetic powder material with plastics (*Japanese*) 0-60829  
R-X-Sn, X=Rh, Ir, Ru, Co, cryst. growth and cryst.-chem. invest, supercond./mag. ternary cpds. 0-100777  
R-Zn, ferromag., parastriction and magnetoelastic coeffs. 0-65996  
 $\text{RAl}_3$ , orbital and spin polarisations of cond. electrons 0-65791  
 $\text{RB}_2$ , thermochemistry and stability 0-97723  
 $\text{RBe}_{13}$ , ESR studies 0-108064  
 $\text{RBe}_{13}$ , XPS, resist, and susceptibility study 0-71565  
 $\text{RCO}_2$ , metamagnetic transitions in internal fields 0-60272  
 $\text{RCO}_3$ , hydride phase synthesis, thermal stability and struct. 0-59438  
 $\text{R}_{1-x}\text{Co}_x$ , amorphous alloys, thermal stability, elec. cond. enthalpy 0-100172  
 $\text{R}_2\text{Co}_3$ , polymorphism of Ce subgroup alloys, eutectic decomposition (*Russian*) 0-66504  
 $\text{R}_{10}\text{Co}_{31}$ , amorphous, mag. props. 0-84590  
 $\text{RFe}_2$ , magnetostrictive, magnetoelast. props, book contrib. 0-75838  
 $\text{R}_2\text{In}$ ,  $\text{R}_3\text{In}$ , R=Gd, Tb, Dy, Ho, Nd, mag. props. 0-108009  
 $\text{R}_2\text{Os}$ , cryst. struct. 0-96475  
 $\text{R}_2\text{Pt}$ , mag. susceptibility meas., mag. transitions obs. 0-60222  
 $\text{RRhSn}_3$ , synthesis, supercond. and mag. props. 0-100547  
 $\text{RT}_x\text{Al}_6$ , T=Cr, Mn, Fe, Cu, cryst. struct. 0-107110

## rare earth compounds

- see also under the individual compounds e.g. cerium compounds  
see also rare earth alloys  
aluminate film coatings, electrophys. props. w.r.t. prep. technology 0-60781  
arsenides, chemical bonding and structural features, coherent alloying theory 0-107101  
binary insulating compounds, exchange interactions, paramag. susceptibility expts. 0-60177  
bismuthides, chemical bonding and structural features, coherent alloying theory 0-107101  
chalcogenides, resonant Raman scattering via virtual exciton 0-71412  
chlorides, glass transition temp. meas., inner-sphere coordination number change effect on soln. props. 0-83239  
chromite based electrode material development for MHD generators 0-84893  
Curie constant rel. to valence bond strength 0-60251  
double orthophosphates with alkali metals, conc. depend. of luminesc. props. 0-100673  
double orthophosphates with alkali metals, spectroscopic obs., struct. and chem. nature 0-100674  
ferrite garnets, phase transitions, field-induced spin-orientational 0-75767  
fluorides, interband, collective and atomic (p,d) excitations, Z-160 eV, fast EELS 0-93443  
germanates, flux-grown, X-ray topography 0-64939  
germanates,  $\text{R}_2\text{O}_3\text{-GeO}_2$  system cpds., physicochem. characts. 0-97469  
group IIIa dihydrides, structs. and stabilities 0-107146  
hydrides, form. by rare earth reaction with  $\text{H}_2\text{O}$  vapour 0-76504  
intermediate valence, models for anomalous cpds. 0-96827  
kaolinite rare-earth complexes, relax., molar free energy of activation for dipole relax. 0-88919  
lanthanide complex, struct. and equil. by time resolved Eu(III) spectrosc. 0-78736  
lanthanide ion bound to macromol., struct. and equil. by time resolved Eu(III) spectrosc. 0-78736  
laser channels, 3 $\mu\text{m}$ , in inorg. materials with  $\text{R}^{3+}$  ions 0-97306  
lead apatites,  $\text{Pb}_{10-2}\text{R}_2\text{M}_8(\text{PO}_4)_6\text{Z}_2$ , M=Na or K and Z=F or Cl, cryst. struct. and IR spectra 0-107167  
mixed valence state, conduction band struct. 0-103624  
multipolar interactions, evidence and origins 0-59935  
nonmetallic compounds, indirect spin-spin coupling, models 0-80238  
orthoferrites, domain wall dynamics 0-65957  
orthoferrites, hyperfine interaction anisotropy, NMR study (*Russian*) 0-66052  
orthoferrites, mag. anisotropy in cryst. field approx. 0-60241  
orthoferrites, muon states, local mag. fields 0-75911  
oxide containing systems, highly refractive, phase equil. and metastable phases 0-97467  
oxides, dielec. const. and loss at low temp. 0-93229  
oxides, interband, collective and atomic (p,d) excitations, Z-160 eV, fast EELS 0-93443  
oxides, segregation study by electron energy-loss spectroscopy 0-79953  
oxides, XPS 0-87170  
oxyphosphates, IR and Raman spectra, vibr. assignments, cryst. struct. characts. 0-97258  
perchlorates, glass transition temp. meas., inner-sphere coordination number change effect on soln. props. 0-83239  
periodicity of atom props. and inorganic cpd. props. 0-96586  
perovskite-like oxides, synthesis, struct., elec. props. 0-65554  
phonons in systems with valence transitions 0-96611  
photoemission, Fano-resonances, surface and bulk effects 0-97405  
pressure effect on mag. ordering temp. 0-100584  
scandate film coatings, electrophys. props. w.r.t. prep. technology 0-60781  
semiconductors, studies in Soviet Union, review 0-96875  
sesquioxides, exchange interactions, paramag. susceptibility expts. 0-60177  
short-arc lamp for Super 8 cinefilm projector using rare-earth halogens 0-62747  
Y-type zeolites, ion exchanged, XPES obs. 0-83421  
zirconate film coatings, electrophys. props. w.r.t. prep. technology 0-60781  
zircon, Jahn-Teller cooperative phase transition, crossover effects 0-88316

## rare earth compounds continued

- $\text{Ba}_2\text{RF}_7$ , (R=Dy, Ho, Er, Tm, Yb, Lu, Y), superstructure phases, prep., thermal characterisation and X-ray powder diff. 0-96494  
 $\text{EuR}_3$ , R=La, Ce, Pr, Nd, Sm, Gd, elec. cond. meas. 0-65555  
 $\text{R}^{3+}$  ions, coord. in aq.  $\text{Cl}^-$  soln., X-ray diff. obs. 0-92445  
 $\text{RAsO}_4$ , ferroelectricity, dielec. meas. 0-60515  
 $\text{RCO}_3$ , catalytic props. 0-66875  
 $\text{RCrO}_3$ , elec. transport 0-70700  
 $\text{RCu}_3\text{Mn}_2\text{O}_{12}$ , R=La to Lu, synthesis and mag. props. 0-75717  
 $\text{RFe}_2(\text{BO}_3)_4$ , cryst. growth from soln.-melt, props. 0-108337  
 $\text{RFeO}_3$ , Raman scatt. from magnons, anisotropy consts. determ. 0-66178  
 $\text{R}_2\text{Ge}_3$ , thermal expansion, phase transition effects 0-70433  
 $\text{RIG}$ , anisotropic, mag. props., high field and low temp. 0-75801  
 $\text{RIG}$ , two-sublattice ferrimagn., mag. polaritons 0-65845  
 $\text{R(III)}$  complexes, cysteinates, thermodynamics of form. 0-89515  
 $\text{RMnO}_3$ , R=La-Eu, catalytic activity 0-71941  
 $\text{RMO}_3\text{S}_2(\text{Se}_2)$ , coexistence of supercond. and mag. ordering (*Russian*) 0-84542  
 $\text{R}_2\text{O}_3\text{-H}_2\text{O}$ , hydrothermal phase equilibria studies 0-104132  
 $\text{R}_2\text{O}_3\text{-P}_2\text{O}_5\text{-M}_2\text{O(M'O')}$ , (M=alkali metal, M'=alkaline earth), metaphosphate glass phosphors, fluoresc. props., activation conc. effect 0-89058  
 $\text{RRh}_2\text{B}_3$ , supercond. and mag. props. 0-97028  
 $\text{RRh}_2\text{B}_3$ , coexistence of supercond. and mag. ordering (*Russian*) 0-84542  
 $\text{RRu}_2\text{B}_3$ , supercond. and mag. props. 0-97028  
 $\text{RTiO}_3$ , bulk mag. and struct. props., ferrimag. order 0-107993  
 $\text{R}_2\text{TiO}_3$ , crystallochem. classification 0-107142  
 $\text{Sm}_{1-x}\text{R}_x\text{S}_2$ , stability of  $\text{Sm}^{2+}$  0-65508  
Th-N rare earth nitride mixed system, quasibinary existence (*German*) 0-91221  
 $\text{ZrF}_4\text{-BaF}_2\text{-ThF}_4\text{-NaF(RF}_3\text{)}$  (R=rare-earth) glass system, anion cond. 0-70460

## rare earth elements see rare earth metals

## rare earth metals

- see also the individual metals e.g. cerium  
abundances in Melrose-b howardite 0-101566  
Archaean metasedimentary rocks from Kambalda, Western Australia, rare earth element geochemistry 0-109143  
atom properties periodicity and inorganic cpd. props. 0-96586  
atomic partition functions, Chebyshev approximations 0-67544  
atoms, Gaussian basis sets calcs. 0-63541  
ceramics, rare earth elements use as dopants (*Polish*) 0-97455  
3d core electron XPS spectra, low-binding-energy satellites, exception of Eu 0-104040  
Cretaceous mid-ocean ridge basalt (MORB), Nd and Sr isotopic comps. and rare earth element abundances 0-94520  
density of 4f states below and above Fermi level, XPS and bremsstrahlung isochromat spectroscopy 0-76140  
electronic sound attenuation anomalies at transition to helical phase, Fermi surface topology (*Russian*) 0-92807  
electronic struct. and magnetism, review 0-70573  
ferromagnetic properties, book contrib. 0-75725  
glass/R. photoacoustic spectrosc. 0-92611  
glass, rare earth elements use as dopants (*Polish*) 0-97455  
identifications in HD 187473, Si star 0-98671  
impurities in Cr, effect on oxidation resist. 0-66703  
impurities in fluorophosphate glasses, magneto-opt. characts. 0-64126  
interband, collective and atomic (p,d) excitations, Z-160 eV, fast EELS 0-93443  
ion source using surface ionisation process 0-68999  
ion spectra, crystal field integral parameters, spin-orbit interaction 0-100447  
lanthanides' ionisation pot. calc., T-value and number of 4f electrons linear correlation (*Chinese*) 0-63850  
liquid heavy rare earths, mag. susceptibility meas. 0-75740  
magnetic excitations, review of neutron scatt. data 0-60227  
magnon dispersions in ferromag. and screw structs., nonlinear s-f exchange interaction effect 0-75746  
radioactive waste, high-level, oxalate precipitation for separation of Am, Cm, and trivalent lanthanides 0-83202  
solar nebula, rare earth element condensation and fractionation 0-72796  
stacking faults and magnetism, transform. effects 0-75840  
SXAPS with sealed-off analyser tube 0-80908  
X-ray 5p emission bands, valence energy band 0-104016  
 $\text{CaF}_2\text{-R}^{3+}$ , elec. dipole-dipole interaction, ionic thermocurrent and EPR study 0-108060  
Ga-Ge-Se-R chalcogenide glasses, elec. props. 0-96885  
 $\text{LaF}_3\text{-R}^{3+}$ , crystal field anal., intensity calcs. 0-100670  
 $\text{LiTmF}_4$ -rare earth, EPR spectra, elec. field effects, cryst. field interactions 0-71176  
 $\text{LiYF}_4$ -rare earth, EPR spectra, elec. field effects, cryst. field interactions 0-71176  
 $\text{R/p-Si(p-GaAs)}$  contacts, surface pot. barrier 0-60086  
 $\text{SrF}_2\text{-R}^{3+}$ , elec. dipole-dipole interaction, ionic thermocurrent and EPR study 0-108060  
 $\text{ZnO}$ -rare earth metals varistors, microstructure-prop. relations 0-100249

## rare gases see inert gases

## rarefied fluid dynamics

- see also atomic beams; Knudsen flow; molecular beams  
conductance for the gas flow of an accelerating tube 0-102359  
gas, nonsteady flow through semipermeable screen to vacuum 0-100029  
gas flow, full solns. for Burnett eqns. c.f. N-S eqns. 0-69876  
low density supersonic gas flow, temp. meas. probe 0-74913  
low density wind tunnel for rarefied gas dynamics 0-96285  
MHD channel flow of rarefied gas, external circuit effects on heat transfer 0-83860  
molecular flow, structure with arbitrary geometry, kinetic anal. method 0-79355  
monatomic gas, rarefied flows in axisymmetric expansion nozzle 0-92182  
nonequilibrium free jet expansion, translational temp. meas. in  $\text{N}_2$  0-64600  
small channels, gas flow, graph and nomograph for anal. eval. 0-106848  
Spacelab pallet, meas. of mol. streaming fields 0-82173  
vehicle hypersonic wake, radiation from injected small particles, free molecular regime 0-64650

## rarefied gas dynamics see rarefied fluid dynamics

## rarefied gas flow see rarefied fluid dynamics

## Rayleigh-Benard instability see flow instability

**Rayleigh law** *see* Rayleigh scattering

**Rayleigh limit** *see* Rayleigh scattering

# Rayleigh scattering

- aniline-cyclohexane solution, depolarised mol. light scatt. near critical exfoliation temp. (*Russian*) 0-108222  
 atmosphere, Rayleigh scattering, optical thickness values 0-90216  
 atmosphere model, scatt. light intensity and polarisation degree, mol. anisotropy effect 0-77104  
 bidirectional optical systems, Rayleigh backscatt. freq. depend. 0-69511  
 bisphenol A-phthalic anhydride epoxy resin, diglycidyl ether, Rayleigh scatt., Brillouin and IR spectra 0-66211  
 central rigid cores, mesogenic power, depolarised Rayleigh scatt. study 0-89012  
 collisional and radiative damping effects in Rayleigh and reson. fluorescence scatt. at high intensities 0-102478  
 diatom + diatom, effect on depolarised light scatt. linewidths 0-58321  
 dielectric cylinder, infinite, randomly oriented, radiation press. 0-58454  
 disperse system, dilute, orientationally induced conservative dichroism 0-102623  
 dust, soil derived atmospheric, IR spectra, Christiansen effect, Rayleigh limit 0-105046  
 Gaussian-Lorentzian light, photon counting distrib. factorial moment, spatial coherence 0-83571  
 Lennard-Jones fluids, orientational and collision induced light scatt. 0-63644  
 low-frequency props. from scattering meas., flaws in solids appls 0-76475  
 2,6-lutidine-water critical mixture, spinodal decomposition, Rayleigh scatt. 0-70416  
 macroparticles; charged spherical, dilute soln., Rayleigh scatt. 0-84748  
 mirror, dielectric, Rayleigh scatt. at 441.6 nm 0-97367  
 molecular scattering of light, spatial dispersion, distributed dipole and local multiple approx. 0-80796  
 molecules, Rayleigh and Raman optical activity, scatt. angle anal. 0-69151  
 molecules adsorbed on rough surfaces, Rayleigh, Mie and Raman scatt. 0-83378  
 myoglobin, atomic vibr. mean square displacement, Rayleigh scatt. of Mossbauer radiation meas. (*Russian*) 0-100665  
 nitrobenzene, liquid and CCl<sub>4</sub> soln. shear waves and translation-rotation coupling obs. by depolarised Rayleigh scattering 0-71432  
 optical waveguide, Rayleigh scatt. of stimulated Raman scatt. Stokes component 0-106569  
 optically isotropic molecules, collision-induced scatt., many-body correls. 0-87127  
 Orientational optic effects from above Rayleigh particles 0-106453  
 particle shape effect on low freq. absorpt. 0-99626  
 plane parallel atmospheres, radiative transfer eqn. soln. 0-67409  
 polymer solution, Rayleigh scattering, intermolecular correlations effect 0-75146  
 polystyrene networks swollen in cyclohexane, swelling equil. and light scatt. at theta conditions 0-107036  
 polystyrene-cyclohexane mixture, Rayleigh and Brillouin scatt. and struct. relaxation 0-63640  
 pyridine-water soln., reorientational relax. and activation energy of pyridine, depolarised Rayleigh scattering 0-76037  
 resonant Rayleigh-type mixing spectroscopy using ps light pulses, ultrafast relax. study 0-91834  
 SAWs, propag. along corrugated solid boundary 0-87600  
 scalar wave scattering by periodic surfaces, general modal theory 0-87271  
 semiconductor, deep impurity centres, elastic light scattering 0-97315  
 spherical particles, colloidal dispersions, refractive index 0-106454  
 tetrafluoromethane, collision-induced scatt., many-body correls. 0-87127  
 1,2,4-trichlorobenzene liq., mol. reorientation, translation and vibr. relax., Rayleigh and Raman spectra 0-95632  
 water-oil microemulsions, optical matching 0-61157  
 Ag electrode, enhanced inelastic light scatt. caused by adatoms 0-89013  
 Ar, cluster formation and homogeneous nucleation, comparison of expt. and theory 0-79925  
 Ar, gas, compressed, Rayleigh-Buillouin spectrum, scaling 0-100062  
 Ar, gas, compressed, Rayleigh-Brillouin spectrum, hydrodynamic region 0-100063  
 Ar, liquid, depolarised Rayleigh scatt. at triple point, mol. dynamics simulation 0-60617  
 BaMnF<sub>4</sub>, spectroscopy near ferroelec. transition, dielec. anomalies near mag. ordering temp. 0-75965  
 CO<sub>2</sub>, near critical point Rayleigh and Raman scatt., Fermi diad 0-80765  
 CS<sub>2</sub>, liquid, Rayleigh and Raman bands, intensities of interaction induced components 0-63645  
 CS<sub>2</sub>, radiation self synchronisation on Rayleigh edge time stimulated scatt. in external resonator (*Russian*) 0-69461  
 He, gas, compressed, Rayleigh-Buillouin spectrum, scaling 0-100062  
 He, gas, compressed, Rayleigh-Brillouin spectrum, hydrodynamic region 0-100063  
 KCl:Pb, impurity distrib., light scatt. and microhardness study, heat treatment 0-96562  
 KD<sub>2</sub>PO<sub>4</sub>, acoustic phonon dispersion, elastic stiffness, light scatt. obs. 0-103966  
 KH<sub>2</sub>PO<sub>4</sub>, Brillouin-Rayleigh scatt. studies near ferroelec. transition temp. 0-76036  
 Ne, gas, compressed, Rayleigh-Buillouin spectrum, scaling 0-100062  
 Ne, gas, compressed, Rayleigh-Brillouin spectrum, hydrodynamic region 0-100063  
 Xe, fluid, near crit. point, correl. range and Rayleigh linewidth 0-93352

**Rayleigh-Taylor instability** *see* flow instability

# Rayleigh waves

- see also surface acoustic waves*  
 anomalous generation from underground nucl. explosion 0-81833  
 China, seismic surface wave study of crust and mantle 0-104916  
 cylindrical cavity in elastic half-space, Rayleigh wave loading, stress spectral representation 0-64453  
 defectoscopy, development of and problems in theory of normal waves, review 0-81265  
 dispersion and damping of Rayleigh wave propagating along rough surface 0-102892  
 dispersion relations for surface waves in cubic crystals 0-102906  
 mantle of Europe and Eurasia, inferences from higher mode seismic data 0-72436  
 metal, SAW mode conversion, by EM generation of US 0-84357

# Rayleigh waves continued

- mode conversion, shear, Lamb and Rayleigh waves, demonstration 0-101687  
 Mountain Crimea region, surface seismic Rayleigh waves, amplitude spectra 0-89969  
 multilayered half space solutions, computer algorithms 0-98260  
 nonlinear interaction in LiNbO<sub>3</sub>-CdS system, expt. investigation 0-102946  
 piezoelectric crystals, elastic surface waves 0-103558  
 piezoelectric medium, semibounded, body waves and quasi-body surface waves 0-107367  
 prism couplers for Rayleigh and Lamb waves, anal. 0-69619  
 propagation over liquid and crystalline layers, effect of crystals. elastic const. 0-76924  
 propagation over liquid and crystalline layers, theory 0-76925  
 quasistationary Rayleigh waves on inhomogeneous anisotropic elastic body surface 0-69721  
 reflection from periodic corrugations of surface in oblique incidence 0-58850  
 San Fernando earthquake, strong ground motion, ray models 0-61762  
 scattering by surface breaking crack, ray analysis 0-69575  
 seismic attenuation in volcanic area of Massif Central, France 0-98264  
 small earthquake mechanism and depth from radiation patterns 0-61764  
 smooth surfaces of arbitrary shape, propag. of waves 0-64272  
 steel, US critical angle reflectivity, near-surface metallic prop. gradient effect 0-70516  
 transmission coeffs. in trench 0-98266  
 upper mantle S-wave velocity model, based on great circle Rayleigh waves 0-109107  
 upper mantle structure, probed by use of higher wave modes 0-104890  
 Si amorphous film, acoustic study using Rayleigh waves 0-75312  
 SiO<sub>2</sub> amorphous films, acoustic study using Rayleigh waves 0-75312  
 YIG, nonreciprocal attenuation of magnetoelastic Rayleigh waves 0-60399

**reactance, electric** *see* electric reactance

# reaction kinetics

- see also catalysis; chemical exchanges; chemical reactions; explosions; potential energy surfaces for collision processes; reaction kinetics theory; reaction rate constants*  
 acetone, adsorbed on ZnO, decomp., IR and kinetic obs. 0-59780  
 activated processes in condensed phases, general kinetic models 0-81281  
 burning rate in engine cylinder, swirl and turbulence effects 0-89492  
 2-butene ion, fragmentation, angular momentum in ion-mol. reacts., RRKM calc. 0-66773  
 calcium oxalate hydrates, crystn. kinetics, comparison for mono-, di-, and trihydrates 0-81528  
 catalysis, advances in TEM obs. 0-85214  
 catalytic processes and stochastic processes of chem. kinetics, historical review 0-105483  
 charge transfer reactions in biological systems, mech. of coupling 0-76889  
 chemical reactions, oscillatory systems, weak coupling 0-66775  
 condensed adsorption layers, effect on electrode reaction rates 0-93769  
 1-cyano-2-methyl-3-(cis-propenyl) cyclopropanes, rotational propensities and bond rupture identity 0-104437  
 diacetylene, photopolymerisation, optical absorpt. spectra, time depend., reaction kinetics 0-85174  
 diffusion equation, nearly degenerate bifurcations, mode interactions 0-85149  
 diffusion system, two chemical species reacting at boundary 0-93733  
 diffusion systems, Chapman-Enskog development of multivariable master eqn. 0-81283  
 dissipative structures, nonlinear reaction-diffusion model, stability of secondary multiple steady states 0-76485  
 dual microcomputer-controlled stopped-flow spectrometer 0-57379  
 electrocatalysis, surfaces modified by metal adatoms, review 0-61110  
 explosion detonation, similarity and differences between conditions for initiation and failure 0-103038  
 fast chemical reaction obs., by pulse radiolysis (*Czech*) 0-81325  
 flames, laminar, premixed, non-adiabatic, nonlinear theory 0-93757  
 free radical reactions, photolytically initiated, high temp. kinetics meas. technique 0-61085  
 fusion chain reactions, kinetics, high electron temps., interactions with D-T plasma 0-68945  
 gas phase chemical reactions in atmosphere, evaluated kinetic and photochemical data 0-101671  
 glass reactions with aq. solns., influence of surface pot. on kinetics 0-108612  
 glow curves and desorption spectra anal. method 0-80053  
 haemoglobin macroporous particle study, photoacoustic spectrometry 0-85543  
 II-VI semiconductors, thin epitaxial layer, direct synthesis (*German*) 0-104070  
 instabilities, stochastic approach, anomalous fluctuation and transient behaviour 0-89465  
 ionospheres, ionic reactions in lab. and planetary atmospheres 0-59168  
 IR laser photolysis of polyat. mols. photochem. appls. 0-66835  
 isopropyl alcohol, adsorbed on ZnO, decomp., IR and kinetic obs. 0-59780  
 laser-chemical reaction kinetic mechanism (*Russian*) 0-101007  
 measurement and control using laser technology, free electron laser appl. 0-81349  
 membrane surfaces, antibody association kinetics with spin-label haptens 0-66787  
 methylundecanhydride hardened phenol formaldehyde resin, hardening kinetics and mech. losses 0-66520  
 microcomputer interfaced spectrophotometer studies 0-62726  
 molecule + molecule, enhancement by collision induced absorpt. of IR laser radiation 0-66798  
 molten carbonate fuel cell, electrolyte comp. effect on electrode kinetics 0-101092  
 optical image phase recording using sensitised photooxidation reactions 0-87350  
 oscillators responding frequency switch 0-108837  
 Petrov equation of chemical kinetics, kinetics of solid state processes 0-97685  
 photoreacts, photochemical reaction rates, intensity depend., kinetic model 0-104452  
 poly(m-xylylene adipamide), molten, gel form. kinetics (*Japanese*) 0-108757



## reaction kinetics continued

- polyethylenepolyamine hardened epoxy resin, hardening kinetics and mech. losses 0-66520  
 precursor intermediates in adsorption, desorption and reaction 0-108731  
 Purex kinetics, U extraction with tributylphosphate (*German*) 0-57937  
 Rochelle salt, dehydration kinetics in ferroelec. and paraelec. phases, surface acoustic waves influence 0-97204  
 roughness fluctuation in layer between two phases 0-85147  
 semiconductor catalytic kinetics, complex mech. of excitation, constant state problems 0-85213  
 solid phase reactions induced by scanning CW laser, reaction rates, analytical model 0-66334  
 spiropyrans, polymer matrix effect on photochromism, thermal decolouration kinetics 0-76537  
 steel, mild, electrodes, in  $\text{H}_2\text{SO}_4$ , H evolution reaction kinetics 0-97630  
 steel, stainless, liq. Li corrosion rate expressions, 600-1000°C 0-93682  
 surface reactions, kinetics and dynamics, conf., La Jolla, CA, USA (Aug 1979) 0-105415  
 surface transport and reaction, stochastic calcs. 0-108736  
 teaching, Faraday balance for studying strong mag. field effects on react. rates 0-57043  
 tetramethyldioxetane, multiphoton dissociation, collisional vibr. relax., rate eqns. model 0-63729  
 thermal boundary layer interactions in shock tube sampling for kinetic obs. 0-104420  
 thermal kinetics meas. using modified commercial stopped flow apparatus 0-86291  
 travelling waves for a model non-linear reaction-diffusion system 0-89476  
 troposphere, lower, modelling, chemical kinetic data needs, conference, Reston, Virginia (1978 May 15 to 17) 0-62383  
 turbulent mixing with react. of miscible reactant streams, simulation 0-64651  
 unimolecular IR multiphoton decomp., energy grained master eqn., approx. model and exact soln. 0-66829  
 AgI/RbI quasibinary system, solid state reactions and transport props. 0-96700  
 Al, reaction with  $\text{H}_2$ , influence of surface reactions on rate (*Russian*) 0-66863  
 $\text{Ar}^* + \text{CO}_2$ ,  $\text{CO}^*$  prod., use in laser systems 0-63824  
 B,C, reaction kinetics with liq. Al, Si, Ni and Fe 0-84344  
 Ba getter film, initial reaction probability with  $\text{O}_2$ , water, CO and  $\text{CO}_2$ , AES obs. 0-61153  
 Ba +  $\text{CO}_2(\text{O}_2)$ , crossed beam kinetics, BaO recoil velocity spectra 0-76500  
 $\text{C}_3 + \text{NO}(\text{O}_2)$ , reaction kinetics, laser induced fluoresc. obs. of allene photolysis 0-66820  
 $\text{CaCO}_3$  crystallisation from aqueous solutions, kinetic study 0-59419  
 $\text{Ca}_{10}(\text{PO}_4)_6(\text{OH})_2$  dissolution kinetics, nucleation-controlled 0-59659  
 $\beta\text{-Ca}_2\text{SiO}_2$ , reaction kinetics with  $\text{CO}_2$  and water vapour 0-76484  
 $\text{Ca}_2\text{SiO}_2$ , reaction kinetics with  $\text{CO}_2$  and water vapour 0-76484  
 Cs sorption in nuclear graphite, sorption kinetics modelling 0-102244  
 DF- $\text{CO}_2$  chemical laser, photon branching in chain reactions, IR radiation initiation 0-91785  
 Fe ore, cold bound pellets, reduction using  $\text{H}_2$  gas, 700 to 900°C (*Japanese*) 0-71907  
 Fe-Ni alloy, fluorination kinetics and fluoride film form., chem. nature obs. 0-101035  
 $\text{H} + \text{CN}(\text{NC})(\text{NSi})$ , bimolecular exchange reactions, dynamical-statistical method calcs. 0-104435  
 $\text{H} + \text{O}_3 \rightarrow \text{HO}_2 + \text{O}(\text{P})$ , yields 0-71900  
 $\text{H}_2$  production by steam reforming of natural gas, chemical kinetics 0-97815  
 $\text{H}_2 + \text{O}_2$ , combustion, kinetic modeling and sensitivity anal. 0-89490  
 $\text{H}_2^+ + \text{D}_2 \rightarrow \text{H} + \text{H}$ , product angular and vel. vector distributions meas. by crossed beam expt. 0-101012  
 HF laser with flow-through chem. active medium, pulsed-periodic regime realisation 0-106513  
 HF, pulsed laser numerical modelling, rot. relax. 0-87388  
 $\text{H}_2\text{SO}_4$  + atmospheric species, collisional reaction probabilities rel. to  $\text{H}_2\text{SO}_4$  aerosols as tropospheric sinks 0-72612  
 $\text{I}_2$ , photolytic cage effect in gas phase 0-81345  
 $\text{K}_2\text{O-Al}_2\text{O}_3\text{-P}_2\text{O}_5\text{-TiO}_2$ , structural role of Ti, kinetic study of chem. destruction 0-88055  
 LaN, form. conditions 0-101019  
 Li/ $\text{SO}_2$  cells, safety studies, kinetics of Li-organic solvent exothermic reactions 0-72030  
 $\text{N}_2$  + methane,  $\text{N}_2$  fixation, catalytic processes in non-equilibrium plasma chemical reactors (*French*) 0-89483  
 $\text{N}_2 + \text{O}_2$ ,  $\text{N}_2$  fixation, catalytic processes in non-equilibrium plasma chemical reactors (*French*) 0-89484  
 $\text{N}_2\text{F}_4$ , collisionless dissociation kinetics in highpower IR radiation field 0-66853  
 $\text{Na}_2\text{WO}_3$  bronzes, reaction with Fe powder, reaction mechanism and reactivity 0-108712  
 Ni (100), kinetics of C deposition from adsorbed CO 0-76553  
 Ni, corrosion, high temp.,  $\text{SO}_4$  induced, studied at 900°C in  $\text{O}_2 + 4.2\% \text{SO}_2$  0-97639  
 O + methane  $\rightarrow$  OH + methyl reaction, photolytically initiated, high temp. kinetics meas. technique 0-61085  
 O( $\text{P}$ ) + dimethyl disulphide, absolute reaction rate const. determ. 0-89472  
 $\text{PF}_3$  dopant for polyacetylene 0-88171  
 $\text{PrO}_{1.714}$ , oxidation, kinetic study 0-108707  
 Pu-Ga (1 wt.%), alloy powder, hydriding kinetics 0-76503  
 Ru (110), kinetics of C deposition from adsorbed CO 0-76553  
 $\text{SiO}_2$ , vitreous, hydroxyl free, reaction with H, diffusion, absorpt. spectra 0-85210  
 $\text{SiO}_2$ -water system, inorg. polymer struct. form., globular crystn. 0-101042  
 SmN, form. conditions 0-101019  
 $\text{TaS}_2\text{-Zn}$  electrodes, topotactic reduction mechanism, neutron diff. obs. and intercalation cpd. form. 0-108748  
 $\text{TiO}_2\text{-TeCl}_4$  system, chem. vapour transport, matrix isolation IR studies 0-93755  
 $\text{V}_2\text{O}_5\text{-AlNbO}_4(\text{GaNbO}_4)(\text{TiNbO}_7)$  systems, interfacial reactions, efficient boundary conditions and solid state reactivity 0-76542  
 $\alpha\text{-Zr}$ , oxidation in  $\text{O}_2\text{-N}_2$  atmospheres 0-104353

## reaction kinetics models and mechanisms see reaction kinetics theory

## reaction kinetics theory

- acetaldehyde, carbonyl addition, model transition states, vibr. anal. 0-71898  
 atom + diatom reactions, semiclassical tunnelling probabilities, trajectory calc. 0-71886  
 Belousov-Zhabotinsky reaction, chem. turbulence, strange attractor representation 0-85148  
 bimolecular exchange reactions, dynamical-statistical method calcs. 0-104435  
 branched chain reactions, thermal nonequilibrium effects 0-76507  
 chemical centre waves, dynamic Pade approx. 0-76486  
 chemical reactions, Brownian dynamics simulation in soln. 0-104422  
 chemical rectifiers, one-way catalysis 0-71901  
 chemical systems, single variable, master eqn. approximation by Fokker-Planck type eqns. 0-77702  
 chemically assisted fracture, general reaction rate theory and thermodynamics 0-64465  
 collinear asymmetric model reaction probabilities quantum and quasiclassical calcs. 0-85145  
 condensed phase chemical dynamics, many-body problems, generalised Langevin theory, modeling 0-76482  
 condensed phase microscopic theory, configuration space eqns. 0-61067  
 condensed phase microscopic theory, pair phase space kinetic eqn. 0-61066  
 desorption, relaxation time approach limitations 0-93795  
 diffusion controlled processes, nonequilibrium decay effects 0-66764  
 diffusion controlled reaction, passage time approach 0-71903  
 diffusion theory of reaction rates, rate consts. and transmission coeffs. calcs. 0-89464  
 diffusional barrier crossing processes, trajectory simulation for kinetics of reacting soln. 0-81280  
 disordered system, donor-acceptor energy transfer, diffusion modulated 0-71888  
 dissipative structures, bifurcation, symmetry and influence of elec. field 0-81289  
 elementary reactions on single crystal surfaces, kinetics 0-108729  
 endoergic reactions, reagent internal excitation effects on rates 0-93731  
 enzyme-catalysed reactions, network thermodynamic modelling 0-89463  
 equilibrium fluctuations, deviations from Poisson behaviour, molecular dynamics 0-86211  
 gas mixture, physical and chemical process modelling 0-71892  
 glassy polymers double NMR, appl. of cross relaxation dynamics in modulated systems 0-71242  
 growth and patterns of spatial organisation 0-81287  
 heterogeneously catalyzed oscillatory reactions 0-108732  
 hot atom + mol. reaction, steady state vel. distrib., Boltzmann eqn. with BGK elastic collision model 0-66856  
 hot atom reactions, nonequilibrium time-depend. theory, model calcs. 0-61125  
 intermicellar kinetics theory, stochastic approach, master equation for, irreversible reactions 0-76561  
 ion-molecule association rate calc. 0-81282  
 liquids, hydrodynamic interactions and pair correl. functions on reaction kinetics, dynamic effect 0-97684  
 maser equation near nonequilibrium transition, stationary solns. 0-89466  
 minimum energy reaction paths, virial theory implications 0-97686  
 multiple stationary point in reacting systems, minimal requirement 0-85146  
 multivariate master equation for reaction-diffusion system 0-95045  
 network structures of a system coded by groups 0-81286  
 non-ideal mixtures, birth and death formalism 0-101006  
 nonadiabatic cage reactions, relaxation hindrance 0-93740  
 nonbimolecular reacting systems, critical bifurcations, scaling and Ginzburg criteria 0-81290  
 nonlinear eqns. for reacting system with physical interactions 0-81288  
 phase transitions, nonequilibrium transient behaviour 0-93732  
 plastic flow, consecutive energy barriers system, reaction kinetics theory 0-106730  
 positive photoresist film exposure, formal kinetics (*German*) 0-104454  
 Rayleigh-Benard instability, n-component reactive fluids 0-69945  
 Rayleigh-Benard instability, reactive binary fluids 0-69944  
 reaction zone propagation, combustion wave structure inversion in porous media 0-89494  
 reaction-diffusion systems, bifurcation theory, classification 0-108713  
 reaction-diffusion systems, dissipative struct., sphere bifurcation numerical determ. 0-76483  
 reactivity-selectivity, bounds derivation 0-66763  
 recombination probability, reactivity depend., scavenger effects 0-76494  
 Schlögl model, transition time statistics 0-89467  
 stationary states, pumped, model for mixing 0-71887  
 sudden rotational approximation, reactive and inelastic, body-fixed frame, exchange reaction extension 0-61073  
 trimer formation from chemical capable of reacting with itself 0-71889  
 unimolecular decomp. kinetics, rot. effects 0-81319  
 unimolecular dynamics, classical trajectory calcs. 0-108692  
 unimolecular reaction, RRKM formula correction by non Boltzmann character factors, Markov eqns. 0-71891  
 $\text{Ba}^+ + \text{D}_2 \rightarrow \text{D} + \text{BaD}^+$ , sequential impulse model, prod. bond dissociation energy and cross section 0-81295  
 $^{18}\text{F} + \text{H}_2$ , hot atom reaction, nonequilibrium time-depend. theory 0-61126
- reaction rate coefficients** see reaction rate constants
- reaction rate constants**  
 acetylperoxy radicals, absorpt. spectrum and reaction kinetics 0-91571  
 anthracenes, exciplex form. with amines, form. kinetics and luminesc. props. 0-66792  
 bis(9-anthryloxy)polyoxaalkanes., intramolecular excimer form. and photodimerisation, kinetic anal., rate constants determ. 0-66800  
 atmospheric photooxidation reactions, rates, reactivity and mechanism for organic compounds reaction with OH radicals 0-72104  
 benzene cation + benzene, trapped ion mass spectra 0-89470  
 2-benzyl-5-benzylidenecyclopentanone, and substituted form, topochem. single-cryst.-to-single-cryst. photodimerisation 0-66819  
 chemical reactions, Brownian dynamics simulation in soln. 0-104422  
 chlorodifluoromethane, unimol. reaction by IR radiation, rate consts. and prod. yield, fluence and intensity depend. 0-97713  
 chlorophyll a, cation radical formation by pulse radiolysis, oxidation and demetalation rate consts. 0-61505  
 chlorophyll-a radical cation lifetime in water-acetonitrile soln. 0-72136  
 complexity and time in physics (*Chinese*) 0-81285

reaction rate constants continued

condensed media, rate processes, master eqns. 0-77687  
coupled multistep chemical reactions, rate const. determ., relax. spectroscopy 0-66766  
cytochrome  $c_3$ -hydrogenase, reduction kinetics, Mossbauer spectra 0-67031  
diffusion systems, quantum statistical theory, multi-channel reactive scatt. 0-81284  
diffusion theory of reaction rates, rate const. and transmission coeffs. calcs. 0-89464  
diffusion-controlled reactions on a two-dimensional lattice 0-71940  
dimethyl sulphide+O( $^3P$ ), fast flow reson. fluoresc. obs. of absolute rate const. 0-61077  
endothermic reaction rate enhancement in EM field 0-66852  
ethyl acetate, gas, radiatively heated by CO<sub>2</sub> laser, cooling mechanism investig. 0-75021  
ethyl cation+alkane reaction, temp. and kinetic energy relative rate const. determ. 0-81299  
ethylene+HBr, low temp. chain hydrobromination, kinetics and mechanism 0-93735  
formaldehyde+Br reactions, rate const. by EPR 0-93736  
formaldehyde+ClO radical, expt. showing no reactivity, stratospheric implications 0-90119  
formaldehyde+F reactions, rate const. by EPR 0-93736  
gas phase chemical reactions in atmosphere, evaluated kinetic and photochemical data 0-101671  
gases, radiatively heated by CO<sub>2</sub> laser, cooling mechanism investig. 0-75021  
H+FH(FD), low barrier quantum model, vibr. deactivation 0-69216  
hydroxymethyl radical + O<sub>2</sub>, rate coefficient meas. by laser magnetic resonance flow tube method 0-66767  
inert gas atom+Ne<sup>2+</sup>(Ar<sup>2+</sup>)(Kr<sup>2+</sup>)(Xe<sup>2+</sup>), low energy reactions, SIFT and drift tube obs. 0-97705  
inert gas mixtures, high-pressure, collisional radiative recomb. 0-63595  
ion+molecule neutralisation rate coefficient parametrisation 0-81301  
ion+molecule association density of quantum states and temp. depend. of rate coeff. 0-101015  
ion+molecule reactions, atmospheric ion chemistry 0-61885  
ion+molecule reactions, low energy, dipole interaction influence 0-89475  
ion kinetics in high-pressure laser plasmas 0-64002  
ion-atom reactions related to interstellar mol. synthesis, rate coeffs. and product ions 0-67812  
ion-molecule association rate calc. 0-81282  
ion-molecule reactions in dilute gases and solutions, electric field effect 0-81315  
Kramer's chemical reaction model, barrier mediated diffusion, generalisation to include viscosity term 0-71890  
metal surface oxidation study, vacuum microbalance investigation 0-76552  
metalloporphyrin, cation radical formation by pulse radiolysis, oxidation and demetalation rate const. 0-61505  
methoxy+NO, reaction rate upper limit, laser induced fluoresc. 0-85200  
methoxy radical+NO, reaction rate meas. 0-76534  
methyl cation+NH<sub>3</sub>, reaction kinetics, 0.04-1 eV (*French*) 0-66768  
methyl ion+H<sub>2</sub>O(He) ternary association reaction in energy range 0.04-0.1 eV 0-71896  
multiphoton dissociation, collisionless, laser pulse shape effect on product yield 0-78667  
naphthylamines, abnormal fluorimetric titration behaviour, kinetic anal., fluoresc. quantum yields and lifetime meas. 0-89560  
phase transitions, Schlogl's chemical model, critical fluctuations near non-equilib. critical point 0-85150  
phenylalanine, hydrated electron impact dissoci., laser flash photolytic investig. 0-58396  
PVC granule morphology during polymerisation, kinetic parameters influence (*German*) 0-85176  
radiative association reactions in dense interstellar clouds, rate coeffs. calcs. 0-82441  
ruthenium tris-bipyridyl, excited state electron transfer quenching, H<sub>2</sub>O photoreduction mediators effects 0-102536  
solid phase chemical reactions, low temp. and fast, mol. motion effect 0-97681  
supercrit. hydrocarbons radiolysis, electron reaction rate const./diffusion coeff. ratio 0-101033  
trimer formation from chemical capable of reacting with itself 0-71889  
unimolecular reaction, thermal, expressions for deriving rate const. 0-85164  
Ag-S+Ln<sub>2</sub>S<sub>3</sub>, powdered mixtures, reaction rate, production of ionic semiconductors 0-93741  
2Ar+Ar<sup>+</sup>(Kr<sup>+</sup>), three body reaction, rate coeffs., temp. depend., 100 to 300K 0-108703  
Ar+Xe<sup>+</sup>, XeAr<sup>+</sup> form., dissoci. energy, reaction equilib. and rate const. 0-61071  
Ba+HF-BaF+H, dual mol. beam excitation difference spectroscopy, state-to-state vibr. resolved dynamics 0-89474  
CCl, reaction rate const. determ. using laser-induced fluoresc. technique 0-97682  
CCl<sub>2</sub>, reaction rate const. determ. using laser-induced fluoresc. technique 0-97682  
CClF, reaction rate const. determ. using laser-induced fluoresc. technique 0-97682  
CCl( $\tilde{X}^1\Pi$ )+methylhalosilanes, reaction rate const. determ. by kinetic absorpt. spectroscopy 0-97683  
CD<sub>4</sub><sup>+</sup>+H<sub>2</sub>(HD)(D<sub>2</sub>), isotopic exchange, interstellar implications 0-61087  
CH+O reaction, absolute rate const. 0-97690  
CH<sub>3</sub><sup>+</sup>+H<sub>2</sub>(HD)(D<sub>2</sub>), isotopic exchange, interstellar implications 0-61087  
CO<sub>2</sub><sup>+</sup><sup>13</sup>C( $\tilde{X}^2\Sigma^+$ )(HCO<sup>+</sup>), isotopic exchange, interstellar implications 0-61087  
CO<sub>2</sub><sup>+</sup>+ethylene, rate coeffs. and product distribution determ. 0-97693  
C<sub>2</sub>O+NO(O<sub>2</sub>)(isobutene), absolute reaction rate const. meas. by laser induced fluoresc. 0-93738  
CO(I)+CO( $\nu$ )-CO(O)+CO( $\nu$ +1), vibr. energy accumulation, reaction rate anal. 0-78692  
CO<sub>2</sub>, CO<sub>2</sub><sup>+</sup>+ethylene, rate coeffs. and product distribution determ., dissoci. energy and heat of form. 0-97693  
CaWO<sub>4</sub>, cryst. growth from solns. in melts, kinetics parameters and thermodynamic props. 0-59424  
Cl+fluoromethane, photochlorination electron and oscill. energy 0-87320  
Cl<sup>+</sup>+molecule, reactions at room temp. 0-93749  
Cl<sub>2</sub>+muonium (H)(D), pot. energy surfaces, inversion calcs. 0-93734  
Cr, corrosion in SO<sub>2</sub>, 700-1000°C 0-97642  
Cu, cementation, on Fe, deposit struct., reaction rates, SEM 0-104421

reaction rate constants continued

Cu-O (0.05 to 0.1 wt.%) liquid alloy, deoxidation kinetics by rotating graphite cylinders 0-61084  
Cu(I) complex, oxidation, fast reactions meas. by pulsed-flow instrument 0-66890  
Cu<sub>2</sub>S+Ln<sub>2</sub>S<sub>3</sub>, powdered mixtures, reaction rate, production of ionic semiconductors 0-93741  
CuSO<sub>4</sub>.5H<sub>2</sub>O monocryst. platelets, dehydration into trihydrate, displacement rate modulation of reaction front 0-108711  
D+FD(FM), low barrier quantum model, vibr. deactivation on chemically reactive potential surfaces 0-69216  
D+H<sub>2</sub> reaction, transition state theory calculations, kinetic isotope effect explanation 0-66784  
D+H<sub>2</sub> rearrangement collision, vibr. excitation effects 0-71910  
D<sub>2</sub>O<sup>+</sup>(D<sub>2</sub>O)<sub>n</sub>+H<sub>2</sub>O(NH<sub>3</sub>), binary reactions, rate coeffs. and product ion distributions determ. 0-81305  
F+HCl(HBr)(DBr)(HI), H abstraction reactions, temp. depend., laser photolysis IR fluoresc. obs. 0-93744  
F+HCl-HF+Cl, time resolved vibr. chemiluminesc. and rate const. 0-61069  
Ge+N<sub>2</sub>O, chemiluminesc. reaction, HTFFR kinetics study 0-76496  
H+D<sub>2</sub> reaction, transition state theory calculations, kinetic isotope effect explanation 0-66784  
H+HCO-H<sub>2</sub>+CO, classical trajectory study 0-93750  
H+O<sub>2</sub>+Ar, HO<sub>2</sub> free radical prod., rate const. calc. 0-101026  
H<sub>2</sub>+Cl(Br)(I)(F), gas phase H-atom transfer reactions, struct.-reactivity correl., pot. energy surfaces 0-104433  
H<sub>2</sub>+O<sub>2</sub>, combustion, kinetic modeling and sensitivity anal. 0-89490  
HCl+Cl(Br)(H), vibr. relaxation and reaction rates determ. 0-108698  
HN<sub>3</sub>, UV photolysis 0-101027  
HN<sub>3</sub>+NH(NH<sub>3</sub>), rate const. from HN<sub>3</sub> UV photolysis data 0-101027  
HO<sub>2</sub>+ClO, free radical reaction rate const. and products at 298K, discharge flow mass spectra 0-67391  
HO<sub>2</sub>+O<sub>2</sub>, reaction kinetics, laser mag. reson. obs. 0-102528  
H<sub>2</sub>O<sup>+</sup>+NO<sub>2</sub>(O<sub>2</sub>)(NO)(CO<sub>2</sub>)(H<sub>2</sub>)(ethylene)(methane), rate constants determ. as function of relative kinetic energy 0-81292  
H<sub>2</sub>O<sup>+</sup>(H<sub>2</sub>O)<sub>n</sub>+D<sub>2</sub>O(NH<sub>3</sub>), binary reactions, rate coeffs. and product ion distributions determ. 0-81305  
2He+He<sup>+</sup>(Ne<sup>+</sup>), three body reaction, rate coeffs., temp. depend., 100 to 300K 0-108703  
He<sup>+</sup>+H<sub>2</sub>(D<sub>2</sub>), dissociative charge transfer, 78-330K 0-61079  
He\*, diatom, optical absorpt. spectra and kinetic behaviour 0-95635  
He\*, inert gas atoms, optical absorpt. spectra and kinetic behaviour 0-95635  
Kr<sup>+</sup>+molecule, <sup>2</sup>P<sub>3/2</sub>(<sup>2</sup>P<sub>1/2</sub>) doublet ground state reactions at 300K 0-108702  
Kr<sup>2+</sup>+H<sub>2</sub>(N<sub>2</sub>)(O<sub>2</sub>)(CO)(CO<sub>2</sub>)(methane), charge transfer reactions, rate coeffs. and product-ion distributions meas. 0-104431  
Mg(NO<sub>3</sub>)<sub>2</sub>-RNO<sub>3</sub> (R=Li, Na, K), thermogravimetric anal. of dehydration processes (*Japanese*) 0-66791  
MoF<sub>6</sub>, reduction by H in the presence of HF (*Russian*) 0-61076  
N<sup>+</sup>+O<sub>2</sub>, branching ratio kinetic energy depend. 0-97703  
N<sub>2</sub>+HgX<sub>2</sub> (X=halide), A<sup>2</sup> $\Sigma_u^+$ -state quenching obs. 0-108693  
N<sub>2</sub>+methylmercury halides, A<sup>2</sup> $\Sigma_u^+$ -state quenching obs. 0-108693  
NF+H(NF), electronically-excited free radical reactions 0-97707  
NF<sub>3</sub>+H(O)(N), electronically-excited free radical reactions 0-97707  
N<sub>2</sub>F<sub>4</sub>, mol. photodissoc. using CO<sub>2</sub>-laser radiation, rate const. meas., mol. fluoresc. and time-resolved UV spectra obs. (*German*) 0-83434  
NH<sub>3</sub>+O<sub>2</sub>, reaction mechanism, flash photolysis obs. 0-104425  
NH<sub>3</sub>+O<sub>2</sub>, reaction rate const., rel. to atmospheric processes 0-85155  
NH<sub>3</sub>-NH<sub>4</sub><sup>+</sup> conversion, in atmosphere, pseudo first-order reaction rate const. 0-94132  
NO, electrocatalytic decomp. on electrochem. reduced zirconia surface 0-61113  
Ne<sup>2+</sup>+H<sub>2</sub>(N<sub>2</sub>)(O<sub>2</sub>)(CO)(CO<sub>2</sub>)(methane), charge transfer reactions, rate coeffs. and product-ion distributions meas. 0-104431  
Ni(CO)<sub>4</sub>, form. reaction rate, substrate mag. phase depend. 0-108737  
O+H<sub>2</sub>, classical trajectory calcs., ab initio surface, singlet state, rate const. 0-66786  
O+H<sub>2</sub>, pot. energy surfaces and reaction rates, ab initio calcs. 0-63531  
O<sup>+</sup>+O<sub>2</sub>->O<sub>2</sub><sup>+</sup>+O, cross section kinetic energy depend., rate const. meas. and Monte Carlo calcs. 0-78701  
O<sub>3</sub> photolysis by sunlight, rate constants at ground level 0-61836  
O<sub>3</sub>+thiirane, autocatalytic reaction, stopped-flow study, reaction rate meas. 0-85152  
O<sup>+</sup>(<sup>4</sup>D)+e-O<sup>+</sup>(<sup>4</sup>S)+e in the thermosphere, rate coeff. meas. 0-94630  
O<sup>+</sup>(<sup>4</sup>D)+N<sub>2</sub>, thermal rate coeff., products and branching ratios in ionosphere 0-82117  
O<sup>+</sup>(<sup>4</sup>D)+N<sub>2</sub> charge exchange, rate coeff. temp. depend. 0-77179  
OH+H<sub>2</sub>O<sub>2</sub>->HO<sub>2</sub>+H<sub>2</sub>O, reaction rate const., laser induced fluoresc. 0-101017  
OH+OCS(CS<sub>2</sub>), lower atmosphere chem. 0-61870  
O(<sup>2</sup>P)+dimethyl disulphide, absolute reaction rate const. determ. 0-89472  
<sup>18</sup>O<sup>16</sup>O, atmospheric photodissoc. rates 0-94559  
SO<sub>2</sub>+Ar, dissoci. rate meas. behind shock wave, laser Schlieren method 0-81296  
SO<sub>2</sub>+O<sub>2</sub>=SO+O<sub>2</sub>, gas phase reaction, rate coeffs. meas. 0-97704  
SbF<sub>5</sub>+benzyl chloride, chemi-ionis. reaction, temp. depend., flow tube investig. 0-108701  
Si, oxidation, solubility and transport behaviour of water, dissolution 0-93801  
T+HD, variational transition field theory and unified statistical model 0-97700  
Ti alloys, hydrogenation at 200-600°C and up to 10000 kPa 0-107435  
Xe+Ne, quenching of excited Xe\*(<sup>3</sup>P<sub>1</sub>, <sup>3</sup>P<sub>1</sub>) states 0-63578  
Xe<sup>+</sup>+molecules, <sup>2</sup>P<sub>3/2</sub>(<sup>2</sup>P<sub>1/2</sub>) doublet ground state reactions at 300K 0-108702  
ZnSb, orientated crystn. conditions during reaction diffusion (*Russian*) 0-70558  
Zr(HPO<sub>4</sub>)<sub>2</sub>.H<sub>2</sub>O, Na<sup>+</sup> transport, gas-solid and solid-solid reaction kinetics 0-61086

reactions (chemical) see chemical reactions

reactions (nuclear) see nuclear reactions and scattering

reactive power

meter for periodical signals in range 50 Hz to 5 kHz (*Spanish*) 0-86339  
three-phase two wattmeters, meas errors (*Croatian*) 0-105677

reactive sputtering

fused silicon substrate, directional reactive ion etching at oblique angles 0-66428



**reactive sputtering continued**

- ion beam, plasma and reactive ion etching, review 0-108621
- refractory carbides, adhesion to metal substrates, improved 0-76481
- AlN film, oriented c-axis, low temp. deposition by reactive magnetron sputtering 0-76180
- AlN films on glass substrate, prep. by reactive DC magnetron sputtering technique, c-axis orientation 0-89146
- Al<sub>2</sub>O<sub>3</sub>-based ceramics, high rate reactive ion etching 0-85070
- Cu, SIMS depth profiling, surface roughening by low energy ion irradiation 0-60727
- FeC<sub>x</sub>-CrC<sub>x</sub>-NiC<sub>x</sub>, stainless steel carbide, graded solar selective surface, magnetron sputtered 0-81485
- FeC<sub>x</sub>-CrC<sub>x</sub>-NiC<sub>x</sub>, stainless steel carbide, sputtered solar selective surface, grading profile 0-81486
- GaAs thin films, reactively sputtered, ESCA/XPS study 0-97430
- In, reactive sputtering in Ar-N<sub>2</sub>, N<sub>2</sub>-O<sub>2</sub> discharges, mechanism, model 0-89109
- InN film growth by reactive sputtering in Ar-N<sub>2</sub> discharge, mechanism 0-89107
- In<sub>2</sub>O<sub>3</sub>, thin film, sputter deposition form., optical and elec. props. 0-60123
- In<sub>2</sub>O<sub>3</sub>-InN film growth by reactive sputtering in N<sub>2</sub>-O<sub>2</sub> discharge, mechanism 0-89108
- Mo-Si, film deposition by reactive sputtering, characteris. (Japanese) 0-93485
- Mo<sub>2</sub>Si<sub>3</sub> films, magnetron DC reactive sputtering, struct. and props. 0-80966
- Si, amorphous, prep. by reactive RF sputtering in Ar-silane mixtures, undoped, n-type and p-type targets 0-76182
- Si, high rate reactive ion etching 0-85070
- Si-Ag-Si heat mirror on plastic sheet for radiation insulation of visible windows 0-95985
- Si<sub>3</sub>N<sub>4</sub> amorphous film deposition by high rate DC reactive sputtering, passivation appl. 0-100784
- Ti, sputtered ion fraction meas. using matrix isolation spectroscopy 0-60738
- TiO<sub>2</sub>-Ag-TiO<sub>2</sub> heat mirror on plastic sheet for radiation insulation of visible windows 0-95985
- ZnO film on glass substrate, high-rate deposition using DC reactive magnetron sputtering 0-80978
- Zr, sputtered ion fraction meas. using matrix isolation spectroscopy 0-60738

**reactive voltamperes** *see* **reactive power****reactively sputtered coatings**

- biological solar cells, photosynthetic bacterial reaction centres on sputtered C and SnO<sub>2</sub> electrodes 0-66981
- closed loop control of deposition using glow discharge mass spectroscopy 0-80973
- steel, stainless, carbide reactively sputtered solar selective absorbers for all-glass tubular evacuated collectors, absorptance and emittance 0-101132
- [α-SiC:H, prepared by reactive sputtering, layer props. (Japanese) 0-60695
- AlN, piezoelectric film, low temp. growth by RF reactive planar magnetron sputtering method 0-76175
- Al<sub>2</sub>O<sub>3</sub> films, DC reactively sputtered, struct. 0-96764
- CdO-SnO<sub>2</sub>, DC reactively sputtered films, elec. and optical props. 0-103763
- Cr<sub>2</sub>C<sub>3</sub>, reactively sputtered solar selective absorbers for all-glass tubular evacuated collectors, absorptance and emittance 0-101132
- Cu<sub>2</sub>S-CdS solar cell fabrication by magnetron reactive sputtering deposition 0-61363
- FeC<sub>x</sub>-CrC<sub>x</sub>-NiC<sub>x</sub>, stainless steel carbide, graded solar selective surface, magnetron sputtered 0-81485
- Fe<sub>2</sub>O<sub>3</sub> films, DC reactively sputtered, for selectively semitransparent photomasks, struct., mech. and chem. props. 0-59835
- Fe<sub>2</sub>O<sub>3</sub> films, DC reactively sputtered, for selectively semitransparent photomasks, deposition conditions and optical props. 0-60782
- Fe<sub>2</sub>O<sub>3</sub> thin films, reactively sputtered, mechanical stresses rel. to deposition conditions 0-80146
- InN film growth by reactive sputtering in Ar-N<sub>2</sub> discharge, mechanism 0-89107
- In<sub>2</sub>O<sub>3</sub>, thin film, sputter deposition form., optical and elec. props. 0-60123
- In<sub>2</sub>O<sub>3</sub>-InN film growth by reactive sputtering in N<sub>2</sub>-O<sub>2</sub> discharge, mechanism 0-89108
- In<sub>2</sub>Si<sub>2</sub>O<sub>7</sub>, thin film, sputter deposition form., optical and elec. props. 0-60123
- NbN, supercond. RF reactively sputtered films, deposition parameter effects on props. 0-80972
- Pb<sub>2</sub>Ge<sub>2</sub>O<sub>7</sub>, sputtered ferroelec. films, prep. struct. and dielec. props. 0-75452
- Si, etching by CF<sub>4</sub>, plasma deposition reactor gas phase charact., mass spectra 0-70566
- Si:H, amorphous, image pickup devices 0-100481
- Si:H, amorphous Schottky solar cells, prep. and charact. of diode RF reactive cathodic sputtered films (French) 0-61347
- Si:H amorphous films, reactively sputtered, prep. and characterisation 0-100785
- Si-H, amorphous, sputtered, photolum. obs. 0-80856
- SiC:H amorphous reactively sputtered film, H content effect on film props. 0-75459
- Si<sub>3</sub>N<sub>4</sub> thin film, reactively sputtered, struct. and elec. props. 0-88656
- SnO<sub>2</sub> films, non-stoichiometric, DC reactively sputtered, elec. props. 0-80415
- Ta-Al-N thin film resistors with improved elec. props. 0-100544
- Ta<sub>2</sub>O<sub>5</sub> on Si, in two-electrode magnetron system, dielectric and optical props. obs. (Bulgarian) 0-89144
- TiN films, reactively RF sputtered, struct. and elec. props., substrate bias effects 0-96763
- TiN layers investigation for solar-cell contacts 0-81461
- ZnO RF sputtered films, post deposition annealing behaviour 0-100416

**reactors (nuclear)** *see* **fission reactors****Read diodes** *see* **IMPATT diodes****read-only storage**

- ferroelectric memory, matrix-addressed analogue, on Gd<sub>2</sub>(MoO<sub>4</sub>)<sub>3</sub> cryst. 0-103926

**read-only storage continued**

- photosensor spectral responsivity calibration microprocessor system 0-86409
  - VMOS dynamic memory, 65536-bit, investigation of alpha-particle induced soft errors 0-88223
- readout, digital** *see* **digital readout**
- real time computer systems** *see* **real-time systems**
- real-time systems**
- see also online operation*
  - air pollution episodes in Venetian region, real-time forecasting via advection-diffusion model 0-77096
  - air pollution episodes in Venetian region, real-time forecasting via Kalman predictor 0-82046
  - edge detection, numerical, optical and hybrid methods compared 0-102662
  - holographic viewing in moving fog 0-102676
  - HTR spent fuel reprocessing facility, real-time data acquisition and processing system (German) 0-106148
  - moire topograms, real-time, video electronic generation 0-67198
  - Pioneer Venus occultation expt., bandwidth reduction for radio science data generation 0-67492
  - solar thermal test facility, 5 MW, real-time computer control 0-72075
  - speech high-performance processor design 0-96144
  - two-beam interference pattern monitoring by phase modulation 0-77844

**reboilers** *see* **boilers****receivers**

- see also acoustic receivers; radio receivers; television receivers; transceivers*
- Josephson junctions, applications in plasma physics 0-103194

**recombination, electron-hole** *see* **electron-hole recombination****recombination, ion** *see* **ion recombination****reconnaissance satellites** *see* **artificial satellites****record players** *see* **gramophones****recorders**

- see also recording; tape recorders*
- atomic probe, field ion microscope with time-of-flight mass spectrometer 0-73520
- automatic digital equipment for recording acoustic emission signals 0-102948
- crack measurement, recording instrument 0-100984
- DNA derivative melting curves, automatic recorder using real time processing (French) 0-104833
- electric dichroism measurement instrument with digital processing 0-82800
- electrical instruments in photometric laboratory, selection, care, and use 0-86283
- electronic transient, use in quarrying for control of noise and vibration emission from explosions 0-67023
- flexible high-resolution film recorder system 0-102827
- Landsat imagery laser film recorder and processor 0-105084
- magnetic circular dichroism recorder calibration at 10.6 μm 0-90876
- Mossbauer spectra recording apparatus, effect of gate setting on spectral parameters 0-90938
- scanning laser beam direct picture printers on photographic paper, appl. in life sciences (French) 0-72119
- strip chart recorder future in laboratory 0-57279
- submarine quantum irradiance and photoperiod meter, with digital recording 0-98474
- surface meas. instrument, modular (German) 0-57283
- system for recording the activation times of pulsed light sources 0-73488
- transient 8 bit recorder using proportional step size tracking A/D converter 0-57269
- transient recorders for acoustic emission studies 0-83717
- unit to record and reproduce acoustic emission signals 0-79039
- waveform, functions and apps. 0-57278

**recording**

- see also audio recording; magnetic recording; video recording*
- astronomy, data recording system for KSC 60 cm reflecting telescope (Japanese) 0-94717
- determination of complete dynamic charact. of recording systems, multi-frequency dynamic charact. method 0-62651
- electrophotography, bit capacity limitation, toner size and deposition 0-62762
- fast processes, photographic and cine methods 0-57413
- flexible high-resolution film recording system design 0-102828
- hologram electronic heterodyne recording and self-interference term rejection 0-91756
- laser recording and information handling, seminar, San Diego, CA, USA (Aug. 1979) 0-101663
- lustre quality meas., recording and evaluation 0-98967
- magnetocardiography recording, props. of ideal system, appl. of ECG theory 0-104700
- optical and strain gauge methods comparison for split Hopkinson press. bar test on C fibre composites 0-85132
- rain, description and field testing of digital recording system for tipping bucket rain gauges 0-77161
- SQUID, appl. to cardiac recording, phase and amplitude relationships of elec. and mag. events 0-104695
- welded joint inspection by X-ray TV intrascope, photographic recording of images 0-86485

**recording instruments** *see* **recorders****recovering** *see* **recovery****recovery**

- see also recovery-creep*
- Al<sub>2</sub> compounds, disordered, reordering kinetics, recovery of supercond. transition temp. 0-96678
- cell wall and lattice misorientation origin during deform. 0-71712
- ductile fracture, strain hardening and damage relationship 0-108564
- grinding, role of elastic and plastic behaviours (Japanese) 0-100868
- internal stress, stochastic model for dip test in steady-state creep 0-58915
- metal, electron irradiation, selfinterstitial atomic defect interaction radii, recovery expts. and error sources 0-65049
- metal, polycrystalline, strain hardening, dislocation link length model 0-84953
- polystyrene, atactic, indentation recovery 0-84988
- steel, HSLA, V and N effect on recovery and recrystn. during and after hot working 0-84973
- steel, low-C, hot deform., austenite strengthening and weakening 0-76282

recovery continued

steel, plastic loosening and deform. defect healing during recovery annealing of 12Kh18N10T (*Russian*) 0-66530  
 Au, deformed, annealing kinetics of vacancies (*Japanese*) 0-88139  
 Au film, adatom surface diffusion at low temps., elec. resist. study (*French*) 0-65376  
 Bi film, adatom surface diffusion at low temps., elec. resist. study (*French*) 0-65376  
 Cu crystals, two-phase, recrystn. retardation, particle size, spacing effects 0-89242  
 Cu, irradiation with O<sub>2</sub> ions, defect production and annealing 0-88214  
 Cu, polycrystalline, recovery and recrystn. kinetics 0-81081  
 Cu-Nb multifilamentary composite, dislocation resistivity 0-70671  
 Fe, irradiated with electrons then annealed, magnetoresistance at 20K (*French*) 0-103677  
 Fe-Al (40 at.%) and Fe-Al (50.5 at.%) ordered alloys, 20K neutron irradiation effects, stoichiometry depend., resist. obs. (*French*) 0-84215  
 GaAs, ion damage, TEM study of laser annealing 0-88215  
 Mg-Ag, ion implanted, recovery stage characterisation by electron irradiation 0-107295  
 Mo-Re(Os)(Ru), recovery after deform. and annealing, destrengthening mechanism (*Russian*) 0-97546  
 NaCl, pure and doped, 20K X-ray irradiation, thermolum. and recovery processes 0-93412  
 Ni, push-pull fatigued polycrystals, point defects, elec. excess resist. meas. 0-100910  
 Ni-Cr-W-Mo-Ti-Al, heat-resist., recovery and recrystn. 0-76268  
 Pt, recovery spectrum after thermal neutron irradiation, resist. obs., Au addition effect and defect conc. depend. 0-65057  
 Si, ion damage TEM study of laser annealing 0-88215  
 Si-Bi, ion implanted, channelling obs. of pulsed Q-switched ruby laser annealing 0-59542  
 steel, Nb, deform., recrystn. and precip. interaction 0-97515  
 UC, quenched-in defects, formation, migration and resistivity 0-64990  
 UCN, quenched-in defects, formation, migration and resistivity 0-64990

recovery-creep

dispersion-strengthened alloys, threshold stress for creep 0-93626  
 polymers, structural, creep and recovery under hydrostatic compression in programmed loading 0-100881  
 polyolefins, ultra-high modulus, production by tensile drawing and hydrostatic extrusion 0-81022  
 polystyrene-tricresyl phosphate solns., viscoelastic props., conc. depend. 0-76299  
 Al<sub>20</sub>Cu<sub>75</sub>Zr<sub>5</sub> metallic glass, inelastic deform., free energy spectra 0-71699  
 Cu-Ni (10 at.%), hardening, recovery, and struct. changes during high temp. creep (*Russian*) 0-89288  
 Cu-SiO<sub>2</sub>, low-temp. recovery creep, Orowan loop accumulation 0-81126  
 Cu<sub>40</sub>Zr<sub>60</sub>, Cu<sub>50</sub>Zr<sub>50</sub>, and Cu<sub>60</sub>Zr<sub>40</sub> metallic glass, inelastic deform., free energy spectra 0-71699  
 Ni alloys, creep transients, friction stress and recovery, dislocation substructure 0-60933  
 Pd<sub>80</sub>Si<sub>20</sub> metallic glass, inelastic deform., free energy spectra 0-71699  
 Si<sub>3</sub>N<sub>4</sub>, hot-pressed, creep and strain recovery 0-100874  
 V<sub>3</sub>Si single cryst., creep deform. 0-71695

recrystallisation

*microstructural processes and features only*  
*see also recrystallisation annealing; recrystallisation texture*  
 brass, recrystallization during induction heating 0-97511  
 camphor, rhombohedral, polycryst., compressive deform. and dynamic recrystn. 0-71698  
 cell wall and lattice misorientation origin during deform. 0-71712  
 crack tip, plastic deform., metallographic anal. by recrystn. 0-85029  
 disilicate, piezoelectric glass ceramic, recrystallisation, pyroelectric response, permittivity 0-80703  
 dry sliding wear, role of dynamic recrystallisation 0-108599  
 grain boundary motion 0-103449  
 low C steel, explosive-thermal treatment, sulphide cracking decrease, hydrogen embrittlement (*Russian*) 0-108477  
 metals, FCC, deformed single crystals, struct. evolution at heating 0-103337  
 photographic emulsion grains, latent image distrib., etching and recrystn. effects of solns. 0-77890  
 polyethylene, high press. phase, US, DTA, and X-ray diffr. study 0-75188  
 quartz in Moine thrust zone, recrystallisation rel. to differential stress 0-85652  
 steel, low alloy, high strength, hot compression dynamic precip. and coarsening of Nb(CN) 0-97514  
 steel, austenitic, explosive-thermal treatment, sulphide cracking decrease, hydrogen embrittlement (*Russian*) 0-108477  
 steel, austenitic stainless, grain boundary struct. during recrystn. and grain growth 0-76270  
 steel, B-Si, grain-oriented, high induction, Cu impurity effects 0-89366  
 steel, Cr-Ni-Mo-V, austenite form. during heating, influence of recrystn. during tempering (*Russian*) 0-104188  
 steel, HSLA, V and N effect on recovery and recrystn. during and after hot working 0-84973  
 steel, low-C, hot deform., austenite strengthening and weakening 0-76282  
 steel, microalloyed, hot-rolled, Nb(C,N) precip. and austenite recrystn. 0-97513  
 steel, multilayered with types St2kp and 10Kh18N10T, secondary recrystallisation props. (*Russian*) 0-66533  
 steel, Nb,(V),(Al), hot-rolling, laboratory simulation, recrystn. of austenite 0-97512  
 steel, pearlitic, struct. variations under plastic strain and subsequent heating, cementite decomp. (*Russian*) 0-84954  
 steel, Si (3 wt.%), struct. and preferred orientation, annealing parameters influence (*Czech*) 0-89248  
 steel, Si (3 wt.%), textured, secondary recrystn., precip. annealing effect (*Japanese*) 0-71662  
 steel, type 20Kh deformed, austenite grain size, inheritance effect with quenching and tempering 0-60881  
 steel, type 34Cr4, post-hot-forming recrystallisation condition, use of NEO-PHOT 2 and EPIQUANT 0-84949  
 steels 4Kh4VMFSSh and 45Kh3V3MFSSh, grain size, hot deform. and austenitising effects 0-76286  
 thermally induced structural changes, specimen surface influence 0-103559  
 thermoelectric recrystallisation, epitaxial film growth rate 0-100424

recrystallisation continued

zinc oxalate, isothermal crystallisation from soln. 0-108336  
 Ag, tensile deformed, dynamic recrystn. (*German*) 0-84959  
 Al alloys, thermomech. treatments, effects on microstruct. 0-100858  
 Al, thermal desorption of oxide film, influence of grain boundaries and recrystn. 0-61023  
 Al-(Mg)(Fe), pure (dilute), large wire drawing plastic deform. 0-108508  
 Al-Li-Mn (2.8, 0.3 wt.%), recrystallised sheet, fracture behaviour, SEM and TEM study 0-97566  
 Al-Zn-Mg-Cu (6.2, xwt.%) type alloy, fatigue crack propag., Cu content and recryst. effect 0-60960  
 BC, sintered, struct. and props. 0-104181  
 Cd<sub>0.7</sub>Hg<sub>0.3</sub>Te recrystallisation for supercooled IR detector production (*German*) 0-86403  
 CdS thin layers, recryst. from CdS-Cr<sub>2</sub>O<sub>3</sub> mixtures, phys. and photoelec. props. 0-96935  
 CdS<sub>x</sub>Te<sub>1-x</sub>, recryst. from CdS<sub>x</sub>Te<sub>1-x</sub>-Cr<sub>2</sub>O<sub>3</sub> mixtures, photocond. props. 0-96936  
 Co-W alloy electrolytic coatings, heat treatment effects on coercivity, hysteresis and structure (*Russian*) 0-60381  
 Cu crystals, two-phase, recrystn. retardation, particle size, spacing effects 0-89242  
 Cu, foils, faulted defect formation by moving boundaries 0-107281  
 Cu pin against steel ring, dry sliding wear, role of dynamic recrystallisation 0-108599  
 Cu, polycrystalline, recovery and recrystn. kinetics 0-81081  
 Cu, polycrystn., strain localisation during hot deform. 0-104195  
 Cu, recrystn. centre growth kinetics, impurity effects (*Russian*) 0-89253  
 Cu, tensile deformed (110) orientated single cryst., recrystn., high voltage electron microscopy study 0-84958  
 Fe, purification, recrystn. temp. and elec. resistivity (*Japanese*) 0-100780  
 Fe, thin foil, extrinsic grain boundary dislocations, low C content influence 0-107273  
 Fe-Cr (9 wt.%), extrinsic grain boundary dislocations, low C content influence 0-107273  
 Fe-Ni, secondary recrystallisation singularities (*Russian*) 0-66528  
 Fe-Ni (4 wt.%), extrinsic grain boundary dislocations, low C content influence 0-107273  
 Fe-Si (3 wt.%), behaviour of disperse inclusions, influence of recrystn. processes (*Russian*) 0-66519  
 Fe-Si (3 wt.%), grain oriented, mag. props., effect of decarburizing (*Chinese*) 0-103821  
 Fe-Si (3wt.%), grain-oriented, secondary recryst., grain growth inhibition 0-89245  
 Fe<sub>80</sub>B<sub>20</sub>, metallic glass, Doppler broadening of positron annihilation  $\gamma$ -radiation and elec. resist. 0-66321  
 Fe<sub>70</sub>Mo<sub>30</sub>B<sub>10</sub>, metallic glass, Doppler broadening of positron annihilation  $\gamma$ -radiation and elec. resist. 0-66321  
 Fe<sub>70</sub>Ni<sub>30</sub>Cr<sub>10</sub>P<sub>10</sub>B<sub>10</sub>, metallic glass, Doppler broadening of positron annihilation  $\gamma$ -radiation and elec. resist. 0-66321  
 Fe<sub>2</sub>O<sub>3</sub> colloidal prep., thermal decomposition of metal chelates 0-71953  
 Gd-Cu, amorphous films, mag. props. ferromag. reson. meas., 20-520°C (*Russian*) 0-97144  
 Li<sub>2</sub>GeO<sub>3</sub>, piezoelectric glass ceramic, recrystallisation, pyroelectric response, permittivity 0-80703  
 Li<sub>2</sub>SiO<sub>4</sub>, piezoelectric glass ceramic, recrystallisation, pyroelectric response, permittivity 0-80703  
 Mo, dislocation structure of diffusional welding zone (*Russian*) 0-96531  
 Mo wire, struct. and high-temp. creep, dopant elements influence 0-66603  
 NaCl:Ca crystals, surface recrystn., moisture effect 0-84950  
 Ni, alloying, influence on recrystn. and grain growth (*Russian*) 0-81071  
 Ni-Cr alloy KhN70MVYu wire, recrystn., optimum heat treatment 0-76278  
 Ni-Cr-W-Mo-Ti-Al, heat-resist., recovery and recrystn. 0-76268  
 Pd, H phase hardened, recrystallisation study 0-60883  
 SbSB glass, IR reflectivity spectra 0-71403  
 Si, amorphous, epitaxial regrowth, structure and impurities effect 0-84401  
 Si, crucible grown, virgin and implanted, laser irradiation effects on surface structure 0-92768  
 Si, implanted crystal, laser induced annealing and diffusion behaviour 0-88202  
 Si, joining and recrystallisation using thermomigration process 0-65298  
 a-Si, laser induced crystallisation mechanism, epitaxial regrowth 0-84962  
 Si, plasma effects during pulsed laser annealing 0-84480  
 Si, polycryst., CVD, recrystn. on heating 0-80107  
 Si solar cells, polycrystalline, from recrystallized plasma deposited thin films 0-104509  
 Si, thin slabs, vibr. freq. calcs., dims. effect 0-60585  
 Si:P, polycrystalline laser recrystallised film on Si substrate, cryst. struct., thermal oxidation 0-65391  
 Si/Al and Si/Al-Si(Cu), Si regrowth minimisation through overlying Al or Al alloy film 0-70569  
 p-Si/Al, ohmic contacts, Si dissoln. and recrystn. effects, computer calc. 0-103749  
 $\beta$ -SiC, thermodynamic props., temp. depend., 5 to 300K 0-96666  
 Si(111):Pb ion implanted amorphous layers, recrystallisation, impurity out-diffusion model (*Chinese*) 0-88363  
 steel, Nb, deform., recrystn. and precip. interaction 0-97515  
 $\beta$ -III<sub>2</sub>O<sub>3</sub> alloy, anal. 0-108470  
 Tm<sub>2</sub>O<sub>3</sub> film, between Al electrodes, prep. and elec. props. 0-60103  
 W wire, struct. and high-temp. creep, dopant elements influence 0-66603

recrystallisation annealing

segregation, nonequilibrium, during pulsed laser annealing, model 0-108451  
 semiconductor, ion implanted, epitaxial regrowth, laser annealing dynamics 0-92548  
 semiconductors, ion-implanted, laser pulse annealing, TEM and channelling study 0-100264  
 steel, C, recrystallization annealing, grain growth, effect of type of deform. 0-100847  
 steel, stainless, Cr-Cu (17, 0.6 to 1.1 wt.%), texture 0-84957  
 Al wire, grain boundary internal friction after recrystn. annealing (*Russian*) 0-66561  
 Al-Ni (6 wt.%) alloy, misorientation between subgrains, second-phase particles role, STEM microdiffr. obs. 0-104415  
 CdS:Cu, C films, photocond. growth and decay time 0-60041  
 Cu, polycrystalline, recovery and recrystn. kinetics 0-81081



**recrystallisation annealing continued**

- Cu, recrystallization annealing, grain growth, effect of type of deform. 0-100847
- Fe powder, recryst. annealing effect on struct. and technological props. (Czech) 0-89250
- Fe, texture, recryst. annealing effect (Czech) 0-89249
- GaAs, amorphous layers, ion-implanted, low-temp. epitaxial regrowth 0-92790
- GaAs, ion-implantation induced damage profile, ellipsometric study, annealing 0-103400
- Ge, strained crystal, annealing effect, recrystn. and struct. (Russian) 0-89252
- Mo-W (30 wt.%), wrought, fracture, characteristic features 0-104278
- Nb-Zr-N biphase alloy, recrystallization annealing 0-104180
- Si, amorphous, implanted, recrystn. induced by scanning CW laser, reaction rates, analytical model 0-66334
- Si, amorphous film, selective laser recrystn. over heavily doped lines 0-84947
- Si amorphous layer recrystallisation by laser beam 0-93566
- Si, amorphous layers, recrystallisation, pulsed laser annealing 0-65404
- Si, deformed, annealed and recrystallized, struct., implications for solar cells 0-60922
- Si, furnace preannealed (111) ion implanted, laser irradi. 0-65015
- Si, implanted with low solubility dopants, laser annealing, TEM study 0-70233
- Si, ion implantation, high dose, solid phase epitaxial regrowth 0-103380
- Si, ion implanted, CW laser annealing 0-92550
- Si, ion implanted, complex annealing behaviour of amorphous layers, TEM obs. of defect struct. 0-107299
- Si, ion implanted, electron beam annealing, surface struct. study using SEM 0-70235
- Si, ion-implanted, annealing using scanning CW laser system 0-100265
- Si, ion-implanted amorphous, laser epitaxial recrystallisation threshold energy 0-70571
- Si, ion-implanted layers, crystn. by ns laser pulses, TEM and RHEED 0-100421
- Si, ion-implanted layers, epitaxial regrowth by laser beam and flash annealing 0-100420
- Si on sapphire, stress-relieved regrowth by laser annealing 0-65389
- Si, strained crystal, annealing effect, recrystn. and struct. (Russian) 0-89252
- Si wafer, thin surface layers, amorphous to cryst. transform., obs. technique 0-107288
- Si:Ar, ion-implanted, epitaxial regrowth by laser annealing, microstruct. 0-84404
- Si:As, ion implanted, pulsed laser annealing, partial solid-state regrowth 0-103591
- Si:As laser annealing, heat and mass transport model 0-92546
- Si:As(Pb), ion-implanted, impurity redistrib. during laser irradi. 0-100280
- Si:B implanted wafers, ionis. assisted annealing and effects 0-100257
- Si:Bi, ion-implanted, solid phase epitaxial growth during annealing, super-saturated solid soln. form. 0-103384
- Si:Ge, recryst. after implantation using different temp. and energy sequences 0-84196
- Si:P, annealing after ion implantation, ellipsometric study 0-65018
- Si:Pt, implanted and laser annealed, segregation and increased dopant solubility 0-65016
- $\alpha$ -Ti, cold rolled, primary recrystn., in situ investig. in HVEM 0-104185
- W, deformed, surface layer struct. effect on polygonisation and recryst., X-ray diffr. anal. and metallographic exam. (Russian) 0-84948
- Zr<sub>3</sub>Al, deformed and irradi., lattice defects obs., superlattice dislocations and defect clusters 0-107261

**recrystallisation texture**

- quartz, naturally deformed, dynamic recrystn. during creep, dislocation substruct., Mg alloy comparison 0-109142
- steel, Cr-Mn type, martensite struct. after quenching and HTMT, X-ray diffr. obs. 0-84975
- steel, high strength, treatment effect on ductility and strength 0-60880
- steel, low-C containing Ti, sheets, recrystn. texture effects on plastic strain ratio and deep-drawing (Chinese) 0-66527
- steel, mild, cold rolled, texture and plastic anisotropy rel. to alloying and precipitation (French) 0-108475
- steel, mild, solderability, annealing effect (Japanese) 0-89244
- Al-Mn (1 wt.%), single crysts., rolled to (123)[412], recrystn. textures 0-104183
- Al-Ni (6 wt.%) alloy, misorientation between subgrains, second-phase particles role, STEM microdiff. obs. 0-104415
- Cu, single crysts., (110) oriented, tensile deformed, HVEM of recrystn., recrystallised state 0-89256
- Cu single crysts., deformed, HVEM study of recrystn. texture 0-104179
- Cu, solderability, annealing effect (Japanese) 0-89244
- Fe-Ni, secondary recrystn. and mag. props. 0-89247
- Fe-Si (3 wt.%) high-permeability grain-oriented steel, quenching effect on primary recrystn. texture development 0-84956
- Ge, strained crystal, annealing effect, recrystn. and struct. (Russian) 0-89252
- Mg alloy, dil., dynamic recrystn. during creep, dislocation substruct., quartz comparison 0-109142
- Mo alloy with dispersed HfN phase, recrystallisation, crystallographic and structure texture (Ukrainian) 0-71668
- Si, strained crystal, annealing effect, recrystn. and struct. (Russian) 0-89252
- $\alpha$ -Ti, cold rolled, primary recrystn., in situ investig. in HVEM 0-104185

**rectangular waveguides**

- Cherenkov radiation source 0-99373
- gas DFB laser waveguide precision calc. and pulse energy obs. 0-58577
- uniaxial anisotropic relativistic warm plasma, EM wave propag. and attenuation 0-59246
- unit power standard for 53.57 to 78.33 GHz 0-90808
- visualization of microwave EM fields using thermooptical effects in liquid crystals 0-62723
- weakly anisotropic rectangular dielec. optical waveguides, wave propag. anal. using coupled modes 0-64154
- CO<sub>2</sub> waveguide laser amplifier with strong discharge tube 0-74398

**rectification**

- alternating current electrode processes, review 0-61107
- full wave, demonstration 0-77598
- IR point-contact diode tunnelling and rectification rel. to electrode geometry 0-57378

**rectification continued**

- metal-vacuum-metal point contact junction characts., Green's function calc. 0-103744
- nonlinear wave rectification, quantum limit 0-83634
- point contact IR detector tunnelling and rectification characteristics, geometrical and multiple image interactions 0-57376
- point contacts between identical metals, HF rectification at low temp. 0-105706
- Al/As<sub>2</sub>SeTe<sub>2</sub>/Sb structures, rectifying effects 0-75654
- GaAs-GaAlAs-GaAs rectifying semicond. struct., prep. by MBE and characts. 0-65657
- GaInAsP, rectifying and ohmic contacts 0-80376
- Se<sub>1-x</sub>Te<sub>x</sub>, Se<sub>1-x</sub>Te<sub>x</sub> junctions, photovoltaic effects and rectification phenomena 0-84506
- Te-Se-Cd, sandwich structure, fabrication and characteristics 0-60089

**rectifier tubes**

No entries

**rectifier valves** *see rectifier tubes***rectifiers**

- see also solid-state rectifiers*
- fusion reactor, Doublet-III, frequency generator-rectifier system performance 0-102326
- solar power satellites microwave power transmission system rectennas, Yagi-Uda receiving elements design, characteristics and economics 0-66938

**rectifying circuits**

- see also rectification; rectifiers*
- burn period plasma current maintenance, rectifying first wall, cct. anal. 0-102307

**recursive functions**

- eclipsing variables, light curves linear analysis, fractional light loss anal. 0-82416
- Ising spin glass, three-dimensional mag. correlations 0-103849
- sound synthesis by continuous spectral transformation (French) 0-79100
- transmission coeff. for 1-D potential barrier, discretisation of Schrodinger eqn. 0-57123

**red giants** *see stars***red shift**

- see also cosmology; Doppler effect; gravitational red shift*
- 1309-216, probable BL Lacertae object with absorpt. red shift 1:49, optical spectrum 0-67856
- 1610-771, QSO with steep optical spectrum red shift 0-94887
- Abell 399/Abell 401, X-ray binary galaxy cluster, radial vels. and mass 0-90546
- Bianchi V type universe, red shift and anisotropic microwave background 0-98744
- 3C 120, underlying galaxy red shift from spectrum of assoc. nebosity 0-67890
- Centaurus I cluster of galaxies, redshift meas. and resolution into two vel. systems 0-77499
- cluster galaxies, redshift determ. using Image Dissector Scanner, visible spectra 0-90544
- clusters of E and S0 galaxies, colour distribution rel. to redshift 0-105361
- conference on high redshift objects, IAU Symposium 92, Los Angeles (August 1979) 0-101669
- extragalactic objects, redshift distrib. rel. to evolution of galaxies 0-90527
- galaxies, bright with low red shift, red shift-magnitude relation 0-101639
- galaxies, compact and bright-nucleus, in S.hemisphere, spectra, redshifts and blueshift 0-94725
- galaxies, elliptical, red shifts and vel. dispersions rel. to mass to light ratios 0-98707
- galaxies, luminosity evolution from 2.2  $\mu$ m of giant ellipticals 0-105358
- galaxies, V-K colours and IR Hubble diagram for giant ellipticals 0-105359
- galaxies in rich clusters 0-85872
- galaxies near late-type spiral NGC 4945, radial vels. and BV photometry 0-109547
- galaxies with double and multiple nuclei, radial vels. of nuclei components 0-67848
- galaxy cluster found by Einstein Observatory, CCD camera study and redshift 0-62315
- galaxy clusters, radial vel. dispersions of real and spurious clusters 0-101643
- hydrogenic ion lines, red shift in plasma 0-103128
- BL Lacertae objects, redshifts upper limits from absence of redshifted C IV absorpt. lines 0-62267
- neutron stars, rotating, max. surface redshifts in bi-metric theory of gravitation 0-90466
- NGC 1023 galaxy group, H I radial vels. rel. to group membership and mass/light ratio 0-82521
- NGC 1023 galaxy group, H I redshifts of subgroups and possible intergalactic H I cloud 0-67886
- NGC 3227, Seyfert galaxy, photoelectric photometry, spectrum and redshift 0-98724
- non-Dopplerian nature, static Euclidean model 0-73081
- objects at the highest redshift 0-105360
- PG 1115+08, triple QSO, spectroscopic obs. and gravit. lens model 0-86012
- photon splitting into 3, cosmological limits, spectral broadening, frequency-dependent and multiple red-shifts 0-77284
- PKS 2155-304, BL Lacertae object, no evidence for redshifted forbidden O III emission 0-73035
- Population II stars at distortion  $\sim 10$ , rel. to distortion of cosmological microwave black body radiation spectrum 0-67915
- protogalaxy formation age and  $\gamma$ -ray background 0-62325
- QSOs, absorpt. line redshift distrib. 0-90563
- QSOs, optically selected, redshift inverse correl. with radio detectability 0-82536
- QSOs, redshifted clouds, 21 cm line studies 0-105389
- QSOs from Molonglo Deep Survey, optical spectra 0-94884
- QSOs near bright galaxies, non-cosmological redshifts 0-105386
- quasar redshifts, teaching consideration 0-90621
- quasar redshifts distributions, periodicity 0-62313
- quasars, cyclic depend. of brightness on parameter  $\ln(1+z)$  0-105382
- quasars, faint red 3C QSO candidates spectrophotometry and red shifts 0-67897
- quasars absorption redshifts, evidence for large-scale uniformity of physical laws 0-73079

**red shift continued**

- quasars assoc. with compact radio sources, apparent magnitude-redshift relations for resolved and unresolved sources (*Chinese*) 0-105380  
 quasars redshifts, relativistic Doppler formula rel. to transverse vels. and distances (*Chinese*) 0-105379  
 radio galaxies, red shift dependence of proper densities and colours 0-62286  
 radio sources, double, redshifts rel. to hot spots behaviour 0-94882  
 radiogalaxies from B2 Catalogue, optical identification, radio positions and redshifts 0-86005  
 Sa type spiral galaxies, redshifted 21 cm line profiles, radio obs. 0-73041  
 Shahbazian I group of galaxies, dynamics from spectroscopic, obs. 0-67878  
 short-pulse laser backscatter from gas target 0-79454  
 star clusters, relativistic, with high central redshift 0-105293  
 Stephan's Quintet, redshifted H I associations 0-67882  
 VV 150, galaxy chain, photoelectric photometry, spectrum and redshift 0-98724  
 H I in field of elliptical galaxy NGC 1052, line profiles and systematic vel. shift 0-98719  
 NaKr, red wing radiation and pot. 0-87180

**reduction (chemical)**

see also oxidation

- chlorophyllide fluorescence quantum yield during photochlorophyllide reduction in etiolated leaves 0-81542  
 clay,  $\text{Al}_2\text{O}_3$  and SiC recovery by C reduction 0-108704  
 cytochrome  $c_3$ -hydrogenase, reduction kinetics, Mossbauer spectra 0-67031  
 electrocatalysis, surfaces modified by metal adatoms, review 0-61110  
 electrolyte, ionic mass transfer in narrow rectangular conduits 0-61105  
 haematite, degree of reduction, potential relaxation due to cracks (*Russian*) 0-66770  
 haematite reduction to magnetite, stress development mechanism (*Russian*) 0-93553  
 iron(II)-A-zeolites, reduction, mag. and Mossbauer study 0-71115  
 kaolinite-C, high temp. reduction reactions, thermodynamic anal. 0-104426  
 metal oxide reduction by electron cyclotron reson. plasma of H, model study on discharge cleaning 0-76548  
 metal powders manufacture by CaH method,  $\text{Ca}(\text{OH})_2$  separation 0-84878  
 Nb, pure, production by carbothermic reduction-electron beam melting combination method 0-89177  
 oxidant impurities elimination, in viologens electrochromic solutions, using Pd catalyst 0-78922  
 quinones-Zn porphyrin, quinones sensitised reduction in vesicle systems 0-71897  
 refractory metals and oxides, reactions of liq. alkali metals, relevance to reactor technology 0-85173  
 refractory oxide development for fusion reactor first walls, chem. environment effects 0-83221  
 ruthenium tris-bipyridyl, excited state electron transfer quenching,  $\text{H}_2\text{O}$  photoreduction mediators effects 0-102536  
 stainless steel, reduction of H by Ar glow discharge, rel. to ultra cold neutron storage 0-104459  
 steel, Al semikilled,  $(\text{Fe}, \text{Mn}_{1-x})\text{O} \cdot \text{Al}_2\text{O}_3$  inclusions, deoxidation, thermodynamic conditions 0-60830  
 steel, Al-Cr,  $\text{FeO}(\text{Al}, \text{Cr}_{1-x})_2\text{O}_3$  inclusions, thermodynamics 0-60831  
 steel powder, high speed, S and O reduction in a  $\text{H}_2$  gas stream 0-61015  
 transition metal oxide catalysts, reduction, cryst. defects influence, in-situ electron microscopy 0-81322  
 $3\text{Al}_2\text{O}_3\text{-GeO}_2\text{-SiO}_2$ , reduction by C, mixed diffusional-kinetic regime (*Russian*) 0-66771  
 $\text{Ag}^+$  reduction in aqueous solns. 0-69148  
 Al-Mg (7 wt.%), bare surface reaction rates in aq. solns. 0-101022  
 $\text{Al}_2\text{O}_3$ , surface microstructural changes due to reduction by C (*Russian*) 0-100378  
 As(III) and As(V), redox stability in aq. soln. 0-61068  
 BaO, reduction by C, kinetics and mechanism (*Russian*) 0-93743  
 BaO- $\text{B}_2\text{O}_3$ - $\text{V}_2\text{O}_5$  glass, oxidation-reduction of V, thermodynamics 0-85169  
 BaTiO<sub>3</sub>, reduction inhibition by impurity ions 0-101018  
 BeO, reduction by C, kinetics and mechanism (*Russian*) 0-93743  
 C polymeric chains, reduced from poly(tetrafluoroethylene), reactivity 0-89488  
 CO<sub>2</sub>, thermochem. reduction using solar energy to provide C-based fuels 0-76610  
 CaO, reduction by C, kinetics and mechanism (*Russian*) 0-93743  
 Cd<sub>3</sub>SnO<sub>4</sub> and Cd<sub>3</sub>SnO<sub>4</sub>:CdO, thin film electrodes in  $\text{H}_2\text{SO}_4$  electrolytes, reduction, AES and SEM 0-65674  
 CdTe electrode, redox reaction due to complex  $\text{M}(\text{CN})_6^{3-/4-}$  (*French*) 0-89482  
 Ce-S-O equilibrium in molten Fe (*Chinese*) 0-104423  
 Cu-O (0.05 to 0.1 wt.%) liquid alloy, deoxidation kinetics by rotating graphite cylinders 0-61084  
 Fe ore, cold bound pellets, reduction using  $\text{H}_2$  gas, 700 to 900°C (*Japanese*) 0-71907  
 Fe ore, reduction degree, chemical anal. calcs. (*Russian*) 0-66769  
 Fe, oxide reduction processes by gases, mathematical modelling (*Russian*) 0-93742  
 Fe, passive film form. in phosphate soln., intensity-following ellipsometry study 0-104345  
 Fe powder, reduction annealing, comminution of sintered cakes 0-66456  
 Fe powder manufacture, collision speed effect 0-84884  
 Fe sheet, cyclic oxidation and reduction kinetics in  $\text{O}_2$ - $\text{H}_2$  atmosphere (*Korean*) 0-71906  
 $\text{Fe}_{0.394}\text{Ti}_{0.606}$ -O-S subsystem, equil. phase data under reducing conditions rel. to ilmenite upgrading 0-76240  
 $\text{Fe}(\text{CN})_6^{4-}$ - $\text{Fe}(\text{CN})_6^{3-}$ , redox reactions, mass transfer at vibr. spheres 0-57220  
 $\text{GeO}_2\text{-SiO}_2$ , reduction by C, mixed diffusional-kinetic regime (*Russian*) 0-66771  
 $\text{H}_2\text{SeO}_4$ , reduction, reaction sequence and CdSe film deposition 0-71603  
 $\text{K}_2\text{Fe}(\text{CN})_6$ , pressure induced reduction, Raman spectra 0-66776  
 $\text{K}_2\text{Fe}(\text{CN})_6$ -KCl, press. induced reduction, IR spectra after pressurization 0-66776  
 LaMnO<sub>3</sub>, stoichiometric manganite form. reaction, thermodynamic characts. 0-108727  
 Li/SOCl<sub>2</sub> primary cells, SOCl<sub>2</sub> reduction mech. in supporting electrolyte 0-108792

**reduction (chemical) continued**

- MgO, reduction by C, kinetics and mechanism (*Russian*) 0-93743  
 MnO, reduction by C, surface reactions, CO regeneration (*Russian*) 0-66772  
 MoCl<sub>5</sub>, by  $\text{H}_2$ , influence of electric field on Mo film deposition 0-93491  
 MoF<sub>6</sub>, reduction by H in the presence of HF (*Russian*) 0-61076  
 MoO<sub>3</sub>, topotactic transform into MoO<sub>2</sub>, electron microscopy, X-ray anal. 0-107417  
 Na<sub>2</sub>O-SiO<sub>2</sub>-(CaO) glass, molten, metal ion diffusion and redox behaviour, electrochemical studies 0-81332  
 NaRhY zeolite, Rh complexes with CO and methyl iodide ligands, spectrosc. obs. 0-85159  
 Na<sub>2</sub>WO<sub>3</sub> bronzes, reaction with Fe powder, reaction mechanism and reactivity 0-108712  
 Nb<sub>2</sub>O<sub>5</sub> and Al<sub>2</sub>O<sub>3</sub> by CaH<sub>2</sub>, Nb<sub>2</sub>Al prep., thermodynamic calc. 0-100809  
 Ni (100), adsorption of O<sub>2</sub> and reduction of surface oxide by H<sub>2</sub> 0-108741  
 NiO ore in segregation roasting process (*Japanese*) 0-71908  
 Sb<sub>2</sub>(O<sub>4</sub>)MoO<sub>3</sub>, synthesis by H<sub>2</sub>/H<sub>2</sub>O reduction of Sb<sub>2</sub>MoO<sub>6</sub>-MoO<sub>3</sub> (*French*) 0-64971  
 Si surface, reduction growth, autoepitaxy (*Russian*) 0-107672  
 SiO<sub>2</sub>/InP interface formation, thermodynamic considerations 0-100529  
 SiO<sub>2</sub>-MgO-CaO-Al<sub>2</sub>O<sub>3</sub>-Ce<sub>2</sub>Fe, redox equilib., expt. 0-85171  
 SrO, reduction by C, kinetics and mechanism (*Russian*) 0-93743  
 SrTiO<sub>3</sub> semicond. electrodes, electroreduction process kinetics, cathodic dark current meas. 0-66807  
 SrTiO<sub>3</sub> surface, oxidation and reduction by D<sub>2</sub>O, H<sub>2</sub><sup>18</sup>O, D<sub>2</sub>, isotope exchange study 0-104461  
 TaS<sub>2</sub>-2H electrodes, topotactic reduction mechanism, neutron diff. obs. and intercalation cpd. form. 0-108748  
 TiC-N<sub>y</sub> powder preparation, physical, chemical props. (*Russian*) 0-76212  
 TiCl<sub>4</sub>, reduction in steady beam-plasma discharge 0-100099  
 TiO<sub>2</sub>/Nb semicond. electrodes, electroreduction process kinetics, cathodic dark current meas. 0-66807  
 TiO<sub>2-x</sub>, reduced, crystallographic shear planes, dislocation struct. 0-107175  
 V<sub>2</sub>O<sub>5</sub> and lower oxides, defect structures and related props., review 0-59454  
 V<sub>2</sub>O<sub>5</sub>, electron beam induced decomposition, appearance pot. spectroscopy 0-85203  
 V<sub>2</sub>O<sub>5</sub>, reduction in butyllithium, ESR study 0-100611  
 V<sub>2</sub>O<sub>5</sub>-AlNbO<sub>4</sub>(GaNbO<sub>4</sub>)(TiNbO<sub>4</sub>) systems, interfacial reactions, efficient boundary conditions and solid state reactivity 0-76542  
 WO<sub>3</sub>, reduction, defect role, in situ HVEM obs. 0-81323  
 WO<sub>3</sub> reduction, in H plasma jet, W powder prep. (*Russian*) 0-76211  
 WO<sub>3</sub>-NiCO<sub>3</sub>-Fe<sub>2</sub>O<sub>3</sub>, reduction alloy form. 0-60801  
 ZnTe electrode, redox reaction due to complex  $\text{M}(\text{CN})_6^{3-/4-}$  (*French*) 0-89482
- redundancy**  
 see also bandwidth compression; data compression; logic design  
 optical coherent processing system, modification to achieve some redundancy 0-106468  
 optical parallel processing 0-95831
- redundancy theory** see redundancy
- reed relays**  
 temperature measurement, using magnetically controlled reed switches (*French*) 0-57291  
 Hg wetted, heat treatment variations effects on Fe-Ni alloys surface conditions and on switch behaviour 0-66547
- reeling** see winding (process)
- references (standards)** see standards
- reflectance** see reflectivity
- reflection**  
 see also acoustic wave reflection; electromagnetic wave reflection; neutron reflection; reflectivity  
 electron beam, relativistic, refl. and transmission by strong mag. field (*Japanese*) 0-91737  
 Mach reflection of solitary wave 0-79340  
 seismic waves, refl. coeffs. rel. to multi-segment traces deconvolution and synthesis 0-77162
- reflection high energy electron diffraction**  
 diamond surface, polished, RHEED pattern 0-65345  
 fluorescent screen, metal-backed, appl. to high temp. RHEED obs. 0-75126  
 specimen transfer device for combined AES/RHEED and TEM obs. 0-70093  
 surface chemical anal. using RHEED-solid state detector method 0-108760  
 surface microstructure determ. and microanalysis by ultrahigh vacuum field emission gun SEM 0-96423  
 surface state resonance effect, obs. by convergent beam RHEED 0-107622  
 Ag film, vacuum deposition on Pb (111), substrate diffusion effects, RHEED, LEED, AES 0-65410  
 Ag thin film, X-ray fluoresc. spectroscopy of surface using RHEED-solid state detector method 0-108760  
 Al, specimen transfer device for combined AES/RHEED and TEM obs. 0-70093  
 AlN films, RF reactive ion-plating, struct. and morphology 0-104074  
 Bi film, structure and electronic props. 0-70562  
 CdS/InP epitaxial thin films on NaCl, HEED and TEM study 0-88446  
 Cu film, vacuum deposition on Pb (111), substrate diffusion effects, RHEED, LEED, AES 0-65410  
 CuInSe<sub>2</sub>, heteroepitaxy on {111} oriented Ge by flash evaporation, struct. 0-108333  
 GaAs, homoepitaxy and epitaxy, surface anal. during growth, using RHEED and Auger spectroscopy 0-66433  
 GaN, initial growth, on Al<sub>2</sub>O<sub>3</sub> and spinel (*German*) 0-107664  
 Ge(111) surface, diffuse scatt. at high temp., RHEED study 0-80043  
 InP, MBE, substrate temp. related degradation mechanisms 0-65385  
 InSb film, grown by MBE, RHEED study 0-100415  
 Nb-NbO<sub>2</sub>-Pb(In) Josephson junctions, props. of Nb<sub>2</sub>O<sub>3</sub> thermally grown tunnel barriers 0-100568  
 Ni/GaAs film contact system, alloying reaction 0-96747  
 NiO, (100) surface interaction with SO<sub>2</sub>, electron diff. and Auger spectrosc. obs. (*French*) 0-97728  
 NiO film, formed by Ni galvanic oxidation in borate buffer soln., struct. 0-100948  
 PbS-Si heterojunction, PbS film growth and struct. 0-96762



**reflection high energy electron diffraction** continued

- Si (111), surface structure, high temp. RHEED obs. using metal-backed fluorese. screen 0-75126  
 Si (111) 7×7 surface structure investigation, RHEED 0-96723  
 Si amorphous layers, glow-discharge, laser-annealed, elec. props. 0-75661  
 Si, CVD, surface anal. during growth, using RHEED and Auger spectroscopy 0-66433  
 Si, epitaxial growth on sapphire by partially ionised vapour deposition, RHEED-AES obs. 0-80985  
 Si ion implanted, amorphous to crystalline transition due to laser irradiation 0-103451  
 Si, ion-implanted layers, crystn. by ns laser pulses, TEM and RHEED 0-100421  
 Si-Pb heterojunction, RHEED, Mossbauer spectroscopy and I-V characts. 0-70828  
 Si-Sn heterojunction, RHEED, Mossbauer spectroscopy and I-V characts. 0-70828  
 ZnO piezoelectric films, RF planar-magnetron sputtered, characterisation 0-96751

**reflection nebulae** *see nebulae***reflection spectra** *see reflectivity; spectra***reflectivity**

- see also electroreflectance; magnetorelectance; piezorelectance; thermorelectance*  
 antireflection coating, multilayer achromatic, extended region of low reflection coeff. values 0-95982  
 antireflection films, on alkali-borosilicate glasses produced by chem. treatment 0-66677  
 B<sub>2</sub>O<sub>3</sub>-Li<sub>2</sub>O-LiCl, ionic conductor, IR refl. Raman study 0-66173  
 blackbody cavities, directional emissivity calc., Monte Carlo method 0-83729  
 brain reflectance, mapping technique using optical fibres 0-72381  
 cholesteric liquid crystal coatings, superimposed left- and right-handed, peak refl. and colour gamut 0-74472  
 clouds, radar reflectivity rel. to cloud dynamics and microphysics 0-61877  
 conjugate interfaces: interfaces between transparent media of the same reflection coefficient for the parallel polarization at the same angle of incidence 0-87299  
 crop and soil bidirectional reflectance factor calibration, remote sensing field research 0-86382  
 4-cyano-4'-n-pentylbiphenyl, refr. index meas. and isotropic-nematic phase transition study, surface plasmon technique 0-84282  
 $\gamma$ -cyclopropyl-bis (1,3,3-trimethylindolenine-2-yl)pentamethinium fluoro-borate, exciton surface polaritons, reflecting faces obs. 0-65645  
 dense scattering media, anisotropy factor 0-87307  
 dichroic beam splitters, high-performance, for DF chem. lasers 0-95932  
 DODCl, saturable absorber, picosecond phase-conjugate refl. 0-95960  
 dye saturable absorbers, picosecond phase-conjugate refl. 0-95960  
 Fabry-Perot cavity, dispersive optical bistability 0-78889  
 films, optical constants, reflection spectra by Kramers Kronig method 0-76099  
 Galilean satellites, water ice existence, IR spectral reflectance obs. 0-82263  
 garnets, IR refl., ATR, Voigt and Faraday expts. 0-66180  
 glass, IR emissivity calc., strongly absorbing media surface refl. 0-107452  
 glasses, high vol. low cost, as solar reflectors, compositions and weathering effects 0-106589  
 gloss paints, reference glossmeter 0-82805  
 Iapetus, relative reflectance meas. at 1.6 and 2.2  $\mu$ m 0-98607  
 illumination and reflection edges, recognition by human visual system 0-94209  
 IR imaging systems, sensibility equation modification (*Chinese*) 0-102806  
 IR spectroscopy of adsorbed layer systems, review, book contrib. 0-84747  
 IR thermography, reflectance errors 0-62661  
 laser plasma, reflectivity and temp., scaling laws 0-87913  
 lustre quality meas., recording and evaluation 0-98967  
 Mars, cloud formations, reflectivity time var., visible photometry obs. 0-72840  
 metal reflectance changes during laser irradiation 0-93261  
 metal-electrolyte interfaces, optical reflectance spectra, interpretation 0-93263  
 metallic rough surface, reflection loss for s and p polarised waves near surface plasmon freq. (*French*) 0-97225  
 metals, specular refl. anomalous behaviour after 10.6  $\mu$ m pulsed laser irradiation 0-93260  
 microwave thermophotoindicators, analysis of diffuse light spectra 0-73457  
 mirror reflectivities from 50-150 eV 0-90966  
 mirrors, dielectric multilayer, reflectance under slight absorpt. conditions 0-83655  
 molecular monolayers, IR absorpt. enhancement by thin metal overlayers, ATR technique 0-88995  
 multilayer highly reflective coating design for wideband 90° phase shift 0-74464  
 multilayer superlattice stacks, very thin nonideal, wavelength variation of transmissivity, refl. 0-100701  
 near IR diffuse reflectance analysis anomalies 0-86383  
 nonlocality effects on optical phenomena in bounded solids, developments 0-93328  
 oil traces, on water surface, continuous detect. system (*German*) 0-72115  
 optical thin film, reflection coefficient partial derivatives, matrix calc. (*French*) 0-89080  
 Osterberg problem and wave prop. in inhomogeneous plasma, numerical study 0-63925  
 phenothiazine derivatives, semicond. elec. props., optical spectra, and EPR 0-103693  
 plasmon surface polariton dispersion curve, optical obs., demonstration 0-101690  
 plastic films, IR reflectance of aluminised thermal screens for energy conservation in greenhouses 0-64351  
 poly-2,4-hexadiyne-1,6-diol bis (p-toluene sulfonate), exciton surface polaritons, reflecting faces obs. 0-65645  
 polycarbonate films, doping effect on elec. cond., chem. and optical props. 0-65572  
 polyamide fibres, differently matted, meas. of diffuse reflectance spectra, using SPEKOL spectrocolorimeter 0-77836  
 powder mixtures, diffuse reflectance, quantitative anal. 0-87308  
 power reflection spectroscopy, analytical techniques 0-62714

**reflectivity** continued

- radiation temperature, reflectivity, emissivity meas. of room temp. materials (*Chinese*) 0-101814  
 rare gas adsorbates on simple metals, optical excitation, configurational switching, charge transfer 0-107643  
 ribbon growth using scanned focused CO<sub>2</sub> laser beams 0-66417  
 rough surface, random, reflectance derived with Fresnel approx. 0-87309  
 rough surfaces, reflection light, division into specular and diffuse components (*Japanese*) 0-106457  
 sapphire and Si surfaces quality determ., using IR and UV specular reflectance meas. 0-108684  
 semiconducting alloys, comp. profile, second derivative wavelength modulation 0-103967  
 semiconductor, optical absorpt. coeff. and minority-carrier diffusion length, differential photocurrent method of meas. 0-96896  
 semiconductor, p-type, infrared absorption and plasma reflection 0-97284  
 semiconductors, optical props. under press., book contrib. 0-84715  
 seminar, optical radiation meas., San Diego, CA, USA (Aug. 1979) 0-86036  
 Shroud of Turin, IR reflectance spectrosc. and thermographic investigations 0-87578  
 Shroud of Turin, spectral props. 0-87577  
 Shroud of Turin, UV-visible reflectance and fluoresc. spectra 0-87579  
 small particle spectral diffuse IR reflectivity meas. 0-68276  
 solid surfaces, non-ideal, optical props., phenomenological models 0-88950  
 spatially dispersive crystal, reflectivity and transmittivity 0-99604  
 specular reflectance standards for visible and infrared region using thin Al film vacuum deposited on optical flats (*Japanese*) 0-102789  
 spherulite, hydrothermal single crystals, feasibility of optical methods for quality control 0-89065  
 TCNQ salt, decamethylferrocenium, monomeric and dimeric, optical and EELS study 0-100660  
 TCNQ salt, n-methyl-n-ethylmorpholinium, unpaired electron states, IR refl. study 0-75491  
 thermal radiation property meas. of materials 0-96181  
 thin film, magnetoresistance, specular reflectivity angular depend. (*Russian*) 0-100453  
 thin films, optical constant volume and surface charge separation, reflection, transmission (*Russian*) 0-66320  
 thin films, optical transmittance and reflectance, bulk optical props. determ. 0-88954  
 (TMTSF)<sub>2</sub>X, (X=PF<sub>6</sub><sup>-</sup>, AsF<sub>6</sub><sup>-</sup>, SbF<sub>6</sub><sup>-</sup>, BF<sub>4</sub><sup>-</sup>, NO<sub>3</sub><sup>-</sup>) highly conducting salts, props. 0-95969  
 topogram sensitivity, wavefront correl. effect 0-69345  
 total, meas. technique using specular-reflectance and diffuse reflectance references 0-73421  
 transition metals, BCC, films, vac. evaporated, optical cond. 0-76100  
 veiling reflections and reflected glare from glossy paper, lighting conditions for visual comfort 0-76733  
 visual acuity screens, reflectance obs. 0-67178  
 waveguide grating, diffraction efficiency, Brewster's law 0-91935  
 Ag film, granular, transmission and reflection spectra, validity of sum rule 0-97358  
 Ag foil, interface with liq., oxide props., refl. and scatt. light spectroscopy 0-60702  
 Ag foil, surface-plasmon resonance, roughness-induced wavelength corrections 0-108288  
 Ag foils, surface plasma-wave reflectance and roughness-induced scatt. 0-66228  
 Ag mirror, Y<sub>2</sub>O<sub>3</sub> coated, for the 0.5 to 14  $\mu$ m region 0-87456  
 Ag<sub>2</sub>HgI<sub>4</sub>, preparation, optical and luminescence spectra 0-104064  
 Al coating reflectivity in vacuum UV, heating effect 0-95981  
 Al plasma, laser produced, reflectance meas. 0-79568  
 Al-Ge-SiO<sub>2</sub> solar selective absorber surfaces, optical behaviour at high temp. 0-101130  
 Al-Si, DC magnetron-sputtered, residual gas influence on props. 0-80968  
 $\alpha$ -Al<sub>2</sub>O<sub>3</sub>, single crystal transmission and reflectance IR phonon spectra, polariton dispersion 0-66170  
 anthracene, polycrystalline, optical props., 3.2-9.3 eV 0-76097  
 Ar, adsorbed on Al, differential refl. spectroscopy, local field effect 0-80811  
 As<sub>2</sub>S<sub>3</sub>-SiO<sub>2</sub>-SiO<sub>2</sub> cryst., ferroelec., soft mode Raman and IR spectroscopy 0-76016  
 Au film, granular, transmission and reflection spectra, validity of sum rule 0-97358  
 Au, optical props., dielec. function, void model, sample effects 0-76048  
 Au/Al thin film, Al diffusion studied by attenuated total reflection method 0-92722  
 Au(Ag)(Cu)-Sn liquid, optical reflectivity spectra of virtual bound states 0-89021  
 BaTiO<sub>3</sub>, ferroelec. cryst., IR and Raman spectra, mode coupling 0-66194  
 BaTiO<sub>3</sub>, ferroelectric mechanisms, anharmonic couplings by scanning IR interferometry 0-75978  
 BaTiO<sub>3</sub>, paraelec. phase, stabilisation of soft mode 0-75985  
 BaTiO<sub>3</sub>, photoelectron and optical spectra derived from self-consistent charge MO and band calcs. 0-96785  
 BaTiO<sub>3</sub>, soft mode spectroscopy IR refl. meas. 0-88982  
 BiTeI, melt and vapour grown, optical props. 0-84746  
 CO chemisorbed on Pt, IR refl.-absorpt. spectra, absorbate island struct. 0-84385  
 CO<sub>2</sub> laser cavity and Ge phase-conjugate 10  $\mu$ m reflection expts. 0-78894  
 CdCr<sub>2</sub>S<sub>4</sub>, ferromag. semicond., IR refl. spectra, phonon props. and dielec. function 0-66191  
 CdF<sub>2</sub>, UPS and XPS spectra, rel. to optical props. 0-66386  
 CdGa<sub>2</sub>S<sub>4</sub>, IR refl. spectra 0-60604  
 Cd<sub>1-x</sub>Mn<sub>x</sub>Se, fundamental optical props. 0-84751  
 CdS, additional waves and polariton dispersion, reflectivity, transmittivity spectra 0-71443  
 CdS, electron-hole plasma, gain and refl. spectra study 0-66227  
 CdS, spectra of refl. and transmission coeffs. near exciton absorpt. line 0-88951  
 CdS/Cu<sub>2</sub>S, polycryst. thin film photovoltaic materials, photon loss anal., expt. determ. 0-93888  
 CdSe, undoped and Cr doped, far IR transmission and reflectance spectra 0-71429  
 CdTe, energy bands and optical props. calc., tight-binding model with spin-orbit interaction 0-65448  
 CdTe:Mn<sup>2+</sup>, exciton refl. spectra and mag. susceptibility 0-66253  
 CeB<sub>6</sub>, mag. and electronic props. 0-71048

reflectivity continued

CeH<sub>3</sub>, phonon features in IR and Raman spectra 0-93310  
CoCl<sub>2</sub>·6H<sub>2</sub>O solution in ethanol, thin absorbing film, nonlinear optical props., Q-switch appl. 0-91836  
CoO-ZnO-MgO ternary systems, solid solns., struct. charact. 0-60629  
Cr film, evaporated, concurrent ion bombard. effects 0-80142  
Cr-Cr<sub>2</sub>O<sub>3</sub> black chrome, commercial, solar absorber coating characterisation 0-80111  
CsPbCl<sub>3</sub>, electronic struct. and optical props. in fundamental absorpt. region 0-93367  
Cu, laser light absorpt. by plasma with very steep density gradient 0-96348  
CuBr(I), reflectance and thermorefectance spectra, electronic struct. 0-71444  
CuCl, refl. spectra, 4.5-30 eV, vel. to band struct. 0-103969  
CuI, single crystals, growth and optical props. 0-93470  
CuInSe<sub>2</sub>, influence of impurities and free carriers on optical props. 0-108225  
Cu<sub>2</sub>S-CdS thin film planar junction devices, quantitative photon loss anal. 0-61362  
Dy-Si, optical props. and electronic struct. in fund. absorpt. region 0-80817  
Dy-Si, vibr. spectra, factor-group anal. 0-80793  
EuO-Gd, pure and doped, elec., mag., and optical props. rel. to electronic conc. 0-96880  
Eu<sub>1-x</sub>Yb<sub>x</sub>Te, (0<x<1), mag. semicond., elec., mag. and optical props. 0-97070  
FeF<sub>2</sub>, dielectric properties, IR spectra, lattice dynamics (*French*) 0-76026  
Fe<sub>2</sub>O<sub>3</sub>, IR refl., ATR, Voigt and Faraday expts. 0-66180  
Fe<sub>2</sub>O<sub>3</sub>, magnetite, optical props. in IR 0-97271  
Ga<sub>1-x</sub>Al<sub>x</sub>Sb, surface oxidation, Raman spectra, residual Sb layers 0-71419  
GaAs anodic oxide films, optical studies using rot. light-pipe reflectometer 0-76096  
Ga<sub>1-x</sub>In<sub>x</sub>As, IR reflectivity, cluster effect on optical phonons 0-97259  
Ga<sub>1-x</sub>In<sub>x</sub>As, P<sub>1-y</sub>, IR refl. spectra 0-60602  
GaP, impurity-containing single crystals, refl. spectra 0-80823  
GaS, infrared optical props., polarisation depend., vibr. modes 0-100658  
GaS<sub>2</sub>, Se<sub>2</sub>, mixed crystals, IR reflectivity spectra 0-66204  
GaSb, bulk and epitaxial, IR reflect. meas., carrier conc. and mobility determ. 0-80769  
p-GaSe, back wall Schottky barrier cells, diffusion length, RT spectral response meas. 0-107806  
GaSe films, optical props. at lattice vibr. freqs., IR and Raman spectra 0-60696  
GaTe, layer cryst., polarised IR refl. spectra 0-97279  
GaTe monocrystal, far IR polarised complex reflectivity obs. 0-60609  
GdFeBi, amorphous ferrimag. films, magneto-optical props., optical spectra 0-76008  
Gd<sub>2</sub>Ga<sub>2</sub>O<sub>7</sub>, IR refl., ATR, Voigt and Faraday expts. 0-66180  
GdIG, IR refl., ATR, Voigt and Faraday expts. 0-66180  
GdN, and GdN<sub>1-x</sub>O<sub>x</sub>, mag. interactions 0-60218  
Ge, black, solar selective absorber characterisation 0-80112  
Ge, high refl. phase conjugation at 10 μm, intracavity CO<sub>2</sub> laser techniques 0-78894  
Ge optical props. in 2.5-15 micron region 0-80775  
Ge surface reflectivity changes and moving diffr. grating efficiency 0-58662  
GeSe<sub>2</sub>, amorphous film, laser induced oscillatory phenomena 0-84711  
GeSe<sub>2</sub>, multimode layer cryst., far IR transmission and reflection spectrosc., comparative merits 0-76019  
p-GeTe, reflectance, and thermoref. spectra 0-80814  
HNO<sub>3</sub>, aqueous soln., reflectance and complex refractive index, IR spectra, vibr. modes 0-66168  
Hg, reflection spectra, electronic density of states, calc. 0-66229  
HgI<sub>2</sub>, IR lattice vibr. and dielec. dispersion 0-76018  
HgSe, two-phonon resonant effect, far-infrared reflectivity 0-108203  
HgTe, energy bands and optical props. calcs., tight-binding model with spin-orbit interaction 0-65448  
In<sub>1-x</sub>Ga<sub>x</sub>As, P<sub>1-y</sub> epitaxial layer, far IR refl. spectra, lattice vibrs. 0-97282  
InP, surface phonon polariton dispersion and damping, frustrated total internal refl. meas. 0-80792  
K double fluorides, IR refl. spectra, vibr. modes, optical vibr. freq., Kramers Kronig anal. 0-66190  
KCN, Cl<sub>1-x</sub>, finite field catastrophe phenomena in spectra 0-92830  
K<sup>+</sup>CN<sub>2</sub><sup>-</sup>Cl<sub>1-x</sub>, influence of structural disorder on exciton spectra 0-108224  
KNO<sub>3</sub>, Raman and IR spectra and lattice vibrs. 0-60565  
KNbO<sub>3</sub>, ferroelec. cryst., IR and Raman spectra, mode coupling 0-66194  
La-Si, optical props. and electronic struct. in fund. absorpt. region 0-80817  
La-Si, vibr. spectra, factor-group anal. 0-80793  
β-LiAl, optical dispersion, room temp. reflectance spectra 0-66195  
Li<sub>10</sub>(Fe<sub>2</sub>O<sub>4</sub>)<sub>2</sub>, magneto-optical Kerr effect, reflectivity spectra 0-66157  
LiH(D), isotope effect on Wannier-Mott exciton levels 0-103633  
LiNbO<sub>3</sub>, ferroelec., dispersive type phase transition, far IR reflection spectra 0-71339  
LiNbO<sub>3</sub>, luminesc. props., Li/Nb ratio effect 0-97323  
Li<sub>2</sub>SO<sub>4</sub>·H<sub>2</sub>O, far IR spectra, H<sub>2</sub>O flipping motion, lattice modes 0-84258  
LiTaO<sub>3</sub>, ferroelec., dispersive type phase transition, far IR reflection spectra 0-71339  
MgO-MgF<sub>2</sub> multilayer stack selective mirror with high reflectivity (*French*) 0-64131  
Mg<sub>2</sub>Zn<sub>1-x</sub>Te, band struct. refl. spectra meas. 0-80813  
MnSi<sub>3</sub>, X=1.72 to 1.75, IR absorpt., transmission, refl. spectra 0-60600  
MoSe<sub>2</sub>, exciton spectra 0-97296  
(NH<sub>4</sub>)<sub>2</sub>BeF<sub>4</sub>, far-infrared and submillimetre dielectric response 0-80782  
Na<sub>2</sub>Al<sub>2</sub>Si<sub>2</sub>O<sub>7</sub>·2NaX<sub>2</sub>·nH<sub>2</sub>O, (X=Cl, Br, I), X-ray irradi., thermal-erase cathodochromism and dihalide mol. centres (*Russian*) 0-66236  
NaNbO<sub>3</sub>, lattice vibrs., order-disorder transform., IR spectra study 0-65176  
Na<sub>2</sub>O-SiO<sub>2</sub> glasses, elementary electronic excitations, refl., luminesc., and photoemission meas. 0-84778  
NdP<sub>2</sub>O<sub>7</sub>, fluoresc. lifetime meas., IR and photoacoustic spectroscopy 0-60652  
Nd-Si, optical props. and electronic struct. in fund. absorpt. region 0-80817  
Nd-Si, vibr. spectra, factor-group anal. 0-80793

reflectivity continued

Ni, anodic passive film form. in NaOH soln., refl. and ellipsometric study 0-104447  
Ni-Co(Fe)(V)(Ti), dil., optical absorpt., electronic struct. 0-108227  
Ni-Ge-SiO<sub>2</sub>, solar selective absorber surfaces, optical behaviour at high temp. 0-101130  
Ni<sub>1-x</sub>Co<sub>x</sub>Si<sub>2</sub>, elec. cond., thermoelec. power and optical meas. 0-59986  
PbCl<sub>2-2x</sub>Br<sub>2x</sub>, luminesc. and reflection spectra (*Russian*) 0-84762  
Pb<sub>1-x</sub>Ge<sub>x</sub>Te magnetoplasma reflectivity and transmission spectra 0-71428  
PbI<sub>2</sub>, first-order 2H-4H polytype transition, exciton spectroscopic study 0-59647  
PbI<sub>2</sub>, photoexciton interaction, luminescence spectra, polariton dispersion diagram 0-93397  
Pb<sub>1-x</sub>Sn<sub>x</sub>Te, hole effective mass near zero bandgap, IR refl. study 0-108205  
RbClO<sub>3</sub>/RbBrO<sub>3</sub> mixed crystals, internal optic modes obs., Raman and IR reflectance spectra 0-76024  
RbHSeO<sub>4</sub>, ferroelec., far IR spectra 0-71404  
Ru (001), adsorption of CO, IR spectra, LEED, and thermal desorption meas. 0-70533  
S, orthorhombic, photogeneration of charge carriers 0-107844  
SbSBr glass, IR reflectivity spectra 0-71403  
SbSI-SbSBr system, ferroelec., anharmonic effects in far IR reflectivity spectra 0-76014  
Se, electronic struct. of cryst. phases and hydrostatic press. effects 0-59865  
Se films, Ag diffusion, effect on interferometric thickness meas. 0-96695  
Si, CVD amorphous films, effect of surface characts. on visible and UV optical props. 0-60698  
Si, optical consts. by unpolarised incident radiation 0-76044  
Si, reflectivity time dependence during pulsed laser annealing 0-66214  
Si ring photodiode reflectometer for cavity reflectance 0-86376  
Si:N(P), ion implanted, IR transmission and refl. spectra study 0-108244  
Si-Si<sub>3</sub>N<sub>4</sub>-SiO<sub>2</sub> non absorbing double layers, optical parameters reflectivity by liquid immersion method 0-71503  
SiC ion implanted, laser induced ordering and defects 0-84754  
SiO amorphous film, optical transmittance and reflectance, bulk optical props. determ. 0-88954  
SiO evaporated film, dielec. function 8 to 33 μm, spectrophotometric and refl. meas. 0-80883  
SiO<sub>2</sub> film, attenuated total reflectance study, impurity spectra 0-97311  
SiO<sub>2</sub> film, on GaP substrate, N ion implantation, optical refl. and EPR meas. 0-84197  
SiO<sub>2</sub> film on Cu substrate, surface EM wave absorpt., optical consts. (*Russian*) 0-108216  
SiO<sub>2</sub>, fused, surface crystn. by Li<sup>+</sup> ion implantation and annealing 0-89383  
Sm<sub>2</sub>S<sub>3</sub> films, refl. and transmission spectra at 300K 0-80889  
SnO<sub>2</sub> films, selective, optical characterisation by thermodynamical method 0-84796  
Sn<sub>2</sub>S<sub>3</sub> mixed valence semiconductor, far IR refl. spectra 0-108191  
SrF<sub>2</sub>, UPS and XPS spectra, rel. to optical props. 0-66386  
Te, electronic struct. of cryst. phases and hydrostatic press. effects 0-59865  
Ti, electropolished, optical props. from 1.8 to 3 eV 0-85088  
TiO<sub>2</sub>, rutile, optoelectronic props., band struct., theory 0-80175  
TiO<sub>2</sub>-SiO<sub>2</sub> multilayer vacuum coatings, optical props. 0-97361  
TiBr, resonant polaron coupling and excitons under mag. field 0-71383  
TiGaTe<sub>2</sub>, TiInTe<sub>2</sub>, and TiInSe<sub>2</sub>, IR refl. spectra 0-60605  
UO<sub>2</sub>, 5f-magnetic semiconductor, spectroscopic data, review 0-97299  
UO<sub>2</sub>, electronic transitions, crystal field effects and phonons, phase transition 0-97303  
US(Se)(Te), electronic struct. and exchange band splitting, optical refl. meas. 0-66226  
V<sub>6</sub>O<sub>13</sub>, semicond., IR vibration spectra 0-88997  
W surface, (110), chemisorpt. effects on dielec. function, refl. spectra 0-75616  
YIG, magneto-optical Kerr effect, reflectivity spectra 0-66157  
YIG:Ga(Sc), magneto-optical Kerr effect, reflectivity spectra 0-66157  
Zn-In-S thin layers, ternary phases, optical props. near long-wavelength intrinsic absorpt. edge 0-80887  
Zn<sub>2</sub>Cd<sub>1-x</sub>Se, exciton reflection spectra anomalies (*Russian*) 0-97304  
ZnO, electron-hole plasma, gain and refl. spectra study 0-66227  
Zn<sub>2</sub>P<sub>2</sub>, optical props., transition energies from transmission and refl. meas. 0-60532  
ZnS evaporated film, refl. loss on UV irradi., ZnO form. 0-99813  
ZnSe, exciton refl. spectra, temp. depend. 0-59886  
ZnTe:Bi, laser annealing, channelling, reflectivity spectra 0-66215  
ZrB<sub>3</sub>, self-consistent band struct., XPS, reflectance, NQR, Hall effect and density of states meas. 0-107689  
ZrO<sub>2</sub> thin film, optical props. rel. to cryst. struct. 0-97357

**reflector antennas**  
far IR antennas for 0.1 to 3.0 mm range, review 0-69553  
radiotelescope construction, light-weight, with prestressed guyed rod 0-109360

**reflex klystrons**  
No entries

**refraction**  
*see also acoustic wave refraction; electromagnetic wave refraction; refractive index*  
seismic waves, refr. index distrib. image reconstruction using iterative ray tracing between boreholes 0-98466

**refractive index**  
*see also photorefractive effect; refractometers*  
acrylic moulding formulations, optical and mech. props. 0-106582  
air, Schlieren photography, detection of abnormal nasal escape 0-64145  
alkali borosilicate system, self-focusing fibres with aperture of 0.18 0-7548  
alkali halides, refractive index calculation 0-88949  
alkali lime germanosilicate GRIN fibre prep., losses and geometrical props. 0-69560  
alkaline earth halides, refractive index, wavelength and temp. derivatives 0-88948  
amplitude-phase holograms, optical parameter dispersion 0-58481  
atmospheres of giant planets VHF refraction 0-98608  
benzene liqs., refractive index, pressure effect 0-71375  
borosilicate glasses, gamma irradiation effect on density, refractive index, thermal expansion 0-79838  
t-butyl acetate, rot. isomerism, dielect. and Raman spectra 0-106328



## refractive index continued

t-butyl formate, rot. isomerism, dielect. and Raman spectra 0-106328  
 butyloxybenzylidene octylaniline film, freely suspended, smectic A layer spacing, optical determ. 0-64883  
 CBOOA film, freely suspended, smectic A layer spacing, optical determ. 0-64883  
 ceramic, KOI, optical homogeneity in terms of refr. index 0-64125  
 chalcogenide glasses, O-free, cooling rate influence on optical consts. 0-88952  
 chalcopyrite crystals, refractive index, temp. depend., appl. to nonlinear devices 0-60555  
 chemical laser, low pressure, line-shape flattening resulting from hyper-sonic nozzle wedge flow 0-91783  
 cholesteric films, absorpt. and contrast in dichroic liq. cryst. displays 0-75155  
 cholesterol esters, molecular-optical, and structural anisotropy 0-84056  
 cholesteryl esters, blue phase, model 0-88030  
 cholesteryl nonanoate, cyclohexanone admixture effect on mesophase order parameter, refr. index meas. 0-100165  
 COOB film, freely suspended, smectic A layer spacing, optical determ. 0-64883  
 crystal optical characteristics, relax. processes exciton dispersion 0-107709  
 crystalline optical material props., symmetries and tensorial relationships 0-108174  
 cubic symmetry cryst., quadrupole exciton theory 0-103632  
 4-cyano-4'-n-pentylbiphenyl, refr. index meas. and isotropic-nematic phase transition study, surface plasmon technique 0-84282  
 p-cyanophenyl p-n-alkyloxybenzoates, nematic, birefringence, polarisability and order parameter 0-100642  
 degenerate four-wave mixing, hysteresis and optical bistability 0-69446  
 DH lasers, phase and group indices 0-64016  
 dielectric fibres, transversely incident beam wave scatt. 0-96004  
 dielectric response function, Kohn singularities near gapless state 0-59904  
 dielectric thin film stack, control by stationarity ratio method, refractive index dispersion influence (*French*) 0-60693  
 differential mode delay rel. to refr. index profile, geometrical optics treatment 0-69529  
 dimethylammonium cadmium tetrachloride, far IR refractive index, extinction coeff. and dichroism obs. 0-66144  
 1,2-dimethylol-sn-glycero-3-phosphoserine multilayers, phase transitions, temp. depend., ellipsometric study 0-108846  
 1,2-dipalmitoyl-sn-glycero-3-phosphocholine multilayers, phase transitions, temp. depend., ellipsometric study 0-108846  
 dispersion staining, in IR and UV 0-76874  
 n-dodecane liqs., refractive index, pressure effect 0-71375  
 Doppler-free two-photon dispersion problem 0-106562  
 education, refractive index, spatially varying, demonstration and theory 0-62425  
 elliptical fibres, near-field correction factor 0-87490  
 elliptical multimode fibres, leaky ray correction factors 0-87487  
 empirical relationship for a nonlinear index coefficient 0-74445  
 fibre lens, gradient index, radiometric props. 0-69481  
 fly ash particles, water accretion, refract. index and accreted layer thickness 0-58462  
 Fresnel's relations in IR, verification and determ. of emissivity and compound index (*French*) 0-84309  
 glass, homogeneity by Christiansen filter method 0-84066  
 glass, refractive index gradient, chromatic variation 0-74471  
 glass, refractive index gradients, form. using ion exchange diffusion 0-64227  
 glass characteristics, electromagnetic, mechanical and thermal props. 0-106587  
 glasses, gradient composition, optical props. 0-88947  
 graded index planar lightguide, electrooptical diffraction 0-78995  
 graded-index curved media, generalised Fresnel power transmission coefficients 0-102815  
 gradient index optical elements and system design 0-106594  
 gradient-index imaging, theory 0-69331  
 gradient-index optics: a review 0-69478  
 gyrotropic media, artificial, EM scattering 0-106423  
 n-heptane liqs., refractive index, pressure effect 0-71375  
 n-hexane liqs., refractive index, pressure effect 0-71375  
 ice, O-H and O-D bond stretching vibrs., Raman spectra at atmospheric press. 0-66166  
 index-matching fluids for long wavelength (1.2-1.6 micron) fibre-optic appls. 0-99841  
 ion exchange, field assisted, for production of graded-index optical materials 0-74447  
 ion implanted layers, complex refr. index profile, ellipsometric meas. 0-93262  
 isotropic dielectric mirror theory 0-102797  
 Langmuir-Blodgett films, lightguiding 0-79006  
 laser amplifier system, small-scale self-focusing 0-106580  
 laser beam refraction at spherical surface, distortion, geometrical optics calc. 0-95929  
 lens, gradient-index rod, aberrations in multimode optical fibre devices 0-69487  
 lens, gradient-index rod, appl. in optical fibre communication systems 0-69488  
 lens, gradient-index rod, evaluation by imaging 0-69485  
 lens, gradient-index spherical, design for optical pickup systems 0-69483  
 lens, photographic gradient singlet, design techniques based on total aberrations 0-69479  
 lens, radial gradient-index, with zero Petzval aberration, third-order aberrations 0-69484  
 lightguides, Maxwell's eqn., numerical soln., refractive indices 0-87520  
 liquid crystals, orientational order parameter, optical birefr. meas., polarisation field problems 0-79688  
 liquid crystals, prep. and phys. props., book 0-105444  
 liquids, cargille PCB-free, refractive index 0-80741  
 luminescence spectroscopy, refractive index correction, quantum efficiencies calc. 0-86444  
 2,6-lutidine-water thick films, interferometric obs. of crit. behaviour 0-93266  
 matching fluids for long wavelength fibre-optic appl. 0-69470  
 methanef-d<sub>4</sub>, liq., Brillouin scatt. and refr. index measurements 0-76035  
 molecular polarizability, anisotropic, optical study (*Rumanian*) 0-74256  
 molecule embedded in dielec. spheroid, Raman and fluoresc. scatt. 0-99507

## refractive index continued

Monsanto X-500 aromatic polyamide hydrazide soln., light scatt. study 0-76038  
 multi-layer optical system, reflection and transmission coeffs. calcs., computer program 0-66316  
 multilayer, electric field distrib. and laser damage reduction 0-87420  
 multilayer multimode optical fibre, ray theory, optimal distrib. of refractive index 0-87489  
 multilayer superlattice stacks, very thin nonideal, wavelength variation of transmissivity, refl. 0-100701  
 nematic liquid crystals, refractive index and birefringence by interference method 0-96440  
 objectives, tolerancing of refr. index heterogeneity 0-78948  
 ocean, internal waves, acoustic refractive index modulation, parabolic moment eqns. 0-83698  
 n-octane liqs., refractive index, pressure effect 0-71375  
 optical fibre, elliptical step-index, tunnelling-radiating effect 0-58714  
 optical fibre, microbending eqns., exact time-dependent, solns. 0-87530  
 optical fibre, modal dispersion of power-law profiles with tails 0-95991  
 optical fibre, multimode, graded index, mode conversion coeff. meas. method 0-99820  
 optical fibre, parabolic index, selective excitation by Gaussian beams 0-95992  
 optical fibre, refractive index profile distortion, stress-induced 0-91889  
 optical fibre, single mode, dispersion characts., correlation between numerical prediction and meas. 0-91890  
 optical fibre, soliton pulse propag. 0-58759  
 optical fibre, step-index, nearly elliptical, with high eccentricity, fabrication for studying modes 0-95989  
 optical fibre, vapour-oxidation fabricated, refractive index modulation, pulse dispersion 0-58756  
 optical fibre, weakly guiding, modes calc. by integral representation technique 0-58758  
 optical fibre array, gradient-index, appl. in copying machine 0-69500  
 optical fibre array, gradient-index, unevenness of illuminance 0-69482  
 optical fibre coupling using graded-index rod lenses 0-91891  
 optical fibre refractive index profile distortion due to thermal stresses 0-58726  
 optical fibres, differential delay time relationship with propagation mode number study by effecting selective mode excitation (*Japanese*) 0-87504  
 optical fibres, piezo-optical effects due to thermal stresses 0-87519  
 optical glass, refr. index tables and calcs. for optical designer 0-83650  
 optical glass, thermally tempered, surface stress meas. by crit. ray method 0-106766  
 optical surface wave at a nonlinear interface 0-91867  
 optical waveguide, refractive index profile calc. from measured coupling angles 0-78954  
 organic compounds usable as solvents in laser saturable absorber, nonlinear refr. index meas. 0-102758  
 orthorhombic crystal, birefr. and refr. index determ., refl. method 0-86380  
 oxide, porous transparent films as antirefl. coatings for glass surfaces, low refr. index 0-74448  
 PET, biaxial orientation, refr. index meas. by Raman and IR spectrosc. 0-60583  
 planar waveguide structure for integrated optics, props. (*Czech*) 0-96018  
 plane parallel optical layer interference props. for radiation parameters control 0-83547  
 polysulfonamide, optically active, synthesised by interfacial polycondensation, mol. wt. determ. 0-99595  
 POPOP solution dye lasers, multiplate reflectors 0-83606  
 quartz glass, Ge and B dopants, OH impurities, preform material and fibre optic waveguide struct. 0-64173  
 radiowave propagation in troposphere waveguide, effect of elevated M-inversion 0-90195  
 rare earth germanates, R<sub>2</sub>O<sub>3</sub>-GeO<sub>2</sub> system cpds., physicochem. characts. 0-97469  
 rare earth oxyorthotitanates, crystallochem. classification 0-107142  
 (rare-earth) Fe<sub>2</sub>(BO<sub>3</sub>)<sub>3</sub> cryst. growth from soln.-melt, props. 0-108337  
 refr. index calcs., 0.365-2.6  $\mu$ m spectral region 0-74444  
 refracted beam formation during light ray motion along optically homogeneous media interface 0-74298  
 rod, tapered gradient-index, geometrical optics 0-69322  
 Selfoc lens, aberration improvement by glass composition and ion exchange process parameter choice 0-69486  
 Selfoc lens as imaging system, chromatic aberration 0-69480  
 semiconductor, Moss formula, refr. index rel. to energy gap 0-108173  
 semiconductors, forbidden gap width, relation to refractive index, single oscillator calcs. (*Russian*) 0-71372  
 semiconductors, mixed and binary, nonlinear polarisability, self-action effects 0-99786  
 single mode and graded-index multimode fibre cable random bend losses 0-58741  
 single mode fibre near- and far-field characteristics, profile-independent representation 0-58739  
 single-mode fibres, axial refr. index dip effect on zero total dispersion wavelength 0-78962  
 smoke aerosols, optical absorption to extinction ratio, photoacoustic determ. 0-58459  
 spheroidal particles, colloidal dispersions, refractive index 0-106454  
 surface tension temp. dependence from triple point to critical point (*German*) 0-100376  
 tetrachloromethane liqs., refractive index, pressure effect 0-71375  
 thin films, optical constant volume and surface change separation, reflection, transmission (*Russian*) 0-66320  
 thin-film multimode waveguides, higher order mode amplification 0-96012  
 TOPOT vapour dye lasers with multiplate reflectors 0-83606  
 uniaxial crystals, refl. ellipsometry nonlinear eqn. inversion 0-95120  
 UV high-power laser material, refractive props. and optical constants 0-106555  
 waveguide, graded-index surface or buried, realized by ion exchange in glass 0-69499  
 AgNO<sub>3</sub>, molten, refr. index and molar refractivity 0-93265  
 (Al,Ga)As: Zn planar stripe lasers with deep Zn diffusion, guiding mechanisms controlled by impurity concs. 0-78853  
 AlF<sub>3</sub> based glasses, chem., thermal and optical props. (*French*) 0-70139  
 Al<sub>2</sub>O<sub>3</sub> porous transparent films as antirefl. coatings for glass surfaces, low refr. index 0-74448  
 Al(PO<sub>3</sub>)<sub>3</sub>-BaF<sub>2</sub>-Al<sub>3</sub> glasses, opt. props., group I-III fluorides effect 0-66143

**refractive index** continued

- anthracene, polycrystalline, optical props., 3.2-9.3 eV 0-76097  
 Ar, gas, liquid, solid, refractive index, density and dielectric const. 0-66138  
 As-S<sub>3</sub> melt struct., orientation birefr., viscosity, refr. index, and density 0-84713  
 AsGe amorphous film, far IR absorpt. spectra, refractive index 0-80785  
 As<sub>2</sub>S<sub>3</sub> film, amorphous, photo-induced dynamical changes 0-66142  
 As<sub>2</sub>S<sub>3</sub> amorphous films, optical props. and photoinduced changes 0-60700  
 Ba film, semitransparent, opt. props. in 2-5.6 eV range, electronic transitions, thickness depend. (*French*) 0-108289  
 BaAl<sub>2</sub>O<sub>9</sub>, refr. index and optical absorpt. 0-66139  
 BaB<sub>2</sub>O<sub>7</sub>-RF<sub>2</sub>, R=Mg, Ca, Sr, Ba, glass form., struct. and props. 0-84077  
 Ba<sub>3</sub>NaNb<sub>2</sub>O<sub>15</sub>, growth layer form., crystallization conditions effect, light diffra., Curie temp. 0-100778  
 BaO-B<sub>2</sub>O<sub>3</sub> glass, refraction, refractive index from 0.365 to 2.50  $\mu$ m 0-88953  
 BaO-La<sub>2</sub>O<sub>3</sub>-B<sub>2</sub>O<sub>3</sub> glass, refraction, refractive index from 0.365 to 2.50  $\mu$ m 0-88953  
 BaR<sub>2</sub>(MoO<sub>4</sub>)<sub>4</sub>, R=rare-earth, struct., optical, mech., spectral and physico-chem. props. 0-84161  
 BiI<sub>3</sub> film, exciton-phonon interaction, optical consts., Faraday effect., permitt. 0-59884  
 C films with high conductivity, prep. and props. 0-80983  
 CO<sub>2</sub> CW laser radiation, freq. conversion in Ti-Cs vapour mixture 0-74438  
 CO<sub>2</sub> ice spheres, IR scatt. and absorpt. props. 0-97269  
 CO<sub>2</sub> solid, IR spectra and refr. index, Martian implications 0-72821  
 CaCeAl<sub>3</sub>O<sub>7</sub>, melilite struct., prep. and props. 0-93524  
 CdGeP<sub>2</sub> thermo-optic coefficient, dispersion 0-71396  
 CdInGaS<sub>4</sub>, layered structure crystals, refractive index meas. method 0-98966  
 CdS plane parallel slab, optical const. determ. methods 0-60531  
 CdS thermo-optic coefficient, dispersion 0-71396  
 CdSe, temp. depend. phase-matched nonlinear optical devices 0-99794  
 CdSe thermo-optic coefficient, dispersion 0-71396  
 CdSe, undoped and Cr doped, far IR transmission and reflectance spectra 0-71429  
 Co-Gd(Tb)(Sm) film, magneto-optic coeff. and refr. index, ellipsometric determ. 0-71501  
 Co-Si interface, glassy layer, ellipsometric charact. 0-103589  
 CsCuCl<sub>3</sub>, phase transition, refr. index, electrooptic coeff., pyroelec. signal, and NQR meas. 0-70386  
 CuGaS<sub>2</sub> thermo-optic coefficient, dispersion 0-71396  
 CuGaTe<sub>2</sub>, refr. indices meas. 0-93259  
 CuInSe<sub>2</sub>, influence of impurities and free carriers on optical props. 0-108225  
 CuInSe<sub>2</sub>, refr. indices meas. 0-93259  
 CuInTe<sub>2</sub>, refr. indices meas. 0-93259  
 DyAsO<sub>4</sub>, first order Jahn-Teller phase transition, sp. ht. and refr. index meas. 0-59645  
 DyAsO<sub>4</sub>, phase transitions obs. 0-70412  
 DyVO<sub>4</sub>, phase transitions obs. 0-70412  
 EuS-Ga<sub>2</sub>S<sub>3</sub>-GeS<sub>2</sub>, chalcogenide glasses, conditions of form. of glassy prod. (*French*) 0-100325  
 Fe-Gd(Tb) film, magneto-optic coeff. and refr. index, ellipsometric determ. 0-71501  
 Fe<sub>2</sub>BO<sub>3</sub>, orthorhombic cryst., birefr. and refr. index determ., refl. method 0-86380  
 GaAs, anodisation at low substrate temp. by low pressure O<sub>2</sub> plasma 0-104314  
 n-GaAs, crystal growth by Czochralski method kinetics, total emittance determ. 0-75193  
 GaAs, ion-implantation induced damage profile, ellipsometric study, annealing 0-103400  
 GaAs:Cr, ion implanted, implantation damage profiles, laser annealing, ellipsometry study 0-79819  
 GaInAsP DH laser emitting at 1.55  $\mu$ m, threshold currents 0-83609  
 Ga<sub>2</sub>S<sub>3</sub> glass (*French*) 0-71369  
 GaSe, thin layers, far IR refractive index 0-80799  
 Ge, far IR photon drag and radiation pressure in refractive media 0-60048  
 Ge-As-Se IR transmitting glass composition, prep. and props. 0-69474  
 GeSe<sub>2</sub> amorphous film, laser induced oscillatory phenomena 0-84711  
 HNO<sub>3</sub>, aqueous soln., reflectance and complex refractive index, IR spectra, vibr. modes 0-66168  
 H<sub>2</sub>O vapour and liquid far IR spectroscopy 0-60610  
 InGaAsP, anodic oxidation, refractive indices 0-97601  
 In<sub>2</sub>O<sub>3</sub>, thin film, sputter deposition form., optical and elec. props. 0-60123  
 InSb, magnetoacoustic wave excitation by acoustic wave propagation 0-88597  
 InSb, optical constants and oxidation with various surface treatment (*Russian*) 0-88955  
 InSb, refractive index and absorpt. coeff., cryst. orientation depend. 0-60536  
 In<sub>2</sub>Si<sub>2</sub>O<sub>7</sub>, thin film, sputter deposition form., optical and elec. props. 0-60123  
 K<sub>2</sub>D<sub>2</sub>H<sub>2</sub>(1-x)PO<sub>4</sub> crystals, 0<x<0.98, light scatt. by polaritons 0-96802  
 K<sub>2</sub>Li<sub>2</sub>Nb<sub>2</sub>O<sub>15</sub> films for optical waveguides epitaxial growth and characterisation 0-79016  
 K<sub>2</sub>O-CaO-BaO-B<sub>2</sub>O<sub>3</sub> glass, refraction, refractive index from 0.365 to 2.50  $\mu$ m 0-88953  
 Kr, gas, liquid, solid, refractive index, density and dielectric const. 0-66138  
 La<sub>2</sub>S<sub>3</sub> glass (*French*) 0-71369  
 LiF, refractive index, effect of ageing, wavelength range 460-1000 nm 0-84707  
 LiNbO<sub>3</sub>, light induced ultrasonic wave velocity change, refractive index 0-97236  
 LiNbO<sub>3</sub> optical waveguides, Ag-Li and Ti-Li ion exchange effects 0-58791  
 LiNbO<sub>3</sub>, optical waveguides by ion implantation 0-106622  
 LiNbO<sub>3</sub>:Ti diffused optical waveguide, guided light scatt. sources 0-78966  
 LiNbO<sub>3</sub>:Ti diffused optical waveguide, efficient tapered gap prism coupling 0-78967  
 Li<sub>2</sub>SO<sub>4</sub> based solid electrolytes, FCC phase transport mechanism studies and uses 0-107525

**refractive index** continued

- Li<sub>2</sub>SO<sub>4</sub>, fast ion conductors, X-ray diffra., neutron diffra., and Brillouin scatt. study 0-107170  
 LiTaO<sub>3</sub> optical waveguides, Ag-Li and Ti-Li ion exchange effects 0-58791  
 LiTaO<sub>3</sub> optical waveguide, Ag-Li ion exchange 0-91888  
 MNbO<sub>3</sub>, tetragonal, electronic struct., optical anisotropy 0-70599  
 Mg-cordierites, synthetic end member, variation of refractive index with water content 0-80739  
 N<sub>2</sub>, liq., high repetition rate stimulated Raman scatt., thermal blooming 0-91865  
 (NH<sub>4</sub>)<sub>2</sub>BeF<sub>4</sub>, linear and nonlinear optical props. in incommensurate phase 0-69452  
 Na<sub>3</sub>AlF<sub>6</sub> film on Si, fused quartz substrates, H<sub>2</sub>O absorpt., IR anal. 0-75446  
 NaCl, amplitude phase hologram recording on colloid type centres (*Russian*) 0-69347  
 Na<sub>2</sub>O-B<sub>2</sub>O<sub>3</sub>-SiO<sub>2</sub> glass, low-loss GRIN fibres, double-crucible prod., loss and bandwidth meas. 0-69559  
 Na<sub>2</sub>O-SiO<sub>2</sub> glass, bridging to non-bridging ratio and correl. to glass density and refr. index, ESCA study 0-84832  
 Nb<sub>2</sub>Al, complex refractive index meas. 0-93264  
 Ni, anodic passive film form. in NaOH soln., refl. and ellipsometric study 0-104447  
 PLZT ferroelectric thin films, epitaxial growth and optical props. 0-70543  
 PbO-containing binary systems, acoustooptic props. from comp. and density 0-76000  
 PbSnTe, optical dielectric const. variation with carrier conc. 0-84709  
 Si amorphous film, anisotropic etching phenomenon, appl. as solar selective absorber surfaces 0-72054  
 Si, anodisation at low substrate temp. by low pressure O<sub>2</sub> plasma 0-104314  
 Si, far IR photon drag and radiation pressure in refractive media 0-60048  
 Si film, low press. CVD prep., struct., elec. and optical props. 0-70548  
 Si, ion implanted, radiation defect production at different temps. 0-103398  
 Si, optical consts. by unpolarised incident radiation 0-76044  
 Si oxides, steam grown, index of refr. ellipsometric meas. 0-75995  
 Si RF sputter-etched surface, cryst. damage, spectroscopic ellipsometry obs. 0-103538  
 Si:B ion implanted layers, light refl. and transmission coeffs., computer program 0-66316  
 a-Si:H, influence of H on optical props., H conc. and H bonds 0-76098  
 a-Si:H alloys, sputter deposited thin film coatings, property-comp. relationships 0-80975  
 Si:N(P), ion implanted, IR transmission and rel. spectra study 0-108244  
 Si-Si<sub>3</sub>N<sub>4</sub>-SiO<sub>2</sub> non absorbing double layers, optical parameters reflectivity by liquid immersion method 0-71503  
 Si-SiO<sub>2</sub> interface, thermally grown oxide, spectroscopic ellipsometric anal. 0-107659  
 SiC, dielectric coating effect on surface polaritons, optical consts. (*Russian*) 0-88489  
 SiC:H amorphous reactively sputtered film, H content effect on film props. 0-75459  
 SiN<sub>x</sub> films, plasma-deposited, radial wafer-to-wafer uniformity 0-104073  
 SiO<sub>2</sub> film, prep. using high press. O<sub>2</sub>, residual stress, chemical etch rate, refr. index and density meas. 0-71768  
 SiO<sub>2</sub> film on 6H-SiC substrate, ellipsometric meas., accuracy and sensitivity 0-77840  
 SiO<sub>2</sub> ion implanted, radiation defects and optical props. 0-107293  
 SiO<sub>2</sub>, thin films on rough polycryst. Si surfaces, oxide thickness and refractive index meas. 0-93422  
 SiO<sub>2</sub> ultrathin layers, refr. index meas. 0-103936  
 SiO<sub>2</sub>-B<sub>2</sub>O<sub>3</sub> glass system, gel hot pressing synthesis and characterisation (*French*) 0-66468  
 SnS<sub>2</sub> thin layer, far IR refractive index 0-93421  
 SnF<sub>2</sub>, thin film, optical props., spectral dependence, 460-1000 nm 0-76094  
 SrTiO<sub>3</sub>, fabrication damage characterisation by internal and external meas. 0-102782  
 Ta<sub>2</sub>O<sub>5</sub> film, reactively sputtered on Si, dielectric and optical props. obs. (*Bulgarian*) 0-89144  
 Ta<sub>2</sub>O<sub>5</sub> film, refractive index 0-84792  
 TiO<sub>2</sub> layers, activated reactive evaporation and absorpt. indices 0-97363  
 TiO<sub>2</sub>-SiO<sub>2</sub> multilayer vacuum coatings, optical props. 0-97361  
 Ti<sub>2</sub>AsSe<sub>3</sub>, refractive index, thermal expansion temp. depend. 0-97223  
 TiInS<sub>2</sub>, layered structure crystals, refractive index meas. method 0-98966  
 V-Si film, optical props. (*Russian*) 0-93418  
 WO<sub>3</sub>, anodic oxide films, quadratic electro-optic and electrostrictive effects, ellipsometry 0-108184  
 Xe, gas, liquid, solid, refractive index, density and dielectric const. 0-66138  
 Yb<sub>2</sub>O<sub>3</sub> thin film on Cr substrate, refr. index depend. on thin film thickness 0-108290  
 ZnB<sub>2</sub>O<sub>4</sub>-RF, R=Mg, Ca, Sr, Ba, glass form., struct. and props. 0-84077  
 ZnGeP<sub>2</sub>, temp. depend. phase-matched nonlinear optical devices 0-99794  
 ZnGeP<sub>2</sub>:Zn 0-71396  
 ZnO-B<sub>2</sub>O<sub>3</sub> glass, refraction, refractive index from 0.365 to 2.50  $\mu$ m 0-88953  
 ZnO-La<sub>2</sub>O<sub>3</sub>-B<sub>2</sub>O<sub>3</sub> glass, refraction, refractive index from 0.365 to 2.50  $\mu$ m 0-88953  
 Zn<sub>3</sub>P<sub>2</sub>, optical props., transition energies from transmission and refl. meas. 0-60532  
 ZnS film on Si, fused quartz substrates, H<sub>2</sub>O absorpt., IR anal. 0-75446  
 ZrO<sub>2</sub> thin film, optical props. rel. to cryst. struct. 0-97357

**refractive index measurement**see also *refractometers*

- Brewster angle determ. by dithered laser beam synchronous detection 0-73422  
 demonstration methods 0-77577  
 dielectric film, refractive index and thickness meas. by optical method 0-82806  
 dielectric films, thickness and refractive index meas. by photoelectric scanning 0-105606  
 diffused channel waveguides, direct index meas. 0-87562  
 ellipsometry data analysis aided by derivative plots in  $n_x$ -space 0-86378  
 fibre, single-mode, cutoff wavelength meas., using refracted power technique 0-99844



**refractive index measurement continued**

- film, nearly transparent, refractive index meas. method 0-68242  
 film optical parameters meas. method, reevaluation 0-104004  
 frozen gas matrix, refr. index determ. by emission spectrosc. 0-90884  
 glass fibre refractive index profile meas. using interf. microscope with freq. shift 0-64175  
 lightguide fibre testing 0-64230  
 liquid, determ. with cell differential refractometer, prism wedge angle effect on meas. error 0-62715  
 liquid, extinction coefficient meas. using coaxial dual channel laser system 0-73425  
 liquids, depend. on concentration at different wavelengths 0-88346  
 monomode fibre selective excitation for differential group delay meas. 0-99876  
 multilayered structure, refr. index difference between adjacent layers, meas. technique 0-101829  
 multimode fibre bandwidth computation from measured index profiles 0-58740  
 optical fibre,  $\gamma$ -irrad., differential interferometric meas. of refr. index changes 0-78952  
 optical fibre attenuation, bandwidth, and refractive index meas. methods compared 0-64190  
 optical fibre preform, refractive index profile and cross-sectional geometry meas. method 0-91893  
 optical fibre preform rod, refractive index profile meas. by transverse differential interferogram 0-64141  
 optical fibre preforms, axially nonsymmetric refr. index distrib., nondes- tructive meas. 0-106601  
 optical fibre preforms, using X-ray absorption measurements (*Japanese*) 0-87506  
 optical fibre profiling using scanning optical microscope 0-87535  
 optical fibre refracted near-field scanning, calibration technique 0-99823  
 optical fibre refractive index profile meas., near-field technique 0-91931  
 optical fibre refractive index profile microdensitometry 0-106632  
 optical fibres, index profile meas. 0-87538  
 optical fibres, measurement techniques for transmission loss and refractive index distribution (*Japanese*) 0-87498  
 tetrafluoroethane, specific refractivity, interferometric meas. 0-95124  
 tetrafluoromethane, specific refractivity, interferometric meas. 0-95124  
 thick planar films, transmission method for index meas., modal effects 0-102862  
 thin films, optical transmittance and reflectance, bulk optical props. determ. 0-88954  
 vacuum automatic ellipsometer for condensing film homogeneity determ. 0-101825  
 CdInGaS<sub>4</sub>, layered structure crystals, refractive index meas. method 0-98966  
 Cl<sub>2</sub>, quadrupole moment determ. by refr. index anisotropy meas. method 0-78722  
 HF in absorption, anomalous dispersion meas. 0-95881  
 He-Ne 3.39  $\mu$ m laser interferometer, length and refr. index meas. 0-68172  
 LiNbO<sub>3</sub>/Ti, planar and channel optical waveguides, anisotropic diffusion expts. 0-64200  
 light-focusing rod refr. index profile determ., Interphako interf. microscopy method 0-101832  
 Si wafers layers, multilayer ellipsometry, layer thickness and refr. index determination of layers 0-95121  
 SiO amorphous film, optical transmittance and reflectance, bulk optical props. determ. 0-88954  
 TiInS<sub>2</sub>, layered structure crystals, refractive index meas. method 0-98966
- refractivity** *see refractive index*
- refractometers**  
 Abbe-type, IRF-454, specification, testing method and facilities 0-73424  
 automatic vee block refractometer design for glass refr. index meas. 0-68243  
 biomedical, IRF-454 and IRF-456 models 0-104715  
 cell differential, for liqs., prism wedge angle effect on meas. error 0-62715  
 laser detector for anal. of liquids 0-101830  
 laser microrefractometer, temperature gradients in liquid, meas. 0-57362  
 optoelectronic refractometers, design, construction and quantitative charac- teristics (*Russian*) 0-62716  
 recording refractometer for optical glasses, 300 to 2600 nm range 0-57363
- refractometry** *see refractive index measurement*
- refractories**  
*see also ceramics; cermets; clay*  
 Bakor 33, refractory, stress relaxation capacity determ. 0-60910  
 borosilicate glass, powder, sintering, foaming by chemical reactions 0-81017  
 cemented carbides, fracture roughness testing 0-104410  
 ceramic coatings, for high temp. use, current status (*Japanese*) 0-71619  
 chamotte concretes, phosphate binder based, strength props. 0-89305  
 development from organosilicon polymers by heat treatment 0-81014  
 dolomite, powders sintering, decarbonisation cycle effect 0-104102  
 double oxides, thermodynamic obs. using galvanic cells with CaF<sub>2</sub> solid electrolyte (*French*) 0-85190  
 elastic moduli measurement, US method for up to 2000K (*French*) 0-104373  
 heat treatment of transformer steel, resistance of refractories in contact 0-66554  
 hot-wire test, critical review and comparison with BS 1902 panel test 0-104409  
 luminescence characteristics of pure surface acted on by flux of field emission electron 0-100695  
 magnesite, refractory concretes, cast. props. 0-89306  
 magnesite, powders sintering, decarbonisation cycle effect 0-104102  
 magnesite artifacts, roasted, props., filler porosity effect 0-104099  
 magnesite refractories, unfired, by resin phosphate binding 0-104101  
 magnesite-dolomite refractories, tar bound, fracture and wear 0-104287  
 metal-Ni(Pd)(Pt)/Si interactions, phase separation 0-65303  
 metals, group V, diffusion of O and N, statistical calcs. on Arrhenius lines 0-59722  
 oxide development for fusion reactor first walls, chem. environment effects 0-83221  
 periclase refractories, props. after testing at over 2000°C 0-104317  
 phosphate containing materials, technological prod. processes, review 0-97452  
 powders, brittle, shock wave disintegration test method 0-66744

**refractories continued**

- quartz sand, high-conc. suspension, prod. principles 0-66463  
 quartzite, vitrified, and quartzite based refractory concretes, prep. and props. 0-89188  
 radiant capacity, calorimetric meas. method 0-65259  
 rare earth chromite based electrode material development for MHD generators 0-84893  
 rare earth oxide containing systems, highly refractive, phase equilib. and metastable phases 0-97467  
 single crystal growth, techniques 0-108341  
 sputtered carbides, adhesion to metal substrates, improved 0-76481  
 strength and thermal properties, automated test system 0-100986  
 surfaces, heat of desorption of alkali metals 0-75430  
 thermal insulation, effective thermal cond., fibre diameter effects 0-104105  
 thermal shock behaviour (*French*) 0-81084  
 thermal stress cracking resistance estimation 0-104288  
 toughness measurement, expt. problems (*French*) 0-104368  
 transition metal silicides for integrated circuits, review 0-100820  
 transition metals and oxides, reactions of liq. alkali metals, relevance to reactor technology 0-85173  
 tridymite, thermal expansion meas. 0-59682  
 AlN films, RF reactive ion-plating, struct. and morphology 0-104074  
 AlN-Si<sub>3</sub>N<sub>4</sub>-Be<sub>3</sub>N<sub>2</sub> system, phase equilibria 0-60844  
 Al<sub>2</sub>O<sub>3</sub> compounds, shrink free, prod./method using slips made from clay, orthophosphoric acid 0-66460  
 Al<sub>2</sub>O<sub>3</sub>, elastic moduli meas., US method for up to 2000K (*French*) 0-104373  
 Al<sub>2</sub>O<sub>3</sub>, fracture, J-integral meas. 0-108537  
 Al<sub>2</sub>O<sub>3</sub>, sintering as function of phase comp. 0-66464  
 Al<sub>2</sub>O<sub>3</sub>, vacuum condensate, struct. and mech. props., second phase effect (*Russian*) 0-71705  
 Al<sub>2</sub>O<sub>3</sub>-SiO<sub>2</sub> refractory, creep, viscosity, resist. to inelastic deform. 0-89309  
 Al<sub>2</sub>O<sub>3</sub>-SiO<sub>2</sub> refractory concrete, elastic props. 0-89280  
 Al<sub>2</sub>O<sub>3</sub>-SiO<sub>2</sub>-ZrO<sub>2</sub> refractories, corrosion behaviour in glassmelting furnaces (*Polish*) 0-71783  
 Al<sub>2</sub>O<sub>3</sub>-ZrSiO<sub>4</sub>, granular corundum-zircon refractory, development 0-66462  
 B<sub>2</sub>C, densification kinetics during hot pressing, 1800-2200°C 0-60817  
 BN, contact reactions with Ti and WC-Co at high pressures 0-61029  
 BaHfO<sub>3</sub>, BaSnO<sub>3</sub> and BaZrO<sub>3</sub>, high-density ceramics prep. and elec. props. 0-60812  
 CaO based refractory from industrial lime, with 5% added electrocorun- dum 0-89184  
 CaO-MgO-Cr<sub>2</sub>O<sub>3</sub>-Al<sub>2</sub>O<sub>3</sub>-ZrO<sub>2</sub>-SiO<sub>2</sub> system, subsolidus region characts. 0-97466  
 CaSnO<sub>3</sub> and CaZrO<sub>3</sub>, high-density ceramics prep. and elec. props. 0-60812  
 Cr<sub>2</sub>C, electrophoretic alloy coatings on C steel, sintered, struct. form., Ni-P undercoat effect 0-61027  
 Cr<sub>2</sub>C, cathodic needle growth, at lower electric fields from Cr(CO)<sub>6</sub> vapour 0-76161  
 CrO<sub>2</sub> semidry refractory, struct. and mech. props., surface-active agents effect 0-89304  
 Cr<sub>2</sub>O<sub>3</sub> sintering behaviour, effect of TiO<sub>2</sub>, C additions 0-66461  
 Cr<sub>2</sub>O<sub>3</sub>-ZrO<sub>2</sub> granules, from spray drying of suspensions 0-104100  
 Cu-BN composite electromachining tools, dynamic hot pressing 0-84889  
 Fe oxides, phase equilibrium and microstructure interpretation 0-60847  
 Fe-Cr-Si, heat resistive films prepared by sputtering, lifetime meas. 0-80132  
 Fe-TiC pseudofused composite magnetoabrasive powders, props. 0-100926  
 HfO<sub>2</sub>, stabilised comps., elastic props. rel. to porosity and temp. 0-81096  
 LaB<sub>6</sub> (100), (110), and (111), surface structs. and work functions 0-70512  
 LaB<sub>6</sub> surfaces, (100), (110) and (111), electron states, UPS study 0-100752  
 LaB<sub>6</sub> synthesis by heating BN with lanthanum citrate hydrate 0-100819  
 La<sub>10</sub>W<sub>2</sub>O<sub>21</sub>, enthalpy and heat capacity at high temp. 0-70424  
 $\alpha$ -La<sub>2</sub>WO<sub>6</sub>, enthalpy and heat capacity at high temp. 0-70424  
 La<sub>2</sub>W<sub>2</sub>O<sub>21</sub>, enthalpy and heat capacity at high temp. 0-70424  
 MgAl<sub>2</sub>O<sub>4</sub> spinel refractory, enthalpy and specific heat determs. 0-88334  
 MgCr<sub>2</sub>O<sub>4</sub> spinel refractory, enthalpy and specific heat determs. 0-88334  
 MgO, sintered; refractories, props. after testing at over 2000°C 0-104317  
 MgO, sintering by activating 3MgCo, Mg(OH)<sub>3</sub>·3H<sub>2</sub>O 0-89183  
 MgO-CaO-FeO-Fe<sub>2</sub>O<sub>3</sub>-SiO<sub>2</sub>-Cr<sub>2</sub>O<sub>3</sub>-Al<sub>2</sub>O<sub>3</sub> spinel refractories, physicochem. prod. conditions 0-89185  
 MgO-NaCl refractory clinkers, Cr containing, densification, thermal treat- ment and phase composition effect (*French*) 0-76219  
 Mo<sub>2</sub>C, cathodic needle growth, at lower electric fields from Mo(CO)<sub>6</sub> vapour 0-76161  
 MoSi<sub>2</sub> film, elastic stiffness and thermal expansion coeffs. 0-107451  
 MoSi<sub>2</sub> refractory formation by As<sup>+</sup> ion beam bombardment 0-107286  
 Nb-Ir(Rh) system glasses, form., crystn. and microhardness, resist. obs. 0-89178  
 NbC fibre reinforced Ni-Cr, eutectic, unidirectional solidification, thermal cycling, temp. range effect on microstruct. 0-89272  
 NbC single cryst., Vickers microhardness, slip mechanism 0-71732  
 NbC, vacuum condensate, struct. and mech. props., second phase effect (*Russian*) 0-71705  
 Ni-Cr-NbC eutectic composite, unidirectional solidification, thermal cycling, temp. range effect on microstructural degradation 0-89272  
 NiTaC, eutectic alloys, chem. incompatibility of ceramic nitrides for direc- tionally solidifying 0-81046  
 Se<sub>2</sub>O<sub>3</sub>, liq. and solid phase elec. cond., high temp. meas. 0-84468  
 SiB<sub>12</sub>, thermam cond., temp. depend., up to 2000K (*French*) 0-70484  
 SiC, controlled nucleation thermochemical deposition, charact. and props. 0-83555  
 SiC, dense, joining by hot pressing, and bond strength 0-66458  
 SiC, fracture toughness and high-temp. slow crack growth 0-81153  
 SiC, HVEM obs. of various polytypes 0-76248  
 SiC microtubes, formation by carburisation of Si whiskers 0-81011  
 SiC, oxide scale microstruct. of oxidised single crystal 0-108613  
 $\beta$ -SiC, polycryst., <sup>31</sup>Si self-diffusion 0-100350  
 SiC polytypes, lattice imaging studies on intergrowth structs. 0-107025  
 SiC, pressureless-sintered, high temp. strength (*Japanese*) 0-104299  
 SiC, reaction-bonded, 'REFEL', microstruct. characterization 0-97490  
 $\beta$ -SiC, sintering, B transport and lattice parameter change 0-108370  
 $\beta$ -SiC, X-ray diffr. study of anisotropic layers in twinned seams 0-107274

# refractories continued

- SiC-AlB<sub>2</sub> (0.61 to 1.2 wt.%), hot pressed, microstruct. 0-93563  
 SiC-Si, wear resist., props. under abrasion and corrosion 0-100927  
 SiN film, elastic stiffness and thermal expansion coeffs. 0-107451  
 SiN powder formation, in high-temp. N flow (*Russian*) 0-100818  
 Si<sub>3</sub>N<sub>4</sub>, bending strength, deformability, elastic moduli and brittleness 0-81191  
 Si<sub>3</sub>N<sub>4</sub> film, elastic stiffness and thermal expansion coeffs. 0-107451  
 Si<sub>3</sub>N<sub>4</sub>, high-speed rolling bearings, fatigue strength 0-93655  
 Si<sub>3</sub>N<sub>4</sub>, hot-pressed, creep and strain recovery 0-100874  
 Si<sub>3</sub>N<sub>4</sub>, hot-pressed, fracture mech. parameters, indentation-precracking and double-torsion methods 0-104364  
 Si<sub>3</sub>N<sub>4</sub>, hot-pressed, fracture toughness determ. using specimens with chevron and straight through notches 0-108538  
 Si<sub>3</sub>N<sub>4</sub>, hot-pressed, strength anisotropy origins 0-89330  
 $\alpha/\beta$ -Si<sub>3</sub>N<sub>4</sub>, phase yields during form., influencing factors 0-108408  
 Si<sub>3</sub>N<sub>4</sub>, reaction bonded, post-sintering, injection moulding applications 0-68087  
 Si<sub>3</sub>N<sub>4</sub>, reaction-bonded, strength, effect of Si purity in production 0-100902  
 Si<sub>3</sub>N<sub>4</sub>, reaction-bonded, theoretical model of manufacture, effect of ambient reaction temp. and compact size 0-108379  
 Si<sub>3</sub>N<sub>4</sub>-MgO, hot-pressed, linear thermal expansion rel. to MgO content 0-70430  
 Si<sub>3</sub>N<sub>4</sub>-ZrO<sub>2</sub>, hot-pressed, compressive surface stresses developed by oxidation induced phase change 0-60992  
 Si<sub>3</sub>N<sub>4</sub>-CeO<sub>2</sub> additive, hot-pressing and oxidation behaviour 0-71618  
 Si<sub>3</sub>N<sub>4</sub>-SiO<sub>2</sub>-Y<sub>2</sub>O<sub>3</sub>, subsolidus phase relations 0-60845  
 SrSnO<sub>3</sub> and SrZrO<sub>3</sub>, high-density ceramics prep. and elec. props. 0-60812  
 Ta-Cr-Si-Al, heat resistive films, prepared by sputtering, lifetime meas. 0-80132  
 Ta-Ir(Rh) system glasses, form., crystn. and microhardness, resist. obs. 0-89178  
 Ta-Ta<sub>2</sub>O<sub>5</sub>-InP thin refractory MIS struct. deposition 0-75647  
 TaB<sub>2</sub>-Cr-Si-Al, heat resistive films prepared by sputtering, lifetime meas. 0-80132  
 TaC and Ta<sub>2</sub>C, self-propag. high-temp. synthesis 0-60815  
 TaSi<sub>2</sub> film, elastic stiffness and thermal expansion coeffs. 0-107451  
 TaSi<sub>2</sub> films, on polycrystalline Si, oxidation characts. 0-97602  
 TaSi<sub>2</sub> refractory formation by As<sup>+</sup> ion beam bombardment 0-107286  
 TiB<sub>2</sub>, TiC, vacuum condensate, struct. and mech. props., second phase effect (*Russian*) 0-71705  
 TiC coated WC-Co cemented carbides, fracture toughness 0-85046  
 TiC coatings, on cemented carbides, struct. and hardness 0-59771  
 TiC coatings on steels and hard alloys 0-76414  
 TiC, deform. at high temps. 0-104239  
 TiC, frictional characts. and contact-zone deform. in homogeneity range 0-66673  
 TiC, wetting by Cr-Ni-Mo-Mn alloy steel, expt. planning investigation 0-60822  
 TiC-(Mo-Cr-Ni-Mn) steel alloy, optimum comp. and manufacture conditions, Mn effect 0-84896  
 TiC<sub>2</sub>, nonstoichiometric, densification during sintering 0-84895  
 TiC<sub>2</sub>N<sub>3</sub>, powder preparation, physical, chemical props. (*Russian*) 0-76212  
 TiN formation, from TiO<sub>2</sub>/Si<sub>3</sub>N<sub>4</sub> reaction in N<sub>2</sub> atmosphere 0-71617  
 TiN, low-energy ion-stimulated deposited, supercond. props. 0-88664  
 TiO<sub>2</sub>-SiO<sub>2</sub>, multilayer vacuum coatings, optical props. 0-97361  
 TiSi<sub>2</sub> film, elastic stiffness and thermal expansion coeffs. 0-107451  
 TiW-TiO<sub>2</sub>-InP thin refractory MIS struct. deposition 0-75647  
 (U,Pu)C, sintering, role of Ni as sintering additive 0-84892  
 UC, sintering, role of Ni as sintering additive 0-84892  
 VC single cryst., Vickers microhardness, slip mechanism 0-71732  
 W, polycryst. surface, heat of desorption of Cs 0-75430  
 WC-Co, contact reaction with BN at high pressures 0-61029  
 WC-Co, STEM anal. of grain boundaries 0-79644  
 WC-Ni hard alloy composite, sintered, void healing 0-60821  
 W<sub>60</sub>Fe<sub>40</sub> glassy alloy, refractory, triode sputtered 0-75185  
 WS<sub>2</sub> film, elastic stiffness and thermal expansion coeffs. 0-107451  
 WS<sub>2</sub> refractory formation by As<sup>+</sup> ion beam bombardment 0-107286  
 Y<sub>2</sub>O<sub>3</sub>, liq. and solid phase elec. cond., high temp. meas. 0-84468  
 ZrO<sub>2</sub>, CaO stabilised, preferred slip system 0-66585  
 ZrO<sub>2</sub>, partially stabilized, props. and appl. to extrusion dies 0-97507  
 ZrO<sub>2</sub>, ZrB<sub>2</sub>, vacuum condensate, struct. and mech. props., second phase effect (*Russian*) 0-71705  
 ZrSiO<sub>4</sub>-Al<sub>2</sub>O<sub>3</sub> (SiO<sub>2</sub>) suspensions for slip casting, prep. and props. 0-104103

# refractory materials see refractories

# refrigeration

- see also cryogenics; freezing; low-temperature production  
 absorption chillers, solar-fired, capacity modulation 0-66952  
 absorption refrigeration machine driven by solar heat for air conditioning, math. modelling 0-76651  
 heat transfer by natural convection with simultaneous frosting on horizontal cylinders in a vertical array (*Japanese*) 0-58890  
 polarised target in high energy physics, horizontal dilution refrigerator with high cooling power 0-73372  
 red blood cell freezing, cryopreservation and refrigeration 0-67262  
 solar, exam. of dry absorption using CaCl<sub>2</sub>-NH<sub>3</sub> 0-61310  
 solar, isothermal dissociation and regeneration of CaCl<sub>2</sub>-NH<sub>3</sub> (*French*) 0-61300  
 solar energy cooling, operating systems and current developments, review 0-85265  
 solar installation for refrigeration and water heating, energy characts. 0-101124  
 He, automatic multirange liquefaction plant 0-57306  
 He liquefiers and refrigerators, cryogenics of Sulzer, Switzerland 0-82769  
 SrTiO<sub>3</sub> ceramic, electrocaloric effects for refrigeration at cryogenic temp. 0-77789

# refrigerators

- dilution refrigerator using centering device, performance characts. 0-77791  
 solar cooling, Rankine-cycle systems, selection of working fluids 0-104515  
 solar evaporation and refrigeration units, assurance of specified energy parameter values, statistical analysis 0-93848  
 solar heating and cooling system for domestic use (*Japanese*) 0-108787

# refrigerators continued

- thermoelectric cooling devices, maximum refrigerating capacity determ. 0-86318  
 N<sub>2</sub>O, thermodynamics and thermoelectric condenser design 0-108809  
 regenerative receivers see radio receivers  
 Regge poles and trajectories  
 $\phi_8^+$  theory, anomalous dimension, Regge cut effect on structure function 0-62847  
 bottomium, potential models, non-relativistic description 0-68426  
 charmonium, potential models, non-relativistic description 0-68426  
 complex energy spectra in Reggeon quantum mechanics with quartic interactions 0-102031  
 cylindrical mixing phenomena in dual topological unitarisation, pomerons, reggeons and gluonic states 0-86696  
 dispersion sum rules and exotic baryon resonances, reggeon scatt., E<sub>55</sub> resonance (*Russian*) 0-101955  
 dual topological expansion, Reggeon and Pomeron slopes 0-102032  
 hard processes, large rapidity separation of baryonic number, partons, and dual topology 0-95255  
 heavy ion+nucleus, orbiting quasimolecular system, nuclear-surface-wave interpretation 0-86914  
 heavy ion+nucleus scattering, Regge pole contrib., forward- and backward-angle, Coulomb and nuclear scatt. functions 0-57788  
 inclusive vector meson production in fragmentation regions of meson at small P<sub>T</sub> 0-105931  
 inelastic diffraction cross section, quark model and three reggeon limit 0-102035  
 interatomic potentials, Regge poles positions and residues, inverse power pots. 0-83439  
 large coupling expansions for eigenenergies and Regge trajectories of the general even-power potential with applications 0-86620  
 magnetic resonances between massive and massless spin-1/2 particles with magnetic moments 0-62895  
 mesons, mass spectrum and Regge trajectories from relativistic quasipot. eqn. (*Russian*) 0-73690  
 non-Abelian gauge theory with many flavours, high energy processes, asymptotical behaviour (*Russian*) 0-101935  
 P+f diffraction model, two component duality and flavouring, Regge fits and pomerons 0-95261  
 perturbation expansion of multichannel Regge poles 0-86623  
 pion exchange at high energies, review 0-95259  
 QCD, string constant, Regge slope and  $\Lambda$  parameter, empirical quarkonium approach 0-91053  
 quantum relativistic strings and the multiplicative dual model (*Russian*) 0-82958  
 quark fragmentation functions for inclusive hadron production, Regge formalism 0-68462  
 quarks, fermion field, nonlinear, origin of four quark flavours, quantum numbers, isosymmetry breaking 0-62920  
 Regge-pole approach to charmonium and bottomium 0-86697  
 Reggeon quantum mechanics with quartic couplings, energy spectrum struct. 0-62889  
 symmetries of 3j and 6j coeffs. 0-86621  
 three gluon integral equation and odd C singlet Regge singularities in QCD 0-101991  
 universal Regge slope  $\alpha'$  from the QCD gluon propagator 0-78026  
 Z(N) strings and hadron structure 0-86572  
 $\gamma p \rightarrow \pi^+ p$ , high energies, semiempirical amplitude anal. dispersion relations and Regge poles 0-86726  
 $K^- p \rightarrow \Lambda^0$ , 6 GeV/c, baryon exchange reactions,  $\eta$ NN coupling constant,  $\Lambda$  polarisation, nucleon-Regge exchange 0-78098  
 $K^- p \rightarrow \Lambda^0$ , 6 GeV/c, baryon exchange reactions,  $\eta$ NN coupling constant,  $\Lambda$  polarisation, nucleon-Regge exchange 0-78098  
 $K^- p \rightarrow \Lambda^0$ , baryon Regge exchange, FESR anal. 0-63022  
 $K^- p \rightarrow \pi^+ \Sigma^+$  and line reversed reaction  $\pi^+ p \rightarrow K^+ \Sigma^+$ , simple Regge pole model 0-78093  
 $K^- p \rightarrow \Sigma^+ \pi^- \pi^+$ , 4.15 GeV/c, nondiffractive A<sub>1</sub> production, double-Regge model 0-78097  
 $K^+ p$ , elastic scatt. and diffractive dissociation, Regge model with  $\alpha_p(0) > 1$  (*Russian*) 0-57630  
 $K^+ p \rightarrow K^+ X$ , triple Pomeron coupling, Reggeon treatment 0-68488  
 np elastic scatt., 70-400 GeV/c, cross sections, simple Regge pole model 0-63032  
 np $\rightarrow$ px, baryonium exchange, triple-Regge couplings 0-86763  
 pp, pp, elastic scatt. and diffractive dissociation, Regge model with  $\alpha_p(0) > 1$  (*Russian*) 0-57630  
 pp, smooth interpolation between Orear- and fixed angle scaling behaviour of the scattering amplitude 0-105873  
 pp $\rightarrow$ cX, pc exotic, triple-Regge formalism, Pomeron exchanges 0-63041  
 pp $\rightarrow$ nX, baryonium exchange, triple-Regge couplings 0-86763  
 pp $\rightarrow$ pp, polarisation structure and Pomeron flip, Regge pole model 0-102073  
 $\pi N$  charge exchange scatt., Regge pole, model calcs. 0-102071  
 $\pi N$  invariant scattering amplitudes, zero trajectories 0-102067  
 $\pi N \rightarrow \pi N$ , finite-energy sum rules, three component duality 0-82996  
 $\pi^- n \rightarrow p X^-$ , 21, 205 and 360 GeV/c, reggeised one-pion-exchange 0-57649  
 $\pi^- p \rightarrow \eta n$ , Regge pole model with phenomenological residue functions 0-102077  
 $\pi^- p \rightarrow p X$ , 12 GeV/c, absorbed Mueller-Regge model for backward inclusive p prod. 0-73752  
 $\pi^- p \rightarrow \pi^- X$ , triple Pomeron coupling, Reggeon treatment 0-68488  
 $\pi^- p \rightarrow \rho^0 \pi^- X$ , diffractive contrib. in multi-Regge factorisation 0-73753  
 $\pi^+ p \rightarrow K^+ \Sigma^+$  and line reversed reaction  $K^- p \rightarrow \pi^- \Sigma^+$ , simple Regge pole model 0-78093  
 $\pi^+ p$ , elastic scatt. and diffractive dissociation, Regge model with  $\alpha_p(0) > 1$  (*Russian*) 0-57630  
 Reggeon field theory  
 non-Abelian gauge theories, high energy behaviour, reggeon field theory, QCD 0-62822  
 O(e<sup>2</sup>) scaling law for d $\sigma$ /dt in the Reggeon field theory 0-101936  
 Reggeization of elementary fermions in arbitrary renormalizable gauge theories 0-68367  
 Reggeon quantum mechanics with quartic couplings, energy spectrum struct. 0-62889  
 relativistic hadron, parton distrib. and Regge field theory parameters (*Russian*) 0-62931  
 region of escape see exosphere  
 regulators see controllers



**Rehinder effect** *see* **mechanical properties of substances; surface phenomena**

**relative density** *see* **density**

**relative humidity** *see* **humidity**

#### relativistic band structure calculations

- APW method, linearised relativistic using approx. pure spin basis functions 0-70581
- crystal slab, 3-D, surface states, relativistic Green matrix method, muffin-tin potential 0-80345
- pseudopotential, norm-conserving, relativistic corrections 0-70584
- Au, energy band structure, X-ray N-emission spectra, relativistic APW calcs. 0-70596
- Au, self-consistent relativistic band struct. 0-75501
- HfC<sub>2</sub>N<sub>2</sub>, X-ray valence photoelectron spectrum, 4f signal calcs. 0-66391
- TiCl<sub>3</sub>, ground-state props., Wannier functions, and electronic struct., ab initio self-consistent calc. 0-80178
- U compounds, NaCl struct. type, relativistic energy bands, LMTO calcs. 0-65442
- U,Th<sub>1-x</sub>As (Sb), electronic struct., relativistic KKR-averaged T-matrix approx. method 0-107702

#### relativistic corrections

- see also* **Lamb shift**
- 1S Lamb shift and 1S-2S isotope shift 0-91464
- approximate relativistic Hartree-Fock eqns., soln. using Slater-type functions 0-58168
- atomic photoionisation anal. using relativistic random phase approximation and multichannel quantum defect theory 0-63602
- atoms,  $70 \leq Z \leq 82$ , K $\alpha$  X-ray linewidths and relative intensities, energy dispersive meas. 0-99483
- atoms, analytical relativistic SCF calcs. 0-83248
- atoms, Hiller-Sucher-Feinberg identity, generalisation, accuracy for approx. wavefunctions 0-63512
- atoms, relativistic energies, perturbation calcs. 0-102453
- channelled relativistic particles emission spectrum, rel. to interplanar pot. 0-65115
- chemistry and relativity, anomalous chemical properties of elements due to high speeds of inner electrons (*French*) 0-93839
- clock synchronisation, India-W.Germany, relativistic corrections 0-95077
- closed-shell atoms, approximate relativistic Hartree-Fock eqns., soln. using Slater-type functions 0-58168
- closed-shell linear molecules, relativistic Dirac-Fock multiconfig. SCF calcs. 0-99455
- closed-shell polyatomic molecules, relativistic Dirac-Fock multiconfig. SCF calcs. 0-99456
- diametric molecules, nucleus-nucleus interaction, Einstein relativistic correction, Born-Oppenheimer approx. 0-91463
- heavy elements, covalent bonding relativistic corrections, kappa valence method 0-91461
- high-Z elements subshells, photoelectron angular distribution 0-99487
- hydrogenic ions, electron capture by charge particles at relativistic energies 0-102565
- Klein-Gordon equation, time-independent, relativistic Stark effect, resonances 0-62890
- many-electron atoms, foundations of relativistic theory, Hamiltonian H<sub>+</sub> and h, and related relativistic HF eqn. derivation 0-99458
- methylene, singlet-triplet excitation energy, relativistic correction 0-69059
- molecules, relativistic Dirac-Fock multiconfig. SCF calcs. 0-99455
- molecules containing heavy atoms, program for calc. electronic struct. by quasirelativistic method 0-69088
- Mossbauer atoms, electron densities at nuclear centre and surface, calcs. using Dirac-Fock eqn. 0-74100
- multicharged ions, transitions between energy levels in strong external field, relativistic calcs. (*Russian*) 0-63547
- multiply charged ions,  $2p_{1/2}3p_{3/2}$  config., level widths, relativistic calc., S-matrix method 0-63546
- one-electron polynuclear systems, Dirac eqn., variational soln. 0-83242
- open-shell molecules, relativistic self-consistent field theory 0-95518
- photoelectron ang. distrib. and spin polarisation, theory 0-91618
- pseudopotential theories and corrections to Hartree-Fock method 0-63523
- Zeeman effect, linear, in Coulomb field 0-102484
- Ag, valence-core electron exchange interactions, local approx. 0-91416
- AgBr, vapour, photoelectron spectrosc., interpretation 0-95679
- AgCl, vapour, photoelectron spectrosc., interpretation 0-95679
- AgI, vapour, photoelectron spectrosc., interpretation 0-95679
- Au<sub>2</sub><sup>+</sup>, ab initio SCF calcs. using relativistic effective core pot. 0-95524
- Cd, electron binding energy and shift, core level XPS 0-87088
- D, 1S Lamb shift and 1S-2S isotope shift 0-91464
- FeBr<sub>2</sub>, transient species, He(I) photoelectron spectrosc. calcs., relativistic corrections 0-95677
- H, infinitely magnetised, ground state relativistic corrections 0-77282
- H, photon emission, Bohr theory covariant eqns., teaching 0-105482
- H, relativistic energy levels in strong mag. fields 0-102454
- H<sub>2</sub>, relativistic Dirac-Fock multiconfig. SCF calcs. 0-99455
- Hf IV, 6s <sup>2</sup>S<sub>1/2</sub>-6p <sup>2</sup>P<sub>1/2,3/2</sub> transition, relativistic oscillator strengths, influence of core polarisation 0-58132
- Hg atoms, elastic electron scatt., relativistic effects 0-102568
- Hg, electron binding energy and shift, core level XPS 0-87088
- Hg, positron scatt. at low energy 0-91670
- Li, isoelectronic sequence, self-consistent relativistic density-functional theory 0-91441
- LiH, relativistic Dirac-Fock multiconfig. SCF calcs. 0-99455
- Lu III, 6s <sup>2</sup>S<sub>1/2</sub>-6p <sup>2</sup>P<sub>1/2,3/2</sub> transition, relativistic oscillator strengths, influence of core polarisation 0-58132
- Lw, ground state config., relativistic prediction, multiconfig. Dirac-Fock calcs. 0-106277
- PbS(PbSe), ab initio SCF calcs. using relativistic effective core pot. 0-95524
- Pd<sub>2</sub>, ab initio relativistic core pot. studies of metal-metal bonding 0-106257
- PdH, ab initio relativistic core pot. studies of metal-H bonding 0-106257
- Pt<sub>2</sub>, ab initio relativistic core pot. studies of metal-metal bonding 0-106257
- PtH, ab initio relativistic core pot. studies of metal-H bonding 0-106257
- Rb, valence-core electron exchange interactions, local approx. 0-91416
- Sn, internal conversion coeffs. for inner shells of atomic ions and relativistic ionic potentials 0-68600
- TeCl<sub>2</sub>, transient species, He(I) photoelectron spectrosc. calcs., relativistic corrections 0-95677

#### relativistic corrections continued

- Tl, oscill. strengths, semiempirical relativistic one-electron central field, model pot. calcs. 0-78575
  - TiH, ab initio SCF calcs. using relativistic effective core pot. 0-95524
  - <sup>92</sup>U, self-consistent relativistic density-functional theory 0-91441
  - UF<sub>6</sub>, relativistic scattered wave calculations 0-63538
  - Yb II, 6s <sup>2</sup>S<sub>1/2</sub>-6p <sup>2</sup>P<sub>1/2,3/2</sub> transition, relativistic oscillator strengths, influence of core polarisation 0-58132
  - Zn, electron binding energy and shift, core level XPS 0-87088
  - Zn XX, energy levels and one electron transitions, relativistic calculations 0-87051
- #### relativistic electron beam tubes
- cylindrical relativistic diode, space charge limited, voltage distrib. and current calc. 0-63437
  - electrically pumped relativistic free-electron wave generators 0-91742
  - EM waves generation and amplification based on Doppler effect 0-63902
  - guiding props. improvement using thin insulated wire 0-74291
  - intense relativistic electron beam generation by foils diodes, simulation 0-63438
  - waveguide containing relativistic electron beam, slow cyclotron wave 0-106983

#### relativistic fluid dynamics

- adiabatic blast wave, gas and cosmic ray acceleration 0-67534
- Bianchi universes, magnetic fields and fluids with conductivity 0-83864
- constrained minimum energy problem in relativistic MHD 0-92238
- Eckart's relativistic temp. gradient 0-103080
- elastic media, dissipative, relativistic electrodynamics 0-73219
- gas, dissociating, relativistic flows, growth and decay of weak waves, shock wave formation 0-69949
- gas dynamics in two dims. 0-83863
- magnetofluid, relativistic, and space-like conformal mappings 0-75001
- magnetofluid dynamics, eqns. of motion for charged particle and charged fluid 0-87821
- perfect fluids flow through channels, self similar solns. and stability rel. to radio galaxies 0-62006
- propagation of the general relativistic blast wave 0-105549
- quantum relativistic hydrodynamics, nonlinear generalised equations 0-68380
- radio sources, formation of knots in relativistic flows as model for compact synchrotron sources variability 0-105369
- shock wave propagation in general relativity, stationary approx. 0-86172
- shock waves, anal. approaches (*French*) 0-96317
- shock waves, plane, relativistic, propag. in slowly moving medium 0-62005
- spherically symmetric relativistic flows, comoving-frame radiative transfer eqn. soln. 0-82181
- suspensions, nonstationary motion in grav. field, volume conc. effect (*Russian*) 0-75002
- variational principle for perfect and imperfect fluids in general relativity 0-90733
- vibrationally relaxing fluid, growth and decay of weak discontinuities 0-69948
- viscous fluids, nonstationary relativistic thermodynamics, hidden variable approach 0-68097

#### relativistic mechanics

- see also* **relativistic fluid dynamics**
- angular scattering of spinor charged particles by a Kerr-Newman field 0-94996
- charge particle free fall acceleration, relation with observed velocity 0-73170
- charged particles, motion in relativistic fields 0-57146
- contraction of metric standards 0-82638
- Dirac Lorentz's equations, relativistic and nonrelativistic, maximally extensive local group of invariance 0-77946
- elastic rotating cylinder, general relativistic formulation 0-82642
- Euclidean space, Galileo transformation 0-62467
- Fokker type relativistic mechanics, single time form with Lagrangian 0-90665
- Fokker type relativistic mechanics, single time Lagrangian form, symmetries, conservation laws 0-90666
- free fall acceleration 0-90672
- gyroscopic weight reduction in left turning due to spontaneous symmetry breaking (*Japanese*) 0-98798
- DI Herculis, eclipsing binary, relativistic motion of periastron 0-94830
- interacting particles, two, Galilei-compatible nonconstrained Hamiltonians 0-73169
- magnetisable media, relativistic models, and energy-momentum tensor of EM field (*Russian*) 0-86180
- mechanical oscillator, relativistic spin quadrupole gravitational effect (*Russian*) 0-68103
- motion in a plane, teaching 0-101686
- Poincare-Cartan integral invariant and canonical transformations for singular lagrangians 0-94956
- polarisable media, relativistic models, and energy-momentum tensor of EM field (*Russian*) 0-86180
- rheometric structure theory, connective differentiation and continuum electrodynamics 0-86087
- rotating systems, Einstein equations 0-68101
- spinning test particle in the manifold of the reference frames 0-62548
- stochastic particles 0-82639
- string moving in uniform static external field, 2-D space-time surface 0-57087

#### relativistic plasmas

- anisotropic plasma, relativistic MHD 0-92380
- Boltzmann theory, reduction of collision integrals 0-79560
- colliding relativistic plasma instabilities with relativistic temps. (*Russian*) 0-83913
- electron beam, inhomogeneous, space charge oscils. 0-78759
- electron magnetised plasma, stability in circularly polarised EM wave field 0-87897
- electron-positron plasma, EM waves, nonlinear generation (*Russian*) 0-106973
- EM wave dispersion relations from hydrodynamical eqns. 0-79559
- EM waves propagating along mag. field in strongly anisotropic relativistic plasma, dispersion props. 0-67542
- excitation spectrum of relativistic quantum plasma, covariant Wigner function approach 0-87938
- magnetoeactive plasma, low frequency waves excitation, relativistic effects (*Russian*) 0-103184
- MHD growth and decay discontinuities 0-92280

relativistic plasmas continued

MHD symmetric flow, eqn. of motion (*Russian*) 0-83992  
modulational instability of nonlinear wave propagation in relativistic plasmas 0-106911  
motion of relativistic charged particle in axisymmetric toroidal system 0-83991  
nonlinear dispersion relation for transverse wave 0-87939  
radio sources, compact, extragalactic, synchrotron and relativistic Maxwellian source models rel. to spectra 0-62299  
resistive hose instability in relativistic electron beam 0-67947  
stochastic heating, relativistic electron generation (*Russian*) 0-83952  
tearing instability in background plasma, relativistic modes 0-62012  
waveguide, rectangular, filled with uniaxial anisotropic relativistic warm plasma, EM wave propag. and attenuation 0-59246

relativistic quantum field theory

4-atomism, theory 0-94967  
 $\lambda\phi^{(4,6)}$  field theory in curved spacetime 0-86556  
 $\lambda\phi^4$  field theory: at finite temp., Casimir effect and topological mass 0-57479  
 $\lambda\phi^4$  self interaction theory, symmetry breaking and mass generation by space-time topology 0-82892  
 $\lambda\phi^4$  theory, conformal symmetry breaking, cosmological particle creation 0-90998  
 $\lambda\phi^4$  theory, renormalisation in nonsimply connected spacetime 0-90999  
 $\sigma$ -model, nonlinear, curved space, spontaneous compactification, Grassmann manifold 0-57467  
acceleration through random classical radiation, thermal effects 0-73191  
Backlund transformation in the classical massive Thirring model 0-57456  
Bianchi type-I cosmologies and spinor fields 0-62347  
Breit equation, Klein paradox 0-57506  
canonical momenta, transformation props. 0-105765  
causality of a wave equation and invariance of its hyperbolicity conditions 0-91000  
charge conservations as concomitant of conformal motions coupled to gauge transforms 0-62835  
composite system, relativistic, light-front wave functions 0-73592  
conformally flat spaces and solutions to Yang-Mills equations 0-57481  
coordinate measurements and operators 0-57458  
covariant derivatives without gauge fields 0-73584  
de Sitter invariant Lagrangian 0-82868  
Dirac Lorentz's equations, relativistic and nonrelativistic, maximally extensive local group of invariance 0-77946  
Dirac particle+two Klein-Gordon particles, relativistic three-body wave equation, preon model 0-73574  
Dirac propagator from path integral quantization of the pseudoclassical spinning particle 0-86577  
directly interacting relativistic particles, positive energy dynamics and scatt. theory 0-82921  
discrete symmetries for scalar and spinor fields in curved space-time 0-68387  
Einstein vacuum and Einstein-Maxwell space-times, infinitesimal holonomy group structure and geometrization 0-73252  
elementary particle modeling in axiomatic relativistic field theories (*German*) 0-91009  
energy-momentum quantised field tensor vacuum means 0-73227  
Euclidean Dirac field, local structure, Green's function method 0-68347  
extended phase space, classical fields 0-86550  
extended phase space, unified meson fields 0-86551  
extended phase space, unified spin 1/2 fields 0-86552  
fiber bundles, sheaf theory, and generalization of differentiable manifolds in physics 0-57459  
Fierz-Pauli field theory, smooth massless limit 0-62843  
finite temp. field theory with boundaries, extensions to curved space, stress tensor and surface action renormalisation, review 0-57455  
free massless scalar field in two-dimensional space-time: revisited 0-105798  
Goldstone theorem generalisation, scalar fields, conserved current and mass spectra struct. 0-68339  
gravitational field and arbitrary gauge field, equations of motion, Heisenberg and classical, force term, spin-curvature coupling 0-57158  
gravity, boson field, equal-time commutator, general relativity, indefinite-metric 0-68119  
hadrons, extended, Lorentz deformation props.,  $O(4)$  and light-cone coordinate systems 0-68354  
Heisenberg Klein Gordon eqn., soln. in space time of const. curvature 0-62829  
kinks and cobordism in field theories, general relativity fermions 0-98835  
Klein-Gordon particles+Dirac particle, relativistic three-body wave equation, preon model 0-73574  
Lagrangian formulation, conservation laws, relativistic gravitation (*Russian*) 0-68337  
large Numbers, explanation via classical unified theory 0-57166  
left-flat space-times, null tetrad and restrictive conditions 0-62545  
light velocity in vacuum, quantised space, special relativity and relativistic field theories 0-82869  
linearization of relativistic nonlinear wave equations 0-62837  
Lorentz basis of quantum fields 0-86565  
low-frequency solutions of the wave equations in Schwarzschild space 0-90743  
Luttinger model, thermodynamic correlation functions, bosonisation of fermion field 0-68356  
 $M_4$  factorisation, spinor algebra, Dirac equation geometrical, interpretation 0-62838  
massive particle production in anisotropic space-times 0-90583  
massive spin-1 particles in external symmetrical tensor field, quantisation and noncausality 0-105790  
massless Euclidean Thirring field, four point Schwinger function, Lorentz group invariant forms (*German*) 0-90980  
massless particle fields, arbitrary spin, Lorentz transformation laws (*French*) 0-62823  
Maxwell-Klein-Gordon fields in (2+1) dims. Minkowski space-time 0-99038  
Minkowski-space formulation of two-pseudoparticle processes 0-95220  
Nelson's stochastic field, tensor field quantisation 0-105574  
neutrino, Weyl, nonlocal position and momentum operators 0-73586  
noninstantaneous  $O(p/c)$  relativistic effects in bound states and a covariant Schrödinger equation 0-73607  
nonpolynomial scalar interactions in four dims., bounded interactions 0-82895

relativistic quantum field theory continued

nonpolynomial scalar interactions in four dims., quartic interaction 0-82894  
null infinity and Killing fields, local isometries, space-times, asymptotic conditions 0-62832  
order, disorder and generalized statistics 0-99055  
particle production by white holes 0-82891  
physical states and observables, relativistic microcausality constraints 0-86589  
Poincare group, mass zero representation extensions 0-57500  
Poincare group representations, momentum and position variables, complete decomposition theory 0-62511  
positronium, relativistic two-fermion equations with instantaneous potential 0-101918  
potential interaction using a metric space 0-82879  
propositional systems in local field theories 0-105799  
QCD, two-dims. with massless fermions in 1-1 dimensions 0-62926  
QED, massless, energy-momentum tensor anomalies in spherical space-time 0-73628  
quadratic lagrangians in a space with torsion and the theory of the spinor gauge field 0-91006  
quantum stress energy in nearly conformally flat spacetimes 0-57170  
regularity constraints and quantised actions 0-73601  
relativistic quantum theory with correct conservation laws 0-82677  
relativistic two fermion equations, Lorentz, parity and charge conjugation invariance 0-90976  
relativistic wave equation and mass spectrum of gluonium 0-73596  
relativistic wavefunctions, approx. near turning point, WKB calcs. for  $Z>137$  0-86598  
Robertson-Walker universe, adiabatic regularisation, arbitrary coupling of scalar field to scalar curvature 0-57461  
rotating system, finite temp. QFT 0-73599  
Schwarzschild-Kruskal space-time, role in developing Maxwell field nonzero vacuum expectation value 0-62828  
self dual SU(2) fields in multicentre spaces 0-73600  
self-dual SU(2) fields in Eguchi-Hanson space 0-57483  
sine-Gordon equation, intrinsic geometry 0-86553  
sine-Gordon equation, supersymmetric, prolongation struct. inverse scatt. formalism 0-99032  
singular state problems, monopole pair energy levels, charged monopole-electron system (*Chinese*) 0-101733  
solitons, charged, stability, relativistic complex scalar field, direct Lyapunov method 0-62827  
space-time, foam-like structure, Bjorken scaling violation due to gravitational field 0-77939  
spin 1/2 fields, tensor description 0-86597  
spin particles, relativistic and Galilean wave eqns. 0-82672  
spinning solutions of classical Yang-Mills theory 0-101937  
spinor models, integrability in two-dims. space-time 0-77935  
SU(2|1) electroweak interactions, implications for 6 extra time dimensions 0-77998  
SU(2) dual charges, 4-D space of constant curvature (*Chinese*) 0-68392  
supersymmetric Dirac particles in external fields 0-82918  
supersymmetry as means to unified field theory 0-91040  
symmetry breakdown and bundle representations of relativity groups 0-86610  
Thirring model, chiral,  $CP^{n-1}$  and  $SU_n$ , exact S-matrix 0-90985  
Thirring model, massive, mass independent renormalisation, dimensional regularisation 0-57463  
twisted scalar and spinor strings in Minkowski spacetime 0-57480  
unified field theories, relativistic, computer field interaction simulation system 0-68412  
vacuum definition in curved space-time 0-73613  
vacuum polarization in a nonsimply connected spacetime 0-57531  
vacuum spacetimes, stationary and axially symmetric, homogeneous Hilbert problem, Kinnerley-Chitre transformations 0-68349  
wave eqns., second-order, causal propagation 0-90986  
wave equation in curved space-time, compact and noncompact sources 0-73571  
Yang-Mills configuration constraint 0-82903  
qq spectra, heavy systems, equaltime relativistic wave eqn. with confining potential 0-77977  
H atom, Dirac and Klein-Gordon relativistic eqns., energy level splitting 0-77938

**relativistic scattering theory**  
*see also elementary particle scattering: quantum field theory of elastic scattering*  
Breit equation, Klein paradox 0-57506  
centre of mass covariant separation for relativistic interacting particles (*Russian*) 0-62891  
directly interacting relativistic particles, positive energy dynamics and scatt. theory 0-82921  
discrete two-variable expansions of scattering amplitudes for particles with spin 0-68397  
eikonal and sudden approx., Moller operators and superoperators 0-86624  
electron+monopole, scatt. through small angles, Dirac-Schwinger monopole 0-68398  
Faddeev equation, product integration, choice of point, convergence 0-68396  
generalised Pade approximation, explicit solns. 0-73623  
Glauber model and time reversal invariance 0-91020  
inverse scattering problem in the eikonal approximation (*Russian*) 0-57522  
Klein-Gordon equation, time-independent, relativistic Stark effect, resonances 0-62890  
mean multiplicity of secondary particles in hadron-nuclear interactions, multiple scatt. theory (*Russian*) 0-68502  
multipartite dynamics, cluster models, Faddeev-Yakubovskii coupling 0-105816  
quasipotential scattering amplitude, analytic props. in complex planes of rapidity and angular momentum 0-68399  
square well potential, separable representation 0-82922  
three hadron systems, resonance peaks, Brayshaw mechanism validity 0-73732  
three-body scattering equations, nonsingular representation, partial-wave anal. 0-91021  
total cross sections, asymptotic upper bound 0-105938  
two point particles, relativistic interaction, singular Lagrangian approach 0-73622



**relativistic scattering theory continued**

- two- and three-particle scatt. for relativistic systems in light front dynamics (*Russian*) 0-62892
- ed elastic scatt. at high momentum transfer 0-82977
- K p, backward elastic scattering, backward differential cross section 0-63024
- K<sup>+</sup>p→K<sup>0</sup>π<sup>+</sup>p, 4.2 GeV/c, multichannel anal. 0-73736
- K p→Σ<sup>+</sup>π<sup>+</sup>, backward differential cross section 0-63024
- pp high energy annihilation in nuclei, multiple scattering models 0-102079
- πd, bound states, scatt. in light front field theory dynamics 0-68477
- πd, relativistic Faddeev calc. 0-102066
- πN, partial wave analysis, S- and P-wave scatt. lengths 0-63019
- π<sup>+</sup>N, in <sup>12</sup>C, 40 GeV/c, one- and multi-nucleon interactions, secondary charged particle multiplicity (*Russian*) 0-83013
- π<sup>+</sup>N in Ne, 25, 50 GeV/c, secondary particle multiplicity and multiple scatt. model anal. (*Russian*) 0-83014
- πNN dynamics, Faddeev approach, 0-1200 MeV pp scatt. 0-57625
- π<sup>+</sup>p, elastic and charge-exchange scatt., partial wave anal., Δ resonances 0-63018
- ππ interactions, dominant resonances, pole positions, partial waves 0-63020

**relativity**

- see also general relativity; light cones; relativistic mechanics; relativistic quantum field theory; relativistic scattering theory; special relativity*
- overtun and continuity of the hypotheses in the framing of the theory of relativity 0-90674
- Planck, Max Karl Ernst Ludwig (1858-1947), quantum and relativity theories 0-68008
- vector laws of physics, reformulation 0-68036

**relaxation**

- for dislocation relaxation see dislocation damping*
- see also anelastic relaxation; chemical relaxation; dielectric relaxation; magnetic relaxation; stress relaxation; ultrasonic relaxation; viscoelasticity*
- noise, 1/f, superposition of relaxation spectra 0-105575
- rate processes in condensed media, master eqns. 0-77687
- Z discharge relaxation between electrodes 0-75089
- CaF:Eu(Gd)(Dy)(Tb), dimer reorientation activation volume 0-107285
- Fe-Ni-P-B, metallic glasses, struct. relax., annealing effects on mag. props. 0-89261
- <sup>4</sup>He, superfluid, flows, healing and relaxation comparison with Khalatnikov-Lebedev theory 0-107587

**relaxation oscillators**

- polymer melt relaxation oscillators (*French*) 0-79361
- symbolic dynamics and relaxation oscillations 0-90719
- van der Pol oscillator, RPA for linewidth 0-68138

**relaxation time, carrier *see carrier relaxation time*****relay control**

- radiation counting rate meter output at threshold, fluctuation and arrival shift by computer simulation 0-106240

**relay protection**

- see also circuit breakers*
- TFTR pulsed loads, AC electrical distribution system protective relaying 0-63387

**relay systems (radio) *see radio links*****relay systems (satellite) *see satellite relay systems*****relays**

- see also reed relays; switches*
- bistable optical fibre switch, construction and performance 0-95994
- gamma spectrometer supply, simple attachment 0-57447
- radioisotope, operation, construction and appl. (*Polish*) 0-106129

**relays (repeaters) *see repeaters*****reliability**

- see also quality control; standards; testing*
- accident at Three Mile Island, lessons learned 0-57929
- Al<sub>0.5</sub>Ga<sub>0.5</sub>As/Al<sub>0.5</sub>Ga<sub>0.5</sub>As heterostructure lasers, prep. characts., and CW reliability 0-58586
- astronomical X-ray telescope, HEAO-2 Observatory, protective design considerations, system reliability 0-61983
- ceramic multilayer capacitors, fracture mechanics approach to structural reliability assessment 0-89328
- computerised nuclear reactor protection systems, reliability anal. using Markov methods 0-91229
- electric insulating oils, composition, physical and chemical props. and determ. of free radicals (*Rumanian*) 0-97745
- equipment reliability under vibration, testing by simulated vibrations, expt. problems 0-58855
- exponential distribution MTBF confidence limits determ. using Epstein and Harters methods 0-98790
- fibre splicing, arc fusion, protection methods 0-69565
- fission reactor auxiliary feedwater systems, fault tree anal. 0-63332
- fission reactors, BWR decay heat removal systems, probabilistic risk assessment, fault and event tree anal. 0-63333
- fission reactors, failure probability distrib. from observed failure data, beta distrib. 0-63335
- fission reactors, operator reliability, Weibull distrib. model 0-63336
- fission reactors, shutdown heat removal systems, reliability fault tree anal. and β-factor method 0-63331
- fossil fuel utilisation, reliability engineering appls. 0-61234
- fusion reactor, BBC CQK 200-4 modulator tube for sustaining neutral beam power supply 0-99290
- lightguide fibre, ensuring mechanical reliability 0-79001
- liquid crystal display elements, principles and applications (*German*) 0-86277
- LMFBR cooling systems 0-57838
- log-normal device optimal burn-in time 0-58743
- metallic structures initial fatigue quality characterisation using equivalent-initial-flaw-size distribution 0-58978
- microcantilever electrostatic deflection system for transmission optical modulator array 0-87512
- micrometer, assessment method (*Rumanian*) 0-68175
- nuclear power engineering materials certification testing for reliability 0-78360
- nuclear power stations, availability of redundant safety systems with common-mode and undetected failures 0-91230
- nuclear power stations, probabilistic methods, safety assessment, Fed. Rep. Germany 0-106124

**reliability continued**

- nuclear power stations, probabilistic methods in safety analysis and regulations in France 0-106123
  - nuclear power stations, structural reliability, conference, Berlin, Germany (Aug. 1979) 0-105422
  - nuclear power stations, unavailability of systems under periodic test and maintenance 0-95368
  - nuclear power stations (*Portuguese*) 0-68844
  - optical fibre cable reliability, deterioration factors, splice point reliability, coating materials, static fatigue life (*Japanese*) 0-99848
  - optical fibre characterisation techniques compared 0-64202
  - optical fibre splicing, connecting and sheath jointing (*Japanese*) 0-87497
  - optical fibre transmission system planning (*French*) 0-87551
  - optical fibres, compound glass, nylon-covered, reliability and verification tests and results (*Japanese*) 0-99866
  - optical fibres, mechanical strength reinforcing and reliability improvement methods of fabrication (*Japanese*) 0-87568
  - photovoltaic modules testing, reliability and performance 0-94063
  - photovoltaic power system reliability assurance methods 0-61315
  - plastic encapsulated and hermetic modules corrosion model 0-100937
  - PWR vessel and primary circuits estimation of reliability, probabilities and adaptive models 0-106125
  - solar, hotwater and heating systems, availability aspects 0-61314
  - solar cell arrays, flat plate PV modules, elec. and environmental testing requirements for terrestrial appls. 0-61368
  - solar cell device reliability estimation using noise spectral density meas. 0-93896
  - solar photovoltaic power systems for rural areas of developing countries, technology, reliability, economics and appls. 0-61286
  - system reliability in face of human (operator) errors, bibliography 0-94940
  - transmission system, semiconductor device reliability tests 0-58573
  - turbogenerators, high capacity, heating reduction measures for enhanced reliability and interval between maintenance (*Russian*) 0-96175
  - underground nuclear waste repositories, risk assessment using reliability models 0-57898
  - vacuum beam diodes, repetitively pulsed 0-63386
  - welded structure reliability estimation, acoustic emission signal appls. 0-93702
  - wind power plant development, low cost approach 0-61268
  - wire fatigue properties, fast testing method using 23 kHz US frequency 0-89460
  - X-ray diffraction powder patterns, indexing reliability 0-87990
  - Ga<sub>1-x</sub>Al<sub>x</sub>As visible diode lasers; degradation due to macroscopic defects (<730 nm) and facet oxidation (>740 nm), life tests 0-99729
  - He-Ne gas lasers, 2 mW and 5 mW, reliability 0-95913
  - InGaAsP/InP injection lasers for long wavelength (1.1 to 1.6 μm) optical communication 0-58582
  - Li-I<sub>2</sub> battery, construction, performance and reliability 0-97771
  - Nd:glass laser performance and reliability developments 0-78869
  - Ni-Cd and maintenance-free Pb accumulator characteristics (*German*) 0-97782
- reliability theory**
- see also statistical analysis*
  - artificial satellites, future applications, reliability and cost considerations (*Italian*) 0-109334
  - optical instrument control life test design 0-87572
  - phased mission analysis, calc. of expected number of failures 0-68851
  - structural system, simulation anal. of reliability and maintenance (*Japanese*) 0-62453
- remenance**
- see also coercive force*
  - Alnico type YuNDK25DA alloy permanent magnets, thermal mag. hysteresis 0-75818
  - ferrimagnetic magnetisation theoretical models, for uniparametric materials 0-65960
  - igneous rock, rot. remanent magnetisation 0-85645
  - ionic compounds, amorphous, exhibiting Mossbauer spectra, magnetic props. (*French*) 0-80490
  - one-dimensional random Glauber model, magnetisation relax. 0-80523
  - Pliensbachian limestone sequence at Bakonyescsere (Hungary), remanent magnetisation 0-90074
  - post-depositional magnetization in Recent tidal-flat sediments 0-101320
  - spin specimens, computer controlled mag. meas. system 0-86346
  - rock, rotational remanent magnetisation, origin 0-61794
  - rock magnetism, post-depositional realignment of sediments, expts. and theory 0-109137
  - sand, specularite-bearing, experimentally deposited, mag. declination and inclination errors 0-90075
  - silicic volcanics, Jurassic, from Nevada, USA, thermochemical remanent magnetisation 0-98310
  - spin glass model, simple, magnetisation decay 0-71073
  - spin glasses, annealing and mag. remanence 0-60308
  - Thetford Mines ophiolites, Quebec, NRM props. and palaeomagnetism 0-61757
  - titanomagnetites, temp. depend. cation distrib., mag. prop. obs. 0-85647
  - transition metal-noble metal spin glass films, mag. props. 0-60306
  - weak, accurate meas. 0-68225
  - Al<sub>0.5</sub>Mn<sub>0.5</sub>Si<sub>0.5</sub>O<sub>2</sub>, amorphous insulating spin glass, susceptibility and magnetisation meas. 0-88765
  - Au-Fe (4 at %), spin glass, magnetisation and energy relax. below T<sub>g</sub> 0-65921
  - Co, ferromagnetic micropowder, cryst. struct., coercivity, remanence, saturation 0-65967
  - Co vacuum condensates, Cr alloying addition effect on texture characts. (*Russian*) 0-108471
  - Co<sub>0.5</sub>Fe<sub>0.5</sub>Ni<sub>0.5</sub>(Si<sub>0.5</sub>B)<sub>20</sub>, amorphous, soft mag. props., switched-mode power supply appls. 0-88850
  - CoO-Al<sub>2</sub>O<sub>3</sub>-SiO<sub>2</sub>, amorphous, remanent magnetisation short time depend. 0-65919
  - Cu-Mn alloy spin glass, macroscopic mag. anisotropy, transverse susceptibility and zero field NMR enhancement 0-80525
  - Fe, ferromagnetic micropowder, cryst. struct., coercivity, remanence, saturation 0-65967
  - Fe-Co, ferromagnetic micropowder, cryst. struct., coercivity, remanence, saturation 0-65967
  - Fe<sub>40</sub>Ni<sub>40</sub>(Mo<sub>0.5</sub>Si<sub>0.5</sub>B)<sub>20</sub>, amorphous, soft mag. props., switched-mode power supply appls. 0-88850
  - Fe<sub>2</sub>O<sub>4</sub> ferrofluids, spin glass behaviour 0-71120

# remanence continued

Gd-Al(Cu)(Ga)(Ni)(Pd)(Rh) alloys, amorphous, mag. and elec. props. 0-80499  
(H<sub>2</sub>O<sub>2</sub>)<sub>0.194</sub>(Al<sub>2</sub>O<sub>3</sub>)<sub>0.227</sub>(SiO<sub>2</sub>)<sub>0.579</sub>, amorphous, low temp. spin glass behaviour 0-60297  
(La,Gd)Al<sub>3</sub> spin glasses, time depend. mag. props. 0-65909  
La<sub>2</sub>MnFeS<sub>8</sub>, antiferromag., mag. props. and mag. struct., neutron diff. and magnetisation meas. 0-65801  
Mn-Al-C, fine-grained cast struct., remanence and coercive force 0-60365  
MnO-Al<sub>2</sub>O<sub>3</sub>-SiO<sub>2</sub>, amorphous, remanent magnetisation short time depend. 0-65919  
Pt-Co system, low temp. susceptibility 0-65920  
Pt-Fe ordered alloy, multiply mag. phase transitions 0-60264  
SmCo<sub>5</sub>, sintered, hard mag. material, magnetisation behaviour 0-75805

# remanent magnetism see remanence

# remote control see telecontrol

# remote control equipment see telecontrol equipment

# remote metering see telemetering

# remote sensing

see also *infrared imaging*; *remote sensing by laser beam*  
active and passive remote sensing of Earth terrain, effects of scattering 0-101435  
aerial photography, stereo viewing, interpretoskop optics, modifications 0-105081  
aerosol, middle atmospheric, remote sensing techniques 0-109269  
aerosol in atmos., mass concentration from Lidar-solar radiometer expt. 0-90171  
Africa CITHARE project, soil thermal inertia and humidity cartography by geostationary satellite 0-76980  
agricultural cover types, separability in spectral channels and wavelength regions 0-98468  
air pollution, pollutant gases monitoring from space using passive microwave techniques 0-76690  
atmosphere, operational vertical sounder on TIROS-N polar-orbiting meteorological satellite 0-77132  
atmosphere, satellite-derived radiance gradient rel. to upper tropospheric/lower stratospheric winds 0-98447  
atmosphere, temp. and press. profiles meas. via solar occultation sounding using narrowband radiometers 0-98452  
atmosphere, turbulent, optical props. determ., He-Ne laser transmitter-receiver appl. 0-98450  
atmosphere acoustic and radio acoustic exploration, effects of sound non-linear absorpt. (*Russian*) 0-94567  
atmosphere boundary layer, acoustic sounder obs. from top of steep mountain 0-98409  
atmosphere IR mosaic background obs. from balloon altitude expt. 0-90222  
atmosphere O<sub>3</sub> total content, determ. using satellite meas. 0-77027  
atmosphere parameters, retrieval from scanning multichannel microwave radiometer obs. 0-90261  
atmosphere remote sensing by satellite, thermal radiation obs. 0-85660  
atmosphere temperature, impact of satellite sounding data on weather forecasts 0-77028  
atmosphere temperature profile, IR remote sounding, error anal. and data acquisition (*Chinese*) 0-109273  
atmosphere temperature profiles, satellite retrieved, error due to aerosol particles effects 0-98449  
atmosphere temperature sounding from TIROS-N, early operational soundings evaluation 0-77133  
atmosphere vacuum UV background, meas. 0-90221  
backscattered pulse shape, small-angle multiple scatt. in random media 0-77079  
Brazil Patanal, drainage network mapping from Landsat-2 imagery 0-81944  
California Current, nutrient upwelling, satellite thermal imagery and chem. anal. 0-101379  
Carpathian Mountains, disjunctive dislocations revealed by interpretation of space television photographs (*Russian*) 0-104958  
city lights obs. by Defense Meteorological Satellite Program 0-104494  
climatology, hydrology, atmospheric research and meteorology from space, conference, Ajaccio, Corsica (1979 November 12 to 16) 0-62397  
cloud winds over oceans, satellite technique verified by aircraft obs. 0-85764  
clouds, 0.35-3  $\mu$ m range detection with aircraft-borne photometer 0-77085  
clouds over NE. Pacific Ocean, Nimbus 6 liq. water data rel. to United States west coast rainfall 0-82005  
cloudy atmospheric parameter determination using microwave radiometric method 0-67435  
coastal photogrammetric mapping 0-104960  
contextual classification of multispectral data, multiprocessor system 0-77149  
crop and soil bidirectional reflectance factor calibration, remote sensing field research 0-86382  
Dakota landforms and drainage patterns, mapping by IR imagery 0-81892  
data analysis of multivariate data set, canonical anal. 0-73333  
digital image change detection 0-102637  
DMSP visible imagery, causes of anomalous grey shades 0-77111  
Earth's atmosphere, optical parameters determ. by aerial photography at sunset 0-90219  
Earth's surface in presence of vegetation cover, microwave radiation spectra 0-68239  
Earth observation programme of ESA 0-109250  
Earth radiance obs. from Miranda (X4) satellite, IR expt. design and performance 0-72745  
Earth remote sensing from space, role of 'smart sensors', book 0-62402  
Earth scene dynamics, satellite-borne mosaic sensor performance 0-90321  
Earth surface, 0.8 cm radiation emission mapping by satellite (*Russian*) 0-77145  
Earth surface UV reflectance, meas. from airborne platform 0-98453  
EM remote sensing, reconstruction algorithms for geophysical applications in noisy environments 0-77168  
EM remote sensing of inhomogeneities in ground, numerical modelling 0-77165  
EM response of Earth surface, aircraft remote sensing (*Chinese*) 0-104859  
flood inundation of agricultural land, LANDSAT digital image anal. 0-61913

# remote sensing continued

geological faults and other linear features, detect. from LANDSAT images 0-77177  
geological IR multispectral aircraft scanner data, image processing 0-98454  
geological problems application 0-109279  
geological structure research, LANDSAT data anal. (*Italian*) 0-109281  
geomagnetic depth sounding by means of oceanographic and aeromagnetic surveys 0-77166  
geomagnetic field variations, at mesospheric heights 0-77124  
geophysical mapping and remote sensing by optical filtering 0-101458  
German Bight, airborne and ground data, Geoscientific Airborne Remote Sensing Programme (*German*) 0-67412  
glacier thickness and water content, radar measurement technique 0-98369  
Great Lakes water quality, remote sensing data interpretation 0-98364  
groundwater in deserts and glaciers using radar subsurface sounding 0-67437  
Gulf Stream rings obs. by satellite tracked drifter buoys 0-90242  
hydrological features, microwave remote sensor development and appl. 0-105082  
image processing applications at IBM Madrid Scientific Center 0-102657  
image scanner technology for digital mapping systems 0-85773  
imagery multiple analysis at JPL's Image Processing Laboratory 0-82219  
IR radiometry, satellite radiometer calibration 0-101440  
IR staring mosaic sensor performance, effect of spacecraft-induced line-of-sight jitter 0-86416  
IR surveillance, continuous-time signal processors 0-78781  
IR technology utilisation, symposium, San Diego, CA, USA (Aug. 79) 0-86037  
lake ice, microwave radar and radiometric remote sensing meas. 0-85691  
Lake Ontario water masses, nonzero subsurface irradi. refl. at 670 nm 0-101387  
lakes, particulate concs. in water 0-105056  
Landsat data, line detection algorithm 0-77150  
LANDSAT image data, evaluation for land-use mapping 0-101443  
Landsat imagery geometrical correction (*French*) 0-81889  
Landsat imagery laser film recorder and processor 0-105084  
lava flow terrain, radar imaged by satellite 0-98285  
light rangefinder and profilometer, high-resolution gas laser 0-102754  
lunar soil, surface refl. characts. for radar, obs. from Luna spacecraft 0-72798  
lunar surface rock comp. remote sensing, regolithic radioactivity in Mare Crisium 0-62045  
machine processing of remotely sensed data, conference, West Lafayette, Indiana (1980 June 3 to 6) 0-82586  
marine chlorophyll a analysis, using aircraft multispectral scanners 0-77164  
marine oil pollution surveillance, microwave remote sensing technology (*Japanese*) 0-76685  
marine wind velocity, remote sensing using oceanic whitecaps 0-72554  
mesosphere and stratosphere, O<sub>3</sub> and temp., satellite IR limb scanning method 0-105086  
METEOSAT project, interactive image system 0-109330  
METEOSAT project overview (*Italian*) 0-109331  
microwave brightness temp. distrib. over Bay of Bengal using SAMIR Satellite Microwave Radiometer data at 19 and 22 GHz 0-104980  
microwave remote sensing expt., operation in Spacelab 0-109332  
microwave sensing from satellites, appl. to meteorological meas. over W. Australia 0-98485  
microwave thermal emission, terrain brightness temp., theory 0-77151  
minerals, near IR spectra for remote sensing of hydrothermally altered areas 0-81871  
MM wave radar system for remotely sensing atmospheric pressure from satellite 0-67443  
MM wave radiometry conducted at Appleton Laboratory 0-67442  
Multi-detector Electro-optical Imaging Scanner for aircraft remote sensing 0-82085  
multiband radiometer for field research 0-90250  
multichannel data sets, integrated optical comparator 0-64213  
multichannel radiometer, programmable, for Earth remote sensing 0-77253  
multispectral scanner, for remote sensing, parametric model 0-77261  
multispectral scanner, high resolution, for Earth obs., optical design 0-82174  
multispectral sensor for satellite, analytical design 0-77262  
ocean, sea level transients obs. by Geos 3 coincident orbits 0-72535  
ocean surface parameters, retrieval from scanning multichannel microwave radiometer obs. 0-90261  
ocean surface sensing equipment, instrument characts. in presence of basic noise (*Russian*) 0-109267  
ocean surface temperature measurements, derivation from Meteosat image data 0-76985  
ocean surface temperature structure, subsurface mesoscale features 0-98347  
ocean surface UV reflectance, meas. from airborne platform 0-98453  
ocean surface waves, radar imaging method using SAR 0-77173  
ocean wave radar monitoring, ground wave and sky wave sensing techniques 0-109256  
oceanic chlorophyll gradient maps from U-2 aircraft platform over Pacific and Atlantic 0-101385  
oceanography, remote sensing appls. to sea ice 0-77176  
oceanography satellite, USA proposal for 1986 launch 0-105088  
optical imaging of surface contrast reduction due to haze with nonuniform albedo 0-101431  
optical preprocessor, use in Earth-resources satellites 0-67430  
optics and optical systems, book 0-101675  
phytoplankton remote sensing from satellite, atm. optical props. 0-77105  
radiative transfer, atmospheric effects, conference, San Diego, California (1979 August 29 to 30) 0-62376  
radio brightness temp. of Earth from Kosmos 243 and Nimbus 5, SHF obs. 0-72521  
radiometric imaging from space, atmosphere effects problems 0-98323  
rain estimation, using geostationary satellite data from extratropical region 0-90244  
rainfall estimation by satellite borne microwave radiometry 0-105085  
rainfall measurement, combined usage of radar and radiometry techniques (*Chinese*) 0-109272  
rainfall rate detect over ocean and land by spaceborne microwave radiometry 0-101423  
random media, active remote sensing, depolarisation effects 0-82090



**remote sensing continued**

- remote sensing and ranging systems from space, conf., Rome, Italy (March 1980) 0-105432
- river pollution distribution determination by remote sensing, study 0-81512
- River Tiber, physical processes related to discharge into sea, aerospatial obs. 0-108831
- Sahel region, Africa, surface albedo vars. investigation during recent drought (1967 to 1974) 0-76981
- Sargasso Sea, surface height vars. from Geos-3 altimetry obs. 0-104969
- satellite-generated radar images of the Earth 0-90249
- scene content measurement from aerial images, appl. to building complex scene 0-78788
- sea ice, Danish studies using Landsat and airborne sensor data 0-94527
- sea ice, remote sensing, appls. 0-77176
- sea ice age category differentiation through location and temp. observations using microwaves 0-67380
- sea surface inhomogeneities sensing via sound scatt., phase function shape in shadowing conditions (*Russian*) 0-94530
- sea surface slope distrib. function determ. from Sun glitter, accuracy (*Russian*) 0-94611
- sea surface waves, remote sensing using one and two freq. microwave techniques 0-94622
- Seasat, altimeter sensor file algorithms 0-94680
- Seasat, radar altimeter, initial performance assessment 0-94679
- Seasat, scanning multichannel microwave radiometer, antenna pattern corrections 0-94683
- Seasat, scanning multichannel microwave radiometer, calibration algorithm development 0-94682
- Seasat, scanning multichannel microwave radiometer, description and performance 0-94681
- Seasat, scatterometer evaluation 0-94684
- Seasat, scatterometer scattering coeff. algorithm 0-94685
- Seasat, synthetic aperture radar system 0-94686
- Seasat, visible and IR radiometer 0-94687
- Seasat artificial oceanographic satellite, microwave instrums. 0-94678
- Seasat Gulf of Alaska experiment, comparison data set winds 0-94570
- Seasat oceanographic satellite, performance evaluation 0-94677
- SEASAT radar altimeter, resolution capability preliminary estimates 0-72645
- Skylab conical multispectral scanner IR data statistics 0-90223
- snow, ice and rain, passive microwave obs. from Nimbus satellites 0-101422
- snow parameters, investigation by radiometry in 3 to 60 mm wavelength region 0-72561
- soil moisture IR thermography remote sensing through agricultural crop 0-109147
- solar Mesosphere Explorer mission description (1981-2), O<sub>3</sub> and related chemistry 0-105096
- solar radiation incident at Earth surface, estimation from geostationary satellite data 0-82006
- space appl. and research, WARC 1979 impact 0-105147
- space-borne remote sensing (*Italian*) 0-109333
- spectral feature enhancement of Landsat data, entropy minimisation (*Italian*) 0-98473
- staring IR sensors, space and reconnaissance appln. 0-86406
- step-stare spaceborne optical system image motion compensation 0-90322
- step-stare spaceborne optical system smear compensation by focal plane manipulation 0-82172
- stratosphere aerosol, satellite monitoring systems, SAM II and SAGE 0-82082
- stratosphere O<sub>3</sub> content, Nimbus 4 UV and IR remote sensing 0-77154
- stratosphere trace molecule Fourier transform spectrometer optical design 0-82099
- subsurface radar using video pulse for deep probing in Earth, pulse propagation, in lossy media using LF window 0-74282
- Sydney Metropolitan area, Landsat data ground control points, stepwise polynomial transformation 0-104961
- synthetic-aperture radar on satellites, digital processing techniques 0-61914
- target discrimination methodology in remote sensing 0-58470
- terrain characterisation, radar scattering 0-101464
- terrestrial surface temperature sensing, emissivity correction for thermal radiation interpretation 0-82092
- texture analysis by hybrid optical/digital system 0-78787
- thermal inertia imagery of Earth surface, model for calibration of survey 0-105083
- thermal inertia mapping by IR imagery, mathematical model 0-109280
- thermosphere, middle, incoherent scatter radar studies 0-72654
- TIROS-N microwave sounder unit for global temp. distribution meas. 0-90265
- trace-gas remote analysis, optoacoustic radiometry limitations 0-108759
- transient EM wave prospecting 0-76905
- troposphere and stratosphere temp., O<sub>2</sub> absorpt. spectra at 60, GHz 0-77172
- Venus atmosphere and surface, investigation by radiosounding from Venera 9 and 10 satellites 0-101543
- vertical magnetic dipole on two-layer Earth 0-76906
- volcanic rock spectral refl., 400-800 nm, obs. to compile reference data 0-90073
- water pollution problems appl. (*Japanese*) 0-94122
- weather forecasting processing of radar and satellite imagery data 0-109252
- wind fields, mesoscale, satellite-derived, covariance anal. 0-82013
- Zendan Fault region, Iran, struct. lineaments, interpretation of Landsat I obs. 0-104941
- O<sub>3</sub>, nighttime concentration (15-68 km), Nimbus 6 obs. comparison with OAO-3 obs. 0-105016
- U, National Uranium Resource Evaluation (NURE) aerial radiometric survey data interpretation via principal components anal. 0-101438

**remote sensing by laser beam**

- airborne lidar system for geophysical and atmospheric expts. (*Italian*) 0-109277
- atmosphere temp. measurement using CO<sub>2</sub> laser radar 0-90225
- atmospheric environmental research, appl. of lasers (*German*) 0-97849
- cigarette smoke, diode laser meas. of methane, ethane and H<sub>2</sub>O vapour concs. 0-97847
- cloud extinction coefficient, estimation from multiwavelength lidar backscatter meas. 0-98446
- cloud seeding studies application of lidar remote sensing 0-109203

**remote sensing by laser beam continued**

- conference, laser and electro-optical systems, San Diego, CA, USA (Feb. 1980) 0-62392
- differential absorption lidars, reference range 0-89700
- dusty IR Test-I lidar obs., transmission meas. 0-99625
- environmental, determ. molecular chem. and biological planet surface composition 0-72651
- ethylene, air pollution monitoring, computer controlled CO<sub>2</sub> laser absorpt. system 0-89699
- gas analysers, freq. modulation appls. 0-85246
- high clouds, cirrostratus emissivity meas. 0-82061
- high ice clouds, visible and LR optical props. from lidar and radiometer meas. 0-82060
- lidar equation for inhomogeneous atmos. (*Russian*) 0-82054
- methanol trace detection using phase fluctuation optical heterodyne spectroscopy 0-68266
- multiple gaseous air pollutants, point monitoring method by tunable laser (*Japanese*) 0-81515
- oil spill detection by airborne laser fluorosensor 0-67024
- optical fibre, use in remote inelastic light scatt. probe 0-58769
- Raman spectroscopy, remote spontaneous, new trends in recording of signals 0-73485
- steel, mild, laser microspectral anal. 0-108769
- vinyl chloride, air pollution monitoring, computer controlled CO<sub>2</sub> laser absorpt. system 0-89699
- water depth measurement using airborne pulsed Ne laser system 0-61908
- CO<sub>2</sub> remote sensing using freq. doubled CO<sub>2</sub> laser radiation 0-67025
- CO<sub>2</sub> IR laser velocimetry, processing techniques and applications 0-87831
- Na enhancement and nightglow, spaced lidar obs. 0-101466
- Nd:YAG laser as source for airborne lidar system for atmospheric expts. (*Italian*) 0-109278
- SF<sub>6</sub>, trace detection using phase fluctuation optical heterodyne spectroscopy 0-68266
- SO<sub>2</sub>, absorption spectrum, meas. using frequency doubled pulsed dye laser 0-87144
- SO<sub>2</sub>, absorption spectrum, meas. using frequency doubled CW dye laser 0-87145
- renormalisation**
- $\lambda_0\phi^4$  field theory, 3 space-time dimensions, renormalisation, analytical continuation to imaginary time 0-86563
- $\lambda_0^4$  field theory at finite temp., Casimir effect and topological mass 0-57479
- $\lambda_0^4$  theory, renormalisation in nonsimply connected spacetime 0-90999
- $\lambda_0^4$  theory, trial wave function renormalisation using effective pot. 0-105791
- $\sigma$  model, SU(3) linear, renormalisation in one loop approx. 0-68368
- $\sigma$ -model, nonlinear, order-parameter relaxation from renormalisation group 0-57504
- $\sigma$ -models, non-linear, and universality in 3-D, scaling limit, and critical behaviour, chirality 0-62824
- $\sigma$ -models, supersymmetric, Kahler geometry and renormalisation 0-105789
- $(\phi^3)_0$  field theory, deep inelastic lepton-headron scatt., cut vertex theory and reciprocity relation 0-57466
- $\phi^{3,6}$  self-interacting theory, three well potential, block spin renormalization 0-57490
- $\phi^4$  model, strong coupling and infrared struct., renormalisation 0-101921
- $\phi^4$  theory, Euclidean, local existence of Borel transform of Schwinger functions 0-77932
- A<sup>+</sup>-coupling in abstract approach of quantum field theory, renormalisation group 0-99033
- Anderson localisation, real-space renormalisation group theory, decimation method 0-88461
- Anderson localisation, scaling theory 0-70646
- antiferroelectrics, multicritical points in structural phase transitions, renormalisation 0-75982
- antiferromagnet, Ising model, crit. props., calc. 0-65946
- antiferromagnet, quantum critical dynamics with mode coupling 0-108024
- antiferromagnet chain, renormalisation group nearest neighbour interactions 0-60357
- antisymmetric tensor fields coupled to gravity, renormalisability 0-90765
- Ashkin-Teller-Potts model, dil., crit. behaviour 0-65897
- asymptotic behaviour in quantum field theory, renormalisation group analysis 0-68378
- asymptotically free SU(5) grand unification, proton stability, renormalisation group 0-82929
- axial vector anomalies, weak-EM interactions nonrenormalisability 0-62859
- charge invariance, QCD, renormalisation group, confining and asymptotically free soln. 0-62881
- condensed matter physics, dynamic correlations, book 0-86046
- cut vertices and dimensional renormalization in non-Abelian gauge theories 0-57484
- deep inelastic leptonproduction, normalising the renormalisation group anal., QCD twist effects 0-86690
- dimensional regularization of composite operators in scalar field theory 0-73573
- dimensional renormalisation, trace and axial anomalies, Zimmermann like identities, massive QED 0-101959
- disordered spin systems, tricrit. behaviour 0-60319
- dynamical systems, critical transition to stochasticity 0-73265
- effective field theories, functional integration, renormalisations 0-86648
- elastic constants crit. behaviour near non-elastic phase transitions 0-100298
- elastically coupled systems at marginal dimensionalities, crit. dynamics and stability 0-101769
- Euclidean quantum field theory, n-point functions, renormalised G-convolution 0-68341
- extended defect system, phase transform., critical props. 0-103455
- extended objects in quantum field theory 0-86557
- ferrodistortive spin-phonon systems, crit. props. 0-88315
- ferroelectric, uniaxial, crit. behaviour, electrostrictive coupling role 0-71329
- ferroelectric antiferromagnets, phase transformations (*Russian*) 0-93114
- ferromagnet, anisotropic, in external mag. field, continuous phase transition existence 0-108011
- ferromagnet, random quenched, crit. behaviour, effective exponents, renormalisation 0-60326

# renormalisation continued

ferromagnets, quantum critical dynamics with mode coupling 0-108023  
Feynman amplitudes, zero-mass behaviour 0-68353  
field operator for unstable particle and complex mass description in local QFT (*German*) 0-90981  
finite temp. field theory with boundaries, extensions to curved space, stress tensor and surface action renormalisation, review 0-57455  
first order phase transitions, droplet models, renormalisation, singularities 0-95050  
free energy derivatives, bounds, upper and lower, renormalisation group methods 0-68162  
 $g\phi^4$  renormalised field theory in limit  $g \rightarrow \infty$ , effective potential 0-99058  
 $g\psi\psi$  theory, trial wave function renormalisation using effective pot. 0-105791  
gauge field models, hard anomalies, cancellation by regularisation independent renormalisation scheme 0-77931  
gauge field phase diagrams, dynamic mass generation and renormalisations 0-68365  
gauge field theories,  $n \neq 4$  axial vector anomaly, noncontribution 0-62858  
gauge theory, renormalisation of ghost and Goldstone fields and ghost symmetries 0-90987  
gauged  $N > 4$  supergravity, vanishing one loop  $\beta$ -function, infinite renormalisation 0-86186  
Gaussian-to-Heisenberg crossover, specific heat, renormalised perturbation theory 0-60356  
hadron polarization operator insuperrenormalizable model, rainbow approx. of  $(\lambda/2)\phi^4$  model 0-105821  
heavy quarkonium decays, renormalisation group approach, exclusive two meson and inclusive decays 0-82972  
Heisenberg, ferromagnet, classical, with dipole-dipole interaction, renormalisation group and crit. exponents 0-60351  
Heisenberg ferromagnet, magnon renormalisation 0-65849  
Heisenberg ferromagnet, spin-wave renormalisation,  $S \geq 1$  0-71070  
Heisenberg metamagnet, collinear, mag. phase diagram 0-71035  
Heisenberg model, randomly dilute, renormalisation group calcs. 0-60321  
Hubbard model, equivalent spin Hamiltonian, for phase transition studies 0-80474  
Hubbard model, Green's function, functional-derivative study 0-75483  
integral formulation divergence elimination, connecting const. renormalisation (*Russian*) 0-68369  
intermediate valence system, local polaron model 0-107717  
inverse problem method, quantum, sine-Gordon model 0-68377  
Ising antiferromag. phase boundaries, hard-core lattice gas calcs. 0-80542  
Ising antiferromagnet, FCC, nearest neighbour interactions, Monte Carlo method 0-80544  
Ising magnet coupled to isotropic elastic medium, first order transition, renormalisation method 0-68151  
Ising model, antiferromag. case, modified Kadanoff variational renormalisation method 0-88710  
Ising model, continuous-variable, real-space renormalisation group method 0-100589  
Ising model, critical dynamics, time-dependent real-space renormalisation group 0-60282  
Ising model, ferromagnetic, band-mixed square-lattice, approx. crit. surface 0-70921  
Ising model, fixed points, determ. by lower bound renormalisation transformation 0-62586  
Ising model, kinetic, reliability of real space renormalisation approach 0-90793  
Ising model, one-dimensional transverse-field, in complex longitudinal field, real-space renormalization group method,  $T=0$  0-103806  
Ising model, two-dimens., in transverse mag. field, renormalisation group studies 0-71042  
Ising model, two-dimensional kinetic, dynamic correlation functions, real space renormalisation group approach 0-62589  
Kellen-Simanzik eqn., correlation function scaling behaviour in phase transitions (*Russian*) 0-57502  
lattice regularised field theory, renormalised and bare coupling constants 0-77960  
lattice theory, percolation, block cluster approach, scaling laws and renormalisation groups 0-62592  
light cone expansion in renormalised perturbation theory 0-99045  
liquid-vapour transition, non-Ising-like effects, eqn. of state, renormalisation group calc. 0-84286  
long polymers in solution, props., direct renormalisation method for study 0-59370  
Luttinger-Thirring model on lattice, real space-time renormalisation 0-62590  
magnetic system, Lifshitz point, phase diagrams and crit. behaviour 0-65928  
magnetically ordered cryst., dislocation drag, magnetoelastic waves 0-103332  
magnets, randomly distributed point defects, critical exponents, renormalisation theory 0-60346  
mass, physical, in  $\phi^4$ -model, renormalisation group and mass generation 0-77948  
membrane models and generalized  $Z_2$  gauge theories, renormalisation props. 0-86587  
metamagnet, compressible, renormalisation group theory of pseudocritical point 0-60337  
methane adsorbed submonolayer on graphite, structural transitions between epitaxially ordered phases 0-96740  
mixed valence model, spinless, coherent-hybridisation states and virtual-bound states 0-107749  
mixed valence model, spinless, isolated f-level problem 0-107750  
non Abelian gauge theories in external electromagnetic fields (*Russian*) 0-57533  
non-Abelian gauge theory, Yang-Mills phase factor renormalisability 0-95211  
nuclear field theory, phonon renormalisation, eigeneqns. and sum rules (*Chinese*) 0-102127  
one loop equivalent gauges, one loop infinities and renormalisation constants 0-62842  
ordering alloys, nonlinear critical relaxation of the Ginzburg Landau field coupled to a conserved density 0-90803  
percolating two-dimens. square lattice, normal-state cond. and crit. current density, crit. exponents 0-84541  
perturbation theory, renormalisation group eqns. and analytic renormalisation 0-82865

# renormalisation continued

perturbation theory, renormalisation group eqns. and analytic renormalisation 0-82866  
perturbative QCD, renormalisation improvement, charmonium decay and scaling violations 0-101993  
perturbative renormalisation theory, general features, quantum action principles, pure Yang-Mills theory 0-105794  
phase transitions, Schlogl's chemical model, critical fluctuations near non-equilib. critical point 0-85150  
polymer, long, short range correlations in solution 0-59367  
polymer chain, direct renormalisation group procedure 0-91712  
polymer chain dynamic critical index calcs. by renormalisation method 0-82756  
polymer solutions, renormalised field theory, polydispersity 0-74270  
Potts lattice gas, crit. and tricrit. exponents using Kadanoff transform. 0-101768  
Potts model, three-state, effects of symmetry-breaking perturbations 0-105579  
Potts model, three-state, first order phase transitions 0-60333  
Potts models, q-state, two-dimens., Monte Carlo renormalisation-group studies 0-77727  
pure Yang-Mills perturbation theory, instanton sector renormalisation, zeroth sector comparison 0-105775  
q-state Potts model multicritical point, singularities and scaling functions 0-57215  
QCD, Migdal approx. and  $1/N$  expansion, string tension 0-101992  
QCD, renormalisation group calcs., cancellation of ambiguities (*Russian*) 0-62930  
QCD corrections at  $Z_0$  for hadron initiated lepton pair prod., renormalisation appl. 0-86678  
QCD renormalisation in two loop approx. in arbitrary gauge 0-102002  
QED, conformal-invariant, Ward identity of dilation current 0-68401  
QED, covariant, renormalised transition amplitudes, gauge independence, Green functions 0-57530  
QED, dimensional renormalisation, coupling constants and masses 0-57523  
QED, heavy particle effects, factorised local operators, renormalisation group 0-62898  
QED, heavy particle effects, factorised local operators, renormalisation group 0-62899  
QED, polarisation operator in ladder approx., renormalisation group 0-73629  
QED, renormalisation group equations, invariant charge function 0-57529  
quadratic lattice, correlated percolation 0-68149  
quantised  $SU(2)$  gauge theory, Monte Carlo study 0-77973  
quantum contour field equations, renormalisation and string like eqn. 0-86581  
quantum field theory, n-point functions, renormalised G-convolution, convergence in Euclidean case 0-77930  
quantum Ising chain, in real or complex field, real space renormalisation group method 0-71050  
quantum renormalisation group, zero temp., appl. to Heisenberg and Ising models 0-80526  
quantum spin model, appl. of projective renormalisation group 0-84607  
quantum spin system, two-dimens., frustration, renormalisation group study 0-80535  
quantum spin systems, ground state energies, renormalisation techniques appls. 0-93132  
quark confinement, bag models, field theoretic, renormalisation and translation invariance 0-62932  
quasi-two-dimensional planar spin system, mag. transition 0-65951  
radiative mass generation in perturbation theory and the renormalization group 0-86611  
random hierarchical model, crit. props. 0-71072  
rare earth zircons, Jahn-Teller cooperative phase transition, crossover effects 0-88316  
rare gas clusters, small, structure, thermodynamic properties 0-88341  
real-space renormalisation group, dimensionality effect 0-77716  
Reggeization of elementary fermions in arbitrary renormalizable gauge theories 0-68367  
relaxational dynamics in systems with many-component order-parameter, scaling fields and variables 0-101772  
renormalons and non-renormalizability for asymptotically and nonasymptotically free theories 0-68366  
Robertson-Walker universe, adiabatic regularisation, arbitrary coupling of scalar field to scalar curvature 0-57461  
selfavoiding random walk problem, direct renormalisation method 0-77703  
semiclassical field theory of gravitation, renormalisation scheme 0-68117  
semiconductors with direct band gaps, exciton-polariton interactions, Green's function approach 0-92831  
site percolation, infinitesimal renormalisation group transform. 0-88525  
soliton solutions, renormalisation and quantum corrections 0-82884  
specific heat, confluent singular term for systems with continuous symmetry, crit. amplitude ratio, calc. to order  $\epsilon^2$  0-57235  
spin Hamiltonian, constant-coupling, higher-order, statics and dynamics 0-60262  
square lattice, critical dynamics and potential moving approx., renormalisation group approach 0-57209  
structural phase transformations, static critical behaviour 0-92640  
 $SU(2)_1 \times U(1)$  theory, radiative corrections, simple renormalisation framework 0-101973  
 $SU(3)_{\text{colour}} \times SU(2) \times U(1)$  gauge, full operator structure of the non-leptonic  $|\Delta S|=1$  weak Hamiltonian 0-99089  
 $SU(5)$ , unification of weak, EM and strong interactions, review 0-105814  
superconductor, renormalisation group recursion relations involving dynamics, in mag. field 0-60137  
surface percolation processes, scaling theory and real space renormalisation group 0-86223  
Thirring model, massive, mass independent renormalisation, dimensional regularisation 0-57463  
three photon vertex in QED, renormalisation group anal., Callan-Symanzik eqn. 0-105822  
three-loop charge renormalization effects due to quartic scalar self-interactions 0-57489  
tricritical behavior in a two-dimensional field theory 0-77726  
two-spin correlation function, dipolar crossover 0-80516  
unified gauge theories, electroweak mixing angle, renormalisation 0-86651  
UV asymptotics and the renormalisation group, review 0-101933



**renormalisation continued**

- UV infinity suppression in gravity modified field theories 0-105787
- wave function renormalisation constants, gauge independ. in gauge field theories 0-82883
- Weinberg-Salam theory, extension to left-right symmetry and quark-lepton unification 0-78002
- Wightman function, two-point, asymptotic behaviour 0-73614
- X-Y model,  $S=1/2$ , phase transitions at  $T=0$ , z-field renormalisation group method 0-71051
- Yang-Mills fields, supersymmetric, Ward identity, one-loop level, renormalisation 0-73597
- Zimmermann identities and renormalization group equation in dimensional renormalization 0-73591
- $\pi$  compositeness from wave function renormalisation constant 0-101997
- $\pi\pi \rightarrow \pi\pi$ , self-interactions, nonperturbative, scatt. amplitudes containing only convergent integrals 0-68480
- $\Sigma^+ \rightarrow p\gamma$ ,  $1/2^-$  resonance poles to parity-violating amplitude, two-quark weak transitions 0-78062
- CeAl<sub>3</sub>, magnetic ordering, 24 component Ginzburg-Landau model 0-97095
- He monolayer, phase diagram, order-disorder transition 0-107604
- <sup>3</sup>He, superfluid, transport parameters, Kubo formulae and BCS-Green's functions 0-88382
- K<sub>2</sub>CuF<sub>4</sub>, layered spin system, planar rotator symmetry, phase transition 0-65951
- Rb<sub>2</sub>CrCl<sub>4</sub>, 2D-ferromag., renormalisation of long wavelength spin waves, neutron scatt. 0-60229
- Si surface, (111), energy states, computer renormalisation-group calc. 0-75617
- TmSe, Kondo lattice model 0-97063

**repackaging** *see packaging***repeaters**

- optical fibre communication advances, materials and techniques 0-102853

**replica techniques**

- biological specimen replication at  $-150^\circ\text{C}$  with improved freeze-fracture apparatus 0-85560
- cord-rubber laminates, two-ply balanced, interlaminar-shear strain study 0-97526
- detaching single-stage C replicas, glue films appl. 0-61038
- freeze-etching improvement using evaporated film 0-85558
- moire contourgraphy, computer-aided replication of human anatomy 0-67189
- PVC, rigid, internal struct. of diamond shaped cavities 0-66628
- rapid aimed preparation, using Pt-C replicas 0-61037
- steel, Cr-Ni-C (3, 1, 0.6 wt.%), grain boundary sulphide precip. and hot ductility (*Japanese*) 0-71654
- steel, ferritic and austenitic, microstruct. study by means of replicas taken from components at  $100^\circ\text{C}$  0-81256
- Wolter lens component replication 0-95972
- C, for TEM investigation of hard nonmetallic materials 0-61034
- Ni-base superalloys, technique for replication of  $\gamma'$  0-79648

**replicas**

- abraded surfaces, topography rel. to contact area and abrasion mechanism 0-58986
- epoxy resin, plastic deform. effect on crack propag. 0-97563

**reproduction (copying)**

- see also photocopying; printing*
- optical fibre array, gradient-index, appl. in copying machine 0-69500

**research and development management**

- electro-optical system manufacture, test and process control changes 0-96044
- energy resources in Britain, general survey (*German*) 0-72000
- India, need for and consequences of technological assessment 0-68017
- lightning strokes, artificial, experimental station in France (*French*) 0-61841
- LMFBRs, national development programmes, status assessment 0-106104

**residual stresses** *see internal stresses***resins** *see polymers***resistance, electric** *see electric resistance***resistance coupled amplifiers** *see d.c. amplifiers***resistance furnaces**

- high-temperature, for drawing out filament light guides 0-74491
- Si<sub>3</sub>N<sub>4</sub> layers deposition, high-temperature, temperature gradient and nitrogen flow influence obs. (*Bulgarian*) 0-80981

**resistance noise** *see thermal noise***resistance thermometers**

- automatic calibration oven 0-98914
- automatic resistance thermometer bridge 0-98913
- automatic temperature measurement with thermojunctions, temperature sensitive ICs and resistance thermometers (*German*) 0-77778
- drift, correction cct. 0-98912
- hermetically sealed, device for measurement of static characteristics 0-77784
- linearisation of bridge measuring circuit for multi-spot temp. check (*Russian*) 0-90847
- semiconductor, for the interval 300K to 0.3K, thermoelectric characts. 0-73359
- standards, GDR, testing (*German*) 0-90842
- thermal inertia compensation (*Russian*) 0-62667
- thermorestive converter error compensation methods (*Russian*) 0-73363
- C resistors for low temp. thermometry 0-86308
- Ge, stability data at 3 temperatures 0-86307
- Pt, effect of oxidation on electrical resistance 0-101794
- Pt, heat leaks effect anal. 0-57296
- Pt, linearisation characts. (*Russian*) 0-82764
- Pt, medium precision, A/D converter appl. 0-86297
- Pt, simple Cu holder for calibration 0-98911
- Pt, TSPN-3 and a carbon thermometer (USSR), stability tests 0-62666
- Pt, temp. range influence on error due to non-linearity (*Russian*) 0-90841
- Pt thin-film temp. sensor (*Japanese*) 0-105645

**resistance welding**

- fusion reactor superconducting magnet joints, resistance welding 0-91259

**resistivity** *see electrical conductivity***resistors**

- see also photoresistors; posistors; thermistors; thin film resistors; varistors*
- alloy selection for cryogenic resistors with low temp. coeff. 0-98922

**resistors continued**

- Speer carbon resistors as pressure gauges 0-95108
- C, high-resistance, He level gauge appl. 0-57277
- C resistors for low temp. thermometry 0-86308
- Si:Sb, low energy ion implantation Schottky barrier diodes and resistors 0-88177

**resolving power (optical)** *see optical resolving power***resonance**

- see also atomic beam electric resonance; circuit resonance; cyclotron resonance; dielectric resonance; Fermi resonance; magnetic resonance; magnetoacoustic resonance; molecular beam electric resonance; optical double resonance; vibrations*
- black holes, rotating, reson. freqs. of free oscills. rel. to gravit. waves 0-105271
- box approach to resonance 0-98824
- combination, parametrically excited oscill. of coupled second order system with nonlinear damping 0-86078
- cylindrical shell, liquid filled under nonlinear resonance conditions, vibration stability 0-99954
- Earth satellite orbits with resonance lunisolar perturbations, dependent on inclination 0-90326
- electrically connected bearing, motion equation (*Russian*) 0-73164
- external friction reduction by forced piezoelec. oscillation 0-92096
- forced damped harmonic oscillators, meas. separation and half-width of components of doublets, high-Q systems 0-74590
- gas, photon echo in a magnetic field at small areas of the exciting pulses 0-95961
- gas, resonance four-photon shift, optimal focusing of high-power pumping 0-95574
- hemispherical monopole surrounded by plasma layer, Tonks-Dattner reson. and input admittance 0-87887
- laboratory equipment for resonance meas. in solids (*Spanish*) 0-86285
- laser-irradiated target, electron accel. by reson. 0-75076
- oscillators, weakly nonlinear, system with slowly varying parameters, resonance 0-62463
- parametric complex objects, multichannel installation for stabilising vibration 0-58990
- piezoelectric transducer, composite, of low freq. acoustic flaw detector, natural freq. calc. 0-89450
- plasma resonances in magnetosphere, JIKIKEN (EXOS-B) satellite stimulated plasma wave expts. (*Japanese*) 0-94649
- pulsating stars, reson. effects on modal selection 0-82372
- Schumann resonances in <sup>3</sup>He-ionosphere cavity, book 0-86050
- spring-loaded mass system vibration analysis (*German*) 0-96224
- stellar surface large-scale pulsations, nonlinear coupling to small-scale deep-seated instabilities 0-62115
- US resonance method, appl. in inspection of symmetrical products 0-89449
- US transducers array, transducer elements tuning 0-87684
- vibrational, math. modelling of built-up structures, using meas. data 0-69718
- viscoelastic cylindrical shell, short, resonance vibrations 0-58962
- waves in rotating gravitating gas cloud, resonant wave wave interaction 0-105154

**resonance reactions and scattering, nuclear** *see nuclear resonance reactions and scattering***resonances, baryon** *see baryon resonances***resonances, meson** *see meson resonances***resonant absorption of gamma-rays** *see Mossbauer effect***resonant cavities** *see cavity resonators***resonant gamma-ray interactions in crystals** *see Mossbauer effect***resonators**

- see also cavity resonators; crystal resonators; resonance*
- aerial ultrasonic generators using metal resonators (*French*) 0-79074
- electromechanical filter resonators, props. of materials used (*Czech*) 0-76318
- low-temperature rectangular resonator for observation of double electron-nuclear resonance in 3 cm range 0-98956
- slotted tube, pulsed ESR and ODMR expts. 0-86360
- toroidal, for EM waves, Maxwell eqns. for toroidal geometry 0-102598

**revaporisation** *see vaporisation***reverberation**

- see also anechoic chambers; architectural acoustics; echo*
- acoustic systems with long reverberation, meas. transfer characts. by narrowband digital signal processing (*Japanese*) 0-64304
- auditoria and studios, reverberation time meas. using digital instrum. (*Japanese*) 0-64321
- Demey metro station, noise level increase due to echoes from passing vehicles (*French*) 0-69600
- derverberation process evaluation by normal and impaired listeners 0-91974
- diffuse-field, shock excitation to determine US absorption in liquids 0-88267
- Fourier transform method for reverberation time measurement 0-74601
- iterative calc. of reverberation time for two-dimens. enclosures 0-102934
- laboratory and domestic environments, relationship between sound power level and sound pressure level, use of noise data 0-74599
- rectangular rooms, reverberation time dependence on wall diffusion and room shape (*German*) 0-102932
- reverberant sound, transmission through orthotropic viscoelastic multilayered plates 0-102884
- room, acoustic wave diffraction at edges of absorbent wall panels, modal analysis (*French*) 0-79060
- room, equivalent absorpt. area (*German*) 0-102931
- speech intelligibility, reverberation effects in cases of presbycusis 0-96139
- underwater, 4 kHz and 20 kHz tone bursts in water filled tank 0-83695

**reverberation chambers**

- acoustic noise insulation, testing of Al tripole-layer wall between two reverberation rooms, road traffic noise 0-69593
- eigenmode analysis of the interference patterns in reverberant sound fields 0-96112
- investigation of sound transmission through pipe walls, presence of flow 0-102883
- multitone decay variance 0-87653
- non-rectangular, resonance freq. and eigenfunctions, calculation by finite element analysis 0-64324

reversible shape memory effect *see shape memory effects*

reviews  
*see also Bibliography Index (special index bound with Author index)*  
1/f noise in electrical conductors, survey 0-107878  
abrasion resist. materials, review 0-108586  
acoustic applications, research over past 50 years 0-96151  
acoustic emission, and its appls. (*Japanese*) 0-93726  
acoustic radiating parametric antenna 0-102898  
acoustical measuring instrums. over past years 0-96152  
acoustical research into life sciences 0-97925  
acoustical research into superconductivity and superfluidity 0-96090  
acoustical research over past 50 years on relation between acoustical behaviour and props. of solids, gases and liquids 0-96089  
acoustics in human communication, evolving ideas about nature of speech 0-96135  
acousto-optics, guided-wave, with appls. to wideband communications and signal processing, progress review 0-58801  
actinide elements and compounds, mag. props., book contrib. 0-75727  
adhesion, surface and interfacial aspects 0-108690  
adhesion, surface chemistry studies, anal. appls. 0-88440  
adsorbed layer, commensurate-incommensurate transition and domain walls 0-107654  
aeroacoustic interaction, turbulent jet noise 0-87765  
AES backscattering effects 0-81398  
agricultural pollutants in runoff water 0-97831  
air pollution, long-range transport modelling 0-108823  
aircraft noise propag., report 0-64258  
Algol, orbit, lightcurve and struct. 0-109460  
alkali metal, vapour states, laser spectroscopy and applic. 0-68260  
alkali metals, liquid, O<sub>2</sub> pot. and O<sub>2</sub> distrib. coeffs. between alkali and struct. metals 0-65231  
alloy, cryogenic, creep, review 0-104222  
alloys, high resoln. diff. and imaging characterisation 0-104050  
alloys, temper embrittlement, impurities and alloying elements role, review 0-66649  
alternating current electrode processes 0-61107  
ambient temperature solid state battery developments, review 0-61328  
amgnetic thin films, amorphous, struct. and mag. props., review 0-93148  
amorphous alloys, struct. and plastic flow 0-84090  
amorphous ferromagnets, book contrib. 0-75743  
amorphous metals and alloys, geometric struct. models and diffraction exam. techniques 0-79700  
amorphous semiconductors, structural and electronic props. 0-64901  
amorphous solids, stochastic geometry, review, book contrib. 0-73269  
anelasticity due to long-range diffusion 0-60904  
anomal plasma membranes, study using freeze-fracture technique 0-104842  
anomalous photovoltaic effect of ferroelectrics 0-65628  
apatite crystal growth in skeletal tissues 0-94181  
asteroid and comet dynamics and evolution 0-82260  
astroblesms on Earth's surface 0-98324  
astronomical gamma-ray burst origin, models review 0-82494  
astronomical observations of faint objects; television detection techniques 0-82208  
astronomical radio spectroscopy (*Japanese*) 0-62031  
atherosclerosis, rheological aspects (*Japanese*) 0-94268  
atmosphere aerosols of Antarctica, origin and props. 0-90197  
atmosphere O<sub>3</sub> layer, transport rel. to chemistry and depletion 0-104534  
atmosphere radar technique, for dynamic struct. of middle atmos. 0-105078  
atmosphere tides, theoretical work since 1970, review 0-94589  
atmospheric pollutants, gaseous, analytical control, review 0-101140  
atom+molecule reaction dynamics, translational energy effect 0-76489  
atom photoionisation, polarisation of photoelectrons 0-78584  
atomic photoionisation, selective, use in laser isotope separation and spectroscopy 0-83332  
atoms, electron scattering, optical pot. methods 0-102569  
auditory evoked response, primary inhibited elements 0-94235  
auditory primary neurons, comparative physiology 0-94224  
aural nonlinearity, two-tone 0-89768  
aurora of dayside cleft, and ionosphere effects 0-94633  
auroral arcs and currents 0-77190  
auroral electrons acceleration mechanisms 0-77210  
auroral forms relationship with high latit. particle precip. 0-77189  
auroral luminosity rel. to geomag. field changes 0-77187  
auroral zone microburst precipitation phenomena 0-77208  
autoguiders and acquisition systems for optical telescopes 0-82206  
autowave processes in distributed kinetic systems 0-101721  
axisymmetric elastic problems, stress function solns. (*Japanese*) 0-64371  
backscattered electron imaging, SEM 0-86513  
baryonium states in QCD, review 0-102001  
binary stars, close, in globular clusters, preliminary report 0-109505  
binary stars, main sequence, absolute dimens. determ., errors requirement review 0-109473  
binocular models, characts. and design features, review 0-74468  
bio-electromagnetic research 0-85444  
biological effects and dosimetric data useful for RF safety standards development 0-67154  
biological effects of ionising radiation, current research in Canada 0-104683  
biological imaging by NMR (*Japanese*) 0-94312  
biological macromolecules, conformation studied by calorimetry 0-97870  
biomedical engineering and materials for orthopaedic implants 0-76862  
biomedical measurements and transducers (*Japanese*) 0-94393  
biomedical X-ray equipment, state of the art 0-81688  
biophysics and bioengineering, book 0-105437  
bipolar spatial filtering, incoherent, review 0-102822  
bistable optical devices: an overview 0-58625  
black foam films stability 0-104463  
blood pressure, indirect meas. method 0-94383  
boiling crisis, nuclear reactor safety and performance, state of the art review 0-63312  
Borrmann-like anomalous effects in volume holography 0-102664  
bright plating, from zincate electrolytes, progress 0-66442  
brittle solids, shock deform., theory 0-72493  
bronchogenic cancer, small cell, undifferentiated, role of radiation therapy in treatment 0-67226  
brush plating, for wear resist. appls. 0-66443  
capillary phenomena for fluid/fluid interfaces 0-70506  
cardiac nuclear medicine, left ventricular edges detect. methods 0-98132

reviews continued  
cardiac fibrillation thresholds for 60 Hz currents and voltages directly applied to heart 0-101301  
cardiac function and anatomy evaluation, complementary role of echocardiography and radionuclide imaging, book contrib. 0-101241  
cardiac nuclear medicine instrumentation, book contrib. 0-101260  
cardiac shunt detection with the short-lived radioactive gases 0-94357  
cardiac US and nuclear medicine, complementary roles 0-98051  
cardiovascular nuclear medicine, an overview 0-85480  
cardiovascular shunts, detection and quantitation with commonly available radioisotopes 0-94356  
cavitation, acoustic field generated 0-74934  
cellular precipitation features in supersaturated solid solns. (*Russian*) 0-84937  
cemented carbides, fracture toughness testing 0-104410  
cemented carbides, physical and chem. nature 0-76265  
ceramics, crack extension micromechanisms 0-108567  
ceramics, high resoln. diff. and imaging characterisation 0-104050  
ceramics, transformation toughening, martensitic transforms. in crack-tip stress fields 0-104154  
CERN, 25 years of physics, review 0-82626  
cervical carcinoma, para-aortic irradiat. 0-72307  
cervix carcinoma, extended field technique complications, correl. of radiation and surgical parameters 0-67225  
chemical lasers oscillating on rot., vibr. and electronic transitions 0-102716  
chemical physics of solids and their surfaces, book 0-82587  
chemisorption on d-band metals, book contrib. 0-107649  
chemisorption on semiconductor surfaces, book contrib. 0-107648  
cholesteric liquid crystals, optical properties, diffraction nature 0-70123  
classical crystal optics, lattice dynamical background 0-97221  
climate variation throughout Earth's history, causal mechanisms 0-82048  
close binary systems, starlight scatt. on gaseous extrastellar material 0-109471  
cluster ions, formation and reactions, SIFT study 0-58435  
coastal circulation and wind-induced currents, review, book contrib. 0-98357  
cochlear micromechanics and anatomy, review 0-76750  
cochlear models-1978 0-94221  
coded aperture imaging, review 0-101914  
collagen molecular organisation and connective tissues props. 0-97858  
collision processes, at. and mol., angular correlations, summary of review papers 0-63757  
collisions, at. and mol. in presence of strong radiation fields 0-63801  
colloidal dispersion dynamics 0-71956  
color geometrodynamics, eightfold way 0-95243  
colour centre physics, last fifty years 0-105487  
combined heat transfer, state of the art review 0-79119  
component development, mag. systems and plasma engineering, programs status 0-99299  
components for optical communication systems, review 0-87539  
composite friction and bearing materials, development, friction and wear theory, review 0-60979  
composite materials, mech. props., theory, review 0-64392  
composite materials, unidirectional, three-dimens. fracture 0-64471  
compound nucleus theory, recent developments, review, book contrib. 0-68636  
computerised tomography, introduction and review of state of the art (*German*) 0-101251  
computerised tomography, quantitative, progress toward 0-81696  
computerised tomography, review and comparison with classical X-ray diagnostic technique (*German*) 0-67239  
computerised tomography, single photon emission 0-81698  
conceptual foundations of the unified theory of weak and electromagnetic interactions 0-95237  
condensed media, vibrational relaxation studied by picosecond or Raman spectroscopy 0-80797  
continuous drawing of liquids to form fibers, review, book contrib. 0-97444  
corona discharge industrial applications, qualitative analysis (*Rumanian*) 0-70061  
cosmic dust in planetary nebulae, observational data 0-109535  
cosmic dust in planetary nebulae 0-109536  
cosmic gamma ray spectroscopy 0-67582  
cosmic ray muon charge ratio, sea level, phenomenological model 0-67487  
creep, irradiation induced, correlation of theory with expt. evidence 0-82255  
creep of metals and plastics under combined stresses. A review 0-59567  
creep rupture data analysis, development of correlation and extrapolation methods 0-58975  
Cretaceous pelagic carbonate rocks, mag. stratigraphy obs. review 0-104876  
critical phenomena at low temperature 0-73297  
critical two-phase flow, bubble nuclei 0-64615  
crystal growth, conference, New Hampshire, USA (July 1977) 0-57008  
crystal growth and graphitization 0-89165  
crystal growth and phase diagrams 0-66407  
crystalline materials, struct. of grain boundaries using diff. techniques 0-59478  
crystalline solids, electronic industry, chem. anal. instrumental methods progress 0-66903  
crystallisation, technical, modern trends, computer modelling 0-66406  
current GaAs laser research 0-83613  
CVD technology, appl. to semiconductor industry 0-66431  
cyclic strain diagrams recording under nonisothermal conditions, review 0-71830  
damage analysis under nonproportional cycling 0-97556  
Danjon astrolabe planetary obs. (*French*) 0-94715  
deep water waves, instabilities, review, book contrib. 0-96274  
density wave theory 0-67873  
derivative spectrophotometry, theory and appls. (*Japanese*) 0-86451  
diagnostic techniques in nuclear medicine, review, book contrib. 0-72322  
diamond, synthesis (*Japanese*) 0-80994  
diatomic molecules, excited states, electronic transition probabilities and lifetimes 0-78658  
dielectric crystal, APR and phonon spectroscopy to study paramagnetic ions 0-84634  
diffraction gratings produced by lasers (*Rumanian*) 0-87542  
diffusion pumps 0-57321  
digital picture processing 0-83562



## reviews continued

- dislocation motion, theory, book contrib. 0-107240  
 dislocations, thermodynamics and thermal activation, book contrib. 0-107241  
 dispersion hardened alloys, strengthening theories 0-97498  
 DNA in conc. solns. of neutral salts, conformational transitions 0-81531  
 drug radioreceptor analysis applications 0-94315  
 duality in field theory and statistical systems 0-73610  
 duodenum, fluid mechanics, review, book contrib. 0-97994  
 dye lasers, book contrib. 0-106517  
 dynamic loading of structures and plastic response 0-83756  
 dynamic self-diffraction of coherent light beams 0-102777  
 Earth albedo, anthropogenic changes and effects on climate 0-81893  
 Earth bow shock, DC mag. field obs. 0-90306  
 Earth bow shock, first evidence and early studies, historical introduction 0-85816  
 Earth heat loss through crust 0-98286  
 Earth sciences, use of electron microscopy 0-105091  
 echocardiograms, 1D and 2D, computer processing (*German*) 0-81665  
 eclipsing binary stars, period variations 0-109474  
 ecology and systematics (book) 0-67945  
 Einstein's part in the development of quantum concepts 0-98781  
 Einstein's theory of gravitation 0-90745  
 elastic constants, third-order, of uniaxial crystals 0-65119  
 electric quadrupole interactions measured by nuclear orientation and NMR on oriented nuclei 0-92868  
 electric vehicle battery systems available and under review (*Dutch*) 0-72025  
 electrical breakdown of gases, prebreakdown stage 0-106868  
 electro-optical and nonlinear-optical materials 0-74450  
 electrocatalysis surfaces modified by metal adatoms 0-61110  
 electrofocusing, current major appls. 0-101306  
 electron energy loss spectroscopy, in electron microscope, review 0-104025  
 electron gas, dielectric constant 0-107731  
 electron microscope, construction, operation and special types 0-86529  
 electron microscope, scanning-transmission, design, operation, capabilities and limitations 0-68300  
 electron microscopy, HV, in situ obs., techniques and appls. (*Japanese*) 0-59351  
 electron microscopy, semiconductor appls., advances 0-101911  
 electron microscopy in metallurgy 0-76458  
 electron microscopy of ferroelectric substances (*Japanese*) 0-71366  
 electron probe microanal. in SEM by means of X-ray spectrometers, review 0-95194  
 electron spectroscopy, inner-shell, for microanal. 0-68303  
 electron theory of metals and geometry 0-103611  
 electronic materials rel. to cryst. growth, device appl. 0-66405  
 electronic transport in insulators (*Spanish*) 0-84464  
 electrons and positrons in dense gases 0-103106  
 elementary particle physics, cosmological approach, review, book contrib. 0-68440  
 elementary particles seen  $J/\psi$  0-57018  
 ellipsometric instrumentation, review 0-101819  
 ellipsometry of clean surfaces, submonolayer and monolayer films 0-103546  
 energy conservation and storage, materials needs 0-66958  
 energy resources, long-term energy systems and the role of nuclear and solar energy 0-66918  
 energy resources, review of alternatives to fossil fuel (*Italian*) 0-66917  
 energy sources for long-term implantable devices 0-98175  
 epithelial mucus, rheology and mol. organisation 0-97959  
 EPR, low symmetry effects 0-71159  
 equipment for the measurement of ions in solution 0-71983  
 equivalence principle, evolution to general relativity 0-98779  
 ethylene-methyl acrylate, random copolymer 0-108330  
 European Space Agency programmes, developmental or operational status 0-72742  
 eutectic alloy, dendrite growth—the coupled zone 0-97489  
 evoked potential and early studies of bioelectricity 0-101158  
 evolution of massive stars 0-82343  
 experimental verification of the general theory of relativity 0-98850  
 far IR IC, antennas and waveguides for integration, review 0-69553  
 fast processes, measurement, present methods in USSR future prospects 0-75271  
 fatigue detection and rating by acoustic emission, review 0-104380  
 fatigue resistance, in metals 0-94907  
 ferrite, transform. kinetics, grain size, alloying element effect, carbide precip. 0-93560  
 ferrites, soft, production and props. 0-88801  
 ferroelectric ceramics, materials and dielec. props. 0-75957  
 ferroelectric liquid crystals, chiral smectic C phase, phys. props. 0-75150  
 ferrofluids, agglomeration 0-61162  
 ferromagnetic particle suspensions in non-conducting and metallic liqs. 0-60372  
 ferromagnetic surface, spin fluctuations and light scatt. 0-84727  
 few nucleon correlations from high energy scatt. (*Russian*) 0-68549  
 fibre optic communication systems, analytical review including survey of commercial systems 0-74489  
 fibre optic communications, prospects for 1 to 1.6  $\mu\text{m}$  spectral range use 0-102848  
 fibre optic connectors, precision and stability developments 0-69523  
 fibre optic market trends, worldwide 0-58699  
 fibre optic systems and field trials, review 0-58700  
 fibre optics, state-of-the-art and available equipment (*German*) 0-87484  
 fibre optics sensors for measurement and control appls. 0-58780  
 fibre optics technology and connector systems, marketing 0-69522  
 filled polymer mechanical properties, particle shape effect, review 0-100864  
 film- and transition-boiling heat transfer to cryogenic fluids 0-92026  
 finite temp. field theory with boundaries, extensions to curved space, stress tensor and surface action renormalisation 0-57455  
 fission barrier props., expt. studies and statistical anal. review 0-102216  
 fission reactor physics 0-63245  
 floating zone, under reduced gravity, Marangoni convection 0-66425  
 flow cytometric data, computerised display and anal., book contrib. 0-109082  
 flow measurement techniques for closed conduits 0-64654  
 fluctuation phenomena, mathematical formulation, review, book contrib. 0-73267

## reviews continued

- fluorescence spectroscopic investigations of the dynamic properties of proteins, membranes and nucleic acids 0-101148  
 fluorescently labelled molecules as probes of living cells struct. and function 0-67321  
 Fourier spectroscopy and multichannel long integration time techniques 0-91751  
 Fourier transform NMR spectroscopy, review 0-104486  
 fracture mechanics 0-64458  
 fracture toughness (*Japanese*) 0-90595  
 free convection in rectangular enclosures filled with fluid and with porous media 0-79115  
 fusion, ETF, engineering challenges 0-95422  
 fusion, international fusion technology program 0-95423  
 fusion, US magnetic fusion program, survey 0-91249  
 fusion hybrid blanket data and development, review, simulation test facilities 0-106170  
 fusion inertial confinement, advanced engineering requirements 0-95421  
 fusion reactor, ASDEX, assembly and commissioning, review 0-102334  
 fusion reactor, Doublet III beamline, review, component relation and config. design constraints 0-99382  
 fusion reactor, large superconducting toroidal field coil program, progress report 0-99335  
 fusion reactor, MFTF, electrical systems, overview 0-91278  
 fusion reactor, Nova, mechanical design, overview 0-91279  
 fusion reactor, PDX, 6 MW Neutral Beam Project, overview 0-106223  
 fusion reactor development, pure and hybrid reactor options 0-63389  
 fusion reactor pellet re-fuelling feasibility 0-91246  
 fusion reactor plasma heating and confinement 0-63388  
 fusion reactors, electron beam driven Tokamaks, review 0-99317  
 fusion reactors, Large Coil Program, superconducting mag. coil struct. design status 0-106189  
 fusion reactors, laser produced nuclear fusion 0-63381  
 fusion reactors, TEXT overview and status report 0-91273  
 fusion research, internat. cooperation (*Japanese*) 0-63371  
 fusion-fission hybrid reactors 0-74019  
 galactic magnetic field review of obs. 0-73042  
 galactic structure from gamma ray obs. 0-98743  
 galaxies, evolution of stars and gas 0-77486  
 galaxies, nearby, radio continuum obs. (*German*) 0-109544  
 galaxies of Magellanic type, review (*German*) 0-105348  
 gas chromatography/mass spectroscopy integrated systems 0-68289  
 gas lasers, atomic and ionic, excitation mechanisms and characts., book contrib. 0-106512  
 gaseous criteria pollutant methodology and standards for USA Clean Air Act 0-94133  
 gases, weakly ionised, electron motion, stochastic theory of homogeneous systems, review, stochastic theory of homogeneous systems 0-77735  
 gauge unification of fundamental forces 0-95238  
 geodetic research, objectives, meas. techniques and data processing methods (*German*) 0-101317  
 geomagnetic coast effect, review 0-94458  
 geomagnetic depth sounding below magnetometer arrays for atmos. research 0-98486  
 geostationary meteorological satellites, role played in Global Weather Expt. 0-77256  
 giant Raman scattering by mols. adsorbed on metals 0-93343  
 gland cells, stimulus-response coupling, book contrib. 0-108864  
 glass, refractive index gradients, form. using ion exchange diffusion 0-64227  
 glass fibre long wavelength optical communication, materials and devices 0-99854  
 glass fibre reinforced plastic, fatigue processes, review 0-81176  
 glass forming melts, crystn. kinetics processes 0-64905  
 glass optical fibre, vapour phase materials and processes, review 0-58825  
 glasses, ESR studies 0-108049  
 glassy metals, structure, transport props., magnetic behaviour 0-70138  
 glassy state and highly viscous liq. rheology 0-70130  
 gradient-index optics: a review 0-69478  
 grain boundaries, cubic materials, intergranular structures, geometrical approach (*French*) 0-59482  
 grain boundary segregation, critical assessment 0-75362  
 gravitational field gauge theories 0-98848  
 gravitational radiation, multiple expansions 0-73240  
 gravitational wave research, current status and future prospects 0-73254  
 hadron interactions, inclusive processes, multiplicity and scaling, resonance production, additive quark model, SU(6) theory 0-63043  
 hadron physics at high  $p_T$  0-73743  
 'He thin film, superfluidity 0-107594  
 heat and mass transfer bibliography—Polish works (1977-1978) 0-57020  
 heat and mass transfer bibliography—Soviet works 0-90618  
 heavy ion collisions, perturbed stationary state method, low energy collision and mol. resons. 0-78320  
 heavy quarks and new particles 0-73661  
 AM Herculis (4U 1814+50), X-ray emitting mag. white dwarf binary, review of props. 0-105403  
 hereditary damage [review] after low-level radiation exposure 0-67165  
 HF current surgery, instruments and problems (*Hungarian*) 0-98172  
 high electrical resistance measurement 0-57331  
 high strain rate processes 0-84864  
 high temperature mechanical behaviour of crystalline solids 0-59568  
 hollow cathode discharges for gas lasers 0-83599  
 hollow cathode discharges for gas lasers 0-99717  
 holographic memories, used for data recording 0-58478  
 hot-wire test, critical review and comparison with BS 1902 panel test 0-104409  
 HTGR development and its process heat, steam-cycle and gas turbine appls. 0-63250  
 HV lines to 800 kV, elec. and mag. field effects on human beings (*French, English*) 0-72209  
 hybrid reactors, fusion driven fissile fuel breeder systems 0-57954  
 hydrodynamic models in star formation (*Polish*) 0-67709  
 hyperon beam physics, book contrib. 0-68503  
 hyperthermia, deep local, induction by US and EM fields, problems and choices 0-94283  
 III-V semiconductors, radiative recomb., optical evaluation review 0-60647  
 Illinois climate centre, review 0-77118  
 image processing in nuclear medicine 0-81694  
 immunological effects of irradiation 0-81660  
 implantable prostheses 0-101292

# reviews continued

implanted semiconductors, laser annealing 0-107301  
impulse/impact noise, current knowledge 0-79056  
impurity centres, electron-phonon coupling from structured optical spectra 0-89038  
inelastic electron-matter interactions 0-104024  
inspection of part quality, coarse struct. materials, LF US methods 0-81264  
intergalactic matter and evolution of galaxies 0-109543  
Interkosmos program and Magion satellite project 0-98535  
intermediate valency compounds, properties and appearance conditions 0-103649  
international architectural acoustics standards (*Japanese*) 0-64294  
International Sun-Earth Explorer (ISEE) mission, review 0-90320  
interstitial alloys, interstitial atomic arrangement and mobility at high degrees of interstice filling (*Russian*) 0-107223  
ion beam, plasma and reactive ion etching 0-108621  
ion implantation, chemical and electrochem. aspects 0-100271  
ionic crystals, defects, computer modelling, review 0-107205  
ionic crystals, dislocations 0-107236  
ionic liquids, structural props. 0-96430  
ionic nitriding thermochemical process, equipment, process details and advantages and prospects (*French*) 0-108641  
ionization phenomena, appls. in medical diagnosis and treatment 0-67240  
ionosphere, time dispersion of EM pulses 0-94645  
ionosphere-magnetosphere system, induced elec. fields 0-94647  
IR and submillimetre astronomy, book (*Russian*) 0-72773  
IR laser systems, for 16  $\mu$ m range (*Rumanian*) 0-87408  
IR non-destructive testing of bonded materials, theory and practice 0-93708  
IR radiation, parametric up-conversion to visible range 0-64104  
IR spectroscopy, reflection-absorption, of adsorbed layer systems, review, book contrib. 0-84747  
IR-ATR spectroscopy, appl. to struct. investigation of biological material in aq. environment 0-61735  
Jovian planet interior heat production 0-98606  
knee biomechanics, review of some basic assumptions 0-94265  
laboratory plasma devices 0-79589  
lake modelling, temperate ecosystem 0-81949  
Large Coil Program, research and development activity 0-99336  
large-scale elec. energy storage 0-89676  
laser applications in biomedical meas. (*Japanese*) 0-94311  
laser applications in nucleus physics, review, book contrib. 0-68504  
laser induced photochem. of vibr. excited mols. 0-71925  
laser ion source, appl. in mass spectrometry 0-89564  
lasers, tunable, principles, characts. and appl. (*Japanese*) 0-74330  
layered superconductors, Josephson coupling effects, review 0-84554  
left ventricular function, radioisotope evaluation with nonimaging probes 0-85484  
left ventricular function assessment using radionuclide techniques, technical considerations, book contrib. 0-101261  
lepton measurements, QED and CPT, CP and T invariance tests 0-77996  
light guide data transmission, review (*German*) 0-95996  
light hadronic spectroscopy, expt. and quark model interpretations, review, book contrib. 0-68438  
light nuclei, alpha transfer reactions, review, book contrib. 0-68699  
light scattering near phase transition pts. in pure and defect containing crystals. 0-93361  
light sources for simulating sunlight 0-87454  
linear elastic beams, shells and plates, elementary theories review 0-69677  
liquefaction cracking during welding, comp. influence 0-66645  
liquid crystals, mol. conformation and orientational order, NMR studies 0-75151  
liquid crystals, X-ray diffr. studies 0-100166  
liquid metal embrittlement micromechanisms 0-108637  
long-range weather forecasting, art and science 0-109184  
Loran-C signal, ground wave propag. theory 0-94580  
lunar highlands crust, origin and comp. and effects of meteorite bombardment 0-109381  
lung cancer, interstitial brachytherapy, 20 year experience 0-72302  
B Lyrae, eclipsing binary system, current knowledge 0-105289  
magnetic bubble materials, props. and preparation models (*Rumanian*) 0-93149  
magnetic bubble wall dynamics 0-75823  
magnetic circular dichroism of biological molecules, book contrib. 0-109080  
magnetic domain walls and bubbles, dynamic props. 0-88784  
magnetic field meas., 1980 status (*French*) 0-95114  
magnetic fluids, mag., optical, and hydrodynamic props., expt. study 0-60376  
magnetic soft and hard materials, garnets, magnetic properties and applications, structural props. 0-65760  
magnetic spectrographs, use in nucl. reaction studies (*Rumanian*) 0-87012  
magnetic surface states, in spin wave resonance, theory 0-84654  
magnetic system, Lifshitz point, phase diagrams and crit. behaviour 0-65928  
magnetosphere, open model plasma populations 0-90295  
mammary carcinoma, primary radiotherapy (*German*) 0-61693  
Mandel'shtam and nonlinear oscillations and wave theory 0-105515  
Mars, as seen at end of Viking mission 0-72839  
martensitic transformations, electron microscope study of cryst. geometry (*Russian*) 0-108441  
mass loss from late-type stars 0-67755  
massive stars evolution, observational review 0-90416  
matched filtering improvements for coherent optical pattern recognition 0-78786  
material properties associated with dynamic deformation of matter, acoustics and the props. of materials 0-64234  
mathematical modelling, vibrational resonances of built-up structures, use of meas. data 0-69718  
matrix isolation studies of high temp. species 0-57399  
medical B-scan US, technical factors influencing the imaging of small anechoic cysts 0-98049  
medical image processing in diagnostic radiology 0-81690  
medical imaging overview 0-98082  
melting, dislocation theory 0-65198  
membrane bilayers, quasitwo dimens., theoretical models 0-76713  
mesomorphic monolayers, quasitwo dimens., theoretical models 0-76713

# reviews continued

metal, ion implanted H(D), interstitial positions and vibr. amplitudes, fast ion channelling study 0-79848  
metal, light element implantation, radiation damage review 0-88219  
metal colloids in ionic cryst., preparation, optical, mag. resonance, elec. props. 0-59459  
metal ion lasers, hollow cathode 0-99708  
metal monolayers, on metal cryst. surfaces, surface struct., review 0-80067  
metal silicides, fabrication technique and characterisation (*Japanese*) 0-60779  
metal vapour lasers, hollow cathode (*Rumanian*) 0-87409  
metal-electrolyte interfaces, optical reflectance spectra, interpretation 0-93263  
metal-H system, hydride formation in high press. range 0-65235  
metallic glass, corrosion behaviour 0-89421  
metallic glass, current exptl. data on struct. 0-88058  
metallic glasses, annealing behaviour, thermal stability and crystn. 0-75167  
metallic glasses, electronic structure rel. to elec. cond., supercond. and mag. props. 0-65429  
metallic glasses, formation, stabilities, and props. 0-64912  
metallic glasses, review 0-88051  
metallic surface, self-consistent electron theory 0-88616  
metallurgical coatings, fabrication, struct., and appls. 0-80121  
metals, BCC, plastic deform., review 0-104213  
metals, dynamical props. of point defects, book contrib. 0-103317  
metals, electronic struct. and magnetism 0-70573  
metals, hydrogen brittleness measurement 0-104291  
metals, point defect diffusion controlled reaction theory, book contrib. 0-103318  
metals, solid and liq., optical props. by spectroscopic ellipsometry, review 0-103929  
metals and alloys, shock wave effect on martensitic transform. (*Russian*) 0-96595  
metastability, rigorous molecular theory, review, book contrib. 0-73271  
metastable microcrystalline alloys, appls. 0-84887  
meteoric nightglow, review of historical obs. 0-94761  
microdosimetry, role in radiobiology 0-61705  
microelectronics and thin film components frontiers 0-73123  
microphones, development and calibration accuracy 0-96167  
micropinch in a high-current diode 0-103183  
microscopic equipment, methods and appls., bibliography 0-62406  
microscopy bibliography 0-90619  
mid-ocean ridges, obs. and implications of ridge crest hot springs 0-98304  
MIM, thin film, use as non-heated source of electrons 0-84516  
modulators, photoelastic radiation polarisation 0-102846  
molecular biology, origins, autobiographical review 0-57052  
molecular emission cavity anal., vapour generating systems, cool flame spectroscopy 0-81396  
molecular laser, optically pumped 0-58519  
molecular radiation biology, time effects 0-72269  
molecules adsorption on oxide surfaces, UPS studies 0-84374  
monocrystals, EM radiation of relativistic positrons and electrons during axial and planar channelling 0-79845  
monolayer on graphite, neutron scatt. studies 0-107655  
Moon, mascon basins: lava filling, tectonics and origin 0-98583  
motion in depth, binocular and monocular stimuli 0-61570  
multielectron target+multiply charged ion, electron capture 0-63812  
multihadron production in nuclear matter and hadron struct., space-time description (*Russian*) 0-68571  
multiply charged ion+one-electron target, electron capture 0-63811  
muon spin rotation method, review (*Polish*) 0-88901  
myocardial blood flow,  $^{133}\text{Xe}$  studies, theoretical, technical and practical aspects 0-94355  
myocardial perfusion imaging, quantitative aspects 0-94358  
narrow gap semiconductors, recombination mechanisms 0-96905  
nature, unity of, as an incentive to research (*German*) 0-77533  
negative ions, at. and mol. collisions electron detachment for energies near threshold 0-63797  
nematic liquid crystal, total internal reflection 0-96445  
neoplasm localisation with radionuclides 0-67215  
nerve impulse conduction, modulation along the axonal tree, book contrib. 0-108872  
neurons, transport of substances 0-89745  
neutral+high Rydberg atom, thermal collisions 0-63756  
neutrino astrophysics, review, book contrib. 0-72769  
neutron absorption radiometric testing of materials, review 0-71860  
neutron activation analysis,  $1/\text{E}^{1/2}$  epithermal neutron spectrum,  $\alpha$ -determ. methods, accuracy 0-71977  
neutron scattering from adsorbed mols., surfaces, and intercalates, review, book contrib. 0-84394  
neutron star X-ray emission models 0-62175  
neutron stars, nonequilibrium shells, role in X-ray emission and nucleosynthesis 0-67774  
NMR applications to phosphoryl transfer enzymes, and metal nuclei of metalloproteins, book contrib. 0-109081  
NMR of solid electrolytes and solid soln. electrodes 0-60432  
noctilucous clouds, advances in space era 0-105095  
non-classical effects in the statistical properties of light 0-99686  
nondestructive evaluation 0-71855  
nonlinear optical resonators, radiation excitation, review 0-69462  
nuclear and particle science, book 0-67940  
nuclear magnetism and ultralow temperature (*Japanese*) 0-86806  
nuclear medical instrumentation, mobile 0-101262  
nuclear medicine in Europe, present status and future trends 0-94331  
nuclear medicine instrumentation, recent developments 0-81692  
nuclear physics, current trends (*Hungarian*) 0-57786  
nuclear physics with synchrotron radiation 0-106216  
nuclear power, environmental impact 0-101143  
nuclear pumped lasers, review of developments at Illinois University 0-63996  
nuclear reaction theory for nuclear engineers (*Japanese*) 0-99155  
nuclear reactor fuel element codes, structural anal. 0-78362  
nuclei far from line of beta stability, mass spectroscopic anal. techniques, book contrib. 0-69014  
nucleic acids and their aggregates, optical activity, book contrib. 0-108847  
obstetric practice, the place of real-time and static B-mode scanning, educational syllabus 0-86057



## reviews continued

- ocean tides 0-98349  
ocean waves of continental shelves, recent advances 0-98348  
optical communication, present and future developments 0-69521  
optical fibre applications outside data transmission and communication 0-74482  
optical fibre preparation methods and performance factors 0-69557  
optical fibres, progress and components (*French*) 0-69524  
optical image processing, analogue and digital, feedback, review 0-102639  
optical instrument design, partial coherence effects 0-78767  
optical microscopes, scanning, imaging props. and appls. 0-82811  
optical properties of rough surfaces, discontinuous films, heterogeneous materials, review 0-103935  
optical rectification effect and meas. appls. 0-91835  
optical waveguide fibre coating technology, overview 0-58828  
optical wavelength division multiplexing transmission technology 0-58727  
organ doses from isotropic  $\gamma$ -ray fields 0-109026  
organic molecular crystals, intermolecular interactions, spectroscopic studies, review 0-103958  
organic solids, vibr. relax. and dephasing, Raman spectra 0-88987  
origin of elements, review 0-62359  
oropharynx, squamous cell carcinomas 0-67925  
OTEC, technology development, US DOE program 0-94098  
OTEC ocean engineering 0-66989  
OTEC power system development and environmental impacts 0-66990  
oxide semiconducting glasses, electronic cond. mechanism 0-65562  
oxides, impurity diffusion and self-diffusion, review and bibliography 0-59719  
oxides, thermally stimulated exoelectron emission (*German*) 0-66404  
Palomar Hale telescope, first 30 years 0-72774  
paralysed, treatment by elec. stimulation (*Slovenian*) 0-81771  
paraplegic patient muscles, provision of functional use by elec. stimulation 0-101289  
particle detectors, methods of detection and appl. of electronics and computer technology 0-106235  
particle motions in a viscous fluid, review, book contrib. 0-96289  
particle properties, leptons, mesons, baryons 0-67944  
particles, massive, with any spin. consistent eqns., Klein-Gordon divisor 0-73577  
passive optical rotation sensors using guided waves, developments 0-58781  
Peers University Biophysics Unit, Hungary, 25 years of radioisotope appls. (*Hungarian*) 0-90647  
percolation theory 0-98868  
phoniatric diagnostics of speech organ disorders, objective acoustic methods 0-104598  
phosphate containing materials, technological prod. processes review 0-97452  
photoacoustic spectroscopy, biological and medical appls., book contrib. 0-109078  
photocells and photomultipliers, USSR 0-57371  
photoelectron spectroscopy, solid-state, with synchrotron radiation, review 0-71570  
photon echo spectroscopy of crystals 0-83648  
photovoltaic materials and devices for terrestrial solar energy applications, R and D status review 0-101112  
physiologic tomography, noninvasive meas. of myocardial metabolism, blood flow and function 0-104730  
pion exchange at high energies 0-95259  
planet interior differentiation processes, trace elements as probes 0-98584  
planetary magnetism 0-98585  
planetary nebulae, advances in optical studies 0-109522  
planetary nebulae, gas dynamics and evolution 0-109533  
planetary nebulae, review of UV obs. 0-109523  
planetary nebulae, spatial and vel. distrib. statistics 0-109518  
planetary nebulae central stars, spectra, temps., binaries and peculiar stars 0-109435  
planetary nebulae chemical abundances 0-109530  
planetary nebulae role in heating stirring and ionisation of interstellar medium 0-109540  
planetary ring systems, review of physical studies 0-72874  
planets, major, pre-Voyager understanding of ionospheres 0-90351  
plasma, low-temp., with nonequilibrium ionisation 0-96343  
plasma chemistry, history, diagnostics, production, organic compd. synthesis 0-61099  
plasma collisionless shocks, simulation and laboratory expts. 0-87893  
plasma heating, neutral beam US development program and review 0-92348  
plasma industrial utilisation, synthesis, powder, metallurgical and surface treatments (*French*) 0-96398  
plasma shock waves, transverse mag. field effects 0-103153  
plasma turbulence, strong, Langmuir, simulations 0-59237  
plasmasphere, large scale elec. fields and currents, related geomag. vars., review 0-105121  
Pluto, long term orbital motion, librational character 0-94753  
Pluto (book) 0-82591  
polar materials, appl. to SAW and other devices 0-66114  
polarised beam experiments, low energy, in nuclear physics, book contrib. 0-68642  
polyester thermoplastic, for electrical insulators 0-103685  
polymer, crack extension micromechanisms 0-108561  
polymer crystallisation, review 0-64925  
polymer dry insulation, for power cables (*Spanish*) 0-81024  
polymer macromolecules, volume interactions, coil-globule transition, statistical physics 0-78737  
polymer systems, crystallisation from solution 0-84105  
polymer systems, crystallisation kinetic data, status of anal. 0-84104  
polymers, dielec. breakdown (*Japanese*) 0-60501  
polymers, electronic structure 0-59860  
polymers, long-term strength prediction, review 0-104226  
polymers, specific fracture surface energy, meas., review (*French*) 0-104275  
polynucleotide electron energy band studies 0-72132  
positive muon probes, metal studies 0-103909  
positron camera system, ring detector, brain research, computed transaxial tomography 0-61739  
powder coatings, in metal finishing, review 0-104330  
powders, phonon electroacoustic echoes, storage mechanisms 0-75606  
principle of maximum entropy and irreversible processes 0-86198  
protein network formation dynamics, review, book contrib. 0-97995

## reviews continued

- proteins involved in active membrane transport, struct., book contrib. 0-108844  
pyrophosphate myocardial imaging 0-94359  
QCD and superdense matter, quark and gluon plasma, hadronic structure, neutron stars, hadron collisions 0-73683  
quantum chemical methods appls. 0-93752  
quantum interference effects in psychology, Schrodinger's cat 0-73158  
QUISTOR, ion kinetic energy calc., survey 0-78468  
radiation damage, mechanisms in semiconductors and insulators 0-107315  
radiation damage by electrons, cryst. and organic materials 0-79840  
radiation protection standards, quantitative risk 0-61708  
radiation science, role of models 0-76144  
radiation therapy, total body techniques for bone marrow transplantation 0-104738  
radiative, (conductive) heat transfer, direct differential methods, review 0-64352  
radioactive waste, decay heat estimation, summation calcs. and Standard eqns. 0-63317  
radioactivity incidents, national arrangements 0-102355  
radiocommunication, propag. problems connected with infinitesimal point source 0-90194  
radiocommunication, propag. problems connected with special source structs. 0-87272  
radiointerferometry, Mandel'shtam's research 0-105488  
radioisotope counting techniques for analytical appls. in biology and medicine 0-81794  
radioisotopes, artificial, 25 years of use and production in Hungary (*Hungarian*) 0-94340  
radioisotopes, development in use (*Hungarian*) 0-90645  
radiolysis of DNA and other bipolymers 0-67163  
radiolysis of heterogeneous inanimate systems, radiobiology appl. 0-66824  
radiomunoassay, book contrib. 0-109021  
radionuclide evaluation of cardiac trauma 0-94361  
rainfall measurement by radar, methods and interpretation of data 0-81969  
Raman spectroscopy, remote spontaneous, new trends in recording of signals 0-73485  
random motion and Brownian rotation 0-73266  
rapid automated nuclear chemistry, short lived fission products, reactor safety 0-81353  
rare earth intermetallic compounds, ferromag. props., book contrib. 0-75726  
rare earth iron intermetallics, RFe<sub>2</sub>, magnetostrictive, book contrib. 0-75838  
rare earth metals and alloys, ferromag. props., book contrib. 0-75725  
rare earth semiconductors, studies in Soviet Union 0-96875  
recording of fast processes, photographic and cine methods 0-57413  
refractory ceramic coatings, for high temp. use, current status (*Japanese*) 0-71619  
remaining creep life for components under stress at elevated temperatures 0-59566  
renormalization group and ultraviolet asymptotics 0-101933  
research uses of early data, from Meteor-1 0-77257  
resonant light scattering from magnetic excitations 0-97290  
retinal research and study, selected review 0-108874  
ring galaxies 0-62281  
rough surface contact, review of expt. work 0-76377  
rubber, natural, crosslinked by dicumyl peroxide, modulus, swelling relations 0-59551  
Rydberg atom + molecule, reaction channels, expt. vs. theory 0-63755  
SAW filter appls. in consumer electronics 0-74675  
scanning Auger microscopy, developments 0-101909  
secondary complex ion emission (*Russian*) 0-108305  
secondary electron emission, angular and energy distrib. 0-100718  
seismology, use of dislocation theory, book contrib. 0-109119  
SEM microanalysis techniques 0-71995  
semi-insulating substrates, monolithic integration of optical and electronic devices 0-58543  
semiconductor, deep levels, review 0-103640  
semiconductor, impact ionization 0-65577  
semiconductor diode lasers, book contrib. 0-106525  
semiconductor film growth, multilayer systems, spectroscopic ellipsometry 0-103603  
semiconductor laser diodes, present status and technology (*German*) 0-58561  
semiconductor step  $I$ - $V$  junction, elec. struct. analytical methods 0-100507  
semiconductors, deep centres, ODMR (*French*) 0-60461  
semiconductors, ion implanted, laser annealing 0-65023  
semiconductors, p-type, spin-flip Raman scattering 0-108209  
semiconductors, temp. depend. electronic cond. 0-59975  
shock acceleration of particles in astrophysical plasma 0-82192  
shock wave interactions with boundary layers, review, book contrib. 0-96283  
Si epitaxy, vapour phase deposition technology 0-75472  
SIMS, quantitative 0-61195  
single crystals under large loads, theoretical elastic behaviour, review and appl. 0-71681  
singular potentials in non-relativistic quantum theory (*Russian*) 0-68345  
soft magnetic materials, meas. methods 0-86345  
solar cell, thin film polycryst. Si, research and develop. overview 0-93921  
solar cell array fabrication, review of present status and future prospects 0-61343  
solar cooling 0-85265  
solar coronal holes, modulation effect on cosmic ray intensity 0-77370  
solar energy conversion, materials science aspect 0-66957  
solar energy conversion technology, assessment and contemporary criteria, 1978-79 0-76650  
solar flare plasma instability and turbulence 0-62100  
Solar Maximum Year project and related space experiments, review 0-90404  
solar passive space heating, review and development of direct, mass wall and attached sun space systems for residential appls. 0-76619  
solar photoelectrochemical cells, review of cell types and electrode props. 0-61385  
solar ponds, nonconvecting 0-61407  
solar radio burst emission mechanisms 0-72917  
Solar System stability and evolution 0-82235  
solar temperature control system, modern control theory appl. 0-66949

## reviews continued

solar wind, plasma fluid aspects 0-90313  
 solar wind, plasmadynamical processes review (*German*) 0-109323  
 solar wind characts. rel. to solar activity, review 0-94777  
 solar wind data measured on lunar surface 0-77556  
 solar wind plasma microinstabilities, review of theory 0-98530  
 solar-H<sub>2</sub> energy systems 0-61447  
 solid polymers, NMR 0-88888  
 solid solutions, polycrystn., rheological study of crystallographic order on creep (*French*) 0-97548  
 solid state dosimetry, tissue-equivalent systems (*Hungarian*) 0-91291  
 solid state lasers, book contrib. 0-106529  
 solid state nuclear track detectors, visualization of latent damage trails etching, decoration and observation techniques 0-91382  
 solid state physics, review of experimentation, undergraduate level (*Spanish*) 0-82624  
 solid surface, microgravimetric-IR study 0-76577  
 solid-solid interface chemistry, characterisation, theory 0-75448  
 solids, acoustic wave emission, absorpt. and propag. in THz range 0-65164  
 solitary waves, review, book contrib. 0-94962  
 solitons, review of concepts and methods in theory (*Polish*) 0-68057  
 solitons in condensed matter: a paradigm 0-77632  
 solution X-ray scattering, review of recent developments, book contrib. 0-109077  
 solvent structure, at polarisable interfaces, mol. models 0-59359  
 somatosensory evoked potentials, review of acquisition and anal. 0-101281  
 sound analysis by the ear 0-104593  
 sound propagation, HF, in metals and semiconductors, nonlinear effects 0-88279  
 space-variant coherent optical processing 0-102638  
 spacecraft solar arrays, in-orbit performance 0-94054  
 spectrally selective solar absorber coatings 0-61404  
 spectrally selective surfaces for photothermal conversion of solar energy 0-101125  
 speech synthesis, current topics (*Japanese*) 0-91973  
 spinodal decomposition, phase transitions via unstable states 0-96657  
 spontaneous symmetry breaking and symmetry defects 0-95231  
 sputtered particles, energy and mass distrib. 0-84822  
 SQUIDS, weak magnetic field meas. 0-86267  
 SS 433, review of obs. and theories 0-72987  
 star formation and protostellar clouds, review 0-101589  
 STARFIRE project, an overview 0-106183  
 stars with anomalous mass, examples 0-72929  
 statistical mechanical theory of the kinetics of phase transitions, review, book contrib. 0-73270  
 statistical methods appl. to planetary surfaces 0-101540  
 steel, austenitic type EI-69, carbide transformations on precipitation of C from austenite (*Russian*) 0-97487  
 steel, clean, review 0-84839  
 steel, Cr-C, structural, struct.-prop. resl., high strength and toughness design criteria 0-97491  
 steel, cryogenic, creep, review 0-104222  
 steel, effect of H<sub>2</sub> on phys. and mech. props. 0-101657  
 steel, fatigue crack propag. near to threshold stress intensity 0-100898  
 steel, ferritic, crack extension, cleavage micromechanisms 0-108562  
 steel, toughness, review of joint tests (*German*) 0-65142  
 steels, nuclear pressure vessel, small specimen predictions of fracture toughness 0-81172  
 steels, solute segregation and intergranular fracture 0-60957  
 stellar chromospheres, review (*German*) 0-109421  
 stethophenendoscopes, design and production 0-104686  
 stochastic gravitational fluctuations in a self-consistent mean field theory 0-90734  
 stochastic processes, review, book contrib. 0-73268  
 stochastic quantisation processes, review, Markov processes, Martingales, quantum dynamics 0-94969  
 Stokeslets and eddies in creeping flow, review, book contrib. 0-96265  
 storage batteries, vehicle and storage appl. 0-72031  
 stratosphere and mesosphere radar studies, UHF and VHF, review 0-90180  
 stratosphere turbulence near tropopause, review of radar obs. 0-90179  
 stratospheric H<sub>2</sub>O, maintenance of extreme aridity 0-105028  
 stress corrosion cracking, role of H<sub>2</sub>, state of art review 0-61017  
 stress corrosion cracking failure, predictive approaches 0-97611  
 structural phase transformations, static critical behaviour 0-92640  
 structural phase transitions, crit. dynamics and quasi-elastic scatt. 0-92641  
 structural phase transitions, Landau theory 0-92639  
 SU(5), unification of weak, EM and strong interactions 0-105814  
 subjective effects of the sound fields and acoustic design of rooms (*Japanese*) 0-64293  
 Sun, active regions, open mag. field lines struct., review 0-85924  
 superconducting band gap anisotropy, Eliashberg eqns. (*Spanish*) 0-84544  
 superconducting magnet stability problem at accelerators under high-energy particle irradiation (*Russian*) 0-68972  
 superconducting metastable alloys, review of current work 0-81002  
 superconducting thin films, vortices, phase transitions 0-88698  
 superconducting transition critical temperature, BCS theory, phonon spectra (*Spanish*) 0-84535  
 superconductivity, inhomogeneous, Ginzburg-Landau theory 0-88672  
 superconductivity and phonons 0-84543  
 superconductor preparation, multifilamentary Nb<sub>3</sub>Sn by 'in situ' and cold powder methods 0-93522  
 superconductors, A15-type, structure and props. 0-70909  
 superconductors, electric field penetration and collective oscillations 0-88678  
 superionic conductors, theoretical models, review 0-107465  
 superluminal motion in compact extra-galactic radio sources 0-77504  
 supersaturated vapour, critical clusters, theory and Monte Carlo simulation 0-82734  
 supersymmetry and supergravity (*Czech*) 0-86183  
 surface anal. tools 0-103540  
 surface analysis techniques appl., electrification phenomena 0-80354  
 surface analytical techniques, quantification 0-65342  
 surface segregation, influence in metallurgical props. (*French*) 0-80045  
 suspensions, rheology, colloidal forces role, review 0-103063  
 suspensions, statistical theory, review, book contrib. 0-96288  
 switches, high press. surface discharge 0-103208

## reviews continued

synaptic slow responses, props. and possible underlying mechs., book contrib. 0-108873  
 synovial joints, immobility effects, pathomechs. of joint contracture 0-97954  
 technical, cooperation among developing countries, evaluating potential of technology transfer 0-82628  
 TEM, advances, catalytic chem. appls. 0-85214  
 terrestrial planets, gravity anomalies and tectonics, review 0-98593  
 tetrahedrally coordinated semiconductors, surface structure, chem. and spectroscopy 0-59764  
 thermocouples, development, pitfalls in their use 0-62664  
 thermodynamic energy conversion efficiencies 0-101081  
 thermometry 0-86305  
 thermonuclear fusion research, economic factors 0-73991  
 thermophysical property research, metallurgical applications 0-97457  
 thin film technology, appls. in energy, optics, and electronics 0-78932  
 thin films, chem. anal. by energy loss spectroscopy 0-104493  
 thin films, deposition techniques 0-80964  
 thin films and interfaces, analytical techniques 0-80120  
 thrombosis, rheological aspects (*Japanese*) 0-94268  
 time domain spectroscopy of dielectrics, survey 0-68212  
 tissue quantitative characterisation by US 0-81670  
 Titan, atmosphere organic chemistry, review 0-90364  
 Tokamak and tandem mirror reactors, neutral beam injection and superconducting magnets 0-63391  
 Tokamak reactors, role of  $\alpha$ -particles 0-86971  
 tomography, transaxial scanners for reconstructing objects from their X-ray projections, review 0-102632  
 topographically trapped waves, review, book contrib. 0-96273  
 transequatorial radiowave propag. over 21 year period, VHF/UHF signals, theories 0-109311  
 transformation of nonlinear variables in construction of statistical models 0-57081  
 transition metal alloys, dilute, spin glasses, mag. ordering, book contrib. 0-75787  
 transition metal chalcogenides, quasi-one-dimens., elec. mag., and supercond. props. (*Russian*) 0-93022  
 transition metal compound surfaces 0-84349  
 transition metal hydrides, H ordering 0-60850  
 transition metal silicides, growth and characterisation 0-66408  
 transition metal silicides, refractory for ICs 0-100820  
 transition metals, 3d, ferromag. props., book contrib. 0-75724  
 transonic plane flows past oscillating airfoils, review, book contrib. 0-96278  
 tribology, material aspects in manufacturing processes 0-81210  
 tRNA in soln., selected topics, book contrib. 0-108839  
 troposphere, radar obs. during clear air conditions, review 0-90178  
 tunnelling MIS structures photovoltaic energy conversion, band struct. 0-92995  
 turbomolecular pumps, advances 0-62676  
 turbulence, 2-D, hydrodynamic and plasma applications, dynamical eqns., diffusion, MHD, superfluidity 0-69769  
 turbulence, current theory and practical examples (*French*) 0-64523  
 two dimensional system, ordering 0-107407  
 two-photon spectroscopy, dipole-forbidden transitions, double excited configurations, CNDO-Cl methods 0-58332  
 ultrapure water, trace metal determ. 0-81394  
 underwater sound scattering by marine organisms, report 0-64269  
 unified gauge theories, grand, asymptotic freedom constraints 0-62914  
 United States fusion power, overview 0-95395  
 unnamed space probes, recent achievements, financial restrictions and their effect on future programmes 0-72743  
 upper atmosphere perturbations assoc. with mag. storms 0-98495  
 urea-formaldehyde resins, book 0-73114  
 SU Ursae Majoris stars, important sub-group of dwarf novae, photometric props. 0-101596  
 US applications in obstetrics and gynecology, safety and pot. hazards 0-67170  
 US defectoscopy, development of and problems in theory of normal waves 0-81265  
 US flaw detection, progress in theory and principles 0-81262  
 US imaging modalities for medical appls. 0-81669  
 US in ophthalmic diagnosis 0-81673  
 US testing 0-104360  
 UV and IR instrument material mech. and thermal props. 0-106584  
 UV high-power laser material, refractive props. and optical constants 0-106555  
 UV radiation physics and the skin 0-81661  
 vapour pressure isotope effects, bibliography 0-77558  
 vapour quenching techniques 0-80977  
 ventricular fibrillation and defibrillation 0-81769  
 ventricular performance, 1st pass radioisotope assess. 0-85482  
 Venus, review of Venera data 0-72804  
 vestibular control of oculomotor and postural mechanisms 0-72151  
 viral infections diagnosis, contrib. of electron microscopy (*Italian*) 0-109024  
 vision, parallel pathways 0-89751  
 vision, pattern recognition functional mechanisms in humans 0-81609  
 visually evoked potentials, speed methods for vision assessment, normal and amblyopic eyes 0-61661  
 vortex methods for flow simulation 0-106801  
 water transport in soils, review, book contrib. 0-96308  
 wave energy converters, materials aspects 0-85262  
 wavelength stabilisation for light interferometry (*German*) 0-57250  
 weak current interactions 0-73654  
 white dwarfs, review 0-82356  
 wind-driven currents on the continental shelf, review, book contrib. 0-98358  
 wustite solid solns., props. connected with localised electron state 0-107734  
 X-ray binary stars, review of types and props. 0-109564  
 x-ray diffraction studies of the heart, book contrib. 0-109079  
 X-ray fluorescence analysis, equations of bond, review 0-66898  
 X-ray spectral analysis, energy dispersive, using semicond. detectors 0-85237  
 X-ray topography assessment of crystals, developments, review 0-64836  
 XUV astronomy, review (*German*) 0-109372  
 yeast, sensitivity to ionising radiations and damage repair 0-81659  
 ZGS, polarised beam results 0-99361



## reviews continued

- ed- $\pi$ , nucleon forces, meson exchange current effects, impulse approx. 0-57603  
 $\mu$  g-factor, ( $g-2$ ) expts., review, book contrib. 0-68403  
 NNN bound-state problems, hyperspherical harmonic expansion 0-91136  
 ( $p, \pi$ ), hopes and realities, review, book contrib. 0-73849  
 pp, neutral particle production in 4 to 2100 GeV interactions (*Russian*) 0-68489  
 pp elastic scatt. at high energies and large momentum transfer, review (*Russian*) 0-105926  
 $\pi p$ , neutral particle production in 4 to 2100 GeV interactions (*Russian*) 0-68489  
 $\pi^+p$ , elastic and charge-exchange scatt., partial wave anal.,  $\Delta$  resonances 0-63018  
 Ag halide crystals, dislocations, survey of post-war research 0-62449  
 Ag halide photographic materials, theory of supersensitisation (*Russian*) 0-62786  
 AgBr, photoexcited electrons and holes in latest image form., review 0-73496  
 and associated metals recovery, from secondary sources, recent developments 0-100800  
 C fibre reinforced composites for spacecraft use, prep., props. and struct. 0-97265  
 C fibre structure, recent advances 0-81069  
 $Ca^{2+}$ , passive and active fluxes across membranes 0-97886  
 CdS solar cells 0-76638  
 Cr, antiferromagnetic structure, mag. field effect, spin density wave model (*Russian*) 0-70953  
 Cu-Fe system, ageing and reversion phenomena study 0-89274  
 EuO(S)(Se)(Te), spin order and fluctuations, Raman scatt. study 0-97273  
 EuO(Se), complex elec. cond. anomalies 0-107812  
 Fe, effect of  $H_2$  on phys. and mech. props. 0-101657  
 Fe-Cr-Mo alloy castings, thick-section, factors affecting 0-108374  
 Fe-Si, grain-oriented sheets, high permeability, low losses, review 0-88790  
 Fe-Si, non-oriented sheets, production and props. 0-88797  
 GaAs, ion implantation review 0-88184  
 $Ga_{0.47}In_{0.53}As$ , photodetector applications 0-95140  
 $Ga_{1-x}In_xAs_{1-x}P_x$ , LPE growth 0-66440  
 $^{67}Ga$ , status in tumour detection 0-98074  
 H $^+$  form. by surface and vol. processes, neg. ion source appl. 0-58375  
 H $_2$  electrolytic production, design and operation of advanced H $_2$ O electrolyzers 0-61449  
 H $_2$  energy research programs in Japan 0-61435  
 H $_2$  high press. afterglows 0-64823  
 H $_2$  photobiological prod., key enzymes and biochem. systems, tech. problems of H $_2$  prod. 0-61446  
 H $_2$  photochemical production by H $_2$  dissociation utilising solar energy 0-61452  
 H $_2$  photoelectrochem. prod., semiconductor-liquid junction systems 0-61453  
 H $_2$  production by biological and biochemical solar energy conversion 0-61454  
 H $_2$  production by direct solar energy conversion at sea 0-61456  
 H $_2$  production by direct thermal decomposition of H $_2$ O utilising solar energy, thermodynamics 0-61450  
 H $_2$  production by H $_2$ O decomposition using solar energy conversion 0-97813  
 H $_2$  solid, fundamentals, static props., review 0-75403  
 H $_2$  storage, transmission and distrib. 0-61439  
 H $_2$  thermochemical prod. by H $_2$ O decomposition utilising solar heat 0-61451  
 H $_2$ O pyrolysis by solar-H $_2$  energy systems, thermodynamics 0-61448  
 He film, adsorbed, NMR measurements 0-107605  
 $^{131}I$ -ortho-iodohippurate absorbed kidney dose calc., literature review 0-76841  
 (In,Ga)(As,P) binary, ternary and quaternary, hydride vapour phase epitaxy, cryst. growth and props. 0-66434  
 KrF, excimer lasers, state of art 0-95879  
 Li solid electrolytes for electrochem. batteries 0-107524  
 LiF thermoluminescent detectors 0-68964  
 Na/S traction batteries, development progress and problems 0-61326  
 Nd:YAG pumped tunable sources, appl. to spectroscopy 0-58576  
 negative ion detachment cross sections for neutral gas targets 0-63796  
 O $_3$ , atmospheric, review of concs. over Australia 0-109223  
 Pd-H and Pd alloy-H systems,  $\alpha$ - $\beta$  phase transform., compositional relationships, hysteresis of press. 0-60859  
 Pu environmental contamination 0-101136  
 Si, (001) and (111), geometrical and electronic struct., review 0-80039  
 Si concentrator solar cells, high efficiency, state-of-the-art design and processing 0-93958  
 Si crystal growth, for electronic devices 0-66419  
 Si epitaxial layer regrowth due to laser annealing mechanism, liquid and solid phase regimes 0-100712  
 Si high efficiency solar cells, laser annealing, reviews 0-93976  
 Si ribbons, edge-defined film-fed growth technique for solar cells 0-89138  
 Si solar cells, current developments 0-108801  
 Si solar cells, perform. parameters of amorphous and polycryst. thin film cells 0-93882  
 Si solar cells, review of physics underlying recent improvements 0-93974  
 Si, thermal oxidation, Cl effects 0-108622  
 SiO $_2$ , vitreous, viscosity meas. 0-103513  
 SiO $_2$ , ion mobility and trapping 0-92985  
 SmB $_6$ , mixed valent semicond., transport props. and electronic struct. 0-96877  
 Ti powder metallurgy, developments 0-100801  
 UO $_2$ , 5f-magnetic semiconductor, spectroscopic data, review 0-97299  
 V-H(D), phase diagrams, struct. studies 0-66491  
 V $_2$ O $_5$  and lower oxides, defect structures and related props. 0-59454  
 YIG crystals, bulk growth from high temp. solns., props. 0-66413

revolution *see* rotationrevolving *see* rotationrewinding *see* winding (process)Reynolds number *see* flowr.f. heating *see* radiofrequency heatingr.f. sputtering *see* radiofrequency sputteringr.f.i. *see* radiofrequency interferenceRHEED *see* reflection high energy electron diffraction

## rhenium

*see also* nuclei with .....

- adsorbed on W (110), long range interatomic interactions with coadsorbed Pd 0-59789  
 adsorption of CO and electronic struct., XPS, UPS, and thermal desorption study 0-71571  
 adsorption of O $_2$ , CO, NO, and H $_2$ O on (0001), XPS, UPS and temp. programmed desorption 0-71574  
 carburised, spectral emissivity at 0.65  $\mu$ m 0-75374  
 electrical resistivity, quadratic contrib., 2 to 40K (*Russian*) 0-92874  
 electrodeposited from fused salts, (1011) texture (*Russian*) 0-92791  
 Fermi surface, Landau quantum oscill. meas. in magnetostriction, stress and strain derivatives 0-107691  
 Fermi surface, RF size effect, temp. depend. 0-65424  
 film, prep. by laser melting 0-84859  
 hydrosols, coagulation under action of US irradiation 0-58853  
 surface, interaction with N $_2^+$  beam, reaction dynamics studied by XPS and thermal desorp. spectrometry 0-93797  
 surface, long range and temp.-depend. interaction with alkali metal atom, theory 0-59802  
 surface (1010), struct., LEED anal. 0-75414  
 TF electron emitters props. obs. 0-66403  
 thermal expansion, 1200 to 2300K 0-103500  
 wear coefficients determ. using pin-on-disc apparatus 0-76366  
 MoO $_3$ :Re, current carrier sign, Fermi surface cross section variations (*Russian*) 0-84420  
 NaReO $_4$ , EPR spectra of paramag. centres and free radicals 0-108072  
 Re-C, work function, graphitic layer formation 0-96966  
 Re:Ir, electric quadrupole orientation of  $^{186,188-190}Ir$  0-78140  
 Re-O-Cl system, gas-transition metal interaction, kinetic model (*French*) 0-108740  
 $^{187}Re$ / $^{186}Os$  in Earth mantle, rel. to use of Os isotopes as petrogenetic and geological tracers 0-89989  
 n-Si-Re Schottky contact barrier height meas. 0-65675

## rhenium alloys

*see also* rhenium compounds

- Cr-Re, phase transformations and magnetostriction (*Russian*) 0-103869  
 Cr-Re (0.18 wt.%), mag. excitations in longitudinal and transverse SDW phases 0-70946  
 Mo-Re, recovery after deform. and annealing, destrengthening mechanism (*Russian*) 0-97546  
 Mo-Re, thermoelec. power, 4.2 to 300K 0-70683  
 ReSi $_2$ , atomic volume deviations and supercond. T $_c$  and elec. cond. 0-75203  
 Re $_2$ Si $_3$ , X-ray cryst. struct. determ., microhardness rel. to Re content 0-84142  
 Rh-W disc bonded to graphite, for X-ray tube rotary anodes (*German*) 0-105760  
 V-Si-SiO $_2$ -Mo $_3$ Re $_2$ , supercond. tunnel junctions 0-107961  
 W-Re alloys, thermal EMF instability, heat treatment effects 0-75553  
 W-Re amorphous alloys, phase-slip and localisation diffusion lengths 0-107747  
 W-Re films, amorphous, one-dimensional quantum localisation 0-80413

## rhenium compounds

*see also* rhenium alloys

- hexaaxy ions, octahedral, mol. const. calcs. 0-106317  
 Co $_3$ RhS $_4$ , mag. semicond., mag. and elec. props. 0-93121  
 FeRh $_2$ S $_4$ , mag. semicond., mag. and elec. props. 0-93121  
 KCl:ReO $_4$ , nonlinear absorption for CO $_2$  laser pulse compression and mode locking 0-74443  
 Re $_2$ Br $_6$ , atomic clusters, electronic struct. and photoelectron spectra 0-69287  
 Re(CO) $_5$ Br-Mn(CO) $_5$ Br, polycryst.,  $\mu$ (CO) vibr. intermol. Raman intensity transfer 0-60564  
 (Re $_2$ Cl $_2$ ) $_3^{3+}$ , atomic clusters, electronic struct. and photoelectron spectra 0-69287  
 Re $_2$ Cl $_6$ , atomic cluster, electronic struct. and photoelectron spectra 0-69287  
 ReO $_3$ , cubic lattice stability, screening effect on vibrs. 0-75356  
 ReO $_3$ , mag. breakdown above compressibility collapse transition 0-103617  
 ReSi $_2$ , atomic volume deviations and supercond. T $_c$  and elec. cond. 0-75203

## rheology

*see also* biorheology; plasticity; viscoelasticity

- Bingham plastic flow through annuli 0-64521  
 biomacromolecules, rigid, modelling approaches of hydrodynamic props. 0-61613  
 bitumen-silica composites, dynamical mechanical props. 0-58996  
 clays, heat treatment, effect on rheological props. of enamel slips 0-60809  
 colloidal dispersion dynamics, review 0-71956  
 dispense system, plastoviscous, cone plastometer for strength props. determ. 0-76426  
 disperse systems, plastic, laminar flow in circular tubes 0-87798  
 dumbbells, nearly-Hookean, dilute soln., rheological equation of state 0-100321  
 electrolyte solutions in glycerol, investigation by US shear strains 0-88266  
 emulsions, concentrated, rheological props. 0-99981  
 forsterite,  $^{18}O$  self-diffusion expts., high-temp. creep implications 0-81870  
 glassy state and highly viscous liq., rheology 0-70130  
 kaolin suspensions, aq., flocculated and dispersed, rheological behaviour in pipe flow 0-64510  
 magnesial refractory concretes, cast. props. 0-89306  
 magnetic micro-rheometer evolution and theory 0-92099  
 metals, rheological interpretation of planar deformed state in extremal friction regime (*Russian*) 0-64385  
 non-Newtonian fluids, mass transfer from cylinders to power law fluids 0-83826  
 non-Newtonian fluids, mass transfer from spheres to power law fluids 0-83825  
 nylon 6.6 in 100% H $_2$ SO $_4$ , primary normal-stress difference coeff., dependence on molecular wt. 0-87752  
 polyacrylamide Separan MG200, aq. soln., rheological props. 0-64507  
 polyaryloxyphosphazene copolymers, thermal, morphological and rheological props. 0-103265

**rheology continued**

- polyethylene, rheological behaviour at high shear strain rates (*French*) 0-66574
- polyethylene film, minimum running thickness, biaxial extensional flow study 0-100993
- polyethyleneterephthalate-polycapraamide melts, two-phase blend, rheological props. (*Russian*) 0-58997
- polymer melt, flow birefringence meas., influence of parasitic birefringences 0-88963
- polymer melts, annular flow, secondary normal stress difference 0-106816
- polymer solns., not infinitely dilute, second-order fluid coeffs., conc. depend. 0-106771
- polymer solution, highly elastic, vel. meas. in die entry region of capillary rheometer 0-99988
- polymer solution rheology based on a finitely extensible bead-spring chain model 0-83775
- polymer solutions, liquid cryst., rheo-optics of shear and elongational flow, quiescent and flow birefringent characts. 0-83773
- polymer substrates, amorphous Se vac. deposited, with dynamic coating device 0-100792
- polypeptides, helical, conc. solns., rheological behaviour and liq. cryst. order 0-83771
- polypropylene-polyethylene blends, capillary flow, rheology and morphology 0-59088
- polypropylene-polyethylene blends, flow behaviour in capillaries 0-59087
- polystyrene melts, flame-retardant high-impact, shear viscosity-temp.-shear rate relationships 0-59691
- polystyrene solns., correlations of network model parameters 0-106772
- polystyrene solution, constitutive models, explt. tests based on birefringence data 0-100015
- PPT in 100% H<sub>2</sub>SO<sub>4</sub>, primary normal-stress difference coeff., dependence on molecular wt. 0-87752
- rheogoniometer, Weissenberg, modification to normal stress meas. unit 0-69750
- Rivlin-Ericksen fluid, dispersion medium on rheological behaviour of dilute suspension of dipolar dumbbells, viscoelastic props. 0-99983
- Rzhanitsyn-Koltunov nucleus, anal. determ., relax. function for shear and stretching 0-58932
- silicone oil, Newtonian, vel. meas. in die entry region of capillary rheometer 0-99988
- simple fluid shear depend. viscosity, central force interactions 0-79970
- simple fluids, small strain oscillatory squeeze film flow, polymeric liquids 0-92765
- styrene-butadiene-styrene block copolymer, melt rheology 0-87751
- styrene-butadiene-styrene block copolymer, stress relax. following steady-state flow, residual shear stress development 0-83772
- styrene/acrylic terpolymers, viscoelastic props. 0-64509
- suspensions, rheology, colloidal forces role, review 0-103063
- viscoelastic droplet break-up, in nonuniform shear flow 0-64588
- viscoelastic fluids, Weissenberg rheogoniometer, R-17, axial compliance reduction 0-106859
- viscoplastic material, mixing process, Bingham model, two-dimens. flow (*German*) 0-92076
- Ag-Mg (18.5 wt.%), rheological study of crystallographic order on creep (*French*) 0-97548
- Al-Si alloy, eutectic, quasiisotropic 0-79165
- Cu-Zn, rheological study of crystallographic order on creep (*French*) 0-97548
- Fe<sub>2</sub>-Al, solid soln., rheological study of crystallographic order on creep (*French*) 0-97548
- Mg<sub>2</sub>SiO<sub>4</sub>, <sup>18</sup>O self-diffusion expts., high-temp. creep implications 0-81870
- MnZn ferrite powders, reactive, mag. materials obtained by compaction 0-89182
- Ni-Al, rheological study of crystallographic order on creep (*French*) 0-97548
- TiO<sub>2</sub> suspension in glycerine, Bingham plastic flow through annuli 0-64521

**rho mesons**

- production in K<sup>-</sup>p→p<sup>-</sup>Y<sup>+</sup>, Y<sup>+</sup>=Σ<sup>+</sup> or Y<sup>++</sup> (1385) 0-82997
- resonance vertex functions and scatt. amplitudes resonance-nucleon scatt.  $\rho$  rescatt. (*Russian*) 0-105918
- e<sup>+</sup>e<sup>-</sup>→p→π<sup>+</sup>π<sup>-</sup>π<sup>+</sup>π<sup>-</sup>, 1.55 GeV 0-82984
- e<sup>+</sup>e<sup>-</sup>→VX, polarisation states and differential cross sections for πA<sub>1</sub> and π<sup>+</sup>ρ<sup>-</sup> (*Russian*) 0-102059
- γp, 30-180 GeV, ρ and φ elastic photoprod. cross sections 0-95278
- γp→π<sup>+</sup>π<sup>+</sup>π<sup>+</sup>p, 20-70 GeV, ωπ<sup>0</sup> state enhancement at 1.25 GeV 0-78078
- γp→π<sup>+</sup>π<sup>+</sup>π<sup>0</sup>π<sup>+</sup>p, ρ<sup>0</sup>(1.6) production 0-102056
- γp→ρ<sup>+</sup>Δ<sup>++</sup>, 2.8 to 4.8 GeV, cross-sections, ρ spin density matrices 0-62999
- γp→ρ<sup>+</sup>π<sup>+</sup>, 2.8 to 4.8 GeV, cross-sections, ρ spin density matrices 0-62999
- γp→π<sup>+</sup>π<sup>+</sup>π<sup>+</sup>p, 20-70 GeV, dipion enhancement, ρ<sup>0</sup>(1600) observation 0-78079
- NN→(π, ρ, ω, f), statistical model 0-102028
- p̄p charged current interaction, inclusive ρ<sup>0</sup> prod. 0-62963
- pp, 405 GeV/c, ρ<sup>0</sup>, f, g<sup>0</sup>, h meson prod., cross sections 0-105930
- p̄p→e<sup>+</sup>e<sup>-</sup>, magnetic nucleon form factor, p-meson type contrbs. 0-57596
- π<sup>+</sup>p→ρ<sup>+</sup>π<sup>+</sup>X, diffractive contrib. in multi-Regge factorisation 0-73753
- π<sup>+</sup>p, 32 GeV/c, π<sup>0</sup> and ρ<sup>0</sup> inclusive prod., f and η cross section estimates (*Russian*) 0-68499
- ππ, ρ-meson contrib. in broken chiral symmetry model, phase shifts and lengths (*Russian*) 0-86756
- ππ interactions, dominant resonances, pole positions, partial waves 0-63020
- ππ→ππ, ρ-resonance production, quasipotential approach, linear σ-model 0-86755
- ρ<sup>+</sup>→π<sup>+</sup>γ, radiative decay width from pion excitation anal. 0-57599
- ρ<sup>0</sup>(1260) existence, vector meson leptonic width, duality between vector mesons and perturbative QCD 0-57589
- ρ<sup>0</sup>(1600) meson resonance from 2- and 4-pion distribs. in photoproduction data 0-95279
- ρ<sup>+</sup>→pπ, current algebra techniques, pole plus remainder model, chiral symmetry breaking and QCD 0-62972

**rhodium**

- see also nuclei with .....  
adsorption, of CO and H<sub>2</sub>, on (111) surface, 2-dimens. phase separation 0-107634

**rhodium continued**

- adsorption of CO, dispersed on Al<sub>2</sub>O<sub>3</sub>, <sup>13</sup>C NMR obs. of adsorbed states 0-96733
- atoms, N<sub>2</sub>/N<sub>2</sub>N<sub>4</sub> super Coster Kronig processes 0-106303
- chemisorption of ethylene and acetylene on (111) surface, EELS, LEED and thermal desorption mass spectrometry 0-80057
- chemisorption of water on (111) surface, effect of adsorbed O, H, or CO, LEED and thermal desorption meas. 0-75435
- core level binding energies 0-71564
- proton-induced L-shell ionisation cross-sections 0-100707
- recovery and use of noble metals from radioactive waste 0-99242
- self powered neutron detectors, influence of Rh burnup on sensitivity 0-63462
- surface, pulsed laser atom-probe FIM, expts. 0-66402
- surface (111), co-adsorption of H<sub>2</sub> and CO segregation of co-adsorbed species 0-65361
- thin films, polycryst., resistivity and temp. coeff. of resistivity 0-88648
- wear coefficients determ. using pin-on-disc apparatus 0-76366
- X-ray emission L-spectra, influence of temp., liq. N<sub>2</sub> temps. (*Russian*) 0-80907
- LiNbO<sub>3</sub>:Rh, Czochralski-grown oxide crystals, fluid-flow effect on gas-bubble entrapment 0-84121
- Rh-H system, energy and electron density of states, improvements to theory 0-70636
- Rh-TiO<sub>2</sub> catalyst, adsorpt. of H<sub>2</sub>, surface states, NMR spectrosc. investig. 0-103891
- rhodium alloys**  
see also rhodium compounds  
rare earth rhodium tin intermetallic cpds., synthesis, supercond. and mag. props. 0-100547
- rare earth-Sn-X, X=Rh, Ir, Ru, Co, cryst. growth and cryst.-chem. invest, supercond./mag. ternary cpds. 0-100777
- Cr-Rh, magnetic transformations, triple point (*Russian*) 0-88747
- Cu-Rh (4 at.%), anneal hardening mechanism 0-60879
- DyRh<sub>1.5</sub>Sn<sub>3.6</sub>, new supercond./mag. cpds., X-ray powder diffr. data 0-100215
- Er<sub>1-x</sub>Ho<sub>x</sub>Rh<sub>4</sub>B<sub>4</sub>, mag. and supercond. transitions, cryst. field effects 0-107950
- ErRh<sub>1.5</sub>Sn<sub>3.6</sub>, new supercond./mag. cpds., X-ray powder diffr. data 0-100215
- ErRh<sub>1.5</sub>Sn<sub>3.6</sub>, synthesis, supercond. and mag. props. 0-100547
- Er<sub>1-x</sub>Tm<sub>x</sub>Rh<sub>4</sub>B<sub>4</sub>, mag. and supercond. transitions, cryst. field effects 0-107950
- Gd-Rh, amorphous, mag. and elec. props. 0-80499
- Gd-Rh, amorphous, mag. props. and ferromag. reson. 0-75862
- GdRh<sub>2</sub>H<sub>2</sub>, struct. and mag. props., Mossbauer and magnetisation meas. 0-71271
- Nb-Rh, σ-phase alloy, superconductivity and resistance behaviour 0-70882
- Nb-Rh system glasses, form., crystn. and microhardness, resist. obs. 0-89178
- NdRh<sub>1.5</sub>Sn<sub>3.6</sub>, new supercond./mag. cpds., X-ray powder diffr. data 0-100215
- Ni-Rh, mag. moment distrib., one-mag.-species model calc. 0-65788
- Pd-Rh-H, hydride formation in high press. range 0-65235
- (Pd<sub>95</sub>Rh<sub>5</sub>)H<sub>x</sub>, elec. resistivity studies 0-59957
- PrRh<sub>2</sub>, hyperfine sp. ht. and magnetisation meas. at 4.2K 0-75775
- PrRh<sub>2</sub>, sp. ht., differential susceptibility and elec. resist. meas., 1.4-40K 0-71063
- PrRh<sub>2</sub>, Sny, crystallography X-ray powder diffr. study 0-100217
- Rh-Cu catalyst, Al<sub>2</sub>O<sub>3</sub> supported, chemisorbed CO, IR spectra (*French*) 0-60559
- Rh-H system, energy and electron density of states, improvements to theory 0-70636
- Rh-Sn-M M=Mg, Ca, Sr, Sc, Y, Zn, Cd, In or Th 0-100777
- Rh<sub>2</sub>MnPb, hyperfine fields, ferromag., NMR and Mossbauer effect studies 0-71259
- Rh<sub>2</sub>MnSb, hyperfine fields, ferromag., NMR and Mossbauer effect studies 0-71259
- Ta-Rh, σ-phase alloy, superconductivity and resistance behaviour 0-70882
- Ta-Rh system glasses, form., crystn. and microhardness, resist. obs. 0-89178
- TbRh<sub>2</sub>Sny, crystallography X-ray powder diffr. study 0-100217
- Zr-Rh-H(D), superconducting transition temp., effect of H(D) conc. 0-84532
- rhodium compounds**  
see also rhodium alloys  
anodic oxide film, two-colour electrochromic system 0-66150
- borides, RRh<sub>2</sub>B<sub>2</sub> (R=rare earth), supercond. and mag. props. 0-97028
- rare earth cpds., RRh<sub>2</sub>B<sub>4</sub>, coexistence of supercond. and mag. ordering (*Russian*) 0-84542
- (Co,Rh,Fe)<sub>2</sub>O<sub>4</sub> film magnetooptical switch for synchronization of CO<sub>2</sub> and red laser beams 0-58615
- ErRh<sub>2</sub>B<sub>4</sub>, ferromag. superconductor, vortex phase 0-80441
- ErRh<sub>2</sub>B<sub>4</sub>, mag. supercond., NMR study of <sup>11</sup>B 0-107957
- ErRh<sub>2</sub>B<sub>4</sub>, superconducting, magnetic dilemma 0-75680
- ErRh<sub>2</sub>B<sub>4</sub>, superconducting thin films, critical mag. field 0-75693
- GdRh<sub>2</sub>B<sub>4</sub>, magnetic and electrostatic props., NMR study 0-93195
- Ho(Ir,Rh<sub>1-x</sub>)<sub>4</sub>B<sub>4</sub> pseudoternary system, supercond. and mag. ordering 0-70876
- LuRh<sub>2</sub>B<sub>4</sub>, magnetic and electrostatic props., NMR study 0-93195
- Mo<sub>4</sub>(Rh,Tc)<sub>3</sub>, synthesis, struct., and elec. props. 0-92877
- NaRhY zeolite, Rh complexes with CO and methyl iodide ligands, spectrosc. obs. 0-85159
- (Rh,V<sub>1-x</sub>)O<sub>3</sub>, impurity doping effects, elec. props. obs. 0-75609
- Richardson effect** see thermionic emission
- ridge waveguides** see rectangular waveguides
- Riemann-Cristoffel tensors** see general relativity; tensors
- Righi-Leduc effect** see thermomagnetic effects
- rigidity** see shear modulus
- ring lasers**  
Brillouin ring laser, fibre-optic, use for inertial sensing 0-87411
- collision model, averaged, in active medium polarizability theory 0-95924
- conference, laser and electro-optical systems, San Diego, CA, USA (Feb. 1980) 0-62392
- differential four frequency laser, precision angle meas. appl. (*Chinese*) 0-64083
- diffraction theory, perturbation method 0-95919



**ring lasers continued**

- dye, optical bistability and first order phase transition 0-95918  
 dye laser, CW, optical diode to enforce one-direction travelling wave operation 0-69427  
 dye laser spectral props., hole-burning effects 0-102718  
 gas laser freq. synchronisation region of colliding waves 0-83620  
 mode competition and anticorrelation calc. and expt. 0-102740  
 multimode, containing saturable absorbers, bistable operation 0-91862  
 open cavity matrix eqns. in diffraction theory 0-69429  
 optical resonator with diaphragmed spherical mirror and spatially inhomogeneous amplifying medium (*Russian*) 0-64082  
 passive resonant ring laser gyroscope design 0-99768  
 perturbed cavity calculations 0-102739  
 rhodamine 6G dye in ethylene glycol, broadband optical diode, one directional traveling wave operation of ring laser 0-58606  
 ruby ring laser with forced mode locking 0-95915  
 self pulsing in dispersive optical bistability in ring cavity 0-78890  
 SHG, computer controlled intracavity, in CW ring dye laser 0-91841  
 solid-state ring laser, single-freq., spontaneous antiphase fluctuations, theory 0-91821  
 travelling wave, mode self-synchronisation 0-83605  
 unidirectional, modes 0-91818  
 GaAlAs DH injection laser, half-ring, room temp. operation 0-58558  
 GaAs-(GaAl)As injection lasers with circular resonator 0-74377  
 He-Ne ring laser, 0.6328  $\mu\text{m}$ , self-pulsing conditions 0-87414  
 He-Ne ring laser, methane stabilised, nonlinear resonance freq. shift due to back scatt. (*Russian*) 0-78874  
 He-Ne ring laser, nonlinear spectroscopic technique 0-91819  
 He-Ne ring laser, nonreciprocal effects with transverse mag. field applied to active medium 0-91820  
 He-Ne-methane ring laser, power resonances 0-99761  
 He-Ne-methane ring laser, freq. synchronisation interval for oppositely directed waves 0-99762  
 Nd garnet ring laser, with return mirror, mode locking 0-99764  
 Nd:glass laser, short pulse mode-locked, using prisms 0-83617

**ringers** *see bells***riometers** *see ionospheric measuring apparatus***riplons**

- conference, Moscow, USSR (Apr. 1978) 0-62378  
 He, liq., phonon coupling of two-dimens. Wigner cryst. with second surface sound (*Russian*) 0-92756  
 He, liq., surface, two-dimens. Wigner cryst., electron-riplon reson. anomalies (*Russian*) 0-92754  
 He liq. surface, cyclotron reson. of two-dimens. electrons (*Russian*) 0-88374

**rivers***see also lakes*

- acidification of headwater stream, New Jersey Pinelands 0-81945  
 Amazon, bed sediment size distrib. 0-101392  
 Amazon, organic C oxidation and transport 0-105007  
 annual floods of E.Australia catchments, freq. distrib. 0-105012  
 annual streamflow record extension by correl. methods 0-81950  
 atmosphere contribution to stream water chem., North Cascade Range, USA 0-61824  
 bank erosion rate, obs. in Devon, England 0-105002  
 Beaton River, British Columbia, regional trend to meander migration 0-101391  
 bed load transport by submerged jets, laboratory expts. 0-81942  
 Bedford Ouse River, systems model of stream flow and water quality 0-81956  
 Black River, Ontario, streamflow record synthesis, feature prediction model appl. 0-98372  
 Brahmaputra river, flood of Aug. 1962, synoptic aspects 0-81939  
 Britain, runoff and water balance, 50000 yr BP to present day 0-72566  
 canyon rivers, rapids characters. 0-72564  
 channel bottom, kinematic characters. of nonuniform flow, limiting stability, erosion 0-94547  
 channel flow resistance due to large obstructing boulders 0-81947  
 cohesionless bottom sediments, limiting stability in turbulent channel flow, erosion 0-94546  
 cohesionless soils on channel bottom and sloping sides, onset of motion 0-94548  
 daily flow, non parametric Markov model, appl. to Cheyenne river 0-81948  
 Dakota drainage pattern mapping IR thermal imagery remote sensing 0-81892  
 Dauguvos, plume influence on Baltic Sea (*Russian*) 0-98345  
 discharge volume estimation, correction for channel and floodplain morphology 0-85695  
 diversion, effect on Mediterranean circulation 0-77014  
 downstream pollution short-term prediction, one-dimensional transient model 0-81496  
 drainage basin characteristics, network power model 0-61823  
 drainage density estimation from topological variables 0-61831  
 drainage network change in Britain 0-81934  
 drainage network mapping of Pantanal Brazil, Landsat-2 imagery 0-81944  
 drought definitions 0-105010  
 drought in streamflow series, statistical chars. 0-105009  
 erodible riverbed, channel deformations, hydraulic modelling 0-77024  
 estuaries, hydrodynamic model using smooth elements, accuracy 0-88356  
 estuaries of variable breadth and depth tidally induced residual currents 0-72544  
 estuarine environment, natural suspended matter flocculation and electro-kinetic pot. (*French*) 0-61817  
 estuary, spread of river jet, models 0-98353  
 estuary, well mixed, buoyancy effects on longitudinal dispersion 0-85681  
 estuary circulation (partially mixed), two-dimens. model 0-109161  
 Euphrates watershed, free water surface evaporation losses 0-81957  
 Finnish river water pollution monitoring network 0-89686  
 flood event real-time predictors, stochastic model 0-67383  
 flood forecasting model from rainfall catchment and evaporation data, retention hysteresis 0-81951  
 flood inundation of agricultural land, LANDSAT digital image anal. 0-61913  
 floods in Plynlimon expt. catchments, Wales, geomorphological effectiveness 0-81932  
 flow prediction, nonlinear feedback system model 0-98375  
 forested watershed streamflow during storm, dominance of flow through soil 0-61825

**rivers continued**

- Fraser River, B.C., Streamflow record synthesis, feature prediction model appl. 0-98372  
 Ganges Basin water supply, groundwater recharge by pumping along rivers 0-81952  
 granular bed material, erosional capacity of smoothly varying streams, particle size 0-94545  
 gulf of St. Lawrence, buoyancy driven current system, mixing and circulation 0-90095  
 high-water peaks, annual recurrence (*French*) 0-77020  
 hydrobiological studies at nuclear sites, conception and main data (*French*) 0-76665  
 Kama Reservoir, USSR, forecasting spring inflow 0-105008  
 longitudinal slope determ. 0-82108  
 Mahanadi basin, India, climatic study of river regime 0-81941  
 meltwater from glacier, elec. resist. obs. showing water origin 0-85689  
 monsoon floods, diluting of industrial pollution in Cochin backwaters 0-76668  
 morphology of river beds 0-77017  
 New England, USA, heavy metal content in non-industrial area 0-61477  
 Nile, climate variation affecting discharge 0-81946  
 old Mangalore port, India, channel siltation study 0-77005  
 Par River estuary, India, pollution transport and abatement methods 0-104521  
 Pee Dee River-Winyah Bay estuary, S.Carolina,  $^{226}\text{Ra}$  behaviour 0-98360  
 pesticides in USSR rivers, 1973-1976 period 0-81495  
 pollution by Pb smelter, trace metal deposition in sediment 0-61475  
 pollution distribution determination by remote sensing, study 0-81512  
 pollution from chlorinated drinking water, effect on organic content 0-97824  
 runoff kernel for basin, mathematical derivation 0-61832  
 S.Saskatchewan River, streamflow record synthesis, feature prediction model appl. 0-98372  
 sediment transport in steady unidirectional flow, scale modelling test 0-81933  
 sediment transport modes in channelised water flows, appl. to Martian outflow channels erosion 0-98363  
 Severn estuary, seasonal and spring neap tidal depend. of axial dispersion coeffs. 0-94534  
 spring-flood forecasting, loss of runoff due to soil water absorpt. 0-109178  
 St. Venant equation modelling (*German*) 0-90103  
 steppe-zone river, spring-runoff norm, estimation method 0-85694  
 stream. water, dissolved forms of trace elements, dialysis cell meas. 0-97851  
 streamflow record synthesis, feature prediction model appl. 0-98372  
 Tiber, physical processes related to discharge into sea, aerospatial obs. 0-108831  
 tidally-generated residual motion in St. Lawrence estuary, numerical model 0-94541  
 tide waves in channel, bottom friction in perturbation method 0-98354  
 Tigris watershed, evaporative losses from free water surface 0-81957  
 tributary junctions, channel geometry changes 0-98376  
 tributary spatial arrangements 0-81929  
 turbid waters, spectral scatt. props. 0-72560  
 USSR rivers, streamflow variation (1961-1976) 0-101394  
 Vellar estuary, Fe precipitation, conc. determ. 0-77015  
 Ventos, plume influence on Baltic Sea (*Russian*) 0-98345  
 wind stress coefficient over water surfaces, new evaluation 0-72603  
 W concentration, in streams draining from agricultural watershed 0-61474  
 Se (-II,0), -(IV) and -(VI) composition of water, by gas chromatography method 0-81928
- RKKY interaction**  
 CuCr, dil., specific heat, impurity contrib. Kondo temp. 0-65903  
 Kondo lattice, impurity interactions, ground state calc., impurity conc. effect 0-65782  
 metals, indirect exchange interaction, partial wave expansion 0-88523  
 Ruderman-Kittel interaction at finite temp. (*Russian*) 0-96835  
 spin glass, RKKY, dil., approach to fully magnetised state 0-60302  
 superconductivity-ferromagnetism coexistence in two-band model (*Russian*) 0-84539  
 Van Vleck compounds, LF dynamics, NMR linewidth, RKKY exchange mechanism role 0-103812  
 AgCr, dil., specific heat, impurity contrib. Kondo temp. 0-65903  
 Au-Cu-Fe spin glass alloys, impurity mag. resist. meas. 0-59972  
 Au-Fe, spin glass, transition temp., freq. depend. 0-97113  
 Au-Fe alloys, spin correlations, neutron diffr. meas. 0-80482  
 Cu-Mn, spin glass, transition temp., freq. depend. 0-97113  
 Cu-Mn-Au(Pt) spin glasses, anisotropic exchange interactions, effect of nonmag. impurities 0-80534  
 Fe, Pd<sub>82</sub>-Si<sub>18</sub> metallic glass, long range interaction and spin wave interactions 0-65949  
 Gd-Al(C)(Cu)(Ga)(Ni)(Pd)(Rh) alloys, amorphous, mag. and elec. props. 0-80499  
 GdNi, mag. interaction and carrier conc. 0-71005  
 GdN<sub>1-x</sub>O<sub>x</sub>, magnetic interaction and carrier conc. 0-71005  
 (Gd<sub>1-x</sub>Al<sub>x</sub>)<sub>2</sub>, ferromag. and spin glass like behaviour, magnetisation meas. 0-75734  
 HgCr<sub>2</sub>Se<sub>4</sub>, n-type ferromag. semicond., galvanomagnetic props. 0-70727  
 PdH<sub>0.003</sub>, Kondo system, local moments, hyperfine fields, Mossbauer study 0-80478  
 PrNi<sub>2</sub>, LF dynamics and  $^{141}\text{Pr}$  thermal relax., coupling parameter and RKKY exchange mechanism 0-103812  
 Sc-Gd, spin glasses, low temp. sp. ht. and magnetisation 0-65913  
 Y-Gd, spin glasses, low temp. sp. ht. and magnetisation 0-65913

**road traffic**

- noise, a socioeconomic approach to subjective responses 0-67022  
 noise, bus noise levels in the New York City and Albany metropolitan areas 0-76684  
 noise, close proximity vehicle noise survey method 0-102926  
 noise, close to light motor vehicles 0-83701  
 noise, computer simulation of traffic flows, road intersections having traffic lights 0-72109  
 noise, control of noise level of moving vehicles 0-99894  
 noise, echoes from vehicles, Demey metro station (*French*) 0-69600  
 noise, highway noise barrier perceived benefit 0-102920  
 noise, highway noise barriers, optimum weight with respect to effectiveness and cost 0-67021

**road traffic continued**

- noise, kerbside study of vehicles 0-79050  
 noise, meas. accuracy using digital instrum. 0-79075  
 noise, meas. radiating height of cars and lorries, effectiveness of sound barriers 0-64325  
 noise, Monte Carlo simulation methods, effect of vehicle spacing on results 0-72110  
 noise, multivariate joint probability expression of general random processes, finite expansion terms 0-69592  
 noise, presentation of statistical results 0-67019  
 noise, reduction by correct building placement, noise emitted by single source in open space 0-87647  
 noise, relationship to air pollution levels 0-69594  
 noise, relationships between multidimens. correlation props. of intensity and higher order information, Stratonovich's stochastic theory for random points system 0-87645  
 noise, subjective annoyance, lab. expt. on students 0-102921  
 noise, traffic passing through road intersections controlled by roundabouts, model 0-64280  
 noise, traffic-induced building vibration 0-96098  
 noise, use of sloped barriers for noise abatement 0-102925  
 noise, use of theoretical and empirical models in prediction (*French*) 0-67020  
 noise, wall insulation, prediction of output probability distribution of noise level 0-69593  
 noise abatement, noise propag. characts. identification under different conditions, Kalman filter theory appl. (*German*) 0-99896  
 Rome road traffic noise, 24-hour obs. and statistical analysis (*Italian*) 0-87651  
 site selected variables effect on human responses to traffic noise 0-61491  
 site selected variables effect on human responses to traffic noise 0-61492  
 CO<sub>2</sub> pollution from road traffic, street level conc. 0-81500

**road vehicles**

- buses, noise levels in New York City and Albany metropolitan areas 0-76684  
 noise radiating height measurement, roadside sound barrier effectiveness calculations 0-64325

**Rochelle salt**

- ammonia Rochelle salt, temp. depend. of optical axis angle, phase transitions (*Russian*) 0-97216  
 ammonium Rochelle salt, thermodynamics of ferroelec. transition 0-84702  
 dehydration kinetics in ferroelec. and paraelec. phases, surface acoustic waves influence 0-97204  
 ferroelectric, Raman and IR study 0-71406  
 ferroelectric phase transitions in pseudo-spin lattice coupled mode model 0-108161  
 (Rochelle salt)<sub>1-x</sub>(ammonium Rochelle salt)<sub>x</sub>, phase transitions, hydrostatic press. effects 0-93246

**rock magnetism**

- see also palaeomagnetism*  
 ash-flow tuffs, microanalytical recognition of TRM components 0-72497  
 basalt, mag. mineral identification by rot. hysteresis loss 0-67428  
 Butte mining district, Montana, palaeomagnetism, rock magnetism and aspects of structural deform. 0-101326  
 Upper Cretaceous limestones from Munster Basin, NW.Germany, magnetisation age 0-89949  
 crustal rocks, magnetisation rel. to long-wavelength mag. anomalies over Canada 0-85594  
 depositional detrital remanent magnetisation of organic mud 0-61795  
 domain structure obs. by Lorentz electron microscopy 0-72502  
 hemollminites, mag. anisotropy, torque balance obs. 0-98309  
 NE Iceland, rock magnetic investigations rel. to  $\Delta Z$  mag. anomalies 0-89951  
 long grains method for palaeomagnetic field strength and direction 0-77148  
 magnetite, magnetisation of immobilised particles, shape factors 0-72499  
 magnetite, weak field TRM is single domain grain, cooling rate effect 0-109139  
 marine ophiolite complexes, evidence for past magnetism 0-109092  
 mineral identification in rocks, mag. rot. hysteresis loss meas. 0-67428  
 palaeointensity determination of laboratory rock sample 0-61917  
 Permian volcanics in western Southern Alps, palaeomag. and rock magnetic props. 0-89948  
 Pliensbachian limestone sequence at Bakonycsérnye (Hungary), remanent magnetisation 0-90074  
 post-depositional realignment of sediments, expts. and theory 0-109137  
 rotational remanent magnetisation, origin 0-61794  
 rotational remanent magnetisation of igneous rock, expt. and theory 0-85645  
 RRM and anhysteretic remanent magnetisation, expts. on laboratory samples 0-90076  
 sand, specularite-bearing, experimentally deposited, mag. declination and inclination errors 0-90075  
 sandstone (Dunnet Head), scattered magnetisation direction, down to small scale 0-90077  
 sediment magnetisation, surface tension effects 0-85644  
 silicic volcanics, Jurassic, from Nevada, USA, thermochemical remanent magnetisation 0-98310  
 single domain grains, mag. blocking temps. during slow cooling 0-90082  
 Thetford Mines ophiolites, Quebec, NRM props. and palaeomagnetism 0-61757  
 titanomagnetites, temp. depend. cation distrib., mag. prop. obs. 0-85647  
 Na<sub>2</sub>(Fe,Mg)<sub>2</sub>Si<sub>2</sub>O<sub>7</sub>(OH)<sub>2</sub>, riebeckite, low temp. Mossbauer obs. of oriented single cryst. behaviour and mag. props. 0-84674

**rocket vehicles *see* rockets****rockets**

- see also missiles; space vehicles; weapons*  
 astronomy and atmosphere programs, conf. Bournemouth, England (1980, Aug.) 0-105433  
 charge neutralisation of rocket payload during electron beam emission, laboratory studies 0-77258  
 electron accelerator expt. on POLAR-5 sounding rocket, for use within aurora 0-77170  
 hydrazine fuel in ambient air CO<sub>2</sub> laser absorption spectra and photoacoustic detection 0-104540  
 impulse recorder for small rocket engines 0-77595  
 ionosphere satellite wake, assessment ion current distrib. 0-101527  
 ionosphere sounding, ion temperature probes system design (*Japanese*) 0-85838

**rockets continued**

- ionosphere sounding rocket, POLAR-5, elec. charge accumulation due to electron expt. 0-77213  
 S-310-5 rocket, ionospheric current obs. (*Japanese*) 0-94635  
 Skylab 1 rocket, 1973-27B, orbit determ. and anal., geopotential resonance 0-67515  
 solid propellant stress transducer evaluation 0-81245  
 Vertical-6 flight results rel. to 1978 International Reference Ionosphere 0-90285  
 Vertical-6 rocket flight results on upper atmosphere parameters 0-90268  
 Al particles produced by rocket launch 0-81503

**rocks**

- see also geology; minerals; rock magnetism*  
 Archaean granulites model for lower continental crust, evidence from mantle Nd-Sr isotopes correl. 0-94498  
 Archaean metasedimentary rocks from Kambalda, Western Australia, rare earth element geochemistry 0-109143  
 basalt, <sup>238</sup>U/<sup>235</sup>U ratio and comparison with chondritic meteorites 0-85903  
 basalt, mag. mineral identification by rot. hysteresis loss 0-67428  
 basalt, naturally occurring, high-temperature quantitative DTA analysis 0-77144  
 basalt glasses from Mid-Cayman Rise spreading centre, geochemical var. and petrogenesis 0-101364  
 basalts from Nauru Basin, trace element abundances 0-94499  
 bentonite, examples of devitrification and early diagenesis 0-81860  
 Blair dolomite, shock wave expts. 0-67362  
 Bohus granite area, SW Sweden, geothermal investigations 0-85631  
 calc-alkaline volcanic rocks of Cerro Galan, NW.Argentina, Sr isotope evidence for crustal contamination 0-98318  
 Caledonian granites of Scotland and N.England, isotopic evidence for provenance 0-109146  
 California rock P-wave velocity, high press. and temp. expts. 0-61783  
 carbonate bearing rocks, fluorite mineralisation dynamic model 0-81876  
 chabazitic tuff, a zeolitic rock for thermal storage of solar energy 0-94117  
 coal, anisotropic elec. props. meas. 0-98312  
 coal seams, approx. seismic wave diffrac. theory for transparent half-planes 0-89974  
 coal-bearing rocks of Bonnet Plume Basin, Yukon Territory, Canada, evaluation from gravity profile 0-76898  
 Upper Cretaceous limestones from Munster Basin, NW.Germany, palaeomagnetism 0-89949  
 Cretaceous mid-ocean ridge basalt (MORB), Nd and Sr isotopic comps. and rare earth element abundances 0-94520  
 Dalradian sediments, Scotland, evidence for Cambrian opening of Iapetus Ocean 0-98299  
 diabase, seismic attenuation rel. to crack and grain boundaries 0-72495  
 dielectric relaxation measurement using blocking layer method 0-103914  
 extension veins of deformed rock, crack-seal mechanism 0-61798  
 failure, role of acoustic fluidisation 0-85653  
 faults and shear zones, assoc. deep focus earthquakes 0-61786  
 fracture, role of crack inertia 0-109138  
 granite, failure expts., pore press. stabilisation 0-90079  
 granite, seismic attenuation rel. to crack and grain boundaries 0-72495  
 granite, static fatigue, effect of confining press. and stress difference 0-81872  
 granite microfracture, source process rel. to earthquake prediction 0-104919  
 granitic magma of Bushveld Complex, crystallisation history as revealed by trace element abundances 0-109145  
 granulitoid rocks, Nd-Sr isotopic relationship and continental crust development, chemical approach to orogenesis 0-94522  
 Green River oil shales, thermal diffusivity depend. on organic content 0-76965  
 groundwater flow through rock, radioactive waste storage study 0-82111  
 half-space, impact of steel cylinder and effects 0-85649  
 high pressure props. of Earth interior, dynamic compression expts. 0-98315  
 high-pressure metamorphic rocks ('knockers') in subduction zones, material transport within accretionary prisms 0-101353  
 hyperthermic magmas, water contents 0-72507  
 Icelandic subglacial volcanic rocks, thermal and physical studies 0-101350  
 igneous, actinide sorption from radioactive waste 0-95367  
 igneous layered rocks, magma double-diffusive crystallization 0-90081  
 impulsive fracture, criteria 0-85646  
 Indian Shield basement rocks, heat prod. meas. from geothermal study of Jharia Gondwana basin 0-98276  
 inorganic gas chromatography for determ. of H<sub>2</sub>O and CO<sub>2</sub> in rocks and minerals 0-85767  
 IR multispectral aircraft scanner data, image processing 0-98454  
 jointed blocks of peridotite xenoliths in basalts and mantle dynamics 0-61796  
 josephinite, Widmanstaetten patterns in metal-bearing rock 0-81887  
 Jurassic rock in N.Armenia, palaeomagnetic directions rel. to remanent magnetisation 0-104870  
 Kayenta Sandstone, deform. in triaxial stress tests 0-81880  
 Kerguelen Islands igneous rocks, Nd isotopic study rel. to enriched oceanic mantle sources 0-98319  
 Kilauca 1977 lava flow, heat transfer meas. 0-85632  
 lava, flowing of South Novo-Tolbachinsky volcano eruption, elec. cond. 0-72498  
 lherzolites, comp. rel. to comp. of Earth mantle 0-76940  
 limestone, dry and saturated, P and S wave attenuation, US obs. 0-72494  
 limestone, seismic attenuation rel. to crack and grain boundaries 0-72495  
 limestone tubes, dynamic torsional failure obs. 0-85648  
 lithosphere petrology and plate tectonics, comparison with Venus tectonics and comp. 0-72805  
 Lithuanian upland and plateau palaeoperiglacial blanket deposit formation (*Russian*) 0-81882  
 magma, solubility and saturation of apatite, laboratory expts. 0-72504  
 Malaysia offshore areas, rocks thermal cond. rel. to heat flow estimation in wells 0-67349  
 mantle xenoliths, equilibrated Nd and unequilibrated Sr isotopic comp. meas. 0-98321  
 metamorphic rocks, quartz c-axis fabrics anal. via photometric method 0-101456



## rocks continued

- Mid-Atlantic Ridge, geology of submarine hydrothermal field at 26°N latit. 0-85641  
 Mid-Atlantic Ridge, rock densities and fracture zones struct. in equatorial Atlantic (*Russian*) 0-104932  
 mineral composition of rocks at great depths, prediction from longit. elastic wave vels. (*Russian*) 0-104956  
 monolithic materials for creating high pressures, anvil device with lune toroid 0-73377  
 Nain anorthositic complex, Labrador, examples of contrasted magmas commingling in plutonic environment 0-104959  
 Neogene trench-slope deposits, Nias Island, Indonesia, sedimentology and palaeobathymetry 0-104950  
 Norwegian eclogites, Caledonian Sm-Nd ages and crustal origin 0-76978  
 obsidian, Japanese, <sup>57</sup>Fe Mossbauer spectra of naturally occurring glasses 0-67364  
 oil shale, dry and saturated, P and S wave attenuation, US obs. 0-72494  
 oil shales of Green River, USA, thermal decomposition rel. to elec. cond. obs. 0-104495  
 olivine, steady state flow creep eqns., implications for mantle rheology 0-104924  
 oolitic limestone, fold strain analysis using elliptical particles 0-61787  
 ophiolite complex of Point Sal, California, seismic vel. struct. 0-109110  
 ophiolites of Pan-African province of Anti-Atlas (Morocco), geodynamic interpretation (*French*) 0-76952  
 pegmatites, U<sup>235</sup> estimation by homogenised fission track anal. using solid state track detector 0-97719  
 pegmatites in Enderby Land, Antarctic U-Pb ages 0-76946  
 peridotite xenoliths of SW Japan island arc, appl. to uppermost mantle differential stress lateral var. determ. 0-98275  
 Permian volcanics in western Southern Alps, palaeomag. and rock magnetic props. 0-89948  
 phosphate fertilizer, specific activity of U and Th rel. to particle size 0-106244  
 physical properties and struct. geol., conf. (1978), Toronto, Canada 0-101666  
 Pliensbachian limestone sequence at Bakonycsérnye (Hungary), remanent magnetisation 0-90074  
 plutonic rock, discrimination and spectral reflectance, visible and IR obs. 0-90083  
 Precambrian metamorphic rocks, from SW Montana, mineral-pair geothermometers 0-81846  
 Late Precambrian rocks of Adelaide Geosyncline, Australia, palaeomagnetism 0-101325  
 pyroxenes from planetary basalt, silicate mineralogy study 0-72802  
 quartz cryst. axes orientation, in metamorphosed volcanic sediment 0-85655  
 Quaternary volcanic rocks across NE Japan, trace element contents, lateral variation 0-104926  
 Rn emanation rate measurement from specimens and powders 0-63494  
 rock salt from New Mexico Salado formation, mech. props. at high-pressure 0-72492  
 S-wave vel. meas. in soil and bedrock using down-hole method 0-98458  
 salt deposits, Upper Triassic, of western N. Atlantic, obs. from Newfoundland Grand Banks 0-94516  
 sandstone, seismic attenuation rel. to crack and grain boundaries 0-72495  
 sandstone, seismic compressional wave absorpt. 0-72433  
 sandstone, U ore assessment by charged particle track analysis 0-91405  
 sandstone (Dunnet Head), scattered magnetisation direction, down to small scale 0-90077  
 sedimentary rocks, Th and U abundances rel. to crustal evolution and sedimentary recycling 0-85654  
 serpentinised pyroxenitic and saxonitic rocks, petrophysical props., factor anal. 0-90087  
 serpentinite diapir W. of Galicia Bank, rel. to Iberian margin ocean-continent boundary 0-94489  
 serpentinite intrusions, origin rel. to deep magmatic diapir folds evolution (*Russian*) 0-104957  
 Setul Limestone (Ordovician-Silurian), NW Peninsular Malaysia, palaeomag. evidence 0-89936  
 shale-sandstone (-limestone), P-, SH- and SV-wave vels. computation 0-98249  
 shear microcrack propag. in triaxially-compressed brittle rocks 0-90080  
 shock deformation of brittle solid, review of theory 0-72493  
 shocked rocks in Goat Paddock cryptoexplosion crater W. Australia, petrology 0-98322  
 Sibley Group, Thunder Bay district, Ontario, Canada, stratigraphy and depositional setting 0-94517  
 spectral reflectance of volcanic rocks, 400-800 nm, for remote sensing studies 0-90073  
 structure analysis, acoustic method (*Russian*) 0-85760  
 tektite-like material in archaeological remains, Indonesia 0-101365  
 thermal conductivity and diffusivity using modified Angstrom or impulse method 0-90085  
 trondhjemitic basement enclave, near Favourable Lake volcanic complex, NW Ontario, Canada, age 0-94518  
 Troodos ophiolite metamorphism, implications for marine mag. anomalies 0-81812  
 Troodos ophiolite complex, major oxide geochemistry and origin 0-98317  
 ultramafic xenolith suite from Tahiti, petrology and genetic significance 0-90086  
 ultramafics from Owen fracture zone, NW Indian Ocean, petrology rel. to nature of oceanic upper mantle 0-94519  
 volcanic ash, examples of devitrification and early diagenesis 0-81860  
 volcanic material from Klyuchevskaya Sopka volcano (1974), chem. anal. 0-101351  
 volcanic rocks, mass fractionation of rare gas isotopes as indicator of gas transport to or from magma 0-98292  
 volcanic rocks from Hess Rise, W. Pacific 0-90026  
 water flow, shear thinning and shear thickening polymer additives 0-72100  
 water-saturated rock, electrically charged, effect on seismic wave propag. and damping coeff. 0-76921  
 weathering by chemical decomposition, rate meas. by now U isotope method 0-77142  
 Fe formation in Early Precambrian Isua supracrustal belt, W. Greenland, cosmic grains discovery 0-72508  
<sup>187</sup>Os/<sup>186</sup>Os in terrestrial samples, rel. to use of Os isotopes as petrogenetic and geological tracers 0-89989

## rocks continued

- U isotope disequilibrium due to  $\alpha$ -recoil and soln. effects 0-98314  
 U, Th contents, rel. to <sup>14</sup>C prod. in groundwater and implications for dating 0-85690  
 Roentgen ray see X-rays  
 rolling  
 see also cold rolling  
 brass, orientation distribution, texturised materials, Ghost effect demonstration 0-70080  
 $\alpha$ -brass, polycryst., deformed in tension or rolling, anneal hardening (*Japanese*) 0-93564  
 brass, rolling texture development and deform. struct., shear bands effect (*Japanese*) 0-84952  
 contact fatigue failure, of rolls of hot strip mills 0-60950  
 ferrite, transform. kinetics, grain size, alloying element effect, carbide precip. 0-93560  
 flat, with spread, cross-section warping (*German*) 0-92064  
 Gauss principle, in rolling theory, deformed and kinematic eqns. (*Russian*) 0-65124  
 granular materials, rolling, granule kinematics 0-84875  
 hot longitudinal, periodically charging sections with flash, pressures calc. (*Polish*) 0-89257  
 metals, longitudinal flow velocity distribution in rolling (*Russian*) 0-93575  
 metals, wave movement, resonance phenomena in deformation zone during rolling (*Russian*) 0-65123  
 powders, agglomerate structure parameters of powders in the incoherent zone in rolling 0-84876  
 steel, alloy, sheet, crack-propag. resist. in heat-affected zone in presence of H, rolling direction and preliminary plastic tensile strain effects 0-60971  
 steel, C, rolling contact fatigue, tufftriding effect on 0.2% C cylindrical specimen 0-100954  
 steel, C-Mn-V-Cb-N, high strength low alloy, controlled-rolled 0-100803  
 steel, Cr-Mn type, martensite struct. after quenching and HTMT, X-ray diff. obs. 0-84975  
 steel, high C, tensile strength, working and heat treatment effects (*Japanese*) 0-104209  
 steel, low C, low alloy, ferritic-pearlitic, high temp. mech. treatment, cooling effect 0-104193  
 steel, machining, 12L14, effect of Pb and Te on hot-shortness mechanism 0-104190  
 steel, microalloyed, hot-rolled, Nb(C,N) precip. and austenite recryst. 0-97513  
 steel, microalloyed, types V1599, V1600, V1286, NbCN precipitation in undeformed austenite 0-89230  
 steel, mild, solderability, annealing effect (*Japanese*) 0-89244  
 steel, Mn-Si-Cr-Mo, dual phase, as-rolled, continuous cooling transformation diagram to optimize composition 0-100829  
 steel, Nb(V), (Al), hot-rolling, laboratory simulation, recryst. of austenite 0-97512  
 steel, rolled, anisotropic, fatigue fracture surface obs. (*Japanese*) 0-108546  
 steel, stainless, Cr-Cu (17, 0.6 to 1.1 wt.%), texture 0-84957  
 steel, stainless, tempering after air hardening from rolling heat (*German*) 0-93571  
 steel, strain-hardened subsurface layer, residual stress change in fatigue 0-81185  
 steel sheet, hot and cold rolled, cold formability, notched tensile test and stretch bend test (*German*) 0-61031  
 steels, induction hardened bearing, rolling contact strength (*Japanese*) 0-93568  
 tubes in round passes, evaluation of moments (*Russian*) 0-97442  
 Al alloy granules, lubricants for rolling 0-60980  
 Al alloys, thermomech. treatments, effects on microstruct. 0-100858  
 Al-Zn-Mg granules and bands rolled from them, heat treatment 0-100862  
 Cr-Al<sub>2</sub>O<sub>3</sub> powder targets for plasma-ion spray deposition of resistance films 0-84897  
 Cu, solderability, annealing effect (*Japanese*) 0-89244  
 Cu-Sn-Al, deform at high temps. (*Polish*) 0-89284  
 Fe-Si-B, high induction, hot rolling treatment 0-89266  
 Ni-containing alloys, hot workability after reheating using S-containing fuel 0-108483  
 Ni-Cr-Al<sub>2</sub>O<sub>3</sub> powder targets for plasma-ion spray deposition of resistance films 0-84897  
 W [310] tip, prep. from rolled sheet 0-97447  
 W brittle alloy rolling, contact stresses (*Russian*) 0-93576  
 Y, plastic deformation props., deformation ageing, plastic flow, dislocation-impurity interactions (*Russian*) 0-66582  
 roots of polynomials see polynomials  
 rotamers see rotational isomerism  
 rotating bodies  
 see also angular velocity measurement; centrifuges; gyroscopes; rotation  
 asteroid 624 Hektor, light curve indicating elongated shape 0-98600  
 asteroids, light curves and rot. periods from photographic photometry during 1977 and 1978 0-72844  
 bar, radially rotating, of variable cross-section, deflection and lateral vibr. (*Japanese*) 0-94954  
 beam with tip mass, vibration 0-58960  
 Bernoulli's principle, spin of balls and coins 0-77592  
 black hole, Kerr metric effect on EM wave plane of polarization 0-94827  
 black holes, rot. rel. to free oscils. reson. freqs. and gravit. waves 0-105271  
 centre of mass rel. to centre of rotation, demonstration 0-77579  
 concave hamburger equilibrium of rotating bodies 0-109422  
 cosmic bodies, ang. momentum-mass relation 0-77528  
 cylindrical gas system, rotating and self gravitating, thermodynamic instability 0-82191  
 disc galaxies, rot. vels. effect on superdense gaseous cores form. 0-90526  
 driven member rotation uniformity test installation 0-92094  
 dust sphere, slowly rotating, maximal slicing condition, initial value equations 0-73246  
 education, infinitesimal rotations, invalidities in usage 0-57036  
 elastic rotating cylinder, general relativistic formulation 0-82642  
 elliptical galaxies, scale free axisymmetric models with little ang. momentum 0-82493  
 45 Eugenia, rot. period and photoelec. light curve determ. 0-72846  
 flexible rotors, basis for a unified balancing method 0-74732  
 fluid mass, axisymmetric, asymptotic estimates 0-98542

rotating bodies continued

galaxies, rotation curves, rel. to nearby galaxy presence (*Russian*) 0-77496  
galaxies, spiral arm development, sufficiency conditions 0-77483  
Galaxy, rot. effect on mag. field leading to corona prod. 0-82492  
gyroscope with tuned elastic suspension, dynamical characts. 0-79133  
gyroscopic eigenvalue problems in elasticity, nonconservative 0-101708  
gyrostatic satellite in Kepler orbit, rot. motions 0-86080  
indenters, rigid, rough, rotating, plane strain collapse theory 0-79172  
interstellar clouds, axially symmetric collapse and protostellar form. 0-77380  
interstellar clouds, rotating, nonaxisymmetric collapse theory rel. to protostellar form. 0-85927  
interstellar clouds, stability against fragmentation from three-dimensional hydrodynamical calcs. 0-62236  
interstellar gravitating gas cloud, wave-wave interactions 0-105154  
Jovian planets, polar moment of inertia determ. 0-94694  
Jupiter, radio emission maps at 2.7 GHz at different rotational phases 0-82272  
Kerr black holes, stable circular orbits of test particles moving in equatorial plane 0-85970  
Kovalevskaya gyroscope, new class of motions 0-68037  
Lake Kinneret (Sea of Galilee), mean flow in rotating basin 0-81937  
68 Leto, rot. period and photoelec. lightcurves determ. for asteroid 0-85994  
magnetic oblique rotator, EM field prod., exact vacuum soln. 0-58442  
Mars, dynamics obs. from Viking lander tracking data anal. 0-77314  
Mars, longit. var. of thermal inertia and 2.8 cm brightness temp. 0-105191  
Mars, rot. period determ. from transits of albedo stations across central meridian (1659 to 1971) 0-98588  
mechanical oscillator, relativistic spin quadrupole gravitational effect (*Russian*) 0-68103  
18 Melpomene, rot. period from photoelec. obs. 0-82258  
metric torsion field effect on spinning particle, equ. of motion 0-62543  
Moon, rotation around centre of mass, historical development of understanding 0-57064  
moving atmosphere simulation by rotating phase plate 0-79021  
moving rigid body, axoid nondevelopable character 0-62460  
Neptune rotation period, correction, photometric and spectroscopic results comparison 0-82301  
NGC 3115, S0 galaxy, rotation and mass of inner 5 kiloparsecs 0-105326  
NGC 488, Sb galaxy, rotation curve from emission line spectra 0-62266  
NGC 5728, barred spiral, vels. and mass distrib. of galaxy 0-94863  
oavalling oscillations of cylindrical shells in cross flow, comments 0-59045  
Periodic Comet Encke, changes in orbital period due to rotation of nucleus 0-62078  
Periodic Comet Schwassmann-Wachmann 1, rotation and outbursts 0-67655  
planets, Coriolis phenomenon and rotational alignment 0-90636  
protostellar cloud, rotating, collapse and stability, turbulent viscosity effect 0-109510  
protostellar cloud ang. momentum problem, mag. breaking 0-82342  
protostellar cloud rotation, mag. braking of aligned rotator during star form., exact time-depend. soln. 0-90493  
relativistic rotating systems, Einstein equations 0-68101  
relativistic spherical mass, effects of rot. on gravit. focusing of light 0-105155  
rigid body rotation in 3D space from body fixed linear acceleration meas. 0-68040  
rigid body, translational-rotational motion of gravit. field of sphere 0-62000  
rigid elastic body system, turning round fixed point, linear viscoelasticity theory (*French*) 0-69646  
rigid shaft rotating in antifriction bearings, motion stability 0-68038  
rotor, partially filled with viscous incompressible fluid, stability anal. 0-64359  
Sc galaxies, rot. props. from major axis visible spectra obs. 0-90517  
shells of revolution, computer program for linear and geometrically nonlinear static analysis (*Japanese*) 0-64500  
solid elastic bodies, ultimate motion of a system gravitating to a fixed point (*Russian*) 0-90664  
spacecraft, spin-stabilised, optimal aerodynamic attitude control 0-77250  
stars, exact solns. for Emden-Chandrasekhar axisymmetric solid-body rotating polytropes with ( $n=0$ , 1 and 5) 0-109419  
strings, elastic, heavy, whirling, nonlinear eigenvalue problems, bifurcating branches of solns. 0-73174  
563 Suleika, rot. period and photoelec. lightcurves determ. for asteroid 0-98594  
three rigid bodies problem, translational motion solns. with uniform rot. (*Russian*) 0-61999  
turntable accessories, for rotational motion phenomena demonstrations 0-77571  
Uranus, rotation period from geometric oblateness and  $J_2$  harmonic of gravity field 0-67649  
Uranus, rotation rate from ellipticity derived from SAO 158687 occultation 0-67648  
Venus, resonance rotation 0-109387  
Venus, spin vector determ. by radar obs. 0-105185

rotation

see also angular velocity measurement; Earth rotation; molecular rotation; optical rotation; rotating bodies; rotational flow; stellar rotation  
angular momentum, operator props. through three-dimens. rot., teaching 0-105469  
asteroids, initial rotation periods and relative formation times (*Chinese*) 0-105182  
Brillouin ring laser, fibre-optic, use for inertial sensing 0-87411  
chemically induced dynamic spin polarisation, orientation depend. 0-63656  
education, eigenvector of general rot., geometrical construction 0-57025  
galaxies, elliptical, rot. vels. and vel. dispersions rel. to equilib. models 0-94865  
galaxies, role of vortex generation in protogalactic medium 0-62360  
Galaxy, rot. models rel. to low-latit. pulsars H I absorpt. meas. and distances 0-101606  
galaxy clusters, rotation as opposed to transverse vel. 0-94876  
IC 342, Scd galaxy, H I rot. curve obs. 0-67857  
Jupiter, fast moving bright spot obs. in North Temperate Current C 0-67640

rotation continued

Moon, peculiarities of translatory-rotatory motion caused by force function third and higher harmonics (*Russian*) 0-90349  
Neptune, equatorial flow model rel. to rot. 0-67653  
NGC 1023, SB0 galaxy, H I obs. rel. to rot. and mass/luminosity ratio 0-67886  
NGC 1055, 681, 4594, galaxies, rot. curves and mass distribis. (*Russian*) 0-90541  
NGC 3115, S0 galaxy, rotation and mass of inner 5 kiloparsecs 0-105326  
NGC 3686 galaxy quartet, spectra and rot. curves rel. to mass distribis. and group stability 0-62297  
NGC 4945, late-type spiral galaxy, mean rot. curve and excited gas kinematics 0-109547  
NGC 741, 1316, 7626, radio galaxies, rot. axes and dynamics 0-94871  
planets, initial rotation periods and relative formation times (*Chinese*) 0-105182  
solar prominences, evidence for rot. mass motions from inclined spectral features 0-62098  
Uranus, equatorial flow model rel. to rot. 0-67653  
vorticity vector, rot. theory 0-82604

rotation by magnetisation see Einstein-de Haas effect

rotational flow

see also vortices  
aerated systems, oblong, flow and mixing, transverse circulating flow of liquid, longitudinal dispersion 0-69900  
annual review of fluid dynamic, book 0-94927  
axisymmetric convection in shallow rotating cylinder, centrifugal acceleration effects 0-96260  
axisymmetric rotating round nosed bodies, flow and heat transfer, buoyancy effects 0-79306  
binary homogeneous mixtures, motion in infinite rot. cylinder, generalised diffusion theory 0-79328  
blades, vibr. due to rotating stall, aerodynamic force meas. 0-92172  
body of revolution with heating and cooling, boundary layer transition and separation 0-64518  
bounded coaxial jets, convective heat transfer in turbulent mixing, swirling 0-64541  
Boussinesq differentially heated fluid, struct. 0-109190  
Boussinesq viscous fluid, inertial instability, appl. to atm. 0-90131  
cascades, annular, secondary flow, shear flow turning or departure of exit flow 0-69842  
centrifugal buoyancy forces from energy considerations 0-82609  
centrifugal instabilities of circumferential flow in finite cylinders, nonlinear theory 0-99989  
circle theorems for inviscid steady flows 0-59043  
cylinder on  $\beta$ -plane, prograde and retrograde rot. flows, boundary layer separation 0-92189  
detached shear layers and boundary currents in rot. liq. 0-81984  
drops, rotating, captive between co-rotating parallel faces, shapes and stability, capillarity eqns. 0-64592  
ducts, rapidly rot., variable area, rectangular, steady flow, inertial perturbations for small divergences 0-59112  
electrically conducting medium, rotation at exit of coaxial MHD channel 0-83853  
energy stability theory of decelerating swirl flows 0-59054  
finite-amplitude thermal convection and geostrophic flow in a rotating magnetic system 0-87813  
flat surface, jet impingement, rotational flow model calcs. 0-64596  
fluid layer heated, turbulent convection 0-100003  
fluid of spherical configuration, wave propagation 0-106804  
gas, perfectly conducting compressible in mag field under gravity, wave dispersion relations (*Chinese*) 0-77276  
gas, strong diverging cylindrical shock propagation 0-79350  
gas turbine combustion chamber flow three-dimens. calc. 0-79405  
geophysical fluid dynamics theory, book 0-105443  
geophysical fluid motion, Rossby and Kelvin waves, open boundary conditions 0-61810  
Hamels spiral flow, temp. and vel. distribis. (*German*) 0-87779  
heat exchange from rotating disc. into unbounded rotating fluid, thermal and hydrodynamic boundary layers 0-59050  
heat transfer, cylinder in stabilised swirl flow having aerodynamic axis parallel to flow, calc. 0-79321  
helical flows in a sphere 0-59052  
hemisphere in MHD rotating stratified fluid 0-100039  
homogeneous turbulence, with internal rotations, theory 0-69772  
inviscid, rotating, compressible fluid, linear stability 0-92161  
liquid film, instability on surface of rot. sphere 0-59006  
magnetic fluids, response to mech., mag. and thermal forces 0-59122  
mean flows driven by weak eddies in rotating systems 0-103032  
measurements of rotating flow around circular cylinder, azimuthal velocity in gas centrifuge 0-74890  
meridional flow of compressible fluid in a rapidly rotating short cylinder 0-106812  
MHD Couette flow, Hall effect in rot. system 0-74991  
Navier-Stokes eqns. numerical solns. (*German*) 0-59057  
non-Newtonian flow classification criteria for rigid motions, viscometric flow and elongational flow 0-69881  
nonequilibrium free jet expansion, rotational temp. meas for  $N_2$  0-69890  
nonuniform grids in finite difference approximations, application to fluid flow problems 0-105507  
nose separation for laminar boundary layers on body of revolution 0-59091  
ocean, exptl. study of nonlinear baroclinic instability and mode selection in large basin 0-85669  
ocean, potential vorticity distrib. rel. to equatorial undercurrent dynamics 0-72558  
ocean, stability of solitary Rossby waves over variable relief, analytical theory 0-101371  
ocean, stability of solitary Rossby waves over variable relief, numerical expts. 0-101372  
ocean, wind driven, new class of steady solns. to wind-driven ocean problem 0-85667  
ocean deep-water channel flow, rotating hydraulics theory 0-94539  
oceanic warm front propag., rotating stratified fluid theory 0-94538  
perforated flat plate over porous medium, turbulence penetration, eddies, mass transfer 0-64528  
pipe flow, rotating pipe of elliptic cross-section 0-92220  
pipe inlets, turbulent local mass and heat transfer, swirling effects 0-64542



**rotational flow continued**

- plate, rotating, 3-D boundary layer turbulence, effects of rotating radial end-plates 0-69843  
 porous disc and rot. disc, fluid flow 0-64569  
 potential flow about body of revolution, axial singularity distrib. 0-64570  
 rapidly rot. gas, free jet expansion, Newtonian thin shock layer approx. 0-74888  
 rotating disc problem, Taylor coefficients, computational methods 0-106802  
 rotating rods and plates, mass transfer and flow regimes 0-79326  
 slow viscous rotation of a sphere on the axis of a circular cone 0-87777  
 stationary flow between porous rotating cylinders in a radial magnetic field 0-83857  
 steady rotating flow over topography, steady  $\beta$ -plane channel, quasi-linear theory 0-92159  
 Stokes flow, slender body theory for viscous incompressible fluid 0-92160  
 Stokes flow, three-dimensional Moffatt-type eddies due to Stokeslet in corner 0-74891  
 stratified fluid, parallel shear flow, baroclinic and barotropic instability 0-98328  
 subsonic rotational and transonic mixed flows, numerical simulation using fast super-dashpot time-dependent technique 0-83813  
 surge and rot. stall, flow instabilities 0-106803  
 swirled flow, sprayed liquid hydrodynamics 0-79325  
 thermally forced stratified rot. fluids, axisymmetric steady motion 0-69844  
 thermoelectric MHD, pipe end problem, boundary layers and rotation 0-69942  
 three dimensional parallel shear flows, stability and transition for rot. disc 0-74887  
 turbulent, velocity vector and stress tensor component measurement (*Russian*) 0-83867  
 two moderately rotating porous discs, heat transfer 0-103028  
 two parallel corotating discs, laminar flow and heat transfer, shear pump appl. (*German*) 0-69840  
 two rotating discs, air flow in gap between 0-92156  
 unsteady axisymmetric 1-dimens. motions of ideal incompressible liquid, small perturbations 0-59004  
 velocity measurements inside a rotating cylindrical cavity with a radial outflow of fluid 0-96275  
 viscoelastic fluid, free surface between cylinders rotating at different speeds 0-59082  
 viscous liquid flow through annular clearance over rotating inner cylinder 0-64626  
 von Karman swirling flows 0-74894  
 water, apparent Weissenberg effect 0-83787  
 wave linear propagation in rotating fluid, critical level absorption and valve effects 0-106805  
 wave/mean flow interaction, mean motion induced by transient inertio-gravity waves 0-105029  
 weak polymer solutions, flow props. in narrow channel between rotating and stationary discs (*Russian*) 0-59089  
 Wedemeyer spin up model, Ekman compatibility conditions, Navier-Stokes eqns. 0-83802  
<sup>3</sup>He, rotating superfluid, equilibrium order parameters, chemical potentials 0-96713  
<sup>4</sup>He, rotating superfluid, equilibrium order parameters, chemical potentials 0-96713  
<sup>4</sup>He, superfluid, nonstationary rot. regime rel. to superfluidity of pulsars 0-98683

**rotational isomerism**

- adamantane, derivatives in solution, mol. motion and methyl group rot. barriers from <sup>13</sup>C NMR relax. times 0-74179  
 n-alkanes, liq., Raman spectra, longit. acoustic modes and gauche-trans energy difference 0-93295  
 alkyl chains, <sup>13</sup>C longitudinal relax. times and nuclear Overhauser enhancement anal. 0-83390  
 aminoborylpolynes, intermolecular interaction through triple bonds, internal rot. 0-106370  
 aminopolynes, intermolecular interaction through triple bonds, internal rot. 0-106370  
 apomyoglobin reconstituted with <sup>111</sup>In(III)mesoporphyrin IX, rot. correl. time determ. 0-76698  
 aromatic polyesters, with S atoms, configurational props. 0-74269  
 benzaldehyde, and isomeric phthalaldehydes, dipole moments meas., config., ab initio MO calc. 0-58410  
 $\Delta^6$ -bicyclo(3,2,0)heptane, conformational mobility 0-99587  
 butane, liq., enthalpy difference between rot. isomers, IR spectrosc. obs. 0-106404  
 t-butyl acetate, rot. isomerism, dielect. and Raman spectra 0-106328  
 t-butyl formate, rot. isomerism, dielect. and Raman spectra 0-106328  
 3-butyn-1-ol, vibr. spectra, assignments, rot. isomerism 0-58257  
 chloro(ethyl)silanes and its C derivatives, Raman spectra, mol. vibr. and rot. isomerism 0-87134  
 1-chloro-2,2-dimethylpropane, IR and Raman spectra, vibr. assignment 0-74169  
 1-chloro-2-methylpropane, IR and Raman spectra, vibr. assignment 0-74169  
 2-chloroethyl radical, struct., ab initio calcs. 0-83252  
 cyclopentadienyl platinum (IV) complexes, mech. spectroscopy to meas. ring rotation 0-74259  
 decylammonium chloride micelles, <sup>13</sup>C longitudinal relax. times and nuclear Overhauser enhancement anal. 0-83390  
 dimethoxymethane, vibr. spectra and rot. isomerism 0-106325  
 dimethylformamide, intramolecular exchange rate determ. from <sup>13</sup>C spin-lattice relax. times 0-69169  
 1,4-disilabutane, rot. isomerism, Raman and IR spectra 0-74168  
 ethane, internal rot. splittings, vibr.-rot.-torsion energy levels perturbations 0-91531  
 ethane, rot. barriers, MS-SCF- $X_\alpha$  calcs. 0-106267  
 ethyl alcohol-d<sub>6</sub>-(d<sub>1</sub>)-(d<sub>1</sub>)-(d<sub>2</sub>), internal rot. and microwave rot. spectra 0-69128  
 ethyl iodide, microwave spectra and internal rot. anal. 0-69130  
 ethyl radical, C-C bond barrier rot., IR spectra 0-76536  
 ethylene, rot. around double bond, four orbital-four-electron model 0-95592  
 ethylenimine, pyrolysis product, microwave spectra, rot. distortion and electric quadrupole const. and rot. barriers determ. 0-78608

**rotational isomerism continued**

- formaldehyde-d<sub>6</sub>-(d<sub>1</sub>)-(d<sub>2</sub>), matrix isolated, IR spectra, monomer absorpt. 0-99503  
 HCl-inert gas mixtures, van der Waals molecules, far IR spectra 0-95610  
 hexafluoroethane, rot. barriers, MS-SCF- $X_\alpha$  calcs. 0-106267  
 inversion geometry, ab initio SCF calcs., basis set effects 0-78532  
 membrane-active complexon fragments, nonrigidity effects calcs. 0-91704  
 2-methoxyethanol, methyl torsional barriers to internal rotation calc. 0-95603  
 2-methoxyethylamine, microwave spectra, H-bond, torsional motion and mol. vibr. obs., rot. isomerism, mol. moments determ. 0-95603  
 methyl acetate, microwave spectra and internal rot. 0-87100  
 methyl azidofornate, microwave rot. spectrum, satellite transitions 0-69127  
 methyl fluoroformate, isomer conformation, CNDO and ab initio STO calcs. 0-58151  
 N-methyl m-fluoroaniline, conformational anal., microwave spectra obs. 0-58247  
 s-methyl nitrite, methyl group rot. barriers in cis and trans forms, ab initio calcs. 0-74111  
 methylamine, membrane-active complexon fragments, nonrigidity effects calcs. 0-91704  
 methylpropylether, trans-trans isomer, microwave spectra, struct., dipole moment and rot. barriers calcs. 0-83348  
 molecular rotational spectra, doublet splittings caused by tunnelling, perturbation treatment 0-91541  
 molecular structures, topological code, modified Morgan algorithm 0-58122  
 molecule, nonrigid, sum of states, isometric group, symmetry no., thermodynamic functions 0-58186  
 monochloroacetic acid, isolated molecules, internal rotation, CNDO/2 calcs., IR spectra 0-69254  
 muonic radicals,  $\mu$ SR spectra obs. 0-69279  
 1- $\beta$ -naphthyl-2-N-piperidinoethane, intramol. exciplex form., ground state conform. control 0-102547  
 nitrocylopropane, vibr. spectra struct. and bonding 0-102520  
 norbornene, derivatives in solution, mol. motion and methyl group rot. barriers from <sup>13</sup>C NMR relax. times 0-74179  
 oxirane cation, struct. rearrangement following vertical ionisation, ab initio CI calc. 0-58191  
 PCIO-INDO method, theory and appls. 0-58153  
 pentane, liq., enthalpy difference between rot. isomers, IR spectrosc. obs. 0-106404  
 polymethylene, short chains, rot. isomeric representation 0-87254  
 polyenes, intermolecular interaction through triple bonds, internal rot. 0-106370  
 propionitriles (-O, NH, S), conformational investig., NMR, IR and semiempirical MO methods 0-95650  
 terpenes, methyl groups internal rotation, <sup>13</sup>C spin lattice relaxation times and force field calcs. 0-74255  
 thiophosgene, vibronic anal. of electronic transition, inversion doubling splittings obs. 0-83388  
 total dipole moment orientation calcs. 0-91705  
 bis-triazolopyridazines, conformation calcs. by mol. mechanics and CNDO/2 method 0-69079  
 bis-triazolyls, conformation calcs. by mol mechanics and CNDO/2 method 0-69079  
 trimethyl-d<sub>3</sub>-vinylsilane, IR and Raman spectra, struct., vibr. assignment, barriers to internal rot. calc. 0-87102  
 trimethylamalgallane, IR and Raman spectra, struct., vibr. assignment 0-95600  
 trimethylvinylsilane, IR and Raman spectra, struct., vibr. assignment, barriers to internal rot. calc. 0-87102  
 Cu complex, Cu(NH<sub>3</sub>)<sub>2</sub>(NCX)<sub>2</sub>, X=O, S, electronic struct., stereochem. 0-58156  
 Ge<sub>2</sub>H<sub>6</sub>, rot. barriers, MS-SCF- $X_\alpha$  calcs. 0-106267  
 H<sub>2</sub>O-HF heterodimer, H bonding, microwave rot. spectrum, mol. geometry and moment 0-99501  
 H<sub>2</sub>PNH<sub>2</sub>, inversion-rot. mechanism, basis set and geometry optimisation effects 0-83273  
 H<sub>2</sub>S<sub>2</sub>, rot. barriers, internal rot. and electronic struct., valence electron study 0-83344  
 H<sub>2</sub>Se<sub>2</sub>, rot. barriers, internal rot. and electronic struct., valence electron study 0-83344  
 H<sub>2</sub>Te<sub>2</sub>, rot. barriers, internal rot. and electronic struct., valence electron study 0-83344  
 (N<sub>2</sub>)<sub>2</sub>, Van der Waals molecule, struct. and internal rot. barriers determ., interaction pot. from ab initio calcs. 0-91626  
 NO<sub>2</sub><sup>-</sup> hydrate clusters, ground-state HF pot., Monte Carlo simulation, energy surfaces and rot. barriers 0-106412  
 SiH<sub>3</sub> radical, in Ar(Kr)(N<sub>2</sub>) matrix, anisotropic ESR spectroscopic parameters 0-63687  
 Si<sub>2</sub>H<sub>6</sub>, rot. barriers, MS-SCF- $X_\alpha$  calcs. 0-106267

**rotator phase in solids** see nuclear magnetic resonance; plastic crystals

**rotatory dispersion power** see optical rotation

**rotors**

- <sup>4</sup>He superfluid, phonon-rotor excitation 0-107586  
<sup>4</sup>He, liq., excited states, variational calcs. 0-80017  
<sup>4</sup>He superfluid, elementary excitations,  $\mu$ eV resolution study by neutron spin echo 0-65327  
<sup>4</sup>He, superfluid, excitation spectrum, RPA calc. involving simple pseudopot. 0-92738  
<sup>4</sup>He superfluid, isotopically pure, roton-driven mech. for nucleation of negatively charged vortex rings 0-59746  
<sup>4</sup>He, superfluid, Landau critical velocity meas., excitations 0-103528  
<sup>4</sup>He, superfluid, neutron spin-echo study of excitations 0-80014  
<sup>4</sup>He, superfluid, roton-rotor interaction for large and zero momentum 0-84336  
<sup>4</sup>He, superfluid, two- and three-dimens., energy spectrum and phase vel. 0-70489

**rotors**

- high speed unequally spaced fan, acoustics and performance anal. 0-96163  
 noise generation by transonic open rotors 0-69599  
 wind turbine aerodynamics, machine performance and rotor aerodynamics 0-74904

roughness measurement *see surface topography measurement*

rovibronic levels *see molecular rotation-vibration*

## RPA calculations

atomic photoionisation anal. using relativistic random phase approximation and multichannel quantum defect theory 0-63602  
CDW distorted solid, quasi-one-dimens., charge density fluctuations and dielec. matrix 0-107726  
deformed nuclei, yrast level ground state correlations, RPA anal. 0-86777  
disordered Heisenberg spin model, magnetisation calc. 0-60167  
electron gas, degenerate, in metal or semicond. slabs, surface plasmon damping 0-88501  
electron gas, interacting, local-field correction to dielectric constant, review 0-107731  
electron gas, spin polarised, correlation energies for local spin density calcs. 0-107725  
electron liquid, spin-dependent, correlation energies for local spin density calcs. 0-107725  
energy weighted sum rules for spin-dependent excitations of nuclei 0-86833  
fast ion in solid, oscillatory wake, trapped electron binding energy, RPA calc. 0-96575  
ferromagnet, itinerant, spin waves, surface effects, RPA calc. 0-60226  
giant monopole vibrs., RPA and collective field description, surface compressibility 0-102100  
gradient approx. anal., nonuniform electronic system 0-96810  
heavy ion+ nucleus, RPA theory, time dependent, quasi-boson approx. 0-57800  
Heisenberg antiferromagnet, Green function theory 0-107975  
Heisenberg ferromagnet, anisotropic, collective Green's function, dynamical RPA 0-70925  
Heisenberg ferromagnet, correlation functions in ferromagnetic and paramagnetic regions, RPA 0-71075  
Heisenberg ferromagnet, surface magnetisation profile and localised magnons 0-70985  
high spin rot. motion, TDHF cranking model and RPA descript. 0-102091  
inelastic positron scatt. in electron gas, plasmon excitation 0-92843  
Jahn-Teller cooperative T-(e+t) system, thermal cond. 0-70479  
metals, classical plasma frequency in long-wavelength limit, quantum correction 0-107728  
metals, simple, quasiparticle props., density functional approx., electron gas calc. 0-96808  
metals, spin fluctuations, mag. field effect, electronic sp. ht. and elec. resist. 0-108026  
mixed valence compounds, dynamic susceptibility, RPA study of Anderson lattice 0-97075  
multipole residual interaction strength, radial depend. in RPA 0-83026  
nuclear structure, pairing rotation and intrinsic Hamiltonian 0-57708  
oscillating dipole-metal surface interaction, jellium model and random phase approx. 0-92955  
rare earth deformed nuclei, high spin region excited rot. bands, RPA calcs. 0-78108  
s-d shell, two nucleon effective interaction, intruder state, RPA correlation 0-57701  
self-consistent quasiparticle RPA in nuclear structure theory 0-86835  
semiconductor, amorphous and liq., Hall conductivity in random-phase model 0-65599  
spin exchange and polarisation changes, RPA breakdown from HF connection 0-99142  
spin glass, Heisenberg mode, RPA approx. 0-65904  
transition metal alloys, dilute ferromagnetic, itinerant d-electron(hole) degenerate, spin stiffness constant 0-70930  
van der Pol oscillator, RPA for linewidth 0-68138  
weak ferromagnet, with easy plane anisotropy correl. functions and magnetisation, temp. depend. (Russian) 0-84581  
X-Y model, biquadratic, spin one, variation of Curie temp. 0-97102  
zero gap semiconductor, thin layer, dielec. response 0-103635  
Ar, outer  $p_{1/2}$  subshell photoionisation, polarised electrons, relativistic RPA calcs. 0-83331  
Bi, gas-liquid type transform. and sound attenuation in strong mag. fields, electron-hole core. effects 0-88598  
 $^{12}\text{C}$ , residual interactions, current conserving RPA calculations 0-57710  
 $^{40}\text{Ca}$ , A=40 to 48, giant multipole resonances, mass dependence of energy weighted sums 0-63144  
 $^{40}\text{Ca}$ , residual interactions, current conserving RPA calculations 0-57710  
 $\text{Co}(\text{C}_6\text{H}_5\text{NO})_2(\text{ClO}_4)_2$  [(BF<sub>4</sub>)<sub>2</sub>], X-Y antiferromagnet, Neel temp., spin correlation functions 0-60345  
 $\text{Cu}_{0.98}\text{Mn}_{0.02}$ , spin glass, Heisenberg mode, RPA approx. 0-65904  
 $\text{ErCo}_2(\text{Fe}_2)$ , mag. excitations, RPA theory 0-65830  
 $\text{EuSr}_{1-x}\text{S}$ , Heisenberg spin glass system, excitations 0-84610  
 $^3\text{He}$ , normal liquid, elementary excitations, density and spin density, zero sound mode, press. depend. RPA model calcs. 0-59749  
 $^4\text{He}$ , superfluid, excitation spectrum, RPA calc. involving simple pseudopot. 0-92738  
Kr, outer  $p_{1/2}$  subshell photoionisation, polarised electrons, relativistic RPA calcs. 0-83331  
 $^{23}\text{Na}$ , A=90,92,94, Gamow-Teller strength distrib., RPA calcs. 0-78218  
 $^{16}\text{O}$ , residual interactions, current conserving RPA calculations 0-57710  
Pb pairing vibr. band, microscopic struct. and wave functions from (p,t), (t,p) 0-91126  
 $^{208}\text{Pb}$ , isobaric analogue states, effects of Coulomb isospin coupling, random-phase method (Russian) 0-86808  
Si, optical spectrum, many particle effects, band struct. 0-89024  
 $\text{UAl}_3$ , spin fluctuations, mag. field effect, electronic sp. ht. and elec. resist. 0-108026  
Xe, outer  $p_{1/2}$  subshell photoionisation, polarised electrons, relativistic RPA calcs. 0-83331

## rubber

ABS-rubber modified, two-phase struct. influence on fracture toughness (German) 0-66666  
acoustic transducer-receiver configuration, flexible, activated by laser 0-83724  
blooming by waxes 0-104109  
cord-rubber laminates, two-ply balanced, interlaminar-shear strain study 0-97526  
crystallising, tensile test specimen prep. 0-71838  
cyclobutene with bisazides, effect of photoresist layer thickness on photosensitivity (Russian) 0-73510

## rubber continued

cylinder, circular, uniformly heated, combined extension and torsion 0-92057  
denture base polymers, fatigue test machine 0-66712  
education, Brownian motion, melting, surface tension and rubber networks, thermodynamic anal. 0-73132  
epoxy-rubber particulate composite, toughness and fracture mech. 0-71727  
ethylene, propylene rubber, effect of electrode profile on dielec. breakdown voltage, epoxy resin insulation system 0-60502  
ethylene-propylene rubber, for dry insulation in power cables (Spanish) 0-81024  
facings, rubber-metal, vulcanisation degree determ.,  $\gamma$ -ray method 0-61043  
fracture in viscoelastic systems under cyclic loading 0-81195  
friction against paper and polymer film surfaces, microroughness effect 0-71763  
latex solids, agglomerating and dewatering 0-104470  
mixtures in range of reversion, vulcanetry, cross-linking model (German) 0-104113  
natural, crosslinked by dicumyl peroxide, modulus, swelling relations 0-59551  
natural rubber vulcanisate, network changes during physical testing 0-60936  
NR, glass-rubber transition, time-temp. superposition, shear creep compliance meas. 0-88309  
oxidation, for prep. of diene oligomers with hydroxyl groups (German) 0-85175  
polybutadiene, dihydroxy-terminated, with unattached styrene-butadiene copolymer, stress relax. 0-104202  
polystyrene, rubber modified, two-phase struct. influence on fracture toughness (German) 0-66666  
polystyrene latexes, monodisperse, model colloid systems 0-89545  
powders, finely dispersed, sedimentometric anal. 0-66883  
protective coating for optical fibres, pressure sensitivity meas. and limitation 0-106605  
PV, glass-rubber transition, time-temp. superposition, shear creep compliance meas. 0-88309  
rubber-metal interface, adhesion mechanism, XPS study 0-65382  
seal technology, advances 0-93730  
silicon-Pb(Zr,Ri,O)<sub>3</sub>Nb flexible composite pyroelectric, dielectric props. 0-80704  
silicone, ring membranes appl., (Slovak) 0-61141  
silicone rubber, arc resistance tests in various gas insulators (Japanese) 0-81250  
silicone rubber substrata, appl. to study of cell locomotion 0-104835

rubbing (abrasion) *see abrasion*

## rubidium

*see also nuclei with .....*  
anions, THF soln., photolysis, appl. to photogalvanic cell 0-85294  
atom,  $^4\text{P}$  photodissoc. product, fine struct. anal. 0-78665  
atom, radiative lifetimes up to  $n=12$  excited states, pulsed dye laser and superradiance excitation 0-83322  
atom, radioisotopes, hyperfine spectroscopy, nucl. props. 0-57677  
atom, situated in external elec. field, near zero energy reson. anal. 0-63563  
atom+atom, radiatively excited states, chemi-ionisation, ionisation rate consts. determ. 0-58363  
atom in Xe, collision-induced dipole transitions, absorpt. meas. 0-95718  
atomic vapour, Doppler-free two-photon dispersion and optical bistability 0-95940  
atoms, valence-core electron exchange interactions, local approx. 0-91416  
crystal struct., van der Waals and repulsive interaction 0-84137  
electrical resistivity, phase transforms. under high press. (German) 0-107763  
erythrocytes, rabbit, increased passive efflux of  $^{22}\text{Na}$  and  $^{86}\text{Rb}$  on microwave irradi. 0-108957  
Fermi surface and quasiparticle props., density functional approx. 0-96771  
Fermi-surface press. dependence 0-96772  
fluorescent excitation anal. of stable Rb, erythrocyte survival determ., rabbits 0-81788  
ground state alkali molecules, mag. shielding and spin-rot. interaction 0-87186  
ground state of solids, spin density functional method, binding energy, compressibility 0-65477  
intercalation compound with graphite, superlattice struct., electron diffraction 0-75214  
liquid, density fluctuations from mol. dynamics simulations 0-100161  
liquid, freq. moment and viscosities calc. 0-88348  
maser oscillator freq. domain meas. of freq. stability 0-83574  
metal impurity effect on residual elec. resistance (Russian) 0-84457  
positronium, formation in positron+alkali metal atom collisions, first Born approx. 0-83525  
positronium formation in positron+alkali metal atom collisions, pseudopot. calcs. 0-83524  
superradiance between degenerate levels, polaris. characts., coupled transitions 0-58493  
vapour, Gaussian pulse propag. under two-photon near reson. conditions 0-87441  
vapour, mag. props. changes under laser irradi., induced EMF obs. 0-100059  
 $\text{KMnF}_3/\text{Rb}$ , phase transition and atomic motions, NMR study 0-75872  
 $^{81,82}\text{Rb}$  production for positron emission tomography 0-98068  
Rb II, lifetimes in  $4p^2\text{S}$  config., precision meas. and calc. 0-102488  
 $\text{Rb}^{2+}$ , dissociation energy from ionisation rate coeffs. of  $\text{Rb}+\text{Rb}$  0-58363  
 $\text{Rb}+\text{H}^+$  (H), single-electron capture total cross sections 0-91656  
 $\text{Rb}+\text{He}$ , quasielastic and inelastic collisions in S and D Rydberg states 0-83462  
 $\text{Rb}+\text{methane}$  (and deuterates),  $5^2\text{P}_{1/2} \rightarrow 5^2\text{P}_{3/2}$  excitation transfer, isotope effects, temp. depend. 0-91630  
 $\text{Rb}+\text{Rb}^{**}$ , freq. shift, line broadening, phase interference effects, Doppler free two photon spectra 0-58200  
 $\text{Rb}_2$ , photodissoc.,  $^2\text{P}$  products, at fine struct. anal. 0-78665  
 $^{81}\text{Rb}$ , excitation functions of proton induced nuclear reactions on  $^{81}\text{Rb}$ , medical appls. 0-78286  
 $^{86}\text{Rb}$ , in molten alkali nitrates, diffusion coeffs. meas. 0-70437  
 $^{87}\text{Rb}+^{129}\text{Xe}$ , spin-exchange cross-section meas. 0-78686  
 $^{85,87}\text{Rb}$ , first excited D-level, hyperfine struct. meas. by cascade, fluorescence spectrosc. 0-69101



**rubidium alloys**

- K-Rb, extreme UV absorpt. spectra 0-97294  
K-Rb, internal energy, heat of mixing, entropy, dielectric function 0-88340

**rubidium compounds**

see also rubidium alloys

- halides, elastic constants, temp. derivatives at constant volume 0-59549  
halides, spin lattice relaxation meas. of  $O_2^-$  centres 0-88863  
Ag/RbAg<sub>4</sub>I<sub>3</sub>/I<sub>2</sub> solid state battery, low temp. degradation 0-61331  
Ag/RbAg<sub>4</sub>I<sub>3</sub>/Ta, solid electrolyte timing cell and coulometer 0-68216  
AgI/RbI quasibinary system, solid state reactions and transport props. 0-96700  
 $\beta$ -Al<sub>2</sub>O<sub>3</sub>-Rb<sub>2</sub>O, single cryst. Raman scatt., cond. mechanism and cryst. struct. 0-66209  
DyF<sub>3</sub>-RbF, phase diagrams and ternary fluorides (*French*) 0-81040  
K<sub>1-x</sub>Rb<sub>x</sub>Cl, impurity centre local vibr., comp. depend. of spectral parameters 0-79898  
LiCl-RbCl, molten, Chemla effect, mol. dynamics simulation, self exchange vel. 0-79967  
MgRb<sub>2</sub>(SeO<sub>4</sub>)<sub>2</sub>·6H<sub>2</sub>O:Mn<sup>2+</sup>, EPR spectra 0-100608  
((NH<sub>4</sub>)<sub>1-x</sub>Rb<sub>x</sub>)<sub>2</sub>SO<sub>4</sub>, isomorphous impurity effect on dielec. and nonlinear optical props. 0-88911  
Rb halides, role of quantum effects in lattice dynamics, Debye temp., shell model calcs. 0-70336  
Rb-tetrahydrofuran solution, polarised photoelectron and loose ion pair (Rb<sup>+</sup>, e) obs., optical-ESR study 0-85196  
RbAg<sub>4</sub>I<sub>3</sub>, contact in solid state cells, electrochem. study 0-76527  
 $\alpha$ -RbAg<sub>4</sub>I<sub>3</sub>, dynamic cage effect 0-107541  
RbAg<sub>4</sub>I<sub>3</sub>, film, thermopower meas. temp. depend., correl. effects role 0-107539  
RbAg<sub>4</sub>I<sub>3</sub>, single particle excitations, inelastic neutron scatt. obs. 0-59599  
RbAg<sub>4</sub>I<sub>3</sub>, solid electrolyte, contrib. of non-Brownian motion to transport props. 0-70453  
RbAg<sub>4</sub>I<sub>3</sub>, solid electrolyte development, Ag<sup>+</sup> cond. 0-107532  
RbAg<sub>4</sub>I<sub>3</sub>, static and dynamic NMR effects at 208K and 122K phase transitions 0-108105  
RbAg<sub>4</sub>I<sub>3</sub>, superionic conductor, phase transition detection by thermoelectric power method 0-92669  
RbAg<sub>4</sub>I<sub>3</sub>, superionic phase transition, dynamical and crit. pt. props. 0-107535  
RbAlF<sub>4</sub>, single cryst., prep. and struct. (*French*) 0-79762  
RbAlF<sub>4</sub>, dissoc. enthalpies, mass spectrometric determ., heat of form. 0-97720  
 $\beta$ -RbAlF<sub>4</sub>, struct. and irreversible and topotactic phase transition  $\beta$ - $\alpha$  mechanism 0-107132  
RbAl(SO<sub>4</sub>)<sub>2</sub>·12H<sub>2</sub>O, spin-Hamiltonian with trigonal S<sup>3</sup>I terms for describing <sup>55</sup>Fe<sup>3+</sup> ENDOR spectra 0-75885  
RbBO<sub>3</sub>, vapour over heated solid, XPS, obs. 0-87171  
RbBr, cation defects creation mechanism 0-75224  
RbBr, F-centre emission, mag. circular polarisation 0-108251  
RbBr, photo-elastic constants and pressure derivatives of shear moduli 0-75284  
RbBr, self trapped exciton form. time at <sup>1</sup>S<sub>u</sub><sup>+</sup> state under pulsed electron beam in ps range 0-97347  
RbBr·I<sup>-</sup>, OH<sup>-</sup>, luminesc. of interstitial atomic H 0-89062  
RbCN, acoustic and optical phonon dispersion at 300K 0-84266  
RbCaCl<sub>3</sub>, Raman scatt. study of phase transitions 0-71411  
RbCaF<sub>3</sub>, cubic to tetragonal phase transition, <sup>87</sup>Rb NMR study 0-70392  
RbCaF<sub>3</sub>, first order improper ferroelastic phase transition at 194K, phenomenological description 0-70397  
RbCaF<sub>3</sub>, phase transitions due to octahedra rots. in perovskite struct., order-disorder model 0-70151  
RbCaF<sub>3</sub>, shift of first order transition under hydrostatic press. 0-59649  
RbCaF<sub>3</sub>:Gd<sup>3+</sup>, struct. phase transition, EPR study 0-71171  
RbCdF<sub>3</sub>:Gd<sup>3+</sup>, struct. phase transition, EPR study 0-71171  
RbCl aqueous solutions, IR absorpt.  $\nu_1$  (CN) band parameter temp., conc. study (*Russian*) 0-80801  
RbCl, cation defects creation mechanism 0-75224  
RbCl, defect modes due to substitutional anion-pair and cation-pair impurities in ionic crystals 0-92540  
RbCl, electron bombard., colour centre photoemission, surface contamination and escape depth 0-66392  
RbCl, F-centre emission, mag. circular polarisation 0-108251  
RbCl films, breakdown on appl. of electric voltage pulses 0-66109  
RbCl, fundamental luminescence at high ionisation levels (*Russian*) 0-103985  
RbCl, photo-elastic constants and pressure derivatives of shear moduli 0-75284  
RbCl, photofragment spectra, bond energies and excited state symmetries 0-87190  
RbCl, positron-trapping colour centre dynamics, positron annihilation study 0-108294  
RbCl:Au<sup>3+</sup>, optical absorpt. bands and MCD, electron-lattice interaction 0-108236  
RbCl:Br<sup>-</sup> (I<sup>-</sup>), interstitial atomic H centres, formation kinetics and struct. MO calc. and EPR studies 0-75854  
RbCl:Ca<sup>2+</sup>, thermolum. and optical absorption studies 0-104002  
RbCl:CoCl<sub>2</sub>, system, precipitate form., ionic cond. meas. 0-96653  
RbCl:Li F<sub>2</sub>(II) centre laser, pumped by flashlamp-pumped dye laser 0-102737  
RbCl(Br)(I), emission band of F-centre 0-76071  
RbClO<sub>3</sub>/RbBrO<sub>3</sub> mixed crystals, internal optic modes obs., Raman and IR reflectance spectra 0-76024  
RbClO<sub>4</sub>, AC elec. cond. temp. and freq. depend., obs. and unified defect struct. model 0-88554  
RbClO<sub>4</sub>, electrical conductivity, frequency dependence 0-65288  
RbCoCr<sub>2</sub>(VO<sub>4</sub>)<sub>3</sub>, synthesis and cryst. struct. 0-88114  
RbCoF<sub>4</sub>, 2-dimens. Ising antiferromag., mag. excitons, Raman scatt. obs. 0-66181  
RbCoF<sub>4</sub>, critical fluctuations near Neel temp., US attenuation study 0-108013  
Rb<sub>2</sub>Co<sub>2</sub>Mg<sub>1-x</sub>F<sub>4</sub> mag.-nonmag. two-dimens. antiferromag. Ising system, spin fluctuations 0-80545  
Rb<sub>2</sub>Co<sub>2</sub>Mn<sub>0.5</sub>F<sub>4</sub>, two dimens. random antiferromag., excitations 0-107997  
RbCrCl<sub>3</sub>,  $\alpha$ - $\beta$  phase transition, dynamical aspects and thermodynamic theory 0-70404  
RbCrCl<sub>3</sub>, Jahn-Teller induced phase transitions 0-70391  
RbCrCl<sub>4</sub>, 2D-ferromag., renormalisation of long wavelength spin waves, neutron scatt. 0-60229

**rubidium compounds continued**

- Rb<sub>2</sub>CrCl<sub>4</sub>, optical absorption intensity, short-range spin correlation 0-108185  
Rb<sub>2</sub>CrCl<sub>4</sub>, planar ferromag., spin waves 0-65835  
Rb<sub>2</sub>CuBr<sub>4</sub>·2H<sub>2</sub>O, dynamic props. in paramag. state, spin-lattice relax. time meas. 0-71214  
(Rb<sub>2</sub>)CuBr<sub>4</sub>·2H<sub>2</sub>O, hyperfine and super-exchange interactions 0-103654  
Rb<sub>2</sub>CuCl<sub>4</sub>·1.5, development of Cu<sup>+</sup> ion cond. 0-107532  
Rb<sub>2</sub>CuCl<sub>4</sub>·2H<sub>2</sub>O, hyperfine and super-exchange interactions 0-103654  
Rb<sub>2</sub>CuCr<sub>2</sub>(VO<sub>4</sub>)<sub>3</sub>, synthesis and cryst. struct. 0-88114  
Rb<sub>2</sub>(SO<sub>4</sub>)<sub>2</sub>, dielec. props. and phase transitions 0-60482  
RbDy<sub>2</sub>F<sub>10</sub>, RbDy<sub>2</sub>F<sub>7</sub> and Rb<sub>2</sub>DyF<sub>6</sub>, cryst. symm. and cell parameters (*French*) 0-81040  
RbF, one electron props., SCF-X-alpha scattered wave method 0-83279  
RbF:Li(Na), F-centres, saddle-point configuration, molecular model parameter 0-107234  
RbF-AlF<sub>3</sub>, ion-molecule equilibria studied by mass spectrometric method, heats of dissoc. and form. calc. 0-104479  
RbFeCl<sub>3</sub>, one-dimens. ferromagnet, lowest excitation, far IR study 0-66186  
RbFeCl<sub>3</sub>, pseudo-one-dimens. singlet ground state ferromag., mag. excitations, neutron scatt. study 0-97064  
RbFeCl<sub>3</sub>·2H<sub>2</sub>O, pseudo-one-dimensional canted Ising antiferromag., spin-cluster excitations 0-70989  
RbFeCl<sub>3</sub>·2H<sub>2</sub>O, rectangular Ising cpd., Mossbauer meas. 0-71252  
RbFeCl<sub>3</sub>·2H<sub>2</sub>O, spin cluster excitation expts. 0-66039  
Rb<sub>2</sub>FeF<sub>4</sub>, antiferromagnet, two-dimensional, mag. excitations 0-80492  
Rb<sub>2</sub>FeF<sub>4</sub>, two-dimensional antiferromagnet, with easy plane anisotropy, mag. excitations and two-magnon Raman scatt. 0-65839  
Rb<sub>2</sub>FeF<sub>4</sub>, mag. struct. and one-dimens. antiferromagnetism 0-60209  
Rb<sub>2</sub>FeF<sub>4</sub>, one-dimensional antiferromag. systems, Mossbauer studies 0-71266  
Rb<sub>2</sub>Fe<sub>2</sub>O(SO<sub>4</sub>)<sub>2</sub>·5H<sub>2</sub>O, cryst. struct. determ. 0-92482  
RbGa(SO<sub>4</sub>)<sub>2</sub>·12H<sub>2</sub>O, spin-Hamiltonian with trigonal S<sup>3</sup>I terms for describing <sup>55</sup>Fe<sup>3+</sup> ENDOR spectra 0-75885  
RbH, structural transition from NaCl to CsCl type under high press. 0-96458  
RbH<sub>2</sub>PO<sub>4</sub>, critical and tricritical phenomena, susceptibility, exponents 0-75976  
RbH<sub>2</sub>PO<sub>4</sub>, electrostrictive effects, US rel. 0-75941  
RbH<sub>2</sub>PO<sub>4</sub>, ferroelec., dielec. props., four-cluster approx. 0-97202  
RbH<sub>2</sub>PO<sub>4</sub>, ferroelec. phase transition, birefringence studies 0-108162  
RbH<sub>2</sub>PO<sub>4</sub>, phase transitions study, role of cryst. struct. determ. 0-75197  
RbH<sub>2</sub>PO<sub>4</sub>, proton modes, dielec. spectroscopy 0-75915  
RbH<sub>2</sub>PO<sub>4</sub>, X-irradiated, hysteresis effects obs. by ESR 0-103928  
RbHSO<sub>4</sub>, ferroelec., dielec. dispersion 0-97179  
Rb<sub>2</sub>H(SO<sub>4</sub>)<sub>2</sub>, dielec. props. and phase transitions 0-60482  
RbHSeO<sub>4</sub>, ferroelec. props. rel. to struct. 0-71345  
RbHSeO<sub>4</sub>, ferroelec., far IR spectra 0-71404  
RbH<sub>2</sub>(SeO<sub>3</sub>)<sub>2</sub> crystal, incommensurate phase, quadrupole moment study 0-97213  
RbH<sub>3</sub>(SeO<sub>3</sub>)<sub>2</sub>, dielec. relax. near ferroelec. Curie temp. 0-97207  
RbH<sub>3</sub>(SeO<sub>3</sub>)<sub>2</sub>, US vel. and absorpt. near ferroelec. Curie temp. 0-97206  
RbH<sub>3</sub>(SeO<sub>3</sub>)<sub>2</sub>:VO<sup>2+</sup>, EPR spectra, spin Hamiltonian parameters 0-100609  
RbI, intra impurity local oscil. composition tone absorpt. band anharmonic peak, broadening (*Russian*) 0-60642  
RbI, luminesc. structure induced by pulsed Ne<sup>+</sup> and electron beams and X-rays 0-80851  
RbI, photo-elastic constants and pressure derivatives of shear moduli 0-75284  
RbI, photostimulated recomb., electron spin polarisation 0-60673  
RbI:Pb, absorpt. spectra of Pb<sup>2+</sup> centres 0-76058  
RbIn(SO<sub>4</sub>)<sub>2</sub>·4H<sub>2</sub>O, refinement of cryst. struct., interatomic distances, bonds 0-59448  
Rb<sub>2</sub>KMoO<sub>4</sub>F<sub>3</sub>, ferroelec., transition obs. 0-75989  
Rb<sub>2</sub>KWO<sub>4</sub>F<sub>3</sub>, ferroelec., transition obs. 0-75989  
RbMgCr<sub>2</sub>(VO<sub>4</sub>)<sub>3</sub>, synthesis and cryst. struct. 0-88114  
RbMnBr<sub>3</sub>, EPR linewidth anisotropies 0-103878  
RbMnCl<sub>3</sub>, specific heat near Neel temp. (*Russian*) 0-100340  
RbMnCl<sub>3</sub>, twinning struct., cryst. domains, orientation mag. transition (*Russian*) 0-107275  
RbMnCl<sub>4</sub>, quasi-2D-antiferromag., linear birefr. and optical absorpt. spectra 0-71385  
RbMnF<sub>3</sub>, Faraday effect mechanism in paramag. phase 0-60552  
RbMnF<sub>3</sub>, Jahn-Teller coupling const., LCAO calc. 0-59940  
RbMnF<sub>3</sub>, spin wave lifetime, theory compared with expt. 0-60228  
RbMnF<sub>3</sub>, spin wave widths 0-97081  
RbMnF<sub>3</sub>:Er<sup>3+</sup>, absorption, emission, excitation and lifetime meas. 0-71460  
RbMnF<sub>3</sub>:Fr, pure and doped, unirradiated and electron irradi., energy transfer 0-108254  
Rb<sub>2</sub>MoO<sub>4</sub>F<sub>3</sub>, ferroelec., transition obs. 0-75989  
RbNO<sub>3</sub>, struct., high temp. phases, neutron diff. study 0-79756  
3RbNO<sub>3</sub>-2Ca(NO<sub>3</sub>)<sub>2</sub>, glass form. from liq., struct. transform., Raman spectrum obs. 0-64916  
Rb<sub>2</sub>NaHoF<sub>6</sub>, NMR spectra of <sup>165</sup>Ho, 1.6 to 13K 0-80620  
RbNaMg<sub>2</sub>M<sub>2</sub>Si<sub>2</sub>O<sub>10</sub> (M=Cu, Fe, Mg), cryst. struct., X-ray diff. and IR spectra (*French*) 0-107158  
Rb<sub>2</sub>NaTbF<sub>6</sub>, NMR spectra of <sup>159</sup>Tb, 1.6 to 13K 0-80620  
Rb<sub>2</sub>Nb<sub>2</sub>O<sub>7</sub>·3H<sub>2</sub>O, cryst. struct. by X-ray diff. (*French*) 0-92503  
RbNbWO<sub>4</sub>, pyrochlore struct., tetragonal to cubic phase transition 0-75355  
RbNbW<sub>2</sub>O<sub>6</sub> crystals, growth and props. 0-104054  
RbNiCl<sub>3</sub>, noncollinear magnetic order and spin wave spectrum in presence of competing exchange interactions 0-65834  
RbNiCr<sub>2</sub>(VO<sub>4</sub>)<sub>3</sub>, synthesis and cryst. struct. 0-88114  
RbNiF<sub>3</sub>, high-temperature mag. sp. ht. (*Russian*) 0-88757  
RbNiF<sub>3</sub> spin lattice, susceptibility, Heisenberg model (*Russian*) 0-65893  
Rb<sub>2</sub>PbCu(NO<sub>2</sub>)<sub>6</sub>, incommensurate Jahn-Teller transition, Huang scatt. 0-70401  
RbPbI<sub>3</sub>·2H<sub>2</sub>O, X-ray cryst. struct. determ. 0-64958  
Rb<sub>2</sub>Pb[Co(NO<sub>2</sub>)<sub>6</sub>], struct. study 0-88106  
RbReO<sub>4</sub>, IR matrix-isolation spectra 0-87108  
Rb<sub>2</sub>Sb<sub>2</sub>O<sub>7</sub>, solid state synthesis (*French*) 0-104438  
RbSbO<sub>3</sub>·1/6RbF, dielec. spectroscopy study, 100 Hz to 10 MHz, 238 to 417K (*German*) 0-108144  
Rb<sub>2</sub>Ta<sub>20</sub>O<sub>70</sub>, layered cryst. struct. 0-107166  
Rb<sub>2</sub>Te<sub>2</sub>, synthesis and cryst. struct. 0-88115  
Rb<sub>2</sub>(Ti<sub>1-x</sub>M<sub>x</sub>)<sub>2</sub>O<sub>7</sub>, M=Nb, Ta, layer compound, cryst. struct., non-stoichiometry 0-64972

**rubidium compounds continued**

- RbTi(SeO<sub>4</sub>)<sub>2</sub>, Rb<sub>3</sub>Ti(SeO<sub>4</sub>)<sub>3</sub>, and Rb<sub>2</sub>Ti(SeO<sub>4</sub>)<sub>4</sub>, cryst. struct. (*French*) 0-84148  
 RbVO<sub>3</sub>:Cr<sup>3+</sup>, study of ESR spectra 0-80601  
 Rb<sub>2</sub>WO<sub>3</sub> bronze, elec. resist. meas., anisotropy 0-75569  
 Rb<sub>2</sub>WO<sub>3</sub>, low lying phonon dispersion curves, neutron scatt. study 0-92622  
 Rb<sub>2</sub>WO<sub>3</sub>F<sub>3</sub>, ferroelec., transition obs. 0-75989  
 Rb<sub>2</sub>ZnBr<sub>4</sub>, ferrielectricity, triple 60 Hz D-E hysteresis loops 0-71365  
 Rb<sub>2</sub>ZnBr<sub>4</sub>, ferroelec., photovoltaic and photorefractive phenomena 0-75598  
 Rb<sub>2</sub>ZnBr<sub>4</sub>, modulated struct., far IR transmission, temp. depend. 0-71408  
 Rb<sub>2</sub>ZnBr<sub>4</sub>, soft modes at phase transforms., far IR spectrum study 0-107398  
 Rb<sub>2</sub>ZnBr<sub>4</sub>, soft modes obs. by Raman scatt. 0-97283  
 Rb<sub>2</sub>ZnBr<sub>4</sub>(Cl<sub>4</sub>), Raman spectra near incommensurate phase transitions 0-76013  
 Rb<sub>2</sub>ZnCl<sub>4</sub>, commensurate-incommensurate phase transition, crit. behaviour, sp. ht. meas. 0-71342  
 Rb<sub>2</sub>ZnCl<sub>4</sub>, commensurate-incommensurate phase transition, <sup>35</sup>Cl NQR study 0-75966  
 Rb<sub>2</sub>ZnCl<sub>4</sub>, dielec. dispersion, 5-900 MHz, near incommensurate-commensurate transition 0-60522  
 Rb<sub>2</sub>ZnCl<sub>4</sub>, ferrielectricity, triple 60 Hz D-E hysteresis loops 0-71365  
 Rb<sub>2</sub>ZnCl<sub>4</sub>, incommensurate phase transition, <sup>87</sup>Rb NMR study 0-75967  
 Rb<sub>2</sub>ZnCl<sub>4</sub>, incommensurate phase transitions, <sup>35</sup>Cl NQR study 0-75968  
 Rb<sub>2</sub>ZnCl<sub>4</sub>, phase transitions, thermal expansion coeff. 0-100638  
<sup>85</sup>RbCl<sub>3</sub>, <sup>85</sup>RbCl isotope enriched cryst., optical registration of EPR F-centres (*Russian*) 0-103886  
 Rb<sub>2</sub>(C<sub>2</sub>O<sub>4</sub>)<sub>2</sub>·D<sub>2</sub>O, neutron profile refinement at 5K 0-88103  
 ZnRb<sub>2</sub>(SeO<sub>4</sub>)<sub>2</sub>·6H<sub>2</sub>O:Mn<sup>2+</sup>, EPR spectra 0-100608

**ruby**

- cross-relaxation to (3d)<sup>1</sup> ions 0-71163  
 crystal, photon echo generation, control method 0-87440  
 crystal, radiation amplification, spatial coherence 0-99737  
 distant nuclei ESR and ENDOR experiments, dipole-dipole reservoir importance 0-71241  
 electric field induced double quantum transitions 0-80595  
 energy transfer between different emitters and spatial diffusion 0-103978  
 fluorescence decay of red R lines used in biological thermometer 0-86306  
 laser, double mode locking using dye saturable absorber 0-99763  
 laser, frequency-stabilised using Fabry-Perot interferometer 0-58566  
 laser, ultrashort pulse generation by internal phase and amplitude modulation 0-106551  
 laser, with electrooptical shutter, emission spectrum narrowing and single freq. giant pulse lasing 0-78877  
 laser, with stimulated Brillouin scatt. complex conjugate mirror 0-87438  
 light echo signal correlation with exciting pulse shape (*Russian*) 0-106576  
 luminescence, absorption of R and N lines, effect of mag. field 0-60550  
 maser, K-band, 500 MHz bandwidth 0-63966  
 optical nutation echoes, Stark switching obs. 0-69467  
 phase modulated conjugate wave generation, hologram model 0-83643  
 phonon spectrum, thermal pulses under diffuse phonon propagation conditions 0-103434  
 polishing features of hard crystals 0-64225  
 pressure calibration system improvement using ruby R<sub>1</sub> fluorescence 0-98928  
 pulsed diode simulators of solid lasers Al<sub>1</sub>Ga<sub>1-x</sub>As and Ga<sub>x</sub>In<sub>1-x</sub>P<sub>1-y</sub>As<sub>y</sub>, solid solns. 0-91816  
 quantum efficiency, photoacoustic meas. 0-73472  
 R<sub>1</sub> zero phonon line, resonance fluoresc. meas. 0-89055  
 radiation-induced optical processes, impurity effects 0-66310  
 resonant scattering and trapping of 29 cm<sup>-1</sup> acoustic phonons in Al<sub>2</sub>O<sub>3</sub>:Cr<sup>3+</sup> 0-93403  
 reversed light echo due to two pulse laser resonance excitation (*Russian*) 0-87439  
 ring laser with forced mode locking 0-95915  
 spatial gratings, transient light-induced, by successive optical coherent pulses 0-64115  
 structural defects due to laser irradi. (*Russian*) 0-100303  
 thermochemical etching, Cr impurity influence 0-88190  
 Al<sub>2</sub>O<sub>3</sub>:Cr<sup>3+</sup>, inhomogeneous spin system, time evolution towards saturated state 0-88869  
 Cr-doped, relaxation behaviour, EPR study, environmental effects 0-66021

**Rudermann-Kittel-Kasuya-Yosida interaction** *see* **RKKY interaction**

**Runge-Kutta methods**

- buoyancy induced flow adjacent to vertical uniform flux surface in cold water 0-69834  
 finitely conducting cross grating theory 0-106635  
 inclined surfaces, wave instability of laminar mixed convection flow 0-69837

**Russell-Saunders coupling**

- atoms, P-state collisions, quantum mechanical treatment, angular momentum coupling 0-99541  
 equivalent electrons, J allowed values in jj coupling, teaching 0-90624  
 inert gas, atomic photoionisation, Dirac-Fock calcs., branching ratios and angular distrib. in p shells 0-63601  
 three-electron systems, transition probabilities calcs. 0-99479  
 Li, optical oscill. strengths calcs. 0-91495  
 O III, electron impact excitation cross sections, independent particle model calcs. 0-63823  
 TmTe, f<sup>12</sup> and f<sup>13</sup> config. photoemission fractional parentage coeffs., intermediate and LS coupling calc. 0-84829

**rust prevention** *see* **corrosion protection**

**ruthenium**

*see also* **nuclei with .....**

- adsorption of CO on (001), temp. depend. ordering processes 0-80773  
 adsorption of CO on (001) surface, IR spectra, LEED, and thermal desorption meas. 0-70533  
 adsorption of O<sub>2</sub>, H<sub>2</sub>, and CO on (1120) surface, ellipsometry-LEED study 0-103570  
 atoms, N<sub>2</sub>N<sub>3</sub>N<sub>4</sub> super Coster Kronig processes 0-106303  
 chemisorption of O<sub>2</sub> on (001) surface, uptake meas., thermal desorpt. spectroscopy and AES 0-108739  
 core level binding energies 0-71564

**ruthenium continued**

- Debye-Waller factor and Lindemann parameter, temp. depend., lattice dynamical model calcs. 0-59610  
 electrical resistivity, quadratic contrib., 2 to 40K (*Russian*) 0-92874  
 kinetics of C deposition from adsorbed CO on (110) surface 0-76553  
 recovery and use of noble metals from radioactive waste 0-99242  
 wear coefficients determ. using pin-on-disc apparatus 0-76366  
 Pt/Ru electrocatalysts for methanol oxidation in acid electrolyte with improved steady state activity for fuel cell appls. 0-76629  
 TiO<sub>2</sub>:Ru<sup>4+</sup>, rutile, EPR and cryst. field const. 0-60415  
 YIG:Ru, optical absorpt. and MCD obs. of Ru<sup>4+</sup> site occupancy 0-71456

**ruthenium alloys**

*see also* **ruthenium compounds**

- Cr-Ru, magnetic transformations, triple point (*Russian*) 0-88747  
 Cr<sub>2</sub>Ru, σ phases, ordering, X-ray cryst. struct. determ. 0-107107  
 Gd-Ru, amorphous, mag. props. and ferromag. reson. 0-75862  
 GdRu<sub>2</sub>H<sub>2</sub>, struct. and mag. props., Mossbauer and magnetisation meas. 0-71271  
 Mo-Ru, recovery after deform. and annealing, destrengthening mechanism (*Russian*) 0-97546  
 Mo-Ru(-Si), amorphous superconductors, prep. by electron beam evaporation and liq. quenching, crit. temp. 0-103776  
 Mo<sub>0.6</sub>Ru<sub>0.4</sub>B<sub>20</sub>, amorphous, local symmetry around glass-former sites, elec. quadrupole effects, NMR 0-80618  
 (Mo<sub>0.6</sub>Ru<sub>0.4</sub>)<sub>0</sub>Si<sub>10</sub>B<sub>10</sub>, amorphous supercond. matrix, flux pinning by MoRu precip. 0-65756  
 Ni-Ru (≤4 at.%), influence of alloying on mag. anisotropy 0-71010  
 PdRu (4.7 at.%), effect of alloying on activation energy of H<sub>2</sub> diffusion 0-107571  
 PrRu<sub>2</sub>, hyperfine sp. ht. and magnetisation meas. at 4.2K 0-75775  
 PrRu<sub>2</sub>, sp. ht., differential susceptibility and elec. resist. meas., 1.4-40K 0-71063  
 PuRu<sub>2</sub>, intermetallic cpd., sublimation thermodynamics 0-96639  
 Ru-Cu clusters, EXAFS study 0-84804  
 Ru-Fe, dil., local magnetisation, Mossbauer meas. 0-66091  
 Ru-Sn-M, m=Mg, Ca, Sr, Sc, Y, Zn, Cd, In or Th 0-100777  
 Ru<sub>2</sub>FeSn, ferromag. Heusler alloys, hyperfine fields at nonmagnetic atoms in various sites, Mossbauer effect and NMR meas. 0-66089  
 Sc-Ru, dil., elec. field gradient, Mossbauer meas. 0-80665  
 Sc-Ru, elec. field gradient and temp. depend. TDPAC meas. 0-60477  
 URu<sub>3</sub>, sublimation thermodynamics 0-97722  
 Y-Ru, elec. field gradient and temp. depend. TDPAC meas. 0-60477  
 Y<sub>2</sub>Ru, cryst. struct. 0-96474  
 Zr-Ru, alloy Zr rich, Ru solubility, eutectic decay, α=β transform., struct. (*Russian*) 0-65227

**ruthenium compounds**

*see also* **ruthenium alloys**

- borides, RRu<sub>2</sub>B<sub>3</sub> (R=rare earth, Y, Th, or U), supercond. and mag. props. 0-97028  
 ruthenium tris-bipyridyl, excited state electron transfer quenching, H<sub>2</sub>O photoreduction mediators effects 0-102536  
 trisbipyridyl ions in surfactant solns., excited state decay kinetics 0-83407  
 Ba<sub>4</sub>NbRuO<sub>12</sub> and Ba<sub>4</sub>TaRuO<sub>12</sub>, (Ru<sub>3</sub>O<sub>12</sub>)<sup>13-</sup> cluster obs. in presence of orbital degeneracy and spin-orbit coupling (*French*) 0-70655  
 Ba<sub>3</sub>Ru<sub>2</sub>MO<sub>9</sub>, (M=Mg, Ca, Sr, Co, Ni, Cu, Zn, Ca), Mossbauer spectra 0-108136  
 Li<sub>0.5</sub>Fe<sub>2.5</sub>O<sub>4</sub> Ru substitution effect on struct. and mag. props., and max. solubility determ. 0-75364  
 Ru complex, [Ru(bpy)<sub>3</sub>]<sup>2+</sup>-Ti (III), photochem. H<sub>2</sub> prod. from aq. soln. 0-85192  
 Ru complexes, [Ru(bipy)<sub>3</sub>(pq)<sub>3</sub>]<sup>2+</sup> mixed-ligand, electronic absorpt. and emission spectra meas. 0-71441  
 Ru<sub>2</sub>Ge<sub>3</sub>Sn<sub>2</sub>, and Ru<sub>2</sub>Ge<sub>3</sub>Si<sub>2</sub>, diffusionless phase transitions, elec. and mag. props. 0-96871  
 Ru(II) complex, carbonyl(pyridine)-phthalocyaninoruthenium(II), optical hole burning, matrix effects 0-102522  
 Ru(NH<sub>3</sub>)<sub>6</sub><sup>3+</sup>, isotopic chem. shift, pseudocontact contrib. 0-91577  
 RuO<sub>2</sub>, thermal conductivity meas., rel. to elec. cond. 0-65317  
<sup>99,101</sup>RuO<sub>2</sub>, NQR spectroscopy 0-63664  
 Ru<sub>2</sub>Ti<sub>1-x</sub>O<sub>2</sub> films, percolation elec. cond. in strong electric fields (*Russian*) 0-84471  
 TiO<sub>2</sub>-RuO<sub>2</sub> surface, photocatalytic decomp. of H<sub>2</sub>O 0-85194

**rutile** *see* **titanium compounds**

**S-matrix theory**

*see also* **dispersion relations; network parameters**

- A<sup>±</sup>-coupling in abstract approach of quantum field theory, renormalisation group 0-99033  
 atom+diatom, sudden approx. of Cross, computational tests, cross section factorisation, scatt. phenomena 0-58352  
 chiral O(N)×O(N) and SU(N)×SU(N) 2-dimens. models, conservation laws and S-matrices 0-68389  
 factorised completely X symmetric S-matrix characterisation, multicomponent field theories 0-105800  
 formal manipulations relating the S-matrix and density matrix formalisms 0-99064  
 gas linear molecules, symmetrised Liouville basis vectors, appl. to spectral linewidths 0-83457  
 gauge singlet operators instead of bound states 0-99063  
 Gross-Neveu model, chiral invariant, S-matrix direct calc. 0-68362  
 hadron+hadron, cluster model, field theoretic, multiperipheral production, Feynman scaling violation 0-57576  
 hadronic targets, spin-1/2, Compton scatt., optimal sum-rule inequalities 0-105815  
 mode-coupled multimode W-fibre, analytical anal., scattering matrix method 0-99872  
 model factorized S matrix and an integrable Heisenberg chain with spin 1 (*Russian*) 0-101767  
 multiply charged ions, 2p<sub>1/2</sub>3p<sub>3/2</sub> config., level widths, relativistic calc., S-matrix method 0-63546  
 NDO in terms of power series expansion in S-matrix 0-69080  
 one-electron atom, rearrangement collisions in laser radiation field 0-74225  
 oscillating potentials, scatt. matrix 0-57126  
 path integral formulation, central scattering potentials 0-82906  
 perturbation expansion of multichannel Regge poles 0-86623  
 quantum field theory, operator ordering, interaction Hamiltonian noncommuting operators, S-matrix expansion, Feynman rules 0-57472



**S-matrix theory** continued

- quantum mechanics, decaying states in rigged Hilbert space formulation 0-62521
- spherically symmetrical coherency strain contrasts, S-matrix theory calcs. 0-100133
- Stiefel manifolds, 2-dimens. nonlinear  $\sigma$ -model, S-matrix regularities 0-86576
- stimulated electron radiation due to wiggled magnetic field 0-58451
- SU(5) without symmetry constraints, unified model of quarks and leptons, conservation laws 0-101968
- Thirring model, chiral,  $CP^{n-1}$  and  $SU_n$ , exact S-matrix 0-90985
- Yukawa potentials, finite sum S-matrix 0-101940
- $\pi NN$  vertex function and off-mass-shell  $\pi N$  scatt. 0-73739
- $CO+H_2$ , rot. excitation, rel. between tensorial cross sections 0-83454

**S-parameters**

- amplifier, fast DC coupled linear pulse, gain and phase response design 0-58088

**safety**

- see also accidents; alarm systems; fission reactor safety; health hazards; protection*
- accidents during work, mapping of reasons using error beams by function sensed computations of admission probabilities (*German*) 0-68027
- air traffic, solar power station hazards, photometric photography of dazzling heliostat mirrors (*French*) 0-61295
- biological effects of radiation, methods of safety estimation and problems encountered (*French*) 0-98003
- biomedical electronics, recommendations for Spanish hospitals (*Spanish*) 0-72350
- clinical engineering safety and technical service centres (*German*) 0-98151
- current nuclear power plant safety issues, 1980 conf. preview 0-95360
- defect evaluation rel. to fracture mech. (*German*) 0-100908
- density of fluid meas., using gamma radiation, theory, practices and appl. 0-73325
- electromedical equipment, safety by monitoring leakage currents (*German*) 0-81749
- electromedical equipment and installations, safety standards (*Croatian*) 0-104795
- fission product decay heat removal with fusion-fission hybrid mobile blanket 0-99282
- fission reactor processing facility, safeguards instrumentation 0-63362
- fission reactors, fast breeder, using uranium-plutonium cycle, Na-cooled, technical and economic viewpoints of application (*German*) 0-99202
- fuel elements recycling and thermal re-irradiation, technical, economic and safety problems (*German*) 0-99269
- fusion reactor, JT-60, grounding system design 0-102313
- fusion reactor, JT-60, grounding system pot. rise during lightning strike, anal. 0-102314
- fusion reactor, safety of superconducting fusion magnets: twelve problem areas 0-102348
- fusion reactors, liquid Li, safety anal. and support facilities 0-63380
- hospital, radioactive, substances, Health and Safety at Work Act 0-98906
- hospital laboratories, general aspects 0-95089
- HV photovoltaic arrays, safety from high reverse voltages 0-93953
- irradiated fuel elements recycling plant design modifications and safety of used nuclear fuel during storage and disposal (*German*) 0-99219
- irradiated LWR fuel, European transport experience 0-63309
- laser applications for discotheque light effects, safety considerations with respect to output power and exposure time, regulations and recommendations (*German*) 0-101224
- laser light dosimeter, health physics evaluation of operating conditions at laser installations 0-76835
- Loviisa-1 Nuclear Power Station, in Finland, safety during design, building, and operating stages (*Russian*) 0-106128
- magneto-inductive flowmeters, installation, earthing, isolation, protection against explosion (*German*) 0-64662
- medical electro-optics, 1980 development trends 0-85464
- MHD test facility safety analysis methodology and documentation system 0-61388
- MPD reduction suggestion to meet requirements of higher safety 0-85499
- nuclear fusion reactor materials, social aspects (*Dutch*) 0-106153
- nuclear medicine department, radiation safety 0-89868
- nuclear medicine laboratory, radiation safety 0-104772
- nuclear power engineering materials certification testing for safety 0-78360
- nuclear power plants, environment protection problems during construction (*French*) 0-76663
- nuclear power plants, environmental studies organisation (*French*) 0-76664
- nuclear power plants, hydrobiological studies, conception and data obtained (*French*) 0-76665
- nuclear power stations, Czechoslovak Research Institute activities (*Slovak*) 0-83188
- nuclear power stations, the need for evacuation to protect public safety at TMI 0-99352
- nuclear power stations (*Portuguese*) 0-68844
- PGFR seismic risk anal. 0-99298
- plutonium, biologically important physicochemical props. and methods of human contamination (*French*) 0-98004
- powder handling, electrostatic spark hazard identification and control 0-69291
- principles underlying IAEA nuclear safety programme 0-95361
- radiation protection, safety standards for X-rays and ionising radiation 0-98146
- radiation safety in laboratories 0-73154
- radioactive materials, IAEA regulations for safe transportation 0-63410
- radioactive materials, IAEA transport information collection system, influence on improved safety measures 0-63413
- radioactive materials, IAEA transport regulations, underlying radiation protection principles 0-63414
- radioactive materials, international regulatory control for safe transportation 0-63411
- radioactive materials, package design, construction and testing for safe transportation 0-63412
- radioactive materials, safe transportation, using type A, exempt and LSA packages 0-63401
- radioactive waste geologic disposal, safety anal., functional relations of risk to input data uncertainties 0-83189

**safety continued**

- RF EM fields, review of effects and dosimetric data, safety standards development 0-67154
- RF EM fields (300 KHz-100 GHz), human exposure safety level 0-89869
- safety and environmental pollution (*German*) 0-63370
- spent fuel transportation, commercial experience in US 0-63310
- underground nuclear waste repositories, risk assessment using reliability models 0-57898
- US applications in obstetrics and gynecology, safety and pot. hazards, review 0-67170
- vacuum technique problems, with modern semiconductor processes (*German*) 0-86330
- Li/SOCl<sub>2</sub>, D cells, optimisation with respect to energy density, storability and safety 0-97775
- Pu fuel facility damage from high winds, risk anal. 0-63356

**safety systems**

*see also alarm systems*

- remote maintenance to comply with new legislation limiting occupational radiation exposure, in United States 0-106210
- thermal imaging with pyroelectric vidicon camera 0-86288
- wind power plant development, low cost approach 0-61268

**salt water conversion** *see desalination***samarium**

*see also nuclei with .....*

- electron radiation damage, elec. resistivity change rates 0-59954
- film, elec. props. 0-107929
- magnetoresistivity and elec. resist., 4.2 to 300K (*Russian*) 0-88539
- praseodymium ethylsulphate:Sm, one-dimens. X-Y system, spin dynamics, electron spin echo meas. 0-66031
- sputtering, thermal and collisional effects influence on energy spectra 0-66370
- surface, valence transition in first atomic layer 0-70652
- surface mixed valence, XPS study 0-60753
- transport properties, low temp., effect of mag. field 0-70679
- CaF<sub>2</sub>:Eu<sup>2+</sup>, Sm<sup>2+</sup>, relaxed resonance acoustic phonons in vibronic anti-Stokes luminescence (*Russian*) 0-93404
- CaF<sub>2</sub>:Sm<sup>2+</sup>, coherent population oscills. and hole burning observed using polarization spectroscopy 0-71457
- CaF<sub>2</sub>:Sm<sup>3+</sup>, VUV absorpt. spectra 0-108230
- CaSO<sub>4</sub>:Sm phosphors, X-irrad., thermoluminesc., charge compensation effects 0-97351
- CdF<sub>2</sub>:Sm<sup>3+</sup>, photoconverted, thermally stimulated relax. 0-84476
- EuO:Sm<sup>3+</sup>, hyperfine field at Sm; TDPAC meas. 0-93215
- Sm, and isotopes, hfs, laser-RF double reson. spectroscopy 0-58170
- SmI, laser atomic beam spectroscopy, isotope shifts, hyperfine struct., transitions 0-102468
- <sup>151</sup>Sm, stopping power in Ni, (Au) 0-70284
- TbF<sub>3</sub>:Sm<sup>3+</sup>, induced visible emission of Sm<sup>3+</sup> 0-97330
- YIG:Sm<sup>3+</sup>, mag. anisotropy, effect of Sm<sup>3+</sup> ferromag. reson. study 0-80615
- ZnO:Sm, electrolum. brightness, field strength and freq. depend. 0-100696

**samarium alloys**

- Ag-Sm system, phase diagram, eutectic temps., microstruct. (*German*) 0-104119
- Co-Sm film, magneto-optic coeff. and refr. index, ellipsometric determ. 0-71501
- Co-Sm crystals, microstruct., homogeneous precip. and nucleation 0-104160
- Dy<sub>1-x</sub>Sm<sub>x</sub>, magnetoresist. of polycryst. specimens in fields up to 44 kOe (*Russian*) 0-92880
- La-Sm-Au, amorphous, surface effects on Sm valence, XPS and X-ray absorption meas. 0-108325
- Sm-Au, amorphous, surface effects on Sm valence, XPS and X-ray absorption meas. 0-108325
- Sm-Co, amorphous, plasma-sprayed, role of Ar or H<sub>2</sub> atm. in mag. props. and crystn., rel. to H<sub>2</sub> storage 0-64898
- Sm-Co ring magnets for BWO, 110 to 170 GHz, design and appl. (*German*) 0-105684
- Sm-Eu, dil., mag. and elec. hyperfine interac., TDPAC obs., paramag. behaviour, exchange integral 0-103908
- Sm<sub>2</sub>Ag<sub>7</sub>, amorphous, sp. ht. at low temp. 0-75780
- SmAl<sub>2</sub>, orbital and spin polarisations of cond. electrons 0-65791
- SmCo<sub>5</sub>, amorphous, supermag.-ferromag. transition and directional crystallisation 0-65891
- SmCo<sub>5</sub>, H<sub>2</sub> absorption in thin film hydriding alloys 0-65238
- SmCo<sub>5</sub>, high coercivity isotropic plasma-sprayed magnet, eutectoid decomp. 0-80568
- SmCo<sub>5</sub>, isotropic plasma-sprayed high coercivity magnet, eutectoid decomp. 0-75810
- SmCo<sub>5</sub>, nucleation of reversed domains at Co<sub>2</sub>Sm<sub>2</sub> precip. 0-75791
- SmCo<sub>5</sub> permanent magnets, crystal texture effects on props. 0-100600
- SmCo<sub>5</sub>, sintered, hard mag. material, magnetisation behaviour 0-75805
- SmCo<sub>5</sub>, sintered, mag. after-effect, expt. and model 0-75816
- SmCo<sub>5</sub> sintered magnets, eutectoid decomp. 0-89219
- Sm<sub>2</sub>Co<sub>7</sub>, coercive force depend. on annealing temp. 0-65964
- Sm<sub>2</sub>Co<sub>7</sub> sintered magnets, coercive force and constitution, annealing temp. depend. (*Russian*) 0-88786
- SmFe<sub>3</sub> and Sm<sub>2</sub>Fe<sub>3</sub>, magnetotstriction, room temp. to 80K 0-65993
- Sm<sub>2</sub>Ir<sub>2</sub>, cryst. struct. 0-96473
- Sm<sub>1-x</sub>La<sub>x</sub>, electron struct., lattice const., X-ray spectral study (*Russian*) 0-100432
- Sm<sub>2</sub>Mn<sub>23-x</sub>Fe<sub>x</sub>, magnetic behaviour, temp. and comp. depend. 0-93090
- SmZn, ferromag., cond. band antiparallel polarisation exceeding 4f moment 0-60207
- Sm<sub>0.91</sub>Zr<sub>0.09</sub>(Co<sub>0.88</sub>Cu<sub>0.10</sub>Fe<sub>0.22</sub>)<sub>6.7</sub>, alloy permanent magnet, coercive force (*Russian*) 0-65966

**samarium compounds**

*see also samarium alloys*

- Ba<sub>1-x</sub>Sm<sub>x</sub>S, electron config. of Sm ions, X-ray L-absorpt. spectroscopy 0-60715
- Ca<sub>1-x</sub>Sm<sub>x</sub>F<sub>2-x</sub>, luminesc. expt. suggesting Sm<sup>3+</sup> ion pairing 0-76065
- Ca<sub>1-x</sub>Sm<sub>x</sub>S, electron config. of Sm ions, X-ray L-absorpt. spectroscopy 0-60715
- EuCl<sub>3</sub>, coord. in aq. Cl<sup>-</sup> soln., X-ray diffr. obs. 0-92445
- Eu<sub>1-x</sub>Sm<sub>x</sub>S, ESR, exchange interaction, susceptibility, elec. cond., thermoelectric power 0-93174
- Eu<sub>1-x</sub>Sm<sub>x</sub>S, electron config. of Sm ions, X-ray L-absorpt. spectroscopy 0-60715

**samarium compounds continued**

- La<sub>0.5</sub>Sm<sub>0.5</sub>B<sub>6</sub>, FIM study 0-71578  
 NaY<sub>1-x</sub>Sm<sub>x</sub>F<sub>4</sub>, luminesc. expt. suggesting Sm<sup>3+</sup> ion pairing 0-76065  
 SMS, band struct. and semicond. metal phase transition 0-80180  
 Sm chalcogenides, semiconductor-metal transition, extended Felicov-Kimball model calcs. 0-70616  
 Sm-H, phase equilibria 0-66492  
 SmB<sub>6</sub>, crystal preparation, elec. resistance, phase transitions 0-97427  
 SmB<sub>6</sub>, FIM study 0-71578  
 SmB<sub>6</sub>, intermediate valence, <sup>11</sup>B NMR study 0-93193  
 SmB<sub>6</sub>, metal insulator transition, cond. processes 0-96787  
 SmB<sub>6</sub>, mixed valence state, conduction band struct. 0-103624  
 SmB<sub>6</sub>, mixed valent semicond., transport props. and electronic struct., review 0-96877  
 SmB<sub>6</sub>, resistivity press. variation, lattice const. 0-100456  
 SmB<sub>6</sub>, surface mixed valence, XPS study 0-60753  
 Sm<sub>1-x</sub>B<sub>x</sub>S, valence transition induced by alloying 0-96829  
 Sm<sub>2</sub>Bi<sub>3</sub>, mixed valence system, X-ray absorption spectroscopic study 0-80906  
 SmBiTe<sub>3</sub>, prep., elec. props., and crystallographic date 0-59981  
 SmCl<sub>3</sub>, coord. in aq. Cl<sup>-</sup> soln., X-ray diff. obs. 0-92445  
 SmCo<sub>5</sub>, mag. domains structure rel. to crystal defects, electron microscopy 0-103856  
 SmCo<sub>5</sub>, permanent magnets, free suspension in const. mag. field with aid of pyrolytic graphite 0-101807  
 Sm<sub>2</sub>CuO<sub>4</sub>, magnetic properties obs. 0-70937  
 SmF<sub>2</sub>, thermal props. (*German*) 0-81355  
 SmFeO<sub>3</sub>, Raman scatt. from magnons, anisotropy const. determ. 0-66178  
 (Sm<sub>1-x</sub>Gd<sub>x</sub>)<sub>2</sub>S<sub>4</sub>, mixed valence compound, elec. cond. transition 0-70777  
 SmI, Zeeman coherence, transient and stationary, polarisation spectroscopy 0-58212  
 SmIG, mag. phase transitions, Mossbauer spectroscopy obs. 0-80509  
 Sm<sub>1-x</sub>La<sub>x</sub>B<sub>6</sub>, valence transition, lattice parameter and mag. susceptibility meas. 0-59929  
 Sm<sub>1-x</sub>La<sub>x</sub>S, magnetoresist. in semicond. and metallic phases 0-96914  
 (SmLu)<sub>2</sub>(FeAl)<sub>2</sub>O<sub>12</sub>, film epitaxial growth on Gd<sub>3</sub>Ga<sub>5</sub>O<sub>12</sub> substrate, mag. props. lattice mismatch 0-65402  
 Sm<sub>2</sub>M<sub>2</sub>CoO<sub>3</sub> (M=Ca, Sr, Ba), catalytic props. 0-66875  
 SmN, form. conditions 0-101019  
 SmN, miscibility with UC (*German*) 0-96654  
 SmO, cryst. field parameters due to 4f<sup>n-1</sup>5d configs. 0-80230  
 Sm<sub>2</sub>O<sub>3</sub>, B-type monoclinic, DC(AC) elec. cond., thermoelectric power, dielectric const., temp. depends. 0-59980  
 Sm<sub>2</sub>O<sub>3</sub>, surface step thickness measurement 0-103555  
 Sm<sub>2</sub>O<sub>3</sub>-Ga<sub>2</sub>O<sub>3</sub> system, garnet-perovskite transform., phase diagram relationships 0-97460  
 SmOsSb<sub>12</sub>, prep. and cryst. struct. 0-100211  
 Sm<sub>3</sub>PO<sub>7</sub>, IR and Raman spectra, vibr. assignments, cryst. struct. characts. 0-97258  
 SmS, electron-phonon interaction, lattice dynamical model 0-96610  
 SmS intermediate valence, low lying states 0-96826  
 SmS, LO phonon freq. softening in semicond. and metallic phases 0-96619  
 SmS, metal insulator transition, cond. processes 0-96787  
 SmS, physical and physicochem. props., review 0-96875  
 SmS, semiconducting, piezoresistance at 80K 0-59990  
 SmS, trivalent rare earth substituted, stability of Sm<sup>2+</sup> 0-65508  
 SmS type semiconductors, electronic struct., influence of point defects 0-70650  
 SmS, valence transition, entropy and phase diagram 0-59877  
 SmS, valence transition, two band model 0-65507  
 Sm<sub>2</sub>S<sub>3</sub> films, refl. and transmission spectra at 300K 0-80889  
 Sm<sub>1-x</sub>As<sub>x</sub>, magnetoresist. in semicond. and metallic phases 0-96914  
 Sm<sub>1-x</sub>P<sub>x</sub>, valence changes, XPS and UPS study 0-97402  
 Sm<sub>3</sub>Se<sub>4</sub>, valence fluctuation, mag. susceptibility meas. 0-97056  
 Sm<sub>2</sub>Ti<sub>2</sub>O<sub>7</sub>, ferroelec., layer type struct., cryst. growth 0-108348  
 Sm<sub>0.4</sub>Y<sub>2.6</sub>Fe<sub>3</sub>Ga<sub>5</sub>O<sub>12</sub> epitaxial films, uniaxial mag. anisotropy, ferrimag. reson. study 0-80577  
 Sm<sub>0.75</sub>Y<sub>0.25</sub>S, mixed-valence, electron-lattice correlations, EXAFS studies 0-76103  
 Sm<sub>1-x</sub>Y<sub>x</sub>S, magnetoresist. in semicond. and metallic phases 0-96914  
 Sm<sub>1-x</sub>Y<sub>x</sub>S, mixed valence system, electron-phonon coupling, theory 0-70343  
 Sm<sub>1-x</sub>Y<sub>x</sub>S, mixed valence, phonon softening and linewidths, calc. 0-75319  
 Sm<sub>1-x</sub>Y<sub>x</sub>B<sub>6</sub>, valence transition, lattice parameter and mag. susceptibility meas. 0-59929  
 Sr<sub>1-x</sub>Sm<sub>x</sub>S, electron config. of Sm ions, X-ray L-absorpt. spectroscopy 0-60715  
 (Y,Sm,Ca)<sub>3</sub>(Fe,Ge)<sub>2</sub>O<sub>12</sub> epitaxial films, mag. props., growth condition effects 0-97124  
 Y-Sm ferrogarnet (*Russian*) 0-71140  
 (YLuSmCa)<sub>3</sub>(FeGe)<sub>2</sub>O<sub>12</sub> garnet film, bubble domain expansion, fuzzy wall struct. 0-71128  
 (YLuSmCa)<sub>3</sub>(GeFe)<sub>2</sub>O<sub>12</sub> garnet films, bubble expansion saturation vel., sampling optical photography 0-75820  
 Y<sub>1-x</sub>Sm<sub>x</sub>Fe<sub>0.5</sub>O<sub>1.5</sub>, <sup>57</sup>Fe film, ion implanted, Mossbauer conversion spectra study 0-80663  
 (YSmLuCa)<sub>3</sub>(FeGe)<sub>2</sub>O<sub>12</sub>, mag. loss and domain wall mobility 0-65980  
 Yb<sub>1-x</sub>Sm<sub>x</sub>S, electron config. of Sm ions, X-ray L-absorpt. spectroscopy 0-60715  
 ZrO<sub>2</sub>/SmF<sub>3</sub> mirror coatings, light scatt. and optical strength in UV range 0-106595

**sand**

- SE.Baltic mainland shore moderately accumulative section morphodynam-ics (*Russian*) 0-67359  
 Baltic underwater coastal slope sand grain size and mineral composition (*Russian*) 0-76963  
 dissolution, during glass melting, kinetic equation for interaction between grain material and liq. 0-84901  
 impact craters in ice and ice-saturated sand, Martian implications 0-67614  
 Mars, sand sea (erg) in north polar region, wind patterns 0-67624  
 specularite-bearing sand 0-90075  
 titanomagnetite sand from New Zealand, density, elec. and mag. prop 0-98311  
 water-saturated, broadband meas. of acoustic attenuation 0-83719

**sapphire**

- crystal growth by edge-defined film-fed growth process 0-104057

**sapphire continued**

- crystal growth from melt by Stepanov's method, axial temp. distrib. 0-103280  
 damage by UV laser radiation, self-focusing mechanisms 0-76110  
 edge dislocation loop obs. by high resolution lattice imaging 0-103346  
 F-centre, fluorescence decay below 75K 0-60664  
 fibre reinforced Mo, strength at rupture 0-104286  
 fibres, strength at rupture 0-104286  
 float zone growth, laser heated, of const. diameter crystals, meniscus angle meas. 0-108347  
 growth angle determ. from cryst. lateral face shape and solidified separation drops 0-103282  
 interface with Pb, heat transfer coeff. meas., 2-80K 0-88419  
 leucosapphire, unique polishing features of hard crystals 0-64225  
 leucosapphire 0-88190  
 neutron bombarded, F-centre fluorescence, photoluminescence 0-100676  
 nondestructive testing, using IR and UV specular reflectance meas. 0-108684  
 optical detection of acoustic phonons at THz freqs. 0-75320  
 ribbon crystals, EFG growth and charact., voids, grain boundaries and dislocations 0-103283  
 ribbon edge-defined film-fed growth, substrate for heteroepitaxial Si 0-108342  
 sapphire-H<sub>2</sub>O interface, SiO<sub>2</sub> sputtered film performance as acoustic antireflection coating 0-106686  
 solid phase Si regrowth in Si-Al-Al<sub>2</sub>O<sub>3</sub> system, Hall effect 0-100413  
 SOS structures, high-field electron transport, drift vel. meas. 0-80387  
 substrate, anthracene ultrathin film deposition 0-59812  
 substrate, single crystalline AlN film, low temp. growth by RF reactive planar magnetron sputtering method 0-76175  
 substrate, with epitaxial Si layer, characterisation, X-ray rocking curves 0-75458  
 substrate crystallisation of amorphous Si layers, RF-sputtered, CW ion laser annealing 0-80109  
 substrate film for Si, laser annealing non-thermal theory expt. test 0-89273  
 substrate for crystallisation of Ni, Ni-B films, struct. evolution (*Russian*) 0-75455  
 substrate for K<sub>2</sub>Li<sub>2</sub>Nb<sub>2</sub>O<sub>7</sub> film for optical waveguide, cryst. struct., dielectric props. 0-79018  
 substrate for Si epitaxial film growth by MBE 0-76186  
 substrate for V, Ta, Mo, W, Nb epitaxial films, growth texture, nucleation texture (*Russian*) 0-75454

**satellite atmospheres** see extraterrestrial atmospheres; planetary satellites

**satellite links**

see also artificial satellites

- Landsat D wideband communications system 0-101529  
 lunar noise effect obs. (*Japanese*) 0-82239  
 microwave Earth-space link, rain cell attenuation 0-94586  
 OTS payload performance, in-orbit RF meas. 0-82167  
 radar reflectivity profile classified by rain types 0-101420  
 rain attenuation above 10 GHz, regression curves for tropical areas, telecommunication, broadcasting systems appl. 0-90111  
 WARC 1979 regulations, impact on space appl. and research 0-105147

**satellite relay systems**

- BWO appl., 110 to 170 GHz, using Sm-Co ring magnets (*German*) 0-105684  
 Interkosmos program and Magion satellite project, reviews 0-98535  
 Meteosat data-collection system, description and appl. 0-77122  
 Ogo 4, VLF signals reception, numerical study using waveguide concepts 0-90282  
 Transit, precise time dissemination system 0-57263

**satellite vehicles** see artificial satellites

**satellites, artificial** see artificial satellites

**satellites, planetary** see planetary satellites

**saturable absorption, optical** see optical saturable absorption

**saturation control** see chemical variables control

**saturation effects, optical** see optical saturation

**saturation measurement** see chemical variables measurement

**Saturn**

- 1966 S 2, positional obs., 1980 March 15 0-85893  
 1980 S 10, precise positions, 1980 March 15 to 16, and relation to Dione 0-85893  
 1980 S 1, 3, 6, 25, new Saturnian satellites, positional obs., (1980 March 9 to 14) 0-94749  
 1980 S 3, 13, positional obs. (1980 March 15 and 16) 0-85893  
 1980 S 7 to 14, Saturnian satellites, obs. (1980 March 13 to April 8) 0-62068  
 A and B rings, surface brightness obs. (*Russian*) 0-72872  
 ammonia and N mixing ratio in troposphere 0-94748  
 atmosphere, Pioneer 11, IR radiometry data 0-82290  
 atmosphere, UV photometry from Pioneer 11 probe 0-82288  
 atmosphere constituents, comparison with Jupiter, visible spectra obs. (*French*) 0-101550  
 atmospheric VHF refraction 0-98608  
 brightness coefficient of disc centre, phase effect 0-98602  
 cosmic ray cutoff rigidities, theory 0-72873  
 E-ring, obs. during (March 1980) 0-67647  
 E-ring radial structure, 1980 March CCD obs. 0-105201  
 E-ring rel. to Enceladus orbit, max. density from CCD obs. 0-94750  
 F-ring, discussion based on Pioneer 11 obs. 0-105202  
 Iapetus, relative reflectance meas. at 1.6 and 2.2  $\mu$ m 0-98607  
 imaging, photometry and polarimetry obs. from Pioneer 11 probe 0-82289  
 interior model for luminosity and mag. determ. 0-109393  
 interior Vashchenko Zubarev formula for Grunescu parameter 0-90030  
 ionosphere, spectral broadening meas. by Pioneer (11) 0-109391  
 IR scans at 7.8 to 25  $\mu$ m, (1977 to 1978) 0-90363  
 limb darkening and brightness temp., 1.30 cm interferometry obs. 0-82279  
 magnetic field, dynamo precession model (*Russian*) 0-94752  
 magnetic field meas., Pioneer 11 obs. 0-82292  
 magnetosphere, bowshock and magnetopause detect. by Pioneer 11, mag. field determ. 0-82283  
 magnetosphere, energetic ions and electrons, Pioneer 11 obs. 0-82286  
 magnetosphere, interactions with satellites and rings 0-82285  
 magnetosphere, trapped radiation, absorpt. by satellites and ring, Pioneer 11 obs. 0-82284



**Saturn continued**

- magnetosphere, trapped radiation belts, particle absorpt., Pioneer 11 obs. 0-82287
- magnetosphere interaction with solar wind, Pioneer 11 obs. 0-82282
- mass determ. from Pioneer 11 trajectory var. carrier freq. Doppler shift 0-82294
- NH<sub>3</sub> abundance from visible obs. 0-82269
- particle flux, Pioneer 11 meteoroid detector obs. 0-82291
- polar moment of inertia determ. 0-94694
- position determ. in 1978 using Double Zeiss Astrograph, Belgian obs. (French) 0-72809
- Rhea, planetary, 1976 to 1979, rel. to possible solar variability detect. 0-98623
- ring detection by focal coronagraph (French) 0-72772
- ring disappearances (1600 to 2100) 0-72876
- ring system, brightness enhancements rel. to existence of supposed satellites (1980 S 7 and 23) 0-94749
- ring system, review of physical studies 0-72874
- ring system, summary of recent research 0-72875
- ring system origin, Roche problem for polytropes in central orbits 0-82179
- ring system-ionosphere interaction 0-94751
- rings, history and perturbation anal. (French) 0-82281
- rings, model constraints from radar obs. of polarisation and albedo 0-82277
- rings, unilluminated side, 20  $\mu$ m brightness temp. 0-109392
- satellite I-IX, astrometry obs. from McDonald Observatory (1975-1976) 0-105199
- satellites, 1966 December and 1980 March positions for five objects 0-94750
- satellites, 1980 March Pic du Midi obs. 0-67646
- satellites, analyses and geodetic/astrometric obs. (1980 March) 0-77346
- satellites, astrometric obs. from McCormick Observatory (1977) 0-105200
- satellites 1966 S 2 and 1980 S 15-18, separations 0-67645
- satellites 1980 S 24 and 1966 S 2, 1980 April obs. 0-82280
- structure and evolution, effect of dense cores 0-98603
- Titan, atmosphere organic chemistry, review 0-90364
- Titan-Hyperion resonances and close approaches, restricted three-body problem anal. 0-77347
- upper atmosphere, struct. from Titan eclipse light curve 0-90362
- upper neutral atm. and ionosphere, vertical struct., Pioneer 11 radio occultation obs. 0-82293
- NH<sub>3</sub> vertical density profiles from IR and radioelectric emissivity data 0-82267
- PH<sub>3</sub> abundance, IR obs. 0-82278

SAW see surface acoustic waves

SC (sudden commencement) see magnetic storms

scale invariance see scaling phenomena

scales (circuits) see scaling circuits

scales see balances

**scaling circuits**

- CMOS ICM 7216B multifunction counter used for time, frequency or period measurement (German) 0-74092

**scaling phenomena**

- see also elementary particle theory; renormalisation
- $\sigma$ -models, non-linear, and universality in 3-D, scaling limit, and critical behaviour, chirality 0-62824
- A<sup>4</sup>-coupling in abstract approach of quantum field theory, renormalisation group 0-99033
- Abelian gauge theories with dynamical symmetry breaking, effective pot., scale and chiral invariance (Russian) 0-57503
- asymptotic freedom infrared instability 0-73678
- Bjorken scaling violation, QCD and models of quarks with substructure 0-105851
- Bose gas, impenetrable, one particle reduced density matrix, Painleve-type eqn. 0-62576
- conference, lepton-hadron physics, Karlsruhe, Germany (Sep. 1978) 0-73098
- covariant derivatives without gauge fields 0-73584
- deep inelastic leptonproduction, meson bound state contrib. to  $\sigma_L/\sigma_T$  0-78029
- elastic hadron-hadron diffraction scatt. processes, scaling, conformal mapping without spurious cut 0-82992
- Euclidean fields, low momentum behaviour scale limit 0-62834
- fermion-fermion high energy scatt., transverse momentum cut-off hypothesis, Yang-Mills theory 0-86575
- form factors of deep inelastic scattering, Tauberian theorems in quantum field theory 0-68375
- hadron+hadron, cluster model, field theoretic, multiperipheral production, Feynman scaling violation 0-57576
- hadron+hadron- $\gamma\gamma$ X, scaling and quark mass dependence, quark parton model 0-73749
- inclusive processes, scaling hypothesis for the rapidity distributions and information theory 0-73747
- Kellen-Simanzik eqn., correlation function scaling behaviour in phase transitions (Russian) 0-57502
- large p<sub>T</sub> photoproduction, gluon fragmentation function extraction, scaling 0-105853
- lattice Hamiltonian field theory, finite-size scaling 0-73580
- lepton+hadron, deep inelastic scatt., quark-parton model with logarithmic scaling violation 0-78071
- Lie groups, compact, simple, rank 2, irreducible representations (Chinese) 0-68391
- minimal metallic cond., localisation scaling theory (Russian) 0-103671
- O( $e^2$ ) scaling law for  $d\sigma/dt$  in the Reggeon field theory 0-101936
- perturbative QCD, renormalisation improvement, charmonium decay and scaling violations 0-101993
- QCD hadron jets, branching processes, multiplicity distrib., KNO scaling (Russian) 0-101998
- QED, conformal-invariant, Ward identity of dilation current 0-68401
- QED, heavy particle effects, factorised local operators, renormalisation group 0-62898
- resonance-saturation picture, scaling violation patterns 0-82940
- space-time, foam-like structure, Bjorken scaling violation due to gravitational field 0-77939
- totally inclusive leptonprod., scaling anal., target mass corrections in QCD parton model 0-102052
- unified scalar-free theory, order-R vacuum functional, with spontaneous scale breaking 0-78003

**scaling phenomena continued**

- $e^+e^-$  collisions, jet prod. and two-photon annihilation, hadron spectra 0-91121
- $e^+e^- \rightarrow \Delta X$ , polarisation effects in nonperturbative parton model, scaling 0-105912
- $e^+e^-$  final states,  $q\bar{q}$  decay, semiclassical model, vacuum polarisation by colour field 0-63011
- $e^+e^- \rightarrow q\bar{q}g$ , (3g), jet-mass spectra, perturbative QCD 0-63006
- K<sup>+</sup>n, inelastic charge exchange scatt., diffraction approach, convergent polynomial expansion, scaling 0-78095
- K<sup>+</sup>p, 130, 200 GeV, jet prod. cross sections, QCD anal. and scale breaking 0-99111
- K<sup>+</sup>p, fireball model, universal scaling function 0-57646
- K<sup>+</sup>p, inelastic charge exchange scatt., diffraction approach, convergent polynomial expansion, scaling 0-78095
- N structure function model from hard consistent quark interactions, scaling violations 0-86719
- $\nu$ N, charged and neutral current interactions, cross sections and scaling variable distrib. 0-57581
- $\nu$ N, heavy-quark production, t and b-quarks, SU(2)×SU(2)×U(1) gauge group mixing angles 0-68445
- Pn-1<sup>+</sup>X, scaling predictions, Drell-Yan model 0-73756
- pp, 53, 63 GeV, massive electron pair prod., T ang. decay, scaling function 0-68495
- pp, 53, 63 GeV, T and  $\psi$  prod., dielectron decay angles 0-68496
- pp, pp, 130, 200 GeV, jet prod. cross sections, QCD anal. and scale breaking 0-99111
- pp, smooth interpolation between Orear- and fixed angle scaling behaviour of the scattering amplitude 0-105873
- pp- $\rightarrow CX, C=\pi^+, K^+, p$ , scaling-in-the-mean hypothesis 0-68497
- pp- $\rightarrow$ hadrons, phase transition in Feynman-Wilson analogue fluid, multiplicities, plateaux, cross-sections 0-73744
- pp- $\mu^+\mu^-X$ , 62 GeV,  $\psi$  and  $\gamma$  cross sections, scaling function 0-105932
- pp scatt. at higher energies, differential cross section ratio scaling 0-73741
- pp scatt. cross section at high momentum transfer, geometrical scaling, energy depend. (Russian) 0-102064
- $\pi$  compositeness from wave function renormalisation constant 0-101997
- $\pi^0$  high p<sub>T</sub> prod. ang. depend., inclusive cross sections, scaling 0-91119
- $\pi^0$ , direct photon prod., Compton and annihilation process contrib. 0-105925
- $\pi$ p, inelastic charge exchange scatt., diffraction approach, convergent polynomial expansion, scaling 0-78095
- $\pi^-p \rightarrow \pi^0 n$ , Regge pole model with phenomenological residue functions 0-102077
- $\pi^+p$ , 130, 200 GeV, jet prod. cross sections, QCD anal. and scale breaking 0-99111
- $\pi^+p$ , fireball model, universal scaling function 0-57646

**scaling tubes see counting tubes****scandium**

see also nuclei with .....

- band structure, density of states, absorpt. spectra, KKRZ calc. 0-70593
- CVD, open-tube technique 0-89128
- Debye-Waller factor and Lindemann parameter, temp. depend., lattice dynamical model calcs. 0-59610
- electronic excitations, charact. energy loss meas. up to 50 eV 0-60723
- interband, collective and atomic (p,d) excitations, Z-160 eV, fast EELS 0-93443
- sputtered excited states, secondary photon emission, role of transition probability 0-102483
- surface, (0001), H adsorption, geometric vs. electronic factor in surface electronic structure 0-70788
- thin films, obtained in vac. of 10<sup>-5</sup>-10<sup>-6</sup> torr, struct. and elec. resist. 0-107931
- S II in  $\zeta$  Ophiuchi interstellar spectrum, abundance upper limit 0-82445
- Sc I, oscill. strength calc. 0-78571
- Sc I to Sc XXI, energy level tables derived from atomic spectra anal. 0-101672
- Sc II, visible spectra and ionisation limit 0-74143
- Sc+NO<sub>2</sub>, chemiluminesc., nonequilib. product distrib. 0-101014
- Si:Sc, photocapacitance and photoconductivity 0-107859
- YIG:Sc, magneto-optical Kerr effect, reflectivity spectra 0-66157

**scandium alloys**

see also scandium compounds

- Al-Sc, elec. resist. determ. 0-92876
- Ce<sub>2</sub>Sc<sub>3</sub>Si<sub>3</sub>, X-ray cryst. struct. determ. 0-92480
- Nb-Ga-Sc, superconducting transition temp., X-ray, microscopic and microprobe anal. (Ukrainian) 0-75667
- Sc, itinerant electron ferromagnet, magnetovolume effects 0-60397
- Sc-Au, dil., elec. field gradient, Mossbauer meas. 0-80665
- Sc-Fe, dil., elec. field gradient, Mossbauer meas. 0-80665
- Sc-Gd, dil., reverse resist. anomaly and negative magnetoresist. 0-84459
- Sc-Gd, spin glasses, low temp. sp. ht. and magnetisation 0-65913
- Sc-Ir, dil., elec. field gradient at <sup>193</sup>Ir, Mossbauer meas. 0-66090
- Sc-Mg, low-temp. heat capacity 0-75370
- Sc-Ru, dil., elec. field gradient, Mossbauer meas. 0-80665
- Sc-Ru, elec. field gradient and temp. depend. TDPAC meas. 0-60477
- Sc-Zr, low-temp. heat capacity 0-75370
- ScAl<sub>2</sub>-Eu, intermediate valence on Eu ions, Mossbauer isomer shift 0-84587
- ScFe<sub>2</sub>, mag. props., 80-1300K (Russian) 0-75750
- ScFe<sub>2</sub>, Mossbauer effect of <sup>57</sup>Fe 0-75903
- ScFe<sub>2</sub>H<sub>2</sub>, Mossbauer effect of <sup>57</sup>Fe 0-75903
- ScGa<sub>2</sub>, atomic structure determ. using single crystal method (Ukrainian) 0-70165
- ScH<sub>2</sub>, electron diffr. investigation 0-107112
- ScH<sub>2</sub>, thin films, struct. and elec. props. 0-107931

**scandium compounds**

see also scandium alloys

- dihydrides, structs. and stabilities 0-107146
- Ba<sub>2</sub>Sc<sub>2</sub>O<sub>9</sub>, Ba<sub>3</sub>Sc<sub>2</sub>WO<sub>9</sub>, and Ba<sub>2</sub>ScTaO<sub>6</sub>, elec. cond. nature, depend. on comp. and medium thermodynamic parameters 0-70773
- Ce<sub>1-x</sub>Sc<sub>x</sub>Pd<sub>3</sub>, intermediate valence of Ce, susceptibility, lattice const., ESR meas. 0-103648
- K<sub>4</sub>Sc<sub>2</sub>(OH)<sub>2</sub>Si<sub>4</sub>O<sub>12</sub>, crystal struct., X-ray diffr. study 0-79763
- Na<sub>2</sub>Sc<sub>2</sub>P<sub>2</sub>O<sub>7</sub>, superionic cond. synthesis, cryst. struct. and ionic cond. 0-107519
- Na<sub>2</sub>YSc[SiO<sub>4</sub>]<sub>2</sub>, crystal struct., atom coordinates, X-ray study 0-59446
- ScBO<sub>3</sub>:Fe<sup>3+</sup>, ESR spectra, lattice parameters 0-93170

**scandium compounds continued**

- Sc<sub>2</sub>C<sub>3</sub>, superconducting phase synthesis at high press. and temp., critical field (*Russian*) 0-65732  
 ScCl<sub>3</sub>-NaCl-CsCl ternary system, cpd. form., thermographic investig. (*Russian*) 0-66490  
 ScH<sub>2</sub>:Er, proton distrib. and site energies, ESR meas. 0-59509  
 ScO, pot. energy curves and dissoc. energy of X<sup>2</sup>Σ state 0-69203  
 Sc<sub>2</sub>O<sub>3</sub> and double oxides, photon multiplication and secondary electron-hole pairs generation (*Russian*) 0-66262  
 Sc<sub>2</sub>O<sub>3</sub>, electronic excitations, charact. energy loss meas. up to 50 eV 0-60723  
 Sc<sub>2</sub>O<sub>3</sub>, interband, collective and atomic (p,d) excitations, Z-160 eV, fast EELS 0-93443  
 Sc<sub>2</sub>O<sub>3</sub>, liq. and solid phase elec. cond., high temp. meas. 0-84468  
 Sc<sub>2</sub>O<sub>3</sub>, solid, enthalpy investig. at high temp. 0-103498  
 Sc<sub>2</sub>O<sub>3</sub>, solid and liq. phases, thermophysical and electrophysical props. 0-103495  
 ScP, thermodynamics and high temp. vaporisation 0-88310  
 ScPO<sub>2</sub>Gd<sup>3+</sup>, zircon struct. EPR investig., rel. to radiation resistance 0-97138  
 ScRh, gaseous, dissociation energies, high temp. mass spectrometric determ. 0-93790  
 Sc<sub>2</sub>S<sub>3</sub>, order-disorder transition, ionic model appl. 0-107096  
 Sc<sub>2</sub>(SO<sub>4</sub>)<sub>3</sub>, aq. soln., dielec. relaxation spectroscopy in microwave region, double-beam interferometry (*German*) 0-71309  
 Sc<sub>2</sub>(WO<sub>4</sub>)<sub>3</sub>:Cr(Eu), and undoped crystals, luminesc. obs. 0-89047

**scanning electron microscope applications**

- biological specimens, macromolecular resolution 0-72401  
 biomedical studies, cathodoluminescence method 0-72400  
 EBIC SEM, stroboscopic principle and resolution enhancement 0-100515  
 electrical conductivity meas., appl. to TTF-TCNQ 0-86507  
 forensic science, backscattered electron detector 0-68319  
 glass micropipettes, comparative calibration by optical microscopy and SEM (*German*) 0-98201  
 mineralogy, backscattered-electron/low vacuum mode appl. 0-82077  
 minority carrier lifetime-meas. technique using SEM-electron beam induced current 0-59999  
 particle track detectors, electron microscopy of etch pits 0-99424  
 SAW device diagnosis, voltage contrast obs. 0-69618  
 surface analysis, corrosion research 0-99004  
 surface roughness measurement methods using SEM techniques, research and development (*German*) 0-105612  
 surface topographical measurements at grazing incidence, alignment problem 0-99014  
 two-dimensional magnetic stray field imaging 0-86514  
 X-ray microtomography in SEM 0-101308

**scanning electron microscope examination of materials**

- see also scanning electron microscopy  
 ? 0-100817  
 adhesion, surface anal. techniques appl. 0-65381  
 AES, ionisation enhanced diffusion effect obs. 0-71497  
 alkali borosilicate glasses, observation of phase separation using SEM-EDX technique 0-76224  
 alloys, embrittling residuals categorisation by Auger electron spectroscopy 0-66739  
 bagasse fibre reinforced phenol formaldehyde, tensile strength and Young's modulus, SEM study 0-60957  
 basalt, cement reinforcing fibre, alkali resist. 0-89377  
 bituminous coal, identification of constituents for petrographic anal. 0-81888  
 [CC] Ag-(100)InP, metal-semicond.cathode contact, metallurgical, physical, chemical processes 0-107911  
 cell membranes, at mol. resoln., introduction 0-104841  
 cellulose diacetate membrane, diffusive permeability 0-104460  
 coal chemical analysis, computer evaluation of SEM images 0-71994  
 coated arc electrodes, identification of types and brands using SEM with energy-dispersive X-ray detector 0-81400  
 collagen fibres, mech. props., role of struct. organisation 0-72207  
 compound eye of *Cicindela tranquebarica* herbst, fine struct. 0-85382  
 α' copper phthalocyanine and chlorinated derivative mol. crystals, radiation damage in electron microscope 0-107328  
 crystal, accelerator irradiation, heavy ion irradiation damage 0-100291  
 crystalline materials, observation of single defects using electron channel imaging 0-64848  
 cyano-biphenyl LC alignment on obliquely evaporated SiO<sub>2</sub> films 0-79677  
 diamond, accelerator irradiation, heavy ion irradiation damage 0-100291  
 diamond, industrial, anal. cathodoluminesc. studies in SEM 0-81410  
 diamond, synthetic, oxidized in fused salts, etch features 0-97604  
 diamond coatings, for increased wear resist. 0-76371  
 disilicate, piezoelectric glass ceramic, recrystallisation, pyroelectric response, permittivity 0-80703  
 epoxy, mica filled, polishing by abrasive papers and lapping cpds. 0-108620  
 etched thin foils, comparative SEM, STEM and TEM analysis 0-10014  
 ethylene-vinyl acetate-vinyl chloride graft copolymers, rel. between morphology and toughness (*German*) 0-66665  
 ferrite, transform. kinetics, grain size, alloying element effect, carbide precip. 0-93560  
 fission reactor mixed oxide fuels, SEM obs. of gas bubble morphology 0-57843  
 fracture surface SEM analysis, microtopography 0-68312  
 fused silicon substrate, directional reactive ion etching at oblique angles 0-66428  
 glass, float, low-Fe, weathered, surface, characterisation 0-93666  
 glass fragments, classification into window and non-window types 0-81401  
 glass rods, compressively clad, residual stresses, comparison of optical and fractographic meas. 0-108539  
 glasses, high vol. low cost, as solar reflectors, compositions and weathering effects 0-106589  
 grain boundary sliding model 0-75237  
 guanidine aluminium sulphate hexahydrate, SEM obs. of ferroelec. domain struct. in single crystals. 0-97219  
 guanidium aluminium sulphate hexahydrate, surface obs., SEM and AES expts. 0-71362  
 III-V multilayer structure, as-grown, assessment of defects by differentiated cathodolum. topography 0-59819  
 Inconel 617, creep, morphological changes of carbides, affect on creep props. 0-108509

**scanning electron microscope examination of materials continued**

- ion etching device for SEM samples 0-82847  
 jute, cement reinforcing fibre, alkali resist. 0-89377  
 kaolin bodies, effect of mineralizers on firing shrinkage, microstruct. and strength 0-97488  
 Kapton, pyrolysed, cond. polymer, transport and mag. props. 0-96887  
 magnetic domain, SEM obs., method of removing fine magnetite particles from surface (*Japanese*) 0-108655  
 magnetic domain imaging by SEM, computer simulation 0-71091  
 material surface texture analysis 0-73548  
 metal cutting, direct SEM obs. of adhesion and frictional sliding 0-104412  
 metal oxide smoke particles prepared by gas evap., morphology and coalescence growth 0-97738  
 metal-C system, spheroidal graphite formation, role of high angle boundaries (*Russian*) 0-81065  
 mild, anodic polarisation behaviour in hot alkaline sulphide solns. 0-100949  
 minority carrier lifetime mapping 0-96903  
 Murchison carbonaceous chondrite meteorites, Si in metal grain, electron probe anal. 0-77363  
 nosean identification, in sodalite and conversion of nosean sodalite 0-84907  
 optical glass diamond grinding kinetics 0-64224  
 orthotropic laminates, torsion strength and shear modulus determ. 0-92587  
 Permalloy thin-film head pole struct., domain configurations, SEM obs. 0-65975  
 phosphosilicate glass coatings, measurement of P content using SEM and energy-dispersive X-ray analyser 0-76588  
 PMMA, quartz- and glass-particle reinforced, abrasive wear 0-97594  
 polyethylene flow crystallisation, in extensional flow developed by convergent capillaries, props. 0-84111  
 porcelain, crack propag. data applicability to failure prediction 0-81154  
 pulmonary fibrosing disease diagnosis, histological section SEM and energy-dispersive X-ray microanalysis 0-72314  
 PVC, oriented mouldings, struct. order 0-60896  
 quartz, surface damage by X-rays, γ-rays, neutrons, SEM study 0-79837  
 quartz crystals, oscillating, surface patterns obs., energy trapping appl. 0-71323  
 quartz high-transmittance antirefl. film, vacuum-etched 0-74449  
 quasi-cleavage fracture, characteristic length parameter, correlation with fracture toughness (*Chinese*) 0-104246  
 reflection electron diffraction method, electron channelling and microdiffraction from surfaces 0-59355  
 semiconductor, SEM electron beam induced current images of dislocations and stacking faults, computer simulation 0-70198  
 semiconductor defects, charge-collection images, contrast formation 0-70087  
 semiconductor diffusion length and lifetime meas. and assessment 0-96902  
 semiconductors depth profiling, using carrier collection models 0-70723  
 spacecraft materials, failure, metallurgical exam. 0-71868  
 steel, 12% W, eutectic carbides struct. and comp. during heating 0-76283  
 steel, (0.36 wt.% C) Ni-Cr-Mo, electroslog refined, fracture toughness and fatigue behaviour 0-81171  
 steel, austenitic stainless, ageing at high temp., effect on creep props. SEM 0-97516  
 steel, austenitic stainless, fretting corrosion of orthopaedic implant materials by bone cement 0-104813  
 steel, austenitic stainless, in boiling MgCl<sub>2</sub> solns., alloying elements effect on stress corrosion cracking and K<sub>ISCC</sub> (*Japanese*) 0-93692  
 steel, austenitic stainless, of type 55 23 33, slow strain rate testing under electrochem. control in high temp. water 0-97650  
 steel, austenitic stainless, rel. between polarisation behaviour and susceptibility to stress corrosion cracking (*Japanese*) 0-93693  
 steel, austenitic stainless, unlubricated, friction, wear and microstruct. of types 304, 316 and Nitronic 60 0-108589  
 steel, austenitic stainless type 304, time-depend. fatigue, mechanistic model 0-100925  
 steel, ball bearing, fatigue damage, influence of dispersed phases in martensitic matrix 0-108549  
 steel, Cr-Mo-P (2.25, 1 wt.%), stress relief cracking, effect of P segregation 0-89324  
 steel, Cr-Mo, oxidised, mechanism of crack decoration of oxides by electrodeposition 0-97560  
 steel, Cr-Mo (10-14, 2-6 wt.%), heat-resist., creep-rupture strengths 0-104271  
 steel, ductile structural, fatigue crack propag. rate and striation spacing 0-93635  
 steel, ferritic stainless, type 444 welds, ductility loss mechanism 0-85002  
 steel, high C, tensile strength, working and heat treatment effects (*Japanese*) 0-104209  
 steel, hot forging die type, fractography (*Japanese*) 0-108547  
 steel, industrial, surface chem. characterisation by SIMS, glow discharge spectrometry and other techniques 0-66907  
 steel, low C, built-up edge form., direct SEM obs. 0-104303  
 steel, low C, fatigue and creep observation using imaging of subgrains 0-66609  
 steel, martensitic stainless, in SO<sub>4</sub> solns., activation pH and susceptibility to H<sub>2</sub> assisted stress corrosion cracking 0-97619  
 steel, medium C, Mn, type 42Mn2 cylinders, flake immunisation by hot working (*Chinese*) 0-66540  
 steel, medium C, Ni-Cr-Mo, overheated, fractographic study (*Chinese*) 0-66616  
 steel, mild and type EN31, eval. of cold rolling oils and boundary lubrication characts. by SEM 0-85068  
 steel, pearlite, deform. and fracture mechanisms, HV SEM obs. 0-104243  
 steel, rail, toughness, effect of Sn, SEM exam. 0-97569  
 steel, rolled, anisotropic, fatigue fracture surface obs. (*Japanese*) 0-108546  
 steel, stainless, 18Cr-2Mo-Ti, atmospheric corrosion 0-85078  
 steel, stainless, emittance meas. rel. to surface roughness parameters 0-100342  
 steel, stainless, Fecralloy, creep-rupture props., 650-800°C 0-97535  
 steel, stainless, stress corrosion testing, slow strain rate, elevated temp. and high press. study 0-97615  
 steel, stainless, type 316, low cycle fatigue props. in vac., fracture mode 0-85021



## scanning electron microscope examination of materials continued

- steel, stainless cast, creep ductility, Auger spectroscopy study 0-60917  
 steel, stainless type 316, thermally aged, accelerated creep-fatigue crack propag. 0-89326  
 steel, structural, impurity effect on crack initiation, dynamical loading (Czech) 0-60955  
 steel, structural, second phase particle effects on impact strength 0-108581  
 steel, V-Nb and Cr-Mo-V-Nb, supercooled austenite isothermal decomp., struct., strength and fracture characts. 0-60966  
 steels, obs. and anal. of sulphides, using non-aqueous electrolyte-potentiostatic etching method (Japanese) 0-84933  
 steels, stainless, surface characterisation rel. to adhesive bonding chem. etching, SEM, AES, XPS and electron probe microanal. 0-88416  
 stretched zone anal. by means of stereo matching method (Japanese) 0-108544  
 superconductors, low temp. SEM appl. 0-80443  
 superconductors, multifilamentary, voids growth obs., via hot stage SEM 0-70089  
 surface microstructure determ. and microanalysis by ultrahigh vacuum field emission gun SEM 0-96423  
 surface potentials visualisation and meas., electron energy analysis 0-68307  
 thermoelectric materials,  $B_4C_x$  and  $(B,Si)_x C_x$  P-type  $LaS_x$  N-type alloys, fabrication and thermoelectric props. 0-107771  
 thinned semiconductor device, SEM, electron beam induced cond. of defects, rel. to TEM 0-107027  
 TTF-TCNQ, elec. cond., SEM technique 0-86507  
 vacuum, ultra-high, secondary electron emission dependence on electron beam density dose, surface interactions from AES and ELS 0-61209  
 volcanic ash, examples of devitrification and early diagenesis 0-81860  
 white Fe castings, morphology of eutectic  $M_2C$  and  $M_7C_3$  0-108427  
 Zircaloy, breakaway mechanism, corrosion kinetics in steam 0-61030  
 Zircaloy-2, mech. props. after exposure to  $I_2$ -methanol solutions, SEM study 0-93689  
 Zircaloy-4, resistance-welded, microstruct. of weld region 0-66549  
 Ag, film, chem. deposited, agglomeration, SEM and TEM obs. 0-59828  
 Ag film growth on Si (111), nucleation and growth modes, SEM study 0-100423  
 Ag on Si and W substrates, UHV-SEM studies of Stranski-Krastanov growth 0-79722  
 Ag-Ni (10 wt.%) wire, plastically deformed, fracture struct. (German) 0-71744  
 Al alloy surfaces anodized in phosphoric acid 0-81241  
 Al and Al alloy anodized oxide films, for adhesive bonding appls., AES and SEM study 0-66689  
 Al, annealed, and sintered powder, sputtering under  $D^+$  and  $He^{++}$  bombardment, microstruct. effects study 0-84821  
 Al, erosion by solid particle impingement at normal incidence, SEM obs. 0-104304  
 Al, fatigue crack initiation, pre-existing subgrain effect 0-97565  
 Al film, deform. under He ion bombardment 0-65073  
 Al, fracture mechanism 0-100903  
 Al sheet surfaces, chem. characterisation by SIMS, glow discharge spectrometry and other techniques 0-66907  
 Al, surface deformation and wear track obs. using analytical electron microscope 0-108687  
 Al-Bi(Cd)(Pb)-Ti, containing low-melting pt. inclusions, mech. props. 0-93632  
 Al-Cu, type 2219-T851, fracture mechanics and surface chemistry of fatigue crack growth 0-81168  
 Al-Cu (4 wt.%), supersaturated and aged conditions, high strain deform. 0-60907  
 Al-Cu-Mg, type RR55, high strength, creep behaviour, effect rel. to anodic coatings, SEM study 0-97542  
 Al-Cu-Mg/mica particulate composite mech. props. 0-100919  
 Al-Li-Mn (2.8, 0.3 wt.%), recrystallised sheet, fracture behaviour, SEM and TEM study 0-97566  
 Al-Si eutectic alloy, banded struct., SEM and optical microscopy 0-104144  
 Al-Si-N-O system, comps. corresponding to  $\beta$ -sialon phase reaction hot-pressing 0-84891  
 Al-Zn-Mg alloy AA-7039, stress corrosion cracking, SEM obs. 0-104323  
 (AlGa)As DH lasers, comparison of 'normal' lasers and lasers exhibiting light jumps 0-106519  
 AlGaAs-GaAs proton irradiated solar cells, deep-level defects, recombination mechanisms, performance characts. 0-81459  
 AlN film, oriented c-axis, low temp. deposition by reactive magnetron sputtering 0-76180  
 AlN films, RF reactive ion-plating, struct. and morphology 0-104074  
 $Al_2O_3$  (96 wt.%), fractographic criteria for subcritical crack growth boundaries 0-81155  
 $Al_2O_3$  substrates, tape-casted, fracture strength analysis 0-60948  
 $3.5Al_2O_3 \cdot 2SiO_2$ , mulitite, decomposition by  $SiO_2$  volatilisation 0-61082  
 Au-Ge contacts on GaAs, SEM and TEM obs. of struct. 0-100522  
 Au-refractory film interdiffusion obs., by combination of scattering techniques 0-65308  
 Au- $Ti_{0.7}W_{0.3}$ , thermal annealing study of metallisation on Si 0-80134  
 $B_2O_3 \cdot SiO_2$ , optical waveguide glass, sintering kinetics 0-84898  
 $B_2O_3 \cdot SiO_2 \cdot Na_2O$  phase-separated glass, creep fracture morphology 0-81151  
 $BaFe_2O_{10}$  particles, magnetic domain study by colloid-SEM method 0-97120  
 $BaFe_2O_{10}$  powders, fast reaction presintering 0-97445  
 $BaMoO_4$  crystals, growth in  $SiO_2$  gel under influence of elec. field 0-93469  
 $BaTiO_3$ , pure and doped crystals, surface and domain struct., AES and SEM expts. 0-71363  
 Be, thick film, amorphous, RF magnetron sputtering 0-80971  
 Bi film, structure and electronic props. 0-70562  
 C fibre, metal-coated with Cu, Co or Ni, coating struct., SEM study 0-97605  
 C, nongraphitizable, catalytic graphitization by  $Cr_2O_3$ ,  $MnO_2$  0-97440  
 $CaF_2$ , cathodoluminescence 0-100700  
 $CaF_2$ :Eu,  $CaF_2$ :Eu,Mn(Gd), single crystal predisintegration phenomena, SEM cathodolum. obs. 0-59502  
 $CaF_2$ :Eu, Mn, stroboscopic cathodoluminescence meas. appl. 0-70088  
 $CaF_2$ :Mn,  $CaF_2$ :Eu,Mn, single crystal predisintegration phenomena, SEM cathodolum. obs. 0-59502  
 $Ca_3(PO_4)_2$  OH bioceramic, material props. 0-93523

## scanning electron microscope examination of materials continued

- $Ca_3ScO_3$ , fracture surfaces, quantitative anal., energy dispersive X-ray spectrometry with Si(Li) diodes (French) 0-89571  
 Cd film on C steel, tribological behaviour 0-89364  
 CdS:Ga crystal cathodoluminescence, SEM analysis 0-97349  
 CdS/Cu<sub>2</sub>S heterojunction solar cells diffusion length determ. using minority carrier SEM 0-61359  
 $Cd_2SnO_4$  and  $Cd_2SnO_4 \cdot CdO$ , thin film electrodes in  $H_2SO_4$  electrolytes, reduction, AES and SEM 0-65674  
 CePd<sub>3</sub>, single crystal Czochralski growth and characterisation 0-60767  
 Cr films, photoresist film on reverse gas plasma etching 0-97634  
 Cr-Cr<sub>2</sub>O<sub>3</sub> black, electroplated solar collector coatings, high temp. optical and struct. degradation 0-66995  
 Cr-Cr<sub>2</sub>O<sub>3</sub> black solar absorber surfaces, microstruct. rel. to electroplating parameters 0-61418  
 Cs/W, work function measurement in SEM 0-80918  
 Cu, cementation, on Fe, deposit struct., reaction rates, SEM 0-104421  
 Cu, erosive wear mechanisms, combined TEM and SEM obs. 0-108601  
 Cu, irradiated with 20 keV  $He^+$ , surface damage and gas trapping profile meas. (French) 0-84219  
 Cu, oxidation kinetics, influence of intermediate annealing treatment 0-89412  
 Cu, polycryst., creep and fracture behaviour, effects of prestrain and O 0-97544  
 Cu, thin film, oxidation, RMEED/SEM studies 0-100968  
 Cu/Sn-Ni/Au tricouples, electrodeposited, interdiffusion obs. 0-84331  
 Cu-Al (14.3 wt.%),  $^{110}Ag$  diffusion in  $\beta/\gamma_2$  interphase boundary 0-79989  
 Cu-Al thin film multistructure,  $Xe^+$  ion beam cratering 0-66708  
 Cu-Al-Sn system, coexistence of different and brass like phases 0-89206  
 Cu-Be, dynode surface, SEM and Auger microanalysis 0-100384  
 Cu-Bi, grain boundary struct. intergranular fracture, segregation role 0-66648  
 Cu-Bi (0.02 wt.%) alloy, intergranular fracture, Kossel X-ray diff. in SEM obs. 0-108579  
 Cu-Ga, binary alloy constituent EDS anal., secondary fluorescence, SEM study (Chinese) 0-85231  
 Cu-mild steel explosively welded interface, SEM examination (German, English) 0-96746  
 Cu-Ni-Zn alloy, surface comp., outdoor exposure influence 0-59770  
 Cu-Sn alloy, surface comp., outdoor exposure influence 0-59770  
 Cu-Zn alloys, surface comp., outdoor exposure influence 0-59770  
 EuTe, high-temperature evaporation and reactivity 0-103469  
 Fe, cast, grey, solidified in oscillatory and rotating moulds, metallographic study 0-89213  
 Fe, free surface and grain boundary  $O_2$  and S chemistry 0-75410  
 Fe, high purity, boriding with cryst. B powder 0-84951  
 Fe, pure, cathodic charging effect on creep and tensile deformation 0-76320  
 Fe, pure, hydrogen-charged, initial cracking obs. 0-108580  
 $\alpha$ -Fe whiskers, pure, ductile fracture initiation, macroscopic obs. of deform. history and failure 0-85043  
 Fe-C-Si, high purity, vacuum melted, nodular graphite form. 0-108452  
 Fe-Cr-Al, HOS 875, oxidation, cyclic, role of thermal shock 0-97640  
 Fe-Cr-Al, scales,  $\alpha$ - $Al_2O_3$ , early stages development at high temp. 0-89413  
 Fe-Cr-Al (7, 5 wt.%), expt. stainless alloys, phys. and mech. props. 0-97637  
 Fe-Cr-Al-Y, oxidation resistance, heat treatment and  $Al^+$  ion implantation 0-71785  
 Fe-Cr-Al-Y, scales,  $\alpha$ - $Al_2O_3$ , early stages development at high temp. 0-89413  
 Fe-Cr-Ti (18, 0.1-0.9 wt.%), high temp. oxidation (Japanese) 0-71806  
 Fe-Ni, secondary recryst. and mag. props. 0-89247  
 Fe-Ni-Cr (30.6, 21.3 wt.%), Alloy 800, high temp. oxidation at low  $O_2$  press., SEM, AES and electron probe microanal. study 0-93688  
 Fe-Ni-Cr-Al-Y, oxidation mechanism, Y addition effect on kinetics and oxide adherence 0-97623  
 Fe-Ti-C, rapidly quenched by splat-cooling 0-84923  
 $(Fe,Cr_{1-x})_2O_3$  corundum-type solid solution single crystal growth, chem. vapour transport 0-93465  
 $Fe_2O_3$  haematite platelets, growth and cross-connection in consolidation of haematite pellet (Chinese) 0-104186  
 $Fe_2Pt$  austenites, ordering kinetics 0-104155  
 GaAs, binary alloy constituent EDS anal., secondary fluorescence, SEM study (Chinese) 0-85231  
 $Ga_{1-x}Al_x$ As visible diode lasers, degradation mechanisms 0-64026  
 GaAs, alloying with Au and Au alloy ohmic contact metallisations, SEM and optical study 0-70820  
 GaAs epitaxial films on strongly doped substrate, basic parameter meas. utilising magnetoresist. and SEM techniques under cathodoluminesc. conditions 0-65728  
 GaAs epitaxial layers on polycryst. GaAs substrates, LPE growth characts. 0-75471  
 GaAs, polycrystalline films, meas. of effective diffusion length by SEM 0-80424  
 GaAs:Se cathodoluminescence decay obs. with SEM and streak camera, 90 to 300K 0-97348  
 GaAs:Se(Zn) polycrystalline film, Hall effect, resistivity meas. 0-96911  
 GaAs:Si defect density before and after Zn diffusion, SEM and TEM obs. 0-96529  
 GaAs:Te Schottky barrier solar cells, diffusion length determ. using minority carrier SEM 0-61359  
 GaAs:Zn, implanted, laser annealing, elect., Rutherford backscattering and SEM meas. 0-100273  
 GaAs-Al,Ga<sub>1-x</sub>As buried-heterostructure lasers, current injection confinement, MBE/LPE hybrid technique 0-74374  
 GaAs-Ga<sub>1-x</sub>Al<sub>x</sub>As DH lasers, electron beam induced current microscopy 0-95899  
 GaAs-Ga<sub>1-x</sub>Al<sub>x</sub>As DH laser material crystal cathodoluminescence, SEM analysis 0-97349  
 GaAs-GaAlAs wafers, defects and degradation, transmission cathodolum. evaluation 0-65395  
 GaP, green cathodolum. from cryst. defects, SEM, TEM study 0-80870  
 GaP LED, SEM study of charge collection and cathodoluminesc. 0-65661  
 GaP, VPE layer structures for LEDs, SEM, and TEM obs. of dislocation density reduction expt. 0-100425  
 GaP:N LED structures, local dopant conc. determ. using SEM cathodolum. spectra 0-101057  
 $\alpha(\beta)$ -Ga<sub>2</sub>Se<sub>3</sub>, cryst. growth, optical, X-ray diff. and SEM study 0-71587

## scanning electron microscope examination of materials continued

- Gd<sub>2</sub>O<sub>3</sub>-Ga<sub>2</sub>O<sub>3</sub> system, phase diagram relationships of garnet-perovskite transform. 0-97460
- Hg lamps, RF-excited, dark film anal. 0-92789
- $\alpha$ -HgS films, sputter-deposited in Hg vapour, growth and props. 0-75467
- In-Bi single crystal, deform. mode under dynamic indentation 0-88163
- K-rich globules in Luna 20 soil, SEM obs. 0-67591
- Li particle size distrib. meas. by SEM 0-101775
- Li, surface characterization of film growth 0-81240
- LiF crystal, contact damage obs. by cathodoluminesc. 0-71728
- Li<sub>2</sub>GeO<sub>3</sub> piezoelectric glass ceramic, recrystallisation, pyroelectric response, permittivity 0-80703
- LiNbO<sub>3</sub> pure and Fe doped, IR induced acousto-photorefractive memory effect 0-80746
- Li<sub>2</sub>SiO<sub>4</sub>, piezoelectric glass ceramic, recrystallisation, pyroelectric response, permittivity 0-80703
- Mg, inclusions, types and size distrib. (*German, English*) 0-97492
- MgCr<sub>2</sub>O<sub>4</sub>-TiO<sub>2</sub>, porous ceramics, humidity-sensitive electrical conduction 0-107782
- MgO crystal, contact damage obs. by cathodoluminesc. 0-71728
- MgO crystal cathodoluminescence, SEM analysis 0-97349
- MgO, smoke particles, size distrib. 0-104471
- Mn micronodules from NW Atlantic, morphology and chemistry 0-81869
- Mo film, evaporated, annealing behaviour, SEM obs. 0-65397
- Mo-base alloy, TZM, blistering under He ion bombard. 0-92567
- Mo-W (30 wt.%), wrought, fracture, characteristic features 0-104278
- Mo-Zr (0.15 wt.%), wrought, fracture, characteristic features 0-104278
- MoO<sub>3</sub> topotactic transform into MoO<sub>2</sub>, electron microscopy, X-ray anal. 0-107417
- Na<sub>2</sub>O-CaO glass, shear deform. under pyramidal indentations 0-84989
- Nb fibre glass composites, new technique for producing fine metal fibres 0-108384
- Nb<sub>40</sub>Fe<sub>60</sub>P<sub>4</sub>B<sub>6</sub>, metallic glass, explosive compaction, mech. props. 0-89176
- Nb<sub>3</sub>Sn, flux density gradient determ. by Faraday effect 0-107969
- Nb<sub>3</sub>Sn-Cu multifilamentary composite wire, Nb<sub>3</sub>Sn filament morphology and grain size 0-100855
- Ni base alloys, IN-702, IN-601, TD-Ni-Cr-Al, B-1900+Hf, oxidation, cyclic, role of thermal shock 0-97640
- Ni, corrosion, high temp., SO<sub>4</sub> induced, studied at 900°C in O<sub>2</sub>+4.2% SO<sub>2</sub> 0-97639
- Ni, erosive wear mechanisms, combined TEM and SEM obs. 0-108601
- Ni, Medicus matrix cathode, surface characts. 0-66378
- Ni, oxidation, high temp., effect of C on cavity form., SEM study 0-97638
- Ni, oxidation kinetics, influence of intermediate annealing treatment 0-89412
- Ni, sintering kinetics, metallographic study 0-93519
- Ni-Al, (2 and 6 wt.%), oxidation,  $\alpha$ -Al<sub>2</sub>O<sub>3</sub> growth, microstruct., precip. 0-108626
- Ni-Al-Cr<sub>2</sub>C<sub>3</sub>, eutectic alloy, directionally solidified resistance, influence of Y 0-89409
- Ni-Co-Al alloys, continuous precip., SEM, TEM, X-ray diffr. study 0-89220
- Ni-Co-W, electrodeposition, surface morphology and cryst. struct. 0-71602
- Ni-Cr, degradation after exposure to 1% H<sub>2</sub>S/H<sub>2</sub> gas mixture at 1000°C 0-89408
- Ni-Cr-NbC eutectic composite, unidirectional solidification, thermal cycling, temp. range effect on microstructural degradation 0-89272
- Ni-Cr-W, oxidation behaviour in air at 1000-1250°C 0-89407
- Ni-Cr-Zr, degradation after exposure to 1% H<sub>2</sub>S/H<sub>2</sub> gas mixture at 1000°C 0-89408
- Ni-ferrite powders, form. in presence of Li<sub>2</sub>SO<sub>4</sub>-Na<sub>2</sub>SO<sub>4</sub> molten salts, prep. and characts. 0-84869
- Ni-Si incongruently subliming system, SEM and TEM obs. of high temp. transitions, temp.-comp. diagrams 0-104136
- Ni-ThO<sub>2</sub>, oxidation, cyclic, role of thermal shock 0-97640
- $\beta$ -NiAl, oxidation,  $\alpha$ -Al<sub>2</sub>O<sub>3</sub> growth and microstruct. 0-108627
- Ni(CO)<sub>4</sub>, form. on single Ni cryst., reaction kinetics and induced surface faceting 0-71948
- NiF: film preparation and characterisation 0-59815
- NiO, stress relief and plastic flow in temp. range 1323-1473K 0-89302
- Pb, film, hillock formation by grain boundary sliding 0-107673
- Pb films, hillock growth upon cycling to cryogenic temps. 0-88448
- PbO, thin film, microstruct. and thermal stress, doping effects 0-88458
- PbS, chem. deposited thin film, effect of morphological struct. on photosensitivity 0-70760
- PbS-Si heterojunction, PbS film growth and struct. 0-96762
- PbTe, effect of pressing and sintering, study of induced defects by SEM 0-59983
- PbTe thermoelectric materials, microstructure anal. using SEM X-ray microanalysis 0-107211
- PbZrTi<sub>1-x</sub>O<sub>3</sub> ceramics, morphotropic phase boundary 0-81035
- Pd coated Si wafers, interference effects on irradi. with laser beam 0-66333
- Pd on UHV-cleaved mica substrate, obs. using scanning Auger microscopy 0-80149
- PtSi surface, and interface with Si, impurity effects 0-80037
- Si, crucible grown, virgin and implanted, laser irradiation effects on surface structure 0-92768
- Si, crystal defects and impurities interaction obs. by electron microscopic methods 0-65003
- Si, Czochralski grown, dislocation free, swirl defect form., doping effect 0-92519
- p-Si, Czochralski grown, microdistrib. of O, SEM and spreading resist. obs. 0-79830
- Si, etching in He-F<sub>2</sub> plasma, etch rates, mass spectra, direct ion sampling study 0-79510
- Si film, MBE, cryst. defect props., substrate treatment effects 0-70551
- Si, ion implanted, electron beam annealing, surface struct. study using SEM 0-70235
- Si, ion-implanted layers, epitaxial regrowth by laser beam and flash annealing 0-100420
- Si, measurements of electron channelling pattern linewidths 0-62805
- Si, near (111), fracture by painted indenter, SEM study 0-71734
- Si phototransistors, slow contamination- and fast surface state effects, SEM study 0-107896
- Si polycrystalline solar cells, recombination, electron-beam-induced current characterisation 0-81470

## scanning electron microscope examination of materials continued

- Si substrate for PMMA electron sensitive layer, 400 Å linewidth electron beam lithography 0-65392
- Si, V-grooves formed by etching, phosphosilicate glass bridge struct. 0-104312
- Si-B radiation damage and minority carrier lifetime, SEM-EBIC obs. 0-96573
- Si-N wafers, Si<sub>3</sub>N<sub>4</sub> layer growth by high dose implantation and annealing, elec. props. 0-70227
- p-Si-Al, ohmic contacts, Si dissoln. and recrystn. effects, computer calc. 0-103749
- Si-Al-Al<sub>2</sub>O<sub>3</sub> system, solid phase Si regrowth on sapphire 0-100413
- Si-CoSi<sub>2</sub>Si, double heteroepitaxy, solid phase and MBE 0-104063
- Si-Pd-Ti, silicide form. in evaporated films 0-80006
- SiAlON, prepared from siliceous sand and Al powder, hot pressing, steatite contamination effects (*Japanese*) 0-93528
- SiC, blistering and flaking due to light ion bombardment (*Japanese*) 0-70264
- SiC particles in EFG ribbon solar cells, EBIC and ion microprobe anal. 0-93838
- SiC, reaction-bonded, impact erosion by ang. Al<sub>2</sub>O<sub>3</sub> particles 0-89362
- SiCl<sub>4</sub>-GeCl<sub>4</sub>-BCl<sub>3</sub> particulate layers consolidation, in fabrication of optical fibre preforms 0-60787
- Si<sub>3</sub>N<sub>4</sub>, bending strength, deformability, elastic moduli and brittleness 0-81191
- Si<sub>3</sub>N<sub>4</sub>, hot-pressed, fracture mech. parameters, indentation-prec cracking and double-torsion methods 0-104364
- Si<sub>3</sub>N<sub>4</sub>, hot-pressed, strength anisotropy origins 0-89330
- Si<sub>3</sub>N<sub>4</sub>-CeO<sub>2</sub> additive, hot-pressing and oxidation behaviour 0-71618
- SiO<sub>2</sub>, etching in He-F<sub>2</sub> plasma, etch rates, mass spectra, direct ion sampling study 0-79510
- SiO<sub>2</sub> fibres, freeze formed from polysilicic acid aq. soln. 0-71609
- SiO<sub>2</sub> films, RF-diode-sputtered, step coverage 0-80117
- SiO<sub>2</sub>, relief, plasma etching, tapered wall prod. 0-97606
- SiO<sub>2</sub> thin films, deposition and characterisation study 0-80133
- Sm<sub>2</sub>O<sub>3</sub>-Ga<sub>2</sub>O<sub>3</sub> system, garnet-perovskite transform., phase diagram relationships 0-97460
- Sn-Pb surfaces, contaminant growth on ageing, SEM 0-108625
- SnO<sub>2</sub> CVD coating on glass, elec. resist. rel. to cryst. microstruct. 0-84520
- Ta single crystal, H<sub>2</sub> embrittlement (*Japanese*) 0-66636
- Te film, surface morphology depend. on vacuum deposition angle 0-103553
- Te film, vacuum deposited, growth and morphology of crystals 0-96766
- Te, vacuum deposited on NaCl, crystallite growth and morphology, electron microscopy 0-65401
- Ti, corrosion in H<sub>2</sub>SO<sub>4</sub>, estimated from weight loss meas. at 270°C and 56 bar (*French*) 0-85080
- $\alpha$ -Ti, fatigue crack growth, influence of grain orientation, SEM study 0-108550
- Ti, fatigue damage, SEM, X-ray diffr. and surface trace anal. 0-85040
- Ti, oxidation behaviour under pure O<sub>2</sub> atmos., temp. range 600-800°C 0-89415
- Ti-Al-V (6, 4 wt.%), fretting corrosion of orthopaedic implant materials by bone cement 0-104813
- Ti-Al-V (6, 4 wt.%),  $\beta$ -annealed, subsurface fatigue crack initiation 0-108553
- Ti-Al-V (6, 4 wt.%), effect of air exposure on fracture characts. 0-100890
- TiC coatings, on cemented carbides, struct. and hardness 0-59771
- $\alpha$ -U, strain rate effect on flow and fracture 0-100887
- $\alpha$ -U, strain rate effect on tensile flow and fracture 0-84992
- W, electron-channelling patterns, crit. voltage effects 0-79647
- W, SEM expts., anomalous patterns (*Chinese*) 0-59349
- W wire, AKS-doped, second phase particle obs. by TEM, SEM and atom probe microanalysis 0-108457
- W, work function measurement in SEM 0-80918
- WC-Co DC and RF sputtered coatings, bias effect, struct., X-ray-Auger study 0-70565
- W<sub>50</sub>Fe<sub>50</sub> glassy alloy, refractory, triode sputtered 0-75185
- YbTe, high-temperature evaporation and reactivity 0-103469
- Zn electrodeposition, on Zn and Al single crystals, from H<sub>2</sub>SO<sub>4</sub> bath, SEM obs. (*Japanese*) 0-93502
- ZnO, CVD of epitaxial films on sapphire, SAW interdigital transducer fabrication 0-66430
- ZnO piezoelectric films, RF planar-magnetron sputtered, characterisation 0-96751
- ZnO RF sputtered films, post deposition annealing behaviour 0-100416
- ZnO:Ba, Co, rare earth metal varistors, microstructure-prop. relations 0-100249
- ZnSe, electron beam induced current study of grain boundaries by SEM 0-59479
- ZnTe, low voltage green LED, struct. double diffusion procedure 0-100697
- Zr, breakaway oxidation kinetics at 623K, SEM study 0-97633
- Zr, foil bending by in situ ion irradi., neutron damage simulation, room temp. oxide growth 0-107342
- ZrO<sub>2</sub>, porous, sintered stabilised microspheres, strength and fracture studies 0-85019
- ZrO<sub>2</sub>-SiO<sub>2</sub>, liquid immiscibility, microstruct. of plasma dissociated ZrSiO<sub>4</sub> 0-107429

## scanning electron microscopes

- see also scanning electron microscopy
- Auger, calc. of effects of backscattered electrons on spatial resolution 0-81412
- Auger, with computerised image processing 0-68304
- Auger microprobe, backscattered electron images, tailored modulation techniques appl. 0-68305
- Auger microscope using microprobe with thermal field emission source 0-68297
- backscattered electron detector, forensic appls. 0-68319
- backscattered electron image, effects of collector take-off angle and energy filtering 0-62802
- backscattered electron image, enhancement of type-2 mag. contrast by lock-in technique 0-62806
- cathodoluminescence, detector system 0-101898
- chopping systems comparison and universal system development 0-68306
- combined deformation/heating stage, acoustic emission rate meas. 0-101892
- contamination buildup, investigations using backscattered electron imaging technique 0-62807



**scanning electron microscopes continued**

- converted backscattered electron detection 0-68318
- development, refinements of lens correction, recording of individual electrons, holography, image quality monitoring (*German*) 0-57430
- electron beam photographic recording system 0-101903
- electron-acoustic microscope, using US imaging 0-95192
- equipotential patterns obtaining, accuracy increase 0-57423
- field emission, high resolution image 0-86520
- field emission electron gun, comparison of cold and thermal types used in the same electron microscope 0-101890
- field emission gun SEM column electron-optical performance obs. and model 0-68328
- field emission micro SEM, for UHV surface anal. 0-86519
- flying spot scanner for conversion of SEM to lithography system 0-86512
- heating stage for the Stereoscan SEM, construction 0-95190
- in-situ gas reaction cell, for field emission SEM 0-81415
- insulating specimen charge neutralization using very low energy ions 0-68309
- ISI Model 7, for research, quality control and teaching (*German*) 0-57429
- lens system design snorkel or condenser-objective 0-57438
- microprobe analyser, scanning cathodolum. 0-81409
- Philips SEM 505 with multifunction detectors 0-101880
- precision SEM image analysis system with full-feature EDXA characterization 0-68311
- stereovision in SEM 0-73532
- teaching methods for short courses 0-73533
- ultra high resolution, with electron optical system and microprocessor control 0-99002
- ultrahigh vacuum field-emission SEM 0-62812
- vacuum system specification and design 0-82779
- MgO coated detector for SEM backscatter to secondary electron conversion 0-68332

**scanning electron microscopy**

- see also scanning electron microscope applications; scanning electron microscope examination of materials; scanning electron microscopes*
- asbestos fibre counting by automatic image analysis 0-73538
- Auger, S/N aspects 0-71993
- Auger electron spectroscopy for analysis of biological material 0-73535
- Auger electron spectroscopy microanalysis 0-101058
- Auger spectroscopy, resolution, quantification and sensitivity 0-81411
- automatic topographical surface reconstruction 0-62803
- backscattered electron conversion to secondary electrons, detector system 0-62804
- backscattered electron image, effects of collector take-off angle and energy filtering 0-62802
- backscattered electron image, enhancement of type-2 mag. contrast by lock-in technique 0-62806
- backscattering theory, using Boltzmann transport equation 0-57439
- biomembrane surface charge visualisation 0-85566
- cathodoluminescence detection of Giemsa stain and its appls. 0-67323
- cell element observations in same sections by light microscopy, TEM and/or SEM 0-85556
- computer-aided topographical analysis 0-70094
- conductive treatment of specimen to prevent charging 0-101883
- conference, Washington, DC, USA (Apr. 79) 0-57003
- contamination buildup in microscopes, investigations using backscattered electron imaging technique 0-62807
- contrast detector and area evaluator, low cost SEM 0-73531
- coordinated, multidiscipline courses 0-67965
- correlative light microscopy, SEM and TEM of argentaffin cells 0-85557
- critical point drying of hydrated specimens, principles and procedures 0-76882
- cryofixation of tissue specimens studied by cooling rate measurements and scanning electron microscopy 0-94430
- dehydration of specimens, bibliography (1974-8) 0-73544
- diffractogram online computation 0-70095
- direct elemental analysis by electron energy loss spectroscopy 0-71998
- dislocation imaging, electron channelling appl. 0-70214
- egg shells, electron microscope embedding medium for pore studies 0-98194
- electron backscattering patterns, in field emission gun SEM 0-100142
- electron beam induced conductivity, determ. defects in thinned semiconductor devices 0-107027
- electron channel imaging used in microscope for observation of single defects in crystals 0-64848
- electron probe, compensation of aberrations, dynamical focusing with stigmator 0-87291
- electron probe microanal. in SEM by means of X-ray spectrometers, review 0-95194
- energy dispersive microanalysis, in SEM, artifacts (*German*) 0-73561
- energy dispersive X-ray spectrometry, qualitative and quantitative analysis problems 0-85249
- environmental particulate exposure in humans, documentation 0-76886
- etching of red blood cells by ion beam sputtering 0-85554
- fissured biological object prep. for SEM, vacuum deposition and cathode sputtering comparison 0-72390
- fracture surface SEM analysis, microtopography 0-68312
- freeze drying technique for SEM 0-104828
- haematopoietic malignancy diagnosis, significance of SEM 0-85529
- imaging techniques, and X-ray microanal. 0-57432
- imaging with backscattered electrons 0-86513
- information representation by equal signal lines 0-95196
- Kossel technique in SEM for crystallographic orientation 0-75133
- low-temperature biological SEM, comprehensive freezing, fracturing and coating system 0-76883
- LSI surface analytical techniques applied to electronic components [Si LSI chip inspection] 0-81392
- material surface texture analysis 0-73548
- measurement of backscattering coefficient and secondary electron yield 0-86515
- microanalysis techniques, review 0-71995
- microscopy equipment, methods, appls. and related topics, bibliography 0-73124
- mineralogical use of energy dispersive X-ray spectrometry with Si(Li) diodes (*French*) 0-85251
- mycoplasma contamination detect., SEM sensitivity 0-85568
- myelinated axon identification, SEM technique 0-85570
- object microrelief analysis by SEM, metallurgy appls. 0-73319
- online topographical analysis in SEM 0-68310

**scanning electron microscopy continued**

- peak-to-background method for quantitative anal. of single particles, with electron probe, developmental progress 0-73541
  - Plato IV network, SEM teaching 0-68003
  - pore size measurement, comparison of methods 0-62622
  - preparation technique for emulsion particles, freeze drying 0-62799
  - reflected, viewing specimens in air 0-82853
  - SAW propag., photographs on TV images of travelling waves using strobed electron beam 0-102894
  - scanning Auger microscopy, developments 0-101909
  - scanning Auger microscopy, effects of backscattering on resolution 0-104021
  - scanning microprobe microscopy, conf., Paris, France (Oct. 1979) 0-82569
  - semiconductor crystal growth and defects, appl. of analytical techniques 0-73546
  - semiconductor layers, thin, theory of lifetime meas. with SEM, transient anal. 0-88573
  - skeletal muscle preparation 0-94431
  - slide/tape modules use in teaching SEM 0-68005
  - solid, backscattering coeff. meas. of 15 to 60 keV electrons at various angles of incidence, rel. to SEM 0-80919
  - specimen coating by ion sputtering deposition 0-76184
  - specimen preparation, metal coating by sputtering, specimen heating (*German*) 0-73338
  - specimen-electron interactions 0-68317
  - stereovision displacement and strain meas. and obs. 0-68314
  - stereoscopic depth perception and measurement 0-68313
  - stereoscopic SEM micrographs, quantitative anal. 0-57433
  - stereoscopic microcomputer-controlled, function testing of bipolar IC and LSI 0-68294
  - subgrains imaged from bulk specimens in study of localized plasticity 0-66609
  - surface anal. tools review 0-103540
  - surface analysis techniques and appls., symposium, Dayton, USA (Jun. 1979) 0-62363
  - surface potential and work function meas. from secondary electron emission energy in SEM 0-66343
  - surfaces and interfaces, analysis by combined Auger, X-ray and SEM studies 0-81413
  - table top SEM for undergraduate training 0-68002
  - teaching methods for short courses 0-73533
  - teaching philosophy and methodology 0-67964
  - thickness measurement of SiO<sub>2</sub> layer 0-57435
  - thin film coating techniques for specimen preparation 0-68308
  - two-surface analysis, of polished sections in scanning electron microscope 0-77912
  - US imaging, appl. in scanning electron microscopy 0-95192
  - video tapes in SEM teaching, evaluation 0-68004
  - voltage contrast in scanning electron probe, device ground level floatation 0-73527
  - voltage contrast in SEM, electron beam current-recording relationship 0-73528
  - X-ray microanalysis, pellet mould for bulk specimens 0-95191
  - X-ray spatial resolution, for SEM and STEM specimens, Monte Carlo methods 0-101066
  - Au coins, surface anal. by X-ray fluores., SEM and scanning Auger spectroscopy 0-89552
  - LaB<sub>6</sub> cathodes for Kohler illum. and brightness meas. 0-68296
  - Ti/Cu/(Au) thin films thermocompression bonds degradation by thermal ageing 0-66546
- scanning radiography**
- see also computerised tomography; radioisotope scanning and imaging*
  - digital image-enhancement, used for human anatomy scanning 0-94408
  - flashing tomosynthesis, 1st clinical results 0-104746
  - flexible scanning industrial X-ray/fluoroscopy inspection 0-89459
  - grid for novel and effective Bucky movement 0-104754
  - laser impled targets, three-dimens. reconstruction of X-ray emission 0-79563
  - microtomography in SEM 0-101308
  - rotation coronary angiography 0-104744
  - scanography with rotation of the rotation of the radiographic tube, new method 0-98130
  - transverse axial film tomography with a therapy simulator 0-81716
  - X-ray topography of large single crystals 0-96415
- scanning-transmission electron microscope examination of materials**
- see also scanning-transmission electron microscopy*
  - catalyst, metal oxide, convergent beam electron microscopy obs. 0-108689
  - composition profiles meas., statistical variation limitation 0-61208
  - diamond, natural type-IIb, single dislocations, cathodoluminescence obs. by STEM 0-80871
  - dislocation core, symmetry of dynamical electron microdiffraction patterns 0-100140
  - dislocations and microplasma sites, STEBIC/STEM/EELS correlation 0-96528
  - etched thin foils, comparative SEM, STEM and TEM analysis 0-100144
  - ferromagnetic thin film, direct determ. of mag. domain wall profiles, using split detector STEM 0-103867
  - fibre, environmental, convergent beam electron microscopy obs. 0-108689
  - field emission gun appl., X-ray analysis of metals and ceramics inhomogeneities 0-59354
  - film, evaporated, metastable phases, convergent beam electron microscopy obs. 0-108689
  - graphite, Fe-catalysed gasification, electron, microscopy 0-104358
  - graphite, zone-axis pattern maps 0-800137
  - natural type-IIb, single dislocations, cathodoluminescence obs. by STEM 0-80871
  - paraffin, single crystal, STEM versus CTEM beam damage 0-103393
  - precipitate free zones, X-ray microanal. 0-108768
  - protein molecular weight and ultrastruct. determ. in STEM 0-85562
  - rare earth oxides, segregation study by electron energy-loss spectroscopy 0-79953
  - semiconductor, STEM spectroscopic techniques for simultaneous electronic and defect obs. 0-100145
  - semiconductor defects, spectroscopic techniques to study of electronic props. 0-84446
  - semiconductor-metal contact, convergent beam electron microscopy obs. 0-108689
  - spot scan TEM technique 0-82846

**scanning-transmission electron microscope examination of materials** continued  
 steel, Cr (10 wt.%), precip. free ferrite form., STEM 0-84941  
 steel, Cr-Mo, ferritic, grain boundary segregation, X-ray microanal. by STEM 0-66740  
 steel, dual phase HSLA, compositional anal., TEM 0-85253  
 steel, ferritic Cr-Mo type, microanalysis of precipitates using TEM 0-108688  
 steel, ferritic stainless, Cr-Mo (12.1wt.%) microstructure influence on localised corrosion behaviour 0-61018  
 steel, stainless, duplex, STEM obs. of localized corrosion 0-104324  
 steel, stainless, ferrite to austenite decomp. 0-93554  
 steel, stainless, precip. obs using convergent beam electron microscopy 0-108689  
 thorium phthalocyanine, phase contrast characteristics in STEM 0-100153  
 transition metal chalcogenide layer compounds, convergent beam electron microscopy obs. 0-108689  
 Al and Al alloy anodised oxide films, for adhesive bonding appls., AES and SEM study 0-66689  
 Al anodising, porous films formed in chromic acid 0-100966  
 Al, small spheres, bulk plasmons damping 0-75561  
 Al, surface deformation and wear track obs. using analytical electron microscope 0-108687  
 Al-Mg-Si, ageing sequence study by electron microdiff. 0-81068  
 Al-Mg-Si alloy, microdiff. obs. of precip. struct. 0-104167  
 Al-Ni (6 wt.%) alloy, misorientation between subgrains, second-phase particles role, STEM microdiff. obs. 0-104415  
 Al<sub>2</sub>O<sub>3</sub>-MgO, grain boundary segregation of Ca and Mg X-ray spectrosc. and STEM study 0-107269  
 Au, thin foil, spatial resolution of X-ray microanalysis 0-101065  
 Cu alloy matrix with Cr and SiO<sub>2</sub> particles, low resolution STEM imaging 0-108685  
 Cu-Be-Co, discontinuous reaction, analytical TEM 0-100842  
 Cu-Ni-Nb (30, 0.9 at.%), precipitate free zones, X-ray microanal. 0-108768  
 Fe-Ni, grain boundary segregation, X-ray microanal. by STEM 0-66740  
 Fe-Ni meteorite, STEM/X-ray microanalysis across  $\alpha/\gamma$  interface 0-105212  
 Fe-Ni(P), phase diagram determ., 700 to 300°C 0-108399  
 Ga<sub>1-x</sub>Al<sub>x</sub>As structures, STEM and scanning deep level transient spectroscopy in defect centre anal, cathodoluminesc. techniques 0-103642  
 Ga<sub>1-x</sub>Al<sub>x</sub>As<sub>1-y</sub>P<sub>y</sub> epitaxial layer heterojunction, nonradiative recombination at misfit dislocations 0-96901  
 MgO, deformed, cathodlum. obs. by STEM 0-76088  
 MgO-NiO, STEM microanal., absorpt. effects 0-80902  
 Nb, electron energy losses due to H, obs. by scanning TEM 0-79850  
 Nb<sub>2</sub>Ge, sputtered on Cu, film-substrate interface obs. by electron microscopy 0-65398  
 Ni superalloy, STEM microanal. of precipitates and their nuclei 0-81067  
 Ni-base superalloy, STEM microanalysis of precipitates 0-104492  
 Si, amorphous, scanning TEM studies of cryst. inclusions 0-79699  
 Si p-n junction depletion layer, electron beam damage inhibition 0-70817  
 Si:As, ion implanted, pulsed laser annealing, partial solid-state regrowth 0-103591  
 V, electron energy losses due to H, obs. by scanning TEM 0-79850  
 V-Ti-C, elemental anal. by EELS 0-101069  
 WC-Co, STEM anal. of grain boundaries 0-79644  
 ZnS, single electron excitation study, cathodoluminescence image contrast using STEM 0-89072

#### scanning-transmission electron microscopes

*see also scanning-transmission electron microscopy*  
 biological specimens, frozen, obs. single heavy atoms 0-89921  
 combined CTEM and STEM, using condenser objective lens and 100 kV LaB<sub>6</sub> gun 0-86516  
 computer driven, image registration 0-104838  
 crystals study, two-dimens. diff. patterns obs. and recording system 0-79650  
 design, operation, capabilities and limitations, review 0-68300  
 electron energy analysis in Vacuum Generators HB5 STEM 0-73543  
 field emission gun, for X-ray microanal. 0-85260  
 foil lens, correction of spherical aberration, appl. to STEM 0-87294  
 future improvements and potential advantages 0-86532  
 HV, detection efficiency and performance estimation 0-101899  
 image formation 0-86399  
 multichannel detector system 0-68331  
 Philips EM400 TEM/STEM performance, with field emission gun and twin lens 0-57441  
 quadrant detector, appls. 0-77914  
 scintillation detector use 0-101897  
 single atom microscopy, instrumental aspects 0-86522  
 spectrograph, recording of energy loss spectra 0-86525

#### scanning-transmission electron microscopy

*see also scanning-transmission electron microscope examination of materials; scanning-transmission electron microscopes*  
 analytical microscopy, contamination reduction 0-68316  
 atomic number contrast, supported catalyst particles 0-79651  
 beam damage sensitivity, STEM versus CTEM 0-103393  
 biological macromolecule observation using CTEM and STEM with negative staining 0-85561  
 bright-field image contrast and resolution 0-95200  
 computer graphics analysis of images 0-73539  
 computerised data recording and replay 0-57440  
 convergent beam, materials science appls. 0-108689  
 crystal structures and cryst. defects, electron microscope imaging 0-88006  
 defocus and astigmatism, automatic correction method 0-68298  
 differential phase contrast role, quadrant and first moment detectors comparison 0-95202  
 displacement energy determ. by electron beam induced conductivity 0-70097  
 EELS, in STEM, multi-channel averaging 0-101061  
 electron beam fabrication, using STEM 0-104104  
 electron energy-loss spectra, progress in quantitation 0-73542  
 electron microdiffraction patterns, point group symmetry from dislocation cores 0-100140  
 grain boundary segregation, critical assessment 0-75362  
 illumination system for thermal cathode; for round beam electron probe systems 0-57436  
 image formation, 2-D computer simulation of heavy atom model compounds 0-75135

**scanning-transmission electron microscopy** continued  
 image formation, partially coherent, two dimens., computer simulation 0-106434  
 images, matching illum. to specimen struct. 0-73551  
 imaging at high resolution, influence of detector geometry 0-62811  
 mass measurements and associated errors 0-73537  
 materials science, appl. combined with energy dispersive X-ray anal. and electron energy loss spectroscopy 0-103228  
 materials science applications 0-76460  
 metallurgical specimen, low resolution imaging problems and soln. 0-108685  
 microanalysis, precipitates in Ni-base superalloy 0-104492  
 multi-signal detection and processing 0-73552  
 non-optimal apertures 0-62801  
 phase contrast characteristics 0-100153  
 plural scattering, influence on image quality of thick amorphous objects 0-86533  
 semiconductor, STEM spectroscopic techniques for simultaneous electronic and defect obs. 0-100145  
 spatial resolution, improved X-ray microanalysis of thin specimens 0-104490  
 split detector, direct determ. of mag. domain wall profiles in ferromag. thin films 0-103867  
 structural and chemical analysis, appls. 0-88003  
 surface originating contamination and its elimination 0-68315  
 thick objects, micrograph anal. 0-82856  
 thin films, chem. anal. by energy loss spectroscopy 0-104493  
 X-ray microanalysis, electron probe dispersion influence on spatial resolution 0-85257  
 X-ray microanalysis, spatial resolution 0-84039  
 X-ray spatial resolution, for SEM and STEM specimens, Monte Carlo methods 0-101066  
 zone-axis pattern formation using four sets of coils 0-70091  
 C film on substrates for supporting specimens, prep. and observation 0-93496  
 LaB<sub>6</sub> cathodes for Kohler illum. and brightness meas. 0-68296

#### scattering

*see also acoustic wave scattering; backscatter; electromagnetic wave scattering; potential scattering*  
 3-body problem with one infinite mass particle, Schrodinger and integral eqn. soln. equivalence 0-77636  
 approximate phase construction by iteration of bounds from unitary integral 0-57142  
 angular scattering of spinor charged particles by a Kerr-Newman field 0-94996  
 approximate coupled equation method 0-73215  
 classical inverse scattering in one dimension 0-82595  
 continental shelf waves, scattering by longshore bottom topography vars. 0-67376  
 education, multiple scatt., elastic and inelastic, two particle system with fixed wall, air track expt. 0-73135  
 elastic waves, scattering by elastic sphere embedded in isotropic elastic medium 0-96214  
 forward or backward scatt. amp. with three constraints, variational pattern 0-94995  
 forward scattering contrasts in multicomponent systems 0-90728  
 high-frequency scattering by a convex soft or a rigid obstacle 0-90727  
 inverse scattering solution for three dimens. three-wave resonant interaction 0-77633  
 ion, comparison of time-of-flight and stripping cell low-energy ion scattering methods 0-73522  
 levinson's theorems in classical scattering 0-90729  
 microwave backscatter, ploughed soil, surface roughness meas. (French) 0-82072  
 multipoles and excitons in higher order coherence 0-82680  
 N-body scattering equation approach using pole decomposition of Green's function 0-62540  
 neutron transport integrals, quadrature sums, Gaussian, orthogonal polynomial method 0-83139  
 nondiffractive scattering from kaledioscopes 0-86155  
 phase of scattering amplitude, uniqueness, variational calc. 0-86156  
 phase space packets, time depend., differential cross sections obtained by superoperator methods 0-105544  
 resonances, scattering theory and rigged Hilbert spaces 0-94987  
 rotated hamiltonians, complex-coordinate rotation and least-squares variational method 0-68075  
 semiconductors, hot electron transverse escape galvanomagnetic effects (Russian) 0-80289  
 solids, chemical bonding studied using scattering theory concepts 0-103289  
 symmetric collision theory, T-operator matrix elements 0-73214  
 theory, propagation of singularities for the transmission problem and application to the inverse problem of scattering (French) 0-94994  
 variational principle for scatt. phase 0-68084  
 wave equation, reduced, fixed incident field, inverse problem 0-62484  
 wave scattering in presence of background slab, algorithm for profile reconstruction 0-94644

**scattering matrix** *see S-matrix theory*

**scattering parameters** *see S-parameters*

#### SCF calculations

*for MS SCF (MS Xalpha) calculations see Xalpha method*  
*see also HF calculations; Xalpha calculations*  
 acetophenones, di- and trisubstituted,  $\pi^*-\pi$  systems, UV electronic absorpt. spectra 0-74132  
 acetophenones, mono substituted, semi empirical II-electron calcs. 0-74131  
 acetophenones, spectrosc. characts. using PPP SCF CI calcs. 0-102448  
 adenine, tautomeric forms protonation, ab initio HF Roothaan SCF calcs. 0-78534  
 n-alkanes, mol. Rydberg S—S and S—T transitions, semi-empirical SCF MO calc. 0-91453  
 allyl radical, restricted SCF and MC SCF calc. of C<sub>2v</sub> and C<sub>s</sub> structs. 0-83289  
 anharmonically coupled oscills., time depend. Hartree theory, susceptibility, absorpt. and Raman spectrum 0-58241  
 ascorbic acid adduct model systems, SCF calc., rel. to protein internal charge transfer 0-69072  
 atom-ion core level shifts,  $\Delta$ SCF calcs. 0-87176  
 atomic quadrupole shielding factors calc. using elec. field variant orbitals 0-106276



## SCF calculations continued

atomic scatt. factors and momentum densities, asymptotic form 0-74105  
 atoms, analytical relativistic SCF calcs. 0-83248  
 atoms, near threshold struct. in K-shell spectra, photoionisation or fast charged particle ionisation 0-87064  
 atoms on semi-infinite linear chain, chemisorption theory and superoperator formalism 0-93800  
 azacyclobutadienes, conjugated mols. electronic struct. and geometry, Hartree-Fock instability 0-69055  
 band structure, optical cond., Compton profile, self consistent calcs. 0-65435  
 benzene, dipole polarisability, finite-field SCF MO calcs. 0-83255  
 trans-butadiene, polarisability, nonlinear elec. susceptibility, SCF calcs. 0-95547  
 butadiene, twisted zwitterionic excited states, SCF calcs. 0-58179  
 closed shell Hartree theory with orthonormal orbitals 0-69051  
 closed-shell linear molecules, relativistic Dirac-Fock multiconfig. SCF calcs. 0-99455  
 closed-shell polyatomic molecules, relativistic Dirac-Fock multiconfig. SCF calcs. 0-99456  
 closed-shell system, polarisability and mag. susceptibility calc. by SCF and CI method 0-99443  
 coupled HF-perturbation theory of atomic and mol. props., correl. corrections 0-106269  
 coupled oscillator system, SCF-state interaction method 0-58239  
 crystals, anharmonic, with complex lattice, equations of state 0-107399  
 cyclic 3- and 4-membered ring cpds., saturated, ab initio struct. anal. 0-58192  
 deoxyhaemoglobin, porphyrin-Fe-imidazole system, SCF-LCAO-ASMO and CI calcs. of low-lying multiplets and excited states 0-94155  
 diatomic mols., one electron props., SCF-Xalpha scattered wave method 0-83279  
 dihydroquinoxalinediones, conjugated mols. electronic struct. and geometry, Hartree-Fock instability 0-69055  
 direct orbital optimisation for MC SCF theory by unitary transformations 0-87049  
 electronic structure calcs., self-consistent, accelerating convergence of iterative process 0-87037  
 electrostatic interactions in liquid state, effect on frontier orbitals and chem. reactivity 0-84046  
 equations of state of crystals with strong sixth-order anharmonicity 0-92637  
 ethane, rot. barriers, MS-SCF-X<sub>α</sub> calcs. 0-106267  
 ethene, dipole polarisability, finite-field SCF MO calcs. 0-83255  
 ethylene, polarisability, nonlinear elec. susceptibility, SCF calcs. 0-95547  
 ethylene ozonide, ab initio gradient and MC SCF calc., conformational anal. 0-83290  
 excited states, perturbation and SCF calcs. 0-102455  
 first-row atoms, SCF calcs. using cusped-Gaussian basis sets, polarisation effects 0-74118  
 first-row transition metal ions, core ionised states, ΔSCF MO calcs. 0-78523  
 floating orbital geometry optimisation with floating outer-shell basis functions 0-95517  
 fluoroformaldehyde, pot. energy surface characts., substitution effect 0-89505  
 formaldehyde, electronic struct., dipole moments, mol. polarisability, force fields, ab initio calcs. 0-78531  
 formaldehyde, mol. Rydberg S→S and S→T transitions, semi-empirical SCF MO calc. 0-91453  
 formamide, force consts. and dipole moment derivatives, ab initio MO calcs. 0-95521  
 formamide-glyoxal, charge transfer theory, Mulliken population, ab initio calc., multiconfiguration scheme 0-106392  
 general SCF coupling operators, arbitrariness 0-99439  
 guanine, tautomeric forms protonation, ab initio HF Roothaan SCF calcs. 0-78534  
 hexafluoroethane, rot. barriers, MS-SCF-X<sub>α</sub> calcs. 0-106267  
 hexatriene, polarisability, nonlinear elec. susceptibility, SCF calcs. 0-95547  
 hydrocarbons, liq., Compton profiles, bond additivity 0-93423  
 hydrocarbyl radicals embedded in naphthalene cryst., optical transition energies and ionisation energies 0-78595  
 β-hydroxy acrolein, lower excited states, electronic struct. and H-bonding, ab initio SCF and CI calcs., photochemical mechanism 0-83278  
 para-hydroxyaniline, mol. complex., electronic struct., basis set and correlation effects 0-91436  
 inversion geometry, ab initio SCF calcs., basis set effects 0-78532  
 iterative sequences, convergence accel. 0-91435  
 k-particle generalisation and new generalisation of SCF type theories 0-102432  
 β-lactam antibiotics, ab initio SCF-MO-LCAO calcs., amidic bond breaking, methoxy substitution effect 0-78533  
 liver alcohol dehydrogenase, proton relay system, SCRF PCE theory, CNDO/2 calcs. 0-83325  
 MCSCF and CI wave functions, two-particle density matrix and graphical unitary group approach 0-63558  
 metal atom cluster compounds, bonding calc. using d-orbital overlap model, SCF-Xα-SW calc. 0-102595  
 metallic ultrathin filaments, dielectric and superconducting fluctuations, Peierls transition (*Russian*) 0-65742  
 methane, core 1s shakeup study, XPS and Xalpha calcs. 0-69064  
 methane, orbital relax. energy for single and double ions. from valence shells 0-106253  
 methane, pot. energy curves, Monte Carlo and SCF LCAO MO calcs. 0-63526  
 methane, SCF calcs. including polaris. functions 0-87034  
 methyl halides, mol. force field at SCF ab initio levels, quantum-mechanical calc., LCAO-MO method 0-106319  
 methylamine, affinities for H<sup>+</sup>(Li<sup>+</sup>)(K<sup>+</sup>)(CH<sub>3</sub><sup>+</sup>), ab initio SCF calculations 0-102443  
 molecular static polarisability, ab initio SCF wave functions 0-74106  
 molecules, relativistic Dirac-Fock multiconfig. SCF calcs. 0-99455  
 molecules involving B and C atoms, self-consistent charge calcs. of core-electron binding energy shifts 0-69084  
 dimolybdenum tetraformate, metal-metal bond energy, SCF-Xα-SW calcs. 0-78538  
 multi-conf. SCF super-CI calc., density matrix formulation 0-78547  
 multiconfigurational Hartree-Fock procedure, second-order, 2-electron integral transformations 0-87045  
 naphthalene, dipole polarisability, finite-field SCF MO calcs. 0-83255

## SCF calculations continued

open-shell system, polarisability and mag. susceptibility calc. by SCF and CI method 0-99443  
 Peierls one dimensional model, exact solution, electron spectra, static lattice deformation (*Russian*) 0-70609  
 periodic systems electronic struct., LCAO SCF ab initio HF calcs. method 0-65419  
 phenol-phenyl complex, electrostatic mol. pot. contour maps, MODPOT and VRDDO calcs. 0-102463  
 polycyclics, fluorinated, electronic struct., tight-binding LCAO-SCF-MO calcs., prep. 0-70591  
 polymers, adsorption of molecules, Green matrix local impurity SCF calcs. 0-92778  
 protein internal charge transfer, ascorbic acid adduct model systems, SCF calc. 0-69072  
 pyridines, monosubst., H<sub>2</sub>O complexes, n-π\* transitions, H bonding, MO theory 0-95550  
 relativistic self-consistent field theory for open-shell molecules 0-95518  
 SCF-Xα-scatt. wave calcs. for photoionisation cross sections and asymmetry parameters 0-63542  
 second-row hydrides, nucl. spin-spin coupling consts., ab initio calcs. 0-95647  
 self-consistency accel. procedure 0-78529  
 semiconductor, deep transition metal impurity states, SCF CNDO cluster calcs. 0-100442  
 semiconductor, defect electronic struct., SCF method 0-80208  
 SiH<sub>4</sub>, SCF calcs. including polaris. functions 0-87034  
 struct. and props., SCF calcs. 0-106260  
 TCNE-benzene, charge transfer theory, Mulliken population, ab initio calc., multiconfiguration scheme 0-106392  
 thioformaldehyde, electronic struct., dipole moments, mol. polarisability, force fields, ab initio calcs. 0-78531  
 thiourea, struct., hydration, ab initio SCF calcs. 0-58142  
 trimethylamine, SCF calcs. including polaris. functions 0-87034  
 twisted conjugated molecule, zwitterionic excited states investig. 0-58179  
 two-level atoms, multiphoton cooperative radiation, SCF approx. calcs. 0-95856  
 Ag (110), electrorreflectance, surface state contrib. 0-80755  
 Al<sub>2</sub>(Al<sub>2</sub>)<sub>2</sub> configurations, ab initio study, LCAO, STO, MO-SCF and CI calcs., binding energy (*French*) 0-91447  
 α-Al<sub>2</sub>O<sub>3</sub>, charge distribution determ., SCF calc., Slater-type orbitals, Madelung type const. 0-107100  
 β-Al<sub>2</sub>O<sub>3</sub>-Na<sub>2</sub>O, adsorption of Na, surface electronic struct. calcs. 0-75431  
 Ar+HHe<sup>+</sup>, ab initio pot. energy data, SCF-LCAO calcs. 0-63530  
 Ar<sub>2</sub> van der Waals dimer, intermol. pot., SCF CI ab initio calcs. 0-106274  
 Ar.HCl, Van der Waals mols., SCF energies and dispersion forces 0-74279  
 Ar.HF, Van der Waals mols., SCF energies and dispersion forces 0-74279  
 Ar.H<sub>2</sub>O, Van der Waals mols., SCF energies and dispersion forces 0-74279  
 AsF<sub>3</sub>, inversion barrier, STO SCF calc. 0-63567  
 Au (110), electrorreflectance, surface state contrib. 0-80755  
 Au<sub>2</sub><sup>+</sup>, ab initio SCF calcs. using relativistic effective core pot. 0-95524  
 BH<sub>3</sub>, electronic wave function determ., genealogical technique using Clebsch-Gordan coeff. 0-95529  
 B<sub>2</sub>O<sub>3</sub>, bipyramidal struct., stability, ab initio SCF-MO calcs. 0-99446  
 Be<sub>4</sub> (Be<sub>4</sub>)<sub>2</sub>, atomic clusters, electronic struct., LCAO-MO-SCF and HF calcs. 0-63880  
 BeO, MCSCF and CI calcs. 0-95526  
 Br<sub>2</sub>, model potential SCF calcs. 0-95528  
 BrF<sub>3</sub>, electronic struct. and ionisation pot., SCF DV Xalpha method 0-69057  
 BrF<sub>5</sub>, electronic struct. and ionisation pot., SCF DV Xalpha method 0-69057  
 C<sub>2</sub>(C<sub>2</sub>)<sup>+</sup> pot. energy curves calc. using SCF, MCSCF and CI methods, dissociation energies, bond lengths, electron affinity 0-95523  
 CH radical, SCF theory, multiconfig., direct orbital optimisation 0-87049  
 C<sub>2</sub>H<sub>3</sub><sup>+</sup>+HF, interaction, struct. and stability, ab initio calcs. 0-58347  
 CO, polarisability derivatives, bond length depend., SCF and CI calcs. 0-58162  
 CO<sub>2</sub>, stretch-stretch interaction force const., electron correlation influence, ab initio CI study 0-58161  
 CO<sub>2</sub>+He, rot. inelastic collision, ab initio SCF, electron gas and pot. energy surfaces 0-83468  
 Ca, forbidden transitions, radiative lifetimes, MCSCF and CI calcs., time of flight spectra for metastable state 0-91498  
 CaH, spin doubling, SCF calcs. 0-95649  
 Cl<sub>2</sub>, model potential SCF calcs. 0-95528  
 Cl<sub>2</sub>, one electron props. and polarisability, SCF and CI calcs. 0-58159  
 ClCO radical, struct. and props. calcs. 0-74112  
 ClO<sub>4</sub><sup>-</sup>, dummy spheres in SCF Xalpha calcs. 0-69056  
 ClO<sub>4</sub><sup>-</sup>, ionisation energies, SCF-Xα transition state calcs. 0-74115  
 ClOO radical, struct. and props. calcs. 0-74112  
 Co, Auger spectrum, ab initio MO LCAO SCF CI calc. many electron contribs. 0-87169  
 CrOCl<sub>3</sub>, electronic structure and valence ionisation energies, obs. by ab initio and SW-Xα methods 0-69073  
 Cs<sub>2</sub><sup>2+</sup>, low-lying states, MC SCF+CI 0-69053  
 Cu (110), electrorreflectance, surface state contrib. 0-80755  
 CuCl<sub>4</sub><sup>-</sup>, ESCA satellite intensity, ab initio SCF calcs. 0-74103  
 CuCl<sub>2</sub>(Cl<sub>4</sub><sup>2-</sup>)(Cl<sub>4</sub><sup>4-</sup>), electronic struct. studies by SCF, MSXα and INDO method 0-74119  
 CuF<sub>4</sub>(F<sub>4</sub><sup>4-</sup>), electronic struct. studies by SCF, MSXα and INDO method 0-74119  
 D<sub>3</sub> Rydberg states, spectroscopic B<sub>0</sub> consts. 0-74109  
 F<sub>2</sub>, electron impact excitation, dissociation of lowest electronic state 0-63839  
 FCO radical, struct. and props. calcs. 0-74112  
 F<sub>2</sub>O, geometry, electron spectrum, vert. ionis. pot. ab initio calc. 0-58187  
 FOO radical, struct. and props. calcs. 0-74112  
 FSO (FOS), struct. and props., SCF calcs. 0-106260  
 FSS, struct. and props., SCF calcs. 0-106260  
 GeH<sub>3</sub><sup>+</sup>, electronic struct., electron affinity, inversion barrier, ab initio SCF Gaussian basis calc. 0-63552  
 Ge<sub>2</sub>H<sub>6</sub>, rot. barriers, MS-SCF-X<sub>α</sub> calcs. 0-106267  
 H atom finite chains, HF solns. stability and symmetry breaking, independent particle model calcs. 0-87035

## SCF calculations continued

- H<sup>+</sup>+CO (<sup>1</sup>Σ), ground state pot. energy surface, ab initio SCF calc., protonated equilib. geometry 0-83301  
H<sub>2</sub> molecule dimer, ab initio SCF intermolecular interaction energy calcs. 0-78537  
H<sub>2</sub>, relativistic Dirac-Fock multiconfig. SCF calcs. 0-99455  
H<sub>2</sub>-H<sub>2</sub> intermol. pair pot., ab initio SCF-CI surface 0-91457  
H<sub>3</sub>, Rydberg states, spectroscopic B<sub>0</sub> consts. 0-74109  
HCN, Fermi and Coulomb correl. holes, SCF and CI wave functions 0-69085  
HCN<sup>+</sup>, <sup>2</sup>Σ<sup>+</sup> and <sup>2</sup>Π states, SCF and CI calcs. for determ. optimum linear geometries, bond angles calc. 0-74114  
HCN-CO complex, charge transfer theory, Mulliken population, ab initio calc., multiconfiguration scheme 0-106392  
HCl, one electron props. and polarizability, SCF and CI calcs. 0-58159  
HF, orbital relax. energy for single and double ions. from valence shells 0-106253  
HF, SCF theory, multiconfig., direct orbital optimisation 0-87049  
HF-HCl, SCF energy hypersurface, stationary points, thermodynamics of form. 0-102436  
HF+Li→LiF+H, pot. energy surface, SCF and CI calcs. 0-71904  
HNC<sup>+</sup>, <sup>2</sup>Σ<sup>+</sup> and <sup>2</sup>Π states, SCF and CI calcs. for determ. optimum linear geometries, bond angles calc. 0-74114  
HO<sub>2</sub>, struct. and props., SCF calcs. 0-106260  
H<sub>2</sub>O affinity for Li<sup>+</sup>(Na<sup>+</sup>)(K<sup>+</sup>), ab initio SCF calcs. 0-58125  
H<sub>2</sub>O, core 1s shakeup study, XPS and Xalpha calcs. 0-69064  
H<sub>2</sub>O, mol. Rydberg S→S and S→T transitions, semi-empirical SCF MO calc. 0-91453  
H<sub>2</sub>O, multiplet states, SCF theory 0-69062  
H<sub>2</sub>O, orbital relax. energy for single and double ions. from valence shells 0-106253  
H<sub>2</sub>O, polarisability and mag. susceptibility calc. by SCF and CI method 0-99443  
H<sub>2</sub>O, SCF calcs. using cusped Gaussian basis sets, polarisation effects 0-74118  
(H<sub>2</sub>O)<sub>3</sub>, geometric config. energies, SCF LCAO MO calcs. 0-63551  
HSS, struct. and props., SCF calcs. 0-106260  
H<sub>2</sub>SiO, electronic struct., dipole moments, mol. polarisability, force fields, ab initio calcs. 0-78531  
He+ArH<sup>+</sup>, ab initio pot. energy data, SCF-LCAO calcs. 0-63530  
He+H<sub>2</sub>, pot. energy surface, ab initio calcs., van der Waals const. determ. 0-106372  
HeCN<sup>+</sup>, SCF calcs., dissoc. energies, rot. and hyperfine const. determ. 0-95531  
I<sub>2</sub>, model potential SCF calcs. 0-95528  
I<sub>2</sub>(I<sub>2</sub><sup>+</sup>)(I<sub>2</sub><sup>+</sup>), HF and SCF calcs., pot. curves, electron affinity and quadrupole moment determ. 0-95527  
Li isoelectronic sequence, self-consistent relativistic density-functional theory 0-91441  
Li<sup>+</sup>-H<sub>2</sub>O complex, charge transfer theory, Mulliken population, ab initio calc., multiconfiguration scheme 0-106392  
Li<sup>+</sup>+ether(thioether)(amide), pair pots., ab initio LCAO SCF MO calcs. 0-58184  
Li<sub>2</sub>, MCSCF and CI calcs. 0-95526  
Li<sub>3</sub>, electronic struct., SCF and SCF-CI calcs. 0-87044  
Li<sub>3</sub>, electronic struct., SCF and SCF-CI calcs. 0-87044  
Li<sub>3</sub>, electronic struct., SCF and SCF-CI calcs. 0-87044  
Li<sub>4</sub>, MCSCF and CI calcs. 0-95526  
LiBr, pair pot., dipole moment, polarisability tensor, bond length depend., finite field SCF calcs. 0-58127  
LiCl(n-1)<sup>+</sup>, energy cluster expansion convergence 0-91715  
LiH, direct optimisation of orbitals for multiconfiguration self-consistent field theory by unitary transformations 0-63544  
LiH, relativistic Dirac-Fock multiconfig. SCF calcs. 0-99455  
LiH, SCF calcs., undergraduate exercise 0-82597  
LiH-NH<sub>2</sub>(ethylene)(acetylene), struct. and props., SCF ab initio calcs. 0-106250  
(LiH)<sub>2</sub> complex, SCF interaction energy nonadditivity 0-91437  
Mg<sub>2</sub>(Mg<sub>2</sub><sup>+</sup>), atomic clusters, electronic struct., LCAO-MO-SCF and HF calcs. 0-63880  
Mo<sub>2</sub>, metal-metal bond energy, SCF-Xα-SW calcs. 0-78538  
Mo<sub>2</sub>Cl<sub>4</sub><sup>4-</sup>, metal-metal bond energy, SCF-Xα-SW calcs. 0-78538  
Mo<sub>2</sub>Cl<sub>6</sub><sup>4-</sup>, complexes, cluster exchange coupling consts. SCF-Xα-SW calcs. 0-74120  
Mo<sub>2</sub>X<sub>8</sub><sup>4+</sup> cluster cpds. (X=F, Cl, Br, I), SCF-SW-Xα calcs. 0-74276  
N<sub>2</sub>, ab initio MO-LCAO-SCF and Gordon-Kim intermolecular pot. for seven different orientations 0-95522  
N<sub>2</sub>, multi-config. SCF super-CI calc., density matrix formulation 0-78547  
N<sub>2</sub> SCF calcs. using cusped Gaussian basis sets, polarisation effects 0-74118  
N<sub>2</sub><sup>2+</sup>, low-lying electronic states, pot. energy curves calcs. by SCF technique, vibr. and ionisation consts. 0-69091  
NH<sub>3</sub>, affinities for H<sup>+</sup>(Li<sup>+</sup>)(K<sup>+</sup>)(CH<sub>3</sub><sup>+</sup>), ab initio SCF calculations 0-102443  
NH<sub>3</sub>, affinity for Li<sup>+</sup>(Na<sup>+</sup>)(K<sup>+</sup>), ab initio SCF calcs. 0-58125  
NH<sub>3</sub>, core 1s shakeup study, XPS and Xalpha calcs. 0-69064  
NH<sub>3</sub>, mol. Rydberg S→S and S→T transitions, semi-empirical SCF MO calc. 0-91453  
NH<sub>3</sub>, orbital relax. energy for single and double ions. from valence shells 0-106253  
NO<sub>2</sub>, ground state pot. surface, ab initio LCAO MO SCF calcs. 0-102461  
NO<sub>2</sub><sup>+</sup>, gas phase equilib. geometry, force consts., vibr. freq., dipole moment function MCSCF/CI calcs. 0-78520  
<sup>14</sup>N quadrupole coupling consts., ab initio calcs. 0-58283  
Ne, temp. perturbed Thomas Fermi eqn., variational principle 0-69074  
NeCN<sup>+</sup>, SCF calcs., dissoc. energies, rot. and hyperfine const. determ. 0-95531  
Ni (100), surface electronic struct., self-consistent local orbital calc. 0-65649  
Ni clusters local densities of states 0-88466  
Ni complex, nickel-bis-dithiolene, pseudopot. MCSCF and limited CI calcs. 0-83292  
Ni surface, adsorbed CO, N<sub>2</sub>, valence band photoemission, SCF MO CNDO calc. 0-100754  
O<sup>n</sup> (n=0 to 2), core binding energy shifts, ΔSCF calcs. 0-95558  
O<sub>2</sub>, Schumann-Runge continuum, oscill. strength and electron impact excitation 0-69121  
O<sub>2</sub>, <sup>2</sup>Σ<sup>+</sup>, state pot. energy curve, MCSCF calcs. 0-63565  
O<sub>4</sub> molecule, equilib. struct., vibr. freqs., SCF closed shell calcs. 0-74101

## SCF calculations continued

- O<sub>4</sub> molecule, SCF-CI calcs. 0-78517  
O<sub>2</sub><sup>2+</sup>, hypothetical, mol. self-consistent study, possible prep. method (French) 0-91717  
ONCl, vibr. freq., anharmonic ab initio/empirical pot. energy functions 0-99457  
PO<sub>3</sub><sup>3-</sup>, ionisation energies, SCF-Xα transition state calcs. 0-74115  
PbS(PbSe), ab initio SCF calcs. using relativistic effective core pot. 0-95524  
Pd<sub>3</sub>, ab initio relativistic core pot. studies of metal-metal bonding 0-106257  
PdH, ab initio relativistic core pot. studies of metal-H bonding 0-106257  
Pt<sub>2</sub>, ab initio relativistic core pot. studies of metal-metal bonding 0-106257  
PtH, ab initio relativistic core pot. studies of metal-H bonding 0-106257  
SO<sub>2</sub><sup>+</sup>, ionisation energies, SCF-Xα transition state calcs. 0-74115  
Si, isolated vacancy, electronic struct., SCF method 0-80208  
Si, solid, electron rearrangement after inner shell ionisation by heavy charge particle impact 0-87043  
Si<sub>2</sub>, electronic struct. and bonding, atomic effective pot. appl. 0-95745  
SiH<sub>4</sub>, SCF calcs. including polaris. functions 0-87034  
SiH<sub>4</sub>, rot. barriers, MS-SCF-Xα calcs. 0-106267  
(SiH<sub>3</sub>)<sub>3</sub>N, SCF calcs. including polaris. functions 0-87034  
SiH<sub>4</sub>(SiF<sub>4</sub>), electron rearrangement after inner shell ionisation by heavy charge particle impact 0-87043  
TCNQ, ab initio SCF LCAO band struct. calc. 0-70608  
TTF, ab initio SCF LCAO band struct. calc. 0-70608  
Te<sub>2</sub><sup>2+</sup>, pseudopot. SCF-MO calcs., spectrum assignments 0-83269  
ThF<sub>4</sub>(Cl<sub>4</sub>), electronic struct., MS-SCF-Xα calcs. and VUV photoelectron spectra 0-63710  
TiCl, ground-state props., Wannier functions, and electronic struct., ab initio self-consistent calc. 0-80178  
TiH, ab initio SCF calcs. using relativistic effective core pot. 0-95524  
<sup>92</sup>U, self-consistent relativistic density-functional theory 0-91441  
UF<sub>6</sub>(Cl<sub>6</sub>), electronic struct., MS-SCF-Xα calcs. and VUV photoelectron spectra 0-63710  
W(001), surface states and surface resonances, self-consistent electronic struct. 0-96960  
Xe, photoabsorption, local field effects 0-74151  
XeCl<sub>2</sub>, electronic structure, MSW-SCF-Xα method 0-78539  
XeF<sub>2</sub>, pseudopotential SCF-MO studies, equilib. struct., stretch-stretch interaction force const. 0-95525  
XeF<sub>4</sub>, pseudopotential SCF-MO studies, equilib. struct., stretch-stretch interaction force const. 0-95525  
XeF<sub>4</sub><sup>+</sup>, pseudopot. SCF MO studies, steric aspects of struct. and force fields, Jahn-Teller effect 0-99444  
XeF<sub>6</sub>, pseudopot. SCF MO studies, steric aspects of struct. and force fields, Jahn-Teller effect 0-99444  
XeF<sub>x</sub>, x=2, 4, 6, electronic structure, MSW-SCF-Xα method 0-78539
- scheduling**  
fusion reactor, TFR, preoperational test plan, manpower loading and scheduling 0-102340
- schizons** see elementary particle weak interactions
- schlieren systems**  
acousto-optic modulator efficiency optimisation, sound diffraction profile model and expt. 0-106615  
dielectric liquid, elec. stressed, motion due to Coulomb, electromech. forces, schlieren image obs. 0-100037  
discharges, selfluminous, schlieren system for time and space resolved photography 0-87471  
hydrophone, multimode, fibre-optic 0-102938  
multiple slit grating, optical inhomogeneity study (Hungarian) 0-69515  
photography of exhaled air, detection of abnormal nasal escape 0-64145  
projector for visualisation for information recorded on photothermoplastic material 0-87544  
refractive index gradient, chromatic variation meas. technique 0-74471  
shell target monitoring by X-ray Schlieren method 0-86263  
sound-intensity meas. by schlieren optical filtering for light diffracted from US beam 0-87672  
supersonic air flow through high press. gas valves into atm., noise and flow pattern obs. 0-59067  
vortex investigations, small inner diameter fluid jets, appl. schlieren photography 0-74935
- Schottky anomaly**  
ytterbium ethyl sulphate, crystal field effects on mag. and hyperfine props. of Yb<sup>3+</sup> 0-97101  
BaCl<sub>2</sub>(F<sub>2</sub>), sp. ht. meas., Schottky-type diffuse phase transitions, defect form. energies and entropies 0-107441  
HoRh<sub>2</sub>B<sub>4</sub>, low temperature magnetic properties 0-88728  
Nd(OH)<sub>3</sub>, heat capacity from 10 to 350K, lattice and Schottky contribs. 0-84300  
PbF<sub>2</sub>, sp. ht. meas., Schottky-type diffuse phase transitions, defect form. energies and entropies 0-107441  
PrIr<sub>2</sub>(Pt<sub>2</sub>)(Rh<sub>2</sub>)(Ru<sub>2</sub>), hyperfine sp. ht. and magnetisation meas. at 4.2K 0-75775  
SrCl<sub>2</sub>, sp. ht. meas., Schottky-type diffuse phase transitions, defect form. energies and entropies 0-107441  
Tb(OH)<sub>3</sub>, heat capacity from 10 to 350K, lattice and Schottky contribs. 0-84300
- Schottky-barrier diodes**  
see also semiconductor-metal boundaries  
charge carrier speed, p-n vs. Schottky diodes, for various appls. (Dutch) 0-65662  
deep impurity levels, spectroscopic determination by compensation method 0-108229  
III-V semiconductor based layered multielectronic systems, electronic process investig. survey (Russian) 0-107891  
interfacial layer theory, surface fixed charge, voltage drops 0-96967  
IR capacitive mixing and detect. at high, intermediate or modulation freqs. 0-77864  
magnetodiode, integrated mag. sensor Si on sapphire 0-68223  
metal-semiconductor junctions, fabrication aspects 0-88632  
one-sided abrupt junctions, normalized representation of avalanche breakdown behaviour 0-65666  
quantum noise at low temperature 0-103733  
resonant tunnelling spectroscopy, deep centre detection 0-96968  
solar cell, doping density effect on efficiency 0-101100  
solar cells, back-illuminated, theoretical performance 0-61345  
solar cells, efficiency depend. on thickness of interface layer 0-76637



**Schottky-barrier diodes continued**

- solar-cells, barrier height change and current transport in presence of interfacial layer 0-61353
- superconducting, space appl. 0-85836
- thermally degenerated Schottky diodes, resonant tunnelling 0-100503
- Al/GaAs contacts, metallization of surfaces covered with adsorbed S (French) 0-107909
- Al-poly-Si Schottky-barrier solar cells, grain boundary effects on electrical behaviour 0-85279
- AlGaAs laser array on Si heat sink, optical power detection 0-74383
- Al<sub>0.5</sub>Ga<sub>0.5</sub>As epitaxial film based device, microstruct., effect on elect. characts. (Russian) 0-107671
- Al<sub>0.5</sub>Ga<sub>0.5</sub>Sb-Pd contacts, struct., preparation elec. props. 0-65684
- Al<sub>0.5</sub>Ga<sub>0.5</sub>Sb-Pd contacts, band gap depend. of barrier height 0-65685
- Au/n-TiO<sub>2</sub> Schottky diodes, I-V and C-V characts. 0-96988
- Au-Al<sub>0.5</sub>Ga<sub>0.5</sub>As -GaAs heterojunction Schottky-barrier solar cells, barrier height enhancement 0-85284
- Au-CdTe, fabrication and characterisation (German) 0-89151
- Au-CdTe-Au structure, current transport props. 0-80408
- Au-Ga<sub>0.5</sub>Al<sub>0.5</sub>As Schottky diodes, band struct. from I-V, C-V meas. 0-96989
- Au-n-AlGaAs-n-GaAs Schottky-barrier solar cells, band readjustment effect 0-81458
- Au-ZnS electrolum. Schottky barrier diode, S<sup>+</sup>-implanted, blue emission 0-76082
- CdS-Cu<sub>2</sub>S junctions, carrier trap density, deep level defects 0-107801
- Cu<sub>2</sub>O-Cu diode junction, Schottky barrier, electronic structure and minority carrier diffusion length (French) 0-65682
- GaAs epitaxial film based device, microstruct., effect on elect. characts. (Russian) 0-107671
- GaAs epitaxial layers, surface impurity gradients, Schottky barrier capacitance meas. 0-70782
- GaAs films for solar cells appl., deposition and characterisation 0-84853
- GaAs Schottky diode, influence of  $\gamma$ - and electron irradiated on recomb. characts. near GaAs surface 0-71478
- GaAs, under high neutron fluence, current transport 0-65679
- GaAs-metal contacts, use of Ga to eliminate large As loss peaks 0-80370
- n-GaP, Schottky barrier height data for several contact systems 0-60080
- Ge-metal Schottky barrier photodetectors, near IR interband transitions and optical parameters 0-73449
- Hg-InP Schottky-barrier diode, contact times, I-V characts. 0-96971
- IrP detector, unbiased, operation in submm. wave region 0-105707
- LiNbO<sub>3</sub>-gap coupled Schottky diode memory correlator, grating coupled optical imaging 0-64143
- Ni-Pt silicide Schottky diodes, current-voltage characts. and comp. profiles 0-84508
- NiSi, parallel contacts, Schottky barrier height meas. 0-96965
- PbS<sub>0.9</sub>Se<sub>0.1</sub>, multispectral photovoltaic IR detectors 0-105710
- Pb<sub>0.9</sub>Sn<sub>0.1</sub>Se, multispectral photovoltaic IR detectors 0-105710
- Pd-W, substrate temp. influence on shallow contact formation on Si 0-96963
- Pt-Si thermally degenerated Schottky diodes, resonant tunnelling 0-100503
- Pt-W, substrate temp. influence on shallow contact formation on Si 0-96963
- PtSi film formation by ion sputtering and annealing, form. and exam. problems 0-100782
- PtSi, parallel contacts, Schottky barrier height meas. 0-96965
- PtSi Schottky-barrier monolithic IRCCD focal plane 0-86427
- Si, electron beam scan annealed, deep levels 0-65481
- Si:H, amorphous, band tail absorpt., photocurrent meas. for Schottky barrier solar cell 0-60032
- Si:H, amorphous, Schottky diodes, elec. props., light-induced effects 0-103741
- Si:H, amorphous Schottky solar cells, prep. and characts. of diode RF reactive cathodic sputtered films (French) 0-61347
- Si:Sb, low energy ion implantation Schottky barrier diodes and resistors 0-88177
- Si/In-(Cd), Si/Cd Schottky contacts, electrochemically deposited 0-88633
- n-Si-Cu Schottky contacts, electrochem. deposition, barrier height and ideality factor 0-75641
- Si-Pd<sub>0.5</sub>Si<sub>0.5</sub>, amorphous, Pd<sub>2</sub>Si layer form., shallow contact 0-103586
- SnO<sub>2</sub>-copper phthalocyanine-Ag systems, elec. and electroluminescent behaviour 0-80864
- ZnAs, Schottky diodes, elec. and photoelec. props., excitons 0-65653
- ZnPt, Schottky diodes, elec. and photoelec. props., excitons 0-65653
- ZnTe single crystal, Schottky-barrier diodes and ohmic contacts props. 0-96987

**Schottky barriers** see *Schottky effect***Schottky defects**

- KCl, ionic cond., defect parameters, diffusion coeffs. 0-79978
- KCl:Sr<sup>2+</sup>(SO<sub>4</sub><sup>2-</sup>), ionic cond., defect parameters, diffusion coeffs. 0-79978
- KCl:Sr<sup>2+</sup>(SO<sub>4</sub><sup>2-</sup>), defect parameters, self-consistent set, ionic cond. meas. 0-107487
- LaF<sub>3</sub>, ionic transport, NMR and cond. studies 0-107555
- NaI:Ca<sup>2+</sup>, pure and doped, lattice defects, entropy and enthalpy of formation and migration 0-96687
- PbBr<sub>2</sub>(Cl<sub>2</sub>)(I<sub>2</sub>), ionic cond. and activation volumes, high press. effects 0-100353
- ZnO, defect struct. calc., doping effects 0-107218

**Schottky effect**see also *work function*

- degenerate semiconductor-metal Schottky barriers, low temp. capacitance 0-60075
- diode, interfacial layer theory, surface fixed charge, voltage drops 0-96967
- grain boundary diffusion, chemical reactions, contamination, AES and SIMS 0-72066
- lead phthalocyanine:O<sub>2</sub>(I), Schottky barrier effect on AC current response 0-75623
- metal-semiconductor contacts with thin interfacial films 0-96969
- metal-semiconductor interface, photoelectron injection, quantum mech. transmission and optical phonon scatt. 0-84511
- metal-semiconductor Schottky barrier junctions, characterisation and appl. 0-92971
- minority carrier lifetime-meas. technique using SEM-electron beam induced current 0-59999
- n-p structure, Schottky-gate, depletion layer, pot. fluctuations 0-88512

**Schottky effect continued**

- polyacetylene films, AsF<sub>6</sub> doped, photocond. and junction props. 0-70770
- semiconductor characterisation, cond. type determ. by pot. profiling 0-73387
- semiconductors, isothermal and non-isothermal C-V deep level meas. using Schottky contacts 0-88515
- silicide contacts on Si, Schottky barriers, elemental description 0-60085
- thin film technology, appls. in energy, optics, and electronics, review 0-78932
- transition metal silicides, refractory for ICs, review 0-100820
- Al-Al<sub>0.5</sub>O<sub>1.5</sub>-GaAs backwall MIS Schottky barrier solar cell, anal. model 0-85289
- Al-SiO<sub>2</sub>-(p-)Si barrier structs., minority carrier injection ratio meas., MIS solar cell model 0-93007
- Al<sub>2</sub>O<sub>3</sub>, MIS Schottky structures, photovoltaic response 0-101115
- Au-AlGaAs-GaAs heterojunction Schottky barrier solar cells, barrier height enhancement 0-94071
- Au-Ga<sub>0.5</sub>Al<sub>0.5</sub>Sb Schottky barriers, barrier height 0-96986
- Au-GaAs Schottky barrier solar cells, effect of interfacial oxide layer on cell characts. 0-61365
- Au-n-Si Schottky barrier solar cells, recombination in space charge region 0-61351
- Au-W-GaAs Schottky barrier, elec. and chem. props., AES 0-96973
- CdS-Au contacts, electronic states, vacuum UV photoelectron spectra 0-70827
- CdSe-Au contacts, electronic states, vacuum UV photoelectron spectra 0-70827
- p-CdTe, barrier heights of metals on etched surface 0-80378
- CdTe-Au contacts, electronic states, vacuum UV photoelectron spectra 0-70827
- Cu-CuGaSe Schottky barriers, electrical and photovoltaic props. 0-92940
- GaAlAs, surface vacancies, bound state energy levels calc., rel. to Schottky barrier formation 0-80340
- GaAs anodic oxide, states, electrochemical meas. 0-80176
- GaAs MIS solar cells, effects of thin oxide layers on characts. 0-89624
- n-GaAs, metal filmed photoelectrochemical cell, energy conversion characts. 0-101118
- GaAs, Schottky barrier electrorefl. meas. by sample rotating technique 0-60544
- GaAs Schottky barrier structure, defects from proton irradiation, thermal transients and optical capacity (French) 0-59534
- p-GaAs, Schottky barriers on polar (111) and (111) surfaces 0-88631
- GaAs Schottky-barrier, linear and quadratic electroreflectance, minicomputer-controlled meas. 0-97241
- n-GaAs, spectra, light induced, electrolyte and Schottky barrier techniques of meas. 0-76046
- GaAs thin film polycrystalline Schottky barrier solar cells, grain boundary chemistry 0-94067
- GaAs:Cr, deep levels, wavelength-modulated photocapacitance spectroscopy 0-76055
- GaAs:Te Schottky barrier solar cells, diffusion length determ. using minority carrier SEM 0-61359
- GaAs/anodic oxide interface, characterisation of proposed model 0-103754
- GaAs-Au polycrystalline Schottky barriers, transition with grain size from electrode-limit to bulk-limited cond. 0-65676
- GaAs-Au(Ag) Schottky barrier solar cells, interface problems, AES, SIMS and XPS study 0-89627
- n-GaAs-metal Schottky barrier, ultrathin native oxide, thickness determ. from C-V and photoresponse meas. 0-70821
- p-GaP, Schottky barriers on polar (111) and (111) surfaces 0-88631
- p-GaSe, back wall Schottky barrier cells, diffusion length, RT spectral response meas. 0-107806
- N-Ge, electrorefl. spectra, light induced, electrolyte and Schottky barrier techniques of meas. 0-76046
- Ge-metal interface, internal photoemission mechanisms 0-60077
- n-Ge-metal Schottky barrier contacts, IR optoelectronic props., quantum detector appls. 0-75640
- Ge-Si<sub>3</sub>N<sub>4</sub> system, potential barriers determ. from photoelectron carriers trapping 0-103756
- Hg-InP Schottky-barrier diode, contact times, I-V characts. 0-96971
- InP, surface vacancies, bound state energy levels calc., rel. to Schottky barrier formation 0-80340
- InP thin films for photovoltaic devices 0-93972
- InP-In<sub>0.5</sub>Ga<sub>0.5</sub>As alloy photocathodes, semiconductor photoemitters, field-assisted, 1-2  $\mu$ m range 0-97396
- LaAl<sub>2</sub>, doped with Tb, Nd, or Pr, crystal field effects, tunnelling within mK range 0-70907
- LaPb<sub>3</sub>, doped with Tb, Nd, or Pr, crystal field effects, tunnelling within mK range 0-70907
- LaSn<sub>3</sub>, doped with Tb, Nd, or Pr, crystal field effects, tunnelling within mK range 0-70907
- NiSi, parallel contacts, Schottky barrier height meas. 0-96965
- PbI<sub>2</sub>-Ag(Au)(Cu), light sensitive, internal photoelectric emission 0-107910
- Pd-W, substrate temp. influence on shallow contact formation on Si 0-96963
- Pt-Si Schottky barriers on Si, laser formation and characts. 0-60079
- Pt-W, substrate temp. influence on shallow contact formation on Si 0-96963
- PtSi, parallel contacts, Schottky barrier height meas. 0-96965
- Si MIS solar cells with Cr, Hf, Be, Sc and Y as barrier forming metals, expt. investigation 0-94077
- Si polycrystalline-metal Schottky barrier solar cells, elec. and photovoltaic contact props. 0-93936
- n-Si wafer, trap centres of self-interstitials 0-75516
- Si:H, amorphous, sputtered Schottky\* barrier solar cells, conduction mechanism 0-104506
- Si-metal contact, transport theory of Schottky barriers 0-80372
- n-Si-Pd<sub>2</sub>Si contact, interface struct. and Schottky barrier height, correl. obs. using TEM 0-100504
- n-Si-Re(Os) Schottky contact barrier height meas. 0-65675
- Si-refractory metal contacts, thermally cleaned surfaces 0-100521
- SiH, amorphous films, internal photoemission, metal contacts 0-96964
- SiO<sub>2</sub> thin film dielec., in MIM struct., interfacial props. rel. to non-stoichiometry 0-80399
- Ta-Ta<sub>2</sub>O<sub>5</sub>-InP thin refractory MIS struct. deposition 0-75647
- Te-Se-Cd rectifying sandwich structs., elec. forming action, Schottky junction form. 0-80371
- TiO<sub>2</sub> film, ion plated, DC cond. study 0-100457
- TiW-TiO<sub>2</sub>-InP thin refractory MIS struct. deposition 0-75647

**Schottky effect continued**

Tm<sub>2</sub>O<sub>3</sub> film, between Al electrodes, prep. and elec. props. 0-60103  
ZnSe layers, cond. type determ. by pot. profiling 0-73387

**Schottky gate field effect transistors**

Josephson FET, hybrid, feasibility 0-80451  
Ga<sub>1-x</sub>Al<sub>x</sub>As low threshold stripe geometry DH laser, Be implanted, on semi-insulating substrate 0-69409  
GaAs, monocrystalline, lateral definition, prep. by MBE 0-108357  
GaAs type FET with buffer, bias effects due to deep centres in struct. (French) 0-107917  
GaAs-W-Au Schottky barrier FET, elec. and chem. props. 0-96973  
InP, VPE growth for MESFET's 0-103602  
SiC, growth techniques of epitaxial layers 0-108360

**Schottky noise** *see random noise***Schrodinger equation**

3-body problem with one infinite mass particle, Schrodinger and integral eqn. soln. equivalence 0-77636  
algebra of three-dimensional generalized functions, associative, involution and differentiation 0-68080  
anharmonic oscillator, three-dimensional, radial Schrodinger eqn. 0-86144  
asymptotic distribution of eigenvalues for the multidimensional Schrodinger equation 0-94985  
atom+diatom, energy correction of infinite order sudden approx., improved phase shift approach 0-95710  
atomic scatt. factors and momentum densities, asymptotic form 0-74105  
atoms, P-state collisions, quantum mechanical treatment, angular momentum coupling 0-99541  
attractive potential,  $r^{-(s+2)}$  type, SL(2,R) acting on quaternions 0-57125  
baryon spectroscopy and photoproduction couplings using new baryon wavefunctions 0-102016  
bistable potentials, diffusion, Schrodinger and Fokker-Planck equations 0-62528  
bound state wavefunctions, normalisation, semiclassical results 0-86128  
bound states in attractive potentials, existence condition (French) 0-57113  
box approach to resonance 0-98824  
Brownian motion interpretation challenged 0-94974  
complex diffusion processes, transforms., and nonrelativistic quantum mechanics 0-82670  
construction of  $L^2$  dependent potentials 0-86129  
continuation property for hamiltonians 0-77642  
continuous singular spectrum of the Schrodinger operator 0-86138  
Coulomb potential, exponential cosine, critical screening parameter 0-82673  
coupled equations, perturbative method, piecewise constant reference potential 0-86111  
diatomic molecule, vibr. energies and functions, cubic splines method calcs. 0-78594  
double well Schrodinger operators 0-90698  
dynamical symmetries, rotationally invariant time-dependent potentials, degeneracy and dynamical algebras 0-62510  
education, Schrodinger eqn. solns. using approximate nucleon-nucleon and A-nucleon pots. 0-62429  
eigenvalues, perturbation theory calc. without complete set of eigenfunctions 0-105519  
eigenvalues of infinite multiplicity, existence theorem 0-94989  
electron nonlinear waves in strongly magnetised plasma 0-79472  
electron reflection and transmission through surface potential barrier 0-87998  
electron wave function in vicinity of planar defect 'on edge' 0-88002  
energy spreading in solns. to nonlinear eqn. 0-86147  
exact solutions for one-dimens. eqn. with continuous plus  $\delta$ -functions 0-98827  
exactly soluble Schrodinger eqn. with bistable pot. 0-67950  
exponential cosine screened Coulomb pot., s-states, Ecker-Weizel approx. calcs. 0-101732  
factorised completely X symmetric S-matrix characterisation, multicomponent field theories 0-105800  
fluid dynamical form of the linear and nonlinear Schrodinger equations 0-90720  
friction, stochastic quantisation, nonlinear wave eqn. 0-98825  
frictional quantum mechanical system, one-dimens. scatt. model for coherence in stopping power problem 0-101736  
functorial geometric quantization and Van Hove's theorem 0-86108  
Galilean invariant Schrodinger eqn., relativistic wave eqn. derivation, Lie algebra 0-105555  
gaseous dipolar media, semiclassical theory, appl. to gas laser 0-83586  
gaseous molecules, persistence of p, d, f and g orbitals, ang. functions, Schrodinger's eqn. and cardinal number anal. 0-102426  
Gel'fand-Levitan equation, non-self adjoint operators, eigenfunctions, spectral representations 0-86131  
Gel'fand-Levitan method as a generalized Jordan-Wigner transformation 0-77962  
harmonic oscillator, three-dimens., Green's function 0-73211  
harmonic oscillator wavefunctions, asymptotic behaviour 0-67979  
Hartree equations, time-dependent, global solutions, and nonlinear Schrodinger eqn. 0-73193  
heavy baryon spectroscopy in the QCD bag model 0-105866  
invariance algebras of Schrodinger and Dirac eqns. (Russian) 0-68081  
inverse scattering, one-dimens. Schrodinger eqn. pot. from S-matrix 0-57127  
inverse scattering in three dims. 0-86130  
inverse scattering problem, incorrect nature 0-86139  
ion cyclotron resonance spectrometry, collisionally damped ion motion 0-57419  
Jost solutions for Yukawa potentials 0-86132  
Langmuir collapse, dimensionality and dissipation 0-87880  
Langmuir plasma, self-magnetised collapse dynamics 0-92327  
layered crystal, wave functions, exciton spectrum, light absorpt. (Russian) 0-100436  
linear potential wavefunctions, generalised hypergeometric functions 0-62512  
local scaled Schrodinger relations and the virial theorem, kinetic energy operator 0-78527  
logarithmic Schrodinger equation, soliton dynamics 0-57130  
many body Schrodinger operators, ground state energy per particle 0-68064  
MISIM struct. inversion layer, symmetrical, carrier conc. calc. 0-75651  
modified Coulomb potentials, bounds for phase-shifts 0-57112

**Schrodinger equation continued**

molecules, composite particle, vibr. amplitude and vibr.-rot. anal. 0-74158  
multi-soliton solutions of a derivative nonlinear Schrodinger equation 0-105528  
multichannel scatt. theory for temp. depend. Hamiltonians, charge transfer problem 0-90695  
N-electron system, Schrodinger eqn. soln. using antisymmetrisation 0-106246  
non-Abelian phase factors, Yang-Mills Hamiltonian 0-73575  
non-Gaussian wave packet time evolution 0-57133  
non-local potentials and positive energy bound states 0-73200  
noninstantaneous  $O(p/c)$  relativistic effects in bound states and a covariant Schrodinger equation 0-73607  
nonlinear, classical systems with infinite set of conservation laws 0-86102  
nonlinear, constrained harmonic motion 0-77625  
nonlinear, in cylindrical symmetry, return and collapse of solns. 0-90711  
nonlinear, three dims. stability of solns. 0-57141  
nonlinear field eqn. and differential Schrodinger eqn. correction (French) 0-77637  
nonlinear field equations, quantum inverse scattering transform method, 2-D ice and ferroelectric lattices 0-68348  
nonlinear focusing and Kelvin-Helmholtz instability 0-83785  
nonlinear mixed eqn. and soliton solns., inverse method 0-68065  
nonlinear waves in cold plasma, classical Vlasov plasma description through quantum numerical methods 0-92288  
nonrelativistic one-dimensional problems, perturbation theory algorithm 0-82671  
nuclear potential, solitons as model 0-83081  
numerical integration leading to Bohr-Sommerfeld formula, alternative to JWKB calcs. 0-86119  
one-body approx., disordered system spectral props., Schrodinger eqn., random fields 0-90696  
one-dimensional model crystals, surface density of states, rel. to adsorbed molecule 0-107889  
one-dimensional motion, relation between phase function and Green's function 0-105543  
operators with long range potentials, spectral representations, book 0-73088  
oscillatory integral approach, semiclassical, linear and parabolic potentials 0-57124  
overlapping avoided crossings, rel. to quantum stochasticity 0-90694  
particle motion in ring shaped potential, spin-orbit coupling 0-101723  
perturbative methods of solution, choosing step sizes 0-86110  
perturbative numerical methods, local and accumulated truncation methods 0-62536  
plasma wave propagation, nonlinear Schrodinger equation, modified Zakharov-Shabat inverse scatt. problem 0-59200  
point spectrum, non-existence of eigenvectors of compact support (French) 0-68063  
potential problems, non-local, Perey effect, WKB method 0-68077  
potential well particle escape, time-depend. Schrodinger eqn. soln. 0-86118  
potential without spherical symmetry, sufficient condition for existence of bound states 0-68070  
prolongation structure for a nonlinear equation with explicit space dependence 0-82664  
quadratic Hamiltonians in phase space and their eigenstates 0-86127  
quantisation of matter without quantising related fields 0-105525  
quantum mechanical perturbation problems, resolution using integral eqn. 0-58112  
quantum three particle system, action-angle variables 0-95708  
quantum tunnelling, reaction coord. method 0-62500  
quark-quark interaction, phenomenological, from s-wave baryon spectrum 0-101984  
quasi-recurring energy leakage in the two-space-dimensional nonlinear Schrodinger equation 0-82676  
radial, fourth-order numerical method of soln. 0-86107  
radial Schrodinger eqn. global numerical soln. by second order perturbation theory 0-68079  
radial Schrodinger equation, eigenvalues, matrix elements, phase shifts 0-86133  
randomly fluctuating interaction term, uncertainty in nature 0-62499  
rearranged perturbation theory, nonlinear transformation 0-105542  
resolvent operator expansion, generalised method, Schrodinger eqn. soln. appl. 0-86126  
resonance theory in indefinite metric spaces 0-101730  
resonant states in the presence of Coulomb interactions, Schrodinger eqn. 0-91161  
scattering matrix for rapidly oscillating potentials 0-57126  
scattering problem with separable potentials 0-90708  
scattering theory and continuous spectra for class of strongly oscillating potentials 0-77638  
Schrodinger's variational quantisation method in stochastic framework 0-105532  
self-focusing of waves on deep water surface (Russian) 0-94536  
solution, hybrid method 0-94968  
spectral and scatt. theory, Schrodinger operator with singular attractive potential 0-86151  
spin particles, relativistic and Galilean wave eqns. 0-82672  
spinning particle in helical mag. field, nonrelativistic quantum theory 0-77651  
stability of self-adjointness of Schrodinger operators under positive perturbations 0-94990  
stationary connected multisoliton formations, Schrodinger eqn. with nonlocal nonlinearity (Russian) 0-57105  
stochastic action integral interpretation of quantum mechanical transformation function 0-77644  
stochastic resolution, analyticity and integrability, existence and uniqueness of soln. (French) 0-73195  
Stormer approach and the solution of two coupled Schrodinger equations 0-62526  
strong coupling QCD, variational approach, Schrodinger eqn. and effective Hamiltonian 0-95245  
three level system, interference between one and two photon processes, occupation probabilities 0-63965  
three-body problem, bound state eigenvalues lower bounds, upper bounds by Rayleigh-Ritz method 0-68068  
three-body problem with hard cores, 1-D, eigenvalue lower bounds 0-68069



**Schrodinger equation continued**

- three-body problem with hard cores, 1-D, reduction to 2-D Helmholtz eqn. 0-62523
- tight lower bounds to eigenvalues of the Schrodinger equation 0-94984
- time evolution operator in quantum mechanics 0-82610
- time recurrent behaviour in the nonlinear Schrodinger equation 0-90704
- transit time measures in scattering theory, time depend. Schrodinger eqn. 0-73194
- transmission coeff. for 1-D potential barrier, discretisation of Schrodinger eqn. 0-57123
- tunnelling phenomena, electronic energy distrib., Schrodinger wave eqn. solutions 0-103743
- von Neumann's measurement theory, phase relationship observation 0-105539
- NNN bound state problems, hyperspherical harmonic expansion, review 0-91136
- qq interactions and nonrelativistic quark model 0-73682
- Ag, electronic and mag. structure calcs. of mag. impurities 0-80213
- Cu, electronic and mag. structure calcs. of mag. impurities 0-80213
- H hyperfine splitting inside paraboloidal surfaces 0-99445
- H. Stark effect, iteration procedure for any field strength 0-69104
- He-He, energy and interaction potential of two ground-state atoms 0-63740
- $^3\text{He}$ , HCP, and adsorbed  $^3\text{He}$  with triangular lattice, exchange and mag. order 0-107606
- $^3\text{He}$ , liq., binding energy and effective interactions, interactions, variational calcs. 0-107596
- Hg atoms, elastic electron scatt., relativistic effects 0-102568
- NaF, quasimolecular struct. characts. of  $\text{NaL}_{\text{I,II,III}}$  absorpt. edge 0-93436

**Schrodinger equation** *see Schrodinger equation***Schwarz-Hora effect**

No entries

**Schwarzschild metric**

*see also cosmology*

- adiabatic accretion onto Schwarzschild black hole 0-77445
- black hole in radiation heat bath, stochastic evolution 0-85971
- black holes, stable circular orbits of test particles moving in equatorial plane 0-85970
- geodesic equation, rel. to Hawking's black hole area theorem 0-90468
- gravitational effects in 6-D general relativity, Schwarzschild metric, orbital precession 0-62550
- low-frequency solutions of the wave equations in Schwarzschild space 0-90743
- neutrino emission from cylindrically symmetric cluster of many gravitating masses 0-94707
- Schwarzschild-Kruskal space-time, role in developing Maxwell field non-zero vacuum expectation value 0-62828
- spherical cavity in an Einstein Universe 0-95013
- three body circular problem, periodic soln. of Schwarzschild's type 0-90730
- transformation to Kruskal-Novikov coordinate system 0-68098

**Schwarzschild space** *see Schwarzschild metric***Schwinger source theory**

- $\theta$ -vacua and confinement in two-dimensional models 0-77990
- $\phi^4$  theory, Euclidean, local existence of Borel transform of Schwinger functions 0-77932
- axial anomaly and meron configurations in 2-dimens. Euclidean Schwinger model 0-86545
- charge confinement, Schwinger model compared with (QED) $_4$  0-62902
- chiral rotations and the fermion-boson equivalence in the Schwinger model 0-101919
- equivalent boson theory, anomaly-free Ward-Takahashi identities 0-82873
- Euclidean Dirac field, local structure, Green's function method 0-68347
- Euclidean QED, on lattice, continuum limit, Schwinger functions, vacuum expectation values 0-73624
- evolution operator, quark struct. of states, two dimensional massless electrodynamics (Russian) 0-73630
- $g\phi^4$  quantum field theory, clusterlike expansion based on static ultralocal approx. 0-62839
- gauge field models, hard anomalies, cancellation by regularisation independent renormalisation scheme 0-77931
- gravitino, axial current anomaly, Faddeev-Popov ghosts 0-68120
- kink solutions on null plane, quantisation of 1+1 dimensional field theory 0-57505
- massless Euclidean Thirring field, four point Schwinger function, Lorentz group invariant forms (German) 0-90980
- multiparticle production in chromoelectric flux tube model in 1+1 dimens. field theory 0-73666
- order, disorder and generalized statistics 0-99055
- phase transitions, structural, first order, anharmonic oscillator model in (1+1) dimensions 0-86239
- QCD, two-dimens. with massless fermions in 1-1 dimensions 0-62926
- Ward identity, fermion axial vector current divergence, chiral invariant regulator field 0-57524
- Yukawa $_2$  model, Schwinger functions, analyticity and Borel type summability (French) 0-73570

**science education** *see education***scientific societies** *see societies***scintillation**

*see also phosphorescence; phosphors*

- astronomical bodies, determ. of stratosphere density inhomogeneity struct., Salyut obs. (Russian) 0-109186
- atmosphere scintillation, theory for millimetre and submillimetre wavebands 0-61884
- atmosphere turbulent boundary layer, scintillation intensity rel. to refr. index struct. charact. (Russian) 0-94597
- auroral zone, nighttime scintillation localised enhancements struct. 0-98506
- film scintillators for extended UV response Si detectors 0-86412
- glycine sulphate:L-alanine, unirradiated, optical spectroscopy of scintillations 0-80863
- inert gases, secondary scintillation under mag. fields, effect in gas proportional counters 0-58055
- interplanetary medium, velocity distrib. from scintillation obs. 0-105143
- interplanetary scintillation, appl. to solar wind recurrence determ. at high heliographic latits. 0-62106
- interplanetary scintillation, obs. rel. to solar wind plasma irregularities anisotropic struct. 0-67489

**scintillation continued**

- interplanetary scintillation spectra, radio spectrograph obs. 0-72741
- interstellar scintillation method for quasar and galaxy superfine radiostructure (Russian) 0-77297
- interstellar scintillation of pulsar radio emission, decorrelation bandwidth rel. to dispersion measure 0-85964
- interstellar scintillation of pulsar radio emission, scale height determ. 0-85965
- ionosphere, auroral zone, irregularities, simultaneous rocket probe, scintillation and incoherent scatter radar obs. 0-94640
- ionosphere, equatorial, scintillation obs. rel. to irregularity patch form., motion and decay 0-67456
- ionosphere, long-term 1.5 GHz amplitude scintillation meas. at mag. equator 0-85792
- ionosphere, scintillation, power law phase screen model, strong scatt. 0-61962
- ionosphere, scintillation, power law phase screen model, weak scatt. 0-61961
- ionosphere, severe disturbances of VHF and GHz waves during mag. storm 0-109302
- ionosphere, spaced scintillation obs. of ionisation irregularity drift motion 0-82133
- ionosphere F-layer, large-scale artificial inhomogeneity spectrum 0-98515
- ionosphere scintillations, assoc. with features of equatorial ionosphere 0-77191
- Jupiter ionosphere, radio spectral broadening obs. under weak scintillation conditions 0-109391
- planetary atmosphere, occulting spacecraft signal, turbulence determin. 0-94734
- pulsars, freq.-time struct., means for detecting interstellar electron density irregularities 0-101608
- quasars 3C 345 and 454.3, 102 MHz obs. of interplanetary scintillations (Russian) 0-94889
- radio sources, extragalactic, interplanetary scintillation rel. to existence of compact sources at low freqs. 0-90553
- radio sources, faint, interpretation of interplanetary scintillation meas. at 81.5 MHz 0-90554
- radio wave scintillation caused by equatorial ionospheric bubbles, model computations 0-94641
- radiowave scattered by 1-D power law phase screen 0-77220
- radiowave scintillation by ionosphere, statistical study 0-109306
- Saturn ionosphere, radio spectral broadening obs. under weak scintillation conditions 0-109391
- SN 1408, evidence for marked scintillation from Japanese guest star record 0-90641
- TGS:L-alanine, unirradiated, optical spectroscopy of scintillations 0-80863
- transionospheric radio wave scintillation, time struct. 0-90281
- VHF scintillation at high-latitude, analytical formulas 0-77224
- VHF scintillation at high-latitude near 70°W 0-77221
- VHF signal scintillation, from ETS-2 satellite, obs. of Waltair and Calcutta 0-109295
- CsI:Ti(Na), light yield under charged-particle bombardment 0-93409
- ZnWO $_4$ , scintillation characts. 0-66256

**scintillation chambers**

*see also scintillation counters*

- plastic ball multi-detector large angle spectrometer for Belavac 0-58028
- Kr photo-ionization proportional scintillation chamber 0-58056

**scintillation counters**

*see also photomultipliers; position sensitive particle detectors*

- analog mean-timer circuit for use with large-volume scintillation counters 0-63477
- bronchoscopic tumour localisation, small radiation detector probes, scintillation and semiconductor detectors 0-61676
- camera collimator image form. 0-89844
- camera field uniformity, global and local, statistical features 0-61677
- computerised tomography, positron emission, crystal size optimisation 0-61681
- computerised tomography, positron emission, data acquisition and processing electronics 0-61690
- EM shower detection in Pb glass blocks and scintillation hodoscope 0-58034
- external standards channels ratio, time-dependent change obs. 0-69036
- fibre-optic data transmission systems for plasma diagnostics 0-79571
- fission reactor loss of coolant studies, gamma densitometer detector comparison 0-57881
- gain stabilising scheme, gated radioactive source and broad digital window 0-63453
- gamma ray appl. to fluid density meas., theory, practices and appl. 0-73325
- gamma ray detection system, 3-D, fabrication and efficiency 0-63483
- gamma-ray astronomy, direction of high energy gamma-rays, active coded aperture imaging 0-62022
- gamma-ray spectrometers; calc. of radioactivity induced during spaceflight 0-102382
- gamma-ray telescope, spark chamber, scintillation counter time-of-flight system 0-62017
- gas proportional scintillation detectors with uniform electric fields, secondary scintillation model 0-74087
- gas scintillation proportional counter, gas fillings, preliminary studies 0-58054
- gas scintillation proportional counters, large vacuum photodiode imaging appl. 0-58050
- high pressure gas scintillation spectrometers for X-ray astronomy 0-105166
- high resolution gas scintillation proportional counter for studying low energy cosmic X-ray sources 0-58052
- imaging gas scintillation counter for X-ray astronomy 0-98551
- inert gases, secondary scintillation under mag. fields, effect in gas proportional counters 0-58055
- large-area gas-scintillation proportional counters for in-vivo measurement of plutonium and americium 0-58086
- liquid,  $^3\text{H}$  filled glass microsphere assay 0-63481
- liquid,  $^{45}\text{Ca}$  and  $^{23}\text{P}$  determination in biological samples by Cherenkov and liq. scintillation counting 0-98183
- liquid scintillation counting, conf., San Francisco, USA (Aug. 1979) 0-58074
- liquid scintillation techniques, appl. in low level activity assessment 0-58082
- liquid scintillation wastings, combustion system (Japanese) 0-63503

**scintillation counters** continued

- liquid scintillation wastings, vaporisation apparatus (*Japanese*) 0-63502  
 liquid-scintillation vial system, biphasic, for radiometry, modifications 0-101253  
 medicine, nuclear, digital filtering and edge detection 0-58065  
 medicine, nuclear, microprocessor systems for data acquisition, image processing, RIA anal., patient data retrieval 0-61670  
 mixed  $\beta$ - $\gamma$  dosimetry, ionisation and scintillation counters 0-57975  
 multiparameter gas-scintillation counter for heavy charged particles 0-58051  
 multistage parallel-serial time averaging filters to reduce time jitter in scintillation counter time meas. 0-102405  
 NE 111 scintillators, timing characts. exam. by single photon counting tech. 0-78494  
 neutron, with electronic device for rapidly changing the multiplication of a photomultiplier 0-74074  
 neutron counter, scintillation, photomultiplier noise characteristics 0-74077  
 neutron detectors with nanosecond time resolution 0-69029  
 optical wave propagating through turbulence, scintillations meas. detector aperture effect (*Slovak*) 0-63921  
 personal monitoring, effect of environmental radiation, thermoluminescent dosimeter (*Japanese*) 0-61707  
 phosphor, detection efficiency and performance estimation, of HV STEM 0-101899  
 Pioneer Venus Orbiter Gamma Burst Detector 0-67505  
 plastic cylinder, preparation gained physical parameters (*Czech*) 0-74076  
 portable microprocessor controlled neutron spectrometer, NE213 organic scintillator 0-58022  
 position sensitive, light signal propag. speed. for spatial resolution determ. 0-69028  
 position sensitive gas scintillation proportional counter for X-ray astronomy 0-58053  
 proportional response photon counter 0-87021  
 pulse shape analyser, effect of pulse pile-up on discrimination between neutrons and gamma rays 0-91402  
 quenching equation for scintillation, relationship between counting rate and quenching agent conc. 0-99411  
 rate dependent photomultiplier gain, time depend. 0-87020  
 sampling grid scintillator, calibrated intensity monitor for intense high energy charged particle beams 0-69034  
 solar gamma ray emissions study, Solar maximum mission, detector assembly and electronic assembly 0-63476  
 spectrometer stabilisation using LED reference light source 0-91365  
 stability analysis 0-99406  
 subnanosecond plastic scintillators 0-69037  
 time-of-flight electronics system for Mark II Detector 0-58093  
 tomograph, positron emission, ring detector, attenuation, scatt. radiation and random coincidences 0-61684  
 ultra-cold neutron scintillation detectors, optimisation 0-74090  
 ultra-fast detectors for laser fusion diagnostics, quenched plastic scintillator with microchannel plate photomultiplier 0-74084  
 X-ray- $\beta$  particle coincidence technique to exam.  $\beta$ -decay of  $^{252}\text{Cf}$  fission fragments 0-74094  
 $\text{Bi}_2\text{Ge}_2\text{O}_7$ , 38 mm scintillator,  $\gamma$ -ray response 0-58048  
 CSF detector, positron emission tomography 0-61688  
 $\text{CaF}_2\text{:Eu}$ , scintillation detector, in STEM 0-101897  
 $\text{CaF}_2\text{(Eu)}$  Phoswich detector, evaluation for  $^{90}\text{Sr}$  in situ anal. 0-58067  
 CsF scintillator, pot. advantages for a time-of-flight positron camera 0-81706  
 Fe scintillator calorimeter, segmented, structure of hadronic and EM showers 0-74078  
 Ge gamma camera, computer controlled, nuclear cardiology appl. 0-61682  
 $^{125}\text{I}$ , variation of  $\gamma$ -counting efficiency with sample composition 0-83238  
 $\text{Li}_2\text{O-MgO-Al}_2\text{O}_3\text{-SiO}_2$  glass scintillator for pulsed neutron detection 0-87019  
 NaI scintillation counter, calc. of self-shielding and detector efficiency 0-99419  
 NaI, scintillator props. in temp. range 125 to 293K 0-58047  
 NaI(Tl) crystals for volume cylindrical sources, efficiency of  $\gamma$ -ray detection 0-63457  
 NaI(Tl) detectors, response functions to terrestrial  $\gamma$ -radiation, computer program 0-83233  
 NaI(Tl) scintillation spectrometer, used simultaneously with Ge(Li) semiconductor, in neutron activation cross-section meas. 0-78485  
 NaI(Tl) scintillation detectors, microprocessor-based multichannel analyser 0-91378  
 NaI(Tl) well-type detectors, photopeak efficiency values, expts. and calcs. 0-63454  
 Na(Tl) scintillator detectors for neutron-gamma discrimination 0-102386  
 Pb-glass total absorption counters, photomultiplier size at high energy 0-74085  
 Pb-scintillator sandwich EM shower detector, perform. characts. 0-102385  
 Si(Li)-NaI spectrometer, L X-rays, meas. of trace radionuclides in soil 0-58020  
 Xe high pressure proportional, scintillation camera for X- and  $\gamma$ -ray imaging 0-99412  
 Xe proportional scintillation detector, energies and angles of emission of  $^{252}\text{Cf}$  fission fragments 0-63488

**scintillation detectors** see *scintillation counters*

**scintillation spectrometers** see *particle spectrometers; scintillation counters*

**scintillators** see *scintillation; scintillation counters*

**scintillometers** see *scintillation counters*

**scorching** see *combustion*

**Scott effect**

No entries

**s.c.r.** see *thyristors*

**screening** see *shielding*

**screening, nuclear** see *nuclear screening*

**screens, fluorescent** see *fluorescent screens*

**screens, phosphorescent** see *fluorescent screens*

**screens (display)**

see also *fluorescent screens*

light transmitting stereo screen (*Russian*) 0-86480

spatial image projection on to lenticular screens with hexagonal structure, raster and holographic projection appl. (*Russian*) 0-86481

**screens (display)** continued

TV, use of cholesteric-nematic phase transitions of liquid crystals (*Chinese*) 0-79922

X-ray film/intensifying screen system, MTF and Wiener spectrum, film and screen quality effect (*German*) 0-73560

**screw dislocations**

- 0-59814  
 absorbing crystals, dislocation contrast in the case of anomalous X-ray transmission 0-100240  
 alloys, single cryst., work hardening phenomena and screw dislocation dipole clusters 0-100845  
 Burgers vector sign determ. for nearly screw dislocations, X-ray dynamical theory applic. 0-59467  
 crack propagation effect of 2- or 3-dimensional macrodefect (*Japanese*) 0-104261  
 crystal face, growth behaviour in presence of screw dislocations 0-103276  
 crystal growth models, attachment energy at habit controlling factor 0-59420  
 diamond, natural type-IIb, single dislocations, cathodoluminescence obs. by STEM 0-80871  
 dislocation motion, lattice resist., effect of impurity interstitials 0-84170  
 FCC anisotropic crystals, extended screw dislocation,  $\{110\}$  misfit defect elastic interactions 0-100232  
 FCC metal, dislocation dissociation 0-107235  
 interface, screw like dislocations behaviour with lattice frictional forces 0-64999  
 magnetically ordered cryst., dislocation drag, magnetoelastic waves 0-103332  
 metal, polycrystalline, strain hardening, dislocation link length model 0-84953  
 metals, atomic mobility under pulsed loading conditions (*Russian*) 0-96684  
 metals, BCC, plastic deform., review 0-104213  
 metals, FCC, misfit defect and extended screw dislocation anisotropic elastic interaction 0-96563  
 monostearine crystals, spiral growth from organic soln. 0-93467  
 nonuniformly moving screw dislocation, transient subsonic motion 0-79790  
 screw subboundaries as dislocation sources, creep 0-100234  
 stearic acid crystals grown from solution, spatial correlation between growth spirals and inclusions 0-96527  
 transition metal oxide catalysts, reduction, cryst. defects influence, in-situ electron microscopy 0-81322  
 transition metals, BCC, interaction energy between self-interstitial and screw dislocation, calc. 0-70248  
 web dendrites, dislocations, stacking faults, X-ray topographic study (*Chinese*) 0-88148  
 Zircaloy-2, irradiation growth, reaction rate theory calcs. 0-88212  
 Al bicrystals, isoaxial, fatigue crack initiation in grain boundary affected regions (*Japanese*) 0-89338  
 Al-Mg (0.3 wt.%) single cryst., dislocations obs. by high voltage electron microsc. 0-79796  
 CdS, acoustic wave attenuation, phonon viscosity and dislocation drag 0-70319  
 CsCl-type lattice,  $\{111\}$  superlattice screw dislocation motion, computer simulation 0-79793  
 Cu alloys, FCC, climb of extended dislocations due to irradiation in HVEM 0-103343  
 Cu, single crystals, neutron irradiated, stresses and secondary slip between overlapping and dislocation arrays 0-88162  
 Cu-Cd (1.0 wt.%) yield stress and flow stress 0-97524  
 Cu-Cr-SiO<sub>2</sub> system, age and dispersion strengthened, dislocation struct. around SiO<sub>2</sub> particles 0-108468  
 Cu-Cr(SiO<sub>2</sub>), single crystals, yield and pre-yield behaviour rel. to aging time 0-81103  
 Fe, effect of H<sub>2</sub> on phys. and mech. props. 0-101657  
 Fe-Cr-Co alloy, spinodally decomposed, micro-twinning 0-92537  
 Fe-N, single cryst., solid soln. softening, effect of interstitial N 0-97496  
 Ga whisker growth from GaN/Ga layered films 0-92800  
 GaSb, acoustic wave attenuation, phonon viscosity and dislocation drag 0-70319  
 Ge, dislocations under high stress, stacking fault energies, TEM study 0-70202  
 $^4\text{He}$  solid-liquid interface mobility under 1 MHz sound wave (*French*) 0-100373  
 KCl, cryst. isolated pore healing under press., dislocation struct. evolution (*Russian*) 0-100245  
 $\text{KH}_2\text{PO}_4$ , Burgers vector sign determ. for nearly screw dislocations, X-ray obs. 0-59467  
 Li, temp. depend. of dislocation behaviour between 90 and 300K 0-88146  
 LiF crystal, contact damage obs. by cathodoluminesc. 0-71728  
 LiF, dislocation structure, influence of variable defect. temp. 0-70211  
 MgO crystal, contact damage obs. by cathodoluminesc. 0-71728  
 MgO crystal, yield strength and dislocation mobility 0-93601  
 MgO crystals, geometrical-statistical parameters of dislocation interactions with point obstacles 0-103341  
 MgO crystals, plastic deform. activation parameters, rel. between macroscopic and in-situ HVEM expts. 0-103355  
 MgO crystals, radiation damage influence on deform. in HVEM 0-103391  
 MgO, single cryst., tensile creep, stress induced dislocation structs. 0-96539  
 MgO single crystals, dislocation processes, obs. by HVEM in-situ deform. 0-103340  
 NaCl, dislocation density in monocrystal deformed under high hydrostatic press. 0-70216  
 NaCl, dislocation mobility under high press., temp. depend. 0-75235  
 NaCl, dislocation ordering influence on integrated X-ray coeff. 0-103357  
 NaCl, electric field gradients near dislocations, resulting NMR lineshapes 0-75225  
 NaClO<sub>3</sub>, dislocations rel. to growth mechanism from aq. soln., X-ray topography 0-59464  
 $\text{PbFe}_{1/2}\text{O}_9$ , dislocation etch pit morphology study (*Chinese*) 0-88150  
 Si,  $\{111\}$  surface structure phase transform, screw dislocations RHEED study 0-88153  
 Si, dislocation generation in local oxidation 0-107245  
 Si, HVEM struct. images of extended 60° and screw dislocations 0-59466  
 Si, screw dislocation networks, TEM study 0-70204



**screw dislocations continued**

- Si:B(P), dislocations under high stress, stacking fault energies, TEM study 0-70202  
 Zn, line energy of basal screw dislocation, exptl. determ. 0-88154  
 Zr alloys, creep and growth, irradiation induced, microstruct. depend. 0-93602  
 Zr, irradiation growth, reaction rate theory calcs. 0-88212

**scrubbing (abrasion) see abrasion****scuffing see abrasion****SDI see information dissemination****sealing see seals (stoppers)****seals (stoppers)****see also glass-metal seals**

- Araldite, high vacuum sealant at liq. N<sub>2</sub> temp. 0-57319  
 bakeable seals development for large noncircular ports on Tokamak fusion test reactor 0-82777  
 elastomer materials, selection for vacuum seals 0-77797  
 electric lead-ins with composite seal for high pressure chambers 0-105665  
 ferrofluid seal against liq. 0-57270  
 fusion reactor, Demonstration Power Tokamak Reactor, vacuum outer containment and metal seals feasibility study 0-95458  
 fusion reactor, TFTR, large noncircular ports, development of bakeable seals 0-95454  
 gasket, large diameter elastic metal gasket for ultra-high vacuum flange connections 0-95106  
 liquid jet vacuum seal, inflow, rel. to electron beam emergence into atmosphere 0-78469  
 lubrication static contact shape and kinetic behaviour 0-97598  
 magnetic fluid, high-speed cryogenic for high-vacuum chambers 0-57314  
 rubber seal technology, advances 0-93730  
 semiconductor packages, hermetically sealed, calibration and anal. of moisture by gas mass spectrometry 0-90928  
 shaft seal, high-speed mag. fluid, heat dissipation 0-59032  
 teflon rope, vacuum sealing material 0-98925  
 thermocouple installation in IR spectroscopy and reaction cells 0-57398  
 vacuum seal design, construction and application 0-82780  
 Al<sub>2</sub>O<sub>3</sub>-glass seals, diffusion of Al, electron microprobe study 0-107577  
 In seal fabrication by prepressing 0-101800

**seawater**

- acoustic absorption, chemical relaxation studies using resonator method 0-96073  
 acoustical props. of laboratory sediments, temp. variation 0-96069  
 N.Atlantic, sea surface temp. year to year changes, (1948 to 1974) 0-67367  
 SE.Baltic coast transit section, suspended load composition in calm and storm (*Russian*) 0-67360  
 Bombay coast region, water pollution physicochemical studies 0-104522  
 boundary layer during evaporation, optical interferometry (*Russian*) 0-61919  
 E.Canadian Arctic, sea ice meltwater, isotope study 0-77002  
 Cariaco Trench, temp. salinity and chemistry 0-98359  
 NW.Caribbean, methane content of deep water indicating seepage 0-81924  
 E.Caribbean, deep water silicate content distrib. 0-76984  
 convective fluxes, temp. and salinity from atm. obs. 0-104986  
 deep water formation in N.Atlantic during last ice age 0-94535  
 density, dependence on temp., salinity and press., math. expressions 0-94540  
 desalination by wind power, anal. 0-108781  
 electrical conductivity and salinity, temp. and press. depend. 0-67368  
 electrical conductivity compared to KCl standard solution, salinity scales 0-72646  
 equation of state at high press. 0-101369  
 Guaymas Basin, <sup>3</sup>He meas. rel. to mantle volatiles injections in Gulf of California 0-85640  
 N.Indian Ocean, dissolved petroleum content 0-98361  
 irradiance attenuation coefficient in a stratified ocean, meas. technique 0-98325  
 Laccadive Sea, chemical oceanography 0-104995  
 Laccadive Sea, trace metals concs. 0-104997  
 Laccadive Sea (Lakshadweep), physical characts. 0-104966  
 Laccadive Sea waters, total Hg concs. 0-104996  
 mixed salt solution approximating seawater composition, dielec. and radiation characts. 0-97184  
 North Sea, sea surface temp. year to year changes, (1948 to 1974) 0-67367  
 Pacific Ocean, December sea surface temps. correl. with spring rains in California 0-77064  
 E.Pacific Ocean, tropical, N<sub>2</sub>O meas. in sea water and marine air 0-94542  
 E.Pacific Rise, hot springs and geophysical expts. 0-101360  
 E.Pacific Rise geothermal system, physical limits on geothermal fluid temp. and role of adiabatic expansion 0-101362  
 permittivity at mm wavelengths 0-66098  
 Practical Salinity Scale 1978, for in-situ meas. of seawater 0-67419  
 salinity measurement, elec. cond. obs., temp. and conc. depend. 0-67421  
 salinity of standard seawater, elec. cond. compared to KCl soln. 0-67420  
 salinity of standard seawater, elec. cond. obs. 0-72647  
 salinity of standard seawater, elec.cond./salinity/temp. relations 0-67422  
 Sargasso Sea, optical props. of seawater (*Russian*) 0-94532  
 sea and beach persistent oil spill identification methods 0-90101  
 sediment-water interface in coastal zone, chem. exchange traced by <sup>222</sup>Rn obs. 0-101386  
 steel, notched specimens in sea water, endurance limit enhancement, specimen size, freq. effects 0-93678  
 sulphate concentrations, indirect anal. by atomic absorpt. 0-89556  
 surface microlayer chemical composition (*Russian*) 0-104998  
 surface temperature, meas. 200 km from land rel. to air-sea heat transfer coeffs. 0-72552  
 temperature fluctuations, small-scale, in upper ocean layer, statistical regularities (*Russian*) 0-94528  
 trace metal composition of N.Pacific, Cd, Ni, Cu, Cd vertical profiles 0-67381  
 upper ocean temperature and salinity structure, obs. during POLE expt. 0-72536  
 warm front, oceanic, propagation, theory with appl. to Sagami Bay Kuroshio phenomenon 0-94538  
 Weddell Sea, bottom water origin, chem. tracer considerations 0-76982  
 Weddell Sea, bottom water variability 0-67366

**seawater continued**

- $\gamma$ -ray field of seawater, meas. method (*Russian*) 0-109268  
 Al content controlled by inorganic processes 0-61815  
 CO<sub>2</sub> solubility temp. coeff. in <sup>13</sup>C air-sea interchange calc. 0-61814  
 Cl, residual, in saline cooling waters, determ. via modified amperometric membrane probes 0-82112  
<sup>137</sup>Cs/<sup>134</sup>Cs radioisotopes in seawater, Cs-selective resin determ. 0-94137  
 H<sub>2</sub> dissolved in N.Atlantic surface water, interchange with air 0-77057  
<sup>3</sup>He excess in Mid-Atlantic Ridge bottom waters, hydrothermal activity 0-101383  
 Mn dissolved in NE.Pacific water 0-101384  
 NaCl, monoelectrolyte, highly mineralised salt soln., dielec. and radiation characts. 0-97184  
 Se (-II,0), (-IV) and (-VI) composition of water, by gas chromatography method 0-81928  
<sup>87</sup>Sr/<sup>86</sup>Sr ancient seawater composition, Jurassic to Pleistocene, Israel groundwater obs. 0-61804  
 T in deep N.Atlantic current, from weapons tests 0-101380  
<sup>234</sup>Th removal from Funka Bay, Japan 0-61803  
 U<sub>2</sub>O<sub>8</sub> recovery from seawater, R and D program 0-99217

**second-order optical susceptibility see nonlinear optical susceptibility****second sound****see also liquid helium sound propagation**

- smectic A LC, second sound excitation in insulating and conducting crystals 0-103244  
 superfluid prop. meas., review 0-96090  
 He, liq., phonon coupling of two-dimens. Wigner cryst. with second surface sound (*Russian*) 0-92756  
 He, sound transmission at liq. solid interface, probe of melting kinetics 0-92734  
<sup>4</sup>He, superfluid, fluctuations in turbulent counterflow, vortex line density fluctuation power spectra 0-84335  
<sup>4</sup>He, superfluid, Kapitza resist. meas. (*Russian*) 0-88375  
<sup>4</sup>He, superfluid, second sound discharge and compression shock wave propagation (*Russian*) 0-103529  
<sup>4</sup>He, superfluid, sound conversion phenomena at free surface, acoustic coeffs. 0-96709

**secondary cells**

- ambient temperature solid state battery developments, review 0-61328  
 battery appls. and developments, conf., Brussels, Belgium (Jan. 1979) 0-72032  
 battery energy storage, 1979 status and prospects (*Japanese*) 0-76655  
 characteristics of Gates' cylindrical, sealed lead-acid cells for float applications 0-66964  
 criteria for electric vehicle and energy storage applications 0-72031  
 developments in electrochemical energy sources (*German*) 0-97770  
 electric vehicle power sources, battery design requirements for commercial use (*Dutch*) 0-72024  
 electric vehicle power sources, fuel cell/secondary battery hybrid appls. (*Dutch*) 0-72037  
 fast ion transport in solids, conf., Lake Geneva, USA (May 1979) 0-57006  
 fast ion transport in solids, conf., Lake Geneva, USA (May 1979) 0-105427  
 galvanic cells, high energy, with molten salt electrolytes (*German*) 0-72036  
 high power batteries, possible use of honeycomb-type structs. 0-72027  
 intercalation compound electrodes, thermodynamic and transport props. 0-66963  
 Na-S batteries, solid electrolyte  $\beta$ -Al<sub>2</sub>O<sub>3</sub> formation from m-Al<sub>2</sub>O<sub>3</sub> by new method 0-89606  
 redox flow battery, quantum parameters separation in continuum of ferromag. liquid insulation 0-61338  
 solar energy plant electricity storage, battery appls. potential 0-72067  
 solid electrolyte, layer and tunnel compounds, fast ion transport and electrochem. storage 0-61324  
 solid solution electrodes, characterisation and performance 0-72033  
 standard cells combination with low temp. coeff. for Josephson voltage standard maintenance 0-101788  
 wind energy conversion system, electricity storage using batteries 0-72008  
 Ag/RbAg<sub>4</sub>I<sub>5</sub>/I<sub>2</sub> solid state battery, low temp. degradation 0-61331  
 Ag/RbAg<sub>4</sub>I<sub>5</sub>/Ta, solid electrolyte timing cell and coulometer 0-68216  
 Ag-H<sub>2</sub> electrochemical cell design using rolled stack configuration 0-101084  
 Al/AlCl<sub>3</sub>-NaCl/FeS<sub>2</sub> secondary cell, preliminary study 0-108793  
 $\beta$ -Al<sub>2</sub>O<sub>3</sub>-Na<sub>2</sub>O, solid electrolyte, behaviour at high current density, sodium heat engine mode 0-61330  
 $\beta$ -Al<sub>2</sub>O<sub>3</sub>-Na<sub>2</sub>O solid electrolyte, strength degradation under electrolytic conditions 0-61329  
 C-air electrodes in alkaline electrolytes, ageing mechanism study 0-101087  
 Fe-air batteries, bifunctional air electrode 0-72028  
 H<sub>2</sub>-Br<sub>2</sub> cell for energy storage appls. 0-72029  
 Li, electrochemistry of amorphous V<sub>2</sub>S<sub>5</sub> 0-76626  
 Li, high energy density, mixed electrolyte solns. of propylene carbonate and dimethoxyethane 0-76627  
 Li long life battery systems, standby power for data retention in volatile memory systems, selection criteria 0-61337  
 Li metal for battery industry, sources and preparation 0-97781  
 Li salt based solid electrolyte, synthesis and characterisation, secondary cell appl. (*French*) 0-72034  
 Li solid cathode cells, Li closoboranes as electrolytes 0-108794  
 Li solid electrolyte materials, review of crystal and electrochem. props. 0-107524  
 Li/SO<sub>2</sub> cells, safety studies, kinetics of Li-organic solvent exothermic reactions 0-72030  
 Li-S, Li exchange current in LiCl-KCl eutectic melt at 400°C 0-93867  
 LiAl/FeS, battery system research developments at ANL 0-61323  
 LiAl/FeS experimental cells with molten salt electrolyte, self-discharge behaviour 0-104501  
 LiAl(Si)/FeS(S<sub>2</sub>) battery developments for electric vehicle propulsion and load levelling appls. 0-61325  
 LiBr, surface characterization of film growth on Li anode 0-81240  
 Li<sub>2</sub>CoO<sub>2</sub>, cathode material for batteries of high energy density 0-101089  
 Li<sub>2</sub>WO<sub>4</sub>/Li<sub>2</sub>TiS<sub>2</sub> cyclable organic electrolyte cell, using 2 intercalation electrodes 0-76625  
 MgO sintered-ceramic separator plate development, Li-Al/LiCl-KCl/FeS battery applications 0-61321  
 Na/S battery, development of  $\beta$ -Al<sub>2</sub>O<sub>3</sub>-N<sub>2</sub>O electrolyte 0-71615

**secondary cells continued**

- Na/S battery, mass transport phenomena in molten S-Na<sub>2</sub>S<sub>2</sub> system 0-72026
- Na/S battery development program at GEC for utility lead levelling with beta alumina solid electrolyte 0-61327
- Na/S cells operating with dissolved catholyte, elec. props. 0-101085
- Na/S load levelling batteries, optimisation of fabrication process of beta Al<sub>2</sub>O<sub>3</sub> solid electrolyte 0-72035
- Na/S traction batteries, development progress and problems, review 0-61326
- Na-Na<sub>2</sub>ErSi<sub>4</sub>O<sub>12</sub>-TiS<sub>2</sub>, electrochem. characts. 0-107518
- Na-S, fabrication of  $\beta''$ -Al<sub>2</sub>O<sub>3</sub> solid electrolyte tubes from cast ceramic tape 0-60819
- Na-S, processing + props. of  $\beta''$ -Al<sub>2</sub>O<sub>3</sub> and NASICON ceramic electrolytes 0-60820
- Na-S battery, appls. (*French, German*) 0-61322
- Ni-Cd accumulators, efficient charger cct. based on Fairchild,  $\mu$ A78S40 IC (*German*) 0-66961
- Ni-Cd, plastic-bonded electrodes positive active layer study 0-101088
- Ni-Cd and maintenance-free Pb accumulator characteristics (*German*) 0-97782
- Ni-Cd batteries, button and cylinder types, self discharge behaviour during storage (*German*) 0-66960
- Ni-Cd batteries for standby power systems 0-104500
- Ni-Cd cells, characts. limitations, future developments 0-89607
- Ni-Cd pocket plate batteries characteristics, solar applications 0-61332
- Ni-Cd sealed battery electrode performance meas. 0-66962
- Ni-H<sub>2</sub> battery for satellite energy storage, prelaunch and orbital performance through one eclipse season 0-81430
- Pb acid battery plants, current and future trends, telecommunications emergency power supply 0-61333
- Pb-acid 'G-cell', construction and design and performance charact. for UPS systems 0-61335
- Pb-acid batteries for electric propulsion (*Dutch*) 0-72025
- Pb-acid battery charging from photovoltaic array energy source, problems and efficiency 0-61336
- Pb-acid cells, PbO<sub>2</sub> formation on Pb and antimonial Pb alloy 0-76628
- Pb-acid storage batteries for uninterrupted power supply appls. 0-61334
- PbO<sub>2</sub> powder, electronic conductivity, separation of particle core and surface resistance 0-104442
- Y<sub>2</sub>O<sub>3</sub> sintered-ceramic separator plate development, LiAl/LiCl-KCl/FeS battery applications 0-61321
- Zn electrode development, dispersed, electric vehicles appl. (*French*) 0-72023
- Zn, props. of alternate electrolytes 0-104502
- Zn-Br, performance anal. in electric vehicle and utility applications 0-101086

**secondary electron emission**

- n-alkanes, conduction band struct., LEED, secondary electron emission and UPS study 0-70601
- angular and energy distrib. 0-100718
- diamonic molecules, N<sub>2</sub> and CO nuclear pumped lasers, electron impact cross section meas. 0-63985
- dielectric theory of secondary electron spectra 0-93442
- ethylene, conduction band struct., LEED, secondary electron emission and UPS study 0-70601
- F 0-60740
- Inconel 625, electron yields under ion bombardment for clean and oxidised surfaces 0-66368
- inert gas nuclear pumped lasers, electron impact cross section meas. 0-63985
- ion induced, energy and angular spectra 0-71547
- kinetic emission from electron and ion bombardment 0-66342
- laser plasma, ion emission, secondary electron emission effects on detect. efficiency 0-100096
- low energy distrib. meas. using double-pass cylindrical mirror analyser 0-68293
- metal surface, appl. to energy anal. of energetic neutrals in plasma diagnostics 0-59278
- metal surface, heterogeneous cluster ion bombardment, secondary electron emission 0-60742
- metal surface, keV neutrals energy determ. method 0-89100
- metals high density collision emission cascades following heavy ion bombard. 0-71531
- piezoelectric insulator, nonlinear interaction of SAW with electron beam 0-70517
- polyethylene, solid liq., secondary electron emission spectroscopy 0-80916
- pulsed surface flashover mechanism involving electron-stimulated desorption 0-70055
- SEM, ultra-high vacuum secondary electron emission dependence on electron beam density dose, surface interactions from AES and ELS 0-61209
- SEM accuracy increase, equipotential patterns obtaining 0-57423
- SEM specimen-electron interactions 0-68317
- single crystals with lowered work function, secondary and Auger electron emission anisotropy 0-100716
- spectroscopy based instrument applic. to rate controlled deposition of alloy films (*German*) 0-89152
- surface analysis techniques and appls., symposium, Dayton, USA (Jun. 1979) 0-62363
- surface potential and work function meas. from secondary electron emission energy in SEM 0-66343
- surface spacings from secondary electron yield 0-66341
- threshold studies from ion-surface impact 0-66360
- trifluoriodomethane nuclear pumped lasers, electron impact cross section meas. 0-63985
- wake-bound electron contrib. to convoy electron vel. distrib., effect of ionic field 0-60729
- water vapour ionised by He<sup>+</sup> and He<sup>2+</sup>, electron yield obs. 0-102562
- yield from ion-surface impact 0-71544
- Zircaloy, breakaway mechanism, corrosion kinetics in steam 0-61030
- Ag coating on refractory metals, energy struct. determ. at two monolayer thickness 0-100392
- Ag, low energy distrib. meas. using double-pass cylindrical mirror analyser 0-68293
- Al, foil, secondary electron emission due to  $\alpha$ -particle irradi. (*Russian*) 0-66344
- Al, ion-induced electron emission, ion charge depend. 0-108315
- Be, slowly oxidised, secondary electron yield changes, and AES characterisation 0-71524

**secondary electron emission continued**

- Be thick film or Au substrate secondary electron emission 0-104022
- CO, adsorbed layer, electron impact, electron impulsive ionisation spectroscopy obs. 0-60720
- Cs/W, work function measurement in SEM 0-80918
- Cu, low energy distrib. meas. using double-pass cylindrical mirror analyser 0-68293
- GaP-Cs-O simultaneous adsorption, oxidation interface chemical struct. 0-103584
- LiNbO<sub>3</sub>, piezoelec., SAW interaction with secondary electrons 0-80708
- MgO coated detector for SEM backscatter to secondary electron conversion 0-68332
- NO, adsorbed layer, electron impact, electron impulsive ionisation spectroscopy obs. 0-60720
- Nb, electron bombardment, high-energy, secondary electron emission 0-80917
- PbS, film, total current spectrum and energy struct. 0-100719
- Pd (111) surface, clean and CO covered, metastable He impact, electron emission, energy and ang. distrib. 0-60744
- SiO<sub>2</sub> layer, thickness measurement by secondary electron emission 0-57435
- UF<sub>6</sub> nuclear pumped lasers, electron impact cross section meas. 0-63985
- V<sub>2</sub>O<sub>5</sub>-P<sub>2</sub>O<sub>5</sub>-Cs<sub>2</sub>O(Na<sub>2</sub>O) glasses, enhanced secondary electron emission yield 0-93441
- W, surface diffusion of adsorbed O, secondary electron emission study 0-76117
- W, work function measurement in SEM 0-80918
- secondary emission**  
see also secondary electron emission; secondary ion emission
- Be, secondary photon emission following ion bombard. 0-71493
- secondary ion emission**  
see also secondary ion mass spectra; secondary ion mass spectroscopy
- caesiated surface, negative ion emission (*French*) 0-108314
- conference, Stanford, USA (Aug. 1979) 0-105419
- desorption, heavy-ion induced, of organic cpds. from solid surfaces 0-100739
- fission fragment and alpha recoil induced secondary ion ejection 0-71533
- review, secondary complex ion emission (*Russian*) 0-108305
- semiquantitative analysis, one fitting parameter approach 0-108762
- silicate glass, silicates, matrix effects in secondary ion emission 0-76125
- silicates, quantitative anal., linear variation of secondary ion yield (*French*) 0-108763
- yield, linear variation, quantitative anal. of mineral silicates (*French*) 0-108763
- Fe-N alloys, secondary ion emission, phase transforms. effect (*Russian*) 0-66347
- Si, Auger electron emission, ion induced and secondary ion emission 0-71546
- secondary ion mass spectra**
- adhesion, surface anal. techniques appl. 0-65381
- ceramics, local in depth anal. by neutral beam SIMS 0-89565
- conference, Stanford, USA (Aug. 1979) 0-105419
- depth profiling, dynamic range of 10<sup>5</sup> 0-107302
- histological section, high mass resolution by ionic analyser (*French*) 0-109069
- implanted ion depth distrib., secondary ion mass spectra 0-79829
- ionic clusters, struct., thermodynamic functions, energy surfaces and SIMS 0-63881
- mass peaks identification in SIMS using computer program 0-101867
- MIS solar cells, interface problems, AES, SIMS and XPS study 0-89627
- molecular ion cluster emission, parity rule applics. in SIMS (*French*) 0-63882
- quantitative, review 0-61195
- semiconductor materials, quantitative anal. 0-101052
- semiconductor microstructure fabrication, ion channeling effects 0-70230
- semiquantitative, one fitting parameter approach 0-108762
- sputtered particles, energy and mass distrib. 0-84822
- stainless steel, in MgCl<sub>2</sub> solutions, Cl distrib. in oxide films (*French*) 0-108765
- stainless steel, neutron dose determ., from isotope abundance ratio, mass spectra obs. 0-61220
- steel, continuously cast, segregation at halfway cracks 0-60869
- surface segregation, effect on metallurgical props, SIMS, XPS and AES (*French*) 0-80045
- Ag, Cu diffusion, SIMS investigations 0-59717
- Ag surface, CO chemisorption, SIMS, XPS study 0-84382
- Al, film and polished bulk specimens, initial stages of oxidation obs. 0-81239
- Cu polycrystals, oxidation, secondary ion energy spectra 0-71788
- Cu, SIMS depth profiling, surface roughening by low energy ion irradi. 0-60727
- Cu-Co-Si (0.36, 0.11 wt.%), surface layer struct. on annealing, SIMS and AES exam. 0-88415
- Fe-Cr, high-temp. oxidation, borate inhibitors 0-66705
- Ga<sub>0.9</sub>Al<sub>0.9</sub>As LPE layers containing low-cond. regions, charging effects in SIMS anal. 0-66348
- GaAs, polycryst., wet and dry oxides, comparative study by AES, SIMS and XPS 0-80116
- GaAs solar cell, polycryst., grain boundary passivation by oxidation, AES, SIMS and XPS obs. 0-81467
- GaAs:Cr, Cr distrib. and heat-treatment migration studies by SIMS 0-107305
- GaAs:Cr capless annealed, under As press., Cr redistrib., SIMS obs. 0-59503
- GaAs:Si, ion implantation, thermal annealing, Hall meas., SIMS atomic profile meas. 0-75243
- GaAs:Sn thermal diffusion from spin-on SnO<sub>2</sub>/SiO<sub>2</sub> source 0-96691
- GaAs-Au(Ag) Schottky barrier solar cells, interface problems, AES, SIMS and XPS study 0-89627
- GaAsP<sub>1-y</sub> alloy, composition effects in growth by MBE 0-59816
- GaP:Cr epitaxial layers, Cr conc. profile determ. 0-65029
- GaSb, diffusion of In, 520 to 712°C 0-79995
- In, chemisorption of O<sub>2</sub>, XPS and static SIM spectral study 0-80055
- InAsP<sub>1-y</sub> alloy, composition effects in growth by MBE 0-59816
- InP, VPE growth for MESFET's 0-103602
- Li<sub>3</sub>N thin film, vacuum evaporation on WO<sub>3</sub>, retarded deposition 0-108351
- Mo, ion bombard., ion and photon yields, CO adsorption effect 0-89098
- Ni (001), azimuthal anisotropies of ejected dimer ions, SIMS expt. 0-60730



**secondary ion mass spectra continued**

- Ni, ion bombard., ion and photon yields, CO adsorption effect 0-89098  
 Ni-Cr(Fe)(Cu) alloy, matrix effect in SIMS anal. using  $O_2^+$  primary beam 0-76576  
 Pd surface, CO chemisorption, SIMS, XPS study 0-84382  
 PdAg surface, CO chemisorption, SIMS, XPS study 0-84382  
 Si, amorphous, epitaxial regrowth, structure and impurities effect 0-84401  
 Si, annealing, using laser pulses, impurity incorporation at melt-cryst. interface 0-59504  
 Si layers amorphized by molecular ions, laser annealing 0-103379  
 Si, multigrained, grain boundary elec. and compositional props., surface anal. 0-76575  
 Si, multigrained, impurity segregation to grain boundaries, AES and SIMS obs. 0-65027  
 Si, oxidation induced by ion or electron bombardment, AES-SIMS study 0-108606  
 Si ribbon, EFG, C contaminant conc. determ. by nuclear techniques and SIMS 0-59506  
 Si:B(Be)(Li) ion implanted, channelling and random equivalent depth distrib. 0-100293  
 Si:B(P)(As)(Sb)(Cu)(Fe), ion implanted, doping profile, pulsed laser annealing effects 0-88197  
 Si:Be, ion implanted, correl. of atomic distrib. and implantation induced damage profiler 0-88199  
 Si:C(O), implant redistribution, annealing effects, SIMS meas. 0-96561  
 Si:Sb, low energy ion implantation, profile determ. 0-88176  
 Si-SiO<sub>2</sub> laminar ion-implanted systems, struct. change investig. by MSSI method (*Russian*) 0-107918  
 SiO<sub>2</sub>, amorphous, <sup>30</sup>Si diffusion (*French*) 0-59696  
 SiO<sub>2</sub>, amorphous, diffusion of <sup>30</sup>Si (*French*) 0-107482  
 SiO<sub>2</sub>-CaO-Na<sub>2</sub>O, glass, layers near surface, anal. using SIMS 0-88041  
 SiO<sub>2</sub>-Li<sub>2</sub>O, glass, layers near surface, anal. using SIMS 0-88041  
 Si(111), ion-bombard., O<sub>2</sub> adsorption, SIMS study 0-70522  
 SnTe, diffusion of <sup>125</sup>Te, diffusion profiles by SIMS meas. 0-84325  
 TiH<sub>4</sub> and TiD<sub>0.9</sub>, surface characts., AES, EELS, SIMS, and XPS study 0-65343  
 W dispenser cathodes, Ba-activated, surface characts., ion scatt. spectrometry and SIMS study 0-66377

**secondary ion mass spectroscopy**

- alloys, surface composition after fabrication by SIMS 0-65351  
 concentration profiles depth differential, evaluation 0-59531  
 conference, Stanford, USA (Aug. 1979) 0-105419  
 crystalline solids, electronic industry, chem. anal. instrumental methods progress 0-66903  
 depth profiles, edge effects, anal. correction 0-80925  
 depth profiling, automatic sequential mass analysis 0-108764  
 depth profiling, dynamic range of 10<sup>6</sup> 0-107302  
 dielectrics, use of Cs<sup>+</sup> beams in secondary ion mass spectra 0-90929  
 electronic material and device characterisation using surface-sensitive analytical techniques 0-65341  
 flint implements, provenance determ. possible appl. of SIMS 0-61197  
 III-V semiconductors, surface and interface anal., secondary ion mass spectrometry technique 0-59763  
 interfacial impurities, quantitative anal. 0-84396  
 ion implantation by laser annealing, characterisation, solar cell applications 0-70247  
 LSI surface analytical techniques applied to electronic components [Si LSI chip inspection] 0-81392  
 MACS mass and charge analysis technique, principle and appl. 0-73521  
 metal oxidation, secondary ion energy spectroscopy 0-71788  
 metallurgical applications of XPS, AES, and SIMS (*French*) 0-81253  
 photovoltaics and absorber/reflector, diffusion, chemical reactions, contamination, AES and SIMS 0-72066  
 quadrupole mass spectrometer, transmission of narrow ion beam (*French*) 0-105747  
 quantitative investigations, results and possibilities (*Hungarian*) 0-73523  
 second-generation ion microanalyser description and performance (*French*) 0-101055  
 semiconductor crystal growth and defects, appl. of analytical techniques 0-73546  
 solid substance surfaces, physico-chemical props. investigations (*Czech*) 0-90927  
 solids, elemental analysis 0-97748  
 specimen charging control for SIMS and AES of insulators 0-101875  
 steel, cold-rolled sheet, surface chemistry 0-61146  
 steel, industrial, surface chem. characterisation by SIMS, glow discharge spectrometry and other techniques 0-66907  
 surface analysis techniques and appls., symposium, Dayton, USA (Jun. 1979) 0-62363  
 surface analytical techniques, quantification, review 0-65342  
 surfaces and thin film studies by combined system of SIMS, AES and XPS 0-86536  
 thin films, surface anal., survey of ESCA, AES, SIMS, and ISS (*Hungarian*) 0-70544  
 Al sheet surfaces, chem. characterisation by SIMS, glow discharge spectrometry and other techniques 0-66907  
 Au-refractory film interdiffusion obs., by combination of scattering techniques 0-65308  
 Fe-Ni-Cr-Al-Y, oxidation mechanism, Y addition effect on kinetics and oxide adherence 0-97623  
 GaAs:Si(s), generation of high mobility n layers 0-103375  
 LiNbO<sub>3</sub>:Ti, planar and channel optical waveguides, anisotropic diffusion expts. 0-64200  
 Si, EFG ribbon, characterisation by ion beam tech. 0-79833  
 Si, grain boundary elec. props./impurity correl. using surface anal. of multigrained samples by SIMS and AES 0-79816

**sedimentation**

- see also disperse systems; sediments; water treatment*  
 aerosol particles growing, gravitational deposition from laminar tube flow 0-59099  
 aerosol particles in flow type chamber, coagulation, deposition 0-69908  
 apatite deposition in Laccadive Sea, rel. to seawater and low F<sup>-</sup> concs. 0-104995  
 Archaean aeon, sedimentary basins development 0-89986  
 Baltic Sea, estuary region, suspension distrib. under river drifts influence (*Russian*) 0-98345  
 Baltic Sea coast sedimentary material differentiation (*Russian*) 0-104951  
 biphase liquid cylindrical vortex, mass force effect on dispersion phase distrib. (*Russian*) 0-79388

**sedimentation continued**

- cohesive sediment entrainment in fresh water 0-90107  
 Deimos, loose material downslope movement obs. 0-94737  
 equilibrium eqns. derivation using hard spheres in Percus-Yevick approximation 0-66884  
 erythrocyte distribution profiles during sedimentation as determ. by HeNe laser light 0-81563  
 erythrocyte sedimentation rate in inclined tubes 0-67048  
 fluorides deposition in Laccadive Sea, rel. to seawater and low F<sup>-</sup> concs. 0-104995  
 gravity, basic theory and experimental demonstrations 0-66885  
 leukocytes of human blood, gravity sedimentation anal. 0-98197  
 longshore sediment transport by tidal current, outside surf zone 0-76961  
 magnetic fluids, barbotage and sedimentation, multiveLOCITY model 0-61161  
 molten metal binary mixtures with wide immiscibility range, gravitational layering of components (*Russian*) 0-104092  
 near-shore and lake sedimentation process, fallout radionuclide tracer obs. 0-81864  
 old Mangalore port, India, channel siltation study 0-77005  
 particulate sedimentation, stability, two-dimens. anal. 0-69768  
 poly-4,4-diphenylphthaleneinterephthalamide, mol. mass distrib., sedimentation and fractionation method meas. (*Russian*) 0-71957  
 polymer solution, sedimentation rates for low mol. wt. materials in dilute region 0-108756  
 polymer systems, sedimentation field-flow fractionation in macromolecule characterization 0-66879  
 polystyrene, solns., sedimentation behaviour, branching effects determ. 0-66887  
 remanent magnetisation, acquisition by settling organic mud 0-61795  
 rubber powders, finely dispersed, sedimentometric anal. 0-66883  
 settling velocity scale 0-81376  
 sulphide deposits of E.Pacific Rise (21°N) physics of geothermal system fluid 0-101362  
 suspensions of charged particles, laminar tube flow, entrance deposition 0-59100  
 urethane elastomer, thermoplastic, dilute soln., viscosity and sedimentation 0-103512  
 AgI hydrosols, kinetics and mechanics of colloid systems formation 0-101045  
 Fe particles, dispersed in Hg, mag. props., aggregate form. 0-60375

**sediments**

*see also rocks; sedimentation*

- acoustical props. of laboratory sediments of seawater, temp. variation 0-96069  
 Amazon River, bed sediment size distrib. 0-101392  
 Arabian Fan of NW.Indian Ocean floor, sediment sound vel. 0-72488  
 S.Atlantic, CaCO<sub>3</sub> and radiolarial distrib. rel. to glacial and interglacial oceanographic conditions 0-72556  
 N.Atlantic, Mesozoic and Cenozoic, calcareous sediments depth distrib. 0-81866  
 Atlantic nuclear waste disposal site, radionuclide redistrib. 0-85309  
 Baltic beach sedimentary material stratification (autumn/winter 1976-7) (*Russian*) 0-76962  
 Baltic coastal beach scouring and accumulation by moderate sea disturbances (*Russian*) 0-81867  
 Baltic Sea coast sedimentary material differentiation (*Russian*) 0-104951  
 Baltimore Canyon, submarine mass-wasting of sediments 0-101354  
 beach changes in S.California, statistical prediction 0-98305  
 beach ridges in S.Australia, palaeomag. chronology rel. to Milankovitch theory of ice ages 0-98307  
 Benguela upwelling system off N.Namibia, late Miocene origin, sediment evidence 0-104993  
 boulders of canyon rivers rapids, resistance to movement rel. to rapids stability 0-72564  
 California-Mexico coastal basins, sediments <sup>241</sup>Pu and <sup>241</sup>Am concs. 0-98303  
 Carpathian region sedimentary cover, elec. conduction 0-89940  
 Chesapeake Bay sediment, time depend. transport, temp. and chloride obs. 0-81863  
 coastal marine sediments, fossil C effect on <sup>14</sup>C ages 0-98308  
 cohesionless bottom sediments, limiting stability in turbulent channel flow, erosion 0-94546  
 continental shelf sediment core, anomalous declination due to slumping 0-76964  
 Cretaceous plankton species extinction due to comet impact 0-76977  
 Cretaceous-Tertiary boundary, plankton extinction and geochem. indicating extraterrestrial event 0-76976  
 dating of marine sediment,  $\alpha$ -scintillation counting of <sup>230</sup>Th 0-72636  
 deep ocean, compressional wave attenuation 0-79033  
 duststorm fallout, Kuwait, summer 1978 obs. 0-81966  
 estuary heavy metal pollution, Mosquito Lagoon, Florida 0-76671  
 estuary sediment containing lead pollution, rel. to flood control measures, California 0-76670  
 gas-bearing, meas. of sound speed and attenuation, gas bubble models 0-87670  
 gas-bearing sediments, characterization of acoustic props. 0-87630  
 glacial sediments of English Lake District, pre-Devonian till 0-94523  
 Great Lakes, inorganic sediment, spectral absorbance and backscattering coeffs. 0-98364  
 Gulf of California, varved sediment core appl. to <sup>32</sup>Si half life determ. 0-91153  
 Gulf of Kutch, geomorphology, sediment and tectonic instability origin 0-76960  
 Holocene lake sediments, N.Poland, palaeomag. records anal. rel. to short period secular geomag. vars. 0-98221  
 Indo-Australian plate, deformed oceanic sediments rel. to plate internal deform. 0-109134  
 Lake Naini Tal, India, metal pollution in water and sediment 0-97828  
 lake sediment pollution records in New York State 0-85311  
 lakes, vertical mixing by turbidic oligochaetes 0-101390  
 lakes of western USA, benzo(a)pyrene conc. 0-61476  
 magnetic remanence, post-depositional realignment of sediments, expts. and theory 0-109137  
 magnetisation, surface tension effects 0-85644  
 marine, radiocarbon dating by benzene variant method aboard ship 0-85770  
 marine laminated diatomaceous sediments of Gulf of California, climate record 0-98351  
 marine sediment heat flow, Indian Ocean equator region 0-76958

## sediments continued

- Matanuska Glacier, Alaska, pebble orientation in ice and deposits 0-98366  
 E-Mediterranean sediments, heavy metal content, off Lebanon coast 0-97830  
 Mid-Atlantic Ridge, submarine hydrothermal deposits at 26°N latit., lithology and struct. 0-85641  
 mid-ocean ridges formations, role of ridge crest hot springs 0-98304  
 natural waters, suspended solids concs. rel. to spectral scatt. props. 0-72560  
 near-shore and lake sedimentation process, fallout radionuclide tracer obs. 0-81864  
 ocean bottom, O<sub>2</sub> penetration into coastal marine sediment 0-104952  
 Pacific Ocean, box cores from Ontong-Java Plateau, radiometric obs. 0-61793  
 E-Pacific Rise, sulphide deposits obs., near 21°N 0-101361  
 Pee Dee River—Winyah Bay estuary, S.Carolina, sediments <sup>226</sup>Ra desorpt. rel. to dissolved <sup>226</sup>Ra behaviour 0-98360  
 periglacial cover formations in Lithuania (*Russian*) 0-98367  
 pore water metal concs. in E. equatorial Pacific sediments 0-101358  
 pore water nutrients and carbonate in E. equatorial Pacific sediments 0-101357  
 Quaternary sediments of N.America, pollen contents rel. to palaeotemps. and palaeoprecip. determ. 0-98438  
 Recent tidal-flat sediments, post-depositional remanent magnetization 0-101320  
 remanent magnetisation, acquisition by settling organic mud 0-61795  
 rigidity effects on ocean bottom underwater sound reflection loss in typical deep sea sediment 0-96083  
 sand, specularite-bearing, experimentally deposited, mag. declination and inclination errors 0-90075  
 sea floor south and west of Iceland, bottom sediment active redistrib. obs. 0-90068  
 Sea of Marmara, evidence for Late Quaternary water exchange 0-81916  
 seafloor, acoustical imaging of buried objects using focused US transducers 0-79036  
 Searles Valley, California, lacustrine sediment core chronology from palaeomagnetic data 0-89955  
 sediment-water interface in coastal zone, chem. exchange traced by <sup>222</sup>Rn obs. 0-101386  
 shear wave effects on ocean bottom refl. loss, ray path anal. 0-96084  
 stream sediment, deposition of trace metals downstream of Pb smelter 0-61475  
 submarine sediments, automatic recognition by sonoprobe survey, acoustic reflection pattern model (*Japanese*) 0-85776  
 sulphide deposits on E-Pacific Rise, assoc. with hot springs 0-101360  
 titanomagnetite sand from New Zealand, density, elec. and mag. prop. 0-98311  
 United States Atlantic continental shelf, US Geological Survey core drilling 0-72511  
 Urazoko Bay, <sup>239</sup>Pu, <sup>137</sup>Cs and <sup>60</sup>Co distrib. and behaviour 0-97825  
 Visakhapatnam coast, Bay of Bengal, clay sediments derived from inland sediments 0-76959  
 viscous sound attenuation in high-porosity marine sediments 0-74577  
 Wastwater, W.Cumbria, Pu and <sup>137</sup>Cs concs. in lake sediment samples 0-108817  
 wave transport of sand sediment, by near bottom orbital motion 0-98306  
<sup>10</sup>B geochemistry in North Pacific during Pliocene 0-101356  
<sup>14</sup>C age of deep-sea sediments, rel. to vertical mixing 0-81865  
<sup>113</sup>Cd<sup>+</sup> in marine organisms and sediment around Marshall Island nuclear test site 0-109174  
 Ce determination method for marine sediments 0-104543  
 Fe precipitation in Vellar estuary, conc. determ. 0-77015  
 Hg loss rate from contaminated estuarine sediments 0-85310  
 Mn nodules, maintenance at surface by bioturbation of infauna 0-101359  
 Pb in subalpine pond sediments, anthropogenic source var. 0-85315  
<sup>210</sup>Pb determination in sediment core from ocean floor off Californian coast 0-72101

## Seebeck effect

- calorimetry, applications of thermoelectric devices in various types of calorimeters 0-105648  
 coefficient measurement of disc-shaped samples by AC method (*Japanese*) 0-73392  
 dilute alloy, Seebeck coefficient, electron-phonon enhancement 0-70685  
 eutectics, HgTe-PbTe and Au-PbTe, prep. and thermoelectric behaviour characts. 0-107774  
 lattice parameters, mag. and elec. props. 0-100578  
 MgAl<sub>2</sub>-Fe<sub>2</sub>O<sub>3</sub> solid solution system, solid state properties study 0-93094  
 rare earth-CrO<sub>2</sub>, elec. transport 0-70700  
 semiconductor, Seebeck and Hall coeffs. Lorenz number; anisotropy, theory (*German*) 0-65608  
 thermocouple, thermometers, voltage generation, calibration 0-57295  
 thermoelectric alloys, phase diagrams, and imperfection chemistry 0-108422  
 thermoelectric materials, B<sub>4</sub>C<sub>2</sub> and (B,Si)<sub>4</sub>C<sub>2</sub> P-type LaS<sub>4</sub> N-type alloys, fabrication and thermoelectric props. 0-107771  
 transition metal chalcogenophosphates, intercalation with n butyl-lithium, possible appl. in Li batteries 0-71446  
 Ag<sub>10</sub>Sb<sub>25</sub>Te<sub>52</sub>, single-phase, thermoelectric efficiency 0-107826  
 δ-Bi<sub>2</sub>O<sub>3</sub>, thermoelectric power, heat of transport of O<sup>2-</sup> ions 0-92713  
 Co<sub>2</sub>Mo<sub>6</sub>S<sub>8</sub>O<sub>2</sub>, O-containing Chevrel phases, synthesis and props. 0-108368  
 Cu<sub>2</sub>Mo<sub>6</sub>S<sub>8</sub>O<sub>2</sub>, O-containing Chevrel phases, synthesis and props. 0-108368  
 Ge-Si alloys, n-type, phosphorous doped, precipitation effects due to heat treatment 0-107833  
 Mo<sub>6</sub>S<sub>8</sub> Chevrel phases with group IIIA metals, Nb, Hg, Pb and Cu, synthesis, stability and characts. 0-71608  
 Mo<sub>6</sub>W<sub>6</sub>Se<sub>2</sub> single cryst. vapour growth, characterisation 0-93466  
 NbSe<sub>2</sub>(2H), low field magnetoresist. and anomalous transport props. 0-65602  
 Ni<sub>2</sub>Mo<sub>6</sub>S<sub>8</sub>O<sub>2</sub>, O-containing Chevrel phases, synthesis and props. 0-108368  
 PbMo<sub>6</sub>S<sub>8</sub>O<sub>2</sub>, O-containing Chevrel phases, synthesis and props. 0-108368  
 Pb,Sn,-O<sub>2</sub>Sb films, DC sputtered, elec. props. 0-80426  
 Si position-sensitive detector for CW and pulsed laser beams 0-78883  
 SiAs, cryst. growth from melt, elec. props. 0-76170  
 Sn-Pb (26%), liq. eutectic alloy Seebeck coeff. 0-84463

## Seebeck effect continued

- Te<sub>50</sub>-Se<sub>50</sub>Sn<sub>3</sub>, thin films, elec. cond. and thermoelectric power meas. (*French*) 0-80335  
 V<sub>2</sub>O<sub>5</sub>-V<sub>2</sub>O<sub>4</sub>-BaZnO<sub>2</sub> glass, V ion states, mag. and elec. props. 0-88556

## segregation

- microstructural processes and features only*  
*see also Guinier-Preston zones; spinodal decomposition*  
 alkali halide, crystal, irradiation-induced defects 0-107316  
 alkali halides, divalent metal impurities, aggregation process, order of reaction, fractional time conc. depend. 0-107308  
 alloy, binary, magnetic, interface struct., Monte Carlo simulation 0-60317  
 alloy, solute redistrib. during in situ irradiation in HVEM 0-107324  
 alloys, binary, surface segregation kinetics 0-80044  
 alloys, embrittling residuals categorisation by Auger electron spectroscopy 0-66739  
 alloys, rapidly quenched crystalline, struct., and heat treatment effects 0-76292  
 alloys, temper embrittlement, impurities and alloying elements role, review 0-66649  
 binary alloys, initial transient segregation during unidirectional solidification in a furnace with thermal damping 0-70146  
 binary alloys, surface conc. profile and surface energy 0-84350  
 α-β brass, interface segregation 0-89231  
 cellular and cellular dendritic growth, general microsegregation eqn. 0-84921  
 ceramics, glassy, struct. and electron beam sensitivity 0-79841  
 concrete, fresh, behaviour under a vibr. action, large particle segregation (*Japanese*) 0-88329  
 Czochralski growth, fluctuating growth rates effect on segregation, back-melt 0-59413  
 dehydrogenation kinetics in ferroelec. and paraelec. phases, surface acoustic waves influence 0-97204  
 dilute solute-binary solvent activity coeffs., statistical mech. theory 0-59663  
 grain boundary, equilib. impurity conc. (*Russian*) 0-103478  
 grain boundary cohesion, resulting from solute segregation, pair bonding theory 0-88166  
 grain boundary segregation, critical assessment 0-75362  
 grain boundary segregation, rel. to free surface segregation 0-71657  
 Hastelloy, H<sub>2</sub>, embrittlement in H<sub>2</sub>S environments, impurity segregation effects 0-71724  
 identification of segregating phases, single crystals, radiographs computer calc. 0-84934  
 Inconel 600, thermal treatment, grain boundary microstruct. and SCC resistance 0-71675  
 interfaces, co-segregation of metallic and non-metallic impurities 0-60868  
 interfacial cohesion, adsorption-induced losses 0-65010  
 metals, atomic binding energy and surface energy rel. to prediction of physical props. 0-59434  
 metals, residuals, impurities and props. 0-66521  
 metals and alloys, non-equilib., review 0-66516  
 metals and alloys, segregation studies by imaging atom probe microscopy 0-66911  
 microsegregation in crystals, anal. 0-59410  
 nonequilibrium, during pulsed laser annealing, model 0-108451  
 opal glasses, phosphate opacified, phase comp. and struct. 0-64919  
 polyether-polyester elastomers, differential scanning calorimetry by using poly(oxy-1,4-butylene glycol) as soft segment (*Japanese*) 0-79916  
 polymer blends, fluctuation dynamics, spinodal decomp. 0-79943  
 rare earth oxides, segregation study by electron energy-loss spectroscopy 0-79953  
 semiconductor, polycrystalline, grain boundary effects, doping tech. for study and control 0-79815  
 solid-solid interface chemistry, characterisation, theory 0-75448  
 steel, alloy, temper embrittlement, comp. influence 0-66658  
 steel, continuously cast, segregation at halfway cracks 0-60869  
 steel, Cr-C (1, 1 wt.%), hot ductility and S segregation 0-66594  
 steel, Cr-Mo-P (2.25, 1 wt.%), stress relief cracking, effect of P segregation 0-89324  
 steel, Cr-Mo, ferritic, grain boundary segregation, X-ray microanal. by STEM 0-66740  
 steel, Cr-Mo (2.25, 1.0 wt.%), temper embrittlement, effect of P, Sn, comp. and carbide precip. 0-85036  
 steel, Cr-Mo (2.25, 1.0 wt.%), temper embrittlement, effect of Mn, Si, comp. and carbide precip. 0-85037  
 steel, grain boundary P segregation, effect after quenching and tempering (*Russian*) 0-81145  
 steel, hardenability, role of B and P segregation 0-97486  
 steel, low alloy, temper embrittlement and ternary equilib. segregation 0-60958  
 steel, low C, cold rolled, graphite precip. and S segregation, AES investigation (*Japanese*) 0-89222  
 steel, low-alloy, impurities, segregation and creep embrittlement 0-66653  
 steel, martensitic, alloying element effect on coarsening behaviour of cementite particles in ferrite 0-66518  
 steel, martensitic 12% Cr, temper embrittlement 0-66650  
 steel, Ni-Cr, Sb doped, solute segregation and brittle fracture 0-85033  
 steel, Ni-Cr, solute segregation and intergranular brittle fracture 0-108568  
 steel, Ni-Cr, temper embrittlement, intermediate tempering treatments 0-60944  
 steel, nonmetallic inclusion segregation during cooling (*Russian*) 0-100330  
 steel, segregation and adsorption of S, influence on carburisation and nitrogenation 0-66701  
 steel, stainless cast, creep ductility, Auger spectroscopy study 0-60917  
 steel, tempered martensitic, type AISI 410, role of C in embrittlement phenomena 0-93652  
 steels, solute segregation and intergranular fracture 0-60957  
 surface chemistry rel. to metallurgical props., SIMS, XPS and AES (*French*) 0-80045  
 surface segregation of mixture, nonequilibrium 0-88325  
 undersaturated alloys, irradiated, solute segregation kinetics, via drift and defect-solute complexes 0-60872  
 void, and interstitial loop evolution in pulsed fusion reactors 0-84217  
 voids, coated, capture efficiency 0-96515  
 web dendrites, dislocations, stacking faults, X-ray topographic study (*Chinese*) 0-88148  
 Al-An (8-25 wt.%), solid solns., residual resist. during clustering 0-97483  
 Al-Cu (1.9 at.%), solute fluctuations, EXAFS study 0-79949



## segregation continued

- Al-Cu dilute alloys, vein closing mechanism in fluidity tests 0-84924  
 Al-Mg-Zn alloys, Al-rich, weld metal comp. effect on microsegregation and eutectic phase segregation (*German*) 0-108455  
 Al-Si eutectic alloy, banded struct., SEM and optical microscopy 0-104144  
 Al-Zn-Mg alloys, grain boundary segregation, implications to stress corrosion cracking 0-84936  
 $\alpha$ -Al<sub>2</sub>O<sub>3</sub>, grain boundary segregation, electron microscopy 0-103361  
 Al<sub>2</sub>O<sub>3</sub> polycrystalline, effects of space charge, grain-boundary segregation and mobility differences on conductivity 0-79979  
 Al<sub>2</sub>O<sub>3</sub>-MgO, grain boundary segregation of Ca and Mg X-ray spectrosc. and STEM study 0-107269  
 Au-Cu, surface conc. profile and surface energy 0-84350  
 Au-Ni, surface segregation, strain effects 0-80042  
 BaTiO<sub>3</sub> ceramics, PTC-type, grain boundary study using TEM 0-107267  
 CaF<sub>2</sub>-Eu, CaF<sub>2</sub>-Eu,Mn(Gd), single crystal predisintegration phenomena, SEM cathodolum. obs. 0-59502  
 CaF<sub>2</sub>-Mn, CaF<sub>2</sub>-Eu,Mn, single crystal predisintegration phenomena, SEM cathodolum. obs. 0-59502  
 Co-Ti(Hf)(Ta)(Mo)(Zr)(Al)(Fe)(Ni), dendritic segregation 0-76260  
 25Cr-20Ni stainless steel dendritic solidification, growth morphology and solute redistrib. (*Japanese*) 0-81045  
 Cu ferrite films, Mn-, Ni- and Al-substituted, LPE growth 0-96752  
 Cu-Ag, surface segregation of S, Auger spectral study diffusion 0-76549  
 Cu-Al(Au)(Ga)(Ni)(Pd)(Rh)(Zn) (4 at.%), anneal hardening mechanism 0-60879  
 Cu-Bi, grain boundary struct. intergranular fracture, segregation role 0-66648  
 Cu-Fe (1.5 wt.%), precipitation-effect on void formation during electron irradiation 0-84211  
 Cu-Ni, evaporation limited segregation 0-70513  
 Cu-Ni, liq., surface conc. profile and surface energy 0-84350  
 EuTe, high-temperature evaporation and reactivity 0-103469  
 Fe, cast, alloyed and unalloyed, microsegregation thermodynamics 0-76261  
 Fe, free surface and grain boundary O<sub>2</sub> and S chemistry 0-75410  
 Fe, segregation and adsorption of S, influence on carburisation and nitrogenation 0-66701  
 Fe, segregation of impurities, physico-chemical aspects (*Czech*) 0-60866  
 Fe, single cryst., segregation behaviour of S, O and P at (100) surface 0-100841  
 Fe surfaces, adsorption, segregation and reactions of non-metal atoms, LEED and AES obs. 0-59783  
 Fe-Co-Ti-Al alloy type YuNDK magnets, metallographic method of distinguishing cracks 0-85096  
 Fe-Cr-Ni (12, 15 wt.%) austenitic alloy, Ni<sup>6+</sup> irradiated, void swelling and phase stability, Si and Ti effects 0-65055  
 Fe-Cu-C, phase equilibria, 950 to 1500°C 0-60836  
 Fe-M-(I) (M=Ni, Cr, V, Ti, Mo; I=Sb, P), co-segregation at free surfaces studied by Auger spectroscopy 0-59767  
 Fe-Mn, as cast, pseudo-composite struct. resulting from interdendritic segregation, cryogenic materials appl. (*French*) 0-93556  
 Fe-Mn cast alloys, homogenisation annealing and chemical diffusion (*Czech*) 0-66551  
 Fe-N, single cryst., solid soln. softening, effect of interstitial N 0-97496  
 Fe-Ni, grain boundary segregation, X-ray microanal. by STEM 0-66740  
 Fe-Ni-Cr-Al-Ti-W-Mo (35, 15, 2.4, 2.3, 2.2 wt.%) wrought superalloy, freckles (*Chinese*) 0-104137  
 Fe-Sb-Ti(V)(Cr)(Mn)(Co)(Ni), interactions and segregations, Mossbauer and X-ray diff. study 0-70415  
 Fe-Ti (0.15 wt.%), Ti distrib., segregation, FIM anal. 0-84200  
 FeTi, surface and mag. props., heat treatment and hydrogenation effects 0-75447  
 Ge single crystals, constitutional supercooling growth conditions, structural and chem. inhomogeneities 0-93473  
 GeO, Cu, amorphous thin film, impurity effects on struct. 0-107054  
 Hg,  $\chi$ cd, Te, segregation, compositional characterisation 0-107434  
 InSb, undoped and Te-doped, anomalous impurity segregation, Hall and mass spectrum meas. (*Chinese*) 0-59501  
 KBr(Cl):Mg<sup>2+</sup>, dopant aggregation and precipitation 0-107306  
 LiF, alkali ion implantation, migration, segregation, effect on optical props. 0-100269  
 Mg-Cu polycrystals, surface study by AES, XPS and X-ray induced AES 0-65346  
 Mo-C (110) surface, segregation, precip. and desorpt. of C, AES and LEED study (*French*) 0-103480  
 NaCl, impurity precipitation and grain boundary diffusion 0-107567  
 NaCl:Eu, secondary Eu phase dissolution, EPR and optical absorpt. study 0-96655  
 NaCl:Mg<sup>2+</sup>(Ba<sup>2+</sup>), dopant aggregation and precipitation 0-107306  
 Nd<sub>2</sub>O<sub>3</sub>-Y<sub>2</sub>O<sub>3</sub> film, segregation obs. by EELS 0-79953  
 Ni dilute alloys, implant profiles modification by radiation enhanced diffusion and segregation 0-88217  
 Ni, oxidation, high temp., effect of C on cavity form., SEM study 0-97638  
 Ni, stress corrosion susceptibility, S segregation effect, Auger spectrosc. study 0-61019  
 Ni-Cr-Ti rapidly solidified superalloys, surface segregation 0-76263  
 Ni-Cu, surface segregation, computerised atom-probe FIM study 0-75412  
 Ni-Ti (1 at.%), surface comp., temp. and O<sub>2</sub> exposure effects, AES study 0-80914  
 Ni<sub>0.96</sub>Sb<sub>0.04</sub>, surface segregation, XPS and AES obs. 0-76135  
 Pb-Au, interstitial and substitutional distrib. 0-84204  
 PbTe thermoelectric materials, microstructure anal. using SEM X-ray microanalysis 0-107211  
 Pt/Fe solid solution crucibles, Fe segregation 0-61192  
 Pt-Au, surface segregation, comp. depth profiles meas. using atom-probe field ion microscope 0-100380  
 Rh (111), co-adsorption of H<sub>2</sub> and CO segregation of co-adsorbed species 0-65361  
 Si, annealing, using laser pulses, impurity incorporation at melt-cryst. interface 0-59504  
 Si, crucible grown, virgin and implanted, laser irradiation effects on surface structure 0-92768  
 p-Si, Czochralski grown, microdistrib. of O, SEM and spreading resist. obs. 0-79830  
 Si, ion implanted, dopant depend. of oxidation rate 0-89384  
 Si, melt grown crystals, impurity incorporation, calcs. 0-79718

## segregation continued

- Si, multigrained, impurity segregation to grain boundaries, AES and SIMS obs. 0-65027  
 Si, polycrystalline, As segregation at grain boundaries, elec. props. meas. 0-75259  
 Si:As, shallow junctions by high-dose implants 0-96694  
 Si:As laser annealing, heat and mass transport model 0-92546  
 Si:As(B), heavy-doping effects and impurity segregation during high-pressure oxidation 0-65014  
 Si:As(Pb), ion-implanted, impurity redistrib. during laser irradiation 0-100280  
 Si:B(P)(As)(Sb)(Cu)(Fe), ion implanted, doping profile, pulsed laser annealing effects 0-88197  
 n-Si:Ga laser doped, segregation, Rutherford backscattering 0-103483  
 Si:In, clustering and precipitation, time-dependent perturbed ang. correlation meas. 0-65234  
 Si:O, A centre, theoretical study 0-75521  
 Si:Pt, implanted and laser annealed, segregation and increased dopant solubility 0-65016  
 Si-Al-O-N ceramic, grain boundary desegregation and intergranular cohesion 0-100872  
 SrF<sub>2</sub>:Dy<sup>3+</sup>, cluster form., IR absorption study (*French*) 0-108240  
 W (100), clustering of Kr, He desorption spectrometry 0-77908  
 W electrodes, C segregation and arc damage 0-64795  
 W-Cu (92.8, 7.2 wt.%), liq.-phase sintered, embrittlement and interfacial impurity segregation 0-66647  
 YIG:(Si), liq. flux growth, SiO<sub>2</sub> segregation and cryst. defects 0-66416  
 YbTe, high-temperature evaporation and reactivity 0-103469  
 ZrO<sub>2</sub>-SiO<sub>2</sub>, liquid immiscibility, microstruct. of plasma dissociated ZrSiO<sub>4</sub> 0-107429
- Seidel theory** see aberrations  
**Seignette salt** see Rochelle salt  
**Seignettelectric materials** see ferroelectric materials  
**seismic waves**  
 see also seismology  
 absorption coefficients of P- and L-waves 0-76915  
 E.African Rift valley, seismic wave travel times 0-98238  
 airborne sound coupling into earth, freq. dependence 0-74567  
 Alpine orogeny, Europe, upper mantle horizontal inhomogeneities, P-wave obs. 0-98268  
 attenuation in aftershock region, example from Off-Izu Peninsula earthquake (1974 May 9) 0-76926  
 body waves, propagation in S.-Kanto Region derived from earthquakes observed initial motion (*Japanese*) 0-94481  
 S California, upper mantle seismic velocity, regional variations 0-109111  
 California rock P-wave velocity, high press. and temp. expts. 0-61783  
 camouflet source of transverse waves, theory 0-101344  
 compressional wave attenuation in partially gas saturated porous rock 0-72434  
 compressional wave propagation in gas saturated porous rock 0-72433  
 compressional wave propagation in porous rock containing gas pockets 0-72432  
 core and mantle elastic wave velocity at high-pressure, using Debye theory of sp. ht. 0-89979  
 core region, attenuation coeff. distrib. 0-90035  
 crack induced velocity anomaly, P-waves for crack estimation 0-98253  
 crustal velocity structure, in Superior-Churchill boundary zone, S.Canada, cooperative surveys 0-89985  
 deep interior, magnetoviscoelastic wave refl. and refr. at welded contact 0-89967  
 diffraction at coal seams, approx. diff. theory for transparent half-planes 0-89974  
 diffraction properties of crust, using Earth crust models 0-98239  
 dislocation source in heterogeneous crust, propag. study using dislocation model 0-101340  
 Earth deformation, mag. field effects 0-109085  
 earthquake energy dissipation during propag., by solid friction 0-109106  
 earthquake foreshocks, waveform anal. rel. to differentiation from earthquake swarms (*Japanese*) 0-67342  
 earthquake parameter determ. computer technique using wave phase data (*Chinese*) 0-77126  
 earthquake swarms, seismic waveform anal. rel. to differentiation from foreshocks (*Japanese*) 0-67342  
 W.Europe, upper mantle P-wave vel., large scale variations 0-109112  
 first arrival of P-waves from quake, nonquadratic distrib. of signs 0-94474  
 Garm region elastic wave vel. temporal changes in 0-104914  
 ground response to weight dropping, wave amplitude and vel. 0-76914  
 Hidaka mountain region, Hokkaido, Japan, unusual seismic waves from shallow quakes (*Japanese*) 0-94477  
 Iceland, body wave vel. correl. with basaltic crust alteration 0-90015  
 inelastic media, propag. theory (*German*) 0-104885  
 initial longitudinal waves of Friuli earthquake, 1976 May 6, polarities anal. and focal mechanism 0-85603  
 inner core PK11KP wave detect. and damping 0-104925  
 inverse problem for normal incidence waves to horizontal layered media 0-98252  
 inversion of microseismic array cross spectra 0-98243  
 limestone, dry and saturated, P and S wave attenuation, US obs. 0-72494  
 long-period oscillations, meas. by borehole long-period seismometer (BELS type 79) with stable period (*Japanese*) 0-67417  
 longitudinal wave velocities in rocks, appl. to mineral comp. prediction for rocks at great depths (*Russian*) 0-104956  
 lower mantle seismic wave vel., meas. method using wide aperture array 0-105071  
 mantle surface waves, vels. in SW flank region of Baikal Rift 0-94503  
 microvibration frequency analysis by 50 m interferometer 0-109276  
 multidimensional velocity generalisation technique, appl. to Black Sea NW shallow and nearby land areas (*Russian*) 0-105068  
 multiple reflected signal attenuation, least squares estimation procedure 0-85596  
 multiple wave suppression on seismic recordings, two methods of soln. 0-77147  
 multiply reflected seismic ray, multi-segment traces deconvolution and synthesis 0-77162  
 multipolar source in layered media, seismic wave emission 0-81816  
 normal mode oscillations of Earth, asymptotic representation of multiplet spectra 0-94459  
 ocean bottom hydrophone array obs. of P and S waves, wave train characteristics 0-104898



## seismic waves continued

- oil shale, dry and saturated, P and S wave attenuation, US obs. 0-72494  
 Onikobe earthquake, Japan, ground motion deduced from damage, source model (*Japanese*) 0-94479  
 onset of waves, detection algorithm for automatic seismometer (*Japanese*) 0-94476  
 ophiolite complex of Point Sal, California, seismic vel. struct. 0-109110  
 P- and S-waves of deep interior, max. vel. amplitudes 0-98262  
 P-wave arrival-time differences for relative epicentre determ. 0-101328  
 P-wave displacement in rectangular fault, spectral amplitude calcs. (*Chinese*) 0-76911  
 P-wave residuals, mantle vel. anomalies below Colorado Rocky Mountains 0-81853  
 P-wave three-dimensional velocity structure for Beijing upper mantle and crust (*Chinese*) 0-104894  
 P-wave travel time anomalies rel. to epicentral distance to African stations 0-98237  
 P-wave vel. determ. from Honshu local earthquake data 0-76937  
 P-wave vel. struct to depth of 150 km, Kanto District, Japan (*Japanese*) 0-94475  
 P-wave vel. structure of metamorphic belt of central California 0-98270  
 P-wave velocities, in uppermost mantle beneath Turkey and Iran 0-72462  
 P-wave velocities in Shikoku district, Japan, rel. to upper crustal struct. (*Japanese*) 0-94508  
 P-waves, vel.-depth model of subcrustal lithosphere beneath Fennoscandia 0-90009  
 P-waves from Rumania earthquake, 1977 March 4, obs. rel. to Moho vel. depth distrib. (*German*) 0-98256  
 P-waves from small earthquakes, anal. rel. to detailed spatial distrib. of foreshock and aftershock activities (*Japanese*) 0-94483  
 P-waves refracted by mantle, hydrophone recordings of underground nuclear explosions 0-98257  
 passing exchange wave effects on inclined interface (*Russian*) 0-85600  
 planar SH wave diffraction, density, rigidity bidimensional perturbation (*French*) 0-76917  
 propagation, Wiechert-Herglotz inversion, as integration on closed contour 0-61766  
 propagation and damping coeff. in electrically charged water-saturated rock 0-76921  
 pulse propag. in media with freq. dependent Q, theory 0-72438  
 ray series method and dynamic ray tracing system for three-dimensional inhomogeneous media 0-98456  
 Rayleigh in trench 0-98266  
 Rayleigh wave attenuation in volcanic area of Massif Central, France 0-98264  
 Rayleigh waves higher modes to determine upper mantle struct. 0-104890  
 raypath reflection model for layered media with source and receiver in different layers 0-83704  
 reflected wave travel-time curve inversion theory 0-89968  
 reflection seismograms, simultaneous spherical divergence correction and optimal deconvolution 0-98258  
 refracted wave correlation method, interpretation accuracy (*Russian*) 0-85758  
 refractive index distribution, image reconstruction via iterative ray tracing between boreholes 0-98466  
 rock seismic wave attenuation, role of crack and grain boundaries 0-72495  
 S-wave anisotropy in the upper mantle under a volcanic area in Japan 0-90024  
 S-wave short-period attenuation under W.United States 0-98242  
 S-wave vel. meas. in soil and bedrock using down-hole method 0-98458  
 San Fernando earthquake, strong ground motion, ray models 0-61762  
 sandstone, dry and saturated, P and S wave attenuation, US obs. 0-72494  
 sandstone, propagation vel. 0-76915  
 seafloor propagation of earthquake wave, theory 0-81843  
 SH wave propag. in heterogeneous media, from line source 0-81842  
 SH waves in anelastic media, ray-synthetic seismograms 0-98241  
 SH-waves incident on cylindrical tunnel dynamic stress anal. of elastic liner 0-79201  
 shear wave recording with geophones 0-101447  
 shear waves excitation and propag. from Melanesia and Banda arcs to Australia 0-104887  
 signal processing using inverse diffraction technique 0-74608  
 soil layer amplifying plane waves arriving at surface 0-76929  
 source location by surface waves, reference point equalisation method 0-72648  
 Sp waves, from upper-lower mantle transition cone, seismogram calcs. 0-104901  
 spectra, explosion earthquakes assoc. with 1973 eruptions of Asama Volcano (*Japanese*) 0-67340  
 spheroidal modes from 1977 Indonesian earthquake, attenuation obs. 0-81815  
 SS shear-wave travel time for Earth struct. 0-81817  
 strong ground motions at short epicentral distance, simulation 0-104906  
 strong motion short period accel. and vel. using fault model 0-104918  
 surface wave crossing a vertical discontinuity, refl. and transmission coeffs. (*German*) 0-76931  
 surface wave dispersion from earthquakes, use in Reykjanes Ridge crest study 0-90021  
 surface waves in three-dimens. struct., finite element matrices 0-61765  
 surface waves propagation over liquid and crystalline layers, elastic consts. of crystals 0-76924  
 surface waves propagation over liquid and crystalline layers, theory 0-76925  
 T waves from Tonga earthquake (June 1977), human perception on Tahiti 0-61769  
 teleseismic P-wave residual anal. at Shillong, India, earthquake prediction 0-104921  
 transversely isotropic media, P-, SH-, and SV-wave vels. computation 0-98249  
 tsunami, island of Hawaii, 1979 November 25, numerical anal. by finite-element method 0-72449  
 tsunami accompanying Tonankai earthquake of 1944, source model (*Japanese*) 0-67344  
 tsunami at Oshima (W.Hokkaido), 1741 August 29, religious monuments (*Japanese*) 0-67345  
 tsunami height rel. to earthquake mag., empirical relation 0-94461  
 tsunami prediction and magnitude, coastal radar system appl. 0-82101

## seismic waves continued

- tsunami wave generation by finite bottom displacement (*Russian*) 0-109113  
 tsunamis in Kanto, 1677 and 1703, behaviour along Kujukuri-hama coast from old monuments (*Japanese*) 0-67339  
 United States, attenuation of strong ground motion 0-81834  
 W.United States, horizontal ground accel. attenuation rel. to magnitude 0-104905  
 upper mantle S-wave velocity model, based on great circle Rayleigh waves 0-109107  
 velocities in lower mantle, evaluation of finite strain eqns. of state using lattice models 0-96620  
 velocity anomalies in Pamirs-Hindu-Kush upper mantle, mapping by graphical method 0-77146  
 velocity change in S.Kanto area, study by Tateyama explosions (*Japanese*) 0-67338  
 velocity changes in deep interior, press. and temp. induced phase transitions 0-90034  
 velocity inversion in upper crust, for synthetic seismogram construction (*Japanese*) 0-94478  
 wavefront curvature theory, for laterally inhomogeneous media 0-104908

## seismographs see seismometers

## seismology

- see also earthquakes; lunar seismology; seismic waves; seismometers  
 abyssal fan sediment in Arabian Sea, acoustic velocity 0-72488  
 acoustic logging data, on-line computer interpretation techniques 0-90239  
 acoustical imaging, US visualization and characterization, conf., vol.8, Key Biscayne, FL, USA (May-June 1978) 0-83720  
 active continental margins, earthquake foci three-dimensional projection 0-72453  
 Adak Canyon region, central Aleutians, seismicity and tectonics 0-61772  
 E.Afghanistan, shallow earthquakes and tectonic activity 0-72444  
 aftershock region of Off-Izu Peninsula earthquake, 1974 May 9, seismic waves attenuation 0-76926  
 aftershock sequences, implications of dilatancy-fluid diffusion theory 0-85604  
 air gun operational method, pulse generation 0-90234  
 Alaskan Seismic Gap, effect of 1979 February 28 earthquake 0-109116  
 central Aleutians, ocean bottom seismograph meas. 0-89978  
 E. Alpine region, seismicity and earthquakes assoc. with Bohemian Massif-Carpathians contact zone 0-104888  
 Alps, longitudinal profile (Judenburg to Hozzuperezsteg), refr. seismic meas. (*German*) 0-76916  
 S.America, earthquake migration, spectral anal. 0-85614  
 N.America, effect of craton on distrib. of seismicity and intraplate stresses 0-98248  
 N.Antolian fault zone, earthquake migration and seismic gaps 0-85613  
 antipodal waves for Earth interior structure determ. 0-89972  
 NE.Atlantic, upper crustal struct., seismic study 0-61784  
 Atotsugawa Fault, Japan, seismicity and focal mechanism of local earthquakes (*Japanese*) 0-94482  
 Australia, plate collision, seismic shear waves excitation and propag. 0-104887  
 Azores, earthquake (1980 January 1), aftershock sequence and present day tectonics 0-104911  
 Azov-Kuban' oil-gas basin structure from seismic data (*Russian*) 0-85601  
 NE.Baikal region, seismicity, interpretation 0-98217  
 SW Baikal Rift, crust and upper mantle struct. according to seismic data 0-94503  
 Black and Azov Sea floors, seismic profiling, techniques and expt. results 0-89970  
 body-wave analysis of St. Elias, Alaska earthquake (1979 February 28) 0-104897  
 body-wave inversion method for Earth struct., using travel time and amplitude data 0-109108  
 Burma and S China, seismicity and tectonics 0-89983  
 S California, upper mantle seismic velocity, regional variations 0-109111  
 California earthquake parameters, statistics and model 0-104891  
 camouflet source of transverse waves, theory 0-101344  
 E.Canada seismic risk, regional assessment 0-61774  
 Canadian seismic risk estimation, probabilistic methods 0-61773  
 Caribbean seismic network, preliminary results 0-61771  
 Carpathian region and Ukrainian shield adjacent slope, basic crustal surfaces, seismic obs. 0-89995  
 S China and Burma, seismicity and tectonics 0-89983  
 Chinese earthquake history, point process anal. 0-85612  
 coal seams fault indication using acoustic array processor 0-85778  
 Colima earthquake, Mexico, Jan. 1973, source mech. and aftershocks 0-81823  
 common-depth-point method, prestack migration method for deformed refl. layer 0-98251  
 conference, New Delhi, India (March 1978), earthquake prediction 0-85602  
 conference, Nov. 1979, New Orleans, USA 0-81891  
 Coral Sea, crustal struct. from seismic data 0-72459  
 core boundary discovery, historical aspects 0-105486  
 core fluid oscillations, transverse motion, Earth rot. effects 0-89965  
 Coso geothermal area, underlying low-vel. body, teleseismic evidence 0-90005  
 Coso Hot Springs, Known Geothermal Resource Area, model 0-90004  
 Coso Range, California, seismicity 0-89971  
 Coyote Lake, California (1979 August 6), local magnitude and seismic moment determ. 0-104904  
 deep interior, magnetoviscoelastic wave refl. and refr. at welded contact 0-89967  
 deep seismic zone, Tohoku, Japan, freq.-magnitude obs. rel. to geochem. changes 0-72447  
 Dellwood knolls, active seismicity rel. to role in triple junction tectonics off northern Vancouver Island 0-90067  
 depth migration after stack, finite-difference method 0-98254  
 depth migration before stack, finite-difference method 0-98255  
 descending slab stress state, anal. of seismic source parameters 0-104946  
 detection probability for weak seismic events, theory 0-67347  
 Diablo Plateau region, W.Texas, preseismic deform. model for tectonic uplift 0-72481  
 diffraction properties of crust, using Earth crust models 0-98239  
 digital generation of accurate synthetic seismograms 0-85779  
 dilatancy induced seismogram polarisation anomalies, and earthquake prediction 0-101342



## seismology continued

- discrimination between induced and natural earthquakes in geothermal area 0-101332  
 dislocation theory appl., book contrib. 0-109119  
 Earth core synthetic seismograms, full wave theory and reflectivity method 0-61777  
 Earth crust, tectonic deform. characts. from seismological data in China (Chinese) 0-76951  
 Earth free oscill., radial mode Q-value using 1977 Indonesia earthquake data 0-67346  
 Earth free oscill. spectra, coupling and attenuation of near reson. multiplets 0-61778  
 Earth interior sounding iterative ray tracing between boreholes for underground image reconstruction 0-98466  
 Earth structure model based on torsional oscill. eigenperiods 0-90044  
 earthquake energy dissipation during propag., by solid friction 0-109106  
 earthquake focal mechanisms, classical study techniques 0-76918  
 earthquake frequencies, stochastic modelling (Japanese) 0-94480  
 earthquake magnitude correl. with focal parameters, theoretical basis 0-101338  
 earthquake precursory seismicity burst, long-term prediction 0-72441  
 earthquake prediction, appl. of geodetic research (German) 0-101317  
 earthquake prediction, based on geochem. meas., conf., San Francisco, USA (Dec. 1980) 0-90606  
 earthquake prediction, workshop, Strasbourg, France, (1980 January 31 to February 1) 0-62396  
 earthquake prediction from pseudo-periodicity of strong after shocks (Chinese) 0-76913  
 earthquake seismic moment tensor elucidation from teleseismic data 0-104915  
 earthquake source mechanism model for thermo-visco-elastic Earth 0-104886  
 earthquake spatial distribution, two-point correl. function 0-89963  
 earthquake swarms, differentiation from foreshocks via similarity of seismic waveform (Japanese) 0-67342  
 W.Europe, upper mantle P-wave vel., large scale variations 0-109112  
 explosion profiling of deep crust struct., 2-D scheme 0-72637  
 explosion radiation pattern, cavity creation in prestressed media, theory 0-61780  
 explosion seismology, appl. to rocks mineral comp. prediction at great depths (Russian) 0-104956  
 explosion seismology, residual static correction problem, iterative soln. anal. 0-101334  
 explosion seismology data analysis method for wave eqn. migration 0-90233  
 Fairbanks, Alaska seismic zone, earthquake migration 0-101330  
 fault location in underground coal seams 0-94613  
 fault strain field, included rectangular fault in semi-infinite media 0-98261  
 faulting, acoustic fluidisation theory 0-85653  
 faulting rupture process, plane shear faulting model of earthquake (Chinese) 0-104893  
 Fennoscandia, subcrustal lithosphere seismic investigations 0-90009  
 foreshocks, differentiation from earthquake swarms via seismic waveform variability (Japanese) 0-67342  
 Fort Ross, California, earthquake sequence, March-April 1978 0-81824  
 free modes excited by Indonesia earthquake, Aug. 19<sup>th</sup> 1977 obs. 0-61767  
 free oscillation of Earth, attenuation of radial modes 0-89966  
 free oscillation of Earth, radial mode, damping by bulk attenuation 0-76928  
 frequency-magnitude relations, in NGSDC earthquake data file 0-81838  
 Friuli, Italy, May 6, 1976, earthquake sequence 0-81822  
 Fuji river, active faults anal. by track etch method (Japanese) 0-109127  
 fusion reactors, JT-60, seismic anal., design changes 0-95425  
 Geotraverse Rhenohertzynikum, fault zones investigation by seismic refl. and refr. studies 0-90046  
 granite terrain weathered zone, appl. of correl. refr. method 0-90230  
 gravimetric and seismic methods combination for initial seismic data crustal vel. sections 0-105070  
 gravitational radiation, seismometer detection possibility 0-86196  
 great earthquake occurrence, chaos theory of fault block behaviour 0-72448  
 great earthquakes, chaotic behaviour, coupled relax. oscillator model, billiard model and electronic circuit model 0-94462  
 Griffith crack-antiplane shear wave interaction at interface of two bonded elastic half-spaces, geophys., seismological appl. 0-92087  
 ground response near Long Beach, California, near surface struct. 0-61775  
 Guadeloupe, seismic profiles of superficial struts. (French) 0-76932  
 Gulf of Papua, crustal struct. from seismic data 0-72459  
 Hengill-Hellisheidi area, SW. Iceland, seismicity obs. 0-89976  
 N. Hida region, Japan, seismicity and focal mechanism of local earthquakes (Japanese) 0-94482  
 Himalaya and Tibet Plateau region, tectonic history 0-72486  
 Hindu Kush region, microearthquake seismicity and fault plane solns. 0-72446  
 Hindukush, Baluchistan arc, seismotectonics and struct. (1890-1970) 0-104922  
 SW. Iceland, axial rift zone, seismic crustal study 0-90014  
 Iceland, seismic structure along RRISP-Profile I 0-90018  
 Iceland, statistical anal. of damaging earthquakes and volcanic eruptions, (1550 to 1978) 0-89975  
 Iceland crust above layer three, seismic structure 0-90015  
 N.Iceland rift zone, seismic study of crust struct. 0-90013  
 Iceland-Faeroe Ridge, crustal struct. 0-90016  
 NE India, teleseismic P-wave residual anal. at Shillong, rel. to earthquake prediction 0-104921  
 Indian geopotential anomaly, seismic and gravity data anal. 0-90037  
 Indo-Australian plate, intraplate seismicity rel. to plate internal deform. 0-109134  
 inverse problem for normal incidence waves to horizontal layered media 0-98252  
 Iran, seismic risk 0-76922  
 Iran, seismic waves from Iranian quakes, excitation and attenuation 0-104900  
 Iran and Turkey, focal and seismicity depth determ. errors 0-61779  
 ISC seismological catalogue, geographical distrib. of detectability 0-109117  
 Italy, precursory seismicity to strong earthquakes 0-104884

## seismology continued

- Izu Peninsula, active faults anal. by track etch method (Japanese) 0-109127  
 Japan, statistics of earthquakes energy release (1915 to 1978) 0-94471  
 Japan seismicity, 1885 to 1925, catalogue of  $M \geq 6$  earthquakes and smaller, damaging, earthquakes (Japanese) 0-67341  
 Japan-Bonin trench, crustal and upper mantle changes 0-72466  
 Japanese earthquakes, 1901 to 1925, instrumental magnitudes (Japanese) 0-94484  
 Japanese Islands region, earthquakes and mechanisms data compilation (Japanese) 0-67332  
 Kane Fracture Zone of Atlantic, seismic study of crust struct. 0-104936  
 S.Kanto area, seismic waves vel. change meas. from Tateyama explosions (Japanese) 0-67338  
 Kanto District, Japan, earthquakes rel. to countercurrent accompanying descending Pacific plate (Japanese) 0-94514  
 S. Kanto Region, Japan, body waves propag. derived from earthquakes observed initial motion (Japanese) 0-94481  
 Kern County, earthquake, precursory seismicity and small quakes 0-104902  
 kinematic data, joint linear external inversion method 0-90240  
 Krafla volcano, Iceland, 1978 July deflation, seismic activity rel. to magma intrusion 0-90054  
 Kuril-Kamchatka trench, seismic study of crust 0-89982  
 Kurile Island earthquake, seismic quiescence precursory 0-85610  
 La Malbaie, Quebec (1924-1978), epicentre relocation 0-104903  
 La Soufriere, Guadeloupe, seismic profiles of superficial struts. (French) 0-76932  
 Lacq, France, petroleum exploitation rel. to non-natural earthquakes (French) 0-104892  
 Lake Jocassee, S.Carolina, seismicity rel. to Rn content of groundwater 0-94466  
 Laramide orogeny, seismic profiles in Wyoming, USA 0-85626  
 large earthquakes, time-predictable recurrence model 0-85598  
 layered media lossless wave eqn. soln., Bremmer Series decomp. 0-89962  
 lower mantle seismic wave vel., meas. method using wide aperture array 0-105071  
 LWR power stations, R and D for improving seismic safety 0-99231  
 magnitude scale based on strong-motion horizontal particle vel. 0-81836  
 Makran region, seismicity var. rel. to large earthquakes 0-85611  
 mantle, seismic vel. variations, origins 0-81854  
 mantle and crust seismic vel. struct., model 0-89990  
 mantle below Colorado Rocky Mountains, seismic vel. anomaly 0-81853  
 mantle earthquakes, spatial distrib. in Japan and Aleutian arcs 0-81820  
 mantle isotropy assumption brought into question 0-90024  
 mantle of W.Pacific, multiple ScS travel times 0-72443  
 mantle seismic waves in Europe and Eurasia, inferences from higher mode data 0-72436  
 Massif Central, France, Rayleigh wave attenuation in volcanic area 0-98264  
 maximum ground acceleration determ. for large earthquakes (Japanese) 0-101453  
 meizoseismal shaking of long-period, for strike-slip event 0-81814  
 Michoacan, Mexico, seismic gap, length of earthquake-free period 0-76919  
 microseismic array cross spectra, inversion 0-98243  
 migration by phase shift-algorithm for array processor 0-72638  
 Miyagiken-oki earthquake, June 1978, aftershock spectral anal. 0-109118  
 Moho, continental, throws and dips sounding by explosion seismology 0-85620  
 Mountain Crimea region, surface seismic Rayleigh waves, amplitude spectra 0-89969  
 multi-segment seismic traces, deconvolution and synthesis 0-77162  
 multidimensional velocity generalisation technique, appl. to Black Sea NW shallow and nearby land areas (Russian) 0-105068  
 multiple reflected signal attenuation, least squares estimation procedure 0-85596  
 multipolar source in layered media, seismic wave emission 0-81816  
 Nankaido earthquakes correl. with Shikoku seismicity characts. 0-101339  
 Nepal Himalaya, body waves from earthquakes, focal mechanism and tectonics 0-72455  
 New Zealand (N.Island), plate boundary microearthquake study 0-109131  
 normal mode oscillations of Earth, asymptotic representation of multiplet spectra 0-94459  
 normal moveout velocity in 3D laterally inhomogeneous media with curved interfaces 0-101336  
 Norris Geyser, Yellowstone Park, USA, microseisms of geothermal area 0-104909  
 North America, S and P station anomalies 0-94460  
 nuclear power stations, seismic qualification of Class 1E eqpt. 0-99234  
 nuclear power stations, seismic qualification tests of elect. eqpt., damage severity factor concept 0-99235  
 nuclear power stations, seismic safety margins research program of the US Nuclear Regulatory Commission 0-99229  
 nuclear power stations, seismic safety of mechanical eqpt., R and D program 0-99232  
 Oaxaca earthquake, Mexico, aftershocks in former seismic gap 0-98265  
 Oaxaca gap, Mexico prediction of earthquakes 0-85609  
 ocean crust sounding, computer processing method of seismograph records 0-85605  
 ocean crust studies, suppression of sea-floor multiples 0-90231  
 ocean-bottom seismograph observation system (Japanese) 0-94615  
 oceanic crust, petrology and porosity, shear vel. struct. 0-72473  
 oceanic type crust as a type of Earth crust 0-89997  
 Okhotsk Sea deep basin, seismic study of crust 0-89982  
 ophiolite complex of Point Sal, California, seismic vel. struct. 0-109110  
 oscillations, split normal modes, theoretical amplitude and Green's dyadics 0-101341  
 Oshima (W.Hokkaido), source area of 1741 tsunami from religious monuments (Japanese) 0-67345  
 E.Pacific Rise, seismic sounding rel. to oceanic crust props. and origin 0-101360  
 Pamir-Hindu Kush region, seismicity and fault plane solns. 0-72445  
 peak acceleration, velocity, and displacement from strong-motion records 0-98246  
 Peruvian earthquakes, seismic gaps and source zones 0-85607  
 Philippine Islands, tectonic struct. revealed by seismicity and volcanicity 0-94511  
 Philippines, microearthquake survey of tectonic features 0-81827  
 plate boundary seismic pot., major boundaries 0-85606

## seismology continued

- Pocotalto Valley earthquake, 1975 March 28, source model 0-104896  
 pulse propag. in media with freq. dependent Q, theory 0-72438  
 q estimates using the coda of local earthquakes 0-104899  
 radial overtones eigenfrequencies, pattern for specified Earth model 0-104889  
 ray method for theoretical seismograms, accuracy 0-67348  
 ray theoretical seismograms of laterally inhomogeneous struts. 0-72450  
 ray tracing, two-point problem, adaptive finite difference method 0-98457  
 Rayleigh waves from nucl. explosion, anomalous generation 0-81833  
 Rayleigh-wave radiation pattern, for small earthquake mechanism 0-61764  
 reflected wave travel-time curve inversion theory 0-89968  
 reflection seismograms, simultaneous spherical divergence correction and optimal deconvolution 0-98258  
 reflection seismology south and west of Iceland, rel. to sea floor morphology and struct. 0-90068  
 reflection surveying, wave eqn. migration with absorbing boundary conditions 0-104907  
 refracted wave correlation method, interpretation accuracy (*Russian*) 0-85758  
 refraction data interpretation, time-term method to simulated crustal struct. 0-61768  
 refraction survey, program for pocket calculator for depth determination 0-82088  
 Reykjanes Ridge, crustal struct. from seismic refr. 0-90020  
 Reykjanes Ridge, Profile I on SE. flank, seismic struct., RRISP 0-90019  
 Reykjanes Ridge, SE.flank, lithosphere evolution, seismic surface wave study 0-90022  
 Reykjanes Ridge at 59°N, microearthquake epicentres and seismic vel. 0-89964  
 Reykjanes Ridge Iceland Seismic Experiment (RRISP 77), for crust and upper mantle struct. 0-90017  
 Rhinegraben area, crustal struct. rel. to gravity anomalies and geothermal implications 0-104852  
 rock layers, adjacent, material const. determ. using seismic refl. (*German*) 0-105054  
 Rumania earthquake, 1977 March 4, P-waves obs. rel. to Moho vel. depth distrib. (*German*) 0-98256  
 San Andreas Fault, crustal strain obs. site for earthquake prediction 0-81832  
 San Andreas fault quakes, precursory rainfall 0-85615  
 San Fernando earthquake, California (1971), dislocation fault model, tectonic significance (*Japanese*) 0-104923  
 seismic gaps, two types of definition 0-85608  
 seismic moment, method of determination from seismological bulletin data 0-89980  
 seismic signals deconvolution, adaptive filter struts. 0-98451  
 seismicity associated with subduction zones, stereoviews 0-72452  
 seismogram inversion, use of generalised Kunetz-type eqns. 0-101337  
 shallow earthquakes, seismic efficiency, radiated seismic energy, fault motion energy balance 0-76927  
 Shikoku district, Japan, upper crustal struct. from seismic anal. (*Japanese*) 0-94508  
 Sitka, Alaska, earthquake, 1972 July 30, changes in direction of mag. vector of short-period geoidal vars. 0-76923  
 small earthquakes, detailed spatial distrib. of foreshock and aftershock activities (*Japanese*) 0-94483  
 source location by surface waves, reference point equalisation method 0-72648  
 Spain, dam and reservoir induced seismicity 0-61776  
 strong ground motions at short epicentral distance, simulation 0-104906  
 strong motion prediction for pot. earthquake fault, barrier model 0-105053  
 strong-motion accelerograms, digitization errors and base line corrections 0-98245  
 strong-motion autoregressive modelling of rock-site accelerogram 0-81835  
 strong-motion Fourier spectra of bedrock 0-81839  
 Sturt Block, Australia, vel. determ. and error anal., seismic refr. obs. 0-90229  
 subduction zone seismicity, Makran coast, Iran 0-85635  
 Sunda trench and forearc basin, seismic study 0-72470  
 Superior-Churchill provinces boundary zone, S.Canada, cooperative seismic surveys 0-89985  
 surface waves propagation over liquid and crystalline layers, elastic consts. of crystals 0-76924  
 survey data analysis, sequential anal. method 0-89981  
 Swabian Jura earthquake of Sept. 1978, macroseismic field obs. 0-72451  
 Sweden, map of maximum seismic intensity using new determ. method 0-105089  
 Sweden earthquakes (1951-76), error anal. of source parameters 0-104920  
 synthetic seismogram of layered media with explosive source 0-98250  
 synthetic seismograms (one dimensional), effect of subsurface sampling 0-72435  
 synthetic seismograms of upper crust involving vel. inversion (*Japanese*) 0-94478  
 T waves from Tonga earthquake (June 1977), human perception on Tahiti 0-61769  
 Tabas-e-Golshan earthquake, Iran, Sept. 1978, mechanism and aftershocks 0-81825  
 Tasmania University seismic net, electronic development 0-82073  
 Tataria, USSR, lithological data from seismic refl. of longit. and transverse waves (*French*) 0-101335  
 tectonic stress directions in Alpine regions, correl. with joint orientations 0-105052  
 telephony appls., underground cables laying, rocks location verification 0-72456  
 teleseismic magnitude relations, extension of Zurich magnitude recommendations (1967) 0-109105  
 Three Forks Basin, Montana, USA, seismicity and tectonics 0-81829  
 Tibet and Himalaya, long-term premonitory seismicity 0-72442  
 time correlation using radio broadcast signals 0-90253  
 Tonankai (Japan) earthquake, 1944, source model for accompanying tsunami (*Japanese*) 0-67344  
 N.Tonga region, earthquake distrib. geometry and complicated subduction closure model 0-90010  
 travel-time inversion method, for earthquake location and vel. struct. 0-109109  
 tree ring growth, affected by Fort Tejon quake, California 0-98259

## seismology continued

- Tsengwen reservoir, Taiwan, seismicity due to fault and lake filling 0-81930  
 Turgen' Geophysical Observatory data for crustal deformations 0-76935  
 W.United States, 3-D mantle struct., P vel. study 0-85621  
 United States, attenuation of strong ground motion 0-81834  
 W.United States, horizontal ground accel. attenuation rel. to magnitude 0-104905  
 W.United States, short-period S-wave attenuation 0-98242  
 Upper Amur region USSR, seismicity, tectonic features and earthquake epicentre confinement 0-101343  
 upper mantle, P-wave vel. profile, eastern USA 0-81818  
 upper mantle physical conditions, Walsh's model 0-90047  
 USSR, correl. between seismicity and underground water regime (*Russian*) 0-104913  
 velocity-depth structure, using waveform inversion method 0-105060  
 vertical seismic profiling, travel-time curves, theory 0-94473  
 vibration generator for seismic surveys, electromagnetic motor type 0-90262  
 vibrator exploration with non-sinusoidal signal 0-82086  
 Vibroseis deconvolution method, noise effects 0-90232  
 vibroseis operation, vibrator-ground forced oscillating system, reson. phenomena (*Hungarian*) 0-105074  
 Virgin Islands, tectonic struct. and earthquake swarms, seismic network obs. 0-89973  
 Voronezh Crystalline Massif, seismic vels. significance of mineral substance inhomogeneous compression 0-94504  
 Vrance earthquake seismic wave travel-time curves 0-89998  
 wave front control method in seismic surveys and shooting data processing 0-90238  
 wavefront curvature theory, for laterally inhomogeneous media 0-104908  
 Weddel Sea, geomagnetic, bathymetric and seismic obs. of crust 0-104929  
 Western Cordillera, Colombia, upper crust seismic vel. 0-81819  
 Yakataga Gap, Alaska, seismic history and earthquake pot. 0-109115  
 S.Yamanashi Prefecture, Central Japan, microearthquake activity (*Japanese*) 0-67343  
 NWSyria, seismic risk to large quakes 0-72454
- seismometers**  
*see also seismology*  
 borehole easy-operation long-period seismometer (BELS type 79) with stable period (*Japanese*) 0-67417  
 geophones for recording shear waves 0-101447  
 intermediate-period field system 0-61910  
 long period seismic wave obs. with 5s period seismometer (*Japanese*) 0-94627  
 ocean-bottom seismograph observation system 0-98479  
 recording network at Campotosto reservoir (*Italian*) 0-101446  
 Tasmania University seismic net, electronic development 0-82073  
 wave onset detection algorithm for automatic seismometer (*Japanese*) 0-94476
- selective dissemination of information** *see information dissemination*
- selenium**  
*see also nuclei with .....*  
 amorphous, bulk, Raman scatt. near T<sub>g</sub> 0-60596  
 amorphous, bulk, reson. Raman scatt. 0-60597  
 amorphous, elec. cond., activation energy, density, cryst. Se effect 0-65548  
 amorphous, electronic struct. and optical props., pseudopot. calc. 0-65428  
 amorphous, high field transport, impact ionisation, carrier mobility 0-80286  
 amorphous, luminescence 0-80862  
 amorphous, photogeneration, thermalisation model calcs., band gap (*French*) 0-75595  
 amorphous, transient electrical transport, general and unified treatment 0-59977  
 amorphous, US attenuation at low temp., internal friction peak 0-65152  
 amorphous, US relaxation and retardation of deform. near T<sub>g</sub> point 0-84256  
 amorphous, vac. deposited on polymeric substrates, with dynamic coating device 0-100792  
 amorphous and liquid state, mol. structure, local atomic arrangement at intrinsic bonding defects 0-59374  
 amorphous and liquid state, Raman spectra, crystn. processes 0-60608  
 amorphous film, dielec. activity obs. near glass transition temp. 0-75933  
 amorphous film, highly disordered, UPS study 0-76148  
 amorphous film, influence of wavelength on optical quenching of photoconductivity 0-60046  
 amorphous film, photocond., dark cond., rel. to crystn. 0-88596  
 amorphous films, evaporated, ageing and crystn., DTA 0-65413  
 amorphous layer, localised states in band gap 0-59928  
 atom, LMM Auger spectra, relative intensity and relaxation energy 0-69115  
 atom+H<sup>+</sup>(D<sup>+</sup>), K shell ionisation, nuclear Coulomb effect 0-91650  
 bonding coordination defects 0-59927  
 charge density, self-consistent OPW and pseudopot. calcs. 0-92813  
 electronic structure of cryst. phases, hydrostatic press. effects 0-59865  
 electrophotographic characts. of films rel. to viscosity of bulk specimens (*Russian*) 0-73505  
 EM wave scattering from crowded Se sphere monolayer, migration imaging film appl. 0-99627  
 film, amorphous, empirical formula for temp. depend. of dielec. loss peaks 0-97197  
 films, Ag diffusion, effect on interferometric thickness meas. 0-96695  
 films, optical constants in visible region 0-97360  
 glassy, localised electronic states, photoluminesc. and ESR studies 0-65501  
 glossy, structural excitation energies of defects, pseudopot. approach 0-107061  
 impurity in Nimonic 105, influence on creep and stress rupture props. 0-66602  
 K-edge dispersion anomalies, meas. using X-ray interferometry 0-90956  
 liquid, dielectric relax. and elec. cond. 0-108150  
 liquid, electronic transport props., equation of state, to 1900K and 1800 bars 0-65574  
 liquid, heat capacity and chem. equilib. 0-103486  
 liquid, viscosity meas. by rot. cylinder method 0-88347  
 liquid and amorphous, struct. modelling using Monte Carlo method 0-59391  
 low-frequency coupled photocurrent and temp. oscillation 0-60044



**selenium** continued

- metallic state, press. induced, elec. cond. meas. 0-96949  
modulated photocurrent, analysed for trap-limited case (*Japanese*) 0-60030  
monolayer, adsorbed on Al (111), angle resolved UPS of 2-dimens. band struct. 0-60059  
photocell optical vibration transducer 0-77768  
photoelectronic behaviour, in glass transition region 0-60045  
photosensitive particle migration, electrophotographic film structure and process 0-101863  
positron lifetimes, positronium form. in trigonal and amorphous Se 0-60711  
powder compacts, sintered, electrical cond. 0-70693  
rhombohedral, IR absorpt. spectrum 0-103949  
SAW vel. and electromech. coupling factor 0-75422  
sea- and river water, Se (-II,0), (-IV), and (-VI) composition, by gas chromatography method 0-81928  
solid, chemical shift and nucl. spin-lattice relax., high temp behaviour 0-60445  
space group C3<sub>2</sub>C<sub>3</sub>2, habit variation 0-107090  
thin film selective absorber coatings, prod. using an oblique vacuum deposition technique 0-81488  
threads in natural mordenite channels, optical absorpt., cond. (*Russian*) 0-89022  
trace amount determ. by hydride generation-nondispersive flame at. fluoresc. spectroscopy 0-89553  
trigonal, acoustoelectric current saturation 0-60053  
trigonal, behaviour of optical gap under press. 0-80171  
trigonal, normal mode calcs. 0-84259  
trigonal, Raman scatt. at very high press. 0-60566  
trigonal, transverse magnetoresistance meas., influence of illumination 0-65607  
trigonal and amorphous, electronic struct. and nonempirical calc. of struct. props. 0-59866  
trigonal and vitreous, sp. ht. and thermal cond., 3 to 300K 0-59676  
xerography applications 0-57415  
BP-Se, epitaxial layers, ion implantation, defects and lattic locations, channelling obs. 0-88179  
GaAs:Cr,Se, ion-implanted, semi-insulating effects of Cr redistrib. on elec. characts. 0-59982  
GaAs:Ge,Se transmutation shallow donor transition obs. 0-59925  
GaAs:Se, Ga, dual species ion implantation, elec. characts. 0-103377  
GaAs:Se, ion-implanted, capless annealing by melt-controlled ambient technique 0-75251  
GaAs:Se, n-type layers, heavily doped, formation by multiple ion implantation 0-88187  
GaAs:Se cathodoluminescence decay obs. with SEM and streak camera, 90 to 300K 0-97348  
GaAs:Se ion implanted samples, Q-switched ruby laser annealing, improvement in elec. props. 0-100460  
GaAs:Se ohmic contacts, pulsed electron beam annealing donor density, mobility 0-65678  
GaAs:Se polycrystalline film, Hall effect, resistivity meas. 0-96911  
GaP:Se, donor bound exciton excited states 0-66284  
He-Se, vapour laser, continuous wave, intensity fluctuations investig. 0-83593  
NaX-Se semiconductor superlattice absorpt. edge, light scatt. (*Russian*) 0-71438  
Se:As, amorphous film, dielec. activity obs. near glass transition temp. 0-75933  
Se:As X-ray plates, electronic transport (*German*) 0-80290  
Se:I, vitreous, crystn, kinetics determ. (*German*) 0-79936  
Se<sub>2</sub>, b<sup>2</sup>Σ<sup>+</sup>→X<sup>3</sup>Σ<sup>-</sup> near IR emission obs. 0-91556  
Se<sub>2</sub>, laser induced fluoresc. in inert gas matrix 0-87161  
<sup>75</sup>Se, neutron activation anal., coincidence counting, biological and soot samples (*Japanese*) 0-97750  
Si:Se, impurity states, A- and B-centres, electron, hole thermionic emission rates 0-96813  
Te-Se-Cd, sandwich structure, fabrication and characteristics 0-60089  
Te-Se-Cd rectifying sandwich structs., elec. forming action, Schottky junction form. 0-80371  
ZnP<sub>2</sub>:Se, optical absorpt. spectra in range 0.5 to 2.2 eV 0-66250

**selenium alloys**

- see also **selenium compounds**  
Mo-Sn-Se system, supercond. crit. temp. and cryst. struct. (*Russian*) 0-107947  
Ni-Se, dil., ferromagnetic, hyperfine field and relax. time obs. of impurity heavy nuclei 0-75533  
Se-Tl-S alloys, liq., dielectric relax. and elec. cond. 0-108150  
Tl-Se, liquid mixtures, press. effect on two-phase region 0-75347

**selenium compounds**

- see also **selenium alloys**  
LMM Auger spectra, relative intensity and relaxation energy 0-69115  
xerographic applications 0-57415  
As-Se-S-Ge chalcogenide amorphous film, computer-generated holograms using electron beam irradi. 0-95846  
As-Se-Sb, crystallised glasses, struct. from Mossbauer spectra 0-64917  
As<sub>2</sub>Sb<sub>2</sub>Se<sub>6</sub> glassy semiconductors, electronic props. 0-103712  
CdSe thin-film solar cells 0-93970  
CuIn<sub>1-x</sub>Ga<sub>x</sub>Se<sub>2(1-x)}</sub>Te<sub>2x</sub> pentenary alloy compounds for photovoltaic solar energy conversion 0-93971  
Ga-Ge-Se chalcogenide glasses, rare earth element doped, elec. props. 0-96885  
Ga-Se system, phase diagram and cryst. struct. of phases (*French*) 0-93544  
GaSe<sub>1-x</sub>Te<sub>x</sub>, Raman spectra, phonon freq. 0-97286  
N-Ge-Bi-Se glass, elec. and optical props. 0-65550  
Ge-S-Se, glass formation 0-103251  
Ge-Sb-Se glass, elec. props, comp. depend. 0-70697  
Ge<sub>10</sub>As<sub>1</sub>Te<sub>10</sub>Se<sub>21</sub>As<sub>2</sub>S<sub>3</sub>, two-layer antirefl. coating, error considerations in design 0-74477  
Mo<sub>2</sub>Se<sub>3</sub>Sn, triple chalcogenide, NMR spectra in supercond. state (*Russian*) 0-93194  
SbSe, amorphous thin film high field charge transport and quasi-Fermi level location 0-70863  
Se-As, photoelectronic behaviour, in glass transition region 0-60045  
Se-Ge amorphous films, obliquely deposited, photoinduced chem. changes 0-76385  
Se-Ge-Te, chalcogenide glass, elec. cond. and dielec. const. 0-75567  
Se-Te single crystals, chem. etching 0-96526

**selenium compounds** continued

- Se-Te-Sb glasses, electronic transport 0-88579  
SeCl<sub>2</sub>, photoelectron spectra 0-69186  
SeCl<sub>2</sub>-SbCl<sub>3</sub> systems, Raman spectra (*German*) 0-93324  
SeCl<sub>2</sub>, photoelectron spectra 0-69186  
SeD, isotope effects, Rydberg levels-ground state transitions, rot. const., VUV spectra obs. 0-58279  
SeF<sub>6</sub>, in Kr matrix, temp. reversible IR spectral changes, site struct. dynamics 0-102505  
SeH, isotope effects, Rydberg levels-ground state transitions, rot. const., VUV spectra obs. 0-58279  
SeH<sub>2</sub>, atomisation in cool H<sub>2</sub>-O<sub>2</sub> flame burning in quartz tube atomiser 0-76581  
SeO, b<sup>2</sup>Σ<sup>+</sup>→X<sup>3</sup>Σ<sup>-</sup> near IR emission obs. 0-91556  
SeO<sub>2</sub>+Ar(N<sub>2</sub>)(CO<sub>2</sub>), radiative lifetime and quenching rates 0-95685  
SeO<sub>2</sub><sup>+</sup>, SeO<sub>2</sub><sup>+</sup>, O K-emission spectra, electron struct. 0-87099  
SeOCl<sub>2</sub>:Pr<sup>3+</sup>(Nd<sup>3+</sup>)(Er<sup>3+</sup>), SbCl<sub>5</sub> acidified, Racah and Judd-Ofelt parameters in laser liqs. 0-106516  
SeS, b<sup>2</sup>Σ<sup>+</sup>→X<sup>3</sup>Σ<sup>-</sup> near IR emission obs. 0-91556  
SeTe/Se multilayer photoreceptor, transient photoconductivity (*Japanese*) 0-75596  
Se<sub>0.95</sub>Te<sub>0.05</sub>, glass crystallisation, effect of an alternating electric field 0-88054  
Se<sub>1-x</sub>Te<sub>x</sub>, amorphous, optical and elec. props. 0-84506  
Se<sub>1-x</sub>Te<sub>x</sub>, amorphous film, photo-crystallisation 0-59839  
Se<sub>1-x</sub>Te<sub>x</sub>-Se<sub>1-x</sub>Te<sub>x</sub>, junctions, photovoltaic effects and rectification phenomena 0-84506  
Se<sub>x</sub>Te<sub>1-x</sub>, acoustoelectric current saturation 0-60053  
Se<sub>x</sub>Te<sub>1-x</sub>, amorphous, structural relaxation and crystallisation kinetics study by DTA 0-59394  
Se<sub>x</sub>Te<sub>1-x</sub>, growth of single crystals by Czochralski method 0-66423  
Se<sub>1/2</sub>Te<sub>3/8</sub>As<sub>2/8</sub>Ge<sub>1/8</sub> semiconductor amorphous films, field effect, trapping 0-84472  
Te-Se liquid mixtures, sound vel. meas., adiabatic compressibility determ. 0-65161  
Te<sub>50-x</sub>Se<sub>50</sub>Sn<sub>x</sub>, thin films, elec. cond. and thermoelectric power meas. (*French*) 0-80335
- self-adjusting systems**  
see also **learning systems**  
nerve nets, fundamental theory, developmental plasticity anal. 0-67062
- self-consistent field calculations** see **SCF calculations**
- self-diffusion**  
see also **self-diffusion in gases**; **self-diffusion in liquids**; **self-diffusion in solids**  
sine-Gordon chain, self diffusion via solitons 0-70443
- self-diffusion in gases**  
dense gases, vel. autocorrelation function, memory function 0-59154  
dilute gas, transport props., simple pair pot. model 0-87835  
dilute gas transport props., logarithmic term in softness expansion 0-83872  
hard sphere gas mixture, vel. autocorrelation function calc. 0-75019  
Kr, Lennard Jones (12,6) pot. distance parameter, transport props. calc. 0-79423  
Ne, Lennard Jones (12,6) pot. distance parameter, transport props. calc. 0-79423  
Xe, Lennard Jones (12,6) pot. distance parameter, transport props. calc. 0-79423
- self-diffusion in liquids**  
benzene, diffusion coeff. meas., Fourier transform NMR, pulsed field gradient system 0-57353  
benzene, isotope-mass effects in self-diffusion 0-92695  
benzene, liq., mol. motion at high press. 0-103509  
benzene, self-diffusion coefficients determ. by gel sectioning technique 0-92694  
cyclohexane, isotope-mass effects in self-diffusion 0-92695  
cyclohexane, liquid, density effect on transport properties 0-65264  
cyclohexane, self-diffusion coefficients determ. by gel sectioning technique 0-92694  
decane-water-Na p-octylbenzene sulphonate-1-pentanol-NaCl, microemulsion system, existence of bicontinuous zone 0-104466  
EABAC, smectic A, nematic, and isotropic phases, NMR and quasielastic neutron scatt. obs. 0-88022  
haemoglobin, mutual and tracer diffusion coeffs., photon correl. obs. 0-72123  
hexafluorobenzene, liq., self-diffusion and density as functions of press. and temp. 0-92696  
hexafluorobenzene-n-paraffins, binary liquid solns., self diffusion, spin echo meas. 0-65263  
latex spheres in H<sub>2</sub>O, photon correlation spectroscopy, diffusion coeffs. determ. 0-93802  
Lennard-Jones mixture, binary, equimolar, static (dynamic) props., mol. dynamics calc. 0-64857  
low conductivity media, unipolar injection, forced diffusion model 0-92692  
microemulsion system, existence of bicontinuous zone 0-104466  
polydisperse systems, photon correlation spectroscopy, diffusion coeffs. determ. 0-93802  
polymer, spherical, in soln, long time tail in diffusion 0-88018  
polymer melts, dynamics, self-diffusion const., relax. time and viscosity 0-64874  
polystyrene, solns., diffusion coeffs. meas., Fourier transform NMR, pulsed field gradient system 0-57353  
serum albumin, bovine, mutual and tracer diffusion coeffs., photon correl. obs. 0-72123  
smectic-A liquid crystals, nucl. spin relax. by translational self diffusion 0-60442  
water, H<sub>2</sub>O and H<sub>2</sub><sup>18</sup>O, self-diffusion, pressure and temp. depend., NMR spin-echo obs. 0-65266  
Ag-In melt system, conc. depend. of component and impurity diffusion coeffs., radioactive isotope method (*Russian*) 0-107454  
Ar, liquid, binary non-additive particle interaction, self diffusion and at. motion, mol. dynamics method 0-59372  
Ar, liquid, diffusion coefficient for model potentials through means square displacement 0-70098  
Co-Ca, liq. alloy form. kinetics (*French*) 0-96652  
InAs, melt, mutual diffusion of components 0-88345  
InGaAs, LPE, diffusion-limited step-cooling technique, layer thickness and composition 0-84402  
InGaAsP, LPE, diffusion-limited step-cooling technique, layer thickness and composition 0-84402

**self-diffusion in liquids continued**

- LiCl-KCl, molten mixture, struct., diffusion, cond., mol. dynamics calc. 0-64871  
 LiCl-RbCl, molten, Chemla effect, mol. dynamics simulation, self exchange vel. 0-79967  
 Na, liquid, diffusion coefficient for model potentials through mean square displacement 0-70098  
 Na<sub>2</sub>S<sub>2</sub>-molten S interface, mass transport phenomena, rel. to Na/S battery 0-72026  
 Pb-Bi liquid alloy, Pb and Bi diffusivities, temp. and conc. depend. (*German*) 0-84311  
 Sn, diffusion coeff. of <sup>113</sup>Sn, <sup>124</sup>Sb, <sup>110</sup>Ag, and <sup>195</sup>Au 0-96676

**self-diffusion in solids**

- see also diffusion creep*  
 alkali halides, matter transport rel. to point defect parameters 0-107488  
 alkaline earth fluoride, doped with trivalent rare earths, migration entropy for bound fluorine motion 0-71303  
 alloy, dispersion hardened, work hardening due to Orowan loops, temp. depend. (*Japanese*) 0-66534  
 cubic lattice, self-diffusion via vacancy mechanism, correl. effect 0-59693  
 n-eicosane, triclinic phase, self-diffusion, 295 to 309K 0-88359  
 faulted dislocation loops induced by elastic interaction, climbing motion 0-75227  
 ferrite-austenite ( $\alpha$ - $\gamma$ ) interface, Fe self-diffusion compared with grain boundaries diffusion 0-65306  
 ice, cubic, D<sub>2</sub>O isolated, H<sup>+</sup> exchange and Bjerrum defect migration, direct spectroscopic obs. 0-88356  
 ionic crystal defects, mag. reson. studies 0-108066  
 ionic solids, diffusion routes and thermal vibrs., calc. method 0-107462  
 lattice defects and diffusion processes in solids, book 0-107207  
 metals, atomic mobility under pulsed loading conditions (*Russian*) 0-96684  
 metals, individual atomic events on surfaces, quantitative examination 0-75409  
 metals, light interstitials diffusion, multiphonon transition modes classification 0-70448  
 metals, point defect diffusion controlled reaction theory, book contrib. 0-103318  
 metals, point defect dynamic props. and diffusion controlled reactions, book 0-101674  
 metals, quenched, vacancy cluster form. process 0-92706  
 metals, radiation creep speed and swelling, self diffusion mechanisms (*Russian*) 0-92955  
 metals, sintering analysis using sintering maps 0-93513  
 NMR spin-lattice relax., effect of correlated atomic diffusion 0-107495  
 nuclear fuels, creep, irradiation induced, transient state, kinetic eqn. treatment 0-88251  
 oxides, impurity diffusion and self-diffusion, review and bibliography 0-59719  
 polymers, NMR, review 0-88888  
 powder, deforming, self-diffusion coeffs. in failure zones and percolation 0-76209  
 proton transport 0-79974  
 rare earth metal silicide thin film formation on (100), (111)Si substrates, backscattering study 0-70542  
 sintering, surface redistribution by grain boundary diffusion 0-84871  
 solid electrolyte, diffusion and ionic cond., correl. factor meas. problems 0-59709  
 solid electrolytes and solid soln. electrodes, NMR investigs., review 0-60432  
 steel, austenitic, of Fe, Cr, and Ni (*Czech*) 0-107464  
 steel, Cr (0.5 wt.%), austenite-pearlite transformation 0-97480  
 steel, ferrite-austenite transition, diffusion const. of C and carburisation rate const., thermopower meas. 0-89216  
 superionic conductor, effects of disorder and mobile particle interactions 0-107536  
 superionic conductor, Haven ratio, temp. depend., correl. effects role 0-107504  
 superionic conductor, hydrodynamic theory for collective excitations 0-107530  
 superionic conductor, interacting Brownian particles in periodic medium model 0-59712  
 Ag halides, matter transport rel. to point defect parameters 0-107488  
 Ag-In-Sn, internal oxidation, solute element and O<sub>2</sub> behaviour (*Japanese*) 0-89479  
 AgBr(Cl), ionic transport, defect form. and migration energies, quasi-harmonic model 0-107538  
 AgCl, ionic mobility, diffusion coeffs., defect mobility energies 0-65284  
 AgF, diffusion, elec. cond. and <sup>19</sup>F relax. T<sub>1</sub> meas. 0-92718  
 $\alpha$ -AgI, diffusion dynamics, quasielastic neut. scatt. expt. 0-107484  
 $\alpha$ -AgI, dynamic cage effect 0-107541  
 $\alpha$ -AgI, ionic motions nature, mol. dynamics calcs. 0-107533  
 $\alpha$ -AgI, structural and dynamical behaviour 0-107544  
 (AgI)<sub>2</sub>(Ag<sub>2</sub>O<sub>3</sub>)<sub>2</sub>·x, amorphous superionic compound, <sup>11</sup>B lineshape and relaxation 0-108107  
 Ag<sub>2</sub>Se, between metal electrodes, current-voltage characts (*French*) 0-97005  
 Al-Al<sub>3</sub>Ti, directionally solidified, thermal stability during annealing, 435-660°C 0-108393  
 Al-Cr, thin film metal contact, sheet resistance changes 0-80356  
 Al-Si (1.2 wt.%), dispersion hardened, work hardening due to Orowan loops, temp. depend. (*Japanese*) 0-66534  
 $\beta$ -Al<sub>2</sub>O<sub>3</sub>-(Na,Li)<sub>2</sub>O, NMR, Raman and IR spectra, and X-ray diffr., heat treatment induced changes 0-107508  
 Al<sub>2</sub>O<sub>3</sub>, single cryst., O self diffusion, ion-probe meas. 0-59701  
 Al<sub>2</sub>O<sub>3</sub>, single cryst., self-diffusion of O, isotope exchange investig. 0-100348  
 $\beta$ -Al<sub>2</sub>O<sub>3</sub>-(Na,K)<sub>2</sub>O, model calcs. of cond. anomalies, pot. energies of cation arrangements 0-107510  
 $\beta$ -Al<sub>2</sub>O<sub>3</sub>-(Na,Li)<sub>2</sub>O, first-order quadrupole NMR obs. of cation distrib. and ion motion 0-108113  
 $\beta$ -Al<sub>2</sub>O<sub>3</sub>-(Na,Li)<sub>2</sub>O, ionic motion obs. using NMR and internal friction 0-108099  
 $\beta$ -Al<sub>2</sub>O<sub>3</sub>-(Na,Li)<sub>2</sub>O solid electrolyte, Li motion and activation obs. using <sup>7</sup>Li NMR 0-108100  
 $\beta$ -Al<sub>2</sub>O<sub>3</sub>-Ag<sub>2</sub>O, Haven ratio, temp. depend., Ag diffusivity and ionic cond. 0-107503  
 $\beta^*$ -Al<sub>2</sub>O<sub>3</sub>-Ag<sub>2</sub>O(K<sub>2</sub>O)(Li<sub>2</sub>O)(Na<sub>2</sub>O)(Rb<sub>2</sub>O), single cryst. Raman scatt., cond. mechanism and cryst. struct. 0-66209  
 $\beta^*$ -Al<sub>2</sub>O<sub>3</sub>-H<sub>3</sub>O<sup>+</sup>(Na<sub>2</sub>O), struct. basis for superionic cond. 0-107498

**self-diffusion in solids continued**

- $\beta$ -Al<sub>2</sub>O<sub>3</sub>-NH<sub>4</sub><sup>+</sup> and  $\beta^*$ -Al<sub>2</sub>O<sub>3</sub>-NH<sub>4</sub><sup>+</sup>-H<sub>3</sub>O, single cryst. PMR and proton motion 0-108101  
 $\beta$ -Al<sub>2</sub>O<sub>3</sub>-Na<sub>2</sub>O, <sup>23</sup>Na NMR obs. of ionic diffusion, 180 to 800K, attempt freq. 0-108097  
 $\beta$ -Al<sub>2</sub>O<sub>3</sub>-Na<sub>2</sub>O, <sup>23</sup>Na NQR and two-dimens. diffusion, model analysis 0-108111  
 $\beta$ -Al<sub>2</sub>O<sub>3</sub>-Na<sub>2</sub>O, <sup>27</sup>Al NMR obs., Na motion and cond. characts. 0-108096  
 $\beta$ -Al<sub>2</sub>O<sub>3</sub>-Na<sub>2</sub>O, anomalous Na behaviour obs. using pulsed and CW NMR 0-108095  
 $\beta$ -Al<sub>2</sub>O<sub>3</sub>-Na<sub>2</sub>O, low-temp. <sup>23</sup>Na satellite spectra, Na ion motion 0-108112  
 $\beta$ -Al<sub>2</sub>O<sub>3</sub>-Na<sub>2</sub>O, motion of charge carrying ions, mol. dynamics simulation 0-107506  
 $\beta^*$ -Al<sub>2</sub>O<sub>3</sub>-Na<sub>2</sub>O, NMR of <sup>23</sup>Na, elec. quad. interaction, 185 to 419K, ion motion obs. 0-108110  
 $\beta^*$ -Al<sub>2</sub>O<sub>3</sub>-Na<sub>2</sub>O, nonstoichiometric, correl. effects in diffusion, Haven ratio, point defect interactions 0-107505  
 Ar, diffusion processes in plastic deform. (*Russian*) 0-92591  
 CaF<sub>2</sub>, cation jump freq., isotope effect, lattice dynamical calc. 0-88357  
 CaF<sub>2</sub>, fast ion transport, computer simulation 0-107485  
 CaF<sub>2</sub>, mol. dynamics studies of superionic conductors 0-107547  
 Cd<sub>2</sub>Hg<sub>1-x</sub>Te, epitaxial growth from stoichiometric melt, crystn. and diffusion 0-75475  
 Cd<sub>2</sub>Hg<sub>1-x</sub>Te, long term stability at 300K, rel. to device appl. 0-59978  
 Co-Zn, physical-chemical metallurgy (*German*) 0-108390  
 CoO, isotope effects in CoO diffusion rel. to vacancies 0-84319  
 Co-ZnO-MgO ternary systems, solid solns., struct. charact. 0-60629  
 Cu film, Gorsky effect, internal friction maxima, atom diffusional mobility (*Russian*) 0-70446  
 Cu, impurity diffusion of V<sup>h</sup> period elements and self-diffusion 0-65301  
 Cu,  $\mu^+$  diffusion data anal., theory of incoherent direct and indirect multiphonon transitions 0-70448  
 Cu-Zn-Mn, steady-state diffusion of Zn and Mn 0-70445  
 CuBr(Cl)(I), LF light scatt. spectra in superionic cond. phases, ion motion obs. 0-108217  
 CuI, ionic motions nature, mol. dynamics calcs., sp. ht. anomaly due to order-disorder transform. 0-107533  
 Cu<sub>2</sub>Mo<sub>2</sub>S<sub>3-y</sub>, mixed conductor, partial Cu ion cond. and chem. diffusion 0-84323  
 CuO-containing glass, Cu<sup>+</sup> diffusion and oxidation 0-79980  
 Cu<sub>2</sub>VS<sub>4</sub>, out of equil. mixed cond., chem. origin of mobile ions, spin-lattice relax. and NQR obs. 0-108104  
 Fe-B metallic glasses, diffusion coeffs. from primary crystn. data 0-100345  
 Fe-Cr (9 wt.%), oxidation studied using C<sup>18</sup>O<sub>2</sub> and D<sub>2</sub>O tracers 0-71784  
 Fe-Mn cast alloys, homogenisation annealing and chemical diffusion (*Czech*) 0-66551  
 Fe-Si-C, austenitic, C diffusivity (*German*) 0-92705  
 Fe-V, <sup>59</sup>Fe self-diffusion (*Czech*) 0-88352  
 Fe-Zn, physical-chemical metallurgy (*German*) 0-108390  
 Fe<sub>2</sub>O<sub>3</sub>, magnetite, cation diffusion, correlation and isotope effects 0-96686  
 Ga-In eutectic system, diffusion coeff. depend. on composition (*Russian*) 0-59695  
 Ga-Zn, eutectic system, diffusion coeff. depend. on composition (*Russian*) 0-59695  
 Ge, activation energy and entropy factors 0-88353  
 H<sub>0.3</sub>MoO<sub>3</sub> and H<sub>1.7</sub>MoO<sub>3</sub> bronzes, NMR relax. obs. at 77<T<450K, H diffusion 0-108089  
 HFV<sub>2</sub>H<sub>2.1</sub>, proton NMR relax. time and Knight shifts, diffusional activation energies meas., sorption props. 0-75871  
 In<sub>2</sub>O<sub>3</sub>-SnO<sub>2</sub> thin film, Hall mobility, temp. depend., grain boundary effects 0-75658  
 K, self-diffusion, high temp. bulk modulus determ. 0-79976  
 KCl, ionic cond., defect parameters, diffusion coeffs. 0-79978  
 KCl:Sr<sup>2+</sup>(SO<sub>4</sub><sup>2-</sup>), ionic cond., defect parameters, diffusion coeffs. 0-79978  
 LaH<sub>2.69</sub> two-phase behaviour, <sup>1</sup>H-NMR evidence 0-93189  
 Li<sub>2</sub>FeP<sub>2</sub>(Se<sub>3</sub>), Li<sub>2</sub>MnPSe<sub>3</sub> and Li<sub>2</sub>NiP<sub>2</sub>(Se<sub>3</sub>), NMR and neutron diffr. obs., mag. props. 0-60433  
 Li<sub>2</sub>N, diffusion processes and struct. NMR study 0-108090  
 Li<sub>2</sub>N, interstitial sites and anharmonic thermal vibrs. in cryst. struct., ionic cond. mechanism 0-107190  
 Li<sub>2</sub>N, ionic hopping model, NMR relax. data anal. 0-92714  
 Li<sub>2</sub>N layer structure with fast ion cond., <sup>6</sup>Li NMR obs. of diffusion 0-108102  
 Li<sub>2</sub>O-SiO<sub>2</sub> glass, thermotransport props. 0-79985  
 Li<sub>2</sub>O-SiO<sub>2</sub> glasses, Li self-diffusion, mass spectrometric method 0-79982  
 Li<sub>2</sub>S(O), cation diffusion NMR investigation up to 800°C 0-108092  
 Li<sub>2</sub>SO<sub>4</sub> based solid electrolytes, FCC phase transport mechanism studies and uses 0-107525  
 Mg, Fe<sub>1-x</sub>O, diffusion of <sup>59</sup>Fe and elec. cond. 0-59700  
 MgO, subgrain boundaries form. obs. by TEM, diffusion coeff. determ. 0-79817  
 Mg<sub>2</sub>SiO<sub>4</sub>, <sup>18</sup>O self-diffusion expts., high-temp. creep implications 0-81870  
 Mg<sub>2</sub>SiO<sub>4</sub>, forsterite, O<sub>2</sub> self-diffusion coeffs. 0-70457  
 MnS, phase transform. at 200°C, diffusive and deformational mechanisms 0-65216  
 Mo<sub>2</sub>Si<sub>3</sub>, layer electrotransfer of Si 0-92708  
 Na, atomic jump processes, quasi-elast. neutron scatt. study 0-84317  
 NaI:Ca<sup>2+</sup>, pure and doped, lattice defects, entropy and enthalpy of formation and migration 0-96687  
 Na<sub>2</sub>S(O), cation diffusion NMR investigation up to 800°C 0-108092  
 Na<sub>2</sub>Zr<sub>2</sub>PSi<sub>2</sub>O<sub>7</sub>, NASICON, <sup>23</sup>Na NMR obs. of ionic diffusion, 180 to 800K 0-108097  
 Nb<sub>3</sub>Sn-Cu multifilamentary composite wire, Nb<sub>3</sub>Sn filament morphology and grain size 0-100855  
 Ni dilute alloys, implant profiles modification by radiation enhanced diffusion and segregation 0-88217  
 Ni, hardness after-effect studied by anelastic relaxation 0-66570  
 Ni surface, single-atom self-diffusion FIM study 0-103548  
 Ni-Al(Si), diffusion, lattice parameter, microhardness, and constitution, effect of Si additions (*Russian*) 0-84316  
 Ni-Cr austenitic alloy, oxidation mechanism, intergranular diffusion effect (*French*) 0-81229  
 Ni-V, solid soln., diffusion and thermodynamic props. 0-65278  
 Ni-Zn, physical-chemical metallurgy (*German*) 0-108390  
 $\beta$ -NiAl, ordered, hardness after-effect studied by anelastic relaxation 0-66570



**self-diffusion in solids continued**

- Ni(NH<sub>3</sub>)<sub>2</sub>, phase transition and rot. excitation 0-96642  
 NiO, diffusion of ion-implanted <sup>18</sup>O 0-107494  
 NiO, nonstoichiometric, near-surface and bulk chem. diffusion 0-80035  
 NiO, undoped and Al doped, Ni self-diffusion, vacancy-impurity complex effects 0-107493  
 Ni<sub>0.5</sub>Zn<sub>0.5</sub>Fe<sub>2</sub>O<sub>4</sub> coarse grain polycryst. ferrite, diffusional creep (*Japanese*) 0-104238  
 Pb, grain boundary self diffusion, microtome serial sectioning anal. 0-79975  
 α-RbAg<sub>4</sub>I<sub>3</sub>, dynamic cage effect 0-107541  
 RbAg<sub>4</sub>I<sub>3</sub>, solid electrolyte development, Ag<sup>+</sup> cond. 0-107532  
 RbCu<sub>2</sub>Cl<sub>3</sub>I<sub>2</sub>, development of Cu<sup>+</sup> ion cond. 0-107532  
 Si, activation energy and entropy factors 0-88353  
 Si, ion implanted, interstitial generation and loop form. during annealing in oxidising medium 0-107225  
 n-Si wafer, trap centres of self-interstitials 0-75516  
 Si:B(P), proton-irrad., impurity uphill diffusion, vacancy mechanism 0-92719  
 β-SiC, polycryst., <sup>30</sup>Si self-diffusion 0-100350  
 SiO<sub>2</sub>, amorphous, <sup>30</sup>Si diffusion (*French*) 0-59696  
 SiO<sub>2</sub>, amorphous, of <sup>30</sup>Si, SIMS (*French*) 0-107482  
 SiO<sub>2</sub>, vitreous, O and Si diffusion-controlled processes 0-79981  
 SnO<sub>2</sub> thin films, O<sub>2</sub> vacancy diffusion 0-107467  
 SnTe, diffusion of <sup>125</sup>Te 0-84325  
 SrCl<sub>2</sub>, fast ion transport 0-107558  
 SrCl<sub>2</sub>, ionic cond., self-diffusion, rel. to defect motion, mol. dynamics study 0-65282  
 SrCl<sub>2</sub>, mass and charge transport 0-100347  
 SrCl<sub>2</sub>, self-diffusion and ionic cond. 0-107489  
 ThO<sub>2</sub>-CaO, and ThO<sub>2</sub>-YO<sub>1.5</sub>, solid solns., defective oxides, ionic cond. 0-107548  
 Ti-Ni-Co, constitution diagram, isothermal section, interdiffusion coeffs. (*Russian*) 0-89200  
 TiC, nonstoichiometric, densification during sintering 0-84895  
 γ-TiH<sub>3</sub>, interstitial H diffusion mechanism, NMR spin-lattice relax. study 0-103515  
 (U,Ce), U self-diffusion 0-92711  
 (U,La)C, U self-diffusion 0-92711  
 (U,Pu)(C,N) and (U,Pu)N, high burn-up simulated, Pu self diffusion 0-92712  
 (U,Y)C, U self-diffusion 0-92711  
 (U,Zr)C, U self-diffusion 0-92711  
 W, self-diffusion, high temp. bulk modulus determ. 0-79976  
 W surface self-diffusion, ion impact induced, FIM study 0-103549  
 ZnTe, self-diffusion profile and trapping of Zn 0-75381  
 ZrMn<sub>2</sub>H<sub>3</sub>, proton NMR relax. time and Knight shifts, diffusional activation energies meas., sorption props. 0-75871  
 ZrO<sub>2</sub>-CaO, and ZrO<sub>2</sub>-YO<sub>1.5</sub>, solid solns., defective oxides, ionic cond. 0-107548

**self-focusing**

- see also electrostriction; Kerr electro-optical effect; optical Kerr effect; optical self-focusing  
 electron beam, self-focused, relativistic, filamentation instability 0-74289  
 nonlinear focusing and Kelvin-Helmholtz instability 0-83785  
 particulate self-focusing and nonlinear-wave mechanics 0-105520

**self-induced transparency**

- breather generation, inverse scatt. technique 0-78913  
 perturbed soliton solns., finite relax. time 0-58643  
 semiconductor, nonlinear coherence phenomena in exciton region 0-99806  
 two-level resonant medium, light pulses propag. 0-64119  
 I atomic vapour, self-induced transparency and reson. self focusing 0-64114  
 Na vapour, soliton interactions, self-induced transparency, numerical plane wave simulations 0-64117

**self inductance** see inductance**self-optimising systems** see self-adjusting systems**self-organising systems** see self-adjusting systems**self-trapping**

- Gaussian laser beam, transverse self-focusing and self-trapping investig., moment method 0-58652  
 lattice vibration TO and LO modes, role in self-trapping of powerful light pulses 0-99809

**SEM** see scanning electron microscopy**semi-insulating materials** see semiconductor materials**semiconductor alloys** see semiconductor materials; semiconductors**semiconductor counters**

- see also position sensitive particle detectors  
 active volume, determ. from gamma ray interactions, Monte Carlo method 0-63448  
 alpha, surface-barrier Au(Si), protective glass walls 0-91374  
 backscattered electron detector, multi-purpose 0-102404  
 bronchoscopic tumour localisation, small radiation detector probes, scintillation and semiconductor detectors 0-61676  
 dielectric-breakdown, heavy-ion counters based on MOS structure 0-69032  
 epitaxial integrated E-dE silicon detector with a buried low-resistive diffused layer 0-58059  
 Ge control detector, dead layer minimisation for Compton-suppression spectrometer 0-99400  
 ion implanted, neutron detection 0-69030  
 long-range charged particle detector, field effect investig. (*Russian*) 0-106234  
 mosaic, characts. and parameters, nuclear radiation detection 0-69031  
 multichannel semiconductor detectors for X-ray transmission computed tomography 0-58058  
 protective surface coatings anal. 0-58057  
 surface barrier detector, peak changes under particle irradi. 0-58077  
 surface barrier detector for beta dosimetry 0-57973  
 surface-barrier photodetectors, registration of pulsed radiation 0-91373  
 telescopic setup for detection of heavy particles produced in electron-nucleus reactions at 4.5 GeV (*Russian*) 0-63461  
 X-ray diffractometry uses and assoc. problems (*French*) 0-84031  
 CdTe detector, performance compared to HgI<sub>2</sub> detector 0-58062  
 CdTe gamma backscatt. assay meter 0-58070  
 CdTe ventricular function monitor, ambulatory, cardiac ejection fraction meas. 0-61680  
 n-GaAs surface barrier diodes for nuclear radiation detection, deep trapping centres 0-92849

**semiconductor counters continued**

- Ge detector, high purity, fast neutron damage 0-59526  
 Ge detector, high purity, fast neutron damage, hole trapping and detrapping 0-63463  
 Ge detector system for inhaled radionuclide detection and meas. 0-57990  
 Ge detectors, high purity, event timing, compared to Ge(Li) detectors 0-69018  
 Ge diode, high purity, buffer ring for edge protection 0-63465  
 Ge intrinsic detector and multichannel analyzer in 5.1 cm borehole probe 0-63451  
 Ge p<sup>+</sup>-n-n<sup>+</sup> structures, charge transport under impurity freezeout conditions 0-92965  
 Ge p<sup>+</sup>-n-n<sup>+</sup> structures, large-scale trap characts. 0-92966  
 Ge X-ray detector, Au contact layer thickness meas. 0-62627  
 Ge(Li) detector, fast neutron damage 0-59525  
 Ge(Li) detector, gamma pulse pileup, random summing losses 0-58023  
 Ge(Li) detector, gamma spect., coincident sum peaks 0-63447  
 Ge(Li) detector efficiency determ. for gas bomb geometries 0-78486  
 Ge(Li) detectors, coaxial, zero cross-over timing 0-69017  
 Ge(Li) detectors, gamma-ray intensity standards for calibration 0-74083  
 Ge(Li) detectors for γ-radioactivity in rocks and soils 0-67418  
 Ge(Li), in situ meas of fission product plateau in HTGR 0-73881  
 Ge(Li), peaks in gamma spectra analysis, analytic approx. 0-102395  
 Ge(Li) semiconductor, used simultaneously with NaI(Tl) scintillation spectrometer, in neutron activation cross-section meas. 0-78485  
 Ge(Li) summing-up effects, optimisation of detector-target geometry for in-beam γ-spectroscopy 0-74070  
 HPGe detector, gamma spect., coincident sum peaks 0-63447  
 HgI<sub>2</sub> detector, performance compared to CdTe detector 0-58062  
 HgI<sub>2</sub> detectors, γ- and X-ray detection, solution grown crystals 0-63452  
 HgI<sub>2</sub> nuclear radiation detector, polarisation reduction 0-58060  
 HgI<sub>2</sub>, soln. grown crystals, low-energy gamma-ray cond. type detectors 0-97418  
 Si detectors and Pb absorber plate, telescope structure, high energy muon flux measurement 0-58061  
 Si diffused junction detector for alpha air monitoring instrumentation 0-58083  
 Si heavy ion surface barrier detector, plasma delay times, electron back-scattered from fission fragment or alpha particle 0-58095  
 Si(Li), peaks in gamma spectra analysis, analytic approx. 0-102395  
 Si(Li), use in energy dispersive X-ray spectrometry of minerals (*French*) 0-85251  
 Si(Li), use in energy dispersive X-ray spectrometry of fracture surfaces (*French*) 0-89571  
 Si(Li) X-ray detector; Au contact layer thickness meas. 0-62627  
 Si(Li)-emulsion shower counter for cosmic ray electron obs. 0-58033

**semiconductor defects** see crystal defects**semiconductor device manufacture**

- Used for commercial manufacture only  
 conference, New York, USA (Oct. 79) 0-73093  
 epitaxial integrated E-dE silicon detector with a buried low-resistive diffused layer 0-58059  
 microelectronics and thin film components frontiers 0-73123  
 optical microscope, large field, for use in semiconductor manufacture 0-82812  
 solar cells, thick film technology applic. 0-93903  
 solar cells automated production, with wraparound contacts 0-76635  
 CdS-Cu<sub>2</sub>S thin-film solar cells, low-cost manufacturing process outline, economic anal. 0-93930  
 Si, single crystal solar cell manufacturing process, laser annealing of implanted area, energy saving 0-97791

**semiconductor device models**

- abrupt p-n junction with one side heavily doped, elec. field max. formulation 0-75629  
 back surface field solar cells, theoretical design considerations 0-93961  
 cascade solar cells design for high-temp. operation using computer modelling 0-81456  
 heterojunction solar cell model, design and evaluation 0-93964  
 IGFET, simulation of semiconductor transport using coupled and decoupled solution techniques 0-65695  
 inversion layer solar cells, numerical modelling 0-81444  
 junction diode, diffused, with deep level traps, negative capacitance 0-96976  
 MIM structure, analytical expressions for tunnel currents 0-60064  
 MIS inversion layer solar cells, two-dimensional model 0-89641  
 MIS structures, analytical expressions for tunnel currents 0-60064  
 MOS, electron mobility in inversion and accumulation layers on thermally oxidised Si surfaces 0-103753  
 MOS inversion layers, freq. response of charge transfer 0-88638  
 MOS structures, quasistatic and nonequilibrium phenomena with constant gate-current bias 0-80385  
 MOST structure, using hybrid computing system, Poisson partial differential equation solution (*Slovak*) 0-75643  
 p<sup>+</sup>-n-n<sup>+</sup> pulsed diodes, forward pulsed case, voltage transient response 0-60071  
 p-n junctions small signal equivalent circuit, finite carrier multiplication 0-65664  
 p-n-insulator metal switching devices, avalanche mode operation 0-70838  
 quasi-monopolar semiconductors, I/V characts., effect of weak diffusion with metal contacts 0-70824  
 Schottky barrier solar cell, doping density effect on efficiency 0-101100  
 solar cell, tandem, low-high junction 0-89626  
 solar cell, tandem junction, Ebers-Moll transistor model 0-93911  
 solar cell, tandem junction, one-dimensional theoretical model 0-81450  
 solar cells, monolithic III-V compound two-junction cascade devices, computer modelling 0-81433  
 solar cells with distributed series resistance, simulation using single diode models 0-93962  
 (Al,Ga)As DH injection lasers, ambipolar transport 0-64025  
 Cu<sub>2</sub>S-Zn<sub>3</sub>Cd<sub>1-x</sub>S heterojunction, improved model of electro-optic behaviour 0-94023  
 GaAs-Al<sub>0.4</sub>Ga<sub>0.6</sub>As heterostructures, real-space electron transfer by thermionic emission, analytical model 0-100512  
 n-Ge-n-GaAs isotype heterojunctions, modelling, characts. 0-103747  
 Si, heavily doped, excess intrinsic carrier density, deionisation of impurities as explanation, bipolar transistor/solar cell models 0-96864  
 Si solar cell I-V charact. meas., effect of voltage ramp, theoretical anal. using linear model 0-61354  
 Si solar cells, fundamental efficiency limitations 0-93963  
 Si solar cells, unified model of fundamental limitations 0-81448



**semiconductor device testing**

- see also *integrated circuit testing*  
 dislocations and microplasma sites, STEBIC/STEM/EELS correlation 0-96528  
 electron beam depth profiling, using carrier collection models 0-70723  
 scanning optical microscope for semicond. materials and devices 0-95136  
 SEM, electron beam induced cond. of defects, rel. to TEM 0-107027  
 SEM voltage contrast obs., electron beam current-recording relationship 0-73528  
 solar cell, automated electronic analysis system 0-93952  
 transmission system, semiconductor device reliability tests 0-58573  
 GaAs-Ga<sub>1-x</sub>Al<sub>x</sub>As DH lasers, electron beam induced current microscopy 0-95899  
 Si ion-implanted laser-annealed solar cells 0-93881  
 Si solar cells with light concentrating lens (*Rumanian*) 0-89620  
 Si terrestrial solar cells, stress tested, contact integrity testing 0-94018

**semiconductor devices**

- see also *field effect devices; Gunn devices; integrated circuits; semiconductor counters; semiconductor diodes; semiconductor junction lasers; space-charge limited devices; thermistors; thyristors; transistors; transit time devices; varistors*  
 applied solid state physics, book 0-94936  
 biomedical pressure transducer (*Japanese*) 0-94394  
 conference, New York, USA (Oct. 79) 0-73093  
 displacement damage, displacement energy determ. by electron beam induced conductivity 0-70097  
 electronics for the physicist with applications, book 0-62403  
 force transducer suitable for use with small muscles 0-72395  
 frequency breakdown, effect of freq. on applied voltage 0-75592  
 microelectronics and thin film components frontiers 0-73123  
 photoelectrochemical cells, energy conversion system, principles and appl. 0-89652  
 radiation effects, dose rate dependent effects of total ionising dose irradiation, annealing 0-70249  
 scanning electron probe voltage contrast, device ground level floatation 0-73527  
 solid state physics, book 0-101676  
 STEM spectroscopic techniques for simultaneous electronic and defect obs. 0-100145  
 GaAlAs-GaAs heteroepitaxial devices, interstitial impurities and degradation, Auger obs. 0-99730  
 Ge sensors, He level gauge appl. 0-57277  
 HgI<sub>2</sub> detectors for X-ray, computerized tomography, evaluation 0-89837  
 Si, photovoltaic cell, absolute spectral sensitivity calibration, radiometry, photometry (*Chinese*) 0-86367  
 Si spectroscopic applications of structures produced by orientation-dependent etching 0-93668  
 p-Si:P semiconductor detector in radiometric inspection problems 0-62819

**semiconductor diode light emitters** see *light emitting diodes***semiconductor diodes**

- see also *avalanche diodes; charge storage diodes; light emitting diodes; photodiodes; Schottky-barrier diodes; solid-state rectifiers; tunnel diodes; varactors; Zener diodes*  
 back diode amplifier, use at low temp. 0-57324  
 junction diodes, fabrication by LPE on Si:B substrates, and characts. 0-80633  
 magnetodiode and magnetoconcentration effects, influence of field effect 0-107903  
 microwave p-i-n diode modulator, transient plasma instability meas. (*German*) 0-87942  
 p<sup>+</sup>-n<sup>+</sup> pulsed diodes, forward pulsed case, voltage transient response 0-60071  
 p-n junctions, variation forward voltage with temp., use as linear temp. transducer 0-57293  
 semiconductor layers, thin, theory of lifetime meas. with SEM, transient anal. 0-88573  
 semiconductor-oxide-semiconductor diodes, tunnel-assisted transport at room temp. 0-92975  
 thermometer system sensor, for use in varying ambient conditions 0-73361  
 thin film glass based structures, surface electron states effect on switching (*Russian*) 0-107887  
 AlGaAs-GaAs mesa diode, deep level defects and hole diffusion length meas. in proton irradiated GaAs 0-60000  
 n-GaAs surface barrier diodes for nuclear radiation detection, deep trapping centres 0-92849  
 GaAs-GaAlAs-GaAs rectifying semicond. struct., prep. by MBE and characts. 0-65657  
 InP:Cd, p<sup>+</sup>-p<sup>+</sup>-n<sup>+</sup> junction form. by diffusion doping 0-84504  
 LiNbO<sub>3</sub>-pn-diode airgap convolver struct. optical scanner using single SAW pulse 0-64144  
 Si, impurity profiles, scanning electron microprobe anal. 0-79832  
 Si ion-controlled diodes, acid-base exposure effects, Si-SiO<sub>2</sub> interface state density 0-96984  
 n-Si, ion-implanted, elec. characts. after laser annealing, mesa diode fabrication 0-88562  
 Si junction diode, diffused, with deep level traps, negative capacitance 0-96976  
 Si p-n junctions, spin depend. surface recomb., electron irradiation effect 0-88627  
 Si:Sb vacuum deposited coating, p-n junction, pulsed electron beam annealing doping, diffusion 0-75480  
 n-Si-Pd diodes, chemical reduction process for fabrication 0-60082  
 Si-SiO<sub>2</sub>-Al MOS surface channel influence on channel-to-contact diode charact. 0-92994  
 p<sup>+</sup>-Si<sub>1-x</sub>Ge<sub>x</sub>-nSi junction diodes, lattice misfit effects on I-V characts. 0-70804

**semiconductor doping**

- see also *doping profiles; ion implantation*  
 amorphous semiconductors, doped, electronic props. 0-80283  
 chalcogenide glasses, memory effect, local doping, switching 0-107873  
 converters, photoelectric, optical methods for checking parameters of semiconductor doped layer 0-93869  
 diamond:Sb, implanted, radiation damage and annealing study 0-100263  
 epitaxial films, model for autoping lateral variation 0-103595  
 grain boundary effects, doping tech. for study and control 0-79815  
 high current ion implanter with hybrid scanning 0-79826  
 highly doped, behaviour of buried O<sub>2</sub> implanted layers 0-59499

**semiconductor doping continued**

- ion implantation by laser annealing, characterisation, solar cell applications 0-70247  
 lightly doped compensated, electric fields at impurity centres (*Russian*) 0-84198  
 MBE for precision doping 0-89156  
 metal-semiconductor contacts with thin interfacial films 0-96969  
 n<sup>+</sup>-p-p<sup>+</sup> bifacial back surface field solar cells, optimisation of p<sup>+</sup> doping level by ion implantation 0-97784  
 one-sided abrupt junctions, normalized representation of avalanche breakdown behaviour 0-65666  
 polyacetylene films, doping effect on elec. cond., chem. and optical props. 0-65572  
 polyacetylene films, doping investigation, insulator-metal transition, optical transmission meas. 0-103729  
 reduction doping using zone recrystn. with temp. gradient 0-104062  
 Schottky barrier solar cell, doping density effect on efficiency 0-101100  
 Si, on sapphire, Schottky magnetodiode, integrated mag. sensor 0-68223  
 solar cell fabrication, laser-induced p-n junction formation 0-93880  
 As<sub>2</sub>Ge<sub>1-x</sub>Te<sub>x</sub>Ag<sub>x</sub> glass, elec. and dielec. props., Ag additions effect 0-65558  
 As<sub>2</sub>S<sub>3</sub> chalcogenide glass films, photographic Ag photodoping to produce negative relief image 0-59490  
 As<sub>2</sub>S<sub>3</sub>:Ag glassy films, optical transmission spectra, photodoping effect 0-66317  
 BP:Zn(Se)(Cd), epitaxial layers, ion implantation, defects and lattice locations, channelling obs. 0-88179  
 Bi<sub>2</sub>Te<sub>3</sub>-Bi<sub>2</sub>Se<sub>3</sub>-Sb<sub>2</sub>Te<sub>3</sub>, solid solution, single crystal, elec. cond., thermoelectric props. 0-88550  
 C:H film, amorphous elec. props., chem. modifications by doping 0-84523  
 CdCr<sub>2</sub>S<sub>4</sub> crystal growth, structural defects, physical properties 0-60759  
 CdInGaS<sub>2</sub>, pure and Cu-doped, electrophotography layers (*Russian*) 0-68282  
 CdS:Cu(Ag), charge and transport mechanism of impurities, electrodiffusion doping 0-59725  
 CdTe, diffusion and solubility of Ge, 630-800°C, prep. conditions depend. 0-103519  
 CdTe:Li(Cl), acceptor states study by donor acceptor pair excitation luminesc. 0-100683  
 CdTi<sub>2</sub>Se<sub>4</sub>:Au, solubility meas. by microhardness method 0-96650  
 CdTi<sub>2</sub>Se<sub>4</sub>(Te<sub>4</sub>):Au, elec. cond., density, dielectric const., changes on fusion 0-88553  
 CuInTe<sub>2</sub> single crystals, directional freezing growth and doping, resist. changes on annealing 0-60768  
 Cu<sub>2</sub>S-CdS heterojunction interface, depth distribution profiles, Auger spectra 0-88622  
 GaAs, semi-insulating and n-type, doping by neutron transmutation 0-96553  
 GaAs, carrier conc. and compensation microprofiles 0-80820  
 GaAs devices, ion implantation damage, characterisation and appl. 0-92551  
 GaAs heavily doped n-type layers, formation by multiple ion implantation 0-59491  
 GaAs ion implantation, semiinsulating materials, role of substrate in elec. props. 0-59488  
 n-GaAs, nature of low temp. field generation of carriers, liberation from surface states 0-92960  
 GaAs, open tube diffusion of Zn 0-84326  
 GaAs, positron annihilation depend. on doping 0-60710  
 GaAs:B, deep levels, optically stimulated transient current method (*French*) 0-59919  
 GaAs:Cr, ion implanted, implantation damage profiles, laser annealing, ellipsometry study 0-79819  
 GaAs:Cr, low temp. gettering 0-96549  
 GaAs:Cr,O semi-insulating monocrystal development and four-level model 0-88191  
 GaAs:Cr,Se, ion-implanted, semi-insulating effects of Cr redistrib. on elec. characts. 0-59982  
 n-GaAs:Ge, film, substrate temp. depend. of Ge incorporation during MBE 0-76196  
 GaAs:Ge,Se transmutation shallow donor transition obs. 0-59925  
 GaAs:Ge film, MBE grown, heavily doped, elec. props. rel. to growth parameters 0-100537  
 GaAs:Ge MBE power FETs with Sn surface impurities 0-80374  
 GaAs:Se, low dose Se<sup>+</sup> ions implanted, DLTS study of laser annealing 0-80204  
 GaAs:Si, accelerated growth rate effect on MBE, Hall mobility and photolum. meas. 0-104067  
 GaAs:Si, activation by multiply scanned electron beams 0-75246  
 GaAs:Si(Sn), ion implanted, laser annealed, high doping levels 0-88181  
 GaAs:Si(s), generation of high mobility n layers, SIMS 0-103375  
 GaAs:Sn thermal diffusion from spin-on SnO<sub>2</sub>/SiO<sub>2</sub> source 0-96691  
 GaAs:Sn(Te), epitaxial film, influence of impurities on stacking fault energy 0-103371  
 GaAs:Zn, implanted, furnace annealed, electrical, Rutherford backscattering and TEM meas. 0-100272  
 GaAs:Zn, implanted, laser annealing, elect., Rutherford backscattering and SEM meas. 0-100273  
 GaAs:Zn(Cr), As precipitation at dislocations, TEM study 0-79820  
 GaAs-Ga<sub>2</sub>Al<sub>0.8</sub>As<sub>0.2</sub>Be, LPE, diffusion of Be into GaAs substrate 0-103517  
 GaAs-Si ion implanted, impurity profiles elec. props. 0-96550  
 GaAs<sub>1-x</sub>P<sub>x</sub>N, photolum. and electrolum. study of N isoelectronic traps 0-89061  
 Ga<sub>1-x</sub>In<sub>x</sub>As:Mn grown by LPE, elect. props. 0-100541  
 GaInAsP/InP lasers, LPE grown, effect of p-doping on carrier lifetime and threshold current density 0-99726  
 GaP:Bi,N, photoluminesc., electroluminesc., 4.2 to 300K, excitons and hole trans 0-108275  
 GaSe, <sup>110</sup>Ag diffusion, temp. depend. and solution (*Russian*) 0-70467  
 GaSe:Sn, <sup>110</sup>Sn diffusion, temp. depend. and Sn solubility (*Russian*) 0-70466  
 GaTe, <sup>110</sup>Ag diffusion, temp. depend. and solution (*Russian*) 0-70467  
 Ge epitaxial film, vac. deposited on GaAs, doping effect of annealed GaAs surface 0-65718  
 Ge:Sb, Ni(Mn), recombination wave spectrum, two-level traps 0-96906  
 Ge:Sn, ion implantation of radioactive <sup>119</sup>Sn 0-59495  
 Ge<sub>2</sub>S<sub>3</sub>:Ag, amorphous, bulk and film forms, doping effect on elec. props. 0-103691  
 n-InAs, photoelectric props., inhomogeneous impurity distrib. 0-107867



**semiconductor doping continued**

- InAs: Cd, Te, donor-acceptor interaction, elec. cond. and Hall coeff. meas. 0-59988  
 p-In<sub>0.53</sub>Ga<sub>0.47</sub>As: Zn on InP, elec. and optical props. 0-75662  
 InP, VPE growth for MESFET's 0-103602  
 InP: Cd, doping by UV laser photodeposition 0-84191  
 InP: Cd, p<sup>+</sup>-p<sup>-</sup>-n<sup>+</sup> junction form. by diffusion doping 0-84504  
 InP: S, SSD growth of low dislocation density crystals 0-89135  
 p-InP-Cd(Zn), ohmic contact formation on InP by laser photochemical doping 0-80369  
 InSb, ion implantation, anomalous radiation disordering 0-92553  
 InSb, morphological and structural changes due to ion bombardment 0-79843  
 InSb: Cd (Zn) (Ge), ion-irradiated, p-n conversion during heat treatment 0-96558  
 InSe, <sup>110</sup>Ag diffusion, temp. depend. and solution (*Russian*) 0-70467  
 PF<sub>3</sub> dopant for polyacetylene 0-88171  
 PH<sub>3</sub> doping, conc. meas. by vacuum UV absorpt. spectra 0-71972  
 Si, amorphous, hydrogenation using DC and HF plasma treatment 0-59497  
 Si, amorphous, ion implantation method, B and P ions 0-100274  
 Si, amorphous, sputtered, resist. control by ion implantation 0-100262  
 Si, BN glass transfer process 0-107459  
 Si, concentrator solar cells, new technology for fabrication 0-81457  
 Si, Czochralski grown, dislocation free, swirl defect form., doping effect 0-92519  
 Si, diffusion of B from CVD BN covered with Si<sub>3</sub>N<sub>4</sub>, appl. to master slice p-MOS IC 0-107564  
 Si, doping impurity distrib., during cryst. growth by Czochralski method (*Russian*) 0-100276  
 Si epitaxial layers, grown in vac. at low temps. P and Sb doping 0-88189  
 Si epitaxial layers, vacuum deposited, conditions for impurity migration from B, P, Sb doped sources (*Russian*) 0-107570  
 Si epitaxy, autodoping effects 0-100259  
 Si film, MBE, cryst. defect props., substrate treatment effects 0-70551  
 Si, heavy ion induced disorder in surface and at shallow depths 0-59535  
 Si, ion implanted, dopant depend. of oxidation rate 0-93834  
 Si, ion implanted, standard for TEM, EELS 0-99017  
 n-Si, ion-implanted, elec. characts. after laser annealing, mesa diode fabrication 0-88562  
 Si ion-implanted dopant redistribution under laser annealing 0-70242  
 a-Si, laser induced crystallisation mechanism, epitaxial regrowth 0-84962  
 Si, migration of Au, electron bombardment effects 0-100362  
 Si, neutron transmutation doping, impediments to use in power device fabrication 0-96560  
 Si, phonon-phonon relaxation investigation for conventional and neutron doped crystals 0-96927  
 Si ribbon solar cells, var. of minority-carrier diffusion length with light intensity, heavy metal doping effects 0-93937  
 Si solar cells, effects of metallic impurities 0-85278  
 Si solar cells, fabrication using continuous or pulsed lasers (*French*) 0-61350  
 Si solar cells, high open circuit voltage, P implantation 0-89642  
 Si solar cells, ion implanted grating type 0-101102  
 Si solar cells, junction formation techniques using spray-on polymer dopants, cost effective, high throughput 0-94014  
 Si solar cells, POCl<sub>3</sub> gettering of Ti, Mo and Fe-contaminated cells 0-94010  
 Si solar cells, realisation by laser induced diffusion of deposited Sb 0-93998  
 Si, surface, pulsed electron beam processing, doping, annealing 0-75254  
 Si thin film, polycryst., CVD, elec. props. 0-107934  
 Si wafers, floating-zone, etch struct. on microdefects as affected by dopants and surface treatment 0-79773  
 Si: Al(Ga), O<sub>2</sub> diffusion, conc. profile meas. 0-79990  
 Si: Al(Ga), spreading resist. calibration using Si: B 0-103690  
 Si: Ar, As, ion implanted, laser annealing, doping profiles, channelling 0-97506  
 Si: As, CVD, doping using SiH<sub>4</sub>-H<sub>2</sub>-AsH<sub>3</sub> system 0-79823  
 Si: As, heavily As-diffused, Hall mobility and resist. rel. to carrier conc. 0-107815  
 Si: As, ion implanted, formation of As complexes 0-59511  
 Si: As, ion implanted, low temp. thermal annealing 0-96552  
 Si: As, scanning electron beam annealing, spreading resistance, junction depth 0-75267  
 Si: As, solid solubility and thermal behaviour of metastable 0-75359  
 Si: As ion implanted layers, annealing by CO<sub>2</sub> laser, doping profile shift 0-84965  
 Si: As<sup>+</sup>, implanted, CW laser annealing, electron-beam induced current 0-100709  
 Si: B, high conc. effects in ion implantation 0-75245  
 Si: B, use of BN source to achieve high surface concentration of B (*Russian*) 0-107639  
 Si: B diffusion at Si-SiO<sub>2</sub> interface, Auger spectra, Rutherford backscattering 0-70471  
 Si: B ion implanted, strain profiles from X-ray rocking curves 0-107290  
 Si: BF<sub>3</sub><sup>+</sup>, ion implantation appl. in semicond. device production 0-103383  
 Si: B(Be)(Li) ion implanted, channelling and random equivalent depth distrib. 0-100293  
 Si: B(P), ion implanted crystalline and amorphous laser annealing 0-97509  
 Si: Be, ion implanted, correl. of atomic distrib. and implantation induced damage profiler 0-88199  
 Si: Bi, ion implanted, channelling obs. of pulsed Q-switched ruby laser annealing 0-59542  
 Si: Co, ion implanted, Co lattice location, channelling meas. 0-88201  
 n-Si: Ga laser doped, segregation, Rutherford backscattering 0-103483  
 a-Si: H, depletion width determ. by analytical model 0-100445  
 Si: H, Li, amorphous, photoluminescence obs. 0-66280  
 a-Si: H film, glow discharge deposited, H profiles, doping level 0-84202  
 a-Si: H: F, depletion width determ. by analytical model 0-100445  
 Si: In, dopant energy levels, Hall meas., interpretation 0-107736  
 p-Si: In, ion implanted, doping profiles from capacitance-voltage characts. 0-88203  
 Si: N, high energy ion implantation of buried insulating layers 0-88188  
 Si: N, implantation at high doses, annealing conditions for homogeneous buried insulating layer (*French*) 0-59498  
 Si: N, ion implanted, oxidation characts. 0-93835  
 Si: P, doping during growth from gas phase, thermodynamic analysis 0-59489

**semiconductor doping continued**

- Si: P, homogeneous nuclear transmutation technique, thyristors appl. 0-70236  
 Si: P, implanted low temp. annealed, elec. activation, damage depend. 0-88182  
 Si: P, incoherent light flash annealing, elec. props., backscattering spectra 0-97504  
 Si: P, neutron transmutation doping, elec. props. rel. to neutron fluence 0-96555  
 Si: P, neutron transmutation doping, resist. homogeneity rel. to compensation ratio 0-96556  
 Si: P, polycryst. films, elec. props., EPR, defect states, doping effects 0-75660  
 Si: P polycrystalline layer, role in lattice defect reduction assoc. with P predeposition 0-70229  
 Si: P(O) p<sup>+</sup>-n<sup>+</sup> solar cells, comparison rel. to resistance to 1.5 MeV electron irradi., majority carrier trapping 0-94087  
 Si: Sb, MBE film, doping technique 0-79821  
 Si: Sb, produced by ion implantation and laser annealing, Sb behaviour above solid solubility 0-88200  
 Si: Sb, P, double implants, residual defect reduction after damage anneal 0-88170  
 Si: Sb vacuum deposited coating, p-n junction, pulsed electron beam annealing doping, diffusion 0-75480  
 Si: Sb(Ga)(Bi)(In), dopant solubility limit, laser irradi. effects 0-84295  
 Si: Te, laser melting, surface Te atom accumulation, profiles 0-100258  
 Si-F-H-P, film, dark cond., struct., Raman scatt. 0-88588  
 Si-SiO<sub>2</sub>, interface, doping depend. of interface states and charges 0-92992  
 SnO<sub>2</sub>: P, CVD films, elec. props., cryst. to amorphous transition effects 0-107933  
 SnO<sub>2</sub>: P, CVD growth and etching characts., doping effects 0-107667  
 TiO<sub>2</sub>, doping processes, influence on photoelectrochem. behaviour 0-79822  
 n-TiO<sub>2</sub>, photoelectrochemical electrodes, effect of Nb doping on quantum efficiency 0-101121  
 YIG: Si single crystals, liq. flux growth, obs. 0-66416  
 ZnO, defect struct. calc., doping effects 0-107218  
 ZnO: Ga sputtered films, props. rel. to deposition conditions 0-107935  
 ZnTe, doping and intrinsic stoichiometric defects, self-compensation 0-59918  
 ZnTe: P(As), ion implanted, cathodoluminescence emission spectrum 0-108281
- semiconductor-electrolyte boundaries**  
 charge transfer via surface states, water photoelectrolysis anal. 0-75636  
 hot carrier injection, tunnelling from semiconductor states in depletion region 0-75637  
 oxide semiconductors in photoelectrochemical conversion of solar energy, use as cell anodes 0-101120  
 photoelectrochemical cells, energy conversion system, principles and appl. 0-89652  
 photoelectrochemical cells with semiconductor electrodes for solar energy conversion and storage (*French*) 0-61386  
 photovoltaic cells, interface charge transfer, recombination rate, C-V characts. 0-70818  
 thin film electrode, photosensitization by cyanine dye in lipid bilayer 0-75639  
 CdS: Te-based photoelectrochem. cell, luminesc., thermal manipulation of deactivation processes 0-81479  
 CdSe, chemically sprayed thin films as photoanode in photoelectrochem. cells, power charact. meas. 0-85293  
 CdSe film photoanodes for electrochem. photovoltaic cells, fabrication and evaluation 0-76641  
 CdSe photoanode improved efficiency by photoelectrochem. etching 0-104512  
 CdSe photoanodes, S substitution during operation and mech. of surface protection 0-107906  
 Cd<sub>2</sub>SnO<sub>4</sub> and Cd<sub>2</sub>SnO<sub>4</sub>: CdO, thin film electrodes in H<sub>2</sub>SO<sub>4</sub> electrolytes, reduction, AES and SEM 0-65674  
 CdTe, minority carrier diffusion length from photocurrent meas. in semicond.-electrolyte boundary 0-65584  
 n-CdTe, semiconductor electrode, electrochem. behaviour in nonaqueous media (*French*) 0-66808  
 Fe<sub>2</sub>O<sub>3</sub>, semicond. anode in aq. electrolyte, electrochem. and electrochem. 0-76080  
 p-GaAs electrode, flatband pot. determ. from differential stress meas. 0-75638  
 n-GaAs, metal filmed photoelectrochemical cell, energy conversion characts. 0-101118  
 p-GaAs/heptyl viologen system, appl. in photoelectrochemical cells and photoelectrochromic displays 0-76640  
 n-GaAs-K<sub>2</sub>Se-K<sub>2</sub>Se<sub>2</sub>-KOH/C thin film solar cell, 7.3% cell efficiency 0-93931  
 n-GaP electrode, photoanodic dissolution rate, effect on surface electronic band energies 0-103748  
 p(GaP): Zn-electrolyte interface, electrochemical LED, luminescence obs. 0-84507  
 N-Ge, electrorefl. spectra, light induced, electrolyte and Schottky barrier techniques of meas. 0-76046  
 Ge surface states, recomb. centres, regularities, electrolyte contact effects (*Russian*) 0-65652  
 H<sub>2</sub>, review 0-61453  
 n-MoSe<sub>2</sub> based liq. junction solar cell, nonaqueous electrolyte system employing Cl<sub>2</sub>/Cl<sup>-</sup> couple 0-81432  
 n-Si, Fe<sub>2</sub>O<sub>3</sub>-coated, heterostruct. photoanode for photoelectrolysis of water 0-61384  
 Si, thermally oxidised-electrolyte system, features of cathodic breakdown (*Russian*) 0-107907  
 Si: H, amorphous, photoelectrochem. behaviour 0-81480  
 p-Si: P(P<sup>+</sup>) photolytic props. in HF 0-89504  
 n-SnO<sub>2</sub>, pigmented solar cell for electrolysis of water, two-photon process 0-93932  
 n-SrTiO<sub>3</sub>, electrode, flatband pot. determ. from differential stress meas. 0-75638  
 SrTiO<sub>3</sub>, semicond. anode in aq. electrolyte, electrochem. and electrochem. 0-76080  
 SrTiO<sub>3</sub> semicond. electrodes, electroreduction process kinetics, cathodic dark current meas. 0-66807  
 SrTiO<sub>3</sub>: H<sub>2</sub>O, H<sub>2</sub>O photoassisted decomp. 0-85202  
 TiO<sub>2</sub>, doping processes, influence on photoelectrochem. behaviour 0-79822

**semiconductor-electrolyte boundaries continued**

- n-TiO<sub>2</sub> electrode, flatband pot. determ. from differential stress meas. 0-75638  
 n-TiO<sub>2</sub> electrode in AlCl<sub>3</sub>-NaCl melt, electrochem. and photoelec. props. 0-81328  
 TiO<sub>2</sub> electrodes, chemically modified, nature of surface states 0-107905  
 n-TiO<sub>2</sub> photoelectrochemical electrodes, effect of Nb doping on quantum efficiency 0-101121  
 TiO<sub>2</sub> semicond. anode in aq. electrolyte, electrolum. and electrochem. 0-76080  
 TiO<sub>2</sub>, sputtering defects, associated surface electron states, UPS, XPS and AES obs. 0-60755  
 TiO<sub>2</sub>/Nb semicond. electrodes, electroreduction process kinetics, cathodic dark current meas. 0-66807  
 n-TiO<sub>2</sub>-electrolyte interface, charge transfer via surface states, water photoelectrolysis anal. 0-75636  
 n-TiO<sub>2</sub>-electrolyte interface impedance, freq. depend., equiv. cct. 0-100516  
 WO<sub>3</sub> semicond. anode in aq. electrolyte, electrolum. and electrochem. 0-76080  
 n-WS<sub>2</sub> electrode in aq. iodide medium, high efficiency photoelectrochemical solar cell 0-72069  
 ZnS crystals in electrolyte, electrolum. and elec. props. 0-93407

**semiconductor electron states** see band structure of crystalline semiconductors and insulators; electron energy states of amorphous solids; electron energy states of liquid semiconductors

**semiconductor epitaxial layers**

- autodoping, lateral variation model 0-103595  
 depth profiling by electron beam induced junction current meas. 0-96977  
 diamond-like semiconductor film epitaxial growth, computer simulation 0-70560  
 doping reduction using zone recrystn. with temp. gradient 0-104062  
 HgCdTe/CdTe, limited diffusion volume photodiode, characterisation 0-75627  
 II-VI semiconductors, direct synthesis (*German*) 0-104070  
 III-V multilayer structure, as-grown, assessment of defects by differentiated cathodolum. topography 0-59819  
 III-V semiconductor based layered multielectronic systems, electronic process investig. survey (*Russian*) 0-107891  
 III-V semiconductor-epitaxial structures as wide-gap substrates, minority carrier diffusion length determ. by photoluminesc. 0-103992  
 ion implanted semiconductor epitaxial regrowth, laser annealing dynamics 0-92548  
 MBE manufacture 0-103593  
 multilayer systems, film growth, spectroscopic ellipsometry, review 0-103603  
 narrow-band semiconductor, growth, activation by UV and IR radiation 0-71598  
 semiconductor thin films, fabrication for device appls. 0-100418  
 Si epitaxy, vapour phase deposition technology 0-75472  
 solar cell fabrication, laser-induced p-n junction formation 0-93880  
 varizional, parameter determ. by photoluminescence method (*Russian*) 0-108291  
 AlGaAs p-n diodes, I-V characts., tunnelling 0-100510  
 AlGaAs-GaAs proton irradiated solar cells, deep-level defects, recombination mechanisms, performance characts. 0-81459  
 Al<sub>0.42</sub>Ga<sub>0.58</sub>As-GaAs-Al<sub>0.42</sub>Ga<sub>0.58</sub>As, etalon, optical bistability and modulation 0-58628  
 Al<sub>0.1</sub>Ga<sub>0.9</sub>As epitaxial layers on GaAs, struct. study by scanning Auger electron microscopy 0-80110  
 Al<sub>0.1</sub>Ga<sub>0.9</sub>As, microstruct., effect on elect. characts. of Schottky diode (*Russian*) 0-107671  
 Al<sub>0.1</sub>Ga<sub>0.9</sub>As, pure and Ge doped, shallow acceptor photoluminescence 0-76064  
 Al<sub>0.1</sub>Ga<sub>0.9</sub>As semitransparent photocathode, LPE, quantum efficiency spectrum 0-76153  
 Al<sub>0.1</sub>Ga<sub>0.9</sub>As-Al<sub>0.1</sub>Ga<sub>0.9</sub>As DH IR-visible (0.89-0.72  $\mu$ m) MBE grown lasers 0-64058  
 AlGaAsSb LPE growth, lattice-matched to GaSb, characterisation 0-60794  
 Al<sub>0.1</sub>Ga<sub>0.9</sub>AsZn-GaAs solar cells by LPE, open circuit voltage, fill factor 0-101108  
 Al<sub>0.1</sub>Ga<sub>0.9</sub>P, LPE, crystallographic obs. and electrolum. 0-88445  
 Al<sub>0.1</sub>Ga<sub>0.9</sub>Sb-Pd contacts, struct., preparation elec. props. 0-65684  
 AlSb solar cell material, epitaxy, ionicity and bond struct. 0-61367  
 AlSb, thin film growth on insulating substrates, by metal organics CVD 0-60786  
 BP:Zn(Se)(Cd), epitaxial layers, ion implantation, defects and lattice locations, channelling obs. 0-88179  
 (Cd,Hg)Te epitaxial structures, comp. profile depend. on deposition parameters 0-100795  
 Cd<sub>0.1</sub>Hg<sub>0.9</sub>Te epitaxial graded gap layers, plasma reflection and magnetoreflection 0-71391  
 Cd<sub>0.1</sub>Hg<sub>0.9</sub>Te, epitaxial growth from stoichiometric melt, crystn. and diffusion 0-75475  
 Cd<sub>0.1</sub>Hg<sub>0.9</sub>Te, epitaxial layer p-n junction, current-voltage characteristics of photovoltaic detectors, 1 to 15  $\mu$ m 0-86407  
 Cd<sub>0.1</sub>Hg<sub>0.9</sub>Te, graded gap epitaxial layers, spectral characts. of photoelectromagnetic effect 0-60022  
 Cd<sub>0.1</sub>Hg<sub>0.9</sub>Te, graded-gap layers, galvanomag. props. at low temp. and in weak mag. field 0-75664  
 Cd<sub>0.1</sub>Hg<sub>0.9</sub>Te, tunnelling effect in p-n junctions 0-75630  
 CdS, epitaxial growth and nucleation, on monocrystrn. ZnS, substrate real struct. influence 0-88455  
 CdS epitaxial layers on sapphire, exciton struct. of absorpt., photoluminesc. and photocond. spectra 0-89027  
 CdS/InP epitaxial thin films on NaCl, HEED and TEM study 0-88446  
 CdSe(Te) films, oriented, epitaxial growth by epitaxial nucleation in sub-microscopic holes method 0-59834  
 CdTe thin films, oriented, VPE growth, infrared transmission, photovoltaic cells 0-59825  
 CdTe-CdS heterojunctions, growth by closed-tube chem. transport, elec. props. 0-60070  
 Cd<sub>0.1</sub>Zn<sub>0.9</sub>S heteroepitaxial single-cryst. layers, photoluminesc. props. 0-100692  
 CuIn<sub>0.7</sub>Ga<sub>0.3</sub>Se, epitaxial layers, on GaAs substrates, struct. and elec. props. 0-107670  
 CuInSe<sub>2</sub>, heteroepitaxy on {111} oriented Ge by flash evaporation, struct. 0-108333  
 CuInTe<sub>2</sub> epitaxial layers, on GaAs, growth and props. 0-108359

**semiconductor epitaxial layers continued**

- EuSe, VPE by hot-wall technique 0-80958  
 (Ga,Al)As:Si (Ge), epitaxial layers, radiative recomb., compensation, cathodolum. study 0-66307  
 n-GaAs epitaxial film, radiative recomb. under influence of mech. stresses 0-66291  
 GaAlAs-GaAs, defects and degradation, transmission cathodolum. evaluation 0-65395  
 GaAlAs-GaAs heteroepitaxial devices, interstitial impurities and degradation, Auger obs. 0-99730  
 Ga<sub>0.1</sub>Al<sub>0.9</sub>As LPE layers containing low-cond. regions, charging effects in SIMS anal. 0-66348  
 Ga<sub>1-x</sub>Al<sub>x</sub>As, LPE layers, electron mobility, scatt. processes 0-84519  
 Ga<sub>1-x</sub>Al<sub>x</sub>As:Zn, acceptor energy level and elec. props. 0-65482  
 Ga<sub>1-x</sub>Al<sub>x</sub>As based layer structures, optimum growth conditions, comp. and struct. perfection 0-104069  
 Ga<sub>1-x</sub>Al<sub>x</sub>As, epitaxial, radiative deep states 0-76061  
 Ga<sub>1-x</sub>Al<sub>x</sub>As-GaAs p-n and p-p-n heterojunction solar cells, high efficiency, prep., eval. and characters (*Japanese*) 0-61342  
 Ga<sub>0.1</sub>Al<sub>0.9</sub>As-GaAs heteroepitaxial layer distortion characterisation by X-ray multiple diff. 0-96754  
 Ga<sub>0.1</sub>Al<sub>0.9</sub>As, photodetector diode on GaAs substrate dark currents, tunnelling, energy gaps, effective masses 0-70805  
 Ga<sub>1-x</sub>Al<sub>x</sub>As<sub>1-y</sub>P<sub>y</sub> epitaxial layer heterojunction, nonradiative recombination at misfit dislocations 0-96901  
 GaAlAsSb-GaSb low bandgap solar subcell for high efficiency multiband-gap converters, LPE growth 0-93927  
 Ga<sub>1-x</sub>Al<sub>x</sub>N heteroepitaxial films, photoluminesc., cathodoluminesc. 0-66292  
 Ga<sub>1-x</sub>Al<sub>x</sub>P:N epitaxial films, ion implanted, cathodoluminescence study 0-60684  
 GaAs antireflecting MOS solar cells, epitaxial and polycryst. using OM-CVD techniques 0-94072  
 GaAs base laminated epitaxial struct., surface plasmon phonon polaritons (*Russian*) 0-59905  
 GaAs compensated VPE thin film, electron Hall mobilities 0-107932  
 GaAs, doping profile degradation due to ion implantation 0-84194  
 GaAs, electron-beam excited, efficient generation of electron-hole plasma 0-76051  
 n-GaAs, epitaxial, high temp. carrier transport 0-65725  
 GaAs epitaxial film, enhanced electrodiffusion purification in mag. field 0-66409  
 n-GaAs epitaxial film, magnetoresist. at low temp., geometric effect 0-93015  
 GaAs epitaxial film, photo-EMF echo at 4.2K 0-60038  
 GaAs epitaxial films on strongly doped substrate, basic parameter meas. utilising magnetoresist. and SEM techniques under cathodoluminesc. conditions 0-65728  
 GaAs epitaxial III-V semiconductor thin film prep. by low temp. CVD 0-60789  
 GaAs, epitaxial layer, nondislocation etch pits 0-92535  
 GaAs epitaxial layers, meas. of doping profiles (*Hungarian*) 0-70545  
 GaAs epitaxial layers, surface impurity gradients, Schottky barrier capacitance meas. 0-70782  
 GaAs, epitaxial layers, electron irradi. deep level trap energy depend. 0-80205  
 GaAs epitaxial layers on polycryst. GaAs substrates, LPE growth characts. 0-75471  
 GaAs epitaxial thin films with neg. electron affinity, photoelectron energy distrib. 0-100755  
 GaAs, epitaxy by metallorganic and chloride depositions, defect characterisation at growth interface 0-59817  
 GaAs, exciton effects in photocond., photoluminesc. 0-96797  
 GaAs films for solar cells appl., deposition and characterisation 0-84853  
 GaAs, gas-phase epitaxy, step stopping centre form. kinetics 0-65407  
 n-GaAs, LPE, deep trapping centre characterisation by Hall and photo-Hall meas. 0-88578  
 GaAs LPE from Ga soln., carrier conc., growth condition depend. 0-71584  
 n-GaAs, low temp. field generation of carriers, liberation from surface states 0-92959  
 n-GaAs, MBE, correl. between electron traps and growth processes 0-65387  
 p-GaAs, MBE grown, As<sub>2</sub> and As<sub>4</sub> effects on photolum. 0-103974  
 GaAs, microstruct., effect on elect. characts. of Schottky diode (*Russian*) 0-107671  
 GaAs, multilayer liquid phase epitaxy, transition to faceting 0-96750  
 GaAs multilayer photocathode structures, TEM obs. of dislocations generated 0-100241  
 GaAs, nonuniform electroconductivity (*Russian*) 0-70753  
 GaAs, organometallic VPE, with varying As/Ga ratios, deep states 0-65480  
 GaAs, photoluminescence, electron gas coding influence in ion-bombarded layers 0-108272  
 GaAs, proton irradiated, low energy, deep level defects and hole diffusion length meas. 0-60000  
 GaAs, residual donor identification by far IR photocond. 0-60047  
 GaAs, residual donor identification by far IR photoconductivity meas. 0-103717  
 GaAs type FET with buffer, bias effects due to deep centres in struct. (*French*) 0-107917  
 GaAs, undoped epitaxial layer growth from nonstoichiometric solns., O<sub>2</sub> contamination sources 0-108362  
 n-GaAs:Ge, substrate temp. depend. of Ge incorporation during MBE 0-76196  
 GaAs:Ge film, MBE grown, heavily doped, elec. props. rel. to growth parameters 0-100537  
 GaAs:Ge MBE power FETs with Sn surface impurities 0-80374  
 GaAs:O epitaxial film, impurity states, photocapacitance spectra 0-65625  
 GaAs:Si, accelerated growth rate effect on MBE, Hall mobility and photolum. meas. 0-104067  
 GaAs:Si, transferred-electron devices by low-level ion implantation 0-92543  
 GaAs:Sn(Te), epitaxial film, influence of impurities on stacking fault energy 0-103371  
 GaAs/GaInP DH, MBE grown, optically pumped laser action at 77K 0-95890  
 GaAs-Al<sub>0.1</sub>Ga<sub>0.9</sub>As n-n heterojunction, LPE grown, cond. band discontinuity, C-V profiling meas. 0-70801  
 GaAs-Al<sub>0.1</sub>Ga<sub>0.9</sub>As DH laser, MBE grown, CW electro-optical props. 0-102725



## semiconductor epitaxial layers continued

- GaAs-Al<sub>x</sub>Ga<sub>1-x</sub>As multilayers, two-dimens. transport at high mag. fields 0-65724  
 GaAs-Ga<sub>1-x</sub>In<sub>x</sub>P heterostructure, elastic stresses and substrate/epitaxial film mismatch, X-ray diff. method 0-92794  
 GaAs-GaAlAs superlattices, metalorganic VPE growth, in sites ellipsometry monitoring 0-70547  
 GaAs-GaInAs structure, dislocation struct., TEM anal., appl. as IR LED 0-70206  
 GaAs-Ge, heterostructure, zincblende-on-diamond type systems, MBE growth, (110) orientation as preferred orientation 0-80099  
 (GaAs)<sub>m</sub>(AlAs)<sub>n</sub> multilayers, MBE, interdiffusion, X-ray diff. study 0-70474  
 GaAs-P<sub>1-x</sub> alloy, composition effects in growth by MBE 0-59816  
 GaAs<sub>1-x</sub>Sb<sub>x</sub> layer on GaAs, dislocation density reduction by improved LPE growth method 0-76202  
 GaInAs-InP, growth by low-pressure metalorganic CVD 0-71595  
 Ga<sub>1-x</sub>In<sub>x</sub>As epitaxial layer growth by organometallic pyrolysis, homojunction LED prep. 0-76194  
 Ga<sub>1-x</sub>In<sub>x</sub>As:Mn grown by LPE, elect. props. 0-100541  
 Ga<sub>1-x</sub>In<sub>x</sub>As, on (111)B InP, LPE growth, characterisation of high purity lattice 0-104082  
 Ga<sub>1-x</sub>In<sub>x</sub>As-InP, MBE film growth, composition control obs. 0-84399  
 Ga<sub>1-x</sub>In<sub>x</sub>As<sub>1-y</sub>P<sub>y</sub>, IR refl. spectra 0-60602  
 Ga<sub>1-x</sub>In<sub>x</sub>As<sub>1-y</sub>P<sub>y</sub>, LPE growth 0-66440  
 Ga<sub>1-x</sub>In<sub>x</sub>P MBE layers, comp., Rutherford scatt. and X-ray diff. meas. 0-75457  
 Ga<sub>1-x</sub>In<sub>x</sub>P solid solns., isothermal liq. epitaxy 0-60793  
 GaN epitaxial films, cathodoluminesc. spectra 0-71496  
 GaN, photoluminesc. spectra, energy distrib. 0-97339  
 GaN, VPE growth rate influence on elec. and luminesc. props. 0-100702  
 GaP, VPE layer structures for LEDs, SEM, and TEM obs. of dislocation density reduction expt. 0-100425  
 GaP:Ce(Dy)(Pr) epitaxial films, photoluminesc. spectra 0-66294  
 GaP:Cr epitaxial layers, Cr conc. profile determ. 0-65029  
 GaP/Si heterostruct., differential thermal contraction, plastic deform., fracture 0-108494  
 GaP-Si, heterostructure, zincblende-on-diamond type systems, MBE growth, (110) orientation as preferred orientation 0-80099  
 GaSb, electroliquid epitaxial growth 0-89160  
 n-GaSb:Te, IR refl. meas., carrier conc. and mobility determ. 0-80769  
 (GaSb)<sub>1-x</sub>Ge<sub>x</sub> films, single-cryst. metastable semicond., growth and phase stability 0-80115  
 Ge epitaxial film, ion implantation and electron beam anneal effects on carrier conc. 0-75255  
 Ge epitaxial film, vac. deposited on GaAs, doping effect of annealed GaAs surface 0-65718  
 Ge, epitaxial growth of very thin electron microscopy specimens 0-100793  
 Ge heteroepitaxial film, ethanol pulsed adsorption effect on elec. cond. 0-93014  
 Ge-GaAs, heteroepitaxial systems, misfit dislocations obs. using HV electron microscopy 0-100242  
 Hg<sub>0.5</sub>Cd<sub>0.5</sub>Te LPE layer growth from Te-, Hg-, and HgTe-rich solns., comparison 0-76199  
 Hg<sub>1-x</sub>Cd<sub>x</sub>Te, epitaxial layers, elec. properties in the range 4.2 to 300K (French) 0-65721  
 Hg<sub>1-x</sub>Cd<sub>x</sub>Te epitaxial layers, elec. props. 0-96910  
 (In,Ga)(As,P) binary, ternary and quaternary, hydride vapour phase epitaxy, cryst. growth and props. 0-66434  
 InAs-P<sub>1-x</sub> alloy, composition effects in growth by MBE 0-59816  
 InGaAs, LPE, diffusion-limited step-cooling technique, layer thickness and composition 0-84402  
 In<sub>1-x</sub>Ga<sub>x</sub>As:Zn, lattice matching to InP, LPE growth conditions 0-70541  
 InGaAsP, anodic oxidation, refractive indices 0-97601  
 InGaAsP avalanche photodiodes, breakdown mechanism, donor conc. effect 0-70710  
 InGaAsP, epitaxial growth by chloride CVD process, thermodynamic anal. 0-64936  
 InGaAsP, LPE, diffusion-limited step-cooling technique, layer thickness and composition 0-84402  
 InGaAsP LPE heterostructs., interface grading, Auger depth profile 0-103585  
 InGaAsP/InP phototransistors, fabrication by LPE, photodetectors 0-95139  
 InGaAsP-InP DH laser, 1.55 μm, low temp. LPE growth for room-temp. CW operation 0-64045  
 InGaAsP-InP DH lasers, perturbed InP growth, photoluminesc. study 0-106518  
 InGaAsP-InP layers, grown by LPE techniques, lattice const., bandgap, thickness and surface morphology meas. 0-59818  
 In<sub>1-x</sub>Ga<sub>x</sub>As<sub>1-y</sub>P<sub>y</sub> epitaxial layer, far IR refl. spectra, lattice vibrs. 0-97282  
 In<sub>1-x</sub>Ga<sub>x</sub>As<sub>1-y</sub>P<sub>y</sub> far IR reflection spectrum 0-60612  
 In<sub>1-x</sub>Ga<sub>x</sub>As<sub>1-y</sub>P<sub>y</sub>, hole mobility over temp. range 77 to 300K 0-60111  
 In<sub>1-x</sub>Ga<sub>x</sub>As<sub>1-y</sub>P<sub>y</sub>/InP 1.5 μm room-temp. CW laser fabrication and operation 0-64070  
 In<sub>1-x</sub>Ga<sub>x</sub>As<sub>1-y</sub>P<sub>y</sub> epitaxial layers, characterisation and relation to lattice matching 0-100540  
 In<sub>1-x</sub>Ga<sub>x</sub>As<sub>1-y</sub>P<sub>y</sub> photodetector diode on InP substrate dark currents, tunnelling, energy gaps, effective masses 0-70805  
 InGaP/InGaAs struct. for transferred electron photocathodes, VPE growth and characterisation 0-76193  
 In<sub>0.3</sub>Ga<sub>0.7</sub>P, N free and implanted, photoluminescence study 0-97322  
 In<sub>1-x</sub>Ga<sub>x</sub>P, compositional inhomogeneity 0-88444  
 InGaPAs LPE layers, compositional inhomogeneity, photoluminesc. obs. 0-75451  
 In<sub>1-x</sub>Ga<sub>x</sub>P<sub>1-y</sub>As<sub>y</sub>, lattice matched to InP, electrorreflectance obs. 0-93416  
 InP epitaxial films, grown on heavily doped substrates, carrier mobility study, magnetoresist. meas. 0-60116  
 n-InP, epitaxial layer, (100) surface chemistry, ESCA study 0-103552  
 InP films, organometallic VPE grown, props. 0-96753  
 InP, MBE, substrate temp. related degradation mechanisms 0-65385  
 InP surface decomposition prevention in LPE growth 0-96749  
 InP, VPE growth for MESFET's 0-103602  
 InP-GaInAsP buried heterostructure layers of 1.5 μm region, fabrication and characts. 0-74388  
 InP-In<sub>1-x</sub>Ga<sub>x</sub>As<sub>1-y</sub>P<sub>y</sub>-InP 1.53 μm single-mode CW ridge-waveguide laser 0-64072  
 InSb<sub>1-x</sub>Bi<sub>x</sub> films, single-cryst. metastable semicond., growth and phase stability 0-80115

## semiconductor epitaxial layers continued

- InSb<sub>1-x</sub>Bi<sub>x</sub>, metastable epitaxial film, phase diagram 0-76238  
 InSb<sub>1-x</sub>Bi<sub>x</sub>, multitarget RF sputtering, metastable phase, conductivity transition 0-76178  
 Pb<sub>1-x</sub>Ge<sub>x</sub>Te magnetoplasma reflectivity and transmission spectra 0-71428  
 PbS, small-angle X-ray scatt. and electron density inhomogeneities 0-96758  
 PbS-PbSe epitaxial bicrystals, direct scatt. of channelled He ions at dislocations 0-65110  
 PbSe films, current carrier conc. and type control, elec. cond., synthesis process (Russian) 0-100412  
 Pb<sub>1-x</sub>Sn<sub>x</sub>Se epitaxial layers, radiative and nonradiative recomb. processes 0-60670  
 Pb<sub>1-x</sub>Sn<sub>x</sub>Se layers obtained by LPE, growth conditions correl. with morphology 0-104079  
 Pb<sub>0.85</sub>Sn<sub>0.15</sub>Te homostructure diode laser, LPE growth, with controlled carrier conc. 0-95903  
 Pb<sub>1-x</sub>Sn<sub>x</sub>Te epitaxial films, adsorption-induced accumulation layer form. on surface 0-60117  
 Pb<sub>1-x</sub>Sn<sub>x</sub>Te LPE film IR detector performance 0-86422  
 Pb<sub>1-x</sub>Sn<sub>x</sub>Te, x=0.2, monocystal, photoelectric props. of p-n structures (Russian) 0-70808  
 n-PbTe, noncubic (111) oriented epitaxial films, weak field magnetoresistance 0-75584  
 PbTe, nonstoichiometric, evap. and growth of epitaxial layers 0-104072  
 Pb<sub>1-x</sub>Te-Pb<sub>1-y</sub>Sn<sub>y</sub>Te (x,y≤0.3), double heterostruct., LPE growth, heterointerface morphology 0-70550  
 Se, SAW vel. and electromech. coupling factor 0-75422  
 Si, amorphous, epitaxial regrowth, structure and impurities effect 0-84401  
 Si, amorphous, substrate orientation effect on regrowth by laser pulses, channeling, backscatter 0-84409  
 Si epitaxial film, containing struct. defects formed during growth, positron annihilation 0-93433  
 Si epitaxial film on sapphire, microtwins, TEM exam. 0-70555  
 Si, epitaxial growth on sapphire by partially ionised vapour deposition, RHEED-AES obs. 0-80985  
 Si, epitaxial layer deposition by ion beam methods 0-100417  
 Si epitaxial layer regrowth due to laser annealing mechanism, liquid and solid phase regimes 0-100712  
 Si, epitaxial layer thickness meas. using phase correction function of substrate resistivity (Rumanian) 0-90812  
 Si epitaxial layers, grown in vac. at low temps. P and Sb doping 0-88189  
 Si, epitaxial layers, stacking defect distrib. anal. using ion channelling tech. 0-100294  
 n-Si epitaxial layers on oppositely conducting substrates, two layer Hall coeff. meas. technique 0-80297  
 Si epitaxial thin film growth on sapphire and spinel by MBE 0-76186  
 Si epitaxy, autoping effects 0-100259  
 Si, etching by CF<sub>4</sub>, plasma deposition reactor gas phase characts., mass spectra 0-70566  
 Si film, MBE, cryst. defect props., substrate treatment effects 0-70551  
 Si, graphoepitaxy on fused SiO<sub>2</sub> using surface micropatterns and laser crystn. 0-70554  
 Si, ion implanted, annealing by ion beam heating 0-103382  
 Si, ion implanted, CW laser annealing 0-92550  
 Si, ion-implanted amorphous, laser epitaxial recrystallisation threshold energy 0-70571  
 Si, ion-implanted layers, crystn. by ns laser pulses, TEM and RHEED 0-100421  
 Si, ion-implanted layers, epitaxial regrowth by laser beam and flash annealing 0-100420  
 Si, ionised-cluster-beam deposited, cryst. and elec. characts. 0-70553  
 Si junction diodes, fabrication by LPE on SiB substrates, and characts. 0-80363  
 Si, meas. of doping profiles (Hungarian) 0-70545  
 Si, metallurgical-grade, fabrication by epitaxial growth or direct diffusion 0-101104  
 Si n/n<sup>+</sup> epitaxial layers, anomalies of Sb distrib. 0-65035  
 Si, on Czochralski sapphire, optimisation of deposition conditions in SiH<sub>4</sub>-H<sub>2</sub> system 0-75464  
 Si, on sapphire, characterisation, X-ray rocking curves 0-75458  
 Si, on sapphire, epitaxial, crystalline quality improvement by ion implantation and furnace regrowth 0-88452  
 Si, saucer pit microdefects reduction by intrinsic gettering 0-75450  
 Si, solid soln. of B, equilib. with B<sub>2</sub>H<sub>6</sub> 0-97721  
 Si, vacuum deposited, conditions for impurity migration from B, P, Sb doped sources (Russian) 0-107570  
 Si wafer, ion implanted, electron beam annealing, computer simulation 0-96569  
 Si:Ar, ion-implanted, epitaxial regrowth by laser annealing, microstruct. 0-84404  
 Si:As, ion implanted, laser annealed, lattice defects, epitaxial regrowth 0-103334  
 Si:Sb, MBE film, doping technique 0-79821  
 Si:Ti substrate for epitaxial solar cells 0-61341  
 Si-CoSi<sub>2</sub>Si<sub>3</sub>, double heteroepitaxy, solid phase and MBE 0-104063  
 Si-SiO<sub>2</sub>, interface, doping depend. of interface states and charges 0-92992  
 SiC (6H), blue-emitting diodes by CVD 0-97439  
 SiC, growth techniques 0-108360  
 SiC p-n junction, epitaxial, grown by sublimation, elec. and struct. props. (Chinese) 0-60067  
 p<sup>+</sup>-Si<sub>1-x</sub>Ge<sub>x</sub>-nSi junction diodes, lattice misfit effects on I-V characts. 0-70804  
 Sn<sub>1-x</sub>Pb<sub>x</sub>Se(Te), Mossbauer effect of <sup>119</sup>Sn, spectral characts., conc. depend. 0-103903  
 Sn<sub>1-x</sub>Pb<sub>x</sub>Se(Te), oxidation rel. to annealing temp. and time, Mossbauer spectra, X-ray and microstruct. obs. 0-104311  
 ZnO, CVD of epitaxial films on sapphire, SAW interdigital transducer fabrication 0-66430  
 ZnO epitaxial film, nonuniform cond. due to H chemisorption (Russian) 0-65723  
 ZnO films, RF sputtered single-cryst., on sapphire, struct. and SAW props. 0-80105  
 ZnS:Cu crystal, powder, epitaxial film, luminescence anomalous thermal 0-76077  
 ZnS,Se<sub>1-x</sub>, VPE on CaF<sub>2</sub> substrate, in flowing H<sub>2</sub>, growth and characterisation (French) 0-107678

**semiconductor epitaxial layers continued**

- ZnSb, orientated crystn. conditions during reaction diffusion (*Russian*) 0-70558  
 ZnSe, epitaxial growth on Ge substrate 0-75469

**semiconductor growth**

- Al,Ga<sub>1-x</sub>As/Al,Ga<sub>1-y</sub>As heterostructure lasers, prep. charact., and CW reliability 0-58586  
 crystal growth and defects, appl. of analytical techniques for observation 0-73546  
 crystal growth and phase diagrams 0-66407  
 diamond-like semiconductor film epitaxial growth, computer simulation 0-70560  
 electronic materials 0-66405  
 II-VI compounds, optimal synthesis conditions for single cryst. growth 0-100776  
 II-VI compounds, optimal synthesis methods for single cryst. growth 0-100764  
 II-VI semiconductors, thin epitaxial layer, direct synthesis (*German*) 0-104070  
 III-V materials bulk crystal growth, LPE and VPE methods (*Czech*) 0-89131  
 MBE for precision doping 0-89156  
 metal chalcogenides, electrodeposition, using nonaqueous solvents 0-76200  
 narrow-band semiconductor, growth of epitaxial layers, activation by UV and IR radiation 0-71598  
 ribbon growth using scanned focused CO<sub>2</sub> laser beams 0-66417  
 shaped crystal growth from melt, meniscus-controlled process 0-107075  
 Si:In growth by Czochralski crystal pulling, characterisation for extrinsic IR detectors, focal-plane arrays 0-76168  
 Si epitaxy, vapour phase deposition technology 0-75472  
 thermoelectric recrystallisation, epitaxial film growth rate 0-100424  
 AgInS<sub>3</sub>, and AgInS<sub>3</sub>, spray pyrolysis, film struct., elec. and optical props. 0-71592  
 AlGaAsSb LPE growth, lattice-matched to GaSb, characterisation 0-60794  
 AlN film, thermodynamics and kinetics of CVD 0-108354  
 AlN films on glass substrate, prep. by reactive DC magnetron sputtering technique, c-axis orientation 0-89146  
 BN, semicond. film, chemical deposition 0-71596  
 Bi<sub>2</sub>Te<sub>3</sub>-Bi<sub>2</sub>Se<sub>3</sub> solid solns., single cryst. growth and thermocouple construct. 0-104056  
 BiTe, melt and vapour grown, optical props. 0-84746  
 (Cd,Hg)Te epitaxial structures, comp. profile depend. on deposition parameters 0-100795  
 Cd<sub>2</sub>As<sub>2</sub> film on NaCl substrate, vacuum deposition, growth morphology, microstructure 0-75479  
 CdCr<sub>2</sub>S<sub>4</sub> crystal growth, structural defects, physical properties 0-60759  
 Cd,Hg<sub>1-x</sub>Te, epitaxial growth from stoichiometric melt, crystn. and diffusion 0-75475  
 Cd(S, Se) film grown on InP substrate, mismatch dislocations and lattice distortion, dangling bond density 0-84406  
 CdS crystal growth from vapour, preferential deposition, elec. field effects 0-84122  
 CdS film spray fabrication, physical props., Cu<sub>2</sub>S-CdS solar cell applications (*French*) 0-60113  
 CdS films, chem. deposited, growth kinetics and polymorphism 0-75463  
 CdS thin films, growth and evaluation for fabrication of high performance photovoltaic solar cells 0-93501  
 CdS thin layers, recryst. from CdS-Cr<sub>2</sub>O<sub>3</sub> mixtures, phys. and photoelec. props. 0-96935  
 CdS/InP epitaxial thin films on NaCl, HEED and TEM study 0-88446  
 CdS,Te<sub>1-x</sub>, recryst. from CdS<sub>1-x</sub>Te<sub>1-x</sub>-Cr<sub>2</sub>O<sub>3</sub> mixtures, photocond. props. 0-96936  
 CdSe film, soln. growth 0-66437  
 CdSe film deposition, and reaction sequence of H<sub>2</sub>SeO<sub>3</sub> reduction 0-71603  
 CdSe(Te) films, oriented, epitaxial growth by epitaxial nucleation in sub-microscopic holes method 0-59834  
 n-CdTe layers, growth and characterisation, heterojunctions and Schottky barriers fabrication (*German*) 0-89151  
 CdTe, low temp. thermal cond., growth parameter influence 0-92725  
 CdTe thin films, oriented, VPE growth, infrared transmission, photovoltaic cells 0-59825  
 CdTe/Hg<sub>1-x</sub>Cd<sub>x</sub>Te multilayers, LPE growth 0-80104  
 CdTe-In system, equilib. phase diagram and liq. phase epitaxial growth of CdTe from In soln. (*Japanese*) 0-71634  
 CdZnS thin films, growth and evaluation for fabrication of high performance photovoltaic solar cells 0-93501  
 Co<sub>3-x</sub>Mo<sub>3-x</sub>O<sub>4</sub> films, prep. struct. and elec. characteris. 0-108353  
 (Cu,Ag)<sub>2</sub>Se/(Bi, Sb)<sub>2</sub>Te<sub>3</sub>, P type selenide segmented element fabrication, thermoelectric props. 0-107835  
 CuInSe<sub>2</sub>, heteroepitaxy on {111} oriented Ge by flash evaporation, struct. 0-108333  
 CuInTe<sub>2</sub> epitaxial layers, on GaAs, growth and props. 0-108359  
 CuInTe<sub>2</sub> single crystals, directional freezing growth and doping, resist. changes on annealing 0-60768  
 Cu<sub>2</sub>-S-CdS p-n heterojunction, copper sulphide growth features during formation (*Russian*) 0-107898  
 Cu<sub>2</sub>S-CdS solar cells, Cu<sub>2</sub>S growth kinetics and composition analysis by absorbance transient and galvanic electrochemical measurements 0-92797  
 CuSb<sub>2</sub> crystals, growth and characterisation 0-60770  
 FeSe, VPE by hot-wall technique 0-80958  
 Eu(Sb<sub>1-x</sub>Te<sub>x</sub>)<sub>2</sub> system cpds., prep., cryst. struct., elec. and mag. characteris. 0-108349  
 (GaAl)As DH laser, threshold current density, growth terraces effect 0-99723  
 (GaAl)As, LPE, GaAs dissolution kinetic in undersaturated isothermal solns. in Ga-Al-As system 0-80106  
 (GaAl)As low-beam-divergence CW DH laser, grown by low press. metal-organic CVD 0-74376  
 GaAlAs-GaAs lasers, channelled substrate, prepared by combination of organometallic pyrolysis and LPE 0-99745  
 Ga<sub>1-x</sub>Al<sub>x</sub>As, appl. of theory of electroepitaxy of multicomponent systems 0-65396  
 Ga<sub>1-x</sub>Al<sub>x</sub>As based layer structures, optimum growth conditions, comp. and struct. perfection 0-104069  
 Ga<sub>1-x</sub>Al<sub>x</sub>As heterostructure, LPE prep., growth and dissolution kinetics, thermodynamic and kinetic models 0-75456

**semiconductor growth continued**

- Ga<sub>1-x</sub>Al<sub>x</sub>As-GaAs p-n and p-p-n heterojunction solar cells, high efficiency, prep., eval. and characters (*Japanese*) 0-61342  
 GaAlAsSb-GaSb low bandgap solar subcell for high efficiency multiband-gap converters, LPE growth 0-93927  
 Ga<sub>1-x</sub>Al<sub>x</sub>P varigap structs., crystallation 0-80993  
 GaAs, cryst. growth from large Ga:As solns., critical cooling rate 0-64938  
 GaAs epitaxial growth, CVD-organometallics method, reactional efficiency in solar cell elaboration 0-93498  
 GaAs epitaxial layers on polycryst. GaAs substrates, LPE growth charact. 0-75471  
 GaAs, epitaxy by metalloorganic and chloride depositions, defect characterisation at growth interface 0-59817  
 GaAs films for solar cells appl., deposition and characterisation 0-84853  
 GaAs, LPE, temperature instability effect, report 0-66446  
 GaAs LPE from Ga soln., carrier conc., growth condition depend. 0-71584  
 n-GaAs, MBE, correl. between electron traps and growth processes 0-65387  
 p-GaAs, MBE grown, As<sub>2</sub> and As<sub>4</sub> effects on photolum. 0-103974  
 GaAs, MBE of doped cryst., thermodynamics and kinetics interplay 0-70144  
 GaAs, monocrystalline, lateral definition, prep. by MBE 0-108357  
 GaAs, polycryst. solar cells, thin film growth and grain size, effect on cell efficiency 0-81471  
 GaAs, undoped epitaxial layer growth from nonstoichiometric solns., O<sub>2</sub> contamination sources 0-108362  
 GaAs, VPE thin layers, thickness uniformity, main factor anal. 0-76197  
 n-GaAs:Ge, film, substrate temp. depend. of Ge incorporation during MBE 0-76196  
 GaAs:Si, accelerated growth rate effect on MBE, Hall mobility and photolum. meas. 0-104067  
 n-GaAs:Sn-p-GaAs:Ge-p-Al,Ga<sub>1-x</sub>As:Ge heterostructure solar cells, LPE growth techniques 0-66977  
 GaAs-Al<sub>0.2</sub>Ga<sub>0.7</sub>As DH lasers grown by MBE, influence of growth conditions on threshold current density 0-58587  
 GaAs-Al,Ga<sub>1-x</sub>As transverse junction lasers with low threshold current prep. by MBE on semi-insulating substrates 0-58588  
 GaAs-Al,Ga<sub>1-x</sub>As, current transverse junction lasers, low threshold, MBE prep. 0-83614  
 GaAs-Al,Ga<sub>1-x</sub>As buried-heterostructure lasers, current injection confinement, MBE/LPE hybrid technique 0-74374  
 GaAs-GaAlAs superlattices, metalloorganic VPE growth, in sites ellipsometry monitoring 0-70547  
 GaAs-GaAlAs-GaAs rectifying semicond. struct., prep. by MBE and charact. 0-65657  
 GaAs-Ge, heterostructure, zincblende-on-diamond type systems, MBE growth, (110) orientation as preferred orientation 0-80099  
 GaAs<sub>1-x</sub>P<sub>x</sub> heterostructure, LPE prep., growth and dissolution kinetics, thermodynamic and kinetic models 0-75456  
 GaAs,P<sub>1-x</sub> alloy, composition effects in growth by MBE 0-59816  
 GaAsSb/GaAlAsSb DH lasers, growth and props. 0-69412  
 GaAs<sub>1-x</sub>Sb<sub>x</sub> layer on GaAs, dislocation density reduction by improved LPE growth method 0-76202  
 GaAs<sub>1-x</sub>Sb<sub>x</sub>, organometallic VPE growth using trimethylantimony 0-60788  
 GaInAs-InP, growth by low-pressure metalloorganic CVD 0-71595  
 Ga<sub>1-x</sub>In<sub>x</sub>As epitaxial layer growth by organometallic pyrolysis, homojunction LED prep. 0-76194  
 Ga<sub>1-x</sub>In<sub>x</sub>As, organometallic VPE growth using trimethylarsenic 0-60788  
 Ga<sub>1-x</sub>In<sub>x</sub>As, on (111)B InP, LPE growth, characterisation of high purity lattice 0-104082  
 Ga<sub>1-x</sub>In<sub>x</sub>As-InP, MBE film growth, composition control obs. 0-84399  
 GaInAsP/InP DH lasers emitting at 1.3 μm, growth and charact. 0-64057  
 GaInAsP/InP DH stripe geometry lasers emitting at 1.3 μm, growth characterisation 0-69410  
 GaInAsP/InP DH lasers, 1.3 μm wavelength, LPE growth and characterisation 0-69411  
 Ga<sub>1-x</sub>In<sub>x</sub>As<sub>1-y</sub>P<sub>1-y</sub>/GaAs structure, LPE growth and lattice const. matching conditions 0-59822  
 Ga<sub>1-x</sub>In<sub>x</sub>As<sub>1-y</sub>P<sub>1-y</sub>/InP DH laser emitting at 1.15 micron grown by low-pressure CVD 0-64052  
 Ga<sub>1-x</sub>In<sub>1-y</sub>As<sub>1-x-y</sub>P<sub>1-x-y</sub> LPE growth 0-66440  
 Ga<sub>1-x</sub>In<sub>1-y</sub>P solid solns., isothermal liq. epitaxy 0-60793  
 Ga<sub>1-x</sub>In<sub>1-y</sub>P,As<sub>1-y</sub>/InP DFB injection laser, one-step LPE 0-58575  
 Ga<sub>1-x</sub>In<sub>1-y</sub>Sb, Ga-rich, prep. by Czochralski technique 0-60771  
 GaN, initial growth, on Al<sub>2</sub>O<sub>3</sub> and spinel (*German*) 0-107664  
 GaN, VPE growth rate influence on elec. and luminesc. props. 0-100702  
 GaP electroluminescent diode struct. prep. by SSD and Czochralski methods, dynamic props. (*Czech*) 0-97425  
 GaP, VPE layer structures for LED's, SEM, and TEM obs. of dislocation density reduction expt. 0-100425  
 GaP-Si, heteroepitaxial growth, electronic and optical props. 0-104075  
 GaP-Si, heterostructure, zincblende-on-diamond type systems, MBE growth, (110) orientation as preferred orientation 0-80099  
 GaSb, electroliquid epitaxial growth 0-89160  
 GaSb films, elemental incorporation probability modification by ion bombard. during growth 0-80118  
 (GaSb)<sub>1-x</sub>Ge<sub>x</sub> films, single-cryst. metastable semicond., growth and phase stability 0-80115  
 α(β)-Ga<sub>2</sub>Se<sub>3</sub>, cryst. growth, optical, X-ray diff. and SEM study 0-71587  
 GaTe, single cryst. prep. and electroabsorpt. spectra investig. 0-103968  
 Gd<sub>2</sub>Se<sub>3</sub>/PbTe, N type selenide segmented element fabrication, thermoelectric props. 0-107835  
 Ge, epitaxial growth of very thin electron microscopy specimens 0-100793  
 Ge ribbon single crystals, grown from melt, dislocation struct. form. under thermal stress 0-107082  
 HgCdTe photodiodes formed by double-layer LPE 0-104078  
 HgCdTe-CdTe photodiode, 1.33 μm, grown by LPE, phys. props. 0-107892  
 Hg<sub>0.4</sub>Cd<sub>0.6</sub>Te LPE layer growth from Te, Hg-, and HgTe-rich solns., comparison 0-76199  
 Hg<sub>0.74</sub>Cd<sub>0.26</sub>Te thin film deposition on Si substrates by RF triode-sputtering, large-area photodetector arrays 0-80965  
 HgI<sub>2</sub>, soln. grown crystals, low-energy gamma-ray cond. type detectors 0-97418  
 In<sub>2</sub>O<sub>3</sub>:Sn, RF magnetron sputtered film, elec. and optical props. 0-104065



## semiconductor growth continued

- (In,Ga)(As,P) binary, ternary and quaternary, hydride vapour phase epitaxy, cryst. growth and props. 0-66434
- In-Ga-P ternary system, low temp. phase diagram rel. to epitaxial growth 0-84916
- InAs,P<sub>1-x</sub> alloy, composition effects in growth by MBE 0-59816
- InGaAs, LPE, diffusion-limited step-cooling technique, layer thickness and composition 0-84402
- In<sub>1-x</sub>Ga<sub>x</sub>As layer on InP, misfit dislocation free, LPE growth 0-108364
- In<sub>1-x</sub>Ga<sub>x</sub>As:Zn, lattice matching to InP, LPE growth conditions 0-70541
- InGaAsP, LPE, diffusion-limited step-cooling technique, layer thickness and composition 0-84402
- InGaAsP-InP CW lasers, 1.5-1.7  $\mu$ m, VPE 0-78861
- InGaAsP-InP DH laser, 1.55  $\mu$ m, low temp. LPE growth for room-temp. CW operation 0-64045
- InGaAsP-InP layers, grown by LPE techniques, lattice const., bandgap, thickness and surface morphology meas. 0-59818
- In<sub>1-x</sub>Ga<sub>x</sub>As,P<sub>1-y</sub>InP 1.5  $\mu$ m room-temp. CW laser fabrication and operation 0-64070
- InGaP/InGaAs struct. for transferred electron photocathodes, VPE growth and characterisation 0-76193
- In<sub>1-x</sub>Ga<sub>x</sub>P<sub>1-y</sub>As, lattice-matched epitaxial layers, LPE growth on GaAs(100), characterisation 0-75465
- In<sub>2</sub>O<sub>3</sub> films, electron beam evaporation, elec. and optical props. (*Japanese*) 0-60784
- In<sub>2</sub>O<sub>3</sub>, pure and Sn-doped, prep. by activated reactive evaporation, and characterisation 0-80989
- InP, epitaxial, kinetics of VPE 0-60790
- InP films, organometallic VPE grown, props. 0-96753
- InP grown by LPE, method for free In removal from surface 0-84860
- InP, MBE, substrate temp. related degradation mechanisms 0-65385
- InP, VPE growth for MESFET's 0-103602
- InP-GaInAsP buried heterostructure lasers of 1.5  $\mu$ m region, fabrication and characts. 0-74388
- InP-In<sub>1-x</sub>Ga<sub>x</sub>As,P<sub>1-y</sub>InP 1.55  $\mu$ m DH room-temp. CW laser fabrication and operation 0-64071
- InP-In<sub>1-x</sub>Ga<sub>x</sub>As,P<sub>1-y</sub>InP 1.53  $\mu$ m single-mode CW ridge-waveguide laser 0-64072
- InSb, convection in melts, and cryst. growth under large inertial accelerations 0-66421
- InSb, crystal growth from melt, facets and twin formation obs. (*Chinese*) 0-59409
- InSb film, grown by MBE, RHEED study 0-100415
- InSb films, elemental incorporation probability modification by ion bombard. during growth 0-80118
- InSb, growth angle determ. from cryst. lateral face shape and solidified separation drops 0-103282
- InSb:Te, cryst. growth from melt, pulling method, US effects on facet growth 0-76169
- InSb<sub>1-x</sub>Bi<sub>x</sub> films, single-cryst. metastable semicond., growth and phase stability 0-80115
- InSb<sub>1-x</sub>Bi<sub>x</sub>, multitarget RF sputtering, metastable phase, conductivity transition 0-76178
- InSe thin film, sputter growth and chem. anal. by XPS/ESCA 0-80976
- PbS-Si heterojunction, PbS film growth and struct. 0-96762
- PbSe film, soln. growth 0-66437
- Pb<sub>1-x</sub>Sn<sub>x</sub>Se epitaxial layers obtained by LPE, growth conditions correl. with morphology 0-104079
- Pb<sub>1-x</sub>Sn<sub>x</sub>Te LPE film IR detector performance 0-86422
- Pb<sub>1-x</sub>Sn<sub>x</sub>Te-PbTe heterostructures, MBE produced on mica and LiNbO<sub>3</sub>, elec. props. study 0-88629
- Pb<sub>1-x</sub>Sn<sub>x</sub>Te<sub>1-x</sub>Se<sub>x</sub>, quaternary solid solns. with const. lattice parameter, cryst. growth and characts. 0-108332
- PbTe, nonstoichiometric, evap. and growth of epitaxial layers 0-104072
- PbTe single crystals, growth from vapour phase under micro-gravity conditions 0-80957
- Pb<sub>1-x</sub>Te-Pb<sub>1-x</sub>Sn<sub>x</sub>Te (x,y $\leq$ 0.3), double heterostruct., LPE growth, heterointerface morphology 0-70550
- (Sb<sub>2</sub>Se<sub>3</sub>)<sub>0.7</sub>(Bi<sub>2</sub>Se<sub>3</sub>)<sub>0.3</sub>, solid soln., prep. and elec. properties of layered crystals 0-70762
- Sb<sub>2</sub>Te<sub>3</sub>-Bi<sub>2</sub>Te<sub>3</sub> solid solns., single cryst. growth and thermocouple construct. 0-104056
- Se<sub>2</sub>Te<sub>1-x</sub>, growth of single crystals by Czochralski method 0-66423
- Si, amorphous, prep. by reactive RF sputtering in Ar-silane mixtures, undoped, n-type and p-type targets 0-76182
- Si, annealing during Czochralski growth, influence on defect density 0-60769
- Si, CVD from SiH<sub>4</sub>-HCl-H<sub>2</sub> system, rate-determining reactions and surface species 0-84405
- Si crystal growth, for electronic devices 0-66419
- Si, Czochralski grown crystal, O precip., nucleation behaviour and dislocation loop form. (*Japanese*) 0-59664
- Si, Czochralski grown crystals, swirl-type defect obs. 0-100236
- Si, deposition on rotating disc, one-dimens. model 0-75461
- Si, effect of C on dissolution of quartz in liq. Si, rel. to melt growth 0-70414
- Si epitaxial films on Czochralski sapphire, optimisation of deposition conditions in SiH<sub>4</sub>-H<sub>2</sub> system 0-75464
- Si, epitaxial growth on sapphire by partially ionised vapour deposition, RHEED-AES obs. 0-80985
- Si, epitaxial layer deposition by ion beam methods 0-100417
- Si epitaxial layer regrowth due to laser annealing mechanism, liquid and solid phase regimes 0-100712
- Si epitaxial thin film growth on sapphire and spinel by MBE 0-76186
- Si film, MBE, cryst. defect props., substrate treatment effects 0-70551
- Si film, polycryst., laser-induced CVD growth from SiCl<sub>4</sub> 0-84852
- Si films, electron beam evaporated, for MIS solar cells 0-93490
- Si films, ribbon-against-drop process, physical and chemical characterisation 0-92798
- Si, graphoepitaxy on fused SiO<sub>2</sub> using surface micropatterns and laser crystn. 0-70554
- Si junction diodes, fabrication by LPE on Si:B substrates, and characts. 0-80363
- Si, liquid, interaction with die material during edge defined film fed growth 0-104060
- Si, melt grown crystals, impurity incorporation, calcs. 0-79718
- Si monocrystalline sheet fabrication for solar cells, CLF Czochralski furnace and enhanced slicing technology 0-93476
- Si multicrystalline solar cell material prep., fast-pulled float zone, CZ and cast ingot and foil methods 0-93483

## semiconductor growth continued

- Si on ceramic, coating with inverted meniscus (SCIM) technique, solar cell appl. 0-89163
- Si, polycryst., deposition as example of pyrolytic CVD process 0-84407
- Si polycrystalline layers on C substrates, RAD process, solar cells appl. 0-89635
- Si, prod. of polySi vapour deposited coatings for solar cells, cost anal. 0-93495
- Si ribbon, dendritic web growth from melt, solar cell module fabrication 0-93478
- Si ribbon, low angle sheet growth technique, direct shaping characts. 0-93480
- Si ribbon crystal growth, 10 cm wide, temp. distrib. meas. in die 0-104059
- Si ribbon crystals, edge-defined film-fed growth technique for solar cells 0-89633
- Si ribbon growth by EFG, thermal sensitivity and stability 0-107080
- Si ribbons, dendritic web for solar cells 0-89634
- Si ribbons, edge-defined film-fed growth technique for solar cells 0-89138
- Si ribbons for solar cells, ultra high speed growth, elec. props. 0-89162
- Si ribbons grown by capillary action shaping technique, surface quality and impurity distrib. 0-108343
- Si sheet, high speed growth, heat transport analysis 0-107669
- Si single crystal, improved horizontal ribbon growth technique 0-108345
- Si single crystal ingot growth from metallurgical grade Si, inhomogeneities 0-59416
- Si solar cell fabrication from multiple ingots using melt replenishment Czochralski method, cell anal. 0-93477
- Si solar cells, capacitance transient spectra of processing- and radiation-induced defects 0-61340
- Si, square single crystals, Czochralski growth 0-97422
- Si surface, reduction growth, autotaxity (*Russian*) 0-107672
- Si thick-film growth using contiguous capillary coating on porous C substrates 0-93507
- Si thin film for solar cells, thermal expansion shear separation technique 0-81439
- Si thin ribbon grown at high speed, thermal stresses, reduced thermal buckling 0-107078
- Si thin-film polycrystalline vacuum-deposited solar cells, TiB<sub>2</sub> bottom electrode, 10% efficiency 0-93489
- Si tube growth by EFG process 0-108344
- Si wide ribbon, high speed edge-defined film-fed growth 0-104058
- Si:As, CVD, doping using SiH<sub>4</sub>-H<sub>2</sub>-AsH<sub>3</sub> system 0-79823
- Si:As, MBE with simultaneous ion implant doping 0-66432
- Si:F, amorphous alloys, RF sputtering prep. in SiF<sub>4</sub>-Ar gas mixture, spectra 0-80772
- Si:H, amorphous thin film, ion plating, IR absorpt. meas. 0-84857
- Si:In extrinsic IR detector material with high responsivity compensated by neutron transmutation, float-zone growth 0-75597
- Si:P, doping during growth from gas phase, thermodynamic analysis 0-59489
- Si/Pd system, solid phase epitaxial growth control by C ion implantation 0-75466
- Si-CoSi<sub>2</sub>, double heteroepitaxy, solid phase and MBE 0-104063
- SiAs, cryst. growth from melt, elec. props. 0-76170
- SiC (6H), blue-emitting diodes by CVD 0-97439
- $\alpha$ -SiC crystals, broad-band semiconductors, growth in Acheson furnace 0-84841
- $\beta$ -SiC form. on Si substrate in RF powered reactor 0-76173
- SiC p-n junction, epitaxial, grown by sublimation, elec. and struct. props. (*Chinese*) 0-60067
- SnO<sub>2</sub>:Sb sprayed film, growth mechanism and cryst. struct. 0-89143
- SnTe, annealed, iodide method of prep., props. meas. 0-71591
- Te, growth of single crystals by Czochralski method 0-66423
- Te-(Bi,Sb)<sub>1-x</sub>Te<sub>x</sub>, eutectic, electrophys. props., directed crystn. conditions influence and comp. depend. 0-107827
- Te-based eutectics, crystn. rate effect on electrophys. props. mutual solubility effect 0-60774
- Te-Se-Cd, sandwich structure, fabrication and characteristics 0-60089
- WSe<sub>2</sub>, chem. vapour transport growth, microstruct. develop. 0-103278
- ZnO films, RF sputtered single-cryst., on sapphire, struct. and SAW props. 0-80105
- ZnSb, oriented crystn. conditions during reaction diffusion (*Russian*) 0-70558
- ZnSe, epitaxial growth on Ge substrate 0-75469
- ZnSe, MBE growth, elec. and optical props. 0-75462
- ZnTe, MBE growth, elec. and optical props. 0-75462
- ZnTe growth from vapour, growth interruption 0-97416

## semiconductor-insulator boundaries

- c Si-SiO<sub>2</sub> layers, physics, electron and ion motion, Cl, Na and K ion effects (*Dutch*) 0-60093
- conductor-insulator-semicond. (CIS) solar cells, noncrystalline (poly and amorphous), interface importance 0-81466
- conference, Durham, England (July 1979) 0-90612
- density of states determ. from field effect data 0-107688
- dielectric-semiconductor structures, surface ion migration, theoretical analysis 0-65700
- III-V semiconductor-oxide interface states, photoemission obs. of energy levels induced by adsorpt. 0-93000
- impurity-band hopping conduction in surface layers 0-75649
- interface electronic struct., microcomputer aided anal. 0-80383
- MOS structure implanted with B ions, radiation defects and impurity activation 0-103757
- polyacetylene-graphite, ohmic control (*Japanese*) 0-96888
- semiconductor, amorphous, field effect and capacitance-voltage meas. anal., localised density of states 0-103686
- semiconductor-oxide-semiconductor diodes, tunnel-assisted transport at room temp. 0-92975
- SOS MOST, electronic props. at Si-sapphire interface 0-96993
- SOS quality determ. using IR and UV specular reflectance meas. 0-108684
- SOS structures, high-field electron transport, drift vel. meas. 0-80387
- CdS-SiO<sub>2</sub>-Si solar cell, I-V characteristics 0-89621
- CdTe film-ferroelectric TGS substrate system, influence of polarisation reversal on elec. cond. of CdTe thin film 0-65720
- p-CdTe-Langmuir film interface, prep., characters, and MIS struct. 0-92998
- GaAs, polycryst., wet and dry oxides, comparative study by AES, SIMS and XPS 0-80116

**semiconductor-insulator boundaries continued**

- GaAs, selective plasma oxidation, interface props. 0-100933  
 GaAs, surface passivation using composite  $\text{Al}_2\text{O}_3$  and native oxide, MIS characts. 0-93004  
 GaAs, surface passivation using  $\text{Si}_3\text{N}_4$ , interface characts. 0-93005  
 GaAs, surface passivation using  $\text{GaO}_x\text{N}_y$  based multiple insulating layers 0-93006  
 GaAs/anodic oxide interface, characterisation of proposed model 0-103754  
 Ge- $\text{Si}_3\text{N}_4$  system, potential barriers determ. from photoinjection carriers trapping 0-103756  
 $\text{In}_2\text{O}_3\text{-SnO}_2\text{-Si}$  SIS solar cells, reverse current-voltage characts. under illumination 0-89622  
 InP, and  $\text{In}_x\text{Ga}_{1-x}\text{As}_y\text{P}_{1-y}$ , binary and quaternary cpds., surface and dielec.-semicond. interface props. 0-93001  
 InP, surface passivation using composite  $\text{Al}_2\text{O}_3$  and native oxide, MIS characts. 0-93004  
 InP- $\text{Si}_3\text{N}_4$  ( $\text{SiO}_2$ ), interface props., plasma deposited dielectrics, n-channel MOSFET action 0-93003  
 InP- $\text{SiO}_2$  interface, CVD problems, ESCA profiles 0-93497  
 $\text{In}_{2-x}\text{Sn}_x\text{O}_{3-y}$  solar cells, majority carrier conduction effects 0-97796  
 $\text{In}_{2-x}\text{Sn}_x\text{O}_{3-y}$ -insulator-poly-Si solar cells, photovoltaic conversion parameters 0-101093  
 $\text{LiNbO}_3\text{-Si}$ , acoustoelectronic memory, effect of band-bending 0-70771  
 Si on sapphire thin film, Hall effect, magnetoresistance (*French*) 0-65601  
 Si shallow junction device, silicide contact 0-70819  
 Si-insulator interface, non-avalanche charge injection, expt. study, charge trapping effects 0-60099  
 Si- $\text{Si}_3\text{N}_4$  interface in MNS capacitors, surface state density investigation 0-60100  
 Si- $\text{SiO}_2$ , influence on frequency-temp. coeff. of SAW devices 0-79066  
 Si- $\text{SiO}_2$ , interface, stress meas. technique 0-84395  
 Si- $\text{SiO}_2$ , MOS interface states density, meas. techniques and model development 0-92988  
 Si- $\text{SiO}_2$ , Si oxidation, solubility and transport behaviour of water, dissolution 0-93801  
 Si- $\text{SiO}_2$ , thermal growth mechanisms of vitreous oxide layers on Si 0-93675  
 Si- $\text{SiO}_2$ , two layer system,  $\text{P}^+$ -ion penetration tails, expt. and computer anal. 0-75249  
 Si- $\text{SiO}_2$  (111) interface,  $\text{H}_2$  effects, AES study 0-65688  
 Si- $\text{SiO}_2$ , abrupt interface form. by very high dose  $\text{O}^+$  ion implantation 0-75253  
 Si- $\text{SiO}_2$ , boundary, relaxation of nonequilibrium capacitance in electrolyte in intense elec. fields 0-70845  
 Si- $\text{SiO}_2$ , boundary, surface charge transport in valence band of Si 0-70789  
 Si- $\text{SiO}_2$ , electrode, electronic cond., luminesc. obs. 0-61111  
 Si- $\text{SiO}_2$ , in MOSFETs, inversion layer carrier mobility, theory 0-60094  
 Si- $\text{SiO}_2$ , interface, (001) vicinal planes, minigaps in inversion layers, far IR absorpt. meas. 0-107919  
 Si- $\text{SiO}_2$ , interface, density of states, theory 0-80395  
 Si- $\text{SiO}_2$ , interface, doping depend. of interface states and charges 0-92992  
 Si- $\text{SiO}_2$ , interface, electronic struct. calc. 0-100531  
 Si- $\text{SiO}_2$ , interface, improved characterisation, refined quasistatic and cond. methods 0-96990  
 Si- $\text{SiO}_2$ , interface, remote polar phonon scatt. in Si inversion layers 0-80095  
 Si- $\text{SiO}_2$ , interface, thermal  $\text{SiO}_2$  sputter induced roughness, Auger sputter profiling study 0-75424  
 Si- $\text{SiO}_2$ , interface, thermally grown, surface pot. inhomogeneities after stress ageing 0-92993  
 Si- $\text{SiO}_2$ , interface, thermally grown oxide, spectroscopic ellipsometric anal. 0-107659  
 Si- $\text{SiO}_2$ , interface, unwanted effects of ions in  $\text{SiO}_2$  layers, review 0-92985  
 Si- $\text{SiO}_2$ , interface in IGFETs, anal. of CVD  $\text{SiO}_2$  on (100) and (111) surfaces, near-ideal structs. 0-100528  
 Si- $\text{SiO}_2$ , interface in MIS structs., effects of crystal defects on generation process 0-65702  
 Si- $\text{SiO}_2$ , interface in MOS structs. low-energy electron beam irradiat., charge accumulation process anal. 0-65701  
 Si- $\text{SiO}_2$ , interface in MOS capacitors, lateral diffusion of  $\text{Na}^+$ , neutralisation 0-92986  
 Si- $\text{SiO}_2$ , interface in MOS device, indirect tunnelling involving intermediate states 0-92994  
 Si- $\text{SiO}_2$ , interface in MOS solar cells, operational characts. and struct. 0-93901  
 Si- $\text{SiO}_2$ , interface of MIS/SIS solar cells, automated surface states anal. 0-93966  
 Si- $\text{SiO}_2$ , interface state density in ion-controlled diodes, acid-base exposure effects 0-96984  
 Si- $\text{SiO}_2$ , interface states, deposition of H containing layers and annealing 0-92991  
 Si- $\text{SiO}_2$ , interfaces, near ideal, props. 0-80382  
 Si- $\text{SiO}_2$ , laminar ion-implanted systems, struct. change investig. by MSSSI method (*Russian*) 0-107918  
 Si- $\text{SiO}_2$ , MOS interface, surface-state density and minority carrier generation rate, meas. by DLTS, hot hole effect 0-100527  
 Si- $\text{SiO}_2$ , MOS interface states density, transient capacitance meas. eval. 0-92989  
 Si- $\text{SiO}_2$ , structures, B ions implanted, energy spectra of shallow traps at various implantation energies 0-80392  
 Si- $\text{SiO}_2\text{-Si}$  capacitor, polycryst., capacitance voltage characterisation 0-70794  
 Si- $\text{SiO}_2\text{-polySi}$  thin film structures, dielectric props. (*Slovak*) 0-75934  
 $\text{SiO}_2$  films, grown in presence of  $\text{O}_2\text{-trichloroethylene}$ , room temp. negative bias instability 0-60102  
 $\text{SiO}_2/\text{InP}$  interface formation, thermodynamic considerations 0-100529  
 $\text{SiO}_2$  ultrathin oxide on Si, struct. obs. by high-resolution electron microscopy 0-103592  
 $\text{SiO}_2\text{-GaAs}$ , vacuum evaporated system, acoustoelec. signal, interface props. 0-75646  
 ZnO/Si SAW structs., anal. of charge injection 0-80049

**semiconductor integrated circuits** see *monolithic integrated circuits***semiconductor junction lasers**

- $\text{Al}_x\text{Ga}_{1-x}\text{As}/\text{Al}_x\text{Ga}_{1-x}\text{As}$  heterostructure lasers, prep. characts., and CW reliability 0-58586  
 AlGaAs laser array with Si detector array for stabilization 0-58817

**semiconductor junction lasers continued**

- analogue video transmission feasibility using laser diode, over 30 km at 1.3  $\mu\text{m}$  0-58737  
 book, quantum electronics 0-105442  
 Bragg mirror, corner-reflector type, laser beam divergence reduction 0-91822  
 buried heterostructure laser, DH multilayer LPE growth on etched substrate, optical read-out appls., longitudinal mode operation 0-99749  
 buried strip geometry DH injection lasers, first derivative of I-V charact. above threshold 0-58533  
 calibration by IR spectra of OCS 0-83363  
 CdS, single crystals, laser emission from surface diffraction grating 0-95900  
 conference, laser and electro-optical systems, San Diego, CA, USA (Feb. 1980) 0-62392  
 correlative data processing system using semiconductor injection laser 0-74307  
 correlator, laser diode lensless MSF holographic optical element 0-102663  
 corrugated waveguides, effective index approach to distrib. feedback, TE polarisation 0-102859  
 coupling from semicond. laser into tapered hemispherical end single-mode fibre 0-99827  
 CW stripe lasers, thermal-impedance ageing characteristics 0-64018  
 DH, single and dual-filament self-sustained oscillations, theoretical model 0-64023  
 DH laser diode, second harmonic distortion for threshold current, anal. (*Korean*) 0-87394  
 DH lasers, current-crowded carrier confinement 0-78854  
 DH lasers, phase and group indices 0-64016  
 DH stripe geometry lasers, three-dimensional anal. of mode props. 0-64020  
 DH stripe-geometry lasers, thermal props., interpretation of thermal resistance measurements 0-64017  
 diode laser, thermal time constant meas. method 0-99731  
 diode laser with spatial thickness var., anal. 0-102723  
 diode lasers as transmitter source in optical communication, modulation, power consumption, optical links 0-102807  
 diode-laser-fibre coupling, effects of fibre propagation loss 0-74484  
 double-current-confinement channelled-substrate struct., near-field and beam-waist position 0-106553  
 electron beam pumped semiconductor laser, use of periodic structs. with special profiles 0-95923  
 electron beam pumping efficiency, coating effect 0-91795  
 electrooptic polarization modulated injection laser 0-58591  
 external cavity, linearized theory 0-69391  
 External cavity operation with complete removal of sub-cavity effects for mode-locking injection lasers 0-58545  
 external optical feedback effect on props. 0-58535  
 fibre bandwidth determination in time domain, OTF meas., laser diode source evaluation 0-79002  
 fibre coupled diode lasers, LF noise meas. 0-58542  
 fibre-optic transmission by laser diode analogue baseband modulation 0-58738  
 Fourier transform spectrosc., new developments—passive heterodyne spectrosc. and diode laser absorpt. spectrosc. 0-95148  
 frequency self-modulation interpretation 0-64028  
 GaAs laser diode power supply control cct. (*German*) 0-78852  
 glass fibre long wavelength optical communication, materials and devices, review 0-99854  
 harmonic distortion analysis of injection lasers 0-58537  
 heterojunction laser diodes, book contrib. 0-99733  
 heterojunction lasers, partially homogeneous broadening and saturation, non-oscillating mode suppression 0-99775  
 high resolution measurement of laser output spectrum 0-95891  
 high-speed optical systems at 0.85  $\mu\text{m}$ , modal noise and optical feedback 0-87323  
 hologram recording using a visible single-mode GaAs/As CW emitted diode laser 0-95839  
 homo- and heterojunction, history and development, new constructions (*Polish*) 0-91794  
 injection, defect-induced pulsations, theory 0-91793  
 injection laser, comprehensive model, current depend. of spontaneous and coherent emission 0-74361  
 injection laser diode mode structure enhancement by backface plating 0-64056  
 injection laser with composite resonator, active region internal parameters determ. 0-106548  
 injection lasers, output depend. on inhomogeneous bonding 0-64015  
 integrated and guided-wave optics, conference, Incline Village, NV, USA, January 1980 0-58772  
 intensity modulation in GHz region, image tube streak camera obs. 0-87417  
 intrinsic noise in optical communication systems 0-69394  
 IR, for 16  $\mu\text{m}$  range, review (*Rumanian*) 0-87408  
 IR emitting diodes and injection lasers, optical communication appls. 0-58563  
 low-threshold-current injection laser with built-in passive waveguiding 0-64029  
 matching of semiconductor sources to thin-film planar and stripe waveguides 0-64174  
 mode locking, simplified theory 0-64021  
 mode locking to external resonator, theory 0-106550  
 modulation, non-linear distortions, communication systems appl. (*German*) 0-69395  
 monolithically integrated lasers and amplifiers using cleaved substrate technique 0-58590  
 narrow double-current-confinement channelled-substrate-planar laser fabrication by double etching 0-64073  
 near IR (1 to 2  $\mu\text{m}$ ) optical communications, colloquium, London, England (May 1980) 0-86040  
 noise phenomena 0-58538  
 optical communication log-normal device optimal burn-in time 0-58743  
 optical fibre communication appl., characteristics and state of art (*Italian*) 0-58569  
 optical fibre communication system components, state-of-the-art survey (*German*) 0-69538  
 optical fibre sources and detectors (*Italian*) 0-69390  
 optical fibre transmission system devices (*Japanese*) 0-58693  
 optical transmitter laser diode module description and performance 0-64069



## semiconductor junction lasers continued

- output stabilization by bevelled-end fibre coupling 0-91806  
 phase-modulated optical carrier detection using conductor laser source 0-64159  
 photopumped, III-V semiconductor, book contrib. 0-99732  
 picosecond pulse generation scheme for injection lasers 0-87418  
 picosecond pulse generation using reson. oscill. 0-87391  
 plano-convex waveguide transverse-mode-stabilised laser, optical quality, static and dynamic characts. 0-69419  
 pressure-tuned diode laser, appl. to high-resolution spectroscopy 0-82835  
 pulsed diode simulators of solid lasers  $\text{Al}_x\text{Ga}_{1-x}\text{As}$  and  $\text{Ga}_x\text{In}_{1-x}\text{P}_{1-y}\text{As}_y$  solid solns. 0-91816  
 review of semiconductor diode lasers, book contrib. 0-106525  
 selection criteria, w.r.t. performance, mounting and appl. 0-69407  
 self-sustained pulsations 0-106522  
 slab waveguide, TE Mode dispersion rel. to DH semiconductor lasers 0-91886  
 spatial coherence and modal struct. 0-87531  
 spectrometer, diode laser dual-beam, long-term temporal and scanning characts. 0-90902  
 stripe geometry semiconductor lasers, transverse mode stabilisation 0-99774  
 super-DFB single-mode laser with periodic stripe width variations 0-58574  
 superlattice structures of semiconductor thin films, laser appl. 0-100418  
 technology and present status (*German*) 0-58561  
 terraced substrate DH laser, fundamental transverse mode oscillation (*Japanese*) 0-78856  
 thermal characteristics determ. method 0-91800  
 thin-film waveguide laser amplifier with lossy cladding 0-64074  
 transients in injection lasers, phase-plane anal., effects of absorbing section 0-64022  
 transmission system, semiconductor device reliability tests 0-58573  
 transport phenomena, junction effects and devices, book 0-98766  
 triggerable laser, light-coupled logic appl. 0-74360  
 tunable diode laser spectrometer, rapid-scanning computer-controlled 0-101854  
 tunable IR diode lasers appls. to high resolution spectroscopy 0-58562  
 wavelength monitoring using fibre interferometer 0-74413  
 window-stripe high power laser, deep Zn-diffused stripe region, characts. 0-69419  
 (Al,Ga)As DH injection lasers, ambipolar transport 0-64025  
 (Al,Ga)As DH lasers, water role in gradual degradation 0-74379  
 (Al,Ga)As DH lasers, superlinear emission characts., negative resist. obs. 0-95895  
 (Al,Ga)As double heterostructure, comparison of deep and shallow proton bombardment fabricated devices 0-99724  
 (Al,Ga)As double-heterostructure lasers degraded, deep-level changes during accelerated ageing at high temps. 0-74356  
 (Al,Ga)As:Zn planar stripe lasers with deep Zn diffusion, guiding mechanisms controlled by impurity concs. 0-78853  
 AlGaAs buried heterostructure lasers, gain and absorpt. spectra meas. 0-91792  
 AlGaAs DH injection phase-locked laser, coherence 0-102726  
 AlGaAs DH laser, self-pulsations due to proton bombarded region self-annealing during ageing 0-99728  
 AlGaAs DH laser epilayer struct. optimization for integrated optical circuits 0-99879  
 (AlGa)As DH lasers, catastrophic optical damage generation mechanism, TEM obs. of dark line defects 0-100239  
 (AlGa)As DH lasers, comparison of 'normal' lasers and lasers exhibiting light jumps 0-106519  
 AlGaAs heterojunction diode as light source for fibre optical communication 0-58653  
 AlGaAs heterojunction laser, lightwave sources and detectors 0-64068  
 AlGaAs injection laser, large optical cavity, with multiple active regions 0-106538  
 AlGaAs laser array on Si heat sink, optical power detection 0-74383  
 (AlGa)As laser system, VPE growth and degradation mechanisms 0-99748  
 AlGaAs lasers, CW high-power single-mode constricted DH lasers with large optical cavity 0-64076  
 AlGaAs mode-locked diode laser, optical pulse generation 0-95907  
 AlGaAs semiconductor lasers, single-mode stabilisation by traps 0-95893  
 (AlGa)As strip buried heterostructure lasers, mode locking using external cavity 0-91791  
 (AlGa)As stripe geometry, proton-bombardment delineated DH laser, lifetime 0-106520  
 AlGaAs stripe-geometry DH laser, filament displacement and refr. losses 0-58536  
 AlGaAs transverse junction stripe laser with distributed Bragg reflector 0-106535  
 Al,Ga<sub>1-x</sub>As CW heterolaser, 10000 hr. lifetime tests, degradation of mirror surfaces 0-106542  
 Al,Ga<sub>1-x</sub>As CW multiwavelength TJS laser, MBE, single-longitudinal modes 0-64049  
 Al,Ga<sub>1-x</sub>As, modified-strip buried-heterostructure lasers, CW electro-optical properties 0-74359  
 Al,Ga<sub>1-x</sub>As solid solution, pulsed diode laser simulator of solid laser 0-91816  
 Al,Ga<sub>1-x</sub>As triggerable semiconductor lasers made by deep proton bombardment 0-69408  
 Al,Ga<sub>1-x</sub>As/Al,Ga<sub>1-y</sub>As DH lasers grown by metalorganic CVD, CW operation in wavelength range 760-780 nm 0-64053  
 Al,Ga<sub>1-x</sub>As-Al,Ga<sub>1-y</sub>As DH IR-visible (0.89-0.72  $\mu\text{m}$ ) MBE grown lasers 0-64058  
 Al,Ga<sub>1-x</sub>As-GaAs, quantum-well heterostructure laser diode, temp. depend. of threshold current 0-87395  
 Al,Ga<sub>1-x</sub>As-GaAs DH injection laser, active region internal parameters determ., composite resonator use 0-106548  
 Al,Ga<sub>1-x</sub>As-GaAs DH laser diode, I-V characts., variation of ideality factor 0-64027  
 Al,Ga<sub>1-x</sub>As-GaAs DH laser operation, phonon contrib. 0-102724  
 Al,Ga<sub>1-x</sub>As-GaAs large-quantum-well heterostructures, induced phonon-sideband laser operation 0-95888  
 Al,Ga<sub>1-x</sub>As-GaAs quantum-well heterostructures, phonon-assisted recomb. and stimulated emission 0-74358  
 AlGaAsSb-GaSb heterojunction injection laser, radiative props. 1.4 to 1.8  $\mu\text{m}$  range 0-91798  
 (Ga, Al)As laser diode, operation and gain meas., importance of gap shrinkage effects 0-66257

## semiconductor junction lasers continued

- (Ga,Al)As narrow double-current-confinement channelled-substrate planar laser fabrication, double etching technique 0-74371  
 GaAlAs actively mode-locked laser, bandwidth limited picosecond pulses 0-95905  
 GaAlAs DH, SiO<sub>2</sub> insulated, characteristics and near field 0-64019  
 GaAlAs DH injection laser, half-ring, room temp. operation 0-58558  
 GaAlAs DH laser, narrow stripe geometry, spontaneous carrier lifetime 0-87392  
 (GaAl)As DH laser, threshold current density, growth terraces effect 0-99723  
 GaAlAs DH laser coherent light, propagating in multimode optical fibre, speckle contrast 0-78978  
 GaAlAs DH laser coupled to LiNbO<sub>3</sub> Ti-diffused optical waveguide, anal. 0-58706  
 GaAlAs DH laser diodes, small signal modulation, junction capacitance effect 0-83625  
 GaAlAs DH laser diode, edge coupling to planar LiNbO<sub>3</sub>:Ti waveguide 0-87559  
 (GaAl)As DH laser wafer, photoluminesc. improvement with buffer layer 0-64014  
 GaAlAs DH lasers, self-sustained pulsation suppression, effect of SiO<sub>2</sub> facet coating films 0-95894  
 GaAlAs injection DH laser and GaAs Schottky-gate FET, monolithic integration 0-58593  
 (GaAl)As injection lasers operating with optical fibre external resonator, characts. 0-58544  
 (GaAl)As injection laser operating in external cavity, intensity self-pulsations 0-64013  
 (GaAl)As injection lasers operating with optical fibre resonators 0-91812  
 GaAlAs laser diode, for heterodyne communication systems, high frequency stability 0-99727  
 GaAlAs laser nonlinearities, harmonic distortion 0-74357  
 (GaAl)As low-beam-divergence CW DH laser, grown by low press. metal-organic CVD 0-74376  
 GaAlAs mode stabilised separated multilayer stripe geometry DH laser, optical waveguide 0-64051  
 GaAlAs terraced substrate laser, visible-light-emitting, characts. 0-106523  
 (GaAl)As:Be DH stripe geometry lasers with current confinement structure 0-58592  
 (GaAl)As:Be implanted DH stripe geometry laser 0-64044  
 GaAlAs/GaAs kink-free narrow-stripe proton-isolated injection DH lasers 0-58534  
 GaAlAs-GaAs heterostructure lasers, interstitial impurities and degradation, Auger obs. 0-99730  
 AlGaAs-GaAs lasers, channelled substrate, prepared by combination of organometallic pyrolysis and LPE 0-99745  
 (GaAl)As-GaAs narrow stripe laser, improved optical communication system performance 0-102733  
 Ga<sub>1-x</sub>Al<sub>x</sub>As DH injection laser, FM at microwave freq. rates 0-58610  
 Ga<sub>1-x</sub>Al<sub>x</sub>As DH laser diode, long-lived, high-power, facet coated 0-58564  
 Ga<sub>1-x</sub>Al<sub>x</sub>As laser, SHG with KNbO<sub>3</sub> 0-74431  
 Ga<sub>1-x</sub>Al<sub>x</sub>As low threshold stripe geometry DH laser, Be implanted, on semi-insulating substrate 0-69409  
 Ga<sub>1-x</sub>Al<sub>x</sub>As visible diode lasers, degradation mechanisms 0-64026  
 Ga<sub>1-x</sub>Al<sub>x</sub>As visible diode lasers, degradation due to macroscopic defects (<730 nm) and facet oxidation (>740 nm), life tests 0-99729  
 Ga<sub>1-x</sub>Al<sub>x</sub>As-GaAs DH injection lasers grown by metalorganic CVD, props. 0-99751  
 Ga<sub>1-x</sub>Al<sub>x</sub>As, hetero-isolation stripe geometry for IR and visible radiation (*Japanese*) 0-83607  
 GaAs, comments on host dispersion in ultra-short pulse generation 0-64024  
 GaAs, current research, fibre optic appl. 0-83613  
 GaAs DH laser diodes stabilised using self-apertured facet coatings 0-58609  
 GaAs degraded lasers, climb asymmetry, TEM obs. 0-79802  
 GaAs double and narrow stripe laser structures 0-64062  
 GaAs, fabrication using double-etching technique 0-74387  
 GaAs heterojunction diode as light source for fibre optical communication 0-58653  
 GaAs, injection laser with localisation of injection current, design and characts. 0-106543  
 GaAs injection lasers, direct modulation enhancement effect of HF noise 0-83608  
 GaAs laser arrays 0-69393  
 GaAs laser diode, spontaneous emission reduction 0-95904  
 GaAs narrow-channel double-current-confinement CSP lasers, current distrib. effect on performance 0-58539  
 GaAs, semi-insulating substrates, monolithic integration of optical and electronic devices, review 0-58543  
 GaAs, semi-insulating substrates, whispering gallery lasers 0-69405  
 GaAs, striped DH lasers, anomalous behaviour at low temp. (*Chinese*) 0-87390  
 GaAs/(Ga,Al)As, DH laser diode, electroluminescence near 1 eV 0-60682  
 GaAs/(Ga,Al)As channelled substrate narrow stripe lasers, with quarter-wavelength facet coatings 0-99746  
 GaAs/GaAlAs crowding effect lasers using whispering gallery mode on semi-insulating GaAs substrates 0-58589  
 GaAs/GaInP DH, MBE grown, optically pumped laser action at 77K 0-95890  
 GaAs/(GaAl)As DH injection laser with pillbox resonator, characts. and fabrication 0-58581  
 GaAs-(GaAl)As injection lasers with circular resonator 0-74377  
 GaAs-Al<sub>0.27</sub>Ga<sub>0.73</sub>As DH lasers grown by MBE, influence of growth conditions on threshold current density 0-58587  
 GaAs-Al<sub>0.3</sub>Ga<sub>0.7</sub>As laser diode, spontaneous radiation transfer 0-91796  
 GaAs-Al<sub>0.3</sub>Ga<sub>0.7</sub>As transverse junction lasers with low threshold current prep. by MBE on semi-insulating substrates 0-58588  
 GaAs-Al<sub>0.3</sub>Ga<sub>0.7</sub>As, current transverse junction lasers, low threshold, MBE prep. 0-83614  
 GaAs-Al<sub>0.3</sub>Ga<sub>0.7</sub>As buried-heterostructure lasers, current injection confinement, MBE/LPE hybrid technique 0-74374  
 GaAs-Al<sub>0.3</sub>Ga<sub>0.7</sub>As DH laser, MBE grown, CW electro-optical props. 0-102725  
 GaAs-Al<sub>0.3</sub>Ga<sub>0.7</sub>As electro-optic frequency- and polarisation-modulated injection laser 0-91810

semiconductor junction lasers continued

GaAs-AlGaAs DH injection laser with stripe contacts, radiation pulse stepped shape 0-91799  
GaAs-AlGaAs DH laser structure, defect assessment by differentiated cathodolum. topography 0-59819  
GaAs-Ga<sub>1-x</sub>Al<sub>x</sub>As DH lasers, electron beam induced current microscopy 0-95899  
GaAs-Ga<sub>1-x</sub>Al<sub>x</sub>As DH laser material crystal cathodoluminescence, SEM analysis 0-97349  
GaAs-GaAlAs bipolar transistor and heterostruct. laser, monolithic integration 0-102558  
GaAs-GaAlAs DH injection lasers, external cavity operated angled-stripe geometry, CW operation 0-64078  
GaAs-GaAlAs DH lasers, strain-enhanced luminesc. degradation, photoluminesc. obs. 0-69392  
GaAs-GaAlAs DH laser, O<sup>+</sup> isolation compared with SiO<sub>2</sub> isolation 0-74382  
GaAs-GaAlAs injection laser, radiation divergence reduction by non-waveguide mode excitation 0-91797  
GaAs-GaAlAs injection lasers, narrow-stripe proton-implanted, high bit-rate modulation 0-91824  
GaAs-InP heterojunction laser output wavelength control 0-74384  
GaAsSb/GaAlAsSb DH lasers, growth and props. 0-69412  
GaInAsP DH laser emitting at 1.55  $\mu$ m, threshold currents 0-83609  
GaInAsP diode lasers, self-sustained pulsations in light output 0-64012  
GaInAsP/InP 1.5-1.6 micron integrated twin-guide lasers with distributed Bragg reflectors 0-74380  
GaInAsP/InP buried heterostruct. laser, 1.6  $\mu$ m, fabrication and room temp. CW operation 0-58568  
GaInAsP/InP DH lasers, room temp. CW operation at 1.5 to 1.6 micron range, fabrication 0-58585  
GaInAsP/InP DH lasers emitting at 1.3  $\mu$ m, growth and characts. 0-64057  
GaInAsP/InP DH stripe geometry lasers emitting at 1.3  $\mu$ m, growth characterisation 0-69410  
GaInAsP/InP DH lasers, 1.3  $\mu$ m wavelength, LPE growth and characterisation 0-69411  
(100)GaInAsP/InP DH lasers, 1.5-1.6  $\mu$ m wavelength, two' phase soln. LPE technique using anti-meltback layer 0-99750  
GaInAsP/InP integrated twin-guide lasers with first order distrib. Bragg reflector, room temp. operation at 1.3  $\mu$ m 0-64077  
GaInAsP/InP integrated twin-guide lasers with distributed Bragg reflector, spectral behaviour 0-74381  
GaInAsP/InP lasers, 1.5  $\mu$ m emitting, high temp. CW operation 0-95889  
GaInAsP/InP lasers, LPE growth, effect of p-doping on carrier lifetime and threshold current density 0-99726  
GaInAsP/InP narrow planar stripe lasers, lasing characts. 0-95897  
GaInAsP/InP terraced substrate DH lasers, fabrication and single transverse mode operation 0-58580  
GaInAsP-InP buried heterostructure lasers, 1.6  $\mu$ m wavelength 0-64055  
GaInAsP-InP integrated twin-guide lasers with first-order distributed Bragg reflectors, 1.3  $\mu$ m 0-58567  
GaInAsP-InP stripe-geometry monolithic laser with etched mirror and monitoring detector 0-64054  
GaInAsP-InP stripe laser, etched mirrors fabricated by wet chem. etch 0-99744  
Ga<sub>1-x</sub>In<sub>x</sub>As<sub>1-y</sub>P<sub>y</sub>/InP DH laser emitting at 1.15 micron grown by low-pressure CVD 0-64052  
Ga<sub>1-x</sub>In<sub>x</sub>As<sub>1-y</sub>Sb<sub>1-z</sub> tunable electron-beam-pumped laser parameters 0-106524  
GaInPAs/InP heterostructure DFB laser under optical pumping, lasing characts. 0-87396  
Ga<sub>1-x</sub>In<sub>x</sub>P<sub>1-y</sub>As<sub>1-y</sub>/InP DFB injection laser, one-step LPE 0-58575  
Ga<sub>1-x</sub>In<sub>x</sub>P<sub>1-y</sub>As<sub>1-y</sub>/solid solution, pulsed diode laser simulator of solid laser 0-91816  
GaP semiconductor Raman laser 0-78864  
InGaAsP DH lasers with etched reflectors, fabrication, current density 0-64050  
(InGa)(AsP) laser system, VPE growth using metal organic sources or halide transports 0-99748  
InGaAsP single-mode CW ridge-waveguide laser emitting at 1.55 micron 0-58584  
InGaAsP strip-buried-heterostructure high-output power laser 0-58540  
InGaAsP strip-buried-heterostructure laser, high output power, operation 0-58559  
InGaAsP/InP buried heterostructure laser diodes for transmission loss meas. of graded-index fibres 0-87486  
InGaAsP/InP DH lasers, temp. depend. characts. 0-58541  
InGaAsP/InP DH stabilised 1.3  $\mu$ m laser diode-isolator module for hybrid optical integrated ckt. 0-58583  
InGaAsP/InP injection lasers for long wavelength (1.1 to 1.6  $\mu$ m) optical communication 0-58582  
InGaAsP-InP buried crescent injection laser emitting at 1.3  $\mu$ m with low threshold current 0-87404  
InGaAsP-InP buried heterostructure lasers emitting at 1.3  $\mu$ m, accelerated ageing characts. 0-95898  
InGaAsP-InP CW lasers, 1.5-1.7  $\mu$ m, VPE 0-78861  
InGaAsP-InP DH lasers, 1.55  $\mu$ m, low temp. LPE growth for room-temp. CW operation 0-64045  
InGaAsP-InP DH lasers, interfacial recomb., influence on oscill. characts. 0-87393  
InGaAsP-InP DH lasers, spatial hole burning, spontaneous emission saturation, direct obs. 0-95892  
InGaAsP-InP DH lasers, temp. dependence of threshold and elect. characts. 0-99725  
InGaAsP-InP DH lasers, perturbed InP growth, photoluminesc. study 0-106518  
InGaAsP-InP DH laser, threshold current, temp. depend. 0-106521  
(InGa)(AsP)-InP laser system, 1  $\mu$ m wavelength, lattice matching techniques 0-99748  
In<sub>1-x</sub>Ga<sub>x</sub>As<sub>1-y</sub>P<sub>y</sub>/InP DH lasers for 1.3 and 1.5  $\mu$ m optical fibre communications 0-91817  
In<sub>1-x</sub>Ga<sub>x</sub>As<sub>1-y</sub>P<sub>y</sub>/InP 1.5  $\mu$ m room-temp. CW laser fabrication and operation 0-64070  
InGaPAs LPE layers, compositional inhomogeneity, photoluminesc. obs. 0-75451  
In<sub>1-x</sub>Ga<sub>x</sub>P<sub>1-y</sub>As<sub>1-y</sub>In<sub>1-x</sub>Ga<sub>x</sub>P<sub>1-y</sub>As<sub>1-y</sub> visible spectrum multiple-quantum-well heterostruct. lasers 0-106537  
In<sub>1-x</sub>Ga<sub>x</sub>P<sub>1-y</sub>As<sub>1-y</sub>InP coupled multiple quantum-well heterostructure laser diodes, threshold current temp. depend. 0-78855

semiconductor junction lasers continued

InP-GaInAsP buried heterostructure lasers of 1.5  $\mu$ m region, fabrication and characts. 0-74388  
InP-In<sub>1-x</sub>Ga<sub>x</sub>As<sub>1-y</sub>P<sub>1-y</sub>-InP 1.55  $\mu$ m DH room-temp. CW laser fabrication and operation 0-64071  
InP-In<sub>1-x</sub>Ga<sub>x</sub>As<sub>1-y</sub>P<sub>1-y</sub>-InP 1.53  $\mu$ m single-mode CW ridge-waveguide laser 0-64072  
InP-InGaPAs heterojunction lasers and LEDs, 1.0 to 1.2  $\mu$ m 0-74362  
Pb salt tunable diode laser-integrating sphere system, output intensity characts. 0-78881  
PbS<sub>1-x</sub>Se<sub>x</sub> (X=0.18) homojunction injection lasers, near-field emission 0-95896  
PbS<sub>1-x</sub>Se<sub>x</sub> diode laser, contact degradation due to diffusion 0-102734  
Pb<sub>0.85</sub>Sn<sub>0.15</sub>Te homostructure diode laser, LPE growth, with controlled carrier conc. 0-95903  
Pb<sub>1-x</sub>Sn<sub>x</sub>Te diode laser, contact degradation due to diffusion 0-102734  
Pb<sub>1-x</sub>Sn<sub>x</sub>Te/PbTe<sub>1-x</sub>Se<sub>x</sub> lattice-matched buried heterostructure lasers with CW single mode output 0-74386

semiconductor junctions  
see also p-n junctions  
depletion region of junction barriers, capture from free-carrier tails 0-70802  
depth profiling by electron beam induced junction current meas. 0-96977  
heterojunction, impact ionisation 0-65663  
heterojunction solar cells 0-61344  
III-V semiconductor (Slovak) 0-88620  
isotype heterojunction barriers, cond. band discontinuity, C-V profiling meas. method 0-70801  
n-n homojunction, calc. of free carrier density profile in a semicond. near ohmic contact 0-70810  
one-sided abrupt junctions, normalized representation of avalanche breakdown behaviour 0-65666  
step 1-h junction, elec. struct. analytical methods, review 0-100507  
Au-n-Ga<sub>1-x</sub>Al<sub>x</sub>As-n-GaP narrow-band variable-gap surface-barrier photo-detector 0-96944  
GaAs-Al<sub>0.3</sub>Ga<sub>0.7</sub>As n-n heterojunction, LPE grown, cond. band discontinuity, C-V profiling meas. 0-70801  
GaAs-AlAs superlattice, folded acoustic phonons obs., Raman scatt. 0-88996  
GaAs-GaAlAs-GaAs rectifying semicond. struct., prep. by MBE and characts. 0-65657  
n-GaAs-n-Al<sub>x</sub>Ga<sub>1-x</sub>As rectifying heterojunction, cond. props. study 0-88626  
GaSb-InAs system, (110) surface and interface electronic struct. 0-100494  
n-Ge-n-GaAs isotype heterojunctions, modelling, characts. 0-103747  
InAs-GaSb superlattices, mag. field induced semimetal-semicond. transition 0-65656  
InGaP/InGaAs struct. for transferred electron photocathodes, VPE growth and characterisation 0-76193  
InSe-SnO<sub>2</sub> n-n heterojunctions, photoelec. props. 0-96945  
PbS-Si heterojunction, PbS film growth and struct. 0-96762  
Se<sub>1-x</sub>Te<sub>x</sub>-Se<sub>1-y</sub>Te<sub>y</sub> junctions, photovoltaic effects and rectification phenomena 0-84506  
n<sup>++</sup>nn<sup>+</sup>Si planar device, hot electron flicker noise at 78K 0-103732  
Si/In<sub>2</sub>O<sub>3</sub>-SnO<sub>2</sub> thin film junctions, polarity dependent memory switching effects 0-70814  
Si-Ge heterojunction form., microscopic aspects, EELS meas. 0-80368  
Si-PbS heterojunction, effect of Si substrate orientation on struct. and interface props. 0-80097  
Si-Si interface, elec. cond. rel. to interface state population 0-65672  
ZnO/Si acoustoelectric devices, magnetron discharge sputtering prep. 0-80332  
ZnSe:Mn/n-GaAs low threshold thin film DC electrolum. cell, pulse-excited characts. 0-76081

semiconductor materials  
see also amorphous semiconductors; degenerate semiconductors; elemental semiconductors; heavily doped semiconductors; II-VI semiconductors; III-V semiconductors; III-VI semiconductors; IV-VI semiconductors; liquid semiconductors; magnetic semiconductors; many-valley semiconductors; narrow band gap semiconductors; organic semiconductors; polar semiconductors; semiconductors; ternary semiconductors  
chalcogenides of ABX<sub>3</sub> type comp., cybernetic prediction of form. possibility 0-101004  
copper quaternary thiospinels, mag. and elec. props. (French) 0-65771  
history, solid state research to semiconductor electronics 0-68015  
multicompositional compound semiconductor materials (Japanese) 0-107778  
oxide semiconductors in photoelectrochemical conversion of solar energy, use as cell anodes 0-101120  
rare earth oxides, perovskite-like, synthesis, struct., elec. props. 0-65554  
rare earth sulphides, EuR<sub>4</sub>, R=La, Ce, Pr, Nd, Sm, Gd, elec. cond. meas. 0-65555  
[ $\alpha$ ]-SiC:H, prepared by reactive sputtering, layer. props. (Japanese) 0-60695  
AgN<sub>3</sub>, high-resist. explosive cpd., elec. and galvanomag. props., temp. depend. 0-103728  
Ag<sub>2</sub>Se, between metal electrodes, current-voltage characts (French) 0-97005  
Al-Ge-SiO<sub>2</sub> solar selective absorber surfaces, optical behaviour at high temp. 0-101130  
AlB<sub>2</sub>,  $\alpha$ - and  $\beta$ -forms, elec. props. at high temps. and in strong elec. fields, thermistor appls. 0-92903  
As chalcogenides, deep levels, photoluminesc. and photocond. 0-70641  
As<sub>2</sub>S<sub>3</sub>, two photon light absorpt. dispersion, induced linear light absorpt. (Russian) 0-66231  
As<sub>2</sub>Se<sub>3</sub>, monoclinic, chem. bonds rel. to electronic and vibr. states 0-64951  
As<sub>2</sub>Se<sub>3</sub>, single crystals, fine struct. of direct gap from electoref. spectra 0-93280  
Ba<sub>2</sub>Sc<sub>2</sub>O<sub>9</sub>, Ba<sub>2</sub>Sc<sub>2</sub>WO<sub>9</sub> and Ba<sub>2</sub>Sc<sub>2</sub>TaO<sub>9</sub>, elec. cond. nature, depend. on comp. and medium thermodynamic parameters 0-70773  
Ba<sub>1-x</sub>Sm<sub>x</sub>S, electron config. of Sm ions, X-ray L-absorpt. spectroscopy 0-60715  
Ba<sub>0.5</sub>Sr<sub>0.5</sub>Nb<sub>2</sub>O<sub>6</sub>, electronic props. and photoresponses 0-92925  
n-BaTiO<sub>3</sub>, ohmic contact form. 0-92969  
(Bi,Sb)<sub>2</sub>(Te,Se), thermoelectric alloys, phase diagrams, and imperfection chemistry 0-108422  
Bi<sub>2</sub>GeO<sub>10</sub> crystals, principal carriers obs., in dark and under laser illumination (Russian) 0-80312



## semiconductor materials continued

- Bi<sub>2</sub>S<sub>3</sub>-Bi<sub>2</sub>Se<sub>3</sub> and Bi<sub>2</sub>Te<sub>3</sub>-Bi<sub>2</sub>Se<sub>3</sub> systems, thermal cond. change during phase transitions 0-100368  
 Bi<sub>0.85</sub>Sb<sub>0.15</sub>, semiconducting transport props., 2 to 100K 0-59989  
 Bi<sub>0.9</sub>Sb<sub>0.1</sub>, magnetophonon effect on hot electrons (*Russian*) 0-107814  
 Bi<sub>1-x</sub>Sb<sub>x</sub>, deformation calculations, band struct. variation, electron phase transitions due to deform. (*Russian*) 0-65137  
 Bi<sub>1-x</sub>Sb<sub>x</sub>, EM wave prop. for rot. of mag. field from Faraday to Voigt config. 0-84419  
 Bi<sub>1-x</sub>Sb<sub>x</sub>, semiconducting alloy, band struct. study, Shubnikov-de Haas effect (*Russian*) 0-80181  
 Bi<sub>0.6</sub>Sb<sub>0.4</sub>Te, single crystal, dispersion of magnetoplasma waves (*Russian*) 0-70739  
 Bi<sub>2</sub>Sb<sub>2</sub>Te<sub>3-x</sub>Se<sub>x</sub>, elec. cond. and thermoelec. props., neutral defects influence 0-60017  
 Bi<sub>12</sub>SiO<sub>20</sub> film, photoelectric props. obs., UV illumination effects (*Russian*) 0-80313  
 Bi<sub>2</sub>Te<sub>3</sub>, anodic film form., in situ ellipsometric study 0-104318  
 Bi<sub>2</sub>Te<sub>3</sub>, surface prep. by etching for electroplating elec. contacts 0-108647  
 Bi<sub>2</sub>Te<sub>3</sub>-Bi<sub>2</sub>Se<sub>3</sub> solid solns., single cryst. growth and thermocouple construct. 0-104056  
 BiTeI, melt and vapour grown, optical props. 0-84746  
 (Bi<sub>2</sub>Te<sub>3</sub>)<sub>0.9</sub>(Sb<sub>2</sub>Te<sub>3</sub>)<sub>0.1</sub>(Sb<sub>2</sub>Se<sub>3</sub>)<sub>0.05</sub> n-type alloy for thermogenerators, thermo-EMF, elec. cond. and thermoelec. efficiency factor, 300-600K 0-70735  
 Ca<sub>1-x</sub>Sm<sub>x</sub>S, electron config. of Sm ions, X-ray L-absorpt. spectroscopy 0-60715  
 CdAs<sub>2</sub>, cryst. struct. and vitrification capacity 0-88126  
 Cd<sub>3</sub>As<sub>2</sub>, energy band structure calc. 0-75504  
 Cd<sub>3</sub>As<sub>2</sub> film on NaCl substrate, vacuum deposition, growth morphology, microstructure 0-75479  
 Cd<sub>3</sub>As<sub>2</sub> films, nucleation processes, on NaCl substrates 0-59813  
 Cd<sub>3</sub>(As<sub>1-x</sub>P<sub>1-x</sub>)<sub>2</sub>, 0 ≤ x ≤ 1.0, band struct. calc. near Brillouin zone centre 0-107703  
 CdF<sub>2</sub>:NaF(AgF), colour centres, IR absorpt. and photocond. after UV irradi. 0-79784  
 Cd<sub>1-x</sub>Mn<sub>x</sub>Se, fundamental optical props. 0-84751  
 Cd<sub>1-x</sub>Mn<sub>x</sub>Te mixed crystals, Raman spectra 0-103961  
 CdO-SnO<sub>2</sub> DC reactively sputtered films, elec. and optical props. 0-103763  
 CdSb:Al, p-n junction formation by laser emission, photoelectric effects (*Russian*) 0-70815  
 CdSb:Al(In)(Ga)(Te), p-n junction formation by laser radiation 0-96983  
 CdSb:Fe, self absorpt. edge, impurity effect (*Russian*) 0-97316  
 Cd<sub>3</sub>SnO<sub>4</sub> and Cd<sub>3</sub>SnO<sub>4</sub>:CdO, thin film electrodes in H<sub>2</sub>SO<sub>4</sub> electrolytes, reduction, AES and SEM 0-65674  
 CdTe-InAs quasi-binary system, temp.-comp. diagram, physicochem. and thermodynamic analysis 0-104127  
 Cs<sub>3</sub>Sb vacuum deposited photoemitter, XPS study 0-89122  
 (Cu<sub>2</sub>Ag)<sub>2</sub>Se/(Bi, Sb)<sub>2</sub>Te<sub>3</sub>, P type selenide segmented element fabrication, thermoelectric props. 0-107835  
 CuB<sub>24</sub>, elec. props. at high temps. and in strong elec. fields, thermistor appls. 0-92903  
 CuBr(I), reflectance and thermoreflectance spectra, electronic struct. 0-71444  
 CuCl, band struct., OPW calc. and X-ray spectra meas. 0-75506  
 CuCl, electron-hole pairs behaviour in energetic ion tracks 0-65457  
 CuCl, electronic struct. by LCAO and LMTO methods, direct gap semiconductor 0-59868  
 CuCl, exciton spatial dispersion determ., two-photon Raman scatt. via excitonic mol. state 0-60595  
 CuCl powder compacts, DC voltage depend. resist. under press. 0-80334  
 CuO, on Al or Cu, solar selective coating, figure of merit 0-72082  
 Cu<sub>2</sub>O, Cu inclusions and annealing, optical and IR absorpt. obs. 0-60630  
 Cu<sub>2</sub>O, photosensitive etching in nonoxidising etchants 0-78813  
 Cu<sub>2</sub>O, reson. Raman scatt. from stress-split forbidden excitons 0-93332  
 Cu<sub>2</sub>O, self-consistent energy bands 0-59869  
 Cu<sub>2</sub>O solar cells, electrical and optical props., photocurrent anal. 0-101116  
 Cu<sub>2</sub>O, uniaxial stress effects on excitons 0-60589  
 Cu<sub>2</sub>O:Ag<sup>+</sup>, exciton-neutral and exciton-charged impurity scatt. cross sections 0-70618  
 Cu<sub>2</sub>O:Mn, photomemory mobility components, charged centre conc. 0-103725  
 Cu<sub>2</sub>-O-Cu diode junction, Schottky barrier, electronic structure and minority carrier diffusion length (*French*) 0-65682  
 Cu<sub>2</sub>S, diffusion length meas. using scanned laser beam tech. 0-93886  
 Cu<sub>2</sub>S films, prpe. methods, appl. to Cu<sub>2</sub>S-CdS solar cells 0-80980  
 Cu<sub>2</sub>S, on Cu, solar selective coating, figure of merit 0-72082  
 Cu<sub>2</sub>S/CdS heterojunction solar cells, diffusion length determ. using minority carrier SEM 0-61359  
 Cu<sub>2</sub>S-CdS heterojunction solar cells, carrier transport, nonmonotonic band profiles 0-61361  
 Cu<sub>2</sub>S-CdS heterojunction interface, depth distribution profiles, Auger spectra 0-88622  
 Cu<sub>2</sub>S-CdS heterophotocells based on CdS films of stoichiometric composition, elec. and photoelec. props. 0-93873  
 Cu<sub>2</sub>S-CdS solar cell fabrication by magnetron reactive sputtering deposition 0-61363  
 Cu<sub>2</sub>S-CdS solar cells, interface recombination phenomena and tunnel effect 0-66978  
 Cu<sub>2</sub>S-CdS solar cells, optical absorption coefficient changes in Cu<sub>2</sub>S 0-93980  
 Cu<sub>2</sub>S-CdS thin film planar junction devices, quantitative photon loss anal. 0-61362  
 Cu<sub>2</sub>S-ZnCd<sub>1-x</sub>S heterojunction, improved model of electro-optic behaviour 0-94023  
 Cu<sub>2-x</sub>S-CdS ceramic solar cells, solar batteries operating characts. 0-93874  
 Cu<sub>2</sub>S evaporated layer growth in vacuum, compositional and optical characterisation, solar cell appls. 0-97437  
 Cu<sub>2</sub>S-CdS solar cells, Cu<sub>2</sub>S growth kinetics and composition analysis by absorbance transient and galvanic electrochemical measurements 0-92797  
 Cu<sub>2</sub>S-CdS solar cells, SCL current 0-76634  
 p-Cu<sub>2</sub>VS<sub>4</sub>, mixed conduction due to cationic interstitials 0-70772  
 Cu<sub>2</sub>VS<sub>4</sub>, out of equil. mixed cond., electronic cond. decrease in ionic soln. 0-107874  
 CuWO<sub>4-x</sub>, prod. from CuO+WO<sub>3</sub> solid state reaction 0-66796

## semiconductor materials continued

- EuGd<sub>2</sub>S<sub>4</sub>, nonstoichiometric, elec. transport props., semicond. and metallic cond. 0-107786  
 Eu<sub>2</sub>Ir<sub>2</sub>O<sub>7</sub>, pyrochlore, sp. ht. below 20K, Debye temp. 0-65241  
 Eu<sub>1-x</sub>Sm<sub>x</sub>S, electron config. of Sm ions, X-ray L-absorpt. spectroscopy 0-60715  
 α-Fe<sub>2</sub>O<sub>3</sub> ceramics, gas sensor for city gas appl. (*Japanese*) 0-61498  
 α-Fe<sub>2</sub>O<sub>3</sub>, elec. resist. and phase transition under shock compression 0-72496  
 Fe<sub>2</sub>O<sub>3</sub>, semicond. anode in aq. electrolyte, electrochem. and electrochem. 0-76080  
 FePS<sub>3</sub>, layered semiconductors, optical and electronic props. 0-70761  
 FeS<sub>2</sub>, natural pyrite, photocond. spectra 0-70758  
 Fe(Sb<sub>1-x</sub>Te<sub>x</sub>)<sub>2</sub> system cpds., prep., cryst. struct., elec. and mag. charact. 0-108349  
 θ-Fe<sub>2</sub>V<sub>2</sub>O<sub>5</sub>, spin glass and paramag. props., susceptibility, EPR and Mossbauer studies 0-75782  
 Ge-Si, electronic structure, short-range order effects, calc. 0-92861  
 Ge-Si, imperfect homopolar cryst., lattice dynamics, IR spectra calc. 0-59601  
 Ge-Si alloys, hot-pressed, fine-grained, boundary scatt. of phonons, lattice thermal cond. 0-107583  
 Ge-Si alloys, hot-pressed, fine-grained, boundary scatt. of phonons, theory 0-107584  
 Ge-Si thermoelectric alloys, phase diagrams, and imperfection chemistry 0-108422  
 GeP, thermodynamic characts. 10-300K, interatomic bond elasticity 0-59677  
 Ge<sub>0.5</sub>Si<sub>0.5</sub>, elec. cond., density of states, impurity and temp. depend 0-65568  
 H<sub>2</sub>WO<sub>4</sub>, bronzes, Anderson transition, XPS 0-107705  
 HgI<sub>2</sub>, IR lattice vibr. and dielec. dispersion 0-76018  
 HgI<sub>2</sub>, soln. grown crystals, low-energy gamma-ray cond. type detectors 0-97418  
 Hg<sub>1-x</sub>Mn<sub>x</sub>Te, non-parabolic zero-gap semicond., indirect exchange interaction 0-80498  
 In<sub>2</sub>O<sub>3</sub>:Sn, RF magnetron sputtered film, elec. and optical props. 0-104065  
 In<sub>2</sub>O<sub>3</sub> films, electron beam evaporation, elec. and optical props. (*Japanese*) 0-60784  
 In<sub>2</sub>O<sub>3</sub>, thermally evaporated film, struct. and elec. props. 0-104066  
 In<sub>2</sub>O<sub>3</sub>:Sn films; vac. deposited, elec. props. 0-100542  
 In<sub>2</sub>O<sub>3</sub>:SnO<sub>2</sub>-CdTe:P, p-n homojunction solar cell, elec., photovoltaic props., photoluminescence 0-81463  
 In<sub>2</sub>O<sub>3</sub>:SnO<sub>2</sub>-Si solar cells, reverse current-voltage characts. under illumination 0-89622  
 In<sub>2-x</sub>Sn<sub>x</sub>O<sub>3-y</sub> solar cells, majority carrier conduction effects 0-97796  
 In<sub>2-x</sub>Sn<sub>x</sub>O<sub>3-y</sub>-Ga<sub>1-x</sub>In<sub>1-x</sub>P-(InP,As<sub>1-y</sub>) heterojunction solar cells, chemistry and prep. 0-94073  
 In<sub>2-x</sub>Sn<sub>x</sub>O<sub>3-y</sub>-insulator-poly-Si solar cells, photovoltaic conversion parameters 0-101093  
 Li<sub>1/3</sub>Si, cryst. struct. and electrochem. anal. (*German*) 0-88132  
 Lu<sub>2</sub>Ir<sub>2</sub>O<sub>7</sub>, pyrochlore, sp. ht. below 20K, Debye temp. 0-65241  
 LuRhO<sub>4</sub>, elec., mag. and photoelectrochemical props. 0-96925  
 Mg<sub>2</sub>Cd<sub>1-x</sub>Te, electroreflection spectra, comp. depend. 0-66230  
 Mg<sub>2</sub>Zn<sub>1-x</sub>Te, band struct. refl. spectra meas. 0-80813  
 MnAs<sub>0.95</sub>P<sub>0.05</sub>, anisotropy of elec. cond. and Hall effect 0-92908  
 Mn<sub>2</sub>Cd<sub>1-x</sub>Se single crystals, photoluminesc., composition depend. 0-80854  
 Mn<sub>2</sub>Cd<sub>1-x</sub>Te, lattice vibrs., Raman and IR spectra meas. 0-93311  
 Mo<sub>2</sub>Ru<sub>2</sub>Se<sub>8</sub>, synthesis, struct., and elec. props. 0-92877  
 MoS<sub>2</sub>, molybdenite band structural props. rel. to supercond. and semicond. 0-96781  
 n-MoSe<sub>2</sub> based liq. junction solar cell, nonaqueous electrolyte system employing Cl<sub>2</sub>/Cl<sup>-</sup> couple 0-81432  
 MoSe<sub>2</sub>, imperfections from TEM study 0-79800  
 Mo<sub>0.5</sub>W<sub>0.5</sub>Se<sub>2</sub> single cryst. vapour growth, characterisation 0-93466  
 NaZnGeO<sub>4</sub>:Mn, electrochem., ionisation domains 0-84787  
 Nb chalcogenides and chalcogenide halides, geometrical struct. and metal-metal bonding 0-80172  
 NbO<sub>2</sub>, on-state decay rel. to recomb. and nonlinear props. 0-84492  
 NbS<sub>2</sub>, electronic struct. and predicted cond. props. 0-92815  
 NbS<sub>2</sub>:Cl<sub>2</sub>(Br<sub>2</sub>)(I<sub>2</sub>), absorpt. edge spectrum, fine struct. 0-66219  
 Ni-Ge-SiO<sub>2</sub>, solar selective absorber surfaces, optical behaviour at high temp. 0-101130  
 NiO, Hall effect anomaly, sign reversal at 600K 0-100471  
 NiPS<sub>3</sub>, layered semiconductors, optical and electronic props. 0-70761  
 NiS<sub>2-x</sub>Se<sub>x</sub>, first-order Raman scattering 0-108206  
 PbI<sub>2</sub>, first-order 2H-4H polytype transition, exciton spectroscopic study 0-59647  
 PbI<sub>2</sub>, photoexciton interaction, luminescence spectra, polariton dispersion diagram 0-93397  
 PbI<sub>2</sub>-Ag(Au)(Cu), light sensitive, internal photoelectric emission 0-107910  
 Pb<sub>1-x</sub>Mn<sub>x</sub>Te, photovoltaic effect, p-n junction, energy gap determ. 0-92931  
 PbS-Sb<sub>2</sub>S<sub>3</sub> semicond., optical and photoelec. behaviour 0-96938  
 PbTe-InTe system, phase interactions and solid soln. form., physicochem. and elec. charact. 0-104129  
 RbMnF<sub>6</sub>:Er<sup>3+</sup>, absorption, emission, excitation and lifetime meas. 0-71460  
 Ru<sub>2</sub>Ti<sub>2</sub>O<sub>7</sub> films, percolation elec. cond. in strong electric fields (*Russian*) 0-84471  
 SMS, band struct. and semicond. metal phase transition 0-80180  
 Sb<sub>2</sub>S<sub>3</sub>, defect dir. in elec. fields and bistable switching 0-92947  
 Sb<sub>2</sub>S<sub>3</sub> film, coevaporated, elec. cond. meas. 0-65726  
 Sb<sub>2</sub>Se<sub>3</sub>-CdSe heterojunction, photoelec. props. 0-70816  
 (Sb<sub>2</sub>Se<sub>3</sub>)<sub>0.7</sub>(Bi<sub>2</sub>Se<sub>3</sub>)<sub>0.3</sub>, solid soln., prep. and elec. properties of layered crystals 0-70762  
 Sb<sub>2</sub>Te<sub>3</sub>, stoichiometric, Hall effect and thermoelec. power studies 0-100470  
 Sb<sub>2</sub>Te<sub>3</sub>-Bi<sub>2</sub>Te<sub>3</sub> and Sb<sub>2</sub>Te<sub>3</sub>-Sb<sub>2</sub>Se<sub>3</sub> systems, thermal cond. change during phase transitions 0-100368  
 Sb<sub>2</sub>Te<sub>3</sub>-Bi<sub>2</sub>Te<sub>3</sub> solid solns., single cryst. growth and thermocouple construct. 0-104056  
 Se<sub>2</sub>Te<sub>2-x</sub>, growth of single crystals by Czochralski method 0-66423  
 Si-Ge, high temperature thermoelectric materials 0-89659  
 SiAs, cryst. growth from melt, elec. props. 0-76170  
 SiC (6H), IR absorpt., UV illumination effects, defect levels 0-66251  
 α-SiC crystals, broad-band semiconductors, growth in Acheson furnace 0-84841  
 SiC devices, epitaxial layer growth techniques 0-108360



## semiconductor materials continued

- SiC, diffusion of B, elec. cond. meas. 0-96696  
 $\beta$ -SiC form. on Si substrate in RF powered reactor 0-76173  
 SiC, laser Raman spin-flip scatt. from excitons, luminesc. 0-80786  
 SiC p-n junction, electroluminesc. 0-97343  
 SiC p-n junction, epitaxial, grown by sublimation, elec. and struct. props. (Chinese) 0-60067  
 SiC p-n junctions, current-voltage characts. 0-60073  
 SiC p-n junctions, electrolum. spectra and kinetics 0-66305  
 SiC particles in EFG ribbon solar cells, EBIC and ion microprobe anal. 0-93838  
 SiC polytypes, free exciton luminesc. meas., phonon energies 0-80852  
 SiC, radiation defect annealing, recovery of LEED maxima 0-65075  
 SiC, spin-flip scatt. of laser light from photoexcited excitons 0-93330  
 SiC thin-film thermistors with high thermal response (Japanese) 0-105629  
 SiC with dielectric coating, surface polaritons, waveguide modes 0-80195  
 SiC:Al,N (6H), ODMR for effective-mass-like acceptor 0-93213  
 SiP, thermodynamic characts. 10-300K, interatomic bond elasticity 0-59677  
 SiP<sub>2</sub> with pyrite struct., Fermi surface calc. 0-65427  
 (SiTe)<sub>1-x</sub>(ATe)<sub>x</sub>, A=Ge, Sn, Pb, solid soln. with small substitution, mag. susceptibility (Russian) 0-70933  
 SmS, LO phonon freq. softening in semicond. and metallic phases 0-96619  
 SmS, piezoresistance at 80K 0-59990  
 SmS, trivalent rare earth substituted, stability of Sm<sup>2+</sup> 0-65508  
 SmS type semiconductors, electronic struct., influence of point defects 0-70650  
 SmS, valence transition, two band model 0-65507  
 SnO<sub>2</sub> CVD coating on glass, elec. resist. rel. to cryst. microstruct. 0-84520  
 SnO<sub>2</sub> gas sensor, fast-detecting, prep. 0-61497  
 SnO<sub>2</sub>, O chemisorption, elec. cond. and EPR meas. correlation 0-84369  
 SnO<sub>2</sub> thin films, O<sub>2</sub> vacancy diffusion 0-107467  
 SnO<sub>2</sub>:P, CVD growth and etching characts., doping effects 0-107667  
 SnO<sub>2</sub>:Sb sprayed film, growth mechanism and cryst. struct. 0-89143  
 SnO<sub>2</sub>/n<sup>+</sup>-Si heterojunction solar cells, fabrication by paint-on-diffusant method 0-94048  
 SnO<sub>2</sub>-based gas sensors, resist. temp. depend. on exposure to CO, H<sub>2</sub>, and propane 0-103694  
 SnO<sub>2</sub>-copper phthalocyanine-Ag systems, elec. and electroluminescent behaviour 0-80864  
 SnO<sub>2</sub>-GaTe(GaSe)(InSe) heterojunctions, photoelec. props. 0-96945  
 SnO<sub>2</sub>-InP heterojunctions, elec. and photovoltaic characts. 0-75628  
 SnO<sub>2</sub>-polySi solar cells, fabrication, grain size effects on device parameters 0-94045  
 SnO<sub>2</sub> films, passivation effect on Si solar cells 0-61360  
 Sn<sub>2</sub>S<sub>3</sub> mixed valence semiconductor, far IR refl. spectra 0-108191  
 SnS<sub>2</sub>-Se<sub>2</sub>, layer cryst., Raman active modes 0-80767  
 Sr<sub>2</sub>Nb<sub>2</sub>O<sub>7</sub>, electronic props. and photoresponses 0-92925  
 Sr<sub>1-x</sub>Sm<sub>x</sub>S, electron config. of Sm ions, X-ray L-absorpt. spectroscopy 0-60715  
 SrTiO<sub>3</sub>, semicond. anode in aq. electrolyte, electrolum. and electrochem. 0-76080  
 SrTiO<sub>3</sub> surface, photosensitizer for water photoassisted decomp. 0-85202  
 Tb(NO<sub>3</sub>)<sub>3</sub>·Fe(NO<sub>3</sub>)<sub>3</sub>·(NH<sub>4</sub>)<sub>2</sub>CO<sub>3</sub>·H<sub>2</sub>O system, cpd. form., comp. and props. 0-100832  
 Te-(Bi,Sb,-)<sub>2</sub>Te<sub>2</sub> eutectic, electrophys. props., directed crystn. conditions influence and comp. depend. 0-107827  
 Te-based eutectics, crystn. rate effect on electrophys. props. mutual solubility effect 0-60774  
 TiO<sub>2</sub>, doping processes, influence on photoelectrochem behaviour 0-79822  
 TiO<sub>2</sub>, electrode, carrier density determ. by optical absorpt. and photoelectrolysis spectra 0-71462  
 n-TiO<sub>2</sub>, electrode, flatband pot. determ. from differential stress meas. 0-75638  
 n-TiO<sub>2</sub>, electrode, photo-oxidation of acetate and iodide 0-81331  
 n-TiO<sub>2</sub>, electrode in AlCl<sub>3</sub>-NaCl melt, electrochem. and photoelec. props. 0-81328  
 TiO<sub>2</sub>, electrodes, chemically modified, nature of surface states 0-107905  
 n-TiO<sub>2</sub>, photoelectrochemical electrodes, effect of Nb doping on quantum efficiency 0-101121  
 TiO<sub>2</sub>, semicond. anode in aq. electrolyte, electrolum. and electrochem. 0-76080  
 TiO<sub>2</sub>, sputtering defects, associated surface electron states, UPS, XPS and AES obs. 0-60755  
 TiO<sub>2</sub>:Nb semicond. electrodes, electroreduction process kinetics, cathodic dark current meas. 0-66807  
 n-TiO<sub>2</sub>-electrolyte interface, charge transfer via surface states, water photoelectrolysis anal. 0-75636  
 n-TiO<sub>2</sub>-electrolyte interface impedance, freq. depend., equiv. cct. 0-100516  
 TiS<sub>2</sub>, band struct., angle-resolved photoemission studies 0-70610  
 Ti-Sn-Te system equilibria, polythermal and isothermal cross sections obs., ternary cpd. form. 0-104128  
 Ti<sub>2</sub>AsSe<sub>3</sub>, refractive index, thermal expansion temp. depend. 0-97223  
 TiCl<sub>4</sub> ground-state props., Wannier functions, and electronic struct., ab initio self-consistent calc. 0-80178  
 Tm<sub>1-x</sub>Eu<sub>x</sub>Se, semicond. with valence instabilities, cryst. chem. considerations 0-100213  
 TmSe<sub>1-x</sub>Te<sub>x</sub>, semicond. with valence instabilities, cryst. chem. considerations 0-100213  
 VO<sub>2</sub>, metal-insulator transition and electronic struct., ion bombard. effects 0-92948  
 VO<sub>2</sub>, single cryst., noise in presence of current filament 0-92952  
 VO<sub>2</sub>, single crystal, elec. switching 0-92946  
 VO<sub>2</sub>, V<sub>2</sub>O<sub>3</sub> and V<sub>2</sub>O<sub>5</sub>, film prep. under equil. conditions, struct. and elec. props. 0-108352  
 VO<sub>2(2n-1)/n</sub>, metal-semicond. transition temps. 0-59876  
 VO<sub>2</sub>, semicond., IR vibration spectra 0-88997  
 WO<sub>3</sub>, semicond. anode in aq. electrolyte, electrolum. and electrochem. 0-76080  
 WSe<sub>2</sub>, chem. vapour transport growth, microstruct. develop. 0-103278  
 Y oxides, perovskite-like, synthesis, struct., elec. props. 0-65554  
 Yb<sub>1-x</sub>Sm<sub>x</sub>S, electron config. of Sm ions, X-ray L-absorpt. spectroscopy 0-60715  
 ZnAs<sub>2</sub>, homogeneity region and electrophys. props. 0-60833  
 ZnAs<sub>2</sub> Schottky diodes, elec. and photoelec. props., excitons 0-65653  
 p-Zn<sub>0.9</sub>Cd<sub>0.1</sub>Sb, thermoelec. anisotropic semicond., carrier kinetics at low temps. 0-92893

## semiconductor materials continued

- Zn<sub>0.1</sub>Cd<sub>0.9</sub>Sb, thermoelectrically isotropic semicond., carrier kinetics in intrinsic cond. range 0-92894  
 ZnP<sub>2</sub>, Brillouin scattering and optical props. meas. 0-76041  
 $\alpha$ -ZnP<sub>2</sub>, doped, single crystal, electrical properties 0-92892  
 $\alpha$ -ZnP<sub>2</sub>, resonant Brillouin scatt. near indirect band gap 0-93350  
 ZnP<sub>2</sub> Schottky diodes, elec. and photoelec. props., excitons 0-65653  
 ZnP<sub>2</sub> tetragonal crystals, polarisation study of photocond. 0-96942  
 ZnP<sub>2</sub>:In(Ga)(Ge)(S)(Se), doped and undoped, optical absorpt. spectra in range 0.5 to 2.2 eV 0-66250  
 ZnP<sub>2</sub>, elec. cond., Hall effect, P interstitial effects 0-84465  
 ZnP<sub>2</sub> thin polycrystalline films for solar photovoltaic cells 0-97797  
 ZnP<sub>2</sub>-metal contacts, photoelectric props. 0-92930  
 ZnSb, orientated crystn. conditions during reaction diffusion (Russian) 0-70558  
 ZnSb, thermoelec. anisotropic semicond., carrier kinetics at low temps. 0-92893  
 ZrC-C composite system, negative magnetoresist. 0-60008  
 ZrS<sub>3</sub>, excitonic transition, reson. Raman spectra, Franck-Condon factors 0-97252  
 ZrS<sub>3</sub>, photolum. from excitons 0-66274  
 ZrS<sub>3</sub>, quasi one-dimens. semicond., elec. transport props. 0-107790  
 ZrSe<sub>2</sub>, photo-intercalation: possible application in solar energy devices 0-108803

## semiconductor-metal boundaries

- see also Schottky-barrier diodes  
 [CC] Ag-(100)InP, metal-semicond. cathode contact, metallurgical, physical, chemical processes 0-107911  
 contact, frequency relationships of photocurrent and photo-EMF (Russian) 0-107908  
 contact investigation by photoelectron spectroscopy 0-100517  
 contact resistance and resistivity meas. 0-105672  
 convergent beam electron microscopy obs. 0-108689  
 degenerate semiconductor-metal Schottky barriers, low temp. capacitance 0-60075  
 diffusion barrier formation, Au film, using laser annealing 0-80373  
 disordered interface, supercond. transition temp. enhancement by bipolaron interface centres 0-84528  
 electronic cond., temp. depend. review 0-59975  
 interfacial film effects on elec. characts. of metal-semiconductor contact 0-96969  
 interfacial reaction, AES study (Japanese) 0-96701  
 lead phthalocyanine:O<sub>2</sub>(I), Schottky barrier effect on AC current response 0-75623  
 metal silicide formation, induced by scanning CW laser, reaction rates, analytical model 0-66334  
 ohmic contact props., factors affecting contact resistance of semiconductors, theoretical model 0-60076  
 photoelectron injection, quantum mech. transmission and optical phonon scatt. 0-84511  
 polariton propagation between semiconductor-metallic screen interface (Spanish) 0-84510  
 polyacetylene-Au, ohmic contact (Japanese) 0-96888  
 quasi-monopolar semiconductors, I/V characts., effect of weak diffusion with metal contacts 0-70824  
 Schottky barrier junction, characterisation and appl. 0-92971  
 Schottky barrier junction, fabrication aspects 0-88632  
 Schottky-barrier diodes, resonant tunnelling spectroscopy, deep centre detection 0-96968  
 n<sup>+</sup>-Si-Al ohmic contacts, metallisation structs. for very shallow n<sup>+</sup>/p junctions 0-60084  
 silicide Schottky barriers, elemental description 0-60085  
 surface barrier structures, two-photon photoelec. effect 0-88594  
 Ag-InP interface, AgP<sub>2</sub> formation during sintering 0-65309  
 Ag-Si interfaces, solar cell contacts 0-92973  
 Al-amorphous Ge-nSi, photoelectric props. 0-70822  
 Al<sub>1-x</sub>Ga<sub>x</sub>-Sb solid soln., electrochem. deposition of Ni and Pd 0-93505  
 Al<sub>1-x</sub>Ga<sub>x</sub>-Sb-Pd contacts, struct., preparation elec. props. 0-65684  
 Al<sub>1-x</sub>Ga<sub>x</sub>-Sb-Pd contacts, band gap depend. of barrier height 0-65685  
 As-Te-Si-Ge amorphous chalcogenide semiconductor, thin film interface, elec. charact. (Korean) 0-97014  
 As<sub>2</sub>Se<sub>3</sub>-Ag photosensitive semiconductor-metal systems, effect of AsS<sub>3</sub> barrier layer (Russian) 0-62777  
 Au/GaSb (110) interface, heat-treated, struct. and chem. state, angle-resolved XPS 0-97400  
 Au/ZnSe:Mn/n-GaAs low threshold thin film DC electrolum. cell, pulse-excited characts. 0-76081  
 Au-Al/GaAs interfaces, atomic interdiffusion, soft XPS studies 0-65302  
 Au-Ga<sub>1-x</sub>Al<sub>x</sub>As Schottky diodes, band struct. from I-V, C-V meas. 0-96989  
 Au-Ga<sub>1-x</sub>Al<sub>x</sub>Sb Schottky barriers, barrier height 0-96986  
 Au-GaAs Schottky barrier solar cells, effect of interfacial oxide layer on cell characts. 0-61365  
 Au-n-Ga<sub>1-x</sub>Al<sub>x</sub>As-n-GaP narrow-band variable-gap surface-barrier photo-detector 0-96944  
 Au-Si interface, critical Au-film thickness obs. for room temp. interfacial reaction 0-75390  
 Au-Si interface, electron energy loss and AES meas. 0-89096  
 Au-Si thin film double layer, silicide form., electron diff. study 0-80005  
 Au-W-GaAs Schottky barrier, elec. and chem. props., AES 0-96973  
 CdGa<sub>2</sub>S<sub>4</sub> double surface-barrier diodes, current-voltage characts. 0-92972  
 Cd<sub>0.175</sub>Hg<sub>0.825</sub>Te-Au(In) contacts, photo-effect in the 77-300K range, barrier height estimation 0-107850  
 CdS-Al(Au) interfaces, bonding and interdiffusion, XPS obs. 0-80000  
 CdS-Au contacts, electronic states, vacuum UV photoelectron spectra 0-70827  
 CdS-Au contacts, electronic states, vacuum UV photoelectron spectra 0-70827  
 CdSnAs<sub>2</sub>-Au(Al), surface barrier junction, elec. props., temp. depend. 0-65686  
 p-CdTe, barrier heights of metals on etched surface 0-80378  
 CdTe-Au contacts, electronic states, vacuum UV photoelectron spectra 0-70827  
 CdTe-Au(In) contacts, photo-effect in the 77-300K range, barrier height estimation 0-107850  
 Co-Si interface, glassy layer, ellipsometric charact. 0-103589  
 Cr-Si interfaces, metallurgical and electrical props. 0-60081  
 Cu-CuGaSe Schottky barriers, electrical and photovoltaic props. 0-92940  
 Cu-n-Si diodes, fabrication by electroless deposition method, characts. 0-100520



## semiconductor-metal boundaries continued

- Ga<sub>1-x</sub>Al<sub>x</sub>As, intervalley energy gaps, temp. junction, exptl. determ. using metal-semicond. contacts 0-80179
- GaAs (110), with Al or Ga overlayers, interfacial electron states, UPS and LEED obs. 0-80377
- GaAs, alloying with Au and Au alloy ohmic contact metallisations, SEM and optical study 0-70820
- GaAs ohmic contacts with Au-Ge, SEM and TEM obs. of struct. 0-100522
- GaAs, Schottky barrier electronef. meas. by sample rotating technique 0-60544
- p-GaAs, Schottky barriers on polar (111) and (111) surfaces 0-88631
- GaAs Schottky diode, influence of  $\gamma$ - and electron irradiated on recomb. characts. near GaAs surface 0-71478
- GaAs:Se ohmic contacts, pulsed electron beam annealing donor density, mobility 0-65678
- GaAs/Au-Ge-Ni alloy metal-semiconductor thermoelectric coolers, effects of contact resist. and dopant conc. 0-81481
- GaAs/metal contacts, recent developments in investigations of preparation and props. (French) 0-107909
- p-GaAs/rare earth metal contacts, surface pot. barrier 0-60086
- GaAs-Au polycrystalline Schottky barriers, transition with grain size from electrode-limit to bulk-limited cond. 0-65676
- GaAs-Au(Ag) Schottky barrier solar cells, interface problems, AES, SIMS and XPS study 0-89627
- GaAs-metal contacts, use of Ga to eliminate large As loss peaks 0-80370
- n-GaAs-metal Schottky barrier, ultrathin native oxide, thickness determ. from C-V and photoresponse meas. 0-70821
- GaInAsP, rectifying and ohmic contacts 0-80376
- p-Ga<sub>1-x</sub>In<sub>x</sub>PyAs<sub>1-y</sub>/Au-Zn, specific contact resist. 0-84509
- n-GaP, Schottky barrier height data for several contact systems 0-60080
- p-GaP, Schottky barriers on polar (111) and (111) surfaces 0-88631
- GaP-Pd contact system, low temp. alloyed contact formation 0-100519
- Ge-metal interface, internal photoemission mechanisms 0-60077
- Ge-metal Schottky barrier photodetectors, near IR interband transitions and optical parameters 0-73449
- n-Ge-metal Schottky barrier contacts, IR optoelectronic props., quantum detector appls. 0-75640
- Hg-InP Schottky-barrier diode, contact times, I-V characts. 0-96971
- Hg<sub>1-x</sub>Cd<sub>x</sub>Te-In contact, diffusion of In 0-103520
- p-InP, ohmic contact using Be-Au metallisation, low contact resist. 0-65677
- InP-Al interface struct., low temp. interaction, AES study 0-107661
- InP-Cu contact system, low temp. alloyed contact formation 0-100519
- InSb-Au contact system, low temp. alloyed contact formation 0-100519
- Ni/GaAs film contact system, alloying reaction 0-96747
- Ni-Si(111), interface, reactivity and struct., ion channelling meas. 0-92788
- Pb-CdS-In junctions, Josephson effect through 0-100558
- Pb<sub>1-x</sub>Ag<sub>x</sub>(Au)(Cu), light sensitive, internal photoelectric emission 0-107910
- PbS<sub>1-x</sub>Se<sub>x</sub> diode laser, contact degradation due to diffusion 0-102734
- Pb<sub>1-x</sub>Sn<sub>x</sub>Te diode laser, contact degradation due to diffusion 0-102734
- PbTe-In contacts, fabrication and props. 0-60078
- Pd coated Si wafers, interference effects on irradi. with laser beam 0-66333
- Pd-Si structure, epitaxial silicide growth, LEED and AES study 0-103590
- Pt-Cr, shallow silicide contact 0-70819
- Pt-Si:As, silicide form. during laser irradi., p-n junctions and ohmic contacts 0-84397
- n-Si, bipolar ohmic contact with macroscopic recomb. centres. 0-80379
- Si, ion implantation, channelled, through metal silicide film 0-70231
- Si, polycrystalline-metal contacts, minority carrier injection 0-103750
- Si polycrystalline-metal Schottky barrier solar cells, elec. and photovoltaic contact props. 0-93936
- Si solar cells, all-plate low cost contact system 0-93992
- Si solar cells, Ni-Cu conductor system 0-93991
- Si:H, amorphous, Pt film growth, AES and LEED study 0-88447
- Si:H, amorphous, Schottky diodes, elec. props., light-induced effects 0-103741
- Si/Al and Si/Al-Si(Cu), Si regrowth minimisation through overlying Al or Al alloy film 0-70569
- p-Si/rare earth metal contacts, surface pot. barrier 0-60086
- Si/refractory metal-Ni(Pd)(Pt) interactions, phase separation 0-65303
- Si-Al, current-voltage characts., oxide film effects 0-70841
- p-Si-Al, ohmic contacts, Si dissoln. and recrystn. effects, computer calc. 0-103749
- Si-Au, interface study using EELS 0-97391
- Si-CoSi<sub>2</sub>, double heteroepitaxy, solid phase and MBE 0-104063
- n-Si-Cu Schottky contacts, electrochem. deposition, barrier height and ideality factor 0-75641
- Si-metal contact, transport theory of Schottky barriers 0-80372
- Si-metal contacts, analytical techniques, review 0-80120
- Si-metal interface, silicide formation, interface marker technique obs. 0-59734
- Si-Mo sputtered contacts, contact resistance 0-92970
- Si-Mo substrate-film interface, reaction on heat treatment, silicide formation 0-79999
- Si-Pb heterojunction, RHEED, Mossbauer spectroscopy and I-V characts. 0-70828
- n-Si-Pd diodes, chemical reduction process for fabrication 0-60082
- n-Si-Pd:Si contact, interface struct. and Schottky barrier height, correl. obs. using TEM 0-100504
- Si-Pd<sub>1-x</sub>Si<sub>x</sub>, amorphous, Pd<sub>2</sub>Si layer form., shallow contact 0-103586
- Si-Pd-Ti, silicide form. in evaporated films 0-80006
- Si-Pt Schottky barrier, laser formation and characts. 0-60079
- n-Si-Re(Os) Schottky contact barrier height meas. 0-65675
- Si-refractory metal contacts, thermally cleaned surfaces 0-100521
- Si-refractory metal structs., interface modification by ion implantation 0-70475
- Si-Sn heterojunction, RHEED, Mossbauer spectroscopy and I-V characts. 0-70828
- SiH<sub>4</sub>, amorphous films, internal photoemission, metal contacts 0-96964
- T-metal, thin film contact, time evolution of photovoltaic effect 0-65687
- Te-Ag, thin film system, stress-relief appearance conditions 0-65416
- Te-Se-Cd, sandwich structure, fabrication and characteristics 0-60089
- Te-Se-Cd rectifying sandwich structs., elec. forming action, Schottky junction form. 0-80371
- W-EuS, amorphous, memory effect in field emission 0-89126
- Zn<sub>3</sub>P<sub>2</sub>, evaporated metal contact barrier heights 0-80375

## semiconductor-metal boundaries continued

- Zn<sub>3</sub>P<sub>2</sub>-metal contacts, photoelectric props. 0-92930
- ZnSe, low resistance ohmic contacts using In-Ga liquid alloy, LED fabrication appl. 0-70823
- ZnTe single crystal, Schottky-barrier diodes and ohmic contacts props. 0-96987
- semiconductor-metal transition *see electrical conductivity transitions; metal-insulator transition*
- semiconductor processing *see semiconductor technology*
- semiconductor storage devices  
*see also integrated memory circuits*  
MNOS p-channel transistor, memory characts., H<sub>2</sub> anneal effects 0-80388
- semiconductor switches  
chalcogenide glasses, memory effect, local doping, switching 0-107873  
diodes, thin film glass based structures, surface electron states effect on switching (Russian) 0-107887  
p-n-insulator metal switching devices, avalanche mode operation 0-70838  
Ag-Sb thin film, switching and Ag movement, point contact technique 0-60107  
EuS, amorphous, on W, memory effect in field emission 0-89126  
Ge-S-Ga amorphous thin film, memory switching effects 0-88605  
Si/In<sub>2</sub>O<sub>3</sub>-SnO<sub>2</sub> thin film junctions, polarity dependent memory switching effects 0-70814
- semiconductor technology  
*See also under specific device headings*  
*see also semiconductor doping; semiconductor growth*  
amorphous Si preparation, hydrogenated 0-80956  
boundary layer theory application, introduction 0-66431  
contactless measurement of sheet conductivity and mobility of semiconductor wafer by using eddy current 0-62693  
crystal growth and defects, appl. of analytical techniques for observation 0-73546  
dielectric-isolated substrates, deform., and control by multilayer poly Si support struct. 0-107681  
diffusion barrier formation, Au film, using layer annealing 0-80373  
electronic material and device characterisation using surface-sensitive analytical techniques 0-65341  
n-GaAs-Ge laser alloying to from ohmic contacts 0-58546  
high dose Sb ion implantation, buried layer appls. 0-88186  
history, solid state research to semiconductor electronics 0-68015  
III-V semiconductor-based layered multielectronic systems, electronic process investig. survey (Russian) 0-107891  
inert gas ion milling processes, etch-rate ratio of oxides to nonoxides, increase using halocarbon gases 0-93663  
ion beam, plasma and reactive ion etching 0-108621  
ion implantation with controlled nonuniformity 0-100261  
ion milling, string segment motion algorithm 0-71779  
LAMEL activities (Italian) 0-60026  
large monocrystal X-ray reflection/scanning and transmission topographic methods 0-96415  
laser applications in materials processing, seminar, San Diego, CA, USA (Aug. 79) 0-90609  
LPCVD-type plasma-enhanced deposition system [for semiconductor wafer processing] 0-60791  
metal-semiconductor Schottky barrier junctions, fabrication aspects 0-88632  
metal-semiconductor thermoelectric coolers, effects of contact resist. and dopant conc. 0-81481  
microelectronics, conf., Calcutta India (Jul. 79) 0-96755  
MOS structures, radiation-induced positive charge, thermal annealing 0-75648  
MOSFET, near-ideal Si-SiO<sub>2</sub> interfaces using CVD, props. 0-80382  
multilayer ellipsometry, layer thickness and refr. index determination of layers 0-95121  
narrow double-current-confinement channelled-substrate-planar laser fabrication by double etching 0-64073  
ohmic contacts to semiconductor, meas. of contact resistance using transmission line model 0-70826  
optoelectronic devices development 0-91902  
packaging hermetically sealed, moisture calibration and anal. by gas mass spectrometry 0-90928  
production processes, vacuum technique problems (German) 0-86330  
purification, by electrodiffusion in mag. field, GaAs epitaxial film appl. 0-66409  
solar cell fabrication, laser-induced p-n junction formation 0-93880  
solar cell fabrication, Si wafer prep., anti-refl. coatings and metallisation, efficiency (Spanish) 0-72059  
solar cells, degradation processes of electrophysical characts. during long-term operation 0-89617  
solar grade Si economic commercial production, problems in cost reduction (Spanish) 0-72058  
solar-cell grade Si prod., recent developments, low-cost processes (Spanish) 0-72061  
spreading-resistance meas. for doping profile determ., preprocessing of data for resistivity calcs. 0-57265  
superlattice structures of semiconductor thin films, laser appl. 0-100418  
thin sample etching for electron microscope exam. 0-86272  
wafer exposure camera, optical, step-and-repeat, with-dark field automatic alignment 0-68283  
X-ray lithography using synchrotron radiation, resist sensitivity 0-62820  
Al plasma etching, undercutting phenomena 0-97635  
CdTe-CdS heterojunctions, growth by closed-tube chem. transport, elec. props. 0-60070  
Cr films, photoresist film on reverse gas plasma etching 0-97634  
GaAlAs injection DH laser and GaAs Schottky-gate FET, monolithic integration 0-58593  
GaAs, laser-induced microscopic etching 0-76379  
GaAs:Cr,Se, ion-implanted, semi-insulating effects of Cr redistrib. on elec. characts. 0-59982  
GaAs(Sb), electrochemical sectioning and surface finishing 0-108611  
InP, laser-induced microscopic etching 0-76379  
p-type InP/Langmuir film MIS diodes, characts. 0-80384  
Ni-Cr/Au films, interdiffusion processes and oxidation phenomena 0-59735  
Si device metallisation, TiN and TaN as diffusion barriers 0-65304  
Si, dislocation generation in local oxidation 0-107245  
Si epitaxial wafer, saucer pit microdefects reduction by intrinsic gettering 0-75450



**semiconductor technology continued**

- Si, etching characts. using reactive ion etching with tetrafluoromethane-  
Cl<sub>2</sub> gas mixture 0-104313  
Si, gettering by ion damage, minority carrier lifetime and backscatt. study  
0-100286  
Si, ion implanted, scanning CW and pulsed laser annealing 0-92549  
Si ion-implanted laser-annealed solar cells 0-93881  
Si, joining and recrystallisation using thermomigration process 0-65298  
Si polycrystalline films, characts. 0-80988  
Si processing technology, appls. of scanning CW lasers and electron beams  
0-100932  
Si, reactive ion beam etching expts., selectivity, anisotropy 0-104308  
Si single crystals., mech. polishing with reagent, activation energy effects  
(*Japanese*) 0-89379  
Si, solar cells, prospects (*Italian*) 0-60024  
Si surface formation during etching of thin thermally grown oxide layers,  
ellipsometric control (*Russian*) 0-104315  
Si, surface treatment by the low-energy ions of plasma accelerators  
0-97608  
Si, V-grooves formed by etching, phosphosilicate glass bridge struct.  
0-104312  
Si wafers, saw damage reduction in lubricant environment 0-108585  
Si:P implanted, multicunning electron beam annealing 0-75242  
SiN<sub>x</sub> films, plasma enhanced CVD, props., meas. and interpretations  
0-80987  
SiN<sub>x</sub> films, plasma-deposited, radial wafer-to-wafer uniformity 0-104073  
SiN<sub>x</sub> films plasma deposition, process and props. 0-80986  
Si<sub>3</sub>N<sub>4</sub>(SiO<sub>2</sub>) plasma etching, plasma processes involved in dry processing  
using CF<sub>4</sub> active etchant species 0-79581  
SiO<sub>2</sub>, HF vapour phase etching, prod. viability for semicond. manufactur-  
ing and reaction model 0-81219  
SiO<sub>2</sub>, masking film in alkaline etching 0-71771  
SiO<sub>2</sub>, plasma-chemical etching, spectroscopy 0-85243  
SiO<sub>2</sub>, reactive ion beam etching expts., selectivity, anisotropy 0-104308  
SiO<sub>2</sub>, relief, plasma etching, tapered wall prod. 0-97606  
SiO<sub>2</sub>, separation below 500°C, state and tendency of chemical gas phase  
separation (*German*) 0-100794  
SiO<sub>2</sub> thin films, radiation-induced trapping centres, rel. to MOS transistor  
technology 0-107804  
YAG laser trimmer for wafer level products 0-87428  
ZnSe, low resistance ohmic contacts using In-Ga liquid alloy, LED  
fabrication appl. 0-70823

**semiconductor thin films**

- for electronic conduction in crystalline and amorphous films, see "elec-  
tronic conduction in crystalline semiconductor thin films" and "electrical  
conductivity of amorphous semiconductors and insulators", respectively  
see also amorphous semiconductors; semiconductor epitaxial layers  
amorphous semiconductor film, laser induced nucleation, long wavelength  
instability 0-84126  
CdTe thin film on ferroelectric TGS, influence of polarisation reversal on  
elec. cond. 0-65720  
chalcogenide glass films, threshold switching 0-96950  
chalcogenide glasses, photoconductivity dependences applied elec. field  
0-107857  
conference, Masnuy-St-Jean, Mons, Belgium, Oct. 1979 0-82570  
conference, New York, USA (Oct. 79) 0-73093  
confining substrate for micron thick liquid films, semicond. films  
0-96722  
diodes, thin film glass based structures, surface electron states effect on  
switching (*Russian*) 0-107887  
energy spectrum in mag. field, size effect, calc. 0-70865  
enhanced conductivity in plasma hydrogenated films, thermionic emission  
0-70692  
exciton light absorption coefficient (*Russian*) 0-71504  
ferroelectric properties, quantum size effect 0-97201  
III-V semiconductor based layered multielectronic systems, electronic  
process investig. survey (*Russian*) 0-107891  
III-V semiconductor thin film prep. by low temp. CVD 0-60789  
inhomogeneous thin amorphous chalcogenide films, reversible switching,  
thermal stability criteria 0-70856  
ion beam milling, amomalous sputter yield behaviour 0-108624  
ion-implanted, laser pulse annealing, TEM and channelling study  
0-100264  
laminar piezoelectric-dimensionally quantised semiconductor film struct.,  
acoustoelectronic effects 0-75607  
laser crystallisation, for production of large grained sheets for solar cells  
0-93570  
lead phthalocyanine:O<sub>2</sub>(I), Schottky barrier effect on AC current response  
0-75623  
magnesium phthalocyanine, depletion layer studies, temp. depend. of LF  
capacitance 0-65617  
microelectronics, conf., Calcutta India (Jul. 79) 0-96755  
microelectronics and thin film components frontiers 0-73123  
multilayer systems, film growth, spectroscopic ellipsometry, review  
0-103603  
multilayer thin film struct. thermolec. props. 0-92964  
oblique cut production by etching 0-104309  
optical coatings, photoacoustic spectroscopy study 0-64124  
optical properties of polycrystalline semiconductor films, grain boundary  
effects 0-80890  
organic, Schrieffer effect 0-60118  
polar semiconductor crystalline thin films, surface vibr. states, IR absorpt.  
spectra obs. (*Russian*) 0-60606  
polaron near-threshold spectrum 0-65471  
polyacetylene, and derivatives, thin polycryst. film, solar cell applie.  
0-92899  
polycrystalline film, photocond. probe studies 0-80326  
polymethine semiconductor films, surface photovoltage 0-70857  
review (*Japanese*) 0-107936  
sapphire film, substrate for Si, laser annealing non-thermal theory expt.  
test 0-89273  
semiconductor thin films, ion implanted, optical and luminesc. props.  
0-60699  
spectrochemical analysis of film on dielec. backing 0-66904  
sulphide black, on Al, solar selective coating, figure of merit 0-72082  
superlattice structures and properties 0-100418  
TEM 90° cross-section and 1° angle-lap specimen prep. 0-71881  
tetracene, depletion layer studies, temp. depend. of LF capacitance  
0-65617  
thin film heterostructure, energy spectrum study 0-70787

**semiconductor thin films continued**

- TTT film, Schrieffer effect 0-60118  
US propagation in quantised elec. field (*Russian*) 0-60050  
zero gap semiconductor, thin layer, dielec. response 0-103635  
[α]-SiC:H, prepared by reactive sputtering, layer props. (*Japanese*)  
0-60695  
AgInS<sub>2</sub> and AgIn<sub>2</sub>S<sub>3</sub>, spray pyrolysis, film struct., elec. and optical props.  
0-71592  
Ag<sub>2</sub>Se thin film, switching and Ag movement, point contact technique  
0-60107  
Al-amorphous GeSe-Al junctions, electrical contact effects on properties  
(*German*) 0-93010  
Al<sub>x</sub>Ga<sub>1-x</sub>As, electron mobility illumination, compensation, space charge  
regions, carrier scatt. 0-70691  
p-Al<sub>x</sub>Ga<sub>1-x</sub>As film, variable-gap photo-EMF 0-65626  
AlN film, oriented c-axis, low temp. deposition by reactive magnetron  
sputtering 0-76180  
AlN films on glass substrate, prep. by reactive DC magnetron sputtering  
technique, c-axis orientation 0-89146  
AlSb, laser pulse annealing, induced nucleation, crystal growth 0-84966  
AlSb, thin film growth on insulating substrates, by metal organics CVD  
0-60786  
As-Se-Ge(-S), photostructural change in Urbach tail 0-76021  
As-Se-S-Ge chalcogenide amorphous film, computer-generated holograms  
using electron beam irradi. 0-95846  
As-Te-Si-Ge amorphous chalcogenide semiconductor, thin film interface,  
electrical charact. (*Korean*) 0-97014  
AsGe amorphous film, far IR absorpt. spectra, refractive index 0-80785  
As<sub>2</sub>S<sub>3</sub> and As<sub>2</sub>S<sub>4</sub> vapour-deposited films, valence states, thermal and  
photo-induced changes UPS study 0-93459  
As<sub>2</sub>S<sub>3</sub> chalcogenide glass films, photographic Ag photodoping to produce  
negative relief image 0-59490  
As<sub>2</sub>S<sub>3</sub>, evaporated, switching effects 0-96952  
As<sub>2</sub>S<sub>3</sub> film, amorphous, photo-induced dynamical changes 0-66142  
As<sub>2</sub>S<sub>3</sub> film, hologram recording using total-internal-refl., polarisation  
depend. 0-106491  
As<sub>2</sub>S<sub>3</sub> film, optical recording, light scatt. enhancement due to coherence  
0-97362  
As<sub>2</sub>S<sub>3</sub>-Ag glassy films, optical transmission spectra, photodoping effect  
0-66317  
As<sub>2</sub>Se<sub>3</sub> amorphous films, optical props. and photoinduced changes  
0-60700  
As<sub>2</sub>Se<sub>3</sub> glassy films, current-voltage characts., temp. depend., SCL current  
0-92902  
As<sub>2</sub>Se<sub>3</sub>-Ge glassy thin films, flash photoresponse 0-107863  
As<sub>2</sub>Te<sub>3</sub> and As<sub>2</sub>Te<sub>2</sub>Ge, amorphous, AC cond. at low temps. 0-80269  
Au-amorphous GeSe-Au junctions, electrical contact effects on properties  
(*German*) 0-93010  
Au-Si thin film double layer, silicide form., electron diffr. study 0-80005  
BP film, high temp. thermolec. power, scattering processes 0-80305  
Bi-Te thin thermoelectric films prep. by solid state reaction method  
0-108361  
BiI, film, exciton-phonon interaction, optical const., Faraday effect.,  
permitt. 0-59884  
Bi<sub>12</sub>SiO<sub>20</sub>, photoelectric props., obs., UV illumination effects (*Russian*)  
0-80313  
C:H films, amorphous, elec. props., chem. modifications 0-84523  
Cd chalcogenides, thin films, VPE, needle-like cryst. growth 0-80148  
Cd<sub>2</sub>As<sub>2</sub> film on NaCl substrate, vacuum deposition, growth morphology,  
microstructure 0-75479  
CdCr<sub>2</sub>Se<sub>4</sub>, energy structure, magnetoptoelectric effects 0-71394  
CdF<sub>2</sub>/NaF thin films, electroluminescence obs. at 77K (*French*) 0-80866  
Cd<sub>2</sub>Hg<sub>1-x</sub>Te films, growth by cathodic sputtering in Hg vapour plasma  
0-97431  
CdO, aqueous-deposited films, struct. and electronic props. for solar cell  
appls. 0-100797  
CdO-P<sub>2</sub>O<sub>5</sub> glass, thin film, elec. cond., high and low fields 0-80427  
Cd(S, Se) film grown on InP substrate, mismatch dislocations and lattice  
distortion, dangling bond density 0-84406  
CdS, aqueous-deposited films, struct. and electronic props. for solar cell  
appls. 0-100797  
CdS film spray fabrication, physical props., Cu<sub>2</sub>S-CdS solar cell applica-  
tions (*French*) 0-60113  
CdS films, chem. deposited, growth kinetics and polymorphism 0-75463  
CdS films, prep. by reactive pulverisation, chemical, crystallographic and  
electronic props. (*French*) 0-60112  
CdS, growth and evaluation for fabrication of high performance photovol-  
taic solar cells 0-93501  
CdS thin film solar cell fabrication, HCl etching 0-81474  
CdS:Mn, vacuum deposited film, Mn migration, EPR and X-ray study  
0-5411  
n-CdS/p-ZnIn<sub>2</sub>Se<sub>4</sub> thin film solar cell, photovoltaic props. 0-89628  
CdS-Cu<sub>2</sub>S junctions, carrier trap density, deep level defects 0-107801  
CdS(Se)(Te), vacuum deposited film, orientation axis tilt rel. to vapour  
angle of incidence 0-88456  
CdSe, chemically sprayed thin films as photoanode in photoelectrochem.  
cells, power charact. meas. 0-85293  
CdSe film photoanodes for electrochem. photovoltaic cells, fabrication and  
evaluation 0-76641  
CdSe film polycryst., thermal diffusion of Cr, 240-400°C 0-80001  
CdSe films, solar energy conversion using electrodeposited films for pho-  
toelectrochemical cell 0-94093  
CdSe, polycrystalline, for solar energy converters 0-93870  
CdSe thin film transistor on Cr substrate, cryst. struct., substrate defect  
effects 0-70563  
CdTe film, exciton spectra, press. and temp. depend. 0-80886  
CdTe film, photogenerated carrier transport props. 0-88590  
n-CdTe layers, growth and characterisation, heterojunctions and Schottky  
barriers fabrication (*German*) 0-89151  
CdTe:Cu films, impurity behaviour, Hall mobility and hole density meas.  
0-80420  
CdZnS, growth and evaluation for fabrication of high performance photo-  
voltaic solar cells 0-93501  
Cd<sub>1-x</sub>Zn<sub>x</sub>S solar cell thin films, microprobe characterisation (*French*)  
0-61349  
Cs<sub>2</sub>Sb vacuum deposited photoemitter, XPS study 0-89122  
CuBr(I), reflectance and thermorefectance spectra, electronic struct.  
0-71444  
CuGaTe<sub>2</sub>, refr. indices meas. 0-93259  
CuIn<sub>0.7</sub>Ga<sub>0.3</sub>Se<sub>2</sub> epitaxial layers, on GaAs substrates, struct. and elec.  
props. 0-107670



## semiconductor thin films continued

- CuInS<sub>3</sub> single phase thin film prep. by flash evaporation 0-100796  
 CuInSe<sub>2</sub> amorphous thin film, flash evaporation, struct., stoichiometry 0-89150  
 CuInSe<sub>2</sub>, refr. indices meas. 0-93259  
 CuInSe<sub>2</sub> thin film fabrication by RF-sputtering for solar cell appls. 0-100786  
 CuInSe<sub>2</sub> thin films, prep. by spray pyrolysis, struct., elect. and optical props. for solar cell appls. 0-100781  
 CuInTe<sub>2</sub> epitaxial layers, on GaAs, growth and props. 0-108359  
 CuInTe<sub>2</sub>, refr. indices meas. 0-93259  
 CuO, on Al or Cu, solar selective coating, figure of merit 0-72082  
 Cu<sub>2</sub>S films, prpe. methods, appl. to Cu<sub>2</sub>S-CdS solar cells 0-80980  
 Cu<sub>2</sub>S, on Cu, solar selective coating, figure of merit 0-72082  
 Cu<sub>2</sub>S-CdS solar cell fabrication by magnetron reactive sputtering deposition 0-61363  
 Cu<sub>2</sub>S-CdS thin film planar junction devices, quantitative photon loss anal. 0-61362  
 Cu<sub>2</sub>S-Zn<sub>1-x</sub>Cd<sub>x</sub>S solar cells, thin film photovoltaic solar energy conversion 0-61379  
 Cu<sub>2</sub>S evaporated layer growth in vacuum, compositional and optical characterisation, solar cell appls. 0-97437  
 Cu<sub>2</sub>S/CdS, sequential evaporation, for solar cell applic. 0-93902  
 EuO, light scatt. from spin waves and magneto-optic hysteresis meas. 0-97244  
 EuO nonstoichiometric film, ESR spectra and exchange interaction 0-93176  
 EuS, light scatt. from spin waves and magneto-optic hysteresis meas. 0-97244  
 $\alpha$ -Fe<sub>2</sub>O<sub>3</sub>, photochem. props. of sintered and doped samples for solar photoelectrochem. cell appls. 0-89651  
 Fe(OH)<sub>3</sub> thin films, elec. cond. var. with temp., amorphous struct. 0-75566  
 GaAs, amorphous layers, ion-implanted, low-temp. epitaxial regrowth 0-92790  
 GaAs base laminated epitaxial struct., surface plasmon phonon polaritons (Russian) 0-59905  
 GaAs epitaxial thin films with neg. electron affinity, photoelectron energy distrib. 0-100755  
 GaAs film, electron scatt., cathodoluminesc. meas., energy depend. of electron deposition depth determ. 0-104023  
 GaAs, polycryst. solar cells, thin film growth and grain size, effect on cell efficiency 0-81471  
 GaAs, polycrystalline films, meas. of effective diffusion length by SEM 0-80424  
 GaAs thin films, reactively sputtered, ESCA/XPS study 0-97430  
 GaAs:Se(Zn) polycrystalline film, Hall effect, resistivity meas. 0-96911  
 GaP films on Si, epitaxial crystallisation by nanosecond laser pulses 0-107674  
 GaSb film, polycrystalline, Hall mobility 0-97015  
 GaSe, far IR refractive index 0-80799  
 GaSe films, optical props. at lattice vibr. freqs., IR and Raman spectra 0-60696  
 $\epsilon$ -GaSe films, optical props. in IR region, metal substrate effect 0-71502  
 GaSe thin films, electroabsorpt. spectra, exciton line splitting 0-107716  
 Ge, amorphous, prepared by evap. or sputtering, AC loss meas. 0-65560  
 Ge amorphous film, crystn. front velocity during scanned laser crystn. 0-107662  
 Ge, amorphous film, DC sputter deposited, effect of trapped Ar on minimum temp. for impulse stimulated explosive crystallisation 0-100422  
 Ge, amorphous film, persistent photoconductivity, dangling bonds 0-84487  
 Ge amorphous films, structural relaxation and crystallisation 0-100170  
 Ge film bolometer, radiation loss from JFT-2 Tokamak, meas. 0-95141  
 Ge, laser pulse annealing, induced nucleation, crystal growth 0-84966  
 Ge thin films on glass substrates, annealing by Ar ion bombardment 0-80136  
 Ge:Al film strain gauges, press. sensor (Japanese) 0-105631  
 Ge:O, Cu, amorphous thin film, impurity effects on struct. 0-107054  
 Ge-Ga amorphous alloy, co-evaporated elec. and optical props. 0-70860  
 Ge-S-Ga amorphous thin film, memory switching effects 0-88605  
 Ge<sub>3</sub>As<sub>2</sub>S<sub>15</sub>Te<sub>25</sub>, chalcogenide thin films, coupled carrier theory test, high field conditions 0-100466  
 Ge<sub>2</sub>S<sub>58</sub>, amorphous, bulk and film forms, elec. props. and ESR study 0-103691  
 GeSe, amorphous, film, thermally induced effects, UPS study 0-104042  
 GeSe<sub>2</sub>, amorphous, film, thermally induced effects, UPS study 0-104042  
 GeSe<sub>2</sub>, amorphous film, laser induced oscillatory phenomena 0-84711  
 Ge<sub>2</sub>Se<sub>3</sub>Te amorphous layers, prep. and elec. props. 0-97436  
 Ge<sub>2</sub>Si<sub>10</sub>Te<sub>3</sub>Ga<sub>10</sub>, chalcogenide thin films, coupled carrier theory test, high field conditions 0-100466  
 Ge<sub>1-x</sub>Sn<sub>x</sub>Te film, amorphous, elec. cond. 0-93016  
 Hg<sub>0.74</sub>Cd<sub>0.25</sub>Te thin film deposition on Si substrates by RF triode-sputtering, large-area photodetector arrays 0-80965  
 HgSe film, anomalous photocond., electron microscope study 0-65623  
 In<sub>2</sub>O<sub>3</sub>:Sn, RF magnetron sputtered film, elec. and optical props. 0-104065  
 In<sub>1-x</sub>Ga<sub>x</sub>Sb films, elec. props., preparation 0-100473  
 InN film growth by reactive sputtering in Ar-N<sub>2</sub> discharge, mechanism 0-89107  
 In<sub>2</sub>O<sub>3</sub> films, electron beam evaporation, elec. and optical props. (Japanese) 0-60784  
 In<sub>2</sub>O<sub>3</sub>, thermally evaporated film, struct. and elec. props. 0-104066  
 In<sub>2</sub>O<sub>3</sub>, thin film, sputter deposition form., optical and elec. props. 0-60123  
 In<sub>2</sub>O<sub>3</sub>-InN film growth by reactive sputtering in N<sub>2</sub>-O<sub>2</sub> discharge, mechanism 0-89108  
 InP film, electron-beam annealed, surface conduction 0-84500  
 InP solar cells, thin film growth tech. and characterisation 0-89631  
 InSb, depletion layer, plasma and vibr. plasma type guided polaritons (Russian) 0-96933  
 InSb, films, X-ray fluoresc. anal. method, long-term stability 0-61212  
 InSb, Raman scattering study of unoxidised Sb in anodic oxide films 0-88985  
 InSb, thin films, electrophysical props. obs. 0-103765  
 InSe thin film, sputter growth and chem. anal. by XPS/ESCA 0-80976  
 In<sub>2</sub>Se<sub>1-x</sub>Sn<sub>2x</sub> amorphous film-SnO<sub>2</sub> system, photovoltaic spectra, annealing effect (Japanese) 0-92926  
 In<sub>2</sub>Si<sub>2</sub>O<sub>7</sub>, thin film, sputter deposition form., optical and elec. props. 0-60123  
 InTe thin films, flash evaporation, electrical props. 0-65722

## semiconductor thin films continued

- Mo-amorphous GeSe-Mo junctions, electrical contact effects on properties (German) 0-93010  
 p-Pb<sub>1-x</sub>Ge<sub>x</sub>Te film, cyclotron reson. above and below struct. phase transition 0-88879  
 PbO, reactively evaporated, photocond., H<sub>2</sub>O induced phase transform. 0-60122  
 PbS, chem. deposited thin film, effect of morphological struct. on photosensitivity 0-70760  
 PbS islands, vacuum deposited, electron microscope obs. 0-103601  
 PbS, polycryst., small-angle X-ray scatt. and electron density inhomogeneities 0-96758  
 PbS, vacuum deposited film, orientation axis tilt rel. to vapour angle of incidence 0-88456  
 PbS-Si heterojunction, space charge capacitance, PbSn film thickness depend. 0-88630  
 PbS-Si heterojunction, PbS film growth and struct. 0-96762  
 PbS(Se), valence band struct. determ. by optical absorpt., size quantization effects 0-59871  
 PbS<sub>1-x</sub>Se<sub>x</sub> thin film, stimulated emission, temp. depend. 0-66232  
 PbSe films, current carrier conc. and type control, elec. cond., synthesis process (Russian) 0-100412  
 Pb<sub>1-x</sub>Sn<sub>x</sub>Se epitaxial layers, radiative and nonradiative recomb. processes 0-60670  
 Pb<sub>1-x</sub>Sn<sub>x</sub>Se, X=0.03-0.07, monocrystal film, edge of intrinsic absorpt. (Russian) 0-71368  
 Pb<sub>0.8</sub>Sn<sub>0.2</sub>Te:La, evaporated thin films, low carrier conc. 0-65414  
 Pb<sub>0.82</sub>Sn<sub>0.18</sub>Te, effect of hydrostatic pressure on props. 0-70862  
 Pb<sub>0.82</sub>Sn<sub>0.18</sub>Te, layers on mica substrate, Hall constant peculiarities 0-75588  
 n-PbTe, noncubic (111) oriented epitaxial films, weak field magnetoresistance 0-75584  
 Pt-Si:As, silicide form. during laser irradi., p-n junctions and ohmic contacts 0-84397  
 Ru<sub>x</sub>Ti<sub>1-x</sub>O<sub>2</sub> films, percolation elec. cond. in strong electric fields (Russian) 0-84471  
 S-based amorphous semicond. film, prep. by plasma decomp. of H<sub>2</sub>S-N<sub>2</sub>-NH<sub>3</sub>, and characterisation 0-80422  
 Se, Ag diffusion, effect on interferometric thickness meas. 0-96695  
 Se, amorphous, influence of wavelength on optical quenching of photoconductivity 0-60046  
 Se, amorphous, localised states in band gap 0-59928  
 Se, amorphous film, dielec. activity obs. near glass transition temp. 0-75933  
 Se, amorphous film, highly disordered, UPS study 0-76148  
 Se, amorphous film, photocond., dark cond., rel. to crystn. 0-88596  
 Se, amorphous films, evaporated, ageing and crystn., DTA 0-65413  
 Se film, amorphous, empirical formula for temp. depend. of dielec. loss peaks 0-97197  
 Se, optical constants in visible region 0-97360  
 Se sphere monolayer, multiple EM wave scatt., migration imaging film appl. 0-99627  
 Se, thin film selective absorber coatings, prod. using an oblique vacuum deposition technique 0-81488  
 Se:As, amorphous film, dielec. activity obs. near glass transition temp. 0-75933  
 Se-Ge amorphous films, obliquely deposited, photoinduced chem. changes 0-76385  
 Se<sub>1-x</sub>Te<sub>x</sub>, amorphous, photo-crystallisation 0-59839  
 Se<sub>1-x</sub>Te<sub>x</sub>As<sub>20</sub>Ge<sub>10</sub> semiconductor amorphous films, field effect, trapping 0-84472  
 Si, amorphous, acoustic study using Rayleigh waves 0-75312  
 Si, amorphous, analytical techniques, review 0-80120  
 Si, amorphous, EELS microanalysis 0-100722  
 Si, amorphous, hydrogenated, electron drift mobility meas. 0-75565  
 Si, amorphous, hydrogenated preparation by SiH<sub>4</sub> decomposition 0-80956  
 Si, amorphous, hydrogenated film, electroreflectance study 0-88967  
 Si, amorphous, sputtered, resist. control by ion implantation 0-100262  
 Si, amorphous evaporated, picosecond optoelectronic detect., sampling and correlation meas. 0-100478  
 Si amorphous film, anisotropic etching phenomenon, appl. as solar selective absorber surfaces 0-72054  
 Si, amorphous film, glow discharge deposition, rate enhancement by mag. field 0-65412  
 Si, amorphous film, RF plasma deposition from SiCl<sub>4</sub>-H<sub>2</sub>, characterisation 0-66435  
 Si, amorphous film, selective laser recrystn. over heavily doped lines 0-84947  
 Si, amorphous film, TSC, density of localised states distrib. 0-65587  
 Si, amorphous films, halogenated and hydrogenated, elec. and optical props. 0-97016  
 Si, amorphous films, RF sputtering prep. at high Ar press., props. obs. 0-80418  
 Si amorphous films, switching, electrothermal model 0-80407  
 Si, CVD amorphous films, effect of surface characts. on visible and UV optical props. 0-60698  
 Si deposition using solar furnace 0-89148  
 Si film, amorphous, glow discharge deposited, for low cost solar cells 0-61355  
 Si film, amorphous, hopping cond. control by ion bombard. induced struct. modification 0-92898  
 Si film, low press. CVD prep., struct., elec. and optical props. 0-70548  
 Si film, polycryst., grain struct. and surface roughness, TEM study 0-70556  
 Si film, polycryst., laser-induced CVD growth from SiCl<sub>4</sub> 0-84852  
 Si films, electron beam evaporated, for MIS solar cells 0-93490  
 Si films, RF sputtered, Ar conc. as function of operation frequency and discharge pressure 0-65393  
 Si films, ribbon-against-drop process, physical and chemical characterisation 0-92798  
 Si, ion bombarded, crystalline-to-amorphous transition, defect-rich film prep. 0-65071  
 Si large grain films on metallurgical Si substrates, chem., struct., elect. and photovoltaic props. 0-61357  
 a-Si, laser induced crystallisation mechanism, epitaxial regrowth 0-84962  
 Si noncrystalline film, struct., interatomic distances, SRO 0-107053  
 Si, on sapphire, quality determ. using IR and UV specular reflectance meas. 0-108684  
 Si photoconductive films, amorphous, undoped, I-V characts. of vacuum deposited films 0-60049

**semiconductor thin films continued**

- Si, polycryst., energy distrib. of trapping states, from impedance of MOSS struct. 0-65691  
 Si, polycryst., layer structure dependence on carrier gas moisture and O<sub>2</sub> content (*Bulgarian*) 0-59811  
 Si, polycrystalline, As segregation at grain boundaries, elec. props. meas. 0-75259  
 Si polycrystalline film, effect of defects/grain boundaries on photovoltaic mech. 0-93883  
 Si, polycrystalline films, meas. of effective diffusion length by surface photovoltage method 0-80424  
 Si, polycrystalline self-supporting, thermal expansion shear separation technique, solar cell appl. 0-81439  
 Si, polycrystalline structure stability, stacking defects, twins grain struct. (*Russian*) 0-100248  
 Si, prod. of polySi vapour deposited coatings for solar cells, cost anal. 0-93495  
 Si solar cells, fabrication using continuous or pulsed lasers (*French*) 0-61350  
 Si solar cells, perform. parameters of amorphous and polycryst. thin film cells 0-93882  
 Si solar cells, polycrystalline, from recrystallized plasma deposited thin films 0-104509  
 Si:Al, polycryst. film, grain boundary diffusion, Auger sputter profiling 0-75388  
 Si:Au, O(H), film, amorphous, elec. cond. meas. 0-80423  
 Si:B, use of BN source to achieve high surface concentration of B (*Russian*) 0-107639  
 Si:B ion implanted layers, light refl. and transmission coeffs., computer program 0-66316  
 Si:F, amorphous, heat resistant, prep., elec. cond., IR absorpt., annealing 0-65719  
 Si:H, amorphous, sputtered on Gd<sub>2</sub>(MoO<sub>4</sub>)<sub>3</sub>, ferroelec. domain wall motion, image scanning 0-83663  
 Si:H, amorphous Schottky solar cells, prep. and characts. of diode RF reactive cathodic sputtered films (*French*) 0-61347  
 Si:H, amorphous thin film, ion plating, IR absorpt. meas. 0-84857  
 Si:H, amorphous thin film solar cells 0-81478  
 Si:H,P amorphous film, elec. cond., thickness and temp. depend. 0-65559  
 a-Si:H alloys, sputter deposited thin film coatings, property-comp. relationships 0-80975  
 Si:H amorphous films, conductivity and temp. dependence of optical gap 0-100462  
 Si:H amorphous films, ESR, optical gap and elec. cond. meas. 0-75842  
 Si:H amorphous films, IR spectrum and struct. 0-97277  
 Si:H film, amorphous, H-associated disorder modes, PMR spin-lattice relax. time meas. 0-93202  
 Si:H film, amorphous, plasma-deposited, small angle X-ray and neutron scatt. studies 0-59826  
 a-Si:H film, glow discharge deposited, H profiles, doping level 0-84202  
 Si:P, polycrystalline laser recrystallised film on Si substrate, cryst. struct., thermal oxidation 0-65391  
 Si:Sb vacuum deposited coating, p-n junction, pulsed electron beam annealing doping, diffusion 0-75480  
 Si/Pd system, solid phase epitaxial growth control by C ion implantation 0-75466  
 Si-Al-Al<sub>2</sub>O<sub>3</sub> system, solid phase Si regrowth on sapphire 0-100413  
 Si-F-H:P, film, dark cond., struct., Raman scatt. 0-88588  
 Si-H, amorphous, sputtered, photolum. obs. 0-80856  
 Si-H:P amorphous film, dark cond., struct., Raman scatt. 0-88588  
 Si-metal contact, transport theory of Schottky barriers 0-80372  
 Si-Pd-Si structure, epitaxial growth, backscattering and transmission electron microscopy studies of layered structures 0-80123  
 Si-Si<sub>3</sub>N<sub>4</sub>-SiO<sub>2</sub>, non absorbing double layers, optical parameters reflectivity by liquid immersion method 0-71503  
 $\beta$ -SiC form. on Si substrate in RF powered reactor 0-76173  
 SiC:H amorphous reactively sputtered film, H content effect on film props. 0-75459  
 Si<sub>1-x</sub>C<sub>x</sub>H glow discharge films, local atomic struct., XPS and AES study 0-93448  
 Si<sub>1-x</sub>C<sub>x</sub>H, amorphous, H content determ. by nuclear reaction analysis 0-59821  
 Si<sub>1-x</sub>C<sub>x</sub>H, film, H content determ. by nuclear reaction analysis 0-59821  
 SiH<sub>4</sub>, amorphous, H content determ. by nuclear reaction analysis 0-59821  
 SiH, film, H content determ. by nuclear reaction analysis 0-59821  
 Si<sub>1-x</sub>H<sub>x</sub>Al, amorphous, co-sputtered Al modification, electronic and optical props. 0-100461  
 SnO<sub>2</sub> films, selective, optical characterisation by thermodynamical method 0-84796  
 SnO<sub>2</sub> gas sensor, fast-detecting, prep. 0-61497  
 SnO<sub>2</sub>, O chemisorption, elec. cond. and EPR meas. correlation 0-84369  
 SnO<sub>2</sub> thin films, O<sub>2</sub> vacancy diffusion 0-107467  
 SnO<sub>2</sub>:P, CVD growth and etching characts., doping effects 0-107667  
 SnO<sub>2</sub>:Sb, amorphous, electrotransport phenomena obs., under DC electric field 0-59840  
 SnO<sub>2</sub>:Sb film on glass substrates, elec. props. 0-88652  
 SnO<sub>2</sub>:Sb sprayed film, growth mechanism and cryst. struct. 0-89143  
 SnO<sub>2</sub> films, passivation effect on Si solar cells 0-61360  
 T-metal, thin film contact, time evolution of photovoltaic effect 0-65687  
 Te film, stability in moist air, rel. to information storage capability, atmospheric corrosion model 0-71774  
 Te film, surface morphology depend. on vacuum deposition angle 0-103553  
 Te, oriented films, semiconducting props., Hall coeff., band structure 0-70854  
 Te, thin film selective absorber coatings, prod. using an oblique vacuum deposition technique 0-81488  
 Te, vacuum deposited, growth and morphology of crystals 0-96766  
 Te-Ag, thin film system, stress-relief appearance conditions 0-65416  
 Te-Bi thin film system, stress-relief appearance conditions 0-65416  
 VO<sub>2</sub>, V<sub>2</sub>O<sub>5</sub> and V<sub>2</sub>O<sub>3</sub>, film prep. under equil. conditions, struct. and elec. props. 0-108352  
 V-O, amorphous film, photochromism and thermochromism 0-93254  
 V-O, amorphous layers, gel deposited, semicond. props. 0-92887  
 Zn chalcogenides, thin films, VPE, needle-like cryst. growth 0-80148  
 Zn-In-S thin layers, ternary phases, optical props. near long-wavelength intrinsic absorpt. edge 0-80887  
 Zn,Cd<sub>1-x</sub>S, optimal synthesis conditions for single cryst. growth 0-100776

**semiconductor thin films continued**

- Zn,Cd<sub>1-x</sub>S, thin solid soln. films, vapour deposited, elec. and optical characts. 0-60110  
 ZnO, aqueous-deposited films, struct. and electronic props. for solar cell appls. 0-100797  
 ZnO RF sputtered films, post deposition annealing behaviour 0-100416  
 Zn<sub>3</sub>P<sub>2</sub>, elec. cond., Hall effect, P interstitial effects 0-84465  
 Zn<sub>3</sub>P<sub>2</sub>, optical props., transition energies from transmission and refl. meas. 0-60532  
 Zn<sub>3</sub>P<sub>2</sub> thin polycrystalline films for solar photovoltaic cells 0-97797  
 ZnS, effect of fabrication parameters on electroluminescence and related props. (*Japanese*) 0-76083  
 ZnS film, defect form. and development 0-96759  
 ZnS, film, intrinsic stress meas. 0-71696  
 ZnS film on Si, fused quartz substrates, H<sub>2</sub>O absorpt., IR anal. 0-75446  
 ZnS films, electrolum., bistable excitation 0-93406  
 ZnS:Cu, Cl, Mn film, AC electrolum. 0-60680  
 ZnS:Mn, Cu, Cl films, AC electrolum. 0-60679  
 ZnS:Mn AC thin film devices, domain electrolum. 0-66303  
 ZnSe films, long wavelength IR polariton emission band thermal shift and broadening 0-92833  
 ZnSe films, reson. Raman spectra 0-80888  
 ZnTe film, exciton spectra, press. and temp. depend. 0-80886  
 ZnTe films, internal stress effect on fund. refl. spectra 0-60701

**semiconductors**

- Generalities and properties of unspecified materials only. For specific materials see semiconductor materials.*  
*see also amorphous semiconductors; degenerate semiconductors; heavily doped semiconductors; magnetic semiconductors; many-valley semiconductors; narrow band gap semiconductors; polar semiconductors; thermoelectric effects in semiconductors and insulators*  
 acoustic domain injection (*Japanese*) 0-91945  
 ambipolar diffusion, electron-hole scatt. effect 0-59976  
 ambipolar hot-carrier size effect kinetics 0-107799  
 amorphous, Mossbauer spectrometry (*French*) 0-80660  
 anisotropic semiconductors, light reflection in interband transition freq. (*Russian*) 0-88945  
 applied solid state physics, book 0-94936  
 Auger recombination rate, nonequilibrium carrier distrib. 0-65578  
 band states temp. depend., book contrib. 0-80182  
 biexcitons, coherent, two-photon nutation in semiconductors 0-80191  
 biexcitons, one-photon radiative recomb. 0-70621  
 carrier relaxation time anisotropy effect on free carrier dispersion studies 0-84474  
 channelling-blocking measurements, (n,α) method for B-depth profiling 0-70276  
 charge carrier density determ. calibrated polarimeters and the Faraday magneto-optical effect 0-60551  
 charge neutrality produced by impurity diffusion 0-59724  
 chemical energy, direct conversion to elec. energy 0-66984  
 chemisorption of mol. complexes, bond orbital model (*German*) 0-59807  
 chemisorption on semiconductor surfaces, review, book contrib. 0-107648  
 coherent biexcitons, two-photon nutation effect (*Russian*) 0-59892  
 compensated semiconductors, low temp. mobility, unscreened charged impurities effects calcs. 0-75562  
 complex energy band under optical excitation, high-frequency negative cond. and population inversion 0-107858  
 composite semiconductor-ferrite struct., surface magnetostatic spin wave interactions (*Russian*) 0-88739  
 composition profile in semicond. alloy, second derivative wavelength modulation 0-103967  
 compound semiconductor, plastically deformed, electronic transport and optical props. of dislocations 0-80212  
 Coulomb collisions between nonequilibrium electrons during interband interaction of high-power optical pulses with semiconductors and insulators 0-76049  
 covalent, cancellation effects in localised orbital theories 0-84445  
 covalent, displacement correlations, adiabatic bond charge model 0-70350  
 covalent semiconductors, electronic interface states in intrinsic stacking-faults 0-75522  
 covalent semiconductors, low temp. galvanomag. effects, shallow attractive traps 0-88575  
 crystal growth aspects of electronic materials 0-66405  
 current fluctuation anisotropy, electron diffusion, quasielastic scatt. (*Russian*) 0-107882  
 cyclic queue models of semiconductor noise and vehicle fleet operations 0-80336  
 deep defects, contrib. to binding energy 0-70634  
 deep impurity centres, elastic light scattering 0-97315  
 deep level carrier trapping and emission, transient spectroscopy, book contribution 0-80216  
 deep level impurity photoionisation cross-section 0-65485  
 deep levels, review 0-103640  
 deep transition metal impurity states, SCF CNDO cluster calcs. 0-100442  
 defect cluster annealing, kinetics 0-84209  
 defect electronic struct., SCF method 0-80208  
 defect electronic structure and lattice config., MO approaches 0-65495  
 defect fermion properties, ionic cond. calcs. 0-59457  
 defect images obs., SEM, charge-collection, contrast formation 0-70087  
 defective surface layer, surface position states 0-75526  
 defects, electronic props. study by spectroscopic techniques 0-84446  
 defects, electronic structure and lattice distortion, Green's function methods (*French*) 0-59917  
 dielectric function, modulation spectroscopy and elec. field effects book contrib. 0-80201  
 diffusion from limited source 0-70444  
 diffusion length, meas. by surface photovoltage method effects of optical beam size 0-60002  
 direct band gap, electronic Raman scatt. of polarised light on donor levels 0-93309  
 direct band gap type, polariton theory of reson. electronic Raman scatt. on neutral donor levels 0-108194  
 direct gap semiconductors, electron-hole droplet condensation 0-103630  
 direct-gap, gain spectrum of electron-hole liquid 0-66279  
 dislocations, structures and elec. props. 0-70201  
 disordered system, low-freq. cond. due to variable range hopping, cluster approx. 0-92886  
 displacement damage, displacement energy determ. by electron beam induced conductivity 0-70097



## semiconductors continued

- donor minus ion, binding energy determ. 0-70645  
 donor-acceptor system, weak wave absorpt. in reson. laser radiation field 0-66252  
 doped, impurity band density in atomic limit 0-107735  
 doped, ionised centre diffusion accel. by electrostatic fields 0-70473  
 doped, metal-insulator transition, anal. 0-88478  
 doped, shallow impurity states, Hubbard bands and donor excitonic states, HF calc. 0-100443  
 doped semiconductor, potential fluctuations, random impurity distribution 0-88512  
 doping profile determ., interpretation of C-V meas. 0-59510  
 drift velocity relation to low-field mobility and high-field saturation velocity 0-75563  
 electroabsorption, interband, in semicond. with complex valence band, polarisation props. 0-66152  
 electron beam depth profiling using SEM 0-70723  
 electron conductivity, temp. and freq. depend., two band model (*Russian*) 0-75564  
 electron emission from surface subband, reduced work function 0-60757  
 electron excitation spectra in field of two travelling waves 0-65514  
 electron microscopy, developments in high resolution imaging 0-99001  
 electron microscopy, semiconductor appls., advances 0-101911  
 electron quantum states, nonequilibrium current fluctuations in quantised mag. fields (*Russian*) 0-107704  
 electron-electron collision effect on current voltage characts. in quantising mag. field 0-103705  
 electron-hole drop formation, phonon wind influence (*Russian*) 0-92825  
 electron-hole liquid, 'neutrality' question of impurities 0-92822  
 electron-hole plasma and elec. field, stratification at low temp. 0-60020  
 electron-phonon interactions, combined phonon resonance (*Russian*) 0-75321  
 electron-phonon interactions, dispersion law in van Hove critical point region 0-70344  
 electron-stimulated absorption of bulk spin waves 0-70992  
 electronic cond., temp. depend. review 0-59975  
 EM wave interaction in weakly nonlinear medium with superlattice 0-93257  
 EM wave propagation in semiconductors with superlattices, magnetic field effect 0-70745  
 exchange interactions in semiconductors and insulators, mean free path and energy gap effects 0-88522  
 exciton and domain luminesc., book 0-82588  
 exciton effect in interband electronic Raman scattering 0-103946  
 exciton-impurity state with low binding energy 0-103646  
 exciton-polariton interactions, Green's function approach for semiconductors with direct band gaps 0-92831  
 excitonic dielectric liquid, Wannier-Mott 0-65458  
 exotic atoms, conf., Erice, Sicily, (1979) 0-67939  
 Fabry-Perot interferometer retuning by optical excitation (*Russian*) 0-98970  
 Fermi level, monotonous shift with increasing temp. 0-92809  
 ferromagnet-semiconductor contact, spin-depend. recomb. and scatt. on electron injection 0-65654  
 forbidden gap width, relation to refractive index, single oscillator calcs. (*Russian*) 0-71372  
 force variation due to charged defects 0-92634  
 four-photon transitions, perturbation theory calc. 0-96786  
 free carrier optical props., book contrib. 0-80738  
 graded-gap, internal photo-effects, excess carrier distrib. 0-107847  
 Gunn diodes, multidomain mode due to charge inhomogeneities 0-70714  
 heat pulse absorpt. in nonquantising mag. fields 0-60054  
 heterogeneous, anisotropic, Hall coeffs., Hall mobility, carrier density (*Russian*) 0-70734  
 HF wave dispersion for complex wave numbers, ordinary waves 0-70740  
 high-frequency ballistic electron transport, AC impedance meas. 0-80306  
 hologram recording by photosensitive etching, attainable spatial frequencies 0-69343  
 homogeneous, nondegenerate, single-level Shockley-Read-Hall recomb. centres, flicker noise 0-70779  
 hopping promoted by electron-electron coupling 0-59987  
 hot electron transverse escape galvanomagnetic effects (*Russian*) 0-80289  
 impact ionisation, Auger recombination involving traps 0-80912  
 impact ionization, review 0-65577  
 imparting states, transition metal, EPR linewidths calc. 0-80599  
 impurities, localised, transition metal, lattice relaxation in optical transition (*Polish*) 0-70345  
 impurities, trace element anal. 0-81399  
 impurity characterisation from thermal carrier meas. 0-65595  
 impurity electron scatt., resonance scatt., Hall and drift mobility 0-65487  
 impurity ion pot., approx. equivalence of Csavinsky and Resta models 0-59901  
 impurity ion screening charge density expansion 0-107780  
 impurity photoionisation, quantum-defect, billiard-ball model comparison 0-65486  
 interimpurity absorption in strong EM wave field (*Russian*) 0-60631  
 intervalley acoustoimpurity resonance 0-107868  
 intrinsic, indirect exchange interaction, finite temp. effects 0-71003  
 ion implanted, laser annealing 0-65023  
 ionic semiconductors, cyclotron resonance, elec. cond., electron-phonon interactions 0-93180  
 ionisation coeffs. of electron and hole multiplication, empirical fit to Baraff's curves 0-96897  
 IR absorpt. and optical relax. time of free carriers 0-66206  
 IR switching, ultrafast optically controlled, in semiconductors 0-58626  
 isothermal and non-isothermal C-V deep level meas. using Schottky contacts 0-88515  
 Kane semiconductor films, thermomag. and thermolec. effects, theory 0-70864  
 large-band-gap, self-compensation, role of impurities 0-92850  
 laser-photoinduced etching, photodissociation of dissolved complexed halogens in soln. 0-100929  
 layer crystals, exciton absorption of light 0-70623  
 light induced electron drift, two-photon transitions (*Russian*) 0-107853  
 light transient scattering by free carriers 0-102766  
 local density of electron states for system with defects or impurities 0-92857  
 localised magnetic moment of transition metal impurities 0-60192  
 localised states near displacive transition 0-70644  
 magnetised plasma, theory of EM surface waves 0-88584

## semiconductors continued

- magnetodiode and magnetoconcentration effects, influence of field effect 0-107903  
 magnetophonon resonance oscils., peak shape, theory 0-107824  
 minority carrier injection in trap free semicond. 0-96904  
 MM wave guiding and control by surface plasmons 0-103713  
 mobility-fluctuation description of 1/f noise 0-84496  
 Moss formula, refr. index rel. to energy gap 0-108173  
 Mott exciton formation in two-dimensional systems in high mag. fields (*Russian*) 0-65467  
 multiphoton spectroscopy, IR tunable laser (*French*) 0-82836  
 muon diffusion and trapping 0-71283  
 n-type, donor-polarizability enhancement as the insulator-metal transition is approached from the insulating side 0-80184  
 n-type, inhomogeneous, nonequilib. carrier diffusion and lifetime 0-60005  
 n-type, lightly doped, hopping acoustoconductivity mechanism 0-65635  
 n-type, nonequilibrium photoelectron distrib. and absolute negative cond. in quantising mag. fields 0-65622  
 negative photoconducting materials, photovoltaic effects 0-96943  
 non-equilibrium, acoustic plasma oscils. generation 0-96811  
 noncoherent interaction of a light pulse 0-106561  
 nondegenerate, thermomagnetic phenomena in quantising mag. field (*Russian*) 0-60014  
 nonequilibrium acoustic phonons, generation by interband light absorption 0-96607  
 nonequilibrium phase transitions, stability and dissipation, teaching 0-105479  
 nonlinear coherence phenomena in exciton region 0-99806  
 nonlinear conductivity, vortex waves, carrier mobility and lifetime 0-96893  
 nonlinear conductor, odd-symmetry two-dimens. Hall effect in alternating elec. field 0-80303  
 nonlinear electroacoustic echo 0-92943  
 nonlinear optical props., book contrib. 0-78899  
 nonlinear polarisability and self-action effects in binary and mixed semiconductors 0-99786  
 nonuniform band structure materials, Shockley like equations for current density and carrier density 0-60001  
 normal transverse waves in longitudinal mag. field 0-80309  
 nuclear polarisation due to anisotropic size effect in weak elec. field 0-71199  
 optical heating, coupled diffusion eqns. for heat and excess carrier density 0-60718  
 optical investigations, vacuumless cryostat 0-73370  
 optical phonon amplification by EM wave field in presence of mag. field 0-65181  
 optical properties, book 0-77554  
 optical properties above band edge, book contrib. 0-84425  
 optical properties due to phonons, book contrib. 0-80805  
 optical properties under press., book contrib. 0-84715  
 optical saturation for high carrier recomb. freq. (*Russian*) 0-88585  
 optical SHG, elec. field induced, theory 0-69457  
 optical waveguide, semiconductor clad, attenuation and propagation coeffs. 0-79004  
 optically anisotropic, magnetoabsorpt., light freq. modulation effect 0-66162  
 optoelectric effect in semicond. with superlattice, theory 0-70768  
 p-type, Faraday effect due to free holes 0-97247  
 p-type, intervalence-band transitions, saturation, theory 0-75997  
 particle complexes,  $N=1$  to  $\infty$ , book contrib. 0-80194  
 percolation level, Monte Carlo calc. for lightly doped compensated semicond. 0-59923  
 phonon cond., three-phonon N- and U-processes 0-65313  
 phonon conduction and relaxation times 0-107585  
 phonon generation by EM wave 0-96606  
 phonon induced hopping between Stark levels 0-92900  
 phonon two-stage drag of electrons, thermoelectric power, scatt. mechanism 0-92919  
 photoconductivity, photoelec. effects, book contrib. 0-84488  
 photoconductivity measurement at UHF and at high excitation levels 0-65627  
 photoexcited hot electrons energy relaxation in near-surface region of semiconductors 0-92928  
 photomagnetolectric effect, injection-level dependent lifetime 0-80319  
 photosensitive area localisation in semiconductors, expt. apparatus 0-75599  
 photosensitive etching in nonoxidising etchants 0-78813  
 photovoltaic effects, semicond. with internal elec. short circuits, calc. 0-65620  
 piezoelectric-semiconductor struct., nonlinear acoustoelectric effects for large amplitude SAW 0-92942  
 planar acoustomagnetoelec. effect, theory 0-60052  
 plasma, longitudinal oscillations with small number of carriers in perpendicular fields 0-88583  
 plasma effects, strongly elongated electron distrib., normal oscils. 0-60021  
 plasma self-oscillations within submillimetre freq. range 0-84473  
 polarised light nonlinear rotation 0-93268  
 polaritons, classical and quantum mechanical aspects (*French*) 0-103634  
 polypeptides, electronic struct., side-chain disorder effect 0-76706  
 population inverted, resonant Brillouin scatt., photoelastic consts. 0-89015  
 powders, semiconducting, band-gap energies, photoacoustic meas. 0-70579  
 power reflection spectroscopy, analytical techniques 0-62714  
 proton semiconductors, with H-bonds, quantum theory of proton cond. 0-65641  
 pyroelectricity, primary and secondary, review 0-93243  
 radiation damage, mechanisms, review 0-107315  
 radiative recombination, book contrib. 0-84784  
 resonant Brillouin scattering of exciton polaritons 0-93357  
 SEM electron beam induced current images of dislocations and stacking faults, computer simulation 0-70198  
 semiconductor surface eval. using SAW convolver 0-97677  
 semiconductor-piezoelectric structure, vol. acoustic wave excitation in nonlinear interaction with surface waves 0-69582  
 shallow impurity centre spectra, isotopic shift of zero-phonon lines 0-66249  
 shielding by electron gas in magnetic field 0-107727  
 size-quantised wires, two-photon interband absorpt. 0-93256  
 solid state physics, 1933-40, contrib. of Sir Nevill Mott 0-57055

**semiconductors continued**

- solid state physics, historical aspects, symposium, London, England (Apr.-May 1979) 0-56999  
 sound propagation, HF, nonlinear effects 0-88279  
 space charge, surface region, semiconductor with arbitrary energy spectrum of trapped states 0-107811  
 space charge region thickness, deep level props., determ. by  $\gamma$ -ray absorpt. 0-59995  
 spatially inhomogeneous magnetic field effect on semiconductor carriers 0-92916  
 sphalerite, hydrothermal single crystals, feasibility of optical methods for quality control 0-89065  
 spin dependent recomb., theory 0-103708  
 spin glass, indirect exchange interaction of localised spins 0-88768  
 spin-dependent recomb. and scatt. in presence of optical orientation of electrons 0-96908  
 sputtering yield, energy depend., semiempirical formula 0-100736  
 Stark and photoabsorption spectra, density of oscillator strengths 0-83318  
 STEM spectroscopic techniques for simultaneous electronic and defect obs. 0-100145  
 submillimetric magneto-optical props., strip line technique 0-60554  
 superlattice, EM wave absorption in quantising electric field 0-108182  
 superlattice, plasma resonant interaction with Stark oscills. 0-107842  
 superlattice, transverse electron effective mass 0-100429  
 superlattices, Stark-cyclotron resonance, Larmor freq. (Russian) 0-60421  
 surface, cyclotron reson., projection operator formalism 0-88524  
 surface, depth profiling, optoacoustic technique 0-65337  
 surface analysis by SIMS (Czech) 0-90927  
 surface and adsorbate states, charge injection into space charge layers 0-100496  
 surface depletion and inversion, arbitrary doping profile, theory 0-107912  
 surface helicons in semiconductor plasma, theory 0-60019  
 surface inversion layers, exchange and correl. 0-75618  
 surface magnetoplasmon type polaritons, LF, existence criterion in Faraday config. 0-96961  
 surface space charge layers, subband struct., perturbation theory 0-84497  
 surface-states concentration profile and capture cross section determ. using SAW convolver 0-80341  
 surfaces, optical props., book contrib. 0-80737  
 tetrahedrally coordinated, temp. depend. of diamagnetic susceptibility (Rumanian) 0-88717  
 thermal domain investigation, Joule heating, current-voltage characts. 0-70711  
 thermal EMF measurement, thermal cell and copper blocks method, more accurate treatment of results 0-77812  
 thermally stimulated conductivity luminescence, defect levels, traps, book contribution 0-80296  
 thermally stimulated relaxation processes, book contribution 0-80295  
 thin film semiconductors (Japanese) 0-107936  
 thin layers, double injection in transverse mag. field, theory 0-80421  
 three-impurity clusters, ionisation energies and electron affinities 0-65496  
 transport properties, Seebeck and Hall coeffs. Lorenz number, anisotropy, theory (German) 0-65608  
 two-dimensional electron gas, CDW 0-65476  
 variable gap semiconductors, carrier transport and fluctuation effects due to changes in gap width 0-107793  
 weakly doped, compensated, IR light absorption by small scale fluctuations (Russian) 0-66255  
 weakly doped compensated, hopping photoconductivity in disordered systems (Russian) 0-65573  
 wurtzite structure, effect of local strain fields on shallow acceptor states 0-96821  
 zero-gap semiconductors, anisotropy of IR absorpt. coeff., k.p. calc. 0-97285  
 Zincblende struct., localised vibr. due to defect complexes, Green's function study 0-79896  
 CuCl, dielectric function for semiconductors with high exciton conc. 0-84443

**semileptonic decays**

- baryon resonances, EM transitions, multipole moments in single quark transition model 0-62985  
 charmed baryons, weak decays, quark model framework 0-62976  
 charmed mesons, semileptonic decays, charged weak current struct. 0-102042  
 heavy meson inclusive semileptonic decays, lifetime estimates, quark-parton model difficulties 0-86704  
 sequential charged lepton, semileptonic branching ratio and lifetime 0-57578  
 $SU_3 \times U_1$  and the origin of the Cabibbo angle, charged gauge boson mixing 0-73639  
 $D \rightarrow K^* \mu \nu$ , in  $e^+e^-$  annihilation, T-odd asymmetry in CP violation model (Russian) 0-105885  
 $D \rightarrow K^* \nu \nu$ , charm-changing weak hadronic current, models 0-57585  
 $D^0$ , lifetime difference from  $D^+$  0-91084  
 $D^0$  nonleptonic and semileptonic decays, isospin selection rule tests 0-73700  
 $K \rightarrow \pi e(\mu) \gamma$ , quark mass ratios 0-105884  
 $K^* \rightarrow \pi \mu \nu$ ,  $\mu$  polarisation and T-odd correlations, Weinberg model of CP violation (Russian) 0-62969  
 $K^* \rightarrow \pi^0 \mu^+ \nu$ ,  $K^* \rightarrow \mu^+ \nu$  decay spectrum and form factors 0-57587  
 $K^* \rightarrow \pi^0 e^+ e^-$ , neutral-current process, strong interaction corrections 0-62968  
 $K_{10}^0 \rightarrow \pi^+ \mu^+ \nu$ , transverse polarisation of  $\mu$ , violation of time-reversal invariance 0-68448  
 $K_{10}^0 \rightarrow \pi^+ \mu^+ \nu$ , form factors 4-momentum depend.,  $\mu e$  universality (Russian) 0-68449  
 $K_{10}$  decay vector form factor (Russian) 0-105900  
 $\Lambda^0 \rightarrow p e^- \bar{\nu}$ , absolute rate,  $\Lambda(\Gamma^0 \rightarrow p e^- \bar{\nu})/\Gamma(\Lambda^0 \rightarrow p \pi^-)$  precise meas. 0-57593  
 $n$ , decay, weak interaction meas., coincidence type ion electron converter detector obs. 0-58100  
 $n \rightarrow H \bar{\nu}$ , atomic decay, scalar and tensor interaction effects (Russian) 0-68455  
 $\Omega \rightarrow \Theta e(\mu) \bar{\nu}$  or  $\Theta^* e(\mu) \bar{\nu}$ , branching ratios and lepton energy spectra 0-73701  
 $\Omega \rightarrow \Xi^* \pi$  ( $\Xi^{*0} \pi^-$ ), nonleptonic hyperon decays, QCD description, PCAC anal. 0-95269  
 p, baryon number nonconservation, expt. status 0-57594

**semileptonic decays continued**

- p decay, flavour goniometry 0-99100  
 $\pi \rightarrow e \nu \gamma$ , isospin-breaking, chiral limit, conserved-vector-current violation,  $\sigma$  model 0-62988  
 $\Sigma^+ \rightarrow p e \nu$ , flavour changing neutral current search 0-105836  
 $\tau \rightarrow \nu_\tau + \text{hadron(s)}$ , decay modes and  $\nu_\tau$ -mass 0-63057  
 $\tau \rightarrow \nu_\tau \pi$ , T-violation effects, neutrino mass (Russian) 0-95294  
 $\tau \rightarrow \nu \rho^0 \pi$ , spin parity anal. 0-105941  
 $\tau \rightarrow \rho \pi \nu$ , quark model, current algebra model, divergence of axial vector current 0-57655  
 $\tau \rightarrow \nu_\tau \pi^+ \gamma$ ,  $\pi$  form factors, axial-vector and structure dependent, vector meson dominance model 0-62989  
 $V \rightarrow \rho \mu^+ \mu^-$ , vector meson decay EM form factors in bag model (Russian) 0-62982  
 $K \rightarrow \pi e^+ e^-$ , six-quark model, CP violation 0-78055  
 pN, 350 GeV in Ne,  $D^+$  prod. cross section and lifetime 0-68494

**semimetallic thin films**

- multilayer thin film struct. thermoelec. props. 0-92964  
 Bi, amorphous film, temp. dependence of SAW attenuation 0-75679  
 Bi, amorphous metal films, crystallisation with and without mag. field 0-70570  
 Bi, ellipsoidal model of textured specimens with uniaxial symm. (Russian) 0-80100  
 Bi film, adatom surface diffusion at low temps., elec. resist. study (French) 0-65376  
 Bi film fast-response photodetector, employing charge carrier photon entrainment 0-73462  
 Bi thin film, structure and electronic props. 0-70562  
 Bi-Te, thin film system, stress-relief appearance conditions 0-65416  
 Sb, elec. cond., grain boundary scatt. effects 0-103766

**semimetals**

- see also *antimony; arsenic; bismuth; semimetallic thin films*  
 degenerate, conduction electron acoustic spin resonance, oscillations of absorbed power 0-108075  
 degenerate, heat conduction, thermal EMF, Lorenz number anisotropy at low temp. 0-75549  
 EPR line shape, magnetoresist. effect 0-84638  
 simultaneous Cooper and insulating pairing, physical states 0-93036  
 AsSb, thermopower, thermomagnetic power, 4.5 to 77K 0-107825  
 BiSb ( $>20$  wt.%), electronic band struct. 0-107698  
 Hg<sub>1-x</sub>Cd<sub>x</sub>Te, Hall coeff., anomalous temp. depend., 4.2 to 70K 0-65604  
 Hg<sub>1-x</sub>Cd<sub>x</sub>Te, optical absorpt., quasiloal acceptor level effects, theory 0-92853  
 Hg<sub>1-x</sub>Cd<sub>x</sub>Te-type semimetals, kinetic props., local acceptor level effects 0-65557  
 LiAl, anomalous elec. resistivity near critical composition 0-103673  
 TiSe<sub>2</sub>, band struct., angle-resolved photoemission studies 0-70610  
 TiSe<sub>2</sub>, impurity effects on elec. props. 0-80263

**Senftleben-Beenakker effect**

- atom-diatom kinetic cross section, ES, CS and IOS approx. with translational-internal coupling, viscomag. effect 0-63764  
 methyl cyanide-Ar mixture, thermal cond. in mag. field 0-100058  
 symmetric top molecules, thermal cond., Senftleben-Beenakker effect 0-100049  
 NH<sub>3</sub>-Ar mixture, thermal cond., viscosity, Senftleben-Beenakker effect 0-100054  
 NH<sub>3</sub>-He mixture, viscosity, Senftleben-Beenakker effect 0-100054

**sensing devices see detectors****sensing devices, electric see electric sensing devices****sensing devices, nonelectric see nonelectric sensing devices****sensitivity**

- focal plane IR detector arrays for planetary missions 0-85862  
 hot-film shear probes, position sensitivity 0-101286  
 Lampard-type electrostatic system, appl. of sensitivity criterion in capacitance meas. 0-98942  
 magnetoencephalography, sensitivity distrib. 0-101246  
 manometers, liq., sensitivity, wetting hysteresis effect 0-98926  
 NMR spectrometers, SQUID-based sensitivity limit 0-98961  
 photographic exposure prediction techniques, still, motion-picture photography appl. 0-66817  
 piezoelectric receivers, amplitude-freq. response determ. for acoustic emission 0-87699  
 pressure transducer, miniature implantable, biomedical appl. IC fabrication techniques 0-76849  
 SEASAT radar altimeter, resolution capability preliminary estimates 0-72645  
 second-generation ion microanalyser description and performance (French) 0-101055  
 Space Telescope spectrograph Digicons 0-85858  
 Si accelerometer, batch fabricated 0-73328

**sensitivity analysis**

- see also *control system analysis; dynamic response; frequency response; transient response*  
 FBR thermal hydraulics, sensitivity theory for general systems of nonlinear equations 0-86954  
 secondary radiation dosimeters, prep., sensitivity anal. and calibration 0-74034

**sensors, nonelectric see nonelectric sensing devices****sensory aids**

- see also *contact lenses; hearing aids*  
 acoustic aid for the blind 0-104810  
 blind aid, image conversion to a tactile presentation 0-94414  
 blind reading aid using conversion of optical images into vibrotactile 0-85533  
 car drivers, work spectacles and functional visual fields (Italian) 0-108875  
 lenses, low-power plus, perceptual effects in emmetropic observers 0-67084  
 ophthalmic correcting cylinder axis, ophthalmometric prediction 0-98174  
 optical reading machine, multifont adaptable automatic, for blind people 0-104814  
 optical-to-tactile converter 0-57041  
 spectacle lens blanks, grinding and polishing using automatic and semi-automatic machines (French) 0-58822  
 spectacle lenses, hard resin, comparative study of bitoric effect 0-91877

**separation**

- see also *desalination; distillation; drying; filtration; isotope separation; magnetic separation*  
 carrier-mediated extraction, development 0-66870



## separation continued

- CHISA international conference, Prague, Czechoslovakia (Aug. 1978) 0-62372  
 gas discharge, DC, time-depend. cataphoretic gas separation with end volumes 0-79603  
 ionic mixtures, phase separation 0-77279  
 leukocytes of human blood, gravity sedimentation anal. 0-98197  
 liquid membranes, emulsion-type, pertraction appls., comparison with double liq.-liq. extraction 0-66869  
 liquid membranes, separation and reaction appls. 0-66871  
 pigment separation and deposition, electron sensitive, by electrophoresis (German) 0-108365  
 poly-4,4-diphenylphthalinterephthalamide, mol. mass distrib., sedimentation and fractionation method meas. (Russian) 0-71957  
 preparative scale thin-film dialysis apparatus 0-101296  
 T separation from Li at low conc. using Y for fusion-reactor appls. 0-83219  
 velocity sedimentation, mammalian cells 0-101293  
 C-O eutectic, form. in C-O white dwarfs 0-77405  
 GeO<sub>2</sub>-Na<sub>2</sub>O borosilicate glass fibre prod. by phase separation and leaching 0-69558  
 H/He separation in interior of Saturn, rel. to energy release 0-77307  
 Pu safeguarding, automated ion-exchange system for rapid Pu separation from impurities 0-78383  
 S-benzene systems, liq.-liq. phase separation 0-96658

## series (mathematics)

- acoustics, approach (Japanese) 0-87658  
 beams flexural-torsional problem by series expansion in eigenfunctions 0-83732  
 blackbody function efficient computation, two-series approach 0-79128  
 boundary layer problem, unsteady, extended series expansion 0-83781  
 EM waves diffraction at surfaces with inhomogeneous admittance 0-69296  
 Ising model, critical temperature, modulated Pade approximant 0-84605  
 optimal control, differential eqn., canonical, functional relation expressed by Volterra series (French) 0-73159  
 Pade approximant, modulated, applied to Ising model critical temperature 0-84605  
 plasma radiation emission spatial distrib. reconstruction in torus 0-103123  
 recurrence technique for confluent singularity analysis of power series 0-73277  
 Taylor-Fourier series, appl. in new exact method for Hill's eqn. of celestial mechanics (Chinese) 0-105152

## serrated yielding

- strain ageing, dynamic, and serrated yielding, mechanism 0-88245  
 Al-Mg (0.3 wt.%) single cryst., dislocations obs. by high voltage electron microsc. 0-79796  
 Pd<sub>90</sub>Si<sub>10</sub> amorphous alloy, skip deform. and crit. shear stress, using tensile testing machine 0-89321

## services, information see information services

## servo systems see servomechanisms

## servomechanisms

- dual capstan drive tape recorder (German) 0-95092  
 fatigue servo-hydraulic testing machines 0-108649  
 linear servo-loop, increasing efficiency at low frequencies (French) 0-86280  
 microscope objective, piezoelec. and electrodynamic automatic focusing servo mechanisms 0-73445  
 wideband optical disc data recorder systems 0-102751

## set theory

- algebras, normal varieties of  $\Omega$ -algebras (Russian) 0-68019  
 foundational studies, A. Mostowski, book 0-57014  
 foundational studies, A. Mostowski, book 0-57015  
 nonstatistical parameter estimation adaptive algorithms 0-91995  
 physical system, model of space-time from set theory concepts 0-82660  
 polygraphic sleep recordings, computerised scoring method 0-109049  
 selective families of sets 0-98784

## sets (mathematics) see set theory

## sferics see atmospheric

## shadow universe see cosmology

## shape memory effects

- alloy, martensite boundaries, lattice imaging study 0-107359  
 alloys, device for testing in bending 0-66723  
 alloys, unidirectional memory effect (French) 0-66606  
 brass, Cu-Zn (39(40) wt.%), shape memory effect and martensitic transform. depend. on heating-cooling cycles (Russian) 0-97482  
 engine, memory alloy, efficiency 0-71648  
 pseudoelastic body, model for first-order phase transition 0-92642  
 thermal efficiency, of ideal shape-recovery cycle 0-108445  
 Cu-Zn-Al,  $\beta'$  martensite crystal crossing rel. to reversible shape memory effect (Japanese) 0-108499  
 Cu-Zn-Al, reversible shape memory effect (Japanese) 0-108500  
 Fe-C-Mn-V, austenite microstruct. memory (German) 0-84977  
 Fe-Ni alloy, reverse martensitic transform., shape deform. reversibility 0-66506  
 Fe-Pd (31.2 wt.%), thermoelastic FCC-FCT martensitic transformation 0-104156  
 In-Sn alloy crystals, phase changes and shape memory effect (Japanese) 0-108502  
 K(D<sub>2</sub>H<sub>1-2</sub>)<sub>2</sub>(SeO<sub>3</sub>)<sub>2</sub>, ferroelastic, anelastic and elastic infra-low freq. props. 0-70304  
 NiTi martensite, struct. characts., TEM 2<sup>1/2</sup> D imaging obs. 0-108446  
 NiTi, premartensitic transformation of B2 phase, shape memory 0-84931  
 Ti-Fe-Ni (67, 30, 3 wt.%), reversible shape alteration (Russian) 0-71647

## shear see crystallographic shear

## shear flow

- see also shear turbulence  
 carboxymethyl cellulose, aqueous soln., diffusion and mass transfer from rotating disc 0-83827  
 cascades, annular, secondary flow, shear flow turning or departure of exit flow 0-69842  
 cement pastes, flow behaviour, specific surface and conc. of solids influence 0-65132  
 cholesteric liquid crystals, steady low shear rate flow normal to helical axis 0-96443  
 cholesterics, shear flow induced propagating domains 0-64887  
 colloidal particles, Poiseuille flow, total particle conc. axial change 0-108752

## shear flow continued

- critical mixtures, shear and critical fluctuations, instantaneous mapping of velocity gradients 0-79420  
 drop deformation and orientation in shear and extensional flow fields, dynamic interfacial props. 0-107611  
 drop dynamics in shear fields, role of dynamic interfacial effects 0-107612  
 drops, long and slender, slow viscous motion 0-79365  
 ducts, rapidly rot., variable area, rectangular, steady flow, inertial perturbations for small divergences 0-59112  
 ducts, sound propagation in parallel sheared flow mode estimation 0-79026  
 fine particles aggregation, mechanism and rate at uniform shear field 0-101046  
 forced oscillations of separated shear layer, appl. to cavity flow-tone effects 0-64256  
 granular material flow from parallel sided bins, thickness of shear zone 0-81279  
 heat or mass transfer rate from freely suspended particle 0-79313  
 inviscid, rotating, compressible fluid, linear stability 0-92161  
 inviscid flow, 2-D, weakly sheared, past circular cylinder 0-74893  
 Jupiter, Great Red Spot, atmosphere baroclinic model, solitary waves on unsymmetric shear flow 0-82266  
 linear, characterisation of acoustic disturbances 0-69848  
 Lorenz attractor behaviour in a continuously stratified baroclinic fluid 0-83806  
 nematic liquid crystals, sinusoidal shearing and temporal sinusoidal standing twist wave 0-84053  
 non-Newtonian liquid with power-law behaviour, flat submerged jet theory 0-59078  
 nylon 6.6 in 100% H<sub>2</sub>SO<sub>4</sub>, primary normal-stress difference coeff., dependence on molecular wt. 0-87752  
 optical fibre coating with conical shape applicator 0-58820  
 parabolic, forces on neutrally buoyant disc, creeping flow approx. 0-92105  
 pentyl-cyano-biphenyl, nematic, hydrodynamic parameters meas. with and without applied elec. field 0-100297  
 plane parallel flow, free convection in Couette and Poiseuille flows, numerical simulation 0-99995  
 plasma shear flow, electrostatic instability theory and appl. to magnetopause and solar wind 0-96359  
 polyacrylamide Separan MG200, aq. soln., rheological props. 0-64507  
 polymer melt containing suspension, cell model theory of shear viscosity 0-103048  
 polymer melt flowing through duct, heat transfer 0-103049  
 polymer melts, annular flow, secondary normal stress difference 0-106816  
 polymer melts, flow indices (Japanese) 0-79360  
 polymer melts, normal stress and Barus effect 0-64589  
 polymer solution, nonlinear response to uniaxial shear flow histories 0-59084  
 polymer solution rheology based on a finitely extensible bead-spring chain model 0-83775  
 polymer solutions, aqueous, diffusion and mass transfer from rotating disc 0-83827  
 polymer solutions, dilute, normal stress difference and shear rate 0-83776  
 polymer solutions, liquid cryst., rheo-optics of shear and elongational flow, quiescent and flow birefringent characts. 0-83773  
 polymer spheres, colloidal suspension, steady state shear flow coupled to conc. fluctuations 0-61170  
 Polyox, drag reduction meas. in square duct, anomalous effects due to polymer degradation 0-83824  
 polypropylene-polyethylene blends, capillary flow, rheology and morphology 0-59088  
 polypropylene-polyethylene blends, flow behaviour in capillaries 0-59087  
 polystyrene solns., correlations of network model parameters 0-106772  
 polystyrene solution, constitutive models, exptl. tests based on birefringence data 0-100015  
 PPT in 100% H<sub>2</sub>SO<sub>4</sub>, primary normal-stress difference coeff., dependence on molecular wt. 0-87752  
 PVC plastisol, flow behaviour at high shear rate (German) 0-92186  
 radio double sources (astronomical), beam and cloud stability, shear layers, two dims. computations 0-67893  
 Reynolds equation at very low spacing, compressible, numerical soln., factored implicit scheme, mag. recording appl. 0-92183  
 rotating Boussinesq viscous fluid, inertial instability, appl. to atm. 0-90131  
 rotating stratified fluid, parallel shear flow, baroclinic and barotropic instability 0-98328  
 simple fluid shear depend. viscosity, central force interactions 0-79970  
 stagnation points on cycloidal boundary in flow with const. shear 0-87755  
 steady rotating flow over topography, steady  $\beta$ -plane channel, quasi-linear theory 0-92159  
 stratified shear flows, internal solitary waves 0-69856  
 streaklines in a shear layer perturbed by two waves 0-59055  
 styrene-butadiene-styrene block copolymer, stress relax. following steady-state flow, residual shear stress development 0-83772  
 styrene/acrylic terpolymers, viscoelastic props. 0-64509  
 suspension, memory impairment, Brownian rotation of spheroids 0-79386  
 three dimensional parallel shear flows, stability and transition for rot. disc 0-74887  
 two-dimensional soft-disc systems, nonlinear viscous flow 0-92102  
 viscoelastic droplet break-up, in nonuniform shear flow 0-64588  
 viscoelastic fluid, stability of steady shearing flows, energy method and parabolic maximum principle 0-74926  
 viscoelastic fluids, Weissenberg rheogoniometer, R-17, axial compliance reduction 0-106859  
 viscous fluid under cyclic deform., self-heating, hydrodynamic thermal explosion 0-58993  
 viscous stratified shear flow, stability eqns., completeness obs. 0-64519  
 wave evolution, nonlinear, in free shear layers, effects of critical layer structure 0-83809

## shear modulus

- abietic acid, transverse US wave propag., glass and liquid transition region 0-79883  
 adatoms, elastic interaction between, near distortive phase transition 0-80080  
 bar, rectangular, torsion crack problem, harmonic function continuation technique soln. 0-99969

**shear modulus continued**

- beam subjected to gravity loading, Timoshenko shear coeff. 0-79159  
 biomembrane material, increase in rigidity during morphogenesis 0-94249  
 butyloxybenzylidene octylaniline, liq. cryst. film, smectic B-A transition, mech. meas. 0-79918  
 chitin (poly-N-acetyl-D-glucosamine), dynamic mech. behaviour, effect of water 0-97522  
 chitosan (poly-D-glucosamine), dynamic mech. behaviour, effect of water 0-97522  
 composite elastic medium, effective bulk and shear moduli 0-99927  
 cubic crystals, response to (111) loading, internal energy, elastic moduli 0-84230  
 elastic deformation, thermodynamics of, eqn. of state for solids 0-96589  
 elastohydrodynamic traction, granular behaviour 0-103008  
 elastohydrodynamic traction, non-Newtonian thermo-viscoelastic, from combined slip and spin 0-103043  
 filled polymers, dynamic shear modulus and acoustic velocity, filler content depend. 0-69900  
 glass fibre reinforced epoxy-phenolic, cyclically deformed under shear, energy dissipation, static tensile-compressive stress effect 0-104225  
 glass fibre reinforced plastics, ageing by boiling in water, effect on physico-mech. props. 0-60892  
 glass-plastic, unidirectional, torsion strength and shear modulus 0-99948  
 laminated anisotropic shells, nonlinear eqns. of Timoshenko-type theory 0-69669  
 matrix analysis of composed bar of open cross section 0-83736  
 metals, constitutive model at high strain-rate, shear modulus, yield strength 0-75292  
 metals, polycryst., relations between shear modulus, bulk modulus and Young's modulus 0-97540  
 orthotropic laminates, torsion strength and shear modulus determ. 0-92587  
 phthalocyanine polymer, dynamic mech. props. and fracture energy 0-100866  
 plasma coatings, elastic properties, acoustic meas. (*Russian*) 0-97519  
 poly(di-n-heptyl itaconate), alkyl side chain independent relax., double glass transition 0-59636  
 polycrystalline materials, effect of grain boundary sliding on anelasticity 0-96592  
 polymer, plasticizer effect on mech. props. (*German*) 0-92467  
 polystyrene, cyclically deformed under shear, energy dissipation, static tensile-compressive stress effect 0-104225  
 rubber, natural, crosslinked by dicumyl peroxide, modulus, swelling relations 0-59551  
 steel, austenitic stainless, N-alloyed 0-108490  
 steel, Cr-Mn (13, 19 wt.%), elastic const. behaviour, anomalous, low temp. 0-97521  
 voids, coated, capture efficiency 0-96515  
 Al-SiC cermet elasticity, porosity meas. by US means 0-81101  
 Al<sub>2</sub>O<sub>3</sub> refractories, fracture, J-integral meas. 0-108537  
 a-As, second and third order elastic consts., ultrasonic velocity meas. 0-103408  
 Cr-Fe, elastic moduli, electron conc., pulse echo overlap meas. 0-59550  
 (Cu-Au)-Co, single crystals, solid soln. and particle strengthening, superposition 0-97495  
 Fe-B(P) amorphous alloys, anomalous thermal expansion,  $\Delta E$  effect, Invar and Elvinar charact., delay time 0-80589  
 Fe-Cr-Al (12, 3 wt.%), strain amplitude-depend. damping and modulus (*Japanese*) 0-92606  
 K(D,H,<sub>1/2</sub>)(SeO<sub>3</sub>)<sub>2</sub>, ferroelastic, anelastic and elastic infra-low freq. props. 0-70304  
 Nb-H(D)(T) system, BCC, US vel. changes caused by H isotope dissolution 0-65117  
 Nb<sub>5</sub>Ta<sub>4</sub>, elastic const. change caused by H addition, hydrostatic press. effect 0-75287  
 Ni, strain amplitude-depend. damping and modulus (*Japanese*) 0-92606  
 Rb halides, photo-elastic constants and pressure derivatives of shear moduli 0-75284  
 Ti-Mo-V-Al-Cr-Fe (4.8, 4.7, 5.2, 1.1, 1.0 wt.%), structural changes during heating up to 1000°C, DTA study (*Russian*) 0-93552  
 Ti-V, elastic moduli, electron conc., pulse echo overlap meas. 0-59550  
 V, elastic const. change caused by H addition, hydrostatic press. effect 0-75287  
 V-H(D)(T) system, BCC, US vel. changes caused by H isotope dissolution 0-65117

**shear strength**

- clays, heat treatment, effect on rheological props. of enamel slips 0-60809  
 colloids, model, elastic moduli, Monte Carlo methods 0-108754  
 concrete, reinforced slabs, punching shear strength under in-plane biaxial tension 0-100876  
 concrete beams, reinforced, shear strength calc. 0-99942  
 concrete reinforced rectangular membranes, torsional stiffness 0-65131  
 cord-rubber laminates, two-ply balanced, interlaminar-shear strain study 0-97526  
 disperse system, plastoviscous, cone plastometer for strength props. determ. 0-76426  
 epoxy resin adhesives, capillary flow and bond strength 0-71883  
 fibre reinforced composites, stress redistribution dynamics during fibre rupture 0-64394  
 glass fibre reinforced epoxy laminates, exp. determ. of nonlinear shear behaviour 0-66575  
 glass fibre reinforced plastic, fracture dynamics 0-100906  
 glass fibre reinforced plastics, shear characteristics of tubular specimens, strain gauge and clamp 0-85114  
 graphite fibre epoxy composites, exposed to high temp., degradation of tensile and shear props. 0-81113  
 graphite fibre filled polyimide composite laminates, space environment, phys. and mech. response 0-81140  
 graphite fibre filled polyimide composite prepreg laminates, room-temp. ageing effect 0-81093  
 hydrodynamic contacts, films, elastic properties 0-88239  
 magnesial refractory concretes, cast, props. 0-89306  
 metal-polymer, ply-separation resist. polymer polarity effect (*Russian*) 0-61064  
 metallic fibre knitted gauze permeable materials, mech. props. 0-66607  
 metallic glasses, friction coeff. determ. using sliding friction rig 0-89355  
 organoplastics, fracture charact., effect on strength 0-66642

**shear strength continued**

- orthotropic laminates, torsion strength and shear modulus determ. 0-92587  
 polycarbonate, glassy, fatigue crack initiation in high strain fatigue tests 0-97564  
 polyethylene, creep during shear deform. with applied hydrostatic press. 0-76324  
 polymer systems for adhesive applications, radiation curing, lap shear strength props. 0-66842  
 polymer-metal adhesive bonds, shear resist., polymer crystn. effect 0-89462  
 polyurethane cement, viscosity and shear strength, components influence (*German*) 0-93729  
 PVC, glassy, fatigue crack initiation in high strain fatigue tests 0-97564  
 spherulastic, spherical shells, supporting capacity 0-87723  
 viscoplastic medium, flow between two noncoaxial circular cylinders under pure shear 0-99938  
 Al, 6061-T6, pressure shear impact in transverse displacement interferometer, plastic flow 0-81137  
 Al<sub>2</sub>O<sub>3</sub>, semisintered, shear strength at high press. 0-76308  
 C fibre reinforced plastics, strength props., effect of SiC coating on fibre 0-104224  
 C-fibre reinforced plastic insert molding strength (*Japanese*) 0-66588  
 Cu-Be (2 at.%), plastic deform. and dislocation substruct. 0-76307  
 Fe<sub>2</sub>O<sub>3</sub>, semisintered, shear strength at high press. 0-76308  
 MgO, semisintered, shear strength at high press. 0-76308  
 Na<sub>2</sub>O-CaO glass, shear deform. under pyramidal indentations 0-84989  
 Ni sintered permeable materials with bidisperse structure, pore-forming additions effect 0-84885  
 ZrO<sub>2</sub>, semisintered, shear strength at high press. 0-76308
- shear turbulence**  
 astrophysical plasmas, mirror instability, mag. field first adiabatic invariant breaking 0-67546  
 axisymmetric turbulent jet initial region, annular free shear layer 0-106826  
 boundary layer, hyperbolic system of eqns., Keller-Cebeci 'box' scheme 0-79274  
 discrete frequency sound generation by fluid flows 0-69812  
 extended pressure strain correlation models for turbulent shear flows 0-69777  
 gas, turbulent boundary layer vel. distrib., probabilistic statistical approach, vortices 0-92123  
 homogeneous, nearly, strongly sheared flow 0-79283  
 hydroacoustics, role of surface shear stress fluctuations 0-69808  
 instability waves, radiation of sound 0-79341  
 inviscid parallel shear flow, instability 0-79265  
 jets and boundary layers, irrotational strain dissipation eqn. sensitisation 0-106794  
 kaolin suspensions, aq., flocculated and dispersed, rheological behaviour in pipe flow 0-64510  
 LMFBF triangular rod array, flow resistance wall shear stress in interior subchannel 0-63244  
 longitudinal blunt circular cylinder, axisymmetric separated and reattached flow, turbulence 0-79285  
 mixing layer, free, axisymmetric, turbulent spot, data processing 0-79280  
 mixing layer, free, axisymmetric, turbulent spot, vorticity and Reynolds stress 0-79281  
 omnidirectional wall shear stress meter 0-106860  
 perforated plate generators in wind tunnels, wake, shear flow and isotropic turbulence prod. 0-69770  
 quasi-standing-wave phenomenon due to oscillating internal flow, vortices in shear layer 0-106809  
 Reynolds shear stress to total intensity ratio, response to additional distortion 0-79282  
 shear layer instability noise produced by various jet nozzle configurations 0-69791  
 sound generation and simulated emission by vortex flows 0-69797  
 spectral theory of stratified turbulent shear flow, interactions between motion fields 0-90114  
 submerged jets impinging on baffle, flow and mass transfer, polymer additive effects 0-92194  
 supersonic boundary layers interacting with cooling wall jets, turbulent and optical characteristics 0-106792  
 supersonic flows, freq. response of constant temp. hot-wire anemometers 0-59149  
 triple correlation of the pressure in subsonic circular jets and nonlinear interaction of instability waves 0-69893  
 two viscous incompressible fluids in parallel uniform shearing motion, hydrodynamic stability 0-59010  
 unsteady flow past semi-infinite porous flat plate with suction, velocity profiles 0-92129  
 CO<sub>2</sub> IR laser velocimetry, processing techniques and applications 0-87831
- shear turbulent flow** *see shear turbulence*  
**sheathing, cable** *see cable sheathing*  
**sheaths, plasma** *see plasma sheaths*  
**shell model (nuclear)** *see nuclear shell model*  
**shielding**  
*see also magnetic shielding; radiation protection*  
 accelerator shielding problems (*Japanese*) 0-99343  
 controlled fusion expt. shielding and earth loop elimination using fibre optics 0-74007  
 electron microscopy, dielectric support film screening effects 0-86504  
 eye shields, individualised, for electron beam therapy and low-energy photon irradiat. 0-109040  
 fusion reactor, Doublet III, vacuum vessel neutral beam armour 0-95462  
 fusion reactor, ISSEC selection and PKA spectra, use of fission reactor test facilities 0-57950  
 fusion reactor Li liq., deuterium activated, shielding 0-99286  
 fusion reactors, shielding and maintainability in an experimental Tokamak 0-99287  
 gamma rays, 6 MeV, penetrating shielding materials, energy and ang. flux density spectra 0-63393  
 gamma-ray buildup factors for Pb/H<sub>2</sub>O stratified radiation shields 0-86994  
 health physics research reactor, neutron spectra meas., various shielding conditions 0-63396  
 improved radiation shielding using packed mixed size Pb particles, nuclear plant maint. appls. (*Japanese*) 0-106207



**shielding continued**

- linear accelerator, local absorber in accelerating section to reduce radiation level 0-83229
- Lipowitz metal shielding thickness for dose reduction of 6-20 MeV electrons 0-76842
- LMFBR, neutron elastic removal cross sections, interference effect of strong scattering resonances 0-68658
- neutron flux self-shielding in activation anal. 0-93835
- organ shielding and localisation in a diverging treatment beam, simple method 0-94317
- proton attenuation lengths in paraffin, concrete and iron around targets 0-102412
- tomography, multi-slice positron emission-computed, design criteria, shielding 0-61673
- X-ray attenuation measurements on Y tung shielding material (*German*) 0-98145
- X-ray tubes, rotary anode, HV insulation, discharges due to back scattered electrons elimination (*German*) 0-105758
- B,C reflector-shield concept for fusion reactor designs 0-102293
- B,C-304 stainless steel cermet for nuclear shielding appls. 0-102352
- B,C-Cu cermet fabrication for neutron shielding appls. 0-102354
- B,C-phenolic fibre reinforced composite for nuclear shielding appls. 0-102353
- <sup>125</sup>I, shielding of (*Japanese*) 0-63404

**shielding, magnetic** *see magnetic shielding***shift registers**

- see also logic circuits*
- dynamic PMOS for self-scanned photodiode array, evaluation for integrated optics spectrum analyser 0-58806
- PtSi Schottky-barrier monolithic IRCCD focal plane 0-86427

**ships**

- see also navigation*
- diesel-engined ships, noise in cabins and engine room, reduction by abatement at source (*Japanese*) 0-79052
- marine corrosion, and its prevention 0-104333
- Navy vessel fracture mechanics and flow separation, instability phenomena 0-99971
- propellers, acoustic wave generation, non-uniform liq. stream 0-96094
- steel, Ni, welded joints on LNG carriers mech. props. and fracture toughness 0-85017
- submarine periscope optical design for laser rangefinding compatibility 0-78987
- submersibles for underwater research, commercially available vessels 0-82104
- surface effect, noise control design problems 0-74598

**shock, thermal** *see thermal shock***shock measurement**

- dynamic shock position measurements using microprocessor-controlled time-domain reflectometer 0-79248
- K-band microwave interferometry for measurements of high surface vels. 0-77761
- laser-produced shock wave optical diagnostic system 0-79421
- temperature meas. of shock compression of solids by optical means 0-86304
- C piezoresistive gauges, shock loading and unloading behaviour up to 5 GPa 0-87750

**shock tubes**

- see also shock waves*
- detonation wave propagation, investigations on suitability of piezoelectric and magnetoelastic detectors (*Polish*) 0-79351
- driver gas flow with fluctuations 0-96282
- Mach wave radiation of hot supersonic jets 0-69894
- pulse-pressure generator, quasistatic method for stepped pressure transducer testing 0-62678
- pulsed gasdynamic shock-tube laser, working time extension 0-99696
- thermal boundary layer interactions in shock tube sampling for kinetic obs. 0-104420
- wall supported shock precursor obs. 0-100011
- Fe+Ar, Fe I reson. line, collisional broadening at high temp. (*German*) 0-106298
- HBO<sub>2</sub>, band strengths, shock tube IR spectrosc. meas. 0-106358
- MgO, electronic transition strengths, shock tube meas. 0-87183
- OBf, band strengths, shock tube IR spectrosc. meas. 0-106358

**shock wave effects**

- Blair dolomite, shock wave expts. 0-67362
- brittle solid deformation, review of theory 0-72493
- Bruderheim meteorite, L6 chondrite, 500 Ma shock event effects on U-Pb age 0-98616
- concrete slab, explosive shock resist., tensile fracture 0-85065
- containment vessel, cylindrical, submerged, dynamic plastic response, design formulae 0-83759
- elastoplastic relaxing media, shock waves struct., distribution model 0-58961
- electrical conductivity of high temp. imperfect gas (*Russian*) 0-100072
- ESR, particle size and lattice microdistortions 0-97140
- Fe, twinning under influence of plane shock wave (*Russian*) 0-92538
- ferroelectrics, converters of shock wave mech. energy into elec. power 0-61429
- frame, plane, impulsively loaded, large deflections, mode approx. technique extension 0-83757
- Goat Paddock cryptexplosion crater, W.Australia struct. and shocked rocks petrology 0-98322
- graphite-diamond, shock induced transform. anal., post shock graphitisation 0-79933
- graphite/epoxy laminates, stress wave damage 0-93611
- ice VI, shock compression expts. for Hugoniot function 0-84248
- interstellar medium, shock enhancement of HCO<sup>+</sup> in supernova remnant (IC 443) 0-82464
- interstellar molecule formation and IR emission in shocks, physical processes 0-62219
- liquids, shock excitation for diffuse-field reverberation studies 0-88267
- manganin foil like gauge calibration in planar shock wave expts. 0-95091
- metal tube, dynamic lateral compression, strain rate effects 0-83758
- metallic shell, explosive expansion, deform. and rupture modes and mechanisms 0-85064
- metallic shell, explosive expansion, rupture behaviour 0-85063
- metals, constitutive model at high strain-rate, shear modulus, yield strength 0-75292
- metals, dislocations and shock compression, thermodynamics 0-100235

**shock wave effects continued**

- metals and alloys, shock wave effect on martensitic transform. (*Russian*) 0-96595
- minerals, dislocations and shock compression, thermodynamics 0-100235
- monatomic three dimensional FCC lattice, solitary wave effect on shock profile 0-79874
- paraboloids of revolution, internal fractures due to stress wave focusing 0-83762
- plate under the effect of a spherical shock wave, stresses and deflections 0-79204
- Plexiglas 0-66592
- PMMA, shock loaded, lateral compressive stresses meas. using Yb piezoresist. gauges 0-103007
- porous solid, generalised p- $\alpha$  model, eqn. of state, sound vel. 0-65154
- powders, brittle, shock wave disintegration test method 0-66744
- power type spectrum for particle accel. at spherical shock wave (*Russian*) 0-72730
- protostellar cloud and formation of solar-type stars in spherical symmetry, accretion shock effects 0-62107
- $\alpha$ -quartz 0-72490
- rock half-space, impact of steel cylinder and effects 0-85649
- silica, fused, temp. in high-press. shock state 0-72490
- single crystals under large loads, theoretical elastic behaviour, review and appl. 0-71681
- solar wind, energetic particles shock accel. in corotating, interaction regions 0-82159
- solar wind, ion acceleration to 40 keV by shock wave disturbances 0-72738
- sonic boom, pressures inside room with open window, effect on plaster/wood walls 0-69602
- steel, high-strength, dynamic yield strengths, phase transition press. and Hugoniot parameters 0-75331
- steel, stainless, austenitic, explosively welded, orientation relationship in martensitic transform. 0-104158
- steel, stainless, shock loaded, residual martensite obs. 0-104414
- stellar winds, shock heating rel. to turbulent mixing with interstellar gas 0-67701
- structural member, dynamic loading and plastic response, review 0-83756
- supernovae, effects of core eqn. of state on outcome of stellar collapse 0-85928
- Textolite 0-66592
- 1,3,5-trinitro 1,3,5-triazacyclohexane, shock-induced intramol. bond breaking, XPS and EPR study 0-76512
- trinitrotoluene, shock-induced intramol. bond breaking, XPS and EPR study 0-76512
- unsteady flow of supersonic gas stream past a slender profile, asymptotic expansion of nonlinear effects 0-69863
- Venus atmosphere, NO prod. by thunder shock waves 0-98587
- wall supported shock precursor obs. 0-100011
- Al aircraft alloy, fatigue resistance improvement by laser shock 0-93654
- Al, elastoplastic stress wave propag. (*Czech*) 0-108507
- Al, shock compression at high press., neutron irradi. (*Russian*) 0-88264
- Al, shock compression at high press. (*Russian*) 0-92608
- Al, shock wave data, 'solid Hugoniot' rel. to 'fluid Hugoniot' 0-65155
- Al-steel mixture, wear resistant, produced by compaction by discrete shock waves 0-84882
- $\beta$ -BaF<sub>2</sub>, stress wave profiles 0-96593
- CO<sub>2</sub> pulsed laser system, acoustic suppression 0-74378
- CS<sub>2</sub>, shock heated, visible emission 0-58274
- Cu, shock wave data, 'solid Hugoniot' rel. to 'fluid Hugoniot' 0-65155
- Cu-concentration junctions with solder, shock-induced elec. response 0-75626
- Cu-Mn alloy, manganin, hysteresis-corrected calibration under shock loading 0-74818
- $\alpha$ -Fe<sub>2</sub>O<sub>3</sub>, elec. resist. and phase transition under shock compression 0-72496
- Fe<sub>2</sub>SiO<sub>4</sub>, fayalite, elec. cond. obs. under shock compression 0-81873
- H<sub>2</sub>O, shock compression at high press. (*Russian*) 0-92608
- (Mg,Fe)<sub>2</sub>SiO<sub>4</sub>, shock deform. expts., Hugoniot data implications 0-94497
- Mg<sub>2</sub>SiO<sub>4</sub>, temp. in high-press. shock state 0-72490
- Mo, shock deformation twinning, shock loaded BCC and FCC metals comparison 0-104413
- NH<sub>4</sub>NO<sub>3</sub>, shock-induced intramol. bond breaking, XPS and EPR study 0-76512
- NO<sub>2</sub>, shock heated, visible emission 0-58274
- Pb, shock compression at high press. (*Russian*) 0-92608
- Pb(Zr,Ti<sub>1-x</sub>)O<sub>3</sub>, meas. of Hugoniot curve with commercial manganin stress gauges 0-70362
- SO<sub>2</sub>, shock heated, visible emission 0-58274
- SO<sub>2</sub>+Ar, dissoc. rate meas. behind shock wave, laser Schlieren method 0-81296
- p-Si, elec. resist., shock wave compression effects 0-80265
- Si on sapphire film, laser annealing non-thermal theory expt. test 0-89273
- SiO<sub>2</sub>, shock compression at high press. (*Russian*) 0-92608
- TiO<sub>2</sub>, rutile phase, shock induced phase transition anisotropic behaviour 0-103475

**shock waves**

- see also detonation; explosions; plasma shock waves; shock tubes; shock wave effects; supersonic flow*
- acceleration of particles in astrophysical plasma 0-82192
- air, atmospheric, cylindrically converging blast waves 0-92180
- arbitrary strength, with viscosity and heat conduction, stability 0-59076
- axially symmetric explosion in magnetogasdynamics 0-62007
- brightness, in air with reduced density 0-86371
- bubble, spherical, pressure waves produced by collapse (*Japanese*) 0-100027
- cavitation bubbles, amplitude distrib. of pulses produced by shock waves 0-64252
- channel, shock wave stationary motion for axial blowing and two-layer detonation 0-92177
- chemically reactive flow, aerodynamic heating of blunt bodies 0-74998
- completely dispersed, in relaxing mixtures, struct. obs. 0-59072
- concave corners, Whitham theory of shock-wave diff. 0-100012
- corner interaction of boundary layer and shock wave, flow separation 0-96287
- Cygnus Loop, fast shock wave detection, optical spectra 0-82467
- cylinders, elliptic 2-D, cavitation shock-noise measurement for different eccentricities 0-79368
- detonation wave, turbulent, boundary-layer treatment 0-106791

## shock waves continued

detonation wave magnification by pulsation energy 0-59075  
 detonation waves, heterogeneous, propagation and blast wave initiation 0-74915  
 dispersed supersonic two-phase flow, shock characts., droplet size depend. at nozzle 0-106815  
 distensible tubes, fluid-filled, biological appl. 0-94272  
 duct, supersonic flow downstream oscillations from abrupt cross section increase, nozzles 0-74976  
 dusty gases, fully dispersed wave struct., Navier-Stokes eqns. 0-69875  
 Earth bow shock, conference, Strasbourg, France (1978 August 31 to September 1) 0-82573  
 Earth bow shock, DC mag. field obs. 0-90306  
 Earth bow shock, first evidence and early studies, historical introduction 0-85816  
 Earth bow shock, initial ISEE mag. field obs. 0-90307  
 Earth bow shock, obs. of backstreaming protons in upstream solar wind 0-90309  
 Earth bow shock, review of upstream energetic-particle meas. 0-90308  
 Earth bow shock, solar wind upstream deceleration rel. to diffuse upstream ions origin 0-98528  
 Earth bow shock, three-dimensional shape 0-85832  
 Earth bow shock, upstream particle events obs. close to shock and 200 R<sub>E</sub> upstream 0-77247  
 Earth bow shock plasma, possible generation mechanisms of low-freq. waves ( $\leq 50$  Hz) 0-90312  
 Earth bow shock vicinity, low-freq. waves obs. 0-90311  
 elastic bars, phase boundary propagation, dynamic elastic bar theory, sound wave interactions 0-69706  
 electrically exploded etched Cu mesh, impulse loading 0-64428  
 energy spectrum characts. of shock processes in fluid 0-103041  
 fusion, inertial confinement, implosion of black body radiation 0-73990  
 galaxies, density wave shocks rel. to wave energy and lifetime and galaxies spiral struct. 0-98715  
 galaxies, two-arm spiral shock prod. by non-linear corrugation waves 0-67859  
 gas, dissociating, relativistic flows, growth and decay of weak waves, shock wave formation 0-69949  
 gas, dissociating, sonic wave propagation, formation of shock waves 0-64672  
 gas, isothermal, strait compression wave due to pressure pulse driven flat piston 0-69873  
 gas, polytropic, synchronous shock waves overtaking each other, disintegration of arbitrary discontinuity 0-69871  
 gas, shock wave under continuous energy supply 0-103042  
 gas compression in heavy piston, hypersonic speed, shock waves 0-69869  
 gas expansion into near vacuum, contact front-primary shock regime, particle path formulation 0-59070  
 gas mixtures, detonating, symmetric piston motion 0-59073  
 gas shock adiabats, props. near Jouguet points 0-92178  
 gas-particle flow in shock tube, finite difference calc. (*Japanese*) 0-79390  
 gasdynamic disturbance in chem. reacting gas mixture, shock wave formation 0-74999  
 graphite, shock wave, prod. by explosion, vel. meas. 0-59074  
 Herbig-Haro object 1, shock wave model rel. to far UV spectrum 0-67714  
 Herbig-Haro objects, stellar wind model 0-85985  
 homothermal shock, prod. by instantaneous monochromatic radiation 0-59159  
 Hugoniot eqn. corollaries, impact heat transfer and shock waves 0-92132  
 hydrodynamic cumulation regimes during lining collapse, cumulative jet 0-69891  
 ideal gas supersonic flow around blunt wedge, sonic line shape 0-64577  
 impact response, two degrees of freedom system, effect of damping 0-74587  
 impacted solid, expt. facility to produce and measure compression and shear waves 0-59581  
 impacted solids, compression and shear wave propag., modelling 0-83755  
 implosive spherical, produced by laser pulses, shadowgraphic detection 0-87529  
 infinite circular cylinder, moderately strong shock wave interaction 0-92176  
 instability in a relaxing medium 0-100013  
 interactions with boundary layers, review, book contrib. 0-96283  
 intergalactic medium, shock waves rel. to giant ellipsoidal shells around normal elliptical galaxies 0-86000  
 interplanetary collisionless shock waves, thickness 0-90314  
 interplanetary shock followed by large solar wind He<sup>+</sup> flux, Imp 7 obs. 0-101520  
 interplanetary shock wave, 1978 January 3 to 4, Prognoz-6 energetic particle and solar wind meas. 0-90315  
 interplanetary shock wave, He<sup>+</sup> obs. in driver gas 0-72735  
 interplanetary shock wave in solar wind, thermal electrostatic noise, LF obs. from ISEE 3 0-101519  
 interstellar bright rimmed molecular clouds, evidence for CH emission from postshock gas 0-62238  
 interstellar cloud, shocked gas dynamics rel. to sequential form. of subgroups in OB associations 0-98696  
 interstellar medium, H II region shock fronts rel. to interstellar clouds form. 0-109506  
 interstellar radiative shocks, thermal instability rel. to maser condensations form. 0-67821  
 interstellar shocks from presupernova stellar wind, rel. to supernova remnant filamentary struct. 0-62249  
 ionising Ar flows, shock wave and laminar boundary layer coupled interaction 0-59071  
 Kelvin-Helmholtz instability in supersonic and super-Alvenic fluids 0-87816  
 laser-produced shock wave optical diagnostic system 0-79421  
 localisation, by shock-capturing results of computation of gas dynamics problems 0-83815  
 Ludwig tube, steady flow duration extension, reservoir orifice method, variable opening area effect 0-64579  
 Mach wave radiation of hot supersonic jets 0-69894  
 magneto-radiative shocks, axisymmetric, equatorial propagation 0-79349  
 magnetosonic wave propag. in warm plasma, appl. to solar atm. MHD fluctuations 0-77275  
 magnetosphere, electrostatic shock waves rel. to ULF elec. field fluctuations in dayside auroral oval 0-98505  
 MHD, generalised polar diagrams of plane-parallel stationary similarity flows, waves 0-96314

## shock waves continued

mobile load on ideally packed material layer 0-99952  
 monotonic three dimensional FCC lattice, solitary wave effect on shock profile 0-79874  
 MSH 11-54, supernova remnant, adiabatic shock wave model rel. X-ray obs. 0-82463  
 multicomponent gas mixture, transport eqns. and distrib. functions 0-64581  
 multidimensional fluid dynamic calcs., artificial viscosity use, Navier-Stokes viscosity 0-92181  
 NGC 7027, planetary nebula, shock model for H<sub>2</sub> emission generation 0-98698  
 nonlinear heat conduction effect on shock wave fronts (*Russian*) 0-79352  
 nonlinear mechanics eqns. and entropy growth across a shock, symmetric form 0-69705  
 nozzles, high enthalpy supersonic flow conversion to hypersonic flow 0-74937  
 ocean blast wave propagation, theory for stratified ocean (*Russian*) 0-81904  
 oceanic warm front propagation, shock wave model with appl. to Sagami Bay Kyucho phenomenon 0-94538  
 particle acceleration by MHD shock turbulence 0-87894  
 piston, magnetic field effect, self-similar magnetogasdynamic problem with radiative heat transfer 0-64578  
 plane relativistic shock waves, propag. in slowly moving medium 0-62005  
 plane wave-plane shock interaction in magnetofluidynamics 0-69931  
 polytropic medium layer on linear elastic substrate, mass-impact generated shock waves 0-69870  
 propagation in general relativity, stationary approx. 0-86172  
 propagation investigations on suitability of piezoelectric and magnetoelastic detectors (*Polish*) 0-79351  
 pseudo-steady single-Mach reflection, reconsideration of shock polar soln. 0-99893  
 radiating gases, sonic wave propag., wave front curvature effects, shocks 0-87784  
 rapidly rot. gas, free jet expansion, Newtonian thin shock layer approx. 0-74888  
 rarefied shock wave existence near thermodynamic critical point of a substance (*Russian*) 0-88263  
 reflection from cylindrical surface, transition from normal to Mach refl. 0-64582  
 reflection from sphere or cylinder, gas parameter distrib. in initial stage 0-96281  
 relativistic blast waves that accelerate 0-67534  
 relativistic fluid with vibrational relaxation, growth and decay of weak discontinuities 0-69948  
 relativistic shock waves, anal. approaches (*French*) 0-96317  
 rotating gas, strong diverging cylindrical shock propagation 0-79350  
 self-similar explosion waves of variable energy at the front 0-103040  
 shell deformation by supersonic gas flow, drag 0-96279  
 shells, two fluid-coupled cylindrical elastic, transient response to incident press. pulse 0-58966  
 slurry explosives, layered medium with liquid-polytropic gas structure, pressure pulse propagation 0-69872  
 solar coronal expansion, hydrodynamic blast wave theory with radiation heat flux 0-90377  
 solar flare generated shock wave, plasma enriched by O<sup>6+</sup> and He<sup>++</sup> 0-72740  
 solid, compression wave interaction, pulsed electron beam initiation 0-79877  
 sonic boom of supersonic transport aircraft, effects on ecological environment 0-106661  
 sphere at supersonic speeds, impulsive motion, shocks, subsonic flow at stagnation point 0-106814  
 spherical imploding shocks, pressure extremes 0-64580  
 sputtering yields, hydrodynamical approach to non-linear effects 0-66374  
 square shaped fluid shock wave pulses with variable time duration 0-74593  
 steady homenergetic compressible flow with finite shocks, variational principle 0-69874  
 stellar atmospheres, soln. for one-dimensional piston problem in non-ideal gas 0-82185  
 strained coordinate method for transonic flows 0-69861  
 supernova, shock accelerated galactic cosmic rays 0-82154  
 supernova blast wave instabilities, adiabatic and isothermal models 0-67814  
 supernova remnant optical emission spectra, effect of shock wave intermediate zone radiative cooling 0-109517  
 supersonic nozzle, pulsed jet wave struct. in nonstationary flow stage 0-59094  
 supersonic separation flow, 2- and 3-dimensl, turbulent boundary layer and shock wave 0-100917  
 thermal boundary layer interactions in shock tube sampling for kinetic obs. 0-104420  
 tracking, subgrid resolution of fluid discontinuities 0-105506  
 translational relaxation at shock wave front in gas mixture 0-74917  
 transonic flow, parabolic regularisation of nonlinear mixed elliptic hyperbolic eqn., finite element anal. 0-83814  
 transonic flow, shock wave interaction with turbulent boundary layer, pressure distrib. 0-74918  
 transonic flow, shock wave interaction with turbulent boundary layer, wall shear stress 0-74919  
 transonic flow, unsteady, turbulence modelling, compression waves developing into shock wave 0-74909  
 turbulent boundary layer interaction 0-74916  
 ultrahigh press. (TPa) shockwave from underground nuclear explosion 0-59580  
 unsteady laminar boundary layers behind blast waves, num. soln. 0-69776  
 viscous compressible flow, hybrid integration scheme, shock tube problem 0-69868  
 viscous materials, heat-conducting, with hidden variables, shock waves and acceleration waves 0-74788  
 W1, supernova remnant, shock wave refl. from small dense cloud rel. to radial vel. field 0-62250  
 water, cavitation expts. using shock tube 0-87789  
 water, explosive shock wave propagation, energy hypothesis 0-92179  
 weakly nonlinear wave propagation due to dispersion and dissipation, long wave approx. 0-57104  
 X-ray induced shocks in stellar winds of massive binaries 0-94784  
 Ar, shock-tube end-wall boundary layer 0-79348



**shock waves continued**

- Fe, Armco, dynamic  $\alpha \rightarrow \epsilon$  transform., stress gauge meas. 0-96594  
 H, ionisation rates, shock tunnel meas. 0-75022  
 \*He, liquid, first sound nonlinear wave distrib. (*Russian*) 0-107588  
 \*He, superfluid, second sound discharge and compression shock wave propagation (*Russian*) 0-103529  
 Xe, condensed at high press., electron-band theory and fluid theory calcs. 0-59875

**shocks, electric** *see electric shocks***short-circuit currents**

- insulators, HV for transmission lines, power arcs occurring in networks and laboratories, comparisons 0-87983  
 LV short-circuit testing station, equipment and measurement methods (*Polish*) 0-77773  
 p-GaSe, back wall Schottky barrier cells, diffusion length, RT spectral response meas. 0-107806  
 Si solar cells, analysis of short-circuit current 0-85285  
 SiH<sub>4</sub>, amorphous, solar cells, short circuit-currents and collection efficiencies 0-94028

**short-range order**

*see also order-disorder transformations*

- adsorbed layers, order-disorder transition, effect on work function 0-59791  
 alloys, binary, constitution diagrams, computer calc. (*Russian*) 0-84909  
 alloys, disordered, residual resistivity due to clustering, ageing effects 0-65521  
 alloys, phase transition premonitory phenomena, exam. by electron diffraction and microscopy (*French*) 0-59651  
 alloys, substitutional, electrical resist., long and short range orders effect 0-107761  
 amorphisation due to ion bombardment, SRO struct. 0-79844  
 amorphous materials, Mossbauer effect, props. and investigation methods (*French*) 0-80652  
 amorphous solid, structural defects, computer simulation study 0-88040  
 antimonates, columbite or trirutile struct., force fields rel. to cryst. struct. (*French*) 0-107104  
 binary linear chain, electronic props. 0-96769  
 copolymer globule model, orientationally-ordered liq. cryst. state (*Russian*) 0-59389  
 disordered structures, two-dimensional, computer program for modelling (*French*) 0-59337  
 disordered system with corrs., density of states at band tail 0-80154  
 distance dependence restrictions, Cowley short-range order parameters 0-103294  
 ethylammoniumtetrachlorochromate, optical absorption intensity, short-range spin correlation 0-108185  
 Heisenberg model, nearest-neighbour spin-spin correl. functions calc. 0-80537  
 hollandites, cryst. growth and structural props. 0-89129  
 magnetic soft and hard materials, garnets, magnetic properties and applications, structural props. 0-65760  
 melts, of a congruently melting substance, single struct. model 0-103233  
 metals, amorphous, structure model, structural changes 0-92462  
 methylammoniumtetrachlorochromate, optical absorption intensity, short-range spin correlation 0-108185  
 niobates, columbite or trirutile struct., force fields rel. to cryst. struct. (*French*) 0-107104  
 nonstoichiometric compounds, physicochem. props. depend. on short-range order struct. 0-100227  
 pentacene, disordered solid layer, absorpt. spectra 0-93417  
 photoemission technique for meas. of magnetic order and spin depend. of electron scatt. 0-60748  
 random anisotropy model in Ising model, Monte Carlo simulation 0-80546  
 rare earth-transition metal alloys, disordered, magnetisation behaviour 0-71099  
 semiconductors, amorphous, short-range order, theory and probes 0-79698  
 structural phase transformations, static critical behaviour 0-92640  
 substitutionally disordered binary systems, existency domain 0-88068  
 tantalates, columbite or trirutile struct., force fields rel. to cryst. struct. (*French*) 0-107104  
 TCNQ salt, TSeF-TCNQ, short-range ordering investigated by XDE 0-59652  
 ternary BCC alloys, ordering process, effect of short-range order (*Russian*) 0-84908  
 tetracene, disordered solid layer, absorpt. spectra 0-93417  
 transition metal alloys, amorphous, mag. props., chem. short-range order 0-75739  
 transition metal alloys, binary, state density curves, relation between short-range order and Fermi level position, CPA calculations 0-107687  
 transition metal-metalloid glasses, short range order of dense-random-packing models 0-64907  
 transition metal-metalloid glasses, struct. end plastic flow, review 0-84909  
 $\beta$ -Al<sub>2</sub>O<sub>3</sub>-Ag<sub>2</sub>O, stoichiometric A phase, X-ray diffuse scatt. obs., sublattice phase transition 0-64944  
 AlZn, disordered, residual resistivity due to clustering, ageing effects 0-65521  
 As<sub>2</sub>S<sub>3</sub>, amorphous, struct., vibr. and electronic spectra 0-64908  
 As<sub>2</sub>Se<sub>3</sub>, glassy defect electron states, tight binding calc. 0-96818  
 Au-Pd (1/50 wt.%), quenched, vacancy annihilation and short-range order formation, elec. resist. 0-108487  
 Au<sub>2</sub>Mn, heat treated, short-range order, diffuse X-ray diffr. study (*German*) 0-88092  
 Au<sub>2</sub>Si<sub>1-x</sub>, amorphous films, phys. studies 0-75476  
 Co<sub>0.9</sub>P<sub>0.1</sub>, noncrystalline ferromagnet, electroless deposited, struct. and microscopic mag. props. 0-88063  
 CsLi<sub>0.5</sub>(Al,Fe), F<sub>0.5</sub> pyrochlore, Mossbauer contrib. to exam. of cationic order (*French*) 0-93224  
 CsLi<sub>0.5</sub>Fe<sub>1-x</sub>F<sub>0.5</sub> pyrochlore, Mossbauer contrib. to exam. of cationic order (*French*) 0-93224  
 CsNiF<sub>3</sub>, one-dimensional ferromagnet, optical absorpt. and static spin correlation functions 0-71415  
 CsNiF<sub>3</sub>, quasielastic neutron scatt. around Neel-point 0-75768  
 CsNiFeF<sub>6</sub> pyrochlore, Mossbauer contrib. to exam. of cationic order (*French*) 0-93224  
 Cu-Al, short range order and static distortion contribution to residual elec. resistivity (*Russian*) 0-70672
- short-range order continued**  
 $\alpha$ -Cu-Al (6 to 17 at.%), short-range order investigated by diffuse X-ray scatt. (*Russian*) 0-104187  
 $\alpha$ -Cu-Al (9.13, 13.56, 14.76, wt.%) short-range ordered, characterisation of locally ordered regions 0-79747  
 Cu-Al(Au) alloys, HV electron microscopy, crit. voltages depend. on comp., temp. and short-range order 0-100146  
 Cu-Au alloys, vacancy and divacancy migration activation energies, elec. cond. meas. 0-88140  
 Cu-Ga (17 wt.%), elec. resist. and TEM studies 0-108604  
 Cu-Si (6.5 at.%), plastic deformation, HVEM study (*French*) 0-66605  
 r-CuMn, annealing ordered phase study by neutron diffr. 0-89265  
 Cu<sub>2</sub>MnIn<sub>1-x</sub>Sn<sub>x</sub> alloy, compositional SRO, hyperfine interactions 0-71065  
 Fe-B, amorphous alloys, compositional study on short-range struct. 0-84095  
 Fe-Ge, amorphous, atomic struct., neutron diffr. study 0-59392  
 Fe-Ni alloy, martensitic transform., influence of thermal and electron irradi. treatment of austenite (*Russian*) 0-66509  
 Fe-Ni-Cr, mag. props. in weak mag. fields (*Russian*) 0-75771  
 $\gamma$ -Fe-Ni-Mn alloys, spin glass state, short and long range order investigation 0-65808  
 Fe-P(Ga)(As)(Sb), dil., short range order, NMR study 0-71237  
 Fe-Sb-Ni(Cr), dil., short range order, NMR study 0-71237  
 Fe<sub>10.82</sub>K<sub>1.55</sub>O<sub>17</sub>, ferrite, cryst. struct., nonstoichiometry, ion-ion correlations 0-88130  
 Fe<sub>40</sub>Ni<sub>40</sub>P<sub>14</sub>B<sub>6</sub>, amorphous, resistometric study of short-range ordering rel. to heat treatment 0-70140  
 Fe<sub>2</sub>Zn<sub>1-x</sub>F<sub>2</sub>, Neel point and short range order, dilution effects, mag. birefr. obs. 0-71019  
 GaPAs<sub>1-x</sub>N<sub>x</sub>, luminesc. of N bound state excitons, local-environment effects 0-100691  
 Ge-Si, electronic structure, short-range order effects, calc. 0-92861  
 GeO<sub>2</sub>, vitreous, struct., contrasted with EXAFS obs. of ZnCl<sub>2</sub> liq. and glass struct. 0-70133  
 HfV<sub>2</sub>D<sub>4</sub>, disordered solid solution, order-disorder transition 0-88321  
 La<sub>2</sub>NiO<sub>4</sub>, La<sub>2</sub>CuO<sub>4</sub>, magnetic properties obs. 0-70937  
 Li<sub>2</sub>O-LiX-B<sub>2</sub>O<sub>3</sub> glass, X=halogen, high anionic cond. of new solid electrolytes 0-107546  
 Mn-Bi mictomagnetic alloy, mag., elec. and elastic props. (*Russian*) 0-108028  
 MnOOH, mag. ordering, fine struct. and crit. behaviour, neutron diffr. meas. 0-65800  
 Mn<sub>2</sub>Zn<sub>1-x</sub>F<sub>2</sub>, Neel point and short range order, dilution effects, mag. birefr. obs. 0-71019  
 Nb<sub>2</sub>Ge(Si), amorphous films, thermally-activated internal friction peaks, structural obs. 0-80147  
 Nb<sub>2</sub>Ge(Si), RF sputtered films, amorphous atomic scale struct. 0-84064  
 Nb<sub>2</sub>O<sub>5</sub>-WO<sub>3</sub> system complex cpds. with TTB type subcells, HV superhigh resolution electron microscopy obs. of struct. 0-103311  
 Nb<sub>2</sub>Sn, Al<sub>15</sub> cpd., normal state, low temp. resist., disorder effects 0-107762  
 Nd<sub>2</sub>NiO<sub>4</sub>, Nd<sub>2</sub>CuO<sub>4</sub>, magnetic properties obs. 0-70937  
 Ni, paramagnetic, mag. form factors in Stoner-like model 0-97061  
 Ni-Cr, (30 wt.%), collective dislocation movements, in situ study 0-100243  
 Ni-Cr (33 at.%), plastic deformation, HVEM study (*French*) 0-66605  
 Ni-Cu, electron-irrad., neutron-scatt. studies 0-75268  
 Ni-Ge, amorphous, atomic struct., neutron diffr. study 0-59392  
 Ni-Mn, permeability, diffusion and solubility of H 0-107573  
 Ni-Pt alloys, magnetic-moment distrib. neutron study 0-97066  
 Ni-Fe alloys, low-temperature specific heat, long and short range order effects 0-100339  
 Ni<sub>40</sub>Ti<sub>60</sub>, amorphous, chem. short-range-order, X-ray and neutron scatt. obs. 0-96447  
 P, amorphous, prepared by chem. transport in low-pressure H<sub>2</sub> plasma, radial distrib. function 0-64899  
 Pb, liquid, short range order amongst cond. electrons 0-107040  
 Pd-Si, amorphous, compositional study on short-range struct. 0-84095  
 Pd<sub>1-x</sub>W<sub>x</sub>, calc. of short-range order parameters from X-ray scatt. data (*Russian*) 0-75367  
 Pr<sub>2</sub>NiO<sub>4</sub>, Pr<sub>2</sub>CuO<sub>4</sub>, magnetic properties obs. 0-70937  
 PtCr, AC susceptibility near percolation limit, ordered and disordered alloy 0-65900  
 Rb<sub>2</sub>CrCl<sub>4</sub>, optical absorption intensity, short-range spin correlation 0-108185  
 Sc-Zr(Mg), low-temp. heat capacity 0-75370  
 short range order amongst cond. electrons Al, liquid, short range order amongst cond. electrons 0-107040  
 Si noncrystalline film, struct., interatomic distances, SRO 0-107053  
 Si<sub>1-x</sub>H<sub>x</sub>, noncrystalline film, struct., interatomic distances, SRO 0-107053  
 SiO<sub>2</sub>, dielec. and optical props., chemical disorder effects 0-80815  
 Sm<sub>2</sub>CuO<sub>4</sub>, magnetic properties obs. 0-70937  
 TeO<sub>2</sub>-P<sub>2</sub>O<sub>5</sub> system, glass struct., neutron diffr. study 0-70128  
 Ti-Fe, equiatomic, heats of form., influence of short-range order (*Russian*) 0-81354  
 V<sub>12</sub>, MCD spectra, interpretation rel. to mag. struct. 0-66222  
 V<sub>12</sub>, mag. struct., long- and short-range order and Mossbauer spectroscopy 0-65803  
 ZnCl<sub>2</sub>, glassy and liq. EXAFS obs. of struct., comparison with vitreous GeO<sub>2</sub> 0-70133  
 ZnCr<sub>2</sub>Se<sub>4</sub>:In, magnetoresist. and elec. resist. above and below Neel temp. (*Russian*) 0-88576  
 Zr(Ca,Y)O<sub>2-x</sub>, local ionic arrangement, X-ray diffr. study 0-100203
- shot noise** *see random noise*
- showers, cosmic ray** *see cosmic ray showers and bursts*
- Shpol'ski spectra**  
 benzenoid aromatics, triplet zero field splitting parameters, ODMR obs., struct. effects 0-78636  
 chloroquinolines, photophys. behaviour, substituent and solvent effects 0-106342  
 multisite luminesc. spectrum deconvolution, vibr. struct. anal. 0-58304  
 porphyrin in n-octane Shpol'ski matrix, defect props., Monte Carlo obs. 0-63533
- shrinkage**  
 coke, shrinkage kinetics during calcination 0-93572  
 concrete, flowing, exp. studies (*Japanese*) 0-89298  
 concrete, high strength, made with a special cement admixture, mech. props. (*Japanese*) 0-89297

**shrinkage continued**

- concrete, strength, shrinkage strain and deterioration down to  $-160^{\circ}\text{C}$  (*Japanese*) 0-100886  
 ethylene-vinyl alcohol copolymer, drawn samples, annealing effect around  $T_g$  temps. on shrinkage and mol. orientation 0-79712  
 graphite, polygranular, flexural strength after heat treatment porosity correl. 0-84996  
 kaolin bodies, effect of mineralizers on firing shrinkage, microstruct. and strength 0-97488  
 magnesite artifacts, roasted, props., filler porosity effect 0-104099  
 polyethylene flow crystallisation, in extensional flow developed by convergent capillaries, props. 0-84111  
 polyethylene terephthalate, oriented, amorphous, stress-induced crystn., shrinkage meas. 0-92466  
 C, polygranular, flexural strength after heat treatment porosity correl. 0-84996  
 C reinforced plastic, degraded, study of strain, 20 to  $1000^{\circ}\text{C}$  0-71680  
 GdCu, electrical resistivity and length changes with temp., hysteretic behaviour 0-97600  
 SiAlON, prepared from siliceous sand and Al powder, hot pressing, steatite contamination effects (*Japanese*) 0-93528  
 YIG, substituted, magnetite nucleation in transitional zone, ionic process, lattice imaging 0-107424  
 $\text{ZrO}_2\text{-CaO(Y}_2\text{O}_3)$  ceramics with grainy structure, props., effect of heating to  $2000^{\circ}\text{C}$  0-104194

**Shubnikov-de Haas effect** see *magnetoresistance*

**Si-Ge alloys** see *Ge-Si alloys*

**SIC** see *monolithic integrated circuits*

**signal acquisition** see *signal detection*

**signal coding** see *encoding*

**signal delay lines** see *delay lines*

**signal detection**

- acoustic, Fourier series method appl. to signal in noise background, comments 0-106671  
 acoustic signals, robust sequential detection of weak signals in undefined noise using acoustic arrays 0-58861  
 auditory detection of intensity increments of narrowband noise signals, amplitude model 0-61591  
 colour vision models, vector magnitude operation, derivation from signal detect. theory 0-101174  
 CW signals in white noise, influence of data window shape 0-64300  
 Gaussian acoustic signal detection using array processors, performance eval. 0-83696  
 hearing, detection of temporally uncertain signals 0-67094  
 hearing, theory of FM detection for low modulation freqs. 0-61586  
 homodyne detection at 100 GHz with a pyroelectric detector 0-105650  
 nonwhite noise, S/N ratio and detail detection 0-102648  
 partially coherent radiation, optical heterodyne detection 0-77871  
 partitioned signal detection by discrete cross-spectrum analysis 0-91966  
 photodetector with automatically adjustable threshold level, design considerations 0-62724  
 proportional chamber, electronic device using K405KhPI IC (USSR) 0-91376  
 shape variation detection, two-component chromatographic peaks resolution 0-71971  
 STEM, multi-signal detection and processing 0-73552  
 zero-crossing statistics utilization 0-74609

**signal processing**

- see also *bandwidth compression; correlation theory; data compression; filtering and prediction theory; picture processing; signal detection*  
 acoustic, bispectrum and its appl. (*Japanese*) 0-91965  
 acoustic, broadband directional reception, US transducer arrays 0-96126  
 acoustic, echolocation in bats 0-108906  
 acoustic, eigenvector decomposition of correlation matrices 0-96118  
 acoustic, element failure and random errors effect on sidelobe level for linear array 0-106670  
 acoustic, estimation of source motion from time delay and time compression measurements 0-58860  
 acoustic, gain limitations of passive vertical line array in shallow water 0-96117  
 acoustic, maximum a posteriori estimation of narrow-band signal parameters 0-96120  
 acoustic, maximum likelihood detection and estimation for harmonic sets 0-96116  
 acoustic, multiple input/output problems anal. 0-96122  
 acoustic, optimum range and bearing estimation with randomly perturbed arrays 0-96119  
 acoustic, phonon echo, recent trends in physical acoustics (*Japanese*) 0-79889  
 acoustic, resolving directions of sources in correlated field incident on array using adaptive beamforming algorithm 0-64297  
 acoustic, schemes for filtering signals propagating through random multipath medium 0-58862  
 acoustic, simplified approach to optimum quadrature sampling 0-79061  
 acoustic, time windows and DFTs (*Japanese*) 0-87658  
 acoustic, underwater sound, average array signal response in two-path medium 0-87657  
 acoustic, unreliability of coherence estimates based on amplitudes of signals reradiated by rough sea surface, unreliability 0-58847  
 acoustic imaging, multiplicative and additive processing comparison 0-64303  
 acoustic signal characterization using spectral microanalysis 0-74607  
 acoustic sounding of ocean-bottom subsurface layered media, spatial parameter estimation 0-77134  
 acoustical communication theory, computation of modulation and carrier functions of an arbitrary audio signal 0-79064  
 acousto-optical processors based on light polarization discrimination techniques 0-74310  
 acousto-optics, guided-wave, with appls. to wideband communications and signal processing, progress review 0-58801  
 analog, instrumentation, book 0-86047  
 atmosphere radar signal processing, for SOUSY-VHF-radar, using preprocessor 0-85774  
 audio, hearing, application of communication theory 0-79063  
 audition, compound PST histogram rel. to neural activity in cochlear 0-94148  
 audition, freq. following pot., appl. of least-square-fit technique 0-94149  
 auditory evoked brain stem pots., effects of analogue and digital filtering 0-89878

**signal processing continued**

- auditory models and signal processing, conf., Munster, Germany (Sep. 1978) 0-90610  
 autoregressive model order selection applied to physiological signals 0-104780  
 beamforming when the sound velocity is not precisely known 0-96123  
 biomedical MEFV curves, smoothing by digital filtering 0-98157  
 bistable optical device development from integrated two-arm interferometer, appls. (*French*) 0-69555  
 compound PST histograms, deconvolution 0-94146  
 conference on acoustics, speech and signal processing, Denver, CO, USA (Apr. 1980) 0-83689  
 convolution equation solution, problems arising, auditory appl. 0-94147  
 correlation methods, signal parameter meas. 0-57241  
 degenerate SAW elastic convolver, theory 0-74628  
 disturbed measuring systems, estimation of signal parameters, autoregressive linear models (*German*) 0-68165  
 ECG, His-bundle activity detect., theoretical anal. of error during signal averaging 0-94392  
 ECG, R-wave enhancement for heart rate determ., abdominal-lead fetal ECG 0-67264  
 EEG, by spatial deconvolution 0-94391  
 EEG, deconvolution procedure for information extraction from average evoked response signals 0-61724  
 electron diffraction patterns convergent-beam type, obtained by beam-rocking method 0-70085  
 evolution systems, meas., rel. to master eqn., Bayesian anal. 0-90782  
 Gaussian signals in Gaussian noise transmitted over digital channel, degradation of S/N ratio 0-64298  
 Hankel transform computation using projections 0-96124  
 heterodyne holographic interferometry, electronic circuitry used for signal preprocessing 0-87352  
 heterodyne interferometers, quasilinear filtration theory appl. to signal processing (*Russian*) 0-82807  
 image processing appl. of multiple bandpass filters 0-109002  
 information processing methodologies, conference, Trieste, Italy (1979 February 23 to 24) (*Italian*) 0-94917  
 integrated and guided-wave optics, conference, Incline Village, NV, USA, January 1980 0-58772  
 integrated optic spectrum analyser, design of Bragg cells 0-74515  
 interaction of determinate packet with random noise, in Burgers' equation 0-106650  
 ion beam co-ordinate monitor, induced noise-like signals processing 0-102607  
 Josephson ultrahigh resolution sampling system 0-90828  
 laser transit anemometer signals, semiclassical processing 0-59145  
 liver pathology characterisation, clinical appl. of a US attenuation coeff. estimation technique 0-76813  
 mechanical speech processing, new results (*Hungarian*) 0-69604  
 medical US, spread energy method, use of time gain control 0-108988  
 meteorological radar equipment, pulse-wise interpretation of echo-signals (*Russian*) 0-67432  
 metrological research on prospective measuring techniques, conf. Wroclaw, Poland, Sept. 1978 (*Hungarian*) 0-86247  
 myoelectric signal processing, expt. demonstration of optimal myoprocessor performance 0-89882  
 myoelectric signal processing, optimal myoprocessor derivation 0-89881  
 myoelectric signals, improved processor 0-104800  
 narrowband digital, meas. transfer characts. of acoustic systems with long reverberation (*Japanese*) 0-64304  
 nerve spike trains, interleaved, in a noisy channel, separation system 0-94424  
 nerve trunk multifibre activity quantitation 0-76853  
 noise and vibration analysis, Cranfield Institute of Technology, SPAG minicomputer system 0-96162  
 noisy acoustic signal sources, optimal meas. of coords. by group of acoustic arrays 0-87659  
 ocean acoustic transfer function impact on coherence of undersea propag. 0-58842  
 period analysis at high noise level 0-73263  
 Pioneer Venus occultation expt., bandwidth reduction for radio science data generation 0-67492  
 post-detection data load prediction for passive sonars 0-96125  
 quantification of stochastic process, principles of quantification noise (*Spanish*) 0-57190  
 quantisation and averaging auditory appl. 0-94145  
 radar signal reflection from sea surface, spatial intensity fluctuations 0-109170  
 radio antenna arrays, incoherent optical 1-bit cross-correlators, radioastron. appls. 0-98555  
 reflection seismograms, simultaneous spherical divergence correction and optimal deconvolution 0-98258  
 remote sensing of Earth from space, role of 'smart sensors', book 0-62402  
 removal of periodic waves from reflecting signals, moving target indicator 0-69585  
 SAW device analogue signal processing technology, transversal filters and resonators 0-87656  
 SAW filter appls. in consumer electronics, review 0-74675  
 SAW signal processor theory and production method (*German*) 0-58867  
 seismic, using inverse diffraction technique 0-74608  
 seismology, deconvolution and synthesis of multi-segment seismic traces 0-77162  
 shape variation detection, two-component chromatographic peaks resolution 0-71971  
 solar spectra, correction function for granulation mean vertical vel. determ. 0-62094  
 sonar, synthetic-aperture sonar systems in turbulent medium 0-96080  
 sonar systems, digital beam forming 0-91950  
 speckle reduction in US B-mode images of human tissue 0-74634  
 spectrograms, detection, estimation and classification 0-64296  
 spectrometer, diode laser dual-beam, long-term temporal and scanning characts. 0-90902  
 spectrophotometers automatic processor for atomic absorption signals 0-105694  
 spectroscopy, noise reduction by low pass filter for DC signal, appl. chlorophyll-a fluoresc. 0-87249  
 speech, phoniatric diagnostics of speech organ disorders, objective acoustic methods 0-104598  
 STEM, multi-signal detection and processing 0-73552  
 time selector for acoustic spectrosc. 0-87660



**signal processing continued**

- tissue structures characterisation, method of obtaining an acoustic impedance profile 0-67171
- underwater acoustic time delay estimation, cross-correl. and smoothed coherence transform methods compared 0-96086
- US data, digital processing by deconvolution 0-106669
- US Doppler returns from foetal heart, processing, valvular timing information extraction 0-101238
- US return signals, correlation with bipolar digital representation of broadcast waveform 0-99897
- visual evoked cortical potential meas., signal optimisation using Kalman filter (*Japanese*) 0-72348
- Walsh spectral estimates with appls. to classification of EEG signals 0-104789
- InSb-LiNbO<sub>3</sub> SAW convolver, efficient struct. realisation, Hall mobility meas. 0-83705

**signal processing, computerised** *see computerised signal processing***signal transformers** *see high-frequency transformers; pulse transformers***silica minerals** *see minerals***silicate glasses** *see glass***silicate minerals** *see minerals***silicon***see also nuclei with .....*

- (1,1,0) direction, channelled particle radiation spectra, emitted quanta angular distrib. 0-96578
- (001) (2×1) reconstructed surface, dimer model self consistent calcs. 0-88613
- (001) substrate for Pd<sub>2</sub>Si epitaxial islands 0-96748
- (100), (111) substrates for rare earth metal silicide thin film formation, backscattering study 0-70542
- (100) inversion layer, electromigration in two dimensional electron gas, driving force 0-84441
- (110) plane, quantum state observation during fast electron channelling (*Russian*) 0-59541
- (111) surface, proton dechannelling under channelling, blocking and double alignment conditions 0-88235
- (111) surface structure phase transform, screw dislocations RHEED study 0-88153
- (111) surface substrate for Al film, struct., props. depend. on vapour flow (*Russian*) 0-75453
- (111) surface substrate for NiSi<sub>2</sub> epitaxial film, interfacial order, backscatter, channelling study 0-65390
- A-centre, theoretical study 0-75521
- adsorption of H on (100), MeV ion scatt. study 0-80071
- adsorption of O<sub>2</sub> on ion-bombard. (111) surfaces, SIMS study 0-70522
- advanced material for space solar cell 0-94007
- ambient effect of O precipitation, self interstitial mechanisms, IR spectra, TEM study 0-66510
- amorphous, co-sputtered doped, photovoltaic material appl. 0-93488
- amorphous, defects, band gap states 0-80215
- amorphous, doped, electronic props. 0-80283
- amorphous, elec. props., ion implantation effects 0-79828
- amorphous, epitaxial regrowth, structure and impurities effect 0-84401
- amorphous, EPR and spin-dependent effects 0-80592
- amorphous, glow discharge deposited, mobility edge calc. 0-80220
- amorphous, glow discharge produced, defect creation, high optical excitation 0-97327
- amorphous, hydrogenated, electron drift mobility meas. 0-75565
- amorphous, hydrogenated and deuterated, struct. 0-103245
- amorphous, hydrogenated film, electroluminescence study 0-88967
- amorphous, ideal surface, definition and characts. 0-107623
- amorphous, implanted, recrystn. induced by scanning CW laser, reaction rates, analytical model 0-66334
- amorphous, ion bombard., etch pit and ripple struct. formation mechanisms 0-66366
- amorphous, ion implantation, negative magnetoresist., localised mag. states 0-70731
- amorphous, ion implantation method, B and P ions 0-100274
- amorphous, Lifshitz constant for calc. of van der Waals force between two solids (*French*) 0-107658
- amorphous, luminescence 0-80862
- amorphous, opaque, surface phonon attenuation, Brillouin scatt. 0-80808
- amorphous, photovoltaic behaviour, solar cell appl. 0-94051
- amorphous, prep. by reactive RF sputtering in Ar-silane mixtures, undoped, n-type and p-type targets 0-76182
- amorphous, pure and H doped, picosecond relax. of optically induced absorption 0-97302
- amorphous, pure and hydrogenated, far IR absorption coeff. meas. 0-108213
- amorphous, random-network model, charge-density variation 0-80165
- amorphous, scanning TEM studies of cryst. inclusions 0-79699
- amorphous, short-range order, theory and probes 0-79698
- amorphous, solar cells, barrier props. determ. by differential I-V characts. meas. 0-94053
- amorphous, solar cells, current collection and electrical shorting problems 0-93969
- amorphous, solar cells design considerations 0-85277
- amorphous, sputtered, resist. control by ion implantation 0-100262
- amorphous, structural and electronic props., review 0-64901
- amorphous, substrate orientation effect on regrowth by laser pulses, channelling, backscatter 0-84409
- amorphous, transient electrical transport, general and unified treatment 0-59977
- amorphous, transport results, interpretation 0-80260
- amorphous, UHV evaporated, annealing behaviour of spin density 0-93163
- amorphous, undoped, photocond., continuous illum. effect 0-84486
- amorphous and crystalline, heating by Q-switched laser radiation 0-84963
- amorphous and crystalline, ion implanted, UPS meas. 0-97411
- amorphous evaporated, picosecond optoelectronic detect., sampling and correlation meas. 0-100478
- amorphous film, acoustic study using Rayleigh waves 0-75312
- amorphous film, analytical techniques, review 0-80120
- amorphous film, anisotropic etching phenomenon, appl. as solar selective absorber surfaces 0-72054
- amorphous film, EELS microanalysis 0-100722
- amorphous film, glow discharge deposited, for low cost solar cells 0-61355

**silicon continued**

- amorphous film, glow discharge deposition, rate enhancement by mag. field 0-65412
- amorphous film, hopping cond. control by ion bombard. induced struct. modification 0-92898
- amorphous film, hydrogenated, fabrication method 0-80956
- amorphous film, RF plasma deposition from SiCl<sub>4</sub>-H<sub>2</sub>, characterisation 0-66435
- amorphous film, selective laser recrystn. over heavily doped lines 0-84947
- amorphous film, TSC, density of localised states distrib. 0-65587
- amorphous films, halogenated and hydrogenated, elec. and optical props. 0-97016
- amorphous films, RF sputtering prep. at high Ar press., props. obs. 0-80418
- amorphous films, switching, electrothermal model 0-80407
- amorphous hydrogenated solar cells, field depend. quantum efficiency, electron-hole recombination 0-66971
- amorphous layer prod. by ion implantation, diffusion broadening, ESR study 0-92552
- amorphous layer recrystallisation by laser beam 0-93566
- amorphous layers, glow-discharge, laser-annealed, elec. props. 0-75661
- amorphous layers, oxidised, supercond. tunnel junction barriers 0-93040
- amorphous layers, recrystallisation, pulsed laser annealing 0-65404
- amorphous layers, RF-sputtered on sapphire, crystallisation by CW ion laser annealing 0-80109
- amorphous p-n junctions, high current, characts. 0-70807
- amorphous Si region obs. in Si-rich CVD SiO<sub>2</sub> films 0-84400
- annealed, photoluminesc. anal. of defects 0-80836
- annealed, TEM and EELS identification of oxide precipitates 0-100723
- annealing, using laser pulses, impurity incorporation at melt-cryst. interface 0-59504
- annealing during Czochralski growth, influence on defect density 0-60769
- anodic oxidation, high electronic current density 0-89386
- anodic oxidation in RF induced O plasma 0-100931
- anodisation at low substrate temp. by low pressure O<sub>2</sub> plasma 0-104314
- anodisation in HF soln., porous layer form. mechanism 0-71769
- anomalous avalanche breakdown 0-80284
- as-grown Czochralski crystal, multiple p-n junction structure obtained by heat treatment, appl. to solar cells 0-101099
- atom, ab initio effective valence shell Hamiltonian for neutral and ionic valence states 0-74117
- atom, excited states lifetimes, fluoresc. decay curves 0-58175
- atomically sharp cracks, TEM study 0-71729
- Auger electron emission, ion induced and secondary ion emission 0-71546
- Auger spectra, KLL and KLV, screening effects and plasmon gains 0-80913
- Auger spectra induced by 100 keV Ar<sup>+</sup> impact 0-84820
- avalanche photodiode, lightwave sources and detectors 0-64068
- back surface field solar cell degradation at high intensity due to base cond. modulation loss 0-94085
- band structure, semi-empirical APW calc. 0-84424
- bent crystal,  $\gamma$ -radiation beam deflection due to 900 MeV channelled electrons 0-84223
- blazed holographic grating fabrication by selective etching 0-74320
- blistering due to 400 to 1800 keV <sup>4</sup>He<sup>+</sup> ions, modal range determ. 0-100289
- Borrmann effect, enhanced, in heat treated Czochralski grown cryst. 0-70191
- bound-exciton spectral lines, conc. broadening at high impurity concs. 0-80826
- brittle fracture in axisymmetric bending, study at room temp., for single cryst. 0-81180
- bulk plasmon dispersion, electron energy loss spectra meas. 0-59899
- c Si-SiO<sub>2</sub> layers, physics, electron and ion motion, Cl, Na and K ion effects (*Dutch*) 0-60093
- C-CD imager, edge enhancement using 3×3 pixel neighbourhood operator functions 0-102644
- carrier capture at amphoteric deep level defects 0-88569
- carrier lifetime depth distrib. due to Ar ion implantation 0-70232
- cast, growth structure and photovolt. props. of solar cells 0-94008
- cast polycrystalline, hydrogenation effects, rel. to p-n solar cells 0-93916
- cast polycrystalline, laser annealed for solar cells 0-93918
- catalyst for water photolysis, I-V model 0-108721
- channelling of relativistic protons in bent crystals, theory 0-96581
- chemisorption of XeF<sub>2</sub> and SiF<sub>4</sub>, XPS and Auger spectra, surface chemistry 0-81358
- chemisorption on semiconductor surfaces, book contrib. 0-107648
- chip manufacture for fibre alignment in lightguide cable connectors 0-64188
- coated with Pd, interference effects on irradiation with laser beam 0-66333
- coherent twin boundaries, struct. by TEM 0-75238
- colar cell arrays, for earth orbital and orbit transfer missions 0-94044
- collision cascade following ion bombard. 0-65069
- compensated by thermal defects, recomb. and optical props. 0-64989
- concentrator solar cells, effects of nonuniform illumination 0-93942
- concentrator solar cells, high efficiency, state-of-the-art design and processing 0-93958
- conductor-insulator-semiconductor solar cells, automated production, outlook 0-94021
- controlled dislocation formation, struct. density (*Russian*) 0-107244
- core exciton binding energies 0-80188
- crack-tip dislocation pattern, X-ray topography (*French*) 0-107253
- cross-slip of isolated dislocations at surface and in bulk 0-70215
- crucible grown, laser irradiation effects on surface structure of virgin and implanted Si 0-92768
- crystal, desorption of SiO<sub>2</sub> films, ellipsometric obs. 0-100410
- crystal, electron and hole effective mass, intrinsic conc., temp. depend. 0-107692
- crystal defects, interaction with impurities, electron microscopy obs. 0-65003
- crystal growth, for electronic devices 0-66419
- crystal growth, improved horizontal ribbon growth technique 0-108345
- crystal microcrack detection by ultrasonprobe 0-66733
- CVD, surface anal. during growth using RHEED and Auger spectroscopy 0-66433
- CVD amorphous films, effect of surface characts. on visible and UV optical props. 0-60698
- CVD based on pyrolytic reaction, polycryst. Si deposition as example 0-84407

## silicon continued

- CVD from  $\text{SiH}_4\text{-HCl-H}_2$  system, rate-determining reactions and surface species 0-84405  
 Czochralski grown, oxide precip. homogeneous nucleation 0-65221  
 Czochralski grown crystal, O precip., nucleation behaviour and dislocation loop form. (*Japanese*) 0-59664  
 Czochralski grown crystals, swirl-type defect obs. 0-100236  
 Czochralski grown wafers, minority carrier transport props., laser beam scan for homogeneity anal., photovoltaic cell appls. 0-92905  
 Czochralski growth, small-angle dislocation boundary form. anal. 0-89136  
 deep centres, continuous energy spectrum, isothermal capacitance relaxation method 0-107741  
 deep impurity levels, activation energy 0-107742  
 deep level defects, struct. bonding, amphoteric centres 0-88506  
 deep-level point defects, effective-mass nature 0-59922  
 defects, divacancy and split 100 interstitial, electronic structure calc. 0-65494  
 deformed, annealed and recrystallized, struct., implications for solar cells 0-60922  
 dendritic web for solar cells 0-89634  
 dense plasma dynamics during pulsed laser annealing, carrier density, recombination 0-84479  
 deposition on rotating disc, one-dimens. model 0-75461  
 depth profiling by electron beam induced junction current meas. 0-96977  
 determination in optical waveguide glass by DC plasma emission spectroscopy 0-87446  
 determination with Al in atmospheric aerosols by neutron activation anal. 0-72116  
 dielectric function spectra, ellipsometric determ., many-particle effects at E<sub>1</sub>-transition 0-93363  
 diffracted X-ray channelling by special deflection. fields 0-100295  
 diffusion, in amorphous  $\text{SiO}_2$  (*French*) 0-107482  
 diffusion and power spectral density and correl. function of vel. fluctuation for electrons 0-65576  
 diffusion coefficient determ. from carrier conc. depth profile 0-107566  
 diffusion in Au-refractory thin film systems obs., by combination of scattering techniques 0-65308  
 diffusion mechanism of P, migration channels along vacancies and interstices 0-79996  
 diffusion of B from CVD BN covered with  $\text{Si}_3\text{N}_4$ , appl. to master slice p-MOS IC 0-107564  
 diffusion of P, elastic deform. relax. and dislocation generation 0-79997  
 diffusion through Au films at low temp., Co effect 0-100361  
 diode, impurity profiles, scanning electron microprobe anal. 0-79832  
 diode radiation detector, stabilisation of radiation damage 0-91377  
 dislocation generation in local oxidation 0-107245  
 dislocation motion from indentation rosette 0-79798  
 dislocation processes, during high temp. deform., in-situ HVEM obs. in single crystals 0-103342  
 dislocation velocity, thermal activation exam. of applied stress and temp. depend., expt. methods (*French*) 0-59474  
 dislocation-free, deep centres formed after high temp. treatment 0-96824  
 dislocations, HVEM struct. images of extended 60° and screw dislocations 0-59466  
 dislocations, noise spectrum 0-107881  
 disordered, effect of disorder on H content 0-75258  
 donor polarizability, multivalency effective mass calc. 0-96817  
 doping impurity distrib., during cryst. growth by Czochralski method (*Russian*) 0-100276  
 edge dislocations, energy spectra 0-70637  
 education, forbidden energy gap meas. in Si and Ge p-n junctions 0-57027  
 effective masses of heavy and light holes, from ohmic mobility data 0-80160  
 elasto-optic constants, real and imaginary, direct absorpt. and Raman scatt. meas. 0-97234  
 electrical conductivity, inertia of electron heating, expt. and theory 0-65613  
 electrical resistivity of crystals after reactor neutron irradi., impurities determ. 0-65563  
 electron beam annealing, beam voltage effect modeling 0-75275  
 electron beam annealing of ion implanted layer, computer simulation 0-96569  
 electron beam evaporated Si films for MIS solar cells 0-93490  
 electron beam irradi., {113} faults, nature and origin 0-70258  
 electron beam scan annealed, deep levels 0-65481  
 electron channel pattern linewidth measurements 0-62805  
 electron diffraction study, ECP contrast, Bloch wave model 0-96419  
 electron drift in high elec. fields, long-time tail of autocorrelation function 0-103702  
 electron microprobe local anal. of light elements, ultrasoft X-ray spectroscopy 0-99027  
 electron optical conditions for struct. image form. in (110) orientation 0-75131  
 electronic interface states in intrinsic stacking-faults 0-75522  
 electrotransfer, in  $\text{Mo}_2\text{Si}_3$  0-92708  
 energy gap, impurity conc. depend., calc. 0-80170  
 energy loss and multiple scattering of non-channelled  $\alpha$ -particles (*German*) 0-59544  
 enhanced conductivity in plasma hydrogenated films, thermionic emission 0-70692  
 epitaxial, on sapphire, characterisation, X-ray rocking curves 0-75458  
 epitaxial (111) surface, etching observation of stacking faults, dislocations, S-pits, etch pits (*Chinese*) 0-70197  
 epitaxial film, containing struct. defects formed during growth, positron annihilation 0-93433  
 epitaxial film, ionised-cluster-beam deposited, cryst. and elec. characts. 0-70553  
 epitaxial film on sapphire, microtwins, TEM exam. 0-70555  
 epitaxial films on Czochralski sapphire, optimisation of deposition conditions in  $\text{SiH}_4\text{-H}_2$  system 0-75464  
 epitaxial growth on sapphire by partially ionised vapour deposition, RHEED-AES obs. 0-80985  
 epitaxial layer deposition by ion beam methods 0-100417  
 epitaxial layer regrowth due to laser annealing mechanism, liquid and solid phase regimes 0-100712  
 epitaxial layer thickness meas. using phase correction function of substrate resistivity (*Rumanian*) 0-90812  
 epitaxial layers, anomalies of Sb distrib. 0-65035  
 epitaxial layers, grown in vac. at low temps. P and Sb doping 0-88189

## silicon continued

- epitaxial layers, meas. of doping profiles (*Hungarian*) 0-70545  
 epitaxial layers, stacking defect distrib. anal. using ion channelling tech. 0-100294  
 epitaxial layers, vacuum deposited, conditions for impurity migration from B, P, Sb doped sources (*Russian*) 0-107570  
 epitaxial solar cell substrate prep., low-cost, unidirectional solidification process 0-93924  
 epitaxial thin film growth on sapphire and spinel by MBE 0-76186  
 epitaxial wafer, saucer pit microdefects reduction by intrinsic gettering 0-75450  
 epitaxy, autodoping effects 0-100259  
 etching, anomalous etch structures using ethylenediamine-pyrocatechol-water based etchants and their elimination 0-81217  
 etching by  $\text{CF}_4$  plasma deposition reactor gas phase characts., mass spectra 0-70566  
 etching characts. using reactive ion etching with tetrafluoromethane- $\text{Cl}_2$  gas mixture 0-104313  
 etching in  $\text{He-F}_2$  plasma, etch rates, mass spectra, direct ion sampling study 0-79510  
 etching in reactive plasmas 0-71778  
 extrinsic IR monolithic focal plane array detectors, I-V characts. of  $\text{p}^+\text{-p-p}^+$  and  $\text{n}^+\text{-p-p}^+$  structs. 0-77863  
 Fabry-Perot couplers for optically pumped far IR lasers 0-69404  
 film emission photocathodes, emission current noise characts. 0-100746  
 film, ion bombarded, crystalline-to-amorphous transition, defect-rich film prep. 0-65071  
 film, low press. CVD prep., struct., elec. and optical props. 0-70548  
 film, MBE, cryst. defect props., substrate treatment effects 0-70551  
 film, polycryst., grain struct. and surface roughness, TEM study 0-70556  
 film, polycryst., laser-induced CVD growth from  $\text{SiCl}_4$  0-84852  
 film, semi-insulating, with 40 at.% O, AES and PES study 0-107939  
 film on sapphire, residual strain effect on elec. props. (*Japanese*) 0-84522  
 film on sapphire, stress-relieved regrowth by laser annealing 0-65389  
 films, amorphous, hopping conduction, dangling bond generation by high temp. annealing 0-60115  
 films, RF sputtered, Ar conc. as function of operation frequency and discharge pressure 0-65393  
 films, ribbon-against-drop, physical and chemical characterisation 0-92798  
 fine structure of lowest exciton state (*Russian*) 0-96801  
 float zone, meas. of deep levels by photovoltage spectroscopy 0-103723  
 float zone, process-induced effects on carrier lifetime and defects 0-81216  
 float zone crystal, dislocation creation and elimination 0-107072  
 foil, computer simulation of high resolution images of defects 0-107208  
 fracture, of single crystals, under several liq. environments 0-81157  
 fracture by painted indentor, on near (111) surface 0-71734  
 free excitons, drift and diffusion, luminesc. obs. 0-84434  
 gettering by ion damage, minority carrier lifetime and backscatt. study 0-100286  
 glide-set 90° and 30° partial dislocations, core struct. 0-96523  
 grain boundaries, high resolution TEM 0-103364  
 grain boundary elec. props./impurity correl. using surface anal. of multi-grained samples by SIMS and AES 0-79816  
 graphoeptaxy on fused  $\text{SiO}_2$  using surface micropatterns and laser crystn. 0-70554  
 ground state props. in density-functional pseudopot. approach 0-92803  
 growth of sheet Si, coating with inverted meniscus (SCIM) technique, solar cell appl. 0-89163  
 guided-wave acousto-optical devices 0-102864  
 half wavelength and stopping power of planar channelled protons 0-65087  
 heavily doped, excess intrinsic carrier density, deionisation of impurities as explanation 0-96864  
 heavily doped, microcreep breakdown 0-97549  
 heavily doped, minority-carrier transport parameters meas. 0-80291  
 heavily doped films, electromigration obs. 0-65295  
 high-resistivity layer form. during electron irradi. 0-80352  
 hole-hole-electron Auger recombination 0-70720  
 hydrogenated amorphous, gap states, comparison of photoemission and photocond. results 0-103724  
 hydrogenated amorphous, laser annealing 0-100713  
 hydrogenation of a-Si using DC and HF plasma treatment 0-59497  
 IGFET, velocity-field curves for surface-free carrier in Si 0-60095  
 implantation, microstruct. fabrication, ion channelling effects 0-70230  
 implantation on Cr-Ni Nb stabilized austenitic stainless steel surface, effect on oxidation behaviour 0-71791  
 implanted, standard for TEM, EELS 0-99017  
 implanted crystal, laser induced annealing and diffusion behaviour 0-88202  
 implanted semiconductors, laser annealing, review 0-107301  
 implanted with low solubility dopants, laser annealing, TEM study 0-70233  
 impurities of O, N, C, trace anal. by proton activation (*Chinese*) 0-81403  
 impurity at glass-metal seal interface, composition and conc. determ. by AES 0-76587  
 impurity content characterisation, exciton luminesc. 0-60653  
 impurity solubility limit after laser induced melting 0-107426  
 impurity states, localised orbital approach 0-92851  
 impurity-doped cryst. plate, as an X-ray monochromator, strain distrib. for 220 reflections 0-100126  
 inversion layers, electronic g-factor, spin-split Landau levels 0-80346  
 inversion layers, mobility temp. depend., Coulomb and surface roughness scatt. 0-80390  
 inversion layers, nonmetallic cond. at low temp. 0-70833  
 inversion layers, phase diagram in strong mag. fields. 0-88492  
 inversion layers, resist. temp. depend. at liq. He temps. 0-80391  
 ion and electron emission following ion impact 0-100729  
 ion beam irradi., defects prod. by individual displacement cascades, TEM study 0-70265  
 ion beam milling, anomalous sputter yield behaviour 0-108624  
 ion bombardment, anomalous surface damage from channelling-backscatt. meas. 0-84222  
 ion bombardment induced defect distrib., IR and electron diff. study 0-65074  
 ion damage, TEM study of laser annealing 0-88215  
 ion etching using Ar, carbide form. 0-81222  
 ion implantation, channelled, through metal silicide film 0-70231  
 ion implantation, channelling, alignment effects 0-88183



## silicon continued

ion implantation, high dose, solid phase epitaxial regrowth 0-103380  
 ion implantation, high-dose Ar, X-ray topographic obs. of strains and damage 0-59496  
 ion implantation by laser annealing, characterisation, solar cell applications 0-70247  
 ion implantation induced disorder in surface and at shallow depths 0-59535  
 ion implantation with  $\text{Si}^+$ , high dose spatial correl. of primary and secondary defect profiles 0-59536  
 ion implanted, amorphous to crystalline transition due to laser irradiation 0-103451  
 ion implanted, annealing by ion beam heating 0-103382  
 ion implanted, annealing of heavy ion cascade damage, channelling meas. 0-89255  
 ion implanted, complex annealing behaviour of amorphous layers, TEM obs. of defect struct. 0-107299  
 ion implanted, CW laser annealing 0-92550  
 ion implanted, damage profiles, Rutherford backscattering 0-100733  
 ion implanted, damage struct. obs. using TEM and cross section specimens 0-107298  
 ion implanted, defect struct., dislocation loops and elongated defects 0-107300  
 ion implanted, dopant depend. of oxidation rate 0-89384  
 ion implanted, electron beam annealing, surface struct. study using SEM 0-70235  
 ion implanted, interstitial generation and loop form. during annealing in oxidising medium 0-107225  
 ion implanted, radiation defect production at different temps. 0-103398  
 ion implanted, scanning CW and pulsed laser annealing 0-92549  
 ion implanted, self implanted, self annealing using high ion current density treatment 0-89254  
 ion implanted by high energy C ions, structural and optical props. 0-107292  
 ion implanted films, optical and luminesc. props. 0-60699  
 ion implanted layers, complex refr. index profile, ellipsometric meas. 0-93262  
 ion penetration, computer program 0-88185  
 ion sputter cleaning, in EM 0-101895  
 ion-controlled diodes, acid-base exposure effects, Si-SiO<sub>2</sub> interface state density 0-96984  
 ion-implanted, annealing using scanning CW laser system 0-100265  
 ion-implanted, impurity activation monitoring by SAW techniques 0-65020  
 ion-implanted, laser pulse annealing, TEM and channelling study 0-100264  
 ion-implanted amorphous, laser epitaxial recrystallisation threshold energy 0-70571  
 ion-implanted dopant redistribution under laser annealing 0-70242  
 ion-implanted laser-annealed solar cells 0-93881  
 ion-implanted layers, crystn. by ns laser pulses, TEM and RHEED 0-100421  
 ion-implanted layers, epitaxial regrowth by laser beam and flash annealing 0-100420  
 IR absorption spectra, Fourier transform obs. 0-60644  
 irradiation induced crystalline to amorphous transition, Gibbs energy 0-70371  
 isolated dislocation motion, velocity determ. (*Chinese*) 0-107243  
 joining and recrystallisation using thermomigration process 0-65298  
 junction diode, diffused, with deep level traps, negative capacitance 0-96976  
 junction diodes, fabrication by LPE on Si:B substrates, and characts. 0-80363  
 Kikuchi patterns, contrast depend. on primary electron beam energy (*Russian*) 0-64844  
 L-shell ionisation by 80 keV electrons, transmission electron energy loss spectrometry 0-60721  
 large monocrystal X-ray reflection/scanning and transmission topographic methods 0-96415  
 laser annealed, nonequilibrium solubility and segregation 0-84296  
 laser annealing, nonlinear dynamic transport processes 0-93437  
 laser annealing for improved stacked-struct. oxide quality 0-65386  
 laser annealing mechanisms, disordered overlayers, crystalln. 0-84967  
 laser annealing of Si on sapphire film, non-thermal theory expt. test 0-89273  
 laser annealing of SiO<sub>2</sub> layers 0-97505  
 laser crystallisation, for production of large grained sheets for solar cells 0-93570  
 laser damage statistics rel. to structural defect statistics 0-91829  
 laser heating of lightly damaged material, carrier diffusion effect 0-84809  
 laser induced dense plasma, dynamics 0-65612  
 laser irradiation of furnace preannealed (111) ion implanted Si 0-65015  
 laser pulsed heating, lattice temp., Raman meas. 0-80780  
 lattice dynamics under press 0-92627  
 lattice images of defects and radiation damage appls. 0-107210  
 lattice parameters and topographic meas., using double-beam triple-cryst. X-ray spectrometer 0-77915  
 lattice strains induced by localized oxidation, high temp. real-time X-ray topographic studies 0-108489  
 layers amorphized by molecular ions, laser annealing 0-103379  
 lightguide connector component characts. 0-69544  
 liquid, dissolution of quartz, effect of C, rel. to melt growth 0-70414  
 liquid, interaction with the material during edge defined film fed growth 0-104060  
 local pseudopotential, Gaussian band charge model 0-88477  
 materials, advanced, preliminary evaluation for space solar cells 0-94006  
 mechano-chemical polishing rate (*Japanese*) 0-89379  
 melt grown crystals, impurity incorporation, calcs. 0-79718  
 in metal grain from Murchison type 2 carbonaceous chondrite 0-77363  
 metal-Si, polycryst., Schottky barrier solar cells, elec. and photovoltaic contact props. 0-93936  
 metallic, superconducting transition temp., press. effects, elec. cond. 0-103777  
 metallic state, press. induced, elec. cond. meas. 0-96949  
 metallisation, TiN and TaN as diffusion barriers 0-65304  
 metallurgical grade, impurity gettering of polycrystalline solar cells 0-81441  
 metallurgical-grade, solar cells 0-101104  
 microcrack detection using US sonoprobe 0-76462

## silicon continued

microdefect density, in dislocation free crystals, quantitative determ. by preferential chem. etching 0-65001  
 migration of Au, electron bombardment effects 0-100362  
 minority carrier lifetime improvement through laser damage gettering 0-65589  
 minority carrier MIS solar cells, AM1 efficiencies 0-93975  
 MIS capacitors, C-V curves, outer oxide surface conditions effects 0-97000  
 MIS negative barrier contact for induced back surface field solar cell 0-101101  
 MIS phototransistors, photoelec. props. at high illum. intensities 0-60101  
 MIS solar cells, comparison of majority and minority-carrier 0-85280  
 MIS solar cells, computer simulation studies rel. to interface state meas. 0-72048  
 MIS solar cells with Cr, Hf, Be, Sc and Y as barrier forming metals, expt. investigation 0-94077  
 MIS structure, photoelectric characts. carrier injection levels (*Russian*) 0-96946  
 MIS/inversion layer solar cells 0-94075  
 monocrystal peripheral fusion channelling under HF heating (*Russian*) 0-59627  
 MOS capacitor, direct current/voltage relns. as function of oxide doping 0-88635  
 MOS capacitor, interface state parameter determ. by DLTS 0-65642  
 MOS capacitors, scanning photovoltage investigation 0-80396  
 MOS device, thermally oxidised surfaces, electron mobility in inversion and accumulation layers 0-103753  
 MOS device irradiation with  $\gamma$ -rays, minority carrier generation, C-V characts. 0-88637  
 MOS diode, dependence of minority carrier bulk generation on HCl concentration 0-88639  
 MOS structure, p-channel, stress effects on elec. props., press. transducer props. 0-100526  
 MOS structure Pt diffused, hysteresis and memory props. 0-96992  
 MOS tunnel junctions, processing condition depend. of props. 0-80380  
 MOS-structure, with adjoining reversed biased p-n junction, charge pumping current and reverse current (*German*) 0-88636  
 MOSFET dopant profile determ., DC method 0-70244  
 Mossbauer spectroscopy of defects, radiation damage and deep levels 0-59533  
 multigrained, grain boundary elec. and compositional props., surface anal. 0-76575  
 multigrained, impurity segregation to grain boundaries, AES and SIMS obs. 0-65027  
 multiple tip field emission photocathode, photokinetics 0-100480  
 muon spin rotation, spin Hamiltonian and anomalous muonium states 0-71286  
 n<sup>+</sup>-p diode,  $\gamma$ -radiation defects, annealing and recomb. props. 0-65045  
 n<sup>+</sup>-p solar cell, forward and reverse bias tunnelling 0-85274  
 n<sup>+</sup>-p solar cells, effect of elec. bus during 1 MeV electron irradiation and isochronal annealing, elec. characts. and deep level pop. 0-94086  
 n-channel inversion layers, mag. susceptibility of electrons in presence of quantising mag. field 0-75650  
 n-type, (111) inversion layers, valley splitting, Shubnikov de Haas oscills 0-65698  
 n-type, bipolar ohmic contact with macroscopic recomb. centres. 0-80379  
 n-type, bound excitons and bound multiexciton complexes, excitation spectra 0-96792  
 n-type, defect charge states, complex form., gamma-ray effects 0-96564  
 n-type, elec. cond. control by hot electron intervalley transfer 0-59993  
 n-type, electron heating by static elec. field 0-96894  
 n-type, Faraday rot. temp. depend., effective mass determ. 0-71392  
 n-type, Fe<sub>2</sub>O<sub>3</sub>-coated, heterostruct. photoanode for photoelectrolysis of water 0-61384  
 n-type, lattice vibr. excitation conditions, vol. charge redistrib. effect (*Russian*) 0-103427  
 n-type, multivalued Sasaki effect 0-107795  
 n-type, piezoresist. rel. to piezothermoelec. power, electron-phonon drag region 0-70737  
 n-type, relaxation of electron energy, carrier-density dependence 0-107809  
 n-type, size-induced magnetoresist. in strong elec. fields 0-65582  
 n-type, wafer, trap centres of self-interstitials 0-75516  
 n-type crystals, phonon-phonon relaxation 0-96609  
 n-type epitaxial layers on oppositely conducting substrates, two layer Hall coeff. meas. technique 0-80297  
 neutron and electron bombard., radiation defect recomb., photoelec. props. meas. 0-60039  
 neutron irradiated and annealed, EPR centre (S=1), characts. 0-71177  
 neutron transmutation doping, impediments to use in power device fabrication 0-96560  
 nitridation, effect of BaF<sub>2</sub> 0-81359  
 non thermal laser induced ordering, plasma life time, phonon interactions 0-84481  
 noncrystalline film, struct., interatomic distances, SRO 0-107053  
 optical constants by unpolarised incident radiation 0-76044  
 optical spectrum, many particle effects, band struct. 0-89024  
 optical waveguides along both sides of groove 0-96006  
 oxidation, growth of vitreous SiO<sub>2</sub> films, role of defect struct. of film 0-65403  
 oxidation, thermal growth mechanisms of vitreous oxide layers 0-93675  
 oxidation in high press. O<sub>2</sub>, residual stress, chemical etch rate, ref. index and density meas. 0-71768  
 oxidation induced by ion or electron bombardment, AES-SIMS study 0-108606  
 oxidation solubility and transport behaviour of water, dissolution 0-93801  
 oxidation stacking faults, shrinkage and growth, bulk O<sub>2</sub> effects 0-96546  
 oxidation-induced Frank sessile dislocation loops, struct. change 0-75228  
 oxidation-induced stacking faults, distinction between clean and decorated faults by etching 0-79818  
 oxide precipitate diffusion limited growth in Czochralski Si 0-97484  
 oxide scale microstruct. of oxidised single cryst. 0-108613  
 oxide structure obs. by high-resolution electron microscopy 0-103592  
 p<sup>+</sup>-n<sup>+</sup> back surface field concentrator solar cells 0-93939  
 p<sup>+</sup>-n<sup>+</sup> back-surface-field solar cells, physics underlying performance 0-85283  
 p-i-n structure, ESR of conduction electrons 0-93179  
 p-n junction, current-voltage characts., misfit dislocations, high press. effects 0-65671  
 p-n junction, electrolytic anodic oxidation method of decoration 0-60069

## silicon continued

p-n junction, reverse bias high voltage, secondary surface breakdown 0-70813  
 p-n junction, small signal equivalent circuit, finite carrier multiplication 0-65664  
 p-n junction, subnanosec. current drops in delayed breakdown 0-75633  
 p-n junction, subnanosec. current drops in delayed breakdown 0-75634  
 p-n junction, voltage-current characts., fast neutron irradi. effects (*Russian*) 0-65659  
 p-n junction depletion layer, electron beam damage inhibition 0-70817  
 p-n junction diodes and solar cells, minority carrier diffusion length 0-107894  
 p-n junctions, avalanche breakdown anisotropy 0-70811  
 p-n junctions, electron emission from depletion layers 0-100509  
 p-n junctions, spin depend. surface recomb., electron irradiation effect 0-88627  
 p-n junctions, thermal emission rates and capture cross sections of majority carriers at V centres 0-96980  
 p-type, anodic etching for discriminating between elec. active and inactive defects 0-108605  
 p-type, conductivity and carrier lifetime, high injection effects 0-70719  
 p-type, Czochralski grown, microdistrib. of O, SEM and spreading resist. obs. 0-79830  
 p-type, electron irradi. effect on Hall mobility temp. depend. 0-60011  
 p-type, heavily doped, intra- and interband Raman scatt. by free carriers 0-108208  
 p-type, heavily doped contact layers on IR detectors, IR transmissivity 0-108190  
 p-type, laser irradi., accumulation of defects, effect on elec. props. 0-107317  
 p-type, odd magnetoresist. under weak carrier heating conditions 0-96917  
 p-type elec. resist., shock wave compression effects 0-80265  
 phase transformation, lattice dynamics, microscopic theory 0-107387  
 phonon-assisted Auger recomb., direct calc. of overlap integrals 0-107808  
 phonon-phonon relaxation investigation for conventional and neutron doped crystals 0-96927  
 photocapacitive MIS IR detector, spectral response, noise characts. 0-75644  
 photoconducting films, amorphous, undoped, I-V characts. of vacuum deposited films 0-60049  
 photodetectors with increased blue sensitivity (*Rumanian*) 0-62720  
 photodiode, avalanche, n<sup>+</sup>p<sup>+</sup>-type, primary photocurrent anal. by noise measurements (*French*) 0-88624  
 photodiode, diffused junction, performance characts. 0-80367  
 photodiode absolute spectral response self-calibration 0-73448  
 photodiode for optical channel waveguides 0-102805  
 photodiode internal quantum efficiency basis for absolute radiometric standard 0-86410  
 photoelectric converters, p-n mesa structure for investigating optical and energy characts. of solar and radiant energy concentrators 0-97783  
 photon drag and radiation press. in refractive media, subMM wavelength 0-60048  
 photon emission due to Ar<sup>+</sup> ion bombard., adsorbed and recoil-implanted O effect 0-80872  
 phototransistors, slow contamination and fast surface state effects, SEM study 0-107896  
 photovoltaic and photomagnetic effects, rel. to intervalley electron transfer 0-60034  
 photovoltaic cell, absolute spectral sensitivity calibration, radiometry, photometry (*Chinese*) 0-86367  
 photovoltaic cells using silicone materials, encapsulation 0-94019  
 photovoltaic concentrator cell for high intensity appl. 0-93940  
 photovoltaic industry, environmental control, economic and ecological requirements 0-94026  
 photovoltaic technology, conf., San Diego, CA, USA (Jan. 1980) 0-86041  
 piezobirefringence in opaque region 0-60541  
 planar semiconductor junctions, disruptive voltage calc., ionisation coeff. (*Rumanian*) 0-103746  
 plasma effects during pulsed laser annealing 0-84480  
 plasma growth of native layers, F-enhanced, Auger profiles 0-93662  
 plastically deformed, dislocation structure with different sample orientation 0-70207  
 plastically deformed, high dislocation density crystals, photoelectret state investigation 0-97191  
 point defects, H passivation 0-75515  
 point defects, laser annealing 0-107224  
 poly-oxide-poly struct., elec. cond., charge distrib. in SiO<sub>2</sub> films 0-92984  
 polycrystalline, anisotropic plasma etching 0-85069  
 polycrystalline, Ar segregation at grain boundaries, elec. props. meas. 0-75259  
 polycrystalline, CVD, recrystn. on heating 0-80107  
 polycrystalline, electrode shape effects on oxide conduction 0-96890  
 polycrystalline, electronic behaviour of grain boundaries, solar cell appl. 0-92859  
 polycrystalline, energy distrib. of trapping states, from impedance of MOSS struct. 0-65691  
 polycrystalline, grain boundary obs. by TEM, solar cell appl. 0-72057  
 polycrystalline, Hall mobility 0-60006  
 polycrystalline, layer structure dependence on carrier gas moisture and O<sub>2</sub> content (*Bulgarian*) 0-59811  
 polycrystalline, layers on C substrates, RAD process, solar cell appl. 0-89635  
 polycrystalline, low cost conversion into sheet by heat exchange method and fixed slicing technique 0-93479  
 polycrystalline, oxidation, morphological aspects 0-76388  
 polycrystalline, p-n junction solar cell, grain-boundary and intragrain recombination currents 0-81442  
 polycrystalline, phenomenological model for mobility 0-65564  
 polycrystalline, solar cells, grain-boundary hydrogenation technique for improvement 0-85273  
 polycrystalline, thermal oxide anomalous stress 0-93661  
 polycrystalline barrier heights and passivation of grain boundaries 0-93890  
 polycrystalline Czochralski-grown, MIS solar cell characterisation using scanned laser response exam. 0-93884  
 polycrystalline film resistivity reduction by Nd:YAG laser annealing 0-100539  
 polycrystalline films, characts. 0-80988  
 polycrystalline films, meas. of effective diffusion length, by surface photovoltage meas. 0-80424

## silicon continued

polycrystalline multilayer support struct., control of deform. in dielec. isolated substrates 0-107681  
 polycrystalline Si-Al Schottky barrier solar cell, grain boundary effects on elec. behaviour 0-85279  
 polycrystalline solar cells fabricated from refined metallurgical-grade Si, impurity gettering 0-94011  
 polycrystalline structure stability, stacking defects, twins grain struct. (*Russian*) 0-100248  
 polycrystalline thin films for solar cells, thermal expansion shear separation technique 0-81439  
 polycrystalline-metal contacts, minority carrier injection 0-103750  
 position-sensitive detector for CW and pulsed laser beams 0-78883  
 positron trapping in electron-irradiated Si crystals, temp. depend. 0-104009  
 precipitation of O, 650°C, IR absorpt. and X-ray diff. 0-76258  
 production process effect on fracture strength 0-93656  
 purification, plasma melting zone technique, optimisation (*French*) 0-89142  
 purification, plasma melting zone technique (*French*) 0-89141  
 purity for semicond. appls., neutron activation anal. 0-71979  
 quasimonolithic and hybrid integrated optical circuits on Si substrates 0-64218  
 radiation damage by 0.5 to 10 keV ions 0-100285  
 radiation defects, influence of dislocations on accumulation, elec. props. 0-92558  
 radiation induced defects in high-voltage electron microscope 0-65048  
 radiative recomb. centre accumulation due to high temp. electron irradi. 0-93394  
 radiometer for storage ring synchrotron radiation 0-86411  
 reaction kinetics of liquid with B<sub>2</sub>C 0-84344  
 reactive ion beam etching expts., selectivity, anisotropy 0-104308  
 reactive ion etching, high rate 0-85070  
 recombination centres and carrier lifetimes after  $\gamma$ -irrad. of n-Si 0-60004  
 reflectivity time dependence during pulsed laser annealing 0-66214  
 removal by plasma etching process, from thin oxides and thin metal films 0-76384  
 residual stress and defects induced by scribing 0-60990  
 ribbon, dendritic web growth from melt, solar cell module fabrication 0-93478  
 ribbon, EFG, C contaminant conc. determ. by nuclear techniques and SIMS 0-59506  
 ribbon, EFG, characterisation by ion beam tech. 0-79833  
 ribbon, high speed edge-defined film-fed growth 0-104058  
 ribbon, low angle sheet growth technique, direct shaping characts. 0-93480  
 ribbon crystal growth, 10 cm wide, temp. distrib. meas. in die 0-104059  
 ribbon crystals, edge-defined film-fed growth technique for solar cells 0-89633  
 ribbon growth by EFG, thermal sensitivity and stability 0-107080  
 ribbon growth by laser zone melting 0-93482  
 ribbon growth using scanned focused CO<sub>2</sub> laser beams 0-66417  
 ribbon solar cells, defect anal. using laser scanner 0-94089  
 ribbon solar cells, var. of minority-carrier diffusion length with light intensity, heavy metal doping effects 0-93937  
 ribbons, edge-defined film-fed growth technique for solar cells 0-89138  
 ribbons for solar cells, ultra high speed growth, elec. props. 0-89162  
 ribbons grown by capillary action shaping technique, surface quality and impurity distrib. 0-108343  
 ring photodiode reflectometer for cavity reflectance 0-86376  
 Schottky barriers, silicide contacts, elemental description 0-60085  
 Schottky magnetodiode, integrated mag. sensor 0-68223  
 screw dislocation networks, TEM study 0-70204  
 selective anodic oxidation of Si in O<sub>2</sub> plasma 0-108610  
 self-diffusion, activation energy and entropy factors 0-88353  
 self-scanned photodiode array, evaluation for integrated optics spectrum analyser 0-58806  
 SEM exam., ultra-high vacuum, secondary electron emission dependence on electron beam dose, surface interactions from AES and ELS 0-61209  
 semicrystalline vs. single crystal, for photovoltaics 0-93917  
 shallow contact formation substrate temp. depend., Pd-W alloys 0-96963  
 shallow contact formation substrate temp. depend., Pt-W alloys 0-96963  
 shallow junction devices, silicide contact 0-70819  
 shaped crystal growth from melt, meniscus-controlled process 0-107075  
 sheet, high speed growth, heat transport analysis 0-107669  
 sheet casting for solar cells 0-89139  
 sheet-form solar cells, efficiency improvement, minority carrier diffusion length limitations 0-93925  
 Si:In growth by Czochralski crystal pulling, characterisation for extrinsic IR detectors, focal-plane arrays 0-76168  
 n<sup>+</sup>-Si-Al ohmic contacts, metallisation structs. for very shallow n<sup>+</sup>/p junctions 0-60084  
 SIMS quantitative anal. 0-101052  
 single cryst., chem.-mech. polishing of low-scatt. optical surface 0-96040  
 single crystal solar cell manufacturing process, laser annealing of implanted area, energy saving 0-97791  
 slip, room temp., TEM obs. 0-79804  
 slip dislocation nucleation during laser annealing 0-84179  
 SOC (Si on ceramic) continuous coating for solar cells 0-93904  
 solar cell, I-V charact. meas., effect of voltage ramp, theoretical anal. using linear model 0-61354  
 solar cell, laser annealing, conversion efficiency improvement (*French*) 0-66976  
 solar cell, n<sup>+</sup>-p, degradation mechanisms associated with Ti impurities 0-81465  
 solar cell, open-circuit voltage at ultrahigh light intensities, plasma reflection effects 0-96928  
 solar cell, p<sup>+</sup>-i-n<sup>+</sup>, field induced junction, conversion efficiency limit in concentrated sunlight 0-85282  
 solar cell arrays, Si, fixed-base, flat panels, possible developments for more competitive power production 0-72050  
 solar cell arrays, technological and economic barriers to be overcome for competitive power production 0-72049  
 solar cell fabrication from multiple ingots using melt replenishment Czochralski method, cell anal. 0-93477  
 solar cell multicyst. material prep., fast-pulled float zone, CZ and cast ingot and foil methods 0-93483  
 solar cell parameters, grain size dependence 0-94049  
 solar cell processing, pulsed laser techniques for annealing ion-implantation damage 0-81453



## silicon continued

- solar cells, all-plate low cost contact system 0-93992  
 solar cells, amorphous and polycryst. thin film solar cells, perform. parameters, review 0-93882  
 solar cells, analysis of short-circuit current 0-85285  
 solar cells, base resist. influence on temp. characts., temp. cycling 0-89618  
 solar cells, capacitance transient spectra of processing- and radiation-induced defects 0-61340  
 solar cells, concentrator, new technology for fabrication 0-81457  
 solar cells, design for limit conversion efficiency 0-93960  
 solar cells, developments and trends for automatic interplanetary stations, Venus-9 and Venus-10, and mooncar program 0-89613  
 solar cells, effect of Ti, Cu and Fe 0-72064  
 solar cells, effects of metallic impurities 0-85278  
 solar cells, fabrication using continuous or pulsed lasers (*French*) 0-61350  
 solar cells, fundamental efficiency limitations 0-93963  
 solar cells, grain boundary defects in thin semicrystalline material 0-93889  
 solar cells, grating minority carrier, design and expt. results 0-81445  
 solar cells, high open circuit voltage, P implantation 0-89642  
 solar cells, HV, multijunction, characts. 0-89615  
 solar cells, inhomogeneities and their influence on cell performance 0-93967  
 solar cells, ion implantation and annealing technology 0-93996  
 solar cells, ion implanted grating type 0-101102  
 solar cells, ion-implanted, expt. study of efficiency controlling factor 0-93997  
 solar cells, ion-implanted, factors controlling efficiency 0-81451  
 solar cells, ion-implanted 0-81452  
 solar cells, junction formation techniques using spray-on polymer dopants, cost effective, high throughput 0-94014  
 solar cells, large grain films on metallurgical Si substrates, chem., struct., elect. and photovoltaic props. 0-61357  
 solar cells, laser annealing, reviews 0-93976  
 solar cells, limit efficiency evaluation 0-93973  
 solar cells, low cost, Ni contacts 0-94017  
 solar cells, low cost processes for fabrication 0-94013  
 solar cells, manufacturing cost anal. of flat plate vs. concentrator solar cells 0-93949  
 solar cells, monocryst. sheet fabrication, CLF Czochralski furnace and enhanced slicing technology 0-93476  
 solar cells, MOS and oxide-charge-induced BSF structs., open-cct. voltage >700 mV, 20% conversion efficiencies 0-81435  
 solar cells, n<sup>+</sup>-p junction, electron irradi., DLTS spectra and defect effects 0-93999  
 solar cells, Ni-Cu conductor system 0-93991  
 solar cells, output power and sunshine conditions, correlation 0-97785  
 solar cells, photoreactance of p-n junction diodes 0-81464  
 solar cells, POCl<sub>3</sub> gettering of Ti, Mo and Fe-contaminated cells 0-94010  
 solar cells, polycryst. surface barrier cells, eval. for terrestrial appls. 0-61376  
 solar cells, polycrystalline, from recrystallized plasma deposited thin films 0-104509  
 solar cells, polycrystalline film, effect of defects/grain boundaries on photovoltaic mech. 0-93883  
 solar cells, polycrystalline p-n junctions, recombination currents, physical models 0-93892  
 solar cells, preparation using laser processing 0-81454  
 solar cells, radiation damage annealing mechanisms and low temp. annealing 0-94003  
 solar cells, radiation damaged, origin of reverse annealing 0-76630  
 solar cells, realisation by laser induced diffusion of deposited Sb 0-93998  
 solar cells, review and current developments 0-108801  
 solar cells, review of physics underlying recent improvements 0-93974  
 solar cells, solid source diffusion process for fabrication 0-93994  
 solar cells, spray-on TiO<sub>2</sub>, antireflection coatings 0-80963  
 solar cells, TiO<sub>2</sub>, AR coating by spray deposition 0-104511  
 solar cells, ultrathin, electron and proton effects 0-94002  
 solar cells, unified model of fundamental limitations 0-81448  
 solar cells, updating limit efficiency 0-81447  
 solar cells, upgraded metallurgical grade substrates, epitaxial growth 0-93905  
 solar cells appl. minority carrier MIS diodes (*Slovak*) 0-97792  
 solar cells proton irradiated, processing influence on elec. performance 0-94001  
 solar cells using minority carrier MISS 0-101103  
 solar cells with fire through contacts printed on anti-reflection coating 0-93993  
 solar cells with screen printed diffusion and metallisation 0-94015  
 solar concentrator cell, effects of nonuniform illumination and temp. profiles under concentrated sunlight 0-93941  
 solar concentrator cells with high efficiency 0-93938  
 solid, electron rearrangement after inner shell ionisation by heavy charge particle impact 0-87043  
 solid solution, of B<sub>2</sub>, equil. with B<sub>2</sub>H<sub>6</sub> 0-97721  
 solid thermal cond. and interface resistance meas. by radiation thermometry 0-86289  
 solubility in Mg, depend. on impurity inclusions (*German, English*) 0-97492  
 solute loss on laser annealing, solute out diffusion 0-100840  
 SOS structures, high-field electron transport, drift vel. meas. 0-80387  
 spectrochemical analysis, atomic-absorption, tubes design with hollow cathode (*Bulgarian*) 0-85232  
 spectroscopic applications of structures produced by orientation-dependent etching 0-93668  
 sputter yields, anomalous, due to cascade mixing 0-76122  
 sputtered atom ang. distrib. for keV Ar<sup>+</sup> bombard. 0-84819  
 sputtering, low energy, H, D and He ions 0-100734  
 square single crystals, Czochralski growth 0-97422  
 stacking faults, dynamic processes associated with deform. twins, HVEM in-situ obs. 0-103369  
 stacking faults, preoxidation gettering by reverse side P diffusion-induced misfit dislocations 0-60988  
 stacking faults, weak-beam contrast in TEM 0-75132  
 static compression in [100] and [111] directions, elec. resist. obs. 0-65637  
 stationary creep depend. on deform. stabilisation of material struct. (*Russian*) 0-100300  
 strained crystal, annealing effect, recrystn. and struct. (*Russian*) 0-89252

## silicon continued

- stressed, one- and two-component electron-hole liq. at T=0 0-80189  
 stretched, lattice vibr. anharmonicity, influence of stress on elastic moduli, Raman spectra 0-80791  
 substrate, Ag film growth modes and nucleation, SEM study 0-100423  
 substrate, thin films of Ag or Al, work function (*French*) 0-80353  
 substrate for Ag, UHV-SEM studies of Stranski-Krastanov growth 0-79722  
 substrate for Al film, annealing effect on eutectic point (*Russian*) 0-100850  
 substrate for epitaxial crystn. of GaP films by ns laser pulses 0-107674  
 substrate for Pd and Pt, silicide formation by laser, electron beam annealing 0-84849  
 substrate for PMMA electron sensitive layer, 400 Å linewidth electron beam lithography 0-65392  
 substrate for Pt-Ni vacuum condensates, X-ray anal. (*Russian*) 0-70559  
 substrate for RF sputtered ferroelectric BaTiO<sub>3</sub> films, ferroelectric props. 0-80697  
 substrate for SiO<sub>2</sub> film, ellipsometric spectra, thickness determ. (*Chinese*) 0-86379  
 substrate for wet thermal oxide film, trap emptying kinetics 0-92983  
 substrate for ZnS, Na<sub>3</sub>AlF<sub>6</sub> films, H<sub>2</sub>O absorpt., IR anal. 0-75446  
 substrate thickness, device design, solar cell processing, empirical study of interaction 0-93995  
 substrates for integrated optics high quantum efficiency waveguide coupled photodetectors 0-58805  
 surface, (100), dimer reconstruction, photoemission obs. 0-80939  
 surface, (111), energy states, computer renormalisation-group calc. 0-75617  
 surface, (111), ion bombard., struct. changes, AES obs. 0-79842  
 surface, (111)-(7×7), and impurity stabilised Si(111)-(1×1) surface, photoemission studies 0-104041  
 surface, adsorbed Br, X-ray standing waves obs. 0-96417  
 surface, band structure, minigaps, magnetoresistance, cond. space charge layers 0-92980  
 surface, cleaved (111), electronic structure following Al adsorption 0-75610  
 surface, depth profiling, optoacoustic technique 0-65337  
 surface, ion bombardment enhanced mixing of Ag layers, Rutherford backscatt. meas. 0-65034  
 surface, laser-annealed, characterisation by ellipsometry 0-103544  
 surface, pulsed electron beam processing, doping, annealing 0-75254  
 surface, pulsed laser atom-probe FIM, expts. 0-66402  
 surface, -reconstructed- Si(111) 7×7 surface superlattices, microdomain model 0-107625  
 surface, reduction growth, autoepitaxy (*Russian*) 0-107672  
 surface, thermal oxidation induced defects, origin and growth (*Chinese*) 0-66681  
 surface (001), high energy ion scatt. study 0-59772  
 surface (100), reconstructed, struct. study using thermal energy He diffr. 0-60731  
 surface (100), vicinal LEED obs. of stepped surface 0-59773  
 surface (111), intermediate oxidation state, core photoelectron absorpt. vs. chemical shifts 0-81220  
 surface (111), nitridation, AES and LEED results 0-80041  
 surface (111), O and CO sorption, ion scatt. obs. 0-59810  
 surface (111), relax., EHT and cluster calcs. (*Chinese*) 0-59762  
 surface (111)(7×7) struct. models, LEED anal. 0-75418  
 surface (111) 7×7, clean and O chemisorbed, valence band density of states from L<sub>23</sub> VV AES 0-100717  
 surface (111) 7×7 struct. determ. using RHEED 0-96723  
 surface (111)-1×1, electronic struct. of surface, model pseudopot. calc. 0-65651  
 surface and films on sapphire quality determ. using IR and UV specular reflectance meas. 0-108684  
 surface crystal damage due to RF sputter etching, spectroscopic ellipsometry obs. 0-103538  
 surface electron beam deposited silicide formation using scanning CW laser beam 0-66862  
 surface formation during etching of thin thermally grown oxide layers, ellipsometric control (*Russian*) 0-104315  
 surface inversion layers, harmonic generation due to hot electrons 0-65694  
 surface layer, on buried SiO<sub>2</sub> layer formed by high-dose, O ion implantation, TEM, AES, and XPS obs. 0-88172  
 surface passivation in solar cells by SnO<sub>x</sub> films, effect on cell transport props. and short circuit current 0-61360  
 surface selective etching relative to SiO<sub>2</sub> by CBrF<sub>3</sub> plasma without undercutting 0-76380  
 surface Si reinforced type U8 steel, metastable phase composition, struct. (*Russian*) 0-92599  
 surface topography changes due to pulsed laser annealing 0-84348  
 surface treatment by the low-energy ions of plasma accelerators 0-97608  
 surface treatment quality control of semicond. plates, using Al spraying technique 0-60989  
 surfaces (001) and (111), geometrical and electronic struct., review 0-80039  
 surfaces etched in CF<sub>4</sub> or CF<sub>4</sub>-O<sub>2</sub> plasma, morphology 0-93671  
 swirl defect formation, doping effect, Czochralski grown dislocation free cryst. 0-92519  
 temperature during CW laser heating, Raman scatt. meas. 0-76109  
 terrestrial solar cells, stress tested, contact integrity testing 0-94018  
 thermal annealing study of Au-Ti<sub>0.3</sub>W<sub>0.7</sub> metallisation 0-80134  
 thermal conductivity calculation for single crystals (*Hungarian*) 0-65311  
 thermal expansion reference data: 1-1000K 0-96669  
 thermal oxidation, role and effect of Cl 0-108622  
 thermal oxidation kinetics, steady-state transport anal. 0-71773  
 thermal oxidation kinetics, theoretical perspective 0-76387  
 thick-film growth using contiguous capillary coating on porous C substrates 0-93507  
 thin film, polycryst., CVD, elec. props. 0-107934  
 thin film deposition using solar furnace 0-89148  
 thin film on sapphire, Hall effect, magnetoresistance (*French*) 0-65601  
 thin p-n junction solar cells, minority carrier mirrors and optical confinement for high efficiency (27%) 0-93933  
 thin slabs, vib. freq. calcs., dimens. effect 0-60585  
 thin-film polycrystalline vacuum-deposited solar cells, TiB<sub>2</sub> bottom electrode, 10% efficiency 0-93489  
 total energy calcs. by r-space method, Wannier functions 0-88503  
 tube growth by EFG process 0-108344

## silicon continued

- uniaxially stressed, excitonic molecule emission spectra, electron valley degeneracy effects 0-60669  
 US eval. of Si wafers using SAW 0-76470  
 UV Propagation in pure and n-type crystals, velocity and attenuation, second and third order elastic moduli 0-70325  
 UV detectors coated with thin film scintillators 0-86412  
 V-grooves formed by etching, phosphosilicate glass bridge struct. 0-104312  
 vacancy, charge states, Jahn-Teller stabilisation energy 0-80209  
 vacancy, electron states, Anderson negative-U system 0-96820  
 vacancy, isolated, electronic struct., SCF method 0-80208  
 vacancy formation and stability due to noncentral force 0-70192  
 vacuum deposition source, with two independent filaments 0-76190  
 vapour deposited coatings for solar cells, prod. by  $\text{SiCl}_4$  reduction, cost anal. 0-93495  
 vapour phase epitaxy technology 0-75472  
 wafer, (001), pyramidal hillocks, TEM obs. during chemical etching 0-70508  
 wafer, slotted mask, direct deposition of metal contact pattern on MIS solar cells 0-97786  
 wafer, thin surface layers, amorphous to cryst. transform., obs. technique 0-107288  
 wafer processing,  $\text{CO}_2$  laser heating dynamics 0-76106  
 wafers, floating-zone, etch struct. on microdefects as affected by dopants and surface treatment 0-79773  
 wafers, saw damage reduction in lubricant environment 0-108585  
 web dendrites, dislocations, stacking faults, X-ray topographic study (Chinese) 0-88148  
 X-ray section topography in the Bragg case 0-79637  
 X-ray source,  $K\alpha$ , sensitivity factors, cross section and resolution data 0-77920  
 X-ray topography and double-crystal diffraction 0-92534  
 Ag-In $_2$ S $_3$ -Si layered struct., Hall effect, I-V characs., surface states (Russian) 0-97001  
 Ag-Si interfaces, solar cell contacts 0-92973  
 Al-Al $_2$ O $_3$ -Si structure, study of charge trapping 0-60097  
 Al-Al $_2$ O $_3$ -SiO $_2$ -Si capacitors, physical and elec. props. of RF plasma grown Al $_2$ O $_3$  0-100530  
 Al-AlN-SiO $_2$ -Si capacitors, physical and elec. props. of RF plasma grown AlN 0-100530  
 Al-amorphous Ge-nSi, photoelectric props. 0-70822  
 Al-In $_2$ S $_3$ -Si layered struct., Hall effect, I-V characs., surface states (Russian) 0-97001  
 Al-Si MIS solar cells, depth conc. profiles, elec. and optical props. of Al films 0-94076  
 Al-Si $_3$ N $_4$ -SiO $_2$ -Si, MNOS structures degradation under UV irradiation effect 0-107923  
 Al-SiO $_2$ -Si, pyroelectricity 0-100524  
 Al-SiO $_2$ -Si MOS solar cells, open-circ. voltage var. with oxide layer thickness 0-81434  
 Al-SiO $_2$ -(p)-Si barrier structs., minority carrier injection ratio meas., MIS solar cell model 0-93007  
 n-Al $_x$ Ge $_{1-x}$ As-Si-GaAs heterojunctions, selectively doped, FET 0-80364  
 Ar $^{+}$  ion implant damage gettered Si, generation lifetime meas. 0-75247  
 Au-nSi Schottky barrier solar cells, recombination in space charge region 0-61351  
 Au-Si interface, electron energy loss and AES meas. 0-89096  
 Au-Si thin film double layer, silicide form., electron diff. study 0-80005  
 Au-SiO $_2$ -nSi, tunnelling MIS struct. 0-92995  
 Au-Ti/SiO $_2$ /p-Si MOS struct., interface state distrib., DC tunnelling spectra determ. 0-75611  
 CdTe:Si, force variation due to charged defects 0-92634  
 Co-Si interface, glassy layer, ellipsometric charact. 0-103589  
 Cr-MIS solar cells, on polycryst. Si, grain boundary effect and conduction mech. 0-93894  
 Cr-Si interfaces, metallurgical and electrical props. 0-60081  
 Cr-SiO $_2$ -Si MIS solar cells, photovoltaic performance and interface states, nucl. radiation effects 0-94004  
 Cu-nSi diodes, fabrication by electroless deposition method, characts. 0-100520  
 (Ga,Al)As:Si, epitaxial layers, radiative recomb., compensation, cathodolum. study 0-66307  
 n-Ga $_x$ Al $_{1-x}$ As:Si, room-temp. cond. and band struct. 0-96869  
 GaAs:Si, accelerated growth rate effect on MBE, Hall mobility and photolum. meas. 0-104067  
 GaAs:Si, activation by multiply scanned electron beams 0-75246  
 n-GaAs:Si, B, IR absorpt. spectra, reson. and localised modes 0-66172  
 GaAs:Si, generation of high mobility n layers, SIMS 0-103375  
 GaAs:Si, IR absorpt. bands, localised modes, Si-related defects 0-76054  
 GaAs:Si, influence of stoichiometry on recomb. processes 0-93396  
 GaAs:Si, ion implantation, thermal annealing, Hall meas., SIMS atomic profile meas. 0-75243  
 GaAs:Si, ion implanted, laser annealed, high doping levels 0-88181  
 GaAs:Si, ion-implanted, capless annealing by melt-controlled ambient technique 0-75251  
 GaAs:Si, Li, IR absorpt., microstruct., charge compensation 0-107565  
 GaAs:Si, n-type layers, heavily doped, formation by multiple ion implantation 0-88187  
 GaAs:Si, stacking fault prod. during heat treatment in As vapour 0-96547  
 GaAs:Si, transferred-electron devices by low-level ion implantation 0-92543  
 GaAs:Si p-n junction LED, electroluminesc. efficiency 0-71491  
 GaAs-Si heterojunction, IR quenching of photocapacitance 0-92968  
 GaAs-Si ion implanted, impurity profiles elec. props. 0-96550  
 GaP-Si heterostruct., differential thermal contraction, plastic deform., fracture 0-108494  
 GaP-Si, heteroepitaxial growth, electronic and optical props. 0-104075  
 GaP-Si, heterostructure, zincblende-on-diamond type systems, MBE growth, (110) orientation as preferred orientation 0-80099  
 Ge-Si sandwich structure, sputter profiling, combined Auger-X-ray anal. 0-66909  
 In $_x$ Ga $_{1-x}$ As:Si p-n structs., electrolum. spectra, 77 to 300K 0-93408  
 In $_2$ O $_3$ -SnO $_2$ /polySi, solar cell response exam. using electron-beam-induced current and scanning light spot tech. 0-81477  
 In $_2$ O $_3$ -SnO $_2$ -Si SIS heterojunction solar cells 0-85281  
 In $_2$ O $_3$ -SnO $_2$ -Si SIS solar cells, reverse current-voltage characts. under illumination 0-89622  
 (In $_x$ ,Sn $_y$ ) $_2$ O $_3$ - $\gamma$ -Si solar cells, degradation 0-94047

## silicon continued

- In $_x$ ,Sn $_y$ O $_3$ -insulator-poly-Si solar cells, photovoltaic conversion parameters 0-101093  
 In $_2$ ,Sn $_2$ O $_3$ -SiO $_2$ -Si SIS solar cells, loss mechanisms study for improvement of efficiency to above 12% 0-94080  
 n-inversion layers, (001),  $K_F$ -depend. of subband energies 0-103738  
 Li-Si, electrode pot., Li utilisation determ. 0-81427  
 LiNbO $_3$ -Si, acoustoelectronic memory, effect of band-bending 0-70771  
 Ni-Si(111), interface, reactivity and struct., ion channelling meas. 0-92788  
 Pb $_1$ ,Hg,Si-Si heterojunctions, elect. props. 0-100513  
 PbS-Si heterojunction, chem. struct., AES anal. 0-76115  
 PbS-Si heterojunction, related optical and IR detector props. 0-77866  
 PbS-Si heterojunction, space charge capacitance, PbSn film thickness depend. 0-88630  
 PbS-Si heterojunction, PbS film growth and struct. 0-96762  
 PbS-Si p-n heterojunctions, AC admittance meas. 0-96979  
 Pd-Si structure, epitaxial silicide growth, LEED and AES study 0-103590  
 Pt-Si interface, low-temp. diffusion, ambient effects 0-100355  
 Pt-Si Schottky barriers on Si, laser formation and characts. 0-60079  
 Pt-Si:As, silicide form. during laser irradi., p-n junctions and ohmic contacts 0-84397  
 Si III, electron impact excitation of  $3s^2\ ^1S$ - $3s3p\ ^3P^0$  transition 0-102578  
 SOS, epitaxial, crystalline quality improvement by ion implantation and furnace regrowth 0-88452  
 Si (III), excitation thresholds and oscillator strength calc. using CI wavefunctions 0-91496  
 n-Si channel (100) inversion layer MOSFET, valley splitting, conductivity 0-70840  
 n-Si, deformed, thermal treatment effect on elec. cond. and dislocation mobility 0-107265  
 Si, elastically bent, strain canc. determ. by microfluorescent densitometry of X-ray topography 0-79245  
 Si II and III, UV line spectrum of active chromosphere star  $\epsilon$  Eridani, models 0-77394  
 Si II homologous ions series, Stark broadening trends 0-105157  
 Si IV interstellar column density towards early-type stars 0-73018  
 Si IV interstellar lines in Wolf-Rayet star spectra, IUE obs. 0-67748  
 a-Si In $_x$ ,Sn $_y$ O $_3$ - $\gamma$ -Si 0-101113  
 n-Si, ion-implanted, elec. characts. after laser annealing 0-88562  
 a-Si, laser induced crystallisation mechanism, epitaxial regrowth 0-84962  
 Si MIS grating solar cells on minority carrier blocking back surface field substrates 0-94078  
 a-Si p-i-n and c-Si p-n junction solar cells, design concept differences 0-94031  
 n $^{100}$ Si planar device, hot electron flicker noise at 78K 0-103732  
 n-Si, quenched, fast electron irradiated, annealing of defects 0-89259  
 Si rich SiO $_2$ -SiO $_2$ -Si rich SiO $_2$  layers for dual electron injector struct. 0-96991  
 Si thin ribbon grown at high speed, thermal stresses, reduced thermal buckling 0-107078  
 Si $^{2+}$ , static dipole quadrupole polarisabilities and shielding factors calc. using HF scheme 0-99450  
 Si: As(Pb), high-dose ion implanted and annealed, implant redistribution 0-107309  
 Si: $^{119m}\text{Sn}$ , impurity lattice dynamics, Mossbauer spectra, Debye temp. 0-84262  
 Si: $^{57}\text{Co}$ ( $^{57}\text{Fe}$ ), implanted, Mossbauer spectra, study of dose dependence 0-75900  
 Si:Al, electron irradi. induced defects, transient capacitance study 0-59516  
 Si:Al, localised exciton bound to isoelectronic trap 0-66283  
 Si:Al, polycryst. film, grain boundary diffusion, Auger sputter profiling 0-75388  
 Si:Al epitaxial layers, nuclear microanalysis of Al impurities  $^{27}\text{Al}(d,\alpha)^{25}\text{Mg}$  0-61193  
 Si:Al(Ga), O $_2$  diffusion, conc. profile meas. 0-79990  
 Si:Al(Ga), spreading resist. calibration using Si:B 0-103690  
 Si:Ar, As, ion implanted, laser annealing, doping profiles, channelling 0-97506  
 Si:Ar, ion-implanted, epitaxial regrowth by laser annealing, microstruct. 0-84404  
 Si:Ar(Ne)(O)(N), ion-implanted, defect reverse annealing, 550-650°C 0-88875  
 Si:As, CVD, doping using SiH $_4$ -H $_2$ -AsH $_3$  system 0-79823  
 Si:As, CW CO $_2$ -laser annealing, comparison with thermal annealing 0-84193  
 Si:As, diffused, laser irradi., stability study 0-65547  
 Si:As, diffusion model, degeneracy and partial ionisation effects 0-96693  
 Si:As, heavily As-diffused, Hall mobility and resist. rel. to carrier conc. 0-107815  
 Si:As, ion implanted, formation of As complexes 0-59511  
 Si:As, ion implanted, laser annealed, lattice defects, epitaxial regrowth 0-103334  
 Si:As, ion implanted, low temp. thermal annealing 0-96552  
 Si:As, ion implanted, pulsed ion beam annealing 0-103395  
 Si:As, ion implanted, pulsed laser annealing, partial solid-state regrowth 0-103591  
 Si:As, laser-doped, impurity distrib., Rutherford backscatt. and channelling anal. 0-59507  
 Si:As, MBE with simultaneous ion implant doping 0-66432  
 Si:As, scanning electron beam annealing, spreading resistance, junction depth 0-75267  
 Si:As, shallow junctions by high-dose implants 0-96694  
 Si:As, solid solubility and thermal behaviour of metastable 0-75359  
 Si:As high-dose implanted single crystals, pulsed electron-beam annealing 0-103373  
 Si:As ion implanted layers, annealing by CO $_2$  laser, doping profile shift 0-84965  
 Si:As ion implanted shallow junction 0-70228  
 Si:As laser annealing, heat and mass transport model 0-92546  
 Si:As $^{+}$ , implanted, CW laser annealing, electron-beam induced current 0-100709  
 Si:As $^{+}$ (P $^{+}$ ) ion implanted, laser annealed, correlation of struct. and elec. props 0-70855  
 Si:As(B), heavy-doping effects and impurity segregation during high-pressure oxidation 0-65014  
 Si:As(P), ion implanted, TEM study after laser and furnace annealing 0-70234



## silicon continued

- Si:As(P)(Sb), donor-polarizability enhancement as the insulator-metal transition is approached from the insulating side 0-80184  
 Si:As(Pb), ion-implanted, impurity redistrib. during laser irradi. 0-100280  
 Si:As(Sb), ion implanted, lattice location of impurities after pulsed laser annealing 0-88196  
 Si:Au, amphoteric centre, struct. bonding of deep level defects 0-88506  
 Si:Au, C-V curves of MIS diode used to examine trapping levels 0-65697  
 Si:Au, EPR spectrum, strong nucl. quadrupole effect 0-93172  
 Si:Au, O(H), film, amorphous, elec. cond. meas. 0-80423  
 Si:Au, P-induced point defects influence on Au gettering mechanism 0-65030  
 Si:Au, precipitation of solid soln., effect of gamma irradiation 0-59515  
 Si:Au deep level parameter determ. by isothermal capacitance transient spectroscopy 0-88507  
 Si:Au p<sup>+</sup>-n junction, small area, acceptor level conc., determ. from TSC curves 0-75631  
 Si:Au planar extrinsic IR detector, use of multiple internal refl. for increased sensitivity 0-77862  
 Si:B, anomalous B profiles prod. by BF<sub>3</sub> implantation 0-75252  
 Si:B, bound many-exciton complexes, luminescence spectra, mag. props. 0-103994  
 Si:B, He<sup>+</sup> irradiation-induced diffusion, effect on impurity distrib. 0-70470  
 Si:B, high conc. effects in ion implantation 0-75245  
 Si:B, implanted, radiation damage and minority carrier lifetime, SEM-EBIC obs. 0-96573  
 Si:B, implanted laser annealed, lattice strain, X-ray study 0-96554  
 Si:B, ion implanted, structure defects formation and behaviour under annealing in various ambients 0-65033  
 Si:B, layer resist. depend. on implanting and annealing conditions (*German*) 0-96551  
 Si:B, P, long range enhancement of B diffusivity by P diffusion 0-103386  
 Si:B, resonant scattering of phonons by bound holes in temp. range 1 to 5K 0-75393  
 Si:B, use of BN source to achieve high surface concentration of B (*Russian*) 0-107639  
 Si:B (0.2 wt.%) ion implanted, B atom displacement due to low temp. irradi. 0-88234  
 Si:B diffusion at Si-SiO<sub>2</sub> interface, Auger spectra, Rutherford backscattering 0-70471  
 Si:B implanted wafers, ionis. assisted annealing and effects 0-100257  
 Si:B ion implanted, strain profiles from X-ray rocking curves 0-107290  
 Si:B ion implanted grazing-type solar cells, var. of junction depth, collection efficiencies 0-93934  
 Si:B ion implanted layers, light refl. and transmission coeffs., computer program 0-66316  
 Si:B photodiode front region collection efficiency models 0-96899  
 Si:BF<sub>3</sub><sup>+</sup>, ion implantation appl. in semicond. device production 0-103383  
 p-Si:B(Al), radiation defect form. and annealing study using Hall effect, cond. and carrier diffusion length 0-84214  
 Si:B(Be)(Li) ion implanted, channelling and random equivalent depth distrib. 0-100293  
 Si:B(P), dislocations under high stress, stacking fault energies, TEM study 0-70202  
 Si:B(P), ion implanted crystalline and amorphous laser annealing 0-97509  
 Si:B(P), proton-irrad., impurity uphill diffusion, vacancy mechanism 0-92719  
 Si:B(P)(As)(Sb)(Cu)(Fe), ion implanted, doping profile, pulsed laser annealing effects 0-88197  
 Si:Be, ion implanted, correl. of atomic distrib. and implantation induced damage profiler 0-88199  
 Si:Bi, ion implanted, channelling obs. of pulsed Q-switched ruby laser annealing 0-59542  
 Si:Bi, ion-implanted, solid phase epitaxial growth during annealing, super-saturated solid soln. form. 0-103384  
 Si:C, impurity determ. by IR absorpt. spectroscopy, room temp. and low temp. meas. comparison 0-108237  
 Si:Co, ion implanted, Co lattice location, channelling meas. 0-88201  
 Si:Co, minority carrier lifetime investigation 0-80292  
 Si:Cr(Mn), spin-lattice relax. of Jahn-Teller centres, coexistence of minima with different symmetries 0-80602  
 Si:Cu, precipitate morphology, IR microscopy study (*Chinese*) 0-103539  
 Si:F, amorphous, heat resistant, prep., elec. cond., IR absorpt., annealing 0-65719  
 Si:F, amorphous alloys, RF sputtering prep. in SiF<sub>4</sub>-Ar gas mixture, spectra 0-80772  
 Si:F,H, amorphous, elec. and optical props. 0-60031  
 Si:F,H, amorphous efficient carrier generation for solar photovoltaic energy conversion 0-92906  
 Si:Fe, ion implanted, laser annealing studies using Mossbauer spectroscopy 0-79827  
 Si:Fe, solubility study by EPR and neutron activation anal. 0-75361  
 Si:Fe(Al), compensated substrates for solar cells, effects of Fe and Al 0-94009  
 Si:Ga, IR absorption of dopant centres, spectral depend. on doping, impurity conc. and temp. 0-76053  
 Si:Ga, laser-doped, impurity distrib., Rutherford backscatt. and channelling anal. 0-59507  
 n-Si:Ga laser doped, segregation, Rutherford backscattering 0-103483  
 Si:Gd(Pr), photoconductivity anomalies due to mag. impurities (*Russian*) 0-103722  
 Si:Ge, recryst. after implantation using different temp. and energy sequences 0-84196  
 Si:H, amorphous, 2p level shift, XPS obs. 0-97401  
 Si:H, amorphous, Auger electron spectrosc. obs. 0-76112  
 Si:H, amorphous, band tail absorpt., photocurrent meas. for Schottky barrier solar cell 0-60032  
 n-Si:H, amorphous, bulk density of deep states, DLTS meas. 0-88518  
 Si:H, amorphous, defect photoluminesc. meas. 0-97334  
 Si:H, amorphous, defect states, luminesc. and ESR obs. 0-76075  
 Si:H, amorphous, depletion width determ. by analytical model 0-100445  
 Si:H, amorphous, discharge prod., optically induced cond. changes 0-96937  
 Si:H, amorphous, geminate recombination model for photoluminescence decay 0-71481  
 Si:H, amorphous, HV photovoltaic cells, design parameters 0-101105  
 Si:H, amorphous, horizontal cascade type integrated photovoltaic cell module 0-94091

## silicon continued

- Si:H, amorphous, image pickup devices 0-100481  
 Si:H, amorphous, optical studies of excess carrier recomb., evidence for dispersive diffusion 0-76059  
 Si:H, amorphous, photoelectrochem. behaviour 0-81480  
 n-Si:H, amorphous, photoelectromagnetic effect 0-107845  
 Si:H, amorphous, Pt film growth, AES and LEED study 0-88447  
 Si:H, amorphous, Schottky diodes, elec. props., light-induced effects 0-103741  
 Si:H, amorphous, solar cells, trap spectroscopy using transient current techniques 0-104508  
 Si:H, amorphous, solar-cells, charge collection and spectral response 0-85275  
 Si:H, amorphous, sputtered on Gd<sub>2</sub>(MoO<sub>4</sub>)<sub>3</sub>, ferroelec. domain wall motion, image scanning 0-83663  
 Si:H, amorphous, sputtered Schottky barrier solar cells, conduction mechanism 0-104506  
 Si:H, amorphous, stacked solar cells, development 0-94050  
 Si:H, amorphous, surface states distribution using MOS tunnel junctions 0-103735  
 Si:H, amorphous, temp. depend. of photolum. 0-89063  
 Si:H, amorphous Schottky solar cells, prep. and characts. of diode RF reactive cathodic sputtered films (*French*) 0-61347  
 Si:H, amorphous thin film, ion plating, IR absorpt. meas. 0-84857  
 Si:H, amorphous thin film solar cells 0-81478  
 a-Si:H, electronic states and bonding config. 0-64900  
 a-Si:H, influence of H on optical props., H conc. and H bonds 0-76098  
 Si:H,B, amorphous, field effect and thermoelec. power 0-96924  
 Si:H,Li, amorphous, photoluminescence obs. 0-66280  
 Si:H,P amorphous film, elec. cond., thickness and temp. depend. 0-65559  
 Si:H alloy, amorphous, dihydride model of vibrational spectra 0-80827  
 Si:H amorphous, solar cell structure, optical absorption by gap states 0-94052  
 Si:H amorphous films, conductivity and temp. dependence of optical gap 0-100462  
 Si:H amorphous films, ESR, optical gap and elec. cond. meas. 0-75842  
 Si:H amorphous films, IR spectrum and struct. 0-97277  
 Si:H amorphous films, reactively sputtered, prep. and characterisation 0-100785  
 Si:H amorphous MIS solar cell, loss mechanisms and photovoltaic parameters, overview 0-93923  
 Si:H film, amorphous, H-associated disorder modes, PMR spin-lattice relax. time meas. 0-93202  
 Si:H film, amorphous, plasma-deposited, small angle X-ray and neutron scatt. studies 0-59826  
 a-Si:H film, glow discharge deposited, H profiles, doping level 0-84202  
 a-Si:H highly homogeneous, for low-cost solar cell fabrication 0-72053  
 Si:H,F, amorphous, depletion width determ. by analytical model 0-100445  
 Si:He, B ion implantation 0-96559  
 Si:In, absorpt. spectra, impurity excited state lines 0-108243  
 Si:In, clustering and precipitation, time-dependent perturbed ang. correlation meas. 0-65234  
 Si:In, dopant energy levels, Hall meas. interpretation 0-107736  
 p-Si:In, ion implanted, doping profiles from capacitance-voltage characts. 0-88203  
 Si:In extrinsic IR detectors with closely compensated residual impurities, model of responsivity temp. depend. 0-73453  
 Si:In extrinsic IR detector material with high responsivity compensated by neutron transmutation, float-zone growth 0-75597  
 Si:K, bound exciton luminescence in mag. field (*Russian*) 0-108278  
 Si:Li, bound-exciton excited states, uniaxial anal. 0-71475  
 Si:Li, defect electronic struct. and config., semi-empirical calc. 0-107739  
 Si:Li, electron-phonon scatt., in intermediate conc. region 0-65180  
 Si:Li, photolum. of bound exciton and bound multiexciton complex, Zeeman effect 0-108265  
 Si:Li, thermal cond., low temp. phonon scatt., internal strain effects 0-96706  
 Si:Li n<sup>+</sup>-p solar cells, electron beam irradi. damage 0-94000  
 Si:Mn,Bi, standard, doubly implanted, Rutherford backscattering meas. at MeV energies, screening corrections 0-88204  
 Si:N, high energy ion implantation of buried insulating layers 0-88188  
 Si:N, implantation at high doses, annealing conditions for homogeneous buried insulating layer (*French*) 0-59498  
 Si:N, ion implanted, oxidation characts. 0-89385  
 Si:N, laser-annealed, Jahn-Teller distorted donor, EPR meas. 0-84642  
 Si:N wafers, Si<sub>3</sub>N<sub>4</sub> layer growth by high dose implantation and annealing, elec. props. 0-70227  
 Si:N(P), ion implanted, IR transmission and rel. spectra study 0-108244  
 Si:O, carrier recomb. processes, role of vacancy-O complexes 0-65592  
 Si:O, Czochralski crystal, oxygen striation and thermally induced microdefects 0-100275  
 Si:O, heat treated, excess carrier recomb. rate, defect levels 0-75579  
 Si:O, IR absorpt. at low temp. (*Chinese*) 0-108228  
 Si:O, incorporation of O during pulsed-laser irradi. 0-96557  
 Si:O, kinetics of donor formation, under heat treatment in 450-900°C range 0-75523  
 Si:O,H amorphous, time resolved luminesc. 0-66288  
 Si:O(C), implant redistribution, annealing effects, SIMS meas. 0-96561  
 Si:O(C) wafers, impurity meas. by Fourier transform IR spectra 0-89030  
 Si:O(C) films, impurity meas. by Fourier transform IR spectra at low temp. 0-89031  
 Si:P, annealing after ion implantation, ellipsometric study 0-65018  
 Si:P, dielec. susceptibility meas., polarisation catastrophe at metal-insulator transition 0-59873  
 Si:P, dislocation disloc. mode obs. by weak-beam TEM 0-107259  
 Si:P, doping during growth from gas phase, thermodynamic analysis 0-59489  
 Si:P, heavily doped semicond., scatt. mechanism, resist. and Hall coeff. maxima 0-75586  
 Si:P, homogeneous nuclear transmutation technique, thyristors appl. 0-70236  
 Si:P, implanted low temp. annealed, elec. activation, damage depend. 0-88182  
 Si:P, incoherent light flash annealing, elec. props., backscattering spectra 0-97504  
 Si:P, ion implanted, regrowth of damage structs. by laser annealing 0-107289  
 Si:P, ion implanted, subsurface damage, TEM and channelled Rutherford backscatt. study 0-107337

## silicon continued

Si:P, ion implanted with small doses, defect annealing by nanosecond laser pulses 0-107297  
 Si:P, luminescence circular polarisation, emission by many exciton complexes 0-93398  
 Si:P, measurement techniques for determining P densities 0-75262  
 Si:P, neutron transmutation doping, elec. props. rel. to neutron fluence 0-96555  
 Si:P, neutron transmutation doping, resist. homogeneity rel. to compensation ratio 0-96556  
 n-Si:P, piezothermoelec. power in electron-phonon drag region, anisotropy 0-70738  
 Si:P, polycryst., channelling of implanted P during MOS device processing 0-65017  
 Si:P, polycryst. films, elec. props., EPR, defect states, doping effects 0-75660  
 Si:P, polycrystalline laser recrystallised film on Si substrate, cryst. struct., thermal oxidation 0-65391  
 Si:P, thermal cond., electron-phonon interaction at low temps. 0-92730  
 Si:P bipolar transistors, interstitial supersaturation and misfit dislocation climb, TEM study 0-70203  
 Si:P film, polycryst., heavily doped, mobility and carrier conc., optical determ. 0-66314  
 Si:P implanted, multicasting electron beam annealing 0-75242  
 p-Si:P implanted films, piezoresist. stress tensors, ion dose depend., -80 to 120°C 0-100538  
 Si:P polycrystalline layer, role in lattice defect reduction assoc. with P predeposition 0-70229  
 p-Si:P semiconductor detector in radiometric inspection problems 0-62819  
 Si:P(As)(B), nonequilibrium solid solutions obtained by heavy ion implantation and laser annealing 0-92544  
 n-Si:P(B), elec. cond. oscills., electron instability effects due to dislocations 0-103704  
 Si:P(O)  $p^+-n-n^+$  solar cells, comparison rel. to resistance to 1.5 MeV electron irradi., majority carrier trapping 0-94087  
 p-Si:P(P<sup>+</sup>) photolytic props. in HF 0-89504  
 Si:Pt, hole capture cross-section at  $E_v+0.34$  eV, capacitance meas. (French) 0-65493  
 Si:Pt, implanted and laser annealed, segregation and increased dopant solubility 0-65016  
 Si:S, deep level characterisation, implantation predeposition technique 0-100444  
 Si:Sb, high dose Sb ion implantation, buried layer appls. 0-88186  
 Si:Sb, ion implanted, Sb diffusion during oxidation, snow-plough effect 0-88366  
 Si:Sb, ion implanted and annealed, influence of implantation temp. on dislocation generation 0-88158  
 Si:Sb, laser doping, evaporation loss and diffusion of Sb, under pulsed laser irradi. 0-59508  
 Si:Sb, low energy ion implantation, profile determ. 0-88176  
 Si:Sb, low energy ion implantation Schottky barrier diodes and resistors 0-88177  
 Si:Sb, MBE film, doping technique 0-79821  
 Si:Sb, Mossbauer spectra of  $^{119}\text{Sn}$  defect struct. 0-97174  
 Si:Sb, produced by ion implantation and laser annealing, Sb behaviour above solid solubility 0-88200  
 Si:Sb,P, double implants, residual defect reduction after damage anneal 0-88170  
 Si:Sb vacuum deposited coating, p-n junction, pulsed electron beam annealing doping, diffusion 0-75480  
 Si:Sb(Ga)(Bi)(In), dopant solubility limit, laser irradi. effects 0-84295  
 Si:Sc, photocapacitance and photoconductivity 0-107859  
 Si:Se, impurity states, A- and B-centres, electron, hole thermionic emission rates 0-96813  
 Si:Sn, Mossbauer study of defects due to  $^{119}\text{In}$  implantation 0-80641  
 Si:Te, laser melting, surface Te atom accumulation, profiles 0-100258  
 Si:Te, Mossbauer spectra of  $^{119}\text{Sn}$  defect struct. 0-97175  
 Si:Ti substrate for epitaxial solar cells 0-61341  
 Si:Y, photoelectric props. 0-107860  
 Si:Zn, minority carrier lifetime investigation 0-80292  
 Si:Al and Si:Al-Si(Cu), Si regrowth minimisation through overlying Al or Al alloy film 0-70569  
 n-Si/As-Te-Ge film, heterojunction, elec. and photovolt. props. 0-100514  
 Si/In<sub>2</sub>O<sub>3</sub>-SnO<sub>2</sub> thin film junctions, polarity dependent memory switching effects 0-70814  
 Si/In(Cd), Si/Cd Schottky contacts, electrochemically deposited 0-88633  
 Si/Ni, Stoneley waves at (001) interface between cubic symm. cryst. 0-100388  
 Si/Pd system, solid phase epitaxial growth control by C ion implantation 0-75466  
 p-Si/rare earth metal contacts, surface pot. barrier 0-60086  
 Si/refractory metal-Ni(Pd)(Pt) interactions, phase separation 0-65303  
 Si/SiO<sub>2</sub> interface, precise wet-chemical etching, using rapidly rotating sample 0-93669  
 Si-Ag-Si heat mirror on plastic sheet for radiation insulation of visible windows 0-95985  
 p-Si-Al, ohmic contacts, Si dissoln. and recrystn. effects, computer calc. 0-103749  
 Si-Al-Al<sub>2</sub>O<sub>3</sub> system, solid phase Si regrowth on sapphire 0-100413  
 Si-Au, interface study using EELS 0-97391  
 Si-Au interface, critical Au-film thickness obs. for room temp. interfacial reaction 0-75390  
 Si-CoSi<sub>2</sub>Si, double heteroepitaxy, solid phase and MBE 0-104063  
 Si-Cr<sub>2</sub>O<sub>3</sub>Al, current-voltage characts., oxide film effects 0-70841  
 n-Si-Cu Schottky contacts, electrochem. deposition, barrier height and ideality factor 0-75641  
 Si-F-H amorphous solar cells, DC glow discharge fabrication 0-72041  
 Si-F-H:P, film, dark cond., struct., Raman scatt. 0-88588  
 Si-GaSe n-p heterojunction, elec. characts., interface states 0-70812  
 Si-Ge heterojunction form., microscopic aspects, EELS meas. 0-80368  
 Si-H, amorphous, spattered, photolum. obs. 0-80856  
 Si-H:P amorphous film, dark cond., struct., Raman scatt. 0-88588  
 Si-In<sub>2</sub>-Sn<sub>2</sub>O<sub>3</sub>-y SIS heterostructure solar cells, spray-deposited 0-101106  
 Si-insulator interface, non-avalanche charge injection, expt. study, charge trapping effects 0-60099  
 Si-metal contact, transport theory of Schottky barriers 0-80372  
 Si-metal contacts, analytical techniques, review 0-80120

## silicon continued

Si-metal interface, silicide formation, interface marker technique obs. 0-59734  
 Si-Mo sputtered contacts, contact resistance 0-92970  
 Si-Mo substrate-film interface, reaction on heat treatment, silicide formation 0-79999  
 Si-on-ceramic solar cells, short-circuit current density meas. using light-beam-induced-current tech. 0-93887  
 Si-Pb heterojunction, RHEED, Mossbauer spectroscopy and I-V characts. 0-70828  
 Si-PbS heterojunction, effect of Si substrate orientation on struct. and interface props. 0-80097  
 n-Si-Pd diodes, chemical reduction process for fabrication 0-60082  
 n-Si-Pd<sub>2</sub>Si contact, interface struct. and Schottky barrier height, correl. obs. using TEM 0-100504  
 Si-Pd<sub>2</sub>Si<sub>20</sub>, amorphous, Pd/Si layer form., shallow contact 0-103586  
 Si-Pd-Si structure, epitaxial growth, backscattering and transmission electron microscopy studies of layered structures 0-80123  
 Si-Pd-Ti, silicide form. in evaporated films 0-80006  
 Si-PtSi interface, impurity effects 0-80037  
 n-Si-Re(Os) Schottky contact barrier height meas. 0-65675  
 Si-refractory metal contacts, thermally cleaned surfaces 0-100521  
 Si-refractory metal structs., interface modification by ion implantation 0-70475  
 Si-Si interface, elec. cond. rel. to interface state population 0-65672  
 Si-Si<sub>3</sub>N<sub>4</sub> interface in MNS capacitors, surface state density investigation 0-60100  
 Si-Si<sub>3</sub>N<sub>4</sub>-SiO<sub>2</sub> non absorbing double layers, optical parameters reflectivity by liquid immersion method 0-71503  
 Si-SiC chemical interaction in rarefied O<sub>2</sub> under pulsed action of concentrated solar radiation 0-71930  
 Si-SiO<sub>2</sub>, influence on frequency-temp. coeff. of SAW devices 0-79066  
 Si-SiO<sub>2</sub> interface, doping depend. of interface states and charges 0-92992  
 Si-SiO<sub>2</sub> interface, stress meas. technique 0-84395  
 Si-SiO<sub>2</sub>, ion implantation through SiO<sub>2</sub> film, recoil implantation of O, EPR study 0-88180  
 Si-SiO<sub>2</sub>, MOS interface states density, meas. techniques and model development 0-92988  
 n-Si-SiO<sub>2</sub>, MOS structures, radiation states 0-103758  
 Si-SiO<sub>2</sub>, recoil implanted O profile after ion implantation through SiO<sub>2</sub> 0-88198  
 Si-SiO<sub>2</sub>, two layer system, P<sup>+</sup>-ion penetration tails, expt. and computer anal. 0-75249  
 Si-SiO<sub>2</sub> (111) interface, H<sub>2</sub> effects, AES study 0-65688  
 Si-SiO<sub>2</sub> abrupt interface form. by very high dose O<sup>+</sup> ion implantation 0-75253  
 Si-SiO<sub>2</sub> boundary, relaxation of nonequilibrium capacitance in electrolyte in intense elec. fields 0-70845  
 Si-SiO<sub>2</sub> boundary, surface charge transport in valence band of Si 0-70789  
 Si-SiO<sub>2</sub> electrode, electronic cond., luminesc. obs. 0-61111  
 Si-SiO<sub>2</sub> in MOSFETs, inversion layer carrier mobility, theory 0-60094  
 Si-SiO<sub>2</sub> interface, (001) vicinal planes, minigaps in inversion layers, far IR absorpt. meas. 0-107919  
 Si-SiO<sub>2</sub> interface, barrier height in MOS tunnelling structures 0-88644  
 Si-SiO<sub>2</sub> interface, density of states, theory 0-80395  
 Si-SiO<sub>2</sub> interface, electronic struct. calc. 0-100531  
 Si-SiO<sub>2</sub> interface, improved characterisation, refined quasistatic and cond. methods 0-96990  
 Si-SiO<sub>2</sub> interface, O<sub>2</sub> plasma effects on elec. props. 0-100523  
 Si-SiO<sub>2</sub> interface, remote polar phonon scatt. in Si inversion layers 0-80095  
 Si-SiO<sub>2</sub> interface, thermal SiO<sub>2</sub> sputter induced roughness, Auger sputter profiling study 0-75424  
 Si-SiO<sub>2</sub> interface, thermally grown, surface pot. inhomogeneities after stress ageing 0-92993  
 Si-SiO<sub>2</sub> interface, thermally grown oxide, spectroscopic ellipsometric anal. 0-107659  
 Si-SiO<sub>2</sub> interface, two-dimensional impurity bands, carrier-density dependence of activation energies associated with hopping 0-88561  
 Si-SiO<sub>2</sub> interface in IGFETs, anal. of CVD SiO<sub>2</sub> on (100) and (111) surfaces, near-ideal structs. 0-100528  
 Si-SiO<sub>2</sub> interface in MIS structs., effects of crystal defects on generation process 0-65702  
 Si-SiO<sub>2</sub> interface in MOS structs. low-energy electron beam irradi., charge accumulation process anal. 0-65701  
 Si-SiO<sub>2</sub> interface in MOS capacitors, lateral diffusion of Na<sup>+</sup>, neutralisation 0-92986  
 Si-SiO<sub>2</sub> interface in MOS solar cells, operational characts. and struct. 0-93901  
 Si-SiO<sub>2</sub> interface states, deposition of H containing layers and annealing 0-92991  
 Si-SiO<sub>2</sub> inversion layer, n-channel, anomalous magnetoresist., model 0-96996  
 Si-SiO<sub>2</sub> laminar ion-implanted systems, struct. change investig. by MSSI method (Russian) 0-107918  
 Si-SiO<sub>2</sub> MIS systems, dynamic props. of switching, appl. to charge transfer devices 0-92997  
 Si-SiO<sub>2</sub> MOS capacitors, relationship between trapped holes and interface states 0-70830  
 Si-SiO<sub>2</sub> MOS interface, surface-state density and minority carrier generation rate, meas. by DLTS, hot hole effect 0-100527  
 Si-SiO<sub>2</sub> MOS interface states density, transient capacitance meas. eval. 0-92989  
 Si-SiO<sub>2</sub> structure, alkali metal ion migration and accumulation, interface struct. 0-107574  
 Si-SiO<sub>2</sub> structures, B ions implanted, energy spectra of shallow traps at various implantation energies 0-80392  
 Si-SiO<sub>2</sub>-Al, interface barrier energies for tunnel oxides, internal photoemission meas. 0-84512  
 Si-SiO<sub>2</sub>-Al, internal photoemission, pot. barrier height determ. 0-65699  
 Si-SiO<sub>2</sub>-Al MOS surface channel influence on channel-to-contact diode charact. 0-92994  
 Si-SiO<sub>2</sub>-Al structures, SiO<sub>2</sub> thin dielec. film elec. props. with DC voltage (Slovak) 0-88634  
 Si-SiO<sub>2</sub>-Al with thick dielec. layer, photoelec. props. 0-92979  
 Si-SiO<sub>2</sub>-Au Schottky barrier solar cells, back-illuminated, theoretical performance 0-61345  
 Si-SiO<sub>2</sub>-Au system, oxide film 16-36 Å thick, tunnel currents 0-70842  
 Si-SiO<sub>2</sub>-CdS solar cell, I-V characteristics 0-89621



## silicon continued

- Si-SiO<sub>2</sub>-Mg-Cu powder compact, nitridation to form Si<sub>3</sub>N<sub>4</sub> whiskers (*Japanese*) 0-93674  
 Si-SiO<sub>2</sub>-Mo-Si<sub>3</sub>N<sub>4</sub>-Al MNOS structures with metal grains, charge transport at SiO<sub>2</sub>-Si<sub>3</sub>N<sub>4</sub> interface 0-65693  
 Si-SiO<sub>2</sub>-Si capacitor, polycryst., capacitance voltage characterisation 0-70794  
 Si-SiO<sub>2</sub>-Si thin film MOS structures, elec. props. with applied DC voltage (*Slovak*) 0-92977  
 Si-SiO<sub>2</sub>-Si<sub>3</sub>N<sub>4</sub> MNOS structure, chem. comp. and electronic states, Auger and energy loss spectra obs. 0-92999  
 Si-SiO<sub>2</sub>-Si MOS structures, charge motion, TSC meas. 0-100534  
 n-Si-SiO<sub>2</sub>-SnO<sub>x</sub> SIS solar cell, transport props., 14% efficiency realisation 0-94079  
 Si-SiO<sub>2</sub>-polySi thin film structures, dielectric props. (*Slovak*) 0-75934  
 Si-SiO<sub>2</sub> interfaces, carrier transport processes, electron states, conference, Durham, England (July 1979) 0-90612  
 Si-Sn heterojunction, RHEED, Mossbauer spectroscopy and I-V characts. 0-70828  
 Si-TiO<sub>2</sub>-Al, current-voltage characts., oxide film effects 0-70841  
 Si-V<sub>2</sub>O<sub>5</sub>-Al, current-voltage characts., oxide film effects 0-70841  
 Si-ZnSe, IR segmented composite window design 0-106621  
 Si+F<sup>-</sup>, inner-shell ionisation, X-ray cross sections 0-58369  
 Si+SF<sub>6</sub>, IR laser induced surface reaction, mol. vibr. and mol. dissoci. obs. 0-93798  
 Si<sub>2</sub>, electronic struct. and bonding, atomic effective pot. appl. 0-95745  
 p<sup>+</sup>-Si<sub>1-x</sub>Ge<sub>x</sub>-nSi junction diodes, lattice misfit effects on I-V characts. 0-70804  
 Si(Li) X-ray detector, Au contact layer thickness meas. 0-62627  
 SiN powder formation, in high-temp. N flow (*Russian*) 0-100818  
 Si(Si<sup>2+</sup>)(Si<sup>3+</sup>), excited levels, radiative lifetimes, beam foil spectra 0-58368  
 Si(111)-Pb ion implanted amorphous layers, recrystallisation, impurity out-diffusion model (*Chinese*) 0-88363  
 Si(111)/Pt/Ni Schottky diodes, current-voltage characts. and comp. profiles 0-84508  
 Si(111)-√3×√3-Ag structure, atomic arrangement, low energy ion scatt. spectroscopy 0-96724  
 SnO<sub>2</sub>/n<sup>+</sup>-pSi heterojunction solar cells, fabrication by paint-on-diffusant method 0-94048  
 SnO<sub>2</sub>-polySi solar cells, fabrication, grain size effects on device parameters 0-94045  
 surface (111), high temp. RHEED Obs. using metal-backed fluoresc. screen 0-75126  
 YIG:Si single crystals., mag. props. 0-107981  
 YIG:Si, effects of nontrigonal cryst. field on spectroscopic props. of Fe<sup>2+</sup> ions 0-92864  
 ZnO/Si acoustoelectric devices, magnetron discharge sputtering prep. 0-80332  
 ZnO/Si SAW struts., anal. of charge injection 0-80049  
 ZnO-SiO<sub>2</sub>-Si SAW device, interface transduction 0-102949

## silicon alloys

- see also Ge-Si alloys  
 Colmonoy, self-weldability in high temp Na (*Japanese*) 0-89392  
 Colmonoy hardfacing materials, friction characts. in high temp. Na (*Japanese*) 0-89356  
 dilute, irradiation softening effect on yield stress 0-76319  
 Hayes alloy no.716, Fe-Cr-Ni-Co-W-Mo-Si-C-B (26, 22, 12, 3.5, 3, 1.2, 1.1, 0.4 wt.%), hardfacing alloy 0-100802  
 irradi., surface effects on precip. morphology 0-104168  
 metal silicides, fabrication technique and characterisation (*Japanese*) 0-60779  
 rare earth-transition metal alloys, RM<sub>2</sub>Si<sub>2-x</sub>Ge<sub>x</sub>, magnetism and hyperfine interactions, magnetisation and Mossbauer effect studies 0-75892  
 steel, B-Si, grain-oriented, high induction, Cu impurity effects 0-89366  
 steel, Cr-Mo, Mn and Si effect on temper embrittlement, comp. and carbide precip. effects 0-85037  
 steel, Cr-Si, oxidation resist. in high pressure CO<sub>2</sub>, Si effect 0-66704  
 steel, Si, grain-oriented, high permeability, dissoln. and precip. of AlN and MnS 0-89223  
 steel, Si, nonoriented sheet prod. with texture of {100} {ovw} 0-89246  
 Stellite, self-weldability in high temp Na (*Japanese*) 0-89392  
 stellite hardfacing materials, friction characts. in high temp. Na (*Japanese*) 0-89356  
 thermally degenerated Schottky diodes, resonant tunnelling 0-100503  
 Al-Cu-Mg-Mn-Si-Fe, torsional vibrations decrement, deformed vol. effect 0-76326  
 Al-Cu-Si-Mg, deform. simulation using torsional test, elastoplastic constitutive eqn. 0-93594  
 Al-Cu-Si-Mn, type 2017S-T4, crack initiation at root of circumferential notch of round bar specimens (*Japanese*) 0-60947  
 Al-Fe-X-Si (X=transition metal), struct. and comp. by electron microscopy 0-88093  
 Al-Mg, Si alloy, void form. under different precip. conditions, after Al ion irradi. 0-59529  
 Al-Mg-Si, ageing sequence study by electron microdiff. 0-81068  
 Al-Mg-Si, STEM microdiff. obs. of precip. struct. 0-104167  
 Al-Mg-Si, cast, precip.-rich zones on grain boundaries, soln. heat treatment conditions effect on mech. props. 0-104176  
 Al-Mg-Si, type 6010, microstruct. characts. influence on formability, heat treatment 0-81090  
 Al-Mg-Si, type 6061-T6, 6063-T6, effective stress range factor in fatigue 0-100924  
 Al-Mg-Si alloy, Mg<sub>2</sub>Si dispersion hardened US waveguides, concentrators (*Polish*) 0-89237  
 Al-Mg-Si alloys, ductile intergranular fracture mechanisms, void formation and nucleation 0-108578  
 Al-Mg(Cu)(Si), (5.0/4.5)/(11.8 wt.%), ingots, vibr. effect during solidification on porosity formation 0-108426  
 Al-Ni(Cd)(Fe)(Si), cold worked, struct. and props. 0-71666  
 Al-Si, DC magnetron-sputtered, residual gas influence on props. 0-80968  
 Al-Si, eutectic, quasiisotropic, rheological deformation theory 0-79165  
 Al-Si, graphite dispersed, wear characts. (*Korean*) 0-93658  
 Al-Si, rapid quenching, struct. and decomp. 0-76244  
 Al-Si (0.57 at.%), Si precipitate dissolution kinetics 0-84935  
 Al-Si (1.2 wt.%), dispersion hardened, work hardening due to Orowan loops, temp. depend. (*Japanese*) 0-66534  
 Al-Si (25.4 wt.%), solidification, high press. effects 0-66499  
 Al-Si (2.4 wt.%), liq. fluidity in solid-liq. zone 0-108429  
 Al-Si eutectic, irregular, branching limited growth 0-81042

## silicon alloys continued

- Al-Si eutectic alloy, banded struct., SEM and optical microscopy 0-104144  
 Al-Si eutectic alloys in screened ohmic contacts for solar cells 0-94090  
 Al-Si melt, microheterogeneity (*Russian*) 0-103238  
 Al-Si melts, spreading behaviour on Fe 0-84345  
 Al-Si-Cu, fracture resistance at low temps. 0-104284  
 Al-Si-Cu-Zr, ageing kinetics (*Russian*) 0-76274  
 Al-Si-Y alloy, phase equilibria in Al rich region (*Russian*) 0-93537  
 Al-Si(Mg), dimensional changes in heat treatment. 0-89271  
 Al-Si(9.3, 12) with graphite particles seizure resistance study using Hohman wear tests 0-89360  
 (Al-Si) Si system, Si regrowth minimisation through overlying Al or Al alloy film 0-70569  
 Au-Ge-Si, influence of struct. on elec. resist. of glass forming alloys 0-65518  
 Au-Si formation at thin film interface, electron diff. study 0-80005  
 Au<sub>7</sub>Ge<sub>13</sub>Si<sub>9.4</sub>, heat of crystn. and viscous behaviour 0-75166  
 Au<sub>35</sub>Si<sub>65</sub>, amorphous vacuum-deposited and liquid-quenched films, diffusion and crystn. 0-84094  
 Au<sub>3</sub>Si<sub>1-x</sub> amorphous alloy, crystallisation, elec. cond. study 0-103246  
 Au<sub>3</sub>Si<sub>1-x</sub> amorphous films, phys. studies 0-75476  
 Au<sub>2</sub>Si<sub>3</sub> m, metastable phase, substruct. unit cell (*German*) 0-88091  
 B-Si, (0 to 14.3 at.%), phase charact., regions of existence (*French*) 0-104117  
 B-Si alloys, B-rich, prep., anal. and cryst. growth (*French*) 0-104091  
 CeCu<sub>2</sub>Si<sub>2</sub>, collective phenomena 0-65933  
 CeNi<sub>5</sub>Si<sub>4.5</sub>, X-ray cryst. struct. determ. 0-88089  
 Ce<sub>2</sub>Si<sub>5</sub>, X-ray cryst. struct. determ. 0-92480  
 Co-B-Si amorphous alloy, liq. quenched, elec. resist. and cyclic deform. 0-59949  
 Co-Fe-Si-B, decomp. of amorphous state during annealing below recryst. temp., electron microscope study (*Russian*) 0-75164  
 Co-Fe-Si-B, ferromag., magneto-optical spectra in amorphous and cryst. states (*Russian*) 0-84749  
 Co-Mn-Ni-Fe-Si-B amorphous alloys, mag. props., low magnetostriction 0-75832  
 Co-Si, surface physicochemical state, Auger electron spectroscopy study 0-100715  
 Co-Si-B, amorphous ribbon, saturation magnetostriction meas. by small-angle magnetisation rot. 0-60391  
 (Co<sub>0.93</sub>Fe<sub>0.07</sub>)<sub>75</sub>-Cr<sub>2</sub>Si<sub>15</sub>B<sub>10</sub> amorphous alloy, thermal stability, Cr conc. effects, DTA expts. 0-59395  
 (Co<sub>0.89</sub>Fe<sub>0.11</sub>)<sub>72</sub>Mo<sub>2</sub>Si<sub>15</sub>B<sub>10</sub>, metallic glass, strain- and field-induced mag. anisotropy 0-108004  
 Co<sub>7</sub>Fe<sub>3</sub>Ni<sub>10</sub>(Si<sub>2</sub>B)<sub>28</sub>, amorphous, soft mag. props., switched-mode power supply appls. 0-88850  
 Co<sub>70</sub>Fe<sub>15</sub>Si<sub>15</sub>B<sub>10</sub>, amorphous, crystn. and thermal stability 0-107057  
 Co<sub>70.4</sub>Fe<sub>4.6</sub>Si<sub>15</sub>B<sub>10</sub>, amorphous, mag. aftereffect spectra and annealing props. 0-88831  
 CoMnSi<sub>1-x</sub>Ge<sub>x</sub>, amg. props. 0-60270  
 Co<sub>73</sub>Mo<sub>2</sub>Si<sub>15</sub>B<sub>10</sub>, metallic glass, strain- and field-induced mag. anisotropy 0-108004  
 Co<sub>2</sub>Pd<sub>80-x</sub>Si<sub>20</sub>, amorphous, structural and mag. heterogeneities 0-80484  
 Co<sub>2</sub>Si, struct. comparison with Co<sub>2</sub>P, PbCl<sub>2</sub>, and SbSi (*French*) 0-84155  
 Co<sub>2</sub>Si<sub>3</sub>B<sub>10</sub>, amorphous, crystn. and thermal stability 0-107057  
 Cr-Fe-Ni-Si, ternary phase equilibria for Cr-Fe-Ni rich portion, lattice stabilities 0-71628  
 Cr-Si, dilute alloy, mag. susceptibility and Neel temp. meas. 0-71017  
 Cr-Si-V, (2, 0.1 at.%), paramag. to commensurate spin density wave transition 0-65875  
 Cr<sub>2</sub>Si, mag. susceptibility, 2 to 300K, rel. to electron energy spectrum 0-60185  
 Cu-Co-Si (0.36, 0.11 wt.%), surface layer struct. on annealing, SIMS and AES exam. 0-88415  
 Cu-Ni-Si, cast, strength and hot ductility, Si effect 0-66595  
 Cu-Si (6.5 at.%), plastic deformation, HVEM study (*French*) 0-66605  
 Cu-Si (7 at.%), dislocation interactions, influence of jogs on extension of dislocation nodes 0-84176  
 Cu-Si (8 wt.%), intrinsic struct. in grain boundaries and boundary mobility 0-103368  
 Cu-V-Si, supercond. props. 0-107945  
 EuCu<sub>2</sub>Si<sub>2</sub>, interconfiguration fluctuation, NMR expts. 0-66069  
 (Fe<sub>2</sub>Co<sub>2</sub>Ni)-Si, amorphous alloy, magnetostriction rel. to soft mag. props. 0-84633  
 Fe-Al-Si (6.22, 9.63 wt.%), bending test under high press., high temp. 0-85057  
 Fe-B-Si, glassy, field-induced mag. anisotropy near eutectic comp. 0-93110  
 Fe-B-Si amorphous alloy, liq. quenched, elec. resist. and cyclic deform. 0-59949  
 Fe-B-Si-C amorphous alloys, prep. and props. 0-88748  
 Fe-C-Si, cast, graphite nodularization during annealing, Mg and S effects (*Japanese*) 0-10087  
 Fe-C-Si, high purity, vacuum melted, nodular graphite form. 0-108452  
 Fe-Ci (3 wt.%), local magnetisation losses, grain orientation effect 0-88817  
 Fe-Co-Si-B, amorphous soft ferromagnet with high mag. induction 0-84619  
 Fe-Co-Si-B, zero magnetostrictive amorphous alloy with high saturation induction, mag. annealing 0-60362  
 Fe-Co-Si(B), amorphous ferromagnet, mag. after effect on soft mag. props. 0-84626  
 Fe-Cr-Mo-Si, amorphous films, corrosion resist. and ion plating use 0-89423  
 Fe-Cr-Ni (12, 15 wt.%) austenitic alloy, Ni<sup>6+</sup> irradiated, void swelling and phase stability, Si and Ti effects 0-65055  
 Fe-Cr-Si, heat resistive films prepared by sputtering, lifetime meas. 0-80132  
 Fe-Cr-Si, oxidation resist. in high pressure CO<sub>2</sub>, Si effect 0-66704  
 Fe-Ni-B-Si, amorphous, mag. props., heat treatment effects 0-89370  
 Fe-Ni-Si, austenite, annealing effect on atom redistrib., Mossbauer anal. (*Russian*) 0-66529  
 Fe-Si, (110) [001] oriented, mag. props., compressive stress effects 0-60392  
 Fe-Si, fatigue fracture fractography in broad strain-amplitude range, in air and vacuum 0-81186  
 Fe-Si, grain oriented, misorientation effects on mag. props. 0-88792  
 Fe-Si, grain oriented, phosphate coating anal. by IR spectroscopy 0-89570  
 Fe-Si, grain oriented sheet, grain struct. by computer mapping 0-88168

## silicon alloys continued

- Fe-Si, grain oriented sheet, AC hysteresis, surface struct. and elastic stress effects 0-88791
- Fe-Si, grain oriented transformer sheets, permeability and magnetostriction, tensile stress effects 0-88843
- Fe-Si, grain-oriented sheets, high permeability, low losses, review 0-88790
- Fe-Si, loss meas. at high flux densities 0-88799
- Fe-Si, mag. props., stress and reannealing effects 0-88844
- Fe-Si, microflow and strain hardening under cyclic loading 0-104182
- Fe-Si, non-oriented sheets, production and props. 0-88797
- Fe-Si, power loss and permeability meas. by means of Hall probes and stochastic ergodic correl. 0-86350
- Fe-Si, rapid cracks self-arrest potential, -196.0°C 0-100911
- Fe-Si, single cryst., mag. domain wall motion, X-ray topography study 0-65953
- Fe-Si, spreading behaviour of liq. Al 0-84345
- Fe-Si, stator core, grain-oriented and non-oriented, magnetic flux and loss distrib. 0-88798
- Fe-Si, transformer steel, high-temp. heat treatment, resist. of refractories in contact 0-66554
- Fe-Si (2.8 wt.%), single crystals, growth striations, X-ray studies 0-79774
- Fe-Si (2.6 wt.%) single cryst., crack propag., controlled plastic crack tip opening rate 0-60943
- Fe-Si (3 at%), deformation and electron bombardment, influence on dislocation struct., 20-500°C (*Russian*) 0-92536
- Fe-Si (3 to 5 wt.%) sinters, mag. props., Si and Fe-Si additions effect 0-71104
- Fe-Si (3 wt.%), behaviour of disperse inclusions, influence of recrystn. processes (*Russian*) 0-66519
- Fe-Si (3 wt.%), domain wall spacing and core loss, forsterite and stress coatings effect 0-88780
- Fe-Si (3 wt.%), electron irradiated, yield strength and elongation 0-76325
- Fe-Si (3 wt.%), ferromag. domains, imaging by neutron interferometry 0-71087
- Fe-Si (3 wt.%), grain oriented, mag. props., effect of decarburizing (*Chinese*) 0-103821
- Fe-Si (3 wt.%), grain-oriented, domain struct. regulation and power loss reduction 0-88779
- Fe-Si (3 wt.%), grain-oriented, domain wall profiles throughout magnetisation cycle 0-88781
- Fe-Si (3 wt.%), grain-oriented, stacking effect on power loss, mag. props. 0-88795
- Fe-Si (3 wt.%), grain-oriented, power loss and domain wall variation with lamination thickness 0-88814
- Fe-Si (3 wt.%), grain-oriented, energy loss reduction by lowering sheet thickness 0-88816
- Fe-Si (3 wt.%), high permeability, use in transformer cores 0-88793
- Fe-Si (3 wt.%), internal friction, instantaneous, depend. on phase of torsional oscils. (*Russian*) 0-71142
- Fe-Si (3 wt.%), losses, demagnetisation freq. and grain orientation depend. 0-88796
- Fe-Si (3 wt.%), mag. anisotropy induced by cold rolling (*Russian*) 0-84595
- Fe-Si (3 wt.%), mag. domain wall contrast in synchrotron X-ray topographs 0-75792
- Fe-Si (3 wt.%), mag. loss and magnetostriction, DC flux alternation effects 0-88794
- Fe-Si (3 wt.%), magnetisation variation during bending oscils., rel. to  $\Delta E$  effect (*Russian*) 0-65983
- Fe-Si (3 wt.%), nonoriented sheets, magnetisation, tensile stress effects 0-88845
- Fe-Si (3 wt.%), oriented, losses and domains, mech. stress effects 0-88852
- Fe-Si (3 wt.%), power losses at extremely low freqs. 0-88815
- Fe-Si (3 wt.%), stripe domain structure, dynamic behaviour at high max. induction values (*Russian*) 0-80553
- Fe-Si (3 wt.%), struct. and preferred orientation, annealing parameters influence (*Czech*) 0-89248
- Fe-Si (3 wt.%), texture, Mossbauer expts. 0-71262
- Fe-Si (3 wt.%) high-permeability grain-oriented steel, quenching effect on primary recrystn. texture development 0-84956
- Fe-Si (3 wt.%) laminations, magnetostriction behaviour associated with closure domain spikes 0-75834
- Fe-Si (3 wt.%) laminations, grain oriented, plastically deformed, anomalous losses 0-88853
- Fe-Si (3.25 wt.%), single cryst. with (007) planes, domain struct. influence on mag. torque 0-108034
- Fe-Si (3 wt.%), grain-oriented, secondary recryst., grain growth inhibition 0-89245
- Fe-Si (6.5 wt.%) filament, formation by modified Taylor technique, and mag. props. 0-75795
- Fe-Si (6.5 wt.%) ribbon, splat-cooled, mag. props. 0-88805
- Fe-Si cast alloy with spheroidal graphite, transform. investigation during tempering (*Russian*) 0-97479
- Fe-Si gas-flame spray deposited protective coating, for C steel heat exchanger 0-61025
- Fe-Si system, melting equilibria study (*German*) 0-66473
- Fe-Si-Al, Sendust, ribbon-form, prep. by rapid quenching, mech. and mag. props. 0-71611
- Fe-Si-Al, surface oxide layer struct., AES study 0-89396
- Fe-Si-Al (2.8-3.4, 0.8-0.86 wt.%) oxidation, annealing 0-89395
- Fe-Si-Al (9.6, 5.4 wt.%) ribbon-form Sendust alloy, mag. props., annealing effects 0-88800
- Fe-Si-Al ribbon-form Sendust alloy made by rapid roll quenching, mag. props., recording head appls. 0-81001
- Fe-Si-B, high induction, hot rolling treatment 0-89266
- Fe-Si-B, magnetic metallic glasses, mag. props. 0-84620
- Fe-Si-B alloy filaments produced by glass-coated melt spinning 0-76213
- Fe-Si-B amorphous alloys, Mossbauer spectroscopy (*French*) 0-80653
- Fe-Si-B glassy alloys, mag. props., comp. effects 0-88752
- Fe-Si-C, austenitic, C diffusivity (*German*) 0-92705
- Fe-Si-C mixed powder, cast Fe powder sintering study (*Japanese*) 0-108373
- Fe-Si-Cr magnetic films, sputtered, corrosion reduction, effect of Cr obs. 0-80573
- Fe-Si-Zn, influence of trace elements on morphology (*German*) 0-108390
- (Fe<sub>100-x</sub>B<sub>x</sub>)<sub>1-x</sub>Si<sub>x</sub>, thin film glasses, mag. props. and corrosion resist. 0-80576

## silicon alloys continued

- Fe<sub>80</sub>B<sub>20-x</sub>Si<sub>x</sub>, amorphous, mag. saturation, spin wave stiffness, temp. depend. 0-75741
- Fe<sub>80</sub>B<sub>20-x</sub>Si<sub>x</sub>, amorphous, size effect of metalloids on mag. props. 0-84594
- Fe<sub>84</sub>B<sub>13</sub>Si<sub>2</sub>, metallic glass, electrical resistivity and crystallisation 0-88526
- Fe<sub>3</sub>C<sub>0.7</sub>B<sub>20</sub>Si<sub>10</sub>Al<sub>1</sub>, stress-induced variation in magnetisation and dynamic magnetostrictive charact. 0-88855
- (Fe<sub>0.07</sub>Co<sub>0.93</sub>)<sub>75-1</sub>Cr<sub>0.05</sub>Si<sub>15</sub>B<sub>10</sub>, amorphous, disaccommodation of mag. permeability and induced anisotropy 0-88741
- (Fe<sub>0.05</sub>Co<sub>0.95</sub>)<sub>75</sub>Si<sub>15</sub>B<sub>14</sub> amorphous ribbon, anomalous mag. aftereffect 0-100602
- (Fe<sub>1-x</sub>Co<sub>x</sub>)<sub>75</sub>Si<sub>10</sub>B<sub>12</sub>, amorphous, roll mag. anisotropy 0-75757
- (Fe<sub>0.01-x</sub>Co<sub>0.99</sub>)<sub>75</sub>Si<sub>10</sub>B<sub>14</sub> amorphous, saturation magnetostriction, strain modulated FMR obs. 0-75863
- Fe<sub>88-x</sub>M<sub>x</sub>Si<sub>10</sub>B<sub>12</sub> (M=refractory metal), glass form. and thermal stability 0-79703
- (FeNi)<sub>80</sub>B<sub>17.5</sub>Al<sub>2</sub>Si<sub>0.5</sub>, stress-induced variation in magnetisation and dynamic magnetostrictive charact. 0-88855
- Fe<sub>40</sub>Ni<sub>40</sub>(Mo<sub>0.5</sub>Si<sub>0.5</sub>)<sub>20</sub>, amorphous, soft mag. props., switched-mode power supply appls. 0-88850
- (Fe<sub>1-x</sub>Ni<sub>x</sub>)<sub>75</sub>Si<sub>10</sub>B<sub>13</sub>, amorphous, Landau-Ginzburg theory, magnetisation and Curie temp. 0-75700
- (Fe<sub>1-x</sub>Ni<sub>x</sub>)<sub>75</sub>Si<sub>10</sub>B<sub>12</sub> amorphous alloys, cold rolled and as-quenched, mag. anisotropy 0-97089
- Fe<sub>80</sub>(P<sub>13</sub>C<sub>7</sub>)<sub>20-x</sub>Si<sub>x</sub>, density, microhardness, and crystn. temp., comp. depend. 0-84093
- Fe<sub>80</sub>P<sub>20-x</sub>Si<sub>x</sub>, amorphous, size effect of metalloids on mag. props. 0-84594
- Fe<sub>80-x</sub>Si<sub>20</sub>, amorphous, structural and mag. heterogeneities 0-80484
- Fe<sub>82-x</sub>Si<sub>18</sub> metallic glass, long range interaction and spin wave interactions 0-65949
- Fe<sub>82-x</sub>Si<sub>18</sub> metallic glass, mag. transitions, weak ferromagnetism 0-100583
- FeSi picture frame single cryst., domain wall motion and magnetisation reversal, time-depend. neutron depolarisation study 0-88782
- FeSi, single crystals, domain struct., temp. and field depend. 0-71085
- FeSi-Ca-V complex alloy oxidation of steel, nonmetallic additions (*Russian*) 0-93685
- $\alpha$ -Fe<sub>1-x</sub>Si<sub>2x</sub>, vacancy ordering, cryst. stabilisation energy aspects 0-103325
- Fe<sub>3</sub>Si, electronic structure, X-ray spectra comparison with band struct. calcs. 0-97383
- Fe<sub>3</sub>Si, electronic structure, magnetic moments 0-107695
- Fe<sub>3</sub>Si<sub>1-x</sub>, amorphous film, magneto-optic Kerr effect 0-66158
- Fe<sub>80</sub>Si<sub>15</sub>B<sub>5</sub>, amorphous, soft mag. props. and potential uses 0-88807
- (Fe<sub>1-x</sub>Si<sub>x</sub>)<sub>1-x</sub>By, metallic glass, mag. props., crystallisation 0-65885
- Gd-Si amorphous films, spontaneous Hall effect and elec. resist. 0-80251
- Li/Si/Fe(Si) battery developments for electric vehicle propulsion and load levelling appls. 0-61325
- MnSi, amorphous, spin glass transition, AC susceptibility meas. 0-75779
- MnSi, electronic energy band struct., self-consistent APW calc. 0-65433
- MnSi-Si system, striations and cryst. struct. of matrix 0-103292
- MnSi<sub>1-1.73</sub> crystal growth and characterisation 0-93474
- MnSi<sub>3</sub>, electronic structure, X-ray spectra comparison with band struct. calcs. 0-97383
- Mo-Ru-Si, amorphous superconductors, prep. by electron beam evaporation and liq. quenching, crit. temp. 0-103776
- (Mo<sub>0.6</sub>Ru<sub>0.4</sub>)<sub>80</sub>Si<sub>10</sub>B<sub>10</sub>, amorphous supercond. matrix, flux pinning by MoRu precip. 0-65756
- Mo<sub>70</sub>Si<sub>20</sub>B<sub>10</sub>, amorphous alloys obtained by liq. quenching, superconductivity 0-75670
- Nb-Ge-Si, compounds with A15 structure, films, TEM study (*French*) 0-80135
- Nb-Si, compounds with A15 structure, films, TEM study (*French*) 0-80135
- Nb-Si(-V)(Zr)(Mo)(Ta)(W)(C)(B)(Ge), ductile amorphous, superconductivity 0-60131
- Nb<sub>3</sub>(AlSi), liq. quenched, supercond. props. 0-84580
- Nb<sub>3</sub>(Nb<sub>1-x</sub>Si<sub>x</sub>), impurity stabilised A15 supercond., transition temp., lattice consts., specific heat 0-93026
- Nb<sub>3</sub>Si A15 phase from amorphous Nb-Si alloys, high-press. synthesis 0-93516
- Nb<sub>3</sub>Si A15 struct., high press. synthesis (*Chinese*) 0-70917
- Nb<sub>3</sub>Si, amorphous films, thermally-activated internal friction peaks, structural obs. 0-80147
- Nb<sub>3</sub>Si, RF sputtered films, amorphous atomic scale struct. 0-84064
- Nb<sub>3</sub>Si, substituted, splat cooling influence on supercond. T<sub>c</sub> and stoichiometry 0-80439
- Ni-Al-Si, diffusion, lattice parameter, microhardness, and constitution, effect of Si additions (*Russian*) 0-84316
- Ni-Cr-Ta-Ti-Si, EP557 precipitation hardening alloy, mech. props., heat treatment effect 0-60877
- Ni-Si, magnetoresistivity anisotropy, spin mixing 0-88538
- Ni-Si melt refining by electric fields, ionic conduction of Ni, Si (*Russian*) 0-65273
- Ni-Si-B, amorphous, thermal stability of ductility 0-76327
- Ni<sub>78-x</sub>M<sub>x</sub>Si<sub>10</sub>B<sub>12</sub> (M=refractory metal), glass form. and thermal stability 0-79703
- NiSi<sub>2</sub>, substrate ion implantation, channelled, through metal silicide film 0-70231
- NpCo<sub>2</sub>Si<sub>2</sub>, mag. struct., neutron diffr. determ. 0-93084
- NpCu<sub>2</sub>Si<sub>2</sub>, mag. struct., neutron diffr. determ. 0-93084
- Pd-Au-Si, influence of struct. on elec. resist. of glass forming alloys 0-65518
- Pd-Cu-Si, glass form., crit. cooling rate 0-75169
- Pd-Ni-Si amorphous alloys, crystn. process during isothermal ageing 0-89275
- Pd-Si, amorphous, compositional study on short-range struct. 0-84095
- Pd-Si, amorphous, struct., crystn. and Hall effect meas. 0-75178
- Pd-Si, amorphous metallic glass, with defined local coordination, struct. model 0-84092
- Pd-Si amorphous alloy, heat treated, low temp. lattice sp. ht. 0-75368
- Pd-Si metallic glass, high-resolution electron microscopy 0-84097
- Pd-Si(-Cu), amorphous, Hall effect meas. and electronic struct. 0-75551
- Pd-Si(-Cu) amorphous ribbons, low temp. sp. ht., density of states trends 0-79957
- (Pd<sub>80</sub>Au<sub>2</sub>Si<sub>18</sub>)<sub>70</sub>/Fe<sub>30</sub>, compositionally modulated amorphous film, diffusion, struct. relax. 0-103518
- Pd<sub>75</sub>Cu<sub>5</sub>Si<sub>16.5</sub>, heat of crystn. and viscous behaviour 0-75166



## silicon alloys continued

- Pd<sub>77</sub>Cu<sub>6</sub>O<sub>16.5</sub> metallic glass, glass transition temp., cooling rate depend. 0-75181  
 PdSi films, on Si, stress obs. 0-80145  
 Pd<sub>2</sub>Si films, on Si, stress obs. 0-80145  
 Pd<sub>2</sub>Si films on Si, lattice imaging obs. of structural details 0-103604  
 Pd<sub>2</sub>Si, form. in Si-Pd-Ti evaporated films 0-80006  
 Pd<sub>2</sub>Si-Si, substrate ion implantation, channelled, through metal silicide film 0-70231  
 Pd<sub>80</sub>Si<sub>20</sub>, amorphous alloy, partial struct. functions, X-ray, electron and neutron diff. studies (*Japanese*) 0-88050  
 Pd<sub>80</sub>Si<sub>20</sub> amorphous alloy, skip deform. and crit. shear stress, using tensile testing machine 0-89321  
 Pd<sub>80</sub>Si<sub>20</sub>, glass, deform. localisation, plastic instabilities and fracture 0-89320  
 Pd<sub>80</sub>Si<sub>20</sub> metallic glass, inelastic deform., free energy spectra 0-71699  
 Pd<sub>80</sub>Si<sub>20</sub> metallic glass, tensile deform., shear band form., high-speed cinematographic obs. 0-89322  
 Pd<sub>80</sub>Si<sub>20</sub>, vapour quenched amorphous alloy, atomic arrangements 0-100173  
 Pd<sub>82</sub>Si<sub>18</sub>, stress/strain rate depend. of homogeneous flow 0-71687  
 (Pd<sub>86</sub>Si<sub>14</sub>)<sub>61</sub>/(Fe<sub>85</sub>B<sub>15</sub>)<sub>39</sub>, compositionally modulated amorphous film, diffusion, struct. relax. 0-103518  
 PdSiCu, amorphous, US attenuation and vel. studies at low temps. 0-88278  
 Pt-Si thermally degenerated Schottky diodes, resonant tunnelling 0-100503  
 Pt-Si:As, silicide form. during laser irradi., p-n junctions and ohmic contacts 0-84397  
 PtSi film formation by ion sputtering and annealing, form. and exam. problems 0-100782  
 PtSi films, on Si, stress obs. 0-80145  
 PtSi, growth rate for form. by Pt film deposition under ultrahigh vac. and controlled impurity atm. 0-65388  
 PtSi Schottky-barrier monolithic IRCCD focal plane 0-86427  
 PtSi, substrate ion implantation, channelled, through metal silicide film 0-70231  
 PtSi surface, and interface with Si, impurity effects 0-80037  
 Pt<sub>2</sub>Si, growth rate for form. by Pt film deposition under ultrahigh vac. and controlled impurity atm. 0-65388  
 ReSi<sub>2</sub>, atomic volume deviations and supercond. T<sub>c</sub> and elec. cond. 0-75203  
 Re<sub>2</sub>Si<sub>3</sub>, X-ray cryst. struct. determ., microhardness rel. to Re content 0-84142  
 Si:H, amorphous, solar cells using ultrathin active layer to increase conversion efficiency 0-94030  
 a-Si:H alloys, sputter deposited thin film coatings, property-comp. relationships 0-80975  
 a-Si:H highly homogeneous, for low-cost solar cell fabrication 0-72053  
 Si-Al C fibre composite technological coatings, liquid phase method preparation (*Russian*) 0-108375  
 Si-Au eutectic alloys, field ion sources 0-97414  
 Si-Au system, ion implanted induced giant gettering, annealing effects 0-88221  
 Si-CoSi<sub>2</sub>Si, double heteroepitaxy, solid phase and MBE 0-104063  
 Si-Cr, dil., spin density wave under high press., neutron diff. study 0-65798  
 Si-Fe-W, dil. alloy, compositional changes on sputtering, projectile energy depend. 0-66362  
 Si-H, amorphous, sputtered, photolum. obs. 0-80856  
 Si-H, amorphous, structural and electronic props., review 0-64901  
 n-Si-Pd<sub>2</sub>Si contact, interface struct. and Schottky barrier height, correl. obs. using TEM 0-100504  
 SiFe sheets, grain-oriented, stray field meas. 0-88775  
 Si<sub>100-3</sub> polycryst. ribbon, prep. by rapid quenching, and props. 0-75803  
 Ta-Cr-Si-Al, heat resistive films prepared by sputtering, lifetime meas. 0-80132  
 Ti-Nb-Si, amorphous alloy, supercond. props. and crystn. behaviour, TEM and DTA study (*Japanese*) 0-84536  
 Ti-Si amorphous alloy, melt-quenched, transform. studies and mech. props. 0-100838  
 TiSi<sub>2</sub>, form. in Si-Pd-Ti evaporated films 0-80006  
 U<sub>10</sub>Co<sub>5</sub>Si<sub>33</sub>, crystal struct., dimensions, space group and coord. (*Russian*) 0-88085  
 U<sub>6</sub>Co<sub>30</sub>Si<sub>19</sub>, X-ray cryst. struct. determ. 0-107111  
 U<sub>3</sub>Si, reversible twinning, in-situ obs. 0-104241  
 (V<sub>1-x</sub>Cr<sub>x</sub>)<sub>3</sub>Si, elastic moduli, 4.2 to 290K, softening near supercond. transition (*Russian*) 0-92582  
 V(Nb)-Si-Cu, rapidly quenched, comp. and phase equilb. 0-76235  
 V<sub>2</sub>Si, Al<sub>5</sub> cpd., hydrogenation effects on supercond. transition temp., lattice parameters 0-103772  
 V<sub>2</sub>Si bridge contacts, nonstationary props. 0-103793  
 V<sub>2</sub>Si, coherence parameter, nonlinear high temp. supercond. elements with A-15 lattice (*Russian*) 0-60127  
 V<sub>2</sub>Si embedded in resin, composite supercond., high transition temp. 0-88660  
 V<sub>2</sub>Si film, optical props. (*Russian*) 0-93418  
 V<sub>2</sub>Si, Gruneisen parameter and thermal expansion eval. at room temp. 0-70351  
 V<sub>3</sub>Si, neutron irradi., grain boundary pinning, field-depend. change of crit. current density 0-65759  
 V<sub>3</sub>Si single cryst., creep deform. 0-71695  
 V<sub>3</sub>Si, supercond. mixed state, low temp. tetragonal-domain-reorientation phenomena, US expts. and thermal props. 0-60141  
 V<sub>3</sub>Si, supercond. props., effect of neutron irradi. 0-80463  
 V<sub>3</sub>Si, supercond. structure and properties (*German*) 0-93631  
 V<sub>3</sub>Si thin film far IR laser thermal spectroscopy 0-60144  
 V<sub>3</sub>Si tunnel junctions, energy gap investigation 0-84569  
 V<sub>2</sub>Si-SiO<sub>2</sub>-Mo<sub>2</sub>Re<sub>2</sub>, supercond. tunnel junctions 0-107961  
 V<sub>2</sub>Si<sub>1-x</sub>Ge<sub>x</sub>, elastic props., 77 to 290K, rel. to supercond. transition temp. (*Russian*) 0-66560  
 V<sub>2</sub>Si<sub>1-x</sub>Ge<sub>x</sub>, solid soln., longitudinal and transverse US wave propag. rate, 4.2 to 300K (*Russian*) 0-103423  
 W<sub>60</sub>Si<sub>40</sub>B<sub>10</sub>, amorphous alloys obtained by liq. quenching, superconductivity 0-75670  
 YbCu<sub>2</sub>Si<sub>2</sub>, interconfiguration fluctuation, NMR expts. 0-66069

## silicon compounds

see also quartz; silicon alloys; silicones

basalt, cement reinforcing fibre, alkali resist. 0-89377

## silicon compounds continued

- bis-methyldisilyl chalcogenide, <sup>1</sup>H and <sup>13</sup>C NMR study, chemical shifts 0-71201  
 bitumen-silica composites, dynamical mechanical props. 0-58996  
 clay, Al<sub>2</sub>O<sub>3</sub> and SiC recovery by C reduction 0-108704  
 kaolinite rare-earth complexes, relax., molar free energy of activation for dipole relax. 0-88919  
 Kovar-silicon oxynitride-aluminium cathode, local electron emission and electroluminesc. patterns obs. 0-108327  
 materials for thermoelectric conversion of solar energy (*French*) 0-89660  
 mullite-corundum ceramics, thread-like crystals reinforced, props. 0-108525  
 optical fibres, 800 Mbit/s optical transmission experiments with dispersion-free fibres at 1.5 μm 0-58680  
 optical fibres, ultracure impurities determ., and behaviour during production by CVD process (*Japanese*) 0-87505  
 oxide precipitates, TEM and EELS identification 0-100723  
 oxides, steam grown, index of refr. ellipsometric meas. 0-75995  
 phthalocyanine, elec. cond. temp. depend. 0-80271  
 plasma etching, gas flow-rate depend. 0-97603  
 porcelain, crack propag. data applicability to failure prediction 0-81154  
 Si<sub>3</sub>N<sub>4</sub>-Ce<sub>2</sub>O<sub>3</sub>-SiO<sub>2</sub> materials: phase relations and strength 0-97465  
 SiH<sub>4</sub>, SCF calcs. including polaris. functions 0-87034  
 silicate gardens, growth morphology, mechanisms 0-100765  
 thin film deposition using solar furnace 0-89148  
 3Al<sub>2</sub>O<sub>3</sub>-GeO<sub>2</sub>-SiO<sub>2</sub>, reduction by C, mixed diffusional-kinetic regime (*Russian*) 0-66771  
 [α]-SiC:H, prepared by reactive sputtering, layer props. (*Japanese*) 0-60695  
 Al/SiO<sub>2</sub>/pSi MIS solar cells, stability 0-85287  
 Al-Al<sub>2</sub>O<sub>3</sub>-SiO<sub>2</sub>-Si capacitors, physical and elec. props. of RF plasma grown Al<sub>2</sub>O<sub>3</sub> 0-100530  
 Al-AlN-SiO<sub>2</sub>-Si capacitors, physical and elec. props. of RF plasma grown AlN 0-100530  
 Al-Ge-SiO solar selective absorber surfaces, optical behaviour at high temp. 0-101130  
 Al-Si<sub>3</sub>N<sub>4</sub>-SiO<sub>2</sub>Si, MNOS structures degradation under UV irradiation effect 0-107923  
 Al-Si<sub>3</sub>N<sub>4</sub>-O-Al thin film cathode, physical model from expt. study 0-100535  
 Al-Si-N-O system, comps. corresponding to β-sialon phase reaction hot-pressing 0-84891  
 Al-SiC cermet elasticity, porosity meas. by US means 0-81101  
 Al-SiO<sub>2</sub> interface in MOS capacitors, conductivity effects of oxidation temperatures 0-100518  
 Al-SiO<sub>2</sub>-Si, pyroelectricity 0-100524  
 Al-SiO<sub>2</sub>-p-Si solar cells, comparison of majority- and minority-carrier silicon MIS solar cells 0-85280  
 Al-SiO<sub>2</sub>-Si MOS solar cells, open-cct. voltage var. with oxide layer thickness 0-81434  
 Al-SiO<sub>2</sub>-(p)-Si barrier structs., minority carrier injection ratio meas., MIS solar cell model 0-93007  
 Al-silicon oxynitride-Al cathode, LF noise sources and reduction 0-108328  
 Al<sub>2</sub>C<sub>3</sub>-Be<sub>2</sub>C-Si system, phase analysis and TEM struct. obs. 0-108420  
 AlN-Si<sub>3</sub>N<sub>4</sub>-Be<sub>2</sub>N<sub>2</sub> system, phase equilibria 0-60844  
 Al<sub>2</sub>O<sub>3</sub>-SiO<sub>2</sub> (3 wt %), J-integral meas. at high temps. (*German*) 0-93624  
 Al<sub>2</sub>O<sub>3</sub>-SiO<sub>2</sub> refractory, creep, viscosity, resist. to inelastic deform. 0-89309  
 Al<sub>2</sub>O<sub>3</sub>-SiO<sub>2</sub> refractory concrete, elastic props. 0-89280  
 Al<sub>2</sub>O<sub>3</sub>-SiO<sub>2</sub> system, evidence for metastable miscibility gap 0-71632  
 Al<sub>2</sub>O<sub>3</sub>-SiO<sub>2</sub>-ZrO<sub>2</sub> refractories, corrosion behaviour in glassmelting furnaces (*Polish*) 0-71783  
 3.5Al<sub>2</sub>O<sub>3</sub>.2SiO<sub>2</sub>, mullite, decomposition by SiO<sub>2</sub> volatilisation 0-61082  
 3Al<sub>2</sub>O<sub>3</sub>.2SiO<sub>2</sub>-ZrO<sub>2</sub> composites, sintered, in situ-reacted, fracture props. 0-81158  
 As-Tc-Si-Ge amorphous chalcogenide semiconductor, thin film interface, elec. charact. (*Korean*) 0-97014  
 Au-SiO<sub>2</sub>-Si system, oxide film 16-36 Å thick, tunnel currents 0-70842  
 Au-SiO<sub>2</sub>-n-Si solar cells, comparison of majority- and minority-carrier silicon MIS solar cells 0-85280  
 Au-SiO<sub>2</sub>-n-Si, tunnelling MIS struct. 0-92995  
 Au-Ti/SiO<sub>2</sub>/p-Si MOS struct., interface state distrib., DC tunnelling spectra determ. 0-75611  
 Be-Si-N system polypeptides, struct. obs. using TEM 0-107192  
 CaF<sub>2</sub>-MgO-SiO<sub>2</sub>, melts, elec. cond., surface tension, viscosity, density (*Russian*) 0-92758  
 CaF<sub>2</sub>-SiO<sub>2</sub>, melts, elec. cond., surface tension, viscosity, density (*Russian*) 0-92758  
 CaO-Al<sub>2</sub>O<sub>3</sub>(B<sub>2</sub>O<sub>3</sub>)-SiO<sub>2</sub> glass-forming additive, effect on Al<sub>2</sub>O<sub>3</sub> ceramics sintering 0-89187  
 CaO-MgO-Cr<sub>2</sub>O<sub>3</sub>-Al<sub>2</sub>O<sub>3</sub>-ZrO<sub>2</sub>-SiO<sub>2</sub> system, subsolidus region characts. 0-97466  
 CaO-V<sub>2</sub>O<sub>5</sub>-SiO<sub>2</sub> system, compatibility triangles 0-81037  
 (CaO)<sub>2</sub>SiO cement pastes, electron microsc. anal. 0-108761  
 CdS-SiO<sub>2</sub> layered system, characts. of phase-velocity dispersion and struct. of surface waves 0-59775  
 CdSe-SiO<sub>2</sub> layered system, characts. of phase-velocity dispersion and struct. of surface waves 0-59775  
 p-CdSiAs<sub>2</sub>, electron irradi. elec. props. annealing, lattice defects 0-100465  
 Cl<sub>2</sub>Si(CH<sub>3</sub>)<sub>4-n</sub>, <sup>35</sup>Cl NQR, geminal and vicinal interactions on substituents electronic effect 0-63663  
 Cl<sub>2</sub>Si(OCH<sub>3</sub>)<sub>4-n</sub>, <sup>35</sup>Cl NQR, geminal and vicinal interactions on substituents electronic effect 0-63663  
 Cr-SiO<sub>2</sub>-Si MIS solar cells, photovoltaic performance and interface states, nucl. radiation effects 0-94004  
 Cs-SiO<sub>2</sub>-Al<sub>2</sub>O<sub>3</sub> system interactions, getter development for radiocaesium 0-83208  
 Cu-Cr-SiO<sub>2</sub> single crystals, yield and pre-yield behaviour rel. to aging time 0-81103  
 Cu-Cr-SiO<sub>2</sub> system, age and dispersion strengthened, dislocation struct. around SiO<sub>2</sub> particles 0-108468  
 Cu-SiO<sub>2</sub>, low-temp. recovery creep, Orowan loop accumulation 0-81126  
 Cu-SiO<sub>2</sub> alloys, internally oxidised, plastically deformed, influence of particle form on primary loop nature (*French*) 0-103344  
 Fe-SiO<sub>2</sub> multilayer films, interface magnetisation 0-88858  
 n-GaAs-SiO<sub>2</sub> interface, MOS capacitors, surface states from conductance and capacitance meas. 0-100533  
 Ge-Si<sub>3</sub>N<sub>4</sub> system, potential barriers determ. from photoinjection carriers trapping 0-103756

# silicon compounds continued

- Ge-Si-S system, glass formation, transition temp., crystallisation and melting 0-100178  
 $\text{GeO}_2\text{-P}_2\text{O}_5\text{-SiO}_2$  graded index optical fibres optimised for 1.3  $\mu\text{m}$  wavelength region, fabrication techniques (*Japanese*) 0-99888  
 $\text{GeO}_2\text{-SiO}_2$ , reduction by C, mixed diffusional-kinetic regime (*Russian*) 0-66771  
 $\text{Ge}_2\text{Si}_3\text{As}_{10}\text{Te}_{15}$  chalcogenide thin films, coupled carrier theory test, high field conditions 0-100466  
 $\text{H}_2\text{SiO}_2$ , electronic struct., dipole moments, mol. polarisability, force fields, ab initio calcs. 0-78531  
 $\text{HfO}_2\text{-SiO}_2$  mirror coatings, light scatt. and optical strength in UV range 0-106595  
InP-SiO<sub>2</sub> interface, CVD problems, ESCA profiles 0-93497  
 $\text{In}_2\text{-Sn}_2\text{O}_3\text{-Si-SiO}_2$  solar cells, loss mechanisms study for improvement of efficiency to above 12% 0-94080  
 $\text{K}_2\text{Se}(\text{OH})_2\text{Si}_2\text{O}_7$ , crystal struct., X-ray diffr. study 0-79763  
 $\text{La}_2\text{Si}_2\text{O}_7\text{N}_2$  single cryst. growth by floating zone method with  $\text{SiO}_2\text{-Si}_3\text{N}_4$  additions 0-93481  
 $\text{Li}_2\text{O} \cdot 2\text{SiO}_2$ , prep. from film forming soln. 0-60811  
 $\text{MgO-CaO-FeO-Fe}_2\text{O}_3\text{-SiO}_2\text{-Cr}_2\text{O}_3\text{-Al}_2\text{O}_3$  spinel refractories, physicochem. prod. conditions 0-89185  
 $\text{Mg}_2\text{SiO}_2\text{-SiO}_2$ , elec. and dielec. props. 400-900°C 0-104953  
Mn-SiO<sub>2</sub>, annealed cermet films, elec. resist., composition depend. 0-97007  
Mn-SiO cermet thin film, DC resist., activation energy, thickness depend. 0-84518  
MnO<sub>2</sub> porous powders, Al<sub>2</sub>O<sub>3</sub> and SiO<sub>2</sub> coated, changes in surface free energy for N adsorption 0-84363  
 $\text{MnO} \cdot \text{Al}_2\text{O}_3 \cdot \text{SiO}_2$ , spin glass materials, mag. field dependence of susceptibility peak 0-103840  
 $\text{Na}_2\text{O-B}_2\text{O}_3\text{-SiO}_2$  glass, fracture toughness, effect of microheterogeneous struct. 0-104256  
 $\text{Na}_2\text{O-CaO-SiO}_2\text{-Cr}_2\text{O}_3$  glass, redox equilibria of Cr ions, impurity effects 0-89477  
 $\text{Na}_2\text{O-CaO-SiO}_2\text{-Fe}_2\text{O}_3$  molten glass, optical props., temp. depend. (*French*) 0-100667  
 $\text{Na}_2\text{O-CaO-SiO}_2\text{-H}_2\text{O}$  system gels, metastable nature 0-71952  
 $\text{Na}_2\text{O-PbO-SiO}_2$ , molten glass, reactions with conducting materials 0-85186  
 $\text{Na}_2\text{O-SiO}_2$  glass containing halogens glass formation 0-103254  
 $\text{Na}_2\text{O-SiO}_2\text{-CuO}$ ,  $\gamma$ -irrad., CuO effects on EPR 0-84645  
 $\text{Na}_2\text{O-SiO}_2\text{-Fe}_2\text{O}_3$  glass, X-ray absorpt. spectra, effective co-ordination charges 0-84805  
 $5\text{Na}_2\text{O} \cdot \text{Fe}_2\text{O}_3 \cdot 8\text{SiO}_2$ , glass crystallisation study by  $\text{Fe}^{3+}$  EPR and Mossbauer spectra 0-64904  
 $\text{Na}_2\text{O-SiO}_2$ , prep. from film forming soln. 0-60811  
 $\text{Na}_2\text{S-SiO}_2$  glass forming region, struct. and ionic cond. 0-88358  
 $\text{Na}_2\text{S-SiO}_2$ , synthesis, structure and ionic conduction (*French*) 0-65291  
Ni-Ge-SiO<sub>2</sub> solar selective absorber surfaces, optical behaviour at high temp. 0-101130  
Ni-SiC coating adhesion to Al alloy, metal interdiffusion (*Russian*) 0-66697  
Ni-SiO multilayer films, interface magnetisation 0-88858  
OSiF<sub>2</sub> prod. from SiO<sub>2</sub>+F<sub>2</sub> matrix reactions, IR spectra and force consts. calcs. (*German*) 0-97718  
2PbO-SiO<sub>2</sub>-xSO<sub>3</sub> melts, crystn. 0-59400  
Pd-SiO<sub>2</sub> amorphous thin films, laser irrad., metastable phases 0-96622  
Pd-SiO<sub>2</sub> interface, work function changes due to adsorbed H<sub>2</sub>, surface and interface dipoles 0-96972  
Pt-Si amorphous thin films, laser irrad., metastable phases 0-96622  
Pt-SiO<sub>2</sub> cermet films, struct. and props. 0-96956  
SiO<sub>2</sub>, Franck-Condon factors rot. depend. 0-58319  
Si biradical, six-coordinate, mol. mobility two-spin probe investig. 0-102529  
Si rich SiO<sub>2</sub>-SiO<sub>2</sub>-Si rich SiO<sub>2</sub> layers for dual electron injector struct. 0-96991  
Si, thermally oxidised-electrolyte system, features of cathodic breakdown (*Russian*) 0-107907  
Si/SiO<sub>2</sub> interface, precise wet-chemical etching, using rapidly rotating sample 0-93669  
Si-Al-Be-C-N system, phase equilibria 0-60839  
Si-Al-O-N ceramic, grain boundary desegregation and intergranular cohesion 0-100872  
Si-Al-O-N system, phase analysis and TEM struct. obs. 0-108420  
Si-Al-O-N system, stable phase cryst. struct. and microstruct. obs. using TEM 0-108421  
Si-B system, DTA, X-ray diffr. and metallographic study (*German*) 0-66484  
Si-O fibres, parametric excitation of anti-Stokes coherent stimulated scatt. (*Russian*) 0-58637  
Si-Si<sub>3</sub>N<sub>4</sub> interface in MNS capacitors, surface state density investigation 0-60100  
Si-Si<sub>3</sub>N<sub>4</sub>-SiO<sub>2</sub> non absorbing double layers, optical parameters reflectivity by liquid immersion method 0-71503  
Si-SiC chemical interaction in rarefied O<sub>2</sub> under pulsed action of concentrated solar radiation 0-71930  
Si-SiO<sub>2</sub>, influence on frequency-temp. coeff. of SAW devices 0-79066  
Si-SiO<sub>2</sub> interface, stress meas. technique 0-84395  
Si-SiO<sub>2</sub> ion implantation through SiO<sub>2</sub> film, recoil implantation of O, EPR study 0-88180  
Si-SiO<sub>2</sub> MOS interface states density, meas. techniques and model development 0-92988  
n-Si-SiO<sub>2</sub>, MOS structures, radiation states 0-103758  
Si-SiO<sub>2</sub>, recoil implanted O profile after ion implantation through SiO<sub>2</sub> 0-88198  
Si-SiO<sub>2</sub> (111) interface, H<sub>2</sub> effects, AES study 0-65688  
Si-SiO<sub>2</sub> abrupt interface form. by very high dose O<sup>+</sup> ion implantation 0-75253  
Si-SiO<sub>2</sub> boundary, relaxation of nonequilibrium capacitance in electrolyte in intense elec. fields 0-70845  
Si-SiO<sub>2</sub> boundary, surface charge transport in valence band of Si 0-70789  
Si-SiO<sub>2</sub> electrode, electronic cond., luminesc. obs. 0-61111  
Si-SiO<sub>2</sub> interface, (001) vicinal planes, minigaps in inversion layers, far IR absorpt. meas. 0-107919  
Si-SiO<sub>2</sub> interface, barrier height in MOS tunnelling structures 0-88644  
Si-SiO<sub>2</sub> interface, density of states, theory 0-80395  
Si-SiO<sub>2</sub> interface, electronic struct. calc. 0-100531  
Si-SiO<sub>2</sub> interface, electron mobility in inversion and accumulation layers 0-103753

# silicon compounds continued

- Si-SiO<sub>2</sub> interface, improved characterisation, refined quasistatic and cond. methods 0-96990  
Si-SiO<sub>2</sub> interface, O<sub>2</sub> plasma effects on elec. props. 0-100523  
Si-SiO<sub>2</sub> interface, remote polar phonon scatt. in Si inversion layers 0-80095  
Si-SiO<sub>2</sub> interface, thermal SiO<sub>2</sub> sputter induced roughness, Auger sputter profiling study 0-75424  
Si-SiO<sub>2</sub> interface, thermally grown oxide, spectroscopic ellipsometric anal. 0-107659  
Si-SiO<sub>2</sub> interface, two-dimensional impurity bands, carrier-density dependence of activation energies associated with hopping 0-88561  
Si-SiO<sub>2</sub> interface in IGFETs, anal. of CVD SiO<sub>2</sub> on (100) and (111) surfaces, near-ideal structs. 0-100528  
Si-SiO<sub>2</sub> interface in MIS structs., effects of crystal defects on generation process 0-65702  
Si-SiO<sub>2</sub> interface in MOS structs. low-energy electron beam irrad., charge accumulation process anal. 0-65701  
Si-SiO<sub>2</sub> interface in MOS capacitors, lateral diffusion of Na<sup>+</sup>, neutralisation 0-92986  
Si-SiO<sub>2</sub> interface in MOS solar cells, operational characts. and struct. 0-93901  
Si-SiO<sub>2</sub> inversion layer, n-channel, anomalous magnetoresist., model 0-96996  
Si-SiO<sub>2</sub> laminar ion-implanted systems, struct. change investig. by MSSI method (*Russian*) 0-107918  
Si-SiO<sub>2</sub> MIS systems, dynamic props. of switching, appl. to charge transfer devices 0-92997  
Si-SiO<sub>2</sub> MOS capacitors, relationship between trapped holes and interface states 0-70830  
Si-SiO<sub>2</sub> MOS interface, surface-state density and minority carrier generation rate, meas. by DLTS, hot hole effect 0-100527  
Si-SiO<sub>2</sub> structure, alkali metal ion migration and accumulation, interface struct. 0-107574  
Si-SiO<sub>2</sub> structures, B ions implanted, energy spectra of shallow traps at various implantation energies 0-80392  
Si-SiO<sub>2</sub>-Al interface barrier energies for tunnel oxides, internal photoemission meas. 0-84512  
Si-SiO<sub>2</sub>-Al, internal photoemission, pot. barrier height determ. 0-65699  
Si-SiO<sub>2</sub>-Al MOS surface channel influence on channel-to-contact diode charact. 0-92994  
Si-SiO<sub>2</sub>-Al with thick dielec. layer, photoelec. props. 0-92979  
Si-SiO<sub>2</sub>-Au Schottky barrier solar cells, back-illuminated, theoretical performance 0-61345  
Si-SiO<sub>2</sub>-CdS solar cell, I-V characteristics 0-89621  
Si-SiO<sub>2</sub>-Mg-Cu powder compact, nitridation to form Si<sub>2</sub>ON<sub>2</sub> whiskers (*Japanese*) 0-93674  
Si-SiO<sub>2</sub>-Mo-Si<sub>3</sub>N<sub>4</sub>-Al MNOS structures with metal grains, charge transport at SiO<sub>2</sub>-Si<sub>3</sub>N<sub>4</sub> interface 0-65693  
Si-SiO<sub>2</sub>-Si capacitor, polycryst., capacitance voltage characterisation 0-70794  
Si-SiO<sub>2</sub>-Si thin film MOS structures, elec. props. with applied DC voltage (*Slovak*) 0-92977  
Si-SiO<sub>2</sub>-Si<sub>3</sub>N<sub>4</sub> MNOS structure, chem. comp. and electronic states, Auger and energy loss spectra obs. 0-92999  
Si-SiO<sub>2</sub>-Si MOS structures, charge motion, TSC meas. 0-100534  
n-Si-SiO<sub>2</sub>-SnO<sub>2</sub> SIS solar cell, transport props., 14% efficiency realisation 0-94079  
Si-SiO<sub>2</sub>-polySi thin film structures, dielectric props. (*Slovak*) 0-75934  
Si-SiO<sub>2</sub> interfaces, carrier transport processes, electron states, conference, Durham, England (July 1979) 0-90612  
Si-Te system, phase diagrams 0-89209  
SiAlON, prepared from siliceous sand and Al powder, hot pressing, steatite contamination effects (*Japanese*) 0-93528  
SiAs, cryst. growth from melt, elec. props. 0-76170  
SiB<sub>2-x</sub>, thermom cond., temp. depend., up to 2000K (*French*) 0-70484  
SiB<sub>2-x</sub> films, anal. of H ratios and profiling using nucl. techniques and Rutherford backscatt. 0-61202  
SiBr<sub>4</sub>, electronic struct., X $\alpha$  SW calcs. 0-102447  
SiBr<sub>n</sub> (n=1,2,3) heats of formation, mass spectrometric determ. 0-89511  
SiC (6H), blue-emitting diodes by CVD 0-97439  
SiC (6H), IR absorpt., UV illumination effects, defect levels 0-66251  
SiC, acoustic props. study at 9.43 GHz 0-65169  
 $\alpha$ -SiC, afterglow stimulated by IR radiation (*Russian*) 0-89066  
SiC, atomically sharp cracks, TEM study 0-71729  
SiC, blistering and flaking due to light ion bombardment (*Japanese*) 0-70264  
SiC ceramic heat exchanger, cost-effective design 0-95341  
SiC coated C fibres, effect on strength props. of C fibre reinforced plastics 0-104224  
SiC coating corrosion by fission product Pd in HTGR coated particle fuels 0-102237  
SiC, controlled nucleation thermochemical deposition, charact. and props. 0-108355  
 $\alpha$ -SiC crystals, broad-band semiconductors, growth in Acheson furnace 0-84841  
SiC, dense, joining by hot pressing, and bond strength 0-66458  
SiC devices, epitaxial layer growth techniques 0-108360  
SiC, dielectric coating effect on surface polaritons, optical consts. (*Russian*) 0-88489  
SiC, diffusion of B, elec. cond. meas. 0-96696  
SiC, effect of crystallographic anisotropy on Knoop microhardness 0-66626  
SiC fibre, development from organosilicon polymers by heat treatment 0-81014  
SiC fibre reinforced Al, thermophys. props. 0-59745  
SiC fibre reinforced Al, plasma-formed semfinished products, props. 0-84890  
SiC fibre reinforced Al, synthesis by liquid pressing method 0-100816  
 $\beta$ -SiC form. on Si substrate in RF powered reactor 0-76173  
SiC fracture stress effects of coated nuclear fuel particle failure 0-73920  
SiC, growth by C ion implantation of Si 0-107292  
SiC, HVEM obs. of various polytypes 0-76248  
SiC heat-exchanger tubing, IR techniques for evaluation 0-76435  
SiC ion implanted, laser induced ordering and defects 0-84754  
SiC LED, defect luminesc. 0-89069  
SiC LEDs prepared by overcompensation method, photon assisted tunnelling 0-97341  
SiC, laser Raman spin-flip scatt. from excitons, luminesc. 0-80786  
SiC microtubes, formation by carburisation of Si whiskers 0-81011



## silicon compounds continued

- SiC, oxide scale microstruct. of oxidised single cryst. 0-108613  
 SiC p-n junction, electroluminesc. 0-97343  
 SiC p-n junction, epitaxial, grown by sublimation, elec. and struct. props. (Chinese) 0-60067  
 SiC p-n junctions, current-voltage characts. 0-60073  
 SiC p-n junctions, electrolum. spectra and kinetics 0-66305  
 SiC particles in EFG ribbon solar cells, EBIC and ion microprobe anal. 0-93838  
 $\beta$ -SiC, polycryst.,  $^{30}\text{Si}$  self-diffusion 0-100350  
 SiC, polycryst., high resolution TEM study of  $\beta$ - $\alpha$  transform. 0-84928  
 SiC, polytype relative stabilities, entropy contribs. 0-100197  
 SiC polytypes, free exciton luminesc. meas., phonon energies 0-80852  
 SiC polytypes, lattice imaging studies on intergrowth structs. 0-107025  
 SiC, pot. curves, ab initio MRD-CI method 0-83293  
 SiC, pressureless-sintered, high temp. strength (Japanese) 0-104299  
 SiC, radiation defect annealing, recovery of LEED maxima 0-65075  
 SiC, radiation resistant substrate materials, for X-ray gratings 0-90960  
 SiC, reaction-bonded, impact erosion by ang.  $\text{Al}_2\text{O}_3$  particles 0-89362  
 SiC, reaction-bonded, 'REFEL', microstruct. characterization 0-97490  
 $\beta$ -SiC, sintering, B transport and lattice parameter change 0-108370  
 SiC smokes, vapour-condensed, 800 to 130 nm extinction and interstellar extinction curve 0-82180  
 p-SiC, spin-flip Raman scattering, review 0-108209  
 SiC, spin-flip scatt. of laser light from photoexcited excitons 0-93330  
 SiC, sputtering, low energy, H, D and He ions 0-100734  
 SiC substrate with  $\text{SiO}_2$  film, ellipsometric meas., accuracy and sensitivity 0-77840  
 SiC, TEM investigation using C replicas 0-61034  
 n-SiC, thermal defects, ESR study 0-88876  
 SiC, thermally thin solids, photoacoustic effect 0-75304  
 $\beta$ -SiC, thermodynamic props., temp. depend., 5 to 300K 0-96666  
 SiC thin-film thermistors with high thermal response (Japanese) 0-105629  
 SiC thread-like crystals reinforced mullite-corundum ceramics, props. 0-108525  
 SiC with dielectric coating, surface polaritons, waveguide modes 0-80195  
 B-SiC, X-ray diffr. study of anisotropic layers in twinned seams 0-107274  
 SiC:AlN (6H), ODMR for effective-mass-like acceptor 0-93213  
 SiC:H amorphous reactively sputtered film, H content effect on film props. 0-75459  
 SiC- $\text{AlB}_2$  (0.61 to 1.2 wt.%), hot pressed, microstruct. 0-93563  
 SiC-ceramic, nondestructive evaluation, scanning photoacoustic microscopy 0-85115  
 SiC-coated C fibre, compatibility with Al (Japanese) 0-71700  
 SiC-Si, wear resist., props. under abrasion and corrosion 0-100927  
 $\text{Si}_{1-x}\text{C}_x$ :H glow discharge films, local atomic struct., XPS and AES study 0-93448  
 $\text{Si}_3\text{C}_{1-x}$ , amorphous, luminescence 0-80862  
 $\text{Si}_3\text{C}_{1-x}\text{H}_x$ , amorphous film, H content determ. by nuclear reaction analysis 0-59821  
 $\text{Si}_3\text{C}_{1-x}\text{H}_x$ , amorphous films, IR absorpt. bands 0-100705  
 $\alpha$ -SiC(6H), radiation defect distrib. anisotropy near (0001) surface, LEED study 0-96577  
 $\text{SiCl}_4$  liquid, angular momentum relaxation, effective collision numbers 0-64873  
 $\text{SiCl}_4$  molecule, NMR relaxation expts. to study molecular reorientation 0-63673  
 $\text{SiCl}_4\text{-GeCl}_4\text{-BCl}_3$  particulate layers consolidation, in fabrication of optical fibre preforms 0-60787  
 SiF, use in chemical lasers 0-64004  
 $\text{SiF}_3$ , bond polarisability and force constants 0-69260  
 $\text{SiF}_4$ , chemisorption on Si surface, chemistry, XPS and Auger spectra 0-81358  
 $\text{SiF}_4$ , electronic struct.,  $X\alpha$  SW calcs. 0-102447  
 $\text{SiF}_3\text{Cl}_{4-n}$  in  $\gamma$ -irradiated solid solution of tetramethylsilane, EPR spectra obs. 0-80611  
 $\text{SiF}_3\text{Cl}_2(\text{Br})(\text{I})$  in  $\gamma$ -irradiated solid solution of tetramethylsilane, EPR spectra obs. 0-80611  
 $\text{Si}_2\text{Ge}_{1-x}\text{O}_2$ , amorphous, electronic struct. 0-80166  
 $\text{SiH}_4$ , emission spectroscopy, in  $\text{H}_2$ - $\text{SiH}_4$  glow discharge 0-69984  
 $\text{SiH}^+$ , oscillator strengths and dissociation energy determ. from time resolved precision spectroscopy 0-82722  
 $\text{SiH}_3$  radical, hyperfine coupling consts., vibr. depend., ab initio calcs. 0-87150  
 $\text{SiH}_3$  radical, in  $\text{Ar}(\text{Kr})(\text{N}_2)$  matrix, anisotropic ESR spectroscopic parameters 0-63687  
 $\text{SiH}_4$ , avoided-crossing molecular-beam spectroscopy, hyperfine and spin rot. const. and rot. g factors determ. 0-78671  
 $\text{SiH}_4$ , Doppler-free optical double reson. spectroscopy using single-freq. laser and modulation sidebands 0-68274  
 $\text{SiH}_4$ ,  $L_{\text{H,III}}$  continuous absorpt. spectrum of Si 0-95645  
 $\text{SiH}_4$ ,  $L_{\text{I}}$  MM Auger spectrum, line width and intensities 0-58325  
 $\text{SiH}_4$ , nucl. spin-spin coupling consts., ab initio calcs. 0-95647  
 $\text{SiH}_4$ , SCF calcs. including polaris. functions 0-87034  
 $\text{SiH}_4$ , second order mag. props., coupled Hartree-Fock perturbation theory 0-87042  
 $\text{SiH}_4$ , amorphous, solar cells, short circuit-currents and collection efficiencies 0-94028  
 $\text{SiH}_4$ , amorphous films, internal photoemission, metal contacts 0-96964  
 $\text{SiH}_4$ , amorphous film, H content determ. by nuclear reaction analysis 0-59821  
 $\text{Si}_{1-x}\text{H}_x$ , noncrystalline film, struct., interatomic distances, SRO 0-107053  
 $\text{Si}_{1-x}\text{H}_x\text{:Al}$ , amorphous, co-sputtered Al modification, electronic and optical props. 0-100461  
 $\text{Si}_2\text{H}_6$ , rot. barriers, MS-SCF- $X_\alpha$  calcs. 0-106267  
 $(\text{SiH}_3)_3\text{N}$ , SCF calcs. including polaris. functions 0-87034  
 $\text{SiH}_4(\text{SiF}_4)$ , electron rearrangement after inner shell ionisation by heavy charge particle impact 0-87043  
 $\text{SiHX}_3$  ( $X=\text{F}, \text{Cl}, \text{Br}, \text{I}$ ), force fields and consts., Redington's method calcs. 0-58130  
 $\text{SiH}_2\text{X}$  ( $X=\text{H}, \text{F}, \text{NH}_2, \text{OH}$ ), coord. bond calcs. 0-58129  
 SiN film, elastic stiffness and thermal expansion coeffs. 0-107451  
 $\text{SiN}^+$ , pot. curves, ab initio MRD-CI method 0-83293  
 SiN, films, plasma enhanced CVD, props., meas. and interpretations 0-80987  
 SiN, films, plasma-deposited, radial wafer-to-wafer uniformity 0-104073  
 SiN, films plasma deposition, process and props. 0-80986

## silicon compounds continued

- $\text{Si}_3\text{N}_4$  amorphous film deposition by high rate DC reactive sputtering, passivation appl. 0-100784  
 $\text{Si}_3\text{N}_4$ , bending strength, deformability, elastic moduli and brittleness 0-81191  
 $\text{Si}_3\text{N}_4$ , ceramic inclusions meas. and characterisation using US 0-76474  
 $\text{Si}_3\text{N}_4$ , cracking characterisation by double torsion test (French) 0-104369  
 $\text{Si}_3\text{N}_4$ , crystalline, N implant. in Si at high doses, buried insulating layer (French) 0-59498  
 $\text{Si}_3\text{N}_4$ , dielectric films made by  $\text{NH}_3$ -silane reaction, TEM study 0-84413  
 $\text{Si}_3\text{N}_4$ , electronic struct., LCAO calc. 0-96776  
 $\text{Si}_3\text{N}_4$  film, elastic stiffness and thermal expansion coeffs. 0-107451  
 $\text{Si}_3\text{N}_4$  film, plasma-activated, passivation (Japanese) 0-85073  
 $\text{Si}_3\text{N}_4$  films, CVD in MNOS and MNS structs., elec. resist. 0-97019  
 $\text{Si}_3\text{N}_4$  films, prep., props. and appls., bibliography 0-94939  
 $\text{Si}_3\text{N}_4$  films, thermally stimulated depolarisation current meas. 0-88643  
 $\text{Si}_3\text{N}_4$  films on Si wafers, O determ. by  $^3\text{He}$  activation anal. 0-71981  
 $\text{Si}_3\text{N}_4$ , high-speed rolling bearings, fatigue strength 0-93655  
 $\text{Si}_3\text{N}_4$ , hot-pressed, creep and strain recovery 0-100874  
 $\text{Si}_3\text{N}_4$ , hot-pressed, fracture mech. parameters, indentation-precracking and double-torsion methods 0-104364  
 $\text{Si}_3\text{N}_4$ , hot-pressed, fracture toughness determ. using specimens with chevron and straight through notches 0-108538  
 $\text{Si}_3\text{N}_4$ , hot-pressed, strength anisotropy origins 0-89330  
 $\text{Si}_3\text{N}_4$  layer form. by high dose implantation and annealing of Si:N wafers 0-70227  
 $\text{Si}_3\text{N}_4$  layers deposition, high-temperature, in resistance furnace, temperature gradient and nitrogen flow influence obs. (Bulgarian) 0-80981  
 $\text{Si}_3\text{N}_4$  layers produced by ion implantation, oxidation inhibition and etching 0-103374  
 $\text{Si}_3\text{N}_4$ , low pressure CVD, thermochemical calcs. 0-108356  
 $\text{Si}_3\text{N}_4$ , MIS struct. form. by reactive deposition on n-InSb substrates, C/V meas. 0-103752  
 $\alpha/\beta\text{-Si}_3\text{N}_4$ , phase yields during form., influencing factors 0-108408  
 $\text{Si}_3\text{N}_4$ , powder metallurgy recent developments, Sweden 0-93514  
 $\text{Si}_3\text{N}_4$ , reaction bonded, post-sintering, injection moulding applications 0-60807  
 $\text{Si}_3\text{N}_4$ , reaction sintered, thermal stress failure mode, effect of data scatter 0-60949  
 $\text{Si}_3\text{N}_4$ , reaction-bonded, strength, effect of Si purity in production 0-100902  
 $\text{Si}_3\text{N}_4$ , reaction-bonded, theoretical model of manufacture, effect of ambient reaction temp. and compact size 0-108379  
 $\text{Si}_3\text{N}_4$ , room temp. CVD on InSb 0-71597  
 $\text{Si}_3\text{N}_4$  sample substrates, high resoln. electron beam fabrication using STEM 0-104104  
 $\text{Si}_3\text{N}_4$ , selective etching rel. to Si by plasma reactive sputter etching 0-81221  
 $\text{Si}_3\text{N}_4$ , Si(LVV) Auger spectra, ion bombardment, electron energy loss spectra 0-80911  
 $\alpha\text{-Si}_3\text{N}_4$ , stable phase in Si-Al-O-N system, cryst. struct. obs. using TEM 0-108421  
 $\text{Si}_3\text{N}_4$ , surface etching by laser-generated free radicals 0-71772  
 $\text{Si}_3\text{N}_4$ , surface passivation of GaAs and interface props. 0-93005  
 $\text{Si}_3\text{N}_4$  thin film, reactively sputtered, struct. and elec. props. 0-88656  
 $\text{Si}_3\text{N}_4\text{:MgO}$ , hot-pressed, linear thermal expansion rel. to MgO content 0-70430  
 $\text{Si}_3\text{N}_4/\text{ZrO}_2$ , hot-pressed, compressive surface stresses developed by oxidation induced phase change 0-60992  
 $\text{Si}_3\text{N}_4\text{-Al}_2\text{O}_3\text{-SiO}_2$  systems, glass forming regions 0-84070  
 $\text{Si}_3\text{N}_4\text{-CeO}_2$  additive, hot-pressing and oxidation behaviour 0-71618  
 $\text{Si}_3\text{N}_4$ -ceramic, nondestructive evaluation, scanning photoacoustic microscopy 0-85115  
 $\text{Si}_3\text{N}_4\text{-InP}$ , interface props., plasma deposited dielectrics, n-channel MOS-FET action 0-93003  
 $\text{Si}_3\text{N}_4\text{-SiO}_2\text{-Y}_2\text{O}_3$ , subsolidus phase relations 0-60845  
 $\text{Si}_3\text{N}_4\text{-Y}_2\text{O}_3\text{-Al}_2\text{O}_3$  (4-17, 4 wt.%), sintering 0-81009  
 $\text{Si}_3\text{N}_4\text{-O}$ , thermal decomp. 0-81311  
 $\text{Si}_3\text{N}_4\text{-O}$ , thin film MIM, use as non-heated source of electrons, review 0-84516  
 SiO amorphous film, optical transmittance and reflectance, bulk optical props. determ. 0-88954  
 SiO evaporated film, dielec. function 8 to 33  $\mu\text{m}$ , spectrophotometric and refl. meas. 0-80883  
 SiO, film, thickness influence on nematic MBBA orientation 0-59384  
 SiO film structure exam., Raman microprobe-microscope appl. 0-62737  
 SiO, interstellar, in  $^2$  state, collisional excitation by  $\text{H}_2$  0-109508  
 $\text{SiO}+\text{F}_2$ , matrix reaction, OSiF $_3$  prod., IR spectra and force consts. calcs. (German) 0-97718  
 $\text{SiO}_2$ , amorphous,  $^{30}\text{Si}$  diffusion (French) 0-59696  
 $\text{SiO}_2$ , amorphous, sp. ht., time-dependent, 0.1 to 1K 0-100338  
 $\text{SiO}_2$ , amorphous, transient electrical transport, general and unified treatment 0-59977  
 $\text{SiO}_2$ , amorphous, very small angle X-ray scatt. before and after thermal neutron irradiation 0-75270  
 $\text{SiO}_2$ , amorphous diffusion of  $^{30}\text{Si}$ , SIMS (French) 0-107482  
 $\text{SiO}_2$ , amorphous film, dye-sensitised steady-state photocond. in Au-dye- $\text{SiO}_2$ -Au struct. 0-107924  
 $\text{SiO}_2$ , amorphous film, Si(LVV) Auger spectra, ion bombardment, electron energy loss spectra 0-80911  
 $\text{SiO}_2$ , amorphous layer in multilayer target for channelled ion stopping power meas. 0-63431  
 $\text{SiO}_2$ , As-implanted, electron trapping and detrapping characts. 0-65692  
 $\text{SiO}_2$ , Auger line shapes, final state correlation effects 0-89095  
 $\text{SiO}_2$ , CVD layer, high current injection from Si rich  $\text{SiO}_2$  film 0-80430  
 $\text{SiO}_2$ , CVD on Si producing near-ideal Si- $\text{SiO}_2$  interfaces, props. 0-80382  
 $\text{SiO}_2$ , coatings on  $\text{SiO}_2$  substrate, cathodoluminescence spectra, electron irradiation 0-76085  
 $\text{SiO}_2$ , colloidal films,  $\text{Cr}^{6+}/\text{Cr}^{3+}$ , on Al, TEM/XPS study 0-85090  
 $\text{SiO}_2$ , cryst. and amorphous, laser-induced breakdown, electron avalanche damage mechanism 0-100711  
 $\text{SiO}_2$ , crystal gyrotropy, meas. in IR region 0-88957  
 $\text{SiO}_2$ , deposited on Ge, optical constants, reflection spectra by Kramers Kronig method 0-76099  
 $\text{SiO}_2$ , dispersed particulate in CVD reactor, correlations with film characts. 0-76192  
 $\text{SiO}_2$ , dissolution rate in molten Si 0-103481  
 $\text{SiO}_2$ , etching by trifluoromethane plasma, optical spectroscopy appl. 0-87940

# silicon compounds continued

SiO<sub>2</sub>, etching characts. in trifluoromethane gas plasma 0-76392  
SiO<sub>2</sub>, etching characts. using reactive ion etching with tetrafluoromethane-Cl<sub>2</sub> gas mixture 0-104313  
SiO<sub>2</sub>, etching in He-F<sub>2</sub> plasma, etch rates, mass spectra, direct ion sampling study 0-79510  
SiO<sub>2</sub>, exciton study, luminescent centres as exciton detectors 0-66278  
SiO<sub>2</sub> fabric, structural stability rel. to brittleness, X-ray diff. and IR spectrosc. studies 0-96634  
SiO<sub>2</sub> facet coating film effect on self-sustained pulsation suppression in GaAlAs DH lasers 0-95894  
SiO<sub>2</sub> fibres, freeze formed from polysilicic acid aq. soln. 0-71609  
SiO<sub>2</sub> fibres, fused, drawn from rods, oxy-H<sub>2</sub> flame, prep., strength, dia. var. 0-102868  
SiO<sub>2</sub> fibres, LF optical phonons, Raman spectra 0-80789  
SiO<sub>2</sub> film, attenuated total reflectance study, impurity spectra 0-97311  
SiO<sub>2</sub> film, charge effects at Al electrodes obs. 0-75625  
SiO<sub>2</sub> film, etching by conical beam of Ar ions (*Russian*) 0-76383  
SiO<sub>2</sub> film, on GaP substrate, N ion implantation, optical refl. and EPR meas. 0-84197  
SiO<sub>2</sub> film, prep. using high press. O<sub>2</sub>, residual stress, chemical etch rate, refr. index and density meas. 0-71768  
SiO<sub>2</sub> film on 6H-SiC substrate, ellipsometric meas., accuracy and sensitivity 0-77840  
SiO<sub>2</sub> film on Cu substrate, surface EM wave absorpt., optical consts. (*Russian*) 0-108216  
SiO<sub>2</sub> films, DC plasma Si anodisation, dielectric const., O<sub>2</sub> pressure influence 0-70564  
SiO<sub>2</sub> films, desorption from Si single cryst., ellipsometric obs. 0-100410  
SiO<sub>2</sub> films, grown in presence of O<sub>2</sub>-trichloroethylene, room temp. negative bias instability 0-60102  
SiO<sub>2</sub> films, growth on Si, role of defect structure 0-65403  
SiO<sub>2</sub> films, RF-diode-sputtered, step coverage 0-80117  
SiO<sub>2</sub> films, Si-rich, amorphous Si region obs. 0-84400  
SiO<sub>2</sub> films, vac. thermal evaporation, parameter stabilisation 0-87571  
SiO<sub>2</sub> films in poly-oxide poly Si structures, elec. cond. and charge distrib. 0-92984  
SiO<sub>2</sub> films on Si, ellipsometric spectra, thickness determ. (*Chinese*) 0-86379  
SiO<sub>2</sub> films sputtered in H-Ar mixed gas, enhanced step coverage 0-75470  
SiO<sub>2</sub>, fused, broken bond defect generation mechanisms 0-88044  
SiO<sub>2</sub>, fused, filter in wide field-of-view SW radiometer for Earth radiation meas. 0-87473  
SiO<sub>2</sub>, fused, for sealed ampoule cryst. growth, thermal transmission function 0-84731  
SiO<sub>2</sub>, fused, He solubility and diffusion above transform. range 0-79965  
SiO<sub>2</sub>, fused, Lamb wave optical detect. 0-106690  
SiO<sub>2</sub>, fused, surface crystn. by Li<sup>+</sup> ion implantation and annealing 0-89383  
SiO<sub>2</sub>, fused silica fibre lightguide, static fatigue transitions 0-58744  
SiO<sub>2</sub> gate insulation on InP MIS inversion FETs, interface props. 0-93002  
SiO<sub>2</sub> gel, BaMoO<sub>4</sub> crystals. grown under influence of elec. field 0-93469  
SiO<sub>2</sub> gel, internal and surface struct. by X-ray scatt. 0-84074  
SiO<sub>2</sub> glass, acoustic and thermal Gruneisen parameters 0-59608  
SiO<sub>2</sub> glass, formation by hydrolysis of Si(OC<sub>2</sub>H<sub>5</sub>)<sub>4</sub> with NH<sub>4</sub>OH and HCl soln., and characterisation 0-71622  
SiO<sub>2</sub> glass, high rate MCVD of optical fibres 0-83671  
SiO<sub>2</sub> glass, low loss optical fibre, radiation-induced IR absorpt. 0-87521  
SiO<sub>2</sub> glass fibre, plastic-coated, liq. N<sub>2</sub> strength 0-58707  
SiO<sub>2</sub> glasses, spectral emittance at high temps. 0-96674  
SiO<sub>2</sub>, HCl-grown oxides, characterisation of surface states using MOS transient currents 0-65696  
SiO<sub>2</sub>, HF vapour phase etching, prod. viability for semicond. manufacturing and reaction model 0-81219  
SiO<sub>2</sub>, hydroxylated amorphous, small-particle dynamics, neutron scatt. 0-79899  
SiO<sub>2</sub>, implanted, in MOS capacitor, direct current/voltage relns. as function of oxide doping 0-88635  
SiO<sub>2</sub> ion implanted, radiation defects and optical props. 0-107293  
SiO<sub>2</sub>, ionicity dependence of defect reactions and negative-U states in glasses 0-88511  
SiO<sub>2</sub> isolated GaAs-GaAlAs DH laser compared with O<sup>+</sup> isolation 0-74382  
SiO<sub>2</sub> layer, thickness measurement by secondary electron emission 0-57435  
SiO<sub>2</sub> layer formation on polycryst. Si, morphological aspects 0-76388  
SiO<sub>2</sub> layer laser annealing in Si 0-97505  
SiO<sub>2</sub> layer used for MOSFETs, electron trapping behaviour 0-92981  
SiO<sub>2</sub> layers in LSI cct. device, cathodoluminesc. obs. 0-80867  
SiO<sub>2</sub> layers on Si, ionis. thresholds of electron traps 0-92983  
SiO<sub>2</sub> light emission from sputtered O atoms or ions 0-58199  
SiO<sub>2</sub> liq. cryst. alignment films prod. by RF plasma beam technique 0-76198  
SiO<sub>2</sub>, low pressure CVD, thermochemical calcs. 0-108356  
SiO<sub>2</sub> MOS capacitor, defect current obs. 0-92987  
SiO<sub>2</sub>, masking film in alkaline etching 0-71771  
SiO<sub>2</sub> massive dielectric target, 5-25 keV electrons penetration characts. 0-70260  
SiO<sub>2</sub>, mobility and trapping of ions, Si-SiO<sub>2</sub> interface states 0-92985  
SiO<sub>2</sub> nucleation of isotactic polystyrene, spherulite radial growth retardation 0-107066  
SiO<sub>2</sub> on BeO surface, effect on TSEE 0-76159  
SiO<sub>2</sub> on Si, MOS interface states density, transient capacitance meas. eval. 0-92989  
SiO<sub>2</sub> optical fibre, three-wave stimulated Raman scatt. obs. (*French*) 0-78902  
SiO<sub>2</sub>, P-doped amorphous, porous and hydrophilic, water adsorpt. and IR spectra obs. 0-80061  
SiO<sub>2</sub> phase equilibrium and microstructure interpretation 0-60847  
SiO<sub>2</sub>, plasma etching with hexafluoroethane in radial flow reactor 0-76391  
SiO<sub>2</sub>, plasma-chemical etching, spectroscopy 0-85243  
SiO<sub>2</sub>, powder support for MnO<sub>2</sub> catalyst, N adsorption obs. of dispersion modes 0-81363  
SiO<sub>2</sub>, proton induced ionisation, energy dependence of K<sub>β</sub>/K<sub>α</sub> intensity ratio 0-60716  
SiO<sub>2</sub>, quantitative anal. with SIMS 0-101052  
SiO<sub>2</sub>, reactive ion beam etching expts., selectivity, anisotropy 0-104308  
SiO<sub>2</sub> relief, plasma etching, tapered wall prod. 0-97606

# silicon compounds continued

SiO<sub>2</sub>, selective etching rel. to Si by plasma reactive sputter etching 0-81221  
SiO<sub>2</sub>, separation below 500°C, state and tendency of chemical gas phase separation (*German*) 0-100794  
SiO<sub>2</sub>, shock compression at high press. (*Russian*) 0-92608  
SiO<sub>2</sub>, space charged particle environment effect 0-69472  
SiO<sub>2</sub> sputtered film performance as acoustic antireflection coating at sapphire-H<sub>2</sub>O interface 0-106686  
SiO<sub>2</sub>, stacked-struct. improved quality by laser annealing of Si 0-65386  
SiO<sub>2</sub> substrate, obliquely evaporated for cyano-biphenyl LC, alignment 0-79677  
SiO<sub>2</sub> substrate for Pt-Ni vacuum condensates, X-ray anal. (*Russian*) 0-70559  
SiO<sub>2</sub>, surface etching by laser-generated free radicals 0-71772  
SiO<sub>2</sub>, surfaces etched in CF<sub>4</sub> or CF<sub>4</sub>-O<sub>2</sub> plasma morphology 0-93671  
SiO<sub>2</sub>, thermal decomposition, appl. to solar energy storage 0-76656  
SiO<sub>2</sub> thermal film, freon ion beam etching, IR study (*Russian*) 0-76095  
SiO<sub>2</sub>, thermally grown films, thicknesses 30-600 Å, defect density meas. 0-84412  
SiO<sub>2</sub> thin dielectric films in MOS structures, elec. props. with DC voltage (*Slovak*) 0-88634  
SiO<sub>2</sub> thin film grating for LiNbO<sub>3</sub>:Ti waveguide mode convertor and reflector 0-64216  
SiO<sub>2</sub> thin films, radiation-induced trapping centres, rel. to MOS transistor technology 0-107804  
SiO<sub>2</sub>, thin films on rough polycryst. Si surfaces, oxide thickness and refractive index meas. 0-93422  
SiO<sub>2</sub> thin thermally grown oxide layers etching in HCl, ellipsometric control of Si surface form. (*Russian*) 0-104315  
SiO<sub>2</sub>, three-component glass, liq. phase separation, with two oxide modifiers 0-103250  
SiO<sub>2</sub>, tunnelling barrier asymmetry to electrons and holes in MOS struct., photocurrent 0-75645  
SiO<sub>2</sub>, ultralow loss optical fibre material, loss mechanism 0-78920  
SiO<sub>2</sub> ultrathin layers, refr. index meas. 0-103936  
SiO<sub>2</sub>, vitreous, charged defect centres 0-107745  
SiO<sub>2</sub>, vitreous, hydroxyl free, reaction with H<sub>2</sub>, diffusion, absorpt. spectra 0-85210  
SiO<sub>2</sub>, vitreous, laser-annealed surface, characterisation by ellipsometry 0-103544  
SiO<sub>2</sub>, vitreous, O and Si diffusion-controlled processes 0-79981  
SiO<sub>2</sub>, vitreous, paramag. centres associated with bonding defects 0-80609  
SiO<sub>2</sub>, vitreous, pure and Ge doped, luminescence centres at 396 and 280 nm 0-103996  
SiO<sub>2</sub>, vitreous, quant. X-ray anal. of cristobalite 0-88049  
SiO<sub>2</sub>, vitreous, thermal expansion reference data: 1-1000K 0-96669  
SiO<sub>2</sub>, vitreous, viscosity meas., review 0-103513  
SiO<sub>2</sub>, vitreous, X-ray compaction efficiency 0-65044  
SiO<sub>2</sub>, vitreous Brillouin scatt., 35 GHz phonon vel. and absorpt. below 1K 0-100664  
SiO<sub>2</sub>, vitreous layers, thermal growth on Si 0-93675  
SiO<sub>2</sub>, with embedded Au particles, thin film solar absorber 0-81490  
SiO<sub>2</sub>/Ag, cryst. and glassy, X-ray induced EPR and luminesc. centre 0-65043  
SiO<sub>2</sub>/As<sup>+</sup> implanted layers in MOS struct., electron trapping and detrapping characts. 0-92982  
SiO<sub>2</sub>/Au(Ag)(Cu), XPS line broadening and extra-atomic relax. energies 0-71561  
SiO<sub>2</sub>/F(BF<sub>2</sub>), ion implanted, F influence on oxidation-induced stacking faults 0-65011  
SiO<sub>2</sub>/GeO<sub>2</sub>-P<sub>2</sub>O<sub>5</sub>, graded-index, optical fibres, frequency characts. 0-58669  
SiO<sub>2</sub>/Ge(P) optical fibre, single-polarisation single-mode, exposed cladding fabrication 0-58725  
SiO<sub>2</sub>/GaAs, interface reaction during high-temp. heat-treatments 0-88439  
SiO<sub>2</sub>/GeO<sub>2</sub> fibre, single-mode, numerical aperture effects on optical and mechanical props. 0-69548  
SiO<sub>2</sub>/InP interface formation, thermodynamic considerations 0-100529  
SiO<sub>2</sub>/P<sub>2</sub>O<sub>5</sub> fibre, single-mode, numerical aperture effects on optical and mechanical props. 0-69548  
SiO<sub>2</sub>-Al<sub>2</sub>O<sub>3</sub> porous catalysts, EPMA quantitative anal., new correction calc. method, modified ZAF method (*Japanese*) 0-93822  
SiO<sub>2</sub>-B<sub>2</sub>O<sub>3</sub> glasses, Brillouin scattering meas. of attenuation and vel. of hypersounds 0-100309  
SiO<sub>2</sub>-coated rutile, adsorption of N<sub>2</sub> and Ar, 77.4K, microcalorimetry obs. 0-80062  
SiO<sub>2</sub>-encapsulated semi-insulating GaAs, Cr redistribution during thermal annealing as function of encapsulant and implant fluence 0-84199  
SiO<sub>2</sub>-InP, interface props., plasma deposited dielectrics, n-channel MOS-FET action 0-93003  
SiO<sub>2</sub>-Li<sub>2</sub>O-Li<sub>2</sub>SO<sub>4</sub>, glass-forming region, struct. and ionic cond. 0-84320  
SiO<sub>2</sub>-MgO porous catalysts, EPMA quantitative anal., new correction calc. method, modified ZAF method (*Japanese*) 0-93822  
SiO<sub>2</sub>-MgO-BaO ceramic, steatite, glass-ceramics technology appl. 0-104097  
SiO<sub>2</sub>-Na<sub>2</sub>O surface, Ca<sub>3</sub>(PO<sub>4</sub>)<sub>2</sub> film form., bonding to bone 0-85212  
SiO<sub>2</sub>-Na<sub>2</sub>O-CaO-P<sub>2</sub>O<sub>5</sub>, BIOGLASS, surface, Ca<sub>3</sub>(PO<sub>4</sub>)<sub>2</sub> film form., bonding to bone 0-85212  
SiO<sub>2</sub>-Na<sub>2</sub>O-Nd<sub>2</sub>O<sub>3</sub> glass, magneto-optical props., absorpt. spectrum 0-88969  
SiO<sub>2</sub>-Si, two-layer system, P<sup>+</sup>-ion penetration tails, expt. and computer anal. 0-75249  
SiO<sub>2</sub>-Si in MOSFETs inversion layer carrier mobility, theory 0-60094  
SiO<sub>2</sub>-Si interface, carrier mobility (*French*) 0-65601  
SiO<sub>2</sub>-Si interface, doping depend. of interface states and charges 0-92992  
SiO<sub>2</sub>-Si interface states, deposition of H containing layers and annealing 0-92991  
SiO<sub>2</sub>-Si interface state density in ion-controlled diodes, acid-base exposure effects 0-96984  
SiO<sub>2</sub>-Si interface thermally grown, surface pot. inhomogeneities after stress ageing 0-92993  
SiO<sub>2</sub>-Si layers, physics, electron and ion motion (*Dutch*) 0-60093  
SiO<sub>2</sub>-TiO<sub>2</sub>, vitreous, US vel. and absorption 0-107380  
SiO<sub>2</sub>-water system, inorg. polymer struct. form., globular crystn. 0-101042  
SiO<sub>2</sub> amorphous films, acoustic study using Rayleigh waves 0-75312  
SiO<sub>2</sub>, dielec. and optical props., chemical disorder effects 0-80815  
SiO<sub>2</sub> semi-insulating polycryst. films, AES and PES studies 0-107939



**silicon compounds continued**

- SiO<sub>2</sub> thin film dielec., in MIM struct., interfacial props. rel. to non-stoichiometry 0-80399  
 SiO<sub>2</sub>, thin film on YZ-LiNbO<sub>3</sub>, SAW props. 0-84356  
 SiO<sub>2</sub> thin films, deposition and characterisation study 0-80133  
 SiO<sub>2</sub> ultrathin oxide on Si, struct. obs. by high-resolution electron microscopy 0-103592  
 SiO<sub>2</sub>-GaAs, vacuum evaporated system, acoustoelec. signal, interface props. 0-75646  
 Si<sub>2</sub>O<sub>6</sub><sup>2-</sup> double chain anion containing anhydrous silicates, synthesis, cryst. chem. 0-59444  
 Si, O<sub>2</sub>, films, anal. of H ratios and profiling using nucl. techniques and Rutherford backscatt. 0-61202  
 SiP, thermodynamic characts. 10-300K, interatomic bond elasticity 0-59677  
 SiP<sub>2</sub> with pyrite struct., Fermi surface calc. 0-65427  
 SiS, chemiluminescent flame spectra, electronic states and rot. struct. obs., vibr. assignments, Franck-Condon factors determ. 0-85179  
 (SiTe)<sub>1-x</sub>(ATe)<sub>x</sub>, A=Ge, Sn, Pb, solid soln. with small substitution, mag. susceptibility (*Russian*) 0-70933  
 SiO<sub>2</sub>/Ge, B, P, optical fibre, radiation induced optical absorpt. spectra, 0.4 to 1.7  $\mu$ m region 0-58761  
 Te<sub>80</sub>Si<sub>20-x</sub>Pb<sub>x</sub> glasses, phase separation, double T<sub>g</sub> presence 0-88306  
 TiO<sub>2</sub>-SiO<sub>2</sub> mirror, dielectric, Rayleigh scatt. at 441.6 nm 0-97367  
 TiO<sub>2</sub>-SiO<sub>2</sub> multilayer vacuum coatings, optical props. 0-97361  
 V<sub>1</sub>Si-SiO<sub>2</sub>-Mo<sub>2</sub>Re<sub>2</sub>, supercond. tunnel junctions 0-107961  
 ZnO-SiO<sub>2</sub> layered system, characts. of phase-velocity dispersion and struct. of surface waves 0-59775  
 ZnO-SiO<sub>2</sub>-Si SAW device, interface transduction 0-102949  
 ZnS-SiO<sub>2</sub> multilayer reflector, reflectance under slight absorpt. conditions 0-83655  
 p-ZnSiAs<sub>2</sub>, electron irradi. elec. props. annealing, lattice defects 0-100465  
 ZrO<sub>2</sub>-SiO<sub>2</sub> liquid immiscibility, microstruct. of plasma dissociated ZrSiO<sub>4</sub> 0-107429  
 ZrSiO<sub>4</sub>, zircon yellow pigment, synthesis (*Polish*) 0-66466  
 ZrSiO<sub>4</sub>-SiO<sub>2</sub> suspensions for slip casting, prep. and props. 0-104103

**silicon controlled rectifiers** *see thyristors***silicon integrated circuits** *see monolithic integrated circuits***silicon-on-sapphire integrated circuits** *see field effect integrated circuits***silicon reference diodes** *see avalanche diodes; Zener diodes***silicones**

- elastomers, dental impression materials, dimens. stability, holographic and interferometric study 0-67204  
 optical compound glass fibres, silicone and glass clad, medium loss 0-69533  
 prosthetic breast, dose obs. 0-98144  
 protective coating for optical fibres, pressure sensitivity meas. and limitation 0-106605  
 transparent silicone-glass hybrid Fresnel lens for solar energy concentration 0-61303

**silver***see also nuclei with .....*

- adsorbed methylpyridines, surface enhanced Raman spectra 0-83376  
 adsorbed on AgCl cryst., luminesc. fatigue 0-66281  
 adsorption of acetic and propanoic acids on (111), LEED obs. 0-80073  
 adsorption of mol. O<sub>2</sub> species on (110) surface 0-103578  
 adsorption of pyridine, UPS, AES and flash desorption meas. 0-92776  
 atom, electron (positron), impact, K- and L-shell ionisation, K $\alpha$  and L X-rays meas. 0-99575  
 atom, K-fluorescence yield determ. from K-Auger electron emission rates 0-95569  
 atom, photoionisation, photoelectron spectra 0-87086  
 atom, photoionisation cross sections, electron-impact inverse mean free paths, and stopping powers for each subshell 0-69113  
 atom solvation in methanol, geometrical model, electron spin-echo modulation obs. 0-63682  
 atoms, polarised photoelectron yields in VUV region 0-106307  
 atoms, valence-core electron exchange interactions, local approx. 0-91416  
 Auger spectra, 4d bandwidth effect 0-89093  
 catalyst for oxidation of rubber, prep. of diene oligomers with hydroxyl groups (*German*) 0-85175  
 [CC] Ag-(100)InP, metal-semicond.cathode contact, metallurgical, physical, chemical processes 0-107911  
 clusters, chemisorption of I, UPS obs. 0-84830  
 coating on refractory metals, energy struct. determ. at two monolayer thickness 0-100392  
 coatings, specimen charging control for SIMS and AES 0-101875  
 cold rolling, inhomogeneous texture 0-89251  
 condensation on Mo(100) and W(100), early stage comparison 0-80072  
 core level binding energies 0-71564  
 corrosion, indoor, rate meas. 0-76404  
 crystal growth on Si and W substrates, UHV-SEM studies of Stranski-Krastanov growth 0-79722  
 Debye temp., X-ray diffr. determ., anharmonic parameters of pot. function 0-100320  
 determination of Au in thin Ag objects by gamma ray differential absorpt. 0-85227  
 diffraction grating, concave, Ag-coated, polarisation anomalies 0-69519  
 diffusion in InSe, GaSe and GaTe crystals, temp. depend. (*Russian*) 0-70467  
 diffusion in PbTe, effect of gamma irradiation 0-59515  
 diffusion of Cu, SIMS investigations 0-59717  
 diffusion through Se, effect on interferometric thickness meas. 0-96695  
 dislocations gliding on (001) planes, bright field and weak-beam images 0-107266  
 electrode, enhanced inelastic light scatt. caused by adatoms 0-89013  
 electrode surface, adsorbed rhodamine B and Pb monomolecular film, anisotropy of optical props. 0-60534  
 electrode surface, adsorption of pyridine on graphitic C overlayer, Raman spectra obs. 0-103954  
 electrodeposition, on (111) face, habit modification caused by Cl<sup>-</sup> 0-71600  
 electron backscattering by bulk target, theoretical model (*French*) 0-60722  
 electron diffraction study, ECP contrast, Bloch wave model 0-96419  
 electron excited L $\alpha$  emission spectra 0-102481  
 electron microscope specimens, noncyanide electropolishing method 0-100967  
 electronic and mag. structure calcs. of mag. impurities 0-80213

**silver continued**

- energy loss of heavy nonrelativistic ions in matter, semiclassical theory 0-84224  
 energy losses and straggling for H<sup>+</sup> and He<sup>+</sup> beams (*Russian*) 0-84226  
 epitaxial film, (111), grown on mica, surface defect struct., LEED study 0-80038  
 epitaxial layer, electron channeling pattern, large angle, generation and appl. 0-100296  
 epitaxially grown film, on Au (111) twin form., LEED detection 0-88442  
 evaporated film, adsorbed CO, enhanced Raman scatt. mechanism in ultrahigh vacuum 0-107645  
 FCC(111) substrate, orientation relationship with Fe vac. deposits 0-59836  
 FCC crystals, compressively activated slip, theoretical latent hardening 0-65128  
 film, chem. deposited, agglomeration, SEM and TEM obs. 0-59828  
 film, defect density, thickness depend., elec. resist. obs. 0-70568  
 film, elec. cond., appl. of percolation theory 0-65712  
 film, ellipsometric response to CO adsorption 0-103571  
 film, energy losses of electrons, microcalorimetric meas. 0-59543  
 film, epitaxial growth on Pd, AES and LEED obs. of growth modes and substrate influences (*French*) 0-84408  
 film, granular, transmission and reflection spectra, validity of sum rule 0-97358  
 film, in situ resistivity meas. 0-97008  
 film, inertialess glow induced by picosecond laser pulses (*Russian*) 0-100714  
 film, interaction with adsorbed dye mol., absorpt. and luminesc. 0-103981  
 film, intrinsic stress meas. 0-71696  
 film, on amorphous C and Si substrates, dispersion force contrib. to adhesion (*French*) 0-59842  
 film, surface roughness, light scatt. meas. 0-107624  
 film, vacuum deposited, Ge coated, electrical resistance and ageing (*Russian*) 0-103759  
 film, vacuum deposited, orientation axis tilt rel. to vapour angle of incidence 0-88456  
 film, vacuum deposition on Pb (111), substrate diffusion effects, RHEED, LEED, AES 0-65410  
 film, void growth, TEM obs. 0-59833  
 film deposition, thermal effects, influence on internal stress meas. 0-96767  
 film for Ga liquid spreading, kinetic eqn. (*Russian*) 0-59376  
 film growth on Pd substrate, interface cpd. form., AES study (*French*) 0-80131  
 film growth on Si (111), nucleation and growth modes, SEM study 0-100423  
 films, effect of Ar- and N-ion bombardment on texture (*Russian*) 0-107338  
 films, thin evaporated, rel. between microstruct. and excess free energy, TEM 0-70427  
 foil, or film, conduction electron spin disorientation at surface 0-75855  
 foil, surface plasma-wave reflectance and roughness-induced scatt. 0-66228  
 foil interface with liquid, oxide props. from reflectance and scatt. light spectroscopy 0-60702  
 Gruneisen number and nonlinearity const., elastic moduli data, US attenuation 0-65165  
 holographic gratings, polystyrene coated, Raman spectra enhancement by plasmon surface polaritons 0-80885  
 interface with <sup>4</sup>He, Kapitza cond. and enhanced power anomaly, 1-2K 0-88378  
 latent image particles, electronic effects 0-82840  
 lattice dynamics on Krieb's model 0-59594  
 Lifshitz constant for calc. of van der Waals force between two solids (*French*) 0-107658  
 magnetic susceptibility, Animalu transition metal model pot. invest. 0-75711  
 melting theory for small particles, Helmholtz free energy 0-59629  
 microcrack propagation and plastic strain 0-81187  
 mirror, Y<sub>2</sub>O<sub>3</sub> coated, for the 0.5 to 14  $\mu$ m region 0-87456  
 monolayer, on Au substrate, adsorbed pyridine giant Raman effect 0-63637  
 multiply twinned particles, internal and surface struct. by electron microscopy 0-84189  
 muon diffusion, LAMPF results 0-71285  
 oriented bicrystal, sintering prod. technique 0-108371  
 particles embedded in dielec. KCl medium, search for maximum metallic resist. 0-107756  
 photographic autotyping of amorphous As<sub>2</sub>S<sub>3</sub> films to produce negative relief image 0-59490  
 pionic, Auger electron emission (*Russian*) 0-69271  
 plasma arc spraying, chem. reaction with plasma gases 0-66427  
 porous metallic electrode, for determ. of Cl<sup>-</sup> ions in nuclear reactor water coolant 0-89577  
 positron annihilation spectra, Doppler-broadened, temp. depend., 9 to 1098K 0-71510  
 powder, ultrafine, sintering, coalescence growth stage 0-89174  
 regeneration from cinefilm waste (*Russian*) 0-105734  
 resistivity and thermoelec. ratio, electron-electron scatt. contrib. 0-70670  
 resonant and nonresonant conduction-electron-spin transmission 0-75857  
 secondary electron low energy distrib. meas. using double-pass cylindrical mirror analyser 0-68293  
 solid-state electro-thermal diffusion into glass to form low-loss optical waveguides 0-58792  
 sorption of pyridine, surface enhanced Raman scatt., mol.-surface separation depend. 0-92775  
 speck nucleation and phase formation in latent image 0-97716  
 sputtering by heavy atomic and molecular ion bombard. 0-71532  
 substrate, electrodeposition of Au film 0-81329  
 surface, <sup>4</sup>He backscatt., Rutherford scatt. cross section correction test 0-66369  
 surface, (100) and (111), positronium form. due to slow positron trapping 0-107748  
 surface, (110), ethylene-O<sub>2</sub> interaction, LEED and AES obs. 0-89520  
 surface, (111), adsorbed I, photoelectron diffr. azimuthal patterns, struct. sensitivity 0-107644  
 surface, (111), ethylene adsorption, XPS and UPS investigation 0-103573  
 surface, adsorbed isoquinoline, surface enhanced Raman spectrum 0-100400

## silver continued

surface, adsorbed pyridine, 210-243  $\text{cm}^{-1}$  mode in surface enhanced Raman scatt. 0-89003  
 surface, adsorbed pyridine, enhanced Raman scatt., ultrahigh vac. study 0-88993  
 surface, adsorbed pyridine and  $\text{CN}^-$ , Raman active librational modes 0-65359  
 surface, CO chemisorption, SIMS, XPS study 0-84382  
 surface, Ne scatt., rainbow effects and energy exchange, calc. 0-84825  
 surface, positronium emission 0-80897  
 surface, scatt. of  $\text{He}$ ,  $\text{H}_2$ , Debye-Waller factors, expt. 0-60736  
 surface, SHG 0-83645  
 surface, time-resolved mol. electronic energy transfer interaction with pyrazine 0-92957  
 surface, vibr. spectrum of CN monolayer using picosec. Raman gain technique 0-91859  
 surface (110), electroreflectance, surface state contrib. 0-80755  
 surface (111) phonon dispersion, He atom scatt. meas. 0-75426  
 surface phenomena, electron microscopy 0-103556  
 surface plasmon dispersion relation in presence of surface roughness 0-65650  
 surface-plasmon resonance, roughness-induced wavelength corrections 0-108288  
 tensile deformed, dynamic recrystn. (*German*) 0-84959  
 thermomodulation study of high-energy interband transitions 0-108226  
 thin film, elec. resist., effect of annealing In electrodes 0-80416  
 thin film, X-ray fluoresc. spectroscopy of surface using RHEED-solid state detector method 0-108760  
 thin film deposited on Si, work function (*French*) 0-80353  
 thin targets, electron transmission below 3 keV (*French*) 0-60725  
 thin-film bicrystals, planar lattice defects and migrating grain boundaries interaction 0-79835  
 wear coefficients determ. using pin-on-disc apparatus 0-76366  
 wear under reversed friction, temp. effect 0-108588  
 X-ray absorption, discontinuities and limits, chem. combination effects 0-93435  
 X-ray emission analysis, particle induced, of Mercury Ag statuette 0-85228  
 Young's modulus depend. on temp. and mech. action (*Russian*) 0-92584  
 $Z$  dependence of thick target  $\beta$ -ray backscattering 0-76118  
 $^{107,109}\text{Ag}$ , stopping power in Ni, (*Au*) 0-70284  
 Ag, adsorption of ethylene and propylene, enhanced Raman spectra obs. 0-95607  
 Ag electrodeposition, on (100) face of single crystal Ag in presence of sulphadiazine 0-89161  
 $\text{Ag}^+$ , addition to  $\text{TiO}_2$  photographic layers for sensitivity enhancement during cuprous development (*Russian*) 0-62780  
 $\text{Ag}^+$  impurity diffusion in molten alkali metal chlorides 0-59685  
 $\text{Ag}^+$ , solvation in methyl cyanide-water (methanol),  $\gamma$ -irrad., ESR obs. 0-97726  
 $\text{Ag:Al}_2\text{O}_3$ :Al tunnel-junction struct., surface polariton mean free path, roughness 0-93008  
 $\text{Ag/RbAg}_{1/2}\text{Ta}$ , solid electrolyte timing cell and coulometer 0-68216  
 Ag-Cs-O photocathode, operation mechanism involving  $\text{Cs}_2\text{O}_2$  0-66384  
 Ag-Cu flex leads, microstruct. study of corrosion 0-76406  
 Ag-Ge Schottky barrier photodetectors, near IR interband transitions and optical parameters 0-73449  
 Ag-H<sub>2</sub> electrochemical cell design using rolled stack configuration 0-101084  
 Ag-In-Si-Si layered struct., Hall effect, I-V characts., surface states (*Russian*) 0-97001  
 Ag-InP interface,  $\text{AgP}_3$  formation during sintering 0-65309  
 Ag-Li ion exchange effects on  $\text{LiNbO}_3$  and  $\text{LiTaO}_3$  optical waveguides 0-58791  
 Ag-Li ion exchange in  $\text{LiTaO}_3$  optical waveguides 0-91888  
 Ag-O-Cs surface, oxidation, role of Cs suboxides in low work function surface layers, XPS 0-76131  
 Ag-Si interfaces, solar cell contacts 0-92973  
 Ag-Sn double films, high-speed superconducting bolometer appl. 0-57368  
 $\text{Ag}^+ \text{H}^+$ , excited X-ray polarisation, Born approx. calcs. (*Russian*) 0-78566  
 $\text{Ag}^+ \text{H}^+$ , K-shell ionisation cross-section, 85 to 790 keV 0-106390  
 Ag<sub>2</sub>, Harris-Pohl selected valence electron split-shell MO calcs. 0-91439  
 Ag-S system, phase diagram, 100-600°C (*German*) 0-97471  
 $^{107}\text{Ag}$  excesses in Santa Clara and Pinon Fe meteorites, meas. 0-85902  
 $^{110}\text{Ag}$  diffusion in  $\beta/\gamma$  interphase boundary of Cu-Al alloy 0-79989  
 $^{110m}\text{Ag}$  diffusion in Cu 0-65301  
 Ag(s)/ $\text{Ag}_2\text{SO}_4$ -Na<sub>2</sub>SO<sub>4</sub>(l) high temp. ref. electrode, study 0-76622  
 As<sub>2</sub>S<sub>3</sub>/Ag glassy films, optical transmission spectra, photodoping effect 0-66317  
 As<sub>2</sub>Se<sub>3</sub>/Ag amorphous, freq. depend. cond. 0-88565  
 As<sub>2</sub>Se<sub>3</sub>-Ag photosensitive semiconductor-metal systems, effect of As<sub>2</sub>S<sub>3</sub> barrier layer (*Russian*) 0-62777  
 CdCr<sub>2</sub>S<sub>4</sub>/Ag magnetic semiconductor growth, structural defects, physical properties 0-60759  
 CdCr<sub>2</sub>Se<sub>4</sub>/Ag, ferromag. reson. and ESR line widths 0-60413  
 CdCr<sub>2</sub>Se<sub>4</sub>/Ag, magneto-optical effects in impurity spectral region 0-97313  
 CdS:Ag, charge and transport mechanism of impurities, electrodiffusion doping 0-59725  
 Cu<sub>2</sub>O:Ag<sup>+</sup>, exciton-neutral and exciton-charged impurity scatt. cross sections 0-70618  
 Ge:Ag, gamma ray effects on impurity states 0-96822  
 Ge<sub>40</sub>Se<sub>60</sub>:Ag, bond struct. and character in Ge-S system, EPR obs. 0-66014  
 Ge<sub>42</sub>Se<sub>58</sub>:Ag, amorphous, bulk and film forms, doping effect on elec. props. 0-103691  
 p-In<sub>0.77</sub>Ga<sub>0.23</sub>As/Ag photocathode, field assisted photoemission to 2.1 microns 0-76130  
 KCl:Ag, X-irrad., thermoluminesc. study of Ag centres 0-80874  
 KCl:Ag positron annihilation and impurity states 0-97375  
 LiCl:Ag, fluoresc. and UV absorpt. spectra 0-80844  
 NaCl:Ag, positron annihilation and impurity states 0-97375  
 Ni:Ag, ion-implanted, laser irrad. effect 0-108306  
 Pb-Cu(Ag) double layers, intermetallic boundary effects, tunnelling 0-88692  
 Pb(Ag) alloys, effect of Ag content on yield strength 0-76322  
 PbI<sub>2</sub>-Ag, light sensitive, internal photoelectric emission 0-107910  
 Si:Ag, ion bombardment enhanced mixing of Ag layers 0-65034  
 Si-Ag-Si heat mirror on plastic sheet for radiation insulation of visible windows 0-95985

## silver continued

SiO<sub>2</sub>:Ag, cryst. and glassy, X-ray induced EPR and luminesc. centre 0-65043  
 SiO<sub>2</sub>:Ag, XPS line broadening and extra-atomic relax. energies 0-71561  
 Si(111)- $\sqrt{3}\times\sqrt{3}$ -Ag structure, atomic arrangement, low energy ion scatt. spectroscopy 0-96724  
 SnO<sub>2</sub>-copper phthalocyanine-Ag systems, elec. and electroluminescent behaviour 0-80864  
 Ta-Ta<sub>2</sub>O<sub>5</sub>-Ag junctions, polarity-depend. tunnelling cond. 0-70846  
 Te-Ag thin film system, stress-relief appearance conditions 0-65416  
 TiO<sub>2</sub>-Ag-TiO<sub>2</sub> heat mirror on plastic sheet for radiation insulation of visible windows 0-95985  
 ZnS:Ag, cathodoluminesc. investig., appl. to cathode ray tube screening 0-108282  
 ZnS:Ag, Tb phosphors, luminesc. props. 0-100690  
 ZnS-CdS:Ag, cathodoluminesc. investig., appl. to cathode ray tube screening 0-108282  
 ZnTe:Ag, elec. field and impurity conc. effect on ionisation energy 0-88514

**silver alloys**  
 dilute, virtual bound states due to 4d- and 5d-transition metal impurities 0-70667  
 electron microscope specimens, noncyanide electropolishing method 0-100967  
 ion-selective electrode membranes development, hot pressed (*Japanese*) 0-61203  
 rare earth-Ag alloy, amorphous, model calcs. of mag. props. 0-84616  
 Ag-Al (26 at.%), massive transform,  $\beta$ - $\beta'$ , crystallography and morphology 0-97475  
 Ag-Au, corrosion in HNO<sub>3</sub> 0-85091  
 Ag-Au alloys, EMF meas. employing Ag-Bi-Al<sub>2</sub>O<sub>3</sub> (*German*) 0-104307  
 Ag-Au-Cu, surface composition change on sputtering with 2 keV Ar ions 0-66365  
 Ag-Bi, liq. alloys, thermodynamic investigation 0-70428  
 Ag-Cd peritectic system, separate crystallisation of phases (*Russian*) 0-66497  
 Ag-Cd-(Nd), internally oxidised, oxide particle size control (*Japanese*) 0-89480  
 Ag-Cu metastable solid soln., form. by ion-beam mixing 0-75244  
 Ag-Cu surface alloyed films, laser melt quenched, microstruct. 0-76423  
 Ag-Ga(Ge)(In),  $\alpha$ -phase, lattice sp. ht. calcs. 0-65246  
 Ag-Ge eutectic alloy, heat capacity meas. over temp. range 800-1200K (*French*) 0-88331  
 Ag-In melt system, conc. depend. of component and impurity diffusion coeffs., radioactive isotope method (*Russian*) 0-107454  
 $\alpha$ -Ag-In solid solutions, lattice dynamics parameters (*Russian*) 0-96477  
 Ag-In-Sn, internal oxidation, precipitation behaviour of oxide (*Japanese*) 0-66515  
 Ag-In-Sn, internal oxidation, solute element and O<sub>2</sub> behaviour (*Japanese*) 0-89479  
 Ag-Mg (18.5 wt.%), solid soln., rheological study of crystallographic order on creep (*French*) 0-97548  
 Ag-Mn, conc. spin glasses, thermopower 0-65538  
 Ag-Mn, dil., valence and core level spectra, XPS study 0-84838  
 Ag-Ni (10 wt.%) wire, plastically deformed, fracture struct. (*German*) 0-71744  
 Ag-Ni supersaturated metastable solid solns. formed by ion beam mixing 0-107425  
 Ag-Pd alloys, inert gas ion bombardment, dynamic surface composition changes, AES obs. 0-60745  
 Ag-Sb alloy coating, electrolytes for deposition (*Bulgarian*) 0-93763  
 Ag-Sm system, phase diagram, eutectic temps., microstruct. (*German*) 0-104119  
 Ag-Sn, liquid alloys, thermodynamic props. (*Japanese*) 0-108396  
 Ag-Sn, splat-quenched, X-ray diff. study 0-81094  
 Ag-Sn alloys and amalgams, electrochem. considerations, corrosion in physiological soln. 0-93760  
 Ag-Sn liquid, optical reflectivity spectra of virtual bound states 0-89021  
 Ag-transition metal, dil., mag. impurities, electronic struct., KKR-Green's function calc. 0-65783  
 Ag-Zn, internally oxidized, elec. contact characts., alloying additions effect (*Japanese*) 0-88619  
 Ag-Zn, molten, EMF meas. of activities using ZrO<sub>2</sub> solid electrolytes (*Japanese*) 0-88339  
 Ag-Zn-Te-(Sn)-(In), internally oxidised, oxide particle size control (*Japanese*) 0-89480  
 Ag<sub>3</sub>Au<sub>1-x</sub>Cu<sub>x</sub>, phase relations, X-ray diff. and differential thermal anal. 0-108395  
 AgCr, dil., specific heat, impurity contrib. Kondo temp. 0-65903  
 AgMg, B2 intermediate phase, slip system, ordering energy and atomic size ratio depend. 0-59471  
 AgMg two phase bicrystal growth, orientation, interface struct. 0-60773  
 AgMg, periodic antiphase boundaries, electron microscopy study (*French*) 0-59481  
 AgNi, dil., mag. susceptibility of isolated Ni atoms 0-65777  
 AgZn, B2 intermediate phase, slip system, ordering energy and atomic size ratio depend. 0-59471  
 AgZn,  $\beta'$ - $\beta$  transformation, effect of additional elements 0-66507  
 $\gamma$ -Ag<sub>2</sub>Zn<sub>3</sub>, high pressure effect on brass struct. 0-107108  
 Al-Ag, force-and-mass disordered alloys, vibr., average local-information transfer approx. 0-88290  
 Al-Ag, rapid quenching, struct. and decomp. 0-76244  
 Al-Ag, type-II superconductor, torque oscillations in mag. field (*Russian*) 0-103800  
 Al-Ag (7.2 wt.%), peculiarities exhibited during fatigue loading (*Chinese*) 0-71723  
 Al-Zn-Mg alloy, Ag addition and pre-precipitation treatment, influence on GP zone growth 0-71658  
 AlAg, Auger spectra, 4d bandwidth effect 0-89093  
 Au-3d transition metal alloys, UPS study, localised states 0-93449  
 Au-Ag, bicryst. thin film couples, interphase interfaces, TEM 0-70540  
 Au-Ag (35 at.%), dechannelling of energetic He ions at dislocations 0-70275  
 Au-Pt-Pd-Ag-Cu, commercial dental alloy, age-hardening characts. 0-89235  
 Au<sub>3</sub>Cu<sub>1-x</sub>Ag<sub>x</sub>, phase relations, X-ray diff. and differential thermal anal. 0-108395  
 Cu-Ag, surface segregation of S, Auger spectral study diffusion 0-76549  
 Cu-Ag (0.1 wt.%), cold-worked, internal friction peaks in kHz range 0-89276



## silver alloys continued

- Cu-Ag (3 at.%), plastically deformed, lattice strain distrib. (*German*) 0-85012  
 Cu-Ag-Au, coherent phase diagram, theoretical calc. 0-70373  
 Cu-Ag-Ge, Hume-Rothery glass form. 0-96449  
 Cu-Ag-O alloys, dil., O-metal interactions, activity coeff. meas. at 1423K 0-93792  
 Cu-Ag-P(6-14, 11-14 wt.%) amorphous, crystn. and elec. props., X-ray diffr., elec. resist. and DTA meas. (*Japanese*) 0-84088  
 Cu-Ti-Ag, wetting of  $\text{Al}_2\text{O}_3$ , alloying effects 0-107617  
 $\text{Cu}_3\text{Ag}_{1-x}\text{Au}_x$ , phase relations, X-ray diffr. and differential thermal anal. 0-108395  
 $\text{CuMnAg}_x$ , hysteresis, spin orbit scatt., effect on anisotropy in spin glass state, rel. to Ag impurity conc. 0-71095  
 $\text{DyAg}_{1-x}\text{In}_x$ , elec. and Hall resist. 0-96844  
 Fe-Ag (50 wt.%), plastic behaviour in compression, deform. rate effect (*French*) 0-71711  
 $\text{GdAg}_{1-x}\text{In}_x$ , elec. and Hall resist. 0-96844  
 La-Ag alloys, amorphous, elec. resist. and supercond. 0-70885  
 $\text{LaAgIn}_{1-x}$ , phonon dispersion, elastic consts. and struct. instability, soft mode behaviour 0-103436  
 Mg-Ag, ion implanted, recovery stage characterisation by electron irradi. 0-107295  
 MgAg, Auger spectra, 4d bandwidth effect 0-89093  
 Mn-Ag, XPS meas., Fermi level to 1000 eV below it 0-66389  
 MnAg alloys, XPS meas. 0-60751  
 NdAg<sub>x</sub>, low temp. mag. meas. 0-107989  
 $\text{Nd}_2\text{Ag}_7$ , and  $\text{Nd}_{50}\text{Ag}_{50}$ , amorphous, mag. props. 0-60182  
 Pb-Ag (0.068 wt.%), Ag precipitation kinetics and activation energy 0-66517  
 Pb(Ag) alloys, effect of Ag content on yield strength 0-76322  
 $\text{Pb}_{1-x}\text{Ag}_x$ , liquid alloys, local fluctuations and quadrupolar relaxation 0-66060  
 Pd-Ag, alloys-H solid solutions, superconducting transition temp. behaviour (*Russian*) 0-70879  
 Pd-Ag electrical contacts in  $\text{H}_2\text{S}$  atmospheres, formation of contaminating layers (*German*) 0-71811  
 Pd-Ag thin-walled tubes, for thermal diffusion apparatus H diffuser 0-100358  
 Pd-Ag-H(D), elastic energy dissipation peak 0-60905  
 PdAg (4.7 at.%), effect of alloying on activation energy of  $\text{H}_2$  diffusion 0-107571  
 PdAg surface, CO chemisorption, SIMS, XPS study 0-84382  
 PrAg<sub>x</sub>, low temp. mag. meas. 0-107989  
 $\text{Pr}_{21}\text{Ag}_{79}$ , amorphous, sp. ht. at low temp. 0-75780  
 $\text{Pr}_{21}\text{Ag}_{79}$ ,  $\text{Pr}_{50}\text{Ag}_{50}$ , and  $\text{Pr}_{10}\text{Lu}_{40}\text{Ag}_{50}$ , amorphous, mag. props. 0-60182  
 $\text{Sm}_{21}\text{Ag}_{79}$ , amorphous, sp. ht. at low temp. 0-75780  
 $\text{TbAg}_{1-x}\text{In}_x$ , elec. and Hall resist. 0-96844  
 Ti-Ag (10 to 17.5 wt.%), eutectoid system,  $\beta$ - $\alpha_m$  transform., nucleation kinetics 0-97474

## silver compounds

- Ag halides, photographic sensitivity, latent image centres, determ. of stability and dimens. (*Russian*) 0-90922  
 AgGa<sub>1-x</sub>In<sub>x</sub>Se<sub>2</sub>, X-ray diffr. cryst. data 0-84147  
 $\alpha$ -AgSbS<sub>2</sub>, crystals, influence of external elec. field on elec. cond. 0-60056  
 connection between the topography of luminescence centres and the latent image (*Russian*) 0-62785  
 halide, glass, kinetics of photochromic processes 0-103930  
 halide crystals, relative dissolution rates meas. by flow calorimetry 0-85220  
 halide crysts., dislocations, survey of post-war research 0-62449  
 halide emulsion,  $\text{Na}_2\text{S}_2\text{O}_3$  digested, red-IR photoluminescence obs. at 77K 0-103982  
 halide emulsions, primitive and  $\text{AgNO}_3$ -digested, IR luminescence obs. at 77K 0-103983  
 halide film physical props., effect of gelatin structure 0-97715  
 halide microcrystal, photoconductivity meas. by microwave technique 0-103719  
 halide optical fibres, extrusion, visible and IR transmission 0-58829  
 halide photochromic glasses, colour centres struct. 0-66254  
 halide photochromic glasses, optical properties, effect of Cu ions 0-93364  
 halide polycrystalline fibre, 10.6  $\mu\text{m}$  transmission loss obs. 0-64197  
 halide sensitised gelatin processing, phase volume hologram form. 0-78797  
 halide thin-film optical recording medium 0-102786  
 halide visible luminescence obs. at or below 77K 0-108263  
 halides, cryst., van der Waals coeffs. calcs. 0-96459  
 halides, fundamental absorpt., nature and function of A-centres determ. the extra band at the long wave edge (*Russian*) 0-76060  
 halides, matter transport rel. to point defect parameters 0-107488  
 halides, NMR chemical shifts 0-74180  
 halides, static dielec. constant, strain derivatives 0-100629  
 polyamine iodide-AgI solid electrolytes, elec. cond. and cryst. struct. 0-107537  
 pyridinium silver iodide, fast ion conductor, phase transitions, thermoelec. power meas. 0-107540  
 stability increase during simultaneous photographic development and fixing (*Russian*) 0-95179  
 TCNQ salt, Ag.TCNQ, cryst. struct. 0-70186  
 (Ag,Nb)Br, ionic transport numbers, polarization cell method 0-59705  
 (Ag,Nb)Cl solid solns., ionic transport numbers, polarization cell method 0-59705  
 Ag complex, DNA-Ag (I) in soln., theoret. interpret. of elec. dichroism obs. 0-85347  
 Ag complex, dioxane perchlorate, cryst. struct., phase transitions, X-ray study 0-59646  
 Ag complexes of 2-amino-5-methyl-1,3,4-thiadiazole and 2,5-dimethyl-1,3,4-thiadiazole, conductometric and IR meas. 0-87121  
 Ag halide crystals, effect of redox potential on photosensitivity (*Russian*) 0-73507  
 Ag halide photochromic glass, darkening mech., temp. depend. 0-87449  
 Ag halide photochromic glasses, optical absorpt. of Ag, optically induced dichroism 0-108177  
 Ag halide photographic materials, theory of supersensitisation, review (*Russian*) 0-62786  
 Ag/RbAg<sub>4</sub>I<sub>3</sub>/I<sub>2</sub> solid state battery, low temp. degradation 0-61331  
 Ag/RbAg<sub>4</sub>I<sub>3</sub>/Ta, solid electrolyte timing cell and coulometer 0-68216  
 Ag-Bi-S, ternary phase diagram, DTA and X-ray diffr. investigation 0-84917

## silver compounds continued

- Ag-Ge-Te system, chalcogenide, phase equilibria and diagrams (*German*) 0-108418  
 Ag-S, liq., mag. susceptibility meas., electron localisation and chem. bonding 0-60178  
 Ag-Se, liq., mag. susceptibility meas., electron localisation and chem. bonding 0-60178  
 Ag-Te, liq., mag. susceptibility meas., electron localisation and chem. bonding 0-60178  
 AgAsS<sub>3</sub>, proustite, parametric upconverter, temp. effects on tangential phase-matching condition 0-99804  
 Ag<sub>3</sub>AsS<sub>3</sub>, proustite, phonons and soft modes at ferroelec. transition 0-60524  
 Ag<sub>3</sub>AsS<sub>3</sub>, Raman spectra obs. of low-temp. phases 0-93327  
 AgBF<sub>4</sub>, ionic radii and chem. shifts, correl. with electronegativity 0-66054  
 AgBi(Cr<sub>2</sub>O<sub>7</sub>), cryst. struct. determ. by X-ray and neutron diffr. (*French*) 0-92492  
 AgBr, connection between the topography of luminescence centres and the latent image (*Russian*) 0-62785  
 AgBr crystal produced by action of free radicals, developability 0-66838  
 AgBr, cyclotron reson. of polarons at high density excitation 0-75859  
 AgBr dispersion in gelatin, adsorbed S and Au, transient absorpt. spectra, latent image form. and decay 0-66837  
 AgBr, electronic dielec. const., vol. depend., Clausius-Mossotti model 0-100630  
 AgBr emulsion grains, adsorbed dyes, light-induced ESR spectra 0-88862  
 AgBr emulsion grains, edge length dependence of ionic conductivity, space charge characteristics 0-88360  
 AgBr emulsion layer with gelatin, IR absorpt. spectra before and after laser exposure (*Russian*) 0-62776  
 AgBr, enhanced defect form., mean field theory 0-107220  
 AgBr evaporated layer response in ionisation semiconductor photographic system (*German*) 0-101859  
 AgBr, Herschel effect, latent image centre struct. changes under laser irradi. 0-77900  
 AgBr, ionic transport, defect form. and migration energies, quasi-harmonic model 0-107538  
 AgBr layer, sensitised, topography of developed centres 0-73491  
 AgBr, luminescence of photographic emulsions sensitised by 1,1'-diethyl-2,2'-cyanine with Ag<sub>2</sub>S clusters (*Russian*) 0-73513  
 AgBr microcrystals, spectrally sensitised, luminesc., effect of hydrophobic organic compounds 0-97331  
 AgBr, NMR chemical shifts 0-74180  
 AgBr, NaBr, thermodynamic props., metastable states and demixing 0-96660  
 AgBr, photo-EMF relaxation, temp. depend. 230 to 316K (*Russian*) 0-73508  
 AgBr, photodiode effect at low temp. (*Russian*) 0-96947  
 AgBr, photoexcited electrons and holes in latent image form., review 0-73496  
 AgBr, photoluminesc. study of excitons in high mag. fields 0-80843  
 AgBr, point defect form. energies, atomistic calc. and surface pot. meas. 0-107221  
 AgBr, vapour, photoelectron spectrosc., interpretation 0-95679  
 AgBr, vapour-deposited epitaxial film, surface structure 0-59814  
 AgBr, very fine grained emulsions, effect of hole and electron acceptors on photosensitivity (*Russian*) 0-73515  
 AgBr:Na<sup>+</sup>(Li<sup>+</sup>), correlated diffusion of impurities, nuclear spin relax. meas. 0-108094  
 AgBr-Ag<sub>2</sub>O-P<sub>2</sub>O<sub>5</sub>, glass formation and ionic conductivity 0-65290  
 AgBr-AgI emulsion sensitivity improved by AgCl shell crystallisation (*German*) 0-104453  
 AgBr-NaBr, phase diagram, miscibility, binodal curve and demixing kinetics, X-ray meas. 0-96659  
 AgCNS, mixed conductor, elec. cond. props. 0-65639  
 AgCdO, powder metallurgy production, for switchgear in power engineering 0-104094  
 AgCl crystal growth in gelatin soln. 0-64942  
 AgCl, electronic dielec. const., vol. depend., Clausius-Mossotti model 0-100630  
 AgCl, enhanced defect form., mean field theory 0-107220  
 AgCl, ionic mobility, diffusion coeffs., defect mobility energies 0-65284  
 AgCl, ionic space charge and dissolution 0-107431  
 AgCl, ionic transport, defect form. and migration energies, quasi-harmonic model 0-107538  
 AgCl, luminescence fatigue, adsorbed Ag atoms 0-66281  
 AgCl, NMR chemical shifts 0-74180  
 AgCl, point defect form. energies, atomistic calc. and surface pot. meas. 0-107221  
 AgCl, vapour, photoelectron spectrosc., interpretation 0-95679  
 AgCl, vapour-deposited epitaxial film, surface structure 0-59814  
 AgCl:Cd<sup>2+</sup>, heavily doped, free energy and point defect distrib., integral eqn. method 0-107219  
 AgCl:Pd<sup>2+</sup>, ESR spectrum, quasistatic Jahn-Teller effect 0-71170  
 AgCl-Ag<sub>2</sub>O-P<sub>2</sub>O<sub>5</sub>, glass formation and ionic conductivity 0-65290  
 AgCl-AgBr mixed crysts., elastic consts. and cryst. symm. 0-70290  
 AgCl(Br), activated photochromic glass, kinetics of thermal decolorisation 0-103931  
 AgF, diffusion, elec. cond. and <sup>19</sup>F relax. T<sub>1</sub> meas. 0-92718  
 AgF, NMR chemical shifts 0-74180  
 Ag<sub>2</sub>F, NMR of <sup>109</sup>Ag and <sup>19</sup>F, modified Korringa relation in two-dimens. metal 0-93199  
 AgGaS<sub>3</sub>, deep level obs. by TSC meas. 0-65590  
 AgGaS<sub>3</sub>:Fe, EPR of Fe-associated defect 0-60412  
 AgGaS<sub>3</sub>-AgGaSe<sub>2</sub> system, phase diagram, lattice consts., and IR spectra 0-60841  
 AgGaSe<sub>2</sub>, two-photon absorpt. and short pulse stimulated recombination 0-89054  
 Ag<sub>2</sub>HgI<sub>4</sub>, preparation, optical and luminescence spectra 0-104064  
 Ag<sub>2</sub>HgI<sub>4</sub>, Raman line shape and ionic cond., coupled mode model 0-66171  
 $\alpha$ -AgI, activation vol. for ionic cond. 0-59711  
 AgI aerosol, ice forming activity, UV irradi. effect 0-71950  
 AgI aerosol, studies of ice-forming activity, verification of theory 0-101406  
 AgI aerosol particle size, struct. rel. to ice forming activity 0-61164  
 AgI colloid, stability, dynamic theory 0-89544  
 $\alpha$ -AgI, cond. mechanisms in superionic phases, neutron diffr. obs. 0-59714  
 $\alpha$ -AgI, diffusion dynamics, quasielastic neut. scatt. expt. 0-107484

## silver compounds continued

- $\alpha$ -AgI, dynamic cage effect 0-107541  
 AgI, EXAFS investigation of struct. and ion motion 0-108302  
 $\alpha$ -AgI, fast ion conductor, phase transitions, thermoelec. power meas. 0-107540  
 AgI group superionic conductor, phase transition detection by thermoelectric power method 0-92669  
 AgI hydrosols, kinetics and mechanics of colloid systems formation 0-101045  
 $\alpha$ -AgI, ionic motions nature, mol. dynamics calcs. 0-107533  
 AgI, lattice dynamics of binary superionic conductors 0-107393  
 AgI, NMR chemical shifts 0-74180  
 $\alpha$ -AgI, solid electrolyte, contrib. of non-Brownian motion to transport props. 0-70453  
 $\alpha$ -AgI, structural and dynamical behaviour 0-107544  
 $\alpha$ -AgI, superionic, anal. of Ag K-XAFS data 0-97377  
 AgI, superionic cond., lattice potential effects 0-65274  
 $\alpha$ -AgI, superionic cond., statistical thermodynamic description (*French*) 0-65281  
 AgI surface, adsorption of water, effective pair pot. model 0-100394  
 $\beta$ -AgI, thermal expansion, 4 to 270K 0-79961  
 AgI, thermal expansion under press. 0-92690  
 AgI, vapour, photoelectron spectrosc., interpretation 0-95679  
 AgI: Cd, polycrystalline, thermoelectric power meas. 0-59698  
 AgI/Ag oxy salt system, vitreous solid electrolytes, conductance mechanism 0-107560  
 AgI/RbI quasibinary system, solid state reactions and transport props. 0-96700  
 AgI-Ag<sub>2</sub>MoO<sub>4</sub> pseudobinary system, superionic cond. glasses, comp. depend. of ionic cond. 0-75380  
 AgI-Ag<sub>2</sub>O-MoO<sub>3</sub> glass glass superionic cond., struct. and transport props. 0-88602  
 AgI-Ag<sub>2</sub>O-P<sub>2</sub>O<sub>5</sub>, glass formation and ionic conductivity 0-65290  
 AgI-Ag<sub>2</sub>O-P<sub>2</sub>O<sub>5</sub>(MoO<sub>3</sub>) glassy electrolyte galvanic cells 0-104513  
 (AgI)<sub>2</sub>(Ag<sub>2</sub>O-B<sub>2</sub>O<sub>3</sub>)<sub>1-x</sub>, amorphous superionic compound, <sup>11</sup>B lineshape and relaxation 0-108107  
 AgIO<sub>3</sub>, chem. prep. and cryst. struct. 0-75207  
 Ag<sub>2</sub>I<sub>2</sub>PD<sub>4</sub>, superionic solid film, surface diffusion coeff. 0-92709  
 Ag<sub>26</sub>I<sub>18</sub>W<sub>2</sub>O<sub>16</sub>, order-disorder type ferroelectric transitions, ionic conductivity meas. 0-66122  
 Ag<sub>26</sub>I<sub>18</sub>W<sub>2</sub>O<sub>16</sub>, solid electrolyte, anisotropic elec. cond., low temp. phase transitions 0-65289  
 AgInS<sub>2</sub>, and AgInS<sub>8</sub>, spray pyrolysis, film struct., elec. and optical props. 0-71592  
 AgN<sub>3</sub>, high-resist. explosive cpd., elec. and galvanomag. props., temp. depend. 0-103728  
 AgNO<sub>3</sub>, single crystal, dielec. const., low temp. meas. 0-71290  
 AgNO<sub>3</sub>, centre of symmetry and cryst. perfection (*French*) 0-107089  
 AgNO<sub>3</sub>, digested AgBr(Cl) emulsions, IR luminesc. obs. at 77K 0-103983  
 AgNO<sub>3</sub> in gelatin layers, phosphorescence kinetics curves (*Russian*) 0-62776  
 AgNO<sub>3</sub>, molten, refr. index and molar refractivity 0-93265  
 AgNO<sub>3</sub> soln., visible luminescence obs. at or below 77K 0-108263  
 AgNO<sub>3</sub>-Ag<sub>2</sub>S system, visible luminescence obs. at or below 77K 0-108263  
 AgNa(NO<sub>2</sub>)<sub>2</sub>, <sup>23</sup>Na elec. field gradient tensor from NMR satellite lines near phase transition 0-71191  
 AgNa(NO<sub>2</sub>)<sub>2</sub>, crit. dynamics, hydrostatic press. effect, dielec. props. meas. 0-71328  
 AgNa(NO<sub>2</sub>)<sub>2</sub>, ferroelec., Raman scatt. and phase transitions 0-71349  
 AgNa(NO<sub>2</sub>)<sub>2</sub>, ferroelec. cryst., Raman spectrum, phase transition, comparative anal. with NaNO<sub>2</sub> 0-88935  
 AgNa(NO<sub>2</sub>)<sub>2</sub>, order-disorder ferroelec., influence of hydrostatic press. on polarisation dynamics 0-103913  
 Ag<sub>2</sub>Na<sub>2-x</sub>Te<sub>2</sub><sup>VI</sup>Te<sub>2</sub><sup>VI</sup>O<sub>4</sub> (x=0.4), mixed tellurate, cryst. chem. and elec. cond. (*French*) 0-107150  
 Ag<sub>2</sub>O, exciton luminesc. spectra, mag. field influence 0-80860  
 Ag<sub>2</sub>O, X-ray absorption, discontinuities and limits, chem. combination effects 0-93435  
 Ag<sub>2</sub>O-Al<sub>2</sub>O<sub>3</sub>-MgO-Na<sub>2</sub>O,  $\beta$ -alumina, structure, X-ray determ. 0-107148  
 Ag<sub>2</sub>O-MgO-Al<sub>2</sub>O<sub>3</sub>, ionic cond. 0-107480  
 Ag<sub>2</sub>O-P<sub>2</sub>O<sub>5</sub> glass ESR of VO<sup>2+</sup> ions 0-100610  
 Ag<sub>2</sub>P, formation at Ag-InP interface during sintering 0-65309  
 Ag<sub>2</sub>PO<sub>4</sub>, anhydrous, struct. relationships w.r.t. fast ion cond. 0-107188  
 Ag<sub>2</sub>Re films, galvanomag. props. and quantum size effects, obs. 0-70866  
 $\beta$ -Ag<sub>2</sub>S, cond. mechanisms in superionic phases, neutron diff. obs. 0-59714  
 $\alpha$ -Ag<sub>2</sub>S, single cryst. growth through capillary tube 0-108331  
 Ag<sub>2</sub>S sols, red-IR photoluminescence obs. at 77K 0-103982  
 Ag<sub>2</sub>S-K<sub>2</sub>SO<sub>4</sub> mixtures, surface comp., AES and XPS obs. 0-81386  
 Ag<sub>2</sub>S+Ln<sub>2</sub>S<sub>3</sub>, powdered mixtures, reaction rate, production of ionic semi-conductors 0-93741  
 Ag<sub>2</sub>SBr, ionic conductivity in temp. range 93-573K, X-ray diff. and DTA 0-79988  
 Ag<sub>2</sub>SBr, superionic conductor, phase transition, struct. 0-107144  
 $\beta$ -Ag<sub>2</sub>SI, anharmonic thermal vibr. of cations 0-65214  
 Ag<sub>2</sub>SI, ionic conductivity in temp. range 93-573K, X-ray diff. and DTA 0-79988  
 Ag<sub>2</sub>SO<sub>4</sub>, anhydrous, struct. relationships w.r.t. fast ion cond. 0-107188  
 Ag<sub>2</sub>SO<sub>4</sub>-K<sub>2</sub>SO<sub>4</sub> mixtures, surface comp., AES and XPS obs. 0-81386  
 Ag<sub>2</sub>Sb<sub>2</sub>O<sub>7</sub>F<sub>2</sub>, ionic conductivity, comparative study with pyrochlore phase AgSbO<sub>3</sub> (*French*) 0-103701  
 $\alpha$ -AgSbS<sub>3</sub>, crystals, photoelectric props. 0-107861  
 Ag<sub>2</sub>SbS<sub>3</sub>, Raman spectra obs. of low-temp. phases 0-93327  
 Ag<sub>2</sub>SbS<sub>3</sub>(AsS<sub>3</sub>), electroacoustic echo, ultrasonic wave attenuation (*Russian*) 0-88280  
 Ag<sub>2</sub>Sb<sub>2</sub>Te<sub>2</sub>, single-phase, thermoelectric efficiency 0-107826  
 Ag<sub>2</sub>Se, between metal electrodes, current-voltage characts (*French*) 0-97005  
 Ag<sub>2</sub>Se, electronic and electrogalvanic props. in  $\alpha$ -phase region (*French*) 0-107820  
 $\alpha$ -Ag<sub>2</sub>Se, single cryst. growth through capillary tube 0-108331  
 Ag<sub>2</sub>Se thin film, switching and Ag movement, point contact technique 0-60107  
 Ag<sub>2</sub>TeO<sub>3</sub>, chem. prep. and cryst. struct. (*French*) 0-79755  
 Ag<sub>2</sub>TlTe(S)(Se), cryst. struct. 0-107156  
 $\beta$ -Al<sub>2</sub>O<sub>3</sub>-Ag<sub>2</sub>O, Haven ratio, temp. depend., Ag diffusivity and ionic cond. 0-107503  
 $\beta$ -Al<sub>2</sub>O<sub>3</sub>-Ag<sub>2</sub>O, ionic cond. at room temp. 0-107513  
 $\beta$ -Al<sub>2</sub>O<sub>3</sub>-Ag<sub>2</sub>O, low-energy excitation spectra, localised modes 0-59606

## silver compounds continued

- $\beta$ -Al<sub>2</sub>O<sub>3</sub>-Ag<sub>2</sub>O, neutron diff. obs. of struct. 0-107512  
 $\beta$ -Al<sub>2</sub>O<sub>3</sub>-Ag<sub>2</sub>O, single cryst. Raman scatt., cond. mechanism and cryst. struct. 0-66209  
 $\beta$ -Al<sub>2</sub>O<sub>3</sub>-Ag<sub>2</sub>O, stoichiometric and nonstoichiometric, structure comparison, phase transitions in stoichiometric compound (*French*) 0-60856  
 $\beta$ -Al<sub>2</sub>O<sub>3</sub>-Ag<sub>2</sub>O, stoichiometric A phase, X-ray diffuse scatt. obs., sublattice phase transition 0-64944  
 As<sub>10</sub>Ge<sub>15</sub>Te<sub>75</sub>Ag<sub>x</sub>, glass, elec. and dielec. props., Ag additions effect 0-65558  
 As<sub>2</sub>Se<sub>3</sub>Ag, glassy semicond. film, prep. by photodiffusion of Ag, negative photocond. 0-92934  
 Cd<sub>1-x</sub>Ag<sub>x</sub>Cr<sub>2</sub>S<sub>4</sub>(Se<sub>4</sub>), electronic struct., mixed valence 0-70612  
 CdF<sub>2</sub>:AgF, colour centres, IR absorpt. and photocond. after UV irradiat. 0-79784  
 (Cu,Ag)<sub>2</sub>Se/(Bi, Sb)<sub>2</sub>Te<sub>3</sub>, P type selenide segmented element fabrication, thermoelectric props. 0-107835  
 Cu<sub>2</sub>Ag<sub>1-x</sub>I crystals, layer structs., X-ray diff. studies 0-96457  
 Cu<sub>2</sub>Ag<sub>15</sub>, superionic cond., pressure effect on phase transitions 0-70405  
 KAg<sub>2</sub>I<sub>5</sub>, superionic phase transition, dynamical and crit. pt. props. 0-107535  
 La<sub>2</sub>S<sub>3</sub>-Ag<sub>2</sub>S-Ga<sub>2</sub>S<sub>3</sub> glass system, prep., thermal and elec. props. (*French*) 0-89192  
 Mg-AgCl seawater battery, performance and EMF at great ocean depths 0-76623  
 NH<sub>4</sub>Ag<sub>4</sub>I<sub>5</sub>, superionic cond., pressure effect on phase transitions 0-70405  
 NH<sub>4</sub>Ag<sub>4</sub>I<sub>5</sub>, superionic solid film, surface diffusion coeff. 0-92709  
 NH<sub>4</sub>Ag<sub>4</sub>I<sub>5</sub>, superionic phase transition, dynamical and crit. pt. props. 0-107535  
 Na<sub>2</sub>O-Ag<sub>2</sub>O-B<sub>2</sub>O<sub>3</sub> glass, Ag<sup>+</sup> ion distrib., X-ray diff. study 0-84076  
 PbI<sub>2</sub>-Ag, photographic mat., photolysis, effect of PbI<sub>2</sub> photo-EMF effect (*Russian*) 0-92939  
 $\alpha$ -RbAg<sub>4</sub>I<sub>5</sub>, dynamic cage effect 0-107541  
 RbAg<sub>4</sub>I<sub>5</sub> film, thermopower meas. temp. depend., correl. effects role 0-107539  
 RbAg<sub>4</sub>I<sub>5</sub>, single particle excitations, inelastic neutron scatt. obs. 0-59599  
 RbAg<sub>4</sub>I<sub>5</sub>, solid electrolyte development, Ag<sup>+</sup> cond. 0-107532  
 RbAg<sub>4</sub>I<sub>5</sub>, static and dynamic NMR effects at 208K and 122K phase transitions 0-108105  
 RbAg<sub>4</sub>I<sub>5</sub>, superionic conductor, phase transition detection by thermoelectric power method 0-92669  
 RbAg<sub>4</sub>I<sub>5</sub>, superionic phase transition, dynamical and crit. pt. props. 0-107535
- SIMS** see secondary ion mass spectra; secondary ion mass spectroscopy
- simulation**  
 see also aerospace simulation; analogue simulation; brain models; digital simulation; hybrid simulation; modelling; physiological models; plasma simulation; semiconductor device models  
 atmosphere, urban, numerical simulation of mixing depths 0-105024  
 auroral arcs global formation, numerical simulation 0-67446  
 Brattle Physiological Synchroniser, simulator for testing respiratory gating function 0-109055  
 coal conversion reactor environments, simulation 0-100831  
 comets, orbital evolution of short-period objects, Monte Carlo simulations 0-62073  
 crystal frequency distribution, simulation taking nuclei distrib. into account 0-100184  
 Darrieus rotar windmill arrays, wake interaction, wind tunnel simulation 0-61245  
 direct solar energy, Markov chain simulation with one minute binning (*French*) 0-61293  
 exospheres of Moon and Mercury, Monte Carlo simulation methods 0-67588  
 exospheres of Moon and Mercury, Monte Carlo simulation methods 0-67589  
 fast breeder test reactor operator training simulator model development 0-91219  
 flow simulation, vortex methods, review 0-106801  
 fluids, simple fluid shear depend. viscosity, central force interactions 0-79970  
 fusion reactor first wall, radiation damage simulation using fission reactor test facilities 0-57950  
 fusion reactor neutral beam injector vacuum system transient simulation anal. 0-95453  
 galaxies fields stochastic simulation 0-62295  
 galaxies in clusters, Monte-Carlo simulation of orientations 0-90528  
 galaxy clustering N-body simulations, fraction in groups as function of density enhancement 0-67879  
 galaxy fields, stochastic simulation 0-90530  
 gas turbine combustion chamber flow three-dimens. calc. 0-79405  
 gravitational system dynamics, two-dimensional simulation rel. to Universe large-scale struct. form. 0-98749  
 Keplerian systems, numerical simulations of collisional evolution 0-109342  
 kinetics of reacting solns., diffusional barrier crossing processes, trajectory simulation 0-81280  
 lens mass production yield estimation by centering tolerance simulation 0-78941  
 light sources for simulating sunlight 0-87454  
 lipid monolayer, simulation using mol. dynamics 0-108838  
 mammography, simulation of X-ray spectra 0-76826  
 Mars, Viking gas exchange reaction simulation on UV irradiated MnO<sub>2</sub> substrate 0-72831  
 nonlinear magnetic field simulator for electromagnetic fields anal. (*Japanese*) 0-95756  
 optical element polishing simulation calc. and results (*German*) 0-87566  
 optical sensor system simulation and evaluation 0-96030  
 planet thermal radiation intensity field modelling; principles 0-62056  
 plasma collisionless shocks, simulation and laboratory expts. 0-87893  
 power system that includes wind energy generators, model based regulation 0-61256  
 solar flares experimental simulation, merging of two current carrying plasma columns (*Japanese*) 0-94775  
 stratosphere sulphate aerosol layer, processes, models, obs. and simulations 0-109212  
 structural system, simulation anal. of reliability and maintenance (*Japanese*) 0-62453  
 system aspects of electro-optics, seminar, Huntsville, AL, USA (May 1979) 0-94921  
 tissue temperature simulation in cryosurgery 0-85355



## simulation continued

- tomography simulator, emission computed, design 0-61672  
tsunami, island of Hawaii, 1979 November 25, numerical anal. by finite-element method 0-72449  
vacuum gap breakdown initiation by microparticle impact 0-96413

## simulation, digital see digital simulation

## simulators see simulation

## Sinanoglu's theory see atomic structure

## single phase rectifiers see rectifiers

## sinks, heat see heat sinks

## sintering

## see also densification

- alloys, binary, marker displacements as result of diffusion 0-92724  
borosilicate glass, powder, sintering, foaming by chemical reactions 0-81017  
bronze powders, electric-pressure sintering onto cylindrical parts in fluidised bed 0-100960  
( $\text{CaO} \cdot 6\text{Fe}_2\text{O}_3 \cdot \text{La}_2\text{O}_3$ ), compounds, effects of  $\text{Nd}_2\text{O}_3$  substitution on magnetic props. (Japanese) 0-108010  
[CC] Ag-(100)InP, metal-semicond. cathode contact, metallurgical, physical, chemical processes 0-107911  
ceramic compounds, lyophilisation parameters, freeze-drying synthesis 0-97453  
control by potentiometric level detector (Russian) 0-90813  
diamond, polycryst. sintered under ultra high press., binary inclusion content effect on thermal stability (Chinese) 0-66453  
diamond, polycryst. with Ni additives, sintering under ultrahigh pressure 0-84870  
diffusion processes in ohmic sintering, temp. distrib. influence 0-92704  
dolomite, powders sintering, decarbonisation cycle effect 0-104102  
FBR oxide fuels, dynamic response of grain boundary cavities to stress and temperature changes under conditions of continuous gas generation 0-66544  
ferrites, soft, spray firing for presintered powder prep. 0-89181  
hard metal powders, electric-pressure sintering onto cylindrical parts in fluidised bed 0-100960  
Inconel 718, grain growth during sintering 0-97449  
liquid phase sintered systems, particle coalescence probability estimation 0-104086  
magnesite, powders sintering, decarbonisation cycle effect 0-104102  
metallic fibre knitted gauze permeable materials, mech. props. 0-66607  
metals, sintering analysis using sintering maps 0-93513  
NASICON solid electrolyte, processing and phys. props. 0-60820  
optical graded-index fibre vapour-phase axial deposition method, fibre characteristics 0-58824  
oriented bicrystal, prod. technique 0-108371  
polymer filled ceramic,  $\text{ZrO}_2$  stabilised, fracture mechanism (Russian) 0-100895  
porous materials, behaviour of pore filled with const. amount of gas 0-66450  
porous solids, gases influence, behaviour of assembly of pores filled with gas 0-84877  
pressure sintering, inhomogeneous flow and effective press. 0-93512  
 $\text{Si}_3\text{N}_4$ - $\text{Ce}_2\text{O}_3$ - $\text{SiO}_2$  materials: phase relations and strength 0-97465  
steel, Cr-W-Mo-Co, high-speed, from atomised powders, mech. and cutting props. 0-66556  
steel, Cu-Ni-Mo (2, 2, 0.25 wt.%), sintering, kinetic characts. 0-60805  
steel, Ni-Mo-C (2.0, 0.2, 0.4 wt.%) sintered, struct. transforms. and mech. props. after quenching 0-66557  
steel, Ni-Mo-C (5, 0.5, 0.5 wt.%), sintered, effects of powder and sintering variables on props. 0-104093  
steel, sintered, fracture of residual pores 0-76352  
steel, stainless, 20Kh13, prep. by diffusion impregnation 0-60803  
steel (alloy)-TiC (70, 30 wt.%) composite, sintered, wear resist. 0-100815  
surface redistribution by grain boundary diffusion 0-84871  
SYNROC-B ceramic for radwaste disposal, feasibility of subsolidus sintering 0-83198  
SYNROC-B sintered ceramics for high-level radwaste fixation, comp. and phase charact. 0-106126  
 $\text{Fe}_2\text{O}_3$ - $\text{Bi}_2\text{O}_3$  sintered material, elec. switching effects due to thermal ionic breakdown (Korean) 0-70776  
Ag powder, ultrafine, sintering, coalescence growth stage 0-89174  
Ag-InP interface,  $\text{AgP}_2$  formation during sintering 0-65309  
Al powders, electric-pressure sintering onto cylindrical parts in fluidised bed 0-100960  
Al-Cu (0-10 wt.%) sintered alloys using composite powder 0-76210  
 $\alpha$ - $\text{Al}_2\text{O}_3$ , ceramic, prod. from etching wastes of Al foils 0-108376  
 $\text{Al}_2\text{O}_3$  ceramics, sintering mechanism and kinetics, glass-forming additives effect 0-89187  
 $\text{Al}_2\text{O}_3$ , semisintered, shear strength at high press. 0-76308  
 $\text{Al}_2\text{O}_3$  sintering, effect of  $\text{SrO}$ ,  $\text{MgO}$  and  $\text{Y}_2\text{O}_3$  additives on  $\alpha$ - $\text{Al}_2\text{O}_3$  mineralisation 0-89186  
 $\text{Al}_2\text{O}_3$  sintering, role of  $\text{MgO}$  0-81010  
 $\text{Al}_2\text{O}_3$ , sintering as function of phase comp. 0-66464  
 $\text{Al}_2\text{O}_3$ , sintering temperature effect of titanate additions 0-60808  
 $\beta''$ - $\text{Al}_2\text{O}_3$ - $\text{Na}_2\text{O}$  solid electrolyte, processing and phys. props. 0-60820  
 $\text{Al}_2\text{O}_3$ -Pt metal-ceramic reaction, micro/macro obs. 0-66467  
 $\text{Al}_2\text{O}_3$ - $\text{Y}_2\text{O}_3$ , sintering kinetics, influence of minor additions of  $\text{Y}_2\text{O}_3$  0-84868  
3 $\text{Al}_2\text{O}_3$ ·2 $\text{SiO}_2$ - $\text{ZrO}_2$  composites, sintered, in situ-reacted, fracture props. 0-81158  
Au powder, ultrafine, sintering, coalescence growth stage 0-89174  
 $\text{Au}_8$  particles, vacuum-deposited, degree of faceting during sintering 0-84411  
B-Si alloys, B-rich, prep., anal. and cryst. growth (French) 0-104091  
BC, sintered, struct. and props. 0-104181  
 $\text{B}_2\text{O}_3$ - $\text{SiO}_2$ , optical waveguide glass, sintering kinetics 0-84898  
 $\text{BaFe}_2\text{O}_{10}$  powders, fast reaction presintering 0-97445  
 $\text{BaO}$ - $\text{Nd}_2\text{O}_3$ - $\text{TiO}_2$ - $\text{Bi}_2\text{O}_3$  system ceramics, high stability low loss dielectric preparation 0-81008  
 $\text{BaTiO}_3$ , reduction inhibition by impurity ions 0-101018  
 $\text{BaTiO}_3$ : $\text{BaTiO}_3$ , dielec. props. and microstruct. 0-60481  
Be, sintered, physicochem. props. anisotropy, BeO inclusions effect 0-60804  
 $\text{C}_2\text{S}$ , influence of polymorphic transform. on sinter stability (Russian) 0-66503  
CaO based refractory from industrial lime, with 5% added electrocorundum 0-89184  
 $\text{Co}_2\text{Z}$  ferroplana form. process peculiarities 0-89368

## sintering continued

- Cr- $\text{Al}_2\text{O}_3$  powder targets for plasma-ion spray deposition of resistance films 0-84897  
 $\text{Cr}_2\text{C}_3$  electrophoretic alloy coatings on C steel, sintered, struct. form., Ni-P undercoat effect 0-61027  
 $\text{Cr}_2\text{C}_3$  electrophoretic coatings on steel, sintering 0-66707  
 $\text{Cr}_2\text{O}_3$ , sintering behaviour, effect of  $\text{TiO}_2$ , C additions 0-66461  
 $\text{Cr}_2\text{O}_3$ - $\text{Al}_2\text{O}_3$  solid soln., Vickers micro-hardness 0-66629  
Cu-Ni, sintering, Kirkendall effect 0-93518  
Fe ore concentrate, sinter quality improvement (Chinese) 0-104089  
Fe powder, reduction annealing, comminution of sintered cakes 0-66456  
Fe powder based sintered porous permeable materials, diffusion chromising 0-100958  
Fe, powder-forged, elastic const., density depend. 0-84987  
Fe, sintered, austenitic nitriding and bainitic hardening 0-85084  
Fe-B, for infiltration of Fe compacts 0-60806  
Fe-C (graphite, 0.3 wt.%), powder-forged, elastic const., density depend. 0-84987  
Fe-Cu: graphite- $\text{BaSO}_4$ - $\text{CuSO}_4$ , friction material, solid state sintering kinetics 0-104096  
Fe-Cu sintered porous materials, machinability 0-66457  
Fe-Mo- $\text{CaF}_2$  sintered composite, struct. and mech. props., heat treatment effect 0-66526  
Fe-Si (3 to 5 wt.%) sinters, mag. props., Si and Fe-Si additions effect 0-71104  
Fe-Si-C mixed powder, cast Fe powder sintering study (Japanese) 0-108373  
 $\beta$ - $\text{Fe}_2\text{Ge}_3$  formation in isothermal sintering, phase transition kinetics 0-89197  
 $\text{Fe}_2\text{O}_3$ , semisintered, shear strength at high press. 0-76308  
 $\text{Fe}_2\text{O}_3$ - $\text{Bi}_2\text{O}_3$  sintered material, elec. switching effects for temp. range 700-850°C (Korean) 0-70775  
 $\text{HfO}_2$ - $\text{PO}_4$ - $4\text{H}_2\text{O}$ , film fabrication and appl. as solid electrolyte in electrochromic displays 0-70462  
 $\text{Li}_{0.5}\text{Fe}_{2.5}\text{O}_4$  milled ferrite powder, substruct. and sinterability 0-84894  
 $\text{Li}_{0.5}\text{Mn}_{0.5}\text{Fe}_{2.5}\text{O}_4$  ferrite cores with rectangular hysteresis loops, pulse parameters, effect of  $\text{Fe}_2\text{O}_3$  heat treatment 0-60370  
 $\text{Li}_3\text{N}$ , Li ion conduction 0-70449  
 $\text{MgO}$ , semisintered, shear strength at high press. 0-76308  
 $\text{MgO}$ , sintered, refractories, props. after testing at over 2000°C 0-104317  
 $\text{MgO}$  sintered-ceramic separator plate development, Li-Al/LiCl-KCl/FeS battery applications 0-61321  
 $\text{MgO}$ , sintering by activating 3 $\text{MgCo}_3$ · $\text{Mg}(\text{OH})_2$ ·3 $\text{H}_2\text{O}$  0-89183  
 $\text{MgO}$ - $\text{Al}_2\text{O}_3$ - $\text{SiO}_2$ , sintered, cordierite, mineralogy and props. 0-60827  
 $\text{MgO}$ -NaCl refractory clinkers, Cr containing, densification, thermal treatment and phase composition effect (French) 0-76219  
 $\text{MgO}$ -Pd metal-ceramic reaction, micro/macro obs. 0-66467  
 $\text{Mg}(\text{OH})_2$ , sintering, IR spectra, X-ray anal. 0-66452  
MnZn ferrite, microstructure and initial permeability, presintering process effect 0-89367  
MnZn ferrites, form. of comp. heterogeneity during high-temp. sintering 0-60818  
MnZn ferrites, post sinter-cooling rates effects 0-89369  
Mo powder, influence of powder reduction processes on props. 0-89175  
Mo, sintered, gas evolution and degassing 0-100814  
Na borosilicate glass microsphere material, sintering, struct., strength props. (Russian) 0-108383  
 $\text{Na}_2\text{O}$ -Ca glass powders, mixed with  $\text{CO}_2$  compounds, cellular-struct. glass fabrication 0-108382  
 $\text{Na}_2\text{O}$ -CaO glass phlogopite mica powders, composite fabrication, cellular struct. 0-84902  
 $\text{Na}_2\text{O}$ - $\text{P}_2\text{O}_5$ - $\text{SiO}_2$  glass, metastable liquid immiscibility 0-100331  
 $\text{Nb}_5\text{Sn}$ , powder metallurgically produced, microstruct. characts. 0-89233  
Ni, carbonyl powder, dislocation density sintering 0-108372  
Ni sintered permeable materials with bidisperse structure, pore-forming additions effect 0-84885  
Ni, sintering kinetics, metallographic study 0-93519  
Ni-Cr-Al sintered alloy, hot vac. pressure, fracture and mech. characts. 0-66667  
Ni-Cr- $\text{Al}_2\text{O}_3$  powder targets for plasma-ion spray deposition of resistance films 0-84897  
Ni-Zn-Co ferrites, synthesis from solid solns. of schoenite-type salts 0-93511  
 $\text{NiFe}_2\text{O}_4$  milled ferrite powder, substruct. and sinterability 0-84894  
NiZn ferrite,  $\text{ZrO}_2$  additions influence on sintering and physicochem. props. 0-108369  
NiZn ferrites, density and mag. props., isostatic pressure effect 0-60816  
 $\text{Pb}_{0.94-x}\text{Zr}_{0.06}\text{Nb}_{0.9-x}\text{O}_3$ , Nb dopant morphology effect on microstructure 0-81005  
PbTe, effect of pressing and sintering, study of induced defects by SEM 0-59983  
Pb(Zr, Ti) $\text{O}_3$  ceramics, low temp. sintering, elec. and mech. props. 0-71616  
Pb(Zr, Ti) $\text{O}_3$  ceramics, DC field sintering preparation, piezoelectric props., ageing behaviour 0-81211  
Pb(Zr, Ti) $\text{O}_3$ : $\text{Cr}_2\text{O}_3$  ceramics, reson. freq. comp. and temp. depend. 0-70413  
Se powder compacts, sintered, electrical cond. 0-70693  
Si solar cells, low cost, Ni contacts 0-94017  
p-Si-Al, ohmic contacts, Si dissoln. and recrystn. effects, computer calc. 0-103749  
SiAlON, prepared from siliceous sand and Al powder, hot pressing, steatite contamination effects (Japanese) 0-93528  
SiC, pressureless-sintered, high temp. strength (Japanese) 0-104299  
 $\beta$ -SiC, sintering, B transport and lattice parameter change 0-108370  
SiC-AIB, (0.61 to 1.2 wt.%), hot pressed, microstruct. 0-93563  
 $\text{Si}_3\text{N}_4$ , reaction bonded, post-sintering, injection moulding applications 0-60807  
 $\text{Si}_3\text{N}_4$ - $\text{Y}_2\text{O}_3$ - $\text{Al}_2\text{O}_3$  (4-17, 4 wt.%), sintering 0-81009  
 $\text{SiO}_2$  glass, formation by hydrolysis of  $\text{Si}(\text{OC}_2\text{H}_5)_4$  with  $\text{NH}_4\text{OH}$  and HCl soln., and characterisation 0-71622  
 $\text{SnO}_2$ - $\text{NiO}(\text{ZnO})(\text{Nb}_2\text{O}_5)$ , activated sintering mechanism 0-60810  
 $\text{Sr}_x(\text{Na}_{0.5}\text{Bi}_{0.5})_{1-x}$  solid solutions, piezoelec. and ferroelec. props. (French) 0-108158  
 $\text{Sr}_x(\text{Na}_{0.5}\text{Bi}_{0.5})_{1-x}\text{TiO}_3$  ferroelec. ceramic, hot pressing, numerical simulation (French) 0-76220  
Ta(C,N)-Ni-VC, sintering behaviour, VC effect 0-93520  
 $\text{Tb}_{0.3}\text{Dy}_{0.7}\text{Fe}_2$ , prep. by powder metallurgy, magnetostrictive props. 0-75826  
(Ti,Cr) $\text{B}_2$ , sintering kinetics and props. 0-100811

# sintering continued

Ti base composite sintered bearing materials, metallic solid lubricant infiltrated, antifriction props. 0-60981  
 TiC, wetting by Cr-Ni-Mo-Mn alloy steel, expt. planning investigation 0-60822  
 TiC<sub>x</sub>, nonstoichiometric, densification during sintering 0-84895  
 (U,Pu)C, sintering, role of Ni as sintering additive 0-84892  
 UC, sintering, role of Ni as sintering additive 0-84892  
 UO<sub>2</sub>, green pellet with zinc stearate as additive, effect on sintering 0-68908  
 UO<sub>2</sub> pellets, sinterability, particle size effect 0-104098  
 W-Cu (92.8, 7.2 wt.%), liq.-phase sintered, embrittlement and interfacial impurity segregation 0-66647  
 WC, sinterability of ultrafine powders obtained by CVD method 0-108378  
 WC-Ni hard alloy composite, sintered, void healing 0-60821  
 YIG, permeability, domain rot. and wall displacement contrib. 0-80564  
 Y<sub>2</sub>O<sub>3</sub> sintered-ceramic separator plate development, LiAl/LiCl-KCl/FeS battery applications 0-61321  
 ZnO nonohmic ceramic, formation mechanism 0-60813  
 ZrN-Al<sub>2</sub>O<sub>3</sub> composites, strength rel. to solid-, liquid-phase sintering 0-100823  
 ZrO<sub>2</sub> ceramic, dense nonstabilized, fabrication by hydrothermal reaction sintering 0-97451  
 ZrO<sub>2</sub>, partially stabilized ceramics, strengthening, post-sintering heat treatment 0-97518  
 ZrO<sub>2</sub>, porous, sintered stabilised microspheres, strength and fracture studies 0-85019  
 ZrO<sub>2</sub>, semisintered, shear strength at high press. 0-76308  
 ZrSiO<sub>4</sub> zircon ceramic with glass-forming additives, sintering and mech. props. 0-60814

# size, particle see particle size

# size effect

disperse systems, solubility increase, phase composition, size effect calcs. 0-70418  
 ferroactive fluids, advanced appls. 0-80714  
 granular materials, size effects in cond. and supercond. 0-77581  
 metal film, size effect in Landau diamagnetism, surface pot. effect (*Russian*) 0-93012  
 metal film, temperature coefficient of total resistance 0-70853  
 metal film, Umklapp processes of charge carriers and anomalous transmittance in RF range (*Russian*) 0-70851  
 metallic films, metal-dielectric boundary thermal resistance, nonlinear elec. resistance (*Russian*) 0-65530  
 metallic films, polycryst., size effects and resist., approximate expressions 0-88645  
 metallic thin film, electrical conductivity measurement, thickness dependence, quantum size effect (*German*) 0-86344  
 metallic thin film, transverse electric quantum wave spectrum (*Russian*) 0-84517  
 piezosemiconductors, second harmonics of acoustoelectric current 0-80329  
 semiconductor, ambipolar hot-carrier size effect kinetics 0-107799  
 semiconductor, nuclear polarisation due to anisotropic size effect in weak elec. field 0-71199  
 semiconductor, piezoelec., degenerate, transverse magnetoresist. in strong field, quantum effect 0-80299  
 semiconductor thin film, energy spectrum in mag. field, size effect, calc. 0-70865  
 semiconductor thin film, polaron near-threshold spectrum 0-65471  
 semiconductor thin films, fabrication for device appls. 0-100418  
 semiconductor thin films, ferroelectric properties, quantum size effect 0-97201  
 semiconductor wires, size-quartised, two-photon interband absorpt. 0-93256  
 steel, tuffrided, type S15CK, fatigue strength, estimation of size effect (*Japanese*) 0-81166  
 thin film heterostructure, energy spectrum study 0-70787  
 Ag<sub>2</sub>Re films, galvanomag. props. and quantum size effects, obs. 0-70866  
 Al, small spheres, bulk plasmons damping 0-75561  
 Al, thin film, thermal cond. meas., size effect 0-65715  
 Au clusters on alkali halide surface, size depend. of valence bands, XPS study 0-65647  
 Au film, quantum size effect, field emission study 0-70849  
 Bi, film, size effect of carrier heating, surface scatt. (*Russian*) 0-100474  
 Bi thin film, structure and electronic props. 0-70562  
 Cu, screening charge density round  $\Delta Z = -1$  impurities, vacancies, NQR study 0-103897  
 Cu wire, negative longitudinal magnetoresist. size effect 0-80252  
 Cu-Ni(Pd)(Pt), dil., screening charge density round  $\Delta Z = -1$  impurities, vacancies, NQR study 0-103897  
 Cu<sub>2</sub>S,  $1 \leq x \leq 2$ , quantum temp. size effect and magnetism (*Russian*) 0-103764  
 Fe alloys, amorphous, saturation magnetisation, Curie temp. and size effect 0-65815  
 Fe films, thickness variations in extraordinary and spontaneous Hall coeffs. 0-97013  
 FeBO<sub>3</sub>, size effect during parametric spin wave excitations (*Russian*) 0-103824  
 Ge, ambipolar hot-carrier size effect kinetics 0-107799  
 Hg, solid, resistivity ratio, 1.65 to 234K 0-59952  
 n-InSb, spin polarisation, anisotropic size effect, effect on CESR signal 0-70743  
 Mo, longwave dopplers, nonlocal Hall effect, surface impedance, size effect (*Russian*) 0-80253  
 PMMA, resonance size effect in space charge relaxation 0-75937  
 Pb, single and polytextured thin films, band struct., tunnelling spectroscopy 0-80169  
 PbS(Se), valence band struct. determ. by optical absorpt., size quantization effects 0-59871  
 Pd film, quantum size effect, field emission study 0-70849  
 Re, Fermi surface, RF size effect, temp. depend. 0-65424  
 W, longwave dopplers, nonlocal Hall effect, surface impedance, size effect (*Russian*) 0-80253

# skin

blood flow, reflex control by skin temp., role of core temp. 0-85427  
 ear, mouse, fractionation effects in response to combined heat and X-rays 0-76805  
 electrocutaneous information transmission system using stimulus energy control device (*Japanese*) 0-101280

# skin continued

exercise thermoregulation after 14 days of bed rest 0-97865  
 keratinocytes, dose-dependent vol. changes after X-irrad. 0-61652  
 light absorption and scatt., theoretical and expt. study, in vivo 0-101219  
 malignant melanoma, thermal neutron capture therapy, in vitro radiobiological anal. 0-104657  
 microwave heating combined with radiation therapy, skin and tumor thermal enhancement ratios 0-67192  
 perfusion, quantitative meas. with <sup>133</sup>Xe 0-81707  
 radiation fibrosis after  $\beta$ -irrad. and attempt at suppression, guinea pig expts. 0-72243  
 resistance measurements, collection and off-line processing (*German*) 0-67273  
 senescent, increased susceptibility to  $\beta$ -irrad., mouse obs. 0-104656  
 temperature rises, thermal props. of dry metal-foil dispersive electro-surgical electrodes 0-98171  
 UV radiation physics and the skin, review 0-81661  
 vasomotor thresholds, squirrel monkey, central and peripheral temp. effects 0-97866  
 water exchange of reptile epidermis, the lipid barrier 0-97875  
 X-irradiation, response to single acute exposures, epidermal cell changes quantification, swine expts. 0-72245  
 X-irradiation and microwave heating, combined effects, pig 0-94290  
 X-irradiation combined with microwave heating, response of pig skin 0-61653  
<sup>137</sup>Cs-irradiation, response of pig skin, various schedules of irrad. 0-72237  
<sup>137</sup>Cs-irradiation response, pig obs. 0-67161  
 Na<sup>+</sup> saturation kinetics in frog skin, compartmental aspects 0-67050

# skin effect

see also anomalous skin effect  
 AC distribution in solid turns with skin effect, calc. (*German*) 0-69319  
 conducting media, EPR line shape, magnetoresist. effect 0-84638  
 doped conducting media, low-freq. props., EM wave reflection 0-103715  
 EM wave penetration into plasma, permittivity sign changes (*Russian*) 0-100477  
 intermediate state dynamics in superconducting wire 0-88697  
 magnetic star polarity reversal, appl. of skin effect approx. 0-62010  
 metal, light refl., nonlinear thermo-optic effect at high intensity 0-93289  
 metallic hydrides, solid echo amplitude and phase, skin effect 0-108115  
 thin metallic plate in strong mag. field, electron scatt. elec. cond. theory (*Russian*) 0-59974  
 Cd film, surface RF impedance in strong mag. fields (*Russian*) 0-92920  
 W film, surface RF impedance in strong mag. fields (*Russian*) 0-92920

# sky

see also night sky; sky brightness  
 altazimuth sky scanner optical system, polarization characts. 0-77123  
 clear sky conditions, solar radiation and illumination simultaneous meas. 0-81985

# sky brightness

see also airglow; twilight  
 aerosol above Black Sea, spectral transmission and sky brightness obs. (*Russian*) 0-94603  
 auroral sky background elimination with stellar chopping photometer 0-72776  
 background estimation on starfield plate 0-67577  
 clear daytime sky, brightness rel. to aerosol scatt. indicatrices determ. in 0.55 to 2.4  $\mu$ m region (*Russian*) 0-94600  
 daytime sky brightness fluctuations, due to aerosol layer (*French*) 0-81959  
 diffuse solar radiation below overcast sky, ang. distrib. 0-85719  
 IR spectroradiometric meas., 7 to 14  $\mu$ m, comparison with LOWTRAN-4 predictions 0-61897  
 meteoric nightglow, review of historical obs. 0-94761  
 night sky, Mitaka, Japan (*Japanese*) 0-82067  
 photon, spectra of gamma rays backscattered by infinite air (skyshine) 0-101436  
 planetary atmosphere, zenithal brightness near terminator due to light scatt. by optically thin atmosphere 0-109382  
 three dimensional spatial autocorrelation function meas. 0-67576

# sky surveys see astronomical catalogues

# Slater-type orbital calculations see STO calculations

# slider-type see calculating apparatus

# sliding contacts, electrical see electrical contacts

# slip

see also kink bands; plastic flow  
 alloys, dislocation stress-velocity depend. 0-96537  
 BCC crystal, cyclic deformation, irreversible glide and shape changes 0-103356  
 binary, ternary oxides, dislocation motion and high temp. plasticity 0-59468  
 brass, rolling texture development and deform. struct., shear bands effect (*Japanese*) 0-84952  
 brass, two phase  $\alpha/\beta$  bicrystal, transgranular slip and fracture across an interface 0-81150  
 $\alpha$ - $\beta$  brass, two phase bicrystal, fatigue 0-108520  
 $\beta$ -brass, uniaxial tension and compression, cyclic stress-strain behaviour 0-97551  
 camphor, rhombohedral, polycryst., compressive deform. and dynamic recryst. 0-71698  
 carbonate minerals, deform. twinning mechanisms 0-79814  
 climb process, of edge dislocation, effect of glide forces 0-70195  
 collective behaviour of dislocations, HVEM study (*French*) 0-65006  
 creep, irrad. induced in transient irrad. environments 0-92598  
 creep, irradiation induced, correlation of theory with expt. evidence 0-88255  
 creep, irradiation induced, dislocation glide enabled by preferred absorption of point defects 0-88250  
 creep and growth, radiation induced, fundamental mechanisms 0-92596  
 crystalline materials, in situ deform. by high voltage electron microscopy 0-103352  
 crystals, photogrammetric obs. method 0-100975  
 cubic crystals, compression test, double slip kinematics 0-65005  
 diamond, synthetic, oxidized in fused salts, etch features 0-97604  
 discrete obstacle model, dislocation and stress field distrib. 0-79794  
 dispersion-strengthened alloys, threshold stress for creep 0-93626  
 earthflow slope formation in Hong Kong 0-109144  
 elastic layer pressed against substrate, separation and slip caused by tensile load 0-96536



## slip continued

- eutectics, single grained, directionally solidified, anisotropic yielding behaviour 0-103412  
 FCC material, irradiation induced creep, climb induced glide model 0-89292  
 fracture along planar slip bands 0-107262  
 grain boundaries, interfacial structure effects on high temp. mechanical behaviour 0-59480  
 ice, dislocation vel. theory, glide plane influence 0-79805  
 II-VI compounds, charged dislocations and plastic deform. 0-107264  
 metal, FCC, dislocation behaviour at high strain rates, US detection method, data analysis basis 0-85136  
 metal, polycrystalline, strain hardening, dislocation link length model 0-84953  
 metallic materials, fatigue life distrib. theoretical obs. near fatigue limit 0-59569  
 metals, FCC, 'brass to copper' transition in rolling textures 0-76246  
 naphthalene single crystals, steady creep obs. 0-75296  
 Nimonic 80A, order hardening, comparison between revised theory and expt. 0-93565  
 oxides, dislocation climb model 0-100230  
 quartz, subgrain boundaries, theoret. predictions and microscopic obs. methods 0-84187  
 Rene 80, dislocation behaviour during plastic deform. (*Japanese*) 0-108504  
 screw subboundaries as dislocation sources, creep 0-100234  
 shift-type packing defects, involving dislocation representations, influence on diff. pattern 0-107239  
 single crystals, homogeneous plastic deform. by dislocation glide (*French*) 0-84232  
 solid free boundary, slip line initial development, elastic-plastic problem 0-96196  
 steel, austenitic stainless, irradi. creep of type 316 in HVEM 0-97523  
 steel, ferritic stainless, embrittlement 0-85041  
 steel, ferritic-martensitic, fatigue crack tip plastic zone (*Japanese*) 0-71738  
 steel, low C, initial stages of plastic deform. (*Japanese*) 0-93618  
 steel, low-alloy, plastic deform. mechanisms under dynamic loading 0-100883  
 steel, microstructure of 0Kh16N15M3B after creep tests in BR-10 reactor, electron, microscope invest. (*Russian*) 0-92531  
 steel, mild, fractography study of shear mode fatigue crack growth by etch pits (*Japanese*) 0-108545  
 steel, pearlite, deform. and fracture mechanisms, HV SEM obs. 0-104243  
 steel, stainless, fracture and crack tip plastic zones, in situ obs. 0-108686  
 steel, stainless, in-situ obs. of deform. in HVEM 0-103338  
 steel, stainless, martensite nucleation mechanisms, HVEM obs. 0-104157  
 steel, stainless type 316, in-situ HVEM studies under ion beam irradiation 0-103396  
 triglycine fluoborillate, deuterated, dislocation line defect X-ray topographic analysis 0-59465  
 web dendrites, dislocations, stacking faults, X-ray topographic study (*Chinese*) 0-88148  
 Zircaloy, textured, interactive creep and growth, upper-bound evaluation 0-89293  
 Ag, dislocations gliding on (001) planes, bright field and weak-beam images 0-107266  
 Ag FCC crystals, compressively activated slip, theoretical latent hardening 0-65128  
 Ag halide crystals, dislocations, survey of post-war research 0-62449  
 Ag-Mg (18.5 wt.%), rheological study of crystallographic order on creep (*French*) 0-97548  
 AgMg, B2 intermediate phase, slip system, ordering energy and atomic size ratio depend. 0-59471  
 AgZn, B2 intermediate phase, slip system, ordering energy and atomic size ratio depend. 0-59471  
 Al bicrystal, plastically deformed, slip heterogeneities 0-79858  
 Al bicrystals, isaxial, fatigue crack initiation in grain boundary affected regions (*Japanese*) 0-89338  
 Al, deformed in uniaxial and equibiaxial tension, dislocation arrangements 0-108516  
 Al FCC crystals, compressively activated slip, theoretical latent hardening 0-65128  
 Al, fatigue crack initiation, pre-existing subgrain effect 0-97565  
 Al, initial stages of plastic deform. (*Japanese*) 0-93618  
 Al single crystal, latent hardening in tension 0-60878  
 Al single crystals, (100) oriented, deform. temp. effect on stage IV deform. (*Japanese*) 0-66587  
 Al single crystals, relation between axial orientation rotating and deform. banding 0-104206  
 Al, stationary creep in HVEM, cell struct. evolution 0-104242  
 Al, work of C. Crussard 0-62443  
 Al-Ag (7.27 wt.%), peculiarities exhibited during fatigue loading (*Chinese*) 0-71723  
 Al-Cu (4 wt.%), supersaturated and aged conditions, high strain deform. 0-60907  
 Al-Mg (0.3 wt.%) single crystal, dislocations obs. by high voltage electron microsc. 0-79796  
 Al-Zn-Mg (3.87, 1.79 wt.%), oriented growth of precipitates on dislocations, TEM obs. 0-108447  
 AlCu-NiCo (5 at.%),  $\theta'$  hardened, creep mechanism 0-85013  
 Al<sub>2</sub>O<sub>3</sub>, alumina, deformed by prismatic slip, HV TEM obs. of dislocations 0-108517  
 Al<sub>2</sub>O<sub>3</sub>, fine grained, basal slip and nonaccommodated grain boundary sliding 0-60916  
 AuMg, B2 intermediate phase, slip system, ordering energy and atomic size ratio depend. 0-59471  
 Bi, crit. resolved shear stress of two slip systems, compression tests, 77-538K 0-59470  
 Bi, strain hardening curve correlation with slip band nucleation stress spectra 0-70217  
 Cd crystals, X-ray topographic examination of basal dislocations during microplastic deformation 0-88156  
 Cd, single crystals, plasticity study during deformation by twisting (*Russian*) 0-93597  
 Cd, Hg<sub>1-x</sub>Te, dislocation motion, effect of lattice defects on microhardness (*Russian*) 0-70220  
 Co, glide ahead of terminating {10 $\bar{1}$ 2} twins 0-96545  
 Co, single crystal, cavitation erosion, role of twinning 0-107272  
 Co, single crystals, {11 $\bar{1}$ 2} twins, accommodation and form. 0-96540

## slip continued

- CsCl-type lattice, (111) superlattice screw dislocation motion, computer simulation 0-79793  
 CsI crystals, relation of struct. and bond type to slip geometry 0-88165  
 Cu, dimple spacing on intergranular creep fracture surfaces with slip band spacing 0-76345  
 Cu, dislocations gliding on (001) planes, bright field and weak-beam images 0-107266  
 Cu, near 29 grain boundary properties, boundary dissociation 0-100251  
 Cu polycrystal, fatigued, interior dislocation struct. 0-88147  
 Cu single crystal, latent hardening in tension 0-60878  
 Cu single crystals, neutron irradiated, secondary slip 0-88161  
 Cu, single crystals, neutron irradiated, stresses and secondary slip between overlapping and dislocation arrays 0-88162  
 Cu, single crystals, deformed in [001] and [111] axes, cell structs., TEM 0-70209  
 Cu single crystals, rel. to Bordoni peak, 10.2 and 30.6 MHz 0-66566  
 Cu, tensile deformed (110) orientated single crystal, recrystn., high voltage electron microscopy study 0-84958  
 Cu-Al (10, 16 at.%), influence of jogs on extension of dislocation nodes 0-84176  
 Cu-Al (11 at.%) single crystal, dislocation reactions during deform. twinning 0-79795  
 Cu-Al (5 wt.%), subjected to tension-compression fatigue, deform. and fracture strength (*Japanese*) 0-93644  
 Cu-Al<sub>2</sub>O<sub>3</sub>(SiO<sub>2</sub>)(TiO<sub>2</sub>) alloys, internally oxidised, plastically deformed, influence of particle form on primary loop nature (*French*) 0-103344  
 Cu-Bi (0.02 wt.%) alloy, intergranular fracture, Kossel X-ray diff. in SEM obs. 0-108579  
 Cu-Cr-SiO<sub>2</sub> system, age and dispersion strengthened, dislocation struct. around SiO<sub>2</sub> particles 0-108468  
 Cu-Cr(SiO<sub>2</sub>), single crystals, yield and pre-yield behaviour rel. to aging time 0-81103  
 Cu-Ni-Al (5, 2.5 at.%), precip. hardening (*Japanese*) 0-71663  
 Cu-Si (7 at.%), influence of jogs on extension of dislocation nodes 0-84176  
 Cu-SiO<sub>2</sub>, in-situ deform. in HVEM 0-103338  
 Cu-SiO<sub>2</sub>, low-temp. recovery creep, Orwin loop accumulation 0-81126  
 Cu-Zn, rheological study of crystallographic order on creep (*French*) 0-97548  
 Cu<sub>3</sub>Au, disordered [001]-orientated single crystals, plastic deform., TEM and slip line studies 0-97541  
 $\alpha$ -Fe whiskers, pure, ductile-fracture initiation, macroscopic obs. of deform. history and failure 0-85043  
 Fe-Al, single crystals, deform. at high temps. 0-81125  
 Fe-Cr-Co, ductile magnet alloys, mech. props. 0-85001  
 Fe-Mo(4.1 wt.%), steady state creep at high temps. 0-89316  
 Fe-N, single crystal, solid soln. softening, effect of interstitial N 0-97496  
 Fe-Ni-Cr based alloy, KhN35VTYu, temp. depend. of energy of fracture, influence of  $\gamma'$  phase (*Russian*) 0-81147  
 Fe-Si, fatigue fracture fractography in broad strain-amplitude range, in air and vacuum 0-81186  
 Fe-Si (3 at.%), deformation and electron bombardment, influence on dislocation struct., 20-500°C (*Russian*) 0-92536  
 Fe-Si (3 wt.%), electron irradiated, yield strength and elongation 0-76325  
 Fe<sub>3</sub>-Al, solid soln., rheological study of crystallographic order on creep (*French*) 0-97548  
 GaAs crystal growth, thermal and elastic const. evaluation 0-92586  
 GaAs, pulled, dislocation generation, thermoelastic anal. 0-79787  
 GaP, crystal, growth conditions rel. to dislocation struct. 0-88151  
 InBi single crystal, deform. mode under dynamic indentation 0-88163  
 InP single crystals, uniaxial compression deform. characts. 0-84991  
 InSb, X-ray topographic evidence of asymmetrical pre-yield behaviour 0-75229  
 KCl, crystal, isolated pore healing under press., dislocation struct. evolution (*Russian*) 0-100245  
 LiF bicrystal, high-angle tilt boundary and edge dislocation intersection effects 0-79836  
 LiF crystals, relation of struct. and bond type to slip geometry 0-88165  
 LiF, dislocation structure, influence of variable deform. temp. 0-70211  
 LiF, strain hardening curve correlation with slip band nucleation stress spectra 0-70217  
 MgO crystals, plastic deform. activation parameters, rel. between macroscopic and in-situ HVEM expts. 0-103355  
 MgO, fracture and crack tip plastic zones, in situ obs. 0-108686  
 MgO single crystal, impact wear characts. 0-76374  
 MgO, single crystal, tensile creep, stress induced dislocation structs. 0-96539  
 MgO-Li, mech. deformed crystals, imprinting of slip bands using Li impurities 0-59473  
 MgO:Al<sub>2</sub>O<sub>3</sub> spinel, plastic deformation at T<1000°C, slip systems 0-108505  
 MgO:Li<sub>2</sub>O spinel, high temp. deform., cryst. orientation effect 0-107263  
 Mo alloys, intercryst. fracture in ductile-brittle transition region, local internal stresses effect 0-81200  
 Mo extinction length  $\xi_{00}$  meas., electron energy influence 0-90935  
 Mo, fatigue of single crystals, dislocation struct. and strain localisation (*Russian*) 0-71741  
 Mo, single and polycrystals, struct. change during work softening, HVEM 0-103336  
 NaCl, dislocation density in monocrystal deformed under high hydrostatic press. 0-70216  
 Na<sub>2</sub>O-CaO glass, shear deform. under pyramidal indentations 0-84989  
 Nb-O system, solid soln. hardening and softening 0-71665  
 NbC single crystal, Vickers microhardness, slip mechanism 0-71732  
 $\gamma$ -NbH<sub>0.82</sub>, fracture, TEM obs. 0-108519  
 Ni, creep, irradi. induced with 17 MeV deuterons 0-93607  
 Ni, dislocations gliding on (001) planes, bright field and weak-beam images 0-107266  
 Ni, slip character, H effect 0-89287  
 Ni, structural changes, creep mechanism, multiple dislocation cross slip (*Russian*) 0-59476  
 Ni-Al, order hardening, comparison between revised theory and expt. 0-93565  
 Ni-Al, rheological study of crystallographic order on creep (*French*) 0-97548  
 Ni-Cr, partial dislocation, stacking fault TEM study (*Chinese*) 0-84174  
 $\gamma$ -Ni<sub>3</sub>(Al,Ti), single crystal, dislocation movement, HVEM obs. (*Japanese*) 0-108503

# slip continued

- Ni<sub>3</sub>Fe, mono- and polycryst., strain hardening, test temp. effects (*Russian*) 0-66531  
 Ni<sub>3</sub>Fe, polycrystalline alloy evolution of slip-line pattern during straining 0-107362  
 Pb, film, hillock formation by grain boundary sliding 0-107673  
 Pb, film, thermal strain, strain relax. above room temp. 0-59841  
 PbS, crystals, relation of struct. and bond type to slip geometry 0-88165  
 Pd<sub>40</sub>Si<sub>20</sub> amorphous alloy, slip deform. and crit. shear stress, using tensile testing machine 0-89321  
 Si, core structure of glide-set 90° and 30° partial dislocations 0-96523  
 Si, crack-tip dislocation pattern, X-ray topography (*French*) 0-107253  
 Si cross-slip of isolated dislocations at surface and in bulk 0-70215  
 Si, crystal defects and impurities interaction obs. by electron microscopic methods 0-65003  
 Si crystals, dynamic processes associated with stacking faults and deform. twins, HVEM in-situ obs. 0-103369  
 n-Si, deformed, thermal treatment effect on elec. cond. and dislocation mobility 0-107265  
 Si, slip, room temp., TEM obs. 0-79804  
 Si, slip dislocation nucleation during laser annealing 0-84179  
 SiC, effect of crystallographic anisotropy on Knoop microhardness 0-66626  
 Te, a-edge dislocated crystals, mobility anisotropy 0-107781  
 Ti, fast neutron irradi., twinning deform. at room temp. 0-65061  
 α-Ti, fatigue crack growth, influence of grain orientation, SEM study 0-108550  
 α-β Ti Widmanstätten alloy interfaces, elastic interact. stresses, effect on plastic flow onset 0-104218  
 Ti-Al-Mo-V (8, 1, 1 wt%), Widmanstätten colonies, fracture toughness 0-85031  
 β-Ti-Mo, thermal instability, hardness and tensile deform. (*Japanese*) 0-71703  
 β-Ti-V metastable alloys, fatigue crack propag. 0-60964  
 VC single cryst., Vickers microhardness, slip mechanism 0-71732  
 V<sub>3</sub>Si single cryst., creep deform. 0-71695  
 Y, polycryst., plastic deform. at different deform. speeds, dislocation glide (*Russian*) 0-93598  
 Y<sub>2</sub>O<sub>3</sub>, dislocation and plasticity dissociation 0-107247  
 YSeF, orthorhombic polytype 140, struct. study (*French*) 0-88102  
 Zn crystal, {1122}{1123} slip system, deform. stress, dislocation density depend. (*Russian*) 0-103353  
 Zn crystals X-ray topographic examination of basal dislocations 0-88156  
 Zn, line energy of basal screw dislocation, expl. determ. 0-88154  
 Zn, pure single cryst., fracture stress 0-104269  
 Zn, single cryst., contribution of basal dislocations to residual elec. resist. (*Russian*) 0-75539  
 Zn, twinning, influence of dislocation drag, mag. field effects 0-59472  
 Zn-Al (0.4 wt.%), intergranular slip during in situ superplastic deform. 0-96538  
 Zr alloys, creep and growth, irradiation induced, microstruct. depend. 0-93602  
 ZrO<sub>2</sub>, CaO stabilised, preferred slip system 0-66585

# small electric machines

- translation motors for position with micron precision (*German*) 0-86271

# small polaron conduction

- glass, high-field ionic and polaronic cond., dielec. relax., Poole-Frenkel theory 0-100351  
 magnetic semiconductors, small polaron form. and motion 0-96882  
 molecular crystals, electronic transport theory, local linear electron phonon coupling 0-65545  
 As<sub>2</sub>Se<sub>3</sub>, amorphous, transient electrical transport, general and unified treatment 0-59977  
 Na<sub>2</sub>O-B<sub>2</sub>O<sub>3</sub>-SiO<sub>2</sub>-As<sub>2</sub>O<sub>3</sub>(As<sub>2</sub>O<sub>5</sub>) glasses, DC and AC resist., bipolaronic hopping cond. 0-88558  
 Ni<sub>1-x</sub>Co<sub>x</sub>S<sub>2</sub>, elec. cond., thermoelec. power and optical meas. 0-59986  
 Ni<sub>2-x</sub>Se<sub>x</sub>, elec. cond., thermoelec. power and Hall effect meas. 0-65561  
 Se, amorphous, transient electrical transport, general and unified treatment 0-59977  
 Se-Te-Sb glasses, electronic transport 0-88579  
 Si, amorphous, transient electrical transport, general and unified treatment 0-59977  
 SiO<sub>2</sub>, amorphous, transient electrical transport, general and unified treatment 0-59977  
 V<sub>2</sub>O<sub>5</sub>-As<sub>2</sub>O<sub>3</sub>-RO, R=Ba, Ca, Pb, semicond. glass, electronic props. 0-88557  
 WO<sub>3</sub>-B<sub>2</sub>O<sub>3</sub>-ZnO semiconducting glasses, DC cond. and optical absorb. 0-107783

# small-size generators see small electric machines

# small-size motors see small electric machines

# smectic liquid crystals

- A phase, nucl. spin relax. by translational self diffusion 0-60442  
 A-phase, oscillatory convective instabilities, caused by heating from below 0-103239  
 A-phase, sub-Rayleigh oscill. 0-87774  
 A-phase, thermooptical recording, echo images 0-91928  
 4-alkanoyloxybenzylidene-4'-cyanoazobenzene series, influence of substituent on reentrant mesophases 0-88027  
 4-alkanoyloxybenzylidene-4'-cyanobiphenyl series, influence of substituent on reentrant mesophases 0-88027  
 4-alkanoyloxybenzylidene-4'-cyanostilbene series, influence of substituent on reentrant mesophases 0-88027  
 p-n-alkoxybenzoates of p-n-alkoxyphenyl, smectic A phases mol. struct. and elastic behaviour 0-59382  
 4-4'-n-alkoxybenzylideneamino-biphenyls, central Schiff's base linkage reversal effect on liq. cryst. props. 0-79683  
 4-4'-n-alkoxybenzylidene-4'-n-alkoxyanilines, reentrant nematic and smectic phases 0-88308  
 N-4-n-alkoxybenzylidene-4-n-alkylanilines, smectic polymorphism, calorimetric study 0-88307  
 2-4-n-alkylphenyl-5-(4-n-alkoxyphenyl)-pyrimidines, smectic polymorphism, calorimetric study 0-88307  
 binary mixtures, phase transitions, entropy, relation to smectic plane tilt angle 0-65203  
 butyloxybenzylidene octylaniline, liq. cryst. film, smectic B-A transition, mech. meas. 0-79918  
 butyloxybenzylidene octylaniline, two- and three-dimensional smectic B liq. cryst. film, long range order 0-96442  
 butyloxybenzylidene octylaniline film, freely suspended, smectic A layer spacing, optical determ. 0-64883

# smectic liquid crystals continued

- CBOOA, smectic-A reentrant nematic transition under press., X-ray obs. 0-59637  
 CBOOA film, freely suspended, smectic A layer spacing, optical determ. 0-64883  
 chiral, optics and electro-optics, kinematical diff. theory 0-92461  
 chiral structure in electric field, dielectric permeability, spontaneous polarisation (*Russian*) 0-75159  
 cholesteryl laurate-cholesteryl caprylate (75 wt.%), polymorphic behaviour, optical, elec. and dielec. meas. 0-65208  
 cholesteryl myristate, smectic A-cholesteric transition, tricritical behaviour, DTA and DSC study 0-65206  
 COOB film, freely suspended, smectic A layer spacing, optical determ. 0-64883  
 cyano compounds, liq. cryst. phases, incommensurate coexistent density fluctuations 0-79691  
 4-cyano-4'-octylbiphenyl, dielectric relax. anal. in nematic and smectic phases 0-108153  
 cyano-biphenyl series, nematogens and smectogens, props. characterised by even-odd effect 0-107046  
 4-cyanobenzoyloxy-4'-pentylstilbene, nematic, smectic A, and orthogonal smectic B phases 0-64890  
 cyanooctylbiphenyl, X-ray diff. study 0-79690  
 disclinations, rotation defects, topology (*French*) 0-79679  
 DOBAMBC, chiral smectic, ferroelec., press. and solute effects 0-103920  
 DOBAMBC, ferroelec. liq. crystals, elec. and optical props., appls. (*Japanese*) 0-88943  
 DOBAMBC, smectic A and ferroelec. smectic phases, <sup>13</sup>C NMR study 0-75153  
 p-n-dodecyl-4'-azobenzylidene p-azophenyl aniline, smectic phases, mol. order, EPR study 0-79693  
 EABAC, smectic A, nematic, and isotropic phases, NMR and quasielastic neutron scatt. obs. 0-88022  
 esters, SLC, ferroelectric behaviour, specific heat, spontaneous polarisation 0-75958  
 ethyl-p-azoxybenzoate, far IR and Raman spectra, smectic polymorphism 0-76022  
 ferroelectric, chiral smectic C phase, phys. props., review 0-75150  
 ferroelectric, fundamentals and display appl. 0-79676  
 ferroelectric, submicrosecond bistable electro-optic switching 0-84051  
 film, dislocation-mediated theory of two-dimens. melting predictions, light scatt. use as probe 0-92651  
 G and H phase code letters, recommendation for use 0-103241  
 4-n-heptyl-d<sub>15</sub>-oxybenzoic acid-d<sub>1</sub>, nematic and smectic phases, mol. and relative segmental order 0-96439  
 heptyloxyazobenzene, filamentary structures 0-107051  
 4-n-heptyloxybenzylidene-4'-n-hexylaniline, nematic and smectic phases, long mol. axis reorientation, LF dielec. dispersion 0-70124  
 4-n-heptyloxybenzylideneamino-4'-cyanobiphenyl, reentrant nematic phase and low temp. smectic phases 0-88031  
 4-n-hexyloxybenzylidene-4'-n-hexylaniline, nematic and smectic phases, long mol. axis reorientation, LF dielec. dispersion 0-70124  
 MBBA, fluorinated analogues, mesomorphic props. 0-70118  
 molecular conformation and orientational order, NMR studies, review 0-75151  
 nonlinear reversible hydrodynamics, external mag. field influence 0-75156  
 p-n-nonyloxybenzoic acid, smectic C phase, electro-optical effect (*Russian*) 0-92458  
 nonyloxybenzoic acid/cholesteric liq. cryst. mixtures, helix pitch, temp. depend. 0-64895  
 4-n-octyl-4'-cyanobiphenyl/4-n-decyl-4'-cyanobiphenyl mixture, dynamic characts. of electrooptical effect with memory 0-108183  
 4-n-octyl-d<sub>15</sub>-oxybenzoic acid-d<sub>1</sub>, nematic and smectic phases, mol. and relative segmental order 0-96439  
 octylcyanobiphenyl, crit. heat. capacity near nematic-smectic A transition 0-100323  
 p-n-octyloxy benzylidene-p-toluidine, mol. order, EPR VAAC probe 0-70114  
 optical properties, diffraction nature, differences between cholesteric and chiral smectic liquid crystals 0-70123  
 organic doublet radicals in nematic and smectic liq. crystals., ENDOR obs. 0-91585  
 p-alkoxybenzylidene-p'-amino-2-chloropropyl-cinnamate, chiral smectic, dielec. props. 0-96441  
 p-nitryl 4-(4-n-dodecyloxybenzylidene-amino)-cinnamate, X-ray studies in smectic I phase 0-70119  
 4-n-pentyl-phenylthiol-4'-n-octyloxybenzoate, smectic A-smectic C phase transition, high-resolution X-ray study 0-79921  
 4-n-pentylbenzenethio-4'-n-alkoxybenzoates, birefr., crit. behaviour near smectic A-C transition 0-80745  
 N-4-n-pentylbenzylidene-4-n-hexylaniline (50.6), unclassified smectic phase 0-75157  
 phase transition, smectic A-nematic, liq. cryst. binary mixture, birefringence study 0-59638  
 4-phenylbenzylidene-4'-n-alkoxyanilines, central Schiff's base linkage reversal effect on liq. cryst. props. 0-79683  
 salicidenanilines, SLC, ferroelectric behaviour, specific heat, spontaneous polarisation 0-75958  
 second sound excitation in insulating and conducting crystals 0-103244  
 smectic layers with tilted molecules, solid and fluid phases 0-96444  
 smectic-C, mol. orientation fluctuations in two-dimens., light scatt. obs. 0-93355  
 surface, statistical thermodynamics, local order parameter 0-88023  
 TBACA, chiral, smectic C\* and H\* phases, mol. orientational ordering, <sup>14</sup>N NQR study 0-75152  
 TBBA, mesophase identification by X-ray diff., review 0-100166  
 TBBA liquid crystal, monoclinic cell parameters of solid, smectic and metastable phases, temp. dependence 0-70122  
 terephthalylidene-bis-(4-n-alkylanilines), smectic polymorphism, calorimetric study 0-88307  
 unified model for bulk smectic-A, nematic and isotropic phases 0-79692  
 X-ray and light scattering obs., high resolution 0-92460  
 X-ray diff. studies, review 0-100166  
 Ni complexes, dithienes, nematic and smectic mesophases, synthesis and characts. 0-70120  
 Ni dithiene complexes, mesomorphic props. 0-88026  
 Pt dithiene complexes, mesomorphic props. 0-88026



**smell (physiological)** *see chemioception*

**smoke**

*see also air pollution; dust*

aerosols, optical absorption to extinction ratio, photoacoustic determ. 0-8459

dusty IR Test-1 lidar obs., transmission meas. 0-99625

metal oxide smoke particles prepared by gas evap., morphology and coalescence growth 0-97738

particle shape effect on low freq. absorpt. 0-99626

silicate smokes, vapour-condensed, 800 to 130 nm extinction and interstellar extinction curve 0-82180

smoke/dust cloud temporal analysis algorithm 0-98484

C smokes, vapour-condensed, 800 to 130 nm extinction and interstellar extinction curve 0-82180

K smoke particles, optical props. 480 to 620 nm, rel. light scatt. cross sections meas. 0-97293

MgO, particle size distrib. 0-104471

SiC smokes, vapour-condensed, 800 to 130 nm extinction and interstellar extinction curve 0-82180

**snap off varactors** *see varactors*

**Snoek effect**

metals, BCC, under elastic stress, Snoek peak height determ. 0-65153

Fe, impure, Snoek peak figures in various strain amplitude ranges 0-66562

$\alpha$ -Fe, neutron irradiated, mobile C atom trapping, anelastic and magnetic relaxations 0-100306

V, determination of effect of H on elastic moduli 0-75288

V-H single crystals, rel. to elastic consts., temp. depend., H effects 0-65663

**Snoek-Koster relaxation** *see anelastic relaxation; dislocation damping*

**snow**

acid precipitation in the Pittsburgh, Pennsylvania area 0-94129

acidity of NW Africa snowfields, 1977-79 obs. 0-98370

education, snow and avalanche phenomena 0-57044

Germany, weather forecast for New Year's Day 1978-9, moist baroclinic model (*German*) 0-77065

Himalaya, snowfall during summer 0-72620

Kashmir region, study of chemical components 0-94594

laser beam, intensity fluctuations in snowfall (*Russian*) 0-94602

measurement of snowfall, dual-gauge and Wyoming shield systems 0-61928

New York State, changes in local snowfall in four cities 0-105044

pack snow water on Mt. Everest, mass spectrometric chem. anal. of D,  $^{17}\text{O}$  and  $^{18}\text{O}$  (*Chinese*) 0-77016

passive microwave obs. from Nimbus satellites 0-101422

permittivity and attenuation, 4-12 GHz 0-85692

pesticides and heavy metals in Bavarian snow 0-61488

pollution, atmospheric, metal and S content in deposited snow, effect of human activity compared to volcanoes (*French*) 0-67018

prediction of snow, with 10-level model 0-82025

radiometry in 3 to 60 mm wavelength region, rel. to snow parameters investigation 0-72561

rollers, form, at Coningsby, Lincolnshire (1979 January 2) 0-72568

snowflake, size and falling velocity meas. using laser Doppler velocimeter 0-68185

water equiv. of dry snow, active and passive microwave response 0-72563

wetness, active and passive microwave response 0-67382

wind interaction with dry snow and bare ice surface 0-109181

**SNR** *see supernova remnants*

**societies**

Illinois climate centre, review 0-77118

optical standard test method development by ASTM 0-74528

**sociological effects** *see economic and sociological effects*

**sockets (electrical)** *see electric connectors*

**sodar** *see sonar*

**sodium**

*see also nuclei with .....*

abundance in M13 red giants, evidence for protocluster gas inhomogeneities 0-82439

adsorbed on Al, adatom valence-level position variation 0-88611

adsorbed on Cu (111), UPS study of surface electronic struct. 0-80350

adsorbed on Ni, photoemission, directional memory effects 0-100753

adsorbed on Ni(001), photoelectron diffr. effects in core-level photoemission 0-76144

adsorbed on Ni(100), photoelectron diffr. aximuthal patterns, struct. sensitivity 0-107644

adsorption on V, effect on Br<sub>2</sub> chemisorption 0-101039

arc lamp, light-induced ignition method 0-77599

atmosphere, enhanced Na and nightglow, space lidar obs. 0-101466

atom,  $^{23}\text{P}$  photodissoc. product, fine struct. anal. 0-78665

atom, adsorption on B-Al<sub>2</sub>O<sub>3</sub>-Na<sub>2</sub>O, surface electronic struct. 0-75431

atom, cyclic interaction with circularly polarised laser radiation 0-78581

atom, D doublet of nightglow, excitation and abundance determ. 0-98497

atom, D-lines, inert gas broadening, photon echo meas. 0-91475

atom, damping const. in acetylene-air flame, Lorentz collisions, mag. field effects 0-66805

atom, effective potentials, energy levels 0-106263

atom, electron elastic and inelastic scatt. 0-91672

atom, excited 4D and 5S state, absolute photoionisation cross-section 0-99488

atom, four- and six-photon resonance spectra (*Russian*) 0-91527

atom, high Rydberg states, quenching in strong 1.06  $\mu\text{m}$  laser field 0-95559

atom, incoherent scatt. factors calc. by direct integration over impulse approx. Compton profiles 0-102475

atom, K-shell ionisation by ultrarelativistic electrons, density effect 0-99576

atom, long range and temp. depend. interaction with Re surface, theory 0-59802

atom, matrix isolated in Ne, absorpt. and emission spectra 0-99465

atom, overlapping autoionisation lines, interference effects 0-91677

atom, photofragment of NaBr, non-Gaussian line shape, level shifting and velocity inversion 0-58182

atom, photoionisation and fluoresc. meas., reson. radiation illum. 0-83314

atom, Rydberg states, millimetre spectrosc. 0-99469

atomic beam, laser beam irradi., reson. fluoresc. intensity, Bloch model calcs. 0-58206

atomic fluorescence, near resonant scatt. and collision induced (*Chinese*) 0-63582

**sodium continued**

atomic fluorescence detection in air-acetylene flame, harmonic saturated spectroscopy method 0-104472

atomic jump processes, quasi-elast. neutron scatt. study 0-84317

atomic vapours, three-level system, collisional effects in saturation spectroscopy 0-78579

atoms,  $3^2\text{S}_{1/2}$ - $3^2\text{P}_{3/2}$ , spectral distrib. and collisional depolarisation of laser light, D<sub>2</sub> fluorescence 0-58209

atoms, excited, electron scatt. at low energy, total cross section 0-63821

atoms, fluoresc. excitation profile, laser saturation broadening in flames obs. 0-95568

atoms, fluoresc. selective detect. by laser radiation 0-83312

atoms, motion in optical freq. radiation trap 0-78818

atoms, saturation spectra, crossover signals, effect of atomic alignment, optical pumping 0-58202

atoms cooling by resonant laser radiation (*Russian*) 0-74155

Auger electron emission due to ion collisions with solid targets (*French*) 0-104031

Auger spectra, KLL and KLV, screening effects and plasmon gains 0-80913

boiling detection in LMFBR, power spectral density surveillance systems 0-68740

classical plasma frequency in long-wavelength limit, quantum correction 0-107728

clouds on Io, form, by micrometeoroid impact 0-77330

colon, turtle, active Na transport via an electrogenic Na-K exchange pump 0-108856

Debye-Waller factors, extended de Launay model calcs. 0-70352

desorbed atoms, ang. and velocity distrib. 0-75428

determination in minerals, electron probe analysis with low temperature sample holder (*French*) 0-85248

diffusion lateral, of ions at Si-SiO<sub>2</sub> interface, neutralisation in presence of Cl 0-92986

doubly occupied Wannier functions, constructive definition 0-75492

education, Rydberg states, anomalous fine struct., perturbation model 0-57035

elastic constants, appl. of model pseudopot. to elastic consts. 0-59845

entropy change on melting of simple substances, thermal expansion, configurational entropy 0-59630

equilibrium struct. and phys. props., pseudopot. method 0-96778

erythrocytes, rabbit, increased passive efflux of  $^{22}\text{Na}$  and  $^{86}\text{Rb}$  on microwave irradi. 0-108957

evaporation from slot type capillary structs., crit. heat fluxes 0-74854

Fermi surface distortions, model pot. 0-80157

filtration of Na-fire aerosols in LMFBR 0-68853

ground state of solids, spin density functional method, binding energy, compressibility 0-65477

Gruneisen parameter, press. depend. 0-65184

Hall coefficient, quasiclassical Boltzmann eqn. calcs. 0-103678

hardfacing materials, friction characts. in high temp. Na (*Japanese*) 0-89356

impurity at glass-metal seal interface, composition and conc. determ. by AES 0-76587

ion implantation in LiF, migration, segregation, effect on optical props. 0-100269

ion source, HF, proton yield increase, influence of various admixtures to H<sub>2</sub> obs. 0-57422

ionisation interference, in Ebert spectrograph with 5 kW ICP unit 0-86453

IR and optical props., surface-plasmon-mediated absorpt. mechanism 0-93308

isoelectronic sequence, X-ray spectra 0-87071

K $_{\alpha}$  X-ray satellite struct. and KLL Auger electron spectra, solid-state effects 0-89089

liquid, boiling hazard in LMFBRs (*French*) 0-78402

liquid, diffusion coefficient for model potentials through mean square displacement 0-70098

liquid, evaporation from capillary-porous struct., capillary restriction in initial stages 0-107609

liquid, interionic interaction theory, pseudopotential calcs. (*Russian*) 0-79675

liquid, linear pot. and elec. resist., calcs. 0-65519

liquid, mean spherical approx. and effective pair pots. 0-70099

liquid, O<sub>2</sub> pot. and O<sub>2</sub> distrib. coeffs. between alkali and struct. metals 0-65231

LMFBR, liquid Na-limestone concrete interaction following HCDA, US meas. 0-78412

LMFBR, molten UO<sub>2</sub> fuel-Na coolant thermal interaction, characterisation of fragmented fuel 0-68774

LMFBR, Na purification system, cold traps and plugging indicator 0-99209

LMFBR Na boiling, two-phase flow calculations in low-pressure systems 0-103068

LMFBR structure materials in liquid Na, capsule type creep tester (*Japanese*) 0-108653

magnetic property volume depend., Knight shifts, electron spin response 0-88729

metal impurity effect on residual elec. resistance (*Russian*) 0-84457

MHD generators, optimisation for maximum electrical efficiency, output and power factor (*Rumanian*) 0-64793

MHD laminar flow, longitudinal dynamic effects determination for Na (*Rumanian*) 0-64792

molecular laser, optically pumped, review 0-58519

molecule, absorpt. and relax. const. determ. by optical laser pumping method 0-102550

molecule, laser-induced dissoc., polarisation of atomic fluorescence obs. 0-78569

molecule, triplet satellite band obs. in self-broadened D-line very far blue wing 0-95688

molecule in free jet expansion, internal-state distribution 0-83403

muonic,  $2s^{1/2}$  level decay channel concurrence, neutral current effects observation (*Russian*) 0-83526

optical properties by spectroscopic ellipsometry, review 0-103929

phonon limited resistivity struct. depend., Umklapp scatt., elastic consts. 0-88532

plasmon satellite struct. in (e,2e) process 0-96809

positronium, formation in positron+alkali metal atom collisions, first Born approx. 0-83525

positronium formation in positron+alkali metal atom collisions, pseudopot. calcs. 0-83524

Rydberg atom, electron collisions 0-63833

## sodium continued

- self-weldability of metals and alloys in high temp. Na (*Japanese*) 0-89392
- solid and liquid eqns. of state, melting curve 0-103448
- sputtering, thermal and collisional effects influence on energy spectra 0-66370
- steel, stainless 304, metallurgical factors on the corrosion and mass transfer in liq. Na (*Japanese*) 0-71804
- thermal expansion, temp. depend., vacancy effects 0-79962
- thermopower and elec. cond., relationship at low temps. (*Russian*) 0-92882
- trace identification in neutral-beam research 0-95401
- vapour, CaF<sub>2</sub> coating apparatus for glass, Na-resistant cell 0-90874
- vapour, IR absorpt. bands 0-102507
- vapour, laser induced population grating 0-69466
- vapour, soliton interactions, self-induced transparency, numerical plane wave simulations 0-64117
- vapour, superradiance, quantum beat spectra 0-106311
- vapour, Zeeman coherence, transient and stationary, polarisation spectroscopy 0-58212
- vapour deposition rates and gas flow patterns in LMFBR 0-68732
- vapour thin cell forward phase conjugation obs. 0-78917
- XPS, plasmon gains as monitor of incomplete relax., interference effects and sudden to adiabatic limits transition 0-66390
- zeolite, hydrated Na-Y, <sup>23</sup>Na pulsed NMR free induction decay 0-84660
- AgBr:Na<sup>+</sup>, correlated diffusion of impurities, nuclear spin relax. meas. 0-108094
- CaF<sub>2</sub>:Na<sup>+</sup>O<sup>2-</sup>, thermal depolarisation obs. of defect clusters 0-71299
- CaS:Ce, Na phosphor, photoluminescence and excitation spectra 0-89049
- CdF<sub>2</sub>:Na, ionic cond. investigation by complex admittance method 0-100352
- CdS:Na, Hagemark theory, green edge emission line intensity 0-75517
- CsF:Na, F-centres, saddle-point configuration, molecular model parameter 0-107234
- CsI:Na, light yield under charged-particle bombardment 0-93409
- CsI:Na, X-ray irradiated, optical and ESR studies in IR absorption band 0-80828
- CsI:Na<sup>+</sup>, luminesc. processes 0-103989
- He+Na<sub>2</sub>, rotational inelastic scatt., uniform semiclassical sudden approx. 0-99544
- KCl cryst., Sr and Na impurities radial distrib., influence of form of crystn. front 0-107312
- KCl:Na, F<sub>B</sub> centre energy levels 0-107738
- LiNbO<sub>3</sub>:Na structure field stability limits, LPE film growth, SAW velocity 0-80102
- LiNbO<sub>3</sub>:Na<sup>+</sup> film, improvement in temp. stability and SAW device appls. 0-75939
- Na I, atomic spectrum, series formulas 0-99466
- Na I lines in solar spectra, non-mag. polarisation, centre-to-limb var. 0-67678
- Na I solar D-lines, non-mag. polarisation 0-63569
- Na II, spectrum, config. superposition and transition probabilities calcs. 0-87082
- Na<sup>+</sup> activity of epithelial cells, liquid-ion exchanger microelectrode estimates, resistive artifacts 0-89909
- Na<sup>+</sup> and Cl<sup>-</sup>, interdependence of transport in dog tracheal epithelium 0-61519
- Na<sup>+</sup>, atomic core states, antishielding effects calcs. 0-83299
- Na<sup>+</sup>, H<sub>2</sub>O affinity, ab initio SCF calcs. 0-58125
- Na<sup>+</sup> intracellular activity rel. to Na<sup>+</sup> transport across a tight epithelium 0-67051
- Na<sup>+</sup>, mobility and longit. diffusion coeffs. in Kr and Xe 0-106866
- Na<sup>+</sup> saturation kinetics in frog skin, compartmental aspects 0-67050
- Na<sup>+</sup>, second order correl. energy, Z depend. of irreducible-pair energies 0-91417
- Na/S battery development program at GEC for utility lead levelling with beta alumina solid electrolyte 0-61327
- Na/S cells operating with dissolved catholyte, elec. props. 0-101085
- Na/S load levelling batteries, optimisation of fabrication process of beta Al<sub>2</sub>O<sub>3</sub> solid electrolyte 0-72035
- Na/S traction batteries, development progress and problems, review 0-61326
- Na-graphite intercalates, preparation, struct. 0-103307
- Na-Hg high-pres. discharge, Na reson. radiation, self-reversed maxima shifts 0-92411
- Na-Xe excimer lasers, high-power discharges, models 0-69373
- Na+H<sup>+</sup>, 2p<sup>3</sup>3s<sup>2</sup>P<sub>3/2</sub> state alignment, collisionally induced, impact parameter calc. 0-83474
- Na+H<sup>+</sup>(H), single-electron capture total cross sections 0-91656
- Na+H(Ne)(Kr) vel.-changing collisions, effect on 2 photon and stepwise absorpt. line shape 0-87221
- Na+He<sup>+</sup>, crossed beams, l-changing collisions, n-depend. 0-58345
- Na+inert gas, non-Lorentzian spectral line shape 0-106297
- Na+inert gas, Rydberg states transitions, broadening cross-sections meas. 0-69110
- Na+methyl iodide, anisotropic interactions from double rainbow struct., interaction pot. meas. 0-99540
- Na+Na, crossed-beam collision, laser-induced Penning and assoc. ionisation, struct. obs. 0-83476
- Na+Na, electronic-field pot. curves determ. for large interatomic distances, excitation cross sections calc. 0-95704
- Na+Ne, potential curves from a model potential (*French*) 0-78685
- Na+Ne(Ar)(Xe), 3<sup>3</sup>P-3<sup>3</sup>D line broadening obs. 0-78684
- Na+t-butyl bromide, anisotropic interactions from double rainbow struct., interaction pot. meas. 0-99540
- Na+t-butyl chloride, anisotropic interactions from double rainbow struct., interaction pot. meas. 0-99540
- Na+t-butyl iodide, anisotropic interactions from double rainbow struct., interaction pot. meas. 0-99540
- Na+Xe+h $\nu$ , collisions in presence of nonresonant lasers 0-99567
- Na<sub>2</sub>, <sup>3</sup>Σ<sub>g</sub><sup>+</sup>-<sup>1</sup>Σ<sub>g</sub><sup>+</sup> excimer emission, ab initio calcs. 0-91608
- Na<sub>2</sub>, molecular electronic struct. for lowest <sup>3</sup>Σ<sub>g</sub><sup>+</sup>, <sup>1</sup>Σ<sub>g</sub><sup>+</sup>, <sup>3</sup>Π<sub>g</sub>, <sup>1</sup>Π<sub>g</sub>, <sup>3</sup>Π<sub>g</sub> and <sup>1</sup>Π<sub>g</sub> states 0-63738
- Na<sub>2</sub>, photodissoc., <sup>2</sup>P products, at. fine struct. anal. 0-78665
- Na<sub>2</sub>, Rydberg state, two-step polarisation labelling 0-87053
- Na<sub>2</sub><sup>+</sup>(H<sub>2</sub>O)<sub>n</sub>, clusters, gas phase, high press. mass spectrometry, atmospheric implications 0-58436
- Na<sub>2</sub>+Ar, differential cross sections meas. for rot. energy transfer process, obs. of halos 0-91643
- Na<sub>2</sub>+He, rot. transitions differential cross sections, laser fluoresc. meas. 0-63771

## sodium continued

- Na<sub>2</sub>+He, rotationally inelastic scatt., state-to-state differential cross sections 0-74234
- Na<sub>2</sub>+Xe rate const., energy corrected scaling laws 0-69225
- <sup>22</sup>NaKr, red wing radiation and pot. 0-87180
- <sup>22</sup>Na injection, testis mass loss obs., mouse 0-67156
- <sup>22</sup>Na injection or X-irrad. of mice, sperm count reduction and abnormal sperm increase 0-108961
- <sup>23</sup>Na in heterogeneous system, nuclear mag. relaxation time determ., rel. with dimensions of colloidal particles 0-75876
- <sup>24</sup>Na, laser induced nuclear orientation 0-57680
- Na<sub>2</sub>\*+Xe, rot. energy transfer, vel. depend. 0-95715
- Na(3<sup>3</sup>P), electronic to vibrational energy transfer in collisions with simple molecules 0-63769
- Na(3<sup>3</sup>P)<sub>1/2,3/2</sub>, laser induced flame chemistry, saturated mode fluoresc. meas. 0-89491
- RbF:Na, F-centres, saddle-point configuration, molecular model parameter 0-107234
- Si-SiO<sub>2</sub>:Na<sup>+</sup>, physics, electron and ion motion (*Dutch*) 0-60093
- SiO<sub>2</sub>:Na, ion trapping and mobility, energy levels 0-92985
- (U,Pu)C LMFBR fuel, Na-bonded, consequences of rapid Na loss on fuel behaviour 0-102238
- sodium alloys**
- Na-Cs, internal energy, heat of mixing, entropy, dielectric function 0-88340
- Na-Cs, liq., struct. factor, free energy of mixing, and electrochem. pot., thermodynamic calc. 0-96436
- Na-K, internal energy, heat of mixing, entropy, dielectric function 0-88340
- Na-K, surface tension theory for liquid mixtures 0-88404
- Na-K liq. alloy, Moelwyn-Hughes parameter calc. from US data 0-59375
- Na-K liquid alloys, struct., X-ray and neutron diff. meas. 0-107041
- Na-K liquid alloys, triplet correlation functions and thermodynamics, solute partial structure factor 0-64881
- NaPb alloy, compound-forming, vol. of mixing, conc. depend. 0-103484
- Pb-Na (8.4 at.%), supercond., surface flux pinning, crit. state model 0-97044
- sodium compounds**
- see also Rochelle salt; sodium alloys
- acid oscalate, neutron inelastic scatt. spectra in 2200-200 cm<sup>-1</sup> range 0-70327
- BO<sub>2</sub>-BO<sub>2</sub> 0-65252
- fluorescein-rhodamine B, energy transfer in luminescent mixed solutions 0-103976
- germanate crystals and glasses, struct. and stability, IR spectra meas. 0-64911
- halides, elastic constants, temp. derivatives at constant volume 0-59549
- β-Na<sub>2</sub>O-Al<sub>2</sub>O<sub>3</sub> low temp. ultrasonic vel. meas., temp. depend. 0-79885
- Na<sub>2</sub>Zn[SiO<sub>3</sub>], X-ray cryst. struct. determ., thermal vibration anisotropy allowance 0-92510
- NaCl, dislocation charge photostimulated variation kinetics (*Russian*) 0-79806
- NASICON solid electrolyte, processing and phys. props. 0-60820
- orthophosphates, anhydrous, struct. relationships w.r.t. fast ion cond. 0-107188
- oxalate:Cu<sup>2+</sup>, EPR studies 0-60408
- salt hydrates for heat storage in a solar heating system 0-67005
- salt hydrates for heat storage in solar heating system, based on extra water principle 0-67006
- sodium bentonite, Wyoming suspension, comparison of optico-optical scattering and birefringence 0-85226
- sodium dodecyl sulphate, polydisperse micellar solns., light scatt., size, shape and aggregation number calcs. 0-89531
- stearate, Langmuir-Blodgett multilayers, comp. and transfer mechanism 0-80125
- steel, low C, electroboronising by superimposed cyclic current, Na<sub>2</sub>CO<sub>3</sub>, B<sub>2</sub>C, NaCl, NaOH activator studies 0-85081
- tetraphenylboron sodium aq. soln., dielec. relaxation spectroscopy in microwave region, double-beam interferometry (*German*) 0-71309
- undecanoate/water system, lyotropic liq. cryst. struct. change due to polymerisation of amphiphilic component 0-59386
- zeolites, -A and -Y type, local coordination of Co(II) ions studied by X-ray absorpt. fine struct. spectroscopy 0-93434
- (Ag,Na)Br, ionic transport numbers, polarization cell method 0-59705
- (Ag,Na)Cl solid solns., ionic transport numbers, polarization cell method 0-59705
- AgBr-NaBr, thermodynamic props., metastable states and demixing 0-96660
- AgBr-NaBr, phase diagram, miscibility, binodal curve and demixing kinetics, X-ray meas. 0-96659
- AgNa(NO<sub>2</sub>)<sub>2</sub>, ferroelec., Raman scatt. and phase transitions 0-71349
- AgNa(NO<sub>2</sub>)<sub>2</sub>, ferroelec. cryst., Raman spectrum, phase transition, comparative anal. with NaNO<sub>2</sub> 0-88935
- AgNa(NO<sub>2</sub>)<sub>2</sub>, order-disorder ferroelec., influence of hydrostatic press. on polarisation dynamics 0-103913
- Ag<sub>2</sub>Na<sub>2-x</sub>Te<sub>2</sub>·<sup>1/2</sup>Te<sub>3</sub>O<sub>14</sub> (x=0.4), mixed tellurate, cryst. chem. and elec. cond. (*French*) 0-107150
- Al<sub>2</sub>O-Al<sub>2</sub>O<sub>3</sub>-MgO-Na<sub>2</sub>O, β'-alumina, structure, X-ray determ. 0-107148
- Al/AlCl<sub>3</sub>-NaCl/FeS<sub>2</sub> secondary cell, preliminary study 0-108793
- AlCl<sub>3</sub>-NaCl melt, n-TiO<sub>2</sub> electrode, electrochem. and photoelec. props. 0-81328
- β-AlO<sub>2</sub>-(Na,Li)<sub>2</sub>O, NMR, Raman and IR spectra, and X-ray diff., heat treatment induced changes 0-107508
- β-Al<sub>2</sub>O<sub>3</sub>-(Na,K)<sub>2</sub>O, equil. distrib. of ionic species 0-107511
- β-Al<sub>2</sub>O<sub>3</sub>-(Na,K)<sub>2</sub>O, model calcs. of cond. anomalies, pot. energies of cation arrangements 0-107510
- β-Al<sub>2</sub>O<sub>3</sub>-(Na,Li)<sub>2</sub>O, first-order quadrupole NMR obs. of cation distrib. and ion motion 0-108113
- β-Al<sub>2</sub>O<sub>3</sub>-(Na,Li)<sub>2</sub>O, ionic cond. and Raman spectra 0-107509
- β-Al<sub>2</sub>O<sub>3</sub>-(Na,Li)<sub>2</sub>O, ionic motion obs. using NMR and internal friction 0-108099
- β-Al<sub>2</sub>O<sub>3</sub>-(Na,Li)<sub>2</sub>O solid electrolyte, Li motion and activation obs. using <sup>7</sup>Li NMR 0-108100
- β-Al<sub>2</sub>O<sub>3</sub>-Li<sub>2</sub>O-Na<sub>2</sub>O, spin-lattice relaxation and Li motion 0-70451
- β'-Al<sub>2</sub>O<sub>3</sub>-Na<sub>2</sub>O, <sup>23</sup>Na NMR obs. of ionic diffusion, 180 to 800K, attempt freq. 0-108097
- β-Al<sub>2</sub>O<sub>3</sub>-Na<sub>2</sub>O, <sup>23</sup>Na NQR and two-dimens. diffusion, model analysis 0-108111



## sodium compounds continued

- $\beta$ -Al<sub>2</sub>O<sub>3</sub>-Na<sub>2</sub>O, <sup>27</sup>Al NMR obs., Na motion and cond. characts. 0-108096
- $\beta$ -Al<sub>2</sub>O<sub>3</sub>-Na<sub>2</sub>O, AC impedance, microstruct. and strength 0-100349
- $\beta$ -Al<sub>2</sub>O<sub>3</sub>-Na<sub>2</sub>O, AC ionic cond., dielec. and NMR relax. 0-59713
- $\beta$ -Al<sub>2</sub>O<sub>3</sub>-Na<sub>2</sub>O, adsorbed water effect on NMR lineshape and spin-lattice relax. time 0-108098
- B-Al<sub>2</sub>O<sub>3</sub>-Na<sub>2</sub>O, adsorbed of Na, surface electronic struct. calcs. 0-75431
- $\beta$ -Al<sub>2</sub>O<sub>3</sub>-Na<sub>2</sub>O, anomalous Na behaviour obs. using pulsed and CW NMR 0-108095
- $\beta$ -Al<sub>2</sub>O<sub>3</sub>-Na<sub>2</sub>O, colour centre ESR by localised tunnelling states 0-108073
- $\beta$ -Al<sub>2</sub>O<sub>3</sub>-Na<sub>2</sub>O, cond. plane struct. and energetics 0-92715
- $\beta$ -Al<sub>2</sub>O<sub>3</sub>-Na<sub>2</sub>O, development for Na/S battery 0-71615
- $\beta$ -Al<sub>2</sub>O<sub>3</sub>-Na<sub>2</sub>O, ENDOR meas. of defects 0-66074
- $\beta$ -Al<sub>2</sub>O<sub>3</sub>-Na<sub>2</sub>O, ionic cond. at room temp. 0-107513
- $\beta$ -Al<sub>2</sub>O<sub>3</sub>-Na<sub>2</sub>O, ionic cond. temp. depend., comparison with NASICON 0-107520
- $\beta$ -Al<sub>2</sub>O<sub>3</sub>-Na<sub>2</sub>O, low-energy excitation spectra, localised modes 0-59606
- $\beta$ -Al<sub>2</sub>O<sub>3</sub>-Na<sub>2</sub>O, low-temp. <sup>23</sup>Na satellite spectra, Na ion motion 0-108112
- $\beta$ -Al<sub>2</sub>O<sub>3</sub>-Na<sub>2</sub>O, motion of charge carrying ions, mol. dynamics simulation 0-107506
- $\beta$ -Al<sub>2</sub>O<sub>3</sub>-Na<sub>2</sub>O, NMR of <sup>23</sup>Na, elec. quad. interaction, 185 to 419K, ion motion obs. 0-108110
- $\beta$ -Al<sub>2</sub>O<sub>3</sub>-Na<sub>2</sub>O, nonstoichiometric, correl. effects in diffusion, Haven ratio, point defect interactions 0-107505
- $\beta$ -Al<sub>2</sub>O<sub>3</sub>-Na<sub>2</sub>O, potential energy distrib. and ionic motion 0-70455
- $\beta$ -Al<sub>2</sub>O<sub>3</sub>-Na<sub>2</sub>O, protonic, conductance and spectroscopy 0-70450
- $\beta$ -Al<sub>2</sub>O<sub>3</sub>-Na<sub>2</sub>O, single cryst. Raman scatt., cond. mechanism and cryst. struct. 0-66209
- $\beta$ -Al<sub>2</sub>O<sub>3</sub>-Na<sub>2</sub>O, single cryst., non-Debye capacitance 0-107497
- $\beta$ -Al<sub>2</sub>O<sub>3</sub>-Na<sub>2</sub>O, solid electrolyte, behaviour at high current density, sodium heat engine mode 0-61330
- $\beta$ -Al<sub>2</sub>O<sub>3</sub>-Na<sub>2</sub>O, struct. basis for superionic cond. 0-107498
- $\beta$ -Al<sub>2</sub>O<sub>3</sub>-Na<sub>2</sub>O, X-ray induced defects, EPR and ENDOR study 0-60456
- $\beta$ -Al<sub>2</sub>O<sub>3</sub>-Na<sub>2</sub>O doped with transition metal ions, complex plane anal. of impedance and admittance 0-70452
- $\beta$ -Al<sub>2</sub>O<sub>3</sub>-Na<sub>2</sub>O solid electrolyte, tube fabrication from cast ceramic tape 0-60819
- $\beta$ -Al<sub>2</sub>O<sub>3</sub>-Na<sub>2</sub>O solid electrolyte, processing and phys. props. 0-60820
- $\beta$ -Al<sub>2</sub>O<sub>3</sub>-Na<sub>2</sub>O solid electrolyte, strength degradation under electrolytic conditions 0-61329
- $\beta$ -Al<sub>2</sub>O<sub>3</sub>-Na<sub>2</sub>O solid electrolyte, heat treatment effects on ionic cond. and microstruct. 0-65293
- Al<sub>2</sub>O<sub>3</sub>-Na<sub>2</sub>O-CaO-SiO<sub>2</sub>-(B<sub>2</sub>O<sub>3</sub>) composite glasses, high strength, prod. by overlaying 0-89193
- Ba<sub>2</sub>NaNb<sub>2</sub>O<sub>7</sub> crystals, in Nd<sup>3+</sup>:YAG laser cavity, AM of optical second harmonic 0-78908
- Ba<sub>2</sub>NaNb<sub>2</sub>O<sub>7</sub>, X-ray powder diffraction data determ. (Chinese) 0-70170
- BaO-Fe<sub>2</sub>O<sub>3</sub>-Na<sub>2</sub>O glasses, high Fe<sub>2</sub>O<sub>3</sub> content, micromagnetic props. 0-65916
- BaO-Fe<sub>2</sub>O<sub>3</sub>-Na<sub>2</sub>O glass, rapidly quenched, mag. and ferrimag. props. 0-75744
- <sup>13</sup>C, CIDNP, obs. in reactions of organic and inorganic radicals during pulse radiolysis 0-63660
- CaCu<sub>2</sub>Ru<sub>2</sub>O<sub>12</sub>, synthesis, cryst. struct., mag. and elec. props. (French) 0-107151
- CaF<sub>2</sub>-AlF<sub>3</sub>-Na<sub>2</sub>AlF<sub>6</sub>-(Al<sub>2</sub>O<sub>3</sub>), phase equilibria, X-ray diffr. and DTA meas. 0-108409
- 10CaO.15Na<sub>2</sub>O.75SiO<sub>2</sub> glass, thermal cond., temp. depend. at low temps. 0-65322
- CdF<sub>2</sub>-NaF, colour centres, IR absorpt. and photocond. after UV irradi. 0-79784
- CdF<sub>2</sub>-NaF thin films, electroluminescence obs. at 77K (French) 0-80866
- EuNa<sub>2</sub>Mg<sub>2</sub>(VO<sub>4</sub>)<sub>3</sub>, disordered, thermal quenching of luminesc. 0-71472
- GeO<sub>2</sub>-Na<sub>2</sub>O, Na<sup>+</sup> partial dissociation investigated by elec. meas. 0-92716
- GeO<sub>2</sub>-Na<sub>2</sub>O borosilicate glass fibre prod. by phase separation and leaching 0-69558
- GeO<sub>2</sub>-Na<sub>2</sub>O glass, Raman spectra, struct. and crystn. 0-92463
- GeO<sub>2</sub>-Na<sub>2</sub>O glasses, equivalent cond., temp. depend., weak electrolyte theory appl. 0-107475
- KCl-CaCl<sub>2</sub>-NaCl, ternary phase diagrams, interactive computer program 0-71629
- KCl-NaCl mixed crystals, contact angles and free energies at solid/melt interface 0-64937
- KMg<sub>2</sub>LiSi<sub>2</sub>O<sub>10</sub>F<sub>2</sub>-NaMg<sub>2</sub>LiSi<sub>2</sub>O<sub>10</sub>F<sub>2</sub>, solid soln., solid solubility and swelling characts. 0-59660
- K<sub>1-x</sub>Na<sub>x</sub>Cl, impurity centre local vibr., comp. depend. of spectral parameters 0-79898
- K<sub>1-x</sub>Na<sub>x</sub>TaO<sub>3</sub> quantum ferroelectric, dielec. susceptibility 0-103922
- (Li<sub>0.63</sub>Na<sub>0.37</sub>)<sub>2</sub>O.2SiO<sub>2</sub>, short range struct. by pulsed neutron scatt. 0-59396
- Li<sub>2</sub>O-Na<sub>2</sub>O-B<sub>2</sub>O<sub>3</sub>-Al<sub>2</sub>O<sub>3</sub>-SiO<sub>2</sub> glass, Young's modulus and density, ion exchange effects 0-84982
- Mg(NO<sub>3</sub>)<sub>2</sub>-RNO<sub>3</sub> (R=Li, Na, K), thermogravimetric anal. of dehydration processes (Japanese) 0-66791
- MgO-NaCl refractory clinkers, R containing, densification, thermal treatment and phase composition effect (French) 0-76219
- Na borosilicate glass microsphere material, sintering, struct., strength props. (Russian) 0-108383
- Na salt of  $\beta$ -ketoaldehydes, configurations of anions in solutions studied by IR spectroscopy, H-bond form. 0-87117
- Na zeolites, electronic struct., quantum chemical study 0-69058
- Na-A zeolite, struct. obs. by high-resolution electron microscopy 0-84175
- Na-Co strip-chain silicates, structural-composition inhomogeneities 0-88122
- Na-Co-O system, synthesis and cryst. struct. determ. 0-107185
- Na-Mn-O system, synthesis of oxides 0-107185
- Na-zeolite, matrix, Te cluster superlattices, N and S type volt-ampere characts., elec. cond. (Russian) 0-70665
- Na<sub>2</sub>- $\beta$ -Al<sub>2</sub>O<sub>3</sub>, far IR absorpt., Bevers-Ross sites, interstitials 0-66241
- NaA neolyte, Hg cluster transition to paramagnetic state due to mag. field (Russian) 0-60183
- NaAlCl<sub>4</sub>, Raman spectra, cryst. struct. (French) 0-60578
- NaAlF<sub>4</sub>, dissoc. enthalpies, mass spectrometric determ., heat of form. 0-97720
- Na<sub>3</sub>AlF<sub>6</sub>, film on Si, fused quartz substrates, H<sub>2</sub>O absorpt., IR anal. 0-75446
- Na<sub>3</sub>AlF<sub>6</sub>-MgF<sub>2</sub> thin film deposits, quenched ageing by chopping 0-97364

## sodium compounds continued

- NaAlH<sub>4</sub> and Na<sub>3</sub>AlH<sub>6</sub>, molar heat capacity and thermodynamic functions, 10 to 300K 0-65243
- Na<sub>6</sub>Al<sub>6</sub>(Si<sub>0.99</sub>Ge<sub>0.01</sub>)<sub>6</sub>O<sub>24</sub>-2NaBr, Ge-doped sodalite powders, UV absorpt. band 0-71452
- Na<sub>6</sub>Al<sub>6</sub>Si<sub>6</sub>O<sub>24</sub>(NaX)<sub>20</sub>, X=Cl, Br or I, sodalites, thermal destruction of colour centres (Russian) 0-84169
- Na<sub>6</sub>Al<sub>6</sub>Si<sub>6</sub>O<sub>24</sub>Cl(Br)(I), cathodochromic sodalites, coloured crystals, tunnel and recomb. luminesc., temp. depend. (Russian) 0-66261
- Na<sub>6</sub>Al<sub>6</sub>Si<sub>6</sub>O<sub>24</sub>NaX<sub>(2-n)</sub>, (X=Cl, Br, I), X-ray irradi., thermal-erase cathodochromism and dihalide mol. centres (Russian) 0-66236
- NaBaZn glass, Eu<sup>3+</sup> centre symm. 0-100447
- Na<sub>2</sub>Be(SiO<sub>3</sub>), X-ray cryst. struct. determ., thermal vibration anisotropy allowance 0-92510
- Na<sub>0.5</sub>Bi<sub>0.5</sub>TiO<sub>3</sub>, phase transition, hysteretic behaviour 0-71330
- NaBr, EXAFS at high press. 0-97376
- NaBr Frenkel pairs, interactions forming enrichment centres 0-96518
- NaBr, gamma and additively coloured, dissolving in pure water, lyoluminesc. mechanism 0-100693
- NaBr, optically activated F-F centre conversion in mag. field 0-108253
- NaBr photodissoc., Na non-Gaussian line shape, level shifting and velocity inversion 0-58182
- NaBrO<sub>3</sub>, cryst., mechanoluminesc. spectra 0-97355
- NaBrO<sub>3</sub>, crystal gyrotropy, meas. in IR region 0-88957
- NaBrO<sub>3</sub>, X-ray Debye temp. 0-103440
- NaCN, multidomain birefr. solid, light scatt. and IR transmission spike 0-60587
- NaCN, Raman diffusion spectra, IR absorpt. in phases II and III (French) 0-84741
- Na<sub>2</sub>CO<sub>3</sub>, phys. props. related to phase transitions 0-96643
- Na<sub>2</sub>Ca<sub>2</sub>SiO<sub>5</sub>[Si<sub>2</sub>O<sub>7</sub>][PO<sub>4</sub>], synthesis conditions, cryst. struct. and IR spectra characts. 0-108335
- NaCl, <sup>3</sup>He ion scatt. spectrometry below 5 keV 0-108313
- NaCl 46 cm window optical evaluation facility 0-74526
- NaCl (Br) aqueous solutions, IR absorpt.  $\nu_1$  (CN) band parameter temp., conc. study (Russian) 0-80801
- NaCl, activation coefficients and solvation numbers in mixed methanol solvents 0-81334
- NaCl, adsorbed Xe on stepped and disordered surfaces, two-dimens. phase transformations 0-103580
- NaCl, amplitude phase hologram recording on colloid type centres (Russian) 0-69347
- NaCl aq. soln., vel. correls., time integral calcs. 0-59360
- NaCl, Born-Mayer parameters of He and Ar, interstitial interaction with neighbouring ions 0-100228
- NaCl, cation defects creation mechanism 0-75224
- NaCl, cleavage faces, evaporation pattern determ. by decoration method in electron microscopy (German) 0-107626
- NaCl, con. effect on pitting corrosion of martensitic cutlery steel 0-100962
- NaCl, cryst., laser irradi., electron emission 0-80948
- NaCl, cryst., triboluminesc. spectra 0-66312
- NaCl crystal rough surface smoothing, during evaporation or condensation 0-103470
- NaCl crystals, electronic and hole centres and surface, quantum-chemical calcs. 0-65489
- NaCl Czochralski crystal growth for large CO<sub>2</sub> laser windows 0-74525
- NaCl, defect fermion properties, ionic cond. calcs. 0-59457
- NaCl, defect modes due to substitutional anion-pair and cation-pair impurities in ionic crystals 0-92540
- NaCl, dislocation density in monocrystal deformed under high hydrostatic press. 0-70216
- NaCl, dislocation mobility under high press., temp. depend. 0-75235
- NaCl, dislocation ordering influence on integrated X-ray coeff. 0-103357
- NaCl, edge dislocation, core struct. and props., theory 0-70194
- NaCl, electric field gradients near dislocations, resulting NMR lineshapes 0-75225
- NaCl, emission band of F-centre 0-76071
- NaCl, eqn. of state to 32 kbar and 500°C, length change meas. 0-70361
- NaCl, F-centers, laser irradi. optical bleaching kinetics 0-66244
- NaCl, fundamental luminescence at high ionisation levels (Russian) 0-103985
- NaCl, gamma and additively coloured, dissolving in pure water, lyoluminesc. mechanism 0-100693
- NaCl gas-droplet counterflow heat exchanger, numerical model (French) 0-61396
- NaCl,  $\gamma$ -irradi., F-stimulated inversion of sign of dislocation charge 0-59475
- NaCl, high resolution TEM and radiation sensitivity, dislocation obs. on deformed crystals 0-107260
- NaCl, high-temp. deformed, dislocation grain subboundaries (Russian) 0-96534
- NaCl, impurity precipitation and grain boundary diffusion 0-107567
- NaCl, inelastic light scattering of localised vibration of interstitial H atom in alkali halides 0-88998
- NaCl, ion and electron emission following ion impact 0-100729
- NaCl, ionic clusters, struct., thermodynamic functions, energy surfaces and SIMS 0-63881
- NaCl, kinetic energies of sputtered excited atoms 0-66373
- NaCl large window continuous polishing 0-74527
- NaCl lattice investigations, start stresses of ensemble leading dislocations 0-92530
- NaCl, Madelung pot. determ. by Ewald method 0-92475
- NaCl, microcrack propagation and plastic strain 0-81187
- NaCl, migration of nonrelaxed holes, self-trapping, ESR and luminesc. obs. (Russian) 0-66033
- NaCl, monatomic step struct., decoration technique 0-103554
- NaCl monodisperse aerosols, appl. in cloud droplet nucleation expts. 0-82003
- NaCl, monoelectrolyte, highly mineralised salt soln., dielec. and radiation characts. 0-97184
- NaCl, Ne<sup>+</sup>, Ar<sup>+</sup>, Kr<sup>+</sup> bombard., sputtering and ionoluminescence 0-96583
- NaCl, optical strength, effect of irradi. in mechanically stressed state 0-80695
- NaCl, phase transformation due to high press. and shear stress 0-75357
- NaCl, photofragment spectra, bond energies and excited state symmetries 0-87190
- NaCl, polarisation caused by charged dislocation motion 0-59463
- NaCl polycryst. containing Al<sub>2</sub>O<sub>3</sub> dispersion, diffusive creep 0-97531

## sodium compounds continued

- NaCl polydisperse aerosol number and mass conc. meas. by elect. aerosol anal. 0-108753  
 NaCl, positron source, temp. depend. 0-93426  
 NaCl, positron-trapping colour centre dynamics, positron annihilation study 0-108294  
 NaCl, pure and doped, 20K X-ray irradiation, thermolum. and recovery processes 0-93412  
 NaCl, self-trapped exciton form. via thermally induced defect reactions 0-60687  
 NaCl single cryst., stress birefr. 0-60542  
 NaCl single crystals, thermomigration of brine inclusions, eval. of radioactive waste repositories 0-99251  
 NaCl solutions, anodic dissol. of Ni-Cr steels and alloys in, at high current densities (*Russian*) 0-76396  
 NaCl solutions, of Zn-nucleotide triphosphate complexes  $^{35}\text{Cl}$  NMR obs. 0-63661  
 NaCl structure, evaluation of finite strain eqns. of state using lattice models 0-96620  
 NaCl, water-HMPT soln., ionic diffusion coeffs. meas. (*French*) 0-65265  
 NaCl window production for Antares CO<sub>2</sub> laser system 0-74524  
 NaCl with divalent impurities, lattice relax. from density meas. 0-70226  
 NaCl:Ag, positron annihilation and impurity states 0-97375  
 NaCl:Ba<sup>2+</sup>, dopant aggregation and precipitation 0-107306  
 NaCl:Ca crystals, surface recrystn., moisture effect 0-84950  
 NaCl:Ca<sup>2+</sup>, dipole concs. determ. considering aggregation, expt. and theoretical comparison 0-59512  
 NaCl:Cd<sup>2+</sup>, dielectric loss following plastic deform. 0-84690  
 NaCl:Cu<sup>+</sup>, electrolytically coloured, electron trapping, optical absorpt. 0-100672  
 NaCl:Eu, secondary Eu phase dissolution, EPR and optical absorpt. study 0-96655  
 NaCl:Ga<sup>3+</sup>, polarisation of Ga<sup>3+</sup> centre A<sub>1</sub> emission, temp. depend. 0-80842  
 NaCl:Mg<sup>2+</sup>, dopant aggregation and precipitation 0-107306  
 NaCl:Mg<sup>2+</sup>(Ca<sup>2+</sup>)(Sr<sup>2+</sup>)(Ba<sup>2+</sup>), defect struct., Mott-Littleton technique study 0-59487  
 NaCl:Mn<sup>2+</sup>, Mg<sup>2+</sup>, doubly doped, ionic thermocurrent study of linear dimer 0-79977  
 NaCl:Mn<sup>2+</sup>, thermolum. spectra, mechanisms 0-80873  
 NaCl:Sr, positron annihilation and trapping in A-centres 0-84802  
 NaCl-gas reactions, atmospheric, in situ TEM studies 0-104544  
 NaCl-KCl, molten, alkaline earth oxides solubility products, potentiometric determ. 0-76488  
 NaCl-KCl novel encapsulant for LEC growth of GaSb single crystals 0-93475  
 NaCl-KCl system, interdiffusion, miscibility, Kirkendall effect 0-107568  
 NaCl-NH<sub>3</sub>-CO<sub>2</sub>-H<sub>2</sub>O system, NaHCO<sub>3</sub> crystn. 0-100771  
 NaCl-NaBr, elastic wave damping, 300 to 1500 MHz, impurity effects 0-92602  
 NaCl-NaBr, mixed crystals, microhardness, theory 0-75298  
 NaCl-ZnCl<sub>2</sub>, molten, US velocity, thermodynamic quantities and struct. (*Japanese*) 0-88270  
 NaCl-ZnCl<sub>2</sub>, molten, US absorption coeffs. and bulk viscosity coeffs. (*Japanese*) 0-88271  
 NaCl<sub>2</sub> on Pt and Ir surfaces, adsorption kinetics 0-84393  
 NaClO<sub>3</sub>,  $^{35}\text{Cl}$  NQR appl. in thermometry below 77K 0-66067  
 NaClO<sub>3</sub>, acoustic activity, inelastic neutron scatt. obs. (*French*) 0-103431  
 NaClO<sub>3</sub>, cryst., mechanoluminescence spectra 0-97355  
 NaClO<sub>3</sub>, crystal gyrotropy, meas. in IR region 0-88957  
 NaClO<sub>3</sub>, dislocations rel. to growth mechanism from aq. soln., X-ray topography 0-59464  
 NaClO<sub>3</sub>, lattice vibrations and sp. ht., neutron spectroscopic study 0-107388  
 NaClO<sub>4</sub> electrolyte influence on lasing props. of rhodamine G solutions 0-91788  
 NaClO<sub>4</sub>/Mn(ClO<sub>4</sub>)<sub>2</sub> in aq. soln., interaction between Mn<sup>2+</sup> and ClO<sub>4</sub><sup>-</sup>, NMR studies 0-71212  
 NaClO<sub>4</sub>-H<sub>2</sub>O, cryst. struct. deform. refinement 0-107123  
 NaCo(CO)<sub>4</sub>, soln., ion sites, cryptand C221 doping effects 0-70102  
 NaCrO<sub>2</sub>, two-dimens. mag. props. rel. to cryst. struct. 0-75776  
 Na<sub>2</sub>Cr<sub>2</sub>(PO<sub>4</sub>)<sub>3</sub>, crystallographic data, ionic conductivity (*French*) 0-88077  
 Na<sub>2</sub>Cr<sub>2</sub>(PO<sub>4</sub>)<sub>3</sub>, crystallographic data, ionic conductivity (*French*) 0-88077  
 NaCu<sub>2</sub>Ru<sub>2</sub>O<sub>12</sub>, synthesis, cryst. struct., mag. and elec. props. (*French*) 0-107151  
 NaD, nightglow spectral intensity changes, correl. with O<sub>2</sub> spectra 0-61932  
 NaD<sub>3</sub>H<sub>2</sub>(<sub>1-3</sub>)(SeO<sub>3</sub>)<sub>2</sub>, ferroelec. dispersion 0-66129  
 NaF, <sup>3</sup>He<sup>+</sup> ion scatt. spectroscopy below 5 keV 0-108313  
 NaF, F<sub>2</sub><sup>+</sup>-like colour centre, room temp. stable, CW laser, 0.99-1.22  $\mu\text{m}$  tunable 0-69399  
 NaF filter material interaction mechanism with Al melt (*Russian*) 0-108743  
 NaF, irradiated at room temp., stored energy 0-79839  
 NaF, isothermal compression at 673K, up to 1.0 GPa, X-ray diff. study 0-59565  
 NaF, one electron props., SCF-Xalpha scattered wave method 0-83279  
 NaF, quasimolecular struct. characts. of NaL<sub>1111</sub> absorpt. edge 0-93436  
 NaF, thermal cond. meas. at high press. 0-75392  
 NaF, X-irrad., colour centres and thermolum. 0-84790  
 NaF:Mn, role of Mn<sup>2+</sup> in thermolum. 0-97353  
 NaF:U, luminesc. spectra, Vib. struct. 0-80840  
 NaF-AlF<sub>3</sub>, ion-molecule equilibria studied by mass spectrometric method, heats of dissoc. and form. calc. 0-104479  
 NaF-SrF<sub>2</sub>-CrF<sub>3</sub>, glass transition, crystn. and melting temps., optical transmission (*French*) 0-64910  
 NaF-UF<sub>6</sub>, ion-molecule equilibria, heat of form. and dissoc. and electron affinities determ. 0-104480  
 Na<sub>2</sub>(Fe,Mg)<sub>2</sub>Si<sub>2</sub>O<sub>7</sub>(OH)<sub>2</sub>, riebeckite, low temp. Mossbauer obs. of oriented single cryst. behaviour and mag. props. 0-84674  
 Na<sub>2</sub>Fe(CN)<sub>5</sub>NO<sub>2</sub>H<sub>2</sub>O, absolute Mossbauer fraction of  $^{57}\text{Fe}$  nuclei 0-80648  
 NaFeF<sub>3</sub>, Mossbauer and low-temp. dilatometry study (*French*) 0-80662  
 NaFeF<sub>4</sub>, amorphous, mag. props. and Mossbauer spectra, speromagnetism and micromagnetism 0-75778  
 Na<sub>2</sub>Fe<sub>2</sub>(PO<sub>4</sub>)<sub>3</sub>, crystallographic data, ionic conductivity (*French*) 0-88077  
 $\alpha$ -Na<sub>2</sub>Fe<sub>2</sub>(PO<sub>4</sub>)<sub>3</sub>, orthophosphate, cryst. and vitreous, Mossbauer spectroscopy and mag. susceptibility (*French*) 0-80657  
 Na<sub>0.70</sub>Ga<sub>0.7</sub>Ti<sub>0.3</sub>O<sub>4</sub>, one-dimens. Na<sup>+</sup> ion cond., cryst. struct. and cond. meas. 0-107521  
 NaGdSiO<sub>4</sub>, single cryst. data and ionic cond. 0-84158

## sodium compounds continued

- NaHCO<sub>3</sub>, crystn. in system NaCl-NH<sub>3</sub>-CO<sub>2</sub>-H<sub>2</sub>O 0-100771  
 Na<sup>+</sup>(H<sub>2</sub>O)<sub>n</sub> (n=1,2,4,6), FSGO-pair-pot. calcs. (*German*) 0-74278  
 NaH<sub>3</sub>(SeO<sub>3</sub>)<sub>2</sub>,  $\beta$  to  $\delta$  ferroelec. transition under press. Raman spectra study 0-80725  
 NaH<sub>3</sub>(SeO<sub>3</sub>)<sub>2</sub>, domain struct. realignment and Barkhausen effect 0-71361  
 NaH<sub>3</sub>(SeO<sub>3</sub>)<sub>2</sub>, ferroelec., proton motion within H bonds, neutron scatt. study 0-75986  
 NaI additives in Hg discharge, high-pressure, line broadening and radiative transport 0-74199  
 NaI crystals, used in nuclear medicine, determ. of cause of breakage 0-98077  
 NaI, optically activated F $\rightarrow$ F' centre conversion in mag. field 0-108253  
 NaI, scintillator props. in temp. range 125 to 293K 0-58047  
 NaI:Ca<sup>2+</sup>, pure and doped, ionic thermocurrents meas. 0-80677  
 NaI:Ca<sup>2+</sup>, pure and doped, lattice defects, entropy and enthalpy of formation and migration 0-96687  
 NaI:F, electron-lattice coupling of F-centres, optical props. 0-60641  
 NaI:Pb, absorpt. spectra of Pb<sup>2+</sup> centres 0-76058  
 NaIO<sub>3</sub>, crystal struct. determ., anisotropic thermal vibr. parameters 0-88123  
 NaIO<sub>3</sub>, nuclear electric hexadecapole interactions 0-65513  
 NaI(Tl) detectors, response functions to terrestrial  $\gamma$ -radiation, computer program 0-83233  
 NaI(Tl) scintillation cameras, image artifacts and counting losses 0-94345  
 NaI(Tl) well-type detectors, photopeak efficiency values, expts. and calcs. 0-63454  
 NaIn(SeO<sub>4</sub>)<sub>2</sub>·6H<sub>2</sub>O, X-ray cryst. struct. determ., H bond system 0-92511  
 NaK, laser induced D $\Pi$ -a $\Sigma$  fluorescence, mol. vibr. 0-87160  
 NaK+K collisions studied using circularly polarised laser fluorescence, molecular reorientation obs. 0-69215  
 NaK+K reactive collisions studied using circularly polarised laser fluorescence 0-69215  
 NaKMg<sub>2</sub>Cu<sub>2</sub>Si<sub>12</sub>O<sub>30</sub>, cryst. struct., X-ray diff. and IR spectra (*French*) 0-107158  
 NaKMg<sub>2</sub>Si<sub>12</sub>O<sub>30</sub>, cryst. struct., X-ray diff. and IR spectra (*French*) 0-107158  
 (Na,K)<sub>2</sub>CO<sub>3</sub>, non-stoichiometric, cryst. struct. (*French*) 0-79761  
 Na<sub>3</sub>La<sub>1-x</sub>Ce<sub>x</sub>Tb<sub>2</sub>(PO<sub>4</sub>)<sub>3</sub>, optical props. (*French*) 0-103991  
 Na<sub>3-x</sub>Li<sub>x</sub>ErSi<sub>4</sub>O<sub>12</sub>, solid electrolytes for Na/TiS<sub>2</sub> cells, synthesis, characts. and utilisation 0-107518  
 Na<sub>1-x</sub>Li<sub>x</sub>NbO<sub>3</sub> mixture, ferroelec.-paraelec. transitions, dielec. props. meas. 0-66125  
 NaLiSO<sub>4</sub>, anhydrous, struct. relationships w.r.t. fast ion cond. 0-107188  
 NaM natural mordenite, Se thread lattice, optical absorpt., cond. (*Russian*) 0-89022  
 NaMgF<sub>3</sub>, defects induced by X- and vacuum UV irr., optical and elec. study 0-107319  
 Na<sub>3</sub>Mg<sub>2</sub>LiSi<sub>7</sub>O<sub>30</sub>, cryst. struct., X-ray diff. and IR spectra (*French*) 0-107158  
 Na<sub>2</sub>Mg<sub>3</sub>M<sub>2</sub>Si<sub>2</sub>O<sub>30</sub> (M=Cu, Fe, Zn, Mg), cryst. struct., X-ray diff. and IR spectra (*French*) 0-107158  
 NaMnCl<sub>3</sub>, antiferromag. insulator, self-trapping of excitons 0-70619  
 NaMnCl<sub>3</sub>, mag. struct. and spin-flip transition, powder neutron diff. exam. 0-60210  
 NaMnCrF<sub>6</sub>, mag. struct., neutron Laue diff. method 0-70951  
 NaNCO, val. band electronic struct., XPS meas., MOC and INDO calc. 0-95520  
 Na<sup>15</sup>N<sub>14</sub>N<sub>15</sub>O<sub>3</sub> mixed crystal, Raman spectra determ. of phonon density of states (*Russian*) 0-93313  
 NaNO<sub>2</sub>,  $^{23}\text{Na}$  elec. field gradient tensor from NMR satellite lines near phase transition 0-71191  
 NaNO<sub>2</sub>, ferroelec., dielec. and thermal behaviour 0-80680  
 NaNO<sub>2</sub>, ferroelec. nuclear quadrupole coupling const. and spontaneous polarisation 0-71229  
 NaNO<sub>2</sub>, incommensurate antiferroelec. phase, Brillouin scatt. freq. shift 0-93349  
 NaNO<sub>2</sub>, investigation of switching characts. using cct. containing bipolar square pulse generator 0-62687  
 NaNO<sub>2</sub>, optical harmonic generation near ferroelec. transition 0-91858  
 NaNO<sub>2</sub>, aqueous soln., X-ray diffraction, radial functions and positional correl. 0-79665  
 NaNO<sub>3</sub>, double quantum nuclear magnetic resonance of  $^{23}\text{Na}$  by double resonance, line shape 0-75886  
 NaNO<sub>3</sub>, electron density distrib. (*German*) 0-92481  
 NaNO<sub>3</sub>, lattice vibration neutron diffusion study (*French*) 0-103429  
 NaNO<sub>3</sub>, lattice vibrs., order-disorder transform., IR spectra study 0-65176  
 NaNO<sub>3</sub>, Nd laser second harmonic stimulated Raman scatt., efficiency in calcite, nitrate crystals. 0-95949  
 NaNO<sub>3</sub>, occupation waves, dispersive modulation, struct. using super-space-group concept 0-79726  
 NaNO<sub>3</sub>(<sub>2</sub>), precipitation from mixed aq. solns. 0-100191  
 NaNbO<sub>3</sub>, elect. cond. mech., resist., Hall coeff. and thermoelec. power meas. 0-65603  
 NaNbO<sub>3</sub>, hydrostatic press. effect on permittivity, phase transition, hysteresis 0-80670  
 Na<sub>2</sub>NIPO<sub>4</sub>, X-ray diff. spectra (*French*) 0-93546  
 Na<sub>2</sub>Ni(PO<sub>4</sub>)<sub>2</sub>, double phosphate, X-ray diff. spectra (*French*) 0-93546  
 NaO+O, nightglow, excitation and abundance of Na 0-98497  
 Na<sub>2</sub>O, cation diffusion NMR investigation up to 800°C 0-108092  
 Na<sub>2</sub>O-2B<sub>2</sub>O<sub>3</sub> molten glass, reactions with conducting materials 0-85186  
 Na<sub>2</sub>O-2CaO-3SiO<sub>2</sub> glass, cryst. nucleation and growth, viscosity, thermodynamic props. 0-84079  
 Na<sub>2</sub>O-3SiO<sub>2</sub>:Fe<sup>2+</sup>, Fe<sup>3+</sup> glasses, Mossbauer and ESR spectra and internal friction 0-100865  
 20Na<sub>2</sub>O-(80-x)B<sub>2</sub>O<sub>3</sub>-xSiO<sub>2</sub> glass system, structure toughness-composition relationship 0-104257  
 Na<sub>2</sub>O-Ag<sub>2</sub>O-B<sub>2</sub>O<sub>3</sub> glass, Ag<sup>+</sup> ion distrib., X-ray diff. study 0-84076  
 Na<sub>2</sub>O-Al<sub>2</sub>O<sub>3</sub>-B<sub>2</sub>O<sub>3</sub>-SiO<sub>2</sub>-AgCl(Br), photochromic glass, kinetics of thermal decolorisation 0-103931  
 Na<sub>2</sub>O-Al<sub>2</sub>O<sub>3</sub>-SiO<sub>2</sub>, glass, nucleation, crystn., ceramic form. 0-84082  
 Na<sub>2</sub>O-Al<sub>2</sub>O<sub>3</sub>-SiO<sub>2</sub>-(K<sub>2</sub>) glasses, ion exchange kinetics and interdiffusion mechanisms 0-80003  
 Na<sub>2</sub>O-B<sub>2</sub>O<sub>3</sub>, ferroelectric glass, phase transition, permittivity, electrochromism, photochromism 0-80719  
 Na<sub>2</sub>O-B<sub>2</sub>O<sub>3</sub>, vitreous and cryst., enthalpy of form., calorimetric study 0-66861  
 Na<sub>2</sub>O-B<sub>2</sub>O<sub>3</sub> glass struct. study using  $^{10}\text{B}$  NMR 0-84658



## sodium compounds continued

- Na<sub>2</sub>O-B<sub>2</sub>O<sub>3</sub>-Cu<sup>2+</sup>, Mn<sup>2+</sup> glasses, Cu<sup>2+</sup>-Mn<sup>2+</sup> interaction studied by ESR 0-93166  
 Na<sub>2</sub>O-B<sub>2</sub>O<sub>3</sub>-B<sub>2</sub>O<sub>3</sub> glass with metallic Bi granules, elec. cond. 0-84493  
 Na<sub>2</sub>O-B<sub>2</sub>O<sub>3</sub>-CuO,  $\gamma$ -irrad., CuO effects on EPR 0-84645  
 Na<sub>2</sub>O-B<sub>2</sub>O<sub>3</sub>-GeO<sub>2</sub> glass-forming melts, thermodynamic props. and vaporisation processes, mass spectrometric study 0-79926  
 Na<sub>2</sub>O-B<sub>2</sub>O<sub>3</sub>-GeO<sub>2</sub> system glass-forming melts, mass spectrometry obs. of thermodynamic props. 0-97468  
 Na<sub>2</sub>O-B<sub>2</sub>O<sub>3</sub>-GeO<sub>2</sub> vitreous melts, thermodynamic props. from mass spectra 0-65253  
 Na<sub>2</sub>O-B<sub>2</sub>O<sub>3</sub>-NiO melts, NiO activity and solubility meas. by EMF method (*Japanese*) 0-92677  
 Na<sub>2</sub>O-B<sub>2</sub>O<sub>3</sub>-P<sub>2</sub>O<sub>5</sub> glass, mech. and elec. props 0-84228  
 Na<sub>2</sub>O-B<sub>2</sub>O<sub>3</sub>-SiO<sub>2</sub> containing halogens glass formation 0-103254  
 Na<sub>2</sub>O-B<sub>2</sub>O<sub>3</sub>-SiO<sub>2</sub> glass fibre, plastic coating influence on strength 0-58697  
 Na<sub>2</sub>O-B<sub>2</sub>O<sub>3</sub>-SiO<sub>2</sub> glass fibre, plastic-coated, liq. N<sub>2</sub> strength 0-58707  
 Na<sub>2</sub>O-B<sub>2</sub>O<sub>3</sub>-SiO<sub>2</sub> glass, low-loss GRIN fibres, double-crucible prod., loss and bandwidth meas. 0-69559  
 Na<sub>2</sub>O-B<sub>2</sub>O<sub>3</sub>-SiO<sub>2</sub> glass-Ni compact, indented, strength and fracture toughness 0-93636  
 Na<sub>2</sub>O-B<sub>2</sub>O<sub>3</sub>-SiO<sub>2</sub> glasses, phase-separated, leaching rate 0-104131  
 Na<sub>2</sub>O-B<sub>2</sub>O<sub>3</sub>-SiO<sub>2</sub> glass, fracture toughness, effect of microheterogeneous struct. 0-104256  
 Na<sub>2</sub>O-B<sub>2</sub>O<sub>3</sub>-SiO<sub>2</sub>-As<sub>2</sub>O<sub>3</sub>(As<sub>2</sub>O<sub>5</sub>) glasses, DC and AC resist., bipolaronic hopping cond. 0-88558  
 Na<sub>2</sub>O-B<sub>2</sub>O<sub>3</sub>-SiO<sub>2</sub> mechanical strength and swelling in liq. 0-85024  
 Na<sub>2</sub>O-BaO-Al<sub>2</sub>O<sub>3</sub>-SiO<sub>2</sub> glass, nucleation, crystn., ceramic form. 0-84082  
 Na<sub>2</sub>O-CaO glass, (K<sub>1</sub>, V) diagram determ. (*French*) 0-108558  
 Na<sub>2</sub>O-CaO glass, shear deform. under pyramidal indentations 0-84989  
 Na<sub>2</sub>O-CaO glass, wettability, effect of cleaning procedures 0-65336  
 Na<sub>2</sub>O-CaO glass phlogopite mica powders, composite fabrication, cellular struct. 0-84902  
 Na<sub>2</sub>O-CaO-Al<sub>2</sub>O<sub>3</sub>-SiO<sub>2</sub> glass, crystn. for the purpose of obtaining vitrocramics (*French*) 0-75163  
 Na<sub>2</sub>O-CaO-SiO<sub>2</sub> glass, formation of colour centres, linear absorption of UV radiation 0-103328  
 Na<sub>2</sub>O-CaO-SiO<sub>2</sub> proof testing 0-108654  
 Na<sub>2</sub>O-CaO-SiO<sub>2</sub> glass, grain-cleaning procedures effect on crushed glass chem. durability tests 0-66678  
 Na<sub>2</sub>O-CaO-SiO<sub>2</sub> glass, vol. relaxation and thermal history during forming process 0-70130  
 Na<sub>2</sub>O-CaO-SiO<sub>2</sub> glass, leaching studies by sputter-induced photon spectrometry 0-80004  
 Na<sub>2</sub>O-CaO-SiO<sub>2</sub> glass, molten, metal ion diffusion and redox behaviour, electrochemical studies 0-81332  
 Na<sub>2</sub>O-CaO-SiO<sub>2</sub> glass, redox phenomena evaluation in melting-finishing process, SO<sub>2</sub> evolution 0-84900  
 Na<sub>2</sub>O-CaO-SiO<sub>2</sub> glass, high-vel. liq. impact, oblique impact anomaly 0-89329  
 Na<sub>2</sub>O-CaO-SiO<sub>2</sub> glass, hot erosion plastic flow and fracture 0-89354  
 Na<sub>2</sub>O-CaO-SiO<sub>2</sub> glass foils, HVEM in-situ straining expts. 0-104216  
 Na<sub>2</sub>O-CaO-SiO<sub>2</sub> glasses, Auger analysis, alkali signal decrease 0-61189  
 Na<sub>2</sub>O-CaO-SiO<sub>2</sub> molten glass, electrolysis reactions 0-89496  
 Na<sub>2</sub>O-CaO-SiO<sub>2</sub>-Cr<sup>3+</sup> glass, absorpt. spectra, Fano antireson. and vibronic Lamb shift 0-71458  
 Na<sub>2</sub>O-CaO-SiO<sub>2</sub>-Cr<sub>2</sub>O<sub>3</sub> glass, redox equilibria of Cr ions, impurity effects 0-89477  
 Na<sub>2</sub>O-CaO-SiO<sub>2</sub>-Fe<sub>2</sub>O<sub>3</sub> molten glass, optical props., temp. depend. (*French*) 0-100667  
 Na<sub>2</sub>O-CaO-SiO<sub>2</sub>-H<sub>2</sub>O system gels, metastable nature 0-71952  
 2Na<sub>2</sub>O-CaO-3SiO<sub>2</sub> glass, cryst. nucleation rate, viscosity, heat treatment 0-84081  
 Na<sub>2</sub>O-Cs<sub>2</sub>O-SiO<sub>2</sub> glasses, thermal diffusivity, heat capacity and thermal cond., laser flash method study 0-65310  
 Na<sub>2</sub>O-Ga<sub>2</sub>O<sub>3</sub> system  $\beta$  and  $\beta''$  phases, fast ion cond., prep. and phase comp. 0-59716  
 Na<sub>2</sub>O-GeO<sub>2</sub>(SiO<sub>2</sub>) glasses, structure toughness-composition relationship 0-104257  
 Na<sub>2</sub>O-K<sub>2</sub>O-Al<sub>2</sub>O<sub>3</sub>-SiO<sub>2</sub>, structure of modified surface layer, internal friction method 0-103258  
 Na<sub>2</sub>O-K<sub>2</sub>O-B<sub>2</sub>O<sub>3</sub>-SiO<sub>2</sub> glass, character of elec. cond. 0-103516  
 Na<sub>2</sub>O-Li<sub>2</sub>O-Al<sub>2</sub>O<sub>3</sub>, local electrode current density and flow decoration 0-100935  
 Na<sub>2</sub>O-Li<sub>2</sub>O-B<sub>2</sub>O<sub>3</sub>-H<sub>2</sub>O, water mol. vibrs., IR and Raman spectra 0-89006  
 Na<sub>2</sub>O-MgO-Al<sub>2</sub>O<sub>3</sub>,  $\beta''$ -alumina, high-resolution electron microscopy 0-75208  
 Na<sub>2</sub>O-MgO-Al<sub>2</sub>O<sub>3</sub>, ionic cond. 0-107480  
 Na<sub>2</sub>O-MgO-B<sub>2</sub>O<sub>3</sub>-Cu<sup>2+</sup>, micro-inhomogeneities, EPR and Raman study 0-84080  
 Na<sub>2</sub>O-P<sub>2</sub>O<sub>5</sub> glass ESR of VO<sup>2+</sup> ions 0-100610  
 Na<sub>2</sub>O-P<sub>2</sub>O<sub>5</sub>-Cr<sup>3+</sup> glass, absorpt. spectra, Fano antireson. and vibronic Lamb shift 0-71458  
 Na<sub>2</sub>O-P<sub>2</sub>O<sub>5</sub>-CuO,  $\gamma$ -irrad., CuO effects on EPR 0-84645  
 Na<sub>2</sub>O-P<sub>2</sub>O<sub>5</sub>-SiO<sub>2</sub> glass, metastable liquid immiscibility 0-100331  
 Na<sub>2</sub>O-P<sub>2</sub>O<sub>5</sub>-SiO<sub>2</sub> glass, substitution of Li<sup>+</sup>, Mg<sup>2+</sup>, Sr<sup>2+</sup>, Ba<sup>2+</sup>, Zn<sup>2+</sup> for Na<sup>+</sup> 0-100332  
 Na<sub>2</sub>O-P<sub>2</sub>O<sub>5</sub>-Y<sub>2</sub>O<sub>3</sub>-Tb<sub>2</sub>O<sub>3</sub> glass, conc. quenching of luminesc. in disordered system with dipolar interaction 0-89059  
 Na<sub>2</sub>O-PbO-SiO<sub>2</sub>, molten glass, reactions with conducting materials 0-85186  
 Na<sub>2</sub>O-PbO-SiO<sub>2</sub> glass-ceramic composite, directionally crystallised 0-107058  
 Na<sub>2</sub>O-SiO<sub>2</sub> glass, acoustic and thermal Gruneisen parameters 0-59608  
 Na<sub>2</sub>O-SiO<sub>2</sub> glass, bridging to non-bridging ratio and correl. to glass density and refr. index, ESCA study 0-84832  
 Na<sub>2</sub>O-SiO<sub>2</sub> glass, bubble gas comp. change 0-79946  
 Na<sub>2</sub>O-SiO<sub>2</sub> glass, conduction and dielec. loss mechanisms, paired interstitial model 0-107468  
 Na<sub>2</sub>O-SiO<sub>2</sub> glass, evaporation by high temp. mass spectrometry 0-79927  
 Na<sub>2</sub>O-SiO<sub>2</sub> glass, fusion process study, EMF meas. (*French*) 0-89190  
 Na<sub>2</sub>O-SiO<sub>2</sub> glass, internal and surface struct. by X-ray scatt. 0-84074  
 Na<sub>2</sub>O-SiO<sub>2</sub> glass, microcracking about NiS inclusions, fracture mech. description 0-89333  
 Na<sub>2</sub>O-SiO<sub>2</sub> glass, molten, metal ion diffusion and redox behaviour, electrochemical studies 0-81332  
 Na<sub>2</sub>O-SiO<sub>2</sub> glass, OH<sup>-</sup> content effect on mech. and other props. 0-89337  
 Na<sub>2</sub>O-SiO<sub>2</sub> glass, scoring, deform. and fracture mech. approach 0-89332

## sodium compounds continued

- Na<sub>2</sub>O-SiO<sub>2</sub> glass containing halogens glass formation 0-103254  
 Na<sub>2</sub>O-SiO<sub>2</sub> glass drops, quenched from liq. state, thermally treated, density profile 0-81085  
 Na<sub>2</sub>O-SiO<sub>2</sub> glass melt, dissoln. of O<sub>2</sub> and CO<sub>2</sub> gas bubbles 0-79945  
 Na<sub>2</sub>O-SiO<sub>2</sub> glasses, Auger analysis, alkali signal decrease 0-61189  
 Na<sub>2</sub>O-SiO<sub>2</sub> glasses, elementary electronic excitations, refl. luminesc. and photoemission meas. 0-84778  
 Na<sub>2</sub>O-SiO<sub>2</sub> glasses, water reactions at elevated temps. and press. 0-81312  
 Na<sub>2</sub>O-SiO<sub>2</sub>-Au+CeO<sub>2</sub>, Au particle nucleation 0-81066  
 Na<sub>2</sub>O-SiO<sub>2</sub>-CuO glass, gamma-irradiated, EPR and optical spectra 0-103885  
 Na<sub>2</sub>O-SiO<sub>2</sub>-CuO,  $\gamma$ -irrad., CuO effects on EPR 0-84645  
 Na<sub>2</sub>O-SiO<sub>2</sub>-Fe<sub>2</sub>O<sub>3</sub> glass, X-ray absorpt. spectra, effective co-ordination charges 0-84805  
 Na<sub>2</sub>O-SiO<sub>2</sub>-MgO(CaO)(BaO) glasses, elec. cond., room temp. to 450°C 0-107473  
 Na<sub>2</sub>O-TiO<sub>2</sub>-Al<sub>2</sub>O<sub>3</sub>-SiO<sub>2</sub> glass,  $\gamma$ -irrad., struct. position of Ti, EPR study 0-84644  
 Na<sub>2</sub>O-TiO<sub>2</sub>-SiO<sub>2</sub> glass, co-ordination of Ti, X-ray emission spectra study 0-84072  
 Na<sub>2</sub>O-ZrO<sub>2</sub>-SiO<sub>2</sub> glass fibres, prep. from metal alkoxides, resistance to NaOH soln. 0-97454  
 NaOD solution in D<sub>2</sub>O, collective excitations in liquid and amorphous state, 77 to 300K 0-92636  
 NaOH, fused, H<sub>2</sub> prod. by H<sub>2</sub>O electrolysis 0-76660  
 NaOH gas-crystal system, isotopic equilibrium near phase transition points (*Russian*) 0-91697  
 NaOH·CrO<sub>2</sub>·(NO<sub>2</sub>)<sub>2</sub>, electron tunnelling, pulse radiolysis 0-108722  
 NaOH·Fe(CN)<sub>6</sub><sup>3-</sup>, electron tunnelling, pulse radiolysis 0-108722  
 5Na<sub>2</sub>O·Fe<sub>2</sub>O<sub>3</sub>·8SiO<sub>2</sub> glass crystallisation study by Fe<sup>3+</sup> EPR and Mossbauer spectra 0-64904  
 Na<sub>2</sub>O-SiO<sub>2</sub>, prep. from film forming soln. 0-60811  
 Na<sub>2</sub>O-SiO<sub>2</sub>-Tb<sub>2</sub>O<sub>3</sub> glass magnetooptical study 0-88976  
 Na<sub>2</sub>O·11Al<sub>2</sub>O<sub>3</sub>·Cr, impurity ion struct., ESR study 0-80605  
 Na<sub>2</sub>O·11Al<sub>2</sub>O<sub>3</sub>, polycrystalline with preferably orientated grains, preparation (*Japanese*) 0-81012  
 Na<sub>2</sub>O·2SiO<sub>2</sub>, short range struct. by pulsed neutron scatt. 0-59396  
 25Na<sub>2</sub>O·75SiO<sub>2</sub> glass, thermal cond., temp. depend. at low temps. 0-65322  
 Na<sub>3</sub>PCr<sub>3</sub>O<sub>7</sub>·3H<sub>2</sub>O, cryst. struct. 0-107154  
 NaPO<sub>3</sub>, mol. identification by matrix isolation IR spectrosc. 0-104485  
 NaPO<sub>3</sub>, mol. identification by matrix isolation IR spectrosc. 0-104485  
 NaPO<sub>3</sub>·Eu<sup>3+</sup>, luminesc. of Eu<sup>3+</sup>, transition probabilities 0-80845  
 (NaPO<sub>3</sub>)<sub>x</sub> glass ceramic, transient heterogeneous nucleation 0-88042  
 Na<sub>2</sub>PO<sub>4</sub>, high temp. fast ion cond. phases, neutron diffr. obs. of struct. 0-107512  
 Na<sub>3</sub>PO<sub>4</sub>·Ni<sub>3</sub>(PO<sub>4</sub>)<sub>2</sub> system, phase equilibrium diagrams, crystallographic study, double orthophosphates (*French*) 0-93546  
 Na<sub>2</sub>Pr(C<sub>2</sub>H<sub>3</sub>O<sub>2</sub>)<sub>2</sub>·2NaClO<sub>4</sub>·6H<sub>2</sub>O, absorpt., circular dichroism, and mag. circular dichroism spectra 0-97243  
 Na<sub>2</sub>R(WNb<sub>2</sub>O<sub>7</sub>)<sub>2</sub>F<sub>3</sub> (R=Y, Nd, Eu, Gd, Dy, Lu), synthesis, cryst.-chem. and dielec. study (*French*) 0-108164  
 Na<sub>2</sub>R(XO<sub>4</sub>)<sub>2</sub> (R=rare earth; X=P, As, V), pressure synthesis (*French*) 0-93509  
 NaReO<sub>4</sub>, EPR spectra of paramag. centres and free radicals 0-108072  
 NaRhy zeolite, Rh complexes with CO and methyl iodide ligands, spectrosc. obs. 0-85159  
 Na<sup>+</sup> cation diffusion NMR investigation up to 800°C 0-108092  
 Na<sub>2</sub>S-P<sub>2</sub>S<sub>5</sub> glass forming region, struct. and ionic cond. 0-88358  
 Na<sub>2</sub>S-SiS<sub>2</sub>(GeS<sub>2</sub>)(P<sub>2</sub>S<sub>5</sub>), synthesis, structure and ionic conduction (*French*) 0-65291  
 Na<sub>2</sub>S-XS<sub>2</sub>, X=Si, Ge, glass forming region, struct. and ionic cond. 0-88358  
 Na<sub>2</sub>S<sub>2</sub>-molten S interface, mass transport phenomena, rel. to Na/S battery 0-72026  
 Na<sub>2</sub>SO<sub>4</sub>-CoSO<sub>4</sub>-H<sub>2</sub>O, phase equilb., activities, Pitzer eqn. calcs. (*Russian*) 0-65190  
 Na<sub>2</sub>S<sub>2</sub>O<sub>3</sub> digested AgX emulsions, red-IR photoluminescence obs. at 77K 0-103982  
 Na<sub>2</sub>S<sub>2</sub>O<sub>3</sub>-picric acid-ethanol-H<sub>2</sub>O etchant for high-strength dual-phase steel 0-100951  
 Na<sub>2</sub>SO<sub>4</sub>·10H<sub>2</sub>O, thermal energy storage for solar heating systems 0-101134  
 Na<sub>2</sub>S<sub>2</sub>O<sub>4</sub>·2H<sub>2</sub>O hydrogenase-catalysed decomposition for biologically assisted H<sub>2</sub> prod. 0-61460  
 NaSbO<sub>3</sub>·1/6NaF, dielec. spectroscopy study, 100 Hz to 10 MHz, 238 to 417K (*German*) 0-108144  
 Na<sub>2</sub>SbS<sub>4</sub>, vibrational spectra, internal SbS<sub>4</sub> vibr. assignments 0-66199  
 Na<sub>2</sub>SbS<sub>4</sub>·9H<sub>2</sub>O(D<sub>2</sub>O), vibrational spectra, internal SbS<sub>4</sub> and H<sub>2</sub>O(D<sub>2</sub>O) vibr. assignments 0-66199  
 Na<sub>3</sub>Sc<sub>2</sub>P<sub>2</sub>O<sub>7</sub>, fast-ion conductor, struct. phase transition 0-88362  
 Na<sub>2</sub>Sc<sub>2</sub>P<sub>2</sub>O<sub>7</sub>, superionic cond. synthesis, cryst. struct. and ionic cond. 0-107519  
 NaTaO<sub>3</sub>, high temp. structs. neutron powder diffr., comparison with SrZrO<sub>3</sub> and NaNbO<sub>3</sub> 0-88094  
 Na<sub>1+x</sub>Ta<sub>1-x</sub>W<sub>1-x</sub>O<sub>6</sub> pyrochlore system, comp. depend. of ionic cond. 0-107517  
 Na<sup>99m</sup>TcO<sub>4</sub> solution, special chambers for production (*Hungarian*) 0-93785  
 Na<sub>2</sub>TeO<sub>3</sub>, chem. prep. and cryst. struct. (*French*) 0-79755  
 Na<sub>2</sub>O·Ti<sub>2</sub>Fe<sub>2</sub>O<sub>4</sub>, short period  $\beta$ -alumina type cpds., cryst. struct. and superionic cond. 0-107499  
 Na<sub>2</sub>Ti<sub>2</sub>O<sub>9</sub>, orthorhombic, unit-cell twinning of monoclinic Na<sub>2</sub>Ti<sub>2</sub>O<sub>9</sub>, cryst. struct. 0-107155  
 Na<sub>2</sub>Ti<sub>2</sub>O<sub>8</sub> bronze, hydrothermal prep., Na ion arrangement 0-75209  
 (Na<sub>2</sub>Ti<sub>2</sub>O<sub>13</sub>)<sub>n</sub>(BaTi<sub>4</sub>O<sub>5</sub>)<sub>m</sub>, tunnel struct. intergrowth, electron, microscopy investigations 0-100218  
 Na<sub>2</sub>TiS<sub>2</sub>, alkali ion ordering, X-ray study 0-107165  
 NaTi<sub>3</sub>(SO<sub>3</sub>)<sub>2</sub>, crystallograms, cryst. struct. determ. method 0-103286  
 NaTi<sub>3</sub>(SO<sub>3</sub>)<sub>2</sub>, heat capacity and thermodynamic functions, 10 to 300K 0-65244  
 Na<sub>2</sub>UO<sub>2</sub>Cl<sub>4</sub> melts and mixtures, thermogravimetric determ. of uranyl cation state 0-101050  
 NaVO<sub>3</sub>-Cr<sup>3+</sup>, study of ESR spectra 0-80601  
 NaV<sub>2</sub>O<sub>5</sub>, monocystal, electronic struct. and X-ray emission spectra anisotropy 0-84807  
 $\beta$ -Na<sub>0.27</sub>V<sub>2</sub>O<sub>5</sub>, heat of form. and sp. ht., 450 to 900K 0-61129  
 $\beta$ -Na<sub>0.33</sub>V<sub>2</sub>O<sub>5</sub>, quasi-one-dimensional conductor, NMR studies 0-93204



sodium compounds continued

Na<sub>2</sub>WO<sub>3</sub>, 0.22 < x < 0.84, low temp. struct., press. effects, NMR study 0-59443  
Na<sub>2</sub>WO<sub>3</sub> bronzes, reaction with Fe powder, reaction mechanism and reactivity 0-108712  
Na<sub>2</sub>WO<sub>3</sub>, surface props. 0-71767  
NaX-Se semiconductor superlattice absorpt. edge, light scatt. (*Russian*) 0-71438  
Na<sub>2</sub>XO<sub>4</sub> (X=S, Cr, Mo, W), anal. and calc. of binary and ternary phase diagrams 0-88299  
Na<sub>2</sub>Y[SiO<sub>3</sub>]<sub>2</sub>, crystal struct., atom coordinates, X-ray study 0-59446  
Na<sub>2</sub>YSiO<sub>4</sub>, crystal structure refinement, X-ray anal. 0-79764  
Na<sub>2</sub>YSiO<sub>3</sub>, Na<sub>2</sub>YSi<sub>2</sub>O<sub>7</sub>, Na<sub>2</sub>YSi<sub>3</sub>O<sub>9</sub> and Na<sub>2</sub>YSi<sub>4</sub>O<sub>12</sub>, single cryst. data and ionic cond. 0-84158  
NaY<sub>1-x</sub>Sm<sub>x</sub>F<sub>4</sub>, luminesc. expt. suggesting Sm<sup>3+</sup> ion pairing 0-76065  
Na<sub>2</sub>Y<sub>2</sub>Zr<sub>2</sub>S<sub>2</sub>, ionic cond. and NMR mobility obs., comp. depend. (*French*) 0-70459  
NaZnGeO<sub>4</sub>:Mn, electrochrom., ionisation domains 0-84787  
Na<sub>2</sub>Zr<sub>2</sub>PSi<sub>2</sub>O<sub>12</sub>, NASICON, <sup>23</sup>Na NMR obs. of ionic diffusion, 180 to 800K 0-108097  
Na<sub>2</sub>Zr<sub>2</sub>Si<sub>2</sub>O<sub>12</sub>, struct. analysis at 300 and 600°C, rel. to ionic cond. 0-107189  
Na<sub>1-x</sub>Zr<sub>x</sub>Si<sub>3-x</sub>O<sub>12</sub>, press. and comp. effect on fast Na<sup>+</sup> ion transport 0-107516  
Na<sub>2</sub>Zr<sub>2</sub>Si<sub>2</sub>PO<sub>12</sub>, NASICON, ionic cond. temp. depend., comparison with β-Al<sub>2</sub>O<sub>3</sub>-Na<sub>2</sub>O 0-107520  
Na<sup>+</sup>H<sub>2</sub>, potential energy surfaces 0-74215  
Na<sub>2</sub>[Ti(Ti<sub>0.9</sub>Nb<sub>0.1</sub>)<sub>2</sub>(Si<sub>0.6</sub>O<sub>1.7</sub>)<sub>2</sub>(OH,Cl)<sub>3</sub>].11H<sub>2</sub>O, zorite, X-ray cryst. struct. determ. 0-92513  
Ni-ferrite powders, form. in presence of Li<sub>2</sub>SO<sub>4</sub>-Na<sub>2</sub>SO<sub>4</sub> molten salts, prep. and characts. 0-84869  
SeCl<sub>3</sub>-NaCl-CsCl ternary system, cpd. form., thermographic investig. (*Russian*) 0-66490  
SiO<sub>2</sub>-Al<sub>2</sub>O<sub>3</sub>-CaO-BaO-SrO-ZnO-Na<sub>2</sub>O-K<sub>2</sub>O-B<sub>2</sub>O<sub>3</sub>, glaze effect of P<sub>2</sub>O<sub>5</sub> additions 0-60824  
SiO<sub>2</sub>-Al<sub>2</sub>O<sub>3</sub>-CaO-Na<sub>2</sub>O:Fe<sup>3+</sup>, optical absorpt. due to Fe<sup>3+</sup> ligand field and charge transfer 0-89020  
SiO<sub>2</sub>-Al<sub>2</sub>O<sub>3</sub>-Na<sub>2</sub>O-BaO-TiO<sub>2</sub>, glass ceramic interaction with Pb borosilicate glaze 0-84398  
SiO<sub>2</sub>-CaO-Na<sub>2</sub>O, glass, layers near surface, anal. using SIMS 0-88041  
SiO<sub>2</sub>-Na<sub>2</sub>O alkali glass, grain-cleaning procedures effect on crushed glass chem. durability tests 0-66678  
SiO<sub>2</sub>-Na<sub>2</sub>O surface, Ca<sub>3</sub>(PO<sub>4</sub>)<sub>2</sub> film form., bonding to bone 0-85212  
SiO<sub>2</sub>-Na<sub>2</sub>O-CaO-MgO float glass, surface SnO<sub>2</sub> distrib., ellipsometry and XPS study 0-84346  
SiO<sub>2</sub>-Na<sub>2</sub>O-CaO-P<sub>2</sub>O<sub>5</sub>, BIOGLASS, surface, Ca<sub>3</sub>(PO<sub>4</sub>)<sub>2</sub> film form., bonding to bone 0-85212  
SiO<sub>2</sub>-Na<sub>2</sub>O-Nd<sub>2</sub>O<sub>3</sub> glass, magneto-optical props., absorpt. spectrum 0-88969  
SiO<sub>2</sub>-NaAlSiO<sub>4</sub> glasses and devitrificates, prep. and vibr. spectroscopy study (*Polish*) 0-93530  
SiO<sub>2</sub>-PbO-B<sub>2</sub>O<sub>3</sub>-Al<sub>2</sub>O<sub>3</sub>-CaO-Na<sub>2</sub>O-K<sub>2</sub>O glaze, interaction with aluminosilicate glass-ceramics 0-84398  
SrBaNaNb<sub>2</sub>O<sub>12</sub>, X-ray powder diffraction data determ. (*Chinese*) 0-70170  
SrCu<sub>2</sub>Ru<sub>2</sub>O<sub>12</sub>, synthesis, cryst. struct., mag. and elec. props. (*French*) 0-107151  
Sr<sub>x</sub>(Na<sub>0.5</sub>Bi<sub>0.5</sub>)<sub>1-x</sub> solid solutions, piezoelec. and ferroelec. props. (*French*) 0-108158  
Sr<sub>x</sub>(Na<sub>0.5</sub>Bi<sub>0.5</sub>)<sub>1-x</sub>TiO<sub>3</sub> ferroelec. ceramic, hot pressing, numerical simulation (*French*) 0-76220  
Sr<sub>2</sub>O<sub>5</sub>Na<sub>0.90</sub>Nb<sub>0.10</sub>O<sub>15</sub>, X-ray powder diffraction data determ. (*Chinese*) 0-70170  
V<sub>2</sub>O<sub>5</sub>-P<sub>2</sub>O<sub>5</sub>-Na<sub>2</sub>O glasses, enhanced secondary electron emission yield 0-93441  
ZnCl<sub>2</sub>-KCl-NaCl, molten system, containing Ni<sup>2+</sup> ions, appl. to electrorefining, polarographic study 0-66810  
ZrF<sub>4</sub>-BaF<sub>2</sub>-NaF, vitreous phases, network formers, modifiers and stabilisers (*French*) 0-64909  
ZrF<sub>4</sub>-BaF<sub>2</sub>-ThF<sub>4</sub>-NaF(RF<sub>3</sub>) (R=rare-earth) glass system, anion cond. 0-70460  
ZrNa<sub>2</sub>H<sub>2-x</sub>(PO<sub>4</sub>)<sub>2</sub>, Na<sup>+</sup> transport, gas-solid and solid-solid reaction kinetics in Zr(HPO<sub>4</sub>)<sub>2</sub>.H<sub>2</sub>O 0-61086

sodium potassium tartrate tetrahydrate see Rochelle salt

sofar see sonar

soft modes

see also dispersive transformations; lattice phonons  
aniline hydrobromide, ferroelastic, acoustic softening near transition temp. 0-96617  
benzil, phase transition, far IR spectroscopy meas. 0-71407  
binary compound, Kohn anomaly in optical phonon branch 0-92626  
cubic crystal, Jahn-Teller effect, soft mode influence 0-59937  
D<sub>2d</sub> crystals, structural phase transitions, soft modes, group theory 0-92638  
diatomic linear chain, ferroelec. soft modes 0-70353  
dipole pseudo-spin glasses, collective excitations 0-59617  
dislocation-soft mode interaction in dispersive transitions (*Russian*) 0-84172  
distortive phase transitions, order-disorder and dispersive regimes, mol. dynamics study 0-75324  
elastic phase transitions, order parameter and mode softening 0-75325  
ferroelastic, dislocation-phonon interactions, phase transition effects 0-59600  
ferroelectrics, improper and incommensurate phase transitions, neutron scatt. studies 0-75974  
ferroelectrics, incommensurate phase transitions 0-75964  
ferroelectrics, quantum transition suppression, pyroelectric, electrocaloric effects, specific heat 0-75984  
ferroelectrics, vibronic, band struct. temp. depend. 0-70598  
Grüneisen parameter and eqn. of state determ. at press. induced phase transition 0-90031  
Ising model with transverse field, phonon relax., soft mode and central peak roles 0-59615  
IV-VI semiconductors, structural phase transitions, anomalous resist., electron-soft phonon interactions 0-108167  
metal, electron-phonon interaction effects on spin susceptibility 0-93108  
FAA, nonlinear soft mode at Rayleigh-Benard instability, neutron cond. spectrosc. obs. 0-79266  
Peierls transition in quantizing mag. field, possibility 0-103441

soft modes continued

quasielastic light scattering near phase transitions 0-93362  
Rochelle salt, ferroelec. phase transition, Raman scatt. study 0-97211  
semiconductor thin films, ferroelectric properties, quantum size effect 0-97201  
structural phase transitions, crit. dynamics and quasi-elastic scatt. 0-92641  
structural phase transitions, Landau theory 0-92639  
sym-triazine, Landau mean field description, second-order phase transition, soft modes 0-108434  
sym-trioxane, phase transition, polarised Raman spectra obs. 0-84742  
thiourea, incommensurate phase, soft modes, condensation of even-order harmonics 0-103313  
thiourea, incommensurate phase transition, X-ray and neutron scatt. study 0-75963  
tris-sarcosine calcium chloride:Mn<sup>2+</sup> ferroelec. dynamics, EPR and ENDOR study 0-75972  
tris-sarcosine calcium chloride, ferroelec. transitions, soft modes, Raman scatt. spectra obs. 0-80763  
Ag<sub>3</sub>AsS<sub>3</sub> and Ag<sub>3</sub>SbS<sub>3</sub>, Raman spectra obs. of low-temp. phases 0-93327  
Ag<sub>3</sub>AsS<sub>3</sub>, proustite, phonons and soft modes at ferroelec. transition 0-60524  
As<sub>2</sub>Sb<sub>2</sub>SI cryst., ferroelec., soft mode Raman and IR spectroscopy 0-76016  
As<sub>2</sub>Sb<sub>2</sub>SI mixed crystals, phonon coupling, ferroelectric phase transition, Raman study 0-108165  
BaMnF<sub>4</sub>, anisotropic order parameter phase fluctuations, light scatt. and thermal diffusivity meas. 0-80807  
Ba<sub>2</sub>NaNb<sub>2</sub>O<sub>15</sub>, incommensurate refls. near ferroelastic transition, neutron and X-ray precession obs. 0-70395  
BaTiO<sub>3</sub>, elastooptic effect near ferroelec. transition, temp. depend. 0-97233  
BaTiO<sub>3</sub>, ferroelectric mechanisms, anharmonic couplings by scanning IR interferometry 0-75978  
BaTiO<sub>3</sub>, paraelec. phase, stabilisation of soft mode 0-75985  
BaTiO<sub>3</sub>, soft mode spectroscopy IR refl. meas. 0-88982  
CeSn<sub>3</sub>, mode softening and elastic const., acoustic vel. meas. 0-88242  
CsCN, inelastic neutron scatt. by coupled rotational and translational modes 0-70333  
Cs<sub>2</sub>CdBr<sub>4</sub>, struct. phase transitions, NQR study 0-71343  
CsCrCl<sub>3</sub>, α-β phase transition, dynamical aspects and thermodynamic theory 0-70404  
Cs<sub>2</sub>PO<sub>4</sub>, pseudo-one-dimensional ferroelec. and antiferroelec. transitions, phase diagram obs., soft modes 0-93245  
CsH<sub>2</sub>PO<sub>4</sub> and CsD<sub>2</sub>PO<sub>4</sub>, pseudo one-dimens. ferroelec. ordering dynamics, <sup>31</sup>P NMR study 0-75971  
α-Fe, vibrational states, phonon dispersion, phonon softening 0-88289  
Fe-Ni (28 at.%), martensitic transformations, Mossbauer scattering evidence of soft modes 0-93223  
Fe-Pd Invar, low temp. FCT phase obs. 0-93538  
Hf, lattice dynamics, phonon dispersion, mode softening 0-107390  
Hg<sub>2</sub>Cl<sub>2</sub>, neutron and Raman scatt. studies, ferroelastic transitions 0-76015  
KCaF<sub>3</sub>, struct. phase transitions, DSC, birefr., and neutron powder diffr. 0-70149  
KD<sub>3</sub>(SeO<sub>3</sub>)<sub>2</sub>, phase transition, neutron scatt. study 0-75351  
KF<sub>2</sub>(MoO<sub>4</sub>)<sub>2</sub>, phase transitions at 312 and 139K 0-70396  
KH<sub>2</sub>PO<sub>4</sub>, Brillouin-Rayleigh scatt. studies near ferroelec. transition temp. 0-76036  
KH<sub>2</sub>PO<sub>4</sub>-KD<sub>2</sub>PO<sub>4</sub> mixed crystals, dielec. spectra, sub-mm wavelengths 0-80724  
KMnF<sub>3</sub>, Mossbauer gamma quanta scattering near 186K transition 0-108126  
K<sub>2</sub>ReCl<sub>6</sub>, elastic constants, softening of acoustic modes, obs. by Brillouin scattering 0-71440  
K<sub>2</sub>SO<sub>4</sub>, longitudinal-acoustic soft mode in phase transition 0-75326  
K<sub>2</sub>SeO<sub>4</sub>, hexagonal-orthorhombic transition, Brillouin scatt. study 0-97208  
K<sub>2</sub>SeO<sub>4</sub>, incommensurate to ferroelec. transition, hydrostatic press. effects, neutron scatt. study 0-108166  
K<sub>2</sub>SeO<sub>4</sub>, Raman spectra, effects of temp., substitutional cations, and stress 0-71405  
K<sub>2</sub>SnCl<sub>6</sub>, elastic constants, softening of acoustic modes, obs. by Brillouin scattering 0-71440  
K<sub>2</sub>ZnCl<sub>4</sub>, incommensurate phase transitions, <sup>35</sup>Cl NQR study 0-75968  
LaAg<sub>2</sub>In<sub>1-x</sub>, phonon dispersion, elastic const. and struct. instability, soft mode behaviour 0-103436  
LaP<sub>2</sub>O<sub>4</sub>, coupling effects between soft optic and acoustic modes at ferroelastic transition 0-70358  
La<sub>2</sub>(Se<sub>4</sub>), structural transitions, symm. anal. 0-92671  
LiNbO<sub>3</sub>, Fourier transform IR spectroscopy of vibr. states at high temp. 0-97256  
LiTaO<sub>3</sub>, Fourier transform IR spectroscopy of vibr. states at high temp. 0-97256  
(ND<sub>4</sub>)<sub>2</sub>BeF<sub>4</sub> and (NH<sub>4</sub>)<sub>2</sub>BeF<sub>4</sub>, incommensurate phase, <sup>9</sup>Be NMR study 0-75973  
NH<sub>4</sub>Cl, acoustic absorption by soft modes of defects 0-59584  
(NH<sub>4</sub>)<sub>2</sub>SiF<sub>6</sub>, elastic constants, softening of acoustic modes, obs. by Brillouin scattering 0-71440  
(NH<sub>4</sub>)<sub>2</sub>SnBr<sub>6</sub>, structural phase transitions study by Raman scatt. 0-93318  
(NH<sub>4</sub>)<sub>2</sub>SnCl<sub>6</sub>, elastic constants, softening of acoustic modes, obs. by Brillouin scattering 0-71440  
NaH<sub>2</sub>(SeO<sub>3</sub>)<sub>2</sub>, β to δ ferroelec. transition under press. Raman spectra study 0-80725  
NbD<sub>0.85</sub>, localised D vibr., temp. depend., neutron inelastic scatt. study 0-107395  
NbH<sub>0.82</sub>, localised H vibr., temp. depend., neutron inelastic scatt. study 0-107395  
Nb<sub>2</sub>Sn, softening of surface phonons in (100) plane 0-107627  
Nb<sub>2</sub>Sn, Young's modulus, 4.2-300K, behaviour near martensitic transition 0-66564  
Pb<sub>2</sub>(P<sub>0.95</sub>As<sub>0.05</sub>)<sub>2</sub>, ferroelastic transition, soft mode, inelastic neutron scatt. study 0-70357  
PbTiO<sub>3</sub>, amorphous, crystallisation process, DTA and Raman spectroscopy meas. 0-75161  
PdH<sub>x</sub>, local, soft modes, superconductivity thermal neutron inelastic scatt. (*Chinese*) 0-70331  
RbCrCl<sub>3</sub>, α-β phase transition, dynamical aspects and thermodynamic theory 0-70404



**soft modes continued**

- RbCrCl<sub>3</sub>, crystals,  $\beta \rightarrow \gamma$  structural phase transition, lattice dynamical anal. 0-84291  
 Rb<sub>2</sub>ZnBr<sub>4</sub>, soft modes at phase transforms., far IR spectrum study 0-107398  
 Rb<sub>2</sub>ZnBr<sub>4</sub>, soft modes obs. by Raman scatt. 0-97283  
 Rb<sub>2</sub>ZnBr<sub>4</sub>(Cl<sub>4</sub>), Raman spectra near incommensurate phase transitions 0-76013  
 Rb<sub>2</sub>ZnCl<sub>4</sub>, incommensurate phase transition, <sup>87</sup>Rb NMR study 0-75967  
 Rb<sub>2</sub>ZnCl<sub>4</sub>, incommensurate phase transitions, <sup>35</sup>Cl NQR study 0-75968  
 SbSI, ferroelec. phase transition and nonlinear props. 0-75988  
 SbSI-SbSBr system, ferroelec., anharmonic effects in far IR reflectivity spectra 0-76014  
 Se, trigonal, Raman scatt. at very high press. 0-60566  
 SmS, LO phonon freq. softening in semicond. and metallic phases 0-96619  
 Sm<sub>1-x</sub>Y<sub>x</sub>S, mixed valence, phonon softening and linewidths, calc. 0-75319  
 Sn<sub>2</sub>P<sub>2</sub>S<sub>6</sub>, ferroelec. semicond., phase transition and lattice dynamics 0-60526  
 Sn<sub>2</sub>P<sub>2</sub>S<sub>6</sub>, soft mode props., Raman scatt. study 0-60525  
 SnTe, dispersive transform., interband electron-phonon interactions, phase diagram 0-93252  
 SrO:Ni<sup>2+</sup>, EPR line splitting rel. to Jahn-Teller coupling and soft localised mode 0-66022  
 Sr<sub>2</sub>Ta<sub>2</sub>O<sub>7</sub>, soft optic phonon responsible for structural phase transition, Raman scatt. meas. 0-96618  
 SrTiO<sub>3</sub>, ferroelectric modes, Raman spectra, neutron scatt. meas. 0-80727  
 SrTiO<sub>3</sub>, heavily reduced, soft mode behaviour 0-71409  
 SrTiO<sub>3</sub>, photolum. and carrier drift mobility at ferroelec. transition 0-71469  
 SrTiO<sub>3</sub>, semiconductor, soft modes, zone boundary mode 0-71357  
 SrTiO<sub>3</sub>:Fe<sup>3+</sup>, order-disorder and central peak behaviour, EPR study 0-75970  
 TaSe<sub>2</sub> (2H), Raman scatt. from CDW 0-93340  
 Te, trigonal, Raman scatt. at very high press. 0-60566  
 TiSe<sub>2</sub> (1T), Raman studies of lattice dynamics 0-103962  
 Ti<sub>2</sub>PSe<sub>4</sub>, phonon dispersion temp. depend. 0-96600

**software (computers)** see computer software

**sogicons** see semiconductor devices

**soil**

- aquifer delayed yield resulting from soil water hysteresis 0-61834  
 crop and soil bidirectional reflectance factor calibration, remote sensing field research 0-86382  
 dust due to soil disturbance, particle absorption contributions to mass extinction coefficients 0-61896  
 groundwater flow pattern in soil using equation of mean 0-81958  
 heat and moisture transport in atmosphere-soil boundary 0-77023  
 heat and water transport, force-restore method for ground surface temp. prediction 0-98469  
 horizontal contact resonances of vibration pickup with rectangular bases on soil surfaces 0-96160  
 hydrophys. charact., determ. method 0-85696  
 IR spectra of hydrothermally altered area, for remote sensing 0-81871  
 machine processing of remotely sensed data, conference, West Lafayette, Indiana (1980 June 3 to 6) 0-82586  
 microwave backscatter from ploughed soil, surface roughness meas. (French) 0-82072  
 moisture content meas., quick drying procedure 0-82109  
 moisture content measurement, remote sensing through agricultural crop 0-109147  
 pollution indication, by humic and fulvic acid chemistry 0-76688  
 pressure meas., using capacitive sensor with polyurethane foam dielectrics (Slovak) 0-86281  
 radioactivity of soil samples from W.Cumbria Pu and <sup>137</sup>Cs concs. and possible maritime effect 0-108817  
 radwaste storage, soil homogeneity evaluation by radionuclide tracer breakthrough curve interpretation 0-97821  
 rain infiltration into soil, theory (German) 0-90102  
 S-wave vel. meas. in soil and bedrock using down-hole method 0-98458  
 spring-flood forecasting and runoff loss due to water absorpt. by soil 0-109178  
 substrate core sampler, lightweight low-friction, ecological survey appls. 0-95090  
 temperatures of soil and ground surface in humid tropics, case study from Sierra Leone 0-109242  
 thermal inertia, cartography in Africa by geostationary satellite (CITHARE project) 0-76980  
 Pu dose to lung and bone from contaminated soils, statistical uncertainties 0-109028

**solar absorber-convertors**

- adiabatic desiccant dehumidifiers for air conditioning, performance predictions, linear modelling 0-85305  
 air heaters, comparative investigation of heat collectors heat-engineering characts. 0-92018  
 algae, living electrode for biophotolysis of water, long-lived photoconverter 0-104510  
 axisymmetric reflector-absorber systems with uniform flux conc. 0-94111  
 bi-coolant wall, heating cycle, thermosiphoning, building heating and cooling 0-72083  
 block unit, thermal characts. experimental investigation 0-97801  
 collector absorption enhancement using multiple reflections 0-76649  
 collector applications for space and water heating in buildings 0-61406  
 collector design and operation for solar-H<sub>2</sub> energy systems 0-61447  
 collector design and suntracking control for PORSHE concept 0-61425  
 collector performance eval. without flow meas. 0-61422  
 collector subsystem operating thresholds, quantitative effect of energy flows 0-85304  
 collectors for space and water heating systems 0-66943  
 collectors with multilayer cylinder heat exchangers, heat balance eqn. and thermal stress anal. 0-58977  
 compound parabolic collector glazings, effective beam rad. incidence angles for determ. of diffuse rad. transmittance 0-94112  
 concentrating collector systems, US DOE Solar Thermal Program, R and D review 0-66998  
 concentrating flat plate solar collectors, graphical determ. of working point (French) 0-61409  
 concentrator-receiver system with selective absorbing surface, heating characts. 0-91874

**solar absorber-convertors continued**

- cooling systems, residential, solar absorption-vapour compression system 0-72017  
 cusp mirror-heat pipe evacuated tubular solar thermal collector 0-94110  
 cylindrical black body receiver design, optical and thermal anal. to reduce thermal losses 0-61428  
 diffusion, chemical reactions, contamination, AES and SIMS 0-72066  
 double glass solar energy collection, convection in vertical rectangular channels (French) 0-85300  
 emittance measurement, emissometer with high accuracy for determination of the total hemispherical emittance of surfaces 0-86309  
 energy collection anal. using information theory 0-97799  
 energy storage area design coefficients for consumer demand and solar radiation (Rumanian) 0-89670  
 equitable performance comparison and economic evaluation of active and passive solar energy systems 0-94101  
 finitely conducting crossed grating applications 0-106636  
 flat plate, 75 to 175°C, thermal perform. predictions and sensitivity anal. 0-94109  
 flat plate, optimal air-flow-rate determ. 0-97805  
 flat plate collector, performance tests using solar simulator 0-61419  
 flat plate collector coatings, perf. comparison of flat black and selective coatings 0-61426  
 flat plate collector glazings, effective beam rad. incidence angles for determ. of diffuse rad. transmittance 0-94112  
 flat plate collector systems for residential water heating 0-61311  
 flat plate collectors, algorithm for solar flux estimates 0-61423  
 flat plate collectors, solar flux calc. for angle of optimum tilt 0-61424  
 flat plate collectors for heating and cooling system for domestic use (Japanese) 0-108787  
 flat plate solar collector with flat specular mirror, optimal tilt angles with seasonal variations 0-72081  
 flat plate solar collector with selective transparent and absorbing plates, thermal anal. 0-61427  
 flat plate solar collectors, meas. of wind speed distribution 0-94108  
 flat-plate collector, temp. distributions under actual unsteady insolation 0-97803  
 flat-plate collector air heaters, efficiency and temp. distrib. (French) 0-66991  
 flat-plate collector efficiency comparisons (French) 0-61408  
 flat-plate solar collector design and sizing, modified Hottel-Whillier-Bliss method 0-97806  
 flat-plate solar collectors, dynamic modelling and verification 0-66992  
 flat-plate solar collectors, laminar mixed convection in fully developed flow (French) 0-61411  
 flat-plate water heating collectors, efficiency determ. using BSE and ASHRAE test procedures 0-85301  
 fluid circulation control in conventional and heat pipe planar solar collectors 0-66994  
 heat collectors, with direct and concentrated radiation, maximum equilibrium temp. determ. 0-92031  
 heat pipe, filled with porous material, glycol water circulation 0-66986  
 heat pump, series, flat-plate collectors, vapour compression, energy conservation 0-72078  
 heat pump assisted solar air heating systems, performance anal. 0-66996  
 heat transfer by natural convection in an isothermal rectangular cavity open on one side (French) 0-61412  
 heating panel system, performance testing and evaluation (Dutch) 0-72079  
 heating systems with salt-water mixture and hot water storage systems 0-67006  
 heating systems with salt-water mixture heat storage 0-67005  
 heliostat solar collectors, meas. of performance characts. 0-85303  
 hot air collectors for domestic hot water heating 0-97768  
 hot water system design 0-104518  
 ideal flux concentrators, intensity variation reduction on absorbers 0-104496  
 internal cusp reflector, optical anal. 0-101127  
 KS-7F solar kitchen, economic effects on economy 0-89590  
 maximally concentrating collectors for solar energy applications, collector performance 0-76648  
 parabolic trough collectors, incidence-angle modifier and average optical efficiency 0-85302  
 photoacoustic determination of absorptance and emittance of solar selective coatings 0-77876  
 photovoltaic/thermal collector performance, comparison of theory and expt. 0-94062  
 plastic, construction, performance and efficiency anal. 0-104516  
 ponds, computer simulation of performance 0-72080  
 ponds, electric power generation at Salton Sea, CA, USA 0-94113  
 ponds, for electric power generation in Israel 0-94114  
 ponds, non-convecting, review 0-61407  
 ponds, salt gradient, computer simulation of thermal behaviour 0-101126  
 power plants, solar high temp., with Stirling engine and solar thermal rocket engine, efficiency improvement by using selective radiation absorption surface 0-89589  
 receiver radiative loss and eye hazard evaluation by Net-Radiometer 0-89673  
 review of solar technology, assessment and contemporary criteria, 1978-79 0-76650  
 salt gradient solar pond for space heating 0-94115  
 seasonal storage devices, economic optimisation of storage capacity and collector area 0-101133  
 selective absorber design, optimal comp. profiles for max. solar absorptance of cermet layers 0-101129  
 selective surfaces, hemispherical emittance of rough metal surfaces 0-70434  
 solar energy system installation suggestions for space heating and water heating (German) 0-94102  
 solar heating systems, optimisation formulation of collector area based on TRNSYS computer code 0-61414  
 solar power plant, direct tracking using two-mirror unit with plane and hyperboloidal counter-reflectors 0-91875  
 solar thermoelectric generator panels, energy characts., estimation 0-101123  
 space heating by solar power, office building in Madrid, use of facade 0-89597  
 space heating system for intermittent heat delivery 0-89669  
 space heating using solar heating installation, technical and operational details (Dutch) 0-72013

# solar absorber-convertors continued

space solar furnaces, for materials-science expts. 0-108786  
spectral selectivity of high-temperature solar absorbers 0-61403  
spectrally selective coatings, physical processes, review 0-61404  
spectrally selective surfaces for photothermal conversion of solar energy 0-101125  
static collector of low-conc., heat losses 0-81487  
static endo-absorbent flat solar collector 0-61421  
steel, stainless, carbide reactively sputtered solar selective absorbers for all-glass tubular evacuated collectors, absorbance and emittance 0-101132  
still, double basin, performance and periodic anal. 0-89671  
stills, inclined-stage type, basic parameters determ. 0-89595  
sulphide black, on Al, solar selective coating, figure of merit 0-72082  
Sun tracker, electronic, for clear or cloudy weather 0-76644  
thermal energy accumulator using stones, operating principles (*German*) 0-72085  
thermal insulation of a low cost solar collector 0-104517  
thermal performance of liquid heating solar collectors, instantaneous collector thermal efficiencies in less time 0-61416  
thermokinetics of glass and semi-transparent materials, radiative and conductive heat transfer (*French*) 0-61410  
thermophotocell, design and calculations 0-97800  
thermophotovoltaic convertor, parametric anal. of emitter temp., conc. ratio and cell reflectance 0-94107  
thermosiphon circulation, flow rate prediction 0-66993  
thermosiphon solar water heaters, transient flow meas. using laser doppler anemometer 0-61413  
thin film prep. for solar energy utilisation 0-84847  
tubular cover solar collectors, performance calcs., transmittance and radiosity 0-61415  
tubular solar collector, design and development 0-76646  
water-trickle type solar collector with massive concrete slab for heat storage 0-108814  
Al-Ge-SiO selective absorber surfaces, optical behaviour at high temp. 0-101130  
C, paint type coating layer with spherical pigment, radiative transfer theory 0-61405  
CO<sub>2</sub>-Br<sub>2</sub>-He mixture, possible gas lasers with solar excitation 0-99695  
CoO<sub>(x)</sub>, black cobalt, solar absorbance of high temp. selective absorbers 0-101131  
CoS<sub>(x)</sub>, black cobalt, solar absorbance of high temp. selective absorbers 0-101131  
Cr-Cr<sub>2</sub>O<sub>3</sub>, black chrome, solar absorbance of high temp. selective absorbers 0-101131  
Cr-Cr<sub>2</sub>O<sub>3</sub>, black chrome selective surface, radiation props. and effect on solar collector 0-85299  
Cr-Cr<sub>2</sub>O<sub>3</sub>, black chrome electrolytic coatings for solar collectors 0-94100  
Cr-Cr<sub>2</sub>O<sub>3</sub> black, electroplated solar collector coatings, high temp. optical and struct. degradation 0-66995  
Cr-Cr<sub>2</sub>O<sub>3</sub> black chrome, commercial, solar absorber coating characterisation 0-80111  
Cr-Cr<sub>2</sub>O<sub>3</sub> black solar absorber surfaces, microstruct. rel. to electroplating parameters 0-61418  
Cr-Cr<sub>2</sub>O<sub>3</sub> black solar selective absorbers, thermal degradation 0-61417  
Cr<sub>2</sub>C<sub>3</sub>, reactively sputtered solar selective absorbers for all-glass tubular evacuated collectors, absorbance and emittance 0-101132  
CuO, black Zn-dust pigmented solar selective coatings for solar photothermal conversion 0-66997  
CuO, on Al or Cu, solar selective coating, figure of merit 0-72082  
CuS, black Zn-dust pigmented solar selective coatings for solar photothermal conversion 0-66997  
CuS-PbS, black Zn-dust pigmented solar selective coatings for solar photothermal conversion 0-66997  
Cu<sub>2</sub>S, on Cu, solar selective coating, figure of merit 0-72082  
FeC<sub>2</sub>-CrC<sub>2</sub>-NiC<sub>2</sub>, stainless steel carbide, solar selective surface, fabrication, magnetron sputtering system description 0-80967  
FeC<sub>2</sub>-CrC<sub>2</sub>-NiC<sub>2</sub>, stainless steel carbide, graded solar selective surface, magnetron sputtered 0-81485  
FeC<sub>2</sub>-CrC<sub>2</sub>-NiC<sub>2</sub>, stainless steel carbide, sputtered solar selective surface, grading profile 0-81486  
Fe<sub>2</sub>O<sub>3</sub>, paint type coating layer with spherical pigment, radiative transfer theory 0-61405  
Ge, black, solar selective absorber characterisation 0-80112  
NH<sub>3</sub>-based solar thermochemical cavity absorber, design and cost anal. 0-81489  
Ni-Ge-SiO<sub>2</sub>, solar selective absorber surfaces, optical behaviour at high temp. 0-101130  
Ni-P coating, electroless, ultra-black surface production by chemical treatment 0-76647  
Pb<sub>1-x</sub>K<sub>x</sub> alloys, fundamental abs. edge, potential as solar convertor 0-101128  
PbS-CuS, black Zn-dust pigmented solar selective coatings for solar photothermal conversion 0-66997  
Se, thin film selective absorber coatings, prod. using an oblique vacuum deposition technique 0-81488  
Si amorphous film, anisotropic etching phenomenon, appl. as solar selective absorber surfaces 0-72054  
Si, CVD amorphous films, effect of surface characts. on visible and UV optical props. 0-60698  
SiO<sub>2</sub>, with embedded Au particles, thin film solar absorber 0-81490  
SnO<sub>2</sub> films, selective, optical characterisation by thermodynamical method 0-84796  
Te, thin film selective absorber coatings, prod. using an oblique vacuum deposition technique 0-81488  
TiO<sub>2</sub>, paint type coating layer with spherical pigment, radiative transfer theory 0-61405  
Zn-dust pigmented solar selective black material for photothermal conversion 0-66997  
ZnSe solar spectrum convertor for GaAs solar cells 0-101117

**solar absorbers** see *solar absorber-convertors*

# solar activity

see also *solar flares*; *solar prominences*; *solar-terrestrial relationships*; *sunspots*  
active centres, longitudinal distrib., effect on geomagnetic var. 0-82330  
active complex with developing secondary region, mag. field struct. and dynamics 0-67685  
active regions, coronal and transition region temp. struct. 0-67692  
active regions, visibility at 408 MHz 0-85922

# solar activity continued

chromosphere active regions, bidimensional spectroscopy obs. with birefringent filter (*Italian*) 0-98568  
chromosphere-corona transition zone of solar active regions, non-thermal velocities (*French*) 0-77371  
conference on nuclear cosmic physics, Leningrad, USSR (Oct. 1978) 0-98755  
corona, heating above active regions by fast electron streams 0-105228  
coronal holes, modulation effect on cosmic ray intensity review 0-77370  
coronal Langmuir turbulence, rel. to quasi-stable particle accel. and type I radio bursts (*Chinese*) 0-105220  
coronal loops in an active region, physical props. XUV obs. 0-90376  
correlation with interplanetary cosmic ray protons 0-77243  
cosmic ray protons at 1 AU from active regions, energy spectra from Pognoz-3 0-101512  
cycle, correl. with geomag. external spherical harmonic coeffs. var. 0-85592  
cycle, correl. with vars. of geomag. field first-degree spherical harmonic components 0-85593  
cycle 20, flares rel. to cosmic ray intensity, model 0-72914  
cycle 20 peak, corona obs. with Solwind coronagraph 0-82325  
cycle minimum, H I Lyman  $\alpha$  flux correlation 0-90393  
cycle of activity rel. to mass motions, torsional oscillator model 0-105217  
eleven year cycle, effects on interplanetary mag. field N-S component configurations in solar wind interaction regions 0-98529  
eleven year cycle, evidence for signal in tropospheric winds 0-72604  
eleven-year cycle, rel. to mag. fields floating-up time 0-101580  
eleven-year cycle, rel. to periodicities of Earth annual polar motion many-year var. (*Chinese*) 0-104848  
EUV flux, changes with solar activity, rel. to ionosphere primary ion-electron prod. rates change 0-72675  
F10.7 index during solar cycle 21, correl. with atmospheric O<sup>+</sup>(<sup>2</sup>P) ionisation freq. vars. 0-77195  
faculae rel. to sunspot cycle 0-90390  
flare distrib. in galactic coord. system (*Russian*) 0-67689  
galactic cosmic ray intensity modulation out to 18 AU Pioneer 10 and 11 obs. 0-90297  
heavy-ion-rich particle events, <sup>3</sup>He/<sup>4</sup>He ratios energy depend. and temporal evolution 0-90299  
ionospheric records over Shanghai, March 1953 to June 1955, correl. of solar activities (*Chinese*) 0-77192  
Lyman  $\alpha$  albedo of Jupiter rel. to solar activity 0-98601  
magnetic field lines from active regions, struct. review 0-85924  
magnetic field of active regions, appl. of new approach to force-free field 0-62011  
McMath 14275, 6 cm obs. of active region and bursts with 6" resolution 0-62096  
McMath region 12417, X-type neutral sheet form., chromospheric activity prod. 0-98642  
McMath region 13043, overlying centimetre-wave sources rapid var. rel. to optical phenomena 0-67688  
McMath region 15403, 5 minute oscills., SHF obs. 0-98639  
noise storm, drift pair bursts, polarisation obs., position and freq. characts. 0-85925  
noise storm, drifting pulsations obs. 0-62105  
photosphere activity, energy transfer to solar wind by elec. currents 0-94768  
plage Ca II K-line, peak separation due to microturbulence 0-109407  
polar solar wind, variation rel. to solar activity 0-90385  
proton event of 1978 May 7, neutron monitor obs. 0-67686  
radio bursts, anal. of obs. at 3.2 and 10 cm at Purple Mountain Observatory (*Chinese*) 0-105223  
Solar Maximum Year project and related space experiments, review 0-90404  
solar wind characts. rel. to solar activity, review 0-94777  
Sun and heliosphere, conference, London, England (1979 April 3 to 4) 0-82574  
sunspot cycle, rel. to occurrence of range and freq. spread-F at Kodai-kanal 0-72676  
sunspot number, rel. to tropopause height 0-77090  
surges, dynamics of descending stage (*Chinese*) 0-105221  
terrestrial effects, thermosphere NO and N conc. depend. on activity 0-77178  
transient activity and interplanetary shock waves, implications of He<sup>+</sup> obs. in driver gas 0-72735  
type III bursts, obs. during JIKIKEN (EXOS-B) satellite initial phase (*Japanese*) 0-94675  
type III bursts, position and polarisation, VHF and HF obs. 0-105214  
type IV radio burst quasiperiodic struct., anal. and interpretation 0-62097  
type V radio bursts, position and polarisation, HF and VHF obs. 0-105215  
UV flux variability over solar cycle, 1175-2100 Å 0-90383  
variations rel. to Earth rotation and atmospheric circulation 0-104853  
young active regions, filaments, comparison of X-ray and visible data 0-72910  
Zurich relative sunspot nos. rel. to solar temp. min. in far IR 0-94769

# solar atmosphere

see also *chromosphere*; *photosphere*  
acoustic waves, flux tubes 0-85911  
active regions magnetic field, appl. of new approach to force-free field 0-62011  
circumsolar plasma, radio signal spectral lines formation 0-92330  
dynamics, optically thick chromospheric line formation 0-94767  
electric currents, generation by solar activity rel. to solar wind energy source 0-94768  
expansion into solar wind, higher order fluid eqns. for multicomponent nonequib. plasma atmosphere 0-105156  
flares, polarisation and directivity of hard X-ray bremsstrahlung from thermal source 0-90374  
gravity waves, trapped, in solar atmosphere, obs. 0-72898  
magnetic fields, force-free fields evolution, nonequib. states and preflare stage 0-105213  
penetrative instabilities in solar atmosphere, effects of thermal dissipation 0-109406  
prominences, H line radiation diffusion 0-67694  
radiative transfer, physical effects in multidimens. media, models 0-72758  
radio burst emission mechanisms 0-72917



**solar atmosphere** continued

- radio bursts, peak flux spectra, statistical anal. source mechanisms 0-98641
- spectral line formation depth in mag. field, theory (*Chinese*) 0-105159
- spectral line shifts, wave effects 0-109408
- surges, dynamics of descending stage (*Chinese*) 0-105221
- temperature minimum, absolute brightness temp. meas. in far IR with balloon-borne interferometer 0-62095
- time intensities, dielectronic recomb. excitation effects 0-82332

**solar batteries** see *solar cells***solar cell arrays**see also *solar power*

- 25 kW Fresnel lens/photovoltaic concentrator application experiment at Dallas-Fort Worth Airport 0-89647
- 25 kW solar photovoltaic flat panel power supply for electrodialysis water desalination unit 0-89643
- aggregating cells in series and parallel, technique 0-93954
- concentrator designs for space vehicle photovoltaic arrays 0-94057
- efficiency of generation, solar energy conc. using Fresnel lenses, spectral adaption and fluoresc. and bifacial concentrators (*Spanish*) 0-72060
- electricity storage in solar energy plant, battery appls. potential 0-72067
- ethylene-vinyl acetate lamination, solar cell encapsulation, double vac. technique 0-93510
- fabrication, review of present status and future prospects 0-61343
- flat plate PV modules, elec. and environmental testing requirements for terrestrial appls. 0-61368
- flat-plate non-tracking ground mounted photovoltaic array structures, cost reduction anal. 0-94038
- flat-plate photovoltaic array design optimisation 0-94037
- HV photovoltaic arrays, safety from high reverse voltages 0-93953
- lightweight hybrid solar arrays, status of development 0-94042
- line-focus parabolic-trough photovoltaic arrays, active and passive cooling 0-93988
- parabolic concentrator arrays, collector end shadowing effects minimisation 0-93987
- photovoltaic, optimisation of total annual energy output from constant/adjustable tilt systems 0-94059
- photovoltaic cells using silicone materials, encapsulation 0-94019
- photovoltaic concentrator array technology, status report 0-94024
- photovoltaic modules and systems, circuit design considerations 0-93955
- photovoltaic power conditioning system for professional services office building 0-89646
- photovoltaic power system reliability assurance methods 0-61315
- photovoltaic powered 20-hp DC/AC irrigation system and 3-kW N generator 0-89645
- photovoltaic systems break-even cost anal. for rural Mexico 0-94027
- photovoltaic transient analysis program for electrical and thermal anal. 0-94061
- photovoltaic village power systems: the minigrd concept 0-66973
- photovoltaic/thermal system powers Texas house, performance data and power conditioning equipment 0-94036
- point-focus Fresnel lens photovoltaic arrays, active and passive cooling 0-93988
- point-focus photovoltaic concentrator arrays, durability, reliability 0-93985
- production, research and development, US DOE photovoltaic program 0-93879
- rural electrification by solar power, photovoltaic arrays efficiency 0-66974
- Si ribbon crystals, edge-defined film-fed growth technique 0-89633
- solar voltaic power systems, comparison to fuel energy, for telecommunications 0-61381
- Solarex two-axis tracking linear concentrating collector system, design and operation 0-93989
- spacecraft, in-orbit performance, review 0-94054
- spectrally selective reflectors for concentrator solar arrays, evaluation 0-94043
- tandem solar cells, detailed balance limit of efficiency 0-72056
- technological and economic barriers to be overcome for competitive power production 0-72049
- terrestrial, development of glass encapsulation technique 0-94020
- testing, standard procedures for terrestrial photovoltaic performance measurements 0-66979
- tracking by microprocessor-based coordinate calc. (*Spanish*) 0-89623
- water pumping solar systems using photovoltaic converter arrays 0-61402
- AlGaAs/GaAs monolithic series-connected arrays 0-97794
- GaAs 20 kW photovoltaic dense array for central receiver concentrator appls. 0-61372
- GaAs, for earth orbital and orbit transfer missions 0-94044
- Si, fixed-base, flat panels, possible developments for more competitive power production 0-72050
- Si, for earth orbital and orbit transfer missions 0-94044
- Si polycrystalline, low cost conversion into sheet by heat exchange method and fixed abrasive slicing technique 0-93479

**solar cells**

- Al<sub>1-x</sub>Ga<sub>x</sub>As-GaAs heterophotoconverters, HV, investigations 0-101097
- amorphous materials appls. 0-107693
- Ansaldo, for parabolic trough concentrator systems with forced cooling 0-93982
- ATS-6 solar cell flight expt., radiation damage, summary results 0-94005
- Auger recombination limit on efficiency at high level of illumination 0-108797
- automated electronic analysis system for solar cells 0-93952
- autonomous solar electric systems (*German*) 0-93875
- back surface field, theoretical design considerations 0-93961
- back surface reflector (BSR) and back surface field (BSF) solar cell technology, compatibility 0-89650
- back surface reflectors, effect on device perform. 0-93908
- back-side-reflection, for future solar arrays, design and qualification 0-94040
- back-surface-field n<sup>+</sup>-p-p<sup>+</sup> and p<sup>+</sup>-n-n<sup>+</sup> solar cells, open-cct. voltage in conc. sunlight 0-61352
- biological photoactive components in PEC, photosynthetic bacterial reaction centres on sputtered C and SnO<sub>2</sub> electrodes 0-66981
- calibration using radiometric determ. of solar radiation spectral distrib. 0-61369
- carrier lifetime measurements from transient elect. photoresponses 0-61346
- cascade, design for high-temp. operation using computer modelling 0-81456

**solar cells** continued

- cascade using two or more junctions, material and device considerations 0-81455
- cast polycrystalline, ion implanted, laser annealed 0-93918
- cast polycrystalline p-n junction, hydrogenation effects 0-93916
- collection grid structure, optimisation of area, shape and spacing 0-72042
- concentrator, thick film conductive ink contacts 0-93957
- conductor-insulator-semicond. (CIS) solar cells, noncrystalline (poly and amorphous), interface importance 0-81466
- conductor-insulator-semiconductor solar cell developments for low cost prod. 0-61378
- conversion efficiency, maximum theoretical efficiency as a function of temp. 0-81469
- CuInSe<sub>2</sub> thin film fabrication by RF-sputtering 0-100786
- DC-AC inverter design, effect of meteorological conditions, computer simulation 0-61373
- development, US DOE National Photovoltaic Program R and D 0-66999
- diffusion, chemical reactions, contamination, AES and SIMS 0-72066
- diffusion equation, surface boundary condition 0-66975
- distributed series resistance effects in photovoltaic devices 0-93968
- cleptic-align V-grooved hyperjunction thin film cell, MIS and SIS device appls. 0-94082
- effective series resist. meas. effects of temp. variations 0-93944
- efficiency of generation, solar energy conc. using Fresnel lenses, spectral adaption and fluoresc. and bifacial concentrators (*Spanish*) 0-72060
- electric power sources, applications overview (*Italian*) 0-72044
- electrical load feeding prospects (*Italian*) 0-60028
- electron beam depth profiling, using carrier collection models 0-70723
- energy analysis and viability of photovoltaic conversion and OTEC 0-61358
- fabrication, laser-induced p-n junction formation 0-93880
- fabrication, photovoltaic process based on thick film technique 0-94016
- failure, life prediction using physical chemical failure progression modelling 0-61370
- fault analysis using scanning light spot and distrib. network model 0-81473
- faulty, scanning light spot anal. 0-89625
- flat plate module design evolution, influence of module requirements 0-94065
- fluorescent planar concentrators, efficiency and stability 0-93986
- fluorescent window for semiconductor-liquid junction solar cells 0-101114
- front surface field solar cell, spectral response, theory 0-76633
- G. Donegani Institute activity (*Italian*) 0-60027
- GaAs, polycrystalline, grain boundary resistance meas. effect on solar cell performance 0-93891
- Galileo works activities (*Italian*) 0-60029
- global calibration of terrestrial reference cells and errors involved in using different irradiance monitoring techniques 0-93951
- heteroface, optimum design theory 0-66972
- heterojunction solar cell model, design and evaluation 0-93964
- heterojunction solar cells 0-61344
- HEWACS, high efficiency wraparound contact solar cells 0-93906
- homojunction, superposition principle 0-81449
- homojunction direct gap, theoretical limit efficiency 0-97795
- hybrid solar photovoltaic/solar thermal electric power system, simulation 0-94025
- integral glass covering of spacecraft solar cells by electrostatic bonding 0-93676
- interdigitated back-contact, tandem junction cell and front-surface field cell 0-89638
- inversion layer, numerical modelling 0-81444
- ion implantation and annealing technology 0-93996
- Italian National Research Council program (*Italian*) 0-72045
- LAMEL activities (*Italian*) 0-60026
- laser annealing, conversion efficiency improvement (*French*) 0-66976
- laser scanning for display of operating characts. and detection of cell defects 0-81460
- low resistivity, open cct. voltage improvement 0-93910
- low-high-junction model developed for tandem cell anal. 0-89626
- mass production technology, cell installation development costs (*German*) 0-72046
- metallisation patterns for higher efficiency, analytical approach 0-93943
- metallisation using screen printing tech. 0-85291
- MIS, computer simulation studies rel. to interface state meas. 0-72048
- MIS, effects of nonuniformity of insulating layer 0-104507
- MIS, interface problems, AES, SIMS and XPS study 0-89627
- MIS, inversion layer, surface passivation 0-101098
- MIS inversion layer, two-dimensional model 0-89641
- MIS negative barrier contact for induced back surface field solar cell 0-101101
- MIS Schottky barrier cells, barrier height change and current transport in presence of interfacial layer 0-61353
- MIS solar cells, etched slotted mask for direct deposition of metal contact pattern 0-97786
- MIS solar cells with diffused back surface field (BSF), and diffused junction solar cells with MIS BSF 0-94074
- MIS/SIS, automated surface states anal. 0-93966
- modular, highly reliable Si cell (*Japanese*) 0-81468
- monolithic III-V compound two-junction cascade solar cells, computer modelling 0-81433
- MOS-inversion layer solar cells, fundamental mechanisms affecting performance 0-61377
- n<sup>+</sup>-p-n<sup>+</sup> double sided, optimal static concentration 0-89639
- n<sup>+</sup>-p-p<sup>+</sup> bifacial back surface field solar cells, optimisation of p<sup>+</sup> doping level by ion implantation 0-97784
- n-i-p, thin Si cells, with high output and low diffusion length damage coeff. 0-93909
- noise spectral density as a device reliability estimator 0-93896
- organic, photovoltaic properties of polymer films 0-60040
- output monitoring, design and utilization of a microprocessor-controlled absolute spectral response system 0-81476
- oxide-semiconductor/base-semiconductor, optimization 0-81440
- P<sup>+</sup>-n, BN glass transfer process appl. for cell fabrication 0-107459
- p<sup>+</sup>-n, n<sup>+</sup>-p structures on polycrystalline material, performance 0-89640
- p-n, polycryst., grain boundary influence on recomb. 0-93913
- p-n heterojunction solar cell, general formulation of current-voltage characts. 0-80361
- p-n junction, determ. of lifetime and recombination currents 0-89637
- p-n junction photodiode terminology 0-70800
- p-type, illumination and-temp. dependence 0-94046
- photo-intercalation: possible application in solar energy devices 0-108803



# solar cells continued

photoelectric, optical methods for checking parameters of semiconductor doped layer 0-93869  
photoelectrochemical cells, energy conversion system, principles and appl. 0-89652  
photoelectrochemical cells, review of cell types and electrode props. 0-61385  
photoelectrochemical cells (*Dutch*) 0-85295  
photoelectrochemical regenerative and storage cells with semiconductor electrodes (*French*) 0-61386  
photogalvanovoltaic cells and photovoltaic cells using glassy carbon electrodes 0-89630  
photovoltaic cells in undersea environment, performance 0-93900  
photovoltaic concentrating systems, optical and tracking systems design, performance characts. 0-72051  
photovoltaic conversion comparative evaluation (*Italian*) 0-60023  
photovoltaic flat panel procurement, qualification test results 0-94064  
photovoltaic material and device meas. workshop, conf. Arlington, VA, USA, June 1979 0-77543  
photovoltaic materials and devices for terrestrial solar energy applications, R and D status review 0-10112  
photovoltaic module utilising parabolic trough concentrators 0-93984  
photovoltaic modules testing, reliability and performance 0-94063  
photovoltaic pilot line of 15 kW under Mexican research and development 0-94022  
photovoltaic power supplies, cost reduction possibilities 0-97793  
photovoltaic power system, design and performance charact. 0-89644  
photovoltaic power system elements, efficiency and terminology summary 0-97790  
photovoltaic receiver for parabolic trough concentrator, optimisation 0-93983  
photovoltaic solar devices, modular system (*German*) 0-89629  
photovoltaic system analysis computer program; SOLCEL-II 0-94058  
photovoltaic system sizing anal. 0-94039  
photovoltaic technology, conf., San Diego, CA, USA (Jan. 1980) 0-86041  
photovoltaic terrestrial systems, protection from lightning effects 0-89648  
photovoltaic/thermal collector performance, comparison of theory and expt. 0-94062  
planar multijunction HV, technical considerations and fabrication 0-89636  
Polka Dot, description and anal. 0-93959  
polyacetylene semiconductor film applic. 0-92899  
polycrystalline, grain and grain boundary effects on drive characts. 0-93914  
polycrystalline, influence of grain boundaries electronic structure on diode characts. 0-94068  
polycrystalline, recomb. at grain boundaries, effect on photoresponse 0-108796  
polycrystalline, relative orientation of grains and nature of grain boundaries 0-93915  
polycrystalline and tandem, for high efficiencies, using compound semiconductors 0-72052  
power plant, orbiting, evaluation of current conductor mass and voltage level required 0-89616  
remote islands telecommunication repeater stations power supply 0-61382  
ribbon growth using scanned focused CO<sub>2</sub> laser beams 0-66417  
satellite solar cell power plant, operating experience 0-94055  
Schottky barrier, doping density effect on efficiency 0-101100  
Schottky barrier, efficiency depend. on thickness of interface layer 0-76637  
Schottky barrier solar cells, back-illuminated, theoretical performance 0-61345  
semiconductor solar cells, state of the art, various installations description (*Dutch*) 0-72063  
semiconductor-liquid junction type, efficiency, evaluation 0-72043  
semicrystalline vs. single crystal Si 0-93917  
single diode models for simulating cells with distributed series resistance 0-93962  
SOC (Si on ceramic) continuous coating 0-93904  
Sophia Antipolis 5 kW photovoltaic power generator for habitat 0-61374  
space qualified, high efficiency solar panel project using multiple antireflective cells 0-94056  
spectral irradiance of solar simulators and its effects on cell meas. 0-93950  
stacked multibandgap monolithic multijunction solar cells, loss evaluation, optimum performance 0-93928  
substrate related problems in RAD solar cells 0-89635  
Sun tracker, electronic, for clear or cloudy weather 0-76644  
superposition principle application to solar cell anal. 0-76631  
surface recombination velocity and diffusion length meas. 0-93965  
tandem, detailed balance limit of efficiency 0-72056  
tandem junction, Ebers-Moll transistor model 0-93911  
tandem-junction, one-dimensional theoretical model 0-81450  
testing, standard procedures for terrestrial photovoltaic performance measurements 0-66979  
thermal and other tests of photovoltaic modules performed in natural sunlight 0-97789  
thermoelectric air conditioner humidifier (SATEACH), solar assisted 0-108802  
thermophotocell, design and calculations 0-97800  
thermophotovoltaic convertor, parametric anal. of emitter temp., conc. ratio and cell reflectance 0-94107  
thermophotovoltaic solar energy conversion, upper limit 0-81446  
thick film technology, applic. to manufacture 0-93903  
thin, advanced module technique 0-94041  
thin film, comparison methodology 0-93920  
thin film, degradation processes of electrophysical characts. during long-term operation 0-89617  
thin film, technical and economical eval. 0-94012  
thin film, unified anal. of potential 0-81436  
thin film polycrystalline, chemical and structural defects 0-93919  
thin film polycrystalline materials, resistivity and Hall effect meas. 0-93899  
thin film polycrystalline Si, research and develop. overview 0-93921  
thin film technology, appls. in energy, optics, and electronics, review 0-78932  
thin film wraparound cell, improved perform. 0-93912  
transparent modules, high-efficiency, with improved glass, adhesives and heat dissipation 0-76636

# solar cells continued

ultrathin high efficiency coplanar back contact, design and fabrication 0-89649  
vertical junction, new developments 0-93907  
wavelength shifting, by powdered fluorescent capping layers 0-85286  
wraparound-contact, use of printed-circuit methods 0-76635  
Ag-Si interfaces, solar cell contacts 0-92973  
Al/SiO<sub>2</sub>/pSi MIS solar cells, stability 0-85287  
Al-Al<sub>2</sub>O<sub>3</sub>-GaAs backwall MIS Schottky barrier solar cell, anal. model 0-85289  
Al-poly-Si Schottky-barrier solar cells, grain boundary effects on electrical behaviour 0-85279  
Al-Si MIS solar cells, depth conc. profiles, elec. and optical props. of Al films 0-94076  
Al-SiO<sub>2</sub>-pSi, comparison of majority- and minority-carrier Si MIS cells 0-85280  
Al-SiO<sub>2</sub>-Si MOS solar cells, open-cct. voltage var. with oxide layer thickness 0-81434  
Al-SiO<sub>2</sub>-(p-)Si barrier structs., minority carrier injection ratio meas., MIS solar cell model 0-93007  
Al-SiO<sub>2</sub>-pSi, comparison between MIS and SIS cells 0-81443  
Al-Si(Ge) eutectic alloys in screened ohmic contacts for solar cells 0-94090  
AlGaAs heterojunction photocell with luminesc. wavelength converter 0-108800  
AlGaAs-GaAs proton irradiated solar cells, deep-level defects, recombination mechanisms, performance characts. 0-81459  
AlGaAs-GaAs proton irradiated solar cells, deep level defects and recombination parameters 0-94032  
Al<sub>0.35</sub>Ga<sub>0.65</sub>As-GaAs cascade solar cell structs., spectral response and junction characts. 0-93926  
Al<sub>0.35</sub>Ga<sub>0.65</sub>As, p-n junction solar cells, effect of interface recombination on photoluminescence and current 0-93893  
p-Al<sub>0.35</sub>Ga<sub>0.65</sub>As-p-GaAs-n-GaAs heterophotocells, optimal parameters for high solar-excitation level 0-93872  
Al<sub>0.35</sub>Ga<sub>0.65</sub>As-ZnGaAs solar cells by LPE, open circuit voltage, fill factor 0-101108  
Al<sub>2</sub>O<sub>3</sub> MIS Schottky structures, photovoltaic response 0-101115  
AlSb Schottky barrier solar cells, characteristics and efficiency of Czochralski-grown crystals 0-61366  
AlSb solar cell material, epitaxy, ionicity and bond struct. 0-61367  
Au-Al<sub>0.35</sub>Ga<sub>0.65</sub>As -GaAs heterojunction Schottky-barrier solar cells, barrier height enhancement 0-85284  
Au-AlGaAs-GaAs heterojunction Schottky barrier solar cells, barrier height enhancement 0-94071  
Au-GaAs Schottky barrier solar cells, effect of interfacial oxide layer on cell characts. 0-61365  
Au-n-AlGaAs-n-GaAs Schottky-barrier solar cells, band readjustment effect 0-81458  
Au-n-Si Schottky barrier solar cells, recombination in space charge region 0-61351  
Au-SiO<sub>2</sub>-n-Si, comparison of majority- and minority carrier Si MIS cells 0-85280  
CdO, aqueous-deposited films, struct. and electronic props. for solar cell appls. 0-100797  
CdS, aqueous-deposited films, struct. and electronic props. for solar cell appls. 0-100797  
CdS, for thin film and ceramic solar energy convertors 0-93870  
CdS photoconductivity, spatial homogeneities exam. using DC and microwave techniques 0-93895  
CdS, review and present status 0-76638  
CdS solar cells, construction, solar photovoltaic systems for remote communications power supply 0-66980  
CdS thin film solar cell fabrication, HCl etching 0-81474  
CdS thin film solar cells, R and D of low cost cells 0-85292  
CdS thin films, growth and evaluation for fabrication of high performance photovoltaic solar cells 0-93501  
CdS thin films on brass substrates, nondestructive resistivity meas. tech. 0-93898  
CdS/Cu<sub>2</sub>S, polycryst. thin film photovoltaic materials, photon loss anal., expt. determ. 0-93888  
CdS/Cu<sub>2</sub>S thin film heterojunctions, photocapacitance meas. of solar cell parameters 0-93897  
CdS/Cu<sub>2</sub>S thin film solar cells, design and fabrication, 9.15% conversion efficiency 0-81438  
n-CdS/n-InP/p-InP heteroface solar cell with ultrathin window layer, computer anal. 0-97788  
n-CdS/p-ZnIn<sub>2</sub>Se<sub>4</sub> thin film solar cell, photovoltaic props. 0-89628  
CdS-CdTe p-n junction screen printed thin film solar cells 0-72055  
CdS-Cu<sub>2</sub>S, design and fabrication, 8.5% conversion efficiency 0-72047  
CdS-Cu<sub>2</sub>S, microstructural study of heterojunction materials 0-93978  
CdS-Cu<sub>2</sub>S, props., characts. and efficiency, development costs (*Spanish*) 0-72062  
CdS-Cu<sub>2</sub>S thin-film solar cells, low-cost manufacturing process outline, economic anal. 0-93930  
CdS-Cu<sub>2</sub>S thin-film solar cells, high open-cct. voltage and low refl. losses 0-94088  
CdS-Cu<sub>2</sub>S, electron diffusion length determ. using spectral response meas. 0-81475  
CdS-Cu<sub>2</sub>S solar cell, prep. and characts. (*Croatian*) 0-93876  
CdS-CuInSe<sub>2</sub> solar cell, polycrystalline thin film, high photocurrent, characts. 0-61339  
CdS-InP(CdTe)(GaAs)(Ge), solar cell heterojunctions, CVD fabrication, photovoltaic response 0-93878  
CdS-SiO<sub>2</sub>-Si solar cell, I-V characteristics 0-89621  
CdSe, chemically sprayed thin films as photoanode in photoelectrochem. cells, power charact. meas. 0-85293  
CdSe film, electrodeposited, for photoelectrochemical cell for solar energy conversion 0-94093  
CdSe film photoanodes for electrochem. photovoltaic cells, fabrication and evaluation 0-76641  
CdSe, for thin film and ceramic solar energy convertors 0-93870  
CdSe thin film, performance 0-93970  
CdSe<sub>0.4</sub>Te<sub>0.35</sub>, polysulphide photoelectrochem. solar cell 0-72073  
CdTe thin film polycrystalline solar cells prepared by electrodeposition 0-93948  
CdTe/SnCl<sub>2</sub>/Pt, solar cell photoelectric props. (*Spanish*) 0-85290  
CdTe-CdS thin film p-n solar cells, spectral response temp. depend. 0-93871  
CdZnS thin films, growth and evaluation for fabrication of high performance photovoltaic solar cells 0-93501



## solar cells continued

- Cd<sub>1-x</sub>Zn<sub>x</sub>S solar cell thin films, microprobe characterisation (*French*) 0-61349
- Cd<sub>1-x</sub>Zn<sub>x</sub>S films, chem. sprayed, carrier density and mobility 0-60121
- Cr-MIS solar cells, on polycryst. Si, grain boundary effect and conduction mech. 0-93894
- Cr-MIS solar cells on p-type wafer poly-Si substrates, high efficiency design 0-93935
- Cr-MIS solar cells on Si, revised process to increase active area efficiency and reproducibility 0-81462
- Cr-SiO<sub>2</sub>-Si MIS solar cells, photovoltaic performance and interface states, nucl. radiation effects 0-94004
- CuGa<sub>0.5</sub>In<sub>0.5</sub>Se<sub>2</sub>/Zn<sub>0.25</sub>Cd<sub>0.75</sub>S heterojunction solar cell, preparation and props. 0-101110
- CuIn<sub>1-x</sub>Ga<sub>x</sub>Se<sub>2</sub>(1-x)Te<sub>2x</sub> pentenary alloy compounds for photovoltaic solar energy conversion 0-93971
- CuInS<sub>2</sub> single phase thin film prep. by flash evaporation 0-100796
- CuInSe<sub>2</sub> thin films, prep. by spray pyrolysis, struct., elect. and optical props. for solar cell appls. 0-100781
- CuInSe<sub>2</sub> thin films for solar cells, radiofrequency sputtering technique, elec. props. 0-93487
- Cu<sub>2</sub>O, electrical and optical props., photocurrent anal. 0-101116
- Cu<sub>2</sub>O MIS, with SiO<sub>2</sub> interfacial layers, semi-transparent layers of Au, Cu, Ag and Al 0-93946
- Cu<sub>2</sub>S, diffusion length meas. using scanned laser beam tech. 0-93886
- Cu<sub>2</sub>S/CdS heterojunction solar cells, diffusion length determ. using minority carrier SEM 0-61359
- Cu<sub>2</sub>S-CdS, interface recombination phenomena and tunnel effect 0-66978
- Cu<sub>2</sub>S-CdS, optical absorption coefficient changes in Cu<sub>2</sub>S 0-93980
- Cu<sub>2</sub>S-CdS, optimised grid patterns 0-108798
- Cu<sub>2</sub>S-CdS, sprayed, fabrication and electrical props. 0-93979
- Cu<sub>2</sub>S-CdS, with interdigitated grid, current-voltage analysis 0-93981
- Cu<sub>2</sub>S-CdS heterojunction solar cells, carrier transport, nonmonotonic band profiles 0-61361
- Cu<sub>2</sub>S-CdS heterophotocells based on CdS films of stoichiometric composition, elec. and photoelec. props. 0-93873
- Cu<sub>2</sub>S-CdS solar cell applications, CdS film spray fabrication, physical props. (*French*) 0-60113
- Cu<sub>2</sub>S-CdS solar cell fabrication by magnetron reactive sputtering deposition 0-61363
- Cu<sub>2</sub>S-CdS solar cells, Cu<sub>2</sub>S film growth methods 0-80980
- Cu<sub>2</sub>S-CdS thin film heterojunction 0-93922
- Cu<sub>2</sub>S-CdS thin film planar junction devices, quantitative photon loss anal. 0-61362
- Cu<sub>2</sub>S-Zn<sub>x</sub>Cd<sub>1-x</sub>S and Cu<sub>2</sub>S-CdS thin film solar cells by solid state reaction, comparison 0-101109
- Cu<sub>2</sub>S-Zn<sub>x</sub>Cd<sub>1-x</sub>S heterojunction, improved model of electro-optic behaviour 0-94023
- Cu<sub>2</sub>S-Zn<sub>x</sub>Cd<sub>1-x</sub>S solar cells, thin film photovoltaic solar energy conversion 0-61379
- Cu<sub>2-x</sub>S-CdS, collection coefficient theoretical anal. at conjunction 0-101094
- Cu<sub>2-x</sub>S-CdS ceramic solar cells, solar batteries operating characts. 0-93874
- Cu<sub>2-x</sub>S-CdS p-n heterojunction, optical energy convertor, struct. and recomb. props. 0-72065
- Cu<sub>2</sub>S evaporated layer growth in vacuum, compositional and optical characterisation, solar cell appls. 0-97437
- Cu<sub>2</sub>S/CdS thin film cell, prep. by sequential evaporation 0-93902
- Cu<sub>2</sub>S-CdS, Cu<sub>2</sub>S growth kinetics and composition analysis by absorbance transient and galvanic electrochemical measurements 0-92797
- Cu<sub>2</sub>S-CdS solar cells, SCL current 0-76634
- Cu<sub>2</sub>S-CdS thin film, using all film vacuum deposited process 0-93977
- α-Fe<sub>2</sub>O<sub>3</sub>, photochem. props. of sintered and doped samples for solar photoelectrochem. cell appls. 0-89651
- GaAlAs on GaAs thin film stacked multiple-bandgap solar cell structs., prep. using CVD techniques 0-94083
- GaAlAs/GaAs, Be and Zn behaviour 0-101111
- GaAlAs/GaAs solar cells, efficiency optimisation at high and low current levels (*French*) 0-61348
- GaAlAs-GaAs heteroface solar cells, high open-cct. voltage, full-factor and efficiency 0-94081
- GaAlAs-GaAs heterojunction solar cells, high temp. props. 25 to 300°C 0-94035
- Ga<sub>1-x</sub>Al<sub>x</sub>As-GaAs p-n and p-p-n heterojunction solar cells, high efficiency, prep., eval. and characters (*Japanese*) 0-61342
- GaAlAsSb-GaSb low bandgap solar subcell for high efficiency multibandgap convertors, LPE growth 0-93927
- GaAs antireflecting MOS solar cells, epitaxial and polycryst. using OM-CVD techniques 0-94072
- GaAs, developments and trends for automatic interplanetary stations, Venus-9 and Venus-10, and mooncar program 0-89613
- GaAs, efficiency improvement using ZnSe solar spectrum convertor 0-101117
- GaAs, electron and proton radiation damage 0-94034
- GaAs epitaxial growth, CVD-organometallics method, reactional efficiency in solar cell elaboration 0-93498
- GaAs films for solar cells appl., deposition and characterisation 0-84853
- GaAs homojunction solar cells, large-grained, passivation method to improve open-circuit voltage 0-94070
- GaAs MIS solar cells, effects of thin oxide layers on characts. 0-89624
- GaAs MOS solar cells by anodisation in active region 0-101107
- GaAs on Ge thin film stacked multiple-bandgap solar cell structs., prep. using CVD techniques 0-94083
- GaAs, polycryst., wet and dry oxides, comparative study by AES, SIMS and XPS and solar cell performance 0-80116
- GaAs, polycryst. solar cells, thin film growth and grain size, effect on cell efficiency 0-81471
- GaAs polycryst. solar cell diagnostics using IR electroluminesc. 0-93885
- GaAs, polycrystalline, props. and prep. with grain boundary edge passivation 0-81437
- GaAs polycrystalline thin film solar cells, fabrication 0-94066
- GaAs, props., characts. and efficiency, development costs (*Spanish*) 0-72062
- GaAs prospects (*Italian*) 0-60025
- GaAs shallow-homojunction solar cells on single crystal GaAs and Ge substrates, CVD fabrication and efficiency 0-61364
- GaAs shallow-homojunction solar cells, electron radiation effects 0-97798
- GaAs, simultaneous radiation damage and annealing 0-94033

## solar cells continued

- GaAs solar cell, polycryst., grain boundary passivation by oxidation, AES, SIMS and XPS obs. 0-81467
- GaAs solar cell polycrystalline conducting substrate, minority carrier diffusion length spatially-resolved meas. 0-94084
- GaAs solar cells, photoreaction of p-n junction diodes 0-81464
- GaAs, thin film, polycrystalline, grain boundary edge passivated 0-94069
- GaAs thin film growth tech. and characterisation 0-89631
- GaAs thin film polycrystalline Schottky barrier solar cells, grain boundary chemistry 0-94067
- n-GaAs-Sn-p-GaAs:Ge-p-Al<sub>0.1</sub>Ga<sub>0.9</sub>As:Ge heterostructure solar cells, LPE growth techniques 0-66977
- GaAs:Te Schottky barrier solar cells, diffusion length determ. using minority carrier SEM 0-61359
- GaAs-AlGaAs, with valley-transferred electrons for voltage and efficiency enhancement 0-93956
- GaAs-AlGaAs solar cells (*Rumanian*) 0-93877
- GaAs-Au(Al) Schottky barrier, interface problems, AES, SIMS and XPS study 0-89627
- GaAs-In<sub>0.25</sub>Sn<sub>0.75</sub>O<sub>3-y</sub> SIS heterostructure solar cells, spray-deposited 0-101106
- n-GaAs-K-Se-K<sub>2</sub>Se<sub>2</sub>-KOH/C thin film solar cell, 7.3% cell efficiency 0-93931
- p-GaSe, back wall Schottky barrier cells, diffusion length, RT spectral response meas. 0-107806
- In<sub>2</sub>O<sub>3</sub>-SnO<sub>2</sub>/polySi, response exam. using electron-beam-induced current and scanning light spot tech. 0-81477
- In<sub>2</sub>O<sub>3</sub>-SnO<sub>2</sub>-CdTe:P, p-n homojunction solar cell, elec., photovoltaic props., photoluminescence 0-81463
- In<sub>2</sub>O<sub>3</sub>-SnO<sub>2</sub>-InP solar cell junctions, efficiency, InP surface props. 0-85288
- In<sub>2</sub>O<sub>3</sub>-SnO<sub>2</sub>-Si SIS heterojunction solar cells 0-85281
- In<sub>2</sub>O<sub>3</sub>-SnO<sub>2</sub>-Si SIS solar cells, reverse current-voltage characts. under illumination 0-89622
- In<sub>2</sub>O<sub>3</sub>-SnO<sub>2</sub>-SiO<sub>2</sub>-pSi, comparison between MIS and SIS solar cells 0-81443
- InP homojunction solar cell, antirefl. coated, high-efficiency 0-104505
- n-InP, MOS, electrical and photovoltaic characteristics 0-85276
- InP n<sup>+</sup>-p-p<sup>+</sup> homojunction solar cells, high efficiency, LPE layer growth, photolithographic fabrication 0-93929
- InP, thin film growth tech. and characterisation 0-89631
- InP thin films for photovoltaic devices 0-93972
- InSe solar cells, photovoltaic conversion efficiency 0-61356
- (In<sub>1-x</sub>Sn<sub>x</sub>)<sub>2</sub>O<sub>3-y</sub> Si solar cells, degradation 0-94047
- In<sub>2-x</sub>Sn<sub>x</sub>O<sub>3-y</sub>, majority carrier conduction effects 0-97796
- In<sub>2-x</sub>Sn<sub>x</sub>O<sub>3-y</sub>-Ga<sub>1-x</sub>P-(In<sub>1-x</sub>As<sub>1-x</sub>) heterojunction solar cells, chemistry and prep. 0-94073
- In<sub>2-x</sub>Sn<sub>x</sub>O<sub>3-y</sub>-insulator-poly-Si solar cells, photovoltaic conversion parameters 0-101093
- In<sub>2-x</sub>Sn<sub>x</sub>O<sub>3-y</sub>-poly Si SIS solar cells 0-97787
- In<sub>2-x</sub>Sn<sub>x</sub>O<sub>3-y</sub>-SiO<sub>2</sub>-Si SIS solar cells, loss mechanisms study for improvement of efficiency to above 12% 0-94080
- n-MoSe<sub>2</sub> based liq. junction solar cell, nonaqueous electrolyte system employing Cl<sub>2</sub>/Cl<sup>-</sup> couple 0-81432
- N<sub>2</sub> reducing solar cells for industrial NH<sub>3</sub> synthesis 0-89632
- Si, advanced material for space solar cell 0-94007
- Si, all-plate low cost contact system 0-93992
- Si, amorphous, barrier props. determ. by differential I-V characts. meas. 0-94053
- Si, amorphous, current collection and electrical shorting problems 0-93969
- Si, amorphous and polycryst. thin film solar cells, perform. parameters, review 0-93882
- Si, amorphous design considerations 0-85277
- Si, amorphous hydrogenated solar cells, field depend. quantum efficiency, electron-hole recombination 0-66971
- Si, amorphous vacuum deposited p/undoped photodiode and diode-voltage variable resistor combination 0-61380
- Si, analysis of short-circuit current 0-85285
- Si, as-grown Czochralski crystal, appl. of multiple p-n junction structure obtained by heat treatment 0-101099
- Si back surface field solar cell degradation at high intensity due to base cond. modulation loss 0-94085
- Si, base resist. influence on temp. characts. 0-89618
- Si based alloys, amorphous, photovoltaic behaviour, solar cell appl. 0-94051
- Si, cast, growth structure and photovolt. props. of solar cells 0-94008
- Si concentrator, effects of nonuniform illumination 0-93942
- Si concentrator, high efficiency, state-of-the-art design and processing 0-93958
- Si concentrator, new technology for fabrication 0-81457
- Si concentrator cells, high efficiency, design, fabrication and meas. 0-93938
- Si conductor-insulator-semiconductor solar cells, automated production, outlook 0-94021
- Si, deformed, annealed and recrystallized, struct., implications for solar cells 0-60922
- Si, degradation processes of electrophysical characts. during long-term operation 0-89617
- Si dendritic web for solar cells 0-89634
- Si, design for limit conversion efficiency 0-93960
- Si, developments and trends for automatic interplanetary stations, Venus-9 and Venus-10, and mooncar program 0-89613
- Si, effect of Ti, Cu and Fe 0-72064
- Si, effects of metallic impurities 0-85278
- Si, effects of nonuniform illumination and temp. profiles under concentrated sunlight 0-93941
- Si, fabrication overview, wafer prep., anti-refl. coatings and metallisation, efficiency (*Spanish*) 0-72059
- Si film, amorphous, glow discharge deposited, for low cost solar cells 0-61355
- Si films, electron beam evaporated, for MIS solar cells 0-93490
- Si, fixed-base, flat panels, possible developments for more competitive power production 0-72050
- Si, fundamental efficiency limitations 0-93963
- Si, grain boundary defects in thin semicrystalline material 0-93889
- Si, grain size dependence of parameters 0-94049
- Si, heavily doped, excess intrinsic carrier density, deionisation of impurities as explanation, bipolar transistor/solar cell models 0-96864
- Si, high efficiency, using minority carrier MISS 0-101103
- Si high efficiency solar cells, laser annealing, reviews 0-93976

## solar cells continued

- Si, high open circuit voltage, P implantation 0-89642  
 Si, high performance back-surface field with fire through contacts 0-93993  
 Si, I-V charact. meas., effect of voltage ramp, theoretical anal. using linear model 0-61354  
 a-Si ITO/ZZ 0-101113  
 Si, inhomogeneities and their influence on cell performance 0-93967  
 Si, ion implantation by laser annealing, characterisation, solar cell applications 0-70247  
 Si, ion implanted grating type 0-101102  
 Si, ion-implanted, expt. study of efficiency controlling factor 0-93997  
 Si, ion-implanted, factors controlling efficiency 0-81451  
 Si, ion-implanted, tailored emitter, low resistivity 0-81452  
 Si ion-implanted laser-annealed solar cells 0-93881  
 Si, junction formation techniques using spray-on polymer dopants, cost effective, high throughput 0-94014  
 Si large grain films on metallurgical Si substrates, chem., struct., elect. and photovoltaic props. 0-61357  
 Si, limit efficiency evaluation 0-93973  
 Si, liquid, interaction with die material during edge defined film fed growth 0-104060  
 Si, low cost, Ni contacts 0-94017  
 Si, low cost processes for fabrication 0-94013  
 Si, low series resistance photovoltaic concentrator 0-93940  
 Si, low-grade, review and current developments 0-108801  
 Si MIS grating solar cells on minority carrier blocking back surface field substrates 0-94078  
 Si MIS solar cells with Cr, Hf, Be, Se and Y as barrier forming metals, expt. investigation 0-94077  
 Si, MIS/inversion layer, high efficiency cell fabrication 0-94075  
 Si, MIS-inversion layer, low cost-high efficiency 0-76632  
 Si MOS and oxide-charge-induced BSF solar cells, open-cct. voltage > 700 mV, 20% conversion efficiencies 0-81435  
 Si, manufacturing cost anal. of flat plate vs. concentrator solar cells 0-93949  
 Si materials, advanced, preliminary evaluation for space solar cells 0-94006  
 Si, metallurgical-grade, fabrication by epitaxial growth or direct diffusion 0-101104  
 Si, minority carrier MIS, design and expt. results 0-81445  
 Si minority carrier MIS solar cells, AM1 efficiencies 0-93975  
 Si, minority carrier MIS diodes appl. (Slovak) 0-97792  
 Si monocrystalline sheet fabrication for solar cells, CLF Czochralski furnace and enhanced slicing technology 0-93476  
 Si multicrystalline solar cell material prep., fast-pulled float zone, CZ and cast ingot and foil methods 0-93483  
 Si multielement photoelectric converters, p-n mesa structure for investigating optical and energy characts. of solar and radiant energy concentrators 0-97783  
 Si, n<sup>+</sup>-p, Li-counterdoped, radiation damage 0-94000  
 Si n<sup>+</sup>-p junction solar cells, electron irradi., DLTS spectra and defect effects 0-93999  
 Si n<sup>+</sup>-p solar cell, forward and reverse bias tunnelling 0-85274  
 Si n<sup>+</sup>-p solar cells, degradation mechanisms associated with Ti impurities 0-81465  
 Si, n<sup>+</sup>-p-p<sup>+</sup> structure with two-sided photosensitivity for terrestrial applications, structure and fabrication technology requirements 0-101096  
 Si n<sup>+</sup>p solar cells, effect of elec. bus during 1 MeV electron irradi. and isochronal annealing, elec. characts. and deep level pop. 0-94086  
 Si, Ni-Cu conductor system 0-93991  
 Si on ceramics, coating with inverted meniscus (SCIM) technique, solar cell appl. 0-89163  
 Si open-circuit voltage at ultrahigh light intensities, plasma reflection effects 0-96928  
 Si, output power and sunshine conditions, correlation 0-97785  
 Si, p<sup>+</sup>-i-n<sup>+</sup>, conversion efficiency limit in concentrated sunlight 0-85282  
 Si p<sup>+</sup>-n-n<sup>+</sup> back surface field concentrator solar cells 0-93939  
 Si p<sup>+</sup>-n-n<sup>+</sup> back surface-field, physics underlying performance 0-85283  
 a-Si p-i-n and c-Si p-n junction solar cells, design concept differences 0-94031  
 Si p-n junction diodes and solar cells, minority carrier diffusion length 0-107894  
 Si, POCl<sub>3</sub> gettering of Ti, Mo and Fe-contaminated cells 0-94010  
 Si photovoltaic industry, environmental control, economic and ecological requirements 0-94026  
 Si, polycryst., p-n junction, grain boundary and intragrain recombination currents 0-81442  
 Si polycryst. and amorphous cell characts. 0-89619  
 Si, polycryst. surface barrier cells, eval. for terrestrial appls. 0-61376  
 Si, polycrystalline, electronic behaviour of grain boundaries 0-92859  
 Si, polycrystalline, grain boundary obs. by TEM, solar cell appl. 0-72057  
 Si, polycrystalline, refined metallurgical-grade, impurity gettering 0-94011  
 Si, polycrystalline, solar cells, grain-boundary hydrogenation technique for improvement 0-85273  
 Si, polycrystalline barrier heights and passivation of grain boundaries 0-93890  
 Si, polycrystalline Czochralski-grown, MIS solar cell characterisation using scanned laser response exam. 0-93884  
 Si polycrystalline film, effect of defects/grain boundaries on photovoltaic mech. 0-93883  
 Si, polycrystalline metallurgical grade, impurity gettering 0-81441  
 Si polycrystalline solar cells, recombination, electron-beam-induced current characterisation 0-81470  
 Si polycrystalline-metal Schottky barrier solar cells, elec. and photovoltaic contact props. 0-93936  
 Si, preparation using laser processing 0-81454  
 Si, prod. of polySi vapour deposited coatings for solar cells, cost anal. 0-93495  
 Si, production process effect on fracture strength 0-93656  
 Si, props., characts. and efficiency, development costs (Spanish) 0-72062  
 Si, prospects (Italian) 0-60024  
 Si, proton irradiated, processing influence on elec. performance 0-94001  
 Si, pulsed laser techniques for annealing ion-implantation damage 0-81453  
 Si, radiation damage annealing mechanisms and low temp. annealing 0-94003  
 Si, radiation damaged, origin of reverse annealing 0-76630  
 Si, realisation by laser induced diffusion of deposited Sb 0-93998

## solar cells continued

- Si, review of physics underlying recent improvements 0-93974  
 Si ribbon, dendritic web growth from melt, solar cell module fabrication 0-93478  
 Si ribbon solar cells, defect anal. using laser scanner 0-94089  
 Si ribbon solar cells, var. of minority-carrier diffusion length with light intensity, heavy metal doping effects 0-93937  
 Si ribbons, edge-defined film-fed growth technique for solar cells 0-89138  
 Si ribbons for solar cells, ultra high speed growth, elec. props. 0-89162  
 Si ribbons grown by capillary action shaping technique, surface quality and impurity distrib. 0-108343  
 Si, screen printed diffusion and metallisation 0-94015  
 Si, second quadrant effects 0-76639  
 Si sheet casting for solar cells 0-89139  
 Si sheet-form solar cells, efficiency improvement, minority carrier diffusion length limitations 0-93925  
 Si single crystal growth from metallurgical grade Si for fabricating terrestrial solar cells 0-59416  
 Si, single crystal solar cell manufacturing process, laser annealing of implanted area, energy saving 0-97791  
 Si, single-crystal, HV, multijunction, parameters and characteristics 0-89615  
 Si solar cell fabrication from multiple ingots using melt replenishment Czochralski method, cell anal. 0-93477  
 Si solar cells, capacitance transient spectra of processing- and radiation-induced defects 0-61340  
 Si solar cells, fabrication using continuous or pulsed lasers (French) 0-61350  
 Si solar cells, photoreaction of p-n junction diodes 0-81464  
 Si solar cells, polycrystalline p-n junctions, recombination currents, physical models 0-93892  
 Si solar cells, polycrystalline, from recrystallized plasma deposited thin films 0-104509  
 Si solar cells with concentrators and heat pump 0-61371  
 Si solar cells with light concentrating lens, test results (Rumanian) 0-89620  
 Si, solar grade material economic commercial production, problems in cost reduction (Spanish) 0-72058  
 Si, solar-cell grade material prod., recent developments, low-cost processes (Spanish) 0-72061  
 Si, solid source diffusion process for fabrication 0-93994  
 Si, spray-on TiO<sub>2</sub> antireflection coatings 0-80963  
 Si substrate, upgraded metallurgical grade, epitaxial growth 0-93905  
 Si substrate prep. for epitaxial solar cells, low-cost, unidirectional solidification process 0-93924  
 Si substrate thinness, device design, solar cell processing, empirical study of interaction 0-93995  
 Si, surface passivation by SnO<sub>x</sub> films, effect on cell transport props. and short cct. current 0-61360  
 Si terrestrial solar cells, stress tested, contact integrity testing 0-94018  
 Si thin film for solar cells, thermal expansion shear separation technique 0-81439  
 Si thin p-n junction solar cells, minority carrier mirrors and optical confinement for high efficiency (27%) 0-93933  
 Si thin-film polycrystalline vacuum-deposited solar cells, TiB<sub>2</sub> bottom electrode, 10% efficiency 0-93489  
 Si, TiO<sub>2</sub> AR coating by spray deposition 0-104511  
 Si, ultrathin, electron and proton effects 0-94002  
 Si, unified model of fundamental limitations 0-81448  
 Si, updating limit efficiency 0-81447  
 Si:B ion implanted grading-type solar cells, var. of junction depth, collection efficiencies 0-93934  
 Si:F,H, amorphous efficient carrier generation for solar photovoltaic energy conversion 0-92906  
 Si:Fe(Al), compensated substrates, effects of Fe and Al 0-94009  
 Si:H, amorphous, band tail absorpt., photocurrent meas. for Schottky barrier solar cell 0-60032  
 Si:H, amorphous, discharge prod., optically induced cond. changes 0-96937  
 Si:H, amorphous, HV photovoltaic cells, design parameters 0-101105  
 Si:H, amorphous, horizontal cascade type integrated photovoltaic cell module 0-94091  
 Si:H, amorphous, solar cells, trap spectroscopy using transient current techniques 0-104508  
 Si:H, amorphous, solar-cells, charge collection and spectral response 0-85275  
 Si:H, amorphous, sputtered Schottky barrier solar cells, conduction mechanism 0-104506  
 Si:H, amorphous, stacked solar cells, development 0-94050  
 Si:H, amorphous, using ultrathin active layer to increase conversion efficiency 0-94030  
 Si:H, amorphous Schottky solar cells, prep. and characts. of diode RF reactive cathodic sputtered films (French) 0-61347  
 Si:H, amorphous thin film solar cells 0-81478  
 Si:H amorphous, solar cell structure, optical absorption by gap states 0-94052  
 Si:H amorphous MIS solar cell, loss mechanisms and photovoltaic parameters, overview 0-93923  
 a-Si:H highly homogeneous, for low-cost solar cell fabrication 0-72053  
 Si:P(O) p<sup>+</sup>-n-n<sup>+</sup> solar cells, comparison rel. to resistance to 1.5 MeV electron irradi., majority carrier trapping 0-94087  
 Si:Ti substrate for epitaxial solar cells 0-61341  
 Si:F-H amorphous solar cells, DC glow discharge fabrication 0-72041  
 Si-Ge, amorphous, tandem multiple gap 0-94029  
 Si-In<sub>2-x</sub>Sn<sub>x</sub>O<sub>3-y</sub> SiS heterostructure solar cells, spray-deposited 0-101106  
 Si-ion-ceramic, short-circuit current density meas. using light-beam-induced-current tech. 0-93887  
 Si-SiO<sub>2</sub> interface in MOS solar cells, operational characts. and struct. 0-93901  
 n-Si-SiO<sub>2</sub>-SnO<sub>x</sub> SIS solar cell, transport props., 14% efficiency realisation 0-94079  
 SiC particles in EFG ribbon solar cells, EBIC and ion microprobe anal. 0-93838  
 Si, Ge<sub>1-x</sub> diffused p-n junction, electric and photoelectric props. 0-101095  
 SiH<sub>x</sub>, amorphous, short circuit currents and collection efficiencies 0-94028  
 Si<sub>3</sub>N<sub>4</sub> antireflection coating for solar cells, reactive plasma process for forming metal grid patterns 0-93990



**solar cells continued**

- SiO<sub>2</sub>, thin films on rough polycryst. Si surfaces, oxide thickness and refractive index meas. 0-93422  
 n-SnO<sub>2</sub> pigmented solar cell for electrolysis of water, two-photon process 0-93932  
 SnO<sub>2</sub>/n<sup>+</sup>-pSi heterojunction solar cells, fabrication by paint-on-diffusant method 0-94048  
 SnO<sub>2</sub>-polySi solar cells, fabrication, grain size effects on device parameters 0-94045  
 TiN layers investigation for solar-cell contacts 0-81461  
 n-WSe, electrode in aq. iodide medium, high efficiency photoelectrochemical solar cell 0-72069  
 Zn<sub>x</sub>Cd<sub>1-x</sub>S-Cu<sub>2</sub>S heterojunction solar cells, props., comp. meas. of interfacial region 0-81472  
 ZnO, aqueous-deposited films, struct. and electronic props. for solar cell appls. 0-100797  
 ZnO transparent films for conductor-insulator-semiconductor (CIS) solar cells 0-93947  
 ZnO-Cu<sub>2</sub>O heterojunction solar cells, prop. by RF sputtering 0-93945  
 Zn<sub>3</sub>P<sub>2</sub> large crystal growth, vapour transport perforated capsule technique, prototype solar cell appls. 0-93464  
 Zn<sub>3</sub>P<sub>2</sub> thin polycrystalline films for solar photovoltaic cells 0-97797

**solar chromosphere** *see* **chromosphere****solar composition**

- He abundance in solar wind, evidence for chemical separation by diffusion 0-77381  
 initial chemical comp. discontinuity and non-radial oscils. 0-82341  
 interior, Fe segregation from H, ionic mixtures phase separation theory 0-77279  
 Fe, conc. in solar interior rel. to coalescence in centre of Sun 0-77373  
 Fe I in photosphere, line broadening, Smirnov Roueff pot. calcs. 0-98632  
 Mn abundance meas. by sun model 0-91501  
 Ni I abundance in photosphere from oscillator strength obs. 0-98625  
 TiO in sunspots, equiv. width meas. theoretical interpretation, line form. process 0-72902  
 Zn, photospheric abundance, discrepancy with meteorite abundance 0-72897

**solar constant** *see* **solar radiation****solar corona**

- active regions, coronal and transition region temp. struct. 0-67692  
 activity, effect on radar meteor rate 0-67662  
 ancient Chinese observations of physical phenomena attending solar eclipses 0-72916  
 chromosphere-corona transition zone of solar active regions, non-thermal velocities (*French*) 0-77371  
 cosmic-ray modulation by coronal holes, during solar cycle 0-94661  
 current instability and mag. fields for origin and energy supply to flares 0-101571  
 electric currents in coronal loops and rays, as solar wind energy source 0-94768  
 electron density distrib. during solar minimum, Helios 2 expt. 0-101578  
 energy storage, importance of photospheric mag. field, solar flare model 0-72906  
 expanding coronal mag. bottle, cosmic ray accel. 0-77244  
 expanding loop system, long decay X-ray event 0-90402  
 expansion, effects of radiation heat flux 0-90377  
 expansion, solar wind accel. by Alfvén wave flux from Sun 0-85923  
 F corona, radial vel. obs. at 1979 February 26 solar eclipse 0-85914  
 F-corona, inner, circumstellar dust cloud, model and composition 0-82162  
 flare model based upon photospheric dynamo action 0-62102  
 heating by fast. electron streams theory 0-105228  
 heating mechanisms, mag. field scaling props. 0-85913  
 hole boundaries, evaluation from He I IR obs. 0-72919  
 holes, identification from 9.1 cm synoptic charts 0-98633  
 holes, limb brightening data anal. for EUV lines in chromosphere-corona region 0-82333  
 holes, link with auroral activity, 1972-1977 equatorial latitude 0-98499  
 holes, modulation effect on cosmic ray intensity, review 0-77370  
 holes, temp. decrease, plasma density effect on wave absorpt. (*Russian*) 0-77374  
 holes, visibility at 408 MHz 0-85922  
 ionisation of prominence material 0-101520  
 Langmuir turbulence over active regions, rel. to quasi-stable particle accel. and type I radio bursts (*Chinese*) 0-105220  
 loop prominence knots, motions, H $\alpha$  line filtergram obs. 0-67693  
 loop structures, temporal var., time-lapse sequence obs. 0-72909  
 loops, low beta model, kink instabilities 0-98636  
 loops in an active region, physical props. XUV obs. 0-90376  
 magnetic field, potential, structs. assoc. with solar proton events and type I (metre wave) radio sources (*Chinese*) 0-105222  
 magnetic field above flocculus, determ. from radio obs. 0-98635  
 magnetic field emergence from active region, assoc. radio burst 0-109412  
 magnetic flux tubes, vibration modes, general dispersion relation 0-94706  
 magnetic instability of coronal arcades as the origin of two-ribbon flares 0-72911  
 McMath region 13043, coronal mag. fields intensification rel. to centimetre-wave sources rapid var. 0-67688  
 MHD fluctuations due to magnetosonic wave propag. in warm plasma 0-77275  
 MHD wave generation and heating by prominence turbulence 0-72907  
 north-south asymmetry from Fe XIV green line (1965-78) 0-77369  
 observations with Solwind coronagraph 0-82325  
 plasma, inhomogeneous, electron flows stabilisation 0-109411  
 plasma flow along sheared magnetic arches, theory 0-62092  
 plasma radiation, direct conversion of Langmuir waves into o-mode waves 0-72896  
 N.polar coronal hole at 1973 June 30 eclipse, density model 0-98627  
 radar signal reflection, efficiency of four-plasmon interactions 0-101582  
 radio spectrograms, magnetoplasma, plasma wave motions (*Dutch*) 0-62101  
 spectrum, intensity ratios of fine-struct. components of H like ions resen. lines 0-101581  
 thermal equilibrium of coronal loops 0-94773  
 thermal stability during fast mode wave heating 0-90397  
 transients at high latitude, 1979 September 27 Solwind obs. 0-94774  
 transition region, C V and O VII emission line ratios interpretation 0-98624  
 transition region, origin for UV and radio fluctuations 0-90398  
 transition region, theoretical network structure for coronal holes 0-85917

**solar corona continued**

- transition region, theoretical network structure for quiet Sun 0-85916  
 transition zone, nonresonant heating mechanism (*Chinese*) 0-85921  
 X-ray bursts, thermal models 0-94766  
 N II, electron impact excitation cross sections, rel. to solar corona abundance 0-58391  
 Ni IX to Ni XII transitions, laboratory wavelengths and identifications in solar spectrum 0-99474  
 S IV observations from Skylab 0-87028
- solar corpuscular radiation** *see* **solar wind**
- solar corpuscular streams** *see* **solar wind**
- solar cosmic ray particles**  
 acceleration in expanding coronal mag. bottle 0-77244  
 determ. from <sup>3</sup>He meas. in lunar rocks 0-98576  
 electron events not assoc. with flares, ISEE 3 obs. 0-67683  
 energy variation in interplanetary space 0-101505  
 flare, particles, intensity variations, depend on interplanetary mag. field and solar wind 0-77372  
 flare accelerated particles, nucl. composition and Coulomb losses 0-72913  
 flare energetic particle abundances, Voyager obs. 0-90382  
 flare particles, prod. by mag. energy direct conversion to plasma kinetic energy (*Japanese*) 0-94775  
 flare particles, tracks in Luna 24 core samples, thermolum. obs. 0-82246  
 flare protons, flux limit due to accel. mechanism saturation effects 0-98645  
 flares, particle accel., injection energy concept 0-101509  
 flares rel. to cosmic ray intensity, model 0-72914  
 flares relativistic electron spectra, inference from meas. of inverse Compton radiation 0-90339  
 interplanetary disturbance, 1978 January 3 to 4, Prognoz-6 energetic particle and solar wind meas. 0-90315  
 interplanetary propagation, cosmic ray flow lines and energy changes 0-82158  
 isotope composition form., effect of ion-sonic turbulence 0-101574  
 low-rigidity cosmic rays, weak turbulence diffusion theory rel. to mean free paths 0-98524  
 modulation by coronal holes, review 0-77370  
 near-Earth radiation hazard due to solar flares, dosage estimation technique 0-67482  
 neutrino flux calcs., neutrino oscils. constraint 0-109410  
 propagation, equivalent diffusion coefficients of solar cosmic rays 0-85825  
 propagation in interplanetary medium, solns. to Fokker-Planck eqn. 0-77242  
 proton event of 1978 May 7, neutron monitor obs. 0-67686  
 proton flare events, relation to type I (metre wave) radio sources (*Chinese*) 0-105222  
 proton generation in solar flares 0-101575  
 protons, high energy, effects on middle atmosphere chemical comp. 0-109213  
 protons at 1 AU from active regions, energy spectra from Prognoz-3 0-101512  
 shock acceleration, in corotating interaction regions in solar wind 0-82159  
 solar flare proton generation 0-109413  
<sup>2</sup>Be production in atm. and transport from Sun, tracer for terrestrial-solar relationship 0-98525  
<sup>3</sup>He rich events during 1976 November to December, Prognoz 5 obs. 0-61972  
<sup>3</sup>He/<sup>4</sup>He in heavy-ion-rich solar energetic particle events, energy depend. and temporal evolution 0-90299  
<sup>3</sup>He/<sup>4</sup>He solar cosmic ray isotopic composition from Venera 9 obs. 0-72725
- solar cosmic ray photons**  
 flare impulsive X-ray burst, spectral anal. analytical method (*Chinese*) 0-85919
- solar disturbances** *see* **solar activity**
- solar eclipses**  
 1919 May 29, gravitational deflection of light, obs. reexamined 0-67553  
 1973 June 30, density model for N.polar coronal hole 0-98627  
 1977 October 12 partial eclipse, VLA 6 cm obs. of quiet Sun 0-72895  
 1979 February 26, F corona radial vel. obs. 0-85914  
 1979 February 26, solar flash spectrum obs. 0-67687  
 ancient Chinese observations of physical phenomena attending solar eclipses 0-72916  
 ionosphere effects, VLF focusing during solar eclipse 0-61965  
 predictions using vector method for intermediate level astronomy courses 0-105452  
 stratosphere, effect of eclipse, on NO<sub>2</sub> and O<sub>3</sub> conc., and atm. temps. 0-105017
- solar-electric power stations** *see* **solar power stations**
- solar energy concentrators**  
 Ansaldo solar cell for parabolic trough concentrator systems with forced cooling 0-93982  
 array of directable mirrors as a photovoltaic solar concentrator, calc. of images 0-76609  
 axicon sun-tracking concentrators for photovoltaic conversion, conc. and cost characts. 0-93858  
 axisymmetric mirror class with uniform flux conc. props. along axes 0-95978  
 axisymmetric reflector-absorber systems with uniform flux conc. 0-94111  
 black Ni electrochemical coatings, characts. investigation 0-95975  
 cassegrain solar concentrators for photovoltaics 0-61304  
 chromatic dispersion concentrator, applied to photovoltaic systems 0-93862  
 collection subsystem of 1 MW solar power station, engineering assessment 0-61305  
 collector absorption enhancement using multiple reflections 0-76649  
 collectors characts. and use (*Italian*) 0-101078  
 compound parabolic concentrator, phase space conservation for incoherent propag. 0-69491  
 concentrator-receiver system with selective absorbing surface, heating characts. 0-91874  
 cylindrical, generalisation of 2-D optical anal. 0-101079  
 design, effect of solar elevation angle probability distribution 0-93860  
 effective series resist. meas. effects of temp. variations 0-93944  
 efficiency of solar concentrators with curvature determined by gravity and a variable density distribution 0-85266  
 energy collection anal. using information theory 0-97799

# solar energy concentrators continued

- fibre optics, developments and applications for concentrated solar energy transmission 0-87481
- flat mirror multivalent solar concentrator 0-61420
- fluorescent planar concentrators, efficiency and stability 0-93986
- Fresnel lenses, fabrication techniques 0-91939
- Fresnel lenses, spectral adaption and fluoresc. and bifacial concentrators (*Spanish*) 0-72060
- G. Donegani Institute activity (*Italian*) 0-60027
- general optical concentrator, max. radiant power density at receiver 0-102794
- generalised optical design technique, consideration of various errors 0-95979
- glasses, high vol. low cost, as solar reflectors, compositions and weathering effects 0-106589
- heat collectors, with direct and concentrated radiation, maximum equilibrium temp. determ. 0-92031
- heat pipe, filled with porous material, glycol water circulation 0-66986
- ideal flux concentrators, intensity variation reduction on absorbers 0-104496
- line-focus parabolic-trough photovoltaic arrays, active and passive cooling 0-93988
- linear Fresnel lens with grooves of finite size, solar radiation concentration 0-106592
- mirror, performance evaluation 0-87457
- nonimaging, optimisation for tubular evacuated receivers aligned north-south 0-72015
- nontracking solar collectors, wide-angle lenses and image collapsing subreflectors 0-76603
- optical and energy characs., determ. using Si multielement photoelect. conductors 0-97783
- parabolic, composite, concentration characteristics 0-102793
- parabolic concentrator arrays, collector end shadowing effects minimisation 0-93987
- parallel plate channel, convective-radiative interaction, air-operated solar collectors appl. 0-96259
- photovoltaic concentrating systems, optical and tracking systems design, performance characs. 0-72051
- photovoltaic concentrator array technology, status report 0-94024
- photovoltaic module utilising parabolic trough concentrators 0-93984
- photovoltaic receiver for parabolic trough concentrator, optimisation 0-93983
- point focusing, effects of tracking errors on performance, statistical anal. of intercept factor 0-61302
- point-focus Fresnel lens photovoltaic arrays, active and passive cooling 0-93988
- point-focus photovoltaic concentrator arrays, durability, reliability 0-93985
- power plants, solar high temp., with Stirling engine and solar thermal rocket engine, efficiency improvement by using selective radiation absorption surface 0-89589
- segmented parabolic mirrors, optical performance anal. by THEK computer code (*French*) 0-61294
- silicone-glass hybrid Fresnel lens for solar energy concentration 0-61303
- solar power plant, direct tracking using two-mirror unit with plane and hyperboloidal counter-reflectors 0-91875
- solar power station, tower-type, concentrating and receiving systems design modelling 0-91873
- Solaxex two-axis tracking linear concentrating collector system, design and operation 0-93989
- space solar furnaces, for materials-science expts. 0-108786
- space vehicle photovoltaic arrays, concentrator design 0-94057
- spectrally selective reflectors for concentrator solar arrays, evaluation 0-94043
- static collector of low-conc., heat losses 0-81487
- thermoelectric generator, attainable efficiency values determ. 0-94094
- thick film conductive ink contacts for concentrator cells 0-93957
- two-stage reflecting convertor, pseudo-Lambertian, optimum configuration anal. 0-97765
- variable-shape, fabricated from polymeric-film membrane 0-76645
- Si concentrator cells, high efficiency, design, fabrication and meas. 0-93938
- Si concentrator solar cells, effects of nonuniform illumination 0-93942
- Si concentrator solar cells, high efficiency, state-of-the-art design and processing 0-93958
- Si, effects of nonuniform illumination and temp. profiles under concentrated sunlight 0-93941
- Si p<sup>+</sup>-n-n<sup>+</sup> back surface field concentrator solar cells 0-93939
- Si photovoltaic low series resistance concentrator for high intensity appl. 0-93940

# solar energy conversion

- see also solar absorber-convertors; solar cells*
- 5 MW test facility, real-time computer control 0-72075
- absorbed radiation heat conversion to chemical energy, upper limit 0-81483
- absorption refrigeration machine driven by solar heat for air conditioning, math. modelling 0-76651
- biological, energy from biomass conversion 0-61391
- biomass, review of possible energy conversion processes (*French*) 0-93843
- biomass energy R and D 0-66922
- biomass options for the Big Island of Hawaii 0-66921
- chemical, photo-induced electron transfer reactions in solution, organised assemblies and at interfaces 0-89677
- chemical conversion and storage of solar energy, book 0-86045
- chemical conversion and storage using norbornadiene-quadracycline photoisomeric interconversion 0-89664
- chemical fuel production, efficiency of the conversion processes 0-61318
- chemical heat pumps for solar energy conversion using LaNi<sub>5</sub> hydrides 0-89667
- chemical storage, chemical bond energy of SiO<sub>2</sub> and ammoniates undergoing thermal decomposition 0-76656
- chemical storage, effect of micellar phase on photo-induced reactions 0-89678
- chemical storage, photosensitization mechanisms for energy storing isomerizations 0-89679
- chemical storage using novel photocyclization reactions of 1-alkenyl-2-pyridones 0-89680
- chlorophyll a dihydrate photoelectrochemical cell 0-61387
- DC-AC inverter design, effect of meteorological conditions, computer simulation 0-61373

# solar energy conversion continued

- desalination plant appl., MSF, technical and economic evaluation 0-61281
- desalination plant utilising reverse osmosis, 2.5 kW solar generator 0-61282
- desalination process appl., demonstration project multistage flash evaporation, demonstration project 0-61283
- direct conversion into electric current (*Italian*) 0-89612
- distillation plant, 5000 lit/day, drinking water production in India 0-61280
- energy analysis and viability of photovoltaic conversion and OTEC 0-61358
- energy conservation and storage, materials needs 0-66958
- flywheel energy storage and conversion system for photovoltaic appl., economic anal. 0-94116
- ground thermal energy conversion, solar power generation 0-61313
- H<sub>2</sub> production by H<sub>2</sub>O pyrolysis, thermodynamics, theory 0-61448
- heat pump for energy storage using ammoniated salts. 0-81484
- heat pump house heating system with low quality thermal flow 0-76617
- heat pump plant for space heating in winter, air conditioning in summer 0-76615
- heat pump system, solar ground coupled heat transfer, expt. and GROCS computer model 0-66987
- heat storage by metal hydride, review 0-61455
- heating and cooling system for domestic use (*Japanese*) 0-108787
- heating of buildings, types, construction and thermal and environmental parameters (*French*) 0-85268
- industrial utilisation of energy, book 0-61222
- low-temp. solar water heaters, tubular heat receptacles screen parameters optimisation 0-92030
- materials science aspects, review 0-66957
- microbial production of energy sources from biomass 0-61392
- Middle Eastern research programmes 0-66939
- oil recovery, enhanced, steam injection, cost model comparison of conventional and solar methods 0-66947
- OTEC, design and construction of a test plant 0-85298
- OTEC, evaluation of alternative energy sources for the Guyana energy crisis 0-61270
- OTEC, NH<sub>3</sub> prod. 0-66988
- OTEC, technology development, US DOE program review 0-94098
- OTEC ocean engineering, status report 0-66989
- OTEC power plant, selection of working fluid (NH<sub>3</sub>, propane and freon) 0-89665
- OTEC power system development and environmental impacts 0-66990
- OTEC system performance study 0-104514
- photoelectrochem. processes 0-72068
- photoelectrochemical cells, use of oxide semiconductors as anodes 0-101120
- photogalvanic, photochem. determ. of efficiency 0-89654
- photosynthesis, hydrocarbons production 0-89661
- photosynthesis, photoelectric response of photosensitive liquid membranes and chloroplast discs 0-81482
- photosynthesis, solar energy conversion and storage using artificial photosynthetic systems 0-89662
- photovoltaic village power systems: the minigrid concept 0-66973
- photovoltaic/thermal solar energy systems, theoretical anal. 0-61375
- R and D by US DoE 0-89674
- rural electrification by solar power, photovoltaic arrays efficiency 0-66974
- Solchem energy system, thermochemical solar energy transport, using CO<sub>2</sub>-methane reforming-methanation cycle 0-94096
- space heating, heat pump and thermal storage system based on CaCl<sub>2</sub> and methanol vapour reaction 0-85307
- storage methods for large-scale appls., eval. 0-89675
- sun-mill, version of dunking-bird, solar-powered, gravity-assisted heat engine 0-89672
- system developments and research aims (*German*) 0-108799
- technology and methods for appl. of solar energy to European agriculture 0-76616
- thermal energy storage in salt hydrates for solar heating systems, storage material props. 0-101134
- thermionic power plant, central thermal receiver tower concept, geometric config. and design 0-61390
- thermochemical, conversion yields using CaCO<sub>3</sub> decarbonation 0-94097
- thermochemical electric power generation, reversible chemical reactions 0-61394
- thermoelectric air conditioner humidifier (SATEACH), solar assisted 0-108802
- thermoelectric generator using tubular heat-pipe with concentrator 0-89658
- transients simulation, solar input and solar data computation for engineering of solar systems 0-94060
- vapour turbine plants using combined thermal-power convertor and photoelectric convertor, thermodynamic efficiency for solar energy conversion 0-89614
- water heaters, rural population demand fulfilment 0-89668
- water pumping solar systems using photovoltaic convertor arrays 0-61402
- wind and wave power, utilisation prospects 0-61269
- Al<sub>2</sub>O<sub>3</sub>-B<sub>2</sub>O<sub>3</sub>-SiO<sub>2</sub> sheet glass, solar energy appl., optical and mech. props. 0-87447
- B-Si materials for thermoelectric conversion of solar energy (*French*) 0-89660
- Bi<sub>2</sub>Te<sub>3</sub> alloy thermocouples for solar thermoelectric conversion 0-94095
- CdS film, chemical bath deposited, solar energy conversion by photoelectrochem. cells 0-108804
- Cu(II) complexes, reversible excited-state electron transfer reactions for solar energy conversion 0-89655
- H<sub>2</sub> biophotolytic production from H<sub>2</sub>O 0-61457
- H<sub>2</sub> and O<sub>2</sub> production from H<sub>2</sub>O using solar energy, eval. of a hybrid process 0-104519
- H<sub>2</sub>, photobiological prod., key enzymes and biochem. systems, tech. problems of H<sub>2</sub> prod., review 0-61446
- H<sub>2</sub>, photochemical production by H<sub>2</sub>O dissociation utilising solar energy, review 0-61452
- H<sub>2</sub>, photochemical production using visible light on aqueous solns. of a Ru complex 0-85192
- H<sub>2</sub> production, review of solar-H<sub>2</sub> energy systems 0-61447
- H<sub>2</sub> production and storage utilising solar energy conversion, book 0-57017
- H<sub>2</sub> production by biological and biochemical solar energy conversion, review 0-61454



**solar energy conversion continued**

- H<sub>2</sub> production by direct solar energy conversion at sea, review 0-61456
- H<sub>2</sub> production by direct thermal decomposition of H<sub>2</sub>O utilising solar energy, thermodynamics, review 0-61450
- H<sub>2</sub> production by H<sub>2</sub>O decomposition, review 0-97813
- H<sub>2</sub> production by H<sub>2</sub>O photolysis using solar radiation, feasibility of large scale generation 0-72095
- H<sub>2</sub> production by methylviologen photo-reduction, adsorbed on cellulose 0-81491
- H<sub>2</sub> production by solar-H<sub>2</sub> systems using metal hydrides 0-61464
- H<sub>2</sub>, review 0-61453
- H<sub>2</sub> thermochemical prod. by H<sub>2</sub>O decomposition utilising solar heat 0-61451
- H<sub>2</sub>O photoelectrolysis, H<sub>2</sub>/hydrocarbon fuel prod. via biomass conversion wastes 0-89653
- H<sub>2</sub>O photolysis using Pt/(chlorophyll a 2H<sub>2</sub>O) reaction for H<sub>2</sub> production 0-89663
- KCl-CuCl eutectic fused salt, potential as intermediate temp. solar heat transfer and storage medium 0-101135
- N<sub>2</sub> reducing solar cells for industrial NH<sub>3</sub> synthesis 0-89632
- NaCl gas-droplet counterflow heat exchanger, numerical model (*French*) 0-61396
- Si solar cells with concentrators and heat pump 0-61371

**solar energy power stations** *see solar power stations***solar flares**

- 1973 September 7, new class of transient events, X-ray, UV and visible obs. anal. 0-98643
- 1974 July 3, quasiperiodic struct. of assoc. type IV burst 0-62097
- 1978 January 1, Prognoz-6 energetic particle and solar wind meas. during assoc. interplanetary disturbance 0-90315
- 1979 March 25, X-ray obs. 0-85915
- accelerated particles, nucl. composition and Coulomb losses 0-72913
- acceleration mechanisms, implications for hard X-ray burst models 0-72912
- active regions, 3 cm radio emission spectral slope, flare-associated variations 0-98630
- activity rel. to auroral activity equatorial latitude 0-98499
- chromosphere flare, 6 cm obs. of assoc. burst source with 6" resolution 0-62096
- chromosphere flares, initial phase parameters determ. method 0-62104
- chromosphere limb flare, 1959 July 25, spectrum rel. to physical conditions 0-105227
- cosmic ray events with high relative <sup>3</sup>He abundances, obs. during 1976 November to December 0-61972
- cosmic ray modulation by 1976 April 30 flare 0-67484
- cosmic ray particle intensity variations, depend on interplanetary mag. field and solar wind 0-77372
- cosmic ray particle prod. and accel. in expanding coronal mag. bottle 0-77244
- cosmic ray proton flux determ. from <sup>3</sup>He in lunar rocks 0-98576
- current layers explanation for X-ray and UV emission 0-101572
- cycle 20, flares rel. to cosmic ray intensity, model 0-72914
- distribution in galactic coord. system (*Russian*) 0-67689
- electron density determ. from X-ray spectra obs. 0-82326
- energetic particle abundances Voyager obs. 0-90382
- energy build-up, appl. of new approach to force-free mag. field 0-62011
- energy source and current layer instability origin 0-101571
- evolution model, link with microwave events magnitude distrib. 0-98640
- exposure of Luna 24 core samples, thermolum. obs. 0-82246
- gamma ray emissions study, Solar maximum mission, detector assembly and electronic assembly 0-63476
- gamma-ray lines, HEAO 1 obs. 0-67682
- geomagnetic effects, summary of 1978 activity 0-72919
- hard X-ray bremsstrahlung, polarisation and directivity of radiation from thermal source 0-90374
- impulsive mm-wave bursts, quasi-quantization 0-94770
- impulsive X-ray burst, spectral anal. analytical method (*Chinese*) 0-85919
- inverse Compton radiation, appl. to inference of relativistic electron spectra 0-90339
- Langmuir turbulence spectrum estimate from X-ray obs. 0-82329
- magnetic fields, force-free fields evolution; nonequilib. states and preflare stage 0-105213
- model based upon photospheric dynamo action 0-62102
- model for photospheric mag. field importance in coronal energy storage 0-72906
- monitoring using global radio solar telescope network 0-82202
- near-Earth radiation hazard due to solar flares, dosage estimation technique 0-67482
- particle acceleration, injection energy concept 0-101509
- plasma, infinitely conducting, pinch effect, dynamical accumulation towards neutral line of magnetic field 0-83977
- plasma instability and turbulence, review 0-62100
- prediction by comparison of X-ray and visible data 0-72910
- proton flare active regions, force free mag. field and force free factor determ. (*Chinese*) 0-77365
- proton flare events, relation to type I (metre wave) radio sources (*Chinese*) 0-105222
- protons, flux limit due to accel. mechanism saturation effects 0-98645
- radiation, EM and particle, generation features 0-101575
- radiation, microwave and protons, generation props. 0-109413
- radio brightness distribution, processing in one-dimensional synthesis (*Italian*) 0-98628
- S-component source spectra, correl. with flare occurrence, EHF obs. 0-101579
- shock wave, solar flare generated, plasma enriched by O<sup>6+</sup> and He<sup>++</sup> 0-72740
- simulation, expt. on merging of two current carrying plasma columns (*Japanese*) 0-94775
- Solar Maximum Year project, space expts. for flare-related sub-programmes 0-90404
- solar wind shock wave, model based on Forbush decrease (*Chinese*) 0-90302
- transient plasma X-ray spectra, electron density and temp. diagnostics 0-77368
- two ribbon flares origin from mag. instability of coronal arcades 0-72911
- UV spectra, O I 1355.6 Å and C I 1355.8 Å lines obs. 0-90381
- X-ray bright points, assoc. with type III bursts 0-67681
- X-ray emission (50-100 keV) directivity 0-105218
- X-ray line spectra from transient plasma 0-98626

**solar flares continued**

- X-ray lines from transient plasma, rate coeffs. determ. 0-72903
- Fe XX, new atomic data for flare spectra 0-67545
- <sup>3</sup>He rich events, description and anal. 0-101585
- <sup>3</sup>He-rich flares, 8666 MHz superfine structure line detection 0-109417

**solar furnaces** *see furnaces***solar interior**

- convection zone, ensemble-averaged eqns. for granulation, supergranulation and giant granules 0-67698
- convection zone, mag. fields floating-up time rel. to solar activity 11-year cycle 0-101580
- convection zone, struct. adjustments rel. to solar luminosity short term fluctuations 0-82321
- convective envelope, linear convective modes 0-62091
- core, rotational constraints 0-101576
- differential rotation, due to latitude depend. convective heat transport 0-90411
- dynamo action, interior differential rot. and meridional circulation effects 0-90378
- magnetic dynamo, role of differential rotation 0-109414
- neutrino flux from standard solar model and stellar evolution calc. programme 0-67703
- neutrino fluxes calcs., neutrino oscills. constraint 0-109410
- non-radial oscills. with initial chemical discontinuity 0-82341
- oscillations with 160 min. period, amplitude modulation from solar rot. (*Russian*) 0-77375
- oscillations with 160 minute period, evidence 0-82324
- plasma diagnostics of solar interior, use of MHD pulses 0-109405
- stability against nonradial thermal modes 0-82322
- structure, implications of solar oscills. obs. 0-82526
- torsional oscillator with 11 year period 0-105217
- Fe, coalescence in centre of Sun 0-77373
- Fe segregation from H, ionic mixtures phase separation theory 0-77279

**solar magnetic fields** *see solar magnetism***solar magnetism**

- active complex with developing secondary region, mag. field struct. and dynamics 0-67685
- active region magnetic field emergence into corona, assoc. radio burst 0-109412
- active regions magnetic field, appl. of new approach to force-free field 0-62011
- convection zone, mag. fields floating-up time rel. to solar activity 11-year cycle 0-101580
- convective element intrinsic mag. field 0-101583
- corona, energy source for flares 0-101571
- corona, magnetic flux tubes, vibration modes, general dispersion relation 0-94706
- corona, plasma flow along sheared mag. arches 0-62092
- corona, potential magnetic field structs. assoc. with solar proton events and type I (metre wave) radio sources (*Chinese*) 0-105222
- corona, X-type mag. configuration rel. to type IV radio burst quasiperiodic struct. 0-62097
- corona and chromosphere, mag. field above flocculus determ. using radio obs. 0-98635
- corona heating mechanisms, mag. field scaling props. 0-85913
- coronal arcades mag. instability, two ribbon flares origin 0-72911
- dynamo, role of differential rotation 0-109414
- dynamo action, interior differential rot. and meridional circulation effects 0-90378
- dynamo model of magnetic field, self-consistent treatment 0-81808
- field components, rel. to model of heliospheric mag. field configuration 0-94670
- flares experimental simulation, mag. field effects on merging of two current carrying plasma columns (*Japanese*) 0-94775
- flux tubes, interaction with acoustic waves 0-85911
- flux tubes in photosphere, downdraught development at sunspot origin 0-72908
- force-free magnetic fields evolution, nonequilib. states and preflare stage 0-105213
- general magnetic field fluctuations, correl. with solar rel. oscills. 0-105226
- loop formation in convective regions 0-109420
- McMath region 12417, mag. feature producing X-type neutral sheet 0-98642
- McMath region 13043, coronal mag. fields intensification rel. to centimetre-wave sources rapid var. 0-67688
- MHD pulses, use as diagnostic technique for Sun 0-109405
- open field lines from active regions, struct. review 0-85924
- photosphere, boundary magnetic field effects on cylindrical prominences 0-90396
- photosphere, mag. field importance for coronal energy storage, solar flare model 0-72906
- photosphere active region, mag. field correl. with circularly polarised 6 cm emission 0-62096
- photosphere magnetic fields, possible explanation for fine struct. 0-98646
- proton flare active regions, force free mag. field and force free factor determ. (*Chinese*) 0-77365
- quietest prominence, equipartition mag. field strength from Ca<sup>+</sup> K-line width and shift 0-77364
- Schluter Temesvary sunspot, vertically orientated mag. flux tubes, exact static equilb. 0-98637
- spectral line formation depth in mag. field, theory (*Chinese*) 0-105159
- sunspot magnetic field gradients determ. from Zeeman line rot. and profiles (*Chinese*) 0-85920
- sunspots, Zeeman line profile, mag. field determ. by radiative transfer method 0-82221
- surges, local mag. field strength rel. to dynamics of descending stage (*Chinese*) 0-105221

**solar noise** *see noise; solar radiofrequency radiation***solar power**

- see also solar energy concentrators*
- absorption chillers, solar-fired, capacity modulation 0-66952
- AEROSOLEC, combined solar-wind power station for telecommunication appls. 0-61306
- air conditioning, LiBr absorption, low and high temp. cycles 0-81425
- air conditioning with solid absorbents, earth and underground water cooling 0-72018
- alternative fuel source, predictions for future and technical-economic possibilities 0-89591

# solar power continued

alternative versus conventional energy sources, economic comparison (*German*) 0-72002  
anisotropic diffuse insolation, calc. of instantaneous flux on tilted surfaces 0-101412  
atmospheric attenuation, effect of O<sub>3</sub> and H<sub>2</sub>O vapour content and atmos. turbidity 0-93855  
autonomous solar electric systems (*German*) 0-93875  
building design for maximum utilization (*German*) 0-93854  
building heating, energy storage and power supply for system, optimal conditions (*French*) 0-61297  
central receiver system, flux density integral for reflected sunlight, numerical anal. 0-93863  
climatological design assessment of solar buildings, interactive computer aided design techniques 0-61289  
climatology of global solar radiation in California and an interpolation technique based on orthogonal functions 0-67402  
coal gasification reactors using solar power, tech. and economic feasibility 0-76613  
cooling, evaporation and refrigeration units, assurance of specified energy parameter values, statistical analysis 0-93848  
cooling, operating systems and current developments, review 0-85265  
cooling, Rankine-cycle systems, selection of working fluids 0-104515  
cooling systems, residential, solar absorption-vapour compression system 0-72017  
cyclonic, solar gas-solid chemical reactor, flash pyrolysis of wood sawdust (*French*) 0-61296  
daily solar total irr. fluctuations, temporal statistical anal. (*French*) 0-61292  
desalination plants for desert pastures irrigation 0-89594  
development, availability, and storage possibilities (*French*) 0-89587  
diffuse irradiance measurement using shadowband, corrections 0-101410  
direct irradiance at the ground, parametric modelling 0-101411  
direct solar air heating, theory and practice of heating strategies in Denmark 0-66945  
direct solar energy, Markov chain simulation with one minute binning (*French*) 0-61293  
district heating system using thermal energy storage, sensitivity anal. 0-67007  
domestic hot water heating using hot air solar collectors 0-97768  
domestic hot water system for telephone exchange 0-66940  
energy accounting study 0-76589  
energy management system 0-66951  
energy resources, review of alternatives to fossil fuel (*Italian*) 0-66917  
energy roof, solar energy utilisation and heat recovery (*German*) 0-61285  
energy storage technology and solar energy use, worldwide trends (*German*) 0-72086  
energy structure distrib. laws for solar-radiation regime, analytic representation 0-98378  
energy system synthesis, soft solar energy option 0-76614  
flat plate collectors, solar flux calc. for angle of optimum tilt 0-61424  
flux calculations, algorithm for plane surfaces 0-61423  
flywheel energy storage and conversion system for photovoltaic appl., economic anal. 0-94116  
generation, system developments and research aims (*German*) 0-108799  
global and sky radiation estimates for Austria 0-93861  
global surface irradiance, effect of aerosol props. and surface reflectivity 0-76611  
greenhouse with subsoil heat storage, formation of microclimate 0-89596  
harnessing, biography of A.B. Mouchot (*French*) 0-105484  
heat exchange in a solar greenhouse with a soil heating system 0-93849  
heat pump, series, flat-plate collectors, vapour compression, energy conservation 0-72078  
heat pump, solar assisted, operation 0-61395  
heat pump plant for space heating in winter, air conditioning in summer 0-76615  
heat storage device, off-peak, ambient temp. observer/predictor control system 0-66950  
heat storage in a solar heating system using Na salt hydrates 0-67005  
heat storage in solar heating system using Na salt hydrates, based on extra water principle 0-67006  
heating, air movement control 0-66946  
heating, collector applications for space and water heating in buildings 0-61406  
heating, rapid implementation effect on USA energy supply 0-104497  
heating and air conditioning 0-61290  
heating expts. for performance prediction and design optimisation 0-61288  
heating of gas circulating in forced convection through porous cavity (*French*) 0-69626  
heating panel system, performance testing and evaluation (*Dutch*) 0-72079  
heating system, performance characts. 0-61309  
heating systems, performance modelling and simulation 0-76618  
heating systems, space and water heating, application of solar energy in dwellings. A technical and economical analysis for the European Community 0-66943  
heliotechnics, basic values, symbols, units and definitions (*Rumanian*) 0-57243  
hot-water supply system for residential building 0-93851  
hotwater and heating systems, availability aspects 0-61314  
hourly diffuse radiation predictions from meas. hourly global rad. on a horizontal surface 0-93864  
HVAC system, thermal storage, materials, labour and insulation costs 0-72088  
industrial process heat supplied by solar energy 0-76606  
industrial solar energy utilisation in UK 0-61301  
industrial utilisation of energy, book 0-61222  
installation development costs, solar cell mass production technology (*German*) 0-72046  
installation for drying tobacco, solar powered 0-93850  
irradiance on horizontal surface, estimation of totals from UK average meteorological data 0-81422  
Israel, estimation of solar radiation and ambient temps. 0-76607  
KS-7F solar kitchen, economic effects on economy 0-89590  
mesoscale mapping of available solar energy at the Earth's surface by use of satellites 0-72613  
microwave power transmission system rectennas, Yagi-Uda receiving elements design, characteristics and economics 0-66938  
Middle Eastern research programmes 0-66939

# solar power continued

Minto solar wheel, effect of material properties on thermal efficiency 0-97769  
monthly mean global solar radiation maps for Japan 0-109185  
passive heating, review and development of direct, mass wall and attached sun space systems for residential appls. 0-76619  
passive measures in building design for utilizing solar energy (*German*) 0-93853  
passive solar space heating for energy conservation 0-66948  
photovoltaic conversion comparative evaluation (*Italian*) 0-60023  
photovoltaic power system reliability assurance methods 0-61315  
photovoltaic systems break-even cost anal. for rural Mexico 0-94027  
photovoltaic transient analysis program for electrical and thermal anal. 0-94061  
plant for hot water supply (*Rumanian*) 0-97766  
radiation flux density, solar and terrestrial radiation dependent on the amount and type of cloud 0-67403  
radiation intercepted by a tilted surface, estimation of daily, clear sky, spatial distrib. 0-81423  
radiation statistics, linear spatial interpolation 0-93859  
refrigeration, exam. of dry absorption using CaCl<sub>2</sub>-NH<sub>3</sub> 0-61310  
refrigeration, isothermal dissociation and regeneration of CaCl<sub>2</sub>-NH<sub>3</sub> (*French*) 0-61300  
remote islands telecommunication repeater stations power supply 0-61382  
rock bed storage for solar energy systems, comparison of meas. and predicted performance 0-67004  
SERI, Solar Energy Research Institute, CO, USA, R and D program, organisation 0-89599  
social implications of energy storage 0-67001  
solar cell arrays, technological and economic barriers to be overcome for competitive power production 0-72049  
solar collector-heat pump installations, meas. of efficiency under operational conditions (*German*) 0-101077  
solar energy and environmental heat utilization for space and water heating (*German*) 0-61284  
solar heating of buildings, numerical simulation of thermal performance 0-66942  
solar irradiance, model for determining the spectral quality of daylight on a horizontal surface at any geographical location 0-93856  
solar Rankine cycle air conditioner (*Japanese*) 0-72076  
solar thermoelectric generators, metallic thermo-electric materials utilisation, economic characts. 0-101122  
solar-radiation meter, automatic 0-89592  
space and water heating, trial (*German*) 0-108788  
space heating, heat pump house heating system with low quality thermal flow 0-76617  
space heating, latent heat diode walls for solar energy collection and storage (*French*) 0-61298  
space heating, office building in Madrid, appl. 0-89597  
space heating, solar collectors combined with ground heat pumps, economic advantages (*German*) 0-76605  
space heating, solar energy collection and storage (*French*) 0-61299  
space heating, solar power utilisation employing solar collectors, absorbers and heat pumps (*German*) 0-76604  
space heating, two-tank storage system using seasonal and diurnal tanks 0-72016  
space heating in winter, solar availability from anal. of SOLMET data (1953 to 1975) 0-81421  
space heating installations, case for dynamic controls on hydronic distribution systems 0-104498  
space heating with air and liquid systems 0-61287  
spectral distrib. determ. using rapid spectral radiometer for solar cell appls. 0-61369  
stations, design of village photovoltaic power systems 0-61307  
stochastic predictions of solar cooling system performance 0-85269  
storage, molten salts, heat transfer salt (*French*) 0-61434  
storage system, ammoniated salt heat pump using MgCl<sub>2</sub>, CaCl<sub>2</sub>, NH<sub>4</sub>Cl 0-81484  
technical-economic validation of resources as energy sources 0-89593  
technology and methods for appl. of solar energy to European agriculture 0-76616  
temperature control systems, modern control theory appl., review 0-66949  
terrestrial solar spectral irradiance distrib. variations, sensitivity of solar transmittance, reflectance and absorptance 0-82739  
thermal Albedo Energy Converter, concept, design and testing for high altitude long endurance platforms 0-108789  
thermal energy storage 0-72089  
thermal storage using chabazitic tuff, a zeolitic rock 0-94117  
thin film deposition using solar furnaces 0-89148  
USA, classification of solar climates 0-76612  
utilisation in northern latitudes, insolation modelling of solar collector with thermal storage 0-66941  
water heaters, rural population demand fulfilment 0-89668  
water heating, residential, combined solar systems, economic anal. 0-61311  
water heating system for domestic appls. 0-93852  
water pump for lift irrigation, thermodynamic anal. and simulation 0-61397  
wood wastes, gasification, using flash pyrolysis and concentrated solar energy (*French*) 0-61226  
CO<sub>2</sub>, thermochem. reduction using solar energy to provide C-based fuels 0-76610  
CaO-Ca(OH)<sub>2</sub> reversible hydration-dehydration for solar energy storage 0-97810  
H<sub>2</sub>O heating, freeze-tolerant heater using crosslinked polyethylene 0-66944  
Ni-Cd pocket plate batteries characteristics, solar applications 0-61332  
Pb-acid battery charging from photovoltaic array energy source, problems and efficiency 0-61336

# solar power stations

10 MW thermal central receiver pilot plant 0-66953  
150 kW pilot solar pond project, Israel 0-94114  
600 to 800000 kW solar pond project at Salton Sea, CA, USA 0-94113  
AEROSOLEC, combined solar-wind power station for telecommunication appls. 0-61306  
central receiver system, flux density integral for reflected sunlight, numerical anal. 0-93863  
central receiver with chemical storage, 100 MWe cogeneration 0-93857



**solar power stations continued**

- collection subsystem of 1 MW solar power station, engineering assessment 0-61305
- combined solar and fossil fuel systems 0-61312
- concentrating collector systems, US DOE Solar Thermal Program, R and D review 0-66998
- desalination plant utilising reverse osmosis, 2.5 kW solar generator 0-61282
- design of village photovoltaic power systems 0-61307
- direct tracking using two-mirror unit with plane and hyperboloidal counter-reflectors 0-91875
- electricity storage, battery appls. potential 0-72067
- flat-plate non-tracking ground mounted photovoltaic array structures, cost reduction anal. 0-94038
- flywheel energy storage and conversion system for photovoltaic appl., economic anal. 0-94116
- hazards to air traffic, photometric photography of dazzling heliostat mirrors (*French*) 0-61295
- hybrid solar photovoltaic/solar thermal electric power system, simulation 0-94025
- hybrid solar-diesel power stations for optimum energy utilisation 0-89598
- multi-gigawatt, in space, progress review in field since 1979 (*German*) 0-81424
- orbiting, American project (*Spanish*) 0-81420
- orbiting, evaluation of current conductor mass and voltage level required 0-89616
- OTEC power plant, selection of working fluid (NH<sub>3</sub>, propane and freon) 0-89665
- OTEC system performance study 0-104514
- photovoltaic flat panel system, design and performance of 100 kW plant 0-61308
- photovoltaic power systems for rural areas of developing countries, technology, reliability, economics and appls. 0-61286
- photovoltaic village power systems: the minigrid concept 0-66973
- photovoltaic/thermal system powers Texas house, performance data and power conditioning equipment 0-94036
- power plants, solar high temp., with Stirling engine and solar thermal rocket engine, efficiency improvement by using selective radiation absorption surface 0-89589
- primary circuit and thermal storage tank transient thermal behaviour 0-85267
- satellite, technical considerations 0-72014
- satellite, theoretical anal. of nonlinear interaction between strong microwaves and ionosphere (*Japanese*) 0-94634
- satellites, effect of transmissions on radio-astronomical research 0-61291
- solar photovoltaic system feeding unusual length radio link, characteristics and design data 0-61383
- solar voltaic power systems, comparison to fuel energy, for telecommunications 0-61381
- Sophia Antipolis 5 kW photovoltaic power generator for habitat 0-61374
- space power plant and solar energy power generator, thermionic converter proposal 0-61389
- space-manufactured satellite power systems, costs anal. using lunar materials 0-97767
- state of art survey in solar energy utilisation (*Dutch*) 0-76608
- thermionic power plant, central thermal receiver tower concept, geometric config. and design 0-61390
- tower-type, concentrating and receiving systems design modelling 0-91873
- vapour turbine, using combined thermal-power convertor and photoelectric convertor, thermodynamic efficiency for solar energy conversion 0-89614
- CaO-Ca(OH)<sub>2</sub> reversible hydration-dehydration for energy storage 0-97810

**solar prominences**

- 1979 February 26, prominence excitation conditions determ. from flash spectrum 0-67687
- ancient Chinese observations of physical phenomena attending solar eclipses 0-72916
- Balmer lines, formation in bright prominences spectra (*Russian*) 0-77377
- cylindrical prominences, photospheric boundary magnetic field effects 0-90396
- electric currents as solar wind energy source, theory 0-94768
- eruptive prominences, rel. to He<sup>+</sup> obs. in interplanetary shock wave 0-72735
- filament, synthesized map at 6 cm with about 15" resolution 0-90380
- loop prominence knots, motions, H $\alpha$  line filtergram obs. 0-67693
- quiescent prominence, influence of spatial resolution on Ca<sup>+</sup> K-line width and shift 0-77364
- quiescent prominence spectra, meas. of Ca<sup>+</sup> 8542, 8498 Å, He 4471 Å and Ti<sup>+</sup> 4468 Å 0-90373
- radiative transfer, H line radiation diffusion 0-67694
- radio brightness temp. depression interpretation, cm and mm data 0-90395
- spectra, inclined features obs. in Ondrejov Observatory spectra 0-62098
- turbulence causing coronal heating and MHD wave generation 0-72907
- He I D<sub>2</sub>-line polarization in quiescent prominences, level-crossings effect 0-94772

**solar radiation**

- see also *solar cosmic ray photons; solar radiofrequency radiation; solar spectra; solar wind; sunlight*
- Alfven wave flux, rel. to solar wind accel. 0-85923
- brightness fluctuations, correl. with solar rel. oscils. 0-105226
- chromosphere, continuum radiative losses 0-72924
- chromosphere-corona transition region, emission measure gradient rel. to energy balance 0-90379
- conference on nuclear cosmic physics, Leningrad, USSR (Oct. 1978) 0-98755
- corona, 1973 June 30, polarised brightness distrib. rel. to N.polar hole density model 0-98627
- corona, effects of radiation heat flux on expansion 0-90377
- EUV bursts, C IV 1548 Å line profiles, OSO-8 obs. 0-90401
- EUV flux during solar cycle 21, correl. with atmospheric O<sup>+</sup>(<sup>2</sup>P) ionisation freq. vars. 0-77195
- EUV flux variations, correl. with ionosphere primary ion-electron prod. rates changes 0-72675
- F-corona, flux bump at 4 solar radii 0-82162
- far IR absolute brightness temperature, meas. by balloon-borne interferometer 0-62095
- far IR brightness temp. minima rel. to sunspot activity 0-62035

**solar radiation continued**

- flare, 1973 September 7, new class of transient events, X-ray, UV and visible obs. anal. 0-98643
- flare impulsive X-ray burst, spectral anal. analytical method (*Chinese*) 0-85919
- flares, acceleration mechanisms, implications for hard X-ray burst models 0-72912
- flares, polarisation and directivity of hard X-ray bremsstrahlung from thermal source 0-90374
- flares, X-ray and UV emission explanation within current layer theory 0-101572
- flares, X-ray emission (50-100 keV) directivity 0-105218
- flares inverse Compton radiation, appl. to inference of relativistic electron spectra 0-90339
- hard X-ray bursts, thermal model dynamic spectral characts. 0-98644
- irradiance determination from Nimbus 7 cavity radiometer obs. 0-105225
- limb darkening function at 5012 Å, possible vars. 0-67677
- luminosity variation (solar const.), direct obs. from rockets 0-90386
- luminosity variations, C I 5380 Å line response, effects of granular convection 0-85910
- luminosity variations, meas. and effect on Earth climate 0-77376
- luminosity variations, possible detect. from photometry of Io, Europa, Callisto and Rhea, (1976 to 1979) 0-98623
- luminosity variations assoc. with gravit. const. cosmological var., re-examination 0-82182
- Lyman  $\alpha$  radiation, high resolution filtergrams obs. 0-82323
- meteorological radiation reference scales 0-109206
- optical continuum brightness, fluctuations rel. to trapped gravity waves in solar atmosphere 0-72898
- photodissociative ionisation of cometary comae mols. 0-90370
- pressure effects on artificial satellite anomalous period 0-77255
- solar constant, no correl. with N.Hemisphere average temps. during Little Ice Age 0-82050
- solar constant fluctuations, prod. by convection zone struct. adjustments 0-82321
- UV and radio fluctuations in transition region, common origin 0-90398
- UV flux, cyclic vars. 0-101577
- UV flux variability over solar cycle, 1175-2100 Å 0-90383
- UV spectrum 140 to 350 nm, NASA meas. using SURF storage ring calibrations 0-94721
- variability, effect on <sup>14</sup>C prod. in atm. 0-85730
- X-ray bursts, thermal models 0-94766
- X-ray long decay event, physics 0-90402
- H I Lyman  $\alpha$  flux near solar minimum 0-90393

**solar radio emission** see *solar radiofrequency radiation*

**solar radiobursts** see *solar radiofrequency radiation*

**solar radiofrequency radiation**

- 3.2 and 10 cm emission, anal. of observational data from Purple Mountain Observatory (*Chinese*) 0-105223
- 10.7 cm flux, vars. during solar cycle and correl. with tropospheric winds 0-72604
- active region and bursts, 6 cm obs. with 6" resolution 0-62096
- active regions, 3 cm radio emission spectral slope, flare-associated variations 0-98630
- brightness temp. in SHF, distrib. on quiet Sun, RATAN-600 obs. (*Russian*) 0-94776
- bursts, peak flux spectra, statistical anal. 0-98641
- centimetre-wave sources above McMath region 13043, rapid var. rel. to optical phenomena 0-67688
- corona, radio spectrograms, magnetoplasma, plasma wave motions (*Dutch*) 0-62101
- decametric storm burst source positions, UTR-2 obs. at 25 MHz 0-90403
- drift pair bursts, polarisation obs., position and freq. characts. 0-85925
- F10.7 index during solar cycle 21, correl. with atmospheric O<sup>+</sup>(<sup>2</sup>P) ionisation freq. vars. 0-77195
- filament, synthesized map at 6 cm with about 15" resolution 0-90380
- flare monitoring using global radio solar telescope network 0-82202
- flares, radiation generation features 0-101575
- flares, radio brightness distrib. processing in one-dimensional synthesis (*Italian*) 0-98628
- fluctuations, correl. with solar rel. oscils. 0-105226
- impulsive mm-wave bursts, quasi-quantization 0-94770
- microwave events, magnitude distrib., link with flare build up phenomenological model 0-98640
- microwave generation from flares 0-109413
- noise storm, drifting pulsations obs. 0-62105
- prominence brightness temp. depression interpretation, cm and mm data 0-90395
- quiet spatial structure during 1977 October eclipse, VLA 6 cm obs. 0-72895
- radio burst emission mechanisms 0-72917
- spectral index determ. of radio emission of individual solar regions 0-94723
- synoptic charts at 9.1 cm, use to identify coronal holes 0-98633
- transition region, origin for UV and radio fluctuations 0-90398
- type I (metre wave) sources, relation to solar proton events (*Chinese*) 0-105222
- type I bursts, meter wave, role of coronal Langmuir turbulence and quasi-stable particle accel. (*Chinese*) 0-105220
- type II and IV bursts assoc. with mag. field emergence into corona 0-109412
- type III bursts, assoc. with flaring X-ray bright points 0-67681
- type III bursts, emitting source size and evolution 0-94771
- type III bursts, obs. during JIKIKEN (EXOS-B) satellite initial phase (*Japanese*) 0-94675
- type III bursts, position and polarisation, VHF and HF obs. 0-105214
- type III bursts, radio spectra obs., effect of interactions in ionospheric plasma 0-72904
- type III bursts, vol. emissivity calc. 0-90384
- type III bursts during decametric storm 0-90399
- type III noise storms, rel. to coronal plasma heating by fast electron streams 0-105228
- type IIb bursts, 25 MHz obs. and theoretical model 0-90400
- type IV radio burst quasisperiodic struct., anal. and interpretation 0-62097
- V radio bursts, position and polarisation, HF and VHF obs. 0-105215

**solar radiofrequency radiation continued**

UHF two dimens. maps of 408 MHz 0-85922  
<sup>3</sup>He 8666 MHz superfine structure line detection of <sup>3</sup>He-rich flares 0-109417

**solar radiowaves** *see solar radiofrequency radiation*

**solar rotation**

background vel. fields, anal. and instrumental effects, visible obs. 0-72915  
convection structure, effect of differential rot., Maunder minimum nature 0-101573  
core, rotational constraints 0-101576  
diagnostics of uniformly rotating ionised medium, appl. of MHD pulses 0-109405  
differential rotation, correl. with mag. fields from dynamo action 0-90378  
differential rotation, due to latitude depend. convective heat transport 0-90411  
differential rotation, gaseous polytropic configurations for const. mass solar model 0-82338  
differential rotation of solar wind, determ. from recurrence period as function of heliographic latit. 0-62106  
effect on relativistic galactic cosmic rays, anisotropies 0-67481  
EUV flux, changes with solar rot. rel. to ionosphere primary ion-electron prod. rates change 0-72675  
induced Doppler spectral shift meas. by scanning Fabry-Perot interferometer 0-77298  
longitudinal distribution of solar activity, refl. in geomagnetic var. 0-82330  
magnetic dynamo, role of differential rotation 0-109414  
photosphere Doppler obs. in visible 0-105219  
pulsars, pulse width-period relation rel. to source of coherent radio emission 0-82403  
spatial displacement pattern precession, effect on 160 min. period solar oscils. (*Russian*) 0-77375  
sunspot data (1967-74), global rotation rate determ. 0-90387  
sunspot group velocities, statistical distrib., depend. on solar activity cycle phase 0-72918  
supergranulation cells, equatorial rotation rate 0-90388  
surface oscillations and pulsations, rotation speeds 0-67676  
torsional oscillator with 11 year period 0-105217

**solar spectra**

*see also solar activity; solar corona; solar radiation*  
absorption lines formation in inhomogeneous medium, rel. to waves and convective motions (*Russian*) 0-72901  
active region McMath 12628, EUV and X-ray obs. 0-67692  
active regions, 3 cm radio emission spectral slope, flare-associated variations 0-98630  
automatic observation and data processing, by double-pass digital monochromator (*Russian*) 0-72777  
Balmer lines, formation in bright prominences spectra (*Russian*) 0-77377  
chromosphere, Ca II lines, vel. and temp. disturbances, weighting functions 0-67679  
chromosphere, optically thick line formation, atmospheric dynamics 0-94767  
chromosphere active regions, bidimensional spectroscopy obs. with birefringent filter (*Italian*) 0-98568  
chromosphere flares, H  $\alpha$  spectra rel. to initial phase parameters determ. 0-62104  
chromosphere limb flare, 1959 July 25, spectrum rel. to physical conditions 0-105227  
chromosphere line profiles from OSO-8 satellite 0-67690  
chromosphere mechanical flux determ. from Ca II lines 0-67680  
chromosphere-corona transition zone of solar active regions, non-thermal velocities (*French*) 0-77371  
corona, 530.3 nm emission line from 1965-78, north-south asymmetry 0-77369  
corona, intensity ratios of fine-struct. components of H like ions reson. lines 0-101581  
coronal loops in an active region, physical props. XUV obs. 0-90376  
damping constant and microturbulent velocities determ., study of errors (*Russian*) 0-72899  
Doppler shift measurements, rel. to solar oscillations and Sun internal struct. 0-105226  
EUV lines in chromosphere-corona region, anal. of coronal hole limb brightening data 0-82333  
F corona, radial vel. obs. at 1979 February 26 solar eclipse 0-85914  
flare, electron density determ. from X-ray spectra obs. 0-82326  
flare, Langmuir turbulence spectrum estimate from X-ray obs. 0-82329  
flare, transient plasma X-ray spectra, electron density and temp. diagnostics 0-77368  
flare Fe XX spectra, new atomic data 0-67545  
flare impulsive X-ray burst, spectral anal. analytical method (*Chinese*) 0-85919  
flare of 1979 March 25, X-ray spectra 0-85915  
flares, O I 1355.6 Å and C I 1355.8 Å lines obs. 0-90381  
flares, transient plasma X-ray lines, rate coeff. determ. 0-72903  
flash spectrum, obs. at 1979 February 26 eclipse 0-67687  
Fourier transform spectroscopy 0-98448  
gamma-ray lines from flare, HEAO 1 obs. 0-67682  
hard X-ray bursts, thermal model dynamic spectral chars. 0-98644  
line formation depth in mag. field, theory (*Chinese*) 0-105159  
line polarisation in VUV, technique and data reduction 0-67691  
line profiles, rough reconstruction from series of narrow-band filtergrams (*Italian*) 0-98564  
line shifts, wave effects 0-109408  
line wings, polarized radiative transfer, excited state interference 0-105158  
photosphere spectrum, granulation vertical motions spatial and temporal behaviour 0-85912  
photosphere, line shifts calc. from granulation vertical motion models 0-90375  
photosphere line asymmetries, appl. to vel. gradients retrieval via linearised approach 0-62093  
photosphere spectra, correction function for granulation mean vertical vel. determ. 0-62094  
plate Ca II K-line, peak separation due to microturbulence 0-109407  
plate fragment temp. gradients determ. from equivalent width 0-98634  
prominence spectra taken at Ondrejov Observatory, inclined spectral features obs. 0-62098  
prominences, H line radiation diffusion 0-67694

**solar spectra continued**

quiescent prominence spectra, meas. of Ca<sup>+</sup> 8542, 8498 Å, He 4471 Å and Ti<sup>+</sup> 4468 Å 0-90373  
radio bursts, peak flux spectra, statistical anal. 0-98641  
radio drift pair bursts, polarisation obs., position and freq. chars. 0-85925  
resonance line polarisation, non-mag., centre-to-limb var. 0-67678  
rotation induced Doppler spectral shift meas. by scanning Fabry-Perot interferometer 0-77298  
sunspot magnetic field gradients determ. from Zeeman line rot. and profiles (*Chinese*) 0-85920  
sunspot umbrae, IR Ca II lines 0-85918  
sunspots, TiO equivalent width meas., theoretical interpretation, line form. process 0-72902  
sunspots, Zeeman line profile, mag. field determ. 0-82221  
time intensities, dielectronic recomb. excitation effects 0-82332  
X-component sources, correl. with flare occurrence, EHF obs. 0-101579  
X-ray line spectra from transient flare plasma 0-98626  
Ba III 4554 Å obs. rel. to five-minute oscils. horizontal energy flows struct. 0-62103  
C I 5380 Å response to solar luminosity vars., effects of granular convection 0-85910  
C IV 1548 Å line profiles of impulsive EUV bursts, OSO-8 obs. 0-90401  
C V emission line ratios for corona transition region interpretation 0-98624  
C<sub>2</sub> rotational temp. and photospheric models 0-62099  
Ca II H-K and Na I D-lines, non-mag. polarisation 0-63569  
Ca II K-line, centre-to-limb obs. of K<sub>2</sub> component (*French*) 0-82331  
Ca II K-line in quiescent prominence, influence of spatial resolution on line width and shift 0-77364  
Co XI-XVII, 3s<sup>2</sup>3p<sup>n</sup>-3s3p<sup>n+1</sup> transition arrays, UV spectra classification 0-63570  
Fe I, gravitational red shift, meas. 0-90391  
Fe I in photosphere, line broadening, Smirnov Roueff pot. calcs. 0-98632  
Fe I lines, damping const. determ. preliminary results (*Russian*) 0-72900  
Fe XXII, coupling energy levels, oscillator strengths, electron collision energies 0-69068  
H I Lyman  $\alpha$  flux near solar minimum 0-90393  
Hz spicules, dynamics at various heights, spectral obs. 0-90392  
He I 58.4 nm line profile, monitoring using resonance absorption spectrometer 0-62019  
He I D<sub>2</sub>-line polarization in quiescent prominences, level-crossings effect 0-94772  
<sup>3</sup>He 8666 MHz superfine structure line detection of <sup>3</sup>He-rich flares 0-109417  
Mg I and II line profiles comparison with theoretical spectra, visible obs. 0-82320  
MgH rotational temp. and photospheric models 0-62099  
N II, electron impact excitation cross sections, rel. to solar corona abundance 0-58391  
Ni I solar photosphere from oscillator strength obs. 0-98625  
Ni IX to Ni XII transitions, laboratory wavelengths and identifications in solar spectrum 0-99474  
Ni XII-XVIII, 3s<sup>2</sup>3p<sup>n</sup>-3s3p<sup>n+1</sup> transition arrays, UV spectra classification 0-63570  
O VII emission line ratios for corona transition region interpretation 0-98624  
S IV in solar atm., data from Skylab obs. 0-87028

**solar system**

*see also celestial mechanics; planets; Sun*  
<sup>29</sup>I/<sup>127</sup>I early solar system chronometer 0-62043  
cold-cold aggregates, chemical energy and meteorite chondrule origin 0-105210  
comet belt beyond Neptune, existence rel. to short-period comets origin 0-94759  
cometary cloud, orbital evolution under perturbing influence of giant planets and nearby stars 0-98613  
cometary orbits, reciprocal semimajor axes accuracy 0-62074  
comets, long-period, distrib. of inclination of perihelion dynamical implications 0-101563  
comets, nearly parabolic orbits, distrib. of nodes and perihelia 0-67661  
comets, primordial, interiors radiogenic melting 0-67659  
comets origin, implications of anomalies of orbital inclinations distrib. of original comets 0-98615  
commensurabilities 0-109418  
computer simulations of planetary system evolution 0-94733  
conference on planetary sciences Rome, Italy (Apr. 1979) 0-77537  
development, chemical and gravitational crystallisation of solar nebulae (*Hungarian*) 0-72795  
proto-Earth, formation of inhomogeneous Earth from nebula 0-90348  
fluid drops as cosmological models, stellar evolution, solar system origin, planetary geology 0-73086  
formation from supernova trigger, implications for Mg and Al isotopic abundances 0-90406  
formation of planetary system, Titius-Bode law 0-62057  
formation theory based on Laplacian hypothesis 0-85876  
interstellar dense clouds encounters, effects on solar wind and comets (*German*) 0-109500  
long-period comet loss, planetary collisions 0-77358  
material distrib., effect of Jupiter close encounter with planet crossing bodies 0-77329  
motion and cosmic background radiation anisotropy 0-105407  
nebula, rare earth element condensation and fractionation 0-72796  
nebula cooling rate, by Allende meteorite I-Xe date 0-67666  
nebular origin NH<sub>3</sub> synthesis, kinetic model 0-62041  
origin, implications of mineralogy and petrology of isotopically unusual Ca-Al rich inclusion HAL in Allende meteorite 0-109399  
origin, late nucleosynthetic event rel. to isotopically anomalous Ag in Santa Clara and Pinon Fe meteorites 0-85902  
origin, numerical simulations of collisions in Keplerian systems 0-109342  
origin, particular soln. of restricted three-body problem in resisting medium (*Italian*) 0-90325  
origin, planets rotation periods and relative formation times (*Chinese*) 0-105182  
origin, role of nearby supernova 0-82232  
origin, tidal model and Roche problem for polytropes in central orbits 0-82179  
outer solar system, mass distrib. and planet form. 0-77349  
planetary system formation models 0-62058



**solar system continued**

- planets rectangular coordinates, approximation via Chebyshev polynomials (*Russian*) 0-62033
- presolar gas components, isotopic anomalies in Murchison C2 chondrite 0-85904
- primitive solar nebula, equilib. chemistry thermodynamics calcs. 0-82231
- primordial refractory metal particles 0-85906
- primordial solar nebula, struct. and evolution 0-62042
- protoplanet, solar wind sputtering rate 0-85835
- protosolar nebula, CO and N<sub>2</sub> reduction in solar nebula, kinetic inhibition 0-85875
- stability and evolution review 0-82235
- stability from origin of Solar System tidal friction considerations 0-82233
- structure beyond Neptune, possible asteroid belt, cosmogony (*Russian*) 0-82237
- Sun and heliosphere, conference, London, England (1979 April 3 to 4) 0-82574
- Sun-Jupiter system, tidal torques theory for asteroid belt truncation 0-98596
- Titius-Bode law for planet distances from Sun 0-82236
- <sup>26</sup>Al from red giant stars rel. to meteorite <sup>26</sup>Mg content 0-67712
- <sup>247</sup>Cm evidence from Allende <sup>238</sup>U/<sup>235</sup>U ratio 0-90347
- He during solar nebula evolution, solar He incorporated into Earth (*Russian*) 0-81856

**solar-terrestrial relationships**

- auroral changes during 18th and 19th centuries, implications for solar wind and sunspot activity long-term vars. 0-98498
- Bombay geomagnetic and climatic (1848-1967) data rel. to sunspot nos. 0-81811
- climate link with solar activity, from tree ring meas. of atm. <sup>14</sup>C 0-101424
- coronal activity effect on radar meteor rate 0-67662
- D-region, solar X-ray control of ionisation 0-77198
- Earth annual polar motion, many-year variation rel. to solar eleven-year cycle (*Chinese*) 0-104848
- easterly gales of N. Atlantic, 1881-1970, rel. to 80-90 yr solar period 0-77101
- F-region peak electron density, diurnal and solar cycle variation 0-61949
- geomagnetic external spherical harmonic coeffs., solar cycle var. 0-85592
- geomagnetic field, solar cycle vars. of first-degree spherical harmonic components 0-85593
- geomagnetic storms and solar flares connection 0-72919
- geomagnetic variations, effect of solar activity longitudinal distrib. 0-82330
- global sensitivity to solar constant vars. effect of ice albedo feedback 0-109245
- ionosphere, equatorial spread-F seasonal and solar cycle vars. in American zone 0-109298
- ionosphere, primary ion-electron prod. rates change with solar EUV flux 0-72675
- ionosphere, range and freq. spread-F occurrence at Kodaikanal rel. to sunspot cycle 0-72676
- ionosphere, SITEM events (1966-1977), rel. to solar flares 0-90276
- ionosphere, topside, electron temp. models for low and medium solar activity conditions 0-67460
- ionosphere, VLF focusing during solar eclipse 0-61965
- ionosphere LF radiowave absorpt., variation during solar cycle 0-77193
- ionospheric records over Shanghai, March 1953 to June 1955, correl. of solar activities (*Chinese*) 0-77192
- Little Ice Age, N. Hemisphere average temps. not correlated with sunspots 0-82050
- magnetic substorms, high-latit., occurrence freq. rel. to sunspot cycle 0-109315
- meteorological phenomena affected by solar flares 0-109230
- Pi 2 pulsations, equatorial, fine struct. depend. on solar cycle 0-72721
- rotation and atmospheric circulation rel. to solar activity 0-104853
- solar constant variation, effect on Earth climate 0-77376
- solar corpuscular activity, correl. with Earth lower atmosphere instability at different seasons 0-61881
- thermosphere, middle, depend. on solar cycle vars. from incoherent scatter radar studies 0-72654
- thermosphere O and N<sub>2</sub> composition, seasonal-latitudinal tidal struct. and mass density, solar activity depend. 0-101467
- tornadoes in UK, rel. to solar mag. sector crossing, 1957-77 period 0-77094
- tropopause height rel. to sunspot activity 0-77090
- troposphere winds, evidence for solar cycle signal 0-72604
- upper atmosphere, O<sup>+</sup>(<sup>2</sup>P) ionisation freq. vars. during solar cycle 21 from airglow meas. 0-77195
- zonal wind speed oscills., solar cycle influence 0-94562
- <sup>7</sup>Be as a tracer for helio-geophysical phenomena 0-98525
- <sup>14</sup>C in atmosphere, variability due to variable Sun 0-85730
- <sup>14</sup>C in wines, abundance vars. with 11-year solar cycle, (1909 to 1952) 0-109249
- N<sub>2</sub><sup>+</sup> upper atmos. photochem. rel. to solar cycle phase 0-85783
- NO and N concs. in thermosphere rel. to solar activity 0-77178
- O atom corona in Earth's upper atmos., during solar max. 0-101469

**solar visible radiation** *see* **sunlight****solar wind**

- see also solar cosmic ray particles*
- acceleration, by Alfvén wave flux from Sun 0-85923
- Alfvén waves, non-linear interaction with compressive fast magnetosonic waves 0-105142
- Alfvén waves in solar wind plasma, non-WKB nature 0-72905
- Alfvénic variations, large amplitude, dynamic mag. struct. 0-72734
- ancient solar wind studied by lunar regolith <sup>15</sup>N/<sup>14</sup>N ratio 0-62046
- anisotropic MHD turbulence in solar wind, obs. 0-94669
- auroral electrojet, empirical relations to interplanetary parameters 0-105118
- cometary plasma acceleration in solar wind, rel. to ion-acoustic turbulence (*Russian*) 0-106923
- corona N.polar hole, electron density and solar wind speed at 1973 June 30 eclipse 0-98627
- coronal expansion, effects of radiation heat flux 0-90377
- corotating energetic particle events, origin 0-82161
- corotating interaction regions, energetic particles shock accel. 0-82159
- corpuscular activity, correl. with Earth lower atmosphere instability at different seasons 0-61881

**solar wind continued**

- corpuscular stream arrivals at Earth and tropospheric instability 0-109416
- Earth bow shock, backstreaming ions interaction with solar wind 0-101499
- Earth bow shock, control by solar wind conditions from initial ISEE obs. 0-90307
- Earth bow shock, interaction with backstreaming ions 0-90287
- Earth bow shock, obs. of backstreaming protons in upstream solar wind 0-90309
- Earth bow shock interaction, backstreaming ions and interplanetary mag. field 0-101500
- Earth bow shock interaction, solar wind upstream deceleration rel. to diffuse upstream ions origin 0-98528
- Earth magnetosphere interaction, mag. curl in front of magnetosphere boundary 0-85804
- electron density fluctuation in solar equator region, radio scintillation obs. 0-61978
- electrons, energetic, of magnetospheric origin, obs. and probable source 0-90310
- electrons, epithermal dumbbell distrib. Prognost 7 obs. following-shock wave 0-109321
- energetic particle coronal transport and interplanetary pitch angle scatt. 0-90305
- energetic particles upstream of Earth bow shock, review of meas. 0-90308
- energy source, direct energy transfer from photospheric activity to solar wind 0-94768
- erosion of planetary and satellite atmospheres, by energetic atomic particles 0-72736
- expansion, higher order fluid eqns. for multicomponent nonequilib. plasma atmosphere 0-105156
- exposure effects measured at lunar surface 0-77556
- geomagnetic pulsations affected by interplanetary medium 0-77228
- heliosphere, model of mag. field configuration 0-94670
- heliosphere H atom ionisation, near Sun trajectories 0-105145
- high speed stream effects on solar cycle 20 cosmic ray modulation 0-72914
- high speed streams origin from coronal holes 0-72919
- high-speed streams, origin 0-105224
- hydrodynamic streams, 3-D model of corotating solar wind 0-72737
- interaction regions, N-S mag. field component solar cycle dependent configurations 0-98529
- interaction with Comet Kohoutek (1973 XII) ion tail, dynamic response 0-85897
- interaction with interstellar neutral gas, critical vel. effect 0-94666
- interaction with Saturn magnetosphere, Pioneer 11 obs. 0-82282
- interactions with lunar surface grains, O<sup>+</sup> role 0-62050
- interplanetary collisionless shock waves, thickness 0-90314
- interplanetary corotating structures, MHD model 0-90304
- interplanetary disturbance, 1978 January 3 to 4, Prognost-6 energetic particle and solar wind meas. 0-90315
- interplanetary flows observed by satellites, 0.6 to 1.6 AU 0-90303
- interplanetary magnetic field, intensity vars. during geomag. storms with gradual commencements (*Russian*) 0-105127
- interplanetary objects sputtered by solar wind 0-85835
- interstellar medium interaction, effects of solar system encounters with dense interstellar clouds (*German*) 0-109500
- interstellar neutral He focused by Sun's gravity, interaction with solar wind 0-105144
- ion acceleration to 40 keV by shock wave disturbances 0-72738
- ion bombardment, lunar surface modification 0-109325
- Jupiter, magnetosheath sunward flow, depend. on solar wind press. 0-72857
- long term vars. in solar wind and sunspots, implications of auroral changes during 18th and 19th centuries 0-98498
- low frequency continuum from ISEE 3, thermal electrostatic noise, LF obs. 0-101519
- lunar rocks interaction, Apollo samples obs. rel. to microcrater and accretionary grain populations 0-94732
- lunar rocks interaction, microcrater and accretionary grain populations temporal development 0-94731
- magnetic field obs. by Isec-1 and -3 0-85895
- magnetic field sector boundaries at 1 AU, (1971-1973) 0-94668
- magnetosheath burst of medium nuclei, obs. from Imp 8 (1974, Feb. 16) 0-101501
- magnetosonic and Alfvén waves, transfer by solar wind 0-67490
- magnetosphere compression, rel. to solar cycle var. in geomag. external spherical harmonic coeffs. 0-85592
- magnetosphere energy coupling to solar wind, geomag. disturbances 0-85821
- magnetosphere interaction, plasma sheet slow convection and field-aligned currents theory 0-109312
- magnetosphere interaction, solar wind ion injections into morning auroral oval 0-98502
- magnetosphere merging with interplanetary field, half-wave rectifier response 0-72710
- magnetosphere micropulsations controlled by solar wind, origination region 0-85823
- magnetosphere-solar wind dynamo, energy coupling function and substorms 0-105134
- magnetosphere-solar wind dynamo affected by IMF vector 0-85824
- magnetospheric storm, interplanetary shock wave with increased solar wind energy deposition 0-77237
- Mars interaction, role of planetary ionosphere and magnetosphere 0-72835
- MHD discontinuities, identification method 0-109322
- MHD turbulence, props. 0-61977
- MHD turbulence 0-85834
- monochromatic non-WKB Alfvén waves, normals evolution 0-101521
- parameter measurement using charged-particle spectrometer, instability of analyzing voltages 0-67565
- particle trapping and acceleration during the August 1972 event 0-98532
- plasma, collisionless, stability of contact discontinuity, solar wind and magnetosphere boundary appls. 0-62002
- plasma fluid aspects, review 0-90313
- plasma irregularities, anisotropic struct. obs. using interplanetary scintillations 0-67489
- plasma microinstabilities, review of theory 0-98530
- plasma pressure rel. to magnetopause current fields 0-105123
- plasmadynamical processes in solar wind, reviews (*German*) 0-109323

**solar wind continued**

- polar solar wind, variation rel. to solar activity 0-90385  
 radio wave propagation in turbulent solar wind plasma, meas. using three satellites 0-101518  
 shock wave, solar flare generated, plasma enriched by  $O^{6+}$  and  $He^{++}$  0-72740  
 shock wave produced by flare, model based on Forbush decrease (*Chinese*) 0-90302  
 solar activity rel. to solar wind characts., review 0-94777  
 spiral structures, geophysical and astrophysical 0-77287  
 spiral waves, effect on sector struct. of interplanetary mag. field 0-85831  
 stream interaction regions, microscale instabilities 0-72739  
 stream-stream interfaces, effects of electrostatic shear flow instability 0-96359  
 Sun and heliosphere, conference, London, England (1979 April 3 to 4) 0-82574  
 terrestrial atmos. vorticity of 500 mb rel. to sector boundary crossing 0-109199  
 turbulence upstream of Earth bow shock, nonlinear plasma processes 0-85833  
 upstream particle events close to bow shock and 200  $R_E$  upstream, ISEE-1 and ISEE-3 obs. 0-77247  
 variation effects on solar flare cosmic ray particle intensity 0-77372  
 velocity, influence on magnetosphere hydromag. energy spectra 0-67476  
 velocity change due to interactions with galactic cosmic rays and interstellar H I 0-101506  
 velocity determ. from interplanetary scintillation effects on 3C 279, SHF obs. (*Russian*) 0-77248  
 velocity recurrence period, depend. on heliographic latit. 0-62106  
 velocity rel. to interplanetary magnetic field vertical component origin and recurrency 0-90369  
 Venus, flow of solar wind behind planet, model 0-98531  
 Venus, magnetosphere press. balance, outside dayside ionopause 0-90353  
 Venus atm. interaction, mag. flux ropes nature (*Russian*) 0-77313  
 Venus interaction, study via plasma analyser expt. on Pioneer Venus Orbiter 0-67498  
 Venus ionosphere interaction, meas. by mass spectrometers on Pioneer Venus Bus and Orbiter 0-67499  
 Venus magnetic tail interaction, unipolar induction effects 0-62060  
 He abundance, evidence for chemical separation by diffusion 0-77381  
 He<sup>+</sup> flux after interplanetary shock, Imp 7 obs. 0-101520  
 He<sup>+</sup>, obs. in driver gas of interplanetary shock wave 0-72735

**soldering**

- ceramic/metal layer adhesion mechanism for metallization of electronic ceramics, elec. props. (*German*) 0-76381  
 inspection using optical projection microscopes (*German*) 0-77849  
 PC fabrication, detrimental effect of aged Sn-Pb surfaces 0-108625  
 permanent joining techniques for vacuum components 0-82782  
 solar cell fabrication, photovoltaic process based on thick film technique 0-94016  
 steel, mild, solderability, annealing effect (*Japanese*) 0-89244  
 Cu, solderability, annealing effect (*Japanese*) 0-89244  
 Cu-constantan junctions with solder, shock-induced elec. response 0-75626  
 Ni-Sn intermetallic phase growth kinetics at liq. Sn-solid Ni interface 0-71638  
 Sn-Pb solder, wettability on Cu and mild steel plates (*Japanese*) 0-89244

**solenoids**

- see also coils; electromagnets  
 implosion generator of very strong mag. fields, solenoid for generation of initial mag. flux 0-105681  
 toroidal solenoids, helically wound, form factor calcs. 0-100091

**solid effect**

No entries

**solid electrolytes** see superionic conducting materials**solid helium**

- melting, at room temp. and high-pressure. 0-80025  
 melting kinetics, sound transmission at liq.-solid interface 0-92734  
 solid-fluid, eqn. of state, melting props. under press. 0-96721  
 solid-superfluid interface, struct., surface tension 0-88380  
 surface tension and contact energy, standing waves (*French*) 0-92753  
<sup>4</sup>He, room temp. melting point, press. depend. calcs. 0-103463  
<sup>3</sup>He, as mag. semicond., analogy to Mott insulator 0-96720  
<sup>3</sup>He, BCC, nucl. mag. order and paramag. susceptibility 0-59757  
<sup>3</sup>He, FCC, vacancy induced spin polarons 0-59756  
<sup>3</sup>He, four spin exchange model and magnetism 0-92752  
<sup>3</sup>He, HCP, exchange and mag. order 0-107606  
<sup>3</sup>He, HCP, vacancy-induced transitions 0-88395  
<sup>3</sup>He, magnet, spin-lattice models 0-88394  
<sup>3</sup>He, phase separation of dil. <sup>4</sup>He impurities 0-88393  
<sup>3</sup>He, solid, mag. phase diagram from static magnetisation meas. 0-84342  
<sup>3</sup>He, solid, ordering obs. at melting press. in high mag. fields 0-84341  
<sup>3</sup>He, spin ordered, melting press. and entropy 0-84340  
<sup>3</sup>He, valence band struct., zero-point motion effect 0-65333  
<sup>3</sup>He-<sup>4</sup>He, HCP, solid, nucl. spin-lattice relax., <sup>4</sup>He impurity effects 0-88396  
<sup>3</sup>He-<sup>4</sup>He, mixture, isotropic phase separation temp. press. depend. 0-92751  
<sup>4</sup>He crystals, nucleation and orientation 0-84339  
<sup>4</sup>He, HCP crystal, roughening transition 0-88397  
<sup>4</sup>He, hypernetted chain generalised eqn. optimal solns. 0-75396  
<sup>4</sup>He, liquid-solid boundary, capillary sound motion, Kapitza resistance (*Russian*) 0-92737  
<sup>4</sup>He, solid-liquid interface mobility under 1 MHz sound wave (*French*) 0-100373  
<sup>4</sup>He, solid-superfluid interface, roughening transition 0-103536  
<sup>4</sup>He, thermal cond., 0.4 to 1.8K (*Russian*) 0-103535  
<sup>4</sup>He, US finite amplitude wave propag. 0-80024

**solid hydrogen**

- colouring problem on randomly occupied lattice, critical conc. existence for long range order 0-80519  
 fundamentals, static props., review 0-75403  
 glass phase, use of NMR (*French*) 0-93190  
 metallic, ground-state energies of liq. and solid phases, variational and Monte Carlo methods 0-70502  
 metallic, high density, thermodynamic props. 0-88337  
 NMR studies on single crystals, dynamic effects 0-107608  
 ortho-para mixtures, vibr. coherence decay 0-78903  
 phase transition of second kind in HCP lattice, orientational ordering 0-70410

**solid hydrogen continued**

- quantum diffusion 0-107607  
 H:T solid, collision induced IR lines caused by T<sub>2</sub> radioactivity 0-84756  
 p-H<sub>2</sub>, constant volume heat capacity and eqn. of state, temp. depend. 0-65334  
 p-H<sub>2</sub>, neutron diff. studies up to 5 kbar 0-59436  
 H<sub>2</sub>, room temp. melting point, press. depend. calcs. 0-103463  
 O-H<sub>2</sub>, solid, quantum diffusion of p-H<sub>2</sub> impurities 0-88398  
 p-H<sub>2</sub>, time-resolved CARS, disorder effects on coherent vibr. states 0-93342  
 p-H<sub>2</sub>, quantum diffusion of O-H<sub>2</sub> impurities 0-96719  
 o-p-H<sub>2</sub>, slow neutron scatt. into external radiation field (*Russian*) 0-59348

**solid lasers**

- see also gamma-ray lasers; Raman lasers; semiconductor junction lasers  
 alkaline earth halides:Eu<sup>3+</sup>, fluorescence lifetime and quantum efficiency for 5d-4f transitions 0-100681  
 book, quantum electronics 0-105442  
 coherent and nonlinear optics, conf., Leningrad, USSR (Jun. 1978) 0-998153  
 colour centre laser pumped by flashlamp-pumped dye laser 0-102737  
 colour-centre lasers, thermal strains in active elements 0-91804  
 conference, laser and electro-optical systems, San Diego, CA, USA (Feb. 1980) 0-62392  
 dynamics, Auger recombination effects 0-69398  
 F<sub>2</sub>-centre, pulsed tunable laser, IR spectral characts., 1.1-1.26  $\mu$  region 0-91805  
 F-centre laser used for IR optogalvanic spectrosc. of He positive column discharge 0-78563  
 fluctuations in laser theories 0-83587  
 fluorophosphate laser glasses, Nd doped, piezoelectric coeffs. meas. 0-99815  
 IR tunable laser for semiconductor multiphoton spectroscopy (*French*) 0-82836  
 multimode, with modulated resonator losses, radiation intensity fluctuations 0-74367  
 Nd:glass multichannel laser with plasma shutter 0-64088  
 NOVA, pulsed power control system, fibre-optic multi-tapped computer bus 0-95443  
 Nova Nd:glass large fusion laser system, mechanical design 0-91279  
 optical delay lines to control solid state laser output characts. 0-99758  
 optical fibre laser plate for digital image processing, all-optical parallel logic operation 0-106463  
 periodic laser with unstable resonator, single-pulse emission characts., active-medium inhomogeneities effect 0-74365  
 phosphate glass lasers, highly repetitive, development 0-69415  
 phosphate laser glass, Nd doped, piezoelectric coeffs. meas. 0-99815  
 pulsed diode simulators of solid lasers Al<sub>x</sub>Ga<sub>1-x</sub>As and Ga<sub>x</sub>In<sub>1-x</sub>P<sub>1-y</sub>As<sub>y</sub> solid solns. 0-91816  
 rare earth ion containing inorg. materials, 3 $\mu$ m band stimulated radiation 0-97306  
 rhodamine 6G dye in quartz glass microcomp. matrix, as tunable solid laser 0-99734  
 ring laser, single-freq., spontaneous antiphase fluctuations, theory 0-91821  
 ruby, frequency-stabilised using Fabry-Perot interferometer 0-58566  
 ruby, ultrashort pulse generation by internal phase and amplitude modulation 0-106551  
 ruby, use of KS glasses as passive shutters for generating subnanosec. pulses 0-102728  
 ruby, with electrooptical shutter, emission spectrum narrowing and single freq. giant pulse lasing 0-78877  
 ruby crystal, radiation amplification, spatial coherence 0-99737  
 ruby laser, double mode locking using dye saturable absorber 0-99763  
 ruby laser, with stimulated Brillouin scatt. complex conjugate mirror 0-87438  
 ruby laser with high-frequency control of lasing conditions 0-74363  
 ruby pulsed laser real-time holographic interferometry 0-74319  
 ruby ring laser with forced mode locking 0-95915  
 semiconductor electron-beam-scanned laser quantoscope, large-screen colour projection TV system 0-99783  
 semiconductor single crystal, CRTs with semiconductor laser screens, scanning optical microscopy appl. 0-86398  
 survey of solid state lasers, book contrib. 0-106529  
 tunable IR solid-state laser characteristics and principles 0-87406  
 CO, solid, CO laser excited, strong vibr. population inversion 0-58547  
 CaF<sub>2</sub> crystal active element for colour-centre laser, thermal strain anal. 0-91804  
 CdS crystals, one-photon pumping, active layer structure, light amplification 0-78858  
 CdS, generation of optical radiation in direction of propag. of streamer 0-69401  
 CdS, highly excited, stimulated emission process at 80K 0-97307  
 CdS monocrystal petal lasers, single-photon excitation (*Russian*) 0-99736  
 CdS platelet laser, emission spectra, optical coupling between partial resonators 0-69400  
 CdS platelet lasers, optically pumped, spatial and spectral distribution of laser emission 0-64032  
 CdS single crystal, lasing action excited by ruby laser picosecond pulses 0-64035  
 CdS<sub>1-x</sub>Se<sub>x</sub> monocrystal petal lasers, single-photon excitation (*Russian*) 0-99736  
 Ce:LaF<sub>3</sub> 286 nm laser, optically pumped 0-99738  
 Co:MgF<sub>2</sub>, tunable transition-metal-doped solid state lasers 0-58549  
 Cu laser with excitation by transverse discharge, construction of cuvette 0-106532  
 Er<sup>3+</sup>:KLu(WO<sub>4</sub>)<sub>2</sub>, room temp. stimulated emission obs. 0-106527  
 Er<sub>3</sub>Al<sub>5-x</sub>Ga<sub>x</sub>O<sub>12</sub>, LPE, spectroscopic props. 0-93419  
 GaAs, electron-beam excited, efficient generation of electron-hole plasma 0-76051  
 GaAs ribbon whiskers, photopumped, laser action 0-91801  
 GaAs:Zn optically pumped ribbon-whisker laser, picosecond pulses 0-99771  
 Ho<sup>3+</sup> in oxygen-containing crystals, stimulated emission at low temps. 0-106526  
 Ho:LiYF<sub>4</sub> laser, TEM<sub>00</sub> mode and Q-switched operation 0-74395  
 Ho<sup>3+</sup>:BaYb<sub>2</sub>F<sub>8</sub> 0-95902  
 Ho<sup>3+</sup>:LiEr<sub>0.945</sub>Tm<sub>0.055</sub>F<sub>4</sub> laser, tuning at 2.06  $\mu$ m 0-83611  
 Ho<sup>3+</sup>:LiYbF<sub>4</sub>, active medium for Nd laser freq. convertor, cascade stimulated emission 0-102727



## solid lasers continued

- KCl crystal active element for colour-centre laser, thermal strain anal. 0-91804  
 KCl:Li ( $F_2^+$ )<sub>A</sub> centres, tunable CW laser action 0-87399  
 KCl:Li  $F_A$ (II) centre laser, pumped by flashlamp-pumped dye laser 0-102737  
 La<sub>2</sub>Be<sub>2</sub>O<sub>7</sub>:Nd<sup>3+</sup>(Pr<sup>3+</sup>), cryst. growth, spectral and laser properties in  $^4F_{3/2}$ - $^4I_{11/2}$  and  $^4F_{3/2}$ - $^4I_{13/2}$  transitions 0-80853  
 LiF crystal active element for colour-centre laser, thermal strain anal. 0-91804  
 LiF, picosecond generation on  $F_2^+$  colour centres, induced mode synchronisation (Russian) 0-64033  
 LiNdP<sub>2</sub>O<sub>12</sub> laser, relaxation oscillations and mode spectra, high density pumping effect 0-69396  
 NaF,  $F_2^+$ -like colour centre, room temp. stable, CW laser, 0.99-1.22  $\mu$ m tunable 0-69399  
 Nd:Cr:Li-La phosphate glass, Nd luminesc. quantum efficiency meas., Nd-Cr nonradiative transfer 0-66296  
 Nd garnet ring laser, with return mirror, mode locking 0-99764  
 Nd laser, excited stimulated Mendelstam-Brillouin scatt. phase fluctuations (Russian) 0-89014  
 Nd laser, stable passive switch using phthalocyanine dye, bleaching and relaxation 0-74368  
 Nd laser Mikron system, ultimate Xe pump lamp module operating conditions 0-91815  
 Nd laser produced plasma, nonlinear scattering of laser radiation by fast ion waves in plasma 0-106916  
 Nd:glass, comparative lasing characts. of silicate and phosphate laser glasses 0-74364  
 Nd:glass, subnanosecond pulse oscillator, investigation by high-speed oscillography 0-74411  
 Nd:glass, ultimate power characts. at high pulse repetition freqs. 0-64036  
 Nd:glass laser, blue tunable picosecond pulse generation by synchronous mixing with sideband radiation in NH<sub>4</sub>H<sub>2</sub>PO<sub>4</sub> 0-87431  
 Nd:glass laser, influence of neutron and  $\gamma$  irradi. on generating characts. (Russian) 0-69402  
 Nd:glass laser, short pulse mode-locked, using prisms 0-83617  
 Nd:glass laser, stable ultrashort light pulses generation (German) 0-91823  
 Nd:glass laser in TI vapour, output conversion from 1.06 micron to 388.1 nm 0-91850  
 Nd:glass laser performance and reliability developments 0-78869  
 Nd:glass laser radiation, spatial coherence of fundamental and second harmonic 0-69442  
 Nd:glass laser rod, pumped, thermal relaxation 0-69397  
 Nd:glass laser six beam system, output characts. (Chinese) 0-83612  
 Nd:glass laser system, beam spatial profile optimization in amplifier channel 0-74407  
 Nd:glass laser system, multichannel, for fusion experiments, model 0-58557  
 Nd:glass laser system, Thompson scattering diagnostics of low density plasmas 0-96388  
 Nd:glass laser UV coherent pulse, 45 GW, for laser fusion 0-69450  
 Nd:glass laser with active mode locking, ultrashort pulses 0-64087  
 Nd:glass laser with numerical programmed control (Russian) 0-91811  
 Nd:glass laser with US Q-switch 0-64034  
 Nd:glass solid state laser, giant emission pulse prod. 0-91803  
 Nd:glass telescopic small-signal amplifier with a Brillouin mirror 0-69420  
 Nd:silicate glass, resonance laser excitation, inhomogeneously broadened emission spectra 0-66295  
 Nd:YAG, electro-optical extraction of ps laser pulse (German) 0-87416  
 Nd:YAG, three-way mixing in low dispersion wavelength region in optical fibre 0-99792  
 Nd:YAG CW laser, mode locking, 30 W average power 0-87419  
 Nd:YAG CW mode-locked laser, negative feedback power stabilization 0-69435  
 Nd:YAG crystal, orientation influence on thermally induced birefringence (Chinese) 0-88958  
 Nd:YAG for 100 Gbit/s transmission rate over optical fibres expt., review (French) 0-69525  
 Nd:YAG giant pulse lasers, energy characts., superradiance effects 0-64031  
 Nd:YAG laser, CW mode-locked and intracavity freq. doubled, anal. 0-58548  
 Nd:YAG laser, intracavity freq. doubling by LiIO<sub>3</sub> long pulse emission 0-102736  
 Nd:YAG laser, Q-switched, pulse stretching using Pockels cell 0-95927  
 Nd:YAG laser, subnanosecond pulse generation at 100K 0-74397  
 Nd:YAG laser as source for airborne lidar system for atmospheric expts. (Italian) 0-109278  
 Nd:YAG laser integration into optical systems 0-78887  
 Nd:YAG passively locked laser, pulse width meas. by SHG method (Chinese) 0-87432  
 Nd:YAG pumped tunable sources, appl. to spectroscopy 0-58576  
 Nd:YAG Q-switched laser, ohmic contacts on n-GaAs produced by laser alloying of Ge films 0-58546  
 Nd:YAG regenerative amplifier, expt. studies 0-95909  
 Nd:YAG laser reflection resonator with hole coupling 0-58597  
 Nd<sup>3+</sup>:glass laser for stimulated Raman scatt. Dewar cell 0-99799  
 Nd<sup>3+</sup>:Gd<sub>2</sub>Ga<sub>2</sub>O<sub>12</sub> pulse-pumped laser action at 1.054  $\mu$ m 0-64030  
 Nd<sup>3+</sup>:glass luminesc. band profile deform. under free-oscillation conditions 0-71487  
 Nd<sup>3+</sup>:YAG, CW, intensity fluctuations in single-freq. mode 0-91802  
 Nd<sup>3+</sup>:YAG, Q-switching mechanism by intracavity stimulated Brillouin scatt. 0-106552  
 Nd<sup>3+</sup>:YAG, stable periodic-pulse, with CW pump 0-74400  
 Nd<sup>3+</sup>:YAG continuous laser, radiation freq. stabilisation system using Fabry-Perot interferometer 0-78871  
 Nd<sup>3+</sup>:YAG laser, high repetition rate electrooptic Q-switching, birefringence 0-69430  
 Nd<sup>3+</sup>:YAG laser, pumping by alkali metal vapour arc discharge 0-78924  
 Nd<sup>3+</sup>:YAG laser active element, linearly polarised light depolarisation due to thermally induced birefr. 0-106528  
 Nd<sup>3+</sup>:YAG laser frequency stability improvement using active interferometer (Russian) 0-64043  
 Nd<sup>3+</sup>:YAG multimode laser radiation noise 0-74366  
 Nd-glass, mode-locked, measurement of picosecond pulses using two-photon photoconductivity detector 0-77872

## solid lasers continued

- Nd,R<sub>1-x</sub>P<sub>2-x</sub>O<sub>4</sub> (R=La, Y: 0.1<x<1), laser quality cryst. growth, morphology 0-66412  
 Nd:YAG, Raman shifted, frequency conversion appl. 0-69451  
 Ni:MgF<sub>2</sub>, tunable transition-metal-doped solid state lasers 0-58549  
 Ni:MgO, heavily doped, defect characterisation rel. to use as laser material 0-65000  
 Ni:MgO, tunable transition-metal-doped solid state lasers 0-58549  
 n-Pb<sub>0.85</sub>Sn<sub>0.15</sub>Te spin flip Raman laser pumped by TE CO<sub>2</sub> laser, characts. 0-87397  
 PrF<sub>3</sub>, laser action of Pr<sup>3+</sup> 0-95901  
 RbCl:Li  $F_A$ (II) centre laser, pumped by flashlamp-pumped dye laser 0-102737  
 YAG laser, trimmer for wafer level products 0-87428  
 YAG:Ho<sup>3+</sup>, spectroscopy, stimulated emission 0-93374  
 Zn<sub>1-x</sub>Cd<sub>x</sub>S monocrystal petal lasers, single-photon excitation (Russian) 0-99736  
 ZnO UV laser, electron-beam pumped 0-99753  
 ZnS UV laser, electron-beam pumped 0-99753  
 ZnSe single cryst., lasing action excited by ruby laser picosecond pulses 0-64035  
 ZnTe single cryst., lasing action excited by ruby laser picosecond pulses 0-64035

## solid-liquid transformations

- see also crystallisation; freezing; melting; solidification  
 CaO-SiO<sub>2</sub>-CO<sub>2</sub>, subsolidus and liquidus phase relationships to 30 kbar 0-85643  
 carbon tetrachloride, dual melting curves and metastability 0-92647  
 cyclohexanol, orientationally disordered phase, Brillouin scatt. study 0-93351  
 equilibrium liq.-solid coexistence line, phase instability and direct correl. function integral eqn. 0-65196  
 hard sphere system in equilibrium 0-86225  
 hard sphere system in three dimens., thermodynamic props. 0-86226  
 interface instability in presence of chemical potential gradients (French) 0-75338  
 kinetic coefficient of two-phase transitional region between A+B melt and crystalline bulk phase A 0-96455  
 leghaemoglobin, thermal denaturing in cryst. and soln. 0-108849  
 method and alloys, liquidus and solidus temperatures, determ. by  $\gamma$ -ray method 0-65193  
 nonergodic hard parallel squares, with Maxwellian vel. distrib., mol. dynamics calcs. 0-100156  
 phospholipid bilayers, low temp. transition from fluid state 0-97871  
 potassium n-alkanoates, thermal behaviour, differential scanning calorimetry obs. 0-92650  
 Al-Si (2.4 wt.%), liq. fluidity in solid-liq. zone 0-108429  
 Bi-Sb (1 at.%) alloy, single cryst. growth solid-liq. interface study 0-107073  
 Ga photoacoustic effect at first order phase transitions at increasing and decreasing temp. 0-70320  
 GaP(As), liquid interaction parameters determ., 580-670°C 0-65197  
 He liquid, plane surface layer, density profiles and pair correlation asymptotics (Russian) 0-88371  
<sup>4</sup>He solid-liquid interface mobility under 1 MHz sound wave (French) 0-100373  
 InP(As), liquid interaction parameters determ., 580-670°C 0-65197  
 Ni-Ni intermetallic phase growth kinetics at liq. Sn-solid Ni interface 0-71638  
 SiO<sub>2</sub>, three-component glass, liq. phase separation, with two oxide modifiers 0-103250  
 Te<sub>0.05</sub>Ge<sub>0.95</sub>Pb<sub>0.05</sub>, DSC sensitivity to controlled ageing in glass transition region 0-71673  
 Zn-Cd alloys, liq. and solid, ultrasound speed and compressibility meas. 0-102941  
 Zn-In alloy, solid-liq. equilb. roughening transition 0-96630

## solid mechanics see mechanics

## solid solubility

- alkali metal alloys, dil., binary, equilb. at. vol. and compressibility 0-70295  
 alloys, rapidly quenched crystalline, struct., and heat treatment effects 0-76292  
 binary system, distribution coeffs., estimation from Van Laar and Hayes-Chipman relations 0-84293  
 cemented carbides, physical and chem. nature 0-76265  
 conference, Masnuy-St-Jean, Mons, Belgium, Oct. 1979 0-82570  
 metals, overbarrier states of H and D, subsystem heat capacity, equilibrium props. (Russian) 0-79998  
 pigeonite, inverted, from SW Norway, precipitation temp. estimation 0-72500  
 precipitate free zones, X-ray microanal. 0-108768  
 restoration carbonisation in one and two phase states (Russian) 0-65225  
 steel, austenitic, strength, ductility and fracture toughness, N and Cr effects 0-100878  
 steel, B concentration and solubility depend. on introduction of rare earth metals (Russian) 0-65226  
 steel, medium C, 40MnB, dissoln. and precipitation of M<sub>23</sub>(C,B)<sub>6</sub> (Chinese) 0-66511  
 steel, stainless, ferrite to austenite decomp. 0-93554  
 steel, stainless Kh18N11, MnS solubility determ. method 0-84910  
 steel, V, N effect on precip. and transform. kinetics 0-97485  
 stress corrosion cracking, role of H<sub>2</sub>, state of art review 0-61017  
 Ag-Ni supersaturated metastable solid solns. formed by ion beam mixing 0-107425  
 AgBr NaBr, thermodynamic props., metastable states and demixing 0-96660  
 AgBr-NaBr, phase diagram, miscibility, binodal curve and demixing kinetics, X-ray meas. 0-96659  
 Al-Zr (1-13 wt.%), rapidly quenched, extended solid solubility, grain refinement and age-hardening 0-76266  
 Au, Co-hardened, characterisation by Mossbauer spectroscopy, Co precip. formation 0-80108  
 B-Si, (0 to 14.3 at.%), phase charact., regions of existence (French) 0-104117  
 BaO.6Fe<sub>2</sub>O<sub>3</sub>, solubility of CaO 0-100333  
 Ca-Mn-S-Se system, multicomponent solubilities 0-108416  
 CdTe, of Ge, 630-800°C, prep. conditions depend. 0-103519  
 CdTe<sub>2</sub>Se<sub>2</sub>:Au, solubility meas. by microhardness method 0-96650



## solid solubility continued

- CeNi<sub>2</sub>-CePt<sub>2</sub> system, structural and mag. studies on valence behaviour of Ce 0-103809  
 Co-WC hard alloys, rapidly quenched struct. 0-76233  
 Cr-Ge system, phase diagram, thermal anal., X-ray diffr., microhardness, and electron probe anal. (French) 0-97462  
 Cu-Cr alloy, laser irradiation, structural changes (Russian) 0-100247  
 Cu-Ni-Nb (30, 0.9 at.%), precipitate free zones, X-ray microanal. 0-108768  
 Eu-B-C ternary and binary boundary systems, preparation techniques, X-ray analysis 0-60840  
 Fe, effect of H<sub>2</sub> on phys. and mech. props. 0-101657  
 Fe, segregation of impurities, physico-chemical aspects (Czech) 0-60866  
 Fe, trapping of H, average trapping depth and trapping sites density 0-84297  
 Fe, white cast, migration of C to the surface, solubility (Russian) 0-92720  
 Fe-C system, FCC, austenite field thermodynamics, re-anal. 0-89201  
 Fe-Cr-Co permanent magnet system, miscibility gap, microstruct. and mag. props. obs. 0-76228  
 Fe-Cr-Co-Mo high energy permanent magnets, mag. props. 0-97119  
 Fe-Nb-V-C-N, equilibrium comp. and solubility in steels, model of ideal solns. (Russian) 0-60832  
 Fe-Ni (6-8 at.%) 0-75888  
 Fe-Pd (1-2 wt.%), solution of <sup>119</sup>Sn, study by Mossbauer spectroscopy 0-75888  
 Fe-Sb-Ti(V)(Cr)(Mn)(Co)(Ni), interactions and segregations, Mossbauer and X-ray diffr. study 0-70415  
 Fe-Ti-V-C-N, equilibrium comp. and solubility in steels, model of ideal solns. (Russian) 0-60832  
 GaAs:Cr, carrier equilibrium effects, impurity states, elec. resistivity 0-65488  
 (GaSb)<sub>1-x</sub>Ge<sub>x</sub> films, single-cryst. metastable semicond., growth and phase stability 0-80115  
 Ge-Cu, solubility and behaviour of Cu, internal friction investigations 0-92678  
 H solid solution with Pd-Cu(Ag)(Au) alloys, superconducting transition temp. behaviour (Russian) 0-70879  
 InAs-CdTe quasi-binary system, temp.-comp. diagram, physicochem. and thermodynamic analysis 0-104127  
 InSb<sub>1-x</sub>Bi<sub>x</sub> films, single-cryst. metastable semicond., growth and phase stability 0-80115  
 InSb<sub>1-x</sub>Bi<sub>x</sub>, metastable epitaxial film, phase diagram 0-76238  
 KMg<sub>2</sub>LiSi<sub>2</sub>O<sub>10</sub>F<sub>2</sub>-NaMg<sub>2</sub>LiSi<sub>2</sub>O<sub>10</sub>F<sub>2</sub>, solid soln., solid solubility and swelling characs. 0-59660  
 Li-Al system, Li solubility and chem. diffusion in Al, electrochem. study 0-107432  
 LiNbO<sub>3</sub>:Na structure field stability limits, LPE film growth, SAW velocity 0-80102  
 Mn-Ga system, X-ray struct. investigation, solubility (Chinese) 0-88084  
 Mo-W-N system, nitrided annealed samples, W replacement of Mo 0-76227  
 NaCl-KCl system, interdiffusion, miscibility, Kirkendall effect 0-107568  
 Na<sub>2</sub>O-CaO-SiO<sub>2</sub> glass, redox phenomena evaluation in melting-fining process, SO<sub>2</sub> evolution 0-84900  
 Na<sub>2</sub>O-Ga<sub>2</sub>O<sub>3</sub> system β and β\* phases, fast ion cond., prep. and phase comp. 0-59716  
 Nb-Pd constitution diagram, metallographic and X-ray diffr. anal. 0-89204  
 Ni, diffusion and solubility of S (Russian) 0-70465  
 Ni, grain boundary internal friction, B solid solubility as function of grain size 0-60903  
 Ni-B, grain boundary internal friction, B solid solubility as function of grain size 0-60903  
 Ni-Mn, permeability, diffusion and solubility of H 0-107573  
 NiO, undoped and Al doped, Ni self-diffusion, vacancy-impurity complex effects 0-107493  
 NiTa eutectic superalloy, casting, furnace atm. effects 0-84880  
 NiZn ferrite, ZrO<sub>2</sub> additions influence on sintering and physicochem. props. 0-108369  
 Pb, diffusion and saturation solubility of Pt, melting curve, conc. profiles 0-88365  
 PbTe-Ga<sub>2</sub>Te<sub>3</sub>, phase interaction, DTA, XPA and microstructural anal. 0-96625  
 PbTe-InTe system, phase interactions and solid soln. form., physicochem. and elec. charac. 0-104129  
 Pb(Zr,Ti)O<sub>3</sub>-Cr<sub>2</sub>O<sub>3</sub> ceramics, resom. freq. comp. and temp. depend. 0-70413  
 Si laser annealed, nonequilibrium solubility and segregation 0-84296  
 Si solubility in Mg, depend. on impurity inclusions (German, English) 0-97492  
 Si:Al(Ga), O, diffusion, conc. profile meas. 0-79990  
 Si:As, solid solubility and thermal behaviour of metastable 0-75359  
 Si:B, high conc. effects in ion implantation 0-75245  
 Si:Fe, solubility study by EPR and neutron activation anal. 0-75361  
 Si:P(As)(B), nonequilibrium solid solutions obtained by heavy ion implantation and laser annealing 0-92544  
 Si:Sb vacuum deposited coating, p-n junction, pulsed electron beam annealing doping, diffusion 0-75480  
 Si:Sb(Ga)(Bi)(In), dopant solubility limit, laser irradiation effects 0-84295  
 Te-based eutectics, crystn. rate effect on electrophys. props. mutual solubility effect 0-60774  
 Ti alloys, hydrogenation at 200-600°C and up to 10000 kPa 0-107435  
 α-Ti/Fe, retrograde solid solubility 0-79950  
 Ti<sub>2</sub>O<sub>3</sub>-Al<sub>2</sub>O<sub>3</sub> (MgTi<sub>2</sub>O<sub>7</sub>), solid solubility, X-ray phase and optical microscopic exam. 0-59657  
 Zr-Ru, alloy Zr rich, Ru solubility, eutectic decay, α↔β transform., struct. (Russian) 0-65227

## solid solution hardening

- (Cu-Au)-Co, single crystals, solid soln. and particle strengthening, superposition 0-97495  
 Fe-N, single crystal, solid soln. softening, effect of interstitial N 0-97496  
 KCl-KBr, solution hardening and softening at low temp. 0-108462  
 Nb-O system, solid soln. hardening and softening 0-71665  
 Pb(Ag) alloys, effect of Ag content on yield strength 0-76322

## solid solutions

- solid solutions such as Au-Cu are indexed under alloys of the named elements i.e. 'gold alloys' and 'copper alloys' in this example  
 see also alloys; solid solubility  
 alkali halide crystals, mixed, impurity centre local vibr., comp. depend. of spectral parameters 0-79898  
 alkali halide solid solns., lattice parameter and heat of form. 0-79739  
 binary alloys, acoustic modes in random and correlated alloys, order-disorder transform. 0-65189  
 binary alloys, two phase region calcs. in solidifying melt (Russian) 0-65195  
 binary triangular lattice solution, phase stratification statistical modeling 0-65239  
 chlorophyll, and related mol., in solid solns., fine-structured vibronic spectra under tunable dye laser excitation (Russian) 0-74164  
 p-dichlorobenzene-naphthalene alloys, solid solns., NQR study 0-66063  
 diffusion equation, during a decomp. process, role of non-linearised terms (Japanese) 0-92723  
 diffusion equation, with non-linear terms, Fourier transform 0-103514  
 dislocation-core movement and frictional stress 0-92529  
 isotropic solid soln. cryst. surfaces, surface stress and chem. equil. 0-107628  
 naphthalene-naphthol solid soln. system, excess thermodynamic functions 0-107445  
 oversaturated solid solution, directed decomposition (Russian) 0-97458  
 solid solution, binary, radiation-induced instability, contrib. of dissipative processes 0-65039  
 steel, B concentration and solubility depend. on introduction of rare earth metals (Russian) 0-65226  
 substitutional solid solutions, new phase nucleation mechanism 0-61135  
 supersaturated, cellular precip. features, review (Russian) 0-84937  
 wustite solid solns., props. connected with localised electron state 0-107734  
 wustite solid solutions, miscibility data rationalisation classification of ternary fields and postsaturation reactions 0-79948  
 XY<sub>1-x</sub>Z<sub>x</sub> mixed crystals, impurity centre local oscill. spectral distribution (Russian) 0-60643  
 3Al<sub>2</sub>O<sub>3</sub>-GeO<sub>2</sub>-SiO<sub>2</sub>, reduction by C, mixed diffusional-kinetic regime (Russian) 0-66771  
 Ag-Cu metastable solid soln., form. by ion-beam mixing 0-75244  
 Ag-Ga(Ge)(In), α-phase, lattice sp. ht. calcs. 0-65246  
 α-Ag-In solid solutions, lattice dynamics parameters (Russian) 0-96477  
 Ag-Mg (18.5 wt.%), rheological study of crystallographic order on creep (French) 0-97548  
 Ag-Ni supersaturated metastable solid solns. formed by ion beam mixing 0-107425  
 AgGaIn<sub>1-x</sub>Se<sub>x</sub>, X-ray diffr. cryst. data 0-84147  
 Ag<sub>2</sub>S+Ln<sub>2</sub>S<sub>3</sub>, powdered mixtures, reaction rate, production of ionic semiconductors 0-93741  
 Al(Mn), effects of Mn on electrode or free corrosion potentials 0-100942  
 Al-Ag, type-II superconductor, torque oscillations in mag. field (Russian) 0-103800  
 Al-C interstitial solid solns., atomic static displacements and deform. interaction (Russian) 0-64953  
 Al-Ni solid, liquid mixture, diffusion processes (Russian) 0-107563  
 Al-Zn (8-25 wt.%), solid solns., residual resist. during clustering 0-97483  
 Al-Zn-Mg granules and bands rolled from them, heat treatment 0-100862  
 Au-3d transition metal alloys, UPS study, localised states 0-93449  
 Au-transition metal alloys, <sup>197</sup>Au Mossbauer isomer shift cellular atomic model 0-84673  
 Au-Cu-Al thin film bilayer system, phase formation, backscattering spectra 0-96728  
 B-Si alloys, B-rich, prep., anal. and cryst. growth (French) 0-104091  
 BaFe<sub>2</sub>O<sub>9</sub>, Ca<sup>2+</sup> substitution effect on hexaferrite lattice and mag. props. 0-60243  
 Ba<sub>1-x</sub>La<sub>x</sub>F<sub>2+x</sub>, enhanced ionic motion in solid solutions 0-107491  
 Ba<sub>2</sub>Sr<sub>1-x</sub>Nb<sub>2</sub>O<sub>6</sub> crystals, defects and their characteristic features 0-88138  
 Bi<sub>1-x</sub>La<sub>x</sub>WO<sub>6</sub>, synthesis and crystallography 0-66459  
 Bi<sub>1-x</sub>Sb<sub>x</sub>Te<sub>2-x</sub>Se<sub>x</sub>, elec. cond. and thermoelec. props., neutral defects influence 0-60017  
 Bi<sub>2</sub>Te<sub>3</sub>-Bi<sub>2</sub>Se<sub>3</sub>-Te<sub>2</sub>, single crystal, elec. cond., thermoelectric props. 0-88550  
 Ca-Mn-S-Se system, multicomponent solubilities 0-108416  
 CaSO<sub>4</sub>·2H<sub>2</sub>O-CaHPO<sub>4</sub>·2H<sub>2</sub>O system, solid solns., IR study (French) 0-66165  
 Cd<sub>1-x</sub>M<sub>x</sub> (M=Mg, Ca, Sr), solid solns., phase equilib. diagrams 0-108412  
 Cd<sub>1-x</sub>Ni<sub>x</sub>Fe<sub>2</sub>O<sub>4</sub>, solid soln., mag. and structural characterisation 0-103906  
 CdO-WO<sub>3</sub>, phase rels. and cryst. struct. 0-108410  
 Ce<sub>2</sub>Dy<sub>1-x</sub>C<sub>x</sub>, solid solns., mag. props. 0-108008  
 CeO<sub>2</sub>-Y<sub>2</sub>O<sub>3</sub> solid soln. phases, synthesis 0-104132  
 Co base alloy, creep-fatigue interaction in aligned eutectic and solid soln. 0-108554  
 Co-Ga binary system, lattice consts., phase transform (Chinese) 0-88108  
 Co-Zn, physical-chemical metallurgy (German) 0-108390  
 Co<sub>2</sub>Mg<sub>1-x</sub>O<sub>3</sub> system, thermodynamic investigation, 1100 to 1300K (German) 0-107430  
 Cr-Fe-Ni, γ-solid soln., thermodynamic activity determ. at 1500K 0-108397  
 Cr-Mo, elec. resist. and thermo-EMF, conc. depend., 4.2 to 1500K (Russian) 0-80247  
 Cr<sub>1-x</sub>Fe<sub>x</sub>OOH, 0≤x≤10, prep., Mossbauer effect, Neel temp. 0-108134  
 Cr<sub>2</sub>Mo<sub>2-x</sub>O<sub>2</sub> (x≤0.5), solid soln., trivalent Cr, X-ray powder diffr. anal. 0-70177  
 CsGa<sub>1-x</sub>Fe<sub>x</sub>S<sub>2</sub>, tetrahedrally coordinated Fe atoms in low spin state, mag. props. and neutron diffr. study (German) 0-88714  
 CsI:Ti, precipitation of Ti solid solns. 0-70419  
 Cu dilute binary solid solutions, enthalpies of mixing and excess free enthalpies (French) 0-107427  
 α-Cu-Al (6 to 17 at.%), short-range order investigated by diffuse X-ray scatt. (Russian) 0-104187  
 Cu-Au single crystals, precipitation hardening by misfitting Co particles 0-97495  
 Cu-Au system, two-phase mixtures, long-period superlattices 0-84140  
 Cu-Be solid solutions, local oscill. conc. depend., impurity bands (Russian) 0-75318



## solid solutions continued

- Cu-Zn, rheological study of crystallographic order on creep (*French*) 0-97548  
 Cu-Zn(Ge)(Ni)(Ga),  $\alpha$ -phase alloys, lattice sp. ht. calcs. 0-65246  
 $\text{Cu}_0.5\text{Fe}_{0.5}\text{O}_4$ -ZnFe $_2\text{O}_4$ , cation distrib., mag. moment, Mossbauer spectra, chem. anal. 0-75210  
 $\text{CuGaIn}_{1-x}\text{Se}_x$ , X-ray diffr. cryst. data 0-84147  
 $\text{Cu}_2\text{S-Ln}_2\text{S}_3$ , powdered mixtures, reaction rate, production of ionic semiconductors 0-93741  
 Eu solid solutions with lanthanides, monosulfides, and oxides, vacant d states, X-ray absorpt. 0-103623  
 $\text{Eu}_{1-x}\text{La}_x\text{S}$ , electron struct., lattice const., X-ray spectral study (*Russian*) 0-100432  
 $\text{Eu}_2\text{O}_3\text{-Y}_2\text{O}_3$  solid soln. phases, synthesis 0-104132  
 $\text{Eu}_{1-x}\text{Sm}_x\text{S}$ , ESR, exchange interaction, susceptibility, elec. cond., thermoelectric power 0-93174  
 Fe-C system, FCC, austenite field thermodynamics, re-anal. 0-89201  
 $\alpha$ -Fe-N, supersaturated solid solns., N atom precip. kinetics, resist. meas. 0-60864  
 Fe-N single crystals, N effect on hardening 0-97496  
 Fe-N single crystals, plastic deform. in temp. range 4.2 to 300K 0-76321  
 Fe-Zn, physical-chemical metallurgy (*German*) 0-108390  
 $\text{Fe}_3\text{Al}$ , solid soln., rheological study of crystallographic order on creep (*French*) 0-97548  
 $\text{Fe}_{1-x}\text{Co}_x\text{Si}$ , solid solution, semiconductor-metal transition 0-103627  
 $(\text{Fe}, \text{Cr}_{1-x})_2\text{O}_3$  corundum-type solid solution single crystal growth, chem. vapour transport 0-93465  
 $\text{FeGaSe}_4$ , elec. cond., mag. susceptibility 0-88301  
 $\text{Fe}_2\text{N}$  growth kinetics in Fe-N system (*Korean*) 0-93540  
 $\text{Fe}_2\text{O}_3\text{-Al}_2\text{O}_3$  mixed oxide, X-ray diffr. and elec. cond. 0-79954  
 $\text{GaIn}_{1-x}\text{As}$ , recombination mechanisms of excess carriers 0-97337  
 GaSb, solid solns., impact ionisation, cond. and valence band effects 0-65583  
 $\text{Ga}_2\text{Se}_3$ , elec. cond. 0-88301  
 $\text{Ga}_2\text{Se}_3\text{-FeSe}$ , phase diagram, elec. cond., mag. susceptibility 0-88301  
 $\text{GaSe}_{1-x}\text{Te}_x$ , Raman spectra, phonon freq. 0-97286  
 $\text{Gd}_2\text{Eu}_{1-x}\text{B}_6$ , solid solns., mag. susceptibility, 80 to 1000K (*Russian*) 0-88713  
 $\text{Gd}_2\text{La}_{1-x}\text{B}_6$ , solid solns., mag. susceptibility, 80 to 1000K (*Russian*) 0-88713  
 $\text{Gd}_2\text{Zr}_{1-x}\text{O}_{2-x/2}$ , fluorite and pyrochlore solid solutions, electrical conductivity meas. 0-65287  
 Ge-Si-Te, solid solns., donor states energy spectrum 0-88516  
 $\text{GeO}_2\text{-SiO}_2$ , reduction by C, mixed diffusional-kinetic regime (*Russian*) 0-66771  
 $\text{GeTe-Sb}_2\text{Te}_3$ , cond., density of states 0-88472  
 H solid solution with Pd-Cu(Ag)(Au) alloys, superconducting transition temp. behaviour (*Russian*) 0-70879  
 $\text{HfV}_2\text{D}_4$ , disordered solid solution, order-disorder transition 0-88321  
 $\text{Hg}_{1-x}\text{Mn}_x\text{Te}$ , transverse magnetoresistance in quantised mag. fields 0-96922  
 $\text{InAs-Sb}_{1-x}$ , recombination mechanisms of excess carriers 0-97337  
 KBr-KI, mixed crystals, microhardness, theory 0-75298  
 $\text{KCl:Ba}^{2+}$ , localised stress relaxation in excess vacancy system, prismatic loops (*Russian*) 0-88160  
 $\text{KCl:Br}^{2+}$ , solid solution periodic precipitation in inhomogeneous conc. field 0-103485  
 KCl-KBr, mixed crystals, microhardness, theory 0-75298  
 KF-ErF $_3$ , phase diagram 0-92645  
 $\text{KMg}_2\text{LiSi}_4\text{O}_{10}\text{F}_2\text{-NaMg}_2\text{LiSi}_4\text{O}_{10}\text{F}_2$ , solid soln., solid solubility and swelling characts. 0-59660  
 $\text{K}(\text{OH})_{0.42}(\text{O}_2)_{0.50}$ , cubic solid soln., structural and mag. study (*French*) 0-107177  
 $\text{La}_2\text{C}_3$ , solid solution, lattice const. and superconducting transition temp. (*Russian*) 0-92496  
 $\text{LaS}_{1.500}\text{-LaS}_{1.333}$ , density meas. 0-95075  
 Li-Al system, Li solubility and chem. diffusion in Al, electrochem. study 0-107432  
 $\text{Li:FeCo}$ , flow stress changes during precipitation 0-92594  
 $\text{Li}_2\text{GeO}_4\text{-Zn}_2\text{GeO}_4$ , solid electrolyte system, phase diagram 0-66489  
 $\text{Li}_2\text{O-Al}_2\text{O}_3\text{-Cr}_2\text{O}_3$  system, subsolidus equilibria 0-60843  
 $\text{Li}_2\text{O-TiO}_2$ , pseudobinary phase rotations, DTA and X-ray anal. 0-108411  
 $\text{Li}_{1+y}\text{Ta}_{1.5}\text{Ti}_{0.5}\text{O}_3$  ( $0 \leq y \leq 0.028$ ), non-stoichiometric phase, crystallographic and dielec. props. 0-75212  
 $\text{Mg}_2\text{Fe}_{1-x}\text{O}$ , diffusion of  $^{59}\text{Fe}$  and elec. cond. 0-59700  
 Mn-Ga system, X-ray struct. investigation, solubility (*Chinese*) 0-88084  
 $\text{Mo-(Zr+V+C)}$  (1.1 wt.%) alloy, phase composition, carbide phase microhardness (*Russian*) 0-60834  
 Mo-Be solid solutions, superconducting transition, temp. changing peculiarity due to press. (*Russian*) 0-70878  
 Mo-N, thermodynamic props., 1618 to 1883K 0-65230  
 Mo-V, elec. resist. and thermo-EMF, conc. depend., 4.2 to 1500K (*Russian*) 0-80247  
 Na-rich plagioclase microstructure and exsolution 0-72501  
 $\text{NaCl-NaBr}$ , mixed crystals, microhardness, theory 0-75298  
 Nb-H system, accommodation effects during hydride precipitation, TEM 0-89218  
 Nb-O system, solid soln. hardening and softening 0-71665  
 $\text{Nb-O(N)}$ , dislocation pinning, impurity interactions, strengthening (*Russian*) 0-92532  
 Nb-Zr-C welding solid solutions, ageing kinetics, influence of inclusion elements (*Russian*) 0-100853  
 $\text{Nd}_{1-x}\text{Ca}_x\text{VO}_3$ , elec. props., thermo-EMF 0-96866  
 $\text{Nd}_2\text{Y}_{1-x}\text{Zn}$  system, solid soln., mag. susceptibility, 77 to 600K (*Russian*) 0-65776  
 $\text{Nd}_2\text{Zr}_{1-x}\text{O}_{2-x/2}$ , fluorite and pyrochlore solid solutions, electrical conductivity meas. 0-65287  
 Ni-Al, rheological study of crystallographic order on creep (*French*) 0-97548  
 $\zeta$ -Ni-Al system, solid soln., interdiffusion (*Japanese*) 0-70476  
 Ni-Co-C solid solution, C precipitation, Ni $_3$ Co ordering, Ni-Co lattice parameter meas. (*Czech*) 0-60867  
 Ni-Cu-X (X=Sn, Nb, Ti), spinodal decomp. alloys, linear expansion coeff. influence on morphological anisotropy (*Japanese*) 0-70431  
 Ni-H, thermally charged, serrated yielding 0-85007  
 Ni-Mn (10-40 wt.%),  $\gamma$  solid soln., interdiffusion 0-100366  
 Ni-Mn-H solid solutions, mag. props. 0-88753  
 Ni-Mo-W, diagram of state, W solubility, dispersion hardening (*Russian*) 0-66477  
 Ni-Ni $_3$ B eutectic, high temp. X-ray anal. 0-71639

## solid solutions continued

- Ni-Ni $_3$ Mo system, deformation microstruct. 0-93591  
 Ni-P, electrodeposited film, thermal anal., occlusion of gases rel. to mag. props. 0-59823  
 Ni-Pd-Mn ternary alloys, mag. characts., use for thermoseed 0-107995  
 Ni-S, electrodeposited film, thermal anal., occlusion of gases rel. to mag. props. 0-59823  
 Ni-S, phase diagram calc. and thermodynamic props. of liq. phase 0-108401  
 Ni-V, solid soln., diffusion and thermodynamic props. 0-65278  
 Ni-Zn-Co ferrites, synthesis from solid solns. of schoenite-type salts 0-93511  
 NiH $_2$ , formation and decomp. studies 0-71626  
 NiO-MgO solid solns., surface comp. study by XPS 0-104035  
 $(\text{Pb}, \text{Sr})_2\text{Ge}_2\text{O}_{11}$ , single crystals, growth and X-ray and dielec. investigations 0-88127  
 $\text{Pb-As}$  ( $\sim 0.01$  wt.%), enhanced precip. phenomena, invest. of mechanism by elec. resist. meas. 0-104162  
 $\text{Pb-Sb-As}$  (1.1-1.8,  $\sim 0.01$  wt.%), enhanced precip. phenomena, invest. of mechanism by elec. resist. meas. 0-104162  
 Pb-Si superconducting solutions, effect of hydrostatic compression on tunnelling (*Russian*) 0-65746  
 Pb-Zn, unmixing alloys, mathematical model for solidification process (*Russian*) 0-81047  
 $\text{Pb(Ag)}$  alloys, effect of Ag content on yield strength 0-76322  
 $\text{xPb}_2\text{Ge}_2(\text{VO}_4)_2$ , (1-x) $\text{Pb}_2\text{SiO}_4(\text{VO}_4)_2$ , solid solution of centrosymmetric crystals, electrically induced optical activity 0-108180  
 $\text{Pb}_2(\text{Ge}_{1-x}\text{Si}_x)_2\text{O}_{11}$ , electrogyration, phase transition and dielectric props. 0-93269  
 $\text{PbSc}_{2/3}\text{Te}_{1/3}\text{O}_3\text{-PbSc}_{2/3}\text{W}_{1/3}\text{O}_3(\text{PbFe}_{2/3}\text{Te}_{1/3}\text{O}_3)$  ferroelec. props. and lattice const. 0-60520  
 $\text{Pb}_{1-x}\text{Sn}_x\text{Se}$  solid solns., photoluminesc. spectra, energy band parameter determ. 0-71484  
 $\text{Pb}_{1-x}\text{Sn}_x\text{Se}$ , transport phenomena in solid solutions with band inversion 0-107792  
 $\text{Pb}_{1-x}\text{Sn}_x\text{Te}$ , hole effective mass near zero bandgap, IR refl. study 0-108205  
 $\text{Pb}_{1-x}\text{Sn}_x\text{Te}_{1-x}\text{Se}_x$  solid solutions with constant lattice parameter, phase comp. 0-108417  
 $\text{Pb}_{0.95}\text{Sr}_{0.05}(\text{Zr}_{1-x}\text{Ti}_x\text{O}_3\text{-Nb}_2\text{O}_5)$ , phase coexistence range, lattice const. 0-92680  
 $\text{PbTe-Ga}_2\text{Te}_3$ , phase interaction, DTA, XPA and microstructural anal. 0-96625  
 $\text{Pb(Ti,Zr)}_3\text{O}_3$  solid solutions, phase coexistence discrepancies 0-96662  
 $\text{xPb(Ti,Zr)}_3\text{O}_3 + (1-x)\text{PbCd}_{1/3}\text{Nb}_{2/3}\text{O}_3$ , phase transition spread, polarisation relaxation, dielectric susceptibility (*Russian*) 0-75922  
 $\text{PbZrO}_3$ , ferroelec. solid solns., atom shifts, polarisation and Curie temps. 0-100636  
 $\text{Pb(Zr}_{1-x}\text{Ti}_x\text{O}_3)$  solid solution, piezoelectric ceramic, prop. improvement by multiple substitution 0-80702  
 $\text{PbZrTi}_{1-x}\text{O}_3$  ceramics, morphotropic phase boundary 0-81035  
 Pd-Ag thin-walled tubes, for thermal diffusion apparatus H diffuser 0-100358  
 Pd-H, H phase hardened, recrystallisation study 0-60883  
 Pd-noble metal solid solns., with dissolved H, thermodynamic props. 0-108402  
 S-Ni-Fe system containing monosulphide solid soln., elec. and struct. relations 0-90038  
 $(\text{Sb}_2\text{Se}_3)_{0.7}(\text{Bi}_2\text{Se}_3)_{0.3}$ , solid soln., prep. and elec. properties of layered crystals 0-70762  
 $\text{SeH}_4$  thin films, struct. and elec. props. 0-107931  
 Si:Al, precipitation of solid soln., effect of gamma irradiation 0-59515  
 Si:Bi, ion-implanted, solid phase epitaxial growth during annealing, supersaturated solid soln. form. 0-103384  
 a-Si:H alloys, sputter deposited thin film coatings, property-comp. relationships 0-80975  
 $\text{Si}_2\text{B}$ , equilib. with  $\text{B}_2\text{H}_6$  0-97721  
 $\text{SiF}_4\text{Cl}_4\text{-n}^-$  in  $\gamma$ -irradiated solid solution of tetramethylsilane, EPR spectra obs. 0-80611  
 $\text{SiF}_4\text{Cl}(\text{Br})^-(\text{I}^-)$  in  $\gamma$ -irradiated solid solution of tetramethylsilane, EPR spectra obs. 0-80611  
 $\text{SiO}_2\text{-BPO}_4$ , glasses and devitrificates prep., IR spectra (*Polish*) 0-71624  
 $(\text{SiTe})_{1-x}(\text{ATe})_x$ , A=Ge, Sn, Pb, solid soln. with small substitution, mag. susceptibility (*Russian*) 0-70933  
 $\text{Sm}_{1-x}\text{La}_x\text{S}$ , electron struct., lattice const., X-ray spectral study (*Russian*) 0-100432  
 $\text{SnS}_{2(1-x)}\text{S}_{2x}$  solid soln. system, long-wavelength optical phonons, Raman scatt. study 0-80794  
 $\text{SrFe}_2\text{O}_{19}$ ,  $\text{Ca}^{2+}$  additives effect on hexaferrite lattice and mag. props. 0-60243  
 $\text{Sr}_x(\text{Na}_{0.5}\text{Bi}_{0.5})_{1-x}$  solid solutions, piezoelec. and ferroelec. props. (*French*) 0-108158  
 $\text{Sr}_{1-x}\text{Na}_x\text{Nd}_{0.1}\text{Ta}_2\text{O}_7$ , solid soln., ferroelectric phase transitions, dielec. constant and thermal expansion rel. to temp. 0-88934  
 Ta-Ga, crystal struct. at high press., polymorphism 0-88112  
 Ta-H, fracture modes (*Japanese*) 0-66636  
 Ta-O(N), dislocation pinning, impurity interactions, strengthening (*Russian*) 0-92532  
 $\alpha$ -Ti/Fe, retrograde solid solubility 0-79950  
 $\text{Ti}_2\text{C}_3$ , X-ray order struct. determ. 0-103295  
 $\text{TiC}_x\text{N}_y$ , powder preparation, physical, chemical props. (*Russian*) 0-76212  
 V-O, dislocation pinning, impurity interactions, strengthening (*Russian*) 0-92532  
 $\alpha\text{-V}_{0.97}\text{O}_{0.03}$ , impurity vibr., inelastic neutron scatt. study 0-92635  
 $\text{V}_2\text{O}_5\text{-Ti}_2\text{O}_5$ , DTA, mag. susceptibility and X-ray diffr. study 0-70970  
 $\text{VSe}_{2-x}\text{S}_x$  ( $0 < x < 2$ ) solid solutions, characterisation 0-88730  
 $\text{Zn}_x\text{Cd}_{1-x}\text{S}$ , thin solid soln. films, vapour deposited, elec. and optical characts. 0-60110  
 $(\text{Zn}_{0.2}\text{Co}_{0.8}(\text{Ni}_{0.8}))\text{OAl}_2\text{O}_3$ , ZnO evaporation in vac. 0-59640  
 $\text{Zn}_x\text{Hg}_{1-x}\text{Se}$ , current carrier scattering mechanism 0-65546  
 $\text{ZnO-WO}_3$ , phase rels. and cryst. struct. 0-108410  
 Zr-Ru, alloy Zr rich, Ru solubility, eutectic decay,  $\alpha \rightleftharpoons \beta$  transform., struct. (*Russian*) 0-65227  
 $\text{ZrO}_2\text{-CaO(Y}_2\text{O}_3)$  ceramics with grainy structure, props., effect of heating to 2000°C 0-104194

## solid-state microwave devices

see also IMPATT diodes

- GaAs Schottky-gate FET and GaAlAs injection DH laser, monolithic integration 0-58593

**solid-state microwave devices continued**

- In-In<sub>2</sub>O<sub>3</sub>-Pb, Josephson tunnel junction fabrication for MM-wave detector 0-100427
- Pb-PbO-Pb, Josephson tunnel junction fabrication for Mm-wave detector 0-100427
- W-Ni(Co) point-contact diodes as harmonic generators and mixers, DC bias dependence 0-75653

**solid-state phase transformations**

see also ageing; decomposition; ferroelasticity; ferroelectric transitions; glass transition; high-pressure solid-state phase transformations; martensitic transformations; order-disorder transformations; polymorphic transformations; precipitation; segregation; spinodal decomposition

- A-15 compounds, density of states model for lattice transforms. 0-65219
- adamantane, plastic and solid-solid transitions, Raman study 0-60590
- adsorbed layers, commensurate-incommensurate transitions, substrate defects effect 0-75437
- alkali peroxides, ionic  $\pi$ -electron systems, magnetogyration 0-93155
- alkylene di-ammonium cadmium tetrachlorides, sp. ht. anomalies at phase transitions 0-70421
- alloys, phase transition premonitory phenomena, exam. by electron diffr. and microscopy (French) 0-59651
- ammonium halides, phase transitions by Monte Carlo method using cubic Ising model 0-70408
- aniline hydrobromide, ferroelastic phase transition, Raman scatt. study 0-108195
- anthracene-phenanthrene-tetracyanobenzene, CT-cryst., mini-excitons and lattice dynamics, ESR, optical and Raman spectra 0-60406
- bainitic transformation, suppression in steels (Russian) 0-76247
- benzene-hexa-n-hexanoate, phase transitions and mesophase form., sp. ht. and IR spectra, 13 to 393K 0-79955
- benzil, phase transition, far IR spectroscopy meas. 0-71407
- 1,1'-biphenyl, heat capacity anomalies due to successive phase transitions 0-96664
- bis-(p-toluene-sulphonate) of 2,4 hexadiyne 1,6 diol, X-ray scattering obs. of polymerisation mechanism and phase transition (French) 0-70399
- bis-p-toluene sulphonate of 2,4-hexadiyne-1,6-diol, X-ray scatt., incommensurable modulated struct. obs. 0-70185
- brittle solids, microfracture resulting from anisotropic shape changes 0-88254
- carbon tetrachloride, phase transform. process, energy-dispersive X-ray diffractometry 0-96631
- carborane, ortho- and para-, phase transition and mol. reorientation, isomer effects, PMR obs. 0-80628
- cholesterol, solid-solid phase transitions, positron annihilation study 0-84289
- cholesteryl oleate, solid-solid phase transitions, positron annihilation study 0-84289
- commensurate-incommensurate transition, Devil's staircase and harmless staircase, oscillating interactions through elastic stairs or other harmonic fields 0-88296
- commensurate and incommensurate charge-density wave states, nearly half-filled Frohlich model 0-107723
- commensurate and incommensurate structural phase transitions in Jahn-Teller system 0-70403
- commensurate phases, spatially modulated, in simple Ising model 0-79909
- commensurate-incommensurate transition in the quasi-one-dimensional Frohlich model with a nearly half-filled band 0-80199
- commensurate-incommensurate transitions, conical points, Lifschitz invariants and superspace group characterisation 0-70367
- conference, Masnuy-St-Jean, Mons, Belgium, Oct. 1979 0-82570
- continuous crystalline transitions, counterexample to maximal subgroup rule 0-59428
- critical dynamics and quasi-elastic scattering, structural phase transitions 0-92641
- crystal orientational disordering, thermodynamic props., stat. mech. model 0-96453
- crystal stability and three-body interactions 0-79740
- Cu, theoretical strength, rel. to FCC=BCC transitions 0-104229
- cubic crystals, tensile deform. induced transitions 0-59653
- defect influence on solid props. near phase transition 0-75334
- di(alkylammonium)CdCl<sub>2</sub>Br<sub>2</sub>, solid-solid phase transitions 0-84290
- diacetylene monocarboxylic acids, multilayers, struct. phase transitions and polymerisability 0-80129
- diamantane, plastic and solid-solid transitions, Raman study 0-60590
- p-dibromo-tetrafluorobenzene mol. cryst., in commensurate phase, quasie-lastic neutron scatt. 0-107386
- diethylammonium cadmium tetrachloride, dielec. props., phase transition 0-80675
- dislocations and lattice transformations, book contrib. 0-107242
- double phase transitions, physical value anomalies (Russian) 0-59622
- elastic constants, crit. behaviour near elastic phase transitions 0-100299
- elastic constants crit. behaviour near non-elastic phase transitions 0-100298
- elastic phase transitions, order parameter and mode softening 0-75325
- ferrite, transform. kinetics, grain size, alloying element effect, carbide precip. 0-93560
- ferrodistortive spin-phonon systems, crit. props. 0-88315
- ferroelectric, BaTiO<sub>3</sub> type, thermodynamic analysis of struct. phase transitions (Russian) 0-103473
- ferroelectric and other structural phase transitions at low temps. 0-75990
- ferroic phase transitions, non-mag., unified classification 0-70387
- fine fragmented crystals, complex struct. analysis by electron microscopy 0-104416
- first order transitions induced by single irreducible representation 0-70365
- first-order transitions, finite-size rounding rel. to entropy, system size 0-59623
- glasses, inorganic, struct. by X-ray scatt. diffr. obs. 0-84069
- graphite-Rb, intercalation cpd., superlattice struct., electron diffr. study 0-75214
- haematite reduction to magnetite, stress development mechanism (Russian) 0-93553
- hard disc thin layer, solid-solid phase transformation 0-79908
- hydroxyapatites, dipolar reorientations, TSC study 0-60491
- incommensurate phase, light scatt., order parameter fluctuation (Russian) 0-93354
- incommensurate structures, defectibility and frustration, devil's stair case transform 0-75333
- incommensurate structures phase transitions (Czech) 0-88294

**solid-state phase transformations continued**

- incommensurate-commensurate transition, Ginzburg criterion and crit. behaviour 0-70368
- Invar, phase stability, spinodal decomposition 0-88327
- ionic crystal defects, mag. reson. studies 0-108066
- isomorphic transformation, characterisation of hysteresis processes (Russian) 0-80562
- J-ferroics, rotational-invariant classification of structural phase transitions 0-70369
- Jahn-Teller system, thermodynamic properties, internal stress effects 0-59679
- Landau theory, thermodynamic potential models, mag. reorientation 0-103456
- Landau theory of structural phase transitions 0-92639
- light scattering near phase transition pts. in pure and defect containing crystals, review 0-93361
- macroscopic quadrupole effects as method of obs. of struct. transforms in crystals. 0-71321
- magnetically ordered cryst., dislocation drag, magnetoelastic waves 0-103332
- malononitrile, cryst., phase transitions, Raman and IR obs. 0-88980
- memory alloy, pseudoelectric, model for first-order phase transition 0-92642
- metal halides, fluorite structure, retarded ionic motion 0-88361
- metals, FCC, 'brass to copper' transition in rolling textures 0-76246
- metals, wave movement, resonance phenomena in deformation zone during rolling (Russian) 0-65123
- metals and alloys, critical temperatures determination, elec. resist. method, IMASH-55-69 installation 0-71827
- methane, solid, phase II, Raman spectrum, vol. and temp. depend. 0-97260
- 5-methyl-1-thia-5-azacyclooctane-1-oxide perchlorate, single cryst. transform., evidence for intermediate state 0-88078
- methylammonium bromide, solid, phase transitions, PMR, DTA study 0-107421
- non-ferroic phase transitions, group theoretical methods 0-70388
- ordered regions near macroscopic defects and percolation phase transform. in crystals (Russian) 0-92665
- Peierls transition in quantizing mag. field, possibility 0-103441
- phase boundaries in first-order phase transitions, dynamics stability 0-107403
- phase diagram with first-order transition close to second-order transition 0-59625
- phase transition to incommensurate excitonic phase 0-75510
- phase transitions, induced by several order parameters, thermodynamic parameters 0-103457
- photoacoustic effect 0-69615
- pigeonite, high-low transformation rel. to antiphase domains exptl. coarsening 0-81886
- poly(vinylidene fluoride) phase II, field induced phase transitions 0-96640
- pyrene crystals, anomalous emission excited near absorption edge 0-100682
- pyridinium silver iodide, fast ion conductor, phase transitions, thermoelec. power meas. 0-107540
- quartz, light scattering polarisation props. at  $\alpha$ - $\beta$  phase transition 0-108220
- quasi-one-dimensional electron-phonon system, electron jump effect on phase transition (Russian) 0-92673
- quasielastic light scattering near phase transitions 0-93362
- rare earth intermetallic cpds., cryst. field effects rel. to mag. props. 0-59933
- rare earth zircones, Jahn-Teller cooperative phase transition, crossover effects 0-88316
- rare-earth germanides, R<sub>3</sub>Ge<sub>3</sub>, thermal expansion, phase transition effects 0-70433
- reinforced plastics, equations of state, taking account of mech. damage 0-97553
- squaric acid, two dimensional antiferroelec., Brillouin scatt. at structural phase transition 0-71430
- steel, 12Cr2MoWVTiB, transformation mechanism and fine structure of (M-A) phase, TEM study (Chinese) 0-66500
- steel, austenitic, Cr-Mn-B-N, phase composition and struct. transformations 0-104171
- steel, austenitic stainless, weld, ferritic-austenitic solidification mode 0-89214
- steel, austenitic type KO 34, microstruct. changes on electron beam welding (Hungarian) 0-104252
- steel, Cr, lower bainite transform., significance of carbide precip. 0-97476
- steel, Cr (0.5 wt.%), austenite-pearlite transformation 0-97480
- steel, Cr-Mo (2.8, 1.6 wt.%), atom probe anal. of bainitic phase boundaries 0-71990
- steel, Cr-Mo-V pressure vessel, microstruct. parameters and yielding rel. to plastic deform. 0-89318
- steel, Cr-W(Mo), quenched, carbide reactions during tempering 0-89229
- steel, En 24, Cr, V, deform. effect on decomp. of austenite, carbide precipitation 0-84938
- steel, Fe-V-C (1, 0.2 wt.%), austenite formation 0-84927
- steel, ferritic, Cr-Mo (2.25, 1 wt.%), C and Nb influence on structural transformations (French) 0-84925
- steel, maraging, Fe-Cr-Co-Mo, phase transforms. during high temp. austenitisation and solid soln. decomp. (Russian) 0-66524
- steel, maraging stainless, phase transformation and mech. props. rel. to heat treatment (Chinese) 0-66501
- steel, Mn-B-V, low alloy, transform. singularities (Russian) 0-104116
- steel, Mn-Si-Cr-Mo, dual phase, as-rolled, continuous cooling transformation diagram to optimize composition 0-100829
- steel, Ni-Mo-C (2.0, 0.2, 0.4 wt.%) sintered, struct. transforms. and mech. props. after quenching 0-66557
- steel, stainless, ferrite to austenite decomp. 0-93554
- steel, stainless, stress relieved, microstruct. transformations resulting from ageing 0-71644
- steel, tempered martensitic, type AISI 410, role of C in embrittlement phenomena 0-93652
- steel, V, precip. and transform. kinetics, effect of N 0-97485
- steel ball bearing, fatigued, phase changes, nomenclature 0-89198
- steel Ni-Cr-Ti-C (2.8, 0.9, 0.2, 0.73 wt.%), ferrite, orientation in pearlite, rel. to austenite (Russian) 0-81072
- structural phase transformations, static critical behaviour 0-92640



## solid-state phase transformations continued

- sulpholan, molecular solid, laboratory frame and rotating frame spin-lattice relax., pulsed NMR meas., phase transitions obs. 0-93197  
 superionic conductor, statics and local dynamics near phase transition 0-107542  
 superionic fluorites, structure and transport 0-84318  
 sym-triazine, Landau mean field description, second-order phase transition, soft modes 0-108434  
 sym-trioxane, phase transition, polarised Raman spectra obs. 0-84742  
 TCNQ ion radical salt, DECA(TCNQ)<sub>2</sub>, IR absorpt. spectra obs. of first-order transition 0-71397  
 tetramethylammonium octahydrotriborate, NMR study of proton and B dynamics 0-93200  
 tetramethylammonium tetrachlorocuprate, incommensurate phase, neutron diff. study 0-79935  
 tetramethylammonium tetrachlorocuprate crystal, incommensurate-ferroelastic (commensurate) phase transition obs. 0-75352  
 tetramethylammonium tetrachlorozincate, incommensurate phase study, ferroelectric-paraelectric phases (French) 0-88318  
 thermal conductivity, anomalous temp. behaviour near structural phase transition (Russian) 0-75394  
 thermal expansion of crystals, book 0-73115  
 thiourea, incommensurate phase transitions, thermodynamic pot. 0-79941  
 triamantane, plastic and solid-solid transitions, Raman study 0-60590  
 TTF-TCNQ, CDW transition with tripling of period along chains 0-96805  
 TTF-TCNQ, Landau theory of phase transitions 0-92666  
 vinylidene fluoride-trifluoroethylene film, cryst. phase transition 0-66120  
 wavevector reversed ultrasound studies 0-75306  
 Ag complex, dioxane perchlorate, cryst. struct., phase transitions, X-ray study 0-59646  
 Ag-Al (26 at.%), massive transform,  $\beta$ - $\gamma$ , crystallography and morphology 0-97475  
 $\alpha$ -AgI, fast ion conductor, phase transitions, thermoelec. power meas. 0-107540  
 AgI group superionic conductor, phase transition detection by thermoelectric power method 0-92669  
 Ag<sub>2</sub>Cl<sub>2</sub>·W<sub>2</sub>O<sub>8</sub>, solid electrolyte, anisotropic elec. cond., low temp. phase transitions 0-65289  
 Ag<sub>3</sub>SBr, ionic conductivity in temp. range 93-573K, X-ray diff. and DTA 0-79988  
 Ag<sub>3</sub>SBr, superionic conductor, phase transition, struct. 0-107144  
 Ag<sub>3</sub>SI, ionic conductivity in temp. range 93-573K, X-ray diff. and DTA 0-79988  
 Al-Al<sub>3</sub>Ti, directionally solidified, thermal stability during annealing, 435-660°C 0-108393  
 Al<sub>3</sub>Mg<sub>2</sub>, diffusionless phase transformation 0-104150  
 $\beta$ -Al<sub>2</sub>O<sub>3</sub>-Ag<sub>2</sub>O, stoichiometric A phase, X-ray diffuse scatt. obs., sublattice phase transition 0-64944  
 Au<sub>11</sub>Mn<sub>2</sub>, ordered phase formation, electron diff. and microscopy study 0-107418  
 BaCl<sub>2</sub>(F<sub>2</sub>), sp. ht. meas., Schottky-type diffuse phase transitions, defect form. energies and entropies 0-107441  
 BaMnF<sub>4</sub>, struct. phase transition, optical parameters obs. 0-100328  
 Ba<sub>2</sub>NaNb<sub>2</sub>O<sub>15</sub>, incommensurate refls. near ferroelastic transition, neutron and X-ray precession obs. 0-70395  
 BaTiO<sub>3</sub>, polycryst., phase transition obs. in -170 to 220°C range (Russian) 0-103474  
 BaTiO<sub>3</sub> type crystal, thermodynamic analysis of struct. phase transitions (Russian) 0-103473  
 BaTiO<sub>3</sub>/Fe<sub>2</sub>O<sub>3</sub>, photoacoustic effect, first order phase transitions at increasing and decreasing temp. 0-70320  
 Ba(V<sub>1-x</sub>Ti<sub>x</sub>)S<sub>3</sub>, synthesis and struct. phase transitions 0-107415  
 Bi<sub>2</sub>MoO<sub>6</sub>, superplasticity during phase transitions 0-108498  
 Bi<sub>2</sub>Se<sub>3</sub>-Bi<sub>2</sub>Se<sub>3</sub> and Bi<sub>2</sub>Te<sub>3</sub>-Bi<sub>2</sub>Se<sub>3</sub> systems, thermal cond. change during phase transitions 0-100368  
 BiVO<sub>4</sub>, ferroelastic domains, electron microscopy and electron diff. obs. 0-100254  
 BiVO<sub>4</sub>, ferroelastic phase transition, birefringence meas. using rotating-analyser method 0-80742  
 Bi<sub>2</sub>WO<sub>6</sub>, superplasticity during phase transitions 0-108498  
 Ca<sub>2</sub>SiO<sub>4</sub>, structurally related phases, high-temp. X-ray powder diff. 0-81050  
 Cd(ClO<sub>4</sub>)<sub>2</sub>·6H<sub>2</sub>O and Cd(ClO<sub>4</sub>)<sub>2</sub>·6D<sub>2</sub>O, single crystals, EPR study of phase transitions 0-66025  
 Cd<sub>2</sub>Hg<sub>1-x</sub>Se, phase transition and elastic const., US vel. study 0-75354  
 Ce, isostructural solid-solid phase transitions, core collapse, cell theory 0-59620  
 Co complex, [Co(NH<sub>3</sub>)<sub>6</sub>]I<sub>3</sub>, enantiotropic phase transition obs. 0-107412  
 Co-Ga binary system, lattice const., phase transform (Chinese) 0-88108  
 Co-Ni-Cr-Mo (35, 20, 10 wt.%), MP35N, TEM study of phase transformations 0-81054  
 CrCl<sub>3</sub>, electronic struct. and struct. phase transition 0-59644  
 CrCl<sub>3</sub>, luminesc. in vac. UV range above and below phase transition temp. 0-93399  
 CsCrI<sub>3</sub>, neutron diff. expts. at 300, 77 and 1.2K 0-107163  
 CsCuCl<sub>3</sub>, Jahn-Teller induced phase transitions 0-70391  
 CsCuCl<sub>3</sub>, phase transition, refr. index, electrooptic coeff., pyroelec. signal, and NQR meas. 0-70386  
 CsInCl<sub>3</sub>, mixed-valence cpd., structural phase transition (German) 0-70406  
 Cs<sub>2</sub>NaM<sup>3+</sup>Cl<sub>6</sub> (M<sup>3+</sup>=Bi,Nd,Pr), ferroelastic phase transitions, thermal expansion, elasticity, and X-ray anal. 0-70393  
 CsPbCl<sub>3</sub>, electronic struct. and optical props. in fundamental absorpt. region 0-93367  
 Cs<sub>2</sub>PbCu(NO<sub>3</sub>)<sub>6</sub>, incommensurate Jahn-Teller transition, Huang scatt. 0-70401  
 Cu-Al films, elec. cond. of vacuum condensates depend. on composition, annealing (Russian) 0-65709  
 Cu<sub>2</sub>S, 1≤x≤2, quantum temp. size effect and magnetism (Russian) 0-103764  
 DyAsO<sub>4</sub>, first order Jahn-Teller phase transition, sp. ht. and refr. index meas. 0-59645  
 DyAsO<sub>4</sub>, phase transitions obs. 0-70412  
 DyCo<sub>2</sub>-DyAl<sub>3</sub> system, mag. and structural studies 0-108006  
 DyVO<sub>4</sub>, cooperative Jahn-Teller phase transition, linear birefr. meas. 0-88960  
 DyVO<sub>4</sub>, phase transitions obs. 0-70412  
 Eu<sub>1-x</sub>La<sub>x</sub>S, electron struct., lattice const., X-ray spectral study (Russian) 0-100432

## solid-state phase transformations continued

- Fe, cast, pearlitic, nodular graphite type, struct. evolution (French) 0-93551  
 Fe-M, (M=Cr,W,Mo,V,Ti), morphology and growth kinetics of  $\delta$ -pearlite formed by carburisation 0-108485  
 Fe-Mn-Ni-V-C (0.5, 3.0, 1.0, 0.2 wt.%), austenite decomp., isothermal transform. characts. 0-97477  
 Fe-Mn-V-C (0.5, 1.0, 0.2 wt.%), austenite decomp., isothermal transform. characts. 0-97477  
 Fe-Ni alloys, enthalpy change between  $\alpha'$ - $\gamma$  and  $\alpha$ - $\gamma$  transformations 0-93550  
 Fe-Ni-C martensite morphology, butterfly-lenticular transition temp., Cr addition effect (Japanese) 0-81053  
 Fe-Si cast alloy with spheroidal graphite, transform. investigation during tempering (Russian) 0-97479  
 (Fe<sub>0.9</sub>Al<sub>0.1</sub>)O<sub>3</sub>, IR spectra, lacunar  $\gamma$ -phase to corundum  $\alpha$ -phase transform. 0-108199  
 (Fe<sub>2</sub>Cr<sub>1-x</sub>Al<sub>x</sub>)O<sub>3</sub>, IR spectra, lacunar  $\gamma$ -phase to corundum  $\alpha$ -phase transform. 0-108199  
 (Fe<sub>0.9</sub>Cr<sub>0.1</sub>)O<sub>3</sub>, IR spectra, lacunar  $\gamma$ -phase to corundum  $\alpha$ -phase transform. 0-108199  
 $\beta$ -Fe<sub>2</sub>Ge<sub>3</sub> formation in isothermal sintering, phase transition kinetics 0-89197  
 Fe<sub>2</sub>O<sub>4</sub>, neutron diffuse scatt. due to molecular polarons 0-88488  
 Fe<sub>2</sub>O<sub>4</sub>, Verwey transition, charge density-phonon condensation 0-65217  
 GaSe<sub>1-x</sub>Te<sub>x</sub>, Raman scatt., optical phonons and phase transition 0-66202  
 GaSe<sub>1-x</sub>Te<sub>x</sub>, Raman spectra, phonon freq. 0-97286  
 GdBr<sub>3</sub>, crystal preparation, elec. resistance, phase transitions 0-97427  
 GdBr<sub>3</sub> single crystals, mag. behaviour and structure change at low temp. 0-71018  
 GdMn<sub>2</sub>-GdAl<sub>3</sub> system, mag. and structural studies 0-108006  
 Gd<sub>2</sub>O<sub>3</sub>-Ga<sub>2</sub>O<sub>3</sub> system, phase diagram relationships of garnet-perovskite transform. 0-97460  
 Ge-Bi-Te system, thermal cond. change during phase transitions 0-100368  
 GeTe, bond orbital model of band struct. 0-59853  
 H<sub>2</sub>, phase transition of second kind in HCP lattice, orientational ordering 0-70410  
 Hg<sub>2</sub>Cl<sub>2</sub>, neutron and Raman scatt. studies, ferroelastic transitions 0-76015  
 InSb<sub>1-x</sub>Bi<sub>x</sub>, metastable epitaxial film, phase diagram 0-76238  
 KB<sub>2</sub>H<sub>3</sub>, NMR study of proton and boron dynamics 0-71210  
 KCaF<sub>3</sub>, struct. phase transitions, DSC, birefr., and neutron powder diff. obs. 0-70149  
 KCl:Ba<sup>2+</sup>, localised stress relaxation in excess vacancy system, prismatic loops (Russian) 0-88160  
 KD<sub>3</sub>(SeO<sub>3</sub>)<sub>2</sub>, phase transition, neutron scatt. study 0-75351  
 KFe(MoO<sub>4</sub>)<sub>2</sub>, phase transitions at 312 and 139K 0-70396  
 KH<sub>2</sub>(SeO<sub>3</sub>)<sub>2</sub>, ferroelastic transition under uniaxial press., EPR study 0-59562  
 KMnF<sub>3</sub>, 185K structural transition, wavevector reversed ultrasound study 0-75306  
 KMnF<sub>3</sub>:Rb, phase transition and atomic motions, NMR study 0-75872  
 K<sub>2</sub>PbCu(NO<sub>3</sub>)<sub>6</sub>, incommensurate Jahn-Teller transition, Huang scatt. 0-70401  
 K<sub>2</sub>ReCl<sub>6</sub>, elastic constants, softening of acoustic modes, obs. by Brillouin scattering 0-71440  
 K<sub>2</sub>SO<sub>4</sub>, longitudinal-acoustic soft mode in phase transition 0-75326  
 K<sub>2</sub>SO<sub>4</sub>, phase transform., mech. of thermal hysteresis, DTA, dilatometry and dielec. meas. 0-75353  
 $\beta$ -K<sub>2</sub>SO<sub>4</sub> type crystals, structural transitions 0-75349  
 K<sub>2</sub>SeBr<sub>6</sub>, rotational phase transitions, cryst. struct., X-ray diff. study 0-70400  
 K<sub>2</sub>SeO<sub>4</sub>, structural transition, polarised Raman spectra 0-75349  
 K<sub>2</sub>SeO<sub>4</sub>, ultrasonic study in temp. range of incommensurate phase transform. 0-88276  
 K<sub>2</sub>SnCl<sub>6</sub>, elastic constants, softening of acoustic modes, obs. by Brillouin scattering 0-71440  
 K<sub>2</sub>SnCl<sub>6</sub>, phase-transition-induced dipolar relax. 0-66107  
 K<sub>2</sub>ZnCl<sub>4</sub>, <sup>51</sup>Cl NQR study of incommensurate phase transition 0-60450  
 LaAg<sub>2</sub>In<sub>1-x</sub>, phonon dispersion, elastic const. and struct. instability, soft mode behaviour 0-103436  
 LaD<sub>3</sub>, stoichiometric, structural phase transform., neutron diffraction evidence 0-88319  
 LaP<sub>2</sub>O<sub>14</sub>, continuous ferroelastic transition elastic and mechanical props. 0-92668  
 LaP<sub>2</sub>O<sub>14</sub>, coupling effects between soft optic and acoustic modes at ferroelastic transition 0-70358  
 LaVO<sub>4</sub>, successive phase transitions, X-ray anal. 0-108437  
 Li<sub>1+x</sub>Ti<sub>2-x</sub>O<sub>4</sub>, high temp. spinel-Ramsdellite transform. 0-70407  
 MgAl<sub>2</sub>O<sub>4</sub> spinel, anomalous thermal expansion, second order transition 0-84307  
 Mg(NH<sub>3</sub>)<sub>6</sub>(ClO<sub>4</sub>)<sub>2</sub>, phase transition, group theoretical anal. 0-65218  
 Mn<sub>2</sub>Ga<sub>1-x</sub>Mn<sub>x</sub>N, perovskite struct., phase transformations (French) 0-81048  
 Mn<sub>2</sub>GaN, sp. ht., 6 to 350K, mag. and crystallographic phase transitions 0-71060  
 Mn<sub>2</sub>GaN<sub>1-x</sub>C<sub>x</sub>, perovskite struct., phase transformations (French) 0-81048  
 Mn<sub>1-x</sub>Mg<sub>x</sub>Se, mag. and struct. phase transitions, mag. susceptibility and X-ray diff. study 0-71022  
 Mn<sub>2</sub>O<sub>4</sub>, hausmannite, tetragonal-cubic transform., X-ray anal. 0-103288  
 MnS, phase transform. at 200°C, diffusive and deformational mechanisms 0-65216  
 $\alpha$ -MnSe, mag. and struct. phase transitions, mag. susceptibility and X-ray diff. study 0-71022  
 Mn<sub>2</sub>Si<sub>3</sub>, elastic moduli, phase transitions, ultrasonic velocity 0-92589  
 Mn<sub>2</sub>ZnN, sp. ht., 6 to 350K, mag. and crystallographic phase transitions 0-71060  
 MoO<sub>3</sub>, topotactic transform into MoO<sub>2</sub>, electron microscopy, X-ray anal. 0-107417  
 N<sub>2</sub>H<sub>6</sub><sup>2+</sup> salts, NMR spin lattice relaxation study, <sup>14</sup>N-<sup>1</sup>H dipole-dipole contrib. to relax. 0-75878  
 NH<sub>4</sub>Br, dislocation influence on phase transition and light scatt. (Russian) 0-95648  
 NH<sub>4</sub>Cl, acoustic absorption by soft modes of defects 0-59584  
 NH<sub>4</sub>Cl, piezoelec. effect near nonferroelastic phase transition 0-66116  
 (NH<sub>4</sub>)<sub>2</sub>SiF<sub>6</sub>, elastic constants, softening of acoustic modes, obs. by Brillouin scattering 0-71440  
 (NH<sub>4</sub>)<sub>2</sub>SnBr<sub>6</sub>, structural phase transitions study by Raman scatt. 0-93318



## solid-state phase transformations continued

- (NH<sub>4</sub>)<sub>2</sub>SnCl<sub>6</sub>, elastic constants, softening of acoustic modes, obs. by Brillouin scattering 0-71440  
 Na<sub>2</sub>SeP<sub>2</sub>O<sub>7</sub>, fast-ion conductor, struct. phase transition 0-88362  
 Na<sub>2</sub>SO<sub>4</sub>, high temp. struct. neutron powder diffn., comparison with SrZrO<sub>3</sub> and NaNbO<sub>3</sub> 0-88094  
 $\beta$ -Na<sub>2</sub>O<sub>3</sub>V<sub>2</sub>O<sub>5</sub>, quasi-one-dimensional conductor, NMR studies 0-93204  
 Nb-H system, phase diagram and transforms., struct. obs. of various phases 0-104125  
 Nb-Pd constitution diagram, metallographic and X-ray diffn. anal. 0-89204  
 Nb-Zr alloy, BCC- $\omega$  phase transition, electronically driven nature 0-103433  
 NbH<sub>3</sub>, coherent  $\alpha$ - $\alpha'$  phase transition 0-71641  
 Nb<sub>2</sub>N<sub>3</sub>, supercond. props. and structural phase transform. induced by C<sup>+</sup> and N<sup>+</sup> implantation 0-107942  
 NbO<sub>3</sub>, Lifshitz point behaviour 0-70402  
 Nb<sub>2</sub>Sn, softening of surface phonons in (100) plane, rel. to structural phase transition 0-107627  
 NdP<sub>2</sub>O<sub>7</sub>, ferroelastic, hydrostatic press. effect on phase transition temp. 0-70293  
 Ni perfect crystal, stability under various stresses 0-104208  
 Ni-Cr-Mo-W-Al-Ti, heat-resist., phase comp. 0-76250  
 Ni-Ti (12 wt.%), early stages of transformation 0-76251  
 Ni(NH<sub>4</sub>)<sub>2</sub>(BF<sub>4</sub>)<sub>2</sub>, phase transition, group theoretical anal. 0-65218  
 Ni(NH<sub>4</sub>)<sub>2</sub>(ClO<sub>4</sub>)<sub>2</sub>, phase transition, group theoretical anal. 0-65218  
 Ni(NH<sub>4</sub>)<sub>2</sub>I<sub>2</sub>, phase transition and rot. excitation 0-96642  
 PbF<sub>2</sub>, sp. ht. meas., Schottky-type diffuse phase transitions, defect form. energies and entropies 0-107441  
 p-Pb<sub>1-x</sub>Ge<sub>x</sub>Te film, cyclotron reson. above and below struct. phase transition 0-88879  
 Pb<sub>1-x</sub>Ge<sub>x</sub>Te solid solns., phase transition influence on elec. props., 77 to 450K 0-103689  
 PbI<sub>2</sub>, direct gap polar semicond., electron hole liquid phase diagram (*Russian*) 0-93314  
 Pb<sub>3</sub>(PO<sub>4</sub>)<sub>2</sub>, ferroelastic, dielectric anomalies, phase transitions, permittivity, relaxation (*Russian*) 0-71293  
 Pb<sub>3</sub>(Fe<sub>0.95</sub>V<sub>0.05</sub>O<sub>7</sub>)<sub>2</sub>, ferroelastic transition, soft mode, inelastic neutron scatt. study 0-70357  
 Pb<sub>3</sub>(Fe<sub>1-x</sub>V<sub>x</sub>O<sub>7</sub>)<sub>2</sub>, ferroelastic phase transition, DTA, dilatometric and Brillouin scatt. study 0-70398  
 Pb<sub>1-x</sub>Sn<sub>x</sub>Te, thermoelectric effects, characteristics at low temps. 0-107831  
 Pb<sub>0.95</sub>Se<sub>0.05</sub>(Zr<sub>0.5</sub>Ti<sub>0.5</sub>)<sub>2</sub>O<sub>7</sub>-Nb<sub>2</sub>O<sub>5</sub>, phase coexistence range, lattice const. 0-92680  
 Pb(Ti<sub>2</sub>Zr)<sub>2</sub> solid solutions, phase coexistence discrepancies 0-96662  
 xPbTiO<sub>3</sub> + (1-x)PbCd<sub>1/3</sub>Nb<sub>2/3</sub>O<sub>3</sub>, phase transition spread, polarisation relaxation, dielectric susceptibility (*Russian*) 0-75922  
 Pb<sub>2</sub>VO<sub>4</sub>, ferroelastic, phase transitions, boundary walls 0-107419  
 Pr(OH)<sub>3</sub>, electronic heat capacity, 0.45 to 4.2K, phase transition at 1.21K 0-59673  
 RbAg<sub>4</sub>I<sub>3</sub>, static and dynamic NMR effects at 208K and 122K phase transitions 0-108105  
 RbAg<sub>4</sub>I<sub>3</sub>, superionic conductor, phase transition detection by thermoelectric power method 0-92669  
 $\beta$ -RbAlF<sub>6</sub>, struct. and irreversible and topotactic phase transition  $\beta$ - $\alpha$  mechanism 0-107132  
 RbCaCl<sub>3</sub>, Raman scatt. study of phase transitions 0-71411  
 RbCaF<sub>3</sub>, cubic to tetragonal phase transition, <sup>87</sup>Rb NMR study 0-70392  
 RbCaF<sub>3</sub>, first order improper ferroelastic phase transition at 194K, phenomenological description 0-70397  
 RbCaF<sub>3</sub>, phase transitions due to octahedra rots. in perovskite struct., order-disorder model 0-70151  
 RbCaF<sub>3</sub>Gd<sup>3+</sup>, struct. phase transition, EPR study 0-71171  
 RbCdF<sub>3</sub>Gd<sup>3+</sup>, struct. phase transition, EPR study 0-71171  
 RbNO<sub>3</sub>, struct., high temp. phases, neutron diffn. study 0-79756  
 Rb-PbCu(NO<sub>2</sub>)<sub>6</sub>, incommensurate Jahn-Teller transition, Huang scatt. 0-70401  
 Rb-ZnBr<sub>3</sub>, incommensurate phase, <sup>87</sup>Rb NMR lineshape 0-93191  
 Rb-ZnBr<sub>3</sub>, soft modes at phase transforms., far IR spectrum study 0-107398  
 Ru<sub>2</sub>Ge<sub>2</sub>-Sn<sub>2</sub> and Ru<sub>2</sub>Ge<sub>2</sub>-Si<sub>2</sub>, diffusionless phase transitions, elec. and mag. props. 0-96871  
 Sb<sub>2</sub>Te<sub>2</sub>-Bi<sub>2</sub>Te<sub>2</sub> and Sb<sub>2</sub>Te<sub>2</sub>-Sb<sub>2</sub>Se<sub>2</sub> systems, thermal cond. change during phase transitions 0-100368  
 Si, (111) surface structure phase transform, screw dislocations RHEED study 0-88153  
 Si, phase transformation, lattice dynamics, microscopic theory 0-107387  
 Sm<sub>1-x</sub>La<sub>x</sub>S, electron struct., lattice const., X-ray spectral study (*Russian*) 0-100432  
 Sm<sub>2</sub>O<sub>3</sub>-Ga<sub>2</sub>O<sub>3</sub> system, garnet-perovskite transform., phase diagram relationships 0-97460  
 SnCl<sub>2</sub>·2H<sub>2</sub>O, Brillouin scatt. and thermal expansion 0-97289  
 SnCl<sub>2</sub>·2H<sub>2</sub>O, isomorphous transition, Landau type thermodynamic potential 0-107413  
 SnTe, bond orbital model of band struct. 0-59853  
 SnTe, structural phase transition threshold instability in strong EM field 0-103477  
 SrCl<sub>2</sub>, sp. ht. meas., Schottky-type diffuse phase transitions, defect form. energies and entropies 0-107441  
 Sr<sub>2</sub>Ta<sub>2</sub>O<sub>7</sub>, soft optic phonon responsible for structural phase transition, Raman scatt. meas. 0-96618  
 SrTiO<sub>3</sub>, critical elastic compliance, acoustic resonance meas. 0-65118  
 SrTiO<sub>3</sub>, semiconductor, soft modes, zone boundary mode 0-71357  
 Ta BCC lattice, strain ordering in interstitial solutions 0-107420  
 Ta-H system, phase diagram and transforms., struct. obs. of various phases 0-104125  
 TaSe<sub>2</sub> (2H), broken hexagonal symm., incommensurate charge-density wave struct. 0-96446  
 TaSe<sub>2</sub> (2H), Raman scatt. from CDW 0-93340  
 (Tb<sub>1-x</sub>Gd<sub>x</sub>)<sub>2</sub>Co, intermetallic epd. mag. props., phase transform. and mag. hysteresis (*Russian*) 0-93113  
 TbVO<sub>4</sub>, co-operative Jahn-Teller transition, low freq. dynamics, light scatt. study 0-88317  
 Te-In system, enthalpies of fusion, peritectic decomp. and allotropic transition, DTA (*French*) 0-76226  
 Te<sub>0.95</sub>Ge<sub>0.05</sub>Sb<sub>0.5</sub>(Bi<sub>0.5</sub>), DSC studies of struct. phase transformation 0-90505  
 Ti-Ag (10 to 17.5 wt.%), eutectoid system,  $\beta$ - $\alpha_m$  transform., nucleation kinetics 0-97474

## solid-state phase transformations continued

- Ti-Al-Mo, type BT22, phase transformations under step-by-step heat treatment (*Russian*) 0-108436  
 Ti-Au, (9.9 wt.%), eutectoid system,  $\beta$ - $\alpha_m$  transform., nucleation kinetics 0-97474  
 Ti-Mo (20 at.%), incommensurate struct., stacking soliton 0-107109  
 Ti-Mo-V-Al-Cr-Fe (4.8, 4.7, 5.2, 1.1, 1.0 wt.%), structural changes during heating up to 1000°C, DTA study (*Russian*) 0-93552  
 TiCl<sub>3</sub>, electronic struct. and struct. phase transition 0-59644  
 Ti<sub>2</sub>PbCu(NO<sub>2</sub>)<sub>6</sub>, incommensurate Jahn-Teller transition, Huang scatt. 0-70401  
 Ti<sub>2</sub>SeO<sub>4</sub>, structural transition, polarised Raman spectra 0-75349  
 $\alpha$ -U, CDW at 43K 0-80198  
 UMN<sub>3</sub>, transport props., influence of lattice distortion 0-100452  
 VCl<sub>3</sub>, electronic struct. and struct. phase transition 0-59644  
 (V<sub>1-x</sub>Cr<sub>x</sub>)<sub>2</sub>O<sub>7</sub>, Raman scatt. and phase transitions 0-71420  
 VO<sub>2</sub>, ferroelastic metal-insulator transition, electronically triggered crystallographic phase transition 0-70614  
 VO<sub>2</sub>, photoacoustic effect at first order phase transitions at increasing and decreasing temp. 0-70320  
 VO<sub>2</sub>:Al, photoacoustic effect study of phase transitions 0-69615  
 V<sub>2</sub>O<sub>5</sub>, impurity doping effects, elec. props. obs. 0-75609  
 VSe<sub>2</sub> (1T), incommensurate periodic lattice distortion, X-ray diffraction study 0-107414  
 V<sub>2</sub>Si, magnetic susceptibility, density of states model for lattice transformation in A-15 compounds 0-65219  
 WO<sub>3</sub>, acoustic instability near monoclinic orthorhombic phase transition, X-ray scatt. 0-65215  
 WO<sub>3</sub>, semiconductor-metal transition, structural phase transition 0-107870  
 YIG, substituted, magnetite nucleation in transitional zone, ionic process, lattice imaging 0-107424  
 Zn, internal friction anomalies in temp. initiated brittle-plastic transition (*Russian*) 0-96648  
 Zn(BF<sub>4</sub>)<sub>6</sub>·6H<sub>2</sub>O:Ni, phase transition study, EPR of diluted Ni<sup>2+</sup>, 98-298K 0-75846  
 Zr-Al (8.6 wt.%), dimensional stability struct. and mech. props, effects of neutron irradi. 0-92563  
 ZrCu, constitutional and struct. studies, by mag. susceptibility, metallography and X-ray diffn. 0-70166

## solid-state plasma

- see also helicons; plasmons  
 charged-particle stream, wave interaction, nonlinear effect 0-80310  
 conference, Masny-St-Jean, Mons, Belgium, Oct. 1979 0-82570  
 dielectric crystal, uniaxial, wave propag., polarisation relations and dispersion eqns. 0-64723  
 direct gap semiconductors, gain spectrum of electron-hole liquid 0-66279  
 dislocations and microplasma sites, STEBIC/STEM/EELS correlation 0-96528  
 doped conducting media, low-freq. props., EM wave reflection 0-103715  
 EM wave penetration into plasma, permittivity sign changes (*Russian*) 0-100477  
 ferromagnets with conduction electron spin, EM wave propagation with discrete spectrum 0-92923  
 HF wave dispersion for complex wave numbers, ordinary waves 0-70740  
 Kolmogorov Arnold Moser theorems, appl. to struct. problems in condensed matter 0-59878  
 magnetised semiconductor plasma, EM wave amplitude modulation and demodulation 0-84482  
 metal conductivity, plasma model 0-80311  
 metal lattice heating by radiation, plasma effects, degenerate electron gas calcs. 0-70742  
 nonlinear surface-wave interaction, in plasmalike media, theory 0-107839  
 one-component plasma in two and three dimensions, static props., semi-analytic theory 0-87853  
 photodiode, switching process and plasma effects, theory 0-65667  
 piezoelectric semiconductor, n-type, magnetoactive, Brillouin instability in magnetostatic field 0-78909  
 piezoelectric semiconductor-plasma, parametric excitation of helicon and acoustic waves 0-107837  
 polar semiconductor, highly excited, optical dielec. function of electron-hole plasma 0-92847  
 $\gamma$ -quanta channelling effect in periodic struct. (*Russian*) 0-96584  
 semiconductor, electron-hole plasma and elec. field, stratification at low temp. 0-60020  
 semiconductor, magnetised plasma, theory of EM surface waves 0-88584  
 semiconductor, non-equilibrium, acoustic plasma oscils. generation 0-96811  
 semiconductor, normal transverse waves in longitudinal mag. field 0-80309  
 semiconductor, plasma self-oscillations within submillimetre freq. range 0-84473  
 semiconductor, with superlattice, plasma resonant interaction with Stark oscils. 0-107842  
 semiconductor plasma, longitudinal oscillations 0-88583  
 semiconductor plasma, strongly elongated electron distrib., normal oscils. 0-60021  
 semiconductor plasma, surface helicons, theory 0-60019  
 semiconductors, narrow-gap, recomb. instability under crossed elec. and mag. fields 0-70712  
 two-valley semiconductor, hot electron instability, intervalley scatt. (*Russian*) 0-92921  
 Bi, EM wave dispersion and damping, Voigt configuration, non-local calcs. 0-100475  
 Bi<sub>96</sub>Sb<sub>4</sub>Te, single crystal, dispersion of magnetoplasma waves (*Russian*) 0-70739  
 Cd<sub>2</sub>Hg<sub>1-x</sub>Te epitaxial graded gap layers, plasma reflection and magnetoreflection 0-71391  
 CdS crystals, electron-hole plasma, carrier optical orientation 0-100689  
 CdS, electron-hole plasma, gain and refl. spectra study 0-66227  
 CdS, highly excited, stimulated emission processes, electron-hole plasma recomb. 0-97307  
 CdSe, single crystals, luminesc. of electron-hole plasma 0-60675  
 GaAs, electron-beam excited, efficient generation of electron-hole plasma 0-76051  
 n-Ge, anomalously enhanced plasma diffusion transverse to mag. field 0-96931  
 Ge, carrier relaxation rate temp. depend. and pair density in large electron-hole drop 0-75509  
 Ge, electron-hole drop freq. depend. damping 0-88482



**solid-state plasma continued**

- Ge, electron-hole droplet cloud kinetics, thermalisation phonons 0-88483  
 Ge, nonequilibrium charge carrier-mag. field interaction electron-hole drops, recombination (*Russian*) 0-75511  
 InP avalanche photodiodes, microplasmas, investigation 0-60018  
 InSb, Auger-governed decay of laser-induced plasma, optical probing 0-76105  
 n-InSb, Brillouin instability in magnetostatic field 0-78909  
 n-InSb, degenerate plasma, Coulomb collision photon absorpt. dynamic screening (*Russian*) 0-92924  
 InSb, depletion layer, plasma and vibr. plasma type guided polaritons (*Russian*) 0-96933  
 InSb, electron-hole plasma instabilities, impact ionisation conditions, microwave emission 0-107840  
 n-InSb, microwave helicon resonances, carrier density, mobility, dielectric const. 0-96930  
 InSb, pinch effect at room temp. 0-65615  
 n-InSb, semiconductors, plasma oscills. within submillimetre freq. range 0-84473  
 Pb<sub>1-x</sub>Ge<sub>x</sub>Te magnetoplasma reflectivity and transmission spectra 0-71428  
 Pb<sub>1-x</sub>Sn<sub>x</sub>Te, lattice and electronic props. and g-value 0-80161  
 Si, dense plasma dynamics during pulsed laser annealing, carrier density, recombination 0-84479  
 Si, non thermal laser induced ordering, plasma life time, phonon interactions 0-84481  
 Si p-n junction, reverse bias high voltage, secondary surface breakdown 0-70813  
 Si, plasma effects during pulsed laser annealing 0-84480  
 Si, reflectivity time dependence during pulsed laser annealing 0-66214  
 Si, solar cell, open-circuit voltage at ultrahigh light intensities, plasma reflection effects 0-96928  
 SnO<sub>2</sub> films, selective, optical characterisation by thermodynamical method 0-84796  
 ZnO, electron-hole plasma, gain and refl. spectra study 0-66227

**solid-state rectifiers**

- see also thyristors*  
 fusion reactors, PDX, shaping field-equilib. field power supply rectifier upgrade study 0-91290  
 mass spectrometer magnetic analyser constant current solid-state power unit 0-86499  
 GaAs-GaAlAs-GaAs rectifying semicond. struct., prep. by MBE and charact. 0-65657  
 Te-Se-Cd, sandwich structure, fabrication and characteristics 0-60089

**solid structure**

- see also crystal structure; long-range order; noncrystalline state structure; short-range order*  
 No entries

**solid theory**

- Froehlich, H., biographical notes rel. to solid state physics develop. 0-57059  
 Gottingen school, contrib., 1920-40 0-57070  
 historical aspects, symposium, London, England (Apr.-May 1979) 0-56999  
 history since first appls. of quantum mechanics 0-57072  
 Pohl, R., recollections of solid state physics 0-57060  
 schools of thought, 1930 to mid 1960s 0-57069  
 Seitz, Frederick, biographical notes on early solid state physics 0-57058

**solid-vapour transformations**

- see also sublimation*  
 plane evaporation boundary instability in laser radiation-matter interactions (*Russian*) 0-76111  
 Van der Waals film adsorbed on graphite, two-dimensional phase transitions 0-107653  
 In<sub>2</sub>Se<sub>3</sub>, vapour press. temp. depend., heat of evap. and form. 0-59642  
 KOH gas-crystal system, isotopic equilibrium near phase transition points (*Russian*) 0-91697  
 NaOH gas-crystal system, isotopic equilibrium near phase transition points (*Russian*) 0-91697  
 Xe adsorbed on Cu, NaCl, stepped and disordered surfaces, two-dimens. phase transformations 0-103580

**solidification**

- see also segregation*  
 alloys, binary dilute, solidification, planar interface stability (*Czech*) 0-89212  
 alloys, multidimensional three-phase free boundary problems 0-75340  
 alloys, rapidly quenched crystalline, struct., and heat treatment effects 0-76292  
 amorphous solid, rapid quenching, techniques for determ. very short room temp. lifetimes 0-84981  
 arc welding, molten pool solidification and bead formation 0-75341  
 arc welding, pool metal solidification kinetics in welding with electromag. stirring 0-71636  
 binary alloy, solidification chemical inhomogeneity (*Russian*) 0-75335  
 binary alloy indirectional solidification, convective and interfacial instabilities 0-60851  
 binary alloys, directional solidification, theory of dendritic growth 0-70145  
 binary alloys, initial transient segregation during unidirectional solidification in a furnace with thermal damping 0-70146  
 binary alloys, two phase region calcs. in solidifying melt (*Russian*) 0-65195  
 cellular and cellular dendritic growth, general microsegregation eqn. 0-84921  
 continuous ingots, two phase zone critical parameters during casting (*Russian*) 0-93549  
 cylindrical ingot, shrinkage effects on solidification rate under radiative heat transfer 0-66493  
 dilute binary alloy, unidirectional growth, morphological stability of planar interface 0-84920  
 Earth core, dynamics of fluid core with inward growing boundaries 0-76934  
 eutectic, irregular, branching limited growth 0-81042  
 FCC crystal-melt interfaces, mol. dynamics simulation 0-79913  
 front propagation, residual stress levels, polymerisation 0-59635  
 heat flow, macroscopic, use of anal. approx. for description 0-104142  
 ingots, cooling regime in conditions of minimal thermal stress, modelling (*Russian*) 0-65194  
 low gravity solidification expts., use of metallic analogue materials 0-71635

**solidification continued**

- low temp. melt spinning device 0-100825  
 melt extraction technology, advances 0-76207  
 meltspinning, theoretical anal. of ribbon thickness formation 0-104143  
 metal, eddy current response to solidification in one dimension 0-104140  
 metal metal system, glass formation 0-64921  
 metallic coatings, electric field atomisation from melt 0-76174  
 metallic glasses, electronic structure rel. to elec. cond., supercond. and mag. props. 0-65429  
 metals, unidirectional solidification, heat flow model 0-79914  
 metals, variational formulation of stationary free boundary problem (*French*) 0-96626  
 pattern selection in non-equilib. processes, marginal stability theory, eutectic solidification model 0-60852  
 polyethylene fibre, high-strength high-modulus, morphology and tensile prop. relations 0-103264  
 polyethylene fractions, quasi-binary systems, solidification and crystn. 0-84108  
 polyethylene-paraffin wax, blends, rapid cooling processing techniques 0-84905  
 polymers, solidification, as dissipative process 0-65205  
 polyvinylidene fluoride, melt-solidified, crystn. and morphology 0-103461  
 radioactive waste, high-level, solidification production facility 0-83201  
 radioactive waste fixation using sol-gel technology 0-83207  
 sapphire, growth angle determ. from cryst. lateral face shape and solidified separation drops 0-103282  
 solid/melt interfacial tension and contact angles of small particles, determ. from crit. vel. of engulfing 0-79915  
 solidifying melt, two phase zone formation, convection (*Russian*) 0-93547  
 steel, 12% W, eutectic carbides struct. and comp. during heating 0-76283  
 steel, austenitic, type 12Kh18N10T, pool metal solidification kinetics in welding with electromag. stirring 0-71636  
 steel, austenitic stainless, weld, ferritic-austenitic solidification mode 0-89214  
 steel, Cr-Ni, pendant drop melt extracted, struct. and props. 0-76242  
 steel, Cr-W(Mo), quenched, carbide reactions during tempering 0-89229  
 steel, high speed, props. after electroslag remelting 0-104139  
 steel, low alloy, S and Mn influence on high temp. strength and ductility after solidification from melt (*German*) 0-81106  
 steel, low impurity, peritectic transformations, influence on initial struct., solidification, grain boundaries (*Russian*) 0-66621  
 steel, low-alloyed, C-content influence on high temp. strength and ductility after solidification from melt (*German*) 0-81105  
 steel, solidification during continuous casting, cooling regime comparison (*Russian*) 0-93548  
 steel shell, mech. behaviour during solidification 0-81043  
 stress, and dislocations, creation during crystal growth (*Russian*) 0-103277  
 supersaturated soln., shape stability of growing cylindrical particle due to diffusion and interface kinetics 0-79720  
 SYNROC-B sintered ceramics for high-level radwaste fixation, comp. and phase charact. 0-106126  
 white Fe castings, morphology of eutectic M<sub>2</sub>C and M<sub>7</sub>C<sub>3</sub> 0-108427  
 Ag-Sn, splat-quenched, X-ray diffr. study 0-81094  
 Al alloys, columnar struct. of alloys solidified in flowing melt in centrifugal casting 0-71640  
 Al binary alloys, rapid quenching, struct. and decomp. 0-76244  
 Al, molten, showering cryst. form. in mould cooled from top (*Japanese*) 0-66498  
 Al, solidification, high press. effects 0-66499  
 Al-Al<sub>2</sub>Pt<sub>3</sub> eutectic alloys, unidirectionally solidified, struct. study 0-108394  
 Al-Al<sub>2</sub>Ti, directionally solidified, thermal stability during annealing, 435-660°C 0-108393  
 Al-Cu, molten, showering cryst. form. in mould cooled from top (*Japanese*) 0-66498  
 Al-Cu, solidification, solid-liq. interface, solute conc. effects 0-59632  
 Al-Cu (33 wt.%) eutectic, solidification under reduced gravity, behaviour of suspended Al<sub>2</sub>O<sub>3</sub> particles (*German*) 0-60853  
 Al-Cu alloy dendritic solidification kinetics 0-81041  
 Al-Cu alloys, coarsening mechanisms of secondary dendrite arm, and organic analogue 0-81049  
 Al-Cu dilute alloys, vein closing mechanism in fluidity tests 0-84924  
 Al-CuAl<sub>2</sub> eutectics, microstruct. after solidification, heat pipe influence 0-76243  
 Al-Cu(Mg), dil. binary alloy, planar interface stability during solidification (*Slovak*) 0-108424  
 Al-Cv (0.3 wt.%), moving solid-liq. interface, diffusion in liq. 0-107456  
 Al-Mg, solidification, solid-liq. interface, solute conc. effects 0-59632  
 Al-Mg, type AMg6, pool metal solidification kinetics in welding with electromag. stirring 0-71636  
 Al-Mg(Cu)(Si), 5.0(4.5)(11.8) wt.%, ingots, vibr. effect during solidification on porosity formation 0-108426  
 Al-Ni (3-18wt.%), gun-quenched from melt, struct. 0-76225  
 Al-Si (25.4 wt.%), solidification, high press. effects 0-66499  
 Al-Si (2.4 wt.%), liq. fluidity in solid-liq. zone 0-108429  
 Al-Si eutectic alloy, banded struct., SEM and optical microscopy 0-104144  
 Al-Ti, molten, showering cryst. form. in mould cooled from top (*Japanese*) 0-66498  
 Al-Zn alloys, interfacial stability of planar solid-liq. interface during solidification 0-104145  
 Al-Zn alloys, interfacial holes distrib. at beginning of interfacial instability in solidification 0-104146  
 Al-Zr (1-13 wt.%), rapidly quenched, extended solid solubility, grain refinement and age-hardening 0-76266  
 Al<sub>2</sub>O<sub>3</sub>-Y<sub>2</sub>O<sub>3</sub>, melting behaviour and metastability determ. by optical DTA 0-92648  
 Cd-Zn eutectics, microstruct. after solidification, heat pipe influence 0-76243  
 Co-WC hard alloys, rapidly quenched struct. 0-76233  
 25Cr-20Ni stainless steel dendritic solidification, growth morphology and solute redistrib. (*Japanese*) 0-81045  
 Cu-Al spherical crystals, grown from drop of melt, topography 0-84353  
 Cu-Al Ni Marmen alloys, rapid solidification and ageing 0-76245  
 Cu-Cu<sub>2</sub>Y eutectic alloy, cast and directionally solidified, struct. and props. (*Russian*) 0-104138  
 Cu-Nb alloy, chill casting, consumable arc melting, ingot prep. techniques 0-84879

**solidification continued**

- CuInTe<sub>2</sub>, single crystals, directional freezing growth and doping, resist. changes on annealing 0-60768  
 Fe, cast, grey, solidified in oscillatory and rotating moulds, metallographic study 0-89213  
 Fe, cast, with spherical graphite, crystn. (*German, English*) 0-97473  
 Fe smelting, Si-Q apparatus for solidification temp., Si correction, %P correction (*German*) 0-76450  
 Fe, splat-quenched, microhardness and martensite 0-76359  
 Fe-B, rapidly quenched, metastable phases 0-76234  
 Fe-B amorphous ribbons formation, high-speed photography investigation 0-76216  
 Fe-C-Si, high purity, vacuum melted, nodular graphite form. 0-108452  
 Fe-Cu-C, phase equilibria, 950 to 1500°C 0-60836  
 Fe-MuS eutectics, unidirectional solidification (*German*) 0-100827  
 Fe-Ni-Cr-Al-Ti-W-Mo (35, 15, 2.4, 2.3, 2.2 wt.%) wrought superalloy, freckles (*Chinese*) 0-104137  
 Fe-Ni-P-B amorphous ribbons, form. by melt spin technique 0-76215  
 Fe-Ti-C, rapidly quenched by splat-cooling 0-84923  
 Fe<sub>2</sub>O<sub>3</sub>, haematite platelets, growth and cross-connection in consolidation of haematite pellet (*Chinese*) 0-104186  
 InSb, growth angle determ. from cryst. lateral face shape and solidified separation drops 0-103282  
 Li<sub>2</sub>O.2SiO<sub>2</sub>, ceramic, prep. of oriented microstructure by unidirectional solidification of melts 0-71614  
 NH<sub>4</sub>Cl-H<sub>2</sub>O, solidification microstructs., effect of reduced gravity 0-96632  
 NH<sub>4</sub>Cl-H<sub>2</sub>O solidification model for showering cryst. form. in molten metal cooling (*Japanese*) 0-66498  
 Na<sub>2</sub>O-PbO-SiO<sub>2</sub>, glass-ceramic composite, directionally crystallised 0-107058  
 Ni base superalloys, rapid solidification, use in gas turbine engines 0-84888  
 Ni-Al-Ta dendritic monocrysts., directionally solidified, coarsening kinetics 0-108425  
 Ni-Cr-NbC eutectic composite, unidirectional solidification, thermal cycling, temp. range effect on microstructural degradation 0-89272  
 Ni-Cr-Ti rapidly solidified superalloys, surface segregation 0-76263  
 Ni-NbC (10 wt.%) eutectic alloy, directional solidification and struct. (*Russian*) 0-84922  
 Ni-Ni<sub>3</sub>B eutectic, high temp. X-ray anal. 0-71639  
 Ni-Ti-Al superalloy, pendant drop melt extracted, struct. and props. 0-76242  
 NiTaC, eutectic alloys, chem. incompatibility of ceramic nitrides for directionally solidifying 0-81046  
 NiTaC eutectic superalloy, casting, furnace atm. effects 0-84880  
 Pb, changes in electron image contrast 0-100147  
 Pb-Sb, temp. regime of crystn. on rapid cooling (*Russian*) 0-66495  
 Pb-Sb, thermal analysis in non-faceted/faceted eutectic systems 0-71637  
 Pb-Sn (20wt.%), eddy current study of solidification 0-104141  
 Pb-Zn, unmixing alloys, mathematical model for solidification process (*Russian*) 0-81047  
 Se, amorphous and liquid state, Raman spectra, crystn. processes 0-60608  
 Si, cast, growth structure and photovolt. props. of solar cells 0-94008  
 Si laser annealed, nonequilibrium solubility and segregation 0-84296  
 Si polycrystalline, low cost conversion into sheet by heat exchange method and fixed abrasive slicing technique 0-93479  
 Si sheet, high speed growth, heat transport analysis 0-107669  
 Si sheet casting for solar cells 0-89139  
 Si single crystal ingot growth from metallurgical grade Si, inhomogeneities 0-59416  
 Si-Te, laser melting, surface Te atom accumulation, profiles 0-100258  
 Sn-Bi, thermal analysis in non-faceted/faceted eutectic systems 0-71637  
 Sn-Bi(Pb)(Ga), temp. regime of crystn. on rapid cooling (*Russian*) 0-66495  
 Te amorphous and liquid state, Raman spectra, crystn. processes 0-60608  
 Te-(Bi,Sb<sub>1-x</sub>)<sub>2</sub>Te<sub>3</sub> eutectic, electrophys. props., directed crystn. conditions influence and comp. depend. 0-107827  
 Te-based eutectics, crystn. rate effect on electrophys. props. mutual solubility effect 0-60774  
 Ti base alloys, melt-extracted polycryst., mech. props. 0-76360  
 Ti, type VT1-0, pool metal solidification kinetics in welding with electro-mag. stirring 0-71636  
 Ti-Ag (10 to 17.5 wt.%), eutectoid system,  $\beta$ - $\alpha_m$  transform., nucleation kinetics 0-97474  
 Ti-Au, (9.9 wt.%), eutectoid system,  $\beta$ - $\alpha_m$  transform., nucleation kinetics 0-97474  
 Zn-Ga, temp. regime of crystn. on rapid cooling (*Russian*) 0-66495  
 ZrO<sub>2</sub>-CaO, stabilised microspheres, structure, mechanical props. (*Russian*) 0-100379  
 ZrO<sub>2</sub>-Y<sub>2</sub>O<sub>3</sub>, stabilised microspheres, structure, mechanical props. (*Russian*) 0-100379

**solids**

- Generalities only; for specific aspects see appropriate headings  
 see also crystals; quantum solids; solid hydrogen; solid structure; solid theory*  
 experimentation in solid state physics, review (*Spanish*) 0-82624

**solitons see transducers****solitons**

- $\tau$ -vacuum for  $\phi^4$  and sine-Gordon theories, stationary solitons (*Chinese*) 0-101932  
 amorphous magnets, disclinations and solitons 0-75786  
 anisotropic ferromagnet, one-dimensional Landau-Lifshits eqn. multi-soliton solutions (*Russian*) 0-71014  
 anisotropic Heisenberg chain, nonlinear excitations 0-70927  
 annual review of fluid dynamic, book 0-94927  
 antiferromagnet, linear-chain, sine-Gordon solitons 0-80543  
 antiferromagnet, magnetoelastic soliton propag. 0-66003  
 antiferromagnet, one-dimens., nonlinear dynamics 0-80521  
 antiferromagnets, nonlinear waves 0-84612  
 Benjamin-Ono equation, higher order, solns. 0-62482  
 Benjamin-Ono solitons, interactions 0-73181  
 breather generation, inverse scatt. technique 0-78913  
 caviton dynamics at crit. density 0-106909  
 charged, stability, relativistic complex scalar field, direct Lyapunov method 0-62827  
 collisionless gravitating systems, gravitational pot. nonlinear eqns. determ., astrophysical appl. 0-67560

**solitons continued**

- commensurate-incommensurate transition, Devil's staircase and harmless staircase, oscillating interactions through elastic stairs or other harmonic fields 0-88296  
 condensation of the vortex solitons in a 2+1 dimensional Abelian Higgs model 0-99048  
 condensed matter, a paradigm, review 0-77632  
 converging ion acoustic soliton excitation in double plasma type device 0-106907  
 coupled non-linear field eqns., soliton solns. 0-68338  
 diffraction by circular island in ocean, shallow-water theory (*French*) 0-83803  
 double quadratic kink soln. to ferroelec. domain wall dynamic polarisability 0-66135  
 driven sine-Gordon chain, periodic and solitary states 0-82881  
 effective-potential approach to the quantization of the sine-Gordon theory in 1+1 dimensions 0-73608  
 Einstein-Maxwell eqn., N soliton solutions (*Russian*) 0-105556  
 Einstein-Podolsky-Rosen paradox, de Broglie's physical waves, solitons 0-90710  
 EM soliton propagation in nonequilibrium dispersive media (*Russian*) 0-106933  
 energy loss of a modified Korteweg-de Vries solitary wave in a varying medium 0-90683  
 equilibrium turbulence, soliton role as liquid drops (*Russian*) 0-98804  
 evolution equations, symplectic operators and hereditary symmetries 0-82650  
 exchange vortices of magnetisation, micromagnetic bubble domains 0-71138  
 extended objects, quantum statistical mech., correl. functions in one-dimens., kink-bearing systems 0-86204  
 extended particle, quantisation, degeneracy of eigenstates 0-73594  
 extension of nonlinear evolution equations of the K-dV (mK-dV) type to higher orders 0-105508  
 fermionic solitons in gauge theories and their quantum corrections 0-101927  
 ferromagnet, one-dimens., algebraic soliton in mag. field directed along anisotropy axis 0-75785  
 ferromagnetic Heisenberg chain, weakly bound magnon states (*Russian*) 0-100591  
 finite depth stratified fluids, internal wave solitons, infinite depth limit 0-64574  
 flexural EM waves in magnetoactive plasma (*Russian*) 0-83918  
 gravitational fields, stationary, axis-symmetric, soliton solutions 0-73253  
 gravity waves, interfacial and internal long, dissipation, Korteweg-de Vries eqns. 0-90686  
 guided lightwave propag., soliton techniques 0-58760  
 guided solitary waves from Boussinesq eqns. 0-92298  
 Hartree eqn., quasiclassical soliton soln., Newtonian interaction with screening 0-68569  
 head on collisions between two solitary waves 0-87780  
 Heisenberg chain, classical, solitons and magnons 0-60161  
 Heisenberg chain, classical continuous, magnon-soliton phase shift 0-107998  
 Heisenberg continuous chain, quantum solitons as magnon bound states 0-60162  
 Heisenberg one-dimensional magnet, classical, nonlinear dynamics 0-71056  
 higher order Korteweg de Vries eqn., Backlund transform 0-105510  
 higher order modified KdV eqns., bilinearisation 0-105509  
 incommensurate Peierls systems, amplitude solitons, implications for TTF-TCNQ 0-92841  
 incommensurate systems, discrete lattice effects 0-107402  
 integrable nonlinear evolution equation, soliton soln. from inverse scatt. method 0-73186  
 interaction dynamics and nontopological stability in nonlinear model of complex scalar field 0-101719  
 internal solitary waves in stratified flows, cubic and quadratic nonlinearity 0-69856  
 inverse method for solving differential-difference and difference-difference eqns. 0-105513  
 ion acoustic soliton reflection and transmission at plasma interface 0-106899  
 ion acoustic solitons in beam plasma system with nonisothermal electrons generated by ion-beam 0-103151  
 ion acoustic waves, diverging cylindrical, recurrence investigation 0-79474  
 ion sound soliton-Langmuir wave interactions (*Russian*) 0-100077  
 ion-acoustic solitons, two-dimens., interaction 0-106908  
 ion-acoustic solitons with a temperature gradient 0-79490  
 Ising model, modulated phase with solitons, phasons and devil's staircase 0-95044  
 Ising model, nonlinear excitations and coherent states in transverse field 0-68143  
 kink theories, approximately straight 0-82871  
 Korteweg de Vries eqn., second modified, exact multi-soliton soln. 0-73180  
 Korteweg-de Vries eqn., initial value problem, soliton region determ. 0-62490  
 Korteweg-de Vries solitary wave, energy loss 0-62489  
 Korteweg-de Vries soliton solutions, perturbations 0-105511  
 Langmuir waves, numerical modelling of 1-D turbulence, acoustic oscillations effect (*Russian*) 0-103135  
 lattice stability in coupled linear chain system 0-73282  
 Liouville equation, nonlinear solutions and their stability 0-68374  
 liquid crystal, thin layer, symmetry defects and solitons, topological classif. 0-107044  
 liquid film solitons, draining behaviour 0-96272  
 logarithmic Schrödinger equation, soliton dynamics 0-57130  
 long waves in dispersive media, solitary wave interaction 0-59062  
 lower hybrid, envelopes in magnetic fields 0-59224  
 Mach reflection of solitary wave 0-79340  
 magnetised collisionless plasma, oblique Langmuir solitons under free path conditions (*Russian*) 0-79477  
 mode converted lower hybrid solitons, stability in parametric regions 0-92303  
 molecular chain, 1-D electron motion, electron-phonon interaction, acoustic solitons 0-70628  
 monatomic three dimensional FCC lattice, solitary wave effect on shock profile 0-79874



## solitons continued

- multi-soliton solutions of a derivative nonlinear Schrodinger equation 0-105528  
 multi-soliton solutions of nonlinear partial differential eqns. 0-105763  
 multidimensional soliton eqns., N-soliton solns. by Hirota's method 0-105797  
 nonlinear magnetostatic modes and twisting modes with magnetic islands 0-106900  
 nonlinear refraction and self-focusing effects (*Russian*) 0-98805  
 nuclear potential, solitons as model 0-83081  
 oblique collision of ion-acoustic solitons 0-83934  
 ocean, stability of solitary Rossby waves over variable relief, analytical theory 0-101371  
 ocean, stability of solitary Rossby waves over variable relief, numerical expts. 0-101372  
 one-dimensional solitary-wave-bearing scalar fields, statistical mechanics, ideal-gas phenomenology 0-105792  
 one-dimensional spin 1/2 chain, soliton excitation in strong spin-phonon interaction 0-103842  
 optical fibre, soliton pulse prop. 0-58759  
 optical waveguides, nonlinear pulse prop. theory 0-83669  
 overtaking solitons of high energy in a one-dimensional Lennard-Jones chain 0-73182  
 particle stability in nonlinear scalar field theory 0-91004  
 Peierls-Frohlich condensate, attracting solitons and discontinuous lock-in transition 0-92840  
 plasma, caviton, dissipative three-dimens. Langmuir soliton, formation (*Russian*) 0-83943  
 plasma, ion-acoustic holes in a two-electron-temperature plasma 0-59205  
 plasma, nonlinear theory of unstable plane waves and solitons 0-87888  
 plasma Langmuir turbulence, numerical modelling, solitons, nonlinear interactions 0-70030  
 plasma media with inverse dispersion, soliton solns. 0-103152  
 plasma wave propagation, nonlinear Schrodinger equation, modified Zakharov-Shabat inverse scatt. problem 0-59200  
 polyacetylene:AsF<sub>5</sub>, soliton doping mechanism, mag. susceptibility meas. 0-107979  
 polyacetylene, continuum model for solitons 0-65472  
 polyacetylene, lightly doped, phenomenological theory of soliton formation 0-103644  
 polyacetylene, mag. soliton defect ESR study 0-80590  
 polyacetylene, metallic, mixed Peierls phase, Hartree-Fock calcs. 0-70689  
 polyacetylene, soliton formation and cis trans isomerization 0-76505  
 polyacetylene, vibr. excitations of charged solitons 0-108201  
 relaxation times in solid-state theory and one-dimensional molecular systems (*Russian*) 0-100640  
 renormalisation and quantum corrections 0-82884  
 review of concepts and methods in theory (*Polish*) 0-68057  
 Schrodinger nonlinear eqn. three dimensions. stability of solns. 0-57141  
 Schrodinger nonlinear mixed eqn. and soliton solns., inverse method 0-68065  
 self-diffusion via sine-Gordon solitons 0-70443  
 semiconductor, ferromag., polaron solitary waves 0-70625  
 semiconductor, soliton formation and cis trans isomerization 0-99806  
 shallow water solitary waves, shelves and Korteweg-de Vries eqn. 0-92166  
 sine-Gordon chain, classical, low freq. dynamics 0-108020  
 sine-Gordon chain, displacement fluctuations, long-time behaviour and dynamic scaling props. 0-101764  
 sine-Gordon chain, long-term behaviour 0-68051  
 sine-Gordon eqn., inverse method for solving differential-difference and difference-difference eqns. 0-105513  
 sine-Gordon eqn. and Laplacian invariant, separable solns., complex solitons 0-90680  
 sine-Gordon equation, 3 and 4 dimens., exact solns. 0-86091  
 sine-Gordon equation, Backlund transform., physical space-time solitons 0-77629  
 sine-Gordon equation, double, multidimensional multisoliton kink solutions 0-73184  
 sine-Gordon equation, rotationally symmetric breather-like solns. 0-77955  
 sine-Gordon solitons, boundary effects 0-62481  
 sine-Gordon system with winding-number density, low temp. soliton gas phenomenology 0-105589  
 single Langmuir solitons, perturbation anal. 0-69999  
 solids, kinks, solitons, and nonlinear transport 0-65421  
 solitary wave transport, nontrivial example soln., numerical method 0-77971  
 solitary waves, review, book contrib. 0-94962  
 space charge ionising waves, high velocity propagation 0-87889  
 static gravitational solitons, singularities, horizons, field behaviour at infinity (*Russian*) 0-73229  
 stationary connected multisoliton formations, Schrodinger eqn. with nonlocal nonlinearity (*Russian*) 0-57105  
 SU<sub>N</sub>/Z<sub>N</sub> gauge invariant theory, phase factor operators and soliton fields 0-77947  
 thallium hexanoate, soliton conduction, elec. cond. field and temp. depend. anomaly (*Russian*) 0-103703  
 TMMC, antiferromag., nuclear spin-lattice relax. by solitons 0-97159  
 Toda lattice, excitation spectrum, molecular dynamics study 0-105588  
 Toda lattice, generalised eqn., solitons 0-95040  
 Toda lattice, wave behaviour in nonlinear LC equivalent circuit 0-105577  
 transparency, self-induced, perturbed soliton solns., finite relax. time 0-58643  
 transverse instability of breathers in resonant media 0-62485  
 wave functionals, soliton sector and asymptotic vacuum states, Creutz quantisation method 0-68340  
 weak ferromagnet, domain wall dynamics, nonlinear waves, mag. solitons (*Russian*) 0-75793  
 weak ferromagnets, Landau-Lifshitz eqn. solutions, moving domain walls, struct. (*Russian*) 0-100596  
 Z(2) and Z(3) cyclic symmetric vector field theories, 1-dimens. solitons 0-77950  
 CsNiF<sub>3</sub>, anisotropic Heisenberg chain, nonlinear excitations 0-70927  
 CsNiF<sub>3</sub>, low frequency dynamics in external mag. field 0-108020  
 CsNiF<sub>3</sub>, nonlinear excitations, 1D-ferromag., neutron scatt. 0-70949  
 CsNiF<sub>3</sub>, one dimensional planar model with symm. breaking fields, thermodynamics, static props. 0-97111  
 CsNiF<sub>3</sub>, stochastic motion of Sine-Gordon-solitons, spin-correlation function 0-93105  
<sup>3</sup>He, superfluid, A to B phase nucleation 0-100371  
<sup>3</sup>He superfluid A-phase, exptl. studies of solitons 0-88386

## solitons continued

- <sup>4</sup>He, superfluid film, solitons at low temps., Korteweg-de Vries eqn. 0-96717  
 K<sub>2</sub>SeO<sub>4</sub>, elastic props. at commensurate-incommensurate transition, Brillouin scatt. and US study 0-93248  
 Na vapour, soliton interactions, self-induced transparency, numerical plane wave simulations 0-64117  
 SbSI, ferroelec. phase transition and nonlinear props. 0-75988  
 TMMC, antiferromagnetic chain, 3-D ordering temp. controlled by solitons and defects, mag. field depend. 0-60275  
 Ti-Mo (20 at.%), incommensurate struct., stacking soliton 0-107109

## sols

- see also colloids; sedimentation  
 gelatin sol-gel transition, viscosity meas. method 0-85219  
 liquid particles, aerosol and hydrosol, separation by size in thermal fields 0-101044  
 polymers, based on oligodienehydrazides and diepoxides, A-copolymerisation, sol-fraction (*Russian*) 0-58431  
 size distributions, transient electric birefringence 0-85223  
 sol-gel transition, US attenuation meas. 0-101043  
 sol-gel transition kinetics 0-85218  
 AgI hydrosols, kinetics and mechanics of colloid systems formation 0-101045  
 Ag<sub>2</sub>S, red-IR photoluminescence obs. at 77K 0-103982

## solubility

- see also phase equilibrium; solid solubility; solutions  
 alcohols in organic solvents, H<sub>2</sub>O absorption 0-66788  
 alkali halides, solubility press. coeffs. and solvent isotope effect 0-96649  
 alkali metals, liquid, O<sub>2</sub> pot. and O<sub>2</sub> distrib. coeffs. between alkali and struct. metals 0-65231  
 anthraquinone pleochroic dyes in liq. cryst. soln., photostability, appl. to liq. cryst. displays 0-88961  
 benzene, vapour, solubility in polystyrene (*Japanese*) 0-59667  
 cryogenic liquid, of light alkanes, IR spectroscopy obs. 0-59654  
 crystallisation from solution, same complex effects 0-100189  
 4-cyanobenzoxyloxy-4'-pentylstilbene, nematic, smectic A, and orthogonal smectic B phases 0-64890  
 dextran fractions, production, characterisation and solution properties 0-59368  
 disperse systems, solubility increase, phase composition, size effect calcs. 0-70418  
 glass, melt, bubble behaviour during refining, math. model 0-81277  
 glass-forming multicomponent systems, phase behaviour, miscibility, tie lines 0-84294  
 H<sub>2</sub> absorption in thin film hydriding alloys, LaNi<sub>5</sub> and SmCo<sub>5</sub> 0-65238  
 liquid metals, solubility of H rel. to that in solid phase (*Russian*) 0-65222  
 liquid phase elution chromatography for determining solubilities of organic liqs. in H<sub>2</sub>O 0-71958  
 medical polymers, chem. problems, conf., Prague, Czechoslovakia (Aug. 1977) 0-56996  
 metal, liq., of oxygen, electrochem. obs. using solid oxide electrolytes 0-59669  
 metals, gas saturation, apparatus 0-61039  
 9-methylanthracene, solubilisation in water by hypercoiled polymethacrylic acid 0-91591  
 micellar systems, solubilisation 0-89546  
 nitrobenzene/n-hexane (n-heptane), critical exponent  $\beta$ , phase coexistence curve anal., viscosity coeff. meas. 0-100327  
 polymer protonated and deuterated mixtures, partial miscibility 0-107037  
 polyquinazolones containing pendant imide groups, prep. and props. (*Japanese*) 0-104111  
 polysiloxene, irradi., linear, IR and solubility obs. 0-93775  
 polyurethane foams, elastic, stability against organic solvents (*German*) 0-85074  
 rubber, blooming by waxes 0-104109  
 segregation, nonequilibrium, during pulsed laser annealing, model 0-108451  
 steel, microalloyed, types V1599, V1600, V1286, NbCN precipitation in undeformed austenite 0-89230  
 ternary and higher order, activity coeff. of nonmetallic solutes 0-107433  
 trivalent metal phosphates, condensed, synthesis in polyphosphoric acid melts, physicochem. equil. considerations 0-97419  
 wustite solid solutions, miscibility data rationalisation classification of ternary fields and postsaturation reactions 0-79948  
 Ag-Bi-S, ternary phase diagram, DTA and X-ray diffr. investigation 0-84917  
 Al chalcogenate and chalcogenite double salts, form. laws and acid-base props. 0-101070  
 BaTiO<sub>3</sub>:C, solubility of C at low O<sub>2</sub> potentials, 800°C 0-100334  
 CdSnAs<sub>2</sub>, solubility in Sn melt, temp. depend., enthalpy of melting 0-59658  
 Ce-S-O equilibrium in molten Fe (*Chinese*) 0-104423  
 Cu-Ni-Ti system, phase equilibria in Cu rich region and Cu-T quasi-binary constitution (*Japanese*) 0-89203  
 Cu-Pb (Fe), liq. thermodynamic props. (*Polish*) 0-89199  
 Fe, liquid, N solubility depend. on added elements, mechanism (*Russian*) 0-65223  
 Fe-Cr alloy, N solubility investigation (*Russian*) 0-92675  
 Fe-Cr-Ti(Al) liquid alloys, thermodynamical anal. of O<sub>2</sub> solubility (*Russian*) 0-92676  
 Fe-Ti, solubility and diffusivity of H and D in mixed crystal phase, elec. cond. meas. (*German*) 0-107575  
 $\alpha$ -Fe<sub>2</sub>O<sub>3</sub> crystal flux growth, solubility and relative supersaturation in Fe<sub>2</sub>O<sub>3</sub>:PbO-V<sub>2</sub>O<sub>5</sub> fluxed melt system 0-64934  
 Fe<sub>2</sub>O<sub>3</sub> films, DC reactively sputtered, for selectively semitransparent photomasks, struct., mech. and chem. props. 0-59835  
 Ga chalcogenate and chalcogenite double salts, form. laws and acid-base props. 0-101070  
 GaSe, <sup>110</sup>Ag diffusion, temp. depend. and solution (*Russian*) 0-70467  
 GaSe:Sn, <sup>113</sup>Sn diffusion, temp. depend. and Sn solubility (*Russian*) 0-70466  
 GaTe, <sup>110</sup>Ag diffusion, temp. depend. and solution (*Russian*) 0-70467  
 Gd-C-N system, isothermal section at 1200°C, X-ray investigation (*German*) 0-93543  
 H<sub>2</sub> in Nb-V system 0-59808  
 In chalcogenate and chalcogenite double salts, form. laws and acid-base props. 0-101070  
 InP surface decomposition prevention in LPE growth 0-96749



**solubility continued**

- KLa(MoO<sub>4</sub>)<sub>2</sub>, solubility in aq. K<sub>2</sub>MoO<sub>4</sub> solns., hydrothermal conditions 0-96651  
 La-H<sub>2</sub> phase equilibria 0-66492  
 LaNi<sub>5</sub>/H system, thermodynamics of H trapping 0-107444  
 LaNi<sub>5</sub>Al, solubility and sorption props. of H<sub>2</sub>, effect of Al 0-103482  
 Li-LiH system, H isotope solubility thermodynamic singularities 0-81356  
 Li<sub>0.5</sub>Fe<sub>0.5</sub>O<sub>4</sub> Ru substitution effect on struct. and mag. props., and max. solubility determ. 0-75364  
 Mg, H<sub>2</sub> dissolution, resistometric study under press. 0-70417  
 Mg-MgNi<sub>2</sub>-Zn, diagram of state, Zn solubility, initial phase precipitation (Russian) 0-66478  
 NaCl-KCl, molten, alkaline earth oxides solubility products, potentiometric determ. 0-76488  
 NaNO<sub>3</sub>, precipitation from mixed aq. solns. 0-100191  
 Na<sub>2</sub>O-B<sub>2</sub>O<sub>3</sub>-NiO melts, NiO activity and solubility meas. by EMF method (Japanese) 0-92677  
 Na<sub>2</sub>O-P<sub>2</sub>O<sub>5</sub>-SiO<sub>2</sub> glass, metastable liquid immiscibility 0-100331  
 Na<sub>2</sub>O-P<sub>2</sub>O<sub>5</sub>-SiO<sub>2</sub> glass, substitution of Li<sup>+</sup>, Mg<sup>2+</sup>, Sr<sup>2+</sup>, Ba<sup>2+</sup>, Zn<sup>2+</sup> for Na<sup>+</sup> 0-100332  
 Nb-D-H, equilb. H/D separation factors 0-59668  
 Nb<sub>5</sub>S<sub>3</sub> film formation, solubility, precipitating processes (Russian) 0-92792  
 Ni-Co-Al alloys, continuous precip., SEM, TEM, X-ray diffr. study 0-89220  
 Ni-Mo-W, diagram of state, W solubility, dispersion hardening (Russian) 0-66477  
 Ni-Ni<sub>3</sub>B eutectic, high temp. X-ray anal. 0-71639  
 Ni<sub>99</sub>M<sub>1</sub>, M=impurity metal, solubility of H<sub>2</sub>, formation of MH(D)-complexes 0-65236  
 Ni(s, l) + NiO(s) + NiX<sub>2</sub>O<sub>4</sub> (X=Al, Ga), chem. potential and solubility of O<sub>2</sub> 0-92679  
 Pb-Fe(Cu), liq., thermodynamic props. (Polish) 0-89199  
 Pd, of H, lattice defects influence, extended core model 0-88326  
 Pd-D-H, equilb. H/D separation factors 0-59668  
 Pd-H system, solvus hysteresis 0-71659  
 Pd<sub>3</sub>P<sub>1-x</sub>, nonstoichiometric, H<sub>2</sub>(D<sub>2</sub>) solubility 0-59662  
 Se-Ge amorphous films, obliquely deposited, photoinduced chem. changes 0-76385  
 Si, impurity solubility limit after laser induced melting 0-107426  
 Si solubility and transport behaviour of water, dissolution 0-93801  
 SiO<sub>2</sub>, fused, He solubility and diffusion above transform. range 0-79965  
 SiO<sub>2</sub>, three-component glass, liq. phase separation, with two oxide modifiers 0-103250  
 Sm-H, phase equilibria 0-66492  
 Tb-O<sub>2</sub>-H<sub>2</sub>PO<sub>4</sub>-H<sub>2</sub>O system, cpd. form., comp. and props. 0-100832  
 TeO<sub>2</sub>-P<sub>2</sub>O<sub>5</sub> system, glass struct., neutron diffr. study 0-70128  
 Ti-Al-Kh18 steel, O, solubility thermodynamical anal. (Russian) 0-92676  
 TiCr<sub>1-x</sub>, H and D soln., enthalpy, solubility and mol. vibr. determ., comparison with soln. in metals and binary alloys 0-79951  
 Ti<sub>2</sub>Te<sub>3</sub>-Ti<sub>3</sub>SnTe<sub>2</sub>-Ti<sub>3</sub>PbTe<sub>2</sub>, phase equilb., DTA, SPA and microhardness meas. 0-96628  
 UC, miscibility with rare earth nitrides (German) 0-96654  
 V<sub>2</sub>O<sub>5</sub>, amorphous semicond., solubility and fibrous texture 0-75162  
 YAG, melting behaviour and metastability determ. by optical DTA 0-92648  
 YAl<sub>3</sub>(BO<sub>3</sub>)<sub>4</sub> solubility in K<sub>2</sub>Mo<sub>2</sub>O<sub>10</sub> melt 0-65211  
 YAlO<sub>3</sub>, melting behaviour and metastability determ. by optical DTA 0-92648  
 Zn-Bi, liquid, inconsistent conjugated liquidus 0-76232  
 ZnO, glaze, liq. phase separation rel. to cryst. in glassy phase 0-103252  
 ZrO<sub>2</sub>-SiO<sub>2</sub>, liquid immiscibility, microstruct. of plasma dissociated ZrSiO<sub>4</sub> 0-107429

**solute clustering** *see segregation***solution annealing**

- steel, stainless 304 sol. of annealed and thermally-aged, high-cycle fatigue behaviour 0-100923  
 steel, stainless 316, soln. annealed, cavity alignment and precipitation during dual ion bombardment 0-70273  
 Al alloy RR58, low cycle fatigue at 423K, prior treatment effect 0-104254  
 Al-Cu-Mg type 2036, thermomech. treatment, flow stress anal., effect in mech. props. 0-93584  
 Co-Ti-C, secondary precipitation and allotropic transform., TEM obs. 0-108453  
 α-Cu-Al (6 to 17 at.%), short-range order investigated by diffuse X-ray scatt. (Russian) 0-104187  
 Cu-Be, SCC in NH<sub>3</sub> 0-104326  
 Fe-Ni-Cr (35, 15 wt.%) superalloy, stress rupture and tensile props., C and B additions effect (Chinese) 0-104244  
 Ni-Fe-Cr superalloy 718, heat treatment effect on room temp. and elevated temp. fracture toughness response 0-100922  
 β-Ti-Mo-Zr-Sn(11.5, 6, 4.5 wt.%), metastable phase III, microstruct. and age hardening response 0-84945

**solution energy** *see heat of solution***solutions**

- see also critical mixtures; Debye-Huckel theory; heat of solution; liquids; polymer solutions; solid solutions; solvation*  
 alkali metal cation pairs, luminesc. with dichromate anion 0-83409  
 anthraquinone-xanthone liq. soln., upper excited singlet state, delayed fluorescence 0-106345  
 aqueous electrolyte solutions, vel. correls., improved representation 0-59360  
 binary solutions of dense liquids and gases, isothermal eqn. of state calcs. (Russian) 0-88292  
 binary system, distribution coeffs., estimation from Van Laar and Hayes-Chipman relations 0-84293  
 chemical reactions, Brownian dynamics simulation in soln. 0-104422  
 concentration, interconversion during crystn. 0-100773  
 Coulomb systems, equilb. distrib. functions expansion in power of density 0-64681  
 diazonium salts in aqueous solns. and polymer matrices, IR absorpt. spectra 0-76030  
 dibenzylketone, photolysis in micellar soln., quantum yield and <sup>13</sup>C enrichment 0-97711  
 difluoroacetic acid, soln., polarisable H bonds, IR spectrosc. obs. 0-58408  
 p-dioxane-H<sub>2</sub>O at 11 and 25°C, US absorption 0-65171  
 DNA, phase transitions in water-ethanol solns. (Japanese) 0-89709  
 EBBA, mematic, orientational order, effect of hexa-n-alkoxy-triphenylene disc-like solutes 0-79682

**solutions continued**

- electrolyte, electron energy 0-66812  
 electrolyte dipolar hard sphere solvent with charged hard spheres, hypernetted chain approx. 0-61130  
 electrolytes and non-electrolytes, aq. soln., apparent molal isochoric heater capacities at 25°C 0-59671  
 fluidised beds, dehydration of solutions and suspensions, rel. to granulation 0-81373  
 formic acid, soln., polarisable H bonds, IR spectrosc. obs. 0-58408  
 glass, complex raw material, hydrothermal prep. 0-104106  
 hard disc fluid, infinite dilution solute chemical pot. by Monte Carlo simulation 0-88009  
 4-isocyanate-trans-stilbenes, donor substituted, anisotropic fluoresc. in low viscosity solvents (German) 0-93401  
 kinetics of reacting solns., diffusional barrier crossing processes, trajectory simulation 0-81280  
 macromolecular, alternating elec. field light scatt., low angle approx. 0-84721  
 macromolecular, dynamic light scatt. by flexible macromols. in fluctuating elec. field 0-84722  
 macromolecular, rigid ellipsoidal macromols. in cond. soln. at low ionic strength, specific Kerr consts. 0-84718  
 macromolecular, rot. diffusion coeff. calc. method w.r.t. mol. struct., elec. birefringence relax. time data interpret. 0-85331  
 macromolecular, transient elec. birefringence in reversing fields of arbitrary strength and duration 0-84719  
 methanol solution in benzene, dielec. relax. time by RF cond. meas. 0-71302  
 methine dyes, spectral props., solvent effects 0-69181  
 micellar systems, solubilisation 0-89546  
 organic solute rejection by reverse osmosis, regular soln. theory appl. (Japanese) 0-101041  
 β-picoline-water solution, light scatt. spectra, ultra- and hypersonic absorpt. (Russian) 0-93353  
 polymethine dye solutions, photochem. transformations and short-wavelength luminesc. 0-100686  
 pyridine N-oxide, in benzene, dipolar assoc. investig. 0-107035  
 pyridine-water soln., reorientational relax. and activation energy of pyridine, depolarised Rayleigh scattering 0-76037  
 ruthenium trisbipyridyl ions in surfactant solns., excited state decay kinetics 0-83407  
 seawater, dissolved trace metals concs. in Laccadive Sea 0-104997  
 surfactant solutions, aggregation, micelle and microemulsion form. 0-89547  
 ternary solution phases, empirical methods of predicting and representing thermodynamic props. 0-70423  
 tetrabutylammonium iodide, alcoholic soln., repulsion phenomena in thin layers 0-107619  
 trans-Pu solvent extraction recovery and purification by trioctylphosphine oxide chromatography 0-93826  
 trifluoroacetic acid, soln., polarisable H bonds, IR spectrosc. obs. 0-58408  
 trifluoromethanesulphonic acid, and salts, electrochem. characts. in nonaqueous solvents 0-89499  
 trioxane, in nitrobenzene soln., polymerisation, polyoxymethylene morphology 0-59403  
 viologens, electrochromic, for display appl., oxidant impurities elimination 0-78922  
 As(III) and As(V), redox stability in aq. soln. 0-61068  
 BaCl<sub>2</sub> aq. soln., vel. correls., time integral calcs. 0-59360  
 BeF<sub>2</sub>, aqueous solns., mag. and quadrupole relax. 0-71226  
 CaCl<sub>2</sub> aq. soln., vel. correls., time integral calcs. 0-59360  
 CuBr<sub>2</sub>(Cl<sub>2</sub>) aq. soln., structural transition, neutron diffr. study 0-64872  
 CuCl<sub>2</sub>(Br<sub>2</sub>) aq. solns., EXAFS meas. 0-60714  
 CuSO<sub>4</sub>/H<sub>2</sub>SO<sub>4</sub> electrolytes, densities, elec. cond., viscosities 0-107455  
 K isotope separation in solution by thermal diffusion 0-87236  
 LiCl aq. soln., vel. correls., time integral calcs. 0-59360  
 LiCl, concentrated aqueous soln., IR absorpt. to high press. and temps. 0-80803  
 NaCl aq. soln., vel. correls., time integral calcs. 0-59360  
 NaCo(CO)<sub>4</sub>, soln., ion sites, cryptand C221 doping effects 0-70102  
 NaNO<sub>3</sub>, aqueous soln., X-ray diffraction, radial functions and positional correl. 0-79665  
 NaOD solution in D<sub>2</sub>O, collective excitations in liquid and amorphous state, 77 to 300K 0-92636  
 NiCl<sub>2</sub> aq. soln., structural transition, neutron diffr. study 0-64872  
 NiCl<sub>2</sub>(Br<sub>2</sub>) aq. solns., EXAFS meas. 0-60714  
 O<sub>2</sub> singlet in solns., luminesc. duration following pulsed laser excitation 0-76070  
 Rb anions, THF soln., photolysis, appl. to photogalvanic cell 0-85294  
 SiO<sub>2</sub>-water system, inorg. polymer struct. form., globular crystn. 0-101042  
 SrBr<sub>2</sub>, aq. solns., EXAFS meas. 0-60714  
 ZnBr<sub>2</sub>, aq. solns., EXAFS meas. 0-60714  
 ZnCl<sub>2</sub> aq. soln., structural transition, neutron diffr. study 0-64872

**solvated electrons**

- diffusion controlled reactions in polar solvents, reaction parameters 0-97687  
 dimethylsulphide, liq., solvated electrons, optical absorpt. spectrum obs. 0-97250  
 electrolyte solutions, electron energy 0-66812  
 ethanol-d<sub>2</sub>(d<sub>2</sub>), glassy state, solvated electron geometry, electron spin echo modulation obs. 0-66009  
 methylamine liquid, 293K, solvated electron decay kinetics obs., IR spectra 0-71928  
 polar solvent mixtures, solvated electron diffusion, 2-absorber model 0-85206  
 in polar solvents, absorpt. spectra, intrasolvent and intersolvent correls. 0-93840  
 positronium formation inhibition by solvated electron precursor scavenging, line shape Doppler broadening, lifetime spectroscopy 0-93784  
 thiamine (vitamin B<sub>12</sub>), aq. soln., radiation induced reactions 0-93779  
 water, liq., electron solvation dynamics 0-85205

**solvated protons** *see hydroxonium ion***solution**

- see also hydroxonium ion; solvated electrons*  
 acetone, macroscopic model for solvated ion dynamics, cation conductance calcs. 0-65261  
 acetonitrile, macroscopic model for solvated ion dynamics, cation conductance calcs. 0-65261



**solvation continued**

- t-butyl acetate, rot. isomerism, dielect. and Raman spectra 0-106328  
 t-butyl formate, rot. isomerism, dielect. and Raman spectra 0-106328  
 chlorophyll, and related mols., in solid solns., fine-structured vibronic spectra under tunable dye laser excitation (*Russian*) 0-74164  
 chlorophyll-a, hydration, field desorpt. mass spectral obs. 0-71936  
 dense fluids, solvation forces between two solids 0-64855  
 ethanol, electron solvation, ps laser study 0-101032  
 glass fibre reinforced cement, durability in wet and dry conditions, fibre length and content effect 0-71726  
 glasses, electron scavenging, hopping controlled time-depend. reaction rates 0-108723  
 hydrides, aq. dissoc., solvation, MINDO/S calcs. solvation theory 0-97708  
 methanol, electron solvation, ps laser study 0-101032  
 methyl cyanide-water (methanol), Ag<sup>+</sup> ion solvation,  $\gamma$ -irrad., ESR obs. 0-97726  
 nucleic acids, bases and base pairs, water struct. in soln., Monte Carlo simulation 0-76709  
 Ornstein-Zernike and Percus-Yevick temperature dependent fluids, solvation forces 0-64862  
 Portland cement, absorbed H<sub>2</sub>O, pulsed NMR study 0-84665  
 postionium formation, inhibition processes, role of solvation properties of solvents 0-93786  
 pyridine, macroscopic model for solvated ion dynamics, cation conductance calcs. 0-65261  
 rare earth chlorides, glass transition temp. meas., inner-sphere coordination number change effect on soln. props. 0-83239  
 rare earth perchlorates, glass transition temp. meas., inner-sphere coordination number change effect on soln. props. 0-83239  
 serine, neutral and zwitterion, water solvation, Monte Carlo simulation 0-76707  
 solutions in alcohols, ultrasonic vel. and density meas. used to calc. compressibility, intermol. free length and solvation no. 0-96150  
 surfactant micelles, hydration 0-89518  
 tetracyanoethylene in acetone-d<sub>6</sub>, anion solvation, electron spin echo modulation 0-63676  
 tetracyanoethylene in dimethylsulphoxide-d<sub>6</sub>, anion solvation, electron spin echo modulation 0-63676  
 tetracyanoethylene in methanol-d<sub>3</sub>(d<sub>1</sub>), anion solvation, electron spin echo modulation 0-63676  
 thiourea, struct., hydration, ab initio SCF calcs. 0-58142  
 Ag atom solvation in methanol, geometrical model, electron spin-echo modulation obs. 0-63682  
 CsCl, activation coefficients and solvation numbers in mixed methanol solvents 0-81334  
 EuCl<sub>3</sub>, coord. in aq. Cl<sup>-</sup> soln., X-ray diffr. obs. 0-92445  
 KBr, activation coefficients and solvation numbers in mixed methanol solvents 0-81334  
 KCl, activation coefficients and solvation numbers in mixed methanol solvents 0-81334  
 KNO<sub>3</sub>, activation coefficients and solvation numbers in mixed methanol solvents 0-81334  
 NH<sub>4</sub>Cl, activation coefficients and solvation numbers in mixed methanol solvents 0-81334  
 NO<sub>2</sub><sup>-</sup> (HNO<sub>3</sub>), clusters, form. studied by mass spectrometer, thermodynamic functions, sol. struct., 0-95754  
 NaCl, activation coefficients and solvation numbers in mixed methanol solvents 0-81334  
 R<sup>3+</sup> ions, coord. in aq. Cl<sup>-</sup> soln., X-ray diffr. obs. 0-92445  
 SmCl<sub>3</sub>, coord. in aq. Cl<sup>-</sup> soln., X-ray diffr. obs. 0-92445

**solvent effects**

- anthracene derivatives in solution, polarisability and dipole moments, emission and absorpt. spectra obs. 0-69256  
 $\beta$ -carotene, excitation profile of  $\nu_2$  line in resonance Raman spectrum, solvent effects 0-74173  
 cellulose acetate, solvent effect on lyotropic mesomorphism 0-70121  
 chain molecule, influence of solvent struct. on conformations 0-91700  
 chlorophyll, and related mols., in solid solns., fine-structured vibronic spectra under tunable dye laser excitation (*Russian*) 0-74164  
 chloroquinolines, photophys. behaviour, substituent and solvent effects 0-106342  
 cholinesterase-acetylcholine soln., anion-cation site interactions, solvent effects on aggregate stability 0-61070  
 Coordination equilibria in non-aqueous solvents. I 0-66860  
 coumarin laser dyes, fluoresc. quantum yields and lifetimes, polar solvent effects 0-87054  
 coumarin laser dyes, solvent effects on photophysical parameters 0-91598  
 p-cyano-N,N-dimethylaniline in polar solvents, double fluorescence, theoretical model 0-58296  
 4-cyanobiphenyl and 4'-alkyl- or 4'-alkoxy-substituted liq. cryst. derivatives, soln., absorpt. and fluoresc. spectra 0-87164  
 cyanomethane-d<sub>0</sub>-d<sub>3</sub>, soln., for IR spectra, band shape and moment anal. 0-8252  
 cyclohexane-d<sub>12</sub>, Raman linewidth and molecular diameter meas. 0-69153  
 dichloromethane-d<sub>0</sub>-d<sub>2</sub>, soln., far IR spectra, band shapes and moment anal. 0-58252  
 1,6-diphenylhexatriene, radiationless transitions and natural lifetimes, solvent effects 0-63622  
 diquinolyl cyanomethane, fluoresc. quantum yields, viscosity effects 0-60646  
 divalent transition metal halides, Coordination equilibria in non-aqueous solvents. I 0-66860  
 electrostatic interactions in liquid state, effect on frontier orbitals and chem. reactivity 0-84046  
 ethyl-furan-2-carboxylate, skeletal vibr. of IR spectra, conformational props., solvent polarity effect 0-87118  
 halobenzenes, in potassium laurate mesophase, NMR, proton distance ratios and order tensor elements calcs. 0-63672  
 hydrides, aq. dissoc., solvation, MINDO/S calcs. solvation theory 0-97708  
 iodide, charge transfer to solvent spectra, spectral shift data, Madelung const. determ. 0-85204  
 liquid crystal nematic to isotropic transition, effect of quasispherical and chainlike solutes 0-65202  
 methine dyes, spectral props., solvent effects 0-69181  
 methyl furan-2-carboxylate, skeletal vibr. of IR spectra, conformational props., solvent polarity effect 0-87118

**solvent effects continued**

- methyl furan-2-thiolcarboxylate, skeletal vibr. of IR spectra, conformational props., solvent polarity effect 0-87118  
 multinuclear magnetic resonance spectroscopy, universal referencing, solvent effects 0-73402  
 organic molecules, C-H Raman stretching bands in soln., vibr. freqs. and linewidth 0-78622  
 oscillatory forces between two solid surfaces arising from struct. in intervening liquid, meas. 0-70521  
 phenyl acetylene, liq., phase relax., vibr. dephasing, Raman spectra obs. 0-91567  
 poly- $\gamma$ -benzyl-L(D)-glutamate, soln., liq. cryst. and pretransitional regions, optical rot. 0-66145  
 poly-L-ornithine solution, <sup>15</sup>N NMR, coil-helix transition, solvent effects and pH depend. 0-74275  
 polybutadiene, dil. soln., viscosity, temp. depend., solvent effects 0-59686  
 polydimethyl siloxane-b-styrene-b-dimethyl siloxane block copolymer, morphology, mech. props. 0-64930  
 polymer chains,  $\theta$ -domain, tritric. props. in poor solvent 0-103450  
 polymer solution, diffusion of a chain, conc. effects 0-70103  
 polystyrene, in solns., intrinsic viscosity rel. to mol. wt., unperturbed dimensions 0-65268  
 polystyrene, solns., sedimentation behaviour, branching effects determ. 0-66887  
 propionitrile-hydrocarbon systems, critical solns., Kerr electrooptical Kerr effect meas. 0-100645  
 protoporphyrin IX, triplet states, flash photolysis, obs. 0-95555  
 protoporphyrin IX dimethyl ester, triplet states, flash photolysis, obs. 0-95555  
 radiative transitions, proximity effects, role of vibronic coupling and static crystal field interactions model 0-69126  
 Schulze-Hardy rule, theory 0-89540  
 trichloromethane-d<sub>0</sub>-d<sub>1</sub>, soln., far IR spectra, band shape and moment anal. 0-8252  
 Br<sub>2</sub> in Ar, solvent effects on equilibrium props. 0-61128  
 Fe<sup>2+</sup> and Fe<sup>3+</sup> hydrate clusters, aq. electron exchange reaction, ab initio RHF MO calc. of inner shell reorganisations, vibr. freq. 0-102564  
<sup>123</sup>I<sub>2</sub>, frozen soln. in o- or p-xylene, Mossbauer effect obs. 0-78637  
 I<sub>2</sub>-quinoline (pyridine) complexes, stability const. determ. by spectrophotometric methods 0-87056  
 Ir(III) complex, cis-dichlorobis(4,4'-dimethyl 2,2'-bipyridine) iridium chloride 0-97319  
 N<sub>2</sub>, liquid, in Kr, methane, and CO, Raman scatt. parameters, high-resolution coherent active spectroscopy 0-66207  
 Pt phthalocyanine, reson. Raman excitation profiles, solvent effects 0-102512

**sonar**

- see also *bioacoustics*; *navigation*; *underwater sound*  
 acoustic Doppler sodar, appl. to atmospheric temp. fluctuations heat flux and struct. functions meas. 0-105023  
 acoustical tracking, ocean current profiling 0-67427  
 air pollution meteorology, use of sodar acoustic echo sounder, low level stability and wind velocity monitors 0-108828  
 array paired element delay meas. with sequential state estimation 0-96128  
 atmosphere acoustic and radio acoustic exploration, effects of sound non-linear absorpt. (*Russian*) 0-94567  
 backscattering cross-sections of live fish, probability density function and aspect 0-64260  
 beamformer, serial phase shift, using charge transfer devices 0-96078  
 beamforming when the sound velocity is not precisely known 0-96123  
 digital beam forming 0-91950  
 holographic piezoelectric integrated acoustic array, system anal. 0-79067  
 identifiable sound source location from time differences of arrival 0-91951  
 interference to propag. by marine organisms, review 0-64269  
 meteorology, sodar appl. to weather analysis and local forecasting 0-85713  
 moving target indicator, removal of periodic waves from reflecting signals 0-69585  
 multisignal time difference estimator for transient sound source location 0-96127  
 ocean-bottom subsurface layered media, spatial parameter estimation 0-71734  
 passive, directional transducer arrays appl., underwater location of acoustic sources (*Spanish*) 0-69586  
 passive, errors in range and bearing estimation 0-79030  
 passive, prediction of post-detection data load 0-96125  
 sea surface inhomogeneities sensing via sound scatt., phase function shape in shadowing conditions (*Russian*) 0-94530  
 sediment refraction of sound, importance for sonar studies 0-81902  
 synthetic-aperture sonar systems in turbulent medium 0-96080  
 target recognition expt., comments 0-58866  
 time delay estimation, cross-correl. and smoothed coherence transform methods compared 0-96086  
 tracking of slowly sinking floats, meas. vertical profiles of oceanic current and Richardson number 0-67378

**sonic boom** see *shock waves***sonic propagation** see *acoustic wave propagation***sonoluminescence**

- bulk solution temperature effect on sonoluminescence intensity 0-76090  
 fluid, radio band pulse radiation due to spark initiated cavity dynamics, sonoluminescence (*Russian*) 0-66313  
 Ar saturated solutions, NO<sub>2</sub><sup>-</sup> effects on spectral distribution and intensity of sonoluminescence 0-76091  
 CdS, single crystals, US luminesc. obs. 0-76092  
 N<sub>2</sub> cryogenic liq., laser sonoluminesc., at elevated hydrostatic press. 0-71498

**Soret effect** see *thermal diffusion in liquids***sorption**

- see also *adsorption*; *chemisorption*; *desorption*; *surface diffusion*  
 contact film absorption on plastic deform. of contacting bodies (*Russian*) 0-93596  
 cryosorption pumping of He by charcoal, cryopump design for fusion reactor 0-105654  
 electron irradiation effects on surface prop. of solids 0-70261  
 gelatin layer, dry, aqueous soln. penetration 0-85221  
 glass fibre reinforced plastics, exposed to liq. media, dynamic high-speed Young's modulus determ. (*German*) 0-85123

**sorption continued**

heterogeneous catalysis, conference, Varna, Bulgaria (Oct. 1979) 0-82578  
 hydrous mixed oxides, sorption props. 0-92781  
 interfacial tension minima, dynamic, equilibration of surface-active solute between two liquid phases 0-80026  
 Invar, absorption of  $H_2$ , mag. props. effects 0-65787  
 laminates, exposed to liq. media, dynamic high-speed Young's modulus determ. (German) 0-85123  
 metal surface, sticking rate, transmission problem, model Hamiltonian 0-107640  
 metal-H system, multiplateau absorpt. isotherms, theory 0-103564  
 metals, gas saturation, apparatus 0-61039  
 molecules, physisorbed on homogeneous surfaces, NMR study 0-97732  
 nitrosamine, air sampling sorbents testing 0-77026  
 piezoelectric quartz cryst. microbalance for sorption studies under dynamic conditions 0-73323  
 Polimal 109, polymer resin laminate, density porosity, water vapour diffusion sorption and permeation (Polish) 0-59665  
 polyester film, cross-linked, low-mol. wt. substance sorption effect on struct. (Russian) 0-59405  
 polyester-E glass composites, types SMC-25, SMC-65 and SMC-30EA, moisture absorpt. 0-93799  
 polyethylene, environmental stress cracking correl. with liq. sorption for low-swelling liqs. 0-81165  
 polymers, water absorption, osmotic effects 0-65366  
 Portland cement, absorbed  $H_2O$ , pulsed NMR study 0-84665  
 Potts model, critical dynamics 0-101766  
 radioactive waste storage Sr, Cs, Co sorption meas. on soil sediment 0-95482  
 rare earth alloys,  $RM_x$  ( $R=La, Ce, Pr, Er, M=Co, Ni$ ),  $H(D)$  sorption at press. up to 1500 atm. 0-97819  
 stearic acid films, evaporated, vac. effects 0-97435  
 steel, hydrogen absorption, anilines surfactants effectiveness, HCl conc. effect 0-108638  
 surface reactions, kinetics and dynamics, conf., La Jolla, CA, USA (Aug 1979) 0-105415  
 transition metal ferrocyanide selective sorbents for alkali metals, sorptive props. w.r.t. struct. 0-101051  
 transition metal intermetallic cpds., H absorption and mag. props. 0-60224  
 zsolite, hydrated Na-Y,  $^{23}Na$  pulsed NMR free induction decay 0-84660  
 $^{239}Pu(V)$  in alkaline freshwater pond, determ. by coprecipitation technique 0-71988  
 Ag, of pyridine, surface enhanced Raman scatt., mol.-surface separation depend. 0-92775  
 Al, reaction with  $H_2$ , influence of surface reactions on rate (Russian) 0-66863  
 $\beta''-Al_2O_3 \cdot Na_2O$ , absorbed water effect on NMR lineshape and spin-lattice relax. time 0-108098  
 $CO_2$  absorption in  $H_2O$ , aq. solns. with interfacial turbulence due to microstirrers 0-64527  
 Ce, gettering of H, mass spectrometry and microgravimetry study, rel. to HTGR gas purification 0-73374  
 Ce-M intermetallic cpds.,  $M=3d$  transition metal, of  $H_2$ , structural charges 0-88429  
 Cs, in nuclear graphite, sorption kinetics modelling 0-102244  
 Cs sorption in Ba-impregnated nuclear graphite, thermodynamic modelling of multicomponent sorption behaviour 0-102243  
 $D_2$ , sticking and accommodation on low-temp. substrate, mol. beam expts. 0-84368  
 Fe-Ti, magnetism and  $H_2$  storage 0-70941  
 FeTi, surface and mag. props., heat treatment and hydrogenation effects 0-75447  
 $H^+$ , energetic beam direct cryosorption pumping 0-105655  
 $H_2$ , sticking and accommodation on low-temp. substrate, mol. beam expts. 0-84368  
 $HfV_2H_{2.1}$ , proton NMR relax. time and Knight shifts, diffusional activation energies meas., sorption props. 0-75871  
 $La_2Co_7$ , mag. props. changes upon  $H_2$  absorpt. 0-71270  
 $La_{0.9}Eu_{0.1}Ni_{1.4}Mn_{0.4}$ , absorption-desorption props. of  $H_2$ , degradation mechanism, Mossbauer study 0-88431  
 $LaNi_5$ ,  $H_2$  absorption in thin film hydriding alloys 0-65238  
 $LaNi_5$ , magnetism and  $H_2$  storage 0-70941  
 $LaNi_5$ , of  $H_2$ , kinetics (Chinese) 0-103561  
 $LaNi_4Al$ , solubility and sorption props. of  $H_2$ , effect of Al 0-103482  
 $LaNi_4B_{0.6}$ ,  $H_2$  absorpt. props. 0-88432  
 $LuFe_2$ , mag. props. changes upon  $H_2$  absorpt. 0-71270  
 $Mg_2Ni$ , magnetism and  $H_2$  storage 0-70941  
 Mn film, vacuum-evaporated,  $H(D)$  uptake kinetics and energetics 0-88430  
 $Na_3AlF_6$  film on Si, fused quartz substrates, absorption of  $H_2O$ , IR anal. 0-75446  
 $Na_2O \cdot B_2O_3 \cdot SiO_2$ , optical waveguide glass, molar absorptivity of water 0-80066  
 Nb-V system,  $H_2$  absorpt. 0-59808  
 Pd membrane, H atom interaction, superpermeability 0-81365  
 Pd membrane, of  $H_2$ , adhesion and penetration probabilities, extreme values 0-101040  
 Pd-D, crystallite size effects, simultaneous sorption and X-ray study 0-65237  
 Re-O-Cl system, gas-transition metal interaction, kinetic model (French) 0-108740  
 $SmCo_5$ ,  $H_2$  absorption in thin film hydriding alloys 0-65238  
 $ThCo_3(Ni_3)$ , effect of absorbed  $H_2$  on mag. behaviour 0-60184  
 Ti, gettering of H, mass spectrometry and microgravimetry study, rel. to HTGR gas purification 0-73374  
 Ti thin films, H absorption and desorption, Tokamak gettering, Auger electron spectrosc. 0-75092  
 $TiCo_{1-x}M_n$ , H absorption-desorption characteristics 0-96735  
 $TiO_2$ , nonstoichiometric anodic films, O incorporation kinetics 0-97733  
 W, of Ne, He, tangential momentum accommodation coeff. meas. by acoustic vel. and absorpt. obs. 0-66867  
 Y, of T, recovery from liq. Li fusion reactor blanket 0-95434  
 Y-M intermetallic cpds.,  $M=3d$  transition metal, of  $H_2$ , structural charges 0-88429  
 ZnS film on Si, fused quartz substrates, absorption of  $H_2O$ , IR anal. 0-75446  
 Zr, gettering of H, mass spectrometry and microgravimetry study, rel. to HTGR gas purification 0-73374

**sorption continued**

Zr pseudo-binary alloys,  $Zr(A_xB_{1-x})_2$  ( $A=V, Cr, Mn; B=Fe, Co$ ),  $H_2$  absorpt. capacity 0-88433  
 Zr-3d Laves phase binary and pseudobinary intermetallics, mag. props. H absorpt. effect 0-88821  
 $ZrMn_2H_x$ , proton NMR relax. time and Knight shifts, diffusional activation energies meas., sorption props. 0-75871  
 $Zr(V_{1-x}Co_x)_2$ , of  $H_2$ , relation between electronic struct. and  $H_2$  storing props. 0-76662  
**SOS integrated circuits** see field effect integrated circuits  
**sound** see acoustic waves; acoustics  
**sound amplification** see acoustic wave amplification  
**sound broadcasting** see radio broadcasting  
**sound field** see acoustic field  
**sound generators** see acoustic generators  
**sound intensity** see acoustic intensity  
**sound measurement** see acoustic variables measurement  
**sound propagation** see acoustic wave propagation  
**sound ranging** see sonar  
**sound reproduction**  
 see also audio acoustics; audio recording; pick-ups  
 accuracy of reproduction determ., w.r.t. ear props. (German) 0-106703  
 artificial head stereophony, tone meas. (German) 0-106702  
 artificial head system, transmission errors causes and improvements (German) 0-106700  
 artificial heads with stereophonic intensity signals, directional effects (German) 0-106701  
 hearing and pain thresholds, cassette recorder noise and music levels (German) 0-81616  
 high fidelity, components and characts. 0-77582  
 impulsive noise reduction on gramophone records 0-87689  
 lip synchronised recording technique for speech translation in cinefilms (Russian) 0-105737  
 loudspeaker design for domestic appls. (Italian) 0-91960  
 motion picture sound track, freq. distortion and two dimens. sound record scatt. (Russian) 0-95175  
 Pfleiderer principle, Hi-Fi music reproduction (German) 0-87685  
 room acoustic effects transmission, uniplanar and biplanar eidophony (German) 0-106699  
**sound waves** see acoustic waves  
**space charge**  
 see also limited space charge accumulation; space-charge-limited conduction; space-charge limited devices  
 air, rod-to-plane gap, impulse voltage meas. (Japanese) 0-87970  
 benzene cation+benzene, fragment ions trapped in electron space charge 0-89470  
 breakdown wave propagation in ionised gas in nanosecond discharges 0-87890  
 carrier traps in polymeric insulating materials, investigation by X-ray induced thermally stimulated current and thermoluminescence methods 0-93240  
 corona, AC, obs. at 50 Hz, DC electric field influence (German) 0-70052  
 corona AC, point-plate arrangement, behaviour near threshold voltage obs. (German) 0-70051  
 dielectric liquid, elec. stressed, motion due to Coulomb, electromech. forces, schlieren image obs. 0-100037  
 dielectrics, field induced thermally stimulated polarisation-depolarisation currents, relaxation, book contribution 0-80687  
 double injection p-n structures in magnetic field 0-107899  
 electric field, variable space charge density, design, between hyperboloidal conic electrode and grounded plate (Czech) 0-87258  
 electro-optic crystals, hologram formation arbitrary transport length anal., photovoltaic effects 0-78802  
 electrographic development, electrostatic calc. 0-77888  
 electron beam broadening effects caused by discreteness of space charge 0-69309  
 electron plasma relax. characts., 3-30 eV 0-79612  
 electrostatic ion analysers for laser prod. plasma detection, space charge effects 0-96392  
 III-V semiconductor based layered multielectronic systems, electronic process investig. survey (Russian) 0-107891  
 ionising waves in plasma, high velocity propagation 0-87889  
 liquid dielectric, Sumoto effect under transient conditions 0-97198  
 MBBA, positive space charge influence on texture, domain form. factor, polarised light study 0-88037  
 MIM systems, TSC, space-charge layer model 0-93009  
 MOS structure, space charge layer physics 0-92980  
 nonlinear free electron laser dynamics with space charge and wiggler effects 0-58500  
 orbitron device, optimum injection condition for electrons, influence of end effects 0-82784  
 p-n heterojunction differential admittance theory in the presence of surface electron states 0-96981  
 p-n junction, diffused, space-charge recombination current 0-88623  
 plasma waves in straight-line electron beam, collective accel. of ions 0-103166  
 polycarbonate films, high temp. relaxations 0-97187  
 polyethylene, space-charge storage under high DC voltage condition, TSC meas. (German) 0-75576  
 polymer, dielec. breakdown theories, mol. and morphological features rel. to elec. strength, review (Japanese) 0-60501  
 polymethine semiconducting films, surface photovoltaic 0-70857  
 positive ion beam dynamic decompensation in absence of mag. field (Russian) 0-106993  
 quadrupole ion store, spatial distribution of ions derived by phase space anal. 0-95185  
 QUISTOR, space charge and ion stability 0-86487  
 relativistic electron beam, inhomogeneous, space charge oscils. 0-78759  
 relativistic free-electron wave generators, electrically pumped 0-91742  
 semiconductor, energy relaxation of photoexcited hot electrons in near-surface region 0-92928  
 semiconductor, phonon induced hopping between Stark levels 0-92900  
 semiconductor, space charge region thickness, deep level props., determ. by  $\gamma$ -ray absorpt. 0-59995  
 semiconductor step p-h junction, elec. struct., analytical methods, review 0-100507  
 semiconductor surface and adsorbate states, charge injection into space charge layers 0-100496



## space charge continued

- semiconductor surface space charge layers, subband struct., perturbation theory 0-84497  
 semiconductor with arbitrary energy spectrum of trapped states, surface region of space charge 0-107811  
 semiconductor-electrolyte junction photovoltaic cells, interface charge transfer, recombination rate, C-V characts. 0-70818  
 semiconductors, deep level carrier trapping and emission, transient spectroscopy, book contribution 0-80216  
 SF<sub>6</sub> discharge inception voltage affected by avalanche growth space charge (*German*) 0-75109  
 swarm in fluid, transient currents 0-106869  
 tetraode system, two-dimens., algorithm for solving space-charge problems with thermally-emitted electrons 0-100743  
 thermally degenerated Schottky diodes, resonant tunnelling 0-100503  
 triode and diode guns, electron optics numerical determ. of beam profile 0-106435  
 very thin films, tunnelling currents, temp. and space charge effects 0-70799  
 AgBr emulsion grains, edge length dependence of ionic conductivity 0-88360  
 AgCl, ionic space charge and dissolution 0-107431  
 Al<sub>x</sub>Ga<sub>1-x</sub>As, electron mobility illumination, compensation, space charge regions, carrier scatt. 0-70691  
 Al<sub>2</sub>O<sub>3</sub> polycrystalline, effects of space charge, grain-boundary segregation and mobility differences on conductivity 0-79979  
 BeO, field-assisted thermally stimulated exoelectron emission 0-100761  
 Bi, liquid, field ion source emission characts. 0-74059  
 CdF<sub>2</sub>, electrical transport limitation by electrodes, polarisation effects 0-96689  
 CdS, quasimonopolar semicond., recombination in near surface space charge region (*Russian*) 0-88574  
 Cu<sub>2</sub>S-CdS heterojunction solar cells, carrier transport, nonmonotonic band profiles 0-61361  
 Ga, liquid, field ion source emission characts. 0-74059  
 Ga liquid metal field emission ion source, characts. 0-108326  
 GaAs, chemisorption of Li, charge injection into space charge layers 0-100496  
 GaAs, electron mobility illumination, compensation, space charge regions, carrier scatt. 0-70691  
 GaAs MOS structures, leakage current for anodic oxide layers, space charge trapping effects 0-60091  
 Gd<sub>2</sub>O<sub>3</sub>, B-type monoclinic, DC(AC) elec. cond., thermoelectric power, dielectric const., temp. depends. 0-59980  
 Ge-Au eutectic alloys, field ion sources 0-97414  
 n-InP, compensated, elec. props., space-charge effects 0-65569  
 InSb n<sup>+</sup>-p junctions, photocurrent spectrum near long wavelength edge of fundamental absorption band 0-100483  
 (Li<sub>1/2</sub>B<sub>1/2</sub>O)<sub>1-x</sub>(WO<sub>3</sub>), dipolar glass, space charge injection, thermally stimulated depolarisation currents 0-66103  
 α-Li<sub>2</sub>O<sub>3</sub>, defects decorated by space charge, X-ray topography study (*Chinese*) 0-107204  
 LiNbO<sub>3</sub>, hologram storage depend. on envelope field, space charge field 0-78801  
 LiNbO<sub>3</sub>-gap coupled Schottky diode memory correlator, grating coupled optical imaging 0-64143  
 MgO crystals, dipolar defects, thermally stimulated depolarisation 0-66101  
 N<sub>2</sub>-methane, rapidly developing discharge, streak camera records interpretation 0-59280  
 NaZnGeO<sub>4</sub>-Mn, electrolum., ionisation domains 0-84787  
 PLZT ceramic, visible light scatt. depend. on photorefractive space charge fields 0-80806  
 PMMA, resonance size effect in space charge relaxation 0-75937  
 PbI<sub>2</sub>, dielectric props., elec. cond., space charge polarisation 0-100631  
 PbS-Si heterojunction, space charge capacitance, PbSn film thickness depend. 0-88630  
 Pb(Zr,Ti)O<sub>2</sub> ceramic, surface barrier electroneffectance, hysteresis, ageing 0-80752  
 Pt-Si thermally degenerated Schottky diodes, resonant tunnelling 0-100503  
 SF<sub>6</sub> and SF<sub>6</sub>-air mixture gas under impulse voltage, discharge phenomena (*Japanese*) 0-96409  
 Si photodiode, avalanche, n<sup>+</sup>prp<sup>+</sup>-type, primary photocurrent anal. by noise measurements (*French*) 0-88624  
 Si, photovoltaic and photomagnetic effects, rel. to intervalley electron transfer 0-60034  
 Si-Au eutectic alloys, field ion sources 0-97414  
 Si-SiO<sub>2</sub>-Al, internal photoemission, pot. barrier height determ. 0-65699  
 Sm<sub>2</sub>O<sub>3</sub>, B-type monoclinic, DC(AC) elec. cond., thermoelectric power, dielectric const., temp. depends. 0-59980  
 Sr<sub>1-x</sub>Ba<sub>x</sub>Nb<sub>2</sub>O<sub>6</sub>, photorefractive in space charge field, phase transitions 0-97229  
 Tb<sub>2</sub>O<sub>3</sub>, B-type monoclinic, DC(AC) elec. cond., thermoelectric power, dielectric const., temp. depends. 0-59980  
 W-EuS, amorphous, memory effect in field emission 0-89126  
 XeF<sub>4</sub> seeded mol. beam, transverse ionisation, space charge, mass spectra and vel. 0-78725

## space-charge-limited conduction

- see also limited space charge accumulation*  
 bulk trap energetic distribution props., space charge limited current meas. use 0-80293  
 concentric spheres, space-charge-flow theory 0-75573  
 current-voltage characts., steady state, validity of anal. eqns. 0-107800  
 gas, low density, space charge limited current flow 0-79605  
 high field conduction in solids, effect of collision ionisation space charge 0-84469  
 insulating particles in insulating liquids, high-field electrophoresis, basic transport mechs. 0-93767  
 MIM struct., space charge controlled cond., transport eqns. 0-97002  
 naphthalene, electron trapping, one-carrier TSC and SCL currents 0-70715  
 perspex, electric conduction and isothermal dielectric relax. 0-80285  
 phthalocyanine metal free films, TSC, ferroelectric-semiconductor transition 0-66105  
 As<sub>2</sub>Se<sub>3</sub> glassy films, current-voltage characts., temp. depend., SCL current 0-92902  
 BN films, humidity sensitive elec. props. and switching characts. 0-107938  
 Cu<sub>2</sub>S-CdS solar cells, SCL current 0-76634

## space-charge-limited conduction continued

- GaAs, DC biased, filamentation of laser radiation 0-74428  
 Sb<sub>2</sub>S<sub>3</sub> film, coevaporated, elec. cond. meas. 0-65726  
 Se powder compacts, sintered, electrical cond. 0-70693  
 SiO<sub>2</sub> MOS capacitor, defect current obs. 0-92987  
 SnO<sub>2</sub>-copper phthalocyanine-Ag systems, elec. and electroluminescent behaviour 0-80864  
 Tm<sub>2</sub>O<sub>3</sub> film, between Al electrodes, prep. and elec. props. 0-60103
- space-charge limited devices**  
*see also limited space charge accumulation*  
 junction lasers, transport phenomena, junction effects and devices, book 0-98766
- space-charge limited solid state diodes** *see space-charge limited devices*  
**space-charge limited solid state triodes** *see space-charge limited devices*
- space communication links**  
*see also satellite links; space vehicles; telemetering*  
 interstellar travel and communication, bibliography 0-101677  
 Voyager project, microwave communications from outer planets 0-77263
- space groups**  
*see also crystal atomic structure*  
 43m symmetry geometric units, cryst. structs. 0-107087  
 cholesteryl ethyl carbonate, unit-cell dimensions and space group 0-84165  
 commensurate-incommensurate transitions, conical points, Lifschitz invariants and superspace group characterisation 0-70367  
 continuous crystalline transitions, counterexample to maximal subgroup rule 0-59428  
 extended unit cell-contracted Brillouin zone model, group-theoretical anal. 0-107093  
 incommensurate crystal phases, symmetry, superspace-group approach, commensurate basic structs. 0-79726  
 incommensurate crystal phases symmetry, incommensurate basic struct., superspace group approach 0-79727  
 independent tensor components enumeration method for trigonal and hexagonal point groups 0-79730  
 magnetic space groups, Clebsch-Gordan coeff. calcs. 0-79731  
 magnetic structure, neutron diffr. study, symm. anal., polarisation effects 0-93083  
 P1 group, and its subgroups, reticular conservation (*French*) 0-107086  
 P2 space group, compensation of excess intensity 0-107088  
 Patterson method, multiple solutions for low symm. systems (*Chinese*) 0-87986  
 thiourea, incommensurate phase, soft modes, condensation of even-order harmonics 0-103313  
 wreath groups, symm. of crystals with struct. distortions 0-75196  
 γ-AlOOH and γ-AlOOD, IR and Raman spectra obs., struct. and D<sub>2h</sub><sup>17</sup> space group anal. 0-89000  
 LaNbO<sub>4</sub>, space group determ. using convergent beam electron diffr. 0-79723  
 La<sub>2</sub>S<sub>4</sub>(Se<sub>4</sub>), structural transitions, symm. anal. 0-92671  
 MnF<sub>2</sub> antiferromag., mag. space groups, Clebsch-Gordan coeff. calcs. 0-79731  
 NdNbO<sub>4</sub>, space group determ. using convergent beam electron diffr. 0-79723  
 TiSe type crystals, possible second-order phase transitions, group-theoretical anal. 0-92672  
 U<sub>10</sub>Co<sub>5</sub>Si<sub>13</sub>, crystal struct., dimensions, space group and coord. (*Russian*) 0-88085
- space heating**  
 domestic, heat pump appls. (*German*) 0-94099  
 domestic, mass spectrometer leak detection probe with He-permeable membrane 0-98994  
 energy roof, solar energy utilisation and heat recovery (*German*) 0-61285  
 fossil fuel heat pumps for domestic, commercial and industrial space heating 0-89666  
 geothermal, coaxial well for space heating and cooling 0-66933  
 geothermal energy, utilisation for thermal and electric energy, geochem. engineering and materials 0-61275  
 heat pump, chemical, hydride conversion and storage system 0-72077  
 hot water supply systems using solar collectors, technical problems (*German*) 0-94106  
 office building in Madrid, solar power appl. 0-89597  
 passive solar space heating for energy conservation 0-66948  
 photovoltaic power conditioning system for professional services office building 0-89646  
 solar, heating and air conditioning 0-61290  
 solar, performance modelling and simulation 0-76618  
 solar, salt gradient solar pond for space heating 0-94115  
 solar, types, construction and thermal and environmental parameters (*French*) 0-85268  
 solar availability for winter space heating, anal. of SOLMET data (1953 to 1975) 0-81421  
 solar collector applications for space and water heating in buildings 0-61406  
 solar collector wall, bi-coolant, heating cycle, thermosiphoning, building heating and cooling 0-72083  
 solar collectors combined with ground heat pumps, economic advantages (*German*) 0-76605  
 solar energy, storage and power supply for building heating, optimal conditions (*French*) 0-61297  
 solar energy and environmental heat utilization for space and water heating (*German*) 0-61284  
 solar energy collection and storage, latent heat diode walls, space heating (*French*) 0-61298  
 solar energy collection and storage, space heating (*French*) 0-61299  
 solar energy system installation suggestions for space heating and water heating (*German*) 0-94102  
 solar heat pump house heating system with low quality thermal flow 0-76617  
 solar heat pump plant for space heating in winter, air conditioning in summer 0-76615  
 solar heating, air movement control 0-66946  
 solar heating, passive systems 0-76619  
 solar heating and cooling system for domestic use (*Japanese*) 0-108787  
 solar heating expts. for performance prediction and design optimisation 0-61288  
 solar heating installation, technical and operational details (*Dutch*) 0-72013  
 solar heating of buildings, numerical simulation of thermal performance 0-66942

**space heating continued**

- solar heating panel system, performance testing and evaluation (*Dutch*) 0-72079
- solar heating storage device, off-peak, ambient temp. observer/predictor control system 0-66950
- solar heating system for dwellings, temp. regime investigations 0-97802
- solar heating systems for heating and hot water (*German*) 0-108788
- solar hot water system design 0-104518
- solar hot-water supply system for residential building 0-93851
- solar hotwater and heating systems, availability aspects 0-61314
- solar house heating system, possibilities of integrating heat pump (*Rumanian*) 0-97804
- solar installations for utilisation of solar radiation and heat from outside air (*German*) 0-94104
- solar power utilisation employing solar collectors, absorbers and heat pumps (*German*) 0-76604
- solar powered system for intermittent heat delivery 0-89669
- solar space and water heating rapid implementation effect on USA energy supply 0-104497
- solar space heating, two-tank storage system using seasonal and diurnal tanks 0-72016
- solar space heating installations, case for dynamic controls on hydronic distribution systems 0-104498
- solar space heating with air and liquid systems 0-61287
- solar systems installation for domestic heating (*German*) 0-94103
- solar thermal energy storage in salt hydrates, material props. 0-101134
- solar transition region and inner corona, energy balance 0-90379
- thermal, waste heat utilization with annual aquifer storage for space heating appls. 0-97809
- water heating system using solar collectors (*German*) 0-94105

**space research**

- see also artificial satellites; astronomy and astrophysics; space vehicles*
- asteroid 1943 Anteros, spacecraft rendezvous potential target, request for photometry and spectrophotometry 0-90356
- astrodynamics conf. (Provincetown, MA, USA, June 1979) 0-82583
- blood viscosity and red cell aggregation at zero and 1G, instrumentation for Space Lab 3 0-61716
- circumsolar plasma, Venera 10 radio signal spectral meas. 0-109326
- conference, COSPAR 22nd plenary meeting (Bangalore, India, May-June 1979) 0-77549
- construction of large structures in space 0-98533
- European Space Agency, status of certain privileged non-member states (*French*) 0-72633
- European Space Agency programmes, developmental or operational status 0-72742
- finance, the role of private funding in European space ventures 0-77121
- geostationary satellite, orbit determ. by single ground station tracking 0-109329
- graphite fibre epoxy composites, eutectic coating moisture barriers 0-81228
- graphite fibre epoxy laminates, low thermal expansivity, design considerations 0-81031
- graphite fibre filled polyimide composite laminates, space environment, phys. and mech. response 0-81140
- gravitational Doppler effect explored using geostationary satellite 0-109351
- Halley-Venus mission, Planet-A project for mag. meas. in interplanetary space (*Japanese*) 0-94672
- industrial projects in space 0-90319
- Jupiter colour pictures from Voyager space probes, 800 line scan TV system, land based receiver systems (*German*) 0-101549
- Mars, Viking gas exchange reaction simulation on UV irradiated MnO<sub>2</sub> substrate 0-72831
- microwave and IR detectors, space appl. of superconductivity 0-85836
- named spacecraft, data acquisition and logging system incl. speech 0-61979
- NASA-ESA mission for Periodic Comets Halley and Tempel 2 rendezvous 0-82168
- near-Earth radiation hazard due to solar flares, dosage estimation technique 0-67482
- Periodic Comet Halley mission (*Polish*) 0-67516
- planet thermal radiation intensity field modelling; principles 0-62056
- planetary exploration by spacecraft 0-105146
- planetary exploration using impact spacecraft imagery, crater morphology investigations 0-62052
- radiation environment of space vehicles electronic components, laboratory simulation 0-94689
- satellites studying wave-particle interactions in magnetosphere, X-ray,  $\gamma$ -ray astronomy, Ariel series, Geos, ISEE, Cos-B satellites 0-90317
- slid programme, Spacelab, weightlessness expts. on man 0-94381
- solar furnaces, for materials-science expts. 0-108786
- Solar Maximum Year project and related space experiments, review 0-90404
- solar wind turbulent plasma, radio wave propag. meas. using three satellites 0-101518
- Soviet lunar and planetary exploration, handbook 0-62398
- Space Shuttle, small planetary missions 0-109339
- Space Shuttle and deep space missions 0-109336
- Space Transportation System, integration with deep space mission 0-109337
- Spacelab of European Space Agency 0-85837
- Spacelab pressurised model development for future space missions 0-90318
- TLD system for meas. of cosmic dose on board a spacecraft 0-109047
- Venus, Pioneer radar data, planet's topography (*German*) 0-105190
- Venus atmosphere, struct., and light, heat and wind regimes from space vehicles 0-62062
- Venus atmosphere and surface, investigation by radiosounding from Venera 9 and 10 satellites 0-101543
- Venus cloud layer, struct. according to Venera 9 televised pictures 0-67604
- Viking Mars, extended mission 0-67514
- Viking mission to Mars, review of planetary data 0-72839
- Voyager images, automatic technique for planet centre location 0-101534
- Voyager mission to Jupiter, Galilean satellites improved ephemerides 0-62066
- Voyager project, microwave communications from outer planets 0-77263
- WARC 1979 regulations impact 0-105147

**space science *see space research*****space-time configurations**

*see also general relativity*

- $\lambda\phi^4$  field theory, 3 space-time dimensions, renormalisation, analytical continuation to imaginary time 0-86563
- $\sigma$ -model, nonlinear, curved space, spontaneous compactification, Grassmann manifold 0-57467
- axial symmetric space-times, canaonical forms 0-105545
- Bianchi model universes, hypersurfaces of transitivity, Riemann curvature 0-67922
- Bianchi type I space-time gravitational field, particles eqn. of state 0-77664
- Bianchi type II exact cosmological model with matter and EM field 0-105560
- Bianchi-V cosmological space-time, Einstein-Weyl equations, neutrino currents 0-86023
- black hole, charged, motion in EM field, EM and gravitational perturb. of Reissner-Nordstrom space time 0-82407
- black hole collisions, time-asymmetric initial data from nonsingular vacuum Cauchy hypersurfaces 0-82408
- black holes, primordial, ingoing Vaidya metric rel. to radiation accretion in early Universe 0-67918
- black-hole, Kerr-Newman, quantised massless field, instability 0-82409
- caustics and singularities, gravitational converging effects 0-77654
- charged fluid sphere, general relativity soln., Einstein-Maxwell eqns. 0-68088
- charged particles, motion in relativistic fields 0-57146
- charm, elementary particle theories, properties (*Spanish*) 0-73681
- colliding plane gravitational waves 0-101741
- colour geometrodynamics, eightfold way, review 0-95243
- conformally flat Einstein-Maxwell spaces, Newman-Penrose formalism 0-62559
- cosmology, Lagrangian or Hamiltonian formulations, shift vector field restrictions, symmetry group 0-67923
- cosmology, space-time metric, quantised field influence, external grav. field (*Russian*) 0-86027
- defect dynamics, field equations, four dimensional space-time setting 0-96521
- differentiation with respect to spinors 0-105551
- diffusion equation, from space-time transport eqn., for anisotropic random media 0-62595
- distribution valued curvature tensors 0-86163
- Einstein equations, [(2+1)+1]-formalism, apparent horizons in space-time with rotational Killing vector 0-73222
- Einstein field equations, plane symmetric static and homogeneous vacuum solns. 0-86164
- Einstein vacuum and Einstein-Maxwell space-times, infinitesimal holonomy group structure and geometrization 0-73252
- Einstein-Maxwell eqn., N soliton solutions (*Russian*) 0-105556
- Einstein-Maxwell equations, EM and gravitational wave spacetimes, similarity solutions 0-57154
- Einstein-Maxwell equations, static electrovac solns., complexification technique 0-68114
- electrovac spacetimes, Kinnersley-Chitre transforms., homogeneous Hilbert problem 0-86162
- EM tensor fields in space-time  $V_4$  of general relativity 0-77674
- empty space-times, four-parametric set of solutions to  $G_{\mu\nu}=0$  0-95007
- fluid cylinders, static, and plane layers, general relativity solns. 0-68090
- foam-like structure, Bjorken scaling violation due to gravitational field 0-77939
- gauge field theory, de Sitter invariant Lagrangian 0-82868
- general relativity, vacuum field equations, fifth dimension, ratio of EM to gravitational force 0-77679
- geodesic balls, volume, and geometry of Riemannian manifold (*French*) 0-68085
- global structure of space-time, classical bremsstrahlung problem 0-105547
- gravitation and dynamical space, geometrical framework, Mach's principle 0-95001
- gravitation and space-time, general relativity 0-68104
- gravitation bimetric theory, flat metric element 0-62004
- gravitational, mass defect in Reissner-Nordstrom metric, charge conservation (*Chinese*) 0-68182
- gravitational bubbles, radiative corrections to covariant massless quartically self-interacting meson theory 0-62826
- gravitational effects in 6-D general relativity, Schwarzschild metric, orbital precession 0-62550
- gravitational field and arbitrary gauge field, equations of motion, Heisenberg and classical, force term, spin-curvature coupling 0-57158
- gravitational fields, axially symmetric, Weyl's class of static vacuum solutions 0-68089
- gravitational wave detection, astrophysical sources, resonant mass, laser interferometer and Doppler ranging methods 0-68122
- gravitational wave field, conformal coupling to curvature 0-68105
- hadrons, extended, Lorentz deformation props.,  $O(4)$  and light-cone coordinate systems 0-68354
- homogeneous cosmologies, dipole and quadrupole anisotropies 0-109572
- homogeneous space-times of the Godel type 0-105553
- instants, gravitational, flavour currents of QCD, Green's functions, foam-like structure of space-time 0-62825
- isotropic universe, particle creation and vacuum polarisation, cosmological models 0-90582
- Kerr metric, angular momentum, separation const. 0-77658
- killing vectors and maximal slicing 0-77667
- left-flat space-times, null tetrad and restrictive conditions 0-62545
- length prescription for generalised radial observer, Schwarzschild and Reissner-Nordstrom line elements 0-73223
- Lie group broken symmetry of transformation generating general relativistic theories 0-98836
- limits, co-ordinate dependent investigation 0-95003
- $M_4$  factorisation, spinor algebra, Dirac equation geometrical, interpretation 0-62838
- magnetofluid, relativistic, and space-like conformal mappings 0-75001
- mass operator in Riemannian spacetimes 0-82683
- massive particle production in anisotropic space-times 0-90583
- Maxwell equations in Riemann-Cartan space, spin-torsion coupling const. 0-82697
- metrical fluctuations induced by cosmic turbulence 0-82557
- Minkowski space, complex, superluminal boost in x-direction, Lorentz transformation, tachyonic connections 0-105497



## space-time configurations continued

- Minkowski space time, real analytic local extension 0-77656  
 motion of continuous medium in given space-time, four-velocity 0-68091  
 negative mass and positive mass matter, hypothetical coexistence, causal paradoxes 0-82685  
 neutron stars, electrodynamics in curved space 0-90465  
 nonhomogeneous space-time in Brans-Dicke cosmology 0-86024  
 noninertial frames, cotangent bundle approach, Lie derivative 0-62468  
 nonlocalisability of space-time events 0-94972  
 Novikov coordinates, equivalent to Kruskal, transformation from Schwarzschild coordinates 0-68098  
 null infinity and Killing fields, local isometries, space-times, asymptotic conditions 0-62832  
 one-electron atom in curved space-time 0-78509  
 particles with isotopic spin, kinematics, geometric quantisation 0-62871  
 physical system, model of space-time from set theory concepts 0-82660  
 plane-symmetric containing perfect fluid, evolution 0-94999  
 point mass space-time singularity 0-82690  
 QED, massless, energy-momentum tensor anomalies in spherical space-time 0-73628  
 quantum field theory, Lagrangian formulation, conservation laws, relativistic gravitation (*Russian*) 0-68337  
 quantum field theory, relativistic, discrete symmetries 0-68387  
 quantum many-particle systems in curved spacetime 0-98751  
 quantum stress energy in nearly conformally flat spacetimes 0-57170  
 quantum theory, physical geometry, group manifold 0-105522  
 Reissner-Nordstrom perturbations, coupled Einstein-Maxwell eqns. 0-68108  
 Riemannian geometry, Onsager-Machlup Lagrangian, functional integration 0-68102  
 Riemannian manifolds, symmetric vectors and algebraic classification 0-68094  
 right translation invariant metrics and variational principles on principal bundle, gauge theories (*Chinese*) 0-101743  
 rigidly rotating relativistic dust cylinder, Riemann tensor, ultrarelativistic case 0-86158  
 Robertson Walker metric, pair prod., propagator method appl. 0-105564  
 rotating systems, Einstein equations 0-68101  
 scalar electrodynamics in nonsimply connected space-time, topological mass generation 0-82924  
 scattering operator, analyticity in nonlinear relativistic classical and quantised field theories 0-73611  
 Schwarzschild space-time, EM waves diffraction theory appl. to gravit. lens 0-90750  
 Schwarzschild space-time, vacuum polarisation induced by-gravitation 0-82410  
 Schwarzschild-Kruskal space-time, role in developing Maxwell field non-zero vacuum expectation value 0-62828  
 sine-Gordon equation, Backlund transform., physical space-time solitons 0-77629  
 singularities in the  $\delta=3$  Tomimatsu-Sato space-time 0-86170  
 spherically symmetric space-times with vanishing curvature scalar 0-68096  
 spinor field theory, generalized spin structures on 4-D space-times 0-62564  
 static general relativistic stellar models, props. 0-86165  
 string moving in uniform static external field, 2-D space-time surface 0-57087  
 SU(2) dual charges, 4-D space of constant curvature (*Chinese*) 0-68392  
 Tomimatsu-Sato  $\delta=3$  metric, Weyl conform tensor, invariants 0-68087  
 topological spaces for formalising representation of discrete space time 0-98837  
 twisted scalar and spinor strings in Minkowski spacetime 0-57480  
 unified field theory, five-dimensional theory of interacting scalar, electromagnetic, and gravitational fields 0-105833  
 unified field theory, nonsymmetric, metric hypothesis, spinor analysis 0-68404  
 unified gauge theory of gravitational and strong interactions 0-95016  
 vacuum definition in curved space-time 0-73613  
 vacuum spacetimes, stationary and axially symmetric, homogeneous Hilbert problem, Kinnersley-Chitre transformations 0-68349  
 vacuum superfluidity near anisotropic singularity, phase transitions (*Russian*) 0-94905  
 Vaidya's metric, complexification, radiative and nonradiative, parts of energy-momentum tensor 0-68093  
 vector field with zero covariant deriv., general metric 0-68092  
 velocity matrix in six-dimensional space-time 0-86171  
 velocity of light Markov process, Klein-Gordon quantum statistic, quantum mechanics 0-98808  
 wave equation in curved space-time, compact and noncompact sources 0-73571  
 Yang-Mills theory, broken symmetry soln., Higgs fields and Einstein gravity action 0-101746  
 zero-mass limit of point-mass space-times 0-82691

## space vehicle power plants

- integral glass covering of spacecraft solar cells by electrostatic bonding 0-93676  
 satellite solar cell power plant, operating experience 0-94055  
 solar arrays, in-orbit performance, review 0-94054  
 solar cells, space qualified multiple antireflective cells 0-94056  
 solar concentrator designs for photovoltaic arrays 0-94057  
 solar energy power generators with advanced thermionic converters for spacecraft applications 0-61389  
 Ni-H<sub>2</sub> battery for satellite energy storage 0-81430

## space vehicles

- see also artificial satellites; rockets; space vehicle power plants  
 aerobraking for planetary orbit missions 0-109338  
 charge neutralisation, electron emitter neutralisation (*Japanese*) 0-94673  
 charging problems in plasma, PICPAB ion source on Spacelab 0-85840  
 cryogenic systems for spacecraft 0-86319  
 dielectric materials, charging and discharging 0-71315  
 dielectric materials, surface discharge arc propagation, and damage 0-71314  
 electric charge build up in sunlight, model of photosheath 0-90316  
 electronic components, space radiation environment effects, laboratory simulation 0-94689  
 fibre reinforced polymer matrix composites, space environmental effects 0-71721  
 flight trajectory between satellite orbits of Earth and Moon, variational problem 0-72754

## space vehicles continued

- Halley-Venus mission, Planet-A project for mag. meas. in interplanetary space (*Japanese*) 0-94672  
 International Comet Mission, proposed fast flyby of P/Halley P/Tempel 2 rendezvous 0-82166  
 International Solar Polar Mission 0-109335  
 ISEE 3 gamma ray burst instrument, first results 0-98546  
 Jupiter atmosphere probe, ballistic and navigation aspects of spacecraft braking problem 0-61981  
 Luna 16-24, equipment and expt. procedures for radar obs. of Moon 0-77302  
 Mariner-5, Venus microrelief irregularities mean height, determination from radio transillumination data 0-72807  
 materials failure, metallurgical exam. 0-71868  
 materials in space environment, conf., Noordwijk, Netherlands (Oct. 1979) 0-67933  
 metal and metal oxide thermal control materials low-energy proton effects 0-70288  
 NASA-ESA mission for Periodic Comets Halley and Tempel 2 rendezvous 0-82168  
 navigation to Venus, distance determ. from radar obs. 0-109386  
 nonstationary spacecraft, coordinate-parametric control via multidimensional asymptotically stable adaptive systems 0-101522  
 optical materials and components, space charged particle environment effect 0-69472  
 particle emission from charged sphere into mag. field, theory 0-69304  
 Pioneer 10 and 11, radio signals spectral broadening by ionospheres of Jupiter and Saturn 0-109391  
 Pioneer 11, meteoroid detector particle flux at Saturn 0-82291  
 Pioneer 11 at Saturn, trajectory var., carrier freq. Doppler shift, Saturn mass determ. 0-82294  
 Pioneer Venus, Solar Flux Radiometer 0-82198  
 Pioneer Venus, Unified Abstract Data Library and Quick Look Data Delivery System 0-67494  
 Pioneer Venus Bus and Orbiter, Bennett ion mass spectrometers 0-67499  
 Pioneer Venus Bus neutral gas mass spectrometer 0-67513  
 Pioneer Venus Differential Long Baseline Interferometry expt. 0-67578  
 Pioneer Venus entry probes, atmosphere structure instruments 0-67562  
 Pioneer Venus Multiprobe entry phase, telemetry recovery 0-67493  
 Pioneer Venus occultation experiment, radio science data generation 0-67492  
 Pioneer Venus Orbiter, electron temp. probe 0-67500  
 Pioneer Venus Orbiter, neutral gas mass spectrometer expt. 0-67502  
 Pioneer Venus Orbiter, planar retarding potential analyser plasma expt. 0-67501  
 Pioneer Venus Orbiter, plasma analyser expt. 0-67498  
 Pioneer Venus Orbiter, plasma wave investigation 0-67497  
 Pioneer Venus Orbiter, radar mapper design and operation 0-67495  
 Pioneer Venus Orbiter fluxgate magnetometer design and operation 0-67496  
 Pioneer Venus Orbiter Gamma Burst Detector 0-67505  
 Pioneer Venus Orbiter radiometer (VORTEX) 0-67504  
 Pioneer Venus Orbiter UV spectrometer, design and operation 0-67503  
 Pioneer Venus small probes net flux radiometer experiment 0-67512  
 Pioneer Venus Sounder and small probes nephelometer instrument 0-67511  
 Pioneer Venus Sounder Probe gas chromatograph 0-67507  
 Pioneer Venus Sounder Probe IR radiometer 0-67509  
 Pioneer Venus Sounder Probe neutral gas mass spectrometer 0-67506  
 Pioneer Venus Sounder Probe Particle Size Spectrometer 0-67510  
 Pioneer Venus Sounder Probe Solar Flux Radiometer 0-67508  
 Pioneer Venus spacecraft, design and operation 0-67491  
 polymer composite matrix materials, space radiation effects evaluation 0-70263  
 polymer materials, electron and proton irradiation effects 0-70262  
 Salyut-6 orbital station, cosmic radiation dose field meas. 0-89876  
 Salyut-6 spacelab, data acquisition and logging system incl. speech 0-61979  
 shuttle operations, stratospheric aerosol modification and climate implications 0-98408  
 Space Shuttle, design of Space Telescope as long-life free flyer 0-109364  
 Space Shuttle, prediction of acoustic environment in payload bay 0-102919  
 Space Shuttle, remote manipulator arm, dynamics of chain of flexible bodies 0-94953  
 Space Shuttle, small planetary missions 0-109339  
 Space Shuttle, X-ray astronomical instruments and expts. 0-109363  
 Space Shuttle and deep space missions 0-109336  
 Space Shuttle carrying reusable satellites 0-61985  
 Space Shuttle technology, payloads and operations 0-101528  
 Space Shuttles, Gamma Ray Observatory launch instruments, and operations 0-109365  
 Space Transportation System, integration with deep space mission 0-109337  
 Spacelab, microwave remote sensing expt. operation 0-109332  
 Spacelab of European Space Agency 0-85837  
 Spacelab pallet, meas. of mol. streaming fields 0-82173  
 Spacelab pressurised model development for future space missions 0-90318  
 spin-stabilised spacecraft, optimal aerodynamic attitude control 0-77250  
 Texus 1 and 2 sounding rockets for Swedish materials science expt. 0-104362  
 thermal control coatings, electron and proton irradiation effects 0-70262  
 unmanned (or manned) vehicles, automatic rendezvous with space station 0-77249  
 unnamed space probes, recent achievements, financial restrictions and their effect on future programmes 0-72743  
 Venera 9 and 10 satellites, Venus atmosphere and surface radiosounding 0-101543  
 Viking, extended mission 0-67514  
 Viking landers 1 and 2, Mars atmospheric pressure annual cycle meas. 0-72812  
 Viking orbiters, radio occultation meas. of Mars atmosphere and topography and atmosphere 0-72836  
 Voyager, electrostatic discharge testing, JPL, Pasadena, USA 0-92415  
 Voyager, Jupiter low energy charged particle expt. results 0-98605  
 Voyager 2, Jupiter magnetosphere, energetic ions and electrons obs. 0-77342  
 Voyager 2, Jupiter magnetosphere HF and LF radio events obs. 0-77344  
 Voyager 2, Jupiter magnetosphere obs., hot plasma environment 0-77341  
 Voyager 2, Jupiter magnetosphere plasma waves, radio obs. 0-77343

**space vehicles continued**

- Voyager 2, plasma obs. near Jupiter 0-77340
- Voyager 2 at Jupiter, 1979 J 1 satellite discovery 0-77334
- Voyager 2 at Jupiter, atm. 2400 Å map 0-77336
- Voyager 2 at Jupiter, H I Lyman  $\alpha$  and Io torus, EUV obs. 0-77338
- Voyager 2 at Jupiter, ionosphere struct. from occultation radio obs. 0-77337
- Voyager 2 at Jupiter, magnetometer obs. of bow shock and magnetosphere 0-77339
- Voyager 2 encounter with Jupiter, trajectory and sequence modifications 0-77265
- Voyager 2 encounter with Jupiter system, IR obs. 0-77335
- Voyager 2 obs. of Jupiter and Galilean satellite/features visible 0-72871
- C fibre reinforced composites for spacecraft use, prep., props. and struct. 0-71625

**spacecraft** *see space vehicles***spallation (nuclear)** *see nuclear spallation***spark chambers**

- see also position sensitive particle detectors*
- beta-ray cameras, gas replacement monitor 0-95502
- demonstration 0-77596
- flash chambers for neutrino detection, construction and performance 0-58026
- gamma-ray telescope, spark chamber, scintillation counter time-of-flight system 0-62017
- high current pulse generator for flash chamber particle detector arrays 0-69039
- highly stabilized hybrid spark chamber for  $\beta$ -ray imaging 0-102398
- imaging alpha detector, radioactive contamination monitoring appl. 0-102384
- magnetic spark spectrometer, high-speed photorecorders 0-87014
- multigap, HV supply cct. for parallel feeding 0-63456
- multilayer  $\gamma$ -telescope spark chamber, 5-200 MeV  $e^+e^-$  track anal. 0-63469
- wide-gap, Tskhra-Tskaro (USSR) 0-87016
- wire spark chambers, capacitive read-out system 0-102407

**spark counters**

No entries

**spark erosion machining** *see spark machining***spark-gap voltmeters** *see voltmeters***spark gaps**

- electrical breakdown of air gaps, 1 to 9 cm, with heated electrodes, investigation (German) 0-107010
- electrodes, acoustic phenomena in erosion 0-64796
- electron beam triggered, characts., investig. 0-107001
- flowing gas, electric breakdown study, improved method 0-64821
- four-electrode field emission pre-ionised triggered spark-gap switches, 10 to 30 kV, parallel operation 0-70075
- HV switching surges, influencing factors (German) 0-87958
- laser triggered vacuum gap for high energy appl. 0-78888
- laser triggering through fiber optics of a low jitter spark gap 0-107000
- long air, disruptive voltage calc. with positive switch voltages (German) 0-87964
- parallel-plane electrode erosion characts. at atmos. and vacuum press. 0-70076
- rod-to-plate system, initial corona voltage calculated according to Townsend's Theory (Czech) 0-87961
- square shaped fluid shock wave pulses with variable time duration 0-74593
- Cs, pulsed vapour source for ion sources in heavy ion accelerators 0-63423
- Cu halide laser driving ccts., parametric study 0-83610
- H arc discharges, laser-triggered, electron density meas. 0-64822
- SF<sub>6</sub>, limiting sparkover voltage values determ. and dielectric strength testing in power equipment (Czech) 0-87962
- SF<sub>6</sub>, spark gap, KrF laser triggered, low jitter timing 0-106999

**spark machining**

- Al-Ti alloy spark alloying, cathode weight change and hardened layer obs. (Russian) 0-61005

**sparks**

- see also electric breakdown; lightning*
- air, multichannel spark form. 0-87976
- electrodynamic mechanisms of limitation of the electron concentration in a laser spark (Russian) 0-59333
- electrostatic, charged powder in container anal., hazards identification and control 0-69291
- electrostatic, detection and characts., by radio methods 0-68217
- electrostatic discharges from body nature and incendiary behaviour obs. 0-72406
- energy determ., using mathematical and physical model 0-70065
- fluid, radio band pulse radiation due to spark initiated cavity dynamics, sonoluminescence (Russian) 0-66313
- fusion, FTFR, neutral beam sources overcurrent protection during spark down 0-102331
- ignition of gas mixture, Kasaev cathode call formation 0-70066
- ion acceleration mechanisms in vacuum spark 0-92417
- laser gap breakdown, shock and ionisation waves, photographic absorpt. obs. 0-87967
- long spark form. mechanism 0-59326
- miniature triggered spark switch, high repetition rate 0-103203
- perfluorocarbon-SF<sub>6</sub> mixtures, sparking C inhibition, decomp. product investig. 0-89478
- pressure wave generation and propagation by spark discharges in liquids (Japanese) 0-70060
- probe investigations of the electric fields produced in air near a laser spark (Russian) 0-59334
- selfluminous, schlieren system for time and space resolved photography 0-87471
- sparkling potential in longit. mag. fields 0-106996
- switches, high repetition rate, with Al and brass electrodes, surface ageing 0-106997
- triggered spark gap switch system, long life, high repetition rate 0-106998
- UV light source, surface spark discharge type, for H<sub>2</sub>/F<sub>2</sub> laser initiation 0-78923
- CO<sub>2</sub> laser gas mixture, vol. photo-preionisation by VUV radiation 0-87966
- H, laser-triggered, electron densities meas. 0-106975

**sparks continued**

- Si, controlled dislocation formation, struct. density (Russian) 0-107244
- Zr VIII spectra, reson. transitions in UV 0-91479

**spatial filters**

- acousto-optical wideband programmable filter 0-102842
- amplitude filtering for superresolution, maximum central irradiance under energy constraint 0-91914
- apertures with triangular and assoc. filters, variable apodisation 0-63914
- applications (Japanese) 0-99851
- biological pattern recognition, rotational matched spatial filter 0-76866
- bipolar, review of techniques appl. to incoherent optical systems 0-95821
- bipolar spatial filtering, incoherent, review 0-102822
- circularly symmetric positive filter function realisation by transparent rings 0-87343
- coherent feedback, flexible filter operations 0-87337
- colour spatial filtering for image enhancement 0-87341
- complex Fourier spectra, interferometric determ. 0-87327
- correlation filtering for increasing diff. efficiency 0-96028
- correlation reduction, spatial filtering and variation of resolution 0-102850
- correlator, nonlinear t-E curve effects for matched spatial filter material 0-95812
- correlator with matched filtering using band-limited illumination 0-69531
- dynamic spatial filtration of coded optical image signals from noise 0-95826
- exponential transformation using film nonlinearity for optical homomorphic filtering 0-58467
- feature enhancement using noncoherent optical processing 0-99651
- feedback systems for analogue and digital optical image processing 0-102650
- frequency plane filtering by dynamic coherent illum. 0-95825
- generalised matched filters for coherent optical pattern recognition 0-99654
- holographic, for electron microscopy image improvement 0-99680
- holographic, invariance of diff. correlators to optical element shifts 0-106471
- holographic pattern recognition of Korean alphabets, discrimination enhancement using phase modulated matched filters 0-95854
- incoherent complex spatial filtering 0-95834
- integrated optical spatial digital filter based on Bragg effect 0-96036
- laser amplifier system, small-scale self-focusing 0-106580
- liquid-crystal devices, variable-grating-mode, optical logic operations on binary images 0-106613
- matched filter, multicapacity, for correlator appl., using birefr. object film 0-74478
- matched filter visibility effects on the correlation function 0-96031
- matched filtering improvements for coherent optical pattern recognition 0-78786
- metallic thin film apodising and attenuating filters, phase shifts and aberrations 0-87552
- multi-aperture system imaging props. 0-87332
- optical pattern recognition, discriminant hypersurface prod. by average filters 0-99649
- optical pattern recognition by thermoplastic complex filter 0-99656
- pattern recognition, multiclass, multivariant technique 0-87320
- periodic structure defect detect. using optical processing 0-95829
- periodic-pattern-defects omnidirectional-spatial-filter optical detection system 0-69333
- pick-up tube aperture distortion correction, optical method 0-95827
- real-time optical processing using the liquid crystal light valve 0-63936
- single-mode optical fiber interferometry 0-73442
- statistical filter for image feature extraction 0-99636
- texture pseudocolouring, single pass by spatial filtering 0-95809
- thin phase structure detection method spatial filtering props., under partially coherent illum. 0-95828
- tunable spatial filtering with a Fabry-Perot etalon 0-58668
- uneven interface of media with different refractive indices, statistical characts. of images 0-87331
- volume holograms for image restoration 0-83566
- wavefront reconstruction, linear filtering influence 0-99670
- Wiener filters, bilinearly distorted image linear restoration 0-83557
- CO<sub>2</sub> laser Antares fusion system power amplifier optics 0-74394
- CO<sub>2</sub> laser Helios fusion system alignment 0-74420

**spatial orientation control** *see attitude control***spatial variables measurement**

- see also angular measurement; area measurement; curvature measurement; diameter measurement; displacement measurement; distance measurement; height measurement; length measurement; level measurement; particle size measurement; position measurement; surface topography measurement; thermal expansion measurement; thickness measurement; volume measurement*
- aerosols, monodisperse, mass concentration, laser monitoring 0-98878
- concentric round parts, profile determ., concentricity errors (German) 0-57249
- gear profile testing, new method for discontinuous kinematic errors 0-95068
- gear tooth profile, portable meas. instrum. for large gears, interchangeable standard profiles 0-57259
- intervertebral joints, painful, meas. of movement by biplanar radiography 0-98079
- linear dimensions, measured on production line by optical techniques 0-82746
- Mekometer additional equipment design, manufacture and calibration for more complete utilisation (Italian) 0-64129
- precision measuring table with hollow rotor asynchronous motor, digital control system 0-105607
- stereophotogrammetry, meas. of deforms. in human body (Croatian) 0-108997
- telemetry system, totally implantable, for dimensions meas., animal physiological research 0-67294
- water depth measurement using airborne pulsed Ne laser system 0-61908

**speakers** *see loudspeakers***special purpose computers**

- see also process computers*
- algorithms and data structs. for array processing 0-83530
- hological microprocessor, design and circuit architecture, functions (French) 0-90822



**special relativity***see also Lorentz transformation*

- Abraham-Minkowski controversy, EM momentum in static fields, teaching 0-101678  
 arbitrary moving frames of reference 0-98797  
 classical special relativity mechanics, classical particles with unusual props. 0-77615  
 coordinate transformation formulas for massive reference frame 0-90673  
 CPT invariance, quantum mechanical interpretation 0-105805  
 creation and gnosiological lessons 0-98780  
 didactical challenge for the future (*German*) 0-101714  
 dilatational degree of freedom, six-dimensional space  $V_6$  0-57088  
 Doppler effect 0-82637  
 EM contributions to energy-momentum tensor 0-105495  
 EM propagation between physical source and constant vel. receiver in vacuo 0-105502  
 EM wave dispersion equations in moving media, relativistic electrodynamics 0-57089  
 equations of motion and radiation reaction 0-73232  
 ether theory, relativistic formula for Doppler effect (*French*) 0-105494  
 fluid system, electric conduction in relativistic thermodynamics 0-105498  
 Lewis-Tolman paradox, soln. in relativistic states 0-86083  
 Lienard-Wiechert eqns., rel. to electron mass (*Spanish*) 0-82654  
 light signals on closed path, relativistic expts. 0-82645  
 light velocity in vacuum, quantised space, special relativity and relativistic field theories 0-82869  
 light velocity measurement, one-way, and light signal synchronisation 0-82644  
 linearity postulate of the 'special theory' of 1905, 1907 0-105503  
 Marinov absolute space, velocity aberrational test method 0-82646  
 measuring instrument readings depend on massive reference system 0-73171  
 mechanics and electrodynamics, Euclidean space, Galileo transformation 0-62467  
 microcosm and macrocosm, discrete modelling 0-82643  
 minimum measurable intervals and classical mechanics 0-90668  
 Newton-Huygens problem of circular rotation 0-105501  
 noninertial frames, cotangent bundle approach, Lie derivative 0-62468  
 null hyperspace initial data 0-101740  
 one way velocity of light, anisotropic effect detection using stellar aberration 0-86081  
 Ott relativistic temperature variation, comment on derivation 0-86084  
 path-dependent Lagrangians in relativistic electrodynamics 0-90670  
 quasars redshifts, relativistic Doppler formula rel. to transverse vels. and distances (*Chinese*) 0-105379  
 radiative transfer, comoving-frame transfer eqn. soln. in spherically symmetric relativistic flows 0-82181  
 relativistic ether hypothesis, generalised Galilean transformations 0-86085  
 rotating disk, uniform motion without tangential strain 0-82641  
 rotating disk problem 0-82640  
 rotating frames, generalised theory 0-57086  
 second postulate of Einstein's theory of special relativity 0-90669  
 simultaneity, distant, conventionality, standard synchronisation 0-77612  
 six-dimensional, centre-of-mass frames of pairs of particles, bradyons, luxons, tachyons 0-77614  
 solid angle, relativistic transformation, teaching 0-101683  
 Synge's triads of null rays 0-73146  
 temperature, special relativistic transformation thought expt. 0-86086  
 theory of motion, electromagnetism, gravitation 0-105500  
 three time dimensions, use in relativity 0-68042  
 three-dimensional time, expt. test 0-105499  
 time spending and space exploring 0-90671  
 transport equation for discontinuity wave amplitude, quasi-linear hyperbolic system (*French*) 0-90667  
 twin paradox teaching 0-105465

**specific gravity** *see density***specific gravity measurement** *see density measurement***specific heat**

- see also Debye temperature; Gruneisen coefficient; specific heat of gases; specific heat of liquids; specific heat of solids*  
 adiabatic calorimeter for continuous specific heat meas. 800 to 1800K, design and calibration 0-57299  
 anharmonic oscillator, classical, variational method test, sp. ht., elec. susceptibility and oscillation freq. (*Portuguese*) 0-77611  
 atomic nuclei, level density rel. to eqn. of state at subnuclear densities 0-77278  
 biological macromolecules, conformation studied by calorimetry, review 0-97870  
 confluent singular term for systems with continuous symmetry, crit. amplitude ratio, calc. to order  $\epsilon^2$  0-57235  
 continuous phase transition, universal combination of critical amplitudes from field theory 0-95051  
 Fermi systems, disordered in two dimensions, interaction effects 0-75655  
 humid materials, diffusivity and specific heat, transient temp. changes (*French*) 0-64355  
 Ising chain, spin-1, sp. ht. in presence of impurities and mag. field 0-93128  
 Ising chain of alternating spins of 1/2, and general S, appl. of transfer matrix method 0-80529  
 Ising model, random-bond, upper bond to sp. ht. on Nishimori's line 0-71068  
 Ising model with competing interactions, critical properties and exact results 0-93129  
 Ising spin glass, three-dimensional mag. correlations 0-103849  
 macromolecular systems, statistical thermodynamic analysis, heat capacity function 0-61514  
 macromolecules, linear, heat capacities, scanning calorimetry meas. 0-61134  
 micellar systems, aqueous, thermochemistry 0-61133  
 third law of thermodynamics, vanishing of specific heat at absolute zero 0-73294  
 two-dimensional Ising system, crossing over to two-dimensional Heisenberg system 0-93123  
 He, adsorbed on graphite, band struct. effects in heat capacity 0-59788

**specific heat at constant pressure** *see specific heat***specific heat at constant volume** *see specific heat***specific heat of gases**

- Bose-gas model, dil. hard sphere, calc. of low density atomic H gas props. 0-87194

**specific heat of gases continued**

- CO, heat capacity, calc. by modified Redlich-Kwong eqn. of state 0-69963  
<sup>4</sup>He, heat capacity of liquids and dense gases at low temps. (*Russian*) 0-65324

**specific heat of liquids**

- t-butyl alcohol, aq. soln. 0-88237  
 electrolytes and non-electrolytes, aq. soln., apparent molal isochoric heater capacities at 25°C 0-59671  
 esters, SLC, ferroelectric behaviour, specific heat, spontaneous polarisation 0-75958  
 n-hexane, superheated, thermodynamic props. from ultrasound speed 0-92036  
 liquid crystals, thermodynamic props. calc. 0-103464  
 liquid-glass transition, glass transition depend. on heating and cooling rates 0-79920  
 mesophase pitch, magnetically-oriented, phys. props., mol. struct. 0-64885  
 nematic liquid cryst., two-dimensional, Monte Carlo simulation 0-100168  
 octylcyanobiphenyl, crit. heat. capacity near nematic-smectic A transition 0-100323  
 octyloxycyanobiphenyl, nematic-smectic A transition, heat capacity study 0-88033  
 polymethylsiloxane-2, liq., thermodynamic props. at high press., US propag. meas. (*Russian*) 0-65157  
 salicidenanilines, SLC, ferroelectric behaviour, specific heat, spontaneous polarisation 0-75958  
 soft discs, two-dimens. melting, phase transition boundary 0-96629  
 transition metals, thermophysical data at high temps., submicrosecond-pulse-heating method 0-103459  
 water, physical props., two-state model approach 0-75144  
 water, random network model, liq. and ice polymorphs enthalpy and heat content 0-64869  
 water, relax. compressibility and heat capacity 0-92580  
 Ag-Ge eutectic alloy, heat capacity meas. over temp. range 800-1200K (*French*) 0-88331  
 D<sub>2</sub>O, liquid, volumetric and derived thermal characteristics at low temp. and high pressure 0-107352  
 Ga, liq., thermal props. at high temp. 0-75536  
 H<sub>2</sub>O-H<sub>2</sub>O<sub>2</sub>, isolation of singular component for heat capacities of super-cooled H<sub>2</sub>O 0-107437  
 H<sub>2</sub>O-N<sub>2</sub>H<sub>4</sub>, isolation of singular component for heat capacities of super-cooled H<sub>2</sub>O 0-107437  
<sup>3</sup>He, liq., exchange model 0-88387  
<sup>3</sup>He, superfluid, sp. ht. jump at superfluid transition and effective mass, press. depend. 0-65331  
<sup>4</sup>He, heat capacity of liquids and dense gases at low temps. (*Russian*) 0-65324  
 In, liq., thermal props. at high temp. 0-75536  
 KCl-CuCl eutectic fused salt, potential as intermediate temp. solar heat transfer and storage medium 0-101135  
 Pb, thermodynamic characterisation, by isobaric expansion meas. 0-103494  
 Pt, thermodynamic characterisation, by isobaric expansion meas. 0-103494  
 Se, heat capacity and chem. equilb. 0-103486  
 Tl, liq., thermal props. at high temp. 0-75536  
 ZnCl<sub>2</sub>-LiCl(NaCl)(KCl)(CsCl), molten, US velocity, thermodynamic quantities and struct. (*Japanese*) 0-88270

**specific heat of solids***see also Schottky anomaly*

- A 15 type superconductors, acoustic phonon spectra, electronic density of state function (*French*) 0-80444  
 adamantane, thermal cond. and heat capacity under press. 0-80008  
 alkali metal halides, ionic crystals, impulse compression temps. 0-100307  
 alkylene di-ammonium cadmium tetrachlorides, sp. ht. anomalies at phase transitions 0-70421  
 amorphous magnet, random anisotropy axis model in the infinite-range limit 0-88761  
 amorphous magnets, random anisotropy axes, high-temp. expansion for sp. ht. 0-71041  
 amorphous solids, vibr. sp. ht. enhancement from force-const. variations 0-88333  
 antiferromagnetic triangular cactus tree, bond-diluted, ordered phase 0-71037  
 benzene-hexa-n-hexanoate, phase transitions and mesophase form., sp. ht. and IR spectra, 13 to 393K 0-79955  
 binary alloys, random, specific heat enhancement and electron-phonon interaction 0-65242  
 1,1'-biphenyl, heat capacity anomalies due to successive phase transitions 0-96664  
 butyloxybenzylidene octylaniline, liq. cryst., phase transitions, calorimetric obs. 0-103466  
 copper, benzoate, one-dimens. antiferromag., heat capacity, field-induced crossover of spin-dimensionality 0-97099  
 covalent semiconductors, displacement correlations, adiabatic bond charge model 0-70350  
 cyclo-hexyl-ammonium-copper-trichloride, specific heat, ferromagnetic chain system 0-103491  
 dielectric, regulated, thermal capacity, strong US waves effects (*Russian*) 0-65240  
 dilute alloy, perturbation expansion for the asymmetric Anderson Hamiltonian 0-80202  
 dimethylammonium copper tetrabromide, quasi two-dimensional antiferromag., mag. behaviour 0-97098  
 electron gas, two-dimensional, internal energy, specific heat effective mass, temp. depend. 0-75513  
 ferroelectric materials for dielectric power conversion, dielectric prop. anal. 0-80712  
 ferroelectrics, quantum transition suppression, pyroelectric, electrocaloric effects, specific heat 0-75984  
 ferromagnet, Ising model, diamond lattice, phase transition, crit. props. 0-93127  
 ferromagnet, itinerant, mag. props., temp. depend., functional integral approach 0-60170  
 ferrous formate dihydrate, paramagnetic specific heat, decoration iteration transformation anal. 0-70938  
 Gaussian-to-Heisenberg crossover, specific heat, renormalised perturbation theory 0-60356  
 glass-ceramic, machinable, elastic const. temp. depend. 0-79852

## specific heat of solids continued

- graphite, frequency distribution based on unfolding technique 0-92619  
 graphite, pyrolytic commercial, high-temp. thermal and mech. props. 0-75372  
 harmonic crystals, thermodynamic props., effects of vacancy defects determ. by cell cluster method 0-79959  
 heat-pulse experiments, nonlinear effects, theory 0-96182  
 Heisenberg, ferromagnet, classical, with dipole-dipole interaction, renormalisation group and crit. exponents 0-60351  
 Heisenberg model magnets, high-temperature specific heat (*Russian*) 0-88757  
 hexamethylenetetramine, thermal cond. and heat capacity under press. 0-80008  
 Hubbard model, one-dimensional, elementary excitation with complex wave vector 0-75783  
 ice, random network model, liq. and ice polymorphs enthalpy and heat content 0-64869  
 intermediate valence, theory, electronic sp. ht. calc. 0-79956  
 iron formate dihydrate, mag. sp. ht.,  $S_z^4$ -term 0-60289  
 Ising chain, with next-nearest neighbour interactions, mag. responses to spin-Peierls transition 0-71054  
 Ising ferromagnet, one-dimens., with phase transition, thermodynamic props. calc. 0-80536  
 Ising model, bond random, ferromagnetic-antiferromag. mixture, triangular cactus tree, statistical theory 0-75702  
 Ising model, spatially nonhomogeneous, correl. functions 0-60314  
 itinerant-electron systems with narrow bands, single-site spin fluctuation theory 0-97049  
 Jahn-Teller system, thermodynamic properties, internal stress effects 0-59679  
 lattice vibrations and cryst. heat capacity, historical review 0-57071  
 liquid-glass transition, glass transition depend. on heating and cooling rates 0-79920  
 lithium thallium tartrate, sp. ht., 0.3 to 25K, second-order ferroelec. transition 0-59674  
 magnetic model systems, computer simulations 0-65924  
 manganese formate dihydrate, Zn- and Mg-substituted, anomalous crit. phenomena 0-60316  
 metallic glass, stability, hole theory of liquids appl. 0-100174  
 metals, nonstationary temperature fields due to moving heat sources, heat capacity, thermal cond. (*Russian*) 0-107448  
 metals, overbarrier states of H and D, subsystem heat capacity, equilibrium props. (*Russian*) 0-79998  
 metals, spin fluctuations, mag. field effect, electronic sp. ht. and elec. resist. 0-108026  
 methane- $d_4$ , solid, tunnel splittings, heat capacity meas. 0-96451  
 mixed valence model, spinless, isolated f-level problem 0-107750  
 molybdenum chalcogenides, multicomponent, physical props. 0-84577  
 Neel ferrimagnets, phase transitions, field-induced spin-orientational 0-75767  
 nitromethane, solid, tunnel states investig. 0-103274  
 ordered regions near macroscopic defects and percolation phase transform. in crystals (*Russian*) 0-92665  
 paramagnet, narrow-band with strong Coulomb correlations, electron. sp. ht. (*Russian*) 0-103487  
 PMMA, Gruneisen const. and thermal props., temp. depend., 4-300K, Brillouin scatt. obs. 0-100662  
 polyethylene, extruded semicryst., thermal cond. and specific heat, <1K 0-59742  
 polyethylene terephthalate, low temp. sp. ht., effect of cooling rate 0-100336  
 pyridinium manganese chloride, anhydrous, quasi one-dimensional mag. behaviour, heat capacity meas. 0-80549  
 pyridinium nickel chloride, anhydrous, quasi one-dimensional mag. behaviour, heat capacity meas. 0-80549  
 quartz, smoky, gamma-irradiated, short-time-scale sp. ht. meas. 0-59672  
 random anisotropy model in Ising model, Monte Carlo simulation 0-80546  
 rare earth alloy, amorphous, ferromag. state, non-axial elec. field gradient effect 0-75728  
 rare earth metals and alloys, ferromag. props., book contrib. 0-75725  
 Rochelle salt, ferroelec. phase transition, Raman scatt. study 0-97211  
 semiconductor, phonon conduction and relaxation times 0-107585  
 silicate glass, containing ZnO and TiO<sub>2</sub>, thermal capacity 0-88335  
 soft discs, two-dimens. melting, phase transition boundary 0-96629  
 solid-on-solid representation, planar model Monte Carlo simulation 0-96727  
 spin glass, infinite-ranged model, mean field theory hypothesis 0-97104  
 spin glasses, dilute ferromagnets, ferromagnetic modes 0-93133  
 spin glasses, free energy, order parameter expansion, random bond model 0-84609  
 squaric acid, antiferroelec., struct. phase transition mechanism 0-75969  
 steel, martensitic, sp. ht. and magnetisation meas. 1.2 to 10K 0-71059  
 superconducting composites, granular, Ginzburg-Landau theory, props. 0-88673  
 superconductors, granular, percolation model, specific heat, elec. resistance 0-93025  
 superconductors, granular, percolation theory, crit. props. 0-84575  
 superconductors, magnetic impurity low temp. behaviour, transition temp., specific heat, free energy 0-88691  
 tetrabromomethane, thermal resistivity, heat capacity and phase diagram under pressure 0-65316  
 TGS, perfect and imperfect, sp. ht. and sound vel., crit. anomalies 0-71331  
 TGS ( $-d_{11}$ ), sp. ht. near ferroelec. phase transition 0-70420  
 TMMC, linear antiferromag., mag. phase diagram, expt. and theoretical study 0-71038  
 3d-transition metal complexes, low spin-high spin paramag. transition, Ising model calc. 0-93073  
 triangular lattice, thermodynamic props., effect of vacancy defects determ. by cell cluster method 0-79959  
 trimethylammonium manganese trichloride, Heisenberg antiferromag. chain, specific heat and EPR 0-65931  
 TTF-TCNQ complex, trans-diethyl-dimethyl TTF-TCNQ, one-dimens. cond. 0-96853  
 uniaxial ferromagnet, domain struct. in mag. field 0-103853  
 vacancy formation parameters from specific heat data 0-75221  
 valence transition, entropy and phase diagram 0-59877  
 vanadocene, order-disorder phase transition, sp. ht. and crystallographic study (*French*) 0-84131

## specific heat of solids continued

- Wolff model, thermodynamic props., local moments in dil. alloys, var. method 0-65781  
 ytterbium ethyl sulphate, crystal field effects on mag. and hyperfine props. of  $Yb^{3+}$  0-97101  
 Zn<sub>3</sub>B<sub>2</sub>O<sub>7</sub>Br, ferroelec. 43m-mm2 phase transition, molar heat capacity meas. 0-93249  
 Ag-Ga(Ge)(In),  $\alpha$ -phase, lattice sp. ht. calcs. 0-65246  
 Ag-Ge eutectic alloy, heat capacity meas. over temp. range 800-1200K (*French*) 0-88331  
 AgBr NaBr, thermodynamic props., metastable states and demixing 0-96660  
 AgCr, dil., specific heat, impurity contrib. Kondo temp. 0-65903  
 Al film, lattice and bulk heat capacity meas. for normal and supercond. states 0-92684  
 Al, superconducting band gap anisotropy and Fermi surface anisotropy (*Spanish*) 0-84544  
 Ar, solid, equilib. props., uncorrel. pairs approx. 0-84303  
 As<sub>2</sub>S<sub>3</sub>, vitreous, thermal capacity, 300 to 600K 0-103492  
 As<sub>2</sub>Se<sub>3</sub>, vitreous, thermal capacity, 300 to 600K 0-103492  
 As<sub>2</sub>Te<sub>3</sub>, vitreous, thermal capacity, 300 to 600K 0-103492  
 Au-Fe (1 at.%), spin glass, specific heat 0-60355  
 B<sub>2</sub>C, thermophysical props. and neutron absorpt. 0-103488  
 BaNi<sub>2</sub>(PO<sub>4</sub>)<sub>2</sub> and BaNi<sub>2</sub>(AsO<sub>4</sub>)<sub>2</sub>, mag. props., neutron diffr. and sp. ht. meas. 0-70948  
 C<sub>60</sub>Rb, intercalated graphite, resistivity and specific heat anomalies 0-107440  
 CaNi<sub>2</sub>, Hauke compounds, low temp. heat capacity, Debye temp. 0-96663  
 CdTe<sub>2</sub>Te<sub>4</sub>, single and polycryst. samples, linear expansion, heat capacity and thermodynamic props. 0-103489  
 (Ce, La)In<sub>3</sub>, heat capacity and elec. resist. 0-71049  
 $\alpha$ -Ce, exchange-enhanced, elec. resist. T<sup>2</sup> depend., press. effect 0-96845  
 CeAl<sub>2</sub>, pure and LaAl<sub>2</sub>(YAl<sub>2</sub>) diluted, collective phenomena 0-65933  
 CeAl<sub>3</sub>, sp. ht., Kondo effect and ferromag. order coexistence 0-65927  
 Ce<sub>3</sub>Al<sub>11</sub>, sp. ht., Kondo effect and ferromag. order coexistence 0-65927  
 CeB<sub>6</sub>, anomalous sp. ht. intrinsic mag. phase transitions obs. 0-108027  
 CeB<sub>6</sub>, mag. and electronic props. 0-71048  
 CeCu<sub>2</sub>Si<sub>2</sub>, collective phenomena 0-65933  
 Ce(In, Sn)<sub>3</sub>, heat capacity and elec. resist. 0-71049  
 CeTi<sub>3</sub>, mag. susceptibility, magnetisation, neutron diffr., elec. resist., and sp. ht. meas. 0-75733  
 Co complex, Co(II)(1,2,4-triazole)<sub>2</sub>(NCS)<sub>2</sub> quasi two-dimens. canted S=1/2 antiferromag. 0-70976  
 CoCl<sub>2</sub>, antiferromag., phase diagram, heat capacity meas. 0-93126  
 CoMn(Cr)(V)(Ti), dil., low temp. specific heat and magnetisation 0-65925  
 CoTi<sub>2</sub>, Al<sub>3</sub>, mag. and electronic props., ferromag. and paramag. state 0-65814  
 Co(urea)<sub>2</sub>Cl<sub>2</sub>·2H<sub>2</sub>O, two-dimens. mag. props., cryst. struct., specific heat 0-75777  
 Cr, enthalpy and specific heat, empirical eqn. (*Russian*) 0-92683  
 Cr-V, itinerant electron antiferromag., spin fluctuations, low temp. specific heat 0-107439  
 Cr<sub>2</sub>B<sub>2</sub>O<sub>7</sub>Cl, ferroelec. 43m-mm2 phase transition, molar heat capacity meas. 0-93249  
 CrCo, dil., low temp. specific heat meas., 1.5 to 4K 0-60328  
 CsMn<sub>2</sub>Co<sub>2</sub>Cl<sub>2</sub>·2H<sub>2</sub>O, random mag. mixture, mag. torque and sp. ht. expts. 0-60323  
 CsNiF<sub>3</sub>, one dimensional planar model with symm. breaking fields, thermodynamics, static props. 0-97111  
 Cu-Zn(Ge)(Ni)(Ga),  $\alpha$ -phase alloys, lattice sp. ht. calcs. 0-65246  
 Cu<sub>2</sub>B<sub>2</sub>O<sub>7</sub>Cl, ferroelec. 43m-mm2 phase transition, molar heat capacity meas. 0-93249  
 CuCr, dil., specific heat, impurity contrib. Kondo temp. 0-65903  
 CuI, ionic motions nature, mol. dynamics calcs., sp. ht. anomaly due to order-disorder transform. 0-107533  
 CuMn spin glass, specific heat and entropy 0-60354  
 Dy-Cu, amorphous, mag. phase diagram, magnetisation and sp. ht. meas. 0-80532  
 DyAsO<sub>4</sub>, first order Jahn-Teller phase transition, sp. ht. and refr. index meas. 0-59645  
 DyAsO<sub>4</sub>, phase transitions obs. 0-70412  
 Dy<sub>2</sub>Ga<sub>2</sub>O<sub>12</sub>, dipolar magnet, sp. ht. and magnetisation meas. 0-60344  
 DyVO<sub>4</sub>, phase transitions obs. 0-70412  
 ErLa<sub>2</sub>Be<sub>13</sub>, mag. sp. ht. and ESR, cryst. field interactions 0-60290  
 ErK<sub>2</sub>B<sub>4</sub>, ferromag. superconductor, vortex phase 0-80441  
 ErRh<sub>1-x</sub>Sn<sub>3+x</sub>, synthesis, supercond. and mag. props. 0-100547  
 EuB<sub>6</sub>, electronic struct., transport and mag. props. 0-96782  
 EuB<sub>6</sub>, ferromag. and antiferromag. sp. ht. meas., 1.8-77K 0-65948  
 Eu<sub>2</sub>Ir<sub>2</sub>O<sub>7</sub>, pyrochlore, sp. ht. below 20K, Debye temp. 0-65241  
 Eu<sub>2</sub>O<sub>3</sub>, thermophysical props. and neutron absorpt. 0-103488  
 Eu<sub>2</sub>Sn<sub>2</sub>S<sub>2</sub>, mag. and thermodynamic props., metamagnetism 0-60273  
 Eu<sub>2</sub>Si<sub>2</sub>-S, Heisenberg spin glass system, excitations 0-84610  
 Eu<sub>2</sub>Si<sub>2</sub>-S, insulating spin glass, sp. ht. near ferromag. onset 0-97106  
 Eu<sub>2</sub>Si<sub>2</sub>-S, spin glass, spin wave modes and low temp. sp. ht. 0-80538  
 Fe complex, Fe(1,2,4-triazole)<sub>2</sub>(NCS)<sub>2</sub>, quasi-2-dimens. S=1/2 antiferromag., mag. props., hidden canting 0-107986  
 Fe-Co-Ti(V)(Cr)(Mn), sp. ht. in ordered and disordered phases 0-71061  
 Fe-Ni-Cr, mag. props. in weak mag. fields (*Russian*) 0-75771  
 Fe-Ti (V)(W), dil., thermophysical props. and elec. cond., temp. depend. 0-96842  
 Fe<sub>2</sub>B<sub>2</sub>O<sub>7</sub>I, ferroelec. 43m-mm2 phase transition, molar heat capacity meas. 0-93249  
 FeCl<sub>3</sub>, metamagnet, scaling props. of magnetisation and heat capacity, test of tricritical scaling 0-60336  
 (Fe<sub>0.8</sub>Cr<sub>0.2</sub>)<sub>79</sub>P<sub>1</sub>B<sub>8</sub> and (Fe<sub>0.8</sub>Cr<sub>0.2</sub>)<sub>79</sub>P<sub>1</sub>B<sub>8</sub>, amorphous, low temp. sp. ht., mag. contribs. 0-80552  
 FeF<sub>2</sub>, mag. sp. ht. near Neel temp. mag. susceptibility meas. 0-60341  
 Fe<sub>0.99</sub>Mn<sub>0.01</sub>Ti<sub>0.9</sub>H<sub>0.1</sub>, localised vibrs., sp. ht. obs., room temp. 0-65248  
 Fe<sub>2</sub>Ni<sub>10-x</sub>Fe<sub>14</sub>B<sub>6</sub>, metallic glass, low temp. sp. ht. for spin-glass and spin-cluster-glass regime 0-71071  
 (Fe<sub>2</sub>Ni<sub>10-x</sub>)<sub>79</sub>P<sub>1</sub>B<sub>8</sub>, metallic glass, low temp. sp. ht. for spin-glass and spin-cluster-glass regime 0-71071  
 Fe<sub>2</sub>TiO<sub>5</sub>, anisotropic spin glass type behaviour 0-60296  
 Ga II, superconducting high pressure phase, sp. ht. 0-70894  
 Gd, ferromagnetic, crit. sp. ht. and thermal expansion 0-60343  
 GdAlO<sub>3</sub>:La, antiferromag., random-field crit. and multicritical behaviour 0-65939  
 Gd<sub>3</sub>Mo<sub>2</sub>Se<sub>8</sub>, coexistence of supercond. and long range antiferromag. order 0-84534



## specific heat of solids continued

- GeP, thermodynamic characts. 10-300K, interatomic bond elasticity 0-59677
- HgCr<sub>2</sub>S<sub>4</sub>, cooling efficiency near 60K mag. refrigerant 0-71034
- HgTe, 1.5 to 30K, thermal expansion and heat capacity meas. 0-59681
- HoRh<sub>2</sub>B<sub>4</sub>, low temperature magnetic properties 0-88728
- HoVO<sub>4</sub>, RF susceptibility below 1K, mag. sp. ht. 0-84585
- Ho<sub>2</sub>-Sb system, magnetisation, elec. resist., and sp. ht. meas. 0-60213
- In-Bi(Tl)(Pb), small  $\kappa$  supercond., phase transitions higher than second order 0-88668
- In<sub>0.65</sub>Tl<sub>0.35</sub>, supercond. transition temp., specific heat, pseudopotential form factor 0-97026
- KAg<sub>16</sub>, superionic phase transition, dynamical and crit. pt. props. 0-107535
- KCl:Cs<sup>+</sup>(I<sup>-</sup>), low-temp. heat capacity enhancement due to impurities 0-107442
- KCl-CuCl eutectic fused salt, potential as intermediate temp. solar heat transfer and storage medium 0-101135
- KFe(MoO<sub>4</sub>)<sub>2</sub>, phase transitions at 312 and 139K 0-70396
- KH<sub>2</sub>PO<sub>4</sub> type ferroelectrics, Green's function theory of phase transitions with pseudo-spin-lattice coupled mode model 0-71354
- KMnF<sub>3</sub>, specific heat near Neel temp. (*Russian*) 0-100340
- KReO<sub>4</sub>, heat capacity and thermodynamic props., 8 to 304K 0-100335
- $\beta$ -K<sub>0.77</sub>V<sub>2</sub>O<sub>5</sub>, heat of form. and sp. ht., 450 to 900K 0-61129
- La, heat capacity and supercond. props. 0-65247
- LaNi<sub>5</sub>, Hauke compounds, low temp. heat capacity, Debye temp. 0-96663
- LaP<sub>2</sub>O<sub>14</sub>, continuous ferroelastic transition elastic and mechanical props. 0-92668
- La<sub>0.6</sub>Tm<sub>0.4</sub>Se, sp. ht. meas., 1.6 to 20K, mag. contrib. 0-65934
- La<sub>10</sub>W<sub>2</sub>O<sub>21</sub>, enthalpy and heat capacity at high temp. 0-70424
- $\alpha$ -La<sub>2</sub>WO<sub>6</sub>, enthalpy and heat capacity at high temp. 0-70424
- La<sub>8</sub>W<sub>2</sub>O<sub>16</sub>, enthalpy and heat capacity at high temp. 0-70424
- LiH, cryst., specific heat at const. vol., isotopic modifications effects 0-103490
- LiNH<sub>4</sub>SO<sub>4</sub> and LiNd<sub>2</sub>SO<sub>4</sub>, dielec. pyroelec., and thermal props. 0-60509
- LiRbSO<sub>4</sub>, order-disorder phase transitions with many-minimum potential, thermodynamic props. 0-96623
- $\beta$ -Li<sub>0.27</sub>V<sub>2</sub>O<sub>5</sub>, heat of form. and sp. ht., 450 to 900K 0-61129
- Lu<sub>2</sub>Ir<sub>2</sub>O<sub>7</sub>, pyrochlore, sp. ht. below 20K, Debye temp. 0-65241
- MgAl<sub>2</sub>O<sub>4</sub> spinel refractory, enthalpy and specific heat determ. 0-88334
- MgCr<sub>2</sub>O<sub>4</sub> spinel refractory, enthalpy and specific heat determ. 0-88334
- MnCl<sub>2</sub>, lattice dynamics, density of states and sp. ht. calc. 0-92624
- Mn<sub>2</sub>Ga<sub>2</sub>N, sp. ht., 6 to 350K, mag. and crystallographic phase transitions 0-71060
- MnP, spin polarised energy band struct., electronic specific heat, APW calcs. 0-65431
- Mn<sub>2</sub>ZnN, sp. ht., 6 to 350K, mag. and crystallographic phase transitions 0-71060
- NH<sub>4</sub>Ag<sub>4</sub>, superionic phase transition, dynamical and crit. pt. props. 0-107535
- NH<sub>4</sub>Br, heat capacity meas. near order-disorder transition 0-88332
- NH<sub>4</sub>Br<sub>2</sub>Cl<sub>2</sub>, heat capacity meas. near order-disorder transition 0-88332
- NH<sub>4</sub>ReO<sub>4</sub>, heat capacity and thermodynamic props., 8 to 304K 0-100335
- (NH<sub>4</sub>)<sub>2</sub>SO<sub>4</sub>(BeF<sub>4</sub>), order-disorder phase transitions with many-minimum potential, thermodynamic props. 0-96623
- NaAlH<sub>4</sub> and Na<sub>2</sub>AlH<sub>6</sub>, molar heat capacity and thermodynamic functions, 10 to 300K 0-65243
- Na<sub>2</sub>CO<sub>3</sub>, phys. props. related to phase transitions 0-96643
- NaClO<sub>3</sub>, lattice vibrations and sp. ht., neutron spectroscopic study 0-107388
- NaNO<sub>2</sub>, ferroelec., dielec. and thermal behaviour 0-80680
- Na<sub>2</sub>O-Cs<sub>2</sub>O-SiO<sub>2</sub> glasses, thermal diffusivity, heat capacity and thermal cond., laser flash method study 0-65310
- Na<sub>3</sub>Sc<sub>2</sub>P<sub>2</sub>O<sub>12</sub>, fast-ion conductor, struct. phase transition 0-88362
- NaTi<sub>2</sub>(SO<sub>4</sub>)<sub>2</sub>, heat capacity and thermodynamic functions, 10 to 300K 0-65244
- $\beta$ -Na<sub>0.27</sub>V<sub>2</sub>O<sub>5</sub>, heat of form. and sp. ht., 450 to 900K 0-61129
- Nb<sub>0.75</sub>Ga<sub>0.25</sub>, A 15 phase high transition temp., sp. ht. determ. 0-60140
- Nb<sub>2</sub>Ge, amorphous film, supercond., flux flow resist., vortex pair dissociation 0-88701
- Nb<sub>3</sub>Nb<sub>1-x</sub>Si<sub>x</sub>(Ge<sub>x</sub>), impurity stabilised A15 supercond., transition temp., lattice const., specific heat 0-93026
- Nb<sub>20</sub>Zr<sub>80</sub>, supercond. and normal, sp. ht. meas., 2-20K 0-70893
- Nd(OH)<sub>3</sub>, heat capacity from 10 to 350K, lattice and Schottky contribs. 0-84300
- Ni-Fe based metallic glasses, Curie pt. anomalies 0-60256
- Ni<sub>2</sub>B<sub>2</sub>O<sub>7</sub>Br, ferroelec. 43m-mm2 phase transition, molar heat capacity meas. 0-93249
- NiCl<sub>2</sub>6NH<sub>3</sub>, low temp. sp. ht. and mag. ordering 0-75784
- Ni<sub>2</sub>Fe alloys, low-temperature specific heat, long and short range order effects 0-100339
- (Ni<sub>0.9</sub>Fe<sub>0.1</sub>)<sub>79</sub>P<sub>11</sub>B<sub>9</sub>, amorphous, low temp. sp. ht., mag. contribs. 0-80552
- NiSe<sub>2</sub>, paramag. props., NMR, mag. susceptibility 0-60175
- $\beta$ -O<sub>2</sub> crystal, thermodynamics of mol. lattice motion (*Russian*) 0-70328
- Pbl<sub>2</sub>-piperidine(aniline)(pyridine), intercalation cpds., heat capacity of low temp., intercalation effect (*Russian*) 0-92682
- Pd-Fe-Mn, ferromagnet-spin glass, thermal expansion forced, magnetisation and magnetisation under high press. 0-65255
- Pd-Si amorphous alloy, heat treated, low temp. lattice sp. ht. 0-75368
- Pd-Si(Cu) amorphous ribbons, low temp. sp. ht., density of states trends 0-79957
- Pr<sub>2</sub>Ag<sub>70</sub>, amorphous, sp. ht. at low temp. 0-75780
- PrIn<sub>3</sub>-Gd, indirect nuclear exchange interactions, ESR-linewidth meas., sp. ht. determ. 0-103825
- PrIr<sub>2</sub>(Pt<sub>2</sub>)(Rh<sub>2</sub>)(Ru<sub>2</sub>), sp. ht., differential susceptibility and elec. resist. meas., 1.4-40K 0-71063
- Pr<sub>2</sub>La<sub>80-x</sub>Al<sub>20</sub>, amorphous, low temp. excitations, specific heat 0-100337
- PrMg<sub>3</sub>, cryst. field study, inelastic neutron scatt. and sp. ht. meas. 0-59939
- Pr(OH)<sub>3</sub>, electronic heat capacity, 0.45 to 4.2K, phase transition at 1.21K 0-59673
- PtMn, spin glass, nonlinear susceptibility and sp. ht. 0-60304
- RbAg<sub>4</sub>I, superionic phase transition, dynamical and crit. pt. props. 0-107535
- RbCaF<sub>3</sub>, first order improper ferroelastic phase transition at 194K, phenomenological description 0-70397
- RbMnCl<sub>3</sub>, specific heat near Neel temp. (*Russian*) 0-100340
- RbNiF<sub>2</sub>, high-temperature mag. sp. ht. (*Russian*) 0-88757

## specific heat of solids continued

- Rb<sub>2</sub>ZnCl<sub>4</sub>, commensurate-incommensurate phase transition, crit. behaviour, sp. ht. meas. 0-71342
- Sc-Gd, spin glasses, low temp. sp. ht. and magnetisation 0-65913
- Sc-Zr(Mg), low-temp. heat capacity 0-75370
- Se, trigonal and vitreous, sp. ht. and thermal cond., 3 to 300K 0-59676
- $\beta$ -SiC, thermodynamic props., temp. depend., 5 to 300K 0-96666
- SiO<sub>2</sub>, amorphous, sp. ht., time-dependent, 0.1 to 1K 0-100338
- SiO<sub>2</sub>, vitreous, low temperature heat capacity enhancement model 0-75369
- SiO<sub>2</sub>-Al<sub>2</sub>O<sub>3</sub>-Cu<sub>2</sub>O glass alkaline durability, corrosion rate, heat capacity and elastic moduli 0-93673
- SIP, thermodynamic characts. 10-300K, interatomic bond elasticity 0-59677
- Sm<sub>2</sub>Ag<sub>29</sub>, amorphous, sp. ht. at low temp. 0-75780
- Sn-Bi(Sb), small  $\kappa$  supercond., phase transitions higher than second order 0-88668
- SnCl<sub>2</sub>·2H<sub>2</sub>O, isomorphous transition, Landau type thermodynamic potential 0-107413
- p-H, solid, constant volume heat capacity and eqn. of state, temp. depend. 0-65334
- SRCl<sub>2</sub>, fast ion cond., specific heat anomaly, mol. dynamics study 0-65283
- Ta, thermophysical props. and neutron absorpt. 0-103488
- Tb(OH)<sub>3</sub>, heat capacity from 10 to 350K, lattice and Schottky contribs. 0-84300
- TbP (As)(Sb)(Bi), mag. transitions, quadrupolar interaction effects 0-80512
- TbPO<sub>4</sub>, zircon struct., cryst. field analysis 0-80232
- Th<sub>3</sub>As<sub>4</sub>, 5-300K 0-88769
- ThC<sub>2</sub>N<sub>2</sub>, NMR, Knight shift and spin-lattice relax. 0-100621
- ThNi<sub>5</sub>, Hauke compounds, low temp. heat capacity, Debye temp. 0-96663
- Ti-Mo-V-Al-Cr-Fe (4.8, 4.7, 5.2, 1.1, 1.0 wt.%), structural changes during heating up to 1000°C, DTA study (*Russian*) 0-93552
- TiC-C composites, hot pressed, thermophys. props. at high temps. 0-59675
- (Ti<sub>1-x</sub>V<sub>x</sub>)<sub>2</sub>O<sub>3</sub>, spin glass, nonlinear susceptibility and sp. ht. 0-60304
- Tl films, supercond. amorphous, effective phonon spectrum and lattice sp. ht. 0-70895
- TlMnCl<sub>3</sub>, specific heat near Neel temp. (*Russian*) 0-100340
- Ti<sub>2</sub>PO<sub>4</sub>, heat capacity and thermodynamic functions, 5 to 320K 0-65245
- UAl<sub>3</sub>, spin fluctuations, mag. field effect, electronic sp. ht. and elec. resist. 0-108026
- U<sub>3</sub>As<sub>4</sub>, 5-300K, ferromag. transition obs. 0-88769
- UO<sub>2</sub>, crystn., specific heat anomaly 0-84299
- U<sub>2</sub>S<sub>3</sub>, sp. ht. at low temps., mag. behaviour 0-60353
- V-Pt, sp. ht. and mag. meas. in ordered and disordered phases 0-70422
- V<sub>2</sub>Hf<sub>2</sub>-Zr<sub>2</sub>, normal and supercond. state, transition temps., mag. susceptibility and specific heat determ. (*Russian*) 0-60132
- V<sub>2</sub>Si, supercond. mixed state, low temp. tetragonal-domain-reorientation phenomena, US expts. and thermal props. 0-60141
- W, relative enthalpy, 273 to 1173K, electronic heat capacity coeff. 0-103496
- Y-Gd, spin glasses, low temp. sp. ht. and magnetisation 0-65913
- Y<sub>2</sub>Mn<sub>23</sub>, low temp. specific heat determ. 0-65896
- Y<sub>2</sub>Mo<sub>2</sub>O<sub>7</sub>, pyrochlore compounds, sp. heat meas. 0-107438
- YNi<sub>3</sub>, magnetism resurgence, neutron diffr. and mag. props. study 0-65819
- YNi<sub>5</sub>, Hauke compounds, low temp. heat capacity, Debye temp. 0-96663
- Y<sub>2</sub>Ru<sub>2</sub>O<sub>7</sub>, pyrochlore compounds, sp. heat meas. 0-107438
- Y<sub>0.8</sub>Tm<sub>0.2</sub>Se, sp. ht. meas., 1.6 to 20K, mag. contrib. 0-65934
- YVO<sub>4</sub>:Nd<sup>3+</sup>, zircon struct., cryst. field analysis 0-80232
- YbGaG, mag. props. between 44-600 mK 0-80517
- Yb<sub>2</sub>Ga<sub>2</sub>O<sub>3</sub>, dipolar magnet, sp. ht. and magnetisation meas. 0-60344
- Zn, mean square displacement of atoms in cryst. lattice, rel. to sp. ht. (*German*) 0-79902
- ZrC-C composites, hot pressed, thermophys. props. at high temps. 0-59675
- ZrI<sub>2</sub>, high-temp. enthalpy, X-ray powder diffr. data 0-107446
- ZrO<sub>2</sub>, enthalpy and heat capacity at 1100-2500K 0-103472
- ZrS<sub>2</sub>, electronic struct., bonding effects, photoelectron spectroscopic and low temp. heat capacity cal. 0-96780

## specific volume see density

## specimen preparation

- see also biological specimen preparation; metallography; replica techniques
- asbestos fibres concentration meas., in air and liquid, analytical methods review 0-72120
- baryta crystal gas-liquid inclusion meas. with microscope heating stage 0-76967
- compact specimen, for plane strain crack arrest toughness testing 0-76433
- decoration technique, surface step struct. determ. 0-103554
- dehydration of specimens, for SEM, bibliography (1974-8) 0-73544
- device for making plane and plane-parallel specimens 0-85104
- device for producing fatigue cracks in specimens 0-61051
- distillation apparatus incorporating vaporizer which induces vapour flow pattern producing centrifugal field 0-86274
- electron microscopy, decoration method, rel. to crystal growth (*German*) 0-103222
- electron microscopy, specimen deposition and fabrication by ion beam sputtering 0-82855
- EPR, CO<sub>2</sub> laser-heated sample holder for high-temp. EPR spectrometer 0-68233
- fatigue and fracture toughness testing, fastening materials 0-61050
- fluorescence microscopy, incident light, specimen prep. method 0-82755
- fluorite crystal gas-liquid inclusion meas. with microscope heating stage 0-76967
- foil mounting technique, wrinkle-free 0-77767
- foil thinning for transmission electron microscopy, monitoring by PP-8 radiometer (USSR) 0-73525
- fracture preservation and cleaning, for fractography 0-71866
- glasses and fragile materials, fracture energy, direct meas. (*French*) 0-104376
- incubator, choice 0-68187
- ion sputtering deposition of coatings for ultrahigh resolution SEM 0-76184

**specimen preparation continued**

- magnetic domain, SEM obs., method of removing fine magnetite particles from surface (*Japanese*) 0-108655  
 metal coatings, electrolytic cell for making standard samples 0-85106  
 metallographic sample preparation, procedures 0-57272  
 metallurgical coke, mech. behaviour charact. (*French*) 0-104371  
 micro-sample handling device, various appl. 0-62642  
 optical fibre characterisation techniques compared 0-64202  
 polymer materials, characterisation, by TEM 0-103270  
 pore-channel marking, electron microscopy of polymer films 0-103271  
 rubber, crystallising, tensile test specimen prep. 0-71838  
 scanning electron microscopy; pellet mould for bulk specimen anal. 0-95191  
 SEM, thin film coating techniques 0-68308  
 SEM conductive treatment of specimen to prevent charging 0-101883  
 SEM insulating specimen charge neutralization using very low energy ions 0-68309  
 SEM preparation technique for emulsion particles, freeze drying 0-62799  
 SEM samples, metal coating by sputtering, specimen heating (*German*) 0-73338  
 semiconductor TEM 90° cross-section and 1° angle-lap specimen prep. 0-71881  
 semiconductor thin sample etching for electron microscope exam. 0-86272  
 steel, low C, mech. characts., specimen size and shape effects 0-66715  
 steel, surface state influence on etching effect 0-81235  
 STEM specimen support using C film, prep. and observation 0-93496  
 TEM, cold cathode ion gun for sputter etching 0-105748  
 TEM, welding technique, grain boundaries in Si 0-103364  
 TEM fine grained coating prep., sputter source design 0-99015  
 Ag and alloy electron microscope specimens, noneyanide electropolishing method 0-100967  
 Au, epitaxially grown bicrystalline thin films, preferred inclinations of (100) grain boundaries 0-103367  
 BaTiO<sub>3</sub>, Mossbauer spectroscopy, sample prep. and results 0-66078  
 Ge, epitaxial growth of very thin electron microscopy specimens 0-100793  
 Mo foils, device for electrolytic thinning from wire, for electron microscopy 0-85105  
 Nb<sub>3</sub>Sn multifilamentary composite supercond. wires, transverse sections prep., ion milling, TEM obs. of grain size 0-101000  
 Ni-base superalloys, technique for replication of  $\gamma'$  0-79648  
 Pr tinted glasses, transparency, dichroism and colour effects (*Polish*) 0-71371  
 SrTiO<sub>3</sub>, Mossbauer spectroscopy, sample prep. and results 0-66078  
 W, polishing technique as prep. for TEM 0-71851

**speckle**

- 1978 P 1, speckle obs. rel. to orbital radius and system mass and density 0-109394  
 analogue video transmission feasibility using laser diode, over 30 km at 1.3  $\mu$ m 0-58737  
 astronomical speckle interferogram masking, holography and phase flipping 0-109373  
 bibliography of laser speckles (1976 to 1978) 0-82593  
 binary stars, obs. by speckle interferometry 0-90477  
 biological objects, electronic speckle pattern interferometry in vivo 0-109083  
 cylindrical surface two-wavelength speckle pattern intensity distrib. at optical transform plane 0-106487  
 deflection contour generation by white light projection speckle method 0-98881  
 deformation measurement, out-of-plane, using holographic interferometry and speckle photography, comparative accuracy 0-78804  
 diffuse object longitudinal motion under Gaussian beam illum., laser speckle dynamic statistical props. 0-99628  
 diffuse object real-time velocity meas. using laser speckle zero-crossings 0-77760  
 diffuser, weak, speckle pattern, spherical aberration effect 0-87476  
 double exposure interferometry through speckle photography (*French*) 0-83568  
 double-exposure speckle photography, analysis using electro-optical readout system 0-62708  
 electronic speckle pattern interferometric system based on a speckle reference beam 0-58472  
 fluid section flow pattern speckle photography 0-103096  
 Fresnel plane interference fringe generation by correlated speckle patterns 0-106462  
 general object deformation decomposition by speckle displacement 0-106486  
 high-resolution astronomical imaging, results 0-82225  
 holographic interferometry and speckle photography, scatt. geometry, topology vector fields theory 0-87347  
 image plane speckle patterns, statistical props. 0-63940  
 image processing technique requiring no reference point 0-98556  
 image subtraction through speckle modulated by Young fringes 0-95813  
 intensity level crossings, expected number in normal speckle pattern 0-99629  
 interference fringes, lens aberration effects 0-105700  
 interferometric analysis of transient phenomena 0-105701  
 interferometric obs. of binary stars with Haute-Provence 1.93 m telescope 0-90475  
 interferometric obs. of Pluto's satellite (1980 June) 0-101553  
 interferometry, electronic, using digital image processing techniques 0-87322  
 interior displacement and strain measurement using white light speckles 0-95064  
 laser beam spatial coherence control by progressive US wave 0-78885  
 laser speckle and surface roughness 0-102622  
 laser speckle reduction in image plane by US modulation of spatial coherence 0-106459  
 laser speckle suppression during magneto-optical tests 0-85093  
 MTF, two-dimensional, meas. by second order speckle statistics calc. 0-63937  
 multimode optical fibres, freq. depend. of modal noise, speckle theory 0-102817  
 multiplex image coding, astronomical IR speckle interferometry appl. (*French*) 0-67580  
 non-Gaussian, contrast variation 0-83554  
 optical coherence applications, seminar, San Diego, CA, USA (Aug. 1979) 0-77542

**speckle continued**

- optical fibres, step-index, modal-noise probability distrib. meas. and anal. 0-99859  
 partially coherent beam intensity fluctuation calc. in turbulent atmosphere 0-78775  
 pattern holographic projection, metrological applications 0-106493  
 phase statistics in coherently superposed Gaussian speckle patterns 0-102626  
 photography, double exposure, anal. technique 0-62718  
 polychromatic speckle pattern, dominant eigenvalues to evaluate intensity probability density function 0-106451  
 polypropylene film, double-exposure speckle pattern obs. of tensile deform., displacement, Poisson's ratio and stress relax. 0-84795  
 Rayleigh-Benard flow, equal velocity fringes by speckle photography 0-75005  
 real-time measurement of in-plane translation and tilt by electronic speckle correlation 0-57252  
 real-time optical processing using the liquid crystal light valve 0-63936  
 rough metal surfaces, diffuse and specular refl., empirical representation 0-87315  
 rough surfaces, reflection light, division into specular and diffuse components (*Japanese*) 0-106457  
 scattering object, coherently illuminated, speckle pattern statistics in diffraction field 0-63924  
 scatterplate interferometer, scalar diffraction theory 0-73432  
 signal and image processing, US Air Force research programme 0-78791  
 space-time optics, speckle phenomena and white light correlations 0-106460  
 space-time random speckle pattern optical analysis 0-102682  
 spatial coherence meas. by correlated diffusers 0-74296  
 spot size estimate in diffraction pattern of scattered field 0-95789  
 statistical props. and coherence aspects 0-78773  
 step height determ. by two-wavelength speckle pattern method 0-105614  
 strain meas. speckle photography with hybrid optical/electronic image processing 0-106768  
 strain measurement by speckle photography, hybrid optical and electronic image processing 0-99976  
 temporal frequency dependence of modal noise in fibres [optical] 0-58687  
 thermal expansion, speckle interferometric meas. apparatus 0-68170  
 topogram sensitivity, wavefront correl. effect 0-69345  
 turbulent atmosphere speckle propag. statistics, log-amplitude covariance function effect 0-82058  
 two-dimensional optical system MTF meas. by second-order speckle statistics computation 0-74304  
 two-dimensional structure in-plane vibr., stress analysis by laser speckle method 0-103006  
 two-scatter-plate low-speckle-noise integrator for atmospheric laser beam transmission meas. 0-90252  
 US B-mode images of human tissue, real-time speckle reduction 0-74634  
 velocity measurement by first order statistics of time-differentiated laser speckles 0-82750  
 velocity measurement using time-space cross-correlation of speckle patterns 0-105623  
 vibrating membrane speckle pattern analysis 0-106769  
 white light image speckle statistical props. 0-106461  
 white light speckle patterns, contrast near image plane 0-102624  
 zero-crossing study on dynamic properties of speckles 0-63923  
 Al plate, thermal strain meas. by one-beam laser speckle interferometry 0-103005  
 GaAlAs DH laser coherent light, propagating in multimode optical fibre, speckle contrast 0-78978

**spectra**

- see also alpha-particle spectra; astronomical spectra; atmospheric spectra; atomic spectra; beam-foil spectra; beta-ray spectra; Brillouin spectra; cosmic ray energy spectra; electron spectra; energy level crossing; gamma-ray spectra; light scattering; luminescence; mass spectra; matrix isolation spectra; microwave spectra; molecular spectra; multiphoton spectra; neutron spectra; nonradiative transitions; optical double resonance; oscillator strengths; proton spectra; quantum beat spectra; Raman spectra; spectra of inorganic liquids and solutions; spectra of organic molecules and substances; spectra of solids; spectral line breadth; spectral line shift; spectrochemical analysis; Stark effect; stimulated scattering; time of flight spectra; time resolved spectra; transition moments; tunnelling spectra; X-ray spectra  
 quantum system, nonintegrable, irregular part of discrete energy spectrum, statistical theory 0-82667

**spectra of diatomic inorganic molecules**

- see also infrared spectra of diatomic inorganic molecules; radiofrequency and microwave spectra of diatomic inorganic molecules; Raman spectra of diatomic inorganic molecules  
 alkali metal chlorides, photofragment spectra, bond energies and excited state symmetries 0-87190  
 bound, hybrid potential function 0-69209  
 diatomic hydrides, quantum mechanically calculated observables, reliability determ. 0-63505  
 AlH<sup>+</sup>, spectrum at 3632 Å, rot. anal. 0-78632  
 AlS, B<sup>1</sup> $\Pi$ -X<sup>2</sup> $\Sigma^+$  transition, assignment of UV bands, vibr. and rot. anal. 0-58278  
 BaO, recoil velocity spectra from form. in crossed beam system 0-76500  
 Br<sub>2</sub>, vac. UV absorpt. cross section 0-91574  
 BrCl laser induced fluoresc., quantum resolved level dynamics in B<sup>1</sup> $\Pi$ (O<sup>+</sup>) state 0-74188  
 BrO, free radical, Ar matrix absorpt. spectra, mol. vibronic states obs., spectroscopic const. determ. 0-83387  
 C<sub>2</sub>, triplet ground state dissociation continuum obs. in UV spectrum of C<sub>2</sub> white dwarf (LP 145-141) 0-67715  
 CH<sup>+</sup>, photodissociation to C<sup>+</sup> and H, wavelength depend. and photofragment kinetic energies, visible obs. 0-58275  
 CN, (A<sup>2</sup> $\Pi$ -X<sup>2</sup> $\Sigma^+$ ) and (B<sup>2</sup> $\Sigma^+$ -X<sup>2</sup> $\Sigma^+$ ) yields from HCN photodissoc. 0-87141  
 CN, B<sup>2</sup> $\Sigma^+$ -A<sup>2</sup> $\Pi$  0-0 and 1-0 bands, laser excitation spectra 0-91588  
 CO, (4+) system, electronic transition probability 0-106332  
 CO, output spectra from CS<sub>2</sub>-O<sub>2</sub>-CO<sub>2</sub>(N<sub>2</sub>O) flame lasers 0-83601  
 CaO, B<sup>1</sup> $\Pi$ -X<sup>2</sup> $\Sigma$  and C<sup>1</sup> $\Sigma$ -X<sup>2</sup> $\Sigma$  electronic transition strengths meas. 0-78602  
 CeO, dissociation energy, rel. band strengths of a<sub>2</sub>-X<sub>2</sub> and b<sub>2</sub>-X<sub>2</sub> systems 0-99495  
 Cl<sub>2</sub>, vac. UV absorpt. cross section 0-91574



## spectra of diatomic inorganic molecules continued

- ClO, free radical, Ar matrix absorpt. spectra, mol. vibronic states obs., spectroscopic const. determ. 0-83387  
 CrO, A<sup>2</sup>Π-X<sup>2</sup>Π transition, rot. anal. laser induced fluoresc. and discharge emission spectra 0-69173  
 Cs<sub>2</sub>, 4800 Å absorpt. band, classical method anal. 0-106330  
 CuCl, mol. emission spectrum, 5900-6800 angstrom, rot. anal. of A-X system 0-58273  
 CuH, UV absorpt. spectra 0-87143  
 DyO, UV emission spectrum, high resolution, band systems and isotopic shifts 0-87146  
 H<sub>2</sub>, predissoc., interference effects, lineshape obs. 0-83432  
 H<sub>2</sub>, free free absorpt. coeffs, dipole length formulation and two-centre close coupling calc. 0-83345  
 H<sub>2</sub>+H, reactions and collisions in IR laser field, collision-induced absorpt. spectra 0-76499  
 HCl, C<sup>2</sup>Π-X<sup>2</sup>Σ<sup>+</sup> system, (0, 0) and (0, 1) bands, oscillator strength determ. and UV spectra 0-91570  
 HCl, overtone vibr.-rot. bands, intracavity dye laser techniques meas. 0-91532  
 HCl(Br)(I), vac. UV absorpt. cross section 0-91574  
 HD, predissoc., interference effects, lineshape obs. 0-83432  
 He<sub>2</sub>, 600 Å emission continuum struct., in 700-900 Å region in glow discharge 0-95641  
 He<sub>2</sub>, laser-driven transitions to high Rydberg states 0-106360  
 He<sub>2</sub> optical absorpt. spectra and kinetic behaviour 0-95635  
 He<sub>2</sub>(1σ<sub>g</sub>)<sup>2</sup>(1σ<sub>u</sub>)np<sup>4</sup> triplet levels, multichannel quantum defect anal. 0-91542  
 I<sub>2</sub>, high-resolution saturated absorpt. spectroscopy with short light pulse coherent trains 0-64110  
 I<sub>2</sub>, in Ar, emission spectrum interpretation 0-95634  
 I<sub>2</sub>, RF optically heterodyned saturation spectroscopy, reson. degenerate four-wave mixing 0-74211  
 I<sub>2</sub>, vac. UV absorpt. cross section 0-91574  
 IF, in solid Ar, emission and excitation visible spectra at 12K 0-87137  
 IO, free radical, Ar matrix absorpt. and emission spectra, mol. vibronic states obs., spectroscopic const. determ. 0-83387  
<sup>129</sup>I<sub>2</sub>, <sup>129</sup>I<sub>2</sub>, <sup>127</sup>I<sub>2</sub>, <sup>127</sup>I<sub>2</sub>, high resolution saturated absorption spectra at 633 nm using He-Ne laser 0-95637  
<sup>129</sup>I<sub>2</sub>, complete hyperfine spectrum obs. at 612 nm 0-95638  
 MgO, electronic transition strengths, shock tube meas. 0-87183  
 N<sub>2</sub>, I<sup>-</sup> system bands, line broadening and shift 0-87138  
 N<sub>2</sub>, first positive system, electronic transition probabilities 0-78603  
 N<sub>2</sub> gas, electron impact ionisation, electronic fluoresc. spectra 0-95664  
 N<sub>2</sub>, liq. and gas, induced absorpt. spectral moment, mol. calcs. 0-63737  
 N<sub>2</sub>, multiphoton absorpt., spectroscopic evidence 0-63726  
 N<sub>2</sub><sup>+</sup>, Meinel system, high resolution spectrum to 11 250 Å 0-99497  
 N<sub>2</sub><sup>+</sup>, spectrum, appl. air arc temp. meas. 0-59314  
 N<sub>2</sub>+Ar, metastable atom excitation of C<sup>3</sup>Π<sub>u</sub> state, symmetry, propensity rules and alternation intensity, rot. spectrum 0-87135  
 N<sub>2</sub><sup>+</sup>(B<sup>2</sup>Σ<sub>u</sub><sup>+</sup>), N<sub>2</sub>(C<sup>3</sup>Π<sub>u</sub>) and N<sub>2</sub>(C<sup>3</sup>Π<sub>g</sub>) molecules, emissions obs. in yellow N<sub>2</sub> afterglow 0-63649  
 ND, singlet-triplet transitions, high resolution spectrosc. with new emission source (French) 0-57383  
 NH, singlet-triplet transitions, high resolution spectrosc. with new emission source (French) 0-57383  
 NO, electronically excited photofragment of VUV photodissoc. methyl nitrite, identification and quantum yield 0-99527  
 NO, γ and β system, electronic transition probability 0-106332  
 NO nonlinear laser spectroscopy, VUV harmonic generation 0-74175  
 NO vibr. overtone band, mag. rot. spectrosc. obs. 0-86446  
 NO+N<sub>2</sub>(CO<sub>2</sub>)(CO)(CH<sub>3</sub>)<sub>2</sub>(Ar), NO γ(0,0) band, oscillator strength and line broadening 0-106356  
 N<sub>2</sub>O, satellite struct. and momentum distrib., binary (e,2e) spectroscopy 0-69125  
 Na<sub>2</sub>, triplet satellite band obs. in self-broadened D-line very far blue wing 0-95688  
 NaKr, red wing radiation and pot. 0-87180  
 O<sub>2</sub>, A<sup>3</sup>Δ<sub>g</sub> state, inversion, presence in nightglow and discharges 0-63616  
 O<sub>2</sub>, atmospheric, electric quadrupole transitions detection in A band 0-85746  
 O<sub>2</sub>, b<sup>2</sup>Σ<sub>g</sub><sup>+</sup> state prod. and deactivation following O(<sup>1</sup>D<sub>2</sub>) quenching 0-76493  
 O<sub>2</sub>, liq. and gas, induced absorpt. spectral moment, mol. calcs. 0-63737  
 O<sub>2</sub>, mag. dipole transitions, line positions and strengths from stratospheric emission spectra 0-78604  
 O<sub>2</sub>, Schumann-Runge continuum, oscill. strength and electron impact excitation 0-69121  
 O<sub>2</sub>, Schumann-Runge system, electronic transition probabilities 0-78603  
 O<sub>2</sub>, spin-forbidden transition intensities, selective heavy atom effects 0-58240  
 OH, (0,0) UV transitions, band oscill. strength 0-69162  
 OH, fundamental vibr. band, mag. rot. spectrosc. obs. 0-86446  
 OH+H<sub>2</sub>O, OH linewidth rot. depend. on UV transitions 0-91606  
<sup>18</sup>O<sup>16</sup>O, Schumann-Runge bands line positions rel. to atmospheric photodissoc. and O<sub>3</sub> prod. 0-94559  
 PN, absorpt. and emission spectra, electronic transition and vibr. obs. 0-91573  
 Sbl, decay branching ratios meas., transition probabilities derivation 0-95642  
 SeH, isotope effects, Rydberg levels-ground state transitions, rot. const., VUV spectra obs. 0-58279  
 SiH<sup>+</sup>, time resolved precision spectroscopy rel. to oscillator strengths and dissociation energy 0-58272  
 Sn<sub>2</sub>, in Ar matrix, absorpt., fluoresc. and reson. Raman spectra 0-95640  
 TiN, electronic absorpt. spectrum, rot. anal. 0-78601  
 TiO, γ<sup>-</sup> system, Franck-Condon factors, r-centroids and Einstein coefficients calcs. 0-74163  
 TiO in Ar matrix, meas. of absorpt. and magnetic circular dichroism spectra 0-86356  
 TI-Hg, excimer band emission from electron beam initiated discharge in TI-Hg 0-78841  
 TI-Xe, excimer band emission from electron beam initiated discharge in TI-Xe 0-78840  
 ZrO, singlet-triplet separation meas. 0-78623

## spectra of inorganic liquids and solutions

- see also Raman spectra of inorganic liquids and solutions  
 alkali-haloid salts, aqueous solutions, IR absorpt. ν<sub>1</sub> (CN) band parameter temp., conc. study (Russian) 0-80801  
 dilute metal solutions in molten salts, optical absorption 0-89023

## spectra of inorganic liquids and solutions continued

- interaction induced light scattering and IR absorption in liquids 0-60561  
 ions in aqueous soln., absolute absorpt. coeff. meas. using photoacoustic spectroscopy 0-82828  
 polar solvents, solvated electron absorpt. spectra, intrasolvent and intersolvent corrls. 0-93840  
 water, turbid, spectral scatt. props. 0-72560  
 water, UV absorpt. spectra 0-76043  
 Ar, liquid, depolarized Rayleigh scatt. at triple point, mol. dynamics simulation 0-60617  
 CaO-Al<sub>2</sub>O<sub>3</sub>-B<sub>2</sub>O<sub>3</sub>-SiO<sub>2</sub>-FeO, glass, IR spectra at room and melt temp. 0-88986  
 CrO<sub>2</sub>Cl<sub>2</sub>+carbon tetrachloride+acetone, intermediate complex form., electronic spectra 0-61075  
 Fe<sup>3+</sup> solutions, UV absorption spectrosc. obs. of equilib. 0-93812  
 HNO<sub>3</sub>, aqueous soln., reflectance and complex refractive index, IR spectra, vibr. modes 0-66168  
 H<sub>2</sub>O vapour and liquid far IR spectroscopy 0-60610  
 He, liq., surface local disorder, for IR transmittance meas. 0-75395  
 H<sub>2</sub>(NO<sub>3</sub>)<sub>3</sub> solns., f-f transitions, intensity anal., correl. with cond. and US absorpt. 0-97292  
 LiCl, concentrated aqueous soln., IR absorpt. to high press. and temps. 0-80803  
 Na<sub>2</sub>O-CaO-SiO<sub>2</sub>-Fe<sub>2</sub>O<sub>3</sub> molten glass, optical props., temp. depend. (French) 0-100667  
 Nd(NO<sub>3</sub>)<sub>3</sub>, aqueous soln., single photon absorpt. band struct., electronic resons. coherent ellipsometry 0-90881  
 Ru complexes, [Ru(bipy)<sub>3</sub>]<sup>2+</sup> mixed-ligand, electronic absorpt. and emission spectra meas. 0-71441  
 SF<sub>6</sub>, soln., cryosystem, vibr. relax. times, pulsed IR absorpt. spectra obs. 0-66188
- spectra of inorganic molecules**  
 see also spectra of diatomic inorganic molecules; spectra of polyatomic inorganic molecules  
 No entries
- spectra of inorganic solids**  
 see also impurity and defect absorption spectra of inorganic solids; infrared spectra of inorganic solids; luminescence of inorganic solids; radiofrequency spectra of inorganic solids; Raman spectra of inorganic solids; visible and ultraviolet spectra of inorganic solids  
 alkali-alumino-phosphate:U, x-ray photoluminesc. and fluoresc., radiative transitions obs. 0-103977  
 ceramic, B content by emission spectrosc. with high freq. plasma excitation (French) 0-76477  
 ferromagnetic semiconductors, s-f interaction on conduction band, red shift effect theory 0-59872  
 CsMnCl<sub>2</sub>·2H<sub>2</sub>O, antiferromag. insulator, self-trapping of excitons 0-70619  
 NaMnCl<sub>3</sub>, antiferromag. insulator, self-trapping of excitons 0-70619  
 NiO, bulk props., initial state MO Ni<sub>2</sub>O<sub>4</sub> and Ni<sub>2</sub>O<sub>14</sub>, cluster model, lattice and force consts., photoemission and CT absorpt. spectra 0-84828  
 Pb<sub>1-x</sub>Sn<sub>x</sub>Se, X=0.03-0.07, monocrystal film, edge of intrinsic absorpt. (Russian) 0-71368  
 Pb<sub>1-x</sub>Sn<sub>x</sub>Te, X=0.62, monocrystal, edge of intrinsic absorpt. (Russian) 0-71368  
 TlBr, resonant polaron coupling and excitons under mag. field 0-71383
- spectra of organic molecules and substances**  
 see also infrared spectra of organic molecules and substances; luminescence of organic solids; radiofrequency and microwave spectra of organic molecules and substances; Raman spectra of organic molecules and substances; Shpolskii spectra  
 absorption bands, vibronic intensification obs., floating-orbital method 0-63619  
 acetone, absorption bands, vibronic intensification obs., floating-orbital method 0-63619  
 acetophenones, di- and trisubstituted, π\*π\* systems, UV electronic absorpt. spectra 0-74132  
 acetylene, excited state, photochem. and spectrosc. investig. 0-95553  
 acetylene, relationships between higher-transition frequencies 0-69119  
 acetylperoxy radicals, absorpt. spectrum and reaction kinetics 0-91571  
 adenine, hydroxy and methoxy derivatives, absorption UV spectroscopy and electronic struct. of ionic and tautomeric forms 0-74177  
 alkylbenzenes, jet-cooled, vibr. relax., absorpt. spectra 0-74236  
 alkylbenzenes, jet-cooled, vibr. relax., fluoresc. spectra 0-78694  
 anthracene:tetracene, electronic absorpt. spectrum, host-cryst. field effect 0-100669  
 anthracene, electronic vibr. spectra, stochastic description, numerical modeling, comparison with expt. 0-63620  
 anthracene, pulsed electron excitation, triplet excitons, spectral and electrical investigations 0-92828  
 anthracene derivatives in solution, polarisability and dipole moments, emission and absorpt. spectra obs. 0-69256  
 anthracene films, optical props., comparison between free and optical contact mounting 0-89079  
 anthracene-pyromellitic dianhydride crystal., refl. and absorpt. spectra of singlet charge transfer excitons 0-71442  
 anthraquinone-xanthone liq. soln., upper excited singlet state, delayed fluoresc. 0-106345  
 azo dyes, UV-visible spectrophotometric 0-61207  
 azulene vapour, IR and CO<sub>2</sub>-laser absorpt. spectra 0-87120  
 bacteriorhodopsin, effect of high press. on absorpt. spectrum and isomeric composition 0-67041  
 benzaldehyde gas, nonradiative electronic transition 0-83413  
 benzaldehyde in methylcyclohexane, nπ\* spectra 0-63627  
 benzene, first-ionisation Rydberg spectrum assignment via John-Teller splitting 0-69155  
 benzene, liq., visible region absorpt. spectra, overtones meas. 0-78625  
 benzene, nanosecond laser photolysis 0-66825  
 benzene, S<sub>0</sub>-S<sub>1</sub> transitions, two-photon absorpt. spectra by nozzle beam-multiphoton ionisation method 0-63728  
 benzene cryst., electron irradi., phenylcyclohexadienyl radical form., absorpt. and fluoresc. spectra study 0-89035  
 benzene excimer, nanosecond laser photolysis 0-66825  
 benzene radical cation in solid Ar, fluorescence spectra obs. 0-83382  
 benzophenone, laser spectroscopy by cascade photoionisation method in mass spectrometer 0-99496  
 benzyl radical, 1<sup>3</sup>B<sub>2</sub>-3<sup>2</sup>B<sub>2</sub> transition in absorpt. spectrum, extinction coeffs. 0-102523

## spectra of organic molecules and substances continued

benzyl radical, in solid Ar, absorption and photodissociation spectra 0-69156  
 benzyl radicals, monomethyl- and dimethyl-substituted, electronic spectra and electron affinity 0-63618  
 biphenyl:tetracene, electronic absorpt. spectrum, host-cryst. field effect 0-100669  
 p-bromofluorobenzene, UV electronic absorption spectrum, band shape and molecular geometry 0-87147  
 bromoform, highly excited vibr. states, thermal lensing spectrosc. and local mode model 0-87140  
 bromotrifluoromethane, vac. UV absorpt. cross section 0-91574  
 bromotrifluoromethane, vac. UV absorpt. cross section 0-91574  
 trans-butadiene,  $B_1^u$ -state dynamics in cooled supersonic expansion, electronic absorpt. spectra obs. 0-78629  
 carbazole:tetracene, electronic absorpt. spectrum, host-cryst. field effect 0-100669  
 carbon tetrachloride, vac. UV absorpt. cross section 0-91574  
 chlorobenzaldehyde,  $a^1A' \rightarrow X^1A'$  phosphoresc., conformations and ground state fundamentals 0-78642  
 chlorobenzene,  $S_0 \rightarrow S_1$  transitions, two-photon absorpt. spectra by nozzle beam-multiphoton ionisation method 0-63728  
 chlorofluorobenzene cations in gaseous phase, emission spectra and lifetimes in  $B(0^+)$  states 0-63711  
 chloroform, highly excited vibr. states, thermal lensing spectrosc. and local mode model 0-87140  
 chlorophyll, and related mol., in solid solns., fine-structured vibronic spectra under tunable dye laser excitation (*Russian*) 0-74164  
 chlorophyll a, absorpt. and fluoresc. spectra, observance of Stepanov relation 0-81554  
 chlorophylls, mag. reson., site selected fluoresc. detection 0-69164  
 cholesteric liquid crystal coatings, superimposed left- and right-handed, peak refl. and colour gamut 0-74472  
 contact charge transfer complexes of organic molecules with  $O_2$ , CNDO/S calcs., absorpt. spectra obs. 0-69076  
 continuous relaxation spectra, direct anal. 0-104831  
 copper (II) complex, bis(dithiocarbamate), HF-Slater-LCAO calcs., mag. coupling parameters and optical spectrum 0-99447  
 4-cyanobiphenyl and 4'-alkyl- or 4'-alkoxy-substituted liq. cryst. derivatives, soln., absorpt. and fluoresc. spectra 0-87164  
 4-cyanobiphenyl/4-cyano-p-terphenyl liq. cryst. mixture, order parameters of dissolved dyes 0-100167  
 cyanodiacetylene cation, gas phase, UV emission spectra of  $A(\pi^-) \rightarrow X(\pi^-)$  band system 0-95636  
 cyclophosphazene-DNA complex, spectrofluorometric and spectrophotometric investig. 0-95643  
 cytosine, hydroxy and methoxy, derivatives, absorption UV spectroscopy and electronic struct. of ionic and tautomeric forms 0-74177  
 diacetylene (TSHD), low temp. photopolymerisation, short chain intermediates obs. 0-93754  
 diazaphthalenes, excited state absorpt. spectra and intersystem crossing kinetics 0-74176  
 dibromomethane, highly excited vibr. states, thermal lensing spectrosc. and local mode model 0-87140  
 1,3- and 1,4-dibromotetrafluorobenzene cations in gaseous state, emission spectra 0-63648  
 dichlorofluoromethyl peroxynitrate, UV absorpt., spectra, photodissoc. lifetime meas. 0-83386  
 dichloromethane, highly excited vibr. states, thermal lensing spectrosc. and local mode model 0-87140  
 3,3'-diethylthiacarbocyanine iodine-rhodamine 6G, energy transfer with increased local conc., Förster mechanism 0-69220  
 4-(2,4'-dinitrobenzyl)-pyridine, photochromism, nanosec. laser absorpt. spectrosc. obs. 0-85193  
 diphenyl anion salts, sublimed layer, electronic and IR absorpt. spectra 0-66189  
 1,6-diphenylhexatriene, radiationless transitions and natural lifetimes, solvent effects 0-63622  
 diphenylpolyene molecules, excited electronic states, vibronic mixing, wave functions, method of fragments anal. 0-63615  
 DNA interactions with cations, UV difference spectrosc. and Marcus theory 0-94153  
 dye in polymer matrices, electrochromic props. and use as probe of matrix softening around  $T_g$  0-84724  
 dye molecules adsorbed on Ag, Au and Cu films, absorpt. and luminesc. study 0-103981  
 ethane, diode laser spectra, baseline variations, elimination by ultra-low freq. filtering 0-90901  
 ethane gas, local mode overtone bands 0-83444  
 ethylcyanodiacetylene cation, gas phase, UV emission spectra of  $A(\pi^-) \rightarrow X(\pi^-)$  band system 0-95636  
 ethylene, vacuum ultraviolet absorption spectra 0-63653  
 N-ethylphthalimide+olefins, photochemical reaction, absorpt., fluoresc., phosphoresc. and triplet-triplet absorpt. spectra 0-85197  
 ferrocene, multiphoton dissociation and ionisation by tuneable dye lasers 0-99524  
 fluorobenzene, multiphoton ionisation spectrum in one-photon wavelength region 0-63727  
 fluorobenzene,  $S_0 \rightarrow S_1$  transitions, two-photon absorpt. spectra by nozzle beam-multiphoton ionisation method 0-63728  
 fluorobenzenes in Ne matrices, molecular cation electronic absorption spectra, new photolytic technique 0-58415  
 formaldehyde, mol., UV absorpt. cross-section, and stratosphere chem. 0-109209  
 formaldehyde, selective laser photolysis for  $^{14}C$  enrichment 0-108720  
 formaldehyde and its isotopic species, rot. spectra of ground vibr. state, rot. const. determ. 0-83350  
 furan, resonantly enhanced multiphoton ionisation 0-106362  
 germanium phthalocyanine, elec. cond. temp. depend. 0-80271  
 glyoxal,  $S_0 \rightarrow S_1$  band, opto-acoustic phase angle meas. 0-68256  
 haematoporphyrine, complexed with chloral and tryptophane, energy spectra, transition moments and intermolecular distances 0-72127  
 halobenzene type ions, high resolution spectrosc. with new emission source (*French*) 0-57383  
 heterocyclic compounds, bond lengths, fifth overtone of C-H stretching vibr. obs. 0-91528  
 hexafluorobenzene, IR multiphoton excitation, vibr. energy redistrib. and hot band spectrum 0-95656  
 hexamethylbenzene in tetrachloromethane soln., local mode overtone bands 0-83444

## spectra of organic molecules and substances continued

1,3,5-hexatriene radical cation, in Ne matrix, laser induced fluoresc. and emission spectra 0-87163  
 1-hydronaphthyl radical, 4.2K absorpt. spectrum (*French*) 0-80809  
 hydronaphthyl radicals embedded in naphthalene cryst., optical transition energies and ionisation energies 0-78595  
 3-iodopropene, rot. spectra, quadrupole hyperfine struct. 0-91545  
 methane, appl. of band-model parameters to Uranus visible and near IR spectrum 0-98609  
 methane, liquid, opto-acoustic study of weak optical absorpt. 0-93278  
 methane-d<sub>2</sub>, high resolution spectra, line intensities, ground-state rot. const. determ. 0-83517  
 methine dyes, spectral props., solvent effects 0-69181  
 methoxy radical UV emission spectra from methanol+Ar(Kr) reactions 0-91572  
 methyl allenyl sulphide, UV absorpt. spectra, role of 3d valence-shell and 4s Rydberg-type atomic orbitals 0-83384  
 3-methyl lumiflavin, in soln., absorpt. spectrum 0-58277  
 methyl peroxynitrate, UV absorpt., spectra, photodissoc. lifetime meas. 0-83386  
 N-methyl pyrrole, resonantly enhanced multiphoton ionisation 0-106362  
 methylbenzenes, 3p Rydberg transitions, multiphoton ionis. spectrosc. obs. 0-95644  
 methylcyanodiacetylene cation, gas phase, UV emission spectra of  $A(\pi^-) \rightarrow X(\pi^-)$  band system 0-95636  
 methylhydroperoxide, UV absorpt. spectra of vap. 0-69159  
 $\beta$ -methylumbelliferone in ethanol solns., spontaneous luminesc. kinetics 0-74192  
 molecular crystals, intermolecular interactions, spectroscopic studies, review 0-103958  
 2(4)-monooxypyrimidines, gaseous, matrix, soln., tautomeric equilib., IR and UV absorpt. spectra 0-58256  
 naphthalene:tetracene, electronic absorpt. spectrum, host-cryst. field effect 0-100669  
 naphthalene, solution, structured UV spectrum obtained by ultrafast two-pulse excitation 0-78630  
 naphthalene- $\beta$ -naphthol, concentration effects in exciton absorption region 0-108241  
 naphthalene- $\beta$ -naphthol mixture, exciton absorpt. depolarisation 0-103972  
 neopentane liq., local mode overtone bands 0-83444  
 neoclozene, multiphoton dissociation and ionisation by tuneable dye lasers 0-99524  
 n-octane-3,4,6,7-dibenzpyrene impurity, fluorescence impurity spectra, phonon free line broadening (*Russian*) 0-108279  
 trans, trans-1,3,5,7-octatetraene, high-resolution one and two photon excitation spectra 0-78669  
 organic molecular crystal, doped, two-particle electronic excitation, optical cooperative excitation 0-93368  
 2-oxophenylbenzoxazol, proton intramolecular transfer, light absorpt. and emission, dichroism, polarised fluoresc. 0-87166  
 pentacene, disordered solid layer, absorpt. spectra 0-93417  
 pentacene in naphthalene (p-terphenyl), mol. mixed crystals, optical dephasing and vibronic relax. 0-95957  
 phenothiazine derivatives, semicond. elec. props., optical spectra, and EPR 0-103693  
 6-phenoxy-5,11-naphthacenequinones, photochromism, molar extinction coefficients, meas. 0-66220  
 phthalocyanine, quasiline emission spectra using low temp. laser luminesc. spectrosc. (*Czech*) 0-86445  
 pinacanol in ethanol, electronic relax., analysing light ps spectroscopy 0-99517  
 PMMA, glassy, optical absorpt., visible region, determ. by laser calorimetry 0-66218  
 poly(2-vinyl pyridine), dil. solns., translational diffusion, chain conformation influence 0-103508  
 polyenes, electronic absorpt. spectra, charact. spectral band criteria 0-63651  
 polymer spectral sensitivity and photochem. stability using Xe high press. lamp (*German*) 0-61119  
 polymethine dye solutions, photochem. transformations and short-wavelength luminesc. 0-100686  
 polypeptide chains, struct. of conduction and valence band 0-76700  
 polystyrene, glassy, optical absorpt., visible region, determ. by laser calorimetry 0-66218  
 polyvinylquinazoline- $I_2$  complexes, absorpt. spectra and elect. cond. 0-92891  
 porphyrin, hypersurface of adiabatic pot. calc. by CNDO/2 method, vibr. freqs., absorpt. spectra calc. 0-95543  
 propioly chloride(-d), 357-333 nm absorpt. system 0-69161  
 propioly fluoride(-d), 290 nm absorpt. system 0-87142  
 protoclrophyl, mag. reson., site selected fluoresc. detection 0-69164  
 protoporphyrin IX, triplet states, flash photolysis, obs. 0-95555  
 protoporphyrin IX dimethyl ester, triplet states, flash photolysis, obs. 0-95555  
 PVC, thermal stabilisation by triazine dithiols (*Japanese*) 0-108386  
 PVC thermal degradation, reinitiation mechanism of HCl catalysis 0-71944  
 pyridines, monosubst.,  $H_2O$  complexes,  $n \rightarrow \pi^*$  transitions, H bonding, MO theory 0-95550  
 pyrimidines, substituted analogues, absorption UV spectroscopy and electronic struct. of ionic and tautomeric forms 0-74177  
 pyrrole, resonantly enhanced multiphoton ionisation 0-106362  
 rhodamine 6G, in rigid matrix, conc. effects in spectra 0-83347  
 rhodamine 6G ethanol soln., absorpt. and luminesc. spectra using picosecond excitation 0-106351  
 silicon phthalocyanine, elec. cond. temp. depend. 0-80271  
 spiropyron solutions, nitro-substituted, electronic state participation in photochromy 0-81347  
 stilbene, pulsed electron excitation, triplet excitons, spectral and electrical investigations 0-92828  
 sucrose, single cryst., absorption spectrum of electron traps, pulse radiolysis obs. 0-93369  
 TCNQ salt, MeDABCO(TCNQ)<sub>2</sub>, optical, elec., and mag. props. 0-65539  
 p-terphenyl cryst., low lying single state 0-97320  
 tetrabenzofila, cd, j, Implevylene evaporated film, crystn., time depend. as function of purity 0-88449  
 tetracene, disordered solid layer, absorpt. spectra 0-93417  
 tetracene, intrastate scrambling in large mol. bound level struct. 0-63696  
 tetrachloromethane, UV laser photolysis 0-66826



**spectra of organic molecules and substances continued**

- tetramethyl-1,3-cyclobutanedithione- $h_{12}$  and - $d_{12}$ , visible spectra,  $\pi\pi^*$  transitions obs., mol. vibr. 0-97297  
 tetramethylbutane in hexachlorobutadiene soln., local mode overtone bands 0-83444  
 tetraphenyldithiopyranilidene mixed valence polyiodides, crystalline struct. and optical props. 0-92516  
 thermotropic polymers, cholesteric with mesogenic moieties and flexible spacers in main chain, synthesis and light reflection 0-88028  
 thiocarbonyl chlorofluoride, second excited singlet state emission spectroscopy, resonance fluorescence obs. 0-69158  
 thionine in sodium lauryl sulphate micellar solns., absorpt. spectra and fluoresc. yield, local dye conc. depend. 0-106343  
 thiophosgene, second excited singlet state emission spectroscopy, Franck-Condon anal. 0-69157  
 thiophosgene, vibronic anal. of electronic transition, inversion doubling splittings obs. 0-83388  
 toluene cation in solid Ar, absorption and photodissociation spectra 0-69156  
 trialkylammonium, iodides, absorpt. and luminesc. spectra of self-localized excitons 0-97340  
 1,3,5-tribromotrifluorobenzene in gaseous state, emission spectra 0-63648  
 trichlorobenzene cation, selectively excited wavelength resolved emission spectra 0-87136  
 trichlorofluoromethane, UV laser photolysis 0-66826  
 trichloromethyl peroxyhydrate, UV absorpt., spectra, photodissoc. lifetime meas. 0-83386  
 trifluorobenzene cation, selectively excited wavelength resolved emission spectra 0-87136  
 trifluoriodomethane, highly excited, intermol. vibr. energy transfer, transient UV absorpt. spectra 0-106381  
 trifluoriodomethane, vac. UV absorpt. cross section 0-91574  
 vinyl copolymers, containing fluorescent groups, optically active 0-102594  
 anthracene, polycrystalline, optical props., 3.2-9.3 eV 0-76097  
 CCO radical, heat of form. calc., geometries excitation energies and vibr. freq. calc. using POL-CI wave functions 0-89512  
 $CH_3PF_4$ , nonrigid mol., tunnelling mechanisms, spectrosc. theory 0-78605  
 $CS_2$  in cooled supersonic expansion, electronic absorpt. spectra obs. 0-78629  
 Cr complex,  $(-)_5$ -tris(ethylenediamine) chromium (III), solid-state circular dichroism spectra, phase modulation spectrosc. obs. 0-93271  
 Cu(II) complex, 2,2',2''-triarniotriethylamine, EPR and optical absorpt. obs. 0-108055  
 Cu(II) complex, hexamethyltriarniotriethylamine, EPR and optical absorpt. obs. 0-108055  
 Cu(II)-DL-proline complex, ESR, magnetic susceptibility and optical absorption 0-93167  
 Ru(II) complex, carbonyl(pyridine)-phthalocyaninoruthenium(II), optical hole burning, matrix effects 0-102522

**spectra of polyatomic inorganic molecules**

- see also infrared spectra of polyatomic inorganic molecules; radiofrequency and microwave spectra of polyatomic inorganic molecules; Raman spectra of polyatomic inorganic molecules*  
 Doppler-limited spectroscopy,  $3\nu_3$  band of  $SF_6$  0-58244  
 transition metal cluster carbonyls, fluxionality, collective oscills. and low energy spectra 0-78738  
 Ar-OCS, liq., dissoci. studies 0-78716  
 $CO_2$  gas, electron impact ionisation, electronic fluoresc. spectra 0-95664  
 $CO_2$ , induced absorpt. spectral moment, mol. calcs. 0-63737  
 $CS_2$ , shock heated, visible emission 0-58274  
 $CIPF_4$ , nonrigid mol., tunnelling mechanisms, spectrosc. theory 0-78605  
 Co complexes, Co II tetraphenylporphyrins, constraint, ESR and optical detect. 0-83394  
 Co complexes, Co(III) mixed complexes, orbital angular momentum reduction,  $^{59}Co$  NMR chemical shift 0-58137  
 $Co_2$ , electrooptical const.,  $2\nu_3$  band induced component 0-78626  
 $D_3$ , emission spectra, rot. struct. obs. mol. const. determ., predissociation 0-106331  
 $H_2$ , emission spectra, rot. struct. obs. mol. const. determ., predissociation 0-106331  
 HCN, photodissoc., photoabsorpt., photoemission and CN form. obs. 0-87141  
 HCN, relationships between higher-transition frequencies 0-69119  
 $H_2O$ , excited stretching vibrs., quantum mechanics 0-91535  
 $H_2O$  vapour, visible absorpt. spectrum, fine struct. acoustooptical determ. 0-86450  
 $H_2O$ , weak spectral absorpt. of vap., visible and near IR 0-82062  
 $HO_2NO$ , UV absorpt., spectra, photodissoc. lifetime meas. 0-83386  
 HSO radical, Doppler-limited dye laser excitation spectroscopy, rot., distortion and spin-rot. interaction const. determ. 0-83383  
 He+OCS, emission spectra in He afterglow 0-87139  
 $HgCl_2(Br_2)(I_2)$ , vac. UV absorpt. cross section 0-91574  
 $NH_3$ , inversion spectrum collisional line broadening, general theory 0-87184  
 $NH_3$ , inversion spectrum press. broadening by He and Ar, linewidths calc. 0-95599  
 $NH_3(ND_3)$  in solid Ar, matrix isolated spectra, temp. dependence 0-63652  
 $NO_2$ , laser spectroscopy by cascade photoionisation method in mass spectrometer 0-99496  
 $NO_2$ , shock heated, visible emission 0-58274  
<sup>15,14</sup> $NO_2$ , predissoc. rot. struct. in 2490 Å band 0-87192  
 $N_2O$  gas, electron impact ionisation, electronic fluoresc. spectra 0-95664  
 $O_3$ , in atmosphere, Chappuis-band absorpt. rel. to conc. determ. 0-77063  
 $O_3$ , UV absorpt. spectra, IR laser induced changes 0-83385  
 $O_3$ , UV absorpt. spectrum, Hartley continuum, IR laser induced changes 0-95639  
 $PH_3$ , conc. meas. by vacuum UV absorpt. spectra 0-71972  
 $SO_2$ , absorption spectrum, meas. using frequency doubled pulsed dye laser 0-87144  
 $SO_2$ , absorption spectrum, meas. using frequency doubled CW dye laser 0-87145  
 $SO_2$ , shock heated, visible emission 0-58274  
 $SO_2$ , UV excitation spectra, mol. fluoresc. meas., mol. predissoc. obs. 0-83389  
 $SO_2^{2-}$ ,  $SO_4^{2-}$ , O K-emission spectra, electron struct. 0-87099  
 $S_2O$ , UV excitation spectra, mol. fluoresc. meas. 0-83389  
 $SeO_2^{2-}$ ,  $SeO_4^{2-}$ , O K-emission spectra, electron struct. 0-87099  
 $TeO_3^{2-}$ ,  $TeO_4^{2-}$ , O K-emission spectra, electron struct. 0-87099

**spectra of polyatomic inorganic molecules continued**

- $ThF_4$ , absorpt. spectrum of vapour, Th reson. localised 5,epsilon f state 0-91467  
 $UF_4$ , absorption spectrum indicating presence of resonantly localised continuum state 0-58173  
 $UF_6$ , multiphoton irradiation, spectra and modeling of laser induced emission 0-69160  
**spectra of solids**  
*see also impurity and defect absorption spectra of solids; luminescence of solids; Shpol'skii spectra; spectra of inorganic solids; spectra of organic molecules and substances*  
 anisotropic transition layer, surface polariton spectra in presence of resonance 0-88484  
 biexcitons, nonlinear laser spectrosc., multiphoton transitions 0-84433  
 conference, basic optical props. of materials, Gaithersburg, MD, USA (May 1980) 0-101668  
 dust, soil derived atmospheric, IR spectra, Christiansen effect, Rayleigh limit 0-105046  
 exciton absorption peak, temp. depend., calc. 0-59885  
 Frenkel biexcitons, eigenstates and transition spectra 0-88480  
 ionic crystals, lattice defects, conference, Canterbury, England (Sept. 1979) 0-105420  
 non-equilibrium phonon distrib., in cryst., spectral line shape theory 0-60530  
 photon echo spectroscopy of crystals, review 0-83648  
 quasi-Jahn-Teller optical absorption line shape due to transition from  $A_{1g}$  to  $(A_{1g} + T_{1u}) \times T_{1u}$  system 0-92862  
 semiconductor, electron excitation spectra in field of two travelling waves 0-65514  
 semiconductor, IR absorpt. and optical relax. time of free carriers 0-66206  
 semiconductors and insulators, nonequib. electron Coulomb collisions during optical pulse interband interaction 0-76049  
 thin film heterostructures, optical transition selection rules 0-66319

**spectral analysers**

- see also spectral analysis; wave analysers*  
 acoustic noise meas., unsteady, from letter-handling machines, automatic classification of noise levels 0-79085  
 coherent light valve processor, two-dimens. optical modulator 0-102840  
 cross-power spectrum analysers, satellite-borne, appl. to ionospheric plasma wave meas. 0-94621  
 Fourier, using light polarization discrimination technique combined with chirp-Fourier transform algorithm 0-74310  
 GenRad 2512, simplicity of operation due to interactive display, technical specifications 0-64326  
 integrated optic, design of Bragg cells 0-74515  
 integrated optics, broadband chirp transducers 0-74514  
 integrated optics version, SAW Broadband modified chirp transducers appl. 0-58802  
 laser output spectrum, high resolution meas. 0-95891  
 optical analogue processing system appl. (Spanish) 0-95822  
 optical line image transmission through single fibre using spectral instrums. 0-102820  
 real time anal., FFT appl. (Spanish) 0-90825  
 SAW integrated optics spectrum analyser, development progress 0-58803  
 SAW spectrum analysers in photon-counting mode, statistical props. 0-105712  
 self-scanned photodiode array, evaluation for integrated optics spectrum analyser 0-58806  
 spectrum analyzer employing SAW chirp filter (Japanese) 0-79065  
 $TeO_2$  time-integrating acousto-optical correlator for chirp spectrum analyses 0-106474

**spectral analysis**

- see also spectral analysers*  
 acoustic noise meas., unsteady, from letter-handling machines, automatic classification of noise levels 0-79085  
 acoustic noise spectrum meas. in ocean for small observation baseline 0-102902  
 acoustic signal characterization using spectral microanalysis 0-74607  
 analogue data processing systems, polarised modulation of light (Russian) 0-91884  
 atmospheric precip.-time struct., daily precip. amounts modelling with Markov-I chain 0-101401  
 autoregressive technique, appl. to astronomy and geodynamics (Chinese) 0-85869  
 biological shape pattern recognition, average similarities of Fourier spectra 0-104818  
 CW signals in white noise, influence of data window shape 0-64300  
 Earth secular polar motion, low frequency spectrum anal. (Chinese) 0-104849  
 EEG, spectral band analysis, contrib. to attentional processes study (French) 0-61721  
 electrostatic sparks detection and characts., by radio methods 0-68217  
 esophageal speech, long-time spectral and intensity characts. 0-74643  
 generalized framework for power spectral estimation 0-83703  
 geomagnetic energy spectra, depend. on solar wind vel. and interplanetary mag. field direction 0-67476  
 HD 101065, Przybylski's star, light variability freq. anal. 0-62152  
 Indian Ocean equatorial waves, evidence for continuous spectrum 0-98331  
 laser Doppler anemometer signals operating in burst mode 0-100041  
 laser Doppler velocimeter with direct spectral anal. for instantaneous vel. meas. 0-99782  
 long-term spectra, computerised meas. method, English and Finnish data comparative study 0-104688  
 method of moments in spectral analysis 0-68137  
 musical complex tone classification according to shape of spectrum envelope 0-102939  
 musical scale, 12-tone, tempered Fourier transform 0-87671  
 narrowband optical signal, spectral width estimation 0-102627  
 optical processor, time- and space-integrating, for spread spectrum appl. 0-78777  
 optical wave, log-amplitude fluctuations spectra, turbulence spectra parameters determ. 0-95797  
 particle size and density determ., bispectral anal. of laser Doppler vibr. meas. 0-98880  
 polished surfaces, smoothness parameter meas. using spectral analysis optical system 0-86261  
 precipitation, seasonal, in Jerusalem, temporal fluctuations 0-72618

## spectral analysis continued

- quasar redshifts distributions, periodicity from correl. and power-spectrum anal. 0-62313  
 randomly sampled signals, variability reduction by filtering out parts of spectral energy 0-57193  
 SEASAT radar altimeter data, spectral coherence rel. to geoid features resolution capability 0-72645  
 seismic waves, of explosion earthquakes assoc. with 1973 eruptions of Asama Volcano (*Japanese*) 0-67340  
 seismic waves, spectral anal. rel. to attenuation in earthquake aftershock region 0-76926  
 space-time optics, speckle phenomena and white light correlations 0-106460  
 spatial frequency analysis with incoherent optical approach, using LED light panel 0-78779  
 spectrograms, detection, estimation and classification 0-64296  
 spoken word recognition method using nonlinear spectral matching (*Japanese*) 0-69605  
 stratigraphic data, spectral density anal. rel. to astronomical theory of climatic fluctuations 0-72509  
 time-delay spectrometry, practical appl. in field of acoustics 0-79082  
 US, using frequency-tracked gated RF pulses 0-79079  
 vibration data, manufacturing machines, failure prediction 0-79048  
 water waves, wind-generated, cross-spectral density rel. to freq. independent phase vels. 0-98333

## spectral line breadth

- see also atomic spectral line breadth; chemical shift; Davydov splitting; Doppler effect; EPR line breadth; molecular spectral line breadth; NMR line breadth; Stark effect; Zeeman effect  
 1309-216, probable BL Lacertae object, absorpt. lines intrinsic widths and red shifts 0-67856  
 A-type supergiant stars, reson. line profiles from IUE and Copernicus spectra 0-90424  
 acetic acid-d<sub>3</sub>(-d<sub>1</sub>), Fermi reson., IR spectra band profiles 0-60569  
 acetylene, He-Ne laser line, high temp. absorpt., anal. by high resolution IR spectra 0-91554  
 alkali halides, photoemission, energies and lineshapes 0-89119  
 alkali intercalated graphite, C XXV Auger lineshape anal. 0-104019  
 alkali-haloid salts, aqueous solutions, IR absorpt.  $\nu_1$  (CN) band parameter temp., conc. study (*Russian*) 0-80801  
 analyte emission characts., inductively coupled plasma, effect of emission spatial profiles 0-89557  
 anthracene, cryst., exciton aggregate possible form. under intense optical pumping, fluoresc. spectra 0-84772  
 R Aquarii, H $\alpha$  and forbidden O III emission line profiles 0-85946  
 atom pairs in solids, cooperative two-photon absorpt. lineshape 0-84706  
 atomic spectra in intense mag. fields, theory and appl. to dense stars atmospheres 0-105160  
 Auger lineshape anal. of molecules and solids 0-76113  
 AR Aurigae, eclipsing binary Hg star, Hg II 3984 Å profile vars. during eclipse 0-98679  
 band shape of IR spectra, slit width effect 0-86463  
 $\xi$  Bootis A, G8 V star, line profiles Fourier deconvolution and mag. field obs. 0-72949  
 3C 120, radio galaxy, search for vars. in emission lines equivalent widths and profiles (*Russian*) 0-90540  
 UW Canis Majoris, O7f supergiant, UV lines P Cygni profiles rel. to mass loss rate 0-67736  
 VV Cephei, Mg II reson. lines profiles and absolute visual magnitude 0-109498  
 chemical laser, low pressure, line-shape flattening resulting from hyper-sonic nozzle wedge flow 0-91783  
 collisional linewidths and shifts determ. by convolution method 0-102541  
 P Cygni, H Paschen  $\alpha$  equivalent width 0-62156  
 V1329 Cygni (HBV 475), symbiotic variable, nebular and Balmer line profiles 0-62148  
 V1500 Cygni (Nova 1975), Balmer line emission profiles evolution in early decline phase 0-82371  
 V1668 Cygni (Nova 1978), H $\alpha$  emission line profiles obs., (1978 to 1979) (*Russian*) 0-109444  
 DFS-8 spectrograph, attachment for oscillographic recording of line shapes 0-105721  
 Doppler broadening, elimination problem, parametric soln. 0-62730  
 S Doradus, Hubble-Sandage variable in LMC, visual line profiles rel. to mass loss 0-101595  
 early-type stars, H and He<sup>+</sup> synthetic line profiles in stellar winds 0-85926  
 electron spectroscopy of core levels in solids, lifetime broadening 0-80938  
 emission line shapes from a rotating ring radiator 0-83998  
 ethane-1,1,1-d<sub>3</sub>, gas-phase IR spectra, rot. fine struct. obs. 0-83359  
 ethylene, He-Ne laser line, high temp. absorpt., anal. by high resolution IR spectra 0-91554  
 ferromagnet, shape of Mossbauer line 0-71251  
 ferromagnetic, thick film, reson. transmission of EM energy via phonons 0-60382  
 fluorescence line narrowing, line-shape deconvolution 0-89039  
 galaxies, IR magnitude/H I vel. width relation rel. to distance scale and Universe expansion rate outside Local Supercluster 0-105325  
 gas, inhomogeneous layer, transmission calc. for spectral line with Voigt profile 0-59164  
 graphite intercalation with Li, Raman scatt. study 0-88999  
 HD 168607 (B9 Ia<sup>+</sup>), S Doradus type star candidate, spectral line profiles (*Russian*) 0-90456  
 heavily doped semicond., photoemission lineshapes of impurity levels, p-wave resonance 0-76154  
 Hercules X-1, X-ray cyclotron line features width calcs. 0-86015  
 high-Z emitters in ultradense plasmas, hydrogenic profiles, perturbing ion effects 0-79566  
 impurity centres, electron-phonon coupling from structured optical spectra, review 0-89038  
 inert gas crystal, lattice vibrs. and radiative transitions of implanted ions (*Russian*) 0-69098  
 interplanetary H I,  $\lambda$  emission profiles reanal. rel. to local interstellar gas temp. and vel. 0-105141  
 interstellar H<sub>2</sub>O (*Russian*) 0-105320  
 iodide, charge transfer to solvent spectra, spectral shift data, Madelung const. determ. 0-85204  
 isopropyl benzene, mol. solid, temp. depend. UPS linewidths 0-89115  
 EV Lacertae, flare star, Balmer emission lines vars. rel. to starspots and rot. period 0-98665

## spectral line breadth continued

- 48 Librae, Be star, shell spectrum line profiles 0-62146  
 line broadening theory, screening process dynamics (*Russian*) 0-69988  
 liquid, Raman band profile, vibr. dephasing and intermolecular interactions 0-60556  
 magnetic DA white dwarfs, spectral line and circular polarisation profiles 0-62123  
 maser with beam of infllying atoms, spectral line broadening mechanism 0-106503  
 metals, narrow-band, Auger line shape 0-60719  
 methane, <sup>12</sup>C and <sup>13</sup>C, line parameters for  $\nu_2$  and  $\nu_4$  bands, isotope shifts, appln. to planetary atmospheres 0-95622  
 molecular crystal IR spectral line shape and polarisation temp. depend. 0-88991  
 Mossbauer line narrowing by resonant filter 0-77922  
 Mossbauer spectra, line-broadening 0-93221  
 N70, giant filamentary shell in LMC, line profiles rel. to dynamics 0-90511  
 naphthalene: pentacene, intermol. interaction dynamics and optical dephasing 0-64112  
 naphthalene, vibr. relax. studied by four wave mixing (CARS), spectral lineshapes obs. 0-80762  
 NGC 604, 5471, giant extragalactic H II regions, P Cygni line profiles in UV spectra 0-77467  
 NGC 604, H II region in M 33, H $\alpha$  line profile width rel. to core-halo struct. 0-85984  
 NGC 6888, ring nebulae around Wolf-Rayet star HD 192163, filaments and smooth gas linewidths (*Russian*) 0-90515  
 non-equilibrium phonon distrib., in cryst., spectral line shape theory 0-60530  
 non-Lorentzian laser lineshape and reversed peak asymmetry in double optical reson. 0-69443  
 nonafluorobutane, IR spectra, spectral bandshape and intensity of C-H chromophore 0-83355  
 nonlinear spectroscopy, recoil effects on Doppler-free lineshapes 0-82829  
 70 Ophiuchi A, K0 V star, line profiles Fourier deconvolution and mag. field obs. 0-72949  
 organic solids, vibr. relax. and dephasing Raman spectra, review 0-88987  
 $\zeta$  Orionis, Reticon obs. of H $\alpha$  P Cygni profile 0-82365  
 $\beta$  Persei (Algol), UV line profiles obs. rel. to primary component rot. 0-72996  
 photosynthetic systems, discovery of phase transitions, Stokes Raman scatt. 0-81539  
 Pioneer 10 and 11 radio signals, spectral broadening by ionospheres of Jupiter and Saturn 0-109391  
 plasma optical transparency evaluation, line broadening effect 0-79453  
 polystyrene-cyclohexane mixture, Rayleigh and Brillouin scatt. and struct. relaxation 0-63640  
 positron annihilation and vacancy formation, Doppler broadening study 0-60708  
 propylene, He-Ne laser line, high temp. absorpt., anal. by high resolution IR spectra 0-91554  
 $\zeta$  Puppis, Reticon obs. of H $\alpha$  P Cygni profile 0-82365  
 quasi-Jahn-Teller optical absorption line shape due to transition from A<sub>1g</sub> to (A<sub>1g</sub>+T<sub>1g</sub>) $\times$ T<sub>1g</sub> system 0-92862  
 radiative transfer, non-LTE, asymptotics of partial redistrib. 0-62008  
 resonance Raman lineshapes study of vibrational and rotational relaxation in soln. 0-60560  
 resonance Raman lineshapes and fluorescence in strong radiation fields 0-87074  
 Rochelle salt, ferroelectric, Raman and IR study 0-71406  
 ruby R<sub>1</sub> zero phonon line, resonance fluoresc. meas. 0-89055  
 semiconductors, luminesc., electron beam or optically excited, quasi-equilib. approx. 0-84779  
 Seyfert galaxies, nearby, H $\beta$  line width correl. with morphology 0-82478  
 solar corona, intensity ratios of fine-struct. components of H like ions reson. lines 0-101581  
 solar Fraunhofer lines, asymmetry rel. to photospheric waves and convective motions (*Russian*) 0-72901  
 solar limb flare, 1959 July 25, Balmer line profiles rel. to physical conditions 0-105227  
 solar photosphere line asymmetries, appl. to vel. gradients retrieval via linearised approach 0-62093  
 solar quiescent prominence spectra, meas. of Ca<sup>+</sup> 8542, 8498 Å, He 4471 Å and Ti<sup>+</sup> 4468 Å 0-90373  
 solar spectra, line profiles, rough reconstruction from series of narrow-band filtergrams (*Italian*) 0-98564  
 solar spectra, local macroturbulent broadening by granulation vertical vel. component 0-62094  
 solar spectrum, photospheric lines damping const. determ. methods errors (*Russian*) 0-72899  
 squaric acid, two-dimens. phase transition, Raman scatt. study 0-71401  
 steel, austenitic, Cr-Ni, ion-implanted N, chem. state study by AES and XPS 0-79825  
 steel, high C, type 7KfNSh, plastic deform. influence of X-ray interference line breadth (*Russian*) 0-93599  
 stellar spectra, line formation in turbulent media 0-77387  
 stellar spectra, line profiles anal. using linear filtering theory (*Italian*) 0-90340  
 Stepanyan's star, eclipsing binary, H $\beta$  emission line width 0-67788  
 Stokes parameters and mag. field vector profiles (*Chinese*) 0-77386  
 strongly coupled Jahn-Teller system, cluster model for optical absorption spectrum 0-89034  
 synchronous excitation spectrofluorometry (*Japanese*) 0-86452  
 DR Tauri, T Tauri star, Balmer line profile changes and inverse P Cygni profiles 0-101591  
 thiourea, ferroelectric, Raman and IR study 0-71406  
 trifluoromethane, IR spectra, spectral bandshape and intensity of C-H chromophore 0-83355  
 tunable diode laser spectrometry for line profile determination in second derivative spectra 0-86435  
 tunable diode laser spectrometry for line profile determination of second derivative spectra, expt. results 0-86436  
 turbulent plasma, magnetised, line shape of optical satellites 0-75098  
 W Ursae Majoris stars, rot. line broadening functions rel. to stellar shapes 0-109494  
 Voigt functions, nonlinear least square algorithm 0-90900  
 Voigt lineshape, evaluation and characterisation 0-73401  
 Voigt profile, expansion into components 0-83427  
 Voigt profile, Lorentz component true halfwidths and line intensities 0-87943



## spectral line breadth continued

- $XY_2$ ,  $Z$  mixed crystals, impurity centre local oscill. spectral distribution (Russian) 0-60643
- $Ag_2HgI_4$ , Raman line shape and ionic cond., coupled mode model 0-66171
- $Al$ , valence band Auger spectra, surface effect 0-80915
- $AlN$ , absorpt. edge shape interpretation, Wannier excitons absorpt. in charge impurity elec. field 0-66233
- $Al_2O_3:Cr^{3+}$ , Jahn-Teller system, zero-phonon line broadening due to non-radiative transitions 0-108258
- $As_0.5Sb_{0.5}Si$  cryst., ferroelec., soft mode Raman and IR spectroscopy 0-76016
- $Bi$ , optical phonon anharmonicity and melting, light scatt. study 0-60621
- $CF_4$ , Nd laser excited stimulated Mendelstam-Brillouin scatt. phase fluctuations (Russian) 0-89014
- $Ca$ , laser saturation broadening in flames, fluoresc. excitation profile obs. 0-95568
- $CaF_2:Sm^{2+}$ , coherent population oscills. and hole burning observed using polarization spectroscopy 0-71457
- $Ca_{1-x}Sr_xF_2:Er^{3+}$  mixed crystal, luminesc. transition, inhomogeneous line broadening calc. 0-97332
- $CdSe$ :Li, pure and doped, reson. Raman and Brillouin scatt., elastic exciton-defect scatt. 0-80788
- $CdTe(Se):Co$ , impurity luminescence no phonon line depend. on temp., Debye temp. 0-66273
- $CsMnCl_2 \cdot 2H_2O$ , subthreshold two-magnon absorpt., depend. on freq., temp. and mag. field, exchange coupling const. (Russian) 0-71184
- $CsNiF_3$ , 1D ferromag., optical absorption and spin dynamics 0-71417
- $Cs_2SO_4:Al_2(SO_4)_3 \cdot 24H_2O$ ,  $^{53}Cr^{3+}$  ENDOR Lines, RF ENDOR power and modulation freq. effects 0-75884
- $Cu$ , prevacancy temperature depend. of positron annihilation, Doppler broadening lineshape parameters 0-60709
- $Cu_2VS_4$ , Raman linewidth of  $A_1$  mode under high press., reson. effects 0-108210
- $EuO$  nonstoichiometric film, ESR spectra and exchange interaction 0-93176
- $Eu_{1-x}Sm_xS$ , ESR, exchange interaction, susceptibility, elec. cond., thermoelectric power 0-93174
- $FeI$ , self-absorption-free spectral lines for temp. meas. in DC C-arc 0-87965
- $GaAs$ , exciton quenching, obs. at room temp. using electrolyte electroreflectance 0-60546
- $n-GaAs$ , spectra, light induced, electrolyte and Schottky barrier techniques of meas. 0-76046
- $GaP$ , complex  $^{119}Sn$  impurity-defect, Mossbauer study 0-75898
- $GaP$ , light scatt. by LO phonons, high-resolution study 0-80798
- $GaSb$ , accumulation layer localised carriers interaction with LO phonons, Raman interference lineshapes 0-93338
- $p-GaSb$ , heavily doped, LO phonon-carrier interaction, Raman interf. lineshapes 0-93319
- $GdRh_2B_4$ , magnetic and electrostatic props., NMR study 0-93195
- $Ge$  (111), spectroscopy of electron subbands 0-71422
- $N-Ge$ , electrorefl. spectra, light induced, electrolyte and Schottky barrier techniques of meas. 0-76046
- $Ge$ , impurity spectral linewidth meas., free electron effects 0-71463
- $H I$  in field of elliptical galaxy NGC 1052, 21 cm emission mapping and line profiles 0-98719
- $H$  plasma, Stark broadening, model microfield methods calcs. 0-92274
- $H$ -bonded systems, frequency shift rel. to IR bandwidth 0-99502
- $H_2$  and  $H_2$  spectral profiles from neutral beams and plasmas in high mag. fields 0-83999
- $HCl$ -inert gas rot.-vibr. line pressure broadening and shift calc. 0-69124
- $He II$  4686 Å line, Stark profile meas. in high density plasma 0-96390
- $He+NO$ , multiphoton ionisation spectra in supersonic expansion, laser entranced collisional effects 0-83459
- $^4He$ , liq., cyclotron reson. of hot electrons 0-88377
- $In$ , laser saturation broadening in flames, fluoresc. excitation profile obs. 0-95568
- $InSb$ , accumulation layer localised carriers interaction with LO phonons, Raman interference lineshapes 0-93338
- $p-InSb$ , heavily doped, LO phonon-carrier interaction, Raman interf. lineshapes 0-93319
- $Ir(III)$  complex, cis-dichlorobis(4,4'-dimethyl 2,2'-bipyridine) iridium chloride 0-97319
- $^{191}Ir$ , excited nuclei mean precession time depend. on  $\gamma$ -spectral width, g-factors (Russian) 0-78211
- $KBr$ , intra impurity local oscill. composition tone absorpt. band anharmonic temp. broadening (Russian) 0-60642
- $KCN$ , dynamics of  $CN^-$  ions near phase transitions at 83K 0-80717
- $3KNO_3 \cdot 2Ca(NO_3)_2$ , glass form. from liq., struct. transform., Raman spectrum obs. 0-64916
- $3KNO_3 \cdot 2ZnCl_2$ , glass form. from liq., struct. transform., Raman spectrum obs. 0-64916
- $K_2SeO_4$ , phase mode in incommensurate phase, Raman scatt. obs. 0-80766
- $LaCl_3:Np^{3+}$ , phonon-induced relax. in excited optical states, linewidth temp. depend. meas. 0-100688
- $Li$ , valence band Auger spectra, surface effect 0-80915
- $LiC_6$ , intercalation compound, electronic struct., XPS meas. 0-59850
- $LuRh_2B_4$ , magnetic and electrostatic props., NMR study 0-93195
- $MgO:Cr$ , high resolution far IR spectroscopy of lower energy levels of  $Cr^{2+}$  0-80822
- $MgO:V^{2+}$ , Jahn-Teller system, zero-phonon line broadening due to non-radiative transitions 0-108258
- $MnO$ , magnon-sideband lineshape, exciton-phonon interaction effects 0-65846
- $NH_3$ , inversion spectrum press. broadening by He and Ar, linewidths calc. 0-95599
- $Na$ , laser saturation broadening in flames, fluoresc. excitation profile obs. 0-95568
- $Na$ , overlapping autoionisation lines, interference effects 0-91677
- $Na+inert$  gas, non-Lorentzian spectral line shape 0-106297
- $NaFeF_2$ , Mossbauer and low-temp. dilatometry study (French) 0-80662
- $NaNO_3$ , lattice vibration neutron diffraction study (French) 0-103429
- $Nd:silicate$  glass, resonance laser excitation, inhomogeneously broadened emission spectra 0-66295
- $Nd:YAG$  laser, subnanosecond pulse generation at 100K 0-74397
- $Nd^{3+}$  glass luminesc. band profile deform. under free-oscillation conditions 0-71487
- $Nd^{3+}:LaCl_3$ , laser-induced fluoresc., hyperfine structs. 0-100677
- $Ni_{0.25}Zn_{0.75}Fe_2O_4$ , Mossbauer study, noncollinear spin struct. 0-60472

## spectral line breadth continued

- $PbTe$ , far IR magnetoref., band struct. 0-76010
- $\beta-PdH_x$ , diffusion-induced reduction of  $^{57}Fe$  Mossbauer fraction 0-108131
- $RbI$ , intra impurity local oscill. composition tone absorpt. band anharmonic temp. broadening (Russian) 0-60642
- $3RbNO_3 \cdot 2Ca(NO_3)_2$ , glass form. from liq., struct. transform., Raman spectrum obs. 0-64916
- $S^{4+}$ , travelling in solids,  $K\alpha$  X-ray spectra 0-100706
- $Sb$ , optical phonon anharmonicity and melting, light scatt. study 0-60621
- $Si$ , bound-exciton spectral lines, conc. broadening at high impurity concs. 0-80826
- $Si$ , dielectric function spectra, ellipsometric determ., many-particle effects at  $E_c$ -transition 0-93363
- $SiO_2:Au(Ag)(Cu)$ , XPS line broadening and extra-atomic relax. energies 0-71561
- $Sr$ , laser saturation broadening in flames, fluoresc. excitation profile obs. 0-95568
- $TiO_2$ , anatase, Raman spectrum, temp. depend. 0-76027
- $Xe$ , fluid, near crit. point, correl. range and Rayleigh linewidth 0-93352
- $Zn$ , optical phonon anharmonicity and melting, light scatt. study 0-60621
- $ZnS:Fe$ , Co Mossbauer sources,  $Fe^{2+}$  transient charge state 0-108128
- $ZnS(Se)(Te):Co$ , impurity luminescence no phonon line depend. on temp., Debye temp. 0-66273
- $ZnSe$ , exciton emission, halfwidths, thermal and optical activation energies obs. (French) 0-66268
- spectral line profiles** see *spectral line breadth*
- spectral line shift**  
see also *chemical shift; isomer shift; isotope shifts; Lamb shift; radiative shifts; red shift; Stark effect; Zeeman effect*  
atom-ion core level shifts,  $\Delta SCF$  calcs. 0-87176  
atomic level field splitting, resonant cooperative light scatt. (Russian) 0-74148  
benzene cryst., electron irradi., phenylcyclohexadienyl radical form., absorpt. and fluoresc. spectra study 0-89035  
collisional linewidths and shifts determ. by convolution method 0-102541  
coumarin 102, excited state interaction dynamics, picosec. time-resolved spectral shift obs. 0-78624  
4-cyanobiphenyl and 4'-alkyl- or 4'-alkoxy-substituted liq. cryst. derivatives, soln., absorpt. and fluoresc. spectra 0-87164  
cyclophosphazene-DNA complex, spectrofluorometric and spectrophotometric investig. 0-95643  
foreign gas induced line shifts, thermodynamics 0-106295  
free-base porphyrin, Zeeman shift meas. by photochem. hole-burning 0-83416  
frequency shifts, determ. by Raman difference spectrosc. 0-78654  
gas pressure depend. 0-87185  
HD 168607 (B9 Ia<sup>+</sup>), S Doradus type star candidate, absorption lines differential shifts (Russian) 0-90456  
heterocyclic compounds, bond lengths, fifth overtone of C-H stretching vibr. obs. 0-91528  
highly excited atoms, blackbody radiation effects 0-58176  
isobutylene, liq., vibr. phase relax. and freq. shifts, density and temp. effects 0-74235  
methanol laser, CW, optically pumped, 170- $\mu m$  emission, press. shift 0-106510  
1-methylindole-n-butanol (ethyl acetate), soln., ground state complex form., fluoresc. spectra, Stokes shift origin 0-58299  
molecular interaction anisotropy, small angle scatt., spectral evidence 0-78600  
molecular solid, intermolecular interactions, laser induced phonon probe 0-79891  
naphthalene, phosphorescence spectra in rare gas matrices, multiplet struct. and pot. energy functions 0-106341  
neutral+high Rydberg atom, thermal collisions, review 0-63756  
neutral atom collisions, hyperfine component broadening and shift of spectral lines 0-74136  
pentacene in naphthalene (p-terphenyl), mol. mixed crystals., optical dephasing and vibronic relax. 0-95957  
pentacene in p-terphenyl, intermolecular interactions, laser induced phonon probe 0-79891  
perylene, intermolecular interactions, laser induced phonon probe 0-79891  
Polaroid K, oriented analogue of polyacetylene, reson. Raman spectroscopy 0-66208  
polyacetylene:1, pure and doped, reson. Raman spectroscopy 0-66208  
predissociated two-channel model, resonances with complex rot. method 0-58327  
protonium, atomic X-ray yields 1s and 2p level shifts and widths, cascades, calc. 0-78730  
quadrupolar nuclei in solids, enhanced resolution NMR interferometric correl. of shifts 0-57355  
rhodamine 6G, in rigid matrix, conc. effects in spectra 0-83347  
rhodamine 6G dye laser, induced radiation spectral characs., effect of vibr. relax. 0-64008  
rhodamine 6G in dimethylsulphoxide, concentrational red shift and luminesc. spectra 0-83426  
Rochelle salt, ferroelectric, Raman and IR study 0-71406  
ruby fluorescence line shift, condensed gas phase transitions obs. in diamond-anvil cell 0-73381  
semiconductors, indirect interzone absorpt. in presence of strong EM waves (Russian) 0-66217  
solar photosphere line shifts, granulation contrib. spatial and temporal depend. 0-85912  
solar photospheric line shifts, calc. from granulation vertical motion models 0-90375  
solar rotation induced Doppler spectral shift meas. by scanning Fabry-Perot interferometer 0-77298  
SS 433, reality of 6-day periodicity in spectral lines wavelengths var. 0-67743  
SS 433, wavelength shifts 164<sup>d</sup> period as precessional motion, massive black hole and pulsar models 0-62138  
Stark, width and shift depend. on ionisation potential 0-58211  
thiourea, ferroelectric, Raman and IR study 0-71406  
TMMC, crossover transition, effects on susceptibility and EPR shift 0-71047  
two-atom resonance fluoresc. spectrum, cooperative effects 0-78570  
two-level atoms, dynamics and spontaneous radiation in bichromatic EM field 0-91502  
 $As_2S_3$ , amorphous, time resolved luminesc. 0-66288

**spectral line shift continued**

- Ca II K-line in quiescent solar prominence, influence of spatial resolution on line width and shift 0-77364  
 Cd,  $5s5p^1P_1-5s^2$   $^1S_0$  intercombination line, press. broadening and shift 0-95564  
 Cr complex, tris(2,2'-bipyridine)Cr(III), excited states, Raman spectra 0-97263  
 CsNiF<sub>3</sub>, one-dimensional ferromagnet, optical absorpt. and static spin correlation functions 0-71415  
 Cu+Cu collisions, K $\alpha$  X-ray energy shifts, target thickness depend. 0-83311  
 Dy, isotope shift meas. using laser atomic beam technique specific mass shift determ. 0-91497  
 GaAs, photoconductivity, impurity induced, low energy edge spectral shift 0-65630  
 H, mesic, atomic X-ray yields 1s and 2p level shifts and widths, cascades, calc. 0-78730  
 H, quasi-stationary states in field of strong monochromatic wave, perturbation theory calcs. (*Russian*) 0-58145  
 HCl-inert gas rot.-vibr. line pressure broadening and shift calc. 0-69124  
 HCl-inert gas, weak collisions, HCl spectral line broadening of IR spectra 0-74161  
 HCl+N<sub>2</sub>(O<sub>2</sub>)(D<sub>2</sub>)(H<sub>2</sub>), HCl  $\nu_0-\nu_1$  band perturbations, linewidth and shifts calcs., IR spectra obs. (*French*) 0-58251  
 He II, Paschen lines, red shift in plasma 0-103128  
 He II plasma, spectral line shifts, electron collision induced 0-106879  
 p-InSb, photoexcited exciton spin-flip scatt. 0-74434  
 K salt of  $\beta$ -ketoaldehyde, configurations of anions in solutions studied by IR spectroscopy, H-bond form. 0-87117  
 Li salt of  $\beta$ -ketoaldehyde, configurations of anions in solutions studied by IR spectroscopy, H-bond form. 0-87117  
 N<sub>2</sub>,  $1^+$  system bands, line broadening and shift 0-87138  
 N<sub>2</sub>-Ar(Kr)(O<sub>2</sub>)(CO)(CH<sub>4</sub>), liquid, high resolution CW CARS spectra 0-63635  
 NH<sub>3</sub>+H<sub>2</sub>, NH<sub>3</sub> inversion transition, linewidths and T<sub>1</sub>/T<sub>2</sub> ratio 0-99499  
 Na salt of  $\beta$ -ketoaldehydes, configurations of anions in solutions studied by IR spectroscopy, H-bond form. 0-87117  
 NaCl, inelastic light scattering of localised vibration of interstitial H atom in alkali halides 0-88998  
 Ne, X-ray line shift for high density laser produced plasma diagnostics 0-64778  
 Ne\* 5882 Å line, Doppler free spectra, press. broadening and shifts, saturation spectroscopy 0-78565  
 Rb+Rb\*, freq. shift, line broadening, phase interference effects, Doppler free two photon spectra 0-58200  
 Si:O:H amorphous, time resolved luminesc. 0-66288  
 Ti, 535.0 nm line shift by H<sub>2</sub> perturber 0-91506

**spectral linewidths** *see spectral line breadth***spectral methods of temperature measurement***see also pyrometers*

- air arc temp. meas. by N<sub>2</sub><sup>+</sup> integrated emission coeffs. 0-59314  
 CARS spectrometer for gases and flames 0-95154  
 chopping pyrometer for remote meas. below 200°C (*German*) 0-86313  
 circuit breaking arcs, HV, AC, switching, spectroscopic measurement of temp. distribution in constant pressure axial air flow (*Czech*) 0-86296  
 contactless, IR techniques and detectors (*German*) 0-86314  
 electric arcs, temperature estimation from self-reversed spectral lines 0-75110  
 flame temperature, meas. using unresolved rot. struct. of mol. spectra 0-86300  
 flame temperature meas., 5 laser-excited fluoresc. methods, theoretical basis 0-101793  
 flame temperature meas. using laser induced fluoresc. spectrosc. of OH 0-90839  
 gas temperature measurement by spectrum line reversal 0-73358  
 NMR meas. at ultra-low tapes, S/N ratio, appl. to thermometry 0-73400  
 NMR thermometer, for multinuclear Fourier transform NMR 0-57292  
 pyrometry, photoelec., radiance temp. direct calc. 0-73367  
 Raman spectroscopy, remote spontaneous, new trends in recording of signals 0-73485  
 solar far IR brightness temp. minima rel. to sunspot activity 0-62035  
 CO<sub>2</sub>-N<sub>2</sub> mixture, temperature measurement by spectrum line reversal 0-73358  
 FeI, self-absorption-free spectral lines for temp. meas. in DC C-arc 0-87965  
 SF<sub>6</sub>, arc, temp. determ. accounting for demixing 0-70057  
 Si, temperature during CW laser heating, Raman scatt. meas. 0-76109  
 W ribbon-filament temperature lamps, radiation error estimation 0-64128

**spectrochemical analysis***see also atomic absorption spectroscopy; atomic emission spectroscopy; X-ray fluorescence analysis*

- air pollutant measurement by absorption spectrum Fourier transform 0-81514  
 air pollution, laser-Raman microprobe anal. of suspended particulates 0-76687  
 alkali tetrachloroaluminate, vapor characterisation by photoelectron spectrosc. 0-81388  
 alkali tetrafluoroaluminate, vapor characterisation by photoelectron spectrosc. 0-81388  
 Allende, S content, neutron capture gamma-ray spectroscopy 0-94728  
 alpha spectrometry using liquid, scintillation methods appl. to nuclear materials safeguards 0-78379  
 ammonium tetrachloroaluminate, vapor characterisation by photoelectron spectrosc. 0-81388  
 analyte emission characs., inductively coupled plasma, effect of emission spatial profiles 0-89557  
 atmospheric pollutant interferential detector 0-108830  
 CARS spectrometer for gases and flames 0-95154  
 ceramic, B content by emission spectrosc. with high freq. plasma excitation (*French*) 0-76477  
 cigarette smoke, diode laser meas. of methane, ethane and H<sub>2</sub>O vapour concs. 0-97847  
 coal and mineral content characterisation by Fourier transform IR spectroscopy 0-104474  
 coherent Raman loss spectroscopy, appl. to conc. meas. and fundamental spectrosc. 0-89580  
 colorimetric techniques, on-line developments 0-81378  
 conduction cooling device for low temp. phosphorimetry 0-90855

**spectrochemical analysis continued**

- derivative spectrophotometry, theory and appls. (*Japanese*) 0-86451  
 dicyclopentadiene, liq., CO<sub>2</sub> laser pulse induced chem. reactions 0-66821  
 differentiation, filtering props. of polynomial methods 0-66900  
 dithiocarbamate complexes of Cr, Mn, Sn and Pb IR, electronic and mass spectra, mag. susceptibility, cond. meas. 0-97270  
 dual-grating direct-reading spectrograph mirror system design and performance 0-81397  
 electrification phenomena obs., surface analysis techniques appl. 0-80354  
 electrothermal atomisation, atom form. and dissipation 0-57388  
 ethylene, air pollution monitoring, computer controlled CO<sub>2</sub> laser absorpt. system 0-89699  
 gas chromatography-IR spectroscopy using Sadler CIRA 101 analyser, vapour phase spectra of liqs. and solids 0-93809  
 graphite cups for solid sample introduction into electrothermal atomiser 0-62734  
 high-concentration alloy analysis by optical emission spectrometers 0-104477  
 hydrocarbons, aromatic, ultrasensitive detection by two-photon photoionisation 0-104473  
 hydrophilic polymers, ESCA evaluation of surface layer water structuring and protein adsorpt. 0-108758  
 ICP background emission, highly structured 0-73467  
 ICP unit, 5 kW, for 3.4 metre Ebert spectrograph, commissioning, operation 0-86453  
 image analysis device, Chromotom 0-83683  
 inductively coupled plasma emission spectrometry, with programmable monochromator, intensity meas., data processing 0-62728  
 information processing, television methods appls. 0-89568  
 internal combustion engine, conc. fluctuation meas. 0-71973  
 internal reflection spectroscopy, effective thickness calc. 0-89558  
 IR absorption gas analyser, portable model, molecular resonance effects (*German*) 0-98990  
 IR laser photolysis of polyat. mols. photochem. appls. 0-66835  
 isotope dilution alpha spectrometry for determ. of Pu concentration in irradi. fuel dissolver solns. 0-78428  
 lanthanide complex, struct. and equilb. by time resolved Eu(III) spectrosc. 0-78736  
 lanthanide ion bound to macromol., struct. and equilb. by time resolved Eu(III) spectrosc. 0-78736  
 laser gas analysers, freq. modulation appls. 0-85246  
 laser microspectral analyser, sample chamber with supply module 0-85241  
 laser microspectral analysis, forensic appl. 0-81385  
 lasers for industrial chemistry 0-87427  
 lunar rock, S content, neutron capture gamma-ray spectroscopy 0-94728  
 matrix isolation Raman spectroscopy, water pollution detect. appl. 0-108829  
 measurement theory, anal. function optimisation, appl. to spectrometry 0-62614  
 Microprobe Mole/plasma chromatograph system, for anal. of compounds on micron scale 0-101049  
 molecular emission cavity anal., vapour generating systems, cool flame spectroscopy 0-81396  
 multielement, using coherent forward scatt. at spectrosc. 0-57389  
 multipass-systems for Raman spectroscopic gas analysis (*German*) 0-81393  
 naphthylamines, abnormal fluorimetric titration behaviour, kinetic anal., fluoresc. quantum yields and lifetime meas. 0-89560  
 near IR diffuse reflectance analysis anomalies 0-86383  
 non-dispersive IR photometer for gas anal., function and design (*German*) 0-108772  
 nuclear energy materials, anal. techniques 0-93834  
 oil spill detection by airborne laser fluorosensor 0-67024  
 online spectroscopic data base system status 0-104475  
 pathological samples, mol. microanal. in situ with laser-Raman microprobe 0-81683  
 pentachlorotoluenes, positional isomers, <sup>13</sup>C Fourier transform NMR spectroscopy, struct. and compositional anal. 0-91576  
 photoacoustic FT IR spectroscopy of liquid and solid samples 0-90911  
 pollution plume transport and diffusion studies using fluorescence lidar 0-101139  
 $\alpha$ -quartz, synthetic, growth, defects induced by seed orientation 0-96454  
 Raman photoluminescence and cathodoluminescence 0-108774  
 Raman spectroscopy, chemical species anal. in conjunction with liq. phase chromatography (*French*) 0-93823  
 reaction products, weak excitation spectra, computerised spectrometer meas. 0-76574  
 resonant ionisation spectroscopy, chem.-physics appls. 0-68259  
 semiconducting film, on dielectric backing, spectrochem. anal. 0-66904  
 semiconductor surface, depth profiling, optoacoustic technique 0-65337  
 Shroud of Turin, IR reflectance spectrosc. and thermographic investigations 0-87578  
 Shroud of Turin, scientific investigation 0-87576  
 Shroud of Turin, spectral props. 0-87577  
 Shroud of Turin, UV-visible reflectance and fluoresc. spectra 0-87579  
 silicate: Yb<sub>2</sub>O<sub>3</sub> glassy film, Yb laser spectral microanalysis 0-76585  
 silver clouds, visible spectroscopic investig. from Salyut-4 orbit 0-82014  
 spectral lines intensity and plasma parameters dependence on Li additive 0-73478  
 spectrographic anal., signal near detect. limit 0-85244  
 steel, bar, and wire rod, small sample prep. and spectrometric anal. (*German*) 0-93704  
 steel, high speed, fixed time integration-emission spectral anal. and employment of high freq. induction melting-centrifugal casting samples (*Japanese*) 0-89567  
 steel, impurity spectral lines, intensity, temp. and conc. effects 0-64774  
 steel, mild, laser microspectral anal. 0-108769  
 steel, trace element UV emission, spectrochem. anal. (*French*) 0-71997  
 steelworks computerised spectrometric analysis and management information system 0-89574  
 stratosphere trace molecule Fourier transform spectrometer optical design 0-82099  
 synchronous excitation spectrofluorometry (*Japanese*) 0-86452  
 techniques, review 0-98989  
 thiosulphate determ. in photographic gelatine, spectrophotometric method (*Hungarian*) 0-66905  
 trace-gas remote analysis, optoacoustic radiometry limitations 0-108759  
 transuranic trace analysis using resonance ionisation spectroscopy of inert gases 0-93833  
 ultrapure water, trace metal determ. 0-81394



**spectrochemical analysis continued**

- vinyl chloride, air pollution monitoring, computer controlled CO<sub>2</sub> laser absorpt. system 0-89699  
 X-ray, specimen particles dimensions effect on X-ray intensity excited by protons 0-85238  
 X-ray, spectral line superpositioning, calc. 0-85240  
 X-ray intensity ratio  $L\beta/L\alpha$ , atomic number dependence 0-62818  
 X-ray microscopy, high resolution, with synchrotron radiation, for chem. microanal. 0-81416  
 X-ray spectral analysis, energy dispersive, using semicond. detectors 0-85237  
 XPS, quantitative, rel. to subshell photoionis. cross-sections and electron mean free path 0-81389  
 Ag statuette of Mercury from Bonn 1896, particle induced X-ray emission analysis 0-85228  
 $\alpha$ -AlPO<sub>4</sub>, berlinite, H<sub>2</sub>O conc. determ. by Raman scatt. 0-76572  
 Au in thin Ag objects, quantitative analysis by  $\gamma$ -ray differential absorpt. 0-85227  
 B, amorphous, microimpurities determ. using hollow cathode discharge 0-85247  
 B-Si alloys, B-rich, prep., anal. and cryst. growth (*French*) 0-104091  
 CO concentration meas. in coal pulverising plant, IR gas analysers 0-89572  
 CO, determ. by portable IR tester 0-89569  
 (Cd,Hg)Te epitaxial structures, comp. profile depend. on deposition parameters 0-100795  
 Cr <sup>0</sup> state, radiative lifetime in matrices, meas. using laser ablation and selective excitation 0-71959  
 Cr in urine, determ. by electrothermal atomic absorpt. spectrophotometry 0-61175  
 Cr-Cr<sub>2</sub>O<sub>3</sub> black chrome, commercial, solar absorber coating characterisation 0-80111  
 CrO<sub>2</sub>Cl<sub>2</sub> + carbon tetrachloride + acetone, intermediate complex form., electronic spectra 0-61075  
 CuF<sub>2</sub>·2H<sub>2</sub>O, synthesis, appl. for carrier-distillation emission spectroscopy 0-89164  
 Fe<sup>3+</sup> solutions, UV absorption spectrosc. obs. of equil. 0-93812  
 Fe-Cr-Al-Y, oxidation resistance, heat treatment and Al<sup>3+</sup> ion implantation 0-71785  
 Fe-Ni alloy, fluorination kinetics and fluoride film form., chem. nature obs. 0-101035  
 Fe-Si, grain oriented, phosphate coating anal. by IR spectroscopy 0-89570  
 HCN in smoke, tunable diode laser meas. 0-89559  
 In-InP, epitaxial layer, (100) surface chemistry, ESCA study 0-103552  
 InP-SiO<sub>2</sub> interface, CVD problems, ESCA profiles 0-93497  
 Mo-Si, film deposition by reactive sputtering, characteris. (*Japanese*) 0-93485  
 N I, detect. using Ar ICP emission spectrosc. 0-91474  
 NO measurements in CH<sub>4</sub>-O<sub>2</sub>-N<sub>2</sub> flame by laser fluorescence 0-61178  
 Na, single atoms, fluoresc. selective detect. by laser radiation 0-83312  
 NaPO<sub>3</sub>, mol. identification by matrix isolation IR spectrosc. 0-104485  
 NaPO<sub>3</sub>, mol. identification by matrix isolation IR spectrosc. 0-104485  
 Ni-base superalloys, emission spectral anal. with fixed time integration technique (*Japanese*) 0-71974  
 OI, detect. using Ar ICP emission spectrosc. 0-91473  
 PH<sub>3</sub>, conc. meas. by vacuum UV absorpt. spectra 0-71972  
 Pu analysis in irradiated fuel reprocessing solns., spectrophotometric determ. in near IR 0-78433  
 Pu, isotope composition, determ. using gamma spectrometry 0-66915  
 Pu, isotopic composition, determ. using thermal ionisation spectrometry with automatic data eval. 0-66913  
 Pu, isotopic composition, determ. using precise absolute gamma spectroscopic meas. 0-66916  
 Re surface, interaction with N<sub>2</sub><sup>+</sup> beam, reaction dynamics studied by XPS and thermal desorpt. spectrometry 0-93797  
 S isotopic composition in CS, spectroscopic meas. (*Russian*) 0-91696  
 Se trace amount determ. by hydride generation-nondispersive flame at. fluoresc. spectroscopy 0-89553  
 SiO<sub>2</sub>, plasma-chemical etching, spectroscopy 0-85243  
 Ti alloys, surface layers examination using vacuum UV spectrograph (*French*) 0-71987  
 Ti, surface layer, study using vac. UV spectrograph (*French*) 0-71987  
 U concentration in fuel reprocessing streams, acid-compensation dual-wavelength spectrochem. anal. 0-78430  
 U safeguarding, determ. of trace amounts by pulsed laser fluorimetry 0-78382  
 V-Ti-C, elemental anal. by EELS 0-101069

**spectrography** *see spectroscopy***spectrometer components and accessories**

- see also mass spectrometer components and accessories*  
 30 MHz amplifier for EPR spectrometer 0-98955  
 acousto-optical tunable filter spectrometer development 0-101848  
 anastigmatic mounting for ellipsoidal concave grating 0-106634  
 appearance pot. spectrometer design, demonstrations 0-105477  
 Bragg mode analyser potassium acid phthalate, Bragg refl. coeff. obs. 0-95204  
 burner system for atomic absorpt. spectrophotometers 0-73468  
 cathode lamps for atomic absorpt. spectrometry, method of modifying used lamps 0-90898  
 chromatographic-IR analyser, appl. to vapour phase spectrosc. 0-93809  
 conduction cooling device for low temp. phosphorimetry 0-90855  
 cooling system for sample introduction in low temperature phosphorimetry 0-87158  
 deuterated polyethylene target holders for (n, $\gamma$ ) studies 0-99402  
 DFS-8 spectrograph, attachment for oscillographic recording of line shapes 0-105721  
 diffuse reflectance Fourier transform IR spectroscopy using diamond anvil cell 0-101855  
 dissector pickup tube operating as a counter 0-95153  
 dual-grating direct-reading spectrograph mirror system design and performance 0-81397  
 duplexing switch with high isolation, for pulsed NMR spectrometer 0-86363  
 Ebert-Fastie monochromator, alignment using He-Ne laser and Fresnel diffraction pattern 0-99853  
 echelle efficiencies, theory and expt. 0-102802  
 electron beam guiding system including automatic capture circuitry 0-99005

**spectrometer components and accessories continued**

- electrostatic cylindrical electron vel. analyser, 127°, relativistic effects 0-86506  
 ellipsoidal mirror display analyzer system for electron energy and angular measurements 0-90908  
 EPR spectrometer attachment for studying materials in 120 to 350K. 1-10<sup>4</sup> atm. range 0-105686  
 Fabry-Perot spectrometer, reference channel for path difference determ. of interfering beams 0-77882  
 far IR modular Fourier interferometer construction, very high resolution 0-57401  
 fixed groove depth lamellar grating Fourier transform spectrometer 0-77885  
 focal plane IR detector arrays for planetary missions 0-85862  
 Fourier transform spectrometer performance, instrumentation for assessment 0-95165  
 gamma spectrometer protection and operation simplification, by relay device attachment 0-57447  
 Girard grille, holographic simulation 0-69337  
 graphite cups for solid sample introduction into electrothermal atomiser 0-62734  
 holographic grating, transparent 0-57395  
 ICP unit, 5 kW, for 3.4 metre Ebert spectrograph, commissioning, operation 0-86453  
 IKS-21, high temp. attachment for reflection and absorption coeff. meas. 0-105720  
 image detector, Si intensified vidicon target tube for inductively coupled plasma emission spectrometer 0-86439  
 image dissector spectrometer, magn. disturbances 0-73476  
 image dissector tube design, with high resolution and large deflection angle 0-73475  
 integrating sphere, for high-resolution UV and visible spectrophotometry of solids 0-61188  
 integrating sphere accessory, spectrosc. meas. of horizontal surface from above 0-86443  
 interferometer, appl. to dual beam Fourier transform spectrometer, sensitivity improvement 0-90910  
 IR detector-preamplifier for cryogenic spectrometer, optimization 0-95164  
 IR spectrophotometer, digital data acquisition/analysis system 0-73482  
 IR spectrophotometer data processing system applications 0-90912  
 IR window mounting for ultrahigh vac. appl. 0-82778  
 large capacity sample changer for fully automated gamma ray spectroscopy 0-58021  
 large spectrometer calibration chamber for SURF-II storage ring 0-91339  
 laser spectrometer based on Pb and Sn tellurides injection lasers 0-102504  
 microreactor assembly to study heterogeneous catalyst system, IR emission spectra anal. 0-98988  
 microspecimens photo-, X-ray and thermally stimulated luminescence obs., installation for specimens  $\geq 0.8$  mm 0-57381  
 monochromator, multiple, construction (*Hungarian*) 0-102812  
 monochromator, programmable, for ICP emission spectrometry, intensity meas. 0-62728  
 monochromator scanning control system using microprocessor, spectral line shift correction (*Japanese*) 0-57384  
 Mossbauer furnace for amorphous alloy investigations 0-98916  
 multichannel analysers for X-ray spectroscopy (*Hungarian*) 0-95205  
 multiparameter focal plane detector, development of capacitively coupled distributed parameter delay lines 0-78491  
 multiplex and high throughput spectroscopy 0-95145  
 NMR low-noise broadband transmit/receive circuit 0-62706  
 NMR thermometer, for multinuclear Fourier transform NMR 0-57292  
 phase splitting circuit, for pulsed NMR spectrometer 0-62704  
 photoacoustic cell for liqs. and solids, one-dimens. model generalisation 0-82827  
 photoacoustic cell for mirror scan Michelson interferometer 0-68277  
 photoelectric systems for recording spectral and temporal characteristics of pulsed light 0-73471  
 photon counter design for low light detection systems, spectroscopy, cathodolum. materials appl. 0-105711  
 potassium acid phthalate 0-95204  
 predisperser for large plane-grating spectrograph 0-73477  
 pressure cell for IR investigations of gases 0-83522  
 pulse field gradient for Fourier transform NMR spectrometer 0-57353  
 quick access sample system for low temp. K-band ESR and ENDOR 0-57352  
 reflection dispersive Fourier interferometer window eliminating backlash error 0-57402  
 RYA-2308 radiospectrometer, attachment for obs. of DNMR in <sup>31</sup>P 0-98957  
 sample chamber with supply module, for laser microspectral analyser 0-85241  
 self-scanned photodiode array as multichannel spectrometric detector 0-73466  
 sequential/parallel track selector, 1  $\mu$ s hardware pre-analyser for CERN Omicron spectrometer 0-91364  
 slotted tube resonator, pulsed ESR and ODMR expts. 0-86360  
 Space Telescope spectrograph Digicons 0-85858  
 spectrograph focal plane counter with sub-mm position resolution 0-91399  
 thermocouple installation in IR spectroscopy and reaction cells 0-57398  
 thyristor temp. regulator for pulsed NMR spectrometer 0-105687  
 triple monochromator a spectrometer in Raman scatt. (*French*) 0-96007  
 tubes design with hollow cathode, for Mo, Fe and Si analysis (*Bulgarian*) 0-85232  
 two-way EPR cavity, for Stark effect meas. on NO, 0-90872  
 unclipped digital correlator constr. for photon correlation spectroscopy 0-57387  
 UV high-resolution optical telescope design 0-90335  
 variable-thickness cell for liquid MM-wave Fourier transform and laser spectroscopy 0-57403  
 Wadsworth improved mounting with aspherical holographic grating 0-99824  
 XL-100 spectrometer, design of voltage-controlled oscillator 0-71211  
 XPS azimuthal angular-depend. studies, using electron spectrometer 0-57428  
 C electrodes, used in emission spectrography, isotopic labelling study (*Hungarian*) 0-106976

**spectrometry components and accessories continued**

- Si  $K\alpha$  source, sensitivity factors, cross section and resolution data 0-77920
- Si spectroscopic applications of structures produced by orientation-dependent etching 0-93668

**spectrometers**

- see also interference spectrometers; magnetic resonance spectrometers; mass spectrometers; microwave spectrometers; particle spectrometers; radiofrequency spectrometers; X-ray spectrometers*
- absorption spectrometer for gas phase samples, computer controlled 0-86459
- acoustooptical laser spectrometer, high resolution, appl. to  $H_2O$  vapour spectrum 0-86450
- aerosol spectrometer using two-pulse Fraunhofer holography, fibrous particle motion anal. 0-58476
- airborne far IR Fabry-Perot spectrometer for astronomical fine structure lines 0-62026
- angle resolved photoelectron spectrometer for atoms and molecules using synchrotron radiation 0-90932
- CARS spectrometer for gases and flames 0-95154
- diode laser dual-beam, long-term temporal and scanning characts. 0-90902
- double-beam single-detector wavelength-modulating, AGC 0-86447
- dual-beam diode laser spectrometer with sweep integration,  $^{12}CH_4$  absolute line strengths meas. 0-101853
- dye laser spectrometer, computer controlled, time averaging to improve sensitivity 0-101850
- field meas. Fourier transform spectrometer 0-86470
- flat-field spectrograph design, holographic grating appl. 0-68264
- Fourier transform far IR spectrometer 0-86461
- grazing incidence, construction, and appl. to extreme UV spectra of light impurity ions in linear pinch plasmas 0-59276
- grazing incidence spectrometer, 1.0 m, photometric calibration for plasma fusion diagnostics 0-92386
- Hadamard spectrometer, curved slits used to increase throughput 0-95149
- high energy electron spectroscopy techniques 0-62740
- image analysis device, Chromatron 0-83683
- inductively coupled plasma, determination of minor impurities and alloying constituents in steel 0-90903
- infrared high resolution spectrometer, used for satellite astronomical measurements, cryogenically cooled 0-90914
- IR, instrumental distortion computation without measuring apparatus function 0-95159
- IR absorption gas analyser, portable model, molecular resonance effects (*German*) 0-98990
- laser spectrometer based on Pb and Sn tellurides injection lasers 0-102504
- Lexan spectrometry, relativistic projectile fragments, imaging and identification 0-63442
- light scattering spectrom., polymer characterisation 0-95753
- magnetic prism beta spectrometer for low energies 0-99403
- magnetic spark, high-speed photorecorders 0-87014
- Michelson Fourier transform stellar spectrometer 0-98552
- microwave-optical, microcomputer-controlled 0-86448
- multiplex and high throughput spectroscopy 0-95145
- near IR mapping spectrometer design and testing for Galileo Jupiter Orbiter 0-90336
- NMR low-noise broadband transmit/receive circuit 0-62706
- optical, instrumental advances and new designs (*Polish*) 0-101847
- optical single-particle-size spectrometer calibration and testing, monofilament fibres as substitute particles 0-58819
- photophoretic, spectral dependence meas. of radiometric force on micron sized particle 0-105719
- Pioneer Venus Orbiter UV spectrometer, design and operation 0-67503
- plasma-optical emission spectrometer, inductively coupled, light scatt. effect 0-86455
- radiation meas. bibliography (1972-76) (*German*) 0-95510
- radio spectrograph, appl. to interplanetary scintillation spectra obs. 0-72741
- remote sensing field research, refl. factor calibration, spectrometer system performance 0-86382
- resonance absorption spectrometer for monitoring profile of solar He I 58.4 nm line 0-62019
- SHG, computer controlled intracavity, in CW ring dye laser 0-91841
- stroboscopic absorpt. spectrometer, dye laser appl. with forced mode synchronisation 0-78873
- telescope-spectrometer combination, optical props. 0-87455
- thin-film spectrograph for guided waves 0-58778
- time- and space-resolved spectrometry, instrumental advances, optical spectrometers (*Polish*) 0-90906
- tunable diode laser spectrometer, rapid-scanning computer-controlled 0-101854
- vacuum grating 3-m IR spectrometer with digital recording, description 0-95157
- vacuum monochromator spectrograph with plane diffraction grating, for 120 to 700 nm region 0-82831

**spectrophotometers**

- see also spectrophotometry*
- 8450A spectrophotometer, microcomputer system based on MC5 SOS processor 0-68272
- absorption bands in solids at low temps., spectrophotometer for meas. 0-86456
- automatic processor for atomic absorption signals 0-105694
- CORAVEL, Cassegrain spectrophotometer for stellar radial vel. determ. 0-82210
- diffuse-reflection spectra recording instrum., 200 to 2500 nm 0-57382
- diver-operable multiwavelength spectroradiometer 0-90251
- double beam atomic absorption spectrophotometer, electronic-mechanical modulator (*Russian*) 0-68262
- dual-wavelength spectrophotometer/fluorometer, high-performance 0-98198
- Hewlett-Packard 8450A UV/Vis, beam director 0-68271
- Hewlett-Packard 8450A UV/Vis, design and performance 0-68267
- Hewlett-Packard 8450A UV/Vis, input section 0-68270
- Hewlett-Packard 8450A UV/Vis, user interface 0-68268
- Hewlett-Packard 8450A UV/Vis optical measurement system 0-68269
- IR, digital data acquisition/analysis system 0-73482
- IR, effective spectral slit width determ. using  $NH_3$  absorpt. line 0-95167
- IR, for small particle spectral diffuse IR reflectivity meas. 0-68276

**spectrophotometers continued**

- IR spectrophotometer data processing system applications 0-90912
- microcomputer interfaced spectrophotometer for kinetic studies 0-62726
- microprocessor controlled spectrophotometric colorimeters (*Hungarian*) 0-101851
- non-dispersive IR photometer for gas anal., function and design (*German*) 0-108772
- optical-null spectrophotometers, photometric scale nonlinearity 0-101816
- optimum colour appearance anal using spectrophotometers in quality assurance laboratories 0-90877
- photopic response sensor, calibration rel. to photopic handbook data 0-62732
- Reticon spectrophotometer at Asiago Observatory, data anal. procedure (*Italian*) 0-98565
- spectral slit width determ., method comparison, IR spectrophotometers 0-86472
- spectrocolorimeter, SPEKOL, meas. of diffuse reflectance spectra, of differently matted polyamide fibres 0-77836
- Spectronic 2000 spectrophotometer, interactive microprocessor-controlled instrument 0-105716
- spectral reflectometer-spectrophotometer, NBS reference, mirror refl. meas. 0-68236
- stray radiation level during 280 to 350 nm region operation, SF-26 spectrophotometer 0-101852
- UV and visible spectra of solids using integrating sphere 0-61188
- UV-visible, high throughput, optical and optomechanical design 0-95155
- UV-visible, HP 8450 system, using reversed opt method 0-68273
- Zeeman effect appls. to atomic absorpt. spectrophotometer, development of spectral-line sources 0-76583

**spectrophotometry**

- see also colorimetry; spectrophotometers*
- alloy colour and colour stability as alloy design criteria 0-101005
- aluminoborate glass, Fe and Cr ion interaction, mag. and spectral props. 0-103883
- atmosphere vacuum UV background, meas. 0-90221
- automatic fluorescence microscopy photometry data processing and display (*German*) 0-86369
- borosilicate glass, Fe and Cr ion interaction, mag. and spectral props. 0-103883
- burner system for atomic absorpt. spectrophotometers 0-73468
- colour science contributions, collection of papers by D.B. Judd 0-98761
- crystalline material optical absorption meas. 0-105718
- derivative spectrophotometry, theory and appls. (*Japanese*) 0-86451
- derivative spectroscopy, understanding its appl. 0-77875
- enzyme-linked immunosorbent assay, apparatus for meas. light absorbance of small vols. of liquids 0-72387
- ethidium bromide E-DNA, intercalated birefringent fibres, microspectrophotometric investig. (*German*) 0-57392
- grating type monochromators, errors caused by polarisation of meas. system (*Japanese*) 0-101815
- internal reflection spectroscopy, effective thickness calc. 0-89558
- IR internal reflection spectroscopy, high reliability, simplified theory 0-105722
- IR spectrophotometers, meas. errors of polarising objects 0-86471
- liquid chromatography effluents on line anal., micro liq. chromatograph-interfaced Fourier transform IR spectrophotometer 0-73483
- modulation excitation, kinetic anal. of multiple lifetime meas. 0-86449
- nitrocellulose fibres, polarised light study 0-80736
- noise meas. in atomic absorpt. flame spectrometry, single and double beam instrum. comparison 0-76584
- optical spectra recording with UR-20 spectrophotometer 0-105693
- rocket instrument for far-UV spectrophotometry of faint astronomical objects 0-62014
- scanning photoluminescence, coupled with IR microscopy 0-73447
- synchronous excitation spectrofluorometry (*Japanese*) 0-86452
- thiosulphate determ. in photographic gelatine (*Hungarian*) 0-66905
- transmission meas. of neutral absorbers of NS glass, when irradiated with laser radiation 0-105692
- Cr in urine, determ. by electrothermal atomic absorpt. spectrophotometry 0-61175
- 1,2-quinoline (pyridine) complexes, stability const. determ. by spectrophotometric methods 0-87056
- Pu analysis in irradiated fuel reprocessing solns., spectrophotometric determ. in near IR 0-78433
- Si, epitaxial layer thickness meas. using phase correction function of substrate resistivity (*Rumanian*) 0-90812
- Si, photovoltaic cell, absolute spectral sensitivity calibration, radiometry, photometry (*Chinese*) 0-86367

**spectroscopes *see spectrometers*****spectroscopic light sources**

- cathode lamps for atomic absorpt. spectrometry, method of modifying used lamps 0-90898
- DC plasma excitation source, interference effects 0-86434
- diode laser, pressure-tuned, appl. to high-resolution spectroscopy 0-82835
- diode lasers, tunable IR, appls. to high resolution spectroscopy 0-58562
- dual-grating direct-reading spectrograph mirror system design and performance 0-81397
- dye laser,  $N_2$ -pumped subnanosecond pulse generation, design 0-87403
- dye laser spectrometer, computer controlled, time averaging to improve sensitivity 0-101850
- dye lasers, single-mode and multimode CW, as sources for obtaining power-squared corrected two-photon spectra 0-78849
- emission source for high resolution spectrosc. (*French*) 0-57383
- high-frequency discharge, appl. to anal. of semicond. film on dielec. backing 0-66904
- high-resolution spectroscopy using tunable lasers 0-101849
- hollow cathode discharge, for spectrochem. anal. of microimpurities in amorphous B 0-85247
- industrial IR instrumentation sources and optical components 0-87453
- IR tunable laser for semiconductor multiphoton spectroscopy (*French*) 0-82836
- laser and electro-optical systems, conf., San Diego, CA, USA (Feb. 1980) 0-62392
- lasers, tunable diode, for far-IR region, optical coupling arrangement 0-73481
- monochromatic, electronically variable wavelength 0-102791
- nanosecond light pulser with Hg vapour, quenching rate constants determ. 0-100111
- plasma continua, laser-produced, for absorpt. spectroscopy in VUV and XUV 0-75094



**spectroscopic light sources continued**

- radiation energy meas., spectral slit width correction 0-96020
- radio-frequency excited pulsed hollow-cathode lamp, absorpt. and emission characteristics 0-89550
- synchrotron radiation sources, props. and characts. 0-62729
- synchrotron radiation used for fast fluoresc. obs. 0-62736
- synchrotron sources for low energy AES 0-77913
- three-electrode DC Ar plasma source for optical emission spectrometry 0-62735
- tunable IR solid-state laser characteristics and principles 0-87406
- UV glow discharge source, appl. in spectrochem. anal. of steel products (French) 0-71997
- D<sub>2</sub> lamps, influence of Ne and Ar on spectral parameters 0-86460
- D<sub>2</sub>-Ne capillary-arc lamp, optimum parameters 0-95971
- KrF\* laser, generation of high-spectral-brightness tunable XUV radiation at 83 nm 0-91846
- Li heat-pipe arc lamp as spectroscopic source 0-102787
- Nd:YAG pumped tunable sources, appl. to spectroscopy 0-58576
- Ne hollow cathode discharge tube, spectral line intensities, rise time 0-103212
- Xe high pressure lamp for polymer spectral sensitivity determ. (German) 0-61119

**spectroscopy**

- see also beam-foil spectroscopy; computerised spectroscopy; electron spectroscopy; Fourier transform spectroscopy; interference spectroscopy; magnetic resonance spectroscopy; mass spectroscopy; matrix isolation spectroscopy; microwave spectroscopy; modulation spectroscopy; optical double resonance; photoacoustic spectroscopy; quantum beat spectroscopy; radiofrequency spectroscopy; Raman spectroscopy; spectroscopy computing; time resolved spectroscopy; tunnelling spectroscopy; two-photon spectroscopy; X-ray spectroscopy*
- alkali metals, vapour states, laser spectroscopy and applic., review 0-68260
- analytical and quality control techniques, review 0-98989
- atomic absorpt. spectroscopy, absorpt. max. in analytical curves 0-86442
- atoms, laser excited, reactive collisions 0-66793
- baseline variations, elimination by ultra-low freq. filtering 0-90901
- beam spectroscopy, Hadamard transform appl. 0-62741
- boride coatings on C and alloy steel, spectroscopic thickness determ. 0-85099
- COCHISE: laboratory spectroscopic studies of atmospheric phenomena with high sensitivity cryogenic instrumentation 0-95166
- coherent and nonlinear optics, conf., Leningrad, USSR (Jun. 1978) 0-98753
- coherent forward scattering atomic spectroscopy for multielement anal. 0-57389
- derivative, understanding its appl. 0-77875
- derivative spectroscopy, spectra differentiation with digital computer 0-77878
- Doppler line convolution by Gaussian instrument function, appl. to diode laser 0-82830
- double collision spectroscopy 0-58378
- double-quantum saturation spectroscopy, laser and RF, appl. to H 0-77880
- education, blackbody radiation and Planck function, derivative spectroscopy expt. 0-77563
- electrothermal atomisation, atom form. and dissipation 0-57388
- environmental samples, spectrometric method for meas. of hard  $\beta$ -emitters 0-94135
- ethane, diode laser spectra, baseline variations, elimination by ultra-low freq. filtering 0-90901
- far IR laser thermal spectroscopy of superconductors 0-60144
- far IR transmission and reflection spectroscopy in layer crystals 0-76019
- fluorescence spectroscopy, rapid scanning of photochemical anthracene in polychlorinated alkanes 0-86440
- four-wave mixing spectroscopy, coherent cancellation of background 0-91842
- Gaussian-Lorentzian light, photon counting distrib. factorial moment, spatial coherence 0-83571
- hole-burning spectroscopy, electron phototransfer in reaction centres of *Chlorella* photosystem I 0-81561
- hook spectra, evaluation limitations 0-90905
- ICP background emission, highly structured 0-73467
- image, dissector tubes, echelle spectrographs, design considerations 0-91918
- integrating sphere accessory, spectrosc. meas. of horizontal surface from above 0-86443
- intracavity spectrosc., enhancement calc. for single mode laser 0-69426
- intracavity spectroscopy, laser stimulation optimisation of gases 0-77881
- IR and millimetric waves and applications, conf., Miami Beach, USA (Dec. 1979) 0-57009
- IR internal reflection spectroscopy, high reliability, simplified theory 0-105722
- IR radiation, parametric up-conversion to visible range, review 0-64104
- IR spectrometric method for meas. of slight heavy water enrichment in natural water (French) 0-104718
- IR spectrum deconvolution beyond the Doppler limit 0-86467
- IR tunable laser for semiconductor multiphoton spectroscopy (French) 0-82836
- IR-ATR spectroscopy, appl. to conduct. investigation of biological material in aq. environment 0-61735
- kinetic IR spectroscopy IR, appl. to biochem. systems 0-98178
- laser absorption spectroscopy, sensitivity enhancement using Faraday effect 0-86446
- laser heterodyne spectroscopy for stratospheric trace constituents meas. 0-109257
- laser spectroscopic methods 0-62739
- laser spectroscopy in intense magnetic fields, appl. to astrophysical spectra and plasma diagnostics 0-62738
- liquid-solid interface transmission IR spectroscopy 0-98985
- low temperature luminescence spectroscopy using pulsed dye laser (Czech) 0-86445
- luminescence spectroscopy, refractive index correction, quantum efficiencies calc. 0-86444
- measurement theory, anal. function optimisation, appl. to spectrometry 0-62614
- mechanical spectroscopy of organometallic complexes, ring rot. meas. 0-74259

**spectroscopy continued**

- metastable atomic or molecular species, multiphoton transition detection 0-58231
- monochromatic atmospheric transmission determination, laser heterodyne spectrometry 0-72653
- monochromators, single, appl. in modern spectroscopy (Hungarian) 0-91905
- monochromators 1980 state and selection criteria (Hungarian) 0-73469
- multiplex and high throughput spectroscopy 0-95145
- nonlinear, recoil effects on Doppler-free lineshapes 0-82829
- nonlinear, resolvent formalism appl. (Japanese) 0-82833
- nonlinear laser spectrosc., multiphoton transitions 0-84433
- optical emission and X-ray spectroscopy developments (French) 0-68263
- optical processor, incoherent, for making 'spectrogram' of 1-D function 0-87528
- optics conference, Los Alamos, NM, USA (May 79) 0-73095
- optics laboratory, undergraduate, in American universities, status 0-62411
- photoflash units, chemical and electronic, temporal spectral characts., meas. method 0-95171
- photon echo spectroscopy of crystals, review 0-83648
- photophoretic spectroscopy, broadband 0-86469
- photothermal deflection technique for absorpt. meas. in optically thin media, thermal lens effect comparison 0-105717
- picosecond spectroscopy using continuous analyzing light, electronic relaxation of pinacyanol in ethanol 0-99517
- plasma-optical emission spectrometer, inductively coupled, light scatt. effect 0-86455
- power reflection spectroscopy, analytical techniques 0-62714
- pressure cell for IR investigations of gases 0-83522
- quantum electronics, conf., New York, USA (Jun. 1980) 0-90614
- resonance ionisation spectroscopy appl. to atoms and mols. in chem.-phys. 0-68259
- resonant Rayleigh-type mixing spectroscopy using ps light pulses, ultrafast relax. study 0-91834
- ring gas laser, freq. synchronisation region of colliding waves 0-83620
- saturation spectroscopy of atomic vapour three level system, collisional effects, appl. to Na 0-78579
- slit width effect on IR band shape spectra 0-86463
- spectrum reconstruction using test response 0-77884
- thermal blooming spectroscopy of dopamine 0-86441
- transient line narrowing, laser spectroscopic technique yielding resolution beyond natural linewidth 0-82834
- tunable diode laser spectrometry for line profile determination in second derivative spectra 0-86435
- tunable diode laser spectrometry for line profile determination of second derivative spectra, expt. results 0-86436
- US, algorithm for relaxation spectra 0-79038
- US spectroscopy appl. in NDT 0-79090
- UV/visible absorption, derivative anal. of component bands 0-98984
- Voigt functions, nonlinear least square algorithm 0-90900
- Ar ICP emission spectroscopy, appl. to OI spectra 0-91473
- CaCl, B<sup>2+</sup>-X<sup>2+</sup> transitions, rot. anal. by laser spectroscopy 0-91536
- spectroscopy applications of computers** *see computerised spectroscopy*
- spectroscopy computing**
  - see also computerised spectroscopy*
  - 168/E microprocessor for offline data analysis 0-58102
  - analytical information processing, television methods appls. 0-89568
  - benzenes, monosubstituted, NMR, high resolution, automated anal. by computer program DAVINS appl. 0-63669
  - chromatographic information processing by computer 0-71970
  - derivative spectroscopy, spectra differentiation with digital computer 0-77878
  - digital isotope ratio meas. system, using programmable calculator with double collector mass spectrometer 0-63845
  - electron energy-loss spectroscopy, as analytical tool, data handling and processing 0-81407
  - gamma-ray spectra analysis of fission products, automatic general-purpose program GSAP (Chinese) 0-69013
  - inductively coupled plasma emission spectrometry, with programmable monochromator, intensity meas., data processing 0-62728
  - IR spectra, standard organic compounds, principal component analysis (Japanese) 0-69143
  - mass spectrometric photoplate processing, microcomputer based system 0-62787
  - multipass-systems for Raman spectroscopic gas analysis (German) 0-81393
  - neutron spectra, SAIPS system, algorithms for spectra determ. w.r.t. measured reaction rates (Russian) 0-102416
  - NMR, high resolution, automated anal., principles and computational strategy 0-58287
  - NMR high resolution, automated anal. by computer program DAVINS appl. 0-63669
  - NMR spectra, computer-aided interpretation, minicomputer based file search system 0-62702
  - NMR spectra, computer-aided interpretation using artificial intelligence system 0-62701
  - online spectroscopic data base system status 0-104475
  - secondary ion mass spectra, mass peaks identification using computer program 0-101867
  - Li<sup>+</sup>-ligand complexes, NMR appl. <sup>7</sup>Li chemical shifts, expt. and ab initio studies 0-63670
  - N<sub>2</sub>, liquid, vibrational dephasing, computer simulation, Raman spectra, pair potential effect 0-63863
  - SiH<sub>3</sub> radical, in Ar(Kr)(N<sub>2</sub>) matrix, anisotropic ESR spectroscopic parameters 0-63687
- spectrum** *see spectra*
- spectrum analysers** *see spectral analysers*
- speech**
  - see also hearing*
  - acoustical research into life sciences, review 0-97925
  - auditory-nerve fibre discharge patterns, representation of speech-like sounds 0-108912
  - automatic parameterization of vocal cord motion from ultra high speed films 0-85419
  - biofeedback training device for speech therapy, portable, microprocessor-based 0-104808
  - chest wall movements prior to phonation 0-76768
  - conference on acoustics, speech and signal processing, Denver, CO, USA (Apr. 1980) 0-83689

**speech continued**

- encoding in auditory nerve, effects of nonlinearities 0-108913
- evolving ideas about nature of speech and relationship with human communication, review 0-96135
- laryngeal activity in Swedish obstruent clusters 0-108920
- loudness discomfort level and acoustic reflex threshold for speech stimuli 0-76762
- low bit-rate coding, signal models 0-106674
- masking effects on articulation in normal speaking adults wearing palatal appliances 0-76766
- noise-tolerant continuously variable slope DM to linear predictive coding conversion 0-96141
- perception, hemispheric specialisation, acoustic change rate, expt. obs. 0-104594
- pharyngeal and velar displacement for selected speech sounds 0-108921
- phonetic categories, acoustic props. 0-106675
- processing by auditory nervous system 0-108911
- real-time speech high-performance processor design 0-96144
- reception threshold, reliability in the determ., psychometric function 0-61657
- sensorineural hearing loss, freq. selectivity and speech discrimination 0-61593
- shimmer in sustained phonation 0-94242
- stuttering, articulatory behaviours, cinefluorographic anal. 0-94240
- stuttering, articulatory dynamics of fluent utterances 0-94239
- stuttering model, movement disorder 0-94241
- subjective loudness measurement, affecting auditory factors (*Japanese*) 0-85409
- vocal cord vibration, continuous model 0-85418
- vocal tract length preservation and vowel production 0-61594

**speech amplifiers** *see audio-frequency amplifiers***speech analysis**

- Attached Processor for Speech 0-96145
- dichotic and monotic masking of consonant-vowels by consonant-vowel second formants 0-79069
- electropalatography, thermo-formed pseudopalates and use of 3D display 0-85511
- esophageal speech, long-time spectral and intensity characts. 0-74643
- fast spectral estimation of speech signal in analytic form 0-83715
- formant transitions using interactive speech anal. synthesis system 0-83712
- fundamental frequency measurement, comparison of contact microphone and electroglottograph 0-109056
- homomorphic filter in ARMA model (*Japanese*) 0-87666
- jaw movement, cineradiographic study of chin marker positioning and implications for strain gauge transduction 0-76764
- least squares glottal inverse filtering from acoustic speech waveform, comments 0-83707
- linear prediction parameter estimation using Kalman filtering (*German*) 0-96134
- long-term spectra, computerised meas. method, English and Finnish data comparative study 0-104688
- mechanical speech processing, new results (*Hungarian*) 0-69604
- nonstatistical parameter estimation adaptive algorithms 0-91995
- oral constriction port, effects of increased vertical dimension on size 0-76765
- parser for segmenting continuous speech into pseudo-syllabic nuclei 0-91985
- phase information preservation 0-83713
- phoniatric diagnostics of speech organ disorders, objective acoustic methods 0-104598
- pitch determ. using nonlinear digital filter (*German*) 0-91972
- pitch extraction method based on peak detection and AMDF (*Korean*) 0-102935
- pole-zero modelling of speech 0-83716
- reflection coeff. calc. of inverse filter of PARCOR anal. lattice without multiplication (*German*) 0-96114
- reflection coefficient estimates based on Markov chain model 0-83710
- scalar parameter quantization methods 0-83711
- Schlieren photography appl. for speech research 0-64145
- sound analyser, undergraduate lab. expts. 0-82600
- spectrographic, identification of vocal diseases (*Japanese*) 0-85455
- spectrographic analysis of children's speech 0-94238
- speech trainer for multihandicapped children, display method and control program (*Japanese*) 0-108922
- spoken word recognition method using nonlinear spectral matching (*Japanese*) 0-69605
- vocal tract cross-sectional area functions, estimated values 0-99900
- vowel duration as cue for voicing distinction in following word-final consonant 0-74642
- vowel roughness effect on harmonic levels 0-76767

**speech compression** *see bandwidth compression***speech intelligibility**

- see also hearing*
- adaptive noise cancellation by short-time Fourier transform 0-91976
- auditory fatigue effect on masked speech intelligibility 0-67096
- broadband compression for improved hearing procedures (*German*) 0-104591
- dereverberation process evaluation by normal and impaired listeners 0-91974
- frequency selectivity of the cochlea for formant peaks at high signal levels 0-97936
- fricative, effects of increased vertical dimension 0-76765
- hearing aids, quality judgments of speech signals processed by hearing aids, multidimensional scaling 0-97933
- lateralization of complex waveforms 0-97931
- linear predictive coded speech digitisers, background noise spectral subtraction 0-96140
- linear predictive coded speech quality problems and expts. 0-91982
- loudness function of artificial speech, for reference equivalent meas. 0-79068
- noise suppression filter for narrowband vocoder 0-91977
- phoneme boundaries meas. in four ways 0-96138
- quality and intelligibility measures and their correlations 0-91978
- quality parametric objective measures correlated with subjective results 0-91980
- quality subjective and objective measures and their correlations 0-91979
- results interpretation of meas. in noise in anechoic room (*German*) 0-91968

**speech intelligibility continued**

- reverberation and noise effects on intelligibility of sentences in cases of presbycusis 0-96139
- time delay effect experiment 0-91996
- time-compressed speech, intonation and intelligibility, English vs. French 0-74644
- waveform coders, objective quality meas. equipment and method 0-91981
- wideband noise reduction by spectral weighting 0-96146

**speech recognition**

- artificial language word boundary detection by pitch contours 0-91991
- Attached Processor for Speech 0-96145
- automatic recognition, effect of speaker's mood on acoustic parameters 0-64306
- automatic speaker recognition, cepstral/spectral and linear prediction techniques compared 0-91993
- automatic speaker verification by cepstral analysis 0-91998
- automatic spoken language identification, finite-state models 0-91987
- Bengali vowels format struct., tracking loop formant extraction system 0-106673
- book 0-73118
- categorical features in speech perception and production 0-64310
- continuous speech recognition system for data base consultation 0-91990
- continuously-read natural language recognition achievements 0-91984
- deaf subjects with cochlear implants, elec. stimulation of auditory nerve 0-108915
- dichotic and monotic masking of consonant-vowels by consonant-vowel second formants 0-79069
- distribution of acoustic cues for stop consonant place of articulation in VCV syllables 0-64309
- formant tracking system toward automatic recognition of speech 0-58872
- French speech understanding system, syntactic-semantic sentence interpretation 0-91989
- microprocessor based speaker verification device 0-102936
- mispronunciations listening tests by segmenting speech into words 0-64308
- multispeaker phoneme classification by canonical correlation analysis 0-91988
- phoneme boundaries meas. in four ways 0-96138
- present and future, study (*Japanese*) 0-87663
- quasistationary processes and universal codes 0-91994
- Russian speech automatic recognition, deductive strategy 0-91997
- segmentation of band-limited speech signals using linear prediction 0-91970
- sentence intonation in Danish utterances 0-58870
- speaker verification algorithm for noisy utterances 0-91992
- speech production measures of speech perception, rapid shadowing of VCV syllables 0-64311
- speech trainer for multihandicapped children, display method and control program (*Japanese*) 0-108922
- spoken word recognition method using nonlinear spectral matching (*Japanese*) 0-69605
- syllable mispronunciation effects on word recognition 0-64307
- syllable-based recogniser for continuous speech 0-91986
- synthetic /bdg/ by hearing-impaired listeners under monotic and dichotic formant presentation 0-58871
- synthetic stop consonant identification, evaluation and integration of acoustic features 0-58869
- voice communication, speech production mechanisms and models (*Spanish*) 0-87665
- voice input and output, implementation and appl. (*Japanese*) 0-87664
- vowel, algorithms using zero crossings (*French*) 0-83708
- word sequences, segmentation for automatic recognition (*German*) 0-91971

**speech synthesis**

- 32 channel multiplex audio response system based on formant vocoder principle (*German*) 0-96133
- compilation, pre-recorded words and phrases for weather reports, expt. system 0-87667
- data compression and digitisation of speech signal, devices and techniques (*German*) 0-91969
- deconvolving speech waveform, maximum peakiness criterion 0-83714
- electronic methods currently available 0-106677
- formant frequency and bandwidth conversion to reflection coefficients 0-91975
- formant representations of parameters for channel vocoder 0-83709
- formant transitions using interactive speech anal. synthesis system 0-83712
- human communications, appls. 0-96110
- human vocal tract, IC technology appl. to speech synthesizers 0-87661
- linear predictive coded speech quality problems and expts. 0-91982
- log likelihood ratio interpretation as measure of waveform code performance 0-83706
- microprocessor for programmable speech synthesis 0-91983
- multimicroprocessor implementation of all-digital speech synthesizer 0-96143
- PARCOR system, description and appl. (*Japanese*) 0-79070
- review of current topics (*Japanese*) 0-91973
- software for cascade/parallel formant synthesizer 0-58868
- speech trainer for multihandicapped children, display method and control program (*Japanese*) 0-108922
- techniques (*Japanese*) 0-87662
- text-to-speech synthesizer for blind and handicapped 0-96142
- voice communication, speech production mechanisms and models (*Spanish*) 0-87665

**speech transmission** *see voice communication***speed** *see velocity***speed control** *see velocity control***speed indicating instruments** *see velocity measurement***speed measurement** *see velocity measurement***spelter** *see zinc***spherical aberration** *see aberrations***spheroidizing**

- modular cast Fe, probability prediction of spheroidisation by parametric diagram of chem. bond (*Chinese*) 0-66543
- steel, 12% W, eutectic carbides struct. and comp. during heating 0-76283
- steel, pearlite, global microstruct. evolution during spheroidization 0-108482



spicules *see solar prominences*

## spin

*see also baryon spin and parity; electron spin; isotopic spin (elementary particles); lepton spin and parity; meson spin and parity; nuclear spin and parity; spin density waves; spin hamiltonians*  
Bernoulli's principle, spin of balls and coins 0-77592  
Galileian formulation of spin, explicit realisations 0-62505  
 $pp \rightarrow \pi^0 X$ , pol. p, 24 GeV/c, high  $p_T$  prod., spin. depend. 0-105935

spin arrangements *see magnetic structure*

spin decoupling (NMR) *see double nuclear magnetic resonance*

## spin density waves

antiferromagnet, itinerant, paramag. impurity effects on Neel temp., calc. 0-60257  
antiferromagnet, neutron scatt. by magnons, modulated spin amplitudes 0-75722  
electron gas, dielectric function, dynamical exchange decoupling, plasmon dispersion, SDW and CDW 0-59900  
ferromagnet, magnetic susceptibility, spin and charge density waves, Curie temp. (*Russian*) 0-100581  
hydrocarbons, cyclic, non alternant, nonsingle instabilities of HF solns. 0-58164  
magnetic order coexistence with charge density waves 0-97096  
phase transition to incommensurate excitonic phase 0-75510  
quasi-one-dimensional systems, spin-lattice Peierls instabilities, static and dynamic aspects 0-71052  
superconductivity-ferromagnetism coexistence in two-band model (*Russian*) 0-84539  
(TMTSF)<sub>2</sub>PF<sub>6</sub> (AsF<sub>6</sub>), linear-chain conductor, semicond.-metal transition in small elc. field 0-103730  
transverse dynamic susceptibility and spin waves in itinerant electron SPW states 0-97076  
Cr alloys, Neel temp. of one dimens. electron gas in spin density wave state 0-65884  
Cr, antiferromag., transverse magnetoresist., electron interference oscils. 0-65534  
Cr, hyperfine interactions on <sup>111</sup>Cd-probe nuclei, TDPAC meas. 0-75904  
Cr, mag. phase diagram, near, spin-flip temp., US attenuation 0-60267  
Cr, Q-vector locking, press. induced hardening 0-103870  
Cr, spin density wave, Nambu-Eliashberg eqns. for k-state electron-hole pairing 0-97050  
Cr, spin density wave phases, domains 0-103871  
Cr, spin density wave state, phenomenological free energy density description 0-75720  
Cr, spin-flip transition temperature, press. depend. from elastic const. meas. 0-65944  
Cr-Co, dil., antiferromag., elec. resist. min., press. and impurity effects 0-59970  
Cr-Fe, dil., antiferromag., elec. resist. min., press. and impurity effects 0-59970  
Cr-Mo, electrical resistivity, spin density wave gap, Neel temp. 0-88534  
Cr-Re (0.18 wt.%), mag. excitations in longitudinal and transverse SDW phases 0-70946  
Cr-Si-V, (2, 0.1 at.%), paramag. to commensurate spin density wave transition 0-65875  
Fe-Cr, dil., spin density wave under high press., neutron diffr. study 0-65798  
 $\gamma$ -Mn, collinear spin structure stability 0-107984  
Si-Cr, dil., spin density wave under high press., neutron diffr. study 0-65798

## spin disorder resistivity

ferromagnet, itinerant, mag. props., temp. depend., functional integral approach 0-60170  
ferromagnetic metal, uniaxial, anisotropic spin fluctuations and anisotropic band struct. effects on resist. near T<sub>c</sub> 0-65543  
ferromagnetic metals, resist. anisotropy, crit. behaviour and temp. depend. 0-96858  
spin glasses, elec. resist., thermal resist. and thermopower 0-65542  
Au-Cu-Fe spin glass alloys, impurity mag. resist. meas. 0-59972  
α-Ce, exchange-enhanced, elec. resist. T<sub>c</sub> depend., press. effect 0-96845  
C<sub>60</sub>Au<sub>20</sub>, metallic glass, mag. ordering and cryst. field effects, speromagnetism 0-80531  
DyAg<sub>1-x</sub>In<sub>x</sub>, elec. and Hall resist. 0-96844  
Gd-Ni, ferromag., elec. resist. temp. depend. 0-96843  
GdAg<sub>1-x</sub>In<sub>x</sub>, elec. and Hall resist. 0-96844  
HgCr<sub>2</sub>Se<sub>4</sub>, n-type ferromag. semicond., galvanomagnetic props. 0-70727  
Nd, transport props., low temp., effect of mag. field 0-70679  
NdSn<sub>3</sub>, elec. cond., cryst. field effect, spin disorder contrib. 0-65540  
Pd-Mn (1-10 wt.%), mag. ordering, influence on resistivity 0-75557  
Pr, transport props., low temp., effect of mag. field 0-70679  
Pt-Cr, disordered, atomic order-disorder transform. effect on resist. min. 0-65911  
Sm, magnetoresistivity and elec. resist., 4.2 to 300K (*Russian*) 0-88539  
Sm, transport props., low temp., effect of mag. field 0-70679  
TbAg<sub>1-x</sub>In<sub>x</sub>, elec. and Hall resist. 0-96844  
TbZn, elec. resist., behaviour at mag. crit. points 0-65901  
TbZn, ferromag., thermoelec. power, temp. depend. and crit. behaviour 0-96852  
Th-Gd(Tb)(Dy)(Ho)(Er)(Tm)(Lu) (1 at.%), Heisenberg exchange, residual resist. meas. 0-75558  
Tm magnetic transitions, effect of H<sub>2</sub> in solid solns., elec. resist. meas. 0-100585  
U<sub>3</sub>P<sub>4</sub>, press. effects on elec. resist. and Curie temp. 0-75559

## spin dynamics

*see also spin density waves; spin disorder resistivity*  
aluminum copper tetrahedra, exchange, mag. anisotropy, and spin diffusion contribs. to EPR linewidth 0-80597  
anisotropic spin-phonon coupling model, exact solutions (*Russian*) 0-100590  
antiferromagnet, impure, Heisenberg model, impurity banding and mag. reson., theory 0-93181  
antiferromagnet, interphase boundary dynamics, domain wall motion and scatt. (*Russian*) 0-108032  
antiferromagnet, magnetic phases, spin configurations in external field 0-70955  
antiferromagnet, one-dimens., nonlinear dynamics 0-80521  
antiferromagnet, quantum critical dynamics with mode coupling 0-108024  
antiferromagnet, rhombohedral, spin-reorientation phase transition (*Russian*) 0-93122

## spin dynamics continued

antiferromagnet,  $s=1/2$  linear Heisenberg, zero-temp. dynamics in mag. field 0-65764  
antiferromagnets, disordered spin flop, bicritical behaviour, critical experiments 0-65899  
α-bis (N-methylsalicylaldehyde) copper II, one-dimens. spin-1/2 Heisenberg antiferromag., high-field spin dynamics 0-71224  
chemically induced dynamic spin polarisation, orientation depend. 0-63656  
classical dynamics, for particles with spin, Hamiltonian and Lagrangian formulation 0-86079  
1,8-dichlorooctane, quadrupolar relax. centres, limited spin diffusion 0-100649  
diethylammonium manganese chloride, Heisenberg magnet, spin diffusion, EPR study 0-66019  
dimethylammonium manganese tetrachloride, antiferromag. and spin-flop resonance obs., 70 to 100 GHz 0-71190  
dynamical plane rotator model, dynamical correl. functions in mol. field approx. 0-88758  
ferromagnet, exact integration of nonlinear Landau-Lifschitz equation 0-80495  
ferromagnetic conducting cryst., dynamics of s-d model in alternating mag. field (*Russian*) 0-65825  
ferromagnetic crystal, spin subsystem thermodynamics, spin-phonon interactions, mag. order parameter 0-103848  
ferromagnetic Heisenberg chain, weakly bound magnon states (*Russian*) 0-100591  
ferromagnetic metals, spin fluctuation theory, Curie temp., mag. susceptibility 0-65937  
ferromagnetic slab, finite thickness, spin correl. functions 0-80522  
ferromagnetic systems, singlet-triplet, excitation spectrum, double-time Green's functions 0-84603  
ferromagnets, quantum critical dynamics with mode coupling 0-108023  
Heisenberg antiferromagnet, one-dimens., autocorrelation function, low freq. temp. and field depend. 0-65929  
Heisenberg bicritical points in antiferromagnets, universality tests 0-84604  
Heisenberg chain, classical, nearest-neighbour, low temp. dynamics 0-80524  
Heisenberg chain, impure classical, dynamics near T=0 for low impurity conc. 0-71055  
Heisenberg ferromagnet, correlation functions in ferromagnetic and paramagnetic regions, RPA 0-71075  
Heisenberg ferromagnet, critical dynamics of impurity spin below T<sub>c</sub> 0-71076  
Heisenberg magnet, correlation theory of static and dynamic properties 0-65765  
Heisenberg magnet, random one-dimens., classical, spin dynamics, neutron scatt. cross section 0-60312  
Heisenberg model, classical, infinite, nonlinear dynamics, quantum time evolution 0-100576  
Heisenberg model, nearest-neighbour spin-spin correl. functions calc. 0-80537  
Heisenberg one-dimensional magnet, classical, nonlinear dynamics 0-71056  
high speed rot., spin diffusion, NMR spin lattice relax. obs. of D 0-66056  
Hubbard model, one-dimensional, elementary excitation with complex wave vector 0-75783  
impurity relaxation in nonresonance field, phonon amplification (*Russian*) 0-100310  
Ising ferromagnet, one-dimens., with phase transition, thermodynamic props. calc. 0-80536  
Ising model, spatially nonhomogeneous, correl. functions 0-60314  
Ising model, with long-range interactions, dynamical props. 0-100593  
magnetic materials, symmetry and macroscopic dynamics 0-107973  
magnetic superconductors, spin fluctuation and US attenuation 0-80445  
magnetically ordered cryst., indirect nuclear spin interactions 0-103847  
magnetically ordered crystals, exchange symm., mag. struct. (*Russian*) 0-65785  
mean-field theory of Peierls and spin-Peierls instabilities—commensurability, harmonics and dimerized-spin pinning 0-108014  
metals, spin fluctuations, mag. field effect, electronic sp. ht. and elec. resist. 0-108026  
metamagnet, two-dimens., tricritical spinodal decomp., Monte Carlo study 0-93117  
mixed-spin paramagnet, dynamics 0-60173  
Neel mode, ferrimagnetic-helical [hh0] mode coupling vector model (*French*) 0-75770  
NiWO<sub>4</sub>, antiferromag., low symmetry exhibited during spin-flop phase transition 0-60263  
NMR, superspin, appl. to ABX system 0-60426  
nuclear spin relax. by translational diffusion in solids, reciprocal-space formalism, mean-field theory 0-71208  
one dimensional randomly dilute Ising ferromagnet, dynamics 0-70922  
one-dimensional Heisenberg magnet, in mag. field, dynamic correlations 0-70926  
one-dimensional random Glauber model, magnetisation relax. 0-80523  
one-dimensional spin 1/2 chain, soliton excitation in strong spin-phonon interaction 0-103842  
paramagnet, anisotropic, spin dynamics, exchange-bond dilution effects 0-88763  
paramagnetic spin system, two-level open system, kinetic theory of resonance and relaxation 0-88859  
paramagnets, low-dimens., EPR spectra 0-71154  
planar spin system with annealed bond disorder 0-57212  
praseodymium ethylsulphate-Sm, one-dimens. X-Y system, spin dynamics, electron spin echo meas. 0-66031  
rare earth orthoferrites, hyperfine interaction anisotropy, NMR study (*Russian*) 0-66052  
RF field effect on spin diffusion 0-93104  
sine-Gordon chain, classical, low freq. dynamics 0-108020  
spin glass, one dimens. ideal, dynamical susceptibility and relax. behaviour 0-65950  
spin glass dynamics, barrier modes and spin waves 0-60293  
spin glasses phase transition, obs. by DC Josephson effect 0-100594  
spin Hamiltonian, constant-coupling, higher-order, statics and dynamics 0-60262  
TCNQ salt, K-TCNQ, EPR linewidth, ang. and freq. depend. 0-80591  
TMMC, Cu-substituted, spin dynamics, neutron scatt. cross section 0-60312

## spin dynamics continued

- TMMC, low-symmetry spin distrib. effect on EPR line 0-66018  
 TMMC, quasi one-dimensional planar ferromag., low temp. NMR study im mag. field 0-97157  
 transition metal, chemisorption of H, effect of surface spin fluctuations 0-75613  
 uniaxial antiferromagnet, nonuniform spin configurations 0-97109  
 uniaxial antiferromagnetic, phase diagram, spin flop transition (*Russian*) 0-100587  
 weak ferromagnet, domain wall dynamics, nonlinear waves, mag. solitons (*Russian*) 0-75793  
 X-Y model, one-dimensional isotropic, dynamics 0-71057  
 $\text{Al}_2\text{O}_3\cdot\text{Cr}^{3+}$ , inhomogeneous spin system, time evolution towards saturated state 0-88869  
 Au-Fe, dil., crit. dynamics 0-60325  
 AuFe spin glass,  $\mu^+$  zero-field spin relax. probe for spin dynamics 0-97177  
 CdS, doped, amorphous antiferromagnet model, susceptibility and spin-flip Raman scatt. meas. 0-97057  
 CdS, pure spin diffusion without charge transport, spin flip Raman scatt. obs. 0-93329  
 $\text{CeIn}_3\cdot\text{Sn}$ , mixed valence system, low-temp. susceptibility, paramagnon study 0-97077  
 $(\text{Ce},\text{La}_{1-x})_2\text{Mg}_3(\text{NO}_3)_{12}\cdot 24\text{H}_2\text{O}$ , adiabatic demagnetisation temp., mag. entropy (*Russian*) 0-65892  
 $\text{Ce}_{0.9-x}\text{La}_{0.1}\text{Th}_{0.1}$ , mixed valence state, static and dynamic mag. response 0-103816  
 $\text{CoBr}_2\cdot 6(0.48\text{D}_2\text{O}, 0.52\text{H}_2\text{O})$  spin-flop system, intermediate phase existence, sublattice magnetisation reorientation 0-80510  
 $\text{CoCl}_2$ , antiferromag., phase diagram, heat capacity meas. 0-93126  
 Cr, mag. phase diagram, near, spin-flip temp., US attenuation 0-60267  
 $\text{CsMnBr}_3$ , EPR linewidth anisotropies 0-103878  
 $\text{CsNiF}_3$ , 1D ferromag., optical absorption and spin dynamics 0-71417  
 $\text{CsNiF}_3$ , low frequency dynamics in external mag. field 0-108020  
 $\text{CsNiF}_3$ , quasi one dimensional planar ferromag., low temp. NMR study im mag. field 0-97157  
 $\text{CsNiF}_3$ , stochastic motion of Sine-Gordon-solitons, spin-correlation function 0-93105  
 $(\text{Cu},\text{Zn})\text{C}_2(\text{SO}_4)_2\cdot 6(\text{H},\text{D})_2\text{O}$  Tutton salt, proton spin-lattice relax. time, proton conc. depend. and spin diffusion role 0-71221  
 Cu-Mn spin glass, spin freezing and exchange narrowing of mag. reson. 0-60411  
 CuMn spin glass,  $\mu^+$  zero-field spin relax. probe for spin dynamics 0-97177  
 $\text{CuSO}_4\cdot 5\text{H}_2\text{O}$ , low freq. spin dynamics, proton relax. study 0-71218  
 $\text{DyFeO}_3$ , field induced spin reorientation, Mossbauer spectroscopy 0-65878  
 $\text{DyFeO}_3$ , spin reorientation transitions induced by magnetic fields, Mossbauer study 0-71246  
 $\text{Dy},\text{Tb}_{1-x}\text{Fe}_2$ , single cryst., torque meas. 0-65877  
 $\text{ErFeO}_3$ , field induced spin reorientation, Mossbauer spectroscopy 0-65878  
 $\text{EuO}(\text{S})(\text{Se})(\text{Te})$ , spin order and fluctuations, Raman scatt. study 0-97273  
 $\text{Eu}_{0.8}\text{Sr}_{0.2}\text{S}$ , spin glass, spin dynamics, neutron scatt. study 0-65907  
 $(\text{Eu},\text{Sr}_{1-x})_2\text{S}$ , very dil., magnetisation dynamics 0-65915  
 Fe, ferromag., dynamic susceptibility calc. 0-80488  
 Fe film, nuclear spin system dynamics Mossbauer study in FMR conditions (*Russian*) 0-80651  
 Fe, magnetic moments, local short range order, high temp. effects 0-65902  
 Fe-Co, 3d ferromagnet nuclear spin-lattice relaxation 0-80627  
 $\text{FeBO}_3$ , spin-reorientation phase transition (*Russian*) 0-93122  
 $\text{Fe}_{1-x}\text{Mn}_x\text{Sn}$ , spin reorientation, Mossbauer study, 77 to 400K 0-97172  
 $^3\text{He}$ , liquid, polarisation potentials, viscosity, thermal cond., spin diffusion 0-88389  
 $^3\text{He}$ , superfluid, A-phase, helical textures, NMR response 0-70496  
 $\text{HoFeO}_3$ , field induced spin reorientation, Mossbauer spectroscopy 0-65878  
 $\text{Ho},\text{Tb}_{1-x}\text{Co}_2$  lase phase compounds, elastic props., temp. and magnetic field dependence 0-60393  
 $\text{p-InSb}$ , photoexcited exciton spin-flip scatt. 0-74434  
 $\text{K}_2\text{CoF}_6$ , two-dimens. Ising antiferromag., nearest neighbour correl. function, birefr. expts. 0-71386  
 $\text{KCuF}_3$ , linear chain Heisenberg antiferromag., nearest neighbour correl. function, birefr. expts. 0-71386  
 $\text{K}_2\text{CuF}_6$ , spin relax., crit. behaviour, high freq. susceptibility meas. 0-65936  
 $\text{K}_2\text{FeO}_4$ , crit. slowing down of spin fluctuations, Mossbauer spectra and relax. theory 0-65882  
 $\text{KMg}_{1-x}\text{Mn}_x\text{F}_3$ , disordered paramagnet,  $^{19}\text{F}$  NMR study 0-71216  
 $\alpha\text{-Mn}$ , localised spin fluctuations, Knight shift obs. 0-60181  
 $(\text{NH}_4)_2\text{ReCl}_6(\text{IrCl}_6)$ , proton relaxation near antiferromagnetic phase transitions 0-80640  
 Ni, ferromag., dynamic susceptibility calc. 0-80488  
 $\text{Ni}_{0.25}\text{Zn}_{0.75}\text{Fe}_2\text{O}_4$ , Mossbauer study, spin fluctuations 0-60471  
 Pd, spin fluctuation model interpretation of mag. susceptibility 0-80477  
 Pt, spin fluctuation model interpretation of mag. susceptibility 0-80477  
 $\text{Rb}_2\text{Co}_2\text{Mg}_{1-x}\text{F}_4$  mag.-nonmag. two-dimens. antiferromag. Ising system, spin fluctuations 0-80545  
 $\text{Rb}_2\text{Co}_2\text{Mn}_{0.5}\text{F}_4$ , two dimens. random antiferromag., excitations 0-107997  
 $\text{Rb}_2\text{CrCl}_4$ , 2D-ferromag., renormalisation of long wavelength spin waves, neutron scatt. 0-60229  
 $\text{Rb}_2\text{CuBr}_4\cdot 2\text{H}_2\text{O}$ , dynamic props. in paramag. state, spin-lattice relax. time meas. 0-71214  
 $\text{RbMnBr}_3$ , EPR linewidth anisotropies 0-103878  
 SiC, laser Raman spin-flip scatt. from excitons, luminesc. 0-80786  
 SiC, spin-flip scatt. of laser light from photoexcited excitons 0-93330  
 TbZn, mag. excitations meas. 0-70979  
 $\text{TmFeO}_3$ , acoustic vel. and attenuation shifts at spin reorientation phase transition 0-65986  
 $\text{UAl}_3$ , spin fluctuations, mag. field effect, electronic sp. ht. and elec. resist. 0-108026  
 V surface, spin fluctuations, finite temp. mag. props. study 0-107994  
 $\text{V}_3\text{Se}_4$ , itinerant antiferromag., spin fluctuations, NMR study 0-75874  
 $\text{V}_3\text{Se}_6$ , itinerant antiferromag., spin fluctuations, NMR study 0-75874  
 $\text{Y}_2\text{Fe}_{1-x}\text{Co}_{1-x}\text{Si}_{2-x}\text{O}_{12}$ , spin reorientation, NMR and ferromag. reson. meas. 0-65890

## spin echo (EPR)

- electron plasma relax. charact., 3-30 eV 0-79612  
 envelope modulation, 2-dimens. Fourier transform 0-63680  
 ethanol- $\text{d}_3(\text{d}_1)$ , glassy state, solvated electron geometry, electron spin echo modulation obs. 0-66009  
 methanol,  $\beta$ -irrad., radical truck struct., electron spin-echo obs. 0-93776  
 nitroxide free radicals in liquids, electron spin-echo obs. 0-63685  
 pentacene in naphthalene, triplet state, EPR study by electron spin-echo and laser flash excitation 0-58172  
 praseodymium ethylsulphate:Sm, one-dimens. X-Y system, spin dynamics, electron spin echo meas. 0-66031  
 tetracyanoethylene in acetone- $\text{d}_6$ , anion solvation, electron spin echo modulation 0-63676  
 tetracyanoethylene in dimethylsulphoxide- $\text{d}_6$ , anion solvation, electron spin echo modulation 0-63676  
 tetracyanoethylene in methanol- $\text{d}_3(\text{d}_1)$ , anion solvation, electron spin echo modulation 0-63676  
 tris-sarcosine calcium chloride: $\text{Mn}^{2+}$  ferroelec. dynamics, EPR and ENDOR study 0-75972  
 Ag atom solvation in methanol, geometrical model, electron spin-echo modulation obs. 0-63682  
 $\text{Cs}_2\text{ZnCl}_4\cdot\text{Cu}^{2+}$  electron spin echo envelope, Fourier transform  $^{133}\text{Cs}$  modulation 0-58291

## spin echo (NMR)

- benzene, diffusion coeff. meas., Fourier transform NMR, pulsed field gradient system 0-57353  
 $\alpha$ -cyclodextrin and  $\alpha,\beta$ -D-xylose, absorption mode spin-echo spectra appl. 0-78634  
 cyclohexane, liquid, density effect on transport properties 0-65264  
 dextran T-10 and  $\alpha$ -cyclodextrin, absorption mode spin-echo spectra appl. 0-78634  
 p-dichlorobenzene,  $^{35}\text{Cl}$  NQR line narrowing by nonreson. RF photon dressing 0-63662  
 dichloromethane- $\text{d}_2$ , spectral densities determ. from spin-lattice relax. and spin-echo decay rates 0-75877  
 hexafluorobenzene, liq., self-diffusion and density as functions of press. and temp. 0-92696  
 hexafluorobenzene-n-paraffins, binary liquid solns., self diffusion, spin echo meas. 0-65263  
 hexamethylenetetramine, mol. ultraslow rot. obs. using D probe spin alignment tech. 0-88890  
 indirectly induced NMR spin echoes in solids 0-71239  
 liquid crystals, NMR magic echo by sample reorientation 0-103899  
 lysozyme, absorption mode spin-echo spectra appl. 0-78634  
 metallic hydrides, solid echo amplitude and phase, skin effect 0-108115  
 nuclear echo formation in spin systems with dynamic freq. shift to NMR 0-93208  
 organic free radicals, solid, selective pulse NMR expts. 0-60452  
 polyethylene, mol. ultraslow rot. obs. using D probe spin alignment tech. 0-88890  
 polystyrene, solns., diffusion coeffs. meas., Fourier transform NMR, pulsed field gradient system 0-57353  
 proteins, globular, in water, proton NMR spin echo decay comparative investigation 0-81541  
 quadrupole, with two-frequency action, amplification and modulation 0-108116  
 solids, D NMR spin echo theory 0-103898  
 three-level NMR system, coherence-transfer rotary echoes prod. by double RF field irradi. 0-66071  
 water,  $\text{H}_2\text{O}$  and  $\text{H}_2^{18}\text{O}$ , self-diffusion, pressure and temp. depend., NMR spin-echo obs. 0-65266  
 $\beta\text{-Al}_2\text{O}_3(\text{Na},\text{Li})_2\text{O}$  solid electrolyte, Li motion and activation obs. using  $^7\text{Li}$  NMR 0-108100  
 Co film, mag. anisotropy study using NMR spin echo method 0-60384  
 Co thin film, nuclear spin echo excitation on subharmonics, and multiple freq. (*Russian*) 0-60454  
 Co-V, Co rich, ferromag. behaviour, mag. moments, Curie temp., and NMR spectrum 0-70964  
 Co-V, ferromag. struct. in nucl. spin echoes 0-60453  
 $\text{Co}_2\text{B}$ , glassy and cryst., hyperfine field distrib.,  $^{59}\text{Co}$  spin echo spectra 0-80635  
 CoV alloys, phase dependent MNR spectra 0-108114  
 $\text{CuCr}_2\text{S}_4\cdot\text{Se}_2$  spinels, NMR spin echo study 0-71238  
 D probe spin alignment for obs. ultraslow mol. rot. 0-88890  
 $\text{Fe-P}(\text{Ga})(\text{As})(\text{Sb})$ , dil., short range order, NMR study 0-71237  
 $\text{Fe-Sb-Ni}(\text{Cr})$ , dil., short range order, NMR study 0-71237  
 $\text{Fe-V}$ , ferromag. struct. in nucl. spin echoes 0-60453  
 $\text{FeBO}_3$ , parametric echo, magnetoelastic NMR excitation (*Russian*) 0-66072  
 $\text{FeV}$  (2 at.%), NMR spin echoes, domain wall effects 0-75883  
 $\text{Gd}_2\text{Co}_{17}$ , NMR spin echo meas., dipolar field anisotropy 0-71236  
 $\text{Gd}(\text{Co}_{1-x}\text{Ni}_x)_2$  compounds, NMR and thermal expansion 0-66070  
 H, gaseous, high-resolution mag. reson. study, 1 to 1.3K 0-95560  
 $\text{HTV}_2\text{H}_{21}$ , proton NMR relax. time and Knight shifts, diffusional activation energies meas., sorption props. 0-75871  
 $\text{KH}_2\text{PO}_4$ , NMR spin echoes, indirectly induced 0-71239  
 Li ferrites, nuclear spin echo excitation on subharmonics, and multiple freq. (*Russian*) 0-60454  
 $\text{MnFe}_2\text{O}_4$ , additional spin echo of  $^{55}\text{Mn}$  nuclei 0-60455  
 $\text{Na}_2\text{WO}_3$ ,  $0.22 < x < 0.84$ , low temp. struct., press. effects, NMR study 0-95443  
 Ni, ferromag. struct. in nucl. spin echoes 0-60453  
 PdNb, dilute, NMR obs. of  $^{93}\text{Nb}$  0-71203  
 PtV, dil. alloys, NMR obs. of  $^{31}\text{V}$  0-71203  
 $\text{VO}_{2.5}$ ,  $^{51}\text{V}$  NMR studies, microscopic mag. props. 0-108086  
 $\text{YCo}_2$  amorphous films,  $^{59}\text{Co}$  spin echo study 0-80636  
 $\text{Y}_2\text{Co}_{17}$ , NMR spin echo meas., dipolar field anisotropy 0-71236  
 $\text{Y}(\text{Fe}_{1-x}\text{Co}_x)_2$ , NMR study 0-75882  
 $\text{Y}_2\text{Fe}_{1-x}\text{Co}_x\text{Si}_{2-x}\text{O}_{12}$ , spin reorientation, NMR and ferromag. reson. meas. 0-65890  
 $\text{Zr}(\text{Fe}_{1-x}\text{Co}_x)_2$ , NMR study 0-75882  
 $\text{ZrMn}_2\text{H}_4$ , proton NMR relax. time and Knight shifts, diffusional activation energies meas., sorption props. 0-75871

## spin glasses

## see also micromagnetism

- alloys, magnetic localisation and charge oscillations 0-75781  
 alloys, magnetoresistance, Boltzmann formalism calcs. 0-88540  
 aluminosilicate glass:Co (14.3 wt.%), AC susceptibility meas. 0-88771  
 amorphous Ising antiferromagnetic model, frustration effects 0-103838



## spin glasses continued

- amorphous magnets, random anisotropy axes, high-temp. expansion for sp. ht. 0-71041  
annealing and mag. remanence 0-60308  
computer simulation 0-60299  
computer simulations of mag. model systems 0-65924  
cubic lattices, fully frustrated, phase transitions, Gaussian and spherical model, free energy calcs. 0-60281  
dilute, conc. expansions at zero temp., Ising model 0-60303  
dilute magnetic alloys, electron sound absorpt., disordered mag. impurities, spin glasses (*Russian*) 0-80503  
diluted Ising and Heisenberg systems with competing interactions, mag. ordering, appl. to  $\text{EuSr}_{1-x}\text{S}$  0-65914  
dipole pseudo-spin glasses, collective excitations 0-59617  
disclinations and solitons 0-75786  
disordered metamagnets, random field effects 0-60318  
dynamics, barrier modes and spin waves 0-60293  
dynamics, partial ferromag. order, antiferromag. spin wave modes 0-93133  
Edwards-Anderson spin glass model in two dimensions, numerical results 0-97100  
electrical resistivity, thermal resist. and thermopower 0-65542  
experimental status, introduction 0-60292  
ferromagnetism onset, mag. inhomogeneity 0-75774  
ferromagnets and spin glasses, supercond. and mag. order 0-93029  
five-dimensional, Edwards-Anderson ordering possibility 0-60295  
free energy, order parameter expansion, random bond model 0-84609  
frustration model, ground states 0-60294  
frustration model, ground states by graph theory matching method 0-100592  
giant moments and spin glasses, order out of disorder (*Dutch*) 0-97107  
Heisenberg mode, RPA approx. 0-65904  
Heisenberg model, excitation spectra, numerical studies 0-60300  
Heisenberg model calc. 0-60301  
ill-condensed matter, summer school, Les Houches, France (July-Aug. 1978) 0-82561  
infinite range model, stability and susceptibility in Parisi's soln. 0-88762  
infinite-ranged model, mean field theory hypothesis 0-97104  
Ising model, Sherrington-Kirkpatrick, white and weighted averages over solns. of Thouless-Anderson-Palmer eqns. 0-108012  
Ising model, two-dimens., ferromagnet-spin glass transition, Monte Carlo calc. 0-60287  
Ising spin glass, glass, Edwards-Anderson order parameter instability 0-71043  
Ising spin glass, d-dimensional, frustration effect 0-108019  
Ising spin glass, d-dimensional, frustration effect and dilution problems 0-108018  
Ising spin glass, three-dimensional mag. correlations 0-103849  
Ising spin glasses, in effective interaction approx. 0-60288  
Ising systems, random mixture, phase boundaries 0-60285  
Israel Physical Society 1980 annual meeting, Rehovot, Israel (April 1980) 0-94909  
layered two dimensional Ising lattice, phase transitions, spin glasses (*Russian*) 0-65945  
low concentration series expansion, dilute spin glasses at zero temperature 0-93131  
lower critical dimensionality for spin glass transition 0-60291  
magnetic field dependence of susceptibility peak 0-103840  
magnetic properties in mean field theory 0-80514  
magnetic properties of Sherrington-Kirkpatrick model, Monte Carlo simulations 0-88774  
magnetic resonance props. 0-71153  
magnetisation decay of single spin glass model 0-71073  
Mattis model, modified, mag. relax. 0-65947  
metastable states, crit. free energy 0-88764  
one dimensional, ideal, dynamical susceptibility and relax. behaviour 0-65950  
one-dimensional random Glauber model, magnetisation relax. 0-80523  
order parameter expansion of free energy, random site model 0-88772  
ordering temperature, beyond mean field value 0-60298  
parametric amplification of spin waves by elastic pumping (*Russian*) 0-65895  
phase transition examination, by DC Josephson effect 0-100594  
principle of minimum free energy 0-88773  
quantum spin glass theory 0-103839  
quenched free energy of mag. systems with random interactions, upper bounds 0-103845  
random energy model, disordered models family-limit 0-90794  
random Glauber chain, relax. of magnetisation, numerical studies 0-60313  
replica theory, Sherrington-Kirkpatrick model, sequence of approximated solutions 0-60284  
RKKY, dil., approach to fully magnetised state 0-60302  
semiconductor, indirect exchange interaction of localised spins 0-88768  
spin glass-ferromagnetic phase, mean field theory 0-103841  
spin waves in amorphous ferromagnets, asperomagnets and spin-glasses 0-75747  
Stoner spin glass, conditions for freezing of spins with itinerant 3d electrons 0-60309  
symmetry and macroscopic dynamics of mag. materials 0-107973  
time translation, spatial scaling and nonexponential relaxation 0-97110  
transition, cumulant expansion of free energy of disordered systems 0-71067  
transition metal alloys, dilute, mag. ordering, book contrib. 0-75787  
transition metal-noble metal spin glass films, mag. props. 0-60306  
transitions, field-induced, masking effects 0-65943  
X-Y and Heisenberg, below four dimensions, vanishing of Edwards-Anderson order parameter 0-60347  
Ag-Mn, conc. spin glasses, thermopower 0-65538  
 $\text{Al}_2\text{Mn}_3\text{Si}_3\text{O}_{12}$ , amorphous insulating spin glass, susceptibility and magnetisation meas. 0-88765  
Au-Co, electron scatt., spin-orbit effects 0-65533  
Au-Cu-Fe spin glass alloys, impurity mag. resist. meas. 0-59972  
Au-Fe, spin glasses, alternating susceptibility 0-65912  
Au-Fe, transition temp., freq. depend. 0-97113  
Au-Fe (1 at.%), spin glass, specific heat 0-60355  
Au-Fe (4.2 at.%), spin glass, magnetisation and energy relax. below  $T_g$  0-65921  
Au-Fe (4.2 at.%), DC magnetisation, field depend. 0-97103  
Au-Fe alloys, spin correlations, neutron diff. meas. 0-80482

## spin glasses continued

- Au-Mn alloys, reversible and irreversible DC magnetisation in spin glass regime 0-65908  
Au-Mn(Cr)(Fe), conc. spin glasses, thermopower 0-65538  
AuFe spin glass,  $\mu^+$  zero-field spin relax. probe for spin dynamics 0-97177  
 $\text{Co}_2\text{Ga}_{1-x}\text{Al}_x$  alloys, cluster spin glass, host and impurity NMR and AC susceptibility 0-71194  
 $\text{CoO-Al}_2\text{O}_3\text{-SiO}_2$ , amorphous, remanent magnetisation short time depend. 0-65919  
Cu-Mn, mag. viscosity below freezing temp. 0-65910  
Cu-Mn, spin glasses, alternating susceptibility 0-65912  
Cu-Mn, transition temp., freq. depend. 0-97113  
Cu-Mn, zero field ESR in spin glass state 0-66017  
Cu-Mn (8 to 75 at.%), spin correl., neutron polarisation anal. study 0-65905  
Cu-Mn alloy, macroscopic mag. anisotropy, transverse susceptibility and zero field NMR enhancement 0-80525  
Cu-Mn spin glass, spin freezing and exchange narrowing of mag. reson. 0-60411  
Cu-Mn-Au(Pt), anisotropic exchange interactions, effect of nonmag. impurities 0-80534  
CuFe solid solns., quenched from vap. phase, mag. props. 0-60307  
CuMn, hysteresis, spin orbit scattering effect on anisotropy in spin glass state 0-71095  
CuMn spin glass, AC susceptibility 0-60305  
CuMn spin glass,  $\mu^+$  zero-field spin relax. probe for spin dynamics 0-97177  
CuMn, spin glass, random moments time correl., zero field muon spin relax. meas. 0-60335  
CuMn spin glass, specific heat and entropy 0-60354  
 $\text{Cu}_{0.98}\text{Mn}_{0.02}$ , spin glass, Heisenberg mode, RPA approx. 0-65904  
 $\text{Eu}_{1-x}\text{Gd}_x\text{S}$  and  $\text{EuSr}_{1-x}\text{S}$ , transition temp., freq. depend. 0-97113  
 $\text{Eu}_{0.4}\text{Sr}_{0.6}\text{S}$ , spin dynamics, neutron scatt. study 0-65907  
 $\text{EuSr}_{1-x}\text{S}$ , Heisenberg spin glass system, excitations 0-84610  
 $\text{EuSr}_{1-x}\text{S}$ , insulating spin glass, sp. ht. near ferromag. onset 0-97106  
 $\text{EuSr}_{1-x}\text{S}$ , mag. clusters, spinodal decomp. trend 0-65923  
 $\text{EuSr}_{1-x}\text{S}$ , spin glass to ferromag. transition, neutron scatt. and susceptibility meas. 0-60254  
 $\text{EuSr}_{1-x}\text{S}$ , spin wave modes and low temp. sp. ht. 0-80538  
 $\text{EuSr}_{1-x}\text{S}$ , spin-glass props. and mag. transition 0-97105  
Fe-Ni-Cr, mag. props. in weak mag. fields (*Russian*) 0-75771  
 $\gamma$ -Fe-Ni-Mn alloys, spin glass state, short and long range order investigation 0-65808  
 $\text{Fe}_x\text{Cr}_{1-x}$ , spin-wave evolution crossing from ferromag. to spin-glass regime 0-97080  
 $\text{FeMgBO}_4$ , and  $\text{FeMg}_2\text{MO}_5$ , imperfect 1D mag. systems, Mossbauer expts. 0-60466  
 $\text{FeNbSe}_2$ , transport props. and mag. ordering 0-65527  
 $\text{Fe}_6\text{Ni}_{12}\text{Mn}_{11}$ , disordered, mag. struct. near ferro-antiferromagnetic transition 0-60211  
 $\text{Fe}_{180}\text{Ni}_{14}\text{B}_{60}$ , metallic glass, low temp. sp. ht. for spin-glass and spin-cluster-glass regime 0-71071  
 $(\text{Fe}_{100-y}\text{Ni}_y)_{75}\text{P}_{13}\text{B}_8$ , metallic glass, low temp. sp. ht. for spin-glass and spin-cluster-glass regime 0-71071  
 $\text{Fe}_2\text{O}_4$  ferrofluids, spin glass behaviour 0-71120  
 $\text{FePd}_{82}\text{Si}_{18}$  metallic glass, long range interaction and spin wave interactions 0-65949  
 $\text{FePd}_{83}\text{Si}_{17}$  metallic glass, mag. transitions, weak ferromagnetism 0-100583  
 $\text{Fe}_2\text{TiO}_5$ , anisotropic spin glass type behaviour 0-60296  
 $\text{Fe}_2\text{TiO}_5$ , spin glass system, cation distrib. Mossbauer spectra 0-71248  
 $\text{Fe}_{3-x}\text{Ti}_x\text{O}_4$ , spin glass behaviour, susceptibility and hysteresis meas. 0-65917  
 $\theta$ - $\text{Fe}_2\text{V}_2\text{O}_5$ , spin glass and paramag. props., susceptibility, EPR and Mossbauer studies 0-75782  
 $\text{Fe}_2\text{V}_2\text{O}_5$ , spin glass transition range, cluster blocking distrib. function 0-80548  
( $\text{Gd}_2\text{Y}_{1-x}\text{Al}_x$ ), ferromag. and spin glass like behaviour, magnetisation meas. 0-75734  
 $\text{H}_2$ , solid, glass phase, use of NMR (*French*) 0-93190  
 $\text{Hg}_{1-x}\text{Zn}_x\text{Cr}_2\text{Se}_4$ , magnetic struct., neutronographic and mag. investigation (*Russian*) 0-88726  
( $\text{Ho}_2\text{O}_3$ ) $_{0.194}$ ( $\text{Al}_2\text{O}_3$ ) $_{0.227}$ ( $\text{SiO}_2$ ) $_{0.579}$ , amorphous, low temp. spin glass behaviour 0-60297  
(La,Gd) $\text{Al}_2$  spin glasses, time depend. mag. props. 0-65909  
La-Gd (8 at.%), FCC, under hydrostatic pressure, resistivity meas., comparison with positive-J spin glasses 0-59958  
 $\text{LaNi}_{1-x}\text{Fe}_x\text{O}_3$ , magnetisation meas. and  $^{57}\text{Fe}$  Mossbauer studies 0-93217  
 $\text{Mn}_3\text{Al}_2\text{Si}_2\text{O}_{12}$ , amorphous, spin-glass, insulating,  $\text{Mn}^{2+}$  mag. reson. 0-65918  
 $\text{MnO-Al}_2\text{O}_3\text{-SiO}_2$ , amorphous, remanent magnetisation short time depend. 0-65919  
 $\text{MnO-Al}_2\text{O}_3\text{-SiO}_2$ , amorphous spin glass, AC susceptibility 0-80520  
 $\text{MnSi(Ge)}$ , amorphous, spin glass transition, AC susceptibility meas. 0-75779  
Ni-Mn alloys, ferromagnetism-to spin glass phase transition and strong mag. field effect 0-75773  
( $\text{Ni}_{99}\text{Fe}_{1}$ ) $_{79}\text{P}_{13}\text{B}_8$ , amorphous, low temp. sp. ht., mag. contribs. 0-80552  
 $\text{PbMnFeF}_3$  and  $\text{PbMnFeF}_3$ , vitreous, insulating, evidence of spin-glass transition 0-97112  
Pd-Fe-Mn, ferromagnet-spin glass, thermal expansion forced, magnetotri-  
tion and magnetisation under high press. 0-65255  
Pd-Mn, ferromagnetism to spin glass behaviour transition 0-71062  
Pd-Mn (1-10 wt.%), mag. ordering, influence on resistivity 0-75557  
( $\text{Pd}_{0.996}\text{Fe}_{0.0035}$ ) $_{1-x}\text{Mn}_x$ , mag. behaviour at Fe sites, Mossbauer effect meas. 0-66085  
 $\text{Pd}_{1-x}\text{Mn}_x\text{H}_x$  alloy, spin glass, transition temp., susceptibility and EPR meas. 0-65930  
Pt-Co, spin system, low temp. susceptibility 0-65920  
Pt-Cr, disordered, atomic order-disorder transition. effect on resist. min. 0-65911  
Pt-Fe(Mn), dil., skew scatt. Hall effect, magnetoresist. and mag. anisotropy, orbital magnetism of impurity 0-70678  
PtCr, AC susceptibility near percolation limit, ordered and disordered alloy 0-65900  
PtMn, spin glass, nonlinear susceptibility and sp. ht. 0-60304  
Sc-Gd, spin glasses, low temp. sp. ht. and magnetisation 0-65913  
( $\text{Ti}_{1-x}\text{V}_x$ ) $_2\text{O}_3$ , spin glass, nonlinear susceptibility and sp. ht. 0-60304  
Y-Gd, spin glasses, low temp. sp. ht. and magnetisation 0-65913



**spin Hamiltonians**

- alkali halide:  $\text{Eu}^{2+}$ , spin-Hamiltonian parameters, superposition model calcs. 0-96830  
 alkali halides, heteronuclear  $\text{XY}^-$  defects, spin Hamiltonian parameter anal. 0-88509  
 alloy, pseudobinary, ferromag, magnon energy derivation 0-107996  
 antiferromagnet, induced staggered magnetic fields, microscopic mech. 0-80527  
 antiferromagnet, linear-chain, sine-Gordon solitons 0-80543  
 constant-coupling, higher-order, statics and dynamics 0-60262  
 dispersive phase transition, S ion spin Hamiltonian parameter dependence on order parameter 0-70356  
 effective Hamiltonian approximation, quenched and annealed random systems 0-93125  
 ESR, magnetic field operator 0-108051  
 ferromagnet, singlet-triplet, Dyson eqn. derivation 0-107974  
 ferromagnetic crystal, spin subsystem thermodynamics, spin-phonon interactions, mag. order parameter 0-103848  
 Heisenberg magnet, correlation theory of static and dynamic properties 0-65765  
 Heisenberg model, classical, infinite, nonlinear dynamics, quantum time evolution 0-100576  
 Hubbard model, equivalent spin Hamiltonian, for phase transition studies 0-80474  
 Kondo Hamiltonians diagonalisation, zero-temp. mag. susceptibility 0-93078  
 Lorentzian lineshapes and isotropic distrib. of molecules, analytical expressions derived for powder samples 0-60401  
 magnesium hexahydrate  $\text{H}_2\text{EDTA}\cdot\text{VO}^{2+}$ , single cryst., ESR spectra and spin Hamiltonian parameters 0-75845  
 metal, indirect coupling between localised mag. moments by narrow band electrons 0-70942  
 one-dimensional compressible Ising chain with general spin 0-90791  
 quantum spin systems, ground state energies, renormalisation techniques appls. 0-93132  
 $\alpha$ -quartz, dynamic interchange among three states of P, EPR obs. 0-66010  
 scheelites, zero-field splitting of  $\text{Mn}^{2+}$  ions 0-75531  
 Schrodinger eqn., exact soln., spinning particle in helical mag. field, non-relativistic quantum theory 0-77651  
 single electron state classification on basis of spin space groups 0-93065  
 sodium oxalate:  $\text{Cu}^{2+}$ , anhydrous spin Hamiltonian and bonding parameters and orbital-reduction factors 0-60408  
 spin glass, Heisenberg model calc. 0-60301  
 transition density matrices, spin variables separation by Fock coordinate function and spin Hamiltonian methods 0-63513  
 transition metal compound, superexchange interaction, effective spin-orbital Hamiltonian 0-70998  
 transition metal compound, superexchange interaction, multielectron theory 0-70997  
 triglycine calcium bromide:  $\text{Cu}^{2+}$ , ESR studies 0-97136  
 $\text{Al}_2\text{O}_3\cdot\text{V}^{3+}$ , spin-phonon coupling, rot. mode role 0-70329  
 $\text{BaO}\cdot\text{P}_2\text{O}_5\cdot\text{Mo}^{3+}$  glass, EPR spectra, computer simulation 0-88872  
 $\text{CaSe}\cdot\text{Sn}^{2+}$ , EPR study of octahedral  $\text{Sn}^{2+}$  centres, 4 to 290K (Russian) 0-84637  
 $\text{CdF}_2\cdot\text{Eu}^{2+}$ , EPR spectra, hydrostatic press. and temp. effects 0-84648  
 $\text{Ce}(\text{SO}_4)_3\cdot 8\text{H}_2\text{O}\cdot\text{Gd}^{3+}$ , single cryst., EPR study, spin Hamiltonians 0-80606  
 Co complex, triazene-1-oxide complexes, EPR spectra in frozen nematic liq. cryst. glass 0-88871  
 Cr-V, itinerant electron antiferromag., spin fluctuations, low temp. specific heat 0-107439  
 Cu complex, triazene-1-oxide complexes, EPR spectra in frozen nematic liq. cryst. glass 0-88871  
 $\text{Fe}(\text{H}_2\text{O})_6^{3+}$  ion, amorphous frozen soln., Mossbauer study, hyperfine struct. 0-80644  
 $\text{Fe}^{3+}$  paramagnetisations, spin lattice relaxation Mossbauer study, dynamic spin Hamiltonian formalism 0-97173  
 $\text{FeTiS}_2$ , mag. struct. and props., neutron diffr. and mag. meas. 0-60201  
 Ge,  $\mu\text{SR}$ , spin Hamiltonian and anomalous muonium states 0-71286  
 $^3\text{He}$ , HCP, and adsorbed  $^3\text{He}$  with triangular lattice, exchange and mag. order 0-107606  
 $^3\text{He}$ , superfluid, p-wave spin triplet pairing Hamiltonian, 5-D spin 0-75400  
 $\text{KMgF}_2$ , spin Hamiltonian parameters for  $\text{Fe}^{3+}$  ions, superposition model anal. 0-108053  
 $\text{KZnF}_2$ , spin Hamiltonian parameters for  $\text{Fe}^{3+}$  ions, superposition model anal. 0-108053  
 $\text{La}_2(\text{SO}_4)_3\cdot 9\text{H}_2\text{O}\cdot\text{Gd}^{3+}$ , single cryst., EPR study, spin Hamiltonians 0-80606  
 $\text{LiAlSiO}_4\cdot\text{Cu}$ ,  $\beta$ -eucryptite solid electrolyte,  $\text{Cu}^{2+}$  EPR obs. of ion exchange props. 0-108056  
 $\text{Mg}(\text{NH}_4)_2(\text{SeO}_4)_2\cdot 6\text{H}_2\text{O}\cdot\text{Mn}^{2+}$ , EPR spectra 0-100608  
 $\text{MgRb}(\text{SeO}_4)_2\cdot 6\text{H}_2\text{O}\cdot\text{Mn}^{2+}$ , EPR spectra 0-100608  
 $\text{Mg}_2\text{TiO}_4\cdot\text{Cu}(\text{Ni})$ , ESR of  $\text{Cu}^{2+}$  and  $\text{Ni}^{2+}$  0-97131  
 $\text{NH}_4\text{Cl}\cdot\text{Ni}^{2+}$ , EPR spectrum, spin Hamiltonian, zero-field splitting effects 0-97135  
 $\text{RbAl}(\text{SO}_4)_2\cdot 12\text{H}_2\text{O}$ , spin-Hamiltonian with trigonal  $\text{S}^1$  terms for describing  $\text{Fe}^{3+}$  ENDOR spectra 0-75885  
 $\text{RbGa}(\text{SO}_4)_2\cdot 12\text{H}_2\text{O}$ , spin-Hamiltonian with trigonal  $\text{S}^1$  terms for describing  $\text{Fe}^{3+}$  ENDOR spectra 0-75885  
 $\text{RbH}(\text{SeO}_4)_2\cdot \text{VO}^{2+}$ , EPR spectra, spin Hamiltonian parameters 0-100609  
 Si,  $\mu\text{SR}$ , spin Hamiltonian and anomalous muonium states 0-71286  
 YCrO<sub>3</sub>, bubble domain struct. temp. depend. 0-71137  
 $\text{Zn}(\text{BF}_4)_2\cdot 6\text{H}_2\text{O}\cdot\text{Ni}$ , phase transition study, EPR of diluted  $\text{Ni}^{2+}$ , 98-298K 0-75846  
 $\text{Zn}(\text{NH}_4)_2(\text{SeO}_4)_2\cdot 6\text{H}_2\text{O}\cdot\text{Mn}^{2+}$ , EPR spectra 0-100608  
 $\text{ZnRb}(\text{SeO}_4)_2\cdot 6\text{H}_2\text{O}\cdot\text{Mn}^{2+}$ , EPR spectra 0-100608  
 $\text{ZnSe}\cdot\text{Ti}^{2+}$ , EPR meas. 0-80594

**spin-lattice relaxation**

- see also electron spin-lattice relaxation: nuclear spin-lattice relaxation  
 anisotropic spin-phonon coupling model, exact solutions (Russian) 0-100590  
 benzene, liq., mol. motion at high press. 0-103509  
 cellulose, mobility of adsorbed water, NMR pulse obs. 0-108835  
 deoxyhaemoglobin, proton NMR, modified DEFT technique for obs. hyperfine shifted line,  $T_1$  values meas. 0-76871  
 dichloromethane- $d_2$ , spectral densities determ. from spin-lattice relax. and spin-echo decay rates 0-75877

**spin-lattice relaxation continued**

- dimethylformamide, intramolecular exchange rate determ. from  $^{13}\text{C}$  spin-lattice relax. times 0-69169  
 mathematical formulation for selecting optimal parameter for meas. of relaxation times 0-62703  
 methylammonium bromide, solid, phase transitions, PMR, DTA study 0-107421  
 muscle, skeletal, water protons NMR relax. times anisotropy obs. 0-85341  
 proton relaxation times prolongation, regionally ischemic dog heart tissue 0-101216  
 terpenes, methyl groups internal rotation,  $^{13}\text{C}$  spin lattice relaxation times and force field calcs. 0-74255  
 tetrafluoromethane, liq., mol. reorientation 0-106320  
 time measurement using saturation, inversion and fast inversion recovery expts. 0-57356  
 tissues, normal and malignant, pulsed NMR obs. 0-94171  
 triplet exciton annihilation rate, magnetic field depend. effect of spin-lattice relaxation 0-65459  
 Cr, antiferromagnetic, muon diffusion, spin relax. and coherent motion 0-71281  
 D probe spin alignment for obs. ultraslow mol. rot. 0-88890  
 $\text{He}^3\text{-He}^4$  mixture, relax. of  $2\text{S}$ , metastable atoms 0-102469  
 $\text{Li}\cdot\text{NH}_3$ , concentrated solution, NMR relaxation of  $^7\text{Li}$  0-108084  
 Mo-Co Kondo alloy, Co impurity susceptibilities, Knight shift 0-88721

**spin-orbit interactions**

- actinide compounds, neutron scatt. studies 0-75716  
 alkali halides, heteronuclear  $\text{XY}^-$  defects, spin Hamiltonian parameter anal. 0-88509  
 alkali metal atoms, spin-polarised, near-reson. two-photon ionis., light polarisation effects 0-106308  
 alkali metal halide crystals, g-tensor anal. of  $\text{S}^-$  and  $\text{Se}^-$  centres, ESR 0-84650  
 anisotropic spin-phonon coupling model, exact solutions (Russian) 0-100590  
 bremsstrahlung by transversely polarised electrons, azimuthal asymmetry due to spin-orbit coupling 0-60705  
 bromobenzene ion fragmentation, photoelectron-photoion coincidence spectra 0-95682  
 N-bromosuccinimide, X-irrad., ESR study of Br and  $\sigma^*$  radical 0-66037  
 chloroquinolines, photophys. behaviour, substituent and solvent effects 0-106342  
 cubic complexes, weak-field coupling scheme 0-92866  
 diatomic alkaline earth halides, multiplet splitting, extended Huckel approach 0-74127  
 diatomic molecules, hydrides, oxides and BeF, spin orbit coupling const., ab initio calcs. 0-63537  
 diazaphthalenes, excited state absorpt. spectra and intersystem crossing kinetics 0-74176  
 dichloronaphthalenes, heavy atom effects on substrates of lowest triplet states, MIDP obs. 0-91594  
 1,8-dichlorooctane, quadrupolar relax. centres, limited spin diffusion 0-100649  
 dimethylbenzaldehydes, in durene single cryst., zero-field splitting, guest and host isotope effects 0-107752  
 disordered electronic systems, spin interaction effects, loop expansion and exact relations among local gauge invariant modes 0-80221  
 electron-photon coincidence expts., interpretation 0-83489  
 equivalent electrons, J allowed values in jj coupling 0-90624  
 ferromagnet, itinerant electron, magnetoresist. and anomalous Hall effect due to electron-phonon interactions 0-70680  
 ferromagnetic metals, resist. anisotropy, crit. behaviour and temp. depend. 0-96858  
 formaldehyde,  $^3\text{A}^*$  state, zero-field splitting param., ab initio CI calcs. 0-99454  
 high-Z elements subshells, photoelectron angular distribution 0-99487  
 hydrogenlike atoms, spin-orbit terms derivation 0-73148  
 inert gas atom, first excited config., intermediate coupling coeff. 0-83450  
 Josephson coupled layered supercond., upper critical field (Russian) 0-100551  
 metals, Kondo effect, Anderson hamiltonian 0-60187  
 molecules, electronic spin orbit interaction, molecular Aharonov-Bohm effect 0-83303  
 particle motion in ring shaped potential, spin-orbit coupling 0-101723  
 quantum scattering theory inverse problem, fixed energy Jost functions (Russian) 0-68082  
 random electronic models with spin-dependent hopping 0-70574  
 random system, 2-D, spin-orbit interaction and magnetoresistance 0-70728  
 rare earth ion spectra, crystal field integral parameters, spin-orbit interaction 0-100447  
 thioformaldehyde,  $\lambda^3\text{A}_2\text{-X}^1\text{A}_1$  IR absorpt. spectra 0-83362  
 transition metal, ferromag., band theory of linear magnetostriiction 0-71141  
 transition metal oxides, second and third-row, XPS 0-87170  
 universal variational functionals of electron densities, first-order density matrices, and natural spin-orbitals and solution of the  $\nu$ -representability problem 0-95516  
 X-ray 5p emission bands, valence energy band 0-104016  
 xanthione, large zero-field splitting of lowest triplet state 0-58171  
 Ag foil, or film, conduction electron spin disorientation at surface 0-75855  
 $\text{AlS}$ ,  $\text{B}^1\Pi\text{-X}^2\Sigma^+$  transition, assignment of UV bands, vibr. and rot. anal. 0-58278  
 $\text{Ar}^+(\text{P}_1)+\text{H}_2(\text{D}_2)$ ,  $\text{Ar}^+$  two spin orbit state, reaction cross section, direct determ. 0-93748  
 $\text{As}_2\text{Se}_3$ , single crystals, fine struct. of direct gap from electronef. spectra 0-93280  
 Au subshell photoelectron branching ratio meas. using synchrotron radiation 0-66397  
 Au-Co, electron scatt., spin-orbit effects 0-65533  
 $\text{Ba}_2\text{NbRuO}_{12}$  and  $\text{Ba}_2\text{TaRuO}_{12}$ ,  $(\text{Ru}_2\text{O}_{12})^{13-}$  cluster obs. in presence of orbital degeneracy and spin-orbit coupling (French) 0-70655  
 BeF, spin orbit coupling const., ab initio calcs. 0-63537  
 $\text{C}(\text{C}_2\text{S}_2)+\text{H}_2(\text{O}_2)$  (ethylene), collisional behaviour, kinetic study 0-74241  
 CdTe, energy bands and optical props. calc., tight-binding model with spin-orbit interaction 0-65448  
 Co, liquid, Hall effect, band struct. and exchange scatt. 0-80250  
 Cs, 6s-electron photoionisation, ab initio calcs. 0-91523



**spin-orbit interactions continued**

- CsBr, (110) surface, electronic struct. of valence bands calc. (*Russian*) 0-75621  
 CsCl, (110) surface, electronic struct. of valence bands calc. (*Russian*) 0-75621  
 CsI, (110) surface, electronic struct. of valence bands calc. (*Russian*) 0-75621  
 $\text{Cs}_2\text{MX}_4$  (M=Se, Te, X=Cl, Br),  $\Gamma_4^-({}^2T_{1u})$  state, Jahn-Teller effect, luminesc. obs. 0-60650  
 $\text{Cs}_2\text{SiF}_6\text{Mn}^{4+}$ , IR absorpt. band, electron-vibr. effect 0-108238  
 $\text{Cs}_2\text{TiF}_6\text{Mn}^{4+}$ , spin-orbit and field splitting, Jahn-Teller effect, Zeeman meas. 0-80234  
 Cu foil, rel. to conduction electron spin disorientation at surface 0-75855  
 Cu-Mn-Au(Pt) spin glasses, anisotropic exchange interactions, effect of nonmag. impurities 0-80534  
 CuMn, hysteresis, spin orbit scattering effect on anisotropy in spin glass state 0-71095  
 $\text{Cu}_2\text{O}$ , self-consistent energy bands 0-59869  
 F, spin-orbit splitting and  ${}^2P_{1/2}$  radiative lifetime, absorpt. spectrosc. meas. 0-87063  
 Fe, fine struct. levels fitting, config. interaction effect, spin-orbit and electrostatic interaction parameters 0-69248  
 Fe, liquid, Hall effect, band struct. and exchange scatt. 0-80250  
 $\text{Fe}_3\text{O}_4$ , magnetite, mag. aftereffects, 4.35K 0-80571  
 GeF, use in chemical lasers 0-64004  
 HBr, photoelectron angular distrib. 0-58318  
 HI, photoelectron angular distrib. 0-58318  
 $\text{H}_2\text{O}^+$ , spin and rot. fine struct., orbital angular momentum 0-83247  
 ${}^1\text{H}(n,n)$ , pol. n, 13.5-16.9 MeV, anal. power and spin-orbit phase parameters 0-78269  
 ${}^3\text{He}$  atom forbidden singlet-triplet anticrossings, D levels 0-99491  
 HgTe, energy bands and optical props. calcs., tight-bonding model with spin-orbit interaction 0-65448  
 InAs and solid solutions, recombination mechanisms of excess carriers, luminesc. obs. 0-97337  
 $\text{KCl:Ca(Yb)}$ ,  $Z_2$  and  $Z_2^+$  centres, excited state, magneto-optical spectra 0-108233  
 $\text{KCl(Br)}$ , F-centre emission, mag. circular polarisation 0-108251  
 $\text{K}_2\text{CoF}_4$ , 2-dimens. Ising antiferromag., mag. excitons, Raman scatt. obs. 0-66181  
 $\text{K}_2\text{FeF}_4$ , two-dimensional antiferromag., cryst. field effects, Mossbauer spectroscopy 0-71254  
 $\text{K}_3\text{Fe}_2\text{F}_7$ , two-dimensional antiferromag., cryst. field effects, Mossbauer spectroscopy 0-71254  
 $\text{KMgF}_3\text{:Co}^{2+}$ ,  ${}^4T_1$ - ${}^4T_2$  transition, zero-phonon lines intensities 0-75529  
 $\text{MgO:Cr}^{2+}$ , APR under applied stress 0-88865  
 $\text{MgS:Ce}^{3+}$  phosphors, emission and excitation spectra (*French*) 0-93380  
 Mn, fine struct. levels fitting, config. interaction effect, spin-orbit and electrostatic interaction parameters 0-69248  
 $\text{Mo}_2\text{N}_2\text{N}_4$ , super Coster Kronig processes 0-106303  
 Mo, X-ray spectra, K $\alpha$  hypersatellites 0-63576  
 $\text{NH}_2$ , spin and rot. fine struct., orbital angular momentum 0-83247  
 $\text{NO}$ , Zeeman spectrum, mol. beam elec. reson. spectrosc. 0-91621  
 $\text{Nb}_2\text{N}_2\text{N}_4$ , super Coster Kronig processes 0-106303  
 Ni, liquid, Hall effect, band struct. and exchange scatt. 0-80250  
 $\text{O}_2$ , spin-forbidden transition intensities, selective heavy atom effects 0-58240  
 ${}^{16}\text{O}(\text{p},2\text{p})$ , cross section, analysing power, energy sharing spectra, distorted wave impulse approx. 0-78291  
 Pb subshell photoelectron branching ratio meas., using synchrotron radiation 0-66397  
 $\text{PbMoO}_4$ , doped and undoped single crystals, polarisation of luminesc. and assignments 0-76069  
 $\text{PbWO}_4$ , doped and undoped single crystals, polarisation of luminesc. and assignments 0-76069  
 Pt porphyrin in n-alkane single cryst.  ${}^3E_g$ - ${}^1A_g$  transition, Zeeman expts. at 4.2K 0-78645  
 Pt subshell photoelectron branching ratio meas., using synchrotron radiation 0-66397  
 rare earth oxides, XPS 0-87170  
 $\text{RbCl(Br)}$ , F-centre emission, mag. circular polarisation 0-108251  
 $\text{RbCoF}_4$ , 2-dimens. Ising antiferromag., mag. excitons, Raman scatt. obs. 0-66181  
 $\text{Rh}_2\text{N}_2\text{N}_4$ , super Coster Kronig processes 0-106303  
 $\text{Ru}_2\text{N}_2\text{N}_4$ , super Coster Kronig processes 0-106303  
 $\text{Sc+NO}_2$ , chemiluminesc., nonequilib. product distrib. 0-101014  
 $\text{SeOCl}_2\text{:Pr}^{3+}(\text{Nd}^{3+})$ , SbCl<sub>5</sub> acidified, Racah and Judd-Ofelt parameters in laser liqs. 0-106516  
 $\text{Si:Al,N}$  (6H), ODMR for effective-mass-like acceptor 0-93213  
 SiF, use in chemical lasers 0-64004  
 Sn, white, Fermi surface, dilatational strain depend., OPW calcs. 0-84418  
 $\text{SnF}_4$ , use in chemical lasers 0-64004  
 SrI, low-lying electronic states, vibr. anal. 0-106315  
 Ti, fine struct. levels fitting, config. interaction effect, spin-orbit and electrostatic interaction parameters 0-69248  
 $\text{UF}_6$ , relativistic scattered wave calculations 0-63538  
 V, fine struct. levels fitting, config. interaction effect, spin-orbit and electrostatic interaction parameters 0-69248  
 $\text{WV}_2\text{O}_8$ , magnetic susceptibility, behaviour in terms of quasi-isolated binuclear units 0-97073  
 Xe subshell photoionisation, multichannel k-matrix calc., spin orbit interactions 0-63600  
 $\text{ZnF}_2\text{:Co}^{2+}$ , Raman tensor calcs. of isolated impurity in diamagnetic matrix 0-76025

**spin-phonon interactions**

- see also *spin-lattice relaxation*  
 anisotropic spin-phonon coupling model, exact solutions (*Russian*) 0-100590  
 antiferromagnet, nuclear spin oscillations, interaction with lattice vibrs. 0-70996  
 ferrodistorive spin-phonon systems, crit. props. 0-88315  
 ferromagnet, shape of Mossbauer line 0-71251  
 ferromagnetic crystal, spin subsystem thermodynamics, spin-phonon interactions, mag. order parameter 0-103848  
 ideal Heisenberg ferromagnet, phonon renormalisation and spin waves 0-88754  
 Ising chain, with next-nearest neighbour interactions, mag. responses to spin-Peierls transition 0-71054  
 Ising spin system, coupled to acoustic and optic lattice modes, critical behaviour 0-71044

**spin-phonon interactions continued**

- one-dimensional spin  $1/2$  chain, soliton excitation in strong spin-phonon interaction 0-103842  
 paramagnetic spin system, two-level open system, kinetic theory of resonance and relaxation 0-88859  
 quantum compressible Ising model, critical behaviour 0-108016  
 rare earth zircons, Jahn-Teller cooperative phase transition, crossover effects 0-88316  
 Rochelle salt, ferroelec. phase transition, Raman scatt. study 0-97211  
 Rochelle salt, ferroelectric, Raman and IR study 0-71406  
 tetramethylammonium(0),  $\text{Li}(\text{CH}_3\text{NH}_2)_4$ , existence, conduction- and localised-electron spin reson. 0-66035  
 thiourea, ferroelectric, Raman and IR study 0-71406  
 $\text{Al}_2\text{O}_3\text{:V}^{3+}$ , Jahn-Teller effects, ground state 0-75528  
 $\text{Al}_2\text{O}_3\text{:V}^{3+}$ , spin-phonon coupling, rot. mode role 0-70329  
 $\text{BaF}_2\text{:Gd}^{3+}$ , spin-lattice coeffs., EPR study 0-66032  
 Eu chalcogenides, spin-dependent Raman scatt. from phonons 0-97274  
 $\text{EuO(S)(Se)(Te)}$ , spin order and fluctuations, Raman scatt. study 0-97273  
 $\text{EuS(S)(Te)}$ , spin-assisted phonon Raman scatt., mag. phase depend. 0-71413  
 EuTe, antiferromag. semicond., Raman scatt., spin-phonon interactions 0-66185  
 $\text{Fe}^{3+}({}^6\text{S})$  paramagnetisations, spin lattice relaxation Mossbauer study, dynamic spin Hamiltonian formalism 0-97173  
 n-InSb, spin-magnetophonon resonance 0-96918  
 $\text{KMgF}_2\text{:Ni}^{2+}$ , acoustic Faraday and Cotton-Mouton effects, theory 0-65987  
 $\text{NiSiF}_6\cdot 6\text{H}_2\text{O}$ , non-Kramers system, spin-lattice relaxation at strong fields 0-100612  
 $\text{VI}_2$ , spin-dependent Raman scatt. from phonons 0-97274  
**spin polarised electron emission**  
 magnetic order and spin depend. of electron scatt. meas. technique using photoemission 0-60748  
 Ar, spin-polarised photoelectrons by circularly polarised synchrotron radiation 0-91516  
 Eu chalcogenides, cond. band spin struct. 0-71577  
 FeTi, surface and mag. props., heat treatment and hydrogenation effects 0-75447  
 Kr, spin-polarised photoelectrons by circularly polarised synchrotron radiation 0-91516  
**spin polarised electron phenomena** see *electron spin polarisation*  
**spin-spin nuclear coupling in molecules** see *molecular nuclear coupling*  
**spin-spin relaxation**  
 blood, normal and pathologic, NMR  $T_2$  relax. time studies 0-81682  
 cellulose, mobility of adsorbed water, NMR pulse obs. 0-108835  
 collagen fibril,  ${}^2\text{H}$  NMR of mol. motion 0-67034  
 cytochrome c<sub>3</sub>, haeme-haeme mag. interaction, Mossbauer obs. 0-108836  
 decacyclene anion, photoexcited quartet state, transient EPR 0-78635  
 dimethylbenzaldehydes, in durene single cryst., zero-field splitting, guest and host isotope effects 0-107752  
 ethylene oxide, rot. relax., double reson. and Stark switching obs. 0-106340  
 free radicals, spin exchange, anisotropic spin-density distrib. 0-102526  
 inhomogeneous systems, line broadening, spin-spin and spin-lattice relax. rate meas. 0-58292  
 muscle, skeletal, water protons NMR relax. times anisotropy obs. 0-85341  
 neopentane adsorbed on graphite, quasi two-dimens. fluid, NMR 0-102525  
 NMR hybrid relaxation and multiple pulse methods for studying chemical, physical and spin exchange 0-80629  
 NMR linewidth, paramagnetic contrbs. calcs. 0-58286  
 nuclear spin relax. by translational diffusion in solids, reciprocal-space formalism, mean-field theory 0-71208  
 paramagnetic system with quadrupole splitting, magneto-optical effects, magnetic resonance saturation 0-60404  
 polyatomic molecules, intramolecular vibr. relax., restricted quantum exchange theory 0-63610  
 polydiethylsiloxane, mol. motion, NMR spin relax. data re-interpret. 0-84664  
 polyurethanes, cross-linked, mol. mobility and struct., thermomechanical and NMR obs. (*Russian*) 0-69285  
 Portland cement, absorbed  $\text{H}_2\text{O}$ , pulsed NMR study 0-84665  
 praseodymium ethylsulphate:Sm, one-dimens. X-Y system, spin dynamics, electron spin echo meas. 0-66031  
 quantum systems, at or spin two level, reson. EM wave excitation, free induction decay oscils. 0-63562  
 rare earth nonmetallic compounds, indirect spin-spin coupling, models 0-80238  
 resonant Rayleigh-type mixing spectroscopy using ps light pulses, ultrafast relax. study 0-91834  
 solid polymers, NMR, review 0-88888  
 TMNC, quasi one dimensional planar ferromag., low temp. NMR study im mag. field 0-97157  
 water mobility in blood plasma, NMR determ., viscosity correl. to  $1/T_2$  0-67176  
 $\text{Al}_2\text{Cl}_6$  molten, nuclear mag. relax., mol. rot. 0-71209  
 $\beta\text{-Al}_2\text{O}_3\text{:NH}_4^+$ , PMR relax. time obs. of ionic motion 0-71213  
 $\beta\text{-Al}_2\text{O}_3\text{:NH}_4^+$  and  $\beta^-\text{-Al}_2\text{O}_3\text{:NH}_4^+\text{-H}_2\text{O}$ , single cryst. PMR and proton motion 0-108101  
 $\beta\text{-Al}_2\text{O}_3\text{:Na}_2\text{O}$ , anomalous Na behaviour obs. using pulsed and CW NMR 0-108095  
 ${}^{13}\text{C}$ , 2D NMR spectra, off-resonance decoupling 0-74182  
 ${}^{13}\text{C}$ , NMR spectra, transition intensities, off-resonance proton spin decoupling influence 0-74183  
 CdI<sub>2</sub>-Cd(I) mixture, molten, nuclear spin relax. 0-88887  
 Cs+Cs, spin destruction, obs. 0-63781  
 $\text{CsNiF}_3$ , quasi one dimensional planar ferromag., low temp. NMR study im mag. field 0-97157  
 HD, spin-dipolar term, spin-spin coupling const. corrections, Fermi contact terms calcs. 0-99448  
 $\text{H}_{0.36}\text{MoO}_3$  and  $\text{H}_{1.7}\text{MoO}_3$  bronzes, NMR relax. obs. at  $77 < T < 450\text{K}$ , H diffusion 0-108089  
 $\text{He}^3\text{-He}^4$  mixture, relax. of  $2^3\text{S}$ , metastable atoms 0-102469  
 ${}^3\text{He}$ , nucl. relax. in gas discharge at liq.  $\text{N}_2$  temp. 0-100114  
 ${}^3\text{He}$ , superfluid A-phase, spin relax. and zero sound attenuation at low temp. 0-107595  
 $\text{HfV}_2\text{H}_2$ , proton NMR relax. time and Knight shifts, diffusional activation energies meas., sorption props. 0-75871

spin-spin relaxation continued

<sup>199</sup>Hg, atom-surface interaction, nucl. relax., temp. depend. 0-88886  
LaF<sub>3</sub>, <sup>19</sup>F NMR study, relaxation times meas. 0-108093  
Mn<sup>2+</sup>, ionic transport, NMR and cond. studies 0-107555  
Mn 11-lectithin lipid-water system, NMR and EPR obs. 0-61168  
Mn(ClO<sub>4</sub>)<sub>2</sub>/NaClO<sub>4</sub> in aq. soln., interaction between Mn<sup>2+</sup> and ClO<sub>4</sub><sup>-</sup>, NMR studies 0-71212  
NH<sub>3</sub>, transverse relax. time, T<sub>2</sub>, of inversion doublets from free induction decay 0-58281  
NaClO<sub>4</sub>/Mn(ClO<sub>4</sub>)<sub>2</sub> in aq. soln., interaction between Mn<sup>2+</sup> and ClO<sub>4</sub><sup>-</sup>, NMR studies 0-71212  
<sup>23</sup>Na in heterogeneous system, nuclear mag. relaxation time determ., rel. with dimensions of colloidal particles 0-75876  
Pb<sub>0.7</sub>Sn<sub>0.3</sub>F<sub>2</sub>, NMR study of F atom motion (*French*) 0-100622  
PdH, Fe<sub>0.003</sub>, Kondo system, local moments, hyperfine fields, Mossbauer study 0-80478  
<sup>87</sup>Rb + <sup>129</sup>Xe, spin-exchange cross-section meas. 0-78686  
Sb<sub>2</sub>O<sub>3</sub>·H<sub>2</sub>O, crystalline, <sup>1</sup>H NMR study of proton transport 0-60446  
<sup>89</sup>V spin-spin relaxation times, pH depend. 0-66059  
ZrMn<sub>2</sub>H<sub>2</sub>, proton NMR relax. time and Knight shifts, diffusional activation energies meas., sorption props. 0-75871

spin systems

see also *magnetic properties of substances; magnetism*  
adamantane powder, dipolar relaxation, short time behaviour, pulse method meas. 0-84667  
anisotropic exchange interactions, effect on singlet ground state system 0-65852  
anisotropic magnet, dil., crit. behaviour near percolation threshold 0-88767  
anisotropic magnets, dil., scaling representation meas. percolation threshold 0-88766  
anisotropic spin-phonon coupling model, exact solutions (*Russian*) 0-100590  
antiferromagnet, magnetic phases, spin configurations in external field 0-70955  
classical spin system with long range interaction, phase transition existence conditions 0-88298  
coherent two-photon NMR, standard-basis operators, coherent averaging 0-82798  
colouring problem on randomly occupied lattice, critical conc. existence for long range order 0-80519  
1,8-dichlorooctane, quadrupolar relax. centres, limited spin diffusion 0-100649  
Dicke maser model-van der Waals spin system thermodynamic equivalence 0-83572  
disordered media, spin wave propagation, nonlinear magnon interactions (*Russian*) 0-80496  
disordered spin systems, tritric. behaviour 0-60319  
DPFH, dil., saturated spin system, spin decoupling effect and variation of dipolar energy reservoir temp. 0-88877  
EPR spin system saturation characs., acoustic wave excitation (*Russian*) 0-66013  
equivalent neighbour model, generalised, derivation of high temp. lattice consts 0-77721  
exchange energy near singular points or lines 0-93106  
ferromagnets, spin wave excitation due to parallel pumping, mag. impurity interactions (*Russian*) 0-80497  
Ga, Al, <sup>75</sup>As, optically oriented electron, nuclei spin instability (*Russian*) 0-70660  
Heisenberg model, anisotropic spin system, S=1/2 frustration effects 0-65763  
Heisenberg model, classical, infinite, nonlinear dynamics, quantum time evolution 0-100576  
Ising chain, with next-nearest neighbour interactions, mag. responses to spin-Peierls transition 0-71054  
Ising spin system, coupled to acoustic and optic lattice modes, critical behaviour 0-71044  
Ising spin systems on union jack lattice, non-universal behaviour of pair or three-spin interactions 0-57206  
magnetically ordered cryst., indirect nuclear spin interactions 0-103847  
magnetism, conference, Munich, Germany (Sep. 1979) 0-56997  
molecular field theory, simple derivation, with correlation 0-80547  
nuclear echo formation in spin systems with dynamic freq. shift to NMR 0-93208  
nuclear magnetic ordering, domains, neutron diffr. patterns, theory 0-100577  
one-dimensional spin 1/2 chain, soliton excitation in strong spin-phonon interaction 0-103842  
polarisation and magnetisation of electronic matter 0-75929  
Potts s-state model on Cayley tree Bethe-Peierls critical coupling 0-103844  
quantum Ising chain, in real or complex field, real space renormalisation group method 0-71050  
quantum spin system, two-dimens., frustration, renormalisation group study 0-80535  
quantum spin systems, ground state energies, renormalisation techniques appls. 0-93132  
quantum spin systems, S=1/2, manifestation of frustration effect 0-65767  
quasi-one-dimensional systems, spin-lattice Peierls instabilities, static and dynamic aspects 0-71052  
quasi-two-dimensional planar spin system, mag. transition 0-65951  
random band square lattice, frustrated plaquettes distrib. 0-108015  
random hierarchical model, crit. props. 0-71072  
random ordered phase, frustration, phenomenological theory 0-60349  
rare earth orthoferrites, hyperfine interaction anisotropy, NMR study (*Russian*) 0-66052  
spin systems, randomly competing, random ordered phase, frustration, phenomenological theory 0-60349  
surface magnetisation profile singularities near critical point 0-103843  
symmetry, wreath groups 0-88724  
transverse dynamic susceptibility and spin waves in itinerant electron SPW states 0-97076  
tricritical behavior in a two-dimensional field theory 0-77726  
uniaxial antiferromagnet, nonuniform spin configurations 0-97109  
uniaxial antiferromagnetic, phase diagram, spin flop transition (*Russian*) 0-100587  
Union Jack lattices, non-universal Ising spin systems 0-68145  
X-Y model, S=1/2, phase transitions at T=0, z-field renormalisation group method 0-71051

spin systems continued

XY one dimensional system containing impurities, static mag. props. (*Russian*) 0-65826  
Al<sub>2</sub>O<sub>3</sub>·Cr<sup>3+</sup>, inhomogeneous spin system, time evolution towards saturated state 0-88869  
CaF<sub>2</sub>, heteronuclear mag. spin system relaxation in many pulse NMR expts. 0-93203  
CaF<sub>2</sub>:Eu<sup>2+</sup>, photoluminesc. mag. circ. polaris. 0-89056  
Fe film, nuclear spin system dynamics Mossbauer study in FMR conditions (*Russian*) 0-80651  
FeBO<sub>3</sub>, parametric echo, magnetoelastic NMR excitation (*Russian*) 0-66072  
<sup>3</sup>He, superfluid, magnetic relaxation and high amplitude spin waves (*Russian*) 0-92749  
LiF, heteronuclear mag. spin system relaxation in many pulse NMR expts. 0-93203  
γ-Mn, antiferromagnetic, self-consistent bandstructure calcs. 0-88475  
α-O<sub>2</sub> crystals, spin ordering effect on light absorpt. (*Russian*) 0-89029

spin tickling (NMR) see *double nuclear magnetic resonance*

spin wave resonance see *ferromagnetic resonance*

spin waves

see also *magnetostatic waves; magnons*  
alloys, ferromagnetic disordered, spin wave and ferromag. reson. linewidth 0-66045  
amorphous ferromagnets, asperomagnets and spin-glasses, spin waves, theory 0-75747  
amorphous ferromagnets, hidden excitations, theory 0-75748  
antiferromagnet, amorphous, spin waves, exchange fluctuations, calc. 0-65847  
antiferromagnet, easy-plane, coupled spin wave branches (*Russian*) 0-93096  
antiferromagnet, IR absorption on impurity excitations near upper edge of spin-wave band 0-80829  
antiferromagnet, long-wavelength, surface spin-waves 0-88737  
antiferromagnet, nuclear spin oscillations, interaction with lattice vibrs. 0-70996  
antiferromagnets, easy-plane, nucl. spin wave relax. 0-65850  
antiferromagnets, magnon damping in zero external mag. fields, mag-non-magnon interactions 0-70988  
biaxial Lifshitz point problem in 3-dimens., spin wave theory 0-88759  
composite semiconductor-ferrite struct., surface magnetostatic spin wave interactions (*Russian*) 0-88739  
disordered magnetic system, spin waves, Heisenberg model 0-71064  
disordered media, spin wave propagation, nonlinear magnon interactions (*Russian*) 0-80496  
EM wave emission at twice freq. of parametrically excited spin waves, line profile depend. on spin wave distrib. 0-60234  
ferrites, ferroelec., coupled ferroelec. and spin waves, exchange interactions 0-70995  
ferrites, frequency tripling of spin waves due to longitudinal pumping excitation (*Russian*) 0-88740  
ferrites, inhomogeneous exchange interaction influence on ferromagnetic resonance line moments 0-75864  
ferrites, parametric spin wave excitation (*Russian*) 0-93099  
ferromagnet, dynamic correlations in condensed matter physics, book 0-86046  
ferromagnet, excitonic, zero-sound excitations, Fermi liq. model 0-93101  
ferromagnet, itinerant, spin waves, surface effects, RPA calc. 0-60226  
ferromagnet, surface, Brillouin light scatt. by spin waves 0-93359  
ferromagnet, surface and bulk nucl. spin waves, Green function formalism 0-70984  
ferromagnetic alloys, surface spin waves, cluster Bethe lattice approach 0-70983  
ferromagnetic conducting cryst., dynamics of s-d model in alternating mag. field (*Russian*) 0-65825  
ferromagnetic semiconductor, energy and mobility of spin polarons 0-70982  
ferromagnetic semiconductors with hot electrons, instability of coupled spin-helical waves 0-107841  
ferromagnetic slab, finite thickness, spin correl. functions 0-80522  
ferromagnetic slab, light scattering from bulk and surface spin waves, theory 0-71389  
ferromagnetic surface, spin fluctuations and light scatt. 0-84727  
ferromagnetic thin films, Brillouin scattering from spin waves 0-65843  
ferromagnets, spin wave excitation due to parallel pumping, mag. impurity interactions (*Russian*) 0-80497  
ferromagnets, spin waves in domain struct. 0-70993  
film, ferromag., dynamics near transition pt. from homogeneous to inhomogeneous magnetis. state 0-108038  
Heisenberg chain, classical, nearest-neighbour, low temp. dynamics 0-80524  
Heisenberg chain, classical, solitons and magnons 0-60161  
Heisenberg chain, impure classical, dynamics near T=0 for low impurity conc. 0-71055  
Heisenberg ferromagnet, critical dynamics of impurity spin below T<sub>c</sub> 0-71076  
Heisenberg ferromagnet, critical dynamics spin wave theory, dynamic scaling hypothesis failure 0-97082  
Heisenberg ferromagnet, spin-wave renormalisation, S≥1 0-71070  
Heisenberg ferromagnetic system with biquadratic exchange interactions, spin wave theory (*Chinese*) 0-88755  
ideal Heisenberg ferromagnet, phonon renormalisation and spin waves 0-88754  
magnetic surface states, in spin wave resonance, review 0-84654  
metal-magnetodielectric layered delay lines, dispersion eqn. (*Russian*) 0-88736  
metallic ferromagnet, antiresonance region, EM wave propag., Maxwells' eqns. sol. 0-66038  
micropolar fluids, thermodynamical aspects, non-linear approach 0-105598  
neutron beam channelling and focusing in ferromagnets (*Russian*) 0-107351  
noncollinear magnetic order and spin wave spectrum in presence of competing exchange interactions 0-65834  
one dimensional anisotropic Heisenberg model, spin 1/2, Ising like antiferromag., dynamic correlation function 0-75704  
parametric excitation, stochastic auto-oscill., Kolmogorov entropy (*Russian*) 0-75749  
parametric wave excitation by incoherent pumping 0-93103



## spin waves continued

- rare earth alloys, amorphous, with random anisotropy axes, spin excitations in paramag. phase 0-80476  
 rare earth metals, magnon dispersions in ferromag. and screw structs., nonlinear s-f exchange interaction effect 0-75746  
 resonant light scattering from magnetic excitations, review 0-97290  
 semiconductor, ferromag., spin polaron props., effect on carrier scatt. 0-60233  
 semiconductor-ferrite plate contact, electron-stimulated absorption of bulk spin waves 0-70992  
 semiconductors, magnetic, spin wave electron amplification theory 0-97083  
 spin glass, parametric amplification of spin waves by elastic pumping (*Russian*) 0-65895  
 spin glass dynamics, barrier modes and spin waves 0-60293  
 spin glasses, dilute ferromagnets, ferromagnetic modes 0-93133  
 strip films, bulk and surface spin oscills., mag. reson. 0-97149  
 systems far from thermodynamic equilib., dissipative structures, broken symm. equilib. phase transition theory 0-65827  
 TMMC, Cu-substituted, spin dynamics, neutron scatt. cross section 0-60312  
 transition metal alloys, dilute ferromagnetic, itinerant d-electron(hole) degenerate, spin stiffness constant 0-70930  
 transition metal alloys, disordered ferromag., spin wave stability 0-70994  
 transition metals, 3d, ferromag. props., book contrib. 0-75724  
 transverse dynamic susceptibility and spin waves in itinerant electron SPW states 0-97076  
 weak ferromagnet, collective excitations in transverse mag. field, AFMR spectrum 0-93100  
 Au, resonant and nonresonant conduction-electron-spin transmission 0-75857  
 CdCr<sub>2</sub>S<sub>4</sub>(Se<sub>4</sub>), spontaneous magnetisation temp. depend., nuclear resonance freq. depend. (*French*) 0-80483  
 CoCO<sub>3</sub>, Brillouin-Mandelstam light scatt. obs. of spin wave spectra 0-93358  
 Cr, antiferromagnetic structure, mag. field effect, spin density wave model (*Russian*) 0-70953  
 CrBr<sub>3</sub>, HF spectra, susceptibility, spin waves in domain walls (*Russian*) 0-80909  
 CsCoBr<sub>3</sub>, ID Ising antiferromagnet, spin dependent Raman scattering from phonons and electronic excitations 0-103948  
 CsCoCl<sub>3</sub>, spin dynamics, neutron scatt. study 0-80493  
 CsMnCl<sub>3</sub>, antiferromagnetic resonance, parametric spin wave excitation (*Russian*) 0-93183  
 CsMnF<sub>3</sub>, antiferromag., variation of spin wave spectrum in interaction between magnons 0-65841  
 Cu, resonant and nonresonant conduction-electron-spin transmission 0-75857  
 ErCo<sub>2</sub>(Fe<sub>2</sub>), mag. excitations, RPA theory 0-65830  
 EuO, light scatt. from spin waves and magneto-optic hysteresis meas. 0-97244  
 EuO, spin wave lifetime, theory compared with expt. 0-60228  
 EuS, ferromag. semicond., high field susceptibility, spin waves 0-75735  
 EuS, light scatt. from spin waves and magneto-optic hysteresis meas. 0-97244  
 EuS, single cryst., high-field susceptibility meas., temp. range 2.5 to 16.5K 0-84589  
 Eu, Sr<sub>1-x</sub>S, spin glass, spin wave modes and low temp. sp. ht. 0-80538  
 Fe alloys, amorphous, mag. saturation, spin wave stiffness, temp. depend. 0-75741  
 Fe, electron tunnelling 0-60104  
 Fe, ferromag., dynamic susceptibility calc. 0-80488  
 Fe-Ni based metallic glass, Metglas 2826 MB, Mossbauer study 0-75897  
 Fe-Ni Invar anomalies, explanation in terms of itinerant electron magnetism 0-75705  
 Fe-Ni(35.4 at.%) Invar alloys, T<sup>2</sup> term contribution to magnetisation 0-71096  
 Fe<sub>3</sub>Pt, ordered ferromagnetic alloy, magnetic excitation obs. 0-70978  
 Fe<sub>30</sub>B<sub>70</sub>, amorphous, Brillouin scatt. from magnons, ferromag. reson. 0-65844  
 Fe<sub>30</sub>B<sub>70</sub> film, amorphous metallic, standing spin waves, Brillouin scatt. obs. 0-97291  
 FeBO<sub>3</sub>, size effect during parametric spin wave excitations (*Russian*) 0-103824  
 Fe<sub>2</sub>Cr<sub>1-x</sub>, spin-wave evolution crossing from ferromag. to spin-glass regime 0-97080  
 Fe<sub>2</sub>, spin waves and two magnon bound states, mag. field IR absorption meas. 0-65840  
 Fe<sub>40</sub>Ni<sub>60</sub>P<sub>14</sub>B<sub>6</sub>, amorphous ferromag., spin wave excitations 0-97079  
 Fe<sub>2</sub>P, spin wave excitations meas. 0-65831  
<sup>3</sup>He, superfluid, magnetic relaxation and high amplitude spin waves (*Russian*) 0-92749  
<sup>3</sup>He-Z near A. phase transition, collective oscill. hybridisation (*Russian*) 0-80020  
 HgCr<sub>2</sub>Se<sub>4</sub>, spontaneous magnetisation temp. depend., nuclear resonance freq. depend. (*French*) 0-80483  
 Ho<sub>2</sub>Co<sub>7</sub>, spin wave excitations, 4.8 and 78K 0-60230  
 KCuF<sub>3</sub>, one-dimens. antiferromag., spin waves, neutron scatt. study 0-65848  
 K<sub>2</sub>FeF<sub>4</sub>, two dimensional easy plane antiferromag., neutron scatt. expts. 0-65838  
 γ-Mn-Cu (10 at.%), spin wave studies using neutron diffraction 0-70991  
 MnF<sub>2</sub>, spin wave lifetime, theory compared with expt. 0-60228  
 MnP, ferro-spiral transition, neutron scatt. studies, spin wave dispersion relations meas. 0-65876  
 Mn<sub>2</sub>Sb, spin-wave dispersion relations, exchange interactions, neutron inelastic scatt. 0-65832  
 Ni, electron tunnelling 0-60104  
 Ni, ferromag., dynamic susceptibility calc. 0-80488  
 Ni-Co, high-field susceptibility, spin-wave spectrum, CPA calc. 0-65818  
 Ni-Cu, high-field susceptibility, spin-wave spectrum, CPA calc. 0-65818  
 Ni-Fe, high-field susceptibility, spin-wave spectrum, CPA calc. 0-65818  
 Ni<sub>2</sub>Fe alloys, low-temperature specific heat, long and short range order effects 0-100339  
 Rb<sub>2</sub>CrCl<sub>4</sub>, 2D-ferromag., renormalisation of long wavelength spin waves, neutron scatt. 0-60229  
 Rb<sub>2</sub>CrCl<sub>4</sub>, planar ferromag., spin waves 0-65835  
 RbMnF<sub>3</sub>, spin wave lifetime, theory compared with expt. 0-60228  
 RbMnF<sub>3</sub>, spin wave widths 0-97081  
 TbZn, mag. excitations meas. 0-70979

## spin waves continued

- W, resonant and nonresonant conduction-electron-spin transmission 0-75857  
 YIG, open die hot pressing, spin wave and FMR line width 0-89170  
 YIG, spin wave parametric excitation threshold at low temp. 0-97084  
 YIG:La(Ga) films, ferromagnetic resonance, ion implantation effect 0-97145  
 Y<sub>2.85</sub>La<sub>0.15</sub>Fe<sub>3</sub>75Ga<sub>1.25</sub>O<sub>12</sub> LPE films, ion implantation effect on spin waves 0-71124  
**spinodal decomposition**  
 alloy, ordered, spinodal decomposition, theoretical basis 0-60862  
 alloys, high resoln. diff. and imaging characterisation 0-104050  
 alloys, phase transitions via unstable states, review 0-96657  
 binary liquid mixture, phase transitions via unstable states, review 0-96657  
 β-brass, spinodally decomposed, morphology and characts. 0-60863  
 FCC alloy, hardening by spinodal modulated structure 0-60874  
 glasses, phase transitions via unstable states, review 0-96657  
 Invar, phase stability, spinodal decomposition 0-88327  
 2,6-lutidine-water critical mixture, spinodal decomposition, Rayleigh scatt. 0-70416  
 magnetic alloys, binary, spinodal decomp., computer simulation study of interface behaviour 0-84913  
 metamagnet, two-dimens., tricritical spinodal decomp., Monte Carlo study 0-93117  
 optical fibres, fabrication using phase separation and leaching method (*French*) 0-106623  
 phase separation kinetics, Boltzmann's transport eqn. calcs. 0-79952  
 polymer blends, fluctuation dynamics, spinodal decomp. 0-79943  
 polymers, solidification, as dissipative process 0-65205  
 statistical mechanical theory of the kinetics of phase transitions, review, book contrib. 0-73270  
 Al-Zn, spinodally decomposing, main wavelength of conc. fluctuations calc. 0-97459  
 Al-Zn (38 at.%), alloy, TEM study of precipitation processes or different microstructures during ageing 0-93561  
 Co-Ti-Fe (3, 1 to 2 wt.%), spinodal decomposition 0-100839  
 Cr-Co-Fe, low Co, phase separation, TEM and Mossbauer spectra obs. 0-71269  
 Cu-Ni-Sn (10, 6 wt.%), spinodal decomposition, X-ray and electron diff. study 0-81063  
 Cu-Ni-Sn (15, 8 wt.%), prior deform. effect on spinodal age hardening 0-108465  
 Eu, Sr<sub>1-x</sub>S, mag. clusters, spinodal decomp. trend 0-65923  
 Fe-Cr-Co alloy, coercive force mechanism 0-71103  
 Fe-Cr-Co alloy, spinodally decomposed, micro-twinning 0-92537  
 Fe-Cr-Co alloys, (5-9 wt.% Co), obtained by slow cooling under mag. field, permanent magnet props. 0-75797  
 Fe-Mo (13-20 at.%) binary alloys, spinodal decomp. on ageing, TEM and X-ray diff. study 0-97503  
 Na-rich plagioclase microstructure and exsolution 0-72501  
 Ni-Cu-X (X=Sn, Nb, Ti), spinodal decomp. alloys, linear expansion coeff. influence on morphological anisotropy (*Japanese*) 0-70431  
**spinor groups** see group theory  
**spirality** see elementary particle theory  
**splines (mathematics)**  
 see also function approximation; interpolation  
 fluid flow problems, incompressible, free surfaces 0-106774  
 magnetisation curves representation by cubic spline functions (*German*) 0-71112  
 radiocardiography, equilibrium left ventricular ejection fraction determ., background noise estimation 0-94365  
 sea model, 3-D numerical, Galerkin method with polynomial basis set 0-72524  
**sponges** see porous materials  
**sponginess** see porosity  
**spontaneous fission**  
 superheavy elements, search for using solid state nuclear track detectors 0-91200  
 superheavy nuclei, evidence from meteorite Xe and Kr isotopes 0-63215  
<sup>248</sup>Cm, spontaneous fission Xe and Kr daughter isotope ratios 0-63215  
<sup>248</sup>Am, A=240,244 actinide spontaneous fission activities from <sup>209</sup>Bi(<sup>56</sup>Fe,X) 0-86937  
<sup>248</sup>Cf, A=234,238, actinide spontaneous fission activities from <sup>209</sup>Bi(<sup>56</sup>Fe,X) 0-86937  
<sup>250</sup>Cf, spontaneous fission Xe and Kr daughter isotope ratios 0-63215  
<sup>252</sup>Cf, far-out asymmetric mass distrib. 0-83132  
<sup>252</sup>Cf fission, neutron deficient fragments, search for positron activity (*Russian*) 0-63218  
<sup>252</sup>Cf spontaneous fission, fission product β spectra (*Russian*) 0-91204  
<sup>252</sup>Cf spontaneous fission, prompt γ-ray differential angular distrib. 0-102220  
<sup>254</sup>Cf spontaneous fission, neutron-rich fragments, even-even products 0-78342  
<sup>242</sup>Cm, prompt neutron multiplicity distrib. meas. 0-83131  
<sup>248</sup>Fm, A=242-246, actinide spontaneous fission activities from <sup>209</sup>Bi(<sup>56</sup>Fe,X) 0-86937  
<sup>235</sup>Np, fission lifetime from <sup>235</sup>U(d,f) reaction 0-63216  
<sup>240</sup>Pu, effect of spontaneous fission on energy release in a nuclear explosive 0-95464  
 UO<sub>2</sub>, burnup determ. in PWR and BWR using NDA of neutron emission rates 0-83148  
**spontaneous magnetisation**  
 Heisenberg ferromagnet, spin-wave renormalisation, S≥1 0-71070  
 Ising system, 2D fully frustrated, correlation functions, on square lattice 0-103805  
 lattice parameters, mag. and elec. props. 0-100578  
 magnetization reversal of the two-dimensional Heisenberg ferromagnet with weak Ising anisotropy 0-107977  
 oxides, RCu<sub>2</sub>Mn<sub>2</sub>O<sub>12</sub>, R=La to Lu, Y, synthesis and mag. props. 0-75717  
 quasi-two-dimensional planar spin system, mag. transition 0-65951  
 rare earth alloy, amorphous, ferromag. state, non-axial elec. field gradient effect 0-75728  
 SQUID magnetometer with temp. control, spontaneous magnetisation and mag. susceptibility meas. 0-68221  
 superconductor, magnetic, shape effects 0-103773  
 vacancy distribution along mag. sublattices in β-brass type ferro and antiferromagnetic alloys (*Russian*) 0-79783

spontaneous magnetisation continued

X-Y model, quantum effects and dynamics at low temps., path integral approach 0-84584  
CdCr<sub>2</sub>Se<sub>4</sub>(Se<sub>4</sub>), spontaneous magnetisation temp. depend., nuclear resonance freq. depend. (*French*) 0-80483  
CoMnSi<sub>1-x</sub>Ge<sub>x</sub>, amg. props. 0-60270  
Fe<sub>3</sub>Pt Invar alloy, thermal expansion and spontaneous magnetisation, Invar anomalies, low spin model 0-71001  
FeTh<sub>2</sub>S<sub>8</sub>, mag. struct. and props., neutron diff. and mag. meas. 0-60201  
Fe<sub>1-x</sub>Ti<sub>x</sub>O<sub>4</sub>, 0.5 ≤ x ≤ 1, mag. props. of antiferromag. phase 0-70960  
HgCr<sub>2</sub>Se<sub>4</sub>, spontaneous magnetisation temp. depend., nuclear resonance freq. depend. (*French*) 0-80483  
K<sub>2</sub>CuF<sub>4</sub>, layered spin system, planar rotator symmetry, phase transition 0-65951  
N<sub>2</sub> complex, Ni(C<sub>6</sub>H<sub>5</sub>NO)<sub>4</sub>(NO<sub>3</sub>)<sub>2</sub>, singlet ground-state systems, field induced mag. long range order 0-60266  
Ni-Fe Invar, thermal expansion and spontaneous magnetisation, Invar anomalies, low spin model 0-71001  
Ni-I single crystals, mag. and dielectric props. 0-93095

spontaneous symmetry breaking

λφ<sup>4</sup> self interaction theory, symmetry breaking and mass generation by space-time topology 0-82892  
λφ<sup>4</sup> theory, conformal symmetry breaking, cosmological particle creation 0-90998  
λφ<sup>4</sup> theory, dynamical mass generation in S<sup>1</sup> × R<sup>3</sup> 0-99046  
Abelian gauge theories with dynamical symmetry breaking, effective pot., scale and chiral invariance (*Russian*) 0-57503  
baryon mass relations in internal SU(6) symmetry 0-82962  
baryons, b-quark, magnetic moments, broken SU(5) symmetry 0-95257  
boson fields, massless, spontaneous symmetry breaking, and Goldstone theorem (*Chinese*) 0-62861  
conceptual foundations of the unified theory of weak and electromagnetic interactions, review 0-95237  
confining theories, chiral symmetry breaking in gauge theories 0-95244  
cosmological ν sea, EM wave propagation, torsionic background 0-77283  
defects and symmetry breaking, review 0-95231  
Dual Topological Unitarisation scheme, flavour symmetry breaking 0-102030  
dynamical cluster properties in the quantum statistical mechanics of phase transitions 0-77693  
dynamically broken gauge models, natural mass hierarchy, unification 0-68409  
E(6) gauge theory, dynamical symmetry breaking 0-86580  
early Universe, horizon problem and the broken-symmetric theory of gravity 0-62344  
Earth gravitational field, local vanishing due to left turning motion (*Japanese*) 0-98798  
education, gauge symmetry breaking, geometrical approach, superconductivity and spontaneous symmetry breaking 0-57028  
electroweak interactions, dynamically broken gauge theories, CP nonconservation without elementary scalar fields 0-86613  
exotic new quarks and dynamical symmetry breaking 0-73669  
fermion masses and hierarchy of symmetry breaking, u and d quarks 0-86618  
fiber bundle structure of gauge field and reduction by the Higgs mechanism 0-82885  
gauge theory, renormalisation of ghost and Goldstone fields and ghost symmetries 0-90987  
grand unification with exceptional group E<sub>6</sub>, symmetry breaking, SU(5) relations, quark masses 0-68407  
grand unified theory from broken SO(8) extended supergravity, SU(5) theory 0-99081  
gravitational bubbles, radiative corrections to covariant massless quartically self-interacting meson theory 0-62826  
gravitational radiative corrections as the origin of spontaneous symmetry breaking 0-86192  
hadrons, charmed, SU(4) mass-breaking, mass sum rules 0-62959  
horizontal symmetries dynamical symmetry breaking and neutrino masses 0-105830  
isotopic cosmological models, vacuum stress energy tensor and particle creation (*German*) 0-94901  
large-N chromodynamics, chiral symmetry breakdown 0-91052  
lattice gauge theories, chiral symmetry dynamical breaking 0-99061  
left-right symmetry breaking and fermion masses 0-105810  
Lie group broken symmetry of transformation generating general relativistic theories 0-98836  
magnetic flux metamorphosis in spontaneously broken gauge theories 0-99047  
mass, physical, in φ<sup>4</sup>-model, renormalisation group and mass generation 0-77948  
meson decay, tensor, current algebra approach, symmetry-breaking Hamiltonian, chiral SU(3) × SU(3) or SU(4) × SU(4) 0-68450  
meson dipion cascade decays, current algebra techniques, pole plus remainder model, chiral symmetry breaking and QCD 0-62972  
models of dynamically broken gauge theories 0-77974  
neutron oscillation phenomenology in gauge model with spontaneously broken B-L symmetry 0-90996  
non Abelian gauge theories in external electromagnetic fields (*Russian*) 0-57533  
O(10) spontaneous symmetry breaking for Higgs fields 0-105812  
QCD, 1+1 dimens., dynamical symmetry breakdown 0-82949  
QCD vacuum in strong external gauge fields, spontaneously, broken chiral symmetries 0-57555  
QED, heavy particle effects, factorised local operators, renormalisation group 0-62898  
QED, heavy particle effects, factorised local operators, renormalisation group 0-62899  
QED, nonlinear approach, conformal invariance and fine-structure constant 0-91023  
quark-quark interaction, phenomenological, from s-wave baryon spectrum 0-101984  
quarks, fermion field, nonlinear, origin of four quark flavours, quantum numbers, isosymmetry breaking 0-62920  
quasiconfinement in colour gauge symmetry, unconfined quarks and gluons 0-86686  
radiative mass generation in perturbation theory and the renormalization group 0-86611  
relativity groups, symmetry breakdown and bundle representations 0-86610

spontaneous symmetry breaking continued

SO(10) unified model, phenomenological group, symmetry breaking chain low energy effects 0-86645  
SO(3,2) de Sitter symmetry, spontaneously broken, gravitational holonomy group 0-57149  
SO(4n+2) gauge theory, dynamical symmetry breaking 0-86580  
space-dispersion approach to the explanation of the Higgs-mechanism 0-90975  
SU<sub>4</sub> × U<sub>1</sub> and the origin of the Cabibbo angle, charged gauge boson mixing 0-73639  
SU(2|1) electroweak interactions, implications for 6 extra time dimensions 0-77998  
SU(2) × (T<sub>3</sub>)<sub>R</sub> × U<sub>V</sub>(1) gauge group, grand unification, symmetry breaking and Z bosons 0-73641  
SU(2) × U(1), strong CP-violating phase, one-loop corrections, Higgs particles 0-62910  
SU(4), symmetry breaking effects on strong coupling const., charmed and uncharmed B BP couplings calc. 0-105802  
SU(4) irreducible tensors and norms, symmetry breaking and energy variation 0-105801  
SU(5), symmetry breaking patterns, Higgs fields 0-101953  
SU(5), unification of weak, EM and strong interactions, review 0-105814  
SU(5) electroweak-strong interaction model, broken colour symmetry and gluon mass 0-73650  
SU(5) unified gauge theory, non-Abelian electric and mag. flux 0-57545  
SU(N) × SU(N) symmetry breaking with extremum constraints 0-68385  
SU(n) gauge theories, spontaneous symmetry breaking pattern 0-95228  
SU(S) based grand unified theory, monopoles and vector bosons, symmetry breaking 0-99079  
supergrand unification in E<sub>8</sub>, quark-lepton assignments, symmetry breaking scheme 0-68408  
superspace affine theory, simple Lagrangian 0-105813  
supersymmetry, OSp(1,4), superfield formulation in anti-de Sitter space 0-57508  
tensor meson radiative decay in SU(6) × O(3) broken symmetry quark model 0-73710  
tumbling gauge theories with chiral fermion fields, symmetry breaking 0-99042  
U(1) chiral symmetry breaking from SU(1) gauge theory 0-86617  
unification of EM, weak and strong interactions, SU(5) group and symmetry breakdown 0-73637  
unified scalar-free theory, order-R vacuum functional, with spontaneous scale breaking 0-78003  
unified theory of elementary-particle forces 0-105827  
UV infinity suppression in gravity modified field theories 0-105787  
vacuum spontaneously broken symmetry of Higgs field and Bose condensation 0-82912  
vector meson radiative decays, vector dominance model in broken SU(3) 0-73711  
vector mesons, EM decay in broken SU(3) 0-82976  
vector mesons, radiative decay, single parameter scheme 0-86720  
Weinberg-Salam model, vacuum instability, cosmology and particle mass constraints 0-78007  
Weinberg-Salam model with two massless Higgs doublets, particle masses, perturbation constraint 0-57541  
Weinberg-Salam theory, extension to left-right symmetry and quark-lepton unification 0-78002  
Yang-Mills theory, broken symmetry soln., Higgs fields and Einstein gravity action 0-101746  
Zee's broken symmetric gravity theory 0-62558  
eN, deep inelastic scatt., quark model, field-theoretic, quark indistinguishability, nucleon structure function 0-62993  
π(η) → γγ, quark model tests 0-78067  
K<sup>0</sup> → K<sup>0</sup> γ, SU(3) and isospin symmetry breaking effects 0-95272  
φ<sup>4</sup> model, free energy, spontaneous symmetry breaking 0-101925  
φ<sup>4</sup>-field model with image mass, spontaneous coherent state transition 0-99057  
πK scattering amplitude, analytic continuation, chiral symmetry breaking 0-63027  
πN σ term in hybrid chiral bag model, PCAC and SU(3) × SU(3) symmetry violation 0-78096  
ππ, ρ-meson contrib. in broken chiral symmetry model, phase shifts and lengths (*Russian*) 0-86756  
Σ<sup>+</sup> → pγ, 1/2<sup>-</sup> resonance poles to parity-violating amplitude, two-quark weak transitions 0-78062

spooling see winding (process)

sporadic-E layer

blanketing E<sub>s</sub>-layers, rel. to equatorial electrojet type 1 radar echoes with double-peaked Doppler spectra 0-67458  
blanketing layer type ionisation irregularities, growth and decay 0-101477  
disturbances, large scale periodic, Faraday fading of satellite 40 MHz signals 0-101475  
E<sub>s</sub>-layer, lossless refls. rel. to global ionospheric absorpt. meas. on board ships 0-98500  
E<sub>s</sub>-layer in equatorial ionosphere, assoc. with radio scintillations 0-77191  
ELF wave propag. at nighttime, sporadic-E effects 0-77202  
gravity waves at E-region heights, obs. of Es 0-72657  
high latitude E<sub>s</sub>-ionisation during quiet and disturbed conditions 0-61941  
metallic ions of meteor origin effect in VHF ionospheric forward scattering, contribution to sporadic-E formation 0-67461  
meteor ionisation creating E<sub>s</sub>, effect of different meteor particle sizes 0-105108  
reflection coefficient at high latitude 0-61922  
reflection coeffs., explanation for cut-off freq. 0-82131  
whistlers at low latitude, banded struct. origin on refl. from sporadic E-layers 0-101476

spray coating techniques

see also electrostatic coating techniques; flame spraying; plasma arc spraying; powder spraying  
plasma industrial utilisation, synthesis, powder, metallurgical and surface treatments, review (*French*) 0-96398  
thin film prep. for solar energy utilisation 0-84847  
AgInS<sub>2</sub> and AgIn<sub>2</sub>S<sub>3</sub>, spray pyrolysis, film struct., elec. and optical props. 0-71592  
CdS film spray fabrication, physical props., Cu<sub>2</sub>S-CdS solar cell applications (*French*) 0-60113  
Cu<sub>2</sub>S-CdS sprayed solar cells, chemical spray deposition 0-93979



**spray coating techniques continued**

- SnO<sub>2</sub> gas sensor, fast-detecting, prep. 0-61497  
 ZnO-CdTe heterojunctions and ZnO films preparation using spray pyrolysis 0-96985

**spray coatings**

- see also electrostatic coatings; flame sprayed coatings; plasma arc sprayed coatings; powder sprayed coatings  
 spectrally selective surfaces for photothermal conversion of solar energy 0-101125  
 AgInS<sub>3</sub> and AgInS<sub>3</sub>S<sub>8</sub>, spray pyrolysis, film struct., elec. and optical props. 0-71592  
 CdS film spray fabrication, physical props., Cu<sub>2</sub>S-CdS solar cell applications (French) 0-60113  
 CdS films, prep. by reactive pulverisation, chemical, crystallographic and electronic props. (French) 0-60112  
 CdSe, chemically sprayed thin films as photoanode in photoelectrochem. cells, power charact. meas. 0-85293  
 Cd<sub>1-x</sub>Zn<sub>x</sub>S films, chem. sprayed, carrier density and mobility 0-60121  
 CuInSe<sub>2</sub> thin films, prep. by spray pyrolysis, struct., elect. and optical props. for solar cell appls. 0-100781  
 Cu<sub>2</sub>S-CdS solar cells, Cu<sub>2</sub>S growth kinetics and composition analysis by absorbance transient and galvanic electrochemical measurements 0-92797  
 GaAs-In<sub>2-x</sub>Sn<sub>x</sub>O<sub>3-y</sub> SIS heterostructure solar cells, spray-deposited 0-101106  
 Si-In<sub>2-x</sub>Sn<sub>x</sub>O<sub>3-y</sub> SIS heterostructure solar cells, spray-deposited 0-101106  
 SnO<sub>2</sub>/Sb sprayed film, growth mechanism and cryst. struct. 0-89143  
 SnO<sub>2</sub>/poly-Si solar cells, fabrication, grain size effects on device parameters 0-94045  
 SnO<sub>x</sub> films, passivation effect on Si solar cells 0-61360  
 TiO<sub>2</sub> AR coating for Si solar cells by spray deposition, review 0-104511  
 TiO<sub>2</sub>, spray-on antireflection coatings for Si solar cells 0-80963  
 Zn<sub>1-x</sub>Cd<sub>x</sub>S films, spray pyrolysis, elec. props. 0-75657

**sprays**

- see also aerosols; drops; jets  
 automatic sprayer with programmable dose for serial expts. (Hungarian) 0-104822

**sputterions** see elementary particles**sputter etching**

- broad beam ion source used for sputtering and etching of Ar, Kr, O<sub>2</sub> and N<sub>2</sub> gases 0-69002  
 carbonaceous materials, directional O ion beam etching, compared with reactive ion etching 0-71781  
 cold-cathode ion gun, discharge characts. and improvements 0-105748  
 combined ion beam deposition and etching for thin film studies 0-71594  
 conical ion beams use in thin film technology (Russian) 0-76383  
 fused silicon substrate, directional reactive ion etching at oblique angles 0-66428  
 holey film preparation by ion-etching method, electron microscopy appls. 0-105751  
 inert gas ion milling processes, etch-rate ratio of oxides to nonoxides, increase using halocarbon gases 0-93663  
 ion beam, plasma and reactive ion etching, review 0-108621  
 ion beam milling, amomalous sputter yield behaviour 0-108624  
 ion etching device for SEM samples 0-82847  
 ion etching for selective erosion of thin film surface layers, cathodic sputtering, overview (Hungarian) 0-66682  
 metallography, appl. (Japanese) 0-93715  
 plasma etching mechanisms, using reactive plasmas 0-71778  
 quartz high-transmittance antiref. film, vacuum-etched 0-74449  
 reactive ion etching of III-V compounds 0-58813  
 red blood cells, by ion beam sputtering, for SEM 0-85554  
 refractory carbides, adhesion to metal substrates, improved 0-76481  
 surface, three-dimens., under ion bombardment 0-104029  
 Al<sub>2</sub>O<sub>3</sub>, CVD film on III-V semicond. substrate, ion beam etching, defect detection 0-89155  
 Al<sub>2</sub>O<sub>3</sub>-based ceramics, high rate reactive ion etching 0-85070  
 BaTiO<sub>3</sub>, surface microrelief after ion irradi. 0-59774  
 Cr films, photoresist film on reverse gas plasma etching 0-97634  
 Cu-Al thin film multistructure, Xe<sup>+</sup> ion beam cratering 0-66708  
 Fe-Cr alloy, sputter etching oxide film, comp. profile, quantitative AES 0-81383  
 GaAlAs DH lasers, self-sustained pulsation suppression, effect of SiO<sub>2</sub> facet coating films 0-95894  
 Gd-Co alloy film, sputter yield ratio, combined ion deposition and etching 0-71594  
 In, sputtering in Ar-N<sub>2</sub> discharge, mechanism, optical spectra study 0-89107  
 P<sub>2</sub>O<sub>5</sub>/SiO<sub>2</sub> glass, selective etching rel. to Si by plasma reactive sputter etching 0-81221  
 PtSi film formation by ion sputtering and annealing, form. and exam. problems 0-100782  
 Si, amorphous, ion bombard., etch pit and ripple struct. formation mechanisms 0-66366  
 Si, Ar ion etching, carbide form. 0-81222  
 Si chip backside removal, technique and fixture 0-76384  
 Si, etching characts. using reactive ion etching with tetrafluoromethane-Cl<sub>2</sub> gas mixture 0-104313  
 Si, high rate reactive ion etching 0-85070  
 Si, polycryst., anisotropic plasma etching 0-85069  
 Si RF sputter-etched surface, cryst. damage, spectroscopic ellipsometry obs. 0-103538  
 Si, selective etching rel. to SiO<sub>2</sub> by CBrF<sub>3</sub> plasma without undercutting 0-76380  
 Si<sub>3</sub>N<sub>4</sub>, selective etching rel. to Si by plasma reactive sputter etching 0-81221  
 SiO<sub>2</sub>, etching characts. using reactive ion etching with tetrafluoromethane-Cl<sub>2</sub> gas mixture 0-104313  
 SiO<sub>2</sub>, selective etching rel. to Si by plasma reactive sputter etching 0-81221  
 SrTiO<sub>3</sub>, surface microrelief after ion irradi. 0-59774

**sputtered coatings**

- see also reactively sputtered coatings  
 combined ion beam deposition and etching for thin film studies 0-71594  
 film on Si substrate, eutectic point displacement on annealing (Russian) 0-100850  
 ion sputtering deposition of coatings for ultrahigh resolution SEM 0-76184

**sputtered coatings continued**

- metallic film characterisation technique, APFIM, time-of-flight spectroscopy 0-75138  
 Permalloy films, RF sputtered on Au, coercivity 0-80575  
 porous metal thermionic cathode with sputtered metal films, emission operating characts. 0-100740  
 rare earth aluminate, scandate and zirconate film coatings, electrophys. props. w.r.t. prep. technology 0-60781  
 refractory carbides, adhesion to metal substrates, improved 0-76481  
 SEM specimen preparation thin film coating techniques 0-68308  
 TEM specimen preparation, fine grained coatings, sputter source design 0-99015  
 thin film deposition process, line-edge profile simulation appl. 0-104068  
 Al film, wave front reversal, holography applications (Russian) 0-58483  
 Al-Cu films, DC sputtered, Cu distrib. 0-80113  
 Al-Si, DC magnetron-sputtered, residual gas influence on props. 0-80968  
 Al-Ta<sub>2</sub>O<sub>3</sub>-Al, healing of defects in dielec. film by anodisation 0-65406  
 Au, electrodeposited and sputtered, hard, reactive softening, X-ray diffr. studies 0-100414  
 Au, thin film, discontinuous, high resist., Hall effect meas. 0-65716  
 Au-Ti<sub>0.3</sub>W<sub>0.7</sub>, thermal annealing study of metallisation on Si 0-80134  
 Au-W-GaAs Schottky barrier, elec. and chem. props., AES 0-96973  
 Ba(Pb,Bi)O<sub>3</sub> perovskites, resputtering effects 0-80969  
 BaTiO<sub>3</sub> RF sputtered ferroelectric film on Si substrate, ferroelectric props. 0-80697  
 Be, thick film, amorphous, RF magnetron sputtering 0-80971  
 Bi<sub>2</sub>SiO<sub>20</sub> film, photoelectric props. obs., UV illumination effects (Russian) 0-80313  
 Cd<sub>2</sub>Hg<sub>1-x</sub>Te films, growth by cathodic sputtering in Hg vapour plasma 0-97431  
 CdSnO<sub>2</sub> films, transparent conducting, deposited by RF sputtering from CdO-SnO<sub>2</sub> target 0-76179  
 Co-Gd-Mo amorphous films, resist. and extraordinary Hall effect, thermal annealing effect 0-70852  
 Co-Gd-Mo films, sputtered, O effects on mag. props. during annealing 0-89374  
 Co<sub>2</sub>Er<sub>3</sub> amorphous alloy, local order and amorphous struct. 0-88061  
 Cr film, obtained by thermo ionic precipitation, phase composition, lattice parameters (Russian) 0-96756  
 Cu, surface morphology influence on sputtered yield angular distribution 0-65338  
 Cu-Fe, explosive plasma sputtered coatings, struct. and props. (Russian) 0-100783  
 CuInS<sub>3</sub> films, RF sputtered, growth and props. 0-80124  
 Fe sputtered film, amorphous, Mossbauer study and electron diffr. obs. 0-75897  
 Fe thin layers, vacuum coated on PMMA, mag. behaviour during mech. stress cycles (German) 0-80581  
 Fe-Al<sub>2</sub>O<sub>3</sub> granular films, superparamagnetism and relax. effects 0-71118  
 Fe-Cr-Si, heat resistive films prepared by sputtering, lifetime meas. 0-80132  
 Fe-Si-Cr magnetic films, corrosion reduction effect of Cr obs. 0-80573  
 Fe<sub>2</sub>C-Cr<sub>2</sub>C-NiC<sub>2</sub>, stainless steel carbide, graded solar selective surface, magnetron sputtered 0-81485  
 GaN/Ga layered films, Ga whisker growth 0-92800  
 GaSb films, elemental incorporation probability modification by ion bombard. during growth 0-80118  
 (GaSb)<sub>1-x</sub>Ge<sub>x</sub> films, single-cryst. metastable semicond., growth and phase stability 0-80115  
 Gd-Co alloy film, sputter yield ratio, combined ion deposition and etching 0-71594  
 Gd-Co based amorphous sputtered films, microstruct. variability and mag. anisotropy, implanted ion effects 0-88459  
 (Gd,Co)<sub>1-x</sub>Ar<sub>x</sub> amorphous films, effective anisotropy field, ferromag. reson. obs. 0-71123  
 Ge, black, solar selective absorber characterisation 0-80112  
 Ge film, amorphous, prepared by evap. or sputtering, AC loss meas. 0-65560  
 Ge, heterodiffusion due to H atom surface recombination stimulation, Cu, Zn, In coated (Russian) 0-59726  
 Hg<sub>0.7</sub>Cd<sub>0.3</sub>Te thin film deposition on Si substrates by RF triode-sputtering, large-area photodetector arrays 0-80965  
 α-HgS films, sputter-deposited in Hg vapour, growth and props. 0-75467  
 In<sub>2</sub>O<sub>3</sub>/Sn, RF magnetron sputtered film, elec. and optical props. 0-104065  
 In<sub>2</sub>O<sub>3</sub>-SnO<sub>2</sub>-CdTe:P, p-n homojunction solar cell, elec., photovoltaic props., photoluminescence 0-81463  
 In<sub>2</sub>O<sub>3</sub>-SnO<sub>2</sub>-InP solar cell junctions, efficiency, InP surface props. 0-85288  
 InSb and InSb<sub>1-x</sub>Bi<sub>x</sub> films, elemental incorporation probability modification by ion bombard. during growth 0-80118  
 InSb<sub>1-x</sub>Bi<sub>x</sub> films, single-cryst. metastable semicond., growth and phase stability 0-80115  
 InSb<sub>1-x</sub>Bi<sub>x</sub>, metastable epitaxial film, phase diagram 0-76238  
 InSe thin film, sputter growth and chem. anal. by XPS/ESCA 0-80976  
 In<sub>2-x</sub>Sn<sub>x</sub>O<sub>3-y</sub>-insulator-poly-Si solar cells, photovoltaic conversion parameters 0-101093  
 In<sub>2-x</sub>Sn<sub>x</sub>O<sub>3-y</sub>-poly-Si SIS solar cells 0-97787  
 K<sub>2</sub>Li<sub>2</sub>Nb<sub>2</sub>O<sub>5</sub> films for optical waveguides epitaxial growth and characterisation 0-79016  
 La-Fe alloy, amorphous, sputtered at high rate, mag. props. 0-75753  
 Mo, elec. resist., annealing and struct. effects 0-60109  
 Mo, thin film deposition by high current ion beam sputtering, struct. and elec. props. 0-59837  
 MoSi<sub>2</sub> film, elastic stiffness and thermal expansion coeffs. 0-107451  
 Nb films, ion beam sputtered, supercond., laser annealing effects 0-97024  
 Nb/Cu, layered ultrathin coherent struts., supercond. props. 0-84525  
 Nb/Cu layered ultrathin coherent struct. 0-80122  
 Nb<sub>2</sub>Al, complex refractive index meas. 0-93264  
 Nb<sub>2</sub>Ge film, high-temp. supercond. phase stabilisation w.r.t. prep. conditions (Russian) 0-70871  
 Nb<sub>2</sub>Ge, sputtered on Cu, film-substrate interface obs. by electron microscopy 0-65398  
 Nb<sub>2</sub>Ge(Si), amorphous films, thermally-activated internal friction peaks, structural obs. 0-80147  
 Nb<sub>2</sub>Ge(Si), RF sputtered films, amorphous atomic scale struct. 0-84064  
 PLZT ferroelectric thin films, epitaxial growth and optical props. 0-70543  
 Pb<sub>2</sub>Sn<sub>1-x</sub>O<sub>2</sub>:Sb films, DC sputtered, elec. props. 0-80426

**sputtered coatings continued**

- Pb(Zr,Ti)O<sub>3</sub> films, ferroelec., ion beam deposition sputtered from multi-component targets 0-80974  
 Pb(Zr,Ti<sub>1-x</sub>)O<sub>3</sub> films, deposition by focused ion beam sputtering 0-76177  
 (Pd<sub>80</sub>Au<sub>20</sub>Si<sub>13</sub>)/Fe<sub>30</sub>, compositionally modulated amorphous film, diffusion, struct. relax. 0-103518  
 (Pd<sub>85</sub>Si<sub>15</sub>)<sub>61</sub>/(Fe<sub>85</sub>B<sub>15</sub>)<sub>30</sub>, compositionally modulated amorphous film, diffusion, struct. relax. 0-103518  
 Pt-SiO<sub>2</sub> cermet films, struct. and props. 0-96956  
 SiO<sub>2</sub> films, electronic struct., reduction processes, photoemission, optical absorpt. and resist. meas. 0-80931  
 PtSi film formation by ion sputtering and annealing, form. and exam. problems 0-100782  
 Si, amorphous, hydrogenated, electron drift mobility meas. 0-75565  
 Si, amorphous, sputtered, resist. control by ion implantation 0-100262  
 Si, amorphous co-sputtered doped, photovoltaic material appl. 0-93488  
 Si:Al, O(H), film, amorphous, elec. cond. meas. 0-80423  
 Si:F, amorphous, heat resistant, prep., elec. cond., IR absorpt., annealing 0-65719  
 Si:H, amorphous, sputtered on Gd<sub>2</sub>(MoO<sub>4</sub>)<sub>3</sub>, ferroelec. domain wall motion, image scanning 0-83663  
 a-Si:H, influence of H on optical props., H conc. and H bonds 0-76098  
 a-Si:H alloys, sputter deposited thin film coatings, property-comp. relationships 0-80975  
 Si:H amorphous films, IR spectrum and struct. 0-97277  
 Si-Al C fibre composite technological coatings, liquid phase method preparation (*Russian*) 0-108375  
 Si<sub>1-x</sub>H<sub>x</sub>Al, amorphous, co-sputtered Al modification, electronic and optical props. 0-100461  
 SiO<sub>2</sub> facet coating film effect on self-sustained pulsation suppression in GaAlAs DH lasers 0-95894  
 SiO<sub>2</sub> films, RF-diode-sputtered, step coverage 0-80117  
 SiO<sub>2</sub> sputtered film performance as acoustic antireflection coating at sapphire-H<sub>2</sub>O interface 0-106686  
 SiO<sub>2</sub> ultrathin layers, refr. index meas. 0-103936  
 SnO<sub>2</sub>, O chemisorption, elec. cond. and EPR meas. correlation 0-84369  
 Ta, thin film deposition by high current ion beam sputtering, struct. and elec. props. 0-59837  
 Ta-Cr-Si-Al, heat resistive films, prepared by sputtering, lifetime meas. 0-80132  
 TaB<sub>2</sub>-Cr-Si-Al, heat resistive films prepared by sputtering, lifetime meas. 0-80132  
 TaSi<sub>3</sub> film, elastic stiffness and thermal expansion coeffs. 0-107451  
 Ta<sub>2</sub>Si<sub>3</sub> and TaSi<sub>2</sub> form. in thin cosputtered (Ta+Si) films on polycryst. Si and SiO<sub>2</sub> 0-70546  
 (Tb,Dy)-Fe amorphous films prep. by cosputtering, magnetoelastic props. 0-97429  
 Tb-Fe amorphous thin films, magnetic after-effect, Kerr magneto-optic effect obs. 0-97123  
 Ti-W films, bias-sputtered, quantitative anal. 0-80114  
 TiSi<sub>2</sub> film, elastic stiffness and thermal expansion coeffs. 0-107451  
 WC, erosive plasma sputtered coatings, struct. and props. (*Russian*) 0-100783  
 WC-Co DC and RF sputtered coatings, bias effect, struct., X-ray-Auger study 0-70565  
 WSi<sub>2</sub> film, elastic stiffness and thermal expansion coeffs. 0-107451  
 WSi<sub>2</sub>, sputtered, props. for MOS IC appl. 0-70831  
 WSi<sub>2</sub>, steam-oxidized, Auger sputter profiling studies 0-107663  
 YCo<sub>3</sub> amorphous films, <sup>59</sup>Co spin echo study 0-80636  
 ZnO film on Corning 7059 glass and Si, SAW transducer appl. 0-80138  
 ZnO film on oxidized Si, optical measure of acoustic quality 0-80893  
 ZnO films, RF sputtered single-cryst., on sapphire, struct. and SAW props. 0-80105  
 ZnO piezoelectric films, RF planar-magnetron sputtered, characterisation 0-96751  
 ZnO sputtered films, undoped and Ga doped, props. rel. to deposition conditions 0-107935  
 ZnS film on Corning 7059 glass and Si, SAW transducer appl. 0-80138

**sputtered layers** *see sputtered coatings***sputtering**

- see also d.c. sputtering; diode sputtering; radiofrequency sputtering; reactive sputtering; sputter etching; triode sputtering*  
 AES composition depth profiling sputtering times, conc. gradient effect (*French*) 0-76116  
 alloys, ion-implanted, integral Gaussian profile determ. method 0-107313  
 atom ejection studies by classical trajectory simulation 0-108311  
 atoms in excited states, vel. meas. 0-63561  
 ceramics, local in depth anal. by neutral beam SIMS 0-89565  
 combined ion beam deposition and etching for thin film studies 0-71594  
 conference, atomic collisions in solids, Hamilton, Canada (Aug. 1979) 0-62375  
 crystal surface, in-situ cleaning by ion sputtering, in EM 0-101895  
 crystal surface morphology development during sputter erosion 0-88414  
 depth profile improvement using two ion guns 0-71964  
 depth profiles, edge effects, anal. correction 0-80925  
 depth resolution in sputter profiling, surface transport effects, calc. 0-97393  
 electron microscopy, specimen deposition and fabrication by ion beam sputtering 0-82855  
 energy, and mass distrib. of sputtered particles 0-84822  
 energy distribution, ion mass and target temp. effects 0-66361  
 energy reflection by backscatt. and sputtering, total yields and ang. distrib. 0-89101  
 fissured biological object prep. for SEM, vacuum deposition and cathode sputtering comparison 0-72390  
 fusion reactor materials, low energy ion erosion expts., Kaufman source appl. 0-68942  
 glass-metal seals, use of AES and ion sputtering in interface study 0-76587  
 heavy ion bombardment, hydrodynamical approach to non-linear effects in sputtering yields 0-66374  
 III-V semiconductor, superlattices and related structures (*Slovak*) 0-88620  
 intensity, from half-space, angle of incidence depend., theory 0-100735  
 ion impact induced shock processes in solids 0-89104  
 ion plating, evaporation sources, gaseous media, and transport modes 0-80984  
 ionisation of atomic particles sputtered from solids, microscopic anal. 0-97392

**sputtering continued**

- low-energy ion sputtering, anal. formula and important parameters 0-84818  
 lunar rocks, solar wind sputtering rel. to microcrater and accretionary grain populations development 0-94732  
 measurement of sputtered ion fractions using matrix isolation spectroscopy 0-60738  
 metal oxidation, secondary ion energy spectroscopy 0-71788  
 metal-semiconductor interfacial reaction, AES study (*Japanese*) 0-96701  
 metals and carbides, sputtering, low energy, H, D and He ions 0-100734  
 minerals, sputtering rates, implications for abundances of solar elements in lunar samples 0-61797  
 monocrystalline metals, low yield sputtering 0-66364  
 negative ions, sputtered, characteristic electronic and vibrational temp., laser photoelectron spectral meas. 0-66346  
 plasma contamination, sputtered particles, energy and mass distrib. 0-84822  
 PMMA, optical damage threshold, alteration methods 0-99814  
 rare earth aluminate, scandate and zirconate film coatings, electrophys. props. w.r.t. prep. technology 0-60781  
 recoil-energy, surface-normal distrib. analysis 0-60733  
 secondary photon emission from sputtered excited states, role of transition probability 0-102483  
 SEM samples metal coating, heating effect (*German*) 0-73338  
 single and multiple component materials, theory 0-80924  
 sputtering induced topography on solids, energetics and kinetics 0-88220  
 steel, stainless, oxidised, sputtering yield meas. by atomic fluoresc. spectroscopy 0-80922  
 surface barrier curvature influence on sputtering characts. 0-60739  
 surface recoil ejection mechanisms, computer studies 0-66363  
 surface-barrier shape effects on sputtering characts. 0-93447  
 target cracking, acoustic emission testing 0-81248  
 TEM specimen preparation, fine grained coatings, sputter source design 0-99015  
 thin films, deposition techniques, review 0-80964  
 thin films fabrication techniques 0-76176  
 Tokamak, metal impurity reduction by working gas injection 0-106963  
 Tokamak fusion test reactor, thermal response of first wall limiters 0-79585  
 track radiography of heavy-ion induced sputtering 0-91404  
 transition metal-O bond energy in O<sub>2</sub> glow discharge, mass spectrometry obs. 0-64808  
 triangular microprofile containing surfaces, oblique incidence sputtering, topographic changes 0-66372  
 yield, energy depend., semiempirical formula 0-100736  
 Ag, Cu diffusion, SIMS investigations 0-59717  
 Ag, sputtering by heavy atomic and molecular ion bombard. 0-71532  
 Ag-Au-Cu, surface composition change on sputtering with 2 keV Ar ions 0-66365  
 Ag-Pd alloys, inert gas ion bombardment, dynamic surface composition changes, AES obs. 0-60745  
 Al, annealed and powder sintered (SAP 895), sputtering under D<sup>+</sup> and <sup>4</sup>He<sup>+</sup> bombardment, microstruct. effects study 0-84821  
 Al, film and polished bulk specimens, initial stages of oxidation obs. using SIMS 0-81239  
 Al foil, solar wind ion bombardment, lunar surface modification 0-109325  
 Al, oxide films, metal and O<sub>2</sub> transport, AES and inert marker, techniques 0-97641  
 Al, oxidised, light emission from sputtered O atoms or ions 0-58199  
 Au cryst., ion bombarded, Ar<sup>+</sup> ions, time-of-flight spectra of sputtered atoms 0-89103  
 Au film, ion bombarded, surface craters induced by displacement cascades 0-107344  
 Au-O bond energy glow discharge, mass spectrometry obs. 0-64808  
 Be, foil, ion bombardment, secondary photon emission, ion energy depend. 0-97346  
 CH radical, sputtered, rotational and vibrational excitation 0-69224  
 CdTe surface, sputter cleaning and dry oxidation, XPS and LEED study 0-108618  
 Cr, photon emission due to Ar<sup>+</sup> ion bombard., adsorbed and recoil-implanted O effect 0-80872  
 Cu polycrystals, oxidation, secondary ion energy spectra 0-71788  
 Cu, SIMS depth profiling, surface roughening by low energy ion irradi. 0-60727  
 Cu, sputtered Cu<sub>1</sub><sup>+</sup> ion energies by low energy inert gas ion bombard. 0-71555  
 Cu, sputtering, binding energies 0-108312  
 Cu<sub>n</sub><sup>+</sup> ion cluster yield intensity from Cu target bombard. by H<sup>+</sup>, Ne<sup>+</sup>, Xe<sup>+</sup>, Kr<sup>+</sup> 0-100728  
 Cu<sub>x</sub>Zn<sub>1-x</sub>, sputtering, binding energies 0-108312  
 Fe<sub>1-x</sub>O powder, wustite, AES study, ion and electron bombard. effects 0-76114  
 α-Fe<sub>2</sub>O<sub>3</sub> powder, hematite, AES study, ion and electron bombard. effects 0-76114  
 Fe<sub>2</sub>O<sub>4</sub> powder, magnetite, AES study, ion and electron bombard. effects 0-76114  
 GaAs-based mixed cryst. form. by ion beam synthesis, vibr. anal. 0-103376  
 Gd-Co alloy film, sputter yield ratio, combined ion deposition and etching 0-71594  
 Ge, ion bombardment-induced photon emission as function of target temp. 0-100698  
 Hg<sub>0.1</sub>Cd<sub>0.9</sub>Te surface, sputter cleaning and dry oxidation, XPS and LEED study 0-108618  
 HgTe surface, sputter cleaning and dry oxidation, XPS and LEED study 0-108618  
 InP (110) surfaces, cleaved and polished-sputtered-annealed, LEED and AES study 0-103550  
 InP/In<sub>0.9</sub>Ga<sub>0.1</sub>As<sub>0.1</sub>P<sub>0.9</sub> interfaces, sputter-profiled, depth resolution degradation by cone form. 0-80094  
 InSe thin film, sputter growth and chem. anal. by XPS/ESCA 0-80976  
 In<sub>2</sub>Si<sub>2</sub>O<sub>7</sub>, thin film, sputter deposition form., optical and elec. props. 0-60123  
 Li, kinetic energies of sputtered excited atoms 0-66373  
 LiF, kinetic energies of sputtered excited atoms 0-66373  
 Mo films, sputtered from cylindrical-post magnetron with Ne, Ar, Kr and Xe, compressive stress and presence of inert-gas obs. 0-80140  
 Mo, thin film deposition by high current ion beam sputtering, struct. and elec. props. 0-59837  
 Na, thermal and collisional effects influence on energy spectra 0-66370



**sputtering** continued

- NaCl, kinetic energies of sputtered excited atoms 0-66373  
 Na<sub>2</sub>O-CaO-SiO<sub>2</sub> glass, leaching studies by sputter-induced photon spectrometry 0-80004  
 Nb-N, superconducting layers, sputtering in high vacuum apparatus (*German*) 0-89147  
 Ni, ang. distrib. and differential sputtering yields for low-energy light-ion irradi. 0-71527  
 Ni, Medicus matrix cathode, surface characts. 0-66378  
 Ni, oxide films, metal and O<sub>2</sub> transport, AES and inert marker, techniques 0-97641  
 Ni, photon emission due to Ar<sup>+</sup> ion bombard., adsorbed and recoil-implanted O effect 0-80872  
 $\beta$ -NiAl, oxide films, metal and O<sub>2</sub> transport, AES and inert marker, techniques 0-97641  
 Pt (100) (5 $\times$ 20) and (1 $\times$ 1) surfaces, stability and reactivity, adsorption of H 0-75434  
 PtSi film formation by ion sputtering and annealing, form. and exam. problems 0-100782  
 Si, anomalous sputter yields of interfacial species, cascade mixing process for interpretation 0-76122  
 Si, epitaxial layer deposition by ion beam methods 0-100417  
 Si, photon emission due to Ar<sup>+</sup> ion bombard., adsorbed and recoil-implanted O effect 0-80872  
 Si, sputtered atom ang. distrib. for keV Ar<sup>+</sup> bombard. 0-84819  
 Si surface, ion bombardment enhanced mixing of Ag layers, Rutherford backscatt. meas. 0-65034  
 Si-Fe-W, dil. alloy, compositional changes on sputtering, projectile energy depend. 0-66362  
 Si-refractory metal structs., interface modification by ion implantation 0-70475  
 SiO<sub>2</sub>, light emission from sputtered O atoms or ions 0-58199  
 Sm, thermal and collisional effects influence on energy spectra 0-66370  
 Ta, thin film deposition by high current ion beam sputtering, struct. and elec. props. 0-59837  
 (Tb,Dy)-Fe amorphous films prep. by cosputtering, magnetoelastic props. 0-97429  
 Ti atoms sputtered from Ti, Ti oxides, photon emission, nonradiative transition effects 0-58208  
 Ti, photon emission due to Ar<sup>+</sup> ion bombard., adsorbed and recoil-implanted O effect 0-80872  
 Ti, sputtered ion fraction meas. using matrix isolation spectroscopy 0-60738  
 TiO<sub>2</sub>, sputtering defects, associated surface electron states, UPS, XPS and AES obs. 0-60755  
 TiW-TiO<sub>2</sub>-InP thin refractory MIS struct. deposition 0-75647  
 U, sputtered atoms, laser fluorescence spectroscopy 0-66359  
 UAl<sub>3</sub>(Co)<sub>2</sub>, surface comp. and electronic struct., photoemission study 0-66382  
 UO<sub>2</sub>, nuclear fuel, sputtering by thermal neutrons, depend. of ejection coeff. on neutron flux 0-83157  
 W, ang. distrib. and differential sputtering yields for low-energy light-ion irradi. 0-71527  
 W, low-energy ion bombardment, depth of sputtering damage obs. by FIM 0-60734  
 W, vacancy structure in near surface depleted zone following ion bombard. 0-70267  
 WSi<sub>2</sub>, steam-oxidized, Auger sputter profiling studies 0-107663  
 Zn, sputtering, binding energies 0-108312  
 Zr, photon emission due to Ar<sup>+</sup> ion bombard., adsorbed and recoil-implanted O effect 0-80872  
 Zr, sputtered ion fraction meas. using matrix isolation spectroscopy 0-60738

**square-wave generators**

- automatic resistance thermometer bridge 0-98913

**SQUIDS** *see superconducting junction devices***stabilisation** *see stability***stabilisers** *see controllers***stability**

- see also flow instability; frequency stability; limit cycles; Lyapunov methods; plasma instability*  
 accelerating two-phase nozzle/diffuser flows, virtual mass effects on numerical stability 0-92204  
 aeroelastic, large wind turbines 0-61249  
 aeroelastic behaviour, large Darrieus rotors derived from behaviour of 5.5 m rotor 0-61251  
 airborne target tracking filter configurations compared 0-96130  
 anharmonic system, superstability, probability estimates for correlation functions 0-82708  
 aqueous film, plane-parallel symmetrical, stability, non-spreading oil droplet effect 0-107620  
 asymptotic stability of resonance systems 0-68031  
 atmosphere, steady states and stability props. of low-order barotropic system 0-72614  
 beam, periodically varying length, instability of motion 0-69716  
 beam on elastic foundation subjected to nonconservative load, stability 0-79191  
 bipedal locomotion, inverted pendulums stabilisation algorithm (*Japanese*) 0-81630  
 black foam films stability, review 0-104463  
 black holes, gravit. wave instability of maximally rotating Kerr soln. 0-105271  
 buckling, bifurcation and limit point instability of dual eigenvalue third order systems 0-87727  
 cantilever panels, in uniform incompressible flow 0-74781  
 cantilevers, flutter load, discontinuity, variational technique 0-58944  
 cm-wave radiometer, with enhanced long-term stability, for solar radio emission obs. 0-109361  
 composite, slab, spatially reinforced, optimisation in stability problem 0-102978  
 composite materials, tension stability, deformation up to failure (*Russian*) 0-75289  
 composite rib stiffened constructions, design criteria 0-102977  
 composite ribbed multilayer cylindrical shells, stability and optimal design 0-58949  
 composites, multilayer, stability under inelastic deformations 0-99944  
 cone cylinder jointed shell, ring stiffened, external hydrostatic pressure, elastic stability (*Chinese*) 0-64412  
 conical models in shock tunnel, static and dynamical stability derivatives (*Chinese*) 0-58941

**stability** continued

- conical shell, skew, truncated, external hydrostatic pressure, elastic stability (*Chinese*) 0-64413  
 contact binary stars structure, secular stability of stemp. inversion layer 0-109493  
 coupled bending-torsion flutter in cascades, aeroelastic stability boundaries 0-64424  
 crack growth stability, in plastic material 0-74810  
 critical loads for elastic bodies, lower bounds, stability 0-79185  
 crystals, monatomic, nonlinearly elastic, twinning 0-58903  
 cylindrical orthotropic shell stability problems, spectrum singularities 0-99950  
 cylindrical plasma filament under axisymmetric perturbation, numerical anal. 0-106853  
 Dead Sea, mixolimnion deepening and water column overturn 0-61822  
 difference schemes for multidimensional equations of acoustics 0-105512  
 drop, incompressible fluid, equilib. and stability analysis 0-59092  
 elastic body, nonlinear relation between stability and continuous dependence at eqn. 0-92063  
 elastic plastic spherical body, instability under uniform loading 0-58946  
 elastic plate stability conditions, variational formulations 0-69701  
 elastic solids, stability, response to finite strain 0-79187  
 electro-optic reflector, controlled, temp. fields, thermal distortions 0-96021  
 EMF of Nicrosil-Nisil thermocouples, 538°C to 1177°C, production furnaces appl. 0-68198  
 eutectic, irregular, branching limited growth 0-81042  
 evolution systems and convection-diffusion, stiffness and stability, Gershgorin theory 0-77626  
 fibre reinforced composite bodies, structure optimisation in stability problems 0-58947  
 fibre reinforced elastic slab subjected to axial loads, instability and buckling 0-64420  
 galaxies, stability against perturbations rel. to nonflat components mass 0-62291  
 gyro-stabilisation platform, nonlinear loss of stability and trembling (*Chinese*) 0-62457  
 H-shaped section cylinder in laminar and turbulent flows, aerodynamic charact. 0-106813  
 horizontal axis wind turbine blades, aeroelastic stability and response 0-61250  
 interstellar clouds, rotating, stability against fragmentation from three-dimensional hydrodynamical calcs. 0-62236  
 interstellar contracting CO clouds, thermal instability and fragmentation 0-67838  
 interstellar gas clouds, non-uniform collapse stability 0-101631  
 interstellar large globules, struct. rel. to gravit. stability 0-62246  
 laminated reinforced elastic shells, stability 0-58948  
 linear thermoelasticity, continuous depend. and instability 0-74783  
 mechanical systems, follower load type, time invariant functionals 0-77609  
 mechanical systems, stability of stationary motion, Lagrangian eqns. and Liapunov's direct method 0-69645  
 membranes, stability of nonlinear oscillations from Liapunov method 0-96212  
 metallic glass, stability, hole theory of liquids appl. 0-100174  
 neutron stars, slowly rotating, radial perturbations, stability 0-98685  
 NGC 3686 galaxy quartet, surface photometry, mass distrib. and group stability 0-62297  
 nonequilibrium steady states, irreversible processes, Lyapunov functions 0-95049  
 one-dimensional self-gravitating isothermal systems, stability 0-73008  
 oscillators, planar, nonlinear, stability of modes 0-74790  
 parametric instability, demonstration and discussion 0-57032  
 pendulum inverted, design and stabilisation control (*Japanese*) 0-73167  
 periodic density patterns as uniform fluid crystallizes 0-107404  
 plastic instabilities and uniaxial tensile ductilities 0-79180  
 plates, periodically varying length, instability of motion 0-69717  
 polyethylene/ethylene vinyl acetate copolymer mixture, rel. between hyper-mol. struct. and stability (*German*) 0-64929  
 position control system for plasma column, stability 0-106982  
 quasi-static potential oscillations of thin conductor, instability 0-87900  
 rapidly rotating compressed rods 0-79189  
 reinforced plastic cylindrical shells, optimal design under dynamic constraints 0-102996  
 rheonomic shell, cylindrical, local stability in creep conditions (*Russian*) 0-92069  
 ribbed plates with large openings, design optimisation, finite element anal. appl. 0-87724  
 rod with clamped ends, axial and transverse loading, stability, plane elasticity theory (*Russian*) 0-79184  
 rotating liquid drops, asymmetric shapes and stability 0-87796  
 rotating viscoelastic tapered cantilever, circulatory force at free end, influence of angle of attack 0-69686  
 rotor, partially filled with viscous incompressible fluid, stability anal. 0-64359  
 satellites attitude control, stability of inertially fixed pitch stabilisation by solar radiation press. 0-101523  
 semiconductors nonequilibrium phase transitions, stability and dissipation, teaching 0-105479  
 shell, cylindrical, isotropic, elastic stability, critical load analysis 0-83744  
 shell, elastic, cylindrical, stability, Liapunov's second method 0-64410  
 shell, three-layer orthotropic cylindrical, with stiffening ribs, stability 0-74784  
 shell formed by truncated cones, stability and deformation 0-69691  
 shell stability during axial compression, hardening beyond elastic limit 0-99931  
 shells, cylindrical, dynamic stability, in-plane inertia and disturbance effects 0-79181  
 shells, Kirchhoff-Love, structural stability, mixed variational principles and non holonomic constraints (*French*) 0-74779  
 shells, spatial stability problems in elastic systems, modified energetic procedure (*Russian*) 0-58943  
 shock wave, impulsive spherical, produced by laser pulses, shadowgraphic detection 0-87529  
 soft mode instability mech. 0-86142  
 Space Telescope pointing control fine guidance subsystem design 0-82201  
 SQUID magnetometer, AC-biased 0-98948  
 stars, distorted, Clairaut coordinates and vibr. stability 0-90408  
 stars, magnetic, convective stability 0-94781

**stability continued**

- stars containing mixed poloidal and toroidal mag. fields, adiabatic stability 0-67706
- stellar systems, prolate, instability 0-101642
- structural instability critical behaviour and broken symm., demonstrations 0-105476
- superconducting magnets, pulsed, stability studies, fusion reactor appls. (*Japanese*) 0-106158
- superconductor, hard, critical state stability and oscillations 0-107959
- supergiant stars, atmospheric instability rel. to brightness limits and corae 0-109432
- suspensions, crystallisation, aggregate stability and effect on purity of product 0-100769
- system with parametric excitations, instability regions determ. 0-90662
- thin tubes conveying fluid, hydroelastic stability, in plane boundary conditions, shearing loads 0-64419
- three-body problem, unrestricted stability of constant Laplace solns. 0-68030
- three-layer plates, circular, stability 0-79188
- troposphere, instability following solar corpuscular stream arrivals 0-109416
- two coupled conductors, stab. anal. 0-96219
- vacuum beam diodes, repetitively pulsed 0-63386
- viscoelastic rods and shells under loads that decrease with time 0-69700
- water film on Fe surface, stability 0-75408
- wavelength multiplexer, single-mode-fibre 0-102816
- white dwarfs undergoing spherically symmetric steady-state accretion, stability 0-77402
- wind induced oscillations, domains of stability 0-64441
- Al-Cu(Si)(Mg) binary and ternary alloys, dimensional changes in heat treatment. 0-89271
- Ge resistance thermometers, stability data at 3 temperatures 0-86307
- $\gamma$ -Mn, collinear spin structure stability 0-107984
- Mo fibre reinforced Cu with weak interfaces, stability of tensile deform. 0-97533
- Ni perfect crystal, stability under various stresses 0-104208
- Xc short-arc lamp, current modulated, arc forms and instability 0-96399

**stability of numerical methods** *see convergence of numerical methods***stacking faults**

- amphiboles, high-resolution electron microscopy 0-75241
- anthracene, orientationally disordered cryst., lattice relax. effect 0-107278
- $\gamma$ - brass type alloys, superstructures and defect obs. 0-107284
- chromites, electron microscopy, high-resolution observations 0-75241
- close-packed structures, with faults, anal. soln. for X-ray diffr. integrated intensities 0-100256
- covalent semiconductors, electronic interface states in intrinsic stacking-faults 0-75522
- crystalline materials, in situ deform. by high voltage electron microscopy 0-103352
- electron microscope resolution improvement for crystal structure imaging and atomic movement dynamic obs. 0-70090
- electron wave function in vicinity of planar defect 'on edge' 0-88002
- FCC metal, dislocation dissociation 0-107235
- film defect growth and nucleation, electron microscopy and diffraction exam. (*French*) 0-59824
- fine fragmented crystals, complex struct. analysis by electron microscopy 0-104416
- ion implanted, F influence on oxidation-induced stacking faults 0-65011
- metal, BCC, twin boundary and stacking fault structs., computer simulation 0-59485
- metal, polycrystalline, strain hardening, dislocation link length model 0-84953
- metals and alloys, stacking faults in HCP and FCC structures, long-range oscillatory interactions and stability 0-65012
- polytype relative stabilities, entropy contribs. 0-100197
- rare earths, light, stacking faults and magnetism, transform. effects 0-75840
- rectorite, stacking and ordered interstratification, high-resolution TEM obs. 0-109140
- SEM imaging, electron channelling appl. 0-70214
- semiconductor, SEM charge-collection images, contrast formation 0-70087
- semiconductor, SEM electron beam induced current images of dislocations and stacking faults, computer simulation 0-70198
- semiconductor defects, spectroscopic techniques to study of electronic props. 0-84446
- silicates, layered, optical filtering of faulted areas in electron micrographs 0-84035
- steel, austenitic stainless, stacking fault energy, effect of N 0-107279
- steel, stainless, austenitic, deform. substruct. and annealing, stacking fault tetrahedra form 0-107282
- steel, stainless, in-situ obs. of deform. in HVEM 0-103338
- steel, stainless, martensite nucleation mechanisms, HVEM obs. 0-104157
- steel, stainless, shock loaded, residual martensite obs. 0-104414
- TEM weak-beam contrast of stacking faults 0-75132
- web dendrites, dislocations, stacking faults, X-ray topographic study (*Chinese*) 0-88148
- Ag, multiply twinned particles, internal and surface struct. by electron microscopy 0-84189
- Ag, thin-film bicrystals, planar lattice defects and migrating grain boundaries interaction 0-79835
- Ag-Sn, splat-quenched, X-ray diffr. study 0-81094
- $\beta^*$ -Al<sub>2</sub>O<sub>3</sub>, Mg- and Li-stabilised, high-resoln. electron microscopy images 0-107277
- Au, multiply twinned particles, internal and surface struct. by electron microscopy 0-84189
- Be-Si-N system polytypes, struct. obs. using TEM 0-107192
- Be<sub>3</sub>N<sub>2</sub>, BeSiN<sub>2</sub> system, crystallography and phase relationships, TEM and electron diffr. study 0-92502
- CdSe thin film transistor on Cr substrate, cryst. struct., substrate defect effects 0-70563
- Co-Ni-Cr-Nb (40, 18, 1.8 wt%), precipitation behaviour of NbC, effect of ageing temp. on morphology 0-89227
- Co-P films with various preferred orientations, mag. props. 0-100604
- Co-Pd film, ordered, stacking fault obs. by TEM and interpret. using many-beam theory 0-107680
- Cr<sub>2.8</sub>V<sub>0.7</sub>Fe<sub>3.4</sub>C<sub>3</sub>, stacking fault study, morphology, comp. and struct. 0-84190
- Cu, foils, faulted defect formation by moving boundaries 0-107281

**stacking faults continued**

- Cu, near  $\Sigma$  grain boundary properties, boundary dissociation 0-100251
- Cu, point and planar defects, computer simulation 0-59455
- Cu-Al, dislocation core cut-off parameter, estimation from stacking fault nodes 0-103370
- Cu-Al alloy, planar faults, faint electron microscopic image contrast obs. 0-107283
- Cu-SiO<sub>2</sub>, in-situ deform. in HVEM 0-103338
- Cu<sub>2</sub>NiZn, comparison between different theories predicting stacking fault energy from extended nodes 0-75240
- Cu<sub>2</sub>NiZn, stacking fault energy determ. from extended nodes 0-107280
- Cu<sub>2</sub>O polycryst., dislocation obs. by electron microscope (*Spanish*) 0-75230
- Fe<sub>2</sub>O<sub>3</sub>/Fe<sub>2</sub>O<sub>4</sub> transformation matrices, higher-order orientation relationships 0-100846
- GaAs:Si, stacking fault prod. during heat treatment in As vapour 0-96547
- GaAs:Sn(Te), epitaxial film, influence of impurities on stacking fault energy 0-103371
- Gd<sub>2</sub>P<sub>2</sub>S<sub>7</sub> defect struct. and tetrahedral precipitates, TEM study 0-107246
- Gd<sub>2</sub>, Dy, Ni, FeB-CrB type stacking variations, cryst. struct. 0-64952
- GdNi<sub>2</sub>YNi, FeB-CrB type stacking variations, cryst. struct. 0-64952
- Ge, dislocations under high stress, stacking fault energies, TEM study 0-70202
- Ge, dissociated dislocations, constriction correlation with jogs 0-79801
- Ge, electron beam irradiat., {113} faults, nature and origin 0-70258
- Ge, faulted dipoles, high-resolution TEM study 0-103345
- MgAl<sub>2</sub>O<sub>4</sub> crystals, flux grown, artificial spinel twin form. by BeAl<sub>2</sub>O<sub>4</sub> addition 0-96542
- MgNi<sub>2</sub>, four-layer, Friauf-Laves phases, stacking variants 0-96468
- MgZn<sub>2</sub>, two-layer, Friauf-Laves phases, stacking variants 0-96468
- MgZn<sub>2</sub>-MgAg<sub>2</sub> system, Friauf-Laves phases, stacking variants 0-96468
- MoS<sub>2</sub>, homogeneity size estimation, stacking fault conc. effect 0-96661
- Ni-Cr, (30 wt%), collective dislocation movements, in situ study 0-100243
- Ni-Cr, partial dislocation, stacking fault TEM study (*Chinese*) 0-84174
- Ni-Ni<sub>4</sub>Mo system, deformation microstruct. 0-93591
- Sb<sub>2</sub>S<sub>3</sub> spherulite crystals, direct lattice resolution obs. of defect struct. 0-107255
- Si (001) wafer, pyramidal hillocks, TEM obs. during chemical etching 0-70508
- Si crystals, dynamic processes associated with stacking faults and deform. twins, HVEM in-situ obs. 0-103369
- Si, electron beam irradiat., {113} faults, nature and origin 0-70258
- Si, epitaxial (111) surface, etching observation of stacking faults, dislocations, S-pits, etch pits (*Chinese*) 0-70197
- Si epitaxial film on sapphire, microtwins, TEM exam. 0-70555
- Si, epitaxial layers, stacking defect distrib. anal. using ion channelling tech. 0-100294
- Si, epitaxial wafer, saucer pit microdefects reduction by intrinsic gettering 0-75450
- Si film, MBE, cryst. defect props., substrate treatment effects 0-70551
- Si foil, computer simulation of high resolution images of defects 0-107208
- Si, HVEM struct. images of extended 60° and screw dislocations 0-59466
- Si, high dose self-irrad., spatial correl. between primary and secondary defect profiles 0-59536
- Si, ion implanted, complex annealing behaviour of amorphous layers, TEM obs. of defect struct. 0-107299
- Si, ion implanted, defect struct., dislocation loops and elongated defects 0-107300
- Si laser annealing of SiO<sub>2</sub> layers 0-97505
- Si, oxidation stacking faults, shrinkage and growth, bulk O<sub>2</sub> effects 0-96546
- Si, oxidation-induced stacking faults, distinction between clean and decorated faults by etching 0-79818
- Si, polycrystalline structure stability, stacking defects, twins grain struct. (*Russian*) 0-100248
- Si surface, thermal oxidation induced defects, origin and growth (*Chinese*) 0-66681
- Si wafer, stacking faults, preoxidation gettering by reverse side P diffusion-induced misfit dislocations 0-60988
- Si(B,P), dislocations under high stress, stacking fault energies, TEM study 0-70202
- Si:P, ion implanted, regrowth of damage structs. by laser annealing 0-107289
- SiC ion implanted, laser induced ordering and defects 0-84754
- SmCo<sub>5</sub>, mag. domains structure rel. to crystal defects, electron microscopy 0-103856
- $\beta$ -Ti-Mo, thermal instability, hardness and tensile deform. (*Japanese*) 0-71703
- W, stacking fault stability determ. 0-96548
- Y<sub>2</sub>O<sub>3</sub>, dislocation and plasticity dissociation 0-107247
- Zn, single cryst. contribution of basal dislocations to residual elec. resist. (*Russian*) 0-75539
- ZnO, irradiation in high voltage electron microscope dislocation loops study 0-88157
- Zr<sub>3</sub>Al, deformed and irradiat., lattice defects obs., superlattice dislocations and defect clusters 0-107261

**staff** *see personnel***stainless steel**

- see also austenitic stainless steel; martensitic steel*
- 304, bend test ductility of irradi. specimens for LMFBR appls. 0-104235
- 316, erosion in cavitating venturi 0-108602
- 316, fatigue behaviour of materials containing significant amounts of irradi.-induced He 0-100917
- 316, oxidation behaviour in the environment, appl. to GCFR fuel claddings 0-104350
- amorphous films, corrosion resist. and ion plating use 0-89423
- atmospheric corrosion, of type 18Cr-2Mo-Ti 0-85078
- carbide and intermetallic phases, quantitative anal. by X-ray diffr. 0-66514
- carbide reactively sputtered solar selective absorbers for all-glass tubular evacuated collectors, absorbance and emittance 0-101132
- cathodic alloying on surface, for increased passivation and corrosion resist. 0-100940
- coating with Ni by detonation powder spray deposition 0-61028
- corrosion and grain boundary penetration on exposure to coal gasification environment 0-61003



## stainless steel continued

corrosion behaviour of composite materials in  $N_2O_4$  oxidising atmospheres (Russian) 0-76421  
 corrosion protective films, surface treatment development 0-66699  
 corrosion testing, type St. 3PS, suitability for power station chimney flue structural material 0-108681  
 Cr-Ni-Mo, phase anal. of carbide phases after isothermal annealing (Czech) 0-89224  
 crack propagation under fatigue-creep conditions and fractography in type 304 (Japanese) 0-104267  
 creep, irradiation induced, correlation of theory with expt. evidence 0-88255  
 creep limit, cyclic load component effect at high temps. 0-104231  
 cutting, by turning, smoothing appl. for plastic pre-straining (Russian) 0-60911  
 deformation, in-situ obs. in HVEM 0-103338  
 deformation, rapid dynamic, at  $-196^\circ C$  0-104220  
 deformation broaching, of type 12Kh1810T bushings 0-108473  
 deuteron bombardment, retention and re-emission of 0.125-1 keV  $D^+$  ions 0-66349  
 diffusion and permeation of  $D_2^+$ , ion beam meas. 0-59492  
 duplex, STEM obs. of localized corrosion 0-104324  
 EBR-II reflector assembly irradi. induced bowing, implications for core restraint design 0-104234  
 electrode, electrical breakdown of water in  $\mu s$  region 0-103917  
 emittance, oxidation and surface roughness effects 0-96673  
 emittance meas. rel. to surface roughness parameters 0-100342  
 explosive loading technique for uniform plastic expansion at high strain rates for type 304 0-81273  
 fast neutron irradiated, solution annealed tubing, residual stress behaviour 0-65054  
 fatigue limit, in bi-freq. loading 0-104289  
 fatigue properties of low-fluence neutron-irradiated stainless steel DIN 1.4948 0-97585  
 FBR blanket facility, gamma-ray heating rate meas. 0-57912  
 ferrite, magnetomechanical acoustic emission for residual stress NDT 0-71149  
 ferritic, cleavage fracture toughness, temp. and strain rate depend. 0-85028  
 ferritic, Cr-Mo-Nb, intergranular corrosion resistance 0-104319  
 ferritic, FeCrAlloy, creep-rupture props., 650-800°C 0-97535  
 ferritic, phosphide analysis using nonaqueous electrolyte potentiostatic etching method (Japanese) 0-89221  
 ferritic Cr-Mo (12,1wt.%) microstructure influence on localised corrosion behaviour 0-61018  
 ferritic stainless, embrittlement 0-85041  
 fixing pins for fractured bones, strength, ultrasound effect 0-71710  
 Fokker-Planck eqn. describing evolution of interstitial loop microstruct. during irradiation 0-107215  
 fracture, of type 12Cr1MoV joint effects of thermal fatigue and creep 0-104297  
 fracture and crack tip plastic zones, in situ obs. 0-108686  
 fracture micromechanism when kept isothermally in sulphur pulp 0-76355  
 fusion reactor materials, design of materials irradiation experiments utilizing spectral tailoring 0-102305  
 global bending response analysis of elastic and viscoplastic nuclear shipping cask structures subjected to impact loading 0-76301  
 heat treated, oxide comp. and corrosion susceptibility of grades 410 and 430, AES study 0-66692  
 Hugoniot parameters to 620 GPa, dynamic yield strengths and phase transition press. 0-75331  
 ion irradiated with heavy ions, type 321 steel, defect cluster obs. 0-107341  
 irradiated, void nucleation, numerical evaluation 0-70252  
 irradiation induced nuclear cladding swelling, empirical development of design equation 0-59527  
 laser induced damage 0-66335  
 laser radiation coupling coeffs. for CW  $CO_2$  laser 0-84811  
 laser surface melting for corrosion protection 0-93698  
 LWR fuel cladding material evaluation 0-99213  
 machine faceted, low-energy ion erosion studies 0-80923  
 maraging stainless, phase transformation and mech. props. rel. to heat treatment (Chinese) 0-66501  
 martensite nucleation mechanisms, HVEM obs. 0-104157  
 microcrystalline, rapidly quenched particulates, appl. 0-84887  
 neutron dose determ. from isotope abundance ratio, mass spectra obs. 0-61220  
 neutron irradi. effects on tensile props. and microstruct., for type 316 steel 0-65059  
 neutron irradiated 304 SS, low-cycle fatigue characteristics 0-97586  
 oxide film, Cl distrib., SIMS (French) 0-108765  
 oxidised, sputtering yield meas. by atomic fluoresc. spectroscopy 0-80922  
 passive state, electron spectroscopy anal. 0-59765  
 pipes, welded branch, stresses calc. 0-108493  
 pitting corrosion in chloride media, electrochem. aspects 0-61007  
 porous sheet, mech. strength, bend and reverse bend tests (Russian) 0-93595  
 porous sheet, pore dimensions, filtration and permeability (Russian) 0-76480  
 precipitate observations using convergent beam electron microscopy 0-108689  
 preparation of 20Kh13 by diffusion impregnation 0-60803  
 radiation damage by 1 MeV electrons, dislocation struct., brittleness (Russian) 0-75226  
 radiation-enhanced  $H_2$  permeation in steel 4301 0-59732  
 reduction of H by Ar glow discharge, rel. to ultra cold neutron storage 0-104459  
 rubbing of cast Fe, surface temperature effect on dry sliding wear 0-60983  
 sensitization, C content and ferrite morphology effect 0-89400  
 sensitized, crack growth in high-temp. water 0-108636  
 shock loaded, residual martensite obs. 0-104414  
 solubility of MnS in Kh18N11, determ. method 0-84910  
 stacking faults, weak-beam contrast in TEM 0-75132  
 steam pipes, 12Cr1MoV, selection of allowable stresses based on minimum possible strength data 0-104237  
 steam turbine casings of susceptibility to brittle struct. and fracture, influence of props. 0-104298  
 steel, ferritic stainless, effect of Cl ions on passive layers 0-59766

## stainless steel continued

steel, stainless, type EP838 ion irradiated, surface structure changes during post-irradiation heating (Russian) 0-75272  
 steel, stainless 316, soln. annealed, cavity alignment and precipitation during dual ion bombardment 0-70273  
 steel, stainless casts, creep ductility, Auger spectroscopy study 0-60917  
 strength down to 4.2K; influence of stress raisers 0-71754  
 stress corrosion cracking and microhardness, effect of bombardment by  $He^+$ ,  $Ni^+$ , and  $Cr^+$  0-85087  
 stress corrosion cracking in  $H_2SO_4$ -NaBr aq. soln. (Japanese) 0-108629  
 stress corrosion cracking in  $H_2SO_4$ -NaI aq. soln. (Japanese) 0-108630  
 stress corrosion cracking in  $MgCl_2$  soln., environment effect on initiation and propag. in type 301 (Japanese) 0-104338  
 stress corrosion susceptibility in high purity water,  $O_2$  and temp. effects 0-61002  
 stress relaxation, in-reactor study at low temps. 0-93588  
 stress relieved, microstruct. transformations resulting from ageing 0-71644  
 substrate, for  $Al_2O_3$  layer, leaky wave generation at interface with water 0-75419  
 surface,  $O_2$  desorpt. during laser irradi., etching, AES study 0-66338  
 surface characterisation rel. to adhesive bonding chem. etching, SEM, AES, XPS and electron probe microanal. 0-88416  
 surface chemistry rel. to metallurgical props., SIMS, XPS and AES (French) 0-80045  
 SUS 316, corrosion behaviour in high temp. impure He gas 0-76402  
 TEM foils, white band contrast 0-75134  
 tempering after air hardening from rolling heat (German) 0-93571  
 tensile testing, of type SUS 304 diffusion welded joints; sound emission (German) 0-61062  
 thin sheet, fracture resist., critical opening of crack criterion 0-61048  
 type 304, creep modelling incorporating initial strain and ageing 0-58939  
 type 304, plastic buckling of cylindrical shells under axial compression 0-74785  
 type 304, rate equations for elevated temperature creep 0-65141  
 type 316 20% cold worked fission reactor fuel cladding, axial stress effects on transient mech. response 0-71743  
 vacuum components, pre-vacuum surface finish influence on electron stimulated desorption in ultrahigh vacuum 0-57320  
 viscoplastic model, uniaxial, based on total strain and overstress 0-64387  
 voids, TEM, diff. contrast 0-75218  
 wear, rubbing on mild steel, mag. field influence 0-60982  
 weld metal AISI 316, high-temp. mech. props. 0-66601  
 welds, type 444 stainless steel, ductility loss investigation 0-85002  
 wire, axial texture after electroplastic drawing, X-ray struct. investigation (Russian) 0-104177  
 $B_4C$ -304 stainless steel cermet for nuclear shielding appls. 0-102352  
 25Cr-20Ni stainless steel dendritic solidification, growth morphology and solute redistrib. (Japanese) 0-81045  
 Cr-Cu (17, 0.6 to 1.1 wt.%), texture 0-84957  
 Cr-Mn (13, 19 wt.%), elastic const. behaviour, anomalous, low temp. 0-97521  
 Cr-Mo-W-V (12, 1, 1, 0.25), stress relax. data anal. using total strain-time parametric method (Japanese) 0-104198  
 Cr-Ni (20, 25 wt.%) steel 0-89414  
 Cr-Ni-Mo-Mn (16.55, 10.23, 2.28, 1.34 wt.%), hardfacing materials, friction characts. in high temp. Na (Japanese) 0-89356  
 Cr-Ni-Mo-Mn-Si (17-20, 8-12, 2.5-3.5, 2, 0.2 wt.%), orthopaedic, type En58J, Mo ion-plating, corrosion fatigue 0-66694  
 Cr-Ni-Mo-W-Nb (19, 9, 1.4, 1.4), stress relax. data anal. using total strain-time parametric method (Japanese) 0-104198  
 Cr-Ni-Mo (26, 5, 1.3 wt.%), ferrite to austenite decomp. 0-93554  
 Cr-Ni-Ti, metallographic detection of (Ti,Ni) $_6$ C 0-66721  
 Cr-(Mo)-(Ni), self-weldability in high temp Na (Japanese) 0-89392  
 10CrNiCuP, suitability for power station chimney flue structural material, corrosion testing 0-108681  
 Fe-Cr-Al (15, 4 wt.%) FeCrAlloy, oxidation behaviour, Al and Y surface ion implantation effect 0-71790  
 f- ferritic, Cr-Mo (10-14, 2-6 wt.%), heat-resist., creep-rupture strengths 0-104271

## standard microphones see microphones

## standardization

audiometric facility at West Middlesex Hospital, London for standardised hearing tests 0-76858  
 neutron radiometers testing, Soviet method 0-99405  
 photochromic glasses, parameter standardisation 0-69476  
 rheograph linear-distortion estimation 0-85502  
 surface roughness meas., hand-held instrument with in-built data processor (German) 0-57255  
 tensile tests, standardization from metal physics viewpoint (German) 0-93711

## standards

see also CAMAC; constants; measurement standards; units (measurement)  
 architectural acoustics, review (Japanese) 0-64294  
 cardiac monitor, heart rate meter and alarm eval., proposed standard test tapes 0-89899  
 colour-reference-standard fluorescent lamp with colour rendering index of 99 0-78925  
 condenser microphone, laboratory (Japanese) 0-79096  
 electrical quantities, units, symbols and definitions (German) 0-86248  
 gloss measurement of paints, reference glossmeter 0-82805  
 heliotechnics, basic values, symbols, units and definitions (Rumanian) 0-57243  
 high-volume preparation of air to standard quality for zeroing analyzers 0-90829  
 image restoration using maximum information norm 0-106476  
 laser applications for discotheque light effects, safety considerations with respect to output power and exposure time, regulations and recommendations (German) 0-101224  
 nuclear energy, quality assurance, international standardisation, FORATOM 0-58008  
 nuclear reactor electrical equipment, qualification concept 0-57883  
 optical standard test method development by ASTM 0-74528  
 pressure vessel code, ASME, seismically qualified piping, failure probability 0-78365  
 radioactive materials, IAEA regulations for safe transportation 0-63410  
 radioactive materials, IAEA transport information collection system, influence on improved safety measures 0-63413



standards continued

radioactive materials, international regulatory control for safe transportation 0-63411  
radioactive materials, package design, construction and testing for safe transportation 0-63412  
radioactivity standards for medical use 0-67232  
regulations and methods for noise measurement (*German*) 0-69610  
safety principles underlying IAEA nuclear safety programme 0-95361  
SI units, guidelines for use, US National Bureau of Standards 0-68167  
simulated neutron tomography for nondestructive assays 0-99218  
spectral reflectance standards for visible and infrared region using thin Al film vacuum deposited on optical flats (*Japanese*) 0-102789  
X-ray diffraction powder patterns, NBS 0-64839  
<sup>244</sup>Pu standard reference material for nuclear materials safeguards appls. 0-78373

standby power supply see emergency power supply

star phase rectifiers see rectifiers

Stark broadening see Stark effect

Stark effect

see also atomic spectra

alkali metal, Stark and photoabsorption spectra, density of oscillator strengths 0-83318  
anthracene in naphthalene crystal, second-order Stark shifts in optical spectrum 0-88966  
atomic level field splitting, resonant cooperative light scatt. (*Russian*) 0-74148  
atomic neutral particles, electrostatic trapping 0-102485  
Bloch electron in step-like elec. pot. 0-59942  
dibromonaphthalene, quasilinear chain excitons, Stark effects 0-97239  
ethylene oxide, rot. relax., double reson. and Stark switching obs. 0-106340  
ethylidenimine, pyrolysis product, microwave spectra, rot. distortion and electric quadrupole const. and rot. barriers determ. 0-78608  
exponential decay 0-91491  
fluoroacetylene-d, Stark and microwave double reson. laser spectra 0-63690  
fluoromethane, <sup>12</sup>C (<sup>13</sup>C), Doppler-free optical double reson. spectroscopy using single-freq. laser and modulation sidebands 0-68274  
forbidden M<sub>1</sub> transitions, parity violation, stray static elec. fields 0-87078  
gas detector appl., all-electric 0-74417  
glass:Nd<sup>3+</sup>, spectral props. (*Chinese*) 0-60645  
highly excited atoms, blackbody radiation effects 0-58176  
homologous ions series, Stark broadening trends 0-105157  
Josephson junction, ultrasmall, dynamic Stark splitting 0-103790  
Klein-Gordon equation, time-independent, relativistic Stark effect, resonances 0-62890  
laser plasma diagnostics using Balmer series transitions Stark broadening 0-64780  
liquid, nuclear quadrupole relaxation of non centre symm. mols. (*Russian*) 0-88889  
methane-d, Doppler-free optical double reson. spectroscopy using single-freq. laser and modulation sidebands 0-68274  
methanol far IR laser line Stark splitting obs. 0-58313  
methanol far IR Stark spectroscopy and 9-P(34) CO<sub>2</sub> laser line 0-69145  
methanol optically pumped 118.8 μm laser line, Stark splitting obs. 0-102710  
methylacetylene, ν<sub>s</sub> band, microwave and IR laser Stark spectrosc. 0-91558  
methylpropylether, trans-trans isomer, microwave spectra, struct., dipole moment and rot. barriers calcs. 0-83348  
NQR, electronics appls. 0-63668  
optical multistability, light self-modulation in double resonance (*Russian*) 0-106560  
optically pumped laser three-photon transition theory 0-102690  
paramagnetic crystal, magnetisation change by light pulse 0-70932  
plasma, Stark shift by inhomogeneous strong E field, X-ray Lyman profile 0-106977  
plasmas, Tormac, Gaussian Hell 4686 Å spectral lines, Doppler and Stark broadening effect, turbulence 0-106980  
rare earth oxyhalides: Eu<sup>3+</sup>, fluorescence spectra obs. (*French*) 0-89042  
rigid symmetric top molecules, dynamic Stark effect spectrum 0-63621  
ruby, optical nutation echoes, Stark switching obs. 0-69467  
semiconductor, phonon induced hopping between Stark levels 0-92900  
semiconductor, Stark and photoabsorption spectra, density of oscillator strengths 0-83318  
semiconductor, with superlattice, plasma resonant interaction with Stark oscils. 0-107842  
semiconductors with superlattices, Stark-cyclotron resonance, Larmour freq. (*Russian*) 0-60421  
silyl acetylene, microwave spectra in ground and ν<sub>10</sub> vibr. state 0-78610  
Stark resonances, stabilisation method calcs., convergence 0-91492  
trifluoromethyl bromide, microwave spectra, mol. rot., isotopic variation in bond lengths, Stark meas., dipole moments determ. 0-74165  
trifluoromethyl iodide, microwave spectra, mol. rot., isotopic variation in bond lengths, Stark meas., dipole moments determ. 0-74165  
trinitromethane, microwave and rot. spectra, effect of twist of NO<sub>2</sub> groups, rot. and centrifugal distortion const. determ. 0-95605  
two-photon double-beam optical bistability 0-64113  
width and shift depend. on ionisation potential 0-58211  
Ar<sup>16,17</sup> filled glass shell, symmetric laser compression 0-64759  
Ar-acetylene van der Waals molecule, radiofreq. spectroscopy and Stark effect meas., equilb. struct. and props. 0-91543  
Ba I, light shift induced zero-field level crossing 0-58220  
BeF<sub>2</sub>-KF-CaF<sub>2</sub>-AlF<sub>3</sub>-EuF<sub>3</sub> fluoroberyllate glass, Eu<sup>3+</sup> fluoresc. linewidth 0-66285  
CdF<sub>2</sub>:Er<sup>3+</sup>, Tm<sup>3+</sup>, evidence for Er<sup>3+</sup>→Tm<sup>3+</sup> energy transfers, fluoresc. exps. 0-60655  
GaAs, field ionisation speed of shallow impurity levels, quantum-mechanical estimates 0-97412  
Ge, internal Stark effect on impurity states, low-temp. magnet. absorption meas. 0-60636  
GeH<sub>4</sub>, Doppler-free optical double reson. spectroscopy using single-freq. laser and modulation sidebands 0-68274  
H<sub>2</sub> is reson., stabilisation method calcs., convergence 0-91492  
H atom, Stark effect, second order correction for energy (*Rumanian*) 0-74147  
H, four dimensional oscillator, rot. invariance of coordinate transform., appln. to Stark problem 0-99436  
H, perturbation theory and Pade approx. in electric field 0-91493  
H plasma, Stark broadening, model microfield methods calcs. 0-92274

Stark effect continued

H, scattering theory methods appl. 0-63586  
H spark, laser-triggered, electron densities meas. 0-106975  
H, Stark and photoabsorption spectrum, density of oscillator strengths, atom c.f. semiconductor spectra 0-83318  
H, Stark effect, high orders of perturbation theory for excited states 0-87079  
H, Stark effect, iteration procedure for any field strength 0-69104  
H, Stark spectrum and field ionisation, density of continuum states, normalised wavefunctions 0-83317  
H<sup>-</sup>, DC Stark broadening of <sup>1</sup>P<sup>o</sup> shape reson. 0-63585  
H<sup>-</sup> resonances in electric field 0-63607  
H<sup>+</sup> solid, collision induced IR lines caused by T<sub>2</sub> radioactivity 0-84756  
H<sub>2</sub>, CARS, optical Stark effect on vibr., and rot. transitions 0-99512  
H<sub>2</sub> and H<sub>3</sub> spectral profiles from neutral beams and plasmas in high mag. fields 0-83999  
H<sub>2</sub>, dynamic Stark effect for elec. field strength meas. in waveguide 0-69103  
HF, laser field interaction, Floquet theory, dynamic Stark shift, broadening 0-63716  
HNO A<sup>1</sup>A<sup>o</sup> excited state dipole moment, optical-optical double reson. Stark spectrosc. obs. 0-106337  
HO<sub>2</sub>, free radical, dipole moments and Stark effects from microwave spectra 0-63623  
Hα and Hβ, Stark profiles, ion-motion effect 0-63592  
He, dynamic Stark effect for elec. field strength meas. in waveguide 0-69103  
He I 447.1 and 492.2 nm lines, ion motion effects on Stark profiles 0-69105  
He II, 4686 Å line, Stark broadening, meas. and calcs. 0-91504  
He II 4686 Å line, Stark profile meas. in high density plasma 0-96390  
He metastable state, two- and three-photon ionisation 0-91518  
I<sub>2</sub>, polarisability anisotropy, laser assisted mol. beam spectroscopy 0-78646  
KY<sub>3</sub>F<sub>10</sub>:Eu<sup>3+</sup>, cryst. field parameters and intensity parameters, J-mixing effects 0-59932  
La<sub>2</sub>Be<sub>2</sub>O<sub>7</sub>:Nd<sup>3+</sup> (Pr<sup>3+</sup>), cryst. growth, spectral and laser properties in <sup>4</sup>F<sub>3/2</sub>→<sup>4</sup>I<sub>11/2</sub> and <sup>4</sup>F<sub>3/2</sub>→<sup>4</sup>I<sub>13/2</sub> transitions 0-80853  
N<sub>2</sub>, CARS, optical Stark effect on vibr., and rot. transitions 0-99512  
NH<sub>3</sub> CW far IR laser lines, CO<sub>2</sub> laser pumping and Stark tuning 0-69382  
NH<sub>3</sub> CW far IR laser lines, CO<sub>2</sub> laser pumping and Stark tuning 0-106508  
NH<sub>3</sub>, stimulated hyper-Raman scatt. via 3-photon process to obtain IR and far IR radiation 0-58633  
NO<sub>2</sub>, Stark effect investig., using two-way EPR cavity system 0-90872  
<sup>14</sup>NH<sub>3</sub>, ground state, microwave inversion lines 0-87098  
<sup>15</sup>NH<sub>3</sub>, Doppler-free optical double reson. spectroscopy using single-freq. laser and modulation sidebands 0-68274  
Nd:silicate glass, resonance laser excitation, inhomogeneously broadened emission spectra 0-66295  
Nd<sup>3+</sup> glass luminesc. band profile deform. under free-oscillation conditions 0-71487  
PH<sub>3</sub>, Doppler-free optical double reson. spectroscopy using single-freq. laser and modulation sidebands 0-68274  
SiH<sub>4</sub>, Doppler-free optical double reson. spectroscopy using single-freq. laser and modulation sidebands 0-68274  
Sn II, cool plasma, isolated lines, Stark broadening, semi-empirical impact approx. calcs. 0-59186  
SrO:Ni<sup>2+</sup>, linear Stark effect for zero-phonon optical absorpt. line 0-80830  
Xe, autoionising reson., Stark effect 0-58198  
YAG:Ho<sup>3+</sup>, spectroscopy, stimulated emission 0-93374  
Yb, 4f<sup>14</sup>6s6p <sup>3</sup>P<sub>1</sub> and <sup>1</sup>P<sub>1</sub> levels, Stark effect, tensor polarisabilities 0-87080

stars

see also stellar .....

see also dwarf stars; giant stars; magnetic stars; multiple stars; neutron stars; novae; Sun; variable stars  
134045+083448, no occultation by Pluto on 1980 April 6, ephemeris 0-62070  
134045+083448, probable occultation by Charon (1978 P 1), (1980 April 6) 0-62071  
A-type stars, effect of C+H<sup>+</sup>→C<sup>+</sup>+H charge transfer on C I 1101 Å absorpt. edge 0-90423  
aberration, classical rel. to relativistic theory 0-67517  
accreting gas, thermodynamics and hydrodynamics 0-67696  
accretion onto compact gravitating object, travelling sound wave behaviour WKB anal. 0-67551  
AGK+19°0599, occultation by 65 Cybele, 1979 October 18, obs. using photoelectric photometer (*Chinese*) 0-105172  
α Andromedae, shell star, lack of linear polarisation variability 0-62157  
θ Aquilae (B9.5 III), abundance anal. from model atmosphere 0-90415  
astrometric analyses of bright nearby stars, from Sproul 61 cm refractor plates 0-61991  
astrometry, stellar absolute declinations system construction for entire sky using high-latit. obs 0-67520  
B5 V-P5 V type stars in Geneva Observatory catalogue, radii, temp. and brightness determ. 0-77396  
B-type stars at high southern galactic latitudes, four colour and Hβ obs. 0-82357  
B-type stars clouds, distrib. of nearly interstellar mols. (*Russian*) 0-105321  
late B-type stars small v sin i values, Ap star determ., visible spectra 0-74049  
BD+10°2179, C rich H deficient star, UVB photometric obs. 0-90437  
Be and shell stars, UV spectrophotometry with TD-1 satellite 0-90438  
Be stars, discoveries in open clusters NGC 3766 and (IC 2581) 0-90445  
Be stars, mag. fields determ. via linear polarisation spectrum (*Russian*) 0-90344  
blue horizontal-branch, He stratification in model atmosphere 0-90409  
α Canis Majoris (Sirius), ghost image on Palomar Sky Survey as hiding place for new star cluster 0-109501  
ν Capricorni (B9.5 V), abundance anal. from model atmosphere 0-90415  
Cassiopeia-Taurus association stars, interstellar 2200 Å feature anomalous strength 0-77469  
3 Cassiopeiae, Flamstead missing star, identification with Cassiopeia A supernova 0-62436  
3 Cassiopeiae rel. to supernova remnant Cassiopeiae A 0-72792  
catalogue in Ptolemy's Syntaxis, position meas. method 0-67586



## stars continued

- Chu's object in Perseus, identification as galactic star with refl. nebula 0-62132  
 classification criteria by statistics from co-occurrence matrix (*Italian*) 0-98574  
 cocoon stars, numerical soln. of radiation transfer eqn. in spherical geometry 0-90329  
 comparison star sequences in six variable star fields, photometry obs. 0-82433  
 configurations and fields, anal. by statistical methods 0-82224  
 coordinate system error reduction using 51 Nemausa posns. 0-72849  
 counts, use in determination of galactic struct. 0-82507  
 Cygnus X-3, evidence for He star companion from period derivative and asymmetric X-ray light curve 0-105394  
 distribution in S. Milky Way 0-85997  
 distribution perpendicular to galactic plane, fine struct. study (*Russian*) 0-73036  
 early type stars complexes in M31 (Andromeda galaxy), assoc. with Cepheid variables (*Russian*) 0-90455  
 early-type, mass loss from radio obs. of 6 cm 0-82347  
 early-type, rapidly rotating models with radiation press., struct. parameters calc. 0-67697  
 early-type stars, H and He<sup>+</sup> synthetic line profiles in stellar winds 0-85926  
 early-type stars and cool stars, UV spectroscopy of outer layers 0-72922  
 early-type stars in LMC open cluster NGC 955, stellar winds rel. to motions in bubble-like nebula N51D 0-105295  
 early-type stars in southern hemisphere, IR photometry 0-94786  
 early-type stars with Balmer emission, near UV (2000-3000 Å) spectra 0-94811  
 emission-line stars misclassified as H planetary nebulae, catalogue 0-109378  
 EUV radiation, point source contribs. to EUV background 0-62324  
 exciting stars in H II regions, mean temp. determ. method 0-73024  
 faint blue stars, southern, UVB photometry 0-82349  
 faint stars in globular cluster M2 (NGC 7089), photometry and colour-magnitude diagram 0-101623  
 faint stellar images, colour-magnitude diagrams and clustering correl. functions rel. to star populations 0-82360  
 field stars of solar neighbourhood, chromospheric Ca II H and K emission survey 0-109423  
 FK4, corrections to zero points from minor planet obs. (*Russian*) 0-82228  
 FK5, equinox and equator of new fundamental reference coord. system 0-109341  
 galaxy disc stars, nonlinear interaction with spiral wave near corotation radius (*Russian*) 0-62289  
 Galaxy disc stars, z-distrib., rel. to local galactic force field 0-62271  
 general magnitude eqn. between FK4 and southern catalogues 0-67705  
 in giant ellipsoidal shells around normal elliptical galaxies, origin 0-86000  
 Greenwich Obs. Time and Latitude Service, Time Report (January to March 1979) 0-72749  
 Greenwich Obs. Time and Latitude Service Time Report (April-June 1979) 0-72750  
 HD 137613, C rich H deficient star, UVB photometric obs. 0-90437  
 HD 192163, Wolf-Rayet star, spectra of filaments and smooth gas in ring nebulae (NGC 6888) (*Russian*) 0-90515  
 HD 200775, Be star, optical and UV extinction by dust in (NGC 7023) 0-109515  
 HD 200775, possible protostar in reflection nebula NGC 7023, optical polarization and IR spectrum 0-85944  
 HD 219150, F0 V star with remarkable UV excess, optical and UV photometry and spectrum 0-90429  
 HD 36665, B1e star, detect. of interstellar CO absorpt. in direction of supernova remnant (S147) 0-67836  
 HD 93250, O3 massive star in η Carinae complex, non-LTE analysis 0-77398  
 Herbig-Haro 2, detection of H<sub>2</sub> vibrationally excited 2 μm lines 0-94853  
 Herbig-Haro objects, stellar wind model 0-85985  
 Herbig-Haro objects 7-11, compact H II region and H<sub>2</sub>O maser sources 0-73019  
 Herbig-Haro objects and surrounding dark clouds, NH<sub>3</sub> 23 GHz obs. 0-72934  
 Herbig-Haro objects exciting stars, 2 micron search 0-67720  
 Herbig-Haro objects in Orion Nebula 0-77397  
 high luminosity stars in SMC, interstellar reddening distrib. functions appl. to total/selective absorption. ratio determ. (*German*) 0-67851  
 I-118, probable Norma OBI assoc. member with anomalous distance modulus 0-62129  
 images, automatic CCD measuring machine (*Japanese*) 0-82212  
 interaction with dense interstellar gas clouds, theoretical aspects (*German*) 0-109500  
 interferometry, first fringe meas. 0-82215  
 IR airborne spectrophotometry, 1.2-5.5 μm, spectra and absolute calibration 0-62117  
 K-type stars, spectroscopic investigations in 4500 to 7500 Å region 0-109430  
 Klemola 23, occultation by Neptune, 1980 August 21, obs. 0-109395  
 Klemola-Marsden 12, occultation by Uranus, 1980 August 15 to 16, reality of additional occultations questioned 0-109396  
 late-type catalogue of revised Mk spectral types 0-82226  
 late-type main-sequence and subgiant stars, HEAO 1 obs. of active cor- nae 0-72925  
 late-type stars, Ca II 8542 Å line as chromospheric activity indicator 0-62108  
 LMC X-1 optical candidate, spectrum and semi-accurate position 0-67908  
 α Lyrae (Vega), obs. with Solar Thermal Test Facility 0-77301  
 M1-2 central star, possible eclipsing binary in planetary nebula 0-105239  
 in M31, galaxy population synthesis models, nonuniqueness 0-82489  
 M32, stellar population spectral synthesis and galaxy age 0-67842  
 main-sequence reddened stars, ANS photometry, UV colours 0-77400  
 main-sequence stars, F to M-type, comparison of activity cycles to old and young stars 0-105235  
 main-sequence stars, Population I, luminosity functions in SA 51, SA 57 and (SA 68) 0-98648  
 mass flux fluctuation theory 0-72923  
 massive main-sequence stars, effects of convective and semiconvective mixing 0-90405  
 metal-deficient stars, subdwarf ionization equilibrium 0-90421

## stars continued

- metal-poor star distrib. in galactic halo- (*German*) 0-94867  
 MWC 349A, near-IR spectrographic obs. 0-94810  
 nearby objects, space astrometry 0-67518  
 nearby stars, gravitational effects on comet orbits evolution 0-98613  
 in NGC 205, stellar content rel. to UV flux 0-98716  
 NGC 6210, planetary nebula, central star, high dispersion EUV obs. and spectral type 0-77466  
 NGC 6494 (M23), open star cluster, membership from astrometry with PDS microdensitometer 0-98697  
 Northern stars, True Visual Magnitude Photographic Star Atlas 0-109376  
 O-type stars, assoc. with nebulosity rel. to galactic struct. 0-105236  
 O-type mass loss rate from UV spectra 0-82346  
 O-type runaway, extreme Population I nature 0-85938  
 O-type star in open cluster, interstellar dust ejection rel. to cluster dynam- ics 0-101622  
 O-type stars, C III 7901 to 9715 Å emission lines obs. 0-77401  
 O-type stars in NGC 7000 (North America Nebula), continuum scatt. rel. to rocket UV imagery 0-82440  
 OB3 type stars in young clusters, circumstellar matter 2200 Å hump interpretation 0-82351  
 OB stars in Circinus-Norma region, search for faint objects 0-62121  
 OB-type stars, radial vels. rel. to distance of Sun from galactic centre 0-101584  
 OB-type stars and interstellar medium, cloud formation theory, effect of eqns. of state 0-109506  
 OB-type stars assoc. with H II region DR15 radio component, obs. 0-94881  
 observation with Solar Thermal Test Facility 0-77301  
 occultation by Uranus and rings, 1980 August 15 to 16, obs. 0-98610  
 occultation of 13th magnitude star by Charon (1978 P 1), light curve obs. 0-94754  
 Of and O stars, reasons for difference in mass loss 0-90413  
 { Ophiuchi, 1980 March emission episode, Hα and He I line behaviour 0-62151  
 { Ophiuchi, interstellar <sup>12</sup>CH<sup>+</sup>/<sup>13</sup>CH<sup>+</sup> abundance ratio meas. 0-67809  
 { Ophiuchi (HR 6175), O-type star, emission line episode 0-72953  
 Orion population stars, OH emission survey 0-67716  
 θ<sup>2</sup> Orionis B, long-slit spectroscopy in rocket UV 0-105297  
 { Persei, interstellar <sup>12</sup>CH<sup>+</sup>/<sup>13</sup>CH<sup>+</sup> abundance ratio meas. 0-67809  
 photometric catalogues: present and future 0-105179  
 Pictis Austrinus, UBVR photoelectric sequence 0-62201  
 planetary nebulae central star, far UV flux determ. from nebula ionisation state 0-72945  
 planetary nebulae central stars, atmospheric models 0-109434  
 planetary nebulae central stars, hot wind model for nebulae refractory elements gas-phase abundances 0-109516  
 planetary nebulae central stars, interpretation of UV continuum radiation 0-109524  
 planetary nebulae central stars, spectra, temps., binaries and peculiar stars 0-109435  
 planetary nebulae nuclei, far UV fluxes rel. to nebulae ionisation and spectra 0-109529  
 planetary nebulae nuclei, He shell flashes rel. to nebulae ionisation 0-73021  
 planetary nebulae nuclei, models rel. to distances determined from ionised mass/radius relation 0-101625  
 planetary nebulae nuclei, stability anal. and short period oscills. prediction 0-77402  
 Population II (pregalactic) stars, rel. to distortion of cosmological micro- wave black body radiation spectrum 0-67915  
 position determ. on Schmidt plate, standard coord. and Stevenson's method 0-82176  
 positions, comprehensive general catalogue construction 0-105178  
 positions, general catalogue compilation, material evaluation 0-109375  
 pre main sequence stars, rapidly rotating, evolution in gravit. contraction phase 0-62133  
 presupernovae, stellar wind as possible cause of supernova remnant filamentary struct. 0-62249  
 protostars, magnetic, quasistatic contraction due to mag. flux leakage 0-98662  
 { Puppis, Reticon obs. of Hα P Cygni profile 0-82365  
 PZT stars, mean posns. and proper motions for 304 stars, obs. at Ondrej- ov 0-82175  
 quark stars, beta decay 0-82398  
 R 136 in 30 Doradus, struct., colour, mass and excitation parameter, photometry obs. (*German*) 0-67825  
 reddened stars, JHK photometry rel. to near IR interstellar reddening 0-94857  
 relativistic stars, struct. and stability of polytropic fluid spheres with negative index (*Chinese*) 0-57143  
 Rubin-152, possible massive O-type star on galactic fringe, spectroscopic obs. 0-98656  
 S-type stars, Keenan band identification problem, IR obs. 0-72946  
 SAO 75392, occultation by 78 Diana, 1980 September 4, predicted central path revision 0-101547  
 SB 21, extremely He rich subdwarf O-star, spectrum 0-98659  
 shell stars in cluster near IC 1805, photometry and spectral classes 0-62214  
 South Celestial Pole stars, extinction and colour coeffs. UBVR photoelec. sequence 0-77456  
 southern standard stars, 320-880 nm energy distrib. 0-62125  
 in spiral galaxies, vel. dispersion determ. (*Chinese*) 0-85995  
 stellar populations in galaxies, mixing processes in galaxy mergers 0-67860  
 stellar wind, theory of classical fluid dynamics 0-90412  
 Stokes' problem, mass transfer effects of MHD free convective flow 0-62003  
 subdwarfs in 47 Tucanae, CN vars. 0-94794  
 20 Tauri, interstellar <sup>12</sup>CH<sup>+</sup>/<sup>13</sup>CH<sup>+</sup> abundance ratio meas. 0-67809  
 T Tauri stars, Hα and Na I D lines high-resolution profiles 0-62116  
 Tokyo Astronomical Obs., Time and Latitude Bulletins (April/June 1979) 0-72752  
 Tokyo Astronomical Obs., Time and Latitude Bulletins (Jul-Sep 1979) 0-82177  
 Tokyo Astronomical Observatory Time and Latitude Service, Bulletin (January to March 1979) 0-72751  
 trigonometric parallaxes, freq. distrib. and systematic effects 0-94785  
 Trumpler 27 star 28, obs. of WC9-type star with large IR excess 0-67738

- stars continued**  
 UV photoelectric sequence for studies of NGC 55 galaxy 0-73007  
 UV spectra of standard stars, IUE photometric calibration 0-77383  
 Vilnius photometric catalogue on mag. tape, description 0-98578  
 WC stars, near IR spectrometry 0-94816  
 winds from OB associations, interaction with interstellar medium to form  
   H I supershells 0-82468  
 Wolf-Rayet, single-line Population I stars, space vel. 0-77415  
 Wolf-Rayet atmospheres, structure and composition 0-98668  
 Wolf-Rayet stars, evolutionary status of high-luminosity (WN7/WN8)  
   stars (*Russian*) 0-109425  
 Wolf-Rayet stars, interstellar N V lines, IUE obs. 0-101634  
 Wolf-Rayet stars, short-lived changes of emission lines (*Russian*)  
   0-72977  
 XUV sources, candidate types review (*German*) 0-109372  
 young stars in galaxy NGC 4314, distrib. from UVB surface photometry  
   of central region 0-77482  
 H $\alpha$  emission line stars in nebulae, rel. to galactic spiral struct. in vicinity  
   of Sun (*Russian*) 0-62290  
 H $\alpha$  stars in NGC 2264 and NGC 7000/IC 5070, slitless spectrographic  
   search 0-62120  
 OH type I maser sources, model 0-90556
- state estimation**  
 nuclear materials accountability enhancement in first solvent extraction  
   cycle, modern techniques 0-83216  
 one dimensional distributed parameter system parameter and state estima-  
   tion, heat conduction experimental result (*Japanese*) 0-83727  
 sonar array paired element delay meas. with sequential state estimation  
   0-96128
- state of the art studies** *see reviews*
- static (atmospherics)** *see atmospherics*
- static electricity** *see electrostatics*
- static electrification**  
*see also triboelectricity*  
 electrostatic charges meas. and localisation, neutralised during lightning  
   flashes 0-77097  
 insulating films, PET and SiO<sub>2</sub>, charge effects at Al electrodes obs.  
   0-75625  
 insulators, expts. with solid rare gases 0-70797  
 metal surface heated, charge separation from electrolyte drops 0-88617  
 moving fluids, progress up to 1979 0-69292  
 paper sheets, charge decay and resistance parameters correlation determ.  
   0-70795  
 polymer surfaces charging injection times obs., with aid of computer  
   0-70796  
 polymers, frictional electrification, temp. and friction speed dependence  
   obs. 0-70798  
 polymers by metals, contact time effect obs. 0-70829  
 spark hazard in charged powder handling, identification and control  
   0-69291  
 surface analysis techniques appl. 0-80354  
 Hg-polymer interface, contact potential and charge exchange meas.  
   0-75642
- statics**  
*see also hydrostatics*  
 No entries
- stations, power** *see power stations*
- statistical analysis**  
*see also demography; measurement errors; probability; random processes; statistical theory of nuclear reactions and scattering*  
 accidents during work, mapping of reasons using error beams by function  
   sensed computations of admission probabilities (*German*) 0-68027  
 acoustic-emission pulse distrib., statistical investigation 0-87638  
 alloys, criteria of chemical inhomogeneity 0-59670  
 analytic theory of extrema, appl. to nonlinear oscillators 0-73160  
 atmosphere visibility trends, appl. of ridit anal. 0-82051  
 autoregressive analysis, a method for detect. of EEG changes in newborns  
   to tones 0-108982  
 bandwidth compression effect on military target observers' detection and  
   recognition performance 0-106484  
 beach changes in S. California, statistical prediction 0-98305  
 binary image statistical modelling, enhancement and recognition (*Russian*)  
   0-63929  
 binary stars, statistical distrib. and evolution (*Chinese*) 0-85975  
 Bingham distrib. function in palaeomagnetic studies 0-72649  
 brittle ceramics, effect of data scatter on apparent thermal stress failure  
   mode 0-60949  
 CECG waveform, statistical algorithm and struct. anal. 0-72341  
 Collinder 140, young open star cluster, membership statistics from spectro-  
   scopic study 0-62211  
 complete computer program in FORTRAN, for analysis of variance and  
   means 0-98792  
 composite materials, stochastic fracture models, and strength test results  
   statistical anal. 0-64470  
 creep, fatigue and fracture data analysis, statistical methods 0-58936  
 creep rupture data analysis, development of correlation and extrapolation  
   methods 0-58975  
 daily solar total irr. fluctuations, temporal statistical anal. (*French*)  
   0-61292  
 data volume determ., based on risk for arbitrary volume of a priori data  
   0-95054  
 earthquakes, damaging, and volcanic eruptions in Iceland, 1550 to 1978,  
   statistical anal. 0-89975  
 EEG, topographical display of epileptiform transients based on a statistical  
   approach 0-108833  
 EEG 0-85504  
 electron microscopy, correlation analysis of radiation damage 0-100282  
 EM wave propagation, in one-dimensional, randomly inhomogeneous  
   medium, with specularly reflecting walls 0-105514  
 EM waves scattering, in nonlinear medium with one-dimensional random  
   nonuniformities 0-106421  
 endogenous and exogenous activity in molluscan neurone, identification by  
   spike train anal. 0-89735  
 error definition for data acquisition systems, in steady and unsteady states  
   0-95056  
 exponential distribution MTBF confidence limits determ. using Epstein  
   and Harters methods 0-98790  
 fatigue test data, statistical anal. (*Japanese*) 0-62452  
 flat galaxies dynamical struct., statistical characts. 0-62269
- statistical analysis continued**  
 fragile materials, mech. props. and fracture mech. (*French*) 0-104274  
 galaxy clustering 0-105363  
 Gaussian function approximation using Weibull's distribution function  
   (*Czech*) 0-57083  
 global solar radiation est. and prediction by stepwise multiple regression  
   anal. for Greece (1961 to 1975) 0-61880  
 Hertzian fracture of Pyrex glass using Weibull distribution function  
   0-66623  
 hierarchical systems, calibration errors influence on end item performance  
   0-98788  
 homogeneous turbulence, with internal rotations, theory 0-69772  
 impact toughness test results, cold brittleness crit. temps. determ.  
   0-100980  
 inviscid flow on sphere, statistical mech., atm. appl. 0-90152  
 jets, two-dimensional water, sensitive to sound, behaviour (*Japanese*)  
   0-79376  
 lifetimes and numbers of groups, predictions from statistical anal.  
   0-82327  
 linear regression model, pollutant gas analysis, defining conc. relationships  
   0-61486  
 linear state estimator design, updating budget, meas. theory 0-95058  
 linear system with nondelta-correlated parameter fluctuations, statistical  
   anal. 0-95036  
 linear systems acted upon by Poisson processes 0-57196  
 LMFBR HCDA analysis, uncertainty in accident consequences calculated  
   by large codes due to uncertainties in input 0-78413  
 materials testing, planning and evaluation by statistical methods (*German*)  
   0-93725  
 mean value test, acceptance charact. with prior knowledge of standard  
   deviation (*German*) 0-77605  
 mechanics, structural steel, type St3S, hardness, random functions  
   0-76329  
 metals, creep limit and long-term strength, parametric eval. method  
   0-100996  
 microgeometry of stylus roughness tested surfaces, influence of stylus tip  
   geometry on meas. (*German*) 0-68182  
 multipath neural systems method 0-101162  
 multiphoton detectors of laser radiation, statistical characts. 0-86408  
 multiple comparisons for Poisson rates 0-98789  
 multivariate joint probability expression of general random processes,  
   finite expansion terms 0-69592  
 nonlinear statistical theories, fluctuation effects, truncation schemes of  
   cumulant hierarchies 0-68133  
 nuclear materials safeguarding, diverse forms of fissile material, large  
   stocks verification 0-73932  
 nuclear materials safeguarding, optimal estimates of inventory and losses  
   using nuclear material accountability data 0-68818  
 nuclear materials safeguarding, statistical anal. of materials accountability,  
   computer simulation 0-73933  
 nuclear power plants, operator performance and response time, stress  
   degradation, Poisson model 0-63415  
 nuclear reactor surveillance, pattern recognition techniques appl. 0-63351  
 ocean high-frequency internal waves, anal. of energy partition among wave  
   modes 0-98330  
 optical fibre signal polarisation statistical meas. 0-99877  
 optical fibres, tensile strength and static fatigue, analysis using Weibull  
   distribution for optimum design 0-85011  
 optical instrument control life test design 0-87572  
 partitioned sub-optimal linear estimator, separate channel implementation  
   0-94949  
 Pb airborne particulate concentration variation at two stations in Perth,  
   1974-76 period 0-94127  
 period analysis at high noise level 0-73263  
 planet surfaces, appl. of statistical methods 0-101540  
 polymers, atmospheric resistance, distrib. function determ. and anal. (*Ger-  
   man*) 0-81225  
 probabilities of error in research statistical interpretation 0-90658  
 quantum chemistry, matching model calcs. with experiment through linear  
   regression 0-58243  
 quantum system, nonintegrable, irregular part of discrete energy spectrum,  
   statistical theory 0-82667  
 quasars brightnesses, correl. anal. of depend. on parameter  $\ln(1+z)$   
   0-105382  
 radioactive waste geologic disposal, safety anal., functional relations of  
   risk to input data uncertainties 0-83189  
 radiological assessment of inactive nuclear sites, statistical design and  
   anal. 0-95473  
 radionuclides, short-lived, meas., counting statistics 0-58098  
 radiosources of intermediate strength, statistical props. 0-62303  
 random vibrations, statistical data digital processing method (*Japanese*)  
   0-64430  
 random-phase screens, deep, interferometric anal. 0-101834  
 reactor cooling channels, flow anomaly diagnosis, autoregressive model  
   appl. (*Japanese*) 0-83146  
 redshift distribution of extragalactic objects, rel. to evolution of galaxies  
   0-90527  
 refractory metals, group V, diffusions of O and N, statistical calculations  
   on Arrhenius lines 0-59722  
 regression line analysis, teaching 0-73144  
 Rome road traffic noise, 24-hour obs. and statistical analysis (*Italian*)  
   0-87651  
 sample sizes for comparing two proportions 0-98791  
 sign test and Wald's sequential analysis, appl. to expt. investigations  
   0-57082  
 Skylab conical multispectral scanner IR data statistics 0-90223  
 solar point focusing concentrators, effects of tracking errors on perfor-  
   mance, statistical anal. of intercept factor 0-61302  
 solar wind velocity recurrence period, depend. on heliographic latit.  
   0-62106  
 solar-radiation regime, energy structure distribution laws analytic  
   representation 0-98378  
 speckle statistical props. and coherence aspects 0-78773  
 spectroscopic binaries, orbital elements statistical anal. 0-82422  
 star fields and configurations 0-82224  
 stars space densities derivation, new method 0-85932  
 steel, alloy X8CrNiNb1613, creep limit and long-term strength, param-  
   etric eval. method 0-100996  
 stellar trigonometric parallaxes, freq. distrib. and systematic effects  
   0-94785  
 surface irregularities, deformation under static loads 0-58985



**statistical analysis continued**

- ternary system compound formation, comp. and props. w.r.t. component electron struct., computer prediction 0-103444
- thin island films, statistical theory for dielectric props. 0-80699
- transformation of nonlinear variables in construction of statistical models, review 0-57081
- transient electrical transport, general and unified treatment 0-59977
- transmission loss estimation of sound absorbent panels, statistical energy analysis 0-64278
- turbulent diffusion, of passive scalar magnitude (*French*) 0-69778
- two-dimensional optical system MTF meas. by second-order speckle statistics computation 0-74304
- Van der Waals equation, statistical anal. of  $RT_c/P_cV_c$  (*Spanish*) 0-74213
- volcanic eruptions and damaging earthquakes in Iceland, 1550 to 1978, statistical anal. 0-89975
- water, compressed, thermodynamic props., evaluation by statistical error anal. 0-92685
- wave propagation in randomly inhomogeneous media, quasi-optical parabolic approx., validity analysis 0-106422
- wave reflected from randomly inhomogeneous layer description, by series satisfying causality condition 0-106420
- Weiner-Einstein processes, Markov, maxima and first-passage-time statistics 0-68134
- wind fields, mesoscale, satellite-derived, covariance anal. 0-82013
- wood, fracture toughness variations with specimen size, statistical approach 0-100889
- Cu, high purity, creep cavitation topology, high temperature region (*Czech*) 0-65138
- H II regions density fluctuations, statistical approach 0-77468
- H+H<sub>2</sub>, reaction probability, max. entropy derivation, statistical theories 0-66781
- H<sub>2</sub>, statistical fluctuations in ionisation yield, rel. to electron degradation spectrum 0-99581
- Pu dose to lung and bone from contaminated soils, statistical uncertainties 0-109028
- Si solar cells, production process effect on fracture strength 0-93656

**statistical distributions** *see statistical analysis; statistics***statistical mechanics**

- see also classical theories of fluid structure; lattice theory and statistics; Liouville equation; liquid theory; master equation; quantum statistical mechanics; renormalisation*
- anharmonic oscillator, classical, variational method test, sp. ht., elec. susceptibility and oscillation freq. (*Portuguese*) 0-77611
- anharmonic system, superstability, probability estimates for correlation functions 0-82708
- antiferromagnet, linear-chain, sine-Gordon solitons 0-80543
- BBGKY system, irreversibility, velocity correlations and non-Hamiltonian dynamics 0-77686
- biodynamics, Hamiltonian content 0-89704
- charge fluctuations in classical Coulomb systems 0-95027
- chemical system, equilibrium fluctuations, deviations from Poisson behaviour, molecular dynamics 0-86211
- classical system with long-range forces, eqn. props., BBGKY eqn., neutrality, screening, sum rules 0-62569
- compressed gas, radial distrib. function hard sphere model 0-69961
- constrained systems, Hamiltonian construction and diffusion eqns. derivation 0-73258
- converse to Koopman's lemma 0-98851
- correlation function, long time asymptotic behaviour, influence of waves on relax. processes (*Chinese*) 0-59195
- Coulomb gas, 2-D, equilibrium props. and phase transition, hard core, neutral dipolar pairs 0-62567
- Coulomb gas 2-D, interaction potential, screening length, critical temp. 0-62571
- Coulomb system, Debye screening 0-73256
- crystal orientational disordering, thermodynamic props., stat. mech. model 0-96453
- deterministic dynamics to probabilistic descriptions 0-68029
- dilute solute-binary solvent activity coeffs., statistical mech. theory 0-59663
- dislocations, thermodynamics and thermal activation, book contrib. 0-107241
- dissipative system, chaotic flow, fractal dimensions, vortex stretching, cascade model 0-73176
- Enskog quasiparticle, non-Hamiltonian dynamics 0-101750
- Fokker-Planck equation with spatial coordinate-dependent moments, path integral soln. 0-77688
- free asymmetric rotors, classical system, second rank tensors, ang. correl. functions 0-64865
- gas, monatomic, time average problem, statistical entropy change over constant energy path 0-68123
- granular materials, random packing, statistical mech. considerations 0-104088
- granular materials, shear deformation, entropy model 0-84233
- hard rods, attractive interactions, scaled particle theory 0-82735
- hard sphere gas mixture, vel. autocorrelation function calc. 0-75019
- hard spheres in thermal eqn., time correlation functions in low-density limit 0-64859
- hard-sphere systems, statistical geometry 0-95028
- harmonic oscillators, flexible and rigid constraints 0-90773
- Henon mapping, topological horseshoe, chaotic behaviour 0-73257
- hydrodynamical fluctuation theory far from equilibrium 0-98856
- infinite crystal, classical statistical mechanics 0-107067
- information theoretic approach, expl. and inherent uncertainties 0-82733
- interionic force pot. in ideal dipolar gas 0-96330
- ionic systems, hard spheres, mean spherical approx. radial distrib. function 0-62570
- kinetic equations from Hamiltonian dynamics: Markovian limits 0-95029
- Landau equation, non-Markovian terms 0-79432
- linear response, approx. method of calc. (*Russian*) 0-77685
- liquid-vapour coexistence and correlations in interface 0-65212
- liquids and mixtures, statistical thermodynamics, book 0-90616
- macromolecular systems, statistical thermodynamic analysis, heat capacity function 0-61514
- macroscopic theory of statistical thermodynamics 0-105567
- Markov process generated by Langevin equations, WKB-type expansion 0-86212
- memory alloy, pseudoelectric, model for first-order phase transition 0-92642

**statistical mechanics continued**

- molecular dissociation, RRKM formula correction by non Boltzmann character factors, Markov eqns. 0-71891
- molecular dynamics simulations at constant pressure and/or temperature 0-64852
- moment and Fokker-Planck eqns. for growth and decay of small objects 0-82709
- multiple approximations, Hilbert-Pade method, appl. to Gaussian function 0-82707
- N interacting particle canonical distrib. from kinetic theory 0-105569
- nonequilibrium fluctuations in driven systems 0-86210
- nonlinear systems, dynamics, heavy damping limit 0-86199
- open systems, eqns. of motion in nonequilibrium. statistical mechanics 0-82710
- periodic density patterns as uniform fluid crystallizes 0-107404
- physical adsorption in condensed phases statistical mechanics 0-84365
- polymer chains, helical wormlike, statistical mechanics, anisotropic light scatt. near the rod limit 0-93346
- polymer solution, osmotic pressure, correlation functions, in grand canonical formalism 0-100159
- polymer solution, Rayleigh scattering, intermolecular correlations effect 0-75146
- polymers in poor solvent, loop expansion of irreducible diagrams 0-100160
- Potts model, hierarchical, three-state, high temp. susceptibilities 0-77723
- principle of maximum entropy and irreversible processes, review 0-86198
- random matrix ensembles, joint eigenvalue distrib. 0-101748
- randomly driven system, strong coupling expansion for classical statistical dynamics 0-105568
- rate processes in condensed media, master eqns. 0-77687
- real fluids, short range repulsions and long range attractions, simple pair pot. model 0-64850
- relation to fluid mechanics, book contrib. 0-94959
- replica method for amorphous materials 0-86197
- Saha equation, elementary derivation, rel. to mol. dissociation 0-82599
- self-avoiding walks with span limitations, cubic lattice, mean square end-to-end distance 0-62568
- simplified hydrodynamic theory of nonlocal stationary state fluctuations 0-98857
- solid state physics, contrib. of Conyers Herring in 1930s 0-57056
- solitons in condensed matter: a paradigm, review 0-77632
- stellar turbulent convection equations, ensemble averaging 0-67698
- sufficiency and its role in the macroscopic description 0-57171
- time-dependent pair distribution in the mean-field approximation 0-77689
- triatomic molecules, C<sub>2</sub>, symm., vector statistical distrib., mol. dynamics computer simulation 0-63734
- vortex-acoustic ion wave turbulence, statistical mechanics 0-92326
- X-ray structure amplitude phases, statistical-thermodynamic determ. 0-84028
- Mn-bearing binary substitutional alloy systems, props., applicability of statistical thermodynamic approach 0-88336
- Ni-S, phase diagram calc. and thermodynamic props. of liq. phase 0-108401

**statistical methods** *see statistical analysis***statistical models**

- additive quark model and multiparticle production off emulsion nuclei at 50 GeV 0-68491
- atmospheric radio noise statistical models for reception in VLF band 0-72611
- bag model, isobaric ensemble and multiplicity distrib. (*Russian*) 0-82952
- bottom meson nonleptonic decay, many body final states, isospin-statistical models 0-62975
- cluster decomposition of many dimens. phase space, appl. to high energy collisions 0-102027
- composite particles, nonrelativistic many-body theory, foundations and statistical mechanics 0-82947
- cumulative hadron production, statistical bootstrap model with strangeness (*Russian*) 0-62948
- diffraction hadronic reactions, statistical description of multipion prod. 0-95260
- double-logarithmic quark and form factors and the evolution of parton jets 0-68421
- fireball model three component, appl. to pp interactions above 9 GeV 0-62946
- fluid droplet model of tachyons in framework of two centres particles 0-105868
- gluon fragmentation, polarised, in  $e^+e^-$ ,  $e^-q$  and hadron scattering 0-82988
- hadron + hadron, cluster model, field theoretic, multiperipheral production, Feynman scaling violation 0-57576
- hadron + nucleus, spatial temporal development, nuclear hadronic cascades 0-63040
- hadron induced multiparticle reactions, S-1500 GeV, resonance prod. correlations, jet model (*German*) 0-91118
- hadron inelastic scatt., secondary hadron multiplicity distribution, Regge like parton model (*Russian*) 0-78100
- hadron interactions, inclusive, large momentum transfer, quark counting, EM form factors 0-68498
- hadron interactions, inclusive processes, multiplicity and scaling, resonance production, additive quark model, SU(6) theory, review 0-63043
- hadron production, inclusive, quark fragmentation and triple Regge models, quark decay functions 0-62921
- hadron scatt. mediated by  $q\bar{q}$ - $q\bar{q}$  and  $g\bar{g}$ - $g\bar{g}$  0-82988
- hadron-induced and  $e^+e^-$  annihilation, multiplicity ratio 0-105877
- hadronic collisions, jet structure, two-jet events, glueball-Pomeron identity, dual field theory 0-63051
- hadronic events, inelastic, non-diffractive, charge correlations in jets, quantum number effects 0-86764
- hadronic lepton pair production, QCD jets 0-62994
- hadronic matter, anisotropic superfluidity, analytic formulation 0-105869
- higher order QCD jets in photoproduction 0-99087
- hydrodynamical model, resonance prod. (*Russian*) 0-62947
- inclusive distribution, transverse momentum correlations for secondaries, rapidity cluster, stat. model 0-73754
- inelastic processes, cluster model with repulsion and correlation anal. (*Russian*) 0-102026
- interacting instanton-antiinstanton system under external colour mag. fields in SU(2) gauge 0-101920

**statistical models continued**

- intermediate vector boson decay, QED and QCD radiative corrections, hadronic jets 0-73759  
 jet decay models, group-theoretical and four-momentum variables 0-73684  
 jet phenomenon and Lorentz deformation 0-105806  
 jet production on nuclei, strong A depend. (*Russian*) 0-102084  
 jet structures of leptons, quarks and gluons, perturbative QCD, process dependence 0-68470  
 jets of quarks and gluons, leading logarithmic approx., parton interpretation 0-68433  
 Kopylov-Podgoretsky-Cocconi formulation modification for hadron-hadron collisions 0-78044  
 lepton+nucleon, quark and gluon jets, Breit frame, QCD 0-62995  
 local number fluctuation in multiparticle production 0-57574  
 nonperturbative gluon jet model, gluon fragments, meson prod. 0-68420  
 pp collisions, high energy, fireball mass, rapidity, spin distrib. 0-57645  
 QCD, parton jet and shower model 0-86663  
 QCD hadron jets, branching processes, multiplicity distrib., KNO scaling (*Russian*) 0-101998  
 QCD jet fragmentation functions in leading log approx. 0-101981  
 qCD scattering processes with hard gluon emission, jet prod. 0-62939  
 quark fragmentation functions for inclusive hadron production, Regge formalism 0-68462  
 quark fragmentation jets in QCD, cascade model 0-78045  
 resonance vertex functions and scatt. amplitudes resonance-nucleon scatt. p rescatt. (*Russian*) 0-105918  
 road traffic noise, relationships between multidimens. correlation props. of intensity and higher order information, Stratonovich's stochastic theory for random points system 0-87645  
 valence quark clusters in nucleon structure functions from neutrino scatt. 0-95252  
 $e^+e^-$  0-63010  
 $e^+e^-$  annihilation, 10 to 40 GeV, hadron multiplicity 0-63007  
 $e^+e^-$  annihilation, hadron multiplicity distribution, Regge like parton model (*Russian*) 0-78100  
 $e^+e^-$  annihilation, jets, colour-singlet subsystems, large rapidity gaps 0-68469  
 $e^+e^-$  annihilation, quark fragmentation in field-theoretic model of composite hadrons 0-82986  
 $e^+e^-$  annihilation and hadron-induced events, multiplicity ratio 0-105877  
 $e^+e^-$  final states, qq decay, semiclassical model, vacuum polarisation by colour field 0-63011  
 $e^+e^-$  jets, particle ratios from quark statistical model 0-73724  
 $e^+e^-$  jets, two-particle distrib. from single-particle fragmentation functions, effects of heavy quark flavours 0-68468  
 $e^+e^-$  qqg, (3g), jet-mass spectra, perturbative QCD 0-63006  
 $e^+e^-$  qqg, gluon fragmentation, polarised 0-82988  
eq-egg, gluon fragmentation, polarised 0-82988  
 $\gamma N$ -jet+X, QCD cross sections 0-73715  
 $\gamma p \rightarrow \pi^+ \pi^- \pi^+ \pi^- p$ , diffractive production, jet-like structure 0-57606  
in deep inelastic scattering, quark jet as trigger for gluon jet 0-62996  
 $K^+p \rightarrow \pi^+ \pi^- X$ , 32 GeV/c, two-pion correlations, Monte Carlo model 0-83008  
 $K^+p$ , fireball model, universal scaling function 0-57646  
 $\mu^-N$ -hadron shower, charm-pair production effects 0-73748  
NN,  $10^{12}$  eV, rapidity gap distrib., Snider multiperipheral cluster model 0-73757  
NN-( $\pi, \rho, \omega, f$ ), statistical model 0-102028  
 $\rho N$ -hadron shower, charm-pair production effects 0-73748  
 $pN$ -hadron shower, charm-pair production effects 0-73748  
pp, probabilistic quark-model approach to p fragmentation 0-63049  
pp annihilation cross sections, corrected differences, fireball model, diffraction cross sections 0-91108  
pp annihilations, multipion distrib., statistical bootstrap model 0-68472  
pp-CX,  $C=\pi^2, K^2, \beta$ , scaling-in-the-mean hypothesis 0-68497  
pp-hadrons, phase transition in Feynman-Wilson analogue fluid, multiplicities, plateaux, cross-sections 0-73744  
pp-mesons, multimeson inclusive spectra and recombination model, multi-quark structure functions 0-73751  
pp multiplicities, viscosity effect in Landau hydrodynamical model 0-63055  
pp-pX, 205 GeV/c, leading p spectrum, random walk hypothesis, geometric bremsstrahlung model 0-68493  
pp-pp, large momentum transfer, multiple-scattering model, three-quark proton 0-63031  
pp-pp, large momentum transfer, multiple-scattering model, three-quark proton 0-63031  
 $\pi^+p$ , fireball model, universal scaling function 0-57646  
 $\pi\pi$  interactions, dominant resonances, pole positions, partial waves 0-63020  
 $T(946)$  orthoquarkonium decay, jet profiles, three gluon structure 0-73698  
 $e^+e^-$  annihilation, quark jets, transverse momentum profile 0-57621  
 $e^+e^-$ , high energy interactions (*Chinese*) 0-78074  
Y-3g, angular patterns and front-back moments, QCD 0-73702

**statistical tests** see statistical analysis**statistical theory** see statistical analysis**statistical theory of nuclear reactions and scattering**

- $\alpha$ -clustering in heavy nuclei, pre-equil. model, nuclear matter NN, N $\alpha$  interactions 0-63111  
 A=24-108, level widths in charged particle induced reactions, stat. anal. 0-68535  
 astrophysics, nuclear reactions in dense plasmas, simple classical fluids theory 0-75141  
 average fluctuation cross section from unitary analytic K-matrix 0-102172  
 baryonic inclusive spectra in hadron-, photon- and HI-nucleus collisions, fireball model 0-86892  
 central nuclear collisions, standard deviation of  $\pi$  multiplicity (*Russian*) 0-73864  
 channel averages and energy averaged cross section relation 0-68634  
 compound nucleus theory, recent developments, review, book contrib. 0-68636  
 compressible nuclei, surface energy 0-83031  
 deformed and superdeformed nuclei from heavy ion reactions,  $\alpha$ -decay amplification 0-102156  
 doubly even nuclei, yrast band B(E2) values, hydrodynamical model and CAP effect 0-86793  
 electric multipole modes in the fluid-dynamical approximation 0-106029

**statistical theory of nuclear reactions and scattering continued**

- energy dissipation in heavy-ion collisions 0-106038  
 entropy approach to statistical nuclear reactions 0-102173  
 equilibration process, master eqn. and closed form approaches 0-99166  
 fission, saddle point, statistical fluctuations, Suzuki's scaling limit 0-86946  
 fission barrier props., expt. studies and statistical anal. review 0-102216  
 fission reactions, fragment excitation, prompt neutron distrib., renormalised gas model calcs. 0-99169  
 fissionability, target mass depend. for  $\pi, \gamma, \alpha, p$ , cascade-evaporation and liquid drop calcs. (*Russian*) 0-106089  
 Glauber approx. anal. of high energy heavy ion collisions 0-106039  
 hadron+nucleus, spatial temporal development, nuclear hadronic cascades 0-63040  
 hadron induced fission, low energy evaporative particle emission from emulsion nuclei (*Russian*) 0-86943  
 hadron-nucleus collision, cascade model, space-time model 0-68633  
 head on heavy ion collisions, compression and temp. extremes, nuclear matter phase changes (*Russian*) 0-83121  
 heavy ion collisions, energy dissipation and the stochastic process 0-106040  
 heavy ion collisions, generalised master eqn., drift and diffusion coeffs. 0-106075  
 heavy ion collisions, mass transfer, kinetic energy, comparison with hydrodynamic and microscopic calcs. 0-57787  
 heavy ion deep inelastic collision processes, optical model description, statistical considerations 0-68687  
 heavy ion fusion reactions, statistical yrast line 0-86948  
 heavy ion reactions, 10-200 MeV/N, Markovian and non-Markovian effects in transition probabilities 0-102175  
 heavy ion reactions, coherence angle and cross section fluctuations correlation function, resonances 0-57790  
 heavy ion-light particle angular correlation, forward peaked, light particle emission from l-windows 0-63142  
 ion-ion interaction pot., real part energy depend., antisymmetrization effects, Fermi gas model 0-83120  
 lepton-nucleus collision, cascade model, space-time model 0-68633  
 level density in large spectroscopic spaces, statistical spectroscopic methods 0-86814  
 many-body problem, classical hydrodynamics and collective motion approx. 0-83027  
 maximum entropy approach, analyticity and ergodicity 0-68635  
 multi-chance high-spin fission, fragment anisotropy, stat. model anal. 0-57812  
 multistep compound cross section from Markovian processes 0-83090  
 multistep compound processes, autocorrelation function, average fluctuation cross section, different theoretical approaches 0-78234  
 neutron capture, total radiative width and degree of freedom, statistical model calcs. 0-57732  
 neutron resonance data, statistical anal. method 0-102174  
 photon-nucleus collision, cascade model, space-time model 0-68633  
 preequilibrium reactions, angular distrib. theoretical models (*Russian*) 0-68690  
 quantum fluctuations and quantum mechanical distrib., heavy ion physics appl. 0-78264  
 relativistic central heavy ion collisions, spherical and linear fluid dynamical models 0-86926  
 relativistic heavy ion collisions, central and peripheral, p emission patterns 0-73860  
 relativistic heavy ion collisions, d prod. mechanism, three models, fireball rate eqns. 0-63198  
 relativistic nuclear collisions, pulsating blobs of quark matter in hydrodynamical model 0-83122  
 relativistic nuclei collisions, multi-hadron prod. mechanism 0-57763  
 stellar environment, nucl. struct. and reactions 0-72765  
 supercharged nucleus screening, relativistic Thomas-Fermi model, comments 0-91170  
 Thomas-Fermi kinetic-energy density with gradient corrections 0-91169  
 ( $\gamma, n$ ), preequilibrium exciton model with evaporative component, photoneutron spectra, giant resonances 0-57762  
 ( $n, \alpha$ ) with resonance neutrons, properties of highly-excited states of nuclei (*Russian*) 0-106053  
 ( $n, \gamma$ ), ( $n, \gamma$ ), low energy  $\gamma$ -transitions between compound states, statistical theory 0-57737  
 ( $n, n$ ), A=90 region, elastic, inelastic and total cross section, statistical model calcs. 0-68674  
 ( $n, n$ ), 14.6 MeV, ang. distrib., preequil. and equil. neutron emission, unified model 0-86891  
 ( $n, X$ ) X=p, 2n, 3n, precompound and compound emission mechanisms 0-102176  
 ( $p, n$ ), A=90 region, reaction cross section, statistical model calcs. 0-68674  
 ( $p, p'$ ), compound nucleus lifetimes from X-ray method, statistical properties 0-78295  
 ( $p, X$ ), 200 GeV/c in emulsion, fireball parameters and  $\pi$  emission 0-95317  
 ( $p, X$ ), hydrodynamic model 0-68671  
 ( $p, X$ ), total reaction cross sections, microscopic description 0-95318  
<sup>21</sup>Al( $n, \alpha$ ), 14.8 MeV, expt. and statistical model determ. of  $\alpha$ -prod. in fusion reactors 0-95397  
<sup>27</sup>Al( $p, n$ )<sup>27</sup>Si, cross sections and thermonuclear reaction rates 0-73852  
<sup>19</sup>Au(<sup>16</sup>O, p)X, 315 MeV, high energy p emission, fireball and preequilibrium anal. 0-91194  
<sup>19</sup>Au(<sup>20</sup>Ne, X), exactly central heavy-ion collisions by nuclear hydrodynamics 0-68690  
<sup>19</sup>Au( $p, ^4$ He x), 72 MeV, pre-equilibrium emission (*German*) 0-68657  
<sup>19</sup>Au( $p, \alpha$ ), 72 MeV, pre-equilibrium emission (*German*) 0-68657  
<sup>208</sup>Bi(<sup>16</sup>Xe, X), deeply inelastic collisions, mass transport, shell effects 0-99188  
<sup>12</sup>C(<sup>12</sup>C, X), two fireball model, pp correlations and inclusive pion spectrum 0-68694  
<sup>12</sup>C(<sup>12</sup>C,  $\alpha$ ), 7-15 MeV, excitation function statistical anal., nonstatistical features 0-99167  
<sup>12</sup>C(<sup>28</sup>Si,  $\alpha$ X), 87-91.5 MeV,  $\alpha$ -HI angular correlations, excitation functions, statistical anal. 0-86915  
<sup>12</sup>C( $p, p$ ), 122 MeV, precritical phenomena 0-83089  
<sup>13</sup>C(<sup>16</sup>O, X), 11.6 MeV, p.t.d., <sup>8</sup>Be ang. distrib., Hauser-Feshbach and DWBA anal. 0-91193  
<sup>40</sup>Ca(d, d), 4.5-5.4 MeV, excited states, excitation functions and ang. distrib., statistical anal. 0-57686



## statistical theory of nuclear reactions and scattering continued

- <sup>41</sup>Ca excited states, excitation functions and ang. distrib., statistical anal. from <sup>40</sup>Ca(d,p) 0-57686  
 Co(p,<sup>3</sup>He x), 72 MeV, pre-equilibrium emission (*German*) 0-68657  
 Co(p,αx), 72 MeV, pre-equilibrium emission (*German*) 0-68657  
<sup>4</sup>Cr(p,p), A=50, 52, 6 MeV, elastic and inelastic differential cross sections, spin flip probability (*Russian*) 0-91187  
<sup>6</sup>Cu(n,α), A=63.65, 14.8 MeV, expt. and statistical model determ. of α-prod. in fusion reactions 0-95397  
<sup>16</sup>Er(<sup>8</sup>K,X), deep inelastic collision, charge drift and dispersion calc., thermal eqn. model based on shell model 0-57798  
<sup>166</sup>Er(<sup>86</sup>Kr,X), 5.1-7.9 MeV/N, deep inelastic neutron emission, pre-equilibrium effects search 0-63200  
<sup>4</sup>Fe(p,p'), A=54, 56, 6 MeV, resonances, spin flip and cross section depends., Hauser-Feshbach anal. (*Russian*) 0-83084  
<sup>56</sup>Fe(<sup>32</sup>Cr, X), entrance channel mass asymmetry effects on reaction mechanism, fission and fusion 0-106077  
<sup>56</sup>Fe(x), isobaric charge distrib., energy loss depend. in damped collisions 0-99182  
<sup>56</sup>Fe(p,p), 6 MeV, elastic and inelastic, quadrupole deformation, IAR excitation, optical pots. (*Russian*) 0-63149  
<sup>252</sup>Fm, pot. energy surface, liquid model, deformation energy formulae (*Chinese*) 0-102106  
<sup>194</sup>Hg, α evaporation spectrum 0-68715  
<sup>252</sup>Mg(p,n)<sup>252</sup>Al, cross sections and thermonuclear reaction rates 0-73852  
<sup>92</sup>Mo(<sup>8</sup>O,X), entrance channel mass asymmetry effects on reaction mechanism, fission and fusion 0-106077  
 (N,X), disintegration by high energy nucleons, α-prod. mechanism from pre-equilibrium fluctuations (*Russian*) 0-106059  
<sup>23</sup>Na high spin states, excitation functions, nonstatistical effects, Hauser-Feshbach anal. of <sup>12</sup>C(<sup>13</sup>N,α) 0-106041  
<sup>20</sup>Ne(<sup>12</sup>C,X), 66.5 MeV, evaporation residue ang. and energy distrib. from statistical model anal. 0-83110  
<sup>4</sup>Ni(<sup>3</sup>He, p), 8, 10 MeV, A=58, 60, 62, p spectra compound nucleus contrib., odd-even effect 0-106061  
<sup>56</sup>Ni from HI reactions, superdeformed nucleus decay, α-decay amplification 0-68608  
<sup>58</sup>Ni(<sup>16</sup>O, X), 70 MeV, compound nuclei charged particle evaporation, moment of inertia 0-57785  
<sup>58</sup>Ni(<sup>40</sup>Ar,X), 280 MeV, deep inelastic, light fragments, thermal equilb., ang. momentum transfer 0-63203  
<sup>4</sup>O(π<sup>+</sup>, π<sup>-</sup>), A=16, 18, cross section and ang. distrib., Glauber and coherent fluctuation models (*Chinese*) 0-102211  
<sup>16</sup>O fragmentation at intermediate energies, statistical fluctuation, fragment momentum distrib. 0-78263  
<sup>16</sup>O level excitation functions, resonances from <sup>12</sup>C(<sup>16</sup>O,<sup>12</sup>C) 0-63146  
<sup>16</sup>O(<sup>16</sup>O, X), fusion limiting ang. momenta, from evaporation, mass distrib. stat. model fit 0-68714  
<sup>16</sup>O(<sup>16</sup>O,X), 55 MeV 0-83110  
<sup>30</sup>P level width isospin depend., excitation functions, statistical anal. of <sup>29</sup>Si(p,α) 0-78152  
<sup>208</sup>Pb(<sup>208</sup>Pb,X), exactly central heavy-ion collisions by nuclear hydrodynamics 0-68690  
<sup>208</sup>Pb(<sup>4</sup>Ne,X), 400 MeV/N, inclusive p, d, t, <sup>3</sup>He cross sections from sequential scatt. model 0-57792  
<sup>4</sup>Rb(n,γ), 550-2100 keV, A=85.87, levels, excitation functions, J<sup>π</sup>, Hauser-Feshbach anal. 0-105982  
<sup>32</sup>S(X), A=59-89, double differential cross section, mass asymmetry, transport model 0-102203  
<sup>32</sup>S resonances and excitation functions, Hauser Feshbach anal. of <sup>20</sup>Ne(<sup>12</sup>C,X), X=p,α 0-78249  
<sup>32</sup>Si(γ,d), below 30 MeV, photodeuteron yield and cross section, meas. and statistical calcs. 0-63171  
<sup>28</sup>Si(α,n)<sup>31</sup>S, cross sections and thermonuclear reaction rates 0-73852  
<sup>29</sup>Si(d,p), 1.1-2.1 MeV, excitation functions, statistical fluctuations anal. 0-95322  
<sup>147</sup>Sm(n,α)<sup>144</sup>Nd, 2 keV, statistical model anal. 0-102186  
<sup>120</sup>Sn(p,n), statistical multistep direct emission, p-h and DWBA calcs. 0-106035  
<sup>181</sup>Ta(p,n)<sup>181</sup>W, multi-step compound and direct reactions, statistical theory 0-57761  
<sup>149</sup>Tb from HI reactions, superdeformed nucleus decay, α-decay amplification 0-68608  
<sup>232</sup>Th(p,p'), 52.5 MeV, fission probability 0-99195  
<sup>169</sup>Tm(n,γ), capture cross section from 10<sup>-5</sup> eV to 2×10<sup>7</sup> eV, statistical model 0-63189  
 U(Ne,X), 250, 400, 800 MeV/N, nuclear matter collective sideward flow, nuclear fluid dynamics 0-57715  
<sup>235</sup>U, pot. energy surface, liquid model, deformation energy formulae (*Chinese*) 0-102106  
<sup>235</sup>U(n,f), thermal, fragment ionisation, charge distrib., stat. and instant perturbation theory (*Russian*) 0-63219  
<sup>238</sup>U fission as multi-dimensional Brownian motion, Fokker-Planck soln. (*Chinese*) 0-99197  
<sup>238</sup>U isomeric and prompt fission, nuclear superfluidity evidence from <sup>235</sup>U(d,pf) 0-68711  
<sup>238</sup>U(<sup>238</sup>U,X), 7.42 MeV/N, mass transport, shell effects, anharmonic pots. 0-99187  
<sup>238</sup>U(<sup>238</sup>U,X) deeply inelastic collisions, mass transport, shell effects 0-99188  
<sup>51</sup>V(p,X), X=γ or n, 0.93-4.47 MeV, cross sections, competition effects, Hauser-Feshbach calcs. 0-91184  
<sup>4</sup>W(e,f), A=182,184,186, 35-55 MeV, fission barriers, pairing strength deformation depend., stat. anal. 0-57810  
<sup>4</sup>Zn, A=64, 66 levels and primary E1 transition strength functions from Cu(p,γ) 0-91149  
<sup>66</sup>Zn\* composite particle emission, ang.-distrib., exciton-coalescence model from (d,X), (<sup>3</sup>He,X), (α,X) 0-78265  
<sup>90</sup>Zr(γ,α) statistical and pre-equilibrium cross sections and multipolarities from (e,α) 0-68646

## statistical thermodynamics see statistical mechanics

## statistics

- see also error statistics; game theory; Monte Carlo methods; probability; queueing theory; time series  
 atmospheric precipitations, statistics of spatial distrib. on Experimental meteorological test range, Ukraine 0-101414  
 earthquakes in and near Japan, energy release statistics (1915 to 1978) 0-94471  
 ECG prototype waveforms generation by piecewise correlational averaging 0-109053

## statistics continued

- education, Poisson statistics demonstration using X-ray tube, electronic 'shot noise' 0-73129  
 entropy, information and statistical, and law of large numbers, opacity of statistics (*French*) 0-73288  
 image segmentation based on second-order grey level statistics 0-99663  
 multisensor image pattern recognition, statistical and deterministic aspects 0-99647  
 ocean upper layer, small-scale temp. fluctuations statistical regularities (*Russian*) 0-94528  
 particle size calculation simplification 0-90814  
 periodic nonstationary Gaussian process, high level crossings (*Russian*) 0-94948  
 phase statistics in coherently superposed Gaussian speckle patterns 0-102626  
 planetary nebulae, spatial and vel. distrib. statistics 0-109518  
 radiative association reactions in dense interstellar clouds, statistical theory 0-82441  
 radio sources, double, statistical props., asymmetry and components flux ratio 0-67892  
 radio sources, faint, interpretation of interplanetary scintillation meas. at 81.5 MHz 0-90554  
 sea surface slope distrib. function determ. from Sun glitter, accuracy (*Russian*) 0-94611  
 sub-poissonian statistics of an anharmonic oscillator in thermal equilibrium 0-82669  
 subcritical cyclostationary nuclear reactor, neutron counting statistics, sinusoidally modulated neutron source 0-99203  
 white light image speckle statistical props. 0-106461  
 wind speed, freq. distrib. of hourly meas. 0-94554
- stators**  
 axial flow compressor blade wake guidevane mean velocity and decay characts. anal. 0-95085  
 quality control using thermovision flaw detector 'Stator-1', meas. channel 0-76449  
 turbogenerator stator core losses simulation, expt. 0-88798  
 windings, failure mechanisms under thermal cycling (*Japanese*) 0-104189
- steady-state theory** see cosmology
- steam**  
 electrolysis, high temperature, H<sub>2</sub> production, fusion reactors, synfuel production 0-72099  
 electrolysis at high temp. for H<sub>2</sub> production 0-61440  
 high pressure steam/water mixture flow through cylindrical channels, obs. 0-79404  
 measuring instrument, steam fraction determ. in flowing air/stream mixtures by meas. of IR rad. attenuation 0-75010  
 MHD generator, production of short bursts of power 0-64789  
 saturated steam parameters in reactor containments with escape of coolant, simplified calc. 0-68764  
 sorption effect on cross-linked polyester film struct. (*Russian*) 0-59405  
 two-phase countercurrent flow, turbulent steam condensation in a horizontal channel 0-106800  
 wet steam, high speed flows, drop dimensions meas. method 0-90817  
 Zircaloy, breakaway mechanism, corrosion kinetics in steam 0-61030
- steam boilers** see boilers
- steam generators** see boilers
- steam plants**  
 see also boilers; condensers (steam plant)  
 chemical washing, aqueous effluent neutralisation by use of ash 0-89486  
 flaw detection in steam generator tubes, EM acoustic transducer 0-76464  
 primary and secondary water chemistry of PWR power stations, European experience 0-106110  
 steel, steam pipes, 12Cr1MoV, selection of allowable stresses based on minimum possible strength data 0-104237
- steam power stations**  
 antiscalse forming effectiveness of seeding crystals in thermal power plant 0-89527  
 boiler feedwater redox potential meas. by Pt thin-layer electrodes 0-89578  
 coal fired, gas-particle conversion obs. in plumes 0-81502  
 phase distribution in two-phase steam flows, effects of probe position 0-87799  
 plant, chemical washing, aqueous effluent neutralisation by use of ash 0-89486  
 steel, stainless type 10CrNiCuP and St. 3PS, suitability for power station chimney flue structural material, corrosion testing 0-108681  
 thermal efficiency, CO<sub>2</sub> fund. condensation cycles, performance characts. 0-63368
- steam turbines**  
 see also turbogenerators  
 200 MW, with accessories, noise reduction research and development 0-91958  
 cascade, two phase flows, mixed and discontinuous, calc. 0-79391  
 cascades, transonic flow computation 0-96276  
 district heating plant, condensing and regenerating equipment 0-92029  
 drop coagulation in cross-over pipe flows of wet steam 0-74982  
 droplet size distribution in liquid phase of two-phase flow effect on characts. 0-103070  
 spontaneously condensing and wet steam discontinuous flows, subsonic, transonic and supersonic, numerical investigation (*Russian*) 0-87800  
 steel casings, 15Cr1Mo1VL, susceptibility to brittle struct. and fracture, influence of props. 0-104298  
 steel turbine casings, residual life determ. 0-93585  
 structural stresses, experimental anal. 0-93727  
 three-dimension transonic flow prediction, characteristic method appl. 0-96277  
 vapour turbine plants using combined thermal-power convertor and photoelectric convertor, thermodynamic efficiency for solar energy conversion 0-89614  
 welds, with the 25000 R/min Linac 0-97656
- steel**  
 see also alloy steel; austenitic steel; carbon steel; stainless steel  
 acoustic emission parameters, brittle fracture, crack propagation in types S13+0Kh13 (*Russian*) 0-93633  
 acoustic emission sources and dislocation patterns 0-61040  
 acoustical method of studying steel microstructure 0-76469  
 age hardened, dynamics of cyclic plasticity (*Czech*) 0-108464  
 aluminising, thermodynamic anal. of phase transforms. 0-76413

- steel continued
- backing plate, hot pressing with powder layer, joint form. kinetics 0-100961
  - bainite formation mechanism 0-108431
  - ball bearing, fatigued, phase changes, nomenclature 0-89198
  - ball bearing rods, inspection installation 0-81268
  - bar, and wire rod, small sample prep. and spectrometric anal. (German) 0-93704
  - bearing rings, optimisation of thermomechanical working parameters (Russian) 0-93579
  - brittle fracture, grain boundary P segregation, effect after quenching and tempering (Russian) 0-81145
  - carburisation process, diffusion modelling 0-108632
  - carburized and quenched, residual stresses (Japanese) 0-89262
  - carburizing, vacuum, case depth 0-100956
  - case depth after quench hardening, inspection using coercimeters 0-104377
  - cast automatic couplings, yield strength, crack propag. resistance and ductile-brittle transition temp. 0-104281
  - cast continuously, segregation at halfway cracks 0-60869
  - casting, calc. method of thermal and thermo-visco-elasto-plastic processes (German) 0-79859
  - cathodes, phosphate pickled mild steel, behaviour during deep electrolytical water enrichment, T meas. 0-93764
  - clean steel, review 0-84839
  - coercimeters with attached electromagnets used for quality control 0-108672
  - cold resistance determination, quick method 0-100997
  - cold strained, defects interaction with carbide strengthening phases, carbide decomp. degree (Russian) 0-84955
  - cold-rolled, isotropic, specific magnetic loss meas. at high frequency 0-101808
  - commercial, type In-787, for use in Arctic, low temp. effects on mech. props. 0-76310
  - constructional, El736, creep, viscosity, resist. to inelastic deform. 0-89309
  - continuous casting, thermal, thermo-visco-elasto-plastic processes (German) 0-81044
  - corrosion inhibitor action ellipsometric obs., of propargyl alcohol, film growth on steel surfaces (Rumanian) 0-60996
  - crack initiation, impurity effects, dynamical loading (Czech) 0-60955
  - crack resistance, -196 to 500°C 0-71750
  - crack-resistance limit and stress analysis in the ductile state 0-81188
  - creep rate mismatch interaction in stress relief cracking 0-97578
  - cryogenic, creep, review 0-104222
  - cylinder impact on rock half-space 0-85649
  - deformation strengthening, of bayanite phase in type KVK (Russian) 0-100851
  - deformed 20Kh type, austenite grain size, inheritance effect with quenching and tempering 0-60881
  - ductile structural, fatigue crack propag. rate and striation spacing 0-93635
  - eddy current losses, estimation method, in large steel plate having one-phase excitation (Polish) 0-93145
  - elastic-plastic plane-strain crack growth, comparison of theory and experiment 0-108560
  - electrical, mag. props. determ. with Epstein hysteresis tester 0-60364
  - electrical steel sheet, systematic and random errors, in wattmeter apparatus for measuring unit losses 0-71858
  - electrodes, pitting corrosion currents rel. to conc. of inhibitive and corrosive anions under corrosion conditions 0-85181
  - electrolytically notched, in direct evidence of active path formation in stress corrosion cracking in Al-alloys 0-85077
  - electron emission depend. on surface mechanical treatment (Russian) 0-100945
  - electron microscopy on etched thin foils, comparative SEM, STEM and TEM analysis 0-100144
  - electrotechnical, single strips, mag. props. meas. using AC compensated permeameter 0-86352
  - embrittlement mechanism, microcrack formation, dislocation model (Russian) 0-65143
  - fatigue, low cycle, hysteresis loops, cyclic strain curves, fatigue diagrams (Polish) 0-66638
  - fatigue, low-cycle, of SW7M at high hardness levels (Polish) 0-89323
  - fatigue and cyclic plasticity rel. to struct. inhomogeneity 0-81184
  - fatigue crack growth rate in air and saltwater, stress ratio effect 0-100952
  - fatigue crack propag. near to threshold stress intensity 0-100898
  - fatigue crack propagation, quantifying the parameters 0-100891
  - fatigue crack tip plastic deform., X-ray diffr. investigation (Russian) 0-104251
  - fatigue damaged, fracture toughness 0-89353
  - fatigue failure of 1Kh17N2Sh, surface finishing influencing 0-60972
  - fatigue life, influence of cyclic loading conditions 0-76350
  - fatigue life estimates, of bluntly notched members 0-100999
  - fatigue limit, static and cyclic loading 0-71755
  - fatigue limit assessment, progressive load methods (German) 0-61058
  - fatigue resistance, of type 1018 in sea water, specimen size and freq. effect 0-93678
  - fatigue strength, low cycle overload effect 0-60967
  - fatigue strength, tempering effect 0-60891
  - ferrite, transform. kinetics, grain size, alloying element effect, carbide precip. 0-93560
  - ferrite grain size, and comp. influence on Ludwik eqn. constants (German) 0-81107
  - ferrite-austenite transition, diffusion const. of C and carburisation rate const., thermopower meas. 0-89216
  - ferritic, clad with austenitic steel 309, US detection of undercladding microcracks (Italian) 0-108683
  - ferritic, crack extension, cleavage micromechanisms, review 0-108562
  - ferritic, creep resist., high-temp. props. residuals effect 0-66600
  - ferritic disc, biaxial fatigue testing under changing temps. (German) 0-71759
  - ferromagnetic 2Kh13, rod, coupled flexural and torsional vibrs., energy dissipation 0-89281
  - fibre reinforced Al, thermophys. props. 0-59745
  - fibre reinforced concrete, vibr. compaction, pressure compaction and curing (Japanese) 0-89179
  - fibrous crack extension, micromechanisms 0-108563
  - fine structure after heat treatment, X-ray diffr. exam. 0-60890
- steel continued
- fission reactor material, defect development in contact area with coolant (Russian) 0-57859
  - foil, microanalysis by energy dispersive X-ray spectrometry (French) 0-85250
  - forgings, untreated surface, US monitoring, sensitivity comparison 0-66751
  - fracture, intergranular, and solute segregation 0-60957
  - fracture initiation moment, I-integrals critical value determ., ultrasonic method 0-61049
  - fracture mechanics parameters, influence of specimen thickness on types RSt 37-2, st52-3, StE70 and 30CrNiMo8 (German) 0-66614
  - fracture mode, determ. from shear lip width 0-60968
  - fracture of Kh18N10T in low-cycle fatigue tests in H<sub>2</sub> (Russian) 0-76332
  - fracture resistance, from impact bending tests and oscillograms 0-61047
  - fracture toughness of nuclear reactor pressure vessels 0-81172
  - friction and wear during hot forging 0-89358
  - friction measuring test for use under conditions of high normal interfacial force 0-76454
  - friction pairs C steel-antifrictional alloys, electrochem.-mech. investigation (Russian) 0-76367
  - Gruneisen parameter and thermal diffusivity, thermoelastic meas. method 0-107581
  - heat resistance, thermal stability, stress-rupture strength, and creep 0-81194
  - heat resistant, tensile strain and endurance, normal and radiation conditions, linear load variation 0-81189
  - heating effect on phase composition, microstruct. and mech. props. 0-100859
  - high permeability grain oriented elec. steels and instrument current transformers 0-88824
  - high speed, props. after electroslag remelting 0-104139
  - high strength, dislocation sweeping model for hydrogen assisted subcritical crack growth 0-97577
  - high strength, failure stress, structural relationships 0-81190
  - high strength, heat resistant, fracture resistance at low temps. 0-104284
  - high strength, subcritical crack growth, role of time delayed H<sub>2</sub> assisted plastic zone growth 0-97576
  - high strength 4340, fatigue crack growth resistance, fracture mechanism effect (Japanese) 0-104265
  - high strength dual phase, martensite/bainite differentiation using improved etching technique 0-100951
  - high strength weld metal, fractography, microstructure and reheated zone toughness effects (Japanese) 0-108543
  - high-speed, fracture toughness, carbides influence (French) 0-108559
  - high-strength, H distrib. and delayed brittle fracture 0-108577
  - high-strength castings, AE study of intercrystalline crack form. 0-104403
  - high-strength tool steel D7KhFN, remelting effect on mech. props. 0-76284
  - hot blooms, US inspection to detect internal pipe 0-97655
  - hot forging die type, fractography (Japanese) 0-108547
  - hot shortness, high-temp. embrittlement, residual and trace elements influence 0-66644
  - hydrogen absorption, anilines surfactants effectiveness, HCl conc. effect 0-108638
  - hydrogen embrittlement, effect of S content in H<sub>2</sub> 0-97562
  - hydrogen embrittlement, effect on band strength 0-104293
  - impact welding to Cu, fundamental parameters 0-97679
  - impact welding to Cu, wavy interface characts. and formation 0-97680
  - impurity spectral lines, intensity, temp. and conc. effects 0-64774
  - inclusion chemistry control for machinability enhancement 0-85067
  - ingots, cooling regime in conditions of minimal thermal stress, modelling (Russian) 0-65194
  - ionic nitriding thermochemical process, equipment, process details and advantages and prospects (French) 0-108641
  - jig brushes, wear resist. (Russian) 0-60977
  - low-alloy, impurities, segregation and creep embrittlement 0-66653
  - magnetic anisotropy of electrical steel sheet, determ. method and laboratory tests (Polish) 0-97071
  - magnetic susceptibility, 4.2 to 300K, and magnetoelasticity of Kh18N(10-25) (Russian) 0-65812
  - maraging, ductility and resist. to deform., -196-1000°C 0-89313
  - martensitic growth 0-108439
  - martensitic transform, stress calcs. using statistical model (Russian) 0-93557
  - melt, interaction with Al<sub>2</sub>O<sub>3</sub>:Zr ceramic 0-104305
  - microstructure of OKh16N15M3B after creep tests in BR-10 reactor, electron microscope invest. (Russian) 0-92531
  - mild, rubbing on brass, magnetic field effect on diffusive wear of cutting tools 0-60985
  - monitoring, with pulsed magnetic analyser, IMA-5 0-104399
  - neutron quasialbedo thickness meas. of single layer product, optimization 0-105611
  - nitrided layer depth, electroinduction meas. method 0-104379
  - nonstationary temperature fields due to moving heat sources, heat capacity, thermal cond. (Russian) 0-107448
  - normalised and strained Ck45, length charges under cyclic load (German) 0-100869
  - notched, cyclic stress/strain behaviour, random fatigue life (German) 0-100907
  - oxidation by Fe-Si-Ca-V complex alloy, nonmetallic inclusions (Russian) 0-93685
  - passivation treatment, of galvanised strip 0-61146
  - pearlitic, heat treatment effect on fracture resistance, microstruct. and mech. props. 0-104191
  - pearlitic, wear behaviour rel. to basic material props. 0-108592
  - pearlitic constructional, K<sub>IIIc</sub> expt. determ. 0-100985
  - pearlitic structural, austenite grains, growth rate during heating 0-100860
  - pipe, flaw detection by US pulse-echo method 0-66756
  - plasma coatings, elastic properties, acoustic meas. (Russian) 0-97519
  - plasma magnetic confinement system, surface problems caused by dissolved H<sub>2</sub> 0-57946
  - plastic deform., density changes (German) 0-60908
  - plate, thick high strength, for press. vessels, low cycle fatigue and notch sensitivity (French) 0-66670
  - platelike parts, quenching, temp. field calc. 0-60889
  - plates, explosively clad, fatigue crack propagation behaviour (Japanese) 0-104262
  - powder metallurgy, recent developments, Sweden 0-93514



## steel continued

- pressure vessels, testing by pendulum impact machines, energy meas. using optical system 0-69746  
 radiographic inspection method, productivity 0-71861  
 radiography, with the 25000 R/min Linac 0-97656  
 restorational carbonisation in one and two phase states (*Russian*) 0-65225  
 ring against Cu pin, dry sliding wear, role of dynamic recrystallisation 0-108599  
 rod, dynamic bending and residual deformation (*Russian*) 0-75293  
 rod, transverse vibrations, energy dissipation, static longitudinal load effect 0-81099  
 rolled, anisotropic, fatigue fracture surface obs. (*Japanese*) 0-108546  
 rolled sheet, thick, metrological peculiarities when inspecting with US shadow flaw detectors 0-81263  
 segregation, solute, and intergranular fracture 0-60957  
 segregation and adsorption of S, influence on carburisation and nitrogenation 0-66701  
 seizure, effect of polymer-containing metal-filled lubricant 0-104301  
 sheet, cold-rolled, surface chemistry 0-61146  
 sheets bonded with low density polyethylene, static fatigue (*French*) 0-108522  
 shell, explosive expansion, deform. and rupture modes and mechanisms 0-85064  
 shell, explosive expansion, rupture behaviour 0-85063  
 shell, mech. behaviour during solidification 0-81043  
 sintered, fracture of residual pores 0-76352  
 sintered ductile fracture, microvoid effects (*Japanese*) 0-108542  
 solidification during continuous casting, cooling regime comparison (*Russian*) 0-93548  
 solubility of O<sub>2</sub> in steel Kh18-Ti-Al alloy (*Russian*) 0-92676  
 spheroidization of pearlite, global microstruct. evolution 0-108482  
 steel sheet, surface anal. by ion etching and atomic absorpt. spectroscopy (*German*) 0-81377  
 strain-hardened subsurface layer, residual stress change in fatigue 0-81185  
 structural, 34KhN3M, heat treatment effect on magnetostriction 0-104306  
 structural, elastic limit determ. by acoustic emission 0-66716  
 structural, high strength type StE47, specimen geometry and plastic deform. effect on fracture mechanics (*German*) 0-66613  
 structural, second phase particle effects on impact strength 0-108581  
 structural, strained in tension after tempering, compression effects on struct. changes (*Russian*) 0-66577  
 structural, supercooled austenite, structural characts. of decomposition 0-60870  
 structural, type St 37, microstruct. rel. to fracture toughness and fracture load of bending specimens (*German*) 0-89352  
 structural, wide plate tensile testing eval. (*German*) 0-100969  
 structural, with yield pt. of about 420 to 720 N/mm<sup>2</sup>, correlation between yield pt./tensile strength ratio and toughness (*German*) 0-66615  
 structural 15KhNMF, resist. to weakening during tempering, high purity effect 0-76279  
 structural changes in types 60 G, ShKh15 near holes and inclusions due to pulsed currents (*Russian*) 0-108459  
 structural ties, NDT by eddy current transducer, optimum parameters and capabilities 0-108669  
 structure after high-speed cold plastic deformation steels 60, 18Kh2N4MA, 17GSND, and 12Kh21NST 0-76316  
 substrate, Sn autocatalytic deposition 0-100965  
 substrate for Cr<sub>2</sub>C<sub>3</sub> electrophoretic coatings, sintering 0-66707  
 substrate limiting temp. during vaporisation and condensation coating in vacuum (*Russian*) 0-100787  
 surface, chem. characterisation by SIMS, glow discharge spectrometry and other techniques 0-66907  
 surface composition, degreasing and batch annealing effects 0-66700  
 surface hardening, ion-carbo-nitriding in CO-N<sub>2</sub>-H<sub>2</sub> gas mixtures, expt. (*Japanese*) 0-71670  
 surface metrology using peak counting, quality control 0-95065  
 surface Si reinforced type U8, metastable phase, composition, struct. (*Russian*) 0-92599  
 surface state influence on etching effect 0-81235  
 tempered, notched, impact bending tests, cold brittleness curves 0-71758  
 thermal fatigue, effects of inclusions 0-81183  
 tin plate, passivation treatment 0-61146  
 tinplate surfaces, Auger depth profiling and anal. 0-59768  
 tool and high-speed, high freq. induction melting and centrifugal casting in instrumental anal. 0-84886  
 tool steel, US vel. meas., 20-900°C 0-70318  
 toughness, effect of Sn, SEM exam. 0-97569  
 toughness, review of joint tests (*German*) 0-65142  
 trace element UV emission, spectrochem. anal. (*French*) 0-71997  
 track autoradiography for N detect. 0-100979  
 US critical angle reflectivity, near-surface metallic prop. gradient effect 0-70516  
 US immersion testing, effects of curved entry surfaces on calibration, steel sample expts. 0-71849  
 US inspection to 1000°C, hot-metal defectoscopy 0-66750  
 US strengthening treatment effect on fatigue resistance 0-81193  
 US velocity, meas. method for isotropic nondispersive solids 0-69616  
 volatile products from reaction with H<sub>2</sub>O-CO<sub>2</sub>, high temp. 0-81233  
 wear characts. of burnished machined surfaces 0-108595  
 wear resistance of low temp. nitriding treatment 0-89357  
 weldable, fatigue data, low and high cycle compatibility (*Czech*) 0-89343  
 welded joints, bead-on-plate, H<sub>2</sub> diffusion and trapping 0-96697  
 welds in plates, flaw classification using microprocessor controlled flaw detector 0-100992  
 white phases structure after heat treatment, steels ShKh15 and 12KhN3A 0-76281  
 wide plate tests, and V-notch bending tests evaluation on basis of materials mechanics (*German*) 0-66571  
 wire, drawn, quantitative texture anal., neutron diff. studies 0-81078  
 wire, US inspection, immersion method 0-66757  
 yield point, research of Cottrell and Bilby, (1945-55) 0-62444  
 yield strength, influence of deform. rate on type 10G2SAF (*Bulgarian*) 0-89315  
 Young's modulus of Fe<sub>3</sub>C phase (*Russian*) 0-76297  
 Al-steel mixture, wear resistant, produced by compaction by discrete shock waves 0-84882  
 C-C interaction energy, thermodynamics of steels 0-93793  
 Cr plated, factors influencing durability 0-108643

## steel continued

- Cr-Ni-Mn, adiabatic shear band determ. by surface obs. 0-97579  
 H<sub>2</sub>, effect on phys. and mech. props. 0-101657  
 Mn-C-Si-Cu (0.95, 0.85, 0.25, 0.16 wt.%), fibrous-banded fracture mechanism 0-104280  
 Ni-Cr-Ti-C (2.8, 0.9, 0.2, 0.73 wt.%) (*Russian*) 0-81072  
 P, deep-drawing, spatial orientation distrib. of crystallites in cold-rolled and in annealed sheets 0-81079  
 Si, nonoriented sheet prod. with texture of {100} {ovw} 0-89246
- steel industry**  
 cooling water flow control in continuous casting process, vortex flowmeters 0-64655  
 induction heating of slabs 0-71672
- steel manufacture**  
 computerised spectrometric analysis and management information system 0-89574
- stellar atmospheres**  
 see also solar atmosphere  
 A-type stars, effect of C+H<sup>+</sup>=C<sup>+</sup>+H charge transfer on C I 1101 Å absorpt. edge 0-90423  
 A-type stars, Lyman α effect on non-LTE model atmospheres 0-90422  
 A-type supergiant stars, mass loss rates from UV reson. line profiles 0-90424  
 accretion, spherical, buoyancy effect 0-109349  
 accretion discs, steady, optically thick, convective vertical energy transport 0-62112  
 accretion discs, viscosity determ. for Hercules X-1 and (SS 433) 0-62110  
 accretion disks, optically thick, pulsational instability to axially symm. oscils. 0-82190  
 Algol, eclipsing binary, X-ray spectra interpretation, corona model 0-105283  
 Algol type systems, secondaries with active chromospheres, possible RS Canum Venaticorum system 0-105276  
 Am-type, binary stars, tidal interaction producing stable atm., evolution 0-67752  
 o Andromedae, Be star, spectroscopic evidence for new shell episode 0-90444  
 Z Andromedae, symbiotic star, atmospheric struct. from IUE obs. 0-109450  
 α and β Aquari, G-type supergiants, evidence for hybrid atmospheres and winds from UV spectra 0-72948  
 α Aquarii (A0 IVs), hot-metallic-line star, abundance anal. from model atmosphere 0-90415  
 R Aquarii (M7+pec), late type variable star, IUE obs. of circumstellar emission 0-82370  
 θ Aquilae (B9.5 III), abundance anal. from model atmosphere 0-90415  
 V603 Aquilae (Nova 1918), accretion disc eclipse model for periodic light vars. 0-82391  
 † Aurigae, eclipsing binary, UV obs. of supergiant atmos. 0-94836  
 ε Aurigae, extinction by circumstellar matter rel. to wavelength-depend. fluctuations 0-62190  
 α Aurigae (Capella), theoretical stellar chromosphere model 0-67718  
 late B dwarf in circumstellar dust cloud, IR source coincident with OH 205.1-14.1 0-101630  
 B-stars of early type, atm. LTE model using opacity sampling technique 0-90414  
 Be and shell stars, UV radiation deficiency correl. with shell existence 0-90438  
 binary star giants, chromospheric activity due to tidal interactions 0-82420  
 close binary systems, atmospheric gas streams effects on radial vel. curves 0-94829  
 black holes, spin-up by thick accretion discs 0-105273  
 black holes, supercritical accretion discs models 0-105272  
 black holes, thick accretion discs models rel. to supercritical luminosities 0-101614  
 blue supergiant with neutron star immersed in envelope 0-98689  
 Z Camelopardalis, dwarf nova, accretion disc models at standstill and in eruption 0-82366  
 UW Canis Majoris, eclipsing binary, mass flow anal. from UV spectrum 0-109429  
 UW Canis Majoris, O7f supergiant, mass loss rate meas. 0-67736  
 α Canis Minoris (Procyon), theoretical stellar chromosphere model 0-67718  
 TX Canum Venaticorum, cataclysmic variable shell and dust emission, visible spectra obs. 0-105249  
 α<sup>2</sup> Canum Venaticorum, line blanketed model atmospheres of Ap-star 0-90440  
 RS Canum Venaticorum binary stars, mag. starspot model for photometric and spectroscopic behaviour 0-109488  
 RS Canum Venaticorum type binaries, Hγ line vars., chromospheric diagnostics 0-62181  
 † Capricorni (B9.5 V), abundance anal. from model atmosphere 0-90415  
 QZ Carinae (HD 93206), O-type quadruple eclipsing system, evidence for mass loss from supergiant 0-105275  
 VX Cassiopeiae, circumstellar shell rel. to photometric variability (*Russian*) 0-72973  
 cataclysmic binaries, circumstellar material geometrical and photometric parameters 0-109492  
 cellular convection in a stratified atmosphere 0-98652  
 α Centauri binary system, sealed solar model atmospheres for spectroscopic anal. 0-62128  
 Centaurus X-3, neutron star accretion disc rel. to spin-up and X-ray luminosity 0-101648  
 U Cephei, accretion discs obs. 0-82412  
 VV Cephei, eclipsing binary, UV spectrum 0-82415  
 9 Cephei (B2 Ib), circumstellar CO obs. 0-94795  
 β Cephei stars, effects of mass loss on instability strip 0-90436  
 o Ceti (Mira) of 1978 max., light scatt. in atm., spectropolarimetry 0-94799  
 Z Chamaeleontis, eruptive binary, accretion disc struct. rel. to photometric behaviour 0-72961  
 chromosphere Ca II emission in main sequence stars, comparison of activity cycles to old and young stars 0-105235  
 chromosphere Ca II H and K emission in field stars of solar neighbourhood, survey 0-109423  
 chromospheres, catalogue of stars with Ca II H and K emission lines (*Polish*) 0-82227  
 chromospheres, review (*German*) 0-109421  
 chromospheres, time dependent ionisation obs. 0-98651

## stellar atmospheres continued

- chromospheres of F, G and K-type stars, radiative losses in continuum 0-72924  
 circumstellar clouds, implications for existence of interstellar Mg lines obs. 0-94782  
 circumstellar dust shells, photoelectric yield of insulating dust grains 0-90507  
 circumstellar dust shells, polarisation by Mie scatt., Monte Carlo anal. 0-98650  
 circumstellar envelopes, Monte Carlo analysis of polarization by Thomson scattering 0-85931  
 circumstellar envelopes scatt., radiation linear polarisation spectrum rel. to mag. field determ. (*Russian*) 0-90344  
 close binaries, energy release, flares and particle acceleration (*Russian*) 0-73005  
 close binaries, light scattering in extrastellar gaseous material, emission line profiles spectropolarimetry obs. 0-109471  
 close binaries, narrow-band photometry and differential effects 0-67780  
 close binary systems, atmospheric gas motions rel. to radial vel. curves anal. 0-90470  
 compact objects, nonrelativistic electrons interaction with radiation in mag. field 0-109354  
 contact binaries, envelope energy transfer model 0-90478  
 cool giant stars, chromosphere mass loss determ. from Mg II UV line obs. 0-85935  
 cool stellar atmospheres, rare-earth elements atomic partition functions 0-67544  
 coronae, low-temperature, contrib. to EUV background 0-62324  
 R, S, T Coronae Austrinae, T Tauri stars, circumstellar shells rel. to long period light vars. 0-82350  
 $\theta$  Coronae Borealis, Be-type star, shell line profile and radial vel. obs. 0-77426  
 R Coronae Borealis, UVRIHKL MN photometry, interpretation 0-67756  
 coronae of late-type main-sequence and subgiant stars, HEAO-1 X-ray obs. 0-72925  
 31 and 32 Cygni, eclipsing binaries, supergiant components atmospheres from UV spectra 0-109499  
 P Cygni, H Paschen  $\alpha$  equivalent width rel. to circumstellar envelope struct. 0-62156  
 CH Cygni, symbiotic star, 1977 outburst, radial vel. and atm. struct. determ. 0-72969  
 CH Cygni, symbiotic star, binary model and hot companion circumstellar envelope struct. 0-62158  
 CI Cygni, symbiotic star, emission lines source regions from UV and optical obs. during eclipse 0-105258  
 V1500 Cygni (Nova 1975), anisotropically radiating condensations rel. to Balmer line emission profiles evolution 0-82371  
 V1500 Cygni (Nova 1975), distance and temp., visible spectral obs. (*Chinese*) 0-85955  
 V1668 Cygni (Nova 1978) envelope, dust form. rel. to multifilter photometry and polarimetry 0-90454  
 HR Delphini (Nova 1967), C and N overabundances in stellar wind from UV spectra 0-109440  
 dense stars atmospheres, atomic spectra in intense mag. fields 0-105160  
 S Doradus, LMC star, evidence for circumstellar envelope and mass loss from IUE and optical obs. 0-101595  
 dwarf stars, degenerate accreting, thermonuclear bursts assoc. with chromosphere flares 0-98684  
 early-type stars, effect of gas-dust envelopes on IR spectral energy distrib. 0-67732  
 early-type stars and cool stars, UV spectroscopy of outer layers 0-72922  
 early-type stars in LMC open cluster NGC 955, stellar winds rel. to motions in bubble-like nebula N51D 0-105295  
 early-type stars with Balmer emission, outer atmospheres props. from near UV spectra 0-94811  
 early-type stellar winds, H and He<sup>+</sup> synthetic line profiles 0-85926  
 eclipsing binaries with extended atmospheres, light curve anal. techniques and appl. to V444 Cygni 0-82417  
 eclipsing binary stars, near IR photometry rel. to mass transfer rates 0-67784  
 ejected envelope <sup>26</sup>Mg, interaction with collapsed core prod. neutrinos, <sup>26</sup>Al prod. (*Russian*) 0-77285  
 $\nu$  Eridani,  $\beta$  Cephei variable atm. parameters from H and He spectral obs. 0-67739  
 $\epsilon$  Eridani, UV line spectrum of active chromosphere star, models 0-77394  
 40 Eridani A(=o<sup>2</sup> Eridani), evidence of corona on X-ray image 0-105282  
 evolved stars expanding envelopes, CO thermal and maser emission 0-82334  
 expanding envelopes, Lyman  $\alpha$  quanta scattering (*Russian*) 0-67556  
 F, G, K-type stars, giants and dwarfs chromospheres, wave dissipation of mechanical energy 0-82340  
 F-type star, main sequence, convection and photospheric granulation 0-90417  
 flare stars chromospheres, electron heating rel. to nature of flares optical continuum (*Russian*) 0-109445  
 G128-7, cool DA white dwarf, atmospheric parameters and evolutionary consequences 0-62126  
 G 165-7, metallic line white dwarf, model atm. code anal. of spectrum 0-85940  
 $\gamma$  Geminorum, differential abundance anal. rel. to  $\alpha$  Lyrae standard 0-82362  
 $\beta$  Geminorum (Pollux), theoretical stellar chromosphere model 0-67718  
 giant stars in globular clusters M5, M13, M3, model atmospheres rel. to chemical comp. 0-67695  
 gravity stratification, perturbation propag. (*Chinese*) 0-85934  
 HC 105056, ON supergiant, spectroscopic evidence for variable stellar wind 0-90427  
 HD 102567, optical counterpart to 4U 1145-61, atm. model from UV obs. 0-105396  
 HD 10783, Ap star, model atmospheres rel. to spectrophotometric obs. 0-98663  
 HD 192163, Wolf-Rayet star in ring nebula HGC 6888, SHF obs. 0-82386  
 HD 206267, exciting star in H II region IC 1396, stellar wind, role in cloud struct. 0-105316  
 HD 4174, symbiotic star, circumstellar envelope model rel. to spectroscopic obs. 0-85945

## stellar atmospheres continued

- HD 44179, binary with surrounding dusty nebula, 3.3 micron feature 0-82466  
 HD 45677, peculiar Be-star 0.12-12.6  $\mu$ m obs. of circumstellar dust shell 0-72957  
 HD 77581 (=Vela X-1), supergiant+neutron star, stellar wind mass transfer, spectral obs. 0-94892  
 HD 93250, O3 massive star in  $\eta$  Carinae complex, non-LTE analysis 0-77398  
 HD 97048 (=HM 18), pre-main sequence star, unidentified IR features obs. 0-85943  
 Henize 715 (4U 1145-61), Be star, circumstellar envelope disappearance (1979-80) 0-72979  
 Herbig-Haro objects, stellar wind model 0-85985  
 Hercules X-1, coronal contrib. to X-ray continuum and Fe line emission during X-ray low state 0-105393  
 $\phi$  Herculis, Hg-Mn star, corona search, UV obs. 0-72986  
 high velocity giant stars, model atmospheres rel. to detailed chemical anal. 0-82352  
 hot coronae, possible detection from XUV emission (*German*) 0-109372  
 hot stars with circumstellar clouds, synthetic UV spectra calcs. 0-77382  
 HR 6127, chemically peculiar star, spectral lines and equivalent width lists, visible obs. 0-82387  
 HR 8752, binary supergiant, photosphere, emission feature variability, visible obs. 0-109463  
 HR 96, Ap-type star, atm. parameters and stellar comp., visible obs. 0-67740  
 EX Hydrae, dwarf nova, accretion disc dimensions from IR and optical light curves 0-67747  
 W Hydrae, form. of carbyne and cyanoacetylenes in stellar atm. 0-67708  
 VW Hydrae, dwarf nova, accretion disc dimensions from IR light curves 0-67747  
 hydromagnetic free convection flow in Stokes problem, for porous vertical limiting surface with const. suction 0-90328  
 HZ 43, white dwarf, He abundance and stellar struct. from soft X-ray spectra 0-72944  
 $\epsilon$  Indi, late type dwarf star, model atmosphere 0-90425  
 IRC+30219, extreme C star, circumstellar envelope optical emission-line phase 0-90569  
 IRC +10216, C star, circumstellar dust cloud size from far IR obs. 0-82539  
 K-type giant stars, evidence of circumstellar shells 0-90420  
 EV Lacertae, evidence for photospheric starspots from photometric and spectroscopic obs. 0-98665  
 late type dwarf stars, temp. minima, chromosphere models 0-67717  
 late-type field stars in S. hemispheric, evidence for chromospheric activity 0-98686  
 late-type stars, Ca II 8542 Å line as chromospheric activity indicator 0-62108  
 late-type young stars in  $\rho$  Ophiuchi dark cloud, photometry obs. 0-72942  
 CW Leonis (IRC+10216), IR C star, circumstellar dust orientation by paramag. relaxation rel. to intrinsic polarisation 0-67730  
 long-period variable stars, photospheric absorpt. and scatt. rel. to narrow-band polarimetry 0-98666  
 M-type dwarf stars in galaxy cluster Abell 2029, coronal X-ray emission rel. to SAS 3 obs. 0-82519  
 magnetic DA white dwarfs, model atmospheres and line profiles 0-62123  
 magnetogasdynamics, axially symmetric explosion 0-62007  
 maser stars, late supergiants and long period variables 0-77410  
 mass flux fluctuation theory 0-72923  
 massive stars, single and binaries, evolution review 0-82343  
 metal-deficient stars, subdwarf ionization equilibrium and model atmospheres 0-90421  
 MHD, unsteady thermal boundary layer problem, numerical treatment 0-92227  
 Milne problem, invariance principles and integral eqns. for radiation fields in plane atmosphere 0-67559  
 Mira type variables atm., OH maser, IR line overlap pumping mechanism 0-72764  
 R Monocerotis, T Tauri star, circumstellar shell changes rel. to long period light vars. 0-82350  
 multicomponent nonequilibrium plasma atmospheres, higher order fluid eqns. 0-105156  
 neutron star, rot. with magnetosphere, effect of elec. field. 0-109453  
 neutron star X-ray emission models 0-62175  
 neutron stars, accreting, thermonuclear bursts assoc. with chromosphere flares 0-98684  
 neutron stars, accretion disc interaction with rot. mag. field 0-62173  
 neutron stars, extended atmosphere form during supercritical time-dependent accretion 0-85967  
 neutron stars, pair annihilation in superstrong magnetic fields 0-85847  
 neutron stars accretion discs and spheres, plasma accretion theory 0-109452  
 neutron stars with mag. fields, radiative heat transfer in surface layers 0-94826  
 nova envelope C enrichment on surface accretion at white dwarf 0-85936  
 nova envelopes, dust form. and ionisation theory 0-98678  
 Nova Serpentis 1978, evolution of dust shell 0-90430  
 novae, effect of expanding envelope interaction with binary companion on outburst 0-82394  
 novae, nonuniform stellar wind manifested in light curves 0-62160  
 O-type star, wind, effect on H II region evolution in mol. clouds 0-94846  
 O-type stars, extended atmospheres rel. to C III 9701 to 9715 Å lines 0-77401  
 OB3 type stars in young clusters, circumstellar matter 2200 Å hump interpretation 0-82351  
 OB stars, stellar wind mass loss determ., UV spectra obs. 0-94789  
 Of and O stars, stochastic accel. in photospheres rel. to difference in mass loss 0-90413  
 70 Ophiuchi A, theoretical stellar chromosphere model 0-67718  
 $\rho$  Ophiuchi cloud, cosmic ray accel. by stellar winds 0-77512  
 $\zeta$  Orionis, Reticon obs. of Ha P Cygni profile rel. to stellar wind vel. law 0-82365  
 $\alpha$  Orionis, supergiant variable, mass loss, visible spectra obs. 0-67755  
 particle discs, infrequently colliding, in binary system, tidal torques and appl. to asteroid belt truncation 0-98596  
 AG Pegasi, symbiotic binary star, circumstellar cloud and stellar winds rel. to spectrum 0-109449  
 X Persei, eclipsing binary, gaseous ring struct., H I alpha obs. 0-109482  
 $\beta$  Persei, eclipsing binary, Mg II 280 nm line profile, calcs. and UV obs. 0-82421



## stellar atmospheres continued

- RY Persei, eclipsing binary, spectroscopy and physical parameters of atmospheres 0-101618  
 X Persei (A 0535+26), stellar wind parameters from Prognost-6 X-ray obs. (*Russian*) 0-109562  
 TX Piscium, disc brightness distrib. and envelope obs. from lunar occultation meas. 0-67725  
 SZ Piscium, RS Canum Veneticorum star, starspots surface distrib. from photometric obs. 0-109490  
 piston problem, one-dimensional, in non-ideal gas, time-dependent soln. 0-82185  
 planetary nebulae central stars, atmospheric models 0-109434  
 planetary nebulae central stars, hot wind model for nebulae refractory elements gas-phase abundances 0-109516  
 presupernovae, stellar wind as possible cause of supernova remnant filamentary struct. 0-62249  
 pulsar magnetosphere, plasma waves propag. along mag. field in strongly anisotropic relativistic plasma 0-67542  
 pulsar magnetosphere, radio wave generation at plasma frequency 0-109451  
 pulsar magnetosphere, relativistic particle curvature radiation 0-77434  
 pulsar open magnetosphere, plasma instabilities as source of coherent radio emission 0-82403  
 pulsars, finite force face cold plasma atm. models, plasma differential rot. 0-77378  
 pulsars axisymmetric magnetospheres, method of soln. of self-consistent description 0-94825  
 pulsating stars asymptotic theory, boundary layer method 0-82389  
 { Puppis, of supergiant, mass flow var., visible and UV obs. 0-90431  
 { Puppis, Of type star, stellar wind model from UV line fit 0-72965  
 { Puppis, Reticon obs. of H $\alpha$  P Cygni profile rel. to stellar wind vel. law 0-82365  
 radiation transfer eqn. in spherical geometry, numerical soln. 0-90329  
 radiative transfer, comoving-frame transfer eqn. soln. in spherically symmetric relativistic flows 0-82181  
 radiative transfer, integral eqn. spectrum calc. for semi-infinite medium 0-67540  
 radiative transfer, key eqn. exact soln., Laplace transform and linear singular operators method 0-72762  
 radiative transfer, polarisation of scattered radiation in presence of internal energy sources 0-67541  
 radiative transfer, synthetic scattering phase function 0-98541  
 radiative transfer, time-dependent, exact soln. of integro-differential eqn. via Laplace transform 0-94703  
 radiative transfer in finite atmosphere, exact soln. of basic eqn. via Laplace transform 0-94702  
 radiative transfer in plane-parallel atmosphere with polynomial emission source distrib. 0-94700  
 red giant envelope composition rel. to evolution 0-105237  
 red giant model atmospheres, opacity sampled models grid 0-82348  
 red giant stars, circumstellar shells chem. struct. 0-105242  
 red giants in M13, Na abundance var., protocluster gas inhomogeneities 0-82439  
 WZ Sagittae, eruptive binary, accretion disc radius from hot spot eclipses anal. 0-72962  
 WZ Sagittae, recurrent nova, accretion disc models comparison with IUE obs. during outburst 0-109448  
 WZ Sagittae, recurrent nova, circumbinary gaseous disc model for superhump phenomena 0-82368  
 V818 Scorpii (Scorpius X-1), atmospheric ionisation vars. rel. to UV, visible, IR and X-ray obs. 0-82541  
 spectral line formation depth in mag. field, theory (*Chinese*) 0-105159  
 spherical accretion onto compact X-ray sources, luminosity thermal limit 0-82546  
 spherical dust shell around central star, two-shell moment method for radiative transfer 0-62001  
 spherical envelopes, line profile computation by three methods 0-85868  
 spherical transonic flow, reson. line radiative transfer 0-94698  
 SS 433, accretion disc model for beam accel., radiation and precession 0-72971  
 Stokes' problem, mass transfer effects of MHD free convective flow 0-62003  
 supergiant stars with stellar winds LMC, luminosity and extinction values, UV obs. 0-77477  
 supergiants instability effects, brightness limits and coronae 0-109432  
 supernovae, distance determ. by Baade's generalised method, appl. to H $\beta$  and  $q_0$  0-73082  
 supernovae, type I, conservative scatt. theory for effects of line overlapping on spectra (*Russian*) 0-105266  
 supernovae, Type I, envelopes, radioactive excitation source model for late time spectra 0-105264  
 symbiotic stars, stellar wind and accretion rates rel. to subclasses 0-62144  
 RW Tauri, eclipsing binary, gaseous ring struct., H I alpha obs. 0-109482  
 SU Tauri, R Coronae Borealis star, circumstellar dust shell discovery from optical and IR photometry 0-101601  
 DR Tauri, T Tauri star, mass flow var. in envelope, visible spectra 0-85939  
 28-BU Tauri (Pleione) Be shell star, 3167 to 4924 Å spectrum atlas 0-98673  
 T Tauri stars, H $\alpha$  emission line core formation in chromosphere 0-94792  
 T Tauri stars in dust cloud Lynds 134, mass loss causing cloud turbulence 0-94845  
 thermal-convective instability of partially ionized plasma, radiative transfer, medium porosity and collisional effects 0-67538  
 transfer, equation, in semi-infinite atmosphere with albedo ( $\omega > 1$ ) 0-82184  
 Trumpler 27 star 28, WC9-star with thermal dust shell 0-67738  
 turbulence, conference, London, Ontario, Canada (1979 August 27 to 30) 0-73102  
 turbulence, effect on spectral line form., finite correl. length 0-77387  
 upper main-sequence peculiar stars, atmospheric stability rel. to radiatively driven diffusion theory 0-82374  
 $\tau$  Ursae Majoris, Am star, microturbulence and metal content determ. 0-82377  
 XY Ursae Majoris, eclipsing binary, observational evidence for large-scale spot activity on primary component 0-109491  
 $\lambda$  Velorum, K-type supergiant, UV spectrum rel. to chromosphere and wind struct. 0-72948  
 $\gamma_2$  Velorum, Wolf-Rayet binary, spectral obs. 0-85950

## stellar atmospheres continued

- CU Virginis (HD 124224), Ap star, model atmospheres rel. to spectrophotometric obs. 0-98663  
 Voigt function computation, path lengths of integration 0-105234  
 white dwarfs, atmosphere structure rel. to composition in hot stars 0-98658  
 white dwarfs, highly magnetised, accretion, role of electron conduction 0-82358  
 wind, radiatively ionised, in emission nebula NGC 6302, direct evidence 0-67835  
 wind from massive close binaries, mass loss 0-90474  
 winds, interaction with interstellar medium, cosmic ray origin and accel. 0-77512  
 winds, relativistic modes of tearing instability in background plasma 0-62012  
 winds, steady state transonic wind model, radiative cooling effects 0-77391  
 winds, theory of classical fluid dynamics 0-90412  
 winds, turbulent mixing with interstellar gas 0-67701  
 Wolf-Rayet stars, late type with circumstellar dust shell, 8-13 micron spectral obs. 0-101599  
 Wolf-Rayet atmospheres, structure and composition 0-98668  
 Wolf-Rayet stars, Roche lobe overflow and stellar wind mass loss 0-105250  
 Wray 977, optical counterpart to X-ray binary pulsar, 4U 1223-62, optical spectra 0-72984  
 X-ray binary sources, pulsating, accretion from Keplerian disc rel. to spin-up 0-67904  
 X-ray induced shocks in stellar winds of massive binaries 0-94784  
 X-ray sources, accretion disc plasma oscils. rel. to radio emission 0-62317  
 X-ray sources, pulsating, accretion disc mag. field calc. for oblique mag. dipole configuration 0-94895  
 young stars in Chamaeleon TI, photometry and spectral obs. 0-72943  
 C stars, form. of carbene and cyanoacetylenes in stellar atm. 0-67708  
 He stratification in model atmosphere of blue horizontal-branch star 0-90409  
 He variable stars, IR excesses rel. to circumstellar matter 0-67733  
 Hg-Mn binary stars, inhibition of atmos. diffusion 0-62153  
 HgMn stars, evidence for Hg in thin atmospheric layer rel. to diffusion model 0-105243

## stellar binaries see binary stars

## stellar clusters and associations

- see also *global star clusters*  
 07021-1940, cluster hidden in ghost image of Sirius on Palomar Sky Survey, discovery 0-109501  
 Berkeley 11, compact open cluster, UVB obs. 0-94840  
 Berkeley 19, anticentre open cluster, age determ. from colour magnitude diagram, BV photometry 0-90486  
 binding energy distrib. of binaries in cluster, homogeneous cluster model 0-62209  
 Cassiopeia-Taurus association stars, interstellar 2200 Å feature anomalous strength 0-77469  
 Cepheus IV star formation region, continuum and recomb. lines, SHF obs. 0-90501  
 Chamaeleon TI, young stars, photometry and spectral obs. 0-72943  
 classification criteria by statistics from co-occurrence matrix (*Italian*) 0-98574  
 cluster around massive black hole, stationary state (*Russian*) 0-67806  
 Collinder 135, nearby field of view, wide and narrow band photometry obs. 0-109504  
 Collinder 140, young open cluster, spectroscopic and statistical study 0-62211  
 Collinder 228 and 232 in Carina Nebula, extinction determ. from UVB photometry obs. 0-90513  
 collinder 228 in Carina Nebula, open clusters distance determ., photometry obs. 0-85977  
 Coma cluster, reddening 0-62222  
 Cygnus OB2 association, connection with Cygnus X-ray superbubble 0-90575  
 Czernik 29 in Puppis open cluster pair, UVB obs. 0-109503  
 dynamical evolution of cluster models with continuous stellar mass loss 0-82438  
 dynamical evolution of Keplerian systems, numerical simulations of collisions 0-109342  
 dynamics, collision integral determ. (*Polish*) 0-67799  
 dynamics, higher order fluid eqns. for multicomponent nonequilibrium systems 0-105156  
 dynamics, stability of one-dimensional self-gravitating isothermal systems 0-73008  
 faint clusters in LMC, colour magnitude diagrams, BV photometry 0-94841  
 formation rel. to universal expansion and big-bang theory (*Dutch*) 0-62212  
 galactic centre region, sources and obscuration 0-77487  
 galactic clusters, Basle catalogues data rel. to interstellar reddening in solar neighbourhood 0-62239  
 Haffner 10 in Puppis open cluster pair, UVB obs. 0-109503  
 Hyades, lunar occultations in 1979 March, stellar angular diameters 0-72921  
 Hyades, reddening, polarimetry and field star photometry 0-62222  
 Hyades metal content and distance rel. to solar colour 0-101569  
 IC 1805 (W4), nearby cluster, spectral classes and photometry 0-62214  
 IC 2581, open cluster, discovery of two Be stars 0-90445  
 An King 13, open cluster, UVB obs. (*German*) 0-77459  
 in LMC, survey, visible obs. 0-73011  
 Loden cluster candidates in S. Milky Way, colour excess, distance and spectral types 0-85997  
 loose stellar clusters in southern Milky Way, spectral type and UVB obs. 0-94839  
 M11, galactic open cluster, age and distance, colour diagram, photometric obs. 0-73012  
 M67, reddening 0-62222  
 Markarian 38, galactic open star cluster, photometric obs. (*German*) 0-73015  
 Monoceros R2, far IR obs. of young assoc. 0-73010  
 NGC 129, open cluster membership from four colour and H $\beta$  photometry 0-90485  
 NGC 1955, open cluster in LMC, early-type stars stellar winds rel. to motions in bubble-like nebula N51D 0-105295

**stellar clusters and associations continued**

- NGC 2264, young star cluster, interstellar OH and NH<sub>3</sub> obs., SHF and UHF 0-94847  
 NGC 2264 and 7000/IC 5070, new H $\alpha$  stars, slitless spectrographic search 0-62120  
 NGC 2547, open cluster in Vela star cloud, photometric survey 0-90482  
 NGC 3293, open cluster, UBVRI photometry and relation to OB complex in Carina 0-90490  
 NGC 3293, uvby  $\beta$  photometry rel. to other young clusters 0-101621  
 NGC 330, in SMC, radial vels. of individual stars 0-67803  
 NGC 3603, compact galactic cluster central star HD 97950, interstellar features, visible obs. 0-101586  
 NGC 3766, open cluster, discovery of twelve Be stars 0-90445  
 NGC 4103, open cluster, membership determ. from proper motions, visible obs. 0-67802  
 NGC 604, 5471, giant extragalactic H II regions, UV spectra rel. to exciting clusters comp. 0-77467  
 NGC 6087, galactic cluster, four-colour and H $\beta$  photometry 0-62208  
 NGC 6231, open cluster, spectral types 0-90492  
 NGC 6494 (M23), open star cluster, membership from astrometry with PDS microdensitometer 0-98697  
 NGC 654, young open cluster, UVB photometric study 0-109502  
 NGC 741, 1316, 7626, radio galaxies, central dense star clusters luminosities rel. to accreting black holes 0-94871  
 NGC 7789, open cluster, blue straggler K1211, photometry and polarimetry obs. 0-109433  
 NGC 957, young open cluster, distance and reddening, RGU photometry 0-85976  
 OB associations, CNO abundances in B-type stars 0-67702  
 OB associations, initial mass function in young objects 0-98695  
 OB associations, interstellar medium interactions, H I supershell form. 0-82468  
 OB associations, sequential form. of subgroups 0-98696  
 OB associations in M31, correl. with spiral struct. in UV image 0-98716  
 OB type stars, Gould belt, local cosmic ray origin 0-77512  
 Oel 352, open cluster, excitation of W4 H II region and form. 0-94843  
 oldest open clusters, galactic distrib. in disk 0-101620  
 open clusters, age determ. methods (*Italian*) 0-90489  
 open clusters, southern, kinematics and dynamics from radial vel. obs. (*German*) 0-94724  
 open clusters assoc. with interstellar gas-dust clouds, dynamics 0-101622  
 $\rho$  Ophiuchi cloud, cosmic ray accel. by stellar winds 0-77512  
 Pismis 13, open cluster, colour magnitude diagram, UVB obs. 0-67805  
 Praesepe radial and nonradial pulsation periods in  $\delta$  Scuti star BT Cancri (38 Cancri) 0-85948  
 protocluster cloud rotation, mag. braking of aligned rotator during star form., exact time-depend. soln. 0-90493  
 Puppis open cluster pair Czernik 29 and Haffner 10, UVB obs. 0-109503  
 relativistic, with high central redshift 0-105293  
 relativistic spherical systems, binding energy criterion for dynamical stability 0-94837  
 Scorpius-Centaurus association, evidence for membership of  $\alpha^1$  Crucis from improved spectroscopic orbit 0-67792  
 Sirius moving group, evidence for existence from chromospheric Ca II H and K emission in field stars of solar neighbourhood 0-109423  
 SMC star cluster colour magnitude diagrams and stellar identification charts 0-73014  
 spherically symmetric model cluster with stars of uniform mass, struct. and dynamics 0-62215  
 star formation evidence from bright star clusters round NGC 5253, visible obs. 0-77489  
 T association in Chamaeleon dark cloud, embedded Be-star, IR obs. 0-85943  
 Trapezium type multiple systems, connection with associations, galactic clusters and emission nebulae 0-67781  
 Trumpler 10, open cluster in Vela star cloud, photometric survey 0-90482  
 Trumpler 14, 15, 16 in Carina Nebula, extinction determ. from UVB photometry obs. 0-90513  
 Trumpler 14, 15 and 16 in Carina Nebula, open clusters distance determ., photometry obs. 0-85977  
 Trumpler 15 in  $\eta$  Carina, open cluster, age and reddening from UBVRI obs. 0-90487  
 Vela star cloud, large scale photometric survey 0-90482  
 young associations in LMC, stars embedded in ring-shaped nebulae 0-77457  
 young clusters, circumstellar matter round OB3 type stars, 2200 Å hump interpretation 0-82351

**stellar composition**

- see also element origin; solar composition*  
 Algol type star, accretion and chem. struct., evolutionary calcs. 0-109481  
 Ap, Am stars, chemical differentiation and abundance spots prod. by diffusion 0-77381  
 Ap stars in spectroscopic binary systems, chemical anomalies surface distrib. 0-62140  
 R Aquarii, symbiotic long-period variable, spectrum and comp. of assoc. nebulosity 0-90450  
 $\sigma$  Aquarii (A0 IVs), hot metallic-line star, abundance anal. from model atmosphere 0-90415  
 $\theta$  Aquilae (B9.5 III), abundance anal. from model atmosphere 0-90415  
 asymptotic giant branch evolution of intermediate-mass stars, post-second dredge-up phase 0-72936  
 B-type stars, CNO abundances in associations and general field 0-67702  
 binary stars, close detached, Ap components, chem. anomalies surface distrib. 0-109475  
 binary stars, He abundances from speckle interferometric obs. 0-90475  
 $\alpha$  Bootis (Arcturus), effects of mag. mixing on C/N and <sup>12</sup>C/<sup>13</sup>C ratios 0-105229  
 $\nu$  Capricorni (B9.5 V), abundance anal. from model atmosphere 0-90415  
 $\epsilon$  Centauri, main sequence stars photometry rel. to He abundance 0-90491  
 $\alpha$  Centauri binary system, spectroscopic chemical anal. 0-62128  
 9 Cephei (B2 Ib), circumstellar CO obs. 0-94795  
 RS Chamaeleontis, eclipsing binary, four-colour photometry rel. to photometric elements, absolute dimensions and He abundance 0-67783  
 XX Cygni, dwarf Cepheid, composition and motion, visible photometric and spectrographic obs. 0-77424  
 V645 Cygni (AFGL 2789), broad absorpt. band obs. and identification 0-73066

**stellar composition continued**

- HR Delphini (Nova 1967), C and N overabundances in stellar wind from UV spectra 0-109440  
 dense stellar cores, chemical comp. oscills. rel. to time-dependent neutrino transport 0-94783  
 early-type stars, envelope mixing of elements, shear flow instability 0-109424  
 early-type stars, He abundance effect on H and He<sup>+</sup> line profiles in stellar winds 0-85926  
 elliptical galaxies, chemical evolution 0-67843  
 F-type supergiants in Magellanic Clouds, Ca abundances 0-98655  
 G128-7, cool DA white dwarf, atmospheric metal abundance and evolutionary consequences 0-62126  
 G 165-7, metallic line white dwarf, abundances, model atm. code anal. of spectrum 0-85940  
 $\gamma$  Geminorum, differential abundance anal. rel. to  $\alpha$  Lyrae standard 0-82362  
 giant stars, Population I, theoretical surface abundances 0-94796  
 giant stars in globular star clusters, Ca II H and K-lines and abundance 0-72940  
 globular cluster stars, He settling and effect on inferred ages 0-73013  
 globular clusters, ages and comp. rel. to fundamental knowledge about galaxies evolution 0-90488  
 halo stars, cool, Al abundance implications for galaxy abundance 0-105232  
 HD 10380, Population I giant, chemical anal. and comparison with high vel. stars 0-82352  
 HD 187473, rare earths in Si star 0-98671  
 HD 25329, subdwarf, metal deficiency from spectroscopic anal. 0-62122  
 heavy element abundance, effects on evolution of stars, struct. of models 0-105231  
 $\alpha$  Herculis A, M-type supergiant, Li abundance in atmosphere (*Russian*) 0-72950  
 high velocity giant stars, detailed chemical anal. 0-82352  
 HR 6127, chemically peculiar star, spectral lines and equivalent width lists, visible obs. 0-82387  
 HR 96, Ap-type star, atm. parameters and stellar comp., visible obs. 0-67740  
 Hyades metal content and distance rel. to solar colour 0-101569  
 W Hydrae, form. of carbyne and cyanoacetylenes in stellar atm. 0-67708  
 HZ 43, white dwarf, He abundance and stellar struct. from soft X-ray spectra 0-72944  
 III-106, CH star in globular cluster M22, CO in IR spectra 0-62131  
 $\epsilon$  Indi, late type dwarf star, model atmosphere and abundance anomalies 0-90425  
 initial chemical comp. discontinuity and non-radial oscills. of 1 M $\odot$  star 0-82341  
 AQ Leonis, homogeneous model of Population II double-mode RR Lyrae star 0-62134  
 LP 145-141, C<sub>2</sub> white dwarf, CO, C<sub>2</sub> and O<sub>2</sub> abundances rel. to strong UV absorpt. 0-67715  
 $\beta$  Lyrae, CNO abundances in atmosphere, IR spectra (*Russian*) 0-67794  
 R Lyrae, M-type supergiant, Li abundance in atmosphere (*Russian*) 0-72950  
 RR Lyrae stars, in 47 Tucanae, membership and metallicity 0-62206  
 M32, metallicity and galaxy age from spectral synthesis 0-67842  
 M5, M13, M3, globular clusters, giant stars chemical comp. 0-67695  
 main sequence galactic disk stars, chem. comp., implications for galaxy 0-109553  
 massive star core collapse, eqn. of state and composition near  $\beta$  equilib. 0-82335  
 massive stars, element abundances rel. to evolution 0-90416  
 metal abundances in galactic disc stars, rel. to gas inflow problem and disc chemical evolution 0-62279  
 metal abundances of F- and G-dwarfs from CORAVEL radial vel. scanner 0-94791  
 metal rich stars, zero age main sequence position 0-109426  
 metallicity gradients in galaxies, weakening during galaxy mergers 0-67860  
 metals in stellar populations in bright galaxy nuclei 0-98708  
 neutron star matter expansion and its final nuclear composition 0-67769  
 NGC 1851, 6624, globular cluster, abundance gradients spectroscopic investigation 0-82437  
 Nova Serpentinis 1978, enhanced C abundance in dust shell 0-90430  
 nucleosynthesis at explosive Ne burning in supernovae 0-94780  
 Orion population stars, OH emission survey 0-67716  
 Pal 12, metal-rich globular cluster in outer galactic halo, optical and IR obs. 0-105290  
 IW Persei, metallic-line close binary, local metallicity surface distrib. 0-62186  
 19 Piscium, C star, violet spectrum line identification and radial vel. 0-82361  
 planetary nebula central star evolutionary scenario towards white dwarf stage 0-109427  
 planetary nebulae central star abundances corrections from UV flux determ. 0-72945  
 planetary nebulae central stars, C abundance rel. to nebulae refractory elements gas-phase abundances 0-109516  
 pulsar outer crust composition, influence of mag. field 0-101610  
 L<sub>2</sub> Puppis, semiregular variable, Ca I uneven distrib. from narrowband polarimetry 0-98666  
 rare earth elements, atomic partition functions, Chebyshev approximations 0-67544  
 red giant of 6 M $\odot$ , envelope composition rel. to evolution 0-105237  
 red giant stars, circumstellar shells chem. struct. 0-105242  
 red giants, convective He shells, s-branch nucleosynthesis during thermal pulses 0-90410  
 red giants in Draco dwarf spheroidal galaxy, metal abundance 0-73030  
 red giants in M13, Na abundance var., protocluster gas inhomogeneities 0-82439  
 Ross 640, He-rich white dwarf, Ca, Mg, S and Fe abundances from UV spectra 0-94790  
 S-type stars, Keenan and Wing bands, IR obs. 0-67722  
 S-type stars, possible presence of ZrO IR spectrum 0-62124  
 FG Sagittae, 1975-8 spectral obs. of peculiar variable 0-72959  
 SB 21, extremely He rich subdwarf O-star, spectrum 0-98659  
 spectroscopic binary stars, He and metal abundances rel. to apsidal motion 0-82413  
 subdwarf stars, odd-Z and r-process elements abundances from spectroscopic anal. 0-62122  
 subdwarfs, 37-45 excess calibration using Fe/H abundances 0-82363



## stellar composition continued

- subdwarfs, photometry rel. to compositions and kinematics 0-82364  
 supernovae, Type I, envelopes, comp. rel. to radioactive excitation source model for late time spectra 0-105264  
 surface composition, effects of interaction with dense interstellar gas clouds (*German*) 0-109500  
 upper main-sequence peculiar stars, chemical and physical props. rel. to radiatively driven diffusion theory 0-82374  
 $\tau$  Ursae Majoris, Am star, microturbulence and metal content determ. 0-82377  
 white dwarf in binary system, outer layer C and O enrichment from companion 0-109465  
 white dwarfs, atmosphere structure rel. to composition in hot stars 0-98658  
 white dwarfs, spectra and atmospheric comps. 0-82356  
 Wolf-Rayet atmospheres, structure and composition 0-98668  
 Wolf-Rayet stars, binary freq. distrib. and chemical comp. 0-105250  
 Wolf-Rayet stars, CNO abundance var. in massive binaries 0-94802  
 young variable stars, absorpt. and emission features, IR spectrophotometry obs. 0-72954  
 C enhancement in nova envelope on surface accretion at white dwarf 0-85936  
 C stars, form. of carbyne and cyanoacetylenes in stellar atm. 0-67708  
 C/N abundances on first giant branch of NGC 6752 globular cluster 0-67719  
 C-O white dwarfs, C-O eutectic model 0-77405  
 $C_2$ ,  $A^1\Pi-X^1\Sigma_g^+$  lines, obs. in carbon stars 0-98661  
 CN variations among main-sequence 47 Tucanae stars 0-94794  
 CO in evolved stars expanding envelopes, thermal and maser emission lines profiles 0-82334  
 Fe I in Ap stars, photoionisation spectrum causing UV absorpt. 0-109437  
 Fe/H abundance, catalogue for 628 stars 0-98579  
 He stratification in model atmosphere of blue horizontal-branch star 0-90409  
 Hg-Mn binary stars, inhibition of atmos. diffusion 0-62153  
 HgMn stars, evidence for Hg in thin atmospheric layer rel. to diffusion model 0-105243

## stellar dimensions

- angular diameter determ. using IR flux method 0-62030  
 angular diameter from lunar occultations, photolec. obs. 0-72920  
 angular diameters from lunar occultations of Hyades photolec. obs. 0-72921  
 KO Aquilae, eclipsing binary, mass ratio and secondary component fractional radius from photoelectric study 0-62198  
 EO Aurigae, eclipsing binary star, revised elements from light curve anal. 0-90471  
 B5 V-P5 V type stars in Geneva Observatory catalogue, radii, temp. and brightness determ. 0-77396  
 binary stars, distances, masses and dias. from speckle interferometric obs. 0-90475  
 binary stars, main sequence, absolute dims. determ., errors requirement review 0-109473  
 BT Cancr (38 Cancr),  $\delta$  Scuti star, multiple periods rel. to radial and nonradial pulsation periods 0-85948  
 $\beta$  Canis Majoris,  $\beta$  Cephei star, pulsations periods from Fourier anal. of radial vel. changes 0-105246  
 OY Carinae, white dwarf cataclysmic, eclipsing binary, parameter determ. 0-82385  
 SU Cassiopeiae, Cepheid variable, temp. and radius determ. rel. to luminosity and mass 0-90435  
 cataclysmic binaries, circumstellar material geometrical and photometric parameters 0-109492  
 VW Cephei, W Ursae Majoris star, rot. line broadening rel. to shape and mass ratio 0-109494  
 Cepheids, stellar pulsation problem, time dependent convection local theories 0-72964  
 XY Ceti, eclipsing binary, masses, radii and luminosities from revised photometric elements 0-109458  
 RS Chamaeleontis, eclipsing binary, four-colour photometry rel. to photometric elements, absolute dimensions and He abundance 0-67783  
 Z Chamaeleontis, eruptive binary, model from photoelectric data anal. 0-72961  
 close binary systems, components dimensions and distortion rel. to radial vel. curves anal. 0-90470  
 AI Crucis, eclipsing binary, photometric mass and radius ratios and configuration 0-109459  
 V380 Cygni, eclipsing binary, masses, radii and luminosities from revised photometric elements 0-109458  
 distorted stars, Clairaut coordinates and vibr. stability 0-90408  
 eclipsing binaries, sd-d and R Canis Majoris type, struct. and dims. 0-82423  
 $\nu$  Eridani,  $\beta$  Cephei star, pulsations periods from Fourier anal. of radial vel. changes 0-105246  
 gravitational radius, equilib. of gravity and elec. forces 0-57152  
 HD 93250, O3 massive star in  $\eta$  Carinae complex, non-LTE analysis 0-77398  
 HDE 245770, optical counterpart to A 0535+26, dims. spectral type and luminosity visible obs. 0-72976  
 TT Hydrae, absolute dimensions of  $\beta$  Persei type eclipsing binary 0-62184  
 EX Hydrae, dwarf nova, accretion disc dimensions from IR and optical light curves 0-67747  
 VW Hydri, dwarf nova, accretion disc dimensions from IR light curves 0-67747  
 IRC +10216, C star, far IR size 0-82539  
 RR Lyrae stars, effects of hydromagnetic cycle on photospheric radius and pulsation period 0-105261  
 neutron stars, mass-radius relation 0-77444  
 1W Persei, metallic-line close binary, primary component fractional radius and local metallicity distrib. 0-62186  
 planetary nebulae central stars, temp. and and radius evolution and relaxation, process 0-67724  
 WZ Sagittae, eruptive binary, accretion disc radius from hot spot eclipses anal. 0-72962  
 $\sigma$  Scorpii,  $\beta$  Cephei star, pulsations periods from Fourier anal. of radial vel. changes 0-105246  
 V701 Scorpii, dimensions and evolution of early-type contact binary 0-62188

## stellar dimensions continued

- surface large-scale pulsations, nonlinear coupling to small-scale deep-seated instabilities 0-62115  
 $\gamma$  Tauri, ang. diameter determ. from lunar occultation obs. 0-62119  
 RW Trianguli, nova-like eclipsing binary radial vels., dims. from visible spectra 0-82418  
 W Ursae Majoris stars, rot. line broadening functions rel. to stellar shapes 0-109494  
 AI Velorum, radius and mass from BVRI photometry and photoelectric radial vels. 0-94815  
 ER Vulpeculae, W Ursae Majoris star, rot. line broadening rel. to shape and mass ratio 0-109494  
 white dwarfs, rapid mass accretion and extended envelope form. 0-67723
- stellar evolution
- 2 to 10 MG stars, effect of heavy element abundance on evolution, struct. of models 0-105231  
 accreting neutron stars, He burning shell evolution 0-85968  
 Algol type star, accretion and chem. struct., evolutionary calcs. 0-109481  
 Am-type, binary stars, tidal interaction producing stable atm., evolution 0-67752  
 anomalous mass stars, evolution on main sequence 0-72929  
 KO Aquilae, eclipsing binary system, evolutionary phase from UVB photoelectric study 0-62198  
 asymptotic giant branch evolution of intermediate-mass stars, post-second dredge-up phase 0-72936  
 EO Aurigae, eclipsing binary star, revised elements and evolutionary stages of components 0-90471  
 axially symmetric star, general relativistic collapse, initial data 0-85960  
 B7 to G4 stars, ages rel. to distrib. perpendicular to galactic plane (*Russian*) 0-73036  
 B-type stars formation is interstellar clouds, effects on distrib. of molecules (*Russian*) 0-105321  
 Be stars, evidence for evolutionary stage from presence in two open clusters 0-90445  
 Berkeley 19, anticentre open cluster, age determ. from colour magnitude diagram, BV photometry 0-90486  
 binaries, wide visual, spectral type, age and uvby $\beta$  photometry 0-94833  
 binary stars, binding energy distrib. in cluster, homogeneous cluster model 0-62209  
 binary stars, detached, evolution to contact binaries involving mass flow 0-109477  
 binary stars, statistical distrib. and evolution (*Chinese*) 0-85975  
 binary system evolution, Roche problem for polytropes in central orbits problem for polytropes in central orbits 0-82179  
 blue stragglers, evolution on main sequence 0-72929  
 blue supergiant with neutron star immersed in envelope 0-98689  
 calculation programme and standard solar model 0-67703  
 RS Canum Venaticorum binary stars, evolutionary status and orbital parameters rel. to starspot phenomena 0-109488  
 $\beta$  Cephei stars, effects of mass loss on instability strip 0-90436  
 $\beta$  Cephei stars, pulsations and evolutionary status 0-85959  
 Cepheids, membership in open clusters from star and cluster age determ. (*Italian*) 0-90489  
 chemical evolution rel. to galactic evolution and nucleosynthesis 0-67847  
 close binaries, intermediate mass, mass transfer for different stars within evolutionary scheme 0-109476  
 close binaries, synchronous systems devel. from tidal are rot. interactions 0-109468  
 close binary stars, low mass, evolution, gravitational wave emission influence 0-82425  
 close binary stars evolution, mass transfer effects on props., obs. and theory comparison 0-62187  
 cluster models with continuous stellar mass loss, dynamical evolution 0-82438  
 Collinder 140, young open cluster, age from spectroscopic study rel. to membership statistics 0-62211  
 contact binaries, solar type, mass ratio evolution function rel. to initial mass ratio distrib. function 0-109496  
 contact binaries with age-zero components, secular stability 0-67786  
 contact binary star, idealised dynamical evolution (*French*) 0-62199  
 convective envelope stars, value of mixing length rel. to stellar evolution sequences 0-77379  
 core collapse, time-dependent neutrino transport theory 0-94783  
 core collapse and overturn with Rayleigh-Taylor unstable gradient 0-94819  
 core collapse outcome, effects of core eqn. of state 0-85928  
 core collapse to neutron star, electron neutrino and antineutrino emission, spectral calcs. 0-109454  
 degenerate C ignition, burning front propag. rel. to core implosion or disruption 0-77390  
 S Doradus, Hubble-Sandage variable in LMC, effect of mass loss on evolution 0-101595  
 BY Draconis stars, angular momentum initial distrib. and evolution 0-85954  
 fluid drops as cosmological models, stellar evolution, solar system origin, planetary geology 0-73086  
 formation, hydrodynamic model reviews (*Polish*) 0-67709  
 formation, protostellar cloud ang. momentum problem, mag. breaking 0-82342  
 formation, role of supernovae 0-82232  
 formation and protostellar clouds, review 0-101589  
 formation evidence from bright star clusters round NGC 5253, visible obs. 0-77489  
 formation from collapsing gas sphere, nonlinear development of gravitational instability 0-62114  
 formation from mol. and at. cloud-cloud collisions 0-94844  
 formation in barred galaxies rel. to nucleus activity 0-105341  
 formation in bright galaxy nuclei, spectra anal. 0-98708  
 formation in Cepheus IV region, continuum and recomb. lines, SHF obs. 0-90501  
 formation in disk galaxies 0-82483  
 formation in expanding molecular shell surrounding Pelican Nebula H II region, evidence from CO obs. 0-105296  
 formation in faint galaxies, spectroscopy and photometry rel. to evolution 0-105353  
 formation in gas clouds in elliptical galaxies 0-67868  
 formation in M82 and NGC 253 nuclei, model constraints 0-82485  
 formation in non-elliptical galaxies, galaxy two colour diagram 0-67875  
 formation in photometry of remote clusters 0-105364  
 formation in primaeval galaxies, high luminosity epoch 0-105354

## stellar evolution continued

- formation of solar-type stars in spherical symmetry, accretion shock effects 0-62107
- formation rate and ionising Lyman continuum photon flux 0-67711
- formation rate in inner Galaxy, IR obs. 0-67704
- formation rel. to spiral galaxy types Sab to Scd luminosity freq. distrib. 0-82482
- G128-7, cool DA white dwarf, atmospheric parameters and evolutionary consequences 0-62126
- in galaxies, review 0-77486
- giant stars, mass loss before envelope ejection due to pulsational instability 0-72935
- giant stars, Population I, evolution from ZAMS rel. to theoretical surface abundances 0-94796
- giant stars as progenitors of planetary nebulae, struct. anal. form. 0-109537
- GL 2591, protostellar source, 3  $\mu$ m ice absorpt. band, linear polarisation obs. 0-105303
- GL 2636, star form. region in Cygnus-X, IR obs. 0-105302
- globular cluster stars inferred ages, effects of He settling 0-73013
- globular clusters, ages and comp. rel. to fundamental knowledge about galaxies evolution 0-90488
- globular clusters, models, props. based on stellar evolution and cluster structure 0-62210
- globular star cluster, relax. degree and evolution, appl. of N-body system numerical integration 0-67808
- globular star cluster age and distance determ. using subdwarf photometry results 0-82435
- gravitational collapse, maximal time slicing condition 0-67554
- gravitational collapse, neutrino trapping effect on nucl. dissoc. 0-90407
- gravitational collapse, neutronisation and lepton escape rel. to hydrodynamics 0-77388
- gravitational collapse, theory 0-77389
- HD 166734, Of binary system, evolutionary state, visible obs. 0-82414
- HD 93250, O3 massive star in  $\eta$  Carinae complex, non-LTE analysis 0-77398
- Hercules X-1 (HZ Herculis) binary system, pre-supernova parameters 0-62318
- K1211, blue straggler in NGC 7789, evolution status and mass, photometry obs. 0-109433
- L 183 (L 134 N) dust cloud, evolution of condensations 0-105307
- late-type stars of solar neighbour emission with age 0-109423
- lifetimes, effects of interaction with dense interstellar gas clouds (*German*) 0-109500
- M11, galactic open cluster, age and distance, colour diagram, photometric obs. 0-73012
- mass loss, fate of loss material in galactic nuclei 0-67858
- mass loss, rel. to white dwarfs form. 0-77281
- massive close binaries with OB components, evolutionary calcs. comparison with obs. 0-90474
- massive close binary stars, effect of stellar evolution on components synchronous rot. 0-62192
- massive main-sequence star, early evolution 0-62113
- massive stars, effect of convective and semiconvective mixing on evolution 0-90405
- massive stars, single and binaries, review 0-82343
- massive stars ( $M \geq 50 M_{\odot}$ ), evolutionary status, mass transfer model (*Russian*) 0-109425
- massive stars evolution, observational review 0-90416
- massive stars formation in dense molecular clouds, radio and IR appearance of dusty H II blisters 0-85979
- TY Mensae, contact eclipsing binary, evolutionary stage from UVB light curve anal. 0-105278
- metal rich stars, zero age main sequence position 0-109426
- models, effect of gravitational const. var. 0-82186
- neutron star X-ray emission models 0-62175
- neutron stars, cooling 0-77443
- neutron stars, quark beta decay and cooling 0-82406
- NGC 3293, open cluster in Carina, UVRI photometry and age 0-90490
- NGC 6397, globular star cluster, age from main sequence turnoff, BV photometry 0-90484
- novalike object in Vulpecula, UV decline and expanding cooling photosphere 0-67741
- O- and Of-type stars, masses and mass loss 0-94793
- Of-type stars as evolved O-type stars, rel. to difference in mass loss 0-90413
- open clusters, age determ. methods (*Italian*) 0-90489
- MW Pavonis, W Ursae Majoris system, evolutionary stage from UVB light curve anal. 0-105278
- $\beta$  Persei (Algol) eclipsing binaries, mass loss and mass transfer theory 0-62191
- planetary nebula central star evolutionary scenario towards white dwarf stage 0-109427
- planetary nebulae, central stars of solar mass, evolution 0-109428
- planetary nebulae central stars, protoplanetary stage of evolution rel. to cool stars 0-109435
- planetary nebulae central stars, temp. and radius evolution and relaxation, process 0-67724
- planetary nebulae central stars, two-wind model for nebulae refractory elements gas-phase abundances 0-109516
- planetary nebulae nuclei, evolutionary tracks rel. to halo white dwarf masses 0-82344
- planetary nebulae nuclei, He shell flashes rel. to nebulae ionisation 0-73021
- protosolar nebula, dust grain motion time evolution 0-82234
- protostars, Barnard globules evolution 0-82462
- protostars, magnetic, quasistatic contraction due to mag. flux leakage 0-98662
- protostellar cloud, solar-type star form. with spherical symmetry 0-85930
- protostellar cloud fragmentation processes, evidence from solar neighbourhood mass distrib. 0-98649
- protostellar clouds fragmentation, three-dimensional hydrodynamical calcs. 0-62236
- protostellar envelope evolution, radiative transfer and spectrum 0-77384
- protostellar formation in rotating interstellar clouds, axially symmetric collapse 0-77380
- protostellar formation in rotating interstellar clouds, nonaxisymmetric collapse 0-85927
- pulsar age, correl. with  $P_1$  period 0-90461

## stellar evolution continued

- pulsars, classification method from period change and radio luminosity (*Chinese*) 0-85963
- pulsars, distribution, birthrate and flux density distrib. 0-98681
- pulsars, evolution rel. to torques, magnetic moment and pair production 0-62169
- quark stars, beta decay 0-82398
- rapidly rotating pre main sequence stars, evolution in gravit. contraction phase 0-62133
- red giant envelope composition rel. to evolution 0-105237
- red giants, IR radiation emission in final stages 0-72931
- red giants in M13, Na abundance var., protocluster gas inhomogeneities 0-82439
- Roberts 22, bipolar nebula with OH emission, obs. rel. to evolutionary status 0-94859
- Rubin-152, possible massive O-type star on galactic fringe, evolutionary stage 0-98656
- FG Sagittae, 1975-8 spectral obs. of peculiar variable 0-72959
- V701 Scorpii, dimensions and evolution of early-type contact binary 0-62188
- in SMC, distrib. and evolution of stellar populations 0-94868
- solar nebula, primordial, struct. and evolution 0-62042
- solar neighbourhood, initial mass function and stellar birthrate 0-62259
- star formation, in giant ellipsoidal shells around normal elliptical galaxies 0-86000
- star formation, mag. braking of aligned rotator, cloud rotation, mag. braking of aligned rotator during star form., exact time-depend. soln. 0-90493
- star formation, numerical calcs. of collapse of nonrotating magnetic gas clouds 0-105299
- star formation, role of interstellar cloud formation induced by OB-type stars 0-109506
- star formation bursts in galaxies of Magellanic type, effects on struct. and colour (*German*) 0-105348
- star formation in barred spiral galaxy NGC 925, correl. with H I distrib. 0-105329
- star formation in central regions of galaxy IC 342, evidence from IR emission 0-62256
- star formation in dark clouds, radio continuum interferometric search for newly formed H II regions 0-98699
- star formation in galaxies, suppression rel. to delayed star form. problem 0-105349
- star formation in galaxy NGC 4314, distrib. from UVB surface photometry of central region 0-77482
- star formation in interstellar dark clouds, implications of radio continuum obs. of young H II regions 0-105301
- star formation in M31 (Andromeda galaxy), depend on interstellar gas density rel. to Cepheid periods radial var. (*Russian*) 0-90455
- star formation in M32, duration from galaxy spectral synthesis 0-67842
- star formation in merging galaxies, influence on population gradients 0-67860
- star formation in NGC 6334, rel. to  $H_2$  O masers 0-73025
- star formation in OB associations, sequential form. of association subgroups 0-98696
- star formation in W3, struct. of OH maser source W3(OH) from VLBI synthesis obs. 0-105368
- star formation in W58, evidence from CO obs. 0-67810
- star formation laws, implication of bright stars luminosity function 0-82499
- star formation regions, rel. to galactic spiral struct. in vicinity of Sun (*Russian*) 0-62290
- star formation sites in W3/W4/W5 direction, correl. with heavy optical obscuration 0-62301
- Sun, neutrino problem and evolution (*French*) 0-72933
- supergiants, early-type, with mass loss, two-core model and evolutionary status (*Russian*) 0-109425
- supergiants in Magellanic Clouds, birthrate and mass function 0-67699
- supernovae, types I and II, evolution rel. to radial distrib. in spiral and elliptical galaxies 0-62163
- supernovae in molecular clouds, spectra and luminosity, evolution 0-82399
- symbiotic stars, evolutionary considerations 0-62144
- T Tauri star formation, regulatory force in dark mol. cloud evolution 0-85980
- thermonuclear explosions 0-72766
- Trapezium type multiple systems, evidence for youth from connection with association and nebulae 0-67781
- white dwarf formation rate, luminosity function determ. 0-90418
- white dwarf in binary system, outer layer C and O enrichment from companion 0-109465
- white dwarfs, He flash and nova evolution 0-72938
- white dwarfs, rapid mass accretion and extended envelope form. 0-67723
- white dwarfs, struct. and evolution theory rel. to EUV obs. and spectra 0-82356
- Wolf-Rayet stars, binary freq. distrib. 0-105250
- Wolf-Rayet stars, CNO abundance var. in massive binaries 0-94802
- Wolf-Rayet stars, evolutionary status of high-luminosity (WN7/WN8) stars (*Russian*) 0-109425
- X-ray bursters, form. of neutron star and low mass main sequence star binary system 0-109455
- young stars in Chamelaon T1, photometry and spectral obs. 0-72943
- young stars with mass accretion 0-101592
- C cores evolution, nuclear energy generation rates and energy dissipation 0-82339
- C shell burning to Fe core collapse, evolution of 15  $M_{\odot}$  star 0-72937
- C-O white dwarf freezing, C-O eutectic model 0-77405

## stellar interiors see stellar internal processes

## stellar internal processes

- see also solar interior: stellar evolution
- asymptotic giant branch evolution of intermediate-mass stars, post-second dredge-up phase 0-72936
- axions, very low mass, astrophysical bounds and stellar-energy loss 0-109353
- Cepheids, stellar pulsation problem, time dependent convection local theories 0-72964
- convection, turbulent, in Boussinesq fluids, viscosity, conductivity and power spectra 0-98543
- convection equations, ensemble averaging 0-67698
- convective and semiconvective mixing in massive stars, effects on struct. and evolution 0-90405



## stellar internal processes continued

- convective envelopes, non-local convection, statistical theory (*Chinese*) 0-85933
- core collapse, neutrino prod. and interaction with ejected envelope <sup>26</sup>Mg, <sup>26</sup>Al prod. (*Russian*) 0-77285
- core collapse and overturn with Rayleigh-Taylor unstable gradient 0-94819
- core collapse outcome, effects of core eqn. of state 0-85928
- core collapse to neutron star, electron neutrino and antineutrino emission, spectral calcs. 0-109454
- core gravitational collapse, shockwave prod., neutrino transport effects 0-94818
- core He flash, models with two-dimensional convection 0-105230
- core homologous collapse, perturbations effects 0-94779
- V1329 Cygni (HBV 475), symbiotic variable, shell flash assoc. with optical outburst 0-62148
- degenerate C ignition, burning front propag. rel. to core implosion or disruption 0-77390
- differential rotation, due to latitude depend. convective heat transport 0-90411
- diffusion, radiatively driven, in upper main-sequence peculiar stars, rel. to chemical and physical props. 0-82374
- diffusion in stars, astrophysical context 0-77381
- dwarfs, degenerate accreting, thermonuclear bursts assoc. with chromosphere flares 0-98684
- early-type stars, envelope mixing of elements, shear flow instability 0-109424
- explosive H burning, <sup>26</sup>Al synthesis 0-85929
- explosive nucleosynthesis 0-72766
- F-type star, main sequence, convection and photospheric granulation 0-90417
- globular cluster stars, He settling and effect on inferred ages 0-73013
- gravitational collapse, neutronisation and lepton escape rel. to hydrodynamics 0-77388
- gravitational collapse, theory 0-77389
- gravitational collapse of stellar core, secondary indications 0-62177
- high Coulomb barrier secondary nucl. reaction rate, ion distrib. effects (*Russian*) 0-64684
- RR Lyrae stars, hydromagnetic processes as cause of period changes 0-105261
- magnetic flux tube, buoyancy and equilib. 0-109420
- main-sequence stars, mag. mixing rel. to CNO isotope abundances and  $\alpha$  Bootis (Arcturus) problem 0-105229
- massive star core collapse, eqn. of state and composition near  $\beta$  equilib. 0-82335
- neutrino transport, time-dependent, out of dense stellar cores, theory 0-94783
- neutrino trapping at stellar collapse, effect on nucl. dissoc. 0-90407
- neutron star, accreting, thermonuclear burning in degenerate envelope 0-109455
- neutron star cores, AC Josephson effect rel. to pulsars emission 0-82404
- neutron star X-ray emission models 0-62175
- neutron stars, accreting, thermonuclear bursts assoc. with chromosphere flares 0-98684
- neutron stars, pion condensate form. rel. to cooling 0-77443
- NGC 7027, planetary nebula, evidence for CNO and  $3\alpha$  processing of nebular material 0-82459
- novae thermonuclear runaways, effect of binary companion on outburst 0-82394
- nuclear reactions, struct. and strong interactions 0-72765
- nuclear reactions associated with nucleosynthesis problem 0-101585
- nuclear reactions in dense plasmas, theory rel. to stellar evolution 0-77281
- nucleosynthesis rel. to element origin, review 0-62359
- oscillations, adiabatic nonradial, freq. splitting by slow differential rot. 0-105233
- planetary nebulae nuclei, He shell flashes rel. to nebulae ionisation 0-73021
- pulsating stars asymptotic theory, boundary layer method 0-82389
- pulsation damping due to interior weak interaction processes 0-77439
- pulsations, nonlinear coupling 0-62115
- r-nuclei production sites 0-72932
- s-process nucleosynthesis, effects of unthermalised isomeric states and time-varying neutron flux on branching ratios 0-90410
- s-process nucleosynthesis, neutron capture time scale from s-process Kr in meteorite 0-73080
- shell flashes, difficulty with <sup>22</sup>Ne as neutron source for solar system s-process 0-72926
- slow novae and symbiotic stars, role of white dwarf H shell flashes 0-94813
- stable method heavy leptons, astrophysical mass constraint, condensation in stars and galaxies (*Russian*) 0-72768
- stellar convection, value of mixing length 0-77379
- supernova collapse, eqn. of state at subnuclear densities 0-77278
- supernova core, Rayleigh-Taylor convective overturn rel. to explosion 0-77429
- supernovae, explosive core overturn and mass ejection 0-72988
- supernovae, Fe group elements prod. through e-process nucleosynthesis, relative abundances (*Russian*) 0-62167
- supernovae, magnetorotational explosion in cylindrical model 0-101605
- supernovae, Mg and Al isotopic yields from C and Ne shells of massive star 0-90406
- supernovae, type I and II, neutrino mechanism of thermonuclear explosion of degenerate C-O cores 0-62162
- supernovae core collapse, neutrino energy equilibration models 0-105265
- symbiotic stars, H shell burning rates and evolutionary considerations 0-62144
- symbiotic stars and slow novae, role of white dwarf H shell flashes 0-94813
- thermonuclear flashes in envelopes of accreting neutron stars 0-67772
- thermonuclear reactions, high energy particle excess, effect on secondary reaction rates (*Russian*) 0-77393
- turbulence, conference, London, Ontario, Canada (1979 August 27 to 30) 0-73102
- SU Ursae Majoris stars, g-mode oscills. rel. to periodicity of supermaxima 0-101596
- weak interaction rates for sd-shell nuclei, appl. to supernovae 0-82336
- white dwarf degenerate cores, thermomagnetic instability conditions 0-77395
- white dwarfs, accreting, instability of steady state nuclear burning 0-77402

## stellar internal processes continued

- white dwarfs, He flash and nova evolution 0-72938
  - white dwarfs, rapid mass accretion rel. to H shell burning and extended envelope form. 0-67723
  - Wolf-Rayet stars, CNO abundance var. in massive binaries 0-94802
  - <sup>26</sup>Al nucleosynthesis, long lived nucl. isomeric states, thermalization 0-85846
  - <sup>11</sup>B, neutrino-induced prod. in stellar C layer 0-82337
  - C cores, evolved, nuclear energy generation rates and energy dissipation 0-82339
  - C shell burning to Fe core collapse, evolution of 15 M $\odot$  star 0-72937
  - C-O white dwarfs, C-O eutectic model 0-77405
  - <sup>42,44</sup>Ca nucl. reaction rates, reactions involving proton and  $\alpha$ -particle absorpt. 0-82183
  - HgMn stars, diffusion model rel. to obs. of Hg in thin atmospheric layer 0-105243
  - <sup>26</sup>Mg(p, $\gamma$ )<sup>27</sup>Al, isotopic anomaly, stellar reaction rate, astrophysical aspects 0-99132
  - Mg(p, $\gamma$ ), 0.3-2.1 MeV, stellar H burning in explosive C burning 0-86875
  - Ne explosive burning in supernovae isotope production 0-94780
  - Si explosive burning, Ca reactions in approach to equilib. phase 0-82183
  - <sup>49</sup>Ti(p, $\gamma$ ), 0.74-3.25 MeV, cross section and thermonuclear reaction rates, nucleosynthesis, IAR effects 0-102187
  - <sup>49</sup>Ti(p,n), 0.74-3.25 MeV, cross section and thermonuclear reaction rates, nucleosynthesis 0-102187
- stellar light curves** *see stellar photometry*
- stellar magnetism**  
*see also solar magnetism*
- Ap, Am stars, mag. fields rel. to chemical differentiation by diffusion 0-77381
  - Ap and Bp stars, surface mag. field intensity rel. to Geneva photometry 0-105248
  - Ap stars, mag. fields meas. techniques and field geometries 0-82213
  - Ap-stars, mag. field obs. using photoelec. method, visible spectra obs. 0-82373
  - R Aquarii, symbiotic long-period variable, magnetically active single star model rel. to nebula spectrum 0-90450
  - atom motion in very strong mag. fields, mass anisotropy effect (*Russian*) 0-67557
  - Be stars, mag. fields determ. via linear polarisation spectrum (*Russian*) 0-90344
  - binary stars, surface nucl. reactions and origin of mag. fields 0-101616
  - $\xi$  Bootis A, late-type dwarf star, mag. field obs. 0-72949
  - RS Canum Venaticorum binary stars, mag. starspot model for photometric and spectroscopic behaviour 0-109488
  - 17 Comae A, Ap star, mag. field meas. and rot. period (*Russian*) 0-90457
  - convective stability in magnetic stars, theory 0-94781
  - $\beta$  Coronae Borealis, obs. with Zeeman analyzer system on McDonald 2.7 m telescope 0-62021
  - Crab pulsar, magnetized cracks in crust rel. to matter flow, radio, X-ray and optical emissions 0-72990
  - DA white dwarfs, mag. field geometries rel. to spectral line profiles 0-62123
  - dense stars, atomic spectra in intense mag. fields 0-105160
  - differential rotation effect on velocity and magnetic fields, superposition of poloidal and toroidal field 0-72928
  - dwarfs, degenerate accreting, thermonuclear bursts effects on mag. field 0-98684
  - dynamo model of magnetic field, self-consistent treatment 0-81808
  - dynamo theorems 0-81810
  - dynamo theory, spherical dynamo with anisotropic  $\alpha$ -effect 0-81809
  - equilibrium structures, of self-gravitating gas masses containing axisymmetric mag. fields 0-94708
  - field line reconnection, relativistic modes of tearing instability in background plasma 0-62012
  - flux tube in star interior, buoyancy and equilib. 0-109420
  - HD 153882, obs. with Zeeman analyzer system on McDonald 2.7 m telescope 0-62021
  - HD 4174 (=EG Andromedae), peculiar M giant, mag. field existence, UV spectra obs. 0-94798
  - Hercules X-1, mag. field rel. to prod. of cyclotron features in X-ray spectrum 0-86015
  - AM Herculis (3U 1809+50), polarimetry and spectrophotometry rel. to mag. field 0-94835
  - AM Herculis (4U 1814+50), mag. white dwarf models for X-ray source 0-105403
  - CW Leonis (IRC+10216), IR C star, circumstellar dust orientation by paramag. relaxation rel. to intrinsic polarisation 0-67730
  - RR Lyrae stars, hydromagnetic processes as cause of period changes 0-105261
  - magnetic star polarity reversal, appl. of skin effect approx. 0-62010
  - main-sequence stars, mag. mixing rel. to CNO isotope abundances and  $\alpha$  Bootis (Arcturus) problem 0-105229
  - neutron stars, accreting, mag. fields rel. to cyclotron emissivity 0-90463
  - neutron stars, accreting, thermonuclear bursts effects on mag. field 0-98684
  - neutron stars, effects of rot. and mag. fields on superfluidity 0-77441
  - neutron stars, electrodynamics in curved space 0-90465
  - neutron stars, electrodynamics of disk accretion, magnetic field structure 0-85973
  - neutron stars, mag. field effects on plasma accretion 0-109452
  - neutron stars, mag. fields and related effects 0-72991
  - neutron stars, mag. fields rel. to radiative heat transfer in surface layers 0-94826
  - neutron stars, pair annihilation in superstrong magnetic fields 0-85847
  - neutron stars, pair formation and electric field boundary conditions at magnetic poles 0-101613
  - neutron stars, props. of condensed matter in huge mag. fields 0-82187
  - neutron stars, radiation source form. mechanism, mag. annihilation (*Chinese*) 0-77440
  - neutron stars, rot. mag. field interaction with accretion disc 0-62173
  - 70 Ophiuchi A, late-type dwarf star, mag. field obs. 0-72949
  - protostars, quasistatic contraction due to mag. flux leakage 0-98662
  - pulsar crust, crust, infinitely magnetised H atom theory 0-77282
  - pulsar magnetosphere, plasma waves propag. along mag. field in strongly anisotropic relativistic plasma 0-67542
  - pulsar open magnetosphere, plasma instabilities as source of coherent radio emission 0-82403
  - pulsars, influence of mag. field on comp. of outer crust 0-101610

**stellar magnetism continued**

- pulsars, mag. field correl. with  $P_3$  period 0-90461
- pulsars, magnetic field similarities with Jupiter, radio emissions (*Russian*) 0-77333
- pulsars axisymmetric magnetospheres, method of soln. of self-consistent description 0-94825
- VV Puppis, AM Herculis type binary, optical absorpt. spectrum, cyclotron interpretation and models 0-73003
- rotating magnetic stars, nonradial oscill. mode splitting 0-77414
- Scorpius X-1, mag. field determ. via linear polarisation spectrum (*Russian*) 0-90344
- spectral line formation depth in mag. field, theory (*Chinese*) 0-105159
- SS 433, magnetic X-ray binary model 0-109447
- stars containing mixed poloidal and toroidal mag. fields, adiabatic stability 0-67706
- Stokes' problem, mass transfer effects of MHD free convective flow 0-62003
- Stokes parameters and mag. field vector profiles (*Chinese*) 0-77386
- supernovae, magnetorotational explosion in cylindrical model 0-101605
- transverse magnetic field, effect on hydromag. free convection flow in Stokes problem 0-90328
- turbulent diffusion of magnetic fields, stochastic phenomena 0-105161
- upper main-sequence peculiar stars, chemical and physical props. rel. to radiatively driven diffusion theory 0-82374
- white dwarfs, highly magnetised, accretion, role of electron conduction 0-82358
- white dwarfs, mag. fields rel. to unexplained spectral features theory 0-82187
- X-ray sources, pulsating, accretion disc mag. field calc. for oblique mag. dipole configuration 0-94895

**stellar mass**

- anomalous mass stars, evolution on main sequence 0-72929
- KO Aquilae, eclipsing binary, mass ratio and secondary component fractional radius from photoelectric study 0-62198
- asymptotic giant branch evolution of intermediate-mass stars, post-second dredge-up phase 0-72936
- T Aurigae (Nova 1891), old nova, primary star mass from photometric and spectroscopic obs. 0-90446
- binary stars, distances, masses and dias. from speckle interferometric obs. 0-90475
- binary stars, spectroscopic, statistical investigation 0-109466
- CC 1299 (BD+27°4120), unresolved astrometric binary, orbital anal., mass and parallax 0-109464
- OY Carinae, white dwarf cataclysmic binary 0-82385
- SU Cassiopeiae, Cepheid variable, pulsation and evolutionary masses from temp. determ. 0-90435
- AB Cassiopeiae, eclipsing binary, masses from light vars. preliminary anal. 0-94831
- Centaurus X-3, neutron star lower mass limit from spin-up and X-ray luminosity meas. 0-101648
- NY Cephei, eclipsing binary, UVB photometry and masses 0-67789
- VW Cephei, W Ursae Majoris star, rot. line broadening rel. to shape and mass ratio 0-109494
- Cepheids in M31 (Andromeda galaxy), masses radial var. rel. to interstellar gas density (*Russian*) 0-90455
- XY Ceti, eclipsing binary, masses, radii and luminosities from revised photometric elements 0-109458
- Z Chamaeleontis, eruptive binary, secondary component relative mass from photometric data anal. 0-72961
- close binaries, intermediate mass, mass transfer for different stars within evolutionary scheme 0-109476
- close binaries with OB components, evolution of massive systems 0-90474
- close binary stars, masses and mass ratios distrib. before and after mass transfer 0-62187
- contact binaries, solar type, initial mass ratio distrib. function 0-109496
- contact binary star, fractional mass var. during dynamical evolution (*French*) 0-62199
- contact binary stars, mass of third component responsible for sudden period changes 0-109497
- continuous loss from cluster models, dynamical evolution 0-82438
- $\sigma$  Coronae Borealis (=ADS 9979), binary, mass and orbital elements (*French*) 0-77449
- AI Crucis, eclipsing binary, photometric mass and radius ratios and configuration 0-109459
- SS Cygni, dwarf nova, white dwarf mass from rapid optical oscills. obs. 0-85947
- V380 Cygni, eclipsing binary, masses, radii and luminosities from revised photometric elements 0-109458
- V1329 Cygni (HBV 475), symbiotic variable, masses from eclipsing binary model 0-62148
- DA white dwarfs, H I Balmer  $\gamma$  line profiles and masses 0-77399
- dense matter star, limiting mass 0-101611
- distribution in solar neighbourhood, Weibull statistical function 0-98649
- G128-7, cool DA white dwarf, mass rel. to atmospheric parameters and evolution 0-62126
- HD 34664 (S 22) in LMC, peculiar emission line supergiant 0-77416
- HD 45088, dK3 spectroscopic binary, mass ratio from double red lines 0-67778
- HD 50896, Wolf-Rayet binary, secondary component mass from linear polarisation periodic vars. 0-72972
- HD 93250, O3 massive star in  $\eta$  Carinae complex, non-LTE analysis 0-77398
- Hercules X-1 (HZ Herculis) system, non-degenerate star pre-supernova mass 0-62318
- DQ Herculis, red and white dwarf eclipsing binary, component mass determ. 0-94800
- high-mass stars ( $M \geq 50 M_{\odot}$ ) masses and space vels. rel. to evolutionary status (*Russian*) 0-109425
- HR 1225,  $\delta$  Scuti star, absolute magnitude, effective temp. and mass from photoelectric study 0-109436
- K1211, blue straggler in NGC 7789, evolution status and mass, photometry obs. 0-109433
- 19 Leonis Minoris, spectroscopic binary, orbital elements and mass ratio 0-62197
- main sequence B-type stars, physical parameter determ. from uvby $\beta$  photometry obs. 0-72952
- main sequence star, max. mass for white dwarf evolutionary stage 0-105237
- massive star core collapse, eqn. of state and composition near  $\beta$  equil. 0-82335

**stellar mass continued**

- massive stars, masses rel. to evolution 0-90416
- massive stars, single and binaries, evolution review 0-82343
- neutron star, model within general relativity, mass evaluation 0-101612
- neutron star formation through stellar core collapse, effects of eqn. of state on mass 0-85928
- neutron stars, mass-radius relation 0-77444
- neutron stars, max. mass determ. from pulsars and compact X-ray sources 0-77442
- neutron stars, rotating, masses in bi-metric theory of gravitation 0-90466
- nova envelopes, mass rel. to dust grains form. 0-98678
- O- and Of-type stars, masses and mass loss 0-94793
- O-type binaries, binary freq. and anomalous mass ratios 0-109478
- OB associations, initial mass function in young objects 0-98695
- $\beta$  Persei (Algol) eclipsing binaries, masses rel. to mass loss and mass transfer theory 0-62191
- planetary nebulae nuclei, masses rel. to nebulae evolution 0-82344
- WZ Sagittae, eruptive binary, masses from hot spot eclipses anal. 0-72962
- V701 Scorpii, masses and mass exchange rates of early-type contact binary 0-62188
- Stepanyan's star, eclipsing binary, relative orbit radius and collapsed component mass 0-67788
- subdwarf stars, no evidence for low spectroscopic masses 0-62122
- Sun, mass/gravit. const. relation rel. to solar luminosity cosmological var. 0-82182
- supergiants in Magellanic Clouds, birthrate and mass function 0-67699
- supernova that produced N63A, lower mass limit 0-62165
- supernovae, type II, mass of ejected matter from light curves analytic solns. 0-77427
- RW Trianguli, nova-like eclipsing binary radial vels., dims. from visible spectra 0-82418
- W Ursae Majoris stars, rot. line broadening functions rel. to mass ratio 0-109494
- AI Velorum, radius and mass from BVRI photometry and photoelectric radial vels. 0-94815
- $\gamma_2$  Velorum, Wolf-Rayet binary, minimum mass from spectra obs. 0-85950
- visual binaries, orbital elements and masses for 18 pairs 0-62180
- ER Vulpeculae, W Ursae Majoris star, rot. line broadening rel. to shape and mass ratio 0-109494
- Wolf Rayet binary, binary freq., mass ratio, low mass companion evidence 0-109479
- Wray 977, optical counterpart to X-ray binary pulsar, 4U 1223-62, optical spectra 0-72984
- X-ray binaries, masses rel. to hard and soft X-ray spectra 0-62316

**stellar models**

- 2 to 10  $M_{\odot}$  stars, effect of heavy element abundance on evolution, struct. of models 0-105231
- A-type stars, Lyman  $\alpha$  effect on non-LTE model atmospheres 0-90422
- accretion disk model, gas flow above alpha disk 0-62161
- Am-type, binary stars, tidal interaction producing stable atm., evolution 0-67752
- R Aquarii, symbiotic long-period variable, magnetically active single star model rel. to nebula spectrum 0-90450
- $\sigma$  Aquarii (A0 IVs), hot metallic-line star, abundance anal. from model atmosphere 0-90415
- $\theta$  Aquilae (B9.5 III), abundance anal. from model atmosphere 0-90415
- V1301 Aquilae (Nova Aquilae 1975), dust grain IR emission model 0-105254
- $\alpha$  Aurigae (Capella), theoretical stellar chromosphere model 0-67718
- T Aurigae (Nova 1891), old nova, cataclysmic binary model from photometric and spectroscopic obs. 0-90446
- axisymmetric rotating fluid, asymptotic estimates 0-98542
- B-stars of early type, atm. LTE model using opacity sampling technique 0-90414
- black holes, supercritical accretion discs models 0-105272
- black holes, thick accretion discs models rel. to supercritical luminosities 0-101614
- Z Camelpardalis, dwarf nova, accretion disc models at standstill and in eruption 0-82366
- UW Canis Majoris, O7f supergiant, warm wind model for mass loss 0-67736
- $\alpha$  Canis Minoris (Procyon), theoretical stellar chromosphere model 0-67718
- $\alpha^2$  Canum Venaticorum, line blanketed model atmospheres of Ap-star 0-90440
- RS Canum Venaticorum binary stars, mag. starspot model for photometric and spectroscopic behaviour 0-109488
- $\nu$  Capricorni (B9.5 V), abundance anal. from model atmosphere 0-90415
- $\alpha$  Centauri binary system, scaled solar model atmospheres for spectroscopic anal. 0-62128
- $\beta$  Cephei stars, line profile variables, pulsational modes 0-85951
- Cepheid variables, double mode, anal. of modal selection pulsating stars 0-82372
- Cepheids, stellar pulsation problem, time dependent convection local theories 0-72964
- multimode Cepheids, two zone rel. to classical models 0-72967
- Z Chamaeleontis, eruptive binary, model from photoelectric data anal. 0-72961
- Circinus X-1, binary model, orbital eccentricity from X-ray and radio obs. 0-98735
- Circinus X-1, binary model, radio emission 0-98736
- cluster models with continuous stellar mass loss, dynamical evolution 0-82438
- contact binaries, envelope energy transfer model 0-90478
- core He flash, models with two-dimensional convection 0-105230
- coronae of late-type main-sequence and subgiant stars, loop model rel. to HEAO 1 obs. 0-72925
- Crab pulsar, magnetized cracks in crust rel. to matter flow, radio, X-ray and optical emissions 0-72990
- CH Cygni, symbiotic star, binary model 0-62158
- V1329 Cygni (HBV 475), symbiotic variable, accreting binary star model 0-62148
- V1500 Cygni (Nova 1975), anisotropically radiating condensations rel. to Balmer line emission profiles evolution 0-82371
- V1500 Cygni (Nova 1975), emission line vars. rel. to central object radiation model 0-82367
- degenerate star-red giant interacting binary stars, compressible fluid flow, accretion 0-67779



## stellar models continued

- dynamo model of magnetic field, self-consistent treatment 0-81808  
 early-type stars, model atmospheres rel. to H and He<sup>+</sup> line profiles in stellar winds 0-85926  
 Emden-Chandrasekhar axisymmetric solid-body rotating polytropes, exact solutions for ( $n=0, 1$  and  $5$ ) 0-109419  
 $\epsilon$  Eridani, UV line spectrum of active chromosphere star, models 0-77394  
 evolution calc. programme and standard solar model 0-67703  
 evolutionary tracks, effect of gravitational const. var. 0-82186  
 $\gamma$  Geminorum, differential abundance anal. rel. to  $\alpha$  Lyrae standard 0-82362  
 $\beta$  Geminorum (Pollux), theoretical stellar chromosphere model 0-67718  
 giant stars in globular clusters M5, M13, M3, model atmospheres rel. to chemical comp. 0-67695  
 HD 10783, Ap star, model atmospheres rel. to spectrophotometric obs. 0-98663  
 HD 93250, O3 massive star in  $\eta$  Carinae complex, non-LTE analysis 0-77398  
 Herbig-Haro objects, stellar wind model 0-85985  
 Hercules X-1, accretion disc viscosity determ. using slaved disc model 0-62110  
 AM Herculis (4U 1814+50), mag. white dwarf models for X-ray source 0-105403  
 high velocity giant stars, model atmospheres rel. to detailed chemical anal. 0-82352  
 $\epsilon$  Indi, late type dwarf star, model atmosphere 0-90425  
 late type dwarf stars, temp. minima, chromosphere models 0-67717  
 late-type stars, Ca II 8542 Å line as chromospheric activity indicator 0-62108  
 AQ Leonis, homogeneous model of Population II double-mode RR Lyrae star 0-62134  
 magnetic DA white dwarfs, model atmospheres and line profiles 0-62123  
 magnetic field, dynamo theorems 0-81810  
 magnetic field, spherical dynamo with anisotropic- $\alpha$  effect 0-81809  
 main sequence intermediate and late type stars, differential rot. models 0-105238  
 massive main-sequence star, early evolution 0-62113  
 massive stars, single and binaries, evolution review 0-82343  
 massive stars ( $M \geq 50 M_{\odot}$ ), binary star mass transfer model rel. to evolutionary status (Russian) 0-109425  
 metal-deficient stars, subdwarf ionization equilibrium and model atmospheres 0-90421  
 neutron star, model within general relativity, mass evaluation 0-101612  
 neutron stars, slowly rotating, models and stability against radial perturbations 0-98685  
 70 Ophiuchi A, theoretical stellar chromosphere model 0-67718  
 $\beta$  Persei, eclipsing binary, Mg II 280 nm line profile, calcs. and UV obs. 0-82421  
 RY Persei, eclipsing binary, visible spectral obs., model 0-67795  
 SZ Piscium, RS Canum Venaticorum star, photometric obs. rel. to starspot model 0-109490  
 planetary nebulae central stars, atmospheric models 0-109434  
 planetary nebulae nuclei, models rel. to distances determined from ionised mass/radius relation 0-101625  
 pulsar emission models, implications of drifting subpulses obs. in CPS 0-67763  
 pulsars, finite force face cold plasma atm. models, plasma differential rot. 0-77378  
 pulsars, gamma-ray production mechanism 0-77433  
 pulsars, pair creation model rel. to source of coherent radio emission 0-82403  
 pulsars axisymmetric magnetospheres, method of soln. of self-consistent description 0-94825  
 VV Puppis, AM Herculis type binary, optical absorpt. spectrum, cyclotron interpretation and models 0-73003  
 $\rho$  Puppis, line profile variable, pulsational mode-typing 0-90432  
 $\zeta$  Puppis, Of type star, stellar wind model from UV line fit 0-72965  
 rapidly rotating models with radiation press., struct. parameters calc. 0-67697  
 red giant model atmospheres, opacity sampled models grid 0-82348  
 red giant of 6  $M_{\odot}$ , envelope composition rel. to evolution 0-105237  
 WZ Sagittae, eruptive binary, model from hot spot eclipses anal. 0-72962  
 WZ Sagittae, recurrent nova, accretion disc models comparison with IUE obs. during outburst 0-109448  
 WZ Sagittae, recurrent nova, model for superhump phenomena 0-82368  
 $\delta$  Scuti, line profile variable, pulsational mode-typing 0-90432  
 FH Serpentis (Nova Serpentis 1970), dust grain IR emission model 0-105254  
 slow novae and symbiotic stars, binary star model from obs. of late-type components 0-94813  
 solar model, constant mass, differentially rotating gaseous polytropes configurations 0-82338  
 spectroscopic binary systems, main-sequence homogeneous stellar models rel. to apsidal motion 0-82413  
 SS 433, accreting black hole model 0-85958  
 SS 433, accretion disc viscosity determ. using slaved disc model 0-62110  
 SS 433, beam models, energetics anal., possible triple system 0-90433  
 SS 433, deviations from standard model 0-98669  
 SS 433, dissipative infall model 0-67749  
 SS 433, general spectral features 0-77421  
 SS 433, magnetic X-ray binary model 0-109447  
 SS 433, massive black hole and pulsar models rel. to precessional motion origin of 164<sup>d</sup> period 0-62138  
 supergiants, early-type, with mass loss, two-core model and evolutionary status (Russian) 0-109425  
 supernovae, magnetorotational explosion in cylindrical model 0-101605  
 supernovae core collapse, neutrino energy equilibration models 0-105265  
 symbiotic stars, models of two subclasses 0-62144  
 symbiotic stars and slow novae, binary star model from obs. of late-type components 0-94813  
 Vela pulsar (PSR 0833-45), radiation model 0-94824  
 CU Virginis (HD 124224), Ap star, model atmospheres rel. to spectrophotometric obs. 0-98663  
 visual surface brightness depend. on colour, model stellar atm. calcs. 0-67707  
 X-ray binaries, recurrent transients model 0-109565  
 X-ray sources, pulsating, oblique mag. dipole configuration model 0-94895  
 C-O white dwarfs, C-O eutectic model 0-77405

## stellar models continued

- He stratification in model atmosphere of blue horizontal-branch star 0-90409  
 HgMn stars, diffusion model rel. to obs. of Hg in thin atmospheric layer 0-105243  
 Mn stars, diffusion model, implications of Hg II line oscillator strength 0-72966
- stellar motion  
*see also celestial mechanics*  
 2A 0311-227, AM Herculis type X-ray binary, optical counterpart, radial vel. obs. 0-94890  
 2A 0526-328 optical counterpart, radial vel. meas. and orbital period 0-90579  
 2A 0526-328 optical counterpart, radial vel. var. 0-77515  
 3A 2252-035, optical counterpart, proper motion and radial vel. determ. 0-82395  
 ADS 1833 and 6871 AB, visual binaries, orbital calc. (French) 0-98690  
 Algol, orbit, lightcurve and struct. review 0-109460  
 algorithms for numerical orbit computation in galaxy models 0-67797  
 CG Andromedae, Si binary star, spectrum variable, short period radial vel. variability determ. 0-72968  
 Ap stars in spectroscopic binary systems, orbital inclinations rel. to chemical anomalies surface distrib. 0-62140  
 AE Aquarii, spectroscopic binary variable, X-ray source, orbital element determ. 0-105288  
 V342 Aquilae, eclipsing binary, period and light curve changes, (1966 to 1976) 0-67791  
 KO Aquilae, eclipsing binary system, period increase from UVB photoelectric study 0-62198  
 T Aurigae (Nova 1891), old nova, orbital elements from photometric and spectroscopic obs. 0-90446  
 BD+29°3805, K-type giant, spectroscopic binary orbit 0-67790  
 binary stars, orbital eccentricity effect on polarimetric obs. 0-109472  
 binary system, close, with mass and ang. momentum loss, period changes 0-72998  
 binary systems, speckle interferometric obs. with Haute-Provence 1.93 m telescope 0-90475  
 CC 1299 (BD+27°4120), unresolved astrometric binary, orbital anal., mass and parallax 0-109464  
 $\beta$  Canis Majoris,  $\beta$  Cephei-star, Fourier anal. of radial vel. changes 0-105246  
 TX Canum Venaticorum, cataclysmic variable, orbit from visible spectra obs. 0-105249  
 OY Carinae, white dwarf cataclysmic, eclipsing binary, parameter determ. 0-82385  
 QZ Carinae (HD 93206), O-type quadruple eclipsing system, spectroscopic and radial vel. study 0-105275  
 cataclysmic binaries, radial vel. data rel. to circumstellar material geometrical and photometric parameters 0-109492  
 cataclysmic binary stars (CBS), critique of polarimetric evidence on physical parameters and orbital inclination 0-109486  
 EM Cephei, eclipsing, binary, UVB photometry rel. to constancy or variability of period 0-105286  
 U Cephei, eclipsing binary, anal. of radial velocity curve of B9 component 0-94829  
 NY Cephei, massive eclipsing binary, orbital period and inclination from UVB photometry 0-67789  
 U Cephei, three colour light curve perturbations and orbital element determ. (French) 0-67787  
 VW Cephei, W Ursae Majoris star, orbital period decrease and B-V colours rel. to physical status 0-109495  
 $\delta$  Ceti,  $\beta$  Cephei variable, spectroscopic binary, radial vels. and period var. 0-82376  
 RS Chamaeleontis, eclipsing binary, four-colour photometry and photometric orbital elements 0-67783  
 RS and RZ Chamaeleontis, photometric elements of detached eclipsing binaries 0-90473  
 Chu's object in Perseus, radial vel. rel. to identification as galactic star 0-62132  
 Circinus X-1, binary model, orbital eccentricity from X-ray and radio obs. 0-98735  
 Circinus X-1, H $\alpha$  emission mean radial vel. rel. to runaway origin 0-67910  
 close binary stars, orbital periods distrib. before and after mass transfer 0-62187  
 close binary systems, radial vel. curves anal. 0-90470  
 cluster, spherically symmetric with stars of uniform mass, struct. and dynamics 0-62215  
 cluster dynamics, higher order fluid eqns. for multicomponent nonequilibrium systems 0-105156  
 contact binaries, orbital periods sudden changes due to third component 0-109497  
 contact binary star, idealised dynamical evolution (French) 0-62199  
 $\sigma$  Coronae Borealis (=ADS 9979), binary, mass and orbital elements (French) 0-77449  
 $\alpha^1$  Crucis, improved spectroscopic orbit 0-67792  
 25  $\gamma$  Crucis (HD 108250), orbital elements from spectrograms 0-82432  
 EM Cygni, cataclysmic variable, red and white dwarf binary, period change, B photometry 0-90434  
 XX Cygni, dwarf Cepheid, composition and motion, visible photometric and spectrographic obs. 0-77424  
 GO Cygni, eclipsing binary, orbital period changes 0-72999  
 SS Cygni, spectroscopic binary variable, X-ray source, orbital element determ. 0-105288  
 CH Cygni, symbiotic star, radial vels. and binary model 0-62158  
 V1329 Cygni (HBV 475), symbiotic variable, radial vel. vars. rel. to eclipsing binary model 0-62148  
 Cygnus X-1, critique of polarimetric evidence on physical parameters and orbital inclination 0-109486  
 Cygnus X-3, period derivative and asymmetric X-ray light curve from HEAO 2 obs. 0-105394  
 HR Delphini (Nova 1967), revised orbital ephemeris from simultaneous X-ray, UV and optical obs. 0-109440  
 disc galaxies, stellar motion following massive objects ejection in plane of stellar disc 0-82495  
 disc galaxies, stellar motion following massive objects ejection out of stellar disc plane 0-82496  
 Draco dwarf spheroidal galaxy, stellar colour magnitude diagram and proper motion 0-73029

## stellar motion continued

- RZ Draconis, eclipsing binary, photoelectric light curve and orbital period study 0-109461  
 dynamical evolution of cluster models with continuous stellar mass loss 0-82438  
 dynamical evolution of Keplerian systems, numerical simulations of collisions 0-109342  
 dynamics, collision integral determ. (*Polish*) 0-67799  
 dynamics, stability of one-dimensional self-gravitating isothermal systems 0-73008  
 dynamics in galaxies, stability rel. to galaxies nonflat components mass 0-62291  
 eclipsing binaries, sd/d nature from radial vels. 0-82423  
 eclipsing binary runaway, orbital data, UV obs. 0-85952  
 ellipsoidal distrib. of vels. in spiral galaxies (*Chinese*) 0-77484  
 $\nu$  Eridani,  $\beta$  Cephei star, Fourier anal. of radial vel. changes 0-105246  
 flat galaxies dynamical struct., statistical characs. 0-62269  
 galaxies, gravitational instability of loosely wound spiral density wave 0-85998  
 galaxy disc stars, nonlinear interaction with spiral wave near corotation radius (*Russian*) 0-62289  
 galaxy mergers, stellar populations mixing processes 0-67860  
 Galaxy stellar orbits, applicability of approximate third integral of motion 0-67798  
 YY Geminorum, eclipsing binary, photometry and orbital period study 0-105287  
 globular clusters in Galaxy, tidal disruption 0-105294  
 H 2252-035, cataclysmic variable, photometry and spectrum rel. to orbital and rot. periods 0-101651  
 HD 105056, ON supergiant, radial vel. study 0-90427  
 HD 108078, spectroscopic binary orbit from photoelec. radial vel. meas. 0-77451  
 HD 127617 (Bidelman's high latitude Be star), photometric and visible spectra obs. 0-77420  
 HD 166734, Of star, spectroscopic binary orbit determ. from visible obs. 0-82414  
 HD 200925 radial vels. of new short period  $\delta$  Scuti star (*French*) 0-90441  
 HD 203631, spectroscopic binary orbit from photoelectric radial vels. 0-105285  
 HD 219150, F0 V star with remarkable UV excess, unsuccessful search for radial vel. var. 0-90429  
 HD 22007 (primary of ADS 16681), spectroscopic binary, radial vel., orbit elements 0-67793  
 HD 27507, proper motion determ. of A-type high-vel. horizontal branch star 0-77407  
 HD 39937, 101379, 155555, 174429, southern RS Canum Venaticorum stars candidates, radial vel. study 0-98686  
 HD 4174, symbiotic star, radial vels. vars. and binary star model 0-85945  
 HD 50896, Wolf-Rayet binary, orbital period and inclination from linear polarisation periodic vars. 0-72972  
 Hercules X-1 (HZ Herculis) system, pre-supernova binary period 0-62318  
 DI Herculis, eclipsing binary, relativistic motion of periastron 0-94830  
 high galactic latitude stars, division into giants and dwarfs by proper motion (*Russian*) 0-109431  
 high-mass stars ( $M \geq 50 M_{\odot}$ ) masses and space vels. rel. to evolutionary status (*Russian*) 0-109425  
 Hipparcos satellite, proposed space-astrometry mission 0-82164  
 HR 6659, spectroscopic binary, radial vel. obs. 0-82430  
 HS Hydrae, photometric elements of detached eclipsing binary 0-90473  
 late-type field stars in S.hemisphere, radial vel. study rel. to possible duplicity 0-98686  
 LB 3479, subdwarf eclipsing binary, evolutionary model comment 0-90426  
 19 Leonis Minoris, spectroscopic binary, orbital elements and mass ratio 0-62197  
 LSI +61°303, supergiant Be star, radio emission and radial vel. periodic vars. 0-62149  
 $\beta$  Lyrae, orbital period variability 0-72997  
 M81, spiral galaxy dynamics, axisymmetric models and stellar density wave 0-105335  
 M87 (NGC 4486), vel. dispersion from a population model 0-77490  
 M87 core dynamics, anisotropic vel. distrib. rel. to supermassive black hole model 0-82500  
 Magellanic Clouds, Wolf Rayet binaries, spectroscopic orbits 0-109479  
 NGC 330, young cluster in SMC, radial vels. of individual stars 0-67803  
 NGC 4103, open cluster, membership determ. from proper motions, visible obs. 0-67802  
 NGC 6494 (M23), open cluster, proper motions and membership from astrometry with PDS microdensitometer 0-98697  
 NGC 741, 1316, 7626, radio galaxies, dynamics 0-94871  
 nonlinear orbital behaviour near corotation in spiral systems 0-98694  
 O-type stars, relation between peculiar vels., assoc. with nebulosity and z-distances 0-105236  
 OB associations subgroups, motion towards parent cloud rel. to sequential form. 0-98696  
 OB-type stars, radial vels. rel. to distance of Sun from galactic centre 0-101584  
 old stars, kinematics rel. to Galaxy initial contraction 0-62204  
 open clusters, southern, kinematics and dynamics from radial vel. obs. (*German*) 0-94724  
 open clusters assoc. with interstellar gas-dust clouds, dynamics 0-101622  
 parallax and proper motion meas. for seven stars 0-62109  
 IW Persei, metallic-line close binary system, spectroscopic orbital elements 0-62186  
 19 Piscium, C star, violet spectrum line identification and radial vel. 0-82361  
 planetary nebulae, spatial and vel. distrib. statistics 0-109518  
 polytropes in central orbits, Roche problem 0-82179  
 Population I O-type runaway stars 0-85938  
 prolate stellar systems, instability 0-101642  
 proper motion stars in direction of galactic centre (*French*) 0-77404  
 proper motions, extrasolar planetary systems, dynamical instability and detection 0-82429  
 proper motions from reduction and repetition of Astrographic Catalogue 0-105178  
 proper motions measurement, sky photography programme with wide-angle astrographs (*Russian*) 0-72747

## stellar motion continued

- proper motions of bright nearby stars, astrometric anal. from Sproul 61 cm refractor plates 0-61991  
 pulsars, periods, positions and proper motion determ. from pulse arrival times, UHF, obs. 0-77431  
 PZT stars, mean posns. and proper motions for 304 stars, obs. at Ondrejov 0-82175  
 radial vel. determ., survey of different methods 0-73006  
 radial vel. determ. with CORAVEL, Cassegrain spectrophotometer 0-82210  
 radial velocity curves of close binary systems, anal. 0-94829  
 resonant 2/1 orbits stellar reson. orbits comparison, 2/1 reson. 0-67796  
 in rotating galaxy gravitational field (*Russian*) 0-94838  
 Rubin-152, possible massive O-type star on galactic fringe, radial vel. and galactic orbit 0-98656  
 FG Sagittae, planetary nebula central star, radial vel. meas. rel. to binary star model 0-98664  
 WZ Sagittae, recurrent nova, radial vels. obs. and model for superhump phenomena 0-82368  
 $\sigma$  Scorpii,  $\beta$  Cephei star, Fourier anal. of radial vel. changes 0-105246  
 V701 Scorpii, radial vels. of early-type contact binary 0-62188  
 semidetached systems, revised photometric elements 0-62193  
 spectroscopic binaries, orbital elements statistical anal. 0-82422  
 spectroscopic binary systems, apsidal motion 0-82413  
 SS 433, radial vel. curve low amplitude section, visible spectra anal. 0-67737  
 stellar system dynamics, field of directions of motion in Contopoulos potential (*Russian*) 0-62205  
 Stepanyan's star, eclipsing binary, eclipses obs. and orbital period refinement 0-62195  
 Stepanyan's star, eclipsing binary, relative orbit radius and collapsed component mass 0-67788  
 subdwarfs, photometry rel. to compositions and kinematics 0-82364  
 CD Tauri, eclipsing binary, orbital element determ., BV photometer obs. 0-73000  
 RW Trianguli, nova-like eclipsing binary radial vels., dims. from visible spectra 0-82418  
 velocity dispersion determ. in spiral galaxies (*Chinese*) 0-85995  
 velocity dispersion inhomogeneities in local spiral arm 0-98653  
 AI Velorum, nature from BVRI photometry and photoelectric radial vels. 0-94815  
 $\gamma_2$  Velorum, Wolf-Rayet binary, orbital element determ. from spectral obs. 0-85950  
 visual binaries with variable components, orbital elements, visible obs. (*Russian*) 0-77455  
 Wolf-Rayet, single-line Population I stars, space vel. 0-77415  
 WRA 977 (4U 1223-62, GX 301-2), binary star orbit determ., X-ray obs. 0-90570  
 Ba II giant stars binary nature from visible radial vel. obs. 0-82355
- stellar multicolour photometry** *see stellar photometry*  
**stellar origin** *see stellar evolution*  
**stellar photometry**  
*see also stellar radiation; stellar spectra*  
 HR 1099, RS Canum Venaticorum type binary, light and colour curve meas. 0-73004  
 A1742-28, transient X-ray source, optical counterpart, visible and IR obs. 0-101653  
 2A 0311-227, AM Herculis type binary star, IR photometry and polarimetry 0-77517  
 2A 0311-227, optical counterpart, AM Herculis type eclipsing binary, V-band obs. 0-101617  
 2A 0311-227 optical counterpart, binary star, light curve Fourier anal. 0-82549  
 2A 0311-227 optical counterpart, high speed photometry 0-82547  
 2A 0311-227 optical counterpart, simultaneous photometric and spectroscopic obs. 0-90572  
 Am stars, evolved, search for photometric variability on lower part of Cepheid instability strip 0-62145  
 BM Andromedae, spectroscopic and photometric obs. of T Tauri-type star 0-62130  
 Ap, Bp stars catalogue of photometric data rel. to surface mag. fields 0-85873  
 Ap and Bp stars, surface mag. field intensity rel. to Geneva photometry 0-105248  
 Ap stars, new  $\Delta\alpha$  photometry and evidence for two-component struct. of 5200 Å feature 0-67734  
 Ap stars, spectrophotometry of broad flux depressions and comparison with synthetic spectra 0-67735  
 $\delta_{1400}$  Ap type stars, excess UV index, photometry obs. 0-72963  
 CY Aquarii, RRs type star, BV photometric obs. (*Italian*) 0-90449  
 $\eta$  Aquilae, Cepheid variable, absolute energy distrib. in radiation spectrum (*Russian*) 0-72974  
 KO Aquilae, eclipsing binary system, UVB photoelectric study 0-62198  
 Arakelyan 120, Seyfert galaxy nuclei, optical variability, UVB obs. 0-73049  
 TT Arietis, nova-like cataclysmic variable, photoelectric photometry 0-82382  
 59 Aurigae,  $\delta$  Scuti star, light curves periodogram anal. 0-62141  
 $\epsilon$  Aurigae, photometry during 1955-57 eclipse rel. to wavelength-depend. fluctuations 0-62190  
 T Aurigae (Nova 1891), old nova, photometric and spectroscopic obs. 0-90446  
 late B dwarf in circumstellar dust cloud, IR source coincident with OH 205.1-14.1 0-101630  
 B-type stars at high southern galactic latitudes, four colour and H $\beta$  obs. 0-82357  
 BD +10°2179, C rich H deficient star, UVB photometric obs. 0-90437  
 BDS 1269 A, metal-poor  $\delta$  Scuti star, pulsation periods from b-band photometry 0-105247  
 Berkeley 11, compact open cluster, UVB obs. 0-94840  
 Berkeley 19, anticentre open cluster, age determ. from colour magnitude diagram, BV photometry 0-90486  
 binaries, wide visual, spectral type, age and uvby $\beta$  photometry 0-94833  
 TZ Bootis, W Ursae Majoris type system, eclipsing binary, photoelec. obs. 0-73001  
 3C 120, Seyfert galaxy nuclei, optical variability, UVB obs. 0-73049  
 Z Camelopardalis, dwarf nova, spectrophotometry at standstill and in eruption 0-82366  
 XX Camelopardalis, R Coronae Borealis star, photometry in optical and IR ranges 0-101601



## stellar photometry continued

- SZ Camelopardalis, semi-detached eclipsing binary, UVB lightcurves 0-85974
- AX Camelopardalis (53 Camelopardalis), Ap star, UVB photoelectric photometry and period of var. (*Italian*) 0-90448
- BT Cancri (38 Cancri)  $\delta$  Scuti star, photometry rel. to radial and nonradial pulsation periods 0-85948
- 38 Cancri in Praesepe cluster,  $\delta$  Scuti variable, pulsation anal. from light curves 0-77419
- VY Carinae, Cepheid, luminosity and membership of assoc., visible obs. 0-94797
- I Carinae, search for comparison stars, uvby $\beta$  photometry, colour excess 0-62136
- SU Cassiopeiae, Cepheid variable, spectrophotometric determ. of effective temp. 0-90435
- VX Cassiopeiae, early-type star, UVB obs. rel. to photometric variability (*Russian*) 0-72973
- AB Cassiopeiae, eclipsing binary with  $\delta$  Scuti primary, light vars. preliminary anal. 0-94831
- UV Cassiopeiae, R Coronae Borealis star, photometry in optical and IR ranges 0-101601
- $\omega$  Centauri, SEC Vidicon photometry of main sequence 0-90491
- 7810 Centauri (HD 101947), yellow variable supergiant near Cepheid instability strip, VBLUW photometry 0-98672
- central star of Abell 46, eclipsing binary 0-73027
- U Cephei, eclipsing binary, light curve, perturbations and orbital element determ. (*French*) 0-67787
- U Cephei, excess light obs. rel. to accretion discs 0-82412
- NY Cephei, massive eclipsing binary star, progress report from UVB photometry 0-67789
- EM Cephei, UVB, photometry rel. to constancy or variability of period 0-105286
- VW Cephei W Ursae Majoris system, period and colour change mass transfer model 0-77453
- Cepheid binary detection from U-V curve obs. 0-98667
- Cepheids, short period, in N.hemisphere, UVB photometry rel. to search for double mode Cepheids 0-94814
- Cepheids, ultrashort period, classification from photometric and astrometric data 0-62135
- sinusoidal Cepheids in LMC, first overtone pulsations, photometry obs. 0-77422
- XY Ceti, eclipsing binary, masses, radii and luminosities from revised photometric elements 0-109458
- UV Ceti stars, photometric features near flare initial phase 0-105252
- Chamaeleon T1, young stars, photometry and spectral obs. 0-72943
- RS Chamaeleontis, eclipsing binary, four-colour photometry rel. to photometric elements, absolute dimensions and He abundance 0-67783
- RS and RZ Chamaeleontis, photometric elements of detached eclipsing binaries 0-90473
- chopping photometer to eliminate auroral sky background 0-72776
- Chu's object in Perseus, UVB photometry and spectrum rel. to identification as galactic star 0-62132
- close binaries, narrow-band photometry and differential effects 0-67780
- close binary stars, H I  $\alpha$  and  $\beta$  line photometry 0-109470
- cluster stars near IC 1805 (W4), spectral classes and photometry 0-62214
- Collinder 135, nearby field of view, wide and narrow band photometry obs. 0-109504
- comparison star sequences in six variable star fields, photometry obs. 0-82433
- R Coronae Borealis, UVBRIHKLMN photometry, interpretation 0-67756
- R Coronae Borealis type variables and related objects, UVB photometric obs. 0-90437
- CPD -62° 1837 (HDE 308122), long-period variable member of triple 0-105260
- AI Crucis, revised photometric elements 0-109459
- EM Cygni, cataclysmic variable, red and white dwarf binary, period change, B photometry 0-90434
- XX Cygni, dwarf Cepheid, composition and motion, visible photometric and spectrographic obs. 0-77424
- V380 Cygni, eclipsing binary, masses, radii and luminosities from revised photometric elements 0-109458
- GO Cygni, eclipsing binary, UVB photometry rel. to period changes 0-72999
- CC Cygni, photometric obs. of RS Canum Venaticorum type binary, interpretation 0-62182
- V1016 Cygni, symbiotic star, IR variability obs. from VJHKL photometry (*Russian*) 0-105263
- V645 Cygni (AFGL 2789), spectroscopic and photometric obs. 0-73066
- V1668 Cygni (Nova 1978), multifilter photometry and polarimetry 0-90454
- V1668 Cygni (Nova 1978), optical light curve, uvby photometry 0-62154
- V1668 Cygni (Nova 1978), spectroscopic and photometric obs., (1978 to 1979) (*Russian*) 0-109444
- V1668 Cygni (Nova Cygni 1978), post-max. short period oscils., photoelectric photometry 0-82380
- Cygnus X-1 (V1357 Cygni), optical photometry (1980 May 25 to July 7) 0-90578
- HR Delphini (Nova 1967), short period light vars. from UVB photometry 0-67744
- $\beta$  Doradus, Cepheid, reddening determ. from nearby star UVB obs. 0-101598
- double stars, focal grating photometer for magnitude difference determ. 0-67567
- CX Draconis, binary Be star, UVB obs. 0-82388
- RZ Draconis, eclipsing binary, photoelectric light curve and orbital period study 0-109461
- E3 (ESO-037-SC 01) dying globular cluster, photometry and stellar content rel. to tidal truncation 0-105291
- early type stars in Hauck-Mermilliod catalogue of four colour data, astrophysical parameter determ. 0-72951
- early-type stars in S. Milky Way, uvby $\beta$  photometry 0-85942
- early-type stars in southern hemisphere, IR photometry 0-94786
- SW eclipsing binary, period study, photometry and spectra obs. 0-82424
- eclipsing binary stars, near IR photometry rel. to mass transfer rates 0-67784
- emission line stars in southern hemisphere, IR obs. 0-90496
- emission-line variable (No.86) in core of M 15, UVB photometry, probably W Virginis star 0-77458
- CD Eridani, photometric soln. for eclipsing binary system 0-62185

## stellar photometry continued

- faint blue stars, southern, UVB photometry 0-82349
- faint clusters in LMC, colour magnitude diagrams, BV photometry 0-94841
- faint stellar images, colour-magnitude diagrams and clustering correl. functions rel. to star populations 0-82360
- YY Geminorum, eclipsing binary, photometry and orbital period study 0-105287
- Geneva photometric boxes as absolute magnitude indicators, comparison with MK spectral types through trigonometric parallaxes 0-77385
- giant stars in Draco dwarf galaxy, effective temp. from photometry and spectral obs. 0-72941
- Gleise 490 AB (BD+36°2322), red dwarf binary, flares and starspots, rot. period determ. 0-77423
- globular clusters, integrated IR photometry and wide field techniques 0-67574
- globular clusters, integrated IR photometry using wide field photometer 0-62029
- globular star cluster age and distance determ. using subdwarf photometry results 0-82435
- globular star clusters, metal abundance and reddening from photometry obs. 0-67800
- H 2252-035, optical counterpart photometry and spectrum 0-101651
- HD 10783, Ap star, spectrophotometric obs. 0-98663
- HD 108078, spectroscopic binary orbit from photoelec. radial vel. meas. 0-77451
- HD 113001, photometric separation of visual binary (*French*) 0-105281
- HD 127617 (Bidelman's high latitude Be star), photometric and visible spectra obs. 0-77420
- HD 129708, new bright short-period Cepheid variable with unusual spectrum, photometric obs. 0-67751
- HD 137613, C rich H deficient star, UVB photometric obs. 0-90437
- HD 153919 (=4U 1700-37), eclipsing binary, supergiant-neutron star, optical variability 0-82419
- HD 159378 (Tr 27-102), yellow variable supergiant near Cepheid instability strip, VBLUW photometry 0-98672
- HD 185332, new  $\delta$  Scuti star, photometric and spectroscopic obs. 0-90451
- HD 192273, EUV flux upper limit, Voyager 1 obs. 0-77406
- HD 21479, brightness microvariability and non-radial pulsations (*Russian*) 0-67754
- HD 219150, F0 V star, with remarkable UV excess, optical and UV photometry and spectrum 0-90429
- HD 77581 (=Vela X-1), supergiant+neutron star, visible obs. 0-94892
- HD 77581 and 153919, polarimetric obs. of massive X-ray binaries 0-98688
- He2-442, UVBK photometry and spectroscopic obs. (*Russian*) 0-94817
- Henize 715 (4U 1145-61), Be-type star, colour and luminosity vars. (1976-1980) 0-72979
- HZ Herculis, 1978 UVB photometry of active state 0-62189
- AH Herculis, dwarf nova outburst, rapid oscils. evolution 0-94805
- DI Herculis, eclipsing binary, photometric obs. anal. rel. to relativistic motion of periastron 0-94830
- u Herculis, eclipsing variable, two new light curves 0-90472
- AM Herculis, polar, IR photometric obs. 0-98687
- AM Herculis, spectrophotometric obs. at min. light min. light 0-98692
- AM Herculis (3U 1809+50), simultaneous three-channel photometry rel. to optical flickering mechanism 0-82411
- HZ Herculis (Hercules X-1), optical and UV obs. 0-109487
- HR 1099 (V711 Tauri), JHK photometry of nonclipping RS Canum Venaticorum type star 0-72995
- HR 1225,  $\delta$  Scuti star, photoelectric study and periodogram anal. 0-109436
- HR 5110, Algol type RS Canum Venaticorum star, H $\alpha$ , yu photometry obs. 0-105276
- HR 5110, RS Canum Venaticorum binary, V photometry near radio outburst time 0-90469
- TT Hydrae, absolute dimensions of  $\beta$  Persei type eclipsing binary 0-62184
- HS Hydrae, photometric elements of detached eclipsing binary 0-90473
- integrated IR photometry, of globular clusters, colours and interstellar reddening 0-67575
- interstellar reddening in solar neighbourhood, anal. 0-62239
- IR bright stars in region of galactic centre, catalogue and photometry 0-77299
- IR sources near Herbig-Haro objects, obs. during search for exciting stars 0-67720
- IRC +10216, C star, far IR photometry and circumstellar dust cloud size 0-82539
- K1211, blue straggler in NGC 7789, evolution status and mass, photometry obs. 0-109433
- K-type giant stars, evidence for circumstellar shells from 0.4 to 20  $\mu$ m photometry 0-90420
- An King 13, open cluster, UVB obs. (*German*) 0-77459
- KUV09313+4052, variable UV excess object, UGR photographic photometry 0-62159
- 12 and 16 Lacertae,  $\beta$  Cephei stars, light var. anal. and photoelec. photometry 0-77412
- EV Lacertae, flare star, photometry and spectrum rel. to starspots and rot. period 0-98665
- SW Lacertae, W Ursae Majoris star, photoelectric obs. and epochs of min. light 0-62196
- late-type stars, anal. of balloon-borne near IR multicolour photometry 0-98654
- late-type young stars in  $\rho$  Ophiuchi dark-cloud, photometry obs. 0-72942
- LMC giants and supergiants, photometric luminosity calibration, visible obs. 0-94797
- loose stellar clusters in southern Milky Way, spectral type and UVB obs. 0-94839
- luminous stars in NGC 6822 and IC 1613, visible spectra and photometry 0-82345
- $\beta$  Lyrae, photoelectric photometry rel. to orbital period variability 0-72997
- M11, galactic open cluster, age and distance, colour diagram, photometric obs. 0-73012
- M2 (NGC 7089), globular cluster, faint stars photometry and colour-magnitude diagram 0-101623
- main sequence B-type stars, physical parameter determ. from uvby $\beta$  photometry obs. 0-72952
- main-sequence reddened stars, ANS photometry, UV colours 0-77400

## stellar photometry continued

- Markarian 38, galactic open star cluster, photometric obs. (*German*) 0-73015
- TY Mensae, contact eclipsing binary, evolutionary stage from UBV light curve anal. 0-105278
- Mira type variables, Me and Se types, UBV photometry 0-82375
- Mira variables, IR Photometry and OH maser pumping efficiency 0-82379
- AU Monocerotis, eclipsing binary, photolec. obs. 0-73002
- multicolour photometric data, comparison with Moscow and Alma-Ata stellar spectrophotometry 0-101590
- MXB 1730-335, X-ray rapid burster, IHKL photometry rel. to search for IR bursts 0-98740
- NGC 129, open cluster membership from four colour and H $\beta$  photometry 0-90485
- NGC 3293, open cluster, UBVR photometry and relation to OB complex in Carina 0-90490
- NGC 3293, uvby  $\beta$  photometry rel. to other young clusters 0-101621
- NGC 6087, galactic cluster, four-colour and H $\beta$  photometry 0-62208
- NGC 6397, globular star cluster, age from main sequence turnoff, BV photometry 0-90484
- NGC 6440, globular cluster, cluster core surface photometry and colour-magnitude diagram 0-82436
- NGC 654, young open cluster, UBV photometric study 0-109502
- NGC 6624, optical counterparts of X-ray burster in core of globular cluster 0-67801
- NGC 6635, globular cluster, colour magnitude diagram, BV photometry 0-90483
- NGC 957, young open cluster, distance and reddening, RGU photometry 0-85976
- S Normae, Cepheid, luminosity and membership of NGC 6087 visible obs. 0-94797
- Nova Serpentis 1978, visible and IR photometry rel. to dust shell evolution 0-90430
- novaklike object in Vulpecula, light curve, photometric and spectroscopic obs. 0-67758
- novaklike object in Vulpecula, photometry, June 1980, and spectral classification 0-94807
- novaklike variable in Virgo, discovery, approximate positions and magnitudes, (1980 July and August) 0-98674
- O-type stars towards Carina Nebula, extinction law 0-105240
- OB stars in Puppis, UBVR photometry 0-85937
- OB stars near Carina arm, UBVR photometry 0-85941
- open cluster reddening, polarimetry and field star photometry of M67, Hyades and Coma cluster 0-62222
- open clusters in Carina Nebula, extinction determ. from UBV photometry obs. 0-90513
- open clusters NGC 2547 and Trumpler 10 in Vela star cloud 0-90482
- open clusters Tr 14, 15, 16 and Cr 228 in Carina Nebula, dist. determ. 0-85977
- Pal 12, metal-rich globular cluster in outer galactic halo, optical and IR obs. 0-105290
- Palomar 2, distance and structural props. of globular cluster 0-62213
- MW Pavonis, W Ursae Majoris system, evolutionary stage from UBV light curve anal. 0-105278
- BB Pegasi, BV photoelectric lightcurve analysis of eclipsing binary 0-62194
- IW Persei, metallic-line close binary star, photometric and spectroscopic obs. 0-62186
- X Persei (4U 0352+30), Be star, photoelectric photometry rel. to 6-year periodicity 0-109446
- $\beta$  Persei (Algol), UV photometry and spectrum rel. to primary component rot. 0-72996
- photoelectric photometry, UBV obs. method and reduction 0-72784
- photographic, digitalised image processing, reduction procedures (*Italian*) 0-98569
- photometer for rapid stellar light variation, microprocessor controlled (*Spanish*) 0-82222
- Pismis 13, open cluster, colour magnitude diagram, UBV obs. 0-67805
- PSR 1913+16, optical candidate, astrometry and high-speed photometry 0-101609
- VV Puppis, polar, IR photometric obs. 0-98687
- Puppis open cluster pair Czernik 29 and Haffner 10, UBV obs. 0-109503
- PZT stars including suspected variables, photolec. UBV photometry obs. 0-77392
- R 136 in 30 Doradus, struct., colour, mass and excitation parameter, photometry obs. (*German*) 0-67825
- red dwarfs in southern hemisphere, absolute magnitude and distance, BVRI photometry 0-90419
- red giants in Draco dwarf spheroidal galaxy, metal abundance 0-73030
- red stars, RSO 1 catalogue cross correl. with IRC, AFGL and EIC catalogues 0-77511
- reddened stars, JHK photometry rel. to near IR interstellar reddening 0-94857
- Roberts 22, bipolar nebula with OH emission, IR photometry of assoc. A2 Ie star 0-94859
- HM Sagittae, symbiotic star, IR variability obs. from VJHKL photometry (*Russian*) 0-105263
- V1437Sagittarii, Population II Cepheid, identification and dist. 0-82396
- $\zeta$  Scorpii (HD 152236), UV spectroscopic and photometric vars. 0-101594
- V818 Scorpii (Scorpius X-1), UV, visible, IR and X-ray obs. 0-82541
- AI, WZ and XX Sculptoris, southern  $\delta$  Scuti stars, photoelectric study 0-90452
- RZ Scuti, eclipsing binary, ephemeris and UBV obs. 0-94832
- RZ Scuti, JKL IR obs., light curves for eclipsing binary 0-101615
- secondary standards, spectrophotometric obs. rel. to Ap stars HD 10783 and CU Virginis 0-98663
- semidetached systems, revised photometric elements 0-62193
- Serpens X-1 (4U 1837+04), burster optical binary counterpart visible spectra and photometry 0-94891
- Y Sextantis, W Ursae Majoris system, UBV obs., light curve soln. by computer program 0-77454
- simultaneous UBV photometry, by fast double head photometer 0-72775
- SMC star cluster colour magnitude diagrams and stellar identification charts 0-73014
- South Celestial Pole stars, extinction and colour coeffs. UBV photolec. sequence 0-77456
- southern double stars, magnitude differences, focal grating photometer obs. 0-67785
- SS 433, JHK photometry rel. to IR variability 0-98676

## stellar photometry continued

- SS 433, light curves, double peak and binary-like period, photometry 0-94804
- SS 433, V band photometry and broad min. prediction (1980 April-May) 0-82390
- standard stars, IUE photometric calibration, UV spectra 0-77383
- subdwarfs, 37-45 excess calibration using Fe/H abundances 0-82363
- subdwarfs, photometry rel. to compositions and kinematics 0-82364
- supernova in NGC 3733, spectrophotometry (1980 March 22) 0-62164
- supernova in NGC 4321, UBVR photometry 0-77428
- symbiotic star candidates in LMC, optical spectroscopy and IR photometry 0-62139
- CD Tauri, eclipsing binary, orbital element determ., BV photometer obs. 0-73000
- SU Tauri, R Coronae Borealis star, photometry in optical and IR ranges 0-101601
- V711 Tauri (HR 1099), RS Canum Venaticorum star, BV light curve during (1978-79) 0-105279
- BL Telescopii A, yellow variable supergiant near Cepheid instability strip, VBLUW photometry 0-98672
- Trapezium-type systems, UBVR photometry 0-82431
- EK Trianguli Australis, SU Ursae Majoris dwarf nova, superhumps, light curve UBV obs. 0-105255
- Trumpler 15 in  $\eta$  Carina, open cluster, age and reddening from UBVR obs. 0-90487
- Trumpler 27 star 28, obs. of WC9-type star with large IR excess 0-67738
- 4U 0115+634, X-ray binary, 1980 Aug. photometry and spectroscopy 0-101650
- UBV for S. Milky Way, stellar distrib. and colour excess obs. 0-85997
- UBV photoelectric sequence for studies of NGC 55 galaxy 0-73007
- UBV system, uniform transitions for extinction coeffs. 0-67408
- UBVR photoelectric sequence in Piscis Austrinus 0-62201
- XY Ursae Majoris, eclipsing binary, photometry and spectrum rel. to spot activity on primary component 0-109491
- UX Ursae Majoris, eclipsing binary, time series photometry 0-77446
- AN Ursae Majoris, polar, IR photometric obs. 0-98687
- US Naval Observatory data associated with stellar parallax determ. 0-72788
- Utrecht photometric system and adopted standard stars 0-62202
- uvby $\beta$  and prediction of MK spectral classification, general case 0-82216
- uvby $\beta$  photoelectric photometric catalogue 0-62036
- uvby $\beta$  photometry appl. spectral classification prediction with assumed luminosity class 0-67700
- AH Velorum, classical cepheid, binary detect., UBV obs. 0-109443
- $\gamma$  Velorum, multiple system, photometric obs. 0-90482
- AI Velorum, nature from BVRI photometry and photoelectric radial vels. 0-94815
- Vilnius photometric catalogue on mag. tape, description 0-98578
- CU Virginis (HD 124224), Ap star, spectrophotometric obs. 0-98663
- visual surface brightness depend. on colour, model stellar atm. calcs. 0-67707
- white dwarfs, HR-diagram and luminosity function determ. (*Chinese*) 0-77403
- II Zw 136, Seyfert galaxy nuclei, optical variability, UBV obs. 0-73049
- C stars, variable, IJHKL photometry obs. 0-98657
- He variable stars, IR photometry and IR excesses 0-67733

## stellar positions see astrometry

## stellar radiation

- see also solar radiation: stellar photography
- 1732-303, 1745-248, new X-ray burst sources, discovery and identifications with globular clusters (Terzan 1, 5) 0-98739
- 2A 0311-227, optical counterpart, AM Herculis type eclipsing binary, V-band obs. 0-101617
- 2A 0311-227, X-ray flux modulation period from HEAO obs. 0-77516
- A-type stars, Lyman  $\alpha$  effect on non-LTE model atmospheres 0-90422
- Abell 46, planetary nebula, eclipsing binary nucleus, hot component UV continuum obs. by IUE 0-98693
- absolute luminosity calibrations, consistency 0-62111
- absolute magnitudes determination, comparison between Geneva photometric boxes and MK spectral types 0-77385
- accretion disks round neutron stars and white dwarfs, flux distrib. and colours 0-94778
- Algol, orbit, lightcurve and struct. review 0-109460
- Am stars,  $\tau$  Ursae Majoris and 15 Vulpeculae, energy distrib. from spectral obs. 0-85949
- amplification by turbulent atm. 0-72782
- $\alpha$  Andromedae, shell star, lack of linear polarisation variability 0-62157
- Z Andromedae, symbiotic star, hot stellar UV continuum identification from IUEobs. 0-109450
- Ap stars broad flux depressions, comparison between synthetic spectra and spectrophotometry 0-67735
- R Aquarii, UV, visible and 85 GHz continuum obs. 0-85946
- R Aquarii (M7+pec), late type variable star, IUE obs. of circumstellar emission 0-82370
- Aquila X-1 (4U 1908+00), optical outburst obs. 0-67909
- Aquila X-1 (4U 1908+00), X-ray outburst obs. 0-77514
- $\eta$  Aquilae, Cepheid variable, absolute energy distrib. in radiation spectrum (*Russian*) 0-72974
- $\eta$  Aquilae, classical Cepheid, UV obs. and companion star detect. 0-90443
- V342 Aquilae, eclipsing binary, period and light curve changes. (1966 to 1976) 0-67791
- V603 Aquilae (Nova 1918), IUE obs. of periodic light vars. 0-105251
- V603 Aquilae (Nova 1918), old nova, eclipses obs. 0-90476
- V603 Aquilae (Nova 1918), periodic light vars. detect. 0-82391
- V1301 Aquilae (Nova Aquilae 1975), dust grain IR emission model 0-105254
- 59 Aurigae,  $\delta$  Scuti star, absolute magnitude, effective temp. and mass from light curves periodogram anal. 0-62141
- KR Aurigae, brightness history from 1890 AD 0-105245
- $\epsilon$  Aurigae, dual aspect of wavelength depend. fluctuations 0-62190
- EO Aurigae, eclipsing binary star, revised elements from light curve anal. 0-90471
- KR Aurigae, X-ray source nearby, X-ray, IR and visible obs. 0-67742
- B5 V-P5 V type stars in Geneva Observatory catalogue, radii, temp. and brightness determ. 0-77396
- B stars, empirical effective temp. determ. 0-101587
- B-type stars at high southern galactic latitudes, four colour and H $\beta$  obs. 0-82357



## stellar radiation continued

- Be and shell stars, UV radiation deficiency, TD-1 satellite obs. 0-90438  
 binary stars, review of X-ray emission 0-109564  
 binary system gravitational radiation, relativistic corrections and spectrum fine structure 0-90479  
 black holes, supercritical accretion discs luminosities 0-105272  
 black holes, thick accretion discs models rel. to supercritical luminosities 0-101614  
 BT Cancri (38 Cancri),  $\delta$  Scuti star, multiple periods rel. to radial and nonradial pulsation periods 0-85948  
 RS Canum Venaticorum, out of eclipse light var. and comparison with similar stars 0-109489  
 RS Canum Venaticorum binary stars, mag. starspot model for photometric and spectroscopic behaviour 0-109488  
 RS Canum Venaticorum type binaries, H $\gamma$  line vars., chromospheric diagnostics 0-62181  
 VY Carinae, Cepheid, luminosity and membership of assoc., visible obs. 0-94797  
 $\gamma$  Carinae, Cepheid variable, Fourier anal. of light var. 0-90442  
 $\gamma$  Cassiopeiae, Be star, rapid linear polarisation variability (*Russian*) 0-77417  
 SU Cassiopeiae, Cepheid variable, spectrophotometric determ. of temp. and luminosity 0-90435  
 VX Cassiopeiae, early-type irregular variable, photometric variability (*Russian*) 0-72973  
 cataclysmic binaries, circumstellar material geometrical and photometric parameters 0-109492  
 cataclysmic binary stars (CBS), critique of polarimetric evidence on physical parameters and orbital inclination 0-109486  
 Centaurus X-3, neutron star characts. from correlated spin-up and X-ray luminosity meas. 0-101648  
 central star of Abell 46, eclipsing binary 0-73027  
 VV Cephei, absolute visual magnitude Mg II reson. lines widths 0-109498  
 U Cephei, excess light obs. rel. to accretion discs 0-82412  
 VW Cephei, W Ursae Majoris star, orbital period decrease and B-V colours rel. to physical status 0-109495  
 $\beta$  Cephei stars, pulsation effect on period-luminosity relation 0-72970  
 Cepheid variables, period-luminosity-colour relation, numerical simulations 0-82393  
 Cepheid variables, phase shift technique for determining incidence of duplicity 0-90453  
 Cepheid variables determ. of colour term in period-luminosity colour relation 0-94812  
 dwarf Cepheids, period changes 0-62142  
 $\delta$  Ceti,  $\beta$  Canis Majoris variable, period meas. and detect. of period decrease 0-105257  
 XY Ceti, eclipsing binary, masses, radii and luminosities from revised photometric elements 0-109458  
 ZZ Ceti stars, constraints on possible long-term variability 0-90428  
 UV Ceti stars, photometric features near flare initial phase 0-105252  
 Z Chamaeleontis, eruptive binary, photometric data anal. 0-72961  
 Z Chamaeleontis, gravitational waves from eclipsing cataclysmic binary 0-90439  
 chromospheres of F, G and K-type stars, radiative losses in continuum 0-72924  
 Circinus X-1, binary model, radio emission 0-98736  
 Circinus X-1, changes in optical, IR and radio emission 0-67910  
 cocoon stars, numerical soln. of radiation transfer eqn. in spherical geometry 0-90329  
 R, S, T Coronae Austrinae, T Tauri stars, long period vars. 0-82350  
 Crab pulsar, magnetized cracks in crust rel. to matter flow, radio, X-ray and optical emissions 0-72990  
 Crab pulsar, model for pulsed  $\gamma$ -ray and X-ray emission 0-62230  
 SS Cygni, dwarf nova, rapid optical oscils., phase variability 0-85947  
 V380 Cygni, eclipsing binary, masses, radii and luminosities from revised photometric elements 0-109458  
 V1500 Cygni, ionising source UV flux rel. to Balmer-line emission profiles evolution 0-82371  
 CH Cygni, symbiotic star, binary model rel. to blue continuum and emission and absorpt. lines 0-62158  
 V1016 Cygni, symbiotic star, IR variability obs. from VJHKL photometry (*Russian*) 0-105263  
 CI Cygni, symbiotic star, UV continuum fading during eclipse 0-105258  
 V1329 Cygni (HBV 475), symbiotic variable, photometric and spectroscopic history 0-62148  
 V1500 Cygni (Nova 1975), emission line vars. rel. to central object radiation model 0-82367  
 V1500 Cygni (Nova 1975), luminosity and distance, light curve obs. 0-72981  
 V1668 Cygni (Nova 1978), optical light curve, uvby photometry 0-62154  
 V1668 Cygni (Nova 1978), UBV photometric search for short term light vars. (*Russian*) 0-109444  
 V1668 Cygni (Nova Cygni 1978), post-max. short period oscils., photoelectric photometry 0-82380  
 Cygnus X-1, critique of polarimetric evidence on physical parameters and orbital inclination 0-109486  
 Cygnus X-1, obs. during high state (1980 June 11 to 27) 0-86017  
 Cygnus X-1, transition from high X-ray state to low X-ray state, 1980 June to July 0-98738  
 Cygnus X-1 (V1357 Cygni), optical light curve vars. rel. to X-ray vars. 0-109560  
 Cygnus X-1 (X-2, X-3), X-ray polarisation obs. from OSO 8 0-90571  
 Cygnus X-3, 34.1 day period, 2-12 keV obs. by COS-B 0-94897  
 Cygnus X-3, period derivative and asymmetric X-ray light curve from HEAO 2 obs. 0-105394  
 HR Delphini (Nova 1967), continuum fluxes, temp. and luminosity from simultaneous X-ray, UV and optical obs. 0-109440  
 HR Delphini (Nova 1967), short period light vars. from UBV photometry 0-67744  
 dense stars, continuum spectrum polarisation in intense mag. fields, atomic physics theory 0-105160  
 disc population stars, luminosity functions in SA 51, SA 57 and (SA 68) 0-98648  
 S Doradus, LMC Hubble-Sandage variable, IUE and ground based spectroscopic obs. 0-101595  
 BY Draconis stars, out of eclipse light var. and comparison with RS Canum Venaticorum stars 0-109489  
 early A stars, empirical effective temp. determ. 0-101587  
 early type stars, luminosity determ. X-ray obs. 0-105241

## stellar radiation continued

- early-type stars, mass loss rel. to luminosity from radio obs. at 6 cm 0-82347  
 early-type stars with Balmer emission, luminosity classes from near UV spectra 0-94811  
 early-type stars with gas-dust envelopes, IR spectral energy distrib. 0-67732  
 eclipsing binaries light curve analysis, new techniques and appl. to V444 Cygni 0-82417  
 eclipsing binary light curves soln. using LIGHT computer program 0-77454  
 eclipsing binary stars, light curve analysis by Fourier techniques 0-72993  
 eclipsing binary stars, light curve analysis by Fourier techniques 0-72994  
 eclipsing variables, light curves linear analysis, fractional light loss anal. 0-82416  
 energy distrib. in Hayes-Latham calibration from spectrophotometric data 0-72790  
 energy distrib. of southern standard stars (320-880 nm) 0-62125  
 EUV radiation, point source contribs. to EUV background 0-62324  
 evolved stars expanding envelopes, CO thermal and maser emission 0-82334  
 expanding envelopes, Lyman  $\alpha$  quanta scattering (*Russian*) 0-67556  
 F-type main-sequence stars, effects of granulation on spectral energy distrib. 0-90417  
 flare stars, flare emission spectrum rel. to fast electron hypothesis 0-67731  
 flare stars, nature of flares optical continuum (*Russian*) 0-109445  
 flare stars in Scorpius-Ophiuchus region, discoveries (*Chinese*) 0-77418  
 U Geminorum, dwarf nova, visual magnitudes during outburst, (1980 May 6 to 9) 0-72978  
 U Geminorum, visual magnitude estimates during outburst (1980 Oct.) 0-109439  
 globular cluster stars, He settling rel. to main sequence turnoff luminosity and inferred ages 0-73013  
 globular clusters, UV energy distrib. from Orbiting Astronomical Observatory photometry 0-73009  
 GX 3+1, X-ray bursts obs., (1980 July 19 to August 18) 0-98739  
 halo population stars, luminosity functions in SA 51, SA 57 and (SA 68) 0-98648  
 HD 101065, Przybylski's star, light variability freq. anal. 0-62152  
 HD 102567, optical counterpart to 4U 1145-61, atm. model from UV obs. 0-105396  
 HD 113001, visual binary absolute magnitude determ. (*French*) 0-105281  
 HD 127617 (Bidelman's high latitude Be star), photometric and visible spectra obs. 0-77420  
 HD 129494, new pulsating  $\delta$  Delphini star, luminosity from period-luminosity-colour relation 0-67750  
 HD 129494, new pulsating  $\delta$  Delphini star, photometric obs. and luminosity 0-67750  
 HD 192273, EUV flux upper limit, Voyager 1 obs. 0-77406  
 HD 200775, possible protostar in reflection nebula NGC 7023, optical polarization and IR spectrum 0-85944  
 HD 21479, brightness microvariability and non-radial pulsations (*Russian*) 0-67754  
 HD 219150, F0 V star with remarkable UV excess, optical and UV photometry and spectrum 0-90429  
 HD 50896, Wolf-Rayet star, linear polarisation periodic vars. rel. to binary star nature 0-72972  
 HD 93250, O3 massive star in  $\eta$  Carinae complex, non-LTE analysis 0-77398  
 HDE 245770, optical counterpart to A 0535+26, dimens. spectral type and luminosity visible obs. 0-72976  
 Henize 715 (4U 1145-61), Be-type star, colour and luminosity vars. (1976-1980) 0-72979  
 Herbig-Haro object 1, far UV continuum obs. rel. to nature of object 0-67714  
 Hercules X-1 (HZ Herculis), X-ray continuum and Fe line emission during X-ray low state 0-105393  
 u Herculis, eclipsing variable, two new light curves 0-90472  
 HZ Herculis, light curve, radiation pressure effects 0-105280  
 AM Herculis, visual magnitude estimates (1980 March-June) 0-82428  
 AM Herculis (3U 1809+50), polarimetry and spectrophotometry rel. to mag. field 0-94835  
 AM Herculis (3U 1809+50), UV continuum radiation and spectrum obs. 0-67782  
 AM Herculis (4U 1814+50), radiation modulation with orbital period 0-105403  
 HZ Herculis (Hercules X-1), IUE obs. spectrum and light var. 0-73069  
 high luminosity stars in SMC, interstellar reddening distrib. functions appl. to total/selective absorption. ratio determ. (*German*) 0-67851  
 high-luminosity stars in nearby galaxies, interstellar reddening distrib. function rel. to reddening law determ. (*German*) 0-67850  
 hot white dwarfs, luminosity function, spectral type anal. 0-90418  
 HR 1225,  $\delta$  Scuti star, absolute magnitude, effective temp. and mass from photoelectric study 0-109436  
 EX Hydrae, dwarf nova, IR and optical light curves 0-67747  
 EX Hydrae, dwarf nova lightcurve, periodic and secular vars. 0-77413  
 VW Hydri, dwarf nova, IR light curves 0-67747  
 illumination of ring-shaped nebulae in LMC by embedded stars 0-77457  
 integrated starlight, synthetic spectrum between 3000 and 10000 Å, discussion 0-62200  
 intensity statistical distrib. resulting from star random distrib. 0-98700  
 interstellar polarisation, fluctuation theory 0-82442  
 interstellar UV radiation, role in interstellar gas heating 0-67839  
 interstellar UV radiation field, obs. from S2/68 sky-survey telescope 0-77523  
 ionising Lyman continuum photon flux and galactic star formation rate 0-67711  
 ionising star in interstellar density gradient, radio and IR appearance of dusty H II blisters 0-85979  
 IR flux method for stellar temps. and diameter determ. 0-62030  
 IRC+10374, IRC+10523, IR stars, H $_2$ O maser emission detect. 0-62298  
 K-type giant stars, IR excesses rel. to presence of circumstellar shells 0-90420  
 Kerr black hole, low-freq. radiation from infalling particle 0-62176  
 Kuwano's novae-like object in Vulpecula, IR photometric obs. 0-62147  
 12 and 16 Lacertae,  $\beta$  Cephei stars, light var. anal. and photoelec. photometry 0-77412  
 SW Lacertae, W Ursae Majoris star, photoelectric obs. and epochs of min. light 0-62196

## stellar radiation continued

- late-type main-sequence and subgiant stars, X-ray obs. of active coronae 0-72925  
 CW Leonis, (IRC+10216), IR C star, intrinsic polarisation origin 0-67730  
 AQ Leonis, Population II double-mode RR Lyrae star, theoretical period ratio 0-62134  
 linear polarisation spectrum of compact thermal sources, appl. to mag. fields determ. (*Russian*) 0-90344  
 LMC bright stars, luminosity function and comparison with galactic luminosity function 0-82499  
 LMC giants and supergiants, photometric luminosity calibration, visible obs. 0-94797  
 long-period variable stars in S.hemisphere, narrowband polarimetry 0-98666  
 LS 1+61°303, variable binary radio star (BI Ib), X-ray emission detect. 0-105400  
 LSI+61°303, supergiant Be star, radio emission and radial vel. periodic vars. 0-62149  
 luminosity classification of ADH objective prism spectra, procedure 0-72930  
 luminous stars in NGC 6822 and IC 1613, visible spectra and photometry 0-82345  
 Luyten proper motion stars, use of Luyten's magnitude estimates of red nearby star spectra selection 0-82353  
 RR Lyrae stars, theoretical period ratios 0-62134  
 RR Lyrae stars light variations, hydromagnetic processes as cause of period changes 0-105261  
 M1-2 central star, possible eclipsing binary in planetary nebula 0-105239  
 M-type dwarf stars in galaxy cluster Abell 2029, coronal X-ray emission rel. to SAS 3 obs. 0-82519  
 magnetic DA white dwarfs, spectral line and circular polarisation profiles 0-62123  
 main-sequence reddened stars, ANS photometry, UV colours 0-77400  
 massive stars, effects of convective and semiconvective mixing on main-sequence luminosity 0-90405  
 massive stars, luminosities and temps. rel. to evolution 0-90416  
 metallic line stars, spectral energy distrib. (*Russian*) 0-72975  
 Mira type stars, luminosity props. from spectra and light curve elements 0-105253  
 AU Monocerotis, mathematical anal. of photometric peculiarities 0-77448  
 R Monocerotis, T Tauri star, long period vars. 0-82350  
 MXB 1730-335, X-ray rapid burster, unsuccessful search for IR bursts 0-98740  
 MXB 1730-335 (Rapid Burster), microwave bursts obs. 0-62320  
 neutrino emission from dense stellar cores, time-dependent neutrino transport theory 0-94783  
 neutron star, accreting, X-ray bursts rel. to thermonuclear flashes in degenerate envelope 0-109455  
 neutron stars, accreting magnetic, cyclotron line form. 0-90463  
 neutron stars, electrodynamics and radiated power in curved space 0-90465  
 neutron stars, luminosity and spectrum from supercritical time-dependent accretion 0-85967  
 neutron stars, neutrino energy loss rel. to cooling 0-77443  
 neutron stars, radiation source form. mechanism mag. annihilation (*Chinese*) 0-77440  
 neutron stars, X-ray bursts radiation spectrum rel. to mass-radius relation 0-77444  
 neutron stars X-ray bursts, radiative heat transfer in surface layers 0-94826  
 NGC 205, stellar content rel. to UV flux 0-98716  
 NGC 741, 1316, 7626, radio galaxies, central dense star clusters luminosities rel. to accreting black holes 0-94871  
 S Normae, Cepheid, luminosity and membership of NGC 6087 visible obs. 0-94797  
 S Normae, Cepheid in NGC 6087, distance and luminosity from cluster four-colour and H $\beta$  photometry 0-62208  
 nova light curves, as manifestation of nonuniform stellar wind 0-62160  
 Nova Serpentis 1978, distance and luminosity from dust shell ang. expansion rate 0-90430  
 novae, effect of binary companion on outburst 0-82394  
 novae, UV radiation rel. to dust form. and ionisation in envelope 0-98678  
 novalike object in Vulpecula, 1980 May-June spectra and magnitudes 0-82392  
 novalike object in Vulpecula, UV decline and expanding cooling photosphere 0-67741  
 novalike object is Vulpecula, visual magnitude estimates (1980 February 2 to May 9) 0-72980  
 O-type stars in NGC 7000 (North America Nebula), continuum scatt. rel. to rocket UV imagery 0-82440  
 O-type stars towards Carina Nebula, extinction law 0-105240  
 OB3 type stars in young clusters, circumstellar matter 2200 Å hump interpretation 0-82351  
 old stars, UV excesses rel. to kinematics and Galaxy initial contraction 0-62204  
 Orion population stars, OH emission survey 0-67716  
 X Persei (4U 0352+30), Be star, evidence for 6-year photometric periodicity 0-109446  
 X Persei (A 0535+26), Prognosz-6 obs. of X-ray fluxes and energy spectra (*Russian*) 0-109562  
 SZ Piscium, RS Canum Venaticorum star, photometric obs. rel. to starspot model 0-109490  
 planetary nebulae central star, far UV flux determ. from nebula ionisation state 0-72945  
 planetary nebulae central stars, colour temps. and spectral classifications 0-109435  
 planetary nebulae central stars, interpretation of UV continuum radiation 0-109524  
 planetary nebulae central stars, temps. and EUV radiation rel. to nebulae H and He II spectra 0-67724  
 planetary nebulae central stars, visual spectra comparison with Zanstra temps. 0-109434  
 planetary nebulae nuclei, far UV fluxes rel. to nebulae ionisation and spectra 0-109529  
 planetary nebulae nuclei, radiation during He shell flashes rel. to nebulae ionisation 0-73021  
 planetary nebulae nuclei, temps. rel. to masses and nebulae evolution 0-82344

## stellar radiation continued

- polarisation of scattered radiation, in medium with internal energy sources 0-67541  
 polarization by Thomson scattering in circumstellar envelopes, Monte Carlo analysis 0-85931  
 Population II (pregalactic) stars, rel. to distortion of cosmological microwave black body radiation spectrum 0-67915  
 pre main sequence stars, rapidly rotating, evolution in gravit. contraction phase 0-62133  
 PSR 0031-07, drifting subpulses obs. and implications for pulsar models 0-67763  
 PSR 0611+22, short time scale integrated pulse shape vars. 0-105267  
 pulsar magnetosphere, relativistic particle curvature radiation 0-77434  
 pulsar radiation, plasma waves propag. along mag. field in strongly anisotropic relativistic plasma 0-67542  
 pulsars, distribution, birthrate and flux density distrib. 0-98681  
 pulsars, radio emission rapid var., mechanism (*Russian*) 0-77437  
 pulsars, source of coherent radio emission 0-82403  
 pulsars, subpulse and micropulse emissions rel. to neutron star crusts torsional oscills. 0-90464  
 pulsars emission mechanism, AC Josephson effect hypothesis 0-82404  
 $\zeta$  Puppis, of supergiant, mass flow var., visible and UV obs. 0-90431  
 red dwarfs in southern hemisphere, absolute magnitude and distance, BVRI photometry 0-90419  
 Rubin-152, possible massive O-type star on galactic fringe, spectrum rel. to luminosity and distance 0-98656  
 WZ Sagittae, eruptive binary, hot spot eclipses rel. to model of system 0-72962  
 WZ Sagittae, recurrent nova, IUE obs. in outburst 0-109448  
 WZ Sagittae, recurrent nova, model for superhump phenomena 0-82368  
 HM Sagittae, symbiotic star, IR variability obs. from VJHKL photometry (*Russian*) 0-105263  
 V701 Scorpii, luminosity ratio of early-type contact binary 0-62188  
 V861 Scorpii, upper limit on X-ray emission, and non-coincidence with (OAO 1653-40) 0-73072  
 V818 Scorpii (Scorpius X-1), bremsstrahlung, model for UV continuum energy distrib. 0-82541  
 Scorpius X-1, Prognosz-6 obs. of X-ray fluxes and energy spectra (*Russian*) 0-109562  
 Scorpius X-1, rapid variability simultaneous X-ray and optical obs. 0-62322  
 VY Sculptoris, novalike variable, faint state occurrence and spectrum 0-98675  
 RZ Scuti, JKL IR obs., light curves for eclipsing binary 0-101615  
 FH Serpentis (Nova Serpentis 1970), dust grain IR emission model 0-105254  
 SN 1979c in NGC 4321 (M100), detect. at 60 nm wavelength 0-82402  
 spectral energy distribution of 16 stars in 3500 to 7500 Å region, absolute calibration 0-67710  
 spectrophotometry, Moscow and Alma-Ata data comparison with multicolour photometric systems 0-101590  
 SS 433, beam acceleration, radiation and precession theory 0-72971  
 SS 433, beam models, energetics anal., possible triple system 0-90433  
 SS 433, emission regions and black hole accretion disk 0-67746  
 SS 433, implications of 13-day variation for mag. X-ray binary model 0-109447  
 SS 433, IR variability obs. 0-98676  
 SS 433, light curves, double peak and binary-like period, photometry 0-94804  
 SS 433, spectral features interpreted a precessing neutron star with jets, possible binary 0-90447  
 SS 433, V band photometry and broad min. prediction (1980 April-May) 0-82390  
 star image at telescope focus, quality, rel. to photoelectric obs. efficiency 0-62034  
 Stepanyan's star, eclipsing binary, eclipses obs. and orbital period refinement 0-62195  
 supergiant stars, brightness limits set by atmospheric instabilities 0-109432  
 supergiants in LMC, IUE obs. of UV spectra and flux distribts. 0-101593  
 supernova, light curve for very distant ( $z=0.5$ ) object 0-94821  
 supernova, nearby, UV and gamma radiation effects on terrestrial atmosphere 0-94584  
 supernova in anonymous galaxy in Centaurus, magnitude (1980 June 30) 0-85962  
 supernova in anonymous galaxy in Grus, discovery and magnitudes (1980 May 23 to July 12) 0-94820  
 supernova in anonymous galaxy near  $\kappa$  Centauri, discovery and magnitudes 0-85962  
 supernovae, Type I, luminosity calcs. 0-82400  
 supernovae, type II, light curves analytic solns. 0-77427  
 supernovae in molecular clouds, spectra and luminosity, evolution 0-82399  
 symbiotic stars, evolutionary considerations and origin of brightness vars. 0-62144  
 $\zeta$  Tauri, Be star, rapid linear polarisation variability (*Russian*) 0-77417  
 SU Tauri, R Coronae Borealis star, IR excess discovery from optical and IR photometry 0-101601  
 SU Tauri, R Coronae Borealis variable, brightening after long minimum, 1980 August to September 0-109438  
 T Tauri star formation, stellar wind as dynamic input into dark mol. clouds 0-85980  
 RW Trianguli, nova-like eclipsing binary radial vels., dimens. from visible spectra 0-82418  
 EK Trianguli Australis, SU Ursae Majoris dwarf nova, superhumps, light curve UVB obs. 0-105255  
 Tycho's supernova (SN 1572), unsuccessful search for optical stellar remnant 0-101603  
 4U 1700-37 (HD 153919), X-ray binary, high-energy X-ray obs. 0-86014  
 4U 1822-37, 2129+42, X-ray fluxes modulation periods from HEAO obs. 0-77516  
 4U 1907+09, X-ray spectrum and variability, position and optical identification 0-82542  
 SU Ursae Majoris stars, important sub-group of dwarf novae, photometric props. 0-101596  
 W Ursae Majoris stars, rot. line broadening functions rel. to gravity brightening and limb darkening 0-109494  
 UV observations by Earth-orbiting satellites of hot components and extended coronas 0-109379



**stellar radiation continued**

- UV radiation field in interstellar clouds, attenuation theory (*Russian*) 0-73026
- V444 Cygni, eclipsing binary, light curve anal. 0-109374
- variable stars, Scorpius-Ophiuchus region, discoveries (*Chinese*) 0-77418
- Vela pulsar (PSR 0833-45), radiation model 0-94824
- visual surface brightness depend. on colour, model stellar atm. calcs. 0-67707
- WC stars H-K colours, effects of near IR emission lines 0-94816
- white dwarfs, EUV and neutrino emission rel. to cooling theory 0-82356
- white dwarfs, HR-diagram and luminosity function determ. (*Chinese*) 0-77403
- X-ray binaries, recurrent transients model 0-109565
- X-ray sources, compact, radio emission origin 0-62317
- X-ray sources, galactic, hard and soft X-ray spectra rel. to physical nature 0-62316
- X-ray sources, time-dependent Comptonisation and X-ray reverberations rel. to rapid time variability 0-86013
- XUV emission, possibility of detect. (*German*) 0-109372
- Ca II H and K emission, chromospheric, in main-sequence stars, comparison of activity cycles to old and young stars 0-105235
- Ca II H and K emission, chromospheric, in field stars of solar neighbourhood, survey 0-109423
- He variable stars, IR excesses obs. 0-67733
- Mn-Hg stars, surface gravity and stellar temp. derivation from uvby $\delta$  data, statistical anal. 0-82397
- OH main line emission from globular clusters, high sensitivity search 0-62207

**stellar rotation**

- see also solar rotation
- Ap, Am stars, slow rot. rel. to chemical differentiation by diffusion 0-77381
- Ap-stars, mag. field rel. to rot. period, visible spectra obs. 0-82373
- axisymmetric rotating fluid, asymptotic estimates 0-98542
- late B-type stars small  $v \sin i$  values, Ap star determ., visible spectra 0-77409
- black holes, rot. rel. to free oscills. reson. freqs. and gravit. waves 0-105271
- black holes, spin-up by thick accretion discs 0-105273
- 53 Camelopardalis, Ap star, Ca II K and H $\delta$  lines vars. in rot. period (*Russian*) 0-90458
- AX Camelopardalis (53 Camelopardalis), Ap star, UVB photoelectric photometry and period of var. (*Italian*) 0-90448
- RS Canum Venaticorum binary stars, rot. rel. to mag. dynamo and star-spot model 0-109488
- Centaurus X-3, neutron star characts. from correlated spin-up and X-ray luminosity meas. 0-101648
- close binaries, synchronous systems devel. from tidal arc rot. interactions 0-109468
- 17 Comae A, Ap star, mag. field meas. and rot. period (*Russian*) 0-90457
- concave hamburger equilibrium of rotating bodies 0-109422
- $\theta$  Coronae Borealis, Be-type star, shell line profile and radial vel. obs. 0-77426
- $\beta$  Coronae Borealis, Ap star, Ca II K and H $\delta$  lines vars. in rot. period (*Russian*) 0-90458
- differential rotation, due to latitude depend. convective heat transport 0-90411
- differential rotation effect on velocity and magnetic fields, superposition of poloidal and toroidal field 0-72928
- differentially rotating gaseous polytropes construction of const. mass solar model 0-82338
- distorted stars, vibr. stability anal. using Clairaut coordinates 0-90408
- BY Draconis stars, angular momentum initial distrib. and evolution 0-85954
- early-type stars, envelope mixing of elements, shear flow instability 0-109424
- Emden-Chandrasekhar polytropes, exact solns. for axisymmetric solid-body rotators with ( $n=0, 1$  and  $5$ ) 0-109419
- Gleise 490 AB (BD+36°2322), red dwarf binary, flares and starspots, rot. period determ. 0-77423
- H 2252-035, X-ray flux modulation, compact star rotation 0-101652
- H 2252-035 cataclysmic variable, white dwarf rot. period from photometry and spectrum 0-101651
- HD 101065, Przybylski's star, rot. vel. from light variability freq. anal. 0-62152
- HD 127617 (Bidelman's high latitude Be star), photometric and visible spectra obs. 0-77420
- HD 45088, BY Draconis binary, surface activity from high rot. vel., visible obs. 0-77425
- HZ Herculis (Hercules X-1), accretion disk precession period 0-73070
- DQ Herculis (Nova 1934), white dwarf rot. period rel. to nova remnant shape 0-105244
- EV Lacertae, flare star, rot. period from photometric and spectroscopic obs. 0-98665
- $\alpha$  Lyrae (Vega) rot. rate determ. from line profile photoelec. obs., Fourier transforms 0-77408
- main sequence intermediate and late type stars, differential rot. models 0-105238
- massive close binary stars, effect of stellar evolution on components synchronous rot. 0-62192
- massive stars, single and binaries, evolution review 0-82343
- neutron star elec. field anal., effect on accretion and radio pulsar model 0-109453
- neutron stars, effects of rot. and mag. fields on superfluidity 0-77441
- neutron stars, effects of rot. on form of quantum vortex filaments 0-67770
- neutron stars, effects of slow rotation on stability against radial perturbations 0-98685
- neutron stars, rot. mag. field interaction with accretion disc 0-62173
- neutron stars, rotating, moments of inertia in bi-metric theory of gravitation 0-90466
- novae, effects of white dwarf rot. on remnants shapes 0-105244
- NP 0532, Crab pulsar, random walk timing noise anal. 0-77432
- NP 0532, rotation parameters, temporal var. 0-62170
- oscillations, adiabatic nonradial, freq. splitting by slow differential rot. 0-105233
- II Pegasi (HD 224085), surface active binary star, H $\alpha$  emission vars. rel. to rot. 0-90480

**stellar rotation continued**

- $\beta$  Persei, eclipsing binary, Mg II 280 nm line profile, calcs. and UV obs. 0-82421
- $\beta$  Persei (Algol), primary component rot. 0-72996
- pre main sequence stars, rapid rot. effect on evolution in gravit. contraction phase 0-62133
- pre main sequence stars rotation, theory of rotating interstellar clouds nonaxisymmetric collapse 0-85927
- PSR 0611+22, short time scale integrated pulse shape vars. 0-105267
- PSR 1913+16, binary pulsar, nature from observational data 0-77435
- pulsars, classification method from period change and radio luminosity (*Chinese*) 0-85963
- pulsars, evolution rel. to torques, magnetic moment and pair production 0-62169
- pulsars, finite force face cold plasma atm. models, plasma differential rot. 0-77378
- pulsars, periods, positions and proper motion determ. from pulse arrival times, UHF, obs. 0-77431
- pulsars, rotational behaviour rel. to superfluidity 0-98683
- pulsars, rotational energy loss, slowing down index and time derivs. 0-67762
- pulsars, self-consistent description of axisymmetric magnetosphere of parallel rotator 0-94825
- VV Puppis, AM Herculis type binary, optical absorpt. spectrum, cyclotron interpretation and models 0-73003
- rapidly rotating models with radiation press., struct. parameters calc. 0-67697
- relativistic spherical mass, effects of rot. on gravit. focusing of light 0-105155
- SS 433, 164<sup>d</sup> period as precessional motion, massive black hole and pulsar models 0-62138
- SS 433, beam acceleration, radiation and precession theory 0-72971
- SS 433, disk-driven precession 0-94803
- SS 433, spectral features interpreted a precessing neutron star with jets, possible binary 0-90447
- supernovae, magnetorotational explosion in cylindrical model 0-101605
- 41 Tauri, Ap star, Ca II K and H $\delta$  lines vars. in rot. period (*Russian*) 0-90458
- V711 Tauri (HR 1099), RS Canum Venaticorum star, rot. rel. to BV light curve during (1978-79) 0-105279
- RW Trianguli, nova-like eclipsing binary radial vels., dims. from visible spectra 0-82418
- upper main-sequence peculiar stars, chemical and physical props. rel. to radiatively driven diffusion theory 0-82374
- W Ursae Majoris stars, rot. line broadening functions rel. to stellar shapes 0-109494
- X-ray binaries, recurrent transients model rel. to spin-up and spin-down timescales 0-109565
- X-ray binary sources, pulsating, spin-up due to accretion from Keplerian disc 0-67904
- stellar size** see stellar dimensions
- stellar spectra**
- see also solar spectra; stellar photometry
- HR 1099, RS Canum Venaticum type binary, light and colour curve meas. 0-73004
- Ap stars, Fe I photoionisation spectrum causing UV absorpt. 0-109437
- 2A 0311-227, AM Herculis type X-ray binary, optical counterpart, radial vel. obs. 0-94890
- 2A 0311-227 optical counterpart, simultaneous photometric and spectroscopic obs. 0-90572
- 2A 0526-328, optical counterpart, eclipsing binary, visible emission line variability 0-73075
- 2A 0526-328 optical counterpart, radial vel. meas. and orbital period 0-90579
- 2A 0526-328 optical counterpart, spectroscopic obs. 0-77515
- 3A 2252-035, optical counterpart, proper motion and radial vel. determ. 0-82395
- A-type stars, effect of  $C+H^+ \rightleftharpoons C^+ + H$  charge transfer on C I 1101 Å absorpt. edge 0-90423
- A-type supergiant stars, reson. line profiles from IUE and Copernicus spectra 0-90424
- Abell 46, planetary nebula, eclipsing binary nucleus, hot component UV continuum obs. by IUE 0-98693
- absorpt. and emission features, IR spectrophotometry obs. 0-72954
- Algol, eclipsing binary, spectral obs., description and interpretation 0-105283
- Algol type stars, H I  $\alpha$  obs. 0-109484
- Am stars,  $\tau$  Ursae Majoris and 15 Vulpeculae, energy distrib. from spectral obs. 0-85949
- $\sigma$  Andromedae, Be star, spectroscopic evidence for new shell episode 0-90444
- CG Andromedae, Si binary star, spectrum variable, short period radial vel. variability determ. 0-72968
- BM Andromedae, spectroscopic and photometric obs. of T Tauri-type star 0-62130
- Ap stars, mag. fields meas. techniques and field geometries 0-82213
- Ap stars 5200 Å feature, evidence for two component struct. from new  $\Delta\alpha$ -photometry 0-67734
- Ap stars broad flux depressions, comparison between synthetic spectra and spectrophotometry 0-67735
- $\delta_{400}$ -Ap type stars, excess UV index, photometry obs. 0-72963
- Ap-stars, mag. field obs. using photoelec. method, visible spectra obs. 0-82373
- Ap-stars, spectral energy distrib., spectrophotometry in 3300 to 7100 Å region 0-85953
- $\alpha$  and  $\beta$  Aquarii, G-type supergiants, evidence for hybrid atmospheres and winds from UV spectra 0-72948
- AE Aquarii, cataclysmic variable, IUE satellite UV obs. 0-72985
- R Aquarii, symbiotic long-period variable, spectrum of assoc. nebulosity 0-90450
- R Aquarii, UV, visible and 85 GHz continuum obs. 0-85946
- $\sigma$  Aquarii (A0 IVs), hot metallic-line star, spectrum and abundance anal. 0-90415
- R Aquarii (M7+pec), late type variable star, IUE obs. of circumstellar emission 0-82370
- Aquila X-1 (4U 1908+00), emission line spectrum obs. during optical outburst 0-67909
- $\eta$  Aquilae, classical Cepheid, UV obs. and companion star detect. 0-90443
- $\theta$  Aquilae (B9.5 III), spectrum and abundance anal. 0-90415

## stellar spectra continued

- T Aquilae (Nova 1891), spectrophotometry of shell 0-72955  
 $\gamma$  Arae, line of sight interstellar cloud, model from spectra anal. 0-105312  
 $\zeta$  Aurigae, eclipsing binary, UV obs. of supergiant atmos. 0-94836  
 AR Aurigae, eclipsing binary Hg star, peculiar spectral var. during eclipse 0-98679  
 RW Aurigae, T Tauri star, far UV spectra, emission measure obs. 0-94788  
 T Aurigae (Nova 1891), old nova, photometric and spectroscopic obs. 0-90446  
 B7 to G4 stars, spectral type depend. of distrib. perpendicular to galactic plane (*Russian*) 0-73036  
 late B-type stars small  $v \sin i$  values, Ap star determ., visible spectra 0-77409  
 B-type supergiant assoc. with GL 2636, IR obs. 0-105302  
 BD+33°2642, galactic halo blue star, mass loss determ. from IUE obs. 0-72947  
 Be and shell stars, UV spectrophotometry with TD-1 satellite 0-90438  
 Be stars, discoveries in open clusters NGC 3766 and (IC 2581) 0-90445  
 Be-stars, IUE obs. 0-82383  
 binaries, wide visual, spectral type, age and uvby $\beta$  photometry 0-94833  
 binary stars, G and K-type giants Ca II H and K lines emission intensity 0-82420  
 binary stars, spectroscopic, spectral obs. with solid state detector 0-109469  
 binary system gravitational radiation, relativistic corrections and spectrum fine structure 0-90479  
 binary X-ray sources, cyclotron line feature identification 0-90577  
 $\alpha$  Bootis, spectrophotometric profile, 3200-3600 Å 0-62118  
 $\xi$  Bootis A, late-type dwarf star, field obs. 0-72949  
 53 Camelopardalis, Ap star, Ca II K and H $\delta$  lines rapid vars. (*Russian*) 0-90458  
 XX Camelopardalis, R Coronae Borealis star, spectral type from optical and IR photometry 0-101601  
 UW Canis Majoris, eclipsing binary, mass flow anal. from UV spectrum 0-109429  
 UW Canis Majoris, O7f supergiant, UV lines P Cygni profiles rel. to mass loss rate 0-67736  
 TX Canum Venaticorum, cataclysmic variable, P Cygni type, visible spectral obs. 0-105249  
 RS Canum Venaticorum binary stars, mag. starspot model for photometric and spectroscopic behaviour 0-109488  
 RS Canum Venaticorum stars, spotted component spectral type rel. to amplitude of out of eclipse light var. 0-109489  
 RS Canum Venaticorum type binaries, H $\gamma$  line vars., chromospheric diagnostics 0-62181  
 $\zeta$  Capricorni, Ba star, white dwarf+giant, UV spectra obs. 0-105284  
 $\nu$  Capricorni (B9.5 V), spectrum and abundance anal. 0-90415  
 QZ Carinae (HD 93206), O-type quadruple eclipsing system, spectroscopic and radial vel. study 0-105275  
 Cassiopeia-Taurus association stars, interstellar 2200 Å feature anomalous strength 0-77469  
 UV Cassiopeiae, R Coronae Borealis star, spectral type from optical and IR photometry 0-101601  
 $\mu$  Centauri (B2 IVe), new circumstellar shell development, spectroscopic obs. (1980 June 10-12) 0-94808  
 $\alpha$  Centauri binary system, spectroscopic chemical anal. 0-62128  
 Centaurus X-4, spectroscopic obs. of visual counterpart, companion type 0-82545  
 VV Cephei, supergiant eclipsing binary UV spectrum 0-82415  
 VV Cephei, UV spectrum obs. during chromospheric eclipse phase 0-109498  
 $\delta$  Ceti,  $\beta$  Cephei variable, spectroscopic binary, radial vels. and period var. 0-82376  
 o Ceti (Mira) at 1978 max., visible spectropolarimetry 0-94799  
 chromospheric spectral lines, primary and secondary indicators of hot envelopes (*German*) 0-109421  
 Chu's object in Perseus, UV photometry and spectrum rel. to identification as galactic star 0-62132  
 Circinus X-1, H $\alpha$  emission vars. 0-67910  
 classification of ADH objective prism spectra, procedure 0-72930  
 close binaries, light scattering in extrastellar gaseous material, emission line profiles spectropolarimetry obs. 0-109471  
 cluster stars near IC 1805 (W4), spectral classes and photometry 0-62214  
 Collinder 140, young open cluster, spectroscopic and statistical study 0-62211  
 17 Comae A, Ap star, mag. field meas. and rot. period (*Russian*) 0-90457  
 R Coronae Austrinae dark cloud stars, interstellar absorpt. spectra rel. to dust grain growth 0-67834  
 $\beta$  Coronae Borealis, Ap star, Ca II K and H $\delta$  lines rapid vars. (*Russian*) 0-90458  
 $\theta$  Coronae Borealis, Be-type star, shell line profile and radial vel. obs. 0-77426  
 $\alpha$  Coronae Borealis, Hg-Mn star, spectroscopic binary, visible spectra obs. 0-72983  
 coronal plasma, EUV spectra and contris. to diffuse EUV background 0-62324  
 CPD -62° 1837 (HDE 308122), long-period variable member of triple 0-105260  
 BI Crucis, new symbiotic star, spectrum 0-109442  
 25 G Crucis (HD 108250), orbital elements from spectrograms 0-82432  
 31 and 32 Cygni,  $\zeta$  Aurigae stars, UV spectroscopic obs. 0-109499  
 XX Cygni, dwarf Cepheid, composition and motion, visible photometric and spectrographic obs. 0-77424  
 $\theta$  Cygni, F-type dwarf star, spectral type of faint distant companion 0-90481  
 P Cygni, H Paschen  $\alpha$  obs. 0-62156  
 59=V832 Cygni, IR emission increase, spectrum scanner obs. 0-94809  
 V1016 Cygni, near-IR spectrographic obs. 0-94810  
 CH Cygni, symbiotic star, 1977 outburst, radial vel. and atm. struct. determ. 0-72969  
 CH Cygni, symbiotic star, binary model rel. to blue continuum and emission and absorpt. lines 0-62158  
 V645 Cygni (AFGL 2789), Ae star, perplexing spectrum 0-73066  
 $\alpha$  Cygni (Deneb), Ca II K-line core asymmetry 0-85981  
 V645 Cygni (GL 2789), IR and EHF spectroscopy 0-72956  
 V1329 Cygni (HBV 475), symbiotic variable, photometric and spectroscopic history 0-62148

## stellar spectra continued

- V1500 Cygni (Nova 1975), Balmer line emission profiles evolution in early decline phase 0-82371  
 V1500 Cygni (Nova 1975), distance and temp., visible spectral obs. (*Chinese*) 0-85955  
 V1500 Cygni (Nova 1975), emission line vars. rel. to struct. of central object 0-82367  
 V1668 Cygni (Nova 1978), spectroscopic and photometric obs., (1978 to 1979) (*Russian*) 0-109444  
 CI Cygni symbiotic star, UV and optical spectral changes during eclipse 0-105258  
 Cygnus X-1, X-ray binary, variable star, SHF obs. 0-73071  
 Cygnus X-2, binary, radial vel. and orbital elements from visible spectra obs. 0-77519  
 DA white dwarfs, H I Balmer  $\gamma$  line profiles and masses 0-77399  
 HR Delphini (Nova 1967), premaximum mass loss rate, H line anal. 0-82378  
 HR Delphini (Nova 1967), simultaneous X-ray, UV and optical obs. 0-109440  
 dense stars, atomic spectrum in intense mag. fields 0-105160  
 S Doradus, LMC Hubble-Sandage variable, IUE and ground based spectroscopic obs. 0-101595  
 double stars, visual, new spectral classification on MK system 0-109462  
 K Draconis, Be star, search for short time scale vars. in H $\alpha$  emission 0-109441  
 early type stars, luminosity determ. X-ray obs. 0-105241  
 early type stars, spectral classification from UV line features 0-72927  
 early-type stars and cool stars, UV spectroscopy of outer layers 0-72922  
 early-type stars with Balmer emission, near UV (2000-3000 Å) spectra 0-94811  
 early-type stellar winds, H and He<sup>+</sup> synthetic line profiles 0-85926  
 SW eclipsing binary, period study, photometry and spectra obs. 0-82424  
 eclipsing binary runaway, orbital data, UV obs. 0-85952  
 $\nu$  Eridani,  $\beta$  Cephei variable atm. parameters from H and He spectral obs. 0-67739  
 $\epsilon$  Eridani, UV line spectrum of active chromosphere star, models 0-77394  
 evolved stars expanding envelopes, CO thermal and maser emission 0-82334  
 F-type supergiants, southern, visible spectra obs. 0-98660  
 F-type supergiants in Magellanic Clouds, spectra and Ca abundances 0-98655  
 fine structure lines, dust UV opacity effects 0-90505  
 flare stars, multichannel spectrophotometry 0-105256  
 G128-7, cool DA white dwarf, spectrophotometry rel. to atmospheric parameters and evolution 0-62126  
 G 165-7, metallic line white dwarf, model atm. code anal. of spectrum 0-85940  
 galactic halo C star possible association with Magellanic Stream, visible obs. 0-77411  
 ingalaxies assoc. with QSOs, spectroscopic search 0-105355  
 giant stars in Draco dwarf galaxy, effective temp. from photometry and spectral obs. 0-72941  
 giant stars in globular clusters M5, M13, M3, spectra and chemical comp. 0-67695  
 $\beta$  Gruis (M2 II), S I emission obs. in EUV spectrum 0-82359  
 H 2252-035, optical counterpart photometry and spectrum 0-101651  
 H 2252-035, spectrophotometry, no periodic linear polarization (1980 Sept.) 0-105401  
 halo stars in galaxy NGC 4565, spectral types radial gradient 0-62261  
 HD 102567, optical counterpart to 4U 1145-61, atm. model from UV obs. 0-105396  
 HD 105056, ON supergiant, radial vel. study 0-90427  
 HD 10783, Ap star, spectrophotometric obs. 0-98663  
 HD 108078, spectroscopic binary orbit from photoelec. radial vel. meas. 0-77451  
 HD 127617 (Bidelman's high latitude Be star), photometric and visible spectra obs. 0-77420  
 HD 129708, new bright short-period Cepheid variable with unusual spectrum, photometric obs. 0-67751  
 HD 166734, Of star, spectroscopic binary orbit determ. from visible obs. 0-82414  
 HD 168607 (B9 Ia<sup>+</sup>), S Doradus type star candidate, spectral line profiles (*Russian*) 0-90456  
 HD 185332, new  $\delta$  Scuti star, photometric and spectroscopic obs. 0-90451  
 HD 187473, rare earths in Si star 0-98671  
 HD 192163, WR star in filamentary nebula NGC 6888, optical spectra calc. 0-105304  
 HD 192273, EUV flux upper limit, Voyager 1 obs. 0-77406  
 HD 200775, Be star, optical and UV extinction spectrum due to dust in (NGC 7023) 0-109515  
 HD 200775, possible protostar in reflection nebula NGC 7023, optical polarization and IR spectrum 0-85944  
 HD 219150, F0 V star with remarkable UV excess, optical and UV photometry and spectrum 0-90429  
 HD 25329, subdwarf, metal deficiency from spectroscopic anal. 0-62122  
 HD 34664 (S 22) in LMC, peculiar emission line supergiant 0-77416  
 HD 36665, B1e star, detect. of interstellar CO absorpt. in direction of supernova remnant (S147) 0-67836  
 HD 39937, 101379, 155555, 174429, southern RS Canum Venaticorum stars candidates, radial vel. study 0-98686  
 HD 4174, symbiotic star, spectroscopic obs. 0-85945  
 HD 4174 (=EG Andromedae), peculiar M giant, UV spectra obs. 0-94798  
 HD 44179, 3.3 micron unidentified feature, high resolution spectra 0-82466  
 HD 45088, BY Draconis binary, surface activity from high rot. vel., visible obs. 0-77425  
 HD 45088, reticon obs. in red of dK3 spectroscopic binary 0-67778  
 HD 45677, peculiar Be-star, 0.12-12.6  $\mu$ m obs. 0-72957  
 HD 77581 (=Vela X-1), supergiant+neutron star, X-ray, UV and visible obs. 0-94892  
 HD 97048 (=HM 18), pre-main sequence star, unidentified IR features obs. 0-85943  
 HD 97950, central star in NGC 3603, interstellar spectral lines, visible obs. 0-101586  
 HDE 226868 (Cygnus X-1), X-ray and UV spectra from HEAO 2 and IUE 0-82543  
 HDE 245770, optical counterpart to A 0535+26, dimens. spectral type and luminosity visible obs. 0-72976



## stellar spectra continued

- He2-442, UVRK photometry and spectroscopic obs. (*Russian*) 0-94817  
 He 2-467, yellow symbiotic star, emission lines and continuum 0-62155  
 Herbig-Haro object, far UV spectrum obs. rel. to nature of object 0-67714  
 Herbig-Haro objects, nearby IR sources optical spectra 0-67720  
 Hercules X-1, implications of cyclotron features in X-ray spectrum 0-86015  
 Hercules X-1 (HZ Herculis), X-ray continuum and Fe line emission during X-ray low state 0-105393  
 Hercules, B3 IV type star, Copernicus, UV spectral atlas 0-67583  
 DQ Herculis, eclipsing binary emission line eclipse phenomena, visible spectra obs. 0-94800  
 AM Herculis, spectrophotometric obs. at min. light min. light 0-98692  
 AM Herculis, X-ray eclipsing binary, UV and visible spectra anal. 0-109563  
 AM Herculis (3U 1809+50), He II 4686 Å photometry vel. to optical flickering mechanism 0-82411  
 AM Herculis (3U 1809+50), polarimetry and spectrophotometry rel. to mag. field 0-94835  
 AM Herculis (3U 1809+50), UV spectrum obs. 0-67782  
 HZ Herculis (Hercules X-1), Ariel V X-ray spectra 0-90580  
 HZ Herculis (Hercules X-1), IUE obs. spectrum and light var. 0-73069  
 HZ Herculis (Hercules X-1), optical and UV obs. 0-109487  
 α Herculis A, M-type supergiant, Li abundance in atmosphere (*Russian*) 0-72950  
 high velocity giant stars, detailed chemical anal. 0-82352  
 hot stars in Magellanic Clouds, UV spectra, evidence for galactic hot gaseous corona 0-82490  
 hot stars with circumstellar clouds, synthetic UV spectra calcs. 0-77382  
 hot subdwarfs in Carnochan and Wilson catalogue, UV spectra 0-82354  
 hot white dwarfs, luminosity function, spectral type anal. 0-90418  
 HR 1099 (V711 Tauri), RS Canum Venaticorum star, Hα line variability, visible spectra obs. 0-105277  
 HR 2142 and 7084, mass loss from UV spectra obs. 0-109485  
 HR 5049, Co II in spectrum of southern magnetic Ap-star 0-82384  
 HR 6127, chemically peculiar star, spectral lines and equivalent width lists, visible obs. 0-82387  
 HR 6659, spectroscopic binary, radial vel. obs. 0-82430  
 HR 8752, binary supergiant, emission feature variability, visible obs. 0-109463  
 HR 96, Ap-type star, atm. parameters and stellar comp., visible obs. 0-67740  
 TT Hydrae, absolute dimensions of β Persei type eclipsing binary 0-62184  
 EX Hydrae, spectra of dwarf nova 0-98670  
 HZ 43, white dwarf, He abundance and stellar struct. from soft X-ray spectra 0-72944  
 III-106, CH star in globular cluster M22, CO in IR spectra 0-62131  
 ε Indi, late type dwarf star, spectrum rel. to model atmosphere and comp. 0-90425  
 integrated starlight, synthetic spectrum between 3000 and 10000 Å, discussion 0-62200  
 interstellar CH<sup>+</sup> line obs., <sup>12</sup>CH<sup>+</sup>/<sup>13</sup>CH<sup>+</sup> abundance ratio meas. 0-67809  
 interstellar extinction feature at 220 nm and diffuse 443 nm band, ANS obs. 0-62244  
 interstellar Mg lines, obs. rel. to existence of circumstellar clouds 0-94782  
 interstellar UV absorption features, in two stars in 30 Doradus 0-85978  
 IR airborne spectrophotometry, 1.2-5.5 μm, spectra and absolute calibration 0-62117  
 IRC+10216, variable C star, IR spectra obs. 0-90568  
 IRC+10374, IRC+10523, IR stars, H<sub>2</sub>O maser emission detect. 0-62298  
 IRC+30219, variable C star, optical emission-line phase obs. 0-90569  
 K dwarfs assoc. with X-ray transients A060-00 to A1742-28, visible and IR obs. 0-101653  
 K-type stars, spectroscopic investigations in 4500 to 7500 Å region 0-109430  
 EV Lacertae, flare star, photometry and spectrum rel. to starspots and rot. period 0-98665  
 late-type catalogue of revised Mk spectral types 0-82226  
 late-type field stars in S.hemisphere, radial vel. study rel. to possible duplicity 0-98686  
 late-type giant stars, H<sub>2</sub>O band absorpt. effect on balloon-borne near IR multicolour photometry 0-98654  
 late-type stars, Ca II 8542 Å line as chromospheric activity indicator 0-62108  
 late-type stars, S I emission in EUV spectra 0-82359  
 late-type young stars in ρ Ophiuchi dark cloud, photometry obs. 0-72942  
 19 Leonis Minoris, spectroscopic binary, orbital elements and mass ratio 0-62197  
 48 Librae, Be star, shell spectrum line profiles 0-62146  
 48 Librae (FX Librae), Be star, search for short time scale vars. in Hα emission 0-109441  
 line formation depth in mag. field, theory (*Chinese*) 0-105159  
 line formation in turbulent media 0-77387  
 line profiles, anal. using linear filtering theory (*Italian*) 0-90340  
 line profiles in spherical envelopes, three computation methods 0-85868  
 LMC X-1 optical candidate, spectrum and semi-accurate position 0-67908  
 long-period variable stars, polarisation vars. across TiO bands and Ca I line 0-98666  
 loose stellar clusters in southern Milky Way, spectral type and UVB obs. 0-94839  
 low dispersion objective prism spectra, automatic reduction (*Italian*) 0-98567  
 LP 145-141, C<sub>2</sub> white dwarf, spectrum, strong UV absorpt. obs. by IUE 0-67715  
 luminous early type stars in giant extragalactic H II regions, IUE UV spectra 0-77467  
 luminous stars in NGC 6822 and IC 1613, visible spectra and photometry 0-82345  
 RU Lupi T Tauri star, far UV spectra, emission measure obs. 0-94788  
 β Lyrae, CNO abundances in atmosphere, IR spectra (*Russian*) 0-67794  
 R Lyrae, M-type supergiant, Li abundance in atmosphere (*Russian*) 0-72950  
 α Lyrae (Vega) rot. rate determ. from line profile photoelec. obs., Fourier transforms 0-77408  
 RR Lyrae stars, in 47 Tucanae, membership and metallicity 0-62206

## stellar spectra continued

- M-type stars, classification from spectral scans 0-62127  
 magnetic DA white dwarfs, spectral line and circular polarisation profiles 0-62123  
 main sequence B-type stars, physical parameter determ. from uvbyβ photometry obs. 0-72952  
 maser stars, late supergiants and long period variables 0-77410  
 Michelson Fourier transform stellar spectrometer 0-98552  
 Mira type stars, luminosity props. from spectra and light curve elements 0-105253  
 Mira type variables atm., OH maser, IR line overlap pumping mechanism 0-72764  
 MK spectral classification from photometric obs., appl. to uvbyβ photometry with assumed luminosity class 0-67700  
 MK spectral classification from uvbyβ photometry, general case 0-82216  
 MK spectral types as absolute magnitude indicators, comparison with Geneva photometric boxes through trigonometric parallaxes 0-77385  
 15=S Monocerotis, interstellar lines, UV obs. 0-90494  
 MWC 349, Be star, radio-source, spectral EHF obs. 0-105262  
 MWC 349A, near-IR spectrographic obs. 0-94810  
 neutron stars, accreting magnetic, cyclotron line form. 0-90463  
 neutron stars, rotating, max. surface redshifts in bi-metric theory of gravitation 0-90466  
 neutron stars, X-ray bursts radiation spectrum rel. to mass-radius relation 0-77444  
 neutron stars, X-ray spectra from accretion column, optically thick region inc. 0-67767  
 NGC 6210, planetary nebula, central star, high dispersion EUV obs. and spectral type 0-77466  
 NGC 6231, open cluster, spectral types 0-90492  
 nova-like stars, cyclotron line search in optical spectra (*Russian*) 0-67753  
 novalike object in Vulpecula, 1980 May-June spectra and magnitudes 0-82392  
 novalike object in Vulpecula, light curve, photometric and spectroscopic obs. 0-67758  
 novalike object in Vulpecula, photometry, June 1980, and spectral classification 0-94807  
 nuclear waste spectrum, means of detecting extraterrestrial civilisations 0-82230  
 O-type stars, C III 7901 to 9715 Å emission lines obs. 0-77401  
 O-type stars, gravity and effective temp. determ. by automatic procedure 0-98557  
 O-type stars, mass loss rate from UV spectra 0-82346  
 OAO 1653-40, 38 s X-ray pulsar, optical counterpart, spectroscopic search 0-73072  
 OB3 type stars in young clusters, circumstellar matter 2200 Å hump interpretation 0-82351  
 OB stars, stellar wind mass loss determ., UV spectra obs. 0-94789  
 OB stars in Circinus-Norma region, search for faint objects 0-62121  
 OB-type stars, search for H Paschen α 0-62156  
 OH 205.1-14.1 in Lynds 1630 dark cloud, coincident IR source obs. 0-101630  
 open cluster stars, southern, radial vel. obs. (*German*) 0-94724  
 † Ophiuchi, 1980 March emission episode, Hα and He I line behaviour 0-62151  
 x and 66 Ophiuchi, Be stars, search for short time scale vars. in Hα emission 0-109441  
 † Ophiuchi, search for interstellar Sc II 0-82445  
 † Ophiuchi (HR 6175), O-type star, emission line episode 0-72953  
 70 Ophiuchi A, late-type dwarf star, mag. field obs. 0-72949  
 ρ Ophiuchi dark cloud stars, interstellar absorpt. spectra rel. to dust grain growth 0-67834  
 Orion population stars, variables light curve characts. and emission line intensities 0-67721  
 † Orionis, Reticon obs. of Hα P Cygni profile 0-82365  
 α Orionis, supergiant variable, mass loss, visible spectra obs. 0-67755  
 θ<sup>2</sup> Orionis B, long-slit spectroscopy in rocket UV 0-105297  
 θ<sup>1</sup> Orionis C and θ<sup>2</sup> Orionis A, UV spectra 0-90499  
 Pal 12, metal-rich globular cluster in outer galactic halo, optical and IR obs. 0-105290  
 AG Pegasi, symbiotic binary system, UV and optical spectrum rel. to nature of components 0-109449  
 II Pegasi (HD 224085), surface-active binary star, spectroscopic obs. 0-90480  
 X Persei, eclipsing binary, gaseous ring struct., H I alpha obs. 0-109482  
 β Persei, eclipsing binary, Mg II 280 nm line profile, calcs. and UV obs. 0-82421  
 RY Persei, eclipsing binary, spectroscopy and physical parameters of atmospheres 0-101618  
 β Persei, eclipsing binary, UV obs. from TD-1A satellite 0-77447  
 RY Persei, eclipsing binary, visible spectral obs., model 0-67795  
 † Persei, interstellar C, rot. fine-struct. lines obs. 0-67811  
 IW Persei, metallic-line close binary star, photometric and spectroscopic obs. 0-62186  
 X Persei (A 0535+26), Prognos-6 obs. of X-ray fluxes and energy spectra (*Russian*) 0-109562  
 β Persei (Algol), UV line profiles obs. rel. to primary component rot. 0-72996  
 19 Piscium, C star, violet spectrum line identification and radial vel. 0-82361  
 planetary nebulae central stars, visual spectra comparison with Zanstra temps. 0-109434  
 protostellar envelope evolution, radiative transfer and spectrum 0-77384  
 pulsars, charact. feature interpretation 0-109451  
 pulsars, infinitely magnetised H atom spectrum 0-77282  
 pulsars, low-latit., H I absorpt. spectra meas. 0-101606  
 VV Puppis, AM Herculis type binary, optical absorpt. spectrum, cyclotron interpretation and models 0-73003  
 ρ Puppis, line profile variable, pulsational mode-typing 0-90432  
 † Puppis, of supergiant, mass flow var., visible and UV obs. 0-90431  
 † Puppis, Of type star, stellar wind model from UV line fit 0-72965  
 † Puppis, Reticon obs. of Hα P Cygni profile 0-82365  
 radial vel. determ., survey of different methods 0-73006  
 radial vel. determ. with CORAVEL, Cassegrain spectrophotometer 0-82210  
 red giants in Draco dwarf spheroidal galaxy, metal abundance 0-73030  
 red giants in M13, Na abundance var., protocluster gas inhomogeneities 0-82439  
 Ross 640, He-rich white dwarf, Ca, Mg, S and Fe abundances from UV spectra 0-94790

## stellar spectra continued

- Rubin-152, possible massive O-type star on galactic fringe, spectroscopic obs. 0-98656
- S-type stars, Keenan and Wing bands, IR obs. 0-67722
- S-type stars, Keenan band identification problem, IR obs. 0-72946
- S-type stars, possible presence of ZrO IR spectrum 0-62124
- FG Sagittae, 1975-8 spectral obs. of peculiar variable 0-72959
- WZ Sagittae, 1978-9 outburst of dwarf nova, spectra 0-94801
- WZ Sagittae, image-tube spectroscopic obs. of 1978 Dec. outburst 0-72958
- FG Sagittae, planetary nebula central star, radial vel. meas. rel. to binary star model 0-98664
- WZ Sagittae, recurrent nova, eclipsing binary, outburst of December 1978, UV obs. 0-72982
- WZ Sagittae, recurrent nova, IUE obs. in outburst 0-109448
- WZ Sagittae, recurrent nova, spectroscopic obs. and model for superhump phenomena 0-82368
- SB 21, extremely He rich subdwarf O-star, spectrum 0-98659
- $\mu^1$  Scorpii, eclipsing binary, UV obs. from TD-1A satellite 0-77447
- $\zeta^1$  Scorpii (HD 152236), UV spectroscopic and photometric vars. 0-101594
- V818 Scorpii (Scorpius X-1), UV, visible, IR and X-ray obs. 0-82541
- Scorpius X-1, binary star, X-ray spectrum 20-75 keV, high sensitivity determ. 0-98741
- Scorpius X-1, binary star X-ray obs. from 20 to 250 keV 0-94893
- Scorpius X-1, Prognoz-6 obs. of X-ray fluxes and energy spectra (Russian) 0-109562
- VY Sculptoris, novalike variable, spectrum during faint state 0-98675
- $\delta$  Scuti, line profile variable, pulsational mode-typing 0-90432
- Serpens X-1 (4U 1837+04), burster optical binary counterpart visible spectra and photometry 0-94891
- W Serpentis stars, long period eclipsing binaries, new class, spectral characts. 0-109483
- slow novae and symbiotic stars, late-type components spectral classifications 0-94813
- SN 1979c in M100, coordinated obs. (1979 April-June) 0-101604
- SN 1979c in M100 (NGC 4321), spectrophotometry 0-62166
- SN in MCG -3-34-61, Type I spectrum revealed (1980 June) 0-82401
- spectrophotometric data processing by large scale interactive one dimens. array processing system 0-82220
- spectroscopic binaries near southern open clusters, radial vel. obs. near southern open clusters (German) 0-94724
- SS 433, general spectral features 0-77421
- SS 433, implications of 13-day variation for mag. X-ray binary model 0-109447
- SS 433, 0-6 day periodicity in 1978 June-1980 Feb. obs. period 0-62150
- SS 433, radial vel. curve low amplitude section, visible spectra anal. 0-67737
- SS 433, reality of 6-day periodicity in spectral lines wavelengths var. 0-67743
- SS 433, search for radio spectral lines in UHF 0-109556
- SS 433, spectral features interpreted a precessing neutron star with jets, possible binary 0-90447
- SS 433, wavelength shifts 164<sup>d</sup> period as precessional motion, massive black hole and pulsar models 0-62138
- SS 433 inside SNR, unique spectrum 0-82381
- SS 433 region of SNR W50, visible obs. relativistic jets interaction with interstellar medium 0-101629
- standard stars, IUE photometric calibration, UV spectra 0-77383
- Stepanyan's star, obs. of G8 V absorpt. spectrum and emission spectrum 0-67788
- Stokes parameters and mag. field vector profiles (Chinese) 0-77386
- subdwarfs, masses and metal abundances from spectroscopic anal. 0-62122
- supergiant stars with stellar winds LMC, luminosity and extinction values, UV obs. 0-77477
- supergiants in LMC, diffuse interstellar 4430 Å feature 0-73033
- supergiants in LMC, IUE obs. of UV spectra and flux distrib. 0-101593
- supernova, possible, in Virgo galaxy cluster, discovery, position and spectrum 0-90460
- supernova in NGC 3733, spectrophotometry (1980 March 22) 0-62164
- supernovae, distance determ. by Baade's generalised method, appl. to H<sub>0</sub> and q<sub>0</sub> 0-73082
- supernovae, gamma-ray emission, continuum intensity and spectrum 0-101602
- supernovae, type I, effects of line overlapping on spectra in conservative scatt. case (Russian) 0-105266
- supernovae, Type I, radioactive excitation source model for late time spectra 0-105264
- supernovae in molecular clouds, spectra and luminosity, evolution 0-82399
- symbiotic star candidates in LMC, optical spectroscopy and IR photometry 0-62139
- symbiotic stars, radio mol. maser line obs. 0-72960
- symbiotic stars and slow novae, late-type components spectral classifications 0-94813
- 41 Tauri, Ap star, Ca II K and H $\delta$  lines rapid vars. (Russian) 0-90458
- RW Tauri, eclipsing binary, gaseous ring struct., H I alpha obs. 0-109482
- $\lambda$  Tauri, eclipsing binary star, mass loss from UV spectra obs. 0-109485
- SU Tauri, R Coronae Borealis star, spectral type from optical and IR photometry 0-101601
- DR Tauri, T Tauri star, Balmer line profile changes and inverse P Cygni profiles 0-101591
- DR Tauri, T Tauri star, mass flow var. in envelope, visible spectra 0-85939
- $\alpha$  Tauri (K5 III), S I emission obs. in EUV spectrum 0-82359
- 28=BU Tauri (Pleione) Be shell star, 3167 to 4924 Å spectrum atlas 0-98673
- T Tauri stars, H $\alpha$  and Na I D lines high-resolution profiles 0-62116
- 4U 0115+634, X-ray binary, 1980 Aug. photometry and spectroscopy 0-101650
- 4U 1700-37 (=HD 153919), eclipsing binary, X-ray obs. 0-86016
- 4U 1700-37 (HD 153919), high-energy obs. rel. to thermal bremsstrahlung X-ray spectrum 0-86014
- 4U 1907+09, optical identification and OB supergiant binary hypothesis 0-82542
- $\tau$  Ursae Majoris, Am star, microturbulence and metal content determ. 0-82377

## stellar spectra continued

- XY Ursae Majoris, eclipsing binary, photometry and spectrum rel. to spot activity on primary component 0-109491
- W Ursae Majoris stars, rot. line broadening functions rel. to stellar shapes 0-109494
- UV spectra, IUE preliminary results, workshop, Udine, Italy (1978 October 12) (Italian) 0-86033
- UV spectra, second OAO atlas 0-72786
- $\lambda$  Velorum, K-type supergiant, UV spectrum rel. to chromosphere and wind struct. 0-72948
- $\gamma_2$  Velorum, Wolf-Rayet binary, orbital element determ. from spectral obs. 0-85950
- $\gamma_2$  Velorum, Wolf-Rayet binary star, UV obs. from TD-1A satellite 0-77447
- CU Virginis (HD 124224), Ap star, spectrophotometric obs. 0-98663
- WC stars, near IR spectrometry 0-94816
- white dwarfs, magnetic, unexplained spectral features theory 0-82187
- white dwarfs, spectra and atmospheric comps. 0-82356
- Wolf-Rayet stars, late type, 8-13 micron spectral obs. 0-101599
- Wolf-Rayet stars, evolution and binary freq. distrib., spectra anal. 0-105250
- Wolf-Rayet stars, interstellar N V lines, IUE obs. 0-101634
- Wolf-Rayet stars, short-lived changes of emission lines (Russian) 0-72977
- Wolf-Rayet stars, Si IV and C IV, absorpt. lines, IUE obs. 0-67748
- Wray 977, optical counterpart to X-ray binary pulsar, 4U 1223-62, optical spectra 0-72984
- X-ray binaries, Fe line emission from Alfvén shell 0-98737
- X-ray sources, galactic, hard and soft X-ray spectra rel. to physical nature 0-62316
- young stars in Chamaeleon TI, photometry and spectral obs. 0-72943
- Ba II giant stars binary nature from visible radial vel. obs. 0-82355
- C<sub>2</sub>, A<sup>+</sup><sub>1</sub>II<sub>g</sub>-X<sup>+</sup><sub>2g</sub> lines, obs. in carbon stars 0-98661
- CN (0,0) 3883 Å band strengths of subdwarfs in 47 Tucanae 0-94794
- Ca II H and K emission, chromospheric, in main-sequence stars, comparison of activity cycles to old and young stars 0-105235
- Ca II H and K emission, chromospheric, in field stars of solar neighbourhood, survey 0-109423
- Ca II H and K emission lines, catalogue (Polish) 0-82227
- Ca II H and K-line, and abundance in globular star cluster giant stars 0-72940
- H I Balmer  $\alpha$  emission line core formation in chromosphere of T Tauri-type variables 0-94792
- H $\alpha$  stars in NGC 2264 and NGC 7000/IC 5070, slitless spectrographic search 0-62120
- He rich stars, intermediate and extreme, spectral atlas in 3700 to 4600 Å range 0-94806
- Hg II line oscillator strength determ. in Ap-type stars, diffusion model implications 0-72966
- HgMn stars, UV spectra rel. to thin Hg layers and diffusion model 0-105243
- Mg II h and k lines in cool giant star chromospheres, mass loss determ. 0-85935
- OH main line emission from globular clusters, high sensitivity search 0-62207

## stellar spectrophotometry see stellar photometry

## stellar structure

- see also solar interior
- 2 to 10 M $\odot$  stars, effect of heavy element abundance on evolution, struct. of models 0-105231
- accreting neutron stars, He burning shell evolution 0-85968
- Algol, orbit, lightcurve and struct. review 0-109460
- AE Aquarii, cataclysmic variable, IUE satellite UV obs. 0-72985
- 59 Aurigae,  $\delta$  Scuti star, pulsation modes from light curves periodogram anal. 0-62141
- BDS 1269 A, metal-poor  $\delta$  Scuti star, pulsation periods from b-band photometry 0-105247
- binary star giants, chromospheric activity due to tidal interactions 0-82420
- 38 Cancri in Praesepe cluster,  $\delta$  Scuti variable, pulsation anal. from light curves 0-77419
- $\beta$  Canis Majoris,  $\beta$  Cephei star, pulsations periods from Fourier anal. of radial vel. changes 0-105246
- cellular convection in a stratified atmosphere 0-98652
- VW Cephei, W Ursae Majoris star, orbital period decrease and B-V colours rel. to physical status 0-109495
- $\beta$  Cephei stars, effects of mass loss on instability strip and pulsation 0-90436
- $\beta$  Cephei stars, line profile variables, pulsational modes 0-85951
- $\beta$  Cephei stars, pulsation effect on period-luminosity relation 0-72970
- $\beta$  Cephei stars, pulsations and evolutionary status 0-85959
- Cepheids, double mode pulsation, iterative treatment 0-82369
- multimode Cepheids, two zone rel. to classical models 0-72967
- sinusoidal Cepheids in LMC, first overtone pulsations, photometry obs. 0-77422
- Cepheids with He enriched inhomogeneous outer layers, three mode reson. 0-101600
- $\delta$  Ceti,  $\beta$  Canis Majoris variable, period meas. and detect. of period decrease 0-105257
- close binaries, energy release, flares and particle acceleration (Russian) 0-73005
- close binary systems, components dimensions and distortion rel. to radial vel. curves anal. 0-90470
- collapsed stars with huge magnetic fields, astrophysical problems 0-82187
- concave hamburger equilibrium of rotating bodies 0-109422
- contact binaries, solar type, initial mass ratio distrib. function 0-109496
- contact binaries, theories of struct. 0-109493
- contact discontinuities, perturbed, junction conditions 0-94787
- convection equations, ensemble averaging 0-67698
- convective cores extant in massive stars, role of convective and semiconvective mixing 0-90405
- convective envelope stars, value of mixing length 0-77379
- convective envelopes, non-local convection, statistical theory (Chinese) 0-85933
- core gravitational collapse, shockwave prod., neutrino transport effects 0-94818
- core homologous collapse, perturbations effects 0-94779
- $\theta$  Coronae Borealis, Be-type star, shell line profile and radial vel. obs. 0-77426



**stellar structure continued**

- Crab pulsar, magnetized cracks in crust rel. to matter flow, radio, X-ray and optical emissions 0-72990  
 AI Crucis, eclipsing binary, photometric mass and radius ratios and configuration 0-109459  
 CH Cygni, symbiotic star, 1977 outburst, radial vel. and atm. struct. determ. 0-72969  
 degenerate C-O cores, degenerate C ignition afterglow 0-77390  
 dense matter star, limiting mass 0-101611  
 dense plasma, form. during stellar evolution 0-77281  
 dense stellar cores, time-dependent neutrino transport dependent neutrino transport 0-94783  
 differentially rotating gaseous polytropes construction of const. mass solar model 0-82338  
 distorted stars, Clairaut coordinates and vibr. stability 0-90408  
 eclipsing binaries, sd-d and R Canis Majoris type, struct. and dimens. 0-82423  
 Emden-Chandrasekhar axisymmetric solid-body rotating polytropes, exact solns. for ( $n=0, 1$  and  $5$ ) 0-109419  
 equilibrium structures, of self-gravitating gas masses containing axisymmetric mag. fields 0-94708  
 $\nu$  Eridani,  $\beta$  Cephei star, pulsations periods from Fourier anal. of radial vel. changes 0-105246  
 F-type star, main sequence, convection and photospheric granulation 0-90417  
 giant stars, mass loss before envelope ejection due to pulsational instability 0-72935  
 giant stars as progenitors of planetary nebulae, struct. anal. form. 0-109537  
 Gleise 490 AB (BD+36°2322), red dwarf binary, flares and starspots, rot. period determ. 0-77423  
 HD 101065, Przybylski's star, pulsation mode identification from light variability freq. anal. 0-62152  
 HD 21479, brightness microvariability and non-radial pulsations (*Russian*) 0-67754  
 HD 45088, BY Draconis binary, surface activity from high rot. vel., visible obs. 0-77425  
 HZ Herculis (Hercules X-1), accretion disk precession period 0-73070  
 hot white dwarf, radial oscill. mode nonlinear calc. 0-67713  
 HR 1225,  $\delta$  Scuti star, pulsation freqs. meas. rel. to absolute magnitude, effective temp. and mass 0-109436  
 HZ 43, He abundance and stellar struct. from soft X-ray spectra 0-72944  
 linear stellar structure model in general relativity 0-94709  
 magnetic stars, convective stability 0-94781  
 magnetic stars containing mixed poloidal and toroidal mag. fields, adiabatic stability 0-67706  
 massive highly evolved star, Ne-rich layers, explosive burning and nucleosynthesis 0-94780  
 massive main-sequence star, early evolution 0-62113  
 massive star core collapse, eqn. of state and composition near  $\beta$  equilib. 0-82335  
 massive star Ne and C zones, supernova explosion producing Mg and Al 0-90406  
 massive stars, single and binaries, evolution review 0-82343  
 massive stars ( $M \geq 50 M_{\odot}$ ), binary star mass transfer model rel. to evolutionary status (*Russian*) 0-109425  
 neutron star torsional oscils., period determ. 0-90464  
 neutron stars, electrodynamics of disk accretion, magnetic field structure 0-85973  
 neutron stars, implications of dense neutron matter physics 0-77277  
 neutron stars, mass-radius relation 0-77444  
 neutron stars, nonradial oscils. and micropulses 0-67766  
 neutron stars, pion condensate form. rel. to cooling 0-77443  
 neutron stars, props. of condensed matter in huge mag. fields 0-82187  
 neutron stars, pulsation damping due to interior weak interaction processes 0-77439  
 neutron stars, rotating, form of quantum vortex filaments 0-67770  
 neutron stars, rotating, moments of inertia in bi-metric theory of gravitation 0-90466  
 neutron stars, slowly rotating, radial perturbations, stability 0-98685  
 neutron stars structure, determ. from pulsars and compact X-ray sources 0-77442  
 non-radial oscils. of  $1 M_{\odot}$  star with initial chemical discontinuity 0-82341  
 novalike object in Vulpecula, UV decline and expanding cooling photosphere 0-67741  
 22 Orionis, nonradial m-mode changes in 53 Persei variable 0-72939  
 polytropes in central orbits, Roche problem 0-82179  
 protostars, magnetic, struct. and quasistatic contraction due to mag. flux leakage 0-98662  
 pulsar crust, crust, infinitely magnetised H atom theory 0-77282  
 pulsars outer crust, influence of mag. field on comp. 0-101610  
 pulsating stars, modal selection theory rel. to double-mode Cepheids 0-82372  
 pulsating stars asymptotic theory, boundary layer method 0-82389  
 pulsations, nonlinear coupling 0-62115  
 $\rho$  Puppis, line profile variable, pulsational mode-typing 0-90432  
 rapidly rotating models with radiation press., struct. parameters calc. 0-67697  
 rapidly rotating pre main sequence stars, struct. and evolution in gravit. contraction phase 0-62133  
 red giants, convective He shells, s-branch nucleosynthesis during thermal pulses 0-90410  
 relativistic stars, struct. and stability of polytropic fluid spheres with negative index (*Chinese*) 0-57143  
 rotating magnetic stars, nonradial oscill. mode splitting 0-77414  
 $\sigma$  Scorpii,  $\beta$  Cephei star, pulsations periods from Fourier anal. of radial vel. changes 0-105246  
 $\delta$  Scuti, line profile variable, pulsational mode-typing 0-90432  
 self accreting stellar winds 0-101588  
 shell flashing stars, core masses rel. to  $^{22}\text{Ne}$  as neutron source for s-process 0-72926  
 superdense celestial bodies, theory 0-67773  
 supergiants, early-type, with mass loss, two-core model and evolutionary status (*Russian*) 0-109425  
 supernova core, Rayleigh-Taylor convective overturn rel. to explosion 0-77429  
 supernova envelope, temp. struct. rel. to  $^{11}\text{B}$  neutrino-induced prod. in C layer 0-82337  
 supernova interior, eqn. of state at subnuclear densities 0-77278

**stellar structure continued**

- supernovae, effects of core eqn. of state on outcome of stellar collapse 0-85928  
 white dwarf in binary system, outer layer C and O enrichment from companion 0-109465  
 white dwarfs, atmosphere structure rel. to composition in hot stars 0-98658  
 white dwarfs, rapid mass accretion and extended envelope form. 0-67723  
 white dwarfs, struct. and evolution theory rel. to EUV obs. and spectra 0-82356  
 white dwarfs undergoing spherically symmetric steady-state accretion, stability 0-77402  
 Wolf-Rayet atmospheres, structure and composition 0-98668  
 C cores, evolved, nuclear energy generation rates and energy dissipation 0-82339  
 C-O white dwarfs, C-O eutectic model 0-77405  
 Mn-Hg stars, surface gravity, and stellar temp. derivation from uvby data, statistical anal. 0-82397
- stellar variables** *see variable stars*
- stellators**
- Asperator NP-3, nonplanar helical mag. axis system, line of force, toroidal effect 0-70020  
 Asperator NP-L stellator, mag. field config. meas. 0-92367  
 CLEO stellator, low and zero current plasma confinement 0-83983  
 current turbulent ion heating, modulation instability 0-79525  
 energy confinement comparison of ohmically heated stellators to Tokamaks 0-92360  
 equations of motion calcs. 0-103198  
 equilibrium and stability calcs. 0-83982  
 fields,  $m=2$  tearing mode, linear growth rate 0-75037  
 helical stellator, Asperator NP-3, toroidal discharge forbidden region 0-79592  
 helical winding geometry modulation and optimisation 0-79549  
 ion temp. and parametric decay development in RF-generated stellator plasma 0-79436  
 JIPP T-II, neutral beam injection system, design and expt. test 0-106226  
 Josephson junctions, applications in plasma physics 0-103194  
 Kharkov stellators, plasma-wall interactions 0-79552  
 L-2 stellator, ohmic heating discharges with gas puffing 0-79593  
 magnetic hill effects on equilibrium 0-79558  
 MHD equilibrium and stability of plasma in toroidal geometry, 3-D computer code 0-70041  
 modular coil design for 2.1 m radius device 0-79548  
 particle orbits and toroidal vacuum fields 0-79450  
 plasma equilibrium currents, effect on separatrix characts. in  $I=3$  stellator 0-64706  
 plasma losses, quasi-neoclassical law 0-79544  
 positional stability of a current-carrying plasma in an  $I=2$  stellator field 0-106906  
 R-OM stellator, MHD resonant HF heating 0-79518  
 research status 0-74013  
 toroidal vacuum fields, particle orbits 0-79445  
 torsatron, superconducting mag. engineering design 0-99297  
 W VII-A, neutral injection 0-83960  
 W VII-A (2.1) tearing mode depend. on stellator field 0-79550  
 W VII-A stellator, neutral injection, heating efficiencies, deposition profiles 0-79524  
 W VII-A stellator, particle and energy transport 0-83222  
 W VII-A stellator, line emission, poloidal and toroidal asymmetry 0-79578  
 WEGA stellator, lower hybrid heating 0-79515  
 Wendelstein VII, neutral beam injectors, HV power supply system, thyristor control 0-99332  
 Wendelstein VII-A, neutral beam injectors, performance 0-99389
- STEM** *see scanning-transmission electron microscopy*
- step motors** *see stepping motors*
- step-recovery diodes** *see charge storage diodes*
- Stepanov method** *see crystal growth from melt*
- stepped motors** *see stepping motors*
- stepping motors**
- drives for use in synchronous interlock systems for cinematographic special effects 0-98991  
 laser grating mount drive unit modification 0-87402  
 multiaxis neutron diffractometer automation 0-102417  
 timber volumetric meter angular displacement control (*Russian*) 0-57253  
 translation motors for position with micron precision (*German*) 0-86271
- stereo amplifiers** *see audio-frequency amplifiers*
- stereoisomerism** *see isomerism*
- stereoscopy** *see vision*
- stiffness constants** *see elastic constants*
- stimulated Brillouin scattering**
- amplitude and phase time oscils. noise (*Russian*) 0-87435  
 carbon tetrachloride, Stokes wave phase fluctuations in stimulated light scatt. (*Russian*) 0-87436  
 laser Q-switching mechanism by intracavity stimulated Brillouin scatt. 0-106552  
 mirror, short high-power pulses obtained by wavefront reversal 0-99801  
 nonmonochromatic radiation stimulated scatt., efficiency depend. on pump radiation statistics 0-95950  
 optical fibre, nonlinear effects, appl. to active and passive device fabrication 0-58638  
 piezoelectric semiconductor, n-type, magnetoactive, Brillouin instability in magnetostatic field 0-78909  
 plasma, Brillouin and dielec. side-scatt. of  $10 \mu\text{m}$  laser light 0-103156  
 plasma, stimulated Brillouin scattering initiated by ponderomotive force density fluctuations 0-103129  
 plasma, stimulated Raman and Brillouin backscattering along mag. field 0-69983  
 plasma jet form. by focusing laser beam on plane target, investigation using wavefront method 0-75103  
 pre-ionised plasma, side- and backscattering 0-92267  
 quartz-liquid  $^4\text{He}$  interface, saturation effects in phonon reflection 0-92736  
 rescattering in plasma 0-87896  
 ruby laser, with stimulated Brillouin scatt. complex conjugate mirror 0-87438  
 three dimensional, for focused Gaussian beam 0-69456  
 wavefront reversal, transverse enhancement of coherence of scatt. field 0-95952

**stimulated Brillouin scattering continued**

- wavefront reversal of beam with incomplete spatial modulation, small-scale distortions 0-95953  
 $\text{CF}_4$  Nd laser excited stimulated Mendelstam-Brillouin scatt. phase fluctuations (*Russian*) 0-89014  
 $\text{CdS}$ , stimulated Mandelstam-Brillouin scatt. on acoustic phonon amplification (*Russian*) 0-71437  
 $n\text{-InSb}$ , Brillouin instability in magnetostatic field 0-78909

**stimulated dielectric relaxation currents** *see thermally stimulated currents***stimulated emission**

- see also laser theory; lasers; population inversion*  
 atoms, multiphoton rate equations, generalised 0-91525  
 Dicke state N two level atom assembly, radiation emission theory 0-69350  
 3,3-diethyl thiadibenzocyanine iodide dye, stimulated fluoresc. and stimulated reson. Raman scatt. relationship 0-91853  
 dye laser, CW, pumped, stable multifreq. picosecond pulse emission, phase-locked radiation pumping 0-91789  
 Fresnel formulas and law of stimulated emission 0-58489  
 highly excited atoms, blackbody radiation effects 0-58176  
 naphthalene, doped, role of nonequilibrium phonons in stimulated radiation emission 0-103971  
 negative light absorption by medium with selective freq. modulation of quantum oscillators 0-106501  
 nonlinear active medium in Gaussian random optical field, stimulated emission statistics 0-58488  
 organic laser dyes, nonlinear transmission including stimulated emission influence 0-99720  
 rare earth ion containing inorg. materials,  $3\mu\text{m}$  band stimulated radiation 0-97306  
 rotating anharmonic oscillators in resonator, stimulated emission power 0-99689  
 semiconductors, photocarrier distrib. and photomagnetolectric effect near stimulated emission threshold 0-80320  
 superradiance waveguide laser, stimulated emission spectrum, leaky modes (*Russian*) 0-87400  
 two-level atom, radiation by intense laser beam, resonance fluorescence, photon antibunching, Doppler shift 0-74146  
 $\text{CdS}$  crystals, one-photon pumping, active layer structure, light amplification 0-78858  
 $\text{CdS}$ , highly excited, stimulated emission process at 80K 0-97307  
 $\text{CdS}$  platelet lasers, optically pumped, spatial and spectral distribution of laser emission 0-64032  
 $n\text{-CdSe}$ , laser excited stimulated emission, optical gain spectrum 0-76050  
 $\text{Er}^{3+}\text{KLu}(\text{WO}_4)_2$ , room temp. stimulated emission obs. 0-106527  
 $\text{Ho}^{3+}$  in oxygen-containing crystals, stimulated emission at low temps. 0-106526  
 $\text{Ho}^{3+}:\text{BaYb}_2\text{F}_6$  0-95902  
 $\text{Ho}^{3+}:\text{LiYbF}_4$ , active medium for Nd laser freq. convertor, cascade stimulated emission 0-102727  
 $\text{La}_2\text{Be}_2\text{O}_7:\text{Nd}^{3+}(\text{Pr}^{3+})$ , cryst. growth, spectral and laser properties in  $^4\text{F}_{3/2} \rightarrow ^4\text{I}_{13/2}$  and  $^4\text{F}_{3/2} \rightarrow ^4\text{I}_{11/2}$  transitions 0-80853  
 $\text{Li}_2\text{Zr}_2\text{Si}_2\text{O}_{10}$  excimer emission, ab initio calcs. 0-91608  
 $\text{Na}_2\text{Zr}_2\text{Si}_2\text{O}_{10}$  excimer emission, ab initio calcs. 0-91608  
 $\text{Nd}^{3+}$ : glass, spectral props. (*Chinese*) 0-60645  
 $\text{PbS}_{1-x}\text{Se}_x$ , thin film, stimulated emission, temp. depend. 0-66232  
 $\text{PrF}_3$ , laser action of  $\text{Pr}^{3+}$  0-95901  
 $\text{Ti I}$ , photodissociative pumping effect 0-58182  
 $\text{Ti}$ , inverted atomic populations, obs. of stimulated level shifting 0-58218  
 $\text{YAG}:\text{Ho}^{3+}$ , spectroscopy 0-93374

**stimulated Raman scattering**

- see also coherent antiStokes Raman scattering*  
 acetone, vibr. dephasing theories, test using selective coherent ps. Stokes scatt. 0-59609  
 anthracene crystals, pre-reson. Raman scatt., 4.2-30K 0-60571  
 chemical reaction wave, propag. of coherent probe light pulse 0-61190  
 Cherenkov type parametric optical oscillator, optical saturation 0-102771  
 combined stimulated Raman scattering and continuum self-phase modulation 0-69460  
 condensed phase fluoresc., double reson. excitation spectroscopy 0-86438  
 3,3-diethyl thiadibenzocyanine iodide dye, stimulated fluoresc. and stimulated reson. Raman scatt. relationship 0-91853  
 difference frequency generation by stimulated Raman scatt. using inhomogeneous electrostatic field 0-95954  
 dimethyl sulphoxide, high efficiency stimulated Raman scatt. source (*Chinese*) 0-87433  
 double resonance Raman amplifier, theory 0-87434  
 fibre Raman lasers 0-102767  
 forbidden rotational and vibr.-rot. transitions in strong optical field, spontaneous and stimulated Raman scatt. 0-74174  
 four-photon spectroscopy of condensed media, nonlinear spectroscopy developments 0-91860  
 free electron laser based on stimulated Raman scatt. by relativistic electron beam, oscill. characts. 0-99688  
 frequency-modulated shot noise limited stimulated Raman gain laser system for monolayer vibr. spectroscopy 0-62744  
 gases, second Stokes component, dispersion effects 0-91857  
 laser plasma, stimulated Raman light scatt. spectrum (*Russian*) 0-106926  
 laser resonator, stimulated combined scattering of light, effect of generation of 'hot' vibrs. 0-58601  
 laser sources frequency conversion 0-69451  
 magneto-optical Raman scattering of Raman-inactive phonon polaritons 0-91843  
 methanol, vibr. dephasing theories, test using selective coherent ps. Stokes scatt. 0-59609  
 molecules, optically active, coherent Raman scatt., quantum theory 0-69150  
 multimode laser steady-state stimulated Raman scatt. 0-99796  
 near-IR stimulated Raman emission in single-mode fibres by Nd-YAG laser pumping in low-dispersion region at  $1.3\mu\text{m}$  0-64100  
 nonmonochromatic radiation stimulated scatt., efficiency depend. on pump radiation statistics 0-95950  
 optical fibre, backscatter of stimulated Raman scatt. 0-64109  
 optical fibre, multimode step-index, forward and backward stimulated Raman scatt. 0-58639  
 optical fibre, nonlinear effects, appl. to active and passive device fabrication 0-58638  
 optical fibre, three-wave stimulated Raman scatt. (*French*) 0-78902  
 optical fibres, Raman scatt., guiding structs. effects on spontaneous and stimulated emission 0-58636

**stimulated Raman scattering continued**

- optical waveguide, stimulated Raman scatt. excitation by wideband pump 0-64108  
 optical waveguide, Stokes components recording opposite to pump wave 0-106569  
 ortho-para mixtures, vibr. coherence decay 0-78903  
 picosecond Raman gain technique for vibr. spectra of mol. monolayers 0-91859  
 plasma, stimulated Raman and Brillouin backscattering along mag. field 0-69983  
 quantum theory 0-106565  
 quartz fibre, Stokes components recording opposite to pump wave 0-106569  
 radiation self-synchronisation during stimulated Raman scatt. in external resonator (*Russian*) 0-102772  
 randomly modulated pump, stimulated Raman scatt., method of successive approxs. 0-95951  
 resonance illumination conditions 0-64105  
 stimulated hyper-Raman scattering in a molecular gas via a three-photon process to obtain IR and far IR radiation 0-58633  
 subnatural linewidth spectra by optical double reson. with two-photon pumping 0-74200  
 transient stimulated Raman scattering in lossy media 0-102768  
 wavefront reconstruction in stimulated light scatt. 0-64107  
 wavefront reversal with freq. shift, based on anti-Stokes stimulated Raman scatt. 0-74440  
 Ba atom, laser excited, ionisation studies 0-83330  
 $\text{Ba}(\text{NO}_3)_2$ , Nd laser second harmonic stimulated Raman scatt., efficiency in calcite, nitrate crystals. 0-95949  
 CN, monolayer on Ag surface, vibr. spectra, picosec. Raman gain technique 0-91859  
 Ca atom, laser excited, ionisation studies 0-83330  
 $\text{CaCO}_3$ , calcite, single-crystal, wave front reconstruction of light 0-93323  
 $\text{CdS}$  electronic two- and one-photon Raman scatt. via biexcitons, stimulated config. obs. mag. field shift 0-103963  
 $\text{CdS}$ , two-photon absorpt. effect on hyper-Raman scatt. 0-74441  
 Cs vapour, threshold for stimulated electronic Raman scatt. determ. using picosecond laser pulses 0-102768  
 $\text{H}_2$  laser, stimulated Raman scatt., appl. to holography 0-91782  
 $\text{H}_2$ , stimulated Raman scatt. gain of Nd laser radiation by rot. levels 0-69464  
 $p\text{-InSb}$ , photoexcited exciton spin-flip scatt. 0-74434  
 K, atomic vapour, resonant interaction with laser, Vavilov-Cherenkov effect (*Russian*) 0-106573  
 $\text{LiIO}_3$  crystal, noncollinear stimulated Raman scatt. using parallel pump beam 0-78912  
 $\text{N}_2$ , liq., ang. distrib. of stimulated Raman scatt. following excitation by two coherent beams 0-106571  
 $\text{N}_2$ , liq., high repetition rate stimulated Raman scatt., thermal blooming 0-91865  
 $\text{N}_2$ , stimulated scattering investigation, 1-4 atm press. range 0-91568  
 $\text{NH}_3$ , far IR CW Raman lasing 0-83595  
 $\text{NH}_3$ , stimulated hyper-Raman scatt. via 3-photon process to obtain IR and far IR radiation 0-58633  
 $\text{NaNO}_3$ , Nd laser second harmonic stimulated Raman scatt., efficiency in calcite, nitrate crystals. 0-95949  
 Nd:YAG pumped tunable sources, appl. to spectroscopy 0-58576  
 $\text{Pb}(\text{NO}_3)_2$ , Nd laser second harmonic stimulated Raman scatt., efficiency in calcite, nitrate crystals. 0-95949  
 $\text{SiO}_2$  optical fibre, three-wave stimulated Raman scatt. obs. (*French*) 0-78902

**stimulated scattering**

- see also stimulated Brillouin scattering; stimulated Raman scattering*  
 EM wave scattering by relativistic electron beam, nonlinear theory (*Russian*) 0-102601  
 light field reconstruction accuracy after stimulated scatt. 0-78911  
 nonmonochromatic radiation stimulated scatt., efficiency depend. on pump radiation statistics 0-95950  
 quartz, fused, photoelastic light scatt. from surface Rayleigh waves 0-97235  
 relativistic free-electron wave generators, electrically pumped 0-91742  
 semiconductors, transient light scatt. by free carriers 0-102766  
 $\text{CS}_2$ , radiation self synchronisation on Rayleigh edge time stimulated scatt. in external resonator (*Russian*) 0-69461

**STO calculations**

- approximate Hartree-Fock methods using density approximations and Coulomb field corrections, testing 0-91422  
 atoms,  $5f^N$  and  $5f^{N+1}$  config., parametric study 0-91444  
 atoms,  $70 \leq Z \leq 82$ ,  $K\alpha$  X-ray linewidths and relative intensities, energy dispersive meas. 0-99483  
 atoms, near threshold struct. in K-shell spectra, photoionisation or fast charged particle ionisation 0-87064  
 closed-shell atoms, approximate relativistic Hartree-Fock eqns., soln. using Slater-type functions 0-58168  
 $\text{Co}_2\text{Sb}_4(\text{CO})_{12}$ , electronic struct. calc. (*Russian*) 0-58136  
 copper (II) complex, bis(dithiocarbamate), HF-Slater-LCAO calcs., mag. coupling parameters and optical spectrum 0-99447  
 diagrammatic perturbation theory, appl. to  $\text{N}_2$ ,  $\text{CO}_2$ , BF 0-58131  
 dicyanoketene, and isomeric forms, heat of form., ab initio STO-3G calcs. 0-58190  
 electron-repulsion integrals evaluation, expansion of Slater-type orbitals 0-99451  
 graphite, electronic struct. exact exchange HF calcs. 0-65438  
 heavy ion + nucleus, RPA theory, time dependent, quasi-boson approx. 0-57800  
 meta-hydroxyaniline, mol. complex., electronic struct., basis set and correlation effects 0-91436  
 magnetic multipole moment integrals for Slater-type orbitals, analytic evaluation 0-58110  
 methane, coord. bond calcs. 0-58129  
 methanol, coord. bond calcs. 0-58129  
 methyl fluoride, coord. bond calcs. 0-58129  
 methyl fluoromate, isomer conformation, CNDO and ab initio STO calcs. 0-58151  
 methylamine, coord. bond calcs. 0-58129  
 pyrrole-acetonitrile, H-bonded complex, ab initio MO calcs. 0-102440  
 rare earth metal ions, 3d and 4f energy level parametrisation, Slater parameters and correl. corrections 0-87041  
 semiempirical theory for ground and excited states, Fock operator expansion, STO-3G and CNDO/S calcs. 0-58154



**STO calculations continued**

- Slater is orbital four centre mol. integrals, Fourier transforms 0-74104  
 Slater-Koster integrals, general expressions in two-centre approx. 0-70585  
 spirohydrocarbons, strained, bond angles, interatomic distances, semiempirical and ab initio calcs. 0-95533  
 three-electron bonds, strengths, ab initio LCAO MO CI calcs. 0-87046  
 transition metal, Racah parameters, atomic screening parameter Slater and Clementi-Raimondi values 0-69071  
 transition metal ions, 3d and 4f energy level parametrisation, Slater parameters and correl. corrections 0-87041  
 two-centre charge distrib., Fourier transform, STO general expression derivation 0-58119  
 unsaturated hydrocarbons, dipole polarisabilities, STO-4G calcs. 0-83255  
 water-imidazole, H bond interrupted chain, cooperative effects, STO-3G ab initio calcs. 0-63535  
 $Al_2(Al_2)_2(Al_2)_2^+$  configurations, ab initio study, LCAO, STO, MO-SCF and CI calcs., binding energy (French) 0-91447  
 $\alpha-Al_2O_3$ , charge distribution determ., SCF calc., Slater-type orbitals, Madelung type const. 0-107100  
 AsF<sub>3</sub>, inversion barrier, STO SCF calc. 0-63567  
 BN, electronic struct., exact exchange HF calcs. 0-65438  
 C, electron excitation cross section calc., Born approx. with Slater wave functions 0-69243  
 CO<sub>2</sub>+Ne, intermol. pot. in repulsive short-range region, ab initio 0-69204  
 CaH, spin doubling, SCF calcs. 0-95649  
 H<sub>2</sub>PNH<sub>2</sub>, inversion-rot. mechanism, basis set and geometry optimisation effects 0-83273  
 HS<sub>n</sub><sup>2-</sup>, n=1-4, electronic struct., ab initio Hartree-Fock-Slater calcs. 0-74107  
 HS<sub>n</sub><sup>2-</sup>, n=1-4, electronic struct., ab initio Hartree-Fock-Slater calcs. 0-74107  
 H<sub>2</sub>S<sub>n</sub>, n=1-4, electronic struct., ab initio Hartree-Fock-Slater calcs. 0-74107  
 Li, electron excitation cross section calc., Born approx. with Slater wave functions 0-69243  
 SiH<sub>3</sub>X (X=H, F, NH<sub>2</sub>, OH), coord. bond calcs. 0-58129

**stochastic processes**

see also random processes

- air pollution episodes in Venetian region, real-time forecasting via advection-diffusion model 0-77096  
 air pollution episodes in Venetian region, real-time forecasting via Kalman predictor 0-82046  
 Alfvén waves, in stochastic mag. field, Khasminskii's theorem 0-59198  
 amorphous solids, stochastic geometry, review, book contrib. 0-73269  
 astrophysics, stochastic phenomena 0-105161  
 betatron oscillation reduction, low-noise wide-band power amplifier system 0-58011  
 Boltzmann equation, stochastic, hydrodynamic fluctuations 0-68158  
 Brownian fluid affected by potential, Maxwell-Boltzmann distrib. in infinite-time limit 0-105573  
 catalytic processes and stochastic processes of chem. kinetics, historical review 0-105483  
 chemical instabilities, stochastic approach, anomalous fluctuation and transient behaviour 0-89465  
 chemical reaction diffusion systems, Chapman-Enskog development of multivariable master eqn. 0-81283  
 chemical systems, single variable, master eqn. approximation by Fokker-Planck type eqns. 0-77702  
 composite materials, stochastic fracture models, and strength test results statistical anal. 0-64470  
 condensed matter physics, dynamic correlations, book 0-86046  
 contracted description of fluctuating systems 0-90781  
 convective cells, stochastic oscill. spatial-time spectra (Russian) 0-103029  
 cooperative cascade emission, linear stochastic theory 0-74326  
 damped harmonic oscillator, quantum friction in c-number picture 0-94980  
 Davidson's generalization of the Fenyès-Nelson stochastic model of quantum mechanics 0-62531  
 discontinuous processes, weak solutions (French) 0-62579  
 discontinuous transitions into chaos after single bifurcation, hysteresis existence 0-73264  
 dynamical systems, critical transition to stochasticity 0-73265  
 earthquake frequencies, stochastic modelling (Japanese) 0-94480  
 Einstein symposium, Berlin, Germany (Mar. 1979) 0-90596  
 electron gas, ground state, stochastic method calcs. 0-95031  
 electron microscopy, correlation analysis of radiation damage 0-100282  
 excitons, diffusive and percolative lattice migration 0-59879  
 fast charged particle, dechannelling from planar channel, stochastic theory 0-96579  
 filtering, nonlinear, conditional laws, smoothness, stochastic calculus of variations (French) 0-68128  
 fission reactor fuel-coolant interactions, temperature noise in one-phase heat transfer: stochastic models 0-68726  
 flood event real-time predictors, stochastic model 0-67383  
 fluctuations, random, moment behaviour of soln. processes for nonlinear stochastic differential eqns. (Japanese) 0-95039  
 fluctuations and nonlinear irreversible processes. II 0-82724  
 four-vortex integrable and chaotic motions 0-103035  
 friction, stochastic quantisation, nonlinear wave eqn. 0-98825  
 functional equations, random, stochastic approx. in Banach space (Japanese) 0-95038  
 galaxies fields stochastic simulation 0-62295  
 gases, weakly ionised, electron motion, stochastic theory of homogeneous systems, review 0-77735  
 generalised representation, of physical situation, appl. to hydrodynamics (Russian) 0-69760  
 gravitational fluctuations in self-consistent mean field theory, review 0-90734  
 great earthquakes, chaotic behaviour, coupled relax. oscillator model, billiard model and electronic circuit model 0-94462  
 gross variables, microdynamics and nonlinear stochastic processes 0-101754  
 inert gas exchange in living organs 0-81520  
 inhomogeneous structures, macroscopic third-order elastic moduli 0-69672  
 intermicellar kinetics theory, stochastic approach, master equation for, irreversible reactions 0-76561  
 internal stress, stochastic model for dip test in steady-state creep 0-58915

**stochastic processes continued**

- IR staring mosaic sensor performance, effect of spacecraft-induced line-of-sight jitter 0-86416  
 Langevin equations, Fokker Planck Dynamics approach 0-57194  
 laser speckle, time-differentiated, first order statistics, vel. meas. 0-82750  
 linear oscillator, nonstationary narrow band response and first passage probability, stochastic process 0-62465  
 loading, random, laminated plates, dynamic response 0-58902  
 measure preserving mapping, stochastic transition, approx. determ. 0-95035  
 mechanical system, with stochastic loading, first crossing probability (German) 0-86219  
 multistationary behaviour systems, stochastic approaches 0-98854  
 n-photon resonance phenomena, finite laser bandwidth effect 0-58230  
 non equilibrium systems, stochastic model, master eqns. (Chinese) 0-68126  
 nonequilibrium thermodynamics, stochastic measures 0-86240  
 nonmonotone stochastic integrals and stochastic differential calculus (French) 0-90779  
 nonstationary, probability characts. of mass flow rate meas. 0-73302  
 Of and O stars, stochastic accel. in photospheres rel. to difference in mass loss 0-90413  
 open dynamic subsystem, nonlinear eqn. with fluctuating parameters derivation 0-94991  
 open dynamical system, equations with fluctuating parameters 0-62584  
 overlapping avoided crossings, rel. to quantum stochasticity 0-90694  
 particle motion in stochastic space, relativistic dynamics 0-82639  
 passive tracking acoustic array evaluation, nonlinear filtering lower bound algorithms 0-96088  
 photon echo spectroscopy of crystals, review 0-83648  
 point process with continuous probability measure, non-parametric test (French) 0-57184  
 point processes, physical background and mathematical model (Chinese) 0-62577  
 pollution modelling, numerical estimation of unknown parameters (Japanese) 0-89702  
 polymer, cross-linked, on basis of oligodienedihydrazides and diepoxides, characts. (Russian) 0-58431  
 polymer chains, Edwards' model, stochastic model 0-68140  
 polymer solutions, dilute, regularly alternant, thermodynamic props. self avoiding random walk calcs. (French) 0-59369  
 quantification of stochastic process, principles of quantification noise (Spanish) 0-57190  
 quantum Heisenberg-ferromagnets and stochastic exclusion processes 0-88712  
 quantum mechanical transformation function, stochastic action integral interpretation 0-77644  
 quantum theory, stochastic electrodynamics formulation (Spanish) 0-82925  
 rainfall, annual, stochastic anal. rel. to effects of urbanisation 0-98407  
 review, book contrib. 0-73268  
 rigid sphere embedded in elastic medium, response to incident stochastic waves 0-64451  
 Schrödinger's variational quantisation method in stochastic framework 0-105532  
 Schrödinger equation, Brownian motion interpretation challenged 0-94974  
 Schrödinger equation, stochastic resolution, analyticity and integrability, existence and uniqueness of soln. (French) 0-73195  
 second order stochastic processes and the dilation theory in Banach spaces 0-90778  
 solar cooling system performance predictions using stochastic weather data 0-85269  
 solar photosphere, stochastic mag. pumping model rel. to mag. fields fine struct. 0-98646  
 soluble-model Boltzmann equations for spatially uniform systems, written in form of stochastic equation 0-95046  
 space dependent stochastic neutron kinetics with Gaussian parametric excitation 0-63223  
 space independent low power model, multigroup energy formalism for reactor stochastic eqns. 0-63224  
 spectral estimates, randomly sampled signals, variability reduction by filtering out parts of spectral energy 0-57193  
 steel, low C, high cycle fatigue, crack initiation model (Japanese) 0-104258  
 stochastic fields from stochastic mechanics 0-95033  
 stochastic mag. field fluctuations, self-consistent model 0-100074  
 stochastic quantisation processes, review, Markov processes, Martingales, quantum dynamics 0-94969  
 stochastic quantum mechanics, dissipative forces, operator algebra 0-98826  
 superfluorescence, two-level atoms system, quantum theory, incl. propag. effects 0-58491  
 superionic conductors, theoretical models, review 0-107465  
 surface transport and reaction, stochastic calcs. 0-108736  
 symmetric or asymmetric many degrees of freedom nonlinear systems, stochastic linearisation 0-77708  
 thermodynamics, irreversible, extended, hydrodynamical fluctuations 0-86235  
 time-dependent statistical props., recording method (German) 0-101706  
 transfer function with several inputs, model, math. methods of investigation identification 0-62451  
 turbulence in the motion of a free particle and de Broglie waves 0-57189  
 turbulent mixing with react. of miscible reactant streams, simulation 0-64651  
 underwater sound, stochastic internal-wave model for deep moving ocean 0-64267  
 unstable state decay, trajectory time spread, laser photon statistics 0-83585  
 wind, stochastic predictors, AR and ARMA models 0-67400  
 CsNiF<sub>3</sub>, stochastic motion of Sine-Gordon-solitons, spin-correlation function 0-93105  
 K<sub>2</sub>Mg<sub>2</sub>Ti<sub>8-x</sub>O<sub>16</sub>, stochastic Langevin dynamics study of correlated ionic motion in 1-D solid electrolytes 0-65279

**stochastic systems**

see also random processes

- Bedford Ouse River, systems model of stream flow and water quality 0-81956  
 Benard problem, R<sup>2</sup> class of mappings, invariant Cantor sets and strange attractors 0-59037

**stochastic systems continued**

- bifurcation and transition toward stochasticity for dissipative dynamical systems 0-57201
- cellular systems, probability model (*German*) 0-90661
- closed loop control systems, appl. to blood pressure control 0-81522
- conference on plasma intrinsic stochasticity, Cargese, France (June 1979) 0-59174
- critical transition to stochasticity 0-57202
- dissipative non-Hamiltonian dynamical system, stochastic props. and strange attractors 0-57200
- dynamic multi-nonlinear systems, action of white noise 0-68135
- galaxy fields, stochastic simulation 0-90530
- intermittancy in turbulence onset 0-59013
- Kolmogorov Arnold Moser theorems, appl. to struct. problems in condensed matter 0-59878
- Lyapunov characteristic exponents and stochasticity 0-59177
- Lyapunov characteristic numbers and Kolmogorov entropy, stochasticity of dynamical systems 0-59178
- nonlinear mixed stochastic integral equations existence, uniqueness and stability of solutions 0-68131
- nonlinear oscillator systems, primary resonances do not overlap 0-59176
- one-variable system, growth of fluctuations from marginal eqn. 0-86213
- optimal control, measurer containing unknown variable parameters (*Russian*) 0-86218
- pendulum, bounce resonance and Kolmogorov entropy 0-57199
- plasma, coupled three wave system, instability saturation, bifurcations and strange attractor 0-59233
- plasma, discrete unstable modes, transition to turbulence, theory and expt. 0-59240
- plasma, electrostatic wave, magnetised plasma charged particle stochastic accel. 0-59230
- plasma, electrostatic wave, stochastic ion motion, mag. field config. depend. 0-59229
- plasma, linearly unstable mode stabilisation by reson. nonlinear coupling to damped modes 0-59234
- plasma, particle stochastic motion in mirror machines 0-59264
- plasma, pulsed RF-trapped particle interaction stochastic effects in tokamak 0-59245
- plasma, self-consistent kinetic theory of stochasticity 0-59179
- plasma, stochastic heating of plasmas in inhomogeneous magnetic fields 0-59231
- plasma, stochastic orbits in Tokamak, statistical description, low freq. fluctuations 0-59265
- plasma, toroidal, overlapping and stochasticity, critical limits 0-59268
- plasma adiabatic to stochastic motion transition, Kolmogorov Arnold Moser surface 0-59175
- plasma magnetic field line trajectory calc., Kolmogorov Arnold Moser surface 0-59263
- plasma particle motion, regular and stochastic, Hamiltonian formalism 0-59167
- plasma wave, electrostatic, perpendicularly propag., vel.-space diffusion 0-59228
- PWR components, using correlation techniques (*German*) 0-79247
- quantum system, nonintegrable, irregular part of discrete energy spectrum, statistical theory 0-82667
- ray and wave optics of integrable and stochastic systems, WKB method 0-59244
- AuFe spin glass,  $\mu^+$  zero-field spin relax. probe for spin dynamics 0-97177
- CuMn spin glass,  $\mu^+$  zero-field spin relax. probe for spin dynamics 0-97177

**Stockbarger method** see crystal growth from melt

**Stokes flow** see flow

**Stokes law (fluid mechanics)** see flow

**Stokes law (optical)** see luminescence

**Stokes lines** see spectra

**Stokes optical law** see luminescence

**stopping of particles** see energy loss of particles

**storage, analogue** see analogue storage

**storage, digital** see digital storage

**storage devices**

- see also energy storage devices; optical storage devices; semiconductor storage devices
- No entries

**storage organisation** see file organisation

**storage rings**

- ACO storage ring, design of undulator, use as free electron laser 0-91334
- Aladdin, status of the Synchrotron Radiation Center of the University of Wisconsin, Madison 0-91326
- BESSY, 800 MeV dedicated light sources, choice of principal parameters and light source 0-91333
- brightness of synchrotron radiation from electron storage rings 0-91330
- CERN, 25 years history and equipment (*French*) 0-98778
- CERN, 25 years of physics, review 0-82626
- CESR, status 0-74047
- CHESSE—the Cornell high energy synchrotron source 0-91328
- CHESSE synchrotron radiation facility, high energy tunable X-ray source 0-68984
- CHESSE synchrotron source, photon position sensitive monitors 0-91336
- design considerations for parasitic use of synchrotron radiation in the infrared 0-91340
- EUV photodiodes for high accuracy location of orbital plane 0-91335
- future technologies in high-energy physics, collective accelerators, laser accelerators, single-pass collectors 0-78466
- ISABELLE full cell, ultrahigh vacuum system 0-77798
- ISABELLE ultrahigh vacuum system, self-modulating ion gauge 0-82786
- LEP, design, tests of unified field theories and quark properties, search for new quarks and leptons 0-74048
- LEP, electron positron storage ring, vac. chamber, glow discharge surface cleaning 0-58010
- LEP colliding beam machine, data handling and standard practices 0-58009
- National Synchrotron Light Source basic design and project status 0-91329
- PETRA, recent results 0-74044
- phase space cooling for pp colliders at CERN and Fermilab 0-99360
- soft X-ray microscopy/lithography branch line at SSRL 0-91344
- SPEAR, crystal ball detector, recent results 0-74046

**storage rings continued**

- SPEAR, Mark II detector, recent results 0-74045
- SPEAR, Stanford Synchrotron Radiation Laboratory, status report 0-91327
- SPEAR, use of wiggler magnets as synchrotron radiation source 0-91332
- SURF II, large spectrometer calibration chamber 0-91339
- SURF II, synchrotron flux meas. using Si radiometer 0-90895
- SURF II storage ring, status report 0-91325
- SURF storage ring calibrations for NASA stratosphere and climate programs 0-94721
- synchrotron radiation, expt. enclosures and beam line safety components 0-91341
- synchrotron radiation sources, nuclear physics appls., review 0-106216
- undulator for the 700 MeV VUV-Ring of the National Synchrotron Light Source 0-91337
- UV beamlines for National Synchrotron Light Source 0-91342
- VEPP-2M storage ring, synchrotron radiation use to test VUV detectors absolute efficiency 0-82824
- VUV beam line instrumentation for National Synchrotron Light Source storage ring 0-91343
- wigglers and undulators, interaction with stored electron beam 0-91331
- Si radiometer for storage ring synchrotron radiation 0-86411

**storage tubes**

see also image storage tubes

- vacuum-deposited layers, formation, use of borosilicate glass intermediate layer 0-80979

**stored program control** see electronic switching systems

**stores (computer)** see digital storage

**storms**

see also magnetic storms; thunderstorms

- N.Atlantic easterly gales, 1881-1970 period 0-77101
- SE.Baltic coast transit section, suspended load composition in calm and storm (*Russian*) 0-67360
- Brahmaputra river, flood of Aug. 1962, synoptic aspects 0-81939
- cold front of midlatitude cyclone, cloud and precipitation struct. 0-109192
- convection currents in axisymmetric cyclone 0-77084
- cyclone development along weak thermal fronts, model soln. 0-81994
- Cyclone Joan 1975, wind and rain meas. over W.Australia by satellite microwave sensing 0-98485
- cyclones, extratropical, with northerly component, rel. to poor summers in British Isles 0-109241
- cyclones, midlatitude, satellite-derived mesoscale wind fields covariance anal. 0-82013
- Darling River system floods, chronological evolution, Nimbus-5 radiometry obs. 0-94543
- dust storm in Israel, dust property obs. 0-90162
- electric field observations of storm clouds (*French*) 0-85712
- extratropical cyclones, mesoscale rainbands, assoc. cloud microphysics and dynamics 0-82030
- flood inundation of agricultural land, LANDSAT digital image anal. 0-61913
- SW.Germany, heavy rainfall from May 22 to 24 (1978) (*German*) 0-61869
- hailstone formation within cloud, microphys. recycling 0-90146
- hailstorm, finger radar echoes, form. mechanism (*Chinese*) 0-109234
- hailstorms of S.Saskatchewan, Canada, climatological characts. 0-109204
- Himalaya, wind and storms during summer 0-72620
- hurricane decedion by Doppler radar for coast of U.S.A. 0-67414
- hurricane forcing of longshore currents in Gulf of Mexico 0-76998
- hurricane formation, tropical storm control by cloud seeding (*German*) 0-90207
- hurricane formation near Cape Verde Islands, general circulation from Meteosat 0-105042
- Hurricane Gladys (1975), subcloud layer energy transformations 0-77089
- hurricane season activity analysis, N.Atlantic (1886-1974) 0-101427
- hurricanes in the USA, speed determ. by Monte Carlo method 0-90209
- Indian summer monsoon, intensity rel. to ocean surface temp. 0-90121
- London area rainstorm of 16-17th Aug. 1977 0-77093
- monsoon circulation over Bay of Bengal, 1976, winter to spring 0-82038
- SW monsoon on W.India coast, aerosol and rain trace constituents 0-81967
- monsoon over Calcutta, rel. to VLF atmospheric anomalies 0-82127
- monsoon over Indian region, energy anal. by baroclinic model 0-77073
- multicellular severe storm simulations, 'three-dimens. cloud model 0-77049
- Nagapattinam cyclone, India, 12 Nov. 1977, radar-synoptic study 0-82026
- W.Norway coast, long barotropic waves and storm surges, model 0-81907
- ocean depths disturbed by surface storm, persistent nature of disturbance (*Russian*) 0-81921
- sandstorm dust fallout, Kuwait, summer 1978 obs. 0-81966
- severe local storms, automated 12 to 36 hour probability forecasts 0-77062
- stationary tropical cyclone, energetics of stratified ocean below (*Russian*) 0-61808
- thunderstorm, precipitation obs. immediately after lightning stroke 0-77055
- thunderstorm gust front, wind shear meas. using pulsed lidar 0-67415
- thunderstorm top, ascent rate obs. 0-61861
- tornadoic storm research, implications for dual-Doppler radar spacing of effective coverage area anal. 0-82093
- tornado activity rel. to precipitation, assessment 0-61882
- tornado over Delhi, of 1978 March 17, sodar obs. 0-109188
- tornado simulation, core radii and peak vel. in modeled vortices 0-90130
- tornado-like vortex, laboratory expt. of swirl ratio effect 0-61862
- tornadoes in UK, rel. to solar mag. sector crossing, 1957-77 period 0-77094
- tropical cyclone, model of ocean-atmos. boundary layer interaction 0-109231
- tropical cyclone generated surges in Bay of Bengal, numerical model 0-81923
- tropical cyclone intensity measurement from tropospheric aircraft 0-67416
- tropical cyclones, preferred mode of Ekman conditional instability of second kind (CISK) 0-72617
- tropical cyclones, radius and frequency of 15 m s<sup>-1</sup> (30 kt) winds 0-105025



**storms continued**

- tropical depression, synoptic scale kinetic energy source, cumulus cloud convection 0-77088
- tropical regions, atm. noise data 0-61875
- typhoon tracks near Taiwan, forecasting using simulations 0-90200
- typhoons anomalous tracks, over East China Sea, mechanism (*Chinese*) 0-82043
- S. Wales floods of late December 1979, meteorological anal. 0-98429
- wave height prediction during gales in North Sea 0-98346
- western disturbances development over India, role of westerly upper air troughs 0-90173

**strain ageing**

- abras, single cryst., yielding behaviour rel. to low temp. annealing treatment (*Japanese*) 0-93582
- dynamic strain ageing, and serrated yielding, mechanism 0-88245
- steel, low C, stress ageing embrittlement under short term thermally stressed cycle (*Russian*) 0-60885
- steel, medium and high C, deformation ageing, entropy, free energy, dislocations (*Russian*) 0-66581
- steel, Mn-V reinforcing type, strain ageing characts. rel. to mech. props. 0-84969
- Cu-Cd (1.0 wt.%), yield stress and flow stress 0-97524
- Cu-Cr( $\text{SiO}_2$ ), single crystals, yield and pre-yield behaviour rel. to aging time 0-81103
- Fe-Mn (1 at.%), strain age hardening 0-108472
- Fe-N, single cryst., solid soln. softening, effect of interstitial N 0-97496
- Y, plastic deformation props., deformation ageing, plastic flow, dislocation-impurity interactions (*Russian*) 0-66582

**strain gauges**

- see also strain measurement
- clamp and strain gauge, for shear characts. determ. of glass reinforced plastic 0-85114
- data logger, for educational purposes 0-73353
- dynamometer system, body of rotation form, non axially symm. load 0-73350
- Langmuir film balance meas. system 0-62659
- load cells and force transducers 0-86276
- manganin foil like gauge calibration in planar shock wave expts. 0-95091
- mass comparator, high precision, using bonded strain gauge load cell 0-57261
- pressure measurement in industrial environments (*Hungarian*) 0-86278
- selection, applications and technical specifications, output signals 0-101790
- semiconductor, acoustic power meas. of US medical probes 0-87679
- semiconductor, method to improve temp. stability 0-87826
- spinal deformities correction, force meas. 0-76861
- split Hopkinson pressure bar test on C fibre composites, opt. and strain gauge methods comparison 0-85132
- thick-film strain gauges and pressure transducers 0-57285
- vibrating wire strain gauges, temp. effect 0-73354
- Cu-Mn alloy, manganin, hysteresis-corrected calibration under shock loading 0-74818
- Cu-Ni/Au-Ni multilayer films, ohmic behaviour, use as strain gauge 0-65713
- Ge/Au film strain gauges, press. sensor (*Japanese*) 0-105631
- Si integrated bridge strain gauges with diffusion piezoresistors, strain sensitivity (*Polish*) 0-73341
- Ta thin film, elec. cond., strain gauge factor, ion bombardment effects 0-80417

**strain hardening** see work hardening**strain measurement**

- see also strain gauges
- accuracy improvement in impact tests 0-81259
- automated method of strain state determination, dividing nets appl. 0-100982
- contactless, laser beam and photoresist grating method (*German*) 0-68195
- crack tip strain meas. by electron micrograph stereoscopy 0-69752
- error due to communication lines, elimination, 20-550°C 0-64499
- extensometric method, for inside nuclear reactor channels 0-100998
- fracture strain measurement at high strain rates, radial expansion technique 0-85134
- fragile materials, at high temperatures, improved clamp for transducer attachment 0-73351
- general object deformation decomposition by speckle displacement 0-106486
- holographic interferometry appls. (*German*) 0-78815
- inclusion spherical strain fields, S-matrix theory calcs. 0-100133
- interior displacement and strain measurement using white light speckles 0-95064
- living cells, stress-strain meas. using cell poker 0-76880
- metal, strong, compressive stress/strain props. meas. at very high strain rates, modified Hopkinson bar system 0-85128
- nuclear reactor pressure vessels, strain measurements 0-79865
- optical fibre cable vibration characteristics, fibre strain and optical loss meas. 0-99870
- residual strains in components, determ. by holographic interferometry 0-99980
- resistance strain gauge-meas. techniques in biomech. expts. (*German*) 0-104819
- SEM, combined deformation/heating stage, acoustic emission rate meas. 0-101892
- speckle photographic technique, hybrid optical and electronic image processing 0-99976
- speckle photography with hybrid optical/electronic image processing 0-106768
- stress-intensity factor determ. by strain-gauge method 0-76445
- truss joint strain meas. by modified Michelson interferometer 0-74821
- two-dimensional structure in-plane vibr., stress analysis by laser speckle method 0-103006
- vibrating wire strain gauges, temp. effect 0-73354
- Al plate, thermal strain meas. by one-beam laser speckle interferometry 0-103005
- Fe-Ni-Ti, preaged martensite, shear strain magnitude, X-ray diffr. method 0-93592
- $\text{Li}_2\text{O-Al}_2\text{O}_3\text{-SiO}_2$  glass, crystallised, grain size and internal strain 0-103259

**strain measurement continued**

- Si, elastically bent, strain conc. determ. by microfluorescent densitometry of X-ray topography 0-79245
- Si impurity-doped cryst. plate, as an X-ray monochromator, strain distrib. for 220 reflection 0-100126

**strange particles**

- see also hyperons; kaons
- flavour changing weak radiative decays, short and long distance effects 0-73712
- $K_S^0 \rightarrow \rho^0 Q^0(Q^0)\rho$ , differential cross section slope, further Deck model anal. 0-73737
- $\nu$ , charmonium and strangeonium, linear+Coulomb pot. study, high  $\alpha$ s regime 0-62935
- $\nu N \rightarrow \mu \mu X$ , neutral strange particle prod. in opposite sign dimuon events 0-57584
- $\bar{p}p$ , 100 GeV/c, inclusive meson and strange particle prod., energy partition 0-95289
- $\pi^+p$ , 100 GeV/c, inclusive meson and strange particle prod., energy partition 0-95289
- $Q_1(1280)$ , mass formulas and selection rules in large SU(3) mixing 0-86700
- $Q_2(1400)$ , mass formulas and selection rules in large SU(3) mixing 0-86700

**strangeness** see strange particles**stratified flow**

- air turbulent flow in heated channel, effect of gravitational field 0-64533
- air-Hg flow, stratified, co-current, in rectangular channel, interfacial wave structure 0-74955
- asymptotic stability of unsteady inviscid stratified flows 0-83832
- atmosphere-ocean system, equilib. Langmuir circulation model for ocean 0-101381
- Boussinesq differentially heated fluid, struct. 0-109190
- channel, open, critical flow conditions for two stably stratified fluids 0-74956
- coastal trapped waves at low latitudes in a stratified ocean 0-90097
- composite mixture, flow through porous medium, Rayleigh-Taylor instability 0-69912
- convective flow, free, over point heat source 0-79323
- convective free flow struct. above heated cylinder 0-79322
- critical flow regime in a stratified medium 0-92200
- decaying turbulence in neutral and stratified fluids 0-96247
- duct, equilibrium breakdown, thermosiphon work (*French*) 0-59114
- ducts, one-dimensional models for transient gas-liquid flows 0-64614
- energy stability of the Eulerian-mean motion in the upper ocean to three-dimensional perturbations 0-92149
- estuaries of variable breadth and depth, tidally induced two-layer residual currents 0-72544
- finite depth stratified fluids, internal wave solitons, infinite depth limit 0-64574
- gas-liquid pipe flow, influence of return bends on velocity ratio 0-74962
- geophysical fluid dynamics theory, book 0-105443
- heated pounds, turbulent boundary layer of stratified airflow, surface waves 0-92133
- hemisphere in MHD rotating stratified fluid 0-100039
- inclined fluid layer, double diffusive instability, linear stability anal. 0-92113
- inclined fluid layer, double diffusive instability, secondary convecting layers 0-92112
- incompressible stably stratified fluid, internal waves, Brunt-Vaisala freq. 0-79343
- incompressible viscoelastic fluid, Rayleigh-Taylor instability 0-79363
- insulated water layer, combined heat transfer, stratified layer, energy eqn., boundary value problem 0-79290
- internal solitary waves in stratified flows, cubic and quadratic nonlinearity 0-69856
- internal wave generation in stratified fluid collapse (*Russian*) 0-74942
- liquid-metal-H<sub>2</sub>O stratified flow, horizontal co-current, interface heat transfer, turbulence model 0-92131
- lorenz attractor behaviour in a continuously stratified baroclinic fluid 0-83806
- LWR safety, condensation heat transfer in stably stratified systems 0-63311
- MHD pulsating viscous flow superposed on steady laminar motion 0-92228
- ocean, realistically stratified, nonlinear energy and enstrophy transfers 0-101370
- oceanic warm front propag., rotating stratified fluid theory 0-94538
- rotating fluid, parallel shear flow, baroclinic and barotropic instability 0-98328
- separated flow models, stratified flow, averaged formulation, high order dispersion effects 0-74960
- spectral theory of stratified turbulent shear flow, interactions between motion fields 0-90114
- stably stratified medium, plane free convection from local heat source 0-96253
- thermally forced stratified rot. fluids, axisymmetric steady motion 0-69844
- turbulence, normal and abnormal turbulent transport in stratified medium (*French*) 0-59095
- two-phase pressure driven stratified laminar pipe flow 0-64609
- two-phase stratified horizontal flow, averaged and local instantaneous formulations, stability 0-64613
- viscous incompressible liquid, heat conductivity problem (*Russian*) 0-69897
- viscous stratified shear flow, stability eqns., completeness obs. 0-64519
- wave/mean flow interaction, mean motion induced by transient inertio-gravity waves 0-105029

**stratosphere**

- see also ozonosphere
- aerosol, modification by supersonic transport and space shuttle operations, climatic implications 0-98408
- aerosol, remote sensing techniques 0-109269
- aerosol content, satellite monitoring systems, SAM II and SAGE 0-82082
- aerosol content var., rel. to atm. transparency and direct solar radiation 0-82035
- aerosol particles, concentration rel. to error in satellite retrieved atmospheric temp. profiles 0-98449
- chemical composition, importance of energetic particle precip. 0-109213
- circulation in circumpolar vortex, model 0-77082

**stratosphere continued**

- cosmic ray variations, evidence for interplanetary modulation processes 0-101508
- density inhomogeneity struct. determ. from Salyut obs. of astronomical scintillation (*Russian*) 0-109186
- dichlorodifluoromethane, height profile meas. at several latits. 0-72601
- dust collected from interplanetary space, optical absorpt. spectra 0-101554
- electron precipitation at high latitude, X-ray bremsstrahlung obs. 0-77205
- environmental decisions in context of large observational uncertainties 0-104535
- equatorial, vertical vel. determ. from Diurnal Experiment 0-77047
- formaldehyde, chem. of stratosphere, UV absorpt. spectra implications 0-109209
- formaldehyde+ClO radical, expt. showing no reactivity, stratospheric implications 0-90119
- gamma-rays, quasi-periodic intensity variations (*Russian*) 0-90177
- gas concentrations from limb sounding radiometry, inversion algorithm 0-82000
- heating and cooling due to aerosol IR radiation scatt., calc. 0-72630
- inclinations of atmospheric layers, determ. from sounding data (*Russian*) 0-72569
- intrusion into troposphere, explanation for <sup>7</sup>Be var. 0-98525
- ion composition and ionisation rates 0-61885
- ion mobility and conc. and ionic conductivity, rocket and balloon obs. 0-72605
- mean meridional circulations of stratosphere and mesosphere, monthly mean planetary wave fluxes 0-109219
- mesosphere at Thumba from in situ UV absorpt. photometry obs. 0-105051
- meteor trail metal ions, chem. reactions 0-72580
- methane, stratosphere content at mid-latitude, simultaneous N and S hemisphere obs. 0-77052
- middle atmosphere, obs. from balloons, rockets and satellites, conference, London, England, (1978 December 12 to 13) 0-77540
- minor constituents transport between troposphere and stratosphere 0-105034
- movements, Lagrangian motion of air parcels in presence of planetary waves 0-109215
- multi-ion complexes, implications for aerosols and trace gases 0-61872
- peroxynitrates, UV absorpt., spectra, photodissoc. lifetime meas. 0-83386
- photodissociation fluxes, tropospheric and stratospheric, Mie scatt. contrib. improved model 0-77103
- planetary wave, radiatively damped, in middle atmosphere, interaction with zonally averaged circulation 0-109217
- planetary wave secondary circulation, vertical air exchange implication 0-72584
- planetary waves in stratosphere global propag. in spherical atmos. 0-90139
- radar echo mechanisms, returns from clear air 0-90181
- radar facility, MST radar at Poker Flat, Alaska 0-90254
- radar for observing middle and upper atmosphere, Yaggi antenna array design 0-90255
- radar signal reflection and scatt. from refr. index structs. 0-90182
- radar studies at VHF and UHF freqs., review of obs. 0-90180
- radar techniques (VHF and UHF) for dynamic struct. 0-105078
- radiation budget affected by N<sub>2</sub>O and methane 0-90211
- radiometric measurements made in situ with superpressure balloon 0-85763
- radiowave backscattering, depolarisation obs. at 50 MHz 0-85729
- reactive N in unpolluted troposphere, stratospheric source 0-94561
- satellite solar occultation sounding of the middle atmosphere 0-105079
- semiannual oscillation in tropical middle atmosphere, review of observational evidence 0-109216
- solar eclipse effect on NO<sub>2</sub> and O<sub>3</sub> conc. and atm. temp. 0-105017
- solar occultation sounding, appl. to press. and temp. profiles meas. 0-98452
- solar UV radiation, absorpt. in mesosphere and stratosphere 0-109248
- solar UV radiation effects, rel. to solar cycle signal in tropospheric winds 0-72604
- southern hemisphere stratosphere, temp. and press. field spring transformation anal. 0-98420
- stable layers obs. by vertical pointing VHF radar 0-90189
- stratosphere-troposphere exchange at polar latits. in summer, from O<sub>3</sub> concs. meas. 0-72599
- sudden stratospheric warming initiated by planetary wave, model 0-90150
- sulphate aerosol, kinetics of growth by condensation in homogeneous medium (*Russian*) 0-94566
- sulphate aerosol layer, processes, models, obs. and simulations 0-109212
- SURF storage ring calibrations for NASA stratosphere and climate programs 0-94721
- temperature, obs. by satellite IR limb scanning method 0-105086
- temperature diurnal variation, 25-65 km altitude equator region 0-82022
- temperature remote sensing by O<sub>2</sub> 60 GHz absorpt. 0-77172
- temperature wave in polar winter upper stratosphere 0-72597
- tide in temperature due to Moon, NIMBUS 5 obs. 0-101405
- trace constituents, laser heterodyne spectroscopy 0-109257
- trace gas analysis method based on in situ ion composition obs. 0-105077
- trace gas concs. during 1976 in N.Hemisphere 0-67016
- trace molecule Fourier transform spectrometer optical design 0-82099
- travelling planetary waves, theory and obs. 0-105030
- trichlorofluoromethane, height profile meas. at several latits. 0-72601
- turbulence struct., 10-30 km altitude, high resolution 430 MHz radar obs. 0-90258
- turbulence struct. near tropopause, review of radar obs. 0-90179
- turbulent layer struct., 2380 MHz radar obs. 0-90191
- Van der Waals molecules comp. of lower atmos. 0-85699
- vertical wind shear from Lagrangian wind field obs. 0-82032
- VHF radar obs. of struct. and dynamics 0-105032
- warming forced by mountain 0-72583
- warmings, interactions with troposphere, thermal and kinetic 0-105031
- water vapour conc. meas. using aircraft-borne UV fluorescence instrument 0-82100
- water vapour vertical profile in stratosphere (*French*) 0-77033
- wave/mean flow interaction, introduction to generalised Lagrangian-mean distribution 0-109214
- wave/mean flow interaction, mean motion induced by transient inertio-gravity waves 0-105029
- waves of short-period, 13-25 km altitude, Doppler radar obs. 0-90192

**stratosphere continued**

- wind diurnal variation, 25-65 km altitude equator region 0-82022
- wind meas. with clear air Doppler radar, vertical component 0-72642
- wind measurement by radar, method for reducing backscatt. data 0-90257
- wind phenomena affecting troposphere circulation pattern 0-82021
- wind profile in troposphere and stratosphere, using Poker Flat MST radar 0-72579
- wind structure over Antarctica 0-81992
- winds in upper troposphere/lower stratosphere rel. to satellite-derived radiance gradient 0-98447
- zonal mean circulation of middle atmosphere, numerical model 0-109218
- zonal mean winds, vars. rel. to planetary wave props. and links with troposphere 0-109225
- zonal wind speed oscills., solar cycle influence 0-94562
- zonal winds effect on Earth rot. 0-81804
- Br chemistry and depletion of O<sub>3</sub> layer 0-98391
- CO, stratosphere content at mid-latitude, simultaneous N and S hemisphere obs. 0-77052
- CO<sub>2</sub>, stratosphere content at mid-latitude, simultaneous N and S hemisphere obs. 0-77052
- ClO composition balloon borne in situ reson. fluoresc. obs. 0-90167
- ClO, conc. vars. at twilight rel. to interperation of solar occultation meas. 0-85756
- ClO+HO<sub>2</sub>, free radical reaction rate const. and products at 298K, discharge flow mass spectra 0-67391
- ClO<sub>2</sub>, possible existence and chemistry 0-77066
- HCl, HF, volume mixing ratios simultaneous meas. 0-72587
- HCl, stratosphere content at mid-latitude, simultaneous N and S hemisphere obs. 0-77052
- HF, stratosphere content at mid-latitude, simultaneous N and S hemisphere obs. 0-77052
- HNO<sub>3</sub> composition, in situ obs. 0-105077
- H<sub>2</sub>O, composition, in situ obs. 0-105077
- H<sub>2</sub>O mixing ratio, in-situ obs. using NOAA UV fluoresc. instrument 0-90137
- H<sub>2</sub>O, stratosphere content at mid-latitude, simultaneous N and S hemisphere obs. 0-77052
- H<sub>2</sub>O structure, maintenance of extreme aridity 0-105028
- H<sub>2</sub>O-H<sub>2</sub>SO<sub>4</sub>-ion aerosol particles, ultrafine, stratospheric form., ion-induced nucleation 0-72608
- NO and NO<sub>2</sub> mixing ratio profiles from IR sunset spectra 0-94563
- NO, conc. vars. at twilight rel. to interperation of solar occultation meas. 0-85756
- NO<sub>2</sub> and H<sub>2</sub>O, mixing ratio profiles from IR solar spectra obs. 0-105015
- NO<sub>2</sub>, stratospheric, ground based obs. 0-85697
- N<sub>2</sub>O mixing ratio, height profile meas. at several latits. 0-72601
- N<sub>2</sub>O, stratosphere content at mid-latitude, simultaneous N and S hemisphere obs. 0-77052
- N<sub>2</sub>O<sub>2</sub>, gaseous, integrated band intensity data, stratospheric detection implications 0-58250
- O<sub>2</sub>, mag. dipole transitions, line positions and strengths from stratospheric emission spectra 0-78604
- O<sub>3</sub> behaviour and thermal structure during S. Hemisphere spring 0-105014
- O<sub>3</sub> composition, effect of chlorofluoromethane photolysis 0-109197
- O<sub>3</sub> depletion in stratosphere, space-time distrib. and UV radiation changes at Earth surface 0-94577
- O<sub>3</sub>, instantaneous global balance including observed NO<sub>2</sub> 0-109211
- O<sub>3</sub> layer depletion by chlorofluorocarbons, calc. using two-dimensional model 0-109221
- O<sub>3</sub> measurement by satellite IR limb scanning method 0-105086
- O<sub>3</sub> net vertical flux from circulation model, implication for troposphere O<sub>3</sub> budget 0-101402
- O<sub>3</sub>, nighttime concentration (15-68 km), Nimbus 6 obs. comparison with OAO-3 obs. 0-105016
- O<sub>3</sub>, obs. of meridional flux by transient eddies in 0 to 30 km height range 0-109224
- O<sub>3</sub>, partial press. profile over Uccle, Belgium, April-June 1979 obs. (*French, Flemish*) 0-98385
- O<sub>3</sub>, partial pressure profile over Uccle, Belgium, 1979 obs. (*French, Flemish*) 0-94571
- O<sub>3</sub> photodissoc., O(<sup>1</sup>S) yield at 1700-2000 Å 0-97714
- O<sub>3</sub>, stratosphere content at mid-latitude, simultaneous N and S hemisphere obs. 0-77052
- O<sub>3</sub> vertical distrib. during polar front passage over Uccle 0-94582
- <sup>18</sup>O/<sup>16</sup>O, photodissociation as source of atmospheric O<sub>3</sub> 0-94559

strays (atmospherics) *see* **atmospherics**

**streak photography**

- Homalite-100 plates, modified compact-tension specimens, dynamic anal. 0-97561
- indigo derivatives, fluorescence decay times, meas. by synchroscan streak camera 0-84759
- photochron picosec. streak cameras for linear photoelec. recording 0-86365
- polycarbonate plates, modified compact-tension specimens, dynamic anal. 0-97561
- pulsed laser real-time holographic interferometry 0-74319
- Shuttle Orbiter re-entry, remote IR imagery and tracking 0-82171
- streak camera, picosecond jitter 0-73486
- time-resolved X-ray spectroscopy of laser-produced plasmas 0-84004
- GaAs:Se cathodoluminescence decay obs. with SEM and streak camera, 90 to 300K 0-97348

**streamer chambers**

- JINR high press. streamer chamber, selection criteria for <sup>3,4</sup>He( $\pi$ , $\pi$ ) elastic interactions 0-102401
- JINR high press. streamer chamber, triggering system efficiency for <sup>3</sup>He( $\pi$ , $\pi$ ) elastic interactions 0-102400
- low energy heavy ion reaction study appl. 0-58035
- particle tracks recording technique using TV 0-69023
- ZGS streamer chamber and kaon physics 0-91308
- $\nu$  detector based on combined operation of streamer chamber and Converse hodoscopic tubes 0-63455

streamers *see* **discharges (electric)**

streaming, acoustic *see* **acoustic streaming**



strength (mechanical) *see* mechanical strength

stress *see* internal stresses; stress effects; stress/strain relations; yield stress

# stress analysis

*see also* bending; crack-edge stress field analysis; photoelasticity; photoelasticity; strain gauges; thermal stresses; torsion; yield strength; yield stress

anti-median elastic problem, N-harmonic solutions 0-99928

axisymmetric elastic problems, stress function solns. (*Japanese*) 0-64371

beams flexural-torsional problem by series expansion in eigenfunctions 0-83732

bending-free torsion condition to define centre of twist 0-79140

bonded wedge shaped stamp apex singularity, Green's functions for elastic half space 0-64489

circular notches and loaded ends, interference effects 0-64365

coiled multilayer shell, stress anal. of elastic and elastoplastic work 0-79156

colliding cylinders, resulting stress field for linearly elastic material (*Russian*) 0-79237

complex loading of materials, plastic deform. 0-99939

composite materials, stretching, stress distrib. 0-58931

cylinder, circular, transversely isotropic, concentrated loads, 3-D anisotropic elasticity theory 0-83734

cylinder, hollow thick-walled, having axial holes and varying section thickness, stress state anal. 0-100879

cylinder, hollow with internal circular crack, axially symmetric torsion determ., numerical results for boundary value anal. 0-64456

cylinders, constrained, elastic stress analysis by special finite element method 0-106718

cylindrical cavity in elastic half-space, Rayleigh wave loading, stress spectral representation 0-64453

cylindrical punch, three-dimensional stress field, photoelastic studies 0-93272

cylindrical tube, isotropic elastic, holographically meas. surface displacement, stress/strain extrapolation 0-64374

discoidal agglomerate, stress pattern, distributed loading effect during diametral compression test 0-60934

drawing, of continuous round ultrasonically perturbed profiles, stressed states at centre of deformation (*Russian*) 0-59557

dynamic stress-optical coeffs. of transparent media, simple interferometric instrum. 0-86394

Earth crust, effect of craton on distrib. of seismicity and stress in N.America 0-98248

Earth crust, plume generated radial stress fields rel. to Hawaiian rifts and recent Icelandic volcanism 0-90051

Earth crust, stress field rel. to dilatancy-fluid diffusion theory and after-shock sequences 0-85604

Earth mantle, convection and subcrustal stresses under Australia 0-72484

Earth uppermost mantle, lateral var. of differential stress across SW Japan island arc 0-98275

edge cracked sheets with mixed boundary conditions, stress intensity factors, displacements, stresses 0-64477

elastic half space, rectangular cylinder penetration, contact problem, stress fields 0-64490

elastic liner in cylindrical tunnel subjected to SH waves, dynamic stresses 0-79201

elastic materials, nonlinear, stress tensor, Kauderer's postulates (*German*) 0-64364

elastic plane with const. tangential stress at free boundary, expt. stress anal. of subdomains 0-99978

elastic waves, scattering by elastic sphere embedded in isotropic elastic medium 0-96214

elastoplastic medium with cylindrical cavity, stress distrib., photoelastic investigations, successive elastic solns. (*Polish*) 0-64391

Fermilab Doubler warm Fe supercond. dipole, stress anal. 0-58012

fibre reinforced plastics, stress distributions along short fibre 0-60913

fusion reactor, compact toroidal ignition experiment, support struct. anal. by numerical code 0-106167

fusion reactor, PDX, toroidal field coil and frame struct., anal., finite element anal. 0-106165

fusion reactor, PDX Tokamak, struct. anal. by finite element method 0-106166

fusion reactor, SLPX TF coil, stress anal. using COSMIC-NASTRAN 0-106168

fusion reactor, toroidal field coil in-plane bending stress, struct. support design 0-106164

fusion reactor toroidal field coil finite element stress anal. 0-91256

glass, tempered, stress analysis, oblique incidence light scattering, birefringence (*Polish*) 0-71374

glass fibre reinforced plastic pipe, thin walled, finned, stress anal. and load bearing capacity 0-81100

half space, elastic field due to ellipsoidal inclusions with uniform dilatational eigenstrains 0-58913

harmonic holes for nonconstant stress fields, deloids and cardeloids 0-64373

heteromaterial materials, stress strain correls. 0-87716

high temperature plant design methods, reference stresses and bounding theorems 0-58937

hip, total prosthesis, 3D stress anal. of femoral stem 0-98176

hydrostatic pressure loaded membrane of revolution 0-64363

infinite plate with doubly periodic hole array, transverse bending, Poisson-Kirchhoff theory 0-58920

integrated load increment method for finite elasto-plastic stress analysis 0-92072

joints, stress concentrations, Modeltech method, full scale models and photoelastic coatings (*Polish*) 0-64369

laminates, angle ply, 3D finite difference soln. of free edge effect 0-79152

laminates, cross-ply, edge effects, traction-free-edge condition satisfaction 0-79151

laminates, damage zone failure analysis 0-85059

laminates, multilayer, thick, hybrid-stress finite element formulation 0-92043

leg-foot, complex, in conditions of lesion and reconstruction, holography 0-67142

loaded construction, randomly loaded, crossing probabilities, numerical anal. (*German*) 0-96186

matrix analysis of composed bar of open cross section 0-83736

metallic materials, fatigue life distrib. theoretical obs. near fatigue limit 0-59569

metals, BCC, under elastic stress, Snoek peak height determ. 0-65153

# stress analysis continued

metals, engineering, multi-axial creep characts. 0-64398

metals, high temp. stress anal. by finite element method 0-96203

Moire thrust zone, differential stress determ. from deformation-induced microstructs. 0-85652

mountain massif, pre-face zone, stressed state, finite difference method (*Ukrainian*) 0-74735

notch stress anal. in elastic bodies, energy variations 0-64378

nuclear fuel, coated HTR particles, failure statistics calc., effect of SiC fracture stress and kernel porosity 0-73920

panels, stiffened, eight-stringer, with rectangular cut-out, stresses and deformations, eccentric tensile load (*Japanese*) 0-64467

photothermoelastic technique, appraisal for transient 2D thermal stress analysis 0-79244

piecewise homogeneous bodies, two-dimens. elasticity theory stress problems 0-74749

pipes, welded branch, stresses calc. 0-108493

plane V-notched specimen, elastic-plastic limit load anal. 0-69684

plate, elastic-plastic, flexed in its plane, stress concentrations, method of small parameter (*Russian*) 0-74759

plate, impact force meas. method 0-79242

plate with two unequal circular holes, stress concentrations 0-92047

plates, annular, clamped edges, asymmetric bending, Ritz method 0-58907

plates, V-notched elastic, symm. loaded, stress intensity factors, caustic method 0-83770

plates and slabs, perforated (*Russian*) 0-74728

plates under uniaxial load, optimum hole shapes, cracks and fracture appl. 0-64479

polycarbonate, glassy, fatigue crack initiation in high strain fatigue tests 0-97564

poroelastic cylinder, twisted pore effect on fluid flow, solid deformation and stress 0-64377

precipitate and dislocation loop strain and stress field calcs. using affine transformations 0-106722

PVC, glassy, fatigue crack initiation in high strain fatigue tests 0-97564

PWR containment vessel optimisation 0-106137

reinforcement material distrib. for specified stress field criteria, plane elasticity hybrid problem 0-64376

remaining creep life for components under stress at elevated temperatures 0-59566

residual, US drawing 0-97674

Reykjanes Ridge, stress directions rel. to ridge crest morphology near 62°N 0-90070

rigid punch bonded to elastic half plane, stress singularities 0-64491

rigid-plastic medium, ideal, surface force strength lower limit under plain strain 0-99937

ring, plane deformation, determ. of stresses and displacements, composite boundary conditions (*Russian*) 0-74738

ring caps, shallow spherical, transverse twisting 0-79139

rod of time hardening (softening) material, thermoelastic stresses 0-92046

rubber covered rolls, contact and deformation nonlinear elastic problem, stress anal. 0-79239

San Andreas fault, stress changes due to creep episodes rel. to local mag. field meas. 0-85629

second order beam theory 0-58908

shear wall with N-rows of openings, stress anal., weighted residuals method (*Chinese*) 0-64362

shell, high-shallow, with rib of equal resistance, contact interaction, tangential stress distrib. (*Russian*) 0-87745

shells, thin, axial compression, mass reduction, stress anal. 0-106716

shells of revolution, computer program for linear and geometrically nonlinear static analysis (*Japanese*) 0-64500

shells of revolution under axisymmetric and asymmetric loadings, linear elastic dynamic analysis program using finite element analysis (*Japanese*) 0-106719

solar collectors with multilayer cylinder heat exchangers, heat balance eqn. and thermal stress anal. 0-58977

solid deformable body, residual stresses by creating holes, holographic interferometry appl. (*German*) 0-79243

solid free boundary, slip line initial development, elastic-plastic problem 0-96196

spheroplastics, mech. characts. calc. 0-60931

steam turbines, structural stresses, experimental anal. 0-93727

steel, crack-resistance limit and stress analysis in the ductile state 0-81188

strip or beam, state of stress, rectilinear thin walled inclusion effects 0-96187

strip with semicircular notches, tensile load conditions at end, interf. effects obs. 0-64455

strips, seizure, elastic stresses, extra loading moments (*Russian*) 0-69664

superconducting fusion magnetic systems, struct. anal. methods and standards 0-86972

telescope, altazimuth mounted, primary mirror deflection and stress anal. 0-58659

tensionless contact without friction between elastic layer and elastic foundation 0-64487

thermal elastoplastic stress analysis based on initial strain method (*Japanese*) 0-77620

thermoelastic cooler, single stage, finite element thermal stress anal. 0-108807

thermoviscoelastic laminate beam, stress anal. (*German*) 0-106727

thin shell theory, stress boundary conditions 0-79137

three-dimensional stress anal., transition finite elements 0-92042

Timoshenko beam, shear coeff. (*German*) 0-106729

transition finite elements for axisymmetric stress analysis 0-92048

transversely isotropic half space, indentation anal. 0-92090

tubes, thick-walled, thermoelastoplastic creep stress anal. 0-58922

US nondestructive inspection system, microprocessor utilization 0-71845

viscoplastic model, cyclic load, stress evolution, asymptotic behaviour (*French*) 0-64382

webs, thin, under partial edge loading, influence of longitudinal stiffening determ. 0-79857

wheel temperature in railroad service, effect of brake shoes 0-93660

wind stress coefficient over water surfaces, new evaluation 0-72603

Bi anisotropic crystal, dislocation wall stress field and strain energy 0-100233

stress birefringence *see* mechanical birefringence

# stress control

PbF<sub>2</sub>-ZnSe multilayer 16  $\mu$ m dichroic mirror, 16  $\mu$ m region, mech. stress compensation 0-74465

# stress corrosion cracking

Admiralty Metal, transgranular stress corrosion crack propag. 0-89402  
 $\alpha$ -brass, stress corrosion fracture surface anal. by AES 0-104321  
 bronze, low-cycle fatigue, NH<sub>3</sub> effect 0-104348  
 BWR coolant pipes, intergranular stress cracking, in-service inspection influences 0-68887  
 ceramic, growth micromechanism in corrosive environment 0-108616  
 conference on electrochem. test methods for stress corrosion cracking, Firminy, France (Sep. 78) 0-94910  
 electrode holder for electrochem. stress corrosion expts. at high temp. and press. 0-61102  
 engineering materials, intergranular fragility index 0-66637  
 failure, predictive approaches 0-97611  
 fracture analysis of failure in service (*Japanese*) 0-104337  
 glass, growth micromechanism in corrosive environment 0-108616  
 glass fibre reinforced polyester crack growth micromechanism in corrosive environment 0-108615  
 glass fibres, crack growth during dynamic fatigue and effect on strength loss for tensile loading 0-89334  
 graphite fibre reinforced composites, damage by moisture, diffusion anal. 0-81227  
 hydrogen effect on stress corrosion cracking, state of art review 0-61017  
 Incoloy 800, stress corrosion cracking in NaOH solns., electrochem. aspects, peening treatment 0-97618  
 Inconel, caustic stress corrosion cracking resistance, processing variables effect 0-71796  
 Inconel 600, small bore tubing, crevice corrosion 0-60999  
 Inconel 600, stress corrosion cracking in NaOH solns., electrochem. aspects, peening treatment 0-97618  
 Inconel 600, thermal treatment, grain boundary microstruct. and SCC resistance 0-71675  
 Inconel 600 alloys, stress corrosion cracking, prediction in 10% NaOH soln. at 315°C 0-97616  
 LWR piping, intergranular stress-corrosion cracking 0-81234  
 micromechanisms of crack extension, conf., Cambridge, England (March 1980) 0-105421  
 Ni-Co, H<sub>2</sub> embrittlement, heat treatment and impurities effect 0-76331  
 optical fibre, dynamic fatigue and strength degradation 0-58719  
 optical fibres, stress corrosion susceptibility constant meas. 0-66680  
 polyethylene, low-density, environmental stress cracking, surfactant soln. effect 0-89376  
 polyethylene, resist. to stress corrosion cracking, ionising radiation effect (*German*) 0-81224  
 sheet materials, failure kinetics, method for investigating under long-term static loading in corrosive medium 0-85110  
 static and dynamic loading, crack kinetics 0-89334  
 steel, alloy, hardened, electrochem. characts. and stress corrosion cracking, ageing and cold treatment effects 0-108639  
 steel, alloy, heat-treated, crack resist. in seawater 0-104347  
 steel, alloy, sheet, crack-propag. resist. in heat-affected zone in presence of H<sub>2</sub>, rolling direction and preliminary plastic tensile strain effects 0-60971  
 steel, austenitic stainless, mechanisms (*Japanese*) 0-104336  
 steel, austenitic, type 316, in MgCl<sub>2</sub>, acidity and applied potential effect on stress corrosion cracking 0-85076  
 steel, austenitic stainless, in boiling MgCl<sub>2</sub> solns., alloying elements effect on stress corrosion cracking and K<sub>ISCC</sub> (*Japanese*) 0-93692  
 steel, austenitic stainless, in MgCl<sub>2</sub> soln., temp. effect (*Korean*) 0-93694  
 steel, austenitic stainless, of type 35 23 33, slow strain rate testing under electrochem. control in high temp. water 0-97650  
 steel, austenitic stainless, rel. between polarisation behaviour and susceptibility to stress corrosion cracking (*Japanese*) 0-93693  
 steel, austenitic stainless, repassivation kinetics study in Ct media 0-97614  
 steel, austenitic stainless, sensitised factors influencing susceptibility 0-97617  
 steel, austenitic stainless, stress corrosion crack growth, electrochem. aspects 0-97620  
 steel, austenitic stainless, SUS 304, stress corrosion cracking in various environments, fractography (*Japanese*) 0-93690  
 steel, austenitic stainless, type SUS 304, welded joint, polarisation behaviour, boiling MgCl<sub>2</sub> soln. (*Japanese*) 0-93695  
 steel, austenitic stainless 304, stress corrosion cracking in MgCl<sub>2</sub> soln., cold working effect (*Japanese*) 0-104339  
 steel, austenitic stainless SUS 301, stress corrosion cracking susceptibility, effect of strain-induced  $\alpha'$ -martensite (*Japanese*) 0-104335  
 steel, austenitic type 304, sensitised, intergranular stress corrosion cracking inhibition study 0-100939  
 steel, C, sulphide cracking resistance 0-108640  
 steel, C and sensitized stainless, crack growth in high-temp. water 0-108636  
 steel, Co-Cr-Mo HY 180M, SCC in NaCl, temp. effect 0-108633  
 steel, Co-Cr-Mo type HY-180M, mech. props. and SCC, overageing effect 0-108634  
 steel, Cr-Mo, H embrittlement in H<sub>2</sub>S environment, Mo effect 0-76415  
 steel, Cr-Ni-Mo, resist. to corrosion and corrosion-fatigue in seawater 0-104346  
 steel, electrolytically notched, in direct evidence of active path formation in stress corrosion cracking in Al-alloys 0-85077  
 steel, high-strength, type 4340, new inhibitors for crack arrestment in corrosion fatigue 0-100941  
 steel, martensitic stainless, in SO<sub>2</sub> solns., activation pH and susceptibility to H<sub>2</sub> assisted stress corrosion cracking 0-97619  
 steel, martensitic-aged, plastic deformation influence in type N17K12MST steel on mech. props. (*Russian*) 0-76305  
 steel, mild, cyclic strain enhanced dissolution in NH<sub>4</sub>NO<sub>3</sub>, corrosion fatigue props. 0-85083  
 steel, mild, transgranular stress corrosion cracking in H<sub>2</sub>SO<sub>4</sub>-KI soln. 0-71797  
 steel, Ni-Cr-Mo-V, corrosion fatigue, crack growth in NaOH soln., cathodic pot. effect 0-89403  
 steel, Ni-Cr-Mo-V, in NaOH soln., corrosion fatigue crack growth rate, applied pot. effect 0-60998  
 steel, stainless, 304, stress corrosion cracking in H<sub>2</sub>SO<sub>4</sub>-NaBr aqu. soln. (*Japanese*) 0-108629

# stress corrosion cracking continued

steel, stainless, 304, stress corrosion cracking in H<sub>2</sub>SO<sub>4</sub>-NaI aqu. soln. (*Japanese*) 0-108630  
 steel, stainless, orthopaedic, type En58J, Mo ion-plating, corrosion fatigue 0-66694  
 steel, stainless, stress corrosion cracking and microhardness, effect of bombardment by He<sup>+</sup>, Ni<sup>+</sup> and Cr<sup>+</sup> 0-85087  
 steel, stainless, stress corrosion susceptibility in high purity water, O<sub>2</sub> and temp. effects 0-61002  
 steel, stainless, stress corrosion testing, slow strain rate, elevated temp. and high press. study 0-97615  
 steel, stainless 301, stress corrosion cracking in MgCl<sub>2</sub> soln., environment effect on initiation and propag. (*Japanese*) 0-104338  
 steel, stainless 304, stress corrosion cracking, classification in various environments (*Japanese*) 0-71805  
 steel, X70, fatigue crack growth rate in air and saltwater, stress ratio effect 0-100952  
 steel Ni-Cr-Mo-V, and Cr-Ni-Mn type 4340, hydrogen bearing environment effect on K<sub>ISCC</sub> 0-104325  
 steels, austenitic stainless, stress corrosion cracking, correl. between electrochem. and mech. parameters 0-97613  
 test machine, design and construction, appl. to Fe-Cr-Ni alloys 0-97649  
 Zircaloy, LWR fuel rod cladding, damage accumulation during I<sub>2</sub>-induced stress corrosion cracking 0-71810  
 Zircaloy, unirrad., I<sub>2</sub>-induced, effect of test temp., alloy comp. and heat treatment 0-97632  
 Zircaloy cladding, stress corrosion cracking, inner surface texture effect 0-66695  
 Zircaloy cladding stress corrosion cracking due to I (*Japanese*) 0-78361  
 Zircaloy-2, mech. props. after exposure to I<sub>2</sub>-methanol solutions, SEM study 0-93689  
 Al alloy V95T1 sheets, failure kinetics, method for investigating under long-term static loading in corrosive medium 0-85110  
 Al-Zn-Mg, crack-arrest markings on intergranular stress corrosion fracture surfaces 0-89405  
 Al-Zn-Mg alloy AA-7039, stress corrosion cracking, SEM obs. 0-104323  
 Al-Zn-Mg alloys, grain boundary segregation, implications to stress corrosion cracking 0-84936  
 Al-Zn-Mg type 7N01-T4, weld, SCC in NaCl-H<sub>2</sub>O<sub>2</sub> soln. (*Japanese*) 0-108631  
 Al-Zn-Mg-Cu (6.2, xwt.%) type alloy, fatigue crack propag., Cu content and recryst. effect 0-60960  
 Al<sub>2</sub>O<sub>3</sub>, bioceramic synthesis, for orthopedic purposes, props. (*Polish*) 0-66465  
 Cu-Be, SCC in NH<sub>3</sub> 0-104326  
 Cu-Be (2 wt.%) , tarnish surface films, formed in ammoniacal Cu(II) solns. 0-97624  
 Fe, H<sub>2</sub> embrittlement and H<sub>2</sub> adsorption 0-89401  
 Fe-Cr-Ni, test machine, design and construction 0-97649  
 LaNi<sub>5</sub>Fe, H<sub>2</sub> absorpt. cracking, acoustic emission characts. (*Japanese*) 0-66631  
 Ni, stress corrosion susceptibility, S segregation effect, Auger spectrosc. study 0-61019  
 Ni-Cr-Al-Ti, stress corrosion cracking, factors influencing susceptibility 0-97617  
 Ni-Cr-Fe, stress corrosion cracking, factors influencing susceptibility 0-97617  
 Ti alloys, corrosion in saline radioactive waste isolation environments 0-104349  
 Ti, commercial, texture depend. stress corrosion cracking 0-104334  
 $\alpha$ -Ti sheet, texture dependent stress corrosion cracking in Br<sub>2</sub>-methanol soln. 0-71803  
 Ti-Al-V (6, 4 wt.%), texture depend. stress corrosion cracking 0-104334  
 Ti-V-Fe-Al (10, 2, 3 wt.%), fracture toughness and stress corrosion resistance 0-100904

# stress effects

*see also* cavitation; deformation; elastic waves; heat treatment; high-pressure phenomena and effects; magnetomechanical effects; materials testing; mechanical properties of substances; mechanical testing; piezoelectric effects; piezoelectricity; piezoresistance; shock wave effects; stress analysis; stress measurement; stress/strain relations; tribology  
 bone remodelling, quantification of stresses 0-85437  
 dislocation mobility in inhomogeneous stress field, hardening effects 0-70219  
 graphite/epoxy laminates, stress wave damage 0-93611  
 paraelastic force on homogeneous cryst. inclusion, theory 0-79777  
 polymer melts, normal stress and Barus effect 0-64589  
 steam turbines, structural stresses, experimental anal. 0-93727  
 AuMn alloy, ordered, vacuum deposited epitaxial films, orientation control by external stress 0-100426  
 CdCr<sub>2</sub>Se<sub>4</sub>, modulated piezoreflection spectra 0-97237  
 CuAl alloy, ordered, vacuum deposited epitaxial films, orientation control by external stress 0-100426  
 Ni perfect crystal, stability under various stresses 0-104208  
 Si p-channel MOS structure, stress effects on elec. props., press. transducer props. 0-100526  
 Ti-Nb-Zr-Ta, superconducting props. comp. depend., stress effects and precipitation behaviour, X-ray scatt. 0-93059

stress field analysis at cracks *see* crack-edge stress field analysis

# stress measurement

birefringent object, isopachics meas. using immersion method polarisation holography 0-99672  
 elastomeric bearings, high-capacity, laminated, finite-element anal. 0-96197  
 ellipsometry, three-dimens., stress meas. in birefringent medium 0-101821  
 extruded billets, nondestructive determ. of residual stress from acoustoelastic meas. 0-76467  
 fragile materials, at high temperatures, improved clamp for transducer attachment 0-73351  
 goniometer, for stress measurement in single crystals and coarse-grained specimens 0-64837  
 internal friction in solids, direct meas. with continuous variation of freq. 0-99979  
 living cells, stress-strain meas. using cell pocker 0-76880  
 metal, textured cubic, residual stress evaluation 0-89435  
 optical glass, thermally tempered, surface stress meas. by crit. ray method 0-106766  
 photoelastic birefringent material stress determ. in single hologram exposure 0-106770



**stress measurement continued**

- PMMA, shock loaded, lateral compressive stresses meas. using Yb piezoresist. gauges 0-103007
- polymer solutions, dilute, normal stress difference and shear rate 0-83776
- porcelain-metal cermet, stress determ., meas. method (*German*) 0-76425
- residual stress measurement, X-ray diffr. equipment, comparison 0-82858
- rheogoniometer, Weissenberg, modification to normal stress meas. unit 0-69750
- sandwich composite beams, stress distrib. meas. under four-point bonding, multilayer builtup theory 0-96190
- single crystals, internal stresses determ. with multicryst. X-ray spectrometer 0-64832
- solid propellant stress transducer evaluation 0-81245
- steel, austenitic stainless, X-ray stress meas., accuracy and method of data treatment (*Japanese*) 0-104365
- steel, Cr-Mo-Ni-V, dynamic stress intensity factor meas., possibilities and limits (*German*) 0-93719
- steel, low C, dynamic stress intensity factor meas., possibilities and limits (*German*) 0-93719
- steel, low C, initial stages of plastic deform. (*Japanese*) 0-93618
- steel, Ni, 11.6%, quenched cylinder residual stresses, boring/turning and X-ray diffr. obs. (*German*) 0-93586
- steel, Ni-Co-Mo, dynamic stress intensity factor meas., possibilities and limits (*German*) 0-93719
- stress-intensity factor determ. by strain-gauge method 0-76445
- structural stress distrib. determ. by remote IR thermometry 0-87749
- Stycast-1266, mechanical props. at low temps. 0-57286
- temporary and residual stresses, high-temps. 0-64498
- two-dimensional structure in-plane vibr., stress analysis by laser speckle method 0-103006
- US nondestructive eval. using bipolar transducers 0-76471
- welding stresses on component surfaces, semi-automatic measuring device 0-68194
- welds, residual stresses, evaluation by Barkhausen noise meas. 0-76436
- wires in steel cables, tension measuring device and method of use (*Russian*) 0-68196
- X-ray integration method, extension of  $\sin^2\psi$  method (*German*) 0-92420
- X-ray stress meas., computer-aided system (*Japanese*) 0-104366
- Al, initial stages of plastic deform. (*Japanese*) 0-93618
- Cu electroplating method, sensitization methods (*Japanese*) 0-68197
- Ni, cold-rolled, anomalous effects during X-ray stress meas. (*German*) 0-104184
- Pb(Zr,Ti)<sub>1-x</sub>O<sub>3</sub>, meas. of Hugoniot curve with commercial manganin stress gauges 0-70362
- Si-SiO<sub>2</sub> interface, stress meas. technique 0-84395

**stress-optical effects** see piezo-optical effects**stress relaxation**

- see also anelastic relaxation; creep; viscoelasticity
- alkali silicate glasses, high temp. relax. mechanisms 0-70134
- articular cartilage in compression, biphasic creep and stress relax., theory and expts. 0-94275
- austempered reinforcing wire, tempering under stress, effect on mech. props. and relaxation resistance 0-100861
- Bakor 33, refractory, stress relaxation capacity determ. 0-60910
- Burgers vector sign determ. for nearly screw dislocations, X-ray dynamical theory applic. 0-59467
- ceramic materials, fine-grained, cyclic plastic deform. as cause for thermal expansion hysteresis 0-89290
- ceramics, cracking characterisation by double torsion test (*French*) 0-104369
- creep, transition between dislocation and diffusion 0-88253
- creep modelling incorporating initial strain and ageing 0-58939
- crystalline materials, fracture, stress relaxation effect 0-88256
- deformation resistance, depend. on hot press. working speed (*Russian*) 0-65126
- elastomers, rel. between relax. behaviour and tensile strength (*German*) 0-66604
- epoxy EDT-10, rigid polymer, thermal stress isothermal relaxation 0-71683
- ethyl acrylate ionomers, stress relax. 0-104200
- gelatin gels, in water and glycerol/water mixtures, dynamic viscoelastic props. 0-64508
- glass, mechanical destruction role of relaxation processes 0-89282
- glass and glass-forming liq., viscoelastic properties, comparison with Lennard-Jones model 0-84983
- glass-metal sealing, set point of glass 0-108423
- glasses, commercial, viscosity and stress relax. in glass transition region 0-93589
- glassy state and highly viscous liq., rheology 0-70130
- lecithin-water system, lamellar phase, rheology 0-89779
- Maxwell fluid, diffusion of vortex line in stagnation point flow 0-74892
- metals and alloys, in-reactor, study at low temps. 0-93588
- modulus, evaluation from response to constant strain rate followed by constant strain 0-74765
- nylon 6-Li halide mixtures, viscoelastic behaviour, stress relaxation 0-58995
- PMMA, rigid polymer, thermal stress isothermal relaxation 0-71683
- PMMA melt, stress relax. at large deformations 0-58994
- PMMA organic glass, stress relax. calc. from creep curves 0-71709
- poly(di-n-heptyl itaconate), alkyl side chain independent relax., double glass transition 0-59636
- polyamide-polyurethane copolymer dispersions, structuring and relax. props., coating from props. 0-76559
- polybutadiene, dihydroxy-terminated, with unattached styrene-butadiene copolymer, stress relax. 0-104202
- polymer latex film composite, glass transition temp. determ. using thermomech. curves 0-75342
- polymer liquid, entangled, phenomenological consequences of Doi-Edwards viscoelasticity theory 0-79250
- polyoxymethylene, transitions and relaxation spectrograph 0-65204
- polypropylene film, double-exposure speckle pattern obs. of tensile deform., displacement, Poisson's ratio and stress relax. 0-84795
- porcelain-metal cermet, stress determ., meas. method (*German*) 0-76425
- relaxation test method, for plastic deform. (*Hungarian*) 0-97661
- Rzhanitsyn-Koltunov nucleus, anal. determ., relax. function for shear and stretching 0-58932
- second phase particle, diffusional relaxation 0-60898
- steel, age hardened, dynamics of cyclic plasticity (*Czech*) 0-108464
- steel, austenitic, Cr-Mn-N, plastic deformation influence on internal friction, relaxation processes (*Russian*) 0-100870

**stress relaxation continued**

- steel, Cr-Mo weld metal, trace element embrittlement suppression by creep strength effects 0-66656
- steel, stainless, type 304, viscoplastic behaviour, strain rate sensitivity, creep, relaxation, tensile tests 0-66727
- steel, stainless, type 304, viscoplastic model, uniaxial, based on total strain and overstress 0-64387
- steel, type 4052Kh, thermomechanical working influence on mech. props. (*Russian*) 0-93578
- steels, alloy, stress relax. data anal. using total strain-time parametric method (*Japanese*) 0-104198
- styrene-butadiene-styrene block copolymer, stress relax. following steady-state flow, residual shear stress development 0-83772
- test device, for variable temp. 0-85113
- textolite glass, stress relax. calc. from creep curves 0-71709
- thermal activation analysis, of plastic deformation and dislocation motion using stress and temp. jumps 0-74771
- trifluoropropylmethylsiloxane fluids, viscoelastic props., mechanical impedance, viscosity and density meas. 0-79249
- viscoelastic fluids, Weissenberg rheogoniometer, R-17, axial compliance reduction 0-106859
- viscoelastic strip, dynamic crack propagation due to antiplane loading 0-64464
- viscoelasticity, time reversal and symmetry relations 0-102970
- Zircaloy, unirrad., stress corrosion cracking, I<sub>2</sub>-induced, effect of test temp., alloy comp. and heat treatment 0-97632
- Zircaloy-4, stress-relieved and cold-worked, stress relaxation in bending at 673K 0-93609
- Al foil, internal friction changes during low temp. plastic deform. (*Russian*) 0-100304
- Al, plastic deformation thermal activation parameters from creep kinetics and stress relaxation 0-71717
- Co, single crystals, {112} twins, accommodation and form. 0-96540
- Cu, plastic deformation thermal activation parameters from creep kinetics and stress relaxation 0-71717
- Cu-SiO<sub>2</sub>, low-temp. recovery creep, Orowan loop accumulation 0-81126
- Cu-Zn (30 wt.%), single crystals, quantitative anal. of stress relax., obstacle strength and athermal stress variation 0-89277
- Cu<sub>60</sub>Zr<sub>40</sub>, amorphous, ductility and stress relief, low-temp. annealing effects 0-76296
- Fe, pure, dislocation relaxation peaks under low temp. deform. (*French*) 0-100867
- Fe-Ni alloys props. of materials used in electromechanical filter resonators (*Czech*) 0-76318
- Fe-Si (2.8 wt.%), single crystals, growth striations, X-ray studies 0-79774
- Fe<sub>80</sub>B<sub>20</sub> metallic glass, crystn. and struct. relax., Mossbauer effect study 0-75182
- KCl:Ba<sup>2+</sup>, localised stress relaxation in excess vacancy system, prismatic loops (*Russian*) 0-88160
- LiF, kinetics analysis of stress relaxation 0-65136
- MgO, photoluminesc. during mechanical deform. 0-60665
- Na<sub>2</sub>O-CaO-SiO<sub>2</sub> glass, vol. relaxation and thermal history during forming process 0-70130
- Nb<sub>2</sub>Sn, hot isostatically pressed, plastic deform. 0-108510
- NiO, stress relief and plastic flow in temp. range 1323-1473K 0-89302
- NiPt, quenched, ordering kinetics and domain struct. form. during isothermal tempering (*Russian*) 0-66502
- Pb, film, thermal strain, strain relax. above room temp. 0-59841
- Pb<sub>0.92</sub>Fe<sub>0.06</sub>Ti<sub>0.47</sub>Zr<sub>0.53</sub>O<sub>3</sub>, piezoelectric ceramic, stress relax., time depend. deformation 0-60899
- Pb(Zr,Ti)O<sub>3</sub>, fracture and deform. 0-79870
- Si<sub>3</sub>N<sub>4</sub>, cracking characterisation by double torsion test (*French*) 0-104369
- Ti-Al-Sn, alloy 6242, dynamic effects of flow and fracture during isothermal forging 0-76343
- W fibre reinforced Cu composites, correl. between thermal cycling-induced microstructural changes at interphase boundaries and tensile behaviour (*Japanese*) 0-71674

**stress wave emission testing** see ultrasonic materials testing**stress/strain curves** see stress/strain relations**stress/strain diagrams** see stress/strain relations**stress/strain relations**

- see also elastic constants; elastic limit; serrated yielding; yield point; yield stress
- p-n-alkoxybenzoates of p-n-alkoxyphenyl, smectic A phases mol. struct. and elastic behaviour 0-59382
- bar-to-block based testing method for materials characteris. in high-vel. tension 0-85133
- biological soft tissues, elastic stress/strain relation based on a struct. model 0-101205
- bounded domain undergoing sequential crystallisation, stress and strain investigation 0-100183
- brass, crack initiation at high strain rates, uniaxial and biaxial tests 0-85141
- brass, cyclic creep under increasing stress condition, constitutive eqn. 0-93593
- brass, plastic deform., stress-strain relation of integral type 0-74754
- $\beta$ -brass, uniaxial tension and compression, cyclic stress-strain behaviour 0-75551
- cable design and testing, optical fibre 0-69551
- cavity growth, by surface diffusion in polycrystn. metals 0-104217
- composite materials, stretching, stress distrib. 0-58931
- composite polymers, viscoelasticity theory, appl. 0-64397
- composite shell structs., stress-strain state, elastic equilib. 0-74748
- concrete, stress-strain relationships, applicable to biaxial tension and compression 0-65133
- cracktip under incipient creep deform., stress field and modified J-integral (*Japanese*) 0-103411
- curve determination at high strain rate in uniaxial compression (*Japanese*) 0-96238
- cyclic strain diagrams recording under nonisothermal conditions, review 0-71830
- cylinder, hollow thick-walled, having axial holes and varying section thickness, stress state anal. 0-100879
- cylinder, rupture under wave conditions, stress-strain state for explosive loading (*Russian*) 0-79220
- cylinder, thick-walled heteromodal, subjected to underwater waves, numerical calc. 0-74746
- cylinder under torsion elastic, spherical cavity effect in stress-strain state 0-101717

## stress/strain relations continued

cylindrical shell, contact problem with ribbed cylinder under axisymmetric loads 0-99974  
 cylindrical three layer pipe, stress-strain state, filler compressibility effects (*Russian*) 0-58901  
 cylindrical tube, isotropic elastic, holographically meas. surface displacement, stress/strain extrapolation 0-64374  
 damage analysis under nonproportional cycling 0-97556  
 deformation and fracture of materials in creep range, effects of nonlinear stress-strain rate relations 0-58938  
 deformation wave processes, corrected nonlinear eqns., stresses and strains 0-102998  
 disc, with crack, stress and strain calcs. (*German*) 0-106760  
 dissipative medium, stress/strain rate relations 0-74736  
 dynamic biaxial loading techniques and apparatus 0-85129  
 dynamic measurements under superimposed high press., torsion bomb machine 0-85130  
 elastic bodies, nonlinear, of different tensile and compression-strengths, stress and strain (*Ukrainian*) 0-69661  
 elastic plane, stress-strain state at brittle crack vertex, geometric non-linearity effects (*Russian*) 0-79221  
 elastic-plastic materials, uniaxial stress/strain relations 0-83739  
 elastic/viscoplastic media, constitutive eqn. covering wide range of strain rates (*Japanese*) 0-79862  
 elasto-plastic stress wave propag. (*Czech*) 0-108507  
 fatigue crack propagation, crack closure, effective stress range factors 0-100924  
 fatigue testing, cyclic stress-strain curve determination (*Czech*) 0-89434  
 fibre crack-reinforced layered composites, moment effects in plane problem 0-64393  
 fibre reinforced composites, deformability characteristics, reinforcement scheme effect 0-58930  
 fibre reinforced composites, reinforcement scheme optimisation with respect to deformability at assigned stresses 0-69689  
 fission reactor materials, thermomechanical transient anal., strain-rate dependent plasticity 0-79864  
 fracture strain measurement at high strain rates, radial expansion technique 0-85134  
 gels of rodlike macromolecules, nonlinear elasticity in condensed state 0-104199  
 glass bead reinforced nylon, design parameters, fibre orientation effect 0-81141  
 glass bead reinforced polycarbonate, design parameters, fibre orientation effect 0-81141  
 glass fibre reinforced epoxy laminates, exp. determ. of nonlinear shear behaviour 0-66575  
 glass fibre reinforced epoxy-phenolic, cyclically deformed under shear, energy dissipation, static tensile-compressive stress effect 0-104225  
 glass fibre reinforced nylon, design parameters, fibre orientation effect 0-81141  
 glass fibre reinforced plastic, cemented joint of cylindrical shell with cover, stressed state 0-69668  
 glass fibre reinforced plastic, fracture dynamics 0-100906  
 glass fibre reinforced plastic, woven-roving type, high-speed punching, failure mechanisms 0-85143  
 glass fibre reinforced plastic laminates, strength and deformability, artificial ageing effect 0-60893  
 glass fibre reinforced plastics, ageing by boiling in water, effect on physico-mech. props. 0-60892  
 glass fibre reinforced plastics, cylindrical shells, compressive and flexural strength (*Japanese*) 0-81115  
 glass fibre reinforced polycarbonate, design parameters, fibre orientation effect 0-81141  
 glass rod, optimum sample shape for compression testing, failure 0-71756  
 glass shell, cylindrical, bearing capacity under axial compression 0-76323  
 glass-fibre reinforced cement, strength study by reliability concept, fibre concept and temp. depend. (*Japanese*) 0-66586  
 Hastelloy-X, low cycle fatigue crack propagation at 25°C and 760°C 0-104270  
 heteromodal materials, stress strain correls. 0-87716  
 high strain rate behaviour, incremental elastic-viscoplastic constitutive eqns. integration 0-85138  
 high strain rate mechanical properties, conf., Oxford, England (Mar. 79) 0-82575  
 hysteresis properties of nonlinear nonideally elastic materials (*Russian*) 0-90675  
 ice, plastic deformation, ultrasonic wave attenuation by dislocations (*French*) 0-59564  
 inelastic deformation, stiff constitutive models, numerical integration 0-96208  
 inorganic glass, effect of liq. medium on process of mechanical destruction 0-89283  
 isotropic stable media, stress tensors and creep-strain rates correl. 0-87722  
 laminated anisotropic shells, nonlinear eqns. of Timoshenko-type theory 0-69669  
 laminates, thin, optimal struct. and strength in two-dimens. stress state 0-64395  
 limestone tubes, dynamic torsional failure obs. 0-85648  
 metal, notched, cyclic stress/strain behaviour, random fatigue life (*German*) 0-100907  
 metal, single crystal, dislocation loop formation, during deformation in quantising mag. fields (*Russian*) 0-103354  
 metal, strong, compressive stress/strain props. meas. at very high strain rates, modified Hopkinson bar system 0-85128  
 metal rods, stress state and fracture in pulsed mag. field 0-81201  
 metallic shell, explosive expansion, rupture behaviour 0-85063  
 metals, inelastic cyclic strain under nonuniform stress state conditions, residual stresses effect 0-81132  
 metals, polycrystn., creep damage and cavity growth, assessment using density meas. 0-104217  
 metals and alloys, strain rate history, endochronic theory of viscoplasticity 0-65122  
 metals during settling, technique using rotation of thin layer (*Russian*) 0-97529  
 Mylar film/adhesive/Al foil laminate, mech. interactions 0-81112  
 nonlinear anisotropic medium 0-98800  
 1-nylon polymers, stress-strain curve 0-60938  
 piecewise-homogeneous plate with slits on elliptic line separating materials 0-99932  
 plastic deform., generalised constitutive eqns. 0-104219

## stress/strain relations continued

plastic fracturing materials, work inequalities and stress-strain relations 0-103000  
 plastic wave theory, comparison of predictions with impact expts. 0-83742  
 plates, rectangular cross-ply laminated, with nonlinear stress-strain behaviour, buckling 0-64415  
 plates, thick, multiply connected, stressed-strain state under nonstationary heat conditions (*Russian*) 0-87714  
 plates and slabs, perforated (*Russian*) 0-74728  
 PMMA, crazing, deform. kinetics 0-84990  
 PMMA, glassy atactic, thermodynamic analysis of plastic deform. modes, 150 to 330K 0-84999  
 PMMA, large deforms. at tip of running crack, opt. interference obs. 0-85062  
 polyacetylene films, tensile props. and partial alignment 0-104210  
 1,2-polybutadiene, crosslinked in states of strain, entanglement networks, swelling anisotropy obs. 0-79666  
 1,2-polybutadiene crosslinked in strain states; entanglement networks, stress-birefr. relations 0-66590  
 polycarbonate, amorphous, yield behaviour in oriented and unoriented condition, effect of temp. 0-97537  
 polycarbonate, rigid plastic, yield behaviour (*Japanese*) 0-93620  
 polycrystalline metals, effect of grain boundary sliding on steady creep 0-96590  
 polycrystals, elastic stress and strain microinhomogeneity, finite element method 0-79155  
 polydimethylsiloxane, crosslinked, stress/strain relations from large compression to high elongation 0-66589  
 polydimethylsiloxane, end-linked chains, model elastomeric networks, Gaussian, nonGaussian and ultimate props. 0-103260  
 polydimethylsiloxane chains, end-linked, swollen model networks, stress/strain isotherms and elastic modulus 0-79668  
 polymeric materials, thin-wall tubes, rupture time determ. 0-64473  
 polypropylene, crystalline, yield behaviour in oriented and unoriented condition, effect of temp. 0-97537  
 polypropylene fibrillated film reinforced cement matrix for low cost sheeting 0-80996  
 polystyrene, cyclically deformed under shear, energy dissipation, static tensile-compressive stress effect 0-104225  
 porous metals, plasticity, stress-strain curves, yield stresses, strain vectors 0-83738  
 powder metallurgy, fatigue strength significance (*German*) 0-60946  
 precipitate and dislocation loop strain and stress field calcs. using affine transformations 0-106722  
 PTFE, stress-time analogy under shear and hydrostatic pressure in creep regime 0-104227  
 PVC, crazing, deform. kinetics 0-84990  
 PVC, rigid plastic, yield behaviour (*Japanese*) 0-93620  
 relaxation modulus, evaluation from response to constant strain rate followed by constant strain 0-74765  
 ribbed plates with large openings, design optimisation, finite element anal. appl. 0-87724  
 rigid-plastic medium, ideal, surface force strength lower limit under plain strain 0-99937  
 shell, cylindrical, three-layered, stress-strain state (*Russian*) 0-90677  
 shell, rotating, stress-strain state for random loading, numerical soln. (*Russian*) 0-90676  
 shell of revolution, orthotropic, thick, stress-strained state, finite element method (*Russian*) 0-87713  
 sitall cylindrical shell reinforced with internal stiffening ribs, stress-strain state under external press. 0-71684  
 split Hopkinson pressure bar application to fracture dynamics 0-85140  
 steel, austenitic stainless, type 304, cyclic creep during unbalanced tension-compression loading at elevated temp. 0-97545  
 steel, austenitic stainless, type SUS 304, low cycle fatigue strength reduction factor (*Japanese*) 0-104259  
 steel, austenitic stainless SUS 301, stress corrosion cracking susceptibility, effect of strain-induced  $\alpha'$ -martensite (*Japanese*) 0-104335  
 steel, austenitic stainless type SUS 316, low cycle fatigue tests, freq. effect on notch sensitivity at elevated temps. (*Japanese*) 0-104260  
 steel, C, crack initiation and propagation life under repeated impact tensile loads (*Japanese*) 0-104264  
 steel, C, type SFV1, low cycle fatigue strength reduction factor (*Japanese*) 0-104259  
 steel, cast, SC49, rel. between rotating and flexural bending strengths (*Japanese*) 0-81117  
 steel, cast automatic couplings, yield strength, crack propag. resistance and ductile-brittle transition temp. 0-104281  
 steel, Cr-Mn, strain hardening, 4.2 to 293K 0-81076  
 steel, Cr-Ni, strain hardening, 4.2 to 293K 0-81076  
 steel, low alloy-high strength, deforms. during cold crack developments in welded joints 0-81142  
 steel, low C, fatigue life, variable strain ranges (*Czech*) 0-60956  
 steel, low C, type En3, high strain deform., struct. and props. 0-89301  
 steel, medium C, microflow and strain hardening under cyclic loading 0-104182  
 steel, mild, plastic flow localisation under dynamic torsional loading, crit. variables 0-85015  
 steel, Ni-Cr-Mo, cyclic creep under increasing stress condition, constitutive eqn. 0-93593  
 steel, pearlitic, wear behaviour rel. to basic material props. 0-108592  
 steel, stainless, austenitic, dynamic uniaxial and biaxial stress-strain relationships 0-81122  
 steel, stainless, type 304, viscoplastic behaviour, strain rate sensitivity, creep, relaxation, tensile tests 0-66727  
 steel, stainless, type 304, viscoplastic model, uniaxial, based on total strain and overstress 0-64387  
 steel, stainless 304 sol. of annealed and thermally-aged, high-cycle fatigue behaviour 0-100923  
 steel, SUS 304 and S15C, creep deform. under reversed cyclic stresses (*Japanese*) 0-81114  
 steel, type SAE 1008, finite fatigue life distrib., various load-time histories 0-97589  
 steel, types S25C and S45C surface damage produced by pulsating impact contact load (*Japanese*) 0-104263  
 steel, weldable, fatigue data, low and high cycle compatibility (*Czech*) 0-89343  
 stiff bending plates, stress-strain states, finite element effectiveness, polynomial approx. (*Russian*) 0-58921



**stress/strain relations continued**

- structural deformation under dynamic loading, state variable description of material behaviour 0-85137  
 superplastic flow, activation enthalpy determ. from strain rate changes in tensile tests 0-81127  
 three-layer cylindrical shells, thermoplastic stress state 0-96204  
 tubes, thick-walled, thermoelastoplastic creep stress anal. 0-58922  
 viscoelastic bar, transient wave propag. 0-106745  
 Zircaloy, annealed, neutron irradiated, inhomogeneous deform. behaviour 0-85014  
 Zircaloy, textured, interactive creep and growth, upper-bound evaluation 0-89293  
 Zircaloy, unirrad., stress corrosion cracking, I<sub>1</sub>-induced, effect of test temp., alloy comp. and heat treatment 0-97632  
 Zircaloy-2, pressure tubes, irradiat. creep and growth, anisotropy factors 0-97536  
 Al alloy, crack initiation at high strain rates, uniaxial and biaxial tests 0-85141  
 Al, commercially pure, stress-strain curves, cyclic loading initial stage (*Japanese*) 0-93617  
 Al notched bars, deform. behaviour and strength having biaxial state of stress at notch root (*Japanese*) 0-81116  
 Al single crystals, {100} oriented, deform. temp. effect on stage IV deform. (*Japanese*) 0-66587  
 Al, ultimate tensile strength for brief impact 0-70309  
 Al-Cu-Mg/mica particulate composite mech. props. 0-100919  
 Al-Cu(Mg), low freq. internal friction during plastic deform. (*Chinese*) 0-103420  
 Al-Mg, dynamic uniaxial tension and compression curves 0-100884  
 Al-Mg-Si, type 6010, microstruct. characts. influence on formability, heat treatment 0-81090  
 Al-Ni (6 wt.%), fine-grained, deform. in tension and torsion 0-85008  
 Al-Ni(Cd)(Fe)(Si), cold worked, struct. and props. 0-71666  
 Al-Zn-Mg, type V-95, ultimate tensile strength for brief impact 0-70309  
 AlN, polycrystalline, stress-strain data up to 1.25 GPa 0-100899  
 Al<sub>2</sub>O<sub>3</sub>, polycrystalline, stress-strain data up to 1.25 GPa 0-100899  
 Al<sub>2</sub>O<sub>3</sub>-SiO<sub>2</sub> (3 wt.%), J-integral meas. at high temps. (*German*) 0-93624  
 BeO, polycrystalline, stress-strain data up to 1.25 GPa 0-100899  
 Bi, crit. resolved shear stress of two slip systems, compression tests, 77-538 K 0-59470  
 Bi<sub>2</sub>MoO<sub>6</sub>, superplasticity during phase transitions 0-108498  
 Bi<sub>2</sub>WO<sub>6</sub>, superplasticity during phase transitions 0-108498  
 C fibre reinforced composite, split Hopkinson press. bar test, opt. and strain gauge methods comparison 0-85132  
 C fibre reinforced nylon, design parameters, fibre orientation effect 0-81141  
 C fibre reinforced polycarbonate, design parameters, fibre orientation effect 0-81141  
 Cu, dynamic uniaxial tension and compression curves 0-100884  
 Cu, high-purity, grain size and strain rate influence on mech. behaviour, precursors existence 0-85016  
 Cu, polycrystn., strain localisation during hot deform. 0-104195  
 Cu, single crystals., deformed in [001] and [111] axes, cell structs., TEM 0-70209  
 Cu-Cd (1.0 wt.%), yield stress and flow stress 0-97524  
 Cu-Cr (0.75 wt.%), deformation characts., fully reversed cyclic strain with fatigue cracks and dislocation struct. 0-81148  
 Cu-Sn (4.9 wt.%), role of mech. twinning on stress/strain behaviour 0-85004  
 Cu<sub>3</sub>Au, disordered [001]-orientated single crystals., plastic deform., TEM and slip line studies 0-97541  
 $\beta$ -CuZn, acoustic emission rel. to stress induced martensitic transformation 0-81061  
 Fe, Armco, microflow and strain hardening under cyclic loading 0-104182  
 Fe, cast flake and nodular, rupture strength, circumferential notch (*Japanese*) 0-93649  
 Fe, pure, cathodic charging effect on creep and tensile deformation 0-76320  
 Fe-N, single cryst., solid soln. softening, effect of interstitial N 0-97496  
 Fe-Si, microflow and strain hardening under cyclic loading 0-104182  
 Fe<sub>40</sub>Ni<sub>40</sub>P<sub>14</sub>B<sub>6</sub>, metallic glass, bending tests, evidence of ideal elastic-plastic deform. 0-97543  
 InP single crystals, uniaxial compression deform. characts. 0-84991  
 K(D,H<sub>1</sub>)<sub>2</sub>(SeO<sub>3</sub>)<sub>2</sub>, ferroelastic, anelastic and elastic infra-low freq. props. 0-70304  
 Mo polycrystn., cyclically deformed, dislocation arrangements 0-108506  
 Mo-Cr-V-P, load curves, structure states boundaries and strain hardening (*Russian*) 0-89241  
 Mo-Ti (3.5 wt.%), load curves, structure states boundaries and strain hardening (*Russian*) 0-89241  
 Nb-O system, solid soln. hardening and softening 0-71665  
 Nb<sub>3</sub>Sn, hot isostatically pressed, plastic deform. 0-108510  
 Ni, polycrystalline, strain hardening, dislocation link length model 0-84953  
 Ni single crystal, compressed, strengthening and dislocation cells (*German*) 0-66536  
 Pd<sub>82</sub>Si<sub>18</sub>, stress/strain rate depend. of homogeneous flow 0-71687  
 239PuO<sub>2</sub>, stoichiometric, high-temp. deformation 0-81111  
 Si, crack-tip dislocation pattern, X-ray topography (*French*) 0-107253  
 Te, strained and unstrained, SHG and propag. of CO<sub>2</sub> laser radiation 0-58641  
 Te-Ag thin film system, stress-relief appearance conditions 0-65416  
 Te-Bi thin film system, stress-relief appearance conditions 0-65416  
 Ti, fast neutron irradiat., twinning deform. at room temp. 0-65061  
 Ti, polycrystal, discontinuous electrical resistivity, low temp. active strain-  
 ing (*Russian*) 0-103666  
 $\alpha$ - $\beta$  Ti Widmanstätten alloy interfaces, elastic interact. stresses, effect on plastic flow onset 0-104218  
 $\alpha$ -U, mech. props. at very high strain rates, double-notch shear test use 0-85131  
 $\alpha$ -U, strain rate effect on tensile flow and fracture 0-84992  
 Zn, pure single cryst., fracture stress 0-104269  
 Zr alloys, creep and growth, irradiation induced, rate theory approach 0-89294  
 Zr-Al (8.6 wt.%), fast neutron irradiated, tensile props. and fracture toughness 0-84994  
 Zr-Nb (2.5 wt.%), pressure tubes, irradiat. creep and growth, anisotropy factors 0-97536
- stresses, internal** *see internal stresses*  
**stretch receptors** *see mechanoreception*  
**striations** *see discharges (electric)*  
**striking** *see impact (mechanical)*  
**strip line components**  
 microstrip microwave biological exposure system 0-89924  
 SAW multistrip coupler, superposition model 0-74674  
 two-dimensional wave beam diffraction by stripline grid 0-87273  
**strip lines**  
 dielectric small standing wave ratio and losses meas. 0-77811  
 optical stripline waveguides, dispersion characts. and radiation fields 0-64155  
 semiconductor, submillimetric magneto-optical props., strip line technique 0-60554  
**stripping reactions**  
 double stripping core independ. 2-nucleon transfer, Tang-Herndon effective interactions, ( $\alpha$ ,d), (t,p) 0-73836  
 heavy ion stripping and pickup reactions on closed shell nuclei, level shifts, DWBA 0-91168  
<sup>40</sup>Ca(<sup>11</sup>B,<sup>10</sup>B), 51.5 MeV, n stripping, DWBA anal. with Woods-Saxon and double folding optical pots. 0-102171  
 Hd( $\alpha$ ,t), <sup>147</sup>Pm, A=143-153, odd-A, spectroscopic factors, shell model anal. 0-78137  
 Nd(<sup>2</sup>He,d), <sup>147</sup>Pm, A=143-153, odd-A, spectroscopic factors, shell model anal. 0-78137  
<sup>20</sup>Ne(d,pol,p), 10 MeV, <sup>21</sup>Ne deduced spectroscopic factors, levels and anal. powers 0-83087  
<sup>16</sup>O(d,X), X=d or N, elastic scatt. and stripping, three body calc. 0-91165  
<sup>208</sup>Pb(<sup>11</sup>d,d), 90 MeV, alpha-cluster transfer from alpha-decaying nuclei 0-91166  
<sup>147</sup>Pm, A=143, 145, proton states and transitions, stripping strength, shell model anal. from Nd(<sup>2</sup>He,d) 0-68508  
<sup>28</sup>Si(<sup>3</sup>He,<sup>2</sup>He), 52 MeV, <sup>28</sup>Si levels, J<sup>+</sup>, spectroscopic factor, DWBA anal. 0-86811  
<sup>28</sup>Si(d,pn), <sup>29</sup>P and <sup>29</sup>Si nucleon unbound states, spin, parity, partial width 0-102118  
**stroboscopes**  
*see also velocity measurement*  
 particle size distribution meas., online stroboscopic microscope apparatus 0-101783  
 sampling stroboscopic convertor identification by Hammerstein model (*Russian*) 0-74495  
 strobe light with variable pulse length over 22-360 Hz frequency range 0-58716  
**strong-coupling superconductors**  
 electronic density of states, variation effect on transition temp. and effective mass. 0-75672  
 Cu<sub>1-x</sub>Mo<sub>x</sub>S<sub>2</sub>, electron tunnelling spectroscopy expts. (*German*) 0-107966  
 Nb, proximity electron tunnelling spectroscopy 0-107964  
 Nb, upper crit. field, temp. depend. and anisotropy 0-80462  
 PbMo<sub>6</sub>, electron tunnelling spectroscopy expts. (*German*) 0-107966  
 Ti films, supercond. amorphous, effective phonon spectrum and lattice sp. ht. 0-70895  
**strong interactions, elementary particle** *see elementary particle strong interactions*  
**strontium**  
*see also nuclei with .....*  
 adsorption by Al<sub>2</sub>O<sub>3</sub>, radioactive waste storage 0-99240  
 atomic quasi-Landau spectrum, semiclassical strong field mixing models 0-63847  
 atoms, excitation series, potential barrier effects, single configuration HFC 0-78558  
 atoms, fluoresc. excitation profile, laser saturation broadening in flames 0-95568  
 atoms, quantum defect param., ab initio calcs. 0-78525  
 basalt isotopic abundance, Earth struct. models 0-72475  
 Duxbury massif (2.5 Ga), Quebec, initial <sup>87</sup>Sr/<sup>86</sup>Sr rel. to remobilised pre 3.0 Ga sialic basement hypothesis 0-76970  
 Earth mantle, Nd-Sr isotope correl. and constraints on continental crust comp. and nature of lower crust 0-94498  
 forced-flow chromatography, detection by photometric method 0-71965  
 four-wave mixing production of CW VUV coherent radiation 0-58640  
 granitoid rocks, Nd-Sr isotopic relationship and continental crust development, chemical approach to orogenesis 0-94522  
 low-level transuranic storage, radwaste Sr, Cs, Co sorption meas. on soil sediment 0-95482  
 superradiant emission, visible, on three-level cascade, coupled transitions 0-58493  
 Eu+Sr, laser induced collisional energy transfer profile, high resolution study 0-83471  
 He-Sr laser, possibility of nucl. pumping, 4305 Å Sr II transition 0-58518  
 KBr(Cl):Sr<sup>2+</sup>:Cu<sup>+</sup>, thermolum. response, extension of two-step reaction model 0-89075  
 KCl cryst., Sr and Na impurities radial distrib., influence of form of crystn. front 0-107312  
 KCl:Sr, positron annihilation and trapping in A-centres 0-84802  
 KCl:Sr crystal, Z<sub>4</sub> colour centre, luminesc. study 0-64993  
 KCl:Sr<sup>2+</sup>, defect parameters, self-consistent set, ionic cond. meas. 0-107487  
 KCl:Sr<sup>2+</sup>, ionic cond., defect parameters, diffusion coeffs. 0-79978  
 NaCl:Sr, positron annihilation and trapping in A-centres 0-84802  
 Sr atomic beam, time correlations between two sidebands of reson. fluoresc. triplet, multiphoton processes 0-95570  
 Sr-Cs mixture, laser induced collisional two-photon ionisation, fluoresc. monitoring 0-91515  
 Sr+Eu absorptive collisional energy transfer, laser induced excitation spectra 0-63584  
 Sr+HF, endothermic reaction, comparison of effectiveness of vibr. and translational excitation 0-93746  
 Sr+inert gas, <sup>1</sup>P<sub>1</sub>-<sup>3</sup>P<sub>1</sub> excitation transfer 0-102559  
 Sr<sub>2</sub> dimer, photoassoc., photoluminesc., collisional dissociation 0-58303  
<sup>85</sup>Sr, uptake in healing bone fracture rel. to blood flow 0-72187  
<sup>85</sup>Sr, use in revascularisation processes study, local blood flow dynamic anal. 0-81684  
<sup>87</sup>Sr/<sup>86</sup>Sr, initial ratios in Archaean rocks of English River subprovince, NW Ontario rel. to crust form. 0-94486

## strontium continued

- <sup>87</sup>Sr/<sup>86</sup>Sr, ratios in Cretaceous mid-ocean ridge basalt (MORB) from DSDP Holes 417D and 418A 0-94520  
<sup>87</sup>Sr/<sup>86</sup>Sr in Bay of Islands ophiolite complex, rel. to midocean ridge basalts source evolution 0-85651  
<sup>87</sup>Sr/<sup>86</sup>Sr in Kerguelen Islands igneous rocks, inferences on enriched oceanic mantle sources 0-98319  
<sup>87</sup>Sr/<sup>86</sup>Sr in mantle xenoliths, unequilibrated isotopic comp. meas. with equilibrated Nd isotopes 0-98321  
<sup>87</sup>Sr/<sup>86</sup>Sr in Norwegian eclogites, rel. to crustal origin 0-76978  
<sup>87</sup>Sr/<sup>86</sup>Sr in Scottish Caledonian granites, isotopic evidence for crustal provenance 0-109146  
<sup>87</sup>Sr/<sup>86</sup>Sr initial ratios and Rb-Sr ages, from Oxford Lake-Knee Lake greenstone belt, N. Manitoba 0-94485  
<sup>87</sup>Sr/<sup>86</sup>Sr ratios in calc-alkaline volcanic rocks from Cerro Galan, NW Argentina, evidence for crustal contamination 0-98318  
<sup>90</sup>Sr bremsstrahlung radiation meas. for well logging using Ge spectrometer 0-94619  
<sup>90</sup>Sr concentrations in pronghorn antelope bones near a nuclear fuel reprocessing plant 0-89875  
Sr\*+HCl, reaction performed under high resolution, luminescence obs. 0-95662

## strontium alloys

- see also strontium compounds  
Sr<sub>2</sub>(Co<sub>1-x</sub>M<sub>x</sub>)<sub>7</sub>, M=Mn, Ti, Zr, powders, influence of substitutes on mag. props. 0-100601  
SrCu, X-ray cryst. struct. determ. 0-92478  
SrPdSn<sub>3</sub>, prep. and crystal structure (German) 0-84138

## strontium compounds

- see also strontium alloys  
ferrite, hexagonal, with M, W and Y structures containing Fe<sup>2+</sup> and Fe<sup>3+</sup> mag. ions, saturation moment and anisotropy 0-71009  
ferrite, plastic magnet appl. based on moulding ferromagnetic powder material with plastics (Japanese) 0-60829  
halides, XY<sub>4</sub> molecules, force consts. by modified Redington and Aljibury method 0-69261  
maleate tetrahydrate, cryst. struct., H-bonding scheme 0-96505  
monochalcogenides, electronic energy band struct., APW calcs. 0-65439  
perovskite compound combination, Mossbauer spectroscopy study (Russian) 0-80666  
perovskites, A<sup>2+</sup>B<sup>3+</sup>U<sup>5+</sup><sub>1/6</sub>O<sub>6</sub>, struct., cation vacancies, X-ray diff. study (German) 0-107147  
Al<sub>2</sub>O<sub>3</sub>:SrTiO<sub>3</sub>, sintering temperature effect of titanate additions 0-60808  
(Ba,Sr)TiO<sub>3</sub>, ferroelec. props., press. depend., anharmonic oscillator model 0-80716  
BaSrCa<sub>1-x</sub>Fe<sub>2</sub>O<sub>6</sub>, substituted hexagonal ferrites, mag. split Mossbauer spectra obs. and X-ray struct. data 0-71250  
Ba<sub>0.6</sub>Sr<sub>0.4</sub>Nb<sub>2</sub>O<sub>6</sub>, electronic props. and photoresponses 0-92925  
Ba<sub>0.8</sub>Sr<sub>0.2</sub>Nb<sub>2</sub>O<sub>6</sub>, photoelectric states in real time spatial light modulators, photorefractive effect 0-80676  
Ba<sub>0.8</sub>Sr<sub>0.2</sub>Nb<sub>2</sub>O<sub>6</sub>:Ce, pure and doped, photoelec. props. and photorefractive 0-60538  
Ba<sub>0.8</sub>Sr<sub>0.2</sub>TiO<sub>3</sub> films, DC conductivity, strong microwave field effect 0-65727  
Ba<sub>0.8</sub>Sr<sub>0.2</sub>TiO<sub>3</sub>, ferroelec. film, heteroepitaxial growth in cathode sputtering 0-93486  
Ba<sub>2-x</sub>Sr<sub>x</sub>TiSi<sub>2</sub>O<sub>8</sub>, piezoelec. crystals, SAW charact. 0-84354  
(Ca,Sr)<sub>2</sub>(PO<sub>4</sub>)<sub>2</sub>Cl, partially substituted chlorapatite, cryst. struct. from X-ray data 0-96478  
CaO-SrO-Fe<sub>2</sub>O<sub>3</sub> system, phase relations, Sr hexaferrite field occurrence 0-93545  
Ca<sub>1-x</sub>Sr<sub>x</sub>Y<sub>2</sub>Ba<sub>2</sub>Zr<sub>1-x</sub>Ti<sub>x</sub>O<sub>10</sub>, ceramic system, dielectric props., microwave resonator application 0-80674  
Ca<sub>1-x</sub>Sr<sub>x</sub>F<sub>2</sub>:Er<sup>3+</sup> mixed crystal, luminesc. transition, inhomogeneous line broadening calc. 0-97332  
Ca<sub>10-x</sub>Sr<sub>x</sub>(PO<sub>4</sub>)<sub>6</sub>(OH)<sub>2</sub>, continuous cation migration, IR spectra study 0-93297  
Cd<sub>1-x</sub>Sr<sub>x</sub>S, solid soln., phase equilb. diagrams 0-108412  
Eu-Sr-S, spin glass materials, mag. field dependence of susceptibility peak 0-103840  
Eu<sub>0.8</sub>Sr<sub>0.2</sub>S, spin glass, spin dynamics, neutron scatt. study 0-65907  
Eu<sub>0.8</sub>Sr<sub>0.2</sub>S, Heisenberg spin glass system, excitations 0-84610  
Eu<sub>0.8</sub>Sr<sub>0.2</sub>S, insulating spin glass, sp. ht. near ferromag. onset 0-97106  
Eu<sub>0.8</sub>Sr<sub>0.2</sub>S, mag. clusters, spinodal decomp. trend 0-65923  
Eu<sub>0.8</sub>Sr<sub>0.2</sub>S, mag. ordering in dil. Ising and Heisenberg systems with competing interactions 0-65914  
Eu<sub>0.8</sub>Sr<sub>0.2</sub>S, paramag. susceptibility, expt. and comparison with high temp. series expansion 0-60176  
Eu<sub>0.8</sub>Sr<sub>0.2</sub>S, spin glass, spin wave modes and low temp. sp. ht. 0-80538  
Eu<sub>0.8</sub>Sr<sub>0.2</sub>S, spin glass, transition temp., freq. depend. 0-97113  
Eu<sub>0.8</sub>Sr<sub>0.2</sub>S, spin glass to ferromag. transition, neutron scatt. and susceptibility meas. 0-60254  
Eu<sub>0.8</sub>Sr<sub>0.2</sub>S, spin-glass props. and mag. transition 0-97105  
(Eu,Sr)<sub>1-x</sub>S, transferred hyperfine fields, NMR 0-71196  
(Eu,Sr)<sub>1-x</sub>S, very dil., magnetisation dynamics 0-65915  
La<sub>1-x</sub>Sr<sub>x</sub>CoO<sub>3</sub> (0.5≤x≤0.9), ferromag., elec. props., itinerant electron model 0-107785  
La<sub>2-x</sub>Sr<sub>x</sub>CoO<sub>4</sub>, mag. behaviour obs. 0-70971  
La<sub>2-x</sub>Sr<sub>x</sub>VO<sub>3</sub>, Anderson transition, elec. resist. and thermopower meas. 0-100488  
NaF-SrF<sub>2</sub>-CrF<sub>3</sub>, glass transition, crystn. and melting temps., optical transmission (French) 0-64910  
(Pb,Sr)<sub>2</sub>Ge<sub>2</sub>O<sub>11</sub>, single crystals, growth and X-ray and dielec. investigations 0-88127  
(Pb,Sr)TiO<sub>3</sub>, ferroelec. props., press. depend., anharmonic oscillator model 0-80716  
Pb<sub>0.9</sub>Sr<sub>0.1</sub>(Zr,Ti,Nb)<sub>2</sub>O<sub>12</sub>, hydrophone ceramic, effect of one-dimensional uniaxial stress 0-80705  
Pb<sub>0.9</sub>Sr<sub>0.1</sub>(Zr<sub>x</sub>Ti<sub>1-x</sub>)O<sub>3</sub>-Nb<sub>2</sub>O<sub>5</sub>, phase coexistence range, lattice consts. 0-92680  
SiO<sub>2</sub>-Al<sub>2</sub>O<sub>3</sub>-CaO-BaO-SrO-ZnO-Na<sub>2</sub>O-K<sub>2</sub>O-B<sub>2</sub>O<sub>3</sub>, glaze effect of P<sub>2</sub>O<sub>5</sub> additions 0-60824  
Sr Nb<sub>2</sub>O<sub>6</sub>, crystallography, polymorphism and isomerism, X-ray diff. and DTA study 0-100216  
Sr-H system, equilb. H<sub>2</sub> press., enthalpies of soln. and formation determ. 0-107428  
SrB<sub>2</sub>O<sub>4</sub>:Eu<sup>2+</sup>, luminesc. of high-pressure phases 0-100680  
SrBaNaNb<sub>2</sub>O<sub>12</sub>, X-ray powder diffraction data determ. (Chinese) 0-70170  
Sr<sub>0.5</sub>Ba<sub>0.5</sub>Nb<sub>2</sub>O<sub>3</sub> piezoelectric transducer, SAW props. 0-79037

## strontium compounds continued

- Sr<sub>0.75</sub>Ba<sub>0.25</sub>Nb<sub>2</sub>O<sub>6</sub>, ceramic ageing, dielec. props. 0-88940  
Sr<sub>1-x</sub>Ba<sub>x</sub>Nb<sub>2</sub>O<sub>6</sub> crystals, defect-free growth 0-108346  
Sr<sub>1-x</sub>Ba<sub>x</sub>Nb<sub>2</sub>O<sub>6</sub>, photorefractive in space charge field, phase transitions 0-97229  
Sr<sub>0.8</sub>Ba<sub>0.2</sub>Nb<sub>2</sub>O<sub>6</sub>, appl. in sub-100 ps pyroelec. detectors, 10.6 μm damage threshold meas. 0-77859  
Sr<sub>0.9</sub>Ba<sub>0.1</sub>Nb<sub>2</sub>O<sub>6</sub>, domain struct. influence on electrooptical props. 0-93283  
Sr<sub>0.8</sub>Ba<sub>0.2</sub>Nb<sub>2</sub>O<sub>6</sub>, high press. phase transitions, Raman scatt. studies 0-71402  
SrBr<sub>2</sub>, aq. solns., EXAFS meas. 0-60714  
SrCl<sub>2</sub>, anion disorder at high temps., neutron diff. obs. 0-59614  
SrCl<sub>2</sub>, anion motion at high temps., quasielastic neutron scatt. obs. 0-59715  
SrCl<sub>2</sub>, fast ion cond., specific heat anomaly, mol. dynamics study 0-65283  
SrCl<sub>2</sub>, fast ion transport 0-107558  
SrCl<sub>2</sub>, in-activated, luminescence studies at 77 and 300K 0-108247  
SrCl<sub>2</sub>, ionic cond., activation volumes and high press. phase transitions 0-70461  
SrCl<sub>2</sub>, ionic cond., self-diffusion, rel. to defect motion, mol. dynamics study 0-65282  
SrCl<sub>2</sub>, mass and charge transport 0-100347  
SrCl<sub>2</sub>, point defect parameters, ionic cond. study 0-107490  
SrCl<sub>2</sub>, pure and doped, disorder and defect props. 0-107217  
SrCl<sub>2</sub>, self-diffusion and ionic cond. 0-107489  
SrCl<sub>2</sub>, sp. ht. meas., Schottky-type diffuse phase transitions, defect form. energies and entropies 0-107441  
SrCl<sub>2</sub>:Cu<sup>2+</sup>, exciton bands, optical absorpt. and MCD spectra 0-80821  
SrCl<sub>2</sub>:Eu<sup>2+</sup>, fluorescence lifetime and quantum efficiency for 5d-4f transitions 0-100681  
SrCl<sub>2</sub>:Gd<sup>3+</sup>, hyperfine interaction, X-band ENDOR 0-60457  
SrCl<sub>2</sub>.6H<sub>2</sub>O:Gd<sup>3+</sup>, evaporation technique prep. of SrCl<sub>2</sub>:Gd<sup>3+</sup>, H<sub>2</sub>O content, EPR powder spectrum obs. 0-60416  
SrCoO<sub>3-x</sub> (0<x<0.5), ferromag., metallic elec. props. 0-70668  
SrCoO<sub>3-x</sub>, mag. and neutron diff. study 0-65805  
SrF<sub>2</sub>, doped with trivalent rare earths, migration entropy for bound fluorine motion 0-71303  
SrF<sub>2</sub>, high-frequency phonon lifetimes 0-70338  
SrF<sub>2</sub>, ionic cond., activation vols., freq. depend. cond., press. effects 0-100354  
SrF<sub>2</sub>, optical detection of acoustic phonons at THz freqs. 0-75320  
SrF<sub>2</sub>, strain induced splitting and oscillator strength anisotropy of IR transverse optic phonon 0-92625  
SrF<sub>2</sub>, thermal props. (German) 0-81355  
SrF<sub>2</sub>, thin film, optical props., spectral dependence, 460-1000 nm 0-76094  
SrF<sub>2</sub>, UPS and XPS spectra, rel. to optical props. 0-66386  
SrF<sub>2</sub>, vaporisation and sublimation thermodynamics (German) 0-81355  
SrF<sub>2</sub>:Ce<sup>3+</sup>, cryst. field energies 0-59941  
SrF<sub>2</sub>:Dy<sup>3+</sup>, cluster form., IR absorption study (French) 0-108240  
SrF<sub>2</sub>:Eu<sup>2+</sup>, fluorescence lifetime and quantum efficiency for 5d-4f transitions 0-100681  
SrF<sub>2</sub>:La, type-I dipole reorientation, activation vol. determ. from dielec. const. 0-88916  
SrF<sub>2</sub>:La<sup>3+</sup>, thermal depolarisation of La<sup>3+</sup>-F<sup>-</sup> defect dipoles 0-75926  
SrF<sub>2</sub>:Ni, X-irradi., optical absorpt. spectra and dichroism meas. 0-108239  
SrF<sub>2</sub>:Pb<sup>2+</sup>, band struct., Jahn-Teller effect, UV luminesc. and optical absorpt. spectra 0-66243  
SrF<sub>2</sub>:rare earth ion, elec. dipole-dipole interaction, ionic thermocurrent and EPR study 0-108060  
SrF<sub>2</sub>:LaF<sub>3</sub>, tentative phase diagram 0-71633  
SrFCl, thermolum. and optical absorption spectra 0-66309  
SrFCl:Eu<sup>2+</sup>, fluorescence lifetime and quantum efficiency for 5d-4f transitions 0-100681  
SrFe<sub>2</sub>Al<sub>2</sub>O<sub>19</sub>, thin film LPE growth and mag. props. 0-80992  
SrFe<sub>12-x</sub>Cr<sub>x</sub>O<sub>19</sub>, hexagonal ferrite series, Mossbauer study 0-71258  
SrFe<sub>2</sub>Ga<sub>2</sub>O<sub>19</sub> ferrite, mag. struct., Mossbauer study 0-93087  
SrFe<sub>2</sub>O<sub>19</sub>, Ca<sup>2+</sup> additives effect on hexaferrite lattice and mag. props. 0-60243  
SrFe<sub>2</sub>O<sub>19</sub>:Si, Sr, second phase effect on elec. and mag. props. 0-60986  
SrFe<sub>2</sub>Ta<sub>2</sub>O<sub>19</sub>, Mossbauer and X-ray diff. studies 0-103905  
Sr<sub>2</sub>Gd<sub>1-x</sub>Tb<sub>x</sub>GaO<sub>5</sub>, Gd<sup>3+</sup>-Tb<sup>3+</sup> energy transfer, emission and excitation spectra (French) 0-84770  
Srl, low-lying electronic states, vibr. anal. 0-106315  
Sr(IO<sub>3</sub>)<sub>2</sub>, complex salts, phase transitions, cryst. struct. (Chinese) 0-70171  
SrI<sub>2</sub>Se<sub>4</sub>, cryst. struct. (German) 0-79760  
SrLaFeO<sub>4</sub>, two-dimens. mag. props. rel. to cryst. struct. 0-75776  
Sr<sub>0.5</sub>La<sub>1.5</sub>Li<sub>0.5</sub>Fe<sub>0.5</sub>O<sub>4</sub>, high spin configuration stabilisation for Fe<sup>4+</sup> (French) 0-88519  
Sr<sub>2</sub>Mg(Co)(Zn)(Mn)(Cd)(Sr)TeO<sub>6</sub>, optical SHG study of acentricity, ferroelec. of low temp. phases 0-71324  
SrMnO<sub>3-x</sub>, O-deficiency induced polymorphs and elec. cond. 0-71643  
SrMoO<sub>4</sub>, centrosymmetric cryst., linear electrogyration study 0-60540  
SrMoO<sub>4</sub>, Davydov splitting of vibr. levels, short range interaction 0-71418  
SrMoO<sub>4</sub>:Mn<sup>2+</sup>, zero-field splitting of Mn<sup>2+</sup> EPR 0-75531  
Sr(NO<sub>3</sub>)<sub>2</sub>, isomorphous crystals, growth defects, X-ray topography 0-70188  
Sr<sub>1</sub>(Na<sub>0.5</sub>Bi<sub>0.5</sub>)<sub>1-x</sub> solid solutions, piezoelec. and ferroelec. props. (French) 0-108158  
Sr<sub>1</sub>(Na<sub>0.5</sub>Bi<sub>0.5</sub>)<sub>1-x</sub>TiO<sub>3</sub>, ferroelec. ceramic, hot pressing, numerical simulation (French) 0-76220  
Sr<sub>0.05</sub>Ba<sub>0.95</sub>Nb<sub>2</sub>O<sub>15</sub>, X-ray powder diffraction data determ. (Chinese) 0-70170  
Sr<sub>0.8</sub>Na<sub>0.1</sub>Nd<sub>0.1</sub>Ta<sub>2</sub>O<sub>7</sub>, solid soln., ferroelectric phase transitions, dielec. constant and thermal expansion rel. to temp. 0-88934  
Sr<sub>2</sub>Nb<sub>2</sub>O<sub>7</sub>, electronic props. and photoresponses 0-92925  
Sr<sub>2</sub>Nb<sub>2</sub>O<sub>7</sub>, ferroelectric phase transitions, dielec. constant and thermal expansion rel. to temp. 0-88934  
Sr<sub>2</sub>Nb<sub>2</sub>O<sub>7</sub>, high press. phase transitions, Raman scatt. studies 0-71402  
Sr<sub>2</sub>Nb<sub>2</sub>O<sub>7</sub>, layered ferroelectric, anomalous photovoltaic effect, photovoltaic current 0-75603  
SrO, cohesive and thermophysical props., role of three-body interactions 0-92477  
SrO, reduction by C, kinetics and mechanism (Russian) 0-93743  
SrO sintering activator, effect on α-Al<sub>2</sub>O<sub>3</sub> mineralisation, alumina heat treatment 0-89186  
SrO, XPS valence bandstruct. 0-89117



**strontium compounds continued**

- SrO:Co, noncentral and interstitial ion complexes, ESR obs. 0-71169  
 SrO:Ni<sup>2+</sup>, EPR line splitting rel. to Jahn-Teller coupling and soft localised mode 0-66022  
 SrO:Ni<sup>2+</sup>, ionic thermocurrent meas. 0-108148  
 SrO:Ni<sup>2+</sup>, linear Stark effect for zero-phonon optical absorpt. line 0-60830  
 SrO-P<sub>2</sub>O<sub>5</sub>, glass, US velocity rel. to elastic props. 0-103425  
 SrO-P<sub>2</sub>O<sub>5</sub>, glass, ESR of VO<sup>2+</sup> ions 0-100610  
 SrS:Mn, Zr phosphor, photodiode effect 0-107848  
 SrS:Nd, phosphorescence decay, trapping levels 0-104003  
 Sr<sub>1-x</sub>Sm<sub>x</sub>S, electron config. of Sm ions, X-ray L-absorpt. spectroscopy 0-60715  
 SrSnO<sub>3</sub>, high-density ceramics prep. and elec. props. 0-60812  
 SrTa<sub>2</sub>O<sub>6</sub>, structural study X-ray diffr., IR absorpt. and Raman spectra (French) 0-107173  
 SrTa<sub>2</sub>O<sub>7</sub>, ferroelectric phase transitions, dielec. constant and thermal expansion rel. to temp. 0-88934  
 Sr<sub>2</sub>Ta<sub>2</sub>O<sub>7</sub>, soft optic phonon responsible for structural phase transition, Raman scatt. meas. 0-96618  
 SrTiO<sub>3</sub>, (100), LEED and UPS studies 0-100747  
 SrTiO<sub>3</sub>, (111), O<sub>2</sub>, H<sub>2</sub> and H<sub>2</sub>O chemisorption, UPS and XPS studies, illum. effects 0-71572  
 SrTiO<sub>3</sub>, adsorption of O<sub>2</sub>, electron energy-loss spectra obs. 0-89521  
 SrTiO<sub>3</sub>, calc. of matrix element effects in freq. dependent dielectric function 0-70632  
 SrTiO<sub>3</sub>, centrosymmetric crystal, phonon polariton hyper-Raman scatt. obs. 0-76028  
 SrTiO<sub>3</sub>, ceramic, electrocaloric effects for refrigeration at cryogenic temp. 0-77789  
 SrTiO<sub>3</sub>, critical elastic compliance, acoustic resonance meas. 0-65118  
 SrTiO<sub>3</sub>, cubic, temp. depend. of X-ray reflection intensities 0-107021  
 SrTiO<sub>3</sub>, disorder manifestation, light scatt. spectra, high temp. 0-76017  
 n-SrTiO<sub>3</sub>, electrode, flatband pot. determ. from differential stress meas. 0-75638  
 SrTiO<sub>3</sub>, fabrication damage characterisation by internal and external meas. 0-102782  
 SrTiO<sub>3</sub>, ferroelectric modes, Raman spectra, neutron scatt. meas. 0-80727  
 SrTiO<sub>3</sub>, ferroelectric, first order structural phase transition, anharmonic oscillator model 0-86239  
 SrTiO<sub>3</sub>, ferroelectric, polarisation reversal, electric field induced phase transform. 0-103925  
 SrTiO<sub>3</sub>, heavily reduced, soft mode behaviour 0-71409  
 SrTiO<sub>3</sub>, K-edge X-ray absorpt., cond. band states 0-97382  
 SrTiO<sub>3</sub>, mean square atomic displacement temp. depend., sublattice vibration anharmonicity 0-79890  
 SrTiO<sub>3</sub>, monodomain, O-D and O-H stretching vibrs., IR spectra 0-71449  
 SrTiO<sub>3</sub>, Mossbauer spectroscopy, sample prep. and results 0-66078  
 SrTiO<sub>3</sub>, optical SHG near phase transition 0-71348  
 SrTiO<sub>3</sub>, photolum. and carrier drift mobility at ferroelec. transition 0-71469  
 SrTiO<sub>3</sub>, prep. from film forming soln. 0-60811  
 SrTiO<sub>3</sub> prism coupler for LiNbO<sub>3</sub> integrated optics very high throughput damage resistant waveguide modulator 0-58788  
 SrTiO<sub>3</sub>, semicond. anode in aq. electrolyte, electrochem. and electrochem. 0-76080  
 SrTiO<sub>3</sub> semicond. electrodes, electroreduction process kinetics, cathodic dark current meas. 0-66807  
 SrTiO<sub>3</sub>, semiconductor, soft modes, zone boundary mode 0-71357  
 SrTiO<sub>3</sub> surface, oxidation and reduction by D<sub>2</sub>O, H<sub>2</sub><sup>18</sup>O, D<sub>2</sub>, isotope exchange study 0-104461  
 SrTiO<sub>3</sub> surface, photosensitizer for water photoassisted decomp. 0-85202  
 SrTiO<sub>3</sub> surface microrelief after ion irradi. 0-59774  
 SrTiO<sub>3</sub>, thermal cond., anomalous temp. behaviour near structural phase transition (Russian) 0-75394  
 SrTiO<sub>3</sub>, undispersive nonlinear dielectric, third harmonic generation (Russian) 0-95955  
 SrTiO<sub>3</sub>, valence band UPS and partial p and d density of states 0-71560  
 SrTiO<sub>3</sub>:Fe<sup>3+</sup>, order-disorder and central peak behaviour, EPR study 0-75970  
 Sr<sub>2</sub>TiO<sub>3</sub>, photoelectric states in real time spatial light modulators, photorefractive effect 0-80676  
 SrWO<sub>4</sub>, Davydov splitting of vibr. levels, short range interaction 0-71418  
 SrWO<sub>4</sub>, slow neutron inelastic scatt. spectra, Debye temp. calcs. (Russian) 0-59347  
 SrWO<sub>4</sub>:Mn<sup>2+</sup>, zero-field splitting of Mn<sup>2+</sup>, EPR 0-75531  
 SrZrO<sub>3</sub>, high-density ceramics prep. and elec. props. 0-60812  
 U-Sr-C FBR nuclear fuels, phase anal., 1400°C 0-66487

**structural transformations** see solid-state phase transformations

**structure (chemical)** see chemical structure

**structure factors (crystals)** see crystal atomic structure

**structure functions**

- $\phi_s^3$  theory, anomalous dimension, Regge cut effect on structure function 0-62847  
 bounds for the ratio of anomalous dimensions, scalar gluon theories 0-57595  
 deep inelastic and semi-inclusive annihilation structure function factorisation in Bjorken limit, mass singularities 0-86713  
 deep inelastic scatt., QCD predictions for singlet case 0-73707  
 deep inelastic structure function behaviour near physical region endpoints, QCD anal. 0-99101  
 deep inelastic structure functions, QCD tests, Bernstein moments 0-101983  
 Drell-Yan processes, asymptotic freedom corrections, Q<sup>2</sup>-dependence 0-62933  
 electron-muon symmetry of Callan-Symanzik function: two-lepton case 0-73627  
 hadron collisions, lepton pair production, qq annihilation within same hadron, structure function anal. validity 0-57622  
 hadronic wave functions at short distances and the operator product expansion, QCD tests 0-57564  
 lepton pair prod. struct. functions, QCD improved quark-parton model 0-73671  
 meson structure function in covariant parton model context 0-78020  
 MIT bag, 1-dimens., structure function L<sub>0</sub> approx. correction 0-101985  
 Nachtmann moments of F<sub>2</sub><sup>N</sup>(x, Q<sup>2</sup>) and energy momentum sum rule 0-57580  
 nucleon structure functions, overview of measurable types 0-73706

**structure functions continued**

- parton distributions, nonsinglet, QCD parametrisation, leading and next-to-leading order corrections 0-68456  
 polarised deep inelastic scatt., parton transverse momenta role, struct. function, QCD evolution 0-78034  
 QCD, gauge independ. approach to hard processes, structure functions, gluons 0-86665  
 QCD at low Q<sup>2</sup>, structure function moments, correspondence relation 0-73673  
 QCD axial gauge, O( $\alpha_s$ ) infra-red divergences, deep inelastic quark struct. function 0-86676  
 QCD higher order effects of structure function moments 0-62979  
 QCD tests and singlet struct. function moments 0-82941  
 spin dependent photon structure functions from Drell-Yan and e<sup>+</sup>e<sup>-</sup> reactions 0-82973  
 unpolarised lepton-lepton collisions, photon 3rd struct. function, QCD implications 0-73708  
 valence quark clusters in nucleon structure functions from neutrino scatt. 0-95252  
 e<sup>+</sup>e<sup>-</sup> → 0-63010  
 e<sup>+</sup>e<sup>-</sup> →  $\Delta X$ , polarisation effects in nonperturbative parton model, scaling 0-105912  
 e<sup>+</sup>e<sup>-</sup> →  $\gamma^* \rightarrow \gamma$  + hadrons, QCD predictions 0-63009  
 e<sup>+</sup>e<sup>-</sup> → VV, polarisation states and differential cross sections for  $\pi A_1$  and  $\rho^+ \rho^-$  (Russian) 0-102059  
 eN, deep inelastic scatt., quark model, field-theoretic, quark indistinguishability, nucleon structure function 0-62993  
 eN, deep inelastic scattering and asymptotic freedom, Q<sup>2</sup> dependence of moments 0-82978  
 ep, deep inelastic scatt., higher order asymptotic freedom corrections 0-105903  
 ep, deep inelastic scatt.,  $\sigma_1/\sigma_T$  ratio from quark model 0-82979  
 $\gamma$  + hadron → lepton pair, perturbative QCD, twist-2 photon operator, parton subprocesses 0-73716  
 K, deep inelastic structure functions in massive quark model 0-86717  
 K structure functions from inclusive prod. data, nonstrange quark distrib. 0-86715  
 K<sup>-</sup>N →  $\mu^+ \mu^- X$ , K<sup>-</sup>/ $\pi^-$  structure function ratio using Drell-Yan process 0-86718  
 kp, large P<sub>T</sub> pion<sup>0</sup> prod., meson structure functions, quark distrib. functions 0-86714  
 $\mu$ N, deep inelastic scattering and asymptotic freedom, Q<sup>2</sup> dependence of moments 0-82978  
 $\mu p$ , deep inelastic scatt., higher order asymptotic freedom corrections 0-105903  
 n, structure function nonsinglet moments from deep inelastic lepton scatt., QCD 0-62980  
 N structure function model from hard consistent quark interactions, scaling violations 0-86719  
 $\nu$ N, deep inelastic scattering and asymptotic freedom, Q<sup>2</sup> dependence of moments 0-82978  
 $\nu$ N, structure functions of deep inelastic scatt., QCD test, high-twist contribs. 0-57579  
 p, higher order asymptotic freedom corrections from deep inelastic scatt. 0-105905  
 p, structure function nonsinglet moments from deep inelastic lepton scatt., QCD 0-62980  
 pp, large P<sub>T</sub> pion<sup>0</sup> prod., meson structure functions, quark distrib. functions 0-86714  
 pp → mesons, multimeson inclusive spectra and recombination model, multi-quark structure functions 0-73751  
 $\pi$ , deep inelastic structure functions in massive quark model 0-86717  
 $\pi$ , modified quark loop model, form factors, struct. functions, radiative decay 0-91088  
 $\pi$ , structure functions from inclusive prod. data, nonstrange quark distrib. 0-86715  
 $\pi$  compositeness from wave function renormalisation constant 0-101997  
 $\pi^- N \rightarrow \mu^+ \mu^- X$ , K<sup>-</sup>/ $\pi^-$  structure function ratio using Drell-Yan process 0-86718  
 $\pi p$ , direct photon prod., Compton and annihilation process contrib. 0-105925  
 $\pi p$ , large P<sub>T</sub> pion<sup>0</sup> prod., meson structure functions, quark distrib. functions 0-86714

**structure of alloys, crystal** see crystal atomic structure of alloys

**structure of elements, crystal** see crystal atomic structure of elements

**student experiments** see demonstrations

**student laboratory apparatus**

- appearance pot. spectrometer design 0-105477  
 beam splitting device for use with smoke chamber ray optics demonstrations 0-67990  
 compact solar camera, student project 0-67975  
 dielectric constant meas., cell, student, research laboratory appls. 0-62433  
 electrostatic potential, laboratory and theoretical comparison 0-105461  
 ESR of KN<sub>3</sub>, undergraduate expt. 0-105471  
 falling objects accel. due to gravity, Doppler effect, student microwave expt. 0-105472  
 Faraday balance for teaching appl., strong mag. field rel. to react. rates 0-57043  
 holography using modified Michelson interferometer, undergraduate expt. 0-105473  
 light polarisation by reflection, apparatus for obs. 0-62434  
 logarithmic amplifier, schematic diagram 0-57047  
 mechanical start-stop gates for air tracks 0-101698  
 microprocessor multichannel analyzer laboratory project 0-101685  
 numerical analysis, interactive teaching package 0-86058  
 optical radiation detector laboratory, graduate-level, expts. 0-62432  
 optical teaching microscope for investigation of transparent biological objects 0-82622  
 physics laboratory experiments, graphic computer simulations 0-105470  
 spark timer circuit 0-67991  
 table top SEM for undergraduate training 0-68002  
 triggered calibrated sweep for AC oscilloscope 0-67987  
 weather forecasting games at American Universities, survey 0-98770  
 Young's modulus meas. using audio generator amplifier and speaker 0-62427

**studios**

see also radio studios  
 acoustic design in recording studios 0-69601

SU<sub>2</sub> theory

$\nu$ -dimensional Yang-Mills and  $(\nu-1)$ -dimens. nonlinear  $\sigma$ -model connection, quark confinement, dual strings 0-90978  
 't Hooft electromagnetic tensor for Higgs fields of arbitrary isospin 0-68364  
 Airy function basis for  $(D_{1/4}^+ + D_{3/4}^+)$  oscill. representation of  $SL(2, \mathbb{R})$  0-82919  
 asymptotic freedom scales calc. using Monte Carlo methods 0-90988  
 charges, dual, 4-D space of constant curvature (*Chinese*) 0-68392  
 classical Yang-Mills eqn., multimeron solns. 0-57477  
 Clebsch-Gordan coeffs., bilinear relns., based on anal. of Poincare, Lorentz and rotation group  $SO(3)$  0-57509  
 coherent state representation, path integrals 0-62502  
 covariant derivatives without gauge fields 0-73584  
 E<sub>7</sub> grand unification, neutral currents problem in  $SU(2) \otimes [U(1)]^3$  gauge theory (*Russian*) 0-62913  
 electroweak gauge models with heavy W bosons,  $SU_2 \times U_1 \times U_1'$  scheme (*Russian*) 0-86652  
 Euclidean space, spherically symmetric self-dual eqns., representation theory and integration 0-77936  
 explosive cascade-decays of leptons, quarks, virtual photons, weak vector bosons and Higgs scalars 0-86641  
 fermion field with broken  $SU_2$  symm., two-dimensional isotopic model (*Russian*) 0-73616  
 fermion masses and hierarchy of symmetry breaking, u and d quarks 0-86618  
 gauge field, Hamiltonian formulation in interaction with external source 0-62850  
 gauge field theory, nonlinear scalar field eqn., spherical symmetric exact solns. (*Chinese*) 0-62886  
 gauge fields coupled to strong gravity, Coulomb like solutions 0-82701  
 gauge theory, external charges, topological classification for Yang-Mills eqns. 0-90977  
 geometrical unification of gauge and Higgs fields 0-99077  
 Gibow vacuum copies in terms of harmonic maps for  $SU_2$  gauge theories 0-57488  
 instanton solutions, Penrose twistor transform and methods of algebraic geometry 0-73612  
 instanton system weakly interacting with anti-instanton system, external electric fields, structure and stability 0-77956  
 interacting instanton-antiinstanton system under external colour mag. fields in  $SU(2)$  gauge 0-101920  
 interaction potentials for multi-quark states from instantons and other background gauge field configurations 0-101995  
 massless QCD<sub>2</sub>, non-Abelian travelling wave solns.,  $SU(2)$  subalgebra 0-57563  
 neutral-current weak interaction without electroweak unification 0-105835  
 nonstationary quantum systems,  $SU(2)$  coherent states (*Russian*) 0-90693  
 QCD vacuum of background  $SU(2)$  gauge field, colour mag. permeability 0-78023  
 quantised  $SU(2)$  gauge theory, Monte Carlo study 0-77973  
 rishon model of quarks and leptons with double  $SU(2)$  symmetry and Dirac magnetic moments 0-82943  
 self dual  $SU(2)$  fields in multicentre spaces 0-73600  
 self-dual  $SU(2)$  fields in Eguchi-Hanson space 0-57483  
 sine-Gordon equation, discrete, on  $SU(2)$  lattice, group theory aspects 0-57486  
 static magnetic  $SU(2)$  Yang-Mills-Higgs system, static axial and mirror symmetric monopoles 0-90992  
 strongly interacting Higgs bosons, gauged nonlinear  $\sigma$ -model,  $SU(2)_1 \times U(1)$  extension 0-86656  
 $SU_2 \times U_1 \times U_1'$  electroweak model, Weinberg-Salam intermediate bosons 0-105831  
 $SU(2)_1(1)$  nonlinear invariant  $\sigma$  model, superconformal group and curved fermionic twistor space 0-62831  
 $SU(2)_1$ , graded Lie algebra, irreducible representations 0-82913  
 $SU(2)_1(1)$  electroweak interactions, implications for 6 extra time dimensions 0-77998  
 $SU(2)_1 \times (T)_R \times U_V(1)$  gauge group, grand unification, symmetry breaking and Z bosons 0-73641  
 $SU(2)_1 \times U(1) \times U(1)_R$  model, chiral symmetry and weak neutral currents 0-101980  
 $SU(2)_1 \times U(1)$  gauge model, mixing angles and CP violation 0-73648  
 $SU(2)_1 \times U(1)$  theory, radiative corrections, simple renormalisation framework 0-101973  
 $SU(2)_1 \times U(1)$  with four flavours, relation between Cabibbo angle and quark masses 0-105872  
 $SU(2)_1 \otimes SU(2)_R \otimes U(1)$  weak model,  $\nu$  mass and spontaneous P nonconservation 0-62884  
 $SU(2)_1 \otimes U(1)$  gauge Weinberg Salam model, lepton number bound 0-82927  
 $SU(2) \times U(1)$ , gauge invariance and fermion mass dimensions 0-62907  
 $SU(2) \times U(1)$  gauge model, muon anomalous mag. moment, charged Higgs boson contrib. 0-78011  
 $SU(2) \times U(1)$  theories, weak isospin breaking, higher order corrections 0-95235  
 $SU(2) \times U(1)$  unified gauge field, Euclidean space and  $O_4$  invariance 0-91031  
 $SU(2) \times U(1)$  unified model, universal Yukawa coupling 0-91032  
 $SU(2) \times U(1)$  Weinberg-Salam model, possible classical solns. 0-86644  
 $SU(2) \otimes U(1)$  standard and  $SU(5)$  grand unification models, neutral current data implications 0-78000  
 $SU(5)$ , gauge invariance and fermion mass dimensions 0-62907  
 $SU(5)$ , symmetry breaking patterns, Higgs fields 0-101953  
 $SU(5) \times SU(2)$  unification, horizontal symmetry due to quantised motion along internal axes 0-62905  
 $SU(S)$  based grand unified theory, monopoles and vector bosons, symmetry breaking 0-99079  
 supersymmetric  $SU(2)$  Yang-Mills fields, Lie groups, chiral coeffs., Baker-Campbell-Hausdorff formula 0-68355  
 twist selection rule, mass zero representation partons 0-78027  
 $U(1) \times SU_2(2) \times SU(3)$  theory, integer charge quarks, lepton hadronic processes (*Russian*) 0-86653  
 $U(1)$  chiral symmetry breaking from  $SU(1)$  gauge theory 0-86617  
 unconfined colour quark models, weak interactions and neutral currents (*Russian*) 0-105841  
 unit tensor operators 0-62873  
 weak gauge boson doubling in standard  $SU(2) \otimes U(1)$  model, W, Z bosons 0-62916

SU<sub>2</sub> theory continued

Weinberg-Salam model, Lagrangian, invariant under  $SU(2)_1$  gauge group and rotations, in 6-D graded space 0-57537  
 Yang's monopole, quaternionic gauge fields on  $S^7$  0-57473  
 Yang-Mills dyons, mag. charge and Pontryagin index equality in  $SU(2)$  0-57562  
 Yang-Mills eqns., elliptic generalization of the one-meron configuration 0-62854  
 Yang-Mills field, quantum string representation,  $SU_2$  gauge group 0-57465  
 Yang-Mills theory, 1<sup>st</sup> and 2<sup>nd</sup> order eqn. equivalence 0-90979  
 Yang-Mills theory, field-strength description of non-Abelian gauge theories 0-62856  
 Yang-Mills theory, finite field eqn. 0-62830  
 Yang-Mills theory, ground state 0-101939  
 Yang-Mills theory, vacuum struct. 0-57501  
 eN, deep inelastic scatt., heavy lepton mixings, Weinberg-Salam model 0-62992  
 en $\rightarrow$ en $\pi$ , pol. e, P-odd asymmetry and cross sections,  $SU(2) \times U(1)$ ,  $SU(3) \times U(1)$  calcs. (*Russian*) 0-62998  
 $\mu$ N, deep inelastic scatt., heavy lepton mixings, Weinberg-Salam model 0-62992

SU<sub>3</sub> theory

$\sigma$  model,  $SU(3)$  linear, renormalisation in one loop approx. 0-68368  
 asymptotic freedom scales calc. using Monte Carlo methods 0-90988  
 baryons, leptonic decays and mag. moments in nonlocal quark model (*Russian*) 0-86711  
 canonical neutral-current predictions from the weak-electromagnetic gauge group  $SU(3) \times U(1)$  0-95242  
 charmed baryon decays, weak hadronic,  $SU(3)$  dynamical scheme 0-68454  
 cluster systems, normalisation kernels,  $SU(3)$  prop., generator coordinate theory 0-73814  
 colour gauge group, coloured monopoles 0-68360  
 colour geometrodynamics, eightfold way, review 0-95243  
 congruence number, a generalization of  $SU(3)$  triality 0-95224  
 CP(N) ( $N \geq 2$ ) chiral theory, 2-dimens., non-selfdual instantons 0-86585  
 forced harmonic oscillator, complete symmetry group 0-90705  
 hadron scattering, non-charmed,  $SU(1,3)$ , dynamical group 0-62883  
 interaction potentials for multi-quark states from instantons and other background gauge field configurations 0-101995  
 $K^0 \rightarrow K^0$  transition in the standard  $SU(3) \otimes SU(2) \otimes U(1)$  scheme (*Russian*) 0-82951  
 leptons,  $SU(3)$  electroweak theory 0-86638  
 low rank group enveloping algebras, reduction and generating function 0-86601  
 meson decay, tensor, current algebra approach, symmetry-breaking Hamiltonian, chiral  $SU(3) \times SU(3)$  or  $SU(4) \times SU(4)$  0-68450  
 particle under repulsive oscillator,  $SU(3, R)$  complete symmetry group, Lie group 0-86602  
 QCD, gauge field propagator and the number of fermion fields 0-62928  
 QDD, quantum dath dynamics,  $SU(3)$  model for composite quarks and leptons 0-91055  
 quark wave eqns. 0-57571  
 quark-quark interaction, phenomenological, from s-wave baryon spectrum 0-101984  
 $SL(3, R)$  algebra, minimal and centred graded spin extensions 0-82910  
 strong interactions in gravitational field 0-91047  
 $SU(3)_{\text{colour}} \times SU(2) \times U(1)$  gauge, full operator structure of the non-leptonic  $|\Delta S|=1$  weak Hamiltonian 0-99089  
 $SU(8)$  grand unification, natural embedding of  $SU(3)$  horizontal symmetry 0-86646  
 subcomponent models of quarks and leptons in  $SU(3)$  subcolour, proton decay 0-78035  
 topless model for grand unification 0-73653  
 $U(1) \times SU_2(2) \times SU(3)$  theory, integer charge quarks, lepton hadronic processes (*Russian*) 0-86653  
 unitary symmetry in baryon-antibaryon systems (*Chinese*) 0-102000  
 vector meson radiative decays,  $SU(3)$  symmetry viewpoint 0-95273  
 vector meson radiative decays, vector dominance model in broken  $SU(3)$  0-73711  
 vector mesons, EM decay in broken  $SU(3)$  0-82976  
 A<sub>1</sub> meson, mass formulas and selection rules in large  $SU(3)$  mixing 0-86700  
 B meson, mass formulas and selection rules in large  $SU(3)$  mixing 0-86700  
 D-meson decay, hadronic, six-quark model, quark-mass dependence, final state interactions, mixing angle effects 0-62973  
 en $\rightarrow$ en $\pi$ , pol. e, P-odd asymmetry and cross sections,  $SU(2) \times U(1)$ ,  $SU(3) \times U(1)$  calcs. (*Russian*) 0-62998  
 $\eta \rightarrow \pi\pi\gamma$ , quark loop model,  $SU(3)$  splitting of quark masses 0-62990  
 $\eta \rightarrow \rho\gamma(\gamma\gamma)$ , C-even meson radiative decay,  $SU(3)$ , and VDM anal. (*Russian*) 0-68460  
 $\eta(957)$  meson, quark model description 0-62970  
 $K^+ \rightarrow K_S^0$ , quark loop model,  $SU(3)$  splitting of quark masses 0-62990  
 $K^* \rightarrow K_S^0 \gamma$ ,  $SU(3)$  and isospin symmetry breaking effects 0-95272  
 $\bar{\nu}_N$ ,  $K^0$  and  $\pi^-$  prod. rates,  $SU(3)$  symmetry violation in quark jet 0-82966  
 $\phi \rightarrow \eta\gamma$ , quark loop model,  $SU(3)$  splitting of quark masses 0-62990  
 $\pi$ -N  $\sigma$  term in hybrid chiral bag model, PCAC and  $SU(3) \times SU(3)$  symmetry violation 0-78096  
 Q<sub>1</sub>(1280), mass formulas and selection rules in large  $SU(3)$  mixing 0-86700  
 Q<sub>2</sub>(1400), mass formulas and selection rules in large  $SU(3)$  mixing 0-86700

SU<sub>4</sub> theory

Franzini-Radicati mass relationship in isobars, Wigner  $SU(4)$  supermultiplet 0-105958  
 hadrons, charmed,  $SU(4)$  mass-breaking, mass sum rules 0-62959  
 Kramers' symbolic method, extension to  $SU_4$  0-86603  
 low rank group enveloping algebras, reduction and generating function 0-86601  
 meson decay, tensor, current algebra approach, symmetry-breaking Hamiltonian, chiral  $SU(3) \times SU(3)$  or  $SU(4) \times SU(4)$  0-68450  
 O(10),  $SU(4)$  colour subgroup, fractional charged gauge boson, proton half-life 0-73644  
 $SU(4)$ , symmetry breaking effects on strong coupling const., charmed and uncharmed B BP couplings calc. 0-105802  
 $SU(6) \times SU(4)$  tensor decomp. of effective interactions in 2s-1d shell,  $SU(4)$  irreducible tensors and norms 0-105801



**SU<sub>4</sub> theory continued**

symmetry breaking and energy variation of SU(4) irreducible tensors and norms 0-105801  
 vector mesons, radiative decay, single parameter scheme 0-86720  
 $e^+e^- \rightarrow O$  particle, decay, mass, prod. from Zweig rule intermediate vector particle model (*Chinese*) 0-73697  
 $\Lambda$ , charmed baryon mass in SU(1,4) dynamical group theory 0-62882  
 $\Sigma$ , charmed baryon mass in SU(1,4) dynamical group theory 0-62882  
 $\Sigma^- \rightarrow p\gamma$ ,  $1/2^-$  resonance poles to parity-violating amplitude, two-quark weak transitions 0-78062

**SU<sub>n</sub> theory**

see also elementary particle symmetry; SU<sub>2</sub> theory; SU<sub>3</sub> theory; SU<sub>4</sub> theory

1/N expansions, singular integral operator 0-57511  
 5-dimensional generation structure, possible signature for SU(5) semi-simple grand unification 0-82930  
 $\alpha$ -model supersymmetric dynamics on pre-QCD level with elementary quarks and composite gluons 0-82886  
 asymptotically free SU(5) grand unification, proton stability, renormalisation group 0-82929  
 baryon magnetic moments, ground-state, SU(6) symmetry 0-78064  
 baryon mass relations in internal SU(6) symmetry 0-82962  
 baryons, b-quark, magnetic moments, broken SU(5) symmetry 0-95257  
 bottom hadrons, masses and allowed decays, SU(5) quark model 0-62954  
 charmed baryons, mass spectrum from SU<sub>1,3</sub> dynamical group theory 0-62956  
 chiral O(N)×O(N) and SU(N)×SU(N) 2-dimens. models, conservation laws and S-matrices 0-68389  
 confinement in SU(N) lattice gauge theories 0-57493  
 Dyon solutions, existence, rigorous results 0-73595  
 fermion generations in grand unified theories, SU(8) model 0-78012  
 fermion-fermion high energy scatt., transverse momentum cut-off hypothesis, Yang-Mills theory 0-86575  
 fermions, light, mass hierarchy, grand unification, SU(N) theory 0-62911  
 flavour unification in SU(11) 0-62912  
 gauge theory with scalar fields, effective Lagrangian 0-82897  
 glueball spectra, prod. and decay for QCD and SU(n) gauge theories 0-62941  
 grand unification with exceptional group E<sub>6</sub>, symmetry breaking, SU(5) relations, quark masses 0-68407  
 grand unification with the exceptional group E<sub>8</sub> 0-105828  
 grand unified model with a stable proton and no axion problem 0-95234  
 grand unified theory from broken SO(8) extended supergravity, SU(5) theory 0-99081  
 group theoretical construction of two-dimensional models with infinite sets of conservation laws 0-99056  
 hadron interactions, inclusive processes, multiplicity and scaling, resonance production, additive quark model, SU(6) theory, review 0-63043  
 Higgs theory, two-dimens., instanton approach 0-99053  
 identical particle indistinguishability, field quantisation Lie algebraic approach 0-77984  
 integer-charged quarks in the SU(5) grand unified theory 0-68410  
 lattice gauge theories, weak to strong coupling crossover 0-95212  
 lattice gauge theories, Z(N) system phase struct., dual variables 0-62848  
 lattice SU(N) gauge theory, vacuum structure, large-scale 0-57470  
 meron pair, introduction, motivation and formalism 0-82861  
 meron pairs, bare activity 0-82862  
 multilevel system, group theoretical method for coherent effects calc. 0-106502  
 net baryon number and CP nonconservation with unified fields 0-62349  
 neutrino number and isotropy of Universe 0-85852  
 non-Abelian gauge theory with many flavours, high energy processes, asymptotical behaviour (*Russian*) 0-101935  
 O(3)-symmetric merons in SU(N) gauge theory 0-82904  
 Q(5)×SU(1,1) symmetric irreducible representations, orthonormal basis, interacting boson model appl. 0-78178  
 order and disorder parameter inequalities 0-99051  
 planar approximation for coupling N×N matrices 0-62872  
 planar diagrams, SU(N) asymmetric model, semiclassical approach 0-77957  
 pre-quarks and fractional charges 0-91048  
 quantum collective field method, planar limit appl., SU(N) theory and harmonic oscillators 0-57468  
 quark-lepton unification in SU(N>5) 0-73646  
 quark-quark interaction, phenomenological, from s-wave baryon spectrum 0-101984  
 Schnurs, combinatorial hierarchy, spin dichotomy and conservation of quantum numbers 0-68383  
 SL(n,C) actions, analytic, real, on spheres and complex projective spaces 0-68382  
 SO(2N) grand unification in an SU(N) basis 0-62906  
 SU<sub>7</sub> grand unification model, two (V-A) and one (V+A) generations of quarks and leptons 0-57538  
 SU<sub>N</sub>/Z<sub>N</sub> gauge invariant theory, phase factor operators and soliton fields 0-77947  
 SU(2)⊗U(1) standard and SU(5) grand unification models, neutral current data implications 0-78000  
 SU(2n) principle models for integrable nonlinear systems, current constraints, conservation laws 0-86619  
 SU(5), gauge invariance and fermion mass dimensions 0-62907  
 SU(5), Higgs scalars number and  $m_h/m_t$  ratio 0-105826  
 SU(5), unification of weak, EM and strong interactions, review 0-105814  
 SU(5)×SU(2) unification, horizontal symmetry due to quantised motion along internal axes 0-62905  
 SU(5)×U(1) unified theory, neutral current anal. 0-73647  
 SU(5) and SO(10) grand unification, flavour mixing and proton instability (*Russian*) 0-68413  
 SU(5) electroweak-strong interaction model, broken colour symmetry and gluon mass 0-73650  
 SU(5) electroweak-strong interaction model, mass relations and mixing angles 0-73649  
 SU(5) grand unification, cosmological baryon asymmetry 0-86640  
 SU(5) grand unification, heavy coloured Higgs scalars, b-quark mass 0-57543  
 SU(5) grand unification, p lifetime and branching ratio, bag model wavefunctions 0-78004  
 SU(5) grand unification, spin from isospin, half integer spin charge monopoles 0-68406

**SU<sub>n</sub> theory continued**

SU(5) grand unification, superheavy fermions and proton lifetime (*Russian*) 0-91036  
 SU(5) grand unified theory, proton lifetime estimate accuracy 0-101967  
 SU(5) invariant theory, B-L nonconservation and neutron oscillation 0-78005  
 SU(5) model, dyons and monopoles 0-82931  
 SU(5) monopoles, magnetic symmetry and confinement 0-99078  
 SU(5) theories with both proton stability and cosmological baryon-number generation 0-86642  
 SU(5) theory, unified theory of elementary-particle forces 0-105827  
 SU(5) unification, Higgs potential, coupling constants, and gauge hierarchy 0-86637  
 SU(5) unified gauge theory, non-Abelian electric and mag. flux 0-57545  
 SU(5) without symmetry constraints, unified model of quarks and leptons, conservation laws 0-101968  
 SU(5/1) supergroup based strong-electroweak unified model with supersymmetry 0-101977  
 SU(8) grand unification, natural embedding of SU(3) horizontal symmetry 0-86646  
 SU(N>5) chiral grand unification 0-91028  
 SU(N)×SU(N) symmetry breaking with extremum constraints 0-68385  
 SU(N) Coulomb and Landau gauge theories vacuum struct., Gribov ambiguities, harmonic anal. 0-68363  
 SU(n) gauge theories, spontaneous symmetry breaking pattern 0-95228  
 SU(n) symmetric quantum dynamical systems, N→∞, energy spectrum for singlet and adjoint states 0-62880  
 SU(N) Yang-Mills field eqns., constant classical solns. for N=∞ 0-73589  
 symmetric versus antisymmetric mass matrices in grand unified theories 0-99082  
 tensor meson radiative decay in SU(6)×O(3) broken symmetry quark model 0-73710  
 Thirring model, chiral, CP<sup>N-1</sup> and SU<sub>n</sub>, exact S-matrix 0-90985  
 twistor theory in Weinberg-Salam and Georgi-Glashow SU(5) model 0-73651  
 unification of EM, weak and strong interactions, SU(5) group and symmetry breakdown 0-73637  
 unified gauge theories, electroweak mixing angle, sequential triplets scheme of fermions 0-86650  
 bb baryons, mag. moment sum rules, in Su(S) 0-78065  
 eN, deep inelastic scatt., quark model, field-theoretic, quark indistinguishability, nucleon structure function 0-62993  
 NN $\rho$  couplings, parity-violating, QCD and MIT bag model,  $1/2^-$  resonance contribs., SU(6)<sub>w</sub> symmetry 0-57540  
 W, mass in SU(5) grand unified theory 0-68411  
 Z, mass in SU(5) grand unified theory 0-68411

**subboundary structure**

cell wall and lattice misorientation origin during deform. 0-71712  
 deformed crystal, theory of X-ray scatt. (*Russian*) 0-70077  
 quartz, naturally deformed, dynamic recrystn. during creep, dislocation substruct., Mg alloy comparison 0-109142  
 quartz, theoret. predictions and microscopic obs. methods 0-84187  
 SEM imaging, in bulk specimens to study localised plasticity 0-66609  
 Ag halide crysts., dislocations, survey of post-war research 0-62449  
 Ag, tensile deformed, dynamic recrystn. (*German*) 0-84959  
 Al, cold rolling of 1100 plates, substruct. development 0-108476  
 Al, fatigue crack initiation, pre-existing subgrain effect 0-97565  
 Al, stationary creep in HVEM, cell struct. evolution 0-104242  
 Al-Ni (6 wt.%) alloy, misorientation between subgrains, second-phase particles role, STEM microdiff. obs. 0-104415  
 Ar, solid, diffusion processes in plastic deform. (*Russian*) 0-92591  
 Cu crystals, two-phase, recrystn. retardation, particle size, spacing effects 0-89242  
 Cu-Ni (10 at.%), creep, substruct. and internal stresses (*Russian*) 0-97527  
 Fe-Mo(4.1 wt.%), steady state creep at high temps. 0-89316  
 Mg alloy, dil., dynamic recrystn. during creep, dislocation substruct., quartz comparison 0-109142  
 MgO, subgrain boundaries form. obs. by TEM, diffusion coeff. determ. 0-79817  
 MgO:Ni, heavily doped, defect characterisation, rel. to use as laser material 0-50000  
 Mo, creep deformed single crysts., subboundary struct. obs., dislocation sets 0-103348  
 Ni, creep, substruct. and internal stresses (*Russian*) 0-97527  
 Y<sub>2</sub>O<sub>3</sub>(Nd) single crystal growth, floating zone method with Xe arc lamp imaging furnace 0-60777  
 Zr alloys, creep and growth, irradiation induced, microstruct. depend. 0-93602

**subgrain structure see subboundary structure****sublimation**

see also heat of sublimation  
 ice nucleation on AgI, expl. verification of ice-forming activity theory 0-101406  
 metals, radiation induced vaporisation, press. behaviour 0-84288  
 naphthalene, external mode one-density states, low freq. Raman scatt. spectra (*French*) 0-76012  
 naphthalene, sublimation, mass transfer at vibr. spheres 0-57220  
 Tokamak fusion test reactor, thermal response of first wall limiters 0-79585  
 C<sub>2</sub> vapour, Swan bands, oscillator strength 0-63712  
 Hg, deposition, on W, two-dimensional condensation 0-107666  
 KCl surface, sublimation kinetics, elec. field influence, terrace-ledge-kink model 0-84287  
 Li<sub>2</sub>N, vaporisation, studied by Knudsen effusion method 0-92662  
 Ni-S incongruently subliming system, SEM and TEM obs. of high temp. transitions, temp.-comp. diagrams 0-104136  
 NiF<sub>2</sub> film preparation and characterisation 0-59815  
 PCl<sub>5</sub>, sublimed phase studied by <sup>31</sup>P NMR, Raman spectra and X-ray diff. 0-100209  
 SnSe<sub>2</sub>, temp. depend. of equilb. constants 0-88312  
 SrF<sub>2</sub>, vaporisation and sublimation thermodynamics (*German*) 0-81355  
 URu<sub>3</sub>, sublimation thermodynamics 0-97722  
 ZnTe growth from vapour, growth interruption 0-97416

**submarine cables**

see also cable laying  
 glass fibre, expt. cable (*German*) 0-58711  
 monomode optical fibre design and fabrication for submerged cable applications 0-91932

submillimetre waves *see* microwaves

suboptimal control *see* optimal control

## subroutines

- biomedical surface mapping, interpolation methods, in FORTRAN 0-81750
- linear prediction in least-squares scheme for max. entropy spectra, Fortran subroutines 0-98465
- molecular structures, topological code, modified Morgan algorithm 0-58122
- ternary phase diagrams, interactive computer program 0-71629

subsets (mathematics) *see* set theory

## substrates

*see also semiconductor device manufacture*

- adsorbed layers, commensurate-incommensurate transitions, substrate defects effect 0-75437
- anthracene surface UV light irr. effect on organic layer nucleation during crystallisation 0-75478
- confining substrate for micron thick liquid films, semicond. films 0-96722
- film-substrate layered systems, characts. of phase-velocity dispersion and struct. of surface waves 0-59775
- fused silicon, directional reactive ion etching at oblique angles 0-66428
- GaAs wafer, dissolution kinetics in undersaturated isothermal solns. in Ga-Al-As systems 0-80106
- glass substrate,  $\text{SnO}_2$ -Sb film, elec. props. 0-88652
- graphite, growth of  $^4\text{He}$  films, vap. press. meas. 0-70499
- graphite for adsorbed methane submonolayer, structural transitions between epitaxially ordered phases 0-96740
- III-V semiconductors for  $\text{Al}_2\text{O}_3$  films, ion beam etching defect detection 0-89155
- incommensurate epitaxies at finite temps., substrate pot. effect 0-88451
- insulating, thin film growth of  $\text{AlSb}$ , by metal organics CVD 0-60786
- LPE growth method to reduce thermal degradation of substrates, appl. to LED fabrication 0-104061
- metal surface, approached by substrate, surface amplitude patterns 0-75620
- Mylar, growth of  $^4\text{He}$  films, vap. press. meas. 0-70499
- optical properties of film-substrate systems, reflectance-aided null ellipsometry 0-101827
- orientation effect on amorphous Si regrowth by laser pulses 0-84409
- polar materials, appl. to SAW and other devices 0-66114
- polyethylene terephthalate, thickness determ. of Al coating using photometry 0-62626
- polymer, amorphous Se vac. deposited, with dynamic coating device 0-100792
- quartz, fused, anthracene ultrathin film deposition 0-59812
- quartz, fused, for  $\text{ZnS}$ ,  $\text{Na}_3\text{AlF}_6$  films,  $\text{H}_2\text{O}$  absorpt., IR anal. 0-75446
- quasimonolithic and hybrid integrated optical circuits on Si substrates 0-64218
- quench-condensed films, superconducting transition temp., elastic stress and strain effects 0-70883
- rough quartz, Al thin films evaporated on rough quartz substrates surface irregularities, light scattering measurements (Polish) 0-88450
- ruby, synthetic, CC  $\text{Nb}_3\text{Pb}$  superconducting film, prep., vac. deposition 0-89149
- sapphire, solid phase Si regrowth in Si-Al- $\text{Al}_2\text{O}_3$  system, Hall effect 0-100413
- sapphire, substrate for V, Ta, Mo, W, Nb epitaxial films, growth texture, nucleation texture (Russian) 0-75454
- sapphire (1012) substrate for Si epitaxial thin film growth by MBE 0-76186
- sapphire film, substrate for Si, laser annealing non-thermal theory expt. test 0-89273
- sapphire for  $\text{K}_3\text{Li}_2\text{Nb}_2\text{O}_5$  film for optical waveguide, cryst. struct., dielectric props. 0-79016
- sapphire ribbon crystals, EFG growth and charact., voids, grain boundaries and dislocations 0-103283
- sapphire ribbon EFG prod., substrate for heteroepitaxial Si 0-108342
- solar cells, RAD process, substrate related problems 0-89635
- spinel (100) substrate for Si epitaxial thin film growth by MBE 0-76186
- steel backing plate, hot pressing with powder layer, joint form. kinetics 0-100961
- steel substrate limiting temp. during vaporisation and condensation coating in vacuum (Russian) 0-100787
- surface temperature measurement during film deposition using thin film thermocouple 0-62668
- uniformity, Kr vapour press. isotherms at 77K as standardized meas. 0-107657
- vacuum coating, surface temp. meas. 0-57297
- Ag, electrodeposition of Au film, substrate effects on film props. 0-81329
- Al (111) surface, Pb, Sn monolayer, double layer growth, struct. 0-70567
- Al, for Zn film deposition, TEM and electron diff. obs. 0-75460
- $\text{Al}_2\text{O}_3$  for Ni-Cr/Au films interdiffusion processes and oxidation phenomena 0-59735
- $\text{Al}_2\text{O}_3$  substrates, tape-casted, fracture strength analysis 0-60948
- Au for evaporated Be thick films, secondary electron emission 0-104022
- Au, with Ag monolayer, adsorbed pyridine giant Raman effect 0-63637
- Cr, refr. index depend. of  $\text{Yb}_2\text{O}_3$  thin film on thickness 0-108290
- Cr substrate for CdSe, thin film transistor, cryst. struct., substrate defect effects 0-70563
- Cu, electrodeposition of Au film, substrate effects on film props. 0-81329
- Cu substrate for  $\text{SiO}_2$  film, surface EM wave absorpt. optical const. (Russian) 0-108216
- GaAs, anodisation in HF  $\text{O}_2$  plasma, oxide film form. mechanism and kinetics (Japanese) 0-93667
- GaAs semi-insulating substrates, monolithic integration of optical and electronic devices, review 0-58543
- GaAs semi-insulating substrates CC GaAs- $\text{Al}_x\text{Ga}_{1-x}\text{As}$  transverse junction lasers with low threshold current by MBE 0-58588
- GaAs semi-insulating substrates, GaAs/GaAlAs crowding effect lasers using whispering gallery mode 0-58589
- GaAs, semi-insulating substrates, whispering gallery lasers 0-69405
- GaSb, LPE growth of lattice-matched  $\text{AlGaAsSb}$  0-60794
- $\text{Gd}_3\text{Ga}_2\text{O}_7$  substrates, LPE of  $\text{Y}_3\text{Fe}_5\text{O}_{12}$ , substrate orientation effect 0-66438
- Ge, epitaxial growth of ZnSe 0-75469
- InP (111), (110) and (001) substrates, Cd(S, Se) film growth, mismatch dislocations and lattice distortion 0-84406
- InSb room temp. CVD of  $\text{Si}_3\text{N}_4$  0-71597

## substrates continued

- $\text{K}_3\text{BiNb}_2\text{O}_5$  for  $\text{K}_3\text{Li}_2\text{Nb}_2\text{O}_5$  film for optical waveguide, cryst. struct., dielectric props. 0-79016
- $\text{LiNbO}_3$  substrates for integrated passive optical rotation sensors using guided waves, developments 0-58781
- $\text{MgO}$ , growth of  $^4\text{He}$  films, vap. press. meas. 0-70499
- Mo (110) surface, molecular adsorbed CO, electronic states, photoemission spectra 0-65363
- Mo substrate limiting temp. during vaporisation and condensation coating in vacuum (Russian) 0-100787
- $\text{NaCl}$ , nucleation process of  $\text{Cd}_3\text{As}_2$  films 0-59813
- Pd, for Ag epitaxial growth, influence on film growth modes (French) 0-84408
- Si (001) substrate for  $\text{Pd}_2\text{Si}$  epitaxial islands 0-96748
- Si (100), (111) substrates for rare earth metal silicide thin film formation, backscattering study 0-70542
- Si, (111) surface substrate for  $\text{NiSi}_2$  epitaxial film, interfacial order, backscattering, channelling study 0-65390
- Si (111) surface substrate for Al film, struct., props. depend. on vapour flow (Russian) 0-75453
- Si and  $\text{SiO}_2$ , for Pt-Ni vacuum condensates, X-ray anal. (Russian) 0-70559
- Si, epitaxial layer thickness meas. using phase correction function of substrate resistivity (Rumanian) 0-90812
- Si, for epitaxial crystn. of GaP films by ns laser pulses 0-107674
- Si for integrated optics high quantum efficiency waveguide coupled photodetectors 0-58805
- Si for wet thermal oxide film, trap emptying kinetics 0-92983
- Si, ion implantation, channelled, through metal silicide film 0-70231
- Si ribbons, edge-defined film-fed growth technique for solar cells 0-91318
- Si, shallow contact formation substrate temp. depend., Pd-W alloys 0-96963
- Si, substrate for Al film, annealing effect on eutectic point (Russian) 0-100850
- Si substrate for PMMA electron sensitive layer, 400 Å linewidth electron beam lithography 0-65392
- Si substrate for Pd and Pt, silicide formation by laser, electron beam annealing 0-84849
- Si substrate for RF sputtered ferroelectric  $\text{BaTiO}_3$  films, ferroelectric props. 0-80697
- Si substrate for  $\text{SiO}_2$  film, ellipsometric spectra, thickness determ. (Chinese) 0-86379
- Si, substrate for  $\text{ZnS}$ ,  $\text{Na}_3\text{AlF}_6$  films,  $\text{H}_2\text{O}$  absorpt., IR anal. 0-75446
- Si substrate prep. for epitaxial solar cells, low-cost, unidirectional solidification process 0-93924
- Si substrate solar cells, upgraded metallurgical grade, epitaxial growth 0-93905
- Si, substrate temp. influence on shallow contact formation on Si, shallow contact formation substrate temp. depend., Pt-W alloys 0-96963
- Si substrate thickness, device design, solar cell processing, empirical study of interaction 0-93995
- Si surface electron beam deposited silicide formation using scanning CW laser beam 0-66862
- Si:Fe(Al), compensated substrates for solar cells, effects of Fe and Al 0-94009
- Si:Ti substrate for epitaxial solar cells 0-61341
- $\text{Si}_3\text{N}_4$  sample substrates, high resoln. electron beam fabrication using STEM 0-104104
- $\text{SiO}_2$  on Si wafer for ZnO low-loss optical waveguides 0-58793
- $\text{SiO}_2$  substrate, obliquely evaporated for cyano-biphenyl LC, alignment 0-79677
- W, deposition of Au film, interface struct., FIM obs. 0-65384
- YAG, as substrate for  $\text{Er}_3\text{Al}_5\text{-Ga}_2\text{O}_{12}$  LPE film for solid laser 0-93419
- ZnS monocrystalline substrate, influence of struct. on CdS epitaxial growth and nucleation 0-88455

sudden commencement *see* magnetic storms

## Suhl effect

- No entries

## sulphur

*see also nuclei with .....*

- 100 MW fluidised bed combustion district heating plant burning high S content residual oils 0-108777
- adlayer effect on CO and  $\text{H}_2$  adsorption and desorption on Fe(100) 0-71573
- adsorbed on AgBr dispersion in gelatin, transient absorpt. spectra, latent image form. and decay 0-66837
- adsorption on Cu vicinal surfaces, LEED study 0-103575
- adsorption on Fe(100), adsorbate coverage determ. by LEED, AES and XPS 0-103566
- adsorption on Pd (110) surface, LEED study (French) 0-88422
- Allende meteorite, S content, neutron capture gamma-ray spectroscopy 0-94728
- alloying addition to Alnico 5 alloy, mag. props. and grindability 0-89375
- atmosphere aerosol, level meas. using continuous flame photometric detect. system 0-81508
- atom, ab initio effective valence shell Hamiltonian for neutral and ionic valence states 0-74117
- atom, photoionisation cross sections and asymmetry parameters, SCF  $X\alpha$  scatt. wave calcs. 0-63542
- chemisorption, on  $\text{Al}_2\text{O}_3$ -supported Ni, thermodynamic parameters meas. 0-88424
- diffusion and solubility in Ni (Russian) 0-70465
- fluidised-bed steam generating system to supply 100000 lb/h of saturated steam burning high S coal 0-108778
- free surface and grain boundary chemistry in Fe alloys 0-75410
- implant fluence, Cr redistribution, during thermal annealing of semi-insulating GaAs 0-84199
- impurity in C steel plates, effect on through-thickness props. 0-66660
- interstellar chemistry 0-101632
- ions in Jupiter magnetosphere, plasma cloud injection from IO 0-90358
- isotopic composition in CS, spectroscopic meas. (Russian) 0-91696
- lunar rock content, neutron capture gamma-ray spectroscopy 0-94728
- Mars lithosphere, possible S overabundance 0-72832
- molecular laser, optically pumped, review 0-58519
- monolayer, adsorbed on Al (111), angle resolved UPS of 2-dimens. band struct. 0-60059
- ordered overlayers on N(001) surface, elec. struct. 0-84835
- orthorhombic, photogeneration of charge carriers 0-107844
- photoelectret state in polycryst. following X-irrad. 0-60485



## sulphur continued

- planetary nebulae, S abundance from IR and visible line meas. 0-82444  
radiation effects, allotropic modifications and activity distrib. 0-70255  
segregated onto Pd surface, state, AES, EELS, UPS and XPS study 0-93452  
segregation and adsorption in Fe and steel, influence on carburisation and nitrogenation 0-66701  
segregation in Cr-C steel 0-66594  
single crystal, photoinjection, electronic transport and Mott-Gurney transition (*Spanish*) 0-84464  
steel, stainless, fracture micromechanism when kept isothermally in sulphur pulp 0-76355  
steel, welded-joints, H<sub>2</sub> induced cracking, S content effect 0-97562  
surface segregation on Cu-Ag alloy, Auger spectral study diffusion 0-76549  
Venus, S chemistry of atmosphere/lithosphere system rel. to oxidation state of atmosphere and crust 0-98586  
Ag-S system, phase diagram, 100-600°C (*German*) 0-97471  
Ce-S-O equilibrium in molten Fe (*Chinese*) 0-104423  
Fe, single cryst., segregation behaviour of S, O and P at (100) surface 0-100841  
GaAs:S, generation of high mobility n layers, SIMS 0-103375  
GaP:S, defect struct. and tetrahedral precipitates, TEM study 0-107246  
GaP:S, donor bound exciton excited states 0-66284  
GaP:S, ground and excited states of bound exciton complex, stress effects 0-65463  
p-GaP:Zn:S, spin polarisation of donors and acceptors in mag. field, optical and microwave study 0-93393  
InAs:S, ion implanted, photocond., photo-EMF, and optical absorpt. spectra 0-70763  
InP:S, SSD growth of low dislocation density crystals 0-89135  
Na/S battery development program at GEC for utility lead levelling with beta alumina solid electrolyte 0-61327  
Na/S cells operating with dissolved catholyte, elec. props. 0-101085  
Na/S load levelling batteries, optimisation of fabrication process of beta Al<sub>2</sub>O<sub>3</sub> solid electrolyte 0-72035  
Na/S traction batteries, development progress and problems, review 0-61326  
Na<sub>2</sub>S<sub>2</sub>-molten S interface, mass transport phenomena, rel. to Na/S battery 0-72026  
Ni passivation, S influence study by Auger and electron spectroscopy 0-65347  
 $\alpha$ -S, attachment energy as habit controlling factor 0-59421  
S I, emission lines obs. in EUV spectra of late-type stars 0-82359  
S II forbidden line emission nebula studies of Jupiter 0-67636  
S II forbidden line emission round Jupiter, distrib. and intensity 0-85885  
S II Jupiter torus emission, longitudinal symmetry, visible spectra 0-82721  
S II ring round Jupiter, var. in characts., link with Io, visible obs. 0-90360  
S III forbidden lines in Omega Nebula (W38, M17, NGC 6618), IR spectra obs. 0-90495  
S IV, 3s<sup>2</sup>3p<sup>2</sup>P-3s3p<sup>2</sup><sup>4</sup>P multiplet, energy levels and transitions, appl. to solar atm. 0-87028  
S<sub>n</sub>, contracted Gaussian basis sets for mol. calcs. 0-83264  
S<sub>n</sub>, charge transfer in diffuse nebulae 0-77463  
S<sub>n</sub><sup>+</sup>, static dipole quadrupole polarisabilities and shielding factors calc. using HF scheme 0-99450  
S<sub>n</sub><sup>+</sup>, travelling in solids, K $\alpha$  X-ray spectra 0-100706  
S-benzene systems, liq.-liq. phase separation 0-96658  
S-He discharges, stability, emission spectra 0-107003  
S+CS<sub>2</sub>(OCS)(CH<sub>3</sub>), electronically excited atom, reson. fluoresce. 0-99476  
S+F<sup>-</sup>, inner-shell ionisation, X-ray cross sections 0-58369  
S<sup>+</sup>+O<sub>2</sub>(Ar)(He), (q=6-16), K X-ray prod., charge-state depend. 0-106391  
S<sub>n</sub>, matrix-isolated, B<sup>3</sup> $\Sigma$ <sup>-</sup> predissoc., relax. processes 0-58329  
S<sub>n</sub>, optically pumped superfluorescence molecular laser 0-63990  
S<sub>n</sub>, vibrational constants, UV absorption and fluorescence spectros. of S<sub>x</sub> vapour, x=3 to 8 0-78631  
S<sub>n</sub>+N<sub>2</sub> (*Russian*) 0-99711  
S<sub>n</sub><sup>+</sup> and S<sub>n</sub><sup>2+</sup>, structure investigation by ab initio calcs. 0-69066  
S<sub>n</sub> vapour, x=3 to 8, UV absorption and fluorescence spectros., vibrational constants of S<sub>2</sub> 0-78631  
S in troilite, enrichment rel. to lunar soil 0-77303  
<sup>35</sup>S diffusion in NiO crystals, simultaneous diffusion by two different modes 0-59720  
Si:S, deep level characterisation, implantation predeposition technique 0-100444  
ZnP<sub>2</sub>:S, optical absorpt. spectra in range 0.5 to 2.2 eV 0-66250

## sulphur compounds

- air pollutants, detection using continuous flame photometric detection system 0-81508  
compressed SF<sub>6</sub>, repeated breakdown field strength in uniform field perturbed by protrusion 0-96406  
ESCA shifts and effective charges 0-78648  
fluoromethane-SF<sub>6</sub>, 496- $\mu$ m optically pumped laser, energy-transfer mechanisms 0-99712  
oxide pollutants, SURE/MAP3S obs. comparison with regional model predictions 0-81501  
SF<sub>6</sub>, buffered, 10.6  $\mu$ m transmission props. for nanosecond pulses 0-58644  
steels, obs. and anal. of sulphides, using non-aqueous electrolyte-potentiostatic etching method (*Japanese*) 0-89433  
sulphate, atmospheric, concs. comparison with analytical diffusion model for pollutants long distance transport 0-94125  
sulphate aerosol, atmospheric, meso-scale transport obs. in rural East Midlands, England 0-94124  
sulphate aerosol layer in stratosphere, processes, models, obs. and simulations 0-109212  
sulphate concentrations in atmosphere, correl. with total nitrate concs. 0-94123  
sulphates, brine sulphate anal. by atomic absorpt. 0-89556  
sulphates, residence times under non-steady-state conditions 0-77092  
sulphates in particulate form, air quality over Los Angeles and New York 0-61483  
sulphide ore deposits in NW.Kola Peninsula, electric near zone field development method testing (*Russian*) 0-85761  
Ar:OCS, liq., dissoc. studies 0-78716

## sulphur compounds continued

- As-S, melt struct., orientation birefr., viscosity, refr. index, and density 0-84713  
As-Se-S-Ge chalcogenide amorphous film, computer-generated holograms using electron beam irradi. 0-95846  
Bi-S liquid soln., S activities meas. by EMF method (*Japanese*) 0-70425  
Ge-S glass, melt-quenched photoinduced ESR, annealing behaviour and glass comp. depend. 0-71156  
Ge-S-Ga amorphous thin film, memory switching effects 0-88605  
Ge-S-Se, glass formation 0-103251  
Ge-Si-S system, glass formation, transition temp., crystallisation and melting 0-100178  
Ge<sub>31</sub>As<sub>27</sub>S<sub>15</sub>Te<sub>25</sub>, chalcogenide thin films, coupled carrier theory test, high field conditions 0-100466  
Ge<sub>25</sub>S<sub>75</sub>Mn, bond struct. and character in Ge-S system, EPR obs. 0-66014  
Ge<sub>40</sub>S<sub>60</sub>Mn (Ag)(Cu), bond struct. and character in Ge-S system, EPR obs. 0-66014  
Ge<sub>42</sub>S<sub>58</sub>, amorphous, bulk and film forms, elec. props. and ESR study 0-103691  
HI-SF<sub>6</sub> system, HF pulsed chemical laser 0-106514  
HI-SF<sub>6</sub> system, HF pulsed chemical laser 0-106515  
H<sub>2</sub>S atmospheres, formation of contaminating layers on elec. contact materials (*German*) 0-71811  
H<sub>2</sub>SO<sub>4</sub> atmosphere-aerosol study of Venus cloud microstructure and optical props. 0-72808  
H<sub>2</sub>SO<sub>4</sub>-SO<sub>2</sub> thermochemical cycle for H<sub>2</sub> prod., electrochem. aspects 0-97812  
KClO<sub>4</sub>:SO<sub>2</sub><sup>2-</sup>, AC elec. cond. and dielec. loss meas. 0-59699  
Li/SO<sub>2</sub> cells, DTA, safety studies 0-81428  
Li/SO<sub>2</sub> cells, safety studies, kinetics of Li-organic solvent exothermic reactions 0-72030  
Li/SOCl<sub>2</sub> cells, high rate discharge characts. 0-72021  
Li/SOCl<sub>2</sub> primary cells, SOCl<sub>2</sub> reduction mech. in supporting electrolyte 0-108792  
Mo<sub>6</sub>S<sub>6</sub>Sn, triple chalcogenide, NMR spectra in supercond. state (*Russian*) 0-93194  
N<sub>2</sub>-SF<sub>6</sub> pulsed discharge laser with CW X-ray preionisation 0-95910  
Ni-S incongruently subliming system, SEM and TEM obs. of high temp. transitions, temp.-comp. diagrams 0-104136  
2PbO-SiO<sub>2</sub>-xSO<sub>3</sub> melts, crystn. 0-59400  
S-based amorphous semicond. film, prep. by plasma decomp. of H<sub>2</sub>S-N<sub>2</sub>-NH<sub>3</sub>, and characterisation 0-80422  
S-N system, inorganic, electronic struct. obs. by photoemission XPS and UPS, CNDO calcs. 0-78653  
S-Ni-Fe system containing monosulphide solid soln., elec. and struct. relations 0-90038  
SBr<sub>2</sub>, Si<sub>2</sub>, matrix isolated, IR spectra 0-58254  
SF<sub>6</sub>+ClF<sub>3</sub>, thermal and photochem. reactions investig. 0-61117  
SF<sub>6</sub>, <sup>19</sup>F NMR vibr. anharmonicity effects 0-91580  
SF<sub>6</sub>, adsorption on Cs ion source, thermionic emission 0-71557  
SF<sub>6</sub> and SF<sub>6</sub>-air mixture gas under impulse voltage, discharge phenomena (*Japanese*) 0-96409  
SF<sub>6</sub>, arc, temp. determ. accounting for demixing 0-70057  
SF<sub>6</sub>, binary collision-induced light scatt., rot. Raman scatt. 0-78660  
SF<sub>6</sub>, binary collisions induced light scatt. 0-83428  
SF<sub>6</sub>, CW CO<sub>2</sub> laser spectroscopy 0-83367  
SF<sub>6</sub>, circuit-breaker, non-LTE plasma props. and at. processes, medium to high press. 0-59170  
SF<sub>6</sub>, corona-stabilised breakdown, computations and obs. 0-64804  
SF<sub>6</sub>, critical isochore, dielectric const. critical anomaly upper bound 0-84679  
SF<sub>6</sub>, discharge and oscill. due to axial injection of impulsive electron beam 0-59316  
SF<sub>6</sub>, Doppler-limited spectroscopy, of 3v<sub>3</sub> band 0-58244  
SF<sub>6</sub>, Doppler-limited spectroscopy of 3v<sub>3</sub> band, rot. const. and anharmonic parameters calcs., mol. photodissoc. 0-83361  
SF<sub>6</sub>, gas, excited molecule vibr. translational relaxation, nonlinear processes (*Russian*) 0-91540  
SF<sub>6</sub>, gas, low press., excitation of nonlinear wave by repeated pulsed electron beam 0-87878  
SF<sub>6</sub>, gaseous saturable absorber effects on eight-beam CO<sub>2</sub> laser fusion system performance 0-106577  
SF<sub>6</sub>, high-current discharge plasma column, radiation charact. and struct. (*Russian*) 0-106989  
SF<sub>6</sub>, IR laser radiation multiphoton absorpt. direct meas. by pyroelec. detector 0-102545  
SF<sub>6</sub>, IR multiphoton dissociation studies, inverse bottle-neck effect 0-87193  
SF<sub>6</sub>, IR multiphotonic excitation, depend. on cell geometry, mol. fluoresce. and decomp. obs. 0-83430  
SF<sub>6</sub>, IR multiple-photon excited molecules, Raman spectroscopy 0-74207  
SF<sub>6</sub>, IR spectra, fine struct. of rot.-vibr. bands 0-102504  
SF<sub>6</sub>, impulse breakdown characteristics for nonuniform field gaps for switchgear design 0-84024  
SF<sub>6</sub>, insulation, under impulse voltage stress, effects of pressure and vol. on firing delay (*German*) 0-87959  
SF<sub>6</sub>, insulation breakdown characts. under operating conditions in HV apparatus 0-96414  
SF<sub>6</sub>, laser, for 16  $\mu$ m range, review (*Rumanian*) 0-87408  
SF<sub>6</sub>, laser pumping in collisional region of nozzle beam, internal excitation, time-of-flight anal. 0-95719  
SF<sub>6</sub>, liq., positronium bubble states, temp. depend. 0-108293  
SF<sub>6</sub>, matrix isolated, IR spectrosc., temp. reversible site structural changes 0-95613  
SF<sub>6</sub>, molecule drift mobility due to IR laser radiation (*Russian*) 0-69192  
SF<sub>6</sub>, multiphoton dissoc. by mol. beam method, energy distribution meas. by time-of-flight spectra, dissoc. dynamics 0-78670  
SF<sub>6</sub>, multiphoton excitation due to vibr.-rot. transitions 0-102546  
SF<sub>6</sub>, multiphoton-excited,  $\nu_3$ + $\nu_4$  absorption and emission 0-63626  
SF<sub>6</sub>, multiple photon absorpt., laser pulse intensity and collisions influence 0-95699  
SF<sub>6</sub>, multiwavelength phase conjugation using multiline CO<sub>2</sub> TEA laser 0-91847  
SF<sub>6</sub>, nonlinear absorpt. of CO<sub>2</sub> laser pulse, computer simulation 0-106575  
SF<sub>6</sub>, pair polarisability anisotropy, point atom polarisability approx. calcs. 0-87244  
SF<sub>6</sub>, partial saturation of  $\nu_3$  ladder in IR absorpt., rate process model 0-58645  
SF<sub>6</sub> plasma interaction with solid polymer, emission-spectra 0-87960

**sulphur compounds continued**

- $\text{SF}_6$  plasma thermodynamic props. at arc extinction temp. and pressures 0-79435  
 $\text{SF}_6$  polyatomic molecule dissociation in IR laser field (*Chinese*) 0-106363  
 $\text{SF}_6$  soln., cryosystem, vibr. relax. times, pulsed IR absorpt. spectral obs. 0-66188  
 $\text{SF}_6$  spark gap, KrF laser triggered, low jitter timing 0-106999  
 $\text{SF}_6$  surface ionisation on W cathode, laser irradiation effects 0-93440  
 $\text{SF}_6$  surface tension temp. dependence from triple point to critical point (*German*) 0-100376  
 $\text{SF}_6$  trace detection using phase fluctuation optical heterodyne spectroscopy 0-68266  
 $\text{SF}_6$  vibr. coupling in collision-induced Raman scatt. 0-83373  
 $^{32}\text{SF}_6$  point group symmetry breakdown, vibr.-rot. state, saturation spectroscopy 0-87116  
 $\text{SF}_6$ -inert gas mixture, high power cylindrical spark discharge, dynamic and visible charact. 0-64816  
 $\text{SF}_6$ -inert gas mixture, formation of inert gas fluorides in AC discharge 0-64817  
 $\text{SF}_6$ - $\text{N}_2$  mixture, electron swarm development, Boltzman eqn. anal. 0-87841  
 $\text{SF}_6$ - $\text{N}_2$  mixtures, attachment coeffs. and ionic mobilities, 1.2-4 eV 0-96338  
 $\text{SF}_6$ -R-He(Ar) ternary mixtures, formation of inert gas fluorides in AC discharge 0-64817  
 $\text{SF}_6$ -fluoromethane, fluoromethane laser, buffer gases collisional narrowing 0-99710  
 $\text{SF}_6$ + $\text{H}_2$  chemical laser, electron beam pumping 0-91784  
 $\text{SF}_6$ + $\text{Li}^+$ ( $\text{H}^+$ ), mode selective vibr. excitation 0-58351  
 $\text{SF}_6$ +methane, vibr.-vibr. relax. 0-99537  
 $\text{SF}_6$ + $\text{N}_2\text{O}$ , vibr.-vibr. energy transfer, fluoresc. 0-78688  
 $\text{SF}_6$ +Rydberg atom, reaction channels, expt. vs. theory 0-63755  
 $\text{SF}_6$ +Si(surface), IR laser induced reaction, mol. vibr. and mol. dissoc. obs. 0-93798  
 $\text{SF}_6$ +Xe(nf), l-changing collisions obs. 0-91633  
 $\text{SH}_3^+$ , bond polarisability and force constants 0-69260  
 $(\text{SN})_x$ , brominated, X-ray absorpt. meas., 5K to room temp. 0-71516  
 $(\text{SN})_x$ , electronic struct., one-electron band theory 0-65450  
 $(\text{SN})_x$ , halogenated, struct. behaviour, TEM obs. 0-70126  
 $(\text{SN})_x$ , supercond. polymer, mag. props. meas. 0-107953  
 $(\text{SN})_x$ , supercond. props. rel. to fibrous morphology 0-84570  
 $(\text{SN})_x$ , Br, ion implantation effect on elec. props. 0-65026  
 $\text{S}_2\text{N}_2$ , gas phase and solid state core level XPS 0-66401  
 $\text{S}_2\text{N}_2$ , photoelectron spectrum, interpretation, Green's function calcs. 0-87175  
 $\text{S}_2\text{N}_4$ , solid state core level XPS 0-66401  
 $(\text{SNBr}_{0.04})_x$  and  $(\text{SNBr}_{0.25})_x$ , solid state core level XPS 0-66401  
 $(\text{SNBr}_{0.4})_x$ , supercond. polymer, mag. props. meas. 0-107953  
 $(\text{SNI})_x$ , crystals, reson. Raman scatt. meas. 0-66203  
 $\text{SO}^+$ ( $\text{A}''\text{-X}''\text{II}_1$ ) emission following  $\text{He}^+$ + $\text{SO}_2$  afterglow reaction 0-95659  
 $\text{SO}_2$ , absorption spectrum, meas. using frequency doubled pulsed dye laser 0-87144  
 $\text{SO}_2$ , absorption spectrum, meas. using frequency doubled CW dye laser 0-87145  
 $\text{SO}_2$ , air pollutant dispersal, Forth Valley, Scotland 0-81497  
 $\text{SO}_2$ , atmospheric, meso-scale transport obs. in rural East Midlands, England 0-94124  
 $\text{SO}_2$ , atmospheric pollutant dosages in urban areas 0-81499  
 $\text{SO}_2$ , atmospheric residence times under non-steady-state conditions 0-77092  
 $\text{SO}_2$  conc. over Netherlands, source areas, dispersion model 0-61482  
 $\text{SO}_2$  evolution in soda-lime glass melting-fining, redox phenomena 0-84900  
 $\text{SO}_2$  frost, IR spectra and implications for Io 0-77331  
 $\text{SO}_2$  ground-level conc. calcs. near a nuclear facility 0-97823  
 $\text{SO}_2$ , harmonic and anharmonic matrix elements comparison, appl. to vibrational energy transfer 0-63760  
 $\text{SO}_2$ , IR multiphoton excitation and inverse electronic relax., mol. vibr. and fluoresc. 0-106349  
 $\text{SO}_2$ , IR spectra, Coriolis intensity perturbations 0-95617  
 $\text{SO}_2$ , interaction with NiO (100) surface, electron diffraction and Auger spectrosc. obs. (*French*) 0-97728  
 $\text{SO}_2$ , microwave spectra, Ku-band Fourier transform spectrometer appl. 0-68265  
 $\text{SO}_2$ , movement in atmosphere (*Dutch*) 0-97844  
 $\text{SO}_2$  on Io, upper limit to global abundance 0-77332  
 $\text{SO}_2$  oxidation to  $\text{SO}_4$  in urban atmosphere 0-81964  
 $\text{SO}_2$  oxidation to sulphate in troposphere, model predictions 0-81963  
 $\text{SO}_2$  pollution episodes in Venetian region, real-time forecasting via advection-diffusion model 0-77096  
 $\text{SO}_2$  pollution episodes in Venetian region, real-time forecasting via Kalman predictor 0-82046  
 $\text{SO}_2$  pollution in Montreal, Canada, anal. of meteorol. and source factors 0-104537  
 $\text{SO}_2$  pollution of industrial area, occurrence affected by wind direction 0-89691  
 $\text{SO}_2$ , pure gas, enthalpy, Carlson-Thodos van der Waals eqn. calcs. 0-83878  
 $\text{SO}_2$ , relative Raman scatt. cross section 0-100061  
 $\text{SO}_2$ , shock heated, visible emission 0-58274  
 $\text{SO}_2$ , single vibronic level fluoresc. spectra 0-91597  
 $\text{SO}_2$ , surface reaction and decomposition on zeolites, resonance Raman study 0-61145  
 $\text{SO}_2$ , T, relax. meas. using budge-type superhet. microwave spectrometer 0-91551  
 $\text{SO}_2$ , UV excitation spectra, mol. fluoresc. meas., mol. predissoc. obs. 0-83389  
 $\text{SO}_2$ , vibr. relax., phase spectrophone method obs. 0-87059  
 $\text{SO}_2$ - $^{18}\text{O}$  mixtures, IR laser pumped, intermol. vibr. energy transfer dynamics obs. 0-87207  
 $\text{SO}_2$ -containing ions, photodestruction 0-63722  
 $\text{SO}_2$ -tetrachloromethane, solns., near critical point, ultrasound absorpt. obs. 0-65160  
 $\text{SO}_2$ +active  $\text{N}_2$ , excited neutral metastable  $\text{SO}_2$  form. mass spectrometric study 0-83300  
 $\text{SO}_2$ +Ar, dissoc. rate meas. behind shock wave, laser Schlieren method 0-81296  
 $\text{SO}_2$ + $\text{CO}_2^*$ , near-reson. energy transfer, fluoresc. obs. 0-106348  
 $\text{SO}_2$ + $\text{O}_2$ = $\text{SO}+\text{O}_2$ , gas phase reaction, rate coeffs. meas. 0-97704

**sulphur compounds continued**

- $\text{SO}_2$ +olefin+thiirane+ $\text{O}_3$  excited neutral metastable  $\text{SO}_2$  form. mass spectrometric study 0-83300  
 $\text{SO}_2^{2+}$ ,  $\text{SO}_2^{2+}$ , O K-emission spectra, electron struct. 0-87099  
 $\text{SO}_4^{2-}$ , ionisation energies, SCF-X $\alpha$  transition state calcs. 0-74115  
 $\text{SO}_4$  removal from atmosphere, by absorption reaction, using MARTZ-CLEAN reagents based on  $\text{NaClO}_2$  and  $\text{K}_2\text{CO}_3$  (*Japanese*) 0-61147  
 $\text{S}_2\text{O}$ , UV excitation spectra, mol. fluoresc. meas. 0-83389  
 $\text{SO}_2\text{Cl}^-$  and  $(\text{SO}_2)_2\text{Cl}^+$ , heats of formation, determ. by mass spectroscopic technique 0-76540  
 $\text{SO}_2\text{F}$ , dye laser excitation of vibr. levels of upper electronic state, mol. fluoresc. meas. 0-83402  
 $\text{SO}(\Sigma^+ \rightarrow \Sigma^-)$ , in O-COS- $\text{O}_2(^1\Delta_g)/\text{O}_2$  system, chemiluminescence 0-66806  
 $\text{SPBr}_3$ , mol. struct., electron diffraction and spectroscopic vibr. amplitude 0-58387  
 $\text{Sf}_6$ , integrated IR band intensities and transition moments 0-95611

**sum rules**

- Adler-Weisberger sum rule and the  $\sigma$ -commutator for the kaon-proton system 0-101956  
Adler-Weisberger sum rule and the  $\sigma$ -commutator for the kaon-neutron system 0-101957  
charmed hadrons, SU(4) mass-breaking, mass sum rules 0-62959  
charmed particles, hadronic props., superconvergence sum rules 0-78043  
class of sum rules for system of identical particles 0-91019  
conserved axial second class current, sum rule, dispersion calc. 0-77986  
dispersion sum rules and exotic baryon resonances, reggeon scatt.,  $E_{55}$  resonance (*Russian*) 0-101955  
doubly closed shell nuclei, isovector giant monopole resonances, sum rule approach 0-78244  
Drell-Yan process higher order corrections, QCD and parton model sum rules 0-95251  
effective NN interaction and exchange current vel. depend., dipole sum rule enhancement 0-63100  
energy momentum sum rule beyond the leading order in QCD 0-78024  
energy weighted sum rules for spin-dependent excitations of nuclei 0-86833  
even-even nuclei, static quadrupole moments of arbitrary excited states, sum rule approach 0-91135  
hadron interactions, effective radius quantum number depend., quark sum rules (*Russian*) 0-102062  
hadronic targets, spin- $1/2$ , Compton scatt., optimal sum-rule inequalities 0-105815  
Nachtmann moments of  $F_2^{pN}(x, Q^2)$  and energy momentum sum rule 0-57580  
nuclear electro-excitation, energy-weighted isoscalar sum rules 0-63174  
nuclear field theory, phonon renormalisation, eigeneqns. and sum rules (*Chinese*) 0-102127  
nuclear matter, correlated, electric dipole sum rule 0-83056  
polynomials, zeros, sum rules 0-57521  
polynomials, zeros, sum rules 0-62888  
QCD spectral function sum rules, EM current flavour components 0-99084  
quarkonium systems, sum rules 0-68423  
d inelastic screening, form factor at  $t \neq 0$  0-91070  
 $\gamma p \rightarrow W^+ n$ , current algebra and sum rules high energy  $W^+$  prod. 0-102039  
 $\mu p \rightarrow \mu n W^+$ , current algebra and sum rules high energy  $W^+$  prod. 0-102039  
 $\nu(\bar{\nu})N \rightarrow N' \gamma e(\bar{e})$ , current algebras and high energy  $\gamma$ -prod., sum rules 0-102039  
 $\pi^0, \pi^\pm$  EM polarisabilities, sum rules, coloured quark field theory 0-57561  
 $\pi N \rightarrow \pi N$ , finite-energy sum rules, three component duality 0-82996  
 $^{56}\text{Fe}(\alpha, e)$ , E2 isoscalar resonance sum rule, DWBA anal. 0-68621  
 $^2\text{He}(\alpha, e)$  energy weighted sum rules (*Russian*) 0-86900  
 $^4\text{He}$  photodisintegration, total, dipole, and quadrupole cross sections, sum rules (*Russian*) 0-83094

**Sun**

- see also solar .....  
see also cosmic ray solar modulation  
Alfven wave flux, rel. to solar wind accel. 0-85923  
angular semidiameter, new meas. from limb darkening function obs. at 5012 Å 0-67677  
centre-to-limb solar observation of Ca II K-line component (*French*) 0-82331  
chromosphere-corona transition zone of solar active regions, non-thermal velocities (*French*) 0-77371  
colour rel. to Hyades metal content and distance 0-101569  
constant mass solar model, differentially rotating gaseous polytropes configurations 0-82338  
convection zone, ensemble-averaged eqns. for granulation, supergranulation and giant granules 0-67698  
diameter, secular decrease, Tobias Mayer obs. refute hypothesis 0-90389  
distance from galactic centre, determ. from radial vels. of O and B stars 0-101584  
ellipsoid of inertia, model rel. to perihelia of inner planets orbits 0-67531  
five-minute oscillations, horizontal energy flows struct. 0-62103  
gravitational red shift, Fe I line meas. 0-90391  
heliosphere H atoms, ionis. by light and solar wind in near Sun region 0-105145  
non-radial oscils. with initial chemical discontinuity 0-82341  
oscillation periods, correl. with cosmic ray short-term fluctuations periods 0-67483  
oscillations, period obs. rel. to internal struct. 0-105226  
oscillations with 160 minute period, evidence 0-82324  
plasma diagnostics of solar interior, use of MHD pulses 0-109405  
position, ephemerides calc. formulae (*German*) 0-77367  
positions, low-precision formulae 0-61990  
quiet spatial structure during 1977 October eclipse, VLA 6 cm obs. 0-72895  
radio antenna using gravitational lens, interstellar communication 0-62040  
secular accel. rel. to Earth-Moon tidal friction, Earth moment of inertia change 0-81803  
solar motion vector, correl. with nodes and perihelia distrib. of nearly parabolic cometary orbits 0-67661  
stability against nonradial thermal modes 0-82322  
standard model and stellar evolution calc. programme 0-67703



**Sun** continued

- Sun and heliosphere, conference, London, England (1979 April 3 to 4) 0-82574
- surface oscillations and pulsations, rotation speeds 0-67676
- temperature minimum in far IR, var. with solar cycle 0-94769
- torsional oscillator with 11 year period 0-105217
- velocity field meas. using Fabry-Perot spectrometer 0-90333

**sunlight**

see also atmospheric optics; sky brightness

- aerosol, solar radiation absorpt., visual photometric meas. technique 0-85750
- airport control tower cab, optical design 0-58661
- anisotropic diffuse insolation, calc. of instantaneous flux on tilted surfaces 0-101412
- atmosphere attenuation, effect of O<sub>3</sub> and H<sub>2</sub>O vapour content and atmos. turbidity 0-93855
- atmosphere extinction, meas. in mountainous regions 0-90202
- atmosphere temp. drop due to airborne volcanic dust 0-85726
- British spring weather, survey (1950 to 1979) 0-98427
- clear sky conditions, solar radiation and illumination simultaneous meas. 0-81985
- climatology of global solar radiation in California and an interpolation technique based on orthogonal functions 0-67402
- daily solar total irradiance, fluctuations, temporal statistical anal. (French) 0-61292
- diffuse irradiance measurement using shadowband, corrections 0-101410
- diffuse solar radiation below overcast sky, ang. distrib. 0-85719
- direct beam solar irradiance and illuminance computation 0-90174
- direct irradiance at the ground, parametric modelling 0-101411
- direct solar energy, Markov chain simulation with one minute binning (French) 0-61293
- Earth satellite orbits, effects of resons. with respect to solar radiation press. perturbations 0-90326
- fluctuations observed at Earth surface rel. to stratosphere aerosol content fluctuations 0-82035
- flux var. rel. to O<sub>2</sub> density in thermosphere 0-72659
- global solar radiation est. and prediction by stepwise multiple regression anal. for Greece (1961 to 1975) 0-61880
- global spectral distrib. determ. using rapid spectral radiometer for solar cell appls. 0-61369
- global surface irradiance, effect of aerosol props. and surface reflectivity 0-76611
- incident solar radiation at Earth surface, estimation from geostationary satellite data 0-82006
- insolation, SOLMET data, 1953 to 1975, anal. rel. to solar availability for winter space heating 0-81421
- irradiance on horizontal surface, estimation of totals from UK average meteorological data 0-81422
- irradiance outside atmosphere, Bouguer method for ozonometer determ. (Russian) 0-61918
- Israel, estimation of solar radiation and ambient temps. 0-76607
- Jupiter atmosphere, UV radiation rel. to hydrocarbon photochemistry and Lyman alpha albedo 0-105194
- light sources for simulating sunlight 0-87454
- luminous efficacy of daylight at Tokyo (Japanese) 0-72631
- measurement, using automatic solar-radiation meter 0-89592
- mesoscale mapping of available solar energy at the Earth's surface by use of satellites 0-72613
- monthly average diffuse radiation, cloudiness index and sunshine duration correlating methods 0-98384
- monthly mean global solar radiation maps for Japan 0-109185
- ocean, diurnal var. of underwater irradiances on horizontal surfaces 0-72549
- pollution affecting solar radiation incident on St. Louis, USA 0-109247
- radiation flux density, solar and terrestrial radiation dependent on the amount and type of cloud 0-67403
- radiation intercepted by a tilted surface, estimation of daily, clear sky, spatial distrib. 0-81423
- radiation pressure, appl. to satellites inertially fixed pitch stabilisation 0-101523
- radiation statistics, linear spatial interpolation 0-93859
- radiative transfer, cloud shape and mutual shading effects 0-101430
- scattered light intensity and polarisation degree in model atm., mol. anisotropy effect 0-77104
- sea surface, Sun glitter pattern appl. to surface slope distrib. function determ. (Russian) 0-94611
- solar central receiver system, flux density integral for reflected sunlight, numerical anal. 0-93863
- solar energy utilisation, global and sky radiation estimates for Austria 0-93861
- solar energy utilisation, prediction of hourly diffuse solar radiation from measured hourly global radiation on a horizontal surface 0-93864
- solar irradiance, model for determining the spectral quality of daylight on a horizontal surface at any geographical location 0-93856
- solar-radiation regime, energy structure distribution laws analytic representation 0-98378
- sunset IR spectra and stratospheric NO and NO<sub>2</sub> mixing ratio profiles determ. 0-94563
- underwater sunlight fluctuations in sea spatial and temporal correlation 0-94533
- United States, solar climates 0-76612
- UV radiation changes at Earth surface, effects of possible O<sub>3</sub> changes 0-94577
- UV radiation in stratosphere, rel. to solar cycle signal in tropospheric winds 0-72604
- UV spectrum 140 to 350 nm, NASA meas. using SURF storage ring calibrations 0-94721
- Venus atmosphere, scattered solar radiation fluxes spectral and altitude distrib. 0-62059
- C I photoionisation by sunlight, C II line excitation 0-58223
- Si solar concentrator cell, effects of nonuniform illumination and temp. profiles under concentrated sunlight 0-93941

**sunshine** see sunlight**sunsports**

see also solar activity

- annual mean no. rel. to Bombay geomagnetic and climatic (1848-1967) data 0-81811
- area on solar disc, effect on solar constant 0-77376
- early records in 'The Book of Changes' (Chinese) 0-77366

**sunsports** continued

- eleven-year cycle, correl. with ionosphere equatorial spread-F occurrence in American zone 0-109298
- equator-crossing spot, development and motion 0-90394
- faculae rel. to sunspot cycle 0-90390
- fine struct., image motion due to atmospheric heat turbulence 0-77108
- global rotation rate determ. using 1967-74 sunspot data 0-90387
- group velocities, statistical distrib., depend. on solar activity cycle phase 0-72918
- lifetimes and numbers of groups, predictions from statistical anal. 0-82327
- long term vars. in solar wind and sunspots, implications of auroral changes during 18th and 19th centuries 0-98498
- magnetic field gradients determ. from Zeeman line rot. and profiles (Chinese) 0-85920
- Maunder Minimum, sunspot numbers not correlated with temps. during Little Ice Age 0-82050
- Maunder minimum nature, explanation of differential rot. effect on convection struct. 0-101573
- McMath 14275, sunspots correl. with 6 cm emission maxima from 6" resolution obs. 0-62096
- McMath region 13043, opposite polarity sunspots collision rel. to centimetre-wave sources rapid var. 0-67688
- numbers, rel. to solar far IR brightness, temp. minima 0-62035
- numbers in current millennium, rel. to <sup>14</sup>C prod. in atm. 0-85730
- origin, strong downdraught development, hydrodynamic anal. 0-72908
- penumbral edge continuum bright spot, characts. 0-98638
- plage fragments, characts. assoc. with photosphere network props. 0-98634
- radio bursts, peak flux spectra, statistical anal. 0-98641
- Schluter Temesvary sunspot, vertically orientated mag. flux tubes, exact static equilib. 0-98637
- umbrac, internal structure 0-82328
- umbrac, IR Ca II lines 0-85918
- umbral dots, dynamic and struct. behaviour for photometry obs. 0-109409
- Wolf relative number, rel. to originating groups and average lifetime 0-67684
- Wolf-Zurich number conversion, reduction factors (German) 0-98631
- Zeeman line profile, mag. field determ. 0-82221
- TiO equivalent width meas., theoretical interpretation, line form. process 0-72902

**superaerodynamics** see rarefied fluid dynamics**superalloys**

- Hastelloy, C-276, H-transport rel. to ageing treatment 0-75384
- Hastelloy, C-276, H-induced crack growth 0-71747
- Hastelloy-X, low cycle fatigue crack propagation at 25°C and 760°C 0-104270
- Hastelloy-X, Ni-Cr-Fe-Mo, cyclic oxidation resist. improvement by high temp. etching treatment 0-97627
- Incoloy 800, nuclear grade boiling tubing superalloy, Co and C content anal. 0-78397
- Inconel 600, nuclear grade boiling tubing superalloy, Co and C content anal. 0-78397
- Inconel 617, creep, morphological changes of carbides, affect on creep props. 0-108509
- Inconel 718, grain growth during sintering 0-97449
- Inconel X-750, deform. and fracture characts., 24-816°C 0-108551
- microcrystalline, rapidly quenched particulates, appl. 0-84887
- Nimonic 80A superalloy, contrast from cavities in HVEM 0-79780
- Rene 80, dislocation behaviour during plastic deform. (Japanese) 0-108504
- Al-Zn-Mg superplastic alloy, cavity growth under creep conditions 0-60940
- Fe base superalloy, type A-286, elevated temp. fracture toughness testing of thin section irradi. materials 0-61063
- Fe-Ni-Al-Co-Cu-Ti YundKT type, S effect on mech. props. 0-60927
- Fe-Ni-Co-Cu-Ti YundKT alloys, impaired mag. props. with C and S additions 0-60368
- Fe-Ni-Cr (35, 15 wt.%) superalloy, stress rupture and tensile props., C and B additions effect (Chinese) 0-104244
- Fe-Ni-Cr-Al-Ti-W-Mo (35, 15, 2.4, 2.3, 2.2 wt.%) wrought superalloy, freckles (Chinese) 0-104137
- Ni base superalloy Nimonic 80A, microstruct. anal. by high-resolution electron microscopy 0-76459
- Ni base superalloys, rapid solidification, use in gas turbine engines 0-84888
- Ni based Rene 80 superalloy, initial stages of pack aluminisation 0-76188
- Ni superalloy, STEM microanal. of precipitates and their nuclei 0-81067
- Ni-(Co)-Cr, aluminate coating, microstruct. and chem. 0-76189
- Ni-Al, (2 and 6 wt.%), oxidation,  $\alpha$ -Al<sub>2</sub>O<sub>3</sub> growth, microstruct., precip. 0-108626
- Ni-base, powder metallurgical, creep-rupture at intermediate temps. 0-97568
- Ni-base, STEM microanalysis of precipitates 0-104492
- Ni-base superalloys, emission spectral anal. with fixed time integration technique (Japanese) 0-71974
- Ni-base superalloys, technique for replication of  $\gamma'$  0-79648
- Ni-base wrought superalloy, creep and stress rupture behaviour in air and vacuum 0-60918
- Ni-based, hot workability, effect of S, Ca, Mg, Y and Zr minor elements 0-66552
- Ni-Cr superalloy, interactions between creep and low cycle fatigue (Chinese) 0-66572
- Ni-Cr-Co-Al super alloy, IN-738, creep failure criteria 0-65150
- Ni-Cr-NbC (18, 10 wt.%) eutectic composite, unidirectional solidification, thermal cycling, temp. range effect on microstructural degradation 0-89272
- Ni-Cr-Ti rapidly solidified superalloys, surface segregation 0-76263
- Ni-Fe-Cr superalloy 718, heat treatment effect on room temp. and elevated temp. fracture toughness response 0-100922
- Ni-Ti-Al superalloy, pendant drop melt extracted, struct. and props. 0-76242
- $\beta$ -NiAl, oxidation,  $\alpha$ -Al<sub>2</sub>O<sub>3</sub> growth and microstruct. 0-108627
- NiTaC eutectic superalloy, casting, furnace atm. effects 0-84880
- Ti-70A superalloy, fusion reactor blanket structures, radiation resistance 0-63379

**superconducting cables**

fusion reactor, induction heating coils, 50 kA prototype superconducting cable, critical current 0-106196  
rows of wires, in transverse mag. field, AC losses (*Japanese*) 0-60143  
Nb-Ti, multifilamentary, Mirror Fusion Test Facility, superconductor core manufacturing and quality 0-93521

**superconducting critical field**

anisotropic superconductors, upper critical field theory 0-75692  
experimental data, anal. for type A and type B superconductors (*Chinese*) 0-60151  
granular superconductors, percolation theory, crit. props. 0-84575  
hard superconductor, flux trapping, penetration depth determ. 0-100572  
Josephson coupled layered supercond., upper critical field (*Russian*) 0-100551  
layered compounds, upper crit. fields and reduced dimensionality 0-70910  
magnetic impurity low temp. behaviour, transition temp., specific heat, free energy 0-88691  
molybdenum chalcogenides, multicomponent, physical props. 0-84577  
molybdenum ternary chalcogenides, structures and properties survey (*Czech*) 0-70870  
periodic structures, crit. fields (*Russian*) 0-88700  
quantum polarisation effect in critical freq. EM field 0-75677  
quasi-one-dimensional superconductor, critical mag. field, transition temp. (*Russian*) 0-93058  
quasi-zero-dimensional superconductor, theory of upper critical field 0-107968  
superconductor, magnetic, shape effects 0-103773  
transition metal chalcogenides, quasi-one-dimens., elec. mag., and supercond. props., review (*Russian*) 0-93022  
transport current effects on superconducting thin-walled cylinder in mag. field (*Russian*) 0-100573  
type II supercond. cylinder, magnetisation change induced by current near upper crit. field 0-70890  
type II superconductor, bounded, intermediate state struct. form. near crit. field, role of surface 0-80465  
type II superconductors, anisotropic, demagnetisation effects on lower critical field 0-97043  
type II superconductors, order parameter change near  $H_{c2}$ , influence of transport current 0-75690  
type-II superconductors, anisotropic, lower crit. field 0-60153  
Al film in microwave radiation field, resistive state transition (*Russian*) 0-93038  
BaPb<sub>1-x</sub>Bi<sub>x</sub>O<sub>3</sub>, superconducting props., Hall coeff. and elec. resist. meas. 0-84531  
Cu-Nb<sub>3</sub>Sn multifilamentary tapes, in situ formed, crit. current density anisotropy 0-84576  
Cu-V<sub>3</sub>Ga, supercond. in situ composites, stress effects on crit. props. 0-65757  
Cu<sub>1-x</sub>La<sub>x</sub>, sputter-cooled, phase diagram and supercond. props. 0-70881  
ErRh<sub>3</sub>B<sub>4</sub>, superconducting thin films, critical mag. field 0-75693  
ErRh<sub>1-x</sub>Sn<sub>3+x</sub>, synthesis, supercond. and mag. props. 0-100547  
Er<sub>2</sub>Y<sub>1-x</sub>Rh<sub>2+x</sub>B<sub>4</sub>, mag. and supercond. transitions 0-70874  
B-Ga, metastable, elec. props. in normal and supercond. states (*Russian*) 0-65520  
In-Bi(Tl)(Pb), small  $\kappa$  supercond., phase transitions higher than second order 0-88668  
In-Pb (7 at %) alloy cylinder, magnetisation change induced by current near upper crit. field 0-70890  
In<sub>2</sub>Sn, tetragonal supercond., lower and upper crit. field, anisotropy and temp. depend. 0-97042  
La, heat capacity and supercond. props. 0-65247  
Mo<sub>70</sub>Si<sub>30</sub>B<sub>10</sub>, amorphous alloys obtained by liq. quenching, superconductivity 0-75670  
Nb, critical current density, deviation from critical state model 0-84578  
Nb, film, critical mag. fields and currents, temp. depend. (*Russian*) 0-103798  
Nb film, struct. and electrophys. props. at 4.2K 0-80436  
Nb, peak effect due to vortex pinning in subsurface layer (*Russian*) 0-93060  
Nb, US attenuation, hysteresis near and below  $H_{c1}$  0-75676  
Nb, upper crit. field, temp. depend. and anisotropy 0-80462  
Nb-Rh,  $\sigma$ -phase alloy, superconductivity and resistance behaviour 0-70882  
Nb-Si(-V)(Zr)(Mo)(Ta)(W)(C)(B)(Ge), ductile amorphous, superconductivity 0-60131  
Nb-Ti, pinning curves, high field  $J_c$  and scaling behaviour 0-93064  
Nb-Ti-Ta, pinning curves, high field  $J_c$  and scaling behaviour 0-93064  
Nb-Ti-Zr ternary system, high-field supercond. 0-97045  
Nb<sub>2</sub>/Sn-Cu composites, in situ processed, supercond. props. 0-75698  
NbN, supercond. RF reactively sputtered films, deposition parameter effects on props. 0-80972  
Nb<sub>3</sub>Sn bronze process, flux pinning scaling law depend. on strain 0-75696  
Nb<sub>3</sub>Sn, supercond. props., effect of neutron irradiation 0-80463  
Pb-Bi alloy, crit. mag. fields, influence of parameters 0-75691  
Pb-Bi-Tl alloy, crit. mag. fields, influence of parameters 0-75691  
Pb-Tl alloy, crit. mag. fields, influence of parameters 0-75691  
PbMo<sub>6</sub>S<sub>8</sub>, supercond., upper crit. field meas. up to 600 kG 0-93057  
PbMo<sub>6</sub>S<sub>8</sub> wire, powder processed, crit. current density and field 0-80466  
(SN)<sub>x</sub>, supercond. props. rel. to fibrous morphology 0-84570  
Se<sub>2</sub>C<sub>3</sub>, superconducting phase synthesis at high press. and temp., critical field (*Russian*) 0-65732  
Sn film, crit. mag. fields, temp. depend., penetration depth thickness depend. 0-70908  
Sn-Bi(Sb), small  $\kappa$  supercond., phase transitions higher than second order 0-88668  
Ta-Rh,  $\sigma$ -phase alloy, superconductivity and resistance behaviour 0-70882  
TaS<sub>2</sub>, intercalated with methylamine, supercond. layer cpd., crit. field enhancement and reduced dimensionality 0-60152  
Ti-Nb-Si, amorphous alloy, supercond. props. and crystn. behaviour, TEM and DTA study (*Japanese*) 0-84536  
Ti-Nb-Zr-Ta, superconducting props. comp. depend., stress effects and precipitation behaviour, X-ray scatt. 0-93059  
TiN, low-energy ion-stimulated deposited, supercond. props. 0-88664  
V columnar films, crit. field anisotropy, depend. on prep. conditions (*Russian*) 0-93056  
V<sub>3</sub>Si, neutron irradiation, grain boundary pinning, field-depend. change of crit. current density 0-65759

**superconducting critical field continued**

V<sub>3</sub>Si, supercond. props., effect of neutron irradiation 0-80463  
W<sub>70</sub>Si<sub>30</sub>B<sub>10</sub>, amorphous alloys obtained by liq. quenching, superconductivity 0-75670  
superconducting critical temperature *see* superconducting transition temperature  
superconducting devices  
*see also* cryotrons  
applied solid state physics, book 0-94936  
bolometer, high-speed, based on Ag-Sn double films 0-57368  
fluxmeter, quantum, with 15 to 20 kHz passband 0-57345  
laser frequency measurement using supercond. point contacts 0-90824  
lens, for imaging organic materials in electron microscope 0-73553  
magnetic flux-free environment creation, cryogenic appl. 0-101797  
positive-sensitive detector of ionizing particles 0-63460  
solenoid with flowthrough opt. cryostat, for magnetoopt. investigations 0-105651  
spheres and current carrying coils, integral representation of inductance 0-80469  
temperature fixed point device, prep. and calibration 0-82770  
NbTi monofilamentary wire in current sharing state, supercond. temp. sensor use 0-57288

**superconducting energy gap**

Al<sub>15</sub> compounds, supercond. crit. temp. for model density of state using Eliashberg gap eqns. 0-93034  
anisotropic superconductors, nonmag. impurities effect on supercond. transition temp. 0-93035  
anisotropy, Eliashberg eqns., review (*Spanish*) 0-84544  
anisotropy, normal layer proximity effect 0-84558  
barium stearate single-layer Langmuir films, elastic and inelastic tunnelling 0-80403  
charge imbalance relaxation freq. depend. near  $T_c$  0-93030  
collective oscillations and electric field penetration, review 0-88678  
Cooper pairs formation, and nature of supercond. currents 0-65736  
energy dependent electronic density of states, gap and crit. temp. 0-84538  
ferromagnetic superconductor, paramagnetic fluctuations, influence on superconductivity 0-70900  
nonequilibrium states, narrow nonequilibrium sources (*Russian*) 0-88687  
nonequilibrium superconductor, high-freq. AC process dynamics 0-88674  
phonon Raman scattering in superconductors 0-100657  
proximity systems with magnetic impurities, DC Josephson effect 0-100554  
quasi-two-dimensional dirty superconductor, nonstationary Josephson effect (*Russian*) 0-100556  
transition metal chalcogenides, quasi-one-dimens., elec. mag., and supercond. props., review (*Russian*) 0-93022  
tunnel junction, nonequilibrium phonon effect on supercond. states with 2 coexisting energy gaps 0-84561  
weak links, order parameter and quasiparticle dynamic props. 0-100555  
Al, narrow superconducting bridges, microwave radiation stimulated  $T_c$  enhancement 0-84537  
Al, superconducting band gap anisotropy and Fermi surface anisotropy (*Spanish*) 0-84544  
Al-Mn(Cr)(V), dil., supercond., nucl. spin relax. and quasiparticle excitations 0-88680  
Cu<sub>1-x</sub>Mo<sub>x</sub>S<sub>8</sub>, electron tunnelling spectroscopy expts. (*German*) 0-107966  
Hg films, superconducting, far-IR and electrodynamic props. meas. 0-103957  
Nb, effect of changes in  $\alpha^2(\Omega)F(\Omega)$  on the zero-temp. energy gap 0-97025  
Nb, superconducting, thermodynamic props. 0-107955  
Nb-NbO<sub>x</sub>-Pb tunnel junction, temp. depend. of effective Nb energy gap 0-80454  
NbSe<sub>2</sub> (2H), Raman scatt. from supercond. gap excitations 0-93340  
NbSe<sub>2</sub> (2H), Raman scatt. by supercond. gap excitations, coupling to CDWs 0-103956  
Nb<sub>3</sub>Sn, effect of changes in  $\alpha^2(\Omega)F(\Omega)$  on the zero-temp. energy gap 0-97025  
Pb, effect of changes in  $\alpha^2(\Omega)F(\Omega)$  on the zero-temp. energy gap 0-97025  
Pb-Cu(Ag) double layers, intermetallic boundary effects, tunnelling 0-88692  
PbMo<sub>6</sub>S<sub>8</sub>, electron tunnelling spectroscopy expts. (*German*) 0-107966  
Sn-KCl granular superconductors, far IR absorpt. 0-84548  
Ta, effect of changes in  $\alpha^2(\Omega)F(\Omega)$  on the zero-temp. energy gap 0-97025  
V<sub>3</sub>Si thin film far IR laser thermal spectroscopy 0-60144  
V<sub>3</sub>Si tunnel junctions, energy gap investigation 0-84569  
superconducting junction devices  
bridge, phase slip dynamics and excess current (*Russian*) 0-103786  
dynamic props. of supercond.-normal-supercond. junction (*Russian*) 0-103785  
FIR detectors, Josephson-junction direct devices and transition edge bolometers, review 0-77865  
fluxons on a Josephson line with loss and bias 0-103794  
gradiometers, for measuring magnetic effects of geophysical origin 0-101463  
granular films as weak link in Josephson devices 0-88685  
granular microbridges, fluctuations and crit. current determ. 0-84562  
Josephson coupled layered supercond., upper critical field (*Russian*) 0-100551  
Josephson current, paramag. impurities effect (*Russian*) 0-70903  
Josephson effect, through locally lowered tunneling barriers 0-100558  
Josephson effect higher harmonics, flux tunnelling, thermodynamic free energy 0-60147  
Josephson effect voltage standard, at zero current bias 0-57245  
Josephson element principles, applications to precision meas. of electric potential and magnetic flux at high freq. (*Norwegian*) 0-80447  
Josephson FET, hybrid, feasibility 0-80451  
Josephson harmonic mixer, freq. meas. of methyl alcohol laser at 4.25 THz 0-95078  
Josephson interferometers, large arrays, device parameter meas. 0-75682  
Josephson junction, coherent radiation induced bistability 0-80453  
Josephson junction, with linear periodic current-phase relations, phase locking and microwave impedance 0-93043  
Josephson junction interferometer, loop inductance 0-97034  
Josephson junction with matched RF source, analogue simulation 0-75683  
Josephson junctions, applications in plasma physics 0-103194  
Josephson junctions, coupled, I-V charact., model calc. 0-84559



**superconducting junction devices continued**

- Josephson junctions fabrication, tunnelling through edge-grown barriers 0-100567
- Josephson parametric amplifiers, gain-dependent noise temp. 0-84552
- Josephson symmetric two-junction interferometers, self-induced reson., theory 0-107962
- Josephson tunnel junction, nonresonant vortex motion 0-97037
- Josephson tunnel junctions of nonuniform width, max DC Josephson current vs. external mag. field charact. calc. 0-65747
- Josephson-junction capacitor, QED theory 0-93049
- magnetopneumographic meas. with SQUID fluxgate magnetometers 0-104711
- microbridge, high-resistance, with Bi crosspiece 0-93050
- microbridges, triggering of phase slip by impact of low-energy atoms 0-93045
- microbridges, with paramag. impurities, Josephson steady-state effect (*Russian*) 0-93042
- microbridges and filaments, high-freq. AC process dynamics 0-88674
- neuromagnetic fields sources location, using SQUID system, comparison with electrical method 0-101190
- non-equilibrium superconductivity characterisation, via Josephson effect 0-100557
- oscillator, current-drive, quantum modelling 0-75687
- parametrically coupled Josephson bridges, resistive state, proximity effect (*Russian*) 0-100550
- point contacts, three-dimens. assembly, crit. currents and penetration depth 0-84560
- proximity effect weak links, steady-state and RF props. 0-84563
- quasiparticle mixers, supercond.-insulator-supercond., conversion gain prediction 0-70901
- quasiparticle superconductor-insulator-superconductor tunnel junctions as microwave detectors 0-65744
- RF biased SQUID, meas. of absolute intensity of weak mag. field 0-82794
- RF SQUID, hysteretic, input noise 0-70905
- RF SQUID, quantum interference in supercond. ring closed by weak link 0-97035
- RF SQUID magnetometer, synchronous demodulation, amplitude- and phase-sensitive detection 0-105679
- RF SQUID structures, topology and theory 0-97036
- SQUID, appl. to cardiac recording, phase and amplitude relationships of elec. and mag. events 0-104695
- SQUID, DC-thin film, magnetocardiogram meas. first order gradiometer 0-89877
- SQUID, operating principles (*Hungarian*) 0-75686
- SQUID, RF, LF noise expt. exam. 0-98947
- SQUID, thermodynamic equilibrium fluctuations generation by Josephson junction, Werthamer theory 0-100564
- SQUID appl. to nuclear gyros and magnetometers, high stability and sensitivity 0-98949
- SQUID appl. to somatically evoked field meas., transient responses to elec. stimulation of median nerve 0-104706
- SQUID applications to weak magnetic field measurement 0-86267
- SQUID based detection systems, mag. field meas., comparison between two methods 0-104712
- SQUID biomedical appl., iron overloaded liver non-invasive diagnosis 0-101244
- SQUID detection, low temp., NMR imaging improvement towards mol. kinetic meas. 0-104723
- SQUID gradiometer, DC, thin-film, design optimisation 0-98951
- SQUID gradiometer, second-derivative, magnetocardiogram meas. 0-104696
- SQUID instrumentation for biomagnetic meas. in unshielded and noisy environments 0-104710
- SQUID magnetometer, 430 MHz, AC-biased, quantum limited 0-101809
- SQUID magnetometer, AC-biased, noise, slew rate and stability 0-98948
- SQUID magnetometer, optomagnetic meas. appl. 0-98950
- SQUID magnetometer, with independent pumping 0-105685
- SQUID magnetometer for meas. of magnetocardiogram and cardiac output 0-104709
- SQUID magnetometer with temp. control, spontaneous magnetisation and mag. susceptibility meas. 0-68221
- SQUID magnetometers, AC-biased, classical to macroscopic quantum transition 0-98953
- SQUID magnetometers, AC-biased, macroscopically quantised, higher harmonics in Josephson effect 0-98952
- SQUID magnetometers, geophysical dewar systems design 0-101462
- SQUID magnetometers, magnetoretinographic meas. of retina injuries in eye 0-104702
- SQUID ring, fluxoid transition mechanisms, quantum vs. thermally excited 0-100565
- SQUID system for low drift high sensitivity magnetisation meas. 0-86347
- SQUID technique for magnetoencephalogram power spectrum estimation of human brain 0-104704
- SQUID used in superconducting shield for magnetoencephalography 0-104708
- SQUID-based NMR spectrometers, sensitivity limits 0-98961
- super-Schottky diode, space appl., microwave and IR detectors 0-85836
- superconductor-insulator-superconductor tunnel junctions, responsivity to microwave radiation 0-100553
- thin film technology, appls. in energy, optics, and electronics, review 0-78932
- tunnel junction, normal conductance change, origin 0-65753
- tunnel junctions, quantum noise effects in 0-1 mV bias range 0-80449
- tunnel-junction refrigerator 0-57311
- weak links, order parameter and quasiparticle dynamic props. 0-100555
- weak links, quasiparticle-injected, simple-heating-induced Josephson effects 0-70904
- Al granular bridges, with different thicknesses and widths, crit. current, temp. depend. 0-88688
- Al, narrow superconducting bridges, microwave radiation stimulated  $T_c$  enhancement 0-84537
- Al shielded room for biomag. meas. 0-104846
- Al/AIO<sub>x</sub>/La-rare earth metal tunnel junctions, cond. meas., cryst. field effects 0-88694
- Au/In proximity effect bridges, square arrays, transition temps. 0-84557
- Au/Pb/In-oxide-PbBi tunnel junctions, supercurrent interference patterns and excess currents 0-100563
- In-In<sub>2</sub>O<sub>3</sub>-Pb, Josephson tunnel junction fabrication for MM-wave detector 0-100427

**superconducting junction devices continued**

- Nb, ion-implanted bridge with thick Pb banks, fabrication and characterisation of film parameters 0-100569
- Nb microbridges, vertical type, fabrication and DC characts. 0-103788
- Nb SQUID, low-noise DC type, with 1  $\mu$ m tunnel junctions 0-80450
- Nb superconducting point contact, singularities of I-V curve and voltage fluctuations 0-93044
- Nb thin film microbridge, video detection of far IR radiation (*Japanese*) 0-97038
- Nb thin-film Josephson tunnel junctions, fabrication and props., in situ ellipsometric meas. 0-65749
- Nb, thin-film SQUID working at 4.2K, fabrication and characterisation 0-100570
- Nb-Nb Josephson junctions, submicron, thermally recyclable, fabrication and characts. 0-100566
- Nb-Nb<sub>2</sub>O<sub>5</sub>-Pb Josephson junction formed on Nb film edge 0-107960
- Nb-Nb<sub>2</sub>O<sub>5</sub>-Pb(In) Josephson junctions, props. of Nb<sub>2</sub>O<sub>5</sub>, thermally grown tunnel barriers 0-100568
- Nb-NbO<sub>x</sub>-Pb Josephson junctions with high current densities, critical current 0-100552
- Nb-NbO<sub>x</sub>-Pb tunnel junctions, oxide tunnelling barriers, ESCA characterisation 0-65745
- Nb-NbO<sub>x</sub>-Pb tunnel junction, temp. depend. of effective Nb energy gap 0-80454
- Nb-Pb, long, magnetic field behaviour of zero field steps 0-100561
- Nb-Te-Pb Josephson junctions, prep. and props. 0-65754
- Nb<sub>2</sub>Ge, bridge contact, Josephson effect 0-70906
- NbN granular microbridges, Josephson effects 0-84556
- NbN weak links, granular, Josephson behaviour 0-75681
- Pb-alloy Josephson tunnel junctions, effect of process variables on elec. props., cryogenic memory appls. 0-65748
- Pb-Cd-Pb junctions, pair pot., mag. field depend., crit. currents meas. 0-84555
- Pb-In(Au) base electrode film Josephson junctions, tunnel barrier oxide struct. 0-65750
- Pb-Nb-Pb bridged, variable thickness, ion implant, coherent vortex motion props. obs. 0-100562
- Pb-PbO-Pb, Josephson tunnel junction fabrication for Mm-wave detector 0-100427
- Pb-Te-Te oxide-Pb Josephson junctions, prep. and props. 0-65754
- Sn-SnO<sub>x</sub>-SN tunnel point contacts, spatially inhomogeneous state under strong injection conditions 0-80457
- Sn-SnO<sub>x</sub>-Sn tunnelling junctions, fabrication by modified RF plasma oxidation method 0-103787
- V-CdS-In Josephson junctions preparation and behaviour obs. 0-100559
- V<sub>3</sub>Si bridge contacts, nonstationary props. 0-103793
- V<sub>3</sub>Si-SiO<sub>x</sub>-Mo<sub>3</sub>Re<sub>2</sub>, supercond. tunnel junctions 0-107961

**superconducting lenses see magnetic lenses****superconducting machines**

- rotary machines as I/O system for superconducting magnetic energy storage system (*Japanese*) 0-85306

**superconducting magnets***see also superconducting machines*

- AC loss measurement, analogue digital double integration joulemeter 0-57325
- energy storage magnet, single layer, design and cost-related parameters 0-108815
- forced flow cooling, numerical anal. of heat-induced transients in He 0-82773
- frictional heating of metal-insulator pairs at cryogenic temps., rel. to supercond. magnet technology 0-66671
- fusion, toroidal field superconducting coil cryogenic stability and field anal., design parameter 0-106200
- fusion magnetic systems, struct. anal. methods and standards 0-86972
- fusion reactor, CC NbTi, pool cooling superconducting test coil, Japanese design 0-99340
- fusion reactor, cluster test facility, design 0-90835
- fusion reactor, ELMO Bumpy Torus Proof-of-Principle, proposed mag. system 0-99296
- fusion reactor, HFCTR, demonstration reactor conceptual design, high force density magnets and modularisation 0-95439
- fusion reactor, high current density superconducting coils, cryostability 0-106201
- fusion reactor, JXFR, superconducting mag. system conceptual design 0-99295
- fusion reactor, Large Coil Program, coil winding development support 0-106190
- fusion reactor, Large Coil Program, General Dynamics Convair/IGC manufacturing engineering 0-106169
- fusion reactor, Large Coil Program, Nb<sub>3</sub>Sn forced flow superconducting test coil, Westinghouse design 0-99337
- fusion reactor, Large Coil Program, NbTi superconducting test coil, General Electric design and manufacture program 0-102319
- fusion reactor, Large Coil Program, Westinghouse superconducting mag. elec. design 0-91250
- fusion reactor, Large Coil Task, CC NbTi forced flow superconducting test coil, Swiss design 0-99341
- fusion reactor, Large Coil Test Facility test stand design description 0-102320
- fusion reactor, large superconducting toroidal field coil program, progress report 0-99335
- fusion reactor, maximum toroidal mag. field value by core constraint 0-102349
- fusion reactor, MFTF, mag. cryostability 0-106198
- fusion reactor, MFTF, superconducting mag. quench vent rate 0-106197
- fusion reactor, multiple mirror, coil design and economic optimisation 0-99284
- fusion reactor, multiple fusion confinement with 2 MA levitated superconducting coil 0-106191
- fusion reactor, press. induced flow cooling, highly stable superconducting mag. systems 0-106192
- fusion reactor, SLPX TF coil, stress anal. using COSMIC-NASTRAN 0-106168
- fusion reactor, STARFIRE project, superconducting poloidal coils design study 0-106185
- fusion reactor, STARFIRE project, toroidal field coil system preliminary assessment 0-106186
- fusion reactor, superconducting toroidal system, force anal. for all fault conditions 0-91258

**superconducting magnets continued**

- fusion reactor, Tandem Mirror Reactor, end plug mag. system design 0-102347
- fusion reactor, torsatron, superconducting mag. engineering design 0-99297
- fusion reactor Large Coil Program, NbTi, superconducting test coil, General Dynamics Convair Division, Intermagnetics General Corp. design 0-99338
- fusion reactor magnetic coil, Large Coil Program, test heater conceptual designs 0-91251
- fusion reactor superconducting magnet joints, resistance welding 0-91259
- fusion reactor superconducting magnets, structural design 0-86974
- fusion reactors, Large Coil Program, low temp. stability, joints, design method 0-106195
- fusion reactors, Large Coil Program, pool boiling mag. quench press. calc. 0-106199
- fusion reactors, Large Coil Program, superconducting mag. coil struct. design status 0-106189
- fusion reactors, large Coil Program, Westinghouse coil cooldown and warmup 0-106193
- fusion reactors, Large Coil Program, Westinghouse coil stability testing, pulsed induction heating 0-106194
- fusion reactors, Large Coil Task, NbTi, forced flow superconducting test coil, EURATOM design 0-99339
- fusion reactors, Large Coil Test Facility, liq. He cooling system 0-102321
- fusion reactors, MFTF superconducting mag. design and construction 0-101008
- fusion reactors, Tokamak and tandem mirror reactors, neutral beam injection and superconducting magnets 0-63391
- fusion reactors, Torsatron T-1, demountable resistive joint for high current superconductors 0-106202
- gyromonotron design, 240 GHz, using supercond. magnet system 0-58498
- high-energy physics appl. 0-68990
- hollow conductors for force-cooled superconducting magnets, fabrication and properties (*Japanese*) 0-90868
- ion source, electron beam type, using supercond. solenoid, low-vel. heavy ions prod. 0-58017
- Large Coil Program, research and development activity 0-99336
- lens system for 500 kV electron microscope 0-68321
- magnetic energy storage system with superconducting rotary machines as 1/O system (*Japanese*) 0-85306
- magnetic flux compression, compression generator, PULSAR, design optimisation 0-68957
- multifilament superconductors, effect of local heat dissipation on stability 0-60156
- neutron irradiation effects on organic insulators at 5K for superconducting magnets 0-107336
- pulsed, stability studies, fusion reactor appls. (*Japanese*) 0-106158
- RST, RF driven steady state toroidal expt., design 0-91276
- safety of superconducting fusion magnets: twelve problem areas 0-102348
- solenoids fields meas., automatic, using NMR 0-57344
- stability problems in accelerators under high energy particle interactions (*Russian*) 0-68972
- structural alloys for superconducting magnets in fusion energy systems, props. at 4K 0-86976
- H<sub>2</sub> atoms trapping and thermal detection using superconducting magnet of low temp. 0-73396
- Nb-Ti, multifilamentary, Mirror Fusion Test Facility, superconductor core manufacturing and quality 0-93521
- Nb-Ti, superconductor optimisation for 12 Tesla toroidal field coils 0-91272
- Nb-Ti coils, for thermonuclear fusion (*French*) 0-95399
- Nb-Ti-Ta, superconductor optimisation for 12 Tesla toroidal field coils 0-91272
- Nb<sub>3</sub>Sn, multifilamentary coils for Lawrence Livermore Laboratory superconducting High Field Test Facility 0-90834

**superconducting materials**

- see also composite superconductors; dirty superconductors; strong-coupling superconductors; superconducting semiconductors; superconducting thin films; type I superconductors; type II superconductors
- internal friction near critical temperature at acoustic frequencies 0-100305
- Israel Physical Society 1980 annual meeting, Rehovot, Israel (April 1980) 0-94909
- layered superconductors, Josephson coupling effects, review 0-84554
- magnetic superconductors, mag. scatt. of neutrons 0-103819
- magnetic superconductors, spin fluctuation and US attenuation 0-80445
- metastable compound synthesis with high supercond. transition temp. 0-93024
- rare earth-Sn-X, X=Rh, Ir, Ru, Co, cryst. growth and cryst.-chem. invest. supercond./mag. ternary cpds. 0-100777
- semifinite sheet, current coil interaction, electrodynamic suspension system (*Russian*) 0-83539
- AH<sub>3</sub>, electronic struct. and electron-phonon interaction, hydrogenation effect, rel. to supercond. 0-107694
- CuCl, interface supercond., piezoelec. hypothesis 0-60128
- (SN)<sub>x</sub>, supercond. polymer, mag. props. meas. 0-107953
- (SnBr<sub>0.4</sub>)<sub>x</sub> 0-107953

**superconducting quantum interference devices** see **superconducting junction devices****superconducting semiconductor materials** see **superconducting semiconductors****superconducting semiconductors**

- metal-insulator transition, electron pairing, effect on optical props. of supercond. 0-60139
- Co<sub>2</sub>Mo<sub>2</sub>S<sub>6</sub>O<sub>2</sub>, O-containing Chevrel phases, synthesis and props. 0-108368
- Cu<sub>2</sub>Mo<sub>2</sub>S<sub>6</sub>O<sub>2</sub>, O-containing Chevrel phases, synthesis and props. 0-108368
- GaSe, press. induced metallic and supercond. state 0-75666
- Ge, supercond. at high press., crit. temp. 0-60130
- GeTe, supercond., metal-insulator transition, electron pairing, effect on optical props. 0-60139
- Ni<sub>2</sub>Mo<sub>2</sub>S<sub>6</sub>O<sub>2</sub>, O-containing Chevrel phases, synthesis and props. 0-108368
- PbMo<sub>4</sub>S<sub>6</sub>O<sub>2</sub>, O-containing Chevrel phases, synthesis and props. 0-108368
- SnTe, supercond., metal-insulator transition, electron pairing, effect on optical props. 0-60139

**superconducting thin films**

- cooper pairs, photon scatt. on plasmons, Landau-Ginzburg theory 0-65738
- critical electric fields and currents in two dimensional systems (*Russian*) 0-107972
- electric field under tunnel injection conditions 0-103792
- Faraday effect obs. in polarising microscope 0-70892
- flux lattice melting, phase diagram 0-84571
- flux pinning in films with periodic thickness modulation 0-88702
- granular films, percolation threshold and crit. current, theory 0-88706
- granular microcylinder, flux quantisation phenomena above T<sub>c</sub> (*Russian*) 0-70899
- inhomogeneous, pair-breaking current, Ginzburg-Landau theory 0-97029
- inhomogeneous film, cond. near superconducting transition temp. 0-93031
- long thin-film, paradox in crossover of mech. causing hysteresis 0-107971
- metastable alloys, review of current work 0-81002
- optically irradiated, phonon spectrum and phonon temp. definition 0-93037
- proximity effect weak links, steady-state and RF props. 0-84563
- quench-condensed films, superconducting transition temp., elastic stress and strain effects 0-70883
- resistivity evidence in Monte Carlo studies 0-80434
- RF complex impedance meas. 0-84573
- supercond. cylinder, order parameter enhancement by microwave irrad. 0-70896
- ultra-thin films, transition temp., interface and fluctuation phenomena 0-84527
- vortices, local mag. flux density and elec. current density 0-84572
- vortices, phase transitions, review 0-88698
- weakly damped collective oscillations, EM excitation, surface impedance (*Russian*) 0-65739
- Al, cylindrical, order-parameter variations meas. 0-103797
- Al film, crit. temp. enhancement (*Russian*) 0-93021
- Al film in microwave radiation field, resistive state transition (*Russian*) 0-93038
- Al, granular, transition to localisation, elec. resist. 0-70877
- Al granular films, inhomogeneous supercond. transitions, microwave meas. 0-103789
- Al granular films, self-ion implantation, supercond. transition temp. enhancement 0-103774
- Al granular films, vortex noise at supercond. transition 0-84530
- Al granular films as weak link in Josephson devices 0-88685
- Al granular superconducting bolometer as mol. beam detector 0-73524
- Al, nonlinear conductivity of thin films in mixed state (*Russian*) 0-80464
- Al, transition to zero vorticity, long-range topological order 0-93039
- Al tunnel junctions, superconductivity enhancement by microwaves 0-107956
- Al<sub>2</sub>O<sub>3</sub>, RF complex impedance meas., dynamic pinning 0-84573
- Al-Cu, superconducting amorphous films of high stability 0-70889
- Al-Formvar-Sn coupled films, Ginzburg's excitonic supercond. model 0-97039
- BaPb<sub>1-x</sub>Bi<sub>x</sub>O<sub>3</sub>, superconducting thin films, RF sputtering prep. 0-76181
- Bi, amorphous film, temp. dependence of SAW attenuation 0-75679
- Bi, superconducting amorphous film, Kosterlitz-Thouless transition 0-88699
- Bi superconducting film, critical temp., thermal equilibrium (*Russian*) 0-80438
- ErRh<sub>4</sub>B<sub>4</sub>, superconducting thin films, critical mag. field 0-75693
- B-Ga, metastable, elec. props. in normal and supercond. states (*Russian*) 0-65520
- Hg films, superconducting, far-IR and electrodynamic props. meas. 0-103957
- Hg-Xe vapour deposited films, cond. transitions, effect of disorder on supercond. 0-88659
- In film, Josephson arrays, proximity effect junctions 0-84553
- In films, crit. temp. enhancement (*Russian*) 0-93021
- In superconducting films, metastable states, supercooling fields 0-97031
- In-In<sub>2</sub>O<sub>3</sub>-Pb, Josephson tunnel junction fabrication for MM-wave detector 0-100427
- Mo-Sn-Se system, supercond. crit. temp. and cryst. struct. (*Russian*) 0-107947
- Nb, critical mag. fields and currents, temp. depend. (*Russian*) 0-103798
- Nb, film, epitaxy, struct. and supercond. props., on (001) surface of fluorophlogopite (*Russian*) 0-80101
- Nb films, ion beam sputtered, supercond., laser annealing effects 0-97024
- Nb granular films, ratio of supercond. transition temps. 0-84529
- Nb granular films as weak link in Josephson devices 0-88685
- Nb, granulated film, critical current temp. depend. (*Russian*) 0-103803
- Nb, ion-implanted bridge with thick Pb banks, fabrication and characterisation of film parameters 0-100569
- Nb layer, ion bombarded, supercond. props. and struct. 0-88671
- Nb, struct. and electrophys. props. at 4.2K 0-80436
- Nb, thin-film SQUID working at 4.2K, fabrication and characterisation 0-100570
- Nb/Cu, layered ultrathin coherent struts., supercond. props. 0-84525
- Nb-Ge, compounds with A15 structure, films, TEM study (*French*) 0-80135
- Nb-Ge-Si, compounds with A15 structure, films, TEM study (*French*) 0-80135
- Nb-N, superconducting layers, sputtering in high vacuum apparatus (*German*) 0-89147
- Nb-Nb<sub>2</sub>O<sub>5</sub>-Pb Josephson junction formed on Nb film edge 0-107960
- Nb-Si, compounds with A15 structure, films, TEM study (*French*) 0-80135
- Nb<sub>3</sub>Al, complex refractive index meas. 0-93264
- Nb<sub>3</sub>Al film, electron-beam coevaporated, prep. and characts. 0-76187
- Nb<sub>3</sub>Ge, amorphous film, supercond., flux flow resist., vortex pair disloc. 0-88701
- Nb<sub>3</sub>Ge coevaporated film, high supercond. transition temp., nucleation and growth 0-76185
- Nb<sub>3</sub>Ge film, superconductivity, relevance of mag. interactions, EPR study 0-100545
- Nb<sub>3</sub>Ge, high-temp. supercond. phase stabilisation w.r.t. prep. conditions (*Russian*) 0-70871
- Nb<sub>3</sub>Ge, sputtered on Cu, film-substrate interface obs. by electron microscopy 0-65398
- Nb<sub>3</sub>Ge, supercond. film, amorphous content, X-ray diffr. study, rel. to transition temp. 0-75668
- NbN granular films, supercond., crit. props. 0-88661



**superconducting thin films continued**

- NbN granular films as weak link in Josephson devices 0-88685  
 NbN, granulated film, critical current temp. depend. (*Russian*) 0-103803  
 Nb<sub>2</sub>N, supercond. props. and structural phase transform. induced by C<sup>+</sup> and N<sup>+</sup> implantation 0-107942  
 Nb<sub>3</sub>Pb superconducting film, prep., vac. deposition 0-89149  
 Nb<sub>3</sub>Sn film formation, solubility, precipitating processes (*Russian*) 0-92792  
 Nb<sub>3</sub>Sn, on LiNbO<sub>3</sub> substrate, US attenuation of SAW in applied mag. field 0-75678  
 Nb<sub>3</sub>Sn, TEM microanalysis 0-104491  
 Pb film, monocryst., heteroepitaxial growth, struct. defects, and elec. props. (*Russian*) 0-84403  
 Pb, film, spatially inhomogeneous state appearance under laser pumping conditions 0-93053  
 Pb granular film, Josephson coupled, resistive transition 0-88683  
 Pb-In film, superconducting tunnel junction, pulsed quasiparticle injection 0-84565  
 Pb-PbO-Pb, Josephson tunnel junction fabrication for Mm-wave detector 0-100427  
 Sn, crit. mag. fields, temp. depend., penetration depth thickness depend. 0-7908  
 Sn film, crit. temp. enhancement (*Russian*) 0-93021  
 Sn film, limitation in microwave stimulation of supercond., crit. current meas. (*Russian*) 0-88695  
 Sn film, metastable supercond. alloys, produced by low temp. ion implantation 0-88670  
 Sn, film, superconducting fluctuations, transition temp. (*Russian*) 0-65740  
 Sn films covered by Ge, effect on excess elec. cond. 0-65741  
 Sn, long film, crit. currents in microwave EM fields 0-70898  
 Sn, nonlinear conductivity of thin films in mixed state (*Russian*) 0-80464  
 Sn, spatially inhomogeneous state under tunnel injection conditions 0-80457  
 Sn-Cu film, metastable supercond. alloys produced by low temp. ion implantation 0-88670  
 Sn-In, nonlinear conductivity of thin films in mixed state (*Russian*) 0-80464  
 Te-Au film, metastable supercond. alloys, produced by low temp. ion implantation 0-88670  
 TiN films, reactively RF sputtered, struct. and elec. props., substrate bias effects 0-96763  
 TiN, low-energy ion-stimulated deposited, supercond. props. 0-88664  
 Ti films, supercond. amorphous, effective phonon spectrum and lattice sp. ht. 0-70895  
 V columnar films, crit. field anisotropy, depend. on prep. conditions (*Russian*) 0-93056  
 V<sub>2</sub>Si film, optical props. (*Russian*) 0-93418  
 V<sub>2</sub>Si thin film far IR laser thermal spectroscopy 0-60144  
 V<sub>2</sub>Si-SiO<sub>2</sub>-Mo<sub>3</sub>Re<sub>2</sub>, supercond. tunnel junctions 0-107961  
 Zn film for energy selective phonon detection 0-92621

**superconducting transition temperature**

- A15 compound, superconducting transition depend. on non-hydrostatic stress 0-107948  
 A15 compounds, disordered, reordering kinetics, recovery of supercond. transition temp. 0-96678  
 A15 compounds, supercond. crit. temp. for model density of state using Eliashberg gap eqns. 0-93034  
 A15-type compounds, review of superconducting props. and structure 0-70909  
 A-15 compounds, disordered, resist. and supercond. transition temp. 0-107944  
 A-15 superconductors, transition temp., d band relative displacement (*Chinese*) 0-103770  
 alloys, binary, supercond. transition temp. lowering by nonmagnetic impurities 0-100546  
 amorphous superconductor, Eliashberg function, tunnelling and crit. temp. anal. 0-80455  
 Anderson impurity ordering, critical temp., Gor'kov eqn. calcs. (*Russian*) 0-65731  
 anisotropic superconductors, nonmag. impurities effect on supercond. transition temp. 0-93035  
 anisotropic superconductors, upper critical field theory 0-75692  
 approximate T<sub>c</sub> formula, Eliashberg eqn. (*Chinese*) 0-107941  
 charge imbalance relaxation freq. depend. near T<sub>c</sub> 0-93030  
 close packed compounds, superconducting T<sub>c</sub>, heterogeneous hybridisation (*Chinese*) 0-107940  
 dirty superconductors, time-depend. Ginzburg-Landau eqns. near supercond. transition temp. 0-70886  
 electric field penetration and collective oscillations, review 0-88678  
 electronic density of states, variation effect on transition temp. and effective mass 0-75672  
 energy dependent electronic density of states, gap and crit. temp. 0-84538  
 ferromagnetic superconductor, paramagnetic fluctuations, influence on superconductivity 0-70900  
 ferromagnets and spin glasses, supercond. and mag. order 0-93029  
 granular, percolation model, specific heat, elec. resistance 0-93025  
 granular composite superconductors, Ginzburg-Landau theory, props. 0-88673  
 granular superconductors, coherence transition, structural disorder effects 0-88657  
 granulated superconductors, phase transitions, Josephson energy (*Russian*) 0-84540  
 graphite-K intercalation compound, effect of H addition on superconducting transition temp. 0-70872  
 high Debye temperature material, theoretical upper limit of crit. temp. 0-60129  
 inhomogeneous film, cond. near superconducting transition temp. 0-93031  
 internal friction near crit. temp. at acoustic freqs. 0-100305  
 Josephson coupled layered supercond., upper critical field (*Russian*) 0-100551  
 Josephson FET, hybrid, feasibility 0-80451  
 lattice instability, high superconducting transition temp. 0-88663  
 magnetic field, weak, meas. of absolute intensity, use of RF biased SQUID 0-82794  
 magnetic impurity low temp. behaviour, transition temp., specific heat, free energy 0-88691

**superconducting transition temperature continued**

- metal-semiconductor disordered interface, supercond. transition temp. enhancement by bipolaron interface centres 0-84528  
 metallic glasses, electronic structure rel. to elec. cond., supercond. and mag. props. 0-65429  
 metallic ultrathin filaments, dielectric and superconducting fluctuations, Peierls transition (*Russian*) 0-65742  
 metastable compound synthesis with high supercond. transition temp. 0-93024  
 micropower-induced enhancement (*Russian*) 0-93023  
 molybdenum chalcogenides, multicomponent, physical props. 0-84577  
 molybdenum ternary chalcogenides, structures and properties survey (*Czech*) 0-70870  
 multiband system, electron pairing, radiation effect 0-88679  
 porous glass:In, effect of press. on transition temp. 0-97027  
 quasi-one-dimensional superconductor, critical mag. field, transition temp. (*Russian*) 0-93058  
 quench-condensed films, superconducting transition temp., elastic stress and strain effects 0-70883  
 rare earth cpds., RMO<sub>2</sub>S<sub>2</sub>(Se<sub>2</sub>) and RRh<sub>2</sub>B<sub>4</sub>, coexistence of supercond. and mag. ordering (*Russian*) 0-84542  
 renormalisation group recursion relations involving dynamics, in mag. field 0-60137  
 resistive state, phase-slip centres, current-voltage characts. (*Russian*) 0-80437  
 review of calc. techniques, BCS theory and phonon spectra (*Spanish*) 0-84535  
 superconducting thin hollow cylinder, mag. field penetration, Ginzburg-Landau calcs. (*Russian*) 0-75674  
 superconductivity-ferromagnetism coexistence in two-band model (*Russian*) 0-84539  
 temperature fixed point device, prep. and calibration 0-82770  
 thermometer referenced by superconducting to normal transition point (*Japanese*) 0-77785  
 transition metal chalcogenides, quasi-one-dimens., elec. mag., and supercond. props., review (*Russian*) 0-93022  
 transition metal compounds, reduced ionisation potentials as parameters in superconducting transition temp. calcs. 0-75671  
 transition metals, Cauchy discrepancy with supercond. transition temp. 0-84533  
 transition metals silicides, atomic volume deviations and supercond. T<sub>c</sub> 0-75203  
 transport current effects on superconducting thin-walled cylinder in mag. field (*Russian*) 0-100573  
 two-dimensional superconductor, resistivity evidence in Monte Carlo studies 0-80434  
 type I superconductors, approximate T<sub>c</sub> formula, Eliashberg eqn. calcs. (*Chinese*) 0-88662  
 ultra-thin films, transition temp., interface and fluctuation phenomena 0-84527  
 Al, defect structure depend. on Ga and Ca implanted ions 0-59494  
 Al film, crit. temp. enhancement (*Russian*) 0-93021  
 Al, film, granular, transition to localisation, elec. resist. 0-70877  
 Al, film, superconducting transition temp. and lattice dynamics 0-93028  
 Al granular films, inhomogeneous supercond. transitions, microwave meas. 0-103789  
 Al granular films, self-ion implantation, supercond. transition temp. enhancement 0-103774  
 Al granular films, vortex noise at supercond. transition 0-84530  
 Al, narrow superconducting bridges, microwave radiation stimulated T<sub>c</sub> enhancement 0-84537  
 Al, nonlinear sound wave interactions, sound attenuation in weak superconducting state (*Russian*) 0-75310  
 Al-Cu, superconducting amorphous films of high stability 0-70889  
 Au/In proximity effect bridges, square arrays, transition temps. 0-84557  
 BaPb<sub>1-x</sub>Bi<sub>x</sub>O<sub>3</sub>, superconducting thin films, RF sputtering prep. 0-76181  
 BaPb<sub>1-x</sub>Bi<sub>x</sub>O<sub>3</sub>, superconducting props., Hall coeff. and elec. resist. meas. 0-84531  
 Be alloys, enhancement of supercond. transition temp. 0-60129  
 Bi, superconducting amorphous film, Kosterlitz-Thouless transition 0-88699  
 Bi, superconducting modification obtained by impact compression (*Russian*) 0-93020  
 Bi superconducting film, critical temp., thermal equilibrium (*Russian*) 0-80438  
 C films with high conductivity, prep. and props. 0-80983  
 Cd-Sn alloy, superconductivity and microstructure 0-107949  
 Co<sub>2</sub>Mo<sub>2</sub>S<sub>2</sub>O<sub>2</sub>, O-containing Chevrel phases, synthesis and props. 0-108368  
 Cs, supercond., elec. resist. and phase transforms. under high press. (*German*) 0-107763  
 Cu-V-Si, supercond. props. 0-107945  
 CuCl, pressure depend. of structural, chemical, elec. and mag. props. 0-96596  
 Cu<sub>2</sub>La<sub>1-x</sub>, splat-cooled, phase diagram and supercond. props. 0-70881  
 Cu<sub>2</sub>Mo<sub>2</sub>S<sub>2</sub>O<sub>2</sub>, O-containing Chevrel phases, synthesis and props. 0-108368  
 Cu<sub>40</sub>Zr<sub>60</sub>, amorphous alloys, supercond. transition temp., press. depend. 0-84524  
 Er<sub>1-x</sub>Hf<sub>x</sub>Rh<sub>2</sub>B<sub>4</sub>, mag. and supercond. transitions, cryst. field effects 0-107950  
 ErRh<sub>2</sub>B<sub>4</sub>, ferromag. superconductor, vortex phase 0-80441  
 ErRh<sub>2</sub>B<sub>4</sub>, superconducting thin films, critical mag. field 0-75693  
 Er<sub>1-x</sub>Tm<sub>x</sub>Rh<sub>2</sub>B<sub>4</sub>, mag. and supercond. transitions, cryst. field effects 0-107950  
 Er<sub>2</sub>Y<sub>1-x</sub>Rh<sub>2</sub>B<sub>4</sub>, mag. and supercond. transitions 0-70874  
 Ga II, superconducting high pressure phase, sp. ht. 0-70894  
 B-Ga, metastable, elec. props. in normal and supercond. states (*Russian*) 0-65520  
 Ga, nonlinear sound wave interactions, sound attenuation in weak superconducting state (*Russian*) 0-75310  
 Ga ultrathin metallic filaments, appearance of dielec. instability, coexistence with supercond. 0-103784  
 GaSe, press. induced metallic and supercond. state 0-75666  
 Ge, supercond. at high press., crit. temp. 0-60130  
 Hg ultrathin metallic filaments, appearance of dielec. instability, coexistence with supercond. 0-103784  
 Hg-Xe vapour deposited films, cond. transitions, effect of disorder on supercond. 0-88659  
 Ho(Ir,Rh<sub>1-x</sub>)<sub>2</sub>B<sub>4</sub> pseudoternary system, supercond. and mag. ordering 0-70876

**superconducting transition temperature continued**

- In films, crit. temp. enhancement (*Russian*) 0-93021  
 In, superconductivity destruction singularities, intermediate state, hysteresis (*Russian*) 0-80460  
 In ultrathin metallic filaments, appearance of dielec. instability, coexistence with supercond. 0-103784  
 In whiskers from Sn-In alloys, current carrying, superconductivity breakdown 0-60133  
 In-Bi(Tl)(Pb), small  $\kappa$  supercond., phase transitions higher than second order 0-88668  
 In-Sb, cryst. struct. after appl. of high press., supercond. transition temp. 0-70169  
 In<sub>0.65</sub>Tl<sub>0.35</sub>, supercond. transition temp., specific heat, pseudopotential form factor 0-97026  
 Ir borides, MIr<sub>2</sub>B<sub>2</sub> (M=La, Th, U), supercond. and mag. props. 0-97028  
 Ir-Y eutectic alloy, supercond. transition enhancement due to lattice softening 0-103775  
 (La,Y)Ce, dil., Kondo supercond., transition temp., susceptibility and resist. 0-65733  
 La-Ag alloys, amorphous, elec. resist. and supercond. 0-70885  
 La-Au, splat-quenched, Mossbauer effect and elec. resist., amorphous struct. 0-84676  
 La<sub>2</sub>C<sub>3</sub>, solid solution, lattice const. and superconducting transition temp. (*Russian*) 0-92496  
 La<sub>80-90</sub>-Pr<sub>10-20</sub>, amorphous, mag. and supercond. props. 0-75713  
 Mo ternary cpds., R<sub>2</sub>Sn<sub>2</sub>Mo<sub>2</sub>S<sub>8</sub> (R=La, Ce, Pr, Eu, Gd, Ho, Lu, Y, In, U), supercond. props. 0-97023  
 Mo-Be solid solutions, superconducting transition, temp. changing peculiarity due to press. (*Russian*) 0-70878  
 Mo-Ru<sub>2</sub>(Si), amorphous superconductors, prep. by electron beam evaporation and liq. quenching, crit. temp. 0-103776  
 Mo-Sn-Se system, supercond. crit. temp. and cryst. struct. (*Russian*) 0-107947  
 Mo<sub>2</sub>PbS<sub>2</sub> embedded in resin, composite supercond., high transition temp. 0-88660  
 (Mo<sub>0.8</sub>Ru<sub>0.2</sub>)<sub>80</sub>Si<sub>10</sub>B<sub>10</sub>, amorphous supercond. matrix, flux pinning by MoRu precip. 0-65756  
 Mo<sub>2</sub>TuTe<sub>2</sub>, synthesis, struct., and elec. props. 0-92877  
 Mo<sub>2</sub>Si<sub>2</sub>B<sub>10</sub>, amorphous alloys obtained by liq. quenching, superconductivity 0-75670  
 Nb, film, epitaxy, struct. and supercond. props., on (001) surface of fluorophlogopite (*Russian*) 0-80101  
 Nb film, struct. and electrophys. props. at 4.2K 0-80436  
 Nb films, ion beam sputtered, supercond., laser annealing effects 0-97024  
 Nb granular films, ratio of supercond. transition temps. 0-84529  
 Nb layer, ion bombarded, supercond. props. and struct. 0-88671  
 Nb, superconductive transition point as reference temp. 0-107943  
 Nb/Cu, layered ultrathin coherent structures, supercond. props. 0-84525  
 Nb/In composite superconductor, transport props. 0-88658  
 Nb-Ga-Se, superconducting transition temp., X-ray, microscopic and microprobe anal. (*Ukrainian*) 0-75667  
 Nb-Ge, amorphous supercond. alloy, resistivity, transition temp. 0-60126  
 Nb-N, superconducting layers, sputtering in high vacuum apparatus (*German*) 0-89147  
 Nb-Rh,  $\sigma$ -phase alloy, superconductivity and resistance behaviour 0-70882  
 Nb-Si(-V)(Zr)(Mo)(Ta)(W)(C)(B)(Ge), ductile amorphous, superconductivity 0-60131  
 Nb<sub>3</sub>(Al,Ge) and Nb<sub>3</sub>(Al,Si), liq. quenched, supercond. props. 0-84580  
 Nb<sub>3</sub>Al film, electron-beam coveoparated, prep. and characts. 0-76187  
 Nb<sub>3</sub>Al, supercond. props. and lattice parameter, comp. and neutron irradi. effects 0-70880  
 Nb<sub>3</sub>(Al,Ga), NQR freq. temp. depend., supercond. transition temp. 0-93207  
 NbC, diffuse, production and superconductive props. (*Bulgarian*) 0-80467  
 Nb<sub>3</sub>C, supercond. critical temp., neutron irradi. effect 0-80433  
 NbC<sub>x</sub>, light element implantation effect on T<sub>c</sub> 0-107951  
 Nb(CN), supercond. critical temp., neutron irradi. effect 0-80433  
 Nb<sub>0.75</sub>Ga<sub>0.25</sub>, A 15 phase high transition temp., sp. ht. determ. 0-60140  
 Nb<sub>3</sub>Ga, transition temp. increase by rapid hardening with annealing 0-76275  
 Nb<sub>3</sub>Ge film, high-temp. supercond. phase stabilisation w.r.t. prep. conditions (*Russian*) 0-70871  
 Nb<sub>3</sub>Ge, low temperature electron, neutron irradi. effects on critical temp. (*French*) 0-75669  
 Nb<sub>3</sub>Ge, supercond. film, amorphous content, X-ray diffr. study, rel. to transition temp. 0-75668  
 Nb<sub>3</sub>Ge<sub>1-x</sub>Al<sub>x</sub>, ternary supercond. alloys, comp. variations 0-97022  
 NbN, diffuse, production and superconductive props. (*Bulgarian*) 0-80467  
 NbN embedded in resin, composite supercond., high transition temp. 0-88660  
 NbN granular films, supercond., crit. props. 0-88661  
 NbN,  $\gamma$ - and  $\delta$ -forms, cryst. growth and supercond. transition temp. 0-107946  
 NbN single crystal preparation, transition temperature determination 0-60776  
 NbN, supercond. RF reactively sputtered films, deposition parameter effects on props. 0-80972  
 Nb<sub>2</sub>N, supercond. props. and structural phase transform. induced by C<sup>+</sup> and N<sup>+</sup> implantation 0-107942  
 NbN<sub>0.7</sub>C<sub>0.3</sub>, cryst. growth and supercond. transition temp. 0-107946  
 Nb<sub>2</sub>Nb<sub>1-x</sub>Si<sub>x</sub>(Ge<sub>x</sub>), impurity stabilised A15 supercond., transition temp., lattice const., specific heat 0-93026  
 NbSe<sub>3</sub>, superconducting transitions and diamagnetism 0-84526  
 Nb<sub>2</sub>Si, substituted, splat cooling influence on supercond. T<sub>c</sub> and stoichiometry 0-80439  
 Nb<sub>3</sub>Sn bronze process, flux pinning scaling law depend. on strain 0-75696  
 Nb<sub>3</sub>Sn, coherence parameter, nonlinear high temp. supercond. elements with A-15 lattice (*Russian*) 0-60127  
 Nb<sub>3</sub>Sn, filaments in Cu matrix, thermal strain effects on superconducting critical temp. 0-93032  
 Nb<sub>3</sub>Sn, supercond. props., effect of neutron irradi. 0-80463  
 NbTi/In composite superconductor, transport props. 0-88658  
 NbTi-Cu, composite superconductor, acoustic emission 0-84546  
 (Nb<sub>0.96</sub>Ti<sub>0.04</sub>)<sub>1-x</sub>Ge<sub>x</sub>, high T<sub>c</sub>, resist. meas. 0-88531  
 Nb<sub>30</sub>Zr<sub>70</sub>, supercond. and normal, sp. ht. meas., 2-20K 0-70893  
 Ni<sub>2</sub>Mo<sub>2</sub>S<sub>8</sub>O<sub>2</sub>, O-containing Chevrel phases, synthesis and props. 0-108368

**superconducting transition temperature continued**

- Os borides, MOs<sub>2</sub>B<sub>2</sub> (M=Lu, U), supercond. and mag. props. 0-97028  
 Pb, strength loss in supercond. state, size factor effect (*Russian*) 0-88677  
 Pb-Bi alloy, T<sub>c</sub> evaluation, from ab initio band struct. calcs. on Pb 0-75502  
 Pb-formvar-Al tunnel junction, excitonic superconductivity, BCS theory, generalised jellium model 0-75684  
 Pb-Sn(Bi)(Ni), strength loss in supercond. transition, nonmag. and paramag. impurities influence (*Russian*) 0-70875  
 PbMo<sub>2</sub>S<sub>8</sub>O<sub>2</sub>, O-containing Chevrel phases, synthesis and props. 0-108368  
 Pd-Cu(Ag)(Au) alloys-H solid solutions, superconducting transition temp. behaviour (*Russian*) 0-70879  
 Pd-Ni-H, hydride formation in high press. range 0-65235  
 PdH, superconducting transition critical temperature, BCS theory, phonon spectra (*Spanish*) 0-84535  
 PdH<sub>x</sub>, superconducting transition temp., inverse isotope effect, Einstein model 0-65734  
 PdH<sub>x</sub>(D<sub>x</sub>), isotope effect (*Russian*) 0-88665  
 (Pd<sub>95</sub>Rh<sub>5</sub>)H<sub>x</sub>, elec. resistivity studies 0-59957  
 Pd<sub>30</sub>Zr<sub>70</sub>, amorphous alloys, supercond. transition temp., press. depend. 0-84524  
 Rh borides, RRh<sub>3</sub>B<sub>2</sub> (R=rare earth), supercond. and mag. props. 0-97028  
 Ru borides, RRu<sub>2</sub>B<sub>2</sub> (R=rare earth, Y, Th, or U), supercond. and mag. props. 0-97028  
 Se<sub>2</sub>C<sub>3</sub>, superconducting phase synthesis at high press. and temp., critical field (*Russian*) 0-65732  
 Si, metallic, superconducting transition temp., press. effects, elec. cond. 0-103777  
 Sn film, crit. temp. enhancement (*Russian*) 0-93021  
 Sn film, metastable supercond. alloys, produced by low temp. ion implantation 0-88670  
 Sn, film, superconducting fluctuations, transition temp. (*Russian*) 0-65740  
 Sn superconducting films, Ge-covered, effect on excess elec. cond. 0-65741  
 Sn ternary intermetallic systems, new supercond./mag. cpds., X-ray powder diffr. data 0-100215  
 Sn ultrathin metallic filaments, appearance of dielec. instability, coexistence with supercond. 0-103784  
 Sn-Bi(Sb), small  $\kappa$  supercond., phase transitions higher than second order 0-88668  
 Sn-Cu film, metastable supercond. alloys produced by low temp. ion implantation 0-88670  
 Sn<sub>2</sub>Mo<sub>2</sub>S<sub>8</sub>, struct. anal. supercond. props. 0-97023  
 Ta, superconductive transition point as reference temp. 0-107943  
 Ta-Rh,  $\sigma$ -phase alloy, superconductivity and resistance behaviour 0-70882  
 TaSe<sub>3</sub>, superconducting transitions and diamagnetism 0-84526  
 Te, superconductivity and Fermi surface calcs. 0-70873  
 Te, high-press. metallic, supercond. transition temp. press. depend. 0-84355  
 Te-Au film, metastable supercond. alloys, produced by low temp. ion implantation 0-88670  
 Th-Cr, supercond., press. meas. to 20 kbar 0-88667  
 Ti-Mo (3 to 35 wt.%), high pressure influence on transition temp. to supercond. 0-107952  
 Ti-Nb-Si, amorphous alloy, supercond. props. and crystn. behaviour, TEM and DTA study (*Japanese*) 0-84536  
 Ti-Nb-Zr-Fe, supercond. and paramag. props., effect of Fe additions (*Russian*) 0-65730  
 TiN, low-energy ion-stimulated deposited, supercond. props. 0-88664  
 TiN, supercond. critical temp., neutron irradi. effect 0-80433  
 Tl films, supercond. amorphous, effective phonon spectrum and lattice sp. ht. 0-70895  
 Tl<sub>0.33</sub>WO<sub>3</sub> bronze, elec. resist. meas., anisotropy, supercond. 0-75569  
 (V<sub>1-x</sub>Cr<sub>x</sub>)<sub>3</sub>Si, elastic moduli, 4.2 to 290K, softening near supercond. transition (*Russian*) 0-92582  
 V<sub>3</sub>Ga, A15 cpd., hydrogenation effects on supercond. transition temp., lattice parameters 0-103772  
 V<sub>3</sub>Ga, supercond. A15 phase, prep. by controlled precip. 0-81000  
 V<sub>3</sub>Ge, A15 cpd., hydrogenation effects on supercond. transition temp., lattice parameters 0-103772  
 V<sub>2</sub>Hf<sub>1-x</sub>Zr<sub>x</sub>, normal and supercond. state, transition temps., mag. susceptibility and specific heat determ. (*Russian*) 0-60132  
 V<sub>2</sub>Si, A15 cpd., hydrogenation effects on supercond. transition temp., lattice parameters 0-103772  
 V<sub>2</sub>Si embedded in resin, composite supercond., high transition temp. 0-88660  
 V<sub>3</sub>Si film, optical props. (*Russian*) 0-93418  
 V<sub>3</sub>Si, supercond. props., effect of neutron irradi. 0-80463  
 V<sub>3</sub>Si, supercond. structure and properties (*German*) 0-93631  
 V<sub>3</sub>Si(Ga), coherence parameter, nonlinear high temp. supercond. elements with A-15 lattice (*Russian*) 0-60127  
 V<sub>3</sub>Si<sub>1-x</sub>Ge<sub>x</sub>, elastic props., 77 to 290K, rel. to supercond. transition temp. (*Russian*) 0-66560  
 V<sub>3</sub>Sn, A-15 cpd., normal-state elec. resist. 0-75542  
 W<sub>70</sub>Si<sub>30</sub>B<sub>10</sub>, amorphous alloys obtained by liq. quenching, superconductivity 0-75670  
 Zn film for energy selective phonon detection 0-92621  
 Zr, H(D) implanted, superconductivity enhancement obs. 0-70884  
 Zr-Rh-H(D), superconducting transition temp., effect of H(D) conc. 0-84532

**superconducting tunnelling**

- see also Josephson effect; proximity effect; superconducting junction devices; tunnelling spectra; tunnelling spectroscopy  
 A15-type compounds, review of superconducting props. and structure 0-70909  
 amorphous superconductor, Eliashberg function, tunnelling and crit. temp. anal. 0-80455  
 current characteristics of supercond. tunnel junctions 0-60150  
 energy gap anisotropy, normal layer proximity effect 0-84558  
 film, electric field under tunnel injection conditions 0-103792  
 granular metal, supercond. transition, increased resistance rel. to quasiparticle tunnelling 0-88689  
 helical order of spins in supercond. 0-70888  
 Josephson junctions fabrication, tunnelling through edge-grown barriers 0-100567  
 junction, nonequilibrium phonon effect on supercond. states with 2 coexisting energy gaps 0-84561



**superconductive tunnelling continued**

- junction, phonon spectroscopy of paramagnetic crystals 0-84634  
 metal-oxide interface, surface states, enhanced tunnel conductivity 0-80456  
 metal-semiconductor disordered interface, supercond. transition temp. enhancement by bipolaron interface centres 0-84528  
 N-S boundary resistivity, tunnelling contact resistance (*Russian*) 0-93048  
 nonequilibrium states, narrow nonequilibrium sources (*Russian*) 0-88687  
 nonequilibrium superconductor, normal component drag by condensate, tunnelling (*Russian*) 0-93051  
 normal conductance change, origin 0-65753  
 order parameter singularities, tunnelling currents, Fermi surface calcs. (*Russian*) 0-80458  
 quantum noise effects in tunnel junctions in 0-1 mV bias range 0-80449  
 quasiparticle mixers, supercond.-insulator-supercond., conversion gain prediction 0-70901  
 quasiparticle superconductor-insulator-superconductor tunnel junctions as microwave detectors 0-65744  
 refrigerator, cooling power and efficiency, tunnelling calc. 0-57311  
 ring with weak links, critical voltage for flux tunnelling 0-75685  
 SQUID ring, fluxoid transition mechanisms, quantum vs. thermally excited 0-100565  
 superconductor-insulator-superconductor tunnel junctions, responsivity to microwave radiation 0-100553  
 Al/AlO<sub>3</sub>/La rare earth metal tunnel junctions, cond. meas., cryst. field effects 0-88694  
 Al-Al<sub>2</sub>O<sub>3</sub>-ferromagnet struct., electron tunnelling into ferromagnetic metals 0-60104  
 Al-Formvar-Sn coupled films, Ginzburg's excitonic supercond. model 0-97039  
 Al-PbBi superconducting tunnel junctions, optically illuminated, quasiparticle energy distribution 0-75688  
 Al<sub>2</sub>O<sub>3</sub>, inelastic electron tunnelling spectroscopy of adsorbates, MgO comparison 0-88686  
 Cu<sub>1-x</sub>Mo<sub>x</sub>S<sub>8</sub>, electron tunnelling spectroscopy expts. (*German*) 0-107966  
 He cryostat design, superconductive tunnelling study (*Spanish*) 0-73347  
 LaAl<sub>3</sub>, doped with Tb, Nd, or Pr, crystal field effects, tunnelling within mK range 0-70907  
 LaPb<sub>3</sub>, doped with Tb, Nd, or Pr, crystal field effects, tunnelling within mK range 0-70907  
 LaSn<sub>3</sub>, doped with Tb, Nd, or Pr, crystal field effects, tunnelling within mK range 0-70907  
 MgO, inelastic electron tunnelling spectroscopy of adsorbates, Al<sub>2</sub>O<sub>3</sub> comparison 0-88686  
 Pb-Cd-Pb, supercond.-normal-metal-supercond. junction, crit. currents 0-107965  
 Pb-Cu(Ag) double layers, intermetallic boundary effects, tunnelling 0-88692  
 Pb-formvar-Al tunnel junction, excitonic superconductivity, BCS theory, generalised jellium model 0-75684  
 Pb-In film, superconducting tunnel junction, pulsed quasiparticle injection 0-84565  
 Pb-Si superconducting solutions, effect of hydrostatic compression on tunnelling (*Russian*) 0-65746  
 PbMo<sub>6</sub>S<sub>8</sub>, electron tunnelling spectroscopy expts. (*German*) 0-107966  
 Si oxidised amorphous layers, supercond. tunnel junction barriers 0-93040  
 Sn, supercond. tunnel junction, quasiparticle excitation by  $\alpha$ -particles 0-103791  
 Sn-SnO<sub>x</sub>-Sn tunnel contacts, spatially inhomogeneous state under strong injection conditions 0-80457  
 TI films, supercond. amorphous, effective phonon spectrum and lattice sp. ht. 0-70895  
 V<sub>3</sub>Si tunnel junctions, energy gap investigation 0-84569

**superconductivity**

- see also BCS theory; coherence length; composite superconductors; Cooper pairs; critical currents; dirty superconductors; fluctuations in superconductors; Ginzburg-Landau theory; Meissner effect; penetration depth (superconductivity); strong-coupling superconductors; superconducting critical field; superconducting devices; superconducting energy gap; superconducting materials; superconducting transition temperature; superconductive tunnelling; type I superconductors; type II superconductors  
 amorphous metals, superconducting properties rel. to ordering 0-65735  
 Bardeen, John, contrib. to solid state physics 0-57057  
 clean superconductor, effect of impurity scatt. on thermally induced charge imbalance 0-60135  
 critical parameters during field emission of electrons 0-88682  
 critical slowing down, dynamic-exponents, Ginzburg-Landau theory 0-103783  
 cryoelectrics, computerised measurement instrumentation 0-98920  
 cryogenics of Sulzer, Switzerland 0-82769  
 edge dislocation screening in metals and superconductors, metal softening (*Russian*) 0-64997  
 education, gauge symmetry breaking, geometrical approach, superconductivity and spontaneous symmetry breaking 0-57028  
 electrodynamic suspension system, current coil interaction with semiinfinite superconducting sheet (*Russian*) 0-83539  
 electrodynamics and quantum field theory 0-60134  
 electrodynamics of superconductors as a consequence of local gauge invariance (*German*) 0-103778  
 electron gas, one-dimens., interacting, ground-state energy in mean field approx. and instabilities 0-88493  
 Eliashberg formulation, electron-phonon density rel. to phonon inverse lifetime, review 0-84543  
 EM wave nonlinear absorpt. near one-photon threshold 0-60142  
 Fermi-liquid, electromagnetic response, formal solutions 0-100548  
 granular, percolation model, specific heat, elec. resistance 0-93025  
 granular materials, size effects in cond. and supercond. 0-77581  
 helical ordering of spins in supercond. 0-88669  
 inhomogeneous, conf., Berkeley Springs, WV, USA, 1979 0-82562  
 inhomogeneous, Ginzburg-Landau theory 0-88672  
 lens, electron microscope appl. 0-86530  
 lysozyme, search for superconducting regions 0-101149  
 magnetic impurities, coexistence of superconductivity and ferromag., BCS and Zener models 0-88676  
 metals, superconductivity studied by electron-phonon and Coulombian e-e coupling strength and quasi particle mass 0-88666  
 nonequilibrium superconductor, with wideband source of quasiparticles, kinetic theory 0-80442

**superconductivity continued**

- phenomenological unifying approach to London and Ginzburg-Landau theories 0-103779  
 physical acoustics and exploration of superconducting state, 1st, 2nd, 3rd, 4th and 5th sound, review 0-96090  
 quantum polarisation effect in critical freq. EM field 0-75677  
 quasi-one-dimensional electron-phonon system, electron jump effect on phase transition (*Russian*) 0-92673  
 renormalisation group recursion relations involving dynamics, in mag. field 0-60137  
 resistive phase-slip states in superconducting channels 0-103780  
 S-wave and P-wave superconductors, absence of proximity effect 0-93033  
 SEM, low temp., appl. to superconductors 0-80443  
 stability, in forced flow He cooling system, numerical anal. of heat-induced transients 0-82773  
 superconductivity-ferromagnetism coexistence in two-band model (*Russian*) 0-84539  
 superfluidity and superconducting phenomena demonstrated with He cryostat (*Polish*) 0-86059  
 theory developments from 1950s to 1980s, w.r.t. elementary particles theories (*Czech*) 0-80440  
 Au-Pd-Au sandwich, obs. of strongly enhanced mag. susceptibility, possibility of p-wave supercond. 0-93076  
 Cr<sub>3</sub>Si phase structure, rel. between phase diagrams and superconductivity 0-88330  
 CuCl, optical absorpt. meas., evidence against intrinsic electron-hole supercond. 0-108172  
 PdH<sub>x</sub>, local, soft modes, superconductivity thermal neutron inelastic scatt. (*Chinese*) 0-70331

**superconductors see superconducting materials; superconductivity****supercooling**

- 4-cyano-4'-n-pentylbiphenyl, refr. index meas. and isotropic-nematic phase transition study, surface plasmon technique 0-84282  
 dilute binary alloy, unidirectional growth, morphological stability of planar interface 0-84920  
 Josephson element principles, applications to precision meas. of electric potential and magnetic flux at high freq. (*Norwegian*) 0-80447  
 liquid, thermal conductivity and viscosity, mode-mode coupling 0-88370  
 2-6-lutidine-water, anomalous supercooling near critical point 0-70384  
 solute redistribution during crystallisation, interface field effects 0-84119  
 steel, structural, supercooled, austenite, structural characts. of decomposition 0-60870  
 water, sound vel. dispersion, struct. relax. effect, Brillouin scatt. obs. 0-107375  
 water, supercooled to -33°C, sound vel. determ. by acoustic levitation method 0-88269  
 $\alpha$ -Fe<sub>2</sub>O<sub>3</sub>, crystal flux growth, solubility and relative supersaturation in Fe<sub>2</sub>O<sub>3</sub>-PbO-V<sub>2</sub>O<sub>5</sub> fluxed melt system 0-64934  
 Ge single crystals, constitutional supercooling growth conditions, structural and chem. inhomogeneities 0-93473  
 In superconducting films, metastable states, supercooling fields 0-97031  
 InGaAsP-InP layers, grown by LPE techniques, lattice const., bandgap, thickness and surface morphology meas. 0-59818  
 Si:Pt, implanted and laser annealed, segregation and increased dopant solubility 0-65016  
 ZrO<sub>2</sub>-SiO<sub>2</sub>, liquid immiscibility, microstruct. of plasma dissociated ZrSiO<sub>4</sub> 0-107429

**superexchange interactions**

- garnets, superexchange operator and cryst. field interactions 0-59931  
 ruby, energy transfer between different emitters and spatial diffusion 0-103978  
 transition metal compound, effective spin-orbital Hamiltonian 0-70998  
 transition metal compound, multielectron theory 0-70997  
 BaLaMRuO<sub>6</sub>, (M=Mg, Fe, Co, Ni, Zn), cubic ordered perovskites, Mossbauer and mag. susceptibility meas. 0-75889  
 CsCuCl<sub>4</sub>·2H<sub>2</sub>O, hyperfine and super-exchange interactions 0-103654  
 CsMnF<sub>4</sub>, planar ferromag., cryst. and mag. struct., Jahn-Teller effect 0-75715  
 Fe complex (2, 9-dimethylphenanthroline) sulphate, mag. props., Mossbauer spectra 0-66081  
 GdN<sub>3</sub>, mag. interaction and carrier conc. 0-71005  
 GdN<sub>1-x</sub>O<sub>x</sub>, magnetic interaction and carrier conc. 0-71005  
 K<sub>2</sub>CuCl<sub>4</sub>·2H<sub>2</sub>O, hyperfine and super-exchange interactions 0-103654  
 MnAs<sub>1-x</sub>P<sub>x</sub>, double exchange ferromag. coupling, magnetisation meas. 0-75751  
 Mn(CN)<sub>3</sub>·(H<sub>2</sub>O)<sub>0.53</sub>, mag. interactions, theory 0-97085  
 Mn<sub>1-x</sub>Cr<sub>x</sub>As, double exchange ferromag. coupling, magnetisation meas. 0-75751  
 (NH<sub>4</sub>)<sub>2</sub>CuBr<sub>4</sub>·2H<sub>2</sub>O, hyperfine and super-exchange interactions 0-103654  
 (NH<sub>4</sub>)<sub>2</sub>CuCl<sub>4</sub>·2H<sub>2</sub>O, hyperfine and super-exchange interactions 0-103654  
 (Rb)<sub>2</sub>CuBr<sub>4</sub>·2H<sub>2</sub>O, hyperfine and super-exchange interactions 0-103654  
 Rb<sub>2</sub>CuCl<sub>4</sub>·2H<sub>2</sub>O, hyperfine and super-exchange interactions 0-103654

**superfluid helium-3**

- A phase, homogeneous case orbital dynamics 0-75399  
 A to B phase nucleation 0-100371  
 A-phase, dissipation of flow, NMR study 0-92745  
 A-phase, helical textures, NMR response 0-70496  
 A-phase, ion mobility tensor, ion-quasiparticle scatt. 0-59753  
 A-phase, longitudinal mag. relax. 0-59751  
 A-phase, mass current, intrinsic orbital angular momentum 0-84338  
 A-phase, microscopic theory for orbital hydrodynamics 0-70494  
 A-phase, orbital angular momentum at finite temps., local plane-wave approx. 0-65330  
 A-phase, orbital angular momentum density at finite temps. 0-59752  
 A-phase, soliton study 0-88386  
 A-phase, spin relax. and zero sound attenuation at low temp. 0-107595  
 B-phase, anisotropic gap distortion due to superflow and departing crit. current 0-88383  
 B-phase, Balian-Werthamer system, stability and inequalities for autocorrelation functions 0-96714  
 B-phase, collective excitations in presence of superflow 0-92744  
 B-phase, first-sound attenuation and viscosity 0-75401  
 B-phase, gap distortion, departing critical currents, all temperatures 0-92743  
 B-phase, HF sound propag. meas. 0-88391  
 B-phase, nonlinear hydrodynamics 0-59750  
 B-phase, shear viscosity, s-p-d wave approximation 0-96715  
 B-phase, zero sound attenuation peak obs. 0-88390  
 B-phase at equilib., formalism 0-88384  
 Barnett effect 0-88388



**superfluid helium-3 continued**

- Bose spectrum nonphonon branches (*Russian*) 0-92750  
collective oscillation hybridisation near A. phase transition (*Russian*) 0-80020  
dissipative current structure, hydrodynamic calcs. (*Russian*) 0-100372  
domain wall energy and spatial conformation in parallel plate geometry 0-96716  
fluid-superfluid transition phase diagram, thermodynamic stability, fluctuations (*Russian*) 0-80023  
interface with nonmagnetic solid, Kapitza resist., quantum perturbation treatment 0-88385  
magnetic relaxation and high amplitude spin waves (*Russian*) 0-92749  
magnetisation, nonlinear motion, parallel ringing 0-107597  
magnetisation, p-wave spin triplet pairing Hamiltonian, 5-D spin 0-75400  
mobility of negative ions, theory 0-107598  
rotating, equilibrium order parameters, chemical potentials 0-96713  
size effect influence on fluid density and transition temp., fourth sound meas. 0-80022  
specific heat jump at superfluid transition and effective mass, press. depend. 0-65331  
spin flow density fluctuations, superfluidity (*Russian*) 0-65328  
superflow, gap functions, critical currents, susceptibilities 0-103531  
transport parameters, Kubo formulae and BCS-Green's functions 0-88382  
<sup>3</sup>He-<sup>4</sup>He mixture superfluid thin film, third sound vel. calc. 0-107602  
<sup>3</sup>He-superfluid <sup>4</sup>He solutions, mag. phases of superfluid <sup>3</sup>He 0-59755

**superfluid helium-4**

- anharmonic effects in US propagation near  $\lambda$  transition 0-96707  
breakdown of superfluidity, excitation emission from negative ions with extreme supercritical vels. 0-65323  
circulation, in <sup>3</sup>He-<sup>4</sup>He dilution refrigerator 0-57304  
coolant, superfluid plug control device 0-82774  
didactic demonstrations of superfluidity and superconductivity phenomena (*Polish*) 0-86059  
elementary excitation, structure factor and phase velocity 0-80012  
elementary excitations,  $\mu$ eV resolution study by neutron spin echo 0-65327  
excitation spectrum, RPA calc. involving simple pseudopot. 0-92738  
fifth sound mode 0-75398  
film, compressible and layered, third sound 0-65325  
film, dynamics 0-59748  
film, solitons at low temps., Korteweg-de Vries eqn. 0-96717  
film, superflow decay, vortex pinning effects 0-84332  
film, third sound propagation, and attenuation (*Russian*) 0-92733  
film growth on graphite, MgO, and Mylar substrates, vap. press. meas. 0-70499  
films, geometry induced third sound splitting 0-96712  
films, vortices and superfluid decay 0-96710  
flow hydrodynamics, normal density component velocity depend. (*Russian*) 0-65326  
flows, healing and relaxation comparison with Khalatnikov-Lebedev theory 0-107587  
fluctuations in turbulent counterflow, vortex line density fluctuation power spectra 0-84335  
fourth sound attenuation 0-100370  
fourth sound phenomenon under adiabatic and isothermal conditions 0-100369  
freely suspended, rot. vel. nonregular variation (*Russian*) 0-88376  
Gorter-Mellink convection in He II, axial heat slow eqn. and dimensions. anal. 0-64545  
hydrodynamical modes when the vapour volume is small 0-88379  
interface with clean Ag, Kapitza cond. and enhanced power anomaly, 1-2K 0-88378  
isotopically pure, rotator-driven mech. for nucleation of negatively charged vortex rings 0-59746  
Kapitza resistance meas. using second sound (*Russian*) 0-88375  
lambda point, light scatt. props., static and dynamic scaling phenomena 0-92739  
Landau critical velocity meas., excitations 0-103528  
low and ultralow temp. cryogenic coolers for space missions 0-77790  
neutron spin-echo study of excitations 0-80014  
nonstationary rotation regime, rel. to superfluidity of pulsars 0-98683  
phonon-rotor excitation 0-107586  
rotating, continuous model of vortex oscils. 0-70490  
rotating, equilibrium order parameters, chemical potentials 0-96713  
rotating, obs. of quantisation of circulation 0-59747  
rotating, vortex position photography technique 0-96708  
rotor-rotor interaction for large and zero momentum 0-84336  
second sound discharge and compression shock wave propagation (*Russian*) 0-103529  
self-consistent description of an interacting Bose gas at T=0K 0-80015  
solid-superfluid interface, roughening transition 0-103536  
solid-superfluid interface, struct., surface tension 0-88380  
sound conversion phenomena at free surface, acoustic coeffs. 0-96709  
spherically confined superfluid, quantised vortices (*Russian*) 0-70487  
static struct. factor and pair correls., neutron diff. study, 1.00 to 4.27K 0-80010  
structure factor, dynamical, two component character, superfluid and normal fluid 0-70488  
thin film, superfluidity 0-107594  
two-dimensional and three-dimensional fluids, energy spectrum and phase vel. 0-70489  
unsaturated films, decay of persistent currents obs. 0-75397  
US finite amplitude wave propag. 0-80024  
vortex form., crit. vel. depend. on oscill. period (*Russian*) 0-92732  
vortex lattice form. relax. times in two-valued vessel subjected to ang. accelerations (*Russian*) 0-92731  
vortex nucleation inhibition by strong electric fields 0-92735  
vortex pinning, surface roughening effects 0-88381  
<sup>3</sup>He-<sup>4</sup>He mixture superfluid thin film, third sound vel. calc. 0-107602

**superfluidity**

- see also quantum fluids; superfluid helium-3; superfluid helium-4; vortices  
Bose-gas model, dil. hard sphere, calc. of low density atomic H gas props. 0-87194  
boson condensate, dynamic eqn. functional formulation, many body theory 0-84334  
hadron superfluidity in neutron stars, determ. from pulsars and compact X-ray sources 0-77442  
hadronic matter, anisotropic superfluidity, analytic formulation 0-105869

**superfluidity continued**

- molecular crystals with several sublattices, exciton-phonon interaction and Bose-Einstein condensation of Frenkel excitons 0-107713  
neutron fluid, stationary flow in <sup>3</sup>P<sub>2</sub> paired state (*Russian*) 0-103527  
neutron stars, rotating, form of quantum vortex filaments 0-67770  
neutron stars, superfluidity 0-77441  
nuclear physics, high spin rotation, collective aspects of heavy ion collisions 0-78309  
physical acoustics and exploration of superfluid state, 1st, 2nd, 3rd, 4th and 5th sound, review 0-96090  
pulsars, rotational behaviour rel. to superfluidity 0-98683  
turbulence, 2-D, hydrodynamic and plasma applications, dynamical eqns., diffusion, MHD, superfluidity, review 0-69769  
two dimensional system, ordering 0-107407  
<sup>3</sup>He, dissipative current structure, hydrodynamic calcs. (*Russian*) 0-100372  
<sup>3</sup>He, liquid, superfluid transition temp. calcs. 0-103530  
<sup>3</sup>He, superflow, gap functions, critical currents, susceptibilities 0-103531  
<sup>3</sup>He-<sup>4</sup>He mixtures, homogeneous phase separation obs. 0-107599  
<sup>3</sup>He-He II dilute solution, fourth sound velocity 0-70498

**supergiant stars**

- A-type supergiant stars, reson. line profiles from IUE and Copernicus spectra 0-90424  
 $\alpha$  and  $\beta$  Aquari, G-type supergiants, evidence for hybrid atmospheres and winds from UV spectra 0-72948  
 $\eta$  Aquilae, Cepheid variable, absolute energy distrib. in radiation spectrum (*Russian*) 0-72974  
 $\epsilon$  Aurigae, dual aspect of wavelength depend. fluctuations 0-62190  
 $\xi$  Aurigae, eclipsing binary, UV obs. of supergiant atmos. 0-94836  
B-type supergiant assoc. IR source GL 2636, IR and visible obs. 0-105302  
blue supergiant+neutron star, evolution 0-98689  
XX Camelopardalis, R Coronae Borealis star, photometry in optical and IR ranges 0-101601  
VY Canis Majoris, irregular variable supergiant, OH maser source, UHF spectra obs. 0-90550  
UW Canis Majoris, O7f supergiant, mass loss rate meas. 0-67736  
 $\alpha$  Canis Minoris (Polaris), interferometry, first fringe meas. 0-82215  
SU Cassiopeiae, Cepheid variable, spectrophotometric determ. of effective temp. 0-90435  
UV Cassiopeiae, R Coronae Borealis star, photometry in optical and IR ranges 0-101601  
V810 Centauri (HD 101947), yellow variable supergiant near Cepheid instability strip, VBLUW photometry 0-98672  
VV Cephei, eclipsing binary, UV spectrum 0-82415  
VV Cephei, UV spectrum obs. during chromospheric eclipse phase 0-109498  
9 Cephei (B2 Ib), circumstellar CO obs. 0-94795  
Cepheid variables determ. of colour term in period-luminosity colour relation 0-94812  
R Coronae Borealis, UBVRIHKLMN photometry, interpretation 0-67756  
31 and 32 Cygni,  $\xi$  Aurigae stars, UV spectroscopic obs. 0-109499  
P Cygni, H Paschen  $\alpha$  line 0-62156  
 $\alpha$  Cygni (Deneb), Ca II K-line core asymmetry 0-85981  
S Doradus, LMC Hubble-Sandage variable, IUE and ground based spectroscopic obs. 0-101595  
early-type mass-losing supergiants, two-core model and evolutionary status (*Russian*) 0-109425  
F-type stars, southern, visible spectra obs. 0-98660  
F-type supergiants in Magellanic Clouds, Ca abundances 0-98655  
HD 105056, ON supergiant, radial vel. study 0-90427  
HD 153919 (=4U 1700-37), supergiant-neutron star, optical variability 0-82419  
HD 159378 (Tr 27-102), yellow variable supergiant near Cepheid instability strip, VBLUW photometry 0-98672  
HD 166734, Of binary system, evolutionary state, visible obs. 0-82414  
HD 168607 (B9 Ia<sup>+</sup>), S Doradus type star candidate, spectral line profiles (*Russian*) 0-90456  
HD 34664 (S 22) in LMC, peculiar emission lines, mass loss and wind 0-77416  
HD 77581 (=Vela X-1), supergiant+neutron star, X-ray, UV and visible obs. 0-94892  
 $\alpha$  Herculis A, M-type supergiant, Li abundance in atmosphere (*Russian*) 0-72950  
HR 8752, binary emission feature variability, visible obs. 0-109463  
I-15, distant B-type object in Norma 0-62129  
instability effects, brightness limits and coronae 0-109432  
late-type stars, anal. of balloon-borne near IR multicolour photometry 0-98654  
late-type supergiant stars, S I emission in EUV 0-82359  
in LMC, luminosity and extinction values, UV obs. 0-77477  
in LMC, photometric luminosity calibration, visible obs. 0-94797  
in LMC, spectra, diffuse interstellar 4430 Å feature 0-73033  
LMC members, IUE obs. of UV spectra and flux distrib. 0-101593  
LS I+61°303, variable binary radio star (B1 Ib), X-ray emission detect. 0-105400  
LSI+61°303, supergiant Be star, radio emission and radial vel. periodic vars. 0-62149  
luminous stars in NGC 6822 and IC 1613, visible spectra and photometry 0-82345  
 $\delta^2$  Lyrae, M-type supergiant, Li abundance in atmosphere (*Russian*) 0-72950  
M-type, classification from spectral scans 0-62127  
M-type maser stars, radial vel. determ. 0-77410  
in Magellanic Clouds, supergiants birthrate and mass function 0-67699  
in NGC 654, young open cluster B to F-type supergiants identification from UV photometric study 0-109502  
OB-type stars, search for H Paschen  $\alpha$  0-62156  
 $\xi$  Orionis, Reticon obs. of Ha P Cygni profile 0-82365  
 $\alpha$  Orionis, variable, mass loss, visible spectra obs. 0-67755  
 $\xi$  Persei, interstellar C<sub>2</sub> rot. fine-struct. lines obs. 0-67811  
 $\xi$  Puppis, of supergiant, mass flow var., visible and UV obs. 0-90431  
Roberts 22, bipolar nebula assoc. with A2 Ie star, radio, IR and visual obs. 0-94859  
FG Sagittae, planetary nebula central star, radial vel. meas. rel. to binary star model 0-98664  
 $\xi$  Scorpii (HD 152236), UV spectroscopic and photometric vars. 0-101594



**supergiant stars continued**

- SU Tauri, R Coronae Borealis star, photometry in optical and IR ranges 0-101601  
 SU Tauri, R Coronae Borealis variable, brightening after long minimum, 1980 August to September 0-109438  
 BL Telescopii A, yellow variable supergiant near Cepheid instability strip, VBLUV photometry 0-98672  
 4U 1907+09, optical identification and OB supergiant binary hypothesis 0-82542  
 $\lambda$  Velorum, K-type supergiant, UV spectrum rel. to chromosphere and wind struct. 0-72948  
 $\gamma_2$  Velorum, Wolf-Rayet binary, orbital element determ. from spectral obs. 0-85950  
 WRA 977 (4U 1223-62, GX 301-2), binary star orbit determ. from X-ray obs. 0-90570  
 Wray 977, optical counterpart to X-ray binary pulsar, 4U 1223-62, optical spectra 0-72984  
 in young galaxies, role in contribution to X-ray background 0-82550  
 C shell burning to Fe core collapse, evolution of 15 M $\odot$  star 0-72937

**supergravity**

- antisymmetric tensor fields coupled to gravity, renormalisability 0-90765  
 classical supersymmetric particles 0-86560  
 conformal supergravity, linear and scalar N=2 multiplets with central charges 0-105562  
 conformal supergravity, ordinary space and superspace connections 0-98844  
 curvature in terms of torsion and covariant derivatives, Bianchi identities 0-62561  
 differential geometry methods in gauge and gravitational theories 0-90768  
 eleven-dimensional supergravity on the mass shell in superspace 0-68116  
 extended supergravity, irreducible representations of extended supersymmetry algebras on superfields 0-98843  
 extended supergravity, N=3,4, meson type classical solns. 0-90755  
 fibre bundles and supersymmetries, super-Poincaré group 0-105559  
 gauge theories, Quantum inequivalence of different field representations, supergravity appl. 0-95214  
 gauged N>4 supergravity, vanishing one loop  $\beta$ -function, infinite renormalisation 0-86186  
 geometrical description, fibre bundle analogy 0-98841  
 geometrical formulation of supergravity theories on orthosymplectic supergroup manifolds 0-95019  
 ghost-free axial gauge in supergravity 0-57162  
 global theory of supermanifolds 0-82911  
 grand unified theory from broken SO(8) extended supergravity, SU(5) theory 0-99081  
 gravitational axial superfield and the formalism of differential geometry (Russian) 0-57164  
 gravitino, axial current anomaly, Faddeev-Popov ghosts 0-68120  
 Higgs effect, gravitino masses and couplings 0-62562  
 N=2 extended supergravity, superfields, auxiliary fields and tensor calculus 0-57157  
 N=2 extended supergravity, superspace constraints, algebraic derivation 0-57159  
 N=2 Poincaré supergravity multiplets, transformation rules 0-73248  
 non-distinguishable field and space variables in QFT, supergravity appl. 0-98845  
 nonlinear realization of graded conformal group 0-105561  
 O(N) model, dynamical mass generation in  $S^1 \times R^3$  0-99046  
 off-shell N=8 supersymmetry with central charges for maximally extended supergravity 0-95230  
 on-shell 11-dimens. supergravity in superspace, eqns. of motion 0-57160  
 Rarita-Schwinger Majorana field, exact soln. and eqns. of motion 0-90756  
 spinning particle in metric-torsion field, eqn. of motion 0-62543  
 spinning strings, the scalar multiplet, and supergravity in (2+2)-dimensional superspace 0-90757  
 SU(2,2/1) superconformal group, Yang-Mills-like Lagrangian 0-62560  
 superspace constraint algebraic origins 0-98842  
 superspace formalism, construction of supervielbeins and superconnections off-shell 0-105558  
 superspace geometry and N=1 non-minimal supergravity 0-57155  
 superspace geometry in supergravity, Riemannian theory reduction, Yang-Mills connections 0-57156  
 supersymmetry and supergravity, review (Czech) 0-86183  
 supersymmetry transformations of noninteracting massless particles 0-95015  
 trivial solution identification, gauge transformation to Einstein vacuum soln. 0-68115  
 twisted supermultiplets, topological effects 0-98839  
 vector multiplets, massless limit 0-73250  
 zero Riemann curvature flat space topology and gravitino eqn. of motion 0-86187

**superheating** *see* heat transfer**superheavy nuclei**

*see also* nuclei with mass number 220 or higher

- <sup>294</sup>110, naturally occurring superheavy element search, alpha emission half-life 0-63139  
<sup>298</sup>114, high spin pot. energy surfaces, fission barrier,  $\alpha$ -,  $\gamma$ -decay half-lives, yrast spectrum 0-73764  
 atomic collision systems, intermediate and superheavy nuclei, UNILAC expts. 0-63751  
 collision system, radiative processes, search for positron emission 0-63752  
 growth points in nuclear physics, book 0-94928  
 ion-atom collisions, quasiats., K-vacancy form., positron emission 0-63753  
 meteorite Kr and Xe isotopes, study of spontaneous fission products 0-63215  
 monazite, from South Indian beach sand, superheavy element search, K X-ray fluoresc. anal. 0-61801  
 search for, using solid state nuclear track detectors 0-91200  
<sup>258</sup>104 prod. from cool compound nucleus formation with oriented heavy ions 0-99179  
<sup>260</sup>106 prod. from cool compound nucleus formation with oriented heavy ions 0-99179  
<sup>235</sup>U fission fragment thermonuclear superheavy nuclei synthesis, prod. cross sections 0-95331

**superheterodyne receivers**

- CMOS ICM 7555 capacitance meter cct., using radio receiver indicator 0-62692

**superionic conducting materials**

*see also* ionic conduction in solids; mixed conductivity

- activation volume for fast ionic cond. in solid and molten salts 0-59711  
 $\beta$ -Al<sub>2</sub>O<sub>3</sub>-Cu<sub>2</sub>O, phys. and chem. props., use in determ. of thermodynamics of Cu-Sn alloys 0-107502  
 alkali glasses, rapidly quenched, alkali ion cond. 0-107559  
 ambient temperature solid state battery developments, review 0-61328  
 B<sub>2</sub>O<sub>3</sub>-Li<sub>2</sub>O-LiCl, ionic conductor, IR refl. Raman study 0-66173  
 battery appls. and developments, conf., Brussels, Belgium (Jan. 1979) 0-72032  
 conductivity measurement, four-probe AC bridge technique 0-57340  
 confined-gas model for ion flow 0-65276  
 correlations among mobile ions role, microscopic model 0-107534  
 diffusion and conductivity, effects of disorder and mobile particle interactions 0-107536  
 EXAFS investigation of struct. and ion motion, excluded vol. model 0-108302  
 excluded volume model, constraints of immobile ion lattice 0-107543  
 fabrication and properties of solid electrolytes 0-70463  
 fast ion transport in solids, conf., Lake Geneva, USA (May 1979) 0-57006  
 fast ion transport in solids, conf., Lake Geneva, USA (May 1979) 0-105427  
 fast ionic transport in solid electrolytes and mixed conductors, material stability and chem. diffusion 0-65292  
 fluoride solid electrolytes 0-70464  
 fluorite structure, activation vol. 0-107557  
 fluorite structures, superionic props., IR spectra 0-107483  
 fluorites, structure and transport 0-84318  
 glass, ionic conductivity, weak electrolyte theory 0-84322  
 glasses as solid electrolytes 0-84321  
 Haven ratio, temp. depend., correl. effects role 0-107504  
 hollandites, cryst. growth and structural props. 0-89129  
 hopping conductivity, freq. depend., model calcs. 0-107507  
 hydrodynamic theory for collective excitations 0-107530  
 interacting Brownian particles in periodic medium model 0-59712  
 ionic crystals, defects, computer modelling, review 0-107205  
 lattice gas, phys. correl. factor in Nernst-Einstein relation 0-105591  
 lattice potential effects on ion flow in superionic conductor 0-65274  
 layer and tunnel compounds, fast ion transport and electrochem. storage 0-61324  
 microscopic models for ionic cond. 0-70454  
 microwave conductivity theory, hopping model 0-59710  
 mobility paths for M<sub>4</sub><sup>3+</sup> clusters, ab initio electronic struct. calc. 0-70458  
 Na-S batteries, solid electrolyte  $\beta$ -Al<sub>2</sub>O<sub>3</sub> formation from m-Al<sub>2</sub>O<sub>3</sub> by new method 0-89606  
 NASICON solid electrolyte, processing and phys. props. 0-60820  
 NMR investigations in solid electrolytes, review 0-60432  
 oxide glasses, fast ion transport 0-107470  
 oxides, standard free energy of formation, by EMF method with solid oxide electrolyte at low temps. (Japanese) 0-88338  
 polyamine iodide-AgI solid electrolytes, elec. cond. and cryst. struct. 0-107537  
 polyether-alkali metal salt adducts, cond. investigation rel. to use as solid electrolytes 0-59708  
 pyridinium pentasilver hexafluoride, solid electrolyte, contrib. of non-Brownian motion to transport props. 0-70453  
 pyridinium silver iodide, fast ion conductor, phase transitions, thermoelec. power meas. 0-107540  
 solid electrolyte, diffusion and ionic cond., correl. factor meas. problems 0-59709  
 solid electrolyte gas sensor developments 0-61217  
 solid electrolyte materials chemistry problems 0-96680  
 solid electrolyte-metal interface adsorption layer capacitance calc. (Russian) 0-59697  
 solid electrolytes containing both mobile and immobile alkali ions 0-96690  
 solid solution electrodes, characterisation and performance, secondary battery appl. 0-72033  
 statics and local dynamics of solid electrolytes near phase transition 0-107542  
 superionic solid film, surface diffusion coeff. 0-92709  
 ternary fluorides, high anion cond. of new solid electrolytes 0-107546  
 tetramethylammonium silver iodide superionic film, electrocodeposition, electrochem. cells 0-107478  
 theoretical models, review 0-107465  
 Ag orthophosphates and sulphates, anhydrous, struct. relationships w.r.t. fast ion cond. 0-107188  
 Ag/RbAg<sub>4</sub>I<sub>3</sub>/I<sub>2</sub> solid state battery, low temp. degradation 0-61331  
 Ag- $\beta$ -Al<sub>2</sub>O<sub>3</sub>, test for solid electrolyte by EMF meas on Ag/Au couples (German) 0-104307  
 Ag-Zn, molten, EMF meas. of activities using ZrO<sub>2</sub> solid electrolytes (Japanese) 0-88339  
 AgBr(Cl), ionic transport, defect form. and migration energies, quasi-harmonic model 0-107538  
 $\alpha$ -AgI, activation vol. for ionic cond. 0-59711  
 $\alpha$ -AgI, cond. mechanisms in superionic phases, neutron diff. obs. 0-59714  
 $\alpha$ -AgI, diffusion dynamics, quasielastic neut. scatt. expt. 0-107484  
 $\alpha$ -AgI, dynamic cage effect 0-70541  
 AgI, EXAFS investigation of struct. and ion motion 0-108302  
 $\alpha$ -AgI, fast ion conductor, phase transitions, thermoelec. power meas. 0-107540  
 AgI group superionic conductor, phase transition detection by thermoelectric power method 0-92669  
 $\alpha$ -AgI, ionic motions nature, mol. dynamics calcs. 0-107533  
 AgI, lattice dynamics of binary superionic conductors 0-107393  
 AgI, lattice potential effects on superionic cond. 0-65274  
 $\alpha$ -AgI, solid electrolyte, contrib. of non-Brownian motion to transport props. 0-70453  
 $\alpha$ -AgI, structural and dynamical behaviour 0-107544  
 $\alpha$ -AgI, superionic, anal. of Ag K-EXAFS data 0-97377  
 $\alpha$ -AgI, superionic cond., statistical thermodynamic description (French) 0-65281  
 AgI/Ag oxysalt system, vitreous solid electrolytes, conductance mechanism 0-107560  
 AgI-Ag<sub>2</sub>MoO<sub>4</sub> pseudobinary system, superionic cond. glasses, comp. depend. of ionic cond. 0-75380  
 AgI-Ag<sub>2</sub>O-MoO<sub>3</sub> glass glass superionic cond., struct. and transport props. 0-88602

## superionic conducting materials continued

- AgI-Ag<sub>2</sub>O-P<sub>2</sub>O<sub>5</sub>(MoO<sub>3</sub>) glassy electrolyte galvanic cells 0-104513  
 (AgI)<sub>1-x</sub>(Ag<sub>2</sub>O-B<sub>2</sub>O<sub>3</sub>)<sub>1-x</sub>, amorphous superionic compound, <sup>11</sup>B lineshape and relaxation 0-108107  
 Ag<sub>2</sub>IPD<sub>2</sub>, superionic solid film, surface diffusion coeff. 0-92709  
 Ag<sub>23</sub>W<sub>18</sub>O<sub>16</sub>, order-disorder type ferroelectric transitions, ionic conductivity meas. 0-66122  
 Ag<sub>23</sub>W<sub>18</sub>O<sub>16</sub>, solid electrolyte, anisotropic elec. cond., low temp. phase transitions 0-65289  
 Ag<sub>2</sub>O-MgO-Al<sub>2</sub>O<sub>3</sub>, ionic cond. 0-107480  
 β-Ag<sub>2</sub>S, cond. mechanisms in superionic phases, neutron diff. obs. 0-59714  
 Ag<sub>2</sub>S+Ln<sub>2</sub>S<sub>3</sub>, powdered mixtures, reaction rate, production of ionic semi-conductors 0-93741  
 Ag<sub>2</sub>SBr, superionic conductor, phase transition, struct. 0-107144  
 βAg<sub>2</sub>Si, anharmonic thermal vibr. of cations 0-65214  
 α-Ag<sub>2</sub>Se, single cryst. growth through capillary tube 0-108331  
 Al solid electrolytic capacitors, pit etching method for improving freq. and temp. characts. 0-100944  
 β-Al<sub>1-x</sub>Mg<sub>x</sub>O<sub>1.6</sub>, X-ray diffuse scatt. obs. of struct. 0-107186  
 β-AlO<sub>2</sub>(Na<sub>2</sub>Li)<sub>2</sub>O, NMR, Raman and IR spectra, and X-ray diff., heat treatment induced changes 0-107508  
 Al<sub>2</sub>O<sub>3</sub>, β- and β'-phases, defect struct. obs. by high resolution TEM, battery ageing relevance 0-107501  
 β-Al<sub>2</sub>O<sub>3</sub>, defect props. and ionic transport 0-107486  
 β'-Al<sub>2</sub>O<sub>3</sub>, Mg- and Li-stabilised, high-resoln. electron microscopy images 0-107277  
 B-Al<sub>2</sub>O<sub>3</sub> solid electrolyte, optimisation of fabrication process, for Na/S load leveling batteries 0-72035  
 β-Al<sub>2</sub>O<sub>3</sub> solid electrolyte based Na/S traction batteries, development progress and problems, review 0-61326  
 β-Al<sub>2</sub>O<sub>3</sub> solid electrolyte for Na/S battery, GEC development program 0-61327  
 β-Al<sub>2</sub>O<sub>3</sub> solid electrolytes, elec. cond. and activation energy (Chinese) 0-79987  
 β-β'-Al<sub>2</sub>O<sub>3</sub> solid electrolytes, resist. obs. 200-1000°C 0-107500  
 β-Al<sub>2</sub>O<sub>3</sub> structures, superionic props., IR spectra 0-107483  
 β-Al<sub>2</sub>O<sub>3</sub>(Na<sub>2</sub>K)<sub>2</sub>O, equil. distrib. of ionic species 0-107511  
 β-Al<sub>2</sub>O<sub>3</sub>(Na<sub>2</sub>K)<sub>2</sub>O, model calcs. of cond. anomalies, pot. energies of cation arrangements 0-107510  
 β-Al<sub>2</sub>O<sub>3</sub>(Na<sub>2</sub>Li)<sub>2</sub>O, β-Al<sub>2</sub>O<sub>3</sub>(K<sub>2</sub>Li)<sub>2</sub>O and β-Al<sub>2</sub>O<sub>3</sub>(K<sub>2</sub>Sn)<sub>2</sub>O, ionic cond. and Raman spectra 0-107509  
 β-Al<sub>2</sub>O<sub>3</sub>(Na<sub>2</sub>Li)<sub>2</sub>O, first-order quadrupole NMR obs. of cation distrib. and ionic motion 0-108113  
 β-Al<sub>2</sub>O<sub>3</sub>(Na<sub>2</sub>Li)<sub>2</sub>O, ionic motion obs. using NMR and internal friction 0-108099  
 β-Al<sub>2</sub>O<sub>3</sub>(Na<sub>2</sub>Li)<sub>2</sub>O solid electrolyte, Li motion and activation obs. using <sup>7</sup>Li NMR 0-108100  
 β-Al<sub>2</sub>O<sub>3</sub>-Ag<sub>2</sub>O, Haven ratio, temp. depend., Ag diffusivity and ionic cond. 0-107503  
 β-Al<sub>2</sub>O<sub>3</sub>-Ag<sub>2</sub>O, stoichiometric A phase, X-ray diffuse scatt. obs., sublattice phase transition 0-64944  
 β-Al<sub>2</sub>O<sub>3</sub>-Ag<sub>2</sub>O(D<sub>2</sub>O)(NH<sub>4</sub><sup>+</sup>) 0-107512  
 β'-Al<sub>2</sub>O<sub>3</sub>-Ag<sub>2</sub>O(H<sub>2</sub>O)(K<sub>2</sub>O)(Li<sub>2</sub>O)(NH<sub>4</sub><sup>+</sup>)(Na<sub>2</sub>O), ionic cond. at room temp. 0-107513  
 β-Al<sub>2</sub>O<sub>3</sub>-Ag<sub>2</sub>O(K<sub>2</sub>O)(Li<sub>2</sub>O)(Na<sub>2</sub>O), low-energy excitation spectra, localised modes 0-59606  
 β'-Al<sub>2</sub>O<sub>3</sub>-Ag<sub>2</sub>O(K<sub>2</sub>O)(Li<sub>2</sub>O)(Na<sub>2</sub>O)(Rb<sub>2</sub>O), single cryst. Raman scatt., cond. mechanism and cryst. struct. 0-66209  
 β-Al<sub>2</sub>O<sub>3</sub>-D<sub>2</sub>O, anhydrous, prep. and struct. of DAl<sub>2</sub>O<sub>3</sub> 0-107187  
 Al<sub>2</sub>O<sub>3</sub>-H<sub>2</sub>O<sup>+</sup>, β and β' phases, protonic, conductance and spectroscopy 0-70450  
 β'-Al<sub>2</sub>O<sub>3</sub>-H<sub>2</sub>O<sup>+</sup>(Na<sub>2</sub>O), struct. basis for superionic cond. 0-107498  
 β-Al<sub>2</sub>O<sub>3</sub>-Li<sub>2</sub>O-Na<sub>2</sub>O, spin-lattice relaxation and Li motion 0-70451  
 β-Al<sub>2</sub>O<sub>3</sub>-NH<sub>4</sub><sup>+</sup>, PMR relax. time obs. of ionic motion 0-71213  
 β-Al<sub>2</sub>O<sub>3</sub>-NH<sub>4</sub><sup>+</sup>, single cryst. characts. and AC cond. obs. 0-107514  
 β-Al<sub>2</sub>O<sub>3</sub>-NH<sub>4</sub><sup>+</sup> and β'-Al<sub>2</sub>O<sub>3</sub>-NH<sub>4</sub><sup>+</sup>-H<sub>2</sub>O, single cryst. PMR and proton motion 0-108101  
 β-Al<sub>2</sub>O<sub>3</sub>-NH<sub>4</sub><sup>+</sup> proton dynamics neutron scatt. study 0-59408  
 β'-Al<sub>2</sub>O<sub>3</sub>-Na<sub>2</sub>O, <sup>23</sup>Na NMR obs. of ionic diffusion, 180 to 800K, attempt freq. 0-108097  
 β-Al<sub>2</sub>O<sub>3</sub>-Na<sub>2</sub>O, <sup>23</sup>Na NQR and two-dimens. diffusion, model analysis 0-108111  
 β-Al<sub>2</sub>O<sub>3</sub>-Na<sub>2</sub>O, <sup>27</sup>Al NMR obs., Na motion and cond. characts. 0-108096  
 β-Al<sub>2</sub>O<sub>3</sub>-Na<sub>2</sub>O, AC impedance, microstruct. and strength 0-100349  
 β-Al<sub>2</sub>O<sub>3</sub>-Na<sub>2</sub>O, AC ionic cond., dielec. and NMR relax. 0-59713  
 β'-Al<sub>2</sub>O<sub>3</sub>-Na<sub>2</sub>O, absorbed water effect on NMR lineshape and spin-lattice relax. time 0-108098  
 β-Al<sub>2</sub>O<sub>3</sub>-Na<sub>2</sub>O, anomalous Na behaviour obs. using pulsed and CW NMR 0-108095  
 β-Al<sub>2</sub>O<sub>3</sub>-Na<sub>2</sub>O, colour centre ESR by localised tunnelling states 0-108073  
 β-Al<sub>2</sub>O<sub>3</sub>-Na<sub>2</sub>O, cond. plane struct. and energetics 0-92715  
 β-Al<sub>2</sub>O<sub>3</sub>-Na<sub>2</sub>O, development for Na/S battery 0-71615  
 β-Al<sub>2</sub>O<sub>3</sub>-Na<sub>2</sub>O, ionic cond. temp. depend., comparison with NASICON 0-107520  
 β-Al<sub>2</sub>O<sub>3</sub>-Na<sub>2</sub>O, low-temp. <sup>23</sup>Na satellite spectra, Na ion motion 0-108112  
 β-Al<sub>2</sub>O<sub>3</sub>-Na<sub>2</sub>O, motion of charge carrying ions, mol. dynamics simulation 0-107506  
 β'-Al<sub>2</sub>O<sub>3</sub>-Na<sub>2</sub>O, NMR of <sup>23</sup>Na, elec. quad. interaction, 185 to 419K, ion motion obs. 0-108110  
 β'-Al<sub>2</sub>O<sub>3</sub>-Na<sub>2</sub>O, nonstoichiometric, correl. effects in diffusion, Haven ratio, point defect interactions 0-107505  
 β-Al<sub>2</sub>O<sub>3</sub>-Na<sub>2</sub>O, potential energy distrib. and ionic motion 0-70455  
 β-Al<sub>2</sub>O<sub>3</sub>-Na<sub>2</sub>O, protonic, conductance and spectroscopy 0-70450  
 β-Al<sub>2</sub>O<sub>3</sub>-Na<sub>2</sub>O, single cryst., non-Debye capacitance 0-107497  
 β'-Al<sub>2</sub>O<sub>3</sub>-Na<sub>2</sub>O, solid electrolyte, behaviour at high current density, sodium heat engine mode 0-61330  
 β-Al<sub>2</sub>O<sub>3</sub>-Na<sub>2</sub>O doped with transition metal ions, complex plane anal. of impedance and admittance 0-70452  
 β'-Al<sub>2</sub>O<sub>3</sub>-Na<sub>2</sub>O solid electrolyte, tube fabrication from cast ceramic tape 0-60819  
 β'-Al<sub>2</sub>O<sub>3</sub>-Na<sub>2</sub>O solid electrolyte, processing and phys. props. 0-60820  
 β'-Al<sub>2</sub>O<sub>3</sub>-Na<sub>2</sub>O solid electrolyte, strength degradation under electrolytic conditions 0-61329  
 β'-Al<sub>2</sub>O<sub>3</sub>-Na<sub>2</sub>O solid electrolyte, heat treatment effects on ionic cond. and microstruct. 0-65293  
 β-Al<sub>2</sub>O<sub>3</sub>-OH<sub>3</sub><sup>+</sup>, proton dynamics neutron scatt. study 0-59408

## superionic conducting materials continued

- Au/solid electrolyte/Au primary cells, charge storage with various electrolytes 0-89605  
 Au-Zn, molten, EMF meas. of activities using ZrO<sub>2</sub> solid electrolytes (Japanese) 0-88339  
 BaCl<sub>2</sub>(F<sub>2</sub>), sp. ht. meas., Schottky-type diffuse phase transitions, defect form. energies and entropies 0-107441  
 δ-Bi<sub>2</sub>O<sub>3</sub>, thermoelectric power, heat of transport of O<sup>2-</sup> ions 0-92713  
 CaF<sub>2</sub>, anion motion at high temps., quasielastic neutron scatt. obs. 0-59715  
 CaF<sub>2</sub>, fast ion transport, computer simulation 0-107485  
 CaF<sub>2</sub>, mol. dynamics studies of superionic conductors 0-107547  
 CaF<sub>2</sub> solid electrolyte use in galvanic cells for thermodynamic obs. on refractory double oxides (French) 0-85190  
 CaF<sub>2</sub>-H<sub>2</sub>, ionic cond. determ. from admittance and dielec. loss meas. (French) 0-107479  
 CeO<sub>2</sub>-Y, slow transient phenomenon 0-107550  
 Cu halides, lattice dynamics of binary superionic conductors 0-107393  
 Cu-Cul-graphite secondary cell, transient ionic current obs. 0-108790  
 Cu-Cul-graphite secondary cell, steady state hole current obs. 0-108791  
 CuBr, superionic behaviour at high temp., EXAFS study 0-107496  
 CuBr(Cl)(I), LF light scatt. spectra in superionic cond. phases, ion motion obs. 0-108217  
 CuCl, superionic behaviour at high temp., EXAFS study 0-107496  
 CuI, EXAFS investigation of struct. and ion motion 0-108302  
 CuI, ionic motions nature, mol. dynamics calcs., sp. ht. anomaly due to order-disorder transform. 0-107533  
 Cu<sub>2</sub>Mo<sub>2</sub>S<sub>8-y</sub>, mixed conductor, partial Cu ion cond. and chem. diffusion 0-84323  
 Cu<sub>2</sub>Mo<sub>2</sub>S<sub>8-y</sub>, mixed conductor, equil. partial thermodynamic props. 0-85270  
 Cu<sub>2</sub>PS<sub>2</sub>Br, cryst. struct. at 293 and 473K, thermal parameters, neutron diff. obs. 0-59450  
 Cu<sub>2</sub>S+Ln<sub>2</sub>S<sub>3</sub>, powdered mixtures, reaction rate, production of ionic semi-conductors 0-93741  
 Cu<sub>2</sub>VS<sub>4</sub>, out of equil. mixed cond., electronic cond. decrease in ionic soln. 0-107874  
 Cu<sub>2</sub>VS<sub>4</sub>, out of equil. mixed cond., off-centre positions and order-disorder transition, ultrafast nucl. relax. obs. 0-108103  
 Cu<sub>2</sub>VS<sub>4</sub>, out of equil. mixed cond., chem. origin of mobile ions, spin-lattice relax. and NQR obs. 0-108104  
 H<sub>2</sub>O<sub>2</sub>AsO<sub>4</sub>·4H<sub>2</sub>O and H<sub>2</sub>O<sub>2</sub>PO<sub>4</sub>·4H<sub>2</sub>O layered cpds., struct. investigs. below antiferroelec. transition temps., H bond ordered structs. 0-107416  
 H<sub>2</sub>O<sub>2</sub>AsO<sub>4</sub>·4H<sub>2</sub>O and H<sub>2</sub>O<sub>2</sub>PO<sub>4</sub>·4H<sub>2</sub>O layered cpds., single and polycryst., proton cond. behaviour w.r.t. antiferroelec. transition temps. 0-107481  
 H<sub>2</sub>n-2UO<sub>2</sub>(IO<sub>3</sub>)<sub>n</sub>·4H<sub>2</sub>O, n=0.5 to 2.0, high proton cond. 0-107562  
 H<sub>2</sub>O<sub>2</sub>PO<sub>4</sub>·4H<sub>2</sub>O, film fabrication and appl. as solid electrolyte in electrochromic displays 0-70462  
 H<sub>2</sub>O<sub>2</sub>PO<sub>4</sub>·4H<sub>2</sub>O solid proton conductor, appl. as electrochromic cell 0-89497  
 H<sub>2</sub>O<sub>2</sub>P(As)O<sub>4</sub>·4H<sub>2</sub>O, water deficiency, enthalpy of dehydration, thermogravimetric anal. 0-65251  
 In<sub>2</sub>ZnI<sub>4</sub> and In<sub>2</sub>CdI<sub>6</sub> solid electrolytes, ion transport mechanism and polarisability role, comparison with Cu<sup>+</sup> and Ag<sup>+</sup> cond. 0-107531  
 KAgI<sub>3</sub>, pressure effect on phase transitions 0-70405  
 KAgI<sub>3</sub>, superionic phase transition, dynamical and crit. pt. props. 0-107535  
 K<sub>1-x</sub>Mg<sub>0.77</sub>Ti<sub>0.23</sub>O<sub>6</sub>, hollandite, one-dimens. superionic cond., transport model 0-107529  
 K<sub>2</sub>Mg<sub>2</sub>Ti<sub>8-x</sub>O<sub>16</sub>, stochastic Langevin dynamics study of correlated ionic motion in 1-D solid electrolytes 0-65279  
 K<sub>2</sub>O-MgO-Al<sub>2</sub>O<sub>3</sub>, ionic cond. 0-107480  
 K<sub>2</sub>OsCl<sub>6</sub>, impurity H<sup>+</sup> ion motion, <sup>35</sup>Cl NQR obs., 77 and 298K 0-60451  
 K<sub>2</sub>OsCl<sub>6</sub>, single cryst. with H<sup>+</sup> interstitials, protonic cond. from dielec. meas. 0-107515  
 K<sub>2</sub>SO<sub>4</sub>, anhydrous, struct. relationships w.r.t. fast ion cond. 0-107188  
 Li salt based solid electrolyte, synthesis and characterisation, secondary cell appl. (French) 0-72034  
 Li solid electrolyte materials, review of crystal and electrochem. props. 0-107524  
 Li-ion conductors in solid electrolytes 0-71610  
 LiAl/FeS, battery system research developments at ANL 0-61323  
 LiAlCl<sub>4</sub>, fast ionic conductor, thermodynamic and phase props. 0-89211  
 LiAlCl<sub>4</sub>, solid and molten electrolyte, thermodynamic stability 0-107447  
 Li<sub>2</sub>AlO<sub>3</sub>, Li<sub>2</sub>FeO<sub>4</sub> and Li<sub>2</sub>GaO<sub>4</sub>, additives and moisture effect on ionic cond. 0-107523  
 LiAlSiO<sub>4</sub>, β-eucryptite one-dimens. fast ion cond., temp. depend. of cryst. struct. 0-107191  
 LiAlSiO<sub>4</sub>-Cu, β-eucryptite solid electrolyte, Cu<sup>2+</sup> EPR obs. of ion exchange props. 0-108056  
 Li<sub>2</sub>GeO<sub>4</sub>-Zn<sub>2</sub>GeO<sub>4</sub>, solid electrolyte system, phase diagram 0-66489  
 LiI-WO<sub>3</sub> solid-state electrochromic cell, fabrication and characts. (Japanese) 0-84717  
 Li<sub>3</sub>N, defect props. and ionic transport 0-107486  
 Li<sub>3</sub>N, diffusion processes and struct. NMR study 0-108090  
 Li<sub>3</sub>N, electron density study using Compton scattering 0-79750  
 Li<sub>3</sub>N, interstitial sites and anharmonic thermal vibrs. in cryst. struct., ionic cond. mechanism 0-107190  
 Li<sub>3</sub>N, ionic hopping model, NMR relax. data anal. 0-92714  
 Li<sub>3</sub>N, ionic transport mechanism and defect props. 0-107528  
 Li<sub>3</sub>N layer structure with fast ion cond., <sup>6</sup>Li NMR obs. of diffusion 0-108102  
 Li<sub>3</sub>N single crystal and sinters, Li ion conduction 0-70449  
 Li<sub>3</sub>N thin film, vacuum evaporation on WO<sub>3</sub>, retarded deposition 0-108351  
 Li<sub>3</sub>N-LiBr(Cl)(I) quasibinary cuts, fast ionic cond. props., 25 to 400°C 0-107527  
 Li<sub>2</sub>O-B<sub>2</sub>O<sub>3</sub> glasses, fast ion transport 0-107470  
 Li<sub>2</sub>O-LiF-B<sub>2</sub>O<sub>3</sub> glasses, fast Li<sup>+</sup> conduction 0-79984  
 Li<sub>2</sub>O-LiF-B<sub>2</sub>O<sub>3</sub>-Li<sub>2</sub>SO<sub>4</sub>, glasses, DC cond. and secondary struct. relax. 0-107469  
 Li<sub>2</sub>O-LiX-B<sub>2</sub>O<sub>3</sub> glass, X=halogen, high anionic cond. of new solid electrolytes 0-107546  
 Li<sub>2</sub>O-TiO<sub>2</sub>, pseudobinary phase rotations, DTA and X-ray anal. 0-108411  
 Li<sub>2</sub>S-P<sub>2</sub>S<sub>5</sub>-LiI, ionic cond. meas. from room temp. to glass transition temp. (French) 0-88355  
 Li<sub>2</sub>SO<sub>4</sub> based solid electrolytes, FCC phase transport mechanism studies and uses 0-107525



## superionic conducting materials continued

- Li<sub>2</sub>SO<sub>4</sub>, fast ion conductors, X-ray diffr., neutron diffr., and Brillouin scatt. study 0-107170  
 Li<sub>2</sub>SO<sub>4</sub>, high temp. fast ion cond. phases, neutron diffr. obs. of struct. 0-107512  
 Li<sub>1-x</sub>Zn(GeO<sub>4</sub>)<sub>x</sub>, LISICON, AC meas. of ionic cond., 298 to 573K 0-107526  
 NH<sub>4</sub>Ag<sub>4</sub>I<sub>5</sub>, pressure effect on phase transitions 0-70405  
 NH<sub>4</sub>Ag<sub>4</sub>I<sub>5</sub>, superionic solid film, surface diffusion coeff. 0-92709  
 NH<sub>4</sub>Ag<sub>4</sub>I<sub>5</sub>, superionic phase transition, dynamical and crit. pt. props. 0-107535  
 NH<sub>4</sub>Cu<sub>4</sub>Cl<sub>3</sub>(I<sub>2</sub>-xCl<sub>x</sub>), highly conducting solid electrolyte 0-65280  
 Na, orthophosphates and sulphates, anhydrous, struct. relationships w.r.t. fast ion cond. 0-107188  
 Na<sub>0.70</sub>Ga<sub>0.72</sub>Ti<sub>0.70</sub>O<sub>8</sub>, one-dimens. Na<sup>+</sup> ion cond., cryst. struct. and cond. meas. 0-107521  
 Na<sub>5-x</sub>Li<sub>x</sub>ErSi<sub>4</sub>O<sub>12</sub>, solid electrolytes for Na/TiS<sub>2</sub> cells, synthesis, characts. and utilisation 0-107518  
 Na<sub>2</sub>O-Ga<sub>2</sub>O<sub>3</sub> system β and β' phases, fast ion cond., prep. and phase comp. 0-59716  
 Na<sub>2</sub>O-Li<sub>2</sub>O-Al<sub>2</sub>O<sub>3</sub>, local electrode current density and flow decoration 0-100935  
 Na<sub>2</sub>O-MgO-Al<sub>2</sub>O<sub>3</sub>, ionic cond. 0-107480  
 Na<sub>3</sub>PO<sub>4</sub>, high temp. fast ion cond. phases, neutron diffr. obs. of struct. 0-107512  
 Na<sub>3</sub>Sc<sub>2</sub>P<sub>2</sub>O<sub>12</sub>, fast-ion conductor, struct. phase transition 0-88362  
 Na<sub>3</sub>Sc<sub>2</sub>P<sub>2</sub>O<sub>12</sub>, synthesis, cryst. struct. and ionic cond. 0-107519  
 Na<sub>0.9</sub>Ti<sub>1.1</sub>Fe<sub>0.9</sub>O<sub>4</sub>, short period β-alumina type cpds., cryst. struct. and superionic cond. 0-107499  
 Na<sub>3</sub>Zr<sub>2</sub>PSi<sub>2</sub>O<sub>12</sub>, NASICON, <sup>23</sup>Na NMR obs. of ionic diffusion, 180 to 800K 0-108097  
 Na<sub>3</sub>Zr<sub>2</sub>Si<sub>2</sub>O<sub>12</sub>, struct. analysis at 300 and 600°C, rel. to ionic cond. 0-107189  
 Na<sub>1-x</sub>Zr<sub>x</sub>Si<sub>3-x</sub>O<sub>12</sub>, press. and comp. effect on fast Na<sup>+</sup> ion transport 0-107516  
 Na<sub>3</sub>Zr<sub>2</sub>Si<sub>2</sub>PO<sub>12</sub>, NASICON, ionic cond. temp. depend., comparison with β-Al<sub>2</sub>O<sub>3</sub>-Na<sub>2</sub>O 0-107520  
 Pb<sub>1-x</sub>Bi<sub>x</sub>F<sub>2+x</sub>, solid soln., struct. and ionic cond. correl., neutron diffr. study (French) 0-84324  
 PbF<sub>2</sub>, anion disorder at high temps., neutron diffr. obs. 0-59614  
 PbF<sub>2</sub>, fast ion conductor, phonon freq. distrib., temp. variation 0-84264  
 PbF<sub>2</sub>, sp. ht. meas., Schottky-type diffuse phase transitions, defect form. energies and entropies 0-107441  
 PbF<sub>2</sub>·Fe<sup>3+</sup>, F<sup>-</sup> motion, ESR study 0-66023  
 PbSnF<sub>4</sub>, high anionic cond. of new solid electrolytes 0-107546  
 Pb<sub>2</sub>Sn<sub>1-x</sub>F<sub>2</sub> solid soln., struct. evolutions (French) 0-96488  
 RbAg<sub>4</sub>I<sub>5</sub>, contact in solid state cells, electrochem. study 0-76527  
 α-RbAg<sub>4</sub>I<sub>5</sub>, dynamic cage effect 0-107541  
 RbAg<sub>4</sub>I<sub>5</sub> film, thermopower meas. temp. depend., correl. effects role 0-107539  
 RbAg<sub>4</sub>I<sub>5</sub>, single particle excitations, inelastic neutron scatt. obs. 0-59599  
 RbAg<sub>4</sub>I<sub>5</sub>, solid electrolyte, contrib. of non-Brownian motion to transport props. 0-70453  
 RbAg<sub>4</sub>I<sub>5</sub>, solid electrolyte development, Ag<sup>+</sup> cond. 0-107532  
 RbAg<sub>4</sub>I<sub>5</sub>, static and dynamic NMR effects at 208K and 122K phase transitions 0-108105  
 RbAg<sub>4</sub>I<sub>5</sub>, superionic conductor, phase transition detection by thermoelectric power method 0-92669  
 RbAg<sub>4</sub>I<sub>5</sub>, superionic phase transition, dynamical and crit. pt. props. 0-107535  
 RbCu<sub>4</sub>Cl<sub>3</sub>I<sub>3</sub>, development of Cu<sup>+</sup> ion cond. 0-107532  
 Sb<sub>2</sub>O<sub>3</sub>·nH<sub>2</sub>O, crystalline, <sup>1</sup>H NMR study of proton transport 0-60446  
 SrCl<sub>2</sub>, anion disorder at high temps., neutron diffr. obs. 0-59614  
 SrCl<sub>2</sub>, anion motion at high temps., quasielastic neutron scatt. obs. 0-59715  
 SrCl<sub>2</sub>, fast ion cond., specific heat anomaly, mol. dynamics study 0-65283  
 SrCl<sub>2</sub>, ionic cond., self-diffusion, rel. to defect motion, mol. dynamics study 0-65282  
 SrCl<sub>2</sub>, sp. ht. meas., Schottky-type diffuse phase transitions, defect form. energies and entropies 0-107441  
 ThO<sub>2</sub>·Ce<sup>4+</sup> (Ce<sup>4+</sup>), mixed ionic and electronic transport 0-107875  
 Ti<sub>2</sub>ZnBr<sub>4</sub>(I<sub>2</sub>), solid electrolytes, ion transport mechanism and polarisability role, comparison with Cu<sup>+</sup> and Ag<sup>+</sup> cond. 0-107531  
 ZrF<sub>4</sub>·BaF<sub>2</sub>·ThF<sub>4</sub>(LaF<sub>3</sub>)(NdF<sub>3</sub>)(PrF<sub>3</sub>), F<sup>-</sup> ion cond. glasses, cond. process 0-107477  
 Zr(HPO<sub>4</sub>)<sub>2</sub>·H<sub>2</sub>O, Na<sup>+</sup> transport, gas-solid and solid-solid reaction kinetics 0-61086  
 ZrO<sub>2</sub>, based solid electrolyte, use for study of O<sub>2</sub> solubility and diffusivity in liq. metals 0-59669  
 ZrO<sub>2</sub>, doped, ionic cond., theoretical model 0-107552  
 ZrO<sub>2</sub>, solid electrolyte, electrochem. reduced, electrocatalytic decomp. of NO 0-61113  
 ZrO<sub>2</sub>/Pt solid electrolyte/porous electrode system, interface polarisation effects 0-61114

## superlattices

- adsorbed layers, general principles of construction of structural models 0-84351  
 antiferromagnet, Ising model, crit. props., calc. 0-65946  
 γ-brass type alloys, superstructures and defect obs. 0-107284  
 derivative lattices, determ. of relationships 0-107012  
 p-dibromo-tetrafluorobenzene mol. cryst., in commensurate phase, quasi-elastic neutron scatt. 0-107386  
 ferroelectric substances, electron microscopy investigations, review (Japanese) 0-71366  
 III-V semiconductor (Slovak) 0-88620  
 image potential enhancement by static elec. field 0-92846  
 lattice image calculations for imperfect crystals., superlattice approach 0-107030  
 layer structures, intercalation with N<sub>2</sub>H<sub>4</sub>, charge density waves or artefacts 0-100221  
 multilayer stacks, very thin nonideal, wavelength variation of transmissivity, refl. 0-100701  
 one-dimensional superlattices, electronic density of states 0-75488  
 partial Patterson function, use for superlattice reflection phase determ. 0-79627  
 plasmons, two-dimens., due to piezoelec. effect 0-92845  
 polymeric series of coverings, symmetry, comparison with layers of real structs., Below subclass development 0-84129

## superlattices continued

- semiconductor, with superlattice, plasma resonant interaction with Stark oscils. 0-107842  
 semiconductor superlattice, transverse electron effective mass 0-100429  
 semiconductor thin films, fabrication for device appls. 0-100418  
 semiconductor with superlattice, optoelectric effect, theory 0-70768  
 semiconductor with superlattice, EM wave propag., mag. field effect 0-70745  
 semiconductors, EM wave absorption in quantising electric field 0-108182  
 semiconductors, EM wave interaction in weakly nonlinear medium with superlattice 0-93257  
 semiconductors with superlattices, Stark-cyclotron resonance, Larmour freq. (Russian) 0-60421  
 single crystal surface, electrochemistry, surface struct., superlattice struct. 0-76519  
 Al<sub>3</sub>(Ni, Co)<sub>3</sub> ternary phase in Al-Ni-Co system, cryst. struct., vacancy controlled phase (Chinese) 0-70164  
 β"-Al<sub>2</sub>O<sub>3</sub>·H<sub>2</sub>O<sup>+</sup>(Na<sub>2</sub>O), struct. basis for superionic cond. 0-107498  
 CdTe-HgTe superlattice on CdTe layers, evanescent states, tight binding calcs. 0-70611  
 CsCl-type lattice, (111) superlattice screw dislocation motion, computer simulation 0-79793  
 Cu-Al alloy, ordered, superlattice fringe images, computer simulation 0-103296  
 Cu-Au system, two-phase mixtures, long-period superlattices 0-84140  
 Cu-Ni-Al (5, 2.5 at.%), precip. hardening (Japanese) 0-71663  
 Cu-Ni-Sn (10, 6 wt.%), spinodal decomposition, X-ray and electron diffr. study 0-81063  
 Cu-Sn alloy system, long period superlattice obs. and impurity effects 0-103297  
 Cu<sub>3</sub>Au, alloys, superlattice-fringe imaging theory, images formed from two beams 0-79649  
 Cu<sub>3</sub>Au, electrical resistivity and LRO, energy gap formation in Fermi surface 0-88533  
 Cu<sub>3</sub>Au, neutron irradi., displacement cascades, direct obs. method 0-107335  
 Cu<sub>3</sub>Au-Ni, antiphase domains morphology 0-108460  
 CuCrS<sub>2</sub>, domain struct. and superstructure, TEM obs. 0-79779  
 r-CuMn, annealing ordered phase study by neutron diffr. 0-89265  
 Cu<sub>2</sub>Pt, antiphase domains morphology 0-108460  
 Fe-Al alloy, ordered, superlattice fringe images, computer simulation 0-103296  
 Fe<sub>2</sub>Al, alloys, superlattice-fringe imaging theory, images formed from two beams 0-79649  
 Fe<sub>2</sub>Al, electrical resistivity and LRO, energy gap formation in Fermi surface 0-88533  
 GaAs-AlAs superlattice, folded acoustic phonons obs., Raman scatt. 0-88996  
 GaAs-AlGaAs heterojunction superlattices, inelastic light scatt. by two-dimens. electron gas 0-93360  
 n-GaAs-Ga<sub>1-x</sub>Al<sub>x</sub>As, heavily doped superlattice, electronic props., perpendicular low temp. mobility 0-65660  
 GaAs-GaAlAs superlattices, metalorganic VPE growth, in sites ellipsometry monitoring 0-70547  
 (GaAs)<sub>m</sub>(AlAs)<sub>n</sub> multilayers, MBE, interdiffusion, X-ray diffr. study 0-70474  
 InAs-GaSb superlattices, mag. field induced semimetal-semicond. transition 0-65656  
 KC<sub>24</sub>, press. induced staging transition 0-79938  
 Na-zeolite, matrix, Te cluster superlattices, N and S type volt-ampere characts., elec. cond. (Russian) 0-70665  
 Na<sub>2</sub>Ti<sub>2</sub>O<sub>8</sub> bronze, hydrothermal prep., Na ion arrangement 0-75209  
 NaX-Se semiconductor superlattice absorpt. edge, light scatt. (Russian) 0-71438  
 Nb/Cu layered ultrathin coherent struct. 0-80122  
 NbS<sub>2</sub>-(pyridine)<sub>1/2</sub> intercalation complex, superlattice struct., NMR meas. 0-70180  
 PdD<sub>0.73</sub>, (1, 1/2, 0)-superlattice reflection splitting near 50K, neutron diffr. studies 0-70168  
 (SN)<sub>x</sub>, halogenated, struct. behaviour, TEM obs. 0-70126  
 Si (111) 7×7 surface structure investigation, RHEED 0-96723  
 Si(111) reconstructed 7×7 surface superlattices, microdomain model 0-107625  
 Zr<sub>3</sub>Al, deformed and irradi., lattice defects obs., superlattice dislocations and defect clusters 0-107261

## supernova remnants

- adiabatic phase, thermal X-ray spectra 0-82475  
 blast model, parameters from X-ray data and SNRs of known age (Chinese) 0-77471  
 blast wave instabilities, adiabatic and isothermal models 0-67814  
 3C 58, comparison of optical and radio emission of plerion 0-73023  
 Cassiopeia A, explanation of secular flattening of radio spectrum 0-101637  
 Cassiopeia A, foreground interstellar HCN absorpt. obs. 0-101624  
 Cassiopeia A, secular decrease in 927 MHz flux, radio flux density obs. 0-67840  
 Cassiopeia A historical records 0-77430  
 Cassiopeiae A, historical records rel. to 3 Cassiopeiae 0-72792  
 Cassiopeiae A, mag. field origin 0-85989  
 catalogue of optical candidates in nearby galaxies 0-62037  
 chemical and isotope fractionation by grain size separates 0-67831  
 cosmic ray acceleration 0-82192  
 Crab, magneto-parametric instabilities, two-fluid model of interaction with pulsar EM waves 0-85851  
 Crab, search for 1-20 MeV gamma rays, balloon-borne obs. 0-67912  
 Crab Nebula, compact source flux density meas. by interferometer 0-62252  
 Crab Nebula, lunar occultation obs. at decametre wavelengths 0-62248  
 Crab Nebula, model 0-62230  
 CTB 1, kinematics and evolution 0-67823  
 CTB 1, UHF emission and radio shell 0-77461  
 Cygnus Loop, abundances and filament shock vel., UV obs. 0-94848  
 Cygnus Loop, ANS X-ray obs. 0-82455  
 Cygnus Loop, fast shock wave detection, optical spectra 0-82467  
 Cygnus Loop, soft X-ray spectra emission line features obs. 0-94849  
 Cygnus Loop, UHF emission and filamentary structure 0-77461  
 Cygnus Loop, UV spectra interpretation using radiating shock wave models 0-90498  
 Cygnus Loop, X-ray spectra var. with position 0-82472

## supernova remnants continued

- Cygnus Loop, X-ray spectrum two component appearance interpretation 0-82475  
 Cygnus X-ray superbubble, multiple supernovae 0-90575  
 in dense molecular clouds, struct. and IR emission 0-82450  
 30 Doradus nebula, supernova remnants contrib. to struct. 0-62226  
 electron acceleration mechanism 0-85988  
 expansion characteristics in mol. cloud 0-94846  
 filamentary structure, prod. by stellar wind from presupernova 0-62249  
 G321.9-0.3, possible assoc. with runaway star (Circinus X-1) 0-67910  
 G74.9+1.2, continuum obs. at 2695 MHz 0-67830  
 G 261.9+5.5, H I 21 cm obs., H I clouds 0-62229  
 G 84.2-0.8, high resolution 1415 and 2695 MHz obs. 0-98702  
 H0207+19, Delphinus soft X-ray source, model, X-ray obs. 0-90576  
 HB 3, kinematics and evolution 0-67823  
 IC 443, shock enhancement of  $\text{HCO}^+$  0-82464  
 interstellar medium heating, rel. to delayed star form. in galaxies 0-105349  
 Kepler's SN 1604 remnant, spectrum 0-85982  
 Kepler's supernova remnant, X-ray obs. from Einstein Observatory 0-82465  
 kinematics and evolutionary sequence in cloudy interstellar medium, interferometry obs. 0-67823  
 in LMC, SHF obs. 0-67864  
 Lupus Loop, X-ray spatial extent and spectrum 0-82457  
 MSH 11-54, X-ray obs. 0-82463  
 N132 D in LMC, rapidly moving material, visible and UV obs. 0-82449  
 N49, LMC supernova remnant, as source of fast intense unusual gamma-ray transient 0-73073  
 N49, LMC supernova remnant, as source of gamma-ray transient event of 1979 March 5 0-73074  
 N49, SNR in LMC, Pioneer Venus Orbiter obs. of 1979 March 5 gamma-ray transient 0-77518  
 N49 and N63 in LMC, UV spectra interpretation using radiating shock wave models 0-90498  
 N49 supernovae remnant as source of March 1979  $\gamma$ -ray burst 0-105270  
 N51D, giant filamentary shell in LMC, nature and dynamics 0-105343  
 N63A, lower limit to mass of original supernova 0-62165  
 N 132D in LMC bar, possible correl. with X-ray source 0-82491  
 in NGC 6946, search for radio emission from four young SNRs 0-77473  
 North Polar Spur, reheated supernova remnant model appl. to X-ray obs. 0-105370  
 North Polar Spur, soft X-ray spectra emission line features obs. 0-94849  
 OA 184, kinematics and evolution 0-67823  
 old supernova remnants in solar neighbourhood, evidence from interstellar He I obs. 0-62234  
 periodicity investigation at 21 cm 0-82529  
 Puppis A, X-ray spectrum two component appearance interpretation 0-82475  
 Puppis A X-ray spectra var. with position 0-82472  
 radio evolution, generalized theoretical approach 0-85990  
 radio supernova remnants, source counts rel. to galactic supernova outbursts frequency 0-62168  
 S147, assoc. CO absorpt. detect. 0-67836  
 shock wave intermediate zone radiative cooling, effect on optical emission spectra 0-109517  
 SN 1006, X-ray spectrum 0-82457  
 SN 1572 (Tycho's supernova), small dia. radio source discovery near centre of remnant 0-98680  
 spectral index distrib. of radio shells 0-77462  
 near SS 433, faint, highly-contorted nebular filament discovery 0-94855  
 Taurus A, secular decrease in 927 MHz flux, radio flux density obs. 0-67840  
 Tycho's SNR (3C 10), distance, Westerbork H I obs. 0-101633  
 Tycho's supernova (SN 1572), unsuccessful search for optical stellar remnant 0-101603  
 type rel. to supernovae type, mag. field effects 0-77474  
 Vela, IUE UV spectrum 0-101635  
 Vela SNR, X- and gamma-ray emission (Russian) 0-94861  
 Vela X, X-ray spectrum two component appearance interpretation 0-82475  
 W1 (S171), optical supernova remnant radial vel. field 0-62250  
 W50, continuum obs. at 2695 MHz 0-67830  
 W50, interstellar medium interaction with SS 433 relativistic jets visible obs. 0-101629  
 W50, optical spectrum of faint filamentary nebula 0-90557  
 W50, probable supernova remnant, relation to (SS 433) 0-72987  
 W50 containing SS 433, object with unique spectrum 0-82381  
 young supernovae remnants, X-ray props. rel. to neutron stars cooling 0-77443

## supernovae

see also *supernova remnants*

- in anonymous galaxy in Canes Venatici discovery obs. 0-67759  
 in anonymous galaxy in Centaurus, discovery, posn. and magnitude 0-85961  
 in anonymous galaxy in Centaurus, magnitude (1980 June 30) 0-85962  
 in anonymous galaxy in Crus, discovery and magnitudes (1980 May 23 to July 12) 0-94820  
 in anonymous galaxy near  $\kappa$  Centauri, discovery and magnitudes 0-85962  
 in binary systems, implications for evolutionary status of stars with  $M \geq 50 M_{\odot}$  (Russian) 0-109425  
 Cassiopeia A supernova, probable Flamsteed observation 0-62436  
 Cassiopeiae A rel. to 3 Cassiopeiae 0-72792  
 core collapse, theory 0-77389  
 core collapse outcome, effects of core eqn. of state 0-85928  
 core gravitational collapse, shockwave prod., neutrino transport effects 0-94818  
 cosmic ray prod., intensity var. at Earth from cosmogenic isotope obs. 0-101503  
 in Cygnus X-ray superbubble, power source 0-90575  
 distance determ. by Baade's generalised method, appl. to  $H_0$  and  $q_0$  0-73082  
 distant ( $z=0.5$ ) supernova light curve, photometric obs. 0-94821  
 education, explosion in binary system, classical mechanics appl. 0-62428  
 expanding envelopes, Lyman  $\alpha$  quanta scattering (Russian) 0-67556  
 expanding shell, site for r-nuclei prod. 0-72932  
 explosive core overturn, rel. to mass ejection 0-72988  
 explosive nucleosynthesis 0-72766  
 extragalactic supernovae, types I and II, radial distrib. in spiral and elliptical galaxies 0-62163

## supernovae continued

- galactic supernova outbursts, frequency estimate 0-62168  
 gamma-ray emission, continuum intensity and spectrum 0-101602  
 guest star of AD 1408, Japanese record 0-90641  
 Hercules X-1 (HZ Herculis) binary system, pre-supernova parameters 0-62318  
 historical records of Cassiopeia A 0-77430  
 interstellar medium heating, rel. to delayed star form. in galaxies 0-105349  
 magnetorotational explosion, one-dimensional cylindrical model 0-101605  
 mass of supernova that produced N63A, lower limit 0-62165  
 massive star, Mg, Al isotope yields from C and Ne zones 0-90406  
 in MCG -3-34-61, discovery of 17 mag. object 0-72989  
 in MCG -3-34-61, Type I spectrum revealed (1980 June) 0-82401  
 mechanism for young galaxy contribution to X-ray background 0-82550  
 in molecular clouds, spectra and luminosity, evolution 0-82399  
 nearby supernova, effects on terrestrial atmosphere 0-94584  
 neutrino energy equilibration, models 0-105265  
 neutrino mediated shocks 0-94818  
 neutrino transport, time-dependent, out of dense stellar cores, theory 0-94783  
 in NGC3733, spectrophotometry (1980 March 22) 0-62164  
 in NGC 4321, UBVR photometry 0-77428  
 in NGC 5253, high supernova rate, previous high luminosity explanation 0-77489  
 nucleosynthesis, mechanisms for explosion and element synthesis (French) 0-72933  
 in OB associations, interaction with interstellar medium to form H I supershells 0-82468  
 piston problem, one-dimensional, in non-ideal gas, time-dependent soln. 0-82185  
 presupernova stellar wind, as possible cause of supernova remnant filamentary struct. 0-62249  
 Rayleigh-Taylor convective overturn of core, rel. to supernova explosion 0-77429  
 Rayleigh-Taylor driven explosion, 2-D numerical study 0-94819  
 relativistic blast waves that accelerate 0-67534  
 shock wave acceleration of Galaxy cosmic rays 0-82154  
 SN 1054, possible European record 0-62437  
 SN 1572 (Tycho's supernova), small dia. radio source discovery and precise position 0-98680  
 SN 1979c in M100, coordinated obs. (1979 April-June) 0-101604  
 SN 1979c in M100 (NGC 4321), gamma-ray emission, continuum intensity and spectrum 0-101602  
 SN 1979C in M100 (NGC 4321), precise position 0-85962  
 SN 1979c in M100 (NGC 4321), spectrophotometry 0-62166  
 SN 1979c in NGC 4321 (M100), detect. at 60 nm wavelength 0-82402  
 solar system formation 0-82232  
 spectra of type I supernovae, effects of line overlapping in conservative scatt. case (Russian) 0-105266  
 thermodynamics of nucleon, lepton, photon mixture, quantum mechanical calcs. 0-77273  
 Tycho's supernova (SN 1572), unsuccessful search for optical stellar remnant 0-101603  
 Type I, luminosity calcs. 0-82400  
 Type I and II, neutrino mechanism of thermonuclear explosion of degenerate C-O cores 0-62162  
 Type I supernovae, radioactive excitation source model for late time spectra 0-105264  
 type II supernovae, light curves analytic solns. 0-77427  
 type rel. to supernova remnants type, mag. field effects 0-77474  
 in Virgo galaxy cluster, discovery 0-90460  
 weak interaction rates for sd-shell nuclei 0-82336  
<sup>26</sup>Al, synthesis in explosive H burning 0-85929  
 C detonation supernovae, evolved C cores energy generation and dissipation 0-82339  
 C layer, <sup>11</sup>B neutrino-induced prod. 0-82337  
 Fe group elements production, relative abundances from e-process nucleosynthesis (Russian) 0-62167  
 H II regions, origin from supernovae explosions 0-67877  
<sup>26</sup>Mg( $\gamma$ ), <sup>27</sup>Al, isotopic anomaly, stellar reaction rate, astrophysical aspects 0-99132  
<sup>22</sup>Ne and <sup>26</sup>Al nucleosynthesis in novae and supernovae outbursts 0-62143

## superparamagnetism

see also *magnetic properties of fine particles*

- glass, magnetic susceptibility measurement, torsional reson. technique 0-82796  
 iron(II)-A-zeolites, reduction, mag. and Mossbauer study 0-71115  
 magnetic moment time development and discrete orientation model of particles 0-60378  
 spin glass materials, mag. field dependence of susceptibility peak 0-103840  
 CoFe<sub>2</sub>O<sub>4</sub> ultrafine particles, prep. and mag. props. 0-71116  
 Co<sub>0.54</sub>Ga<sub>0.46</sub>, frequency depend. magnetisation, superparamagnetic behaviour 0-84624  
 Cu-Mn-Al, Heusler alloys, ferromag. inclusions, mag. props. and struct. study (Russian) 0-80570  
 Eu-Sr<sub>1-x</sub>S<sub>x</sub> spin-glass props. and mag. transition 0-97105  
 Fe-Al<sub>2</sub>O<sub>3</sub> granular films, superparamagnetism and relax. effects 0-71118  
 Fe-Ti, magnetism and H<sub>2</sub> storage 0-70941  
 FeMoS<sub>4</sub>, Mossbauer investigation, Neel point, superparamag. effects 0-97170  
 Fe<sub>1.6</sub>Ni<sub>0.8</sub>B<sub>10</sub>P<sub>10</sub> metallic glass, superparamag. behaviour, chem. inhomogeneities role 0-84625  
 Fe<sub>2</sub>O<sub>3</sub> amorphous layer on graphite, Mossbauer spectra, superparamag. props. 0-60474  
 Fe<sub>2</sub>O<sub>3</sub> ultrafine particles in PTFE matrix, EPR and Mossbauer study 0-100625  
 $\alpha$ -Fe<sub>2</sub>O<sub>3</sub>-Cr<sub>2</sub>O<sub>3</sub> solid solution, Mossbauer effect studies 0-71249  
 Fe<sub>3-x</sub>Ti<sub>x</sub>O<sub>4</sub>, spin glass behaviour, susceptibility and hysteresis meas. 0-65917  
 (H<sub>2</sub>O)<sub>0.194</sub>(Al<sub>2</sub>O<sub>3</sub>)<sub>0.227</sub>(SiO<sub>2</sub>)<sub>0.579</sub>, amorphous, low temp. spin glass behaviour 0-60297  
 LaNi<sub>5</sub>, magnetism and H<sub>2</sub> storage 0-70941  
 Mg<sub>2</sub>Ni, magnetism and H<sub>2</sub> storage 0-70941  
 MnO-Al<sub>2</sub>O<sub>3</sub>-SiO<sub>2</sub>, amorphous spin glass, AC susceptibility 0-80520  
 Ni<sub>0.2</sub>Zn<sub>0.75</sub>Fe<sub>0.05</sub>Al<sub>0.0</sub>, Mossbauer study, spin fluctuations 0-60471  
 SmCo<sub>5</sub>, amorphous, supermag.-ferromag. transition and directional crystallisation 0-65891



**superplasticity**

- activation enthalpy determ. from strain rate changes in tensile tests 0-81127
- alloys, cavity growth 0-93627
- brass, recrystallization during induction heating 0-97511
- cavity growth anal. during superplasticity 0-60923
- microcrystalline alloys, metastable, rapidly quenched particulates, props. appl. and production 0-84887
- region I characteristics 0-107357
- Al-Ca-Zn (5.5 wt.%) superplastic sheet alloy, mechanical properties, superplastic forming behaviour 0-60920
- Al-Zn-Mg superplastic alloy, cavity growth under creep conditions 0-6940
- Be-Ni(Y), plastic deform., flow stresses, fracture (*Russian*) 0-108496
- Bi<sub>2</sub>MoO<sub>6</sub>, transform. superplasticity 0-108498
- Bi<sub>2</sub>WO<sub>6</sub>, transformational superplasticity 0-108498
- Fe-Mn-C, struct. superplasticity 0-76317
- Mg-Mn-Ce (1.5, 0.3 wt%), superplasticity role of diffusional creep (*Russian*) 0-97528
- Pb, film, hillock formation by grain boundary sliding 0-107673
- Ti-Al-V (6.4 wt.%) superplastic alloy, maximum attainable ductility 0-60919
- Zn-Al (0.4 wt.%), intergranular slip during in situ superplastic deform. 0-96538
- Zn-Al (1.1 wt.%) superplastic alloy, grain size determ. (*Czech*) 0-81118
- Zn-Al (22 wt.%), eutectoid, low stress and superplastic creep behaviour 0-81120
- Zn-Al (22 wt.%) superplastic alloy, grain growth texture 0-81075
- Zn-Al (22 wt.%), alloy sheet, superplastic, cold-rolling effects on mech. props. and microstructure (*Japanese*) 0-71671

**superradiance**

- see also *acoustic superradiance*
- atomic state, superradiant, excitation by pulse of quantum field 0-87359
- backward Raman amplifier for excimer laser pulse compression, parasitic superfluoresc. suppression 0-69453
- coherence properties, initiating noise source obs., intrinsic delay time quantum fluctuations 0-58492
- collective processes in slightly inverted and absorbing media 0-87367
- computerised analysis, collaboration collection report 0-73106
- cooperative cascade emission, linear stochastic theory 0-74326
- cooperative cascade emission theory, nonlinear evolution 0-74327
- Dicke state N two level atom assembly, radiation emission theory 0-69350
- dye solution, amplified spontaneous emission, effect of O<sub>2</sub> 0-95885
- dynamical behaviour in model mag. insulator 0-87358
- gas superluminescence in high-current discharge, polarisation due to Zeeman splitting 0-10060
- metal atom lasers, finely dispersed metal particle active medium 0-91777
- multilevel system, group theoretical method for coherent effects calc. 0-106502
- non-centresymmetric media, phase transitions into spontaneous coherent state (*Russian*) 0-69353
- RF, optical pulse generated under photon-echo conditions 0-95858
- spatial variation with time, numerical anal. (*Russian*) 0-78821
- superfluorescence, delay-time statistics and inhomogeneous line broadening 0-99684
- superfluorescence beats, theory incl. quantum fluctuations and finite sample size 0-102686
- superfluorescent pulse fluctuation 0-58490
- superluminescence, spatial coherence 0-99683
- thin-film waveguide laser amplifier with lossy cladding 0-64074
- three-level systems, superradiance and subradiance 0-83570
- two-level atoms, inhomogeneously broadened, superfluoresc. and amplified spontaneous emission 0-106499
- two-level atoms system, quantum theory, incl. propag. effects 0-58491
- two-level molecules, gauge-invariant system, superradiant state, phase transition 0-69352
- Wannier excitons, radiative decay in thin crystal fields 0-92823
- waveguide laser, stimulated emission spectrum, leaky modes (*Russian*) 0-87400
- CDs crystals, one-photon pumping, active layer structure, light amplification 0-78858
- Cu vapour pulsed laser, spectral comp. of superradiance, stimulated and spontaneous radiation 0-102713
- He<sup>2+</sup> + Li collisions, soft X-ray emission obs. 0-83591
- InGaAsP-InP DH lasers, spatial hole burning, spontaneous emission saturation, direct obs. 0-95892
- KH<sub>2</sub>PO<sub>4</sub>, ultrashort light pulse parametric transform. under optimum interaction conditions 0-99791
- N<sub>2</sub>, superfluorescent UV laser, demonstration 0-105475
- Na vapour, superradiance, quantum beat spectra 0-106311
- Nd:YAG giant pulse lasers, energy characts., superradiance effects 0-64031
- Rb, radiative lifetimes up to n=12 excited states, pulsed dye laser and superradiance excitation 0-83322
- Rb, superrad. between degenerate levels, polaris. characts., coupled transitions 0-58493
- S<sub>2</sub>, optically pumped superfluorescence molecular laser 0-63990
- Sr, visible emission on three-level cascade, coupled transitions 0-58493
- Xe 3.51  $\mu$ m laser amplifiers, spectral narrowing and saturation induced rebroadening optical heterodyne obs. 0-63976
- Xe-He, 3.51  $\mu$ m laser amplifiers, spectral narrowing and saturation induced rebroadening optical heterodyne obs. 0-63976

**supersaturation control** see *chemical variables control***supersaturation measurement** see *chemical variables measurement***supersonic flow**

- see also *shock waves*
- air flow through high press. gas valves into atm., noise and flow pattern obs. 0-59067
- annular jets for supersonic and sonic flow 0-100019
- atomic O<sub>2</sub>, supersonic nozzle beam source development 0-58016
- base influence on supersonic flow around a cone, power-law injection 0-100010
- boundary layer, free interaction with supersonic flow, dispersion eqn. solutions 0-69867
- boundary layers, supersonic, interacting with cooling wall jets, turbulent and optical characteristics 0-106792
- chemically reacting gas mixture, thermal crisis suppression by laser radiation 0-75000

**supersonic flow continued**

- compressible flow problems, modified FLIC method, finite element anal. 0-74911
- conical crossflow sonic line, flow patterns and bubble props. 0-69862
- corner interaction of boundary layer and shock wave, flow separation 0-96287
- CW supersonic chemical laser, porous nozzle, chemically reacting boundary layer 0-100022
- degeneration of supersonic flow due to interaction of centered compression and rarefaction waves 0-69864
- dispersed supersonic two-phase flow, shock characts., droplet size depend. at nozzle 0-106815
- duct, supersonic flow downstream oscillations from abrupt cross section increase, nozzles 0-74976
- excess noise from supersonic underexpanded jets in flight 0-69815
- gas, shock wave under continuous energy supply 0-103042
- gas jet blowing into supersonic flow without 3-dimens. boundary layer separation, nozzle shape 0-100009
- gas stream, supersonic, stationary, conical flow about plane wedge and circular cone 0-74912
- hot wire anemometry, rarefied gas flow vel. meas. 0-100040
- hot-wire anemometer freq. response, comments on determination and optimization 0-87832
- hot-wire anemometers, freq. response of constant temp. anemometers 0-59149
- ideal gas flow around blunt wedge, sonic line shape 0-64577
- Kelvin-Helmholtz instability in supersonic and super-Alvenic fluids 0-87816
- laminar separation, second order asymptotic soln. 0-83828
- low density supersonic gas flow, temp. meas. probe 0-74913
- Mach wave radiation of hot supersonic jets 0-69894
- molecular beam nozzle, use of pulsed valve 0-100045
- Navier-Stokes equations, parabolic, implicit finite-difference method using fractional steps technique 0-69866
- nonequilibrium gas relaxation in supersonic nozzle, analysis method 0-74941
- nozzle, pulsed jet wave struct. in nonstationary flow stage 0-59094
- nozzle in different jet regimes, internal and external flows, separation and wakes 0-100023
- plate with periodic suction and injections in supersonic region, boundary layers (*German*) 0-59069
- self-similar explosion waves of variable energy at the front 0-103040
- separation flow, 2- and 3-dimens.; turbulent boundary layer and shock wave 0-100017
- shell deformation by supersonic gas flow, drag 0-96279
- spontaneously condensing and wet steam discontinuous flows in steam turbines, numerical investigation (*Russian*) 0-87800
- steady flow about blunt bodies, finite difference methods 0-96280
- turbulent shear layer, instability waves, radiation of sound 0-79341
- two-phase flow, nonequib. condensation, boundary condition numerical anal. 0-64565
- unsteady flow of supersonic gas stream past a slender profile, asymptotic expansion of nonlinear effects 0-69863
- upstream perturbation propagation, supersonic flow, self-induced press. boundary layer on moving surface 0-74914
- Ar, cluster formation and homogeneous nucleation, comparison of expt. and theory, for supersonic nozzle flow 0-79925
- Ar, nonequilibrium condensation and surface tension in supersonic jet flow (*Russian*) 0-65210
- Ar, supersonic pulsed flow from conical nozzle 0-103056
- H supersonic flames, chemical kinetics and unmixedness effects on burning 0-64649
- N<sub>2</sub> jet, freely expanding, quantum effects in rot. relax. 0-58355

**supersonics** see *supersonic flow***supersymmetry**

- see also *supergravity*
- $\sigma$ -model, nonlinear, supersymmetric, Ricci-flat Kahler manifolds and supersymmetry 0-90994
- $\sigma$ -model, U(N,r), supersymmetric, and O(2) extended supersymmetry 0-82878
- $\sigma$ -model supersymmetric dynamics on pre-QCD level with elementary quarks and composite gluons 0-82886
- $\sigma$ -model supersymmetric extensions, dynamical conservation laws, symmetric space valued fields 0-95227
- $\sigma$ -models, nonlinear, supersymmetric, nonlocal conserved currents and instanton-like solutions 0-86544
- $\sigma$ -models, supersymmetric, Kahler geometry and renormalisation 0-105789
- A(0,n) Lie superalgebra, Fock space representation 0-86606
- BRS supersymmetry, non-trivial realisation 0-82882
- chiral field, supersymmetric, 1/N perturbation theory and quantum conservation laws 0-68373
- classical particles with spin, supersymmetry model (*Russian*) 0-101946
- classical supersymmetric particles 0-86560
- CP<sup>N-1</sup> model, (2+1) dims. supersymmetric, supersymmetry algebra and central charge 0-86568
- CP<sup>N-1</sup> supersymmetric model, central charge, superalgebra and Dirac brackets 0-99044
- differential geometry methods in gauge and gravitational theories 0-90768
- dimensional regularisation, supersymmetric form inconsistency 0-91013
- Dirac particles in external fields 0-82918
- dynamical Bose-Fermi supersymmetries in complex nuclei 0-57703
- dynamical growth of supersymmetry 0-105809
- extended N=4 supersymmetric gauge theories, off-mass-shell formulation 0-77959
- extended supergravity, irreducible representations of extended supersymmetry algebras on superfields 0-98843
- extended supersymmetric Yang-Mills theories, superfield formulation, auxiliary component fields 0-90995
- gauge theories, supersymmetric and non-supersymmetric regularisation by dimensional reduction 0-77951
- gauge theory, developments (*Chinese*) 0-77978
- gauging Lie superalgebras 0-73618
- global theory of supermanifolds 0-82911
- Grassmann character, explicit solns. 0-91015
- Hilbert superspaces and Grassmann numbers, Fermi oscillator system appl. 0-95223
- massless Wess-Zumino model in 4-dimens., asymptotic estimates 0-82877

**supersymmetry continued**

- N=2 extended supergravity, superspace constraints, algebraic derivation 0-57159
- N=4 supersymmetric Yang-mills theory, 3-loop  $\beta$  function zero value 0-105783
- Noether's theorem in superspace 0-73621
- off-shell N=8 supersymmetry with central charges for maximally extended supergravity 0-95230
- OSp(1,4), superfield formulation in anti-de Sitter space 0-57508
- QED, supercurrent gauge invariance,  $\alpha$ -independ. 0-95233
- QED, supersymmetric, renormalised supercurrents and scale anomaly 0-105818
- radiative mass generation in perturbation theory and the renormalization group 0-86611
- real simple Lie superalgebras, finite-dimens., classification 0-57516
- renormalisation theory, perturbative, general features, quantum action principles, pure Yang-Mills theory 0-105794
- sine-Gordon equation, supersymmetric, prolongation struct. inverse scatt. formalism 0-99032
- SL(3,R) algebra, minimal and centred graded spin extensions 0-82910
- spin-1 fields, supersymmetric non-polynomial vector multiplets and causal propagation 0-91012
- spl(2,1), basic superalgebra representations 0-82908
- spl(2,1) superalgebra, irreducible representations, tensor product 0-82909
- SU(2,1) nonlinear invariant  $\sigma$  model, superconformal group and curved fermionic twistor space 0-62831
- SU(2) supergroups, Yang-Mills, Lie groups, chiral coeffs., Baker-Campbell-Hausdorff formula 0-68355
- SU(5/1) supergroup based strong-electroweak unified model with supersymmetry 0-101977
- super  $(\phi^4)_2$  model, large order perturbation theory 0-82876
- super sine-Gordon eqn., supergroup geometrical interpretation, supersymmetric extension 0-57475
- super Yang-Mills theory, anomalies and supersymmetric regularisation by dimensional reduction 0-82916
- superalgebra in (0,1) integration of supersymmetrical Liouville eqn. (*Russian*) 0-101947
- superfields and supersymmetric linear multiplet (*Chinese*) 0-101950
- supergrand exceptional unification and quark-lepton constituents 0-91030
- supergrand unification in  $E_6$ , quark-lepton assignments, symmetry breaking scheme 0-68408
- supergravity, fibre bundles and supersymmetries, super-Poincare group 0-105559
- supergravity, global supersymmetry transformations of noninteracting massless particles 0-95015
- supergravity, super Higgs effect, gravitino masses and couplings 0-62562
- supergravity, superspace constraint algebraic origins 0-98842
- supergravity and supersymmetry, review (*Czech*) 0-86183
- superspace affine theory, simple Lagrangian 0-105813
- superspace as family of concrete spinor structures 0-95225
- superspace gauge theories, superspace Maxwell and Yang-Mills actions 0-86582
- superspace geometry and N=1 non-minimal supergravity 0-57155
- three-loop charge renormalization effects due to quartic scalar self-interactions 0-57489
- two-dimensional supersymmetric models, group theoretical construction 0-99069
- unification of EM, weak and strong interactions, extension to gravity 0-73637
- unified field theory applications 0-91040
- Weinberg-Salam model, Lagrangian, invariant under SU(2/1) gauge group and rotations, in 6-D graded space 0-57537
- Yang-Mills field theory, point splitting regularisation, superformal anomaly 0-91014
- Yang-Mills fields, Ward identity, one-loop level, renormalisation 0-73597
- Yang-Mills theory in Wess-Zumino gauge, supersymmetric regulators and supercurrent anomalies 0-86614
- zero-mass representations of Poincare supersymmetries with arbitrary spinor generators 0-99065
- pp, heavy lepton prod. and decay, supersymmetrical model of weak and EM interactions (*Russian*) 0-86748

**supply systems (electric)** see power systems

**supports**

- fusion reactor, compact toroidal ignition experiment, support struct. anal. by numerical code 0-106167
- fusion reactor, RST, support struct. 0-102342
- fusion reactor, TFTR toroidal field coil support restraint struct. 0-95428
- fusion reactor, toroidal field coil in-plane bending stress, struct. support design 0-106164
- fusion reactors, TFTR neutral beam support system 0-102376

**suppressors (surge)** see surge protection

**surface acoustic wave devices**

- see also acoustic microwave devices; acoustic parametric amplifiers; acoustic parametric devices; acoustic parametric oscillators
- 2.148 GHz SAW oscillator using  $\text{AlN}/\text{Al}_2\text{O}_3$  delay line 0-74680
- 2-D separated media semiconductor convolver for acoustic Fourier transforms of optical images 0-74308
- acousto-optic signal processors 0-102640
- acousto-optic signal processors using multichannel SAW correlation and convolution 0-74611
- acousto-optic time integrating correlator 0-64295
- analogue signal processing technology, transversal filters and resonators 0-87656
- automatic response measurements for large time-bandwidth SAW devices 0-74677
- band-pass filter, with three-transducer configuration 0-74610
- broadband chirp transducers for integrated optics spectrum analyzers 0-74514
- Broadband modified chirp transducers for integrated optics spectrum analyser 0-58802
- chirp filters, spectrum analyser appl. (*Japanese*) 0-79065
- combined bandpass and rejection filters, design and eval. (*Russian*) 0-83718
- compensated filter used in wide spread MSK waveform generator 0-74670
- conference, New Orleans, LA, USA 0-73101
- convolver, degenerate elastic, nonlinear interactions 0-64254
- convolver for surface-states concentration profile and capture cross section determ. 0-80341
- degenerate elastic convolver, theory 0-74628

**surface acoustic wave devices continued**

- delay lines, towards an ideal photon correlator 0-68252
- doubly-rotated-cut, numerical anal. 0-74616
- driven equilibrium Fourier transform sensor operating at 100 MHz 0-74612
- echo-tomographic imaging with SAW processing, ultrafast 0-74639
- electronically-addressed bulk acoustic wave Fourier transform device 0-74637
- electrostatic voltage sensor (*Japanese*) 0-105632
- filter, L-band low loss SAW filters 0-74673
- filter appls. in consumer electronics, review 0-74675
- filter design, low-sideband cascaded 0-74679
- filter design applied to group-delay equaliser in TV rebroadcast transmitters 0-74676
- filter design using optimisation technique 0-74671
- filter design with diffraction compensation 0-74672
- gap-coupled Schottky diode array/ $\text{LiNbO}_3$  imager for scanning of optical images 0-74632
- grating-array reflectors and transducers 0-58884
- gratings, theoretical anal. of stored energy 0-74622
- IDT, Al evaporation conditions 0-92007
- IDT, bulk wave radiation suppression, theoretical investigation of crystal-line orientation 0-58886
- in-line reflective array compressor 0-74626
- integrated optic spectrum analyser, design of Bragg cells 0-74515
- integrated optics spectrum analyser, development progress 0-58803
- Israel Physical Society 1980 annual meeting, Rehovot, Israel (April 1980) 0-94909
- metal powder on piezoelec. substrate, dynamic SAW reflecting struct. 0-74565
- multistrip coupler, superposition model 0-74674
- multistrip coupler for coupling of surface skimming bulk waves 0-74630
- periodic dot arrays, selective reflection of SAW 0-74624
- phase shifter with 3 interdigital transducers 0-79062
- photoacoustic surface wave generation system using CW laser, NDT appl. 0-87683
- photoresists, standing waves and other interference elimination 0-69614
- piezoelectric transducers, characterization of RF sputtered ZnO and ZnS films by X-ray diffraction anal. 0-80138
- polymer materials, appl. to SAW and other devices 0-66114
- polyvinylidene fluoride transducers, evaluation of performance 0-74617
- prism couplers for Rayleigh and Lamb waves, anal. 0-69619
- propagation velocity meas. on  $\text{LiNbO}_3$  0-92003
- quartz powder on piezoelec. substrate, dynamic SAW reflecting struct. 0-74565
- quartz with metallic overlay films for temp. compensation, SAW device appls. 0-79043
- reflection gratings, theoretical investigations of energy storage effects and 2nd harmonic responses 0-74621
- reflector, determination of centre freq. and intrinsic refl. coeff. 0-74620
- reflector-array-compressor devices, effects of temperature-dependent anisotropy and use of Y-cut quartz 0-74625
- resonators, fundamental mode oscillators, narrowband filter at 1.43 GHz 0-87687
- resonators, radiation losses formed by interdigital type reflectors 0-69603
- resonators, transverse mode anal. 0-96169
- SEM diagnosis, voltage contrast obs. 0-69618
- shallow bulk acoustic wave devices, recent developmental advances 0-74629
- signal processor theory and production method (*German*) 0-58867
- single-channel reduced-bandwidth processor for US imaging 0-74636
- spectrum analysers in photon-counting mode, statistical props. 0-105712
- surface charge on unapodized periodic IDI 0-91947
- surface skimming bulk wave bandpass filters using Y-rotated quartz 0-74583
- surface skimming shear-wave guidance by corrugated surface 0-74582
- Swazawa wave broadband thin-film interdigital transducers 0-74681
- temperature compensation techniques 0-74614
- temperature effects of devices integrated on Si 0-79066
- temperature stable oscillators employing parallel-connected SAW resonators 0-74615
- thermal shearing effects on the temperature stability 0-69613
- tilted-finger chirp transducer for design of wideband guided-wave acousto-optic Bragg deflector 0-74510
- transducer array for surface defect imaging in metals 0-74660
- transducers, apodized, radiation conductance 0-96174
- transducers, charge distribution for non-periodic transducers using cct. model 0-74691
- transducers, parameter calc. with power scattering coeffs. (*Russian*) 0-64317
- transducers based on layered systems, calc. of electromech. coupling coeff. squared 0-87690
- transducers on Si substrates with polyvinylidene fluoride films 0-74618
- underwater sound sensor using SAW resonator-controlled oscillators 0-74631
- unidirectional transducers, 3-phase equivalent cct. model 0-74627
- US surface wave velocimeter, phase sensitive 0-102947
- ZnO/Si acoustoelectric devices 0-80332
- AlN, piezoelectric film, low temp. growth by RF reactive planar magnetron sputtering method 0-76175
- InSb thin films for acoustoelectronics 0-103765
- InSb- $\text{LiNbO}_3$  SAW convolver, efficient struct. realisation, Hall mobility meas. 0-83705
- Y-Z  $\text{LiNbO}_3$ , acoustic effects of filamentary defects 0-75314
- Y-Z  $\text{LiNbO}_3$ , filamentary defects visualisation at wafer inspection stage 0-75315
- $\text{LiNbO}_3$ , temp. coeff. of freq. determ. 0-75316
- $\text{LiNbO}_3:\text{Na}^+ (\text{Co}^{2+}, \text{Zr}^{4+})$  film, improvement in temp. stability and SAW device appl. 0-75939
- $\text{LiNbO}_3$ -gap coupled Schottky diode memory correlator, grating coupled optical imaging 0-64143
- $\text{LiNbO}_3$ -pn-diode airgap convolver struct. optical scanner using single SAW pulse 0-64144
- $\text{LiTaO}_3$  crystals for commercial SAW TV IF filters, fabrication 0-80961
- $\text{LiTaO}_3$ , single cryst. prep. for surface acoustic wave device appls. (*Japanese*) 0-60772
- Ni film, evaporated, for use as variable delay SAW device, magnetostrictive effects 0-71144
- PVF, thin film SAW transducers for 8 MHz delay line 0-58876
- Si guided-wave acousto-optical devices 0-102864



**surface acoustic wave devices continued**

- ZnO, CVD of epitaxial films on sapphire, SAW interdigital transducer fabrication 0-66430  
 ZnO/quartz for device materials, expt. study of props. 0-80050  
 ZnO/Si structs., anal. of charge injection 0-80049  
 ZnO-SiO<sub>2</sub>-Si SAW device, interface transduction 0-102949

**surface acoustic waves**

*see also acoustic waves; Rayleigh waves; surface acoustic wave devices; surface phenomena*

- anomalous sound absorpt. for fluid-fluid interface 0-74562  
 attenuation of waves propag. along boundary with periodic inhomogeneities 0-102905  
 backward waves and acoustic scanning, nonlinear interaction of vol. and surface waves 0-79040  
 bandpass filter design, use of charge distribution model 0-74678  
 Brillouin scattering by Stoneley waves, elasto-optic and surface ripple mechanisms 0-71435  
 ceramics, surface cracks, acoustic surface wave meas. 0-61055  
 ceramics containing volatiles mechanisms for attenuation 0-74560  
 coherent optics methods appl. to acoustic field investigations 0-106691  
 dispersion relations for Rayleigh waves in cubic crystals 0-102906  
 elastic body, attenuation of surface Rayleigh acoustic waves travelling along periodically surface 0-80047  
 generation by means of CW laser, NDT appl. 0-87683  
 grating coupling between SAWs and plate modes 0-102895  
 interdigital transducer on piezoelectric half space, spectrum of emanating acoustic waves 0-79044  
 Lamb wave diffraction by finite crack in elastic layer 0-64244  
 layered systems, direction control of acoustic wave propagation 0-103557  
 layered systems, film-substrate characts. of phase-velocity dispersion and struct. of waves 0-59775  
 LiNbO<sub>3</sub>, finite difference anal. 0-75423  
 Love waves propag. along cylindrical surface, excitation 0-102907  
 magnetoelastic wave velocity on magnetised ferrite substrate, non-reciprocity 0-80587  
 metal, mode conversion, by EM generation of US 0-84357  
 nonlinear propag. characts. of finite amplitude SAWs excited by monochromatic line source 0-96091  
 optical heterodyne method for SAW study using laser beams (Russian) 0-64271  
 optical probing of HF guided wave surface displacements with arbitrary profile 0-69612  
 particle motion fields anal. 0-79042  
 in periodically corrugated piezoelectric medium, Bleustein-Gulyaev surface waves behaviour 0-87616  
 photographs on TV images of travelling waves using strobed electron beam 0-102894  
 photoinduced surface storage of SAW patterns in LiNbO<sub>3</sub> 0-74309  
 piezoelectric crystal, plasmon transformation into SAW 0-59903  
 piezoelectric crystals, shear surface waves, generalised 0-92770  
 piezoelectric insulator, nonlinear interaction of SAW with electron beam 0-70517  
 piezoelectric medium, semibounded, body waves and quasi-body surface waves 0-107367  
 piezoelectric-semiconductor struct., nonlinear acoustoelectric effects for large amplitude SAW 0-92942  
 propagation along X-axis on Y-cut plate of Se 0-75313  
 quartz, doubly-rotated cuts 0-74584  
 quartz, effects of the ion implantation on SAW propag. 0-75421  
 quartz, fused, photoelastic light scatt. from surface Rayleigh waves 0-97235  
 quartz, propag. meas. by acoustoelectric methods 0-84359  
 quartz with zero temp. coeff. of delay, SAW propag. characts. 0-75420  
 Rayleigh wave nonlinear interaction in LiNbO<sub>3</sub>-CdS system, expt. investigation 0-102946  
 Rayleigh wave propagating along rough surface, dispersion and damping 0-102892  
 Rayleigh wave reflection from periodic corrugations of surface in oblique incidence 0-58850  
 Rayleigh waves on smooth surfaces of arbitrary shape 0-64272  
 Rochelle salt, dehydration kinetics in ferroelec. and paraelec. phases, surface acoustic waves influence 0-97204  
 scanning of optical images using acoustoelectric memory correlator struct. 0-74632  
 semiconductor surface eval. using SAW convolver 0-97677  
 semiconductor-piezoelectric structure, vol. acoustic wave excitation in nonlinear interaction with surface waves 0-69582  
 shear SAW in high permittivity three-layer system (Russian) 0-80048  
 solid insulator interface, parametric interaction with EM waves in microwave field, 0-92771  
 solids, transverse SAW in microwave field 0-92945  
 structure, properties and appls. of SAW, overview (Italian) 0-69574  
 surface skimming bulk wave propag. in Y-rotated quartz 0-74583  
 surface skimming bulk waves, coupling with multistrip coupler 0-74630  
 surface skimming shear-wave guidance by corrugated surface 0-74582  
 transverse modes in SAW resonators 0-96169  
 ultrasonic wave transmission through rough surface (Russian) 0-100387  
 viscous heat conducting fluid, acoustic boundary layer 0-107377  
 visualisation, by acousto-optical holography (German) 0-70515  
 Al, Brillouin spectra, light scatt. cross section for surface ripples 0-71434  
 AlN, piezoelectric film, low temp. growth by RF reactive planar magnetron sputtering method 0-76175  
 α-AlPO<sub>4</sub> as SAW substrate material, piezoelec. props. 0-80710  
 Ba<sub>2</sub>-, Sr-TiSi<sub>3</sub>O<sub>8</sub>, piezoelec. crystals, SAW characts. 0-84354  
 Bi, amorphous film, temp. dependence of SAW attenuation 0-75679  
 Bi<sub>2</sub>SiO<sub>20</sub> crystal, piezoelec. and saw props. 0-75949  
 ErFeO<sub>3</sub>, SAW meas. of magnetoelastic effects 0-75839  
 GaAs, Brillouin spectra, light scatt. cross section for surface ripples 0-71434  
 Gal, Brillouin spectra, light scatt. cross section for surface ripples 0-71434  
 LiO, single crystal, surface acoustic wave parameter meas., coherent optics method 0-106691  
 LiO<sub>3</sub>, transverse gap elastic waves, expt. 0-59576  
 LiNbO<sub>3</sub>, aluminum-coated YZ, measurements of SAW attenuation 0-74619  
 LiNbO<sub>3</sub> crystals, velocity and propag. loss meas. of surface shear waves 0-74581  
 LiNbO<sub>3</sub>, effects of the ion implantation on SAW propag. 0-75421  
 LiNbO<sub>3</sub>, piezoelec., SAW interaction with secondary electrons 0-80708

**surface acoustic waves continued**

- LiNbO<sub>3</sub> pure and Fe doped, IR induced acousto-photorefractive memory effect 0-80746  
 LiNbO<sub>3</sub>, SAW, suppression of harmonic generation by ZnO thin-film loading 0-84355  
 LiNbO<sub>3</sub>/Na structure field stability limits, LPE film growth, SAW velocity 0-80102  
 LiNbO<sub>3</sub>-CdSe layer structure, SAW absorpt., elec. field effects 0-65355  
 LiTaO<sub>3</sub>, propagation with arbitrary cut (Japanese) 0-92769  
 NH<sub>4</sub>H<sub>2</sub>PO<sub>4</sub>, Z-cut, SAW velocity, electromechanical coupling coeff. 0-84358  
 Nb<sub>2</sub>Sn, on LiNbO<sub>3</sub> substrate, US attenuation of SAW in applied mag. field 0-75678  
 Nb<sub>2</sub>Sn, softening of surface phonons in (100) plane 0-107627  
 Ni, Brillouin spectra, light scatt. cross section for surface ripples 0-71434  
 Se, SAW vel. and electromech. coupling factor 0-75422  
 Si, ion-implanted, impurity activation monitoring by SAW techniques 0-65020  
 Si wafers eval. using SAW 0-76470  
 SiO<sub>2</sub>, thin film on YZ-LiNbO<sub>3</sub>, SAW props. 0-84356  
 SiO<sub>2</sub>-GaAs, vacuum evaporated system, acoustoelec. signal, interface props. 0-75646  
 Sr<sub>0.5</sub>Ba<sub>0.5</sub>Nb<sub>2</sub>O<sub>7</sub> piezoelectric transducer, SAW props. 0-79037  
 ZnO films, RF sputtered single-cryst., on sapphire, struct. and SAW props. 0-80105  
 ZnO piezoelectric films, RF planar-magnetron sputtered, characterisation 0-96751  
 ZnO/quartz for SAW device materials, expt. study of props. 0-80050

**surface activity** *see surface energy***surface-atomic beam collisions** *see atom-surface impact***surface chemistry**

- see also chemisorption; corrosion; oxidation*  
 adhesion, surface chemistry studies, anal. appls. 0-88440  
 adsorbed atoms thermal desorption, one dimens. microscopic model, weak binding case 0-96729  
 adsorbed species, surface reactions, dipole interactions effects 0-61143  
 anthracene, in atmosphere, photooxidation on particulate matter 0-61487  
 anticatalytic forming effectiveness of seeding crystals in thermal power plant 0-89527  
 boiler inlet temps. and corrosion product deposits, water chemistry effects 0-89528  
 1-butene, adsorbed on δ-Al<sub>2</sub>O<sub>3</sub>, isomerisation, IR study 0-76554  
 1-butene adsorption on delta alumina, microgravimetric-IR study 0-75432  
 ceramics, local in depth anal. by neutral beam SIMS 0-89565  
 colloidal systems, surface forces, direct meas., elastic deform. effect 0-93805  
 condensed adsorption layers, effect on electrode reaction rates 0-93769  
 α-cyanoacrylate adhesive in first monolayer on bulk Al surface, IR spectra, H-bond form., stretching vibr. 0-87119  
 diffusion-controlled reactions on a two-dimensional lattice 0-71940  
 electrochemistry, steady-state conversion rate rel. to surface reaction process, catastrophe theory 0-108717  
 elementary reactions on single crystal surfaces, kinetics 0-108729  
 EXAFS obs. 0-108735  
 fatigue crack growth, surface reaction and transport controlled, model 0-75299  
 float glass, attack by water, behaviour of Al traces (French) 0-89378  
 formic acid, on Ni surface, decomp., dipole interactions effects 0-61143  
 E-glass fibre, silane coupling agent deposited on surface, hydrolysis and drying effect on siloxane bonds 0-85072  
 glaze/glass-ceramic, interface reactions, electron microprobe anal. 0-84398  
 glow curves and desorption spectra anal. method 0-80053  
 graphite, conditioning of surface by atomic H 0-93665  
 graphite monolayer on Ni (110) surface, oxidation mechanism 0-101037  
 heterogeneous catalysis, conference, Varna, Bulgaria (Oct. 1979) 0-82578  
 hydrazine, decomp. on Ir(111) surface, N<sub>2</sub> emission, ang. depend. 0-97731  
 hydrocarbon formation on interstellar graphite grain surfaces 0-82458  
 hydrocarbons, on activated C, rel. between adsorption and polarizabilities 0-76558  
 ion implantation, chemical and electrochem. aspects, review 0-100271  
 IR photoacoustic spectroscopy of solids and surface species 0-90909  
 metal oxides, nonstoichiometric, work function and near-surface chem. diffusion 0-80034  
 metal surface oxidation study, vacuum microbalance investigation 0-76552  
 metallic surface, catalysed thermal desorption and dissociation processes, microscopic theory 0-75439  
 mineral surface interactions with organic solutes, groundwater vel. determ. 0-98492  
 organometallic decomposition by reaction with photoelectron, appl. to metal film deposition 0-71599  
 plasma magnetic confinement system, surface problems caused by dissolved H<sub>2</sub> 0-57946  
 polymer, degradation, reaction product volatility effect on thermogravimetric anal. 0-104316  
 polymers, high-temp. pyrolysis, heat transfer processes at gas/solid surface (Russian) 0-61152  
 PVC, Cu evaporated film, electron-induced metallochromic reaction for metal image formation 0-86476  
 PVC surfaces, natural and stabilised, composition, ageing, oxidation and weathering, ESCA obs. (French) 0-61139  
 reactions, kinetics and dynamics, conf., La Jolla, CA, USA (Aug 1979) 0-105415  
 Rochelle salt, dehydration kinetics in ferroelec. and paraelec. phases, surface acoustic waves influence 0-97204  
 segregation, effect on metallurgical props., SIMS, XPS and AES (French) 0-80045  
 semiconductor, direct conversion of chem. to elec. energy 0-66984  
 semiconductor, tetrahedrally coordinated, review of surface struct., chem. and spectroscopy 0-59764  
 silicate glass, hydration in steam atmosphere 0-85211  
 silicate glass surface, Ca<sub>3</sub>(PO<sub>4</sub>)<sub>2</sub> film form., bonding to bone 0-85212  
 single crystal surface, electrochemistry, surface struct., superlattice struct. 0-76519  
 solid surface, mol. dynamic processes interaction with laser radiation 0-71943

## surface chemistry continued

- solid surfaces, surface processes, and solid/gas interactions 0-73125  
 solid-solid interface chemistry, characterisation, theory 0-75448  
 stable surface chemical reactions, interfacial hydrodynamic instability 0-66874  
 steel, cold-rolled sheet, surface chemistry 0-61146  
 steel, ferrite-austenite transition, diffusion const. of C and carburisation rate const., thermopower meas. 0-89216  
 steel, hydrogen absorption, anilines surfaces effectiveness, HCl conc. effect 0-108638  
 steel, industrial, surface chem. characterisation by SIMS, glow discharge spectrometry and other techniques 0-66907  
 steel, mild, electrodes, in  $\text{H}_2\text{SO}_4$ , H evolution reaction kinetics 0-97630  
 steel, stainless, surface chem. rel. to metallurgical props., SIMS, XPS and AES (*French*) 0-80045  
 steel, type AISI 316, thermal passivation in controlled vacuum 0-76276  
 theory, aims and recent accomplishments 0-75413  
 thermal desorption mass spectroscopy, computer control, data acquisition, apps. 0-61181  
 transition metal sulphides, ion bombardment damage, XPS obs. 0-97404  
 transition metals, on Si, silicide form. at interface, interface marker technique obs. 0-59734  
 transport and reaction, stochastic calcs. 0-108736  
 $\gamma\text{-Al}_2\text{O}_3$ , physisorption and reaction of  $\text{Mo}(\text{CO})_6$ , IR spectra obs. 0-80064  
 Ag (110), ethylene- $\text{O}_2$  interaction, LEED and AES obs. 0-89520  
 AgI/RbI quasibinary system, solid state reactions and transport props. 0-96700  
 Al, reaction with  $\text{H}_2$ , influence of surface reactions on rate (*Russian*) 0-66863  
 Al-Cu, type 2219-T851, fracture mechanics and surface chemistry of fatigue crack growth 0-81168  
 Al-Mg (7 wt.%), bare surface reaction rates in aq. solns. 0-101022  
 $\gamma\text{-Al}_2\text{O}_3$ , OH layer, IR spectra, outgassing temp. effects 0-66175  
 $\eta\text{-Al}_2\text{O}_3$  outgassed at 400, 650°C, heat of adsorp. of pyridines from soln., surface acidity 0-61154  
 $\text{Al}_2\text{O}_3$ , surface microstructural changes due to reduction by C (*Russian*) 0-100378  
 Al(100) oxidised surface structure anal., extended appearance potential fine struct. study. 0-75411  
 Au surface, clean, hydrophilic nature 0-80029  
 $\text{B}_2\text{C}$ , reaction kinetics with liq. Al, Si, Ni and Fe 0-84344  
 Ba getter film, initial reaction probability with  $\text{O}_2$ , water, CO and  $\text{CO}_2$ , AES obs. 0-61153  
 CO, catalytic oxidation on ferrites, IR spectrosc. investig. 0-89524  
 CO, on CoO, catalytic oxidation 0-71945  
 CO oscillatory oxidation over Pt, theory 0-85215  
 CO oscillatory oxidation over Pt, theory 0-85216  
 Ca-Mg-Ni-B, hydriding behaviour 0-71942  
 Co (0001), adsorption and reactivity of NO, LEED, AES, and thermal desorption study 0-80090  
 Co, adsorption-desorption kinetics of CO, surface carbide form. effects 0-103574  
 Cu (100), adsorbed formate and acetate species, EELS study 0-76120  
 Cu-Ag, surface segregation of S, Auger spectral study diffusion 0-76549  
 EuTe, high-temperature evaporation and reactivity 0-103469  
 Fe, adsorption, segregation and reactions of non-metal atoms, LEED and AES obs. 0-59783  
 Fe dissolution kinetics, and passivation depend. on temp. and ionic strength 0-97626  
 Fe, evaporated, adsorbed acetylacetone, XPS study 0-76133  
 Fe, free surface and grain boundary  $\text{O}_2$  and S chemistry 0-75410  
 Fe-Ni alloy, fluorination kinetics and fluoride film form., chem. nature obs. 0-101035  
 GaP:Cs-O simultaneous adsorption, oxidation interface chemical struct. 0-103584  
 $\text{H}_2+\text{N}_2\text{O}$ , HO radical form. on Pt surface, laser-induced fluoresc. obs. 0-108738  
 $\text{H}_2\text{SO}_4$  bulk surfaces, reactions with atmospheric species rel. to aerosols role as tropospheric sinks 0-72612  
 InAs, thermal oxidation, growth rate and chem. comp., temp. depend. 0-108619  
 n-InP, epitaxial layer, (100) surface chemistry, ESCA study 0-103552  
 Ir film, CO oxidation, IR absorpt. spectroscopy 0-71398  
 Li, surface characterization of film growth 0-81240  
 LiH, effect of surface hydrolysis to LiOH on IR absorption, X-ray luminesc. and EPR spectra 0-60660  
 MnO, reduction by C, surface reactions, CO regeneration (*Russian*) 0-66772  
 Mo (111) planes, adsorption of  $\text{NH}_3$ , preferential nitriding, FEM study 0-66877  
 $\text{NO}_2$  on Cu, ultrahigh vacuum ESR studies 0-97729  
 $\text{NO}_2(\text{N}_2\text{O}_4)$  surface decomposition, resonance and spontaneous Raman spectra 0-61144  
 Ni (100), interaction of adsorbed  $\text{H}_2$ , CO, and methanol, temp. programmed desorption study 0-66876  
 Ni (100), kinetics of C deposition from adsorbed CO 0-76553  
 Ni, corrosion, high temp.,  $\text{SO}_4$  induced, studied at 900°C in  $\text{O}_2+4.2\%\text{SO}_2$  0-97639  
 Ni, evaporated, adsorbed acetylacetone, XPS study 0-76133  
 Ni films, adsorption and decomp. of ethylene, coverage depend. meas. 0-96743  
 Ni/ $\text{Al}_2\text{O}_3$  catalysts, coprecipitated methanation type, metal-support interaction, XPS obs. 0-80936  
 $\text{Ni}^{2+}+\text{MoO}_3$  catalyst on  $\text{Al}_2\text{O}_3$ , Raman spectrum 0-108742  
 $\text{Ni}(\text{CO})_4$  form. on single Ni cryst., reaction kinetics and induced surface facetting 0-71948  
 $\text{Ni}(\text{CO})_4$  form. reaction rate, substrate mag. phase depend. 0-108737  
 NiO, (100) surface interaction with  $\text{SO}_2$ , electron diffr. and Auger spectrosc. obs. (*French*) 0-97728  
 NiO, doped and undoped, elec. props. and surface characts. 0-65571  
 NiO, nonstoichiometric, near-surface and bulk chem. diffusion 0-80035  
 NiO- $\text{Al}_2\text{O}_3$  reaction at film-substrate interface, Rutherford backscatt. obs. 0-97533  
 Ni(001), reaction of CO and  $\text{H}_2$ , extended muffin-tin orbital theory 0-76557  
 Ni(100) oxidised surface structure anal., extended appearance potential fine struct. study. 0-75411  
 Pb electrode, in situ surface phase study by laser Raman spectroscopy 0-103542

## surface chemistry continued

- Pt, adsorption of  $\text{O}_2$  on (110) surface,  $\text{Ar}^+$  bombardment effects on reactivity 0-89099  
 Pu, oxidation, binding energies, Auger and X-ray photoelectron spectra study 0-76550  
 Pu-Ga (1 wt.%), alloy powder, hydriding kinetics 0-76503  
 Re, adsorption, oxidation, and hydrogenation of CO, XPS, UPS, and thermal desorption study 0-71571  
 Re surface, interaction with  $\text{N}_2^+$  beam, reaction dynamics studied by XPS and thermal desorp. spectrometry 0-93797  
 Re-O-Cl system, gas-transition metal interaction, kinetic model (*French*) 0-108740  
 Ru (110), kinetics of C deposition from adsorbed CO 0-76553  
 S interstellar molecule formation, ion reactions at grain surfaces 0-101632  
 $\text{SF}_6+\text{Si}(\text{surface})$ , IR laser induced reaction, mol. vibr. and mol. dissociation obs. 0-93798  
 $\text{SO}_2$  surface reaction and decomposition on zeolites, resonance Raman study 0-61145  
 Si, amorphous, hydrogenation using DC and HF plasma treatment 0-59497  
 Si, chemisorption of  $\text{XeF}_2$  and  $\text{SiF}_4$ , XPS and Auger spectra, surface chemistry 0-81358  
 Si, multigrained, grain boundary elec. and compositional props., surface anal. 0-76575  
 Si, solubility and transport behaviour of water, dissolution 0-93801  
 Si surface electron beam deposited silicide formation using scanning CW laser beam 0-66862  
 $\text{SiO}_2$ , HF vapour phase etching, prod. viability for semicond. manufacturing and reaction model 0-81219  
 $\text{SiO}_2$ , vitreous, hydroxyl free, reaction with H, diffusion, absorpt. spectra 0-85210  
 $\text{SiO}_2/\text{InP}$  interface formation, thermodynamic considerations 0-100529  
 $\text{SrTiO}_3$  surface, oxidation and reduction by  $\text{D}_2\text{O}$ ,  $\text{H}_2^{18}\text{O}$ ,  $\text{D}_2$ , isotope exchange study 0-104461  
 $\text{SrTiO}_3$  surface, photosensitizer for water photoassisted decomp. 0-85202  
 Ta, simultaneous interactions with  $\text{Cl}_2$  and  $\text{O}_2$  under low press. and high temp. 0-71938  
 $\text{TaS}_2\text{-2H}$  electrodes, topotactic reduction mechanism, neutron diffr. obs. and intercalation cpd. form. 0-108748  
 Ti alloys, surface layers examination using vacuum UV spectrograph (*French*) 0-71987  
 Ti, surface layer, study using vac. UV spectrograph (*French*) 0-71987  
 $\text{TiO}_2\text{-Ni}$  (100) interface, electronic props., struct., comp., chemical bonding 0-84499  
 $\text{Ti}_2\text{V}_{1-x}\text{H}_x$  system, reaction and press.-composition isotherms meas. 0-108391  
 V surface, chemisorption of  $\text{Br}_2$ , struct., Na adsorption effects 0-101039  
 YbTe, high-temperature evaporation and reactivity 0-103469  
 Zn, surface oxidation, Auger spectrosc. obs. 0-97388  
 $\text{Zr}(\text{BH}_4)_3$  catalytic reactions on  $\text{Al}_2\text{O}_3$ , inelastic electron tunnelling spectra 0-75425

## surface composition see surface structure

## surface conductivity

- see also surface scattering  
 chemisorption kinetics, determ. from substrate current fluctuations 0-84383  
 hexafluoropropylene-tetrafluoroethylene copolymer, surface component of vac. absorpt. and resorp. currents, source of dielec. loss 0-70792  
 insulator-semicond. interface, impurity-band hopping conduction in surface layers 0-75649  
 metal, surface impedance near anomalous skin-effect limit, electron-electron N processes 0-100497  
 metal film, cond. electron focusing by inhomogeneous mag. field (*Russian*) 0-70850  
 paper sheets, charge decay and resistance parameters correlation determ. 0-70795  
 polymers, surface component of vacuum absorpt. and resorp. currents, surface charge accumulation 0-60063  
 polymers, surface component of vacuum absorpt. and resorp. currents, origin and magnitude 0-70791  
 polystyrene particles, monodisperse, dil. and conc. aqueous dispersions, elec. cond., surface cond. and double-layer polarisation 0-89533  
 semiconductor, ambipolar hot-carrier size effect kinetics 0-107799  
 semiconductor, magnetodiode and magnetoconcentration effects, influence of field effect 0-107903  
 semiconductor surface eval. using SAW convolver 0-97677  
 solar cell, diffusion equation, surface boundary condition 0-66975  
 solid disperse systems, electro-osmotic mass transfer, surface cond. influence (*Russian*) 0-76546  
 superconductor film, weakly damped collective oscillations, EM excitation, surface impedance (*Russian*) 0-65739  
 $\gamma\text{-Al}_2\text{O}_3$  interface with electrolyte solns, adsorption of ions, surface conductance, ion mobility and surface pot. 0-75622  
 BN glass transfer process 0-107459  
 CdS:Cu(Cl) thin films, surface and bulk photoconc. 0-88653  
 n-GaAs, low temp. field generation of carriers, liberation from surface states 0-92959  
 n-GaAs, nature of low temp. field generation of carriers, liberation from surface states 0-92960  
 GaAs, photomag. effect anomalies and state of surface layer 0-100482  
 GaAs, surface photogalvanic effect, polarisation depend. photocurrents (*Russian*) 0-80322  
 Ge, ambipolar hot-carrier size effect kinetics 0-107799  
 Ge heteroepitaxial film, ethanol pulsed adsorption effect on elec. cond. 0-93014  
 Ge, illumination influence on surface cond. irreversible elec. cond. increase (*Russian*) 0-92963  
 Ge, surface, Hall effect study, channel cond. (*Russian*) 0-92909  
 He, liq. surface, electron liq., high freq. cond. electron correlation effects 0-107589  
 InP film, electron-beam annealed, surface conduction 0-84500  
 InSb (110), cleaved, gap states, field effect meas. 0-84501  
 Si, high-resistivity layer form. during electron irradi. 0-80352  
 Si MIS capacitors, C-V curves, outer oxide surface conditions effects 0-97000  
 Si surface, MOS struct. band structure, minigaps, magnetoresistance, cond., space charge layers 0-92980  
 Si:B, use of BN source to achieve high surface concentration of B (*Russian*) 0-107639



**surface conductivity continued**

- ZnO polar surfaces, H and O<sub>2</sub> exposed, ion irradi., and heat treated, cond., EELS study 0-71525  
ZnSe, minority carriers diffusion length by surface photovoltage method 0-60003

**surface contours**

*see also surface structure; surface topography measurement*

- abraded surfaces, topography rel. to contact area and abrasion mechanism 0-58986  
atom-surface impact, roughness effect on capture of gas atoms 0-60726  
carbon tetrachloride drops falling through H<sub>2</sub>O, surfactants rel. to deform., oscill. (French) 0-66880  
deformation of surface irregularities under static loads 0-58985  
diamond turning precision machine tool system 0-69568  
liquid, transient behaviour due to pulsed US transducers 0-95073  
rainbow holographic contour generation 0-63948  
triangular microprofile containing surfaces, oblique incidence sputtering, topographic changes 0-66372  
Al-Cu, high strength, type 2024-T3, crack growth, fatigue induced surface deform., holographic detect. 0-85120  
Cu-Be, dynode surface, SEM and Auger microanalysis 0-100384  
MgO, smoke particles, size distrib. 0-104471  
NaClO<sub>3</sub>, dislocations rel. to growth mechanism from aq. soln., X-ray topography 0-59464  
Ni coatings, detonation powder spray deposition 0-61028  
Te-Ag thin film system, stress-relief appearance conditions 0-65416  
Te-Bi thin film system, stress-relief appearance conditions 0-65416

**surface diffusion**

*see also sorption*

- adatom mobility on metal surface, density functional approximation calc. 0-103577  
adsorbed gases on solid surfaces, mobile and localized adsorption, theory 0-65379  
adsorbed species 0-80070  
amorphous surface, energy profile and binding energy, computer simulation 0-100381  
Burton-Cabrera-Frank surface diffusion model, 0-59415  
CIDEF, two-dimens., surface diffusion and spin polarisation, asymptotic Green's function method appl. 0-91584  
cutting tools, diffusive wear, mag. field effect 0-60985  
diffusion-controlled reactions on a two-dimensional lattice 0-71940  
electron irradiation effects on surface prop. of solids 0-70261  
electron microscope contamination by surface diffusion of adsorbed hydrocarbon mols., theory 0-99013  
gas desorption from solid, two diffusion mechanisms 0-92784  
ice surface viscosity, activation energy, vacancy migration 0-107458  
lattice defects and diffusion processes in solids, book 0-107207  
liquid films, dynamic behaviour, surface mobility effects 0-88409  
metal oxides, nonstoichiometric, work function and near-surface chem. diffusion 0-80034  
metal surface electrochemical smoothing, roughness, diffusional pre-electrode layer (Russian) 0-76401  
metals, carburising, surface-gaseous medium interaction laws 0-76411  
metals, individual atomic events on surfaces, quantitative examination 0-75409  
molecule desorption and surface diffusion from critical deposition rate 0-92786  
polyurethane foams, elastic, stability against organic solvents (German) 0-85074  
sintering, surface redistribution by grain boundary diffusion 0-84871  
solid surface, mol. dynamic processes interaction with laser radiation 0-71943  
solid surfaces, surface processes, and solid/gas interactions 0-73125  
sputter profiling, depth resolution, surface transport effects, calc. 0-97393  
steel, Cr, carburising kinetics, in endothermal atm. 0-76410  
steel, Cr, carburising with high-activity carburiser 0-76412  
steel, high-C, carburising kinetics, in endothermal atm. 0-76410  
steel carburisation process, diffusion modelling 0-108632  
superionic solid film, surface diffusion coeff. 0-92709  
supersaturated soln., shape stability of growing cylindrical particle due to diffusion and interface kinetics 0-79720  
tetramethyltin, adsorbed on graphite, nature of 2 D diffusion, Mossbauer meas. 0-84372  
three-phase system, diffusion laws 0-107310  
Ag film, void growth, TEM obs. 0-59833  
Ag<sub>14</sub>PD<sub>4</sub>, superionic solid film, surface diffusion coeff. 0-92709  
Al, oxide films, metal and O<sub>2</sub> transport, AES and inert marker, techniques 0-97641  
Au film, adatom surface diffusion at low temps., elec. resist. study (French) 0-65376  
Bi film, adatom surface diffusion at low temps., elec. resist. study (French) 0-65376  
C, activated, adsorption in countercurrent flow 0-70524  
Cu, friction surface structural investigation, O<sub>2</sub> surface diffusion (Russian) 0-96726  
Fe, Armcro, carburising kinetics, in endothermal atm. 0-76410  
Fe, polycrystalline, H<sub>2</sub> adsorpt. and embrittlement, work function changes 0-96741  
Fe-Ti, C induced amorphous surface layers 0-107287  
Fe-Ni alloy, fluorination kinetics and fluoride film form., chem. nature obs. 0-101035  
NH<sub>4</sub>Ag<sub>14</sub>, superionic solid film, surface diffusion coeff. 0-92709  
Ni<sub>2</sub>O-(CaO)-SiO<sub>2</sub>, diffusion controlled attack by aq. solns. 0-81218  
Ni, oxide films, metal and O<sub>2</sub> transport, AES and inert marker, techniques 0-97641  
Ni surface, single-atom self-diffusion FIM study 0-103548  
β-NiAl, oxide films, metal and O<sub>2</sub> transport, AES and inert marker, techniques 0-97641  
NiO, nonstoichiometric, near-surface and bulk chem. diffusion 0-80035  
Pb (111) surface, vacuum deposition of Cu, Ag, substrate diffusion effects, RHEED, LEED, AES 0-65410  
Si, CVD from SiH<sub>4</sub>-HCl-H<sub>2</sub> system, rate-determining reactions and surface species 0-84405  
Si-B, P, long range enhancement of B diffusivity by P diffusion 0-103386  
Si-B, use of BN source to achieve high surface concentration of B (Russian) 0-107639  
Ti, friction surface structural investigation, O<sub>2</sub> surface diffusion (Russian) 0-96726

**surface diffusion continued**

- W (110) mobility and two-dimens. compressibility of adsorbed Xe, field emission current fluctuation method 0-80089  
W (110) plane, tunnelling of H in surface diffusion 0-75416  
W {123} plane, clean and H saturated, surface diffusion of single W atoms 0-80081  
W, diatomic cluster migration on W {100} plane, elementary displacement steps 0-88436  
W, surface diffusion of adsorbed O, secondary electron emission study 0-76117  
W surface self-diffusion, ion impact induced, FIM study 0-103549  
Zr, adsorption and absorpt. of CO, NO, N<sub>2</sub>, O<sub>2</sub>, and D<sub>2</sub>, dissoci. and diffusion 0-80085

**surface discharges**

*see also corona*

- dielectric conduction and breakdown, conf., Gainesville, FL, USA (Oct.-Nov. 1979) 0-82564  
dielectric materials spacecraft, surface discharge arc propag. and damage 0-71314  
dielectric surface, photoinduced surface discharge 0-88929  
fast insulator surface flashover, investigation using electro-optical elec. field meas. 0-64820  
fast insulator surface flashover in vacuum, mechanism, electro-optical investig. 0-103206  
plasma switches, high press. surface discharge, review 0-103208  
pulsed surface flashover mechanism involving electron-stimulated desorption 0-70055  
UV light source, surface spark discharge type, for H<sub>2</sub>/F<sub>2</sub> laser initiation 0-78923  
Cu cathodes, broad area type, electrolum. regions, current-voltage characteristics 0-84019

**surface electron states**

*see also interface electron states; surface scattering*

- adatom density of states, impurity atom effects 0-92958  
adatom valence-level position variation on metal surface 0-88611  
adatoms, correlation effects, s-d hybridization in substrate 0-107886  
adsorbate and clean surfaces, electronic props. (French) 0-80344  
adsorbed atoms surface band splitting, theory, with appl. to He/graphite 0-60058  
adsorbed layer, electronic transforms, near boundary separating mag. and nonmag. states 0-92961  
adsorption of atoms on metals, Green's function formalism for studying electronic struct., local density of states calc. 0-107884  
alloy thin film, thickness depend. of CPA electronic densities of states 0-65644  
anisotropic continuum, with anisotropic surface layer, coeff. of attenuated total reflection 0-60535  
anthracene films, optical props., comparison between free and optical contact mounting 0-89079  
anthracene surface, Ar impact, Penning ionisation electron spectra and photoelectron spectra 0-66352  
bixenion in polar semicond., binding energy calc. 0-96796  
cathode material choice methodology to obtain low work function 0-100500  
chemisorption, image charge effects, surface plasmons 0-84381  
chemisorption, image charge effects on adsorbate valence spectra, perturbational study 0-84380  
conference, New York, USA (Oct. 79) 0-73093  
copper phthalocyanine film, electron acceptor surface states due to O<sub>2</sub> adsorption 0-88586  
crystal slab, 3-D, surface states, relativistic Green matrix method, muffin-tin potential 0-80345  
4-cyano-4'-n-pentylbiphenyl, refr. index meas. and isotropic-nematic phase transition study, surface plasmon technique 0-84282  
γ-cyclopropyl-bis (1,3,3-trimethylindolenine-2-yl)pentamethinium fluoroborate, excitation surface polaritons, reflecting faces obs. 0-65645  
degenerate electron liquid, skipping orbit cyclotron resonance, surface state transitions 0-103889  
desorption, multiphonon processes, quantum-statistical theory 0-107641  
diodes, thin film glass based structures, surface electron states effect on switching (Russian) 0-107887  
disordered solids, surface states 0-103736  
electron gas, degenerate, in metal or semicond. slabs, surface plasmon damping 0-88501  
ellipsometry of clean surfaces, submonolayer and monolayer films, review 0-103546  
exciton energies and radii 0-92829  
ferroelectric semiconductor, band bending in surface layer 0-60061  
ferromagnetic semiconductor, surface localised low energy electron-magnon states (Russian) 0-88734  
graphite, adsorbed He, band struct. and thermodynamic props. 0-80349  
graphite (0001), scattering and selective adsorption of H<sub>2</sub> (D<sub>2</sub>) 0-71553  
III-V compounds, (110) surface, energy distrib. of dangling-orbital surface states 0-80347  
III-V semiconductor based layered multielectronic systems, electronic process investig. survey (Russian) 0-107891  
impurities, near-surface, adiabatic potential, symmetry props., group theory methods 0-70786  
jellium, chemisorption, effective-medium theory of chem. binding 0-65367  
laser irradiation effects 0-84812  
lattice and symmetrical description of surface bands 0-70785  
magnetoplasmon type polaritons, LF, existence criterion in Faraday config. 0-96961  
metal, electrodynamics, optical refl. coeffs. and surface plasmon dispersion law 0-75619  
metal, gradient approx, anal. appl. 0-96810  
metal, surface dipole barrier, calc. 0-96958  
metal oxide, molecular adsorption, UPS studies, review 0-84374  
metal surface, approached by substrate, surface amplitude patterns 0-75620  
metal surface, force on moving charge, spatial dispersion effects 0-65646  
metal surface, sticking rate, transmission problem, model Hamiltonian 0-107640  
metal surface region, electrostatic energy and screened charge interaction for different Fermi surface shape 0-70631  
metal-insulator-semiconductor struct., magnetooptic interband absorption by semicond. surface layer 0-93288  
metal-semiconductor contact, frequency relationships of photocurrent and photo-EMF (Russian) 0-107908

## surface electron states continued

- metallic rough surface, reflection loss for s and p polarised waves near surface plasmon freq. (*French*) 0-97225
- metallic surface, self-consistent electron theory, review 0-88616
- metallic surface energy, exchange and correl. contrib., wave-vector decomp. 0-75615
- metallic thin films (*French*) 0-60692
- MIS structure, fast surface states density, photoelectric methods of determ. 0-70835
- MISIM struct. inversion layer, symmetrical, carrier conc. calc. 0-75651
- MNOS p-channel transistor, memory characts., H<sub>2</sub> anneal effects 0-80388
- MOS pulsed capacitor, minority carrier lifetime meas. influence of Si-wafer surface state density 0-60098
- MOS structure, surface state spectrum meas. by pulsed C-V method 0-88641
- MOS structures, inversion layer near electrode edge, pot. and charge density distribution 0-88642
- nickel phthalocyanine film, electron acceptor surface states due to O<sub>2</sub> adsorption 0-88586
- one-dimensional mol. crystals, surface density of states, rel. to adsorbed molecule 0-107889
- one-dimensional semiinfinite systems, surface state energies 0-88607
- oscillating dipole-metal surface interaction, jellium model and random phase approx. 0-92955
- p-n heterojunction differential admittance theory in the presence of surface electron states 0-96981
- perovskites, d-band, concepts of surface states and chemisorption, book contrib. 0-107651
- photoelectron spectroscopy, solid-state, with synchrotron radiation, review 0-71570
- piezoelectric crystal, surface polaron states, polaron-phonon interactions 0-70790
- plasmareons, effect of finite thickness of accumulation layer, theory 0-103636
- plasmon dispersion relation at short wavelengths 0-96962
- polariton motion in thin surface layer, nonstationary phenomenological theory (*German*) 0-88608
- polaritons, theory and spectroscopy uses 0-92835
- polareons, electrons in surface phonon field 0-107885
- poly-2,4-hexadiyne-1,6-diol bis (p-toluene sulfonate), exciton surface polaritons, reflecting faces obs. 0-65645
- polystyrene coated Ag holographic grating, Raman spectra enhancement by plasmon surface polaritons 0-80885
- $\alpha$ -quartz surface, XPS study 0-93451
- Raman scattering, surface enhanced, surface plasmon 0-108211
- semiconducting surface inversion layers, exchange and correl. 0-75618
- semiconductor, electron emission from surface subband, reduced work function 0-60757
- semiconductor, localised states near disclacive transition 0-70644
- semiconductor, MM wave guiding and control by surface plasmons 0-103713
- semiconductor, surface-states concentration profile and capture cross section determ. using SAW convolver 0-80341
- semiconductor, tetrahedrally coordinated, review of surface struct., chem. and spectroscopy 0-59764
- semiconductor plasma, surface helicons, theory 0-60019
- semiconductor space charge layers, subband struct., perturbation theory 0-84497
- semiconductor surface, chemisorption of mol. complexes, bond orbital model (*German*) 0-59807
- semiconductor surface, instrument for angle-resolved UV photoemission spectroscopy (*Japanese*) 0-93455
- semiconductor surface and adsorbate states, charge injection into space charge layers 0-100496
- semiconductor surface eval. using SAW convolver 0-97677
- semiconductor surfaces, optical props., book contrib. 0-80737
- semiconductor-electrolyte interface, charge transfer via surface states, water photoelectrolysis anal. 0-75636
- semiconductor/adsorbate system, local density of states calcs. (*German*) 0-60062
- semiconductors, amorphous, doped, electronic props. 0-80283
- Si (111), surface relax., EHT and cluster calcs. (*Chinese*) 0-59762
- simple metals, density functional theory of chemisorption, book contrib. 0-107647
- solid surfaces, non-ideal, optical props., phenomenological models 0-88950
- sputtering characteristics, surface-barrier shape effects 0-93447
- superlattice, image pot. enhancement by static elec. field 0-92846
- surface plasmon dispersion relation in presence of surface roughness 0-65650
- surface-atom polarisability derivation from field-ion energy deficits 0-76155
- synchrotron radiation techniques 0-80945
- theory, aims and recent accomplishments 0-75413
- thin film, 11-layered, CPA calc. of local density of electronic states 0-65643
- thin film heterostructure, energy spectrum study 0-70787
- transition and noble metals, d-band metals, chemisorption, book contrib. 0-107649
- transition metal, chemisorption of H, effect of surface spin fluctuations 0-75613
- transition metal cpds., rock salt struct., surface energy bands, Shockley surface states, bonding 0-92956
- transition metals, core levels between surface and bulk atoms, variation of binding energy shifts 0-88615
- two dimens. Brillouin zone and Wigner-Seitz cell integrations, special point formulae generation 0-70783
- two-dimensional electron gas in mag. field polarisability 0-107888
- virtual, simple modelistic treatment 0-103739
- virtual surface states, Green function theory 0-80342
- voids and particles, Van der Waals energy between them, from asymptotic to close contact 0-80351
- Ag (100) and (111) surfaces, positronium form. due to slow positron trapping 0-107748
- Ag (110), electoreflectance, surface state contrib. 0-80755
- Ag foil, surface-plasmon resonance, roughness-induced wavelength corrections 0-108288
- Ag foils, surface plasma-wave reflectance and roughness-induced scatt. 0-66228

## surface electron states continued

- Ag surface, time-resolved mol. electronic energy transfer interaction with pyrazine 0-92957
- Ag, surface plasmon dispersion relation in presence of surface roughness 0-65650
- Ag-In<sub>2</sub>S<sub>3</sub>-Si layered struct., Hall effect, I-V characts., surface states (*Russian*) 0-97001
- Al (001), enhanced photoexcitation 0-80937
- Al (111), angle-resolved UPS obs. of 2-dimens. band structs. of S, Se and Te 0-60059
- Al (111), bonding of O, electronic struct. calcs., rel. to UPS data 0-59801
- Al, valence band Auger spectra, surface effect 0-80915
- Al-In<sub>2</sub>S<sub>3</sub>-Si layered struct., Hall effect, I-V characts., surface states (*Russian*) 0-97001
- $\beta$ -Al<sub>2</sub>O<sub>3</sub>-Na<sub>2</sub>O, adsorption of Na, surface electronic struct. calcs. 0-75431
- Au (110), electoreflectance, surface state contrib. 0-80755
- Au clusters on alkali halide surface, size depend. of valence bands, XPS study 0-65647
- Au, surface dipole moment calc. 0-60060
- BaO, monolayer on W (110), film struct. and electron state 0-100498
- BaTiO<sub>3</sub> (001), LEED and UPS studies 0-100747
- BaTiO<sub>3</sub>, photoelectron and optical spectra derived from self-consistent charge MO and band calcs. 0-96785
- BaTiO<sub>3</sub>, XPS and UPS from surface defects 0-76136
- Bi thin film, structure and electronic props. 0-70562
- C:Ni, X-ray photoemission studies 0-76138
- n-Cd,Hg<sub>1-x</sub>Te, recombination due to surface excitation, photoconductivity, impurity states (*Russian*) 0-60042
- CdS, surface energy struct. changes during ion cleaning and thermal annealing 0-92962
- CdS, surface photovoltage, characterisation 0-60033
- Co-Si, surface physicochemical state, Auger electron spectroscopy study 0-100715
- CsBr, (110) surface, electronic struct. of valence bands calc. (*Russian*) 0-75621
- CsCl, (110) surface, electronic struct. of valence bands calc. (*Russian*) 0-75621
- CsI, (110) surface, electronic struct. of valence bands calc. (*Russian*) 0-75621
- Cu (001), M-point surface state, high-resolution angle resolved photoemission study 0-108322
- Cu (001), O<sub>2</sub> chemisorption, Cu3d-O2p interaction study by angular-resolved photoemission using synchrotron radiation 0-84836
- Cu (100), electronic struct., self-consistent local-orbital calc. 0-80348
- Cu (110), electoreflectance, surface state contrib. 0-80755
- Cu (111) surface, positronium form. due to slow positron trapping 0-107748
- Cu, bulk and (001) film, extended tight-binding calcs. 0-70592
- Cu surface, (001), O<sub>2</sub> adsorption effect on surface barrier, LEED study 0-84378
- Cu surface, (110), adsorbed pyridine, photoemission selection rules 0-100751
- Cu, surface states, (100) and (111), polarisation depend. photoemission 0-100495
- CuCl (100), obs. of p- and d-like surface states, angle resolved UPS study 0-100405
- Fe, ferromag. film, surface states, surface magnetisation and electron spin polarisation 0-65648
- Fe-Ni, electronic struct. calc., effects of chemisorption; contact pot. and surface magnetisation 0-103734
- Fe<sub>2</sub>O<sub>3</sub>, semicond. anode in aq. electrolyte, electrolum. and electrochem. 0-76080
- GaAlAs, surface vacancies, bound state energy levels calc. 0-80340
- GaAs (110), chemisorption of O and Al, ab initio theory 0-75612
- GaAs (110), surface core-level binding-energy shifts 0-103737
- GaAs (110), surface electronic struct. calcs. 0-80343
- GaAs base laminated epitaxial struct., surface plasmon phonon polaritons (*Russian*) 0-59905
- GaAs, chemisorption of Li, charge injection into space charge layers 0-100496
- n-GaAs, low temp. field generation of carriers, liberation from surface states 0-92959
- n-GaAs, nature of low temp. field generation of carriers, liberation from surface states 0-92960
- GaAs, photoemission modulation by IR illumination, surface band bending height interpret. 0-108318
- GaAs, surface excitation energy 0-92829
- GaAs, surface recomb. vel., psec. optical techniques 0-70784
- n-GaP electrode, photoanodic dissolution rate, effect on surface electronic band energies 0-103748
- GaP, electron-hole drops, self-consistent surface calculation 0-65464
- GaSb (110), surface core-level binding-energy shifts 0-103737
- GaSb-InAs system, (110) surface and interface electronic struct. 0-100494
- Ge (100), density of states, simple modelistic treatment of virtual surface states 0-103739
- Ge (111), electron struct., photoelec. props. 0-100493
- Ge (111), spectroscopy of electron subbands 0-71422
- Ge heteroepitaxial film, ethanol pulsed adsorption effect on elec. cond. 0-93014
- Ge surface states, recomb. centres, regularities, electrolyte contact effects (*Russian*) 0-65652
- Ge:Pd and pure, photoelectric props., surface states (*Russian*) 0-60043
- H, chemisorbed atom, surface charge fluctuations effect on spectral density 0-65368
- He, adsorbed on graphite, band struct. effects in heat capacity 0-59788
- He atom-surface scattering pot., surface electron density depend. 0-104027
- He, liq., local disorder, for IR transmittance meas. 0-75395
- He, liq., two-dimens. electron gas, CDW 0-65476
- He liq. surface, cyclotron reson. of two-dimens. electrons (*Russian*) 0-88374
- <sup>3</sup>He, liquid, electrostatic image force depend. on spatial dispersion, energy spectrum (*Russian*) 0-107593
- <sup>3</sup>He-<sup>4</sup>He, liquid solution, bound impurity pair effect on surface tension (*Russian*) 0-65332
- <sup>4</sup>He, liquid, electrostatic image force depend. on spatial dispersion, energy spectrum (*Russian*) 0-107593



## surface electron states continued

- InAs, two dimensional accumulation layer, Anderson localisation 0-107871  
 In<sub>2</sub>O<sub>3</sub>-SnO<sub>2</sub>-InP solar cell junctions, efficiency, InP surface props. 0-85288  
 InP, and InGa<sub>1-x</sub>AsP<sub>1-y</sub> binary and quaternary cpds., surface and dielec.-semicond. interface props. 0-93001  
 InP, surface recomb. vel., psec. optical techniques 0-70784  
 InP, surface vacancies, bound state energy levels calc. 0-80340  
 InSb (110), cleaved, gap states, field effect meas. 0-84501  
 Ir, (111) surface states, surface Umklapp effects, photoelectron spectra 0-93457  
 KI microcrystals, UV spectra by diffuse reflectance technique, surface electronic transitions obs. 0-75614  
 LaB<sub>6</sub> surfaces, (100), (110) and (111), electron states, UPS study 0-100752  
 Li, valence band Auger spectra, surface effect 0-80915  
 LiNbO<sub>3</sub> surfaces, ion and electron bombard., photoelectron spectroscopy and electronic props. 0-71559  
 LiNbO<sub>3</sub>, XPS and UPS from surface defects 0-76136  
 N<sub>2</sub> film, on metal or sapphire substrates, luminescence and nonradiative energy transfer to surfaces 0-97350  
 Na, adsorbed on Al, adatom valence-level position variation 0-88611  
 Na, IR and optical props., surface-plasmon-mediated absorpt. mechanism 0-93308  
 NaCl crystals, electronic and hole centres and surface, quantum-chemical calcs. 0-65489  
 NbC, rock salt struct., surface energy bands, Shockley surface states, bonding 0-92956  
 Ni (001) surface, electronic struct. of ordered S overlayers 0-84835  
 Ni (100), surface electronic struct., self-consistent local orbital calc. 0-65649  
 Ni (111), chemisorption and reaction of NH<sub>3</sub>, LEED, desorption and photoemission expts. 0-59799  
 Ni (111) and (110), laser-induced charge transfer to adsorbed CO, photoemission expts. 0-59798  
 Ni, adsorption of N<sub>2</sub>, photoemission and electronic struct., cluster calcs. 0-97403  
 Ni clusters local densities of states 0-88466  
 Ni, ferromag. film, surface states, surface magnetisation and electron spin polarisation 0-65648  
 Ni films, electronic struct. calc., effects of chemisorption; contact pot. and surface magnetisation 0-103734  
 Ni, surface vibrs., chemisorbed O influence 0-84361  
 Ni(001) surface states, surface magnetisation, electron spin polarisation 0-88612  
 Ni(110), mag. exchange splitting of electronic surface states 0-88610  
 O<sub>2</sub> monolayers, on graphite, mag.  $\alpha$ -phase and  $\alpha$ - $\beta$ -phase transition 0-70530  
 Pd film, work function changes due to adsorbed H<sub>2</sub>, surface and interface dipoles 0-96972  
 Pd surface, segregated S state, AES, EELS, UPS and XPS study 0-93452  
 Pt 6(111)×(100), clean and O<sub>2</sub>-covered, UPS studies 0-76151  
 Pt, surface dipole moment calc. 0-60060  
 Sc (0001), H adsorption, geometric vs. electronic factor in surface electronic structure 0-70788  
 Si, (001) (2×1) reconstructed surface, dimer model self consistent calcs. 0-88613  
 Si, (001) and (111), geometrical and electronic struct., review 0-80039  
 Si (100), dimer reconstruction, photoemission obs. 0-80939  
 Si (111), intermediate oxidation state, core photoelectron absorpt. vs. chemical shifts 0-81220  
 Si (111) 7×7 clean surface and O chemisorbed stage valence band density of states from L<sub>23</sub>VV Auger spectra 0-100717  
 Si (111) surfaces, cleaved, electronic structure following Al adsorption 0-75610  
 Si (111)-1×1, electronic struct. of surface, model pseudopot. calc. 0-65651  
 n-Si inversion layers, electronic g-factor, spin-split Landau levels 0-80346  
 Si MOSFET, surface quantum states, two-dimensionality of many-body effects 0-103740  
 Si phototransistors, slow contamination and fast surface state effects, SEM study 0-107896  
 Si surface, (111), energy states, computer renormalisation-group calc. 0-75617  
 Si surface, MOS struct. band structure, minigaps, magnetoresistance, cond., space charge layers 0-92980  
 Si:H, amorphous, surface states distribution using MOS tunnel junctions 0-103735  
 n-Si-SiO<sub>2</sub>, MOS structures, radiation states 0-103758  
 Si-SiO<sub>2</sub> MOS interface, surface-state density and minority carrier generation rate, meas. by DLTS, hot hole effect 0-100527  
 SiC with dielectric coating, surface polaritons, waveguide modes 0-80195  
 SiO<sub>2</sub>, HCl-grown oxides, characterisation of surface states using MOS transient currents 0-65696  
 Si(111)-(7×7), and impurity stabilised Si(111)-(1×1) surface, photoemission studies 0-104041  
 Sm, surface mixed valence, XPS study 0-60753  
 SmB<sub>6</sub>, surface mixed valence, XPS study 0-60753  
 Sn, positron annihilation in fine particles, surface trapped states 0-84800  
 SrTiO<sub>3</sub>, (100), LEED and UPS studies 0-100747  
 SrTiO<sub>3</sub>, semicond. anode in aq. electrolyte, electrolum. and electrochem. 0-76080  
 Ti (0001), H adsorption, geometric vs. electronic factor in surface electronic structure 0-70788  
 Ti, band struct. effect on photon emission from sputtered Ti atoms 0-58208  
 TiH<sub>x</sub> and TiD<sub>0.9</sub>, surface characts., AES, EELS, SIMS, and XPS study 0-65343  
 TiO, TiO<sub>2</sub> band struct. effect on photon emission from sputtered Ti atoms 0-58208  
 TiO<sub>2</sub>, semicond. anode in aq. electrolyte, electrolum. and electrochem. 0-76080  
 TiO<sub>2</sub>, sputtering defects, associated surface electron states, UPS, XPS and AES obs. 0-60755  
 n-TiO<sub>2</sub>-electrolyte interface, charge transfer via surface states, water photoelectrolysis anal. 0-75636  
 W faces, simultaneous adsorption of Ba and Cu atoms, work function changes 0-65378

## surface electron states continued

- W surface, (110), chemisorpt. effects on dielec. function, refl. spectra 0-75616  
 W, surface dipole moment calc. 0-60060  
 WO<sub>3</sub>, semicond. anode in aq. electrolyte, electrolum. and electrochem. 0-76080  
 W(001), electronic surface reson. and thermally induced struct. transition 0-88614  
 W(001), surface states and surface resonances, self-consistent electronic struct. 0-96960  
 ZnO epitaxial film, nonuniform cond. due to H chemisorption (*Russian*) 0-65723  
 ZnTe clean and adsorbed O<sub>2</sub> (110) surfaces, UV photoemission spectra (*Japanese*) 0-93456
- surface energy**  
 see also surface electron states; surface energy measurement  
 adsorption, intermolecular surface forces in plane densely packed hexagonal model 0-59785  
 n-alkanes, anisotropic London dispersion forces, surface effects 0-74214  
 binary alloys, surface conc. profile and surface energy 0-84350  
 p-n-butyl-p'-heptanoyloxazoxybenzene oriented on NaCl MgF<sub>2</sub> coated NaCl, surface phenomena and IR spectra 0-79678  
 covalent or ionic-covalent crystals, dislocation-free contact 0-80096  
 crack tip lattice trapping, relation between macroscopic and microscopic thermodynamic surface energies 0-59572  
 cracks, discrete dislocation analysis 0-84236  
 drops, rotating, captive between co-rotating parallel faces, shapes and stability, capillarity eqns. 0-64592  
 electron-hole liquids, relation between bulk compressibility and surface energy 0-65465  
 fracture stress obtained from the elastic crack tip enclave model 0-71730  
 grain boundaries decohesion energy, solute adsorption influence 0-65009  
 graphite fibre, surface anal. by XPS and polar/dispersive free energy anal. 0-65340  
 haemoglobin equilibria in soln., surface free energy model 0-81535  
 interfaces separating compressible bulk phases, stability 0-107610  
 interfacial tension var. with supersaturation, one-layer adsorpt. model 0-103563  
 isotropic solid soln. cryst. surfaces, surface stress and chem. equilib. 0-107628  
 liquid crystal surface, statistical thermodynamics, local order parameter 0-88023  
 liquid layer, insulating, cellular deformation mechanism, charge flux (*French*) 0-70507  
 liquid phase sintered systems, particle coalescence probability estimation 0-104086  
 metal, adsorption of metal atoms, enthalpy calc. 0-100406  
 metal, exchange and correl. contrib., wave-vector decomp. 0-75615  
 metallic surface, self-consistent electron theory, review 0-88616  
 metals, atomic binding energy and surface energy rel. to prediction of physical props. 0-59434  
 naphthalene, surface dynamics, calc. 0-92772  
 nematic liquid crystals, surface and anchoring energies, van der Waals contrib. 0-92455  
 nematic liquid crystals, molecular alignment using alkoxyisilanes, rel. to surface energy 0-100164  
 nonionic surfactants, stabilisation of bubble nuclei in agarose gels 0-76562  
 oscillatory forces between two solid surfaces arising from struct. in intervening liquid, meas. 0-70521  
 poly(dihydroxypropyl methacrylate), surface charact., by contact angle methods 0-61140  
 poly(hydroxyethyl methacrylate), surface charact., by contact angle methods 0-61140  
 polymer, surface free energy determination (*Polish*) 0-84362  
 polystyrene interfacial colloidal crystals, microscopic obs. 0-97737  
 solid surfaces and interfaces, elastic energy of point defects and inclusions 0-73272  
 supersaturated soln., shape stability of growing cylindrical particle due to diffusion and interface kinetics 0-79720  
 surfactant, insoluble, adsorpt. on monolayer-covered surface, Gibbs eqn. calcs. 0-59781  
 surfactant micelles, hydration 0-89518  
 surfactant solutions, aggregation, micelle and microemulsion form. 0-89547  
 surfactant solutions, review of concepts 0-89542  
 thermodynamics equilib. forms of crystals 0-107629  
 Au, vacancy size effect, surface energy in small particles and bulk specimens 0-75223  
 Au-Cu, surface conc. profile and surface energy 0-84350  
 BaTiO<sub>3</sub> polymorph, hexagonal, low temp. and surface CO<sub>2</sub> adsorption and desorption 0-80713  
 Ca<sub>10</sub>(PO<sub>4</sub>)<sub>6</sub>(OH)<sub>2</sub> dissolution kinetics, nucleation-controlled 0-59659  
 Cu-Au system, two-phase mixtures, long-period superlattices 0-84140  
 Cu-Ni, liq., surface conc. profile and surface energy 0-84350  
 Fe-B, metallic glasses and vapour deposited films, amorphous to cryst. transition 0-88048  
 He crystals, meas. of surface tension and contact energy, standing waves (*French*) 0-92753  
 In, vacancy size effect, surface energy in small particles and bulk specimens 0-75223  
 MnO<sub>2</sub> porous powders, Al<sub>2</sub>O<sub>3</sub> and SiO<sub>2</sub> coated, changes in surface free energy for N adsorption 0-84363  
 Na<sub>2</sub>O-B<sub>2</sub>O<sub>3</sub>-SiO<sub>2</sub>, mechanical strength and swelling in liq. 0-85024  
 SiO<sub>2</sub> thin films, deposition and characterisation study 0-80133  
 UO<sub>2</sub>, surface energy, determ. by Hertzian indentation 0-93641  
 Zn, pure single cryst., fracture stress 0-104269
- surface energy measurement**  
 film balance of wide range (80 dynes/cm) and high sensitivity (10<sup>-3</sup> dyne/cm) 0-98910  
 polymers, specific fracture surface energy, meas., review (*French*) 0-104275
- surface hardening**  
 boriding of high purity Fe with cryst. B powder 0-84951  
 boronising, powder, physicochem. characts. 0-61024  
 glass fibre reinforced epoxy laminate, metallization by Cu and chem. treatment by H<sub>2</sub>CrO<sub>4</sub> (*German*) 0-93670  
 HF cyclically operated generator appls., characts. (*German*) 0-81070  
 laser surface transformation hardening, heat flow model for cylinder 0-93700

**surface hardening continued**

- metals, carburising, surface-gaseous medium interaction laws 0-76411  
 steel, C, rolling contact fatigue, tufftriding effect on 0.2% C cylindrical specimen 0-100954  
 steel, C-Cr (1.0, 1.5 wt.%), 52100 bearing steel, control of surface residual stress by heat treatment 0-75701  
 steel, Cr, carburising with high-activity carburiser 0-76412  
 steel, ferritic, by gas nitriding, process improvements 0-97499  
 steel, hot forging die type, fractography (*Japanese*) 0-108547  
 steel, ion-carbo-nitriding in CO-N<sub>2</sub>-H<sub>2</sub> gas mixtures, expt. (*Japanese*) 0-71670  
 steel, low C, electroboronising by superimposed cyclic current, Na<sub>2</sub>CO<sub>3</sub>, B<sub>2</sub>C, NaCl, NaOH activator studies 0-85081  
 steel, mild, surface hardness improvement by dynamic recoil implantation 0-61008  
 steel, types S25C and S45C surface damage produced by pulsating impact contact load (*Japanese*) 0-104263  
 Al-Ti alloy spark alloying, cathode weight change and hardened layer obs. (*Russian*) 0-61005  
 Cu, polycryst., surface layer hardening by multiple impact 0-108469  
 Fe, cast, grey, fracture kinetics, surface hardening effect 0-76354  
 Fe, ion-carbo-nitriding in CO-N<sub>2</sub>-H<sub>2</sub> gas mixtures, expt. (*Japanese*) 0-71670  
 Fe, sintered, austenitic nitriding and bainitic hardening 0-85084  
 Fe-M, (M=Cr, W, Mo, V, Ti), morphology and growth kinetics of  $\delta$ -pearlite formed by carburisation 0-108485  
 $\alpha$ -Fe-Ti, ion implanted, microstruct., ion beam anal. and TEM study 0-107294  
 Ti-Al-V alloy, friction coeff. reduction on injection with TiC particles 0-85086  
 (W, Mo)C, hard-facing applications, effect of Mo on struct and hardness of WC 0-108474

**surface-ion beam collisions** *see ion-surface impact***surface ionisation**

- ion source using surface ionisation process 0-68999  
 Mo, coadsorption of O<sub>2</sub> and Cs, electron emission props., thermal stability 0-66878  
 Pd surface, adsorbed CO, Penning ionisation by metastable He beam, theory 0-60735  
 Re surface, long range and temp.-depend. interaction with alkali metal atom, theory 0-59802  
 SF<sub>6</sub>, negative ion form. on W cathode, laser irradi. effects 0-93440

**surface-molecular beam collisions** *see molecule-surface impact***surface phenomena**

- see also surface....*  
*see also atom-surface impact; capillarity; crazing; crystal surface and interface vibrations; emissivity; field evaporation; interface phenomena; ion-surface impact; magnetic surface phenomena; molecule-surface impact; sorption; surface acoustic waves*  
 adhesion, surface and interfacial aspects, review 0-108690  
 adsorbed monolayer parameter determ. by full current spectroscopy method (*Russian*) 0-70539  
 anthraquinone, UV light effect on nucleation during crystallisation on anthracene surface 0-75478  
 anthrone, UV light effect on nucleation during crystallisation on anthracene surface 0-75478  
 atomic and surface physics, conf., Salzburg, Austria (Feb. 1980) 0-57010  
 chemical physics of solids and their surfaces, book 0-82587  
 conference, general congress, Societe Francaise de Physique, Toulouse, France (June 1979) 0-77536  
 crystal surface elastic props., surface tension tensor, volume stress (*Russian*) 0-100389  
 crystal surface morphology development during sputter erosion 0-88414  
 diatomic molecules, laser-induced predissoc., surface mag. field effect 0-106365  
 elastic interface wave guided by thin film between two solids 0-100385  
 interatomic forces, theories 0-107632  
 metal surface, mol. vibr. energy transfer, classical EM theory 0-96806  
 metal surface chemisorption theory, electron localisation, surface interactions 0-84376  
 metal surface heated, charge separation from electrolyte drops 0-88617  
 metal surface laser beam irradi., effective absorpt. coeff., temp. field determ. (*Russian*) 0-76108  
 metal surface molecule enhanced Raman scatt., rough surface spheroidal model 0-84744  
 metals, cyclotron resonance depend. on surface, anomalous skin effect (*Russian*) 0-75860  
 metals, surface positronium formation, stopping distance, positron-phonon interactions 0-96582  
 meteors surface layer, thermal fracture and detached particles mean dia. 0-62081  
 molecular clusters adsorbed on conductor surfaces (*Russian*) 0-80078  
 molecular ion formation on molecular cryst. surface UV laser irradi. (*Russian*) 0-71521  
 n-nitroaniline, UV light effect on nucleation during crystallisation on anthracene surface 0-75478  
 percolation problem and surface effects in semi-infinite medium repulsive wall case 0-62588  
 percolation processes, scaling theory and real space renormalisation group 0-86223  
 PMMA moist surface mech. strength reduced by electric charge (*Russian*) 0-60486  
 Raman scattering by forced surface oscils. in liquid drop 0-92763  
 slab, surface displacements for high speed rubs 0-83767  
 solid state physics, contrib. of Conyers Herring in 1930s 0-57056  
 spherical particle, surface enhanced Raman scatt. by molecules 0-95629  
 supersaturated vapour, critical clusters, theory and Monte Carlo simulation, review 0-82734  
 surface and colloid science, conf., Stockholm, Sweden (Aug. 1979) 0-86035  
 surface magnetisation profile singularities near critical point 0-103843  
 thermal coupling of 2.8- $\mu$ m laser radiation to metal targets 0-76107  
 thermally induced structural changes, specimen surface influence 0-103559  
 thermodynamics, fundamental eqns. 0-107630  
 ultrasonic wave transmission through rough surface (*Russian*) 0-100387  
 Al melt-NaF filter material interaction mechanism (*Russian*) 0-108743  
 Al-Li-Mg-Be alloys, phase composition of surface films, oxidation protection mechanism (*Russian*) 0-65417  
 Cr-Ni compressor disk, surface plastic deform., optimal method 0-60924

**surface phenomena continued**

- (FeNi)PB amorphous wires, surface oxidation and annealing influence on induced anisotropy 0-100957  
 Ga ionisation mechanism on W field emitter 0-76156  
 Ge, heterodiffusion due to H atom surface recombination stimulation, Cu, Zn, In coated (*Russian*) 0-59726  
 He liquid, plane surface layer, density profiles and pair correlation asymptotics (*Russian*) 0-88371  
 He, liquid, surface liquid-crystal transition in two dimensional electronic system 0-88303  
<sup>3</sup>He, liquid, electrostatic image force depend. on spatial dispersion, energy spectrum (*Russian*) 0-107593  
<sup>4</sup>He, liquid, electrostatic image force depend. on spatial dispersion, energy spectrum (*Russian*) 0-107593  
<sup>4</sup>He liquid, localised ion states, effective mass, binding energy, surface displacement 0-84333  
 LiNbO<sub>3</sub>:Fe, photoinduced refractive index discontinuities at surface 0-75999  
 LiNbO<sub>3</sub>:Ti optical waveguide, surface wave mode conversion, static strain-optic effect 0-87561  
 Pt (111) surface, backscattering, channelling spectra, H adsorption, surface relaxation 0-71552  
 SiC, dielectric coating effect on surface polaritons, optical consts. (*Russian*) 0-88489  
 SiO<sub>2</sub> film on Cu substrate, surface EM wave absorpt., optical consts. (*Russian*) 0-108216  
 Ti-Al-Mo-Zr, compressor disk, surface plastic deform., optimal method 0-60924  
 W, (110) surface, conduction electron interaction with diffracting electrons (*Russian*) 0-79643  
 W-Zr field emitter, time-of-flight atom-probe study 0-80949

**surface phonons** *see crystal surface and interface vibrations***surface potential**

- axisymmetric field problem soln. by Gaussian surface charge simulation 0-95758  
 biological particle surface, elec. double layer phenomena (*Rumanian*) 0-94144  
 C-CD, signal charge and surface pot., steady-state distrib. calc. 0-100525  
 desorption, multiphonon processes, quantum-statistical theory 0-107641  
 dipole layers, forces between plates 0-70793  
 electron gun, surface charge method, computer anal. of characteristics 0-101891  
 electrophotographic films, surface charge meter using electrostatic induction (*Japanese*) 0-77886  
 glass reactions with aq. solns., influence of surface pot. on kinetics 0-108612  
 guanidinium aluminium sulphate hexahydrate, surface obs., SEM and AES expts. 0-71362  
 guarded electrode design which has small gap between electrode and guard ring 0-68215  
 III-V semiconductor based layered multielectronic systems, electronic process investig. survey (*Russian*) 0-107891  
 insulators, XPS, binding energy, surface pot. and work function calcs. 0-89113  
 metal film, size effect in Landau diamagnetism, surface pot. effect (*Russian*) 0-93012  
 metal oxides and binary metal oxides, spinel struct., isolectric point meas. 0-88609  
 MOS capacitor, interface state parameter determ. by DLTS 0-65642  
 MOS structures, inversion layer near electrode edge, pot. and charge density distribution 0-88642  
 photostimulated field emission, triangular barrier pot. model 0-100759  
 polyethylene films, corona charged, charge trapping 0-88571  
 polyvinylidene fluoride, corona-charged, surface effects 0-66102  
 quartz resonator surface patterns obs., using SEM 0-71323  
 SEM meas., electron energy analysis 0-68307  
 sputtering characteristics, surface barrier curvature influence 0-60739  
 virtual surface states, Green function theory 0-80342  
 work function and surface pot. meas. from secondary electron emission energy in SEM 0-66343  
 AgBr emulsion grains, edge length dependence of ionic conductivity, space charge characteristics 0-88360  
 AgCl(Br), point defect form. energies, atomistic calc. and surface pot. meas. 0-107221  
 $\gamma$ -Al<sub>2</sub>O<sub>3</sub> interface with electrolyte solns, adsorption of ions, surface conductance, ion mobility and surface pot. 0-75622  
 CdS, surface photovoltage, characterisation 0-60033  
 Cs/W, work function measurement in SEM 0-80918  
 GaAs, surface passivation using composite Al<sub>2</sub>O<sub>3</sub> and native oxide, MIS characts. 0-93004  
 p-GaAs/rare earth metal contacts, surface pot. barrier 0-60086  
 HgI<sub>2</sub>:CdS binder layer photoreceptor, surface charge characts. thickness depend. 0-57409  
 InP, surface passivation using composite Al<sub>2</sub>O<sub>3</sub> and native oxide, MIS characts. 0-93004  
 Ni films, electronic struct. calc., effects of chemisorption; contact pot. and surface magnetisation 0-103734  
 Ni-Fe, electronic struct. calc., effects of chemisorption; contact pot. and surface magnetisation 0-103734  
 Pt-Cr(Si) interface, low-temp. diffusion, ambient effects 0-100355  
 p-Si/rare earth metal contacts, surface pot. barrier 0-60086  
 Si-SiO<sub>2</sub> interface, thermally grown, surface pot. inhomogeneities after stress ageing 0-92993  
 TiO<sub>2</sub> electrodes, chemically modified, nature of surface states 0-107905  
 W, work function measurement in SEM 0-80918  
 ZnO, adsorbing p- and n-type dyes, surfaces pot., UV light illum. effect 0-75624

**surface scattering**

- used for carrier scattering by surfaces*  
*see also surface conductivity*  
 defects at surfaces and interfaces, electronic struct. 0-84498  
 metal cylindrical wire, elec. resist., scatt. processes, Monte Carlo calc. 0-75560  
 metallic films, ultrasound attenuation, size magnetoacoustic effect (*Russian*) 0-107869  
 metallic thin films, grain boundary and surface scatt., statistical model 0-103762  
 multilayer thin film struct. thermoelec. props. 0-92964  
 Al foil, electrical conduction, electron mean free path, surface scatt. 0-88535



## surface scattering continued

- Bi bounded semimetals, phonon two-stage drag of electrons, thermoelectric power, scatt. mechanism 0-92919
- Bi, film, size effect of carrier heating, surface scatt. (*Russian*) 0-100474
- n-GaAs-Ga<sub>1-x</sub>Al<sub>x</sub>As, heavily doped superlattice, electronic props., perpendicular low temp. mobility 0-65660
- Mo, elec. resist., quadratic contrib., 2 to 40K (*Russian*) 0-92874
- Mo film, sputtered, elec. resist., annealing and struct. effects 0-60109
- Re, elec. resist., quadratic contrib., 2 to 40K (*Russian*) 0-92874
- Ru, elec. resist., quadratic contrib., 2 to 40K (*Russian*) 0-92874
- Si inversion layers, mobility temp. depend., Coulomb and surface roughness scatt. 0-80390
- Si-SiO<sub>2</sub> boundary, surface charge transport in valence band of Si 0-70789
- W, elec. resist., quadratic contrib., 2 to 40K (*Russian*) 0-92874

## surface structure

- see also interface structure; surface texture
- 0-59814
- adsorbed layers, general principles of construction of structural models 0-84351
- adsorbed layers, photoelectron diffr. aximuthal patterns, struct. sensitivity 0-107644
- alloys, binary, surface segregation kinetics 0-80044
- alloys, machining damage, depth of surface layers determ. 0-85094
- alloys, surface composition after fabrication by SIMS 0-65351
- amorphous surface, energy profile and binding energy, computer simulation 0-100381
- analysis by combined Auger, X-ray and SEM studies 0-81413
- analysis techniques and appls., symposium, Dayton, USA (Jun. 1979) 0-62363
- analytical techniques, quantification, review 0-65342
- anodised films on metals, ellipsometer obs. interpretation using film form. models 0-101828
- atomic beam diffraction from solid surfaces, struct. studies 0-65349
- atomically clean surfaces, instruments for anal. and imaging 0-105749
- atoms as structural components in metallurgy (*Dutch*) 0-96465
- Auger electron spectroscopy microanalysis, in SEM 0-101058
- binary alloys, surface conc. profile and surface energy 0-84350
- bisphenol A-phthalic anhydride epoxy resin, diglycidyl ether, Rayleigh scatt., Brillouin and IR spectra 0-66211
- brittle materials, water drop impacted, damage thresholds 0-81149
- carbon tetrachloride, surface study, ellipticity coeff., ellipsometric method 0-84343
- [CC] Ag-(100)InP, metal-semicond.cathode contact, metallurgical, physical, chemical processes 0-107911
- chemisorbed layers, surface defects and thermodynamics 0-80068
- conference, New York, USA (Oct. 79) 0-73093
- crystal surface morphology development during sputter erosion 0-88414
- crystalline solids, electronic industry, chem. anal. instrumental methods progress 0-66903
- cycano-biphenyl LC alignment on obliquely evaporated SiO<sub>2</sub> films 0-79677
- diamond surface, polished, RHEED pattern 0-65345
- differential geometry, distortion, torsion, Burgers circuit 0-64996
- dislocations, universal concept, rel. to disclinations and grain boundaries 0-100231
- electron capture spectroscopy, technique for surface science and ferromagnetism 0-92766
- electronic material and device characterisation using surface-sensitive analytical techniques 0-65341
- ellipsometry, metallic films and surfaces, nonlocal effects, theory 0-104006
- ellipsometry of clean surfaces, submonolayer and monolayer films, review 0-103546
- EXAFS from X-ray refl. meas 0-71512
- faceted surfaces, investigation by slow electron diffraction 0-100377
- field emission micro SEM, for UHV surface anal. 0-86519
- glass, adsorption of Au, AES study, electron bombardment effects 0-65380
- glass, float, low-Fe, weathered, surface, characterisation 0-93666
- glass, surface damage by abrasive contact, effect on strength 0-85066
- graphite, Fe-catalysed gasification, electron, microscopy 0-104358
- graphite fibre, surface anal. by XPS and polar/dispersive free energy anal. 0-65340
- graphite surface, adsorbed Cs, dissolution, lamellar cpd. form. (*French*) 0-100399
- graphite thin film, high resolution phase contrast electron microscopy 0-103224
- guanidinium aluminium sulphate hexahydrate, surface obs., SEM and AES expts. 0-71362
- Hastelloy B-2, corroded surface, electron bombardment effect during Auger electron anal. 0-61014
- heterogeneous catalysis, conference, Varna, Bulgaria (Oct. 1979) 0-82578
- ice, surface transition layer, ellipsometric study 0-103545
- III-V compounds, surface comp., low-energy ion scatt. spectrometry 0-100382
- III-V semiconductors, surface and interface anal., secondary ion mass spectrometry technique 0-59763
- interface roughness, calc. (*Russian*) 0-103587
- ion beam surface crystallography, channelling and blocking effects, double alignment backscattering 0-65350
- ion bombardment of three-dimens. surface 0-104029
- ion scattering spectrometry and secondary ion mass spectrometry for surface anal. 0-103541
- laser-annealed surfaces, characterisation by ellipsometry 0-103544
- LEED intensity meas., reliability determ. 0-92424
- LEED technique, accuracy-limiting factors 0-75127
- liquid of charged particles in equilib. with vapour, surface dipole layer and surface tension 0-70505
- MBBA, isotropic, surface-induced ordering 0-108176
- meson transfer reactions in solids, surface struct. effects 0-104015
- metal, electrodynamics, optical refl. coeffs. and surface plasmon dispersion law 0-75619
- metal, ion beam induced desorption of overlayers 0-59786
- metal monolayers, on metal cryst. surfaces, surface struct., review 0-80067
- metal oxide, molecular adsorption, UPS studies, review 0-84374
- metallic thin films (*French*) 0-60692

## surface structure continued

- metals, individual atomic events on surfaces, quantitative examination 0-75409
- micro Auger analysis, using field emission source 0-104020
- microfractography (*Japanese*) 0-71841
- microstructure determ. and microanalysis by ultrahigh vacuum field emission gun SEM 0-96423
- multilite-corundum ceramics, electron microscopy of damaged surface 0-88413
- multicomponent surface phase, comp. determ. from gas adsorption data 0-88417
- neutron scattering from adsorbed mols., surfaces and intercalates, review, book contrib. 0-84394
- nitriding in glow discharges, influence on phase comp. and plasticity of diffusion layer (*Russian*) 0-76400
- optical fibre, fracture surface anal. 0-58754
- organic surface contaminants, anal. by plasma chromatography-mass spectrometry, and Raman microprobe technique 0-108773
- PDX Tokamak, surface analysis station 0-79586
- photoacoustic reflection-absorpt. spectroscopy for IR anal. of surface species 0-105723
- photoelectron spectroscopy, solid-state, with synchrotron radiation, review 0-71570
- point defect-edge dislocation interaction near solid surface 0-79834
- polyacrylic acid film, structurisation and mech. props., EM obs. (*Russian*) 0-59406
- polymer, supramol. struct. characterisation, use of C X-radiation 0-79705
- positron apparatus 0-86500
- PVC surfaces, natural and stabilised, composition, ageing, oxidation and weathering, ESCA obs. (*French*) 0-61139
- pyrocarbon coatings, refl. anisotropy and struct. determ. by perpendicular incidence microellipsometer 0-101824
- quartz, single crystals, Ar and O<sub>2</sub> interaction at high temp., surface struct. changes (*German*) 0-96725
- quartz, surface damage by X-rays,  $\gamma$ -rays, neutrons, SEM study 0-79837
- $\alpha$ -quartz surface, XPS study 0-93451
- secondary electron yield, determ. of surface spacings 0-66341
- section topograph technique, high resolution, applicable to synchrotron radiation sources 0-57449
- segregation, effect on metallurgical props., SIMS, XPS and AES (*French*) 0-80045
- SEM appl., field emission, electron channelling and microdiffraction from surfaces 0-59355
- semiconductor, tetrahedrally coordinated, review of surface struct., chem. and spectroscopy 0-59764
- semiconductor microcharacterisation, using electron microscopy, review 0-101911
- semiconductor surface, depth profiling, photoacoustic technique 0-65337
- Si (111), surface relax., EHT and cluster calcs. (*Chinese*) 0-59762
- silicate gardens, growth morphology, mechanisms 0-100765
- silicate glasses, polishing, surface characts. using grazing X-ray reflection (*French*) 0-65353
- single crystal surface, electrochemistry, surface struct., superlattice struct. 0-76519
- solid surface, microgravimetric-IR study 0-76577
- solid surface, physicochemical props. investigation by SIMS (*Czech*) 0-90927
- solid surfaces, surface processes, and solid/gas interactions 0-73125
- sputter profiling, depth resolution, surface transport effects, calc. 0-97393
- stainless steel, in MgCl<sub>2</sub> solutions, Cl distrib. in oxide films, SIMS (*French*) 0-108765
- stainless steel, machine faceted, low-energy ion erosion studies 0-80923
- steel, austenitic, Cr-Ni, ion-implanted N, chem. state study by AES and XPS 0-79825
- steel, austenitic, friction in vacuum of type U8 steel under microshock loading (*Russian*) 0-108583
- steel, austenitic 30KhGSA, white phases structure after heat treatment 0-76281
- steel, cold-rolled sheet, surface chemistry 0-61146
- steel, Cr, cold roll, frictional heating surface damage 0-76289
- steel, ferritic stainless, effect of Cl ions on passive layers 0-59766
- steel, industrial, surface chem. characterisation by SIMS, glow discharge spectrometry and other techniques 0-66907
- steel, low C structural, fracture toughness and X-ray diffr. obs. of surface (*Japanese*) 0-66634
- steel, medium C, Ni-Cr-Mo, overheated, fractographic study (*Chinese*) 0-66616
- steel, mild and type EN31, eval. of cold rolling oils and boundary lubrication characts. by SEM 0-85068
- steel, Ni-P plated, electroless, fatigue strength and plated layer microstruct. (*Japanese*) 0-93645
- steel, segregation and adsorption of S, influence on carburisation and nitrogenation 0-66701
- steel, stainless, austenitic, oxidation mechanism, oxide thickness, comp. and growth, nuclear technique study 0-61022
- steel, stainless, type 316, surface comp. rel. to crevice corrosion initiation 0-93680
- steel, stainless, type EP838 ion irradiated, surface structure changes during post-irradiation heating (*Russian*) 0-75272
- steel, trace element UV emission, spectrochem. anal. (*French*) 0-71997
- steel, type 40 Kh, electron emission depend. on surface mechanical treatment (*Russian*) 0-100945
- steel, types 60G, ShKh15, structural changes near holes and inclusions due to pulsed currents (*Russian*) 0-108459
- steel sheets, surface composition, degreasing and batch annealing effects 0-66700
- steels, stainless, passive state, electron spectroscopy anal. 0-59765
- steels ShKh15 and 12KhN3A, white phases structure after heat treatment 0-76281
- STEM, single atom microscopy, instrumental aspects 0-86522
- step densities, two-dimens. random probability model 0-80036
- step structure, decoration technique 0-103554
- step thickness measurement, TEM 0-103555
- surface state resonance effect, obs. by convergent beam RHEED 0-107622
- synchrotron radiation techniques 0-80945
- theory, aims and recent accomplishments 0-75413
- thin films, surface anal., survey of ESCA, AES, SIMS, and ISS (*Hungarian*) 0-70544
- thin films and interfaces, analytical techniques, review 0-80120

## surface structure continued

- tinplate surfaces, Auger depth profiling and anal. 0-59768  
 tools for surface anal., review 0-103540  
 transition metal compound surfaces, review 0-84349  
 ultrasonic wave transmission through rough surface (*Russian*) 0-100387  
 vacuum deposited film, orientation axis tilt rel. to vapour angle of incidence 0-88456  
 Ag (110), ethylene-CO interaction, LEED and AES obs. 0-89520  
 Ag (111), epitaxially grown on mica, surface defect struct., LEED study 0-80038  
 Ag, (111) surface electron microscopy 0-103556  
 Ag evaporated film, adsorbed CO, enhanced Raman scatt. mechanism in ultrahigh vacuum 0-107645  
 Ag, multiply twinned particles, internal and surface struct. by electron microscopy 0-84189  
 Ag thin film, X-ray fluoresc. spectroscopy of surface using RHEED-solid state detector method 0-108760  
 Ag:Al<sub>2</sub>O<sub>3</sub>:Al tunnel-junction struct., surface polariton mean free path, roughness 0-93008  
 Ag-Au, corrosion in HNO<sub>3</sub> 0-85091  
 Ag-Cu surface alloyed films, laser melt quenched, microstruct. 0-76423  
 Ag-Pd alloys, inert gas ion bombardment, dynamic surface composition changes, AES obs. 0-60745  
 AgBr layer, sensitised, topography of developed centres 0-73491  
 Ag-S-K<sub>2</sub>SO<sub>4</sub> mixtures, surface comp., AES and XPS obs. 0-81386  
 Al, (111) surface, adsorbed O, surface struct., LEED and SEXAFS data 0-92782  
 Al, annealed and powder sintered (SAP 895), sputtering under D<sup>+</sup> and <sup>4</sup>He<sup>+</sup> bombardment, microstruct. effects study 0-84821  
 Al, film on Si(111) substrate, struct., props. depend. on vapour flow, ionisation (*Russian*) 0-75453  
 Al, foil, influence of O<sub>2</sub>-pressure on oxidation rate, TEM study 0-104355  
 Al foil electrolytic perforation, surface film phase composition obs. (*Russian*) 0-61004  
 Al sheet surfaces, chem. characterisation by SIMS, glow discharge spectrometry and other techniques 0-66907  
 Al-Ag (7.27 wt.%), peculiarities exhibited during fatigue loading (*Chinese*) 0-71723  
 Al-Mg, foil, oxidation in O<sub>2</sub> atm., TEM study 0-104356  
 Al-Mg (2.5wt.%) sheet, surface oxide state and weldability 0-59769  
 Al<sub>2</sub>O<sub>3</sub>, anodic oxide film, behaviour of emulsion particles during electrodeposition 0-104357  
 γ-Al<sub>2</sub>O<sub>3</sub>, OH layer, IR spectra, outgassing temp. effects 0-66175  
 Al<sub>2</sub>O<sub>3</sub> rod, damaged, mech. strength, surface defects effect, appl. as insulators (*German*) 0-76330  
 Al<sub>2</sub>O<sub>3</sub>, surface microstructural changes due to reduction by C (*Russian*) 0-100378  
 Al<sub>2</sub>O<sub>3</sub>:SiO<sub>2</sub> glass ceramic, surface streaks and blisters, UV fluoresc. study 0-84347  
 Al(100) oxidised surface structure anal., extended appearance potential fine struct. study. 0-75411  
 Al(111), oxide layer amorphous to cryst. surface transition, slow positron obs. 0-75417  
 Ar, liquid, surface study, ellipticity coeff., ellipsometric method 0-84343  
 Au (100) surface, reconstruction, superstruct., model 0-103551  
 Au, (111) surface electron microscopy 0-103556  
 Au, chemisorption of I, AES and LEED study 0-100405  
 Au coins, surface anal. by X-ray fluoresc., SEM and scanning Auger spectroscopy 0-89552  
 Au evaporated film, adsorbed CO, enhanced Raman scatt. mechanism in ultrahigh vacuum 0-107645  
 Au film, ion bombarded, surface craters induced by displacement cascades 0-107344  
 Au film (001), high resolution TEM 0-100383  
 Au, multiply twinned particles, internal and surface struct. by electron microscopy 0-84189  
 Au surface, clean, hydrophilic nature 0-80029  
 Au, surface dipole moment calc. 0-60060  
 Au-Cu, surface conc. profile and surface energy 0-84350  
 Au-Ni, surface segregation, strain effects 0-80042  
 B, CVD, morphologies, influencing factors, temp. range 1390-1640K 0-89154  
 BaTiO<sub>3</sub> (001), LEED and UPS studies 0-100747  
 BaTiO<sub>3</sub>, pure and doped crystals, surface and domain struct., AES and SEM expts. 0-71363  
 BaTiO<sub>3</sub>, surface microrelief after ion irradi. 0-59774  
 BaTiO<sub>3</sub>, surface study using AES and ion scatt. spectroscopy 0-65339  
 Be, irradiated with He<sup>+</sup> at 20 keV, surface damage and gas trapping profile meas. (*French*) 0-84218  
 Be, slowly oxidised, secondary electron yield changes, and AES characterisation 0-71524  
 Bi, intervalley scattering processes, surface struct., transverse electron focusing study (*Russian*) 0-84352  
 C fibre, metal-coated with Cu, Co or Ni, coating struct., SEM study 0-97605  
 C, on Fe(100), adsorbate coverage determ. by LEED, AES and XPS 0-103566  
 Ca<sub>2</sub>SiO<sub>3</sub>, fracture surfaces, quantitative anal. using energy dispersive X-ray spectrometry (*French*) 0-89571  
 CdTe surface, sputter cleaning and dry oxidation, XPS and LEED study 0-108618  
 Co-Si, surface physicochemical state, Auger electron spectroscopy study 0-100715  
 CsSn<sub>3</sub>I<sub>3</sub>, surface props., Auger study, elec. cond. meas., photochem. study 0-66339  
 Cu (001), surface barrier struct., LEED study 0-65354  
 Cu (100) surface crystallography, LEED I-V profile anal. 0-75415  
 Cu, (111), low-energy positron diff. 0-70511  
 Cu, (111) surface electron microscopy 0-103556  
 Cu, cementation, on Fe, deposit struct., reaction rates, SEM 0-104421  
 Cu, electrochem. nucleation and growth on Te and Al, TEM 0-104451  
 Cu, electron emission depend. on surface mechanical treatment (*Russian*) 0-100945  
 Cu, friction surface structural investigation, O<sub>2</sub> surface diffusion (*Russian*) 0-96726  
 Cu, irradiated with 20 keV He<sup>+</sup>, surface damage and gas trapping profile meas. (*French*) 0-84219  
 Cu, pyramidal structures, development on ion bombarded surfaces 0-84177  
 Cu stepped and disordered surfaces, adsorbed Xe, two-dimens. phase transformations 0-103580

## surface structure continued

- Cu surface, (001), adsorbed c(2×2)CO layer, struct. 0-88428  
 Cu, surface (100), adsorption of O<sub>2</sub>, LEED study 0-100408  
 Cu, surface topographical features formed by ion bombard., crystallographic depend. 0-70266  
 Cu, thin film, oxidation, RMEED/SEM studies 0-100968  
 Cu vicinal surfaces, LEED study, S, O and Pb adsorption effects 0-103575  
 Cu-Ag, surface segregation of S, Auger spectral study diffusion 0-76549  
 Cu-Al spherical crystals, grown from drop of melt, topography 0-84353  
 Cu-Au, corrosion in HNO<sub>3</sub> 0-85091  
 Cu-Be, dynode surface, SEM and Auger microanalysis 0-100384  
 Cu-Co-Si (0.36, 0.11 wt.%), surface layer struct. on annealing, SIMS and AES exam. 0-88415  
 Cu-Fe, explosive plasma sputtered coatings, struct. and props. (*Russian*) 0-100783  
 Cu-Ni, evaporation limited segregation 0-70513  
 Cu-Ni, liq., surface conc. profile and surface energy 0-84350  
 Cu-Ni-Sn (9, 2 wt.%), surface comp., Auger electron spectroscopy study, manufacture and storage influence 0-65348  
 Cu-Ni-Zn (18, 27 wt.%), surface comp., Auger electron spectroscopy study, manufacture and storage influence 0-65348  
 Cu-Ni-Zn alloy, surface comp., outdoor exposure influence 0-59770  
 Cu-Sn alloy, surface comp., outdoor exposure influence 0-59770  
 Cu-Zn alloys, surface comp., outdoor exposure influence 0-59770  
 CuAl<sub>2</sub>O<sub>4</sub>, pure and NiO promoted catalysts, surface oxidation state and comp., XPS study 0-76134  
 CuFeS<sub>2</sub>, superficial degradation in air and water, XPS obs. (*French*) 0-89110  
 EuTe, high-temperature evaporation and reactivity 0-103469  
 Fe (110), atomic struct., LEED anal. 0-88410  
 Fe, free surface and grain boundary O<sub>2</sub> and S chemistry 0-75410  
 Fe, oxidation, FIM obs. 0-89388  
 Fe, reaction with methane at 750 C micro Auger anal. 0-104020  
 Fe, segregation and adsorption of S, influence on carburisation and nitrogenation 0-66701  
 Fe, sintered, austenitic nitriding and bainitic hardening 0-85084  
 Fe zone refined crystals, cryst. orientation and distrib. of stray grains 0-70509  
 Fe-Cr-Ni, foil, in situ oxidation in HVEM 0-104354  
 Fe-Cr-Ti (18, 0.1-0.9 wt.%), high temp. oxidation (*Japanese*) 0-71806  
 α-Fe-Ni (3-12 wt.%), structure and γ-α polymorphic transform. kinetics 0-71645  
 Fe-Ni (50 wt.%), surface comp. and oxide film thickness after various surface treatments, AES study 0-66693  
 Fe-Si, grain oriented sheet, AC hysteresis, surface struct. and elastic stress effects 0-88791  
 Fe-Si (2-8 wt.%), single crystals, growth striations, X-ray studies 0-79774  
 Fe-Si-Al, surface oxide layer struct., AES study 0-89396  
 Fe-Ti (0.15 wt.%), Ti distrib., segregation, FIM anal. 0-84200  
 FeS<sub>2</sub>, superficial degradation in air and water, XPS obs. (*French*) 0-89110  
 FeTi, surface and mag. props., heat treatment and hydrogenation effects 0-75447  
 GaAs (110), chemisorption of O and Al, ab initio theory 0-75612  
 GaAs (110), order-disorder interaction with O<sub>2</sub>, LEED anal. 0-75445  
 GaAs (110), surface electronic struct. calcs. 0-80343  
 GaAs, (110) surface structure, rotational relaxation, cluster model (*Chinese*) 0-107621  
 GaAs epitaxial layers on polycryst. GaAs substrates, LPE growth characts. 0-75471  
 GaAs epitaxial multilayer photocathode structures, TEM obs. of dislocations generated 0-100241  
 GaAs, homoepitaxy and epitaxy, surface anal. during growth, using RHEED and Auger spectroscopy 0-66433  
 GaAs, multilayer liquid phase epitaxy, transition to faceting 0-96750  
 GaAs, surface cryst. regularity by X-ray photoelectron diff. 0-89112  
 GaAs:Cr, semi-insulating, Cr redistrib. during thermal annealing as function of encapsulant and implant fluence 0-84199  
 GaAs:Cr semi-insulating wafer, heat treatment technique for no thermal conversion 0-100857  
 GaAs(-GaP) single crystal, defect distrib. near abraded surface 0-92533  
 GaP single crystal, defect distrib. near abraded surface 0-92533  
 Gd<sub>2</sub>(MoO<sub>4</sub>)<sub>3</sub>, surface study using AES and ion scatt. spectroscopy 0-65339  
 Ge (100), dimer reconstruction, photoemission obs. 0-80939  
 Ge, amorphous, ideal surface, definition and characts. 0-107623  
 Ge, black, solar selective absorber characterisation 0-80112  
 Ge surface, (111), ion-bombarded and annealed, spectroscopic ellipsometry study 0-103543  
 Ge(111) surface, diffuse scatt. at high temp., RHEED study 0-80043  
 Hg<sub>0.8</sub>Cd<sub>0.2</sub>Te surface, sputter cleaning and dry oxidation, XPS and LEED study 0-108618  
 HgTe surface, sputter cleaning and dry oxidation, XPS and LEED study 0-108618  
 InGaAsP-InP layers, grown by LPE techniques, lattice const., bandgap, thickness and surface morphology meas. 0-59818  
 InP (110) surfaces, cleaved and polished-sputtered-annealed, LEED and AES study 0-103550  
 n-InP, epitaxial layer, (100) surface chemistry, ESCA study 0-103552  
 InP film, electron-beam annealed, surface conduction 0-84500  
 n-InP, heat treatment in controlled P vapour 0-88137  
 InP surface decomposition prevention in LPE growth 0-96749  
 InSb (110), surface struct. by elastic LEED, comparison with GaAs(110) and ZnTe(110) 0-80040  
 InSb (110) surface, LEED intensity dynamical anal. 0-88412  
 InSb, single crystal, chem. and ion etching, surface changes (*French*) 0-108614  
 Ir (100) surface, reconstruction, superstruct., model 0-103551  
 K, on Fe(100), adsorbate coverage determ. by LEED, AES and XPS 0-103566  
 KCl surface, sublimation kinetics, elec. field influence, terrace-ledge-kink model 0-84287  
 K<sub>2</sub>SO<sub>3</sub>-Ag<sub>2</sub>SO<sub>4</sub> mixtures, surface comp., AES and XPS obs. 0-81386  
 LaB<sub>6</sub> (100), (110), and (111), surface structs. and work functions 0-70512  
 LaB<sub>6</sub> (210) surface, work function, struct. and chemisorpt. stability, XPS, UPS and LEED 0-65344  
 LaB<sub>6</sub> and La<sub>0.58</sub>Sm<sub>0.42</sub>B<sub>6</sub>, FIM study 0-71578  
 LaB<sub>6</sub> single crystal cathode, thermionic emission, surface struct. 0-97395



## surface structure continued

- $\alpha$ -LiO<sub>2</sub>, surface defect layer struct. due to mechanical working (*Russian*) 0-100238  
 MgO, atomic C anal. by <sup>12</sup>C(d,p)<sup>13</sup>C method 0-108766  
 MgO single crystals, surface atomic steps obs. by electron microscopy, dark- and bright-field techniques 0-84040  
 MnZn ferrites, form. of comp. heterogeneity during high-temp. sintering 0-60818  
 Mo foil electrolytic perforation, surface film phase composition obs. (*Russian*) 0-61004  
 Mo surface, adsorbed Ga and Sn, struct., FIM obs. 0-103576  
 Mo:C (110) surface, segregation, precip. and desorpt. of C, AES and LEED study (*French*) 0-103480  
 Mo-base alloy, TZM, blistering under He ion bombard. 0-92567  
 Mo(001), clean and H chemisorbed, atomic displacements, LEED obs. 0-70514  
 NaCl, cleavage faces, evaporation pattern determ. by decoration method in electron microscopy (*German*) 0-107626  
 NaCl stepped and disordered surfaces, adsorbed Xe, two-dimens. phase transformations 0-103580  
 Na<sub>2</sub>O-K<sub>2</sub>O-Al<sub>2</sub>O<sub>3</sub>-SiO<sub>2</sub> structure of modified surface layer, internal friction method 0-103258  
 Na<sub>2</sub>O-SiO<sub>2</sub> glass, internal and surface struct. by X-ray scatt. 0-84074  
 Nb<sub>2</sub>Sn, flux density gradient determ. by Faraday effect 0-107969  
 Ni (001), adsorption of N<sub>2</sub>, c(2×2) struct. form 0-80083  
 Ni (001), azimuthal anisotropies of ejected dimer ions, SIMS expt., struct. effects 0-60730  
 Ni (100) surface, coadsorption of Sn on Pb, P or O contaminated surface, AES study 0-88437  
 Ni (110), adsorbed H, adatom configuration, He diff. study 0-103569  
 Ni (110), surface damage induced by bombard. with 3-30 keV noble gas ions 0-60728  
 Ni {100} and Ni {100} with O overlayer, crystallographic effects in low energy ion scatt., local ion-atom neutralisation 0-84377  
 Ni alloys, heat resistant E1437B and E1929, surface condition, air stream effect 0-76409  
 Ni foil electrolytic perforation, surface film phase composition obs. (*Russian*) 0-61004  
 Ni, Medius matrix cathode, surface characts. 0-66378  
 Ni passivation, S influence study by Auger and electron spectroscopy 0-65347  
 Ni surface, (001), adsorbed c(2×2)CO layer, struct. 0-88428  
 Ni-Al, (2 and 6 wt.%), oxidation,  $\alpha$ -Al<sub>2</sub>O<sub>3</sub> growth, microstruct., precip. 0-108626  
 Ni-Co-W, electrodeposition, surface morphology and cryst. struct. 0-71602  
 Ni-Cr-Ti rapidly solidified superalloys, surface segregation 0-76263  
 Ni-Cu, surface segregation, computerised atom-probe FIM study 0-75412  
 Ni-Th (1 at.%), surface comp., temp. and O<sub>2</sub> exposure effects, AES study 0-80914  
 $\beta$ -NiAl, oxidation,  $\alpha$ -Al<sub>2</sub>O<sub>3</sub> growth and microstruct. 0-108627  
 Ni(CO)<sub>4</sub>, form. on single Ni cryst., reaction kinetics and induced surface faceting 0-71948  
 NiO (001) surface, chemisorption of H, surface and second-layer defect effects 0-65369  
 NiO (100) surface, LEED expt. and calc. down to 60 eV 0-92767  
 NiO-MgO solid solns., surface comp. study by XPS 0-104035  
 Ni<sub>99</sub>Sb<sub>0.04</sub>, surface segregation, XPS and AES obs. 0-76135  
 NiSi<sub>3</sub>, epitaxial film on (111) Si substrate, interfacial order, backscatter, channelling study 0-65390  
 Ni(001) surface N adsorption due to ion beam irr., surface struct. LEED study (*Chinese*) 0-84364  
 Ni(100) oxidised surface structure anal., extended appearance potential fine struct. study. 0-75411  
 O, on Fe(100), adsorbate coverage determ. by LEED, AES and XPS 0-103566  
 Pb, deposition on Au, quantitative Auger electron spectroscopy, substrate and instrumental effects 0-71523  
 Pb electrode, in situ surface phase study by laser Raman spectroscopy 0-103542  
 PbSe, superficial degradation in air and water, XPS obs. (*French*) 0-89110  
 PbSe films, current carrier conc. and type control, elec. cond., synthesis process (*Russian*) 0-100412  
 Pb<sub>1-x</sub>Sn<sub>x</sub>Se epitaxial layers obtained by LPE, growth conditions correl. with morphology 0-104079  
 Pd (110) surface, adsorption of S, characterised by LEED (*French*) 0-88422  
 Pd, (111) surface electron microscopy 0-103556  
 Pd coated Si wafers, interference effects on irr. with laser beam 0-66333  
 Pt (100) (5×20) and (1×1) surfaces, stability and reactivity, adsorption of H 0-75434  
 Pt (100) surface, reconstruction, superstruct., model 0-103551  
 Pt (997) surface, partial faceting, He beam scatt. and LEED study 0-103547  
 Pt, adsorption of O<sub>2</sub> on (110) surface, Ar<sup>+</sup> bombardment effects on reactivity 0-89099  
 Pt crucibles, surface changes rel. to Fe anal. 0-61192  
 Pt surface, chemisorbed CO, IR refl.-absorpt. spectra, adsorbate island struct. 0-84385  
 Pt, surface dipole moment calc. 0-60060  
 Pt-Au, surface segregation, comp. depth profiles meas. using atom-probe field ion microscope 0-100380  
 PtSi, impurity effects 0-80037  
 Re (1010), LEED anal. 0-75414  
 Re, electrodeposited from fused salts, (1011) texture (*Russian*) 0-92791  
 S, on Fe(100), adsorbate coverage determ. by LEED, AES and XPS 0-103566  
 Sb, cleavage faces, evaporation pattern determ. by decoration method in electron microscopy (*German*) 0-107626  
 Sb<sub>2</sub>Te<sub>3</sub>, cleavage faces, evaporation pattern determ. by decoration method in electron microscopy (*German*) 0-107626  
 Si (001), high energy ion scatt. study 0-59772  
 Si (001) and (111), geometrical and electronic struct., review 0-80039  
 Si (100), H adsorption, MeV ion scatt. study 0-80071  
 Si (100), vicinal, LEED obs. of stepped surface 0-59773  
 Si (100) reconstructed surface struct. study using thermal energy He diff. 0-60731  
 Si (111), ion bombard., struct. changes, AES obs. 0-79842

## surface structure continued

- Si (111), nitridation, AES and LEED results 0-80041  
 Si (111), surface structure, high temp. RHEED obs. using metal-backed fluoresc. screen 0-75126  
 Si (111) 7×7 surface structure investigation, RHEED 0-96723  
 Si, (111) surface structure phase transform, screw dislocations RHEED study 0-88153  
 Si (111) surfaces, cleaved, electronic structure following Al adsorption 0-75610  
 Si, amorphous, ideal surface, definition and characts. 0-107623  
 Si, CVD, surface anal. during growth using RHEED and Auger spectroscopy 0-66433  
 Si, crucible grown, virgin and implanted, laser irradiation effects on surface structure 0-92768  
 Si, epitaxial (111) surface, etching observation of stacking faults, dislocations, S-pits, etch pits (*Chinese*) 0-70197  
 Si, heavy ion induced disorder in surface and at shallow depths 0-59535  
 Si, ion implanted, electron beam annealing, surface struct. study using SEM 0-70235  
 Si, lattice strains induced by localized oxidation, high temp. real-time X-ray topographic studies 0-108489  
 Si phototransistors, slow contamination and fast surface state effects, SEM study 0-107896  
 Si, purity for semicond. appls., neutron activation anal. 0-71979  
 Si RF sputter-etched surface, cryst. damage, spectroscopic ellipsometry obs. 0-103538  
 Si ribbons grown by capillary action shaping technique, surface quality and impurity distrib. 0-108343  
 Si, slip dislocation nucleation during laser annealing 0-84179  
 Si, surface topography changes due to pulsed laser annealing 0-84348  
 Si wafer, thin surface layers, amorphous to cryst. transform., obs. technique 0-107288  
 Si wafers, saw damage reduction in lubricant environment 0-108585  
 Si:B(P)(As)(Sb)(Cu)(Fe), ion implanted, doping profile, pulsed laser annealing effects 0-88197  
 Si:P, ion implanted, subsurface damage, TEM and channelled Rutherford backscatt. study 0-107337  
 Si:Sb, laser doping, evaporation loss and diffusion of Sb, under pulsed laser irr. 0-59508  
 Si-Al-Al<sub>2</sub>O<sub>3</sub> system, solid phase Si regrowth on sapphire 0-100413  
 SiC, radiation defect annealing, recovery of LEED maxima 0-65075  
 $\alpha$ -SiC(6H), radiation defect distrib. anisotropy near (0001) surface, LEED study 0-96577  
 SiCl<sub>4</sub>-GeCl<sub>4</sub>-BCl<sub>3</sub>, particulate layers consolidation, in fabrication of optical fibre preforms 0-60787  
 Si<sub>3</sub>N<sub>4</sub> films on Si wafers, O determ. by <sup>3</sup>He activation anal. 0-71981  
 SiO<sub>2</sub>, fused, surface crystn. by Li<sup>+</sup> ion implantation and annealing 0-89383  
 SiO<sub>2</sub> gel, internal and surface struct. by X-ray scatt. 0-84074  
 SiO<sub>2</sub>-Na<sub>2</sub>O-CaO-MgO float glass, surface SnO<sub>2</sub> distrib., ellipsometry and XPS study 0-84346  
 Si(111) reconstructed 7×7 surface superlattices, microdomain model 0-107625  
 Si(111)-(7×7), and impurity stabilised Si(111)-(1×1) surface, photoemission studies 0-104041  
 Si(111)-√3×√3-Ag structure, atomic arrangement, low energy ion scatt. spectroscopy 0-96724  
 Si(111)-(7×7) surface models, LEED anal. 0-75418  
 SmB<sub>6</sub>, FIM study 0-71578  
 Sn-O<sub>2</sub>, surface step thickness measurement 0-103555  
 Sn-Pb surfaces ageing, detrimental effect in PC fabrication 0-108625  
 SnO<sub>2</sub> CVD coating on glass, elec. resist. rel. to cryst. microstruct. 0-84520  
 SnO<sub>2</sub>:Sb film on glass substrates, elec. props. 0-88652  
 SrTiO<sub>3</sub> (100), LEED and UPS studies 0-100747  
 SrTiO<sub>3</sub>, fabrication damage characterisation by internal and external meas. 0-102782  
 SrTiO<sub>3</sub>, surface microrelief after ion irr. 0-59774  
 Te film, surface morphology depend. on vacuum deposition angle 0-103553  
 Te(1010), LEED intensities anal. 0-88411  
 Ti alloys, electrochemical working, film form. and surface roughness (*Russian*) 0-76397  
 Ti alloys, surface layers examination using vacuum UV spectrograph (*French*) 0-71987  
 Ti foil electrolytic perforation, surface film phase composition obs. (*Russian*) 0-61004  
 Ti, friction surface structural investigation, O<sub>2</sub> surface diffusion (*Russian*) 0-96726  
 Ti, serrated {1012} twin interfaces 0-84182  
 Ti, surface layer, study using vac. UV spectrograph (*French*) 0-71987  
 Ti-Al, elec. spark Al doping of VT-18, surface struct. and props. (*Russian*) 0-76398  
 Ti-N<sub>2</sub>, condensate formed by plasma flow precipitation in vacuum, cryst. and surface props. (*Russian*) 0-100788  
 TiC coatings, on cemented carbides, struct. and hardness 0-59771  
 TiH<sub>2</sub> and TiD<sub>0.9</sub>, surface characts., AES, EELS, SIMS, and XPS study 0-65343  
 TiO<sub>2</sub>, rutile, superficial constitutive water, NMR study 0-88881  
 TiTe, melt, elec. cond., surface tension, microhardness, influence of impurities 0-88551  
 UAl<sub>3</sub>(Co)<sub>3</sub>, surface comp. and electronic struct., photoemission study 0-66382  
 V surface, chemisorption of Br<sub>2</sub>, struct., Na adsorption effects 0-101039  
 V<sub>2</sub>O<sub>5</sub> and lower oxides, electronic, optical, structural and surface props., review 0-88120  
 W (001), displacive transition, H adsorpt. effects, theoretical model 0-65352  
 W (100), surface reconstruction kinetics in presence of O half-monolayer 0-65375  
 W (110) surface, adsorbed Pd, growth, struct., stability, desorption 0-59794  
 W, (110) surface, low energy ion scatt. features, inelastic loss and surface crystallography 0-66371  
 W crystal-atom and W(001) surface, low-energy positron diffraction, theoretical study 0-84034  
 W, deformed, surface layer struct. effect on polygonisation and recryst., X-ray diff. anal. and metallographic exam. (*Russian*) 0-84948  
 W dispenser cathodes, Ba-activated, surface characts., ion scatt. spectrometry and SIMS study 0-66377

**surface structure continued**

- W faces, simultaneous adsorption of Ba and Cu atoms, work function changes 0-65378  
 W monocrystals in alkaline electrolyte, surface orientation, effect on anode current (*Russian*) 0-75360  
 W surface, adsorbed W, Ga, Sn, struct., FIM obs. 0-103576  
 W, surface dipole moment calc. 0-60060  
 WC, explosive plasma sputtered coatings, struct. and props. (*Russian*) 0-100783  
 WC-Co DC and RF sputtered coatings, bias effect, struct., X-ray-Auger study 0-70565  
 W(001), electronic surface reson. and thermally induced struct. transition 0-88614  
 W(100), I adsorption at room temp., LEED and AES study 0-84389  
 W(100) surface, instability, distortion and dynamics 0-84360  
 W[001] (1×1) surface structure, pseudo-relativistic LEED calcs. and R-factor anal 0-70510  
 YbTe, high-temperature evaporation and reactivity 0-103469  
 Zn, electron emission depend. on surface mechanical treatment (*Russian*) 0-100945  
 ZnS ion beam etching, topographic changes, amorphisation, luminescence study 0-76078  
 ZnS, superficial degradation in air and water, XPS obs. (*French*) 0-89110  
 Zr, serrated {1012} twin interfaces 0-84182  
 Zr-N<sub>2</sub>, condensate formed by plasma flow precipitation in vacuum, cryst. and surface props. (*Russian*) 0-100788  
 ZrO<sub>2</sub>-CaO, stabilised microspheres, structure, mechanical props. (*Russian*) 0-100379  
 ZrO<sub>2</sub>-Y<sub>2</sub>O<sub>3</sub>, stabilised microspheres, structure, mechanical props. (*Russian*) 0-100379

**surface tension**

- adsorption, intermolecular surface forces in plane densely packed hexagonal model 0-59785  
 n-alkanes, anisotropic London dispersion forces, surface effects 0-74214  
 body loading with cracks, energy conditions for brittle failure (*Russian*) 0-96234  
 bronchial collapsibility of excised dog lungs, effect of lung surface tension 0-67118  
 charged particles, two-component liquid, in equilib. with vapour, surface dipole layer and surface tension 0-70505  
 colloidal systems, surface forces, direct meas., elastic deform. effect 0-93805  
 crystal surface elastic props., surface tension tensor, volume stress (*Russian*) 0-100389  
 cytoplasm spherical drop with effective surface tension influenced by oscillating enzymatic reactions 0-108862  
 demonstration, teaching aids, convention of secondary school physics teachers (*Hungarian*) 0-67957  
 density functional theory for simple liquids, appl. to liq. metals 0-103537  
 drop, incompressible fluid, equilib. and stability analysis 0-59092  
 drop deformation and orientation in shear and extensional flow fields, dynamic interfacial props. 0-107611  
 drop dynamics in shear fields, role of dynamic interfacial effects 0-107612  
 drops, liquid, rotating, held together by surface tension, equilibrium shapes and stability 0-79367  
 education, Brownian motion, melting, surface tension and rubber networks, thermodynamic anal. 0-73132  
 flow of liq. film down vertical or inclined surface, surface tension effects 0-106778  
 fluid dynamics, free boundary flow, surface tension effects, finite element fluid flow simulators 0-82647  
 fluid/liquid interfaces, capillary phenomena, review 0-70506  
 hard sphere system, surface tension, compressibility, bulk modulus press. coeffs. and Rao's acoustical parameter 0-80027  
 horizontal crystal ribbon growth, meniscus stability 0-103281  
 inhomogeneous charged fluids, density functional theory, rel. to molten salts surfaces 0-79660  
 interface instability in presence of chemical potential gradients (*French*) 0-75338  
 interfacial tension minima, dynamic, equilibration of surface-active solute between two liquid phases 0-80026  
 isobutyric acid-H<sub>2</sub>O, liquid-vapour surface tension near liquid-liquid consolute point 0-107613  
 isotropic solid soln. cryst. surfaces, surface stress and chem. equilib. 0-107628  
 jets, Newtonian, axisymmetric, die-swell, Galerkin finite element method 0-83830  
 lattice systems, phase transition and surface tension 0-77713  
 liquid binary metallic systems, rule for surface enrichment 0-75406  
 liquid crystal surface, statistical thermodynamics, local order parameter 0-88023  
 liquid ionic salts, melting transition statistical model, dielectric const., surface tension 0-70378  
 liquid mixtures, theory 0-88404  
 liquids, potential and flux conserving static equilibria in elec. or mag. fields, determ. 0-88399  
 metals, atomic binding energy and surface energy rel. to prediction of physical props. 0-59434  
 microcluster formation, free energy, curvature-depend. surface tension effect 0-100056  
 nematic liquid crystals., molecular alignment using alkoxysilanes, rel. to surface energy 0-100164  
 Newton black film, line tension, determ. by cnt. bubble method 0-88406  
 Newton black films, line tension determ. by diminishing bubble method 0-88407  
 nitrothane-3-methylpentane, liquid-vapour surface tension near liquid-liquid consolute point 0-107613  
 optical fibre coating with conical shape applicator 0-58820  
 optical glass, melting, fining, surface tension, diffusion, nucleation in microgravity 0-81016  
 oscillatory flow in U-tube manometers, effect of drag reducing polymer additives 0-64584  
 overstability in horizontal layer of binary liq. mixture with Soret effect 0-106782  
 polyalkylene isophthalates, by sessile bubble method (*Japanese*) 0-75405  
 porous materials, sintering, behaviour of pore filled with const. amount of gas 0-66450

**surface tension continued**

- positive surface tension gradients, Rayleigh-Benard convection (*French*) 0-75404  
 solid-liquid metallic binary alloy, interfacial tension, chem. adsorption and temp. depend. 0-59777  
 solid/melt interfacial tension and contact angles of small particles, determ. from crit. vel. of engulfing 0-79915  
 tetrabutylammonium iodide, alcoholic soln., repulsion phenomena in thin layers 0-107619  
 thermo-optical converter with liq. modulating medium 0-91927  
 thin liquid films in emulsions, tension and contact angles 0-92761  
 water, cavitation expts. in steel Berthelot tube 0-87788  
 water, normal and heavy, surface tension from Skeleton table (*German*) 0-75407  
 water-toluene-sodium dodecyl sulphate-butanol 1 mixture, interface light scatt., interface tension meas. 0-76039  
 Ar, liquid-vapour interface, surface of tension near triple point, theory 0-100375  
 Ar, nonequilibrium condensation and surface tension in supersonic jet flow (*Russian*) 0-65210  
 CaF<sub>2</sub>, melts, elec. cond., surface tension, viscosity, density (*Russian*) 0-92758  
 CaF<sub>2</sub>-MgO-SiO<sub>2</sub>, melts, elec. cond., surface tension, viscosity, density (*Russian*) 0-92758  
 CaF<sub>2</sub>-MgO(SiO<sub>2</sub>), melts, elec. cond., surface tension, viscosity, density (*Russian*) 0-92758  
 Ce, surface and volume props., flow props., surface layer thickness (*Russian*) 0-59760  
 Cu, liquid, dissolved O below 0.02 wt.% effect on surface tension 0-107618  
 F, liquid, hard sphere model with attractive interactions 0-96434  
 Fe ore concentrate, sinter quality improvement (*Chinese*) 0-104089  
 Fe-As melts, surface tension, density, adsorption (*Russian*) 0-92757  
 He crystals, meas. of surface tension and contact energy, standing waves (*French*) 0-92753  
<sup>3</sup>He, liquid, surface fluctuation influence on free energy, surface tension (*Russian*) 0-92746  
<sup>3</sup>He-<sup>4</sup>He, liquid solution, bound impurity pair effect on surface tension (*Russian*) 0-65332  
<sup>4</sup>He, HCP crystal, roughening transition 0-88397  
<sup>4</sup>He, solid-superfluid interface, struct., surface tension 0-88380  
 La, surface and volume props., flow props., surface layer thickness (*Russian*) 0-59760  
 LiH, liq., density and surface tension, 982-1280K 0-59548  
 LiH, liq., surface tension investigation, 964-1300K 0-70503  
 Mg-SiO<sub>2</sub>, floating zone method growth, interface shapes 0-60775  
 Nd, surface and volume props., flow props., surface layer thickness (*Russian*) 0-59760  
 Nd<sub>2</sub>Ga<sub>2</sub>O<sub>7</sub>, floating zone method growth, interface shapes 0-60775  
 Pr, surface and volume props., flow props., surface layer thickness (*Russian*) 0-59760  
 TlTe, melt, elec. cond., surface tension, microhardness, influence of impurities 0-88551  
 Tl<sub>2</sub>Te, melt, resistivity, surface tension, microhardness, influence of impurities 0-88552  
 W, molten drop break up in gas flow, surface drag, capillary excitation (*Russian*) 0-100024  
 YFeO<sub>3</sub>, floating zone method growth, interface shapes 0-60775  
 YIG, floating zone method growth, interface shapes 0-60775
- surface tension measurement**  
 Langmuir film balance meas. system 0-62659  
 liquid metals, apparatus for 0-59759  
 temperature dependence from triple point to critical point (*German*) 0-100376
- surface texture**  
 adsorbed molecules, Raman and fluoresc. enhancement by surface roughness 0-102511  
 ceramic/metal layer adhesion mechanism for metallization of electronic ceramics, elec. props. (*German*) 0-76381  
 elastic body, attenuation of surface Rayleigh acoustic waves travelling along periodically surface 0-80047  
 electrode surface roughness, effect on electric breakdown in air 0-84018  
 electron reflection from metal surfaces, surface roughness, IR absorpt. 0-71526  
 flat plate streaming potential investigations: hydrodynamics and electrokinetic equivalency 0-106777  
 grinding, role of elastic and plastic behaviours (*Japanese*) 0-100868  
 laser speckle and surface roughness 0-102622  
 liquid crystals, nematic and cholesteric, surface and bulk configurations, topology 0-59381  
 metal surface, rough, hemispherical emittance 0-70434  
 metals, elastic constants and moduli of axial textures 0-75286  
 molecules adsorbed on rough surfaces, Rayleigh, Mie and Raman scatt. 0-83378  
 optical glass diamond grinding kinetics 0-64224  
 optical pattern recognition by diffraction pattern sampling 0-99643  
 optical properties of rough surfaces, discontinuous films, heterogeneous materials, review 0-103935  
 Raman scattering, surface enhanced, surface roughness effect 0-83377  
 rough surface, random, reflectance derived with Fresnel approx. 0-87309  
 rough surface contact, review of expt. work 0-76377  
 rubber, friction against paper and polymer film surfaces, microroughness effect 0-71763  
 scattering object, coherently illuminated, speckle pattern statistics in diff. field 0-63924  
 silicate glasses, polishing, surface characts. using grazing X-ray reflection (*French*) 0-65353  
 steel, stainless, emittance, oxidation and surface roughness effects 0-96673  
 steel, stainless, emittance meas. rel. to surface roughness parameters 0-100342  
 surface plasmon dispersion relation in presence of surface roughness 0-65650  
 thin-wall cylinder cold rolling method 0-66535  
 topography, correlation with profile statistical parameters 0-88418  
 waveguide scattering problem, comparison of two perturbation theories 0-83662  
 X-ray imaging system, surface roughness and scatt. effects 0-77921  
 Zircaloy cladding, stress corrosion cracking, inner surface texture effect 0-66695



## surface texture continued

- Ag film, surface roughness, light scatt. meas. 0-107624  
 Ag foil, surface-plasmon resonance, roughness-induced wavelength corrections 0-108288  
 Ag foils, surface plasma-wave reflectance and roughness-induced scatt. 0-66228  
 Ag surface, adsorbed pyridine, enhanced Raman scatt., ultrahigh vac. study, surface roughness depend. 0-88993  
 Ag, surface plasmon dispersion relation in presence of surface roughness 0-65650  
 Al laser target, multiple-pulse thermal coupling at 3.8  $\mu\text{m}$  wavelength 0-96371  
 Al, surface deformation and wear track obs. using analytical electron microscope 0-108687  
 Be, thick film, amorphous, RF magnetron sputtering 0-80971  
 CdS thin film solar cell fabrication, HCl etching 0-81474  
 Cu, cementation, on Fe, deposit struct., reaction rates, SEM 0-104421  
 Cu, erosive wear mechanisms, combined TEM and SEM obs. 0-108601  
 Cu film, diffuse optical scattering from variable roughness surfaces 0-100704  
 Cu, surface morphology influence on sputtered yield angular distribution 0-65338  
 GaAs(Sb), electrochemical sectioning and surface finishing 0-108611  
 \*He, superfluid, vortex pinning, surface roughening effects 0-88381  
 InP/In<sub>0.5</sub>Ga<sub>0.5</sub>As<sub>0.5</sub>P<sub>0.5</sub> interfaces, sputter-profiled, depth resolution degradation by cone form. 0-80094  
 Mo alloys (MChVP and TSM10VD), erosion, effect of ion bombardment dose and previous surface treatment 0-89419  
 Mo, film on sapphire substrate, orientational growth, epitaxial textures, nucleation textures (*Russian*) 0-75454  
 Nb, film on sapphire substrate, orientational growth, epitaxial textures, nucleation textures (*Russian*) 0-75454  
 Ni, erosive wear mechanisms, combined TEM and SEM obs. 0-108601  
 Se, thin film selective absorber coatings, prod. using an oblique vacuum deposition technique 0-81488  
 Si, CVD amorphous films, effect of surface characts. on visible and UV optical props. 0-60698  
 Si film, polycryst., grain struct. and surface roughness, TEM study 0-70556  
 Si, polycryst., oxidation, morphological aspects 0-76388  
 Si solar cells, proton irradiated, processing influence on elec. performance 0-94001  
 Si, surface, pulsed electron beam processing, doping, annealing 0-75254  
 Si:P, polycrystalline laser recrystallised film on Si substrate, cryst. struct., thermal oxidation 0-65391  
 Si:Sb vacuum deposited coating, p-n junction, pulsed electron beam annealing doping, diffusion 0-75480  
 SiC, reaction-bonded, impact erosion by ang. Al<sub>2</sub>O<sub>3</sub> particles 0-89362  
 SiO<sub>2</sub>, thin films on rough polycryst. Si surfaces, oxide thickness and refractive index meas. 0-93422  
 Ta, film on sapphire substrate, orientational growth, epitaxial textures, nucleation textures (*Russian*) 0-75454  
 Te, thin film selective absorber coatings, prod. using an oblique vacuum deposition technique 0-81488  
 Ti, coatings, electrolytically deposited, texture, anti-corrosional props. (*Russian*) 0-66532  
 Ti, emittance, during nonstationary high temp. heating by Ar flow (*Russian*) 0-84308  
 Ti metal-metal interface, adhesion energy, surface treatment and ion implantation effects 0-107660  
 Ti-Al-Mo-Zr, compressor disk, surface plastic deform., optimal method 0-60924  
 V, film on sapphire substrate, orientational growth, epitaxial textures, nucleation textures (*Russian*) 0-75454  
 V, radiance temperature at melting point, surface roughness depend. 0-59683  
 W, film on sapphire substrate, orientational growth, epitaxial textures, nucleation textures (*Russian*) 0-75454

## surface topography measurement

- ceramic surface metrology using peak counting, quality control 0-95065  
 component profile inspection equipment 0-105608  
 contactless laser interferometer sweep gauge for diamond-turned surfaces 0-73441  
 dark-field surface inspection using total internal reflection 0-74519  
 deflection contour generation by white light projection speckle method 0-98881  
 diamond turned surface production, interferometric test repeatability 0-74538  
 diffusing surface optical autocorrelation 0-99646  
 fracture surface SEM analysis, microtopography 0-68312  
 holographic contouring, of surface topography and contact rigidity study of rough surfaces 0-64494  
 holographic interferogram quantitative evaluation procedures (*German*) 0-87344  
 interferograms, two wave, sensitivity improvement process (*French*) 0-98968  
 interferometer design, construction and interferogram processing, optical testing appl. 0-79020  
 interferometric examination of lenses, mirrors and optical systems, 3D display 0-69497  
 interferometry at 10.6  $\mu\text{m}$  0-86385  
 large monocrystal X-ray reflection/scanning and transmission topographic methods 0-96415  
 laser dot matrix space-coded surface topographical mapping 0-98885  
 laser speckles, bibliography (1976 to 1978) 0-82593  
 light rangefinder and profilometer, high-resolution gas laser 0-102754  
 liquid, transient behaviour due to pulsed US transducers 0-95073  
 machine part, rotating, surface finish, laser method for determ. 0-89454  
 metal surfaces, shape and deformations, holographic contour immersion method (*Polish*) 0-62630  
 moire, computer generated, for profile testing 0-105689  
 moire contourgraphy, computer-aided replication of human anatomy 0-67189  
 Moire photography, appl. to human face mapping 0-85462  
 multilayer dielectric mirror, light scattering due to surface roughness 0-58460  
 online topographical analysis in SEM 0-68310  
 opaque surface, roughness determ., photometric method 0-95072  
 optical element flatness, interferometric examination techniques 0-69498

## surface topography measurement continued

- optical Nomarski microscopy, differential interf. contrast, for topography quantitative determ. 0-73318  
 optical shop computer-controlled interferometry, in-process production tool 0-74531  
 patient's surface contour measuring device 0-104717  
 ploughed soil, microwave backscatter determ. (*French*) 0-82072  
 polished surfaces, smoothness parameter meas. using spectral analysis optical system 0-82661  
 profile from horizontal light source reflection, calc. from observed image 0-101777  
 profile from horizontal light source reflection, image calc. 0-101776  
 rough surfaces, characterisation by meas. of single roughness constant 0-82624  
 roughness, influence of stylus tip geometry on meas. (*German*) 0-68182  
 roughness measurement, electrical stylus tip instrums. 0-90818  
 roughness measurement methods using SEM techniques, research and development (*German*) 0-105612  
 roughness measurement using improved pneumatic Wheatstone bridge 0-62629  
 SEM, automatic topographical surface reconstruction 0-62803  
 SEM analysis of object microrelief, metallurgy appls. 0-73319  
 SEM computer-aided topographical analysis 0-70094  
 SEM in analysis of material surface texture 0-73548  
 SEM topographical measurements at grazing incidence, alignment problem 0-99014  
 signal processing and analysing device, Herbert-Sigma (*French*) 0-57254  
 site tolerance, and surface roughness, standard rel. 0-62634  
 standardised hand-held instrument, with in-built data processor (*German*) 0-57255  
 stylus tip instrums., standards and calibration (*German*) 0-101782  
 three-dimensional topographic mensuration, laser electro-optic system 0-99784  
 tools for surface anal., review 0-103540  
 two-wavelength contouring with automated thermoplastic holographic camera 0-74318  
 universal instrument, modular with indicator and strip recorder (*German*) 0-57283  
 wavefront correlation effect on topogram sensitivity 0-69345  
 X-ray mirror profile meas. machine 0-69496  
 Zygo interferometer system 0-73437  
 Al surface damage, meas. and detect. after static contact loading 0-64495  
 Al thin films evaporated on rough quartz substrates (*Polish*) 0-88450  
 Al-Cu, high strength, type 2024-T3, crack growth, fatigue induced surface deform., holographic detect. 0-85120  
 CaHPO<sub>4</sub>, powder and granules with starch mucilage binder, surface topography variation under compression 0-80998
- surface treatment**  
*see also etching; polishing; surface hardening*  
 alkali-borosilicate glasses, antireflection film production by heat and chem. treatment 0-66677  
 alloy surface composition modification by high-power CW lasers 0-93699  
 anticale forming effectiveness of seeding crystals in thermal power plant 0-89527  
 boride coatings on C and alloy steel, spectroscopic thickness determ. 0-85099  
 chemothermal treatment, mathematical modelling 0-100955  
 crystal, in-situ cleaning by ion sputtering in EM 0-101895  
 dielectric surface, charge accumulation, losses, electron-beam treatment (*Russian*) 0-75931  
 film cleaning by ultrasonic liquid cavitation and acceptable solvents 0-62769  
 fracture preservation and cleaning, for fractography 0-71866  
 fused silicon substrate, directional reactive ion etching at oblique angles 0-66428  
 E-glass fibre, silane coupling agent deposited on surface, hydrolysis and drying effect on siloxane bonds 0-85072  
 glass surfaces, cracked layer thickness determ., chemical method 0-64226  
 graphite, conditioning of surface by atomic H 0-93665  
 high pressure boiler in-service scavenging by intermittent dosing with chelating agent 0-89485  
 Inconel 625, organic contamination removal by plasma cleaning and etching 0-97645  
 instrumentation engineering, laser beam appls. in drilling, welding, cutting, definite abrasion and surface treatment (*German*) 0-108608  
 integral glass covering of spacecraft solar cells by electrostatic bonding 0-93676  
 ion bombardment by low-energy ions of plasma accelerators 0-97608  
 ion sputter gun, in-situ cleaning of crystal surfaces in EM 0-101895  
 ionic nitriding thermochemical process, equipment, process details and advantages and prospects (*French*) 0-108641  
 laser applications in materials processing, seminar, San Diego, CA, USA (Aug. 79) 0-90609  
 metal surface, plasma cleaning and etching, removal of C 0-97645  
 metal surfaces, radioactive contamination 0-68771  
 moderator surface preparation for increased slow positron yield 0-61011  
 nitrided layer, fracture toughness determ. from hardness impressions (*German, English*) 0-97575  
 nitriding in glow discharges, influence on phase comp. and plasticity of diffusion layer (*Russian*) 0-76400  
 optical coating removal by Al<sub>2</sub>O<sub>3</sub> powder and NH<sub>4</sub>HF<sub>2</sub> soln. 0-74521  
 optical fibre, furnace drawn, tensile strength 0-58751  
 plasma industrial utilisation, synthesis, powder, metallurgical and surface treatments, review (*French*) 0-96398  
 porous materials, effects of different methods of prep. on reproducing surface 0-60995  
 powder coatings, in metal finishing, review 0-104330  
 quartz plates, surface irregularities due to mechanical treatment (*Polish*) 0-89380  
 quartz wafer cleaning, surface contaminant estimation methods (*Polish*) 0-89381  
 stainless steel, laser surface melting for corrosion protection 0-93698  
 steel, alloy, quenched carbonitrided, multicycle fatigue failure 0-104283  
 steel, alloy, surface quality improvement, thermomech. treatment 0-61020  
 steel, carburized and quenched, residual stresses (*Japanese*) 0-89262  
 steel, carburizing, vacuum, case depth 0-100956  
 steel, chemothermal treatment, diffusional basis 0-104343  
 steel, Cr, carburising kinetics, in endothermal atm. 0-76410

**surface treatment continued**

- steel, friction and wear during hot forging 0-89358  
 steel, galvanised strip, passivation treatment 0-61146  
 steel, high-C, carburising kinetics, in endothermal atm. 0-76410  
 steel, low-alloy, oxidation resist., N effect 0-66706  
 steel, mild, descaling by HCl (*French*) 0-108642  
 steel, nitrided layer depth, electroinduction meas. method 0-104379  
 steel, powder forged, fatigue, surface treatment effect 0-85048  
 steel, SC49, tufridized, surface treatment effect on cast, SC49, rel. between rotating and flexural bending strengths (*Japanese*) 0-81117  
 steel, segregation and adsorption of S, influence on carburisation and nitrogenation 0-66701  
 steel, stainless, highly protective film development by surface treatment 0-66699  
 steel, stainless, type 316, surface comp. rel. to crevice corrosion initiation 0-93680  
 steel, stainless, vacuum components, pre-vacuum surface finish influence on electron stimulated desorption in ultrahigh vacuum 0-57320  
 steel, stainless 304, metallurgical factors on the corrosion and mass transfer in liq. Na (*Japanese*) 0-71804  
 steel, type 40 K, electron emission depend. on surface mechanical treatment (*Russian*) 0-100945  
 steel, US critical angle reflectivity, near-surface metallic prop. gradient effect 0-70516  
 steel, W-Mo-Cr-V tool, laser surface melted, struct., heat treatment effect 0-76424  
 steel, wear characts. of burnished machined surfaces 0-108595  
 steel, wear resistance of low temp. nitriding treatment 0-89357  
 steel 1Kh17N2Sh, fatigue failure, surface finishing influence 0-60972  
 steel carburisation process, diffusion modelling 0-108632  
 steel powder, high speed, S and O reduction in a H<sub>2</sub> gas stream 0-61015  
 steel sheets, surface composition, degreasing and batch annealing effects 0-66700  
 thermoplastic layers, isothermal smoothing of surface deformation (*Russian*) 0-76394  
 tinplate, passivation treatment 0-61146  
 vacuum deposition equipment cleaning, practical procedures 0-57318  
 Al, laser strengthening, struct., hardness and dislocation density (*Russian*) 0-76399  
 Al surface, plasma cleaning and etching, removal of C 0-97645  
 Al, TEM/XPS study of Cr<sup>3+</sup>/Cr<sup>2+</sup> colloidal SiO<sub>2</sub> surface films 0-85090  
 Al, thermal desorption of oxide film, influence of grain boundaries and recrystn. 0-61023  
 Al-Cu-Mg, type RR55, high strength, creep behaviour, effect rel. to anodic coatings, SEM study 0-97542  
 Al-Mg (2.5wt.%) sheet, surface oxide state and weldability 0-59769  
 Al-Mg alloy, nitridation process study 0-61013  
 CdTe surface, sputter cleaning and dry oxidation, XPS and LEED study 0-108618  
 Cr-Ni compressor disk, surface plastic deform., optimal method 0-60924  
 Cu, electron emission depend. on surface mechanical treatment (*Russian*) 0-100945  
 Cu pickling in HCl waste free system 0-71795  
 Cu surface, plasma cleaning and etching, removal of C 0-97645  
 Cu-Be(2 wt.%), tarnish surface films, formed in ammoniacal Cu(II) solns. 0-97624  
 FE-Zn, prep. and phase diagrams (*French*) 0-76231  
 Fe, Armcro, carburising kinetics, in endothermal atm. 0-76410  
 Fe, H<sub>2</sub> permeation, rel. to embrittlement, organic inhibitors, surface treatment 0-108635  
 $\alpha$ -Fe, nitrided, aging at room temp. 0-71679  
 Fe, segregation and adsorption of S, influence on carburisation and nitrogenation 0-66701  
 Fe, sintered, austenitic nitriding and bainitic hardening 0-85084  
 Fe-Cr, high-temp. oxidation, borate inhibitors 0-66705  
 Fe-Ni (50 wt.%), surface comp. and oxide film thickness after various surface treatments, AES study 0-66693  
 Fe-Si (3 wt.%), grain oriented, mag. props., effect of decarburizing (*Chinese*) 0-103821  
 FeS<sub>2</sub>, acid bacterial leaching, lixiviant alteration by fungal absorpt. of Fe 0-108617  
 Hg<sub>0.9</sub>Cd<sub>0.1</sub>Te surface, sputter cleaning and dry oxidation, XPS and LEED study 0-108618  
 HgTe surface, sputter cleaning and dry oxidation, XPS and LEED study 0-108618  
 InP (110) surfaces, cleaved and polished-sputtered-annealed, LEED and AES study 0-103550  
 Li, surface characterization of film growth 0-81240  
 NaCl crystal rough surface smoothing, during evaporation or condensation 0-103470  
 Na-O-CaO glass, wettability, effect of cleaning procedures 0-65336  
 Si (111), nitridation, AES and LEED results 0-80041  
 Si processing technology, appls. of scanning CW lasers and electron beams 0-100932  
 Si, residual stress and defects induced by scribing 0-60990  
 Si semiconductor plates, control of quality of surface treatment, using Al spraying technique 0-60989  
 Si, surface, pulsed electron beam processing, doping, annealing 0-75254  
 Si-SiO<sub>2</sub>-Mg-Cu powder compact, nitridation to form Si<sub>3</sub>N<sub>4</sub> whiskers (*Japanese*) 0-93674  
 SiO<sub>2</sub>, fused, surface crystn. by Li<sup>+</sup> ion implantation and annealing 0-89383  
 SiO<sub>2</sub>-B<sub>2</sub>O<sub>3</sub>-Na<sub>2</sub>O-K<sub>2</sub>O glass, strengthening by partial leaching 0-60993  
 SiO<sub>2</sub>-Na<sub>2</sub>O, alkali, grain-cleaning procedures effect on crushed glass chem. durability tests 0-66678  
 steel, Cr plated, factors influencing durability 0-108643  
 Ti alloy VT3-1, fatigue failure, surface finishing influence 0-60972  
 Ti metal-metal interface, adhesion energy, surface treatment and ion implantation effects 0-107660  
 Ti-Al-Mo-Zr, compressor disk, surface plastic deform., optimal method 0-60924  
 W, porous, chromising 0-100959  
 W-Cu pseudoalloy, porous, chromising 0-100959  
 Zn, electron emission depend. on surface mechanical treatment (*Russian*) 0-100945  
 Zr, ion-implanted polycryst., thermal oxidation 0-71786

**surface vibrations** *see crystal surface and interface vibrations***surface waves (fluid)**

- see also liquid waves; oceanography*  
 axisymmetric waves on the surface of viscous fluids 0-96266

**surface waves (fluid) continued**

- capillary waves, progressive, periodic, finite-amplitude 0-79339  
 diffraction by object, integral formulation of Helmholtz eqn. 0-81919  
 gravity wave diffraction, in shallow water, optimal control problem (*Russian*) 0-74896  
 gravity wave diffraction over underwater channel of varying depth (*Russian*) 0-79333  
 gravity wave horizontal asymmetry (*Russian*) 0-74897  
 gravity waves, interaction with arbitrarily disposed submerged inhomogeneities (*Russian*) 0-79334  
 gravity waves, vertical asymmetry over a limited depth (*Russian*) 0-79337  
 heated ponds, turbulent boundary layer of stratified airflow, surface waves 0-92133  
 incipient wave propagation on shallow water (*Russian*) 0-74895  
 induced atmospheric pressure field above spectrum of surface gravity waves 0-92168  
 irrotational free-surface flow, time-dependent, formation of sharp corners 0-83808  
 irrotational free-surface flow, time-dependent 0-83807  
 Langmuir circulations, wave-current interaction theories 0-100004  
 linearised interface-wave problems for superposed inviscid liquids 0-87782  
 liquid dispersion, suspended impurities effects on wave excitation in sound field 0-81372  
 nonlinear baroclinic waves, exptl. study of instability and mode selection in large basis 0-85669  
 shear layers, nonlinear evolution of waves 0-83809  
 shoaling of finite-amplitude surface waves on water of slowly-varying depth 0-69853  
 short crested waves, boundary layer vels. and mass transport 0-92169  
 short gravity waves, phase speeds of upwind and downwind travelling waves 0-98332  
 solitary waves, review, book contrib. 0-94962  
 stationary waves at the surface of a magnetizable liquid in a stream impinging on a point barrier 0-83805  
 steep wind waves, amplitude modulation 0-103036  
 steepness over a limited depth (*Russian*) 0-79336  
 thermally induced surface fluctuations on simple fluids 0-88403  
 topographically trapped waves, review, book contrib. 0-96273  
 turbulent boundary layer, wave generation on elastic surfaces, expt. study 0-78443  
 two-layer 'shallow water' model 0-59061  
 underwater ridge, wave guide properties for surface waves 0-96268  
 uniform depth ocean, energy transmission by surface waves through an opening 0-61811  
 wave height spectrum of two-component composite waves in surf-zone (*Japanese*) 0-100006  
 wave spectrum changes due to shoaling and breaking, -3 power law (*Japanese*) 0-100007  
 wind-generated water waves, spatial correls. rel. to freq. independent phase vels. 0-98333
- surge absorbers** *see surge protection*
- surge protection**  
*see also surges*  
 GaAs laser diode power supply control cct. (*German*) 0-78852
- surge suppressors** *see surge protection*
- surgery**  
 coronary artery bypass graft patient recovery trajectory classification algorithm 0-94411  
 diathermy indifferent electrodes, performance electrodes. 0-72367  
 electrosurgical dispersive electrodes, dry metal-foil, thermal props., skin temp. rises 0-98171  
 HF current surgery, instruments and problems (*Hungarian*) 0-98172  
 laser medicine in Japan, current status (*German*) 0-98059  
 spinal deformities correction, force meas. 0-76861  
 tissue temperature simulation in cryosurgery 0-85355
- surges**  
*see also overvoltage; transients*  
 spark gaps, HV switching surges, influencing factors (*German*) 0-87958  
 spark gaps, long air, disruptive voltage calc. with positive switch voltages (*German*) 0-87964
- surgical operations** *see surgery*
- surveying**  
 atmosphere refraction correction to levelling (*Russian*) 0-77127  
 densification of ground control networks, computer program package (*German*) 0-94452  
 geodetic free nets, modification of Helmert-Wolf's soln. (*German*) 0-94453  
 hybrid distance-direction networks, Helmert-type variance-covariance-component estimator appl. 0-101318  
 levelling networks, Helmert-type variance-covariance-component estimator appl. 0-101318  
 objectives of surveying, meas. techniques and data processing methods (*German*) 0-101317  
 scale and orientation in combined Doppler and triangulation nets 0-101311  
 trilateration network, adjustments to account for meteorological conditions 0-77131  
 U, National Uranium Resource Evaluation (NURE) aerial radiometric survey data interpretation via principal components anal. 0-101438
- susceptance, electric** *see electric admittance*
- susceptance, electric, measurement** *see electric admittance measurement*
- susceptibility, dielectric** *see optical susceptibility*
- susceptibility, magnetic** *see magnetic susceptibility*
- susceptibility, optical** *see optical susceptibility*
- suspensions**  
 absorbing particles, simultaneous meas. of dichroism and birefringence in elec. field., photocurrent signal obs. 0-82801  
 bacteria, E.coli strains in aq. suspension, polarisability anisotropy and aminoglycoside antibiotic effects 0-85441  
 Baltic Sea, estuary region, suspension distrib. under river drifts influence (*Russian*) 0-98345  
 benzene, liq., laser pulsation kinetics, optical damage effects 0-58614  
 blood, red cells, rheological props. meas. by Couette viscometer 0-97992  
 blood suspension aggregation in Couette flow (*French*) 0-97991  
 channel flow, two dimensional model of steady laminar flow 0-106834  
 charged particles, laminar tube flow, entrance deposition 0-59100



**suspensions continued**

- conducting fluid with spherical particle suspension oscillating flow in mag. field 0-79408  
 continuum two-phase theory, volume averaged balance eqns. (*German*) 0-92212  
 deposition in entrance of parallel-plate channel, gravity effect 0-83834  
 dipalmitoylphosphatidylcholine, changes in vol. mag. susceptibility at the phase transition 0-76770  
 electric polarisability, anisotropy, length depend. of ionic contrib. 0-85224  
 electric polarisability, stability 0-85222  
 estuarine environment, natural suspended matter flocculation and electrokinetic pot. (*French*) 0-61817  
 extensional viscosity of a dilute suspension of spherical particles at intermediate microscale Reynolds numbers 0-106835  
 ferromagnetic suspension, residual magnetisation 0-84623  
 ferromagnetic suspension serving as a liquid magnet 0-84622  
 flow, memory impairment, Brownian rotation of spheroids 0-79386  
 flow in cylindrical pipe, using ultrasonic debimetry Doppler spectra (*French*) 0-96303  
 fluidised beds, dehydration of solutions and suspensions, rel. to granulation 0-81373  
 gas-liquid ascending flow, monodispersed, function stress on wall, bubble size effect 0-59098  
 glass, complex raw material, hydrothermal prep. 0-104106  
 glass beads in polystyrene soln., suspension, time depend. viscoelastic behaviour 0-99982  
 graphite, in liq. dicyclopentadiene, CO<sub>2</sub> laser pulse induced chem. reactions 0-66821  
 graphite, suspensions, particle shape influence on light absorpt. in mag. field 0-60549  
 impulsive motion, effect of antisymmetric stresses and particle rotation, two-phase continuum theory 0-106833  
 kaolin suspensions, aq., flocculated and dispersed, rheological behaviour in pipe flow 0-64510  
 laminar tube flow, gravitational deposition of growing aerosol particles 0-59099  
 laser pulsation kinetics, optical damage effects in liqs. 0-58614  
 latex solids, agglomerating and dewatering 0-104470  
 liquid dispersion, suspended impurities effects on wave excitation in sound field 0-81372  
 motion of particles suspended in stationary turbulent medium at large Reynolds number 0-83836  
 nonstationary motion in grav. field, volume conc. effect (*Russian*) 0-75002  
 particle motions in a viscous fluid, review, book contrib. 0-96289  
 particle size meter using laser light scatt. spectroscopy 0-77754  
 particles in dilute suspension in general flow, mass flow and density meas. 0-101784  
 percolation, sol-gel transitions, stirred percolation, and laminar flows of passive suspensions (*French*) 0-77724  
 Polirrit suspension, factors reducing polishing ability 0-74543  
 Polirrit suspension for optical component polishing, chem. antifoaming agents 0-74542  
 polymer melt containing suspension, cell model theory of shear viscosity 0-103048  
 polystyrene spheres suspended in air jets, effect of particle proximity on drag force 0-96306  
 power reflection spectroscopy, analytical techniques 0-62714  
 purple membrane fragment suspensions, elec. dichroism obs., trimer model interpret. 0-89728  
 quartz sand, high-conc. suspension, prod. principles 0-66463  
 rigid spherical particle suspension, two-phase theory, volume averaging and governing eqn. (*German*) 0-87801  
 seawater, particulate trace metals concs. in Laccadive Sea 0-104997  
 sepiolite, electric polarisability, anisotropy, length depend. of ionic contrib. 0-85224  
 small particles suspended in turbulent fluid, convection, mass transfer 0-87793  
 sodium bentonite, Wyoming suspension, comparison of optico-optical scattering and birefringence 0-85226  
 solid particle suspension in compressible fluid, wave propag. 0-69858  
 statistical theory, review, book contrib. 0-96288  
 suspensions, crystallisation, aggregate stability and effect on purity of product 0-100769  
 suspensions, rheology, colloidal forces role, review 0-103063  
 viscoelastic fluid, motion of rigid particles 0-103044  
 viscosity, modified cell model approach 0-74944  
 viscous sound attenuation 0-74577  
 Al<sub>2</sub>O<sub>3</sub> suspended particles, behaviour on solidification of Al-Cu (33%) under reduced gravity (*German*) 0-60853  
 C black particles, simultaneous meas. of dichroism and birefringence in elec. field, photocurrent signal obs. 0-82801  
 CdS, monodisperse particles form. from soln., light scatt. theory use in size estimation 0-76560  
 Cr<sub>2</sub>O<sub>3</sub>-ZrO<sub>2</sub> granules, from spray drying of suspensions 0-104100  
 PbI<sub>2</sub> suspension, chem. sensitization 0-73492  
 TiO<sub>2</sub> in glycerine, Bingham plastic flow through annuli 0-64521  
 TiO<sub>2</sub> suspension, adsorption-desorption of IO<sub>3</sub> 0-93804  
 ZrSiO<sub>4</sub>-Al<sub>2</sub>O<sub>3</sub> (SiO<sub>2</sub>) suspensions for slip casting, prep. and props. 0-104103

**swelling**

- creep, swelling and growth, radiation induced, bias factors estimated from self-consistent model 0-88249  
 N,N-diethylacrylamide, cross-linked copolymer, improved mech. props. 0-61091  
 epoxy/graphite composite and cured epoxy resin, thermal expansion and swelling 0-92450  
 extrudate swell, thermally induced, Galerkin method 0-79312  
 fibrin, modification by synthetic polymers 0-61090  
 fission fuel grain boundary loss terms, use in fission gas release and swelling models 0-63257  
 fuel pins, fast breeder, fuel-cladding mech. interaction, obs. and anal. 0-86959  
 fusion reactor materials, irradiation creep by the climb-controlled glide mechanism in Tokamaks 0-102304  
 gel, heterogeneous two-phase, permeability 0-76563  
 LMFBR advanced MX-type fuels, fission gas swelling, temp. depend. 0-57842

**swelling continued**

- LMFBR advanced MX-type fuels, low-temp. microscopic swelling, phenomenological model 0-57851  
 LMFBR advanced MX-type fuels, swelling mechanism anal. 0-57850  
 LMFBR fuel disruption following LOF accident, in-pile expt. using high-speed cinematography 0-78366  
 LMFBR highly-rated MX-type fuels, fission gas release and microscopic swelling 0-57848  
 metals, radiation creep speed and swelling, self diffusion mechanisms (*Russian*) 0-92595  
 Nimonic PE-16, electron irradi. in HVEM, void growth, vacuum environment influence 0-107323  
 nuclear fuel, gas release and swelling, operational model, grain boundary gas 0-95346  
 nuclear fuels, fission gas precipitation into intra- and intergranular porosity, theory 0-57849  
 nuclear fuels, role of fission gas swelling and release in reactor accidents 0-57854  
 Nylon 6 film, prior high-pressure treatment effects, weight swelling, density, IR crystallinity, X-ray and viscosity obs. 0-81025  
 optical materials and components, space charged particle environment effect 0-69472  
 oxide nuclear fuel, fission gas release and swelling, simple operational model 0-92565  
 PMMA, reactor irradi., growth of macroscopic radiolytic gas bubbles, diffusion model 0-65058  
 polyethylene-polypropylene blend, extruded, thermal swelling and mech. characterisation 0-81110  
 1,2-polybutadiene, crosslinked in states of strain, entanglement networks, swelling anisotropy obs. 0-79666  
 polydimethylsiloxane chains, end-linked, swollen model networks, stress/strain isotherms and elastic modulus 0-79668  
 polydimethylsiloxane end-linked chains, nonGaussian effects 0-65127  
 polymer chain, scaling props., excluded vol. expansion, Monte Carlo study 0-96435  
 polymers, struct. determ. from elastostomometric parameters 0-64923  
 polymethacrylic acid, swollen networks, viscoelastic photoelastic behaviour 0-59366  
 polystyrene latex particles, swollen, aggregation studied by photon correlation spectrosc. 0-66886  
 polystyrene networks swollen in cyclohexane, swelling equil. and light scatt. at theta conditions 0-107036  
 polyvinyl alcohol networks, swelling equil. with dil. salt solns., thermoelastic behaviour, hydroxyl group interact. 0-79667  
 polyvinyl alcohol swollen in aqueous glycol, network thermoelasticity, interactions 0-104201  
 PTFE grafted membranes, struct.-properties relationships (*French*) 0-61136  
 rubber, natural, crosslinked by dicumyl peroxide, modulus, swelling relations 0-59551  
 sink strengths for thin film surfaces and grain boundaries 0-88207  
 steel, austenitic stainless, neutron dose rate depend. of swelling in fission reactors 0-104233  
 steel, austenitic-ferritic stainless, radiation swelling in fission reactors 0-65063  
 steel, stainless, cladding dimensional changes in FBR (U,Pu)O<sub>2</sub> fuel pins due to swelling and inelastic strain 0-104296  
 steel, stainless, EBR-II reflector assembly irradi. induced bowing, implications for core restraint design 0-104234  
 steel, stainless, fast neutron irradiated, solution annealed tubing, residual stress behaviour 0-65054  
 steel, stainless 316, soln. annealed, cavity alignment and precipitation during dual ion bombardment 0-70273  
 steel, stainless type 316, irradi. induced nuclear cladding swelling, empirical development of design equation 0-59527  
 styrene-divinylbenzene copolymers, porosity variation and swelling 0-97493  
 void swelling, nucleation theory 0-65038  
 void volume, swelling, errors in determ. by TEM 0-84208  
 Zircaloy-2, irradiation growth, shape and volume changes 0-92562  
 Al, Al ion irradiated, void swelling and annealing of voids, electron microscopy study 0-88216  
 Al film, deform. under He ion bombardment 0-65073  
 Al-Mg, Si alloy, void form. under different precip. conditions, after Al ion irradi. 0-59529  
 Cu-Fe (1.5 wt.%), precipitation-effect on void formation during electron irradiation 0-84211  
 Fe-Cr-Ti-Mo-Ti<sub>2</sub>O<sub>3</sub> (13, 3.5, 1.5, 2 wt.%) dispersion hardened, void swelling 0-65046  
 KMg<sub>2</sub>LiSi<sub>4</sub>O<sub>10</sub>F<sub>2</sub>-NaMg<sub>2</sub>LiSi<sub>4</sub>O<sub>10</sub>F<sub>2</sub>, solid soln., solid solubility and swelling characts. 0-59660  
 Na<sub>2</sub>O-B<sub>2</sub>O<sub>3</sub>-SiO<sub>2</sub>, mechanical strength and swelling in liq. 0-85024  
 Nb, He blistering, large swelling meas., gas press. model 0-88218  
 Nb, swelling correlation with local gas concentration following He irradi. 0-70271  
 Ni, ion irradi. with 20 and 500 keV <sup>4</sup>He<sup>+</sup>, depth distrib. of cavities and dislocation damage 0-107346  
 Ti-Al-V (6.4 wt.%), ion irradiated, microstruct. study using TEM 0-96572  
 Ti-Fe-C-Ni, ion irradiated, microstruct. study using TEM 0-96572  
 (U, Pu) C, nuclear fuel, irradiation induced creep meas. 0-93605  
 (U,Pu)C<sub>1-x</sub>N<sub>x</sub> LMFBR MX-type fuels, fission gas release and microscopic swelling 0-73921  
 (U,Pu)O<sub>2</sub>, reactor fuels, fission gas swelling, temp. and burnup depend. 0-63252  
 UO<sub>2</sub>, reactor fuels, fission gas swelling, temp. and burnup depend. 0-63252  
 Zr alloys, creep and growth, irradiation induced, rate theory approach 0-89294  
 Zr, void swelling during electron irradi., HVEM study 0-92559

**swept-frequency reflectometry**

No entries

**switchboxes** see *switchgear***switches**see also *relays; semiconductor switches*

- digital beam switch for agile beam laser radar 0-58620  
 duplexing switch with high isolation, for pulsed NMR spectrometer 0-86363  
 electron beam switch, microwave energy compression 0-96396  
 fibre, single-mode, optimised design 0-106607

**switches continued**

- fibre-optic, crossbar 0-74497
- fusion reactor, High Voltage Switch Tube, for Neutral Beam Power System 0-99291
- high voltage opening switch using spoiled electrostatic confinement 0-103205
- high-voltage water switches, streamer model 0-107002
- integrated astable optical multivibrator using Mach-Zehnder interferometric optical switches 0-87560
- Kalousek electromechanical switch, for potentiostatic conditions 0-85236
- laser triggering through fiber optics of a low jitter spark gap 0-107000
- liquid crystal electro-optic switch, four-port, for unpolarized fibre light 0-58715
- miniature triggered spark switch, high repetition rate 0-103203
- multimode 3×2 fibre optical matrix switch 0-58764
- optical bypass switch for fibre-optic data bus systems 0-99826
- plasma switches, high press. surface discharge, review 0-103208
- polarisation-conversion wavelength-selective fibre switches 0-58736
- polarisation-independent optical switch using weighted directional coupler 0-58798
- spark switches, high repetition rate, with Al and brass electrodes, surface ageing 0-106997
- triggered spark gap switch system, long life, high repetition rate 0-106998
- Hg wetted reed, heat treatment variations effects on Fe-Ni alloys surface conditions and on switch behaviour 0-66547

**switchgear**

- see also circuit breakers; switches*
- SF<sub>6</sub>-insulated substations, insulation design and co-ordination 0-100102

**switchgear testing**

- fusion reactors, interrupter and hybrid-switch testing 0-99289
- HV four-electrode field emission pre-ionised triggered spark-gap switches, 10 to 30 kV, parallel operation 0-70075
- SF<sub>6</sub>-insulated metal-clad, arcing, decomposition products and pressure rise 0-100101

**switching**

- see also electrical conductivity transitions; ferroelectric switching; magnetic switching; switches*
- bistable nonlinear Fabry-Perot resonator switching speed and energy calc. 0-64095
- fuel cell electrodes, galvanostatic switching curve shapes 0-66965
- MHD devices, plasma ionization instability, dynamic suppression, switching modelling 0-59308
- PMMA film in small area lateral MIMS device, cond., switching 0-97003
- semiconductor, IR switching, ultrafast optically controlled 0-58626
- Si-SiO<sub>2</sub> MIS systems, dynamic props. of switching, appl. to charge transfer devices 0-92997

**switching circuits**

- see also choppers (circuits); switching networks; trigger circuits*
- temperature regulator for inductive loads using IC zero voltage switch U 106 BS with triac (German) 0-77779

**switching equipment, telephone** *see telephone switching equipment***switching networks**

- see also minimisation of switching nets*
- matrix switching network for fibre-optic communication 0-58735

**switching systems**

- see also electronic switching systems*
- fusion reactor, MFTF, sustaining neutral beam power supply, shunt pre-conditioner, IBM-ASTAP anal. 0-102332
- integrated optical switching system with input modulator 0-99884
- optical fibre communication systems, low loss 4×4 switching network 0-58718

**switching transitions** *see electrical conductivity transitions***symbols** *see nomenclature and symbols***synchrocyclotrons**

- general orbit theory for accelerated particles in cyclotrons, appl. to synchrocyclotrons and omegatrons 0-74052
- injector, functional generator of controlling voltage of energy modulator 0-68975
- neutron beams of the Leningrad Institute of Nuclear Physics synchrocyclotron 0-87003

**synchronisation**

- biotelemetry system, with time division of channels 0-94386
- circuit for gas laser and camera synchronisation 0-73489
- clock synchronisation, India-W.Germany, relativistic corrections 0-95077
- clocks, Symphonie satellite appl. 0-68184
- diagnostic and treatment techniques 0-61727
- fast solid-state camera for high-speed event diagnostics 0-78985
- LASSO experiment on Spiro-2 spacecraft laser synchronisation from stationary orbit 0-82211
- lip synchronised recording technique for speech translation in cinefilms (Russian) 0-105737
- PCM encoding and decoding for optical memories 0-102658
- single mode fibre 1.1-1.3  $\mu$ m dispersion meas. by pulse synchronisation 0-64192
- sound triggered electronic photo flash unit, using variable time delay 0-57407

**synchronism** *see synchronisation***synchronous machines**

- rotary machines as I/O system for superconducting magnetic energy storage system, appl. (Japanese) 0-85306

**synchroscopes** *see cathode-ray oscilloscopes***synchrotron radiation**

- ACO storage ring, design of undulator, use as free electron laser 0-91334
- Aladdin storage ring, status of the Synchrotron Radiation Center of the University of Wisconsin, Madison 0-91326
- angle resolved photoelectron spectrometer for atoms and molecules 0-90932
- angular and spectral distrib., modified Bessel functions of fractional order 0-91738
- application to EXAFS and angle resolved photoemission spectros. (Korean) 0-74453
- atomic physics with synchrotron radiation 0-63583
- BESSY storage ring, 800 MeV dedicated light sources, choice of principal parameters and light source 0-91333

**synchrotron radiation continued**

- BESSY SX/700: a monochromator system covering the spectral range 3 eV  $\leq h\nu \leq 700$  eV 0-90952
- betatron oscillation linear coupling depend. 0-91345
- brightness of synchrotron radiation from electron storage rings 0-91330
- Cassiopeia A, supernova remnant, explanation of secular flattening of radio spectrum 0-101637
- channelled electrons in crystals quasi-synchrotron radiation characts. 0-92572
- CHESS—the Cornell high energy synchrotron source 0-91328
- CHESS synchrotron radiation facility, high energy tunable X-ray source 0-68984
- CHESS synchrotron source, photon position sensitive monitors 0-91336
- Compton scattering in sources with synchrotron reabsorption, rel. to quasars 0-72761
- Daresbury SRS, VUV and soft X-ray monochromators 0-90942
- flux measurement from SURF II storage ring using Si radiometer 0-90895
- galactic cosmic rays, contrib. to diffuse X-ray flux in 2 to 7 keV range 0-98745
- galactic nonthermal radio spectrum, rel. to cosmic ray electrons spectrum and gamma-rays prod. 0-62257
- galactic radio spectrum, influence of primordial black holes 0-62179
- galaxies, nearby, nonthermal radio continuum emission obs. (German) 0-109544
- grazing incidence for UV monochromators using toroidal holographic gratings 0-90946
- grazing incidence monochromators, optimisation for synchrotron radiation 0-90943
- grazing incidence monochromators with holographic toroidal gratings, 10 to 150 eV 0-90947
- holographic transmission diffraction gratings for soft X-rays 0-90965
- instrumentation, conf. Gaithersburg, MD, USA, June 1979 0-90607
- instrumentation utilising surface photoelect. effect 0-92927
- inverse synchrotron radiation, energy exchange between focused laser beam and free relativistic electron 0-74286
- LURE Rowland circle grazing incidence monochromator, performance 110 to 280 eV 0-90945
- molecular dynamics and photochem., synchrotron radiation obs. appls. 0-66830
- monochromator with three-wave Bragg diffr. 0-87993
- monochromators, conical diffraction mounting 0-91910
- monolithic monochromators for synchrotron radiation, 1 to 4 Å, order sorting, focusing and polarising 0-90955
- National Synchrotron Light Source basic design and project status 0-91329
- normal incidence monochromator, 2m high throughput, for SURF II storage ring 0-90951
- nuclear physics appls., review 0-106216
- optical synchrotron radiation interference effects 0-63906
- photodiode detector calibration using synchrotron radiation 0-90810
- photoelectron spectroscopy, solid-state, with synchrotron radiation, review 0-71570
- radiationless transitions, synchrotron radiation obs. 0-63706
- radio sources, compact, extragalactic, interpretation of spectra 0-62299
- radio sources, form. of universal and diffusion regions of relativistic electrons non-linear spectra 0-109555
- radiometry, synchrotron radiation as an absolute standard source 0-90879
- rare earth germantes, flux-grown, X-ray topography 0-64939
- section topograph technique, high resolution, applicable to synchrotron radiation sources 0-57449
- soft X-ray microscopy/lithography branch line at SSRL 0-91344
- sources, props. and characts. 0-62729
- spectra, radio and electron, effect of interstellar mag. field inhomogeneities 0-85849
- spectrometer for 100 to 130 nm 0-90953
- spectroscopic applications, properties, characteristics as radiation source (Norwegian) 0-63420
- spectroscopy of fast fluoresc., nanosec. range 0-62736
- Stanford Synchrotron Radiation Laboratory, status report 0-91327
- storage ring design considerations for parasitic use of synchrotron radiation in the infrared 0-91340
- storage rings, expt. enclosures and beam line safety components 0-91341
- straight groove toroidal grating monochromators, 10 to 500 Å, design optimisation for synchrotron radiation 0-90944
- SURF II storage ring, status report 0-91325
- surface atomic and electronic struct. studied with synchrotron radiation 0-80945
- time resolved X-ray scattering, synchrotron radiation camera and data acquisition system 0-99023
- transition rates in intense-field regime 0-77991
- ultra-high-vacuum double crystal monochromator beam line for studies in the spectral range 500-4000 eV 0-90957
- undulator for the 700 MeV VUV-Ring of the National Synchrotron Light Source 0-91337
- UV beamlines for National Synchrotron Light Source 0-91342
- vacuum UV circular dichroism spectroscopy using synchrotron radiation 0-91575
- Vela pulsar (PSR 0833-45), synchrotron radiation model for optical and gamma-ray emission 0-94824
- VEPP-2M storage ring, synchrotron radiation use to test VUV detectors absolute efficiency 0-82824
- VUV 4 m normal incidence monochromator 0-90950
- VUV beam line instrumentation for National Synchrotron Light Source storage ring 0-91343
- VUV monochromators, 10 to 300 Å for synchrotron radiation, evaluation 0-90907
- VUV monochromators with toroidal holographic gratings, Strehl criterion 0-90949
- wiggler magnets, use as synchrotron radiation source at SPEAR storage ring 0-91332
- X-ray focusing mirror 0-90961
- X-ray interferometry, appl. of synchrotron radiation 0-90954
- X-ray lithography using synchrotron radiation, resist sensitivity 0-62820
- X-ray microscopy, high resolution, for chem. microanal. 0-81416
- X-ray monochromator development for synchrotron radiation facilities 0-91351
- x-ray monochromator geometry for focusing synchrotron radiation above 10 keV 0-90958



**synchrotron radiation continued**

- X-ray monochromators, channel-cut, identification of spurious reflections 0-90959
- X-ray topography, appl. of synchrotron radiation from electron storage rings 0-64830
- X-ray topography, developments, review 0-64836
- X-ray transmission diffraction gratings for synchrotron rad. sources, modelling 0-90964
- XUV mirror reflectivities from 50-150 eV 0-90966
- XUV monochromator design for use with synchrotron radiation sources 0-90940
- Al-Cu, type 1100, synchrotron radiation microradiography 0-85121
- Al-Cu-Mn, type 2219, synchrotron radiation microradiography 0-85121
- Ar, K inner-shell level energies, absorpt. spectroscopy with synchrotron radiation 0-99583
- Ar, spin-polarised photoelectrons by circularly polarised synchrotron radiation 0-91516
- Kr, K inner-shell level energies, absorpt. spectroscopy with synchrotron radiation 0-99583
- Kr, spin-polarised photoelectrons by circularly polarised synchrotron radiation 0-91516
- LiF, anisotropic Compton scattering using synchrotron radiation 0-60703
- OH(A<sup>2</sup>Σ<sup>+</sup> → X<sup>2</sup>Π<sub>g</sub>) yields from H<sub>2</sub>O photodissoc. 0-71927
- Si radiometer for storage ring synchrotron radiation 0-86411
- Se, L<sub>1</sub>, L<sub>2</sub>, L<sub>3</sub> inner-shell level energies, absorpt. spectroscopy with synchrotron radiation 0-99583
- Xe<sup>2+</sup>, synchrotron radiation excited, time resolved spectroscopy 0-69092

**synchrotrons***see also cosmotrons*

- AES sources for use at low energy 0-77913
- chromaticity correction in KEK main ring 0-74049
- KEK synchrotron, proton attenuation lengths in paraffin, concrete and iron around targets 0-102412
- large multiwire proportional chambers for experiment NA3 at the CERN SPS 0-102388
- optical reflector for energy extraction 0-78467
- proton, magnetisation of ferrites in tunable accelerating resonators 0-68983
- Saturne experimental facilities, energies and types of particle (French) 0-78465
- SIRIUS, experimental study of the spectral, angular and polarization properties of undulator radiation 0-91338
- ZGS, 30" bubble chamber 0-91304
- ZGS, conception to turn-on 0-91298
- ZGS, construction history 0-91299
- ZGS, design engineer's view 0-91315
- ZGS, early adventures 0-91301
- ZGS, Effective Mass Spectrometer 0-91310
- ZGS, experimental area operations 0-91316
- ZGS, external proton beams 0-91307
- ZGS, highlights and speculations 0-91324
- ZGS, history, conference, Argonne, IL, USA (Sept. 1979) 0-90600
- ZGS, history as seen from Washington 0-91323
- ZGS, non high energy physics programs 0-91320
- ZGS, operations 0-91319
- ZGS, polarised beam history 0-91311
- ZGS, polarised beam program 0-91312
- ZGS, polarised beam results, review 0-99361
- ZGS, polarised targets 0-91309
- ZGS, role in high energy physics 0-91306
- ZGS, scientific program start-up 0-91302
- ZGS, strong interaction counter expts. 0-91305
- ZGS, superconducting magnet bubble chambers, history 0-91368
- ZGS, technical history 0-91313
- ZGS, the peak years 0-91303
- ZGS, titanium vacuum chamber installation 0-91317
- ZGS, universities role in the seventies 0-91322
- ZGS, visual reminiscences 0-91321
- ZGS as seen from the midnight shift 0-91314
- ZGS history, the early stages 0-91297
- ZGS history, universities' role 0-91300
- ZGS streamer chamber and kaon physics 0-91308
- ZGS technician's view of high energy physics 0-91318

**synoptic climatology** *see climatology***synthetic rubber** *see rubber***system failure and recovery***see also operating systems (computers)*

- optical long focal length aerial reconnaissance system response to thermal shock 0-78939

**system recovery** *see system failure and recovery***system theory**

- see also artificial intelligence; identification; information theory; modelling; pattern recognition; simulation*
- biology and medicine, systems theory, importance and motivations (Spanish) 0-104549
- energy system synthesis, solar energy system 0-76614
- materials science, concept of system 0-101003
- measurement techniques, error anal. using information, signal and system theory (German) 0-68164

**systems analysis**

- wear, systems anal. and description (German) 0-103417

**systems design** *see systems analysis***systems engineering***see also systems analysis*

- electro-optics, systems aspects, seminar, Huntsville, AL, USA (May 1979) 0-94921
- heat transfer, artificially intelligent problem solver, system design outline 0-99916
- holographic one-tube goggle 0-78988
- measurement engineering development trends (German) 0-86243
- optical design, fabrication and operation 0-95986

**systems programming** *see systems analysis***systems software***see also operating systems (computers); program processors*

- cephalometric tracing processing system, software development (Japanese) 0-94409

**Szillard-Chalmers reactions** *see radiochemistry***T invariance**

- cosmic matter-antimatter asymmetry and gravitational force 0-90586

**T invariance continued**

- Glauber model and time reversal invariance 0-91020
- massive particles with any spin. consistent eqns., Klein-Gordon divisor, review 0-73577
- mechanical systems, follower load type, time invariant functionals 0-77609
- nucleon decay, T violation possibility and consequences in superunified theories 0-82917
- Poincare group, irreducible representations of groups containing subgroup of finite index 0-68384
- quantum field theory, relativistic, discrete symmetries 0-68387
- quantum gravity and time reversibility 0-82704
- Racah time reversal and K<sub>2</sub><sup>0</sup> decay problems 0-78056
- superheavy boson decay, neutrino number and isotropy of Universe in grand unified theories 0-85852
- D → K\*μν, in e<sup>+</sup>e<sup>-</sup> annihilation, T-odd asymmetry in CP violation model (Russian) 0-105885
- K<sub>2</sub><sup>0</sup> → Kπ, k=2 or 3, Racah time reversal, a C,P,T scheme 0-78056
- K<sub>1</sub><sup>0</sup> → π<sup>+</sup>μ<sup>+</sup>μ<sup>-</sup>, transverse polarisation of μ, violation of time-reversal invariance 0-68448
- μ decay correlations and lifetime meas. 0-77996
- τ → K\*πν, in e<sup>+</sup>e<sup>-</sup> annihilation, T-odd asymmetry in CP violation model (Russian) 0-105885
- τ → μνππ, T-violation effects, neutrino mass (Russian) 0-95294
- <sup>191</sup>Ir 129 keV transition, atomic screening, time reversal violation 0-106011

**Ta** *see tantalum***table lookup***see also data handling*

- formant frequency and bandwidth conversion to reflection coefficients 0-91975
- truth-table look-up optical processing utilizing binary and residue arithmetic 0-69334

**table-top computers** *see minicomputers***tables (data)** *see collections of physical data***tachometers***see also angular velocity measurement*

- digital, error analysis 0-90832
- optical, with contamination prevention 0-73344

**tachyons**

- classical special relativity mechanics, classical particles with unusual props. 0-77615
- fluid droplet model in framework of two centres particles 0-105868
- massless 't Hooft model, tachyonic modes, vanishing of scalar density 0-77949
- Minkowski space, complex, superluminal boost in x-direction, Lorentz transformation, tachyonic connections 0-105497
- relativity, special, 6-D, centre-of-mass frames of pairs of particles, bradyons, luxons, tachyons 0-77614
- superluminal Lorentz transformations, imaginary units, motion of tachyon 0-86082
- two-body interactions, tachyon exchange 0-82960

**tackiness** *see adhesion***TADMR** *see microwave-optical double resonance***tandem accelerators** *see particle accelerators***tantalum***see also nuclei with .....*

- atom, 5d level open shell interactions, 304 Å photoelectron spectrum 0-87087
- atom, L-shell internal excitation accompanying L-capture 0-95726
- BCC lattice, strain ordering in interstitial solutions 0-107420
- diffusion of H<sub>2</sub>, isotope effects, crystal field stabilisation 0-59728
- diffusion of H and trapping 0-70447
- diffusion of O and N, statistical calcs. on Arrhenius lines 0-59722
- electrical resistivity due to interstitial H (D) 0-96848
- electron-phonon interaction, relativistic, APW calc. 0-92837
- electronic structure, thermoreflectance studies 0-76047
- film on sapphire substrate, orientational growth, epitaxial textures, nucleation textures (Russian) 0-75454
- films, vac. evaporated, optical cond. 0-76100
- high temp. radiative props., expt. determ., spectral emissivities 0-74718
- hydrogen embrittlement, effect on ductility (Japanese) 0-66636
- ion induced continuum emission 0-89025
- ion plated with Pd and Ni, prep., H<sub>2</sub> absorption and desorption rate (Japanese) 0-108358
- lattice dynamics, local frequency spectrum, mean thermal displacement of H 0-59604
- luminescence characteristics of pure surfaces acted on by flux of field emission electrons 0-100695
- SEM exam., ultra-high vacuum, secondary electron emission dependence on electron beam dose, surface interactions from AES and ELS 0-61209
- shear elastic constant, anomalous temp. behaviour, US study 0-79855
- sputtering, low energy, H, D and He ions 0-100734
- superconductive transition point as reference temp. 0-107943
- superconductor, effect of changes in α<sup>2</sup>(Ω)/Ω(Ω) on the zero-temp. energy gap 0-97025
- surface, nonstationary heating and oxidation in low temp. plasma flow, heat and charge transfer obs. (Russian) 0-104341
- surface, simultaneous interactions with Cl<sub>2</sub> and O<sub>2</sub> under low press. and high temp. 0-71938
- surface (111), electroluminescence in 200 to 630 nm range 0-103997
- thermal cond. and emissivity meas. using imaging furnace 0-103667
- thermal conductivity, 4.5 to 200K (Russian) 0-103665
- thermophysical props. and neutron absorpt. 0-103488
- thin film, elec. cond., strain gauge factor, ion bombardment effects 0-80417
- thin film deposition by high current ion beam sputtering, struct. and elec. props. 0-59837
- Ag/RbAg<sub>4</sub>I<sub>5</sub>/Ta, solid electrolyte timing cell and coulometer 0-68216
- Ni-Ta, ion-implanted, laser irradi. effect 0-108306
- Ta, resistivity due to H incorporation 0-70666
- Ta-Nb superimposed metallic layers, ionic movements during anodization, Rutherford backscatt. and nuclear microanal. 0-71913
- Ta-Si, interface modification by ion implantation 0-70475
- Ta-Ta<sub>2</sub>O<sub>5</sub>-Ag junctions, polarity-depend. tunnelling cond. 0-70846
- Ta-Ta<sub>2</sub>O<sub>5</sub>-InP thin refractory MIS struct. deposition 0-75647

**tantalum** continued

- <sup>182</sup>Ta Mossbauer sources (*French*) 0-74064  
 TiO<sub>2</sub>-Ta, slightly doped, elec. cond. and defect struct., charge compensation, point defect model 0-75568

**tantalum alloys**

- see also *tantalum compounds*  
 magnetic susceptibility and Knight shift meas., d-metal alloys 0-66055  
 Co-Ta, dendritic segregation 0-76260  
 Fe-Co-Mo-Ta semihard mag. alloy, mag. props., thermal expansion, elec. resistivity and hardness (*Japanese*) 0-88789  
 Fe-Mo-Ta, ternary Laves phase strengthening 0-108466  
 Fe-Ta, nuclear mag. moment of <sup>182</sup>Ta NMR-ON study 0-78139  
 Nb-Ta, resistivity due to H incorporation 0-70666  
 Nb-Ta alloys, H diffusion at 296K 0-84329  
 Nb-Ta-Si, ductile amorphous, superconductivity 0-60131  
 Nb-Ti-Ta, pinning curves, high field J<sub>c</sub> and scaling behaviour 0-93064  
 Nb-Ti-Ta, superconductor optimisation for 12 Tesla toroidal field coils 0-91272  
 Nb-W-Zr-Ta (90, 4.5, 3.5, 2 wt.%) creep and creep limit in super vac. at 1100°C, heat treatment effect 0-81133  
 Nb<sub>3</sub>Ta<sub>4</sub>, effects of hydrostatic pressure on changes in elastic consts. caused by addition of H 0-75287  
 Ni-Al-Ta dendritic monocrysts., directionally solidified, coarsening kinetics 0-108425  
 Ni-based TaC eutectic, directionally solidified, elastic moduli 0-84984  
 Ni-Cr-Al-TaC, eutectic composite, microstructure, fatigue props. 0-85038  
 Ni-Cr-Co-Al-W-Mo-Ti-Ta, heat resist. and struct., Ta effect 0-76312  
 Ni-Cr-Ta system, phase equilib. of Ni rich region at 1523 and 1273K 0-93541  
 Ni-Cr-Ta-Ti-Si, EP557 precipitation hardening alloy, mech. props., heat treatment effect 0-60877  
 Ni-Ta (70, 30 wt.%) metallic glass, struct. and crystn. (*Russian*) 0-70136  
 NiTaC eutectic superalloy, casting, furnace atm. effects 0-84880  
 Ni<sub>3</sub>Ta<sub>0.5</sub>, conservative domain struct., TEM study 0-79776  
 Ta-Al-C phase diagram and lattice constants, X-ray diff. method 0-89207  
 Ta-Cr-Si-Al, heat resistive films, prepared by sputtering, lifetime meas. 0-80132  
 Ta-Ga, crystal struct. at high press., polymorphism 0-88112  
 Ta-H, fracture modes (*Japanese*) 0-66636  
 Ta-H, physical properties, plastic deformation, H ordering (*Ukrainian*) 0-71689  
 Ta-H system, acoustic emission induced by hydride formation 0-76257  
 Ta-H system, phase diagram and transforms., struct. obs. of various phases 0-104125  
 Ta-Ir(Rh) system glasses, form., crystn. and microhardness, resist. obs. 0-89178  
 Ta-N(O)(C) system, specimen prep. for metallography (*German, English*) 0-89439  
 Ta-Rh,  $\sigma$ -phase alloy, superconductivity and resistance behaviour 0-70882  
 Ta-W, thermoelec. power, 4.2 to 300K 0-70684  
 TaB<sub>2</sub>-Cr-Si-Al, heat resistive films prepared by sputtering, lifetime meas. 0-80132  
 Ta(C,N)-Ni-VC, sintering behaviour, VC effect 0-93520  
 $\alpha$ -TaH<sub>3</sub>, electronic struct., thermoreflectance studies 0-76047  
 Ta<sub>20</sub>Nb<sub>80</sub>, Abrikosov vortex formation kinetics (*Russian*) 0-93055  
 Tb-Ta, dil. elec. quadrupole interaction, temp. and press. depend., TDPAC meas. 0-60469  
 Ti-Nb-Zr-Ta, superconducting props. comp. depend., stress effects and precipitation behaviour, X-ray scatt. 0-93059  
 Ti-Ta (4.37 wt%), oxidation kinetics, 1258-1473K, and at pressure of 0.013, 0.133 and 1.0 bar 0-89411

**tantalum compounds**

- see also *tantalum alloys*  
 minerals, cryst. struct., X-ray powder diff. study 0-107169  
 siltal cylindrical shell reinforced with internal stiffening ribs, stress-strain state under external press. 0-71684  
 Al-anodised Ta<sub>2</sub>O<sub>5</sub>/native oxide-n-GaAs MOS structure evaluation 0-84514  
 Al-Ta<sub>2</sub>O<sub>5</sub>-Al, heating of defects in dielec. film by anodisation 0-65406  
 Ba<sub>4</sub>TaRu<sub>3</sub>O<sub>12</sub> (Ru<sub>2</sub>O<sub>12</sub>)<sup>13-</sup> cluster obs. in presence of orbital degeneracy and spin-orbit coupling (*French*) 0-70655  
 Fe-TaS<sub>2</sub>, metallic, mag. susceptibility at low temp. 0-70972  
 KTa<sub>1-x</sub>Nb<sub>x</sub>O<sub>3</sub>, holographic storage using photorefractive effect, dielectric const. 0-78800  
 K<sub>1+x</sub>Ta<sub>1-x</sub>W<sub>1-x</sub>O<sub>6</sub> pyrochlore system, comp. depend. of ionic cond. 0-107517  
 Li-TaS<sub>2</sub>, chem. diffusivity of Li at 30°C 0-59737  
 Na<sub>1+x</sub>Ta<sub>1-x</sub>W<sub>1-x</sub>O<sub>6</sub> pyrochlore system, comp. depend. of ionic cond. 0-107517  
 (Nb,Ta)<sub>2</sub>N<sub>3</sub>, cryst. struct. determ. (*German*) 0-107145  
 Rb<sub>10</sub>Ta<sub>20</sub>O<sub>78</sub>, layered cryst. struct. 0-107166  
 Ta-Al-N thin film resistors with improved elec. props. 0-100544  
 Ta-H(D), anelasticity due to long-range diffusion 0-60904  
 Ta-H(D), H ordering, review 0-60850  
 Ta-O(N), dislocation pinning, impurity interactions, strengthening (*Russian*) 0-92532  
 Ta-Ta<sub>2</sub>O<sub>5</sub>-Ag junctions, polarity-depend. tunnelling cond. 0-70846  
 Ta-Ta<sub>2</sub>O<sub>5</sub>-InP thin refractory MIS struct. deposition 0-75647  
 TaB<sub>2</sub>-Cr-Si-Al, heat resistive films prepared by sputtering, lifetime meas. 0-80132  
 TaC and Ta<sub>2</sub>C, self-propag. high-temp. synthesis 0-60815  
 TaC, etchant for revealing microstructure 0-85097  
 TaC, pressing regime influence on high-temp. creep (*Russian*) 0-100852  
 TaC, sputtering, low energy, H, D and He ions 0-100734  
 TaN diffusion barrier in Si device metallisation 0-65304  
 TaN, energy band struct. calc., symmetrised APW method 0-96784  
 TaN<sub>3</sub>, films, thermal oxidation and resist. 0-60125  
 Ta<sub>2</sub>N, films, thermal oxidation and resist. 0-60125  
 Ta<sub>2</sub>N, thin film deposition by closed anode bias sputtering (*Japanese*) 0-93484  
 2Ta<sub>2</sub>O<sub>5</sub> thin film, FCC cell struct. investigation 0-92796  
 Ta<sub>2</sub>O<sub>5</sub>, amorphous and cryst., elec. cond. mechanism, admittance meas. 0-70705  
 Ta<sub>2</sub>O<sub>5</sub> film, reactively sputtered on Si, dielectric and optical props. obs. (*Bulgarian*) 0-89144  
 Ta<sub>2</sub>O<sub>5</sub> film, refractive index 0-84792

**tantalum compounds** continued

- Ta<sub>2</sub>O<sub>5</sub> film capacitive humidity sensor Panahume (*Japanese*) 0-105658  
 Ta<sub>2</sub>O<sub>5</sub> film on Al, Cu, Au, Ag electrode, electric strength of MIS system 0-96999  
 Ta<sub>2</sub>O<sub>5</sub> inversion layers for Si solar cells 0-94075  
 Ta<sub>2</sub>O<sub>5</sub>, with hexagonal lattice in thin layers, atomic struct., electron diff. 0-84160  
 TaS<sub>2</sub>, 1T and 1H polytypes, fast neutron irradi., defect prod., effects on resist. and charge density waves 0-65060  
 TaS<sub>2</sub> (1T) electron irradiated, lattice contraction 0-59520  
 TaS<sub>2</sub> intercalate with tetraalkylammonium hydroxide, prep. and struct. 0-79752  
 TaS<sub>2</sub> intercalated with methylamine, supercond. layer cpd., crit. field enhancement and reduced dimensionality 0-60152  
 TaS<sub>2</sub> intercalated with organic cpds., upper crit. fields and reduced dimensionality 0-70910  
 TaS<sub>2</sub>-2H electrodes, topotactic reduction mechanism, neutron diff. obs. and intercalation cpd. form. 0-108748  
 TaS<sub>3</sub>, monoclinic form, cryst. struct. determ., Peierls type transition obs. (*French*) 0-88109  
 TaS<sub>2</sub>(NH<sub>3</sub>) and TaS<sub>2</sub>(NH<sub>3</sub>)<sub>1/3</sub>(H<sub>2</sub>O)<sub>2/3</sub>, incoherent inelastic neutron spectra 0-84163  
 TaSi<sub>1.5</sub>Se<sub>0.4</sub>, pure and intercalated with organic cpds., upper crit. fields and reduced dimensionality 0-70910  
 TaS<sub>2-x</sub>Se<sub>x</sub> (1T), transport props. 0-103710  
 2H-TaSe<sub>2</sub>, 2D dispersive modulation, struct. using superspace-group concept 0-79726  
 TaSe<sub>2</sub> (2H), CDW and discommensurations, <sup>77</sup>Se NMR study 0-88883  
 TaSe<sub>2</sub> (2H), Raman scatt. from CDW 0-93340  
 TaSe<sub>2</sub> (2H) CDW, reentrant lock in transition at high press. 0-88320  
 TaSe<sub>2</sub>, superconducting transitions and diamagnetism 0-84526  
 TaSi<sub>3</sub> film, elastic stiffness and thermal expansion coeffs. 0-107451  
 TaSi<sub>3</sub> films, on polycrystalline Si, oxidation characts. 0-97602  
 TaSi<sub>3</sub> refractory formation by As<sup>+</sup> ion beam bombardment 0-107286  
 Ta<sub>2</sub>Si<sub>3</sub> and TaSi<sub>3</sub> form. in thin computerized (Ta+Si) films on polycryst. Si and SiO<sub>2</sub> 0-70546  
 Ta<sub>1-x</sub>Ti<sub>x</sub>S<sub>2</sub> (1T), magnetoresistance in the Anderson localized states near the metal-nonmetal transition 0-88479  
 Ta<sub>1-x</sub>Ti<sub>x</sub>S<sub>2</sub> (1T), magnetoresist. near metal-nonmetal transition at ultra low temps. 0-88600  
 TiH, ab initio SCF calcs. using relativistic effective core pot. 0-95524  
 Ti<sub>1+x</sub>Ta<sub>1-x</sub>W<sub>1-x</sub>O<sub>6</sub> pyrochlore system, comp. depend. of ionic cond. 0-107517  
 ZrO<sub>2</sub>-YO<sub>1.5</sub>-Ta<sub>2</sub>O<sub>5</sub>, cubic fluorite phase, elec. cond. 0-107551  
 6.14ZrO<sub>2</sub>-Ta<sub>2</sub>O<sub>5</sub>, elec. cond. meas. 0-100463

**tantalum electrolytic capacitors** see *electrolytic capacitors***tape recorders**

- see also *magnetic heads; magnetic recording*  
 bat detection instruments 0-69609  
 biomedical ECG recording, correction of timing errors due to tape speed variation 0-72354  
 dual capstan drive tape recorder (*German*) 0-95092  
 EEG recording system, portable pulse-interval modulation telemetry/multiplexing system, home use 0-67261  
 read head for magnetic tape recorders using magneto-resistance principle 0-87688  
 smoking pattern recorder, portable 0-94385  
 thresholds of pain and hearing, cassette recorder noise and music levels (*German*) 0-81616  
 time reference signal for tape recording, IRIG and NASA code formats 0-57262

**taste** see *chemicoception***Taylor instability** see *flow instability***t.d.m.** see *time division multiplexing***teaching**

- see also *demonstrations; education; student laboratory apparatus; training*  
 Abraham-Minkowski controversy, EM momentum in static fields 0-101678  
 AC power line, reasons for grounding (earthing) 0-77594  
 aids and materials 0-94942  
 alkali metals, cohesive energy 0-90630  
 analytical chemistry, role of audio-visual learning aids laboratory 0-94944  
 approximation methods for 0-105474  
 astronomy, infrared, 3K cosmic background radiation, star form., nuclei of active galaxies 0-67958  
 astronomy, use of computers in schools 0-73126  
 ball and spring, elliptical motion 0-82613  
 bi-lingual audio-visual aids for technical education in developing Arab countries 0-94943  
 blind students, musical acoustics course 0-77584  
 Born's discovery of the quantum-mechanical matrix calculus 0-82615  
 Brewster angle in semi-infinite dielectric moving perpendicularly to interface 0-57034  
 Bronx High School of Science, physics teaching 0-77562  
 Brownian motion, melting, surface tension and rubber networks, thermodynamic anal. 0-73132  
 centrifugal buoyancy forces from energy considerations 0-82609  
 circular motion with friction, numerical and analytical solns. 0-57029  
 classical inverse scattering in one dimension 0-82595  
 classical mechanics gauge invariance, derivation of Maxwell's eqns. 0-73131  
 classical mechanics operator formulation, wave packets in config. space 0-73137  
 college astronomy and physics texts, readability 0-77583  
 continuity equation, 1-dimens., for unsteady flow 0-82598  
 Coriolis phenomenon in nuclei and planets, rot. alignment 0-90636  
 deep one-dimens. periodic pot., zero energy gaps, Kronig-Penney model 0-62426  
 degree-day measurements 0-77574  
 dimensional analysis, modification and generalisation in physics teaching 0-105481  
 dipole relaxation in electric field 0-90625  
 dynamic load line construction 0-67963  
 dynamics, infinitesimal rotations, invalidities in usage 0-57036  
 eigenvector of general rot., geometrical construction 0-57025  
 Einstein's General Theory of Relativity and press reaction 0-57075  
 electromotive force: Volta's forgotten concept 0-73143



## teaching continued

- electron microscopy, autotutorial methods utilizing sound-on-slide presentations 0-73534  
 electron optics, charged particle trajectory calc. in electrostatic field 0-90635  
 electronics, undergraduate laboratory course 0-105478  
 electronics study group, integrated circuit appls. (*German*) 0-67970  
 elementary particles since  $J/\psi$  review 0-57018  
 emission from blackbody, thermodynamic laws 0-105451  
 equivalence principle, monkey and hunter demonstration 0-67984  
 equivalent electrons,  $J$  allowed values in jj coupling 0-90624  
 exponential growth factors, determ. by Mangelsdorf's method 0-67980  
 exterior algebra and exterior differential forms for electromagnetic problems 0-57037  
 feedback, sequential test methods and quality criteria (*German*) 0-67968  
 Feynman path integral and gauge invariance 0-82601  
 Fraunhofer diffraction patterns, from apertures illuminated with nonparallel light 0-67983  
 Fresnel's eqn. for light reflection and refraction 0-101688  
 gauge symmetry breaking, geometrical approach, superconductivity and spontaneous symmetry breaking 0-57028  
 geometrical optics, advanced, for engineers, matrix algebra methods 0-62415  
 geometrical optics, lens Fourier transform properties 0-57024  
 geophysics, applied MSc programme in Nigeria 0-105463  
 granular materials, size effects in cond. and supercond. 0-77581  
 Gurney's ballistics calc. 0-67946  
 Hamilton's principle for canonical equations of motion 0-105464  
 harmonic oscillator wavefunctions, asymptotic behaviour 0-67979  
 harmonic plane waves, particle displacement 0-73138  
 holography, intensity ratio setting method 0-77588  
 Hooke's law, potential energy curve 0-67961  
 human body, live, thermodynamics of cooling for treatment purposes 0-73128  
 hydrogenlike atoms, spin-orbit terms derivation 0-73148  
 improper integrals, programmable pocket calculator calcs. 0-101696  
 interference fringes of Fresnel double mirror, localised and unlocalised, theory extended to wedge 0-67960  
 international organisations for physics teaching 0-77561  
 isotropy of light velocity convention 0-101689  
 Joule's constant determination, large scale 19<sup>th</sup> century expt. method 0-77572  
 Kepler ellipse, symmetry prop. of vel. 0-101694  
 lateral-angular magnification relationship for simple magnifier 0-57031  
 light reflection and refraction, analogue model 0-67948  
 light velocity meas., nuclear timing technique 0-90637  
 linear programming, introduction and appl. to simple cct. 0-73136  
 liquid crystals, crystal display, cyclobiphenyl compounds 0-67962  
 localised interference fringes 0-101680  
 Lorentz transformation, accel. 0-90639  
 magnetic multipole expansion 0-105456  
 magnetic objects, current loops, thermodynamics 0-90633  
 mathematics, remedial work for university students in engineering courses 0-86054  
 mathematics module, description and evaluation 0-86056  
 mathematics teaching by computer, long-division practice program in BASIC 0-98775  
 matrix optics, principal plane concept generalisation 0-73140  
 mesh analysis using graph theory, generalised procedure 0-101681  
 metrological research on prospective measuring techniques, conf. Wroclaw, Poland, Sept. 1978 (*Hungarian*) 0-86247  
 microcomputers in education, hardware, software and personnel problems 0-98771  
 microcomputers in schools, software and equipment choice 0-98772  
 microscopy, course at North Carolina State University 0-95135  
 momentum flow as force, alternative conceptualisation for teaching mechanics 0-67993  
 Moseley's expts.:  $K\alpha$  line freqs., rel. to at. number, reinterpretation 0-82616  
 musical complex tones, interval-based representations 0-101684  
 N-body disintegration theory, Maxwellian distrib., nuclear appls. 0-57033  
 nonequilibrium phase transitions, stability and dissipation 0-105479  
 nonspreading wave packets, physical interpretation of Berry Balazs wave function 0-57040  
 numerical analysis, interactive teaching package 0-86058  
 one-dimensional oscillator systems, density of states-frequency theorem 0-82602  
 operational amplifier behaviour, review 0-67959  
 operator props. through three-dimens. rot. 0-105469  
 optics, faculty of Inst. of Optics, profile 0-62422  
 optics, graduate training at Optical Sciences Centre, programmes 0-62418  
 orbital angular momentum and parity 0-77564  
 orbital angular momentum eigenvalues, integrality calcs. 0-67977  
 orbital motion on an interactive-graphics terminal, teaching appl. 0-73152  
 paradoxes in teaching 0-105453  
 particle collisions, conservation of energy and conservation of vector momentum 0-101693  
 particles, angular momentum in centre-of-mass frame 0-90631  
 performance assessment, sequential test method in physics (*German*) 0-67969  
 PET 2001, multidisciplinary summer course for schoolchildren 0-98774  
 photon emission from mol. and electronic transitions, quantum dynamics, semiclassical description 0-105466  
 physics, changes in methods, emphasis and subject matter 0-77587  
 physics, dialectical approach (*German*) 0-68006  
 physics, performance assessment and control (*German*) 0-73127  
 physics, performance assessment rel. to syllabus (*German*) 0-67967  
 physics, practical exercises (*German*) 0-68007  
 physics, use of models, pedagogical approach rel. to history of science 0-77567  
 physics 13: teaching modern physics through science fiction 0-90626  
 physics computer-aided teaching, hinted finding scheme, simulation appls. (*French*) 0-98777  
 physics homework solutions, recording methods 0-77573  
 physics students, mathematics ability 0-77591  
 physics teaching aids, convention of secondary school physics teachers (*Hungarian*) 0-67957  
 physics teaching and personality development assessment (*German*) 0-67966

## teaching continued

- physics teaching using SWTP 6800 system in BASIC 0-98776  
 Piagetian-type testing, engineering and liberal arts majors at Cornell, performance 0-67955  
 planar electrostatics 0-90623  
 plasma waves, delay line simulation, wave propag. in dispersive and attenuating media 0-82606  
 probability games, modelling stellar evolution and fusion 0-77590  
 proportional navigation 0-82611  
 pseudostationary wave, anal. 0-82605  
 quantum clocks, time meas. 0-90632  
 quantum pendulums, classical, semiclassical and quantum aspects 0-101679  
 quasar redshifts, teaching consideration 0-90621  
 radiation safety in laboratories 0-73154  
 radioactive dating and population growth by dice game 0-57030  
 regression line analysis 0-73144  
 relativistic motion in a plane 0-101686  
 relativity, physicists' reactions and popular attitudes, historical account 0-77602  
 resistance variation with temperature 0-77575  
 rotation operators, time-depend. aspects 0-90634  
 Rutherford's scattering formula via the Runge-Lenz vector 0-73141  
 Saha equation, elementary derivation, rel. to mol. dissociation 0-82599  
 SCF calculations on LiH for undergraduates 0-82597  
 schools specialised in physics and mathematics (*Hungarian*) 0-67956  
 Schrodinger eqn. solns. using approximate nucleon-nucleon and  $\Lambda$ -nucleon pots. 0-62429  
 science, use of models 0-77566  
 SEM, methods for short courses 0-73533  
 SEM, slide/tape modules 0-68005  
 SEM, video tape appls. 0-68004  
 SEM teaching philosophy and methodology 0-67964  
 semiclassical scattering theory, spurious excitation 0-73142  
 SI metric units, in college phys. texts 0-101697  
 simple DC circuits, student concepts 0-77569  
 single slit diffraction, theory testing expt. 0-77568  
 snow and avalanche phenomena 0-57044  
 solid angle, relativistic transformation 0-101683  
 solid state physics, review of experimentation, undergraduate level (*Spanish*) 0-82624  
 sound reproduction systems, high fidelity, components and characts. 0-77582  
 speed, Galilean and Einsteinian concepts, vel., rapidity and celerity 0-73130  
 speed and displacement relations for tire skids, program for PET 0-57038  
 spin-1 matrices, props. 0-101695  
 spiral spring, (nonhelical) simple harmonic motion, Bessel functions, closed form solns. 0-57026  
 stationary waves 0-67999  
 supernovae in binary systems: an application of classical mechanics 0-62428  
 supply and demand phenomena, math. anal. 0-77589  
 Sygne's triads of null rays 0-73146  
 time evolution operator in quantum mechanics 0-82610  
 TRS-80, teaching at Keene High School 0-98773  
 twin paradox in special relativity 0-105465  
 $v=gt$  expression, origins of derivation 0-77593  
 vectors in physics teaching (*German*) 0-82623  
 vibrating strings, intrinsic nonlinear effects 0-82607  
 video monitor, large screen, for computer output display 0-77597  
 vorticity vector, rot. theory 0-82604  
 wave and particle descriptions of light, equivalence, rel. to radar freq. shift 0-101692  
 H, one-dimens.,  $\Psi(x)=\Psi(-x)$  even states 0-90638  
 H, photon emission, Bohr theory covariant eqns. 0-105482  
 He-Ne laser wavelength drift 0-67978  
 Na Rydberg series, anomalous fine struct., perturbation model 0-57035
- teaching approaches to particular topics** see *teaching*  
**teaching demonstrations** see *demonstrations*  
**teaching machines** see *computer-aided instruction*  
**technetium**  
 see also *nuclei with* .....  
 EHDP labelled with  $^{99m}\text{Tc}$ , uptake quantification in sacroiliac scintigraphy, comparative study 0-94326  
 heparin labelled with  $^{99m}\text{Tc}$  for imaging of acute myocardial infarcts, dog expts. 0-81733  
 HIDA labelled with  $^{99m}\text{Tc}$ , synthesis of 5 new isomers and comparison with  $^{99m}\text{Tc}$ -(2,6-dimethyl)HIDA 0-72323  
 internal conversion, scattered-wave cluster technique 0-107696  
 MDP labelled with  $^{99m}\text{Tc}$ , lymphography appl. (*Japanese*) 0-94352  
 MDP labelled with  $^{99m}\text{Tc}$ , quantitative assessment of bone scans in diffuse alterations 0-72287  
 radioisotope adsorption by minerals 0-83203  
 recovery and use of noble metals from radioactive waste 0-99242  
 superconductivity and Fermi surface calcs. 0-70873  
 $^{99m}\text{Tc}$ , intrahepatic lithiasis detection, sequential scintiphotography 0-72309  
 $^{99m}\text{Tc}$ , assay of radioactive impurity in pertechnetate eluted from  $^{90}\text{Mo}$ - $^{99m}\text{Tc}$  generator (*Japanese*) 0-81735  
 $^{99m}\text{Tc}$ , beta-decay and dose calcs. 0-91154  
 $^{99m}\text{Tc}$  contamination of laboratory personnel, its degree and routes 0-98147  
 $^{99m}\text{Tc}$  generators, operational assessment by performance indices 0-94332  
 $^{99m}\text{Tc}$ , improved labelling of proteins by stannous tartrate reduction of pertechnetate 0-72324  
 $^{99m}\text{Tc}$  labelled (Sn)DTPA, comparison of 4 commercial preps. in glomerular filtration rate meas. 0-81704  
 $^{99m}\text{Tc}$  labelled (p-butyl) iminodiacetic acid, clinical evaluation in hepatobiliary imaging (*Japanese*) 0-67236  
 $^{99m}\text{Tc}$  labelled DTPA and MDP, compensative value on brain lesion (*Japanese*) 0-67235  
 $^{99m}\text{Tc}$  labelled pyrophosphate, changes in bone imaging after X-irrad. 0-72239  
 $^{99m}\text{Tc}$ , left ventricular function evaluation by myocardial scintigraphy and radionuclide angiocardigraphy (*Japanese*) 0-81724  
 $^{99m}\text{Tc}$  manipulated in syringes, radiation exposure obs. 0-67252  
 $^{99m}\text{Tc}$  methylene diphosphonate, immediate renal imaging and renography, clinical evaluation 0-98126



**technetium continued**

- <sup>99m</sup>Tc, pyrophosphate and hydroxymethylene diphosphonate carriers, comparison in acute myocardial infarction 0-94342
- <sup>99m</sup>Tc scintiangiograms, importance in optimum radiation schedule in treatment of superior vena caval obstruction 0-72334
- <sup>99m</sup>Tc-E-HIDA, characts. in hepatobiliary scintigraphy (*Japanese*) 0-81729
- <sup>99m</sup>Tc-hepatobiliary agents, absorbed dose estimation 0-72330
- <sup>99m</sup>Tc-labelled erythrocytes, spleen scanning in humans 0-67230
- <sup>99m</sup>Tc-microspheres, bladder wall dose after administration 0-109030

**technetium alloys**

see also *technetium compounds*

- Tc-Fe, dil., local magnetisation, Mossbauer meas. 0-66091

**technetium compounds**

see also *technetium alloys*

- <sup>99m</sup>TcBr<sub>6</sub><sup>2-</sup>, preparation problems, decay const. 0-106020
- <sup>99m</sup>TcCl<sub>6</sub><sup>3-</sup>, preparation problems, decay const. 0-106020
- <sup>99m</sup>TcI<sub>6</sub><sup>3-</sup>, preparation problems, decay const. 0-106020
- <sup>99m</sup>TcO<sub>4</sub>, thyroid scintigraphy, clinical comparative study with <sup>123</sup>I-Na (*Japanese*) 0-81728

**technical information centres** see *information services***technical presentation**

No entries

**technicians** see *personnel***technological forecasting**

see also *research and development management*

- cooperation among developing countries, evaluating potential of technology transfer 0-82628
- energy forecasting models and their validity 0-89582
- energy resources, projections to 2050 (*Dutch*) 0-61221
- European thermonuclear fusion programme, role of technology 0-86982
- fusion, ETF, engineering challenges 0-95422
- fusion, international fusion technology program 0-95423
- fusion, US magnetic fusion program, survey 0-91249
- fusion inertial confinement, advanced engineering requirements 0-95421
- India, need for and consequences of technological assessment 0-68017
- interferometric optical testing status and prospects 0-74529
- optical fibre communications, appls., techniques and predictions 0-87472
- optical fibres, future developments, impact on 'next generation' of electronic equipment, data ring concept 0-102808
- UK energy modelling 0-72003
- wavelength division multiplexing technology status and prospects 0-64203

**tectonics**

- active continental margins, earthquake foci three-dimensional projection 0-72453
- Adak Canyon region, central Aleutians, seismicity and tectonics 0-61772
- Adelaide Geosyncline, Australia, Late Precambrian palaeomagnetism rel. to sigmoidal structural trends 0-101325
- Afar triangle, geotectonic evidence for rifting, model for vertical displacements 0-98295
- Afghan Pamir, geology and tectonics of Himalayas 0-72513
- Afghanistan, shallow earthquakes and tectonic activity 0-72444
- S.Africa, kimberlites, palaeomagnetic obs. and tectonic implications 0-109093
- E.African Rift, cross-cut by volcanic chain in N.Tanzania, gravity survey 0-98301
- Alpine region, tectonic stress directions, correl. with joint orientations 0-105052
- S.Alps, Late Mesozoic pelagic limestone, megatectonic obs. from palaeomagnetism obs. 0-109095
- S.Alps, Permian volcanics palaeomag. props. rel. to S.Alpine block plate tectonics 0-89948
- N.America, effect of craton on distrib. of seismicity and intraplate stresses 0-98248
- N.Anatolian fault zone, Plio-Pleistocene reversal of displacement 0-94512
- anisotropic Earth model, appl. of tensor spherical harmonics to Navier eqn. of dynamic elasticity 0-98296
- Anti-Atlas, Morocco, Pan-African province geodynamic interpretation from geology and geochronology (*French*) 0-76952
- Appalachians, structural trends NE of Newfoundland and Trans-Atlantic correlation 0-85656
- aquifer water extraction leading to land deformation 0-105003
- arc-trench gap accretion, rel. to episodic plutonism in magmatic arcs 0-76956
- Archaean greenstone belts, tectonic hypothesis rel. to Agnew belt, Australia 0-94507
- Archaean tectonism, numerical models of vertical tectonism in greenstone belts 0-81861
- Arctic Ocean Basin, form. by circum-Arctic plate accretion and Pacific plate fragments isolation 0-98294
- Arctic Ocean Basin, plate tectonic evolution 0-76953
- N.Armenia, motion on plate from Jurassic rock palaeomagnetic obs. 0-104870
- N.Atlantic region Upper Triassic tectonics, implications of salt deposits on Newfoundland Grand Banks 0-94516
- Atotsugawa Fault, Japan, seismicity and focal mechanism of local earthquakes (*Japanese*) 0-94482
- Australia, plate collision, seismic shear waves excitation and propag. 0-104887
- Australia, tectonic, igneous and metallogenic provinces rel. to mantle convection and subcrustal stresses 0-72484
- Azores, earthquake (1980 January 1), aftershock sequence and present day tectonics 0-104911
- back-arc basins, asymmetric spreading 0-85636
- Balei gold region (E.Transbaikalia), structural features and tectonics 0-98300
- bedding tilt and rotation correction in palaeomagnetic studies 0-109097
- bending of subducting plate in central Aleutians, ocean bottom seismograph meas. 0-89978
- Bering Island, tectonic struct. of mountainous region 0-90045
- Bering Sea, crustal heat flow and tectonic explanation 0-109123
- Blue Mountains, Oregon, Jurassic plutons tectonic rot., palaeomagnetic obs. 0-109099
- British Columbia, north-central, northward displacement during late Cretaceous/early Tertiary 0-76955
- Burma and S.China, seismicity and tectonics 0-89983
- Butte mining district, Montana, palaeomagnetism, rock magnetism and aspects of structural deform. 0-101326
- Caledonian orogeny, subduction tectonics rel. to Norwegian eclogites crustal origin 0-76978

**tectonics continued**

- California, crust tectonic tilt rate, lake level obs. 0-90065
- Cambrian Arden Pluton tectonic history, palaeomagnetic study 0-61752
- Canada, vertical crustal movements, map 0-109130
- Carpathian Mountains, disjunctive dislocations revealed by interpretation of space television photographs (*Russian*) 0-104958
- chelonian cycles in continental crust evolution (*Chinese*) 0-89984
- Chile, Camaraca Formation of Middle Jurassic, palaeomag. and plate rotation 0-85586
- China, tectonic deform. characts. from seismological data (*Chinese*) 0-76951
- S.China and Burma, seismicity and tectonics 0-89983
- Chuko fault, Taiwan, underlying Tsengwen reservoir, seismicity 0-81930
- conference on plateau uplifts, Flagstaff, Arizona (August 1978) 0-57004
- continental drift of islands, effect on Earth rotation period 0-94445
- Coso Range, California, tectonics and stress field 0-90003
- crust and mantle tect. explainable by plate tectonic processes 0-81855
- crust gravity gliding tectonics, orogenic wave simulation, model 0-94506
- crustal deformation analysis, models for estimation of parameters (*German*) 0-101319
- crustal deformation due to volcanic eruptions, piezomag. field assoc. with Mogi model 0-67334
- crustal stress state, statistical anal. 0-81852
- Dead Sea Rift and N.Israel, mag. and gravity obs. and interpretation 0-98233
- deep seismic zone, Tohoku, Japan, freq.-magnitude obs. rel. to geochem. changes 0-72447
- Dellwood knolls, role in triple junction tectonics off northern Vancouver Island 0-90067
- descending plate lithospheric split, obs. from N Apennines 0-85639
- descending slab stress state, anal. of seismic source parameters 0-104946
- Diablo Plateau region, W.Texas, new evidence for tectonic uplift 0-72481
- Djibouti Republic, magnetic anomaly map and tectonic interpretation 0-61753
- Earth sciences frontiers, orthodoxy and creativity, symposium, Hobart, Tasmania (1977 February 7 to 10) 0-62380
- earthquake fault model (stochastic) 0-109114
- earthquake precursory rock cracking, size estimation of preparation zone 0-76930
- earthquake prediction based on tilt anomaly 0-104917
- earthquake prediction rel. to plate tectonics (*German*) 0-98267
- earthquakes in and near Japan, energy release statistics (1915 to 1978) 0-94471
- Eurasian and North American plates, relative rot. pole determ. 0-85637
- Farallon plate beneath Western USA, seismol. study 0-85621
- fault gouge deformation, simulation expts. on sandstone 0-81880
- fault rupture propagation, theory 0-104910
- fault strain field, included rectangular fault in semi-infinite media 0-98261
- fault termination deformation, normal fault in shade 0-90048
- fault unstable slippage, facing media of different elastic consts. 0-72506
- France, heat flow rel. to deep struct. and mantle convection 0-98291
- Franciscan formation, California, pedestrians guide to rock exposures 0-81849
- Friuli aftershocks during 1977 0-85597
- Friuli earthquake, 1976 May 6, focal mechanism 0-85603
- Fuji river, active faults anal. by track etch method (*Japanese*) 0-109127
- Galapagos Islands, t, spreading centre jumps 0-104877
- Gondwana configuration in Early Palaeozoic, palaeomag. study of Argentina 0-89938
- Gondwanaland, east-west fit from palaeomagnetic data 0-61792
- Gondwanaland reconstruction, Antarctic Napier complex rel. to S. India 0-76946
- gravity anomalies and tectonics, review 0-98593
- great earthquake occurrence, chaos theory of fault block behaviour 0-72448
- E.Greenland, southern Caledonian fold belt polyorogenic nature from isotopic age study 0-76938
- Guaymas Basin spreading axis, high-temp. hydrothermal deposit 0-101355
- Gulf of Aqaba, sinistral movement rel. to Red Sea opening 0-76954
- Gulf of Elat (Aqaba), continental breakup evidence 0-72485
- Hawaiian volcanoes, rift zones as expressions of plume generated radial stress fields 0-90051
- Hess Rise, W.Pacific, plate tectonic history 0-90026
- N. Hida region, Japan, seismicity and focal mechanism of local earthquakes (*Japanese*) 0-94482
- W.Himalaya, Central Crystallines, geology and tectonics 0-72516
- Himalaya, two intracrustal boundary thrusts 0-104948
- Himalaya, uplift and cooling rates from geochronological data 0-85627
- Himalaya and Tibet Plateau region, tectonic history 0-72486
- Himalayan Suture Zone, Landsat picture obs. 0-76948
- Himalayas region, conf., Mar. 1978, Katmandu, Nepal 0-72523
- Hindu Kush region, microearthquake seismicity and fault plane solns. 0-72446
- Hindukush, Baluchistan arc, seismotectonics and struct. (1890-1970) 0-104922
- Iapetus Ocean, evidence for Cambrian opening 0-98299
- Iberian margin ocean-continent boundary struct., discovery of serpentinite diapir W. of Galicia Bank 0-94489
- Iceland, continuum model of crustal generation, kinematic aspects 0-90059
- N.Iceland, gravity and height vars. during present rifting episode 0-90060
- N.Iceland, vertical crustal movements from height meas., (1965 to 1977) 0-89931
- N.Iceland fissures, relative movements and tile changes 0-90062
- Iceland Plateau, tectonic synthesis from sea floor morphology and mag. anomalies N of Iceland 0-89953
- NE Iceland rift zone, geotect. meas. and horizontal crustal movements 0-89930
- Icelandic volcanism, rift zones as expressions of plume generated radial stress fields 0-90051
- India, Bouguer gravity anomaly map and tectonics 0-61791
- India, peninsular, fan faults rel. to origin of Himalayas 0-85630
- Indian Ocean, seafloor spreading history 0-61790
- Indian/Pacific plate boundary, microearthquake study of New Zealand 0-109131
- Indo-Australian plate, evidence for internal deformation. 0-109134
- intra-plate volcanism during Cainozoic, rel. to mantle convection 0-98293



**tectonics continued**

- intracratonic basin, formation model involving deep metamorphism 0-85618  
 island arc development, obs. expts. and speculations 0-98298  
 isostatic compensation and viscosity differences between crust and asthenosphere 0-104947  
 isostatic tilting, post-glacial, induction of regional trend to river meander migration 0-101391  
 Israel, Mesozoic palaeomag. results and inferences for microplate struct. in Lebanon 0-61760  
 Izu Peninsula, active faults anal. by track etch method (*Japanese*) 0-109127  
 SW Japan island arc, uppermost mantle differential stress lateral var. 0-98275  
 Krafla Caldera, NE Iceland, gravity and elevation changes caused by magma movement 0-90052  
 Krafla fissure swarm, Iceland, surface deform. in rifting events 0-90061  
 Krafla volcano area, N. Iceland, horizontal magma flow rel. to subsidence events, (1975 to 1979) 0-90053  
 Kurile trench-Hokkaido rise system, flexure profile by plate model 0-72482  
 Laramide orogeny, seismic profiles in Wyoming, USA 0-85626  
 liquid-filled vertical crack propagating due to hydrostatic press. 0-72505  
 lithosphere creep deformation model, deformation due to geologic load 0-104939  
 lower mantle convection, inferred from low Q zone 0-76944  
 magmatic diapir folds tectonic evolution, influence of temp. and heat exchange with crustal rocks (*Russian*) 0-104957  
 mantle, seismic vel. variations, origins 0-81854  
 mantle, thermal convection, time dependent simulation 0-101352  
 mantle, thermoconvective waves, propag. without attenuation 0-90064  
 mantle convection, internal radiogenic heating rel. to oceanic bathymetry flattening 0-85642  
 mantle convection, rel. to inertia and gravity asymmetry 0-98269  
 mantle convection driven by radioactive energy, model for decaying source 0-72461  
 mantle convection rolls, stability anal. 0-76957  
 mantle convection with moving surface plates, model 0-85634  
 mantle convective instability, thermomechanical model 0-90063  
 mantle creep (steady state), anal. of olivine eqns. of state 0-104924  
 melt production in mantle, by viscous dissipation 0-72463  
 Messina Layered Intrusion, Limpopo Mobile Belt, S.Africa, tectonic setting, geology and age 0-76969  
 Mid-Atlantic Ridge, median valley tectonic model from gravity obs. 0-90071  
 Mid-Cayman Rise spreading centre, tectonic setting rel. to basalt glasses geochemical var. and petrogenesis 0-101364  
 mid-ocean ridge spreading rate, petrological evidence 0-109135  
 midocean ridge, existence of mantle double partial melt zone 0-104940  
 Moine thrust zone, differential stress determ. from deformation-induced microstructs. 0-85652  
 Mongolo-Okhotsk mobile belt, rift formation and tectonic history 0-90066  
 Nepal, basic intrusions of volcanic origin 0-72477  
 W. Nepal, gravel deposits indicating tectonic uplift 0-72487  
 Nepal Himalaya, body waves from earthquakes, focal mechanism and tectonics 0-72455  
 Nepal Himalaya, struct. geology of Kusma-Sirkang section 0-72478  
 Newfoundland, Early Palaeozoic plate tectonic model 0-94509  
 Nias Island, Indonesia, Neogene trench-slope deposits palaeobathymetry and tectonic uplift 0-104950  
 Nias Island, Indonesia, structural geology implications for subduction zone tectonics 0-109120  
 North Sea basin, subsidence in post-mid-Cretaceous 0-109133  
 oceanic fracture zones of equatorial Atlantic (7 to 10°N), lithosphere struct. (*Russian*) 0-104932  
 orogenesis, chemical approach to Nd-Sr isotopic relationship in granitoid rocks and continental crust development 0-94522  
 orogenic volcanism caused by thermal runaways? 0-90057  
 orogeny, caused by tidal deformation of crust 0-85625  
 SW Pacific, Eocene subduction zone, disruptive ophiolitic belt evidence 0-104949  
 Pacific plate subduction (*Japanese*) 0-94514  
 E. Pacific Rise spreading centre, geophysical expts. and hot springs 0-101360  
 Pamir-Hindu Kush region, seismicity and fault plane solns. 0-72445  
 passive continental margin, evolution in light of drilling results 0-76942  
 Philippine Islands, tectonic struct. revealed by seismicity and volcanicity 0-94511  
 plate boundary seismic pot., major boundaries 0-85606  
 plate relative motion problem, linear formulation 0-72480  
 plate tectonics, appl. of geodetic research to geodynamic problems (*German*) 0-101317  
 plate tectonics, role of C in Earth upper mantle 0-81845  
 plate tectonics and lithosphere petrology, comparison with Venus tectonics and comp. 0-72805  
 plate triple junction, of type TTT(b), stability condition (*Japanese*) 0-94513  
 post glacial uplift mechanism, phase boundary reaction to medium press. changes 0-90058  
 postglacial uplift of crust, mechanism 0-104943  
 postseismic surface stress, viscoelastic model 0-98278  
 postseismic viscoelastic surface deform. and stress, theory 0-94496  
 pretertiary continental configuration, palaeomag. data from NW France 0-72414  
 Reykjanes Ridge, fracture zones obs. south of 60°N rel. to evolution between 40 and 12 Myr BP 0-90069  
 Reykjanes Ridge, SE flank, lithosphere evolution, seismic surface wave study 0-90022  
 Reykjanes Ridge, stress directions rel. to ridge crest morphology near 62°N 0-90070  
 rock deformation, crack-seal mechanism causing extension veins 0-61798  
 salt glaciers of Iran, seasonal movement obs. 0-104942  
 San Andreas Fault, crustal strain obs. site for earthquake prediction 0-81832  
 San Andreas fault, fault creep obs. rel. to local mag. field meas. 0-85629  
 San Andreas Fault, geodetic tilt obs. 0-81800  
 San Andreas fault, satellite laser ranging system 0-61984  
 San Andreas Fault, wire strainmeter data subject to meteorological noise 0-81831  
 San Andreas transform, geometry of subducted slab 0-98297

**tectonics continued**

- San Fernando earthquake, California (1971), dislocation fault model, tectonic significance (*Japanese*) 0-104923  
 Sanbagawa Metamorphic Belt, Shikoku, Japan, evidence for recent tectonic uplift from crustal struct. anal. (*Japanese*) 0-94508  
 sea-floor topography, tectonic model using vol. expansion coeff. 0-90072  
 sea-mount loads affecting crust, isostatic compensation and geoid anomalies 0-109132  
 sedimentary basins, development in Archaean rel. to lithosphere thickness 0-89986  
 sedimentary basins, form. with finite crustal extension rates 0-89987  
 sedimentary rock faulting and folding, strain hardening theory 0-85628  
 seismic faulting, acoustic fluidisation theory 0-85653  
 seismic fracture zones, effects of groundwater hydrostatic press. vars. on seismicity (*Russian*) 0-104913  
 seismology, implications of dilatancy-fluid diffusion theory for aftershock sequences 0-85604  
 SE Siberia, crust struct. and role of Archaean folded ovals 0-101349  
 Sibley Group (Neohelikian), Ontario, stratigraphy and depositional setting rel. to Keweenaw rift failed arm 0-94517  
 Souss Basin, S.W. Morocco, mag. survey and crustal struct. 0-89958  
 St. Elias earthquake, Alaska, Feb. 1979, 1974-9 tilt obs. 0-81841  
 St. Vincent's Gulf, South Australia, regional tectonic setting rel. to geomag. vars. 0-72426  
 structural geology, conf. (1978), Toronto, Canada 0-101666  
 subducted lithosphere, correl. with positive geoid height anomalies 0-90056  
 subducting lithosphere, heat transfer with continental asthenosphere 0-94510  
 subducting slab undergoing upper surface melting, thermal field 0-85638  
 subduction of young slabs, consequences 0-81862  
 subduction process segmentation, evidence from Petatlan, Mexico, earthquake (1979 March 14) 0-76920  
 subduction zone seismicity, Makran coast, Iran 0-85635  
 subduction zones, material transport within accretionary prisms and 'knocker' problem 0-101353  
 subduction zones, three-dimensional struct. from stereoviews of seismicity 0-72452  
 sublithospheric upwelling distrib. leading to mantle hot spots 0-109126  
 Sulawesi (E Indonesia) western arc, palaeomag. studies and fission-track dating rel. to tectonic history 0-89957  
 Surkhob fault zone, USSR, tidal deform. determ. for crustal movement anal. 0-104944  
 Tabas-e-Golshan earthquake, Iran, Sept. 1978, faulting and bedding thrust 0-81826  
 N. Thailand, hot springs and geothermal gradients extensional tectonic activity 0-94495  
 Three Forks Basin, Montana, USA, seismicity and tectonics 0-81829  
 tidal forces deforming crust, causing orogeny 0-85625  
 N. Tonga region, Wadati-Benioff zone morphology and complicated subduction closure model 0-90010  
 Transantarctic Mountains, evidence to suggest uplift by Early Miocene 0-98287  
 Triassic Hound Island Volcanics, Alaska, crustal movement from palaeomagnetic obs. 0-89945  
 Upper Amur region USSR, seismicity, tectonic features and earthquake epicentre confinement 0-101343  
 W. USA, vertical crustal movement, anal. of levelling survey 0-72409  
 Virgin Islands, tectonic struct. and earthquake swarms, seismic network obs. 0-89973  
 visco-elastic modelling of tectonic systems, by finite element anal. 0-104930  
 Xingtai earthquake, 1966 March, aftershock freq., possible tectonic stress monitor (*Chinese*) 0-76912  
 S. Yamanashi Prefecture, Central Japan, crustal movements changes rel. to microearthquake activity (*Japanese*) 0-67343  
 Yellowstone caldera, Wyoming, USA, vertical crust movement 0-81859  
 Zendan Fault region, Iran, struct. lineaments, interpretation of Landsat 1 obs. 0-104941  
 CO<sub>2</sub> release due to tectonic activity and earthquake prediction 0-94470

**tektites see meteorites****telecommunication cables**

- see also coaxial cables; submarine cables; telephone lines; underground cables*  
 concatenated fibre-optic cable, cumulative baseband frequency response models 0-78983  
 optical fibre, stress-strain behaviour 0-69551  
 optical fibre cable comprising 48 fibres, design and characts. (*Japanese*) 0-58688  
 optical fibre cable comprising 8 fibres, design and characts. (*Japanese*) 0-58689  
 optical fibre cable splice methods (*Japanese*) 0-58690  
 optical fibre cables, historical development (*Japanese*) 0-87494  
 optical fibre splicing, connecting and sheath jointing (*Japanese*) 0-87497  
 optical fibre transmission, applications and cable techniques (*Japanese*) 0-87493  
 optical fibres, fabrication and construction of secondary coating for optimised design (*Japanese*) 0-87567  
 optical fibres, history and basic principles 0-69543  
 optical fibres, multicore, high density, design and manufacture, characts. (*Japanese*) 0-87501  
 optical fibres microbend charact. and mech. prop. for design, applicational examples (*Japanese*) 0-87500  
 single fibre connectors and cable splice hardware, optical coupling theory 0-64187

**telecommunication theory see information theory****telecontrol**

- see also alarm systems; telemetering*  
 Barnwell Nuclear Fuel Plant, remote handling systems, overview 0-68920  
 fusion reactor, MFTF, exception handling control system 0-99325  
 HTGR, surveillance robot for fuel and reflector element inspection 0-68873  
 PWR irradiated fuel assemblies, remote operations 0-68918  
 teleoperator systems for reactor maintenance, technology assessment 0-68872  
 US decontamination system for reactor fuel transfer pool, remotely operated 0-68916

**telecontrol equipment**

- fibre-optic remote control system for 1.5 MeV heavy-ion fusion pre-accelerator 0-73993
- lantern slide projector remote control using IR-60 infrared system (*German*) 0-95169

**telemetering**

- biotelemetry, conf., Sapporo, Japan (June 1980) 0-90604
- perinatal radio telemetry 0-104722
- Pioneer Venus Multiprobe entry phase, telemetry recovery 0-67493

**telemetering equipment**

- biomedical temperature biotelemetry, modular, expandable, implantable 0-67191
- chronically implanted device, controlled transcutaneous powering 0-98152
- Doppler flowmeters, directional, totally implantable, for animal research 0-67293
- IC implantable systems for animal expts. 0-76887
- physiological measurements, integrated power controllers and RF data transmitters for totally implantable telemetry 0-67295
- temperature multiplexers, types of unit and configurations 0-82577
- temperature telemetry transmitter, crystal-controlled, surgically implantable, for animal expts. 0-72393
- thermometer, transistorised, with remote indication, up to 150°C (*German*) 0-73356

**telemetering systems**

- animal physiological research, totally implantable dimension meas. system 0-67294
- avian ECG, radiotelemetry system 0-98202
- EEG recording system, portable pulse-interval modulation telemetry/multiplexing system, home use 0-67261
- integrated circuit approach to totally implantable telemetry systems 0-67291
- medical research, chronic, appls. of totally implantable systems 0-67296
- RF-powered cage system for implant biotelemetry 0-94422
- synchronisation of biotelemetry system, with time division of channels 0-94386
- telemetry system, implantable, multichannel, for physiological research 0-67292
- temperature telemetry system with interference suppression, implantable, long-life, animal expts. appl. 0-101302

**telemeters** *see telemetering***telemetry** *see telemetering***telephone exchanges**

- solar-collection system for domestic hot water 0-66940

**telephone lines**

- fibre-optic, interconnection using compound-lens devices 0-74493
- optical fibre systems, developments 0-58678

**telephone switching equipment**

- microelectronic appls., conf., Calcutta, India (Jul. 79) 0-96755

**telephone transmitters**

- EL2, electret technology development 0-83723

**telephony**

- cables laying, underground, seismology appl., rocks location verification 0-72456
- ECG telephone transmission, analogue and digital, errors and noise 0-94398
- optical fibre cables, design, manufacture, laying and jointing (*Italian*) 0-99838

**telephotography** *see facsimile***telescopes**

- see also astronomical telescopes*
- aplanatic two mirror telescope from near-normal to grazing incidence, comparative performance anal. 0-58654
- binocular models, characts. and design features, review 0-74468
- collimating system, laser radiation directivity pattern axis spatial location 0-102748
- compensated levels, high-precision, geodetic appl. 0-101813
- image vergence variation with object distance change, general case 0-63934
- lensless scanning telescope, MTF 0-58655
- multianode microchannel array photon-counting detectors 0-77869
- parabolic telescope and spectrometer combination, optical props. 0-87455
- parallax problems in telescopic systems 0-99818
- primary mirror manufacture, monitored null corrector 0-78946
- Shuttle Orbiter re-entry, remote IR imagery and tracking 0-82171
- trihedron optical system, for linear displacement meas., accuracy estimation 0-101780
- two-mirror objective systems, field lens group corrector 0-78945
- visual instruments, optical component contamination, effect on visibility of extended objects 0-64137
- CO<sub>2</sub> laser Helios fusion target positioning with orthogonal telescopes 0-74421
- CO<sub>2</sub> laser Helios fusion system beam diagnostics 0-78882

**teletypes** *see interactive terminals***television**

- see also colour television; video signals*
- usable subject contrast range definition, TV colour films appl. (*German*) 0-57408

**television applications**

- astronomical observations of faint objects, television detection techniques 0-82208
- astronomical observatory, focal reducer for integrating TV system 0-67568
- astronomy, SEC Vidicon photometry of  $\omega$  Centauri main sequence 0-90491
- biological micro-object geometric feature determination, TV set 0-85538
- biological objects, electronic speckle pattern interferometry in vivo 0-109083
- chromosome classification system, banding technique 0-67320
- education, vibrating string, tuning guitar by television 0-73134
- electron microscopy, digital storage and processing system for aposteriori image accumulation 0-101901
- EM, image recording system, detection quantum efficiency 0-99009
- flaw detector with automatic mechanical scanning, TV signal form. on basis of digital memory 0-71864
- holographic interferogram anal. with TV picture system 0-106489
- to interaction with environment, Jupiter Voyager imagery analysis 0-105197

**television applications continued**

- Jupiter colour pictures from Voyager space probes, 800 line scan TV system, land based receiver systems (*German*) 0-101549
- laser dot matrix space-coded surface topographical mapping 0-98885
- medical X-ray video images, enhancement 0-94353
- optical feedback processing by TV-optical method 0-87335
- optical incoherent feedback using TV 0-87334
- particle tracks in streamer chamber, recording technique 0-69023
- real-time holographic viewing in moving fog 0-102676
- sapphire crystal float zone growth, meniscus angle meas., TV viewing system obs. 0-108347
- spectroanalytical information processing, television methods appls. 0-89568
- thermal imaging with pyroelectric vidicon camera 0-86288
- underwater TV, wide angle correcting lens 0-91883
- Venus cloud layer structure, determ. from Venera 9 televised pictures 0-67604
- vibrating membrane speckle pattern analysis 0-106769
- vibration measuring system using interf. fringes TV detect. and electronic image processing 0-103004
- videodensitometry in angiography 0-104745
- virtual image position determ., demonstration using TV camera 0-67992
- X-ray images, quantitative anal. by TV image analyser 0-109008

**television broadcasting**

- object-related colour reproduction in film scanning [TV broadcasting], matrix, electronic masking appl. (*German*) 0-105726
- time and freq. meas., users' manual 0-94934

**television camera tubes***see also image storage tubes*

- image dissector tube design, with high resolution and large deflection angle 0-73475
- laser spatial profile meas. by pyroelectric vidicon camera 0-87425
- pyroelectric vidicons, figures of merit, material parameters 0-77855
- SEC Vidicon photometer, appl. to photometry of  $\omega$  Centauri main sequence 0-90491
- triglycine sulphate, deuterated, reticulated target for pyroelectric vidicon, IR imaging 0-77858
- vidicons for X-ray diffraction topographic patterns, spectral sensitivity of TV system for visualisation (*Russian*) 0-62814
- Si:H, amorphous, image pickup devices 0-100481

**television cameras***see also colour television cameras*

- Fabry-Perot-interferometer imaging system for thermospheric temp. and wind meas. 0-101441
- imagery, 2-D sampled, aliasing and blurring effects 0-99635
- optical microscope combined with TV equipment for teaching and quality control 0-82817
- precision image isocoon X-ray TV camera 0-101263
- video interferogram analysis by TV camera-microprocessor system 0-73440

**television equipment**

- biological micro-object geometric feature determination, TV set 0-85538
- external synchronization of electric drive SA-120 when shooting combine pictures with TV images (*Russian*) 0-86484
- films, 16 mm Fujicolor reversal film RT 500 and RT125 0-106585
- large-screen virtual display, fabrication of parabolic mirror by rotational method 0-87465
- laser beam scanner, rotating mirror, development programme (*Japanese*) 0-74369
- optical microscope combined with TV equipment for teaching and quality control 0-82817
- scintigraphic TV displays, 4 standard types, comparative study 0-109005
- screens, use of cholesteric-nematic phase transitions of liquid crystals (*Chinese*) 0-79922

**television interference**

- windpower systems, TV interference aspects 0-61238

**television picture tubes**

- see also cathode-ray tubes; colour television picture tubes; fluorescent screens*
- aperture distortion correction, optical method 0-95827

**television receivers**

- ceramic filters appl., using  $\text{Pb}(\text{Zn}_{1/3}\text{Nb}_{2/3})\text{O}_3\text{-PbTiO}_3\text{-PbZrO}_3$  and  $\text{Pb}(\text{Mg}_{1/3}\text{Nb}_{2/3})\text{O}_3\text{-PbTiO}_3\text{-PbZrO}_3$  (*Japanese*) 0-60507
- LiTaO<sub>3</sub> crystals for commercial SAW TV IF filters, fabrication 0-80961

**television signals** *see video signals***television systems**

- see also closed circuit television*
- large screen TV aspherical plastic lens optical design and evaluation 0-78937
- X-ray diffraction topographic patterns, spectral sensitivity of TV system for visualisation (*Russian*) 0-62814

**television transmitters**

- SAW filter design applied to group-delay equaliser in TV rebroadcast transmitters 0-74676

**tellurium***see also nuclei with .....*

- acousto-optical props. at wavelength of 10.6  $\mu\text{m}$  0-76001
- adsorbed on Ni(001), photoelectron diff. effects in core-level photoemission 0-76144
- amorphous, electronic struct. and optical props., pseudopot. calc. 0-65428
- amorphous and liquid state, Raman spectra, crystn. processes 0-60608
- cluster superlattices in Na-type X zeolite matrix, N and S type volt-ampere characts. (*Russian*) 0-70665
- core level binding energies 0-71564
- crystal growth by Czochralski method 0-66423
- cyclotron resonance in pulsed high mag. fields, cond. band struct. 0-59867
- electronic structure of cryst. phases, hydrostatic press. effects 0-59865
- film, microstructure 0-103598
- film, stability in moist air, rel. to information storage capability, atmospheric corrosion model 0-71774
- film, surface morphology depend. on vacuum deposition angle 0-103553
- film, vacuum deposited, growth and morphology of crystals 0-96766
- film, vacuum deposited on NaCl, crystallite growth and morphology, electron microscopy 0-65401
- films, elec. and galvanomag. props., microstruct. 0-70859
- films, oriented, semiconducting props., Hall coeff., band structure 0-70854
- Hall coefficient, magnetoresistance, two types of carriers 0-60013



## tellurium continued

- high-pressure metallic, supercond. transition temp. press. depend. 0-80435  
 impurity in Nimonic 105, influence on creep and stress rupture props. 0-66602  
 impurity spectroscopy 0-65499  
 Kikuchi patterns, of non-centrosymmetrical crystal 0-100202  
 metallic state, press. induced, elec. cond. meas. 0-96949  
 mobility anisotropy in a-edge-dislocated crystals. 0-107781  
 molecular laser, optically pumped, review 0-58519  
 monolayer, adsorbed on Al (111), angle resolved UPS of 2-dimens. band struct. 0-60059  
 Mossbauer spectra under press. up to 8000 MPa 0-80647  
 multilayer thin film struct. thermoelec. props. 0-92964  
 negative photoconductivity, intraband absorpt. (*Russian*) 0-107854  
 photoconductivity in strong mag. fields, doping effects, impurity levels 0-75602  
 SHG, 60% efficiency, 12.8  $\mu\text{m}$   $\text{NH}_3$  laser pumping 0-83640  
 space group  $\text{C}_{32}\text{-C}_{32}$ , habit variation 0-107090  
 strained and unstrained crystal, SHG and prop. of  $\text{CO}_2$  laser radiation 0-58641  
 surface, (1010), struct., LEED intensities anal. 0-88411  
 thermal etch pits shape, on cleavage faces 0-107251  
 thin film selective absorber coatings, prod. using an oblique vacuum deposition technique 0-81488  
 trigonal, Raman scatt. at very high press. 0-60566  
 trigonal and amorphous, electronic struct. and nonempirical calc. of struct. props. 0-59866  
 $\text{Bi}_{1-x}\text{Sb}_x\text{Te}$ , single crystal, dispersion of magnetoplasma waves (*Russian*) 0-70739  
 $\text{CdS:Te}$ -based photoelectrochem. cell, luminesc., thermal manipulation of deactivation processes 0-81479  
 $\text{CdS:Te}$ , p-n junction formation by laser radiation 0-96983  
 $\text{Cu-Te}$  thin film couples, room temperature interactions 0-96699  
 $\text{GaAs:Cu}$ ,  $\text{Te}$ , photoelec. props. 0-92936  
 $\text{GaAs:Te}$ , epitaxial film, influence of impurities on stacking fault energy 0-103371  
 $\text{GaAs:Te}$ , ion implant depth distrib., AES and glow discharge optical spectroscopy meas. 0-65028  
 $\text{GaAs:Te}$  Schottky barrier solar cells, diffusion length determ. using minority carrier SEM 0-61359  
 $\text{GaAs:Cu:Ti}$ , cathode luminescence spectra, Hall effect, cryst. defects 0-76087  
 $\text{GaAs}_{1-x}\text{P}_x\text{(Te)}$ , bound exciton stress depend., piezoluminescence, photoluminescence 0-80206  
 $\text{n-GaSb:Te}$ , epitaxial, IR refl. meas., carrier conc. and mobility determ. 0-80769  
 $\text{Ge-Si:Te}$ , solid solns., donor states energy spectrum 0-88516  
 $\text{InAs:Te,Cd}$ , donor-acceptor interaction, elec. cond. and Hall coeff. meas. 0-59988  
 $\text{InSb:Te}$ , anomalous impurity segregation Hall and mass spectrum meas. (*Chinese*) 0-59501  
 $\text{InSb:Te}$ , cryst. growth from melt, pulling method, US effects on facet growth 0-76169  
 $\text{Nb-Te-Pb}$  Josephson junctions, prep. and props. 0-65754  
 $\text{Pb-Te}$  oxide-Pb Josephson junctions, prep. and props. 0-65754  
 $\text{Si:Te}$ , ion implanted, annealing of heavy ion cascade damage, channelling meas. 0-89255  
 $\text{Si:Te}$ , laser melting, surface  $\text{Te}$  atom accumulation, profiles 0-100258  
 $\text{Si:Te}$ , Mossbauer spectra of  $^{119}\text{Sn}$  defect struct. 0-97175  
 $\text{T-metal}$ , thin film contact, time evolution of photovoltaic effect 0-65687  
 $\text{Te VII}$ ,  $4d^6s$  configuration spectrum obs., line identifications 0-106289  
 $\text{Te VIII}$ ,  $4d^8s$ ,  $4d^8p$  and  $4d^44d^{10}$  config. spectrum obs., line identifications 0-106289  
 $\text{Te:Cu}$  films, elec. transport props. 0-60120  
 $\text{Te-Ag}$  thin film system, stress-relief appearance conditions 0-65416  
 $\text{Te-Bi}$ , thin film system, stress-relief appearance conditions 0-65416  
 $\text{Te-Se-Cd}$ , sandwich structure, fabrication and characteristics 0-60089  
 $\text{Te-Se-Cd}$  rectifying sandwich structs., elec. forming action, Schottky junction form. 0-80371  
 $\text{Te}_2$ ,  $\text{B}_0^+ - \text{b}^2_8$  system, transition assignment, IR and visible spectra obs. 0-58298  
 $\text{Te}_2$  laser induced fluoresc. in inert gas matrix 0-87161  
 $\text{Te}_4^{2+}$ , pseudopot. SCF-MO calcs., spectrum assignments 0-83269  
 $^{123\text{m}}\text{Te}$ -labelled adrenal-imaging agents, radiation dosimetry 0-101268

## tellurium alloys

- see also tellurium compounds  
 $\text{Ag-Zn-Te-(Sn)-(In)}$ , internally oxidised, oxide particle size control (*Japanese*) 0-89480  
 $\text{Bi-Sb-Te}$  melt, Sb and Te distribution coeffs. during crystallisation (*Russian*) 0-93472  
 $\text{Bi}_2\text{Te}_3$  alloy thermocouples for solar thermoelectric conversion 0-94095  
 $\text{Pb}_{1-x}\text{Te}_x$ , liquid alloys, local fluctuations and quadrupolar relaxation 0-66060  
 $\text{Sn-Te}$ , molten, elec. cond. and phase diagram 0-84454  
 $\text{Te-Au}$  film, metastable supercond. alloys, produced by low temp. ion implantation 0-88670  
 $\text{Te-In}$  system, enthalpies of fusion, peritectic decomp. and allotropic transition, DTA (*French*) 0-76226  
 $\text{Te}$ -transition metal, liq. semicond., elec. props. 0-96870

## tellurium compounds

- see also tellurium alloys  
 electron spectroscopic studies (*French*) 0-108770  
 eutectics,  $\text{Te}$ -based, crystn. rate effect on electrophys. props. mutual solubility effect 0-60774  
 $\text{Ag-Ge-Te}$  system, chalcogenide, phase equilibria and diagrams (*German*) 0-108418  
 $\text{Ag}_{10}\text{Sb}_2\text{Te}_{12}$ , single-phase, thermoelectric efficiency 0-107826  
 $\text{As-Ge-Te}$ , chalcogenide glass, elec. cond. and dielec. const. 0-75567  
 $\text{As-Te-Ge-n-Si}$ , film on cryst., heterojunction, elec. and photovolt. props. 0-100514  
 $\text{As-Te-In}$ , glass-forming, density and microhardness 0-103257  
 $\text{As-Te-Si-Ge}$  amorphous chalcogenide semiconductor, thin film interface, electrical charact. (*Korean*) 0-97014  
 $\text{As}_{10}\text{Ge}_5\text{Te}_5\text{Ag}_x$  glass, elec. and dielec. props., Ag additions effect 0-65558  
 $\text{CuIn}_{1-x}\text{Ga}_x\text{Se}_{2(1-x)}\text{Te}_{2x}$  pentenary alloy compounds for photovoltaic solar energy conversion 0-93971  
 $\text{FeBr}_2$ , transient species,  $\text{He(I)}$  photoelectron spectrosc. calcs., relativistic corrections 0-95677

## tellurium compounds continued

- $\text{Ge}_{10}\text{As}_{17}\text{Te}_{20}\text{Se}_{22}\text{As}_2\text{S}_3$ , two-layer antirefl. coating, error considerations in design 0-74477  
 $\text{Ge}_{10}\text{Sb}_{10}\text{As}_{10}\text{Te}_{10}\text{Ga}_{10}$ , chalcogenide thin films, coupled carrier theory test, high field conditions 0-100466  
 $\text{HgCdTe}$ , ion implantation, junction form. 0-100260  
 $\text{HgTe}$ ,  $\Gamma_8$  symm. acceptor centre hole mag. props. (*Russian*) 0-88733  
 $\text{MgTeMoO}_6$ , prep., cryst. struct., and catalytic props. 0-108709  
 $\text{xMnO} \cdot (100-x)[19\text{TeO}_2 \cdot \text{PbO}]$ , EPR studies of  $\text{Mn}^{2+}$  ion distribution 0-71167  
 $\text{Pb}_{1-x}\text{Sn}_x\text{Te:Ge}$ , anomalous behaviour of impurity centres under press. (*Russian*) 0-65491  
 $\text{Se-Ge-Te}$ , chalcogenide glass, elec. cond. and dielec. const. 0-75567  
 $\text{Se-Te-Sb}$  glasses, electronic transport 0-88579  
 $\text{Se}_{95}\text{Te}_{05}$ , glass crystallisation, effect of an alternating electric field 0-88054  
 $\text{Se}_{1-x}\text{Te}_x$ , amorphous, optical and elec. props. 0-84506  
 $\text{Se}_{1-x}\text{Te}_x$ , amorphous film, photo-crystallisation 0-59839  
 $\text{Se, Te}_{1-x}$ , acoustoelectric current saturation 0-60053  
 $\text{Se, Te}_{1-x}$ , amorphous, structural relaxation and crystallisation kinetics study by DTA 0-59394  
 $\text{Se, Te}_{1-x}$ , growth of single crystals by Czochralski method 0-66423  
 $\text{Se}_{1-x}\text{Te}_{99}\text{As}_{29}\text{Ge}_{10}$  semiconductor amorphous films, field effect, trapping 0-84472  
 $\text{Si-Te}$  system, phase diagrams 0-89209  
 $\text{TaSe}_2$  (2H), broken hexagonal symm., incommensurate charge-density wave struct. 0-96646  
 $\text{Te-(Bi,Sb)}_{1-x}\text{Te}_x$  eutectic, electrophys. props., directed crystn. conditions influence and comp. depend. 0-107827  
 $\text{Te-Se}$  liquid mixtures, sound vel. meas., adiabatic compressibility determ. 0-65161  
 $\text{TeCl}_2$ , transient species,  $\text{He(I)}$  photoelectron spectrosc. calcs., relativistic corrections 0-95677  
 $\text{TeCl}_4$  gas phase transport agent, chemical transport growth of  $\text{NpO}_2$  single crystals (*French*) 0-60760  
 $\text{TeCr}_2\text{O}_6$ , exchange interactions within binuclear entity ( $\text{Cr}_2\text{O}_{10}$ )<sup>14-</sup> 0-60236  
 $\text{Te}_{80}\text{Ge}_{20-x}\text{As}_x$  glasses, rapid melt cooled, glass transition and stability range 0-75170  
 $\text{Te}_{80}\text{Ge}_{15}\text{Pb}_5$ , DSC sensitivity to controlled ageing in glass transition region 0-71673  
 $\text{Te}_{80}\text{Ge}_{20-x}\text{Sb}_x(\text{Bi}_x)$ , DSC studies of struct. phase transformation 0-66505  
 $\text{TeO}_2$  acousto-optical tunable filter with microcomputer control 0-102833  
 $\text{TeO}_2$ , crystal gyrotropy, meas. in IR region 0-88957  
 $\text{TeO}_2$ , Czochralski-grown oxide crystals, fluid-flow effect on gas-bubble entrapment 0-84121  
 $\text{TeO}_2$ , ferroelectric glass, phase transition, permittivity, electrochromism, photochromism 0-80719  
 $\text{TeO}_2$ , multifer. acousto-optic diffraction 0-74300  
 $\text{TeO}_2$ , paratellurite, single crystals, third-order elastic constants 0-88243  
 $\text{TeO}_2$  shear wave acousto-optical device with polarisation filtering 0-106619  
 $\text{TeO}_2$  thin films, dielec. props. rel. to fabrication conditions 0-97199  
 $\text{TeO}_2$  time-integrating acousto-optical correlator for chirp spectrum analyses 0-106474  
 $\text{TeO}_2$  two coord. deflector, anisotropic diffraction and wide band scatt. 0-91920  
 $\text{TeO}_2\text{-MoO}_3\text{-V}_2\text{O}_5$ , phase comp. determ. using X-ray diffr., electron microscopy and DTA (*German*) 0-88046  
 $\text{TeO}_2\text{-P}_2\text{O}_5$  system, glass struct., neutron diff. study 0-70128  
 $\text{TeO}_2 + \text{NiMoO}_4(\text{FeMoO}_4)$ , solid state reaction 0-108709  
 $\text{TeO}_2^{2-}$ ,  $\text{TeO}_2^{2-}$ , O K-emission spectra, electron struct. 0-87099  
 $\text{TeO}_2\text{Cl}_2$ , thermal decomposition, matrix isolation IR and mass spectra 0-81306  
 $\text{Te(OH)}_6\text{Cs}_2\text{HPO}_4$ , cryst. struct. 0-64975  
 $\text{Te(OH)}_6\text{Cs}_2\text{HPO}_4 \cdot 2\text{CsH}_2\text{PO}_4$ , cryst. struct. 0-64975  
 $\text{Te}_{50-x}\text{Se}_{50}\text{Sn}_x$ , thin films, elec. cond. and thermoelectric power meas. (*French*) 0-80335  
 $\text{Te}_{90}\text{Si}_{10-x}\text{Pb}_x$  glasses, phase separation, double  $T_g$  presence 0-88306  
 $\text{TiO}_2\text{-TeCl}_4$  system, chem. vapour transport, matrix isolation IR studies 0-93755  
 $\text{Ti-Ge-Te}$  glass formation 0-103255
- TEM** see transmission electron microscopy
- temper brittleness** see brittleness
- temperature**  
 see also atmospheric temperature; boiling point; critical points; Debye temperature; ferroelectric Curie temperature; magnetic transition temperature; melting point; superconducting transition temperature; temperature scales  
 acoustical props. of laboratory sediments 0-96069  
 dew point temp. change with pressure, calc., nomogram 0-77607  
 Earth surface temperature, determ. of diurnal var. in mountainous terrain 0-82011  
 interstellar clouds, effects of temp. and activation energies on gas phase chemistry 0-105298  
 interstellar gas of solar neighbourhood, temp. and vel. determ. from interplanetary H I  $\text{Ly}\alpha$  emission profiles 0-105141  
 interstellar medium, local, temp. from interstellar He I obs. 0-62234  
 interstellar medium, local, temp. rel. to ionisation state 0-90502  
 Mars, longit. var. of thermal inertia and 2.8 cm brightness temp. 0-105191  
 E.Pacific Rise geothermal system, physical limits on geothermal fluid temp. and role of adiabatic expansion 0-101362  
 PHL 1092, narrow line quasar, Fe II emission region electron density and temp. 0-77508  
 planetary nebulae central stars, comparison of Zanstra He II temps. and temps. from visual spectra 0-109434  
 planetary nebulae central stars, temps. determ. rel. to nebulae evolution 0-67724  
 sea surface, temp. field rel. to poleward heat flux by oceanic gyre 0-85668  
 Venus upper mantle, temp. rel. to planet tectonics and comp. 0-72805
- temperature compensation** see compensation
- temperature control**  
 see also thermostats  
 biological media temperature stabilisation, electronic device 0-85539  
 calorimeter, automated, high precision, for 200K to 400K, temp. controller design 0-86310  
 constant temp. water bath using simple thermal/vapour barrier 0-86290

**temperature control continued**

- cryogenic, use of ICs 0-90856  
 crystalline thermal treatment, control thermocouple (*Spanish*) 0-73362  
 electronic temperature controller 0-86282  
 electronic thermostat, with 0.1°C accuracy and economical operation, photography appl. 0-77774  
 heat storage device, off-peak, ambient temp. observer/predictor control system 0-66950  
 inductive load temperature regulator, using IC zero voltage switch U 106 BS with triac. (*German*) 0-77779  
 laboratory, modified window air conditioner, thermistor bridge circuit 0-68192  
 LPE, multi-layer, furnace design and fabrication (*Japanese*) 0-108366  
 multiplexers, temperature applications, types of unit and configurations 0-82757  
 optoelectronic temperature profile recorder 0-105642  
 photographic developing bath, thermostatic control (*Spanish*) 0-77898  
 physiomechanical testing, low temperature, temp. control for tests in liquid coolant vapours 0-81260  
 solar energy systems, modern control theory appl. reviews 0-66949  
 spacecraft heat rejection improvements using thermoelectric devices 0-108810  
 SQUID magnetometer with temp. control, spontaneous magnetisation and mag. susceptibility meas. 0-68221  
 TEM specimen freeze drier, all-glass design 0-82854  
 thermocouple reference junction box, used for vacuum chamber 0-90844  
 thyristor temp. regulator for pulsed NMR spectrometer 0-105687

**temperature distribution**

- aquifer, temp. field due to hydrothermal convection, numerical calcs. 0-90105  
 N.Atlantic, sea surface temp. year to year changes, (1948 to 1974) 0-67367  
 S.Atlantic Ocean, glacial and interglacial temp. conditions from  $\text{CaCO}_3$  and radiolarian distrib. 0-72556  
 atmosphere, thermal radiation obs. from ground (*Chinese*) 0-82041  
 atmosphere boundary layer temp. profile determ. from ground-based 60 GHz radiometry (*German*) 0-82097  
 Baltic Sea, estuary region, suspension distrib. under river drifts influence (*Russian*) 0-98345  
 benthic ocean, temp. distrib. and flow struct. 0-72532  
 Boussinesq fluids in turbulent convection, power spectra of temp. and vel. fluctuations 0-98543  
 circular cylinder, local heat transfer by turbulence of free-stream flow of viscous liquid, theoretical determ. of influence (*Russian*) 0-96252  
 cloudy atm., long distance meas. by radiometry 0-90196  
 contact binary stars structure, secular stability of temp. inversion layer 0-109493  
 R Coronae Austrinae interstellar molecular cloud, for IR study and dust temp. profiles 0-62237  
 dielectric liquid, elec. stressed, motion due to Coulomb, electromech. forces, schlieren image obs. 0-100037  
 early universe, density-temp. fluctuations present observability 0-82554  
 Earth crust, temp. distrib. in Ukrainian Shield rel. to search for fracture waters (*Russian*) 0-104935  
 emission measure for UV spectra of RW Aurigae and RV Lupi 0-94788  
 face effect, with paraboloidal or ellipsoidal isotherm effect 0-107085  
 free burning arc characteristic formulae 0-70068  
 free convection flow past vertical porous plate set in impulsive motion 0-69818  
 glass container forming, mould surface temp. meas. 0-82767  
 Gulf Stream and the north east Atlantic temperature anomaly (*German*) 0-85684  
 Hamels spiral flow, temp. and vel. distrib. (*German*) 0-87779  
 heat conduction problems, soln. method (*German*) 0-74705  
 heat pipes, rotating, temperature and heat load distrib. 0-64341  
 heat resistant monocrystal growth apparatus, heat regimes, crystallisation (*Russian*) 0-107071  
 heat-emitted pipe, with surface boiling, temp. fluctuations (*Russian*) 0-102962  
 high-current free burning arcs, approximate model 0-70069  
 IC 1396 interstellar molecular cloud, for IR study and dust temp. profiles 0-62237  
 Indian Ocean, modern and ice-age surface water zonal temp.-anomaly maps 0-77007  
 Indian Ocean, temp. meas. rel. to continuous spectrum of equatorial waves 0-98331  
 intense electric fields in needle/cylinder electrodes, space temp. and thermal model (*Rumanian*) 0-63885  
 interstellar giant molecular clouds, density inhomogeneities temps. rel. to gravit. field 0-62242  
 Kirin meteorite, temp. gradient prod. in atm. passages, thermolum. obs. 0-67672  
 Kirishima volcanoes, Japan, surface temp. distrib. from geothermal survey (*Japanese*) 0-67357  
 Laccadive Sea (Lakshadweep), temp. and salinity characts. 0-104966  
 lakes, surface water temps. appl. to latent and sensible heat fluxes 0-72562  
 lakes in Wyoming, bathymetry and temp. 0-94550  
 laser surface transformation hardening, heat flow model for cylinder 0-93700  
 liquid film, viscous, between two nearly parallel walls, temp. distrib., convection effects 0-83801  
 living tissues, simulated, temp. distrib. in EM irrad. 0-85354  
 long rod, direct-heating meas., interpretation 0-102964  
 MHD forced convection in channel bounded by plate and permeable bed, Hall effects 0-69934  
 microwave brightness temp. distrib. over Bay of Bengal using SAMIR Satellite Microwave Radiometer data at 19 and 22 GHz 0-104980  
 NDT of delamination and inclusion flaws, ID anal. 0-71820  
 nontransparent medium, bounded flat layer effective temp. determ. 0-69638  
 North Sea, sea surface temp. year to year changes, (1948 to 1974) 0-67367  
 ocean surface temperature, meas. 200 km from land rel. to air-sea heat transfer coeffs. 0-72552  
 ocean thermocline, small-scale turbulence (*Russian*) 0-61807  
 ocean upper layer, small-scale temp. fluctuations statistical regularities (*Russian*) 0-94528  
 Pacific Ocean, annual var. in slope of 14°C isotherm along equator 0-72537

**temperature distribution continued**

- Pacific Ocean, December sea surface temps. correl. with spring rains in California 0-77064  
 plate, heated, semiinfinite, vertical, with heat sources and sinks natural convection 0-59035  
 polymerisation in flow-through reactor, low-temp. conditions 0-61092  
 S140 interstellar molecular cloud, for IR study and dust temp. profiles 0-62237  
 sapphire crystal grown by Stepanov's method, axial temp. distrib. 0-103280  
 sea surface temp. anomaly gradient in N.Pacific 0-85674  
 Shuttle Orbiter re-entry, remote IR imagery and tracking 0-82171  
 solar collector, flat-plate, temp. distributions under actual unsteady insolation 0-97803  
 solar transition zone, nonresonant heating mechanism (*Chinese*) 0-85921  
 spent nuclear fuel elements, intermediary storage, stationary temp. level determ. calc. method 0-91223  
 steel, platelike parts, quenching, temp. field calc. 0-60889  
 structural stress distrib. determ. by remote IR thermometry 0-87749  
 Sun under quiet conditions, SHF brightness temp. distrib., RATAN-600 obs. (*Russian*) 0-94776  
 thermoelectric cooling equipment, welded joints, heat emission effects on temp. distrib. (*Russian*) 0-69635  
 trapped flux removal by thermal gradient technique 0-75694  
 upper ocean temperature and salinity structure, obs. during POLE expt. 0-72536  
 Venus, IR brightness temp., daytime minima 0-77309  
 Venus atmosphere, struct., and light, heat and wind regimes from space vehicles 0-62062  
 Weddell Sea, bottom water temp. and salinity variability 0-67366  
 Al billet, hot extrusion, nonsteady state temp. distrib., numerical method 0-60886  
 Al-Al<sub>3</sub>Ni eutectic, temp. gradients, microstructural changes 0-84971  
 GaAs-Al<sub>0.3</sub>Ga<sub>0.7</sub>As laser diode, spontaneous radiation transfer 0-91796  
 Ge ribbon single crystals, grown from melt, dislocation struct. form. under thermal stress 0-107082  
<sup>3</sup>He-<sup>4</sup>He dilution refrigeration system, choice of tube lengths and diameters 0-57308  
 Li<sub>2</sub>O pellets, neutron irradiated, temp. distrib. 0-86968  
 Si ribbon crystal growth, 10 cm wide, temp. distrib. meas. in die 0-104059  
 Si wide ribbon, high speed edge-defined film-fed growth 0-104058  
 Si<sub>3</sub>N<sub>4</sub> layers deposition, high-temperature, in resistance furnace, temperature gradient and nitrogen flow influence obs. (*Bulgarian*) 0-80981

**temperature measurement**

- see also pyrometers; spectral methods of temperature measurement; temperature scales; thermocouples; thermometers  
 A/D converters TL505/507 and microprocessor TMS1000 measurement system (*French*) 0-57290  
 AC circuits for low temperature measurement with semiconductor thermometers (*Polish*) 0-82766  
 atmosphere temperature meas. in fog and stratus, shipboard use of low-level atmospheric thermograph 0-105073  
 band radiation pyrometry for error reduction in transmission coeff. calc. of IR radiation energy depend. on atmospheric props. (*German*) 0-105649  
 bench for metrological certification and testing of radiant-flux sensors (RFS) 0-98977  
 biomedical temperature biotelemeter, modular, expandable, implantable 0-67191  
 biomedical thermometry, use of salt-hydrate transition temps. as fixed points 0-104801  
 bipolar IC temperature transducer, intrinsic bandgap voltage as reference, Fahrenheit, Celsius or arbitrary scale operation 0-82761  
 blood temperature monitoring during extracorporeal circulation, noncontact transducer 0-85513  
 body, ATP-12M infrared imaging system (USSR) 0-67280  
 bridge measuring circuit, linearisation (*Russian*) 0-90847  
 degree-day measurements 0-77574  
 dilatometer for PVT meas. of liquids and plastic crystals at low temperature 0-68208  
 Earth's atmosphere, remote meas. of 3-D temp. distrib. using TIROS-N microwave sounder unit 0-90265  
 electric motors, ribbed frames with external fans, heat transfer coefficient measurements (*Hungarian*) 0-87709  
 electronic excitation and ionisation temp. meas. in ICP Ar source, H<sub>2</sub>O vapour effects 0-75028  
 fibre optical interferometers for length, temp., pressure and force meas. 0-98971  
 flame, swirling, temp. distrib. 0-61098  
 fluid, laser interferometry appl. 0-75018  
 fluidic temperature sensors 0-73342  
 formaldehyde, molecular beam rotation temp. meas. (*French*) 0-78724  
 frequency thermoconverter dynamic error electrical correction (*Russian*) 0-57242  
 gas, thermal probe for high stationary temperatures 0-95101  
 glass, IR thermometry, readings interpretation 0-82765  
 glass container forming, mould surface temp. meas. 0-82767  
 human body-temp. sensor-environment system, analogue model of interaction 0-104783  
 IC temperature sensors used in thermocouple cold junction compensation circuits 0-77777  
 in-reactor fuel temperature, transient response of centreline thermocouples, appl. to fuel modelling 0-95372  
 International Practical Temperature Scale revision, thermodynamic temperature in range 0 to 1064°C 0-62669  
 IR battery operated portable thermometer (*German*) 0-57289  
 liquid metal, thermal conductivity meas. in Spacelab, temp. meas. device for control (*German*) 0-57303  
 liquid-crystal optical fibre temp. probe rel. to thermometry and dosimetry of heat 0-98204  
 loudspeaker moving coil temp. meas. systems (*Hungarian*) 0-106698  
 low density supersonic gas flow, temp. meas. probe 0-74913  
 magnetically controlled reed switches, used for temp. meas. (*French*) 0-57291  
 metal, molten, digital device for determining temp. (*Russian*) 0-90846  
 metal fixed points, limitations caused by trace impurities 0-105644  
 metal objects, moving, temperature meas. by thermoelectrical thermometer (*Russian*) 0-90848  
 metals and alloys, critical temperatures determination, elec. resist. method, IMASH-5S-69 installation 0-71827



**temperature measurement continued**

- MHD combustor and channel, microprocessor-based Na reversal instrument 0-73364  
 monitoring with remote indication, up to 150°C (*German*) 0-73356  
 multiplexers, temperature applications, types of unit and configurations 0-82757  
 NTC thermistor sensors, cct. designs and design calculation tables 0-68201  
 optical, based on fibre optics and phosphors 0-73360  
 optoelectronic temperature profile recorder 0-105642  
 photographic developing bath, thermostatic control (*Spanish*) 0-77898  
 pyrometer, for use in solar furnaces 0-86312  
 resistance thermometer thermal inertia compensation (*Russian*) 0-62667  
 resistance thermometers, thermojunctions and temperature sensitive ICs for automatic meas. (*German*) 0-77778  
 review 0-86305  
 sea ice age category differentiation through location and temp. observations using microwaves 0-67380  
 sea-surface, derivation from Meteosat image data 0-76985  
 seawater, microprocessor-based instrument 0-67440  
 semiconductor thermometer, providing six point temp. meas. (*French*) 0-68200  
 shock compression of solids, temp. meas. by optical means 0-86304  
 SI units fundamentals (*French*) 0-95059  
 specular reflection, use for radiation thermometry (*Japanese*) 0-101795  
 standard temperature lamps, with W ribbon filaments 0-95102  
 standards and thermometers in the USSR 0-62618  
 steel, mild, laser microspectral anal. 0-108769  
 still-shade-temperature meter for use in assessing personnel cold stress 0-81764  
 superconducting temperature sensor, NbTi monofilamentary wire in current sharing state 0-57288  
 superconductive temperature fixed point device, prep. and calibration 0-82770  
 surface temperature in fluidised beds, infrared photoresistors (*Russian*) 0-82763  
 surface temperature measurement using temperature indicating materials, crayons 0-86301  
 surface temperature measurement using thin film thermocouple 0-62668  
 telemetry system with interference suppression, implantable, long-life, animal expts. appl. 0-101302  
 telemetry transmitter, crystal-controlled, surgically implantable, for animal expts. 0-72393  
 TEM, temperature calibration standards using graphite-halogens 0-86510  
 terrestrial surface temperature sensing, emissivity correction for thermal radiation interpretation 0-82092  
 thermal imaging with pyroelectric vidicon camera 0-86288  
 thermal inertia mapping by IR imagery, mathematical model 0-109280  
 thermocouple slip-ring assembly for measurement of temperature of rotating bodies 0-86294  
 thermocouple thermal inertia (*Russian*) 0-62665  
 thermocouples, modern design, avoiding errors 0-62664  
 thermoelectric needle probe for medical and biological temp. meas. 0-101299  
 thermophysical properties, thermometric method determ., harmonic action of heat flow (*Russian*) 0-69642  
 transducer, digital, solid-state, using automatically balanced Wheatstone bridge (*Rumanian*) 0-57287  
 transducer with thermal feedback, operational principles (*Russian*) 0-86299  
 transducers, semiconductor diode junctions, variation of forward voltage with temp. 0-57293  
 transistor temperature transducers, Motorola MTS IC series, appls. (*French*) 0-73357  
 TTF-chloranil visual pressure or temperature indicator 0-87443  
 turbulent temp. fluctuations recording, with detector dynamic response correction, dynamic errors determ. 0-77781  
 two-phase flow, nonequilibrium, phase temp. meas. 0-74950  
 US thermometry, nuclear appls. 0-73365  
 vacuum coating, substrate and film surface temp. meas. 0-57297  
 Venus ionosphere, electron temp. probe on Pioneer Venus Orbiter 0-67500  
 viscosimeter solar radiation tracking sensor 0-86295  
 Ar, compressed gas, PVT meas. at high press. 0-98927  
 C resistors for low temp. thermometry 0-86308  
 CePd<sub>3</sub>-Er, dil. low field mag. susceptibility, electro-nuclear effects, rel. to thermometry 0-60189  
 D<sub>2</sub>, sticking and accommodation on low-temp. substrate, mol. beam expts. 0-84368  
 H<sub>2</sub>, sticking and accommodation on low-temp. substrate, mol. beam expts. 0-84368  
 NbTi-Cu, supercond. composite, use in temp. and heat transfer coeff. meas. 0-77780  
 Pt resistance thermometers, heat leaks effect anal. 0-57296  
<sup>119</sup>Sn, <sup>117</sup>Sn, low temp. NMR thermometry 0-82775

**temperature scales**

- fixed point, triple point of water 0-59626  
 methane 0-95099  
 standards and thermometers in the USSR 0-62618  
 superconductive temperature fixed point device, prep. and calibration 0-82770  
 thermodynamic, gas thermometer reference standard 0-77782  
 thermometry, review 0-86305  
 Ar triple point sealed cells using stainless steel envelope 0-95099  
 Nb, superconductive transition point as reference temp. 0-107943  
 Ta, superconductive transition point as reference temp. 0-107943

**tempering**

- alloys, temper embrittlement, impurities and alloying elements role, review 0-66649  
 austempered reinforcing wire, tempering under stress, effect on mech. props. and relaxation resistance 0-100861  
 ceramics containing metastable tetragonal ZrO<sub>2</sub>, grinding induced tempering 0-89260  
 glass, annealed and tempered, impact damage, strength 0-85025  
 optical glass, thermally tempered, surface stress meas. by crit. ray method 0-106766  
 steel, alloy, cementite phase dispersion change during tempering (*Russian*) 0-93577  
 steel, alloy, heat-treated, crack resist. in seawater 0-104347

**tempering continued**

- steel, alloy, high-speed, struct. changes investigation by hot hardness and quench dilatometry (*French*) 0-76249  
 steel, austenitic, strength, ductility and fracture toughness, N and Cr effects 0-100878  
 steel, austenitic stainless, supercond. magnets, mech. and phys. props. at 4K 0-86976  
 steel, austenitic type EI-69, carbide transformations on precipitation of C from austenite (*Russian*) 0-97487  
 steel, Cr-Mo (2.25, 1.0 wt.%), temper embrittlement, effect of P, Sn, comp. and carbide precip. 0-85036  
 steel, Cr-Mo (2.25, 1.0 wt.%), temper embrittlement, effect of Mn, Si, comp. and carbide precip. 0-85037  
 steel, Cr-Mo weld metal, trace element embrittlement suppression by creep strength effects 0-66656  
 steel, Cr-Mo-Mn-Si-W (3, 1.95, 1.55, 1.45, 0.95 wt.%), struct. and props. 0-104175  
 steel, Cr-Mo-Ni-WV (6, 4, 3, 2 wt.%), tempering and secondary hardening, TEM obs. (*Chinese*) 0-104245  
 steel, Cr-Mo-V pressure vessel, microstruct. parameters and yielding rel. to plastic deform. 0-89318  
 steel, Cr-Ni-Mo-V, austenite form. during heating, influence of recrystn. during tempering (*Russian*) 0-104188  
 steel, Cr-Si-Mn-Ni-Mo-C, resist. to deform. and fracture, C effect 0-71757  
 steel, Cr-W(Mo), quenched, carbide reactions during tempering 0-89229  
 steel, CrMoV, creep resistant, quantitative struct. parameter use in props. prediction (*Czech*) 0-108481  
 steel, high C, investigation of transformations during tempering by nuclear gamma resonance method (*Russian*) 0-76256  
 steel, high C, type 7KhFNSh, plastic deform. influence of X-ray interference line breadth (*Russian*) 0-93599  
 steel, high strength, failure stress, structural relationships 0-81190  
 steel, high strength, treatment effect on ductility and strength 0-60880  
 steel, high strength weld metal, fractography, microstructure and reheated zone toughness effects (*Japanese*) 0-108543  
 steel, high-speed, low temp. mag. cycling effects on ferromag. struct. 0-100928  
 steel, high-speed tool, splat quenching, props. and struct. 0-76294  
 steel, low alloy, isothermal tempering effect on acoustic emission during ductile fracture 0-85047  
 steel, low alloy, temper embrittlement and ternary equilib. segregation 0-60958  
 steel, low Si, martensite struct. and mech. props. (*Korean*) 0-93614  
 steel, low-alloy structural 16G2 and 16GFR, struct. and props. after quenching and tempering 0-76280  
 steel, maraging stainless, phase transformation and mech. props. rel. to heat treatment (*Chinese*) 0-66501  
 steel, martensitic, alloying element effect on coarsening behaviour of cementite particles in ferrite 0-66518  
 steel, Mn-B-V, low alloy, transform. singularities (*Russian*) 0-104116  
 steel, Mn-C-Si-Cu (0.95, 0.85, 0.25, 0.16 wt.%), fibrous-banded fracture mechanism 0-104280  
 steel, Ni, high-strength, impact fatigue strength, heat treatment conditions effect 0-76285  
 steel, Ni-Co-Cr, high-strength medium C, Cr effect on props. 0-76339  
 steel, Ni-Cr, temper embrittlement, intermediate tempering treatments 0-60944  
 steel, Ni-Mo-C (5, 0.5, 0.5 wt.%), sintered, effects of powder and sintering variables on props. 0-104093  
 steel, pearlitic, heat treatment effect on fracture resistance, microstruct. and mech. props. 0-104191  
 steel, stainless, tempering after air hardening from rolling heat (*German*) 0-93571  
 steel, structural, 34KhN3M, heat treatment effect on magnetostriction 0-104306  
 steel, structural, strained in tension after tempering, compression effects on struct. changes (*Russian*) 0-66577  
 steel, structural 15KhNMFA, resist. to weakening during tempering, high purity effect 0-76279  
 steel, tempered, notched, impact bending tests, cold brittleness curves 0-71758  
 steel, tempered martensitic, type AISI 410, role of C in embrittlement phenomena 0-93652  
 steel, tempering effect on fatigue strength 0-60891  
 steel, type 20Kh deformed, austenite grain size, inheritance effect with quenching and tempering 0-60881  
 steel, types 60G, ShKh15, structural changes near holes and inclusions due to pulsed currents (*Russian*) 0-108459  
 steel, W-Co-Mo-Cr-V-C (8.5, 8.1, 4.5, 3.5, 2.2, 1.02 wt.%), phase composition, struct. and props. 0-104163  
 steel (*French*) 0-66670  
 steel 40 G, coercimeters with attached electromagnets used for quality control 0-108672  
 steel bearing rings, optimisation of thermomechanical working parameters (*Russian*) 0-93579  
 steel fine structure after heat treatment, X-ray diffr. exam. 0-60890  
 steels, heat treatment of 30KhN2MFA and 40Kh, nondestructive mag. quality control method 0-108662  
 Al alloys, (5083, 6061, 2219), supercond. magnets, mech. and phys. props. at 4K 0-86976  
 Al-Cu(Si)(Mg) binary and ternary alloys, dimensional changes in heat treatment. 0-89271  
 Al-Mg-Si, type 6010, microstruct. characts. influence on formability, heat treatment 0-81090  
 Co-Fe, soft mag. props. rel. to metallurgical aspects 0-88810  
 Cr-Ni-Mo 40KhN2MA, magnetostriction used in inspection after heat treatment 0-108673  
 Cu-Ni-Fe, magnetic properties, heat treatment and compressive stress effects 0-60367  
 Fe cast with spheroidal graphite, fine cryst. struct. on tempering (*Russian*) 0-96476  
 Fe-Ni-C, intercrystalline embrittlement in tempered martensite, elimination by reautenitization (*Slovak*) 0-108548  
 Fe-Si cast alloy with spheroidal graphite, transform. investigation during tempering (*Russian*) 0-97479  
 Fe<sub>40</sub>Ni<sub>40</sub>P<sub>14</sub>B<sub>6</sub> amorphous alloy, temper embrittlement 0-76295  
 Na<sub>2</sub>O-SiO<sub>2</sub> glass, microcracking about NiS inclusions, fracture mech. description 0-89333  
 Ni-Fe, soft mag. props. rel. to metallurgical aspects 0-88810

**tempering continued**

- Ni-Fe-Nb-Mo-Al, head material for mag. recording, DC and AC mag. props. 0-88812
- NiPt, quenched, ordering kinetics and domain struct. form. during isothermal tempering (*Russian*) 0-66502
- steels, Cr-C-Mn(Ni), struct. prop. rel., design of struct. steels for high strength and toughness 0-97491
- Ti-Al-Mo-Cr alloy weldment containing orthorhombic martensite, auto-tempering behaviour and alpha precip. strengthening 0-84976

**tenacity** *see* **tensile strength****tensile strength**

- see also fracture; yield strength*
- acrylourethane coatings, radiation curable, tensile, elongation and modulus props. appl. techniques 0-66847
- bagasse fibre reinforced phenol formaldehyde, tensile strength and Young's modulus, SEM study 0-60952
- ceramic, proof testing 0-104207
- ceramic, proof testing 0-108654
- coating struct., SEM study 0-97605
- coke, metallurgical, industrial strength meas. methods, critique 0-85117
- coke, metallurgical, strength and struct. relationship 0-84997
- cokes, metallurgical, struct. and strength 0-93610
- composites, single fibre-brittle zone model, fracture behaviour 0-97570
- concrete, flowing, expt. studies (*Japanese*) 0-89298
- concrete, high strength, made with a special cement admixture, mech. props. (*Japanese*) 0-89297
- concrete, impact bending capacity (*Japanese*) 0-89341
- concrete, strength, shrinkage strain and deterioration down to  $-160^{\circ}\text{C}$  (*Japanese*) 0-100886
- concrete, tensile testing device, axial 0-61054
- creep in circular specimen subject to pure bend, ultimate tensile and compressive strength (*Russian*) 0-74768
- CVD optical fibre, long length strength 0-58752
- elastomers, rel. between relax. behaviour and tensile strength (*German*) 0-66604
- empirical determination, cleavage fracture in plane waves 0-96225
- ethylene-Co copolymers and  $-\text{SO}_2$  copolymers prep. by catalysis and  $^{60}\text{Co}$   $\gamma$ -radiation, mech. props. 0-66841
- ethylene-vinyl acetate copolymers, extrusion and heavy duty films, radiation crosslinking, struct. effect 0-66844
- fibre, single-mode, numerical aperture effects 0-69548
- fibre reinforced composites, struct. parameters depend. 0-65134
- fibre reinforced laminated hybrid, tensile first cracking strain and strength 0-81175
- fibres, optical, fatigue characts. improvement, using surface compression cladding 0-69549
- filaments, elastic, tensile test method, and treatment of expt. data 0-85111
- flat sheets, tensile deformation analysis 0-96198
- galvanic coatings, tensile testing device 0-100988
- glass fibre reinforced cement, durability in wet and dry conditions, fibre length and content effect 0-71726
- glass fibres, crack growth during dynamic fatigue and effect on strength loss for tensile loading 0-89334
- glass-fibre reinforced cement, strength study by reliability concept, fibre concept and temp. depend. (*Japanese*) 0-66586
- graphite, pyrolytic commercial, high-temp. thermal and mech. props. 0-75372
- graphite fibre epoxy composites, exposed to high temp., degradation of tensile and shear props. 0-81113
- graphite fibre filled polyimide composite laminates, space environment, phys. and mech. response 0-81140
- laminates, damage zone failure analysis 0-85059
- ligaments of small animals, gripping device for tensile testing 0-81791
- metal, electronic work function under tension, 20 to  $1200^{\circ}\text{C}$  0-76448
- metals and alloys, mech. props. electric current effect, test device for 4.2-300K 0-66719
- natural rubber vulcanisate, network changes during physical testing 0-60936
- optical fibre, furnace drawn, tensile strength 0-58751
- optical fibre, modified CVD prep., optical and mechanical props. reproducibility 0-69535
- optical fibres,  $\text{GeO}_2\text{-B}_2\text{O}_3\text{-SiO}_2$ , ageing effects of moisture on fatigue and tensile strength 0-66539
- optical fibres, mech. reliability 0-91909
- optical fibres, tensile strength and static fatigue, analysis using Weibull distribution for optimum design 0-85011
- organoplastics, fracture characts., effect on strength 0-66642
- polyacetylene films, tensile props. and partial alignment 0-104210
- polyamides, extended chain aromatic, fibres, tensile strength and moduli 0-81021
- polydimethyl siloxane-b-styrene-b-dimethyl siloxane block copolymer, morphology, mech. props. 0-64930
- polyester resin concrete, effects of styrene-unsaturated polyester ratio on props. (*Japanese*) 0-89299
- polyethylene, high density, solid state coextrusion, geometric factors effect 0-71704
- polyethylene, high density, solid state coextrusion, technique for ultradrawing thermoplastics 0-84979
- polyethylene, high-density, solid-state coextrusion, mol. wt. distrib. effect 0-104212
- polyethylene fibre, high-strength high-modulus, morphology and tensile prop. relations 0-103264
- polyethylene ribbons, flow-induced crystn. from melt, in dies fed by single screw extruder 0-84110
- polyethylene surface-growth fibres, hot drawing 0-97517
- polyethylenes, extrusion and heavy duty films struct. parameters influence on cross-linking by radiation 0-66844
- polyphenylene sulphide, high mol. wt. soluble resin, prep., mech. props. 0-60828
- polypropylene, flow-induced crystn. from melt, in dies fed by single screw extruder 0-84110
- polyurethane foams, elastic, stability against organic solvents (*German*) 0-85074
- power cables, HV, Rb coverings quality estimation using mechanical tests (*Polish*) 0-97525
- PVC, oriented mouldings, struct. order 0-60896
- refractories, thermal stress cracking resistance estimation 0-104288
- rubber, crystallising, tensile test specimen prep. 0-71838
- sheet material, method for strength meas. under biaxial tension 0-66717

**tensile strength continued**

- spherulastic, spherical shells, supporting capacity 0-87723
- steel, alloy, deformation, rapid dynamic, at  $-196^{\circ}\text{C}$  0-104220
- steel, alloy, tensile test, regulated, strength and deform. characteristic values, consistency (*German*) 0-93712
- steel, austenitic, strength, ductility and fracture toughness, N and Cr effects 0-100878
- steel, austenitic, tensile strength, elec. current impulse effect down to  $4.2\text{K}$  0-81131
- steel, austenitic stainless, cathodically charged,  $\text{H}_2$  embrittlement,  $\alpha'$  martensite effect 0-71725
- steel, austenitic stainless, supercond. magnets, mech. and phys. props. at  $4\text{K}$  0-86976
- steel, C, low temperature strength, preliminary plastic deform. effect 0-81128
- steel, C, residual elements, effect on props. 0-66643
- steel, C, tensile fracture surface in high press.  $\text{H}_2$  at room temp. (*Japanese*) 0-108540
- steel, C, tensile props. in high press.  $\text{H}_2$  at room temp. (*Japanese*) 0-108501
- steel, Co-Cr-Mo type HY-180M, mech. props. and SCC, overageing effect 0-108634
- steel, Cr-Mo, effect of Mo on high-temp. props. 0-85005
- steel, Cr-Mo (2.25, 1 wt.%) pipe, high temp. fatigue and creep strength 0-85060
- steel, Cr-Si-Mn-Ni-Mo-C, resist. to deform. and fracture, C effect 0-71757
- steel, eutectoid, mech. behaviour, thermomech. treatment effects 0-84970
- steel, heat resistance, thermal stability, stress-rupture strength, and creep 0-81194
- steel, heat resistant, tensile strain and endurance, normal and radiation conditions, linear load variation 0-81189
- steel, high alloy Cr-Mo-W, splat quenched, formation of metastable austenite 0-84974
- steel, high C, tensile strength, working and heat treatment effects (*Japanese*) 0-104209
- steel, high strength, failure stress, structural relationships 0-81190
- steel, high-strength tool steel D7KhFN, remelting effect on mech. props. 0-76284
- steel, hot forging die type, fractography (*Japanese*) 0-108547
- steel, lamellar pearlite, containing proeutectoid cementite, brittle fracture study (*Japanese*) 0-93648
- steel, low alloy, strength, Cr and N effects 0-104277
- steel, low C, dual-phase, law of mixtures, applicability 0-89346
- steel, low C, mech. characts., specimen size and shape effects 0-66715
- steel, low C, type En3, high strain deform., struct. and props. 0-89301
- steel, low-alloy, bearing, mech. props., carbide behaviour effect (*Korean*) 0-93615
- steel, low-alloy, plastic deform. mechanisms under dynamic loading 0-100883
- steel, low-alloy, residual elements, effect on props. 0-66643
- steel, microalloyed, types V1599, V1600, V1286, NbCN precipitation in undeformed austenite 0-89230
- steel, Mn-Mo, castings, mech. props., Cu and Sn trace elements effect 0-66596
- steel, Mn-V reinforcing type, strain ageing characts. rel. to mech. props. 0-84969
- steel, Ni, welded joints on LNG carriers mech. props. and fracture toughness 0-85017
- steel, powder forged, fatigue, surface treatment effect 0-85048
- steel, rail, toughness, effect of Sn, SEM exam. 0-97569
- steel, stainless, AISI 316, high-temp. mech. props. 0-66601
- steel, stainless, deformation, rapid dynamic, at  $-196^{\circ}\text{C}$  0-104220
- steel, stainless, type 316, neutron irradi. effects on tensile props. and microstruct. 0-65059
- steel, stainless type SUS 304, diffusion welded joints, sound emission during tensile testing (*German*) 0-61062
- steel, structural, type St3S, hardness, random functions 0-76329
- steel, structural, wide plate tensile testing eval. (*German*) 0-100969
- steel, toughness, review of joint tests (*German*) 0-65142
- steel, type IN-787, for use in Arctic, low temp. effects on mech. props. 0-76310
- steel, types A533B and KAS, fracture toughness meas. using elect. potential method (*Japanese*) 0-93722
- steels, nitrided age-hardened, for blanking punches, chipping resist. props. (*Japanese*) 0-89340
- steels, types SS41, SB42, SM50A, STK55, liq. Zn embrittlement (*Japanese*) 0-81164
- steels, wide plate and V-notch bending tests evaluation on basis of materials mechanics (*German*) 0-66571
- steels, with yield pt. of about 420 to 720 N/mm<sup>2</sup>, correlation between yield pt./tensile strength ratio and toughness (*German*) 0-66615
- strip with semicircular notches, tensile load conditions at end, interf. effects obs. 0-64455
- Stycast-1266, mechanical props. at low temps. 0-57286
- tensile test, uniaxial, for plastic deform. (*Hungarian*) 0-97657
- vertebrae, human, mech. props. 0-72206
- viscoelastic material, failure and instability in tension 0-87720
- water under tension monitoring, Berthelot-Bourdon tube method 0-88238
- wires in steel cables, tension measuring device and method of use (*Russian*) 0-68196
- Zircaloy, annealed, neutron irradiated, inhomogeneous deform. behaviour 0-85014
- Zircaloy-2, mech. props. after exposure to  $\text{I}_2$ -methanol solutions, SEM study 0-93689
- Ag-Ni (10 wt.%) wire, plastically deformed, fracture struct. (*German*) 0-71744
- Al alloy with different props. in tension and compression, creep 0-81129
- Al alloy-mica particle composite, cast prep. and mech. props., bearing appl. 0-71613
- Al alloys, (5083, 6061, 2219), supercond. magnets, mech. and phys. props. at  $4\text{K}$  0-86976
- Al single crystals, relation between axial orientation rotating and deform. banding 0-104206
- Al, stability and strength of FCC metal using Morse pot. 0-59430
- Al, ultimate tensile strength for brief impact 0-70309
- Al-Ca-Zn (5.5 wt.%) superplastic steel alloy, mechanical properties, superplastic forming behaviour 0-60920
- Al-Cu-Mg type 2036, thermomech. treatment, flow stress anal., effect in mech. props. 0-93584
- Al-Cu-Mg/mica particulate composite mech. props. 0-100919



**tensile strength continued**

- Al-Cu(0.10 wt.%) sintered compacts, mech. props. rel. to sintering 0-76210
- Al-Mg-Si, type 6061-T6, 6063-T6, effective stress range factor in fatigue 0-100924
- Al-Mg-Si alloys, cast, precip.-rich zones on grain boundaries, soln. heat treatment conditions effect on mech. props. 0-104176
- Al-Ni (6 wt.%), fine-grained, deform. in tension and torsion 0-85008
- Al-Zn-Mg, type V-95, ultimate tensile strength for brief impact 0-70309
- Al-Zn-Mg alloy, Ag addition and pre-precipitation treatment, influence on GP zone growth 0-71658
- Al-Zn-Mg-Cu alloys, heat treatment optimisation 0-60888
- Al-Zn-Ti(Mn), mech. props., Ti or Mn addition effect (*Korean*) 0-93613
- $\alpha$ -Al<sub>2</sub>O<sub>3</sub> fibre FP, manufacture, strength and modulus 0-81013
- $\alpha$ -Al<sub>2</sub>O<sub>3</sub> fibre FP reinforced Al and Mg composites, fabrication and props. 0-81004
- B fibre reinforced epoxy composites, notched, tensile strength and failure modes 0-81205
- Be, sintered, physicomech. props. anisotropy, BeO inclusions effect 0-60804
- C fabric reinforced plastic laminates, tensile and compressive strength determ., 20-1500°C 0-100880
- C fibre, tensile strength, heat treatment and flaw effects 0-81173
- C fibre composite, aligned, prep. and theoretical strength agreement 0-84906
- C fibre derived from mesophase-pitch, Young's modulus and tensile strength, struct. flow elimination 0-80995
- C fibre reinforced composites for spacecraft use, prep., props. and struct. 0-71625
- C fibre structure, recent advances 0-81069
- Cd, warm rolled, texture and grain size depend. of tensile props. 0-71720
- Cd-Ge broken lamellar eutectic composite, tensile and compressive props. 0-71694
- Co-Mo-B metallic glass ribbons, tensile strength, crystn. temp. 0-89173
- Cu, cold rolled sheet, anisotropy of elastic and strength props. 0-81077
- Cu, theoretical strength 0-104229
- Cu-Be (2 at.%), plastic deform. and dislocation substruct. 0-76307
- Fe, cast, tensile strength, Al addition effects (*Korean*) 0-71736
- Fe, cast flake and nodular, rupture strength, circumferential notch (*Japanese*) 0-93649
- Fe, cast with spherical graphite, SiC-Q apparatus for tensile strength meas. (*German*) 0-76450
- Fe-B(Si) alloy filaments produced by glass-coated melt spinning 0-76213
- Fe-Co-V(Ni), annealing effect on microstruct. rel. to mag. and mech. props. 0-89267
- Fe-Cr-Al (7, 5 wt.%), expt. stainless alloys, phys. and mech. props. 0-97637
- Fe-Cr-Ni (18.14 wt.%),  $\gamma$  to  $\epsilon$  to  $\alpha$  martensitic transform., external stress effect, double tensile deform. exam. 0-108438
- Fe-Mn-Ni-V-C (0.5, 3.0, 1.0, 0.2 wt.%), austenite decomp., isothermal transform. characts. 0-97477
- Fe-Mn-V-C (0.5, 1.0, 0.2 wt.%), austenite decomp., isothermal transform. characts. 0-97477
- Fe-Mo-B metallic glass ribbons, tensile strength, crystn. temp. 0-89173
- Fe-Mo-Ta, ternary Laves phase strengthening 0-108466
- Fe-Ni-Al(Cu) (12, 0.5, 0.5 to 3 wt.%), Cu addition strengthening at 77K, mech. props. 0-60875
- Fe-Ni-Cr (35, 15 wt.%) superalloy, stress rupture and tensile props., C and B additions effect (*Chinese*) 0-104244
- Fe-Ni-Ti(Cu) (12, 0.25, 2 wt.%), Cu addition strengthening at 77K, mech. props. 0-60875
- Fe-Ni-V(Cu) (12, 2, 2 wt.%), Cu addition strengthening at 77K, mech. props. 0-60875
- Fe-Ni(Cu) (12, 0.5 to 3 wt.%), Cu addition strengthening at 77K, mech. props. 0-60875
- GeTe, stoichiometry deviations influence on mech. props., 25-500°C 0-103410
- KH<sub>2</sub>PO<sub>4</sub>, filiform crystals at low temp., tensile strength determ. 0-100877
- Li<sub>2</sub>O-SiO<sub>2</sub>-P<sub>2</sub>O<sub>5</sub> glass ceramic fibres, heat treatment, crystn., tensile strength 0-84995
- Mo powder, influence of powder reduction processes on props. 0-89175
- NH<sub>4</sub>H<sub>2</sub>PO<sub>4</sub>, filiform crystals at low temp., tensile strength determ. 0-100877
- Na<sub>2</sub>O-B<sub>2</sub>O<sub>3</sub>-SiO<sub>2</sub> glass fibre, plastic-coated, liq. N<sub>2</sub> strength 0-58707
- Na<sub>2</sub>O-CaO-SiO<sub>2</sub>, proof testing 0-108654
- Nb:He, mech. props. and microstruct. 0-85003
- Ni alloy, heat resistant, fatigue limit comparison in torsion and tension-compression 0-81181
- Ni films, adhesion on graphite 0-80141
- Ni-Cr, high temp. thermomech. treatment effect on tensile diagrams of KhN77TYuR (*Russian*) 0-60884
- Ni-Cr-Al (20, 4 wt.%), tensile stress effect on high temp. oxidation (*Japanese*) 0-89393
- Ni-Cr-Al sintered alloy, hot vac. pressure, fracture and mech. characts. 0-66667
- Ni-Cr-Ta-Ti-Si, EP557 precipitation hardening alloy, mech. props., heat treatment effect 0-60877
- Ni-Mo-B metallic glass ribbons, tensile strength, crystn. temp. 0-89173
- Ni<sub>3</sub>Fe<sub>2</sub>Cr<sub>14</sub>P<sub>12</sub>B<sub>6</sub> metallic glass, mech. props. and thermal stability 0-76362
- Pd-H, mech. props., influence of dissolved H<sub>2</sub> (*Russian*) 0-81109
- 239PuO<sub>2</sub>, stoichiometric, high-temp. deformation 0-81111
- Si, stretched, lattice vibr. anharmonicity, influence of stress on elastic moduli, Raman spectra 0-80791
- SiC fibre reinforced Al, synthesis by liquid pressing method 0-100816
- SiC-coated C fibre, compatibility with Al (*Japanese*) 0-71700
- SiO<sub>2</sub> fibre lightguides, fused, zero stress strength reduction and transitions in static fatigue 0-87523
- SiO<sub>2</sub> glass fibre, plastic-coated, liq. N<sub>2</sub> strength 0-58707
- steels, Cr-C-Mn(Ni), struct. prop. rel., design of struct. steels for high strength and toughness 0-97491
- Ta single crystal, H<sub>2</sub> embrittlement (*Japanese*) 0-66636
- Ti alloy, heat resistance, thermal stability, stress-rupture strength, and creep 0-81194
- Ti base alloys, melt-extracted polycryst., mech. props. 0-76360
- Ti-Al-Mo-Cr (4.5, 5, 1.5 wt.%), weld metal,  $\alpha/\beta$  interface sliding 0-108512
- Ti-Al-Mo-Zr, type VT-9, creep eqns. rel. to extension and compression props. 0-100875

**tensile strength continued**

- Ti-Al-V (6.4 wt.%) cast alloy, with improved microstruct., mech. props. (*Japanese*) 0-71701
- Ti-V-Fe-Al (10, 2, 3 wt.%), fracture toughness and stress corrosion resistance 0-100904
- W fibre reinforced Cu composites, correl. between thermal cycling-induced microstructural changes at interphase boundaries and tensile behaviour (*Japanese*) 0-71674
- Zircaloy-2, effect of simulated fission products on mech. props. 0-73922
- Zircaloy-4, deformation behaviour between 77 and 900K 0-71686
- Zn-Al-Cu casting alloys, mech. props. and dendritic morphology, Al content effect (*Korean*) 0-93612
- Zn-Al(Cu), mech. and technological props. (*Polish*) 0-89286
- Zr-Al (8.6 wt.%), dimensional stability struct. and mech. props, effects of neutron irradi. 0-92563
- tensimeters** see vapour pressure measurement
- tensors**
- crystal physics, multivector analysis, comparison with tensor algebra 0-100195
- crystal physics, multivector analysis, comparison with vector anal. 0-100196
- crystal rotational symmetry, and tensor props., 1-, 2- and 4-fold principal symmetry, trigonal, and hexagonal groups 0-100193
- crystal rotational symmetry, and tensor props., method for group 3(3,) 0-100192
- dynamic elasticity, tensor spherical harmonics appl. to Navier eqn. 0-98296
- Einstein tensor in scalar curvature Finsler spaces 0-77655
- EM transmission structures, relativistic foundation and network formalisms 0-58446
- failure analysis of damage zone in laminates 0-85059
- irreducible isotropic tensors of rank six, complete set 0-91419
- plasticity, field theory, integral presentations of second-rank tensors 0-69690
- stress tensors and creep-strain rates correl., correl. for isotropic stable media 0-87722
- terbium**
- see also nuclei with .....
- atom, L-shell internal excitation accompanying L-capture 0-95726
- ferromagnetic domain structures down to 95K 0-71080
- impurities in fluorophosphate glasses, magneto-opt. characts. 0-64126
- impurity in metallic hosts, exchange interaction, electrical resistivity 0-84453
- magnetisation, AC susceptibility and microwave absorption meas. 0-60221
- magnetisation in basal plane, calc. 0-70969
- magnetisation intensity in antiferromag. state and mag. field induced phase transforms. (*Russian*) 0-65811
- neutron elastic scattering, high-angle, anal. 0-80480
- silicite thin film formation on (100) and (111)Si substrate, backscattering study 0-70542
- Bi<sub>2</sub>Al<sub>2</sub>O<sub>5</sub>Tb<sup>3+</sup>, luminesc. expts. 0-60656
- CaF:Tb, dimer reorientation activation volume 0-107285
- Mg<sub>2</sub>SiO<sub>4</sub>:Tb, thermolum. phosphor, photolum. and absorpt. spectra, thermolum. mechanisms 0-97321
- Tb<sup>3+</sup>, aqueous soln., radioluminescence intensity conc. depend. 0-87055
- Tb<sup>3+</sup>+UO<sub>2</sub><sup>2+</sup> solution, nuclear pumped liq. lasers, LASL program 0-64011
- ZnO:Tb phosphor, electrolum. brightness, voltage and freq. depend. 0-60681
- ZnS:Tb, Cu(Ag) phosphors, luminesc. props. 0-100690
- terbium alloys**
- Co-Tb film, magneto-optic coeff. and refr. index, ellipsometric determ. 0-71501
- Dy<sub>2</sub>Tb<sub>1-x</sub>Fe<sub>2</sub>, single cryst., torque meas. 0-65877
- Fe-Tb, magnetoelastic hysteresis, elastic stress and mag. field depend. (*Russian*) 0-65982
- Fe-Tb film, magneto-optic coeff. and refr. index, ellipsometric determ. 0-71501
- Gd-Tb, ferromag., magnetisation and microwave absorpt. 0-65816
- Gd<sub>70</sub>Tb<sub>30</sub>, magnetisation, AC susceptibility and microwave absorption meas. 0-60221
- Ho<sub>2</sub>Tb<sub>1-x</sub>Co<sub>2</sub>, lase phase compounds, elastic props., temp. and magnetic field dependence 0-60393
- (Ho<sub>0.55</sub>Tb<sub>0.45</sub>Dy<sub>0.25</sub>)Fe<sub>2</sub>, microwave mag. props. 0-65860
- La alloys, supercond., Tb-doped, crystal field effects, tunnelling within mK range 0-70907
- La-Tb/AlO<sub>x</sub>/Al tunnel junctions, cond. meas., cryst. field effects 0-88694
- La<sub>1-x</sub>Tb<sub>x</sub>Al<sub>3</sub>, competing paramag. anisotropy from cryst. field and indirect quadrupole coupling 0-60180
- Mg-Tb, dil., macroscopic shape effect due to quadrupole orientation, magnetostriction and thermal expansion meas. 0-60396
- (Tb,Dy)-Fe amorphous films prep. by cosputtering, magnetoelastic props. 0-97429
- Tb-Fe amorphous thin films, magnetic after-effect, Kerr magneto-optic effect obs. 0-97123
- Tb-Ta(Cd), elec. quadrupole interaction, temp. and press. depend., TDPAC meas. 0-60469
- TbAg<sub>1-x</sub>In<sub>x</sub>, elec. and Hall resist. 0-96844
- TbAu<sub>3</sub>, mag. phase diagram 0-75761
- TbBi, mag. transitions, quadrupole interaction effects 0-80512
- TbCo<sub>2</sub>, magnetocrystalline anisotropy and spontaneous magnetostriction 0-75831
- TbCo<sub>3</sub>, sublattice magnetisation, temp. depend., neutron diff. anal. (*Russian*) 0-103815
- Tb<sub>1-x</sub>Co<sub>x</sub>, amorphous alloys, thermal stability, elec. cond. enthalpy 0-100172
- Tb<sub>0.37</sub>Dy<sub>0.7</sub>Fe<sub>2</sub>, vertically zoned, magnetomechanical coupling and magnetostriction 0-65999
- Tb<sub>0.5</sub>Dy<sub>0.5</sub>Fe<sub>2</sub>, prep. by powder metallurgy, magnetostrictive props. 0-75826
- TbFe<sub>2</sub> and Tb<sub>2</sub>Fe<sub>23</sub>, magnetostriction, room temp. to 80K 0-65993
- TbGd<sub>2</sub>, noncollinear magnetic order and spin wave spectrum in presence of competing exchange interactions 0-65834
- Tb<sub>1-x</sub>Gd<sub>x</sub>Al<sub>3</sub>, effective mol. field at <sup>159</sup>Tb, NMR meas. 0-71197
- (Tb<sub>1-x</sub>Gd<sub>x</sub>)<sub>2</sub>Co, intermetallic cpd. mag. props., phase transform. and mag. hysteresis (*Russian*) 0-93113
- Tb<sub>2</sub>In, mag. props. 0-108009
- Tb<sub>2</sub>Ir<sub>2</sub>, cryst. struct. 0-96473

**terbium alloys continued**

- ( $\text{ Tb}_{1-x}\text{La}_x$  ) $\text{Be}_{13}$ , mag. struct., cryst. field effects, neutron diffraction study 0-65789  
 $\text{Tb}_{99}\text{Ni}_{31}$ , amorphous, Curie temp., mag. susceptibility and coercive force, 4.2 to 300K 0-93092  
 $\text{Tb}_2\text{O}_3$ , cryst. struct. 0-96474  
 $\text{TbPt}_5$ , low temp. mag. susceptibility 0-93075  
 $\text{Tb-Pt}$ , mag. susceptibility meas., mag. transitions obs. 0-60222  
 $\text{TbRh}_2\text{Sny}$ , crystallography X-ray powder diffraction study 0-100217  
 $\text{TbZn}$ , elec. resist., behaviour at mag. crit. points 0-65901  
 $\text{TbZn}$ , ferromag., thermoelec. power, temp. depend. and crit. behaviour 0-96852  
 $\text{TbZn}$ , mag. excitations meas. 0-70979  
 $\text{Tb-Tb}$  (1 at.%), Heisenberg exchange, residual resist. meas. 0-75558  
 $\text{Y}_{1-x}\text{ Tb}_x\text{Co}_{5+0.1x}$ , ferrimag., magnetisation, exchange interactions, mag. anisotropy 0-80565  
 $\text{Y}_{1-x}\text{ Tb}_x\text{Pd}_3$ , magnetisation, magnetostriction, and inelastic neutron spectra 0-65998

**terbium compounds**

- see also *terbium alloys*  
 $\text{LiTbF}_6$ , uniaxial dipolar ferromag., critical behaviour, mag. susceptibility meas. 0-80528  
 $\text{LiTbO}_5\text{Y}_2\text{F}_4$ , uniaxial dipolar ferromag., critical behaviour, mag. susceptibility meas., effect of  $\text{Y}^{3+}$  dilution 0-80528  
 $\text{Na}_2\text{La}_{1-x}\text{Ce}_x\text{Tb}_x(\text{PO}_4)_3$ , optical props. (French) 0-103991  
 $\text{Na}_2\text{O-P}_2\text{O}_5\text{-Y}_2\text{O}_3\text{-Tb}_2\text{O}_3$ , glass, conc. quenching of luminesc. in disordered system with dipolar interaction 0-89059  
 $\text{Na}_2\text{O-SiO}_2\text{-Tb}_2\text{O}_3$  glass magnetooptical study 0-88976  
 $\text{TbAG}$ , reson. electronic Raman effect, interferences, lifetime meas. 0-93294  
 $\text{TbAs}$ , mag. transitions, quadrupolar interaction effects 0-80512  
 $\text{TbAsO}_4$ , ferroelectricity, dielec. meas. 0-60515  
 $\text{TbBiTe}_3$ , prep., elec. props., and crystallographic data 0-59981  
 $\text{TbCl}_3$ , vapour press. and sublimation thermodynamics, mass loss effusion meas. 0-88313  
 $\text{TbCoSi}_2$ , mag. props. 0-107988  
 $\text{TbD}_{2-x}$ , mag. susceptibility conc. depend. 0-70968  
 $\text{TbF}_3$  thin films, AC conduction obs. 0-70868  
 $\text{TbF}_3\text{Sm}^{3+}$ , induced visible emission of  $\text{Sm}^{3+}$  0-97330  
 $\text{TbFe}_2$ , elastic modulus magnetic field dependence 0-87698  
 $\text{TbFeO}_3$ , mag. susceptibility, temp. depend., effective field at Tb ion sites 0-75742  
 $\text{Tb-Ge-O}_7$ , flux-grown, X-ray topography 0-64939  
 $\text{TbH}_{2-x}$ , mag. susceptibility conc. depend. 0-70968  
 $\text{TbIG}$ , [111] magnetoelastic props., rel. to Cotton-Mouton birefringence, 90-500K 0-103876  
 $\text{TbIG}$ , spontaneous Faraday rot. rel. to sublattice magnetisation 0-66159  
 $\text{Tb}(\text{MoO}_4)_3$ , cryst. struct. in ferroelec., ferroelastic, antiferroelec. and paraelectric phases 0-75205  
 $\text{Tb}(\text{MoO}_4)_3$ , improper ferroelectric, dielectric props., IR radiation pyroelectric detection 0-80711  
 $\text{Tb}(\text{NO}_3)_3\text{-Fe}(\text{NO}_3)_3\text{-(NH}_4)_2\text{CO}_3\text{-H}_2\text{O}$  system, cpd. form., comp. and props. 0-100832  
 $\text{TbNi}_2\text{Si}_2$ , mag. props., 4.2-200K 0-84602  
 $\text{Tb}_2\text{O}_3$ , B-type monoclinic, DC(AC) elec. cond., thermoelectric power, dielectric const., temp. depends. 0-59980  
 $\text{Tb}_2\text{O}_3\text{-H}_2\text{PO}_4\text{-H}_2\text{O}$  system, cpd. form., comp. and props. 0-100832  
 $\text{Tb}_2\text{O}_3\text{-P}_2\text{O}_5\text{-MO}$  system glasses, (M=Mg, Ca, Sr, Ba or Pb), photoluminesc. under X-ray excitation 0-89060  
 $\text{Tb}(\text{OH})_3$ , dynamical effects of interaction between 4f electrons and optical phonons 0-108196  
 $\text{Tb}(\text{OH})_3$ , heat capacity from 10 to 350K, lattice and Schottky contris. 0-84300  
 $\text{TbP}$ , mag. transitions, quadrupolar interaction effects 0-80512  
 $\text{TbPO}_4$ , zircon struct., cryst. field analysis 0-80232  
 $\text{TbSb}$ , mag. transitions, quadrupolar interaction effects 0-80512  
 $\text{TbTiO}_3$ , bulk mag. and struct. props., ferrimag. order 0-107993  
 $\text{TbVO}_4$ , co-operative Jahn-Teller transition, low freq. dynamics, light scatt. study 0-88317  
 $\text{Tb}_{20}\text{Y}_{274}\text{Fe}_{10}\text{O}_{12}$  garnet, mag. transition, mag. props. anomaly 0-93120  
 $(\text{YEuTm})_3(\text{GaFe}_2\text{O}_{12})$  ferrite garnet films, mag. bubbles, translational motion, mechanism for inertial effects 0-100606  
 $\text{YIG:Tb}$  garnet, Faraday effect in strong mag. field (Russian) 0-100651  
 $\text{Y}_{1-x}\text{ Tb}_x\text{Al}_{0.65}\text{Fe}_{1.35}\text{O}_{12}$  garnet thin films, magnetisation orientation, temp. depend. 0-71125

**terminals, interactive** see *interactive terminals***ternary semiconductors**

- for *pseudobinary semiconductors*, see *II-VI semiconductors*, *III-V semiconductors*, *III-VI semiconductors*, *IV-VI semiconductors* and *semiconductor materials*  
 see also *chalcogenide glasses*  
 $\alpha\text{-AgSbS}_2$  crystals, influence of external elec. field on elec. cond. 0-60056  
 chalcopyrite crystals, refractive index, temp. depend., appl. to nonlinear devices 0-60555  
 computer prediction of system cpd. form., comp. and props. w.r.t. component electron struct. 0-103444  
 $\text{AgGaS}_2$ , deep level obs. by TSC meas. 0-65590  
 $\text{AgGaS}_2\text{:Fe}$ , EPR of Fe-associated defect 0-60412  
 $\text{AgGaS}_2\text{-AgGaSe}_2$  system, phase diagram, lattice consts., and IR spectra 0-60841  
 $\text{AgGaSe}_2$ , two-photon absorpt. and short pulse stimulated recombination 0-89054  
 $\text{AgInS}_3$ , and  $\text{AgInS}_6$ , spray pyrolysis, film struct., elec. and optical props. 0-71592  
 $\alpha\text{-AgSbS}_3$  crystals, photoelectric props. 0-107861  
 $\text{CdCr}_2\text{S}_4$  crystal growth, structural defects, physical properties 0-60759  
 $\text{CdCr}_2\text{S}_4$ , ferromag. semicond., IR refl. spectra, phonon props. and dielec. function 0-66191  
 $\text{CdCr}_2\text{S}_4(\text{Se}_4)$ , pure and Ag doped, electronic struct., mixed valence 0-70612  
 $\text{CdCr}_2\text{Se}_4$ , ferromag. semicond., conc. anomalies rel. to red shift of absorpt. edge 0-70732  
 $\text{CdCr}_2\text{Se}_4\text{:Cu(Ag)}$ , ferromag. reson. and ESR line widths 0-60413  
 $\text{CdGa}_2\text{S}_4$  double surface-barrier diodes, current-voltage characs. 0-92972  
 $\text{CdGa}_2\text{S}_4$ , IR refl. spectra 0-60604  
 $\text{CdGa}_2(\text{S}_{1-x}\text{Se}_x)_4$  solid solns., band struct. behaviour w.r.t. comp. (French) 0-107699  
 $\text{CdGa}_2\text{S}_4(\text{Se}_4)$ , band struct., pseudopot. method 0-92816

**ternary semiconductors continued**

- $\text{CdGeAs}_2$  crystals, Bridgman grown, optical props. rel. to  $\text{O}_2$  content of starting materials 0-81213  
 $\text{Cd}_2\text{GeO}_4$  anode for  $\text{H}_2\text{O}$  photoelectrolysis 0-108716  
 $\text{n-Cd}_2\text{GeO}_4$ , electronic and cond. props. rel. to prep. conditions and defect struct. 0-107787  
 $\text{Cd}_{1-x}\text{Hg}_x\text{Ga}_{2-x}\text{S}_4$  solid solns., band struct. behaviour w.r.t. comp. (French) 0-107699  
 $\text{CdInGaS}_4$  crystal, Raman scattering spectra, polarisation meas. (Russian) 0-71410  
 $\text{CdInGaS}_4$ , layered structure crystals, refractive index meas. method 0-98966  
 $\text{CdInGaS}_4$ , pure and Cu-doped, electrophotography layers (Russian) 0-68282  
 $\text{CdInO}_4$  anode for  $\text{H}_2\text{O}$  photoelectrolysis 0-108716  
 $\text{CdIn}_2\text{S}_4$ , Brillouin scatt., elastic and photoelastic consts. determ. 0-60619  
 $\text{CdIn}_2\text{S}_4$ , partial inverse spinel struct., detection by Fourier transform spectroscopy 0-108197  
 $\text{CdIn}_2\text{S}_4$  single crystals, recombination process and localised levels 0-93383  
 $\text{CdIn}_2\text{Se}_4$ , high resolution electron microscopic study of polytypism 0-88119  
 $\text{n-CdS/p-ZnIn}_2\text{Se}_4$  thin film solar cell, photovoltaic props. 0-89628  
 $\text{p-CdSiAs}_2$ , electron irradi. elec. props. annealing, lattice defects 0-100465  
 $\text{CdSiP}_2$ , electronic struct., X-ray spectroscopic investigation 0-108300  
 $\text{p-CdSnAs}_2$ , heavily doped, elec. transport props. under elastic deformation 0-96915  
 $\text{CdSnAs}_2$ , solubility in Sn melt, temp. depend., enthalpy of melting 0-95658  
 $\text{CdSnAs}_2\text{-Au(Al)}$ , surface barrier junction, elec. props., temp. depend. 0-65686  
 $\text{CdSnAs}_2\text{-InP}$ , n-p heterojunction, elec. props., electroluminesc., band struct. 0-75632  
 $\text{Cd}_2\text{SnO}_4$  anode for  $\text{H}_2\text{O}$  photoelectrolysis 0-108716  
 $\text{CdTe}_2\text{Se}_4\text{:Au}$ , solubility meas. by microhardness method 0-96650  
 $\text{CdTe}_2(\text{Te}_2)\text{:Au}$ , elec. cond., density, dielectric const., changes on fusion 0-88553  
 $\text{CuCr}_2\text{S}_4(\text{Se}_4)$ , electronic struct., mixed valence 0-70612  
 $\text{CuCr}_2\text{Se}_4$ , mag. reson. and valence state of Cu and Cr ions 0-60413  
 $\text{CuGaSe}_2$ , evidence of donor-acceptor type transition 0-93375  
 $\text{CuGaSe}_2$  single crystals, electrical and photovoltaic props. 0-92940  
 $\text{CuGaSe}_2$ , thermal expansion obs. 0-70432  
 $\text{CuGaTe}_2$ , refr. indices meas. 0-93259  
 $\text{CuIn}_{0.9}\text{Ga}_{0.1}\text{Se}_2$ , epitaxial layers, on GaAs substrates, struct. and elec. props. 0-107670  
 $\text{CuInS}_2$  films, RF sputtered, growth and props. 0-80124  
 $\text{n-CuInS}_2$ , mag. props., obs. 0-70939  
 $\text{CuInSe}_2$ , amorphous thin film, flash evaporation, struct., stoichiometry 0-89150  
 $\text{CuInSe}_2$ , heteroepitaxy on {111} oriented Ge by flash evaporation, struct. 0-108333  
 $\text{CuInSe}_2$ , influence of impurities and free carriers on optical props. 0-108225  
 $\text{CuInSe}_2$ , refr. indices meas. 0-93259  
 $\text{p-CuInSe}_2$ , thermal props. 0-96705  
 $\text{CuInSe}_2$  thin films for solar cells, radiofrequency sputtering technique, elec. props. 0-93487  
 $\text{CuInSe}_2\text{-CdS}$  solar cell, polycrystalline thin film, high photocurrent, characs. 0-61339  
 $\text{CuInTe}_2$ , epitaxial layers, on GaAs, growth and props. 0-108359  
 $\text{CuInTe}_2$ , refr. indices meas. 0-93259  
 $\text{CuInTe}_2$  single crystals, directional freezing growth and doping, resist. changes on annealing 0-60768  
 $\text{CuSbS}_2$  crystals, growth and characterisation 0-60770  
 $\text{CuTiS}_2$ , melting heat and melting entropy (Russian) 0-70374  
 $\text{InSeI}$ , X-ray cryst. struct. determ. (German) 0-100214  
 $\text{InTeI}$ , X-ray cryst. struct. determ. (German) 0-100214  
 $\text{Ti-Bi-Sb-Te}$  system, peritectic reactions in  $\text{TbBiTe}_2\text{-TiSbTe}_2$  cross section, cryst. character 0-108406  
 $\text{TiGaSe}_2$ , monocrystal, processes of recombination and trapping levels, photocond. meas. (Russian) 0-70751  
 $\text{TiGaTe}_2$ ,  $\text{TlInTe}_2$ , and  $\text{TlInSe}_2$ , IR refl. spectra 0-60605  
 $\text{TlInSe}_2$ , monocrystal, photoelec. props. (Russian) 0-70752  
 $\text{Zn-In-S}$  thin layers, ternary phases, optical props. near long-wavelength intrinsic absorpt. edge 0-80887  
 $\text{ZnCr}_2\text{Se}_4$ , electroconductivity, thermoelectromotive force, Hall effect (Russian) 0-70694  
 $\text{ZnCr}_2\text{Se}_4$ , screw spin structure, method of controlling the sense, polarised neutron diffraction study 0-70944  
 $\text{ZnGa}_2\text{S}_4$ , band struct., pseudopot. method 0-92816  
 $\text{ZnGeP}_2$ , bandgap absorption edge, spectra, electron transitions (Russian) 0-97305  
 $\text{ZnGeP}_2$ , p-n homodiode, polarisation photosensitivity and photopleochroism spectra 0-107866  
 $\text{ZnGeP}_2$ , temp. depend. phase-matched nonlinear optical devices 0-99794  
 $\text{ZnIn}_2\text{S}_4$  crystals, switching effect, electric field distribution 0-107872  
 $\text{ZnIn}_2\text{S}_4$ , Raman scatt., hydrostatic press. effect 0-84745  
 $\text{ZnIn}_2\text{S}_4$ , S-type negative resist. and switching effects 0-65581  
 $\text{ZnIn}_2\text{S}_4$ , vibr. spectrum, Raman study 0-97278  
 $\text{p-ZnSiAs}_2$ , electron irradi. elec. props. annealing, lattice defects 0-100465  
 $\text{ZnSiP}_2$ , electronic struct., X-ray spectroscopic investigation 0-108300  
 $\text{ZnSiP}_2(\text{As}_2)$ , thermal expansion coeffs. meas. (Russian) 0-65258  
 $\text{p-ZnSnAs}_2$ , LPE, electronic struct. obs. by laser excited photolum. 0-60654

**terrestrial age** see *geochronology***terrestrial atmosphere**

- see also *air*; *clouds*; *stratosphere*; *troposphere*; *upper atmosphere*  
 ancient atmosphere, fate of  $\text{OH}$  and  $\text{O}_3$  origin 0-77116  
 climate variation throughout Earth's history, causal mechanisms 0-82048  
 comet impact, explanation of Cretaceous species extinction 0-76977  
 conference, New Delhi, India (Jan. 1979) 0-94912  
 cosmic ray penetration into atmos., calc. for energetic heavy nuclei 0-85826  
 early atmosphere,  $\text{NH}_3$  photochemically produced in small quantities 0-109208  
 escape of ions to space, ion chem. and low altitude accel. effects 0-85798  
 gas exchange with magmas, determ. from mass fractionation of rare gas isotopes in volcanic rocks 0-98292  
 inert gas composition, Earth's origin from solar nebula 0-61785  
 inert gases, accretion from protoplanetary nebula 0-109385



**terrestrial atmosphere continued**

- IR mosaic background obs. from balloon altitude expt. 0-90222
- meteoroids atmospheric breakup, effects on crater field form. 0-94760
- middle atmosphere, obs. from balloons, rockets and satellites, conference, London, England, (1978 December 12 to 13) 0-77540
- numerical dynamic model atmosphere on a spherical Earth, used in forecasting 0-101416
- optical parameters determ. by aerial photography at sunset 0-90219
- origin of atmosphere (*Russian*) 0-81857
- palaeoclimate of S.Hemisphere since 80 Myr BP, causes for change (*Russian*) 0-98440
- palaeotemperature, O isotopes of mid-Wisconsin limestone cave deposits 0-82069
- radiation budget at top of atmos., influence of cloud cover 0-98398
- radiation problems, thermal struct. 0-82016
- response to heat sources and perturbations (*Chinese*) 0-85748
- secular polar motion excitation function, low freq. spectrum anal. (*Chinese*) 0-104849
- supernovae, nearby, effects on terrestrial atmosphere 0-94584
- vacuum UV background, meas. 0-90221
- Ar degassed from shungite, isotope composition of ancient atmos. 0-85749
- CO<sub>2</sub> model run in tandem with climate model, 1800-2100 AD 0-98381

**terrestrial composition** *see Earth composition***terrestrial electricity**

- Adirondak mountains, deep crustal elec. cond. obs. 0-89946
- Alaska oil pipeline, elec. current induced by electrojet 0-61756
- Alaska oil pipeline, induced elec. currents meas. by gradient fluxgate and SQUID magnetometers 0-98231
- N.America, E. coastal region, EM induction model 0-98235
- apparent resistivity curves for parallel layer Earth, difference algorithm 0-89937
- central Australia, elec. conc. profile from geomag. induction meas. 0-72424
- Carpathian region sedimentary cover, elec. conduction 0-89940
- Carpinian regional lithosphere, geoelectric model from data along deep seismic sounding profile (*Russian*) 0-104934
- coal, anisotropic elec. props. meas. 0-98312
- conductive cylinder, anomalous mag. field, induced by elec. current (*Chinese*) 0-104858
- core, monosulphide solid soln. in Fe-Ni-S system 0-90038
- Coso Range, California, reconnaissance electrical surveys 0-89944
- cross-borehole EM probing, location of high-contrast anomaly 0-72639
- currents in bottom and shore of Barents Sea, EM field 0-104864
- DC concentration on E.Sierran Front, shallow crustal conductors under Coso Range 0-89942
- depth sounding by induction arrow representation, review 0-98486
- dipole-dipole deep geoelectric soundings over geological structures 0-101449
- Earth's negative charge, supply mechanism 0-61758
- Earth electrical parameters, determination from horizontal antennas input impedance meas. 0-90259
- electrical sounding, elec. fields in random cond. layered Earth 0-77171
- electrokinetic props. of rocks, seismic wave propag. effects 0-76921
- electromagnetic sounding, hybrid-rat approx. 0-72412
- electromagnetic sounding transient pulse induction method, one-loop version 0-101448
- EM depth sounding interpretation, master tables, book 0-86043
- EM field above two-dimensional inhomogeneous struct., boundary conditions 0-85595
- EM field eqns., transient time-domain EM method 0-98227
- EM induction effects of ocean coast 0-76908
- EM induction in layered Earth by surface loop, transient response 0-72410
- EM induction of laterally inhomogeneous anisotropic ground, VLF method 0-85754
- EM response of dipping half plane embedded in conducting rock 0-90236
- EM response of Earth surface, aircraft remote sensing (*Chinese*) 0-104859
- EM sounding, detectability of intermediate layers, time domain anal. 0-72641
- EM sounding, iterative ray tracing between boreholes for underground image reconstruction 0-98466
- EM sounding, VLF-EM profiles, topographic correction based on model studies 0-101452
- EM sounding of buried axial conductor, time-domain response 0-105059
- EM sounding of conductive circular cylinder, expt. and theoretical results 0-105058
- EM soundings, multifrequency, topographic and misorientation effects study 0-101451
- EM surface impedance, N-layered half space theory 0-76909
- Foedobrogen area, USSR abyssal elec. cond. 0-90000
- geoelectric sounding, controlled-source DC pot. problem by self-pot. Green's function 0-77136
- geomagnetic coast effect, review 0-94458
- geomagnetic dynamo and secular variation, damping of Hide's mag. waves 0-98218
- geomagnetic transfer functions at pulsation periods 0-72417
- geothermal energy resources in Oregon, USA, elec. and EM sounding obs. 0-97761
- horizontally multilayered Earth models, recurrence formulae for layer eigenfunctions 0-90246
- NE.Iceland, elec. resist. model from magnetotelluric obs., correl. with temp. 0-89954
- induced polarisation (IP) sounding, effects of EM coupling in electrode arrays over uniform half-space 0-101324
- induced polarisation methods for ore body tracing (*German*) 0-82084
- inhomogeneities of geoelectric structure, position determination by variable geomag. field method 0-89956
- NW.Kola Peninsula, near zone field development method testing (*Russian*) 0-85761
- magnetic induced polarisation techniques, effect of large cond. contrasts 0-98461
- magnetic secular variation, modelled on mantle elec. cond. inhomogeneity (*German*) 0-81806
- magneto-telluric response dispersion relations, inversion problem theory 0-104861
- magnetotelluric apparent resistivity, effect of localised source 0-72429
- magnetotelluric sounding, fundamental model 0-77167

**terrestrial electricity continued**

- Mantle, elec. cond., effect of partial melting 0-76936
- mantle conductivity, constraints due to secular mag. variations 0-61754
- mantle conductivity rel. to geomagnetic secular variation impulse 0-98236
- meltwater from glacier, elec. resist. obs. showing water origin 0-85689
- metallic mineral deposits of Australia mag. induced polarisation survey results 0-98223
- mining tectonic forecast maps, geoelectric bed sounding method (*Hungarian*) 0-105075
- New Brunswick, resistivity and induced polarisation (IP) survey for delineating saline water and fresh water zones 0-104867
- ocean bottom current formation by water movement 0-104863
- ocean current induced EM fields, theory 0-61805
- ocean electric current induced by Sq, around land masses 0-72413
- ocean EM induction affecting Sq during IGY 0-72428
- ocean water motion due to geomagnetic variation, theory 0-104962
- E.Pacific Rise, active elec. sounding rel. to oceanic crust props. and origin 0-101360
- peninsular loop current, ULF wave generation 0-90247
- plasmaphere, magnetospheric and ionospheric elec. field simultaneous obs. 0-105110
- potential field around subsurface electrically excited conductors, mathematical model 0-98230
- probing of underground struct. (*German*) 0-82089
- SW.Queensland, telluric currents assoc. with anomalous geomag. vars. 0-109089
- reciprocal geoelectric section appl. to vertical elec. sounding data 0-90237
- resistivity and induced polarisation surveys, topographic effects 0-98224
- resistivity anomalies over buried conducting dykes, model tank expts. 0-85582
- resistivity sounding, direct, interpretation by accumulation of layers 0-101322
- resistivity sounding, variable resist. with depth Earth model 0-85583
- resistivity sounding by bipole-dipole method, theory 0-101450
- resistivity sounding curves, numerical interpretation (*Chinese*) 0-89934
- resistivity sounding for layered transitional Earth 0-85584
- Rio Grande rift, USA, deep crust struct., magnetotelluric interpretation 0-104878
- Scotland, electrical model of crust and upper mantle 0-98234
- Senegal, telluric current variation obs. (*French*) 0-76903
- Sierra Nevada batholith, elec. conductivity of crust 0-72411
- South Novo-Tolbachinsky volcano, flowing lava elec. cond. 0-72498
- St. Vincent's Gulf, South Australia, Island and coast effect in geomag. vars. 0-72426
- subsurface EM field propagation from horizontal elec. dipoles, comprehensive study 0-98229
- sulphide prospect in California copper belt, broadband EM study 0-72503
- surface geoelectric section effects on deep magnetotelluric sounding (*Russian*) 0-85588
- surface geology sensed by ground mode radiowave propag., glaciated area of USA 0-76979
- Travale-Radicondoli geothermal area (Tuscany), dipole elec. sounding method appl. 0-97762
- Vancouver Island region, terrestrial EM induction 0-104879
- wave detection in volcanic region of Armenia, elec. profiling and sounding 0-85753
- wave tilt sounding of multilayered structures 0-61926
- well logging, electric, geometrical factors determ. from electrostatic field successive approx. (*Chinese*) 0-105057

**terrestrial heat***see also volcanology*

- Archaean crust, geothermal heating rel. to vertical tectonism in greenstone belts 0-81861
- Atlantis II Deep, geothermal brine system 0-94526
- Australia, geophysical profile along 29°S 0-72460
- Australia, heat-flow data correction, glaciation effects 0-72457
- back-arc basins, thermal effects of ridge crest migration rel. to asymmetric spreading 0-85636
- Baikal region hot springs (*Russian*) 0-94551
- Bering Sea, crustal heat flow and tectonic explanation 0-109123
- Bohus granite area, SW Sweden, geothermal investigations 0-85631
- Brazilian Highlands, crustal heat flow obs. 0-109124
- Bullaren lineament, SW.Sweden, heat extraction potential 0-76602
- Cerro Prieto geothermal field, conf. at San Diego, (Sept. 1978) 0-94911
- Cesano geothermal field, Italy, geological study 0-76975
- conference, Nov. 1979, New Orleans, USA 0-81891
- continental heat flow, tectonic age and thermal evolution effects 0-72472
- continental heat flow affected by erosion 0-89991
- convective models and radiogenic heat production constraints 0-90006
- cooling rate of Earth, reappraisal 0-76943
- core, temp. distrib., using Gruncisen's parameter vol. depend. theory 0-90033
- core and mantle thermal eqn. of state 0-90029
- Coso, California, geothermal well water, chemical analyses 0-90104
- Coso geothermal area, California, heat flow 0-90001
- Coso geothermal area, underlying low-vel. body, teleseismic evidence 0-90005
- Coso Hot Springs, Known Geothermal Resource Area, model 0-90004
- Coso Range, California, geothermal system 0-90049
- Coso Range, California, Quaternary rhyolite domes rel. to geothermal anomaly 0-90002
- crust hot spots, and sublithospheric upwelling distrib. 0-109126
- crust radiogenic heat production, vertical distrib. 0-85619
- crustal heat flow, global scale pattern (*Russian*) 0-98284
- crustal heat loss of Earth, review 0-98286
- crustal radiogenic heat production, depth depend. modelling by variational approach 0-72464
- crustal rocks, lateral temp. vars. rel. to long-wavelength mag. anomalies over Canada 0-85594
- degassing and thermal history, simple calcs. 0-98282
- dike burial depth estimation by mag. palaeogeobarometric method 0-98220
- Earth mantle, infinite Prandtl number thermal convection in a spherical shell 0-59033
- Earth thermal evolution, theory 0-89988
- Earth thermal history, implications of Archaean sedimentary basins development 0-89986

**terrestrial heat continued**

energy resources in Oregon, USA, elec. and EM sounding obs. 0-97761  
 energy resources in USA, National Exploration Program 0-72011  
 NE.England, granite plutons effecting surface heat flow 0-94490  
 evolution of Earth's interior, heat generation and heat-mass transfer 0-90040  
 France, heat flow rel. to deep crust. and mantle convection 0-98291  
 Galapagos Rift hydrothermal fields, struct. and morphology of seafloor 0-72489  
 geothermal energy extraction from penny-shaped reservoir made in hot dry rock 0-108784  
 geothermal energy recovery from hot dry rock, use of weighted brine 0-101076  
 geothermal energy resource exploitation, conf. Sept., Landerello, Italy 0-81418  
 geothermal reservoir, liquid dominated, fault zone controlled charging model 0-81935  
 geothermal technology, development into an exact science 0-61781  
 Geotraverse Rhenohertzynikum, crustal temp.-viscosity regime rel. to fault zones depth, seismic obs. 0-90046  
 Geysers geothermal area, California, induced versus natural earthquakes 0-101332  
 Gruneisen parameter, melting curve and adiabatic gradient of core and mantle 0-90028  
 Gulf of California, temp., salinity and  $^3\text{He}$  meas. rel. to geothermal heating and mantle volatiles 0-85640  
 Hawaii, ground Rn survey of Puna geothermal area 0-85657  
 Hawaii Geothermal Project, groundwater geochem. study 0-72567  
 Himalaya, uplift and cooling rates from geochronological data 0-85627  
 hot dry rock geothermal reservoir fracture mapping techniques 0-81419  
 hot spring deposits of Roosevelt thermal area, hydrothermal alteration 0-76974  
 Hungary, image of geothermal energy for non-elec. purposes 0-76601  
 hydrothermal activity on Mid-Atlantic Ridge,  $^3\text{He}$  excess in bottom waters 0-101383  
 hydrothermal flows, two-phase, in permeable media, struct. 0-85693  
 hydrothermal system, temp. measurement scale based on chem. comp. of gas fraction 0-98277  
 NE.Iceland, elec. resist. model from magnetotelluric obs., correl. with temp. 0-89954  
 Icelandic subglacial volcanisms, thermal and physical studies 0-101350  
 Icelandic thermal area rock stress implication for oceanic lithosphere 0-90012  
 Indo-Australian plate, abnormally high heat flow rel. to plate internal deform. 0-109134  
 Japanese Islands, compilation of eleven new heat flow meas. 0-67350  
 Japanese Islands region, heat flow data compilation (*Japanese*) 0-67332  
 Jharla Gondwana sedimentary basin, India, heat flow meas. and basement rocks heat prod. 0-98276  
 Juan de Fuca ridge system, heat flow meas., water circulation 0-72468  
 Kilauea 1977 lava flow, heat transfer meas. 0-85632  
 Kirishima volcanoes, Japan, geothermal survey (*Japanese*) 0-67357  
 Lepontine Alps, temporal changes in heat flow distrib. assoc. with metamorphism 0-101347  
 logging instrumentation, borehole measurements, developments 0-61909  
 lower mantle convection, inferred from low Q zone 0-76944  
 magmatic diapiir folds, heat exchange with crustal materials rel. to evolution (*Russian*) 0-104957  
 Malaysia, heat flow estimation in exploration wells in offshore areas 0-67349  
 mantle, radiogenic heating in convecting mantle rel. to oceanic bathymetry flattening 0-85642  
 mantle, thermal convection, time dependent simulation 0-101352  
 mantle convection driven by radioactive energy, model for decaying source 0-72461  
 mantle convection model, finite element method 0-67354  
 mantle convective instability, thermomechanical 0-90063  
 mantle hotspots, correl. with positive geoid height anomalies 0-90056  
 mantle of old platforms, heat flow 0-89996  
 mantle radiative cond. from shock compressed  $\text{Fe}^{2+}$  bearing MgO absorpt. spectrum 0-90039  
 mantle temperature implied from elec. cond. assumptions 0-61754  
 mantle thermal struct., convective regime with moving plates 0-85634  
 mantle with differentiation, thermal evolution 0-98288  
 marine sediment heat flow, equatorial Indian Ocean 0-76958  
 melt production in mantle, by viscous dissipation 0-72463  
 Mesozoic and Cainozoic heat flow 0-76941  
 Mid-Atlantic Ridge, geology of submarine hydrothermal field at 26°N latit. 0-85641  
 mid-ocean ridges, obs. and implications of ridge crest hot springs 0-98304  
 mineral cooling rates, implications of antiphase domains exptl. coarsening in pigeonite 0-81886  
 SW.Montana, Precambrian metamorphic rocks, mineral-pair geothermometers 0-81846  
 Nain anorthositic complex, lower crust heating rel. to contrasted magmas commingling in plutonic environment 0-104959  
 Nepal, geothermal springs 0-72476  
 Norris Geyser, Yellowstone Park, USA, microseisms of geothermal area 0-104909  
 E.Pacific Rise, hot springs and geophysical expts. 0-101360  
 E.Pacific Rise, hydrothermal heat flux of black smoker vents 0-94488  
 E.Pacific Rise geothermal system, physical limits on geothermal fluid temp. and role of adiabatic expansion 0-101362  
 permafrost thermal behaviour, surface heat balance simulation 0-67385  
 plutons, thermal evolution, parameterised approach 0-90042  
 Precambrian shield of Liberia, heat flow 0-98279  
 radiogenic heat generation in old platform crusts 0-89996  
 radiogenic heat source content and whole planet cooling 0-90007  
 Reykjanes Ridge, new heat flow obs. 0-90011  
 Rhinegraben area, gravity anomalies and geothermal implications 0-104852  
 Rhinegraben area, heat transfer and distrib. in upper mantle 0-104927  
 Rhinegraben geothermal anomaly at Landau oil-field, model 0-98281  
 rocks, thermal cond. and diffusivity using modified Angstrom or impulse method 0-90085  
 Roosevelt Hot Springs Thermal area, Utah, heat flow and hydrothermal alteration enthalpy 0-90008  
 SW. Scottish Highlands, temporal changes in heat flow distrib. assoc. with metamorphism 0-101347  
 sea floor of Scotia, S.Atlantic and Weddell Seas, heat flow 0-94491

**terrestrial heat continued**

sedimentary basins, heat flow and subsidence histories with finite crustal extension rates 0-89987  
 St. Lucia, Sulphur Springs geothermal field model 0-94494  
 steamflow in geothermal reservoir, Kawah Kamojang, Java 0-77018  
 subducting lithosphere, heat transfer with continental asthenosphere 0-94510  
 subducting slab undergoing upper surface melting, thermal field 0-85638  
 subsurface temperatures from surface heat flow data, theory of inverse problem 0-104928  
 TAG hydrothermal field,  $^3\text{He}$  excess in bottom waters as activity indicator 0-101383  
 N.Thailand, hot springs and geothermal gradients, temp. obs. 0-94495  
 Travale-Radicondoli geothermal area (Tuscany), dipole elec. sounding method appl. 0-97762  
 Turkey-Iran, Moho temp. from 0-72462  
 Ukrainian Shield, geothermal survey peculiarities rel. to search for fracture waters (*Russian*) 0-104935  
 E.United States, low-temp. geothermal resources 0-85264  
 Wyoming, heat flow and radioactivity 0-72469

**terrestrial magnetic field** *see geomagnetism*

**terrestrial magnetism** *see geomagnetism*

**test equipment**

*see also automatic test equipment*  
 autocollimation instrument for checking angles and pyramidity of AR-90° prisms during manufacturing process 0-87570  
 burn-test apparatus, for fibre reinforced composites 0-76441  
 clamp and strain gauge, for shear characts. determ. of glass reinforced plastic 0-85114  
 component profile inspection equipment 0-105608  
 creep testing, device for producing constant stress 0-71835  
 deformation processes in complex profile shells, installation UDM-1 0-81261  
 denture base materials, multi-station machine for fatigue testing 0-108648  
 driven member rotation uniformity test installation 0-92094  
 dynamic biaxial loading techniques and apparatus, cruciform specimen, elec. motor and hydropneumatic based devices 0-85129  
 electrodes, screening, discharge phenomena with UHV positive and negative lightning and switching pulses for dimensioning (*German*) 0-87963  
 failure analysis tools comparison and selection 0-71865  
 fatigue servo-hydraulic testing machines 0-108649  
 gamma-gamma method, multibeam sonde, stand for adjusting 0-85103  
 glass tubing dia. and wall thickness meas., P-329M instrum. 0-86262  
 hydraulic universal testing machine, K value determ. (*German*) 0-90836  
 LMFBF structure materials in liquid Na, capsule type creep tester (*Japanese*) 0-108653  
 LV short-circuit testing station, equipment and measurement methods (*Polish*) 0-77773  
 NDT laboratory and field equipment in India 0-108650  
 plastometer for multistage incremental compression testing of hot metals 0-85135  
 resistance thermometers, device for measurement of static characteristics 0-77784  
 respiration rate meter tester 0-81758  
 sinewave generator, simultaneous supply of fifty strain transducers, ship vibration testing 0-62652  
 static tensile-compressive testing, smooth tubular specimens, grip for 0-66724  
 stress relaxation test device, for variable temp. 0-85113  
 thickness gauges metrological provisions, 1979 status in USSR 0-77749  
 torsion bomb machine for dynamic stress/strain measurements under superimposed high press. 0-85130  
 US test unit for abrasive granular materials, failure characts. in US field 0-85112  
 volume stressed material under static or low-cycle load, testing device 0-71834  
 Ni-Cd and maintenance-free Pb accumulator characteristics (*German*) 0-97782

**test facilities**

*see also aerospace test facilities; anechoic chambers; reverberation chambers*  
 Alpha-Gamma Hot Cell Facility at Argonne-East 0-68779  
 audiometric facility at West Middlesex Hospital, London for standardised hearing tests 0-76858  
 Babcock & Wilcox hot cell facility 0-68910  
 Battelle Hot Cell Laboratory 0-68913  
 Fuels and Materials Examination facility, design and construction 0-73986  
 fusion hybrid blanket data and development, review, simulation test facilities 0-106170  
 Fusion Materials Irradiation Test Facility, Li liq., deuteron activated, shielding 0-99286  
 Fusion Materials Irradiation Test Facility 0-91361  
 fusion reactor, cluster test facility, design 0-90835  
 fusion reactor, Doublet III, neutral beam test tank design 0-99301  
 fusion reactor, Large Coil Test Facility test design description 0-102320  
 fusion reactor, TFTR, blanket module expts., engineering test station design 0-102338  
 fusion reactor, TFTR, neutral beam injector test facility construction 0-102336  
 fusion reactors, Large Coil Test Facility, liq. He cooling system 0-102321  
 General Atomic Hot Cell modification and refurbishment 0-68786  
 Hanford hot cell facility 0-68911  
 hot cell measurement and test equipment, calibration control 0-68787  
 Hot Fuel Examination Facility Complex, history and status 0-68909  
 Large Coil Test Facility, instrumentation system design 0-95446  
 Lawrence Livermore Laboratory superconducting High Field Test Facility 0-90834  
 LMFBF structural materials, development of an instrumented materials irradiation test for FFTF 0-57858  
 LMFBF structural materials, development of an instrumented materials irradiation test for FFTF 0-68797  
 LV short-circuit testing station, equipment and measurement methods (*Polish*) 0-77773  
 MHD test facility safety analysis methodology and documentation system 0-61388



**test facilities continued**

- Neutral Beam System Test Facility, TFTR, neutral beam line final design 0-99309  
 neutron production by neutral beam sources, shielding design criteria for fusion program 0-99387  
 Nippon Nuclear Fuel Development Co. hot laboratory, present status 0-68781  
 O-arai Engineering Centre post irradiation examination facilities 0-68780  
 Oak Ridge, hot cell facilities, history 0-68784  
 Oak Ridge National Laboratory Ceramic Fuels Alpha Facility 0-68783  
 ORNL Radioactive Materials Analytical Laboratory 0-68785  
 ORNL Transuranium Processing Plant, current status 0-68915  
 reactor fuels, post-irradiation examination, hot cell complex test facilities in Japan (*Japanese*) 0-63255  
 solar thermal receiver, 5 MW, real-time computer control 0-72075  
 Vallecitos Nuclear Center Hot Cells 0-68912  
 Whiteshell Nuclear Research Establishment Hot Cell facility 0-68914  
 Winfrith Hot Cells-1964-1979 0-68782

**testers** *see test equipment***testing**

- see also automatic testing; electron device testing; electronic equipment testing; environmental testing; impulse testing; inspection; integrated circuit testing; machine testing; materials testing; mechanical testing; nondestructive testing; optical testing; production testing; switchgear testing; transformer testing*  
 60 kW experimental wind power plant in Sweden, test results 0-61253  
 acousto-optical correlator, with two-dimensional reference transparency 0-106485  
 diffraction theory, spectral domain approach for testing Albertsen's corner diffr. coeff. 0-87304  
 exponential distribution MTBF confidence limits determ. using Epstein and Harters methods 0-98790  
 fission reactors, BWR, Enrico Fermi-2, system turnover, test and startup program 0-63338  
 flowmeters, design principles for comparative testers 0-96319  
 fusion reactor, neutral beam ion source, core snubber network design, fabrication and testing 0-102378  
 fusion reactor, TFTR, preoperational test plan, manpower loading and scheduling 0-102340  
 fusion reactors, Large Coil Program, Westinghouse coil stability testing, pulsed induction heating 0-106194  
 long arc simulated lightning attachment testing using 150 kW Tesla coil 0-70074  
 measuring instruments, determ. of valid interval between tests values 0-57284  
 radiometer, neutron, testing techniques standardisation, in Soviet Union 0-99405  
 speech and language prostheses evaluation 0-76864  
 tachometric flowmeters, volumetric dynamic flowmeter installation 0-96324  
 wind turbine, variable pitch vertical axis, 2.4 m dia. prototype 0-61265

**testing apparatus** *see test equipment***testing equipment** *see test equipment***testing machines** *see test equipment***tetramethylammonium manganese chlorides** *see organic compounds***tetraneutrons** *see neutrons***tetrodes**

- fusion reactor, BBC CQK 200-4 modulator tube for sustaining neutral beam power supply 0-99290  
 fusion reactor, High Voltage Switch Tube, for Neutral Beam Power System 0-99291  
 inverse reflex tetrode, high power ion beam generation 0-68986  
 two-dimensional, algorithm for solving space-charge problems with thermally-emitted electrons 0-100743

**textile fibres** *see fibres***textile industry**

- lustre quality meas., recording and evaluation 0-98967  
 periodic structure defect detect. using optical processing 0-95829

**texture**

- see also recrystallisation texture; surface texture*  
 Al thick probes, neutron transmission curves near Bragg-edge for grain size and texture eval. (*German*) 0-71667  
 4-4'-n-alkoxybenzylidencamino-biphenyls, central Schiff's base linkage reversal effect on liq. cryst. props. 0-79683  
 brass, cold rolling, inhomogeneous texture 0-89251  
 brass, orientation distribution, textured materials, Ghost effect demonstration 0-70080  
 brass, rolling texture development and deform. struct., shear bands effect (*Japanese*) 0-84952  
 coatings, textured, crystallites faces determ. 0-64846  
 electron diffraction patterns, of textures, reflection sphere curvature influence on reflection location geometry 0-87996  
 ferroelectric liquid crystals, chiral smectic C phase, phys. props., review 0-75150  
 ferromagnetic material, polycryst., magnetic texture anal. 0-108002  
 fir-tree textures, possible existence 0-76269  
 goniometer alignment of Schulz reflection technique, method for testing 0-81272  
 grain orientation, of neighbours, disorientation description 0-79725  
 hybrid optical/digital texture analysis 0-78787  
 II-VI semiconductors, thin epitaxial layer, direct synthesis (*German*) 0-104070  
 image segmentation and texture unit cell size determ. 0-95817  
 isopermalloy, permeability stability calc. rel. to texture (*Chinese*) 0-65959  
 liquid crystal, cholesteric, long pitch type, with homeotropic boundary alignment, elongated and spherulitic domain struct. 0-107047  
 liquid crystals, nematic and cholesteric, surface and bulk configurations, topology 0-59381  
 magnetic texture analysis, generalisation of dispersion theory 0-80556  
 materials, data acquisition and processing 0-64828  
 metal, textured cubic, residual stress evaluation 0-89435  
 metals, cubic, crystallographic orientations distribution function, computer calc. 0-64827  
 metals, cubic, heavily deform., development of lattice curvature 0-81136  
 metals, ellipsoidal model of textured specimens with uniaxial symm. (*Russian*) 0-80100  
 metals, FCC, 'brass to copper' transition in rolling textures 0-76246  
 multicomponent axial, quantitative evaluation 0-85100

**texture continued**

- natural terrain scenes, segmentation-based boundary-modelling processor 0-99661  
 neutron diffraction anal., time of flight vs. conventional method on drawn steel wire 0-81078  
 orientation distribution function analysis from incomplete pole figures normalised by iterative method 0-59344  
 orientation distribution of textured materials, demonstration of ghost effect 0-70080  
 petroleum feedstocks and cokes, graphitisability 0-93580  
 4-phenylbenzylidene-4'-n-alkoxyanilines, central Schiff's base linkage reversal effect on liq. cryst. props. 0-79683  
 polyethylene melt, cryst. kinetics during cooling, nucleation density effect 0-100181  
 steel, alloy, corrugated texture perfection, mag. anal. 0-88745  
 steel, austenitic stainless, welded explosively, induced martensites morphology 0-104153  
 steel, Ni, ferrite, orientation in pearlite, rel. to austenite (*Russian*) 0-81072  
 steel, P, deep-drawing, spatial orientation distrib. of crystallites in cold-rolled and in annealed sheets 0-81079  
 steel, Si, nonoriented sheet prod. with texture of {100} (ovw) 0-89246  
 steel, Si (3 wt.%), struct. and preferred orientation, annealing parameters influence (*Czech*) 0-89248  
 steel, Si (3 wt.%), textured, secondary recrystn., precip. annealing effect (*Japanese*) 0-71662  
 steel, stainless, Cr-Cu (17, 0.6 to 1.1 wt.%), texture 0-84957  
 steel sheet, hot and cold rolled, cold formability, notched tensile test and stretch bend test (*German*) 0-61031  
 Zircaloy, textured, interactive creep and growth, upper-bound evaluation 0-89293  
 Zircaloy-2, irradiation growth, shape and volume changes 0-92562  
 Zircaloy-2, pressure tubes, irradi. creep and growth, anisotropy factors 0-97536  
 Ag, cold rolling, inhomogeneous texture 0-89251  
 Ag films, effect of Ar- and N-ion bombardment on texture (*Russian*) 0-107338  
 Al, cold rolling, inhomogeneous texture 0-89251  
 Al single crystals, relation between axial orientation rotating and deform. banding 0-104206  
 Al<sub>2</sub>O<sub>3</sub>, fine grained, basal slip and nonaccommodated grain boundary sliding 0-60916  
 Bi film, ellipsoidal model of textured specimens with uniaxial symm. (*Russian*) 0-80100  
 C, filamentous catalytic, rel. crystallographic orientations of C and metal 0-89240  
 Cd, warm rolled, texture and grain size depend. of tensile props. 0-71720  
 Co-Cr mag. film, crystallographic texture formation effects on props. (*Russian*) 0-108471  
 Co-Fe, soft mag. props. rel. to metallurgical aspects 0-88810  
 Cr, hyperfine interactions on <sup>111</sup>Cd-probe nuclei, TDPAC meas. 0-75904  
 Cu, cold rolled sheet, anisotropy of elastic and strength props. 0-81077  
 Cu, plastically deformed, lattice strain distrib. (*German*) 0-85012  
 Cu, tensile deformed (110) orientated single cryst., recrystn., high voltage electron microscopy study 0-84958  
 Cu thick probes, subthermal neutron transmission curves, for Bragg grain size and texture eval. (*German*) 0-71667  
 Cu, wire, axial texture after electroplastic drawing, X-ray struct. investigation (*Russian*) 0-104177  
 Cu-Ag (3 at.%), plastically deformed, lattice strain distrib. (*German*) 0-85012  
 Fe polycrystals, grain misalignment, electron microscope determ. (*Russian*) 0-103358  
 Fe, texture, recryst. annealing effect (*Czech*) 0-89249  
 Fe thick probes, subthermal neutron transmission curves, for Bragg grain size and texture eval. (*German*) 0-71667  
 Fe vacuum deposits on Ni(Cu)(Ag) (111) FCC substrates, orientation relationships 0-59836  
 Fe-Co-Ni Perminvar, mag. props. singularities in region of mag. anisotropy (*Russian*) 0-84614  
 Fe-Mn,  $\epsilon$ -martensite, preferred orientation and constitution, reverse pole figures (*Russian*) 0-104178  
 Fe-Ni-C alloy with single-component martensite texture,  $\alpha \rightarrow \gamma$  transform., changes in shape (*Russian*) 0-104152  
 Fe-Si, non-oriented sheets, production and props. 0-88797  
 Fe-Si (3 wt.%), texture, Mossbauer expts. 0-71262  
 Fe<sub>2</sub>O<sub>3</sub>/Fe<sub>3</sub>O<sub>4</sub> transformation matrices, higher-order orientation relationships 0-100846  
<sup>3</sup>He, superfluid, A-phase, helical textures, NMR response 0-70496  
 LiNbO<sub>3</sub> single crystals grown by automatic diameter control, power striations (*Chinese*) 0-81080  
 MgCd wire, elongation during disorder-order transform. (*Russian*) 0-104148  
 Mo polycrystals, grain misalignment, electron microscope determ. (*Russian*) 0-103358  
 Na<sub>2</sub>O-CaO-Al<sub>2</sub>O<sub>3</sub>-SiO<sub>2</sub> glass, crystn. for the purpose of obtaining vitroceramics (*French*) 0-75163  
 Na<sub>2</sub>O.11Al<sub>2</sub>O<sub>3</sub>, polycrystalline with preferably orientated grains, preparation (*Japanese*) 0-81012  
 Nb, mono- and polycrystn., crystallographic orientation, etching technique determ. 0-71814  
 Nb<sub>3</sub>Sn multifilamentary supercond. composites, crystallographic texturing 0-71669  
 NbTi films, effect of Ar- and N-ion bombardment on texture (*Russian*) 0-107338  
 Ni-Fe, soft mag. props. rel. to metallurgical aspects 0-88810  
 Re, electrodeposited from fused salts, (101) texture (*Russian*) 0-92791  
 Ti, commercial, texture depend. stress corrosion cracking 0-104334  
 $\alpha$ -Ti, fatigue crack growth, influence of grain orientation, SEM study 0-108550  
 $\alpha$ -Ti sheet, texture dependent stress corrosion cracking in Br<sub>2</sub>-methanol soln. 0-71803  
 Ti-Al-V (6, 4 wt.%), texture depend. stress corrosion cracking 0-104334  
 V<sub>2</sub>O<sub>5</sub>, amorphous semicond., solubility and fibrous texture 0-75162  
 W, vapour deposited, dislocation struct., rel. to texture (*Russian*) 0-65394  
 Zn-Al (0.4 wt.%), intergranular slip during in situ superplastic deform. 0-96538  
 Zn-Al (1.1 wt.%) superplastic alloy, grain size determ. (*Czech*) 0-81118  
 Zn-Al (22 wt.%) superplastic alloy, grain growth texture 0-81075

## texture continued

- Zr alloys, creep and growth, irradiation induced, rate theory approach 0-89294  
 Zr alloys, creep and growth, irradiation induced, microstruct. depend. 0-93602  
 Zr-Nb (2.5 wt.%), pressure tubes, irradi. creep and growth, anisotropy factors 0-97536

## texture, surface see surface texture

## thallium

- see also nuclei with .....  
 atom, 535.0 nm line shift by  $H_2$  perturber 0-91506  
 atom, autoionisation reson. determ. from photoelectron polarisation meas. 0-58221  
 atom, electron affinity, meas. by dissociation of  $TlBr$ ,  $TlI$  (French) 0-63849  
 atom, oscill. strengths, semiempirical relativistic one-electron central field, model pot. calcs. 0-78575  
 atom, photodissociative pumping effect 0-58182  
 atomic, inverted populations, obs. of stimulated level shifting 0-58218  
 atoms, ionisation limit and oscill. strength in VUV absorpt. spectra 0-74152  
 atoms, VUV photoelectron spectra, pseudo-atomic beam technique 0-58225  
 core level binding energies, UPS obs. 0-66388  
 films, supercond. amorphous, effective phonon spectrum and lattice sp. ht. 0-70895  
 impurity in Nimonic 105, influence on creep and stress rupture props. 0-66602  
 liquid,  $O_2$  activity from electrochemical meas. 0-104123  
 liquid, thermal props. at high temp. 0-75536  
 liquid, thermoelectric power, pseudopotential calc. 0-59959  
 parity non-conservation effect 0-68395  
 phase diagram and high press. phase transforms., DTA study (Russian) 0-66474  
 phonon spectrum from Krasko-Gurskii pseudopot. calc. 0-96608  
 underpotential adsorption, cathodic deposition, on  $Ag(111)$  and  $(100)$  (German) 0-108363  
 vapour, backward Raman amplifier, parasitic superfluoresc. suppression 0-69453  
 vapour, He-Ne laser radiation freq. conversion 1.15  $\mu m$  to 377.6 nm 0-95948  
 vapour, Nd-glass laser output conversion from 1.06 micron to 388.1 nm 0-91850  
 Ba-Tl laser optically pumped by pair-absorption transitions, 1.5  $\mu m$  emission obs. 0-58517  
 CsI:Tl, light yield under charged-particle bombardment 0-93409  
 CsI:Tl, precipitation of Tl solid solns. 0-70419  
 Hg-Tl discharges, 50 Hz, axial segregation effect on elec. field strength 0-59320  
 KBr:Tl, 480K thermal glow peak,  $Tl^+$  centres 0-108284  
 KBr:Tl, electroluminescence, spectra and quantum yield activator conc. depend., cond. changes 0-89070  
 KBr:Tl, luminesc., decay model for  $A_T$  and  $A_X$  emissions 0-93379  
 KCl:Tl, electroluminescence, spectra and quantum yield activator conc. depend., cond. changes 0-89070  
 KCl:Tl, temp. depend. of cathodolum. (Russian) 0-80868  
 KCl:Tl (0.003 to 0.27 mol.%), electrolum. 0-71490  
 $KD_3PO_4:Tl^{2+}$ , EPR of ferroelec. and paraelec. phases 0-66012  
 $KH_2PO_4:Tl^{2+}$ , EPR of ferroelec. and paraelec. phases 0-66012  
 KI:Tl, decay of fast component of impurity luminesc. excitation in A-absorption band (Russian) 0-84767  
 KI:Tl, polarised luminesc. of  $(Tl^+)$ , centres 0-71473  
 $NH_4Br:Tl$ , and pure crystals, luminesc., VUV irradiated at 80K (Russian) 0-84763  
 NaI(Tl) detectors, response functions to terrestrial  $\gamma$ -radiation, computer program 0-83233  
 NaI(Tl) scintillation cameras, image artifacts and counting losses 0-94345  
 NaI(Tl) well-type detectors, photopeak efficiency values, expts. and calcs. 0-63454  
 PbS:Tl, self-compensation of acceptors by vacancies, Hall coeff. meas. 0-92913  
 PbSe:Tl, self-compensation of acceptors by vacancies, Hall coeff. meas. 0-92913  
 PbTe:Tl, absorpt. coeff. spectral depend. 0-93370  
 Tl-Cs vapour mixture,  $CO_2$  CW laser radiation freq. conversion 0-74438  
 Tl-Hg, excimer band emission from electron beam initiated discharge in Tl-Hg 0-78841  
 Tl-Li ion exchange effects on  $LiNbO_3$  and  $LiTaO_3$  optical waveguides 0-58791  
 Tl-Xe, excimer band emission from electron beam initiated discharge in Tl-Xe 0-78840  
 Tl+Ba, dipole-quadrupole radiative collisional fluoresc. 0-83315  
 Tl+Ba, radiative collisional fluoresc. obs. from thermally excited atoms 0-102480  
 Tl+Cs, Tl  $6^2P_{1/2}$ -state relax., NMR obs. 0-95653  
 Tl $_2$ -Te liquid system, conc. fluctuation, time-of-flight quasielastic neutron scatt. obs. 0-88324  
 $Tl_2ZnBr_4$ , solid electrolytes, ion transport mechanism and polarisability role, comparison with  $Cu^+$  and  $Ag^+$  cond. 0-107531  
 $^{201}Tl$  myocardial imaging, subtraction imaging using  $^{201}TlCl$  and  $^{99m}TcO_4$  0-72318  
 $^{201}Tl$ , myocardial uptake, correl. with local perfusion, dog expts. (French) 0-104740  
 $^{201}Tl$ , transverse computerised axial tomography of the myocardium 0-67222  
 $^{201}Tl$ , tumour and organ affinity 0-67234  
 $^{204}Tl$   $\beta$ -particle excitation of external bremsstrahlung spectra from thick targets 0-84797  
 $^{204}Tl(p,5n)^{201}Pb$ ,  $^{201}Tl$ , yields and excitation functions for Pb radioactivities, medical appls. 0-67249

## thallium alloys

- see also thallium compounds  
 Cd-Tl binary alloy system at high press. 0-97461  
 Ce-Tl, phase equilibrium and cryst. struct. 0-66483  
 Tl $_2$ , mag. susceptibility, magnetisation, neutron diffn., elec. resist., and sp. ht. meas. 0-75733  
 Hg-Tl, phase limits, determ. by enthalpy functions along liquidus (French) 0-84911  
 Hg-Tl amalgam, viscosity meas. 0-88349

## thallium alloys continued

- In-Tl, single crystal containing Li, X-ray study of FCC $\rightleftharpoons$ FCT transform. (Japanese) 0-108435  
 In-Tl, small  $\kappa$  supercond., phase transitions higher than second order 0-88668  
 $In_{0.69}Tl_{0.31}$ , supercond. transition temp., specific heat, pseudopotential form factor 0-97026  
 Pb-Bi-Tl, supercond., crit. mag. fields, influence of parameters 0-75691  
 Pb-Tl, supercond., crit. mag. fields, influence of parameters 0-75691  
 $Pb_{1-x}Tl_x$ , liquid alloys, local fluctuations and quadrupolar relaxation 0-66600  
 $Pr_3Tl$ , thermal expansion and transverse elastic const. near mag. phase transition 0-60394  
 Se-Tl-S alloys, liq., dielectric relax. and elec. cond. 0-108150  
 Tl-Pb, in solid and liquid state, specific electric resistance 0-103662  
 Tl-Se, liquid mixtures, press. effect on two-phase region 0-75347  
 $Tm_2Ir_3$ , cryst. struct. 0-96473

## thallium compounds

- see also thallium alloys  
 halides, cryst., van der Waals coeffs. calcs. 0-96459  
 halides, static dielec. constant, strain derivatives 0-100629  
 hexanoate, soliton conduction, elec. cond. field and temp. depend. anomaly (Russian) 0-103703  
 lithium thallium tartrate, sp. ht., 0.3 to 25K, second-order ferroelec. transition 0-59674  
 $AgTlTe(S)(Se)$ , cryst. struct. 0-107156  
 As-S-Tl, glass, viscosity and elastic props. 0-100180  
 $CdTl_2Se_4(Te_4):Au$ , elec. cond., density, dielectric const., changes on fusion 0-88553  
 $CdTl_2Te_4$ , single and polycryst. samples, linear expansion, heat capacity and thermodynamic props. 0-103489  
 CuTlS, melting heat and melting entropy (Russian) 0-70374  
 $LiTmF_4$ , van-Vleck paramagnet, giant magnetostriction (Russian) 0-103872  
 $NaTl_2(SO_4)_2$ , heat capacity and thermodynamic functions, 10 to 300K 0-65244  
 Tl complex of lasalocid (X-537A),  $^{205}Tl$  NMR study 0-58288  
 Tl-Bi-Sb-Te system, peritectic reactions in  $TlBiTe_2$ - $TlSbTe_2$  cross section, crystn. character 0-108406  
 Tl-Ge-Te, glass formation 0-103255  
 Tl-Sn-Te system equilibria, polythermal and isothermal cross sections obs., ternary cpd. form. 0-104128  
 $TlAlF_6$ , single cryst., prep. and struct. (French) 0-79762  
 $TlAsS_3$ , glass, crystallisation, effect of an alternating electric field 0-88054  
 $TlAsS_3(Se_2)(Te_2)$ , vitreous, crystn. kinetics 0-64918  
 $Tl_3AsSe_5$ , refractive index, thermal expansion temp. depend. 0-97223  
 TlBr, electron impact dissociation, ionisation, Tl electron affinity meas. (French) 0-63849  
 TlBr, polymorphism, XPS obs. 0-97398  
 TlBr, resonant polaron coupling and excitons under mag. field 0-71383  
 TlBr-TlI KRS-5 fibre crystals floating zone growth, for IR optical waveguides 0-79019  
 TlBr-TlI(Cl) crystals, photoelastic moduli 0-97230  
 $Tl_2CO_3$ +8-hydroxyquinoline, solid state reaction 0-108708  
 TlCl, ground-state props., Wannier functions, and electronic struct., ab initio self-consistent calc. 0-80178  
 TlCl, phonon difference band absorpt., far IR laser spectroscopy 0-93325  
 TlCl, polymorphism, XPS obs. 0-97398  
 TlCl-TlBr, KRS-6, ultralow loss optical fibre material, loss mechanism 0-78920  
 $TlCoCr_2(VO_4)_3$ , synthesis and cryst. struct. 0-88114  
 $TlCuCr_2(VO_4)_3$ , synthesis and cryst. struct. 0-88114  
 $TlD_3PO_4$ , antiferroelectricity, permittivity, electric field double hysteresis loops 0-60512  
 TlF+Ar, sudden approx. of Cross, computational tests, cross section factorisation, scatt. phenomena 0-58352  
 $TlF_2(Cl_2)$ , molcs., assignment of vibr. Raman and IR spectra bands 0-82686  
 $TlGaSe_2$ , monocrystal, processes of recombination and trapping levels, photocond. meas. (Russian) 0-70751  
 $TlGaTe_2$ , IR refl. spectra 0-60605  
 TlI additives in Hg discharge, high-pressure, line broadening and radiative transport 0-74199  
 TlI, atomic fluorescence,  $D_2$  pressure effect on width and shift 0-99475  
 TlI, electron impact dissociation, ionisation, Tl electron affinity meas. (French) 0-63849  
 TlI laser window films, stoichiometry, Rutherford backscatt. study 0-59831  
 TlI, photodissoc., Tl 535.0 nm line shift by  $H_2$  perturber 0-91506  
 TlI-Hg, excimer band emission from electron beam initiated discharge 0-78841  
 TlI-Xe, excimer band emission from electron beam initiated discharge 0-78840  
 $Tl_4M_2(I_4)^{2+}$ , ( $M=Pb, Ag, Au, (BiO_3)TlO_3$ ), struct., rel. to phonon spectra 0-71425  
 $TlInS_2$ , layered structure crystals, refractive index meas. method 0-98966  
 $TlInSe_2$ , IR refl. spectra 0-60605  
 $TlInSe_2$ , monocrystal, photoelec. props. (Russian) 0-70752  
 $TlInTe_2$ , IR refl. spectra 0-60605  
 $TlMgCr_2(VO_4)_3$ , synthesis and cryst. struct. 0-88114  
 $TlMnCl_3$ , specific heat near Neel temp. (Russian) 0-100340  
 $Tl_2Mo_6S_{11}$ , X-ray cryst. struct. determ.,  $Mo_{12}$  and  $Mo_6$  isolated clusters (French) 0-92490  
 $Tl_2Mo_6S_{11}$ , prep. and struct.,  $Mo_{12}$  cluster in  $Mo_{12}S_{14}$  unit 0-107168  
 $Tl_2Mo_6S_8$  Chevrel phase, synthesis, stability and characts. 0-71608  
 $Tl_2Mo_6S_9$ , superconducting chalcogenides containing  $Mo_6$  and  $Mo_9$  clusters 0-103804  
 $Tl_2Mo_6Se_6$ , X-ray cryst. struct. determ., monodimensional clusters ( $Mo_6/2$ ) $^\infty$  (French) 0-96482  
 $TlMo_6Se_3(Te_3)$ , synthesis and struct. 0-92498  
 $TlNiCr_2(VO_4)_3$ , synthesis and cryst. struct. 0-88114  
 TlO-GeO $_2$  system, structure of thallium I germanates (French) 0-79754  
 $Tl_2PO_4$ , heat capacity and thermodynamic functions, 5 to 320K 0-65245  
 $Tl_2PS_4$ , optical phonons, Raman spectra study 0-80790  
 $Tl_2PSe_4$ , phonon dispersion temp. depend. 0-96600  
 $Tl_2PbCu(NO_2)_6$ , incommensurate Jahn-Teller transition, Huang scatt. 0-70401  
 $TlReO_4$ , IR matrix-isolation spectra 0-87108



**thallium compounds continued**

- TlSe type crystals, possible second-order phase transitions, group-theoretical anal. 0-92672  
 Tl<sub>2</sub>SeO<sub>4</sub>, structural transition, polarised Raman spectra 0-75349  
 Tl<sub>2</sub>SnSe<sub>3</sub>, X-ray cryst. struct. determ. (*French*) 0-107171  
 Tl<sub>2</sub>TaSe<sub>4</sub>, optical phonons, Raman spectra study 0-80790  
 Tl<sub>1-x</sub>Ta<sub>1+x</sub>W<sub>1-x</sub>O<sub>6</sub> pyrochlore system, comp. depend. of ionic cond. 0-105717  
 TlTe, melt, elec. cond., surface tension, microhardness, influence of impurities 0-88551  
 Tl<sub>2</sub>Te, melt, resistivity, surface tension, microhardness, influence of impurities 0-88552  
 Tl<sub>2</sub>Te-Tl liquid system, conc. fluctuation, time-of-flight quasielastic neutron scatt. obs. 0-88324  
 Tl<sub>2</sub>Te<sub>2</sub>-Tl<sub>2</sub>SnTe<sub>2</sub>-Tl<sub>2</sub>PbTe<sub>2</sub>, phase equilib., DTA, SPA and microhardness meas. 0-96628  
 Tl<sub>2</sub>(Te<sub>2</sub>Se<sub>2</sub>)<sub>x</sub> mixtures, liq., electrical conductivity, magnetic susceptibility 0-88715  
 Tl<sub>1-x</sub>(Tl<sub>1-x</sub>Nb<sub>1+x</sub>)O<sub>5</sub>, layer compound, cryst. struct., nonstoichiometry 0-64972  
 Tl<sup>III</sup>(SeO<sub>4</sub>)<sub>2</sub>, Tl<sup>III</sup>(SeO<sub>4</sub>)<sub>3</sub>, and Tl<sup>III</sup>(SeO<sub>4</sub>)<sub>4</sub>, cryst. struct. (*French*) 0-84148  
 TlVO<sub>4</sub>, synthesis and thermal props. (*French*) 0-97443  
 Tl<sub>2</sub>V<sub>2</sub>S<sub>6</sub> single crystal growth, Bridgman-Stockbarger technique 0-89132  
 Tl<sub>0.33</sub>WO<sub>3</sub> bronze, elec. resist. meas., anisotropy, supercond. 0-75569  
 Tl<sub>2</sub>ZnI<sub>4</sub>, solid electrolytes, ion transport mechanism and polarisability role, comparison with Cu<sup>+</sup> and Ag<sup>+</sup> cond. 0-107531  
 Tl<sub>2</sub>[Fe(CN)<sub>5</sub>(NO)], X-ray cryst. struct. determ., heavy atom method 0-92495

**thawing see melting****The Galaxy**

- accretion of intergalactic matter in solar neighbourhood 0-67863  
 anticentre, 21 cm obs. of H I stream 0-90524  
 bright stars, XX LMC luminosity function 0-82499  
 bulge X-ray sources, radio continuum obs. at 2.7, 4.8 and 10.7 GHz 0-101619  
 Carina arm region, OB stars, UVB photometry 0-85941  
 central region, formaldehyde and molecular clouds 0-94852  
 central region, Prognos-6 obs. of X-ray fluxes and energy spectra (*Russian*) 0-109562  
 central region, sources and obscuration 0-77487  
 central region gas distribution, barlike model based on improved H I data 0-67845  
 centre, black hole mass from X-ray flux and radiation spectrum of accreted gas 0-90467  
 centre, nearest Cepheid, V1437 Sagittarii distance 0-82396  
 centre region, H radio recombination line obs. of arc-like source 0-82498  
 centre region, high-energy X-ray detection 0-67854  
 centre region, IR bright stars catalogue and photometry 0-77299  
 Cepheid variables, long-period, absence from Galaxy rel. to obs. of yellow variable supergiants 0-98672  
 chemical evolution, role of planetary nebulae 0-109541  
 chemical evolution from main sequence disk star calcs. 0-109553  
 chemical evolution of galactic disc, inflow problem 0-62279  
 chemical evolution rel. to stellar evolution and nucleosynthesis 0-67847  
 Circinus-Norma region, faint OB star search 0-62121  
 comet orbital elements distrib., effect of galactic forces (*Russian*) 0-77353  
 corona, plasma parameters and heating mechanism 0-82492  
 cosmic ray acceleration by supernova shock waves 0-82154  
 cosmic ray electrons, energy spectrum and fundamental props. (*Chinese*) 0-105138  
 cosmic rays, energy dependent diffusion in dynamic halo model 0-82156  
 cosmic rays origin, appl. of galactic models with halo to proton nucleon component 0-61971  
 diffuse EUV flux, rel. to local interstellar medium ionisation state 0-90502  
 disc, local K<sub>r</sub>-force field rel. to interstellar matter z-distrib. 0-62271  
 disc, obs. between -45° < l < 45° in 80 keV to 8 MeV energy range 0-82540  
 disc population stars, luminosity functions in SA 51, SA 57 and (SA 68) 0-98648  
 early-type stars in S. Milky Way, uvby photometry 0-85942  
 EUV background, point source contribs. 0-62324  
 evolution and abundance from obs. of globular clusters 0-90484  
 galactic bulge wind, interaction with gas disc, hydrodynamic model 0-77476  
 galactic plane far IR emission, obs. at galactic longit. (l = 27.5°) 0-62231  
 gamma-ray burst origin, models review 0-82494  
 gamma-ray obs. with COS-B (*Danish*) 0-82544  
 globular cluster system, state of inferred fundamental knowledge about Galaxy 0-90488  
 globular clusters in Galaxy, tidal disruption 0-105294  
 globular clusters near galactic centre, IR studies 0-82434  
 globular star clusters, metal abundance and reddening from photometry obs. 0-67800  
 GX 1-4, galactic centre X-ray source, X-ray obs. periodicity 0-105399  
 halo, extent from props. of stellar images at faint magnitudes 0-82360  
 halo, metal-poor star distrib. (*German*) 0-94867  
 halo, obs. of metal-rich distant globular cluster (Pal 12) 0-105290  
 halo, regular magnetic field component (*Russian*) 0-67872  
 halo population stars, luminosity functions in SA 51, SA 57 and (SA 68) 0-98648  
 integrated starlight, synthetic spectrum between 3000 and 10000 Å, discussion 0-62200  
 interstellar cosmic ray acceleration models, inconsistencies 0-82155  
 interstellar dust distrib. within 3 kpc in galactic plane 0-109512  
 interstellar extinction, average model, from planetary nebulae obs. 0-62221  
 interstellar hot gas in Galaxy outer halo, evidence from IUE UV obs. of (3C 273) detailed UV obs. with IUE 0-94886  
 interstellar reddening in solar neighbourhood, anal. 0-62239  
 interstellar UV radiation, role in interstellar gas heating 0-67839  
 interstellar UV radiation field, obs. from S2/68 sky-survey telescope 0-77523  
 isotopic species, stable, galactic distrib. from interstellar mol. obs. 0-109550  
 kinematics of old stars, rel. to Galaxy initial contraction 0-62204
- The Galaxy continued**  
 light metal synthesis, evidence from Al abundance in cool halo stars 0-105232  
 local spiral arm, stellar velocity dispersion inhomogeneities 0-98653  
 M33 direction, H I 21 cm emission/absorp. obs. 0-62262  
 magnetic field, review of obs. 0-73042  
 magnetic field components from pulsar rot. meas. 0-85966  
 magnetic field fluctuations, correl. length and fluctuating angle from starlight polarisation theory 0-82442  
 magnetic field interaction with hot intergalactic gas, magnetosphere existence 0-67876  
 metal abundance vars. from young cluster photometry 0-101621  
 molecular cloud complexes, origin, lifetimes and mass 0-82453  
 northern galactic plane, galaxies on POSS E prints obs. through transparent regions 0-62280  
 Northern stars, True Visual Magnitude Photographic Star Atlas 0-109376  
 O-stars, association with nebulosity in spiral arms 0-105236  
 open cluster distrib. in disk 0-101620  
 peculiar motion, rel. to Hubble const. local value determ. from Sb galaxies luminosity classification 0-62339  
 Perseus arm member NGC 957, young open cluster, RGU photometry 0-85976  
 planetary nebulae, central stars masses rel. to galactic disc or halo membership 0-82344  
 planetary nebulae, distances and galactic distrib. 0-67819  
 planetary nebulae, spatial and vel. distrib. statistics 0-109518  
 planetary nebulae near galactic centre, VLA and optical search 0-90506  
 planetary nebulae of galactic halo, photoionisation models and chemical abundances of K 648, 49+88.1° and (108-76.1°) 0-109507  
 planetary nebulae spatial distrib. and luminosity function, evidence from obs. in (M31) 0-109520  
 polar regions, nonthermal radio spectrum rel. to cosmic ray electrons spectrum and γ-rays prod. 0-62257  
 Population I O-type runaway stars, nature and galactic distrib. 0-85938  
 positions, primary source, prod. rate, and escape probability 0-109319  
 Puppis area, spiral arm struct. in third quadrant 0-85937  
 r-nuclei production sites 0-72932  
 radio and soft X-ray emissivity, anticorrelation, plasma cloud interpretation 0-82514  
 radio emission spectrum, influence of primordial black holes 0-62179  
 radio sources, H110α line and formaldehyde absorpt. line obs., SHF obs. 0-77472  
 Rubin-152, possible massive O-type star on galactic fringe, spectroscopic obs. 0-98656  
 Sagittarius B2, galactic centre H II region, He recombination line obs. interpretation 0-62300  
 solar neighbourhood, initial mass function and stellar birthrate 0-62259  
 spiral structure, effect of sound wave propagation in hot gas 0-109511  
 spiral structure, gaseous theory of origin 0-82517  
 spiral structure, in vicinity of Sun (*Russian*) 0-62290  
 spiral structure, mol. clouds as a tracer, 2.6 mm CO survey 0-105346  
 stability of galactic disc as rotating spheroidal stellar system 0-62203  
 star distribution perpendicular to galactic plane, fine struct. study (*Russian*) 0-73036  
 star formation, suppression rel. to delayed star form. problem 0-105349  
 star formation in inner regions, IR obs. 0-67704  
 star formation rate and ionising Lyman continuum photon flux 0-67711  
 stars space densities derivation, new method 0-85932  
 stellar disc central hole, rel. to evolution 0-62268  
 structure from gamma ray obs., review 0-98743  
 structure from star counts 0-82507  
 structure in S. Milky Way, stellar distrib. and colour excess obs. 0-85997  
 Sun, distance from galactic centre determined from radial vels. of O and B stars 0-101584  
 supergiants, comparison with Magellanic Clouds 0-67699  
 supernova outbursts, frequency estimate 0-62168  
 tidal forces, rel. to truncation of dying globular cluster E3 (ESO-037-SC 01) 0-105291  
 turbulent interstellar medium rel. to planetary nebulae extinction 0-62220  
 Wolf-Rayet, single-line Population I stars, distance from galactic plane 0-77415  
 X-ray emission, contrib. to diffuse X-ray flux in 2 to 7 keV range 0-98745  
 X-ray source distrib. 0-67905  
 X-ray sources, space distrib. and physical nature 0-62316  
 Ar, galactic nucleosynthesis rel. to low Ar abundances in three halo planetary nebulae 0-82443  
 H I absorpt. in seven low-latit. pulsars, meas. 0-101606  
 H I absorption in galactic centre direction 0-77465  
 H I emission and absorpt. towards extragalactic radio sources 0-94854  
 H I stream in galactic anticentre, 21 cm obs. 0-90524  
 H I survey, brightness temp. contour maps, 21 cm obs. 0-85986  
 H I survey, photographic presentation 0-62241  
 H II regions, origin from supernovae explosions 0-67877  
 H II regions in Perseus and local spiral arms, H166α line obs. 0-90512  
 H<sub>2</sub>O masers, 22 GHz galactic plane survey, 14 new sources 0-77464  
 O enrichment of Galaxy, evidence from O/H ratios in planetary nebulae 0-105328
- theoretical mechanics see mechanics**
- thermal analysis**  
 alkali metal chloride melts and mixtures, thermogravimetric determ. of uranyl cation state 0-101050  
 alkali silicate glasses, secondary relax. transitions 0-88261  
 alkali silicate glasses, struct. and thermal props. 0-84075  
 N-4-n-alkyloxybenzylidene-4-n-alkylanilines, smectic polymorphism, calorimetric study 0-88307  
 2-4-n-alkylphenyl-5-(4-n-alkyloxyphenyl)-pyrimidines, smectic polymorphism, calorimetric study 0-88307  
 amorphous alloys, thermal stability, crystn., DSC and elec. resist. study 0-107060  
 basalt, naturally occurring, high-temperature quantitative DTA analysis 0-77144  
 binary alloys, initial transient segregation during unidirectional solidification in a furnace with thermal damping 0-70146  
 cholesterol myristate, smectic A-cholesteric transition, tricritical behaviour, DTA and DSC study 0-65206

## thermal analysis continued

- dextran fractions, production, characterisation and solution properties 0-59368  
 dickite, unusual crystal habit, structural disorder 0-59445  
 F 0-100329  
 ferrocene, orthorhombic low-temp. cryst. phase, characterisation 0-96507  
 graphite fibre filled phthalocyanine composites, cure cycle investigation 0-81030  
 graphite fluorides, (CF)<sub>n</sub> and (C<sub>2</sub>F)<sub>n</sub>, prep., struct., discharge characts., electrode props. 0-89502  
 high-temperature quantitative DTA analysis, appl. to basalt 0-77144  
 laser beam heat flux and power profiling, using swept null point calorimetry 0-69439  
 lunar regolith samples from Lunar-24, X-ray diffr. and thermogravimetric obs. 0-67598  
 metallic glass, stability, hole theory of liquids appl. 0-100174  
 metallic glasses, crystn., thermosonimetric investigation 0-75180  
 5-methyl-1-thia-5-azacyclooctane-1-oxide perchlorate, single cryst. transform., evidence for intermediate state 0-88078  
 nonisothermal devitrification kinetics 0-92465  
 plastics, thermosetting, characterisation by thermal anal. 0-61204  
 Polimal 142, polyester moulding material, hardening (Polish) 0-66523  
 poly(di-n-heptyl itaconate), alkyl side chain independent relax., double glass transition 0-59636  
 polyaryloxyphosphazene copolymers, thermal, morphological and rheological props. 0-103265  
 polycarbonate, glassy state, enthalpy relax., thermal density fluctuations 0-59678  
 polydioxolan, crystn. kinetics, dilatometric analysis and microscopy obs. 0-79706  
 polydiphenylsiloxane, thermodynamics of fusion 0-84280  
 polyester, temp. index, rapid determ. by dynamic thermogravimetry 0-85101  
 polyether-polyester elastomers, differential scanning calorimetry, crit. points (Japanese) 0-75344  
 polyether-polyester elastomers, differential scanning calorimetry by using poly(oxy-1,4-butylene glycol) as soft segment (Japanese) 0-79916  
 polyethylene, high press. phase, US, DTA, and X-ray diffr. study 0-75188  
 polyethylene, high-density, solid-state coextrusion, mol. wt. distrib. effect 0-104212  
 polyethylene, low density, melting and crystallisation, DSC characterisation 0-64927  
 polyethylene flow crystallisation, in extensional flow developed by convergent capillaries, props. 0-84111  
 polyethylene melt, cryst. kinetics during cooling, nucleation density effect 0-100181  
 polyethylene terephthalate, oriented, amorphous, stress-induced crystn., shrinkage meas. 0-92466  
 polyimides, temp. index, rapid determ. by dynamic thermogravimetry 0-85101  
 polymer, degradation, reaction product volatility effect on thermogravimetric anal. 0-104316  
 polymer concretes, hydrothermally stable, hydraulic cement-type fillers 0-85144  
 polymer glasses, enthalpy relax., scanning calorimetry technique 0-90851  
 polyphenylacetylene cis-trans isomers, rel. mol. wt. distrib., heating effect 0-106409  
 polypropylene, isotactic, low temp. annealing, differential scanning calorimetry obs. 0-60895  
 polyurethane, segmented, domain struct., deform. effect 0-93623  
 polyvinyl acetal, temp. index, rapid determ. by dynamic thermogravimetry 0-85101  
 potassium n-alkanoates, thermal behaviour, differential scanning calorimetry obs. 0-92650  
 PTFE,  $\gamma$ -ray effects on 19 and 30°C phase transitions, Fourier transform IR spectroscopy 0-103387  
 radiation effects on material determ., thermal defect meas. using total-absorption calorimeters 0-99427  
 resins, prepreps and composites, charact. by differential scanning calorimetry 0-71869  
 rutile structure fluorides, high temp. polymorphism and thermal props. 0-75199  
 silicate glass, hydration in steam atmosphere 0-85211  
 solar power plant, transient thermal behaviour of primary circuit and thermal storage tank 0-85267  
 steel, austenitic types AISI 316, 347 and Eshete 1250, corrosion in molten SO<sub>2</sub> deposits 0-97625  
 steel, cold strained, defects interaction with carbide strengthening phases, carbide decomp. degree (Russian) 0-84955  
 steel, maraging 18%Ni, calorimetric anal. of ageing (Japanese) 0-89264  
 steel casting, calc. method of thermal and thermo-visco-elasto-plastic processes (German) 0-79859  
 steel continuous casting, thermal, thermo-visco-elasto-plastic processes (German) 0-81044  
 terephthalylidene-bis-(4-n-alkylanilines), smectic polymorphism, calorimetric study 0-88307  
 2,2,2,6-tetramethyl-piperidino-oxy, cryst. growth and polymorphism 0-96645  
 thermogravimetry, balance inclination and specimen temp. error sources 0-98887  
 1,1,1-trichloroethane, polymorphism under high pressure (French) 0-96644  
 Zircaloy-2, hot-pressed, influence of diffused C on structure and oxidation 0-61016  
 Ag-Bi-S, ternary phase diagram, DTA and X-ray diffr. investigation 0-84917  
 Ag-Sm system, phase diagram, eutectic temps., microstruct. (German) 0-104119  
 Ag<sub>2</sub>(Au)<sub>1-x</sub>Cu<sub>x</sub>, phase relations, X-ray diffr. and differential thermal anal. 0-108395  
 AgGaS<sub>2</sub>-AgGaSe<sub>2</sub> system, phase diagram, lattice consts., and IR spectra 0-60841  
 Ag-S-Ln<sub>2</sub>S<sub>3</sub>, powdered mixtures, reaction rate, production of ionic semiconductors 0-93741  
 AgSBr, ionic conductivity in temp. range 93-573K, X-ray diffr. and DTA 0-79988  
 AgSI, ionic conductivity in temp. range 93-573K, X-ray diffr. and DTA 0-79988  
 AgZn,  $\beta'$ - $\beta''$  transformation, effect of additional elements 0-66507

## thermal analysis continued

- Al-Cu (2-5 wt.%), precipitation total surface influence on resistivity (French) 0-71650  
 Al-Mg-Zn-Cu, type 7050, calorimetric study of fatigue induced microstructural changes 0-85034  
 Al-Zn-Mg, TEM and calorimetric study 0-76290  
 AlF<sub>3</sub> based glasses, chem., thermal and optical props. (French) 0-70139  
 Al<sub>2</sub>Mg<sub>3</sub>, diffusionless phase transformation 0-104150  
 Al<sub>2</sub>O<sub>3</sub>, ultrafine gel particle form. from NH<sub>4</sub>-AlCl<sub>3</sub> solution 0-93807  
 $\beta$ -Al<sub>2</sub>O<sub>3</sub>-NH<sub>4</sub><sup>+</sup>, single cryst. characts. and AC cond. obs. 0-107514  
 As-Te-In, glass-forming, density and microhardness 0-103257  
 As<sub>2</sub>S<sub>3</sub>100-x, amorphous films, optical props. and photoinduced changes 0-60700  
 Au<sub>2</sub>Cu<sub>1-x</sub>Ag<sub>x</sub>, phase relations, X-ray diffr. and differential thermal anal. 0-108395  
 BaTiO<sub>3</sub>:C, solubility of C at low O<sub>2</sub> potentials, 800°C 0-100334  
 BeF<sub>2</sub> glass, glass transition temp. and thermal expansion 0-64902  
 BeO, heated on W, thermal anal. using mass spectrometric, technique, vapourisation behaviour 0-79932  
 Bi-MnBi eutectic region, of Bi-Mn phase diagram 0-81034  
 Bi<sub>2</sub>O<sub>3</sub>, polymorphic transformation and elec. resistivity (Japanese) 0-93555  
 CaCu<sub>2</sub>,  $\gamma$ -phase in Ca-Cu system, calorimetric determ. of enthalpy of form. (French) 0-84915  
 CaF<sub>2</sub>-AlF<sub>3</sub>-Na<sub>2</sub>AlF<sub>6</sub>(-Al<sub>2</sub>O<sub>3</sub>), phase equilibria, X-ray diffr. and DTA meas. 0-108409  
 CaO, heated on W, thermal anal. using mass spectrometric, technique, vapourisation behaviour 0-79932  
 CdTe-In system, equilib. phase diagram and liq. phase epitaxial growth of CdTe from In soln. (Japanese) 0-71634  
 Ce-In, phase equilibrium and cryst. struct. 0-66483  
 Ce-Tl, phase equilibrium and cryst. struct. 0-66483  
 Co-Ge binary system, phase diagram rel. to that of Ni-Ge (French) 0-97463  
 Co-P, electrodeposited alloys, heat-induced structural changes (Japanese) 0-89263  
 Co<sub>1-x</sub>Al<sub>x</sub>, ordered  $\beta$ -phase, enthalpy of formation are defect struct. descript. 0-89519  
 Co<sub>90</sub>Zr<sub>10</sub>, ferromag. amorphous alloy, crystn. and domain struct. study 0-107056  
 Cr-Ge system, phase diagram, thermal anal., X-ray diffr., microhardness, and electron probe anal. (French) 0-97462  
 Cs-SiO<sub>2</sub>-Al<sub>2</sub>O<sub>3</sub> system interactions, getter development for radiocaesium 0-83208  
 Cu-Ag-Ge, Hume-Rothery glass form. 0-96449  
 Cu-Ag-P(6-14, 11-14 wt.%) amorphous, crystn. and elec. props., X-ray diffr., elec. resist. and DTA meas. (Japanese) 0-84088  
 Cu-Ni, adsorption of H<sub>2</sub>+CO on (110) surface, TDS and UPS obs. 0-80052  
 Cu<sub>2</sub>Ag<sub>1-x</sub>Au<sub>x</sub>, phase relations, X-ray diffr. and differential thermal anal. 0-108395  
 Cu<sub>2</sub>S-Ln<sub>2</sub>S<sub>3</sub>, powdered mixtures, reaction rate, production of ionic semiconductors 0-93741  
 DyF<sub>3</sub>-CsF, phase diagrams and ternary fluorides (French) 0-81040  
 DyF<sub>3</sub>-RbF, phase diagrams and ternary fluorides (French) 0-81040  
 EuTe, high-temperature evaporation and reactivity 0-103469  
 $\beta$ -FeOOH, Mossbauer spectra obs., chemical and thermal anal., X-ray diffr., saturation magnetisation 0-88896  
 Fe, cast, with spheroidal graphite, crystn. (German, English) 0-97473  
 Fe-(Co)-B and Fe-Ni-B(P), amorphous, crystn. 0-79704  
 Fe-B, metallic glasses and vapour deposited films, amorphous to cryst. transition 0-88048  
 Fe-B metallic glasses, struct., stability and crystn. 0-75173  
 Fe-Mo system, thermomech. props. 0-89208  
 Fe-Ni alloys, enthalpy change between  $\alpha'$ - $\gamma$  and  $\alpha$ - $\gamma$  transformations 0-93550  
 Fe-Ni-P-B, metallic glasses, struct. relax., annealing effects on mag. props. 0-89261  
 Fe-Ni-P-B metallic glass, crystallisation temperature values from isothermal transformation times 0-59397  
 Fe-Ti-C, rapidly quenched by splat-cooling 0-84923  
 Fe<sub>32</sub>Ni<sub>36</sub>Cr<sub>14</sub>P<sub>12</sub>B<sub>6</sub> metallic glass, crystn. kinetics by TEM 0-75186  
 Fe<sub>40</sub>Ni<sub>40</sub>P<sub>14</sub>, glass transition, viscous flow and differential scanning calorimetry meas. 0-96635  
 FeO<sub>x</sub>, wustite field, thermodynamic props. and subphases, thermogravimetry, 1100-1300°C 0-76239  
 $\alpha$ -Fe<sub>2</sub>O<sub>3</sub> crystal flux growth, solubility and relative supersaturation in Fe<sub>2</sub>O<sub>3</sub>-PbO-V<sub>2</sub>O<sub>5</sub> fluxed melt system 0-64934  
 Fe(OH)<sub>3</sub>, thin films, Mossbauer spectra obs., chemical and thermal anal., X-ray diffr., saturation magnetisation 0-88896  
 $\beta$ -FeOOH, dehydration 0-79767  
 Fe<sub>2</sub>O(OH)<sub>4</sub>, Mossbauer spectra obs., chemical and thermal anal., X-ray diffr., saturation magnetisation 0-88896  
 Fe<sub>2</sub>VS<sub>2</sub> (0.20 < x < 1.00), phase diagram and order-disorder transition of vacancies 0-81039  
 Ga-Se<sub>2</sub>-FeSe, phase diagram, elec. cond., mag. susceptibility 0-88301  
 Gd<sub>2</sub>O<sub>3</sub>-Ga<sub>2</sub>O<sub>3</sub> system, phase diagram relationships of garnet-perovskite transform. 0-97460  
 GeO<sub>2</sub> glass, nonisothermal devitrification kinetics 0-92465  
 HfO<sub>2</sub>As<sub>2</sub>O<sub>4</sub>·4H<sub>2</sub>O and HfO<sub>2</sub>PO<sub>4</sub>·4H<sub>2</sub>O layered cpds., struct. investigs. below antiferroelec. transition temps., H bond ordered structs. 0-107416  
 Hf<sub>1-x</sub>Fe<sub>x</sub>, amorphous alloys, formation, crystallisation and electrical resistivity 0-96838  
 HfO<sub>2</sub>(P(As))O<sub>4</sub>·4H<sub>2</sub>O, water deficiency, enthalpy of dehydration, thermogravimetric anal. 0-65251  
 InAs-CdTe quasi-binary system, temp.-comp. diagram, physicochem. and thermodynamic analysis 0-104127  
 KCaF<sub>3</sub>, struct. phase transitions, DSC, birefr., and neutron powder diffr. obs. 0-70149  
 KD<sub>2</sub>PO<sub>4</sub>, transparent dielec., thermal analysis of laser-induced damage 0-66336  
 KF-ErF<sub>3</sub>, phase diagram 0-92645  
 KMg<sub>2</sub>LiSi<sub>4</sub>O<sub>10</sub>F<sub>2</sub>-NaMg<sub>2</sub>LiSi<sub>4</sub>O<sub>10</sub>F<sub>2</sub>, solid soln., solid solubility and swelling characts. 0-59660  
 KOH-KO<sub>2</sub>, phase diagram (French) 0-107177  
 K<sub>2</sub>SO<sub>4</sub>, phase transform., mech. of thermal hysteresis, DTA, dilatometry and dielec. meas. 0-75353  
 KYBHP<sub>2</sub>O<sub>10</sub>, thermal decomp., thermogravimetric and X-ray obs. 0-101013  
 La<sub>2</sub>NbO<sub>7</sub>, synthesis and cryst. growth 0-71590  
 Li/SO<sub>2</sub> cells, DTA, safety studies 0-81428



**thermal analysis continued**

- Li-Pt, phase diagram for comp. range 0-40 at.% Pt, mag. and elec. props. (*German*) 0-84912
- LiCl-Li<sub>2</sub>O-P<sub>2</sub>O<sub>5</sub> glass system, vitreous domain, struct., elec. cond. (*French*) 0-70135
- Li<sub>2</sub>O-2SiO<sub>2</sub> glass, DTA study, Kissinger plot 0-84084
- Li<sub>2</sub>O-TiO<sub>2</sub>, pseudobinary phase rotations, DTA and X-ray anal. 0-108411
- Li<sub>1+x</sub>2P<sub>2</sub>O<sub>5</sub>, polyphosphate, melting and crystallisation 0-70376
- Mg-MgNi<sub>2</sub>-Zn, diagram of state, Zn solubility, initial phase precipitation (*Russian*) 0-66478
- Mg(NO<sub>3</sub>)-RNO<sub>3</sub> (R=Li, Na, K), thermogravimetric anal. of dehydration processes (*Japanese*) 0-66791
- MgO, heated on W, thermal anal. using mass spectrometric, technique, vaporisation behaviour 0-79932
- Mo oxides, low-grade, soda roasting study (*Korean*) 0-93508
- NaF-SrF<sub>2</sub>-CrF<sub>3</sub>, glass transition, crystn. and melting temps., optical transmission (*French*) 0-64910
- (Na,Ky).CO<sub>3</sub>, non-stoichiometric, cryst. struct. (*French*) 0-79761
- Na<sub>2</sub>O-PbO-SiO<sub>2</sub> glass-ceramic composite, directionally crystallised 0-107058
- Na<sub>2</sub>PO<sub>4</sub>-Ni<sub>3</sub>(PO<sub>4</sub>)<sub>2</sub> system, phase equilibrium diagrams, crystallographic study, double orthophosphates (*French*) 0-93546
- Ni, electrodeposited film, thermal anal., occlusion of gases rel. to mag. props. 0-59823
- Ni-Cr-Al-TaC, eutectic composite, microstructure, fatigue props. 0-85038
- Ni-Ge binary system, phase diagram rel. to that of Co-Ge (*French*) 0-97463
- Ni-P, electrodeposited film, thermal anal., occlusion of gases rel. to mag. props. 0-59823
- Ni-S, electrodeposited film, thermal anal., occlusion of gases rel. to mag. props. 0-59823
- Ni-Ta (70, 30 wt.%) metallic glass, struct. and crystn. (*Russian*) 0-70136
- Ni<sub>1-x</sub>Cr<sub>x</sub>S, elec. transport, mag. susceptibility and DTA meas. 0-96954
- Ni<sub>3</sub>Fe<sub>3</sub>Cr<sub>14</sub>P<sub>12</sub>B<sub>6</sub> metallic glass, mech. props. and thermal stability 0-76362
- (Ni<sub>0.9</sub>PD<sub>0.1</sub>)<sub>18</sub> amorphous alloy, liquid-quenched, crystn. kinetics, nucleation 0-100176
- Pb-Sb, thermal analysis in non-faceted/faceted eutectic systems 0-71637
- PbI<sub>2</sub>, high press. phase diagram to 3.5 GPa 0-104126
- 2PbO.SiO<sub>2</sub> melt, coding rate influence on constitution of silicate anions, crystn. kinetics 0-103248
- Pb<sub>2</sub>(P<sub>1-x</sub>V<sub>x</sub>-O<sub>4</sub>)<sub>2</sub>, ferroelastic phase transition, DTA, dilatometric and Brillouin scatt. study 0-70398
- PbS-In<sub>2</sub>S<sub>3</sub>, phase investigation 0-66488
- PbSnF<sub>3</sub>, allotropic transformations 0-84926
- PbTe-Ga<sub>2</sub>Te<sub>3</sub>, phase interaction, DTA, XPA and microstructural anal. 0-96625
- PbTe-InTe system, phase interactions and solid soln. form., physicochem. and elec. characteris. 0-104129
- PbTiO<sub>3</sub>, amorphous, crystallisation process, DTA and Raman spectroscopy meas. 0-75161
- Pd-Ni-Si amorphous alloys, crystn. process during isothermal ageing 0-89275
- Sb-S-I glasses, activation energy of crystn. 0-64920
- Se, amorphous films, evaporated, ageing and crystn., DTA 0-65413
- Se, liq., heat capacity and chem. equilb. 0-103486
- Se, Te<sub>1-x</sub> amorphous, structural relaxation and crystallisation kinetics study by DTA 0-59394
- Si ribbon growth by EFG, thermal sensitivity and stability 0-107080
- Si-B system, DTA, X-ray diffr. and metallographic study (*German*) 0-66484
- Si-Na-B-O-N glass, synthesis and characterisation 0-108381
- SiO<sub>2</sub>-water system, inorg. polymer struct. form., globular crystn. 0-101042
- Sm<sub>2</sub>O<sub>3</sub>-Ga<sub>2</sub>O<sub>3</sub> system, garnet-perovskite transform., phase diagram relationships 0-97460
- Sn-Bi, thermal analysis in non-faceted/faceted eutectic systems 0-71637
- Sr Nb<sub>2</sub>O<sub>6</sub>, crystallography, polymorphism and isomerism, X-ray diffr. and DTA study 0-100216
- SrF<sub>2</sub>, vaporisation and sublimation thermodynamics (*German*) 0-81355
- Tb(NO<sub>3</sub>)<sub>3</sub>-Fe(NO<sub>3</sub>)<sub>3</sub>-(NH<sub>4</sub>)<sub>2</sub>CO<sub>3</sub>-H<sub>2</sub>O system, cpd. form., comp. and props. 0-100832
- Tb<sub>2</sub>O<sub>3</sub>-H<sub>3</sub>PO<sub>4</sub>-H<sub>2</sub>O system, cpd. form., comp. and props. 0-100832
- Te-In system, enthalpies of fusion, peritectic decomp. and allotropic transition, DTA (*French*) 0-76226
- Te<sub>60</sub>Ge<sub>40</sub>Pb<sub>60</sub>, DSC sensitivity to controlled ageing in glass transition region 0-71673
- Te<sub>60</sub>Ge<sub>40</sub>-Sb<sub>60</sub>(Bi<sub>4</sub>), DSC studies of struct. phase transformation 0-66505
- TeO<sub>2</sub>-MoO<sub>3</sub>-V<sub>2</sub>C<sub>5</sub>, phase comp. determ. using X-ray diffr., electron microscopy and DTA (*German*) 0-88046
- Te<sub>60</sub>Si<sub>40</sub>-Pb, glasses, phase separation, double T<sub>g</sub> presence 0-88306
- Ti-Mo-V-Al-Cr-Fe (4.8, 4.7, 5.2, 1.1, 1.0 wt.%), structural changes during heating up to 1000°C, DTA study (*Russian*) 0-93552
- Ti-Nb-Si, amorphous alloy, supercond. props. and crystn. behaviour, TEM and DTA study (*Japanese*) 0-84536
- Tl, phase diagram and high press. phase transforms., DTA study (*Russian*) 0-66474
- Tl-Bi-Sb-Te system, peritectic reactions in TiBiTe<sub>2</sub>-TiSbTe<sub>2</sub> cross section, crystn. character 0-108406
- Tl-Sn-Te system equilibria, polythermal and isothermal cross sections obs., ternary cpd. form. 0-104128
- Tl<sub>2</sub>Te<sub>3</sub>-Ti<sub>2</sub>SnTe<sub>3</sub>-Ti<sub>2</sub>PbTe<sub>3</sub>, phase equilb., DTA, SPA and microhardness meas. 0-96628
- U-Co(Ce)(Fe)(Mn)(Ni)(V) metallic glasses, glass form. and thermal stability 0-75183
- UO<sub>2</sub> nuclear fuel preparation, emanation thermal anal. for characterisation of uranyl gel microspheres 0-95391
- V-H(D), phase diagrams, struct. studies 0-66491
- V<sub>2</sub>O<sub>5</sub>-Ti<sub>2</sub>O<sub>5</sub>, DTA, mag. susceptibility and X-ray diffr. study 0-70970
- YAG, melting behaviour and metastability determ. by optical DTA 0-92648
- Y(OH)CO<sub>3</sub>, ancylite like phase, hydrothermal cryst. growth (*French*) 0-108340
- YbTe, high-temperature evaporation and reactivity 0-103469
- Zn-Cd alloys, liq. and solid, ultrasound speed and compressibility meas. 0-102941
- ZnCl<sub>2</sub> glass, glass transition temp. and thermal expansion 0-64902

**thermal analysis continued**

- ZnCl<sub>2</sub>(NCR)<sub>2</sub>, R=CH<sub>3</sub> or C<sub>2</sub>H<sub>5</sub>, thermal decomp., thermogravimetric and differential thermal anal. (*Chinese*) 0-81291
- Zr-Ti-Be metallic glass, phase separation 0-97464
- thermal capacity see specific heat**
- thermal conductivity**
- see also Kapitza resistance; Lorenz number; thermal conductivity of gases; thermal conductivity of liquids; thermal conductivity of solids; thermal diffusivity; thermal insulating materials

air water downflow through packed beds, effective thermal conductivity 0-74952

Boussinesq fluids, turbulent viscosity and conductivity in turbulent convection 0-98543

chemical reaction, solid, endothermic, unsteady heat conduction, thermal conductivity change 0-76511

composite bodies, nonstationary thermal conduction processes, numerical simulation (*Russian*) 0-92016

dispersed medium, effective viscosity and heat cond. coeffs. 0-89537

eutectics, HgTe-PbTe and Au-PbTe, prep. and thermoelectric behaviour characts. 0-107774

fibrosarcoma, para-7, hamster, local thermal conductivity obs. 0-104562

fin, nonlinear problems, 1-D conduction, initial value problem 0-83726

hyperthermia, role of thermal conduction 0-104558

laminar film boiling heat transfer, thermal conductivity and convection effects 0-74864

LWR Sphere-Pac oxide fuel, eval. of thermal conductivity 0-102234

nonlinear, variational formulation, counter functional, exactness of soln. (*Russian*) 0-90800

plasma transport, anomalous, electron temp. gradient instability 0-75034

heat-protective coating, temperature distrib., finite element anal. (*Russian*) 0-74701

thermoelectric energy conversion, heat losses compensation due to thermal cond. through Peltier heat 0-107773

thermophysical property research, metallurgical applications 0-97457
- thermal conductivity measurement**
- automatic thermal conductivity meter with digital readout 0-106714

binary gas mixtures anal. cell using miniature thin film printed cct. 0-105640

cast insulation materials measuring apparatus 0-86293

cylindrical probe improvement 0-92033

fluids, absolute technique 0-101792

gases, meas. in undergraduate physics lab. 0-82614

hot-plate meas., errors associated with imperfect surfaces 0-95098

insulating mechanical supports, appl. to meas. thermal conductance 0-82772

liquid metals, in Spacelab, design and terrestrial testing of measuring cell (*German*) 0-57303

low temperature thermal conductivity measurements under uniaxial compression 0-105653

plate apparatus, guard ring width effect on meas. accuracy (*German*) 0-90837

solid thermal cond. and interface resistance meas. by radiation thermometry 0-86289

thermoelectric materials, thermal conductivity determ. heat losses, direct method 0-62662

thin films 0-68199
- thermal conductivity of gases**
- binary gas mixture, drop thermophoresis 0-93806

binary gas mixture, kinetic theory collision integrals, generalised phase shift approach 0-83874

binary gas mixtures, thermal cond. calc. method 0-79427

binary gas mixtures anal. cell using miniature thin film printed cct. 0-105640

corresponding states model 0-69964

dilute gas transport props., logarithmic term in softness expansion 0-83872

homothermal shock, prod. by instantaneous monochromatic radiation 0-59159

Kr-Ag-N gas mixture, thermal conduction coefficient calculational methods (*Russian*) 0-96335

measurement in undergraduate physics lab. 0-82614

methyl cyanide-Ar mixture, thermal cond. in mag. field 0-100058

optical lens, thermal pulse source 0-95968

symmetric top molecules, thermal cond., Senftleben-Beenakker effect 0-100049

Ar, at high press. 0-103099

D<sub>2</sub> gas, thermal cond. meas., 2-36 MPa 0-64668

H<sub>2</sub> gas, thermal cond. meas., 2-36 MPa 0-64668

H<sub>2</sub>-D<sub>2</sub> gas, thermal cond. meas., 2-36 MPa 0-64668

H<sub>2</sub>-He, thermal cond. meas., up to 14 MPa 0-64669

He, at high press. 0-103099

Kr, at high press. 0-103099

Kr, Lennard Jones (12,6) pot. distance parameter, transport props. calc. 0-79423

NH<sub>3</sub>-Ar mixture, thermal cond., viscosity, Senftleben-Beenakker effect 0-100054

Ne, at high press. 0-103099

Ne, Lennard Jones (12,6) pot. distance parameter, transport props. calc. 0-79423

Xe, at high press. 0-103099

Xe, Lennard Jones (12,6) pot. distance parameter, transport props. calc. 0-79423
- thermal conductivity of liquids**
- corresponding states model 0-69964

n-decane, thermal cond., meas. by transient hot-wire technique 0-103522

dielectric fluid, Debye absorption at crit. liq.-vapour transition 0-100322

dielectrics, thermal performance estimation 0-88582

fluids, one and two dimensional, hydrodynamics, viscosity, heat conductivity, kinetics (*Russian*) 0-79972

fluids, simple, thermally induced surface fluctuations 0-88403

metals, in Spacelab, design and terrestrial testing of measuring cell (*German*) 0-57303

n-octane, meas. by transient hot-wire technique 0-103522

organic compounds, comparison of predicted values with experimental results at different temps. 0-103523

supercooled liquid, thermal conductivity and viscosity, mode-mode coupling 0-88370

toluene, high-precision meas. by obs. technique 0-101792

water, thermal conductivity at high pressures, meas. with Ag co-axial cylinder cell (*Japanese*) 0-80007

thermal conductivity of liquids continued

Ar, at high press. 0-103099  
Cu alloys, and elec. resistivity 0-103661  
Cu, and elec. resistivity 0-103661  
Ga, liq., thermal props. at high temp. 0-75536  
He, at high press. 0-103099  
<sup>3</sup>He, liquid, polarisation potentials, viscosity, thermal cond., spin diffusion 0-88389  
<sup>3</sup>He, superfluid, transport parameters, Kubo formulae and BCS-Green's functions 0-88382  
<sup>3</sup>He, thermal conductivity at very low temps., press. depend. 0-92742  
<sup>4</sup>He layered films on ZYX graphite, thermal resist. below 2K 0-70500  
<sup>4</sup>He, liq., Kapitza heat-transfer model for boundary with solid 0-107591  
<sup>4</sup>He, superfluid, sound conversion phenomena at free surface, acoustic coeffs. 0-96709  
In, liq., thermal props. at high temp. 0-75536  
Kr, at high press. 0-103099  
N<sub>2</sub>O<sub>4</sub>, viscosity and thermal cond., approx. polynomials (*Russian*) 0-59739  
Ne, at high press. 0-103099  
Ti, liq., thermal props. at high temp. 0-75536  
Xe, at high press. 0-103099

thermal conductivity of solids

see also thermal magnetoresistance  
adamantane, thermal cond. and heat capacity under press. 0-80008  
alkali metals, electron-electron scatt., thermal and elec. resistivity 0-59956  
antiferromagnetic insulators, lattice thermal cond. 0-65319  
brass, lattice thermal cond. component, 30 to 300K, microscopic mechanisms 0-107758  
brass, lattice thermal cond. component, 4.2 to 30K, microscopic mechanisms 0-107757  
cast insulation materials measuring apparatus 0-86293  
composite materials, slender nearly-perfect conductors, dilute, bulk thermal properties 0-103525  
composites, short-fibre, unidirectional, effective thermal cond. bounds 0-92727  
diamond, synthetic powder, thermal wave propagation delay method 0-96702  
diamond, thermal conductivity, high temp., electron irradi. effects 0-65318  
dispersed materials, effective thermal conductivity meas. (*Japanese*) 0-70485  
electronic contribution, mobility threshold effects 0-65570  
ferroelectric, H-bonded, central peak, thermal cond. 0-93250  
ferroelectrics, dispersive and order-disorder type, thermal cond. at low temps. 0-75391  
fibre-reinforced materials, slender, non-dilute, thermal and mechanical props. 0-103524  
fibreglass insulating materials, radiative heat transfer rel. to optical props. 0-100367  
glass-metal composite, heat conduction, memory switching 0-96703  
graphite, pyrolytic commercial, high-temp. thermal and mech. props. 0-75372  
graphite, thermal conductivity, effect of porosity 0-65314  
heat flow rate, effect of asymmetry 0-102959  
heat-pulse experiments, nonlinear effects, theory 0-96182  
hexamethylenetetramine, thermal cond. and heat capacity under press. 0-80008  
hot-wire test, critical review and comparison with BS 1902 panel test 0-104409  
insulating mechanical supports, appl. to meas. thermal conductance 0-82772  
insulator, lattice thermal cond., point defect scatt. relax. rate role 0-70478  
Jahn-Teller cooperative T-(e+t) system, thermal cond. 0-70479  
lattice, anomalous temp. behaviour near structural phase transition (*Russian*) 0-75394  
low temperature thermal conductivity measurements under uniaxial compression 0-105653  
magnetite artifacts, roasted, props., filler porosity effect 0-104099  
metal, electron Boltzmann eqn. solns., energy depend. 0-88537  
metal, pseudoacoustic effects of phonons in heat cond., high temp. region 0-70326  
metallic films, metal-dielectric boundary thermal resistance, nonlinear elec. resistance (*Russian*) 0-65530  
metals, electrical and thermal resistance, influence of static atomic displacements 0-103674  
metals, nonstationary temperature fields due to moving heat sources, heat capacity, thermal cond. (*Russian*) 0-107448  
metals, phonon-phonon scatt. role in lattice thermal cond., phonon drag, elec. cond. 0-70483  
metals, radiation induced vapourisation, press. behaviour 0-84288  
Mott's formula for thermopower and for Wiedemann-Franz law 0-84462  
multilayer insulation, simple struct. insulating material props. for low temp. appl. 0-57307  
multilayer thin film struct. thermoelec. props. 0-92964  
nonuniform systems, effective conductivity from percolation and conduction theory 0-62597  
periodically nonuniform solids, effective thermal cond. 0-70486  
PMMA, Gruneisen const. and thermal props., temp. depend., 4-300K, Brillouin scatt. obs. 0-100662  
polyethylene, extruded semicryst., thermal cond. and specific heat, <1K 0-59742  
pulse methods for investigating thermal diffusivity and conductivity in solids, theoretical models (*Polish*) 0-92728  
quartz, fused, thermal cond., temp. depend. at low temps. 0-65322  
 $\alpha$ -quartz, heat transfer at low temps., lattice thermal cond. 0-92729  
refractory thermal insulation effective thermal cond., fibre diameter effects 0-104105  
ruby, phonon spectrum, thermal pulses under diffuse phonon propagation conditions 0-103434  
sapphire-Pb interface, heat transfer coeff. meas., 2-80K 0-88419  
schist containing clay and sand, integrated normal emissivity with low heat conductivity coeffs. 0-103504  
schist dust, integrated normal emissivity with low heat conductivity coeffs. 0-103504  
selenide thermoelectric materials, thermal conductivity, long-term stability and other props. experimental anal. 0-107834  
semiconductor, phonon conduction and relaxation times 0-107585

thermal conductivity of solids continued

semiconductor injection lasers, output depend. on inhomogeneous bonding 0-64015  
semiconductors and insulators, phonon cond., three-phonon N- and U-processes 0-65313  
semimetals, degenerate, heat conduction, thermal EMF, Lorenz number anisotropy at low temp. 0-75549  
solid thermal cond. and interface resistance meas. by radiation thermometry 0-86289  
spin glasses, elec. resist., thermal resist. and thermopower 0-65542  
steel, type Kh23N18, integrated normal emissivity with low heat conductivity coeffs. 0-103504  
steel fibre reinforced Al, thermophys. props. 0-59745  
tetrabromomethane, thermal resistivity, heat capacity and phase diagram under pressure 0-65316  
TGS, nitroaniline admixture effect on thermal parameters 0-107580  
turbogenerator rotor and stator core thermal conductivity solution using integral representation method (*Russian*) 0-100451  
Ag<sub>19</sub>Sb<sub>29</sub>Te<sub>52</sub>, single-phase, thermoelectric efficiency 0-107826  
Al, thin film, thermal cond. meas., size effect 0-65715  
Al<sub>2</sub>O<sub>3</sub>Mn<sup>2+</sup>, Jahn-Teller Mn<sup>2+</sup> ions, phonon spectroscopy and thermal cond. meas. 0-88282  
Ar, at high press. 0-103099  
B fibre reinforced Al, thermophys. props. 0-59745  
B<sub>2</sub>C, thermophysical props. and neutron absorpt. 0-103488  
Bi, thermoelectric power, electronic thermal cond., in mag. field 0-60015  
Bi<sub>2</sub>GeO<sub>20</sub>, thermal cond. and absorptivity 0-70480  
Bi<sub>2</sub>S<sub>3</sub>-Bi<sub>2</sub>Se<sub>3</sub> and Bi<sub>2</sub>Te<sub>3</sub>-Bi<sub>2</sub>Se<sub>3</sub> systems, thermal cond. change during phase transitions 0-100368  
BiSb (>20 wt.%), electronic band struct. 0-107698  
CaF<sub>2</sub>, fluoride, use as standard specimen 0-96704  
10CaO.15Na<sub>2</sub>O.75SiO<sub>2</sub> glass, thermal cond., temp. depend. at low temps. 0-65322  
CdTe, low temp. thermal cond., growth parameter influence 0-92725  
CdTe:Fe<sup>2+</sup>, reson. relax. time for impurity electrons and localised phonons interaction, appl. to thermal cond. 0-59590  
Co-Cr-C eutectic alloy, thermal conductivity and electric resist. at high temp. 0-103668  
CsMnCl<sub>3</sub>·2H<sub>2</sub>O, thermal cond. in mag. field 0-70481  
Cu, compressed powder, thermal cond. meas. (*German*) 0-70669  
Cu, high purity, identification of imperfections by thermal resistivity meas. 0-59951  
Cu powder, sp. ht. cond. and sp. elec. cond. meas., Wiedemann Franz Lorenz law (*German*) 0-92872  
CuCl, mech. vibrs. in piezoelec. solid, excitation by light pulses 0-75305  
p-CuInSe<sub>2</sub>, thermal cond. 0-96705  
Cu<sub>2</sub>S, Cu<sub>1.8</sub>S,  $\alpha$ - $\beta$  transition, thermographic investigation of heats, entropies and activation energies 0-88314  
Eu<sub>2</sub>O<sub>3</sub>, thermophysical props. and neutron absorpt. 0-103488  
Fe-Ti (V)(W), dil., thermophysical props. and elec. cond., temp. depend. 0-96842  
FeCl<sub>2</sub>, antiferromag., magnon-phonon interactions in thermal cond. 0-65315  
Fe<sub>2</sub>S<sub>4</sub>, pyrrhotite, thermocond. and thermoelec. power 0-96926  
GaAs crystal growth, thermal and elastic const. evaluation 0-92586  
GaAs, lattice thermal cond., point defect scatt. relax. rate role 0-70478  
GaSb based eutectics, thermal cond. and diffusivity, 300-700K, phonon mechanism 0-103526  
Gd, thermal conductivity critical behaviour near Curie point 0-75540  
Ge, thermal conductivity of semiconductors, quantum acoustical method, thermal phonon lifetimes 0-65312  
n-Ge, thermal phonon scatt., piezo-thermal cond. 0-70482  
Ge/Ga, resonant scattering of phonons by bound holes in temp. range 1 to 5K 0-75393  
Ge:P, charact. temp. and lattice thermal cond. 0-59743  
Ge-Bi-Te system, thermal cond. changed during phase transitions 0-100368  
Ge-Si alloys, hot-pressed, fine-grained, boundary scatt. of phonons, lattice thermal cond. 0-107583  
Ge-Si alloys, hot-pressed, fine-grained, boundary scatt. of phonons, theory 0-107584  
He, at high press. 0-103099  
<sup>4</sup>He, single crystal, 0.4 to 1.8K (*Russian*) 0-103535  
Hg<sub>1-x</sub>Cd<sub>x</sub>Te-type semimetals, kinetic props., local acceptor level effects 0-65557  
InSb based eutectics, thermal cond. and diffusivity, 300-700K, phonon mechanism 0-103526  
InSb, thermal cond., elec. cond., and thermoelec. power, press. depend. 0-59744  
InSb:Cd, thermal conductivity down to 0.38K 0-107582  
K-Cs, thermal conductivity determ. 0-107760  
KH<sub>2</sub>PO<sub>4</sub> and KD<sub>2</sub>PO<sub>4</sub>, thermal cond., anomalous temp. behaviour near structural phase transition (*Russian*) 0-75394  
Kh<sub>2</sub>AsO<sub>4</sub>, anomalous temp. behaviour near structural phase transition (*Russian*) 0-75394  
Kr, at high press. 0-103099  
La-Eu-B<sub>6</sub> solid solns., thermal cond., 300 to 2000K 0-59741  
Li-Mg, Mathiessen's rule, elec. and thermal deviations, impurity scatt. 0-88536  
LiF,  $\gamma$ -irrad. pure and Mg-doped, phonon scatt. and interstitial clusters 0-70254  
Li<sub>2</sub>O, porosity, dependence on thermal diffusivity and thermal conductivity, 200-900°C 0-92726  
MgO:Cr<sup>2+</sup>(Fe<sup>2+</sup>), reson. relax. time for impurity electrons and localised phonons interaction, appl. to thermal cond. 0-59590  
MnCl<sub>2</sub>·4H<sub>2</sub>O, antiferromag., low temp. thermal cond. 0-65320  
MnS, thermal cond., temp. depend., paramag.-antiferromag. transition effects 0-65321  
Mo, high purity single crystals, thermal conduct. in temp. range 2-70K 0-75545  
NaCl-NaBr, elastic wave damping, 300 to 1500 MHz, impurity effects 0-92602  
NaF, thermal cond. meas. at high press. 0-75392  
Na<sub>2</sub>O-CaO glass phlogopite mica powders, composite fabrication, cellular struct. 0-84902  
Na<sub>2</sub>O-Cs<sub>2</sub>O-SiO<sub>2</sub> glasses, thermal diffusivity, heat capacity and thermal cond., laser flash method study 0-65310  
25Na<sub>2</sub>O.75SiO<sub>2</sub> glass, thermal cond., temp. depend. at low temps. 0-65322  
Nd, transport props., low temp., effect of mag. field 0-70679  
Ne, at high press. 0-103099



**thermal conductivity of solids continued**

- PbTe film, electronic thermal cond. and thermoelec. power 0-93018  
 Pr, transport props., low temp., effect of mag. field 0-70679  
 RuO<sub>2</sub>, thermal conductivity meas., rel. to elec. cond. 0-65317  
 Sb<sub>2</sub>Te<sub>3</sub>-Bi<sub>2</sub>Te<sub>3</sub> and Sb<sub>2</sub>Te<sub>3</sub>-Sb<sub>2</sub>Se<sub>3</sub> systems, thermal cond. change during phase transitions 0-100368  
 Se, trigonal and vitreous, sp. ht. and thermal cond., 3 to 300K 0-59676  
 Si, single crystals, thermal conductivity calculation (*Hungarian*) 0-65311  
 Si:As laser annealing, heat and mass transport model 0-92546  
 Si:B, resonant scattering of phonons by bound holes in temp. range 1 to 5K 0-75393  
 Si:Li, electron-phonon scatt., in intermediate conc. region 0-65180  
 Si:Li, thermal cond., low temp. phonon scatt., internal strain effects 0-96706  
 Si:P, thermal cond., electron-phonon interaction at low temps. 0-92730  
 SiP<sub>12</sub>, thermam cond., temp. depend., up to 2000K (*French*) 0-70484  
 SiC fibre reinforced Al, thermophys. props. 0-59745  
 SiO<sub>2</sub>, fused, for sealed ampoule cryst. growth, thermal transmission function 0-84731  
 72SiO<sub>2</sub> window glass, thermal cond., temp. depend. at low temps. 0-65322  
 Sm, transport props., low temp., effect of mag. field 0-70679  
 Sn thin film, anomalous transmittance of metal-insulator interface for thermally radiated phonons (*Russian*) 0-103664  
 SrTiO<sub>3</sub>, anomalous temp. behaviour near structural phase transition (*Russian*) 0-75394  
 Ta, 4.5 to 200K (*Russian*) 0-103665  
 Ta, thermal cond. and emissivity meas. using imaging furnace 0-103667  
 Ta, thermophysical props. and neutron absorpt. 0-103488  
 Xe, at high press. 0-103099  
 YAG:Cr, optical detection of phonons 0-92630  
 YAG:Er, elastic wave damping, 300 to 1500 MHz, impurity effects 0-92602  
 ZnS:Fe<sup>2+</sup>, reson. relax. time for impurity electrons and localised phonons interaction, appl. to thermal cond. 0-59590  
 ZrO<sub>2</sub> coating on Zircaloy-2, thermal cond. meas. 0-80009

**thermal convection see convection****thermal decomposition see pyrolysis****thermal diffusion**

- see also thermal diffusion in gases; thermal diffusion in liquids*  
 cooled electric probes in dense plasma, thermal diffusion effects 0-92384  
 mass transport and assoc. failures 0-59694  
 tissue perfusion measurements made with thermal diffusion probe, effect of probe geometry 0-104802  
 Al-Al<sub>3</sub>Ni eutectic, temp. gradients, microstructural changes 0-84971  
 Ge, single cryst., <sup>18</sup>F penetration, charged particle activation anal. 0-93828  
 H thermal diffusion, apparatus 0-100358  
 Li<sub>2</sub>O-SiO<sub>2</sub> glass, thermotransport props. 0-79985  
 Si, joining and recrystallisation using thermomigration process 0-65298
- thermal diffusion in gases**  
 binary gas mixture, drop thermophoresis 0-93806  
 drop dynamics in mixture with uniform temp., thermal diffusion effects 0-103097  
 heat pipe, spectroscopic, operation 0-106708  
 ice crystal morphology, vapour growth, influence of vapour diffusion and heat diffusion 0-64933  
 inert gas binary mixture, thermal diffusion factor meas. 0-79425  
 mixtures, marginal comp., thermal diffusion column performance evaluation (*German*) 0-59157  
 non equilibrium light gas, heavy impurity thermal diffusion under laser irradi. 0-64667  
 thermal diffusion flame, two dimens. cellular struct. formation 0-69947  
 Venus ionosphere, thermal diffusion calcs. 0-72806  
 BCl<sub>3</sub>-N<sub>2</sub> mixtures, thermomigration props., effect of resonant excitation of mol. vibr. by laser, isotope separation 0-100047  
<sup>78</sup>Kr/<sup>86</sup>Kr, isotope separation (*Rumanian*) 0-86988  
 N<sub>2</sub>-Co, mixtures, marginal comp., thermal diffusion column performance evaluation (*German*) 0-59157

**thermal diffusion in liquids**

- binary liq. layer, microgravity, thermosconvective stability 0-74866  
 drop dynamics in mixture with uniform temp., thermal diffusion effects 0-103097  
 linear convective stability, Soret effect, horizontal quiescent layer of two-component fluid 0-92144  
 non-Newtonian liquid mixture separation by thermal diffusion in parasitic convection 0-64587  
 overstability in horizontal layer of binary liq. mixture with Soret effect 0-106782  
 K isotope separation in solution by thermal diffusion 0-87236

**thermal diffusivity**

- Green River oil shales, thermal diffusivity depend. on organic content 0-76965  
 pulse methods for investigating thermal diffusivity and conductivity in solids, theoretical models (*Polish*) 0-92728  
 TGS, nitroaniline admixture effect on thermal parameters 0-107580  
 thermoelectric meas. method 0-107581  
 thermophysical property research, metallurgical applications 0-97457  
 Ba<sub>2</sub>C, thermophysical props. and neutron absorpt. 0-103488  
 BaMnF<sub>4</sub>, anisotropic order parameter phase fluctuations, light scatt. and thermal diffusivity meas. 0-80807  
 Bi-Bi<sub>2</sub>O<sub>3</sub> black layer, on polyvinylidene fluoride film, pyroelec. camera tube for IR imaging 0-57369  
 Eu<sub>2</sub>O<sub>3</sub>, thermophysical props. and neutron absorpt. 0-103488  
 Fe-Ti (V)(W), dil., thermophysical props. and elec. cond., temp. depend. 0-96842  
 Ga, liq., thermal props. at high temp. 0-75536  
 GaAs crystal growth, thermal and elastic const. evaluation 0-92586  
 GaSb based eutectics, thermal cond. and diffusivity, 300-700K, phonon mechanism 0-103526  
 In, liq., thermal props. at high temp. 0-75536  
 InSb based eutectics, thermal cond. and diffusivity, 300-700K, phonon mechanism 0-103526  
 Li<sub>2</sub>O, porosity, dependence on thermal diffusivity and thermal conductivity, 200-900°C 0-92726  
 Na<sub>2</sub>O-Cs<sub>2</sub>O-SiO<sub>2</sub> glasses, thermal diffusivity, heat capacity and thermal cond., laser flash method study 0-65310  
 Si, laser annealing, nonlinear dynamic transport processes 0-93437  
 SiP<sub>12</sub>, thermam cond., temp. depend., up to 2000K (*French*) 0-70484  
 Ta, thermophysical props. and neutron absorpt. 0-103488

**thermal diffusivity continued**

- TiC-C composites, hot pressed, thermophys. props. at high temps. 0-59675  
 Ti<sub>4</sub>, thermal diffusivity, near FCC to BCC transition 0-59740  
 Ti, liq., thermal props. at high temp. 0-75536  
 ZrC-C composites, hot pressed, thermophys. props. at high temps. 0-59675

**thermal effects in magnetism see magnetocaloric effects****thermal expansion**

- see also Grunelsen coefficient*  
 A15 compound, superconducting transition depend. on non-hydrostatic stress 0-107948  
 alkali halides, doped, thermal expansion at low temps. 0-96672  
 alkali metal halide mixed crystals, volume thermal coeff. of expansion, calc. 0-96671  
 alkali metaphosphate, M<sub>2</sub>O-R<sub>2</sub>O<sub>3</sub>-P<sub>2</sub>O<sub>5</sub> (R=Y or rare earth), glass transition temps. and coeffs. of linear thermal expansion 0-88343  
 alkaline earth metaphosphate, MO-R<sub>2</sub>O<sub>3</sub>-P<sub>2</sub>O<sub>5</sub> (R=Y or rare earth), glass transition temps. and coeffs. of linear thermal expansion 0-88343  
 alkaline earth oxides, cohesive and thermophysical props., role of three-body interactions 0-92477  
 blood and its constituents, coeff. of thermal expansion (*German*) 0-104556  
 Born model, electrostriction rel. to dielec. and thermoelastic props. 0-71322  
 borosilicate glasses, gamma irradiation effect on density, refractive index, thermal expansion 0-79838  
 ceramic materials, fine-grained, cyclic plastic deform. as cause for thermal expansion hysteresis 0-89290  
 coke, shrinkage kinetics during calcination 0-93572  
 crystals, book 0-73115  
 density changes during melting by X-ray absorption 0-103462  
 electro-optical reflector, controlled, temp. fields, thermal distortions 0-96021  
 entropy change on melting of simple substances, thermal expansion, configurational entropy 0-59630  
 epoxy resin/particle composites, particle size effect in thermal expansion, filler effects on T<sub>g</sub> 0-84305  
 epoxy/graphite composite and cured epoxy resin, thermal expansion and swelling 0-92450  
 extrudate swell, thermally induced, Galerkin method 0-79312  
 ferromagnetic metals, magneto-volume effect, Invar phenomena 0-66007  
 fibre reinforced polymer matrix composites, space environmental effects 0-71721  
 filled polymer mechanical properties, particle shape effect, review 0-100864  
 glass, thermal expansion at low temps. 0-96672  
 glass-metal sealing, set point of glass 0-108423  
 graphite, polygranular, flexural strength after heat treatment porosity correl. 0-84996  
 graphite, pyrolytic commercial, high-temp. thermal and mech. props. 0-75372  
 graphite fibre epoxy laminates, low thermal expansivity, design considerations 0-81031  
 insulating materials, thermal expansion, Morse pot. model 0-107449  
 insulator, thermal expansion, empirical determ. with no exptl. input 0-107450  
 Invar, Fe-Ni (36 wt.%), alloy 36N, effect of melting conditions on thermal expansion coeff. 0-65256  
 Invar, magnetic structure, depend. on absorbed H, Stoner's band model calcs., Mossbauer spectra 0-65787  
 metallic thin films, thermoelectric power, thermal stress effects, theory 0-65714  
 metals, Morse potential appl. in molecular-metallic framework 0-79742  
 metals, positron response to thermal expansion 0-84306  
 Nafion, densities and expansion coeffs. as function of various parameters 0-79711  
 NASICON solid electrolyte, processing and phys. props. 0-60820  
 phosphate glass-Al alloys seals, elec. and mech. props., glass transition 0-81018  
 PMMA, Grunelsen const. and thermal props., temp. depend., 4-300K, Brillouin scatt. obs. 0-100662  
 polycarbonate, bisphenol A, WAXS pattern, temp. effect and thermal history 0-93583  
 polymethylsiloxane-2, liq., thermodynamic props. at high press., US prog. meas. (*Russian*) 0-65157  
 porcelain-metal cermet, stress determ., meas. method (*German*) 0-76425  
 quartz, thermal expansion near  $\alpha$ - $\beta$  transition under uniaxial stresses 0-70429  
 rare-earth germanides, R<sub>5</sub>Ge<sub>3</sub>, thermal expansion, phase transition effects 0-70433  
 reference data: 1-1000K 0-96669  
 refractories, thermal stress cracking resistance estimation 0-104288  
 silicate glasses, longit. and transverse elastic wave vels., temp. and comp. variations 0-88258  
 slab, surface displacements for high speed rubs 0-83767  
 steel, austenitic, heavily doped, linear expansion meas. 0-103501  
 steel, martensitic, heavily doped, linear expansion meas. 0-103501  
 steel, nonmetallic inclusion segregation during cooling (*Russian*) 0-100330  
 steel fibre reinforced Al, thermophys. props. 0-59745  
 TGS, crit. behaviour of thermal expansion, neutron diff. study 0-75371  
 transition metal silicides, refractory for ICs, review 0-100820  
 transition metals, thermophysical data at high temps., submicrosecond-pulse-heating method 0-103459  
 tridymite, thermal expansion meas. 0-59682  
 unidirectional fibre composites, anisotropic constituents, effect elastic moduli and other props. 0-58911  
 uniaxial crystals, third-order elastic consts., low temp. limit of thermal expansion 0-65119  
 vacancy effects, temp. depend. of thermal expansion coeff. 0-79962  
 vanadocene, order-disorder phase transition, sp. ht. and crystallographic study (*French*) 0-84131  
 water, liquid, physical props., two-state model approach 0-75144  
 $\alpha$ -Ag-In solid solutions, lattice dynamics parameters (*Russian*) 0-96477  
 AgI, thermal expansion, 4 to 270K 0-79961  
 AgI, thermal expansion under press. 0-92690  
 Al, molten, thermal expansion meas. to 1300K 0-65254  
 $\beta$ -Al<sub>2</sub>O<sub>3</sub>-Na<sub>2</sub>O solid electrolyte, processing and phys. props. 0-60820  
 Ar, solid, equilib. props., uncorrel. pairs approx. 0-84303

thermal expansion continued

Ar, solid, high-temp. thermal expansion characts. 0-59680  
As-SrTi, glass, viscosity and elastic props. 0-100180  
Au, fine particles, gas evaporation technique for prep., X-ray diffr. study 0-75327  
B fibre reinforced Al, thermophys. props. 0-59745  
Ba<sub>2</sub>C, thermophysical props. and neutron absorpt. 0-103488  
Ba<sub>2</sub>O<sub>3</sub> and alkali borate glasses, Raman study at high temps. 0-93306  
Ba<sub>2</sub>O<sub>3</sub>-V<sub>2</sub>O<sub>5</sub>-P<sub>2</sub>O<sub>5</sub>, glass, mech. and elec. props 0-84228  
(Ba,Sr)TiO<sub>3</sub>, ferroelec. props., press. depend., anharmonic oscillator model 0-80716  
BaR<sub>2</sub>(MoO<sub>4</sub>)<sub>4</sub>, (R=Nd,Eu), struct., optical, mech., spectral and physico-chem. props. 0-84161  
Be intermetallics, MBe<sub>13</sub>, (M=Y, La, Ce, Lu, Th), lattice spacings and susceptibilities 0-65778  
Be, sintered, physicochem. props. anisotropy, BeO inclusions effect 0-60804  
Be-Cu, vibr. characteristics at low temp., effect of substitution impurities (Russian) 0-103439  
BeF, glass, glass transition temp. and thermal expansion 0-64902  
C fibre reinforced composites for spacecraft use, prep., props. and struct. 0-71625  
C, polygranular, flexural strength after heat treatment porosity correl. 0-84996  
C reinforced plastic, degraded, study of strain, 20 to 1000°C 0-71680  
CaCeAl<sub>3</sub>O<sub>7</sub>, melilite struct., prep. and props. 0-93524  
CaF<sub>2</sub>, fluorite, use as standard specimen 0-96704  
Ca<sub>2</sub>Nb<sub>2</sub>O<sub>7</sub>, ferroelectric phase transitions, dielec. constant and thermal expansion rel. to temp. 0-88934  
Cd<sub>2</sub>As<sub>2</sub> and CdAs<sub>2</sub>, molten, thermal expansion and atomic bond strength parameters 0-65257  
CdTi<sub>2</sub>Te<sub>4</sub>, single and polycryst. samples, linear expansion, heat capacity and thermodynamic props. 0-103489  
CeB<sub>6</sub>, magnetostriction, US absorpt. and thermal expansion 0-66004  
Cr-Co, phase transformations and magnetostriction (Russian) 0-103869  
Cr-Re, phase transformations and magnetostriction (Russian) 0-103869  
CsMnCl<sub>2</sub>·2H<sub>2</sub>O, diagonal elastic const., thermal expansion coeffs., ultrasonic velocity meas., 0-79853  
Cs<sub>2</sub>NaM<sup>3+</sup>Cl<sub>6</sub> (M<sup>3+</sup>=Bi,Nd,Pr), ferroelastic phase transitions, thermal expansion, elasticity, and X-ray anal. 0-70393  
CuGaSe<sub>2</sub>, thermal expansion obs. 0-70432  
Cu<sub>2</sub>S, 1≤x≤2, quantum temp. size effect and magnetism (Russian) 0-103764  
DyCo<sub>2</sub>-DyAl<sub>3</sub> system, mag. and structural studies 0-108006  
EuB<sub>6</sub>, X-ray method, room temp. to 1300 K 0-96670  
Eu<sub>2</sub>O<sub>3</sub>, thermophysical props. and neutron absorpt. 0-103488  
Fe, high-purity single crystals, X-ray topography and double-crystal diffraction 0-92534  
Fe, pure and alloyed, density and thermal expansion in liq. and solid states 0-96668  
Fe-B(P) amorphous alloys, anomalous thermal expansion, ΔE effect, Invar and Elinvar characts., delay time 0-80589  
Fe-Co-Mo-Nb(Ta) semihard mag. alloy, mag. props., thermal expansion, elec. resistivity and hardness (Japanese) 0-88789  
Fe-Ni (308-44.1 at%) Invar alloys, anomalous mag. anisotropy and thermal expansion 0-75755  
Fe-Ni Invar anomalies, explanation in terms of itinerant electron magnetism 0-75705  
Fe-Pd Invar alloys, elec. and mag. props. and thermal expansion 0-75732  
Fe<sub>6</sub>(Ni<sub>2</sub>xMn)<sub>1</sub>, disordered, mag. struct. near ferro-antiferromagnetic transition 0-60211  
Fe<sub>3</sub>Pt Invar alloy, thermal expansion and spontaneous magnetisation, Invar anomalies, low spin model 0-71001  
GaAs crystal growth, thermal and elastic const. evaluation 0-92586  
GaP, thermal expansion below room temp. 0-79963  
GaP/Si heterostruct., differential thermal contraction, plastic deform., fracture 0-108494  
Gd, ferromagnetic, crit. sp. ht. and thermal expansion 0-60343  
Gd(Co<sub>1-x</sub>Ni<sub>x</sub>)<sub>2</sub> compounds, NMR and thermal expansion 0-66070  
GdMn<sub>2</sub>-GdAl<sub>3</sub> system, mag. and structural studies 0-108006  
He, liq., anharmonic effects in US propagation near λ transition 0-96707  
He, superfluid, sound conversion phenomena at free surface, acoustic coeffs. 0-96709  
HfO<sub>2</sub>, stabilised comps., elastic props. rel. to porosity and temp. 0-81096  
HgBr<sub>2</sub>, nonintrinsic ferroelastic, thermal expansion and thermodynamic potential 0-88344  
HgTe, 1.5 to 30K, thermal expansion and heat capacity meas. 0-59681  
HoRh<sub>2</sub>B<sub>4</sub>, low temperature magnetic properties 0-88728  
Ir, thermophysical props. at temps. up to 7000K 0-103497  
(K<sub>1/4</sub>Bi<sub>1/4</sub>)(Zn<sub>1/6</sub>Nb<sub>5/6</sub>)O<sub>3</sub>, cation disordered perovskite, elastic const. and thermal expansion 0-96587  
KCl, X-ray irradiated, vacancy conc. determ., thermal expansion meas. 0-79782  
KH<sub>2</sub>PO<sub>4</sub>, crit. behaviour, dilatometric study 0-92689  
K<sub>2</sub>SO<sub>4</sub>, phase transform., mech. of thermal hysteresis, DTA, dilatometry and dielec. meas. 0-75353  
Kr, solid, high-temp. thermal expansion characts. 0-59680  
LaB<sub>6</sub>, X-ray method, room temp. to 1300 K 0-96670  
LaP<sub>2</sub>O<sub>4</sub>, continuous ferroelastic transition elastic and mechanical props. 0-92668  
Li<sub>2</sub>O-B<sub>2</sub>O<sub>3</sub>-P<sub>2</sub>O<sub>5</sub>, glass, mech. and elec. props 0-84228  
Li<sub>2</sub>O·2SiO<sub>2</sub>, ceramic, prep. of oriented microstructure by unidirectional solidification of melts 0-71614  
Mg-Tb(Dy)(Ho)(Tm), dil., macroscopic shape effect due to quadrupole orientation, magnetostriction and thermal expansion meas. 0-60396  
MgAl<sub>2</sub>O<sub>4</sub> spinel, anomalous thermal expansion, second order transition 0-84307  
Mn-Ni, thermal expansion, mag. susceptibility, lattice const. 0-100341  
MoSi<sub>2</sub>, film, elastic stiffness and thermal expansion coeffs. 0-107451  
N<sub>2</sub>, solid struct., and thermodynamic props. (Russian) 0-88083  
Na<sub>2</sub>O-B<sub>2</sub>O<sub>3</sub>-P<sub>2</sub>O<sub>5</sub>, glass, mech. and elec. props 0-84228  
Na<sub>2</sub>O-B<sub>2</sub>O<sub>3</sub>-SiO<sub>2</sub>, two-phase, stresses arising during leaching 0-81086  
Nb<sub>2</sub>O<sub>5</sub>, x+y=0.73 to 0.88, thermal expansion coefficients 0-103502  
Ni-Cu-X (X=Sb, Nb, Ti), spinodal decomp. alloys, linear expansion coeff. influence on morphological anisotropy (Japanese) 0-70431  
Ni-Fe Invar, thermal expansion and spontaneous magnetisation, Invar anomalies, low spin model 0-71001  
Ni-Ti, heavily doped, linear expansion meas. 0-103501  
Ni<sub>2</sub>B, linear thermal expansion 0-71639

thermal expansion continued

NiF<sub>2</sub>, thermal expansion and magnetostriction, 55K to room temp. 0-80586  
(Pb,Sr)TiO<sub>3</sub>, ferroelec. props., press. depend., anharmonic oscillator model 0-80716  
Pb, molten, thermal expansion meas. to 1300K 0-65254  
Pb<sub>3</sub>(GeO<sub>4</sub>)(VO<sub>4</sub>)<sub>2</sub>, Pb<sub>3</sub>(SiO<sub>4</sub>)(VO<sub>4</sub>)<sub>2</sub>, and Pb<sub>3</sub>GeO<sub>11</sub>, elastic nonlinearity and acoustic losses 0-59554  
Pb(Mg<sub>1/3</sub>Nb<sub>2/3</sub>)O<sub>3</sub>, cation disordered perovskite, elastic const. and thermal expansion 0-96587  
Pb,MgNb<sub>2</sub>O<sub>6</sub>-PbTiO<sub>3</sub>, relaxor ferroelectrics, electrostrictive effects 0-66112  
Pb(NO<sub>3</sub>)<sub>2</sub>, thermal expansion study to test sensitivity of X-ray powder goniometer (French) 0-79631  
PbO-B<sub>2</sub>O<sub>3</sub> glass-forming melt, specific volume and viscosity, temp. depend. 0-84073  
Pb<sub>3</sub>(P<sub>1</sub>V<sub>1-x</sub>O<sub>4</sub>)<sub>2</sub>, ferroelastic phase transition, DTA, dilatometric and Brillouin scatt. study 0-70398  
Pb(Zn<sub>1/3</sub>Nb<sub>2/3</sub>)O<sub>3</sub>, cation disordered perovskite, elastic const. and thermal expansion 0-96587  
Pd-Fe-Mn, ferromagnet-spin glass, thermal expansion forced, magnetostriction and magnetisation under high press. 0-65255  
Pd-Ni, thermal expansion and magnetostriction meas. near crit. conc. for ferromagnetism 0-65881  
PrSn<sub>3</sub>, thermal expansion and transverse elastic const. near mag. phase transition 0-60394  
Pr<sub>2</sub>Tl, thermal expansion and transverse elastic const. near mag. phase transition 0-60394  
Pt, liq., thermodynamic characterisation, by isobaric expansion meas. 0-103494  
Rb<sub>2</sub>ZnCl<sub>4</sub>, phase transitions, thermal expansion coeff. 0-100638  
Re, thermal expansion, 1200 to 2300K 0-103500  
Si, temperature during CW laser heating, Raman scatt. meas. 0-76109  
SiC fibre reinforced Al, thermophys. props. 0-59745  
SiN film, elastic stiffness and thermal expansion coeffs. 0-107451  
Si<sub>3</sub>N<sub>4</sub> film, elastic stiffness and thermal expansion coeffs. 0-107451  
Si<sub>3</sub>N<sub>2</sub>:MgO, hot-pressed, linear thermal expansion rel. to MgO content 0-70430  
SiO<sub>2</sub>-B<sub>2</sub>O<sub>3</sub> glass system, gel hot pressing synthesis and characterisation (French) 0-66468  
Sn, molten, thermal expansion meas. to 1300K 0-65254  
SnCl<sub>2</sub>·2H<sub>2</sub>O, Brillouin scatt. and thermal expansion 0-97289  
SrF<sub>2</sub>:La, type-I dipole reorientation, activation vol. determ. from dielec. const. 0-88916  
Sr<sub>1-x</sub>Na<sub>0.1</sub>Nd<sub>0.1</sub>TaO<sub>7</sub>, solid soln., ferroelectric phase transitions, dielec. constant and thermal expansion rel. to temp. 0-88934  
Sr<sub>2</sub>Nb<sub>2</sub>O<sub>7</sub>, ferroelectric phase transitions, dielec. constant and thermal expansion rel. to temp. 0-88934  
Sr<sub>2</sub>Ta<sub>2</sub>O<sub>7</sub>, ferroelectric phase transitions, dielec. constant and thermal expansion rel. to temp. 0-88934  
Ta, thermophysical props. and neutron absorpt. 0-103488  
TaSi, film, elastic stiffness and thermal expansion coeffs. 0-107451  
Ti-Mo-V-Al-Cr-Fe (4.8, 4.7, 5.2, 1.1, 1.0 wt.%), structural changes during heating up to 1000°C, DTA study (Russian) 0-93552  
TiFe<sub>2</sub>Co<sub>1-x</sub>, thermal expansion and magnetoelectric effects 0-80585  
TiO<sub>2</sub>-Al<sub>2</sub>O<sub>3</sub>-SiO<sub>2</sub> system, ternary glass-forming region and phys. props. 0-84919  
TiSi<sub>2</sub>, film, elastic stiffness and thermal expansion coeffs. 0-107451  
Ti<sub>3</sub>AsSe<sub>4</sub>, refractive index, thermal expansion temp. depend. 0-97223  
V, thermophysical props. at temps. up to 7000K 0-103497  
V<sub>2</sub>Ge(Si), Gruneisen parameter and thermal expansion eval. at room temp. 0-70351  
WSi<sub>2</sub> film, elastic stiffness and thermal expansion coeffs. 0-107451  
YbCuAl, mixed-valent cpd., thermal expansion and magneto-volume effects 0-66005  
ZnAs<sub>2</sub> and ZnAs<sub>3</sub>, molten, thermal expansion and atomic bond strength parameters 0-65257  
ZnCl<sub>2</sub> glass, glass transition temp. and thermal expansion 0-64902  
α-ZnP<sub>2</sub>, lattice parameters and thermal expansion, 80-320K, X-ray obs. 0-75373  
ZnS(Se)(Te), thermal expansion and lattice dynamics under press. 0-100316  
ZnSe films, long wavelength IR polariton emission band thermal shift and broadening 0-92833  
ZnSiAs<sub>2</sub>, thermal expansion coeffs. meas. (Russian) 0-65258  
ZnSiP<sub>2</sub>, thermal expansion coeffs. meas. (Russian) 0-65258  
ZnTe, 1.5 to 30K, thermal expansion and Gruneisen parameter meas. 0-59681  
Zr(Fe<sub>1-x</sub>Co<sub>x</sub>)<sub>2</sub>, ferromag. and micromag., thermal expansion and forced volume magnetostriction 0-75830  
ZrO<sub>2</sub>, partially stabilized, props. and appl. to extrusion dies 0-97507

**thermal expansion measurement**  
automatic linear expansion coefficient meter with digital readout 0-106713  
coefficient, steel gauge blocks, meas. in climatic chamber (German) 0-68171  
contactless, by double Michelson interferometer 0-73317  
dilatometer, meas. thermal dilatation of metallic amorphous ribbons 0-86258  
dilatometer based on mechanotron 0-105639  
dilatometric measurements, high temp. method accuracy 0-73308  
dilatometric measurements, high-temp., systematic and fiducial error estimation 0-101796  
speckle interferometric meas. apparatus 0-68170  
C fibres, thermal expansion coeff. meas. using TEM fitted with furnace 0-102966

**thermal fatigue** see thermal stress cracking

**thermal insulating materials**  
see also thermal conductivity  
heat mirror on plastic sheet for radiation insulation of visible windows 0-95985  
mechanical supports, app. to meas. thermal conductance 0-82772  
multilayer insulation, simple struct. insulating material props. for low temp. appl. 0-57307  
multilayer insulation materials, ambient temp. outgassing rate 0-84370  
refractory, effective thermal cond., fibre diameter effects 0-104105

**thermal insulation**  
foam plastics, crack inspection using dye solution or X-ray opaque solution 0-76440



**thermal insulation** continued

- multilayer, simple struct. insulating material props. for low temp. appl. 0-57307
- solar energy collector design for low capital costs and least steady-state heat losses 0-104517
- thermal sensation evaluation, comfort chart (*Japanese*) 0-81545
- thickness meas., using easily calibrated eddy-current meter 0-73316
- trunk pipeline systems, oil and gas, investigation and optimisation of thermal regimes 0-107579

**thermal magnetoresistance**

- alkali metals, elec. and thermal cond. in weak mag. fields 0-65535
- CsMnCl<sub>3</sub>·2H<sub>2</sub>O, thermal cond. in mag. field 0-70481
- K, saturation of longitudinal thermal magnetoresist. obs. 0-88541
- Nd, transport props., low temp., effect of mag. field 0-70679
- Pr, transport props., low temp., effect of mag. field 0-70679
- Sm, transport props., low temp., effect of mag. field 0-70679

**thermal noise**

- 600 MHz to 1 GHz coaxial thermal noise standard 0-98875
- frequency standard, thermal noise effect meas. on amplitude of oscillation 0-98898
- laser frequency measurement using supercond. point contacts 0-90824
- measurement, zero point energy noise term presence 0-68213
- nonlinear oscillator with fluctuating parameters, dynamics, thermal noise 0-101729
- pyroelectric 0-82820
- pyroelectric detector materials, thermal noise and dielec. response 0-75952
- resistance fluctuations, anal. independ. of thermal voltage noise 0-84495
- thin films, substrate supported, temp. fluctuation noise 0-92949
- n-InSb, hot electron noise temp., Monte Carlo calc. 0-107877
- Nb superconducting point contact, singularities of I-V curve and voltage fluctuations 0-93044

**thermal properties of substances**

- see also magnetocaloric effects; Scott effect; specific heat; thermal conductivity; thermal diffusivity; thermal expansion; thermal variables measurement
- alkaline earth difluorides, thermal props. (*German*) 0-81355
- composite material, mechanical behaviour, book 0-94935
- diethyl ether, field ionisation, thermal energy distribution and energy deposition 0-95732
- EMF, semiconductors, thermal cell and copper blocks method, more accurate treatment of results 0-77812
- glass characteristics, electromagnetic, mechanical and thermal props. 0-106587
- graphite fibre filled phthalocyanine composites, cure cycle investigation 0-81030
- hexanes, isomeric, 0-95732
- Mars, radar, visual and thermal characts. of rough planar surfaces 0-98589
- metastable superheated water, specific vols. and P-V-T props. 0-92032
- optical fibres, jacketed, thermal characts. of phase shift 0-58670
- optical material physical props., seminar, San Diego, CA, USA (Aug. 79) 0-105423
- quartzite, vitrified, and quartzite based refractory concretes, prep. and props. 0-89188
- rare earth difluorides, thermal props. (*German*) 0-81355
- refractories, strength and thermal properties, automated test system 0-100986
- thermometric method determ., harmonic action of heat flow (*Russian*) 0-69642
- thermophysical coefficients, integral characts. method (*Russian*) 0-69643
- UV and IR instrument material mech. and thermal props. 0-106584
- Mo-based metallic glass development 0-89172
- U-Co(Ce)(Fe)(Mn)(Ni)(V) metallic glasses, glass form. and thermal stability 0-75183
- Zr gels, thermal and related studies 0-71937

**thermal quenching** see quenching (thermal)**thermal radiation** see heat radiation**thermal resistance**

- thin-walled bodies, variable nonideal contact, coupled heat-conduction solutions 0-102961
- Ga<sub>1-x</sub>Al<sub>x</sub>As laser diode, hetero-isolation stripe geometry for IR and visible radiation (*Japanese*) 0-83607

**thermal resistance measurement**

- DH stripe-geometry lasers, thermal props., interpretation of thermal resistance measurements 0-64017
- solid thermal cond. and interface resistance meas. by radiation thermometry 0-86289

**thermal resistivity** see thermal conductivity**thermal shock**

- graphite, neutron irradiation effects on thermal shock resist. and fracture toughness (*Japanese*) 0-66622
- graphite shell, thin, cylindrical, orthotropic, thermal stresses and displacements due to instantaneous thermal shock 0-92060
- Incoloy 800, clean and steam oxidised, T<sub>2</sub> permeation 0-88364
- optical long focal length aerial reconnaissance system response 0-78939
- optical system response to thermal shock, meas. on long focal length reconnaissance lenses 0-77892
- pellet fusion reactor, thermomech. dynamic behaviour of solid wall 0-95396
- Sanicro 31, T<sub>2</sub> permeation 0-88364
- Fe-Cr-Al, HOS 875, oxidation, cyclic, role of thermal shock 0-97640
- Ni base alloys, IN-702, IN-601, TD-Ni-Cr-Al, B-1900+Hf, oxidation, cyclic, role of thermal shock 0-97640
- Ni-ThO<sub>2</sub>, oxidation, cyclic, role of thermal shock 0-97640
- ZrSiO<sub>4</sub>, zircon ceramic with glass-forming additives, sintering and mech. props. 0-60814

**thermal shock failure** see thermal stress cracking**thermal spikes** see crystal defects; radiation effects**thermal stress cracking**

- brittle ceramics, effect of data scatter on apparent thermal stress failure mode 0-60949
- ellipsoidal cavity, triaxial, collapse to crack, thermoelastic stresses 0-92061
- fusion welding of Al alloys, weld susceptibility to hot cracking 0-81143
- graphite, thermal shock resistance and fracture toughness during graphitising heat treatment (*Japanese*) 0-71843
- meteors thermal fracture, detached particles mean dia. 0-62081

**thermal stress cracking** continued

- mulite-corundum ceramics, thread-like crystals reinforced, props. 0-108525
- multilayer welds, high temp. internal deformations development and effects on crack formation 0-81082
- penny-shaped cracks, in elastic sphere embedding in infinite elastic space, thermal stresses 0-64460
- periclase refractories, props. after testing at over 2000°C 0-104317
- refractories, thermal stress cracking resistance estimation 0-104288
- slab containing annular crack, thermal stresses, integral transform techniques 0-96229
- steel, 12Cr1MoV, thermal fatigue and creep effect in fracture 0-104297
- steel, austenitic stainless, thermal fatigue, fractographic features of failure 0-76349
- steel, Cr-Mo (2.25, 1 wt.%) pipe, high temp. fatigue and creep strength 0-85060
- steel, heat resistance, thermal stability, stress-rupture strength, and creep 0-81194
- steel, thermal fatigue, effects of inclusions 0-81183
- thermodynamics appl. in mathematical anal. 0-108530
- Fe, cast, US study of sections undergoing deform. or thermal cycling 0-104285
- MgO, sintered, refractories, props. after testing at over 2000°C 0-104317
- Mo, fusion reactor appl., quick heating thermal fatigue test, ultra-high vac. environment (*Japanese*) 0-93716
- Ni-Cr-W-Co-Ti, thermal fatigue, effects of inclusions 0-81183
- Ti alloy, heat resistance, thermal stability, stress-rupture strength, and creep 0-81194
- Y<sub>2</sub>O<sub>3</sub> ceramics, strength under mech. and thermal actions 0-97554
- Zn, crack form. at grain and twin boundaries at low temp. (*Russian*) 0-66620

**thermal stresses**

## see also thermal stress cracking; thermoelasticity

- after-effects in thermo-elasticity 0-106724
- ceramics, brittle, heat-transfer variables effect as thermal stress resist., meas. by quenching expts. 0-79871
- ceramics, brittle, partially absorbing, thermal stress anal. subjected to symmetric radiation heating 0-59570
- clad-glass fibres, thermal stresses 0-107360
- contact, frictionally heated, thermoelastic deform. 0-83764
- cylinder, circular, three-dimensional transient thermal stresses under nonaxisymmetric temp. distrib. 0-92054
- cylinder, hollow, heated on outer surface, cooled on inner surface, temp. and thermal stresses (*Russian*) 0-74712
- cylinder, thermal displacements and stresses, determ. by computer-assisted classical methods (*Rumanian*) 0-92066
- elastoplastic stress analysis based on initial strain method (*Japanese*) 0-77620
- epoxy EDT-10, rigid polymer, thermal stress isothermal relaxation 0-71683
- epoxy resin composites, cooldown residual thermal stresses, viscoelastic response 0-60941
- fusion reactor, BBC CQK 200-4 modulator tube for sustaining neutral beam power supply 0-99290
- graphite shell, thin, cylindrical, orthotropic, thermal stresses and displacements due to instantaneous thermal shock 0-92060
- heat memory materials, dynamic thermoelasticity of infinite cylindrical rod (*Russian*) 0-74752
- infinite medium containing periodic ribbon-like inclusions, local intensification of thermal stresses (*Japanese*) 0-96195
- ingots, cooling regime in conditions of minimal thermal stress, modelling (*Russian*) 0-65194
- laminated plates, symmetric, specially orthotropic, thermoelastic anal. 0-92058
- metallic thin films, thermoelectric power, thermal stress effects, theory 0-65714
- optical fibre, refractive index profile distortion, stress-induced 0-91889
- optical fibre refractive index profile distortion due to thermal stresses 0-58726
- optical fibres, piezo-optical effects due to thermal stresses 0-87519
- optical glass, tolerancing of refr. index heterogeneity in objectives 0-78948
- photothermoelastic technique, appraisal for transient 2D thermal stress analysis 0-79244
- plate, cylinder, sphere, temperature (one-dimensional) and thermal stress fields, inverse problems 0-79134
- plate, reinforced strip, 2-dimens. nonsteady temperature stresses 0-74734
- PMMA, rigid polymer, thermal stress isothermal relaxation 0-71683
- reinforced plastics, load-bearing capacity, effect of one-sided heating 0-81135
- rubber cylinder, circular, uniformly heated, combined extension and torsion 0-92057
- semiinfinite plate, heat transfer effect 0-96193
- shells, cylindrical, anisotropic, quasistatic thermoelastic eqns. 0-92059
- solar collectors with multilayer cylinder heat exchangers, heat balance eqn. and thermal stress anal. 0-58977
- stator windings, failure mechanisms under thermal cycling (*Japanese*) 0-104189
- steel, alloy, 15KhM1 and 20KhM1, plastic deform. with thermal cycling 0-89310
- steel, medium, C, US attenuation, mag. field effect 0-89428
- steel, platelike parts, quenching, temp. field calc. 0-60889
- steel, stainless, type 316 20% cold worked fission reactor fuel cladding, axial stress effects on transient mech. response 0-71743
- steel casting, calc. method of thermal and thermo-visco-elasto-plastic processes (*German*) 0-79859
- steel continuous casting, thermal, thermo-visco-elasto-plastic processes (*German*) 0-81044
- thermoelastic cooler, single stage, finite element thermal stress anal. 0-108807
- unsteady thermal stress problems in a doubly connected domain by conformal mapping 0-69652
- viscoelastic materials, stress waves generated by internal heating in Voigt and Maxwell materials (*Japanese*) 0-69693
- C reinforced plastic, degraded, study of strain, 20 to 1000°C 0-71680
- CdS, dislocation motion due to heating by electron beam in TEM 0-79799
- Cu-Zn (30 wt.%), single crystals, quantitative anal. of stress relax., obstacle strength and athermal stress variation 0-89277
- Fe-C-Mn-V, austenite microstruct. memory (*German*) 0-84977

thermal stresses continued

Fe<sub>2</sub>O<sub>3</sub> thin films, reactively sputtered, mechanical stresses rel. to deposition conditions 0-80146  
GaAs crystal growth, thermal and elastic const. evaluation 0-92586  
GaAs, pulled, dislocation generation, thermoelastic anal. 0-79787  
GaP/Si heterostruct., differential thermal contraction, plastic deform., fracture 0-108494  
GaS, elastic prop. anisotropy, Debye temp. (*Russian*) 0-88244  
Ge ribbon single crystals, grown from melt, dislocation struct. form. under thermal stress 0-107082  
LiI<sub>2</sub>O crystal, SHG, thermoelastic stresses and nonlinear refract. effect 0-74437  
Nd:glass laser rod, pumped, thermal relaxation 0-69397  
Pb, film, hillock formation by grain boundary sliding 0-107673  
Pb, film, thermal strain, strain relax. above room temp. 0-59841  
PbO, thin film, microstruct. and thermal stress, doping effects 0-88458  
Si on sapphire, stress-relieved regrowth by laser annealing 0-65389  
Si single crystal growth, Czochralski method, small-angle dislocation boundary form. anal. 0-89136  
Si thin ribbon grown at high speed, thermal stresses, reduced thermal buckling 0-107078  
Si<sub>3</sub>N<sub>4</sub>, bending strength, deformability, elastic moduli and brittleness 0-81191  
U<sub>3</sub>Si, reversible twinning, in-situ obs. 0-104241

thermal transformations see phase transformations

thermal variables measurement

see also bolometers; calorimeters; calorimetry; temperature measurement; thermal conductivity measurement; thermocouples; thermometers  
colour temperature characs. of cholesteric liquid crystals, using temperature wedge method 0-57359  
conducting thin films, covered with electrolytic deposit, thermoelec. props., appl. to thermal flux meas. (*French*) 0-59961  
fluxmeter, multiple thermoelectric junctions on thin conducting sheet (*French*) 0-86286  
heat-pulse experiments, nonlinear effects, theory 0-96182  
high intensity local heat flow, meas. errors anal. (*Russian*) 0-74865  
liquids, opaque and diathermanous, total normal emissivity meas. at high temp. 0-102965  
liquids, thermophysical properties measurement (*Russian*) 0-77776  
long rod, direct-heating meas., interpretation 0-102964  
nonstationary heat flux measurement by auxiliary wall sensors 0-86287  
nonstationary thermal fluxes, in converter, meas. 0-74724  
reaction kinetics meas. using modified commercial stopped flow apparatus 0-86291  
temperature gradients in liquid, using laser microrefractometer 0-57362  
thermoelectromotive force and temperature, study of kinetic phenomena of charge transfers 0-57330  
thermophysical process ambiguous data gathering and processing optimisation (*Russian*) 0-73335  
He, melting at room temp., high high-press. cell 0-80025

thermally stimulated capacitor discharge see thermally stimulated currents

thermally stimulated currents

alkali halides, thermally stimulated depolarisation of NCO<sup>-</sup> centres 0-80678  
alkyl halide, amorphous, depolarisation thermocurrents and dielectric relaxation time distrib. (*French*) 0-60490  
apatites, dipolar reorientations, TSD study 0-107068  
carrier traps in polymeric insulating materials, investigation by X-ray induced thermally stimulated current method 0-93240  
cellulose, dielec. relax. studies, TSD meas. 0-88907  
chloranil pellets, thermally stimulated discharge current and dielectric studies 0-93236  
dielectric conduction and breakdown, conf., Gainesville, FL, USA (Oct.-Nov. 1979) 0-82564  
dielectrics, solid, dipolar relaxation time, trap levels and ionic space charge polarisation 0-84685  
electrets, thermally stimulated discharge 0-80683  
exosmion phenomena, TSC, thermionic emission, book contribution 0-80954  
field induced thermally stimulated polarisation-depolarisation currents, relaxation, book contribution 0-80687  
hydroxyapatites, dipolar reorientations, TSC study 0-60491  
many-body model of universal dielec. response 0-75927  
methacrylic polymers, multiple dielectric relaxations, investigation by thermally stimulated current method 0-93238  
MIM systems, TSC, space-charge layer model 0-93009  
naphthalene, electron trapping, one-carrier TSC and SCL currents 0-70715  
novolac and novolac allyl ether electrets, thermal depolarisation, chem. struct. effect 0-71297  
nylon 6, water effects 0-75925  
photoresist, KTFR, thermally stimulated discharge current studies 0-75924  
phthalocyanine metal free films, TSC, ferroelectric-semiconductor transition 0-66105  
poly-p-xylylene films, carrier traps, X-ray induced TSC, thermolum. and dielec. loss study 0-88570  
polycarbonate, and charge-transfer complex modifications, TSC 0-88572  
polyethylene, dielectric props., investigation for morphology changes created by mechanical drawing and annealing 0-84697  
polyethylene, elec. cond. of high and low density samples, oxidation effects 0-107784  
polyethylene, space-charge storage under high DC voltage condition, TSC meas. (*German*) 0-75576  
polyethylene terephthalate, TSC and thermolum. due to electron detrapping by local mol. motions 0-96898  
polymer, generation mechanism and characs. (*Japanese*) 0-60488  
polymers, frictional electrification, temp. and friction speed dependence obs. 0-70798  
polystyrene:I films, thermally stimulated discharge, I conc. and polarisation temp. depend. 0-107937  
polystyrene film, thermally stimulated discharge currents 0-71300  
polystyrene thin films, TSC and surface charge meas. 0-103769  
polystyrenes, anionic, TSC obs. of T<sub>g</sub> and T<sub>h</sub> transitions 0-84686  
polyvinylbutyral, elec. and dielec. props., mol. wt. effect on charge storage 0-97192  
polyvinylidene fluoride, X-ray induced TSC 0-75578  
relaxation kinetics, transport phenomena in solids, book 0-77553  
semiconductors, deep level carrier trapping and emission, transient spectroscopy, book contribution 0-80216

thermally stimulated currents continued

semiconductors, thermally stimulated conductivity luminescence, defect levels, traps, book contribution 0-80296  
semiconductors, thermally stimulated relaxation processes, book contribution 0-80295  
Teflon FEP, N implanted, TSC spectra 0-88912  
trap depth, determ. from TSC, theory 0-70716  
trap depth determ. from TSC 0-59998  
trapping levels, effect on TSC, calc. 0-60489  
AgGaS<sub>2</sub>, deep level obs. by TSC meas. 0-65590  
Al-SiO<sub>2</sub>:Si MOS structures, charge motion, TSC meas. 0-100534  
Al<sub>2</sub>O<sub>3</sub>, anodic films, trapping levels study using TSC 0-103768  
Al<sub>2</sub>O<sub>3</sub>:Cr, pure and doped, electron irradi. induced cond., TSC and EPR study 0-80277  
Ba<sub>1-x</sub>La<sub>x</sub>F<sub>2+x</sub>, enhanced ionic motion in solid solutions 0-107491  
CaF<sub>2</sub> thin films, initial ionic thermocurrent meas. 0-97018  
CaF<sub>2</sub>:alkali metal cation, thermal depolarisation study 0-108147  
CaF<sub>2</sub>:O<sup>2-</sup>, CaF<sub>2</sub>:Na<sup>+</sup>, O<sup>2-</sup> and CaF<sub>2</sub>:Y<sup>3+</sup>, O<sup>2-</sup>, thermal depolarisation obs. of defect clusters 0-71299  
CaF<sub>2</sub>:Y<sup>3+</sup>, ionic cond. and thermal depolarisation obs. of defect clustering 0-71298  
CdF<sub>2</sub>, electrical transport limitation by electrodes, polarisation effects 0-96689  
CdF<sub>2</sub>:Sm<sup>3+</sup>, photoconverted, thermally stimulated relax. 0-84476  
CdS thin layers, recryst. from CdS-Cr<sub>2</sub>O<sub>3</sub> mixtures, phys. and photoelec. props. 0-96935  
CdS:Li(Cu), pure and doped, electrodiffusion of shallow donors, photocurrent, TSC, and exciton luminesc. meas. 0-79992  
Cd<sub>1-x</sub>Zn<sub>x</sub>S films, thermal evaporation prep., phys. props. 0-84410  
FeF<sub>3</sub> thin film, polarisation mechanism, AC and TSC study 0-66104  
GaAs:O, semi-insulating, excitation temp. effect on TSC 0-70717  
GaP crystals, radiation defects, TSC obs. 0-65588  
α-HgS, trapping parameters determ. by TSC meas. 0-59997  
InP:Fe shallow trap thermally stimulated cond. spectroscopy, photocond. spectrum under DC conditions 0-65585  
K<sub>2</sub>FeF<sub>4</sub>, charge transport and polarisation 0-80681  
K<sub>2</sub>ZnF<sub>4</sub>, charge transport and polarisation 0-80681  
Li<sub>2</sub>B<sub>4</sub>O<sub>7</sub>, ferroelectric glass, phase transition, permittivity, electrochromism, photochromism 0-80719  
(Li<sub>2</sub>B<sub>4</sub>O<sub>7</sub>)<sub>1-x</sub>(WO<sub>3</sub>)<sub>x</sub>, dipolar glass, space charge injection, thermally stimulated depolarisation currents 0-66103  
LiF:Mg, Z<sub>2</sub><sup>-</sup> and associated Z-centres, elec. cond., ionic thermocurrent, and optical absorpt. meas. 0-107229  
LiH, defect form. at low temp., EPR, thermolum. and TSC study 0-107222  
MgAl<sub>2</sub>O<sub>4</sub>, γ-irradiated crystal, TSC, thermoelec. power, thermolum. and afterglow 0-75583  
MgO crystals, dipolar defects, thermally stimulated depolarisation 0-66101  
NaCl:Mn<sup>2+</sup>, Mg<sup>2+</sup>, doubly doped, ionic thermocurrent study of linear dimer 0-79977  
NaI:Ca<sup>2+</sup>, pure and doped, ionic thermocurrents meas. 0-80677  
NaMgF<sub>3</sub>, defects induced by X- and vacuum UV irradi., optical and elec. study 0-107319  
Sb<sub>2</sub>S<sub>3</sub>, defect drift in elec. fields and bistable switching 0-92947  
Si, amorphous film, TSC, density of localised states distrib. 0-65587  
Si, amorphous layers, recrystallisation, pulsed laser annealing 0-65404  
Si, high dislocation density crystals, photoelectret state investigation 0-79191  
Si:Au p<sup>+</sup>-n junction, small area, acceptor level conc., determ. from TSC curves 0-75631  
Si-SiO<sub>2</sub> structures, B ions implanted, energy spectra of shallow traps at various implantation energies 0-80392  
Si<sub>3</sub>N<sub>4</sub> films, thermally stimulated depolarisation current meas. 0-88643  
SiO<sub>2</sub>, HCl-grown oxides, characterisation of surface states using MOS transient currents 0-65696  
SrO:Ni<sup>2+</sup>, ionic thermocurrent meas. 0-108148  
TeO<sub>2</sub>, ferroelectric glass, phase transition, permittivity, electrochromism, photochromism 0-80719  
ZnO non-ohmic ceramic, degradation props. under AC and DC bias 0-80262  
ZnSe, heat-treated in controlled partial press. of Zn or Se, TSC 0-59910  
ZnTe, elec. field and impurity conc. effects on ionisation energy of impurities, appl. to acceptors 0-88514

thermally stimulated depolarisation see thermally stimulated currents

thermally stimulated discharge see thermally stimulated currents

thermally stimulated ionic currents see thermally stimulated currents

thermally stimulated polarisation see thermally stimulated currents

thermally stimulated relaxation currents see thermally stimulated currents

thermionic cathodes

design using heat flow optimisation 0-71558  
field emission source for high resolution, high current e-beam microprobes 0-68297  
impregnated and coated powder cathodes, reactivation following shelf-life poisoning, comparison 0-76128  
impregnated-cathode behaviour, emission, and lifetime, expt. study 0-84827  
porous metal thermionic cathode with sputtered metal films, emission operating characs. 0-100740  
semiconductor, fluctuations of velocity of emitted electrons 0-66380  
LaB<sub>6</sub>, illumination system, for round beam electron probe systems 0-57436  
LaB<sub>6</sub> mounting methods and operating characs. 0-57437  
LaB<sub>6</sub>, single crystal, of <100> and <110 orientations, brightness meas. from 1500 to 1950K 0-62808  
Ni, Medicus matrix cathode, surface characs. 0-66378  
W dispenser cathodes, Ba-activated, surface characs., ion scatt. spectroscopy and SIMS study 0-66377  
Zr-O-W (100) thermal field emitters, operational experience 0-71576

thermionic conversion

alkali metals, vapour states, laser spectroscopy and applic., review 0-68260  
solar energy power generators with advanced thermionic converters for space craft applications 0-61389  
solar thermionic power plant, central thermal receiver tower concept, geometric config. and design 0-61390  
thermionic triode, oscils. in low press. inert gas discharge 0-79590  
uniform-temperature thermionic generator, model 0-85296



**thermionic conversion continued**

- Cs vapour source, thermionic energy convertor with Cs-He gas controlled heat pipe 0-64791  
 Mo, low-temperature thermionic converter with an expanded-area collector 0-70045

**thermionic electron emission**

see also *Schottky effect*; *thermionic cathodes*

- alkali halide, photo- and thermostimulated electron emission under ultrahigh vacuum conditions (*Russian*) 0-66383  
 cadmium arachidate mixed with cyanine dyes, mol. layers, photoelec. props. 0-80401  
 conduction electron retrapping probability, depend. of sums of thermally stimulated electron emission on heating rates (*Russian*) 0-84826  
 elliptic emission functions used in calc. of electron emission from surfaces 0-89124  
 exoemission phenomena, TSC, thermionic emission, book contribution 0-80954  
 metallic heated cathodes, physics of electron emission (*French*) 0-104033  
 orbitron device, optimum injection condition for electrons, influence of end effects 0-82784  
 porous metal thermionic cathode with sputtered metal films, emission operating characts. 0-100740  
 semiconductor cathodes, fluctuations of velocity of emitted electrons 0-66380  
 tetrode system, two-dimens., algorithm for solving space-charge problems with thermally-emitted electrons 0-100743  
 ultrahigh vacuum setup for photo- and thermostimulated electron emission and luminesc. obs. (*Russian*) 0-66383  
 Ag-Cs-O photocathode, operation mechanism involving  $\text{Cs}_2\text{O}_2$  0-66384  
 $\text{Ba}_2\text{Sc}_2\text{O}_6$ ,  $\text{Ba}_2\text{Sc}_2\text{WO}_6$  and  $\text{Ba}_2\text{Sc}_2\text{TaO}_6$ , elec. cond. nature, depend. on comp. and medium thermodynamic parameters 0-70773  
 $\text{K}_2\text{O-Al}_2\text{O}_3\text{-}2\text{SiO}_2\text{-BaO}$  plasma emitter 0-96368  
 $\text{LaB}_6$  cathodes, single crystal, of  $\langle 100 \rangle$  and  $\langle 110 \rangle$  orientations, brightness meas. from 1500 to 1950K 0-62808  
 $\text{LaB}_6$  single cryst. tips with  $[100]$ ,  $[110]$ ,  $[111]$  and  $[210]$  orientations, thermionic emission patterns 0-66379  
 $\text{LaCrO}_3\text{-MgO}$ , LC20M electrode material in open cycle MHD systems, thermionic emission characts. 0-97394  
 LiF, cryst., laser irradi., electron emission 0-80948  
 Mo, coadsorption of  $\text{O}_2$  and Cs, electron emission props., thermal stability 0-66878  
 NaCl, cryst., laser irradi., electron emission 0-80948  
 Si:Se, impurity states, A- and B-centres, electron, hole thermionic emission rates 0-96813  
 $\text{TiO}_2$ , nonstoichiometry study, thermal emission of electrons 0-108317  
 W single cryst., dislocation effects on thermionic emission and work function 0-76129  
 $\text{Y}_2\text{O}_3$ , nonstoichiometry study, thermal emission of electrons 0-108317

**thermionic emission**

see also *thermionic electron emission*; *thermionic ion emission*

- MIS negative barrier contact for induced back surface field solar cell 0-101101  
 $\text{CdS-Cu}_2\text{S}$  junctions, carrier trap density, deep level defects 0-107801  
 $\text{GaAs-AlGa}_{1-x}\text{As}$  heterostructures, real-space electron transfer by thermionic emission, analytical model 0-100512  
 $\text{LaB}_6$  single crystal cathode, thermionic emission, surface struct. 0-97395  
 $\text{LiNbO}_3$ , thermionic emission characts. 0-104034  
 Si, enhanced conductivity in plasma hydrogenated films, thermionic emission 0-70692

**thermionic generators** see *thermionic conversion***thermionic ion emission**

- alkaline earth oxides, emission props. in  $\text{CO}_2$  stream 0-100742  
 alkaline earth oxides, surface emission active centres 0-100741  
 exoemission phenomena, TSC, thermionic emission, book contribution 0-80954  
 polystyrene film, graft, positive-ion emission in thermal destruction 0-66381  
 Cs, ion source, thermionic emission in  $\text{SF}_6$  mol. gas 0-71557  
 $\text{K}_2\text{O-Al}_2\text{O}_3\text{-}2\text{SiO}_2\text{-BaO}$  plasma emitter 0-96368

**thermionic power generation** see *thermionic conversion***thermionic tubes**

- see also *cathode-ray tubes*; *electron-wave tubes*; *gas-discharge tubes*; *rectifier tubes*  
 triode, oscills. in low press. inert gas discharge 0-79590

**thermionic valves** see *thermionic tubes***thermistors**

- anemometer application, thermally compensated, math. models (*French*) 0-90227  
 biological effects of US, use of thermistor probes to mean. energy distrib. 0-109075  
 laboratory temperature control, bridge cct., modified window air conditioner 0-68192  
 NTC sensors, cct. designs and design calculation tables 0-68201  
 $\text{AlB}_{12}$ ,  $\alpha$ - and  $\beta$ -forms, elec. props. at high temps. and in strong elec. fields, thermistor appls. 0-92903  
 $\text{B}$ ,  $\beta$ -rhombohedral, elec. props. at high temps. and in strong elec. fields, thermistor appls. 0-92903  
 $\text{CuB}_{24}$ , elec. props. at high temps. and in strong elec. fields, thermistor appls. 0-92903  
 SiC thin-film thermistors with high thermal response (*Japanese*) 0-105629

**thermo-optical effects**

see also *thermoreflectance*

- acoustic field excitation in liquid by periodic train of laser pulses 0-103945  
 acoustic pulses, short thermooptically excited, exptl. study of propagation 0-102891  
 chalcopyrite crystals, refractive index, temp. depend., appl. to nonlinear devices 0-60555  
 colour-centre lasers, thermal strains in active elements 0-91804  
 image convertor, thermo-optical, with liq. modulating medium 0-91927  
 lasers for industrial chemistry, thermal lensing effect 0-87427  
 liquid crystals, thermooptical effects used to visualise EM fields 0-62723  
 long focal length aerial reconnaissance system response to thermal shock 0-78939  
 military optical system temperature effects and counter-measures 0-78938  
 parametric effects anal., in optics 0-102619

**thermo-optical effects continued**

- phosphate glasses, non-alkaline, transition states, phys. effects of fluors, phase diagrams and optical effects (*German*) 0-88045  
 quartz, cryst., birefringence, temp. depend., intracavity method meas. 0-78931  
 smectic A liquid crystals, thermooptical recording, echo images 0-91928  
 TTF-chloranil visual pressure or temperature indicator 0-87443  
 US generation due to moving laser thermoopt. source in liquid 0-102903  
 UV high-power laser material, refractive props. and optical constants 0-106555  
 $\text{CdGeP}_2$  thermo-optic coefficient, dispersion 0-71396  
 $\text{CdS}$  thermo-optic coefficient, dispersion 0-71396  
 $\text{CdSe}$  thermo-optic coefficient, dispersion 0-71396  
 $\text{CuGaS}_2$  thermo-optic coefficient, dispersion 0-71396  
 $\text{CuSO}_4$  solution, thermooptical excitation of sound by ns. laser pulses 0-79884  
 $\text{LiF:Mg}$  cryst., Mg electron colour centers 0-100229  
 $\text{LiNbO}_3$  crystal in laser resonator, thermo-optical effect (*Chinese*) 0-106546  
 $\text{Nd}^{3+}$ :YAG laser active element, linearly polarised light depolarisation due to thermally induced birefr. 0-106528  
 $\text{V}_2\text{O}_5$  amorphous film, photochromism and thermochromism 0-93254  
 $\text{WO}_3\text{-B}_2\text{O}_3\text{-ZnO}$  semiconducting glasses, DC cond. and optical absorpt. 0-107783  
 YAG:Nd crystal, orientation influence on thermally induced birefringence (*Chinese*) 0-88958  
 $\text{ZnGeP}_2$  thermo-optic coefficient, dispersion 0-71396

**thermochemistry**

see also *chemical reactions*

- metal oxide cycles for  $\text{H}_2$  prod. using fusion energy 0-76658  
 micellar systems, aqueous, thermochemistry 0-61133  
 solar thermochemical cavity absorber based on  $\text{NH}_3$  dissociation, design and cost anal. 0-81489  
 solar thermochemical electric power generation, reversible chemical reactions 0-61394  
 $\text{CO}_2$ , thermochem. reduction using solar energy to provide C-based fuels 0-76610  
 $\text{CO}_2$ -methane reforming-methanation cycle for Solchem thermochemical solar energy transport 0-94096  
 $\text{CaCO}_3$ , decarbonation for solar energy thermochemical conversion 0-94097  
 $\text{CaO-Ca(OH)}_2$  reversible hydration-dehydration for solar energy storage 0-97810  
 Fe, sintered, austenitic nitriding and bainitic hardening 0-85084  
 Fe-Mo system, thermomech. props. 0-89208  
 $\text{H}_2$ , thermochemical compression for hydride thermosorption, theory (*Ukrainian*) 0-76657  
 $\text{H}_2$ , thermochemical production, plasmachemical  $\text{H}_2\text{O}$  decomposition using nuclear energy source 0-61436  
 $\text{H}_2$ , thermochemical production by Mark-13 cycle, development of laboratory-scale plant 0-76659  
 $\text{H}_2\text{O}$ , thermochemical decomposition utilising solar heat for  $\text{H}_2$  prod. 0-61451  
 $\text{TiO}_2\text{:TeCl}_4$  system, chem. vapour transport, matrix isolation IR studies 0-93755  
 Zr gels, thermal and related studies 0-71937

**thermoclines** see *temperature distribution***thermocouples**

see also *thermopiles*

- automatic temperature measurement with thermojunctions, temperature sensitive ICs and resistance thermometers (*German*) 0-77778  
 calibration on-site 0-90840  
 calibrations, comparison, fixed point and melting wire methods 0-86252  
 cold junction compensation circuits using IC temperature sensors 0-77777  
 cylindrical, with plane frontal area, recovery factor in turbulent subsonic flow (*German*) 0-74882  
 fission reactor loss of fluid test program, 2200°C fuel centerline thermocouples 0-57877  
 gas temperature meas., high, stationary, thermal probe 0-95101  
 glass container forming, mould surface temp. meas. 0-82767  
 heat pulse technique for bonding thermoelectric modules contacts 0-107904  
 high temperature in-fuel thermocouples for FBR fuel pin safety expts. 0-102283  
 in-reactor fuel temperature, transient response of centreline thermocouples, appl. to fuel modelling 0-95372  
 IR windows, insertion of thermocouples for IR spectroscopy and reaction cells 0-57398  
 liquid-friction bearing temperature measurement, new bearing tester 0-64503  
 meas. errors, due to windings heating (*German*) 0-95096  
 measurement error avoidance, temp. meas. 0-62664  
 mounting method for thermocouple gauge tubes 0-77795  
 multiple thermoelectric junctions, thin conducting sheet, near heat flux-meter (*French*) 0-86286  
 Nicrosil-Nisil, in production furnaces, 538°C to 1177°C 0-68198  
 reference junction box, used for vacuum chamber 0-90844  
 rotating bodies temperature measurement, thermocouple slip ring assembly 0-86294  
 semiconductor resistance thermometers, for the interval 300K to 0.3K, thermoelectric characts. 0-73359  
 standards, GDR, testing (*German*) 0-90842  
 surface temperature measurement using thin film thermocouple 0-62668  
 thermal inertia meas. (*Russian*) 0-62665  
 thermoelectric cooling devices, maximum refrigerating capacity determ. 0-86318  
 thermometers, voltage generation, calibration 0-57295  
 universal extension leads, geometry of connection 0-57294  
 vacuum gauge, gas analyser appl. 0-61183  
 $\text{Bi}_2\text{Te}_3$  alloy thermocouples for solar thermoelectric conversion 0-94095  
 $\text{Bi}_2\text{Te}_3\text{-Bi}_2\text{Se}_3$  solid solns., single cryst. growth and thermocouple construct. 0-104056  
 Cr-Al thermocouple, temp. control system design (*Spanish*) 0-73362  
 N, nonequilibrium plasma, thermocouple diagnostics 0-103188  
 Ni-Fe thermocouple, appl. to surface temperature measurement 0-62668  
 $\text{Sb}_2\text{Te}_3\text{-Bi}_2\text{Te}_3$  solid solns., single cryst. growth and thermocouple construct. 0-104056  
 Si-Ge thermoelectric generators, approximation errors when using averaged properties solutions for required heat rates estimation 0-108808



**thermoelectricity** see *thermal diffusion*  
**thermodynamic changes of state** see *phase transformations*  
**thermodynamic cooling** see *cooling*  
**thermodynamic equations of state** see *equations of state*  
**thermodynamic potential** see *free energy*  
**thermodynamic properties**  
see also *critical points; enthalpy; entropy; free energy; Gruneisen coefficient; latent heat; specific heat*  
acetone-chloroform-methyl isobutyl ketone, ternary phase diagrams, interactive computer program 0-71629  
acetone-toluene-tetrachloromethane, mol. interaction and thermodynamic props. 0-71935  
acetonitrile-toluene-benzene, mol. interaction and thermodynamic props. 0-71935  
alcohols, vapour-liq. equilib. and heats of mixing, simplified group method anal. 0-96637  
alkali halides,  $V_1$ -centres, vibr. modes, calc. 0-84269  
alkanes, vapour-liq. equilib. and heats of mixing, simplified group method anal. 0-96637  
alloy, binary thermodynamic data 0-104121  
antiferromagnets, pseudo-one-dimens., thermodynamic variables 0-65935  
binary dense gaseous mixtures, struct. and thermodynamic props., molecular dynamics study 0-64866  
binary liquid solutions, struct. and thermodynamic props., molecular dynamics study 0-64866  
 $\text{BO}_2$ , 0-65252  
t-butyl alcohol, mixtures, assoc., thermodynamic study using 2-constant model 0-66789  
chemical potentials of structural elements of compounds and face or dislocation specificity, thermodynamic parameters 0-96514  
chloroalkanes, vapour-liq. equilib. and heats of mixing, simplified group method anal. 0-96637  
o-chlorophenol-acetone (ethyl methyl ketone), thermodynamic and transport props. 0-92686  
cis-1-chlorobutadiene-1,3, microwave spectrum, struct., nuclear quadrupole coupling, distortion const., thermodynamic functions calc. 0-99500  
conduction electrons, thermodynamic method for quantitative anal. 0-59946  
critical behaviour, correction-to-scaling amplitudes, crit. exponents 0-57233  
critical behaviour, correction-to-scaling amplitudes on coexistence curve 0-57234  
cyclopropane( $d_6$ ), centrifugal distortion const. and thermodynamic functions calc. 0-95582  
dilute solute-binary solvent activity coeffs., statistical mech. theory 0-59663  
dipolar hard sphere solvent with charged hard spheres, hypernetted chain approx. 0-61130  
divalent Sr, Ba, Ca, Zn, Cd iodates, complex salts, phase transitions, cryst. struct. (Chinese) 0-70171  
double oxides, thermodynamic obs. using galvanic cells with  $\text{CaF}_2$  solid electrolyte (French) 0-85190  
dynamic living polymers, thermodynamic enhancement of oligomers, end-group interactions 0-58423  
Earth mantle elements compounds and modifications, high press. and temp. thermodynamics 0-81874  
electron system, two-dimensional, melting curve, phase diagram 0-57179  
extended defect system, phase transform., critical props. 0-103455  
ferroelectric semiconductors, props., book 0-82590  
ferromagnet, uniaxial two-sublattice, anisotropic, thermodynamic and mag. props. 0-65866  
film on Si substrate, eutectic point displacement on annealing (Russian) 0-100850  
fluids, perturbation theory and thermodynamic props., CRIS model 0-92430  
fluids, perturbation theory and thermodynamic props., inverse power and 6-12 pots. 0-92431  
fluids, perturbation theory and thermodynamic props. 0-92429  
gaseous ions, thermodynamic props. calcs., dimens. model 0-96334  
gaseous molecules, thermodynamic props. calcs., dimens. model 0-96334  
germylacetylene( $d_8$ ), centrifugal distortion const. and thermodynamic functions calc. 0-95581  
graphite surface, adsorbed He, band struct. and thermodynamic props. 0-80349  
hard rods, attractive interactions, scaled particle theory 0-82735  
hard sphere system in three dimens., thermodynamic props. 0-86226  
hard spheres mixtures, equations of state for calc. thermodynamic props. 0-84301  
hard-particle fluids, general scaled-particle-like descriptions 0-103231  
hard-particle fluids, general  $y$ -expansion-like descriptions 0-107032  
heterogeneous nonideal chemically reacting system, comp., thermodynamic props. calcs. 0-76492  
hexafluorocyclopentane, centrifugal distortion const. and thermodynamic functions calc. 0-95582  
n-hexane, superheated, thermodynamic props. from ultrasound speed 0-92036  
III-V semiconductors, point defects and deep traps, thermodynamic history, model 0-59908  
 $\alpha$ -In $_2$ Te $_3$ , I phase, order-disorder transform. for  $\text{DO}_{22}$  struct., thermodynamic study 0-70155  
inhomogeneous charged fluids, density functional theory, rel. to molten salts surfaces 0-79660  
iodide, charge transfer to solvent spectra, spectral shift data, Madelung const. determ. 0-85204  
ionic clusters, struct., thermodynamic functions, energy surfaces and SIMS 0-63881  
kaolinite-C, high temp. reduction reactions, thermodynamic anal. 0-104426  
liquid boundary layers, struct. and thermodynamic peculiarities 0-88408  
liquid metal, perturbation theory extension to dense partially ionised plasmas 0-75500  
liquid-vapour transition, non-Ising-like effects, eqn. of state, renormalisation group calc. 0-84286  
MBBA-n-heptane, nematic soln., lattice model, thermodynamic functions (Russian) 0-64896  
metal-insulator transition, chemical mechanism, thermodynamics, vacancies 0-103626  
metals, dislocations and shock compression, thermodynamics 0-100235  
metals, melting theory for small particles, Helmholtz free energy 0-59629

**thermodynamic properties continued**  
metastable superheated water, specific vols. and P-V-T props. 0-92032  
methanol-ethanol (n-propanol)(n-butanol) binary systems, excess vol. of mixing, dilatometric meas. 0-59656  
minerals, dislocations and shock compression, thermodynamics 0-100235  
mixtures, binary and ternary, activity coeffs. rel. to excess Gibbs free energies 0-96665  
mixtures, simple, non-equilib. thermodynamics 0-76543  
molecule, nonrigid, sum of states, isometric group, symmetry no., thermodynamic functions 0-58186  
Mott transition in Hubbard long range model, isostructural instability, thermodynamic props. (Russian) 0-65454  
multicomponent systems, intensive parameters, thermodynamic props. depend., stability conditions (Russian) 0-65186  
multicomponent systems, phase diagrams and thermodynamic data, electrochem. determ. 0-71922  
naphthalene-m nitroaniline eutectic, excess thermodynamic functions 0-107445  
NMR, double-quantum, cross-polarization, in solids, theory 0-100623  
plasma, non-LTE, props. and at. processes, medium to high press. 0-59170  
PMMA, glassy atactic, thermodynamic analysis of plastic deform. modes, 150 to 330K 0-84999  
poly-arylate-dimethyl siloxane, polyblock copolymers, struct., thermodynamic stability (Russian) 0-64931  
polyacrylamide, aq. soln., thermodynamic props., light scatt. obs. (Russian) 0-71439  
polyethylene, low density, morphology and props. 0-64926  
polyethylene terephthalate, solid and molten, press. effects on compressibility and crystal., thermodynamic interpret. 0-84102  
polymer chain statics and dynamics, Lennard-Jones interaction, calcs. 0-58425  
polymer solutions, dilute, regularly alternant, thermodynamic props. self avoiding random walk calcs. (French) 0-59369  
polymer spheres, colloidal suspension, steady state shear flow coupled to conc. fluctuations 0-61170  
primitive model electrolytes, symmetrical, canonical Monte Carlo calcs. 0-92428  
quartic anharmonic oscillator, semiclassical and quasiclassical particle function 0-99434  
rare gas clusters, small, structure, thermodynamic properties 0-88341  
semiconductors, temp. depend. electronic cond. 0-59975  
silicate glass, hydration thermodynamics 0-81313  
single phase liquids, thermodynamic stability limit and eqns. of state 0-92037  
small metal particles, thermodynamic props. of electrons 0-59844  
solid, non-hydrostatically stressed, thermodynamics 0-84304  
solid electrolytes and mixed conductors, materials stability and chem. diffusion 0-65292  
spin glass-ferromagnetic phase, mean field theory 0-103841  
steel, mild, laser microspectral anal. 0-108769  
superheated binary solns., flashing kinetics, nucleation and critical bubble 0-92035  
TCNQ complexes, disordered, thermodynamics of random exchange models 0-103826  
temperature in range 0 to 1064°C, International Practical Temperature Scale revision 0-62669  
ternary phase diagrams, interactive computer program 0-71629  
ternary solution phases, empirical methods of predicting and representing thermodynamic props. 0-70423  
unsaturated two-component associated vapour, press., comp., thermodynamic calcs. (Russian) 0-64671  
Van der Waals gases, adiabatic and isothermal spinodal curves 0-92034  
water, compressed, thermodynamic props., evaluation by statistical error anal. 0-92685  
water, Monte Carlo simulation of struct. and thermodynamic props. 0-88017  
water, ordinary and heavy, US vels. thermodynamic props. calc. 0-65156  
Ag-Sn, liquid alloys, thermodynamic props. (Japanese) 0-108396  
AgBr-NaBr, thermodynamic props., metastable states and demixing 0-96660  
 $\alpha$ -AgI, superionic cond., statistical thermodynamic description (French) 0-65281  
Ar, solid, equil. props., uncorrel. pairs approx. 0-84303  
 $\text{BaTiO}_3$ :C, solubility of C at low  $\text{O}_2$  potentials, 800°C 0-100334  
Bi-S liquid soln., S activities meas. by EMF method (Japanese) 0-70425  
BiLi, gas phase thermodynamics, Knudsen effusion mass spectrosc. 0-100057  
 $\text{CaO} \cdot 6\text{Al}_2\text{O}_3$ , thermodynamic stability, reaction with Ti, Cr and Zr oxides 0-92687  
Cd-P, p-T-x phase diagram 0-88300  
 $\text{Co}_{1-x}\text{Al}_x$ , ordered  $\beta$ -phase, enthalpy of formation are defect struct. descript. 0-89519  
 $\text{Co}_2\text{Mg}_{1-x}\text{O}$  system, thermodynamic investigation, 1100 to 1300K (German) 0-107430  
Cr-Fe-Ni,  $\gamma$ -solid soln., thermodynamic activity determ. at 1500K 0-108397  
Cr-Ni-Fe, ternary phase diagrams, interactive computer program 0-71629  
Cr-W-O, phase relations, thermodynamic props. of  $\text{CrWO}_4$  and  $\text{Cr}_2\text{WO}_6$  0-104120  
Cs halides, Gruneisen and Anderson-Gruneisen parameter determ. 0-59611  
 $\text{Ca-SiO}_2$ - $\text{Al}_2\text{O}_3$  system interactions, getter development for radiocaesium 0-83208  
Cu-Ag-O alloys, dil., O-metal interactions, activity coeff. meas. at 1423K 0-93792  
Cu-Au-O alloys, dil., O-metal interactions, activity coeff. meas. at 1423K 0-93792  
Cu-M-O ternary liquid alloys, thermochem. calcs. 0-85209  
Cu-Ni-S, molten, thermodynamic props. 0-104122  
Cu-Pb (Fe), liq., thermodynamic props. (Polish) 0-89199  
Cu-Pt-O alloys, dil., O-metal interactions, activity coeff. meas. at 1423K 0-93792  
Cu-Sn alloy, thermodynamics of Cu and Sn solns. using copper  $\beta$ -alumina solid electrolyte, 800-1100K 0-107502  
 $\text{Cu}_{1-x}\text{Cr}_x\text{Se}_2$ , influence of excess Cu on physical props. 0-103836  
 $\text{Cu}_3\text{Mo}_2\text{S}_8$ , mixed conductor, equil. partial thermodynamic props. 0-85270  
 $\text{EuF}_3$ , thermodynamic data compared with  $\text{SrF}_2$  (German) 0-81355  
EuTe, high-temperature evaporation and reactivity 0-103469



**thermodynamic properties continued**

- Fe-C system, FCC, austenite field thermodynamics, re-anal. 0-89201  
 Fe-Co-Ni-C, activity coeff. of C at 1273K 0-96667  
 Fe-Mo system, thermomech. props. 0-89208  
 Fe-O system, thermodynamics of viustite-haematite alloy melt (*Russian*) 0-65249  
 Fe<sub>3</sub>O<sub>4</sub>, wustite field, thermodynamic props. and subphases, thermogravimetry, 1100-1300°C 0-76239  
 H, spin-polarised, Bose-Einstein condensation 0-77698  
 H<sub>2</sub>, solid, metallic, high density, thermodynamic props. 0-88337  
 HCl, polar liqs. models, mol. polarisability effect 0-92444  
 HF, polar liqs. models, mol. polarisability effect 0-92444  
 H<sub>2</sub>O, acoustic relaxation in critical region (*Russian*) 0-92609  
 I<sub>2</sub>-quinoline (pyridine) complexes, stability const. determ. by spectrophotometric methods 0-87056  
 I<sub>1-x</sub> mixtures, high-temp. solids and melts, struct., thermodynamic props., Raman spectra obs. 0-66174  
 In, liquid O<sub>2</sub> activity from electrochemical meas. 0-104123  
 KCl-CaCl<sub>2</sub>-NaCl, ternary phase diagrams, interactive computer program 0-71629  
 KReO<sub>4</sub>, heat capacity and thermodynamic props., 8 to 304K 0-100335  
 Li-LiH liq.-vap. equilib., activity coeff. 0-103468  
 Li-LiH system, H isotope solubility thermodynamic singularities 0-81356  
 LiF-AlF<sub>3</sub> mixture at 1293K, thermodynamic function 0-104134  
 LiH<sub>2</sub>(LiD<sub>2</sub>)(LiT<sub>2</sub>), pot. surfaces, fundamental freqs. and thermodynamic functions 0-69205  
 Li<sub>2</sub>H(Li<sub>2</sub>D)(Li<sub>2</sub>T), pot. surfaces, fundamental freqs. and thermodynamic functions 0-69205  
 β-Li<sub>2</sub>V<sub>2</sub>O<sub>7</sub> bronze, thermodynamics of ordering 0-84302  
 Mn-bearing binary substitutional alloy systems, props., applicability of statistical thermodynamic approach 0-88336  
 Mo-N solid solution, thermodynamic props., 1618 to 1883K 0-65230  
 NH<sub>4</sub>ReO<sub>4</sub>, heat capacity and thermodynamic props., 8 to 304K 0-100335  
 NO<sub>3</sub>·(HNO<sub>3</sub>)<sub>n</sub> clusters, form. studied by mass spectrometer, thermodynamic functions, sol. struct. 0-95754  
<sup>15</sup>N<sub>2</sub>, solid struct., and thermodynamic props. (*Russian*) 0-88083  
 Na-Cs, liq., struct. factor, free energy of mixing, and electrochem. pot., thermodynamic calc. 0-96436  
 Na-K liquid alloys, triplet correlation functions and thermodynamics, solute partial structure factor 0-64881  
 Na<sub>2</sub>O-B<sub>2</sub>O<sub>3</sub>-GeO<sub>2</sub> glass-forming melts, thermodynamic props. and vapourisation processes, mass spectrometric study 0-79926  
 Na<sub>2</sub>O-B<sub>2</sub>O<sub>3</sub>-GeO<sub>2</sub> vitreous melts, thermodynamic props. from mass spectra 0-65253  
 Na<sub>2</sub>SO<sub>4</sub>-CoSO<sub>4</sub>-H<sub>2</sub>O, phase equilib., activities, Pitzer eqn. calcs. (*Russian*) 0-65190  
 NaTi<sub>3</sub>(SO<sub>4</sub>)<sub>2</sub>, heat capacity and thermodynamic functions, 10 to 300K 0-65244  
 Nb, superconducting, thermodynamic props. 0-107955  
 Ni chemisorption of S on Al<sub>2</sub>O<sub>3</sub>-supported surface, thermodynamic parameters meas. 0-88424  
 Ni-S, phase diagram calc. and thermodynamic props. of liq. phase 0-108401  
 Ni-V, solid soln., diffusion and thermodynamic props. 0-65278  
 Pb-Fe(Cu), liq., thermodynamic props. (*Polish*) 0-89199  
 PbLi, gas phase thermodynamics, Knudsen effusion mass spectrosc. 0-100057  
 Pd-noble metal solid solns., with dissolved H, thermodynamic props. 0-108402  
 SF<sub>6</sub> plasma thermodynamic props. at arc extinction temp. and pressures 0-79435  
 Sb, liquid, diffusion of O<sub>2</sub>, activity coeff. 0-65267  
 SiO<sub>2</sub>-water system, inorg. polymer struct. form., globular crystn. 0-101042  
 SrF<sub>2</sub>, vapourisation and sublimation thermodynamics (*German*) 0-81355  
 Te-In system, enthalpies of fusion, peritectic decomp. and allotropic transition, DTA (*French*) 0-76226  
 Tl, liquid, O<sub>2</sub> activity from electrochemical meas. 0-104123  
 Tl<sub>2</sub>PO<sub>4</sub>, heat capacity and thermodynamic functions, 5 to 320K 0-65245  
 URu<sub>3</sub>, sublimation thermodynamics 0-97722  
 V-W-O system, phase diagram and thermodynamic props. at high temps., in region W-WO<sub>3</sub>-VO<sub>2</sub>-V<sub>2</sub>O<sub>5</sub> 0-104133  
 V<sub>2</sub>O<sub>5</sub>-AlNbO<sub>4</sub>(GaNbO<sub>4</sub>)(TiNbO<sub>4</sub>) systems, interfacial reactions, efficient boundary conditions and solid state reactivity 0-76542  
 Y<sub>3</sub>Fe<sub>5</sub>-Al<sub>2</sub>O<sub>3</sub>, mixed garnet, cation distrib., temp. depend., magnetisation study 0-79831  
 Y<sub>3</sub>Fe<sub>5</sub>-Ga<sub>2</sub>O<sub>12</sub>, mixed garnet, cation distrib., temp. depend., magnetisation study 0-79831  
 YbTe, high-temperature evaporation and reactivity 0-103469  
 Zn-Sn-Bi, ternary phase diagrams, interactive computer program 0-71629  
 ZnCl<sub>2</sub>-LiCl(NaCl)(KCl)(CsCl), molten, US velocity, thermodynamic quantities and struct. (*Japanese*) 0-88270

**thermodynamics**

- see also *atmospheric thermodynamics; critical phenomena; entropy; equations of state; Joule-Thomson effect; statistical mechanics*  
 ϕ<sup>4</sup> lattice field theory, d-dimens., thermodynamic props. near Ising limit 0-82860  
 acceleration through random classical radiation, thermal effects 0-73191  
 adsorption phenomena, thermodynamic theory 0-93794  
 amorphous Heisenberg and Ising chains, thermodynamics 0-108022  
 atomic system, two-level, collective behaviour in external field, thermodynamics 0-86236  
 BBGKY system, irreversibility, velocity correlations and non-Hamiltonian dynamics 0-77686  
 binary mixtures near critical state, gravitational distrib. of thermodynamic props. (*Russian*) 0-88241  
 binary solutions of dense liquids and gases, isothermal eqn. of state calcs. (*Russian*) 0-88292  
 black planet, surface Contact interaction 0-85877  
 blackbody cavities, directional emissivity calc., Monte Carlo method 0-83729  
 boundary conditions, spherical, for computer experiment 0-105597  
 chain subduction criterion, continuous phase transform, Landau thermodynamic methods 0-62606  
 charge fluctuations in classical Coulomb systems 0-95027  
 chemically assisted fracture, general reaction rate theory and thermodynamics 0-64465  
 coal conversion reactor environments, simulation 0-100831

**thermodynamics continued**

- complex solids, energy-momentum tensor, nonequilibrium relativistic dynamic eqns. (*Russian*) 0-57236  
 compressed gas, radial distrib. function hard sphere model 0-69961  
 conductors, rigid, thermodynamic anal., hyperbolic heat conduction eqn. 0-64334  
 contact transformations and brackets in classical thermodynamics 0-95048  
 continuous media, intrinsic parameters schematising shape and stress, Lagrangian formulation (*French*) 0-73173  
 coupled heat and mass transfer, stability, inertial wave effects calcs. 0-105593  
 cryogenic He cycles, minimal losses due to thermodynamic irreversibility 0-86320  
 crystal lattice stability and deform. phase transitions under press. 0-59624  
 cycle operating between positive and negative absolute temps. (*Chinese*) 0-62610  
 cylindrical gas system, rotating and self gravitating, thermodynamic instability 0-82191  
 Dicke maser model-van der Waals spin system thermodynamic equivalence 0-83572  
 differential type media with internal variables, thermodynamic theory 0-99923  
 dipole relaxation in electric field, teaching 0-90625  
 dislocations, thermodynamics and thermal activation, book contrib. 0-107241  
 dissipative flux and Onsager-Machlup function fluctuations 0-76544  
 Eckart's relativistic temp. gradient 0-103080  
 education, human body, live, thermodynamics of cooling for treatment purposes 0-73128  
 elastic-plastic constitutive theory, thermodynamic treatment 0-64390  
 elastically coupled systems at marginal dimensionalities, crit. dynamics and stability 0-101769  
 entropy prod. of extended irreversible thermodynamics, invariant transforms. 0-73293  
 enzyme-catalysed reactions, network thermodynamic modelling 0-89463  
 equilibrium chemistry in primitive solar nebula 0-82231  
 eutectoids(ic), lamellar, stability principles 0-89195  
 FCC crystal-melt interfaces, mol. dynamics simulation 0-79913  
 ferroactive thin films, physical prop. optimisation 0-80698  
 ferroelectrics, incommensurate polar phase form. 0-71344  
 ferromagnet, magnetic susceptibility, spin and charge density waves, Curie temp. (*Russian*) 0-100581  
 ferromagnetic crystal, spin subsystem thermodynamics, spin-phonon interactions, mag. order parameter 0-103848  
 fluid system, electric conduction in relativistic thermodynamics 0-105498  
 Fokker-Planck model, transport equation renormalisation 0-82732  
 foreign gas induced line shifts, thermodynamics 0-106295  
 Frisch-Lloyd random system, low-lying electronic tail spectrum by path integral method and coherent state representation variational method 0-105580  
 gas flows, entropy prod. determ. using Boltzmann's H-theorem, Knudsen effusion 0-106867  
 generalised mean suggested by equilib. temp. 0-86237  
 generalised one-dimens. oscillator, second order Wigner-Kirkwood semiclassical partition function and thermodynamic functions 0-62601  
 geothermal technology, development into an exact science 0-61781  
 glasses, dielectric relax., order parameter model appl. 0-108151  
 hard sphere system in equilibrium, two-dimens. hard disk system 0-107033  
 heat engines, chemically driven, finite time thermodynamics 0-76541  
 heat engines using liquids, thermodynamic principles 0-83730  
 heat flux fluctuations, Fokker Planck eqn. in extended irreversible thermodynamics 0-86205  
 heater gas in cylinder with piston, maximum work production determ. 0-79129  
 industrial gaseous environment characterisation, Brinkley method 0-93817  
 information theoretic approach, exptl. and inherent uncertainties 0-82733  
 interstitial defects, migration kinetics and thermodynamics 0-107461  
 irreversible, internal variable theory, Lagrangian formulation 0-73291  
 irreversible, near equilib., metric geometry 0-62604  
 irreversible thermodynamics, extended, hydrodynamical fluctuations 0-86235  
 laser pumping system, thermodynamic calc. method 0-58551  
 lattice gas, phys. correl. factor in Nernst-Einstein relation 0-105591  
 lattice systems, thermodynamic limitations, on interaction topologies 0-57217  
 linear microscopic equations in irreversible thermodynamics, eigenvalue problem 0-57227  
 liquid crystals, generalised Suzuki formula application (*Chinese*) 0-107045  
 liquids, dielectric relax., order parameter model appl. 0-108151  
 liquids, simple, thermodynamically self-consistent theories, radial distrib. function, functional derivative 0-92435  
 liquids and mixtures, statistical thermodynamics, book 0-90616  
 macroscopic theory of statistical thermodynamics 0-105567  
 magnetic objects, current loops, thermodynamics, teaching 0-90633  
 Markovian processes and irreversibility, hydrodynamic equations, stress tensor and local eqn. 0-82720  
 Markovian processes and irreversibility, hydrodynamic equations from constitutive equations 0-82721  
 materials with memory, thermodynamics 0-64356  
 mathematical inequality derivation from first and second laws 0-57229  
 memory alloy engine, efficiency 0-71648  
 metastable states close to instability, phase transition parameter eqn. of motion 0-57230  
 micropolar fluids, thermodynamical aspects, non-linear approach 0-105598  
 N<sub>2</sub>O refrigerator, thermodynamics and thermoelectric condenser design 0-108809  
 negative ions, sputtered, characteristic electronic and vibrational temp., laser photoelectron spectral meas. 0-66346  
 neutrino emission from blackbody, thermodynamic laws, teaching 0-105451  
 non-equilibrium thermodynamic systems theory 0-105595  
 nonequilibrium steady states, irreversible processes, Lyapunov functions 0-95049  
 nonequilibrium open systems, state variable contraction 0-105600



**thermodynamics continued**

nonequilibrium superconductor, normal component drag by condensate, tunnelling (*Russian*) 0-93051  
 nonequilibrium systems with memory, vector-valued actions 0-86232  
 nonequilibrium thermodynamics, stochastic measures 0-86240  
 nonisothermal rigid shell theory using fundamental laws of thermodynamics 0-87712  
 one component classical charged particle gas, thermodynamic grand function using collective coordinates 0-73289  
 one-dimensional solitary-wave-bearing scalar fields, statistical mechanics, ideal-gas phenomenology 0-105792  
 Onsager-Casimir symmetry, Markovian processes and irreversibility. The Onsager-Casimir symmetry 0-62580  
 open quasi-free systems, time evolution 0-95030  
 open system, current-carrying states in quantum statistics 0-90802  
 open systems, definitions of heat, internal energy transfer by convection 0-69644  
 Ott relativistic temperature variation, comment on derivation 0-86084  
 partition function, modified Lippmann-Schwinger variational principle 0-86233  
 permafrost on Mars 0-67621  
 phase transitions, group theoretical methods rel. to problems of classical Landau theory 0-73292  
 phase transitions, induced by several order parameters, thermodynamic parameters 0-103457  
 phase transitions with two order parameters, Landau theory, mag. reorientation 0-103456  
 photon emission from blackbody, thermodynamic laws, teaching 0-105451  
 plasma, low-temp., with nonequilibrium ionisation, review 0-96343  
 polydisperse solution of rodlike particles, isotropic-nematic phase transition, Onsager theory 0-100324  
 polymers, stressed, thermodynamically controlled cryst. orientation 0-84112  
 porous media models using thermodynamics of mixtures 0-96184  
 principle of maximum entropy and irreversible processes, review 0-86198  
 principles, book 0-73122  
 PTFE grafted membranes, struct.-properties relationships, bifunctionality (*French*) 0-61137  
 quadratic mass action system, irregular oscills. 0-62611  
 quantum channelling theory, channelled particle multiple scatt. by electrons, contrib. to dechannelling rate 0-107350  
 quantum harmonic oscill. chain, relaxation dynamics (*Russian*) 0-94992  
 rarefied shock wave existence near thermodynamic critical point of a substance (*Russian*) 0-88263  
 relations of continuum mechanics for irreversible processes 0-101715  
 resonance phase transition in two-level lattice system, thermodynamics 0-69351  
 reversible state space, geometric invariant representation (*Chinese*) 0-101771  
 rotational like degrees of freedom system, phase transitions, thermodynamic props. 0-77737  
 Saha equation, elementary derivation, rel. to mol. dissoc. 0-82599  
 semiconductors, thermally stimulated relaxation processes, book contribution 0-80295  
 simple fluid, struct. and thermodynamics, Monte Carlo calcs. 0-59365  
 size effect, thermodynamical model for constrained and unconstrained bodies 0-58900  
 solar coronal loops, thermal equilibrium 0-94773  
 solar water pump for lift irrigation, thermodynamic anal. and simulation 0-61397  
 solid lattice thermodynamics, two-temp. Debye approx. (*Russian*) 0-77728  
 solid-fluid interface, wetting and adhesion, thermodynamic aspects 0-89525  
 stars containing mixed poloidal and toroidal mag. fields, adiabatic stability 0-67706  
 steel powder, high speed, S and O reduction in a H<sub>2</sub> gas stream 0-61015  
 stress corrosion cracking failure, predictive approaches 0-97611  
 superconductor nonequilibrium state stability with respect to finite fluctuations 0-103782  
 supernovae, thermodynamic of nucleon, lepton, photon mixture, quantum mechanical calcs. 0-77273  
 surface thermodynamics, fundamental eqns. 0-107630  
 systems far from thermodynamic equilib., dissipative structures, broken symm. equilib. phase transition theory 0-65827  
 theory of constrained mixtures with multiple temperatures 0-62600  
 thermal cycling, thermodynamics appl. in mathematical anal. 0-108530  
 thermodynamic energy conversion efficiencies 0-101081  
 thin films, precipitation and nuclei form. in presence of condensation centres, thermodynamic model 0-103594  
 thiourea, incommensurable phase transitions. thermodynamic pot. 0-79941  
 two dimensional real matter, low density free energy in canonical thermodynamics plasmas 0-87852  
 type I superconductor, magnetisation in thermodynamic and metastable phases 0-93027  
 vacuum bubble evaporation and thermodynamics, surface oscill. consideration 0-62608  
 viscous fluids, nonstationary relativistic thermodynamics, hidden variable approach 0-68097  
 water, Brillouin light scatt., temp. gradient induced 0-100663  
 Weinhold's length, significance 0-98866  
 BaO-B<sub>2</sub>O<sub>3</sub>-V<sub>2</sub>O<sub>5</sub> glass, oxidation-reduction of V, thermodynamics 0-85169  
 BaTiO<sub>3</sub> type crystal, thermodynamic analysis of struct. phase transitions (*Russian*) 0-103473  
 C-C interaction energy, thermodynamics of steels 0-93793  
 Cu liquid, thermodynamic study of O<sub>2</sub> 0-88342  
 Fe-Cr-Ti(Al) liquid alloys, thermodynamical anal. of O<sub>2</sub> solubility (*Russian*) 0-92676  
 GaAs, homogeneity region calc. 0-92681  
 GaSb, defect concentration determ. model, Hall effect 0-103385  
 HF-HCl, SCF energy hypersurface, stationary points, thermodynamics of form. 0-102436  
 H<sub>2</sub>O pyrolysis, solar-H<sub>2</sub> energy systems, theory 0-61448  
<sup>3</sup>He fluid-superfluid transition phase diagram, thermodynamic stability, fluctuations (*Russian*) 0-80023  
 Si-Au system, ion implanted induced giant gettering, annealing effects 0-88221  
 Si<sub>3</sub>N<sub>4</sub>, low pressure CVD, thermochemical calcs. 0-108356

**thermodynamics continued**

SiO<sub>2</sub>, low pressure CVD, thermochemical calcs. 0-108356  
 $\alpha$ -Ti/Fe, retrograde solid solubility 0-79950  
 TiO<sub>2</sub>:TeCl<sub>4</sub> system, chem. vapour transport, matrix isolation IR studies 0-93755

**thermoelasticity**

see also *thermal stresses*  
 after-effects in thermo-elasticity 0-106724  
 anisotropic media, uniqueness theorem for generalised thermoelasticity equations 0-92062  
 Barber, boundary conditions for thermoelastic contact, heat flows 0-69745  
 bodies with wavy surfaces, thermoelastic contact, heat conduction 0-64492  
 Born model, electrostriction rel. to dielec. and thermoelastic props. 0-71322  
 boundary value problems, exterior, 2-D (*French*) 0-79144  
 cavity, ellipsoidal, triaxial, thermoelastic stresses 0-92061  
 circular plates with piecewise-constant thickness 0-99935  
 contact, frictionally heated, thermoelastic deform. 0-83764  
 contact, thermoelastic, involving a sharp corner 0-83766  
 coupled dynamic thermoelasticity problem for a half space with thermal 'memory', thermoelastic waves 0-83753  
 cracks, penny-shaped, in elastic sphere embedding in infinite elastic space, thermal stresses 0-64460  
 crystal growth, creation of stress and dislocations (*Russian*) 0-103277  
 cylinder, circular, three-dimensional transient thermal stresses under nonaxisymmetric temp. distrib. 0-92054  
 deformation, second order effects 0-92051  
 diffraction problems in exterior domain, existence and uniqueness theorems, series expansion of potentials (*French*) 0-64366  
 dynamic theory, based on causality principle 0-69657  
 dynamical properties of thermoelasticity problems solutions (*Ukrainian*) 0-69663  
 elastic wave excitation by laser beam, through thermoelastic effect 0-103503  
 elastohydrodynamic traction, non-Newtonian thermo-viscoelastic, from combined slip and spin 0-103043  
 epoxy resin and glass, thermoelastic phenomena (*Polish*) 0-93724  
 graphite shell, thin, cylindrical, orthotropic, thermal stresses and displacements due to instantaneous thermal shock 0-92060  
 Gruneisen parameter and thermal diffusivity, thermoelastic meas. method 0-107581  
 half-space, dynamic response to energy flux, stress wave evolution (*French*) 0-74795  
 hard sphere crystal, thermoelasticity in relation to melting 0-107353  
 heat memory materials, dynamic thermoelasticity of infinite cylindrical rod (*Russian*) 0-74752  
 infinite medium containing periodic ribbon-like inclusions, local intensification of thermal stresses (*Japanese*) 0-96195  
 laminated plates, symmetric, specially orthotropic, thermoelastic anal. 0-92058  
 laminates, residual thermoelastic stresses 0-106721  
 linear, continuous depend. and instability 0-74783  
 memory alloy engine, efficiency 0-71648  
 micropolar thermoelastic space, travelling discontinuities 0-92055  
 noble metals, thermoelastic relax., interaction of thermal and acoustic phonons calcs. for US longitudinal waves 0-65165  
 plates, thick, multiply connected, stressed-strain state under nonstationary heat conditions (*Russian*) 0-87714  
 polyvinyl alcohol networks, swelling equil. with dil. salt solns., thermoelastic behaviour, hydroxyl group interact. 0-79667  
 polyvinyl alcohol swollen in aqueous glycol, network thermoelasticity, interactions 0-104201  
 rod of time hardening (softening) material, thermoelastic stresses 0-92046  
 rubber cylinder, circular, uniformly heated, combined extension and torsion 0-92057  
 second order thermo-microelasticity 0-74742  
 second-order phase transitions in crystals, equilibrium configurations, thermoelasticity theory 0-70364  
 semifinite plate, thermal stresses, heat transfer effect 0-96193  
 shell of revolution, corrugated, thermoelastic plastic deform. at finite displacements 0-74772  
 shells, cylindrical, anisotropic, quasistatic thermoelastic eqns. 0-92059  
 size effect, thermodynamical model for constrained and unconstrained bodies 0-58900  
 slab, flat, steady state thermoelastic boundary value problem 0-92052  
 slab containing annular crack, thermal stresses, integral transform techniques 0-96229  
 sphere sliding on plane, transient thermoelastic contact 0-83765  
 stationary vibrations in 2-dimensional micropolar thermoelasticity 0-74793  
 Stepanov method shaped cryst. growth, physical problems, thermoelastic stresses 0-103279  
 strain driven thermoelastic instability toward brittle fracture 0-103415  
 thermoelastic cracks in plane, boundary integral eqn. method (*German*) 0-106761  
 thermomechanical constraint, internal, constitutive equations, material anisotropy 0-58897  
 thermoviscoelastic laminate beam, stress anal. (*German*) 0-106727  
 thin walled elements, unbound quasistatic random thermoelastic fields, oscillations 0-69673  
 three-layer cylindrical shells, thermoplastic stress state 0-96204  
 transition, thermoelastic, from line to point contact 0-83768  
 tubes, thick-walled, thermoelastoplastic creep stress anal. 0-58922  
 uniqueness theorem and variational principle 0-92056  
 water, vapourisation and thermoelastic press. due to CO<sub>2</sub> laser pulse 0-84227  
 Fe-Ni-Cr-Ti-Al, with thermoelastic control coeff., comp. and heat treatment influence on props. (*French*) 0-81074  
 Fe-Pd (31.2 wt.%), thermoelastic FCC-FCT martensitic transformation 0-104156  
 GaAs, pulled, dislocation generation, thermoelastic anal. 0-79787  
 GaP, crystal, growth conditions rel. to dislocation struct. 0-88151  
 GaS, elastic prop. anisotropy, Debye temp. (*Russian*) 0-88244  
 GaS(Te)(Se), elastic characteristics, Debye temp., ultrasonic study (*Russian*) 0-79872  
 Ge ribbon single crystals, grown from melt, dislocation struct. form. under thermal stress 0-107082



**thermoelasticity continued**

- LiO<sub>3</sub> crystal, SHG, thermoelastic stresses and nonlinear refract. effect 0-74437
- $\alpha$ -Ti, strain driven thermoelastic instability toward brittle fracture 0-103415
- Zn, growth from melt, conditions influencing dislocation struct. (*Russian*) 0-97424

**thermoelectrets**

- cellulose, dielec. relax. studies, TSD meas. 0-88907
- diamagnetic anisotropy of thermoelectret and magnetolectret states 0-97053

**thermoelectric conversion**

- see also *thermoelectric devices*
- alloys, thermoelectric, phase diagrams and imperfection chemistry 0-108422
- attainable efficiency values determ. 0-94094
- heat pumps, two-stage, design criteria anal. for cool-down speed maximisation 0-108812
- isotopic microgenerator design and construction optimisation due to min. power 0-108813
- materials for thermoelectric conversion of solar energy (*French*) 0-89660
- multijunction thermal converters for AC-DC transfer standards 0-98874
- multijunction thermal converter AC/DC transfer, Thomson effect error reduction 0-103679
- Peltier effect, heat losses due to thermal cond. 0-107773
- selenide thermoelectrics, analytical model for performance and degradation predictions 0-108805
- solar thermoelectric generator panels, energy characts., estimation 0-101123
- solar thermoelectric generator using tubular heat-pipe with concentrator 0-89658
- solar thermoelectric generators, metallic thermo-electric materials utilisation, economic characts. 0-101122
- solid state energy conversion, appl. of solid state cooling to spaceborne IR focal planes 0-107772
- thermal Albedo Energy Converter, concept, design and testing for high altitude long endurance platforms 0-108789
- thermoelectric devices, design, construction and characteristics for high efficiency 0-108806
- thermoelectric energy conversion, conf., Arlington, TX, USA 0-107779
- thermophotocell, design and calculations 0-97800
- Bi-Te thin thermoelectric films prep. by solid state reaction method 0-108361
- $\delta$ -Bi<sub>2</sub>O<sub>3</sub>, thermoelectric power, heat of transport of O<sup>2-</sup> ions 0-92713
- Bi<sub>2</sub>Te<sub>3</sub> alloy thermocouples for solar thermoelectric conversion 0-94095
- (Bi<sub>2</sub>Te<sub>3</sub>)<sub>0.9</sub>(Sb<sub>2</sub>Te<sub>3</sub>)<sub>0.5</sub>(Sb<sub>2</sub>Se<sub>3</sub>)<sub>0.05</sub> n-type alloy for thermogenerators, thermo-EMF, elec. cond. and thermoelec. efficiency factor, 300-600K 0-70735
- GaAs/Au-Ge-Ni alloy metal-semiconductor thermoelectric coolers, effects of contact resist. and dopant conc. 0-81481
- Si-Ge, high temperature thermoelectric materials 0-89659
- Si-Ge thermoelectric generators, approximation errors when using averaged properties solutions for required heat rates estimation 0-108808

**thermoelectric devices**

- see also *thermocouples; thermoelectric conversion; thermopiles*
- calorimetry, applications of thermoelectric devices in various types of calorimeters 0-105648
- cooler, single stage, finite element thermal stress anal. 0-108807
- cooling equipment, welded joints, heat emission effects on temp. distrib. (*Russian*) 0-69635
- design, construction and characteristics for high efficiency 0-108806
- Gipospast-1, thermoelec. apparatus for local hypothermia 0-104807
- heat pumps, cross flow, anal. of operation and performance using mathematical model 0-107836
- heat pumps, single-stage, simplified method for optimization 0-108811
- heat pumps, two-stage, design criteria anal. for cool-down speed maximisation 0-108812
- metal-semiconductor thermoelectric coolers, effects of contact resist. and dopant conc. 0-81481
- N<sub>2</sub>O refrigerator, thermodynamics and thermoelectric condenser design 0-108809
- needle probe for medical and biological temp. meas. 0-101299
- spacecraft heat rejection improvements using thermoelectric devices 0-108810
- thermoelectric energy conversion, conf., Arlington, TX, USA 0-107779
- thermometer, Pt-Rh, 1300 to 1700°C, errors obs. and analysis 0-77783
- thermometer, temperature meas. of moving metal objects (*Russian*) 0-90848
- type RTN (USSR), construction and characts. 0-57372
- BiSb (>20 wt.%), electronic band struct. 0-107698

**thermoelectric effect** see *thermoelectricity***thermoelectric effects in metals and alloys**

- alkali metals, liq., Fermi energy, density of states, electronic props., exchange and correl. effects 0-96774
- alkali metals, thermopower and elec. cond., relationship at low temps. (*Russian*) 0-92882
- amorphous alloys, mag. and nonmag., thermoelec. power, 15 to 580K 0-80255
- antiferromagnetic metal, thermoelec. power in mag. field 0-70686
- dilute alloy, perturbation expansion for the asymmetric Anderson Hamiltonian 0-80202
- dilute alloy, Seebeck coefficient, electron-phonon enhancement 0-70685
- eutectics, HgTe-PbTe and Au-PbTe, prep. and thermoelectric behaviour characts. 0-107774
- liquid metals of groups IIB, IIIB, and IV, thermoelectric power, pseudo-potential calc. 0-59959
- polycrystalline-thin metal films, thermoelectric power, mean free path model 0-107770
- semimetals, degenerate, heat conduction, thermal EMF, Lorenz number anisotropy at low temp. 0-75549
- spin glasses, elec. resist., thermal resist. and thermopower 0-65542
- steel, ferrite-austenite transition, diffusion cons. of C and carburisation rate cons., thermopower meas. 0-89216
- thermoelectric devices, design, construction and characteristics for high efficiency 0-108806
- thermoelectric energy conversion, conf., Arlington, TX, USA 0-107779
- thermoelectric materials, B<sub>2</sub>C<sub>3</sub> and (B<sub>2</sub>Si)<sub>2</sub>C<sub>3</sub> P-type LaS<sub>x</sub> N-type alloys, fabrication and thermoelectric props. 0-107771
- thin films, conductor covered with electrolytic deposit, thermoelectric props., thermal flux meas. (*French*) 0-59961

**thermoelectric effects in metals and alloys continued**

- thin films, grain boundary and surface scatt., statistical model 0-103762
- thin films, thermoelectric power, thermal stress effects, theory 0-65714
- Ag, low temp. resist. and thermoelec. ratio, electron-electron scatt. contrib. 0-70670
- Ag, virtual bound states due to 4d- and 5d-transition metal impurities 0-70667
- Ag-Mn, conc. spin glasses, thermopower 0-65538
- Al, low temp. resist. and thermoelec. ratio, electron-electron scatt. contrib. 0-70670
- Al, pure and dil. alloys, diffusion thermopower, inelastic electron-phonon interaction 0-96851
- Au, low temp. resist. and thermoelec. ratio, electron-electron scatt. contrib. 0-70670
- Au, virtual bound states due to 4d- and 5d-transition metal impurities 0-70667
- Au-Mn(Cr)(Fe), conc. spin glasses, thermopower 0-65538
- Bi, thermal EMF giant quantum oscils. (*Russian*) 0-59960
- Bi-Sb, thermal EMF giant quantum oscils. (*Russian*) 0-59960
- Co<sub>x</sub>(Ni<sub>0.5</sub>Cu<sub>0.5</sub>)<sub>1-x</sub>Fe<sub>2</sub>O<sub>4</sub> ferrite, relation between elec. cond. and mag. anisotropy 0-75548
- Cr-Mo, elec. resist. and thermo-EMF, conc. depend., 4.2 to 1500K (*Russian*) 0-80247
- Cu, low temp. resist. and thermoelec. ratio, electron-electron scatt. contrib. 0-70670
- Cu-concentration junctions with solder, shock-induced elec. response 0-75626
- Eu, electrical resistivity of solid and liquid phases, thermopower, melting temp. 0-59955
- EuGd<sub>2</sub>S<sub>4</sub>, nonstoichiometric, elec. transport props., semicond. and metallic cond. 0-107786
- EuO(Se), complex elec. cond. anomalies 0-107812
- Eu<sub>1-x</sub>Sm<sub>x</sub>S, ESR, exchange interaction, susceptibility, elec. cond., thermoelectric power 0-93174
- Fe-Cr-Al, Kanthal films, vac. deposited, evaporation characts., comp. struct. and elec. props. 0-88646
- Fe-Ni films, on glass substrate, thermoelec. effect 0-107769
- Fe<sub>2</sub>Ni<sub>80-x</sub>B<sub>20</sub> glass, resist., magnetoresist., and thermoelec. power 0-70681
- Fe<sub>2</sub>Ni<sub>80-x</sub>P<sub>14</sub>B<sub>6</sub> glass, resist., magnetoresist., and thermoelec. power 0-70681
- In, supercond., expt. study of thermoelectricity 0-60138
- Ir-Fe, spin fluctuation alloy, thermopower peak diffusion origin 0-88542
- K, low temp. resist. and thermoelec. ratio, electron-electron scatt. contrib. 0-70670
- Li-Pt, phase diagram for comp. range 0-40 at.% Pt, mag. and elec. props. (*German*) 0-84912
- Mo-Nb (Re), thermoelec. power, 4.2 to 300K 0-70683
- Mo-V, elec. resist. and thermo-EMF, conc. depend., 4.2 to 1500K (*Russian*) 0-80247
- Nb-Zr, thermoelec. power, 4.2 to 300K 0-70683
- Ni(Fe,Cr) and Ni<sub>2</sub>(Fe,Cr), electron states density model and mag. characts. calcs. (*Russian*) 0-92804
- Os, thermal EMF quantum oscils. (*Russian*) 0-88543
- Pb, pure and dil. alloys, diffusion thermopower, inelastic electron-phonon interaction 0-96851
- Pd-Co (0.1-45.7 at.%), thermo EMF at 4.2-300K (*Russian*) 0-92881
- Pd-Fe (0.54-8.0 at.%), thermo EMF at 4.2-300K (*Russian*) 0-92881
- Pd-Ni, spin fluctuation alloy, thermopower peak diffusion origin 0-88542
- Pd-Ni (15-90 at.%), thermo EMF at 4.2-300K (*Russian*) 0-92881
- ScAl<sub>2</sub>-Eu, intermediate valence on Eu ions, Mossbauer isomer shift 0-84587
- Si-Ge thermoelectric generators, approximation errors when using averaged properties solutions for required heat rates estimation 0-108808
- Ta-W, thermoelec. power, 4.2 to 300K 0-70684
- TbZn, ferromag., thermoelec. power, temp. depend. and crit. behaviour 0-96852
- $\alpha$ -Ti alloys VT1 and VT5, struct. and phys. props., H<sub>2</sub> effect 0-108576
- UMn<sub>2</sub>, transport props., influence of lattice distortion 0-100452
- W-Re alloys, thermal EMF instability, heat treatment effects 0-75553
- Y, electrical resistivity of solid and liquid phases, thermopower, melting temp. 0-59955
- YIG:Ca, oxidising effects of high temp. annealing in reducing atmosphere 0-66696

**thermoelectric effects in semiconductors and insulators**

- ambipolar semiconductors, thermoelectric redistribution of carriers 0-107830
- amorphous semiconductors, electronic transport mechanisms and coeffs. 0-80282
- anisotropic thermoelement, synthetic media, thermo-EMF 0-92918
- graphite, thermoelectric power, low temperature, anomaly rel. to phonon drag 0-65610
- heat pulse technique for bonding thermoelectric modules contacts 0-107904
- Kane semiconductor films, thermomag. and thermoelec. effects, theory 0-70864
- multilayer thin film struct. thermoelec. props. 0-92964
- polyacetylene:AsF<sub>6</sub>, thermopower and transport props. 0-65611
- polyacetylene, doped, elec. cond. and thermopower 0-96951
- polyacetylene, variable density, synthesis, elec. cond., thermopower 0-60016
- polypyrrole films, electrochemical prep., chem. and phys. characterisation 0-70708
- proton semiconductors, with H-bonds, quantum theory of proton cond. 0-65641
- rare earth chalcobismuthites, RBiTe<sub>3</sub>, prep., elec. props., and crystallographic data 0-59981
- ruthenates, ACu<sub>3</sub>Ru<sub>4</sub>O<sub>12</sub>, A=Na,Ca,Sr,Cd,La,Pt,Nd, synthesis, cryst. struct., mag. and elec. props. (*French*) 0-107151
- selenide thermoelectric materials, thermal conductivity, long-term stability and other props. experimental anal. 0-107834
- semiconducting thermoelement as a medium containing hot electrons 0-107829
- semiconductor, photothermal cond., low temp. depend. 0-70756
- semiconductors, amorphous, doped, electronic props. 0-80283
- semiconductors, thermoelectrically anisotropic, carrier kinetics at low temp. 0-92893
- semiconductors, thermoelectrically anisotropic 0-92894
- TiCN salt, dibenzo-TTF-TiCNQCl<sub>2</sub>, one-dimens. mag. semicond., mag. and elec. props. 0-88601



# thermoelectric effects in semiconductors and insulators continued

thermoelectric heat pumps, cross flow, anal. of operation and performance using mathematical model 0-107836

AgI group superionic conductor, phase transition detection by thermoelectric power method 0-92669

AgI-Cd, polycrystalline, thermoelectric power meas. 0-59698

Ag<sub>2</sub>Sb<sub>2</sub>Te<sub>3</sub>, single-phase, thermoelectric efficiency 0-107826

As<sub>2</sub>S<sub>3</sub> glasses, DC elec. cond. and thermo-elec. power 0-96865

As<sub>2</sub>Sb<sub>1-x</sub>, semimetal, thermopower, thermomagnetic power, 4.5 to 77K 0-107825

As<sub>2</sub>Sb<sub>2</sub>Se<sub>3</sub> glassy semiconductors, electronic props. 0-103712

B-Si materials for thermoelectric conversion of solar energy (French) 0-89660

BP film, high temp. thermoelec. power, scattering processes 0-80305

Bi bounded semimetals, phonon two-stage drag of electrons, thermoelectric power, scatt. mechanism 0-92919

Bi, thermoelectric power, electronic thermal cond., in mag. field 0-60015

δ-Bi<sub>2</sub>O<sub>3</sub>, thermoelectric power, heat of transport of O<sup>2-</sup> ions 0-92713

δ-Bi<sub>2</sub>O<sub>3</sub>, thermoelectric power rel. to fast ionic conduction 0-107549

δ-(Bi<sub>2</sub>O<sub>3</sub>)<sub>1-x</sub>(Y<sub>2</sub>O<sub>3</sub>)<sub>x</sub>, thermoelectric power rel. to fast ionic conduction 0-107549

Bi<sub>0.85</sub>Sb<sub>0.15</sub>, semiconducting transport props., 2 to 100K 0-59989

Bi<sub>2</sub>-Sb<sub>2</sub>Te<sub>3-y</sub>Se<sub>y</sub>, elec. cond. and thermoelec. props., neutral defects influence 0-60017

Bi<sub>2</sub>Te<sub>3</sub>-Bi<sub>2</sub>Se<sub>3</sub> solid solns., single cryst. growth and thermocouple construct. 0-104056

Bi<sub>2</sub>Te<sub>3</sub>-Bi<sub>2</sub>Se<sub>3</sub>-Sb<sub>2</sub>Te<sub>3</sub>, solid solution, single crystal, elec. cond., thermoelectric props. 0-88550

(Bi<sub>2</sub>Te<sub>3</sub>)<sub>0.9</sub>(Sb<sub>2</sub>Te<sub>3</sub>)<sub>0.5</sub>(Sb<sub>2</sub>Se<sub>3</sub>)<sub>0.05</sub> n-type alloy for thermogenerators, thermo-EMF, elec. cond. and thermoelec. efficiency factor, 300-600K 0-70735

p-CdSnAs<sub>3</sub>, Hall effect, thermo EMF, thermomagnetic effects 0-107822

Cd<sub>2</sub>Zn<sub>1-x</sub>S films, chem. sprayed, carrier density and mobility 0-60121

Co<sub>2</sub>RhS<sub>4</sub>, mag. semicond., mag. and elec. props. 0-93121

(Cu<sub>2</sub>Ag)<sub>2</sub>Se/(Bi<sub>2</sub>Sb)<sub>2</sub>Te<sub>3</sub>, P type selenide segmented element fabrication, thermoelectric props. 0-107835

p-CuInSe<sub>2</sub>, thermal props. 0-96705

CuWO<sub>4</sub>, elec. cond., thermoelectric power and dielectric constant temp. depend. 0-96886

EuB<sub>6</sub>, electronic struct., transport and mag. props. 0-96782

EuGd<sub>2</sub>S<sub>4</sub>, nonstoichiometric, elec. transport props., semicond. and metallic cond. 0-107786

FeRh<sub>2</sub>S<sub>4</sub>, mag. semicond., mag. and elec. props. 0-93121

Fe<sub>2</sub>S<sub>3</sub>, pyrrhotite, thermocond. and thermoelec. power 0-96926

GaAs, electrical conductivity and thermoelectric power charge due to melting 0-100490

GaAs, H<sup>+</sup> irradiation, effect on electrical props. 0-65567

Ga<sub>1-x</sub>Mn<sub>x</sub>Sb, elec. cond., mag. susceptibility, Hall const., and thermo-EMF, 80 to 1000K (Russian) 0-88549

Gd<sub>2</sub>O<sub>3</sub>, B-type monoclinic, DC(AC) elec. cond., thermoelectric power, dielectric const., temp. depends. 0-59980

Gd<sub>2</sub>Se<sub>3</sub>/PbTe, N type selenide segmented element fabrication, thermoelectric props. 0-107835

G, photothermal cond., low temp. depend. 0-70756

n-Ge, thermoelec. power in quantising mag. field, phonon-phonon interactions 0-107832

Ge:P, phonon drag thermoelectric power at low temp. 0-107828

N-Ge-Bi-Se glass, elec. and optical props. 0-65550

Ge<sub>20</sub>Bi<sub>80-x</sub> semicond. glass, resist., thermoelec. power, optical absorpt. 0-88555

Ge<sub>20</sub>Bi<sub>80-x</sub>Te<sub>10</sub>, semicond. glass, resist., thermoelec. power, optical absorpt. 0-88555

Hg<sub>1-x</sub>Cd<sub>x</sub>Te-type semimetals, kinetic props., local acceptor level effects 0-65557

InAs, electrical conductivity and thermoelectric power charge due to melting 0-100490

In<sub>1-x</sub>Ga<sub>x</sub>Sb films, elec. props., preparation 0-100473

Inf, electron transport props., mag. field and temp. depend. 0-92888

InSb, thermal cond., elec. cond., and thermoelec. power, press. depend. 0-59744

InTe thin films, flash evaporation, electrical props. 0-65722

LuRhO<sub>3</sub>, elec., mag. and photoelectrochemical props. 0-96925

MgAl<sub>2</sub>O<sub>4</sub>, γ-irradiated crystal, TSC, thermoelec. power, thermolum. and afterglow 0-75583

Mo<sub>0.5</sub>W<sub>0.5</sub>Se<sub>2</sub> single cryst. vapour growth, characterisation 0-93466

NaNbO<sub>3</sub>, elec. cond. mech., resist., Hall coeff. and thermoelec. power meas. 0-65603

Nd<sub>1-x</sub>Ca<sub>x</sub>VO<sub>3</sub>, solid solutions, elec. props. 0-96866

Ni<sub>1-x</sub>Co<sub>x</sub>S<sub>2</sub>, elec. cond., thermoelec. power and optical meas. 0-59986

NiS<sub>2</sub>-Se<sub>2</sub>, elec. cond., thermoelec. power and Hall effect meas. 0-65561

NiWO<sub>4</sub>, AC elec. conductivity, thermoelec. power and dielec. const. 0-70736

Pb<sub>1-x</sub>Ge<sub>x</sub>Te solid solns., phase transition influence on elec. props., 77 to 450K 0-103689

Pb<sub>1-x</sub>Sn<sub>x</sub>Se, transport phenomena in solid solutions with band inversion 0-107792

Pb<sub>1-x</sub>Sn<sub>x</sub>Te, thermoelectric effects, characteristics at low temps. 0-107831

PbTe film, electronic thermal cond. and thermoelec. power 0-93018

RbAg<sub>4</sub>I<sub>3</sub>, superionic conductor, phase transition detection by thermoelectric power method 0-92669

S-based amorphous semicond. film, prep. by plasma decomp. of H<sub>2</sub>S-N<sub>2</sub>-NH<sub>3</sub>, and characterisation 0-80422

Sb<sub>2</sub>Se<sub>3</sub> crystals, mag. and elec. props. 0-96873

Sb<sub>2</sub>Te<sub>3</sub>, stoichiometric, Hall effect and thermoelec. power studies 0-100470

Sb<sub>2</sub>Te<sub>3</sub>, thermoelectric properties and phase transition, under hydrostatic pressure up to 9 GPa 0-65609

Sb<sub>2</sub>Te<sub>3</sub>-Bi<sub>2</sub>Te<sub>3</sub> solid solns., single cryst. growth and thermocouple construct. 0-104056

Se, liq., electronic transport props., equation of state, to 1900K and 1800 bars 0-65574

Se-Te-Sb glasses, electronic transport 0-88579

Si, amorphous, transport results, interpretation 0-80260

Si, phonon-phonon relaxation investigation for conventional and neutron doped crystals 0-96927

n-Si, piezoresist. rel. to piezothermoelec. power, electron-phonon drag region 0-70737

Si:H,B, amorphous, field effect and thermoelec. power 0-96924

n-Si:P, piezothermoelec. power in electron-phonon drag region, anisotropy 0-70738

# thermoelectric effects in semiconductors and insulators continued

Si-Ge, high temperature thermoelectric materials 0-89659

Sm<sub>2</sub>O<sub>3</sub>, B-type monoclinic, DC(AC) elec. cond., thermoelectric power, dielectric const., temp. depends. 0-59980

Tb<sub>2</sub>O<sub>3</sub>, B-type monoclinic, DC(AC) elec. cond., thermoelectric power, dielectric const., temp. depends. 0-59980

Te-(Bi<sub>2</sub>Sb)<sub>1-x</sub>Te<sub>x</sub> eutectic, electrophys. props., directed crystn. conditions influence and comp. depend. 0-107827

Te-based eutectics, crystn. rate effect on electrophys. props. mutual solubility effect 0-60774

Te<sub>0.9</sub>-Se<sub>0.1</sub>Sn<sub>0.1</sub>, thin films, elec. cond. and thermoelectric power meas. (French) 0-80335

V<sub>2</sub>O<sub>5</sub>-As<sub>2</sub>O<sub>3</sub>-RO, R=Ba, Ca, Pb, semicond. glass, electronic props. 0-88557

V<sub>2</sub>O<sub>5</sub>-V<sub>2</sub>O<sub>4</sub>-BaZnO<sub>2</sub> glass, V ion states, mag. and elec. props. 0-88556

VTe, mag. and elec. transport props. 0-92897

ZnAs<sub>2</sub>, homogeneity region and electrophys. props. 0-60833

Zn<sub>0.9</sub>Cd<sub>0.1</sub>-xS films, spray pyrolysis, elec. props. 0-75657

Zn<sub>0.1</sub>Cd<sub>0.9</sub>Sb, thermoelectrically isotropic semicond., carrier kinetics in intrinsic cond. range 0-92894

ZnCr<sub>2</sub>Se<sub>4</sub>, electroconductivity, thermoelectromotive force, Hall effect (Russian) 0-70694

ZnS, ion implantation effects on luminesc., thermo-EMF 0-88178

ZnSb, and p-Zn<sub>0.1</sub>Cd<sub>0.9</sub>Sb, thermoelec. anisotropic semicond., carrier kinetics at low temps. 0-92893

ZrS<sub>3</sub>, quasi one-dimens. semicond., elec. transport props. 0-107790

**thermoelectric generators** see thermoelectric conversion

**thermoelectricity**

see also Peltier effect; Seebeck effect; thermocouples; thermoelectrets; thermoelectric effects in metals and alloys; thermoelectric effects in semiconductors and insulators; thermomagnetic effects; thermopiles; Thomson effect

high pressure chamber designed according to opposed anvil principles, thermoelectric force meas. (German) 0-90863

measurement of thermoelectromotive force and resistance, study of kinetic phenomena of charge transfers 0-57330

Mott's formula for thermopower and for Wiedemann-Franz law 0-84462

pyridinium silver iodide, fast ion conductor, phase transitions, thermoelec. power meas. 0-107540

TCNQ complexes, elec. resist. and thermoelec. power meas. 0-107777

TCNQ salt, MeDABCO(TCNQ)<sub>2</sub>, optical, elec., and mag. props. 0-65539

TCNQ salts, ETTP (TCNQ)<sub>2</sub> and DEPE (TCNQ)<sub>4</sub>, thermoelec. power 0-59966

thermal conductivity determ. heat losses, direct method for thermoelectric materials 0-62662

(TMTSF)<sub>2</sub>X, (X=PF<sub>6</sub><sup>-</sup>, AsF<sub>6</sub><sup>-</sup>, SbF<sub>6</sub><sup>-</sup>, BF<sub>4</sub><sup>-</sup>, NO<sub>3</sub><sup>-</sup>) highly conducting salts, props. 0-59969

wustite solid solns., props. connected with localised electron state 0-107734

α-AgI, fast ion conductor, phase transitions, thermoelec. power meas. 0-107540

FeS, pressure effect on elec. resist. and thermoelec. power 0-70308

La<sub>1-x</sub>Sr<sub>x</sub>VO<sub>3</sub>, Anderson transition, elec. resist. and thermopower meas. 0-100488

RbAg<sub>4</sub>I<sub>3</sub> film, thermopower meas. temp. depend., correl. effects role 0-107539

**thermography** see infrared imaging

**thermogravimetry** see thermal analysis

**thermoluminescence**

alkali halide, dynamics of nonrelaxed and self-trapped holes (Russian) 0-80607

alkali halides, irradiated, formation of Z centre 0-103326

alkali halides, Z<sub>1</sub>-centres, peculiarities of thermolum. 0-103999

alkali metal halides, X-ray induced colour centre and halogen aggregate form. 0-96565

carrier traps in polymeric insulating materials, investigation by thermoluminescence method 0-93240

ceramic materials, thermoluminesc. dating, comparison of results 0-84791

dating methods using thermoluminescence (German) 0-105076

dielectric, solid thermally stimulated characts., dipolar relaxation time, trap levels and ionic space charge polarisation 0-84685

glow curves and desorption spectra anal. method 0-80053

lunar soil samples from Luna-24, radioactivity and cosmic ray dose rate, thermolum. obs. 0-67596

meteorites from Jilin shower 0-90372

microspecimens obs., with size ≥0.8 mm, installation for 300 to 1100 mm range 0-57381

plagioclases, volcanic, thermoluminescence dating 0-98475

poly-p-xylylene films, carrier traps, X-ray induced TSC, thermolum. and dielec. loss study 0-88570

polyethylene terephthalate, TSC and thermolum. due to electron detrapping by local mol. motions 0-96898

ruby, radiation-induced optical processes, impurity effects 0-66310

semiconductors, thermally stimulated conductivity luminescence, defect levels, traps, book contribution 0-80296

semiconductors, thermally stimulated relaxation processes, book contribution 0-80295

thermally stimulated luminescence application, radiation dosimetry, book contribution 0-80882

thermally stimulated relaxation in solids, transport phenomena, book 0-77553

trap depth, method of determ. 0-80211

ultrahigh vacuum setup for photo- and thermostimulated electron emission and luminesc. obs. (Russian) 0-66383

xanthone, in n-pentane, heat pulse induced delayed phosphorescence 0-83404

Al<sub>2</sub>O<sub>3</sub>:Cr photoexcited crystals, cooperative thermoluminescence quenching (Russian) 0-80881

Ba<sub>2</sub>NaNb<sub>2</sub>O<sub>7</sub>, ferroelectric, local states, thermoluminesc. study 0-60690

CaCO<sub>3</sub>, luminesc. under N<sub>2</sub> laser excitation, and appl. to archaeological dating 0-60685

CaF<sub>2</sub>:Mn(Co)(Ni), X-irrad., thermolum. 0-60686

CaS<sub>2</sub>:Pd phosphors, trap and luminescent centre location, photo-, thermo- and electroluminescence studies 0-71482

CaSO<sub>4</sub>:Dy, phototransferred TL studies 0-80875

CaSO<sub>4</sub>:Dy, thermoluminescent glow peaks, post γ-irrad. annealing study 0-89077

CaSO<sub>4</sub>:Dy ribbon, dosimetric props. study 0-63395



**thermoluminescence continued**

- CaSO<sub>4</sub>:Dy sintered pellets, thermolum. response 0-93411  
 CaSO<sub>4</sub>:Sm phosphors, X-irrad., thermoluminesc., charge compensation effects 0-97351  
 CdF<sub>2</sub>:Sm<sup>3+</sup>, photoconverted, thermally stimulated relax. 0-84476  
 CsBr(Cl):Cu<sup>+</sup>,  $\gamma$ -irradiated, thermolum. emission 0-104001  
 Fe, ferromagnetic, partial circular polarisation of thermal emission in mag. field 0-71387  
 KBr, cation defects creation mechanism 0-75224  
 KBr, self-trapped exciton form. via thermally induced defect reactions 0-60687  
 KBr:Ti, 480K thermal glow peak, Ti<sup>+</sup> centres 0-108284  
 KBr(Cl):Sr<sup>2+</sup>, Cu<sup>+</sup>, thermolum. response, extension of two-step reaction model 0-89075  
 KCl, thermoluminesc., halogen and alkali impurity effects 0-97352  
 KCl:Ag, X-irrad., thermoluminesc. study of Ag centres 0-80874  
 KCl:Ca<sup>2+</sup>, Z<sub>2</sub>-centre thermolum. 0-80879  
 KCl:Li, X-irrad., F<sub>A</sub> centres, thermolum. studies 0-80878  
 KCl:Br<sub>1-x</sub> mixed crystals, thermolum. and optical absorption studies 0-104000  
 KI, self-trapped exciton form. via thermally induced defect reactions 0-60687  
 Li<sub>2</sub>Ba<sub>2</sub>O<sub>7</sub>, non-universality of TL-LET response, effect of high-temp. TL 0-99348  
 LiCl single crysts.,  $\gamma$ -irrad., thermolum. meas. 0-80880  
 LiCl, thermolum., order of kinetics 0-89074  
 LiF, non-universality of TL-LET response, effect of high-temp. TL 0-99348  
 LiF TLD phosphor,  $\gamma$ -irrad. induced sensitisation, UV effects 0-108286  
 LiF TLD phosphor, residual thermoluminescence effect on sensitisation 0-108287  
 LiF, thermolum., trapping mechanism based on Z-centres 0-76089  
 LiF:Mg,Ti, defect states, ESR and ionic cond. study 0-108058  
 LiH, defect form. at low temp., EPR, thermolum. and TSC study 0-107222  
 LiH, formation and annihilation of Li colloids and H bubbles 0-107228  
 LuYScO<sub>3</sub>:Er<sup>3+</sup>(Tm<sup>3+</sup>)(Ho<sup>3+</sup>), thermolum. meas. 0-97354  
 MgAl<sub>2</sub>O<sub>4</sub>,  $\gamma$ -irradiated crystal, TSC, thermoelec. power, thermolum. and afterglow 0-75583  
 MgO doped powder phosphors, photo- and thermostimulated luminesc. obs. (*Russian*) 0-66263  
 MgO:Al, and nominally pure single crystal, thermally stimulated luminesc. rel. to temp., and EPR (*Russian*) 0-84789  
 MgO-Al<sub>2</sub>O<sub>3</sub>-P<sub>2</sub>O<sub>5</sub> system glass, heat treatment of aluminium metaphosphate influence on thermolum. 0-108285  
 Na<sub>3</sub>Al<sub>3</sub>(Si<sub>6</sub>O<sub>24</sub>)(NaX)<sub>2n</sub>, X=Cl, Br or I, sodalites, thermal destruction of colour centres (*Russian*) 0-84169  
 NaCl, pure and doped, 20K X-ray irradiation, thermolum. and recovery processes 0-93412  
 NaCl, self-trapped exciton form. via thermally induced defect reactions 0-60687  
 NaCl:Mn<sup>2+</sup>, thermolum. spectra, mechanisms 0-80873  
 NaCl(Br), X-ray or UV irradiated, cation defects creation mechanism 0-75224  
 NaF, X-irrad., colour centres and thermolum. 0-84790  
 NaF:Mn, role of Mn<sup>2+</sup> in thermolum. 0-97353  
 NaMgF<sub>3</sub>, defects induced by X- and vacuum UV irrad., optical and elec. study 0-107319  
 RbCl:Ca<sup>2+</sup>, thermolum. and optical absorption studies 0-104002  
 RbCl(Br), cation defects creation mechanism 0-75224  
 SrFCl, thermolum. and optical absorption spectra 0-66309  
 SrS:Nd, phosphorescence decay, trapping levels 0-104003  
 Y<sub>2</sub>O<sub>3</sub>:Zr<sup>4+</sup>, F-centre charge state, ESR and thermally stimulated luminesc. obs. 0-60418  
 ZnO, single cryst., photo- and thermoluminescence 0-66311  
 Zn<sub>3</sub>P<sub>2</sub>, thermoluminescence glow curve method for radiation induced traps 0-60689  
 Zn<sub>3</sub>(PO<sub>4</sub>)<sub>2</sub>, thermoluminescence glow curve method for radiation induced traps 0-60689  
 ZnS, low-temp. trap anal. thermally stimulated luminesc. model extension 0-80877  
 ZnS, thermoluminescence at different excitation levels 0-93413  
 ZnS:Tb, Cu(Ag) phosphors, luminesc. props. 0-100690  
 ZnSe, donor-acceptor pair emissions characts. (*French*) 0-108249  
 ZrS<sub>2</sub>O<sub>4</sub>, X-irradiated, trapping and emission centres, thermolum. meas. 0-89076  
 ZrSiO<sub>4</sub>, X-irrad., trapping and emission centres, OH<sup>-</sup> ion contribution 0-80876

**thermoluminescent dosimeters**

- archaeological dating, evaluation of internal beta-dose rate 0-98478  
 cards, expected useful lifetime 0-86989  
 depth dose and off-axis characts. of TLD in therapeutic pion beams 0-101271  
 element, effect of mounting condition on meas. (*Japanese*) 0-95471  
 energy dependence of response, method for reducing using filters 0-106206  
 fast neutron sensitivities 0-102413  
 gamma radiation monitoring, automated TLD system 0-57964  
 orientation effects, multivariate anal. 0-89862  
 personal monitoring, effect of environmental radiation (*Japanese*) 0-61707  
 personal monitoring, use of TLDs, judgement of abnormal value by glow curve (*Japanese*) 0-106208  
 personnel dosimeter TLD badge based on CaSO<sub>4</sub>:Dy teflon TLD discs 0-57959  
 reader, microcomputer controlled 0-69044  
 sensitised TLD phosphors, photon energy dependence 0-78498  
 space research system for meas. of cosmic dose on board a spacecraft 0-109047  
 transmitted information of TLD elements, entropy method 0-89860  
 CaF<sub>2</sub>:Dy, TLD-200, thermolum. phosphor, photolum. and absorpt. spectra, thermolum. mechanisms 0-97321  
 CaSO<sub>4</sub>:Dy, TLD-900, thermolum. stability at low radiation doses 0-101272  
 CaSO<sub>4</sub>:Dy ribbon, dosimetric props. study 0-63395  
 CaSO<sub>4</sub>:Dy TLD, low exposure rate depend. meas. 0-102408  
 CaSO<sub>4</sub>:Dy TLD phosphor,  $\gamma$  radiation changes in glow curve 0-60688  
 CaSO<sub>4</sub>:Dy Teflon TL dosimeters, thin, development for  $\beta$ -dosimetry in personnel monitoring 0-63399

**thermoluminescent dosimeters continued**

- CaSO<sub>4</sub>:Dy(Tm), thermolum. thermolum. phosphor, photolum. and absorpt. spectra, thermolum. mechanisms 0-97321  
 Li<sub>2</sub>Ba<sub>2</sub>O<sub>7</sub>:Mn, thermolum. response to pions 0-101270  
 Li<sub>2</sub>Ba<sub>2</sub>O<sub>7</sub>, non-universality of TL-LET response, effect of high-temp. TL 0-99348  
 LiF detectors, survey 0-68964  
 LiF, high energy dependence in low Z media obs. 0-61700  
 LiF, non-universality of TL-LET response, effect of high-temp. TL 0-99348  
 LiF, response to <sup>99m</sup>Tc  $\gamma$ -rays 0-89854  
 LiF, TLD-700, superlinearity of peak 5 and peak 6, C-hit trap struct. 0-99347  
 LiF, thermolum. response to pions 0-101270  
 LiF:Mg, dependence of optical absorpt. on temp. during X-ray irrad. 0-66237  
 LiF:Mg, TLD-100, thermolum. phosphor, photolum. and absorpt. spectra, thermolum. mechanisms 0-97321  
 LiF-polytetrafluoroethane thermolumin. dosimeters, absorbed dose assessment 0-95470  
 LiF(TLD-600), unannealed, fading for thermal neutrons and  $\gamma$ -rays 0-83225  
 Mg<sub>2</sub>SiO<sub>4</sub>:Tb, thermolum. phosphor, photolum. and absorpt. spectra, thermolum. mechanisms 0-97321  
 Rn monitoring, TLD, passive detector, U mill field 0-57963

**thermomagnetic effects**

- alkali metals, elec. and thermal cond. in weak mag. fields 0-65535  
 Ettingshausen device, transient cooling effects, theory 0-80304  
 nondegenerate semiconductor, thermomagnetic phenomena in quantising mag. field (*Russian*) 0-60014  
 Permalloy-Mn film, diffusion aftereffect causing mag. state change (*Russian*) 0-103860  
 semiconductor films, Kane dispersion, thermomag. and thermoelec. effects, theory 0-70864  
 single domain grain assembly, theory for magnetisation processes 0-88828  
 solid state energy conversion, appl. of solid state cooling to spaceborne IR focal planes 0-107772  
 superconductor, hard, critical state stability and oscillations 0-107959  
 As<sub>2</sub>Sb<sub>1-x</sub>, semimetal, thermopower, thermomagnetic power, 4.5 to 77K 0-107825  
 Bi<sub>0.88</sub>Sb<sub>0.12</sub>, semiconducting, transport props., 2 to 100K 0-59989  
 Cd<sub>0.1</sub>Hg<sub>0.9</sub>Te, photothermomagnetic effect in mm range 0-92932  
 p-CdSnAs<sub>2</sub>, Hall effect, thermo EMF, thermomagnetic effects 0-107822  
 Fe-Si cast alloy with spheroidal graphite, transform. investigation during tempering (*Russian*) 0-97479  
 n-Ge, thermoelec. power in quantising mag. field, phonon-phonon interactions 0-107832  
 InP, electron transport props.; mag. field and temp. depend. 0-92888  
 Pb<sub>1-x</sub>Ge<sub>x</sub>Te solid solns., phase transition influence on elec. props., 77 to 450K 0-103689  
 Pb<sub>1-x</sub>Sn<sub>x</sub>Se, transport phenomena in solid solutions with band inversion 0-107792  
 YIG, thermomag. anal. by electron diffraction 0-108035

**thermomagnetic recording**

- Permalloy films with band domain struct., resolving power (*Russian*) 0-75769  
 two-layer mag. structures, thermomag. recording 0-100588  
 MnBi films, prep. by ionised-cluster beam deposition technique, magnetooptical props. 0-100790

**thermomagnetic torque** *see Scott effect***thermomagnetic treatment**

- see also magnetic annealing; magnetocaloric effects*  
 composite superconductor, flux jumps and training 0-70911  
 Fe-Cr-Co, magnetic domain walls, Lorentz microscopy 0-103854  
 Fe-Ni alloys, heat treatment variations effect on surface conditions and on Hg wetted switch behaviour 0-66547  
 Li-Co ferrite, mag. anisotropy induced by thermomag. treatment, ionic order effect, magnetostriction meas. 0-103830

**thermomechanical processing** *see thermomechanical treatment***thermomechanical treatment**

- see also hot pressing; hot working*  
 alkali silicate glasses, secondary relax. transitions 0-88261  
 diamond synthesis by graphitisation of carbon materials at high press. and temp., Ni influence 0-60795  
 fission reactor materials, thermomechanical transient anal., strain-rate dependent plasticity 0-79864  
 polycapromide, oriented filaments, mech. props. 0-66550  
 polymer latex film composite, glass transition temp. determ. using thermomech. curves 0-75342  
 refractories, subjected to severe thermomech. stress, behaviour (*French*) 0-81084  
 steel, alloy, surface quality improvement, thermomech. treatment 0-61020  
 steel, Cr-Mn type, martensite struct. after quenching and HTMT, X-ray diffraction obs. 0-84975  
 steel, eutectoid, mech. behaviour, thermomech. treatment effects 0-84970  
 steel, type 12Kh1MF, dislocation struct. changes after thermomechanical treatment (*Russian*) 0-66545  
 steel, type 34Cr4, post-hot-forming recrystallisation condition, use of NEO-PHOT 2 and EPIQUANT 0-84949  
 steel, type 4052Kh, thermomechanical working influence on mech. props. (*Russian*) 0-93578  
 steel, type KVK, deform. strengthening of bayanite phase (*Russian*) 0-100851  
 steel bearing rings, optimisation of thermomechanical working parameters (*Russian*) 0-93579  
 steel casting, calc. method of thermal and thermo-visco-elasto-plastic processes (*German*) 0-79859  
 steel continuous casting, thermal, thermo-visco-elasto-plastic processes (*German*) 0-81044  
 steel fine structure after heat treatment, X-ray diffraction exam. 0-60890  
 steel turbine casings, residual life determ. 0-93585  
 Al alloy RR58, low cycle fatigue at 423K, prior treatment effect 0-104254  
 Al alloys, thermomech. treatments, effects on microstruct. 0-100858  
 Al-Cu-Mg type 2036, thermomech. treatment, flow stress anal., effect in mech. props. 0-93584  
 Cu, polycrystn., strain localisation during hot deform. 0-104195

**thermomechanical treatment** continued

- Mo, fusion reactor appl., quick heating thermal fatigue test, ultra-high vac. environment (*Japanese*) 0-93716
- Ni-Cr, high temp. thermomech. treatment effect on tensile diagrams of KhN77TYuR (*Russian*) 0-60884
- Ni-Cr-NbC eutectic composite, unidirectional solidification, thermal cycling, temp. range effect on microstructural degradation 0-89272

**thermometers**

- see also pyrometers; resistance thermometers; temperature measurement; thermocouples; thermopiles*
- electronic digital, for long-term patient monitoring 0-90849
- fluorescent decay thermometer with biological applications, using ruby sample 0-86306
- gas, reference standard, 273.15 to 1337.58K range 0-77782
- glass, IR thermometer, readings interpretation 0-82765
- industrial IR thermometer using fibre-optic lightguides 0-86302
- IR battery operated portable thermometer (*German*) 0-57289
- low-temperature gas thermometer, parameter calc. allowing for actual state of He 0-105641
- metal objects, moving, temperature meas. by thermoelectrical thermometer (*Russian*) 0-90848
- Motorola MTS 102 transistor temperature transducer, using LM10 IC op amp (*French*) 0-86298
- non-contact thermometer based on infrared detector (*Polish*) 0-90845
- photoluminescent thermometer probes, temp. meas. in microwave fields 0-104721
- semiconductor diode sensor, for use in varying ambient conditions 0-73361
- semiconductor instruments, providing six point temp. meas. (*French*) 0-68200
- solid thermal cond. and interface resistance meas. by radiation thermometer 0-86289
- superconductive thermometer referenced by superconducting to normal transition point (*Japanese*) 0-77785
- surface contact thermometers, dynamic behaviour (*German*) 0-90843
- temperature transducers, semiconductor diodes, variation of forward voltage with temp. 0-57293
- thermocouple, thermometers, voltage generation, calibration 0-57295
- thermoelectric, Pt-Rh, 1300 to 1700°C, errors obs. and analysis 0-77783
- transistorised, with remote indication, up to 150°C (*German*) 0-73356
- <sup>3</sup>He gas thermometer secondary standard for 0.5 to 40K 0-82762
- KClO<sub>3</sub>, <sup>35</sup>Cl NQR appl. in thermometer below 77K 0-66067
- NaClO<sub>3</sub>, <sup>35</sup>Cl NQR appl. in thermometer below 77K 0-66067
- OH A<sup>2</sup>Σ<sup>+</sup> state, laser excited, vibr. energy transfer, flame thermometer appls. 0-58349
- <sup>117</sup>Sn, <sup>119</sup>Sn, low temp. NMR thermometer 0-82775

**thermometric conductivity** *see thermal diffusivity*

**thermonuclear devices** *see plasma devices*

**thermonuclear reactions** *see nuclear reactions and scattering*

**thermopiles**

- multiple thermoelectric junctions, thin conducting sheet, near heat flux-meter (*French*) 0-86286
- radiometer for Earth radiation meas., fused silica filter performance 0-87473
- selenide thermoelectric materials, thermal conductivity, long-term stability and other props. experimental anal. 0-107834
- type RTN (USSR), construction and characts. 0-57372

**thermoreflectance**

- metal, light refl., nonlinear thermo-optic effect at high intensity 0-93289
- Ag, thermomodulation spectra of high-energy interband transitions 0-108226
- Au, thermomodulation spectra of high-energy interband transitions 0-108226
- CdCr<sub>2</sub>S<sub>4</sub>(Se<sub>4</sub>), thermoreflectance, photoconductance, Raman scatt. near mag. phase transition 0-97298
- Cu, thermomodulation spectra of high-energy interband transitions 0-108226
- CuBr(I), reflectance and thermoreflectance spectra, electronic struct. 0-71444
- EuO(S), ferromagnetic electronic structure, absorption, thermoreflection and thermotransmission spectra (*French*) 0-97300
- EuSe(Te), magnetic phase transitions, thermal modulation spectroscopy study (*French*) 0-97301
- p-GeTe, reflectance, and thermorefl. spectra 0-80814
- HgCr<sub>2</sub>Se<sub>4</sub>, thermoreflectance, photoconductance, Raman scatt. near mag. phase transition 0-97298
- Nb, electronic struct. 0-76047
- β-NiAl, electronic struct. and optical props. 0-97228
- Pd, thermomodulation spectra of high-energy interband transitions 0-108226
- Pt, thermomodulation spectra of high-energy interband transitions 0-108226
- Ta, and α-TaH<sub>x</sub>, electronic struct. 0-76047
- V, electronic struct. 0-76047

**thermosphere**

- compositional modelling taking account of airglow tidal variation 0-109288
- eddy diffusion, models for mesosphere and lower thermosphere 0-109198
- heating by solar UV, efficiency at mid-latitude 0-85780
- incoherent scatter radar studies of daytime middle thermosphere 0-72654
- ionosphere sublayer origin in lower thermosphere 0-61956
- lower thermosphere gravity wave obs., 5-90 minute period 0-61930
- mass density and seasonal-latitudinal tidal struct. of O and N<sub>2</sub> 0-101467
- meteor region, winter motions meas. in S. hemisphere 0-109287
- middle atmosphere, obs. from balloons, rockets and satellites, conference, London, England, (1978 December 12 to 13) 0-77540
- movements and electric currents in lower thermosphere, symposium, Seattle, Washington, 1977 August to September 0-62371
- radiative cooling, IR emission from NO 0-72656
- spectral absorption, Lyman-α extinction by O<sub>2</sub> 0-77180
- temperature and composition, empirical model 0-77183
- temperature and ion chemistry at nighttime, 400-450 km altitude, Ogo 6 data 0-90267
- temperature and wind measurement Fabry-Perot-interferometer imaging system appl. 0-101441
- thermosphere wind causing ionosphere disturbance dynamo 0-82134
- tidal dynamics model with O-N<sub>2</sub> diffusion effects 0-101465
- tides in equatorial region, semidiurnal and terdiurnal 0-82119
- turbulent structure, spectral range (*Chinese*) 0-105092
- wind as cause of ionospheric disturbance dynamo 0-82134

**thermosphere** continued

- wind influences on F-region TIDs 0-109305
- winds in N.Polar Cap thermosphere 0-67445
- H distribution, UV dayglow obs. 0-109290
- N and NO conc. depend. on solar activity 0-77178
- N<sub>2</sub> in equatorial thermosphere, seasonal and diurnal variation 0-85782
- NO<sub>2</sub> ultraviolet spectral absorpt. in lower thermosphere and density profile 0-85781
- O atom corona, of fast atoms during solar max., airglow obs. 0-101469
- O I(³P) in lower thermosphere, nighttime conc. obs., using new rocket borne instrument 0-105066
- O profile of mesosphere and lower thermosphere 0-72660
- O<sub>2</sub> density, solar flux var. 0-72659
- O<sub>2</sub>(¹D), quenching by electrons 0-94630
- O(¹D) formed by N(²D)+O<sub>2</sub> reaction in thermosphere, 6300 Å dayglow implications 0-90270

**thermostats**

- see also cryostats; temperature control; thermistors*
- device for measurement of static characteristics of resistance thermometers 0-77784
- electron thermostat, ion prod. stationary nonequilibrium distrib. (*Russian*) 0-64684
- electronic, with 0.1°C accuracy and economical operation, photography appl. 0-77774
- photographic developing bath, thermostatic control (*Spanish*) 0-77898
- precision, capacitor enclosure, maintaining the unit of capacitance 0-95063
- vital microscopy, electronic thermostatic system 0-85537

**theta pinch** *see pinch effect*

**thick film circuits**

No entries

**thick film devices**

- strain gauges and pressure transducers 0-57285

**thick films**

- concentrator solar cells, thick film conductive ink contacts 0-93957
- solar cell fabrication, photovoltaic process based on thick film technique 0-94016
- solar cell manufacture, thick film technology applic. 0-93903
- BeO black tarnish film, on Cu-Be alloy, Auger electron spectroscopy anal. 0-97624
- Be(OH)<sub>2</sub> black tarnish film, on Cu-Be alloy, Auger electron spectroscopy anal. 0-97624
- Si solar cells with screen printed diffusion and metallisation 0-94015

**thickness control**

- optical thin film coating manufacture, automated deposition control system, design principles 0-64220
- vacuum deposited layers, thickness monitoring techniques (*Japanese*) 0-60783
- welds and castings, differential method of balancing out thickness-variation effects in radiography 0-66748

**thickness measurement**

- achromatic antireflection coatings, thin-layer, layer thickness calcs. 0-87468
- alloy foils, X-ray microanal. technique 0-85256
- amorphous layer thickness meas. by electron back scattering method 0-100721
- boride coatings on C and alloy steel, spectroscopic thickness determ. 0-85099
- coatings industrial meas., 1979 status in USSR 0-77749
- contact media for US thickness meas. and defect inspection over wide temp. range 0-104395
- dielectric film, refractive index and thickness meas. by optical method 0-82806
- dielectric films, thickness and refractive index meas. by photoelectric scanning 0-105606
- electrodeposits, multi-layer, using decade counter (*Czech*) 0-95071
- epoxy resin bond layer, prep. methods, ultimate thickness 0-71884
- ferromagnetic films of high conductivity, magnetic reluctance thickness gauge 0-68178
- galvanic coatings, profilography 0-85095
- glass surfaces, cracked layer thickness determ., chemical method 0-64226
- glass thickness automatic measurement by laser beam 0-82744
- glass tubing dia. and wall thickness meas., P-329M instrum. 0-86262
- insulation, using easily calibrated eddy-current meter 0-73316
- liquid films, conductometric method 0-77751
- metallic film, single layer and multilayer, thickness determ. by X-ray fluoresc. 0-68180
- metallic film, using nondestructive radioisotopic technique 0-68179
- metallic layer thickness measurement using X-ray fluorescence principle (*German*) 0-93705
- metals, thickness meas. by backscatt. γ radiation 0-101781
- microprocessor based film thickness measurement system (*German*) 0-57260
- multilayer Ni deposits, simultaneous thickness and electrochemical potential determination for individual layers 0-71813
- optical, sheet metal, using dynascope visual projector (*French*) 0-82745
- plastic films, using differential electronic circuit 0-73315
- projected inertial confinement fusion reactor target evaluation by buoyancy analysis 0-78442
- shell target monitoring by X-ray Schlieren method 0-86263
- steel, neutron quasi-absolute thickness meas. of single layer product, optimization 0-105611
- thin film, by electron backscattering 0-101904
- thin samples, mass thickness and chem. composition determ., by TEM and X-ray anal. 0-103227
- vacuum deposited layers, thickness monitoring techniques (*Japanese*) 0-60783
- Al coating on polyethylene terephthalate, using photometry 0-62626
- Fe-Cr alloys, in acid and neutral solns., thickness and optical constants of passive and transpassive films 0-66698
- GaAs native oxide layer, determ. from C-V and photoresponse meas. on Schottky barrier 0-70821
- Ge X-ray detector, Au contact layer thickness meas. 0-62627
- PbO layer vapour deposition, structure, and props. 0-65408
- Se films, Ag diffusion, effect on interferometric thickness meas. 0-96695
- Si, epitaxial layer thickness meas. using phase correction function of substrate resistivity (*Rumanian*) 0-90812
- Si(Li) X-ray detector, Au contact layer thickness meas. 0-62627
- SiO<sub>2</sub> layer, measurement by secondary electron emission 0-57435



**thin film capacitors**

- stearic acid, vacuum evaporated film, for low-loss capacitors 0-71317  
 Al-stearic acid-Al structure, dielectric behaviour 0-71317  
 Bi<sub>2</sub>O<sub>3</sub>, thin film capacitor elec. props. under reduced press. 0-80397  
 Si-SiO<sub>2</sub>, MOS interface states density, transient capacitance meas. eval. 0-92989  
 Ta<sub>2</sub>O<sub>5</sub>, film on Al, Cu, Au, Ag electrode, electric strength of MIS system 0-96999

**thin film circuits**

No entries

**thin film devices**

see also *magnetic thin film devices*

- amorphous materials appls. 0-107693  
 gas-sensitive sensor with ultrathin particle film deposited on monolithic IC chip (*Japanese*) 0-105630  
 optical disc for integrated optics 0-106641  
 solar cell, comparison methodology 0-93920  
 solar cell, polycryst., chemical and structural defects 0-93919  
 solar cell, polycryst., research and develop. overview 0-93921  
 solar cells, degradation processes of electrophysical characts. during long-term operation 0-89617  
 solar cells, thin film, technical and economical eval. 0-94012  
 solar cells, unified anal. of potential 0-81436  
 thermoelectric needle probe for medical and biological temp. meas. 0-101299  
 Al-Si-N-O-Al thin film cathode, physical model from expt. study 0-100535  
 CdS/Cu<sub>2</sub>S thin film solar cells, design and fabrication, 9.15% conversion efficiency 0-81438  
 CdSe solar cells 0-93970  
 CdTe thin film polycrystalline solar cells prepared by electrodeposition 0-93948  
 CuInSe<sub>2</sub> thin films for solar cells, radiofrequency sputtering technique, elec. props. 0-93487  
 Cu<sub>2</sub>S-CdS heterojunction solar cell 0-93922  
 Cu<sub>2</sub>S-N<sub>2</sub>Cd<sub>1-x</sub>S and Cu<sub>2</sub>S-CdS thin film solar cells by solid state reaction, comparison 0-101109  
 Cu<sub>2</sub>S/CdS solar cell, prep. by sequential evaporation 0-93902  
 Cu<sub>2</sub>S-CdS thin film solar cells, using all film vacuum deposited process 0-93977  
 GaAs polycrystalline thin film solar cells, fabrication 0-94066  
 GaAs thin film polycrystalline solar cells, props. and prep. 0-81437  
 GaAs thin film polycrystalline Schottky barrier solar cells, grain boundary chemistry 0-94067  
 GaAs thin film polycrystalline solar cells, grain boundary edge passivated 0-94069  
 Ge:Au film strain gauges, press. sensor (*Japanese*) 0-105631  
 InP thin films for photovoltaic devices 0-93972  
 Pt thin-film temp. sensor (*Japanese*) 0-105645  
 a-Si solar cells, current collection and electrical shorting problems 0-93969  
 SiC thin-film thermistors with high thermal response (*Japanese*) 0-105629  
 Ta strain gauge, effects of Ar ion bombardment on elec. props. 0-80417  
 Ta<sub>2</sub>O<sub>5</sub> film capacitance humidity sensor Panahume (*Japanese*) 0-105658
- thin film resistors**
- photoexcitation effects during laser trimming of resistors on Si 0-64093  
 Fe-Cr-Si, heat resistive films prepared by sputtering, lifetime meas. 0-80132  
 Ta-Al-N thin film resistors with improved elec. props. 0-100544  
 Ta-Cr-Si-Al, heat resistive films, prepared by sputtering, lifetime meas. 0-80132  
 TaB<sub>2</sub>-Cr-Si-Al, heat resistive films prepared by sputtering, lifetime meas. 0-80132  
 Ta<sub>2</sub>N, deposition by closed anode bias sputtering (*Japanese*) 0-93484

**thin film transistors**

- CdTe thin film on ferroelectric TGS, influence of polarisation reversal on elec. cond. 0-65720  
 CdSe thin film transistor on Cr substrate, cryst. struct., substrate defect effects 0-70563

**thin film triodes** see *thin film transistors***thin films**

- see also *coatings; dielectric thin films; epitaxial layers; insulating thin films; magnetic thin films; metallic thin films; semiconductor thin films; semimetallic thin films; sputtered coatings; substrates; vapour deposited coatings*
- absorbing film, damage by high-power optical pulses, two-phase model 0-93438  
 absorbing films, laser-induced removal, two-phase mechanism 0-97384  
 absorbing films, laser-induced removal, two-phase mechanism 0-97385  
 adhesion, meas. device 0-66720  
 adhesion determination, electron and laser beam appls. 0-71833  
 alloy, thickness depend. of CPA electronic densities of states 0-65644  
 analytical techniques, review 0-80120  
 anthracene films, optical props., comparison between free and optical contact mounting 0-89079  
 Brillouin scattering by Love waves, theory 0-66212  
 chemical analysis, by energy loss spectroscopy 0-104493  
 trans-1,4-chlorobromocyclohexane, liquid, crystalline and amorphous state, conformation and vibr. spectra, IR obs. 0-60568  
 trans-1,4-chloriodocyclohexane, liquid, crystalline and amorphous state, conformation and vibr. spectra, IR obs. 0-60568  
 condensates coalescence, influence on morphological changes, modelling 0-107676  
 CPA calc. of local density of electronic states, for 11-layered thin film 0-65643  
 crystal symmetry, cubic and non-cubic, distinguished by weak field galvanomagnetic meas. 0-60009  
 defect growth and nucleation, electron microscopy and diffraction exam. (*French*) 0-59824  
 deposition model, correlated percolation 0-107679  
 deposition techniques, review 0-80964  
 electron probe analysis, charact. fluoresc. effects calc. 0-81408  
 ellipsometry of transparent films on transparent substrates, theory 0-104007  
 grain boundary migration, effect on thin film diffusion behaviour, simulation 0-88460  
 hard disc thin layer, solid-solid phase transformation 0-79908  
 high resolution phase contrast electron microscopy imaging 0-103224

**thin films continued**

- holey film preparation by ion-etching method, electron microscopy appls. 0-105751  
 island film growth, cluster size distrib. 0-107665  
 island films, statistical model 0-92795  
 magnetoresistance, specular reflectivity angular depend. (*Russian*) 0-100453  
 multilayers, ultrathin, optical characts. 0-104005  
 nondestructive microhardness testing of near-surface layers 0-71829  
 nucleation kinetics, of thin films under complete condensation conditions 0-88453  
 optical constant volume and surface change separation, reflection, transmission (*Russian*) 0-66320  
 optical constants, reflection spectra by Kramers Kronig method 0-76099  
 optical parameters meas. method, reevaluation 0-104004  
 optical properties of film-substrate systems, reflectance-aided null ellipsometry 0-101827  
 optical transmittance and reflectance, bulk optical props. determ. 0-88954  
 photoacoustic reflection-absorpt. spectroscopy for IR anal. of surface species 0-105723  
 photothermal deflection technique for absorpt. meas. in optically thin media, thermal lens effect comparison 0-105717  
 polycrystalline films, rate of mixing depend. on grain boundary struct. 0-107578  
 roller-plate technique, for thin film prep. from melt 0-71607  
 sink strengths for thin film surfaces and grain boundaries 0-88207  
 size-quantised films, sound amplification under ESR conditions 0-70322  
 solar energy utilisation, deposition techniques 0-84847  
 sputter profiling, combined Auger-X-ray anal. 0-66909  
 surface analysis, survey of ESCA, AES, SIMS and ISS techniques, appls. (*Hungarian*) 0-70544  
 surface films on solids, TEM study method 0-65409  
 surface layer selective erosion using ion etching, cathodic sputtering, overview (*Hungarian*) 0-66682  
 TEM, X-ray anal., mass thickness and chem. composition determ. 0-103227  
 tetramethylammonium silver iodide superionic film, electrocodeposition, electrochem. cells 0-107478  
 thermal conductivity measurement 0-68199  
 thickness measurement, by electron backscattering 0-101904  
 tunnelling currents through very thin films, temp. and space charge effects 0-70799  
 C<sub>60</sub> for STEM specimen support, prep. and observation 0-93496  
 C/Pt-W (8 wt.%), desorption of K from C film surfaces 0-59784  
 ErD<sub>2</sub> thin film, degradation during film processing, investigation 0-101047  
 Fe-Cr alloy, sputter etching oxide film, comp. profile, quantitative AES 0-81383  
 IrO<sub>2</sub> film, A-C response 0-107926  
 LiF film, surface phonons and thickness variation, EELS meas. 0-92774  
 Li<sub>2</sub>N thin film, vacuum evaporation on WO<sub>3</sub>, retarded deposition 0-108351  
 Mo<sub>2</sub>Si<sub>3</sub>, electrotransfer of Si 0-92708  
 NH<sub>3</sub> solid film, absorpt. coeffs. determ. 50 to 7000 cm<sup>-1</sup> 0-97356  
 4NbO<sub>0.76</sub> thin film, FCC cell struct. investigation 0-92796  
 SrF<sub>2</sub>, optical props., spectral dependence, 460-1000 nm 0-76094  
 2Ta<sub>2</sub>O<sub>3</sub> thin film, FCC cell struct. investigation 0-92796
- third-order optical susceptibility** see *nonlinear optical susceptibility*
- thixotropy**
- No entries
- Thomas-Fermi model**
- atomic scatt. factors and momentum densities, asymptotic form 0-74105  
 atoms, multistage ionisation in strong EM fields, Thomas-Fermi calcs. (*Russian*) 0-58226  
 graphite intercalation cpds., electrostatic interactions and staging, nonlinear Thomas-Fermi eqns. 0-107732  
 metals, simple, static props., Thomas-Fermi-pseudopotential approach 0-75514  
 nucleon matter, Thomas-Fermi model rel. to eqn. of state at subnuclear densities 0-77278  
 relativistic generalisation for the atom, scaling and critical charge 0-63554  
 Ne, temp. perturbed Thomas Fermi eqn., variational principle 0-69074
- Thomson effect**
- multijunction thermal convertor AC/DC transfer, Thomson effect error reduction 0-103679  
 neutron stars, magnetic, Thomson scatt. rel. to radiative heat transfer in surface layers 0-94826  
 thermoelectric energy conversion, heat losses compensation due to thermal cond. through Peltier heat 0-107773
- thorium**
- see also *nuclei with .....*
- atom reson. localised 5<sub>f</sub> continuum state, giant reson. 0-91467  
 FBR Th-based metal alloy fuels, determ. of solidus temperature 0-104124  
 field ion microscopy study of structure 0-59437  
 Funka Bay, Japan, <sup>234</sup>Th removal from seawater 0-61803  
 geochemical prospecting 0-72635  
 interband, collective and atomic (p,d) excitations, Z-160 eV, fast EELS 0-93443  
 luminescence characteristics of pure surfaces acted on by flux of field emission electrons 0-100695  
 nondestructive measurement of U and Th conc. and quantities using XFA and gamma spectrometry 0-71877  
 nuclear, fuel cycles, nonproliferation aspect of <sup>232</sup>U presence in <sup>233</sup>U-Th fuel cycle 0-57839  
 phonon dispersion relations, non-central electron fluid model 0-100312  
 phosphate fertilizer, specific activity of U and Th rel. to particle size 0-106244  
 photoelectron spectra study, core and valence levels 0-66394  
 sedimentary rocks, Th and U abundances rel. to crustal evolution and sedimentary recycling 0-85654  
 valence and 5f states, XPS and bremsstrahlung isochromat spectroscopy 0-66393  
 X-ray emission following H and O ion impact, parameter depend. 0-66327  
 CaF<sub>2</sub>:Th, electron irradi. defect aggregates, ordering, impurity effects 0-75216  
 Th-W, TF electron emitters props. obs. 0-66403

thorium compounds

phthalocyanine, phase contrast characteristics in STEM 0-100153  
HfF<sub>4</sub>-BaF<sub>2</sub>-ThF<sub>4</sub>-(ZrF<sub>4</sub>) glass system, IR transmitting, synthesis and props. 0-71623  
Nb-Th, eutectic composition 0-100828  
(Th,U)C advanced FBR fuels, radiological assessment of reprocessing 0-73983  
(Th,U)O<sub>2</sub>, burnup simulated, high O<sub>2</sub> pot., chem. state 0-91220  
(Th,<sup>235</sup>U)O<sub>2</sub> HTGR fuels, radiological implications of use 0-68777  
Th-C-N system, existence of new β' ThCn' phase, struct. and thermodynamic study (*French*) 0-92499  
Th,As<sub>4</sub>, heat capacity, 5-300K 0-88769  
ThC<sub>0.963</sub>, cryst. struct. and lattice dynamics 0-88088  
ThC<sub>0.9</sub>N<sub>0.9</sub>, NMR, Knight shift and spin-lattice relax. 0-100621  
ThC<sub>n</sub>(n=1 to 6), Knudsen effusion mass spectrometric investigations, enthalpies and heat of formation calcs. 0-66858  
Th<sub>1-x</sub>Co<sub>x</sub>, amorphous alloys, thermal stability, elec. cond. enthalpy 0-100172  
ThF<sub>4</sub>, absorpt. spectrum of vapour, Th reson. localised 5,epsilon f state 0-91467  
ThF<sub>4</sub>, interband, collective and atomic (p,d) excitations, Z-160 eV, fast EELS 0-93443  
ThF<sub>4</sub>(Cl<sub>4</sub>), electronic struct., MS-SCF-Xα calcs. and VUV photoelectron spectra 0-63710  
ThIr<sub>3</sub>B<sub>2</sub>, supercond. and mag. props. 0-97028  
ThN, photoelectron spectra study, core and valence levels 0-66394  
ThN-rare earth nitride mixed system, quasibinary existence (*German*) 0-91221  
ThNi<sub>3</sub>, Hauke compounds, low temp. heat capacity, Debye temp. 0-96663  
ThO<sub>2</sub>, crucible material, Cu-Nb alloy prep. 0-84879  
ThO<sub>2</sub>, crystallite growth from oxide plasmas, growth morphology 0-59417  
ThO<sub>2</sub>, microspheres, coated, coating permeability meas. 0-95343  
ThO<sub>2</sub>:Ce<sup>3+</sup> (Ce<sup>4+</sup>), mixed ionic and electronic transport 0-107875  
ThO<sub>2</sub>-CaO, and ThO<sub>2</sub>-YO<sub>1.5</sub>, solid solns., defective oxides, ionic cond. 0-70548  
Ti-Th, eutectic composition 0-100828  
U-Pu-Zr-(Th) LMFBR metal fuel elements, development and performance 0-57856  
U,Th<sub>1-x</sub>As (Sb), electronic struct., relativistic KKR-averaged T-matrix approx. method 0-107702  
U,Th<sub>1-x</sub>As, mag. phase diagram, magnetisation meas. 0-60271  
U,Th<sub>1-x</sub>Sb, valence change of U accompanied by singlet-ground-state ferromag. 0-70965  
ZrF<sub>4</sub>-BaF<sub>2</sub>-ThF<sub>4</sub>, vitreous phases, network formers, modifiers and stabilisers (*French*) 0-64909  
ZrF<sub>4</sub>-BaF<sub>2</sub>-ThF<sub>4</sub> F<sup>-</sup> ion cond. glasses, cond. process 0-107477  
ZrF<sub>4</sub>-BaF<sub>2</sub>-ThF<sub>4</sub>-NaF(RF<sub>3</sub>) (R=rare-earth) glass system, anion cond. 0-70460  
ZrF<sub>4</sub>-ThF<sub>4</sub>-BaF<sub>2</sub> glass, IR-transparent, synthesis using reactive atm. processing technique 0-100826

three-phase flow see multiphase flow

three phase rectifiers see rectifiers

three-photon spectra see multiphoton spectra

throat microphones see microphones

thulium

see also nuclei with .....

ferrogarnet film, cylindrical mag. domain motions, domain boundary oscills. (*Russian*) 0-71140  
impurity in metallic host, exchange interaction, electrical resistivity 0-84453  
magnetic transitions, effect of H<sub>2</sub> in solid solns., elec. resist. meas. 0-100585  
CaF<sub>2</sub>:Tm<sup>3+</sup>, <sup>19</sup>F NMR studies 0-60429  
CaF<sub>2</sub>:Tm<sup>3+</sup>, ultra-low nuclear spin temp., low field behaviour, EPR study 0-100614  
CaSO<sub>4</sub>:Tm, thermolum. phosphor, photolum. and absorpt. spectra, thermolum. mechanisms 0-97321  
CdF<sub>2</sub>:Er<sup>3+</sup>, Tm<sup>3+</sup>, evidence for Er<sup>3+</sup>⇌Tm<sup>3+</sup> energy transfers, fluoresc. expts. 0-60655  
LuYScO<sub>4</sub>:Tm<sup>3+</sup>, thermolum. meas. 0-97354  
Tm I, hyperfine struct., high resolution spectrosc. meas. 0-87238  
Tm IV, 3d and 4f energy level parametrisation, Slater parameters and correl. corrections 0-87041  
ZnS:Tm<sup>3+</sup>, charge compensation and polytypism influences on fluorescence 0-89051

thulium alloys

Er<sub>1-x</sub>Tm<sub>x</sub>Rh<sub>4</sub>B<sub>4</sub>, mag. and supercond. transitions, cryst. field effects 0-107950  
Mg-Tm, dil., macroscopic shape effect due to quadrupole orientation, magnetostriction and thermal expansion meas. 0-60396  
Th-Tm (1 at.%), Heisenberg exchange, residual resist. meas. 0-75558  
Tm-3d transition metal intermetallics, <sup>169</sup>Tm Mossbauer effect 0-71261  
Tm-Zn, paramagnetism, mag. excitations, exchanges interactions 0-88718  
TmFe<sub>2</sub> and Tm<sub>2</sub>Fe<sub>3</sub>, magnetostriction, room temp. to 80K 0-65993  
TmPt<sub>3</sub>, low temp. mag. susceptibility 0-93075  
TmZn<sub>2</sub>, Mossbauer effect meas. in antiferromag. and paramag. states 0-71265

thulium compounds

see also thulium alloys

phthalocyanine, mol. image in high resolution electron microscopy, radiation damage effect 0-107203  
(BiTm)<sub>3</sub>(FeGa)<sub>3</sub>O<sub>12</sub>, ion implanted epitaxial garnet film, bubble domains, cryst. struct. disorder 0-93150  
(Gd,Tm,Y)<sub>3</sub>(FeGa)<sub>3</sub>O<sub>12</sub> LPE garnet thin films, magnetocrystalline anisotropy 0-93147  
(LaTmCa)<sub>3</sub>(FeGe)<sub>3</sub>O<sub>12</sub>, mag. loss and domain wall mobility 0-65980  
La<sub>0.8</sub>Tm<sub>0.2</sub>Se, sp. ht. meas., 1.6 to 20K, mag. contrib. 0-65934  
TmAg, XX 0-66082  
TmBiFe<sub>3</sub>, prep., elec. props., and crystallographic date 0-59981  
Tm<sub>1-x</sub>Eu<sub>x</sub>Se, semicond. with valence instabilities, cryst. chem. considerations 0-100213  
TmF<sub>2</sub>, thermal props. (*German*) 0-81355  
TmFeO<sub>3</sub>, acoustic vel. and attenuation shifts at spin reorientation phase transition 0-65986  
Tm<sub>2</sub>Ga<sub>2</sub>O<sub>12</sub>, Mossbauer study of crystal field props. 0-66082  
Tm<sub>1-x</sub>Lu<sub>x</sub>VO<sub>4</sub>, Jahn-Teller system, thermodynamic properties, internal stress effects 0-59679  
TmNi<sub>2</sub>Si<sub>2</sub>, mag. props., 4.2-200K 0-84602  
Tm<sub>2</sub>O<sub>3</sub> film, between Al electrodes, prep. and elec. props. 0-60103

thulium compounds continued

TmO<sub>2</sub>S<sub>8</sub>, low temp. Mossbauer study and mag. susceptibility 0-80656  
TmSe and its mixed crysts., valence instabilities, phase diagram 0-70651  
TmSe, Anderson lattice resist. for antiferromag. ordering 0-65556  
TmSe, Curie constant rel. to valence bond strength 0-60251  
TmSe, elec. resist. under press. at very low temp. 0-96878  
TmSe, first obs. of negative elastic const. 0-103409  
TmSe, intermediate valence cpd., susceptibility, single-ion approach 0-70935  
TmSe, Kondo lattice model 0-97063  
TmSe, mag. ordering under press., neutron diffr. obs. 0-70947  
TmSe, mag. props. 0-97086  
TmSe, metal insulator transition, cond. processes 0-96787  
TmSe, mixed valence, X-ray absorption study 0-76102  
TmSe, valence mixing, mag. props. obs. 0-70648  
TmSe-TmTe(EuSe), semiconductor-metal transitions 0-96953  
TmSe, magnetoresist. and Hall effect, stoichiometry effects 0-65597  
TmSe<sub>1-x</sub>Te<sub>x</sub>, semicond. with valence instabilities, cryst. chem. considerations 0-100213  
TmTe, f<sup>12</sup> and f<sup>13</sup> config. photoemission fractional parentage coeffs., intermediate and LS coupling calc. 0-84829  
TmTiO<sub>3</sub>, bulk mag. and struct. props., ferrimag. order 0-107993  
TmVO<sub>4</sub>, enhanced nuclear cooling and spin-lattice relax. time 0-80632  
YGd<sub>2</sub>TmFe<sub>4</sub>Ga<sub>7</sub>O<sub>12</sub> epitaxial films, bubble-domain lattices with specified parameters 0-60386  
(YGdTm)<sub>3</sub>(FeGa)<sub>3</sub>O<sub>12</sub> epitaxial film, formation of lattice of cylindrical mag. domains from stripe domains (*Russian*) 0-80579  
Y<sub>0.8</sub>Tm<sub>0.2</sub>Se, sp. ht. meas., 1.6 to 20K, mag. contrib. 0-65934

thunderstorms

see also lightning

1975 July 9, elec. fields, electron precip. and VLF radiation during simultaneous substorm and thunderstorm 0-67392  
Asia, thunderstorm location by single station techniques, improved method, radiowave propag. effects 0-67438  
clouds, charge separation laboratory meas., associated with secondary ice crystal production 0-72623  
electric charge generation and field parameter throughout storm 0-72595  
electric charge separation, model 0-77076  
electric field and precipitation regions, airborne and ground obs. 0-85725  
electrification, field expt. 0-72622  
electrification process, charge separation laboratory meas., associated with secondary ice crystal production 0-72623  
ice nuclei generation in surface outflow 0-90135  
location errors anal., thunderstorms in Asia 0-101421  
point discharge from ground surface objects, annual charge change per km<sup>2</sup> 0-77077  
prediction, automated 12 to 36 hour probability forecasts 0-77062  
propagation of thunder through atmosphere, status of current research 0-87618  
streamer velocities meas., positive, in quasi-uniform electric fields 0-72625  
tropical, cloud to ground and intracloud discharge 0-85705  
tropical regions, atm. noise data 0-61875  
updraft splitting and mesovortex couplet evolution, model 0-98395  
N fixation by lightning 0-90147

thyatrons

Pockels cell driver of fast rise time and high repetition rate using thyatron 0-69537  
Cu halide laser driving ccts., parametric study 0-83610

thyristor applications

dual slide projector fader control cct., using a triac dimmer 0-69489  
fusion reactor, TEXT, motor-generator power supply system 0-99292  
fusion reactor, TEXT, toroidal field coil power supply, thyristor controlled 0-91289  
microtrons, thyristor modulator circuit and construction 0-63422  
photographic flash sequencer, using thyristor control 0-62749  
slide projector, dissolve control unit provides cross-fading and operational sequence recording 0-77833  
temperature regulator for inductive loads using IC zero voltage switch U 106 BS with triac (*German*) 0-77779  
temperature regulator for pulsed NMR spectrometer 0-105687  
X-ray pulse generator supply 0-57446

thyristors

No entries

ticking stars see pulsars

tidal power stations

dams, flexible water barriers, energy conversion to compressed air energy 0-61273  
energy accounting study 0-76589  
evaluation of alternative energy sources for the Guyana energy crisis 0-61270  
Korea, prefereability study 0-61271  
technical details and operating experience 0-72009

tides

atmosphere, solar modulation of lunar tide 0-94593  
atmosphere, solar semidiurnal tide, zonal motion and meridional temp. gradient effects 0-98399  
atmosphere, solar semidiurnal tide influenced by zonal wind, theory 0-61853  
atmosphere, solar semidiurnal tide influenced by zonal wind, theory 0-61854  
atmosphere, surface press. oscill. obs. 0-77054  
atmosphere, temp. tide in stratosphere due to Moon, NIMBUS 5 obs. 0-101405  
atmosphere, theoretical work since 1970, review 0-94589  
atmosphere, tidal dynamics model of thermosphere, with O-N<sub>2</sub> diffusion 0-101465  
atmosphere semi-diurnal tides, upward propag. rel. to ionospheric equatorial anomaly in E.Asia and India 0-109301  
atmosphere tide at meteor altitude, CTOP radar obs. 0-77181  
Bristol Channel, tidal regime by numerical model 0-85670  
Bristol Channel tides, analytical wedge model 0-85671  
connected basin natural oscillation, theory 0-61806  
Cook Inlet, Alaska, tidal currents meas. by two-site HF Doppler radar system 0-72533  
crust deformation by tidal forces, and orogeny 0-85625  
crustal tilt obs. in N.Wales mine, strain-tilt coupling and Earth model 0 89926  
day length and zonal tides, effect of core-mantle coupling 0-104850



## tides continued

- E-region luni-solar tides, electron density distortion meas. using group and phase height meas. 0-109299  
 Earth gravity intensity variations, use of AChF-3 pendulum clock 0-104856  
 Earth tide, dynamic shear modulus influence 0-76901  
 Earth tide, influence of mantle anelasticity 0-76900  
 Earth tide, review (*Chinese*) 0-89925  
 Earth tide recorder photoelec. compensation method to acquire data 0-77129  
 Earth tides, meas. by borehole long-period seismometer (BELS type 79) with stable period (*Japanese*) 0-67417  
 Earth tides, theoretical study assuming Earth viscoelastic body 0-67333  
 Earth-Moon system, tidal evolution 0-82240  
 Earth-Moon system tidal friction, changing Earth moment of inertia 0-81803  
 Earth-Moon system tidal friction theory 0-81802  
 electrojet influenced by lunar tide, semimonthly variation 0-61937  
 estuaries of variable breadth and depth tidally induced residual currents 0-72544  
 estuary, well mixed, buoyancy effects on longitudinal dispersion 0-85681  
 estuary circulation (partially mixed), two-dimens. model 0-109161  
 Florida Current, fluctuations in transport at periods between tidal and two weeks 0-72551  
 geocentric position variation due to terrestrial fluid mass motion 0-76894  
 gravimetric tidal loading computed from integrated Green's functions 0-89928  
 gravity obs. of tides made in Gt. Britain 0-94446  
 gravity perturbation due to ocean tide, series computation 0-104857  
 Greater Cook Strait, New Zealand,  $M_2$  tidal effects 0-90093  
 hemispherical ocean centred on equator, numerical model 0-72528  
 ionosphere, lower, semidiurnal and diurnal tides rel. to wind obs. by Kyoto meteor radar 0-67444  
 ionospheric records over Shanghai, March 1953 to June 1955, influence of atmospheric tides (*Chinese*) 0-77192  
 Knight Inlet, British Columbia, stratified flow tidal interaction with sill 0-101368  
 longshore sediment transport by tidal current, outside surf zone 0-76961  
 lower thermosphere, compositional modelling taking account of airglow tidal variation 0-109288  
 Messina Strait, tidal currents 0-81917  
 Messina Strait, tidal currents 0-81918  
 meteorological tide, energy transfer from atmos. to ocean (*Russian*) 0-76988  
 Narara Bet, Gulf of Kutch, coastal currents, temp. and salinity 0-76990  
 New Hebrides arc, tidal tilt from localized ocean loading 0-98211  
 North Sea,  $M_2$  tidal elevations and currents, hydrodynamic model 0-104973  
 ocean, barotropic and baroclinic tides over continental slope and shelf off Oregon 0-72543  
 ocean, effect on Earth gravity at Aburatsubo Crustal Movement Observatory 0-101316  
 ocean, oscillating three-dimensional tide generating currents struct. 0-72542  
 ocean, semidiurnal internal tide rel. to upper ocean temp. and salinity struct. 0-72536  
 ocean, turbulent Ekman bottom boundary layer, effect of diurnal tidal currents 0-104977  
 ocean shelf edge tides, variable-depth Green's function 0-81915  
 Onslow Bay, eastern USA, existence of continental shelf waves 0-72529  
 Par River estuary, India, effects of tides on pollution rel. to abatement methods 0-104521  
 residual motion, tidally-generated, in St. Lawrence estuary, numerical model 0-94541  
 review of tidal research 0-98349  
 Severn estuary, seasonal and spring neap tidal depend. of axial dispersion coeffs. 0-94534  
 shallow water waves in rot. basin, integral formulation 0-81920  
 simulation on sphere, geodesic finite-difference method for curved domains 0-109153  
 solar-lunar forces calc. accuracy (*Russian*) 0-61813  
 St Kilda shelf, tidal regime, press. gradient obs. 0-85666  
 Surkhob fault zone, USSR, tidal deform. determ. for crustal movement anal. 0-104944  
 thermosphere, seasonal-latitudinal tidal struct. 0-101467  
 thermosphere, winter semi-diurnal and diurnal tides in S.hemisphere meteor region 0-109287  
 thermosphere tides, semidiurnal and terdiurnal 0-82119  
 upper atmosphere, local winds rel. to ionospheric equatorial anomaly in E.Asia and India 0-109301  
 waves in channel, bottom friction in perturbation method 0-98354

## tight-binding calculations

- alloy thin film, thickness depend. of CPA electronic densities of states 0-65644  
 alloys, substitutional, self consistent cluster theory for off diagonal disordered systems 0-84272  
 binary compound, Kohn anomaly in optical phonon branch 0-92626  
 binary linear chain, electronic props., short-range order effects 0-96769  
 central peak in the density of states of a disordered linear chain 0-100428  
 degenerate narrow bands, intraatomic Coulomb and exchange energies 0-84452  
 disordered electronic systems, spin interaction effects, loop expansion and exact relations among local gauge invariant modes 0-80221  
 disordered systems, systematic approach, averaged Green functions calc. 0-80150  
 ferromagnet, tight binding model, surface magnetisation 0-103807  
 finite perturbed chains, g-factor, use of exact one electron solution (*French*) 0-59858  
 glasses, defect reactions, ionicity dependence, negative-U states 0-88510  
 graphite intercalated with  $\text{AsF}_5$ , quantum oscillatory phenomena 0-107823  
 itinerant magnets, band struct., mag. props. and local moments 0-70929  
 metal, tight-binding, electronic struct. and kinetic props. at high temp. 0-59848  
 metal, vacancy-dislocation interaction, tight-binding calc. 0-92554  
 metals, narrow-band, Auger line shape 0-60719  
 one-dimensional conductivity, with arbitrary bandfilling, Peierls instability 0-59968

## tight-binding calculations continued

- one-dimensional conductor, lattice stability, phonon dispersion, Kohn anomaly 0-96603  
 one-dimensional electron system, distorted, dynamical elec. cond. calc. 0-59962  
 polyacetylenes, fluorinated, electronic struct., tight-binding LCAO-SCF-MO calcs., prep. 0-70591  
 $\alpha$ -quartz, electronic struct., local disorder influence 0-59870  
 random binary alloys, quantum percolation 0-80156  
 random electronic models with spin-dependent hopping 0-70574  
 recursion method for the extended impurity problem 0-96814  
 semiconductor surface, chemisorption of mol. complexes, bond orbital model (*German*) 0-59807  
 semiconductors, EM wave interaction in weakly nonlinear medium with superlattice 0-93257  
 semiempirical method, relationship with HF method in band struct. calcs. 0-75495  
 thin film, 11-layered, CPA calc. of local density of electronic states 0-65643  
 transition metal, surface atom vibrations, self-consistent calc. 0-103560  
 transition metal-metalloid band structure, nonorthogonality and tight-binding fit 0-59852  
 transition metals, BCC, interaction energy between self-interstitial and screw dislocation, calc. 0-70248  
 transition metals, ferromag., dil. H electronic struct. 0-70638  
 transition metals, generalisation of modified tight-binding approximation 0-88288  
 $\text{AgF}(\text{AgI}, \text{AgBr}, \text{AgCl})$ , NMR chemical shifts 0-74180  
 $\text{As}_2\text{Se}_3$ , glassy defect electron states, tight binding hopping calc. 0-96818  
 $\text{BaTiO}_3$ , band struct. calc., interpretation of XPS and UPS spectra 0-70597  
 $\text{BaTiO}_3$ , photoelectron and optical spectra derived from self-consistent charge MO and band calcs. 0-96785  
 $\text{CdS:In}$ , impurity resist., Matsubara-Toyozawa theory extension 0-80264  
 CdTe, energy bands and optical props. calc., tight-binding model with spin-orbit interaction 0-65448  
 CdTe-HgTe superlattice on CdTe layers, evanescent states, tight binding calcs. 0-70611  
 $\text{CrCl}_3$ , electronic struct. and struct. phase transition 0-59644  
 Cu, bulk and (001) films, extended tight-binding calcs. 0-70592  
 Cu-Ni, density of states of d-electrons, tight binding approx. calcs. 0-59863  
 Fe, magnetism at high temps., total electronic band struct. energy calc. 0-75721  
 GaSb-InAs system, (110) surface and interface electronic struct. 0-100494  
 H atoms, chemisorbed on cluster, indirect interactions, Grimley-Pisani model and tight-binding calc. 0-65370  
 HgTe, energy bands and optical props. calcs., tight-binding model with spin-orbit interaction 0-65448  
 $\text{LiC}_6$  and  $\text{LiC}_{12}$ , intercalation cpds., electronic struct. calcs. 0-70613  
 $\text{MnBO}_3$ , tetragonal, electronic struct., optical anisotropy 0-70599  
 $\text{NbSe}_3$ , electronic struct., chem. interpret. of geom. deform., oxidation state formalism 0-107690  
 Ni, metallic particles, stability and electronic struct. (*French*) 0-80155  
 Pd-H dilute alloy, impurity elec. struct. 0-103643  
 Pd-H system containing d impurities, chem. binding energies of point defects 0-107214  
 Se, bonding coordination defects 0-59927  
 Se, trigonal and amorphous, electronic struct. and nonempirical calc. of struct. props. 0-59866  
 Si, deep level defects, struct. bonding, amphoteric centres 0-88506  
 Si, defects, divacancy and split 100 interstitial, electronic structure calc. 0-65494  
 Si surface, (111), energy states, computer renormalisation-group calc. 0-75617  
 SmS type semiconductors, electronic struct., influence of point defects 0-70650  
 Te, trigonal and amorphous, electronic struct. and nonempirical calc. of struct. props. 0-59866  
 $\text{TiCl}_3$ , electronic struct. and struct. phase transition 0-59644  
 $\text{VCl}_3$ , electronic struct. and struct. phase transition 0-59644  
 $\text{V}_2\text{O}_5$  and lower oxides, electronic, optical, structural and surface props., review 0-88120  
 $\text{V}_2\text{O}_5$ , energy band structure, tight-binding method 0-70602  
 tilting control see attitude control  
 timber see wood  
 time and latitude  
 see also Earth rotation; time measurement  
 equinox and equator determ. using hypothetical asteroid obs. 0-94742  
 Greenwich Obs. Time and Latitude Service, Time Report (January to March 1979) 0-72749  
 Greenwich Obs. Time and Latitude Service Time Report (April-June 1979) 0-72750  
 latitude observations, props. of local non-polar terms (*Chinese*) 0-77266  
 latitude variation, polar motion and declination, effects of Oppolzer terms (*Chinese*) 0-76891  
 local non-polar terms determ. by Okuda's method, discussion (*Chinese*) 0-85842  
 mean latitude non-polar var., techniques anal. (*Chinese*) 0-85841  
 Tokyo Astronomical Obs., Time and Latitude Bulletins (April/June 1979) 0-72752  
 Tokyo Astronomical Obs., Time and Latitude Bulletins (Jul-Sep 1979) 0-82177  
 Tokyo Astronomical Observatory Time and Latitude Service, Bulletin (January to March 1979) 0-72751  
 zenith telescope, use as astrolabe for time and latitude meas. 0-98550

## time bases

- oscilloscope low repetition trigger cct., for high speed pulse observation (*Spanish*) 0-62657

## time delay circuits see delay circuits

## time delays see delays

## time division multiplexing

- ECG multichannel recording 0-101283

## time-domain analysis

- glass fibre drawing process, characterization and control 0-58826  
 LF dielectric measurements using time-domain technique, 20 Hz to 10 kHz 0-57329  
 space-time random speckle pattern optical analysis 0-102682

# time-domain reflectometry

- benzyl alcohol, dielectric time-domain spectrosc., short and refl. method 0-101805
- chlorobenzene, dielectric time-domain spectrosc., short and refl. method 0-101805
- lumped capacitance method, spectrosc. data treatment 0-82788
- microprocessor-controlled TDR for dynamic shock position measurements 0-79248
- optical fibre connector loss evaluation by backscattering 0-58721
- optical fibre loss estimation using backscatter technique, time domain reflectometry theoretical assumptions 0-74508
- optical fibre parameter measurement using optical time domain reflectometer 0-58755
- optical fibre splice insertion loss meas., backscattering method 0-58720
- optical time domain reflectometry by photon counting 0-95122
- polarisation optical time domain reflectometry, optical fibre technique 0-78959
- travelling wave optical modulator using a directional coupler LiNbO<sub>3</sub> waveguide 0-96035

# time interval measurement *see time measurement*

## time measurement

- see also clocks; frequency measurement; streak photography; time and latitude; time resolved spectroscopy*
- Airy, G.B., Astronomer Royal 1835-81, contrib. to horology 0-86061
- atomic time and frequency standards development at Shanghai observatory, China 0-105617
- atomic time scale instability, contrib. of computation algorithm 0-98890
- atomic time scales, construction and comparison with other time scales 0-82749
- automated time keeping system of Van Swinden Lab. 0-98891
- clock synchronisation, India-W.Germany, relativistic corrections 0-95077
- clock synchronization using Symphonie satellite 0-68184
- decade counter for measuring thickness of multilayer electrodeposits (Czech) 0-95071
- electrolyte timing cell and coulometer 0-68216
- electromagnetic meas., precision, conf., Braunschweig, Germany (Jun. 1980) 0-98903
- errors, accuracy of watches and clocks, time standard 0-90821
- flow, automatic capillary, viscometer, accuracy one part in five million 0-87825
- GDR atomic time scale 0-98892
- International Atomic Time Scale, problems of generation, quality and availability 0-98889
- magnetic tape recording, time reference signal, IRIG and NASA code formats 0-57262
- mechanical start-stop gates for air tracks 0-101698
- multichannel high resolution time analyser scale instability (Russian) 0-73326
- multistage parallel-serial time averaging filters to reduce time jitter in scintillation counter time meas. 0-102405
- optical fact directional coupler switch/modulators, novel ps optical pulse sampling method 0-58784
- portable quartz clocks, accuracy in comparing time scales 0-101786
- quantum clocks, time meas., teaching 0-90632
- quartz clock, accuracy, radio signal control (French) 0-95079
- radio time-signal codes in Italy (Italian) 0-98888
- reaction timer cct., using bipolar transistors and LEDs 0-81781
- seismic events, radio broadcast signals appl. 0-90253
- standards comparison, improved accuracy 0-95062
- time-interval indicator (Russian) 0-105619
- Transit satellite system for precise time dissemination 0-57263
- users' manual on time and freq. meas. 0-94934

# time of flight mass spectra

- benzaldehyde molecules, photoionisation mass-spectrometry with excimer KrF laser 0-95691
- benzene, multiphoton ionisation mass spectra 0-57420
- benzene molecules, photoionisation mass-spectrometry with excimer KrF laser 0-95691
- 1,5-hexadiyne, time-depend. mass spectra, ionisation efficiency and breakdown curves 0-95747
- metal clusters, 2 to 500 atoms, nucleation, mass spectra 0-102596
- nuclear materials analysis using plasma desorption mass spectrometry, isotope ratio determ. using TOF mass spectrometry 0-78375

# time of flight spectra

- see also atom probe field ion microscopy; time of flight mass spectra*
- alkali metal chlorides, photofragment spectra, bond energies and excited state symmetries 0-87190
- 1-chloropropyne cation, internal energy decay studied by photoelectron-photoion coincidence spectroscopy 0-69185
- difluoroethene, cis- and trans-, photoelectron-photoion coincidence study, fluoresc. obs. 0-95678
- fragments, produced via IR laser-excitation 0-74257
- gases, molecular, total scatt. cross sections for intermediate-energy positrons 0-91692
- molecular beams, sources, gasdynamic, use of lasers, time-of-flight and detection techniques 0-69264
- neutron diffraction for quantitative texture analysis, comparison with conventional method 0-81078
- neutron diffractometry studies of time-depend. phenomena (Japanese) 0-70083
- Ar total scattering cross sections for low-energy electrons 0-58417
- Au crst., ion bombarded, Ar<sup>+</sup> ions, time-of-flight spectra of sputtered atoms 0-89103
- Au, ion bombardment by Ar<sup>+</sup>, focused ejection 0-104028
- BaO, recoil velocity spectra from form. in crossed beam system 0-76500
- Ca, forbidden transitions, radiative lifetimes, MCSCF and CI calcs., time of flight spectra for metastable state 0-91498
- Cr<sub>4</sub>(OH)<sub>6</sub>(NH<sub>3</sub>)<sub>2</sub>Cl<sub>4</sub>·4H<sub>2</sub>O, exchange coupled mol. Cr<sup>3+</sup> tetramers, inelastic neutron scatt. 0-65792
- Cu surface, fast D<sub>2</sub> desorpt. mechanism, time-of-flight spectra 0-84379
- Fe<sub>40</sub>Ni<sub>40</sub>P<sub>14</sub>B<sub>6</sub>, amorphous ferromag. spin wave excitations 0-97079
- H<sub>2</sub>, total cross sections meas. for electron scatt. at very low energies 0-58398
- He, total scatt. cross sections for low-energy electrons 0-58417
- He<sup>+</sup>+O<sub>2</sub>, charge transfer product state distrib., time of flight obs. 0-87223
- <sup>3</sup>He(<sup>4</sup>He) clusters, metastable electronic states, electron impact excitation, time of flight spectra 0-106411
- Ir, adsorbed gases, field desorption from field ion tips 0-59793

# time of flight spectra continued

- K+H<sub>2</sub>S(DS), collisional ionisation, positive and negative ion energy spectra obs. 0-63775
- Ne, metastable electronic states, electron impact excitation, time of flight spectra 0-106411
- OH+Br<sub>2</sub>, hydroxyl radicals reactive scatt. 0-85172
- Pd, surface, fast D<sub>2</sub> desorpt. mechanism, time-of-flight spectra 0-84379
- SF<sub>6</sub>, laser pumping in collisional region of nozzle beam, internal excitation, time-of-flight anal. 0-95719
- SF<sub>6</sub> multiphoton dissoci. by mol. beam method, energy distribution meas. by time-of-flight spectra, dissoci. dynamics 0-78670
- SF<sub>6</sub>+Li<sup>+</sup>(H<sup>+</sup>), mode selective vibr. excitation 0-58351
- Se, appl. to xerography 0-57415
- Se-As alloys, appl. to xerography 0-57415
- W, adsorbed gases, field desorption from field ion tips 0-59793
- W, direct inelastic and trapping-desorpt. scatt. of N<sub>2</sub>, elementary steps in N<sub>2</sub> chemisorpt. 0-60737

# time of flight spectrometers

- atom probe, for metallurgical appl. 0-86498
- cold neutron time of flight spectrometer at Studsvik, Sweden 0-63444
- electronic mass spectrometer with separator for metal cluster research 0-77907
- Fourier time-of-flight spectroscopy, higher-harmonics contamination in slow-neutron spectra, theory 0-74072
- gas-phase reactions, anal. using computer interfaced time-of-flight mass spectrometer 0-71967
- ion energy and momentum spectrometer with high resolution 0-86495
- neutron, detector containing <sup>3</sup>He 0-63441
- neutron time of flight single diffractometer using a position sensitive detector 0-99404
- position sensitive transmission time detector, for heavy ions 0-63466
- positron scattering experimental system, for meas. of angular distrib. of scattered slow positrons and electrons 0-86496
- resonance ionization source for mass spectroscopy appl. isotope anal. and time of flight spectrometer 0-81380
- reverse neutron time of flight method, slow neutron spectrometry with Fourier beam choppers 0-106230
- Xe, gas, two-body time correl., Van Hove scatt. function meas. 0-100053

# time resolved spectra

- acetylene, He-Ne laser line, high temp. absorpt., anal. by high resolution IR spectra 0-91554
- anthracene, cryst., heat pulse propag., exciton condensation, time-resolved fluoresc. spectra 0-84771
- apomyoglobin reconstituted with <sup>111</sup>In(III)mesoporphyrin IX, rot. correl. time determ. 0-76698
- atoms, two photon excitation, time depend. emitted light spectra, perturbation theory 0-63605
- benzene, nanosecond laser photolysis 0-66825
- benzene excimer, nanosecond laser photolysis 0-66825
- chrysenes, excited triplet state time-resolved vibr. Raman scatt. 0-58264
- coumarin 102, excited state interaction dynamics, picosec. time-resolved spectral shift obs. 0-78624
- coumarin dye molecules, CH stretching modes, population lifetime meas. 0-58185
- p-dichlorobenzene-p-dibromobenzene mixed crst., triplet exciton migration, time resolved emission spectroscopy 0-89052
- S,p-difluorobenzene, time resolved fluoresc. spectra, direct view of intramolecular vibr. redistribution 0-83341
- ethylene, He-Ne laser line, high temp. absorpt., anal. by high resolution IR spectra 0-91554
- fibrinogen, bovine, high energy-induced aggregation, time resolved spectra 0-61655
- formaldehyde S<sub>1</sub> levels, collisionless single rot. level lifetimes, elec. field depend. 0-63566
- haemoglobin, nanosec. probe of dynamics using time resolved reson. Raman scatt. 0-94162
- heteroexcimers, intramolecular, picosecond time-resolved fluorescence studies 0-83401
- hydrogenic and atomic observables, time resolved spectra, time reversal symm. 0-91418
- III-V semiconductors, radiative recomb., optical evaluation review 0-60647
- immunoglobulin, human, high energy-induced aggregation, time resolved spectra 0-61655
- iodomethyl radical, vibr. excited, photofragmentation IR emission obs. 0-87162
- methyl halide-inert gas mixtures, vibr. energy relax., opto-acoustic obs. 0-95711
- methyl halides, vibr. energy relax., opto-acoustic obs. 0-95711
- methyl radical, vibr. excited, photofragmentation IR emission obs. 0-87162
- optical Autler-Townes effect, time depend., finite bandwidth laser appl. theory 0-91499
- photosynthetic reaction centre spectroscopy by tunable picosec. parametric oscillators 0-61513
- plasma-electrode contact processes, microplasma diagnostics 0-59325
- PMMA film, doped, time resolved absorpt. spectra, decay kinetics of exciplex state 0-84098
- poly-N-vinyl carbazole, pulsed laser excitation, time resolved fluoresc. 0-89041
- propylene, He-Ne laser line, high temp. absorpt., anal. by high resolution IR spectra 0-91554
- pyrene, mol. ionisation pot., two photon ionisation, micellar interface effects on ionisation threshold 0-91609
- Quinacrine Mustard, time-resolved fluoresc. spectrum 0-87165
- quinones, triplet quenching by organometal cpds., time resolved CIDEP and ESR obs. 0-95654
- rhodamine 6G, in ethanol, time-depend. fluoresc. spectrum, using synchrotron radiation 0-62736
- serum albumin, bovine, high energy-induced aggregation, time resolved spectra 0-61655
- steel, mild, laser microspectral anal. 0-108769
- stilbene, cis and trans, transient spectra, radiative lifetimes and quantum yield 0-78640
- triphenylmethane dye soln., electronic relax., viscosity-depend., using picosec. flash photolysis 0-66258
- water, liq., electron solvation dynamics 0-85205
- xanthenes dyes in n-alcohols (ethylene glycol) (glycerol), rot. relax., time-resolved fluoresc. depolaris. obs. 0-58300



## time resolved spectra continued

- Ar atoms in Ne matrix, radiative and nonradiative lifetimes in excited states 0-69106  
 Ar, excitation by pulsed electric discharge, luminescence obs., time resolved spectra meas. 0-102482  
 Ar+Kr, (4p<sup>5</sup>Sp) and (4p<sup>5</sup>Sp) states, radiative lifetimes and two-body collisional deactivation rate consts. 0-95572  
 As<sub>2</sub>S<sub>3</sub>, amorphous, time resolved luminesc. 0-66288  
 BaO, spectra of fluorescence meas. using photon correlator 0-87250  
 CO-myoglobin, mol. tunnelling, isotope effect, time resolved IR Fourier transform obs. 0-72126  
 CuGaSe<sub>2</sub>, evidence of donor-acceptor type transition 0-93375  
 F+HCl→HF+Cl, time resolved vibr. chemiluminesc. and rate consts. 0-61069  
 GaAs, electron-spin relaxation and recomb. kinetics, time-resolved luminesc. study 0-108074  
 GaAs, Raman scattering from nonequilibrium LO phonons with picosecond resolution 0-80779  
 p-H<sub>2</sub>, solid, time-resolved CARS, disorder effects on coherent vibr. states 0-93342  
 H<sub>2</sub>+D(O)(Cl)(Br), relax. and chem. reaction, time resolved IR fluoresc. and mass spectrometry obs. 0-69177  
 HCl+D(O)(Cl)(Br), relax. and chem. reaction, time resolved IR fluoresc. and mass spectrometry obs. 0-69177  
 HF+HCl(CO<sub>2</sub>)(N<sub>2</sub>O)(CO)(N<sub>2</sub>O<sub>2</sub>), HF(v=3) relax. and rate consts. 0-61069  
 He, collisional excitation transfer for 3<sup>1</sup>P and D states 0-106387  
 Kr, 6p levels, two-photon excitation, time resolved fluoresc., quenching, lifetimes and photoionisation cross section 0-78587  
 Kr atoms in Ne matrix, radiative and nonradiative lifetimes in excited states 0-69106  
 Mo impurity flux, time resolved, in DITE Tokamak 0-63373  
 α-N<sub>2</sub> solid, time-resolved CARS, disorder effects on coherent vibr. states 0-93342  
 N<sub>2</sub>F<sub>4</sub>, mol. photodissoc. using CO<sub>2</sub>-laserradiation, rate const. meas., mol. fluoresc. and time-resolved UV spectra obs. (German) 0-83434  
 NO electronically excited photofragment of VUV photodissoc. methyl nitrite, identification and quantum yield 0-99527  
 NO<sub>2</sub>, discrete reson. CARS emission, temporal and spectral props. 0-95630  
 Ne pulsed transverse discharge, spectrosc. absorpt. investig. with nanosec. time resolution (Russian) 0-64782  
 O+H<sub>2</sub>O→OH+OH, energy partitioning 0-101009  
 OH+NO(NO<sub>2</sub>)(O<sub>2</sub>), OH(v=1) relax., time resolved spectra 0-74240  
 POCl<sub>3</sub>:Pr<sup>3+</sup>, fluoresc. and lifetimes of excited states 0-71466  
 Si:O<sub>2</sub>H amorphous, time resolved luminesc. 0-66288  
 Ti impurity flux, time resolved, in DITE Tokamak 0-63373  
 UF<sub>6</sub>, multiphoton irradiation, spectra and modeling of laser induced emission 0-69160  
 Xe atoms in Ne matrix, radiative and nonradiative lifetimes in excited states 0-69106  
 Xe<sub>2</sub><sup>+</sup>, synchrotron radiation excited, time resolved spectroscopy 0-69092

## time resolved spectroscopy

- see also streak photography  
 acridine orange, fluoresc. decay meas. by high repetition rate gated photon counting 0-86402  
 anthracene dianions in dimethyl ether, rotational diffusion meas. 0-65262  
 discharges, selfluminous, schlieren system for time and space resolved photography 0-87471  
 fluorescence spectroscopy using pulsed lasers 0-57393  
 Fourier transform spectrometer, double-pass rapid-scanning, for plasma diagnostics 0-103190  
 instrumental advances in time- and space-resolved spectrometry, optical spectrometer (Polish) 0-90906  
 IR photographic technique using freq. upconversion, methyl isocyanide isomerisation obs. 0-57400  
 laser saturation spectroscopy, time-resolved, free induction decay of two-level resonances 0-102775  
 laser-produced plasmas, time-resolved X-ray spectrosc. 0-84004  
 linear accelerator with S-band subharmonic prebuncher for picosecond single electron pulse (Japanese) 0-78460  
 low loss dielectric measurements using time domain spectroscopy 0-98983  
 optical fibres, subpicosecond response meas. 0-78961  
 optical spectrometers, instrumental advances and new designs (Polish) 0-101847  
 pentacene dianions in dimethyl ether, rotational diffusion meas. 0-65262  
 phenol, aq. soln., electron ejection, picosec. obs. 0-87187  
 phenolate, aq. soln., electron ejection, picosec. obs. 0-87187  
 pyrimidine, vapour, phosphoresc. 0-83408  
 rapid scanning Fourier transform time resolved spectroscopy, practical aspects 0-86464  
 soft X-ray diagnostics, high efficiency CsI and CuI photocathode evaluation 0-57442  
 steel, impurity spectral lines, intensity, temp. and conc. effects 0-64774  
 streak camera, picosecond jitter 0-73486  
 synchrotron radiation used for fast fluoresc. obs. 0-62736  
 tetracene dianions in dimethyl ether, rotational diffusion meas. 0-65262  
 transient dispersion and absorption, bridge type superhet. microwave spectrometer investig. 0-91551  
 tris(bipyridine)ruthenium(II)dichloride, fluoresc. decay meas. by high repetition rate gated photon counting 0-86402  
 unipolar pulsed LCD discharge, spectrum, time scanning 0-64774  
 velocity-changing collisions, study by time resolved saturated absorption 0-82832  
 AgBr, cyclotron reson. of polarons at high density excitation 0-75859  
<sup>13</sup>C, 2D NMR spectra, off-resonance decoupling 0-74182  
 Cd, n<sup>2</sup>S<sub>0</sub> and n<sup>2</sup>D<sub>2</sub> levels lifetimes, time-resolved spectrosc. obs. (French) 0-102456  
 KI, growth time of π emission in picosecond range 0-76067  
 N, (2<sup>2</sup>S<sub>1/2</sub>), kinetic study by time resolved atomic resonance fluorescence 0-95557

## time series

- conference, Nottingham, England (Mar. 1977) 0-82580  
 groundwater, trend of hydrographs 0-85687  
 maximum entropy spectral estimation of frequency and arrival angle 0-96129  
 weather prediction, normalised variance anal. for meteorological time series, F-distribution (Chinese) 0-67388  
 wind, stochastic predictors, AR and ARMA models 0-67400

## timing see time measurement

## timing circuits

- CMOS ICM 7216B multifunction counter used for time, frequency or period measurement (German) 0-74092  
 digital timer with memory, appl. to dynamics experiments, principles of electronic circuitry 0-67994  
 exposure meter and development timer, used for photographic enlarger 0-101856  
 illumination timer for hobby photography (German) 0-98992  
 photographic enlarger digital timer, 0.1 second steps of 0.1 minute steps 0-77893  
 photographic flash sequencer, using thyristor control 0-62749  
 photographic print timer, using ring of LEDs 0-77899  
 spark timer circuit 0-67991  
 timer, touch controlled, photography appls. (Spanish) 0-86478

## tin

- see also nuclei with .....  
 (100) surface, clean and O<sub>2</sub> exposed, slow positron studies, positronium formation 0-93429  
 adsorbed on W and Mo (001), struct., FIM obs. 0-103576  
 coadsorption on Pb, P, or O contaminated Ni surface, AES study 0-88437  
 coatings on steel, Ni, Cu, polypropylene and ABS, autocatalytic deposition 0-100965  
 core level binding energies 0-71564  
 diffusion in bottom surface of float glass, synthesis 0-79993  
 Fermi surface, dilational strain depend., elastic moduli and torque obs. 0-70586  
 film, anomalous transmittance of metal-insulator interface for thermally radiated phonons (Russian) 0-103664  
 film, limitation in microwave stimulation of supercond., crit. current meas. (Russian) 0-88695  
 film, metastable supercond. alloys, produced by low temp. ion implantation 0-88670  
 film, superconducting, crit. currents in microwave EM fields, for long film 0-70898  
 film, superconducting fluctuations, transition temp. (Russian) 0-65740  
 film, vacuum deposited, substrate and substrate temp. effects on struct. 0-107677  
 foils, 1-3.5 GeV electron impact, transition X-ray emission, comparison with theory (Russian) 0-60794  
 galvanomagnetic props., temp. depend. meas. in single cryst. 0-96850  
 grey, lattice dynamics 0-107389  
 hollow cathode, emission obs. from Sn II, I transitions 0-106509  
 impurities in low alloy steels, effect on neutron irradiation embrittlement 0-85055  
 impurity in Cr-Mo-V low-alloy steel, effect on high-temp. ductility and crack growth 0-66652  
 impurity in Mn-Mo steel, effect on mech. props. 0-66596  
 impurity in Nimonic 105, influence on creep and stress rupture props. 0-66602  
 infiltrated Ti base composite sintered bearing materials, antifriction props. 0-60981  
 internal conversion coeffs. for inner shells of atomic ions and relativistic ionic potentials 0-68600  
 ion bombardment-induced photon emission near melting point 0-100699  
 ion polarisation and point defect resistivity in metals 0-103672  
 laser radiation absorption in craters on metal targets 0-97386  
 liquid, diffusion coeff. of <sup>113</sup>Sn, <sup>123</sup>Sb, <sup>110</sup>Ag, and <sup>195</sup>Au 0-96676  
 liquid, impurity diffusion, shear cell assembly meas. (French) 0-75375  
 liquid, optical props., 0.62-3.7 eV 0-75996  
 liquid, optical props. by spectroscopic ellipsometry, review 0-103929  
 magnetic breakdown orbits 0-103615  
 MHD laminar flow, longitudinal dynamic effects determination for Sn (Rumanian) 0-64792  
 molten, thermal expansion meas. to 1300K 0-65254  
 monolayer, double layer with Pb on Al (111), layer growth, struct. 0-70567  
 nonlinear conductivity of thin films in mixed state (Russian) 0-80464  
 pitting corrosion in aq. solns., influence of Cl<sup>-</sup>, ClO<sub>4</sub><sup>2-</sup>, and NO<sub>3</sub><sup>-</sup> (French) 0-89389  
 polycrystalline films, elec. props. and crystallite size, 4.2K to room temp. (Russian) 0-93011  
 positron annihilation in fine particles, surface trapped states 0-84800  
 quench-condensed films, superconducting transition temp., elastic stress and strain effects 0-70883  
 superconducting film, crit. mag. fields, temp. depend., penetration depth thickness depend. 0-70908  
 superconducting thin film, crit. temp. enhancement (Russian) 0-93021  
 superconducting thin films covered by Ge, effect on excess elec. cond. 0-65741  
 thermally induced vacancies, positron trapping 0-89083  
 ultrathin metallic filaments, appearance of dielec. instability, coexistence with supercond. 0-103784  
 white, band masses and deformation pots., OPW pseudopotential model 0-100430  
 white, Fermi surface, dilational strain depend., OPW calcs. 0-84418  
 white, nuclear acoustic reson., Knight shift 0-71204  
 Young's modulus and internal friction, 20°C to melting point (Russian) 0-89278  
 Z dependence of thick target β-ray backscattering 0-76118  
 Ag-Sn double films, high-speed superconducting bolometer appl. 0-57368  
 Al-Formvar-Sn coupled films, Ginzburg's excitonic supercond. model 0-97039  
 Bi<sub>2</sub>SiO<sub>2</sub>Sn, Raman scatt. spectra, impurity effect 0-80795  
 CaSe:Sn<sup>3+</sup>, EPR study of octahedral Sn<sup>3+</sup> centres, 4 to 290K (Russian) 0-84637  
 Cu-Sn thin film couples, room temperature interactions 0-96699  
 Fe<sub>3</sub>Pt-Sn Invar alloy, Mossbauer shift temp. depend. 0-100626  
 GaAs:Ge MBE power FETs with Sn surface impurities 0-80374  
 GaAs:Sn, epitaxial film, influence of impurities on stacking fault energy 0-103371  
 GaAs:Sn, ion implanted, laser annealed, high doping levels 0-88181  
 GaAs:Sn thermal diffusion from spin-on SnO<sub>2</sub>/SiO<sub>2</sub> source 0-96691  
 GaAs:Sn<sup>3+</sup>, impurity-defect complex from <sup>119</sup>In implantation, Mossbauer study 0-59486  
 n-GaAs:Sn-p-GaAs:Ge-p-AlGa<sub>1-x</sub>As:Ge heterostructure solar cells, LPE growth techniques 0-66977  
 GaP:Sn, complex impurity-defect, Mossbauer study 0-75898  
 GaSb:Sn, p-n junction, electroluminesc. and photoluminesc. 0-66306

## tin continued

- p-GaSe:Sn, majority carrier drift mobility meas. 0-92895  
 Ge:<sup>119m</sup>Sn, impurity lattice dynamics, Mossbauer spectra, Debye temp. 0-84262  
 Ge:Sn, ion implantation of radioactive <sup>119</sup>Sn 0-59495  
 IN<sub>2</sub>O<sub>3</sub>:Sn, RF magnetron sputtered film, elec. and optical props. 0-104065  
 InAs:Sn, single crystals, defect formation 0-88606  
 InO<sub>3</sub>:Sn transparent conducting films, homeotropic orientation of liquid crystals (*Russian*) 0-108181  
 In<sub>2</sub>O<sub>3</sub>:Sn, films, activated reactive evaporation technique of prep. 0-80989  
 In<sub>2</sub>O<sub>3</sub>:Sn films; vac. deposited, elec. props. 0-100542  
 PbTe:In, Shubnikov-de Haas oscillatory effects, quasilocal impurity level 0-92912  
 Si:<sup>119m</sup>Sn, impurity lattice dynamics, Mossbauer spectra, Debye temp. 0-84262  
 Si:Sn, Mossbauer study of defects due to <sup>119</sup>In implantation 0-80641  
 Sn II, cool plasma, isolated lines, Stark broadening, semi-empirical impact approx. calcs. 0-59186  
 Sn II homologous ions series, Stark broadening trends 0-105157  
 α-Sn, ion implanted, defect struct., Mossbauer spectra 0-80214  
 Sn, supercond. tunnel junction, quasiparticle excitation by α-particles 0-103791  
 β-Sn, transverse magnetoresist., temp. depend. in mag. field (*Russian*) 0-107765  
 α-Sn:<sup>119m</sup>Sn, impurity lattice dynamics, Mossbauer spectra, Debye temp. 0-84262  
 Sn/Au thin film couples, evaporated, TEM study 0-59832  
 Sn/Au thin film diffusion couples, Kirkendall void form. 0-96698  
 Sn/Cu electroplated bimetallic films, interfacial reaction 0-96765  
 Sn-KCl granular superconductors, far IR absorpt. 0-84548  
 Sn-Si heterojunction, RHEED, Mossbauer spectroscopy and I-V characts. 0-70828  
 Sn-Sn<sub>2</sub>O<sub>3</sub>:Sn long Josephson tunnel junction, flux flow, crit. conditions 0-80452  
 Sn-SnO<sub>2</sub>-Sn tunnel contacts, spatially inhomogeneous state under strong injection conditions 0-80457  
 Sn-SnO<sub>2</sub>-Sn tunnelling junctions, fabrication by modified RF plasma oxidation method 0-103787  
 Sn+He(C)(N)(O), inner-shell multiple ionisation systematics, X-ray obs. 0-63790  
 Sn<sub>2</sub>, in Ar matrix, absorpt., fluoresc. and reson. Raman spectra 0-95640  
<sup>113</sup>Sn, diffusion in Cu 0-65301  
<sup>119</sup>Sn, hyperfine mag. fields in Cr<sub>1-x</sub>Mn<sub>2</sub>O<sub>2</sub> Mossbauer study 0-71260  
<sup>119</sup>Sn temp. depend. isomer shift, pseudopot. approach 0-84675  
<sup>119</sup>Sn<sup>1</sup>, total mass absorpt. coeff. of gamma quanta, chem. binding influence, determ. using Mossbauer effect 0-99467

## tin alloys

## see also tin compounds

- Admiralty Metal, transgranular stress corrosion crack propag. 0-89402  
 bronze, diffusion of Ga in V<sub>3</sub>Ga layer, grain boundaries (*Russian*) 0-65297  
 bronze, low-cycle fatigue, NH<sub>3</sub> effect 0-104348  
 bronze, powders, electric-pressure sintering onto cylindrical parts in fluidised bed 0-100960  
 Dispersalloy, Sn-Hg amalgam, γ<sub>2</sub> precip. suppression and gettering kinetics 0-71651  
 intermetallic ternary systems, new supercond./mag. cpds., X-ray powder diff. data 0-100215  
 rare earth rhodium tin intermetallic cpds., synthesis, supercond. and mag. props. 0-100547  
 rare earth-Sn-X, X=Rh, Ir, Ru, Co, cryst. growth and cryst.-chem. invest, supercond./mag. ternary cpds. 0-100777  
 steel, rail, toughness, effect of Sn, SEM exam. 0-97569  
 Zircaloy, annealed, neutron irradiated, inhomogeneous deform. behaviour 0-85014  
 Zircaloy, breakaway mechanism, corrosion kinetics in steam 0-61030  
 zircaloy, nuclear microprobe methods for investigating oxidative corrosion 0-71787  
 Zircaloy cladding, stress corrosion cracking, inner surface texture effect 0-66695  
 Zircaloy-2, anodic oxidation kinetics, in 0.05M oxalic acid (aq. and alcoholic) 0-104331  
 zircaloy-2, plastic deformation, generalised constitutive eqns. 0-104219  
 Zircaloy-2, yield pts. obtained by ageing at two stresses 0-81091  
 Zircaloy-4, creep rupture at superimposed non-stationary stress and temp. loading 0-66630  
 Zircaloy-4, elastic props., O additions effect 0-66565  
 Ag-In-Sn, internal oxidation, precipitation behaviour of oxide (*Japanese*) 0-66515  
 Ag-In-Sn, internal oxidation, solute element and O<sub>2</sub> behaviour (*Japanese*) 0-89479  
 Ag-Sn, liquid alloys, thermodynamic props. (*Japanese*) 0-108396  
 Ag-Sn, splat-quenched, X-ray diff. study 0-81094  
 Ag-Sn alloys and amalgams, electrochem. considerations, corrosion in physiological soln. 0-93760  
 Ag-Zn-Te-Sn-(In), internally oxidised, oxide particle size control (*Japanese*) 0-89480  
 Au-Sn, zeta and AuSn phases, heats of form. and heat contents 0-60837  
 Au(Ag)(Cu)-Sn liquid, optical reflectivity spectra of virtual bound states 0-89021  
 BaPdSn<sub>3</sub>, prep. and crystal structure (*German*) 0-84138  
 Bi-Sn, eutectic, contact melting kinetics (*Russian*) 0-70377  
 CaSn<sub>3</sub>, powdered, de Haas-van Alphen effect 0-59857  
 Cd-Sn alloy, superconductivity and microstructure 0-107949  
 Cd-Sn binary system, high press. study 0-93539  
 Ce(In, Sn)<sub>3</sub>, heat capacity and elec. resist. 0-71049  
 Ce(In, Sn)<sub>3</sub>, mag. susceptibility, temp. depend., intermediate valence 0-65779  
 CeIn<sub>3</sub>-Sn, mixed valence system, low-temp. susceptibility, paramagnon study 0-97077  
 CeSn<sub>3</sub>, intermediate valence cpd., search for phonon anomalies, inelastic neutron scatt. 0-100317  
 CeSn<sub>3</sub>, mixed valence cpd., electronic struct. and mag. props. 0-70649  
 CeSn<sub>3</sub>, mode softening and elastic consts., acoustic vel. meas. 0-88242  
 Co-Sn system, phase Co<sub>3</sub>Sn obtained by splat cooling (*German*) 0-104147  
 Co-Sn-M, n=Mg, Ca, Sr, Se, Y, Zn, Cd, In or Th, cryst. growth and cryst.-chem. invest, supercond./mag. ternary cpds. 0-100777

## tin alloys continued

- Cu/Sn-Ni/Au tricouples, electrodeposited, interdiffusion obs. 0-84331  
 Cu-Al-Sn system, coexistence of different and brass like phases 0-89206  
 Cu-Nb<sub>3</sub>Sn multifilamentary tapes, in situ formed, crit. current density anisotropy 0-84576  
 Cu-Ni-Sn (10, 6 wt.%), spinodal decomposition, X-ray and electron diff. study 0-81063  
 Cu-Ni-Sn (15, 8 wt.%), prior deform. effect on spinodal age hardening 0-108465  
 Cu-Ni-Sn (9, 2 wt.%), surface comp., Auger electron spectroscopy study, manufacture and storage influence 0-65348  
 Cu-Sn, thermodynamics of Cu and Sn solns. using copper β-alumina solid electrolyte, 800-1100K 0-107502  
 Cu-Sn, vacuum condensed, reflecting surface absorpt. coeffs. at 10.6 μm 0-95984  
 Cu-Sn (4.9 wt.%), role of mech. twinning on stress/strain behaviour 0-85004  
 Cu-Sn binary system, wettability and interaction between solids and liqs. (*Japanese*) 0-92760  
 Cu-Sn industrial bronzes, Sn diffusion in deform. zone influence on wear resistance, friction (*Russian*) 0-108582  
 Cu-Sn system, long period superlattice obs. and impurity effects 0-103297  
 Cu-Sn-Al, deform at high temps. (*Polish*) 0-89284  
 Cu<sub>2</sub>MnAl<sub>1-x</sub>Sn<sub>x</sub>, Mossbauer effect study 0-60473  
 Cu<sub>2</sub>MnIn<sub>1-x</sub>Sn<sub>x</sub> alloy, compositional SRO, hyperfine interactions 0-71065  
 Cu<sub>2</sub>NiSn, Heusler alloy, elec. resist., 4.2 to 300K 0-75547  
 DyRh<sub>1-x</sub>Sn<sub>3x</sub>, new supercond./mag. cpds., X-ray powder diff. data 0-100215  
 ErRh<sub>1-x</sub>Sn<sub>3x</sub>, new supercond./mag. cpds., X-ray powder diff. data 0-100215  
 ErRh<sub>1-x</sub>Sn<sub>3x</sub>, synthesis, supercond. and mag. props. 0-100547  
 Fe-Ni (6.8 at.%) 0-75888  
 Fe-Pd (1-2 wt.%), solution of <sup>119</sup>Sn, study by Mossbauer spectroscopy 0-75888  
 Fe<sub>1-x</sub>Mn<sub>x</sub>Sn, spin reorientation, Mossbauer study, 77 to 400K 0-97172  
 Fe<sub>2</sub>Sn<sub>1-x</sub> amorphous alloy, elec. resist. 0-80246  
 Fe<sub>2</sub>Sn<sub>1-x</sub> amorphous film, struct. and mag. props. 0-65972  
 In-Sn alloy crystals, phase changes and shape memory effect (*Japanese*) 0-108502  
 β-In<sub>2</sub>Sn, decomposition, X-ray powder diff. study 0-89196  
 In<sub>3</sub>Sn, tetragonal supercond., lower and upper crit. field, anisotropy and temp. depend. 0-97042  
 Ir-Sn-M, M=Mg, Ca, Sr, Sc, Y, Zn, Cd, In or Tl, cryst. growth and cryst.-chem. invest, supercond./mag. ternary cpds. 0-100777  
 (La,Nd)Sn<sub>3</sub>, reverse Kondo effect in presence of crystalline elec. field splitting 0-103684  
 La<sub>2</sub>Co<sub>2</sub>Sn<sub>7</sub>, prep. and crystal structure (*German*) 0-84138  
 LaSn<sub>3</sub>, doped with Tb, Nd, or Pr, crystal field effects, tunnelling within mK range 0-70907  
 MnSn<sub>1-x</sub>Sn<sub>x</sub>, films, Faraday rotation, optical absorpt. coeffs. 0-97242  
 Mo-Sn-Se system, supercond. crit. temp. and cryst. struct. (*Russian*) 0-107947  
 Nb<sub>3</sub>/Sn-Cu composites, in situ processed, supercond. props. 0-75698  
 Nb<sub>3</sub>Sn A15 composite superconductors, hydrostatic extrusion (*French*) 0-104090  
 Nb<sub>3</sub>Sn, A15 cpd., normal state, low temp. resist., disorder effects 0-107762  
 Nb<sub>3</sub>Sn based multifilamentary superconductors, bronze process fabrication, voids growth obs., via hot stage SEM 0-70089  
 Nb<sub>3</sub>Sn bronze process, flux pinning scaling law depend. on strain 0-75696  
 Nb<sub>3</sub>Sn, coherence parameter, nonlinear high temp. supercond. elements with A-15 lattice (*Russian*) 0-60127  
 Nb<sub>3</sub>Sn composite, superconducting transition depend. on non-hydrostatic stress 0-107948  
 Nb<sub>3</sub>Sn, composite superconducting wire, critical current-bend strain relationships 0-93063  
 Nb<sub>3</sub>Sn, effect of changes in α<sup>2</sup>(Ω)F(Ω) on the zero-temp. energy gap 0-97025  
 Nb<sub>3</sub>Sn, filaments in Cu matrix, thermal strain effects on superconducting critical temp. 0-93032  
 Nb<sub>3</sub>Sn film formation, solubility, precipitating processes (*Russian*) 0-92792  
 Nb<sub>3</sub>Sn, flux density gradient determ. by Faraday effect 0-107969  
 Nb<sub>3</sub>Sn forced flow superconducting test coil, Westinghouse design for fusion reactor large coil program 0-99337  
 Nb<sub>3</sub>Sn, hot isostatically pressed, plastic deform. 0-108510  
 Nb<sub>3</sub>Sn microfilamentary superconducting composite, critical currents, fracture props. 0-107970  
 Nb<sub>3</sub>Sn, monofilaments, radiation-enhanced diffusion growth, crit. current density 0-65758  
 Nb<sub>3</sub>Sn, multifilamentary coils for Lawrence Livermore Laboratory superconducting High Field Test Facility 0-90834  
 Nb<sub>3</sub>Sn multifilamentary composite supercond. wires, transverse sections prep., ion milling, TEM obs. of grain size 0-101000  
 Nb<sub>3</sub>Sn multifilamentary supercond. composites, crystallographic texturing 0-71669  
 Nb<sub>3</sub>Sn, multifilamentary superconductor preparation by 'in situ' and cold powder methods, review 0-93522  
 Nb<sub>3</sub>Sn, on LiNbO<sub>3</sub> substrate, US attenuation of SAW in applied mag. field 0-75678  
 Nb<sub>3</sub>Sn, powder metallurgically produced, microstruct. characts. 0-89233  
 Nb<sub>3</sub>Sn, softening of surface phonons in (100) plane 0-107627  
 Nb<sub>3</sub>Sn, supercond. composite, residual stress state, crit. currents 0-80468  
 Nb<sub>3</sub>Sn, supercond. props., effect of neutron irradi. 0-80463  
 Nb<sub>3</sub>Sn, superconductor for Large Coil Program, low temp. stability, joints, design method 0-106195  
 Nb<sub>3</sub>Sn, Young's modulus, 4.2-300K, behaviour near martensitic transition 0-66564  
 Nb<sub>3</sub>Sn-Cu multifilamentary composite wire, Nb<sub>3</sub>Sn filament morphology and grain size 0-100855  
 (Nb<sub>0.99</sub>Zr<sub>0.01</sub>)<sub>3</sub>Sn, AC power losses in parallel AC and DC mag. fields 0-97041  
 NdRh<sub>1-x</sub>Sn<sub>3x</sub>, new supercond./mag. cpds., X-ray powder diff. data 0-100215  
 NdSn<sub>3</sub>, elec. cond., cryst. field effect, spin disorder contrib. 0-65540  
 Ni-Cu-X (X=Sn, Nb, Ti), spinodal decomp. alloys, linear expansion coeff. influence on morphological anisotropy (*Japanese*) 0-70431



## tin alloys continued

- Ni-Sn intermetallic phase growth kinetics at liq. Sn-solid Ni interface 0-71638  
 Pb-Sn, strength loss in supercond. transition, nonmag. and paramag. impurities influence (*Russian*) 0-70875  
 Pb-Sn (20wt.%), eddy current study of solidification 0-104141  
 Pb-Sn binary alloy, unidirectional solidification, convective and interfacial instabilities 0-60851  
 Pb<sub>1-x</sub>Sn<sub>x</sub>, liquid alloys, local fluctuations and quadrupolar relaxation 0-66060  
 Pd<sub>2</sub>MnIn<sub>1-x</sub>Sn, Heusler alloy, mag. order, disorder effects 0-88723  
 Pd<sub>2</sub>Mn<sub>1-x</sub>V<sub>x</sub>Sn, Heusler alloy, structural disorder, Mossbauer study 0-80650  
 Pd<sub>2</sub>Sn<sub>1-x</sub> (x=0.95, y=0.05; x=3, y=1), Mossbauer spectra, high press. effects, force consts. 0-84669  
 PrRh<sub>3</sub>Sn<sub>2</sub>, crystallography X-ray powder diffr. study 0-100217  
 PrSn<sub>3</sub>, thermal expansion and transverse elastic const. near mag. phase transition 0-60394  
 Pt<sub>3</sub>Sn, L<sub>1</sub> ordered alloy, positive temp. depend. on strength, phase destabilization 0-81203  
 Ru-Sn-M, m=Mg, Ca, Sr, Sc, Y, Zn, Cd, In or Th 0-100777  
 Ru<sub>2</sub>FeSn, ferromag. Heusler alloys, hyperfine fields at nonmagnetic atoms in various sites, Mossbauer effect and NMR meas. 0-66089  
 Sn-Bi, crystallisation temp., overcooling temp. (*Russian*) 0-97472  
 Sn-Bi, small  $\kappa$  supercond., phase transitions higher than second order 0-88668  
 Sn-Bi, thermal analysis in non-faceted/faceted eutectic systems 0-71637  
 Sn-Bi(Pb)(Ga), temp. regime of crystn. on rapid cooling (*Russian*) 0-66495  
 Sn-Cd-Pb system, contacting layer struct. and phase composition (*Russian*) 0-66475  
 Sn-Cu film, metastable supercond. alloys produced by low temp. ion implantation 0-88670  
 Sn-In, nonlinear conductivity of thin films in mixed state (*Russian*) 0-80464  
 Sn-La(Ce)(Y) systems, heats of form. 0-89517  
 Sn-Ni electrodeposited equatonic alloy, cryst. struct., X-ray, electron diffr. anal. 0-79748  
 Sn-Pb (26%), liq. eutectic alloy Seebeck coeff. 0-84463  
 Sn-Pb alloys electroplating, comparison with Au (*French*) 0-89158  
 Sn-Pb solder, wettability on Cu and mild steel plates (*Japanese*) 0-89244  
 Sn-Pb surfaces ageing, detrimental effect in PC fabrication 0-108625  
 Sn-Pb-Bi-(Cd) infiltrated Ti base composite sintered bearing material, antifricition props. 0-60981  
 Sn-Pb-(Bi) infiltrated Ti base composite sintered bearing material, antifricition props. 0-60981  
 Sn-Sb, small  $\kappa$  supercond., phase transitions higher than second order 0-88668  
 Sn-Te, molten, elec. cond. and phase diagram 0-84454  
 Sn-Zn, use as evaporant source for Zn bearing thin film alloy prep. 0-100789  
 Sn<sub>90</sub>Cu<sub>10</sub>, quench-condensed films, superconducting transition temp., elastic stress and strain effects 0-70883  
 SnMg<sub>2</sub>, <sup>119</sup>Sn temp. depend. isomer shift, pseudopot. approach 0-84675  
 SrPdSn<sub>3</sub>, prep. and crystal structure (*German*) 0-84138  
 TbRh<sub>3</sub>Sn<sub>2</sub>, crystallography X-ray powder diffr. study 0-100217  
 Ti-Al-Sn, alloy 6242, dynamic effects of flow and fracture during isothermal forging 0-76343  
 $\alpha$ -Ti-Al-Sn, alloy Ti-679, electron diffr. anal. of Ti<sub>3</sub>Si phase (*Chinese*) 0-64845  
 Ti-Al-Sn-Zr, Ti-680, O contamination under high temp. (*Chinese*) 0-66688  
 Ti-Al-Sn-Zr-Mo {6,2,4,6 wt.%} fusion weldment, substruct. characts. 0-84183  
 Ti-Al-V-Sn (5.5, 5.5, 2 wt.%), crack growth, slow, H-induced 0-104272  
 Ti-Al-V-Sn (6.6, 2 wt.%), fusion weldment, substruct. characts. 0-84183  
 Ti-Mo-Zr-Sn (11.5, 6.0, 4.5 wt.%), mech. property, microstruct. relationships 0-84961  
 Ti-Mo-Zr-Sn (11.5, 6.0, 4.5 wt.%) alloy, struct. as affected by processing history 0-84972  
 $\beta$ -Ti-Mo-Zr-Sn(11.5, 6, 4.5 wt.%), metastable phase III, microstruct. and age hardening response 0-84945  
 V(Nb)-Sn-Cu, rapidly quenched, comp. and phase equilb. 0-76235  
 V<sub>2</sub>Sn, A-15 cpd., normal-state elec. resist. 0-75542  
 YbSn<sub>3</sub>, powdered, de Haas-van Alphen effect 0-59857  
 Zircaloy-4, deformation behaviour between 77 and 900K 0-71686  
 Zn-Sn-Bi, ternary phase diagrams, interactive computer program 0-71629  
 Zr-Nb-Sn (3.0, 1.0 wt.%), high temp. oxidation in flowing O<sub>2</sub>, 873-1173K 0-93687  
 Zr-Sn, Zr-Sn-Mo, creep characts., influence of Sn and Mo (*Czech*) 0-81119  
 Zr-Sn (1.5 wt.%), electron irradiation damage, direct obs. 0-84212  
 Zr-Sn-Fe-Ni (1.5, 0.1, 0.15 wt.%), electron irradiation damage, direct obs. 0-84212  
 Zr-Sn(Fe)(Ni) (0.15 wt.%), electron irradiation damage, direct obs. 0-84212

## tin compounds

- see also tin alloys  
 halides, XY<sub>4</sub> molecules, force consts. by modified Redington and Aljibury method 0-69261  
 hexahalo ions, octahedral, mol. consts. calcs. 0-106317  
 ternary compounds, R<sub>3</sub>Sn<sub>2</sub>Mo<sub>2</sub>S<sub>8</sub> (R=La, Ce, Pr, Eu, Gd, Ho, Lu, Y, In, U), supercond. props. 0-97023  
 $\beta$ -Al<sub>2</sub>O<sub>3</sub>-(K,Sn)<sub>2</sub>O, ionic cond. and Raman spectra 0-107509  
 Ca<sub>2</sub>Gd<sub>2-x</sub>Sn<sub>2-x</sub>Sb<sub>2-x</sub>O<sub>7</sub>, pyrochlore struct. form. 0-92504  
 CdO-SnO<sub>2</sub>, DC reactively sputtered films, elec. and optical props. 0-103763  
 p-CdSnAs<sub>2</sub>, Hall effect, thermo EMF, thermomagnetic effects 0-107822  
 CdSnAs<sub>2</sub>, solubility in Sn melt, temp. depend., enthalpy of melting 0-59658  
 CdTe/SnCl<sub>2</sub>/Pt, solar cell photoelectric props. (*Spanish*) 0-85290  
 Co(H<sub>2</sub>O)<sub>6</sub>(SnF<sub>3</sub>)<sub>2</sub>, crystal structure (*French*) 0-59441  
 Ge<sub>1-x</sub>Sn<sub>x</sub>Te film, amorphous, elec. cond. 0-93016  
 In<sub>2</sub>O<sub>3</sub>-SnO<sub>2</sub> thin film, Hall mobility, temp. depend., grain boundary effects 0-75658  
 In<sub>2</sub>O<sub>3</sub>-SnO<sub>2</sub>/polySi, solar cell response exam. using electron-beam-induced current and scanning light spot tech. 0-81477  
 In<sub>2</sub>O<sub>3</sub>-SnO<sub>2</sub>-CdTe:P, p-n homojunction solar cell, elec., photovoltaic props., photoluminescence 0-81463

## tin compounds continued

- In<sub>2</sub>O<sub>3</sub>-SnO<sub>2</sub>-InP solar cell junctions, efficiency, InP surface props. 0-85288  
 In<sub>2</sub>O<sub>3</sub>-SnO<sub>2</sub>-Si SIS heterojunction solar cells 0-85281  
 In<sub>2</sub>O<sub>3</sub>-SnO<sub>2</sub>-Si SIS solar cells, reverse current-voltage characts. under illumination 0-89622  
 In<sub>2</sub>Se<sub>1-x</sub>SnO<sub>2-x</sub> amorphous film-SnO<sub>2</sub> system, photovoltaic spectra, annealing effect (*Japanese*) 0-92926  
 In<sub>2</sub>Si<sub>2</sub>O<sub>7</sub>, thin film, sputter deposition form., optical and elec. props. 0-60123  
 In<sub>2-x</sub>Sn<sub>x</sub>O<sub>3-y</sub> solar cells, majority carrier conduction effects 0-97796  
 In<sub>2-x</sub>Sn<sub>x</sub>O<sub>3-y</sub>-Ga<sub>1-x</sub>P-(InP,As<sub>1-y</sub>) heterojunction solar cells, chemistry and prep. 0-94073  
 In<sub>2-x</sub>Sn<sub>x</sub>O<sub>3-y</sub>-SiO<sub>2</sub>-Si SIS solar cells, loss mechanisms study for improvement of efficiency to above 12% 0-94080  
 KCl:SnCl<sub>2</sub>, photostimulated hole recombination luminesc. (*Russian*) 0-80833  
 (NH<sub>4</sub>)<sub>2</sub>SnBr<sub>6</sub>, structural phase transitions study by Raman scatt. 0-93318  
 PbSnF<sub>4</sub>, anionic conductor, thin films and ceramics 0-107556  
 PbSnF<sub>4</sub>, high anionic cond. of new solid electrolytes 0-107546  
 Pb<sub>0.9</sub>Sn<sub>0.1</sub>F<sub>2</sub>, NMR study of F atom motion (*French*) 0-100622  
 Pb<sub>0.8</sub>Sn<sub>0.2</sub>F<sub>2</sub> solid soln., struct. evolutions (*French*) 0-96488  
 Pb<sub>0.8</sub>Sn<sub>0.2</sub>Sb films, DC sputtered, elec. props. 0-80426  
 Pb<sub>1-x</sub>Sn<sub>x</sub>Se epitaxial layers, radiative and nonradiative recomb. processes 0-60670  
 Pb<sub>1-x</sub>Sn<sub>x</sub>Se epitaxial layers obtained by LPE, growth conditions correl. with morphology 0-104079  
 Pb<sub>1-x</sub>Sn<sub>x</sub>Se solid solns., photoluminesc. spectra, energy band parameter determ. 0-71484  
 Pb<sub>1-x</sub>Sn<sub>x</sub>Se, transport phenomena in solid solutions with band inversion 0-107792  
 Pb<sub>1-x</sub>Sn<sub>x</sub>Se, X=0.03-0.07, monocrystal film, edge of intrinsic absorpt. (*Russian*) 0-71368  
 Pb<sub>0.8</sub>Sn<sub>0.2</sub>Se, multispectral photovoltaic IR detectors 0-105710  
 PbSnTe, optical dielectric const. variation with carrier conc. 0-84709  
 Pb<sub>0.78</sub>Sn<sub>0.22</sub>Te, Pb<sub>0.9</sub>Sn<sub>0.09</sub>Se, radiative and nonradiative recombination 0-80849  
 Pb<sub>0.8</sub>Sn<sub>0.2</sub>Te:Ce, influence of Cd doping on high field magnetoresist. and Hall effect 0-75590  
 Pb<sub>0.8</sub>Sn<sub>0.2</sub>Te:La, evaporated thin films, low carrier conc. 0-65414  
 Pb<sub>0.82</sub>Sn<sub>0.18</sub>Te, film, effect of hydrostatic pressure on props. 0-70862  
 Pb<sub>0.82</sub>Sn<sub>0.18</sub>Te, layers on mica substrate, Hall constant peculiarities 0-75588  
 Pb<sub>0.85</sub>Sn<sub>0.15</sub>Te homostructure diode laser, LPE growth, with controlled carrier conc. 0-95903  
 n-Pb<sub>0.88</sub>Sn<sub>0.12</sub>Te spin flip Raman laser pumped by TE CO<sub>2</sub> laser, characts. 0-87397  
 Pb<sub>1-x</sub>Sn<sub>x</sub>Te diode laser, contact degradation due to diffusion 0-102734  
 Pb<sub>1-x</sub>Sn<sub>x</sub>Te epitaxial films, adsorption-induced accumulation layer form. on surface 0-60117  
 Pb<sub>1-x</sub>Sn<sub>x</sub>Te, growth of epitaxial layers, activation by UV and IR radiation 0-71598  
 Pb<sub>1-x</sub>Sn<sub>x</sub>Te, hole effective mass near zero bandgap, IR refl. study 0-108205  
 Pb<sub>1-x</sub>Sn<sub>x</sub>Te LPE film IR detector performance 0-86422  
 Pb<sub>1-x</sub>Sn<sub>x</sub>Te, lattice and electronic props. and g-value 0-80161  
 Pb<sub>1-x</sub>Sn<sub>x</sub>Te, narrow gap semicond., theory of mag. susceptibility 0-93070  
 Pb<sub>1-x</sub>Sn<sub>x</sub>Te, thermoelectric effects, characteristics at low temps. 0-107831  
 Pb<sub>1-x</sub>Sn<sub>x</sub>Te, x=0.2, monocrystal, photoelectric props. of p-n structures (*Russian*) 0-70808  
 Pb<sub>1-x</sub>Sn<sub>x</sub>Te, X=0.2, monocrystal, edge of intrinsic absorpt. (*Russian*) 0-71368  
 Pb<sub>1-x</sub>Sn<sub>x</sub>Te:Ce(In), solid solutions, impurity states in photoluminescence spectra (*Russian*) 0-97333  
 Pb<sub>1-x</sub>Sn<sub>x</sub>Te:Ge, anomalous behaviour of impurity centres under press. (*Russian*) 0-65491  
 Pb<sub>1-x</sub>Sn<sub>x</sub>Te:In, dielectric state, avalanche breakdown in strong elec. fields (*Russian*) 0-92901  
 Pb<sub>1-x</sub>Sn<sub>x</sub>Te:In, Hall effect and photoconductivity (*Russian*) 0-103720  
 Pb<sub>1-x</sub>Sn<sub>x</sub>Te:In, impurity influence on photoluminescence at large excitation levels (*Russian*) 0-93384  
 Pb<sub>1-x</sub>Sn<sub>x</sub>Te:In, tunnelling impurity self-localisation, anomalous props. nature (*Russian*) 0-59915  
 Pb<sub>1-x</sub>Sn<sub>x</sub>Te/PbTe<sub>1-x</sub>Se, lattice-matched buried heterostructure lasers with CW single mode output 0-74386  
 Pb<sub>1-x</sub>Sn<sub>x</sub>Te-PbTe heterostructures, MBE produced on mica and LiNbO<sub>3</sub>, elec. props. study 0-88629  
 Pb<sub>1-x</sub>Sn<sub>x</sub>Te<sub>1-y</sub>Se<sub>y</sub>, quaternary solid solns. with const. lattice parameter, cryst. growth and characts. 0-108332  
 Pb<sub>1-x</sub>Sn<sub>x</sub>Te<sub>1-y</sub>Se<sub>y</sub>, solid solutions with constant lattice parameter, phase comp. 0-108417  
 n-PbTe-p-Pb<sub>1-x</sub>Sn<sub>x</sub>Te, heterojunctions, heavily doped, current-flow mechanisms 0-96974  
 PbTe-Pb<sub>1-x</sub>Sn<sub>x</sub>Te n-p<sup>+</sup> heterojunction photodetector, hot wall evaporation technique 0-65673  
 a-Si In<sub>2-x</sub>Sn<sub>x</sub>O<sub>3-y</sub>/ZZ 0-10113  
 Si/In<sub>2</sub>O<sub>3</sub>-SnO<sub>2</sub> thin film junctions, polarity dependent memory switching effects 0-70814  
 n-Si-SiO<sub>2</sub>-SnO<sub>x</sub> SIS solar cell, transport props., 14% efficiency realisation 0-94079  
 (SiTe)<sub>x</sub>(SnTe)<sub>1-x</sub> solid soln., mag. susceptibility meas. (*Russian*) 0-70933  
 Sn-Se, liq., mag. susceptibility meas., electron localisation and chem. bonding 0-60178  
 Sn-SnO<sub>2</sub>-Sn long Josephson tunnel junction, flux flow, crit. conditions 0-80452  
 Sn-SnO<sub>2</sub>-Sn tunnel contacts, spatially inhomogeneous state under strong injection conditions 0-80457  
 Sn-SnO<sub>2</sub>-Sn tunnelling junctions, fabrication by modified RF plasma oxidation method 0-103787  
 Sn-Te, liq., mag. susceptibility meas., electron localisation and chem. bonding 0-60178  
 SnBaO<sub>3</sub>, resonantly scatt. gamma radiation from <sup>119</sup>Sn, energy spectrum with time parameters 0-108122  
 SnCl<sub>4</sub>+K<sub>2</sub>(C<sub>2</sub>), ionisation reactions, absolute cross sections 0-99565  
 SnCl<sub>4</sub>, X-ray cryst. struct. determ., Patterson synthesis (*French*) 0-96480  
 SnCl<sub>2</sub>·1.5H<sub>2</sub>O single cryst., <sup>35</sup>Cl NQR, cryst. struct. 0-60449  
 SnCl<sub>2</sub>·2H<sub>2</sub>O, Brillouin scatt. and thermal expansion 0-97289

## tin compounds continued

- SnCl<sub>2</sub>·2H<sub>2</sub>O, isomorphous transition, Landau type thermodynamic potential 0-107413  
 SnF<sub>4</sub>, use in chemical lasers 0-64004  
 SnF<sub>2</sub>, cryst. struct. of  $\beta$ - and  $\gamma$ -phases 0-92500  
 SnF<sub>2</sub>, phase transitions, X-ray diffr., elec. cond. and thermal anal. studies 0-100329  
 SnF<sub>2</sub>, second order  $\beta \rightarrow \gamma$  transition, neutron diffr. and NMR obs. 0-107095  
 SnF<sub>2</sub>, solid electrolyte, conducting and activation energy 0-70464  
 SnH<sub>2</sub>, struct. determ., restricted HF calcs. 0-87030  
 SnH<sub>4</sub>, force consts. by modified Redington and Aljibury method 0-69261  
 SnI<sub>2</sub>, <sup>121</sup>I NQR freqs. meas. 0-58285  
 SnI<sub>4</sub>, attachment energy as habit controlling factor 0-59421  
 Sn<sub>1-x</sub>Mn<sub>x</sub>Te, electronic struct., transport props., mag. ordering effects 0-65441  
 SnMo<sub>2</sub>S<sub>8</sub>, Chevrel phase, mag. interactions, LMT0 energy band studies 0-70606  
 Sn, MoS<sub>2</sub>, struct. anal. supercond. props. 0-97023  
 SnO<sub>2</sub>, aerosols, Lamb-Mossbauer factor (French) 0-81375  
 SnO<sub>2</sub>, CVD coating on glass, elec. resist. rel. to cryst. microstruct. 0-84520  
 SnO<sub>2</sub>, electrode reactions with molten glass 0-85186  
 SnO<sub>2</sub>, electrodes, effect of DC on corrosion in lead glass melt 0-85075  
 SnO<sub>2</sub>, exciton luminescence spectra, absorpt. spectra 0-89064  
 SnO<sub>2</sub> films, selective, optical characterisation by thermodynamical method 0-84796  
 SnO<sub>2</sub> gas sensor, fast-detecting, prep. 0-61497  
 SnO<sub>2</sub>, O chemisorption, elec. cond. and EPR meas. correlation 0-84369  
 n-SnO<sub>2</sub> pigmented solar cell for electrolysis of water, two-photon process 0-93932  
 SnO<sub>2</sub>, surface impurity in SiO<sub>2</sub>-Na<sub>2</sub>O-CaO-MgO float glass, ellipsometry and XPS study 0-84346  
 SnO<sub>2</sub> thin films, O<sub>2</sub> vacancy diffusion 0-107467  
 SnO<sub>2</sub>-P, CVD films, elec. props., cryst. to amorphous transition effects 0-107933  
 SnO<sub>2</sub>-P, CVD growth and etching characts., doping effects 0-107667  
 SnO<sub>2</sub>-Sb film, amorphous, electrotransport phenomena obs., under DC electric field 0-59840  
 SnO<sub>2</sub>-Sb film on glass substrates, elec. props. 0-88652  
 SnO<sub>2</sub>-Sb sprayed film, growth mechanism and cryst. struct. 0-89143  
 SnO<sub>2</sub>/n<sup>+</sup>-pSi heterojunction solar cells, fabrication by paint-on-diffusant method 0-94048  
 SnO<sub>2</sub>-based gas sensors, resist. temp. depend. on exposure to CO, H<sub>2</sub>, and propane 0-103694  
 SnO<sub>2</sub>-copper phthalocyanine-Ag systems, elec. and electroluminescent behaviour 0-80864  
 SnO<sub>2</sub>-Cu<sub>2</sub>S-ZnS-Mn<sub>2</sub>Cu<sub>2</sub>Al<sub>2</sub>O<sub>3</sub>-Al<sub>2</sub>O<sub>3</sub>, light-emitting struct., cond. and electrolum., heat treatment 0-97345  
 SnO<sub>2</sub>-GaTe(GaSe)(InSe) heterojunctions, photoelec. props. 0-96945  
 SnO<sub>2</sub>-InP heterojunctions, elec. and photovoltaic characts. 0-75628  
 SnO<sub>2</sub>-NiO(ZnO)(Nb<sub>2</sub>O<sub>5</sub>), activated sintering mechanism 0-60810  
 SnO<sub>2</sub>-polySi solar cells, fabrication, grain size effects on device parameters 0-94045  
 SnO<sub>2</sub> films, non-stoichiometric, DC reactively sputtered, elec. props. 0-80415  
 SnO<sub>2</sub> films, passivation effect on Si solar cells 0-61360  
 Sn<sub>2</sub>P<sub>3</sub>S<sub>6</sub>, ferroelec. semicond., phase transition and lattice dynamics 0-60526  
 Sn<sub>2</sub>P<sub>3</sub>S<sub>6</sub>, investigation of p-T diagram near a singular point (Russian) 0-88937  
 Sn<sub>2</sub>P<sub>3</sub>S<sub>6</sub>, soft mode props., Raman scatt. study 0-60525  
 Sn<sub>2</sub>P<sub>3</sub>(Se<sub>1-x</sub>S<sub>x</sub>)<sub>6</sub>, ferroelec. tritric. phase transform., light transmission study 0-71355  
 Sn<sub>1-x</sub>Pb<sub>x</sub>Se(Te) films, Mossbauer effect of <sup>119</sup>Sn, spectral characts., conc. depend. 0-103903  
 Sn<sub>1-x</sub>Pb<sub>x</sub>Se(Te) films, oxidation rel. to annealing temp. and time, Mossbauer spectra, X-ray and microstruct. obs. 0-104311  
 SnS<sub>2</sub> thin layer, far IR refractive index 0-93421  
 SnS<sub>2</sub> mixed valence semiconductor, far IR refl. spectra 0-108191  
 SnS<sub>1-x</sub>S<sub>x</sub>, solid soln. system, long-wavelength optical phonons, Raman scatt. study 0-80794  
 SnS<sub>2</sub>, Se<sub>x</sub>, layer cryst., Raman active modes 0-80767  
 Sn(S<sub>1-x</sub>Se<sub>x</sub>)<sub>2</sub>, valence band states, composition depend., photoemission spectra study 0-100434  
 SnSe<sub>2</sub>, sublimation, temp. depend. of equilb. constants 0-88312  
 SnTe, <sup>119</sup>Sn temp. depend. isomer shift, pseudopot. approach 0-84675  
 SnTe, annealed, iodide method of prep., props. meas. 0-71591  
 SnTe, bond orbital model of band struct. 0-59853  
 SnTe, cubic semicond. with ellipsoidal valleys, magnetoresist. 0-80300  
 SnTe, diffusion of <sup>125</sup>Te 0-84325  
 SnTe, dispersive transform., interband electron-phonon interactions, phase diagram 0-93252  
 SnTe, mechanochem. and thermal oxidation comparison, Mossbauer obs. 0-104310  
 SnTe, strongly anisotropic polar semicond., electron-hole liq. in mag. field 0-59890  
 SnTe, structural phase transition threshold instability in strong EM field 0-103477  
 SnTe, supercond., metal-insulator transition, electron pairing, effect on optical props. 0-60139  
 SnTe:Mn, NMR shift meas. 0-97154  
 Te<sub>50-x</sub>Se<sub>50-x</sub>Sn<sub>x</sub>, thin films, elec. cond. and thermoelectric power meas. (French) 0-80335  
 Ti-Sn-Te system equilibria, polythermal and isothermal cross sections obs., ternary cpd. form. 0-104128  
 Ti<sub>2</sub>Te<sub>3</sub>-Ti<sub>4</sub>SnTe<sub>3</sub>-Ti<sub>4</sub>PbTe<sub>3</sub>, phase equilb., DTA, SPA and microhardness meas. 0-96628

## titanium

- see also nuclei with .....  
 $\alpha$ -titanium, plastic deformation, anharmonicity Grüneisen parameter 0-88246  
 adsorption, on (110), (121) and (111) faces of W 0-100411  
 air at Ti surface, optical breakdown, interferometric investigation 0-100064  
 atom, 4s3d<sup>3</sup> and 3d<sup>4</sup> states, HF descriptions, alternative orbital config. 0-63534  
 atom, fine struct. levels fitting, config. interaction effect, spin-orbit and electrostatic interaction parameters 0-69248

## titanium continued

- atoms, neutral and ion val. states, electron correlation, ab initio effective val. Hamiltonian calc. 0-99449  
 band struct., cryst. pot. anisotropy effect (Russian) 0-88474  
 cathodic alloying on surface, for increased passivation and corrosion resist. 0-100940  
 coatings, electrolytically deposited, texture, anti-corrosional props. (Russian) 0-66532  
 cold rolled  $\alpha$ -phase, primary recrystn., in situ investig. in HVEM 0-104185  
 composite sintered bearing materials, metallic solid lubricant infiltrated, antifriction props. 0-60981  
 contact reaction with BN at high pressures 0-61029  
 corrosion, by hot perfluoropolyether 0-93684  
 corrosion in H<sub>2</sub>SO<sub>4</sub>, estimated from weight loss meas. at 270°C and 56 bar (French) 0-85080  
 discontinuous electrical resistivity, low temp. active straining of polycrystal Ti (Russian) 0-103666  
 electrochemical machining, electrolytes development, electrochem. in static solns. 0-85182  
 electrochemical machining, electrolytes development, electrochem. studies in flowing solns. 0-85183  
 electropolished, optical props. from 1.8 to 3 eV 0-85088  
 emittance, during nonstationary high temp. heating by Ar flow (Russian) 0-84308  
 energy loss of heavy nonrelativistic ions in matter, semiclassical theory 0-84224  
 energy loss spectra of C<sup>2+</sup> ions in Ti targets 0-65114  
 fatigue crack growth, influence of grain orientation, SEM study 0-108550  
 fatigue crack growth micromechanisms at low stress intensities in  $\alpha$ -phase 0-108570  
 film, EELS, anomalous L<sub>2</sub>/L<sub>1</sub> white-line ratios 0-93444  
 foil electrolytic perforation, surface film phase composition obs. (Russian) 0-61004  
 friction surface structural investigation, O<sub>2</sub> surface diffusion (Russian) 0-96726  
 getter for TFTR Flexibility Modification, in-torus surface pumping 0-95451  
 gettering of H, mass spectrometry and microgravimetry study, rel. to HTGR gas purification 0-73374  
 impurity, in Si n<sup>+</sup>-p solar cell, associated degradation mechanism 0-81465  
 impurity flux, time resolved, in DITE Tokamak 0-63373  
 K-shell X-ray prod. by <sup>14</sup>N<sup>+</sup> bombardment 0-91482  
 liquid, elec. resist., melting pt. to boiling pt., temp. depend. 0-96839  
 liquid, viscosity at melting point, free energy (Russian) 0-92699  
 metal-metal interface, adhesion energy, surface treatment and ion implantation effects 0-107660  
 microflow parameters, determ. from compression tests for  $\alpha$ -phase 0-66584  
 Moon, Fe and Ti surface distrib., orbital  $\gamma$ -ray spectra 0-94727  
 neutron irradiated, characterization of dislocation loops 0-88155  
 neutron irradiated, twinning deform. at room temp. 0-65061  
 oxidation, linear, O diffusion coeff. depend. on rutile layer struct. (French) 0-104328  
 oxidation behaviour under pure O<sub>2</sub> atmos., temp. range 600-800°C 0-89415  
 photon emission due to Ar<sup>+</sup> ion bombard., adsorbed and recoil-implanted O effect 0-80872  
 pit nucleation in bromide media, ion beam anal. 0-93683  
 plasma arc spraying, chem. reaction with plasma gases 0-66427  
 powder metallurgy, developments 0-100801  
 pure, type VT1-0, pool metal solidification kinetics in welding with electromag. stirring 0-71636  
 ruby:Ti<sup>3+</sup>, cross-relax. 0-71163  
 shell, explosive expansion, deform. and rupture modes and mechanisms 0-85064  
 solar quiescent prominence spectra, meas. of Ca<sup>+</sup> 8542 and 8498 Å He 4471 Å and Ti<sup>+</sup> 4468 Å 0-90373  
 spallogenic isotopes in Fe meteorites, radial distrib. 0-67488  
 spongy metallic protective gettered coating for thermonuclear reactor walls (Russian) 0-106154  
 sputtered excited states, secondary photon emission, role of transition probability 0-102483  
 sputtered ion fraction meas. using matrix isolation spectroscopy 0-60738  
 sputtered Ti atoms, photon emission, nonradiative transition effects 0-58208  
 sputtering, low energy, H, D and He ions 0-100734  
 strain driven thermoelastic instability toward brittle fracture 0-103415  
 stress corrosion cracking, texture dependence 0-104334  
 stress relaxation, in-reactor study at low temps. 0-93588  
 sublimation pump, methane outgassing 0-77796  
 surface (0001), H adsorption, geometric vs. electronic factor in surface electronic structure 0-70788  
 surface layer, study using vac. UV spectrograph (French) 0-71987  
 thin films, H absorption and desorption, Tokamak gettering, Auger electron spectrosc. 0-75092  
 Tokamak plasma, atomic struct., highly ionized Ti 0-75086  
 twin interfaces [1012], serrated 0-84182  
 twinning deformation, neutron irradiation effects 0-75236  
 volume changes and defect healing due to plastic deform. (Russian) 0-81139  
 X-ray reflectivity, near L<sub>2,3</sub> absorpt. edge 0-71513  
 yield points, obtained by ageing at two stresses 0-81091  
 B-Ti composite material, for loudspeaker's diaphragm, preparation by physical vapour deposition (Japanese) 0-58883  
 CdS:Ti<sup>2+</sup>, superhyperfine interact., ENDOR study at 4.2K 0-80639  
 Fe:Ti, C induced amorphous surface layers 0-107287  
 GaP:Ti, positron annihilation meas. rel. to deep levels study 0-60712  
 LiF:Mg:Ti, defect states, ESR and ionic cond. study 0-108058  
 LiNbO<sub>3</sub>:Ti, coupled waveguided TE/TM mode splitter 0-64142  
 LiNbO<sub>3</sub>:Ti, planar and channel optical waveguides, anisotropic diffusion expts. 0-64200  
 LiNbO<sub>3</sub>:Ti, planar optical waveguides, processing and props. 0-78965  
 LiNbO<sub>3</sub>:Ti 3-dB optical waveguide mode convertor using chirped gratings, power transfer 0-79014  
 LiNbO<sub>3</sub>:Ti channel waveguide high-speed cutoff modulator 0-64195  
 LiNbO<sub>3</sub>:Ti diffused optical waveguide, guided light scatt. sources 0-78966



## titanium continued

- LiNbO<sub>3</sub>:Ti diffused optical waveguide, efficient tapered gap prism coupling 0-78967  
 LiNbO<sub>3</sub>:Ti diffused strip waveguide, optical propag. losses and coupling losses 0-58664  
 LiNbO<sub>3</sub>:Ti electro-optic TE-TM mode converter structure 0-64215  
 LiNbO<sub>3</sub>:Ti electro-optic branching waveguide, characts. 0-83681  
 LiNbO<sub>3</sub>:Ti optical waveguides, Ti diffusion process and control, waveguide characts. 0-58790  
 LiNbO<sub>3</sub>:Ti phase-matched waveguide electro-optic TE-TM mode converter 0-58749  
 LiNbO<sub>3</sub>:Ti planar waveguide, edge coupling to GaAlAs DH laser diode 0-87559  
 LiNbO<sub>3</sub>:Ti strip waveguide, SHG 0-102773  
 LiNbO<sub>3</sub>:Ti waveguide electro-optic TE-TM mode converter-wavelength filter 0-64210  
 LiNbO<sub>3</sub>:Ti Z-cut crystals, Ti diffusion process parameters 0-102849  
 Nb-Ti-Ta, superconductor optimisation for 12 Tesla toroidal field coils 0-91272  
 Pr covered Ti electrodes for cathodic protection for small plant (German) 0-100943  
 Ru complex, [Ru(bpy)<sub>3</sub>]<sup>2+</sup>-Ti (III), photochem. H<sub>2</sub> prod. from aq. soln. 0-85192  
 Si:Ti contaminated solar cells, POCl<sub>3</sub> gettering 0-94010  
 Si:Ti substrate for epitaxial solar cells 0-61341  
 Si-Pd-Ti, silicide form. in evaporated films 0-80006  
 Ti electrodes, RuO<sub>2</sub> coated, corrosion during O evolution rel. to electrode prep. (French) 0-76420  
 Ti, fatigue damage, SEM, X-ray diffr. and surface trace anal. 0-85040  
 Ti, oscillator strengths from combined hook and emission expts. 0-87081  
 Ti III, 3d and 4f energy level parametrisation, Slater parameters and correl. corrections 0-87041  
 Ti III, IV, V, radiative lifetime meas. using beam-foil technique, 700 to 1900 Å 0-78574  
 Ti, pionic, pion mass high accuracy meas. from transitions 0-106406  
 α-Ti sheet, texture dependent stress corrosion cracking in Br<sub>2</sub>-methanol soln. 0-71803  
 Ti XX 0-100067  
 Ti<sup>2+</sup>, doped ion in divalent metal cpds., correl. between Szigeti charge and hyperfine coupling consts. 0-96832  
 Ti:D, implanted, deuteride imaging using scanning Auger spectroscopy 0-89092  
 Ti:D, implanted, nucleation and growth of TiD<sub>2</sub> 0-97717  
 Ti:D, ion implanted, depth profiles, temp. depend. 0-100270  
 Ti:Pd, ion implanted, corrosion behaviour and Rutherford backscatt. anal. 0-71792  
 Ti+H<sup>+</sup> (He ions), K-shell ionisation cross-section, 85 to 790 keV 0-106390  
 Ti<sup>4+</sup>+Ne highly charged very slow Ne recoil ions, K X-ray transition 0-91649  
 Ti<sup>q+</sup>+O<sub>2</sub>(Ar)(He), (q=8-19), K X-ray prod., charge-state depend. 0-106391  
 TiXIV (TiXV) (TiXVII), Tokamak discharge, ground state, mag. dipole transitions, UV spectra obs. 0-63575  
 ZnSe:Ti<sup>2+</sup>, EPR meas. 0-80594

## titanium alloys

## see also titanium compounds

- Alnico 5 alloy, S and Ti additions effect rel. to non-metallic inclusions, coercive force and grindability 0-89375  
 crack initiation on planar shear bands, H<sub>2</sub> assisted 0-71749  
 delayed brittle fracture, H<sub>2</sub> effect 0-100912  
 electrochemical working, film form. and surface roughness (Russian) 0-76397  
 fatigue failure of VT3-1, surface finishing influence 0-60972  
 Fermi sphere limiting electronic capacitance, Brillouin zones (Russian) 0-92808  
 heat resistance, thermal stability, stress-rupture strength, and creep 0-81194  
 hydrogenation at 200-600°C and up to 10000 kPa 0-107435  
 Inconel X-750, deform. and fracture characts., 24-816°C 0-108551  
 lubrication by chloroparaffins, friction and wear (Russian) 0-93657  
 martensitic transformations, reversibility (Russian) 0-108442  
 recrystallization of β III type 0-108470  
 rotating discs, hysteresis losses and mag. phenomena 0-75695  
 steel, Al-Ti-(Mo), Al-Ti-V-(Mo), Al-Ti-Nb-(Mo) and Al-V-(Mo) low-alloy, toughness improvement through Ti additions 0-66525  
 steel, austenitic (03KH18N10T), heat treatment for fission reactor appls. 0-66454  
 steel, stainless, Cr-Ni-Ti, metallographic detection of (Ti,Ni)<sub>6</sub>C 0-66721  
 stress corrosion cracking, role of H<sub>2</sub>, state of art review 0-61017  
 structure and physical properties, H<sub>2</sub> effect on α-VT5 and VT1 0-108576  
 surface layers examination using vacuum UV spectrograph (French) 0-71987  
 TZM-Mo alloy, mech. props., effect of exposure to high temp. He containing O<sub>2</sub>, room temp. study 0-93639  
 US flaw detection of ingots, struct. effect 0-66722  
 VT6 Ti alloy, diffusion welding with constrained deformation 0-81104  
 Widmanstätten α-β alloy interfaces, elastic interact. stresses, effect plastic flow onset 0-104218  
 Al-Al<sub>3</sub>Ti, directionally solidified, thermal stability during annealing, 435-660°C 0-108393  
 Al-Bi(Cd)(Pb)-Ti, containing low-melting pt. inclusions, mech. props. 0-93632  
 Al-Ti, mechanical props. improvement, by work hardening (French) 0-97502  
 Al-Ti, molten, showering cryst. form. in mould cooled from top (Japanese) 0-66498  
 Al-Ti alloy spark alloying, cathode weight change and hardened layer obs. (Russian) 0-61005  
 Al-Ti system, interdiffusion coeffs. determ. 0-70477  
 Al-Zn-Ti, mech. props., Ti or Mn addition effect (Korean) 0-93613  
 Au-Ti/SiO<sub>2</sub>/p-Si MOS struct., interface state distrib., DC tunnelling spectra determ. 0-75611  
 CC NbTi, pool cooling superconducting test coil, Japanese design for fusion reactor large coil task 0-99340  
 Co-Ti, dendritic segregation 0-76260  
 Co-Ti-C, secondary precipitation and allotropic transform., TEM obs. 0-108453  
 Co-Ti-Fe (3, 1 to 2 wt.%), spinodal decomposition 0-100839

## titanium alloys continued

- Co(GaTiV) alloys, ferromag. onset, electron conc. depend. 0-60203  
 CoTi, dil., low temp. specific heat and magnetisation 0-65925  
 CoTi<sub>1-x</sub>Al<sub>x</sub>, mag. and electronic props., ferromag. and paramag. state 0-65814  
 Co<sub>2</sub>TiAl, hyperfine fields of Fe impurities, Mossbauer spectra 0-71255  
 Cu-Ni-Ti, ordering within precipitates, TEM obs. 0-108461  
 Cu-Ni-Ti system, phase equilibria in Cu rich region and Cu-T quasi-binary constitution (Japanese) 0-89203  
 Cu-Ni-Ti system, reactions with melt in Cu-rich region (Japanese) 0-89202  
 Cu-Ti, strengthened by modulated structs., anomalous age hardening effects 0-97497  
 Cu-Ti-Al(Ga)(Au)(In)(Ag)(Ni), wetting of Al<sub>2</sub>O<sub>3</sub>, alloying effects 0-107617  
 Cu<sub>40</sub>Nb<sub>30</sub>X<sub>30</sub> (X=Ti, Zr, Hf), superconductors with metastable ordered structs. 0-108484  
 Fe-Co-Al-Cu-Ti (40, 14, 7.5, 4.5 wt.%), metastable equilibrium, high coercive state (Russian) 0-66476  
 Fe-Co-Ti, sp. ht. in ordered and disordered phases 0-71061  
 Fe-Co-Ti-Al alloy type YuNDK magnets, metallographic method of distinguishing cracks 0-85096  
 Fe-Cr-Ni (12, 15 wt.%) austenitic alloy, Ni<sup>6+</sup> irradiated, void swelling and phase stability, Si and Ti effects 0-65055  
 Fe-Cr-Ti (18, 0.1-0.9 wt.%), high temp. oxidation (Japanese) 0-71806  
 Fe-Cr-Ti liquid alloy, thermodynamical anal. of O<sub>2</sub> solubility (Russian) 0-92676  
 Fe-Cr-Ti-Mo-TiO<sub>2</sub> (13, 3.5, 1.5, 2 wt.%) dispersion hardened, void swelling 0-65046  
 Fe-Ni-Al-Co-Cu-Ti YuNDK type, S effect on mech. props. 0-60927  
 Fe-Ni-Co-Cu-Ti YuNDK alloys, impaired mag. props. with C and S additions 0-60368  
 Fe-Ni-Co-Ti, coherent particles effect inherited by martensite on α-γ transformation (Russian) 0-108443  
 Fe-Ni-Cr-Al-Ti-W-Mo (35, 15, 2.4, 2.3, 2.2 wt.%) wrought superalloy, freckles (Chinese) 0-104137  
 Fe-Ni-Cr-Ti-Al, with thermoelectric control coeff., comp. and heat treatment influence on props. (French) 0-81074  
 Fe-Ni-Ti, preaged martensite, shear strain magnitude, X-ray diffr. method 0-93592  
 Fe-Ni-Ti-(Cu) (12, 0.25, 2 wt.%), Cu addition strengthening at 77K, mech. props. 0-60875  
 Fe-Sb-Ti, interactions and segregations, Mossbauer and X-ray diffr. study 0-70415  
 α-Fe-Ti, ion implanted, microstruct., ion beam anal. and TEM study 0-107294  
 α-Fe-Ti, ion implanted, with C impurity, microstruct. of TiC precip. 0-66513  
 Fe-Ti, magnetism and H<sub>2</sub> storage 0-70941  
 Fe-Ti, O containing, mag. aftereffect and disaccommodation meas., time depend., activation energy, and ageing props. 0-88836  
 Fe-Ti, solubility and diffusivity of H and D in mixed crystal phase, elec. cond. meas. (German) 0-107575  
 Fe-Ti, thermophysical props. and elec. cond., temp. depend. 0-96842  
 Fe-Ti, Ti as H trap for embrittlement control 0-66662  
 Fe-Ti (W), dil., thermophysical props. and elec. cond., temp. depend. 0-96842  
 Fe-Ti (0.15 wt.%), Ti distrib., segregation, FIM anal. 0-84200  
 Fe-Ti-C, rapidly quenched by splat-cooling 0-84923  
 Fe-Ti-V-C-N, equilibrium comp. and solubility in steels, model of ideal solns. (Russian) 0-60832  
 Fe-TiC pseudofused composite magnetoabrasive powders, props. 0-100926  
 Fe<sub>0.45</sub>Mn<sub>0.05</sub>Ti<sub>0.5</sub>H<sub>2</sub>, localised vibrs., sp. ht. obs., room temp. 0-65248  
 FeTi, surface and mag. props., heat treatment and hydrogenation effects 0-75447  
 FeTiH, solar energy storage by metal hydride 0-61455  
 Gd-Ti amorphous films, spontaneous Hall effect and elec. resist. 0-80251  
 Mn-Cr-Ti layers on low C steel, composite, residual stresses rel. to arc-spraying parameters (German) 0-104077  
 Mo-Nb-Ti-N alloy, with dispersed second phase, ductile-brittle transition 0-93653  
 Mo-Ti (3.5 wt.%), load curves, structure states boundaries and strain hardening (Russian) 0-89241  
 Mo-Ti-N alloy, with dispersed second phase, ductile-brittle transition 0-93653  
 Mo-Ti-Zr, TZM, corrosion behaviour in high temp. impure He gas 0-76402  
 Mo-TiC, eutectic formation of regular struct., crystn. (Russian) 0-66496  
 Nb-Ti, AC loss minimum, pinning, flux distribution 0-84574  
 Nb-Ti, multifilamentary, Mirror Fusion Test Facility, superconductor core manufacturing and quality 0-93521  
 Nb-Ti, pinning curves, high field J<sub>c</sub> and scaling behaviour 0-93064  
 Nb-Ti, resistivity due to H incorporation 0-70666  
 Nb-Ti, superconductor optimisation for 12 Tesla toroidal field coils 0-91272  
 Nb-Ti (50%), supercond., cryostat design for magnetisation study (Spanish) 0-75673  
 Nb-Ti multifilaments, effect of mech. and thermal treatments of supercond. props. 0-104197  
 Nb-Ti superconducting coils, for thermonuclear fusion (French) 0-95399  
 Nb-Ti superconducting single layered multifilamentary coil, eddy current loss depend. on demagnetisation 0-97040  
 Nb-Ti-Ta, pinning curves, high field J<sub>c</sub> and scaling behaviour 0-93064  
 Nb-Ti-Zr ternary system, high-field supercond. 0-97045  
 NbTi filaments for position-sensitive superconducting detector of ionizing particles 0-63460  
 NbTi films, effect of Ar- and N-ion bombardment on texture (Russian) 0-107338  
 NbTi, forced flow superconducting test coil, EURATOM design for fusion reactor Large Coil Task 0-99339  
 NbTi forced flow superconducting test coil, Swiss design for fusion reactor Large Coil Task 0-99341  
 NbTi monofilamentary wire in current sharing state, supercond. temp. sensor use 0-57288  
 NbTi, superconducting test coil, General Dynamics Convair Division, Intermagnetics General Corp. design for fusion reactor Large Coil Program 0-99338  
 NbTi superconducting test coil, General Electric design and manufacture program, for fusion reactors 0-102319  
 NbTi/In composite superconductor, transport props. 0-88658

## titanium alloys continued

- NbTi-Cu, composite superconductor, acoustic emission 0-84546  
 NbTi-Cu, supercond. composite, use in temp. and heat transfer coeff. meas. 0-77780  
 NbTi-In granular supercond. composites, mag. field-induced dissipation 0-84545  
 $(\text{Nb}_{0.99}\text{Ti}_{0.01})_{1-x}\text{Ge}_x$ , high  $T_c$ , resist. meas. 0-88531  
 Ni-Co-Cr-Mo-Al-Ti (17.5, 15.1, 4.9, 4.15, 3.25 wt.%), creep and stress rupture behaviour in air and vacuum 0-60918  
 Ni-Cr-Al-Ti, stress corrosion cracking, factors influencing susceptibility 0-97617  
 Ni-Cr-Co-Al-W-Mo-Ti-Ta, heat resist. and struct., Ta effect 0-76312  
 Ni-Cr-Co-Ti-Mo-W-Al (14, 9.8, 5, 4, 3.9, 3 wt.%), low cycle fatigue, prior heat treatment effect 0-60962  
 Ni-Cr-Mo-W-Al-Ti, heat-resist., phase comp. 0-76250  
 Ni-Cr-Ta-Ti-Si, EP557 precipitation hardening alloy, mech. props., heat treatment effect 0-60877  
 Ni-Cr-Ti rapidly solidified superalloys, surface segregation 0-76263  
 Ni-Cr-W-Co-Ti, high-temp. sulphide corrosion 0-76408  
 Ni-Cr-W-Co-Ti, thermal fatigue, effects of inclusions 0-81183  
 Ni-Cr-W-Mo-Ti-Al, heat-resist., recovery and recrystn. 0-76268  
 Ni-Cu-X (X=Sn, Nb, Ti), spinodal decomp. alloys, linear expansion coeff. influence on morphological anisotropy (Japanese) 0-70431  
 Ni-Fe-Co-Ti, electron microscopy and mag. meas. 0-71097  
 Ni-Fe-Cr-Mo-Ti-Al, PE 16, thermally activated domain wall motion 0-88777  
 Ni-Ti, dil., optical absorpt., electronic struct. 0-108227  
 Ni-Ti, heavily doped, linear expansion meas. 0-103501  
 Ni-Ti (12 wt.%), early stages of transformation 0-76251  
 Ni-Ti/Cu composite, plastic deform. influence on internal friction (Russian) 0-100871  
 Ni-Ti-Al superalloy, pendant drop melt extracted, struct. and props. 0-76242  
 Ni-Ti-P, amorphous, corrosion behaviour, immersion tests and electrochem. meas. (Japanese) 0-85085  
 $\gamma$ -Ni<sub>3</sub>(Al,Ti), single crystal, dislocation movement, HVEM obs. (Japanese) 0-108503  
 NiTi alloy single crystals, ferromag. reson., g-value and linewidth 0-71186  
 NiTi equiatomic alloy, single cryst. elastic consts. near martensitic transform. 0-75283  
 NiTi martensite, shape memory effect, struct. characts., TEM  $2\frac{1}{2}$  D imaging obs. 0-108446  
 NiTi, premartensitic transformation of B2 phase, shape memory 0-84931  
 NiAgTi<sub>60</sub>, amorphous, chem. short-range-order, X-ray and neutron scatt. obs. 0-96447  
 Ni<sub>3</sub>Ti<sub>0.5</sub>Ta<sub>0.5</sub>, conservative domain struct., TEM study 0-79776  
 Pd<sub>2</sub>Ti, L<sub>12</sub> ordered alloy, positive temp. depend. on strength, phase destabilization 0-81203  
 Pt<sub>3</sub>Ti, L<sub>12</sub> ordered alloy, positive temp. depend. on strength, phase destabilization 0-81203  
 Sr<sub>2</sub>(Co<sub>1-x</sub>Ti<sub>x</sub>)<sub>17</sub>, powders, influence of substitutes on mag. props. 0-100601  
 (Ti,Cr)B<sub>2</sub>, sintering kinetics and props. 0-100811  
 Ti powder metallurgy, developments 0-100801  
 $\alpha$ -Ti/Fe, retrograde solid solubility 0-79950  
 Ti-50A and TiCode-12 0-104349  
 Ti-70A superalloy, fusion reactor blanket structures, radiation resistance 0-63379  
 Ti-Ag (10 to 17.5 wt.%), eutectoid system,  $\beta$ - $\alpha_m$  transform., nucleation kinetics 0-97474  
 Ti-Al, elec. spark Al doping of VT-18, surface struct. and props. (Russian) 0-76398  
 Ti-Al-C, ternary system, phase relationships 0-76230  
 Ti-Al-Cr-Mo, type VTZ-1, machinability, using different abrasive materials (Russian) 0-97593  
 Ti-Al-Cr-Mo-V, VT22 alloy, metastable  $\beta$ -phase decay under continuous heating, plastic strain effect (Russian) 0-71656  
 Ti-Al-Cr-Mo-V(Fe), low cycle fatigue in repeated tension 0-76348  
 Ti-Al-Kh18 steel, O<sub>2</sub> solubility thermodynamical anal. (Russian) 0-92676  
 Ti-Al-Mo, type BT22, phase transformations under step-by-step heat treatment (Russian) 0-108436  
 Ti-Al-Mo, type VT14, machinability, using different abrasive materials (Russian) 0-97593  
 Ti-Al-Mo-Cr, weldment containing orthorhombic martensite, auto-tempering behaviour and alpha precip. strengthening 0-84976  
 Ti-Al-Mo-Cr (4.5, 5, 1.5 wt.%), weld metal,  $\alpha/\beta$  interface sliding 0-108512  
 Ti-Al-Mo-V (8, 1, 1 wt.%), Widmanstätten colonies, fracture toughness 0-85031  
 Ti-Al-Mo-Zr, compressor disk, surface plastic deform., optimal method 0-60924  
 Ti-Al-Mo-Zr, type VT-9, creep eqns. rel. to extension and compression props. 0-100875  
 Ti-Al-Sn, alloy 6242, dynamic effects of flow and fracture during isothermal forging 0-76343  
 $\alpha$ -Ti-Al-Sn, alloy Ti-679, electron diffraction anal. of Ti<sub>3</sub>Si phase (Chinese) 0-64845  
 Ti-Al-Sn-Zr, Ti-680, O contamination under high temp. (Chinese) 0-66688  
 Ti-Al-Sn-Zr (6.19, 1.92, 1.43 wt.%), fatigue fracture facet investigation by selected area electron channelling 0-89344  
 Ti-Al-Sn-Zr-Mo (6,2,4,6 wt.%) fusion weldment, substruct. characts. 0-84183  
 Ti-Al-V, friction coeff. reduction on injection with TiC particles 0-85086  
 Ti-Al-V, fusion reactor blanket structures, radiation resistance 0-63379  
 Ti-Al-V (6, 4 wt.%), fretting corrosion of orthopaedic implant materials by bone cement 0-104813  
 Ti-Al-V (6, 4 wt.%), texture depend. stress corrosion cracking 0-104334  
 Ti-Al-V (6.4 wt.%), cyclic temp. creep, transition effect 0-97539  
 Ti-Al-V (6.4 wt.%),  $\beta$ -annealed, subsurface fatigue crack initiation 0-108553  
 Ti-Al-V (6.4 wt.%), effect of air exposure on fracture characts. 0-100890  
 Ti-Al-V (6.4 wt.%), H related fatigue fracture 0-76344  
 Ti-Al-V (6.4 wt.%), ion irradiated, microstruct. study using TEM 0-96572  
 Ti-Al-V (6.4 wt.%), microstruct. effect of base metals on diffusion welding (Japanese) 0-89296  
 Ti-Al-V (6.4 wt.%), porous compacts, determ. of effective stress in hot pressing 0-100807  
 Ti-Al-V (6.4 wt.%) superplastic alloy, maximum attainable ductility 0-60919

## titanium alloys continued

- Ti-Al-V (6.4 wt.%) cast alloy, with improved microstruct., mech. props. (Japanese) 0-71701  
 Ti-Al-V-Be-B, melt-extracted polycryst., mech. props. 0-76360  
 Ti-Al-V-Fe-Cu, melt-extracted polycryst., mech. props. 0-76360  
 Ti-Al-V-Sn (5.5, 5.5, 2 wt.%), crack growth, slow, H-induced 0-104272  
 Ti-Al-V-Sn (6.6, 2 wt.%) fusion weldment, substruct. characts. 0-84183  
 Ti-Al-Zr-Mo-Si (5.97, 4.73, 0.49, 0.34 wt.%), fatigue fracture facet investigation by selected area electron channelling 0-89344  
 Ti-Al-Zr-Mo-Si (6, 5, 0.5, 0.25 wt.%),  $\beta$ -processed, fatigue props., hold time effect 0-60961  
 Ti-Al(Mo), phase relations 0-108398  
 Ti-Au, (9.9 wt.%), eutectoid system,  $\beta$ - $\alpha_m$  transform., nucleation kinetics 0-97474  
 Ti-Cr, diffuse electron scatt. (Russian) 0-103438  
 Ti-Er(Y), effects of Er and Y additives on deformation behaviour 0-81121  
 Ti-Fe, equiatomic, heats of form., influence of short-range order (Russian) 0-81354  
 Ti-Fe, H storage material, Mossbauer surface studies, Fe clusters 0-97167  
 Ti-Fe (1.4 wt.%), polymorphic transform. due to plastic deform., positron annihilation 0-79939  
 Ti-Fe-Al(Mn), homogeneity and lattice parameters, Mn and Al effect on hydriding compd. FeAl 0-108400  
 Ti-Fe-C, type 50A, pitting resist. in low salinity geothermal brines 0-93681  
 Ti-Fe-C-N, ion irradiated, microstruct. study using TEM 0-96572  
 Ti-Fe-Ni (67, 30, 3 wt.%), reversible shape alteration (Russian) 0-71647  
 Ti-Ir, dil., elec. field gradient at <sup>193</sup>Ir, Mossbauer meas. 0-66090  
 Ti-Mo, diffuse electron scatt. (Russian) 0-103438  
 Ti-Mo, structure associated with BCC to omega transform. (Russian) 0-108432  
 $\beta$ -Ti-Mo, thermal instability, hardness and tensile deform. (Japanese) 0-71703  
 Ti-Mo (V), metastable diffusionless equilibria, high press. conditions 0-71627  
 Ti-Mo (20 at.%), incommensurate struct., stacking soliton 0-107109  
 Ti-Mo (3 to 35 wt.%), high pressure influence on transition temp. to supercond. 0-107952  
 Ti-Mo alloy, thin anodic oxide, AES depth profile 0-71801  
 Ti-Mo alloys, structural stability under high-pressure soaking 0-104151  
 Ti-Mo-V-Al-Cr-Fe (4.8, 4.7, 5.2, 1.1, 1.0 wt.%), structural changes during heating up to 1000°C, DTA study (Russian) 0-93552  
 Ti-Mo-Zr-Sn (11.5, 6.0, 4.5 wt.%), mech. property, microstruct. relationships 0-84961  
 Ti-Mo-Zr-Sn (11.5, 6.0, 4.5 wt.%) alloy, struct. as affected by processing history 0-84972  
 $\beta$ -Ti-Mo-Zr-Sn(11.5, 6, 4.5 wt.%), metastable phase III, microstruct. and age hardening response 0-84945  
 Ti-Mo-Zr-Al (15, 5 (3) wt.%), quenched and aged metastable  $\beta$ -phase, crystallography, morphology and decomposition 0-76262  
 Ti-Nb, diffuse electron scatt. (Russian) 0-103438  
 Ti-Nb (4.32 wt.%), high temp. oxidation kinetics under 1 bar pressure, 1255-1471K 0-89410  
 Ti-Nb-Si, amorphous alloy, supercond. props. and crystn. behaviour, TEM and DTA study (Japanese) 0-84536  
 Ti-Nb-Zr-Fe, supercond. and paramag. props., effect of Fe additions (Russian) 0-65730  
 Ti-Nb-Zr-Ta, superconducting props. comp. depend., stress effects and precipitation behaviour, X-ray scatt. 0-93059  
 Ti-Ni, internal friction and US props. (Russian) 0-84247  
 Ti-Ni, martensitic transform., monoclinic to triclinic phase (Russian) 0-81058  
 Ti-Ni, multiplicity of structural transitions, phase diagrams, elec. cond. meas. 0-71649  
 Ti-Ni (48 to 53 at.%), heat treatment and deviation from stoichiometry 0-104192  
 Ti-Ni amorphous alloys, glass transition and ductility, O additions effect 0-75168  
 Ti-Ni-Co, constitution diagram, isothermal section, interdiffusion coeffs. (Russian) 0-89200  
 Ti-Ni-Fe, multiplicity of structural transitions, phase diagrams, elec. cond. meas. 0-71649  
 Ti-Ni-Mo, TiCode 12, pitting resist. in low salinity geothermal brines 0-93681  
 Ti-Si amorphous alloy, melt-quenched, transform. studies and mech. props. 0-100838  
 Ti-Ta (4.37 wt.%), oxidation kinetics, 1258-1473K, and at pressure of 0.013, 0.133 and 1.0 bar 0-89411  
 Ti-Th, eutectic composition 0-100828  
 Ti-V, elastic moduli, electron conc., pulse echo overlap meas. 0-59550  
 Ti-V (10 at.%),  $\alpha$ - $\omega$  transformation, electron diffraction evidence of intermediate BCC phase 0-81051  
 $\beta$ -Ti-V metastable alloys, fatigue crack propag. 0-60964  
 Ti-V-Cr-Mo, fracture resistance at low temps. 0-104284  
 Ti-V-Fe-Al (10, 2, 3 wt.%), fracture toughness and stress corrosion resistance 0-100904  
 Ti-W films, bias-sputtered, quantitative anal. 0-80114  
 TiBe<sub>2</sub>, de Haas-van Alphen effect, Fermi surface, theory 0-103614  
 TiBe<sub>1.8</sub>Cu<sub>0.2</sub>, ferromag., magnetisation density 0-103817  
 TiBe<sub>2-x</sub>Cu<sub>x</sub>, high press. study of Curie temp. and mag. susceptibility 0-84600  
 Ti<sub>50</sub>Be<sub>40</sub>Zr<sub>10</sub>, amorphous, crystn. temp., press. and heating rate depend. 0-70132  
 TiC-(Mo-Cr-Ni-Mn) steel alloy, optimum comp. and manufacture conditions, Mn effect 0-84896  
 TiC-alloy steel (30, 70 wt.%) composite, sintered, wear resist. 0-100815  
 Ti<sub>9</sub>C<sub>3</sub>, X-ray order struct. determ. 0-103295  
 Ti<sub>70</sub>Co<sub>20</sub>B<sub>10</sub>, amorphous alloys, crystn. behaviour, TEM study (Japanese) 0-84087  
 TiCo<sub>1-x</sub>Mn<sub>x</sub>, H absorption-desorption characteristics 0-96735  
 TiCr<sub>1.8</sub>H and D soln., enthalpy, solubility and mol. vibr. determ., comparison with soln. in metals and binary alloys 0-79951  
 Ti(Fe, Co), off-stoichiometric alloy, inverse mag. susceptibility rel. to defect conc. 0-60216  
 Ti(Fe,Co)H<sub>x</sub>, mag. and <sup>57</sup>Fe Mossbauer studies 0-71272  
 TiFe hydrides for bulk H<sub>2</sub> storage 0-61463  
 Ti(Fe,Co), itinerant electron ferromagnet, magnetovolume effects 0-60397



## titanium alloys continued

- Ti<sub>70</sub>Fe<sub>20</sub>B<sub>10</sub>, amorphous alloys, crystn. behaviour, TEM study (*Japanese*) 0-84087  
 TiFe<sub>0.8</sub>Be<sub>0.2</sub> alloys for H<sub>2</sub> storage 0-97817  
 TiFe<sub>1-x</sub>Co<sub>x</sub>, electronic struct. and mag. moment calcs. 0-65821  
 TiFeCo<sub>1-x</sub>, thermal expansion and magnetoelectric effects 0-80585  
 TiMn<sub>1.5</sub>, hydrogen storage appl. (*Japanese*) 0-61443  
 TiN, hard coating on soft Al alloy, tribological anal. 0-108600  
 Ti<sub>70</sub>Ni<sub>20</sub>B<sub>10</sub>, amorphous alloys, crystn. behaviour, TEM study (*Japanese*) 0-84087  
 TiSi<sub>2</sub>, form. in Si-Pd-Ti evaporated films 0-80006  
 Ti<sub>1-x</sub>V<sub>x</sub>-H<sub>2</sub> system, reaction and press.-composition isotherms meas. 0-108391  
 TiW-TiO<sub>2</sub>-InP thin refractory MIS struct. deposition 0-75647  
 Ti<sub>0.3</sub>W<sub>0.7</sub>, thermal annealing study of metallisation on Si 0-80134  
 Ti<sub>1-x</sub>Zr<sub>x</sub>M<sub>12-y</sub>Cr<sub>y</sub>V<sub>2</sub>, hydrogen storage appl. (*Japanese*) 0-61443  
 V-Nb-Ti-N alloy, with dispersed second phase, ductile-brittle transition 0-93653  
 V-Ti (42 at.%), ultrasonic vel. in mixed state 0-75689  
 V-Ti-C, elemental anal. by EELS 0-101069  
 V-Ti-C, high temp. carbide form., electron microscopy study 0-89228  
 Zr-Ti-Be metallic glass, phase separation 0-97464

## titanium compounds

see also titanium alloys

- halides, XY<sub>4</sub> molecules, force consts. by modified Redington and Aljibury method 0-69261  
 hollandites, cryst. growth and structural props. 0-89129  
 oxide reduction by electron cyclotron reson. plasma of H, model study on discharge cleaning 0-76548  
 oxides, sputtered Ti atoms, photon emission, nonradiative transition effects 0-58208  
 phosphide precipitates, obs. in ferritic stainless and C steels (*Japanese*) 0-89221  
 photodecomposition over Pt/TiO<sub>2</sub> catalysts 0-81337  
 titanomagnetites, temp. depend. cation distrib., mag. prop. obs. 0-85647  
 Al<sub>2</sub>O<sub>3</sub>-TiC, composite, fracture behaviour in three-point bending 0-60951  
 Al<sub>2</sub>O<sub>3</sub>-TiO<sub>2</sub> powder, plasma-prepared, morphology and phase constitution 0-100833  
 B-C-Ti, paramagnetic centre struct. and defect form. 0-66034  
 BaO-Nd<sub>2</sub>O<sub>3</sub>-TiO<sub>2</sub>-Bi<sub>2</sub>O<sub>3</sub> system ceramics, high stability low loss dielectric preparation 0-81008  
 BaO-TiO<sub>2</sub>-Al<sub>2</sub>O<sub>3</sub> system, subsolidus equilibria, X-ray powder diff. 0-108413  
 Ba(V<sub>1-x</sub>Ti<sub>x</sub>)S<sub>3</sub>, synthesis and struct. phase transitions 0-107415  
 Cs<sub>2</sub>TiF<sub>6</sub>Mn<sup>4+</sup>, spin-orbit and field splitting, Jahn-Teller effect, Zeeman meas. 0-80234  
 Cu-coated TiO<sub>2</sub> particles, prep. for composites 0-89159  
 Cu-TiO<sub>2</sub> alloys, internally oxidised, plastically deformed, influence of particle form on primary loop nature (*French*) 0-103344  
 Fe-Cr-Ti-Mo-TiO<sub>2</sub> (13, 3.5, 1.5, 2 wt.%) dispersion hardened, void swelling 0-65046  
 Fe<sub>0.394</sub>Ti<sub>0.606</sub>-O-S subsystem, equil. phase data under reducing conditions rel. to ilmenite upgrading 0-76240  
 Fe<sub>3-x</sub>Ti<sub>x</sub>O<sub>4</sub>, spin glass behaviour, susceptibility and hysteresis meas. 0-65917  
 Fe<sub>2</sub>TiS<sub>2</sub>, lattice dynamics and hyperfine interactions, Mossbauer spectra study 0-108135  
 K<sub>2</sub>O-Al<sub>2</sub>O<sub>3</sub>-P<sub>2</sub>O<sub>5</sub>-TiO<sub>2</sub>, structural role of Ti, kinetic study of chem. destruction 0-88055  
 Li/TiS<sub>2</sub>, cell with solvate melt, discharge characts. and lack of rechargeability 0-72022  
 Li/Ti<sub>2</sub>(TiSe<sub>2</sub>)(Ti<sub>1-x</sub>S<sub>x</sub>), electrochem. obs. of Li intercalation 0-61216  
 Li<sub>2</sub>O-Al<sub>2</sub>O<sub>3</sub>-SiO<sub>2</sub>-TiO<sub>2</sub> glass, phase separation at initial stages of sitalization 0-88053  
 Li<sub>2</sub>O-TiO<sub>2</sub>, pseudobinary phase rotations, DTA and X-ray anal. 0-108411  
 Li<sub>2</sub>O-TiO<sub>2</sub>-Al<sub>2</sub>O<sub>3</sub>-SiO<sub>2</sub> glass,  $\gamma$ -irrad., struct. position of Ti, EPR study 0-84644  
 Li<sub>2</sub>TiS<sub>3</sub>, chem. diffusivity of Li at 30°C 0-59737  
 Li<sub>2</sub>TiS<sub>3</sub> electrodes, thermodynamic and transport props. 0-66963  
 MgCr<sub>2</sub>O<sub>4</sub>-TiO<sub>2</sub>, porous ceramics, humidity-sensitive electrical conduction 0-107782  
 MgO-TiO<sub>2</sub>-Al<sub>2</sub>O<sub>3</sub>-SiO<sub>2</sub> glass,  $\gamma$ -irrad., struct. position of Ti, EPR study 0-84644  
 Mo-TiC lamellar eutectic composite, deformation and strength, room temp. to 2073K (*Japanese*) 0-71702  
 Na<sub>2</sub>O-TiO<sub>2</sub>-Al<sub>2</sub>O<sub>3</sub>-SiO<sub>2</sub> glass,  $\gamma$ -irrad., struct. position of Ti, EPR study 0-84644  
 Na<sub>2</sub>O-TiO<sub>2</sub>-SiO<sub>2</sub> glass, co-ordination of Ti, X-ray emission spectra study 0-84072  
 Na<sub>9</sub>Ti<sub>11</sub>Fe<sub>9</sub>O<sub>4</sub>, short period  $\beta$ -alumina type cpds., cryst. struct. and superionic cond. 0-107499  
 Na<sub>2</sub>Ti<sub>2</sub>O<sub>4</sub> bronze, hydrothermal prep., Na ion arrangement 0-75209  
 Pb(Ti,Zr)O<sub>3</sub> solid solutions, phase coexistence discrepancies 0-96662  
 Rh-TiO<sub>2</sub> catalyst, adsorpt. of H<sub>2</sub>, surface states, NMR spectrosc. investig. 0-103891  
 Si-TiO<sub>2</sub>-Al, current-voltage characts., oxide film effects 0-70841  
 SiO<sub>2</sub>-Al<sub>2</sub>O<sub>3</sub>-MgO-TiO<sub>2</sub> devitrificates, microstruct. and props. (*Polish*) 0-70141  
 SiO<sub>2</sub>-Al<sub>2</sub>O<sub>3</sub>-Na<sub>2</sub>O-BaO-TiO<sub>2</sub>, glass ceramic interaction with Pb borosilicate glaze 0-84398  
 SiO<sub>2</sub>-Al<sub>2</sub>O<sub>3</sub>-Y<sub>2</sub>O<sub>3</sub>-La<sub>2</sub>O<sub>3</sub>-TiO<sub>2</sub> glasses with high elastic moduli, alkaline durability 0-85071  
 SiO<sub>2</sub>-TiO<sub>2</sub>, vitreous, US velocity and absorption 0-107380  
 Ta<sub>1-x</sub>Ti<sub>x</sub>S<sub>2</sub> (1T), magnetoresistance in the Anderson localized states near the metal-nonmetal transition 0-88479  
 Ta<sub>1-x</sub>Ti<sub>x</sub>S<sub>2</sub> (1T), magnetoresist. near metal-nonmetal transition at ultra low temps. 0-88600  
 (Ti,Ni)<sub>2</sub>C, metallographic detection in 12Kh18N10T steels 0-66721  
 Ti-N<sub>2</sub>, condensate formed by plasma flow precipitation in vacuum, cryst. and surface props. (*Russian*) 0-100788  
 TiB<sub>2</sub>, fusion reactor material, low energy ion erosion expts., Kaufman source appl. 0-68942  
 TiB<sub>2</sub> thick film on low C steel substrate, CVD in US field, crystallite size 0-84854  
 TiB<sub>2</sub>, vacuum condensate, struct. and mech. props., second phase effect (*Russian*) 0-71705  
 TiC, abrasive, effect on machinability of Ti alloys (*Russian*) 0-97593  
 TiC, CVD, deposition rate meas., rel. to mass transport model 0-103599  
 TiC coated WC-Co cemented carbides, fracture toughness 0-85046

## titanium compounds continued

- TiC coatings, on cemented carbides, struct. and hardness 0-59771  
 TiC coatings on steels and hard alloys 0-76414  
 TiC, deform. at high temps. 0-104239  
 TiC, electron irradi. damage, electron microsc. study 0-84210  
 TiC, electronic structure, PES study 0-70594  
 TiC, frictional characts. and contact-zone deform. in homogeneity range 0-66673  
 TiC, laser CVD, coating characterisation 0-93494  
 TiC particles injection into Ti-Al-V alloy surface for wear resist. improvement 0-85086  
 TiC, plasma arc spraying, chem. reaction with plasma gases 0-66427  
 TiC, precipitates in Ni-base superalloy, STEM microanal. 0-81067  
 TiC precipitates in Ti-implanted Fe, microstruct. 0-66513  
 TiC, sputtering, low energy, H, D and He ions 0-100734  
 TiC, vacuum condensate, struct. and mech. props., second phase effect (*Russian*) 0-71705  
 TiC, wetting by Cr-Ni-Mo-Mn alloy steel, expt. planning investigation 0-60822  
 TiC whisker, TF electron emitters, props. obs. 0-66403  
 TiC, whisker growth in CVD 0-59843  
 Ti-C composites, hot pressed, thermophys. props. at high temps. 0-59675  
 TiC<sub>x</sub>, nonstoichiometric, densification during sintering 0-84895  
 TiC<sub>x</sub>N<sub>1-x</sub>, electronic struct., KKR-ATA method 0-65447  
 TiC<sub>x</sub>N<sub>1-x</sub>, powder preparation, physical, chemical props. (*Russian*) 0-76212  
 TiC<sub>x</sub>O<sub>1-x</sub>, electronic struct., KKR-ATA method 0-65447  
 TiCl<sub>3</sub>, electronic struct. and struct. phase transition 0-59644  
 TiCl<sub>4</sub>, reduction in steady beam-plasma discharge 0-100099  
 Ti<sub>0.9</sub>, surface characts., AES, EELS, SIMS, and XPS study 0-65343  
 TiD<sub>2</sub>, nucleation and growth in D<sub>2</sub><sup>+</sup> implanted Ti, TEM study 0-97717  
 $\gamma$ -TiH<sub>3</sub>, interstitial H diffusion mechanism, NMR spin-lattice relax. study 0-103515  
 $\gamma$ -TiH<sub>3</sub>, NMR spin-lattice relax., effect of correlated atomic diffusion 0-107495  
 TiH<sub>x</sub>, surface characts., AES, EELS, SIMS, and XPS study 0-65343  
 TiH<sub>4</sub>, thermal diffusivity, near FCC to BCC transition 0-59740  
 TiN diffusion barrier on Si device metallisation 0-65304  
 TiN, electronic absorpt. spectrum, rot. anal. 0-78601  
 TiN films, reactively RF sputtered, struct. and elec. props., substrate bias effects 0-96763  
 TiN formation, from TiO<sub>2</sub>/Si<sub>3</sub>N<sub>4</sub> reaction in N<sub>2</sub> atmosphere 0-71617  
 TiN layers investigation for solar-cell contacts 0-81461  
 TiN, low-energy ion-stimulated deposited, supercond. props. 0-88664  
 TiN, supercond. critical temp., neutron irradi. effect 0-80433  
 TiN, whisker growth in CVD 0-59843  
 TiN<sub>x</sub>, substoichiometric, electronic density of states, CPA method calcs. 0-88464  
 TiN<sub>0.32</sub>H<sub>0.19</sub>, cryst. struct., neutron diff. anal. (*Russian*) 0-64965  
 TiN<sub>0.1</sub>, electronic struct., KKR-ATA method 0-65447  
 (TiNbO<sub>3</sub>)<sub>x</sub> oxide layers, intercalation of alkylammonium ions 0-64985  
 TiO, Franck-Condon factors rot. depend. 0-58319  
 TiO,  $\gamma$ -system, Franck-Condon factors, r-centroids and Einstein coefficients calcs. 0-74163  
 TiO in Ar matrix, meas. of absorpt. and magnetic circular dichroism spectra 0-86356  
 TiO in sunspots, equiv. width meas. theoretical interpretation, line form. process 0-72902  
 TiO  $\Phi$  system, near IR emission spectrum 0-69131  
 TiO<sub>2</sub> AR coating for Si solar cells by spray deposition, review 0-104511  
 TiO<sub>2</sub>, addition to Cr<sub>2</sub>O<sub>3</sub> effect on sintering behaviour 0-66461  
 TiO<sub>2</sub>, anatase, Raman spectrum, temp. depend. 0-76027  
 TiO<sub>2</sub>, brookite synthesis from Ti in NaF or Ti compounds, form. mechanism (*Japanese*) 0-93529  
 TiO<sub>2</sub>, core levels, cryst.-field splitting, X-ray emission study 0-66328  
 TiO<sub>2</sub>, crystal structure, stability compared with CaF<sub>2</sub> (*Russian*) 0-64945  
 TiO<sub>2</sub>, decomp. of CaO(Al<sub>2</sub>O<sub>3</sub>)<sub>2</sub> 0-92687  
 TiO<sub>2</sub>, doping processes, influence on photoelectrochem. behaviour 0-79822  
 TiO<sub>2</sub>, electrode, carrier density determ. by optical absorpt. and photoelectrolysis spectra 0-71462  
 n-TiO<sub>2</sub> electrode, flatband pot. determ. from differential stress meas. 0-75638  
 n-TiO<sub>2</sub> electrode, photo-oxidation of acetate and iodide 0-81331  
 n-TiO<sub>2</sub> electrode in AlCl<sub>3</sub>-NaCl melt, electrochem. and photoelec. props. 0-81328  
 TiO<sub>2</sub> electrodes, chemically modified, nature of surface states 0-107905  
 TiO<sub>2</sub>, exciton luminescence spectra, absorpt. spectra 0-89064  
 TiO<sub>2</sub> film, ion plated, DC cond. study 0-100457  
 TiO<sub>2</sub>, in silicate glass, thermal capacity 0-88335  
 TiO<sub>2</sub>, interionic repulsive short-range interaction pot., lattice energy calc. 0-96466  
 TiO<sub>2</sub> layers, activated reactive evaporation and absorpt. indices 0-97363  
 TiO<sub>2</sub>, Mn<sup>3+</sup> ion electron spin-lattice relaxation 0-108054  
 TiO<sub>2</sub>, nonstoichiometric anodic films, O incorporation kinetics 0-97733  
 TiO<sub>2</sub>, nonstoichiometry study, thermal emission of electrons 0-10317  
 TiO<sub>2</sub>, paint type coating layer with spherical pigment, radiative transfer theory 0-61405  
 n-TiO<sub>2</sub> photoelectrochemical electrodes, effect of Nb doping on quantum efficiency 0-101121  
 TiO<sub>2</sub>, photographic layers, sensitivity enhancement by addition of Ag<sup>+</sup> during cupric development (*Russian*) 0-62780  
 TiO<sub>2</sub>, porosity-permittivity relations, depolarising factors determ. and pore effects (*Japanese*) 0-97189  
 TiO<sub>2</sub>, rutile, electron mean free path, four-step transition and Auger spectra investig. 0-97389  
 TiO<sub>2</sub>, rutile, first order Raman spectrum, uniaxial stress effects 0-66196  
 TiO<sub>2</sub>, rutile, first-order Raman spectrum, uniaxial-stress depend. 0-60586  
 TiO<sub>2</sub>, rutile, K-edge X-ray absorpt., cond. band states 0-97382  
 TiO<sub>2</sub>, rutile, optoelectronic props., band struct., theory 0-80175  
 TiO<sub>2</sub>, rutile, pure and SiO<sub>2</sub>-coated, adsorption of N<sub>2</sub> and Ar, 77.4K, microcalorimetry obs. 0-80062  
 TiO<sub>2</sub>, rutile, Raman study at high press. 0-89002  
 TiO<sub>2</sub>, rutile, superficial constitutive water, NMR study 0-88881  
 TiO<sub>2</sub>, rutile phase, shock induced phase transition anisotropic behaviour 0-103475  
 TiO<sub>2</sub>, semicond. anode in aq. electrolyte, electrochem. and electrochem. 0-76080  
 TiO<sub>2</sub>, spray-on antireflection coatings for Si solar cells 0-80963  
 TiO<sub>2</sub>, sputtering defects, associated surface electron states, UPS, XPS and AES obs. 0-60755  
 TiO<sub>2</sub> surface, photocatalytic decomp. of H<sub>2</sub>O 0-85194



## titanium compounds continued

- TiO<sub>2</sub> suspension, adsorption-desorption of IO<sub>3</sub><sup>-</sup> 0-93804  
 TiO<sub>2</sub> suspension in glycerine, Bingham plastic flow through annuli 0-64521  
 TiO<sub>2</sub>, thermally stimulated exoelectron emission (*German*) 0-66404  
 TiO<sub>2</sub>:Cr(Ta), slightly doped, elec. cond. and defect struct., charge compensation and point defect model 0-75568  
 TiO<sub>2</sub>:Fe<sup>3+</sup>, 86-88 GHz low-noise TW maser 0-69354  
 TiO<sub>2</sub>:Mo<sup>4+</sup>, interstitial EPR, g-tensor and hyperfine tensor 0-84647  
 TiO<sub>2</sub>:Nb semicond. electrodes, electroreduction process kinetics, cathodic dark current meas. 0-66807  
 TiO<sub>2</sub>:Ru<sup>4+</sup>, rutile, EPR and cryst. field const. 0-60415  
 TiO<sub>2</sub>:TeCl<sub>4</sub> system, chem. vapour transport, matrix isolation IR studies 0-93755  
 n-TiO<sub>2</sub>/Au Schottky diodes, I-V and C-V characts. 0-96988  
 TiO<sub>2</sub>-Ag-TiO<sub>2</sub> heat mirror on plastic sheet for radiation insulation of visible windows 0-95985  
 TiO<sub>2</sub>-Al<sub>2</sub>O<sub>3</sub>-SiO<sub>2</sub> system, ternary glass-forming region and phys. props. 0-84919  
 n-TiO<sub>2</sub>-electrolyte interface, charge transfer via surface states, water photoelectrolysis anal. 0-75636  
 n-TiO<sub>2</sub>-electrolyte interface impedance, freq. depend., equiv. cct. 0-100516  
 TiO<sub>2</sub>-Ni (100) interface, electronic props., struct., comp., chemical bonding 0-84499  
 TiO<sub>2</sub>-PbO, acoustooptic props. from comp. and density 0-76000  
 TiO<sub>2</sub>-RuO<sub>2</sub> surface, photocatalytic decomp. of H<sub>2</sub>O 0-85194  
 TiO<sub>2</sub>-SiO<sub>2</sub> glass form. by low temp. chem. polymerisation 0-84899  
 TiO<sub>2</sub>-SiO<sub>2</sub> glass system, Raman and hyper-Raman light scatt. spectra 0-66187  
 TiO<sub>2</sub>-SiO<sub>2</sub> mirror, dielectric, Rayleigh scatt. at 441.6 nm 0-97367  
 TiO<sub>2</sub>-SiO<sub>2</sub> multilayer vacuum coatings, optical props. 0-97361  
 TiO<sub>2</sub>-x reduced, crystallographic shear planes, dislocation struct. 0-107175  
 TiO<sub>2</sub>, struct. vacancies in unit cell 0-107213  
 Ti<sub>2</sub>O<sub>3</sub>, electron density distrib., deform. density at 295K, X-ray anal. 0-107117  
 Ti<sub>2</sub>O<sub>3</sub>-Al<sub>2</sub>TiO<sub>5</sub> (MgTi<sub>2</sub>O<sub>5</sub>), solid solubility, X-ray phase and optical microscopic exam. 0-59657  
 Ti<sub>4</sub>O<sub>7</sub>, Verwey transition, cond. processes 0-96787  
 TiS, disordered structures, two-dimensional, computer program for modelling (*French*) 0-59337  
 TiS<sub>2</sub>, band struct., angle-resolved photoemission studies 0-70610  
 TiS<sub>2</sub>, fast ion transport and electrochem. storage, Li reactions 0-61324  
 TiS<sub>2</sub>, valence density of states, Gilat-Raubenheimer method 0-88465  
 TiS<sub>2</sub>, linear chain compound, lattice, props., Raman spectral study 0-71421  
 TiSe<sub>2</sub> (1T), Raman studies of lattice dynamics 0-103962  
 TiSe<sub>2</sub>, band struct., angle-resolved photoemission studies 0-70610  
 TiSe<sub>2</sub>, impurity effects on elec. props. 0-80263  
 TiSe<sub>2</sub>, valence density of states, Gilat-Raubenheimer method 0-88465  
 TiSi<sub>2</sub>, film, elastic stiffness and thermal expansion coeffs. 0-107451  
 Ti<sub>1-x</sub>V<sub>x</sub>C, electronic struct. and X-ray emission spectra, cluster MO calc. 0-65444  
 (Ti<sub>1-x</sub>V<sub>x</sub>)<sub>2</sub>O<sub>3</sub>, O<x<0.1, magnetisation and mag. moments 0-65772  
 (Ti<sub>1-x</sub>V<sub>x</sub>)<sub>2</sub>O<sub>3</sub>, spin glass, nonlinear susceptibility and sp. ht. 0-60304  
 (Ti<sub>1-x</sub>V<sub>x</sub>)<sub>2</sub>O<sub>3</sub>, impurity doping effects, elec. props. obs. 0-75609  
 Ti<sub>1-x</sub>V<sub>x</sub>Se<sub>2</sub>, mag. susceptibility, 4.2-300K 0-60188  
 (Ti<sub>1-x</sub>V<sub>x</sub>)<sub>2</sub>O<sub>3</sub>, metallic antiferromag. struct., neutron studies 0-65797  
 TiW-TiO<sub>2</sub>-InP thin refractory MIS struct. deposition 0-75647  
 V<sub>2</sub>O<sub>5</sub>-TiNb<sub>2</sub>O<sub>7</sub> system, interfacial reactions, efficient boundary conditions and solid state reactivity 0-76542  
 V<sub>2</sub>O<sub>5</sub>-Ti<sub>2</sub>O<sub>3</sub>, DTA, mag. susceptibility and X-ray diffr. study 0-70970

## Tokamak devices

- Alcator C, design and discharge parameters, review 0-79533  
 Alcator C far IR emission diagnostics of electron temp. 0-59291  
 Alcator high density Tokamak, ion temp. profile reconstruction (*Russian*) 0-106959  
 ASDEX, assembly and commissioning, review 0-102334  
 ASDEX, extraction grid for high power ion source 0-102372  
 ASDEX, neutral beam injection, beam line design 0-99395  
 ASDEX, neutral beam injectors, HV power supply system, thyristor control 0-99332  
 bakeable seals development for large noncircular ports on Tokamak fusion test reactor 0-82777  
 blanket, liq. Li module stresses due to changing poloidal mag. field 0-95435  
 blanket and first wall design concept, thermal and hydraulic anal. 0-95460  
 burn period plasma current maintenance, rectifying first wall, cct. anal. 0-102307  
 chopper system, UHV compatible, for meas. of energy spectrum of neutral D atoms 0-79587  
 commercial Tokamak hybrid reactor, blanket and shield design 0-106179  
 commercial Tokamak Hybrid Reactor, reference design 0-106171  
 compact ignition test reactor, engineering design using Bitter type magnet 0-102310  
 conference, New York, USA (Oct. 79) 0-73093  
 confinement time meas. 0-87945  
 contacts for pulsed high currents, design and testing 0-70029  
 control systems, construction and simulation study (*Japanese*) 0-100100  
 controlled Tokamak plasma, simulation 0-59269  
 cooling pattern of acceleration grids meas. by IR scanning 0-86303  
 corpuscular diagnostics by charge exchange of plasma ions at artificial target, in Tokamak T-4 (*Russian*) 0-83968  
 CT6B Tokamak, measurement of plasma column displacement 0-84001  
 CT-6 Tokamak device, development, test operation (*Chinese*) 0-87919  
 CT-6 Tokamak plasma props. (*Chinese*) 0-103159  
 current disruption effects 0-74012  
 cylindrical plasma filament under axisymmetric perturbation, numerical anal. 0-106853  
 Demonstration Power Tokamak Reactor, vacuum outer containment and metal seals feasibility study 0-95458  
 diagnostic Fourier transform spectrometer calibration by liquid N<sub>2</sub> cooled microwave absorber 0-59304  
 disruptions in Tokamaks and small scale turbulence 0-59266  
 DITE, behaviour review including injection and bundle divertor 0-74021  
 DITE, low Q discharges 0-92374  
 DITE, neutral injection heating 0-92347  
 DITE Tokamak, beam driven current meas. 0-106940

## Tokamak devices continued

- DITE Tokamak bundle divertor, Mk.II design 0-91268  
 DITE-II, neutral beam ion source particle beam identification 0-99397  
 DIVA Tokamak, q=1 mag. surface noncircular cross-section, in low-q discharge 0-100090  
 divertor mag. piston action, elec. AC power direct generation 0-102324  
 divertorless Tokamaks, limiter pumping system 0-95463  
 Doublet III, computer control system 0-99321  
 Doublet III, limiter performance, design and material selection 0-106162  
 Doublet III, neutral beam injection system, two-gap magnet design and performance 0-92379  
 Doublet III, neutral beam injector system, instrumentation and control 0-99322  
 Doublet III, neutral beam interlock system using IR detector 0-106228  
 Doublet III, neutral beam test tank design 0-99301  
 Doublet III, ohmic heating E-coil vacuum breaker system, function and operation 0-102323  
 Doublet III, plasma density, shaping and characteristics 0-74018  
 Doublet III, plasma shape control, 1.5 Megawatt DC chopper power supply 0-102333  
 Doublet III, possible Dee configs. 0-91269  
 Doublet III, toroidal field coils, Cu alloy plate defect size restrictions 0-91257  
 Doublet III, vacuum vessel neutral beam armour 0-95462  
 Doublet III beamline, review, component relation and config., design constraints 0-99382  
 Doublet III beamline calorimeter, three dims. heat transfer anal. 0-99381  
 Doublet III neutral beam injector system, outgassing rate meas. and residual gas anal., coating props. 0-95457  
 Doublet-III, frequency generator-rectifier system performance 0-102326  
 DTHR, advanced bundle divertor design 0-99281  
 electrically isolated target, formation of arcing, role of runaway electrons 0-64764  
 electron beam driven Tokamaks, review 0-99317  
 energy confinement comparison of ohmically heated stellarators to Tokamaks 0-92360  
 energy confinement scaling, Frascati Torus results 0-79536  
 enhanced plasma-frequency radiation (*Chinese*) 0-59185  
 ETF, design considerations 0-95438  
 ETF, engineering challenges, review 0-95422  
 far IR laser collective scatt. system 0-59300  
 filament ellipticity, energy lifetime in T-8 apparatus (*Russian*) 0-87930  
 FILTOR-D, T breeding blanket, Monte Carlo calcs. 0-99283  
 first wall blanket, cylindrical module, reference design 0-106181  
 FT Tokamak, non-thermal electron distrib. function 0-83891  
 FT Tokamaks, expt. results 0-74014  
 FT-1 Tokamak, discharges in low density plasma (*Russian*) 0-106958  
 FT-1 Tokamak, electron cyclotron heating expt. 0-75071  
 FT-1 Tokamak, lower hybrid heating, energy balance 0-79523  
 FTR, equilib. field coils, electrical supply system, optimisation and computer aided performance anal. 0-91288  
 fueling and thermonuclear instability, cold plasma layer surface fueling source 0-59196  
 fusion reactor, high mode number ballooning instabilities, max.  $\beta$ -value 0-73995  
 fusion reactor first wall, radiation damage simulation using fission reactor test facilities 0-57950  
 HFCTR, demonstration reactor conceptual design, high force density magnets and modularisation 0-95439  
 high- $\beta$  Tokamak equilibrium, second order effects 0-70024  
 hybrid shielding, radiation heating rates, two-dims. transport anal. 0-106178  
 impurity transport (*Russian*) 0-106957  
 induction heating coils, 50 kA prototype superconducting cable, critical current 0-106196  
 ISX-B, electron cyclotron microwave heating 0-99329  
 ISX-B, high power neutral beam injection studies 0-79545  
 ISX-B, neutral beam power system 0-91283  
 ISX-B, neutral beam system 0-99388  
 ISX-B, with bundle divertor, structural anal. 0-91254  
 ISX-B neutral beam injector expt. on prototype beam line 0-74039  
 ISX-B tokamak, design of bundle divertor expt. 0-102341  
 ISX-B Tokamak, expt. program, review 0-78435  
 ISX-B toroidal field coil finger joints, fatigue life, structural evaluation 0-91253  
 Japanese Tokamak research, impurity control, low-q discharge, scaling law, RF heating 0-74015  
 JET, extraction element design for long pulse multi-megawatt neutral beam 0-102373  
 JET, far IR interferometer design 0-59295  
 JET, neutral injector overvoltage injection system 0-99398  
 JET, periplasmatron ion source for intense neutral beam 0-99380  
 JET-2, origin of arcing 0-92414  
 JET-2 Tokamak, impurity ion sputtering 0-79554  
 JET-2 tokamak radiation loss meas. with Ge film bolometer 0-95141  
 JIPP T-II, horizontal plasma position control by feedforward-feedback system with digital computer 0-75093  
 JIPP T-II, neutral beam injection system, design and expt. test 0-106226  
 JT-60, CAMAC system, microprocessor based 0-59309  
 JT-60, fault current anal. in grounding system 0-99307  
 JT-60, grounding system design 0-102313  
 JT-60, grounding system pot. rise during lightning strike, anal. 0-102314  
 JT-60, poloidal field DC power supply developments 0-102325  
 JT-60, poloidal field power supply system, AC voltage behaviour, simulation 0-91287  
 JT-60, prototype neutral beam injector unit 0-106225  
 JT-60, seismic anal., design changes 0-95425  
 JXFR, superconducting mag. system conceptual design 0-99295  
 Large Coil Program, insulation system cryogenic elec. test 0-91263  
 Large Coil Program, Westinghouse superconducting mag. elec. design 0-91250  
 large magnetic field ripples, electric probe meas. 0-83976  
 LARTS, extended burn operation, physics, engineering and economics 0-95440  
 low power Tokamak experimental fusion power plant, scoping studies with empirical scaling, SISYFUS code 0-102309  
 low Z coating development program 0-106182  
 low-pass interference filters for Tokamak plasma diagnostics 0-64783  
 lower hybrid wave propag. and damping in Tokamak plasma, numerical study 0-64698



**Tokamak devices continued**

- LPTT, engineering design 0-102308  
 maintenance design requirements and economics 0-99285  
 maximum toroidal mag. field value by core constraint 0-102349  
 MHD equilb., var. method in Tokamak (*Russian*) 0-106960  
 Microtor Tokamak, LF microturbulence, far IR laser scatt. 0-96362  
 mobile diaphragm operation mode in Tokamak and CTR reactors (*Russian*) 0-83966  
 motion of relativistic charged particle in axisymmetric toroidal system 0-83991  
 neutral beam injection reionisation power losses in duct, model 0-99385  
 neutral beam ion source, core snubber network design, fabrication and testing 0-102378  
 non-circular Tokamak field shaping coils, current optimisation 0-95426  
 noncircular Tokamak, time evolution of elongation ratio and Mirnov oscill. 0-64763  
 nonlinear perturbation in Tokamak, feedback effect (*Russian*) 0-83967  
 ORNL/TNS and ETF, tokamak reactor poloidal field system study 0-95436  
 PDX, 6 MW Neutral Beam Project, overview 0-106223  
 PDX, assembly, description 0-99308  
 PDX, data acquisition systems, networking and distrib. processing improvements 0-99318  
 PDX, flexible work platform and balcony design 0-106161  
 PDX, initial operation 0-79555  
 PDX, large Tokamak, design and future use 0-79534  
 PDX, neutral beam elec. power system, ion source supply upgrade 0-102330  
 PDX, ORNL prototype neutral beam injection system, ion source development 0-99391  
 PDX, toroidal field coil and frame struct., anal., finite element anal. 0-106165  
 PDX neutral beam injector, ion accel. structural anal. 0-102375  
 PDX neutral beam injector, multi-aperture ion accel. electrodes thermal anal. 0-102371  
 PDX neutral beam injector development 0-99375  
 PDX power test results, struct. finite element anal. 0-91265  
 PDX Tokamak, finite element anal. using computer graphics 0-95424  
 PDX Tokamak, struct. anal. by finite element method 0-106166  
 PDX Tokamak, surface analysis station 0-79586  
 PDX toroidal field coil joint fatigue testing 0-91252  
 pellet refuelling of a divertor Tokamak 0-91247  
 PETULA Tokamak, lower hybrid heating expts. 0-83958  
 PGFR seismic risk anal. 0-99298  
 PHIBEX, poloidal field power supply for ignition, computer based cct. anal. 0-102329  
 plasma current profile meas. by neutral beam probe (*Japanese*) 0-96397  
 plasma diagnostic double-pass rapid-scanning Fourier transform spectrometer 0-59299  
 PLT, D<sub>2</sub> flux and energy incident on probe, power balance, impurity generation 0-79553  
 PLT, data acquisition systems, networking and distrib. processing improvements 0-99318  
 PLT, electron cyclotron radiation Fourier transform diagnostics 0-59292  
 PLT, fusion neutron yield during D neutral beam injection 0-79522  
 PLT, ICRF heating for two-ion regime 0-83959  
 PLT, neutral beam duct reionisation losses, obs. and power loss model 0-99383  
 PLT, neutral beam heating 0-106950  
 PLT, neutral beam injection, power input and plasma temp. reconciliation 0-106224  
 PLT, neutral beam injection and ICRF heating, charge exchange meas. 0-83892  
 polarization and millisecond spectral measurements of electron cyclotron emission from DITE Tokamak 0-92396  
 position instability analysis, effective mode approx. in Tokamak 0-103145  
 power reactor, electron cyclotron reson. heating by gyrotrons 0-99331  
 PRETEXT, poloidal field coil code, expt. verification 0-92377  
 Pulsator Tokamak, electron density limitation 0-96385  
 Pulsator Tokamak discharges with AC modulation 0-96386  
 pulsed RF-trapped particle interaction stochastic effects in tokamak 0-59245  
 RINGBOOG II, toroidal discharges with cold blankets 0-83901  
 RST, RF driven steady state toroidal expt., design 0-91276  
 RST, support struct. 0-102342  
 shielding and maintainability in an experimental Tokamak 0-99287  
 SLPX, Superconducting Long-Pulse Experiment, scoping study 0-91275  
 SLPX TF coil, stress anal. using COSMIC-NASTRAN 0-106168  
 solid breeding blanket for commercial Tokamak reactors, materials and design 0-95441  
 STARFIRE project, an overview 0-106183  
 STARFIRE project, design parameters 0-106184  
 STARFIRE project, first wall and blanket design 0-106188  
 STARFIRE project, impurity control system 0-102345  
 STARFIRE project, maintenance considerations 0-102346  
 STARFIRE project, superconducting poloidal coils design study 0-106185  
 STARFIRE project, T handling and vacuum requirements 0-106187  
 STARFIRE project, toroidal field coil system preliminary assessment 0-106186  
 steady state resistive toroidal field coils 0-91264  
 stochastic orbits in Tokamak, statistical description, low freq. fluctuations 0-59265  
 superconducting toroidal system, force anal. for all fault conditions 0-91258  
 T-10 Tokamak, electron cyclotron emission meas. 0-92375  
 T-10 Tokamak, stainless steel limiter expts. in ohmic heating region (*Russian*) 0-83969  
 TEXT, assembly plan 0-99305  
 TEXT, motor-generator power supply system 0-99292  
 TEXT, poloidal field power systems, design and anal. 0-102328  
 TEXT, toroidal field coil fabrication 0-91267  
 TEXT, toroidal field coil power supply, thyristor controlled 0-91289  
 TEXT overview and status report 0-91273  
 TEXTOR, mag. diagnostics and monitoring systems data acquisition 0-99320  
 TEXTOR, poloidal coil system power distrib. system 0-102327  
 TFR, extraction grid for high power ion source 0-102372  
 TFR, far IR Fourier transform spectroscopic Michelson interferometer 0-59294  
 TFR 600 Tokamak, electron heat transport anomaly 0-79449

**Tokamak devices continued**

- TFR 600 Tokamak, soft X-ray meas., mag. topology near  $q=1$  surface 0-79580  
 TFTR, assembly 0-102335  
 TFTR, blanket module expts., engineering test station design 0-102338  
 TFTR, eddy current theory for structural materials 0-95427  
 TFTR, electrical power blanket module, conceptual design 0-102339  
 TFTR, energy conversion and storage systems, fault detection and protection 0-95431  
 TFTR, field coils cooling water system 0-106160  
 TFTR, gas injection assembly 0-99342  
 TFTR, general arrangement of diagnostics 0-95445  
 TFTR, high energy heat sink, ion beam dump and calorimeter 0-99394  
 TFTR, high power direct energy converters for beams and plasma 0-99334  
 TFTR, High Voltage Switch Tube, for Neutral Beam Power System 0-99291  
 TFTR, hollow cathode mag. multipole ion source 0-102369  
 TFTR, large noncircular ports, development of bakeable seals 0-95454  
 TFTR, large section water cooled Cu conductor, brazing joints 0-91260  
 TFTR, neutral beam injector prototype, construction and performance 0-99390  
 TFTR, neutral beam injector test facility construction 0-102336  
 TFTR, neutral beam line final design 0-99309  
 TFTR, neutral beam power system 0-91282  
 TFTR, neutral beam source, arc current modulator design 0-102379  
 TFTR, neutral beam sources overcurrent protection during spark down 0-102331  
 TFTR, neutral beam-torus connecting duct 0-99302  
 TFTR, neutron spectrometer mech. design 0-95498  
 TFTR, power line, variable freq. AC harmonic content 0-99293  
 TFTR, preoperational test plan, manpower loading and scheduling 0-102340  
 TFTR, T gas injection system transient response 0-102337  
 TFTR, tritium breeding test blanket module design 0-99304  
 TFTR, vacuum pumping system 0-95447  
 TFTR, vacuum vessel bellows, strength and fatigue anal. 0-95455  
 TFTR energy conversion system simulation 0-99303  
 TFTR Flexibility Modification, in-torus surface pumping, Ti and Zr/Al gettering 0-95451  
 TFTR mag. field coil electrical insulation system and test results 0-95429  
 TFTR neutral beam support system 0-102376  
 TFTR outer poloidal-field coil insulation and mould design 0-91261  
 TFTR poloidal field coil system, characts. 0-95430  
 TFTR poloidal field coils, tooling and manufacture 0-91262  
 TFTR toroidal field coil support restraint struct. 0-95428  
 Thor Tokamak, wall conditioning by cleaning H discharges 0-78440  
 TM-1-MH Tokamak, HF heating expts. 0-79527  
 TNS, electron cyclotron heating startup system, design 0-99330  
 Tokamak fusion reactor vacuum vessel, eddy currents when plasma current is disrupted, calc. (*German*) 0-68937  
 Tokamak fusion test reactor, thermal response of first wall limiters 0-79585  
 Tokamak fusion test reactor, transient getter scheme 0-79584  
 toroidal field coil finite element stress anal. 0-91256  
 toroidal field coil in-plane bending stress, struct. support design 0-106164  
 toroidal field coils, EM parameters calcs. of current paths in homogeneous media (*Japanese*) 0-106155  
 TOSCA,  $\beta$  optimisation studies 0-83990  
 USA Tokamak fusion research 0-74017  
 C bonding to Tokamak walls, XPS studies 0-80942  
 D, thermal desorption meas. of H-isotope retention in Alcator-A Tokamak 0-79588  
 Fe XV, line intensity and linewidths at high electron density, generalised population ratio 0-99481  
<sup>2</sup>H-<sup>3</sup>H fuel pellet electrostatic injection (*Japanese*) 0-78434  
 O bonding to Tokamak walls, XPS studies 0-80942  
 W radiation generation in Tokamak, Ag I isoelectronic sequence identification 0-83981

tomography, computerised *see* computerised tomographytool steel *see* steel**tools***see also* hand tools; machine tools

optical fibre cutting tool and automatic splicing machine 0-87575

**topology***see also* catastrophe theory; graph theory

biomedical surface mapping, interpolation methods 0-81750

chemical systems, topological model and orbital mapping 0-78512

crystal growth, topological modelling techniques 0-59418

fibre bundles and topology 0-105793

Henon mapping, topological horseshoe, chaotic behaviour 0-73257

liquid, ideal incompressible flow, topological measuring of canonical

Clebsch variables 0-69758

liquid crystal, thin layer, symmetry defects and solitons, topological classif.

0-107044

molecular structures, topological code, modified Morgan algorithm

0-58122

molecular topological spaces, structs. 0-91701

molecules, composite particle, vibr. amplitude and vibr.-rot. anal.

0-74158

nerve fields, topographic organisation 0-89742

quantum mechanical model, Borel summation appl. 0-90718

representation of groups, semigroups, and categories, book 0-57016

RF SQUID structures, topology and theory 0-97036

soap foam, arrangement of cells in a net rel. to grain sections of polycryst.

0-70225

speckle photography and holographic interferometry, scatt. geometry,

topology, vector fields, theory 0-87347

thermal electrocyclic reactions, anal. using topological model 0-78512

thermodynamics, irreversible, near equilb., metric geometry 0-62604

visual difference thresholds modelling, appl. of ordered topological vector

spaces 0-104587

Cu, high purity, creep cavitation topology, high temperature region

(*Czech*) 0-65138**torque***see also* Scott effect

fibres, biaxial rotation fatigue testing, torque development 0-71840

Nimonic 80A, creep rupture under non-proportional loading 0-108518

- torque continued**  
 steel, friction measuring test for use under conditions of high normal interfacial force 0-76454  
 Fe-Si (3.25 wt.%) alloy, single cryst. with (007) planes, domain struct. influence on mag. torque 0-108034  
 NdCo<sub>2</sub>, magnetocrystalline anisotropic props., torque meas. 0-108003
- torque measurement**  
*see also dynamometers*  
 No entries
- torque meters** *see torque meters*
- torquemeters**  
 pulse-phase, magnetically coupled pulse transducer with electronic phasemeter 0-74819
- Torrey oscillations (NMR)** *see double nuclear magnetic resonance*
- torsion**  
*see also stress analysis*  
 bar, rectangular, torsion crack problem, harmonic function continuation technique soln. 0-99969  
 bars, prismatic, St. Venant's torsion problem, method of singularities (*German*) 0-73163  
 beam, annular, torsional oscillations (*German*) 0-106752  
 beams flexural-torsional problem by series expansion in eigenfunctions 0-83732  
 bending-free torsion condition to define centre of twist 0-79140  
 cellulose nitrate, nonlinear viscoelastic deform., hydrostatic press. and third invariant of deviatoric stress tensor 0-93587  
 colour geometrodynamics, eightfold way, review 0-95243  
 composite beams, effects of fibre orientations on free vibrations 0-87734  
 composite materials, fibre reinforced, rectangular rods, elastic wave propagation (*French*) 0-83749  
 concrete reinforced rectangular membranes, torsional stiffness 0-65131  
 cosmological  $\nu$  sea, EM wave propagation, torsional background 0-77283  
 coupled bending-torsion flutter in cascades, aeroelastic stability boundaries 0-64424  
 cylinder, hollow with internal circular crack, axially symmetric torsion determ. 0-64456  
 cylinder under torsion elastic, spherical cavity effect in stress-strain state 0-101717  
 cylindrical rod, periodic structure, torsional vibrations, interfacial elastic parameters 0-96215  
 disc, axisymmetrically variable thickness, deflection by conc. lateral load (*Japanese*) 0-96194  
 dynamic stress/strain measurements under superimposed high press., torsion bomb machine 0-85130  
 elastic bar under tension, torsion appl., 2nd order effects, energy method 0-79158  
 elastic cylinder with inserts and holes, torsion problem, integral eqn. soln. method 0-106717  
 elastic sphere torsion by elastic punches 0-99929  
 EM field in space with torsion, semi-minimal coupling principle 0-77675  
 glass-plastic, unidirectional, torsion strength and shear modulus 0-99948  
 inhomogeneous elastic layer, torsion investigation by approx. methods 0-98799  
 limestone tubes, dynamic torsional failure obs. 0-85648  
 matrix analysis of composed bar of open cross section 0-83736  
 metal, thin-walled cylinder, elongation upon torsion 0-64386  
 Nimonic 80A, creep rupture under non-proportional loading 0-108518  
 optical fibre, single-mode, for current meas. system, birefr. induced by bends and twists 0-99832  
 orthotropic laminates, torsion strength and shear modulus determ. 0-92587  
 pendulum, with anelastic solid of discrete relaxation spectra, resonant system 0-69687  
 phthalocyanine polymer, dynamic mech. props. and fracture energy 0-100866  
 piezoelectric cylindrical shell, inhomogeneous, torsional wave motion 0-60506  
 pipe elbow element, linear anal., bending axial and torsional displacements, ovalisation 0-79177  
 polycarbonate, rigid plastic, yield behaviour (*Japanese*) 0-93620  
 prismatic bar of linearly elastic material, maximum theorem appl. for complementary energy functional 0-83733  
 PVC, rigid plastic, yield behaviour (*Japanese*) 0-93620  
 quartz, torsional vibration frequency temp. depend. 0-70294  
 rod, thin elastic, non-conservative torsion (*German*) 0-106723  
 rod of rate-sensitive material, elastic-plastic tension-torsion analysis 0-83741  
 rods, prismatic, torsion with internal constraints (*Russian*) 0-69647  
 rods, prismatic, torsion with internal constraints (*Russian*) 0-69648  
 rubber, natural, crosslinked by dicumyl peroxide, modulus, swelling relations 0-59551  
 rubber cylinder, circular, uniformly heated, combined extension and torsion 0-92057  
 spinning charge, torsion contrib. to magnetic field 0-77676  
 spinning particle in metric-torsion field, eqn. of motion 0-62543  
 steel, C, unnotched, fatigue life estimation, under combined torsion and bending (*Japanese*) 0-93647  
 steel, mild, plastic flow localisation under dynamic torsional loading, crit. variables 0-85015  
 test method, for plastic deform. (*Hungarian*) 0-97659  
 US vibrations in metals, measurement of absorpt. 0-58856  
 viscoelastic rod, standard linear body, free torsional oscils. 0-99940  
 Al-Ag (7.27 wt.%), peculiarities exhibited during fatigue loading (*Chinese*) 0-71723  
 Al-Cu-Mg-Mn-Si-Fe, torsional vibrations decrement, deformed vol. effect 0-76326  
 Al-Cu-Si-Mg, deform. simulation using torsional test, elastoplastic constitutive eqn. 0-93594  
 Al-Ni (6 wt.%), fine-grained, deform. in tension and torsion 0-85008  
 Al-Zn-Mg-Cu (6, 2.5, 1.5 wt.%), deform. simulation using torsional test, elastoplastic constitutive eqn. 0-93594  
 Cu, annealed polycryst., torsional vibrations decrement, deformed vol. effect 0-76326  
 Fe whiskers, inverse Wiedemann effect, torsional strain and azimuthal mag. field influence 0-108045  
 Fe-Si (3 wt.%), internal friction, instantaneous, depend. on phase of torsional oscils. (*Russian*) 0-71142  
 Ni alloy, heat resistant, fatigue limit comparison in torsion and tension-compression 0-81181  
 Ni, ductility and fracture, nonmetallic inclusions effect 0-104221
- torsion continued**  
 Ni, internal friction, instantaneous, depend. on phase of torsional oscils. (*Russian*) 0-71142  
 Ni thin-walled cylinder, elongation upon torsion 0-64386  
 V wire, deformed in torsion, internal friction, H effect 0-76300  
 Zn, line energy of basal screw dislocation, exptl. determ. 0-88154
- torsion loading** *see torsion*
- total energy systems**  
 25 kW Fresnel lens/photovoltaic concentrator application experiment at Dallas-Fort Worth Airport 0-89647  
 energy cascading principles (*French*) 0-76621
- touch** *see mechanoeception*
- Townsend coefficient** *see Townsend discharge*
- Townsend discharge**  
 avalanche, vacuum UV spectra 0-64810  
 mechanisms, of single-avalanche, Townsend and channel discharges (*Polish*) 0-79609  
 rod-to-plate system, initial corona voltage calculated according to Townsend's Theory (*Czech*) 0-87961
- tracers**  
*see also radioactive tracers*  
 hydrodispersive transfer in aquifers 0-98374  
 stratosphere tracer transport mechanisms, Lagrangian motion of air parcels in presence of planetary waves 0-109215  
 Fe-Cr (9 wt.%), oxidation studied using C<sup>18</sup>O<sub>2</sub> and D<sub>2</sub>O tracers 0-71784
- track visualisation, particle** *see particle track visualisation*
- tracking**  
*see also radar*  
 conference on satellite Doppler tracking and geodetic appl., London, England (Oct. 1978) 0-77264  
 cumulus clouds, satellite tracking and derived mesoscale wind fields covariance anal. 0-82013  
 IR staring mosaic sensor background suppression and tracking 0-86415  
 Mars, dynamics obs. from Viking lander tracking data anal. 0-77314  
 mosaic IR image differencing for track assembly 0-86420  
 optical signals using SAW spectrum analyser in photon-counting mode 0-105712  
 projectiles, continuous-wave transmitting, passive array 0-94955  
 satellite photographic tracking, astronomical method (*Chinese*) 0-77254  
 solar power plant, direct tracking using two-mirror unit with plane and hyperboloidal counter-reflectors 0-91875  
 spatial pattern recognition by spectral feature classification and coherent optical correlation 0-99644
- tracking (insulation)** *see surface discharges*
- tracking (sonar)** *see sonar*
- tracking systems**  
*see also ground support systems; radar systems*  
 airborne target tracking filter configurations compared 0-96130  
 charge injection device as stellar tracking sensor 0-85861  
 geostationary orbit determ., by single-ground-station tracking 0-109329  
 laser tracking system testing by 1 m unobscured IR collimator 0-78991  
 near-millimetric wavelength military systems 0-86428  
 passive tracking acoustic array evaluation, nonlinear filtering lower bound algorithms 0-96088  
 Shuttle Orbiter re-entry, remote IR imagery and tracking 0-82171  
 step-state spaceborne optical system smear compensation by focal plane manipulation 0-82172  
 Sun tracker, electronic, for clear or cloudy weather 0-76644  
 tracking by microprocessor-based coordinate calc. (*Spanish*) 0-89623  
 underwater acoustic tracking system for divers, PATS 0-91949  
 wideband optical disc data recorder systems 0-102751
- tracks, particle** *see particle tracks*
- traction**  
 electric traction units, driving axle oscillations damping using seismic dampers (*German*) 0-62458  
 Na/S traction batteries, development progress and problems, review 0-61326
- traction current collection**  
 high speed ground transportation vehicles gas-flow-controlled arcs for power collection 0-70054
- tractive effort** *see traction*
- trade fairs** *see exhibitions*
- trade shows** *see exhibitions*
- training**  
*see also education; teaching*  
 Ann Arbor school of astronomers, foundation, 1852-63 0-86062  
 biomedical engineers and technicians in developing countries 0-62408  
 electrical and electronic engineering design education and training conference, London, England 0-67971  
 electron microscopy, autotutorial methods utilizing sound-on-slide presentations 0-73534  
 engineering education, importance of research and design for satisfying industrial needs 0-67974  
 fast breeder test reactor operator training simulator model development 0-91219  
 fibre optical communications, course status and effectiveness 0-62413  
 nuclear power station Czechoslovak Research Institute activities personnel (*Slovak*) 0-83188  
 optics, faculty of Inst. of Optics, profile 0-62422  
 optics, graduate education at Optical Sciences Centre, programmes 0-62418  
 safety, hospital laboratories, general aspects 0-95089  
 SEM, teaching methods for short courses 0-73533
- trams** *see road vehicles*
- transceivers**  
 US inspection unit receiver-transmitter 0-89458
- transducers**  
*see also accelerometers; acoustic transducers; actuators; extensometers; Hall effect transducers; piezoelectric transducers; pressure transducers; strain gauges*  
 AC voltage meas., analogue, checking and calibration methods in USSR 0-98872  
 amplifier interconnection, analog signal processing, book 0-86047  
 biomedical measurements and transducers, review (*Japanese*) 0-94393  
 bipolar IC temperature transducer, intrinsic bandgap voltage as reference, Fahrenheit, Celsius or arbitrary scale operation 0-82761  
 blood temperature monitoring during extracorporeal circulation, noncontact transducer 0-85513



**transducers continued**

capacitive, of torsional oscills., for oscill. type viscometer 0-64656  
 capacitive parametric, for displacements under dynamic damping 0-105626  
 cellular elastomer selection for use in biomechanical capacitive force transducers, measuring device (*German*) 0-85545  
 complex shape product inspection, local eddy current transducer 0-108671  
 cryogenics, linear variable differential transformer displacement transducer optimisation 0-86323  
 displacement measuring fast precision capacitance transducer, design procedure (*Russian*) 0-98884  
 double-ended eddy current transducers, signal calc. for nonferromag. cylindrical products 0-89443  
 eddy current transducer with electrical commutation of excitation field, NDT 0-105633  
 eddy-current, mounted, correct. of errors in coating thickness inspection 0-77775  
 eddy-current feed-through transducer, approx. calc. of mag. field, nonferromag. media 0-78746  
 eddy-current flaw detect., suppression of interf. parameters 0-89442  
 EL2 electret telephone transmitter, technology development 0-83723  
 electric variables meas., third-generation, Czechoslovak (Metra Blansko) range (*Czech*) 0-73340  
 electrical conductivity, threshold sensitivity meas. 0-62688  
 electrocapillary acceleration meters, electrolyte composition selection 0-73331  
 electrocapillary acceleration meters with electrolyte in gel form 0-73330  
 electronics-aided meas. transducers (*Dutch*) 0-105634  
 error analysis, dynamic, using conversion factor 0-77770  
 feed through eddy current transducer, numerical anal. or operating mode during ferromagnetic rod inspection 0-108670  
 ferromagnetic object inspection, method of higher harmonics, difference schemes 0-89444  
 fibre optics sensors for measurement and control appls. 0-58780  
 flow, with steady and pulsating flows, computerised flowmeter system 0-79416  
 inductive, selection, applications and technical specifications, output signals 0-101790  
 interfacing and analogue signal conditioning, book 0-86048  
 liquid-crystal image transducer, normal incidence, on-state optical performance 0-99852  
 low-reactive meas. of motion, transducer effects on body under investigation (*German*) 0-105621  
 matrix eddy-current, with magnetic circuit, design and construction 0-68228  
 membranes appl., silicone rubber, physical props. (*Slovak*) 0-61141  
 metallic objects with complex shape, eddy-current inspection 0-89446  
 modular, third-generation, individual and group arrangements, NC series (*Czech*) 0-62645  
 moving magnet transducer, dynamic props. 0-57276  
 n-type InSb based low-temperature UHF detector, with low noise preamplifier 0-68230  
 nematic liquid crystals, dynamic scatt., pre-excitation 0-88021  
 ohmic resistance, appl. in internal friction test device for thin-walled tubular specimens 0-71836  
 optical path meas. using fibre optics, theoretical investigations of path transducers (*German*) 0-106608  
 optotransducers, electronic compensation for dirty lenses 0-68189  
 orientation system in screen methods of NDT 0-66745  
 passive optical rotation sensors using guided waves, developments 0-58781  
 semiconductor force transducer suitable for use with small muscles 0-72395  
 solid propellant stress transducer evaluation 0-81245  
 straight-through screened circular primary, between multilayer cylinder and tube, EM field 0-71856  
 temperature, digital, solid-state, using automatically balanced Wheatstone bridge (*Rumanian*) 0-57287  
 temperature, p-n junction diode as linear temp. transducer 0-57293  
 temperature with thermal feedback, operational principles (*Russian*) 0-86299  
 time-interval indicator (*Russian*) 0-105619  
 transistor temperature transducers, Motorola MTS IC series, appls. (*French*) 0-73357  
 vibrating capacitor displacement transducer, eqn. of state 0-57281  
 vibration, meas. errors due to surface compliance of vibrating body (*Japanese*) 0-79046  
 vibrational meas., dynamics (*Russian*) 0-105638  
 weighing system, electronic, digital transducer instruments 0-95076  
 MgCr<sub>2</sub>O<sub>4</sub>-TiO<sub>2</sub> porous ceramic humidity sensors 0-86325  
 Se photocell optical vibration transducer 0-77768

**transfer functions**

see also optical transfer function  
 acoustic insulating material complex elastic modulus meas. and transfer function theory (*Hungarian*) 0-106765  
 arbitrarily electrodeposited piezoelec. plate acoustic spatial response determ. 0-99910  
 flaws, 2D, irregularly shaped, fracture mechanics transfer function 0-99970  
 flowmeters, determination using hydromulsator 0-103083  
 gas analysis, by mass spectrometer, dynamic error determ. by transfer functions 0-61194  
 geomagnetic short-period variations, transfer function changes before 1972 Sitka, Alaska, earthquake 0-76923  
 in-duct acoustic props. meas., transfer function method, expt. 0-106688  
 in-duct acoustic props. meas., transfer function method, theory 0-106644  
 model of with several inputs, math. methods of investigation identification 0-62451  
 ocean acoustic transfer function impact on coherence of undersea propag. 0-58842  
 propeller cavitation tunnel hydroacoustic transfer function, meas. and anal. (*Croatian*) 0-92002

**transferred electron devices** see *Gunn devices***transferred electron effects** see *Gunn effect***transferred electron oscillators** see *Gunn oscillators***transfluxors** see *magnetic cores***transformations, phase** see *phase transformations***transformer insulation**

see also insulating oils

current transformers, oil insulated, parameters influencing heating assessment using sensibility matrix (*Hungarian*) 0-87708  
 liquid dielectrics, thermal performance estimation 0-88582  
 oil diagnosis by chromatographic analysis, computerised evaluation of results (*Czech*) 0-97744  
 oil electrohydrodynamic flow, jet dynamic pressure obs. (*Russian*) 0-59117  
 oil immersed transformers, dissolved gas causes and phenomena, anal. (*German*) 0-76570  
 power transformers, electromagnetic testing of partial discharges for failure and breakdown prevention (*Russian*) 0-97743

**transformer magnetic circuits**

Ar-air, transformer plasmatron, LF discharge, electrical and energy props. 0-103200

**transformer testing**

power transformers, electromagnetic testing of partial discharges for failure and breakdown prevention (*Russian*) 0-97743  
 preventive, by analysis of gases dissolved in transformer oil (*German*) 0-71969

**transformers**

see also current transformers; high-frequency transformers; potential transformers; power transformers; pulse transformers  
 arc snubber using transformer core, theory 0-59315  
 core, mag. field distrib., graph-theoretic model appl. 0-87260  
 cores, use of high permeability Fe-Si materials 0-88793  
 heart, human, elec. and mag. events, phase and amplitude relationship recording 0-104695  
 linear differential, profile meas. of two concentric round parts, concentricity errors (*German*) 0-57249  
 single-phase, calc. of inrush current 0-88787

**transforms**

see also Fourier transforms; Laplace transforms; Z transforms

Backlund transformation in the classical massive Thirring model 0-57456  
 Backlund transformations in several variables, differential geometric anal. 0-86073  
 closed time path Green's functions, transform. props. (*Chinese*) 0-105491  
 conformal transformations combined with numerical techniques, with applications to coupled-bar problems 0-83538  
 constrained Hamiltonian systems, generators of symmetry transformations 0-57138  
 coordinate transformation formulas for massive reference frame 0-90673  
 distributed type associative memory model with quantised Hadamard transform 0-108867  
 Eckart Hamiltonian, transformation approach 0-101726  
 Hadamard transform appl. to beam spectroscopy 0-62741  
 Hankel, computation using projections 0-96124  
 Kustanheimo-Stiefel transformation osculating variables, perturbed motion, differential eqns. 0-109344  
 Miura transformation of Kaup and Mikhailov eqns. 0-57103  
 Poincare-Cartan integral invariant and canonical transformations for singular lagrangians 0-94956  
 sound synthesis by continuous spectral transformation (*French*) 0-79100  
 spectral transform method for solving evolution equations and conservation laws 0-62488  
 thermal stresses in slab containing annular crack, integral transform techniques 0-96229  
 transformation group techniques appl. to nonlinear fluid and plasma eqns. (*French*) 0-77623  
 two-electron integral transformations for 2nd order multiconfig. Hartree-Fock method 0-87045  
 weighted line-finding algorithm for digitised picture 0-99660

**transient response**

electrochemical reactor characterisation, marker pulse method improvements 0-76524  
 fusion reactor, FTFR, T gas injection system transient response 0-102337  
 H-polarised EM wave by isotropic moving plasma 0-64731  
 injection lasers, phase-plane anal., effects of absorbing section 0-64022  
 linear system mean square response to nonstationary random excitation 0-57085  
 p<sup>+</sup>-n-n<sup>+</sup> pulsed diodes, forward pulsed case, voltage transient response 0-60071  
 rivers downstream pollution, one-dimensional transient model for short-term prediction 0-81496  
 tsunami, island of Hawaii, 1979 November 25, numerical anal. by finite-element method 0-72449  
 vibrations, transient response of thin elastic spherical shells 0-96217  
 GaAs, carrier diffusion in transient response regime 0-103688  
 GaAs, self-scattering in Monte Carlo calcs. of transient dynamic response 0-103687  
 Hc cooled reactor turbine control experiences Fort St. Vrain HTGR (*German*) 0-57927

**transient stability** see *stability***transient voltages** see *transients***transients**

see also surges

Darrieus rotor, aerodynamic analyses comparison 0-61264  
 meas. instruments random errors analysis, based on instantaneous frequency response 0-77741  
 multiple lifetime measurements analysis modulation methods, excitation spectrophotometer 0-86449  
 thermoelectric heat pumps, two-stage, design criteria anal. for cool-down speed maximisation 0-108812  
 time dependent heat conduction, partial differential equations solution 0-106707  
 transient input processes reconstruction, from output and dynamic props. 0-77742  
 voltage and current, fast digital technique (*Polish*) 0-86340  
 Cu-CuI-graphite secondary cell, transient ionic current obs. 0-108790  
<sup>3</sup>He-<sup>4</sup>He mixture, optical pumping, transients theory 0-91509  
 SF<sub>6</sub> insulation, under impulse voltage stress, effects of pressure and vol. on firing delay (*German*) 0-87959

**transistors**

see also bipolar transistors; phototransistors; thin film transistors  
 No entries

**transit time devices**

see also *IMPATT diodes*

No entries

**transit time noise** see *random noise***transition metal alloys**

see also *alloys of individual transition metals e.g. nickel alloys*

see also *copper alloys; gold alloys; silver alloys; transition metal compounds*

absorption of H and mag. props. 0-60224

amorphous, mag. props., chem. short-range order 0-75739

amorphous, mag. props., structure and preparation 0-75737

amorphous ferromagnets, mag. props., book contrib. 0-75743

binary, state density curves, relation between short-range order and Fermi level position, CPA calculations 0-107687

cohesive properties, and press.-vol. relation 0-92476

dilute, spin glasses, mag. ordering, book contrib. 0-75787

dilute ferromagnetic, itinerant d-electron(hole) degenerate, spin stiffness constant 0-70930

disordered ferromagnetic, spin wave stability 0-70994

elastic-plastic transition behaviour model (*German*) 0-75295

failure, statistical model, in conditions of monotonous cyclic loading (*Bulgarian*) 0-70296

ion polarisation and point defect resistivity in metals 0-103672

metallic glass, micromag. calcs. and props. 0-80501

metallic glass, splat cooled, mag. props. 0-80491

metallic glasses, short range order of dense-random-packing models 0-64907

metallic glasses, transition metal-metalloid glasses, struct., compositional effects (*Japanese*) 0-84086

nonstoichiometric compounds, physicochem. props. depend. on short-range order struct. 0-100227

rare earth alloys, amorphous, electronic and mag. props. 0-93093

rare earth alloys,  $RM_2Si_{2-x}Ge_x$  and  $RM_{4-x}Al_{8-x}$ , magnetism and hyperfine interactions, magnetisation and Mossbauer effect studies 0-75892

rare earth-transition metal alloys, amorphous, ferrimag., spin arrangements in large fields 0-75718

rare earth-transition metal alloys, disordered, magnetisation behaviour 0-71099

silicide formation at Si-metal interface, obs. using interface marker technique 0-59734

silicides, atomic volume deviations and supercond.  $T_c$  0-75203

solid solutions, diffusion equation, during a decomp. process, role of non-linearised terms (*Japanese*) 0-92723

superconductivity, relevance of mag. interactions 0-100545

transition metal-metalloid glasses, struct. and plastic flow, review 0-84090

transition metal-nonmetal glasses, with defined local coordination, struct. model 0-84092

XPS asymmetry of core electrons and electronic struct. parameters 0-93460

Ag-transition metal, dil., mag. impurities, electronic struct., KKR-Green's function calc. 0-65783

Al-Fe-X-Si (X = transition metal), struct. and comp. by electron microscopy 0-88093

Au-transition metal alloys,  $^{197}\text{Au}$  Mossbauer isomer shift cellular atomic model 0-84673

Ce-M intermetallic cpds., M = 3d transition metal, sorption of  $\text{H}_2$ , structural charges 0-88429

Cu-transition metal, dil., mag. impurities, electronic struct., KKR-Green's function calc. 0-65783

Fe-M, dil., hyperfine fields for transition metal impurities 0-80237

Fe-M, dil., impurity electronic struct., multiple scatt. approach 0-92856

M-noble metal spin glass films, mag. props. 0-60306

Pd-noble metal solid solns., with dissolved H, thermodynamic props. 0-108402

Pt-transition metal, dil., impurity resist. 0-92875

Te-M, liq. semicond., elec. props. 0-96870

Y-M intermetallic cpds., M = 3d transition metal, sorption of  $\text{H}_2$ , structural charges 0-88429

**transition metal compounds**

see also *compounds of individual transition metals e.g. nickel compounds*

see also *copper compounds; gold compounds; silver compounds; transition metal alloys*

arsenides (Ti, V, Cr, Mn, Fe, Co, Ni, Cu), oxidation, hardness and electromechanical polishing response 0-71776

band structure of transition metal-metalloid compound, nonorthogonality and tight-binding fit 0-59852

borides (Ti, V, Cr, Mn, Fe, Co, Ni), oxidation, hardness and electromechanical polishing response 0-71776

carbides, oxidation of  $\text{H}_2$  0-104462

carbides, separation layer in X-ray tubes, C diffusion from graphite to W coating prevention (*German*) 0-105759

carbides (Ti, V, Cr, Mn, Fe), oxidation, hardness and electromechanical polishing response 0-71776

chalcogenide layer compounds, convergent beam electron microscopy obs. 0-108689

chalcogenides, quasi-one-dimens., elec. mag., and supercond. props., review (*Russian*) 0-93022

chalcogenides, reversible electrodes appls. 0-61112

chalcogenophosphates, intercalation with n butyl-lithium, possible appl. in Li batteries 0-71446

chlorates, neutron activated, radiation annealing 0-93569

cluster carbonyls, fluxionality, collective oscils. and low energy spectra 0-78738

complexes, electron densities, local orbital populations, polarised neutron diffraction 0-88725

complexes, lattice energies calc. methods 0-107099

3d complexes, low spin-high spin paramag. transition, Ising model calc. 0-93073

conference, Stuttgart, Germany, 12-16 June 1979 0-57002

dichalcogenides, phenomenological theory of CDW state, trigonal-prismatically coordinated layers 0-80200

dihalides, layer struct., lattice dynamics, calc. 0-65177

divalent halides, Coordination equilibria in non-aqueous solvents. I 0-66860

ferrocyanide selective sorbents for alkali metals, sorptive props. w.r.t. struct. 0-101051

halides, cryst. field stabilisation and lattice energy 0-75201

hydrides, binary, heats of form. 0-97725

**transition metal compounds continued**

hydrides, H ordering, review 0-60850

metal-insulator transitions 0-59874

molecule, SINDO/F theory of electronic struct. 0-69075

monoxides, 3d, ground state electronic struct., atomic sphere approx. 0-59855

monoxides, 3d metal, specific vol. and mag. moment calcs. 0-65822

oxide catalysts, reduction, cryst. defects influence, in-situ electron microscopy 0-81322

oxides, (100) coincidence twist boundaries energy 0-107270

oxides, cryst. field stabilisation and lattice energy 0-75201

oxides, d-band perovskites, concepts of surface states and chemisorption, book contrib. 0-107651

oxides, Li incorporated, topochem. reactions, chem. prep. and characterisation 0-61115

oxides cryst. growth, using  $\text{K}_2\text{S}_2\text{O}_7$  as flux material 0-71582

pnictides, displacive and mag. transitions 0-59616

reduced ionisation potentials as parameters in superconducting transition temp. calcs. 0-75671

refractory metals and oxides, reactions of liq. alkali metals, relevance to reactor technology 0-85173

rock salt struct., surface energy bands, Shockley surface states, bonding 0-92956

second row oxides, XPS 0-87170

silicides, atomic volume deviations and supercond.  $T_c$  0-75203

silicides, growth and characterisation 0-66408

silicides, refractory for ICs, review 0-100820

sulphides, displacive transitions, theory 0-59616

sulphides, ion bombardment damage, XPS obs. 0-97404

sulphides (Fe, Co, Ni, Cu), oxidation, hardness and electromechanical polishing response 0-71776

superexchange interaction, effective spin-orbital Hamiltonian 0-70998

superexchange interaction, multielectron theory 0-70997

surface properties, review 0-84349

tetrahedral complex ions, F NMR chem. shifts, outer sphere cation effects 0-102527

XPS asymmetry of core electrons and electronic struct. parameters 0-93460

third row oxides, XPS 0-87170

**transition metals**

see also *the individual transition metals e.g. nickel*

see also *copper; gold; silver*

3d impurities in Al, self-consistent spin density functional calcs. 0-70635

amorphous, exhibiting Mossbauer spectra, mean mag. props. (*French*) 0-80489

atom, Racah parameters, atomic screening parameter Slater and Clementi-Raimondi values 0-69071

atoms, neutral and ion val. states, electron correlation, ab initio effective val. Hamiltonian calc. 0-99449

BCC, interaction energy between self-interstitial and screw dislocation, calc. 0-70248

BCC, neutron spectroscopy of fast H diffusion 0-59731

Cauchy discrepancy with supercond. transition temp. 0-84533

chemisorption of  $\text{H}_2$  and  $\text{O}_2$ , chemisorpt. energy trends 0-107631

chemisorption of H, effect of surface spin fluctuations 0-75613

cohesive energies, many-electron systems, self-interaction corrected approach, beyond local spin density approx. 0-92844

core levels between surface and bulk atoms, variation of binding energy shifts 0-88615

correlation effects, perturb. treatment within Hubbard model 0-70582

correlation effects, perturbation treatment 0-59897

corrosion due to  $\text{V}_2\text{O}_5$  melts (*Japanese*) 0-93691

d-band metals, chemisorption, book contrib. 0-107649

deep impurities in semiconductors, SCF CNDO cluster calcs. 0-100442

elastic-plastic transition behaviour model (*German*) 0-75295

electronic struct. and magnetism, review 0-70573

failure, statistical model, in conditions of monotonous cyclic loading (*Bulgarian*) 0-70296

ferromagnetic, band theory of linear magnetostriction 0-71141

ferromagnetic, dil. H electronic struct. 0-70638

film, on Si, silicide form. at interface, interface marker technique obs. 0-59734

first-row ions, core ionised states,  $\Delta\text{SCF}$  MO calcs. 0-78523

glass:M, photoacoustic spectrosc. 0-92611

impurity states in semiconductors, EPR linewidth calc. 0-80599

3d-ions, s-doublet struct., appl. of exchange correlation mass operator approx. 0-106266

itinerant and localised d-electrons, positron annihilation data 0-93428

magnetism of Fe group metals, mol. Jahn-Teller reson. states as possible antecedents 0-75701

paramagnetic state, itinerant electron model 0-65769

paramagnetic susceptibility, phonon instability, mixed localised-collective electron states 0-103811

refractory metals and oxides, reactions of liq. alkali metals, relevance to reactor technology 0-85173

superconductivity, relevance of mag. interactions 0-100545

surface atom vibrations, self-consistent calc. in tight-binding model 0-103560

thermophysical data at high temps., submicrosecond-pulse-heating method 0-103459

tight-binding approximations, modified, generalisation 0-88288

transition metal-O bond energy in  $\text{O}_2$  glow discharge, mass spectrometry obs. 0-64808

universal LCAO parameters 0-75503

XPS asymmetry of core electrons and electronic struct. parameters 0-93460

**transition moments**

atoms, monovalent, transition probabilities calcs. (*Russian*) 0-63594

1,6diazaspiro[4,4]nonane-2,7-dione, optical rot. strength calcs. 0-95793

DNA, Hg (II) and Ag (I) complexes in soln., theoret. interpret. of elec. dichroism obs. 0-85347

haematoporphyne, complexed with chloranil and tryptophane, energy spectra, transition moments and intermolecular distances 0-72127

local mode mols., normal mode spectra 0-95687

optical rotatory strength, gradient matrix eqn. of motion calcs. 0-95793

purple membrane fragment suspensions, elec. dichroism obs., chromophore transition moment 0-89728

$\text{ArH}^+$ , transition moments, perturbation calcs. 0-102542

$\text{BaO}$ , excited electronic states, lifetimes and transition moments 0-87177

$\text{CH}^+$ ,  $a''\text{II-b}''\Sigma^-$  transition moment, ab initio calcs. 0-87047



**transition moments continued**

- CO, (4+) system, electronic transition probability 0-106332  
 CO<sub>2</sub>, dipole moment functions 0-87094  
 H<sub>2</sub>O<sub>2</sub>, twisted mol., optical rot. strength calcs. 0-95793  
 NO,  $\gamma$  and  $\beta$  system, electronic transition probability 0-106332  
 N<sub>2</sub>O, dipole moment functions 0-87094  
 O<sub>2</sub>, line position and intensities of  $2\nu_3$ ,  $\nu_1 + \nu_3$  bands 0-87181  
 OH<sup>+</sup>, rot.-vibr. bands, line positions,  $\nu_1$  strengths transition probabilities 0-67828  
 Pr<sup>3+</sup>, anomalous hypersensitive  $^3H_4 \rightarrow ^3P_2$  transition 0-106296  
 Si<sub>6</sub>, integrated IR band intensities and transition moments 0-95611

**transition probability** *see radiative lifetimes***transition probability, nuclear** *see nuclear energy level transitions***transition radiation**

- charged particle motion at vac.-medium interface, transient radiation emission spectral distrib. 0-63901  
 intensity derivation 0-106430  
 soft X-ray transition radiation observation from medium energy electrons 0-76104  
 X-ray source, relativistic charged particles passing through periodic struct. 0-69303  
 Sn foils, 1-3.5 GeV electron impact, transition X-ray emission, comparison with theory (Russian) 0-60704

**translators (repeaters)** *see repeaters***transmission**

- see also acoustic wave transmission; light transmission; power transmission*  
 electron beam, relativistic, refl. and transmission by strong mag. field (Japanese) 0-91737  
 spatially dispersive crystal, reflectivity and transmittivity 0-99604

**transmission electron microscope examination of materials**

- see also transmission electron microscopy*  
 adhesion, surface anal. techniques appl. 0-65381  
 Al-Zn-Mg (5.1 wt.%), decomp. process, TEM study 0-71660  
 9-anthraldehyde, struct. by TEM 0-79771  
 9-anthronitrile, struct. by TEM 0-79771  
 brass, nondestructive determ. of in-depth profile 0-93836  
 $\gamma$ -brass type alloys, superstructures and defect obs. 0-107284  
 carbonate minerals, deform. twinning mechanisms 0-79814  
 cell membranes, at mol. resoln., introduction 0-104841  
 ceramics, microcracks, and thin intergranular films obs. by TEM 0-68295  
 compound eye of Cicindela tranquebarica herbst, fine struct. 0-85382  
 crystal, accelerator irradiation, heavy ion irradiation damage 0-100291  
 diamond, accelerator irradiation, heavy ion irradiation damage 0-100291  
 dislocation cell form. during plastic deform., TEM obs. 0-60935  
 etched thin foils, comparative SEM, STEM and TEM analysis 0-100144  
 ethylene-vinyl acetate-vinyl chloride graft copolymers, rel. between morphology and toughness (German) 0-66665  
 F 0-76244  
 faulted dislocation loops induced by elastic interaction, climbing motion 0-75227  
 ferrite, transform. kinetics, grain size, alloying element effect, carbide precip. 0-93560  
 film, thermal strain, strain relax. above room temp. 0-59841  
 film/substrate interface, misfit dislocation obs. using electron microscopy 0-103605  
 films, elec. and galvanomag. props., microstruct. 0-70859  
 glasses and ceramics, characterisation with analytical electron microscope 0-84068  
 grain boundaries, interfacial structure effects on high temp. mechanical behaviour 0-59480  
 graphite, Fe-catalysed gasification, electron, microscopy 0-104358  
 graphite, ion bombarded, light gases, structural study using TEM 0-92570  
 graphite, sources of background X-radiation 0-101908  
 graphite, thin film, high resolution phase contrast imaging 0-103224  
 graphite, zone-axis pattern maps 0-100137  
 Incoloy 901, foil prep. for TEM exam. 0-88001  
 Inconel X-750, deform. and fracture characts., 24-816°C 0-108551  
 layer structures, intercalation with N<sub>2</sub>H<sub>4</sub>, charge density waves or artefacts 0-100221  
 metal crystallites characterisation by selected-zone and weak-beam dark field TEM 0-79654  
 metal oxide smoke particles prepared by gas evap., morphology and coalescence growth 0-97738  
 metal particles, small, possible vibrations associated with twins 0-100253  
 metal powder, method for TEM study 0-84038  
 metal-C system, spheroidal graphite formation, role of high angle boundaries (Russian) 0-81065  
 metals, deformation structure during cutting, investigation by TEM (Japanese) 0-70086  
 micropipette electrode tips, beveled, non-destructive electron microscopic exam. 0-89915  
 microscope specimens, investigation of morphology of damage due to field corrosion 0-57425  
 mineral, Burgers vector characterisation method using electron microscope contrast simulations 0-109141  
 mineral crystallographic defects, high-resolution TEM obs. 0-72517  
 mineral fibre characterisation using energy dispersive X-ray spectrometry in TEM (French) 0-82857  
 PbO-Nb<sub>2</sub>O<sub>5</sub> system, X-ray and electron microscopic phase and struct. determ. (French) 0-92508  
 pigeonite, antiphase domains exptl. coarsening 0-81886  
 polyethylene, single crystal, fold domain boundaries 0-107065  
 polyethylene spherulites, thin melt-cast films, high density, deform. process in non-equatorial regions 0-81124  
 trans-1,4-polyisoprene crystals, press. effect on growth rate 0-88064  
 trans-1,4-polyisoprene crystals, press. effect on melting temp. and lamellar thickness, press. crystn. 0-88302  
 polymer blends, selective staining method for TEM obs. of morphology 0-84103  
 protein adsorbed layers on field-emitter tips, removal by UV radiation 0-104836  
 PVC, rigid resin, TEM studies of morphology, processing effects 0-108385  
 quartz, dislocations, electron irradi. induced vitrification 0-107252  
 $\alpha$ -quartz, electron irradi., defect struct. and radiolysis 0-107321  
 quartz, naturally deformed, dynamic recrystn. during creep, dislocation substruct., Mg alloy comparison 0-109142

**transmission electron microscope examination of materials continued**

- quartz, subgrain boundaries, theoret. predictions and microscopic obs. methods 0-84187  
 rectorite, stacking and ordered interstratification, high-resolution TEM obs. 0-109140  
 semiconductors, ion-implanted, laser pulse annealing, TEM and channelling study 0-100264  
 silicates, layered, optical filtering of faulted areas in electron micrographs 0-84035  
 solid-solid interface chemistry, characterisation, theory 0-75448  
 stacking faults, weak-beam contrast in TEM 0-75132  
 steel, 12Cr2MoWVTiB, transformation mechanism and fine structure of (M-A) phase, TEM study (Chinese) 0-66500  
 steel, austenitic stainless, phase identification, 2<sup>1</sup>/2D imaging techniques 0-96424  
 steel, austenitic stainless, stacking fault energy, effect of N 0-107279  
 steel, austenitic stainless, unlubricated, friction, wear and microstruct. of types 304, 316 and Nitronic 60 0-108589  
 steel, austenitic stainless, welded explosively, induced martensites morphology 0-104153  
 steel, cold worked, original struct. effect on softening during heating 0-60882  
 steel, Cr, lower bainite transform., significance of carbide precip. 0-97476  
 steel, Cr-Mo (2.25, 1.0 wt.%), temper embrittlement, effect of P, Sn, comp. and carbide precip. 0-85036  
 steel, Cr-Mo (2.25, 1.0 wt.%), temper embrittlement, effect of Mn, Si, comp. and carbide precip. 0-85037  
 steel, Cr-Mo-Ni-WV (6, 4, 3, 2 wt.%), tempering and secondary hardening, TEM obs. (Chinese) 0-104245  
 steel, Cr-W(Mo), quenched, carbide reactions during tempering 0-89229  
 steel, dual phase HSLA, compositional anal., TEM 0-85253  
 steel, Fe-V-C (1, 0.2 wt.%), austenite formation 0-84927  
 steel, ferritic stainless, embrittlement 0-85041  
 steel, high alloy Cr-Mo-W, splat quenched, formation of metastable austenite 0-84974  
 steel, low C, type En3, high strain deform., struct. and props. 0-89301  
 steel, maraging, intermetallic phases precip. study by electron microscopy (Polish) 0-89217  
 steel, Mo, energy structure X-ray anal. using TEM 0-84036  
 steel, Ni-P plated, electroless, fatigue strength and plated layer microstruct. (Japanese) 0-93645  
 steel, pearlitic, creep-induced microprobe healing kinetics of 12MKh and 15Kh1MIF, TEM obs. (Russian) 0-71690  
 steel, stainless, austenitic, deform. substruct. and annealing, stacking fault tetrahedra form 0-107282  
 steel, stainless, austenitic, explosively welded, orientation relationship in martensitic transform. 0-104158  
 steel, stainless, austenitic Ni-Cr type, creep deformed, dislocation multipole obs. 0-107258  
 steel, stainless, ferrite to austenite decomp. 0-93554  
 steel, stainless, fracture and crack tip plastic zones, in situ obs. 0-108686  
 steel, stainless, martensite nucleation mechanisms, HVEM obs. 0-104157  
 steel, stainless, shock loaded, residual martensite obs. 0-104414  
 steel, stainless, TEM foils, white band contrast 0-75134  
 steel, stainless, type 316, neutron irradi. effects on tensile props. and microstruct. 0-65059  
 steel, stainless, voids, TEM, diff. contrast 0-75218  
 steel, stainless 316, soln. annealed, cavity alignment and precipitation during dual ion bombardment 0-70273  
 steel, stainless type 316, in-situ HVEM studies under ion beam irradiation 0-103396  
 steel, structural, second phase particle effects on impact strength 0-108581  
 steel, tempered martensitic, type AISI 410, role of C in embrittlement phenomena 0-93652  
 steel foil, microanalysis by energy dispersive X-ray spectrometry (French) 0-85250  
 steel SW7M, low-cycle fatigue at high hardness levels (Polish) 0-89323  
 stretched zone anal. by means of stereo matching method (Japanese) 0-108544  
 surface films on solids, TEM study method 0-65409  
 thin specimens, X-ray microanal. in TEM up to 1000 kV 0-101063  
 thinned semiconductor device, SEM, electron beam induced cond. of defects, rel. to TEM 0-107027  
 thulium phthalocyanine, mol. image in high resolution electron microscopy, radiation damage effect 0-107203  
 titanomagnetites, exsolution microstructures, magnetic significance 0-98313  
 tooth enamel crystallites, contrast effects 0-85572  
 void contrast aid void vol. determ. 0-75217  
 void volume, swelling, errors in determ. by TEM 0-84208  
 Zircaloy, annealed, neutron irradiated, inhomogeneous deform. behaviour 0-85014  
 Zircaloy-2, electron irradiation damage, direct obs. 0-84212  
 Zircaloy-2, hydride precipitation and growth at crack tips, electron optical obs. 0-108449  
 Zircaloy-2, neutron irradi. damage, TEM characts. 0-107332  
 Ag, dislocations gliding on (001) planes, bright field and weak-beam images 0-107266  
 Ag film, chem. deposited, agglomeration, SEM and TEM obs. 0-59828  
 Ag film, void growth, TEM obs. 0-59833  
 Ag thin evaporated films, rel. between microstruct. and excess free energy, TEM 0-70427  
 Ag, thin-film bicrystals, planar lattice defects and migrating grain boundaries interaction 0-79835  
 Ag-Au, corrosion in HNO<sub>3</sub> 0-85091  
 Ag-Cu metastable solid soln., form. by ion-beam mixing 0-75244  
 Al alloys, age-hardenable, precipitation and dissolution processes, positron annihilation and X-ray small-angle scattering comparison 0-89238  
 Al anodic films, flaw obs. 0-93696  
 Al bicrystal, high resolution electron microscopy obs. of dislocations 0-103347  
 Al, cold rolling of 1100 plates, substruct. development 0-108476  
 Al, deformed in uniaxial and equibiaxial tension, dislocation arrangements 0-108516  
 Al film, deform. under He ion bombardment 0-65073  
 Al foil,  $\alpha$ -particle irradi. under fusion reactor conditions, He bubble alignment during deform. 0-107345  
 Al, foil, influence of O<sub>2</sub>-pressure on oxidation rate, TEM study 0-104355  
 Al, grain boundary migration, TEM obs. on mechanism 0-79812



## transmission electron microscope examination of materials continued

- Al, implanted Xe behaviour during anodic oxidation 0-71800  
 Al, pipe diffusion along segment of faulted dislocation loops during annealing 0-107256  
 Al, specimen transfer device for combined AES/RHEED and TEM obs. 0-70093  
 Al, stationary creep in HVEM, cell struct. evolution 0-104242  
 Al, surface deformation and wear track obs. using analytical electron microscope 0-108687  
 Al-Sb(Zn), ion implanted electron beam annealing, ion backscatt. and TEM meas. 0-59500  
 Al/Cu thin film couples, TEM study of intermetallic nucleation at interface 0-65305  
 Al/Pd thin film couples, thermal reactions 0-59830  
 Al-(Mg)(Fe), pure (dilute), large wire drawing plastic deform. 0-108508  
 Al-Bi(Cd)(Pb)-Ti, containing low-melting pt. inclusions, mech. props. 0-93632  
 Al-Cu (3.97 wt.%) alloy containing Guinier-Preston zones, high resolution lattice images 0-107114  
 Al-Cu (4 wt.%), supersaturated and aged conditions, high strain deform. 0-60907  
 Al-Cu (4 wt.%) alloy, high temp. cyclic deform.,  $\theta'$  particle dissolution obs. 0-108515  
 Al-Cu (4 wt.%) alloy, neutron irradi., weak-beam dark-field obs. of dislocations near  $\theta'$  precipitates 0-107333  
 Al-Cu (4.3 wt.%) alloy, containing Guinier-Preston zones, high resolution lattice images 0-107115  
 Al-Cu (4.6 wt.%), cold work and ageing influence on ductility and fracture behaviour (*Japanese*) 0-89295  
 Al-Li-Mn (2.8, 0.3 wt.%), recrystallised sheet, fracture behaviour, SEM and TEM study 0-97566  
 Al-Mg, foil, oxidation in O<sub>2</sub> atm., TEM study 0-104356  
 Al-Mg, Si alloy, void form. under different precip. conditions, after Al ion irradi. 0-59529  
 Al-Mg-Si, type 6010, microstruct. characts. influence on formability, heat treatment 0-81090  
 Al-Mg-Si alloys, cast, precip.-rich zones on grain boundaries, soln. heat treatment conditions effect on mech. props. 0-104176  
 r-Al-Mn-C, permanent magnetism and microstruct. 0-75811  
 Al-Ni(Cd)(Fe)(Si), cold worked, struct. and props. 0-71666  
 Al-Zn-Mg, TEM and calorimetric study 0-76290  
 Al-Zn-Mg (3.87, 1.79 wt.%), oriented growth of precipitates on dislocations, TEM obs. 0-108447  
 Al-Zn-Mg alloy, TEM characteris. of precipitates 0-104166  
 Al-C<sub>3</sub>-Be<sub>2</sub>-C-SiC system, phase analysis and TEM struct. obs. 0-108420  
 Al-Cu-NiCo (5 at.%),  $\theta'$  hardened, creep mechanism 0-85013  
 (AlGa)As DH lasers, catastrophic optical damage generation mechanism, TEM obs. of dark line defects 0-100239  
 Al<sub>2</sub>O<sub>3</sub>, alumina, deformed by prismatic slip, HV TEM obs. of dislocations 0-108517  
 Al<sub>2</sub>O<sub>3</sub>, atomically sharp cracks, TEM study 0-71729  
 Al<sub>2</sub>O<sub>3</sub>,  $\beta$ - and  $\beta'$ -phases, defect struct. obs. by high resolution TEM, battery ageing relevance 0-107501  
 Al<sub>2</sub>O<sub>3</sub> films, DC reactively sputtered, struct. 0-96764  
 Al<sub>2</sub>O<sub>3</sub>, sapphire, edge dislocation loop obs. by high resolution lattice imaging 0-103346  
 Al<sub>2</sub>O<sub>3</sub> substrates, tape-casted, fracture strength analysis 0-60948  
 Al<sub>2</sub>O<sub>3</sub>-Pt metal-ceramic reaction, micro/macro obs. 0-66467  
 3Al<sub>2</sub>O<sub>3</sub>-2SiO<sub>2</sub>-ZrO<sub>2</sub> composites, sintered, in situ-reacted, fracture props. 0-81158  
 Au, bicrystalline thin films, faceting of [001] grain boundaries 0-70222  
 Au crystal, images of inner struct. of atoms 0-103229  
 Au, epitaxially grown bicrystalline thin films, preferred inclinations of {100} grain boundaries 0-103367  
 Au film, ion bombarded, surface craters induced by displacement cascades 0-107344  
 Au film, twin boundary struct. and migration, atomic scale electron microscopy obs. 0-107276  
 Au film (001), surface struct., high resolution TEM 0-100383  
 Au, grain boundary structure 0-100255  
 Au, heavy ion irradi., cascade energy density effect on defect cluster type 0-107340  
 Au particles, small single cryst., habit plane characterisation 0-79733  
 Au, quenched polycryst., vacancy loss at grain boundaries 0-59477  
 Au/Cu, bilayers, interdiffusion phenomena, lattice dislocations, TEM obs. 0-59736  
 Au/Cu, initial epitaxial growth at room temp. 0-59829  
 Au/Sn thin film couples, evaporated, TEM study 0-59832  
 Au-Ag, bicryst. thin film couples, interphase interfaces, TEM 0-70540  
 Au-Ge contacts on GaAs, SEM and TEM obs. of struct. 0-100522  
 Au-Pd, bicryst. thin film couples, interphase interfaces, TEM 0-70540  
 Au-Si thin film double layer, silicide form., electron diffr. study 0-80005  
 B<sub>4</sub>C, TEM investigation using C replicas 0-61034  
 BN, TEM investigation using C replicas 0-61034  
 B<sub>2</sub>O<sub>3</sub>-Nb<sub>2</sub>O<sub>5</sub> system, phase equil. and phase struct. obs. by high resolution TEM 0-108419  
 BaO-B<sub>2</sub>O<sub>3</sub>-V<sub>2</sub>O<sub>5</sub> glass, oxidation-reduction of V, thermodynamics 0-85169  
 BaTiO<sub>3</sub> ceramics, PTC-type, grain boundary study using TEM 0-107267  
 Ba<sub>2</sub>YbF<sub>7</sub>, single crystals, electron diffr. cryst. struct. anal. (*French*) 0-92507  
 Be ingot, high-purity, TEM obs. of BeO dispersion 0-104165  
 Be-Si-N system polytypes, struct. obs. using TEM 0-107192  
 Be<sub>3</sub>N<sub>2</sub>-BeSiN<sub>2</sub> system, crystallography and phase relationships, TEM and electron diffr. study 0-92502  
 Bi film, structure and electronic props. 0-70562  
 C, amorphous, catalytic oxidation by Pd particles, TEM obs. 0-76555  
 C fibres, thermal expansion coeff. meas. using TEM fitted with furnace 0-102966  
 C, filamentous catalytic, rel. crystallographic orientations of C and metal 0-89240  
 C films with high conductivity, prep. and props. 0-80983  
 Ca<sub>2</sub>(Al,Fe,Cr)O<sub>5</sub> solid soln., planar interfaces, TEM obs. 0-65008  
 Ca<sub>2</sub>(Mg,Fe)<sub>2</sub>(Si<sub>4</sub>O<sub>11</sub>)<sub>2</sub>(OH)<sub>2</sub>, amphibole nephrite, planar defects termination, high resol. electron microscopy 0-79772  
 (CaO)<sub>2</sub>SiO cement pastes, electron microsc. anal. 0-108761  
 Cd chalcogenides, thin films, VPE, needle-like cryst. growth 0-80148  
 Cd<sub>2</sub>As<sub>2</sub> films, nucleation processes, on NaCl substrates 0-59813  
 CdS, dislocation motion, TEM obs. 0-79799  
 CdS/InP epitaxial thin films on NaCl, HEED and TEM study 0-88446

## transmission electron microscope examination of materials continued

- CdSe thin film transistor on Cr substrate, cryst. struct., substrate defect effects 0-70563  
 Co, electrodeposited, influence of soln. pH on microstruct. 0-65399  
 Co, glide ahead of terminating {1012} twins 0-96545  
 Co, particle formation by evap., electron microscopy obs. of interaction processes 0-104053  
 Co, single crystals, {1121} twins, accommodation and form. 0-96540  
 Co vacuum deposited coatings on metal substrates, cryst. struct. and stability 0-75481  
 Co-Ni-Cr-Mo (35, 20, 10 wt.%), MP35N, TEM study of phase transformations 0-81054  
 Co-P, electrodeposited alloys, heat-induced structural changes (*Japanese*) 0-89263  
 Co-Ti-C, secondary precipitation and allotropic transform., TEM obs. 0-108453  
 Co-Ti-Fe (3, 1 to 2 wt.%), spinodal decomposition 0-100839  
 CoFe<sub>2</sub>O<sub>4</sub> mag. fluid particles, comp., struct., and mag. props. 0-60374  
 Co<sub>2</sub>Pd film, ordered, stacking fault obs. by TEM and interpret. using many-beam theory 0-107680  
 Co<sub>2</sub>Sm crystals, microstruct., homogeneous precip. and nucleation 0-104160  
 Co<sub>90</sub>Zr<sub>10</sub>, ferromag. amorphous alloy, crystn. and domain struct. study 0-107056  
 Cr containing Cr<sub>2</sub>O<sub>3</sub>, film struct., oxide percentage determ. and temp. coeff. of resist. 0-103607  
 Cr thin films, formation from Cr(CO)<sub>6</sub> dielec. breakdown 0-84881  
 Cr<sup>6+</sup>/Cr<sup>3+</sup> colloidal SiO<sub>2</sub> surface films on Al, TEM/XPS study 0-85090  
 Cr-Cr<sub>2</sub>O<sub>3</sub> black solar absorber surfaces, microstruct. rel. to electroplating parameters 0-61418  
 CrO<sub>2</sub> and Cr(OH)<sub>3</sub>, fine particle obs. of cryst. morphology and topotaxy 0-65969  
 Cr<sub>2</sub>S<sub>3</sub>V<sub>0.5</sub>Fe<sub>3.4</sub>C<sub>3</sub>, stacking fault study, morphology, comp. and struct. 0-84190  
 Cu, dislocations gliding on (001) planes, bright field and weak-beam images 0-107266  
 Cu, electrochem. nucleation and growth on Te and Al, TEM 0-104451  
 Cu, erosive wear mechanisms, combined TEM and SEM obs. 0-108601  
 Cu foils, near  $\Sigma 9$  grain boundary properties, boundary dissociation 0-100251  
 Cu, friction surface structural investigation, O<sub>2</sub> surface diffusion (*Russian*) 0-96726  
 Cu, grain boundary migration, TEM obs. on mechanism 0-79812  
 Cu HCP film, uniaxial, mag. domain struct. 0-60385  
 Cu, ion bombard. by 5 keV Ar<sup>+</sup>, sub-surface damage 0-103399  
 Cu, near  $\Sigma 9$  grain boundary, structure and dislocation interactions 0-79808  
 Cu, near  $\Sigma 9$  grain boundary, props., identification by image matching of Burgers vectors 0-79810  
 Cu polycrystal, fatigued, interior dislocation struct. 0-88147  
 Cu, proton-irradiated, H<sub>2</sub> gas-bubble struct., study at 300K 0-92569  
 Cu single crystals, [100]- and [111], dislocation density meas. using TEM 0-79803  
 Cu single crystals, neutron irradiated, secondary slip 0-88161  
 Cu, single crystals, deformed in [001] and [111] axes, cell structs., TEM 0-70209  
 Cu-Al, linear dislocation multipoles, weak-beam TEM 0-75233  
 Cu-Al alloy, irradi. in HVEM, climb of dissociated dislocations and point defect absorpt. 0-107257  
 Cu-Al alloy, planar faults, faint electron microscopic image contrast obs. 0-107283  
 Cu-Al-Sn system, coexistence of different and brass like phases 0-89206  
 Cu-Au, corrosion in HNO<sub>3</sub> 0-85091  
 Cu-Be (1.8 wt.%) alloy, discontinuous precip. form. and growth 0-104169  
 Cu-Be (2 at.%), plastic deform. and dislocation substruct. 0-76307  
 Cu-Be (2 wt.%), precipitation sequence, TEM obs. 0-108450  
 Cu-Be-Co, discontinuous reaction, analytical TEM 0-100842  
 Cu-Cr (0.75 wt.%), deformation characts., fully reversed cyclic strain with fatigue cracks and dislocation struct. 0-81148  
 Cu-Cr-SiO<sub>2</sub> system, age and dispersion strengthened, dislocation struct. around SiO<sub>2</sub> particles 0-108468  
 Cu-Ga (17 wt.%), elec. resist. and TEM studies 0-108604  
 Cu-Ni-Sn (15, 8 wt.%), prior deform. effect on spinodal age hardening 0-108465  
 Cu-Ni-Ti, ordering within precipitates, TEM obs. 0-108461  
 Cu-Sn alloy system, long period superlattice obs. and impurity effects 0-103297  
 Cu<sub>3</sub>Au, disordered [001]-oriented single crystals, plastic deform., TEM and slip line studies 0-97541  
 Cu<sub>3</sub>Au, neutron irradi., displacement cascades, direct obs. method 0-107335  
 Cu<sub>3</sub>Au-Ni, antiphase domains morphology 0-108460  
 CuCr<sub>2</sub>S<sub>4</sub>, domain struct. and superstructure, TEM obs. 0-79779  
 Cu<sub>40</sub>Nb<sub>30</sub>X<sub>30</sub> (X=Ti, Zr, Hf), superconductors with metastable ordered struct. 0-108484  
 Cu<sub>3</sub>Pt, antiphase domains morphology 0-108460  
 CuZn, planar faults, faint electron microscopic image contrast obs. 0-107283  
 Fe, epitaxial growth on Au platelets, dislocations 0-96760  
 Fe, particle formation by evap., electron microscopy obs. of interaction processes 0-104053  
 Fe vacuum deposits on Ni(Cu)(Ag) (111) FCC substrates, orientation relationships 0-59836  
 Fe-(Co)-B and Fe-Ni-B(P), amorphous, crystn. 0-79704  
 Fe-Al alloy, planar faults, faint electron microscopic image contrast obs. 0-107283  
 Fe-B, metallic glasses and vapour deposited films, amorphous to cryst. transition 0-88048  
 Fe-B amorphous alloy, annealed, microstruct. and mag. domain changes 0-75790  
 Fe-C (1.6 wt.%) martensite habit plane poles, statistical TEM trace anal. 0-97494  
 Fe-Cr-Co, magnetic domain walls, Lorentz microscopy 0-103854  
 Fe-Cr-Co alloy, spinodally decomposed, micro-twinning 0-92337  
 Fe-Cr-Ni (12, 15 wt.%) austenitic alloy, Ni<sup>2+</sup> irradiated, void swelling and phase stability, Si and Ti effects 0-65055  
 Fe-Cu, lath martensite habit planes, TEM study 0-84942  
 Fe-Mn (0.5 wt.%) alloy, Burgers vector of dislocation determ. by weak-beam image in HVEM 0-103351  
 Fe-Mn (1 at.%), strain age hardening 0-108472



## transmission electron microscope examination of materials continued

- Fe-Mn-Ni-V-C (0.5, 3.0, 1.0, 0.2 wt.%), austenite decomp., isothermal transform. characts. 0-97477  
 Fe-Mn-V-C (0.5, 1.0, 0.2 wt.%) austenite decomp., isothermal transform. characts. 0-97477  
 Fe-Mo (13-20 at.%) binary alloys, spinodal decomp. on ageing, TEM and X-ray diffr. study 0-97503  
 Fe-Mo(4.1 wt.%), steady state creep at high temps. 0-89316  
 $\alpha$ -Fe-Ni (3-12 wt.%), structure and  $\gamma$ - $\alpha$  polymorphic transform. kinetics 0-71645  
 Fe-Ni alloys, enthalpy change between  $\alpha'$ - $\gamma$  and  $\alpha$ - $\gamma$  transformations 0-93550  
 Fe-Ni film, amorphous, martensite form. time and struct. 0-104159  
 Fe-Ni-Cr alloy, carbide form. by C diffusion, precip. distrib. and morphology 0-104164  
 Fe-Ni-Mn (20, 5 wt.%), rel. orientation between adjacent martensite laths 0-76254  
 Fe-Ni(Al) (Ti) (V)-(Cu), Cu addition strengthening at 77K, mech. props. 0-60875  
 Fe-Si (3wt.%), grain-oriented, secondary recryst., grain growth inhibition 0-89245  
 $\alpha$ -Fe-Ti, ion implanted, microstruct., ion beam anal. and TEM study 0-107294  
 $\alpha$ -Fe-Ti, ion implanted, with C impurity, microstruct. of TiC precip. 0-66513  
 Fe-Ti-C, rapidly quenched by splat-cooling 0-84923  
 Fe-X-C (X=Cr, Mo, W), quenched rapidly from melts, nonequilib. phases (*Japanese*) 0-71630  
 Fe<sub>83</sub>B<sub>16</sub>, amorphous, mag. props. and microstruct., cooling rate and melt overheating effects 0-65965  
 Fe<sub>80</sub>(C<sub>1</sub>-B<sub>2</sub>)<sub>20</sub> amorphous alloy,  $\alpha$ -Fe crystn., morphology 0-70129  
 FeCo, planar faults, faint electron microscopic image contrast obs. 0-107283  
 FeNi amorphous films, fast phase transition investigation by TEM method 0-107029  
 Fe<sub>23</sub>Ni<sub>35</sub>Cr<sub>14</sub>P<sub>12</sub>B<sub>6</sub> metallic glass, crystn. kinetics by TEM 0-75186  
 Fe<sub>2</sub>O<sub>3</sub> mag. fluid particles, comp., struct., and mag. props. 0-60374  
 $\beta$ -FeOOH, lattice imaging and pore struct., high resolution electron microscopy obs. 0-103310  
 $\delta$ -FeO(OH), study of thermal decomp. by X-ray diffr., electron diffr. and TEM 0-66790  
 Fe<sub>2</sub>Pt austenite, long range order parameter, temp. depend. discussion 0-97481  
 GaAs degraded lasers, climb asymmetry, TEM obs. 0-79802  
 GaAs, dislocation-free, point defects and rad. damage 0-88141  
 GaAs epitaxial multilayer photocathode structures, TEM obs. of dislocations generated 0-100241  
 GaAs, ion damage, TEM study of laser annealing 0-88215  
 GaAs, ion implanted, laser annealing 0-107296  
 GaAs, proton-bombarded, observation of radiation damage 0-75276  
 GaAs:Si, ion implantation, thermal annealing, Hall meas., SIMS atomic profile meas. 0-75243  
 GaAs:Si, Li, IR absorpt., microstruct., charge compensation 0-107565  
 GaAs:Si defect density before and after Zn diffusion, SEM and TEM obs. 0-96529  
 GaAs:Zn, implanted, furnace annealed, electrical, Rutherford backscattering and TEM meas. 0-100272  
 GaAs:Zn, ion implanted, TEM study after laser and furnace annealing 0-70234  
 GaAs:Zn(Cr), As precipitation at dislocations, TEM study 0-79820  
 GaAs-GaInAs structure, dislocation struct., TEM anal., appl. as IR LED 0-70206  
 GaAs-(GaP) single cryst., defect distrib. near abraded surface 0-92533  
 GaAsP<sub>1-x-y</sub> alloy, composition effects in growth by MBE 0-59816  
 GaP, green cathodolum. from cryst. defects, SEM, TEM study 0-80870  
 GaP single cryst., defect distrib. near abraded surface 0-92533  
 GaP, VPE layer structures for LEDs, SEM, and TEM obs. of dislocation density reduction expt. 0-100425  
 GaP:S, defect struct. and tetrahedral precipitates, TEM study 0-107246  
 GaTe, cryst. struct., TEM and X-ray diffr. study 0-79757  
 Ge, atomically sharp cracks, TEM study 0-71729  
 Ge bicrystal, high resolution electron microscopy obs. of dislocations 0-103347  
 Ge bicrystals, high angle tilt boundaries, TEM (*French*) 0-70224  
 Ge, dislocations under high stress, stacking fault energies, TEM study 0-70202  
 Ge, dissociated dislocations, constriction correlation with jogs 0-79801  
 Ge epitaxial film, ion implantation and electron beam anneal effects on carrier conc. 0-75255  
 Ge, faulted dipoles, high-resolution TEM study 0-103345  
 Ge foil, [110] oriented, seven-beam lattice images of defects 0-107209  
 Ge, ion beam irradi., defects prod. by individual displacement cascades, TEM study 0-70265  
 Ge, lattice images of defects and radiation damage applies. 0-107210  
 HF with interstitial O, quantitative TEM obs. of small agglomerates 0-107227  
 InAs films, MBE grown on GaAs, electron mobilities, lattice mismatch effect 0-80419  
 InAsP<sub>1-x-y</sub> alloy, composition effects in growth by MBE 0-59816  
 InGaAsP-InP DH LED, high temp. aged, dark-spot defects, TEM obs. 0-66300  
 InP film, electron-beam annealed, surface conduction 0-84500  
 InP single crystals, uniaxial compression deform. characts. 0-84991  
 InP, Zn diffused single-crystal, substitutional dopant and hole conc. meas. 0-75260  
 KNO<sub>3</sub> calcite-type crystals, topotaxial decomp. TEM obs. 0-108710  
 LaPO<sub>4</sub> catalyst crystals, high resolution electron microscopy, morphological characts. rel. to catalytic activity 0-107193  
 Li, temp. depend. of dislocation behaviour between 90 and 300K 0-88146  
 (Mg,Fe)<sub>2</sub>SiO<sub>4</sub>, dislocation recovery rate affected by high-press. 0-94515  
 Mg alloy, dil., dynamic recrystn. during creep, dislocation substruct., quartz comparison 0-109142  
 Mg-Al-Zn (94.3, 3.9, 1.8 wt.%), precip. on dislocations, weak-beam TEM 0-76264  
 Mg-Mn-Ce (1.5, 0.3 wt.%), superplasticity role of diffusional creep (*Russian*) 0-97528  
 MgAl<sub>2</sub>O<sub>4</sub>, faulted defect aggregates prod. by neutron-irrad. 0-107331  
 Mg<sub>1.86</sub>Al<sub>1.67</sub>Si<sub>2.47</sub>O<sub>3.19</sub>N<sub>3.81</sub>, 12H polytype, intergranular phases and compositional variations 0-79645  
 MgO, crack tip dislocations and dislocation-free zones 0-96533

## transmission electron microscope examination of materials continued

- MgO, electron irradiation damage, cryst. defects 0-107320  
 MgO, fracture and crack tip plastic zones, in situ obs. 0-108686  
 MgO, single cryst., tensile creep, stress induced dislocation structs. 0-96539  
 MgO, smoke particles, size distrib. 0-104471  
 MgO, subgrain boundaries form. obs. by TEM, diffusion coeff. determ. 0-79817  
 MgO:Ni, heavily doped, defect characterisation, rel. to use as laser material 0-65000  
 MgO-Pd metal-ceramic reaction, micro/macro obs. 0-66467  
 Mn-Zn ferrites, grain boundary exam. using TEM and AES 0-107268  
 Mo, creep deformed single crystals, subboundary struct. obs., dislocation sets 0-103348  
 Mo, fracture and crack tip plastic zones, in situ obs. 0-108686  
 Mo, ion irradi., defect anal., electron microscopy, appl. of theory of non-edge loop image contrast 0-70200  
 Mo, shock deformation twinning, shock loaded BCC and FCC metals comparison 0-104413  
 MoS<sub>2</sub>, lattice images of defects and radiation damage applies. 0-107210  
 MoSe<sub>2</sub>, imperfections from TEM study 0-79800  
 NH<sub>4</sub>Cl, submicron particles, density, morphology 0-61166  
 Na-rich plagioclase microstructure and exsolution 0-72501  
 NaCl, high resolution TEM and radiation sensitivity, dislocation obs. on deformed crystals 0-107260  
 NaCl-gas reactions, atmospheric, in situ TEM studies 0-104544  
 Nb, ion bombard. by 5 keV Ar<sup>+</sup>, sub-surface damage 0-103399  
 Nb, voids, elastic side band imaging 0-75219  
 Nb:He, mech. props. and microstruct. 0-85003  
 Nb-Ge, compounds with Al<sub>5</sub> structure, films, TEM study (*French*) 0-80135  
 Nb-Ge-Si, compounds with Al<sub>5</sub> structure, films, TEM study (*French*) 0-80135  
 Nb-H system, accommodation effects during hydride precipitation, TEM 0-89218  
 Nb-H system, phase diagram and transforms., struct. obs. of various phases 0-104125  
 Nb-Si, compounds with Al<sub>5</sub> structure, films, TEM study (*French*) 0-80135  
 $\beta$  NbH<sub>0.82</sub>, fracture, TEM obs. 0-108519  
 Nb<sub>48</sub>Ni<sub>52</sub>, amorphous, produced by Ni<sup>+</sup> implantation, damage distrib. 0-107062  
 Nb<sub>2</sub>O<sub>3</sub>-WO<sub>3</sub> system complex cpds. with TTB type subcells, HV superhigh resolution electron microscopy obs. of struct. 0-103311  
 Nb<sub>3</sub>Sn multifilamentary composite supercond. wires, transverse sections prep., ion milling, TEM obs. of grain size 0-101000  
 Nb<sub>3</sub>Sn-Cu multifilamentary composite wire, Nb<sub>3</sub>Sn filament morphology and grain size 0-100855  
 Ni and alloys, heavy ion irradi., defect cluster obs. 0-107341  
 Ni, carbonyl powder, dislocation density sintering 0-108372  
 Ni, dislocations gliding on (001) planes, bright field and weak-beam images 0-107266  
 Ni electrodeposition on Cu (001), three-dimens. epitaxial crystallites, TEM image contrast 0-88457  
 Ni, erosive wear mechanisms, combined TEM and SEM obs. 0-108601  
 Ni, grain boundary defect structure, hardening effects 0-103365  
 Ni, in situ rare gas ion irradi., cluster creation obs. by electron microscopy 0-107343  
 Ni, ion irradi. with 20 and 500 keV <sup>4</sup>He<sup>+</sup>, depth distrib. of cavities and dislocation damage 0-107346  
 Ni, particle formation by evap., electron microscopy obs. of interaction processes 0-104053  
 Ni-Al-Mo (12.7, 21.6 wt.%), directionally solidified eutectic composite, precipitation 0-108454  
 Ni-Al(Si) foils, ion irradi., surface effects on precip. morphology 0-104168  
 Ni-base superalloys, powder metallurgical, creep-rupture at intermediate temps. 0-97568  
 Ni-base wrought superalloy, creep and stress rupture behaviour in air and vacuum 0-60918  
 Ni-Co-Al alloys, continuous precip., SEM, TEM, X-ray diffr. study 0-89220  
 Ni-Co-Cr TEM foils, white band contrast 0-75134  
 Ni-Cr, partial dislocation, stacking fault TEM study (*Chinese*) 0-84174  
 Ni-Cr-Co superalloy, combined TEM, FIM, atom probe microanalysis of precipitates and carbide phase comp. 0-100844  
 Ni-Cr-Fe alloys, radiation enhanced precip. and dissolution of precipitates, point defect kinetics and dislocation obs. 0-108467  
 Ni-Fe superalloy type 718, heat treatment effect on room temp. and elevated temp. fracture toughness response 0-100922  
 Ni-Fe-Nb-Al (11.2, 8.09, 79.66 wt.%), modulated struct. growth process rel. to ageing (*Chinese*) 0-66541  
 Ni-Ge-Au evaporated contacts on GaAs, TEM obs. 0-75449  
 Ni-Ni<sub>4</sub>Mo system, deformation microstruct. 0-93591  
 Ni-Si incongruently subliming system, SEM and TEM obs. of high temp. transitions, temp.-comp. diagrams 0-104136  
 NiAl, nonstoichiometric, interstitial defect cluster obs. 0-107226  
 $\beta$ -NiAl, oxidation,  $\alpha$ -Al<sub>2</sub>O<sub>3</sub> growth and microstruct. 0-108627  
 NiFe<sub>2</sub>O<sub>4</sub> mag. fluid particles, comp., struct., and mag. props. 0-60374  
 NiTi martensite, shape memory effect, struct. characts., TEM 2<sup>1/2</sup> D imaging obs. 0-108446  
 Ni<sub>3</sub>Ti<sub>0.5</sub>Ta<sub>0.5</sub>, conservative domain struct., TEM study 0-79776  
 PbO, thin film, microstruct. and thermal stress, doping effects 0-88458  
 Pb-In-(Au) base electrode film Josephson junctions, tunnel barrier oxide struct. 0-65750  
 Pd<sub>2</sub>Si epitaxial islands on Si (001) substrate 0-96748  
 Pd<sub>2</sub>Si films on Si, lattice imaging obs. of structural details 0-103604  
 Pt, ion irradi. damage, temp. depend., electron microscopy obs. of defect kinetics 0-107339  
 PtSi surface, and interface with Si, impurity effects 0-80037  
 (SN)<sub>x</sub>, halogenated, struct. behaviour, TEM obs. 0-70126  
 Sb, electron microscope irradiation effects, agglomeration of point defects, dislocation climb and loops (*French*) 0-59518  
 Sb<sub>20</sub>(<sub>20</sub>)<sub>4</sub>MoO<sub>3</sub>, synthesis, struct. and oxidation state (*French*) 0-64971  
 Sb<sub>2</sub>S<sub>3</sub> spherulite crystals, direct lattice resolution obs. of defect struct. 0-107255  
 Si (001) wafer, pyramidal hillocks, TEM obs. during chemical etching 0-70508  
 Si, ambient effect of O precipitation, self interstitial mechanisms, IR spectra, TEM study 0-66510  
 Si, atomically sharp cracks, TEM study 0-71729



**transmission electron microscope examination of materials continued**

- Si, coherent twin boundaries, struct. by TEM 0-75238  
 Si, crystal defects and impurities interaction obs. by electron microscopic methods 0-65003  
 Si, Czochralski grown, oxide precip. homogeneous nucleation 0-65221  
 Si, Czochralski grown, oxide precipitates, diffusion-limited growth 0-97484  
 Si, Czochralski grown crystal, O precip., nucleation behaviour and dislocation loop form. (*Japanese*) 0-59664  
 Si, Czochralski grown crystals, swirl-type defect obs. 0-100236  
 Si, dislocation generation in local oxidation 0-107245  
 Si epitaxial film on sapphire, microtwins, TEM exam. 0-70555  
 Si, epitaxial wafer, saucer pit microdefects reduction by intrinsic gettering 0-75450  
 Si film, low press. CVD prep., struct., elec. and optical props. 0-70548  
 Si film, polycryst., grain struct. and surface roughness, TEM study 0-70556  
 Si foil, computer simulation of high resolution images of defects 0-107208  
 Si, grain boundaries, high resolution TEM 0-103364  
 Si, identification of oxide precipitates 0-100723  
 Si, implanted with low solubility dopants, laser annealing, TEM study 0-70233  
 Si, ion beam irradi., defects prod. by individual displacement cascades, TEM study 0-70265  
 Si, ion damage TEM study of laser annealing 0-88215  
 Si, ion implantation, high dose, solid phase epitaxial regrowth 0-103380  
 Si, ion implantation by laser annealing, characterisation, solar cell applications 0-70247  
 Si, ion implanted, complex annealing behaviour of amorphous layers, TEM obs. of defect struct. 0-107299  
 Si, ion implanted, damage struct. obs. using TEM and cross section specimens 0-107298  
 Si, ion implanted, defect struct., dislocation loops and elongated defects 0-107300  
 Si, ion implanted, interstitial generation and loop form. during annealing in oxidising medium 0-107225  
 n-Si, ion-implanted, elec. characts. after laser annealing 0-88562  
 Si, ion-implanted layers, crystn. by ns laser pulses, TEM and RHEED 0-100421  
 Si, ion-implanted layers, epitaxial regrowth by laser beam and flash annealing 0-100420  
 Si, lattice images of defects and radiation damage applics. 0-107210  
 Si layer, on buried SiO<sub>2</sub> layer formed by high-dose, O ion implantation, TEM, AES, and XPS obs. 0-88172  
 Si n<sup>+</sup>-p solar cells, degradation mechanisms associated with Ti impurities 0-81465  
 Si, oxidation-induced Frank sessile dislocation loops, struct. change 0-75228  
 Si, oxidation-induced stacking faults, distinction between clean and decorated faults by etching 0-79818  
 Si, oxide scale microstruct. of oxidised single cryst. 0-108613  
 Si, polycryst., oxidation, morphological aspects 0-76388  
 Si, polycrystalline, grain boundary obs. by TEM, solar cell appl. 0-72057  
 Si, screw dislocation networks, TEM study 0-70204  
 Si, slip, room temp., TEM obs. 0-79804  
 Si wafers, saw damage reduction in lubricant environment 0-108585  
 Si:Ar, As, ion implanted, laser annealing, doping profiles, channelling 0-97506  
 Si:Ar, ion-implanted, epitaxial regrowth by laser annealing, microstruct. 0-84404  
 Si:As, ion implanted, laser annealed, lattice defects, epitaxial regrowth 0-103334  
 Si:As, ion implanted, pulsed laser annealing, partial solid-state regrowth 0-103591  
 Si:As<sup>+</sup>(P<sup>+</sup>) ion implanted, laser annealed, correlation of struct. and elec. props 0-70855  
 Si:As(P), ion implanted, TEM study after laser and furnace annealing 0-70234  
 Si:B(P), dislocations under high stress, stacking fault energies, TEM study 0-70202  
 Si:Ge, recryst. after implantation using different temp. and energy sequences 0-84196  
 Si:P, dislocation dissoc. mode obs. by weak-beam TEM 0-107259  
 Si:P, incoherent light flash annealing, elec. props., backscattering spectra 0-97504  
 Si:P, ion implanted, regrowth of damage structs. by laser annealing 0-107289  
 Si:P, ion implanted, subsurface damage, TEM and channelled Rutherford backscatt. study 0-107337  
 Si:P bipolar transistors, interstitial supersaturation and misfit dislocation climb, TEM study 0-70203  
 Si:P polycrystalline layer, role in lattice defect reduction assoc. with P predeposition 0-70229  
 Si:Sb, ion implanted, annealed, dislocation generation, channelling and Rutherford backscatt. meas. 0-88158  
 Si-Al-Al<sub>2</sub>O<sub>3</sub> system, solid phase Si regrowth on sapphire 0-100413  
 Si-Al-O-N system, phase analysis and TEM struct. obs. 0-108420  
 Si-Al-O-N system, stable phase cryst. struct. and microstruct. obs. using TEM 0-108421  
 Si-Cr interfaces, metallurgical and electrical props. 0-60081  
 Si-Na-B-O-N glass, synthesis and characterisation 0-108381  
 n-Si-Pd:Si contact, interface struct. and Schottky barrier height, correl. obs. using TEM 0-100504  
 Si-Pd<sub>90</sub>Si<sub>10</sub> amorphous, Pd:Si layer form., shallow contact 0-103586  
 Si-Pd:Si structure, epitaxial growth, backscattering and transmission electron microscopy studies of layered structures 0-80123  
 Si-SiO<sub>2</sub> interface, thermal SiO<sub>2</sub> sputter induced roughness, Auger sputter profiling study 0-75424  
 Si-SiO<sub>2</sub> interface in MOS capacitors, lateral diffusion of Na<sup>+</sup>, neutralisation 0-92986  
 SiC, atomically sharp cracks, TEM study 0-71729  
 SiC, HVEM obs. of various polytypes 0-76248  
 SiC, oxide scale microstruct. of oxidised single cryst. 0-108613  
 SiC, polycryst., high resolution TEM study of  $\beta$ - $\alpha$  transform. 0-84928  
 SiC, TEM investigation using C replicas 0-61034  
 Si<sub>3</sub>N<sub>4</sub>, dielectric films made by NH<sub>3</sub>-silane reaction, TEM study 0-84413  
 SiO<sub>2</sub>/GaAs, interface reaction during high-temp. heat-treatments 0-88439  
 SiO<sub>2</sub>, thin films, deposition and characterisation study 0-80133

**transmission electron microscope examination of materials continued**

- Sm<sub>2</sub>O<sub>3</sub>, surface step thickness measurement 0-103555  
 Sn film, vacuum deposited, substrate and substrate temp. effects on struct. 0-107677  
 Sn/Au thin film diffusion couples, Kirkendall void form. 0-96698  
 Sn-Ni electrodeposited equatonic alloy, cryst. struct., X-ray, electron diffraction. 0-79748  
 steels, Cr-C-Mn(Ni), struct. prop. rel., design of struct. steels for high strength and toughness 0-97491  
 Ta-H system, phase diagram and transforms., struct. obs. of various phases 0-104125  
 Te film, microstructure 0-103598  
 Te film, vacuum deposited, growth and morphology of crystals. 0-96766  
 Te, vacuum deposited on NaCl, crystallite growth and morphology, electron microscopy 0-65401  
 Th-pyromellitate, growth processes, TEM 0-103229  
 $\alpha$ -Ti, cold rolled, primary recrystn., in situ investig. in HVEM 0-104185  
 Ti, corrosion in H<sub>2</sub>SO<sub>4</sub>, estimated from weight loss meas. at 270°C and 56 bar (*French*) 0-85080  
 Ti, friction surface structural investigation, O<sub>2</sub> surface diffusion (*Russian*) 0-96726  
 Ti, neutron irradiated, characterization of dislocation loops 0-88155  
 Ti-Al-V (6.4 wt.%), ion irradiated, microstruct. study using TEM 0-65572  
 Ti-Fe-C-N, ion irradiated, microstruct. study using TEM 0-96572  
 Ti-Mo alloys, structural stability under high-pressure soaking 0-104151  
 Ti-Mo-Zr-Sn (11.5, 6, 4.5 wt.%),  $\beta$  III, mech. props. rel. to heat treatment 0-84961  
 Ti-Mo-Zr-(Al) (15, 5 (3) wt.%), quenched and aged metastable  $\beta$ -phase, crystallography, morphology and decomposition 0-76262  
 Ti-Nb-Si, amorphous alloy, supercond. props. and crystn. behaviour, TEM and DTA study (*Japanese*) 0-84536  
 Ti<sub>70</sub>Co<sub>20</sub>B<sub>10</sub>, amorphous alloys, crystn. behaviour, TEM study (*Japanese*) 0-84087  
 TiD<sub>2</sub>, nucleation and growth in D<sub>3</sub><sup>+</sup> implanted Ti, TEM study 0-97717  
 Ti<sub>70</sub>Fe<sub>20</sub>B<sub>10</sub>, amorphous alloys, crystn. behaviour, TEM study (*Japanese*) 0-84087  
 Ti<sub>70</sub>Ni<sub>20</sub>B<sub>10</sub>, amorphous alloys, crystn. behaviour, TEM study (*Japanese*) 0-84087  
 TiO<sub>2</sub>, reduced, crystallographic shear planes, dislocation struct. 0-107175  
 UO<sub>2</sub>, intragranular fission gas bubbles, size and distrib. 0-57840  
 U<sub>3</sub>Si, reversible twinning, in-situ obs. 0-104241  
 V/Cu-Ga, composite superconductor, V<sub>3</sub>Ga phase form., TEM obs. (*Russian*) 0-84933  
 V-H(D), phase diagrams, struct. studies 0-66491  
 V<sub>2</sub>O<sub>5</sub>, wedge shaped cryst., electron lattice image interpret. 0-103319  
 V<sub>3</sub>Si, neutron irradi., grain boundary pinning, field-depend. change of crit. current density 0-65759  
 W, high resolution phase contrast imaging 0-103224  
 W, polishing technique as prep. for TEM 0-71851  
 W wire, AKS-doped, second phase particle obs. by TEM, SEM and atom probe microanalysis 0-108457  
 W<sub>50</sub>Fe<sub>50</sub> glassy alloy, refractory, triode sputtered 0-75185  
 WO<sub>3</sub> film, amorphous, struct. and crystn. 0-103606  
 WO<sub>3</sub> polymorph, hexagonal, cryst. struct. imaging by high-resolution electron microscopy 0-103309  
 Y<sub>2</sub>GdIG film, amorphous, mag. bubbles obs. and structural transformation 0-75824  
 YIG, substituted, magnetite nucleation in transitional zone, ionic process, lattice imaging 0-107424  
 Zn chalcogenides, thin films, VPE, needle-like cryst. growth 0-80148  
 Zn film deposition on Al, TEM and electron diffraction. obs. 0-75460  
 ZnO, irradiation in high voltage electron microscope dislocation loops study 0-88157  
 ZnS, twist boundary struct., atomic scale electron microscopy obs. 0-107276  
 Zr and alloys, neutron irradi. at 573 to 923K, damage struct. 0-107334  
 Zr, electron irradiation damage, direct obs. 0-84212  
 Zr, hydride precipitation and growth at crack tips, electron optical obs. 0-108449  
 Zr, thin film, sources of background X-radiation 0-101908  
 Zr-H formation, of  $\delta$ - $\gamma$  transformation 0-84929  
 Zr-H formation, of  $\delta$ - $\epsilon$  transformation 0-84930  
 Zr-Nb (2.5 wt.%), cold-worked, pressure tubing, metallography and mech. props. 0-89269  
 Zr-Nb (2.5 wt.%), hydride precipitation and growth at crack tips, electron optical obs. 0-108449  
 Zr-Nb (97.5, 2.5 wt.%) nuclear reactor pressure tube material, H embrittlement study by TEM 0-76363  
 Zr-Sn(Fe)(Ni) (0.15 wt.%), electron irradiation damage, direct obs. 0-84212  
 Zr-Ti-Be metallic glass, phase separation 0-97464  
 Zr<sub>3</sub>Al, deformed and irradi., lattice defects obs., superlattice dislocations and defect clusters 0-107261  
 Zr<sub>3</sub>Al ordered alloy, ion bombardment damage, TEM 0-100287  
 ZrO<sub>2</sub>-CaO (15 mol.%) precipitation and ordering 0-100837  
 ZrO<sub>2</sub>-Y<sub>2</sub>O<sub>3</sub> (9 mol.%) precipitation and ordering 0-100837

**transmission electron microscopes**

- see also *transmission electron microscopy*  
 analytical, sources of background X-radiation 0-101908  
 cold trap assembly, liq. N<sub>2</sub>, for contamination reduction in analytical microscopy 0-101056  
 combined CTEM and STEM, using condenser objective lens and 100 kV LaB<sub>6</sub> gun 0-86516  
 development, refinements of lens correction, recording of individual electrons, holography, image quality monitoring (*German*) 0-57430  
 electron probe X-ray microanalysis, quantitative investigation of thin specimens 0-101068  
 electrostatic energy filter, telescopic, with cylindrical mirror analysers 0-87296  
 energy filter, mag. prism design 0-86523  
 field emission electron gun, comparison of cold and thermal types used in the same electron microscope 0-101890  
 liquid He cooled environmental cell 0-68323  
 magnetic energy filter, without second-order aberrations 0-86524  
 magnetic imaging filter, electron optical experiments 0-87295  
 microdensitometer system for use in TEM 0-95197  
 objective lens, with compensated axial chromatic aberration 0-87293  
 on-line electron-optical correlation computing 0-99008



**transmission electron microscopes continued**

- Philips EM400 TEM/STEM performance, with field emission gun and twin lens 0-57441  
 raster mode of image form. 0-101887  
 spectrometer attachment for energy-loss analysis, theory and instrum. 0-81405  
 stray X-rays from Cu and Mo components in JEM-100C microscope, reduction 0-73550  
 telescopic, with cylindrical mirror analysers 0-87296  
 tilting high temperature gas reaction chamber 0-101894  
 vacuum pump system, simplified low-cost design for use with ZEISS microscope 0-99012

**transmission electron microscopy**

- see also transmission electron microscope examination of materials; transmission electron microscopes*  
 amorphous materials, tilting and defocus effects in high resolution dark field images 0-79652  
 amorphous objects, filtered electron image contrast for elastic scatt., calc. 0-107026  
 analytical, contamination reduction using liq. N<sub>2</sub> cold trap assembly 0-101056  
 atmospheric interaction, between aerosols and gases 0-104544  
 biological macromolecule observation using CTEM and STEM with negative staining 0-85561  
 bipolar transistors, emitter-push effect, analysis of isolated dislocation helices 0-70203  
 bright field TEM, partially coherent attenuation envelope shape 0-101885  
 bright-field image contrast and resolution 0-95200  
 Burgers vector characterisation method for minerals 0-109141  
 catalysis, advances in TEM obs. 0-85214  
 cell element observations in same sections by light microscopy, TEM and/or SEM 0-85556  
 cold-cathode ion gun for sputter etching of specimens 0-105748  
 contrast, fold domain boundaries and microsectors in polyethylene single crystals 0-107065  
 correlative light microscopy, SEM and TEM of argentaffin cells 0-85557  
 critical voltage effect in zone axis patterns, theory 0-59352  
 crystal atomic structure imaging technique and applications 0-105752  
 crystal orientation, determ. by zone axis method, appl. to grain boundaries 0-103226  
 CTEM image recording using CCD 0-68329  
 cubic crystal, image contrast of dislocation loops, elastic anisotropy depend. 0-103349  
 digital image enhancement 0-82852  
 direct elemental analysis by electron energy loss spectroscopy 0-71998  
 dislocation core images, optical filtering for noise removal 0-107254  
 dislocation loop analysis and identification using black-white contrast images 0-103350  
 dislocation motion obs., work of Hirsch et al., (1946-56) 0-62445  
 EELS, chemical analysis, filtered images 0-101062  
 EELS, standard, implanted Si 0-99017  
 electron energy loss spectroscopy, in electron microscope, review 0-104025  
 energy-loss analysis, single crystals, in TEM, diff. conditions influence 0-81406  
 energy-loss spectral resolution optimisation using electron lenses between TEM specimen and electron spectrometer 0-101886  
 epitaxially sandwiched macromolecules, contrast 0-85565  
 field emission, sub-angstrom resolution 0-82851  
 fine fragmented crystals, complex struct. analysis by electron microscopy 0-104416  
 foil thinning, monitoring by PP-8 radiometer (USSR) 0-73525  
 freeze drier, all-glass design 0-82854  
 HEED atomic string approximation use in obtaining dispersion surfaces 0-100143  
 high resolution, welding technique, grain boundaries in Si 0-103364  
 high resolution phase contrast, imaging of single atoms and amorphous state 0-103224  
 image and electron energy loss spectrum display by self-scanned linear Si photodiode arrays 0-68330  
 image contrast from single-electron excitation 0-59353  
 image enlargement and rotation (Czech) 0-73526  
 in-situ techniques, problems and appls. 0-76461  
 incoherent illumination method with conventional electron microscope, granular noise elimination 0-95201  
 lattice defects, characterisation 0-103320  
 lattice defects, SEM, electron beam induced conductivity, thinned semiconductor devices 0-107027  
 lattice images of defects, aberration and cryst. misorientation effects, radiation damage appls. 0-107210  
 lattice images of defects, computer simulation of high resolution images 0-107208  
 metallurgy, review 0-76458  
 microanalysis, appl. to Nb<sub>3</sub>Sn thin films 0-104491  
 microscopic equipment, methods, appls. and related topics, bibliography 0-73124  
 misfit dislocation observations at film/substrate interface 0-103605  
 optical filtering of faulted areas in layered silicate micrographs 0-84035  
 particle track detectors, electron microscopy of etch pits 0-99424  
 plural scattering, influence on image quality of thick amorphous objects 0-86533  
 polymer materials, characterisation 0-103270  
 quantitative elemental analysis 0-101060  
 semiconductor crystal growth and defects, appl. of analytical techniques 0-73546  
 semiconductor TEM 90° cross-section and 1° angle-lap specimen prep. 0-71881  
 single atoms, in molecules and crystals, TEM obs. 0-103229  
 specimen preparation, fine grained coatings, sputter source design 0-99015  
 specimen transfer device for combined AES/RHEED and TEM obs. 0-70093  
 staining method using mercuric trifluoroacetate for polymer blend morphology obs. 0-84103  
 steel, austenitic stainless, phase identification, 2<sup>1/2</sup>D imaging techniques 0-96424  
 surface step thickness measurement 0-103555  
 temperature calibration standards using graphite-halogens 0-86510  
 thin films, chem. anal. by energy loss spectroscopy 0-104493

**transmission electron microscopy continued**

- thin samples, mass thickness and chem. composition determ., by TEM and X-ray anal. 0-103227  
 X-ray analysis, energy selective, TEM appls. 0-84036  
 X-ray microanalysis, in TEM up to 1000 kV 0-101063  
 X-ray production, theoretical and expl. 0-85258  
 Al-Zn (38 at.%), precipitation process study 0-93561  
 FeNi amorphous films, fast phase transition investigation by TEM method 0-107029

**transmission line theory**

- ohmic contacts to semiconductor, meas. of contact resistance using transmission line model 0-70826

**transmission lines**

- see also cables (electric); power transmission lines; waveguides*  
 instantaneous frequency measurement of micro-wave range by two different point detected signals (Japanese) 0-73327  
 magnetically insulated, Compton scattering of photons from electrons 0-68982  
 metallic-conductor, far IR antenna appls., review 0-69553  
 US transmission line of probe for hot metal inspection, spurious signals 0-66754

**transmitters**

- see also television transmitters; transceivers*  
 optical transmitter laser diode module description and performance 0-64069

**transmitting see transmission****transonic flow**

- axisymmetric flow past slender body of revolution, integral equation method 0-74910  
 compressed gas, nonsteady transonic flow, modified Khokhlov method study 0-79347  
 compressible flow problems, modified FLIC method, finite element anal. 0-74911  
 compressor, prediction using characteristic method 0-96277  
 detached flows past a cylinder with a flat end, subsonic and transonic vels. 0-92187  
 dispersive compressible fluid, transonic nozzle flows 0-69895  
 gas flow, optical excitation of intense acoustic waves 0-74564  
 mixed flows, numerical simulation using fast super-dashpot time-dependent technique 0-83813  
 noise generation by transonic open-rotors 0-69599  
 oblique wing as a lifting line problem in transonic flow 0-59065  
 plane flows past oscillating airfoils, review, book contrib. 0-96278  
 shock wave interaction with turbulent boundary layer, pressure distrib. 0-74918  
 shock wave interaction with turbulent boundary layer, wall shear stress 0-74919  
 small-disturbance transonic flow, nonlinear mixed elliptic hyperbolic eqn., finite element anal. 0-83814  
 spontaneously condensing and wet steam discontinuous flows in steam turbines, numerical investigation (Russian) 0-87800  
 stellar atmospheres, spherical transonic flow, reson. line radiative transfer 0-94698  
 strained coordinate method for transonic flows 0-69861  
 supercritical compressor and turbine cascades, computation 0-96276  
 turbulence modelling, compression waves developing into shock wave 0-74909  
 unsteady 3-dimens. compressible flow, implicit finite difference simulations, transonic appl. 0-64576

**transparency see transparency****transparency**

- see also light transmission; optical constants; self-induced transparency*  
 aerosol particle size measuring device, using spectral transparency and small angle scatt. methods 0-95069  
 atmosphere, transparency, meas. on Maidanak mountain during autumn and winter (1977 to 1978) (Russian) 0-72627  
 benzene, liq., laser pulsation kinetics, optical damage effects 0-58614  
 correlation reduction, spatial filtering and variation of resolution 0-102850  
 defect crystal structure determination, light interference, diffraction and scattering 0-103316  
 dispersive system, spectral transparency approx. by Legendre polynomials, distrib. density of particle size 0-95800  
 eclipsing binary stars atmospheres, light curve anal. with allowance for transparency effects 0-82417  
 fibre material selection criteria for  $\lambda > 1.8 \mu\text{m}$  0-87554  
 holographic grating, in spectrograph 0-57395  
 liquids, laser pulsation kinetics, optical damage effects 0-58614  
 MBBA-EBBA, controllable liq. cryst. transparency, electrooptical characts. 0-78996  
 nematic liquid cryst., ZhK-440, transparency, electrooptical characts. 0-78996  
 oxide, porous transparent films as antirefl. coatings for glass surfaces, low refr. index 0-74448  
 particle size distribution, spectral transparency method, improvements 0-86254  
 plane-parallel absorbing layer, nonlinear optical props. 0-58631  
 plasma optical transparency evaluation, line broadening effect 0-79453  
 polyethylene ribbons, flow-induced crystn. from melt, in dies fed by single screw extruder 0-84110  
 polypropylene, flow-induced crystn. from melt, in dies fed by single screw extruder 0-84110  
 solar energy absorbers, thermokinetics of glass and semi-transparent materials (French) 0-61410  
 soot conglomerate destruction dynamics in pulsed laser radiation field 0-58617  
 Al<sub>2</sub>O<sub>3</sub> porous transparent films as antirefl. coatings for glass surfaces, low refr. index 0-74448  
 Al<sub>2</sub>O<sub>3</sub>, transparent hot-pressed, transparent and translucent properties 0-60533  
 BaF<sub>2</sub>, ultralow loss optical fibre material, loss mechanism 0-78920  
 CdGeAs<sub>2</sub> crystals, Bridgman grown, optical props. rel. to O<sub>2</sub> content of starting materials 0-81213  
 CdSnO<sub>2</sub> films, transparent conducting, deposited by RF sputtering from CdO-SnO<sub>2</sub> target 0-76179  
 CsI, ultralow loss optical fibre material, loss mechanism 0-78920  
 Fe<sub>2</sub>O<sub>3</sub> films, DC reactively sputtered, for selectively semitransparent photomasks, deposition conditions and optical props. 0-60782  
 Fe<sub>2</sub>SiO<sub>4</sub>, fayalite, Czochralski growth under controlled O<sub>2</sub> fugacity conditions 0-84843

## transparency continued

- $\text{In}_2\text{O}_3$ , films, activated reactive evaporation technique of prep. 0-80989  
 $\text{In}_2\text{O}_3$  films, reactively evaporated, elec. props. 0-84521  
 $\text{In}_2\text{O}_3/\text{Sn}$ , films, activated reactive evaporation technique of prep. 0-80989  
 KCl, ultralow loss optical fibre material, loss mechanism 0-78920  
 KCl:OH, absorpt. in high-transparency region 0-89037  
 LiF, ultralow loss optical fibre material, loss mechanism 0-78920  
 $\text{Na}_2\text{O}:\text{SiO}_2\text{-Tb}_2\text{O}_3$  glass magnetooptical study 0-88976  
 PLZT ferroelectric thin films, epitaxial growth and optical props. 0-70543  
 Pr tinted glasses, transparency, dichroism and colour effects (*Polish*) 0-71371  
 $\text{SiO}_2$ , ultralow loss optical fibre material, loss mechanism 0-78920  
 TiCl-TiBr, KRS-6, ultralow loss optical fibre material, loss mechanism 0-78920  
 ZnTe:Cu films, high cond., elec. and optical props. 0-88651  
 $\text{ZrF}_4\text{-THF}_4\text{-BaF}_2$  glass, IR-transparent, synthesis using reactive atm. processing technique 0-100826

## transpiration

- see also flow through porous media  
 No entries

## transport see transportation

## transport equation see Boltzmann equation

## transport phenomena see transport processes

## transport processes

- see also biotransport; Boltzmann equation; cellular transport and dynamics; cosmic ray propagation; diffusion; electrical conductivity; Liouville equation; master equation; neutron transport theory; photon transport theory; plasma transport processes; Senfleben-Beenakker effect; thermal conductivity; thermal diffusivity; viscosity  
 adjoint space in heat transport theory 0-58887  
 air pollution transport, air quality models development for limited wind fetch 0-104533  
 alloys, random, equilb. and transport props., single-site approxs. 0-92801  
 artificial membranes, transport regulation by environmental  $\text{H}^+$  conc. 0-89725  
 atmosphere, eddy diffusion models for mesosphere and lower thermosphere 0-109198  
 atmosphere, obs. of  $\text{O}_3$  flux by transient eddies in 0 to 30 km height range 0-109224  
 atmosphere turbulent boundary layer, finite-element numerical modelling 0-77061  
 charged particle transport, multigroup formalism to solve Fokker-Planck eqn. 0-68159  
 dilute gas, transport props., simple pair pot. model 0-87835  
 droplet transport in gases and liquids, gravitational and thermophoretic contribs. 0-100052  
 eigenvalues of Fokker-Planck operators 0-98863  
 energy transport equation, exact soln. for plane source in an infinite medium 0-82729  
 F-region, interhemispheric ion transport induced by neutral zonal winds 0-98509  
 fission reactor materials, ion penetration distance calculations with multigroup transport computer codes 0-102246  
 Florida Current transport, fluctuations at periods between tidal and two weeks 0-72551  
 fluidised system, heterogeneous, aerodynamic aspects of transfer processes, crit. state 0-79394  
 gas, electron and hole drift velocity 0-57223  
 gas, electron and hole transport theory, free-path method, orders of approx. 0-62598  
 gas, weakly ionised, electron distrib. function, isotropic component, collision source 0-62599  
 gas, weakly ionised, electron distribution function, steady-state conditions and elastic collisions 0-57224  
 gas, weakly ionised, electron drift velocity and distrib. function 0-57225  
 gas, weakly ionised, electron transport quantities, divergences 0-57222  
 gas transport in magma, determ. from mass fractionation of rare gas isotopes 0-98292  
 gases weakly ionised, electron motion, stochastic theory of homogeneous systems, review 0-77735  
 Helmholtz eqn., 1-dimens., refined Maslov-WKB technique appl. 0-90795  
 hopping model, exact solns. for neutral particles 0-98865  
 hybrid shielding, radiation heating rates, two-dimens. transport anal. 0-106178  
 infinite dimensional Riccati eqns. from transport theory, strong solns. 0-73287  
 ionic crystals, lattice defects, conference, Canterbury, England (Sept. 1979) 0-105420  
 I 0-57221  
 linear transport equation, continuously varying spatial media, elementary solns. 0-86229  
 Liouville problem, quasi-particle dynamics from a given kinetic eqn., inverse 0-101749  
 liquids, momentum transfer, cooperative effects 0-68160  
 magnetic semiconductors, conference, Montpellier, France (Sept. 79) 0-94916  
 Markovian processes and irreversibility. The Onsager-Casimir symmetry, Onsager Casimir symmetry 0-62580  
 membrane transport, active, for anions, synthetic membrane synthesis 0-61142  
 multicomponent gas mixture, transport eqns. and distrib. functions 0-64581  
 multidimensional diffusion equation, class of general boundary conditions 0-90796  
 multiple band electron-phonon transport eqn. derivation 0-100318  
 objective and regular differentiation and integration, constitutive law and transport (*French*) 0-7090  
 ocean, realistically stratified, nonlinear energy and enstrophy transfers 0-101370  
 Purex kinetics, U extraction with tributylphosphate (*German*) 0-57937  
 radionuclide chain transport through heterogeneous media 0-99250  
 reduced equations of motion for generalized fluxes and forces in the continued-fraction expansion 0-105594  
 retardation of electrolytic mass transport in collinear electric-magnetic fields 0-104443  
 sediment transport modes in channelised water flows, appl. to Martian outflow channels erosion 0-98363

## transport processes continued

- semiconductor, electron and hole drift velocity 0-57223  
 semiconductor, electron and hole transport theory, free-path method, orders of approx. 0-62598  
 semiconductor, intrinsic, electron distribution function, steady-state conditions and elastic collisions 0-57224  
 semiconductor, intrinsic, electron drift velocity and distrib. function 0-57225  
 solid particle systems, high Reynolds number, momentum transfer. Karman-Pohlhausen method 0-74947  
 solids, kinks, solitons, and nonlinear transport 0-65421  
 solutes, movement through aqueous fissures in porous rock 0-94553  
 stratospheric tracer transport mechanisms, Lagrangian motion of air parcels in presence of planetary waves 0-109215  
 surface transport and reaction, stochastic calcs. 0-108736  
 theory of constrained mixtures with multiple temperatures 0-62600  
 thermosphere, middle, incoherent scatter radar studies rel. to energy and mass transport 0-72654  
 two-group integral transport equation, variational method 0-68156  
 ultracold neutrons, lifetime in traps, film-substrate model calcs. 0-106098  
 water pollution in Par River estuary, India, transport and abatement methods 0-104521  
 LiCl aqueous solns., dynamical props. by ultrasonic propag. meas. 0-76517  
 $\text{O}_3$ , of stratospheric origin, measured over Pacific Ocean, source and large-scale wave transport 0-72600  
 S compounds, atmospheric, meso-scale transport obs. in rural East Midlands, England 0-94124
- transport properties see transport processes  
 transport theory see transport processes  
 transport theory of neutrons see neutron transport theory  
 transport through biomembranes see biomembrane transport
- transportation
- see also aircraft; marine systems; rail traffic; road traffic  
 hydraulic coal trunk pipeline transport systems, methods of improving economic effectiveness 0-106837  
 irradiated LWR fuel, European transport experience 0-63309  
 liquefied natural gas, nonsteady-state flow calculations in horizontal pipeline systems 0-106838  
 pipeline systems, problems in fluid mechanics for hydraulic transport of solid materials 0-106836  
 radioactive materials, IAEA transport regulations, underlying radiation protection principles 0-63414  
 radioactive materials, international regulatory control for safe transportation 0-63411  
 radioactive materials, package design, construction and testing for safe transportation 0-63412  
 radioactive waste, low level, transport regulations, proposed changes 0-68896  
 spent fuel transportation, commercial experience in US 0-63310
- transportation networks see transportation  
 transportation services see transportation  
 transportation systems see transportation  
 transverse rupture strength see bending strength
- trapped electron centres see F-centres  
 trapped free radicals see free radicals  
 trapped hole centres see V-centres  
 traps, electron see electron traps
- travelling-wave-tubes
- see also backward-wave tubes  
 EM waves generation and amplification based on Doppler effect 0-63902  
 microwave spectrometer using TWT prior to crystal detection for sensitivity increase 0-82822
- treatment, heat see heat treatment  
 treatment, patient see patient treatment  
 treatment, surface see surface treatment  
 treatment, water see water treatment
- trees (mathematics)
- dielectric breakdown tracks in polymethylmethacrylate 0-100633  
 diffusion in random networks near percolation threshold, ant in labyrinth problem 0-77732  
 fault tree analysis for fission reactor risk assessment 0-63330  
 fault tree analysis of fission reactor auxiliary feedwater systems 0-63332  
 fault tree analysis of fission reactor cooling system (*Spanish*) 0-57870  
 fault tree analysis of fission reactor decay heat removal system 0-63333  
 fault tree analysis of fission reactor shutdown heat removal system failure 0-63334  
 topological indices for branching of tree-like graphs 0-57076
- triboelectric emission see electron emission
- triboelectricity
- see also static electrification  
 No entries
- tribology
- see also friction; lubrication; mechanical contact; wear  
 parameter prediction, for evaluation of surfaces 0-64496
- triboluminescence
- alkali halide crystals, triboluminesc. spectra 0-66312  
 polymethyl methacrylate, subthreshold luminesc. 0-93414  
 Fe, burning particles, flashes, spectrographic obs. 0-89078  
 LiF, cryst., triboluminesc. spectra 0-66312  
 NaBrO<sub>3</sub>, cryst., mechanoluminesc. spectra 0-97355  
 NaCl, cryst., triboluminesc. spectra 0-66312  
 NaClO<sub>3</sub>, cryst., mechanoluminesc. spectra 0-97355
- trigger circuits
- see also flip flops; multivibrators  
 photographic flashlamp trigger circuit 0-62750  
 sound triggered electronic photo flash unit, using variable time delay 0-57407  
 triggered calibrated sweep for AC oscilloscope 0-67987
- triode sputtering
- high-rate vapour quenching techniques and use in amorphous phase prep. 0-80977  
 W<sub>18</sub>Fe<sub>30</sub> glassy alloy, refractory, triode sputtered 0-75185  
 ZnO low-loss optical waveguides on amorphous substrates 0-58793
- triodes
- ion beam prod., high current 0-99372



## triods continued

reflection triode, prod. of high current ion beams (*Russian*) 0-83230  
thermionic triode, oscils. in low press. inert gas discharge 0-79590

triplet point *see critical points*triplet absorption detection of magnetic resonance *see microwave-optical double resonance*

## triplet state

acetylene, triplet state quenching by foreign gases 0-91596  
alkali cyanides, mol. excitons, X-ray excited emission spectra obs. 0-66287  
n-alkanes, mol. Rydberg S<sub>1</sub>-S and S<sub>1</sub>-T transitions, semi-empirical SCF MO calc. 0-91453  
aniline, in p-xylene host cryst., phosphoresc. triplet state, ESR and MIDP obs. 0-66077  
anthracene, pulsed electron excitation, triplet excitons, spectral and electrical investigations 0-92828  
anthracene-amine cation radicals, electron transfer with heterocyclic and carbonyl anion radicals, triplet state electrogeneration 0-63803  
9,10-anthraquinone, lower triplet states, interactions and position, matrix isolation spectra 0-63634  
aromatic compounds in benzene polycrystalline host; active N<sub>2</sub> induced chemilum., 77K 0-60691  
aromatic systems, alternant, sign-alternation rule for triplet state 0-102420  
aryl cations, triplet state, multiple site splitting, ESR obs. 0-97126  
azaaromatics, neutral and protonated, excited singlet and triplet states, charge densities, INDO calcs. 0-58152  
azaphenanthrenes, lowest triplet state zero field splitting parameters calcs. 0-83391  
benzene, excitation spectra, cluster configuration method appl. 0-78546  
benzene-d<sub>6</sub>-(d<sub>8</sub>), radiationless triplet decay, non-Condon effects 0-83405  
benzenoid aromatics, triplet zero field splitting parameters, ODMR obs., struct. effects 0-78636  
benzil, cryst., excited triplet state spin-lattice relax. probabilities, temp. depend. (*Russian*) 0-88860  
benzophenone, migration of triplet excitons, EPR profiles and phosphoresc. decay data 0-84641  
benzophenone vapour, fluoresc. and phosphoresc., nonradiative transitions between triplet and singlet state obs. 0-99516  
biacetyl, triplet  $n \rightarrow \pi^*$  and  $\pi \rightarrow \pi^*$  transitions studied by low-energy electron diff. 0-83502  
butadiene, excitation spectra, cluster configuration method appl. 0-78546  
carbonyl anion radicals, electron transfer with anthracene-amine cation radicals, triplet state electrogeneration 0-63803  
cell surface component rotational diffusion, time-resolved phosphoresc. anisotropy 0-97885  
chemically induced magnetic polarization by S-T<sub>1</sub> mixing in strong mag. field 0-83515  
chlorophylls, mag. reson., site selected fluoresc. detection 0-69164  
chloroquinolines, photophys. behaviour, substituent and solvent effects 0-106342  
chrysene, excited singlet and triplet state, CARS obs. 0-83374  
conjugated molecules, electronic transitions, S-II separability 0-58124  
copper phthalocyanine-iodine, amorphous cpd. prep. by I<sub>2</sub> diffusion in polycryst., triplet EPR signals obs. (*Russian*) 0-66016  
coronene, triplet state, photomagnetism 0-97125  
deoxyhaemoglobin, porphyrin-Fe-imidazole system, SCF-LCAO-ASMO and CI calcs. of low-lying multiplets and excited states 0-94155  
diacetyl vapour, fluoresc. and phosphoresc., nonradiative transitions between triplet and singlet state obs. 0-99516  
diacetylene, low temp. photochemical polymerisation, decay kinetics, ESR spectra obs. 0-100616  
3,6-diaminophthalimide vapour, mol. electronic excitation energy degradation path depend. on pentane 0-74195  
diazonium salts in aqueous solns. and polymer matrices, IR absorpt. spectra 0-76030  
p-dichlorobenzene-p-dibromobenzene mixed crystals, triplet exciton migration, time resolved emission spectroscopy 0-89052  
4,4'-dichlorobenzophenone single crystals, mutual annihilation of triplet excitons, 1.5 and 4.2K, phosphoresc. obs. 0-80850  
dichloronaphthalenes, heavy atom effects on substrates of lowest triplet states, MIDP obs. 0-91594  
dye lasers, metastable state relaxation time determ. 0-102719  
EEDOR triplet state zero-field transition energy, spectral diffusion 0-88893  
ethylene, diatomics-in-mols., semiempirical valence bond  $\pi$ -electron theory 0-99461  
N-ethylphthalimide+olefins, photochemical reaction, absorpt., fluoresc., phosphoresc. and triplet-triplet absorpt. spectra 0-85197  
fluorene:pyrene-d<sub>10</sub>, single cryst., host-guest triplet pairs, mag. field effect 0-60649  
formaldehyde, mol. Rydberg S<sub>1</sub>-S and S<sub>1</sub>-T transitions; semi-empirical SCF MO calc. 0-91453  
glyoxal, singlet-triplet radiationless processes in mag. field 0-106347  
glyoxal, triplet  $n \rightarrow \pi^*$  and  $\pi \rightarrow \pi^*$  transitions studied by low-energy electron diff. 0-83502  
heterocyclic anion radicals, electron transfer with anthracene-amine cation radicals, triplet state electrogeneration 0-63803  
hexatriene, excitation spectra, cluster configuration method appl. 0-78546  
hole burning, photophysical and photochemical theories 0-58322  
lowest triplet state zero field splitting parameters calcs. 0-83391  
molecular triplet states under optical spin orientation conditions, microwave energy transfer 0-74187  
naphthalene, phosphorescence spectra in rare gas matrices, multiplet struct. and pot. energy functions 0-106341  
naphthalene, singlet and triplet excimer interactions, exciton resons. 0-95535  
naphthalene, singlet and triplet exciton percolation, tunnelling and thermalisation 0-84432  
naphthalene-d<sub>8</sub>-(d<sub>9</sub>), radiationless triplet decay, non-Condon effects 0-83405  
nucleic acids bases, excited state dipole moments and geometries 0-95738  
octafluoronaphthalene crystalline complexes with naphthalene and durene, triplet exciton emissions 0-84760  
organic scintillators, vap. phase dye laser media, photophysical parameters 0-95884  
pentacene in naphthalene, triplet state, EPR study by electron spin-echo and laser flash excitation 0-58172  
phenanthrene, lowest triplet state zero field splitting parameters calcs. 0-83391

## triplet state continued

p-phenylphenol in stretched polyvinyl alcohol film, phosphorescent triplet states, ESR spectra obs. 0-83393  
p-phenylphenolate ion in stretched polyvinyl alcohol film, phosphorescent triplet states, ESR spectra obs. 0-83393  
photosynthetic reaction centre chromophore organisation, high-resolution magnetophotoselection 0-97880  
photosynthetic reaction centres, triplet population, mag. field and g-factor differences effect 0-97879  
photosystem I of spinach chloroplasts and subchloroplast particles, EPR obs. 0-85344  
poly(vinyl cinnamate), excited state, low-energy EELS and INDO/S calcs. 0-106407  
poly-N-vinylcarbazole-biacetyl, triplet exciton quenching, exciton trapping model 0-66267  
polyenes, photoisomerisation, triplet pot. energy surfaces and normal mode anal. 0-108700  
porphyrins in liquid crystal, oriented photoexcited triplets, EPR study 0-84636  
protochlorophyll, mag. reson., site selected fluoresc. detection 0-69164  
protoporphyrin IX, triplet states, flash photolysis, obs. 0-95555  
protoporphyrin IX dimethyl ester, triplet states, flash photolysis, obs. 0-95555  
pyrene, distinction of delayed fluorescence S<sub>1</sub>-S<sub>0</sub> and S<sub>2</sub>-S<sub>0</sub> by selective quenching of S<sub>1</sub>-S<sub>0</sub> 0-69175  
pyrene, triplet state, excitonic energy transfer, phosphoresc. and delayed fluoresc., 2 to 300K 0-84776  
quinones, triplet quenching by organometal cpds., time resolved CIDEP and ESR obs. 0-95654  
singlet-triplet energy difference and singlet generalised oscillator strength Lassetter-Dillon relation 0-63508  
spiropyron solutions, nitro-substituted, electronic state participation in photochromy 0-81347  
stilbene, pulsed electron excitation, triplet excitons, spectral and electrical investigations 0-92828  
1,2,4,5-tetrachlorobenzene, exciton states in crystals and dimers 0-70620  
1,2,4,5-tetrachlorobenzene, mol. solid, heat pulses, phonon-induced delocalisation of trapped excited triplet states 0-89053  
1,2,4,5-tetrachlorobenzene, triplet excitons, zero field ODMR 0-88891  
tetramethyl pyrazine in durene, phosphorescent mols., quantum beats in triplet states 0-58312  
triplet exciplexes, rapid rot., spin-selective depopulation of sublevels, heavy atom-induced mag. field effect 0-95552  
triplet exciton annihilation rate, magnetic field depend. effect of spin-lattice relaxation 0-65459  
xanthione, large zero-field splitting of lowest triplet state 0-58171  
zinc pyrochlorophyllide in nematic liquid crystals, oriented photoexcited triplets, EPR study 0-84636  
 $\mu\text{p} + \text{p}$ , elastic scattering cross section of muonic H atoms 0-69278  
Ar, excitation by pulsed electric discharge, luminescence obs., time resolved spectra meas. 0-102482  
Ar(<sup>3</sup>P<sub>0,2</sub>) + H(S), energy transfer collisions, Lyman- $\alpha$  emission profile obs., in microwave discharge and reaction cell 0-58359  
CO<sub>2</sub> lowest triplet state, Ar matrix isolation spectra 0-91569  
Cd + N<sub>2</sub>, vap., creation of inverse population of atomic Cd 6'S and 5'<sup>2</sup>P<sub>2</sub> levels 0-58219  
Cd(<sup>3</sup>P<sub>0,1</sub>) + CO(CO<sub>2</sub>)(NO), absolute quenching cross section, phase-shift method 0-58340  
Cd(<sup>3</sup>P<sub>1</sub>) radiation imprisonment lifetime, inert gas effect, phase-shift method 0-58213  
Cs<sub>2</sub>, <sup>3</sup>A<sub>2</sub>-state detect. by reson. enhanced multiphoton ionis. spectrosc. 0-95551  
Cs<sub>2</sub>, dimer and higher polymer IR absorpt. bands, triplet state 0-63629  
Cs<sub>2</sub>MX<sub>2</sub> (M=Se, Te, X=Cl, Br),  $\Gamma_4^-$ (<sup>3</sup>T<sub>1u</sub>) state, Jahn-Teller effect, luminesc. obs. 0-60650  
Cu complex, bis(triphenylphosphine) phenanthroline copper (I), luminesc. spectra, decay times 0-60648  
H<sub>2</sub>, lowest singlet and triplet states, interactions, electronic force calcs. 0-63742  
H<sub>2</sub>, triplet state, molecular polarisability, ab initio calcs. 0-63860  
HCN, intravalence triplet-triplet electronic transition, geometrical struct. and rel. energies determ. 0-99586  
H<sub>2</sub>O, mol. Rydberg S<sub>1</sub>-S and S<sub>1</sub>-T transitions, semi-empirical SCF MO calc. 0-91453  
He, 2S metastable states, singlet and triplet; two and three photon ionisation cross section, absolute determ. 0-83329  
He like atoms, dipole transitions, transition integral cancellation 0-69052  
He triplet states, doubly excited, spectrum and polarisation 0-99472  
He-like ions, triplet-state, electron impact excitation cross sections obtained by Coulomb Ochkur Rudge approx. 0-102576  
<sup>3</sup>He(<sup>3</sup>He) clusters, metastable electronic states, electron impact excitation, time of flight spectra 0-106411  
He<sub>2</sub>(1 $\sigma_g$ )<sup>2</sup>(1 $\sigma_u$ )nPa triplet levels, multichannel quantum defect anal. 0-91542  
KCl, F-centre formation at highly excited triplet states of self-trapped excitons 0-76066  
KCl, Z<sub>2</sub> centres in triplet state, EPR study 0-108068  
Li<sup>+</sup>, <sup>2</sup>P and <sup>3</sup>S states, fine (hyperfine) struct., dye laser saturation spectroscopy, beam expt. 0-58169  
NH<sub>3</sub>, mol. Rydberg S<sub>1</sub>-S and S<sub>1</sub>-T transitions, semi-empirical SCF MO calc. 0-91453  
Na<sub>2</sub>, triplet satellite band obs. in self-broadened D-line very far blue wing 0-95688  
NaBr(I), optically activated F $\rightarrow$ F' centre conversion in mag. field 0-108253  
Ne, metastable electronic states, electron impact excitation, time of flight spectra 0-106411  
Ne(<sup>3</sup>P<sub>0,2</sub>) + Ne, differential cross sections 0-58370  
Ne(<sup>3</sup>P<sub>2</sub>) elastically scattered, metastable, ang. distrib., conventional rel. to Doppler shift methods 0-58418  
Pt porphyrin in n-alkane single cryst. <sup>3</sup>E<sub>g</sub>-A<sub>1g</sub> transition, Zeeman expts. at 4.2K 0-78645  
S<sub>2</sub>, matrix-isolated, B<sup>3</sup> $\Sigma_g^-$  predissoc., relax. processes 0-58329  
Sr atomic beam, time correlations between two sidebands of reson. fluoresc. triplet, multiphoton processes 0-95570  
Yb, highly excited levels, odd and even parity spectra, multichannel quantum defect anal. 0-58133

## tritium

air contamination monitoring using centralized control (*French*) 0-63407

**tritium continued**

- N.Atlantic Ocean, deep western boundary current core,  $^3\text{H}$  conc. obs. 0-101380  
 breeding fusion blanket with boiling water coolant 0-99274  
 breeding in TFTR, tritium breeding test blanket module design 0-99304  
 breeding performance of Tokamak blankets, comparative eval. of Li,  $\text{Li}_2\text{O}$ ,  $\text{Li}_2\text{Pb}$ , 0-95398  
 cells exposed to HTO, T distrib. obs. 0-72142  
 diffusion in BCC metals, phonon-assisted quantum-mechanical tunnelling of interstitials 0-59730  
 E. coli, damage induced by T decay, secondary lethality under nongrowth conditions 0-104654  
 fusion reactor, FINTOR-D, T breeding blanket, Monte Carlo calcs. 0-99283  
 fusion reactor blanket design, effect of module size on T breeding 0-102295  
 fusion reactor solid breeder blankets for D-T reactors, operating temp. limits for T release and recovery 0-102294  
 gas, container prep. effect on growth of protium and methane impurities 0-78436  
 gas injection system transient response in TFTR 0-102337  
 glass micropheres, T-filled, assay by liquid scintillation. counting 0-63481  
 permeation through Croloy steel for LMFBR steam generator 0-68775  
 permeation through Incolloy 800 and Sanicro 31 0-88364  
 radioactive pollution from nuclear facilities, T population dose in the Northern Hemisphere 0-104779  
 recovery from liq. Li blanket by Y 0-95434  
 separation from Li at low conc. using Y for fusion reactor appls. 0-83219  
 solid breeding blanket for commercial Tokamak reactors, materials and design 0-95441  
 STARFIRE project, T handling and vacuum requirements 0-106187  
 water, deep electrolytical enrichment for T meas. behaviour of phosphate pickled mild steel electrodes 0-93764  
 $\beta$  radiative atomic recombination, antiprotonic atoms 0-83527  
 D-T, liq., dielectric constant and elec. cond. 0-84680  
 H-T solid, collision induced IR lines caused by  $T_2$  radioactivity 0-84756  
 $^2\text{H}$ - $^3\text{H}$  fuel pellet electrostatic injection (Japanese) 0-78434  
 $^2\text{H}$ - $^3\text{H}$  ionised plasma, fast  $\alpha$  particle energy deposition, transport eqn. 0-100071  
 $^3\text{H}$ - $\beta$  spectrum in valine molecule,  $m_e$  mass 0-91158  
 T+ $\text{H}_2$  reactions, accurate pot. energy surface, isotope effects, quasiclassical trajectory study 0-97698  
 T+HD, variational transition field theory and unified statistical model 0-97700  
 T+ $\text{H}_2$  reactions, accurate pot. energy surface, isotope effects, quasiclassical trajectory study 0-97698  
 T $_2$ +H(D), H-exchange studied by crossed molecular beam experiments 0-93747  
 T $_2$ +Y, high temp. equilb. meas. 0-66780

**tritium compounds**

- TOT, vibr. intensities, ab initio and empirical calcs. 0-78592  
 TOT, vibr. intensities, ab initio and empirical calcs., band strengths 0-78593

**triton interactions** *see triton-nucleus reactions***triton-nucleus reactions**

- for inelastic triton-nucleus scattering, *see "triton-nucleus scattering"*  
*see also nuclear fusion*  
 (1p), double stripping core independ. 2-nucleon transfer, Tang-Herndon effective interactions 0-73836  
 $^{48}\text{Ca}(t,p)$ , exact finite range DWBA calcs., realistic triton and nuclear wave functions 0-63191  
 $^{170}\text{Er}(t,p)$  15 MeV,  $^{172}\text{Er}$  levels, bands,  $J^\pi$  and transitions 0-83038  
 $^{56}\text{Fe}(t,p)$  pol.t., 17 MeV,  $^{58}\text{Fe}$  levels,  $J^\pi$ , anal. powers and cross sections 0-68539  
 $^{152}\text{Gd}(t,p)$ , 15 MeV,  $^{154}\text{Gd}$  levels, bands,  $J^\pi$ , DWBA anal. 0-78110  
 $^A\text{Ge}(t,p)$ , pol.t.,  $A=70,72$ , octupole oscillations modes from anal. powers,  $3_1^-$  octupole transition 0-102142  
 $^1\text{H}(t,dn)$ , 2.5 GeV/c,  $4\pi$  geometry, pole approx. description 0-68678  
 $^2\text{H}(\mu,n\mu)^4\text{He}$ , muon catalysed fusion, neutron yield, muonic molecules 0-106095  
 $^7\text{Li}(t,^7\text{Li})^1\text{H}$ , near threshold anomaly, S-matrix formalism,  $^{10}\text{Li}$  neutron binding energy (Russian) 0-105961  
 $^{90}\text{Mo}(t,p)$ , pol.t., cross section and anal. powers, struct. depend., DWBA anal. 0-78272  
 $\text{Mo}(t,p)$ , pol.t., 17 MeV,  $^A\text{Mo}$ ,  $A=98,102$ , anal. powers, transitions, shape coexistence states, DWBA anal. 0-86895  
 $\text{Nd}(t,\alpha)$ ,  $^A\text{Pm}$ ,  $A=143-153$ , odd-A, spectroscopic factors, shell model anal. 0-78137  
 $\text{Ni}(t,p)$  pol.t., 17 MeV,  $^{60,62,66}\text{Ni}$  levels,  $J^\pi$ , anal. powers and cross sections 0-68539  
 $^{16}\text{O}(t,n)^{18}\text{F}$ , 2.73 MeV, triton recoil and  $^{18}\text{F}$  yields 0-68677  
 $\text{Pb}(t,p)$ , pairing vibr. band, microscopic struct. and wave functions 0-91126  
 $^{100}\text{Pd}(t,p)$ , pol.t., cross section and anal. powers, struct. depend., DWBA anal. 0-78272  
 $^{150}\text{Sm}(t,\alpha)$ ,  $^{153}\text{Pm}$   $5/2^-$   $h_{11/2}$  dominated band, anomalous ang. distribns., CCBA calcs. 0-86788  
 $^{128}\text{Te}(t,p)$ , pol.t., cross section and anal. powers, struct. depend., DWBA anal. 0-78272  
 $^{186}\text{W}(t,\alpha)$ , pol.t., 17 MeV,  $^{185}\text{Ta}$  single proton states and rot. bands,  $J^\pi$  0-91130  
 $^{90}\text{Zr}(t,p)$ , exact finite range DWBA calcs., realistic triton and nuclear wave functions 0-63191

**triton-nucleus scattering**

No entries

**triton scattering** *see triton-nucleus scattering***tritons**

- relativistic nuclear collisions, p, d, and t inclusive energy spectra 0-63199  
 $^3\text{H}_\alpha$ , binding energy, Fadeev equation in coord. space, Lambda-nucleon potential 0-63120

**trolleybuses** *see road vehicles***troposphere**

- see also atmospheric boundary layer; tropospheric electromagnetic wave propagation*  
 aerosols, trace gases in summer, background levels in Greenland 0-72609  
 chemical modelling of lower troposphere, conference, Reston, Virginia (1978 May 15 to 17) 0-62383

**troposphere continued**

- circulation in N.Pacific rel. to sea surface temp. anomaly gradient 0-85674  
 circulation patterns, affected by stratosphere wind spring reversal date 0-82021  
 circulation patterns, influenced by stratosphere winter strength 0-82021  
 cloud condensation initiation by gravity waves 0-90159  
 dichlorofluoromethane pollution, conc. obs. in background troposphere air 0-97843  
 formaldehyde, in marine air and rainwater, wet season obs. 0-85703  
 front formation over central Europe, internal processes 0-81979  
 general circulation of midlatitude troposphere, NCAR and GFDL models 0-61856  
 geopotential height fluctuations, geographic variation of vertical struct. 0-90132  
 heating and cooling due to aerosol IR radiation scatt., calc. 0-72630  
 N.hemisphere, press. distrib. assoc. with poor summers in British Isles 0-109241  
 inclinations of atmospheric layers, determ. from sounding data (Russian) 0-72569  
 instability following solar corpuscular stream arrivals 0-109416  
 intertropical convergence zone, interaction with upper westerly waves rel. to Zambian weather during rainy season 0-90175  
 intrusion of stratosphere air mass, explanation for 'Be var. 0-98525  
 IR radiative energy exchange from six-layer general circulation model 0-101432  
 jet stream, VHF radar obs. 0-90187  
 jet stream and associated  $\text{O}_3$  enhancement (Russian) 0-94568  
 jet stream-frontal systems, pot. vorticity, role of turbulence 0-77044  
 Kelvin-Helmholtz instability, jet stream generated, radar obs. and model 0-90165  
 lunar tide in atmosphere, influence of local weather on solar modulation 0-94593  
 methane, troposphere vertical profile, eastern USA in winter 0-77035  
 methylhydroperoxide, UV absorpt. spectra of vap. 0-69159  
 minor constituents transport between troposphere and stratosphere 0-105034  
 moist convection, six-component spectral model 0-61859  
 particulate nitrate in marine air of equatorial Pacific 0-85702  
 photochemical tropospheric  $\text{O}_3$  transport, effect on pollution at rural site 0-61481  
 planetary waves, effect on eddy momentum and heat fluxes 0-85720  
 pollutant gases, monitoring from space using passive microwave techniques 0-76690  
 pollutant transport and struct., in lower troposphere 0-85319  
 radar echo mechanisms, returns from clear air 0-90181  
 radar facility, MST radar at Poker Flat, Alaska 0-90254  
 radar observations during clear air conditions, review 0-90178  
 radar observations of velocities and irregularities, spaced antenna VHF method 0-90185  
 radar signal reflection and scatt. from refr. index structs. 0-90182  
 radar techniques (VHF and UHF) for dynamic struct. 0-105078  
 radiation budget affected by  $\text{N}_2\text{O}$  and methane 0-90211  
 radiative cooling rate and flux, theory 0-85711  
 reactive N in unpolluted troposphere, stratospheric source 0-94561  
 stable layers obs. by vertical pointing VHF radar 0-90189  
 stratosphere air intrusion near tropopause break,  $\text{O}_3$  vertical distrib. study 0-94582  
 stratosphere-troposphere coupling, implications of zonal mean winds vars. and planetary waves 0-109225  
 stratosphere-troposphere exchange at polar latits. in summer, from  $\text{O}_3$  concs. meas. 0-72599  
 sulphate and nitrate mixing ratios obs. near tropopause 0-61835  
 temperature remote sensing by  $\text{O}_3$  60 GHz absorpt. 0-77172  
 tropical cyclone, intensity inferred from troposphere temp. 0-67416  
 tropopause, position identification by VHF radar, vertical pointing 0-90189  
 tropopause height rel. to sunspot activity 0-77090  
 turbulence, influence on radio-interferometric differential meas. of astrominimal coordinates 0-67581  
 turbulence struct. near tropopause, review of radar obs. 0-90179  
 Van der Waals molecules comp. of lower atmos. 0-85699  
 warnings in stratosphere, effect on troposphere 0-105031  
 waves in tropical upper troposphere, dynamical anal. 0-98388  
 waves of short-period, 13-25 km altitude, Doppler radar obs. 0-90192  
 westerly upper air troughs, rel. to western disturbances development over India 0-90173  
 wind, radar obs. made at Kwajalein Atoll, equatorial Pacific 0-90188  
 wind at 300 mb, scale-interaction study with horiz. filtering method 0-98423  
 wind meas. with clear air Doppler radar, vertical component 0-72642  
 wind measurement by radar, method for reducing backscatt. data 0-90257  
 wind profile in troposphere and stratosphere, using Poker Flat MST radar 0-72579  
 wind structure over Antarctica 0-81992  
 wind velocity indicated by cumulus motion across sky 0-98418  
 winds in upper troposphere/lower stratosphere rel. to satellite-derived radiance gradient 0-98447  
 $\text{CO}$ , troposphere vertical profile, eastern USA in winter 0-77035  
 $\text{H}_2$  mixing ratio over N.Atlantic 0-77057  
 $\text{HNO}_3$  in marine air of equatorial Pacific 0-85702  
 $\text{H}_2\text{O}$  isotopic sampling apparatus for troposphere (French) 0-94614  
 $\text{H}_2\text{S}$  in troposphere, photochem. production reactions 0-90112  
 $\text{H}_2\text{SO}_4$  aerosols, heterogeneous atmospheric reactions and role as tropospheric sinks 0-72612  
 N fixation by lightning 0-90147  
 N fixation in lightning channels, theory 0-90148  
 $\text{NH}_3$  fluxes into free atmosphere over W.Germany evaluation 0-94132  
 $\text{NH}_3$ , vertical distrib. by photochem. model 0-85701  
 $\text{NH}_3$  vertical profile, daily and seasonal variation 0-85700  
 $\text{NO}_3$ , detect. in polluted troposphere by differential optical absorpt. 0-77036  
 $\text{NO}_3$  in troposphere, obs. of content in mountain air 0-72582  
 $\text{O}_3$  budget, effect of lower stratosphere  $\text{O}_3$  net vertical flux 0-101402  
 $\text{O}_3$  conc. rel. to general weather situation 0-101397  
 $\text{O}_3$ , evidence for significant in situ photochemical source 0-72619  
 $\text{O}_3$ , obs. of meridional flux by transient eddies in 0 to 30 km height range 0-109224  
 $\text{O}_3$ , partial press. profile over Uccle, Belgium, April-June 1979 obs. (French, Flemish) 0-98385



**troposphere** continued

- O<sub>3</sub>, partial pressure profile over Uccle, Belgium, 1979 obs. (*French, Flemish*) 0-94571  
 O<sub>3</sub> transport mechanisms, general circulation model 0-109196  
 OH+gaseous S compounds, lower atmos. chem. 0-61870  
 S aerosol, of S. American troposphere 0-67401  
 SO<sub>2</sub> oxidation to sulphate in troposphere, model predictions 0-81963

**tropospheric electromagnetic wave propagation**

- angular scattering of water drops and ice particles [electromagnetic interference], freq. above 10 GHz appl. 0-109183  
 clear air radar returns, review of obs. 0-90178  
 clouds, radar reflectivity rel. to cloud dynamics and microphysics 0-61877  
 ducted EM wave propagation, roots of modal eqn. 0-72607  
 extinction cross section for single particles at 100 GHz 0-82116  
 hailstorm, finger radar echoes, form. mechanism (*Chinese*) 0-109234  
 IR transparency window, 10-13  $\mu$ m, H<sub>2</sub>O and aerosol effects in winter and summer (*Russian*) 0-105048  
 long-distance propag., multiple scatt. effect 0-109229  
 microwave attenuation due to precip. of water vapour in atmosphere, meteorological data, raindrop spectral distrib. (*German*) 0-90176  
 microwave propagation at 10, 11 GHz, radiometric measurement of rain attenuation 0-67397  
 nonuniform radio wave guide, coupled mode anal. 0-94587  
 photodissociation fluxes, tropospheric and stratospheric, Mie scatt. contrib. improved model 0-77103  
 precipitation properties using radar polarisation techniques 0-61925  
 radar echo mechanisms, returns from clear air 0-90181  
 radar echoes from distributed targets, averaging of time, angle and range 0-109264  
 radar reflectivity profile classified by rain types 0-101420  
 radar scatter from waves of short-period, 13-25 km altitude 0-90192  
 radar signal reflection and scatt. from refr. index structs. 0-90182  
 radio communication, book 0-62400  
 radio waves, propag. rel. to radar-interferometric differential meas. of astronomic coordinates 0-67581  
 radiothermal sounding of press. and geopotential (*Russian*) 0-77038  
 radiowave propagation in troposphere waveguide, effect of elevated M-inversion 0-90195  
 radiowave propagation studied by FM-CW radar 0-90186  
 rain attenuation, radiometric determ. at millimetre wavelengths, multiple-scatt. effects metric determ. at millimetre wavelengths, multiple-scatt. effect 0-90260  
 rain attenuation above 10 GHz, regression curves for tropical areas, telecommunication, broadcasting systems appl. 0-90111  
 rain attenuation above 11 GHz, radar links appl. 0-98410  
 rain attenuation prediction methods comparative analysis, radiowave propagation appl. 0-109182  
 semi-empirical theory 0-90220  
 trans-horizon propagation path over sea, transmission loss due to ducting at 1.8 GHz 0-105041  
 water vapour studies at 22.235 GHz using microwave radiometer 0-72610

**truth tables** see logic design**TSC** see thermally stimulated currents**TSCD** see thermally stimulated currents**TSD** see thermally stimulated currents**tubes (electronic)** see electron tubes**tuners** see tuning**tungsten**

- see also nuclei with .....  
 (100), H adsorbate low energy electron vibrational excitation 0-84375  
 (110) surface, conduction electron interaction with diffracting electrons (*Russian*) 0-79643  
 adatoms on (110), substrate strain induced interaction 0-96744  
 adsorbed H on (100) surface, angle-resolved and variable impact energy electron vibr. excitation spectroscopy 0-76119  
 adsorbed O, surface diffusion, secondary electron emission study 0-76117  
 adsorbed on W(001), struct., FIM obs. 0-103576  
 adsorbed on W (110), long range interatomic interactions with coadsorbed Pd 0-59789  
 adsorbed Xe on (110) plane, mobility and two-dimens. compressibility, field emission current fluctuation method 0-80089  
 adsorbed He layer, accommodation coeffs. calcs. 0-66866  
 adsorption, of Ba and Ti, work function meas. 0-100411  
 adsorption of Be on (110) surface, film growth and struct. 0-75477  
 adsorption of Dy, Ho, Er, field emission electron study 0-100393  
 adsorption of I on (100) at room temp., LEED and AES study 0-84389  
 adsorption of N<sub>2</sub> on (001) surface, effect on LEED electron spin polarisation and intensity profiles 0-65377  
 adsorption of NO and NO<sub>2</sub>, FEM obs. 0-84390  
 adsorption-desorption behaviour of KCl on (110) and (111) surfaces 0-75442  
 atom, high resolution phase contrast electron microscopy imaging 0-103224  
 atom, multiphoton ionisation and absorpt. 0-95575  
 atomic density, effect on proton energy loss and dechannelling 0-65088  
 BCC, interaction energy between self-interstitial and screw dislocation, calc. 0-70248  
 chemisorbed H<sub>2</sub>, vibr. spectra charact., adsorption sites 0-70535  
 chemisorption of cyclic hydrocarbons on (100) surface 0-59782  
 clustering of adsorbed Kr, He desorption spectrometry 0-77908  
 coadsorption of Ba and Cu atoms, work function changes 0-65378  
 coadsorption of La and B, field emission and field ion microscopy 0-104049  
 composite W-PVC material, fabrication and performance, acoustic properties 0-76218  
 condensation of Cu and Ag on (100), early stage comparison with Mo(100) 0-80072  
 deformed, surface layer struct. effect on polygonisation and recryst., X-ray diff. anal. and metallographic exam. (*Russian*) 0-84948  
 desorption, of Cs-O<sub>2</sub>, activation energy 0-103562  
 desorption, photon-stimulated, angle-resolved, of O<sup>+</sup> from (111) surface 0-88434  
 diatomic cluster migration on W {100} plane, elementary displacement steps 0-88436  
 diffusion of Li, Cs, vacancy and divacancy mechanisms (*Russian*) 0-70472

**tungsten** continued

- dispenser cathodes, Ba-activated, surface charact., ion scatt. spectrometry and SIMS study 0-66377  
 elastic wave scatt. from oblate spheroidal WC inclusion 0-65151  
 electrical resistivity, quadratic contrib., 2 to 40K (*Russian*) 0-92874  
 electrode reactions with molten glass 0-85186  
 electrodes, C segregation and arc damage 0-64795  
 electron stimulated desorption of O from (110) stepped surface, atomic steps and defects influence 0-80091  
 electron stimulated desorption patterns from O<sub>2</sub> on (100) and (111), computer simulations 0-75443  
 electron-channelling patterns, crit. voltage effects 0-79647  
 emissivity, total hemispherical, of W (100), sensitivity to O<sub>2</sub> adsorption 0-79964  
 enhanced penetration of low energy He along (100) channel 0-65093  
 enthalpy, relative, 273 to 1173K, electronic heat capacity coeff. 0-103496  
 epitaxy on W(110) substrate, work function meas., LEED investigation 0-80103  
 fibre reinforced Cu composites, correl. between thermal cycling-induced microstructural changes at interphase boundaries and tensile behaviour (*Japanese*) 0-71674  
 field emission, mag. field effects 0-93463  
 field emission anomalies in mag. field (*Russian*) 0-93462  
 field emitter, Cs VPE, FEM obs. 0-70552  
 filament lamp, polarization characteristics 0-95970  
 film, support, for electron microscopy, Fourier spectrum analysis of phase contrast 0-95199  
 film, surface RF impedance in strong mag. fields (*Russian*) 0-92920  
 films, vac. evaporated, optical cond. 0-76100  
 fine tip cathode, field emission stability, rel. to passivation 0-100760  
 ISSEC selection for fusion reactor 0-57950  
 laser heating in air by obliquely incident radiation 0-71815  
 liquid, elec. resist., melting pt. to boiling pt., temp. depend. 0-96839  
 longwave dopplers, nonlocal Hall effect, surface impedance, size effect (*Russian*) 0-80253  
 luminescence characteristics of pure surfaces acted on by flux of field emission electrons 0-100695  
 molten drop break up in gas flow, surface drag, capillary excitation (*Russian*) 0-100024  
 monocrystals in alkaline electrolyte, surface orientation, effect on anode current (*Russian*) 0-75360  
 needle crystal growth, discharge-induced decomp. of hexacarbonyltungsten mols. 0-84414  
 needles, mechanism of cathodic growth, decomp. of W(CO)<sub>6</sub> under high field conditions 0-76162  
 neutron sources with 10 MeV electron beams 0-83231  
 oxidation, WO<sub>3</sub> amorphous anodic film growth in acidic soln. 0-81232  
 oxidation mechanism, 773 to 973K 0-108644  
 particle formation, ultrafine, via pulsed laser breakdown of W(CO)<sub>6</sub> 0-84881  
 phonon dispersion relations, modified tensor force model 0-103428  
 photon and electron stimulated desorption ion energy and angular distributions for O<sup>+</sup> 0-96734  
 plane {123}, clean and H saturated, surface diffusion of single W atoms 0-80081  
 plasma arc spraying, chem. reaction with plasma gases 0-66427  
 plastically deformed single cryst., mag. susceptibility (*Russian*) 0-93074  
 PLED results for W (100) using appl. of GaAs spin-polarized electron source 0-69000  
 polishing technique as prep. for TEM 0-71851  
 porous, chromising 0-100959  
 powder, gas adsorption and desorption (*Russian*) 0-75429  
 powder preparation by WO<sub>3</sub> reduction in H plasma jet (*Russian*) 0-76211  
 proton-induced L-shell ionisation cross-sections 0-100707  
 radiation generation in Tokamak, Ag I isoelectronic sequence identification 0-83981  
 resonant and nonresonant conduction-electron-spin transmission 0-75857  
 ribbon-filament temperature lamps, radiation error estimation 0-64128  
 self-diffusion, high temp. bulk modulus determ. 0-79976  
 self-weldability in high temp Na (*Japanese*) 0-89392  
 SEM expts., anomalous patterns (*Chinese*) 0-59349  
 single cryst., high temp. creep and dislocation struct. 0-71715  
 sputtering, low energy, H, D and He ions 0-100734  
 sputtering damage due to low-energy ion bombardment, depth of damage, FIM obs. 0-60734  
 sputtering yields, ang. distrib. and differential, for low-energy light-ion irradi. 0-71527  
 stacking fault stability determ. 0-96548  
 substrate, deposition of Au film, interface struct., FIM obs. 0-65384  
 substrate for Ag, UHV-SEM studies of Stranksi-Krastanov growth 0-79722  
 surface, (001), and crystal-atom, energy positron diffraction, theoretical study 0-84034  
 surface, (001), electronic surface reson. and thermally induced struct. transition 0-88614  
 surface, (100), chemisorbed H,  $\nu$ , vibrational mode, IR study 0-60582  
 surface, (100), instability, distortion and dynamics 0-84360  
 surface, (100), photon and electron stimulated desorpt. of O 0-100397  
 surface, (100) adsorbed N<sub>2</sub>, vibr. spectra, bonding struct., LEED study 0-84387  
 surface, (100) and (110), theoretical Debye-Waller factors 0-92773  
 surface, (110), chemisorpt. effects on dielec. function, refl. spectra 0-75616  
 surface, (110), low energy ion scatt. features, inelastic loss and surface crystallography 0-66371  
 surface, (110), Pd coadsorbed with Re, W, long range interatomic interactions 0-59789  
 surface, (110) plane, tunnelling of H in surface diffusion 0-75416  
 surface, adsorbed CO, electron-stimulated desorption, photoemission, relax. energy 0-100401  
 surface, adsorbed CO, electron-stimulated ion desorption 0-59797  
 surface, adsorbed gases, field desorption from field ion tips 0-59793  
 surface, adsorbed Hg, thermal desorption kinetics, theory 0-59792  
 surface, adsorbed K layer, field emission flicker noise power 0-59795  
 surface, Ar beam direct inelastic scatt., vel. distrib. meas. 0-66351  
 surface, direct inelastic and trapping-desorpt. scatt. of N<sub>2</sub>, elementary steps in N<sub>2</sub> chemisorpt. 0-60737  
 surface, He, Ne, tangential momentum accommodation coeff. meas. by acoustic vel. and absorpt. obs. 0-66867

## tungsten continued

- surface, physisorbed  $O_2$  layer,  $Ar^+(Ar^{+m})(Ar^{2+})$  impact, electron emission obs. 0-60740  
 surface, polycryst., heat of desorption of Cs 0-75430  
 surface, polycryst.,  $N_2$  adsorption states 0-100404  
 surface, pulsed laser atom-probe FIM, expts. 0-66402  
 surface [100], anisotropy of inelastic electron refl., energy loss effects 0-79642  
 surface (001), displacive transition, H adsorpt. effects, theoretical model 0-65352  
 surface (001) states and surface resonances, self-consistent electronic struct. 0-96960  
 surface (100) reconstruction kinetics in presence of O half-monolayer 0-65375  
 surface (110), Pd adsorbed layer, growth, struct., stability, desorption 0-59794  
 surface (111), field adsorption of He, array model 0-59800  
 surface adsorbed W, Ga, Sn, struct., FIM obs. 0-103576  
 surface adsorption processes following electron excitation, cathodoluminescence studies 0-100390  
 surface dipole moment calc. 0-60060  
 surface ionisation of  $SF_6$ , laser irradi. effects 0-93440  
 surface self-diffusion, ion impact induced, FIM study 0-103549  
 surface structure, pseudo-relativistic LEED calcs. and R-factor anal. 0-70510  
 surface-atom polarisability derivation from field-ion energy deficits 0-76155  
 thermal expansion reference data: 1-1000K 0-96669  
 thermionic emission and work function, dislocation effects, for single crystals. 0-76129  
 thermophysical data at high temps., submicrosecond-pulse-heating method 0-103459  
 tip, [310], prep. from rolled sheet 0-97447  
 vacancy structure in near surface depleted zone following ion bombard. 0-70267  
 vapour deposited, dislocation struct., rel. to texture (*Russian*) 0-65394  
 volt ampere characteristics during electron melting process (*Russian*) 0-75336  
 wire, AKS-doped, second phase particle obs. by TEM, SEM and atom probe microanalysis 0-108457  
 wire, struct. and high-temp. creep, dopant elements influence 0-66603  
 wire, US inspection, immersion method 0-66757  
 work function measurement in SEM 0-80918  
 XPS, angle-resolved, from valence bands, obs. of strong temp. depend. and direct-transition effects 0-60752  
 Z dependence of thick target  $\beta$ -ray backscattering 0-76118  
 Au-W-GaAs Schottky barrier, elec. and chem. props., AES 0-96973  
 Cs/W, work function measurement in SEM 0-80918  
 GaAs:W<sup>2+</sup>, radiative transitions, photoluminesc. obs. 0-108271  
 Mo, film on sapphire substrate, orientational growth, epitaxial textures, nucleation textures (*Russian*) 0-75454  
 W bicrystals, crack propag. across grain boundaries, crack speed meas. technique appl. 0-108575  
 W<sup>3+</sup> field ion evaporated from ionic bonding states, appearance energies 0-89125  
 W<sup>3</sup>He, implanted ion positions, determ. using mol. deuteron beam 0-70240  
 W/Cu, Stoneley waves at (001) interface between cubic symm. cryst. 0-100388  
 W-EuS, amorphous, memory effect in field emission 0-89126  
 W-Zr field emitter, time-of-flight atom-probe study 0-80949  
 W(100) TF electron emitters props. obs. 0-66403  
 Zr-O-W (100) thermal field emitters, operational experience 0-71576

## tungsten alloys

see also tungsten compounds

- brittle alloy rolling, contact stresses (*Russian*) 0-93576  
 Hastelloy, C-276, H-induced crack growth 0-71747  
 Hayes alloy no.716, Fe-Cr-Ni-Co-W-Mo-Si-C-B (26, 22, 12, 3.5, 3, 1.2, 1.1, 0.4 wt.%), hardfacing alloy 0-100802  
 steel, 12% W, eutectic carbides struct. and comp. during heating 0-76283  
 steel, Cr-Mu-W, carbide form., W effect 0-76259  
 steel, Cr-W-Mo-Co, high-speed, from atomised powders, mech. and cutting props. 0-66556  
 steel, microstruct. and hardness, splat quenching effect 0-76293  
 steel, W-Mo-Co, high-speed tool, struct. and props., cooling rate effect at primary crystn. temp. 0-76241  
 steel, W-Mo-Cr-V tool, laser surface melted, struct., heat treatment effect 0-76424  
 steel turbine casings, residual life determ. 0-93585  
 Stellite, self-weldability in high temp Na (*Japanese*) 0-89392  
 stellite hardfacing materials, friction characts. in high temp. Na (*Japanese*) 0-89356  
 Stellite-6, XPS obs. of aqueous oxidation, surface comp. and gaseous oxidation effect 0-81238  
 C/Pt-W (8 wt.%), desorption of K from C film surfaces 0-59784  
 Co-W alloy electrodeposition, influence of  $MgSO_4$  and gum arabic additives (*Russian*) 0-80991  
 Co-W alloy electrolytic coatings, heat treatment effects on coercivity, hysteresis and structure (*Russian*) 0-60381  
 Co-WC hard alloys, rapidly quenched struct. 0-76233  
 Cr-W, anodic dissoln. at high current densities (*Russian*) 0-76395  
 Cr-W-O, phase relations, thermodynamic props. of  $CrWO_4$  and  $Cr_2WO_6$  0-104120  
 Fe-Ni-Co-W (18.65, 8.99, 4.87 wt.%), ageing characts., 380-530°C 0-60876  
 Fe-Ni-Cr-Al-Ti-W-Mo (35, 15, 2.4, 2.3, 2.2 wt.%) wrought superalloy, freckles (*Chinese*) 0-104137  
 Fe-W, Gibbs energy of form. of phases (*German*) 0-97724  
 Fe-W, thermophysical props. and elec. cond., temp. depend. 0-96842  
 Fe-W-Cr-Mo system, mag. and mech. props. rel. to production methods (*Japanese*) 0-71107  
 Ir-W (0.3%), grain boundary comp., trace element additions effect 0-66661  
 Mo-W (30 wt.%), wrought, fracture, characteristic features 0-104278  
 Mo-W alloy type MW25N, crystallisation form, globular dendrites, grain boundaries (*Russian*) 0-66494  
 Mo-W-N system, nitrated annealed samples, W replacement of Mo 0-76227

## tungsten alloys continued

- Nb-W-Mo-Zr (5, 2.1, 0.92 wt.%), creep resist., high temp. ageing in vacuum 0-71716  
 Nb-W-Si, ductile amorphous, superconductivity 0-60131  
 Nb-W-Zr-N alloy, with dispersed second phase, ductile-brittle transition 0-93653  
 Nb-W-Zr-Ta (90, 4.5, 3.5, 2 wt.%) creep and creep limit in super vac. at 1100°C, heat treatment effect 0-81133  
 Ni-Co-W, electrodeposition, surface morphology and cryst. struct. 0-71602  
 Ni-Cr-Co-Al-W-Mo-Ti-Ta, heat resist. and struct., Ta effect 0-76312  
 Ni-Cr-Co-Ti-Mo-W-Al (14, 9.8, 5, 4, 3.9, 3 wt.%), low cycle fatigue, prior heat treatment effect 0-60962  
 Ni-Cr-Mo-W-Al-Ti, heat-resist., phase comp. 0-76250  
 Ni-Cr-W, oxidation behaviour in air at 1000-1250°C 0-89407  
 Ni-Cr-W-Co granules type ZhS6U, EP741, hot hydrostatic pressing 0-60796  
 Ni-Cr-W-Co-Ti, thermal fatigue, effects of inclusions 0-81183  
 Ni-Cr-W-Co-(Al)(Ti)(Mo), high-temp. sulphide corrosion 0-76408  
 Ni-Cr-W-Mo-Ti-Al, heat-resist., recovery and recrystn. 0-76268  
 Ni-Mo-W, diagram of state, W solubility, dispersion hardening (*Russian*) 0-66477  
 Pd-W, substrate temp. influence on shallow contact formation on Si 0-96963  
 Pd<sub>1-x</sub>W<sub>x</sub>, calc. of short-range order parameters from X-ray scatt. data (*Russian*) 0-75367  
 Pt-W, substrate temp. influence on shallow contact formation on Si 0-96963  
 Rh-W disc bonded to graphite, for X-ray tube rotary anodes (*German*) 0-105760  
 Si-Fe-W, dil. alloy, compositional changes on sputtering, projectile energy depend. 0-66362  
 Ta-W, thermoelec. power, 4.2 to 300K 0-70684  
 Th-W, TF electron emitters props. obs. 0-66403  
 Ti-W films, bias-sputtered, quantitative anal. 0-80114  
 TiC coated WC-Co cemented carbides, fracture toughness 0-85046  
 TiW-TiO<sub>2</sub>-InP thin refractory MIS struct. deposition 0-75647  
 Ti<sub>10</sub>W<sub>90</sub>, thermal annealing study of metallisation on Si 0-80134  
 W-Cu (92.8, 7.2 wt.%), liq.-phase sintered, embrittlement and interfacial impurity segregation 0-66647  
 W-Cu pseudobinary, porous, chromising 0-100959  
 W-Ni-Fe system, reduction kinetics and alloy form. 0-60801  
 W-Ni(Co) point-contact diodes as harmonic generators and mixers, DC bias dependence 0-75653  
 W-Re alloys, thermal EMF instability, heat treatment effects 0-75553  
 W-Re amorphous alloys, phase-slip and localisation diffusion lengths 0-107747  
 W-Re films, amorphous, one-dimensional quantum localisation 0-80413  
 WC/Co cemented carbides, fracture toughness testing 0-104410  
 WC-Co, contact reaction with BN at high pressures 0-61029  
 WC-Co, STEM anal. of grain boundaries 0-79644  
 WC-Co alloys, fracture toughness model 0-84243  
 WC-Co hard alloys, hot-pressed, wear resist. under abrasive friction, heat treatment effect 0-66555  
 WC-Co sphere, erosion of Al by solid particle impingement at normal incidence 0-104304  
 WC-Ni hard alloy composite, sintered, void healing 0-60821  
 W<sub>50</sub>Fe<sub>50</sub> glassy alloy, refractory, triode sputtered 0-75185  
 W<sub>70</sub>Si<sub>20</sub>B<sub>10</sub>, amorphous alloys obtained by liq. quenching, superconductivity 0-75670

## tungsten compounds

see also tungsten alloys

- tungstates, alkaline earth, U activated, scheelite struct. luminesc. props. vibr. modes and quenching temp. 0-60651  
 tungstates, U-doped, perovskite struct., luminesc. quenching, QMSCC calcs. 0-71470  
 BaO-WO<sub>3</sub>-P<sub>2</sub>O<sub>5</sub> glass, struct. and IR spectra 0-64914  
 Ba(PO<sub>3</sub>)<sub>2</sub>-WO<sub>3</sub>, electron-absorpt. spectra and structure of W centres 0-88873  
 Fe-W-O(C), Gibbs energy of form. of phases (*German*) 0-97724  
 LaCrO<sub>3</sub>-W eutectics, prep. and microstruct. 0-108380  
 La<sub>10</sub>W<sub>2</sub>O<sub>31</sub>, enthalpy and heat capacity at high temp. 0-70424  
 α-La<sub>2</sub>WO<sub>6</sub>, enthalpy and heat capacity at high temp. 0-70424  
 La<sub>6</sub>W<sub>2</sub>O<sub>15</sub>, enthalpy and heat capacity at high temp. 0-70424  
 Li-W<sub>2</sub>O<sub>5</sub>, electrochem. and chem. Li incorporation, cryst. struct. 0-88131  
 Mo<sub>5</sub>W<sub>5</sub>Se<sub>2</sub>, single cryst. vapour growth, characterisation 0-93466  
 Nb<sub>2</sub>O<sub>5</sub>-WO<sub>3</sub> system complex cpds. with TTB type subcells, H<sub>2</sub> superhigh resolution electron microscopy obs. of struct. 0-103311  
 PbO-WO<sub>3</sub>-Mo system, M=Ca, Ba, Mg, Sr, perovskite type cpds. detection 0-108404  
 Pb(Z,Ti,Mg,W)O<sub>3</sub>, low-Q ceramics, props. and transducer appl. 0-75944  
 V-W-O system, phase diagram and thermodynamic props. at high temps., in region W-WO<sub>3</sub>-VO<sub>2</sub>-V<sub>2</sub>O<sub>5</sub> 0-104133  
 (W, Mo)C, hard-facing applications, effect of Mo on struct and hardness of WC 0-108474  
 WB, abrasive, effect on machinability of Ti alloys (*Russian*) 0-97593  
 W<sub>2</sub>B<sub>8</sub>, abrasive, effect on machinability of Ti alloys (*Russian*) 0-97593  
 WC, explosive plasma sputtered coatings, struct. and props. (*Russian*) 0-100783  
 WC, sinterability of ultrafine powders obtained by CVD method 0-108378  
 WC, sputtering, low energy, H, D and He ions 0-100734  
 WC-Co DC and RF sputtered coatings, bias effect, struct., X-ray-Auger study 0-70565  
 W(CO)<sub>6</sub>, decomp. under high field conditions, cathodic growth of W needles 0-76162  
 W(CO)<sub>6</sub>, MCD spectra, charge transfer transitions 0-95658  
 W(CO)<sub>6</sub>, photodissoc., W prod. 0-95575  
 WCr<sub>2</sub>O<sub>6</sub>, exchange interactions within binuclear entity (Cr<sub>2</sub>O<sub>10</sub>)<sup>4-</sup> 0-60236  
 WCs, preparation method effects on catalytic activity for H<sub>2</sub> evolution 0-101024  
 WF<sub>6</sub>, CW CO<sub>2</sub> laser spectroscopy 0-83367  
 WO<sub>2</sub> film characterisation technique, APFIM, time-of-flight spectroscopy 0-75138  
 WO<sub>3</sub>, acoustic instability near monoclinic orthorhombic phase transition, X-ray scatt. 0-65215  
 WO<sub>3</sub> amorphous anodic film growth on W in acidic soln. 0-81232  
 WO<sub>3</sub> electrodes, electrochromic processes, digital simulation model 0-76518



**tungsten compounds continued**

- WO<sub>3</sub>, electronically induced lattice distortion, screening effect on vibr. 0-75356  
 WO<sub>3</sub> film, amorphous, struct. and crystn., TEM obs. 0-103606  
 WO<sub>3</sub> film, Au surface layer effect on electrochromic behaviour 0-76004  
 WO<sub>3</sub> film, electrochem. injection kinetics of Li, LF AC meas. 0-57339  
 WO<sub>3</sub> polymorph, hexagonal, cryst. struct. imaging by high-resolution electron microscopy 0-103309  
 WO<sub>3</sub>, reduced, elastic strain energy in cryst. shear planes 0-75239  
 WO<sub>3</sub>, reduction, defect role, in situ HVEM obs. 0-81323  
 WO<sub>3</sub>, reduction, in H plasma jet, W powder prep. (Russian) 0-76211  
 WO<sub>3</sub>, semicond. anode in aq. electrolyte, electrochem. and electrochem. 0-76080  
 WO<sub>3</sub>, semiconductor-metal transition, structural phase transition 0-107870  
 WO<sub>3</sub> smoke particles prepared by gas evap., morphology and coalescence growth 0-97738  
 WO<sub>3</sub> substrate, Li<sub>3</sub>N film, vacuum evaporation, retarded deposition 0-108351  
 WO<sub>3</sub> thin film, Li diffusion, appl. of AC techniques 0-70468  
 WO<sub>3</sub>-B<sub>2</sub>O<sub>3</sub>-ZnO semiconducting glasses, DC cond. and optical absorpt. 0-107783  
 WO<sub>3</sub>-electrolyte electrochromic cells, proton injection phenomena 0-71448  
 WO<sub>3</sub>-LiI, solid-state electrochromic cell, fabrication and characts. (Japanese) 0-84717  
 WO<sub>3</sub>-NiCO<sub>3</sub>-Fe<sub>2</sub>O<sub>3</sub>, reduction alloy form. 0-60801  
 WO<sub>3</sub>-P<sub>2</sub>O<sub>5</sub> glass, AC cond. and dielec. props. 0-92717  
 WO<sub>3</sub>+CuO, solid state reaction kinetics, CuWO<sub>4-x</sub> formation study 0-66796  
 WO<sub>3</sub>, anodic oxide films, quadratic electro-optic and electrostrictive effects, ellipsometry 0-108184  
 WS<sub>2</sub> (2H), layered cpd., Raman scatt. 0-103960  
 WS<sub>2</sub> solid lubricant, antifriction and elec. props. depend. on oxidation temp., dopant influence 0-108584  
 WSe<sub>2</sub>, chem. vapour transport growth, microstruct. develop. 0-103278  
 n-WSe<sub>2</sub>, electrode in aq. iodide medium, high efficiency photoelectrochemical solar cell 0-72069  
 WSi<sub>2</sub> film, elastic stiffness and thermal expansion coeffs. 0-107451  
 WSi<sub>2</sub>, refractory formation by As<sup>+</sup> ion beam bombardment 0-107286  
 WSi<sub>2</sub>, sputtered, props. for MOS IC appl. 0-70831  
 WSi<sub>2</sub>, steam-oxidized, Auger sputter profiling studies 0-107663  
 WY<sub>2</sub>O<sub>6</sub>, exchange interactions within binuclear entity (V<sub>2</sub>O<sub>10</sub>)<sup>14-</sup> 0-60236  
 WY<sub>2</sub>O<sub>6</sub>, magnetic susceptibility, behaviour in terms of quasi-isolated binuclear units 0-97073  
 α-W<sub>2</sub>O<sub>5</sub>, paramag. defect study by ESR 0-103881  
 YCrO<sub>3</sub>-W eutectics, prep. and microstruct. 0-108380

**tuning**

- see also laser tuning; receivers; resonance*  
 acousto-optical noncollinear UV tunable filter 0-102832  
 birefringent filter mechanical tuning techniques 0-102834  
 education, vibrating string, tuning guitar by television 0-73134  
 electro-optical polarisation conversion and interference tunable filters 0-102829  
 electro-optical tunable filters, programmable 0-102830  
 multicavity IR electro-optical tunable filter 0-102831  
 resonators of H masers, automatic 0-95859  
 semiconductor Fabry-Perot interferometer retuning by optical excitation (Russian) 0-98970  
 US transducers array, transducer elements tuning 0-87684  
 H maser autotuning systems, theoretical anal. based on freq. or phase method 0-83575  
 TeO<sub>2</sub> acousto-optical tunable filter with microcomputer control 0-102833

**tuning forks** *see vibrating bodies***tunnel diode oscillators**

- <sup>3</sup>He gas thermometer secondary standard for 0.5 to 40K 0-82762

**tunnel diode storage devices** *see semiconductor storage devices; tunnel diodes***tunnel diodes**

- see also tunnelling*  
 MIS structures, photovoltaic energy conversion, band struct. 0-92995  
 MIS tunnel diode, minority-carrier, pot. barrier height 0-96998  
 MIS tunnel structure, injection and extraction effects, self-consistent model 0-92996  
 phototransistors accompanied by impurity scatt. 0-107901  
 quantum noise at low temperature 0-103733  
 AlGaAs p-n diodes, I-V characts., tunnelling 0-100510

**tunnel effect** *see tunnelling***tunnel triodes** *see thin film transistors***tunnelling**

- see also superconductive tunnelling; tunnelling spectra; tunnelling spectroscopy*  
 alkali halides, doped, thermal expansion at low temps. 0-96672  
 associated liquids, mechanism of structural dielectric relaxation 0-107034  
 atom+diatom reactions, semiclassical tunnelling probabilities, trajectory calc. 0-71886  
 barium stearate single-layer Langmuir films, elastic and inelastic tunnelling 0-80403  
 cyanine dye monolayer assemblies with Al and Ba electrodes, photovolt., dark cond. and photocond. 0-80400  
 diatomic molecule, neutron scatt. induced electronic transitions, tunnelling 0-63844  
 p-dichlorobenzene-p-dibromobenzene mixed crystals., triplet exciton migration, time resolved emission spectroscopy 0-89052  
 dipole pseudo-spin glasses, collective excitations 0-59617  
 disordered materials, fluctuation-induced tunnelling cond. 0-65516  
 disordered systems, spontaneous echoes, spectral diffusion decay 0-84270  
 double well damped motion, proton tunnelling, transfer rate temp. depend. (German) 0-87058  
 electron tunnelling, thermal and photoassisted, theory, fast charge separation in photosynthesis 0-89730  
 electronic energy distrib., Schrodinger wave eqn. solutions 0-103743  
 ferroelectric, H-bonded, central peak, thermal cond. 0-93250  
 ferroelectrics, order-disorder, displacive transformations, tunnelling, phonons 0-75975  
 field-evaporated ions, post-ionisation by tunnelling into substrate 0-80951  
 glass, thermal expansion at low temps. 0-96672  
 glasses, non-radiative recombination at valence-alternation pairs 0-89048

**tunnelling continued**

- IR point-contact diode tunnelling and rectification rel. to electrode geometry 0-57378  
 metal, H(D) diffusion, role of tunnelling, reson./nonreson. approaches 0-59718  
 metal-barrier-metal diodes, I-V characts., nonlinear mechanism in low voltage region 0-88618  
 metal-semiconductor interface, photoelectron injection, quantum mech. transmission and optical phonon scatt. 0-84511  
 metal-tunnel oxide-Si junctions, processing condition depend. 0-80380  
 metal-vacuum-metal point contact junction characts., Green's function calc. 0-103744  
 metallic glass, tunnelling states, struct. model 0-70137  
 metallic glasses, tunnelling two-level system, Kondo-like state 0-88547  
 metals, BCC, diffusion of H<sub>2</sub> and its isotopes, phonon-assisted quantum-mechanical tunnelling of interstitials 0-59730  
 metals, surface positronium formation, stopping distance, positron-phonon interactions 0-96582  
 methane-d<sub>4</sub>, solid, rot. tunnelling, neutron scatt. obs., isotope effect 0-92468  
 methane-d<sub>4</sub>, solid, tunnel splittings, heat capacity meas. 0-96451  
 methyl groups, spin symmetry species, neutron scatt. transitions 0-92470  
 4-methyl-2,6-di-tert-butylphenol, methyl group reorientation, classical dynamics, NMR relax. and inelastic neutron scatt. 0-88066  
 methyl-d groups, reorienting or tunnelling spin-lattice relax. 0-97156  
 methylcyclohexane glasses, γ-irradiated in presence of naphthalene, isothermal luminesc. 0-93388  
 3-methylpentane glasses, γ-irradiated in presence of naphthalene, isothermal luminesc. 0-93388  
 MIM, structure, resonant tunnelling, IV characteristics, comments 0-70847  
 MIM, thin film, use as non-heated source of electrons, review 0-84516  
 MIM structures, analytical expressions for tunnel currents 0-60064  
 MIM tunnel junction, magnetically doped, hopping model of zero-bias tunnelling anomalies, comparison with expt. 0-65703  
 MIS structures, analytical expressions for tunnel currents 0-60064  
 MIS structures, photovoltaic energy conversion, band struct. 0-92995  
 molecular chain, 1-D electron motion, electron-phonon interaction, acoustic solitons 0-70628  
 molecular rotational spectra, doublet splittings caused by tunnelling, perturbation treatment 0-91541  
 MOS diodes, tunnel-assisted transport at room temp. 0-92975  
 muon spin rotation method, review (Polish) 0-88901  
 naphthalene, singlet and triplet exciton percolation, tunnelling and thermalisation 0-84432  
 nitromethane, solid, tunnel states investig. 0-103274  
 nonadiabatic leakage of particles from mag. mirror trap, multiple lifetimes 0-106968  
 optical fibre, elliptical step-index, tunnelling-radiating effect 0-58714  
 p-n tunnel junctions, photoinduced transitions, theory 0-65669  
 p-n tunnel junctions, phototransistors accompanied by impurity scatt. 0-107901  
 point contact IR detector tunnelling and rectification characteristics, geometrical and multiple image interactions 0-57376  
 polyacetylene, doped, fluctuation-induced tunnelling cond. in metallic regime 0-65516  
 PVC films, soln. grown, DC cond. mechanisms, field and temp. depend. 0-97021  
 PVC-C composite, fluctuation-induced tunnelling cond. 0-65516  
 quantal tunneling through a rectangular barrier using |ψ|<sup>2</sup> and flux, education 0-105457  
 quantum tunnelling, reaction coord. method 0-62500  
 resonance differential negative resistance in the Fredkin-Wannier inhomogeneous field model 0-80355  
 scattering resonances, tunnelling decay, absorbing boundary layer 0-57121  
 semiconductor-electrolyte boundary, hot carrier injection, tunnelling from semiconductor states in depletion region 0-75637  
 semiconductor-oxide-semiconductor diodes, tunnel-assisted transport at room temp. 0-92975  
 semiconductors, temp. depend. electronic cond. 0-59975  
 tetramethylgermanium, Zeeman spin-lattice relaxation rate maxima 0-84666  
 meso-tetraphenylporphyrine, NH H<sup>+</sup> tunnelling rate 0-97158  
 thermally degenerated Schottky diodes, resonant tunnelling 0-100503  
 transmission coeff. for 1-D potential barrier, discretisation of Schrodinger eqn. 0-57123  
 tropolone, π-π\* singlet state, H<sup>+</sup> tunnelling dynamics and equilib. geometry 0-102539  
 very thin films, tunnelling currents, temp. and space charge effects 0-70799  
 Ag:Al<sub>2</sub>O<sub>3</sub>:Al tunnel-junction struct., surface polariton mean free path, roughness 0-93008  
 Al tunnel junctions, superconductivity enhancement by microwaves 0-107956  
 Al-insulator-In<sub>1-x</sub>Mg<sub>x</sub> film tunnel junction, resistance zero-bias anomalies 0-107925  
 AlGaAs p-n diodes, I-V characts., tunnelling 0-100510  
 β-Al<sub>2</sub>O<sub>3</sub>-Na<sub>2</sub>O, colour centre ESR by localised tunnelling states 0-108073  
 Au/oxide/n-GaAs struct., photocurrent relax. 0-92978  
 Au-SiO<sub>2</sub>-Si system, oxide film 16-36 Å thick, tunnel currents 0-70842  
 CH<sub>3</sub>PF<sub>6</sub>, nonrigid mol., tunnelling mechanisms, spectrosc. theory 0-78605  
 CO-myoglobin, mol. tunnelling, isotope effect, time resolved IR Fourier transform obs. 0-72126  
 CaF<sub>2</sub>, ionic clusters, struct., thermodynamic functions, energy surfaces and SIMS 0-63881  
 Cd<sub>2</sub>Hg<sub>1-x</sub>Te, tunnelling effect in p-n junctions 0-75630  
 CdS-InP(CdTe)(GaAs)(Ge), solar cell heterojunctions, CVD fabrication, photovoltaic response 0-93878  
 CIPF<sub>4</sub>, nonrigid mol., tunnelling mechanisms, spectrosc. theory 0-78605  
 Cr, antiferromagnetic, muon diffusion, spin relax. and coherent motion 0-71281  
 CrOOH(D), barrier to proton or deuteron tunnelling 0-70156  
 Cu<sub>2</sub>S-CdS heterojunctions, role of deep levels in controlling photovoltaic props. 0-92941  
 Cu<sub>2</sub>S-CdS solar cells, interface recombination phenomena and tunnel effect 0-66978  
 Fe, electron tunnelling 0-60104  
 Fe, quantum diffusion of positive muons, 3 to 300K 0-75909

**tunnelling continued**

- Ga<sub>2</sub>Al<sub>1-x</sub>As<sub>x</sub> photodetector diode on GaAs substrate dark currents, tunnelling, energy gaps, effective masses 0-70805  
 GaAs, heavily doped, fluctuation-induced tunnelling cond. 0-65516  
 n-GaAs, nature of low temp. field generation of carriers, liberation from surface states 0-92960  
 GaAs:Si p-n junction LED, electroluminesc. efficiency 0-71491  
 p-GaAs/rare earth metal contacts, surface pot. barrier 0-60086  
 Ga<sub>0.47</sub>In<sub>0.53</sub>As p-n junctions, band-to-band tunnelling current 0-107895  
 Ge, acceptor complex spectra, tunnelling H systems 0-89036  
 H<sub>2</sub><sup>+</sup> system, quantum oscillations in tunnelling, oscill. freq., tunnelling currents (*Russian*) 0-60065  
 He, adsorbed on graphite, band struct. effects in heat capacity 0-59788  
 Hg<sub>1-x</sub>Cd<sub>x</sub>Te photodiodes, long cutoff wavelength, effect of trap tunnelling on IR detector performance 0-73451  
 In<sub>0.53</sub>Ga<sub>0.47</sub>As photodiodes with dark current limited by generation-recombination and tunneling 0-107893  
 In<sub>0.53</sub>Ga<sub>0.47</sub>As p-n junctions, band-to-band tunnelling current 0-107895  
 InP inversion-type MISFET with SiO<sub>2</sub> gate insulation interface props., elec. drift 0-93002  
 n-InSb based MIS struct., carrier generation under nonequilibrium conditions 0-88640  
 KBr, recomb. in ionic crystals, defect interaction 0-84206  
 KBr:CN<sup>-</sup>, neutron scatt. studies of (CN)<sup>-</sup> defects 0-92620  
 KBr:CN<sup>-</sup> tunnelling motion of dipolar impurities, absorption spectra 0-66239  
 KCl:Eu<sup>2+</sup> crystals, photostimulated afterglow investigation at room temp. 0-108259  
 K<sub>2</sub>PO<sub>3</sub>-type ferroelectrics, parametric tunnelling-like reson. 0-66119  
 KH<sub>2</sub>AsO<sub>4</sub>, ferroelectric phase transition under high hydrostatic press., mol. dynamics, NQR study 0-75880  
 KH<sub>2</sub>PO<sub>4</sub>-type ferroelectrics, tunnelling integral 0-70156  
 (NH<sub>4</sub>)<sub>2</sub>ReCl<sub>6</sub>(IrCl<sub>6</sub>), proton relaxation near antiferromagnetic phase transitions 0-80640  
<sup>15</sup>N, spin-lattice relax. time, quantum effect of NH<sub>4</sub><sup>+</sup> ion rot. 0-75875  
 Na-zeolite, matrix, Te cluster superlattices, N and S type volt-ampere charact., elec. cond. (*Russian*) 0-70665  
 Na<sub>8</sub>Al<sub>6</sub>Si<sub>6</sub>O<sub>24</sub>Cl(Br)(I), cathodochromic sodalites, coloured crystals, tunnel and recomb. luminesc., temp. depend. (*Russian*) 0-66261  
 Na<sub>2</sub>O-B<sub>2</sub>O<sub>3</sub>-SiO<sub>2</sub>-As<sub>2</sub>O<sub>3</sub>(As<sub>2</sub>O<sub>3</sub>) glasses, DC and AC resist., bipolaronic hopping cond. 0-88558  
 NaOH:CrO<sub>4</sub><sup>2-</sup> (NO<sub>3</sub><sup>-</sup>), electron tunnelling, pulse radiolysis 0-108722  
 NaOH:Fe(Cn)<sub>6</sub><sup>3-</sup>, electron tunnelling, pulse radiolysis 0-108722  
 Nb single crystals, for tunnel meas., annealing in ultra high vac. device (*German*) 0-89169  
 Ni, electron tunnelling 0-60104  
 Ni(NH<sub>3</sub>)<sub>6</sub>I<sub>2</sub>, phase transition and rot. excitation 0-96642  
 PdSiCu, amorphous, US attenuation and vel. studies at low temps. 0-88278  
 Pt-Si thermally degenerated Schottky diodes, resonant tunnelling 0-100503  
 Si n<sup>+</sup>-p solar cell, forward and reverse bias tunnelling 0-85274  
 Si:H, amorphous, geminate recombination model for photoluminescence decay 0-71481  
 Si:H, amorphous, surface states distribution using MOS tunnel junctions 0-103735  
 p-Si/rare earth metal contacts, surface pot. barrier 0-60086  
 Si-SiO<sub>2</sub> interface, barrier height in MOS tunnelling structures 0-88644  
 Si-SiO<sub>2</sub> MIS systems, dynamic props. of switching, appl. to charge transfer devices 0-92997  
 Si-SiO<sub>2</sub>-Al, interface barrier energies for tunnel oxides, internal photoemission meas. 0-84512  
 Si-SiO<sub>2</sub>-Al MOS surface channel influence on channel-to-contact diode charact. 0-92994  
 Si-SiO<sub>2</sub>-Mo-Si<sub>3</sub>N<sub>4</sub>-Al MNOS structures with metal grains, charge transport at SiO<sub>2</sub>-Si<sub>3</sub>N<sub>4</sub> interface 0-65693  
 Si-SiO<sub>2</sub> interfaces, carrier transport processes, electron states, conference, Durham, England (July 1979) 0-90612  
 SiC LEDs prepared by overcompensation method, photon assisted tunnelling 0-97341  
 SiH<sub>3</sub> radical, in Ar(Kr)(N<sub>2</sub>) matrix, anisotropic ESR spectroscopic parameters 0-63687  
 SiO<sub>2</sub>, amorphous, sp. ht., time-dependent, 0.1 to 1K 0-100338  
 SiO<sub>2</sub> tunnelling barrier asymmetry to electrons and holes in MOS struct., photocurrent 0-75645  
 Ta-Ta<sub>2</sub>O<sub>5</sub>-Ag junctions, polarity-depend. tunnelling cond. 0-70846  
 W (110) plane, tunnelling of H in surface diffusion 0-75416  
 ZnTe, elec. field and impurity conc. effects on ionisation energy of impurities, appl. to acceptors 0-88514

**tunnelling spectra**

- Schottky-barrier diodes, resonant tunnelling spectroscopy, deep centre detection 0-96968  
 thermally degenerated Schottky diodes, resonant tunnelling 0-100503  
 Al<sub>2</sub>O<sub>3</sub>, inelastic electron tunnelling spectroscopy of adsorbates, MgO comparison 0-88686  
 Au-Ti/SiO<sub>2</sub>/p-Si MOS struct., interface state distrib., DC tunnelling spectra determ. 0-75611  
 CO chemisorbed on Fe, low energy vibr. modes studied by tunnelling spectroscopy 0-78590  
 MgO, inelastic electron tunnelling spectroscopy of adsorbates, Al<sub>2</sub>O<sub>3</sub> comparison 0-88686  
 Pb, single and polytextured thin films, band struct., tunnelling spectroscopy 0-80169  
 Pb-Si superconducting solutions, effect of hydrostatic compression on tunnelling (*Russian*) 0-65746  
 Pt-Si thermally degenerated Schottky diodes, resonant tunnelling 0-100503  
 Zr(BH<sub>4</sub>)<sub>4</sub> catalytic reactions on Al<sub>2</sub>O<sub>3</sub>, inelastic electron tunnelling spectra 0-75425

**tunnelling spectroscopy**

- adhesion, surface chemistry studies, anal. appls. 0-88440  
 inelastic electron tunnelling spectroscopy, appl. to study of lubrication 0-70302  
 Raman spectroscopy of mol. monolayers in inelastic electron tunnelling spectroscopy junctions 0-93344  
 Al, corrosion by carbon tetrachloride, IETS obs. 0-81230  
 Al<sub>2</sub>O<sub>3</sub> thin film used in inelastic electron tunnelling spectroscopy, X-ray photoelectron spectrum 0-108319

**tunnels, wind** *see wind tunnels***turbidimeters** *see turbidimetry***turbidimetry**

- electrooptical nephelometry, characterisation of nonspherical atm. aerosol particles 0-77106  
 multichannel electrooptical turbidity meter 0-67423  
 nephelometer on Pioneer Venus Sounder and small probes 0-67511  
 oil-fired boilers, opacimeter use possibilities (*Rumanian*) 0-87483  
 photoelectric nephelometer for liquids 0-101812

**turbidity***see also turbidimetry*

- aerosol size distribution by inverting spectral turbidity data 0-95796  
 CBNA, nematic-isotropic transition at high press., turbidity meas. 0-92655  
 EBBA, nematic-isotropic transition at high press., turbidity meas. 0-92655  
 Funka Bay, Japan, <sup>234</sup>Th removal from seawater 0-61803  
 hydrological instrument to meas. light absorpt. coeff. 0-82076  
 MBBA, nematic-isotropic transition at high press., turbidity meas. 0-92655  
 natural waters, turbidity rel. to spectral scatt. props. 0-72560  
 ocean, instrument to meas. light absorpt. coeff. 0-82076  
 polystyrene-diethyl malonate, strongly opalescent critical isochore, scattered light intensity 0-71436  
 soot conglomerate destruction dynamics in pulsed laser radiation field 0-58617

**turbine generators** *see turbogenerators***turbines**

- see also compressors; gas turbines; hydraulic turbines; steam turbines; turbogenerators; wind turbines*  
 airflow through cascade of turbine blades, laser anemometry 0-59146  
 axial turbine blades, spatial streamline flow calcs. using pot. flux of incompressible liq. 0-59000  
 blades, three-dimens. annular array, aerodynamic forces with nonsteady flow 0-99991  
 blades nondestructive testing, using scanning laser acoustic microscopes, comparison with SEM and optical microscopy results 0-58875  
 boundary layer charact., influence of external flow turbulence 0-87811  
 jet flow hydrodynamic model 0-79369  
 rotor shaft, US testing, sensitivity multiplication factor 0-85125  
 Ni-Cr-Co based alloy, IN-738 turbine blades, hot isostatically pressed investment castings, effect of heat treatment on grain boundary struct. 0-89270

**turboalternators** *see turbogenerators***turbogenerators**

- bearing oil film damping and stiffness coefficients determ. for dynamic behaviour stability study (*Italian*) 0-106762  
 high capacity, heating reduction measures for enhanced reliability and interval between maintenance (*Russian*) 0-96175  
 rotor and stator core thermal conductivity solution using integral representation method (*Russian*) 0-100451  
 stator core losses simulation, expt. 0-88798  
 tidal power stations, technical details and operating experience 0-72009

**turbulence**

- see also atmospheric turbulence; boundary layer turbulence; cavitation; laminar to turbulent transitions; plasma turbulence; shear turbulence; turbulent diffusion; vortices*  
 acoustic modes, high order, turbulence-generated noise in pipes with various fittings 0-74849  
 acoustic radiation from bodies in unsteady flows 0-69799  
 acoustic tones in side-branch pipe resonators, flow-induced 0-64243  
 acoustic wave propagation on turbulent jets using organ pipe flue 0-91946  
 aeroacoustics of advanced turbopropellers, noise prediction 0-69598  
 aerodynamic sound generation by unsteady subsonic flows around rigid bodies 0-69798  
 aerodynamics of parallel circular cylinders, finite height 0-103013  
 aerothermal turbulent channel, meas. of multi-orders velocity-temp. correls. 0-79268  
 air-Hg flow, stratified, co-current, in rectangular channel, interfacial wave structure 0-74955  
 aircraft noise, basic aeroacoustic research, industrial appl. 0-69596  
 airfoil trailing edge noise, near-wave struct. and unsteady pressures at trailing edge 0-69794  
 airfoil trailing edge noise, pressure field at trailing edge: effect on radiated noise 0-69795  
 atmospheric sound generated by Al plate excited by free turbulent jet (*German*) 0-102908  
 Belousov-Zhabotinsky reaction, chem. turbulence, strange attractor representation 0-85148  
 benthic ocean, bottom mixed layer turbulence 0-72532  
 blades, three-dimens. annular array, aerodynamic forces with nonsteady flow 0-99991  
 blood, extracorporeal circulation connectors, turbulence obs. 0-81641  
 bounded coaxial jets, convective heat transfer in turbulent mixing, swirling flow 0-64541  
 Boussinesq fluids, viscosity, conductivity and power spectrum of turbulent convection 0-98543  
 branch-to-trunk area ratio, effect on transition to turbulent flow, cardiovascular system appls. 0-67108  
 bubbly flow, drift velocity, analytical model of distrib. mechanisms 0-99992  
 burning rate in engine cylinder, swirl and turbulence effects 0-89492  
 channel blockage and turbulence influence on water transverse flow past cylinder (*Russian*) 0-79401  
 chaotic turbulent flows, scaling behaviour, Lyapunov characteristic exponent 0-86217  
 closure relations for the pressure-strain correlation of turbulence 0-59011  
 compressible axisymmetric jet sound radiation by instability waves 0-69792  
 conditional eddies in isotropic turbulence, higher order estimates 0-92119  
 confined coaxial jets with and without swirl, vel. charact., recirculation regions 0-103055  
 confined turbulent coaxial jet, vel. charact. 0-64601  
 cosmic turbulence, primordial, spectrum evolution 0-90589  
 cosmological turbulence theory, observational tests 0-98747  
 Couette flow, plane, resonance mechanism, small 3-D disturbances 0-79269



## turbulence continued

cylindrical thermocouple with plane frontal area, recovery factor in turbulent subsonic flow (*German*) 0-74882  
 decaying turbulence in neutral and stratified fluids 0-96247  
 description and quantification using information theory (*German*) 0-106789  
 direct interaction approximation, higher corrections 0-92118  
 discontinuous transitions into chaos after single bifurcation, hysteresis existence 0-73264  
 dissipation rate for turbulent plane and circular jets 0-69889  
 distensible tube damping effects on turbulent flow, cardiovascular system implications 0-103076  
 double grid of cylinders with opposite grid motion, turbulence decay 0-96246  
 dynamical systems, critical transition to stochasticity 0-73265  
 electrically conducting media with nonlinear heat release, turbulence props. 0-103024  
 electrostatic precipitator, particle velocity, laser Doppler anemometry study 0-59144  
 engine intake noise, high freq., ray-theory approach 0-69595  
 equilibrium turbulence, soliton role as liquid drops (*Russian*) 0-98804  
 excess noise from supersonic underexpanded jets in flight 0-69815  
 extensional viscosity of a dilute suspension of spherical particles at intermediate microscale Reynolds numbers 0-106835  
 external noise effect on transition to turbulent convection 0-96263  
 f reactor coolant interchannel interaction for prolonged flow around bunches of rods 0-73888  
 field-coherence four-point function in turbulent medium 0-87319  
 film rupture in laminar and turbulent lubrication, inertia forces effect 0-74813  
 finite turbulence spatial scale effect, turbulence amplification by a contracting stream 0-87760  
 flame ionisation detector, meas. fluctuating conc., in turbulent flows 0-92240  
 flames, laser Doppler vel. meas. using spark discharge particle generator 0-59139  
 flames, local turbulence props., Raman spectroscopy meas. 0-64648  
 flat plate moving in homogeneous or isotropic turbulence 0-106790  
 flat plate streaming potential investigations: hydrodynamics and electrokinetic equivalency 0-106777  
 flight effect of Michalke and Michel vis-a-vis Lighthill's model 0-59018  
 flocculation, mathematical model (*Japanese*) 0-79389  
 flow, turbulent mixing, velocity biasing resulting from non-uniform seeding 0-59143  
 flow in pipes, temp. field struct. 0-69923  
 flow-field investigations using triple-sensor probes 0-100043  
 fluctuations of intensity at two wavelengths in turbulent medium 0-87318  
 free convection heat transfer from vertical thin wire to air, laminar-turbulent transitions (*Japanese*) 0-92152  
 free convection in mag. field, statistical characs., vortices 0-79310  
 free turbulent heat exchange surface, free convection liquid flow 0-64543  
 free turbulent jet directed against a flat surface, phenomena accompanying the impact, diversion, and distribution (*German*) 0-106827  
 free turbulent mixing in streamwise press. gradients, linearised k- $\epsilon$  anal., wakes 0-59039  
 friction factor, calc. by TI-57, binary-search method 0-83788  
 gas, nonsteady flow through semipermeable screen to vacuum 0-100029  
 gas transported dust, discrete particle phase effect on turbulence intensity (*Russian*) 0-79384  
 gas turbine combustion chamber flow three-dimens. calc. 0-79405  
 gas-liquid ascending flow, monodispersed, function stress on wall, bubble size effect 0-59098  
 gas-liquid interaction in turbulent reacting flows, mathematical model 0-83862  
 gas-solid flow in cyclone, turbulent swirl velocity, particle sizes and concentrations 0-69902  
 grid generated turbulence, uniform strain effect on thermal fluctuations 0-103026  
 grid-generated, vibration of rod in annular downstream region, reactor cooling appl. 0-74836  
 H-shaped section cylinder in turbulent flows, aerodynamic charact. 0-106813  
 heat emission of a rough-surfaced tube in turbulent water flow (*Russian*) 0-74837  
 heat transfer, nonstationary, finite element calcs. 0-83795  
 heat transfer of tubes closely spaced in an in-line bank 0-59026  
 heated flows, fine scale turbulence, hot and cold wire sensitivity corrections 0-69956  
 homogeneous 0-69772  
 homogeneous isotropic turbulence, inertial convective region, scalar fluctuation spectrum (*German*) 0-92120  
 hydrodynamic instabilities and turbulence, flow states, examples and meas. methods 0-92116  
 inclined open channel, stability of permanent roll waves 0-64629  
 incompressible fluid, isotropically turbulent stream, probability distrib. of vel. and temp. differences 0-79273  
 incompressible liquid in planar channel, axial curvature effects 0-87762  
 instability, post-, in class of smooth functions, mathematical model 0-69649  
 intermittency in turbulence onset 0-59013  
 intermittent transitions to turbulence, intermittency in dissipative dynamical systems 0-106781  
 interplanetary magnetic field, turbulence rel. to mean free path of low-rigidity cosmic rays 0-98524  
 interplanetary turbulence, rel. to Earth bow shock theory 0-85816  
 interstellar contracting clouds, influence of turbulence on solid particles growth 0-62251  
 interstellar gas turbulence, effects on grain collisions 0-77470  
 inviscid flow on sphere, statistical mech., atm. appl. 0-90152  
 ionosphere, heating by powerful radio emission with random modulation of carrier freq. 0-109310  
 isotropic and homogeneous self-similar behaviour (*French*) 0-74838  
 isotropic vorticity theory, appl. to adverse pressure gradient flow 0-59047  
 iterative approach to strong turbulence theory 0-92117  
 jet, subsonic and supersonic, laser velocimeter correlation meas. 0-106785  
 jet mixing noise generation, eval. of Lighthill analogy using LV turbulence, source location and spectral noise data 0-69803  
 jet noise, aeroacoustic interaction, review 0-87765  
 jet noise, cross-spectral densities, extension of Ribner's theory 0-69804  
 jet noise in flight, prediction, importance of jet temp. 0-69814

## turbulence continued

jet noise prediction, nonlinear Lilley equation 0-69805  
 jet on cylinder wall, heat transfer and fluid mechanism study (*Japanese*) 0-83800  
 jets, film cooling performance 0-79272  
 jets, influence of drag reducing polymers on cavitation inception 0-106823  
 jets, two-dimensional water, sensitive to sound, behaviour (*Japanese*) 0-79376  
 laser Doppler anemometry on transparent turbulent electromagnetically driven flow 0-103090  
 laser radiation thermal self-interaction in turbulent absorbing liq. medium 0-91868  
 laser-Doppler anemometry and photon correlation for turbulence length scales 0-87828  
 Lorenz model, Feigenbaum sequence of bifurcations 0-83783  
 Lorenz model, turbulence in dissipative dynamical systems 0-90784  
 low dimensional chaotic dynamical system for turbulent flow, time series geometry 0-103014  
 low frequency sound radiation due to the interaction of unsteady flows with a jet pipe 0-69787  
 low Mach number aerodynamic noise theory 0-69796  
 low Reynolds turbulent flow, vel. distribution anal. using hydrogen bubble method (*Japanese*) 0-106788  
 Lucke's theory of turbulence 0-99990  
 Mach wave radiation of hot supersonic jets 0-69894  
 MHD, turbulence, development and generation (*French*) 0-79407  
 mist formation in turbulent convection field, critical supersaturation model 0-64611  
 mixing with react. of miscible reactant streams, simulation 0-64651  
 Navy vessel fracture mechanics and flow separation, instability phenomena 0-99971  
 noise generation by transonic open rotors 0-69599  
 noise source mechanisms, expt. determ. in gas turbine combustors 0-69597  
 non-Newtonian fluids, turbulent flow in absence of anomalous wall effects 0-69880  
 nonisothermal turbulent heterogeneous jet entering air filled half space 0-64599  
 nonsteady one-dimensional liquid flow, analytic method calcs. 0-59009  
 nuclear reactor, two-phase flow in pin bundle, two fluid model 0-91209  
 nuclear reactor wire-wrapped core assemblies, turbulent flow split modelling and expts. 0-95370  
 ocean, exptl. study of nonlinear baroclinic instability and mode selection in large basin 0-85669  
 ocean, realistically stratified, nonlinear energy and enstrophy transfers 0-101370  
 ocean, wind-induced turbulence energy distrib. rel. to mixed layer evolution (*Russian*) 0-94529  
 ocean solitary Rossby waves over variable relief, transition to turbulent behaviour from numerical expts. 0-101372  
 optical beams in randomly inhomogeneous media, strong fluctuations of fields 0-99634  
 optical wave, log-amplitude fluctuations spectra, turbulence spectra parameters determ. 0-95797  
 optical wave propagating through turbulence, scintillations meas. detector aperture effect (*Slovak*) 0-63921  
 particle acceleration by MHD shock turbulence 0-87894  
 particle beams, charge density vol. distrib. in turbulent stream (*Russian*) 0-74288  
 perforated plate generators in wind tunnels, wake, shear flow and isotropic turbulence prod. 0-69770  
 period doubling and turbulence onset, analytical estimate of Feigenbaum ratio 0-87761  
 pipe flow, use of eddy viscosity expressions for vel. profiles in Newtonian, non-Newtonian and drag-reducing flows 0-83789  
 pipes, smooth, turbulent velocity profile, zero centreline velocity gradient 0-74974  
 plane channel flow, subcrit. turbulence transition 0-106787  
 plane horizontal turbulent buoyant jet, parameter calcs. (*Russian*) 0-79373  
 plane parallel flow, free convection in Couette and Poiseuille flows, numerical simulation 0-99995  
 polydispersed flows, Doppler signal spectrum 0-103081  
 polyisobutylene in toluene solution, effect of capillary materials on drag reduction (*German*) 0-87785  
 pulsed laser radiation intensity fluctuations, thermal selfinteraction in turbulent medium 0-102781  
 quadratic structure functions describing random tilted phase fields 0-95799  
 radiation properties of a turbulent jet excited by a sinusoidal acoustic disturbance 0-69789  
 random flow statistics analysed by photon correlation anemometry 0-64522  
 Rayleigh-Benard convection, turbulence and intermittency, expt. 0-99998  
 review, current theory and practical examples (*French*) 0-64523  
 rotating fluid layer, heated, turbulent convection 0-100003  
 rotational flow avoidance, Navier-Stokes eqns. numerical solns. (*German*) 0-59057  
 round free jet, aerodynamic noise, propagation of wavelike disturbances 0-69806  
 shadow methods for studying turbulence using reflection from a mirror in the medium 0-95801  
 shield-hot turbulent jet interaction, nonstationary heat transfer 0-92136  
 small particles suspended in turbulent fluid, convection, mass transfer 0-87793  
 small scale magnetic fields in turbulence, Saffman's approx. 0-106851  
 smoke-motion, numerical anal. by finite-element method (*Japanese*) 0-69910  
 solar convection zone, turbulent viscosity rel. to mag. fields floating-up time and 11-year cycle 0-101580  
 solar corona, prominence turbulence causing heating and MHD wave generation 0-72907  
 solar photosphere, microturbulent vels. and damping const. determ. errors (*Russian*) 0-72899  
 solar transition region, turbulence rel. to nonthermal motions and energy balance 0-90379  
 solar wind plasma, turbulence spectrum from three-satellite radio wave propag. meas. 0-101518  
 sonar, synthetic-aperture sonar systems in turbulent medium 0-96080

**turbulence continued**

- sound generation and propagation in flows, inhomogeneous convected wave equation 0-69813
- sound generation by flow-acoustic coupling 0-69793
- sound generation by head-on collision of two vortex rings 0-69801
- sound generation by turbulence, mean flow calcs. of large eddy struct. and flow-acoustic interaction 0-69785
- sound generation in flows, conf. Gottingen, Germany (Aug. 1979) 0-67937
- sound radiation from a simulated jet flow, calc. of vortex configuration and sound field 0-69786
- sound source location techniques 0-69802
- sound spectra radiated by gas jets, influence of closely located solid surfaces 0-69800
- spherical solids melting in turbulent carrier fluid, deformation and breakup 0-92646
- stagnation flow turbulence about circular cylinder, visual study 0-96248
- stars, massive, convective and semiconvective mixing 0-90405
- statistical dynamics of chaotic flows 0-106786
- steam, wet, drop coagulation in cross-over pipe flows 0-74982
- steel pipe corrosion, mass transfer coeffs. under isothermal flow conditions 0-97628
- stellar turbulence, conference, London, Ontario, Canada (1979 August 27 to 30) 0-73102
- stellar turbulent convection equations, ensemble averaging 0-67698
- stellar winds, turbulent mixing with interstellar gas 0-67701
- stratified medium, normal and abnormal turbulent transport (*French*) 0-59095
- streaklines in a shear layer perturbed by two waves 0-59055
- subsonic, jet-mainstream interaction 0-79271
- supercritical He I, heat transfer to turbulent flow 0-69631
- surface discharging heated turbulent jet, 3D finite difference model, turbulent diffusivities 0-74845
- surface noise from turbulent hot jet, temperature effects 0-69782
- suspensions, flow in cylindrical pipe, using ultrasonic debimetry Doppler spectra (*French*) 0-96303
- suspensions, motion of particles suspended in stationary turbulent medium at large Reynolds number 0-83836
- tensorial volume of turbulence 0-59012
- thermal convection at high Rayleigh number, variation of Nusselt number 0-79300
- three-wave decay interaction, steady-state turbulence spectrum 0-96249
- transition to aperiodic behavior in turbulent systems, recursive method 0-105493
- two dimensional turbulent mixing layer, spanwise struct., vortices 0-69771
- two rotating discs, air flow in gap between 0-92156
- two-dimensional, computational method 0-74839
- two-dimensional random field model for image structural analysis (*Russian*) 0-63932
- two-dimensional turbulence, hydrodynamic and plasma applications, dynamical eqns., diffusion, MHD, superfluidity, review 0-69769
- two-phase countercurrent flow, turbulent steam condensation in a horizontal channel 0-106800
- two-phase gas-liquid flow, turbulent characts., determ. method 0-96300
- Universe model, homogeneous, isotropic, close to cosmological singularity, long-wave disturbances 0-73078
- variable density turbulent subsonic flow, pressure pulsation and vel. divergence correlations 0-100008
- viscosity coefficient, calc. in semiempirical formulae (*Russian*) 0-79267
- viscous flows with no-slip walls, incompressible Navier-Stokes eqn., pseudospectral method 0-69924
- viscous liquid film instability under the influence of an adjacent gas flow 0-92110
- volumentrically heated fluid layer, combined natural turbulent convection and radiation 0-74871
- vortex flow meas. by laser Doppler anemometer, meas. of turbulent vortex flow 0-79412
- vortex pairing in jet noise generation 0-69807
- vortices caused by slender bodies, high angles of attack to medium of travel (*French*) 0-59041
- water jets sensitive to sound, two-dimensional, velocity fluctuations behaviour (*Japanese*) 0-100020
- H supersonic flames, chemical kinetics and unmixedness effects on burning 0-64649
- <sup>4</sup>He, superfluid, fluctuations in turbulent counterflow, vortex line density fluctuation power spectra 0-84335
- Hg, transition and turbulent flow in curved channels under transverse mag. field 0-79396
- TiO<sub>2</sub> suspension in glycerine, Bingham plastic flow through annuli 0-64521

**turbulence, atmospheric** *see atmospheric turbulence*

**turbulence in shear flow** *see shear turbulence*

**turbulent diffusion**

- air, Fourier transformation of space-time transport equation 0-62595
- convection, nonlinear double-diffusive, low Prandtl number, boundary layer method 0-69816
- direct optical meas. of vel. gradients 0-59132
- eulerian-lagrangian turbulent diffusivity relation 0-103018
- invariant props. of fluctuation distribts., contaminant cloud appl. 0-59017
- passive scalar magnitude (*French*) 0-69778
- pipe, asymmetrically heated, turbulent transport and thermal diffusivities 0-64636
- pipe fluid flow, solid particle impurity propag. 0-64630
- plasma strong turbulence and anomalous diffusion in mag. field 0-59239
- Rayleigh-Bernard convection, forced phase diffusion 0-103019
- superimposed miscible liquids, dynamic stabilization, turbulent transport through diffuse boundary layer 0-74844
- surface discharging heated turbulent jet, 3D finite difference model, turbulent diffusivities 0-74845
- tracer gas axial dispersion through tube constrictions 0-64625
- transonic flow, unsteady, turbulence modelling, compression waves developing into shock wave 0-74909
- two-dimensional turbulence, hydrodynamic and plasma applications, dynamical eqns., diffusion, MHD, superfluidity, review 0-69769
- wavefronts in reaction-diffusion systems, instability and turbulence 0-106855
- CO<sub>2</sub> laser amplifiers, porous tube generated flow field, heat and mass diffusion 0-63969

**turbulent flow** *see turbulence*

**Turing machines**

quantum mechanical microscopic Hamiltonian model 0-101727

**TV** *see television*

**twilight**

*see also night sky*

- airglow spectrum, new diffuse emission bands obs. 0-72662
- NO<sub>2</sub>, stratospheric, ground based obs. 0-85697
- O atom corona, of fast atoms during solar max., airglow obs. 0-101469

**twin boundaries**

- dimethylammonium cadmium tetrachloride, far IR refractive index, extinction coeff. and dichroism obs. 0-66144
- ferroelectric substances, electron microscopy investigations, review (*Japanese*) 0-71366
- metal, BCC, twin boundary and stacking fault structs., computer simulation 0-59485
- metal particles, small, possible vibrations associated with twins 0-100253
- metal-C system, spheroidal graphite formation, role of high angle boundaries (*Russian*) 0-81065
- metals, FCC, dislocation barriers at coherent twin boundaries, anisotropic elasticity solns. 0-96522
- plane coalescence, at grain boundaries 0-70221
- steel, austenitic stainless, precipitation of M<sub>23</sub>C<sub>6</sub> type carbide on twin boundaries 0-89226
- steel, Cr-Mo-Ni-WV (6, 4, 3, 2 wt.%), tempering and secondary hardening, TEM obs. (*Chinese*) 0-104245
- steel, stainless, shock loaded, residual martensite obs. 0-104414
- Ag thin evaporated films, rel. between microstruct. and excess free energy, TEM 0-70427
- Au, atomic struct. of large angle {001} twist boundary, determ. by computer modelling and X-ray diffr. study 0-70162
- Au film, twin boundary struct. and migration, atomic scale electron microscopy obs. 0-107276
- Au, quenched polycryst., vacancy loss at grain boundaries 0-59477
- Be<sub>2</sub>SiO<sub>4</sub>, phenakite, flux grown single crystals, twinning study by hydrothermal etching and X-ray diffr. 0-107271
- Cu, point and planar defects, computer simulation 0-59455
- Fe<sub>40</sub>Ni<sub>40</sub>P<sub>14</sub>B<sub>6</sub>, metallic glass, crystn. 0-70127
- Mo, shock deformation twinning, shock loaded BCC and FCC metals comparison 0-104413
- Ni-Cr, partial dislocation, stacking fault TEM study (*Chinese*) 0-84174
- NiTi martensite, shape memory effect, struct. characts., TEM 2<sup>1</sup>/<sub>2</sub> D imaging obs. 0-108446
- Si, coherent twin boundaries, struct. by TEM 0-75238
- Si crystals, dynamic processes associated with stacking faults and deform. twins, HVEM in-situ obs. 0-103369
- Si, deformed, annealed and recrystallized, struct., implications for solar cells 0-60922
- Si, grain boundaries, high resolution TEM 0-103364
- Si single crystal ingot growth from metallurgical grade Si, inhomogeneities 0-59416
- Ti, serrated {10 $\bar{1}$ 2} twin interfaces 0-84182
- Zn, crack form. at grain and twin boundaries at low temp. (*Russian*) 0-66620
- Zr, serrated {10 $\bar{1}$ 2} twin interfaces 0-84182

**twinning**

*see also twin boundaries*

- brass, rolling texture development and deform. struct., shear bands effect (*Japanese*) 0-84952
- camphor, rhombohedral, polycryst., compressive deform. and dynamic recrystn. 0-71698
- carbonate minerals, deform. twinning mechanisms 0-79814
- derivative lattices, determ. of relationships 0-107012
- dislocations and lattice transformations, book contrib. 0-107242
- elastic monatomic crystals, nonlinear, global instabilities 0-58903
- electron microscope resolution improvement for crystal structure imaging and atomic movement dynamic obs. 0-70090
- Fe, twinning under influence of plane shock wave (*Russian*) 0-92538
- film defect growth and nucleation, electron microscopy and diffraction exam. (*French*) 0-59824
- graphite, ion bombarded, light gases, structural study using TEM 0-92570
- HCP metals, atom movement in twinning, {10 $\bar{1}$ 1}, {10 $\bar{1}$ 3} twins, {10 $\bar{1}$ 1} {10 $\bar{1}$ 2} double twinning, new model 0-100252
- merohedry detection, based on intensity statistics 0-100246
- metal particles, small, possible vibrations associated with twins 0-100253
- metals and alloys, HCP struct., relative orientation of cryst. lattices 0-84181
- $\beta$ -phycoerythrin crystals, twinned by merohedry, diffr. data treatment 0-108845
- quartz, light scattering polarisation props. at  $\alpha$ - $\beta$  phase transition 0-108220
- ruby, structural defects due to laser irradi. (*Russian*) 0-100303
- single crystals under large loads, theoretical elastic behaviour, review and appl. 0-71681
- steel, alloy 10G2S1 welds, fracture, subjected to low-temp. fatigue 0-89350
- steel, austenite, carbide strain hardened, strength and plasticity, effect of Mn content (*Russian*) 0-97500
- steel, stainless type 316, in-situ HVEM studies under ion beam irradiation 0-103396
- steel, V, precip. and transform. kinetics, effect of N 0-97485
- texture transformations, 'brass to copper' in FCC metals 0-76246
- tris (3-mercaptop-1, 3-diphenyl-2-propen-1-onato) Co(III), multiple twinning 0-100250
- Ag epitaxially grown film, on Au (111), twin form., LEED detection 0-88442
- Ag, multiply twinned particles, internal and surface struct. by electron microscopy 0-84189
- Ag, tensile deformed, dynamic recrystn. (*German*) 0-84959
- Ag, thin-film bicrystals, planar lattice defects and migrating grain boundaries interaction 0-79835
- Al-Ni(Pt)(Zn), rapidly solidified, twinned dendrites 0-70572
- Au films, vac. condensed at oblique vapour incidence, oriented cryst. growth, electron diffr. study 0-97432
- Au, multiply twinned particles, internal and surface struct. by electron microscopy 0-84189
- BC, sintered, struct. and props. 0-104181
- BaTiO<sub>3</sub>, ferroic materials, fracture processes 0-79869



**twinning continued**

- Be<sub>3</sub>N<sub>2</sub>-BeSiN<sub>2</sub> system, crystallography and phase relationships, TEM and electron diffr. study 0-92502  
 Be<sub>2</sub>SiO<sub>4</sub>, phenakite, flux grown single crystals, twinning study by hydrothermal etching and X-ray diffr. 0-107271  
 Bi, charge carrier interaction with twinning planes in strong transverse mag. fields (*Russian*) 0-88577  
 Bi, twin shape variation under long period loads (*Russian*) 0-65007  
 Co, glide ahead of terminating {1012} twins 0-96545  
 Co, single crystal, cavitation erosion, role of twinning 0-107272  
 Co, single crystals, {1121} twins, accommodation and form. 0-96540  
 CsCl-type lattice, (111) superlattice screw dislocation motion, computer simulation 0-79793  
 CsLiSO<sub>4</sub>, crystal structures of I and III phases, twins 0-70181  
 Cu epitaxially grown film on Au (111), twin form., LEED detection 0-88442  
 Cu films, vac. condensed at oblique vapour incidence, oriented cryst. growth, electron diffr. study 0-97432  
 Cu, single crystals, (110) oriented, tensile deformed, HVEM of recrystn., recrystallised state 0-89256  
 Cu single crystals, deformed, HVEM study of recrystn. texture 0-104179  
 Cu-Al (11 at.%) single crystal, dislocation reactions during deform. twinning 0-79795  
 Cu-Sn (4.9 wt.%), role of mech. twinning on stress/strain behaviour 0-85004  
 Fe zone refined crystals, cryst. orientation and distrib. of stray grains 0-70509  
 Fe-Cr-Co alloy, spinodally decomposed, micro-twinning 0-92537  
 Fe-Mn, mechanical twinning of close-packed hexagonal  $\epsilon$ -phase during plastic deform. (*Russian*) 0-60909  
 Fe-Ni-C (30, 0.5 wt.%) single crystal, stress induced martensitic transform. 0-60860  
 Fe-Ni-C austenitic alloy, banded struct. formed by deform. 0-71713  
 Fe-Si (3 at.%), deformation and electron bombardment, influence on dislocation struct., 20-500°C (*Russian*) 0-92536  
 Fe-Si (3 wt.%), electron irradiated, yield strength and elongation 0-76325  
 Fe<sub>2</sub>O<sub>3</sub>/Fe<sub>3</sub>O<sub>4</sub> transformation matrices, higher-order orientation relationships 0-100846  
 Ge, strained crystal, annealing effect, recrystn. and struct. (*Russian*) 0-89252  
 In-Sn alloy crystals, phase changes and shape memory effect (*Japanese*) 0-108502  
 InBi single crystal, deform. mode under dynamic indentation 0-88163  
 InP, MBE, substrate temp. related degradation mechanisms 0-65385  
 InP single crystals, uniaxial compression deform. characts. 0-84991  
 InSb, crystal growth from melt, facets and twin formation obs. (*Chinese*) 0-59409  
 KTi<sub>2</sub>Ta<sub>2</sub>O<sub>7</sub>, chemically twinned rutile struct., X-ray study 0-107149  
 MgAl<sub>2</sub>O<sub>4</sub> crystals, flux grown, artificial spinel twin form. by BeAl<sub>2</sub>O<sub>4</sub> addition 0-96542  
 Mo, shock deformation twinning, shock loaded BCC and FCC metals comparison 0-104413  
 MoO<sub>3</sub> topotactic transform into MoO<sub>2</sub>, electron microscopy, X-ray anal. 0-107417  
 NH<sub>4</sub>LiSO<sub>4</sub>, point group symm. at high press. phase 0-70150  
 Na<sub>2</sub>Ti<sub>2</sub>O<sub>9</sub>, orthorhombic, unit-cell twinning of monoclinic Na<sub>2</sub>Ti<sub>2</sub>O<sub>9</sub>, cryst. struct. 0-107155  
 Pb(Zr,Ti)O<sub>3</sub>, ferroic materials, fracture processes 0-79869  
 RbMnCl<sub>3</sub>, twinning struct., cryst. domains, orientation mag. transition (*Russian*) 0-107275  
 (SN)<sub>x</sub>, halogenated, struct. behaviour, TEM obs. 0-70126  
 Si crystals, dynamic processes associated with stacking faults and deform. twins, HVEM in-situ obs. 0-103369  
 Si epitaxial film on sapphire, microtwins, TEM exam. 0-70555  
 Si, ion implanted, complex annealing behaviour of amorphous layers, TEM obs. of defect struct. 0-107299  
 Si, ion implanted, damage struct. obs. using TEM and cross section specimens 0-107298  
 Si, polycrystalline, grain boundary obs. by TEM, solar cell appl. 0-72057  
 Si, polycrystalline structure stability, stacking defects, twins grain struct. (*Russian*) 0-100248  
 Si, strained crystal, annealing effect, recrystn. and struct. (*Russian*) 0-89252  
 Si-Al-O-N system, phase analysis and TEM struct. obs. 0-108420  
 B-SiC, X-ray diffr. study of anisotropic layers in twinned seams 0-107274  
 Ti, fast neutron irradiation, twinning deform. at room temp. 0-65061  
 Ti, twinning deformation, neutron irradiation effects 0-75236  
 Ti-Al-Mo-V (8, 1, 1 wt.%), Widmanstätten colonies, fracture toughness 0-85031  
 $\beta$ -Ti-Mo, thermal instability, hardness and tensile deform. (*Japanese*) 0-71703  
 Ti-Mo-Zr-Sn (11.5, 6.0, 4.5 wt.%) alloy, struct. as affected by processing history 0-84972  
 $\beta$ -Ti-V metastable alloys, fatigue crack propag. 0-60964  
 U<sub>3</sub>Si, reversible twinning, in-situ obs. 0-104241  
 V-O alloys, quenched, local ordering of O, electron microscopy and diffr. 0-59453  
 V<sub>16</sub>N<sub>15</sub> solid solution, quenched, ordered structure (*Russian*) 0-88086  
 Zn, twinning, influence of dislocation drag, mag. field effects 0-59472

**two-phase flow**

- accelerating two-phase nozzle/diffuser flows, virtual mass effects on numerical stability 0-92204  
 aerated systems, oblong, flow and mixing, transverse circulating flow of liquid, longitudinal dispersion 0-69900  
 aerosol particles in flow type chamber, coagulation, deposition 0-69908  
 aerosols, flowing, attachment of <sup>222</sup>Rn decay products using aerosol centrifuge 0-61167  
 aggregates, solid, aerosols, dynamic shape factors meas. appls. 0-61165  
 air bubble entrainment in self-aerated flow, channel or pipe flow 0-106832  
 air water downflow through packed beds, apparent wall heat transfer coeff. 0-74953  
 air water downflow through packed beds, effective thermal conductivity 0-74952  
 air water two phase flow in pipe, regime map 0-69901  
 air-H<sub>2</sub>O, two phase upflow across horizontal tube bundles, void fraction and flow pattern 0-92201

**two-phase flow continued**

- air-Hg flow, stratified, co-current, in rectangular channel, interfacial wave structure 0-74955  
 air-liquid flow, liquid droplet disintegration mechanisms 0-74959  
 air-water flow, transverse intraphase vel. profiles and phase fraction distrib. influence 0-96295  
 air-water two-phase flow in a helically coiled tube 0-92206  
 air/water mixture mass flow meas. by drag devices and  $\gamma$  densitometer 0-79385  
 annular two-phase, two-component flow, quasi-stationary model in three-group approx. (*Bulgarian*) 0-69911  
 boiling calculations in low-pressure systems, appl. to LMFBR Na boiling 0-103068  
 bubble oscillations of large amplitude in fluid of infinite extent 0-96298  
 bubbles, evaporating, of low-boiling liq., surface condensation of high-boiling mixture vapours 0-59021  
 bubbles detection in insulating liquid flow, using spiral delay line 0-79415  
 BWR pressure-suppression system, steam chugging anal., heat transfer and fluid mechanics characts. 0-95339  
 cavitation, acoustic field generated, review 0-74934  
 chlorobenzene drops falling freely through water, breakup 0-69899  
 computerised tomography meas. technique 0-59135  
 condensation heat transfer, nonequilibrium temp. profiles, mass transfer engineering calc. 0-63227  
 condensation-driven fluid motions, nuclear reactor safety 0-63228  
 continuum two-phase theory, volume averaged balance eqns. (*German*) 0-92212  
 countercurrent flow, turbulent steam condensation in a horizontal channel 0-106800  
 critical two-phase flow, bubble nuclei 0-64615  
 critical two-phase flow models, nuclear reactor safety 0-63229  
 dichloroethane drops falling freely through water, breakup 0-69899  
 discrete phase variable particle size, Euler and Lagrange methods 0-92203  
 disperse ore in a gas flow, mixing stage calcs. (*Russian*) 0-106829  
 dispersed powder interaction in high temp. gas flow (*Russian*) 0-106830  
 dispersed phase holographic analysis 0-103061  
 dispersed supersonic two-phase flow, shock characts., droplet size depend. at nozzle 0-106815  
 dispersed two-phase flow; relationship between radiation transmissivity and void fraction (*Japanese*) 0-100026  
 dispersion phase distribution, mass force effect in biphasic liq. cylindrical vortex (*Russian*) 0-79388  
 drift flux formulations and calculational methods 0-103067  
 drop deformation and orientation in shear and extensional flow fields, dynamic interfacial props. 0-107611  
 drop dynamics in shear fields, role of dynamic interfacial effects 0-107612  
 drop formation hydrodynamics, macroencapsulation 0-64603  
 droplet size distribution in liquid phase of two-phase flow effect on characts. 0-103070  
 ducts, one-dimensional models for transient gas-liquid flows 0-64614  
 dust laden gas flow over plate, combined heat transfer, thermal fluxes 0-79289  
 dust particles and liquid in circular pipe, two-phase flow heat transfer 0-64607  
 dusty fluid, flow past wavy moving wall 0-96299  
 dusty fluid, laminar boundary layer flow, 2-D stagnation point near oscillating plate 0-64606  
 dusty gases, fully dispersed wave struct., Navier-Stokes eqns. 0-69875  
 emulsion, dilute, straining motion, effect of inertia on dynamic viscosity 0-87797  
 ethane, flow continuity in arterial capillary systems in cryogenic heat pipes 0-64536  
 finite element method, nonlinear test case 0-96293  
 fission reactor coolant depressurisation studies, transient density, press., temp. variations, during discharge 0-57833  
 fission reactor safety, stability analysis and characts. for two-phase flow eqn. systems with viscous terms 0-59103  
 flame advection and propagation in fluid 0-59097  
 flooding phenomena in inclined circular pipe flow 0-96302  
 flow film boiling, void fraction meas. 0-92207  
 fluidised beds, instability waves and bubble origin, two-fluid eqns. 0-92205  
 fluidised beds, theoretical bounding relations, for bubble void fraction 0-96296  
 foam stability relation to structure, criteria derivation w.r.t. drainage stage 0-69904  
 foam with high press. gradients, syneresis in Plateau-Gibbs channels, capillary press. 0-74948  
 free liquid surface oscillations, gas bubble motion 0-100025  
 free motion transition criteria for single bubbles and drops 0-64605  
 Freon-12, annular mist flow in tube, wall film mass flow rate 0-69905  
 gas bubble, rise and cooling in viscous fluid (*Russian*) 0-74949  
 gas bubbles in liquid, nonlinear acoustic disturbances 0-59104  
 gas bubbles in low-viscosity liquids, US attenuation 0-58849  
 gas injection into liquid through porous plate, squeezing out of liq. 0-64622  
 gas transported dust, discrete particle phase effect on turbulence intensity (*Russian*) 0-79384  
 gas-liquid, response of small pitot tubes 0-92209  
 gas-liquid, turbulent characts., determ. method 0-96300  
 gas-liquid ascending flow, monodispersed, function stress on wall, bubble size effect 0-59098  
 gas-liquid flow in horizontal and inclined pipes, flow pattern transition 0-74958  
 gas-liquid interaction in turbulent reacting flows, mathematical model 0-83862  
 gas-liquid mixture, outflow from large container with a slit 0-74951  
 gas-liquid pipe flow, influence of return bends on velocity ratio 0-74962  
 gas-liquid two-phase flow, flow pattern prediction, quantitative indication method 0-79377  
 gas-particle flow in shock tube, finite difference calc. (*Japanese*) 0-79390  
 gas-solid flow in cyclone, turbulent swirl velocity, particle sizes and concentrations 0-69902  
 gas-solid flow in pipe, expansion on deceleration 0-69909  
 gas-solid mixture entering curved duct, particle trajectories 0-96304  
 granular materials, flow round obstacles 0-103064  
 heat flux-flow coupling effects in the stability of vapour generators (*German*) 0-74967

**two-phase flow continued**

heterogeneous fluidised system, aerodynamic aspects of transfer processes, crit. state 0-79394  
 heterogeneous porous medium, two-phase flow, multidimensional problem (*Chinese*) 0-64608  
 high loading ratio slurries, pressure flow, pressure drop calcs. in pipes 0-92202  
 high pressure steam/water mixture flow through cylindrical channels, obs. 0-79404  
 high speed flows, verification calcs. of fundamental eqns. (*Japanese*) 0-69907  
 horizontal gas-liquid stream, flow vel. meas. 0-96301  
 horizontal stratified, 1-D two-fluid eqns. 0-91226  
 horizontal two-phase flow across tube banks, pressure drop predictions 0-103062  
 hydrothermal flows, two-phase, in permeable media, struct. 0-85693  
 immiscible liquid two-phase flow in porous media, unstable displacement 0-92213  
 inclusions in gas-liquid mixture, effect on interphase heat and mass exchange 0-103059  
 instrumentation for safety anal. of LWR LOCA 0-102259  
 isotopic computerised tomography meas. 0-59136  
 laminar liquid film, falling, O<sub>2</sub> adsorpt. with zero order react. in entrance region 0-64652  
 laminar tube flow, gravitational deposition of growing aerosol particles 0-59099  
 liquefied natural gas, nonsteady-state flow calculations in horizontal pipeline systems 0-106838  
 liquid films, vertically falling in circular tube, longitudinal flow characteristics 0-74957  
 low velocity vertical steam-water flow, void fraction in pipes 0-74964  
 LWR LOCA, anal. of LOFT drag disc turbine meter rates 0-102260  
 LWR LOCA, modelling of press. and temp. changes in two-phase, two-component flow (*Bulgarian*) 0-68904  
 mass flow instrumentation performance, during LOFT nonuclear test series 0-69952  
 measurement techniques, recent progress (*French*) 0-79411  
 modelling, theoretical foundation, appl. to fission reactor fluid flow and heat transfer 0-103065  
 molten drop break up in gas flow, surface drag, capillary excitation (*Russian*) 0-100024  
 multicomponent system interface, mass transfer relations (*German*) 0-74966  
 nonequilibrium, phase temp. meas. 0-74950  
 nonequilibrium models, anal. using method of characteristics 0-103069  
 nozzle flows from separate phase model 0-74938  
 nuclear reactor, two-phase flow in pin bundle, two fluid model 0-91209  
 nuclear reactor two-phase-flow instrumentation development at Brookhaven National Laboratory 0-102261  
 nuclear reactors, two-phase flow operating conditions (*French*) 0-78348  
 oil-bearing layer with input parameter correction, discrete dynamic model 0-83778  
 one component, single substance flows, probe method for phase concentration determ. 0-74954  
 optical instrumentation methods for two-phase reactor flows 0-63313  
 oscillating vessel with liquid containing compressible sphere, finely disperse inclusion motion 0-74963  
 particles dispersion variation process study using theoretical kinetic methods 0-106839  
 particulate sedimentation, stability, two-dimens. anal. 0-69768  
 pattern characterisation by electrical conductance probe 0-106857  
 periodic capillary tube, two phase fluid flow and hysteresis 0-107615  
 periodic capillary tube, two phase fluid flow and hysteresis 0-107616  
 phase distribution in two-phase steam flows, effects of probe position 0-87799  
 pipe, annular two-phase flow, downtake turbulent film and gas flows, pressure drop 0-92218  
 pipe fluid flow, solid particle impurity propag. 0-64630  
 pipe lines, on-line holdup or quality meter 0-106858  
 polymeric liquid, viscoelastic, gas bubble pulsations and assoc. dissipation effects 0-59079  
 polystyrene, ordered monodisperse latexes, viscoelasticity and flow props. 0-85992  
 porous media, diffusion-convection eqn., mixed finite element method, water flooding 0-74969  
 pressure driven stratified laminar pipe flow 0-64609  
 pressure drop in bends, eval. of two-phase multiplier 0-92208  
 PWR, two phase flow modelling for LOCA (*French*) 0-78349  
 PWR boiler steam generators, two-phase flow problems in low press. transients (*French*) 0-78350  
 PWR LOCA, pump behaviour conveying two-phase flow (*French*) 0-78351  
 reactor cooling channels, flow anomaly diagnosis, autoregressive model appl. (*Japanese*) 0-83146  
 reactor thermal-hydraulics, quality influence on the departure from nucleate boiling in cross flows through bundles 0-95340  
 rigid spherical particle suspension, two-phase theory, volume averaging and governing eqn. (*German*) 0-87801  
 semi-implicit two-fluid calculational methods 0-103066  
 separated flow models, stratified flow, averaged formulation, high order dispersion effects 0-74960  
 separated two-phase flow, pressure drop and sonic vel. 0-106840  
 simple bodies in two-phase flow, aerodynamic drag 0-96294  
 smoke-motion, numerical anal. by finite-element method (*Japanese*) 0-69910  
 space averaging in continuum mechanics, macrostress tensor symmetry 0-92210  
 space averaging in continuum mechanics, symmetry of macrostress tensor 0-96297  
 sphere in presence of plane fluid-fluid interface, exact soln. of Stokes' eqn. 0-79251  
 spherical solids melting in turbulent carrier fluid, deformation and breakup 0-92646  
 spontaneously condensing and wet steam discontinuous flows in steam turbine cascades, subsonic, transonic and supersonic, numerical investigation (*Russian*) 0-87800  
 spouted beds of spherical particles, spout termination, parameters 0-64621  
 stagnation flow at a heated curved wall, ignition condition 0-96242  
 steam, 2-D two-phase flow, nucleating and wet steam, time-marching method 0-69906

**two-phase flow continued**

steam, wet, drop coagulation in cross-over pipe flows 0-74982  
 steam generating channel, nonuniform heat release, heat transfer crisis location 0-64534  
 steam turbine cascade, mixed and discontinuous, calc. 0-79391  
 stratified fluids in open channel, critical flow conditions 0-74956  
 stratified horizontal flow, averaged and local instantaneous formulations, stability 0-64613  
 submerged gas injection into liquids, flow regimes 0-59101  
 supersonic two-phase flow, nonequilibrium condensation, boundary condition numerical anal. 0-64565  
 suspension, memory impairment, Brownian rotation of spheroids 0-79386  
 suspension of rigid spherical particles, impulsive motion, effect of antisymmetric stresses and particle rotation 0-106833  
 suspensions of charged particles, laminar tube flow, entrance deposition 0-59100  
 tensor formulation of the fluid-solid interaction force for multidimensional, two-phase flow within tube arrays 0-92211  
 unsteady-state gas absorption/desorption, mass transfer product 0-79381  
 vaporisation channels, rough and smooth, heat transfer in post dry-out region 0-96255  
 vapour bubbled through liquid pool, fractional vapour content 0-106831  
 vapour-liquid mixture, outflow from large container with a slit 0-74951  
 vapour-liquid mixture, propagation of acoustic disturbances, model 0-103058  
 variable cross-section channel, quasi-one-dimensional flow, numerical investigation 0-79403  
 viscous fluid, deform. of falling elastic particle 0-79149  
 viscous fluid with suspended particles, motion in a curved tube 0-83835  
 water, annular mist flow in tube, wall film mass flow rate 0-69905  
 water-air plug-train system, press. wave propag. characts. 0-59058  
 water-air two phase flow, oscillatory flow instabilities 0-83833  
 wet steam, high speed flows, drop dimensions meas. method 0-90817  
 CO<sub>2</sub>-water, saturated two phase flow system, non-equilibrium state transient process 0-59096  
 H<sub>2</sub>O vapour under point corona discharge, microprocessor control for vapour generator and EHD phenomena 0-106852  
 He, two-phase mixture, circulation using jet pumps 0-82771  
 N<sub>2</sub> gas jet injection into Hg, interaction at submerged orifice 0-59102  
 NaCl gas-droplet counterflow heat exchanger, numerical model (*French*) 0-61396  
 TiO<sub>2</sub> suspension in glycerine, Bingham plastic flow through annuli 0-64521  
 U enrichment by photochemical laser, two-phase flow with condensation, mathematical model (*French*) 0-74029

**two-photon spectra**

absorptivities, CNDO/S-CI calc. with second order time depend. perturbation eqns. 0-74122  
 absorptivity, ion cyclotron reson. photodissoc. spectra, CNDO/S-CI-perturbation theory 0-74123  
 atom, quantum beats in two-photon resonance fluorescence 0-91488  
 atom, two-photon resonance in coherent fields 0-63606  
 atom pairs in solids, cooperative two-photon absorpt. lineshape 0-84706  
 atomic levels, two-photon transitions 0-83333  
 atomic two-level system, spontaneous emission in bichromatic reson. field 0-69093  
 atoms, two photon excitation, time depend. emitted light spectra, perturbation theory 0-63605  
 benzene, liquid, polarised light two photon thermal blooming near UV spectra 0-66216  
 benzene, mol. cryst., reson. four-wave mixing, third order susceptibilities 0-100654  
 benzene, S<sub>0</sub>-S<sub>1</sub> transitions, two-photon absorpt. spectra by nozzle beam-multiphoton ionisation method 0-63728  
 biphenyl, mol. cryst., reson. four-wave mixing, third order susceptibilities 0-100654  
 chlorobenzene, S<sub>0</sub>-S<sub>1</sub> transitions, two-photon absorpt. spectra by nozzle beam-multiphoton ionisation method 0-63728  
 Doppler-free two-photon dispersion problem 0-106562  
 fluorobenzene, S<sub>0</sub>-S<sub>1</sub> transitions, two-photon absorpt. spectra by nozzle beam-multiphoton ionisation method 0-63728  
 fluoromethane-<sup>13</sup>C, pulsed far IR emission 0-69370  
 hydrocarbons, aromatic, ultrasensitive detection by two-photon photoionisation 0-104473  
 lineshapes of three-level spectra in intense laser field, theory 0-69109  
 mixtures, two-component, two photon isotope separation, dynamics 0-102584  
 molecules, two-photon spectroscopy, dipole-forbidden transitions, double excited configurations, CNDO-CI methods 0-58332  
 naphthalene, mol. cryst., reson. four-wave mixing, third order susceptibilities 0-100654  
 naphthalene molecular ion, two-photon absorpt. dissoc. 0-74210  
 trans, trans-1,3,5,7-octatetraene, high-resolution one and two photon excitation spectra 0-78669  
 orthopositronium quenching by O<sub>3</sub>, meas. by two-photon coincidence rate difference technique 0-74262  
 partially oriented molecules, uniaxial, two-photon processes, polarised spectrosc. 0-74209  
 phenanthrene, two-photon excitation spectra, exciton-phonon and intramol. vibronic coupling 0-84774  
 positronium formation and quenching in Ar-O<sub>2</sub> mixtures, orthopositronium quenching cross section determ. 0-74261  
 propynal, IR-microwave double reson. and two-photon expts. 0-83396  
 pyrene in n-heptane solution, laser two-photon ionisation spectroscopy, photoionisation threshold determ. 0-78668  
 semiconductor wires, size-quantised, two-photon interband absorpt. 0-93256  
 subnatural linewidth spectra by optical double reson. with two-photon pumping 0-74200  
 three-level system, 2-photon reson. fluoresc. 0-87077  
 three-state atom, saturated two-photon absorpt. in perturber gas 0-106310  
 acetaldehyde, multiphoton ionisation meas., two-photon polarisation ratio of n-3s transition 0-91610  
 AgGaSe<sub>2</sub>, two-photon absorpt. and short pulse stimulated recombination 0-89054  
 As<sub>2</sub>S<sub>3</sub>, two photon light absorpt. dispersion, induced linear light absorpt. (*Russian*) 0-66231  
 As<sub>2</sub>S<sub>3</sub>, Se<sub>2</sub>, amorphous, picosecond relax. of optically induced absorption 0-97302



**two-photon spectra continued**

- Ca,  $4p^2 \rightarrow S_0-4s4p \rightarrow P_1-4s^2$   $S_0$  cascade rate, two photon coincidence meas. technique 0-95576  
 CdS, nonlinear self-action effect and absolute two-photon absorption coeff. 0-83649  
 Cs I,  $n^2S_{1/2}$  and  $n^2D_{3/2,5/2}$  states, energies 0-87066  
 Cs, two photon ionisation, destructive interference effect 0-74153  
 CuBr, biexciton dispersion, two-photon absorpt. 0-76045  
 CuCl, exciton spatial dispersion determ., two-photon Raman scatt. via excitonic mol. state 0-60595  
 D<sub>2</sub>O, pulsed opto-acoustic spectroscopy 0-62743  
 H in planetary nebulae, two-photon emission contrib. to UV continuum 0-109523  
 H<sub>2</sub>,  $E,F^2\Sigma^+$  state, collisional and radiative props. 0-58357  
 H<sub>2</sub>O, pulsed opto-acoustic spectroscopy 0-62743  
 He, Doppler-free two-photon high resolution spectroscopy 0-58197  
 Hg, two photon excitation, time resolved spectroscopy 0-87075  
<sup>129</sup>Xe, energy levels near B-state dissociation limit, two-photon spectrosc. obs. 0-106367  
 Kr, 6p levels, two-photon excitation, time resolved fluoresc., quenching, lifetimes and photoionisation cross section 0-78587  
 $\alpha$ -Li<sub>2</sub>O<sub>3</sub>, two-photon absorption spectra, energy struct. anal. 0-99785  
 LiNbO<sub>3</sub>, two-photon absorption spectra, energy struct. anal. 0-99785  
 NH<sub>3</sub> laser transitions, CW, two-photon pumped 0-99702  
 NO nonlinear laser spectroscopy, VUV harmonic generation 0-74175  
 Na+H(Ne)(Kr) vel.-changing collisions, effect on 2 photon and stepwise absorpt. line shape 0-87221  
 Ne, dipole dynamic polarisabilities and two-photon photoionisation cross section calc., R-matrix approach 0-102444  
 Pb stable isotopes, 2-photon spectroscopy, isotope shift of  $6-2 \rightarrow 7p \rightarrow 3P_0$  transition 0-87070  
 Rb vapour, Doppler-free two-photon dispersion and optical bistability 0-95940  
 Rb+Rb<sup>+</sup>, freq. shift, line broadening, phase interference effects, Doppler free two photon spectra 0-58200  
 U atomic beam, two laser irradiation, two photon reson. effects., visible spectra 0-63604  
 Yb highly excited levels, reson., visible two photon absorpt. spectra obs. 0-58228  
 ZnSe, band-edge photoluminesc., far-below band-gap excitation 0-76063

**two-photon spectroscopy**

- atomic cascade rate absolute meas. using two photon coincidence technique, appl. to Ca 0-95576  
 coherent background noise elimination from saturation spectrosc. signals using freq. offset pump 0-62733  
 coherent two-photon NMR, standard-basis operators, coherent averaging 0-82798  
 condensed phase fluoresc., double reson. excitation spectroscopy 0-86438  
 dye lasers, single-mode and multimode CW, as sources for obtaining power-squared corrected two-photon spectra 0-78849  
 high resolution two-photon FM laser spectroscopy of gas atoms, free of Doppler broadening 0-95748  
 nozzle-beam mol. multiphoton ionisation method for determ. two-photon absorpt. spectra 0-63728  
 photoconductivity detector for measurement of picosecond light pulses from Nd-glass laser 0-77872  
 resonant third-harmonic generation with ultrashort pulses, index mismatching, detuning and spectral effects 0-101844

**TWT see travelling-wave-tubes****Tyndallometry see turbidimetry****type I superconductors***see also intermediate state*

- approximate  $T_c$  formula, Eliashberg eqn. (Chinese) 0-107941  
 approximate  $T_c$  formula, Eliashberg eqn. calcs. (Chinese) 0-88662  
 critical field, anal. of expt. data (Chinese) 0-60151  
 cylindrical superconducting domain lattice dynamics (Russian) 0-93052  
 magnetic flux-free environment creation, cryogenic appl. 0-101797  
 magnetisation in thermodynamic and metastable phases 0-93027  
 mixed state, Josephson condition, phase jumps (Russian) 0-107967  
 soft thin superconductors, static paramagnetic response 0-84550  
 surface impedance, anomalous skin effect, surface supercond. regime (Russian) 0-80459  
 Al film, crit. temp. enhancement (Russian) 0-93021  
 Al film, lattice and bulk heat capacity meas. for normal and supercond. states 0-92684  
 Al film, order-parameter variations meas. 0-103797  
 Al film, superconducting transition temp. and lattice dynamics 0-93028  
 Al film in microwave radiation field, resistive state transition (Russian) 0-93038  
 Al granular films, self-ion implantation, supercond. transition temp. enhancement 0-103774  
 Al granular inhomogeneous, supercond. 0-103795  
 Al, nonlinear conductivity of thin films in mixed state (Russian) 0-80464  
 Al, nonlinear sound wave interactions, sound attenuation in weak superconducting state (Russian) 0-75310  
 Al, superconducting band gap anisotropy and Fermi surface anisotropy (Spanish) 0-84544  
 Al tunnel junctions, superconductivity enhancement by microwaves 0-107956  
 Al-Formvar-Sn coupled films, Ginzburg's excitonic supercond. model 0-90739  
 Bi crosspiece in high-resistance supercond. microbridge 0-93050  
 Bi, superconducting modification obtained by impact compression (Russian) 0-93020  
 Bi superconducting film, critical temp., thermal equilibrium (Russian) 0-80438  
 Cs, supercond., elec. resist. and phase transforms. under high press. (German) 0-107763  
 Ga II, superconducting high pressure phase, sp. ht. 0-70894  
 B-Ga, metastable, elec. props. in normal and supercond. states (Russian) 0-65520  
 Ga, nonlinear sound wave interactions, sound attenuation in weak superconducting state (Russian) 0-75310  
 Hg films, superconducting, far-IR and electrodynamic props. meas. 0-103957  
 In films, crit. temp. enhancement (Russian) 0-93021  
 In, mixed state, two-dimensional effect study, destruction current (Russian) 0-93054  
 In, supercond., expt. study of thermoelectricity 0-60138  
 In superconducting films, metastable states, supercooling fields 0-97031

**type I superconductors continued**

- In-Bi(Tl)(Pb), small  $\kappa$  supercond., phase transitions higher than second order 0-88668  
 In-In<sub>2</sub>O<sub>3</sub>-Pb, Josephson tunnel junction fabrication for MM-wave detector 0-100427  
 In-Sb, cryst. struct. after appl. of high press., supercond. transition temp. 0-70169  
 Pb, effect of changes in  $\alpha^2(\Omega)F(\Omega)$  on the zero-temp. energy gap 0-97025  
 Pb film, monocryst., heteroepitaxial growth, struct. defects, and elec. props. (Russian) 0-84403  
 Pb foil, crit. current density, pinning force density, shadow electron microscopy obs. 0-88696  
 Pb intermediate state, Meissner effect investigation by muon technique (Russian) 0-107954  
 Pb slabs, magnetisation and migration field, reversible stage 0-65737  
 Pb, strength loss in supercond. state, size factor effect (Russian) 0-88677  
 Pb-Cu(Ag) double layers, intermetallic boundary effects, tunnelling 0-88692  
 Pb-PbO-Pb, Josephson tunnel junction fabrication for Mm-wave detector 0-100427  
 Pb-sapphire interface, heat transfer coeff. meas., 2-80K 0-88419  
 Sn film, crit. mag. fields, temp. depend., penetration depth thickness depend. 0-70908  
 Sn film, crit. temp. enhancement (Russian) 0-93021  
 Sn film, limitation in microwave stimulation of supercond., crit. current meas. (Russian) 0-88695  
 Sn, film, superconducting fluctuations, transition temp. (Russian) 0-65740  
 Sn, nonlinear conductivity of thin films in mixed state (Russian) 0-80464  
 Sn, supercond. tunnel junction, quasiparticle excitation by  $\alpha$ -particles 0-103791  
 Sn-Bi(Sb), small  $\kappa$  supercond., phase transitions higher than second order 0-88668  
 Th-Dy, dil., paramag. Dy moment relax., Mossbauer spectra study 0-65755  
 Zn film for energy selective phonon detection 0-92621

**type II superconductors***see also mixed state*

- A15 compounds, disordered, reordering kinetics 0-96678  
 A15-type compounds, review of superconducting props. and structure 0-70909  
 A 15 type superconductors, acoustic phonon spectra, electronic density of state function (French) 0-80444  
 A-15 compounds, density of states model for lattice transforms. 0-65219  
 A-15 compounds, disordered, resist. and supercond. transition temp. 0-107944  
 A-15 superconductors, transition temp., d band relative displacement (Chinese) 0-103770  
 anisotropic, demagnetisation effects on lower critical field 0-97043  
 anisotropic, lower crit. field 0-60153  
 anisotropic superconductors, upper critical field theory 0-75692  
 antiferromagnetic, isolated vortex line 0-70912  
 bounded, intermediate state struct. form. near crit. field, role of surface 0-80465  
 critical field, anal. of expt. data (Chinese) 0-60151  
 current density distrib. in type II supercond. with normal inclusions, theory 0-80461  
 cylinder, magnetisation change induced by current near upper crit. field 0-70890  
 F 0-76235  
 flux-line-cutting threshold 0-88705  
 granular, Josephson junction array, phase transition 0-88684  
 granular, percolation theory, crit. props. 0-84575  
 granular films, percolation threshold and crit. current, theory 0-88706  
 granular metal, supercond. transition, increased resistance rel. to quasiparticle tunnelling 0-88689  
 graphite-K intercalation compound, effect of H addition on superconducting transition temp. 0-70872  
 hard superconductor, flux trapping, penetration depth determ. 0-100572  
 layered superconductors, Josephson coupling effects, review 0-84554  
 long ferromag. supercond., metastable supercond. state 0-103771  
 longitudinal current, continuous vortex cutting 0-88704  
 longitudinal currents in a system of Abrikosov vortices, Ginzburg-Landau eqn. anal. 0-70914  
 magnetic superconductor, shape effects 0-103773  
 metallic glasses, electronic structure rel. to elec. cond., supercond. and mag. props. 0-65429  
 metastable alloys, review of current work 0-81002  
 molybdenum chalcogenides, multicomponent, physical props. 0-84577  
 molybdenum ternary chalcogenides, structures and properties survey (Czech) 0-70870  
 nonideal, with dense pinning centres, threshold criterion 0-88703  
 nonideal type II supercond. wire, flux penetration in transverse mag. field (Japanese) 0-60154  
 order parameter change near  $H_{c2}$ , influence of transport current 0-75690  
 phonon Raman scattering in superconductors 0-100657  
 quasi-one-dimensional superconductor, critical mag. field, transition temp. (Russian) 0-93058  
 rare earth cpds.,  $R\text{Mo}_2\text{S}_8(\text{Se}_8)$  and  $\text{RRh}_2\text{B}_4$ , coexistence of supercond. and mag. ordering (Russian) 0-84542  
 rare earth rhodium tin intermetallic cpds., synthesis, supercond. and mag. props. 0-100547  
 superconducting order parameter perturbation flux pinning 0-103801  
 (TMTSF)<sub>2</sub>PF<sub>6</sub>, quasi-dimens. cond., diamagnetic AC susceptibility 0-103781  
 transition metal chalcogenides, quasi-one-dimens., elec. mag., and supercond. props., review (Russian) 0-93022  
 transition metals and alloys, superconductivity, relevance of mag. interactions 0-100545  
 transition metals silicides, atomic volume deviations and supercond.  $T_c$  0-75203  
 vortex pinning at edge dislocations, electrostatic mechanism 0-103802  
 wires, general crit. state model in two dimensions and zero applied field, uniqueness theorem 0-93062  
 zero-gap dirty, cond. electron spin resonance theory 0-103888  
 Al granular films, inhomogeneous supercond. transitions, microwave meas. 0-103789  
 Al granular films as weak link in Josephson devices 0-88685  
 Al, granular supercond., normal state cond. 0-88529

## type II superconductors continued

- Al:O supercond. film, RF complex impedance meas., dynamic pinning 0-84573
- Al-Ag, torque oscillations in mag. field (*Russian*) 0-103800
- Al-Cu, superconducting amorphous films of high stability 0-70889
- Ba<sub>2</sub>Mo<sub>3</sub>Se<sub>10</sub>, superconducting chalcogenides containing Mo<sub>6</sub> and Mo<sub>9</sub> clusters 0-103804
- BaPb<sub>1-x</sub>Bi<sub>x</sub>O<sub>3</sub>, superconducting thin films, RF sputtering prep. 0-76181
- BaPb<sub>1-x</sub>Bi<sub>x</sub>O<sub>3</sub>, superconducting props., Hall coeff. and elec. resist. meas. 0-84531
- Be alloys, enhancement of supercond. transition temp. 0-60129
- Cd-Sn alloy, superconductivity and microstructure 0-107949
- Co-Nb-C, obtained by liq. quenching, superconductivity 0-75699
- Co<sub>2</sub>Mo<sub>3</sub>S<sub>2</sub>O<sub>7</sub>, O-containing Chevrel phases, synthesis and props. 0-108368
- Cr<sub>3</sub>Si structure, rel. between phase diagrams and superconductivity 0-88330
- Cu-Nb<sub>3</sub>Sn multifilamentary tapes, in situ formed, crit. current density anisotropy 0-84576
- Cu-NbTi, composite conductor, acoustic emission 0-97032
- Cu-V-Si, supercond. props. 0-107945
- Cu<sub>1-x</sub>La<sub>x</sub>, sput-cooled, phase diagram and supercond. props. 0-70881
- Cu<sub>1-x</sub>Mo<sub>x</sub>S<sub>8</sub>, electron tunnelling spectroscopy expts. (*German*) 0-107966
- Cu<sub>2</sub>Mo<sub>3</sub>S<sub>2</sub>, constitution diagram, 11-2000K 0-108407
- Cu<sub>2</sub>Mo<sub>3</sub>S<sub>2</sub>O<sub>7</sub>, O-containing Chevrel phases, synthesis and props. 0-108368
- Cu<sub>96</sub>Nb<sub>30</sub>X<sub>30</sub> (X=Ti, Zr, Hf), superconductors with metastable ordered structs. 0-108484
- Cu<sub>96</sub>Zr<sub>30</sub>, amorphous alloys, supercond. transition temp., press. depend. 0-84524
- DyRh<sub>1-x</sub>Sn<sub>3-x</sub>, new supercond./mag. cpds., X-ray powder diffr. data 0-100215
- Er<sub>1-x</sub>Ho<sub>x</sub>Rh<sub>4</sub>B<sub>4</sub>, mag. and supercond. transitions, cryst. field effects 0-107950
- ErMo<sub>6</sub>Se<sub>8</sub>, mag. supercond., neutron scatt. obs. 0-70952
- ErRh<sub>2</sub>B<sub>4</sub>, ferromag. superconductor, vortex phase 0-80441
- ErRh<sub>2</sub>B<sub>4</sub>, long ferromag. supercond., metastable supercond. state 0-103771
- ErRh<sub>2</sub>B<sub>4</sub>, mag. supercond., NMR study of <sup>11</sup>B 0-107957
- ErRh<sub>2</sub>B<sub>4</sub>, superconducting, magnetic dilemma 0-75680
- ErRh<sub>2</sub>B<sub>4</sub>, superconducting thin films, critical mag. field 0-75693
- ErRh<sub>1-x</sub>Sn<sub>3-x</sub>, new supercond./mag. cpds., X-ray powder diffr. data 0-100215
- ErRh<sub>1-x</sub>Sn<sub>3-x</sub>, synthesis, supercond. and mag. props. 0-100547
- Er<sub>1-x</sub>Tm<sub>x</sub>Rh<sub>4</sub>B<sub>4</sub>, mag. and supercond. transitions, cryst. field effects 0-107950
- Er, Y<sub>1-x</sub>Rh<sub>x</sub>B<sub>4</sub>, mag. and supercond. transitions 0-70874
- EuMo<sub>6</sub>S<sub>8</sub>, Chevrel phase, mag. interactions, LMTO energy band studies 0-70606
- Gd<sub>2</sub>Mo<sub>3</sub>Se<sub>8</sub>, coexistence of supercond. and long range antiferromag. order 0-84534
- Hg-Ge vapour deposited films, cond. transitions, effect of disorder on supercond. 0-88659
- Ho(Ir,Rh)<sub>1-x</sub>B<sub>4</sub>, pseudoternary system, supercond. and mag. ordering 0-70876
- HoMo<sub>6</sub>S<sub>8</sub>(Se<sub>8</sub>), mag. supercond., neutron scatt. obs. 0-70952
- In film, Josephson arrays, proximity effect junctions 0-84553
- In superconducting films, metastable states, supercooling fields 0-97031
- In, superconductivity destruction singularities, intermediate state, hysteresis (*Russian*) 0-80460
- In whiskers from Sn-In alloys, current carrying, superconductivity breakdown 0-60133
- In-Bi, mixed state, pinning centre distrib. statistics, I-V characts. (*Russian*) 0-100571
- In-Bi(Tl)(Pb), small  $\kappa$  supercond., phase transitions higher than second order 0-88668
- In-Pb (7 at.%) alloy cylinder, magnetisation change induced by current near upper crit. field 0-70890
- In<sub>2</sub>Mo<sub>3</sub>Se<sub>10</sub>, superconducting chalcogenides containing Mo<sub>6</sub> and Mo<sub>9</sub> clusters 0-103804
- In<sub>2</sub>Sn, tetragonal supercond., lower and upper crit. field, anisotropy and temp. depend. 0-97042
- In<sub>0.69</sub>Tl<sub>0.31</sub>, supercond. transition temp., specific heat, pseudopotential form factor 0-97026
- Ir borides, MIr<sub>2</sub>B<sub>3</sub> (M=La, Th, U), supercond. and mag. props. 0-97028
- Ir-Y eutectic alloy, supercond. transition enhancement due to lattice softening 0-103775
- K<sub>2</sub>Mo<sub>3</sub>S<sub>9</sub>, superconducting chalcogenides containing Mo<sub>6</sub> and Mo<sub>9</sub> clusters 0-103804
- K<sub>2</sub>Mo<sub>3</sub>Se<sub>10</sub>, superconducting chalcogenides containing Mo<sub>6</sub> and Mo<sub>9</sub> clusters 0-103804
- (La<sub>1-x</sub>Y<sub>x</sub>)Ce, dil., Kondo supercond., transition temp., susceptibility and resist. 0-65733
- La, heat capacity and supercond. props. 0-65247
- La-Ag alloys, amorphous, elec. resist. and supercond. 0-70885
- La-Au, sput-cooled, Mossbauer effect and elec. resist., amorphous struct. 0-84676
- LaAl<sub>3</sub>, doped with Tb, Nd, or Pr, crystal field effects, tunnelling within mK range 0-70907
- LaAl<sub>3</sub>, supercond. and normal states, anomalous US attenuation and velocity change 0-80446
- La<sub>2</sub>C<sub>3</sub>, solid solution, lattice const. and superconducting transition temp. (*Russian*) 0-92496
- LaM<sub>2</sub>-Gd, M=transition metal, correl. between g-shift and stability, EPR study 0-88874
- LaPb<sub>3</sub>, doped with Tb, Nd, or Pr, crystal field effects, tunnelling within mK range 0-70907
- La<sub>90-x</sub>Pr<sub>x</sub>Au<sub>20</sub>, amorphous, mag. and supercond. props. 0-75713
- La<sub>2</sub>Se<sub>3</sub>(Se<sub>4</sub>), structural transitions, symm. anal. 0-92671
- LaSn<sub>3</sub>, doped with Tb, Nd, or Pr, crystal field effects, tunnelling within mK range 0-70907
- Mo ternary cpds., R<sub>2</sub>Sn<sub>2</sub>Mo<sub>6</sub>S<sub>8</sub> (R=La, Ce, Pr, Eu, Gd, Ho, Lu, Y, In, U), supercond. props. 0-97023
- Mo-Be solid solutions, superconducting transition, temp. changing peculiarity due to press. (*Russian*) 0-70878
- Mo-Ru(Si), amorphous superconductors, prep. by electron beam evaporation and liq. quenching, crit. temp. 0-103776
- Mo-Sn-Se system, supercond. crit. temp. and cryst. struct. (*Russian*) 0-107947
- Mo<sub>2</sub>PbS<sub>6</sub> embedded in resin, composite supercond., high transition temp. 0-88660

## type II superconductors continued

- (Mo<sub>0.6</sub>Ru<sub>0.4</sub>)<sub>90</sub>Si<sub>10</sub>B<sub>10</sub>, amorphous supercond. matrix, flux pinning by MoRu precip. 0-65756
- Mo<sub>2</sub>RuTe<sub>8</sub>, synthesis, struct., and elec. props. 0-92877
- MoS<sub>2</sub>, molybdenite band structural props. rel. to supercond. and semicond. 0-96781
- Mo<sub>6</sub>S<sub>8</sub> Chevrel phases with group IIIa metals, Nb, Hg, Pb and Cu, synthesis, stability and characts. 0-71608
- Mo<sub>6</sub>S<sub>8</sub>Sn, triple chalcogenide, NMR spectra in supercond. state (*Russian*) 0-93194
- Mo<sub>6</sub>Se<sub>8</sub>Sn, triple chalcogenide, NMR spectra in supercond. state (*Russian*) 0-93194
- Mo<sub>70</sub>Si<sub>20</sub>B<sub>10</sub>, amorphous alloys obtained by liq. quenching, superconductivity 0-75670
- Nb, critical current density, deviation from critical state model 0-84578
- Nb, effect of changes in  $\alpha^2(\Omega)F(\Omega)$  on the zero-temp. energy gap 0-97025
- Nb, film, critical mag. fields and currents, temp. depend. (*Russian*) 0-103798
- Nb, film, epitaxy, struct. and supercond. props., on (001) surface of fluorophlogopite (*Russian*) 0-80101
- Nb film, struct. and electrophys. props. at 4.2K 0-80436
- Nb films, ion beam sputtered, supercond., laser annealing effects 0-97024
- Nb granular films, ratio of supercond. transition temps. 0-84529
- Nb granular films as weak link in Josephson devices 0-88685
- Nb, granulated film, critical current temp. depend. (*Russian*) 0-103803
- Nb layer, ion bombarded, supercond. props. and struct. 0-88671
- Nb, peak effect due to vortex pinning in subsurface layer (*Russian*) 0-93060
- Nb, single crystals, fluxoid pinning by small nitride precip. 0-70913
- Nb, superconducting, thermodynamic props. 0-107955
- Nb, superconducting state influence on dislocation motion (*Russian*) 0-70208
- Nb, superconductive transition point as reference temp. 0-107943
- Nb, US attenuation, hysteresis near and below H<sub>c2</sub> 0-75676
- Nb, upper crit. field, temp. depend. and anisotropy 0-80462
- Nb/Cu, layered ultrathin coherent structs., supercond. props. 0-84525
- Nb/In composite superconductor, transport props. 0-88658
- Nb-Al-Ge-Cu, rapidly quenched, comp. and phase equilib. 0-76235
- Nb-Al(Ga, Si, Ge, Sn)-Cu, rapidly quenched, comp. and phase equilib. 0-76235
- Nb-Ga, A15 phase, chem. deposition on Hastelloy substrate, for superconducting tape (*German*) 0-104071
- Nb-Ga-Sc, superconducting transition temp., X-ray, microscopic and microprobe anal. (*Ukrainian*) 0-75667
- Nb-Ge, amorphous supercond. alloy, resistivity, transition temp. 0-60126
- Nb-Ge, compounds with A15 structure, films, TEM study (*French*) 0-80135
- Nb-Ge-Si, compounds with A15 structure, films, TEM study (*French*) 0-80135
- Nb-N, superconducting layers, sputtering in high vacuum apparatus (*German*) 0-89147
- Nb-Nb<sub>2</sub>O<sub>5</sub>-Pb Josephson junction formed on Nb film edge 0-107960
- Nb-Pb supercond. tunnel junction proximity effect, theory 0-65752
- Nb-Pb tunnel junction, crit. Josephson current, proximity effect model 0-93047
- Nb-Rh,  $\sigma$ -phase alloy, superconductivity and resistance behaviour 0-70882
- Nb-Si, compounds with A15 structure, films, TEM study (*French*) 0-80135
- Nb-Si(-V)(Zr)(Mo)(Ta)(W)(C)(B)(Ge), ductile amorphous, superconductivity 0-60131
- Nb-Ti, pinning curves, high field J<sub>c</sub> and scaling behaviour 0-93064
- Nb-Ti (50%), supercond., cryostat design for magnetisation study (*Spanish*) 0-75673
- Nb-Ti multifilaments, effect of mech. and thermal treatments of supercond. props. 0-104197
- Nb-Ti superconducting single layered multifilamentary coil, eddy current loss depend. on demagnetisation 0-97040
- Nb-Ti-Ta, pinning curves, high field J<sub>c</sub> and scaling behaviour 0-93064
- Nb-Ti-Zr ternary system, high-field supercond. 0-97045
- Nb-Ti(Mo), AC loss minimum, pinning, flux distribution 0-84574
- Nb-V<sub>2</sub>Ge mixed state, Meissner effect investigation by muon method (*Russian*) 0-107954
- Nb-Zr, crit. current, flow-flow resist. depend., allowance for superheating (*Russian*) 0-93061
- Nb<sub>3</sub>/Sn-Cu composites, in situ processed, supercond. props. 0-75698
- Nb<sub>3</sub>(Al,Ge) and Nb<sub>3</sub>(Al,Si), liq. quenched, supercond. props. 0-84580
- Nb<sub>3</sub>Al, A-15 struct., converted from cold worked BCC struct., crit. currents 0-75697
- Nb<sub>3</sub>Al, complex refractive index meas. 0-93264
- Nb<sub>3</sub>Al film, electron-beam coevaporated, prep. and characts. 0-76187
- Nb<sub>3</sub>Al, supercond. props. and lattice parameter, comp. and neutron irradiation effects 0-70880
- Nb<sub>3</sub>Al(Ga), NQR freq. temp. depend., supercond. transition temp. 0-93207
- NbC, diffuse, production and superconductive props. (*Bulgarian*) 0-80467
- NbC, supercond. critical temp., neutron irradiation effect 0-80433
- NbC<sub>x</sub>, supercond. transition temp., light element implantation effect 0-107951
- Nb(CN), supercond. critical temp., neutron irradiation effect 0-80433
- Nb<sub>0.75</sub>Ga<sub>0.25</sub>, A 15 phase high transition temp., sp. ht. determ. 0-60140
- Nb<sub>3</sub>Ga, transition temp. increase by rapid hardening with annealing 0-76275
- Nb<sub>3</sub>Ge coevaporated film, high supercond. transition temp., nucleation and growth 0-76185
- Nb<sub>3</sub>Ge film, high-temp. supercond. phase stabilisation w.r.t. prep. conditions (*Russian*) 0-70871
- Nb<sub>3</sub>Ge film, superconductivity, relevance of mag. interactions, EPR study 0-100545
- Nb<sub>3</sub>Ge, low temperature electron, neutron irradiation effects on critical temp. (*French*) 0-75669
- Nb<sub>3</sub>Ge, sputtered on Cu, film-substrate interface obs. by electron microscopy 0-65398
- Nb<sub>3</sub>Ge, supercond. film, amorphous content, X-ray diffr. study, rel. to transition temp. 0-75668
- Nb<sub>3</sub>Ge,Al<sub>1-x</sub>, ternary supercond. alloys, comp. variations 0-97022
- Nb<sub>3</sub>Ge(Si), amorphous films, thermally-activated internal friction peaks, structural obs. 0-80147



## type II superconductors continued

- NbN, diffuse, production and superconductive props. (*Bulgarian*) 0-80467
- NbN embedded in resin, composite supercond., high transition temp. 0-88660
- NbN granular films, supercond., crit. props. 0-88661
- NbN granular films as weak link in Josephson devices 0-88685
- NbN, granulated film, critical current temp. depend. (*Russian*) 0-103803
- NbN,  $\gamma$ - and  $\delta$ -forms, cryst. growth and supercond. transition temp. 0-107946
- NbN single crystal preparation, transition temperature determination 0-60776
- NbN, supercond. RF reactively sputtered films, deposition parameter effects on props. 0-80972
- NbN<sub>1-x</sub>C<sub>0.3</sub>, cryst. growth and supercond. transition temp. 0-107946
- Nb<sub>3</sub>Nb<sub>1-x</sub>Si<sub>x</sub>(Ge<sub>x</sub>), impurity stabilised A15 supercond., transition temp., lattice consts., specific heat 0-93026
- Nb<sub>3</sub>Pb superconducting film, prep., vac. deposition 0-89149
- NbSe<sub>2</sub> (2H), Raman scatt. from supercond. gap excitations 0-93340
- NbSe<sub>2</sub> (2H), Raman scatt. by supercond. gap excitations, coupling to CDWs 0-103956
- NbSe<sub>2</sub>, upper crit. fields and reduced dimensionality 0-70910
- NbSe<sub>2</sub>, CDW form., supercond. and Fermi surface determ., press. study 0-70891
- NbSe<sub>2</sub>, superconducting transitions and diamagnetism 0-84526
- Nb<sub>3</sub>Si A15 phase from amorphous Nb-Si alloys, high-press. synthesis 0-93516
- Nb<sub>3</sub>Si A15 struct., high press. synthesis (*Chinese*) 0-70917
- Nb<sub>3</sub>Si, substituted, splat cooling influence on supercond. T<sub>c</sub> and stoichiometry 0-80439
- Nb<sub>3</sub>Sn A15 composite superconductors, hydrostatic extrusion (*French*) 0-104090
- Nb<sub>3</sub>Sn bronze process, flux pinning scaling law depend. on strain 0-75696
- Nb<sub>3</sub>Sn, coherence parameter, nonlinear high temp. supercond. elements with A-15 lattice (*Russian*) 0-60127
- Nb<sub>3</sub>Sn composite, superconducting transition depend. on non-hydrostatic stress 0-107948
- Nb<sub>3</sub>Sn, composite superconducting wire, critical current-bend strain relationships 0-93063
- Nb<sub>3</sub>Sn, effect of changes in  $\alpha^2(\Omega)F(\Omega)$  on the zero-temp. energy gap 0-97025
- Nb<sub>3</sub>Sn, filaments in Cu matrix, thermal strain effects on superconducting critical temp. 0-93032
- Nb<sub>3</sub>Sn film formation, solubility, precipitating processes (*Russian*) 0-92792
- Nb<sub>3</sub>Sn, flux density gradient determ. by Faraday effect 0-107969
- Nb<sub>3</sub>Sn microfilamentary superconducting composite, critical currents, fracture props. 0-107970
- Nb<sub>3</sub>Sn, monofilaments, radiation-enhanced diffusion growth, crit. current density 0-65758
- Nb<sub>3</sub>Sn multifilamentary composite supercond. wires, transverse sections prep., ion milling, TEM obs. of grain size 0-101000
- Nb<sub>3</sub>Sn multifilamentary supercond. composites, crystallographic texturing 0-71669
- Nb<sub>3</sub>Sn, multifilamentary superconductor preparation by 'in situ' and cold powder methods, review 0-93522
- Nb<sub>3</sub>Sn, on LiNbO<sub>3</sub> substrate, US attenuation of SAW in applied mag. field 0-75678
- Nb<sub>3</sub>Sn, supercond. composite, residual stress state, crit. currents 0-80468
- Nb<sub>3</sub>Sn, supercond. props., effect of neutron irradi. 0-80463
- Nb<sub>3</sub>Sn, Young's modulus, 4.2-300K, behaviour near martensitic transition 0-66564
- Nb<sub>3</sub>Sn-Cu multifilamentary composite wire, Nb<sub>3</sub>Sn filament morphology and grain size 0-100855
- NbTi monofilamentary wire in current sharing state, supercond. temp. sensor use 0-57288
- NbTi/In composite superconductor, transport props. 0-88658
- NbTi-Cu, supercond. composite, use in temp. and heat transfer coeff. meas. 0-77780
- (Nb<sub>0.99</sub>Ti<sub>0.01</sub>)<sub>1-x</sub>Ge<sub>x</sub>, high T<sub>c</sub>, resist. meas. 0-88531
- Nb<sub>2</sub>Zr<sub>30</sub>, supercond. and normal, sp. ht. meas., 2-20K 0-70893
- (Nb<sub>0.99</sub>Zr<sub>0.01</sub>)<sub>3</sub>Sn, AC power losses in parallel AC and DC mag. fields 0-97041
- NdRh<sub>2</sub>Si<sub>4</sub>, new supercond./mag. cpds., X-ray powder diff. data 0-100215
- Ni-Nb-C, obtained by liq. quenching, superconductivity 0-75699
- Ni<sub>2</sub>Mo<sub>2</sub>S<sub>6</sub>O<sub>8</sub>, O-containing Chevrel phases, synthesis and props. 0-108368
- Os borides, MO<sub>3</sub>B<sub>2</sub> (M=Lu, U), supercond. and mag. props. 0-97028
- Pb creep, low-temp., thermal heating and quantum mechanisms, supercond. transition effects 0-79868
- Pb, film, spatially inhomogeneous state appearance under laser pumping conditions 0-93053
- Pb granular film, Josephson coupled, resistive transition 0-88683
- Pb-Bi alloy, crit. mag. fields, influence of parameters 0-75691
- Pb-Bi alloy, T<sub>c</sub> evaluation, from ab initio band struct. calcs. on Pb 0-75502
- Pb-Bi-Tl alloy, crit. mag. fields, influence of parameters 0-75691
- Pb-Bi(Ni), creep, low-temp., thermal heating and quantum mechanisms, supercond. transition effects 0-79868
- Pb-In film, superconducting tunnel junction, pulsed quasiparticle injection 0-84565
- Pb-Na (8.4 at.%), surface flux pinning, crit. state model 0-97044
- Pb-Si superconducting solutions, effect of hydrostatic compression on tunnelling (*Russian*) 0-65746
- Pb-Sn(Bi)(Ni), strength loss in supercond. transition, nonmag. and paramag. impurities influence (*Russian*) 0-70875
- Pb-Tl alloy, crit. mag. fields, influence of parameters 0-75691
- PbMo<sub>3</sub>S<sub>8</sub>, supercond., upper crit. field meas. up to 600 kG 0-93057
- PbMo<sub>3</sub>S<sub>8</sub>, electron tunnelling spectroscopy expts. (*German*) 0-107966
- PbMo<sub>3</sub>S<sub>8</sub> wire, powder processed, crit. current density and field 0-80466
- PbMo<sub>3</sub>S<sub>6</sub>O<sub>2</sub>, O-containing Chevrel phases, synthesis and props. 0-108368
- Pd-Cu(Ag)(Au) alloys-H solid solutions, superconducting transition temp. behaviour (*Russian*) 0-70879
- Pd-Ni-H, hydride formation in high press. range 0-65235
- PdH, superconducting transition critical temperature, BCS theory, phonon spectra (*Spanish*) 0-84535
- PdH<sub>2</sub>, local, soft modes, superconductivity thermal neutron inelastic scatt. (*Chinese*) 0-70331

## type II superconductors continued

- PdH<sub>2</sub>, superconducting transition temp., inverse isotope effect, Einstein model 0-65734
- (Pd<sub>0.8</sub>Rh<sub>0.2</sub>)<sub>3</sub>H<sub>2</sub>, elec. resistivity studies 0-59957
- Pd<sub>30</sub>Zr<sub>70</sub>, amorphous alloys, supercond. transition temp., press. depend. 0-84524
- Rh borides, RRh<sub>3</sub>B<sub>2</sub> (R=rare earth), supercond. and mag. props. 0-97028
- Ru borides, RRu<sub>3</sub>B<sub>2</sub> (R=rare earth, Y, Th, or U), supercond. and mag. props. 0-97028
- (SN)<sub>x</sub>, supercond. props. rel. to fibrous morphology 0-84570
- Sc<sub>2</sub>C<sub>3</sub>, superconducting phase synthesis at high press. and temp., critical field (*Russian*) 0-65732
- Sn film, metastable supercond. alloys, produced by low temp. ion implantation 0-88670
- Sn-Bi(Sb), small  $\kappa$  supercond., phase transitions higher than second order 0-88668
- Sn-Cu film, metastable supercond. alloys produced by low temp. ion implantation 0-88670
- Sn-In, nonlinear conductivity of thin films in mixed state (*Russian*) 0-80464
- Sn-Sn<sub>2</sub>O<sub>3</sub>-Sn long Josephson tunnel junction, flux flow, crit. conditions 0-80452
- SnMo<sub>3</sub>S<sub>8</sub>, Chevrel phase, mag. interactions, LMTO energy band studies 0-70606
- Sn<sub>2</sub>Mo<sub>3</sub>S<sub>8</sub>, struct. anal. supercond. props. 0-97023
- Ta, effect of changes in  $\alpha^2(\Omega)F(\Omega)$  on the zero-temp. energy gap 0-97025
- Ta, superconductive transition point as reference temp. 0-107943
- Ta-Rh,  $\sigma$ -phase alloy, superconductivity and resistance behaviour 0-70882
- Ta<sub>20</sub>Nb<sub>10</sub>, Abrikosov vortex formation kinetics (*Russian*) 0-93055
- TaSe<sub>2</sub> intercalated with methylamine, supercond. layer cpd., crit. field enhancement and reduced dimensionality 0-60152
- TaSe<sub>2</sub>, intercalated with organic cpds., upper crit. fields and reduced dimensionality 0-70910
- TaSe<sub>2</sub>, pure and intercalated with organic cpds., upper crit. fields and reduced dimensionality 0-70910
- TaSe<sub>2</sub>, superconducting transitions and diamagnetism 0-84526
- Tc, superconductivity and Fermi surface calcs. 0-70873
- Te-Au film, metastable supercond. alloys, produced by low temp. ion implantation 0-88670
- Ti-Mo (3 to 35 wt.%), high-pressure influence on transition temp. to supercond. 0-107952
- Ti-Nb-Si, amorphous alloy, supercond. props. and crystn. behaviour, TEM and DTA study (*Japanese*) 0-84536
- Ti-Nb-Zr-Fe, supercond. and paramag. props., effect of Fe additions (*Russian*) 0-65730
- Ti-Nb-Zr-Ta, superconducting props. comp. depend., stress effects and precipitation behaviour, X-ray scatt. 0-93059
- TiN films, reactively RF sputtered, struct. and elec. props., substrate bias effects 0-96763
- TiN, low-energy ion-stimulated deposited, supercond. props. 0-88664
- TiN, supercond. critical temp., neutron irradi. effect 0-80433
- Ti<sub>2</sub>Mo<sub>15</sub>Se<sub>19</sub>, superconducting chalcogenides containing Mo<sub>6</sub> and TiN clusters 0-103804
- Ti<sub>0.33</sub>WO<sub>3</sub>, bronze, elec. resist. meas., anisotropy, supercond. 0-75569
- TmO<sub>2</sub>S<sub>8</sub>, low temp. Mossbauer study and mag. susceptibility 0-80656
- V columnar films, crit. field anisotropy, depend. on prep. conditions (*Russian*) 0-93056
- V, electron-phonon coupling constant calc. (*Russian*) 0-70624
- V, small particles, crystal structure, magnetic and superconducting props. 0-97121
- V-(Ti), rotating discs, hysteresis losses and mag. phenomena 0-75695
- (V<sub>1-x</sub>Cr<sub>x</sub>)<sub>3</sub>Si, elastic moduli, 4.2 to 290K, softening near supercond. transition (*Russian*) 0-92582
- V<sub>3</sub>Ga, A15 cpd., hydrogenation effects on supercond. transition temp., lattice parameters 0-103772
- V<sub>3</sub>Ga, supercond. A15 phase, prep. by controlled precip. 0-81000
- V<sub>3</sub>Ge, A15 cpd., hydrogenation effects on supercond. transition temp., lattice parameters 0-103772
- V<sub>3</sub>Ge(Si), Gruneisen parameter and thermal expansion eval. at room temp. 0-70351
- V<sub>3</sub>Hf<sub>1-x</sub>Zr<sub>x</sub>, normal and supercond. state, transition temps., mag. susceptibility and specific heat determ. (*Russian*) 0-60132
- V<sub>3</sub>Si, A15 cpd., hydrogenation effects on supercond. transition temp., lattice parameters 0-103772
- V<sub>3</sub>Si embedded in resin, composite supercond., high transition temp. 0-88660
- V<sub>3</sub>Si film, optical props. (*Russian*) 0-93418
- V<sub>3</sub>Si, magnetic susceptibility, density of states model for lattice transformation in A-15 compounds 0-65219
- V<sub>3</sub>Si, neutron irradi., grain boundary pinning, field-depend. change of crit. current density 0-65759
- V<sub>3</sub>Si, supercond. props., effect of neutron irradi. 0-80463
- V<sub>3</sub>Si tunnel junctions, energy gap investigation 0-84569
- V<sub>3</sub>Si-SiO<sub>2</sub>-Mo<sub>3</sub>Re<sub>2</sub>, supercond. tunnel junctions 0-107961
- V<sub>3</sub>Si(Ga), coherence parameter, nonlinear high temp. supercond. elements with A-15 lattice (*Russian*) 0-60127
- V<sub>3</sub>Si<sub>1-x</sub>Ge<sub>x</sub>, elastic props., 77 to 290K, rel. to supercond. transition temp. (*Russian*) 0-66560
- V<sub>3</sub>Si<sub>1-x</sub>Ge<sub>x</sub>, solid soln., longitudinal and transverse US wave propag. rate, 4.2 to 300K (*Russian*) 0-103423
- W-Re amorphous alloys, phase-slip and localisation diffusion lengths 0-107747
- W<sub>70</sub>Si<sub>30</sub>B<sub>10</sub>, amorphous alloys obtained by liq. quenching, superconductivity 0-75670
- YM<sub>2</sub>-Gd, M=transition metal, correl. between g-shift and stability, EPR study 0-88874
- YbMo<sub>3</sub>S<sub>8</sub>, low temp. Mossbauer study and mag. susceptibility 0-80656
- Zr, H(D) implanted, superconductivity enhancement obs. 0-70884
- Zr-Rh-H(D), superconducting transition temp., effect of H(D) conc. 0-84532
- ZrV<sub>2</sub>, anomalous softening at martensitic transform. 0-93630

## U-centres

- alkali halide: H<sup>-</sup> (D<sup>-</sup>), local modes and colour centre absorpt. bands, analogy 0-60632
- alkali halide crystals, mixed, impurity centre local vibrs., comp. depend. of spectral parameters 0-79898
- alkali halides, mixed, U-centre localised modes 0-100319

U-centres continued

alkali halides, U-centre electronic struct. cluster-Bethe lattice calc. 0-107737  
KBr(I):D, inelastic light scattering of localised vibration of interstitial H atom in alkali halides 0-88998  
metal-semiconductor disordered interface, supercond. transition temp. enhancement by bipolaron interface centres 0-84528  
KBr(Cl):OH<sup>-</sup>, cc U<sub>2</sub> to H<sub>2</sub>O<sup>-</sup> defects conversion after UV photodecomp. 0-107230  
KCl<sub>1-x</sub>Br<sub>x</sub> impurity centre local vibrs., comp. depend. of spectral parameters 0-79898  
K<sub>1-x</sub>Na<sub>x</sub>Cl and K<sub>1-x</sub>Rb<sub>x</sub>Cl, impurity centre local vibrs., comp. depend. of spectral parameters 0-79898

UBV photometry *see stellar photometry*

u.h.f. tubes *see ultra-high-frequency tubes*

ultimate tensile strength *see tensile strength*

ultra-high-frequency tubes

*see also microwave tubes*

No entries

ultracentrifuges *see centrifuges*

ultrafiltration *see filtration*

ultrasonic absorption

abietic acid, transverse US wave propag., glass and liquid transition region 0-79883  
acrylamide aqueous solution, ultrasonic investigation (*Chinese*) 0-107371  
algorithm for relaxation spectra in US spectroscopy 0-79038  
aniline-cyclohexane, hypersound velocity, absorption temp. depend (*Russian*) 0-75303  
anthracene, mol. crystal, meas. of US attenuation coeff. by optoacoustical methods (*French*) 0-70317  
attenuation meas., diffraction corrections for finite size of source and receiver 0-96153  
austenite cladding layers, damping of ultrasound 0-104390  
binary liquid mixtures, containing one rotational isomeric relaxing liquid 0-70315  
biological cells, intracellular temp. distrib. 0-61623  
biological tissue, dependence on constituent proteins 0-61621  
cyclohexanol, orientationally disordered phase, Brillouin scatt. study 0-93351  
defect-containing crystals, US absorpt. near displacive phase transitions, anomalous temp. depend. 0-92612  
dichloromethane-cyclohexane, liq. mixture, intermol. vibrational energy transfer, US study 0-70313  
dielectric plate, dimensional effects in ultrasonic wave absorpt. coeff. (*Russian*) 0-70321  
p-dioxane-H<sub>2</sub>O at 11 and 25°C, US absorption 0-65171  
dioxane-water solvent, mixed, with addition of 1-1-valent electrolyte 0-87632  
electrolytic solution, ionic drift from 50 Hz supply, pulse echo technique 0-70314  
erythrocyte membranes in 12 to 68 MHz range 0-89727  
ferroelectric, uniaxial, crit. behaviour, electrostrictive coupling role 0-71329  
ferroelectrics, structural phase transitions, ultrasonic velocity and attenuation meas. 0-75977  
furan-cyclohexane, liq. mixture, intermol. vibrational energy transfer, US study 0-70313  
gases, resonant tube for sound absorption meas. at low freq./press. ratios 0-96156  
graphite fibre reinforced epoxy, US attenuation as an indicator of fatigue life 0-85118  
n-hexane-perfluoro-n-hexane mixtures, US vel. and absorpt. mixtures 0-88281  
ice, plastic deformation, ultrasonic wave attenuation by dislocations (*French*) 0-59564  
insulators, high-intensity US wave vel., phonon-phonon interaction effects 0-70323  
interferometry, US attenuation or velocity meas. 0-58874  
isopropanol-n-propanol aq. mixtures, US relax., US absorpt. and vel. meas. (*French*) 0-103426  
liquid systems, 10 to 30 MHz, 25 to 60°C, undergraduate expt. using 2-transducer RF pulse method 0-69608  
liquids, shock excitation for diffuse-field reverberation studies 0-88267  
liver pathology characterisation, clinical appl. of a US attenuation coeff. estimation technique 0-76813  
low-viscosity liquids containing electrolytically-generated gas bubbles 0-58849  
magnetic fluids, US attenuation, MHD approach 0-60389  
magnetic superconductors, spin fluctuation and US attenuation 0-80445  
metal, FCC, dislocation behaviour at high strain rates, US detection method, data analysis basis 0-85136  
metal, quantum oscills. with dislocations under press. (*Russian*) 0-88273  
metallic films, ultrasound attenuation, size magnetoacoustic effect (*Russian*) 0-107869  
3-methylpentane-nitroethane critical binary liquid mixture, US absorpt. 0-107376  
microemulsion, sound velocity and absorption 0-81374  
naphthalene, mol. crystal, meas. of US attenuation coeff. by optoacoustical methods (*French*) 0-70317  
nematic liquid crystals, acoustic props., rotating mag. field study 0-88034  
nitrobenzol-n-hexane, hypersound velocity, absorption temp. depend (*Russian*) 0-75303  
noble metals, interaction of thermal and acoustic phonons thermoelastic relaxation, calcs. for US longitudinal waves 0-65165  
 $\beta$ -picoline-water solution, light scatt. spectra, ultra- and hypersonic absorpt. (*Russian*) 0-93353  
piezoelectric nondegenerate semicond., magnetoacoustic effects of nonparabolic band struct. 0-96948  
polyacrylamide aqueous solution, ultrasonic investigation (*Chinese*) 0-107371  
polydimethyl siloxane solns., attenuation meas. 0-107372  
polyethylene, high press. phase, US, DTA, and X-ray diffr. study 0-75188  
polymers, filled, cumulative internal damage, US assessment 0-97653  
polystyrene solution, differential meas. of ultrasonic velocity (*French*) 0-75302  
polyvinylidene fluoride films, HF meas., 300 to 1500 MHz 0-74667  
pulse echo waveform rel. to acoustic characteristics of continuous medium 0-67145  
PVA, aq. solns., US absorpt., acetate groups effects (*Russian*) 0-65162

ultrasonic absorption continued

rare earth metals, electronic sound attenuation anomalies at transition to helical phase, Fermi surface topology (*Russian*) 0-92807  
semiconductor film, US propagation in quantised elec. field (*Russian*) 0-60050  
sol-gel transition, US attenuation meas. 0-101043  
solids, acoustic wave emission, absorpt. and propag. in THz range 0-65164  
steel, medium, C, US attenuation, mag. field effect 0-89428  
steel, type AC/HT-2, grain diameters, US attenuation 0-89429  
superconducting and superfluid substances, role of physical acoustics in investigations, review 0-96090  
superconductor, nonequilib., with wideband source of quasiparticles, kinetic theory 0-80442  
superconductors, nonequilibrium states, narrow nonequilibrium sources (*Russian*) 0-88687  
suppression of finite-amplitude primary wave attenuation, parametric acoustic arrays, use of bubbles 0-74563  
torsional vibrations in metals 0-58856  
water-alcohol mixtures, attenuation meas., method of streaming 0-88272  
Ag<sub>3</sub>SbS<sub>3</sub>(AsS<sub>3</sub>), electroacoustic echo, ultrasonic wave attenuation (*Russian*) 0-88280  
Al alloy sheets, type 7075-T6 used in aircraft, early detection of fatigue cracks 0-66730  
Al, superconducting band gap anisotropy and Fermi surface anisotropy (*Spanish*) 0-84544  
Ar, liquid, compressional viscosity and vibrational relaxation 0-70311  
Bi film, amorphous, temp. dependence of SAW attenuation 0-75679  
Bi, giant quantum attenuation anomalies of sound waves at high mag. field, temp. and freq. depend. 0-70587  
Bi, giant quantum attenuation anomalies of sound waves at high mag. field, extra attenuation peaks 0-70588  
CdS crystals, orientational depend. of photoacoustic effect (*Russian*) 0-65167  
CeB<sub>6</sub>, magnetostriction, US absorpt. and thermal expansion 0-66004  
Cr, antiferromagnetic, US attenuation and phase diagram 0-103831  
Cr, mag. phase diagram, near, spin-flip temp., US attenuation 0-60267  
Ge crystals, orientational depend. of photoacoustic effect (*Russian*) 0-65167  
Ge, electron-hole drop drag by ultrasound (*Russian*) 0-100437  
Ge, pure and n-type, US velocity and attenuation, second and third order elastic moduli 0-70325  
Ge, spectral diffusion in acceptor-hole system at low temp., ultrasonic hole-burning expt. 0-92610  
Ho(NO<sub>3</sub>)<sub>3</sub> solns., f-f transitions, intensity anal., correl. with cond. and US absorpt. 0-97292  
In<sub>2</sub>Bi, pre-melting absorption of sound 0-88277  
K, ultrasonic attenuation at low temp., spherical Fermi surface model 0-84255  
K<sub>2</sub>Ba(NO<sub>3</sub>)<sub>2</sub>, elastic props. 0-96588  
K(H<sub>1-x</sub>D<sub>x</sub>)<sub>2</sub>PO<sub>4</sub>, polarisation relaxation time and Landau kinetic coeff. rel. to degree of deuteration 0-84251  
KMnF<sub>3</sub>, critical dynamics of sound 0-103424  
LaAl<sub>2</sub>, supercond. and normal states, anomalous US attenuation and velocity change 0-80446  
Li single crystal, attenuation measurement in vicinity of martensitic phase transformation 0-75358  
Mo, longwave dopplers, nonlocal Hall effect, surface impedance, size effect (*Russian*) 0-80253  
NH<sub>4</sub>Cl, acoustic absorption by soft modes of defects 0-59584  
Nb, mixed state, hysteresis of US attenuation 0-84549  
Nb, US attenuation, hysteresis near and below H<sub>c2</sub> 0-75676  
Nb<sub>2</sub>Sn, on LiNbO<sub>3</sub> substrate, US attenuation of SAW in applied mag. field 0-75678  
Pb<sub>2</sub>Ge<sub>2</sub>O<sub>11</sub>, ferroelec. transition, US and elasto-optic props. 0-60527  
Pb<sub>5</sub>(GeO<sub>4</sub>)(VO<sub>4</sub>)<sub>2</sub>, Pb<sub>5</sub>(SiO<sub>4</sub>)(VO<sub>4</sub>)<sub>2</sub>, and Pb<sub>2</sub>GeO<sub>11</sub>, elastic nonlinearity and acoustic losses 0-59554  
PdSiCu, amorphous, US attenuation and vel. studies at low temps. 0-88278  
RBH<sub>3</sub>(SeO<sub>3</sub>)<sub>2</sub>, US vel. and absorpt. near ferroelec. Curie temp. 0-97206  
SO<sub>2</sub>-tetrachloromethane, solns., near critical point, ultrasound absorpt. obs. 0-65160  
Si, amorphous, US attenuation at low temp., internal friction peak 0-65152  
Si, pure and n-type, US vel. and attenuation, evaluation using elastic moduli 0-70325  
SiC, acoustic props. study at 9.43 GHz 0-65169  
SiO<sub>2</sub>, vitreous Brillouin scatt., 35 GHz phonon vel. and absorpt. below 1K 0-100664  
SiO<sub>2</sub>-Al<sub>2</sub>O<sub>3</sub>, vitreous US vel. and absorption 0-107380  
SiO<sub>2</sub>-B<sub>2</sub>O<sub>3</sub> glasses, Brillouin scattering meas. of attenuation and vel. of hypersounds 0-100309  
SiO<sub>2</sub>-TiO<sub>2</sub>, vitreous, US vel. and absorption 0-107380  
Ta, shear elastic constant, anomalous temp. behaviour, US study 0-79855  
Ti-Ni, internal friction and US props. (*Russian*) 0-84247  
TmFeO<sub>3</sub>, acoustic vel. and attenuation shifts at spin reorientation phase transition 0-65986  
V<sub>2</sub>Si, supercond. mixed state, low temp. tetragonal-domain-reorientation phenomena, US expts. and thermal props. 0-60141  
W, longwave dopplers, nonlocal Hall effect, surface impedance, size effect (*Russian*) 0-80253  
ZnCl<sub>2</sub>-LiCl(NaCl)(KCl)(CsCl), molten, US absorption coeffs. and bulk viscosity coeffs. (*Japanese*) 0-88271  
ZnCl<sub>2</sub>-PbCl<sub>2</sub>, molten, US velocity and absorpt., thermodynamic quantities and bulk viscosity (*Japanese*) 0-84249

ultrasonic applications

*see also biomedical ultrasonics; ultrasonic materials testing; ultrasonic welding*  
acoustic imaging, phase sampler, improved image quality (*French*) 0-79088  
acoustic imaging with nematic liquid crystals (*French*) 0-69617  
blood flow detection in human heart, US pulsed Doppler flowmeter system, microcomputer based 0-104690  
conference, New Orleans, LA, USA 0-73101  
correlation of return signals with bipolar digital representation of broadcast waveform 0-99897  
data collection aperture, based on long-wavelength imaging system 0-99905



**ultrasonic applications continued**

- film cleaning by ultrasonic liquid cavitation and acceptable solvents 0-62769
- heat transfer systems 0-74723
- HF probing method for investigation of hydrodynamic cavitation in viscous liquid 0-87676
- imaging, visualization and characterization, conf., Houston, TX, USA (Dec. 1979) 0-106672
- laser beam spatial coherence control by progressive US wave 0-78885
- microelectronic appls., use of broadband vibratory systems 0-74613
- optical coherence modulation by US waves, partial coherence depend. on US parameters 0-58453
- scanning electron microscopy, US imaging technique 0-95192
- spectroscopy appl. in NDT 0-79090
- transmission tomography 0-94301
- washing and drying of multiwire chambers 0-105624
- wideband Fresnel focusing array response, echography appls. 0-74640

**ultrasonic delay lines**

- capillary tubing delay lines for operation at 20 MHz 0-74654
- GHz bandwidth bulk acoustic delay line using mosaic transducers and stagger tuning 0-74657
- metal film-coated, measurements of SAW attenuation 0-74619
- SAW tapped delay-line for US imaging 0-74636
- SAW transduction on Si substrates with polyvinylidene fluoride films 0-74618
- AlN/Al<sub>2</sub>O<sub>3</sub> for fabrication 2.148 GHz SAW oscillator 0-74680
- PVF<sub>2</sub> Lamb wave delay line, highly temp. dependent 0-106687
- Si-SiO<sub>2</sub> influence on frequency-temp. coeff. of SAW devices 0-79066
- SiC, acoustic props. study at 9.43 GHz 0-65169

**ultrasonic devices**

- see also *ultrasonic delay lines; ultrasonic transducers*
- 2-D separated media semiconductor convolver for acoustic Fourier transforms of optical images 0-74308
- acousto-optic tunable filter, programmable 0-74511
- aerial ultrasonic generators using metal resonators (French) 0-79074
- broadband vibratory systems for microelectronic appls. 0-74613
- driven equilibrium Fourier transform sensor operating at 100 MHz 0-74612
- flowmeter, multichannel 0-103089
- flowmeter, PLL oct. (Japanese) 0-79414
- integrated optic spectrum analyser, design of Bragg cell 0-74515
- memory correlator based on photoinduced surface storage of SAW patterns in LiNbO<sub>3</sub> 0-74309
- multistrip coupler for coupling of surface skimming bulk waves 0-74630
- nuclear materials safeguards, ultrasonically identified security seals for CANDU safeguard systems 0-63297
- prism couplers for Rayleigh and Lamb waves, anal. 0-69619
- Q-switch, ultrasonic, for Nd:glass laser 0-64034
- reflective dot array for high-performance signal processing, development 0-74623
- signal processors using multichannel SAW correlation and convolution 0-74611
- transmission scanning acoustic microscope, single lens 0-87669
- tuning fork for HF operation, second-mode, finite element anal. and expts. 0-102980
- US-optical correlator for spatial freq. meas. 0-95995
- PVF<sub>2</sub> polymer probe for mapping pressure field from arrays 0-74669

**ultrasonic diffraction**

- diffraction corrections for finite size of source and receiver in US vel. and attenuation meas. 0-96153
- large aperture bowl transducers, diffraction pattern 0-58833
- US flaw detection, diffraction of normal modes by a compliant disk 0-87603
- welded joint, US reflection from irregularities 0-104389

**ultrasonic dispersion**

- binary alloys, acoustic modes in random and correlated alloys, order-disorder transform. 0-65189
- isobutytic acid-water critical mixtures, US hypersonic study 0-88268
- water, supercooled, sound vel. dispersion, struct. relax. effect, Brillouin scatt. obs. 0-107375

**ultrasonic effects**

- bean roots, non-thermal inhibition of growth and detect. of acoustic emissions, 1 MHz US 0-104643
- cavitation at a fluid-solid boundary, cleaning and erosion 0-65158
- cavitation in liquid crystals. 0-87633
- cavitation intensity in liquids, organic comparisons 0-106820
- Chinese hamster V-79 cells, US lethality obs. 0-85443
- coagulation of Re hydrosols 0-58853
- cochlear, struct. and functional changes following US irradi. 0-89791
- collagen synthesis stimulation, human fibroblasts, role of US-induced cavitation 0-85442
- conducting media, ultrasound excitation, varying EM fields 0-87635
- crystallising bar, oscillations, EM excitation 0-84845
- dielectric, regulated, thermal capacity, strong US waves effects (Russian) 0-65240
- diffraction of laser light, nonlinear liquids 0-64270
- drawing, of continuous round ultrasonically perturbed profiles, stressed states at centre of deformation (Russian) 0-59557
- Drosophila eggs, killing on exposure to traveling and standing US wave fields 0-101223
- E. coli, effect of US at 1.5 MHz 0-72212
- Elodea, cell death thresholds for 0.45-10 MHz US 0-67149
- gamma-quantum coherent scatt. in field of US waves, kinematic theory 0-80649
- hydrodynamic wave excitation at tangential discontinuity by high-intensity US beams 0-58851
- hyperthermia, deep local, induction by US and EM fields, problems and choices 0-94283
- hyperthermia in tissue-like substances, EM and US induction 0-98012
- laser speckle reduction in image plane by US modulation of spatial coherence 0-106459
- light diffraction, adjacent US beams 0-87629
- light wave diffraction by complex spectral composition US 0-95939
- lymphocyte cell DNA damage by US diagnosis 0-67148
- mammalian cells, in vitro US irradi. at hyperthermic temps. 0-94282
- Mossbauer absorption spectra variations induced by LF excitations 0-102904
- oedema experimentally induced in rats by AgNO<sub>3</sub>, effect of US on response 0-104642

**ultrasonic effects continued**

- piezoelectric probe, radiation and reception field investigations, pulsed mode, Kirchhoff approx. 0-87636
- pregnant mice, acute US exposure at different stages of gestation 0-94284
- steel, stainless, fixing pins for fractured bones, strength, ultrasound effect 0-71710
- thermocytetes, rat, US-induced changes in rates of influx and efflux of K<sup>+</sup> in vitro 0-89793
- transkull transmission of an intense focused US beam, lesion production at 500 kHz 0-89792
- vapour bubble growth in US field 0-87608
- InSb:Te, cryst. growth from melt, pulling method, US effects on facet growth 0-76169
- TiB<sub>2</sub> thick film on low C steel substrate, CVD in US field, crystallite size. 0-84854

**ultrasonic equipment**

- acoustic imaging with electronic ccts., book 0-99899
  - B-scan imaging with automated water-delay system 0-98041
  - biomedical, Aberdeen phased array, real-time US scanner with dynamic focus 0-72276
  - biomedical real-time scanner with pulsed Doppler and T-M facilities, obstetrical appls. 0-67172
  - blood pressure analysis system for treadmill stress testing 0-81674
  - Brillouin scattering cell for liquids 0-106694
  - bubble quantification system, appl. to decompression of animals and man 0-76869
  - concentrators, optimum geometry 0-102952
  - decontamination system for reactor fuel transfer pool, remotely operated 0-68916
  - delay lines, transducer bonding material investigations (Japanese) 0-79097
  - dynamically focused electronic sector scanner based on CCDs 0-98042
  - Echosimulator, function generator for meas. of US diagnostic equipment characts. (German) 0-104685
  - fission reactor materials safeguarding, fuel assembly identification using US signatures, statistical aspects 0-69620
  - fission reactor materials safeguarding, US signatures for remote-controlled identification of fuel assemblies 0-63296
  - fission reactor primary coolant flowmeter 0-73912
  - flow-meters, compensation-type, development of structs. (Russian) 0-83866
  - flowmeter, wide beam 0-106856
  - flowmeters, recal. of characts. and calibration 0-103086
  - focusing probes for flaw detection 0-104383
  - immersion apparatus for determination of HF storage and loss moduli for polymers and polymeric composites 0-74668
  - improvements in ultrasonic testing, narrow-band transmitter pulses of continuously variable wavelength 0-93706
  - Indian status in 1979, industry and medicine appl. 0-81668
  - intraoesophageal imaging, heart dynamics 0-94303
  - microsphere probe for pressure field meas. up to 10 MHz 0-96159
  - neonatal peripheral circulation, human, characterisation by US pulsed Doppler technique 0-76815
  - oscillating US heavy plate body testing equipment, computer controlled, working experience (German) 0-93720
  - scanner for imaging appls. in medicine 0-72388
  - shadow flaw detectors, metrological peculiarities when inspecting thick rolled steel sheet 0-81263
  - signal shape anal., ultrasonic pulsed measuring instrums. 0-87678
  - sloped probe for angular type reflector, US inspection appl. 0-104391
  - sonoprobe for Si crystal microcracks detection 0-74662
  - test unit for abrasive granular materials, failure characts. in US field 0-85112
  - transceiver for US inspection units 0-89458
  - transducer manipulator outside link of coupling fluid in US expts. 0-106693
  - viewing system for reactor fuel assemblies under liquid Na 0-57875
  - waterfilled US testing tanks, appl. of filled rubber material system to echo absorpt. 0-96059
  - Al-Mg-Si alloy, dispersion hardened, concentrators, US waveguides appl. (Polish) 0-89237
- ultrasonic materials testing**
- acoustic defectoscopes, low freq., elec. simulation of compound piezoelec. transducers 0-102956
  - acoustic emission signal, amplitude distrib., information context 0-108666
  - acoustic emission test apparatus 0-61041
  - acoustic wave probing techniques 0-71855
  - AE location, receiving channels, selection of number 0-108676
  - AMUR-6 instrument to detect defects and indicate their location 0-104402
  - austenite cladding layers, damping of ultrasound 0-104390
  - automated ultrasonic testing system for piping in nuclear power plant (Japanese) 0-71839
  - bond evaluation, anal. of problem 0-71847
  - brass wire, US inspection, immersion method 0-66757
  - butt welded joint defects inspection 0-81244
  - capacitative excitation of elastic oscillations 0-71862
  - ceramic, piezoelectric, US instrument for determ. characts. 0-66752
  - ceramic inclusions meas. and characterisation, Si<sub>3</sub>N<sub>4</sub> 0-76474
  - coarse-structure materials, inspection of part quality using LF US methods, review 0-81264
  - composite aircraft materials 0-81274
  - composite piezotransducer for LF acoustic inspection using electrical models 0-104393
  - computer-controlled system for measuring two-dimensional acoustic velocity fields in solid samples 0-76468
  - concrete quality assessment, US pulse vel. meas. practical use 0-100991
  - conducting media, ultrasound excitation, varying EM fields 0-87635
  - contact media for US thickness meas. and defect inspection over wide temp. range 0-104395
  - crack depth measurement by US techniques 0-71859
  - data acquisition system for processing and recording of acoustic emission signals, on-line 0-57266
  - defectoscopy, development of and problems in theory of normal waves, review 0-81265
  - deposited metal, US echo inspection procedure 0-89425
  - echo pattern and amplitude, construction of AVG diagrams (German) 0-108657
  - echo-mirror method with transform. of elastic waves 0-108663

**ultrasonic materials testing continued**

- extruded billets, residual stress determ. from acoustoelastic meas. 0-76467
- fatigue crack growth investigation, testing equipment 0-81247
- fatigue cracks, US visualization, advantages over pulse-echo methods 0-66738
- fatigue damage, procedure for early detect. and remaining life prediction 0-71848
- flaw detection, diffraction of normal modes by a compliant disk 0-87603
- flaw detection, focusing probes 0-104383
- flaw detection, progress in theory and principles 0-81262
- flaw parameters determ., plastic strain and growing cracks identification 0-81252
- flaw width investigation by inclined scanner with regulated directivity diagram 0-89452
- flow detectors, tuning methods for time depend. sensitivity control unit 0-108667
- forgings, untreated surface, US monitoring, sensitivity comparison 0-66751
- fusion reactor vacuum vessel welds, ultrasonic scanner 0-99288
- granular materials, abrasive, failure and strength characts. in US field, test unit 0-85112
- graphite fibre reinforced epoxy, US attenuation as an indicator of fatigue life 0-85118
- hologram numerical reconstruction in NDT (*German*) 0-97667
- hydraulic liquids, cavitation-erosion props. assessment using ultrasonic disperser 0-71832
- imaging system, digitally controlled electronically scanned and focused 0-74659
- immersion testing, effects of curved entry surfaces on calibration, steel sample expts. 0-71849
- immersion type, dead-zone minimization and data-bearing parameters of ultrasonic echo signals 0-66753
- immersion unit for inspecting thin wire and fibres 0-66757
- improvements in ultrasonic testing, narrow-band transmitter pulses of continuously variable wavelength 0-93706
- inclusion cleanliness assessment (*French*) 0-104411
- industrial, Indian 1979 status 0-81668
- ingots, struct. effect on flaw detection 0-66722
- inspection of metallic atomic power station equip., portable unit 0-104394
- insulators, acoustic emission detection prior to elec. breakdown 0-88924
- interface waves between bonded solids, optical meas. of US waves 0-71825
- large aperture bowl transducers, diffr. pattern 0-58833
- leak detection, threshold sensitivity eval. criteria 0-104401
- LMFBR, liquid Na-limestone concrete interaction following HCDA, US meas. 0-78412
- magnetized samples, defects, magnetostrictive conversion of US waves into EM fields 0-66008
- material deformation parameters measurement, ultrasonic fatigue systems, new technique 0-97676
- metal, acoustic signal shape produced by high density electron fluxes 0-108674
- metal, FCC, dislocation behaviour at high strain rates, US detection method, data analysis basis 0-85136
- metal fatigue crack detection using nondestructive evaluation (NDE) methods 0-71826
- metallurgical noise reduction in austenitic welds testing 0-76466
- metals, echo-mirror method with transform. of elastic waves 0-108663
- methylundecanhydride hardened phenol formaldehyde resin, hardening kinetics and mech. losses 0-66520
- microprocessor utilization in ultrasonic nondestructive inspection systems 0-71845
- microscopic defects in stressed materials, rel. between acoustic emission and defect development 0-85127
- n 0-76464
- near-surface defects, US detection and analysis (*German*) 0-93728
- nuclear reactor pressure vessels, thick steel sections, inspection by US nondestructive examination 0-102258
- oscillating US heavy plate body testing equipment, computer controlled, working experience (*German*) 0-93720
- piezoelectric probe, conversion ratios 0-69624
- piezoelectric radiators, heat-treatment method for improved resolu. 0-104196
- piezoelectric transducer, contactive, spectrum of natural freqs. 0-69623
- piezoelectric transducer, surface excited, US field 0-64331
- piezoelectric transducers, broadband, production 0-61044
- plate, flaw reconstruction by automatic US testing (*German*) 0-61059
- polycyclic aromatic hydrocarbons sorbed on fly ash, recovery for quantitative determ. 0-61177
- polyethylenepolyamine hardened epoxy resin, hardening kinetics and mech. losses 0-66520
- polymers, filled, cumulative internal damage, US assessment 0-97653
- porous layer, angle dependence of impedance of polyurethane foam 0-81243
- pressure and interference fields (*German*) 0-89436
- production inspection of parts, automatic noise-blanking, pulse-timing discriminator 0-76472
- PTFE and filled PTFE, nonlinear creep, compression bulk modulus 0-66593
- raw kaolin, acoustical investigations of the effect of additives on elastic props. 0-66559
- receiver-transmitter for ultrasonic inspection units 0-89458
- refractories, elastic moduli meas., US method for up to 2000K (*French*) 0-104373
- residual stress drawing 0-97674
- resonance method, appl. in inspection of symmetrical products 0-89449
- review 0-104360
- rolled sheet, artificial surface cracks, reflection of normal shear waves 0-89448
- SAW transducer array for surface defect imaging in metals 0-74660
- semiconductor surface eval. using SAW convolver 0-97677
- shadow flaw detectors, metrological peculiarities when inspecting thick rolled steel sheet 0-81263
- signal shape anal., ultrasonic pulsed measuring instrums. 0-87678
- sloped probe for angular type reflector 0-104391
- solids, visualisation using Schlieren photoelastic apparatus (*Italian*) 0-88274
- sonoprobe for Si crystal microcracks detection 0-76462
- sputter target cracking, acoustic emission testing 0-81248

**ultrasonic materials testing continued**

- steel, acoustic emission sources and dislocation patterns 0-61040
- steel, alloy, mechanical props. meas. by acoustic methods, chem. composition influence 0-104384
- steel, austenitic stainless, butt welds, US exam. 0-93710
- steel, ball bearing rods, inspection installation 0-81268
- steel, Co-Cr-Mo, type HY 180 correl. between advanced NDT evaluation methods and fracture mech. parameters 0-97675
- steel, Cr-Ni-Mn, AISI 4340, correl. between advanced NDT evaluation methods and fracture mech. parameters 0-97675
- steel, ferritic, clad with austenitic steel 309, US detection of undercladding microcracks (*Italian*) 0-108683
- steel, fracture initiation moment, I-integrals critical value determ., ultrasonic method 0-61049
- steel, high-strength castings, AE study of intercrystalline crack form. 0-104403
- steel, hot blooms, US inspection to detect internal pipe 0-97655
- steel, medium, C, US attenuation, mag. field effect 0-89428
- steel, mild, US detect. of H embrittlement 0-71822
- steel, stainless austenitic welds, US inspection 0-71821
- steel, type AC/HT-2, grain diameters, US attenuation 0-89429
- steel, US critical angle reflectivity, near-surface metallic prop. gradient effect 0-70516
- steel, US inspection to 1000°C, hot-metal defectoscopy 0-66750
- steel microstructure study 0-76469
- steel pipe, flaw detection by US pulse-echo method 0-66756
- steel pressure vessel plates, US examination, PISC project 0-57861
- steel pressure vessel US examination, PISC trials result anal. scheme 0-57863
- steel wire, US inspection, immersion method 0-66757
- stratified medium reflection coeffs. estimation by signal processing techniques (*French*) 0-81242
- structural ceramic components eval. 0-76473
- Temp-1 system for the ultrasonic inspection of bulky aluminium alloy plates 0-66755
- test piece defects, quantitative meas. (*German*) 0-85122
- tone-burst spectroscopy, influence of phase cancellation and pulse shape artifacts 0-81276
- transmission line of probe for hot metal inspection, spurious signals 0-66754
- turbine rotor shaft, US testing, sensitivity multiplication factor 0-85125
- UD-24 instrument, piezoelec. US transducers 0-108664
- ultrasonic and eddy current testing of welded titanium tubes (*Japanese*) 0-108651
- ultrasonic pulse echo technique for location of discrete flaws in metal components 0-74548
- underwater testing of materials by ultrasonics (*German*) 0-97670
- unipolar transducers for nondestructive eval. 0-76471
- US flaw detector, microprocessor controlled, for flaw classification in welded plates 0-100992
- US spectroscopy appl. in NDT 0-79090
- weld inspection system for Space Shuttle external fuel tank, automatic, interim report 0-76463
- weld inspections with freq. scanned SH waves 0-76465
- welded joint, US reflection from irregularities 0-104389
- welded joints in sugar extraction diffusion apparatus 0-93703
- welded structure reliability estimation, acoustic emission signal appls. 0-93702
- wire fatigue properties, fast testing method using 23 kHz US frequency 0-89460
- wood, standing trees, US pulse echo method for flaw detection 0-66731
- Al alloy sheets, type 7075-T6 used in aircraft, early detection of fatigue cracks 0-66730
- Al<sub>2</sub>O<sub>3</sub>, elastic moduli meas., US method for up to 2000K (*French*) 0-104373
- B fibre, US inspection, immersion method 0-66757
- Cd thermal neutron filter, in-cell US inspection 0-68791
- Fe, cast, US flaw detection by boxcar integration 0-89437
- Fe, cast, US study of sections undergoing deform. or thermal cycling 0-104285
- Fe nodular parts, comparison of sonic-resonance and US velocity techniques for quality control 0-97654
- Fe-Ni, sintered, porosity determ. by US attenuation and sound vel. meas. (*German*) 0-76437
- Fe<sub>30</sub>B<sub>20</sub>, Metglas 2605, Young's modulus meas. using piezoelectric US composite oscillator technique 0-108656
- Mo wire, US inspection, immersion method 0-66757
- Ni alloy ZrH<sub>2</sub>Si<sub>6</sub>U, US method of porosity detection 0-71828
- PVF<sub>2</sub> thin film SAW transducers for 8 MHz delay line 0-88876
- Si crystal microcrack detection by ultrasonoprobe 0-66733
- Si wafers eval. using SAW 0-76470
- Si<sub>3</sub>N<sub>4</sub>, bending strength, deformability, elastic moduli and brittleness 0-81191
- W wire, US inspection, immersion method 0-66757

**ultrasonic measurement**

- see also *ultrasonic velocity measurement*
- absolute calibration of piezoelectric transducers 0-79099
- air bubble growth meas. by rectified diffusion at 22.1 kHz 0-96155
- densitometer development for two-phase flow density meas. in pressurised water reactor 0-77759
- elastic const. changes in V<sub>a</sub> and Nb<sub>53</sub>Ta<sub>47</sub> caused by addition of H, effects of hydrostatic pressure 0-75287
- gases, resonant tube for sound absorption meas. at low freq./press. ratios 0-96156
- inertialess sensing with US measurement systems 0-64315
- larynx height and vocal fold vibratory pattern 0-98184
- liquid level measurements using longitudinal, shear extensional and torsional waves 0-77757
- medical probe power, use of semiconductor strain gauges 0-87679
- microsphere probe for pressure field meas. up to 10 MHz 0-96159
- nuclear appls. of US thermometry 0-73365
- particle motion 3D sensing via multibeam laser system 0-83722
- piezotransducers, surface-excited, calc. and meas. of US fields 0-102957
- polydimethyl siloxane solns., attenuation meas. 0-107372
- SAW, particle motion fields anal. 0-79042
- spectrum anal. using frequency-tracked gated RF pulses 0-79079
- standing and travelling waves in water-filled wedge, obs. by frequency-shift holography 0-79089
- tethered float radiometer for US therapy equipment output power meas. 0-104691



**ultrasonic measurement continued**

Al-SiC cermet elasticity, porosity meas. by US means 0-81101  
LiCl aqueous solns., dynamical props. by ultrasonic propag. meas. 0-76517

**ultrasonic paramagnetic resonance** *see acoustic paramagnetic resonance***ultrasonic propagation**

*see also ultrasonic diffraction; ultrasonic dispersion; ultrasonic reflection; ultrasonic refraction; ultrasonic relaxation; ultrasonic scattering; ultrasonic transmission*

acrylamide aqueous solution, ultrasonic investigation (Chinese) 0-107371  
anisotropic crystals, 3-D representations of bulk acoustic wave props. 0-75311

caster oil, calculation of nonlinearity parameters thermodynamic method 0-79880

ceramic piezoelectric transducer, anomalous radiation pattern due to parasitic Lamb wave generation 0-96170

composites, random particulate, US wave propagation, velocity as function of frequency and volume fraction of inclusions 0-59583

condensed matter, conf., Zilina, Czechoslovakia (Sept. 1978) 0-82563

conducting media, ultrasound excitation, varying EM fields 0-87635

defectoscopy, development of and problems in theory of normal waves, review 0-81265

dispersive media, pulse propagation in human soft tissues 0-81644

glass fibre reinforced plastics, ageing by boiling in water, effect on physicochem. props. 0-60892

light beam diffraction, phase geometry variation analysis 0-106441

liquid mixtures, US propag. parameters, effective Debye temp. 0-79882

mammalian tissues, compilation of literature on empirical US props. 0-98007

Mossbauer spectrum, ultrasonic sideband intensity depend. on acoustic field statistics 0-75905

nonlinear effects in cavitating liquids, optical visualisation 0-106651

nonlinearity parameter for solids, relationship with Gruneisen parameter 0-74561

nonreciprocal effect, during light passage through US beam 0-106443

organ-puncture needles, needle surface and tissue propag. 0-96052

periodically corrugated piezoelec. cryst., Bleustein-Gulyaev waves behaviour 0-96115

$\beta$ -picoline-water solution, light scatt. spectra, ultra- and hypersonic absorpt. (Russian) 0-93353

polyacrylamide aqueous solution, ultrasonic investigation (Chinese) 0-107371

polydimethyl siloxane solns., attenuation meas. 0-107372

polydimethylsiloxane-2, liq., thermodynamic props. at high press., US propag. meas. (Russian) 0-65157

polyvinylidene fluoride films, SH and Lamb waves propag. 0-75948

rays, curvature limitations for computerised tomography 0-94301

SAW propagation along X axis on Y-cut plate of Se 0-75313

shear velocity of muscle tissues, mech. props. determ. 0-108930

solids, acoustic wave emission, absorpt. and propag. in THz range 0-65164

solids, visualisation using Schlieren photoelastic apparatus (Italian) 0-88274

spherically curved transducers, anal. of focusing action 0-64332

steel, alloy, mechanical props. meas. by acoustic methods, chem. composition influence 0-104384

TGS, ferroelec. single crystal, low freq. nonlinear effects 0-84490

TGS and deuterated cpd., ferroelec. US relax. time constant 0-84257

thermo-optical US generation due to moving laser source in liquid 0-102903

wavevector reversed ultrasound studies of phase transitions 0-75306

Bi:Te(Sn,Sb,Pn), US attenuation meas. 0-92614

Ge, pure and n-type, US velocity and attenuation, second and third order elastic moduli 0-70325

<sup>4</sup>He, solid and liq., US finite amplitude wave propag. 0-80024

MnO, antiferromag., temp. depend. of elastic consts., US study 0-79854

Rb<sub>2</sub>CoF<sub>6</sub>, critical fluctuations near Neel temp., US attenuation study 0-108013

Si, pure and n-type, US vel. and attenuation, evaluation using elastic moduli 0-70325

Ti-Ni, internal friction and US props. (Russian) 0-84247

V<sub>2</sub>Si<sub>1-x</sub>Ge, solid soln., longitudinal and transverse US wave propag. rate, 4.2 to 300K (Russian) 0-103423

**ultrasonic radiation** *see ultrasonic waves***ultrasonic reflection**

angular type defect, methods of calc. 0-104391

beam displacement of US transverse wave, reflection at free boundary surface (German) 0-87580

dead-zone minimization and data-bearing parameters of ultrasonic echo signals 0-66753

foam, US characts. of open-cell polyurethane foam layers for airborne appls. 0-96597

intensity profiles of reflected beams near Rayleigh angle, numerical integration method 0-64242

nonspecular reflection effects for liquid-solid-liquid layered media 0-102882

porous layer, angle dependence of impedance of polyurethane foam 0-81243

pulses from surfaces, appl. to location of discrete flaws in metal components 0-74548

SAW reflection from quartz powder on piezoelec. substrate 0-74565

steel, US critical angle reflectivity, near-surface metallic prop. gradient effect 0-70516

stratified medium reflection coeffs. estimation by signal processing techniques (French) 0-81242

tissues, inhomogeneous media model 0-108981

welded joint, US reflection from irregularities 0-104389

Al<sub>2</sub>O<sub>3</sub> layer on stainless steel in water, leaky wave generation 0-75419

**ultrasonic refraction**

isotropic nondispersive solid, meas. method for vel. of sound 0-69616

**ultrasonic relaxation**

algorithm for relaxation spectra in US spectroscopy 0-79038

benzene, mean free path meas., US relax. 0-59585

binary liquid mixtures, containing one rotational isomeric relaxing liquid 0-70315

condensed matter, conf., Zilina, Czechoslovakia (Sept. 1978) 0-82563

dichloromethane, mean free path meas., US relax. 0-59585

p-dioxane-H<sub>2</sub>O at 11 and 25°C, US absorption 0-65171

uran, liq., US phase vel. decay in space and time 0-99891

uran, mean free path meas., US relax. 0-59585

**ultrasonic relaxation continued**

n-hexane-perfluoro-n-hexane mixtures, US vel. and absorpt. mixtures 0-88281

isobutyric acid-water critical mixtures, US and hypersonic study 0-88268

isopropanol-n-propanol aq. mixtures, US relax., US absorpt. and vel. meas. (French) 0-103426

nitrobenzene and n-heptane critical mixture, US and hypersonic acoustical props. 0-65170

noble metals, interaction of thermal and acoustic phonons thermoelastic relaxation, calcs. for US longitudinal waves 0-65165

pyridine, mean free path meas., US relax. 0-59585

steel, US critical angle reflectivity, near-surface metallic prop. gradient effect 0-70516

TGS and deuterated cpd., ferroelec. US relax. time constant 0-84257

thiophene, mean free path meas., US relax. 0-59585

Bi:Te(Sn,Sb,Pn), US attenuation meas. 0-92614

K(H<sub>1-x</sub>D<sub>x</sub>)<sub>2</sub>PO<sub>4</sub>, polarisation relaxation time and Landau kinetic coeff. rel. to degree of deuteration 0-84251

O<sub>2</sub>-CO<sub>2</sub> mixture, temp. difference of molecular vibr. relaxation freq. from 300 to 675K 0-74238

O<sub>2</sub>-H<sub>2</sub> mixture, temp. difference of molecular vibr. relaxation freq. from 300 to 675K 0-74238

O<sub>2</sub>-He mixture, temp. difference of molecular vibr. relaxation freq. from 300 to 675K 0-74238

Pb<sub>3</sub>(GeO<sub>4</sub>)(VO<sub>4</sub>)<sub>2</sub>, Pb<sub>3</sub>(SiO<sub>4</sub>)(VO<sub>4</sub>)<sub>2</sub>, and Pb<sub>3</sub>GeO<sub>11</sub>, elastic nonlinearity and acoustic losses 0-59554

Se, amorphous, retardation of deform. near T<sub>g</sub> point 0-84256

**ultrasonic scattering**

backscattering measurements in laboratory waveguide 0-64259

forward sound scatt. by small nylon cylinders in water 0-96054

liver, human, theoretical modelling 0-89785

Rayleigh wave scattering by surface breaking crack, ray analysis 0-69575

SAW propag. along boundary with periodic inhomogeneities 0-102905

scanning laser probe for acoustic wave phenomena observation at liquid-solid interfaces 0-100386

theory, scatt. by single objects 0-99892

turbulence in water, interaction with 1 MHz waves 0-87619

**ultrasonic transducers**

absolute calibration of piezoelectric transducers 0-79099

acoustic vibrating systems, use of nonlinear phenomena for IC microwelding appls. 0-74656

acoustooptic effect calc., integrated 0-91944

arbitrarily electroded piezoelec. plate acoustic spatial response determ. 0-99910

array, transducer elements tuning 0-87684

arrays, broadband directional reception 0-96126

axisymmetric transducers, under various conditions of baffle, nearfield radiation patterns determ. 0-99909

baffled planar, calc. of acousto-optic (Raman-Nath) parameter for entire sound field 0-74689

bonding material investigations, US delay lines (Japanese) 0-79097

broadband chirp transducers for integrated optics spectrum analyzers 0-74514

broadband matching of piezo-transducers for acousto-optical devices (Russian) 0-64329

capacitive excitation of elastic oscillations 0-71862

ceramic piezoelectric transducer, anomalous radiation pattern due to parasitic Lamb wave generation 0-96170

charge distribution for non-periodic transducers using cct. model 0-74691

circular piston, Gaussian-Laguerre description of US fields 0-64239

computer-controlled system for measuring two-dimensional acoustic velocity fields in solid samples 0-76468

conical solid horn with flange, FEM analysis of free vibrations (Japanese) 0-79045

cylindrical transducer scatter scanner for medical ultrasonographic imaging 0-96154

diffraction corrections for US vel. and attenuation meas. 0-96153

electronically-addressed bulk acoustic wave Fourier transform device 0-74637

fibre-optic pressure sensor 0-58878

field intensity distribution measurement, liquid-surface relief method, transient behaviour for pulsed transducers 0-95073

film cleaning by ultrasonic liquid cavitation and acceptable solvents 0-62769

focused, for acoustical imaging of objects buried in seafloor sediment 0-79036

Greens function method for quasi-static anal. of interdigital transducers 0-69621

high-efficiency narrowband transducers and arrays, development 0-58880

imaging biomedical piezoelectric micro-array technology for improved image quality (German) 0-98052

large aperture bowl transducers, diff. pattern 0-58833

loading, monitoring by impedance bridge technique, effect of US field geometry 0-102950

magnetically tunable ultrasonic transducers for shear waves 0-74682

manipulator outside tank of coupling fluid in US expts. 0-106693

measurement systems, inertialess sensing 0-64315

medical ultrasonics, transmitters and receivers from piezoelectric materials 0-76819

multiphase interdigital transducers and the crossed-field model 0-92006

optical determ. of low US powers of circular piston transducers 0-64319

optically-controlled acoustic transducers, piezoelect. and electrostrictive 0-74638

opto-acoustic transducer structs., recent investigations 0-74688

opto-acoustic transducers, improved equivalent cct. 0-74658

piezoceramic aperiodic transducer, mech. load study 0-87700

piezoceramic transducers, transient charact. 0-106704

piezoelectric, included scanner for corner reflector acoustic channel 0-106705

piezoelectric discs, radial vibrs. 0-96166

piezoelectric radiator of longitudinal acoustic waves with an inhomogeneous elec. field 0-87693

piezoelectric shear-mode acoustic wave receiving, transfer characts. 0-87696

piezoelectric surface excited, thick, transient, pulse and amplitude-frequency charact. 0-102958

piezoelectric transducers of tall, narrow elements of acoustic imaging array 0-74690

**ultrasonic transducers continued**

- polyvinylidene fluoride film appl., poled, short duration unipolar stress pulse detection, generation 0-106695  
 polyvinylidene fluoride film polymer transducer, with US appl., durable lead attachment techniques 0-79094  
 polyvinylidene fluoride SAW transducers, evaluation of performance 0-74617  
 pulsed, sound field description, evolution equations 0-87682  
 quartz X-cut crystal transducer, laser intensity distrib. meas. using US diff. 0-64092  
 radiation patterns of acoustical arrays with quantized time delays 0-74566  
 receiving array having power response 0-74653  
 SAW, apodized, radiation conductance 0-96174  
 SAW, parameter calc. with power scattering coeffs. (*Russian*) 0-64317  
 SAW IDT, Al evaporation conditions 0-92007  
 SAW IDT, bulk wave radiation suppression, theoretical investigation of crystalline orientation 0-58886  
 SAW transducer array for surface defect imaging in metals 0-74660  
 SAW transducers on Si substrates with polyvinylidene fluoride films 0-74618  
 sonic transducer, Langevin type, made from  $\text{Pb}(\text{Zr,Ti})\text{O}_3$  type 1 ceramic, performance characts. 0-79095  
 speckle reduction in US B-mode images of human tissue, using transducer and signal processor 0-74634  
 spherically curved transducers, anal. of focusing action 0-64332  
 surface charge on unapodized periodic IDI 0-91947  
 surface excited thick piezoelectric transducer, output current form 0-87701  
 Swzawa wave broadband thin-film interdigital transducers 0-74681  
 thermographic-photographic technique for US intensity pattern characterisation 0-106689  
 thickness-extensional trapped energy mode transducer array, increased bandwidths and mode shapes 0-74633  
 tilted-finger chirp transducer for design of wideband guided-wave acousto-optic Bragg deflector 0-74510  
 Tonpilz piezoelec. transducer design using nonlinear goal programming 0-106696  
 unipolar transducers for nondestructive eval. 0-76471  
 velocity-of-propagation meter, based on interferometer 0-79084  
 vibrations of very small amplitude, measurement using laser probe 0-73443  
 $\text{FeBO}_3$ , magnetically tunable ultrasonic transducers for shear waves 0-74682  
 PVF<sub>2</sub>, Lamb wave delay line, highly temp. dependent 0-106687  
 PVF<sub>2</sub>, thin film SAW transducers for 8 MHz delay line 0-58876  
 $\text{Pb}(\text{Zr,Ti,Mg,W})\text{O}_3$ , low-Q ceramics, props. and transducer appl. 0-75944  
 $\text{ZnO}$ , CVD of epitaxial films on sapphire, SAW interdigital transducer fabrication 0-66430  
 $\text{ZnO}$  film concave transducers for scanning acoustic microscopes 0-74663  
 $\text{ZnO-SiO}_2$ -Si SAW device, interface transduction 0-102949

**ultrasonic transmission**

- foam, US characts. of open-cell polyurethane foam layers for airborne appls. 0-96597  
 liquid-solid-liquid layered media 0-102882  
 transmission line of probe for hot metal inspection, spurious signals 0-66754

**ultrasonic velocity**

- see also *ultrasonic dispersion*  
 abietic acid, transverse US wave prop., glass and liquid transition region 0-79883  
 acetic acid, vapour, chem. reaction effect on speed of sound 0-103100  
 aniline hydrobromide, ferroelastic, acoustic softening near transition temp. 0-96617  
 aniline-cyclohexane, hypersound velocity, absorption temp. depend (*Russian*) 0-75303  
 binary liquid mixture, energy of vaporisation evaluation 0-65209  
 biological tissue, dependence on constituent proteins 0-61621  
 brass, meas. method for isotropic nondispersive solids 0-69616  
 t-butyl alcohol, aq. soln. 0-88237  
 composites, random particulate, US wave propagation, velocity as function of frequency and volume fraction of inclusions 0-59583  
 cyclohexanol, orientationally disordered phase, Brillouin scatt. study 0-93351  
 dichloromethane-cyclohexane, liq. mixture, intermol. vibrational energy transfer, US study 0-70313  
 elastic waves in crystals, invariance relations 0-84250  
 electrolytic solution, ionic drift from 50 Hz supply, pulse echo technique 0-70314  
 ferroelectrics, structural phase transitions, ultrasonic velocity and attenuation meas. 0-75977  
 ferromagnet, itinerant electron, magnetoelastic contribs. to US vel., elastic const., and susceptibility 0-75829  
 furan, liq., US phase vel. decay in space and time 0-99891  
 furan-cyclohexane, liq. mixture, intermol. vibrational energy transfer, US study 0-70313  
 glass-ceramic, machinable, elastic const. temp. depend. 0-79852  
 graphite fibre reinforced epoxy, US attenuation as an indicator of fatigue life 0-85118  
 n-hexane-perfluoro-n-hexane mixtures, US vel. and absorpt. mixtures 0-88281  
 insulators, high-intensity US wave vel., phonon-phonon interaction effects 0-70323  
 isopropanol-n-propanol aq. mixtures, US relax., US absorpt. and vel. meas. (*French*) 0-103426  
 liquid binary mixtures of organic chemicals, excess internal pressure and Van der Waals' constant, Flory's theory 0-70310  
 liquid mixtures, binary, hydrogen bond interactions 0-79881  
 liquids, repulsive exponent, Rao's and Kuzner's relations 0-79878  
 magnetoelastic SAW velocity on magnetised ferrite substrate, non-reciprocity 0-80587  
 metal, FCC, dislocation behaviour at high strain rates, US detection method, data analysis basis 0-85136  
 methane( $-d_4$ ), liq., Brillouin scatt. and refr. index measurements 0-76035  
 3-methylpentane-nitroethane critical binary liquid mixture, US absorpt. 0-107376  
 microemulsion, sound velocity and absorption 0-81374  
 $\beta\text{-Na}_2\text{O-Al}_2\text{O}_3$  low temp. ultrasonic vel. meas., temp. depend. 0-79885  
 nitrobenzol-n-hexane, hypersound velocity, absorption temp. depend (*Russian*) 0-75303

**ultrasonic velocity continued**

- organic ternary liquid systems, intermolecular interaction, US vel. meas. 0-79879  
 piezoelectric nongenerate semicond., magnetoacoustic effects of nonparabolic band struct. 0-96948  
 polyesterimides, solns., ultrasonic vel. and Rao formalism 0-103422  
 polyethylene, high press. phase, US, DTA, and X-ray diff. study 0-75188  
 polymer films, Brillouin scatt. at transitions 0-70312  
 polymers, filled, cumulative internal damage, US assessment 0-97653  
 polystyrene solution, differential meas. of ultrasonic velocity (*French*) 0-75302  
 polyurethane, foaming parameters determ. from US wave vel. 0-71885  
 porous medium, US bulk compressional wave obs. 0-64235  
 raw kaolin, acoustical investigations of the effect of additives on elastic props. 0-66559  
 tris-sarcosine calcium chloride, elastic props., US damping 0-84229  
 steel, meas. method for isotropic nondispersive solids 0-69616  
 steel, tool, US vel. meas., 20-900°C 0-70318  
 steel, US critical angle reflectivity, near-surface metallic prop. gradient effect 0-70516  
 TGS, perfect and imperfect, sp. ht. and sound vel., crit. anomalies 0-71331  
 US velocity in crit. region water 0-59582  
 water, calc. based on Brownian motion theory and counteracting molecular forces, 25 to 80°C 0-88265  
 water, supercooled, sound vel. dispersion, struct. relax. effect, Brillouin scatt. obs. 0-107375  
 water, supercooled to -33°C, sound vel. determ. by acoustic levitation method 0-88269  
 water, superheated, ordinary, heavy, US velocities, thermodynamic props. 0-65156  
 Al, meas. method for isotropic nondispersive solids 0-69616  
 Al, US velocity, temp. depend., stress effects 0-75307  
 a-As, second and third order elastic const., ultrasonic velocity meas. 0-103408  
 $\text{BaMnF}_4$ , spectroscopy near ferroelec. transition, dielec. anomalies near mag. ordering temp. 0-75965  
 $\text{BaO-P}_2\text{O}_5$ , glass, US velocity rel. to elastic props. 0-103425  
 $\text{Bi}_2\text{GeO}_{20}$ , third-order elastic moduli determ., US vel. meas. 0-65121  
 $\text{Bi}_2\text{SiO}_{20}$ , third-order elastic moduli determ., US vel. meas. 0-65121  
 $\text{CaO-P}_2\text{O}_5$ , glass, US velocity rel. to elastic props. 0-103425  
 $\text{CdF}_2$ , ionic conducting fluoride fluoride, US velocity meas. 0-107381  
 $\text{Cd,Hg}_{1-x}\text{Se}$ , phase transition and elastic const., US vel. study 0-75354  
 $\text{CsMnCl}_3 \cdot 2\text{H}_2\text{O}$ , diagonal elastic const., thermal expansion coeffs., ultrasonic velocity meas. 0-79853  
 Cu, US velocity, temp. depend., stress effects 0-75307  
 Fe-Ni, sintered, porosity determ. by US attenuation and sound vel. meas. (*German*) 0-76437  
 Fe-rare earth alloys, amorphous, magnetoelasticity and moment rot., US vel. calc. and neutron scatt. meas. 0-65992  
 $\text{Fe}_2\text{TiO}_5$ , anisotropic spin glass type behaviour 0-60296  
 Ge, pure and n-type, US velocity and attenuation, second and third order elastic moduli 0-70325  
 $^4\text{He}$ , solid-fluid, eqn. of state, melting props. under press. 0-96721  
 $\text{Ho,Tb}_{1-x}\text{Co}_2$  rare phase compounds, elastic props., temp. and magnetic field dependence 0-60393  
 $\text{K,Ba}(\text{NO}_3)_2$ , elastic props. 0-96588  
 $\text{KH}_2(\text{SeO}_3)_2$  and  $\text{KD}_3(\text{SeO}_3)_2$ , ferroelastic phase transition, mech. stress effect 0-70394  
 $\text{K}_2\text{SeO}_4$ , elastic props. at commensurate-incommensurate transition, Brillouin scatt. and US study 0-93248  
 $\text{K}_2\text{SeO}_4$ , ultrasonic study in temp. range of incommensurate phase transform 0-88276  
 $\text{K}_2\text{SnCl}_6$ , elastic const., inelastic neutron scatt. and US meas. 0-59553  
 $\text{LaAl}_3$ , supercond. and normal states, anomalous US attenuation and velocity change 0-80446  
 $\text{LiNbO}_3$ , light induced ultrasonic wave velocity change, refractive index 0-97236  
 $\text{Li}_2\text{O-Al}_2\text{O}_3\text{-SiO}_2$ , glass, study of elastic props. 0-104205  
 $\text{MgO-P}_2\text{O}_5$ , glass, US velocity rel. to elastic props. 0-103425  
 $\text{Mn}_2\text{Si}$ , elastic moduli, phase transitions, ultrasonic velocity 0-92589  
 $(\text{NH}_4)_2\text{BeF}_6$ , elastic props., US damping 0-84229  
 $\text{NaClO}_3$ , lattice vibrations and sp. ht., neutron spectroscopic study 0-107388  
 $\text{Na}_2\text{O-SiO}_2$  glass, acoustic and thermal Gruneisen parameters 0-59608  
 Nb-H(D)(T) system, BCC, US vel. changes caused by H isotope dissolution 0-65117  
 $\text{PbF}_2$ , US vel. near press. induced cubic-to-orthorhombic transform. 0-103476  
 $\text{Pb}_3\text{Ge}_2\text{O}_{11}$ , ferroelec. transition, US and elasto-optic props. 0-60527  
 $\text{Pb}_3(\text{GeO}_4)(\text{VO}_4)_2$ ,  $\text{Pb}_3(\text{SiO}_4)(\text{VO}_4)_2$ , and  $\text{Pb}_3\text{GeO}_{11}$ , elastic nonlinearity and acoustic losses 0-59554  
 $\text{PbO-SiO}_2$  glass, acoustic and thermal Gruneisen parameters 0-59608  
 $\text{PdSiCu}$ , amorphous, US attenuation and vel. studies at low temps. 0-88278  
 $\text{RbH}_2\text{PO}_4$ , electrostrictive effects, US rel. 0-75941  
 $\text{RbH}_2(\text{SeO}_3)_3$ , US vel. and absorpt. near ferroelec. Curie temp. 0-97206  
 $\text{SO}_2$ -tetrachloromethane, solns., near critical point, ultrasound absorpt. obs. 0-65160  
 Si, pure and n-type, US vel. and attenuation, evaluation using elastic moduli 0-70325  
 SiC delay line at 9.43 GHz, acoustic props. study 0-65169  
 $\text{SiO}_2$ , glass, acoustic and thermal Gruneisen parameters 0-59608  
 $\text{SiO}_2$ , vitreous Brillouin scatt., 35 GHz phonon vel. and absorpt. below 1K 0-100664  
 $\text{SiO}_2\text{-Al}_2\text{O}_3$ , vitreous US vel. and absorption 0-107380  
 $\text{SiO}_2\text{-B}_2\text{O}_3$  glasses, Brillouin scattering meas. of attenuation and vel. of hypersounds 0-100309  
 $\text{SiO}_2\text{-TiO}_2$ , vitreous, US vel. and absorption 0-107380  
 $\text{SrO-P}_2\text{O}_5$ , glass, US velocity rel. to elastic props. 0-103425  
 $\text{TmFeO}_3$ , acoustic vel. and attenuation shifts at spin reorientation phase transition 0-65986  
 V-H(D)(T) system, BCC, US vel. changes caused by H isotope dissolution 0-65117  
 V-Ti (42 at.%), ultrasonic vel. in mixed state 0-75689  
 $\text{V}_2\text{Si}_{1-x}\text{Ge}_x$  solid soln., longitudinal and transverse US wave prop. rate, 4.2 to 300K (*Russian*) 0-103423



**ultrasonic velocity continued**

- ZnCl<sub>2</sub>-LiCl(NaCl)(KCl)(CsCl), molten, US velocity, thermodynamic quantities and struct. (*Japanese*) 0-88270  
 ZnCl<sub>2</sub>-PbCl<sub>2</sub>, molten, US velocity and absorpt., thermodynamic quantities and bulk viscosity (*Japanese*) 0-84249

**ultrasonic velocity measurement**

- bone, temp. range of room temp. to 90°C 0-76787  
 ceramic, piezoelectric, US instrument for determ. chars. 0-66752  
 continuous meas. of changes in US velocity 0-87675  
 diffraction corrections for finite size of source and receiver 0-96153  
 femur, human, pulse-echo technique for US vel. meas. in vivo 0-89812  
 filled polymer materials, simple approx. method, acoustic impedance 0-64314  
 interferometry, US attenuation or velocity meas. 0-58874  
 isotropic nondispersive solid, meas. method for vel. of sound 0-69616  
 liquid metals, pulse-echo overlap technique 0-99906  
 liquid systems, 10 to 30 MHz, 25 to 60°C, undergraduate expt. using 2-transducer RF pulse method 0-69608  
 liquids, pulse technique, monostable multivibrator and oscilloscope technique 0-64313  
 liquids and small biological tissue specimens, phase meas. 0-76786  
 longitudinal US vibrations meas., based on interferometer 0-79084  
 pulse superposition technique, apparatus assembled from discrete instruments 0-74650  
 signal shape anal., ultrasonic pulsed measuring instrums. 0-87678  
 solutions in alcohols, ultrasonic vel. and density meas. used to calc. compressibility, intermol. free length and salvation no. 0-96150  
 steel, austenitic, type 304, 304L, 316L, US wave vel. meas. rel. to cold working 0-99908  
 steel, low alloy, 38NiCrMo<sub>4</sub>, US wave vel. meas. rel. to cold working 0-99908  
 superheated water, Brillouin scatt., sound velocity meas. 0-95631  
 surface wave velocimeter, phase sensitive 0-102947  
 Fe nodular parts, comparison of sonic-resonance and US velocity techniques for quality control 0-97654  
 Li single cryst., measurement in vicinity of martensitic phase transformation 0-75358  
 LiNbO<sub>3</sub>, SAW propag. velocity meas. 0-92003  
 V, determination of effect of H on elastic moduli 0-75288  
 Zn-Cd alloys, liq. and solid, ultrasound speed and compressibility meas. 0-102941

**ultrasonic wave propagation** *see ultrasonic propagation***ultrasonic waves**

- see also surface acoustic waves; ultrasonic propagation*  
 diamond, sound excitation orientational effect due to channelled electrons 0-84254  
 generation by focused modulated electron beam, appl. to US imaging in scanning electron microscopy 0-95192  
 generation in insulators, detection prior to breakdown 0-88924  
 metals, generalised Gruneisen tensor from solid nonlinearity parameters 0-84275  
 molecular crystal, optical rotation induced by ultrasonic wave (*Russian*) 0-93270  
 Mossbauer spectrum, ultrasonic sideband intensity depend. on acoustic field statistics 0-75905  
 piezoelectric transducer, surface excited, US field 0-64331  
 standing and travelling in water-filled wedge, obs. by frequency-shift holography 0-79089  
 transmission through rough surface (*Russian*) 0-100387  
 GaS(Te)(Se), elastic characteristics, Debye temp., ultrasonic study (*Russian*) 0-79872  
 Ge, electron-hole drop drag by ultrasound (*Russian*) 0-100437  
 PbMoO<sub>4</sub>, elastic wave excitation and amplification by laser radiation 0-103419

**ultrasonic welding**

- IC microwelding using nonlinear phenomena of acoustic vibratory systems 0-74656

**ultrasonics**

- see also acousto-optical effects; ultrasonic applications; ultrasonic devices; ultrasonic equipment; ultrasonic waves*  
 conference, New Orleans, LA, USA 0-73101  
 n-hexane, superheated, thermodynamic props. from ultrasound speed 0-92036  
 minerals, ultrasonic damping due to internal friction, freq. depend. (*German*) 0-90078

**ultraviolet astronomical observations**

- 1309-216, probable BL Lacertae object with absorpt. red shift 1.49, optical spectrum 0-67856  
 2A 0311-227 optical counterpart, simultaneous photometric and spectroscopic obs. 0-90572  
 2A 2251-179, X-ray quasar, UVB photometry 0-82349  
 A-type supergiant stars, reson. line profiles from IUE and Copernicus spectra 0-90424  
 Abell 46, planetary nebula, eclipsing binary nucleus, hot component UV continuum obs. by IUE 0-98693  
 active galaxies, implications of UV obs. 0-105390  
 Am stars,  $\tau$  Ursae Majoris and 15 Vulpeculae, energy distrib. from spectral obs. 0-85949  
 Z Andromedae, symbiotic star, IUE obs. of UV spectrum 0-109450  
 $\alpha$  and  $\beta$  Aquari, G-type supergiants, evidence for hybrid atmospheres and winds from UV spectra 0-72948  
 AE Aquarii, cataclysmic variable, IUE satellite UV obs. 0-72985  
 R Aquarii, symbiotic long-period variable, spectrum of assoc. nebulosity 0-90450  
 $\sigma$  Aquarii (A0 IVs), hot metallic-line star, spectrum and abundance anal. 0-90415  
 R Aquarii (M7+pec), late type variable star, IUE obs. of circumstellar emission 0-82370  
 $\eta$  Aquilae, classical Cepheid, companion star detect. and distance determ. 0-90443  
 KO Aquilae, eclipsing binary system, UVB photoelectric study 0-62198  
 $\theta$  Aquilae (B9.5 III), spectrum and abundance anal. 0-90415  
 V603 Aquilae (Nova 1918), periodic light vars. detect. 0-82391  
 59 Aurigae,  $\delta$  Scuti star, light curves periodogram anal. 0-62141  
 $\zeta$  Aurigae, eclipsing binary, UV obs. of supergiant atmos. 0-94836  
 T Aurigae (Nova 1891), old nova, photometric and spectroscopic obs. 0-90446  
 BD+10°2179, C rich H deficient star, UVB photometric obs. 0-90437  
 BD+33°2642, galactic halo blue star, mass loss determ. from IUE obs. 0-72947

**ultraviolet astronomical observations continued**

- Be and shell stars, UV spectrophotometry with TD-1 satellite 0-90438  
 Berkeley 11, compact open cluster, UVB obs. 0-94840  
 $\alpha$  Bootis, spectrophotometric profile, 3200-3600 Å 0-62118  
 3C 120, Seyfert galaxy, spectrophotometric obs. of assoc. nebulosity 0-67890  
 3C 273, quasar, detailed UV obs. with IUE 0-94886  
 3C 273, UVB obs., (1975 to 1979) 0-62309  
 Z Camelopardalis, dwarf nova, spectrophotometry at standstill and in eruption 0-82366  
 AX Camelopardalis (53 Camelopardalis), Ap star, UVB photoelectric photometry and period of var. (*Italian*) 0-90448  
 UW Canis Majoris, O7f supergiant, UV lines P Cygni profiles rel. to mass loss rate 0-67736  
 RS Canum Venaticorum, out of eclipse light var. and comparison with similar stars 0-109489  
 $\zeta$  Capricorni, Ba star, white dwarf+giant, UV spectra obs. 0-105284  
 $\nu$  Capricorni (B9.5 V), spectrum and abundance anal. 0-90415  
 QZ Carinae (HD 93206), O-type quadruple eclipsing system, spectroscopic and radial vel. study 0-105275  
 SU Cassiopeiae, Cepheid variable, spectrophotometric determ. of effective temp. 0-90435  
 VX Cassiopeiae, early-type irregular variable, photometric variability (*Russian*) 0-72973  
 AB Cassiopeiae, eclipsing binary with  $\delta$  Scuti primary, light vars. preliminary anal. 0-94831  
 $\omega$  Centauri, SEC Iidene photometry of main sequence 0-90491  
 $\mu$  Centauri (B2 IVe), new circumstellar shell development, spectroscopic obs. (1980 June 10 to 12) 0-94808  
 V810 Centauri (HD 101947), yellow variable supergiant near Cepheid instability strip, VBLUV photometry 0-98672  
 NY Cephei, massive eclipsing binary star, progress report from UVB photometry 0-67789  
 VV Cephei, supergiant eclipsing binary UV spectrum 0-82415  
 EM Cephei, UVB, photometry rel. to constancy or variability of period 0-105286  
 VV Cephei, UV spectrum obs. during chromospheric eclipse phase 0-109498  
 9 Cephei (B2 Ib), circumstellar CO obs. 0-94795  
 Cepheids, short period, in N.hemisphere, UVB photometry rel. to search for double mode Cepheids 0-94814  
 RS Chamaeleontis, eclipsing binary, four-colour photometry rel. to photometric elements, absolute dimensions and He abundance 0-67783  
 Chu's object in Perseus, UVB photometry and spectrum rel. to identification as galactic star 0-62132  
 Comet Bennett (1970 II), CN (0-0) band brightness profile obs. rel. to CN prod. 0-82303  
 Comet Bradfield (1979I), UV spectrum, UE obs. 0-90371  
 Comet West (1976 VI), CN (0-0) band brightness profile obs. rel. to CN prod. 0-82303  
 cool giant stars, chromosphere mass loss determ. from Mg II UV line obs. 0-85935  
 R Coronae Borealis type variables and related objects, UVB photometric obs. 0-90437  
 BI Crucis, new symbiotic star, spectrum 0-109442  
 31 and 32 Cygni,  $\zeta$  Aurigae stars, UV spectroscopic obs. 0-109499  
 GO Cygni, eclipsing binary, UVB photometry rel. to period changes 0-72999  
 V1668 Cygni (Nova 1978), multifilter photometry and polarimetry 0-90454  
 V1668 Cygni (Nova 1978), spectroscopic and photometric obs., (1978 to 1979) (*Russian*) 0-109444  
 CI Cygni symbiotic star, UV and optical spectrum changes during eclipse 0-105258  
 Cygnus Loop, SNR, abundances and filament shock vel., UV obs. 0-94848  
 Cygnus X-1 (V1357 Cygni), optical light curve vars. rel. to X-ray vars. 0-109560  
 Cygnus X-1 (V1357 Cygni), optical photometry (1980 May 25 to July 7) 0-90578  
 HR Delphini (Nova 1967), short period light vars. from UVB photometry 0-67744  
 diffuse sky background, D2B satellite ELZ photometer survey 0-105404  
 S Doradus, LMC Hubble-Sandage variable, IUE and ground based spectroscopic obs. 0-101595  
 30 Doradus nebular complex, chemical comp. and struct. obs. 0-62226  
 E3 (ESO-037-SC 01) dying globular cluster, photometry and stellar content rel. to tidal truncation 0-105291  
 early-type stars, interstellar C IV and Si IV column densities 0-73018  
 early-type stars and cool stars, UV spectroscopy of outer layers 0-72922  
 early-type stars with Balmer emission, near UV (2000-3000 Å) spectra 0-94811  
 SW eclipsing binary, period study, photometry and spectra obs. 0-82424  
 eclipsing binary runaway, orbital data, UV obs. 0-85952  
 emission-line variable (No.86) in core of M 15, UVB photometry, probably W Virginis star 0-77458  
 $\epsilon$  Eridani, UV line spectrum of active chromosphere star, models 0-77394  
 faint blue stars, southern, UVB photometry 0-82349  
 Fairall 160, 182, UVB photometry 0-82349  
 galactic halo, evidence for hot gaseous component from IUE UV obs. of (3C 273) 0-94886  
 galaxies, UVB photoelectric photometry and photometric parameters 0-67855  
 galaxies with UV continuum, twelfth list 0-67585  
 galaxies with UV excess, second list 0-67584  
 galaxies with UV excess and double and multiple nuclei, spectral study 0-67848  
 globular clusters, UV energy distrib. from Orbiting Astronomical Observatory photometry 0-73009  
 $\beta$  Gruis (M2 II), S I emission obs. in EUV spectrum 0-82359  
 H 2252-035, optical counterpart photometry and spectrum 0-101651  
 HD 102567, optical counterpart to 4U 1145-61, atm. model from UV obs. 0-105396  
 HD 105056, ON supergiant, radial vel. study 0-90427  
 HD 137613, C rich H deficient star, UVB photometric obs. 0-90437  
 HD 159378 (Tr 27-102), yellow variable supergiant near Cepheid instability strip, VBLUV photometry 0-98672  
 HD 192273, UV flux upper limit, Voyager 1 obs. 0-77406  
 HD 200775, Be star, optical and UV extinction by dust in (NGC 7023) 0-109515





**ultraviolet astronomical observations continued**

- BL Telescopii A, yellow variable supergiant near Cepheid instability strip, VBLUW photometry 0-98672
- Uranus, UV albedo meas. 0-82295
- XY Ursae Majoris, eclipsing binary, observational evidence for large-scale spot activity on primary component 0-109491
- Vela SNR, IUE UV spectrum 0-101635
- Vela X-1 (HD 77581), binary source, spectral obs. 0-94892
- $\lambda$  Velorum, K-type supergiant, UV spectrum rel. to chromosphere and wind struct. 0-72948
- $\gamma_2$  Velorum, Wolf-Rayet binary, orbital element determ. from spectral obs. 0-85950
- $\gamma_3$  Velorum, Wolf-Rayet binary star, UV obs. from TD-1A satellite 0-77447
- Venus dayglow spectrum, 1250 to 1430 Å, Pioneer Venus obs. 0-77311
- Venus polarisation, wavelength depend. obs. rel. to UV cloud model 0-82250
- VV 150, galaxy chain, photoelectric and spectroscopic study 0-98724
- VV 493 (UGC 07910), unusual extragalactic object, morphology and spectrum rel. to probable nature 0-98718
- Wolf-Rayet stars, interstellar N V lines, IUE obs. 0-101634
- Wolf-Rayet stars, Si IV and C IV, absorpt. lines, IUE obs. 0-67748
- H II regions near nucleus of spiral galaxy NGC 3310, exploratory investigation 0-62235
- HgMn stars, UV spectra rel. to thin Hg layers and diffusion model 0-105243

**ultraviolet astronomy**

see also *ultraviolet sources (astronomical)*

- diffuse sky background, D2B satellite ELZ photometer survey 0-105404
- dust, UV opacity effects on stellar spectra 0-90505
- EUV instruments, computer aided calibration technique 0-85839
- extragalactic work with IUE 0-105357
- galactic neutrinos and decay to UV photons 0-109566
- high-resolution optical telescope design 0-90335
- International Ultraviolet Explorer (IUE) second European conference (Tubingen, Germany, 1980 March 26 to 28) 0-82584
- IUE preliminary results, workshop, Udine, Italy (1978 October 12) (*Italian*) 0-86033
- Jupiter, Lyman  $\alpha$  albedo rel. to solar activity 0-98601
- Lyman  $\alpha$  camera, for high resolution solar Lyman  $\alpha$  filtergrams 0-82323
- Pioneer Venus Orbiter UV spectrometer, design and operation 0-67503
- planetary nebulae, advances in UV obs. 0-109524
- Salyut 6 200-260 nm UV receiver 0-67566
- satellites, Earth-orbiting, study of hot components and extended coronas 0-109379
- sky survey project EXUV 10-1000 Å waveband, proposed mission 0-82165
- solar UV flux, cyclic vars. 0-101577
- solar UV spectrum, 140 to 350 nm, NASA meas. using SURF storage ring calibrations 0-94721
- spectrophotometry of faint astronomical objects, rocket instrument description 0-62014
- stellar spectra, second OAO atlas 0-72786
- Wolter-Schwarzschild optics for Berkeley stellar spectrometer and EUV Explorer 0-82197
- XUV astronomy, review (*German*) 0-109372

**ultraviolet communication** see *optical communication***ultraviolet detectors**

- C-CD, thinned back-illuminated, for extreme UV direct detect. 0-77852
- light-flux generated by single-lens illuminator, spectral composition for UV region 0-87450
- liquid chromatograph detector for high concentration and flows 0-71960
- seminar, optical radiation meas., San Diego, CA, USA (Aug. 1979) 0-86036
- Spectroline DM series, UV appl. 0-77854
- VUV detectors absolute efficiency, meas. using VEPP-2M storage ring synchrotron radiation 0-82824
- water vapour instrum. for stratospheric aircraft using UV fluorescence 0-82100
- Si UV detectors coated with thin film scintillators 0-86412

**ultraviolet lamps** see *lamps***ultraviolet radiometry** see *photometry***ultraviolet sources** see *light sources***ultraviolet sources (astronomical)**

- 3C 273, quasar, detailed UV obs. with IUE 0-94886
- EUV point sources, contrib. to diffuse EUV background 0-62324
- galactic UV radiation, role in interstellar gas heating 0-67839
- HD 192273, EUV flux upper limit, Voyager 1 obs. 0-77406
- HD 219150, F0 V star with remarkable UV excess, optical and UV photometry and spectrum 0-90429
- hot subdwarfs in Carnochan and Wilson catalogue, UV spectra 0-82354
- interstellar UV radiation field, obs. from S2/68 sky-survey telescope 0-77523
- KUV09313+4052, variable UV excess object, discovery, position and photometry 0-62159
- observations by Earth-orbiting satellites of hot components and extended coronas 0-109379
- planetary nebulae, advances in UV obs. 0-109524
- planetary nebulae, review of UV obs. 0-109523
- Seyfert galaxies, nonthermal UV sources vars. rel. to dust thermal emission vars. 0-67865
- supernova, nearby, UV and gamma radiation effects on terrestrial atmosphere 0-94584
- T Tauri, Lyman continuum energy spectrum rel. to nebula ionisation and emission line spectrum 0-67820

**ultraviolet spectra of inorganic solids** see *visible and ultraviolet spectra of inorganic solids***Umklapp process**

- commensurate and incommensurate structural phase transitions in Jahn-Teller system 0-70403
- Peierls transition in quantizing mag. field, possibility 0-103441
- FeCl<sub>2</sub>, antiferromag., magnon-phonon interactions in thermal cond. 0-65315
- Ir, (111) surface states, surface Umklapp effects, photoelectron spectra 0-93457
- K, ultrasonic attenuation at low temp., spherical Fermi surface model 0-84255
- Li, phonon limited resistivity struct. depend., Umklapp scatt., elastic consts. 0-88532

**Umklapp process continued**

- Na, phonon limited resistivity struct. depend., Umklapp scatt., elastic consts. 0-88532
- $\beta$ -Zr, phonon dispersion, modified Sharma-Joshi model 0-100311

**uncertainty principle** see *indeterminancy***underground cables**

see also *cable laying*

- telephone cables laying, seismology appl., rocks location verification 0-72456

**underwater acoustics** see *underwater sound***underwater cables** see *submarine cables***underwater sound**

see also *hydrophones; oceanography; sonar*

- absorption, chemical relaxation studies using resonator method 0-96073
- acoustic array design, environmental influences 0-83721
- acoustic pulse reflected from water surface, spectrum 0-87627
- acoustical imaging, US visualization and characterization, conf., vol.8, Key Biscayne, FL, USA (May-June 1978) 0-83720
- ambient noise in low-loss, shallow water channel, theoretical model 0-64265
- AMTE/OUEL underwater jet noise rig, working report for 1977/78 0-79286
- AMTE/OUEL underwater jet noise rig, working report for 1978/79 0-79287
- backscattering cross-sections of live fish, probability density functions and aspect 0-64260
- beam displacement, cycle distances, and attenuations for rays and normal modes 0-74580
- bubble oscillations of large amplitude 0-96298
- bubble swarm acoustics, insertion loss of a layer on a plate 0-96072
- cavitation threshold meas. for polyalkylene glycol and castor oil 0-107374
- cavitation tunnel hydroacoustic transfer function, meas. and anal. (*Croatian*) 0-92002
- clustered sensor array, turbulent boundary layer induced noise suppression 0-96121
- coherence estimates based on amplitudes of signals reradiated, by rough sea surface, unreliability 0-58847
- compound random process for underwater ambient acoustic noise 0-83699
- compressional wave attenuation in deep ocean sediments 0-79033
- computer model for generating World ocean sound velocity profile 0-87624
- correlation of pseudonoise signals in reflection from layered ocean bottom 0-87626
- correlator compensation requirements for passive time-delay estimation with moving source or receivers 0-58843
- crossing rate statistics for finite bandwidth or modulated multipath signals 0-64262
- CW coherence meas. at low freq. for long underwater paths 0-106654
- cylindrical steel shells in water, thick-walled, distrib. of normal surface vel. and acoustic radiation (*German*) 0-102899
- detonation wave, reflection from water surface 0-87628
- detection finding device for bearing determ. of whale sounds, real-time device 0-96079
- Eckart's formulation, surface correlation effect on average scattered pressure 0-96070
- element failure and random errors effect on sidelobe level for linear array 0-106670
- environmental-acoustic model for deep moving ocean, stochastic 0-64267
- explosive acoustic waves, empirical and theoretical laws comparison (*Russian*) 0-109150
- fish backscattering cross section, swimbladder effect in gadoid and mackerel 0-89787
- gain limitations of passive vertical line array in shallow water 0-96117
- Gaussian acoustic signal detection using array processors, performance eval. 0-83696
- geometric construction of multipaths 0-74575
- Helmholtz resonator as high-power deep-submergence LF source 0-74576
- horizontal acoustic refraction through ocean mesoscale eddies and fronts 0-96085
- horizontal directionality estimation considering array tilt and noise field vertical arrival structure 0-64302
- hydrophone signal phase stability, meas. using moving source 0-87623
- imaging of objects buried in seafloor sediment using focused US transducer 0-79036
- intensity fluctuations and fourth-order coherence function in random media 0-78774
- intensity fluctuations spectrum in internal wave freq. range 0-64268
- LF propag. off Mission Beach, California 0-79035
- marine meas. technology appl. (*Japanese*) 0-87625
- measurement of acoustic noise effects on behaviour of marine organisms 0-106657
- multipath anal. of explosive source signals in ocean 0-79034
- multipath channels, comments on coherence estimates 0-58832
- multipath separation and passive localisation using horizontal wavenumber spectrum 0-91952
- noise correlation functions for arbitrary receiver orientation and steering direction in vertically anisotropic, azimuthally isotropic noise fields 0-58864
- noise spectra produced by fishing boats affecting albacore catch, comment 0-58844
- nondirectional sound sources in layer of fresh-water reservoir, determination of strength 0-58845
- normal modes in bottom, effect on ocean acoustic field 0-106653
- ocean, long-range acoustic transmission variability of NW Atlantic 0-90091
- ocean, two-point coherence function models with inhomogeneous background and anisotropy 0-81922
- ocean acoustic multipaths, stability and identification 0-83697
- ocean acoustic transfer function impact on coherence of undersea propag. 0-58842
- ocean bottom and surface reflections, correlation measurement of coeff. 0-58848
- ocean bottom-reflected pseudonoise signals, correlation with transmitted signal 0-58846
- ocean channel with linear sound speed, effects of class of random currents 0-87621
- ocean ducts, range dependent, acoustic flux formulae 0-96075
- ocean eddies, calcs. of acoustic transmission 0-64264

**underwater sound continued**

- ocean subbottom data analysis through simulation, theoretical vertical and lateral model 0-74571
- ocean surface probing for measurement of directional-frequency spectrum 0-79032
- ocean-surface directional-frequency spectra, inverse scattering problem 0-79031
- oceanic background in high-gain acoustic array, nonstationary and nonuniform 0-64263
- oceanic guided waves, acoustic flux methods 0-96077
- oceanic sound transmission, calc. of strength and diffraction parameters 0-74572
- optimum range and bearing estimation with randomly perturbed arrays 0-96119
- parametric acoustic arrays with intermediate directivity in water, expt. study 0-74569
- passive tracking acoustic array evaluation, nonlinear filtering lower bound algorithms 0-96088
- Pekeris model, uniform asymptotic evaluation of continuous spectrum contrib. 0-87622
- plane-wave refl. coeff. of ocean bottom, meas. technique 0-96081
- pulsation noise damping from small air bubbles in water 0-64253
- ray-phase perturbations due to ocean-environmental variations, simplified calculation 0-64266
- receiver-source motion at intermediate ranges in deep ocean, anal. of acoustical effects 0-96082
- refl. from bottom with sound vel. and density gradients 0-102901
- reverberation of 4 kHz and 20 kHz tone bursts in water filled tank 0-83695
- rough interface between two fluids, coherent acoustic scatter 0-96074
- sand, water-saturated, broadband meas. of acoustic attenuation 0-83719
- SAW hydrophone system using resonator-controlled oscillators 0-74631
- scattering by finite elastic cylinder in water 0-96062
- scattering by large sea surface inhomogeneities, phase function shape in shadowing conditions (*Russian*) 0-94530
- scattering by layered elastic and viscoelastic obstacles in water 0-96061
- scattering by marine organisms, review 0-64269
- sea surface scattering, mechanism 0-106656
- sea-floor reflectivity obs. 0-98302
- sediment refraction of sound, for sonar studies 0-81902
- sediment rigidity effect on ocean bottom reflection loss in typical deep sea sediment 0-96083
- sediment shear wave effects on ocean bottom refl. loss, ray path anal. 0-96084
- seismic signal processing using inverse diffraction technique 0-74608
- shallow sea, influence of bottom on formation of acoustic field 0-102900
- shallow-water propag. over low-velocity bottom 0-74579
- shell of revolution immersed in liquid, freq. distribution function 0-69587
- ships, prediction of post-detection data load for passive sonars 0-96125
- signal response, in two-path medium, average array 0-87657
- single-mode transmission and backscatter measurements in laboratory waveguide 0-64259
- sonar appl., passive, use of directional transducer arrays (*Spanish*) 0-69586
- source location and motion estimation, joint reduction of bias and variance 0-96087
- source micromotion effects on acoustic signal in freq., time, and space domains 0-74574
- source motion effects on acoustic signal in freq., time, and space domains 0-74573
- spatial noise spectrum meas. in ocean for small observation baseline 0-102902
- static pressure influence on operation of hydrodynamic radiating system 0-102954
- submerged plate with finite number of reinforcing ribs, acoustic backscattering 0-74586
- submerged plate with one reinforcing rib, acoustic backscattering 0-74585
- surface generated noise in stratified ocean, spatial correlation 0-87620
- surface-duct propag., evaluation of models of effects of surface roughness 0-64261
- temperature variation of acoustical props. of laboratory sediments 0-96069
- testing of materials by ultrasonics (*German*) 0-97670
- time delay estimation, cross-correl. and smoothed coherence transform methods compared 0-96086
- tracking system for divers, PATS 0-91949
- US scattering by turbulence 0-87619
- velocity inversion in a stratified medium with separated source and receiver 0-96071
- viscous attenuation in suspensions and high-porosity marine sediments 0-74577
- wave-theory peaks in range-averaged channels of uniform sound velocity 0-96076
- wedge-shaped ocean with penetrable bottom 0-74578
- wind-generated noise produced by impact of spray with ocean surface, low freq. 0-106655

**undulator radiation**

- coherent radiation from electrons in transverse periodic fields 0-78748
- coherent X-ray emission from relativistic electron beam 0-91739
- electron beam self-bunching in resonantly absorbing medium, radiation amplification feasibility 0-102605
- irregularity effects 0-99614
- polarization characteristics 0-69305
- relativistic charged particles, in irregular undulator, radiation spectra (*Russian*) 0-63900
- relativistic electron emission characts. from Sirius electron synchrotron 0-63904
- SIRIUS synchrotron, experimental study of the spectral, angular and polarization properties of undulator radiation 0-91338

**unified field theories**

- see also *supergravity; Weinberg model*
- 5-dimensional generation structure, possible signature for SU(5) semi-simple grand unification 0-82930
- affine manifolds, 3-D, existence of metric 0-82695
- asymptotic freedom constraints, review 0-62914
- asymptotically free SU(5) grand unification, proton stability, renormalisation group 0-82929
- axial vector anomalies, weak-EM interactions nonrenormalisability 0-62859

**unified field theories continued**

- axions, very low mass, astrophysical bounds and stellar-energy loss 0-109353
- B-L conservation and B nonconservation in unified models of quarks and leptons 0-95229
- baryon production through primordial black holes in grand unified theories 0-101970
- baryon/photon ratio bounds due to human existence, grand unification 0-62345
- Bianchi type II exact cosmological model with matter and EM field 0-105560
- canonical neutral-current predictions from the weak-electromagnetic gauge group  $SU(3) \times U(1)$  0-95242
- charged fluid sphere, general relativity soln., Einstein-Maxwell eqns. 0-68088
- charm, elementary particle theories, properties (*Spanish*) 0-73681
- conceptual foundations of the unified theory of weak and electromagnetic interactions, review 0-95237
- conformally flat Einstein-Maxwell spaces, Newman-Penrose formalism 0-62559
- development and expansion 0-95239
- direct lepton generation in strong interactions, unified model, colour quark state (*Russian*) 0-82933
- dynamically broken gauge models, natural mass hierarchy, unification 0-68409
- $E_6$  model of unified interactions, asymptotically free, mass relations and interactions 0-73642
- $E_7$  grand unification, neutral currents problem in  $SU(2) \otimes [U(1)]^3$  gauge theory (*Russian*) 0-62913
- effective field theories, functional integration, renormalisations 0-86648
- effective hamiltonian for  $\Delta C=1$  nonleptonic interactions in the Kobayashi-Maskawa model 0-86667
- eight-lepton and eight-quark unification based on Grassmann algebra 0-105824
- Einstein's impact on theoretical physics 0-77677
- Einstein's non-symmetric unified field theory, universal symmetry and Klotz metric 0-62555
- Einstein nonsymmetric unified theory, nonsingular particle solns. 0-57163
- Einstein symposium, Berlin, Germany (Mar. 1979) 0-90596
- Einstein vacuum and Einstein-Maxwell space-times, infinitesimal homology group structure and geometrization 0-73252
- Einstein-Cartan theory in the spin coefficient formalism 0-101742
- Einstein-Maxwell equations, EM and gravitational wave spacetimes, similarity solutions 0-57154
- Einstein-Maxwell equations, inhomogeneous stationary cosmological solns. 0-62556
- Einstein-Maxwell equations, static electrovac solns., complexification technique 0-68114
- Einstein-Maxwell field equations, charging transforms 0-95017
- Einstein-Maxwell fields, stationary solns. by combining Demianski algorithm with Kinnersley method 0-90758
- Einstein-Maxwell stationary field eqns. 0-98840
- Einstein-Maxwell system, covariant quantum field theory 0-68119
- Einstein-Maxwell theory, cosmological model with gravitational, electromagnetic, and scalar waves 0-86188
- electron anapole moment, static parity violating coupling to EM field, unified gauge theory 0-68390
- electroweak and strong interactions without the t quark 0-73640
- electroweak gauge models with heavy W bosons,  $SU_2 \times U_1 \times U_1$  scheme (*Russian*) 0-86652
- electroweak gauge models with sequential W and Z bosons 0-101971
- electroweak interaction model based on  $U_L(2) \otimes U_R(2)$  left-right symmetric gauge group 0-57544
- electroweak interactions, dynamically broken gauge theories, CP nonconservation without elementary scalar fields 0-86613
- electroweak mixing angle, renormalisation 0-86651
- electroweak symmetry group, B-L  $U(1)$  generator and quark-lepton symmetry 0-57549
- elementary particle forces identical at  $10^{-29}$  cm 0-105827
- elementary particle interactions, advances towards a unified theory 0-91039
- elementary particle interactions, unified theories from non-Abelian gauge theories 0-62903
- EM, weak and strong interactions, massless fermions coupling to vector mesons 0-73637
- EM and weak interactions, generalised unified theory, local gauge invariance and P invariance 0-82928
- EM approach to fundamental states of matter, book 0-73103
- EM field in space with torsion, semi-minimal coupling principle 0-77675
- EM fine struct., Fermi weak coupling, Newtonian grav. constants, unified relation 0-101974
- EM phenomena induced by weak grav. fields, possible gravitational wave detector 0-82692
- explosive cascade-decays of leptons, quarks, virtual photons, weak vector bosons and Higgs scalars 0-86641
- extended phase space, unified meson fields 0-86551
- extended phase space, unified spin 1/2 fields 0-86552
- extended technicolour scalarless theories 0-78001
- Extended Technicolour scalarless models 0-73636
- fermion generations in grand unified theories, SU(8) model 0-78012
- fermion masses and hierarchy of symmetry breaking, u and d quarks 0-86618
- fermions, light, mass hierarchy, grand unification, SU(N) theory 0-62911
- five-dimensional theory of interacting scalar, electromagnetic, and gravitational fields 0-105833
- flavour unification in SU(11) 0-62912
- Free vector field in a homogeneous space with torsion 0-90759
- fundamental constituents of matter and unification of weak and electromagnetic interactions 0-62940
- gauge theories 0-73652
- gauge unification of fundamental forces, review 0-95238
- general relativity, vacuum field equations, fifth dimension, ratio of EM to gravitational force 0-77679
- generalized Einstein-Maxwell field theory, asymptotic behaviour 0-86184
- geometric unification of classical gravitational and EM interactions 0-57165
- geometrical unification of gauge and Higgs fields 0-99077
- geometrisation of physics or physicalisation of geometry 0-90760
- grand unification, neutron oscillations and massive neutral Majorana leptons, baryon number 0-91033



## unified field theories continued

grand unification from neutral currents in gauge models 0-78009  
 grand unification with exceptional group  $E_6$ , symmetry breaking,  $SU(5)$  relations, quark masses 0-68407  
 grand unification with the exceptional group  $E_8$  0-105828  
 grand unified gauge theories, running coupling constants and unifying mass scale 0-91029  
 grand unified model with a stable proton and no axion problem 0-95234  
 grand unified theories, compatibility with big bang cosmology, superheavy monopoles 0-86647  
 grand unified theories, mag. monopoles and cosmological implications 0-86643  
 grand unified theory from broken  $SO(8)$  extended supergravity,  $SU(5)$  theory 0-99081  
 grand unified wave function for quarks and leptons 0-91034  
 gravitation-electromagnetism unification, Planck length, five dimensional principal  $U_1$  bundle theory (*Chinese*) 0-86181  
 gravitational and fine struct. consts., grand unification and proton quasis-tability (*Russian*) 0-77680  
 gravitational and strong interactions, unified gauge theory 0-95016  
 gravitational field, nonlocalisation, connection with geometrical theory of gauge fields 0-82696  
 gravitational field and arbitrary gauge field, equations of motion, Heisen-berg and classical, force term, spin-curvature coupling 0-57158  
 gravitational trace anomaly renormalisation in QED 0-57532  
 heavy Majorana particles, cosmological and astrophysical implications 0-90331  
 hierarchical fermion masses from grand unification 0-105832  
 horizontal symmetries dynamical symmetry breaking and neutrino masses 0-105830  
 infrared attractive fixed points, gauge symmetries, QED and anti-grandunification 0-95213  
 integer spin zero-rest-mass field, irreducible representation of Lorentz group 0-68110  
 integer-charged quarks in the  $SU(5)$  grand unified theory 0-68410  
 Kerr-Newman metric, perturb. equations, EM test fields 0-62557  
 large Numbers, explanation via classical unified theory 0-57166  
 left-right symmetric gauge models, parameter constraints from neutral current data 0-86588  
 left-right symmetric model from general horizontal symmetry, Cabibbo angle, CP violation 0-101972  
 LEP, design, tests of unified field theories and quark properties, search for new quarks and leptons 0-74048  
 lepton structure model 0-91063  
 leptons,  $SU(3)$  electroweak theory 0-86638  
 lh theory of leptons and hadrons, unification in  $GA_{4,R}$  gauge 0-86639  
 local B-L symmetry of electroweak interactions, Majorana neutrinos, and neutron oscillations 0-73643  
 mathematical origins of general relativity and of unified field theories 0-95009  
 Maxwell equations in Riemann-Cartan space, spin-torsion coupling const. 0-82697  
 milliweak gauge models of CP violation 0-73633  
 minimal  $O(10)$  grand unification,  $\nu$  mass 0-57546  
 MIT bag model, static electroweak props., PCAC 0-73645  
 mixing matrix and CP violation for  $n$  quark generations 0-101986  
 net baryon number and CP nonconservation with unified fields 0-62349  
 neutral currents, strength limit at PETRA energies 0-105839  
 neutral-current weak interaction without electroweak unification 0-105835  
 neutrino, oscillations, mass and mixing scales 0-105823  
 neutrino number and isotropy of Universe 0-85852  
 neutrino oscillations, Majorana and Dirac mass mixing 0-101969  
 neutrino oscillations of weak interactions 0-105825  
 nonlocal neutrino gravitational interaction and field self interaction 0-91037  
 nonsymmetric unified field theory, metric and local invariance group 0-90754  
 nonsymmetric unified field theory, metric hypothesis, spinor analysis 0-68404  
 nucleon decay, T violation possibility and consequences in superunified theories 0-82917  
 $O(10)$ ,  $SU(4)$  colour subgroup, fractional charged gauge boson, proton half-life 0-73644  
 Pati-Salam model, higher order parton transition effects in deep inelastic scatt. 0-78008  
 Pontecorvo neutrino oscillations for Dirac and Majorana masses, CP non-conservation 0-105829  
 pre-quarks and fractional charges 0-91048  
 primordial baryons, generation by black holes 0-98750  
 primordial magnetic monopoles in unified gauge theories 0-91035  
 proton and neutron disintegration, concepts of leptons and quarks (*French*) 0-91038  
 QCD contributions to vacuum polarization 0-105834  
 quantum gravity, choral of symmetries in general relativity 0-105565  
 quark mass, electroweak contrib. 0-101990  
 quark structure model 0-91063  
 quark-lepton unification in  $SU(N>5)$  0-73646  
 quarks, mass differences of up and down quarks, grand unification 0-62978  
 Reggeization of elementary fermions in arbitrary renormalizable gauge theories 0-68367  
 Reissner-Nordstrom perturbations, coupled Einstein-Maxwell eqns. 0-68108  
 relativistic discrete unified field theories, computer field interaction simulation system 0-68412  
 relativity, seven-dimensional, 4-D gravity coupled to Yang-Mills fields 0-82699  
 relic monopoles from big bang, cosmological problem for standard unified theories 0-77532  
 right translation invariant metrics and variational principles on principal bundle, gauge theories (*Chinese*) 0-101743  
 scalar free unified theory, order-R vacuum functional, with spontaneous scale breaking 0-78003  
 $\sin^2\theta_w$ , grand unified gauge theories and proton decay 0-73634  
 $SO_{10}$ , soft CP violation and complex Majorana mass relations 0-78010  
 $SO(10)$  unification, composite structs., quark and lepton composite models 0-57547  
 $SO(10)$  unified model, phenomenological group, symmetry breaking chain low energy effects 0-86645  
 $SO(2N)$  grand unification in an  $SU(N)$  basis 0-62906

## unified field theories continued

some electrovac models of homogeneous gravitational force fields in general relativity 0-95014  
 spin 3/2 field interacting with EM field, quantisation 0-82698  
 spin (10) grand unified theory, monopole mass 0-99080  
 spin-2 gluon-graviton model with baryon-number nonconservation 0-57565  
 spin-2-gravity coupling, consistency problems 0-77681  
 standard electroweak gauge model with light W and Z bosons 0-95236  
 stationary Einstein-Maxwell equations, gravitational and EM potentials 0-86185  
 strong gravity, field equations, strong interactions, de Sitter microsphere idea of hadrons 0-68111  
 strongly interacting Higgs bosons, gauged nonlinear  $\sigma$ -model,  $SU(2)_L \times U(1)$  extension 0-86656  
 $SU_2 \times U_1$  and the origin of the Cabibbo angle, charged gauge boson mixing 0-73639  
 $SU_2$  grand unification model, two (V-A) and one (V+A) generations of quarks and leptons 0-57538  
 $SU(2,1)$ , graded Lie algebra, irreducible representations 0-82913  
 $SU(2,1)$  electroweak interactions, implications for 6 extra time dimensions 0-77998  
 $SU(2)_L \times (T_3)_R \times U_V(1)$  gauge group, grand unification, symmetry breaking and Z bosons 0-73641  
 $SU(2)_L \times U(1)$ , strong CP-violating phase, one-loop corrections, Higgs particles 0-62910  
 $SU(2)_L \times U(1)$  gauge theory, four flavours, Cabibbo angle natural relations and bounds 0-57550  
 $SU(2)_L \otimes SU(2)_R \otimes U(1)$  weak model,  $\nu$  mass and spontaneous P non-conservation 0-62884  
 $SU(2) \times U(1)$ , gauge invariance and fermion mass dimensions 0-62907  
 $SU(2) \times U(1)$  gauge model, chiral  $SU(2) \times SU(2)$  symmetry and electron mass 0-57542  
 $SU(2) \times U(1)$  gauge model, muon anomalous mag. moment, charged Higgs boson contrib. 0-78011  
 $SU(2) \times U(1)$  model, fermion and Higgs multiplet structure, universality 0-62909  
 $SU(2) \times U(1)$  theories, weak isospin breaking, higher order corrections 0-95235  
 $SU(2) \times U(1)$  unified gauge field, Euclidean space and  $O_4$  invariance 0-91031  
 $SU(2) \times U(1)$  unified model, universal Yukawa coupling 0-91032  
 $SU(2) \otimes U(1)$  standard and  $SU(5)$  grand unification models, neutral current data implications 0-78000  
 $SU(3) \times U(1)$  electroweak model, strong extension, flavour and colour gauge exchange symmetries (*Chinese*) 0-101975  
 $SU(3) \times U(1)$  gauge theory, electro-weak interaction, helicity mixed representation 0-78013  
 $SU(5)$ , gauge invariance and fermion mass dimensions 0-62907  
 $SU(5)$ , Higgs scalars number and  $m_b/m_\tau$  ratio 0-105826  
 $SU(5)$ , unification of weak, EM and strong interactions, review 0-105814  
 $SU(5) \times SU(2)$  unification, horizontal symmetry due to quantised motion along internal axes 0-62905  
 $SU(5) \times U(1)$  unified theory, neutral current anal. 0-73647  
 $SU(5)$  and  $SO(10)$  grand unification, flavour mixing and proton instability (*Russian*) 0-68413  
 $SU(5)$  electroweak-strong interaction model, broken colour symmetry and gluon mass 0-73650  
 $SU(5)$  electroweak-strong interaction model, mass relations and mixing angles 0-73649  
 $SU(5)$  gauge model, masses, mixing angles, CP violation and b-quark decay 0-78006  
 $SU(5)$  grand unification, cosmological baryon asymmetry 0-86640  
 $SU(5)$  grand unification, heavy coloured Higgs scalars, b-quark mass 0-57543  
 $SU(5)$  grand unification, p lifetime and branching ratio, bag model wave-functions 0-78004  
 $SU(5)$  grand unification, spin from isospin, half integer spin charge monopoles 0-68406  
 $SU(5)$  grand unification, superheavy fermions and proton lifetime (*Russian*) 0-91036  
 $SU(5)$  grand unified theory, proton lifetime estimate accuracy 0-101967  
 $SU(5)$  grand unified theory weak vector boson masses 0-68411  
 $SU(5)$  invariant theory, B-L nonconservation and neutron oscillation 0-78005  
 $SU(5)$  model, dyons and monopoles 0-82931  
 $SU(5)$  monopoles, magnetic symmetry and confinement 0-99078  
 $SU(5)$  theories with both proton stability and cosmological baryon-number generation 0-86642  
 $SU(5)$  unification, Higgs potential, coupling constants, and gauge hierarchy 0-86637  
 $SU(5)$  unified gauge theory, non-Abelian electric and mag. flux 0-57545  
 $SU(5)$  without symmetry constraints, unified model of quarks and leptons, conservation laws 0-101968  
 $SU(5)/1$  supergroup based strong-electroweak unified model with supersymmetry 0-101977  
 $SU(8)$  grand unification, natural embedding of  $SU(3)$  horizontal symmetry 0-86646  
 $SU(N>5)$  chiral grand unification 0-91028  
 $SU(N)$  based grand unified theory, monopoles and vector bosons, symmetry breaking 0-99079  
 subquark model of leptons and quarks, unification, currents and exotic states 0-86683  
 superconducting early Universe, cosmological baryon prod., CP invariance grand unification 0-90592  
 supergrand exceptional unification and quark-lepton constituents 0-91030  
 supergrand unification in  $E_6$ , quark-lepton assignments, symmetry breaking scheme 0-68408  
 supersymmetry as means to unified field theory 0-91040  
 superunified theories,  $\Delta B \neq 0$  processes 0-73635  
 symmetric versus antisymmetric mass matrices in grand unified theories 0-99082  
 topless model for grand unification 0-73653  
 twistor theory in Weinberg-Salam and Georgi-Glashow  $SU(5)$  model 0-73651  
 $U(1) \times SU_L(2) \times SU(3)$  theory, integer charge quarks, lepton hadronic processes (*Russian*) 0-86653  
 Universe, closed or open, Fornax system density profile, strong gravitational interactions 0-90587  
 Universe baryon asymmetry, left-right symmetric grand unified models 0-82559

**unified field theories continued**

- universe ultimate fate, effect of finite proton lifetime 0-82560
- weak gauge boson doubling in standard SU(2)@U(1) model, W, Z bosons 0-62916
- Weyl-Dirac theory with torsion, complex Dirac field, conservation equations 0-68112
- $e^+e^- \rightarrow$  jets, transversely polarised annihilation, charged gluon jets, Pati-Salam model 0-86739
- $e^+e^- \rightarrow \gamma X$ , angular asymmetries, weak contribs. 0-101976
- $e^-e^-e^+$ , pol. e, P-odd asymmetry and cross sections, SU(2)xU(1), SU(3)xU(1) calcs. (Russian) 0-62998
- $e^-N \rightarrow e^- \Delta(3/2, 3/2)$ , P-odd asymmetry, P nonconserving neutral current interaction 0-57611
- $n-\bar{n}$  oscillations in nuclei, detectable annihilation rate, grand unification 0-101966
- p decay, flavour gonimetry 0-99100

**unimolecular layers** *see monolayers***uninterruptible power supply** *see emergency power supply***units (measurement)**

- see also constants; dimensions; measurement; nomenclature and symbols*
- ampere, absolute meas. using NMR 0-98941
- ampere, realization expts. at NBS 0-98938
- ampere realization and gyromag. ratio of proton meas. at NPL 0-98940
- ampere realization by means of current balance at NPL 0-105678
- conference on metrology and fundamental constants, Varenna, Italy (July 1976) 0-105603
- derived SI radiation dosimetrical, phys. quantities used in radiation safety monitoring 0-99344
- electrical quantities, units, symbols and definitions (German) 0-86248
- electrical unit reproduction at German ASMW, developments 0-98944
- heliotechnics, basic values, symbols, units and definitions (Rumanian) 0-57243
- historical review and current systems in use (German) 0-68166
- medical measurements, SI units (Croatian) 0-104797
- pressure measurement, definitions of units 0-77745
- radiation effects meas., units selection 0-98870
- radiation units in SI system, conversion problems 0-57244
- SI, fundamentals (French) 0-95059
- SI, guidelines for use, US National Bureau of Standards 0-68167
- SI metric units, in college phys. texts 0-101697
- volt, method and equipment for realization based on fundamental physical constns. and superconductivity phenomenon 0-98943
- volt dissemination method and standard cell enclosure design 0-98876

**universe** *see cosmology***universe models** *see cosmology***untuned power amplifiers** *see power amplifiers***unwinding** *see winding (process)***upper atmosphere**

- see also exosphere; ionosphere; magnetosphere; mesosphere; radiation belts; thermosphere*
- aurora, dayside morphology from large scale obs. at 6300 Å, 5577 Å and 3914 Å 0-85786
- auroral zone electric currents, ground-based obs. using two-dimensional magnetometer array 0-90245
- conference, New Delhi, India (Jan. 1979) 0-94912
- cosmic rays, short-term fluctuations obs. 0-67483
- density distribution, from Cactus accelerometer flight results in Castor satellite 0-77251
- diffusion equations, coupled time-dependent, numerical method using self-diffusion coeff. 0-109285
- discrete auroras near midnight, occurrence and lifetimes 0-67447
- drag perturbations on artificial satellite orbits 0-67522
- electrical coupling to lower atmos., quasi-static model 0-61865
- electrojet induced press. and vel. fluctuations 0-82118
- electron beam scattering in atoms, sounding rocket expt. (POLAR-5) 0-77212
- escape of ions to space, ion chem. and low altitude accel. effects 0-85798
- gravity wave propagation, 'potential' well treatment 0-67396
- gravity waves, possible effect on Loran-C 100 kHz signals 0-109304
- gravity waves at E-region heights, obs. of Es 0-72657
- gravity waves in ionosphere, radar obs. of electron density 0-77182
- gravity waves in nighttime F-region, TID distrib. and occurrence 0-77206
- IR brightness obs. 0-94629
- IR emission at high latitudes from Meteor satellite, radiometer obs. 0-72655
- IR radiation flux in upper atmosphere, meas. in 4 to 6  $\mu$ m spectral range 0-61929
- lunar tide influencing equatorial electrojet 0-61937
- meteor region, winter motions meas. in S. hemisphere 0-109287
- meteors ionisation columns, initial radii meas. 0-94762
- mountain ridge, causing upper atm. perturbations (Russian) 0-105018
- neutral atmosphere, dynamics rel. to ionosphere primary ion-electron prod. rates change 0-72675
- neutral temperature at 100-120 km altitude, compared to  $T_e$  0-77211
- neutral wind profiles between 115 and 175 km altitude in dayside auroral oval 0-98494
- nightglow, rocket meas. of O<sub>2</sub> atmospheric system and OH Meinel bands (Japanese) 0-94631
- noctilucent clouds over W. Europe (during 1979) 0-109289
- perturbations caused by mag. storms, review of obs. 0-98495
- polar wind morphology in mag. quiet conditions (Russian) 0-72713
- radar for observing middle and upper atmosphere, Yagci antenna array design 0-90255
- radar meas. 0-72661
- radar meteors rate depend. on geomag. activity and coronal activity 0-67662
- Rossby neutral mode, secular stability 0-81983
- rotation rate and density, obs. of satellite orbit 0-85785
- sunrise effect on elec. pot. near ground, origin in upper atmos. 0-61866
- temperature, measured using near aperture for interferometry of airglow 0-82075
- temperature and ion chemistry at nighttime, 400-450 km altitude, Ogo 6 data 0-90267
- thermosphere, lower, electric current and atmospheric motion, symposium, Seattle, Washington, 1977 August to September 0-62371
- tide (solar semidiurnal), zonal motion and meridional temp. gradient effects 0-98399
- tides, theoretical work since 1970, review 0-94589

**upper atmosphere continued**

- tides at meteor altitudes, CTOP radar obs. 0-77181
- tides in equatorial thermosphere, semidiurnal and terdiurnal 0-82119
- UV fluoresc. excited by electron beam, POLAR-5 rocket expt. at 391.4 nm 0-77214
- Vertical-6 rocket flight results 0-90268
- VUV solar scatt. radiance, aurora and nightglow, satellite obs. 0-90272
- wind, meas. with airglow Fabry-Perot spectrometer 0-77156
- wind as cause of ionospheric disturbance dynamo 0-82134
- wind in lower ionosphere, obs. by Kyoto meteor radar 0-67444
- wind in neutral atmos. at F-region height, servo model of ionosphere 0-101486
- wind in upper mesopause, diurnal variation of zonal and meridional components 0-109284
- winds in meteor region, periodic fluctuations of recurrent nature 0-90266
- N<sub>2</sub> production, photochem. model, far UV dayglow 0-90271
- N<sub>2</sub> gas, electron energy degradation, Monte Carlo study 0-69969
- N<sub>2</sub> photochem. rel. to solar cycle phase, 285-375 km altitude 0-85783
- N<sub>2</sub><sup>+</sup> 1 NG emissions from proton aurora, anomalous vibr. distrib. 0-67448
- NO<sub>2</sub> density profile from airglow obs., 72-120 km altitude 0-105094
- NO<sub>2</sub><sup>+</sup> cluster ion formation in D-region, temp. control by ion obs. 0-61931
- N(P) in auroral arc, excitation and collisional deactivation processes 0-72658
- Na enhancement at 95 km altitude, airglow and lidar obs. 0-101466
- O, 557.7 nm spectral emission mechanism at 100 km altitude 0-61933
- O, airglow intensity of green line rel. to atom density (Chinese) 0-90269
- O atoms in exposure, polar corona atom distrib. 0-82120
- O<sup>+</sup> + N<sub>2</sub>, charge exchange collision, rate coeff. and ionosphere implications 0-87224
- O<sup>+</sup> + O<sub>2</sub>, charge exchange collision, rate coeff. and ionosphere implications 0-87224
- O<sub>2</sub>, (0-1) spectral emission band in upper atmos. 0-61933
- O<sub>2</sub> density at D-region altitude, obs. of Lyman- $\alpha$  extinction 0-77180
- O<sub>2</sub><sup>+</sup>(<sup>2</sup>D) + N<sub>2</sub> charge exchange, rate coeff. temp. depend. 0-77179

**uranium***see also nuclei with .....**see also fission of uranium*

- alkali-alumino-phosphate:U, rontgenoluminesc. and fluoresc., radiative transitions obs. 0-103977
- assay, experimental comparison of the active well coincidence counter with the random driver 0-78503
- assay of natural samples, meas. of gamma- or neutron activity of short-lived fission products 0-61179
- atom + <sup>3</sup>He(<sup>4</sup>He)(Ne), collisional relax. of highly excited states, laser-induced fluoresc. obs. 0-38205
- atom + molecule, collisional relax. of highly excited states, laser-induced fluoresc. obs. 0-58205
- atomic beam, two laser irradi., two photon reson. effects., visible spectra 0-63604
- bronchogenic carcinoma among former U mine workers at Port Radium, Canada 0-89802
- content in some Indian coal and flyash samples 0-104547
- dental porcelains, determ. of U content and dose to oral mucosa 0-89830
- distribution of speculative uranium resources 0-78369
- Earth mantle, U conc. rel. to Earth thermal evolution 0-89988
- Edwards carbonate aquifer, Texas, U isotopes fractionation rel. to aquifer oxidation/reduction 0-98362
- enriched U, lower costs 0-106111
- enrichment, centrifuge process, LWR fuel (German) 0-68905
- enrichment by laser isotope separation (Japanese) 0-68960
- enrichment by photochemical laser, two-phase flow with condensation, mathematical model (French) 0-74029
- exploration, <sup>222</sup>Rn gas detection using Track Etch system 0-98488
- exploration and prospecting methods 0-85768
- extraction by transfer between liq. phases, laser radiation effect 0-66795
- Fermi surface and effective masses of  $\alpha$ -phase, de Haas-van Alphen meas. 0-65426
- fissile material accountability using controlled potential coulometry 0-63298
- fission track dating using U glasses, error analysis 0-95503
- fuel elements recycling and thermal re-irradiation, technical, economic and safety problems (German) 0-99269
- gas-discharge fission reactor, fuel element component conc., plasma temp. profile instabilities 0-63253
- gaseous, U fueled reactor, use as power supply for nuclear pumped laser system 0-63247
- geochemical prospecting methods 0-72635
- geological exploration by Rn mapping, exclusion of <sup>220</sup>Rn signal 0-61916
- geophysical prospecting, <sup>222</sup>Rn mapping using mat to avoid hole drilling 0-82087
- geophysical prospecting by  $\gamma$ -ray logging of borehole, factors affecting resolution 0-98463
- Hugoniot data, ultrahigh press. (TPa) shockwave from underground nuclear explosion 0-59580
- interband, collective and atomic (p,d) excitations, Z-160 eV, fast EELS 0-93443
- international resources assessment 0-99215
- ion source using surface ionisation process 0-68999
- irradiation growth during fission fragment and proton bombard. 0-92568
- isotopic analysis by resin-bead mass spectrometry for materials safeguards 0-78392
- isotopic composition, determ. using precise absolute gamma spectroscopic meas. 0-66916
- isotopic composition, determ. using thermal ionisation spectrometry with automatic data eval. 0-66913
- isotopic composition, determ. using thermal ionisation mass spectrometry 0-66914
- mechanical properties of  $\alpha$ -phase crystals., very high strain rates, double-notch shear test use 0-85131
- minor isotope concentration meas. for safeguarding U enrichment cascade 0-63283
- molybdates, alkaline earth, U activated, scheelite struct. luminesc. props. vibr. modes and quenching temp. 0-60651
- National Uranium Resource Evaluation (NURE) programme, aerial radiometric survey data interpretation via principal components anal. 0-101438
- neutron activation delayed analysis, U content in Hueco and Guadalupe Mountain Indian ceramics 0-85230



## uranium continued

- nondestructive element and isotope assay 0-71870  
 nondestructive measurement of U and Th conc. and quantities using XFA and gamma spectrometry 0-71877  
 nuclear fuel, impact of fusion-fission hybrid reactors on world demand 0-95404  
 nuclear fuel conversion plant, nondestructive assay 0-66761  
 optical absorption meas. 0.15 to 2.0 eV, polycryst.  $\alpha$ -U 0-108223  
 ore detection, Rn gas concentration meas. using alpha sensitive plastic detectors 0-94617  
 ore detection using integrated meas. of long-distance transport of  $^{220}\text{Rn}$  0-98476  
 ore exploration, Rn gas conc. meas. using alpha sensitive plastic films 0-94618  
 particle etch track technique determ. of U trace content in normal human blood 0-89910  
 phosphate fertilizer, specific activity of U and Th rel. to particle size 0-106244  
 photoelectron spectra study, core and valence levels 0-66394  
 prospecting by active neutron logging, evaluation models 0-98480  
 prospecting of sandstone-type ores, charged particle track analysis 0-91405  
 Purex kinetics, U extraction with tributylphosphate (*German*) 0-57937  
 resources, optimisation of LWR and FBR power prod. strategy 0-99253  
 resources and accessibility, reliability of nuclear fuel supply 0-99216  
 rocks, isotope disequilibrium, due to  $\alpha$ -recoil and soln. effects 0-98314  
 safeguarding, 5 to 20 mg determ. by constant current coulometric titration 0-78381  
 safeguarding, determ. of trace amounts by pulsed laser fluorometry 0-78382  
 safeguarding, determ. of U and Pu content of fuels using isotope correl. tech. 0-68834  
 safeguarding using resin bead mass spectroscopy 0-73984  
 safeguards, computerised nondestructive assay for materials management 0-78388  
 safeguards accountability, NDA of crated waste by gamma-ray and neutron coincidence counting 0-83166  
 sedimentary rocks, Th and U abundances rel. to crustal evolution and sedimentary recycling 0-85654  
 spectrochemical analysis, U concentration in fuel reprocessing streams, determ. using acid-compensated dual-wavelength tech. 0-78430  
 sputtered atoms, laser fluorescence spectroscopy 0-66359  
 St. Severin chondrite, U and Pu distrib. 0-72889  
 symbiotic energy system, U fuelled, economic anal. using SYMECON code 0-106172  
 symbiotic system, managing fusion burn, economic analysis 0-106173  
 tungstates, alkaline earth, U activated, scheelite struct. luminesc. props. vibr. modes and quenching temp. 0-60651  
 tungstates, U-doped, perovskite struct., luminesc. quenching, QMSCC calcs. 0-71470  
 valence and 5f states, XPS and bremsstrahlung isochromat spectroscopy 0-66393  
 $\text{CaF}_2$ -U, electron irradi. defect aggregates, ordering, impurity effects 0-75216  
 $\text{CaF}_2$ - $\text{U}^{3+}$ , anomalous magnetooptic props., optical detection of ESR and cross-relax. resonances 0-93287  
 $\text{LaCl}_3$ - $\text{U}^{3+}$ , cryst., spectrum anal., cryst. field parameters 0-76057  
 $\text{NaF}$ -U, luminesc. spectra, Vibr. struct. 0-80840  
 $\alpha$ -U, CDW at 43K 0-80198  
 U III, IV, line identification on relative intensity basis 0-95561  
 $\alpha$ -U, strain rate effect on flow and fracture 0-100887  
 $\alpha$ -U, strain rate effect on tensile flow and fracture 0-84992  
 $\text{U}^{4+}$ , electron configuration from nuclear information 0-58146  
 $^{92}\text{U}$ , self-consistent relativistic density-functional theory 0-91441  
 $\text{U}^{238}\text{Pu}^{237}\text{Np}$  GCRF fuel cycle to produce isotopically denatured Pu for LWR 0-78427  
 $\text{U}^{+} + \text{O}_2(\text{CO})(\text{CO}_2)(\text{COS})(\text{CS}_2)(\text{D}_2\text{O})$ , reaction cross-sections, ion beam apparatus study 0-97691  
 $\text{U}^{40+} + \text{Ne}$ , highly charged very slow Ne recoil ions, K' X-ray transition 0-91649  
 UI plasma, absolute emission coeff. 0-64693  
 UI, precision isotope shifts meas. in visible, near IR 0-63587  
 UV, energy levels and UV spectral anal. 0-106290  
 $^A\text{U}$ ,  $A=235,238$ , muonic atom lifetimes from muon induced fission 0-69269  
 $^{235}\text{U}$  safeguards, expt. nondestructive assay using a random driver 0-83164  
 $^{235}\text{U}$ , transuranic trace analysis using resonance ionisation spectroscopy of inert gases 0-93833  
 $^{235}\text{U}$  burn-up determ. by mass spectrochemical anal. 0-71989  
 $^{235}\text{U}$  fission product  $\gamma$  radiation for short irradi. times, energy distrib. 0-73929  
 $^{235}\text{U}$ , ground and 1st excited states, hfs, laser fluoresc. and laser-RF double reson. spectroscopy 0-58170  
 $^{235}\text{U}$ , nondestructive active assay in  $(\text{U,Pu})\text{O}_2$  fuels 0-71873  
 $^{235}\text{U}$ , nondestructive assay, appl. to decommissioning of fuel reprocessing facility 0-81269  
 $^{235}\text{U}$ , nondestructive assay techniques for control and accountability 0-81270  
 $^{235}\text{U}$ , recovery from enrichment plant tailings by laser isotope separation 0-83212  
 $^{235}\text{U}/^{238}\text{U}$  isotope ratio determ. in  $\text{UF}_6$  samples using gas quadrupole mass spectroscopy 0-78376  
 $^{235}\text{U}$ -fission track micromapping, exam. of U mobilisation processes in Precambrian sediments 0-98477  
 $^{238}\text{U}/^{235}\text{U}$  in Allende meteorite rel. to early Solar System  $^{247}\text{Cm}$  0-90347  
 $^{238}\text{U}/^{235}\text{U}$  in chondritic meteorites, search for isotopic anomalies 0-85903

## uranium alloys

- shell, explosive expansion, deform. and rupture modes and mechanisms 0-85064  
 shell, explosive expansion, rupture behaviour 0-85063  
 Th-Pu-U-Zr (20, 4, 8 wt.%) metal fuels, compatibility with cladding alloys for FBR appls. 0-102242  
 Th-U (20 wt.%) metal fuels, compatibility with cladding alloys for FBR appls. 0-102242  
 U-Co(Ce)(Fe)(Mn)(Ni)(V) metallic glasses, glass form. and thermal stability 0-75183  
 U-Mo (2 wt.%), depleted, effect of microstruct. on mech. props. 0-108497  
 U-Nb (14 at.%), martensitic and polymorphic transformations 0-60861

## uranium alloys continued

- U-Pu-Zr(Th) LMFBR metal fuel elements, development and performance 0-57856  
 $\text{UAl}_3$ , spin fluctuations, mag. field effect, electronic sp. ht. and elec. resist. 0-108026  
 $\text{UAl}_3$ , dispersion nuclear fuels, development and irradi. performance 0-78368  
 $\text{UAl}_3(\text{Co})$ , surface comp. and electronic struct., photoemission study 0-66382  
 $\text{UB}_3$ , thermochemistry and stability 0-97723  
 $\text{U}(\text{Co}_{1-x}\text{Fe}_x)_2$ , ferromag. onset, susceptibility and resist. meas. 0-70967  
 $\text{U}_{10}\text{Co}_3\text{Si}_{13}$ , crystal struct., dimensions, space group and coord. (*Russian*) 0-88085  
 $\text{U}_6\text{Co}_3\text{Si}_{19}$ , X-ray cryst. struct. determ. 0-107111  
 $\text{UFe}_2$ , giant magnetoelastic deform. of cryst. struct. mag. props. (*Russian*) 0-93159  
 $\text{UMn}_2$ , transport props., influence of lattice distortion 0-100452  
 $\text{UNi}_2$ , mag. phase transition, elec. resist. meas. 0-97094  
 $\text{URu}_3$ , sublimation thermodynamics 0-97722  
 $\text{U}_3\text{Si}$ , reversible twinning, in-situ obs. 0-104241

## uranium compounds

- see also uranium alloys  
 thermal reactor fuel cycles, actinide wastes toxicity limitations (*German*) 0-99220  
 uranyl complexes, IR spectra and bond distances 0-74167  
 $\text{CO-UF}_6$  nuclear pumped laser, expansion cooled, vibr. excitation distrib. 0-63997  
 $\text{Cu}_2\text{U}_6\text{S}_{13}(\text{Se}_2)_3$ , cryst. struct. and magnetic props. (*French*) 0-96496  
 $\text{HfO}_2\text{AsO}_4\cdot 4\text{H}_2\text{O}$  and  $\text{HfO}_2\text{PO}_4\cdot 4\text{H}_2\text{O}$  layered cpds., struct. investigs. below antiferroelec. transition temps., H bond ordered structs. 0-107416  
 $\text{HfO}_2\text{AsO}_4\cdot 4\text{H}_2\text{O}$  and  $\text{HfO}_2\text{PO}_4\cdot 4\text{H}_2\text{O}$  layered cpds., single and polycryst., proton cond. behaviour w.r.t. antiferroelec. transition temps. 0-107481  
 $\text{H}_{n-2}\text{UO}_2(\text{IO}_6)_n\cdot 4\text{H}_2\text{O}$ ,  $n=0.5$  to 2.0, high proton cond. 0-107562  
 $\text{HfO}_2\text{PO}_4\cdot 4\text{H}_2\text{O}$ , film fabrication and appl. as solid electrolyte in electrochromic displays 0-70462  
 $\text{HfO}_2\text{PO}_4\cdot 4\text{H}_2\text{O}$  solid proton conductor, appl. as electrochromic cell 0-89497  
 $\text{HfO}_2\text{P}(\text{As})\text{O}_4\cdot 4\text{H}_2\text{O}$ , water deficiency, enthalpy of dehydration, thermogravimetric anal. 0-65251  
 (Th,U)C advanced FBR fuels, radiological assessment of reprocessing 0-73983  
 (Th,U) $\text{O}_2$ , burnup simulated, high  $\text{O}_2$  pot., chem. state 0-91220  
 (U,Ce), U self-diffusion 0-92711  
 (U,La)C, U self-diffusion 0-92711  
 (U,Pu)C, nuclear fuel, irradiation induced creep meas. 0-93605  
 (U,Pu)(C,N) and (U,Pu)N, high burn-up simulated, Pu self diffusion 0-92712  
 (U,Pu)C FBR fuel pins, irradi. behaviour w.r.t. fission gas release, fuel/clad compatibility, Pu migration 0-57847  
 (U,Pu)C LMFBR fuel, Na-bonded, consequences of rapid Na loss on fuel behaviour 0-102238  
 (U,Pu)C, pellet and sphere-pac nuclear fuels, comparative irradi. tests 0-78367  
 (U,Pu) $\text{C}_{1-x}\text{N}_x$  LMFBR MX-type fuels, fission gas release and microscopic swelling 0-73921  
 (U,Pu) $\text{O}_2$ , 0-63252  
 (U,Pu) $\text{O}_2$ , fission gas release and retention in irradi. nuclear fuels 0-57841  
 (U,Pu) $\text{O}_2$  fuel pin behaviour during FFTF 3c/s reactivity insertion event, TREAT expt. anal. 0-102240  
 (U,Y)C, U self-diffusion 0-92711  
 (U,Zr)C, U self-diffusion 0-92711  
 U-Ba-C FBR nuclear fuels, phase anal., 1400°C 0-66487  
 U-Pr-C FBR nuclear fuels, phase anal., 1400°C 0-66486  
 U-Sr-C FBR nuclear fuels, phase anal., 1400°C 0-66487  
 U-Y-C FBR nuclear fuels, phase anal., 1400°C 0-66485  
 UAs, search for lattice distortions at low temps. 0-79759  
 $\text{U}_3\text{As}$  13a 3-5-5-3a, heat capacity, 5-300K, ferromag. transition obs. 0-88769  
 $\text{U}_3\text{As}_4$ , ferromag., mag. field induced phase transitions 0-65887  
 $\text{U}(\text{BH}_4)_4$  in  $\text{Hf}(\text{BH}_4)_4$ , excited state assignments and E-symmetry ground state, near IR MCD obs. 0-66153  
 $\text{UBr}_3$ , cryst. field levels, neutron scatt. determ. 0-65509  
 U(C,N), N vapour pressures and thermodynamic props. 0-84918  
 UC, chemical compatibility with Cr-Fe-Ni cladding alloys, thermodynamic model 0-63263  
 UC, creep, irradiation induced, transient state, kinetic eqn. treatment 0-88251  
 UC, electronic struct., comparison with photoemission spectra 0-91450  
 UC, miscibility with rare earth nitrides (*German*) 0-96654  
 UC, nuclear fuels, irradi. induced kinetics, diffusion and fission gas resolu. 0-59523  
 UC, quenched-in defects, formation, migration and resistivity 0-64990  
 UC, sintering, role of Ni as sintering additive 0-84892  
 UC,  $\text{UC}_2$ ,  $\text{U}_2\text{C}_3$ , and UC+ $\text{UC}_2$ , elec. resist., 4 to 1900K 0-59953  
 $\text{UC}_x$ , partial molar thermodynamic quantities, semi-invariant cumulants method 0-65250  
 UCN, quenched-in defects, formation, migration and resistivity 0-64990  
 $\text{UF}_4$ , absorption spectrum indicating presence of resonantly localised continuum state 0-58173  
 $\text{UF}_4$ , inner conversion electron spectra, electron orbit hybridisation (*Russian*) 0-87227  
 $\text{UF}_4$ , interband, collective and atomic (p,d) excitations, Z-160 eV, fast EELS 0-93443  
 $\text{UF}_4$ , vapourisation behaviour 0-84283  
 $\text{UF}_4$ - $\text{CF}_4$  mixture, gas core fission reactor, fission based plasma engine 0-63366  
 $\text{UF}_4$ -LiF(KF) molten binary mixtures, viscosity meas. 0-65270  
 $\text{UF}_4$ -MF (M=Na or K), ion-molecule equilibria, heat of form. and dissociation and electron affinities determ. 0-104480  
 $\text{UF}_6$ , arc emission discharges, compared to UI plasma emission coeff. 0-64693  
 $\text{UF}_6$ , CW  $\text{CO}_2$  laser spectroscopy 0-83367  
 $\text{UF}_6$ , conversion for nuclear fuel appls. 0-99266  
 $\text{UF}_6$ , gaseous fuel reactor applications 0-63367  
 $\text{UF}_6$ , high temp. fissioning plasma core reactors, fluid mechanical confinement 0-63248  
 $\text{UF}_6$ , laser chemistry 0-69198  
 $\text{UF}_6$ , matrix isolated, vibronic fine struct. in fluoresc. spectrum 0-83406

## uranium compounds continued

- $UF_6$  molecular dissociation by  $DF_4$  laser radiation 0-91619  
 $UF_6$  molecule dissociation in two-frequency IR laser field 0-66855  
 $UF_6$ , multiphoton irradiation, spectra and modeling of laser induced emission 0-69160  
 $UF_6$ , nucl. lasing, population inversion mechanism 0-63980  
 $UF_6$  nuclear pumped lasers, electron impact cross section meas. 0-63985  
 $UF_6$ , photodissoc. through light scatt. of  $UF_5$  particles, influence of  $N_2$  as collisional partner 0-95698  
 $UF_6$ , quenching action in  $N_2$ -He ion nuclear pumped lasers 0-64001  
 $UF_6$ , reactions inducing plasmas, neutron irradiation UV and visible spectra obs. 0-64784  
 $UF_6$ , relativistic scattered wave calculations 0-63538  
 $UF_6$ , safeguarding of enriched  $UF_6$  bulk transfers 0-68814  
 $UF_6$ ,  $UF_6$ - $H_2$  gas dissociation in pulsed IR and UV laser fields 0-91620  
 $UF_6$ - $H_2$ /HF nuclear pumped laser, characts. 0-78847  
 $UF_6$ + $K_2(CS_2)$ , ionisation reactions, absolute cross sections 0-99565  
 $UF_6$ + $K(CS)$ , ionisation reactions, absolute cross sections 0-99565  
 $UF_6$ +Ar,  $UF_6$  internal excitation 0-106386  
 $UF_6(Cl_4)$ , electronic struct., MS-SCF-X $\alpha$  calcs. and VUV photoelectron spectra 0-63710  
 $UF_6B_7(B_2)$ , Mossbauer effect of  $^{57}Fe$  nuclei, mag. props. 0-103907  
 $U(Fe_{1-x}Mn_x)_2$ , Curie temp. and saturation moment at 4.2K 0-70966  
 $UIr_3B_2$ , supercond. and mag. props. 0-97028  
UN, electronic struct., comparison with photoemission spectra 0-91450  
UN, N vapour pressures and thermodynamic props. 0-84918  
UN, photoelectron spectra study, core and valence levels, antiferromag. transition effects 0-66394  
UN, relativistic energy bands, LMTO calcs. 0-65442  
UN, search for lattice distortions at low temps. 0-79759  
UN, synthesis from  $UO_3$  through carbide 0-73980  
UN-ZrN, Young's modulus antiferromagnetic anomaly 0-92583  
 $U_{1-x}Nd_xS$ , mag. phase diagram 0-71027  
 $UO^{+}+Ar$ , collision-induced dissociation cross section and threshold 0-95706  
 $UO^{+}+O_2(CO)(CO_2)(COS)(CS_2)(D_2O)$ , reaction cross-sections, ion beam apparatus study 0-97691  
 $UO_2$  0-63252  
 $UO_2$ , 5f-magnetic semiconductor, spectroscopic data, review 0-97299  
 $UO_2$ , burnup determ. in PWR and BWR using NDA of neutron emission rates 0-83148  
 $UO_2$ , creep, irradiation induced, transient state, kinetic eqn. treatment 0-88251  
 $UO_2$ , crystallite growth from oxide plasmas, growth morphology 0-59417  
 $UO_2$ , crystn., specific heat anomaly 0-84299  
 $UO_2$ , dense microsphere production by sol-gel technique (Czech) 0-68906  
 $UO_2$ , electronic distributions by X-ray spectroscopy 0-97407  
 $UO_2$ , electronic transitions, crystal field effects and phonons, phase transition 0-97303  
 $UO_2$ , fission gas release and retention in irradiated nuclear fuels 0-57841  
 $UO_2$ , fuel-coolant interaction, film boiling and vapor explosion phenomena 0-95363  
 $UO_2$ , gas bubble mobility 0-91222  
 $UO_2$ , green pellet with zinc stearate as additive, effect on sintering 0-68908  
 $UO_2$ , high burnup nuclear fuels, relation between fission product release and fuel microstruct. 0-57845  
 $UO_2$ , low enriched coated fuel particles for HTGR, anal. of  $O_2$  partition equilibrium 0-68769  
 $UO_2$ , Mg K $\alpha$  and He(II) photoelectron spectra, origin from multi-configurational Dirac-Fock calcs. 0-66387  
 $UO_2$ , molten LMFBR fuel, characterization of fragmented fuel from a thermal fuel-sodium interaction 0-68774  
 $UO_2$ , nuclear fuel, exam. of neutron yield on  $O(\alpha,n)$  reaction 0-86912  
 $UO_2$ , nuclear fuel preparation, emanation thermal anal. for characterisation of uranyl gel microspheres 0-95391  
 $UO_2$ , nuclear fuels, fission gas release at high burn-ups 0-57852  
 $UO_2$ , nuclear fuels, irradiation induced kinetics, diffusion and fission gas resol. 0-59523  
 $UO_2$  pellets, sinterability, particle size effect 0-104098  
 $UO_2$ , photoelectron spectra study, core and valence levels 0-66394  
 $UO_2$  powder compaction, force transmission and friction 0-71620  
 $UO_2$ , single-cryst. neutron diffraction data, reanal. using third cumulants 0-100130  
 $UO_2$ , surface energy, determ. by Hertzian indentation 0-93641  
 $UO_2$ , volatilization pot. of metallic inclusions in irradiated nuclear fuel during LOF overheating transients 0-57895  
 $UO_2$ -PuO $_2$  fuel pin, hyperstoichiometric, post irradiation examination 0-63258  
 $UO_2$ -UC microspheres, coated, coating permeability meas. 0-95343  
 $UO_2$ -Zr high burnup nuclear fuel rods, Xe, Kr, He release 0-57846  
 $UO_2^{+}+Ar$ , collision-induced dissociation cross section and threshold 0-95706  
 $\gamma$ - $UO_2$ , inner conversion electron spectra, electron orbit hybridisation (Russian) 0-87227  
 $UO_4^{6-}$ , octahedral uranate group, charge transfer transition and luminesc. 0-97324  
 $U_3O_8$  aggregates, solid, aerosols, dynamic shape factors meas. 0-61165  
 $U_3O_8$  demand projections using a disaggregated market penetration model 0-99214  
 $U_3O_8$  enrichment standards, gamma-ray spectra 0-78378  
 $U_3O_8$  recovery from seawater, R and D program 0-99217  
 $U_3O_8$  two near-term alternatives for improved nuclear fuel utilization in PWR 0-95347  
 $U_3O_{8-x}$  phase transition to  $U_3O_{21+x}$ , study by elec. cond. meas. 0-100489  
 $U_3O_2Cl_3$ , prep. and cryst. struct. (French) 0-84150  
 $UO_3B_2$ , supercond. and mag. props. 0-97028  
 $U_3P_4$ , press. effects on elec. resist. and Curie temp. 0-75559  
 $U_{1-x}Pr_xS$ , mag. phase diagram 0-71027  
 $U_{0.77}Pu_{0.23}O_{2+x}$ , oxygen potential in temp. range 1523 to 1822K 0-106113  
US, electronic struct. and exchange band splitting, optical refl. meas. 0-66226  
US, relativistic energy bands, LMTO calcs. 0-65442  
 $U_3S_3$ , sp. ht. at low temps., mag. behaviour 0-60353  
USb, relativistic energy bands, LMTO calcs. 0-65442  
USb, search for lattice distortions at low temps. 0-79759  
USc, electronic struct. and exchange band splitting, optical refl. meas. 0-66226  
 $U_2Sn_2Mo_6S_8$ , supercond. props. 0-97023  
UTe, crit. exponents, neutron and magnetisation meas. 0-88823

## uranium compounds continued

- UTE, electronic struct. and exchange band splitting, optical refl. meas. 0-66226  
UTE, relativistic energy bands, LMTO calcs. 0-65442  
 $U,Th_{1-x}As$  (Sb), electronic struct., relativistic KKR-averaged T-matrix approx. method 0-107702  
 $U,Th_{1-x}As$ , mag. phase diagram, magnetisation meas. 0-60271  
 $U,Th_{1-x}Sb$ , valence change of U accompanied by singlet-ground-state ferromag. 0-70965  
 $UZr_2FO_{14}$ , X-ray cryst. struct. determ. and refinement (French) 0-107122  
 $U,Zr_{1-x}Fe_2$ , Curie temp. and saturation moment at 4.2K 0-70966  
 $^{238}UO_3$  grains distrib. in graphite matrix, effect on resonance integral 0-68768  
 $UF_6$ , mass spectrometric determ. of  $^{235}U$  content 0-68961

## Uranus

- albedo and brightness temp., 5  $\mu m$  IR obs. 0-82300  
albedo and spectral features from IR obs. 0-82299  
atmosphere, ammonia and water vapour contents 0-90366  
atmosphere, appl. of methane band-model parameters to visible and near IR spectrum 0-98609  
atmosphere, D/H ratio from visible spectra obs. 0-82296  
geometric oblateness from digitized photographs, Stratoscope II balloon obs. 0-67649  
magnetic field, hydromagnetic dynamo in core 0-90365  
polar moment of inertia determ. 0-94694  
positions, reduction of 19th century obs., method comparison 0-94691  
radius and ellipticity from SAO 158687 occultation obs. 0-67648  
ring, form, and stability 0-82302  
ring system, review of physical studies 0-72874  
ring system, struct. from photoelec. obs. of SAO 158687 occultation 0-77348  
ring system, summary of recent research 0-72875  
rings, occultation obs. (French) 0-82281  
rotation, equatorial flow theory 0-67653  
satellites, astrometric obs. 0-67654  
stellar occultation, 1980 August 15 to 16, reality of additional occultations questioned 0-109396  
stellar occultation by Uranus and rings, 1980 August 15 to 16, obs. 0-98610  
structure and evolution in three-layer interior model 0-72877  
UV albedo, meas. 0-82295

u.v. astronomy see ultraviolet astronomy

u.v. detectors see ultraviolet detectors

## V-centres

see also H-centres

- alkali halide, dynamics of nonrelaxed and self-trapped holes (Russian) 0-80607  
alkali halides, gamma and additively coloured, dissolving in pure water, lyoluminesc. mechanism 0-100693  
alkali halides,  $V_K$ -centres, vibr. modes, calc. 0-84269  
alkali metal halides, F-colouring role of impurities 0-64995  
alkali metal halides, hole self-localization and capture, temp. depend. 0-92526  
ionic crystal, exciton mechanism model for defect form. 0-80187  
trialkylammonium, iodides, absorpt. and luminesc. spectra of self-localized excitons 0-97340  
 $CaF_2:M$ ,  $M=Mn, Fe, Co, Ni$ , X-irrad., impurity effects on defect prod. 0-92525  
 $CaF_2:Ni$ , X-irradiated, optical and EPR meas. 0-108235  
 $CsI:Na$ , X-ray irradiated, optical and ESR studies in IR absorption band 0-80828  
KBr, cation defects creation mechanism 0-75224  
KBr, defect accumulation under electron irradiation at 4K 0-107233  
KBr, X-irrad. crystals, halogen aggregation, absorpt. spectra obs. (Russian) 0-66234  
KBr(I), photostimulated recomb., electron spin polarisation 0-60673  
KCl and  $KCl:NO_2$ , X-irrad. crystals,  $Cl_3^-$  centres photodissoc., optical anisotropy and creation mechanisms (Russian) 0-66235  
 $KCl:SnCl_3$ , photostimulated hole recombination luminesc. (Russian) 0-80833  
 $MgAl_2O_4$ ,  $\gamma$ -irradiated crystal, TSC, thermoelec. power, thermolum. and afterglow 0-75583  
MgO crystals, dipolar defects, thermally stimulated depolarisation 0-66101  
NaCl crystals, electronic and hole centres and surface, quantum-chemical calcs. 0-65489  
 $NaCl:Mn^{2+}$ , thermolum. spectra, mechanisms 0-80873  
 $NaCl(Br)$ , X-ray or UV irradiated, cation defects creation mechanism 0-75224  
NaF:U, luminesc. spectra, Vibr. struct. 0-80840  
NaMgF $_3$ , defects induced by X- and vacuum UV irradiation, optical and elec. study 0-107319  
RbCl(Br), cation defects creation mechanism 0-75224  
RbI, luminesc. spectra induced by pulsed  $Ne^+$  and electron beams and X-rays 0-80851  
RbI, photostimulated recomb., electron spin polarisation 0-60673  
 $Si:Ar(Ne)(O)(N)$ , ion-implanted, defect reverse annealing, 550-650°C 0-88875

 $V_H$ -centres see H-centres $V-VI$  semiconductors see semiconductor materials

## vacancies (crystal)

- see also Frenkel defects; impurity-vacancy interactions; Schottky defects; vacancy condensation loops; vacancy-dislocation interactions  
A15 compounds, disordered, reordering kinetics 0-96678  
adamantane, cryst., vacancy formation energy, positron annihilation study 0-60706  
alkali halide:Eu $^{2+}$  cation vacancy complexes, binding energies 0-96513  
alkali halide, crystal, irradiation-induced defects 0-107316  
alkali halide crystals, defect fermion properties, ionic cond. calcs. 0-59457  
alkali halides, polarization, photoinduced, rel. to exchange between vacancy and impurity 0-59914  
alkaline earth fluoride based solid solns., ion transport 0-107545  
alloy, dispersion hardened, work hardening due to Orowan loops, temp. depend. (Japanese) 0-66534  
binary alloys, quenched, vacancy concs. 0-107212  
 $\beta$ -brass, vacancy form., ordering effect, positron annihilation obs. 0-93427  
brass, vacancy formation energies in mixed  $\alpha+\beta'$  phase 0-59456



## vacancies (crystal) continued

- brass-like alloys, constitutional vacancies 0-84168  
 cavity growth anal. during superplasticity 0-60923  
 chemical potentials of structural elements of compounds and face or dislocation specificity, thermodynamic parameters 0-96514  
 creep, irradi. induced in transient irradi. environments 0-92598  
 creep, swelling and growth, radiation induced, bias factors estimated from self-consistent model 0-88249  
 creep and growth, irradiation induced, solute effects on defect precip. rate 0-88252  
 creep and growth, radiation induced, fundamental mechanisms 0-92596  
 cubic lattice, self-diffusion via vacancy mechanism, correl. effect 0-59693  
 defect diffusion coeffs., site blocking, correlated defect motion 0-84315  
 depth distribution of vacancies produced by ion implantation 0-65024  
 diamond, defect electronic struct. and lattice config., MO approaches 0-65495  
 diamond, thermal conductivity, high temp., electron irradi. effects 0-65318  
 diamond-type crystals, vacancy formation and stability due to noncentral force 0-70192  
 diffusion processes in ohmic sintering, temp. distrib. influence 0-92704  
 disperse systems, solubility increase, phase composition, size effect calcs. 0-70418  
 edge dislocation screening in metals and superconductors, metal softening (Russian) 0-64997  
 n-eicosane, triclinic phase, self-diffusion, 295 to 309K 0-88359  
 Fick's equations solutions for impurity diffusion, dislocations, interstitials, vacancies 0-70469  
 formation energy and vibr. freq. of atom in dislocation core region 0-103322  
 formation parameters from specific heat data 0-75221  
 graphite, irradi., lattice expansion, vacancies and interstitials contrib., bond order role 0-65042  
 harmonic crystals, Helmholtz free energy, vacancy defects interactions calc. by cell cluster method 0-107443  
 harmonic crystals, thermodynamic props., effects of vacancy defects determ. by cell cluster method 0-79959  
 ice surface viscosity, activation energy, vacancy migration 0-107458  
 intermetallic phases, B2 struct., substitutional and triple defects, enthalpies of formation 0-96520  
 ion implantation, net recoil density 0-88175  
 ion polarisation and point defect resistivity in metals 0-103672  
 ionic crystal with vacancies, coherent neutron scatt., calc. 0-59346  
 ionic crystals, migration volumes calc. 0-103324  
 ionic crystals, thermodynamic ion-vacancy complexes (Spanish) 0-75222  
 irradiation growth, contrib. of grain shape to anisotropy 0-92556  
 irradiation-induced, recombination rate with interstitials 0-96516  
 kinks, solitons, and nonlinear transport in solids 0-65421  
 liquid alloys, positron annihilation due to vacancy trapping, simplified model (Russian) 0-71511  
 metal, BCC, effective valence, from phonon data, rel. to vacancy formation energies 0-79781  
 metal halides, fluorite structure, retarded ionic motion 0-88361  
 metal-insulator transition, chemical mechanism, thermodynamics, vacancies 0-103626  
 metals, atomic binding energy and surface energy rel. to prediction of physical props. 0-59434  
 metals, defect chemistry, He desorption spectrometry (Dutch) 0-96737  
 metals, dynamical props. of point defects, book contrib. 0-103317  
 metals, interstitial loop growth, pulsed irradi. effects 0-88210  
 metals, melting temp., press. depend., vacancy mechanism 0-103460  
 metals, point defect diffusion controlled reaction theory, book contrib. 0-103318  
 metals, point defect dynamic props. and diffusion controlled reactions, book 0-101674  
 metals, quenched, vacancy cluster form. process 0-92706  
 metals, submicroscopic defects, influence on HVEM in-situ expts. 0-103392  
 metals, two and one interstitial model explanation of elec. cond. variations 0-88143  
 metals, void growth and time-lag, statistical theory 0-88208  
 metals and alloys, stress relaxation, in-reactor study at low temps. 0-93588  
 NaCl, dislocation charge photostimulated variation kinetics (Russian) 0-79806  
 NMR spin relaxation, motion-induced, in low temp. HF limit 0-60443  
 NMR spin-lattice relax., effect of correlated atomic diffusion 0-107495  
 nonstoichiometric compounds, physicochem. props. depend. on short-range order struct. 0-100227  
 nuclear fuel, gas release and swelling, operational model, grain boundary gas 0-95346  
 nuclear fuels, creep, irradiation induced, transient state, kinetic eqn. treatment 0-88251  
 ordered binary crystals, characts. of equil. distrib. of vacancies 0-59458  
 perovskite oxides, point defects, elec. cond., and electron energy spectra 0-70706  
 perovskites,  $A_2^{2+}B^{3+}U_{5/6}^{6+}v_{1/6}O_6$ , struct., cation vacancies, X-ray diff. study (German) 0-107147  
 point-defect clustering during irradiation 0-92521  
 porphyrin in n-octane Shpol'ski matrix, defect props., Monte Carlo obs. 0-63533  
 precipitate free zones, X-ray microanal. 0-108768  
 precipitate re-solution in low dose irradiations 0-93559  
 $\alpha$ -quartz, CNDO/2 calcs., electronic props. of perfect cluster, EPR parameters of O<sup>-</sup> vacancy 0-107701  
 radiation defect production, exact solns. of models for continuous and pulsed irradi., implications for stability and fluctuations 0-65041  
 rare gas, crystal, quasi-atomic and quasi-molecular exciton states (Russian) 0-103628  
 resistance fluctuations, anal. independ. of thermal voltage noise 0-84495  
 semiconductor, deep levels, review 0-103640  
 semiconductor, with defects or impurities, local density of electron states 0-92857  
 semiconductor defects, electronic structure and lattice distortion, Green's function methods (French) 0-59917  
 solid solution, binary, radiation-induced instability, contrib. of dissipative processes 0-65039  
 steel, austenitic, Cr-Mn-N, plastic deformation influence on internal friction, relaxation processes (Russian) 0-100870  
 strain ageing, and serrated yielding, mechanism 0-88245  
 superionic fluorites, structure and transport 0-84318

## vacancies (crystal) continued

- surface and interface defects, electronic struct., scatt. theory 0-84498  
 thermal expansion, temp. depend., vacancy effects 0-79962  
 transition metal ferrocyanide selective sorbents for alkali metals, sorptive props. w.r.t. struct. 0-101051  
 triangular lattice, thermodynamic props., effect of vacancy defects determ. by cell cluster method 0-79959  
 vacancy distribution along mag. sublattices in  $\beta$ -brass type ferro and antiferromagnetic alloys (Russian) 0-79783  
 voids, coated, capture efficiency 0-96515  
 Zircaloy-2, irradiation growth, reaction rate theory calcs. 0-88212  
 Zircaloy-2, irradiation growth, shape and volume changes 0-92562  
 Ag (100) and (111) surfaces, positronium form. due to slow positron trapping 0-107748  
 Ag film, defect density, thickness depend., elec. resist. obs. 0-70568  
 Ag film, void growth, TEM obs. 0-59833  
 Ag, positron annihilation spectra, Doppler-broadened, temp. depend., 9 to 1098K 0-71510  
 AgCl(Br), point defect form. energies, atomistic calc. and surface pot. meas. 0-107221  
 AgI: Cd, polycrystalline, thermoelectric power meas. 0-59698  
 Al, dislocation loops, interstitial, size distrib. for metal irradiated in high voltage electron microscope (Russian) 0-103335  
 Al, foil, influence of O<sub>2</sub>-pressure on oxidation rate, TEM study 0-104355  
 Al, positron annihilation and vacancy formation, Doppler broadening study 0-60708  
 Al-Mg, dilute, dislocation loops, interstitial, size distrib. for metal irradiated in high voltage electron microscope (Russian) 0-103335  
 Al-Mg, foil, oxidation in O<sub>2</sub> atm., TEM study 0-104356  
 Al-Mg, Si alloy, void form. under different precip. conditions, after Al ion irradi. 0-59529  
 Al-Si (1.2 wt.%), dispersion hardened, work hardening due to Orowan loops, temp. depend. (Japanese) 0-66534  
 Al-Zn, X-ray diff. after omnidirectional compression (Russian) 0-88262  
 Al-Zn (10 wt.%), ageing at low temp., effects of fluctuation of solute conc. 0-76287  
 Al-Zn (10 wt.%), ageing at low temp., effects of fluctuation of solute conc. 0-76288  
 Al-Zn-Mg superplastic alloy, cavity growth under creep conditions 0-60940  
 Al<sub>x</sub>Ga<sub>1-x</sub>As: Cu, variable-gap semicond., impurity props., carrier recomb. 0-96907  
 Al<sub>3</sub>(Ni, Co)<sub>3</sub> ternary phase in Al-Ni-Co system, cryst. struct., vacancy controlled phase (Chinese) 0-70164  
 $\beta'$ -Al<sub>2</sub>O<sub>3</sub>-Na<sub>2</sub>O, nonstoichiometric, correl. effects in diffusion, Haven ratio, point defect interactions 0-107505  
 Ar, solid, vacancy conc., X-ray study at const. vol. 0-64991  
 Au, deformed, annealing kinetics of vacancies (Japanese) 0-88139  
 Au, heavy ion irradi., cascade energy density effect on defect cluster type 0-107340  
 Au, quenched polycryst., vacancy loss at grain boundaries 0-59477  
 Au, vacancy size effect, surface energy in small particles and bulk specimens 0-75223  
 Au-Pd (150 wt.%), quenched, vacancy annihilation and short-range order formation, elec. resist. 0-108487  
 BaTiO<sub>3</sub>, reduction inhibition by impurity ions 0-101018  
 BaTiO<sub>3</sub>: C, solubility of C at low O<sub>2</sub> potentials, 800°C 0-100334  
 Ca fluorapatites, carbonated, B-type, EPR of F<sup>+</sup>-centre after X-irrad. (French) 0-108065  
 CaF<sub>2</sub>:Eu(Gd)(Dy)(Tb), dimer reorientation activation volume 0-107285  
 CaF<sub>2</sub>, cation jump freq., isotope effect, lattice dynamical calc. 0-88357  
 CaF<sub>2</sub>:alkali metal cation, thermal depolarisation study 0-108147  
 CaF<sub>2</sub>:Li(Na)(K)(Rb), dielec. relax., activation energy, rel. to vacancy pair reorientation 0-88917  
 CdF<sub>2</sub>:NaF thin films, electroluminescence obs. at 77K (French) 0-80866  
 Cd<sub>2</sub>Hg<sub>1-x</sub>Te, long term stability at 300K, rel. to device appl. 0-59978  
 Cd<sub>2</sub>Hg<sub>1-x</sub>Te, vacancy electron states, acceptor behaviour, electron mobility 0-70193  
 CdS, electron and hole trapped centres, EPR, photoluminescence, photoconductivity study 0-108071  
 CdTe: Cu films, impurity behaviour, Hall mobility and hole density meas. 0-80420  
 CeO<sub>2</sub>:CaO(Y<sub>2</sub>O<sub>3</sub>), oxygen ion cond. and defect struct. 0-107553  
 Co-Al, X-ray K-absorption spectrum 0-97378  
 CoO, isotope effects in CoO diffusion rel. to vacancies 0-84319  
 Cr condensates, lattice const., internal stresses (Russian) 0-107141  
 Cu (111) surface, positronium form. due to slow positron trapping 0-107748  
 Cu, electron-irradiated, monovacancy migration during stage III annealing, NQR study 0-107576  
 Cu, ion bombard. by 5 keV Ar<sup>+</sup>, sub-surface damage 0-103399  
 Cu, oxidation kinetics, influence of intermediate annealing treatment 0-89412  
 Cu, point and planar defects, computer simulation 0-59455  
 Cu, prevacancy temperature depend. of positron annihilation, Doppler broadening lineshape parameters 0-60709  
 Cu, quenched, Hall coefficient, relaxation times, Fermi surface 0-84460  
 Cu, screening charge density round  $\Delta Z = -1$  impurities, vacancies, NQR study 0-103897  
 Cu, vacancy form. enthalpy, positron annihilation meas. 0-97371  
 Cu-Au alloys, vacancy and divacancy migration activation energies, elec. cond. meas. 0-88140  
 Cu-Co (1.5 and 4 wt.%) alloy, coherent Co-rich separations obs. by positron annihilation (Russian) 0-89082  
 Cu-Ni-Nb (30, 0.9 at.%), precipitate free zones, X-ray microanal. 0-108768  
 CuH dilute alloy, Hall coefficient, relaxation times, Fermi surface 0-84460  
 EuO nonstoichiometric film, ESR spectra and exchange interaction 0-93176  
 Fe, electron-irradiated, positron lifetime meas. 0-93431  
 $\alpha$ -Fe, neutron irradiated, mobile C atom trapping, anelastic and magnetic relaxations 0-100306  
 Fe, pure and doped, electron irradi., mag. aftereffect 0-88838  
 Fe, volume changes and defect healing due to plastic deform. (Russian) 0-81139  
 $\alpha$ -Fe: C, electron irradi., vacancy-C interaction, positron lifetime meas. 0-75264  
 Fe: Y, ion implanted, deep D traps due to Y-vacancy complex 0-103372  
 Fe-C, electron-irradiated, positron lifetime meas. 0-93431  
 Fe<sub>1-x</sub>O, wustite, defect struct. 0-107216



## vacancies (crystal) continued

- Fe<sub>3</sub>O<sub>4</sub>, magnetite, cation diffusion, correlation and isotope effects 0-96686  
 Fe<sub>3</sub>O<sub>4</sub>, substituted magnetite, correl. between IR spectra, X-ray diffr., and struct. vacancy distrib. 0-84753  
 $\alpha$ -Fe<sub>2</sub>Si<sub>2</sub>, vacancy ordering, cryst. stabilisation energy aspects 0-103325  
 Fe<sub>2</sub>VS<sub>2</sub> (0.20 < x < 1.00), phase diagram and order-disorder transition of vacancies 0-81039  
 GaAlAs, surface vacancies, bound state energy levels calc. 0-80340  
 GaAs:Se, Ga, dual species ion implantation, elec. characts. 0-103377  
 GaAs:Sn<sup>+</sup>, impurity-defect complex from <sup>119</sup>In implantation, Mossbauer study 0-59486  
 GaAs-Cu:Ti, cathode luminescence spectra, Hall effect, cryst. defects 0-76087  
 GaP:Fe, double Fe-thermal acceptor centre, energy states 0-96823  
 GaSb, defect concentration determ. model, Hall effect 0-103385  
 Gd<sub>2</sub>Zr<sub>1-x</sub>O<sub>2-x/2</sub>, elec. cond. of ceramic solid solutions 0-107554  
 Ge, self-diffusion, activation energy and entropy factors 0-88353  
 Ge, vacancy formation and stability due to noncentral force 0-70192  
 GeTe, stoichiometry deviations influence on mech. props., 25-500°C 0-103410  
<sup>3</sup>He, FCC, vacancy induced spin polarons 0-59756  
<sup>3</sup>He, HCP, vacancy-induced transitions 0-88395  
<sup>3</sup>He, solid, as mag. semicond., analogy to Mott insulator 0-96720  
 HgTe, vacancy electron states, acceptor behaviour, electron mobility 0-70193  
 In, vacancy size effect, surface energy in small particles and bulk specimens 0-75223  
 InP, surface vacancies, bound state energy levels calc. 0-80340  
 KCl crystals, Eu<sup>2+</sup> concentration effect on lattice parameter and density of crystals 0-88169  
 KCl, fine structure of X-ray absorption spectra 0-71514  
 KCl, X-ray irradiated, vacancy conc. determ., thermal expansion meas. 0-79782  
 KCl:Sr, positron annihilation and trapping in A-centres 0-84802  
 KCl(l), electron range-energy relation, thermally created lattice vacancies effect 0-92574  
 KHSO<sub>4</sub>:Fe<sup>3+</sup>, DC cond. meas., mechanism 0-65285  
 Kr, solid, vacancy conc., X-ray study at const. vol. 0-64991  
 (La<sub>0.9</sub>Ca<sub>0.1</sub>)MnO<sub>3+y</sub>, non-stoichiometry and lattice const. 0-100212  
 LaF<sub>3</sub>, ionic transport, NMR and cond. studies 0-107555  
 LiF,  $\gamma$ -irrad. induced defects, positron capture and annealing obs. 0-60707  
 LiF:OH:Mg,  $\gamma$ -irrad. induced oxyhydride complexes 0-92555  
 LiInS<sub>2</sub>, blue-band emission 0-76062  
 Li<sub>3</sub>N, ionic transport mechanism and defect props. 0-107528  
 LiNbO<sub>3</sub>, XPS and UPS from surface defects 0-76136  
 Mg, HCP, vacancy clusters and interstitials, computer simulation study 0-64992  
 Mg-H<sup>+</sup> 2p<sub>1/2</sub>, vacancy alignment electron capture role 0-83465  
 Mg:Fe<sub>2</sub>O<sub>3</sub>, diffusion of <sup>59</sup>Fe and elec. cond. 0-59700  
 Mo cryst., radiation induced vacancies and D<sub>2</sub><sup>+</sup> implantation 0-65076  
 Mo, diffusion of Li, Cs, vacancy and divacancy mechanisms (*Russian*) 0-70472  
 NH<sub>4</sub>Cl, acoustic absorption by soft modes of defects 0-59584  
 NaCl:Sr, positron annihilation and trapping in A-centres 0-84802  
 NaF:Ca<sup>2+</sup>, pure and doped, ionic thermocurrents meas. 0-80677  
 NaF:Ca<sup>2+</sup>, pure and doped, lattice defects, entropy and enthalpy of formation and migration 0-96687  
 Nb, ion bombard. by 5 keV Ar<sup>+</sup>, sub-surface damage 0-103399  
 NbC<sub>x</sub>, supercond. transition temp., light element implantation effect 0-107951  
 Nb<sub>2</sub>Sn, supercond. props., effect of neutron irradiation 0-80463  
 Nd<sub>2</sub>Zr<sub>1-x</sub>O<sub>2-x/2</sub>, elec. cond. of ceramic solid solutions 0-107554  
 Ni and alloys, heavy ion irradiation, defect cluster obs. 0-107341  
 Ni, hardness after-effect studied by anelastic relaxation 0-66570  
 Ni, in situ rare gas ion irradiation, cluster creation obs. by electron microscopy 0-107343  
 Ni, oxidation kinetics, influence of intermediate annealing treatment 0-89412  
 Ni, positron lifetime meas., 4.2 to 1700K, monovacancy form. enthalpy 0-97370  
 Ni, push-pull fatigued polycrystals, point defects, elec. excess resist. meas. 0-100910  
 Ni, volume changes and defect healing due to plastic deform. (*Russian*) 0-81139  
 $\beta$ -NiAl, ordered, hardness after-effect studied by anelastic relaxation 0-66570  
 Ni<sub>3</sub>Al(Ga), off-stoichiometric alloy, inverse mag. susceptibility rel. to defect conc. 0-60216  
 NiO (001) surface, chemisorption of H, surface and second-layer defect effects 0-65369  
 NiO, diffusion of <sup>35</sup>S by two different modes 0-59720  
 NiO, dipole orientation from bound polaron hopping 0-84437  
 PLZT, diffuse phase transitions, Curie temp., dielectric props. 0-75979  
 (Pb,Ba)(Zr,Ti)O<sub>3</sub>, diffuse phase transitions, Curie temp., dielectric props. 0-75979  
 Pb-As (~0.01 wt.%), enhanced precip. phenomena, invest. of mechanism by elec. resist. meas. 0-104162  
 Pb-Au, interstitial and substitutional distrib. 0-84204  
 Pb-Sb-As (1.1-1.8, ~0.01 wt.%), enhanced precip. phenomena, invest. of mechanism by elec. resist. meas. 0-104162  
 PbF<sub>2</sub>, based solid solns., ion transport 0-107545  
 PbSe:Ti, self-compensation of acceptors by vacancies, Hall coeff. meas. 0-92913  
 PbSe:Ti, self-compensation of acceptors by vacancies, Hall coeff. meas. 0-92913  
 Pd<sub>2</sub>PO<sub>8</sub>, pure and deuterated, cryst. struct., neutron diffr. study 0-84152  
 Pt, recovery spectrum after thermal neutron irradiation, resist. obs., Au addition effect and defect conc. depend. 0-65057  
 R<sub>1-x</sub>Co<sub>x</sub>, rare earth amorphous alloys, thermal stability, elec. cond. enthalpy 0-100172  
 Si, amorphous layer prod. by ion implantation, diffusion broadening, ESR study 0-92552  
 Si, crucible grown, virgin and implanted, laser irradiation effects on surface structure 0-92768  
 Si, Czochralski grown, dislocation free, swirl defect form., doping effect 0-92519  
 Si, deep level defects, struct. bonding, amphoteric centres 0-88506  
 Si, deep-level point defects, effective-mass nature 0-59922

## vacancies (crystal) continued

- Si, defects, divacancy and split 100 interstitial, electronic structure calc. 0-65494  
 Si, diffusion mechanism of P, migration channels along vacancies and interstices 0-79996  
 Si, electron-irradiated crystals, positron trapping, temp. depend. 0-104009  
 Si, isolated vacancy, electronic struct., SCF method 0-80208  
 n-Si, quenched, fast electron irradiated, annealing of defects 0-89259  
 Si, self-diffusion, activation energy and entropy factors 0-88353  
 Si, thermal oxidation kinetics, steady-state transport anal. 0-71773  
 Si, thermal oxidation kinetics, theoretical perspective 0-76387  
 p-Si, vacancy, charge states, Jahn-Teller stabilisation energy 0-80209  
 Si vacancy, electron states, Anderson negative-U system 0-96820  
 Si, vacancy formation and stability due to noncentral force 0-70192  
 Si:Al, electron irradiation induced defects, transient capacitance study 0-59516  
 Si:B (0.2 wt.%) ion implanted, B atom displacement due to low temp. irradiation 0-88234  
 p-Si:B(Al), radiation defect form. and annealing study using Hall effect, cond. and carrier diffusion length 0-84214  
 Si:O, heat treated, excess carrier recomb. rate, defect levels 0-75579  
 Si:Sn, Mossbauer study of defects due to <sup>119</sup>In implantation 0-80641  
 n-SiC, thermal defects, ESR study 0-88876  
 SiO<sub>2</sub>, vitreous, luminescence centres at 396 and 280 nm 0-103996  
 $\alpha$ -Sn, ion implanted, defect struct., Mossbauer spectra 0-80214  
 Sn, thermally induced vacancies, positron trapping 0-89083  
 SnO<sub>2</sub>, CVD coating on glass, elec. resist. rel. to cryst. microstruct. 0-84520  
 SnO<sub>2</sub> thin films, O<sub>2</sub> vacancy diffusion 0-107467  
 SrCl<sub>2</sub>, ionic cond., self-diffusion, rel. to defect motion, mol. dynamics study 0-65282  
 SrCl<sub>2</sub>, point defect parameters, ionic cond. study 0-107490  
 SrTiO<sub>3</sub>, ferroelectric modes, Raman spectra, neutron scatt. meas. 0-80727  
 SrTiO<sub>3</sub>, semiconductor, soft modes, zone boundary mode 0-71357  
 ThO<sub>2</sub>-CaO, and ThO<sub>2</sub>-YO<sub>1.5</sub>, solid solns., defective oxides, ionic cond. 0-107548  
 Ti, neutron irradiated, characterization of dislocation loops 0-88155  
 Ti, volume changes and defect healing due to plastic deform. (*Russian*) 0-81139  
 Ti(Fe, Co), off-stoichiometric alloy, inverse mag. susceptibility rel. to defect conc. 0-60216  
 TiO<sub>2</sub>, nonstoichiometry study, thermal emission of electrons 0-108317  
 TiO<sub>2</sub>, struct. vacancies in unit cell 0-107213  
 U, irradiation growth during fission fragment and proton bombard. 0-92568  
 UC, quenched-in defects, formation, migration and resistivity 0-64990  
 UCN, quenched-in defects, formation, migration and resistivity 0-64990  
 V, electron-irradiated, positron annihilation study 0-70259  
 V<sub>2</sub>O<sub>5</sub> and lower oxides, defect structures and related props., review 0-59454  
 V:Si, supercond. props., effect of neutron irradiation 0-80463  
 W, diffusion of Li, Cs, vacancy and divacancy mechanisms (*Russian*) 0-70472  
 W, vacancy structure in near surface depleted zone following ion bombard. 0-70267  
 YFe<sub>2-x</sub>Al<sub>2</sub>O<sub>12</sub>, impurity redistrib. kinetics, temp. depend., vacancy effects 0-75263  
 YFe<sub>2-x</sub>Ga<sub>2</sub>O<sub>12</sub>, impurity redistrib. kinetics, temp. depend., vacancy effects 0-75263  
 YIG:Ca, oxidising effects of high temp. annealing in reducing atmosphere 0-66696  
 Y<sub>2</sub>O<sub>3</sub>, nonstoichiometry study, thermal emission of electrons 0-108317  
 Zn, growth from melt, conditions influencing dislocation struct. (*Russian*) 0-97424  
 Zn,Hg<sub>1-x</sub>Te, vacancy electron states, acceptor behaviour, electron mobility 0-70193  
 ZnO, irradiation in high voltage electron microscope dislocation loops study 0-88157  
 ZnS, ion implantation effects on luminesc., thermo-EMF 0-88178  
 ZnS, ODMR of Zn vacancy obs. 0-108121  
 ZnS,Se<sub>1-x</sub>, electron trap associated with anion vacancy, DLTS study 0-80210  
 ZnSe, electron trap associated with anion vacancy, DLTS study 0-80210  
 ZnSe, heat-treated in controlled partial press. of Zn or Se, TSC 0-59910  
 Zn alloys, creep and growth, irradiation induced, rate theory approach 0-89294  
 Zr alloys, creep and growth, irradiation induced, microstruct. depend. 0-93602  
 Zr, irradiation growth, reaction rate theory calcs. 0-88212  
 ZrO<sub>2</sub>-CaO, and ZrO<sub>2</sub>-YO<sub>1.5</sub>, solid solns., defective oxides, ionic cond. 0-107548  
 ZrO<sub>2</sub>-YO<sub>1.5</sub>-TaO<sub>2.5</sub>, cubic fluorite phase, elec. cond. 0-107551

## vacancy condensation loops

see also prismatic dislocations

- capture efficiency of dislocation loops, effect of nonlinear elasticity 0-59461  
 faulted dislocation loops induced by elastic interaction, climbing motion 0-75227  
 metals, irradiation, mechanism of formation of vacancy dislocation loops (*Russian*) 0-65053  
 Al, creep behaviour, at high temp., influence of oxidation 0-97538  
 Al, neutron damage, positron annihilation 0-65056  
 Al-Mg (0.1 at.%), neutron damage, positron annihilation 0-65056  
 KCl:Ba<sup>2+</sup>, localised stress relaxation in excess vacancy system, prismatic loops (*Russian*) 0-88160  
 Mo, ion irradiation, defect anal., electron microscopy, appl. of theory of non-edge loop image contrast 0-70200  
 Ni and alloys, heavy ion irradiation, defect cluster obs. 0-107341  
 Ni, in situ rare gas ion irradiation, cluster creation obs. by electron microscopy 0-107343  
 Pt, ion irradiation, damage, temp. depend., electron microscopy obs. of defect kinetics 0-107339  
 Pt, neutron damage, positron annihilation 0-65056  
 Ti, neutron irradiation, characterization of dislocation loops 0-88155  
 Zr and alloys, neutron irradiation, at 573 to 923K, damage struct. 0-107334

## vacancy-dislocation interactions

- edge superdislocations, resist. to motion, temp. depend. expressions (*Russian*) 0-79789



**vacancy-dislocation interactions continued**

- FCC anisotropic crystals, extended screw dislocation, (110) misfit defect elastic interactions 0-100232  
 mass flux, irradiation enhanced, dislocation interactions 0-88206  
 metal, vacancy-dislocation interaction, tight-binding calc. 0-92554  
 Au, deformed, annealing kinetics of vacancies (*Japanese*) 0-88139  
 Au, polycrystn., deformed, computer simulation of vacancy annihilation to dislocations (*Japanese*) 0-88205  
 Cu-Ni alloys, chemical interdiffusion under uniaxial stress 0-65307  
 GeTe, stoichiometry deviations influence on mech. props., 25-500°C 0-103410  
 MgO, interaction energies, atomistic model calcs. 0-59513  
 Si, radiation defects, influence of dislocations on accumulation, elec. props. 0-92558

**vacuum apparatus**

- includes apparatus for producing, maintaining and handling vacuum per se*  
*see also vacuum gauges; vacuum pumps; vacuum techniques*  
 adhesion strength meas. of organic coatings 0-105663  
 Boersch's electron optical bench, modifications 0-87286  
 camera, vacuum-cold, appl. to astronomical near IR photography 0-90341  
 cell for saturating specimens with liq., true and apparent density determ. of ceramics 0-62636  
 chamber-bell jar with built-in cooling body 0-90860  
 deposition equipment cleaning, practical procedures 0-57318  
 electron microscope, high resolution, obs. at liq. He temps. 0-86517  
 ferrite, 350 NNI, for use in superhigh vacuum systems 0-108478  
 field emission micro SEM, for UHV surface anal. 0-86519  
 field emission scanning electron microscope 0-86520  
 flanged joints, appls. in cryogenic and vacuum technology (*German*) 0-101801  
 fusion reactor, Demonstration Power Tokamak Reactor, vacuum outer containment and metal seals feasibility study 0-95458  
 fusion reactor, Doublet III, vacuum vessel neutral beam armour 0-95462  
 fusion reactor, ETA-BETA II RFP, vacuum system design and operation 0-95450  
 fusion reactor, neutral beam injection reionisation power losses in duct, model 0-99385  
 fusion reactor, PLT, neutral beam duct reionisation losses, obs. and power loss model 0-99383  
 fusion reactor, TFTR, large noncircular ports, development of bakeable seals 0-95454  
 fusion reactor, TFTR, neutral beam-torus connecting duct 0-99302  
 fusion reactor, TFTR, vacuum vessel bellows, strength and fatigue anal. 0-95455  
 fusion reactor, TMX, config., liq. N<sub>2</sub> supply and operation of vacuum system 0-95448  
 fusion reactor blanket, NOEL (No External Leak), thermal anal. and tests 0-95459  
 fusion reactor neutral beam injector vacuum system transient simulation anal. 0-95453  
 fusion reactor vacuum vessel, large, ultra high vacuum, design and manufacturing problems 0-99276  
 fusion reactors, TMX, installation and operation of cryolines in vacuum system 0-95449  
 fusion reactors Doublet III neutral beam injector system, outgassing rate meas. and residual gas anal., coating props. 0-95457  
 gap breakdown initiation by microparticle impact 0-96413  
 gasket, large diameter elastic metal gasket for ultra-high vacuum flange connections 0-95106  
 hermetically sealed box, dynamic testing system, vacuum or controlled environment (*French*) 0-61060  
 high vacuum chamber for thermokinetic studies of solid surface thermal shock 0-73373  
 high-vacuum, for degassing studies 0-100814  
 high-vacuum system control and diagnosis by monitoring total press. and per cent N content 0-95105  
 IR window mounting for ultrahigh vac. appl. 0-82778  
 knife-edge flange, sealing after high temp. vacuum firing 0-77793  
 magnetic discharge cells with nonuniform periodic magnetic field 0-101799  
 O-ring type gaskets in metal vacuum systems, replacement for Au gaskets 0-57316  
 PDX vacuum vessel, glow discharge conditioning 0-79607  
 permeation cell for studying H desorption from Fe into ultrahigh vac. system 0-86326  
 piezoelectric quartz cryst. microbalance for sorption studies under dynamic conditions 0-73323  
 sample manipulation and rotation using ultra high vacuum angle resolving photoemission chamber 0-57317  
 sample transfer mechanism 0-77765  
 seal design, construction and application 0-82780  
 SEM vacuum system specification and design 0-82779  
 Spacelab pallet, meas. of mol. streaming fields 0-82173  
 steel, stainless, vacuum components, pre-vacuum surface finish influence on electron stimulated desorption in ultrahigh vacuum 0-57320  
 system construction material selection and degassing 0-82783  
 teflon rope, vacuum sealing material 0-98925  
 thermocouple reference junction box, used for vacuum chamber 0-90844  
 transfer system, 15 cm diameter ultrahigh vac. type, for remote plasma-wall interaction expts. 0-86327  
 ultra high vacuum device, for annealing of Nb single crystals. (*German*) 0-89169  
 ultra-high vacuum evaporation apparatus for deposition of metallic thin films 0-100791  
 ultrahigh vacuum setup for photo- and thermostimulated electron emission and luminesc. obs. (*Russian*) 0-66383  
 ultrahigh vacuum system for ISABELLE full cell 0-77798  
 universal ultrahigh-vacuum system 0-105664  
 valve, baffle and trap design and construction 0-82781  
 variable aperture, externally operable, for ultrahigh vac. appl., design 0-77799  
 He desorption spectrometer, clustering of Kr in W (100) obs. 0-77908

**vacuum control**

- compressor, air, reciprocating, capacity control system 0-90859

**vacuum deposited coatings**

- anthracene, ultrathin films on fused quartz and sapphire 0-59812  
 dielectric coatings, optical characts., effect of electric field during film condensation 0-69539

**vacuum deposited coatings continued**

- dielectric thin film stack, control by stationary ratio method, refractive index dispersion influence (*French*) 0-60693  
 diphenyl anion salts, sublimed layer, electronic and IR absorpt. spectra 0-66189  
 film on Si substrate, eutectic point displacement on annealing (*Russian*) 0-100850  
 films, elec. and galvanomag. props., microstruct. 0-70859  
 graded-thickness, filters for solar corona obs. appl. 0-76164  
 n-hexatriacontane film, vacuum deposited on alkali halide crystals, structure and heat treatment 0-103600  
 ion beam milling, amorphous sputter yield behaviour 0-108624  
 metal film, thickness meas., using nondestructive radioisotopic technique 0-68179  
 monochromatic Maximeter control system for thin multielectric films, stopping criterion (*French*) 0-60694  
 multilayer superlattice stacks, very thin nonideal, wavelength variation of transmissivity, refl. 0-100701  
 orientation axis tilt rel. to vapour angle of incidence 0-88456  
 parylene, electronics appl. 0-108607  
 porphyrin films, methine bridge substituted, surface photovolt. depend. on fabrication method 0-60119  
 a-Si:H highly homogeneous, for low-cost solar cell fabrication 0-72053  
 spectrally selective surfaces for photothermal conversion of solar energy 0-101125  
 squarylium dye films, surface photovolt. 0-75594  
 stable structure formation use of borosilicate glass intermediate layer 0-80979  
 stearic acid, film, for low-loss capacitors 0-71317  
 stearic acid films, evaporated, vac. effects 0-97435  
 surface temperature measurement, on thin films 0-57297  
 p-terphenyl, hopping cond. among localised states 0-70861  
 tetrabenz[a, cd, j, i]perylene evaporated film, crystn., time depend. as function of purity 0-88449  
 tetracene, disordered, vapour deposited on glass substrate, fluoresc. and energy transfer 0-84761  
 tetracene, hopping cond. among localised states 0-70861  
 thickness monitoring techniques (*Japanese*) 0-60783  
 transition metals, BCC, films, vac. evaporated, optical cond. 0-76100  
 Ag, defect density, thickness depend., elec. resist. obs. 0-70568  
 Ag film, adsorbed CO, enhanced Raman scatt. mechanism in ultrahigh vacuum 0-107645  
 Ag film, Ge coated, electrical resistance and ageing (*Russian*) 0-103759  
 Ag film, surface roughness, light scatt. meas. 0-107624  
 Ag film deposition, thermal effects, influence on internal stress meas. 0-96767  
 Ag film growth on Pd substrate, interface cpd. form., AES study (*French*) 0-80131  
 Ag, specimen charging control for SIMS and AES 0-101875  
 Ag, thin film, elec. resist., effect of annealing in electrodes 0-80416  
 Ag-Ni supersaturated metastable solid solns. formed by ion beam mixing 0-107425  
 AgBr(Cl) vapour-deposited epitaxial film, surface structure 0-59814  
 Ag<sub>2</sub>Se thin film, switching and Ag movement, point contact technique 0-60107  
 Al film, H incorporation effect on stress and electromigration 0-80139  
 Al foils, high strength, vapour deposited on curved surfaces, quantitative characterisation 0-80144  
 Al, on CdS, bonding and interdiffusion, XPS obs. 0-80000  
 Al, thin film, elec. resist., effect of annealing in electrodes 0-80416  
 Al<sub>2</sub>O<sub>3</sub>, vacuum condensate, struct. and mech. props., second phase effect (*Russian*) 0-71705  
 As<sub>2</sub>S<sub>3</sub> film, optical recording, light scatt. enhancement due to coherence 0-97362  
 Au, evap., temp. change and gas adsorpt. effect on opt. const's., ellipsometric obs. (*German*) 0-89081  
 Au film, adsorbed CO, enhanced Raman scatt. mechanism in ultrahigh vacuum 0-107645  
 Au film deposition, thermal effects, influence on internal stress meas. 0-96767  
 Au, on CdS, bonding and interdiffusion, XPS obs. 0-80000  
 Au, thin film, elec. resist., effect of annealing in electrodes 0-80416  
 Au/Sn thin film couples, evaporated, TEM study 0-59832  
 Au<sub>3</sub> particles, vacuum-deposited, degree of faceting during sintering 0-84411  
 AuMn alloy, ordered, vacuum deposited epitaxial films, orientation control by external stress 0-100426  
 Au<sub>3</sub>Mn thin films, electron diff. study 0-92793  
 Au<sub>3</sub>Si<sub>6</sub>, amorphous vacuum-deposited and liquid-quenched films, diffusion and crystn. 0-84094  
 Au<sub>3</sub>Si<sub>11</sub>, amorphous films, phys. studies 0-75476  
 B, evaporated, electronic struct., XPS, SXS and isochromat investig. 0-76143  
 Ba getter film, initial reaction probability with O<sub>2</sub>, water, CO and CO<sub>2</sub>, AES obs. 0-61153  
 CaF<sub>2</sub> thin films, initial ionic thermocurrent meas. 0-97018  
 Cd<sub>3</sub>As<sub>2</sub> film on NaCl substrate, vacuum deposition, growth morphology, microstructure 0-75479  
 Cd<sub>3</sub>As<sub>2</sub> films, nucleation processes, on NaCl substrates 0-59813  
 CdS:Cu, Cl films, photocond. growth and decay time 0-60041  
 CdS:Mn, vacuum deposited film, Mn migration, EPR and X-ray study 0-65411  
 n-CdS/p-In<sub>2</sub>Se<sub>3</sub> thin film solar cell, photovoltaic props. 0-89628  
 CdSe film photoanodes for electrochem. photovoltaic cells, fabrication and evaluation 0-76641  
 CdSe film polycryst., thermal diffusion of Cr, 240-400°C 0-80001  
 CdTe, electron mean free path, 350-1450 eV 0-103707  
 Co vacuum condensates, Cr alloying addition effect on texture characts. (*Russian*) 0-108471  
 Co vacuum deposited coatings on metal substrates, cryst. struct. and stability 0-75481  
 Co-CoO films, evaporated, exchange anisotropy 0-88841  
 CoP amorphous alloy, heat treatments influence on opt. props., struct. and DC resist. obs. 0-80892  
 Co<sub>3</sub>Pd film, ordered, stacking fault obs. by TEM and interpret. using many-beam theory 0-107680  
 Cr containing Cr<sub>2</sub>O<sub>3</sub> film struct., oxide percentage determ. and temp. coeff. of resist. 0-103607  
 Cr film, evaporated, concurrent ion bombard. effects 0-80142  
 Cr, on polycryst. CdS, thermal diffusion, 240-400°C 0-80001  
 Cs<sub>2</sub>Sb vacuum deposited photoemitter, XPS study 0-89122

## vacuum deposited coatings continued

- Cu film, on Au substrate, oxidation and interfacial behaviour, ion scatt. spectroscopy study 0-66691  
 Cu film deposition, thermal effects, influence on internal stress meas. 0-96767  
 Cu, ion bombardment induced preferential orientation 0-100290  
 Cu on Fe (001) substrate, orientation relationship 0-65415  
 Cu, thin film, elec. resist., effect of annealing in electrodes 0-80416  
 Cu-Al films, elec. cond. of vacuum condensates depend. on composition, annealing (*Russian*) 0-65709  
 Cu-Al thin film multistructure, Xe<sup>+</sup> ion beam cratering 0-66708  
 Cu-Ni thin films, ferromag., Hall effect meas. 0-80428  
 Cu-Ni/Au-Ni multilayer films, ohmic behaviour, use as strain gauge 0-65713  
 Cu-Sn(Al)(Ga) reflecting surface absorpt. coeffs. at 10.6  $\mu\text{m}$  0-95984  
 CuAu alloy, ordered, vacuum deposited epitaxial films, orientation control by external stress 0-100426  
 CuBr(l), reflectance and thermorefectance spectra, electronic struct. 0-71444  
 CuInSe<sub>2</sub> amorphous thin film, flash evaporation, struct., stoichiometry 0-89150  
 Cu<sub>2</sub>S evaporated layer growth in vacuum, compositional and optical characterisation, solar cell appls. 0-97437  
 EuS films, mag. and elec. props. rel. to stoichiometry and defects 0-97122  
 Fe, epitaxial growth on Au platelets, dislocations 0-96760  
 Fe, evaporated, adsorbed acetylacetone, XPS study 0-76133  
 Fe film, coated, interface magnetism by Mossbauer spectroscopy 0-75890  
 Fe vacuum deposits on Ni(Cu)(Ag) (111) FCC substrates, orientation relationships 0-59836  
 Fe-B, amorphous to cryst. transition 0-88048  
 Fe-Cr-Al, Kanthal films, vac. deposited, evaporation characts., comp. struct. and elec. props. 0-88646  
 $\alpha$ -Fe<sub>2</sub>O<sub>3</sub>, photochem. props. of sintered and doped samples for solar photoelectrochem. cell appls. 0-89651  
 Fe<sub>2</sub>O<sub>3</sub> films, electron microscopy and energy-loss spectroscopy 0-80137  
 Ge epitaxial film, vac. deposited on GaAs, doping effect of annealed GaAs surface 0-65718  
 Ge thin films on glass substrates, annealing by Ar ion bombardment 0-80136  
 Ge-Ga amorphous alloy, co-evaporated elec. and optical props. 0-70860  
 Ge-Sc<sub>2</sub>, vitreous, evaporation kinetics and amorphous film deposition 0-97434  
 Ge<sub>2</sub>Se<sub>2</sub>Te amorphous layers, prep. and elec. props. 0-97436  
 Hg-Xe vapour deposited films, cond. transitions, effect of disorder on supercond. 0-88659  
 In electrode, annealing, effect on elec. resist. of metallic thin film 0-80416  
 In-PbTe contacts, fabrication and props. 0-60078  
 In<sub>2</sub>O<sub>3</sub> films, reactively evaporated, elec. props. 0-84521  
 In<sub>2</sub>O<sub>3</sub>, thermally evaporated film, struct. and elec. props. 0-104066  
 InP-Al interface struct., low temp. interaction, AES study 0-107661  
 InSb thin films for acoustoelectronics 0-103765  
 InTe thin films, flash evaporation, electrical props. 0-65722  
 KI microcrystals, UV spectra by diffuse reflectance technique, surface electronic transitions obs. 0-75614  
 LiF film, intrinsic stress meas. 0-71696  
 MgF<sub>2</sub>-Na<sub>3</sub>AlF<sub>6</sub> thin film deposits, quenched ageing by chopping 0-97364  
 Mn, deposited in elec. field, resist., struct. 0-103761  
 Mn film, elec. resist., deposition rate effect 0-97010  
 Mn film, H(D) uptake kinetics and energetics 0-88430  
 Mn-SiO<sub>2</sub>, annealed cermet films, elec. resist., composition depend. 0-97007  
 MnBi films, prep. by ionised-cluster beam deposition technique, magneto-optical props. 0-100790  
 Mo, evaporated, annealing behaviour, SEM obs. 0-65397  
 Mo film, evaporated, grain size and resist. 0-88650  
 Nb, thin-film SQUID working at 4.2K, fabrications and characterisation 0-100570  
 Nb/Cu, layered ultrathin coherent structs., supercond. props. 0-84525  
 NbC, vacuum condensate, struct. and mech. props., second phase effect (*Russian*) 0-71705  
 NbPb superconducting film, prep., vac. deposition 0-89149  
 Ni based Rene 80 superalloy, initial stages of pack aluminisation 0-76188  
 Ni, evaporated, adsorbed acetylacetone, XPS study 0-76133  
 Ni film, evaporated, elec. resist. and galvanomagnetic props. 0-80411  
 Ni films, adhesion on graphite 0-80141  
 Ni on Fe (001) substrate, orientation relationship 0-65415  
 Ni-(Co)-Cr, aluminide coating, microstruct. and chem. 0-76189  
 Ni-Ge-Au evaporated contacts on GaAs, TEM obs. 0-75449  
 NiF<sub>2</sub> film preparation and characterisation 0-59815  
 NiP amorphous alloy, heat treatments influence on opt. props., struct. and DC resist. obs. 0-80892  
 PbI<sub>2</sub>:KI alloys, fundamental abs. edge, potential as solar converter 0-101128  
 PbO, reactively evaporated, photocond., H<sub>2</sub>O induced phase transform. 0-60122  
 PbS islands, vacuum deposited, electron microscope obs. 0-103601  
 PbS, polycryst. and epitaxial, small-angle X-ray scatt. and electron density inhomogeneities 0-96758  
 PbS-PbO vacuum evaporated films, elec. cond. and photocond. 0-75656  
 PbSnF<sub>4</sub>, anionic conductor, thin films and ceramics 0-107556  
 Pd-Si structure, epitaxial silicide growth, LEED and AES study 0-103590  
 Pt film, growth on amorphous Si-H, AES and LEED study 0-88447  
 Pt-Ni vacuum condensates on Si and SiO<sub>2</sub>, thermally treated, X-ray anal. (*Russian*) 0-70559  
 Se thin films, obtained in vac. of 10<sup>-5</sup>-10<sup>-6</sup> Torr, struct. and elec. resist. 0-107931  
 Se, amorphous, localised states in band gap 0-59928  
 Se, amorphous, vac. deposited on polymeric substrates, with dynamic coating device 0-100792  
 Se, amorphous film, highly disordered, UPS study 0-76148  
 Se, thin film selective absorber coatings, prod. using an oblique vacuum deposition technique 0-81488  
 Si, amorphous, epitaxial regrowth, structure and impurities effect 0-84401  
 Si, amorphous evaporated, picosecond optoelectronic detect., sampling and correlation meas. 0-100478

## vacuum deposited coatings continued

- Si, amorphous vacuum deposited p/undoped photodiode and diode-voltage variable resistor combination 0-61380  
 Si epitaxial layers, vacuum deposited, conditions for impurity migration from B, P, Sb doped sources (*Russian*) 0-107570  
 Si film, amorphous, glow discharge deposited, for low cost solar cells 0-61355  
 Si films, electron beam evaporated, for MIS solar cells 0-93490  
 Si photoconducting films, amorphous, undoped, I-V characts. of vacuum deposited films 0-60049  
 Si solar cells, realisation by laser induced diffusion of deposited Sb 0-93998  
 Si:Sb vacuum deposited coating, p-n junction, pulsed electron beam annealing doping, diffusion 0-75480  
 Si-Pd-Ti, silicide form. in evaporated films 0-80006  
 SiO evaporated film, dielec. function 8 to 33  $\mu\text{m}$ , spectrophotometric and refl. meas. 0-80883  
 SiO, film, thickness influence on nematic MBBA orientation 0-59384  
 SiO<sub>2</sub>-GaAs, vacuum evaporated system, acoustoelec. signal, interface props. 0-75646  
 Sm<sub>2</sub>S<sub>3</sub> films, refl. and transmission spectra at 300K 0-80889  
 Sn film, substrate and substrate temp. effects on struct. 0-107677  
 SnO<sub>2</sub>:Sb film on glass substrates, elec. props. 0-88652  
 SnO<sub>2</sub>-copper phthalocyanine-Ag systems, elec. and electroluminescent behaviour 0-80864  
 T-metal, thin film contact, time evolution of photovoltaic effect 0-65687  
 Ta thin film, elec. cond., strain gauge factor, ion bombardment effects 0-80417  
 TaF<sub>3</sub> thin films, AC conduction obs. 0-70868  
 Te film, surface morphology depend. on vacuum deposition angle 0-103553  
 Te, growth and morphology of crystals 0-96766  
 Te, on NaCl, crystallite growth and morphology, electron microscopy 0-65401  
 Te, thin film selective absorber coatings, prod. using an oblique vacuum deposition technique 0-81488  
 Ti-N<sub>2</sub>, condensate formed by plasma flow precipitation in vacuum, cryst. and surface props. (*Russian*) 0-100788  
 TiB<sub>2</sub>, TiC, vacuum condensate, struct. and mech. props., second phase effect (*Russian*) 0-71705  
 TiN, low-energy ion-stimulated deposited, supercond. props. 0-88664  
 TiO<sub>2</sub> layers, activated reactive evaporation and absorpt. indices 0-97363  
 TiO<sub>2</sub>-SiO<sub>2</sub> multilayer vacuum coatings, optical props. 0-97361  
 V film, vac. evaporated, elec. props. 0-80414  
 V<sub>2</sub>O<sub>5</sub> amorphous film, photochromism and thermochromism 0-93254  
 V-Si-SiO<sub>2</sub>-Mo-Re<sub>2</sub>, supercond. tunnel junctions 0-107961  
 WO<sub>3</sub> electrodes, electrochromic processes, digital simulation model 0-76518  
 WO<sub>3</sub> film, amorphous, struct. and crystn., TEM obs. 0-103606  
 WO<sub>3</sub> thin film, Li diffusion, appl. of AC techniques 0-70468  
 Yb<sub>2</sub>O<sub>3</sub> thin film on Cr substrate, refr. index depend. on thin film thickness 0-108290  
 ZnS evaporated film, refl. loss on UV irradi., ZnO form. 0-99813  
 ZnS film, defect form. and development 0-96759  
 ZnS:Cu, Cl, Mn film, AC electrolum. 0-60680  
 Zr-N<sub>2</sub>, condensate formed by plasma flow precipitation in vacuum, cryst. and surface props. (*Russian*) 0-100788  
 ZrO<sub>2</sub> thin film, optical props. rel. to cryst. struct. 0-97357  
 ZrO<sub>2</sub>, ZrB<sub>2</sub>, vacuum condensate, struct. and mech. props., second phase effect (*Russian*) 0-71705
- vacuum deposited thin films** see *vacuum deposited coatings*
- vacuum deposition**  
 used for EVAPORATED layer production in vacuum  
 see also *electron beam deposition*  
 alloy film, rate controlled deposition using electron impact emission spectroscopy based instrument (*German*) 0-89152  
 borosilicate glass intermediate layer, stable structure formation 0-80979  
 cold light mirror multilayer coating deposition 0-87464  
 conference, New York, USA (Oct. 79) 0-73093  
 equipment cleaning, practical procedures 0-57318  
 fissured biological object prep. for SEM, vacuum deposition and cathode sputtering comparison 0-72390  
 graded-thickness film, optical filter appl. 0-76164  
 metallic thin films, vacuum deposition, ultra-high vac. technique 0-100791  
 microelectronics and thin film components frontiers 0-73123  
 optical component rotation in vac. system, using linear asynchronous motor drive system 0-102874  
 optical thin film coating manufacture, automated deposition control system, design principles 0-64220  
 organic thin film prep. methods in ultrahigh vacuum (*Japanese*) 0-84851  
 SEM specimen preparation thin film coating techniques 0-68308  
 solar furnace application for thin film production 0-89148  
 substrate and film surface temp. meas. 0-57297  
 thin film prep. for solar energy utilisation 0-84847  
 thin films, deposition techniques, review 0-80964  
 tubular-type evaporator, radiation-heated, ZnS film deposition 0-76191  
 Ag film, vacuum deposition on Pb (111), substrate diffusion effects, RHEED, LEED, AES 0-65410  
 Ag film growth on Si (111), nucleation and growth modes, SEM study 0-100423  
 Al-Zn thin film, prep. using Sn-Zn evaporant source 0-100789  
 Au film, integrated condensation coeff. on NaCl cleavage faces, Rutherford ion backscatt. obs. 0-59827  
 Au film growth on Mo (110) surface, AES, LEED, thermal desorption study 0-80130  
 Au films, vac. condensed at oblique vapour incidence, oriented cryst. growth, electron diff. study 0-97432  
 Au-Cd,Hg<sub>1-x</sub>Te(CdTe) contacts, photo-effect in the 77-300K range, barrier height estimation 0-107850  
 n-CdTe layers, growth and characterisation, heterojunctions and Schottky barriers fabrication (*German*) 0-89151  
 Cu film, vacuum deposition on Pb (111), substrate diffusion effects, RHEED, LEED, AES 0-65410  
 Cu films, vac. condensed at oblique vapour incidence, oriented cryst. growth, electron diff. study 0-97432  
 Cu<sub>2</sub>S films, prpe. methods, appl. to Cu<sub>2</sub>S-CdS solar cells 0-80980  
 Cu<sub>2</sub>S/CdS, sequential evaporation, for solar cell appl. 0-93902  
 Ge, epitaxial growth of very thin electron microscopy specimens 0-100793



**vacuum deposition continued**

Ge<sub>2</sub>Se<sub>3</sub>, vitreous, evaporation kinetics and amorphous film deposition 0-97434  
 In-Cd,Hg<sub>1-x</sub>Te(CdTe) contacts, photo-effect in the 77-300K range, barrier height estimation 0-107850  
 Li<sub>3</sub>N thin film, vacuum evaporation on WO<sub>3</sub>, retarded deposition 0-108351  
 Nb-Nb Josephson junctions, submicron, thermally recyclable, fabrication and characts. 0-100566  
 Si, source, with two independent filaments 0-76190  
 Si thin-film polycrystalline vacuum-deposited solar cells, TiB<sub>2</sub> bottom electrode, 10% efficiency 0-93489  
 SiO<sub>2</sub> films, vac. thermal evaporation, parameter stabilisation 0-87571  
 Te-Se-Cd, sandwich structure, fabrication and characteristics 0-60089  
 TiO<sub>2</sub> layers, activated reactive evaporation and absorpt. indices 0-97363

**vacuum gauges**

see also barometers; ionisation gauges; manometers; vacuum measurement  
 calibration, by expansion-reduction method 0-77807  
 Granville-Phillips, series 275, Convectron, sensitivity to various gases 0-77804  
 ionisation vacuumometers, cold or hot cathode, with automatic control (Czech) 0-73376  
 leak detector, mass spectrometer, meas. range extension 0-73375  
 McLeod gauge, capillary depression phenomena, Hg vapour drag effect 0-98923  
 partial pressure measurement and gauges for ultrahigh vacuum meas. 0-57323  
 Pirani gauges, performance reproducibility 0-77806  
 spinning rotor gas friction gauge, calibration against fund. vac. press. standard 0-82787  
 thermocouple, gas analyser appl. 0-61183  
 ultrahigh vacuum system for ISABELLE full cell 0-77798  
 vapour pressure meas. gauge of <sup>3</sup>He for use up to 0.3K 0-68207

**vacuum measurement**

see also vacuum gauges  
 impedance probe calibration, for vacuum meas. in single component two-phase mixture (Italian) 0-62677  
 ionisation vacuumometers, cold or hot cathode, with automatic control (Czech) 0-73376  
 mass spectrometer materials, set up for meas. released gas 0-105746  
 mean sojourn time of molecules on surfaces, meas. in practical vacuum system (Japanese) 0-57315  
 partial pressure measurement and gauges for ultrahigh vacuum meas. 0-57323  
 standards intercomparison,  $8 \times 10^{-5}$ - $8 \times 10^{-2}$  Pa 0-86333  
 supersonic molecular beam source, simple calibration method 0-82845

**vacuum polarisation** see quantum electrodynamics**vacuum pumps**

see also cryopumping; diffusion pumps; ion pumps  
 absorption, magneto-optical cryostat, optical meas. at 0.4K 0-73369  
 CVD, problems with creating vacuum (French) 0-101803  
 electron microscope backing pump system, high-performance oil-free design 0-99011  
 fusion reactor, TFTR, vacuum pumping system 0-95447  
 fusion reactor, TFTR Flexibility Modification, in-torus surface pumping, Ti and Zr/Al gettering 0-95451  
 gas mixtures, pumping in high vacuum region 0-95107  
 oil, rotational, function, construction and operation (Slovak) 0-68206  
 plasma etching, problems with creating vacuum (French) 0-101803  
 pumpdown time eqn. and system selection 0-82785  
 roots pump and oil-sealed mechanical pump combination for low backstreaming 0-57322  
 semiconductor production problems and safety precautions (German) 0-86330  
 turbomolecular pumps, advances, review 0-62676  
 Ti sublimation pump, methane outgassing 0-77796

**vacuum sintering** see sintering**vacuum techniques**

includes techniques for producing, maintaining and handling vacuum per se  
 see also cryopumping; getters  
 Araldite, high vacuum sealant at liq. N<sub>2</sub> temp. 0-57319  
 bakeable seals development for large noncircular ports on Tokamak fusion test reactor 0-82777  
 biological specimen replication at -150°C with improved freeze-fracture apparatus 0-85560  
 chopper system, UHV compatible, for meas. of energy spectrum of neutral D atoms 0-79587  
 crossed fields nitriding in air atm. 0-84867  
 cryostats, twin-chamber flexible vacuum connection 0-73368  
 degassing metals for extreme low pressures 0-98924  
 deposition equipment cleaning, practical procedures 0-57318  
 education, advanced undergraduate expts. in vacuum physics and mass spectrometry 0-73153  
 elastometer materials, selection for vacuum seals 0-77797  
 etching, vac. colour, for investigating hot plastic deform. of C steel 0-61036  
 fast pulsed gas valve for injecting gas pulses 0-62675  
 fusion reactor, Heliotron E, vacuum chamber construction using electron beam welding 0-106180  
 fusion reactor, STARFIRE project, T handling and vacuum requirements 0-106187  
 fusion reactor vacuum vessel welds, ultrasonic scanner 0-99288  
 heat treatment, efficiency 0-81089  
 high-vacuum system control and diagnosis by monitoring total press. and per cent N content 0-95105  
 leak testing with search gases, He leak detectors with mass spectrometer anal. (German) 0-101802  
 LEP, electron positron storage ring, vac. chamber, glow discharge surface cleaning 0-58010  
 liquid jet vacuum seal, inflow, rel. to electron beam emergence into atmosphere 0-78469  
 mean sojourn time of molecules on surfaces, meas. in practical vacuum system (Japanese) 0-57315  
 metallurgy, vacuum, using electron beam techniques, technical problems (German) 0-84850  
 microbalance, Cahn RG-2000, improvement in sensibility 0-77794  
 microweighing techniques and use of beam microbalance, book 0-62401

**vacuum techniques continued**

molecular sieves, adsorp. of atmospheric gases, comparison of 13X and 4A at low temp., press. (German) 0-88423  
 mounting method for thermocouple gauge tubes 0-77795  
 multilayer insulation materials, ambient temp. outgassing rate 0-84370  
 Nb, pure, production by carbothermic reduction-electron beam melting combination method 0-89177  
 outgassing meas. of noncryst. materials, diffusion theory (Chinese) 0-57313  
 permanent joining techniques 0-82782  
 protection of internal components from contaminants of large systems 0-105666  
 pumpdown time eqn. and system selection 0-82785  
 seals, high-speed cryogenic mag. fluid for high-vacuum chambers 0-57314  
 SEM, secondary electron emission dependence on electron beam density dose, surface interactions from AES and ELS 0-61209  
 Spacelab pallet, meas. of mol. streaming fields 0-82173  
 thermal fatigue testing, in ultra high vac. environments (Japanese) 0-93716  
 UHV fatigue drive, design and performance 0-86328  
 ultrahigh vacuum system for ISABELLE full cell 0-77798  
 He desorption spectrometer, clustering of Kr in W (100) obs. 0-77908  
 in seal fabrication by prepressing 0-101800  
 Nb single crystals, for tunnel meas., annealing in ultra high vac. device (German) 0-89169

**valence bands**

alkaline earth fluorides, orbital binding energy and ionicity relations, XPS meas. 0-97399  
 exchange interactions in semiconductors and insulators, mean free path and energy gap effects 0-88522  
 graphite, diamagnetism with quasilinear dispersion law, orbital susceptibility, valence bands (Russian) 0-80475  
 graphite intercalation compound, interaction between one or two s orbitals (French) 0-65440  
 intrinsic semiconductors, indirect exchange interaction, finite temp., valence bands and energy gaps effect 0-59943  
 p-n heterojunctions, forward-biased, charge accumulation 0-107902  
 polyacetylene:1, electronic structure, XPS and UPS meas. 0-66385  
 polypeptide chains, struct. of conduction and valence band 0-76700  
 polypeptides, electronic struct., side-chain disorder effect 0-76706  
 $\alpha$ -quartz, CNDO/2 calcs., electronic props. of perfect cluster, EPR parameters of O<sup>-</sup> vacancy 0-107701  
 rare earth aluminate, scandate and zirconate film coatings, electrophys. props. w.r.t. prep. technology 0-60781  
 rare earth metals, X-ray 5p emission bands, valence energy band 0-104016  
 semiconductor, direct band gap, electronic Raman scatt. of polarised light on donor levels 0-93309  
 semiconductor, intrinsic, indirect exchange interaction, finite temp. effects 0-71003  
 semiconductor, p-type, Faraday effect due to free holes 0-97247  
 semiconductor, p-type, infrared absorption and plasma reflection 0-97284  
 semiconductor, p-type, intervalence-band transitions, saturation, theory 0-75997  
 transition metals, alloys, and cpds., XPS asymmetry of core electrons and electronic struct. parameters 0-93460  
 tunnelling MIS structures photovoltaic energy conversion, band struct. 0-92995  
 Ag-Mn, dil., valence and core level spectra, XPS study 0-84838  
 Al, valence band Auger spectra, surface effect 0-80915  
 Al-Mn(Ni)(Cu), dil., core and valence band spectra, XPS study 0-84837  
 Al<sub>2</sub>O<sub>3</sub>, corundum, band struct. calc. using semiempirical Mulliken-Rudenberg method 0-80177  
 As<sub>x</sub>Si<sub>100-x</sub>(Se<sub>100-x</sub>), localised states density near valence band edge (Russian) 0-103638  
 Au clusters on alkali halide surface, size depend. of valence bands, XPS study 0-65647  
 Au film, photoelectron emission, intershell interaction influence on 3d and 5d branching ratio 0-104038  
 Au subshell photoelectron branching ratio meas. using synchrotron radiation 0-66397  
 Au-Fe(Co)(Ni), dil., valence and core level spectra, XPS study 0-84838  
 Au(111), A-line valence bands, angle-resolved photoemission determ. 0-108323  
 B, evaporated, electronic struct., XPS, SXS and isochromat investig. 0-76143  
 BaO, XPS valence bandstruct. 0-89117  
 BaTiO<sub>3</sub>, band struct. calc., interpretation of XPS and UPS spectra 0-70597  
 BaTiO<sub>3</sub>, photoelectron and optical spectra derived from self-consistent charge MO and band calcs. 0-96785  
 BaTiO<sub>3</sub>, valence band UPS and partial p and d density of states 0-71560  
 C:Ni, X-ray photoemission studies 0-76138  
 CaO, XPS valence bandstruct. 0-89117  
 CdGa<sub>2</sub>Se<sub>4</sub>(Se<sub>4</sub>), band struct., pseudopot. method 0-92816  
 CdIn<sub>2</sub>S<sub>4</sub>, single crystals, recombination process and localised levels 0-93383  
 CdSiP<sub>2</sub>, electronic struct., X-ray spectroscopic investigation 0-108300  
 CoS<sub>2</sub>(Se<sub>2</sub>), core-level and valence-band XPS 0-93450  
 CsBr, (110) surface, electronic struct. of valence bands calc. (Russian) 0-75621  
 CsCl, (110) surface, electronic struct. of valence bands calc. (Russian) 0-75621  
 CsI, (110) surface, electronic struct. of valence bands calc. (Russian) 0-75621  
 Cu film, photoelectron emission, intershell interaction influence on 3d and 5d branching ratio 0-104038  
 Cu-Fe(Co)(Ni), dil., valence and core level spectra, XPS study 0-84838  
 Cu<sub>2</sub>O, self-consistent energy bands 0-59869  
 CuPd, chemical shift effects and origin of Pd 3d core level satellite 0-104039  
 CuZr, photoemission study 0-104046  
 FeB and Fe<sub>2</sub>B, ESCA and mag. spin data, electronic struct., isomer shifts, valence bands and chemical bonding 0-75489  
 Fe<sub>0.5</sub>Cu<sub>0.5</sub>Cr<sub>2</sub>S<sub>4</sub>, ESR spectra, elec. and mag. props., Curie temp. 0-97137  
 Fe<sub>1-x</sub>(P,B)<sub>x</sub>, amorphous and crystalline, photoemission and band structure 0-60754  
 FeS<sub>2</sub>, core-level and valence-band XPS 0-93450

**valence bands continued**

- GaAs, valence-band dispersions, electron and hole lifetimes, angle-resolved photoemission 0-80947  
 GaAs:Cr, carrier equilibrium effects, impurity states, elec. resistivity 0-65488  
 GaAs:Sb, resonance levels of isoelectronic impurities 0-107740  
 GaN, electron struct., ESCA study 0-89116  
 GaS<sub>2</sub>Se<sub>1-x</sub>, valence band states, composition depend., photoemission spectra study 0-100434  
 GaSb, solid solns., impact ionisation, cond. and valence band effects 0-65583  
 Ge, electron-hole drop freq. depend. damping 0-88482  
 Ge/GaAs (110) heterojunction, valence band discontinuity in XPS spectra, precise determ. 0-84834  
 H<sub>2</sub>WO<sub>3</sub>, bronzes, Anderson transition, XPS 0-107705  
<sup>3</sup>He, solid, valence band struct., zero-point motion effect 0-65333  
 HgSe, interband  $\Gamma_6$ - $\Gamma_8$  magnetoabsorption, temp. study 0-76032  
 Li, valence band Auger spectra, surface effect 0-80915  
 LiNbO<sub>3</sub>, valence band UPS and partial p and d density of states 0-71560  
 MgO, XPS valence bandstruct. 0-89117  
 MgSiP<sub>2</sub>, electronic struct., X-ray spectroscopic investigation 0-108300  
 MnS<sub>2</sub>(Se<sub>2</sub>), core-level and valence-band XPS 0-93450  
 NbS<sub>2</sub> and Nb<sub>2</sub>S<sub>4</sub>, electronic struct. and predicted cond. props. 0-92815  
 Ni (001) surface, electronic struct. of ordered S overlayers 0-84835  
 Ni, photoemission spectra, valence band and core level satellite due to excitation of d electron 0-97408  
 NiS<sub>2</sub>(Se<sub>2</sub>), core-level and valence-band XPS 0-93450  
 PbS(Se), valence band struct. determ. by optical absorpt., size quantization effects 0-59871  
 Pb<sub>1-x</sub>Sn<sub>x</sub>Te, hole effective mass near zero bandgap, IR refl. study 0-108205  
 Pb<sub>1-x</sub>Sn<sub>x</sub>Te:Ge, anomalous behaviour of impurity centres under press. (Russian) 0-65491  
 Pd, photoemission spectra, valence band and core level satellite due to excitation of d electron 0-97408  
 PdZr, photoemission study 0-104046  
 Pt band-structure determ., angle-resolved photoemission 0-66398  
 Pt subshell photoelectron branching ratio meas. using synchrotron radiation 0-66397  
 Pt(111), A-line valence bands, angle-resolved photoemission determ. 0-108323  
 Pu, oxidation, binding energies, Auger and X-ray photoelectron spectra study 0-76550  
 Se, trigonal and amorphous, electronic struct. and nonempirical calc. of struct. props. 0-59866  
 Se-Te-Sb glasses, electronic transport 0-88579  
 Si (111) 7×7 clean surface and O chemisorbed stage valence band density of states from L<sub>23</sub>VV Auger spectra 0-100717  
 Si on sapphire, residual strain effect on elec. props. (Japanese) 0-84522  
 Si-SiO<sub>2</sub> boundary, surface charge transport in valence band of Si 0-70789  
 SmS<sub>1-x</sub>P<sub>x</sub>, valence changes, XPS and UPS study 0-97402  
 Sn(S<sub>2</sub>Se<sub>2</sub>), valence band states, composition depend., photoemission spectra study 0-100434  
 SnTe, cubic semicond. with ellipsoidal valleys, magnetoresist. 0-80300  
 SrO, XPS valence bandstruct. 0-89117  
 SrTiO<sub>3</sub>, valence band UPS and partial p and d density of states 0-71560  
 Te, trigonal and amorphous, electronic struct. and nonempirical calc. of struct. props. 0-59866  
 TiS<sub>2</sub>(Se<sub>2</sub>), valence density of states, Gilat-Raubenheimer method 0-88465  
 TiBr<sub>3</sub>, polymorphism, XPS obs. 0-97398  
 TiCl<sub>3</sub>, polymorphism, XPS obs. 0-97398  
 UAl<sub>2</sub>(Co<sub>2</sub>), surface comp. and electronic struct., photoemission study 0-66382  
 V<sub>2</sub>O<sub>5</sub>, energy band structure, tight-binding method 0-70602  
 W, XPS, angle-resolved, from valence bands, obs. of strong temp. depend. and direct-transition effects 0-60752  
 ZnGa<sub>2</sub>S<sub>4</sub>, band struct., pseudopot. method 0-92816  
 ZnSe(Te), photolum. excitation spectra of tightly bound holes, valence band contrib. 0-60658  
 ZnSiP<sub>2</sub>, electronic struct., X-ray spectroscopic investigation 0-108300  
 ZnTe clean and adsorbed O<sub>2</sub> (110) surfaces, UV photoemission spectra (Japanese) 0-93456  
 Zr-Co, amorphous and crystalline, d-band struct., alloying effects 0-59862  
 Zr-Ni, amorphous and crystalline, d-band struct., alloying effects 0-59862  
 ZrS<sub>2</sub>(Se<sub>2</sub>), valence density of states, Gilat-Raubenheimer method 0-88465

**valence band calculations** *see VB calculations***valency**

- brass-like alloy phases, binding and cryst. struct., valence arguments 0-88081  
 metal, BCC, effective valence, from phonon data, rel. to vacancy formation energies 0-79781  
 metallic phase structures, dimensional analysis, bonding information from valency effects appearing as artefacts 0-96471  
 CeNi<sub>2</sub>-CePt<sub>3</sub> system, structural and mag. studies on valence behaviour of Ce 0-103809  
 Cs<sub>2</sub>Au<sub>2</sub>Cl<sub>6</sub>, electronic state of Au at high press., Mossbauer spectra 0-60467  
 CuCr<sub>2</sub>Se<sub>4</sub>, mag. reson. and valence state of Cu and Cr ions 0-60413  
 EuB<sub>6</sub>, valence state of Eu, X-ray line displacement meas. 0-70633  
 EuPt<sub>3</sub> compounds, partial valence change, <sup>151</sup>Eu Mossbauer and magnetisation obs. 0-70167  
 $\alpha$ -Fe:B(C)(N)(O), valency effect of interstitials 0-65502  
 La-Sm-Au, amorphous, surface effects on Sm valence, XPS and X-ray absorption meas. 0-108325  
 Sm metal, valence transition at surface of Sm 0-70652  
 Sm-Au, amorphous, surface effects on Sm valence, XPS and X-ray absorption meas. 0-108325  
 YIG:Ru, optical absorpt. and MCD obs. of Ru<sup>4+</sup> site occupancy 0-71456

**value analysis** *see value engineering***value engineering**

- see also optimisation; quality control*  
 Co permanent magnet material savings (German) 0-103851

**valve voltmeters** *see voltmeters***valves**

*see also diaphragms*

- compressible gas flow through exhaust valve, analytical calc. using flux analysis method (Japanese) 0-69896  
 dual pilot operated valve for switching the flow of a cryogenic liquid 0-98918  
 fast pulsed gas valve for injecting gas pulses into vacuum system 0-62675  
 high pressure gas valves, supersonic air flow noise and flow pattern obs. 0-59067  
 pressure regulators, self-contained, selecting and sizing 0-82759  
 RF sputtering systems, discharge suppression within piezoelectric gas admission valves 0-100110  
 self-opening, for N<sub>2</sub> decanting siphon 0-57310  
 switch valve, lightweight, remotely actuated, for rebreathing exercise studies 0-101278  
 vacuum valve, baffle and trap design and construction 0-82781  
 wedge-gate valve of cast Fe with stainless steel trim for under water use, corrosion protection by dip-applied coating 0-93677

**valves (electronic)** *see electron tubes***Van Allen radiation** *see radiation belts***Van Allen radiation belts** *see radiation belts***Van de Graaff accelerators**

- hoops, circular and oval, stress multiplying factor 0-74043  
 tandem, appl. to meas. of <sup>10</sup>B distrib. in geophysical samples 0-61924  
 tandem, appl. to radioisotope detection in terrestrial and extraterrestrial samples 0-61923

**Van de Graaff generators**

No entries

**Van der Pol oscillators** *see relaxation oscillators***Van der Waals forces**

- alkali halides, repulsive hardness parameters, crystal-independent 0-64947  
 film adsorbed on graphite, two-dimensional phase transitions 0-107653  
 fluoride crystals, rutile-type, interionic pots., cohesive energy, bulk modulus, calc. 0-79741  
 HCl-inert gas mixtures, van der Waals molecules, far IR spectra 0-95610  
 inert gas dimers, electron impact ionis. 0-58400  
 Lifshitz constant for calc. of van der Waals force between two solids (French) 0-107658  
 membrane bilayers, quasitwo dimens., theoretical models 0-76713  
 mesomorphic monolayers, quasitwo dimens., theoretical models 0-76713  
 methyl iodide, van der Waals mol., electron self-scavenging 0-95727  
 molecular interactions, two-body van der Waals coeff., combination rules 0-78677  
 nematic liquid crystals, surface and anchoring energies, van der Waals contrib. 0-92455  
 neutral atom collisions, hyperfine component broadening and shift of spectral lines 0-74136  
 neutral atom scattering, long range, from solid cylinders, quantum theory 0-71549  
 nucleotide base stacking interactions in vacuum, field mass spectrometry 0-81526  
 oxide crystals, rutile-type, interionic pots., cohesive energy, bulk modulus, calc. 0-79741  
 palmitic acid-choleic acid complex, cryst. struct. and van der Waals energy 0-64983  
 pure gas, enthalpy, Carlson-Thodos van der Waals eqn. calcs. 0-83878  
 solvent-rod mixture, two phase, interfacial free energies, quartic van der Waals theory 0-59377  
 spectral line broadening, growth curves 0-102548  
 tris(ethylenediamine)metal(III), H bonding (French) 0-87241  
 TTF dimer, nonbonding intermolecular forces 0-83443  
 Van der Waals constant, liquid, binary mixtures of organic chemicals, US velocity and excess internal pressure, Flory's theory 0-70310  
 Van der Waals equation, statistical anal. of RT/P.V. (Spanish) 0-74213  
 voids and particles, Van der Waals energy between them, from asymptotic to close contact 0-80351  
 Ag film, on amorphous C and Si substrates, dispersion force contrib. to adhesion (French) 0-59842  
 Ag halides, cryst., van der Waals coeffs. calcs. 0-96459  
 Al film, on amorphous C and Si substrates, dispersion force contrib. to adhesion (French) 0-59842  
 Ar-acetylene van der Waals molecule, radiofreq. spectroscopy and Stark effect meas., equilib. struct. and props. 0-91543  
 Ar-HBr, intermol. pot. energy surfaces calcs. 0-91625  
 Au film, on amorphous C and Si substrates, dispersion force contrib. to adhesion (French) 0-59842  
 Cs, crystal struct., van der Waals and repulsive interaction 0-84137  
 Cu film, on amorphous C and Si substrates, dispersion force contrib. to adhesion (French) 0-59842  
 H<sub>2</sub>-H<sub>2</sub> intermol. pair pot., ab initio SCF-CI surface 0-91457  
 He+H<sub>2</sub>, pot. energy surface, ab initio calcs., van der Waals const. determ. 0-106372  
<sup>3</sup>He-<sup>4</sup>He mixture, adsorbed film, systematic exptl. study 0-107603  
<sup>4</sup>He, superfluid film, solitons at low temps., Korteweg-de Vries eqn. 0-96717  
 K, crystal struct., van der Waals and repulsive interaction 0-84137  
 Kr-HCl, intermol. pot. energy surfaces calcs. 0-91625  
 (N<sub>2</sub>)<sub>2</sub>, Van der Waals molecule, struct. and internal rot. barriers determ., interaction pot. from ab initio calcs. 0-91626  
 Na-Hg high-pressure discharge, Na reson. radiation, self-reversed maxima shifts 0-92411  
 Rb, crystal struct., van der Waals and repulsive interaction 0-84137  
<sup>87</sup>Rb+<sup>129</sup>Xe, spin-exchange cross-section meas. 0-78686  
 TI halides, cryst., van der Waals coeffs. calcs. 0-96459  
 Tl, atomic fluorescence, D<sub>2</sub> pressure effect on width and shift 0-99475  
 Xe+Cl<sub>2</sub>, classical trajectory calcs., energy threshold for collision induced dissoc. determ., 0-95709

**Van der Waals molecules** *see quasimolecules***vanadium**

*see also nuclei with .....*

- APS thresholds, extended fine struct., effect of central atom pot. 0-66329  
 atom, fine struct. levels fitting, config. interaction effect, spin-orbit and electrostatic interaction parameters 0-69248



## vanadium continued

- columnar films, crit. field anisotropy, depend. on prep. conditions (*Russian*) 0-93056  
 Compton profiles, anisotropic 0-97368  
 creep rate in vacuum, grain size effect 0-108514  
 dehydrogenation by annealing with Zr foils 0-96736  
 diffusion of H<sub>2</sub>, isotope effects, crystal field stabilisation 0-59728  
 diffusion of H and trapping 0-70447  
 diffusion of O and N, statistical calcs. on Arrhenius lines 0-59722  
 elastic consts., changes caused by addition of H and effects of hydrostatic pressure 0-75287  
 elastic moduli, determination of effect of H based on US vel. meas. 0-75288  
 electrical resistivity due to interstitial H (D) 0-96848  
 electron energy losses due to H, obs. by scanning TEM 0-79850  
 electron-irradiated, positron annihilation study 0-70259  
 electron-phonon coupling constant calc. (*Russian*) 0-70624  
 electronic structure, model potential calcs. (*Russian*) 0-100431  
 electronic structure, thermoreference studies 0-76047  
 film, vac. evaporated, elec. props. 0-80414  
 film on sapphire substrate, orientational growth, epitaxial textures, nucleation textures (*Russian*) 0-75454  
 films, vac. evaporated, optical cond. 0-76100  
 ISSEC selection for fusion reactor 0-57950  
 lattice dynamics, local frequency spectrum, mean thermal displacement of H 0-59604  
 liquid, elec. resist., melting pt. to boiling pt., temp. depend. 0-96839  
 liquid, viscosity at melting point, free energy (*Russian*) 0-92699  
 luminescence characteristics of pure surfaces acted on by flux of field emission electrons 0-100695  
 magnetic susceptibility, model pot. theory 0-75710  
 muon diffusion, LAMPF results 0-71285  
 photoelectric cross sections at 52.4, 60, 72.2 and 84.4 keV 0-69187  
 powder, crystal structure, magnetic and superconducting props. 0-97121  
 radiance temperature at melting point, surface roughness depend. 0-59683  
 ruby:V<sup>3+</sup>, cross-relax. 0-71163  
 spallogenic isotopes in Fe meteorites, radial distrib. 0-67488  
 superconducting, rotating discs, hysteresis losses and mag. phenomena 0-75695  
 surface, chemisorption of Br<sub>2</sub>, struct., Na adsorption effects 0-101039  
 surface, spin fluctuations, finite temp. mag. props. study 0-107994  
 thermophysical props. at temps. up to 7000K 0-103497  
 volt ampere characteristics during electron melting process (*Russian*) 0-75336  
 wire, deformed in torsion, internal friction, H effect 0-76300  
 ZnS:V<sup>2+</sup>, impurity states by Green's function method 0-92855  
 Al<sub>2</sub>O<sub>3</sub>:V<sup>3+</sup>, hyperfine splitting and magnetoelectric consts., freq. crossing spectroscopy 0-107392  
 Al<sub>2</sub>O<sub>3</sub>:V<sup>3+</sup>, Jahn-Teller effects, ground state 0-75528  
 Al<sub>2</sub>O<sub>3</sub>:V<sup>3+</sup>, spin-phonon coupling, rot. mode role 0-70329  
 α-Al<sub>2</sub>O<sub>3</sub>:V<sup>3+</sup>(V<sup>4+</sup>), optically and thermally stimulated reactions, absorpt. spectra 0-80825  
 GaAs:V ion implanted, luminesc., level splitting 0-97338  
 MgO:V<sup>2+</sup>, Jahn-Teller system, zero-phonon line broadening due to non-radiative transitions 0-108258  
 MgO:V<sup>3+</sup>, HF phonon spectroscopy using supercond. tunnel junctions 0-65178  
 MnO<sub>2</sub>:V, Zn<sup>2+</sup> ion specific adsorpt. kinetics, <sup>65</sup>Zn γ-ray scintillation investigation 0-70529  
 MoO<sub>3</sub>:V, current carrier sign, Fermi surface cross section variations (*Russian*) 0-84420  
 Si-V p-n junctions, thermal emission rates and capture cross sections of majority carriers at V centres 0-96980  
 V VII, VIII, IX, X, 3s-3p and 3p-3d transitions, oscillator strength and energy levels calcs. 0-83251  
 V<sup>2+</sup>, doped ion in divalent metal cpds., correl. between Szegedi charge and hyperfine coupling consts. 0-96832  
 V-CdS-In preparation and behaviour obs. Josephson junctions 0-100559  
<sup>50</sup>V, nucl. quadrupole moments from laser-RF double reson. spectroscopy 0-57682

## vanadium alloys

- see also vanadium compounds  
 magnetic susceptibility and Knight shift meas., d-metal alloys 0-66055  
 steel, Al-Ti-(Mo), Al-Ti-V-(Mo), Al-Ti-Nb-(Mo) and Al-V-(Mo) low-alloy, toughness improvement through Ti additions 0-66525  
 steel, Cr-Mo-V, strength and ductility in creep, purity influence 0-66598  
 steel, Cr-Mo-V austenitic, creep resist., high-temp. props. residuals effect 0-66600  
 steel, Cr-Mo-V low-alloy, high-temp. ductility and crack growth, impurities effect 0-66652  
 steel, Cr-Mo-V low-alloy, mech. props. and stress relief cracking, effects of impurities and deoxidation practice 0-66599  
 steel, Cr-Mo-V low-alloy, prior austenite grain boundary embrittlement by B 0-66657  
 steel, Cr-Mo-V low-alloy, stress relief cracking, impurity and alloy content effects 0-66654  
 steel, Cr-Mo-V low-alloy with high residual element content, cavitation control 0-66663  
 steel, Mn-V reinforcing type, strain ageing characs. rel. to mech. props. 0-84969  
 steel, Nb(V), (Al), hot-rolling, laboratory simulation, recrystn. of austenite 0-97512  
 steel, Ni-Cr-Mo-V low-alloy, additive remedy for temper brittleness 0-66659  
 steel, V, precip. and transform. kinetics, effect of N 0-97485  
 steel, V-Nb, supercooled austenite isothermal decomp., struct., strength and fracture characs. 0-60966  
 steel, W-Mo-Cr-V tool, laser surface melted, struct., heat treatment effect 0-76424  
 U-V metallic glasses, glass form. and thermal stability 0-75183  
 Al-V, dil., supercond., nucl. spin relax. and quasiparticle excitations 0-88680  
 Au-V, UPS study, localised states 0-93449  
 Co<sup>48</sup>V, nucl. orientation of <sup>48</sup>V, γ-ray anisotropy obs. 0-97169  
 Co-Fe-V-Ni, mag. and mech. props., heat treatment and stress effects 0-60363  
 Co-V, Co rich, ferromag. behaviour, mag. moments, Curie temp., and NMR spectrum 0-70964  
 Co-V, ferromag. struct. in nucl. spin echoes 0-60453

## vanadium alloys continued

- Co(GaTiV) alloys, ferromag. onset, electron conc. depend. 0-60203  
 CoV, dil., low temp. specific heat and magnetisation 0-65925  
 CoV, phase dependent MNR spectra 0-108114  
 Co<sub>2</sub>Al, hyperfine fields of Fe impurities, Mossbauer spectra 0-71255  
 Cr-Fe(Co)-V, dil., antiferromag., elec. resist. min., press. and impurity effects 0-59970  
 Cr-Mo-V-Nb, supercooled austenite isothermal decomp., struct., strength and fracture characs. 0-60966  
 Cr-Si-V, (2, 0.1 at.%), paramag. to commensurate spin density wave transition 0-65875  
 Cr-V, itinerant electron antiferromag., spin fluctuations, low temp. specific heat 0-107439  
 Cr<sub>2.5</sub>V<sub>0.7</sub>Fe<sub>3.4</sub>C<sub>3</sub>, stacking fault study, morphology, comp. and struct. 0-84190  
 Cu-V-Si, supercond. props. 0-107945  
 Fe<sup>48</sup>V, nucl. orientation of <sup>48</sup>V, γ-ray anisotropy obs. and NMR meas. 0-97169  
 Fe-Co-V-(Ni), annealing effect on microstruct. rel. to mag. and mech. props. 0-89267  
 Fe-Co<sub>2</sub>-V, (49, 2 wt.%), solid soln., rheological study of crystallographic order on creep (*French*) 0-97548  
 Fe-F, thermophysical props. and elec. cond., temp. depend. 0-96842  
 Fe-Mn-Ni-V-C (0.5, 3.0, 1.0, 0.2 wt.%), austenite decomp., isothermal transform. characs. 0-97477  
 Fe-Mn-V-C (0.5, 1.0, 0.2 wt.%), austenite decomp., isothermal transform. characs. 0-97477  
 Fe-Nb-V-C-N, equilibrium comp. and solubility in steels, model of ideal solns. (*Russian*) 0-60832  
 Fe-Ni-V-(Cu) (12, 2, 2 wt.%), Cu addition strengthening at 77K, mech. props. 0-60875  
 Fe-Sb-V, interactions and segregations, Mossbauer and X-ray diffr. study 0-70415  
 Fe-Ti-V-C-N, equilibrium comp. and solubility in steels, model of ideal solns. (*Russian*) 0-60832  
 Fe-V, <sup>59</sup>Fe self-diffusion (*Czech*) 0-88352  
 Fe-V, dilute, irradiation softening effect on yield stress 0-76319  
 Fe-V, ferromag. struct. in nucl. spin echoes 0-60453  
 FeSi-Ca-V complex alloy oxidation of steel, nonmetallic additions (*Russian*) 0-93685  
 FeV (2 at.%), NMR spin echoes, domain wall effects 0-75883  
 (Fe<sub>100-x</sub>V<sub>x</sub>)<sub>2</sub>P<sub>13</sub>B<sub>3</sub> amorphous alloys, splat cooled, mag. and transport props. 0-84593  
 Gd-V amorphous films, spontaneous Hall effect and elec. resist. 0-80251  
 HfV<sub>2</sub>H<sub>2</sub>, proton NMR relax. time and Knight shifts, diffusional activation energies meas., sorption props. 0-75871  
 Mo-(Zr+V+C) (1.1 wt.%) alloy, phase composition, carbide phase microhardness (*Russian*) 0-60834  
 Mo-Cr-V-P, load curves, structure states boundaries and strain hardening (*Russian*) 0-89241  
 Mo-V, elec. resist. and thermo-EMF, conc. depend., 4.2 to 1500K (*Russian*) 0-80247  
 Nb-V, resistivity due to H incorporation 0-70666  
 Nb-V system, H<sub>2</sub> absorpt. 0-59808  
 Nb-V<sub>3</sub>Ga mixed state, Meissner effect investigation by muon method (*Russian*) 0-107954  
 Nb-V-Si, ductile amorphous, superconductivity 0-60131  
 Ni-V, dil., optical absorpt., electronic struct. 0-108227  
 Ni-V, solid soln., diffusion and thermodynamic props. 0-65278  
 Pd<sub>2</sub>Mn<sub>1-x</sub>V<sub>x</sub>Sn, Heusler alloy, structural disorder, Mossbauer study 0-80650  
 PtV, dil. alloys, NMR obs. of <sup>51</sup>V 0-71203  
 Ta(C,N)-Ni-VC, sintering behaviour, VC effect 0-93520  
 Ti-Al-Mo-V (8, 1, 1 wt.%), Widmanstätten colonies, fracture toughness 0-85031  
 Ti-Al-V, friction coeff. reduction on injection with TiC particles 0-85086  
 Ti-Al-V, fusion reactor blanket structures, radiation resistance 0-63379  
 Ti-Al-V (6, 4 wt.%), fretting corrosion of orthopaedic implant materials by bone cement 0-104813  
 Ti-Al-V (6, 4 wt.%), texture depend. stress corrosion cracking 0-104334  
 Ti-Al-V (6.4 wt.%), cyclic temp. creep, transition effect 0-97539  
 Ti-Al-V (6.4 wt.%), β-annealed, subsurface fatigue crack initiation 0-108553  
 Ti-Al-V (6.4 wt.%), effect of air exposure on fracture characs. 0-100890  
 Ti-Al-V (6.4 wt.%), H related fatigue fracture 0-76344  
 Ti-Al-V (6.4 wt.%), ion irradiated, microstruct. study using TEM 0-96572  
 Ti-Al-V (6.4 wt.%), microstruct. effect of base metals on diffusion welding (*Japanese*) 0-89296  
 Ti-Al-V (6.4 wt.%), porous compacts, determ. of effective stress in hot pressing 0-100807  
 Ti-Al-V (6.4 wt.%) superplastic alloy, maximum attainable ductility 0-60919  
 Ti-Al-V (6.4 wt.%) cast alloy, with improved microstruct., mech. props. (*Japanese*) 0-71701  
 Ti-Al-V-Be-B, melt-extracted polycryst., mech. props. 0-76360  
 Ti-Al-V-Fe-Cu, melt-extracted polycryst., mech. props. 0-76360  
 Ti-Al-V-Sn (5.5, 5.5, 2 wt.%), crack growth, slow, H-induced 0-104272  
 Ti-Al-V-Sn (6.6, 2 wt.%) fusion weldment, substruct. characs. 0-84183  
 Ti-Mo-V-Al-Cr-Fe (4.8, 4.7, 5.2, 1.1, 1.0 wt.%), structural changes during heating up to 1000°C, DTA study (*Russian*) 0-93552  
 Ti-V, elastic moduli, electron conc., pulse echo overlap meas. 0-59550  
 Ti-V, metastable diffusionless equilibria, high press. conditions 0-71627  
 Ti-V (10 at.%), α-ω transformation, electron diffr. evidence of intermediate BCC phase 0-81051  
 β-Ti-V metastable alloys, fatigue crack prop. 0-60964  
 Ti-V-Cr-Mo, fracture resistance at low temps. 0-104284  
 Ti-V-Fe-Al (10, 2, 3 wt.%), fracture toughness and stress corrosion resistance 0-100994  
 Ti<sub>1-x</sub>H<sub>2</sub> system, reaction and press.-composition isotherms meas. 0-108391  
 V<sub>3</sub>/Cu-Ga, composite superconductor, V<sub>3</sub>Ga phase form., TEM obs. (*Russian*) 0-84933  
 V-Al-Cu, ternary system, phase relationships 0-76230  
 V-Al(Ga, Si, Ge, Sn)-Cu, rapidly quenched, comp. and phase equilib. 0-76235  
 V-CO(Ni) sigma phase alloys, NMR and electric-field gradients 0-108109  
 V-H single crystals, elastic consts., temp. depend., H effects 0-66563  
 V-H(D/T) system, BCC, US vel. changes caused by H isotope dissolution 0-65117



## vanadium alloys continued

- V-Mo (25 wt.%), corrosion behaviour in high temp. impure He gas 0-76402  
 V-N(O)(C) system, specimen prep. for metallography (*German, English*) 0-84939  
 V-Nb-Ti-N alloy, with dispersed second phase, ductile-brittle transition 0-93653  
 V-O alloys, quenched, local ordering of O, electron microscopy and diff. 0-59453  
 V-Pt, sp. ht. and mag. meas. in ordered and disordered phases 0-70422  
 V-Ti, supercond., rotating discs, hysteresis losses and mag. phenomena 0-75695  
 V-Ti (42 at.%), ultrasonic vel. in mixed state 0-75689  
 V-Ti-C, elemental anal. by EELS 0-101069  
 V-Ti-C, high temp. carbide form., electron microscopy study 0-89228  
 VBe<sub>12</sub>, fusion reactor material, low energy ion erosion expts., Kaufman success appl. 0-68942  
 (V<sub>1-x</sub>Cr<sub>x</sub>)<sub>2</sub>Si, elastic moduli, 4.2 to 290K, softening near supercond. transition (*Russian*) 0-92582  
 V<sub>2</sub>Ga, Al<sub>5</sub> cpd., hydrogenation effects on supercond. transition temp., lattice parameters 0-103772  
 V<sub>2</sub>Ga layer on bronze, diffusion of Ga (*Russian*) 0-65297  
 V<sub>2</sub>Ga, supercond. Al<sub>5</sub> phase, prep. by controlled precip. 0-81000  
 V<sub>2</sub>Ga-Cu, supercond. in situ composites, stress effects on crit. props. 0-65757  
 V<sub>2</sub>Ge, Al<sub>5</sub> cpd., hydrogenation effects on supercond. transition temp., lattice parameters 0-103772  
 V<sub>2</sub>Ge, Gruneisen parameter and thermal expansion eval. at room temp. 0-70351  
 V<sub>2</sub>(Hf,Zr), NMR and mag. susceptibility, density of states determ. (*Russian*) 0-66053  
 V<sub>2</sub>Hf<sub>1-x</sub>Zr<sub>x</sub>, normal and supercond. state, transition temps., mag. susceptibility and specific heat determ. (*Russian*) 0-60132  
 V<sub>16</sub>Ni<sub>15</sub> solid solution, quenched, ordered structure (*Russian*) 0-88086  
 V<sub>2-x</sub>Nb<sub>x</sub>Hf, NMR of <sup>51</sup>V and mag. susceptibility, 20-300K (*Russian*) 0-93192  
 α-V<sub>0.97</sub>O<sub>0.03</sub> solid soln., impurity vibr., inelastic neutron scatt. study 0-92635  
 V<sub>2</sub>Si, Al<sub>5</sub> cpd., hydrogenation effects on supercond. transition temp., lattice parameters 0-103772  
 V<sub>2</sub>Si bridge contacts, nonstationary props. 0-103793  
 V<sub>2</sub>Si embedded in resin, composite supercond., high transition temp. 0-88660  
 V<sub>2</sub>Si film, optical props. (*Russian*) 0-93418  
 V<sub>2</sub>Si, Gruneisen parameter and thermal expansion eval. at room temp. 0-70351  
 V<sub>2</sub>Si, neutron irradi., grain boundary pinning, field-depend. change of crit. current density 0-65759  
 V<sub>2</sub>Si single cryst., creep deform. 0-71695  
 V<sub>2</sub>Si, supercond. mixed state, low temp. tetragonal-domain-reorientation phenomena, US expts. and thermal props. 0-60141  
 V<sub>2</sub>Si, supercond. props., effect of neutron irradi. 0-80463  
 V<sub>2</sub>Si, supercond. structure and properties (*German*) 0-93631  
 V<sub>2</sub>Si thin film far IR laser thermal spectroscopy 0-60144  
 V<sub>2</sub>Si tunnel junctions, energy gap investigation 0-84569  
 V<sub>2</sub>Si-SiO<sub>2</sub>-Mo<sub>3</sub>Re<sub>2</sub>, supercond. tunnel junctions 0-107961  
 V<sub>2</sub>Si(Ga), coherence parameter, nonlinear high temp. supercond. elements with A-15 lattice (*Russian*) 0-60127  
 V<sub>2</sub>Si<sub>1-x</sub>Ge<sub>x</sub>, elastic props., 77 to 290K, rel. to supercond. transition temp. (*Russian*) 0-66560  
 V<sub>2</sub>Si<sub>1-x</sub>Ge<sub>x</sub> solid soln., longitudinal and transverse US wave propag. rate, 4.2 to 300K (*Russian*) 0-103423  
 V<sub>2</sub>Sn, A-15 cpd., normal-state elec. resist. 0-75542  
 ZrV<sub>2</sub>, anomalous softening at martensitic transform. 0-93630  
 ZrV<sub>2</sub>, Knight shift vs. susceptibility plot 0-75712  
 Zr(V<sub>1-x</sub>Co<sub>x</sub>)<sub>2</sub>, relation between electronic struct. and H<sub>2</sub> storing props. 0-76662  
 ZrV<sub>2</sub>D<sub>4</sub>(H<sub>2</sub>), site occupation modes and cryst. struct., neutron diff. study 0-59440  
 Zr(V<sub>x</sub>M<sub>1-x</sub>)<sub>2</sub> (M=Fe, Co), H<sub>2</sub> absorpt. capacity 0-88433

## vanadium compounds

- see also vanadium alloys  
 oxides, change in phonon damping due to metal-insulator transition 0-103625  
 BaO-V<sub>2</sub>O<sub>5</sub>-P<sub>2</sub>O<sub>5</sub>, glass, mech. and elec. props 0-84228  
 BaO-V<sub>2</sub>O<sub>5</sub>-CuO semiconducting glasses, impurity effects, elec. resist. and EPR study 0-103692  
 BaVS<sub>3</sub>:Fe, Mossbauer and mag. studies, electronic state of Fe 0-108130  
 Ba(V<sub>1-x</sub>Ti<sub>x</sub>)S<sub>3</sub>, synthesis and struct. phase transitions 0-107415  
 CaO-V<sub>2</sub>O<sub>5</sub>-SiO<sub>2</sub> system, compatibility triangles 0-81037  
 Cu<sub>3</sub>VS<sub>4</sub>, out of equil. mixed cond., off-centre positions and order-disorder transition, ultrafast nucl. relax. obs. 0-108103  
 Cu<sub>3</sub>VS<sub>4</sub>, out of equil. mixed cond., chem. origin of mobile ions, spin-lattice relax. and NQR obs. 0-108104  
 Fe<sub>2</sub>O<sub>3</sub>-PbO-V<sub>2</sub>O<sub>5</sub> fluxed melt system, solubility and relative supersaturation meas. 0-64934  
 θ-Fe<sub>2</sub>V<sub>2</sub>O<sub>5</sub>, spin glass and paramag. props., susceptibility, EPR and Mossbauer studies 0-75782  
 HfV<sub>2</sub>D<sub>4</sub>, disordered solid solution, order-disorder transition 0-88321  
 Li<sub>2</sub>VSe<sub>4</sub>, intercalation cpds., electron chem., ionicity 0-89501  
 Mg(NH<sub>4</sub>)(SO<sub>4</sub>)<sub>6</sub>H<sub>2</sub>O:VO(H<sub>2</sub>O)<sub>2</sub><sup>2+</sup>, proton ENDOR meas. used to determine hyperfine coupling tensors 0-66075  
 Nb<sub>2</sub>O<sub>5</sub>-V<sub>2</sub>O<sub>5</sub>-P<sub>2</sub>O<sub>5</sub>, glasses and glass ceramics, elec. cond., struct. 0-84466  
 Nb<sub>1-x</sub>V<sub>x</sub>Se<sub>2</sub>, elec. and mag. anomalies at CDW transition 0-107722  
 RbH<sub>2</sub>(SeO<sub>4</sub>)<sub>2</sub>:VO<sup>2+</sup>, EPR spectra, spin Hamiltonian parameters 0-100609  
 Si-V<sub>2</sub>O<sub>5</sub>-Al, current-voltage characts., oxide film effects 0-70841  
 TeO<sub>2</sub>-MoO<sub>3</sub>-V<sub>2</sub>O<sub>5</sub>, phase comp. determ. using X-ray diff., electron microscopy and DTA (*German*) 0-88046  
 Ti<sub>2</sub>V<sub>1-x</sub>C<sub>x</sub>, electronic struct. and X-ray emission spectra, cluster MO calc. 0-65444  
 (Ti<sub>1-x</sub>V<sub>x</sub>)<sub>2</sub>O<sub>3</sub>, O<x<0.1, magnetisation and mag. moments 0-65772  
 (Ti<sub>1-x</sub>V<sub>x</sub>)<sub>2</sub>O<sub>3</sub>, spin glass, nonlinear susceptibility and sp. ht. 0-60304  
 (Ti<sub>1-x</sub>V<sub>x</sub>)<sub>2</sub>Se<sub>2</sub>, mag. susceptibility, 4.2-300K 0-60188  
 (Ti<sub>1-x</sub>V<sub>x</sub>)<sub>2</sub>Se<sub>2</sub>, metallic antiferromag. struct., neutron studies 0-65797  
 V complexes, <sup>51</sup>V quadrupole coupling tensors from EPR meas. 0-88866  
 V-Ge, thermophysical props., at elevated temp. 0-103493  
 V-H(D), anelasticity due to long-range diffusion 0-60904  
 V-H(D), hydrogen ordering, review 0-60850

## vanadium compounds continued

- V-H(D), phase diagrams, struct. studies 0-66491  
 V-O, dislocation pinning, impurity interactions, strengthening (*Russian*) 0-92532  
 V-W-O system, phase diagram and thermodynamic props. at high temps., in region W-WO<sub>3</sub>-VO<sub>2</sub>-V<sub>2</sub>O<sub>5</sub> 0-104133  
 VB, nuclear quadrupole parameters 0-103896  
 VBr<sub>2</sub> growth on V due to Br<sub>2</sub> chemisorption 0-101039  
 VC single cryst., Vickers microhardness, slip mechanism 0-71732  
 VCl<sub>3</sub>, electronic struct. and struct. phase transition 0-59644  
 (V<sub>1-x</sub>Cr<sub>x</sub>)<sub>2</sub>O<sub>3</sub>, Raman scatt. and phase transitions 0-71420  
 (V<sub>1-x</sub>Cr<sub>x</sub>)<sub>2</sub>O<sub>3+y</sub>, elec. props. and struct. 0-84494  
 VD<sub>0.68</sub>, anisotropic Compton profiles 0-97368  
 α-VO<sub>2</sub>, vibrations of interstitial D, coherent neutron scatt. 0-96612  
 V<sub>2</sub>, MCD spectra, interpretation rel. to mag. struct. 0-66222  
 V<sub>2</sub>, mag. 'Bragg' scatt. obs. through Raman scatt. 0-66179  
 V<sub>2</sub>, mag. struct., long- and short-range order and Mossbauer spectroscopy 0-65803  
 V<sub>2</sub>, mag. superlattice, neutron oscill. and Weissenberg photography 0-65802  
 V<sub>2</sub>, noncollinear magnetic order and spin wave spectrum in presence of competing exchange interactions 0-65834  
 V<sub>2</sub>, single crystals, growth from vapour phase 0-66410  
 V<sub>2</sub>, spin-dependent Raman scatt. from phonons 0-92724  
 VN, V(CN), VC, particle coarsening reactions in low alloy steels, effect of cold deform. 0-71664  
 VO, investigation of Fermi surface from electron energy spectrum (*Russian*) 0-75496  
 VO<sup>2+</sup> ion impurities, in hydrated crystals, EPR obs. 0-97130  
 VO<sub>1.25</sub>, <sup>51</sup>V NMR studies, microscopic mag. props. 0-108086  
 VO<sub>2</sub>, ferroelastic metal-insulator transition, electronically triggered crystallographic phase transition 0-70614  
 VO<sub>2</sub> film prep. under equil. conditions, struct. and elec. props. 0-108352  
 VO<sub>2</sub>, magnetic susceptibility in insulating and metallic phases, electron-electron and electron-lattice interactions 0-96788  
 VO<sub>2</sub>, metal-insulator transition, electron correls. and spin dimerization, thermodynamic study 0-70615  
 VO<sub>2</sub>, metal-insulator transition and electronic struct., ion bombard. effects 0-92948  
 VO<sub>2</sub>, photoacoustic effect at first order phase transitions at increasing and decreasing temp. 0-70320  
 VO<sub>2</sub> single cryst., noise in presence of current filament 0-92952  
 VO<sub>2</sub> single crystal, elec. switching 0-92946  
 VO<sub>2</sub> thin films, light modulation appls., optical props. at metal-insulator transition 0-87547  
 VO<sub>2</sub>:Al, photoacoustic effect study of phase transitions 0-69615  
 VO<sub>2(n-1)/n</sub>, metal-semicond. transition temps. 0-59876  
 V<sub>2</sub>O<sub>3</sub>, electron-density studies, deform. density at 295K, metal-metal bonds 0-107118  
 V<sub>2</sub>O<sub>3</sub>, film prep. under equil. conditions, struct. and elec. props. 0-108352  
 V<sub>2</sub>O<sub>3</sub>, impurity doping effects, elec. props. obs. 0-75609  
 V<sub>2</sub>O<sub>3</sub>, Raman scatt. and phase transitions 0-71420  
 V<sub>2</sub>O<sub>3</sub>, amorphous film, photochromism and thermochromism 0-93254  
 V<sub>2</sub>O<sub>3</sub>, amorphous layers, gel deposited, semicond. props. 0-92887  
 V<sub>2</sub>O<sub>3</sub>, amorphous semicond., solubility and fibrous texture 0-75162  
 V<sub>2</sub>O<sub>3</sub> and lower oxides, defect structures and related props., review 0-59454  
 V<sub>2</sub>O<sub>3</sub>, core levels, cryst.-field splitting, X-ray emission study 0-66328  
 V<sub>2</sub>O<sub>3</sub>, electron beam induced decomposition, appearance pot. spectroscopy 0-85203  
 V<sub>2</sub>O<sub>3</sub>, electronic, optical, structural and surface props., review 0-88120  
 V<sub>2</sub>O<sub>3</sub>, energy band struct. rel. to expt. studies 0-70603  
 V<sub>2</sub>O<sub>3</sub>, energy band structure, tight-binding method 0-70602  
 V<sub>2</sub>O<sub>3</sub>, fast ion transport and electrochem. storage, Li reactions 0-61324  
 V<sub>2</sub>O<sub>3</sub>, ferroelec. semicond., dielec. and elec. meas. 0-60516  
 V<sub>2</sub>O<sub>3</sub>, reduction in butyllithium, ESR study 0-100611  
 V<sub>2</sub>O<sub>3</sub>, thermally stimulated exoelectron emission (*German*) 0-66404  
 V<sub>2</sub>O<sub>3</sub>, wedge shaped cryst., electron lattice image interpret. 0-103319  
 V<sub>2</sub>O<sub>3</sub>-AlNbO<sub>4</sub>(GaNbO<sub>4</sub>)(TiNb<sub>2</sub>O<sub>7</sub>) systems, interfacial reactions, efficient boundary conditions and solid state reactivity 0-76542  
 V<sub>2</sub>O<sub>3</sub>-As<sub>2</sub>O<sub>3</sub>-RO, R=Ba, Ca, Pb, semicond. glass, electronic props. 0-88557  
 V<sub>2</sub>O<sub>3</sub>-CuO-BaO glass, unpaired electron localisation, ESR study 0-66026  
 V<sub>2</sub>O<sub>3</sub>-P<sub>2</sub>O<sub>5</sub>-Cs<sub>2</sub>O(Na<sub>2</sub>O) glasses, enhanced secondary electron emission yield 0-93441  
 V<sub>2</sub>O<sub>3</sub>-P<sub>2</sub>O<sub>5</sub>-Nb<sub>2</sub>O<sub>5</sub> glasses, switching 0-88604  
 V<sub>2</sub>O<sub>3</sub>-PbO, acoustooptic props. from comp. and density 0-76000  
 V<sub>2</sub>O<sub>3</sub>-V<sub>2</sub>O<sub>4</sub>-BaZnO<sub>2</sub> glass, V ion states, mag. and elec. props. 0-88556  
 V<sub>2</sub>O<sub>3</sub>, film prep. under equil. conditions, struct. and elec. props. 0-108352  
 V<sub>2</sub>O<sub>3</sub>, low-temp. modification, cryst. struct. and valency distrib., importance of very weak reflections 0-92493  
 V<sub>2</sub>O<sub>3</sub>-Ti<sub>2</sub>O<sub>3</sub>, DTA, mag. susceptibility and X-ray diff. study 0-70970  
 V<sub>2</sub>O<sub>3</sub>, defect structures and related props. of V<sub>2</sub>O<sub>3</sub> and lower oxides 0-59454  
 V<sub>2</sub>O<sub>3</sub>, electronic, optical, struct. and surface props., review 0-88120  
 V<sub>2</sub>O<sub>3</sub>, defect structures and related props. of V<sub>2</sub>O<sub>3</sub> and lower oxides 0-59454  
 V<sub>2</sub>O<sub>3</sub>, electronic, optical, struct. and surface props., review 0-88120  
 V<sub>2</sub>O<sub>3</sub>, semicond., IR vibration spectra 0-88997  
 V<sub>2</sub>O<sub>3</sub>, metal-insulator transition, external mag. field effects 0-92819  
 2-VOPO<sub>4</sub>, IR absorpt. spectra, bond freqs. 0-108192  
 (VO)<sub>2</sub>P<sub>2</sub>O<sub>7</sub>, IR absorpt. spectra, bond freqs. 0-108192  
 β-V<sub>2</sub>O<sub>5</sub>·5H<sub>2</sub>O, X-ray cryst. struct. determ. and refinement (*French*) 0-107121  
 VPO<sub>4</sub>, IR absorpt. spectra, bond freqs. 0-108192  
 V<sub>4</sub>(P<sub>2</sub>O<sub>7</sub>)<sub>3</sub>, IR absorpt. spectra, bond freqs. 0-108192  
 V<sub>2</sub>S<sub>5</sub>, amorphous, electrochemistry in Li cells 0-76626  
 V<sub>2</sub>S<sub>4</sub>, itinerant antiferromag. spin fluctuations, NMR studies 0-93198  
 V<sub>2</sub>S<sub>5</sub>, itinerant antiferromag. spin fluctuations, NMR studies 0-93198  
 V<sub>2</sub>S<sub>5</sub>:Fe, Mossbauer and mag. studies, electronic state of Fe 0-108130  
 VSe<sub>2</sub> (1T), incommensurate periodic lattice distortion, X-ray diffraction study 0-107414  
 VSe<sub>2</sub>, fast ion transport and electrochem. storage, Li reactions 0-61324  
 V<sub>2</sub>Se<sub>4</sub>, itinerant antiferromag. spin fluctuations, NMR study 0-75874  
 V<sub>2</sub>Se<sub>5</sub>, itinerant antiferromag. spin fluctuations, NMR study 0-75874  
 VSe<sub>2-x</sub>S<sub>x</sub> (0<x<2) solid solutions, characterisation 0-88730  
 V<sub>2</sub>Si, mixed state, hysteresis in elastic characteristics (*Russian*) 0-103799  
 VTe, mag. and elec. transport props. 0-92897



**vanadium compounds continued**

- WV<sub>2</sub>O<sub>6</sub>, magnetic susceptibility, behaviour in terms of quasi-isolated binuclear units 0-97073  
 $\alpha$ -W<sub>2</sub>V<sub>2</sub>O<sub>8</sub>, paramag. defect study by ESR 0-103881

**vanadium phosphate semiconductor glasses** *see amorphous semiconductors vapourisation*

- see also boiling; evaporation; heat of vaporisation; sublimation*  
 binary liquid mixture, US evaluation of excess energy of vaporisation 0-65209  
 compound conductors, impulse heating, Cu vapour conc. determ. 0-75346  
 fluoride-opacified glass melt, time depend. of volatilisation losses 0-70381  
 Freon-113, correlation properties near phase-separation boundary, gravitational field effect 0-107410  
 laser vaporisation of metals for prod. of low energy metal neutral beams 0-77910  
 liquid scintillation wastings, vaporisation apparatus (*Japanese*) 0-63502  
 metal film vaporisation by laser, vaporisation front relativistic velocities (*Russian*) 0-66337  
 pentane-benzene solution, vapour-liquid equilibrium study, vaporisation critical state (*Russian*) 0-79931  
 superheated liquid discharge from nozzle, pressure calc. 0-92199  
 water, vaporisation and thermoelastic press. due to CO<sub>2</sub> laser pulse 0-84227  
 Al fracture speed during phase explosion due to electron beam irradiation (*Russian*) 0-76336  
 Al, rhodamine 6G laser radiation interaction 0-97387  
 3.5Al<sub>2</sub>O<sub>3</sub>·2SiO<sub>2</sub>, mullite, decomposition by SiO<sub>2</sub> volatilisation 0-61082  
 CdS single cryst., vaporization and form. of negative whiskers 0-92659  
 Cr, volt ampere characteristics during electron melting process (*Russian*) 0-75336  
 Cu fracture speed during phase explosion due to electron beam irradiation (*Russian*) 0-76336  
 KD<sub>3</sub>PO<sub>4</sub>, transparent dielec., thermal analysis of laser-induced damage 0-66336  
 K<sub>2</sub>Mo<sub>2</sub>O<sub>10</sub> melt volatility, solubility of YAl<sub>3</sub>(BO<sub>3</sub>)<sub>4</sub> 0-65211  
 Mo, volt ampere characteristics during electron melting process (*Russian*) 0-75336  
 Na<sub>2</sub>O-B<sub>2</sub>O<sub>3</sub>-GeO<sub>2</sub> glass-forming melts, thermodynamic props. and vaporisation processes, mass spectrometric study 0-79926  
 Nb, volt ampere characteristics during electron melting process (*Russian*) 0-75336  
 Ni-Si melt refining by electric fields, ionic conduction of Ni, Si (*Russian*) 0-65273  
 Ni-V, solid soln., diffusion and thermodynamic props. 0-65278  
 ScP, thermodynamics and high temp. vaporisation 0-88310  
 UO<sub>2</sub> volatilization pot. of metallic inclusions in irradiated nuclear fuel during LOF overheating transients 0-57895  
 V, volt ampere characteristics during electron melting process (*Russian*) 0-75336  
 W, volt ampere characteristics during electron melting process (*Russian*) 0-75336

**vaporising** *see vaporisation***vapour density** *see density of gases***vapour deposited coatings**

- see also CVD coatings; plasma deposited coatings; sputtered coatings; vacuum deposited coatings*  
 ceramics, glazing with gaseous P<sub>2</sub>O<sub>5</sub> 0-108609  
 3,4-dimethyl-1,2,5-thiadiazol plasma polymerised film for holographic recording 0-106490  
 diphenyl anion salts, sublimed layer, electronic and IR absorpt. spectra 0-66189  
 film, evaporated at oblique incidence, columnar grains inclination angle 0-75468  
 metastable phases, convergent beam electron microscopy obs. 0-108689  
 pentacene, disordered solid layer, absorpt. spectra 0-93417  
 screen printing, in solar cell metallisation 0-85291  
 tetracene, disordered solid layer, absorpt. spectra 0-93417  
 Al, film and polished bulk specimens, initial stages of oxidation obs. using SIMS 0-81239  
 Al thin films evaporated on rough quartz substrates, surface irregularity, light scattering measurements (*Polish*) 0-88450  
 Al-Cu (0.5 wt.%), evaporated layers, electromigration, linewidth depend. 0-65277  
 As<sub>2</sub>S<sub>3</sub> and As<sub>2</sub>S<sub>4</sub>, valence states, thermal and photo-induced changes UPS study 0-93459  
 C films with high conductivity, prep. and props. 0-80983  
 CaF<sub>2</sub>, Na-resistant glass cell, coating apparatus 0-90874  
 CdSe thin film transistor on Cr substrate, cryst. struct., substrate defect effects 0-70563  
 Cu on Mo and steel, substrate limiting temp. during vaporisation and condensation coating in vacuum (*Russian*) 0-100787  
 CuInS<sub>2</sub> single phase thin film prep. by flash evaporation 0-100796  
 Fe-Cr-Mo and Fe-Cr-Mo-Si alloys, amorphous films, corrosion resist. and ion plating use 0-89423  
 Fe<sub>3</sub>Ni<sub>36</sub>Cr<sub>14</sub>P<sub>12</sub>B<sub>6</sub>, Metglas amorphous films, corrosion resist. and ion plating use 0-89423  
 Ge film, amorphous, prepared by evap. or sputtering, AC loss meas. 0-65560  
 Hg lamps, RF-excited, dark film anal. 0-92789  
 In-In<sub>2</sub>O<sub>3</sub>-Pb, Josephson tunnel junction fabrication for MM-wave detector 0-100427  
 In<sub>1-x</sub>Ga<sub>x</sub>Sb films, elec. props., preparation 0-100473  
 In<sub>2</sub>O<sub>3</sub> films, activated reactive evaporation technique of prep. 0-80989  
 In<sub>2</sub>O<sub>3</sub>-Sn, films, activated reactive evaporation technique of prep. 0-80989  
 MnBi film, electrical props., in situ annealing effect 0-65708  
 Nb layer, ion bombarded, supercond. props. and struct. 0-88671  
 Ni film, evaporated, chemisorpt. of CO, ellipsometric investig. (*German*) 0-61156  
 Pb-PbO-Pb, Josephson tunnel junction fabrication for MM-wave detector 0-100427  
 PbIn films strengthening, by preventing formation of misfit dislocations 0-84858  
 PbO layer vapour deposition, structure, and props. 0-65408  
 Pb<sub>0.8</sub>Sn<sub>0.2</sub>Te:La, evaporated thin films, low carrier conc. 0-65414  
 Pd-Si, amorphous thin films, laser irradiation, metastable phases 0-96622  
 Pt-Si, amorphous thin films, laser irradiation, metastable phases 0-96622  
 RbAg<sub>4</sub>I film, thermopower meas. temp. depend., correl. effects role 0-107539  
 Se, amorphous films, evaporated, ageing and crystn., DTA 0-65413

**vapour deposited coatings continued**

- Se, thin film selective absorber coatings, prod. using an oblique vacuum deposition technique 0-81488  
 Si large grain films on metallurgical Si substrates, chem., struct., elect. and photovoltaic props. 0-61357  
 Te, thin film selective absorber coatings, prod. using an oblique vacuum deposition technique 0-81488  
 Y<sub>2</sub>O<sub>3</sub>, in MIM struct., electroforming props. 0-65705  
 Zn<sub>1-x</sub>Cd<sub>x</sub>-S, thin solid soln. films, vapour deposited, elec. and optical characteristics 0-60110

**vapour deposited thin films** *see vapour deposited coatings***vapour deposition**

- see also chemical vapour deposition; crystal growth from vapour; electron beam deposition; ion plating; plasma deposition; sputtering; vacuum deposition*  
 alkali-halide crystals, two-dimens. nucleation and hole nucleation, mol. beam method (*German*) 0-93499  
 composite material, B-Ti, for loudspeaker's diaphragm (*Japanese*) 0-58883  
 diffusion barrier layer evaporation, improved Cr-Zr source 0-76163  
 GaAs solar cells, thin film growth tech. and characterisation 0-89631  
 glass optical fibre, vapour phase materials and processes, review 0-58825  
 high-rate vapour quenching techniques and use in amorphous phase prep. 0-80977  
 metallic thin films, deposition by organometallic cpd. decomp. 0-71599  
 molecule desorption and surface diffusion from critical deposition rate 0-92786  
 optical fibre cable made by vapour phase axial deposition, characts. (*Japanese*) 0-58691  
 optical fibre fabrication, OH-free 0-99887  
 optical fibre preparation methods and performance factors 0-69557  
 optical fibre with ultra wide bandwidth, fabrication by vapour axial deposition method 0-69508  
 optical fibres, 30.4 km graded index vapour-phase axial deposited fibre, props. 0-64149  
 optical fibres, single-mode, fabrication by VAD 0-83687  
 optical fibres, ultimately low OH content achievement, by optimised dehydration 0-99845  
 optical fibres manufactured by MCVD and VAD for transmission system (*Japanese*) 0-58692  
 review of basic technique, chemistry, materials and applications (*Italian*) 0-89153  
 Al, coating prod. by thermal decomp. of Al alkyls 0-104076  
 Au-Si<sub>3</sub>N<sub>4</sub> amorphous alloy, crystallisation, elec. cond. study 0-103246  
 B<sub>2</sub>O<sub>3</sub>-SiO<sub>2</sub>, optical waveguide glass, sintering kinetics 0-84898  
 CaF<sub>2</sub> on glass, Na-resistant cell, coating apparatus 0-90874  
 CdS thin films, growth and evaluation for fabrication of high performance photovoltaic solar cells 0-93501  
 CdZnS thin films, growth and evaluation for fabrication of high performance photovoltaic solar cells 0-93501  
 Co, particle formation by evap., electron microscopy obs. of interaction processes 0-104053  
 Cu alloy, precipitation strengthened compositions with oxide particles, condensed, struct. criteria and thin layer possibilities (*Russian*) 0-89236  
 CuInS<sub>2</sub> single phase thin film prep. by flash evaporation 0-100796  
 Cu<sub>2</sub>S-CdS solar cells, Cu<sub>2</sub>S growth kinetics and composition analysis by absorbance transient and galvanic electrochemical measurements 0-92797  
 Fe, particle formation by evap., electron microscopy obs. of interaction processes 0-104053  
 In<sub>2</sub>O<sub>3</sub>, pure and Sn-doped, prep. by activated reactive evaporation, and characterisation 0-80989  
 InP solar cells, thin film growth tech. and characterisation 0-89631  
 KCl, two-dimens. nucleation rate on the (100) surfaces, mol. beam method, 289-343°C (*German*) 0-93500  
 Na vapour deposition rates and gas flow patterns in LMFBR 0-68732  
 Ni alloy, precipitation strengthened compositions with oxide particles, condensed, struct. criteria and thin layer possibilities (*Russian*) 0-89236  
 Ni, particle formation by evap., electron microscopy obs. of interaction processes 0-104053

**vapour-liquid transformations** *see liquid-vapour transformations***vapour phase epitaxial growth**

- see also molecular beam epitaxial growth*  
 epitaxial films, condensed from vapour or molecular ion beams, impurity distrib. 0-65032  
 n-hexatriacontane film, vacuum deposited on alkali halide crystals, structure and heat treatment 0-103600  
 II-VI semiconductors, thin epitaxial layer, direct synthesis (*German*) 0-104070  
 III-V semiconductor, superlattices and related structures (*Slovak*) 0-88620  
 III-V semiconductors prep. (*Czech*) 0-89131  
 naphthalene crystal nucleation on anthracene microcrystals suspended in vapour-gas stream 0-76165  
 narrow-band semiconductor, growth of epitaxial layers, activation by UV and IR radiation 0-71598  
 semiconductor film growth, multilayer systems, spectroscopic ellipsometry, review 0-103603  
 Si epitaxy, vapour phase deposition technology 0-75472  
 Ag film, on Pd, AES and LEED obs. of growth modes and substrate influences (*French*) 0-84408  
 (AlGa)As laser system, VPE growth and degradation mechanism 0-99748  
 Al<sub>0.5</sub>Ga<sub>0.5</sub>-As/Al<sub>0.5</sub>Ga<sub>0.5</sub>-As DH lasers grown by metalorganic CVD, CW operation in wavelength range 760-780 nm 0-64053  
 AuMn alloy, ordered, vacuum deposited epitaxial films, orientation control by external stress 0-100426  
 Ba<sub>2</sub>Sr<sub>1-x</sub>TiO<sub>3</sub>, ferroelec. film, heteroepitaxial growth in cathode sputtering 0-93486  
 (Cd,Hg)Te epitaxial structures, comp. profile depend. on deposition parameters 0-100795  
 Cd chalcogenides, thin films, VPE, needle-like cryst. growth 0-80148  
 CdS, epitaxial growth and nucleation, on monocryst. ZnS, substrate real struct. influence 0-88455  
 CdS/InP epitaxial thin films on NaCl, HEED and TEM study 0-88446  
 CdS-InP(CdTe)(GaAs)(Ge), solar cell heterojunctions, CVD fabrication, photovoltaic response 0-93878  
 CdSe(Te) films, oriented, epitaxial growth by epitaxial nucleation in sub-microscopic holes method 0-59834

## vapour phase epitaxial growth continued

- CdTe thin films, oriented, VPE growth, infrared transmission, photovoltaic cells 0-59825
- CdTe-CdS heterojunctions, growth by closed-tube chem. transport, elec. props. 0-60070
- Cs, VPE on W emitter, FEM obs. 0-70552
- CuAu alloy, ordered, vacuum deposited epitaxial films, orientation control by external stress 0-100426
- CuIn<sub>0.7</sub>Ga<sub>0.3</sub>Se, epitaxial layers, on GaAs substrates, struct. and elec. props. 0-107670
- CuInSe<sub>2</sub>, heteroepitaxy on {111} oriented Ge by flash evaporation, struct. 0-108333
- CuInTe, epitaxial layers, on GaAs, growth and props. 0-108359
- EuSe, VPE by hot-wall technique 0-80958
- Fe, epitaxial growth on Au platelets, dislocations 0-96760
- $\gamma$ -Fe, FCC film, epitaxial growth on CuAu (111) surfaces, strong ferro-magnetism 0-70557
- GaAlAs on GaAs thin film stacked multiple-bandgap solar cell structs., prep. using CVD techniques 0-94083
- GaAlAs-GaAs lasers, channelled substrate, prepared by combination of organometallic pyrolysis and LPE 0-99745
- Ga<sub>1-x</sub>Al<sub>x</sub>As based layer structures, optimum growth conditions, comp. and struct. perfection 0-104069
- Ga<sub>1-x</sub>Al<sub>x</sub>As-GaAs DH injection lasers grown by metalorganic CVD, props. 0-99751
- GaAs antireflecting MOS solar cells, epitaxial and polycryst. using OM-CVD techniques 0-94072
- GaAs compensated VPE thin film, electron Hall mobilities 0-107932
- GaAs epitaxial growth, CVD-organometallics method, reactional efficiency in solar cell elaboration 0-93498
- GaAs, epitaxial layers, electron irradi. deep level trap energy depend. 0-80205
- GaAs, epitaxy by metallorganic and chloride depositions, defect characterisation at growth interface 0-59817
- GaAs films for solar cells appl., deposition and characterisation 0-84853
- GaAs, gas-phase epitaxy, step stopping centre form. kinetics 0-65407
- GaAs, homoepitaxy and epitaxy, surface anal. during growth using RHEED and Auger spectroscopy 0-66433
- GaAs on Ge thin film stacked multiple-bandgap solar cell structs., prep. using CVD techniques 0-94083
- GaAs optical waveguides, oxide confined, formed by lateral epitaxial growth 0-58815
- GaAs type FET with buffer, bias effects due to deep centres in struct. (French) 0-107917
- GaAs, VPE thin layers, thickness uniformity, main factor anal. 0-76197
- GaAs-GaAlAs superlattices, metallorganic VPE growth, in sites ellipsometry monitoring 0-70547
- GaAs<sub>1-x</sub>Sb<sub>x</sub>, organometallic VPE growth using trimethylantimony 0-60788
- Ga<sub>1-x</sub>In<sub>x</sub>As epitaxial layer growth by organometallic pyrolysis, homojunction LED prep. 0-76194
- Ga<sub>1-x</sub>In<sub>x</sub>As, organometallic VPE growth using trimethylarsenic 0-60788
- Ga<sub>0.9</sub>In<sub>0.1</sub>As, P<sub>1-x</sub>In<sub>x</sub> DH laser emitting at 1.15 micron grown by low-pressure CVD 0-64052
- GaN, growth rate influence on elec. and luminesc. props. 0-100702
- GaN, initial growth, on Al<sub>2</sub>O<sub>3</sub> and spinel (German) 0-107664
- GaP, layer structures for LED's, SEM, and TEM obs. of dislocation density reduction expt. 0-100425
- GaP-Si, heteroepitaxial growth, electronic and optical props. 0-104075
- Ge epitaxial film, vac. deposited on GaAs, doping effect of annealed GaAs surface 0-65718
- Ge, epitaxial growth of very thin electron microscopy specimens 0-100793
- InGaAs-InP punch-through type photodetector fabricated by VPE 0-68253
- InGaAsP, epitaxial growth by chloride CVD process, thermodynamic anal. 0-64936
- (InGa)(AsP) laser system, VPE growth using metal organic sources or halide transports 0-99748
- InGaP-P-InP CW lasers, 1.5-1.7  $\mu$ m, VPE 0-78861
- InGaP/InGaAs struct. for transferred electron photocathodes, VPE growth and characterisation 0-76193
- InP, epitaxial, kinetics of VPE 0-60790
- InP films, organometallic VPE grown, props. 0-96753
- InP, VPE growth for MESFET's 0-103602
- Mo, film on sapphire substrate, orientational growth, epitaxial textures, nucleation textures (Russian) 0-75454
- Nb, film, epitaxy, struct. and supercond. props., on (001) surface of fluo-rophlogopite (Russian) 0-80101
- Nb, film on sapphire substrate, orientational growth, epitaxial textures, nucleation textures (Russian) 0-75454
- Nb<sub>3</sub>Al film, electron-beam coevaporated, prep. and characts. 0-76187
- PLZT ferroelectric thin films, epitaxial growth and optical props. 0-70543
- Pb film, monocryst., heteroepitaxial growth, struct. defects, and elec. props. (Russian) 0-84403
- Pb<sub>0.8</sub>Sn<sub>0.2</sub>Te:La, evaporated thin films, low carrier conc. 0-65414
- Pb<sub>1-x</sub>Sn<sub>x</sub>Te,  $x=0.2$ , monocrystal, photoelectric props. of p-n structures (Russian) 0-70808
- PbTe, nonstoichiometric, evap. and growth of epitaxial layers 0-104072
- PbTe-Pb<sub>1-x</sub>Sn<sub>x</sub>Te n-p<sup>+</sup> heterojunction photodetector, hot wall evaporation technique 0-65673
- Si, deposition on rotating disc, one-dimens. model 0-75461
- Si epitaxial films on Czochralski sapphire, optimisation of deposition conditions in SiH<sub>4</sub>-H<sub>2</sub> system 0-75464
- Si, epitaxial growth on sapphire by partially ionised vapour deposition, RHEED-AES obs. 0-80985
- Si, epitaxial layer deposition by ion beam methods 0-100417
- Si-epitaxial film, ionised-cluster-beam deposited, cryst. and elec. characts. 0-70553
- SiC (6H), blue-emitting diodes by CVD 0-97439
- $\alpha$ -SiC crystals, broad-band semiconductors, growth in Acheson furnace 0-84841
- SiC epitaxial layers, growth techniques 0-108360
- SiC p-n junction, epitaxial, grown by sublimation, elec. and struct. props. (Chinese) 0-60067
- Ta, film on sapphire substrate, orientational growth, epitaxial textures, nucleation textures (Russian) 0-75454
- V, film on sapphire substrate, orientational growth, epitaxial textures, nucleation textures (Russian) 0-75454
- VBr<sub>2</sub> growth on V due to Br<sub>2</sub> chemisorption 0-101039
- vapour phase epitaxial growth continued**
- W, film on sapphire substrate, orientational growth, epitaxial textures, nucleation textures (Russian) 0-75454
- Zn chalcogenides, thin films, VPE, needle-like cryst. growth 0-80148
- ZnO, CVD of epitaxial films on sapphire, SAW interdigital transducer fabrication 0-66430
- ZnS<sub>0.9</sub>Se<sub>0.1</sub> VPE on CaF<sub>2</sub> substrate, in flowing H<sub>2</sub>, growth and characterisation (French) 0-107678
- vapour pressure**
- see also humidity; vaporisation
- Bo<sub>2</sub>-BO<sub>2</sub> 0-65252
- dielectric gases and gas mixtures, maximum electric strength and vapour pressure relationships 0-92249
- n-heptane/3-pentanone mixture, vap. press. meas., thermodynamic functions calcs. 0-75345
- n-hexane/3-pentanone(acetone) mixtures, vap. press. meas., thermodynamic functions calcs. 0-75345
- isotope effects, bibliography 0-77558
- prediction, using equation of state 0-103443
- pure substances, vapour-press. curves, conic section representation 0-92658
- salinity gradient power utilising vapour pressure differences in water 0-76652
- TCNQ, enthalpy of sublimation and vapour press. meas. 0-92661
- TTF, enthalpy of sublimation and vapour press. meas. 0-92661
- TTF-TCNQ, enthalpy of sublimation and vapour press. meas. 0-92661
- vacuum system construction material selection and degassing 0-82783
- Al<sub>4</sub>C<sub>3</sub>, vapors, thermodynamics, 1321-1607K 0-66859
- Ar, solid, high-temp. thermal expansion characts. 0-59680
- Cr-SiO<sub>2</sub>-Al<sub>2</sub>O<sub>3</sub> system interactions, getter development for radiocaesium 0-83208
- Cs<sub>2</sub>CrO<sub>4</sub>, mol. beam obs. of evap., saturated vapour press., 656.8 to 1151K 0-107411
- DyCl<sub>3</sub>, vapour press. and sublimation thermodynamics, mass loss effusion meas. 0-88313
- Fe-Zn, homogeneous phases, Gibbs free energies of form., Knudsen effusion method 0-66481
- GdCl<sub>3</sub>, vapour press. and sublimation thermodynamics, mass loss effusion meas. 0-88313
- H<sub>2</sub>SO<sub>4</sub>, tropospheric or stratospheric gas-particle conversion 0-94560
- <sup>4</sup>He film growth on graphite, MgO, and Mylar substrates, vap. press. meas. 0-70499
- <sup>4</sup>He layered films on ZYX graphite, thermal resist. below 2K 0-70500
- In<sub>2</sub>Se<sub>3</sub>, vapour press. temp. depend., heat of evap. and form. 0-59642
- Kr, solid, high-temp. thermal expansion characts. 0-59680
- La<sub>2</sub>S<sub>3</sub>, unsaturated and saturated vapour press., 673-1173K, thermal dissociation 0-104457
- Na<sub>2</sub>O-B<sub>2</sub>O<sub>3</sub>-GeO<sub>2</sub> system glass-forming melts, mass spectrometry obs. of thermodynamic props. 0-97468
- Na<sub>2</sub>O-B<sub>2</sub>O<sub>3</sub>-GeO<sub>2</sub> vitreous melts, thermodynamic props. from mass spectra 0-65253
- Ne-H<sub>2</sub> liq. mixtures, phase equilib. effects, thermodynamic perturb. theory (Russian) 0-92663
- PbIn<sub>2</sub>S<sub>4</sub>, computer-automated meas. by simultaneous Knudsen torsion-effusion method 0-73334
- Si-Te system, phase diagrams 0-89209
- SnSe<sub>2</sub>, sublimation, temp. depend. of equilib. constants 0-88312
- SrF<sub>2</sub>, vaporisation and sublimation thermodynamics (German) 0-81355
- TbCl<sub>3</sub>, vapour press. and sublimation thermodynamics, mass loss effusion meas. 0-88313
- U(C,N), N vapour pressures and thermodynamic props. 0-84918
- UF<sub>4</sub>, vaporisation behaviour 0-84283
- UN, N vapour pressures and thermodynamic props. 0-84918
- vapour pressure measurement**
- computer-automated meas. by simultaneous Knudsen torsion-effusion method 0-73334
- pyridine N-oxide, in benzene, dipolar assoc. investig. 0-107035
- unsaturated two-component associated vapour, press., comp., thermodynamic calcs. (Russian) 0-64671
- water vapour sensor of P<sub>2</sub>O<sub>5</sub> type 0-98907
- He vapour pressure scale determ. using paramag. salt thermometer and NPL-75 gas thermometer scale 0-95060
- <sup>3</sup>He, high precision, capacitive gauge for use up to 0.3K 0-68207
- vapour-solid transformations** see solid-vapour transformations
- variables**
- No entries
- variable stars**
- see also eclipsing binary stars
- HR 1099, RS Canum Venaticorum type binary, light and colour curve meas. 0-73004
- 2A 0311-227 optical counterpart, binary star, light curve Fourier anal. 0-82549
- 2A 0311-227 optical counterpart, high speed photometry 0-82547
- 2A 0311-227 optical counterpart, simultaneous photometric and spectroscopic obs. 0-90572
- 2A 0526-328 optical counterpart, spectroscopic obs. 0-77515
- A 0538-66, X-ray burster position and optical candidate in LMC 0-73076
- $\alpha$  Andromedae, Be star, spectroscopic evidence for new shell episode 0-90444
- CG Andromedae, Si binary star, spectrum variable, short period radial vel. variability determ. 0-72968
- BM Andromedae, spectroscopic and photometric obs. of T Tauri-type star 0-62130
- Z Andromedae, symbiotic star, IUE obs. of UV spectrum 0-109450
- EG Andromedae (HD 4174), symbiotic star, spectroscopic obs. 0-85945
- AE Aquarii, cataclysmic variable, IUE satellite UV obs. 0-72985
- CY Aquarii, RR type star, BV photometric obs. (Italian) 0-90449
- R Aquarii, symbiotic long-period variable, spectrum of assoc. nebulosity 0-90450
- R Aquarii, symbiotic star, radio mol. maser line obs. 0-72960
- R Aquarii, UV, visible and 85 GHz continuum obs. 0-85946
- R Aquarii (M7+pec), late type variable star, IUE obs. of circumstellar emission 0-82370
- Aquila X-1 (4U 1908+00), optical outburst obs. 0-67909
- $\eta$  Aquilae, Cepheid variable, absolute energy distrib. in radiation spectrum (Russian) 0-72974
- $\eta$  Aquilae, classical Cepheid, companion star detect. and distance determ. 0-90443
- T Aquilae (Nova 1891), spectrophotometry of shell 0-72955



## variable stars continued

- V603 Aquilae (Nova 1918), IUE obs. of periodic light vars. 0-105251  
 V603 Aquilae (Nova 1918), old nova, eclipses obs. 0-90476  
 V603 Aquilae (Nova 1918), periodic light vars. detect. 0-82391  
 V1301 Aquilae (Nova Aquilae 1975), dust grain IR emission model 0-105254  
 TT Arietis, nova-like cataclysmic variable, photoelectric photometry 0-82382  
 59 Aurigae,  $\delta$  Scuti star, light curves periodogram anal. 0-62141  
 KR Aurigae, brightness history from 1890 AD 0-105245  
 $\epsilon$  Aurigae, dual aspect of wavelength depend. fluctuations 0-62190  
 AR Aurigae, eclipsing binary Hg star, peculiar spectral var. during eclipse 0-98679  
 RW Aurigae, T Tauri star, far UV spectra, emission measure obs. 0-94788  
 KR Aurigae, X-ray source nearby, X-ray, IR and visible obs. 0-67742  
 T Aurigae (Nova 1891), old nova, photometric and spectroscopic obs. 0-90446  
 SS Aurigae star fields, comparison star sequences, photometry obs. 0-82433  
 BDS 1269 A, metal-poor  $\delta$  Scuti star, pulsation periods from b-band photometry 0-105247  
 53 Camelopardalis, Ap star, Ca II K and H $\delta$  lines rapid vars. (Russian) 0-90458  
 Z Camelopardalis, dwarf nova, spectrophotometry at standstill and in eruption 0-82366  
 XX Camelopardalis, R Coronae Borealis star, photometry in optical and IR ranges 0-101601  
 AX Camelopardalis (53 Camelopardalis), Ap star, UVB photoelectric photometry and period of var. (Italian) 0-90448  
 BT Cancri (38 Cancri),  $\delta$  Scuti star, multiple periods rel. to radial and nonradial pulsation periods 0-85948  
 38 Cancri in Praesepe cluster,  $\delta$  Scuti variable, pulsation anal. from light curves 0-77419  
 VY Canis Majors, late supergiants to maser star, radial vel. determ. 0-77410  
 $\beta$  Canis Majoris,  $\beta$  Cephei star, Fourier anal. of radial vel. changes 0-105246  
 VY Canis Majoris, irregular supergiant, OH maser source, UHF spectra obs. 0-90550  
 TX Canum Venaticorum, cataclysmic variable, P Cygni type, visible spectral obs. 0-105249  
 RS Canum Venaticorum, out of eclipse light var. and comparison with similar stars 0-109489  
 RS Canum Venaticorum stars, H $\alpha$  line variability, visible spectra obs. 0-105277  
 VY Carinae, Cepheid, luminosity and membership of assoc., visible obs. 0-94797  
 I Carinae, Cepheid variable, Fourier anal. of light var. 0-90442  
 I Carinae, search for comparison stars, uvby $\beta$  photometry, colour excess 0-62136  
 $\gamma$  Cassiopeiae, Be star, rapid linear polarisation variability (Russian) 0-77417  
 SU Cassiopeiae, Cepheid variable, spectrophotometric determ. of effective temp. 0-90435  
 VX Cassiopeiae, early-type irregular variable, photometric variability (Russian) 0-72973  
 AB Cassiopeiae, eclipsing binary with  $\delta$  Scuti primary, light vars. preliminary anal. 0-94831  
 $\gamma$  Cassiopeiae, IUE obs. of Be-star 0-82383  
 UV Cassiopeiae, R Coronae Borealis star, photometry in optical and IR ranges 0-101601  
 cataclysmic binaries, circumstellar material geometrical and photometric parameters 0-109492  
 cataclysmic binaries, role of white dwarf component 0-82356  
 cataclysmic binary stars (CBS), critique of polarimetric evidence on physical parameters and orbital inclination 0-109486  
 cataclysmic variables, period change due to mass transfer 0-82425  
 cataclysmic variables, XUV emission (German) 0-109372  
 cataclysmic variables in globular clusters, preliminary report 0-109505  
 $\mu$  Centauri (B2 IVe), new circumstellar shell development, spectroscopic obs. (1980 June 10 to 12) 0-94808  
 V810 Centauri (HD 101947), yellow variable supergiant near Cepheid instability strip, VBLUW photometry 0-98672  
 EM Cephei, UVB, photometry rel. to constancy or variability of period 0-105286  
 $\beta$  Cephei instability strip, effects of stellar mass loss 0-90436  
 $\beta$  Cephei stars, line profile variables, pulsational modes 0-85951  
 $\beta$  Cephei stars, pulsation effect on period-luminosity relation 0-72970  
 $\beta$  Cephei stars, pulsations and evolutionary status 0-85959  
 Cepheid binary detection from U-V curve obs. 0-98667  
 Cepheid instability strip, lower part, search for photometric variability in evolved Am stars 0-62145  
 Cepheid variables, incidence of duplicity 0-90453  
 Cepheid variables, long-period, absence from Galaxy rel. to obs. of yellow variable supergiants 0-98672  
 Cepheid variables determ. of colour term in period-luminosity colour relation 0-94812  
 Cepheids, double mode, in N.hemisphere, search using new UVB photometry 0-94814  
 Cepheids, double mode pulsation, iterative treatment 0-82369  
 Cepheids, membership in open clusters from star and cluster age determ. (Italian) 0-90489  
 dwarf Cepheids, period changes 0-62142  
 Cepheids, period-luminosity-colour relation, numerical simulations 0-82393  
 Cepheids, stellar pulsation problem, time dependent convection local theories 0-72964  
 multimode Cepheids, two zone rel. to classical models 0-72967  
 Cepheids, ultrashort period, classification from photometric and astrometric data 0-62135  
 sinusoidal Cepheids in LMC, first overtone pulsations, photometry obs. 0-77422  
 Cepheids in M31, use in determ. of S4 spiral arm struct. (Russian) 0-82515  
 Cepheids in M31 (Andromeda galaxy), assoc. with interstellar gas and star complexes (Russian) 0-90455  
 Cepheids with He enriched inhomogeneous outer layers, three mode reson. 0-101600  
 $\delta$  Ceti,  $\beta$  Canis Majoris variable, period meas. and detect. of period decrease 0-105257

## variable stars continued

- $\delta$  Ceti,  $\beta$  Cephei variable, spectroscopic binary, radial vels. and period var. 0-82376  
 $\circ$  Ceti (Mira) at 1978 max., visible spectropolarimetry 0-94799  
 ZZ Ceti stars, constraints on possible long-term variability 0-90428  
 UV Ceti stars, photometric features near flare initial phase 0-105252  
 ZZ Ceti white dwarfs, non-radial oscils. theory 0-82356  
 RS Chamaeleontis,  $\delta$  Scuti variable and eclipsing binary, four-colour photometry 0-67783  
 Z Chamaeleontis, eruptive binary, model from photoelectric data anal. 0-72961  
 Z Chamaeleontis, gravitational waves from eclipsing cataclysmic binary 0-90439  
 Circinus X-1, changes in optical, IR and radio emission 0-67910  
 17 Comae A, Ap star, mag. field meas. and rot. period (Russian) 0-90457  
 R, S, T Coronae Austrinae, T Tauri stars, long period vars. 0-82350  
 $\beta$  Coronae Borealis, Ap star, Ca II K and H $\delta$  lines rapid vars. (Russian) 0-90458  
 R Coronae Borealis, UBVRHKLMN photometry, interpretation 0-67756  
 R Coronae Borealis type variables and related objects, UVB photometric obs. 0-90437  
 CPD -62° 1837 (HDE 308122), long-period variable member of triple 0-105260  
 BI Crucis, new symbiotic star, spectrum 0-109442  
 CSV 6110 in Taurus,  $\circ$  Ceti type variable, visible obs. 0-67745  
 $\chi$  Cygni, diameter of Mira-type star from speckle interferometry 0-67728  
 XX Cygni, dwarf Cepheid, composition and motion, visible photometric and spectrographic obs. 0-77424  
 SS Cygni, dwarf nova, rapid optical oscils. phase variability 0-85947  
 P Cygni, H Paschen  $\alpha$  obs. 0-62156  
 59+V832 Cygni, IR emission increase, spectrum scanner obs. 0-94809  
 V1016 Cygni, near-IR spectrographic obs. 0-94810  
 R Cygni, S-type star, Keenan band identification problem, IR obs. 0-72946  
 SS Cygni, spectroscopic binary variable, X-ray source, orbital element determ. 0-105288  
 CH Cygni, symbiotic star, 1977 outburst, radial vel. and atm. struct. determ. 0-72969  
 CH Cygni, symbiotic star, binary model 0-62158  
 V1016 Cygni, symbiotic star, IR-variability obs. from VJHKL photometry (Russian) 0-105263  
 V645 Cygni (AFGL 2789), Ae star, perplexing spectrum 0-73066  
 V1357 Cygni (Cygnus X-1), critique of polarimetric evidence on physical parameters and orbital inclination 0-109486  
 V1357 Cygni (Cygnus X-1), optical light curve vars. rel. to X-ray vars. 0-109560  
 V1357 Cygni (Cygnus X-1), optical photometry (1980 May 25 to July 7) 0-90578  
 V645 Cygni (GL 2798), IR and EHF spectroscopy 0-72956  
 V1329 Cygni (HBV 4175), symbiotic variable, photometric and spectroscopic history 0-62148  
 V1500 Cygni (Nova 1975), Balmer line emission profiles evolution in early decline phase 0-82371  
 V1500 Cygni (Nova 1975), emission line vars. rel. to struct. of central object 0-82367  
 V1500 Cygni (Nova 1975), luminosity and distance, light curve obs. 0-72981  
 V1500 Cygni (Nova 1975), radio obs. and analysis 0-67726  
 V1668 Cygni (Nova 1978), multifilter photometry and polarimetry 0-90454  
 V1668 Cygni (Nova 1978), optical light curve, uvby photometry 0-62154  
 V1668 Cygni (Nova 1978), spectroscopic and photometric obs., (1978 to 1979) (Russian) 0-109444  
 V1668 Cygni (Nova Cygni 1978), post-max. short period oscils., photoelectric photometry 0-82380  
 CI Cygni symbiotic star, UV and optical spectrum changes during eclipse 0-105258  
 Cygnus X-1 X-ray binary, SHF obs. 0-73071  
 HR Delphini (Nova 1967), premaximum mass loss rate, H line anal. 0-82378  
 HR Delphini (Nova 1967), short period light vars. from UVB photometry 0-67744  
 HR Delphini (Nova 1967), simultaneous X-ray, UV and optical obs. 0-109440  
 $\beta$  Doradus, Cepheid, reddening determ. from nearby star UVB obs. 0-101598  
 S Doradus, LMC Hubble-Sandage variable, IUE and ground based spectroscopic obs. 0-101595  
 K Draconis, Be star, search for short time scale vars. in H $\alpha$  emission 0-109441  
 CX Draconis, binary Be star, UVB obs. 0-82388  
 AB Draconis star fields, comparison star sequences, photometry obs. 0-82433  
 BY Draconis stars, angular momentum initial distrib. and evolution 0-85954  
 BY Draconis stars, out of eclipse light var. and comparison with RS Canum Venaticorum stars 0-109489  
 early-type stars with gas-dust envelopes, IR spectral energy distrib. 0-67732  
 emission-line variable (No.86) in core of M 15, UVB photometry, probably W Virginis star 0-77458  
 $\nu$  Eridani,  $\beta$  Cephei star, Fourier anal. of radial vel. changes 0-105246  
 $\nu$  Eridani,  $\beta$  Cephei variable atm. parameters from H and He spectral obs. 0-67739  
 40 Eridani C, X-ray image of dM4e flare star 0-105282  
 flare stars, flare emission spectroscopy rel. to fast electron hypothesis 0-67731  
 flare stars, multichannel spectrophotometry 0-105256  
 flare stars, nature of flares optical continuum (Russian) 0-109445  
 flare stars in Pleiades, spatial distrib. using recovery method (Russian) 0-94722  
 flare stars in Scorpius-Ophiuchus region, discoveries (Chinese) 0-77418  
 flare stars in Taurus Cloud, comparison with  $\rho$  Ophiuchi flare stars, visible obs. (Chinese) 0-85957  
 G 208-44/45, possible double flare star, spectral obs. 0-67727  
 U Geminorum, dwarf nova, visual magnitudes during outburst, (1980 May 6 to 9) 0-72978  
 U Geminorum, visual magnitude estimates during outburst (1980 Oct.) 0-109439

## variable stars continued

- H 2252-035, cataclysmic variable, photometry and spectrum rel. to orbital and rot. periods 0-101651  
H 2252-035, spectrophotometry, no periodic linear polarization (1980 Sept.) 0-105401  
H 2252-035, X-ray flux modulation, compact star rotation 0-101652  
HD 101065, Przybylski's star, light variability freq. anal. 0-62152  
HD 102567 (4U 1145-61), IUE obs. of Be-star 0-82383  
HD 10783, Ap star, spectrophotometric obs. 0-98663  
HD 129494, new pulsating  $\delta$  Delphini star, photometric obs. and luminosity 0-67750  
HD 129708, new bright short-period Cepheid variable with unusual spectrum, photometric obs. 0-67751  
HD 159378 (Tr 27-102), yellow variable supergiant near Cepheid instability strip, VBLUV photometry 0-98672  
HD 185332, new  $\delta$  Scuti star, photometric and spectroscopic obs. 0-90451  
HD 200925 radial vels. of new short period  $\delta$  Scuti star (*French*) 0-90441  
HD 21479, brightness microvariability and non-radial pulsations (*Russian*) 0-67754  
HD 4174 (=EG Andromedae), peculiar M giant, UV spectra obs. 0-94798  
HD 45088, BY Draconis binary, surface activity from high rot. vel., visible obs. 0-77425  
HD 45677, peculiar Be-star, 0.12-12.6  $\mu$ m obs. 0-72957  
He2-442, UVRK photometry and spectroscopic obs. (*Russian*) 0-94817  
He 2-467, yellow symbiotic star, emission lines and continuum 0-62155  
Henize 715 (4U 1145-61), Be-type star, colour and luminosity vars. (1976-1980) 0-72979  
AH Herculis, dwarf nova outburst, rapid oscils. evolution 0-94805  
AM Herculis, polar, IR photometric obs. 0-98687  
AM Herculis (3U 1809+50), simultaneous three-channel photometry rel. to optical flickering mechanism 0-82411  
DQ Herculis (Nova 1934), white dwarf rot. period rel. to nova remnant shape 0-105244  
 $\alpha$  Herculis A, M-type supergiant, Li abundance in atmosphere (*Russian*) 0-72950  
AH Herculis star fields, comparison star sequences, photometry obs. 0-82433  
HR 1099, 10 GHz radio emission from RS Canum Venaticorum binary 0-82427  
HR 1099 (V711 Tauri), RS Canum Venaticorum star, H $\alpha$  line variability, visible spectra obs. 0-105277  
HR 1225,  $\delta$  Scuti star, photoelectric study and periodogram anal. 0-109436  
EX Hydrae, dwarf nova, IR and optical light curves 0-67747  
EX Hydrae, dwarf nova lightcurve, periodic and secular vars. 0-77413  
EX Hydrae, spectra of dwarf nova 0-98670  
VW Hydri, dwarf nova, IR light curves 0-67747  
IRC+10216, C star, IR obs. 0-90568  
IRC+30219, variable C star, optical emission-line phase obs. 0-90569  
KU09313+4052, variable UV excess object, discovery, position and photometry 0-62159  
Kuwan's novae-like object in Vulpecula, IR photometric obs. 0-62147  
12 and 16 Lacertae,  $\beta$  Cephei stars, light var. anal. and photoelec. photometry 0-77412  
EV Lacertae, flare star, photometry and spectrum rel. to starspots and rot. period 0-98665  
AQ Leonis, Population II double-mode RR Lyrae star, theoretical period ratio 0-62134  
CW Leonis (IRC+10216), Mira variable and IR C star, intrinsic polarisation origin 0-67730  
48 Librae, Be star, shell spectrum line profiles 0-62146  
48 Librae (FX Librae), Be star, search for short time scale vars. in H $\alpha$  emission 0-109441  
long period variable maser stars, radial vel. determ. 0-77410  
long period variables in globular clusters, high sensitivity search for main-line OH emission 0-62207  
long-period variable stars in S.hemisphere, narrowband polarimetry 0-98666  
RU Lupi T Tauri star, far UV spectra, emission measure obs. 0-94788  
MV Lyrae, cyclotron lines in spectrum of nova-like star (*Russian*) 0-67753  
 $\delta^2$  Lyrae, M-type supergiant, Li abundance in atmosphere (*Russian*) 0-72950  
RR Lyrae stars, hydromagnetic processes as cause of period changes 0-105261  
RR Lyrae stars, in 47 Tucanae, membership and metallicity 0-62206  
RR Lyrae stars, kinematics rel. to Galaxy initial contraction 0-62204  
RR Lyrae stars, theoretical period ratios 0-62134  
in M4, discoveries (*Chinese*) 0-77418  
main-sequence stars, F to M-type, comparison of activity cycles to old and young stars 0-105235  
Mira type stars, luminosity props. from spectra and light curve elements 0-105253  
Mira type variables, Me and Se types, UVV photometry 0-82375  
Mira type variables atm., OH maser, IR line overlap pumping mechanism 0-72764  
Mira variables, IR Photometry and OH maser pumping efficiency 0-82379  
15-S Monocerotis, interstellar lines, UV obs. 0-90494  
AU Monocerotis, mathematical anal. of photometric peculiarities 0-77448  
R Monocerotis, T Tauri star, long period vars. 0-82350  
MWC 349, Be star, spectral EHF obs. 0-105262  
in NGC 6584, globular cluster, new objects 0-62137  
S Normae, Cepheid, luminosity and membership of NGC 6087 visible obs. 0-94797  
S Normae, Cepheid in NGC 6087, distance and luminosity from cluster four-colour and H $\beta$  photometry 0-62208  
nova light curves, as manifestation of nonuniform stellar wind 0-62160  
Nova Serpentis 1978, evolution of dust shell 0-90430  
novae, dust formation and ionisation in envelopes 0-98678  
novae, effect of binary companion on outburst 0-82394  
novae, effects of white dwarf rot. on remnants shapes 0-105244  
novae-like object in Vulpecula, 1980 May-June spectra and magnitudes 0-82392  
novae-like object in Vulpecula, light curve, photometric and spectroscopic obs. 0-67758

## variable stars continued

- novae-like object in Vulpecula, photometry, June 1980, and spectral classification 0-94807  
novae-like object in Vulpecula, visual magnitude estimates (1980 February 2 to May 9) 0-72980  
novae-like variable in Virgo, discovery, approximate positions and magnitudes, (1980 July and August) 0-98674  
 $\chi$  and 66 Ophiuchi, Be stars, search for short time scale vars. in H $\alpha$  emission 0-109441  
Orion population stars, light curve characts. and emission line intensities 0-67721  
22 Orionis, nonradial m-mode changes in 53 Persei variable 0-72939  
 $\alpha$  Orionis, supergiant, mass loss, visible spectra obs. 0-67755  
V380 Orionis, T Tauri star, struct. of assoc. refl. nebula (NGC 1999) 0-94856  
AG Pegasi, symbiotic binary system, UV and optical spectrum rel. to nature of components 0-109449  
II Pegasi (HD 224085), surface-active binary star, spectroscopic obs. 0-90480  
RU Pegasi star fields, comparison star sequence, photometry obs. 0-82433  
X Persei, IUE obs. of Be-star 0-82383  
IW Persei, metallic line ellipsoidal variable, photometric and spectroscopic obs. 0-62186  
X Persei (4U 0352+30), Be star, evidence for 6-year photometric periodicity 0-109446  
X Persei (A 0535+26), Prognos-6 obs. of X-ray fluxes and energy spectra (*Russian*) 0-109562  
TZ and UV Persei star fields, comparison star sequences, photometry obs. 0-82433  
19 Piscium, C star, violet spectrum line identification and radial vel. 0-82361  
TX Piscium, disc brightness distrib. and envelope obs. from lunar occultation meas. 0-67725  
UV Piscium, RS Canum Venaticorum star, identification with X-ray source H0118+067, X-ray obs. 0-101654  
SZ Piscium, RS Canum Venaticorum star, photometric obs. rel to starspot model 0-109490  
pulsating stars, modal selection theory rel. to double-mode Cepheids 0-82372  
pulsating stars asymptotic theory, boundary layer method 0-82389  
pulsations, nonlinear coupling 0-62115  
 $\rho$  Puppis, line profile variable, pulsational mode-typing 0-90432  
VV Puppis, polar, IR photometric obs. 0-98687  
L<sub>2</sub> Puppis, semiregular variable, Ca I uneven distrib. from narrowband polarimetry 0-98666  
PZT suspected variables photoelec. UVV photometry obs. 0-77392  
FG Sagittae, 1975-8 spectral obs. of peculiar variable 0-72959  
WZ Sagittae, 1978-9 outburst of dwarf nova, spectra 0-94801  
WZ Sagittae, eruptive binary, model from hot spot eclipses anal. 0-72962  
WZ Sagittae, image-tube spectroscopic obs. of 1978 Dec. outburst 0-72958  
FG Sagittae, planetary nebula central star, radial vel. meas. rel. to binary star model 0-98664  
WZ Sagittae, recurrent nova, IUE obs. in outburst 0-109448  
WZ Sagittae, recurrent nova, spectroscopic obs. and model for superhump phenomena 0-82368  
HM Sagittae, symbiotic star, IR variability obs. from VJHKL photometry (*Russian*) 0-105263  
V1437 Sagittarii, Population II Cepheid, identification and dist. 0-82396  
 $\alpha$  Scorpii,  $\beta$  Cephei star, Fourier anal. of radial vel. changes 0-105246  
W879 Scorpii, M-type long period variable, visible obs. (*Chinese*) 0-85956  
V818 Scorpii (Scorpius X-1), Prognos-6 obs. of X-ray fluxes and energy spectra (*Russian*) 0-109562  
V818 Scorpii (Scorpius X-1), rapid variability simultaneous X-ray and optical obs. 0-62322  
V818 Scorpii (Scorpius X-1), UV, visible, IR and X-ray obs. 0-82541  
Scorpius-Ophiuchus region, discoveries (*Chinese*) 0-77418  
VY Sculptoris, novae-like variable, precise position 0-101597  
VY Sculptoris, novae-like variable, spectrum during faint state 0-98675  
AI, WZ and XX Sculptoris, southern  $\delta$  Scuti stars, photoelectric study 0-90452  
 $\delta$  Scuti, line profile variable, pulsational mode-typing 0-90432  
 $\delta$  Scuti stars, period changes in dwarf Cepheids 0-62142  
FH Serpentis (Nova Serpentis 1970), dust grain IR emission model 0-105254  
slow novae and symbiotic stars, late-type components spectral classifications 0-94813  
SS 433, 164<sup>d</sup> period as precessional motion, massive black hole and pulsar models 0-62138  
SS 433, 180 mm interferometric obs. of triple structure 0-105259  
SS 433, accreting black hole model 0-85958  
SS 433, accretion disc viscosity determ. using slaved disc model 0-62110  
SS 433, beam acceleration, radiation and precession theory 0-72971  
SS 433, beam models, energetics anal., possible triple system 0-90433  
SS 433, change in radio struct., 1980 January to June, from VLBI obs. 0-109557  
SS 433, deviations from standard model 0-98669  
SS 433, disk-driven precession 0-94803  
SS 433, dissipative infall model 0-67749  
SS 433, emission regions and black hole accretion disk 0-67746  
SS 433, general spectral features 0-77421  
SS 433, IR variability obs. 0-98676  
SS 433, light curves, double peak and binary-like period, photometry 0-94804  
SS 433, magnetic X-ray binary model 0-109447  
SS 433, models of supercritical accretion discs around black holes 0-105272  
SS 433, nearby faint, highly-contorted nebular filament discovery 0-94855  
SS 433, no 6-day periodicity in 1978 June-1980 Feb. obs. period 0-62150  
SS 433, radial vel. curve low amplitude section, visible spectra anal. 0-67737  
SS 433, reality of 6-day periodicity in spectral lines wavelengths var. 0-67743  
SS 433, review of obs. and theories 0-72987  
SS 433, search for radio spectral lines in UHF 0-109556  
SS 433, spectral features interpreted a precessing neutron star with jets, possible binary 0-90447



## variable stars continued

- SS 433, V band photometry and broad min. prediction (1980 April-May) 0-82390  
 SS 433 inside SNR, unique spectrum 0-82381  
 Stepanyan's star, obs. of G8 V absorpt. spectrum and emission spectrum 0-67788  
 Stepanyan's star, possible cataclysmic variable, eclipses obs. and orbital period refinement 0-62195  
 symbiotic star candidates in LMC, optical spectroscopy and IR photometry 0-62139  
 symbiotic stars, evolutionary considerations 0-62144  
 symbiotic stars and slow novae, late-type components spectral classifications 0-94813  
 symbiotic stars variations, rel. to stability of white dwarfs undergoing spherically symmetric steady-state accretion 0-77402  
 41 Tauri, Ap star, Ca II K and H $\delta$  lines rapid vars. (*Russian*) 0-90458  
 $\zeta$  Tauri, Be star, rapid linear polarisation variability (*Russian*) 0-77417  
 T Tauri, Lyman continuum energy spectrum rel. to nebula ionisation and emission line spectrum 0-67820  
 SU Tauri, R Coronae Borealis star, photometry in optical and IR ranges 0-101601  
 SU Tauri, R Coronae Borealis variable, brightening after long minimum, 1980 August to September 0-109438  
 DR Tauri, T Tauri star, Balmer line profile changes and inverse P Cygni profiles 0-101591  
 DR Tauri, T Tauri star, mass flow var. in envelope, visible spectra 0-85939  
 V711 Tauri (HR 1099), RS Canum Venaticorum star, BV light curve during (1978-79) 0-105279  
 28=BU Tauri (Pleione) Be shell star, 3167 to 4924 Å spectrum atlas 0-98673  
 T Tauri star formation, regulatory force in dark mol. cloud evolution 0-85980  
 T Tauri stars, H $\alpha$  emission line core formation in chromosphere 0-94792  
 T Tauri stars  $\rho$  Ophiuchi dark cloud, photometry obs. 0-72942  
 T Tauri stars among new H $\alpha$  stars in NGC 2264 and NGC 7000/IC 5070 regions 0-62120  
 T Tauri stars in dust cloud Lynds 134, mass loss causing cloud turbulence 0-94845  
 T Tauri stars in mol. cloud in NGC 2264, nearby OH and NH $_3$  obs. 0-94847  
 T Tauri stars near Herbig-Haro objects, obs. during search for exciting stars 0-67720  
 BL Telescopii A, yellow variable supergiant near Cepheid instability strip, VBLUW photometry 0-98672  
 EK Trianguli Australis, SU Ursae Majoris dwarf nova, superhumps, light curve UVB obs. 0-105255  
 UX Ursae Majoris, eclipsing nova-like variable, time-series photometry 0-77446  
 AN Ursae Majoris, polar, IR photometric obs. 0-98687  
 SU Ursae Majoris, soft X-ray halo around dwarf nova 0-98677  
 SU Ursae Majoris stars, important sub-group of dwarf novae, photometric props. 0-101596  
 V1341 Cygni (Cygnus X-2), X-ray polarisation obs. from OSO 8 0-90571  
 V1357 Cygni (Cygnus X-1), X-ray polarisation obs. from OSO 8 0-90571  
 V80 in dwarf spheroidal galaxy in Ursa Minor, eclipsing binary star with RRc primary 0-109505  
 AH Velorum, classical cepheid, binary detect., UVB obs. 0-109443  
 AI Velorum, nature from BVRI photometry and photoelectric radial vels. 0-94815  
 EQ Virginis, late type dwarf flare star, temp. minima, chromosphere model 0-67717  
 CU Virginis (HD 124224), Ap star, spectrophotometric obs. 0-98663  
 visual binaries with variable components, orbital elements, visible obs. (*Russian*) 0-77455  
 Wray 977, optical counterpart to X-ray binary pulsar, 4U 1223-62, optical spectra 0-72984  
 X-ray sources optical counterparts, appl. of simultaneous fast double head UVB photometer 0-72775  
 young stars, absorpt. and emission features, IR spectrophotometry obs. 0-72954  
 C stars, form. of carbyne and cyanoacetylene in stellar atm. 0-67708  
 C stars, IJHKL photometry obs. 0-98657  
 He rich stars, intermediate and extreme, spectral atlas in 3700 to 4600 Å range 0-94806  
 He variable stars, IR excesses obs. 0-67733

## variational calculus see variational techniques

## variational techniques

- (2+1) dimensional compact QED, combined WKB-variational method, vacuum tunnelling 0-101960  
 acoustic deformation pot. polarons, linear energy-momentum relations 0-80196  
 Anderson model, ground state, var. trial function approach 0-59913  
 Anderson model, impurity pair interactions, local moment form., var. method 0-92854  
 anharmonic oscillator, classical, variational method test, sp. ht., elec. susceptibility and oscillation freq. (*Portuguese*) 0-77611  
 anharmonic oscillator, trial Hamiltonians for quantum statistical treatment 0-77652  
 atomic Rydberg states, Coulomb and Yukawa pot., wave functions and quantum defects, Schwinger's var. principle 0-63549  
 atoms, perturbation var. calc. with contact interaction, effect of approx. zero order wavefunctions 0-58107  
 atoms, two-body correls., variational approach 0-91455  
 atoms and molecules, second-order properties, coupled perturbed Hartree-Fock method improvement 0-58148  
 atoms of Group IIb, dipole polarisabilities from compact variational trial functions 0-63568  
 bending of plates, finite difference variational method 0-92045  
 benzene, dynamic polarisabilities, calcs., superposition method of excited configs., nonstationary perturbation theory eqns. 0-69257  
 boson mixtures, binary, ground state configs. 0-105570  
 bound polaron, non-perturbative variational method 0-88485  
 boundary problems in static elasticity, distortion trivector pot., variational principle (*Russian*) 0-79146  
 buckling, unilateral, of thin plate, variational techniques (*French*) 0-74780  
 celestial mechanics, ELP soln. of Moon main problem (*French*) 0-62044

## variational techniques continued

- classical systems, particle distrib. function, theoretical method 0-64856  
 closed-shell atoms, Jastrow wave functions, var. calcs. 0-83249  
 complementary variational principles for Maxwell's equations 0-99603  
 container subjected to forced pitching oscillation, liquid motion, nonlinear anal. 0-96270  
 convex analysis and variational inequalities (*Japanese*) 0-77606  
 cosmological principle appl. to variation methods for Friedmann universes (*French*) 0-77529  
 cosmology, Lagrangian or Hamiltonian formulations, shift vector field restrictions, symmetry group 0-67923  
 creep, generalised variational principles, Lagrange multiplier method applied to flow theory (*Chinese*) 0-79171  
 dam seepage, variational inequality appl. to flow through porous media 0-100028  
 deformation potential polaron, perturbation theory breakdown 0-84440  
 density operators, time depend., var. principle, rel. to linear decoupling procedures for propagators 0-63514  
 diatomic molecule, electron scatt., low energy, multichannel variational calcs., static exchange approx. 0-83483  
 diatomic molecule, vibr. energies and functions, cubic splines method calcs. 0-78594  
 diatomic transition operators, L $^2$  basis expansions 0-63519  
 dielectrics, hyperelastic, with saturated polarisation, variational and invariance principles 0-74730  
 Earth crust radiogenic heat production, depth depend. modelling by variational approach 0-72464  
 effective action, quantum mechanical definition using time depend. variational principle 0-57457  
 elastic plate stability conditions, variational formulations 0-69701  
 elastic plates, annular, clamped edges, asymmetric bending, Ritz method 0-58907  
 elastic shell, cylindrical, closed, laminated, longitudinal crack, elastic eqn., energy approach (*Russian*) 0-87740  
 elastic stability, cantilevers, flutter load, discontinuity, variational technique 0-58944  
 elastic stress analysis of constrained cylinders by special finite element method 0-106718  
 elastic wave propagation in fibre reinforced composite rectangular rods (*French*) 0-83749  
 elasticity, beam bending on Pasternak foundation, reciprocal variational inequalities 0-92091  
 elastoplasticity, finite strain, rate problems, energy theorems, Lagrangians 0-74766  
 electromagnetic fields, static and stationary, determ. using variation calculus (*Hungarian*) 0-87259  
 electron-ion scattering, Schwinger's variational principle, Rydberg states 0-78713  
 electrons in surface phonon field 0-107885  
 EM induction, irregularly shaped plates, slow ramped field, eddy current heating, anal. 0-91722  
 EM waves propagation, ray surface equation and Fermat's principle, in moving anisotropic media 0-106425  
 Fermi limit, hard-sphere, energy and momentum distrib., Jastrow variational wave functions 0-73261  
 Feynman's variational method applied to the randomly forced Duffing equation 0-73201  
 filtering, nonlinear, conditional laws, smoothness, stochastic calculus of variations (*French*) 0-68128  
 fluid dynamics, complementary variational principles for steady and unsteady Poiseuille flow in porous pipe 0-92225  
 force-free magnetic fields, variational approach and appl. to solar active regions mag. field 0-62011  
 fracture, brittle, energy release rate, equivalent to Rice integral (*French*) 0-64457  
 free convection boundary layer flow and heat transfer, variational technique 0-106796  
 free energy derivatives, bounds, upper and lower, renormalisation group methods 0-68162  
 Frisch-Lloyd random system, low-lying electronic tail spectrum by path integral method and coherent state representation variational method 0-105580  
 fusion reactor neutronics analysis using generalised variational principles 0-57947  
 general relativity, perfect and imperfect fluids, variational principle 0-90733  
 geodesy, Helmholtz type variance-covariance-component estimator props. 0-101318  
 Green function complex pole calc. by variational technique 0-98822  
 hard core fluid with two-Yukawa tail, appl. to Ar 0-59618  
 Hashin-Shtrikman bounds, effective elastic moduli, hexagonal, trigonal and tetragonal polycrystals 0-75282  
 Hashin-Shtrikman bounds, effective elastic moduli, monoclinic polycrystals 0-70291  
 heat and mass transfer, non-stationary, coupled, with convective motion and relaxation, variational principle 0-106797  
 heat conductivity, nonlinear problems, variational formulation (*Russian*) 0-74700  
 heterogeneous mixtures, variational hydrodynamic model in Euler- and Euler-Lagrange formulations 0-92100  
 Hubbard model, single band, magnetic phase diagram, cluster variational calc. 0-60340  
 hybrid deformation elements for elastic media 0-92049  
 hydrodynamic lubrication, free boundary problem, variational inequalities 0-62475  
 inhomogeneous medium, effective cond., iteration series and variational estimates, Herring method 0-70663  
 integrated load increment method for finite elasto-plastic stress analysis 0-92072  
 intermediate valence system, local polaron model 0-107717  
 ion-dipole capture in noncentral field, variational and trajectory investigation 0-63739  
 Ising model, antiferromag. case, modified Kadanoff variational renormalisation method 0-88710  
 Ising model, two-dimens., in transverse mag. field, renormalisation group studies 0-71042  
 Lagrangian-Hamiltonian systems, partial quantisation (*Portuguese*) 0-77653  
 lattice instability theory of fracture 0-84244  
 magnetic impurities in metals, appl. of variational method 0-103814  
 magnetisation of easy plane amorphous wire, variational calc. 0-71098

## variational techniques continued

- magnetofluid dynamics, relativistic, eqns. of motion for charged particle and charged fluid 0-78721  
 many component plasmas with self consistent field, variational principles and canonical theory 0-87856  
 maximum entropy spectral estimation of frequency and arrival angle 0-96129  
 mechanics, mountain massif, pre-face zone, stressed state, finite difference method (*Ukrainian*) 0-74735  
 metal solidification, variational formulation of stationary free boundary problem (*French*) 0-96626  
 metal-insulator transition region, narrow energy bands, electron correlation, Gutzwiller variational method 0-84426  
 molar molecule heat and mass transfer phenomena, generalised variational principle 0-79104  
 molecular polarisabilities calcs., superposition method of excited config., nonstationary perturbation theory eqn. 0-69257  
 molecules, direct CI calcs. with multiconfigurational reference state 0-63506  
 nematic liquid crystals, tridimensional variational approximated model, existence, uniqueness and regularity of solns. 0-59379  
 neutral bound excitons, accurate binding energies, variational method calc. 0-107715  
 non-associated plasticity and elastoplasticity, rate boundary value problems, variational principles 0-87726  
 nuclear structure,  $^{40}\text{Ca}$  ground-state energy, nonunitary model operator approach 0-83030  
 one-electron polynuclear systems, Dirac eqn., variational soln. 0-83242  
 optical directional couplers with graded index profile, variational analysis 0-96037  
 partially coherent beam intensity fluctuation calc. in turbulent atmosphere 0-78775  
 partition function, modified Lippmann-Schwinger variational principle 0-86233  
 plasma drift waves in sheared mag. field, variational method calcs. 0-106910  
 plastic flow, isotropic body, finite element method for volume integration 0-74770  
 plates, large deformation anal., variational formulations 0-92067  
 plates on elastic foundations, variational approach 0-79160  
 Poiseuille flow, complementary variational principles 0-96310  
 polaron energy, bound to Coulomb potential 0-88487  
 positive column with two-step ionisation 0-70056  
 post-buckling behaviour of structures using a finite element-nonlinear eigenvalue technique 0-92078  
 primitive wave function in theory of intermolecular interactions 0-95703  
 principle of least action, minimal interpretation, variational calcs. 0-68039  
 quantum energy levels, statistical mechanics method, perturbative variational approach 0-82513  
 quark-quark interaction, phenomenological, from s-wave baryon spectrum 0-101984  
 right translation invariant metrics and variational principles on principal bundle, gauge theories (*Chinese*) 0-101743  
 rotated hamiltonians, complex-coordinate rotation and least-squares variational method 0-68075  
 scalar field, exterior case, identification of variational principles (*French*) 0-73220  
 scattering amplitude, phase, uniqueness, variational calc. 0-86156  
 scattering phase, variational principle 0-68084  
 Schrodinger's variational quantisation method in stochastic framework 0-105532  
 Schrodinger equations, three-body problem, bound state eigenvalues lower bounds, upper bounds by Rayleigh-Ritz method 0-68068  
 Schwinger and Kohn variational phase shift calculations, comparison 0-78672  
 semiclassical two electron atom, appl. of semiclassical equivalent of Hylleraas var. method 0-58111  
 semiconductor, three-impurity clusters, ionisation energies and electron affinities 0-65496  
 shallow shell bending, mixed variational eqn. 0-77618  
 shell, cylindrical, with spiral groove, Kirchhoff's boundary conditions deduced from energy principle 0-74741  
 shells, flexible, self checking stepping calc. process 0-68044  
 shells, Kirchhoff-Love, structural stability, mixed variational principles and non holonomic constraints (*French*) 0-74779  
 Slater determinants, energy functional, extremum problem, Hartree-Fock equations, gradient method 0-62573  
 spectral filter, optimisation for arbitrary criterion by method of basic extremals 0-96011  
 standard sample homogeneity evaluation, optimal obs. planning 0-93721  
 steady homenergetic compressible flow with finite shocks, variational principle 0-69874  
 strong coupling QCD, variational approach, Schrodinger eqn. and effective Hamiltonian 0-95245  
 thermal conductivity, nonlinear, variational formulation, counter functional, exactness of soln. (*Russian*) 0-90800  
 thermodynamics, irreversible, internal variable theory, Lagrangian formulation 0-73291  
 thermoelasticity, uniqueness theorem and variational principle 0-92056  
 thermoplasticity, time evolution under quasistatic conditions, existence theorems 0-74764  
 Tokamak, plasma MHD equilib., var. method (*Russian*) 0-106960  
 toroidal plasmas, equilib. energy principle with global invariants 0-92366  
 transport theory, two-group integral transport equation, variational method 0-68156  
 underwater acoustic source location and motion estimation, joint reduction of bias and variance 0-96087  
 unified field theory, five-dimensional theory of interacting scalar, electromagnetic, and gravitational fields 0-105833  
 unified theory of atoms and atomic aggregates, self consistent theory 0-102418  
 universal variational functionals of electron densities, first-order density matrices, and natural spin-orbitals and solution of the  $\nu$ -representability problem 0-95516  
 viscoelastic fluid, stability of steady shearing flows, energy method and parabolic maximum principle 0-74926  
 Weyl-Dirac theory with torsion, complex Dirac field, conservation equations 0-68112  
 Z(2) lattice gauge theory, variational approach, two phase struct., phase transition 0-68361

## variational techniques continued

- BH, elec. polarisabilities and dipole moments, var. perturbation obs. 0-63527  
 $^{42}\text{Ca}$ , collective states, quasi-degenerate intrinsic Hamiltonian, variational methods 0-68505  
 Cs halides, F-centre energy levels, ion-size effects, calc. 0-96519  
 GaAs, excitons in arbitrary mag. fields 0-96798  
 GaP, donor states theory, camel's back struct. influence 0-59921  
 Ge, donor polarizability, multivalley effective mass calc. 0-96817  
 H bound states in strong mag. field 0-99438  
 H, electron impact excitation of  $n=2$  to  $n=3$  transition, algebraic variational method close coupling calcs. 0-91678  
 H<sub>2</sub>, dynamic polarisabilities, variation-perturbation calcs. 0-87243  
 H<sub>2</sub>, electron scatt., iterative approach to Schwinger variational principle 0-99580  
 H<sub>2</sub>, electron scatt., Schwinger variational principle, static-exchange approx. 0-63820  
 H<sub>2</sub>, mag. susceptibility vector pot. variational method, gradient transform. function selection 0-69258  
 H<sub>2</sub>, metallic, ground-state energies of liq. and solid phases, variational and Monte Carlo methods 0-70502  
 H<sub>2</sub><sup>+</sup> bound states in strong mag. field 0-99438  
 HD, perturbation var. calc. with contact interaction, effect of approx. zero order wavefunctions 0-58107  
 HD, spin-spin coupling constant convergence, comparative study 0-63536  
 He, appl. of semiclassical equivalent of Hylleraas var. method appls. 0-58111  
 He, Pade type variational functions, appln. to ground state 0-87025  
<sup>3</sup>He, liq., binding energy, variational calcs. by Pandharipande's method 0-101752  
<sup>3</sup>He, liq., binding energy and effective interactions, interactions, variational calcs. 0-107596  
<sup>4</sup>He ground state binding energy, near threshold behaviour in 2 and 3 dims. 0-91716  
<sup>4</sup>He, liq., binding energy, variational calcs. by Pandharipande's method 0-101752  
<sup>4</sup>He, liq., excited states, variational calcs. 0-80017  
<sup>4</sup>He, liq., ground state, self consistent description of long- and short-range correlations 0-107592  
<sup>4</sup>He, threshold condition for forming atomic trimer 0-63741  
<sup>4</sup>He( $\alpha,\alpha$ ), size change of  $\alpha$  effect on phase shift, generator coordinate and variational methods (*Chinese*) 0-68683  
<sup>4</sup>He(d,d), distortion effects, orthogonality condition model 0-63190  
 Ne, temp. perturbed Thomas Fermi eqn., variational principle 0-69074  
 O<sub>2</sub>, line and band strengths in IR spectra, variational calcs. 0-87112  
 O<sub>2</sub>, molecule, equilib. struct., vibr. freqs., SCF closed shell calcs. 0-74101  
 Si, donor polarizability, multivalley effective mass calc. 0-96817  
 SmS intermediate valence, low lying states 0-96826

## varistors

- ZnO ceramic varistors, thermal breakdown 0-88928  
 ZnO varistor ceramics, current-voltage characts., inhomogeneities and single barriers 0-80273  
 ZnO:Ba, Co, rare earth metal varistors, microstructure-prop. relations 0-100249  
 ZnO-grainboundary-ZnO junction in ceramic varistor, capacitance-voltage characts. 0-65689

## varnish

No entries

Vavilov-Cherenkov radiation *see* Cherenkov radiation

## VB calculations

- atom, one-centre integrals of exact effective valence shell Hamiltonian 0-74128  
 self consistent electron pair theory, perfect pairing valence bond generalisation 0-63532  
 ArH, excited states, theoretical pot. curves 0-95548  
 BeH,  $^2\Sigma^+$  states, spin-coupled valence bond theory of molecular electronic struct. 0-83285  
 C, one-centre integrals of semiempirical theories of valence, ab initio calcs. 0-102441  
 CH, one-centre integrals of semiempirical theories of valence, ab initio calcs. 0-102441  
 H<sub>2</sub>, electronic struct., valence bond model, pairwise correlation 0-78543  
 H<sub>2</sub>, electronic struct., valence bond orbital method appl. 0-106268  
 H<sub>2</sub>, pot. energy surfaces, valence bond calcs. 0-74129  
 LiH, electronic struct., valence bond orbital method appl. 0-106268  
 Si<sub>2</sub>, electronic struct. and bonding, atomic effective pot. appl. 0-95745

vector diagrams *see* vectors

## vector meson dominance model

- hadronic gauge couplings in meson decays 0-102037  
 radiative decays of vector mesons, single parameter scheme 0-86720  
 tensor meson dominance, internal symmetries, and meson mixing for the new particles 0-102036  
 vector meson radiative decays, vector dominance model in broken SU(3) 0-73711  
 weak nucleon formfactors in modified vector dominance model (*Russian*) 0-68437  
 $\beta$ -decay, strong meson dominance model and second class currents 0-63132  
 D meson parity violating nonleptonic decays, vector meson dominance model 0-78058  
 $\eta \rightarrow \rho\gamma(\gamma\gamma)$ , C-even meson radiative decay, SU(3), and VDM anal. (*Russian*) 0-68460  
 F parity violating nonleptonic decays, vector meson dominance model 0-78058  
 $\gamma p$ , heavy quark particle photoprod., QCD model, vector dominance implications 0-86730  
 $\kappa$  charge radius, coloured quark field theory 0-62945  
 $\pi$  charge radius, coloured quark field theory 0-62945  
 $\tau \rightarrow \mu \pi \gamma$ ,  $\pi$  form factors, axial-vector and structure dependent, vector meson dominance model 0-62989

vector mesons *see* meson resonances

## vectors

- atoms, general adiabatic-diabatic transformation matrix, electronic non-adiabatic transitions 0-93751  
 crystal physics, multivector analysis, comparison with vector anal. 0-100196  
 general relativity, killing vectors and maximal slicing 0-77667  
 generalised representation, of physical situation, appl. to hydrodynamics (*Russian*) 0-69760



**vectors continued**

- hologram interferometry, sensitivity vector determ., two known object rots. 0-95840
- physics teaching, vector concept (*German*) 0-82623
- plane to spherical wave conversion by volume holograms, vector effects 0-106496

**vehicles**

- see also *electric vehicles; locomotives; road vehicles; space vehicles*
- dynamic interaction with structures, simulation using Lagrange multipliers 0-64357

**velocity**

- see also *acoustic wave velocity; ion mobility; light velocity*
- education, speed, Galilean and Einsteinian concepts, vel., rapidity and celerity 0-73130
- Hamels spiral flow, temp. and vel. distrib. (*German*) 0-87779
- quasars, transverse motions determ. from relativistic Doppler formula for redshift (*Chinese*) 0-105379
- radio galaxies components, fly away velocities upper limits (*Russian*) 0-62306
- solar granulation, mean vertical vel. 0-62094
- solar photosphere, vel. gradients retrieval from line asymmetries, linearised approach 0-62093
- solar wind, particle vel. distrib. rel. to plasmadynamical processes (*German*) 0-109323
- superluminal velocities in compact radio sources, role of spontaneous form. of knots in relativistic flows 0-105369

**velocity analyzers** see *particle separators***velocity control**

- wind turbines, vertical axis, tilting using overspeed control 0-97757

**velocity measurement**

- see also *acoustic wave velocity measurement; anemometers; angular velocity measurement; flow measurement; flowmeters; laser velocimeters; light velocity measurement; stroboscopes*
- anemograph, digital, for wind direction and average speed meas. (*Czech*) 0-77174
- axial flow compressor stator blade wake guidevane, method 0-95085
- blood, pulse-wave vel. meas. in humans (*German*) 0-81751
- blood intravascular mean vel. meas. using crosscorrel. technique 0-81763
- capillary blood flow, dual beam laser velocimeter anal. 0-75015
- diffuse object real-time velocity meas. using laser speckle zero-crossings 0-77760
- digital, error calc. (*Russian*) 0-86266
- dust particles, charged, vel. meas. using laser Doppler velocimeter 0-95083
- electrodiffusion velocity sensor, freq. characts. calcs. 0-96675
- flow mean velocity very close to a wall, hot-wire anemometer meas. errors 0-79413
- graphite, shock wave, prod. by explosion, vel. meas. 0-59074
- high surface vels. using K-band microwave interferometry 0-77761
- horizontal gas-liquid stream, flow vel. meas. 0-96301
- impact, internal meas. of shear and compression waves, gauge lead effects 0-74817
- laboratory's absolute velocity meas. 0-95081
- laser Doppler blood velocimetry (*Japanese*) 0-94310
- laser Doppler velocimeter with direct spectral anal., for instantaneous vel. meas. 0-99782
- laser speckle, time-differentiated, first order statistics, vel. meas. 0-82750
- laser surface speed measurement by correlation, industrial paper machine test (*French*) 0-95082
- liquid velocity measurement and flow trajectory, using image sensor, appl. to stirred vessel 0-69950
- low-reactive meas. of motion, transducer effects on body under investigation (*German*) 0-105621
- mucociliary tracheal clearance vel., radiological method for determ. 0-104727
- non-contact velocimeter for moving objects using statistical method 0-105622
- optical Doppler microscope 0-68251
- polymer soln. highly elastic, vel. meas. in die entry region of capillary rheometer 0-99988
- speckle, dynamic props., zero-crossing study 0-63923
- speckle pattern time-space cross-correlation for in-plane vel. meas. 0-105623
- sputtered particles, vel. meas. by Doppler-shift laser spectrometer 0-62638
- turbine-vane passage, laser Doppler velocimeter appl. 0-95086
- velocity gradients and laminar and turbulent diffusion, direct optical meas. 0-59132
- vibrating string, wave velocity propag. meas., mass tension ratio (*Spanish*) 0-74592
- vibrational, using analogue photoelectric velocities, systematic errors determ. 0-79246
- wind velocity meas. near wind power plant in Sweden 0-61883

**velocity meters** see *velocity measurement***velocity microphones** see *microphones***velocity-modulation tubes**

- No entries

**velocity spectrometers** see *mass spectrometers***Veneziano model**

- space-time anomalous dimension in Veneziano and Neveu-Schwarz models (*Russian*) 0-68434

**ventilating** see *ventilation***ventilation**

- see also *air conditioning*
- BWR, heating, ventilation and air conditioning systems (*Japanese*) 0-91212
- modified window air conditioner, laboratory temperature control 0-68192
- noise abatement for induction motors in air/air heat-exchangers for ventilation (*Hungarian*) 0-102923
- PWR nuclear power station, heating, ventilating and air conditioning systems (*Japanese*) 0-91213
- solar energy collection and storage, space heating (*French*) 0-61299

**ventilators** see *ventilation***Venus**

- atmosphere, aerosol model 0-101545
- atmosphere, C and N species prod. by thunderstorms 0-98587
- atmosphere, greenhouse effect 0-101544
- atmosphere, O<sub>2</sub>, <sup>1</sup>Δg→<sup>3</sup>Σg band prod. mechanisms 0-82251

**Venus continued**

- atmosphere, O<sub>2</sub>, Ar, CO abundances, error of Pioneer Venus chromatography obs. 0-105189
- atmosphere, O spectral line shape following mol. dissociative excitation 0-105097
- atmosphere, radiance meas. using Pioneer Venus Solar Flux Radiometer 0-82198
- atmosphere, response to heat sources and perturbations (*Chinese*) 0-85748
- atmosphere, review of Venera data 0-72804
- atmosphere, scattered solar radiation fluxes spectral and altitude distrib. 0-62059
- atmosphere, struct., and light, heat and wind regimes from space vehicles 0-62062
- atmosphere structure instruments on Pioneer entry probes 0-67562
- atmospheric constitution, struct. and dynamics 0-105186
- cloud layer, struct. according to Venera 9 televised pictures 0-67604
- cloud microstructure, optical props., H<sub>2</sub>SO<sub>4</sub> atmosphere-aerosol study 0-72808
- clouds, IR absorption and scattering, particle size dispersion effect 0-109384
- dark face, atmospheric constitution, pictures from NASA Venus Pioneer space vehicle (*French*) 0-94735
- dayglow spectrum, 1250 to 1430 Å, Pioneer Venus obs. 0-77311
- distance from Earth determ. using radar, appl. to space craft navigation 0-109386
- exosphere, hydrogen Lyman α emission 0-105188
- gravity anomalies and tectonics, review 0-98593
- gravity field, by line of sight tracking of orbiting craft 0-77312
- inert gases in atmosphere, accretion from protoplanetary nebula 0-109385
- ionosphere, ionic reactions in lab. and planetary atmospheres, probe data 0-59168
- ionosphere, mag. flux ropes nature (*Russian*) 0-77313
- ionosphere, thermal diffusion calcs. 0-72806
- ionosphere composition, meas. by ion mass spectrometers on Pioneer Venus Bus and Orbiter 0-67499
- IR brightness temp., daytime minima 0-77309
- magnetic tail, unipolar induction effects 0-62060
- magnetosphere press. balance, outside dayside ionopause 0-90353
- microrelief irregularities mean height, determination from radio transillumination data 0-72807
- occultation by Moon 5 October 1980, positions 0-67605
- oxidation-state of Venus atmosphere and crust, Pioneer Venus results 0-98586
- Pioneer radar data, planet's topography (*German*) 0-105190
- Pioneer Venus, Unified Abstract Data Library and Quick Look Data Delivery System 0-67494
- Pioneer Venus Bus neutral gas mass spectrometer 0-67513
- Pioneer Venus Differential Long Baseline Interferometry expt. 0-67578
- Pioneer Venus Multiprobe entry phase, telemetry recovery 0-67493
- Pioneer Venus occultation experiment, radio science data generation 0-67492
- Pioneer Venus Orbiter, electron temp. probe 0-67500
- Pioneer Venus Orbiter, neutral gas mass spectrometer expt. 0-67502
- Pioneer Venus Orbiter, planar retarding potential analyser plasma expt. 0-67501
- Pioneer Venus Orbiter, plasma analyser expt. 0-67498
- Pioneer Venus Orbiter, plasma wave investigation 0-67497
- Pioneer Venus Orbiter, radar mapper design and operation 0-67495
- Pioneer Venus Orbiter fluxgate magnetometer design and operation 0-67496
- Pioneer Venus Orbiter radiometer (VORTEX) 0-67504
- Pioneer Venus Orbiter UV spectrometer, design and operation 0-67503
- Pioneer Venus small probes net flux radiometer experiment 0-67512
- Pioneer Venus Sounder and small probes nephelometer instrument 0-67511
- Pioneer Venus Sounder Probe gas chromatograph 0-67507
- Pioneer Venus Sounder Probe IR radiometer 0-67509
- Pioneer Venus Sounder Probe neutral gas mass spectrometer 0-67506
- Pioneer Venus Sounder Probe Particle Size Spectrometer 0-67510
- Pioneer Venus Sounder Probe Solar Flux Radiometer 0-67508
- Pioneer Venus spacecraft, design and operation 0-67491
- polarisation, wavelength depend. obs. rel. to UV-cloud model 0-82250
- radiowaves attenuation in atmosphere of Venus by bistatic radar method 0-62061
- resonance rotation 0-109387
- solar wind circulation behind planet, model 0-98531
- Soviet lunar and planetary exploration, handbook 0-62398
- spin vector determ. by radar obs. 0-105185
- surface dust detected by Venera 9 and 10, radiant flux obs. 0-72803
- surface reflections of Pioneer Venus descent vehicles radio emission, atm. data 0-105187
- tectonics and composition, theory 0-72805
- upper atmosphere, aerosol layer obs. from polarimetry 0-90352
- upper atmosphere, N detect. 0-77310
- Venera 9 and 10 satellites, Venus atmosphere and surface radiosounding 0-101543

**Verdet constant** see *Faraday effect***Verneuil process** see *crystal growth from melt***vertex functions**

- see also *elementary particle interactions; elementary particle theory; quantum field theory of interactions*
- ( $\phi^3$ )<sub>h</sub> field theory, deep inelastic lepton-headron scatt., cut vertex theory and reciprocity relation 0-57466
- $\phi^4$  theory, Euclidean, local existence of Borel transform of Schwinger functions 0-77932
- many-body problem, vertex function and crossing symmetry 0-62515
- parton model interpretation of cut vertex formalism 0-86566
- QED tests of electron propagator, vacuum polarisation 0-77994
- quantum field theory, n-point functions, renormalised G-convolution, convergence in Euclidean case 0-77930
- renormalised Feynman amplitude, high energy behaviour 0-86555
- superconducting Fermi-liquid, electromagnetic response, formal solutions 0-100548
- D-Krlw, charm-changing weak hadronic current, models 0-57585
- dnp vertex form factor, ed elastic scatt. at high momentum transfer 0-82977
- $\gamma$ NN vertex form factor, ed elastic scatt. at high momentum transfer 0-82977

## vertex functions continued

- NN $\rho$  couplings, parity-violating, QCD and MIT bag model,  $1/2^-$  resonance contribs., SU(6) $_v$  symmetry 0-57540
- pp $\rightarrow$ pp+N clusters, multiperipheral process, interference terms in transition, amplitudes, correlation expansions 0-62953
- $\pi$ NN vertex function and off-mass-shell  $\pi$ N scatt. 0-73739
- QQ systems, two gluon decay widths, short range quark gluon effective vertex 0-86669

## vibrating bodies

- see also elastic waves; pendulums; piezoelectric oscillations; vibrations
- annular plates, uniform in-plane compressive forces, free flexural vibrations 0-106741
- arbitrarily-shaped membrane, fund. freq. 0-106743
- bar, radially rotating, of variable cross-section, deflection and lateral vibr. (Japanese) 0-94954
- beam, annular, torsional oscillations (German) 0-106752
- beam, dynamically loaded circular, on elastic foundation, natural freqs. 0-79209
- beam, periodically varying length, instability of motion 0-69716
- beam, random vibration against stops 0-74796
- beam, Timoshenko, curved, with internal damping, steady state in-plane response 0-64429
- beam structures, thermally induced vibrations and heat conduction problem, numerical method 0-64427
- beam subjected to gravity loading, Timoshenko shear coeff. 0-79159
- beams, effect of support flexibility on fundamental frequency 0-69591
- beams, stationary random oscillations, covariant anal. (German) 0-106753
- beams, elastic, under tension, nonlinear transverse vibrs. 0-74803
- bowed violin strings, investigation of oscillations (German) 0-64312
- buckled beams and plates, nonlinear vibration studies, magnetoelectric strange attractor 0-87735
- buildings, damping by natural rubber mounts 0-87643
- buildings, traffic-induced vibration 0-96098
- built-up structures, math. modelling of resonances using meas. data 0-69718
- cantilever beam chattering against a stop, Bernoulli-Euler beam theory treatment, photographic meas. of deflections 0-83752
- cantilever plates, extended transfer matrix-finite element method 0-102984
- circular annular plates of parabolically varying thickness, buckling and vibrs. 0-69698
- circular pipes, mode-selective energy transfer to walls from internal sound propag. 0-87586
- circular plate driven by noncentral force, clamped 0-64274
- circular plates, arbitrary thickness, free vibration 0-102990
- circular plates, transverse vibrations, non-uniform edge constraints 0-96210
- circular segment shaped plates vibration anal. 0-58957
- clamped beam with branched elastic arm carrying concentrated mass, steady-state free and forced vibrations (Japanese) 0-83745
- clamped rhombical plates, upper and lower bounds for vibration freqs., method not using boundary conditions 0-79200
- clamped square plates, vibration analysis by Rayleigh-Ritz method, modified Bolotin method 0-69720
- closed circular cylindrical shells freq. formula for variety of boundary conditions 0-102989
- complex plates, anal. non-stationary random vibrations 0-102991
- complex vibrators, mean-value method of predicting dynamic response 0-64273
- component mode analysis of nonlinear and nonconservative systems 0-79211
- composite beams, effects of fibre orientations 0-87734
- concrete plates, sound transmission at junctions 0-87652
- conical solid horn with flange, FEM analysis of free vibrations (Japanese) 0-79045
- continuous beams with concrete slabs under load, vibration problems of method proposed for crack prevention in slab (Japanese) 0-83760
- continuous curved beams, natural freqs. of out-of-plane vibrations 0-74588
- coupled plates, in situ determ. coupling loss, power injection method 0-102983
- curvilinear elastic rods, vibrations 0-57095
- cylinder dynamic behaviour in the vicinity of the fundamental radial-mode frequency (Ukrainian) 0-69709
- cylindrical shell, liquid filled under nonlinear resonance conditions, vibration stability 0-99954
- cylindrical shell, reinforced laminar, intrinsic oscill. 0-99957
- cylindrical shells within initial imperfections, resonance phenomena in nonlinear vibrations 0-99958
- damped plates, vibratory modes 0-69715
- diesel engines, piston slap, assessment of contribution to overall noise and vibration 0-79055
- drives, rotational, damping of torsional vibrations, experimental determ. (Russian) 0-74816
- eccentrically stiffened plates, large amplitude flexural vibration 0-58959
- education, student expt., vibrating plate reson. charact., quality factor and nonlinearity 0-73133
- education, vibrating string, tuning guitar by television 0-73134
- elastic plates, viscoelastic material coated, transverse vibrations (French) 0-79215
- elastic shell, appl. FEM to coupled structural-acoustic radiation system 0-83691
- elastically-restrained prestressed annular plates, flexible core links, resonance freq. and mode shapes 0-69714
- electrodes on vibrating sphere, mass transfer 0-61106
- elliptical plates, nonlinear vibration, use of von Karman and Galerkin methods 0-102992
- flexible structures, dynamic simulation by substructure synthesis 0-87733
- flexible thread in transverse flow with varying vel. (Russian) 0-74789
- floating rod with loaded end, damping during transverse vibr. 0-79205
- fluid carrying pipes, elasticity of supports and critical velocity calc. (German) 0-58914
- fluid-loaded panels, line transfer and line drive admittance approx. 0-64432
- fundamental frequency of vibration of a rectangular plate on a nonlinear elastic foundation 0-69712
- gear wheel, free vibration anal. 0-102993
- hinged-hinged beam, material damping in terms of mode of vibration (Japanese) 0-91954

## vibrating bodies continued

- ideal string, extremal solutions of inverse eigenvalue problems with finite spectral data 0-101712
- idealized straight beam, free and harmonically forced vibration with dynamic friction 0-96220
- impact response, two degrees of freedom system, effect of damping 0-74587
- infinite periodic structures, response to harmonic loads 0-83751
- insonified thick elastic plate, displacement field examination 0-102987
- inverse problems under loading 0-99955
- laser fusion reactor, cylindrical shell, thermal vibrs., general soln. 0-95433
- lightly damped tubular arrays, damping props, flow induced vibr. tests 0-68760
- linear displacement meas. accuracy meas. accuracy improvement under vibration 0-90815
- linear oscillatory systems, stability with proportional damping (German) 0-106751
- loudspeaker surrounds, stiffness at fund. reson. freq. (Japanese) 0-92009
- membrane speckle pattern analysis 0-106769
- metal rods and metal plates, US transducers, piezoelectric discs, radial vibrs. 0-96166
- metallic bar, 30 MeV proton excitation of reson. oscils. 0-64431
- Mindlin plates, Rayleigh-Ritz vibration anal. 0-96218
- modal analysis, general introduction for managers 0-91955
- motor car horn diaphragms, free vibr. anal. 0-74687
- multiple responses, interdependence of spectral densities 0-96221
- non-circular cylindrical panels, arbitrary boundary conditions 0-96222
- nonlinear systems, multi-degree-of-freedom, harmonic excitation, instability 0-73162
- numeric displays, effect of vibration on reading 0-104582
- orthotropic circular plates elastically restrained against rotation, large amplitude axisymmetric vibrations 0-83750
- orthotropic polygonal plates, determ. fund. freq. 0-106739
- oscillation rods in viscous fluids, added mass and damping, finite element anal. 0-58967
- oscillations of firmly clamped, end-stiffened, right circular cylindrical shells (German) 0-106750
- oscillator with non-linear spring, numerical soln. for free vibr. 0-68034
- phase relationships for damped and undamped systems (German) 0-106746
- piezoelectric crystals, vibrations, waves, flexure, fracture, fundamental equations 0-60505
- pipes and beams, structure-borne power flow, cross spectral density methods 0-106742
- plate, annular, variable thickness, free vibration, spline technique method 0-79195
- plate, thin isotropic rectangular, with edge beams, vibrs. 0-79193
- plate, two-layered, with imperfect bonding, resting on fluid half-space, vibrations 0-74792
- plate, vertical, free convection boundary layers and heat transfer 0-59002
- plate rectangular, with eccentric circular inner boundary, transverse vibration 0-106737
- plate with intermediate continuous elastic supports subjected to initial membrane forces 0-106744
- plate with straight line boundaries, method for solving vibration problems, Fourier expansion 0-64433
- plates, periodically varying length, instability of motion 0-69717
- plates, rectangular, with internal rigid support, bending vibration 0-102981
- plates, unconstrained layer damping treated, response to random acoustic excitation 0-74798
- plates, unconstrained layer damping treated, response to random acoustic radiation 0-74799
- plates, varying thickness, natural freq., numerical integration (German) 0-106747
- point loaded beam, vibrs. with coupling between different wave types (German) 0-102979
- porous materials, acoustic radiations anal. 0-87640
- porous plates in fluids, sound absorpt. props. of plates near rigid walls 0-87730
- power press, relationship between force waveform and sound radiation 0-74596
- radial impeller blades, unsteady aerodynamic forces and moments, singularity method obs. 0-58952
- radiation impedance of circular plates subject to various edge conditions 0-102913
- random excitation of system with autoparametric interaction 0-73165
- rectangular plates, edges having different degrees of rotational restraint, free vibrations 0-69713
- rectangular plates, free vibration, generalized orthogonality relations for modes of vibration 0-102988
- rectangular vibrating plates separated by liquid filled gaps, viscosity friction calc. (German) 0-105504
- reflection charact. of torsional waves in semi-infinite cylindrical rod connected to elastic half space 0-96095
- regular polygonal and circular plates, stepped thickness over a concentric circular subdomain, fundamental freq. of vibration 0-87732
- resonance phenomena with incidence of acoustic waves on a sphere (Russian) 0-58965
- resonance phenomena with incidence of waves on a cylinder (Russian) 0-58964
- ribbed cylindrical shell immersed in liquid, dispersion curves and coeffs. of distribution function 0-87736
- ribbed cylindrical shell with solid body, free oscill. 0-99956
- rigid sphere vibrating parallel to plane wall, acoustic near field and impedance 0-102910
- rods with nonlinear elasticity relation and nonlinear internal friction, parametrically excited oscils. 0-99947
- rotating beam with tip mass, vibration 0-58960
- rotating viscoelastic tapered cantilever, circulatory force at free end, influence of angle of attack on stability 0-69686
- rotationally periodic large space structures, finite element transfer matrix dynamic analysis, 100 m parabolic dish 0-74731
- rotationally periodic structures, vibr. behaviour, forced response to rot. force 0-69730
- rotor systems, characteristic behaviour (German) 0-106748
- segmental cylindrical shells vibrations, Fourier series component mode anal. 0-58958
- shell, elastic cylindrical, ribbed, with weight on springs, free vibr. freqs. 0-69725



**vibrating bodies continued**

- shells, cylindrical, finite element anal., solid of rev., thin shell and interphase elements 0-74744
- shells, cylindricals, composite, buckling and vibrational response to axial compression 0-64423
- shells, thick hyperelastic, spherical, large amplitude free and forced oscillations 0-74794
- shells, truncated conical, natural vibr. freqs. and modes, rib effects 0-69726
- simply supported circular plates, accurate natural freqs. determ. 0-102986
- simply supported circular plates, partial elastic boundary constraints 0-106740
- slightly bent slender beams, lateral vibration, axial end displacement 0-74797
- small free vibrations of shell of revolutions in an ideal liquid (*Russian*) 0-73168
- sound radiation by plane structures with diffuse flexural-wave field 0-102912
- spheres, mass transfer, horizontal transverse vibr. effects 0-57220
- spherical shells, transient response of thin elastic spherical shells 0-96217
- spring-loaded mass system vibration analysis (*German*) 0-96224
- springs, helical, cylindrical, natural frequencies of transverse vibrations 0-77630
- steady-state response of internally damped circular plates 0-106658
- stiff string with piezoelec. polymer film, vibration mode meas. 0-99959
- stiffened panels, acoustic noise transmission 0-102922
- stretched strings, intrinsic nonlinear effects 0-82607
- string, vibrating, motion above a concave obstacle, second order hyperbolic problem with unilateral constraints 0-57101
- strip radiator, power output considerations 0-69577
- submerged spherical shell, axisymmetric free vibration 0-74546
- thin annular plate having parabolic thickness variation, flexural vibrations 0-69719
- thin elastic plate with arbitrary shape, method for solving problems 0-87641
- thin electroelastic sheets, fluttering, thermodynamic effects (*German*) 0-106749
- thin infinite panel, sound insulation dependence on effective loss coeff. 0-87737
- tip heavy beam, vibration anal. by Dunkerley's method 0-102994
- transducer, performance calc. 0-77771
- transverse, circular plates of linearly varying thicknesses, soln. by polynomial coord. functions 0-64425
- tube bundle in turbulent water crossflow, bent tube vibrations 0-92124
- tuning fork, generalised, vibration mode anal. 0-96097
- tuning fork for HF operation, second-mode, finite element anal. and expts. 0-102980
- two coupled conductors, stab. anal. 0-96219
- two dimensional distributed resonator, math. model 0-64275
- unconstrained discrete systems, determ. lowest freq., extended bound formula method 0-102985
- vibration insulation, natural rubber in transport engineering 0-96099
- vibration of thin plates using the Ritz method 0-64426
- wedge, free oscillations in a tight cavity (*Russian*) 0-58953
- wide-band plane wave scattering and transmission by fluid loaded plates 0-106646
- Al plate excited by free turbulent jet, generation of vibrs. and atmospheric sound (*German*) 0-102908

**vibration control**

- see also damping*
- buildings, use of natural rubber mounts 0-87643
- cantilevered bench, vibration isolation for balances 0-68183
- IR detector balanced common module coolers 0-95142
- machine, power flow through isolation systems 0-64436
- machine, wave propagation and power flow, beam-stiffened foundation plates 0-64435
- machines and power transmission mechanisms, approximate analyses of beam and plate foundations 0-64434
- natural rubber in transport engineering 0-96099
- structure-borne sound source data, prediction of vibration isolation efficiency 0-102909

**vibration measurement**

- see also seismometers*
- acceleration sensor device for recording vibrations of tall structures 0-95084
- axial flow compressor stator blade wake guidevane, method 0-95085
- drives, rotational, damping of torsional vibrations, experimental determ. (*Russian*) 0-74816
- cardrum vibration meas. using electronic speckle pattern interferometry 0-67209
- explosions, quarrying, use of electronic transient recorders for meas. explosion noise and vibration 0-67023
- free damped mech. vibration logarithmic decrement, optoelectronic meas. 0-92095
- hearing mechanism, vibr. characts. obs. by holographic interferometry with optical fibres 0-76879
- heterodyning two laser beams, meas. small mech. displacements 0-73309
- hologram interferometry, time-averaged, for vibr. anal. 0-63953
- holographic interferometry, linearised subfringe, modulation errors effect 0-78803
- by holographic interferometry (*German*) 0-91759
- holographic interferometry appl., real-time, using finite fringe field of background (*Czech*) 0-58989
- holographic interferometry with swirl type shutter, stroboscopic and time-average methods (*Japanese*) 0-69748
- horizontal contact resonances of vibration pickup with rectangular bases on soil surfaces 0-96160
- interference fringe method, TV detect. and electronic image processing 0-103004
- laboratory equipment for resonance meas. in solids (*Spanish*) 0-86285
- manufacturing machines, spectral analysis of vibration data, failure prediction 0-79048
- membrane speckle pattern analysis 0-106769
- modal analysis techniques, prediction of point mobility plots 0-106659
- moire fringes holography vibration anal., facilitation of fringes counting 0-64504
- multiple shaker testers, production and military applications 0-64276
- multiplied moire fringes holography, vibration anal., expansion of meas. limitation 0-64505

**vibration measurement continued**

- nuclear power plant, PWR, constructional elements, vibrations due to cooling medium flow (*Hungarian*) 0-63304
- parametric resonance in complex objects, multichannel installation for stabilising vibration 0-58990
- particle size and density determ., bispectral anal. of laser Doppler vibr. meas. 0-98880
- plate vibration analysis by time-averaged projection-moire method 0-79241
- production testing, multiple shaker considerations 0-79047
- PWR components, using correlation techniques (*German*) 0-79247
- quartz resonator tangential vibrations, using SEM 0-71323
- seismic microvibration frequency analysis by 50 m interferometer 0-109276
- sinewave generator, simultaneous supply of fifty strain transducers, ship vibration testing 0-62652
- skull and auditory ossicle vibr. anal., human preps., using holographic interferometry 0-67210
- structure-borne sound, procedure for meas. sensitivity of building structures to stationary excitation (*German*) 0-64287
- testing by simulated vibrations, expt. problems 0-58855
- transducer dynamics (*Russian*) 0-105638
- transducers, meas. errors due to surface compliance of vibrating body (*Japanese*) 0-79046
- two-dimensional structure in-plane vibr., stress analysis by laser speckle method 0-103006
- tympanic membrane investigations in living man using holographic interferometry 0-67207
- tympanic membrane vibr. studies in living man using holographic interferometry 0-67208
- US transducers, measurement of vibrations of very small amplitude using US probe 0-73443
- vibrometers, photoelectric, analogue, systematic errors determ. 0-79246
- waveform measurement using temporally modulated holography, in biomedical appl. 0-67212
- Bi<sub>2</sub>SiO<sub>20</sub>, photorefractive, vibr. struct. mode pattern visualisation, phase conjugation and dynamic holography 0-95938
- Se photocell optical vibration transducer 0-77768

**vibrational states in disordered systems**

- acetone, vibr. dephasing theories, test using selective coherent ps. Stokes scatt. 0-59609
- alkali halides, molten, mode coupling theory of charge fluctuation spectrum 0-92451
- alloys, force-and-mass disordered, average local-information transfer approx. 0-88290
- alloys, substitutional, self consistent cluster theory for off diagonal disordered systems 0-84272
- amorphous solids, vibr. sp. ht. enhancement from force-const. variations 0-88333
- biphonon spectra, CPA calc. 0-70341
- biphonon spectra, light absorpt. coeff. and density of states, CPA calc. 0-84271
- t-butyl bromide, vibr. relax. in pure liq. and soln., Raman spectra 0-66167
- t-butyl chloride, vibr. relax. in pure liq. and soln., Raman spectra 0-66167
- 4-cyanobiphenyl and 4'-alkyl- or 4'-alkoxy-substituted liq. cryst. derivatives, soln., absorpt. and fluoresc. spectra 0-87164
- ethyl-p-azobenzoate, far IR and Raman spectra, smectic polymorphism 0-76022
- liquid, ionic, binary mode coupling theory of charge fluctuation spectrum 0-92451
- liquids, vibr. energy relax., nonMarkovian effects 0-74230
- liquids, vibrational relaxation studied by picosecond or Raman spectrosc. 0-80797
- MBBA, Raman spectra in cryst., frozen glassy, and liq. cryst. states 0-60601
- methanol, vibr. dephasing theories, test using selective coherent ps. Stokes scatt. 0-59609
- n-paraffin, longitudinal acoustic mode, perturbing forces 0-70348
- phonon modes, lattice Green function expansion method 0-79900
- PMMA, C-H stretching and bending vibrs. in Raman spectra 0-93300
- polyacetylene, vibr. excitations of charged solitons 0-108201
- polyethylene, phase characterisation, Raman spectra study (*French*) 0-93303
- polyethylene, phase orientation by stretching, Raman study (*French*) 0-93304
- polymer, longitudinal acoustic mode, perturbing forces 0-70348
- polymers, Raman active longitudinal-acoustical mode spectra interpretation 0-103950
- polymethylene crystals, lattice vibrations 0-59607
- polypyrrolenes, iso- and syndio-tactic, Raman tacticity bands, vibr. spectrum 0-66193
- quinizarin in alcohol, glasses, electron-phonon coupling, photochemical hole burning 0-97265
- semiconductors, amorphous, short-range order, theory and probes 0-79698
- shell models, CPA calc. 0-70347
- spontaneous echoes in disordered systems, spectral diffusion decay 0-84270
- trans-polyacetylene, intrinsic, electron-phonon coupling 0-79901
- AgI, lattice dynamics of binary superionic conductors 0-107393
- (AgI)<sub>x</sub>(Ag<sub>2</sub>O B<sub>2</sub>O<sub>3</sub>)<sub>1-x</sub>, amorphous superionic compound, <sup>11</sup>B lineshape and relaxation 0-108107
- Al, liq., density fluctuations, neutron scatt. anal. 0-70349
- Al-Ag, force-and-mass disordered alloys, vibrs., average local-information transfer approx. 0-88290
- AlF<sub>3</sub>-M<sub>2</sub>F glasses, M=alkaline earth, density-of-states and structural forms, Raman spectra study 0-97255
- As-Se-Ge(-S), photostructural change in Urbach tail 0-76021
- As<sub>2</sub>Se<sub>3</sub> glass, mol. struct. model 0-100179
- As-Se-GeSe<sub>2</sub> glasses, bulk and impurity IR absorpt. 0-71455
- CaO-Al<sub>2</sub>O<sub>3</sub>-SiO<sub>2</sub> glasses, density-of-states and structural forms, Raman spectra study 0-97255
- Cu halides, lattice dynamics of binary superionic conductors 0-107393
- α-Fe, vibrational states, phonon dispersion, phonon softening 0-88289
- Ge amorphous film, disorder induced phonon absorpt. meas. using double beam Fourier spectrometer 0-105725
- HNO<sub>3</sub>, aqueous soln., reflectance and complex refractive index, IR spectra, vibr. modes 0-66168

**vibrational states in disordered systems continued**

- La-B, amorphous, B-rich, low freq. modes, Raman scatt. obs. 0-108202  
 Na<sub>2</sub>O-SiO<sub>2</sub> glass, acoustic and thermal Gruneisen parameters 0-59608  
 NaOD solution in D<sub>2</sub>O, collective excitations in liquid and amorphous state, 77 to 300K 0-92636  
 PbO-SiO<sub>2</sub> glass, acoustic and thermal Gruneisen parameters 0-59608  
 PbO-SiO<sub>2</sub> glasses, density-of-states and structural forms, Raman spectra study 0-97255  
 Pd-Si amorphous alloy, heat treated, low temp. lattice sp. ht. 0-75368  
 SbCl<sub>3</sub>/AlCl<sub>3</sub> molten mixtures, Raman spectra 0-93305  
 SbSBr glass, IR reflectivity spectra 0-71403  
 Se, trigonal and vitreous, sp. ht. and thermal cond., 3 to 300K 0-59676  
 Si:F, amorphous alloys, RF sputtering prep. in SiF<sub>4</sub>-Ar gas mixture, spectra 0-80772  
 Si:H alloy, amorphous, dihydride model of vibrational spectra 0-80827  
 Si:H amorphous films, IR spectrum and struct. 0-97277  
 Si:H film, amorphous, H-associated disorder modes, PMR spin-lattice relax. time meas. 0-93202  
 SiO<sub>2</sub> fibres, LF optical phonons, Raman spectra 0-80789  
 SiO<sub>2</sub> glass, acoustic and thermal Gruneisen parameters 0-59608  
 SiO<sub>2</sub>, hydroxylated amorphous, small-particle dynamics, neutron scatt. 0-79899  
 SiO<sub>2</sub>, vitreous Brillouin scatt., 35 GHz phonon vel. and absorpt. below 1K 0-100664  
 TiO<sub>2</sub>-SiO<sub>2</sub> glass system, Raman and hyper-Raman light scatt. spectra 0-66187  
 Y-B, amorphous, B-rich, low freq. modes, Raman scatt. obs. 0-108202

**vibrations**

- see also lattice dynamics; molecular vibration; vibrating bodies*  
 AF, buildings, transmission by columns 0-74602  
 annular plate, radially stiffened, free vibr. studied by Ritz method 0-69707  
 axisymmetric free vibration of submerged spherical shell 0-74546  
 beams, buckling loads and fundamental freqs. improved lower bounds 0-64416  
 cavitating orifice under reattached flow conditions, noise and vibration characteristics 0-83829  
 composite materials, fibre reinforced, rectangular rods, elastic wave propagation (*French*) 0-83749  
 concrete, fresh, behaviour under a vibr. action, large particle segregation (*Japanese*) 0-88329  
 continuous viscoelastic structural members, transient dynamic response 0-64442  
 coupled bending-torsion flutter in cascades, aeroelastic stability boundaries 0-64424  
 crane bridge, damping calc. 0-101711  
 crystal resonators with increased immunity to acceleration fields in any shock/vibration environment 0-91953  
 curved beams, nonlinear dynamic anal., finite element method 0-96213  
 cylindrical rod, periodic structure, torsional vibrations, interfacial elastic parameters 0-96215  
 diffuse vibration field propag. in structs. with periodic inhomogeneities 0-86093  
 dynamic shear loading at boundary between elastic space and cylindrical rigid enclosure (*German*) 0-58896  
 elastic mechanical systems, vibr. damping by dampers with filled voids (*Russian*) 0-58954  
 elastic-viscoplastic frames, dynamic responses, strain hardening effects 0-79178  
 elasticity, contact problem, vibration of partially adhering stamp 0-69656  
 electron microscope, HV 3 MV type, mech. vibr. sources and effects (*French*) 0-82848  
 fibre reinforced composite waveguides, axisymm. elastic vibrs. 0-102995  
 flexural, accel. meas., effect of strain sensitivity of piezoelectric accelerometers 0-58991  
 floor, acceptability scales for occupant-induced vibrations 0-91956  
 floor, footfall-induced, effect on sensitive instruments 0-64277  
 floor, pneumatic isolators with two-chamber damping systems, isolation of very sensitive meas. apparatus (*German*) 0-69590  
 frame, plane, impulsively loaded, large deflections, mode approx. technique extension 0-83757  
 free, non-linear oscillator, numerical soln. 0-68034  
 gyro-stabilisation platform, nonlinear loss of stability and trembling (*Chinese*) 0-62457  
 Hamiltonian systems satisfying the Rosenberg conditions for normal modes 0-64444  
 hysteretic systems under random excitation, equivalent linearisation 0-79210  
 instability regions determ. in system with parametric excitation 0-90662  
 interferometer, data handling in high vibration environment 0-95132  
 interferometer design for high vibration environment 0-95131  
 isolation, machines and power transmission mechanisms, approximate analyses of beam and plate foundations 0-64434  
 loudspeaker cones, effect of voice-coil and surround on vibration and sound pressure level 0-96172  
 machine, power flow through isolation systems 0-64436  
 machine, wave propagation and power flow, beam-stiffened foundation plate 0-64435  
 membrane with both curved and straight line boundaries, dynamic response 0-64440  
 metal particles, small, possible vibrations associated with twins 0-100253  
 modal damping bounds by component modes method using Lagrange multipliers, natural freqs. 0-79213  
 non-Newtonian fluid exit flow through capillaries, effect of vibrations 0-79358  
 nonlinear oscillator and reflectors, periodic vibr. and impact characteristics 0-92089  
 nonstationary random vibrations of multiple-mass systems 0-69728  
 nuclear reactor component vibration investigation using fast Fourier transform analysers 0-63315  
 ore-mill foundation, prevention of vibration by damping and stiffness addition 0-69588  
 oscillatory flow induced vibration, linearisation eqns. 0-64449  
 out-of-plane, natural freqs. of continuous curved beams 0-74588  
 panels, induced edge crack growth rates, excited by convected random pressure fields 0-69737  
 plate, annular, elastically supported, with central rigid mass, free vibrations (*Japanese*) 0-96226  
 plate, circular, elastically supported, with conc. mass at centre, large amplitude vibrs. (*Japanese*) 0-96227

**vibrations continued**

- plate, variable thickness, on elastic foundation, bending, closed form soln. 0-79179  
 plates, anisotropic skew, large amplitude vibrs., transverse shear, rot. inertia, theory 0-79207  
 plates, anisotropic skew, large amplitude vibrs., transverse shear and rot. inertia, numerical results 0-79208  
 plates, continuous, with arbitrary number of equal spans, eigenfreqs. 0-64438  
 plates, laminated anisotropic composite, penalty plate bending element 0-96200  
 poroelastic cylinders, torsional vibrs., wavelength, phase and group vel. 0-79214  
 PWR core barrels with and without holes, various edge conditions, hydrodynamic vibrations 0-78406  
 quartz plates, rotated-Y-cuts, high frequency vibrations 0-96216  
 random, statistical data digital processing method (*Japanese*) 0-64430  
 rectangular laminated plate, free vibrs., freq. and shape determ., complex boundary conditions 0-79203  
 rectangular parallelepiped, natural vibrs. from 3D elasticity and plate theory (*Russian*) 0-79199  
 reinforced plastic cylindrical shells, optimal design under dynamic constraints 0-102996  
 rigid sphere embedded in elastic medium, response to incident stochastic waves 0-64451  
 rods, elastic, high-freq. long wave vibrs. 0-96211  
 self-excited vibrations in lubricated friction 0-58984  
 shell, cylindrical, under external press., vibr. and buckling 0-102975  
 shell, cylindrical elastic, dynamic response in potential fluid 0-64446  
 shells, conical, axisymmetric torsional vibrs. from tangential inertial force 0-64443  
 single mass vibroimpact system, response to white noise random excitation 0-64454  
 small free vibrations of shell of revolutions in an ideal liquid (*Russian*) 0-73168  
 stars, distorted, Clairaut coordinates and vibr. stability 0-90408  
 stationary vibrations in 2-dimensional micropolar thermoelasticity 0-74793  
 steel, austenitic, rod, coupled flexural and torsional vibrs., energy dissipation 0-89281  
 steel, ferromag., rod, coupled flexural and torsional vibrs., energy dissipation 0-89281  
 steel rod, transverse vibrations, energy dissipation, static longitudinal load effect 0-81099  
 string, wave velocity propag. meas., mass tension ratio (*Spanish*) 0-74592  
 torsional, iterative methods of finding natural freqs., change of stiffness method 0-74589  
 torsional wave propag. in infinite piezoelec. cylinder (622) cryst. class 0-87642  
 tuning fork oscillator internal random disturbances (*Russian*) 0-62459  
 upper bounds for amplitudes of harmonic components of excitation 0-64445  
 US torsional vibrations in metals, measurement of absorpt. 0-58856  
 vibroisolation parameter selection method and stability for two machines on elastic beam 0-87738  
 viscoelastic cylindrical shell, short, resonance vibrations 0-58962  
 wedge, plane composite, singular eigenfunctions for plane harmonic problems 0-79206  
 Al-Cu-Mg-Mn-Si-Fe, torsional vibrations decrement, deformed vol. effect 0-76326  
 Al-Mg(Cu)(Si), (5.0(4.5)(11.8) wt.%), ingots, vibr. effect during solidification on porosity formation 0-108426  
 Cu, annealed polycryst., torsional vibrations decrement, deformed vol. effect 0-76326  
 Mn-Cu (25 wt.%) rod, transverse vibrations, energy dissipation, static longitudinal load effect 0-81099  
 Mn-Cu (75, 25 wt.%) rod, coupled flexural and torsional vibrs., energy dissipation 0-89281
- vibrations, crystal lattice** *see lattice dynamics*  
**vibrations, molecular** *see molecular vibration*  
**vibrations of crystal lattices** *see lattice dynamics*  
**vibrometers** *see vibration measurement*  
**vibronic states of molecules** *see molecular vibronic states*  
**video recording**  
 biomedical US data recording method using videotape (*German*) 0-81666  
 digital holographic storage of TV signals 0-87353  
 disc master recording, high density, replication by contact printing 0-62761  
 echocardiograph signals, M-mode, analogue storage using video tape 0-94298  
 gradient-index imaging, theory 0-69331  
 holographic interferogram anal. with TV picture system 0-106489  
 image quality transfer 0-68279  
 laser scanning system, He-Ne, for information identification (*German*) 0-106557  
 lens, gradient-index spherical, design for optical pickup systems 0-69483  
 materials for optical recording (*Japanese*) 0-105730  
 microscopy, applications 0-98972  
 movie camera, laser based, operation and applications 0-57405  
 time control system, Q-Lock, for editing, dubbing, VTR appl. 0-68278
- video signals**  
 analogue video transmission feasibility using laser diode, over 30 km at 1.3  $\mu$ m 0-58737  
 bandwidth compression effect on military target observers' detection and recognition performance 0-106484  
 edge detection, numerical, optical and hybrid methods compared 0-102662  
 fibre-optic transmission by laser diode analogue baseband modulation 0-58738  
 interferogram analysis by TV camera-microprocessor system 0-73440  
 SEM information representation by equal signal lines 0-95196  
 strain meas. speckle photography with hybrid optical/electronic image processing 0-106768  
 PtSi Schottky-barrier monolithic IRCCD focal plane 0-86427
- vidicons** *see television camera tubes*  
**viewing screens** *see screens (display)*



virial coefficients *see* equations of state

virtuons (virtual phonons) *see* phonons

## viscoelasticity

*see also* creep; internal friction; stress relaxation

aging viscoelastic contact 0-64486  
 amylopectin, glycerin impregnated, dynamic viscoelasticity (Japanese) 0-104203  
 amylose, glycerin impregnated, dynamic viscoelasticity (Japanese) 0-104203  
 articular cartilage, normal, quasi-linear viscoelastic props. 0-108937  
 articular cartilage, viscoelastic properties (Japanese) 0-101215  
 bitumens, oil sand, rheological props. 0-64506  
 blood, rheological behaviour, viscoelastic model (French) 0-76779  
 blood, viscoelastic properties, transient flow obs. 0-97980  
 blood plasma, normal and haemophilic, coagulation kinetics study 0-67107  
 blood rheology, erythrocyte rigidity effects on viscoelastic dilatancy 0-61610  
 bone viscoelastic behaviour, anal. on basis of microstruct. 0-85429  
 bubble translational motion in a viscoelastic liquid, retarded motion approx. 0-83777  
 cardiac muscle, passive, viscoelastic theory and obs. 0-94273  
 cellulose nitrate, nonlinear viscoelastic deform., hydrostatic press. and third invariant of deviatoric stress tensor 0-93587  
 composite material, mechanical behaviour, book 0-94935  
 composite polymers, viscoelasticity theory, appl. 0-64397  
 composites, spatially reinforced, viscoelastic props. determ. using averaging methods 0-102973  
 constrained viscoelastic damping composites, noise and vibration insulation 0-83743  
 continuous viscoelastic structural members, transient dynamic response 0-64442  
 crack growth kinetics under cyclic loads in viscoelastic bodies (Russian) 0-87739  
 crack growth law derivation, linear viscoelastic solids, fracture process zone concept 0-92088  
 cracks in viscoelastic body, durability calcs. 0-79227  
 deformation wave processes, corrected nonlinear eqns., stresses and strains 0-102998  
 N,N-diethylacrylamide, cross-linked copolymer, improved mech. props. 0-61091  
 discontinuity propagation, non-homogeneous thermoviscoelastic media 0-102972  
 disturbances under transient tangential force and mag. field 0-92070  
 droplet break-up, in nonuniform shear flow 0-64588  
 dynamic response of a slab of elastic-viscoplastic material that exhibits induced plastic anisotropy 0-83737  
 Earth, viscoelastic model appl. to Earth tides theoretical study 0-67333  
 Earth interior, pulse propag. in viscoelastic medium with freq. depend. Q 0-72438  
 ebonite, viscoelastic, linearity conservation 0-108492  
 elastic/viscoplastic media, constitutive eqn. covering wide range of strain rates (Japanese) 0-79862  
 elastico-viscous liquid flow in axisymmetric pipe of slowly varying cross-section 0-83774  
 elastohydrodynamic lubrication, non-Newtonian effects of volume relaxation 0-103009  
 elastohydrodynamic traction, non-Newtonian thermo-viscoelastic, from combined slip and spin 0-103043  
 electrolyte solutions in glycerol, investigation by US shear strains 0-88266  
 emulsion, dilute, straining motion, effect of inertia on dynamic viscosity 0-87797  
 emulsions, concentrated, rheological props. 0-99981  
 epoxy resin composites, cooldown residual thermal stresses, viscoelastic response 0-60941  
 ethyl acrylate ionomers, stress relax. 0-104200  
 failure and instability in tension 0-87720  
 filled polymer mechanical properties, particle shape effect, review 0-100864  
 flow, cooperative phenomenon, theory 0-69878  
 fluid, laminar flow, combined generalised measure approach, pseudoplasticity 0-64586  
 fluid, motion of rigid particles 0-103044  
 fluid, stability of steady shearing flows, energy method and parabolic maximum principle 0-74926  
 fluid lubrication, viscoelastic, slider-bearing config., non-Newtonian normal stresses 0-69753  
 fluids, axial compliance reduction, in a R-17 Weissenberg rheogoniometer 0-106859  
 fluids, shear-thinning, elastic, Carreau viscosity eqn., creeping motion of spheres 0-87753  
 fluids, third grade, viscometric flows 0-69883  
 gelatin gels, in water and glycerol/water mixtures, dynamic viscoelastic props. 0-64508  
 glass, viscous deformation during heating and cooling 0-89314  
 glass and glass-forming liq., viscoelastic properties, comparison with Lennard-Jones model 0-84983  
 glass beads in polystyrene soln., suspension, time depend. viscoelastic behaviour 0-99982  
 glass fibre reinforced polycapromide, viscoelastic, linearity conservation 0-108492  
 glasses, commercial, viscosity and stress relax. in glass transition region 0-93589  
 infinite power law viscoelastic body, crack propag. by rigid wedge, stress intensity 0-64476  
 layered composites, wave propag., dispersion and dissipation effects 0-102982  
 linear, finite element method variant 0-69692  
 linear viscoelastic media, dynamic problems, approx. soln. 0-69679  
 liquid, viscoelastic, boundary-layer flow past symmetric wedge or right circular cone 0-64513  
 Maxwell fluids, immiscible, hydrodynamic flow through non-conducting rectangular channel 0-100038  
 membrane, circular, nonlinear viscoelastic material 0-64380  
 non-Newtonian fluid, viscoelastic boundary-layer flow past a parabola and a paraboloid 0-83817  
 nylon 6-Li halide mixtures, viscoelastic behaviour, stress relaxation 0-58995

## viscoelasticity continued

orientable polymer fluid, Ericksen's anisotropic fluids theory extension 0-79359  
 perfluorinated polymer, Krytox 143-AB, viscous, viscoelastic and dielectric properties 0-70440  
 plant cell walls, viscoelastic props. 0-67106  
 plate, guided harmonic waves 0-79194  
 plate, viscoelastic, heated, bending, Kelvin Voigt model 0-106731  
 PMMA, craze zones at crack tips, validity of Dugdale model 0-108534  
 poly(spiro[2,4]hepta-4,6-diene) molecular characterisation, glassy state props. 0-64928  
 polyamide, viscoelastic, linearity conservation 0-108492  
 polyamide-polyurethane copolymer dispersions, structuring and relax. props., coating from props. 0-76559  
 1,2-polybutadiene, crosslinked in states of strain, entanglement networks, swelling anisotropy obs. 0-79666  
 1,2-polybutadiene, dynamic viscoelastic props. in curing process 0-76298  
 polycarbonate, secondary flow and stress birefringence patterns in pressure hole 0-64590  
 polycrystalline materials, effect of grain boundary sliding on anelasticity 0-96592  
 polydimethylsiloxane chains, end-linked, swollen model networks, stress/strain isotherms and elastic modulus 0-79668  
 polymer chains with rigid bonds, local relax. times, mol. dynamics study (Russian) 0-59373  
 polymer diffusion equation with hydrodynamic interaction, equiv. normal coord. 0-79966  
 polymer liquid, entangled, phenomenological consequences of Doi-Edwards viscoelasticity theory 0-79250  
 polymer melts, normal stress and Barus effect 0-64589  
 polymer solution, elastic, load bearing capacity of squeeze film flow 0-103051  
 polymer solution rheology based on a finitely extensible bead-spring chain model 0-83775  
 polymer solutions, dilute, normal stress difference and shear rate 0-83776  
 polymer solutions, dilute, production, pulsation and damping of air bubbles 0-69879  
 polymer spherulite, cryst. lattice strains, mech. behaviour, X-ray diffr. detect. 0-59558  
 polymer spherulites, deformation mechanism, linear isothermal viscoelasticity theory 0-58924  
 polymeric liquid, gas bubble-pulsations and assoc. dissipation effects 0-59079  
 polymers, creep under plane stress, nonlinear viscoelasticity models appl. 0-89308  
 polymers, electrification by metals, contact time effect obs. 0-70829  
 polymers with various atomic composition and viscoelastic props., laser damage 0-104017  
 polymethacrylic acid, swollen networks, viscoelastic photoelastic behaviour 0-59366  
 polypeptides, helical, conc. solns., rheological behaviour and liq. cryst. order 0-83771  
 polystyrene, bimodal mol. wt. blends, recoverable compliance 0-66568  
 polystyrene, ordered monodisperse latexes, viscoelasticity and flow props. 0-58992  
 polystyrene, viscoelastic, linearity conservation 0-108492  
 polystyrene-tricresyl phosphate solns., viscoelastic props., conc. depend. 0-76299  
 polyurethane solid foams, creep laws (German) 0-65139  
 polyvinyl alcohol networks, swelling equil. with dil. salt solns., thermoelastic behaviour, hydroxyl group interact. 0-79667  
 protein dispersions, viscoelastic effects, shear viscosity and primary normal stress difference 0-87754  
 pulsed NMR technique for meas. radiation effects in polymer 0-66051  
 rate type constitutive eqns., free energy of viscoelastic and viscoplastic materials 0-79168  
 red blood cells, viscoelastic study of aggregation 0-97960  
 red cell membrane, human, surface elasticity and viscosity 0-61608  
 relaxation modulus, evaluation from response to constant strain rate followed by constant strain 0-74765  
 resonance vibrations in short viscoelastic cylindrical shell 0-58962  
 rigid elastic body system, turning round fixed point, linear viscoelasticity theory (French) 0-69646  
 Rivlin-Ericksen fluid, dispersion medium on rheological behaviour of dilute suspension of dipolar dumbbells, viscoelastic props. 0-99983  
 rods with nonlinear elasticity relation and nonlinear internal friction, parametrically excited oscils. 0-99947  
 rubber, fracture in viscoelastic systems under cyclic loading 0-81195  
 shell, spherical, interaction with acoustic medium, pressure  $\delta$ -impulse (Ukrainian) 0-69681  
 sputum, meas. using conventional dynamic and raised cosine pulse methods (Japanese) 0-67132  
 stability of viscoelastic rods and shells under loads that decrease with time 0-69700  
 standard linear body, free torsional oscils. 0-99940  
 starch, glycerin impregnated, dynamic viscoelasticity (Japanese) 0-104203  
 steel, stainless, global bending response analysis of elastic and viscoplastic nuclear shipping cask structures subjected to impact loading 0-76301  
 steel, stainless, type 304, viscoplastic behaviour, strain rate sensitivity, creep, relaxation, tensile tests 0-66727  
 steel casting, calc. method of thermal and thermo-visco-elasto-plastic processes (German) 0-79859  
 steel continuous casting, thermal, thermo-visco-elasto-plastic processes (German) 0-81044  
 steel shell, mech. behaviour during solidification 0-81043  
 strain wave propagation in viscoelastic bars due to longitudinal impacts anal. (Japanese) 0-96223  
 stress clock function in viscoelasticity 0-99941  
 stress waves generated by internal heating in Voigt and Maxwell materials Laplace transform anal. (Japanese) 0-69693  
 strip, dynamic crack propagation due to antiplane loading 0-64464  
 styrene-butadiene-styrene block copolymer, stress relax. following steady-state flow, residual shear stress development 0-83772  
 styrene/acrylic terpolymers, viscoelastic props. 0-64509  
 tendon, viscoelastic deform. obs. 0-101211  
 thermoviscoelastic laminate beam, stress anal. (German) 0-106727  
 thin plate, optimal cool down in linear viscoelasticity 0-79176  
 time reversal and symmetry relations in finite linear viscoelasticity 0-102970  
 transient wave propag. in viscoelastic bar 0-106745



# viscoelasticity continued

- trifluoropropylmethylsiloxane fluids, viscoelastic props., mechanical impedance, viscosity and density meas. 0-79249  
tube, viscoelastic-plastic, successive deformation under cyclic, temp. variation 0-92074  
two-dimensional wave problem, Volterra method solns. 0-69727  
uterine muscle, isotropy and anisotropy during labour contract. 0-94257  
viscoplasticity theory based on infinitesimal total strain and nonlinear viscoelasticity 0-79164  
viscous fluid under cyclic deform., self-heating, hydrodynamic thermal explosion 0-58993  
wave propagation, integration contour deform. for Laplace transform inversion 0-74801  
Al, 2618, creep under step stress changes, viscous viscoelastic model 0-81138  
As-S-Tl, glass, viscosity and elastic props. 0-100180  
LiCl, hypersonic relaxations studied by Brillouin light scatt. techniques, viscoelastic effects obs. 0-83375  
Si<sub>3</sub>N<sub>4</sub>, hot-pressed, creep and strain recovery 0-100874

# viscometers

- see also viscosity measurement  
air-bearing viscometer, transient rheology study 0-59152  
automatic capillary, accuracy one part in five million 0-87825  
capillary viscometer and obs. of low shear rate blood viscosity 0-98180  
capillary-type closed, stabilized flow 0-59156  
Couette viscometer for short time shearing of blood 0-98179  
Couette viscometry, meas. of rheological props. of red blood cells 0-97992  
Couette-type, capacitor assembly for meas. small rotational vels. 0-100046  
high-temperature melt, torsional cylinder oscils. type 0-79418  
lifting liquid type, accelerated, theory and exptl. design (Japanese) 0-83870  
oscillation type, capacitive transducer of torsional oscils. 0-64656  
solar radiation tracking sensor 0-86295  
vibrating wire, adaptation for liquids 0-87827

# viscoplasticity see plasticity

# viscosimeters see viscometers

# viscosity

- see also electroviscous effect; internal friction; viscosity of gases; viscosity of liquids  
alkali borate glasses, single and mixed, viscosities 0-92701  
asthenosphere, kinematic viscosity rel. to median valley of Mid-Atlantic Ridge 0-90071  
atmosphere turbulent boundary layer, eddy viscosity coeff. for finite-element numerical modelling 0-77061  
blood cells, stored, rheological behaviour obs. (French) 0-67110  
Boussinesq fluids, turbulent viscosity and conductivity in turbulent convection 0-98543  
cement pastes, flow behaviour, specific surface and conc. of solids influence 0-65132  
clays, heat treatment, effect on rheological props. of enamel slips 0-60809  
concretes, further development of 2 point test for workability and extension of its range 0-66728  
constructional materials, creep, viscosity, resist. to inelastic deform. 0-89309  
cytoplasm spherical drop with effective surface tension influenced by oscillating enzymatic reactions 0-108862  
dispersed medium, effective viscosity and heat cond. coeffs. 0-89537  
Earth mantle, viscosity rel. to Earth thermal evolution 0-89988  
Earth mantle viscosity, rel. to Earth tides theory assuming Earth as viscoelastic body 0-67333  
elastico-viscous liquid flow in axisymmetric pipe of slowly varying cross-section 0-83774  
emulsion, dilute, straining motion, effect of inertia on dynamic viscosity 0-87797  
emulsions, concentrated, rheological props. 0-99981  
erythrocyte membranes, fluidity change after X-irrad., pyrene excimer fluorescence, obs. 0-72622  
extensional viscosity of a dilute suspension of spherical particles at intermediate microscale Reynolds numbers 0-106835  
gelatin sol-gel transition, viscosity meas. method 0-85219  
glass and glass-forming liq., viscoelastic properties, comparison with Lennard-Jones model 0-84983  
glasses, commercial, viscosity and stress relax. in glass transition region 0-93589  
glasses, industrial, temp. depend. at const. struct. temp. 0-65271  
glassy state and highly viscous liq., rheology 0-70130  
Hercules X-1, accretion disc viscosity determ. using slaved disc model 0-62110  
hydroxyethyl cellulose, polymer segments, fluoresc. depolarisation on conjugated spin labels 0-91711  
ice surface viscosity, activation energy, vacancy migration 0-107458  
incompressible viscous fluid, slow motion of small sphere outside cylinder 0-96239  
laminar flow through rough wall cracks, friction factor formula (Rumanian) 0-69925  
laminar viscous flow down an open inclined channel with naturally permeable bed 0-69764  
linear Newtonian viscosity, calculative props. 0-68048  
Nylon 6 film, prior high-pressure treatment effects, weight swelling, density, IR crystallinity, X-ray and viscosity obs. 0-81025  
polyamide-polyurethane copolymer dispersions, structuration and relax. props., coating from props. 0-76559  
polydimethyl siloxane-b-styrene-b-dimethyl siloxane block copolymer, morphology, mech. props. 0-64930  
polyester resin, unsaturated, chalk filled, props. (German) 0-104228  
polyethylene oxide, polymer segments, fluoresc. depolarisation on conjugated spin labels 0-91711  
polyurethane cement, viscosity and shear strength, components influence (German) 0-93729  
protein dispersions, viscoelastic effects, shear viscosity and primary normal stress difference 0-87754  
PVC plastisol, flow behaviour at high shear rate (German) 0-92186  
pyrene derivatives, micelle-embedded, rot. relax., time-resolved fluorescence, obs. 0-58300  
simple fluid shear depend. viscosity, central force interactions 0-79970  
solar convection zone, turbulent viscosity rel. to mag. fields floating-up time and 11-year cycle 0-101580

# viscosity continued

- SS 433, accretion disc viscosity determ. using slaved disc model 0-62110  
stability analysis and characts. for two-phase flow eqn. systems with viscous terms 0-59103  
steel E1736, creep, viscosity, resist. to inelastic deform. 0-89309  
stellar accretion discs, viscosity determ. for Hercules X-1 and (SS 433) 0-62110  
suspensions, effective viscosity, modified cell model approach 0-74944  
thermo-viscous materials, with hidden variables, shock waves and acceleration waves 0-74788  
thermodynamics, relativistic, nonstationary, hidden variable approach 0-68097  
turbulent pipe flow, use of eddy viscosity expressions for vel. profiles in Newtonian, non-Newtonian and drag-reducing flows 0-83789  
viscoplastic material, mixing process, Bingham model, two-dimens. flow (German) 0-92076  
Al<sub>2</sub>O<sub>3</sub>-SiO<sub>2</sub> refractory, creep, viscosity, resist. to inelastic deform. 0-89309  
B<sub>2</sub>O<sub>3</sub>-SiO<sub>2</sub>, optical waveguide glass, sintering kinetics 0-84898  
Fe ore concentrate, sinter quality improvement (Chinese) 0-104089  
Fe<sub>40</sub>Ni<sub>40</sub>P<sub>14</sub>B<sub>6</sub>, amorphous, steady-state creep rate, cryst. effect 0-81102  
Na<sub>2</sub>O-2CaO-3SiO<sub>2</sub> glass, cryst. nucleation and growth, viscosity, thermodynamic props. 0-84079  
2Na<sub>2</sub>O-CaO-3SiO<sub>2</sub> glass, cryst. nucleation rate, viscosity, heat treatment 0-84081  
Na<sub>2</sub>O-SiO<sub>2</sub> glass, OH<sup>-</sup> content effect on mech. and other props. 0-89337  
Ni alloy KhN56VMKYu, creep, viscosity, resist. to inelastic deform. 0-89309  
SiO<sub>2</sub>, vitreous 0-103513  
Tb-Fe amorphous thin films, magnetic after-effect, Kerr magneto-optic effect obs. 0-97123  
UF<sub>4</sub>-LiF(KF) molten binary mixtures, viscosity meas. 0-65270

# viscosity measurement

- see also viscometers  
amalgam preparation without O<sub>2</sub>, apparatus to measure viscosity 0-59150  
blood, red cells, rheological props. meas. by Couette viscometer 0-97992  
electrolyte solutions in glycerol, investigation by US shear strains 0-88266  
fatty acid monolayers, light scatt. meas. 0-89011  
high pressure viscosity meas. method 0-69955  
liquid, 25 to 100 C, up to 500 MPa, falling body instrument 0-103510  
liquid metals, apparatus for 0-59759  
liquids, capillary method determ. 0-82619  
metal, liquid, viscosity determination by oscillating vessel method (Japanese) 0-70439  
PVC, thermal stabilisation by triazine dithiols (Japanese) 0-108386  
supercooled liquids, Couette-type viscometer with capacitor assembly for meas. small rotational vels. 0-100046  
water, mobility in blood plasma, NMR determ., viscosity correl. to 1/T<sub>2</sub> 0-67176  
Fe<sub>40</sub>Ni<sub>40</sub>P<sub>14</sub>B<sub>6</sub>, metallic glass, glass transition, viscous flow and differential scanning calorimetry meas. 0-96635

# viscosity of gases

- binary gas mixture, kinetic theory collision integrals, generalised phase shift approach 0-83874  
binary gas mixture, transport properties in applied mag. field 0-83873  
dilute gas, transport props., simple pair pot. model 0-87835  
dilute gas transport props., logarithmic term in softness expansion 0-83872  
heat pipe, spectroscopic, operation 0-106708  
Ar, viscosity meas. at very high press. 0-59155  
Kr, Lennard Jones (12,6) pot. distance parameter, transport props. calc. 0-79423  
Kr, viscosity, vibr. disc method meas. 0-75020  
NH<sub>3</sub>-Ar mixture, thermal cond., viscosity, Senfleben-Beenakker effect 0-100054  
NH<sub>3</sub>-He mixture, viscosity, Senfleben-Beenakker effect 0-100054  
Ne, Lennard Jones (12,6) pot. distance parameter, transport props. calc. 0-79423  
Xe, Lennard Jones (12,6) pot. distance parameter, transport props. calc. 0-79423

# viscosity of liquids

- see also lubrication  
acrylamide aqueous solution, ultrasonic investigation (Chinese) 0-107371  
atomic liquids, shear viscosity determ. by nonequilib. mol. dynamics 0-79971  
benzene, liq., mol. motion at high press. 0-103509  
biomacromolecules, rigid, modelling approaches of hydrodynamic props. 0-61613  
bitumens, oil sand, rheological props. 0-64506  
blood plasma viscosity in sickle-cell anaemia 0-94250  
blood rheology, erythrocyte rigidity effects on viscoelastic dilatancy 0-61610  
blood viscosity and red cell aggregation changes after haemodilution 0-97952  
blood viscosity at low shear rate, capillary viscometer and obs. 0-98180  
capillary method determ. 0-82619  
cellulose acetate butyrate, in soln., hydrodynamic behaviour 0-64876  
channel flow, plane, shear rate dependent viscosity, effect on stability (German) 0-87809  
o-chlorophenol-acetone (ethyl methyl ketone), thermodynamic and transport props. 0-92686  
cholesteric liq. crystals, isotropic phase, pretransitional viscosity 0-84312  
classical fluid, dynamic scaling for crit. viscosity 0-59689  
colloidal dispersion dynamics, review 0-71956  
crown ether-containing polymers, in alkali salt solns., complexation, viscosity obs. 0-64877  
crystallisation from solution, same complex effects 0-100189  
cyclohexane, liquid, density effect on transport properties 0-65264  
dextran fractions, production, characterisation and solution properties 0-59368  
diquinoly cyanomethane, fluoresc. quantum yields, viscosity effects 0-60646  
drop deformation and orientation in shear and extensional flow fields, dynamic interfacial props. 0-107611  
drop dynamics in shear fields, role of dynamic interfacial effects 0-107612



## viscosity of liquids continued

- elastic fluids, shear-thinning, Carreau viscosity eqn., creeping motion of spheres 0-87753  
 elasto-hydrodynamic traction, granular behaviour 0-103008  
 electrolyte solutions in glycerol, investigation by US shear strains 0-88266  
 fluids, one and two dimensional, hydrodynamics, viscosity, heat conductivity, kinetics (*Russian*) 0-79972  
 glass and glass-forming liq., viscoelastic properties, comparison with Lennard-Jones model 0-84983  
 glass forming liquids, vol. relax. 0-96429  
 n-hexane-cyclohexane mixture, 25 to 100 °C, up to 500 MPa 0-103510  
 high pressure viscosity meas. method 0-69955  
 hydroxyethyl cellulose, microviscosity, mobility profile 0-91710  
 Invar, Fe-Ni (36 wt.%), alloy 36N, effect of melting conditions on thermal expansion coeff. 0-65256  
 Kramer's chemical reaction model, barrier mediated diffusion, generalisation to include viscosity term 0-71890  
 Lennard-Jones fluid, nonequilibrium molecular dynamics,  $t^{-3/2}$  long-time tail for stress-stress time correlation 0-70100  
 lipid hydrocarbon chain, biomembrane, rot. motion and fluidity 0-76714  
 liquid crystal, viscosity, anomalous properties near  $N \rightarrow S_A$  transition point (*Chinese*) 0-84052  
 liquid crystals, NMR spin-lattice relax. time near phase transitions 0-71222  
 liquid crystals, prep. and phys. props., book 0-105444  
 measurement with oscillation type viscometer, capacitive transducer of torsional oscils. 0-64656  
 metal, liquid, viscosity determination by oscillating vessel method (*Japanese*) 0-70439  
 metallic glass, heat of crystn. and viscous behaviour 0-75166  
 metallic melts, viscous flow due to high overheating, quasipolycrystalline model 0-70110  
 methyl iodide, liq., mol. reorientation, dielec. and viscosity meas. 0-100157  
 nitrobenzene, liquid and  $CCl_4$  soln. shear waves and translation-rotation coupling obs. by depolarised Rayleigh scattering 0-71432  
 nitrobenzene/n-hexane (n-heptane), critical exponent  $\beta$ , phase coexistence curve anal., viscosity coeff. meas. 0-100327  
 non-Newtonian fluids, mass transfer from cylinders to power law fluids 0-83826  
 non-Newtonian fluids, mass transfer from spheres to power law fluids 0-83825  
 nonisothermal flow of viscous fluid in pipes, crit. phenomena 0-103074  
 pentyl-cyano-biphenyl, nematic, hydrodynamic parameters meas. with and without applied elec. field 0-100297  
 perfluorinated polymer, Krytox 143-AB, viscous, viscoelastic and dielectric properties 0-70440  
 phosphatidylcholine bilayers, fluidity changes and phase transitions, intramol. excimer fluoresc. obs. 0-85342  
 pitch and bitumen, viscosity, temp. depend. up to 500°C 0-92698  
 polar molecules, viscosity activation energy and relax. time, RF cond. meas. 0-96677  
 poly-L-glutamic acid-Na, cooperativity parameter determ. from viscometry 0-75147  
 poly-m-phenylene-isophthalamide in dimethylacetamide, flow birefringence (*Russian*) 0-66148  
 poly-p-tert-butylphenylmethacrylate, soln., viscometric behaviour 0-88016  
 polyacrylamide aqueous solution, ultrasonic investigation (*Chinese*) 0-107371  
 polybutadiene, dil. soln., viscosity, temp. depend., solvent effects 0-59686  
 polydicarboxylic acids, electrophoretic and viscometric props. 0-66811  
 polymer, entangled, phenomenological consequences of Doi-Edwards viscoelasticity theory 0-79250  
 polymer, flexible ring, intrinsic viscosity 0-103511  
 polymer melt containing suspension, cell model theory of shear viscosity 0-103048  
 polymer melts, dynamics, self-diffusion const., relax. time and viscosity 0-64874  
 polymer melts, flow indices (*Japanese*) 0-79360  
 polymer solns., not infinitely dilute, second-order fluid coeffs., conc. depend. 0-106771  
 polymer solutions, dil., coherent scattering law, continued fraction formalism 0-103234  
 polymer solutions, transport properties, conc. effects 0-64875  
 polymerisation in flow-through reactor, low-temp. conditions 0-61092  
 polypeptides, helical, conc. solns., rheological behaviour and liq. cryst. order 0-83771  
 polystyrene, in solns., intrinsic viscosity rel. to mol. wt., unperturbed dimensions 0-65268  
 polystyrene, polymer chain, internal friction range, HF viscosity theory (*French*) 0-79968  
 polystyrene in benzene or cyclohexane, zero shear-rate intrinsic viscosities 0-75376  
 polystyrene melts, flame-retardant high-impact, shear viscosity-temp.-shear rate relationships 0-59691  
 polystyrene monodisperse latex, anomalous viscosity in disordered state 0-74822  
 polysulfonamide, optically active, synthesised by interfacial polycondensation, mol. wt. determ. 0-99595  
 polyvinyl acetate, and conc. solns., viscosity meas. 0-65269  
 ribonuclease A, microviscosity, mobility profile 0-91710  
 silicone oil, ionic behaviour, carrier mobility and viscosity 0-107453  
 simple fluids, fluctuation expressions for nonequilib. distrib. functions in adiabatic flows 0-92441  
 soft-sphere dense fluid, bulk viscosity, nonequilib. and equilb. mol. dynamics calcs. 0-79663  
 square-well fluid, viscosity below critical density, molecular dynamical calcs. 0-79661  
 trans-stilbene, soln., lifetime and anisotropic fluoresc., viscosity effects (*German*) 0-106352  
 styrene/acrylic terpolymers, viscoelastic props. 0-64509  
 supercooled liquid, thermal conductivity and viscosity, mode-mode coupling 0-88370  
 surface, free, charged, isolated, exptl. study of deform. (*French*) 0-88240  
 thin film, viscous, between two nearly parallel walls, temp. distrib., convection effects 0-83801  
 trifluoropropylmethylsiloxane fluids, viscoelastic props., mechanical impedance, viscosity and density meas. 0-79249  
 triphenylmethane dye soln., electronic relax., viscosity-depend., using picosec. flash photolysis 0-66258

## viscosity of liquids continued

- unsaturated polyester resins, gelation, viscosity meas. (*Polish*) 0-59690  
 urethane elastomer, thermoplastic, dilute soln., viscosity and sedimentation 0-103512  
 variable resistance boundary layers, frictional resist. effects on motion of bodies 0-96243  
 vibrating wire viscometer, adaptation for liquids 0-87827  
 viscoelastic fluid lubrication, slider-bearing config., non-Newtonian normal stresses 0-69753  
 viscous fluid, shear processes, local order theory 0-59687  
 viscous liquid flow through annular clearance over rotating inner cylinder 0-64626  
 water, mobility in blood plasma, NMR determ., viscosity correl. to  $1/T_2$  0-67176  
 water-alcohol mixtures, US attenuation meas., method of streaming 0-88272  
 water-methanol mixtures, viscosity at 25°C, isotope substitution effects 0-92700  
 water-toluene-sodium dodecyl sulphate-butanol 1 mixture, interface light scatt., interface tension meas. 0-76039  
 xanthene dyes in n-alcohols (ethylene glycol) (glycerol), rot. relax., time-resolved fluoresc. depolaris. obs. 0-58300  
 Al-Cu, liq. alloys, with zero superheat, fluidity 0-70289  
 Al-Cu dilute alloys, vein closing mechanism in fluidity tests 0-84924  
 Al-Si (2.4 wt.%), liq. fluidity in solid-liq. zone 0-108429  
 Ar, hole theory, compressional viscosity and vibrational relaxation 0-70311  
 As-S, melt struct., orientation birefr., viscosity, refr. index, and density 0-84713  
 Au<sub>77</sub>Ge<sub>13</sub>Si<sub>9</sub>, heat of crystn. and viscous behaviour 0-75166  
 CaF<sub>2</sub>, melts, elec. cond., surface tension, viscosity, density (*Russian*) 0-92758  
 CaF<sub>2</sub>-MgO-SiO<sub>2</sub>, melts, elec. cond., surface tension, viscosity, density (*Russian*) 0-92758  
 CaF<sub>2</sub>-MgO(SiO<sub>2</sub>), melts, elec. cond., surface tension, viscosity, density (*Russian*) 0-92758  
 CuSO<sub>4</sub>, aq. solns., densities, viscosities, elec. cond. meas., 20 to 70°C 0-59688  
 CuSO<sub>4</sub>/H<sub>2</sub>SO<sub>4</sub> electrolytes, densities, elec. cond., viscosities 0-107455  
 Fe particles, dispersed in Hg, mag. props., aggregate form. 0-60375  
 Fe<sub>40</sub>Ni<sub>40</sub>P<sub>14</sub>B<sub>6</sub> glass, viscosity near T<sub>g</sub>, using rapid heating, and fusion characts. 0-70438  
<sup>3</sup>He, liquid, polarisation potentials, viscosity, thermal cond., spin diffusion 0-88389  
<sup>3</sup>He, sound propag. at elevated densities, 0.35 to 1.4K (*Russian*) 0-92741  
<sup>3</sup>He, superfluid, B-phase, first-sound attenuation and viscosity 0-75401  
<sup>3</sup>He, superfluid, transport parameters, Kubo formulae and BCS-Green's functions 0-88382  
<sup>3</sup>He, superfluid B-phase, shear viscosity, s-p-d wave approximation 0-96715  
 Hf, liquid, viscosity at melting point, free energy (*Russian*) 0-92699  
 Hg-In (3, 15, 30, 45 at.%) amalgam, viscosity meas. near melting point 0-70441  
 Hg-Tl amalgam, viscosity meas. 0-88349  
 N<sub>2</sub>O<sub>4</sub>, viscosity and thermal cond., approx. polynomials (*Russian*) 0-59739  
 (Ni<sub>0.5</sub>Pd<sub>0.5</sub>)<sub>82</sub>P<sub>18</sub> amorphous alloy, liquid-quenched, crystn. kinetics, nucleation 0-100176  
 PMMA, polymer chain, internal friction range, HF viscosity theory (*French*) 0-79968  
 PbO-B<sub>2</sub>O<sub>3</sub> glass-forming melt, specific volume and viscosity, temp. depend. 0-84073  
 Pd<sub>77</sub>Cu<sub>23</sub>Si<sub>16.5</sub>, heat of crystn. and viscous behaviour 0-75166  
 Rb, liquid, freq. moment and viscosities calc. 0-88348  
 Rn, calc. of critical density 0-59547  
 Se, viscosity meas. by rot. cylinder method 0-88347  
 SiO<sub>2</sub>-B<sub>2</sub>O<sub>3</sub>, viscosity meas. up to 1840°C (*French*) 0-79969  
 Ti, liquid, viscosity at melting point, free energy (*Russian*) 0-92699  
 V, liquid, viscosity at melting point, free energy (*Russian*) 0-92699  
 Zn, liquid, viscosity determination by oscillating vessel method (*Japanese*) 0-70439  
 ZnCl<sub>2</sub>-LiCl(NaCl)(KCl)(CsCl), molten, US absorption coeffs. and bulk viscosity coeffs. (*Japanese*) 0-88271  
 Zr, liquid, viscosity at melting point, free energy (*Russian*) 0-92699

## visibility

- see also atmospheric optics; brightness; light transmission  
 astronomical seeing, atmosphere surface layer optical inhomogeneities investigation by acoustic method 0-67434  
 astronomical seeing, influence of spatial resolution on Ca<sup>+</sup> K-line width and shift in solar prominence 0-77364  
 astronomical seeing, meas. at Kitt Peak 0-61899  
 atmosphere, fog and haze microphysics, visual range obs. 0-109195  
 atmosphere, Harmattan dust deposition rel. to visibility, wind and solar rad. 0-94578  
 atmosphere, light scatt. coeff. of marine boundary layer 0-82052  
 atmosphere, transparency, meas. on Maidan mountain during autumn and winter (1977 to 1978) (*Russian*) 0-72627  
 atmosphere, visibility, turbidity and light scatt. obs. 0-105047  
 atmosphere, visibility at ground level, two meas. methods 0-82078  
 comets, visibility conditions rel. to discovery probability and reality of concentration of perihelia 0-67660  
 foveal increment threshold, lateral effect of oscill. of peripheral luminance gratings 0-108904  
 illumination system, optical design 0-64135  
 interference transfer function with quadratic detect., coherent illum. 0-78782  
 laser beacon visibility in fog, range extension technique 0-101434  
 mountain shadow phenomena, spike seen by off-summit observer 0-78761  
 phase contrast microscope attachment for weak phase object visibility 0-86396  
 photometric contrast as basic value for visibility meas. (*German*) 0-95118  
 radiographical visibility and sharpness of lung struct. at 90, 140 and 350 kV 0-98124  
 Sargasso Sea, optical props. of seawater (*Russian*) 0-94532  
 spatial frequency tuning studies, psychometric curves description by probability summation 0-61576  
 trends in atmos. visibility due to air quality change, appl. of ridit anal. 0-82051

## visibility continued

- visual instruments, optical component contamination, effect on visibility of extended objects 0-64137  
AlGaAs DH injection phase-locked laser, coherence 0-102726

## visible and ultraviolet spectra of inorganic solids

- alkali halide:  $H^+(D^-)$ , local modes and colour centre absorpt. bands, analogy 0-60632  
alkali halide crystals, activated, physical phenomena and optical data processing appl. (Russian) 0-80819  
alkali halides, emission band of F-centre 0-76071  
alkali metal halides, hole self-localization and capture, temp. depend. 0-92526  
alkali metal halides, X-ray induced colour centre and halogen aggregate form. 0-96565  
ceramic translucent systems, absorpt. and scatt. coeffs for visible light, Kubelka-Munk theory 0-60627  
ceramics, piezoelectric, photoacoustic effect 0-84252  
diamond, GR1 band, anal. of satellite lines by quadratic Jahn-Teller computing 0-97295  
diamond, Jahn-Teller coupling at neutral vacancy 0-71453  
diamond, uniaxial stress splitting of E to E transitions at trigonal centres in cubic crystals 0-97312  
electrode surface, anisotropy of optical props. 0-60534  
ferroelectric semiconductors, props., book 0-82590  
glass:  $Cr^{3+}$ , absorpt. spectra, Fano antireson. and vibronic- Lamb shift 0-71458  
glasses, elec., mag., and optical props., conference, Troy, NY, USA (Aug. 1979) 0-105417  
glasses, electron scavenging, hopping controlled time-depend. reaction rates 0-108723  
metallic glass, prep. and phys. props. development 0-81003  
3-methylpentane glassy matrix, localised electrons, cavity model 0-107743  
optical fibres, glass and plastic, neutron irradiated, optical absorpt. spectra 0.7 to 1.1  $\mu m$  0-58762  
pnictide amorphous semiconductors, absence of photodarkening 0-103970  
polydiacetylene-toluene-sulphonate, photocond. meas., 0.62-3.1 eV 0-70757  
praseodymium ethyl sulphate, phase transition under pressure, absorpt. spectra (Russian) 0-92667  
rocks of volcanic origin, refl. charact., 400-800 nm 0-90073  
ruby, luminescence, absorption of R and N lines, effect of mag. field 0-60550  
semiconducting alloys, comp. profile, second derivative wavelength modulation 0-103967  
semiconductors, amorphous, optical absorption, theory 0-80818  
semiconductors, deep level carrier trapping and emission, transient spectroscopy, book contribution 0-80216  
silicate smokes, vapour-condensed, 800 to 130 nm extinction and interstellar extinction curve 0-82180  
sphalerite, hydrothermal single crystals, feasibility of optical methods for quality control 0-89065  
(TMTSF) $_2X$ , ( $X=PF_6^-$ ,  $AsF_6^-$ ,  $SbF_6^-$ ,  $BF_4^-$ ,  $NO_3^-$ ) highly conducting salts, props. 0-59969  
transition metal chalcogenophosphates, intercalation with n butyl-lithium, possible appl. in Li batteries 0-71446  
X-irrad., optical absorpt. spectra and dichroism meas. 0-108239  
[ $\alpha$ ]SiC:H, prepared by reactive sputtering, layer props. (Japanese) 0-60695  
Ag foil interface with liquid, oxide props. from reflectance and scatt. light spectroscopy 0-60702  
Ag foils, surface plasma-wave reflectance and roughness-induced scatt. 0-66228  
Ag halide photochromic glasses, optical properties, effect of Cu ions 0-93364  
Ag, thermomodulation spectra of high-energy interband transitions 0-108226  
AgBr dispersion in gelatin, adsorbed S and Au, transient absorpt. spectra, latent image form. and decay 0-66837  
AgGaSe $_2$ , two-photon absorpt. and short pulse stimulated recombination 0-89054  
Ag $_2$ HgI $_4$ , preparation, optical and luminescence spectra 0-104064  
AgInS $_3$ , and AgInS $_3$ , spray pyrolysis, film struct., elec. and optical props. 0-71592  
Al ultrafine particles, optical props., 0.3-2.5  $\mu m$  0-76020  
Al-Ge-SiO solar selective absorber surfaces, optical behaviour at high temp. 0-101130  
AlN, absorpt. edge shape interpretation, Wannier excitons absorpt. in charge impurity elec. field 0-66233  
 $\alpha$ -Al $_2$ O $_3$ , polarised luminescence in neutron- and proton-irradiated single crystals 0-66271  
 $\alpha$ -Al $_2$ O $_3$ :V $^{3+}$ (V $^{4+}$ )(Co $^{3+}$ )(Co $^{2+}$ ), optically and thermally stimulated reactions, absorpt. spectra 0-80825  
Al $_2$ O $_3$ -B $_2$ O $_3$ -SiO $_2$  sheet glass, solar energy appl., optical and mech. props. 0-87447  
Al $_2$ O $_3$ -SiO $_2$ -MO-Fe $_2$ O $_3$  glass, M=Ca, Mg, Ba, Sr, UV and EPR absorpt. spectra 0-89018  
AlPO $_4$ , synthetic berlinite, electron irrad. effects, ESR, ENDOR, optical spectral study 0-80608  
Ar, adsorbed on Al, differential refl. spectroscopy, local field effect 0-80811  
 $\alpha$ -As $_2$ S $_3$ , energy gap meas., by Faraday rotation 0-66161  
As $_2$ S $_3$ , glassy, photoinduced defects, EPR and absorpt. spectra 0-59398  
As $_2$ S $_3$ , two photon light absorpt. dispersion, induced linear light absorpt. (Russian) 0-66231  
As $_2$ S $_3$ :Ag glassy films, optical transmission spectra, photodoping effect 0-66317  
As $_2$ S $_3$ , amorphous, struct., vibr. and electronic spectra 0-64908  
As $_{100-x}$  amorphous films, optical props. and photoinduced changes 0-60700  
As $_2$ S $_3$ -Se $_2$ , amorphous, picosecond relax. of optically induced absorption 0-97302  
As $_2$ Sb $_2$ Se $_2$  glassy semiconductors, electronic props. 0-103712  
As $_2$ Se $_3$ , cryst., electroabsorption on indirect gap 0-80812  
Au, optical props., dielec. function, void model, sample effects 0-76048  
Au, thermomodulation spectra of high-energy interband transitions 0-108226  
Au(Ag)(Cu)-Sn liquid, optical reflectivity spectra of virtual bound states 0-89021  
BaAl $_2$ O $_9$ , refr. index and optical absorpt. 0-66139

## visible and ultraviolet spectra of inorganic solids continued

- BaF $_2$ , ultralow loss optical fibre material, loss mechanism 0-78920  
BaF $_2$ :Pb $^{2+}$ , band struct., Jahn-Teller effect, UV luminesc. and optical absorpt. spectra 0-66243  
BaMnF $_4$ , struct. phase transition, optical parameters obs. 0-100328  
BaO-B $_2$ O $_3$ -V $_2$ O $_5$  glass, oxidation-reduction of V, thermodynamics 0-85169  
Ba(PO $_3$ ) $_2$ -WO $_3$ , electron-absorpt. spectra and structure of W centres 0-88873  
BaTiO $_3$ , photoelectron and optical spectra derived from self-consistent charge MO and band calcs. 0-96785  
BeF $_2$  glass, IR and UV transmission spectra 0-89019  
BiI $_3$ , structure, exciton states and physicochem. characteristics (Russian) 0-100435  
C smokes, vapour-condensed, 800 to 130 nm extinction and interstellar extinction curve 0-82180  
CaF $_2$ :Dy, TLD-200, thermolum. phosphor, photolum. and absorpt. spectra, thermolum. mechanisms 0-97321  
CaF $_2$ :Er, defect structure, quenching effect, dielec. relax. and optical absorption 0-65031  
CaF $_2$ :Eu $^{2+}$ (Sm $^{3+}$ ), VUV absorpt. spectra, dopant clustering 0-108230  
CaF $_2$ :M, M=Mn, Fe, Co, Ni, X-irrad., impurity effects on defect prod. 0-92525  
CaF $_2$ :Mn, low temp. X-irrad., Mn centres, optical absorpt. and emission props. 0-60635  
CaF $_2$ :Ni, X-irrad., optical absorpt. spectra and dichroism meas. 0-108239  
CaF $_2$ :Ni, X-irradiated, optical and EPR meas. 0-108235  
CaF $_2$ :Pb $^{2+}$ , band struct., Jahn-Teller effect, UV luminesc. and optical absorpt. spectra 0-66243  
CaF $_2$ :U $^{3+}$ , anomalous magnetooptical props., optical detection of ESR and cross-relax. resonances 0-93287  
Ca $_2$ Fe $_2$ Ge $_2$ O $_{12}$  garnet, light absorpt. spectral study 0-93322  
Ca $_2$ O $_2$ :Dy(Tm), thermolum. thermolum. phosphor, photolum. and absorpt. spectra, thermolum. mechanisms 0-97321  
CaWO $_4$ :Nd $^{3+}$  absorpt. spectra, hypersensitivity of  $^4I_{9/2}$  to  $^6G_{5/2}$ ,  $^2G_{7/2}$  transition 0-97309  
CaWO $_4$ :Pr $^{3+}$ , anomalous hypersensitive  $^3H_4 \rightarrow ^3P_2$  transition 0-106296  
CdBr $_2$ :Co $^{2+}$ , exchange-coupled Co $^{2+}$  pairs, optical absorpt. and Zeeman studies 0-66242  
CdCr $_2$ S $_4$ (Se $_4$ ), thermorefectance, photoconductance, Raman scatt. near mag. phase transition 0-97298  
CdCr $_2$ Se $_4$ , energy structure, magnetooptical effects 0-71394  
CdF $_2$ , UPS and XPS spectra, rel. to optical props. 0-66386  
Cd $_{1-x}$ Mn $_x$ Se, fundamental optical props. 0-84751  
CdS, additional waves and polarisation dispersion, reflectivity, transmittivity spectra 0-71443  
CdS, electron-hole plasma, gain and refl. spectra study 0-66227  
CdS epitaxial layers on sapphire, exciton struct. of absorpt., photoluminesc. and photocond. spectra 0-89027  
CdS, spectra of refl. and transmission coeffs. near exciton absorpt. line 0-88951  
CdS:Ni $^{2+}$ , Zeeman effect at Ni impurities 0-60633  
CdSe, fundamental absorpt. edge, influence of laser radiation intensity (Russian) 0-71445  
CdSnO $_4$  films, transparent conducting, deposited by RF sputtering from CdO-SnO $_2$  target 0-76179  
CdTe, energy bands and optical props. calc., tight-binding model with spin-orbit interaction 0-65448  
CdTe film, exciton spectra, press. and temp. depend. 0-80886  
CdTe:Mn $^{2+}$ , exciton refl. spectra and mag. susceptibility 0-66253  
Cd $_{1-x}$ Zn $_x$ S films, thermal evaporation prep., phys. props. 0-84410  
Co-Fe-Si-B, ferromag., magneto-optical spectra in amorphous and cryst. states (Russian) 0-84749  
CoCO $_3$ , two-sublattice noncollinear antiferromag., exciton-magnon light absorpt. mechanisms (Russian) 0-89017  
CoCO $_3$ , weakly ferromag., light absorpt. dichroism and mag. config. 0-66223  
CoO-ZnO-MgO ternary systems, solid solns., struct. charact. 0-60629  
CoP amorphous alloy, heat treatments influence on opt. props., struct. and DC resist. obs. 0-80892  
Cr-Cr $_2$ O $_3$  black chrome, commercial, solar absorber coating characterisation 0-80111  
CsBr, F-centre absorpt., uniaxial stress effects 0-60634  
CsBr:Cu $^{+}$ , excitation and absorpt. spectra 0-108255  
CsI, ultralow loss optical fibre material, loss mechanism 0-78920  
CsMnF $_3$ , exciton-magnon interactions in optical transition, absorpt. and emission spectra meas. 0-70981  
CsPbCl $_3$ , electronic struct. and optical props. in fundamental absorpt. region 0-93367  
Cs $_2$ ZrBr $_6$ , PtBr $_6^{2-}$ -PtBr $_6^{2-}$  doped, mixed valence, absorpt. spectra, vibronic struct. 0-97308  
Cu, thermomodulation spectra of high-energy interband transitions 0-108226  
CuBr, biexciton dispersion, two-photon absorpt. 0-76045  
CuBr(I), reflectance and thermorefectance spectra, electronic struct. 0-71444  
CuCl, refl. spectra, 4.5-30 eV, vel. to band struct. 0-103969  
CuI, single crystals, growth and optical props. 0-93470  
CuInSe $_2$ , influence of impurities and free carriers on optical props. 0-108225  
Cu $_2$ O, Cu inclusions and annealing, optical and IR absorpt. obs. 0-60630  
Dy $_2$ S $_3$ , optical props. and electronic struct. in fund. absorpt. region 0-80817  
EuO, transmission and resistivity, stress modulation effect near Curie temperature 0-96874  
EuO(S), ferromagnetic electronic structure, absorption, thermorefectance and thermotransmission spectra (French) 0-97300  
EuSe(Te), magnetic phase transitions, thermal modulation spectroscopy study (French) 0-97301  
Eu $_2$ Sr $_{1-x}$ S, magneto-optical redshift in absorpt. and photoluminesc., mag. short-range order 0-71388  
Eu $_{1-x}$ Yb $_x$ Te, ( $0 < x < 1$ ), mag. semicond., elec., mag. and optical props. 0-97070  
Fe-Ni-B-(P), ferromag., magneto-optical spectra in amorphous and cryst. states (Russian) 0-84749  
FeBO $_3$ , mag. linear dichroism and absorpt. spectra, exciton-magnon absorpt. mechanism 0-66160  
 $\alpha$ -Fe $_2$ O $_3$ , photochem. props. of sintered and doped samples for solar photoelectrochem. cell apps. 0-89651  
Fe $_2$ O $_3$ , dielec. function and polar Kerr rotation, 0.5-3.6 eV 0-66221



## visible and ultraviolet spectra of inorganic solids continued

- Fe<sub>2</sub>SiO<sub>4</sub>, fayalite, Czochralski growth under controlled O<sub>2</sub> fugacity conditions 0-84843  
 Fe<sub>1-x</sub>Zn<sub>x</sub>F<sub>2</sub>, dil. antiferromag., electronic and mag. props., Raman scatt. and optical absorpt. study 0-108207  
 GaAs anodic oxide films, optical studies using rot. light-pipe reflectometer 0-76096  
 GaAs, exciton quenching, obs. at room temp. using electrolyte electroreflectance 0-60546  
 n-GaAs, spectra, light induced, electrolyte and Schottky barrier techniques of meas. 0-76046  
 GaAs thin films, reactively sputtered, ESCA/XPS study 0-97430  
 GaP, impurity-containing single crystals, refl. spectra 0-80823  
 GaP:Fe, optical absorption spectrum and Faraday effect 0-108245  
 GaS(Se), reson. Brillouin scatt. 0-89010  
 p-GaSe, back wall Schottky barrier cells, diffusion length, RT spectral response meas. 0-107806  
 GaSe, exciton-phonon quasibound states, photocond. and luminesc. study 0-96800  
 GaSe thin films, electroabsorpt. spectra, exciton line splitting 0-107716  
 GaTe, single cryst. prep. and electroabsorpt. spectra investig. 0-103968  
 GdFeBi, amorphous ferrimag. films, magneto-optical props., optical spectra 0-76008  
 N-Ge, electrorefl. spectra, light induced, electrolyte and Schottky barrier techniques of meas. 0-76046  
 Ge optical props. in 2.5-15 micron region 0-80775  
 N-Ge-Bi-Se glass, elec. and optical props. 0-65550  
 Ge-Ga amorphous alloy, co-evaporated elec. and optical props. 0-70860  
 GeS, absorpt. spectra, electron-phonon interactions 0-80810  
 GeS, physical basis for Urbach's rule 0-93366  
 p-GeTe, reflectance, and thermoref. spectra 0-80814  
 H<sub>1/2</sub>MoO<sub>3</sub>, electronic props., mag. susceptibility and spectra 0-80266  
 Hg, reflection spectra, electronic density of states, calc. 0-66229  
 Hg<sub>1-x</sub>Cd<sub>x</sub>Te, optical absorpt., quasilocal acceptor level effects, theory 0-92853  
 HgCr<sub>2</sub>Se<sub>4</sub>, thermorefectance, photoconductance, Raman scatt. near mag. phase transition 0-97298  
 HgTe, energy bands and optical props. calcs., tight-binding model with spin-orbit interaction 0-65448  
 InAsS(Mg), ion implanted, photocond., photo-EMF, and optical absorpt. spectra 0-70763  
 In<sub>1-x</sub>Ga<sub>x</sub>P<sub>1-x</sub>As<sub>x</sub>, lattice matched to InP, electroreflectance obs. 0-93416  
 InP, Faraday interband effect subjected to quantising mag. fields 0-97246  
 InP, press. depend. of direct absorption edge 0-93365  
 InSe, photo-absorption of green exciton 0-80816  
 K smoke particles, optical props. 480 to 620 nm, rel. light scatt. cross sections meas. 0-97293  
 K-Cs, extreme UV absorpt. spectra 0-97294  
 K-Rb, extreme UV absorpt. spectra 0-97294  
 KBr, colour centre form. under polarised UV irradi., dichroism in absorption spectra 0-107232  
 KBr, X-irrad. crystals, halogen aggregation, absorpt. spectra obs. (Russian) 0-66234  
 KBr(Cl):OH<sup>-</sup>, cc U<sub>2</sub> to H<sub>2</sub>O<sup>-</sup> defects conversion after UV photodecomp. 0-107230  
 K<sup>+</sup>CN<sub>2</sub><sup>-</sup>Cl<sup>-</sup><sub>1-x</sub>, influence of structural disorder on exciton spectra 0-108224  
 KCl, additively coloured photochromic crystals, spectral sensitivity (Russian) 0-91871  
 KCl and KCl:NO<sub>2</sub>, X-irrad. crystals, Cl<sub>2</sub><sup>-</sup> centres photodissoc., optical anisotropy and creation mechanisms (Russian) 0-66235  
 KCl, γ-irrad., F-centre absorpt., flash-stimulated changes 0-92524  
 KCl surface, VUV irradi., colour centre layer, angle-of-incidence derivative ellipsometry and reflectometry 0-73420  
 KCl, ultralow loss optical fibre material, loss mechanism 0-78920  
 KCl:Ca<sup>2+</sup>, Z-centre thermolum. 0-80879  
 KCl:Ca(Yb), Z<sub>2</sub> and Z<sub>2</sub><sup>+</sup> centres, excited state, magneto-optical spectra 0-108233  
 KCl:Cu<sup>+</sup>, excitation and absorpt. spectra 0-108255  
 KCl:Cu<sup>+</sup>, exciton bands, optical absorpt. and MCD spectra 0-80821  
 KCl:Li, (F<sub>2</sub><sup>-</sup>)<sub>A</sub> centres, optical props. 0-89026  
 KCl:Pb<sup>2+</sup>, pure and doped, electrolytically coloured, elec. cond. and optical absorpt. meas. 0-100668  
 KCl:Pb<sup>2+</sup>, X-ray irradi., electron-trapped centres, Pb<sup>+</sup> and Pb<sup>0</sup>, optical absorpt. spectra 0-71461  
 KCl:Br<sub>2</sub>, mixed crystals, thermolum. and optical absorption studies 0-104000  
 KCl(Br)(I):Zn<sup>+</sup>, optical absorpt. bands rel. to charge transfer 0-66245  
 KD<sub>2</sub>H<sub>2</sub>(1-x)PO<sub>4</sub> crystals, 0<x<0.98, light scatt. by polaritons 0-96802  
 KI microcrystals, UV spectra by diffuse reflectance technique, surface electronic transitions obs. 0-75614  
 KI, oscillator strengths of defects, Smakula eqn. generalisation 0-108232  
 KI:Cu<sup>+</sup>, exciton bands, optical absorpt. and MCD spectra 0-80821  
 KI:Pb, absorpt. spectra of Pb<sup>2+</sup> centres 0-76058  
 KMnF<sub>3</sub>, Faraday effect mechanism in paramag. phase 0-60552  
 KZnF<sub>3</sub>, exchange interactions of transition metal ions in orbitally degenerated excited states 0-65512  
 LaAlO<sub>3</sub>, exchange interactions of transition metal ions in orbitally degenerated excited states 0-65512  
 LaCl<sub>3</sub>:U<sup>3+</sup>, cryst., spectrum anal., cryst. field parameters 0-76057  
 LaF<sub>3</sub>:Pr<sup>3+</sup>, ultraslow optical depasing 0-58648  
 La<sub>2</sub>S<sub>3</sub>, optical props. and electronic struct. in fund. absorpt. region 0-80817  
 β-LiAl, optical dispersion, room temp. reflectance spectra 0-66195  
 LiCl:Ag, fluoresc. and UV absorpt. spectra 0-80844  
 LiF, alkali ion implantation, migration, segregation, effect on optical props. 0-100269  
 LiF, ultralow loss optical fibre material, loss mechanism 0-78920  
 LiF:Mg, dependence of optical absorpt. on temp. during X-ray irradi. 0-66237  
 LiF:Mg, TLD-100, thermolum. phosphor, photolum. and absorpt. spectra, thermolum. mechanisms 0-97321  
 LiF:Mg, X-irrad., colour centres, ESR and UV absorpt. meas. 0-108069  
 LiF:Mg, X-irrad. induced sensitisation mechanism, optical absorpt. spectra 0-60637  
 LiF:Mg, Z<sub>2</sub>- and associated Z-centres, elec. cond., ionic thermocurrent, and optical absorpt. meas. 0-107229  
 Li<sub>0.5</sub>Fe<sub>2.5</sub>O<sub>4</sub>, magneto-optical Kerr effect, reflectivity spectra 0-66157  
 LiH, formation and annihilation of Li colloids and H bubbles 0-107228  
 LiH(D), isotope effect on Wannier-Mott exciton levels 0-103633

## visible and ultraviolet spectra of inorganic solids continued

- LiI:Pb, absorpt. spectra of Pb<sup>2+</sup> centres 0-76058  
 LiNbO<sub>3</sub>:Ni optical absorpt. spectra 0-71450  
 Li<sub>2</sub>O, neutron irradi. effects, optical absorpt. spectra 0-75271  
 LiYF<sub>4</sub>, electron-irrad. induced defects, optical and EPR study, impurity effects 0-66238  
 MgAl<sub>2</sub>O<sub>4</sub>, radiation damage, optical absorpt., F-centres 0-64994  
 Mg<sub>2</sub>Cd<sub>1-x</sub>Te, electroreflection spectra, comp. depend. 0-66230  
 MgO:Cr<sup>3+</sup>, emission and excitation spectra 0-93387  
 MgO:Li, mech. deformed crystals, imprinting of slip bands using Li impurities 0-59473  
 MgO-Fe<sup>2+</sup>, shock compressed absorpt. spectrum, appl. to Earth mantle 0-90039  
 Mg<sub>2</sub>SiO<sub>4</sub>:Tb, thermolum. phosphor, photolum. and absorpt. spectra, thermolum. mechanisms 0-97321  
 Mg<sub>2</sub>Zn<sub>1-x</sub>Te, band struct. refl. spectra meas. 0-80813  
 MnAu<sub>2</sub>, helical antiferromag., optical absorpt., density of states 0-66224  
 Mn(CN)<sub>3</sub>(H<sub>2</sub>O)<sub>0.57</sub>, mag. interactions, theory 0-97085  
 Mn<sub>2</sub>Fe<sub>1-x</sub>O<sub>4</sub>, dielec. function and polar Kerr rotation, 0.5-3.6 eV 0-66221  
 MnO, magnon-sideband lineshape, exciton-phonon interaction effects 0-65846  
 MoSe<sub>3</sub>, exciton spectra 0-97296  
 (NH<sub>4</sub>)<sub>2</sub>SO<sub>4</sub>:MnO<sub>4</sub><sup>-</sup>, X-ray irradi. damage, optical absorpt. spectra study 0-66246  
 Na<sub>2</sub>Al<sub>2</sub>(Si<sub>0.98</sub>Ge<sub>0.01</sub>)<sub>6</sub>O<sub>24</sub>.2NaBr, Ge-doped sodalite powders, UV absorpt. band 0-71452  
 Na<sub>6</sub>Al<sub>3</sub>Si<sub>6</sub>O<sub>24</sub>.NaX<sub>2</sub>(X=Cl, Br, I), X-ray irradi., thermal-erase cathodochromism and dihalide mol. centres (Russian) 0-66236  
 NaCl, F-centers, laser irradi. optical bleaching kinetics 0-66244  
 NaCl:Cu<sup>+</sup>, electrolytically coloured, electron trapping, optical absorpt. 0-100672  
 NaF, X-irrad., colour centres and thermolum. 0-84790  
 NaF-SrF<sub>2</sub>-CrF<sub>3</sub>, glass transition, crystn. and melting temps., optical transmission (French) 0-64910  
 NaI:F, electron-lattice coupling of F-centres, optical props. 0-60641  
 NaI:Pb, absorpt. spectra of Pb<sup>2+</sup> centres 0-76058  
 NaMgF<sub>3</sub>, defects induced by X- and vacuum UV irradi., optical and elec. study 0-107319  
 Na<sub>2</sub>O-SiO<sub>2</sub> glasses, elementary electronic excitations, refl., luminesc., and photoemission meas. 0-84778  
 Na<sub>2</sub>O-SiO<sub>2</sub>:CuO glass, gamma-irradiated, EPR and optical spectra 0-103885  
 Na<sub>2</sub>Pr(C<sub>6</sub>H<sub>5</sub>O<sub>2</sub>), 2NaClO<sub>4</sub>.6H<sub>2</sub>O, absorpt., circular dichroism, and mag. circular dichroism spectra 0-97243  
 NaRhy zeolite, Rh complexes with CO and methyl iodide ligands, spectrosc. obs. 0-85159  
 Nb, electronic struct., thermorefectance studies 0-76047  
 NbS<sub>2</sub>.Cl<sub>2</sub>(Br<sub>2</sub>)(I<sub>2</sub>), absorpt. edge spectrum, fine struct. 0-66219  
 Nd<sub>2</sub>S<sub>3</sub>, optical props. and electronic struct. in fund. absorpt. region 0-80817  
 Ni Tutton salts, cryst. field spectra in visible and near IR regions, solid dilution effect 0-100666  
 Ni-Co(Fe)(V)(Ti), dil., optical absorpt., electronic struct. 0-108227  
 Ni-Ge-SiO<sub>2</sub>, solar selective absorber surfaces, optical behaviour at high temp. 0-101130  
 β-NiAl, electronic struct. and optical props. 0-97228  
 NiF<sub>2</sub> film preparation and characterisation 0-59815  
 Ni<sub>2</sub>Mn thin films, transmission spectra, structural order depend. 0-66318  
 NiP amorphous alloy, heat treatments influence on opt. props., struct. and DC resist. obs. 0-80892  
 α-O<sub>2</sub>, antiferromagnetic polycrystal, splitting of exciton absorpt. lines in mag. field (Russian) 0-103943  
 α-O<sub>2</sub>, cryst., exciton, exciton-magnon, and biexciton absorpt. at 1.5K 0-84750  
 α-O<sub>2</sub> crystals, absorption line biexciton polarisation (Russian) 0-89028  
 α-O<sub>2</sub> crystals, spin ordering effect on light absorpt. (Russian) 0-89029  
 PLZT ferroelectric thin films, epitaxial growth and optical props. 0-70543  
 PbI<sub>2</sub>, first-order 2H-4H polytype transition, exciton spectroscopic study 0-59647  
 PbI<sub>2</sub>, photoexciton interaction, luminescence spectra, polariton dispersion diagram 0-93397  
 PbI<sub>2</sub>:KI alloys, fundamental abs. edge, potential as solar convertor 0-101128  
 PbI<sub>2</sub>:PbBr<sub>2</sub> mixed systems, cryst. growth, struct. and optical props. (German) 0-96499  
 PbO, visible absorpt. spectra rel. to indirect exciton transitions 0-60628  
 PbS(Se), valence band struct. determ. by optical absorpt., size quantization effects 0-59871  
 PbTe:Ti, absorpt. coeff. spectral depend. 0-93370  
 Pd, thermomodulation spectra of high-energy interband transitions 0-108226  
 Pt, thermomodulation spectra of high-energy interband transitions 0-108226  
 RbCl:Ca<sup>2+</sup>, thermolum. and optical absorption studies 0-104002  
 RbI:Pb, absorpt. spectra of Pb<sup>2+</sup> centres 0-76058  
 Rb<sub>2</sub>MnCl<sub>4</sub>, quasi-2D-antiferromag., linear birefr. and optical absorpt. spectra 0-71385  
 RbMnF<sub>3</sub>, Faraday effect mechanism in paramag. phase 0-60552  
 RbMnF<sub>3</sub>:Er<sup>3+</sup>, absorption, emission, excitation and lifetime meas. 0-71460  
 Ru complexes, [Ru(bipy)<sub>3</sub>](pq)<sub>3</sub><sup>2+</sup> mixed-ligand, electronic absorpt. and emission spectra meas. 0-71441  
 S, orthorhombic, photogeneration of charge carriers 0-107844  
 Se, band structure, density of states, absorpt. spectra, KKRZ calc. 0-70593  
 Se, threads in natural mordenite channels, optical absorpt., cond. (Russian) 0-89022  
 Si, amorphous, pure and H doped, picosecond relax. of optically induced absorption 0-97302  
 Si, amorphous film, RF plasma deposition from SiCl<sub>4</sub>-H<sub>2</sub>, characterisation 0-66435  
 Si, amorphous films, halogenated and hydrogenated, elec. and optical props. 0-97016  
 Si, dielectric function spectra, ellipsometric determ., many-particle effects at E<sub>r</sub>-transition 0-93363  
 Si, high dose self-irrad., spatial correl. between primary and secondary defect profiles 0-59536  
 Si, optical const. by unpolarised incident radiation 0-76044  
 Si, optical spectrum, many particle effects, band struct. 0-89024

**visible and ultraviolet spectra of inorganic solids continued**

- Si, reflectivity time dependence during pulsed laser annealing 0-66214  
 Si:F:H, amorphous, elec. and optical props. 0-60031  
 a-Si:H, influence of H on optical props., H conc. and H bonds 0-76098  
 Si:P film, polycryst., heavily doped, mobility and carrier conc., optical determ. 0-66314  
 SiC ion implanted, laser induced ordering and defects 0-84754  
 SiC smokes, vapour-condensed, 800 to 130 nm extinction and interstellar extinction curve 0-82180  
 SiO<sub>2</sub>, fused, for sealed ampoule cryst. growth, thermal transmission function 0-84731  
 SiO<sub>2</sub>, ultralow loss optical fibre material, loss mechanism 0-78920  
 SiO<sub>2</sub>-Al<sub>2</sub>O<sub>3</sub>-CaO-Na<sub>2</sub>O-Fe<sup>3+</sup>, optical absorpt. due to Fe<sup>3+</sup> ligand field and charge transfer 0-89020  
 SiO<sub>2</sub>-Na<sub>2</sub>O-Nd<sub>2</sub>O<sub>3</sub> glass, magneto-optical props., absorpt. spectrum 0-88969  
 SiO<sub>2</sub>, dielec. and optical props., chemical disorder effects 0-80815  
 SiO<sub>2</sub>:Ge, B, P, optical fibre, radiation induced optical absorpt. spectra, 0.4 to 1.7  $\mu$ m region 0-58761  
 Sm<sub>2</sub>S<sub>3</sub> films, refl. and transmission spectra at 300K 0-80889  
 Sn<sub>2</sub>P<sub>2</sub>(Se<sub>2</sub>S<sub>2</sub>)<sub>6</sub>, ferroelec. tricitric. phase transform., light transmission study 0-71355  
 SrCl<sub>2</sub>:Cu<sup>2+</sup>, exciton bands, optical absorpt. and MCD spectra 0-80821  
 SrF<sub>2</sub>, thin film, optical props., spectral dependence, 460-1000 nm 0-76094  
 SrF<sub>2</sub>, UPS and XPS spectra, rel. to optical props. 0-66386  
 SrF<sub>2</sub>:Pb<sup>2+</sup>, band struct., Jahn-Teller effect, UV luminesc. and optical absorpt. spectra 0-66243  
 SrFCl<sub>2</sub>, thermolum. and optical absorption spectra 0-66309  
 SrO:Ni<sup>2+</sup>, linear Stark effect for zero-phonon optical absorpt. line 0-80830  
 Ta, and  $\alpha$ -TaH<sub>x</sub>, electronic struct., thermoreflectance studies 0-76047  
 Ta ion induced continuum emission 0-89025  
 TbVO<sub>4</sub>, co-operative Jahn-Teller transition, low freq. dynamics, light scatt. study 0-88317  
 Ti, and Ti alloys, surface layer, study using vac. UV spectrograph (*French*) 0-71987  
 TiO<sub>2</sub>, rutile, optoelectronic props., band struct., theory 0-80175  
 TiCl-TiBr, KRS-6, ultralow loss optical fibre material, loss mechanism 0-78920  
 $\alpha$ -U, polycryst., optical absorption meas. 0.15 to 2.0 eV 0-108223  
 UO<sub>2</sub>, 5f-magnetic semiconductor, spectroscopic data, review 0-97299  
 UO<sub>2</sub>, electronic transitions, crystal field effects and phonons, phase transition 0-97303  
 US(Se)(Te), electronic struct. and exchange band splitting, optical refl. meas. 0-66226  
 V, electronic struct., thermoreflectance studies 0-76047  
 V<sub>2</sub>, MCD spectra, interpretation rel. to mag. struct. 0-66222  
 VO<sub>2</sub>, metal-insulator transition and electronic struct., ion bombard. effects 0-92948  
 W surface, (110), chemisorpt. effects on dielec. function, refl. spectra 0-75616  
 WO<sub>3</sub>-B<sub>2</sub>O<sub>3</sub>-ZnO semiconducting glasses, DC cond. and optical absorpt. 0-107783  
 YIG, magneto-optical Kerr effect, reflectivity spectra 0-66157  
 YIG:Ga, oxidising effects of high temp. annealing in reducing atmosphere 0-66696  
 YIG:Ga(Sc), magneto-optical Kerr effect, reflectivity spectra 0-66157  
 YIG:Ru, optical absorpt. and MCD obs. of Ru<sup>3+</sup> site occupancy 0-71456  
 Y<sub>2</sub>O<sub>3</sub>:Nd<sup>3+</sup>, absorpt. spectra, hypersensitivity of <sup>4</sup>I<sub>9/2</sub> to <sup>4</sup>G<sub>5/2</sub>, <sup>2</sup>G<sub>7/2</sub> transition 0-97309  
 Zn-In-S thin layers, ternary phases, optical props. near long-wavelength intrinsic absorpt. edge 0-80887  
 Zn,Cd<sub>1-x</sub>Se, exciton reflection spectra anomalies (*Russian*) 0-97304  
 ZnCr<sub>2</sub>O<sub>4</sub>, antiferromag. spinel, absorpt. and luminesc. spectra 0-66225  
 ZnGeP<sub>2</sub>, bandgap absorption edge, spectra, electron transitions (*Russian*) 0-97305  
 ZnO, electron-hole plasma, gain and refl. spectra study 0-66227  
 ZnO:Ni<sup>2+</sup>, Zeeman effect at Ni impurities 0-60633  
 Zn<sub>2</sub>P<sub>2</sub>In(Ga)(Ge)(S)(Se), doped and undoped, optical absorpt. spectra in range 0.5 to 2.2 eV 0-66250  
 Zn<sub>3</sub>P<sub>2</sub>, optical props., transition energies from transmission and refl. meas. 0-60532  
 ZnS, reson. Brillouin scatt. and piezobirefringence 0-93348  
 ZnS:Cu, spectral distrib., rise and decay behaviour (*German*) 0-60625  
 ZnS:Ni, IR luminesc. and absorpt. spectroscopy 0-108261  
 ZnS:Ni<sup>2+</sup>, Zeeman effect at Ni impurities 0-60633  
 ZnS(Se):Ni, optical absorpt., impurity ionisation, optical phonon coupling 0-88505  
 ZnSe crystals, doped and undoped, optical absorption edge 0-60626  
 ZnTe film, exciton spectra, press. and temp. depend. 0-80886  
 ZnTe films, internal stress effect on fund. refl. spectra 0-60701  
 ZnTe:Bi, laser annealing, channelling, reflectivity spectra 0-66215

**visible astronomical observations**

- 1308+32, BL Lacertae object, rapid optical outburst, 1980 June to July 0-98733  
 1309-216, probable BL Lacertae object with absorpt. red shift 1.49, optical spectrum 0-67856  
 1966 S 2, positional obs., 1980 March 15 0-85893  
 1978 P 1, speckle interferometric obs. (1980 June) 0-101553  
 1978 P 1, speckle obs. rel. to orbital radius and system mass and density 0-109394  
 1979 J 1 discovery by Voyager 2 camera 0-77334  
 1979 J 1-3, satellite periods from Voyager 1 and 2 data 0-105196  
 1980 LB, precise posns., orbital elements and ephemeris (1980 June-July) 0-82259  
 1980 PA, fast-moving asteroidal object, discovery and semi-accurate positions (1980 August 6 to 7) 0-94745  
 1980 PA, positions, 1980 August 8 to 17, improved orbital elements and ephemeris 0-89597  
 1980 PA, posns., elements and ephemeris (1980 August) 0-94746  
 1980 PA, precise posns., improved elements and ephemeris (1980 Sept.-Oct.) 0-101548  
 1980 QA, fast-moving asteroidal object in Capricornus, discovery and positions (1980 August 16 to 18) 0-98598  
 1980 S 10, precise positions, 1980 March 15 to 16, and relation to Dione 0-85893  
 1980 S 1, 3, 6, 25, new Saturnian satellites, positional obs., (1980 March 9 to 14) 0-94749

**visible astronomical observations continued**

- 1980 S 3, 13, positional obs. (1980 March 15 and 16) 0-85893  
 1980 S 7 to 14, Saturnian satellites, obs. (1980 March 13 to April 8) 0-62068  
 A0620-00, transient X-ray source, optical counterpart, visible and IR obs. 0-101653  
 A1742-28, transient X-ray source, optical counterpart, visible and IR obs. 0-101653  
 2A 0311-227, AM Herculis type X-ray binary, optical counterpart, radial vel. obs. 0-94890  
 2A 0311-227 optical counterpart, high speed photometry 0-82547  
 2A 0311-227 optical counterpart, simultaneous photometric and spectroscopic obs. 0-90572  
 2A 0526-328, optical counterpart, eclipsing binary, visible emission line variability 0-73075  
 2A 0526-328 optical counterpart, radial vel. meas. and orbital period 0-90579  
 2A 0526-328 optical counterpart, spectroscopic obs. 0-77515  
 2A 2251-179, X-ray quasar, UVB photometry 0-82349  
 Abell 30 emission nebula, ejecta from central star 0-82474  
 Abell 399/Abell 401, X-ray binary galaxy cluster, mass 0-90546  
 Algol type stars, H I  $\alpha$  obs. 0-109484  
 Am stars,  $\tau$  Ursae Majoris and 15 Vulpeculae, energy distrib. from spectral obs. 0-85949  
 Am stars, evolved, search for photometric variability on lower part of Cepheid instability strip 0-62145  
 $\alpha$  Andromedae, Be star, spectroscopic evidence for new shell episode 0-90444  
 $\alpha$  Andromedae, shell star, lack of linear polarisation variability 0-62157  
 BM Andromedae, spectroscopic and photometric obs. of T Tauri-type star 0-62130  
 Ap stars, new  $\Delta\alpha$ -photometry and evidence for two-component struct. of 5200 Å feature 0-67734  
 Ap stars, spectrophotometry of broad flux depressions and comparison with synthetic spectra 0-67735  
 Ap-stars, mag. field obs. using photoelec. method, visible spectra obs. 0-82373  
 Ap-stars, spectral energy distrib., spectrophotometry in 3300 to 7100 Å region 0-85953  
 CY Aquarii, RRs type star, BV photometric obs. (*Italian*) 0-90449  
 R Aquarii, symbiotic long-period variable, spectrum of assoc. nebulosity 0-90450  
 $\sigma$  Aquarii (A0 IVs), hot metallic-line star, spectrum and abundance anal. 0-90415  
 Aquila X-1 (4U 1908+00), 1978 summer X-ray and optical outburst 0-73068  
 Aquila X-1 (4U 1908+00), optical outburst obs. 0-67909  
 V342 Aquilae, eclipsing binary, period and light curve changes, (1966 to 1976) 0-67791  
 KO Aquilae, eclipsing binary system, UVB photoelectric study 0-62198  
 $\theta$  Aquilae (B9.5 III), spectrum and abundance anal. 0-90415  
 T Aquilae (Nova 1891), spectrophotometry of shell 0-72955  
 V603 Aquilae (Nova 1918), IUE obs. of periodic light vars. 0-105251  
 V603 Aquilae (Nova 1918), old nova, eclipses obs. 0-90476  
 Arakelyan 120, Seyfert galaxy nuclei, optical variability, UVB obs. 0-73049  
 asteroid 624 Hektor, light curve indicating elongated shape 0-98600  
 asteroid position determination in April 1979, data reduction (*French*) 0-72845  
 asteroid positions in 1978, visible obs. 0-67630  
 asteroids, astrometric 1978 positions from ESO and GPO obs. 0-72841  
 asteroids, astrometry 1975-1978 from Uppsala southern station 0-85883  
 asteroids, astrometry in 1978 April, ESO obs. 0-85882  
 asteroids, Minor Planet Circulars 5333-5390, 623 precise posns. 0-77325  
 asteroids, Minor Planet Circulars 5189-5248, 1389 precise posns. 0-67631  
 asteroids, Minor Planet Circulars 5249-5286, 1112 precise posns. 0-67632  
 asteroids, Minor Planet Circulars 5287-5332, 1045 precise posns. 0-67633  
 asteroids, Minor Planet Circulars 5391-5422, 577 precise posns. 0-85884  
 asteroids, Minor Planet Circulars 5423-5454, 798 precise posns. 0-98599  
 asteroids, Munich meridian obs. (1941-61), orbital elements determ. (*German*) 0-77306  
 asteroids, photographic photometry with Schmidt telescope during 1977 and 1978 0-72844  
 asteroids, precise posns. for 74 objects in 1977, Swedish obs. 0-62065  
 asteroids, Trojan group, discovery of new members, orbital elements and ephemerides 0-72847  
 astrometric obs. with Photographic Zenith Tube at Tokyo Observatory, anal. of errors 0-98547  
 59 Aurigae,  $\delta$  Scuti star, light curves periodogram anal. 0-62141  
 AR Aurigae, eclipsing binary Hg star, peculiar spectral var. during eclipse 0-98679  
 T Aurigae (Nova 1891), old nova, photometric and spectroscopic obs. 0-90446  
 B-type stars, CNO abundances in associations and general field 0-67702  
 late B-type stars small  $v \sin i$  values, Ap star determ., visible spectra 0-77409  
 BD+10°2179, C rich H deficient star, UVB photometric obs. 0-90437  
 BD+29°3805, K-type giant, spectroscopic binary orbit 0-67790  
 BDS 1269 A, metal-poor  $\delta$  Scuti star, pulsation periods from b-band photometry 0-105247  
 Be stars, discoveries in open clusters NGC 3766 and (IC 2581) 0-90445  
 Be stars, mag. fields determ. via linear polarisation spectrum (*Russian*) 0-90344  
 Berkeley 11, compact open cluster, UVB obs. 0-94840  
 binary stars, G and K-type giants, Ca II H and K lines emission intensity 0-82420  
 binary stars, obs. by speckle interferometry 0-90477  
 binary systems, speckle interferometric obs. with Haute-Provence 1.93 m telescope 0-90475  
 $\xi$  Bootis A, late-type dwarf star, mag. field obs. 0-72949  
 bright galaxy nuclei, optical and radio survey, sample selection and obs. 0-73039  
 SC1 radio sources, optical identification by photographic photometry and spectra 0-77503  
 3C 120, radio galaxy, vars. in optical spectrum (*Russian*) 0-90540  
 3C 120, Seyfert galaxy, spectrophotometric obs. of assoc. nebulosity 0-67890  
 3C 120, Seyfert galaxy nuclei, optical variability, UVB obs. 0-73049



## visible astronomical observations continued

- 3C 273, UVB obs., (1975 to 1979) 0-62309  
 3C 351, quasar, VLA maps and outer lobe optical emission search 0-105376  
 3C 446, 1980 June outburst, UVB photometry 0-86010  
 California Nebula (NGC 1499), visual extinction uniformity across nebula 0-62225  
 53 Camelopardalis, Ap star, Ca II K and H $\delta$  lines rapid vars. (*Russian*) 0-90458  
 Z Camelopardalis, dwarf nova, spectrophotometry at standstill and in eruption 0-82366  
 AX Camelopardalis (53 Camelopardalis), Ap star, UVB photoelectric photometry and period of var. (*Italian*) 0-90448  
 BT Cancri (38 Cancri)  $\delta$  Scuti star, photometry rel. to radial and nonradial pulsation periods 0-85948  
 $\alpha$  Canis Minoris (Polaris), interferometry, first fringe meas. 0-82215  
 TX Canum Venaticorum, cataclysmic variable, visible spectra obs. 0-105249  
 RS Canum Venaticorum, out of eclipse light var. and comparison with similar stars 0-109489  
 RS Canum Venaticorum type binaries, H $\gamma$  line vars., chromospheric diagnostics 0-62181  
 $\nu$  Capricorni (B9.5 V), spectrum and abundance anal. 0-90415  
 I Carinae, Cepheid variable, Fourier anal. of light var. 0-90442  
 I Carinae, search for comparison stars, uvby $\beta$  photometry, colour excess 0-62136  
 QZ Carinae (HD 93206), O-type quadruple eclipsing system, spectroscopic and radial vel. study 0-105275  
 SU Cassiopeiae, Cepheid variable, spectrophotometric determ. of effective temp. 0-90435  
 VX Cassiopeiae, early-type irregular variable, photometric variability (*Russian*) 0-72973  
 AB Cassiopeiae, eclipsing binary with  $\delta$  Scuti primary, light vars. preliminary anal. 0-94831  
 $\omega$  Centauri, SEC Vidicon photometry of main sequence 0-90491  
 $\mu$  Centauri (B2 IVe), new circumstellar shell development, spectroscopic obs. (1980 June 10 to 12) 0-94808  
 V810 Centauri (HD 101947), yellow variable supergiant near Cepheid instability strip, VBLUV photometry 0-98672  
 $\alpha$  Centauri binary system, spectroscopic chemical anal. 0-62128  
 Centaurus I cluster of galaxies, redshift meas. and resolution into two vel. systems 0-77499  
 Centaurus X-4, spectroscopic obs. of visual counterpart, companion type 0-82545  
 Centaurus X-4, transient X-ray burst, optical counterpart discovered 0-67906  
 central star of Abell 46, eclipsing binary 0-73027  
 NY Cephei, massive eclipsing binary star, progress report from UVB photometry 0-67789  
 EM Cephei, UVB, photometry rel. to constancy or variability of period 0-105286  
 VW Cephei, W Ursae Majoris star, rot. line broadening rel. to shape and mass ratio 0-109494  
 Cepheids, short period, in N.hemisphere, UVB photometry rel. to search for double mode Cepheids 0-94814  
 Cepheids in M31 (Andromeda galaxy), assoc. with interstellar gas and star complexes (*Russian*) 0-90455  
 Ceres, diameter, interferometric meas. (*Russian*) 0-67634  
 Cernis-Petraskas (1980k), positions, (1980 August 10 and 17) 0-101556  
 $\delta$  Ceti,  $\beta$  Canis Majoris variable, period meas. and detect. of period decrease 0-105257  
 $\sigma$  Ceti (Mira) at 1978 max., spectropolarimetry 0-94799  
 ZZ Ceti stars, constraints on possible long-term variability 0-90428  
 RS Chamaleontis, eclipsing binary, four-colour photometry rel. to photometric elements, absolute dimensions and He abundance 0-67783  
 Charon (1978 P 1), posns. in 1980 April rel. to probable occultation 0-67651  
 Charon (1978 P 1), probable stellar occultation, 1980 April 6, min. dia. 0-62071  
 Charon (1978 P 1), satellite of Pluto, positions and dynamical parameters 0-62069  
 Charon (1978 P 1), stellar occultation obs., 1980 April 6, rel. to satellite dia. and struct. 0-94754  
 Chu's object in Perseus, UVB photometry and spectrum rel. to identification as galactic star 0-62132  
 cluster galaxies, alignment study 0-90516  
 cluster stars near IC 1805 (W4), spectral classes and photometry 0-62214  
 cluster galaxies, redshift determ. using Image Dissector Scanner, visible spectra 0-90544  
 Collinder 140, young open cluster, spectroscopic and statistical study 0-62211  
 17 Comae A, Ap star, mag. field meas. and rot. period (*Russian*) 0-90457  
 GQ Comae Berenices, QSO or N galaxy, spectrophotometry obs. 0-77488  
 Comet Bowell (1980b), precise positions, elements and ephemeris (1980 March-July) 0-62075  
 Comet Cernis-Petraskas (1980k), antitail, precise posns., parabolic elements and ephemeris 0-105206  
 Comet Cernis-Petraskas (1980k), positions, 1980 August 2 to 16, orbital elements and ephemeris 0-98614  
 Comet Cernis-Petraskas (1980k), total visual mag. and coma dia. (1980 Aug.-Sept.) 0-101561  
 Comet Chelnikh-Petraskas, discovery posn. (1980 July) 0-94756  
 Comet Kohler (1977m), precise positions, (1977 October 5 to 19) 0-105203  
 Comet Kohoutek (1972 XII), Swan Cloud, 1974 January 11, rel. to cometary plasma tails general morphology 0-98612  
 Comet Kohoutek (1973 XII), CN violet (0,0) spectra 0-82308  
 Comet Meier (1978 XXI), position from 1979 April 21 to 30, meas. and reduction (*French*) 0-72884  
 Comet Meier (1978f), precise positions meas. at ESO, La Silla, in (April 1979) 0-105204  
 comet on Palomar Sky Survey, discovery and semi-accurate position 0-77352  
 Comet Russell (1980l), discovery posns. and ephemeris (1980 September) 0-101557  
 Comet Russell (1980l), precise positions, 1980 September 6 to 8, and ephemeris 0-101559  
 comet tails, H $_2$ O $^+$  surface brightness rel. to CO $^+$  0-72880  
 Comet Torres, discovery and positions, 1980 June 13 and 14 0-82306

## visible astronomical observations continued

- Comet Torres (1980e), 1980 June 17 semi-accurate posn. 0-85898  
 Comet Torres (1980e), precise posns., elements and ephemeris (1980 June-July) 0-85900  
 Comet West (1976 VI), coma mols. and dust distrib., visible emission profiles 0-101562  
 comets, Minor Planet Circular 5333-5390, 51 precise posns. for eight objects 0-77325  
 comets, Minor Planet Circulars 5189-5248, 69 precise posns. for 13 objects 0-67631  
 comets, Minor Planet Circulars 5249-5286, 63 precise posns. for six objects 0-67632  
 comets, Minor Planet Circulars 5287-5332, 44 precise posns., for eight objects 0-67633  
 comets, Minor Planet Circulars 5391-5422, 64 precise posns. for eight objects 0-85884  
 comets, Minor Planet Circulars 5423-5454, 25 precise posns. for seven objects 0-98599  
 compact galaxies in fields near M3 and M92, selection, statistics and photometry with two telescopes 0-77485  
 R, S, T Coronae Austrinae, T Tauri stars, long period vars. 0-82350  
 $\beta$  Coronae Borealis, Ap star, Ca II K and H $\delta$  lines rapid vars. (*Russian*) 0-90458  
 $\theta$  Coronae Borealis, Be-type star, shell line profile and radial vel. obs. 0-77426  
 $\alpha$  Coronae Borealis, Hg-Mn star, spectroscopic binary, visible spectra obs. 0-72983  
 $\beta$  Coronae Borealis, obs. with Zeeman analyzer system on McDonald 2.7 m telescope 0-62021  
 R Coronae Borealis type variables and related objects, UVB photometric obs. 0-90437  
 cosmic dust in spiral galaxies, optical anal. method, visible obs. 0-101638  
 CPD -62 $^{\circ}$  1837 (HDE 308122), long-period variable member of triple 0-105260  
 3CR radiosources quasars and galaxies, optical identification 0-90555  
 $\alpha$  Crucis, improved spectroscopic orbit 0-67792  
 BI Crucis, new symbiotic star, spectrum 0-109442  
 25 G Crucis (HD 108250), orbital elements from spectrograms 0-82432  
 CSV 6110 in Taurus,  $\sigma$  Ceti type variable, visible obs. 0-67745  
 65 Cybele, occultation of AGK+19 $^{\circ}$ 0599, 1979 October 18, obs. using photoelectric photometer (*Chinese*) 0-105172  
 $\chi$  Cygni, diameter of Mira-type star from speckle interferometry 0-67728  
 XX Cygni, dwarf Cepheid, composition and motion, visible photometric and spectrographic obs. 0-77424  
 SS Cygni, dwarf nova, rapid optical oscils. phase variability 0-85947  
 GO Cygni, eclipsing binary, UVB photometry rel. to period changes 0-72999  
 CC Cygni, photometric obs. of RS Canum Venaticorum type binary, interpretation 0-62182  
 59=V832 Cygni, spectrum scanner obs. 0-94809  
 CH Cygni, symbiotic star, 1977 outburst, radial vel. and atm. struct. determ. 0-72969  
 CH Cygni, symbiotic star, binary model 0-62158  
 V1016 Cygni, symbiotic star, IR variability obs. from VJHKL photometry (*Russian*) 0-105263  
 $\alpha$  Cygni (Deneb), Ca II K-line core asymmetry 0-85981  
 V1500 Cygni (Nova 1975), Balmer line emission profiles evolution in early decline phase 0-82371  
 V1500 Cygni (Nova 1975), distance and temp., visible spectral obs. (*Chinese*) 0-85955  
 V1668 Cygni (Nova 1978), multifilter photometry and polarimetry 0-90454  
 V1668 Cygni (Nova 1978), optical light curve, uvby photometry 0-62154  
 V1668 Cygni (Nova 1978), spectroscopic and photometric obs., (1978 to 1979) (*Russian*) 0-109444  
 CI Cygni symbiotic star, UV and optical spectrum changes during eclipse 0-105258  
 Cygnus Loop, fast shock wave detection, optical spectra 0-82467  
 Cygnus X-1 (V1357 Cygni), optical light curve vars. rel. to X-ray vars. 0-109560  
 Cygnus X-1 (V1357 Cygni), optical photometry (1980 May 25 to July 7) 0-90578  
 Cygnus X-2, binary, radial vel. and orbital elements from visible spectra obs. 0-77519  
 DA white dwarfs, H I Balmer  $\gamma$  line profiles and masses 0-77399  
 dark nebulae in M31, catalogue 0-72787  
 Deimos, loose material downslope movement obs. 0-94737  
 Deimos, photometry from Viking orbiter images 0-72838  
 HR Delphini (Nova 1967), short period light vars. from UVB photometry 0-67744  
 78 Diana, astrometric obs. rel. to central path of occultation of SAO 75392, (1980 September 4) 0-101547  
 diffuse gaseous nebulae, H $\alpha$  photoelectric photometry (*French*) 0-62240  
 S Doradus, LMC Hubble-Sandage variable, IUE and ground based spectroscopic obs. 0-101595  
 30 Doradus nebula in LMC, optical obs. of bright core 0-67827  
 30 Doradus nebular complex, chemical comp. and struct. obs. 0-62226  
 double stars, position angles and separation, Venezuelan obs. (*French*) 0-77450  
 double stars, separation and position angle obs. 0-98691  
 DR15, H II region, optical emission assoc. with 408 to 2695 MHz radio sources 0-94881  
 Draco dwarf spheroidal galaxy, stellar colour magnitude diagram and proper motion 0-73029  
 K Draconis, Be star, search for short time scale vars. in H $\alpha$  emission 0-109441  
 RZ Draconis, eclipsing binary, photoelectric light curve and orbital period study 0-109461  
 E3 (ESO-037-SC 01) dying globular cluster, photometry and stellar content rel. to tidal truncation 0-105291  
 early-type stars in Norma 0-62129  
 Earth-Moon libration points, search for natural or artificial objects 0-98647  
 SW eclipsing binary, period study, photometry and spectra obs. 0-82424  
 elliptical galaxies, normal, giant ellipsoidal shells discovery 0-86000  
 elliptical galaxies assoc. with B2 radiosources, orientation 0-77501  
 emission line galaxies, spatial distrib. rel. to clusters, visible spectra obs. 0-73046  
 emission-line variable (No.86) in core of M 15, UVB photometry, probably W Virginis star 0-77458  
 CD Eridani, photometric soln. for eclipsing binary system 0-62185

**visible astronomical observations continued**

- ES type galaxies, UV photometry obs. 0-73053  
ESO 2612-PN 02, spectroscopic obs. of southern planetary nebula 0-10626  
45 Eugenia, rot. period and photoelec. light curve determ. 0-72846  
extragalactic faint blue objects, nature and distrib. 0-82476  
extragalactic radio sources, optical identifications 0-105373  
F (Chinese) 0-85957  
F corona, radial vel. obs. at 1979 February 26 solar eclipse 0-85914  
F-type supergiants, southern, visible spectra obs. 0-98660  
F-type supergiants in Magellanic Clouds, Ca abundances 0-98655  
faint blue stars, southern, UV photometry 0-82349  
faint star clusters in LMC, survey, visible obs. 0-73011  
faint stellar images, colour-magnitude diagrams and clustering correl. functions rel. to star populations 0-82360  
Fairall 160, 182, UV photometry 0-82349  
flare stars, multichannel spectrophotometry 0-105256  
flare stars in Scorpius-Ophiuchus region, discoveries (Chinese) 0-77418  
Fornax cluster, membership determ. by photographic photometry 0-82523  
FXP 0520-66, flaring X-ray pulsar, nature and optical identification (Russian) 0-77521  
G128-7, cool DA white dwarf, spectrophotometry rel. to atmospheric parameters and evolution 0-62126  
G 208-44/45, possible double flare star, spectral obs. 0-67727  
galactic halo C star possible association with Magellanic Stream, visible obs. 0-77411  
galaxies, compact and bright-nucleus, in S. hemisphere, spectroscopic survey 0-94725  
galaxies, elliptical, extended radio sources, optical positions 0-105331  
galaxies, elliptical, vel. dispersions rel. to mass to light ratios 0-98707  
galaxies, southern late type and irregular, visible survey 0-105334  
galaxies, UV photoelectric photometry and photometric parameters 0-67855  
galaxies assoc. with QSOs, spectroscopic search 0-105355  
galaxies in rich clusters, morphological types 0-85872  
galaxies near late-type spiral NGC 4945, radial vels. and BV photometry 0-109547  
galaxies surface distribution, comparison with galaxy fields stochastic simulation 0-90530  
galaxies with UV continuum, twelfth list 0-67585  
galaxies with UV excess, second list 0-67584  
galaxies with UV excess and double and multiple nuclei, spectral study 0-67848  
galaxy morphology in rich clusters, implications for galaxies form. and evolution 0-62255  
Galilean satellites, photometry of Io, Europa and Callisto, 1976 to 1979, possible solar variability detect. 0-98623  
Galilean satellites, surface features from Voyager 2 obs. 0-72871  
U Geminorum, dwarf nova, visual magnitudes during outburst, (1980 May 6 to 9) 0-72978  
YY Geminorum, eclipsing binary, photometry and orbital period study 0-105287  
U Geminorum, visual magnitude estimates during outburst (1980 Oct.) 0-109439  
giant stars in globular star clusters, Ca II H and K-lines and abundance 0-72940  
globular clusters, energy distrib. from Orbiting Astronomical Observatory photometry 0-73009  
Greenwich Obs. Time and Latitude Service, Time Report (January to March 1979) 0-72749  
Greenwich Obs. Time and Latitude Service Time Report (April-June 1979) 0-72750  
H 2252-035, optical counterpart photometry and spectrum 0-101651  
H 2252-035, spectrophotometry, no periodic linear polarization (1980 Sept.) 0-105401  
halo stars, cool, Al abundance from spectral obs. 0-105232  
HD 101065, Przybylski's star, light variability freq. anal. 0-62152  
HD 10380, Population I giant, chemical anal. and comparison with high vel. stars 0-82352  
HD 105056, ON supergiant, radial vel. study 0-90427  
HD 108078, spectroscopic binary orbit from photoelec. radial vel. meas. 0-77451  
HD 127617 (Bidelman's high latitude Be star), photometric and visible spectra obs. 0-77420  
HD 129494, new pulsating  $\delta$  Delphini star, photometric obs. and luminosity 0-67750  
HD 129708, new bright short-period Cepheid variable with unusual spectrum, photometric obs. 0-67751  
HD 137613, C rich H deficient star, UV photometric obs. 0-90437  
HD 153882, obs. with Zeeman analyzer system on McDonald 2.7 m telescope 0-62021  
HD 159378 (Tr 27-102), yellow variable supergiant near Cepheid instability strip, VBLUV photometry 0-98672  
HD 166734, Of star, spectroscopic binary orbit determ. from visible obs. 0-82414  
HD 168607 (B9 Ia<sup>+</sup>), S Doradus type star candidate, spectral line profiles (Russian) 0-90456  
HD 185332, new  $\delta$  Scuti star, photometric and spectroscopic obs. 0-90451  
HD 200775, Be star, optical and UV extinction by dust in (NGC 7023) 0-109515  
HD 200775, possible protostar in reflection nebula NGC 7023, optical polarization and IR spectrum 0-85944  
HD 200925 radial vels. of new short period  $\delta$  Scuti star (French) 0-90441  
HD 203631, spectroscopic binary orbit from photoelectric radial vels. 0-105285  
HD 22007 (primary of ADS 16681), spectroscopic binary, radial vel., orbit elements 0-67793  
HD 39937, 101379, 155555, 174429, southern RS Canum Venaticorum stars candidates, radial vel. study 0-98686  
HD 4174, symbiotic star, spectroscopic obs. 0-85945  
HD 45088, BY Draconis binary, surface activity from high rot. vel., visible obs. 0-77425  
HD 45088, reticon obs. in red of dK3 spectroscopic binary 0-67778  
HD 50896, Wolf-Rayet star, linear polarisation periodic vars. rel. to binary star nature 0-72972  
HD 77581 and 153919, polarimetric obs. of massive X-ray binaries 0-98688

**visible astronomical observations continued**

- HD 93250, O3 massive star in  $\eta$  Carinae complex, non-LTE analysis 0-77398  
HD 97048 (=HM 18), pre-main sequence star, unidentified IR features obs. 0-85943  
HD 97950, central star in NGC 3603, interstellar spectral lines, visible obs. 0-101586  
HDE 245770, optical counterpart to A 0535+26, dimens. spectral type and luminosity visible obs. 0-72976  
He2-442, UVRK photometry and spectroscopic obs. (Russian) 0-94817  
He 2-467, yellow symbiotic star, emission lines and continuum 0-62155  
Henize 715 (4U 1145-61), Be-type star, colour and luminosity vars. (1976-1980) 0-72979  
Herbig-Haro objects, nearby IR sources optical spectra 0-67720  
Herbig-Haro objects in Orion Nebula 0-77397  
AH Herculis, dwarf nova outburst, rapid oscils. evolution 0-94805  
DI Herculis, eclipsing binary, photometric obs. anal. rel. to relativistic motion of periastron 0-94830  
DQ Herculis, eclipsing binary emission line eclipse phenomena, visible spectra obs. 0-94800  
u Herculis, eclipsing variable, two new light curves 0-90472  
AM Herculis, spectrophotometric obs. at min. light min. light 0-98692  
AM Herculis, visual magnitude estimates (1980 March-June) 0-82428  
AM Herculis, X-ray eclipsing binary, UV and visible spectra anal. 0-109563  
AM Herculis (3U 1809+50), polarimetry and spectrophotometry rel. to mag. field 0-94835  
AM Herculis (3U 1809+50), simultaneous three-channel photometry rel. to optical flickering mechanism 0-82411  
HZ Herculis (Hercules X-1), optical and UV obs. 0-109487  
 $\alpha$  Herculis A, M-type supergiant, Li abundance in atmosphere (Russian) 0-72950  
high velocity giant stars, detailed chemical anal. 0-82352  
high-resolution astronomical imaging, results 0-82225  
hot white dwarfs, luminosity function, spectral type anal. 0-90418  
HR 1099 (V711 Tauri), RS Canum Venaticorum star, H $\alpha$  line variability, visible spectra obs. 0-105277  
HR 1225,  $\delta$  Scuti star, photoelectric study and periodogram anal. 0-109436  
HR 5049, Co II in spectrum of southern magnetic Ap-star 0-82384  
HR 6127, chemically peculiar star, spectral lines and equivalent width lists, visible obs. 0-82387  
HR 6659, spectroscopic binary, radial vel. obs. 0-82430  
HR 8752, binary supergiant, emission feature variability, visible obs. 0-109463  
HR 96, Ap-type star, atm. parameters and stellar comp., visible obs. 0-67740  
TT Hydrae, absolute dimensions of  $\beta$  Persei type eclipsing binary 0-62184  
EX Hydrae, dwarf nova, IR and optical light curves 0-67747  
EX Hydrae, dwarf nova lightcurve, periodic and secular vars. 0-77413  
EX Hydrae, spectra of dwarf nova 0-98670  
Iapetus, visible and IR obs. rel. to relative reflectance at 1.6 and 2.2  $\mu$ m 0-98607  
IC 418, planetary nebula C abundance from visible and IUE obs. 0-82451  
 $\epsilon$  Indi, late type dwarf star, spectrum rel. to model atmosphere and comp. 0-90425  
interstellar  $^{12}\text{CH}^+ / ^{13}\text{CH}^+$  abundance ratio, meas. towards 20 Tauri,  $\xi$  Persei and  $\zeta$  Ophiuchi 0-67809  
interstellar large globules, absorpt. meas. rel. to struct. and dynamics 0-62246  
interstellar matter in Magellanic Clouds, giant and supergiant shells obs. 0-94858  
IR bright stars in region of galactic centre, catalogue and photometry 0-77299  
IRC+30219, variable C star, optical emission-line phase obs. 0-90569  
Jupiter, atmosphere constituents, comparison with Saturn, visible spectra obs. (French) 0-101550  
Jupiter, fast moving bright spot obs. in North Temperate Current C 0-67640  
Jupiter, H Lyman- $\alpha$  brightness, longit. asymm. 0-72852  
Jupiter, methane and NH<sub>3</sub> bands, longitudinal variability, visible obs. 0-82270  
Jupiter, NH<sub>3</sub> abundance from visible obs. 0-82269  
Jupiter, S II forbidden line emission nebula studies 0-67636  
Jupiter, S II forbidden line emission round planet, distrib. and intensity 0-85885  
Jupiter, S II ring, var. in charact., link with Io, visible obs. 0-90360  
Jupiter, S II torus, longitudinal asymmetry visible spectra 0-82271  
Jupiter, satellites 1979 J 1 and 2, Voyager 1 imagery analysis 0-67639  
Jupiter, wind vector, eddy mmtm. and energy conversion obs. 0-72851  
Jupiter and Galilean satellites, astrometric position determ. (1977) (French) 0-77326  
Jupiter and Galilean satellites, astrometric position determ. 0-77327  
K648, halo planetary nebula, Ar III line obs. and low Ar abundance meas. 0-82443  
K-type giant stars, evidence for circumstellar shells from 0.4 to 20  $\mu$ m photometry 0-90420  
K-type stars, spectroscopic investigations in 4500 to 7500  $\text{\AA}$  region 0-109430  
Kepler's SN 1604 remnant, spectrum 0-85982  
216 Kleopatra, photometry rel. to comp., diameter, elongated shape and possible stellar occultations 0-94743  
KUV09313+4052, variable UV excess object, discovery, position and photometry 0-62159  
EV Lacertae, flare star, photometry and spectrum rel. to starspots and rot. period 0-98665  
SW Lacertae, W Ursae Majoris star, photoelectric obs. and epochs of min. light 0-62196  
BL Lacertae objects, polarisation, visual and IR photometry and polarimetry 0-77480  
BL Lacertae objects, search for rapid brightness variability 0-90567  
late-type field stars in S. hemisphere, radial vel. study rel. to possible duplicity 0-98686  
CW Leonis (IRC+10216), IR C star, intrinsic polarisation obs. and origin 0-67730  
19 Leonis Minoris, spectroscopic binary, orbital elements and mass ratio 0-62197  
68 Leo, rot. period and photoelec. lightcurves determ. 0-98594  
48 Librae, Be star, shell spectrum line profiles 0-62146



## visible astronomical observations continued

- 48 Librae (FX Librae), Be star, search for short time scale vars. in H $\alpha$  emission 0-109441  
 LMC X-1 optical candidate, spectrum and semi-accurate position 0-67908  
 long-period variable stars in S.hemisphere, narrowband polarimetry 0-98666  
 LSI+61°303, supergiant Be star, radio emission and radial vel. periodic vars. 0-62149  
 luminous stars in NGC 6822 and IC 1613, visible spectra and photometry 0-82345  
 lunar occultations from University of Illinois Prairie Observatory (1977-1978) 0-105148  
 lunar occultations of stars, diameter meas., photoelec. obs. 0-72920  
 $\delta^2$  Lyrae, M-type supergiant, Li abundance in atmosphere (*Russian*) 0-72950  
 $\beta$  Lyrae, photoelectric photometry rel. to orbital period variability 0-72997  
 $\alpha$  Lyrae (Vega) rot. rate determ. from line profile photoelec. obs., Fourier transforms 0-77408  
 RR Lyrae stars, in 47 Tucanae, membership and metallicity 0-62206  
 M1-2 central star, possible eclipsing binary in planetary nebula 0-105239  
 M2 (NGC 7089), globular cluster, faint stars photometry and colour-magnitude diagram 0-101623  
 M31, disc colour gradient photoelec. surface photometry obs. 0-73032  
 M4-18, spectroscopic obs. of compact planetary nebula 0-67829  
 M5, M13, M3, globular clusters, giant stars chemical comp. 0-67695  
 M82, optical polarisation wavelength depend. 0-67861  
 M 2-9, planetary nebula structural changes (1952-78) 0-82456  
 M-type stars, classification from spectral scans 0-62127  
 Magellanic Clouds, planetary nebulae, identification, luminosity function and numbers 0-67815  
 main sequence B-type stars, physical parameter determ. from uvby $\beta$  photometry obs. 0-72952  
 main-sequence stars, F to M-type, comparison of activity cycles to old and young stars 0-105235  
 Markarian 231, Seyfert galaxy, substructure with UV excess, UV and visible obs. 0-82512  
 Markarian 325, irregular galaxy, emission clumps observational props. 0-67869  
 Markarian 3, class 2 Seyfert, visible spectra obs. 0-85999  
 Markarian 59, supergiant H II region in SBm galaxy NGC 4861 spectrum and struct. 0-98705  
 Mars, cloud formations, reflectivity time var., visible photometry obs. 0-72840  
 Mars, diurnal props. of clouds over Tharsis volcanoes 0-94738  
 Mars, north polar cap, 1975-1978 photographic obs. 0-72823  
 Mars, north polar cap, 1977-1978 regression obs. 0-72825  
 Mars, orbit determination on basis of radar and visible observations 0-90323  
 Mars, positions, with Danjon astrolabe at San Fernando Observatory (Jan. to Feb. 1978) (*French*) 0-94736  
 Mars, rot. period determ. from transits of albedo stations across central meridian (1659 to 1971) 0-98588  
 Mars, surface colour change at Viking landing site 0-72829  
 Mars, topography, photogrammetric portrayal 0-67609  
 Mars, Viking lander sample field obs., current status 0-67626  
 Mars, visual characts. of rough planar surfaces from Viking Orbiter images 0-98589  
 Mars dust storm of 1971, cloud form., multicolour TV photometry obs. 0-101546  
 Mars northern plains, polygonal troughs obs. and origin 0-98590  
 maser stars, late supergiants and long period variables 0-77410  
 MCG-6-30-15, type I Seyfert galaxy, X-ray and optical obs. 0-82479  
 MCS 141, 232, 275, quasars, spectra interpretation 0-90562  
 18 Melpomene, rot. period from photoelec. obs. 0-82258  
 metallic line stars, spectral energy distrib. (*Russian*) 0-72975  
 meteor trajectories, orbits 0-72887  
 meteors, optical brightness rel. to ionised trail props. 0-77354  
 minor planets, 1978, April, astrometric positions determ., ESO GPO obs. 0-77319  
 minor planets, positions from Torino Observatory (1977-1979) 0-94739  
 minor planets, positions in August 1977 from Observatorio Nacional, Rio de Janeiro (*French*) 0-94740  
 AU Monocerotis, mathematical anal. of photometric peculiarities 0-77448  
 R Monocerotis, T Tauri star, long period vars. 0-82350  
 Moon, disc brightness distrib. rel. to photometric props. and dimensional scatt. indicatrix 0-101538  
 Moon, photometric anomalies from 1962 obs., possible transient phenomena 0-67587  
 MR 2251-178, nearby QSO in cluster of galaxies 0-67900  
 MXB 1636-536, binary nature from simultaneous X-ray and optical obs. 0-82548  
 N132 D, SNR in LMC, rapidly moving material, visible and UV solns. 0-82449  
 N51D, bubble-like nebula in LMC, internal motions obs. 0-105295  
 N51D, giant filamentary shell in LMC, nature and dynamics 0-105343  
 N70, giant filamentary shell in LMC, Ca II K absorpt. line profile rel. to dynamics 0-90511  
 Neptune, limb brightening in 7300 Å methane band, photometry obs. 0-82297  
 Neptune, obs. by Galileo, (1612 and 1613) 0-105485  
 Neptune, stellar occultation obs. (1980 August 21) 0-109395  
 NGC 1055, 681, 4594, galaxies, rot. curves and mass distrib. (*Russian*) 0-90541  
 NGC 1068, type 2 Seyfert, recombination spectrum and reddening 0-90519  
 NGC 1275 (Perseus A), correl. between optical and radio variability (*Russian*) 0-77505  
 NGC 1316 (Fornax A), optical study of giant radiogalaxy 0-77479  
 NGC 1672 and 2997, nuclei morphology, H $\alpha$  obs. 0-67867  
 NGC 1851, 6624, globular cluster, abundance gradients spectroscopic investigation 0-82437  
 NGC 1999, reflection nebula, optical polarisation map and struct. 0-94856  
 NGC 2264, H II region, classification of optical, IR and radio obs. data 0-67818  
 NGC 2366 H II region visible and radio obs. 0-77475  
 NGC 2536, spiral galaxy, radial vars. of emission line ratios 0-82497

## visible astronomical observations continued

- NGC 253, barred spiral galaxy, detailed surface photometric study 0-105327  
 NGC 2903, spiral galaxy, nucleus identification and visual energy distrib. 0-62273  
 NGC 2997, morphology and hot spots around nucleus of galaxy 0-62282  
 NGC 3115, S0 galaxy, rotation and mass of inner 5 kiloparsecs 0-105326  
 NGC 3227, Seyfert galaxy, photoelectric and spectroscopic study and comparison with galaxy chain (VV 150) 0-98724  
 NGC 330, young cluster in SMC, radial vels. of individual stars 0-67803  
 NGC 3516, SBO type Seyfert galaxy, extended nebulosity, UV and visible obs. 0-82487  
 NGC 3686 galaxy quartet, surface photometry, mass distrib. and group stability 0-62297  
 NGC 3928 C (Markarian 190), identification as miniature spiral galaxy 0-105347  
 NGC 4103, open cluster, membership determ. from proper motions, visible obs. 0-67802  
 NGC 4314, barred spiral galaxy, UBV surface photometry of central region 0-77482  
 NGC 4565, edge-on spiral galaxy, grid photography of halo 0-62261  
 NGC 488, Sb galaxy, rotation curve from emission line spectra 0-62266  
 NGC 4945, late-type spiral galaxy, excited gas kinematics, obs. 0-109547  
 NGC 5236, spiral galaxy peculiar nucleus continuum and reddening 0-73031  
 NGC 5253, surrounding star clusters, fossil evidence for star form. burst, visible obs. 0-77489  
 NGC 5728, barred spiral, vels. and mass distrib., spectral obs. 0-94863  
 NGC 5866, edge-on galaxy, luminosity obs., BV photometry 0-82511  
 NGC 604, H II region in M 33, H $\beta$  photometry and Fabry-Perot interferometry rel. to core-halo struct. 0-85984  
 NGC 6087, galactic cluster, four-colour and H $\beta$  photometry 0-62208  
 NGC 6231, open cluster, spectral types 0-90492  
 NGC 6440, globular cluster, surface photometry of cluster core 0-82436  
 NGC 6494 (M23), open star cluster, membership from astrometry with PDS microdensitometer 0-98697  
 NGC 654, young open cluster, UBV photometric study 0-109502  
 NGC 6584, new variable stars in globular cluster 0-62137  
 NGC 6624, optical counterparts of X-ray burster in core of globular cluster 0-67801  
 NGC 6752, first giant branch, C/N abundances in globular cluster 0-67719  
 NGC 6888, ring nebulae around Wolf-Rayet star HD 192163, spectra of filaments and smooth gas (*Russian*) 0-90515  
 NGC 7000 (North America Nebula), visual and rocket UV imagery 0-82440  
 NGC 741, 1316, 7626, radio galaxies, optical spectra and dynamics 0-94871  
 NGC 7541, rotation curve and mass distrib. in spiral galaxy (*Russian*) 0-94874  
 Nova Serpentis 1978, visible and IR photometry rel. to dust shell evolution 0-90430  
 nova-like stars, cyclotron line search in optical spectra (*Russian*) 0-67753  
 novalike object in Vulpecula, 1980 May-June spectra and magnitudes 0-82392  
 novalike object in Vulpecula, light curve, photometric and spectroscopic obs. 0-67758  
 novalike object in Vulpecula, photometry, June 1980, and spectral classification 0-94807  
 novalike object in Vulpecula, visual magnitude estimates (1980 February 2 to May 9) 0-72980  
 novalike variable in Virgo, discovery, approximate positions and magnitudes, (1980 July and August) 0-98674  
 OAO 1653-40, 38 s X-ray pulsar, optical counterpart, spectroscopic search 0-73072  
 OB stars in Circinus-Norma region, search for faint objects 0-62121  
 open cluster reddening, polarimetry and field star photometry of M67, Hyades and Coma cluster 0-62222  
 $\zeta$  Ophiuchi, 1980 March emission episode, H $\alpha$  and He I line behaviour 0-62151  
 $\chi$  and 66 Ophiuchi, Be stars, search for short time scale vars. in H $\alpha$  emission 0-109441  
 $\zeta$  Ophiuchi (HR 6175), O-type star, emission line episode 0-72953  
 70 Ophiuchi A, late-type dwarf star, mag. field obs. 0-72949  
 Orion Nebula, C abundance from visible and IUE obs. 0-82451  
 Orion Nebula, macroscopic motions from atomic line vels. 0-62243  
 Orion population stars, variables light curve characts. and emission line intensities 0-67721  
 22 Orionis, nonradial m-mode changes in 53 Persei variable 0-72939  
 $\zeta$  Orionis, Reticon obs. of H $\alpha$  P Cygni profile 0-82365  
 $\alpha$  Orionis, supergiant variable, mass loss, visible spectra obs. 0-67755  
 Pal 12, metal-rich globular cluster in outer galactic halo, optical and IR obs. 0-105290  
 parallax and proper motion meas. for seven stars 0-62109  
 BB Pegasi, BV photoelectric lightcurve analysis of eclipsing binary 0-62194  
 AG Pegasi, symbiotic binary system, UV and optical spectrum rel. to nature of components 0-109449  
 II Pegasi (HD 224085), surface-active binary star, spectroscopic obs. 0-90480  
 Period Comet Brooks 2 (1980f), recovery, positions and perihelion passage correction 0-85899  
 Periodic Comet Borrelly (1980i), recovery and approximate positions, (1980 July 9 and 21) 0-94755  
 Periodic Comet Encke, precise posn. for 1980 Oct. 8 and perihelion passage correction 0-109398  
 Periodic Comet Encke, semiaaccurate posn. and appearance (1980 August 8) 0-94758  
 Periodic Comet Harrington (1980m), recovery and precise positions (1980 September 4 to 9) 0-101558  
 Periodic Comet Honda-Mrkos-Pajdusakova (1980c), independent recovery 0-67658  
 Periodic Comet Honda-Mrkos-Pajdusakova (1980c), recovery and positions (1980 May 1 and 6) 0-67656  
 Periodic Comet Kohoutek (1980j), recovery and approximate positions (1980 August 6 and 7) 0-94757  
 Periodic Comet Reinmuth 2 (1980n), recovery posns. and appearance (1980 Sept.) 0-101560



## visible astronomical observations continued

- Periodic Comet Schwassmann-Wachmann 1, CO<sup>+</sup> obs. near minimum brightness 0-82305  
 Periodic Comet Schwassmann-Wachmann 1 (1974 II), outburst and CO<sup>+</sup> detect. spectrophotometric obs. 0-72881  
 Periodic Comet Stephan-Oterma (1980g), recovery positions, elements and ephemeris 0-82307  
 Periodic Comet Stephan-Oterma (1980g), total visual magnitudes and coma diameters, (1980 September 7 to 11) 0-109397  
 Periodic Comet Tuttle (1980h), recovery and precise position (1980 July 14) 0-85901  
 Periodic Comet Wild 3 (1980d), discovery posns., orbital elements and ephemeris (1980 April-June) 0-67657  
 Periodic Comet Wild 3 (1980d), precise positions, (1980 May 9 to 17) 0-72885  
 X Persei, eclipsing binary, gaseous ring struct., H I alpha obs. 0-109482  
 RY Persei, eclipsing binary, spectroscopy and physical parameters of atmospheres 0-101618  
 RY Persei, eclipsing binary, visible spectral obs., model 0-67795  
 IW Persei, metallic-line close binary star, photometric and spectroscopic obs. 0-62186  
 PG 1115+08, triple QSO, spectroscopic obs. and gravit. lens model 0-86012  
 PHL 1092, narrow line quasar, discovery of extreme Fe II emission 0-77508  
 Phobos, photometry from Viking orbiter images 0-72838  
 TX Piscium, disc brightness distrib. and envelope obs. from lunar occultation meas. 0-67725  
 SZ Piscium, RS Canum Venaticorum star, photometric obs. rel. to starspot model 0-109490  
 PK 108-76°1, 49+88°1, halo planetary nebulae, Ar III line obs. and low Ar abundances meas. 0-82443  
 PKS 2155-304, BL Lacertae object, no evidence for redshifted forbidden O III emission 0-73035  
 planetary nebulae, O/H ratios meas. rel. to Galaxy O enrichment 0-105328  
 planetary nebulae, S abundance from IR and visible line meas. 0-82444  
 planetary position determ., Mars, Jupiter, Saturn, Jovian satellites (*French*) 0-72809  
 planets, Munich meridian obs. (1941-61), orbital elements determ. (*German*) 0-77306  
 Pluto, apulse on 1980 Qpril 6, no occultation from S.England 0-67650  
 Pluto, astrometry (1973 to 1979) 0-85894  
 PN 173+3.1, planetary nebula near galactic anticentre, coords., radial vel. and orbit 0-105309  
 PSR 1913+16, optical candidate, astrometry and high-speed photometry 0-101609  
 16 Psyche, opposition effect and surface structure (*Russian*) 0-67635  
 ρ Puppis, line profile variable, pulsational mode-typing 0-90432  
 ζ Puppis, of supergiant, mass flow var., visible and UV obs. 0-90431  
 ζ Puppis, Reticon obs. of Ha P Cygni profile 0-82365  
 L<sub>2</sub> Puppis, semiregular variable, Ca I uneven distrib. from narrowband polarimetry 0-98666  
 PZT stars, mean posns. and proper motions for 304 stars, obs. at Ondrejov 0-82175  
 Q0353-383, QSO abundance anomalies, UV and visible spectral obs. 0-82532  
 Q0957+561, double quasar, components brightness ratio var. 0-77509  
 QSO 0957+561, double quasar, visible spectrophotometry, gravitational lens interpretation 0-82533  
 quasars, CTIO Curtis Schmidt survey -40° zone, discoveries and spectrophotometry 0-73064  
 quasars, low redshift X-ray selected, visible spectra and UDVr photometry 0-105397  
 quasars, Lyman α absorpt. line distrib., intergalactic origin 0-67899  
 quasars, search for rapid brightness variability 0-90567  
 quasars assoc. with compact radio sources, apparent magnitude-redshift relations for resolved and unresolved sources (*Chinese*) 0-105380  
 quasars in CTIO 4 m survey, visible and UV spectrophotometry 0-86009  
 radio galaxies, elliptical, minor axes orientations rel. to radio sources orientations 0-82527  
 radiogalaxies from B2 Catalogue, optical identification, radio positions and redshifts 0-86005  
 radio sources, galaxies and quasars, optical counterparts, astrometry 0-90551  
 red giants in M13, Na abundance var., protocluster gas inhomogeneities 0-82439  
 Rhea, planetary, 1976 to 1979, rel. to possible solar variability detect. 0-98623  
 Rubin-152, possible massive O-type star on galactic fringe, spectroscopic obs. 0-98656  
 SO galaxies, surface photometry, luminosity struct. 0-62258  
 2S 1702-363 optical counterpart, UV photometry 0-82349  
 FG Sagittae, 1975-8 spectral obs. of peculiar variable 0-72959  
 WZ Sagittae, 1978-9 outburst of dwarf nova, spectra 0-94801  
 WZ Sagittae, image-tube spectroscopic obs. of 1978 Dec. outburst 0-72958  
 FG Sagittae, planetary nebula central star, radial vel. meas. rel. to binary star model 0-98664  
 WZ Sagittae, recurrent nova, spectroscopic obs. and model for superhump phenomena 0-82368  
 HM Sagittae, symbiotic star, IR variability obs. from VJHKL photometry (*Russian*) 0-105263  
 V1357 Sagittarii, case for eclipsing binary, visible obs. 0-77452  
 Saturn, atmosphere constituents, comparison with Jupiter, visible spectra obs. (*French*) 0-101550  
 Saturn, E-ring density and satellite posns. (1966 Dec. and 1980 Mar.) 0-94750  
 Saturn, E-ring radial structure, 1980 March CCD obs. 0-105201  
 Saturn, NH<sub>3</sub> abundance from visible obs. 0-82269  
 Saturn, satellite analyses and electronographic obs. (1980 March) 0-77346  
 Saturn, satellites, 1980 March Pic du Midi obs. 0-67646  
 Saturn, satellites, astrometric obs. from McCormick Observatory (1977) 0-105200  
 saturn, satellites 1966 S 2 and 1980 S 15-18, separations 0-67645  
 Saturn, satellites 1980 S 24 and 1966 S 2, 1980 April obs. 0-82280  
 Saturn, satellites and rings, imaging, photometry and polarimetry obs. from Pioneer 11 probe 0-82289  
 Saturn, satellites I-IX, astrometry obs. from McDonald Observatory (1975-1976) 0-105199

## visible astronomical observations continued

- Saturn A and B rings, surface brightness obs. (*Russian*) 0-72872  
 Saturn E-ring, obs. during (March 1980) 0-67647  
 Saturn rings, new ring detection by focal coronagraph (*French*) 0-72772  
 SB 21, extremely He rich subdwarf O-star, spectrum 0-98659  
 Sc galaxies, rot. props. from major axis visible spectra obs. 0-90517  
 SchuWe-3, spectroscopic obs. of southern planetary nebula 0-101626  
 V879 Scorpii, M-type long period variable, visible obs. (*Chinese*) 0-85956  
 Scorpius X-1, rapid variability simultaneous X-ray and optical obs. 0-62322  
 VY Sculptoris, novalike variable, precise position 0-101597  
 VY Sculptoris, novalike variable, spectrum during faint state 0-98675  
 AI, WZ and XX Sculptoris, southern δ Scuti stars, photoelectric study 0-90452  
 RY Scuti, eclipsing binary, ephemeris and UVB obs. 0-94832  
 δ Scuti, line profile variable, pulsational mode-typing 0-90432  
 seeing, meas. at Kitt Peak 0-61899  
 Serpens X-1 (4U 1837+04), burster optical binary counterpart visible spectra and photometry 0-94891  
 Seyfert 1 galaxies, O I 8446 Å emission excitation mechanism, visible and IR obs. 0-85991  
 Seyfert 1 galaxy 1224+04, discovery from spectrophotometry obs. 0-77488  
 Seyfert 2 X-ray galaxies, nucleus spectra and photometry obs. 0-98712  
 Seyfert galaxies, nearby, photographic study of morphology 0-82478  
 Sh2-156 (IC 1470), morphology, excitation and structure of bright galactic nebula 0-67826  
 Shahbazian 1 group of galaxies, dynamics from spectroscopic, obs. 0-67878  
 SMC, stellar populations, distrib. and evolution 0-94868  
 SN 1979C in M100 (NGC 4321), precise position 0-85962  
 SN 1979c in M100 (NGC 4321), spectrophotometry 0-62166  
 SN in anonymous galaxy in Canes Venatici, discovery obs. 0-67759  
 SN in anonymous galaxy in Centaurus, discovery, posn. and magnitude 0-85961  
 SN in MCG -3-34-61, Type I spectrum revealed (1980 June) 0-82401  
 solar atmosphere, evidence for trapped gravity waves 0-72898  
 solar chromosphere limb flare, 1959 July 25, spectrum rel. to physical conditions 0-105227  
 solar corona, 1973 June 30, polarised brightness distrib. rel. to N.polar hole density model 0-98627  
 solar eclipse 1919 May 29, gravitational deflection of light, obs. reexamined 0-67553  
 solar eclipses, ancient Chinese obs. 0-72916  
 solar flash spectrum, obs. at 1979 February 26 eclipse 0-67687  
 solar granulation structure, vertical motions spatial and temporal behaviour obs. 0-85912  
 solar limb darkening function at 5012 Å, possible vars. 0-67677  
 solar prominence spectra taken at Ondrejov Observatory, inclined spectral features obs. 0-62098  
 solar quiescent prominence, influence of spatial resolution on Ca<sup>+</sup> K-line width and shift 0-77364  
 solar quiescent prominence spectra, meas. of Ca<sup>+</sup> 8542 and 8498 Å He 4471 Å and Ti<sup>+</sup> 4468 Å 0-90373  
 solar spectral lines, high-resolution meas. using scanning Fabry-Perot interferometer 0-77298  
 solar spectrum, absorpt. lines asymmetry (*Russian*) 0-72901  
 southern standard stars, 320-880 nm energy distrib. 0-62125  
 spiral and irregular galaxies, brightest superassociations as distance indicators 0-62260  
 spiral galaxies, early-type, multiperture UVB photometric props. 0-98706  
 SS 433, light curves, double peak and binary-like period, photometry 0-94804  
 SS 433, nearby faint, highly-contorted nebular filament discovery 0-94855  
 SS 433, no 6-day periodicity in 1978 June-1980 Feb. obs. period 0-62150  
 SS 433, radial vel. curve low amplitude section, visible spectra anal. 0-67737  
 SS 433, V band photometry and broad min. prediction (1980 April-May) 0-82390  
 SS 433, visible and IR photometry rel. to IR variability 0-98676  
 SS 433 in SNR W50, relativistic jets interaction with interstellar medium 0-101629  
 star cluster hidden in ghost image of Sirius on Palomar Sky Survey, discovery 0-109501  
 star image at telescope focus, quality, rel. to photoelectric obs. efficiency 0-62034  
 stars, bright, nearby, astrometric anals. from Sproul 61 cm refractor plates 0-61991  
 stars near southern open clusters, relative radial vels. (*German*) 0-94724  
 stars of solar neighbourhood, chromospheric Ca II H and K emission survey 0-109423  
 stellar parallaxes, US Naval Observatory data 0-72788  
 stellar spectral energy distribution in 3500 to 7500 Å region, absolute calibration 0-67710  
 Stepanyan's star, eclipsing binary, eclipses obs. and orbital period refinement 0-62195  
 Stepanyan's star, obs. of G8 V absorpt. spectrum and emission spectrum 0-67788  
 subdwarfs in 47 Tucanae, CN vars. 0-94794  
 563 Suleika, rot. period and photoelec. lightcurves determ. 0-98594  
 Sun, Ba II 4554 Å obs. rel. to five-minute oscils. horizontal energy flows struct. 0-62103  
 Sun, C I, 5380 Å response to solar luminosity vars., effects of granular convection 0-85910  
 Sun, Ca II K-line, centre-to-limb obs. of K<sub>2</sub> component (*French*) 0-82331  
 Sun, chromosphere line profiles from OSO-8 satellite 0-67690  
 Sun, coronal obs. with Solwind coronagraph 0-82325  
 Sun, coronal transients at high latitude, 1979 September 27 Solwind obs. 0-94774  
 Sun, equator-crossing spot, development and motion 0-90394  
 Sun, Fe I line meas. of gravitational red shift 0-90391  
 Sun, global rotation rate determ. using 1967-74 sunspot data 0-90387  
 Sun, Ha spicules, dynamics at various heights, spectral obs. 0-90392  
 Sun, loop prominence knots, motions, Ha line filtergram obs. 0-67693  
 Sun, Mg I and II line profiles comparison with theoretical spectra, visible obs. 0-82320



## visible astronomical observations continued

- Sun, oscillations of 160-min. period, no terrestrial atmospheric extinction effects 0-105216
- Sun, oscills. period obs. rel. to internal struct. 0-105226
- Sun, photosphere, solar rot. from Doppler obs. 0-105219
- Sun, photospheric granulation, 2-dimens. power spectrum analysis, data processing 0-101570
- Sun, reson. line polarisation, non-mag. polarisation, centre-to-limb var. 0-67678
- Sun, rotation, background vel. fields, anal. and instrumental effects, visible obs. 0-72915
- Sun, secular diameter decrease, Tobias Mayer obs. refute hypothesis 0-90389
- Sun, sunspot umbral dots, dynamic and struct. behaviour for photometry obs. 0-109409
- Sun, young active regions, filaments, and flares 0-72910
- supergiant, B-type, assoc. IR source GL 2636, IR and visible obs. 0-105302
- supergiants in LMC, spectra, diffuse interstellar 4430 Å feature 0-73033
- supernova, possible, in Virgo galaxy cluster, discovery, position and spectrum 0-90460
- supernova in anonymous galaxy in Centaurus, magnitude (1980 June 30) 0-85962
- supernova in anonymous galaxy in Grus, discovery and magnitudes (1980 May 23 to July 12) 0-94820
- supernova in anonymous galaxy near  $\kappa$  Centauri, discovery and magnitudes 0-85962
- supernova in MCG -3-34-61, discovery of 17 mag. object 0-72989
- supernova in NGC 3733, spectrophotometry (1980 March 22) 0-62164
- supernova in NGC 4321, UBVR photometry 0-77428
- supernova remnants, kinematics and evolutionary sequence in cloudy interstellar medium, interferometry obs. 0-67823
- supernovae at great distance, luminosity and temporal var. as cosmological probes 0-94821
- $\gamma$  Tauri, ang. diameter determ. from lunar occultation obs. 0-62119
- 41 Tauri, Ap star, Ca II K and H $\delta$  lines rapid vars. (*Russian*) 0-90458
- RW Tauri, eclipsing binary, gaseous ring struct., H I alpha obs. 0-109482
- SU Tauri, R Coronae Borealis variable, brightening after long minimum, 1980 August to September 0-109438
- DR Tauri, T Tauri star, Balmer line profile changes and inverse P Cygni profiles 0-101591
- DR Tauri, T Tauri star, mass flow var. in envelope, visible spectra 0-85939
- V711 Tauri (HR 1099), RS Canum Venaticorum star, BV light curve during (1978-79) 0-105279
- 28=BU Tauri (Pleione) Be shell star, 3167 to 4924 Å spectrum atlas 0-98673
- T Tauri stars, H $\alpha$  and Na I D lines high-resolution profiles 0-62116
- BL Telescopii A, yellow variable supergiant near Cepheid instability strip, VBLUW photometry 0-98672
- 115 Thyræ, astrometry and orbit improvement (*German*) 0-85881
- Titan eclipse by Saturn, light curve obs. rel. to Saturn upper atmosphere struct. 0-90362
- Tokyo Astronomical Obs., Time and Latitude Bulletins (April/June 1979) 0-72752
- Tokyo Astronomical Obs., Time and Latitude Bulletins (Jul-Sep 1979) 0-82177
- Tokyo Astronomical Observatory Time and Latitude Service, Bulletin (January to March 1979) 0-72751
- Tololo emission line galaxies, size, morphology and spectroscopy, visible obs. 0-73044
- Trumpler 27 star 28, obs. of WC9-type star with large IR excess 0-67738
- Tycho's supernova (SN 1572), unsuccessful search for optical stellar remnant 0-101603
- 4U 0115+634, X-ray binary, 1980 Aug. photometry and spectroscopy 0-101650
- 4U 1907+09, optical identification using HEAO-1 scanning modulation collimator position 0-82542
- Uranus, D/H ratio from visible spectra obs. 0-82296
- Uranus, geometric oblateness from digitized photography, Stratoscope II balloon obs. 0-67649
- Uranus occultation of SAO 158687, planetary radius and ellipticity determ. 0-67648
- Uranus satellites, astrometric obs. 0-67654
- Uranus stellar occultation, 1980 August 15 to 16, reality of additional occultations questioned 0-109396
- XY Ursae Majoris, eclipsing binary, observational evidence for large-scale spot activity on primary component 0-109491
- UX Ursae Majoris, eclipsing binary, time series photometry 0-77446
- UV galaxies, double nuclei, visible spectra obs. (*Russian*) 0-77495
- variable stars, Scorpius-Ophiuchus region, discoveries (*Chinese*) 0-77418
- AI Velorum, BVRI photometry and photoelectric radial vels. rel. to nature of variable star 0-94815
- $\gamma_2$  Velorum, Wolf-Rayet binary, orbital element determ. from spectral obs. 0-85950
- Venus, exosphere, hydrogen Lyman  $\alpha$  emission 0-105188
- Venus, surface dust detected by Venera 9 and 10 radiant flux obs. 0-72803
- Venus cloud layer, struct. according to Venera 9 televised pictures 0-67604
- Venus polarisation, wavelength depend. obs. rel. to UV cloud model 0-82250
- Vesta, diameter, interferometric meas. (*Russian*) 0-67634
- visual binaries with variable components, orbital elements, visible obs. (*Russian*) 0-77455
- ER Vulpeculae, W Ursae Majoris star, rot. line broadening rel. to shape and mass ratio 0-109494
- VV 126, multicomponent interacting galaxies, visible spectroscopy obs. (*Russian*) 0-77494
- VV 150, galaxy chain, photoelectric and spectroscopic study 0-98724
- VV 493 (UGC 07910), unusual extragalactic object, morphology and spectrum rel. to probable nature 0-98718
- VV 794 H II regions, photographic and spectral obs. (*Russian*) 0-77493
- W1 (S171), optical supernova remnant radial vel. field 0-62250
- 19 W32, 43 and 109, galactic centre planetary nebulae search 0-90506
- W3/W4/W5 region, heavy optical obscuration obs. 0-62301
- W50, supernova remnant, optical spectrum 0-90557
- Wolf-Rayet stars, short-lived changes of emission lines (*Russian*) 0-72977

## visible astronomical observations continued

- Wray 977, optical counterpart to X-ray binary pulsar, 4U 1223-62, optical spectra 0-72984
- X-ray source fields from Einstein Observatory, RI photometry with CCD camera 0-62315
- II Zw 136, Seyfert galaxy nuclei, optical variability, UVB obs. 0-73049
- Ba II giant stars binary nature from visible radial vel. obs. 0-82355
- H II regions in barred spiral galaxies NGC 1313, 5236 and 7552 visible obs. 0-82510
- H II regions near nucleus of spiral galaxy NGC 3310, exploratory investigation 0-62235
- He rich stars, intermediate and extreme, spectral atlas in 3700 to 4600 Å range 0-94806
- vision**
- see also colour vision; eye; vision defects; visual perception
- accommodation, reaction and response times obs. 0-67073
- accommodative responsiveness rel. to contrast sensitivity for sinusoidal gratings 0-61552
- acuity assessment through linear extrapolation to threshold of bar grating evoked responses 0-67080
- acuity for letters in rows or columns, advantage to rows 0-89761
- acuity screens, reflectance obs. 0-67178
- adaptation, technique for estimating the contrib. of photomech. responses 0-85547
- aftereffects derived from inspection of orthogonally moving patterns 0-104589
- airport control tower cab, optical design 0-58661
- Alopec process: Visual receptive fields by response feedback, trigger features 0-61546
- alpha-contingent visual stimulation, detect. of cerebral lateralisation of function 0-94190
- apparent contrast matching, narrow-band spatial mechanism 0-61571
- aquatic eyes, retinoscopy, refractive error considerations 0-61750
- associative learning model, voltage-dependent Ca<sup>2+</sup> and K<sup>+</sup> conductances 0-72166
- auditory deprivation effects on vision, common intermodal and intramodal factors 0-89754
- bibliography, British university dissertations and theses, 1972-7 0-105449
- bifoveate retina of lizard, light microscopic study 0-101165
- binocular, constant curvature assumption, theory 0-94214
- binocular interactions, suprathreshold, effects of prolonged monocular occlusion 0-67085
- binocular summation, fusion and tolerances 0-104588
- binocular vision deprived humans, binocular interactions tuned to size and orientation 0-81606
- blinking and suppression of visual stimulation 0-97909
- brain, mag. evoked field mapping 0-104705
- Broca-Sulzer effects, asymmetry in brightness and darkness effects 0-101185
- car drivers, work spectacles and functional visual fields (*Italian*) 0-108875
- checkerboard-evoked multichannel pot. fields, reference-free components identification 0-108887
- complexity estimation of visual search, for objects against nonuniform backgrounds 0-67086
- compound gratings, phase and detect. obs. 0-61558
- cone, computer-driven hardware model, response obs. 0-72402
- contrast, successive and simultaneous obs. 0-76742
- contrast sensitivity as a function of position on the retina 0-61561
- contrast thresholds versus border enhancement, scatt. light effect 0-94213
- cortical neurons, optimality of bar and grating stimuli 0-85391
- cortical plasticity in monocularly deprived immobilized kittens, eye movement dependence 0-81588
- dark-adaption, comments on the testing of 2 prominent hypotheses 0-108896
- detection, effect of photon noise 0-61559
- detection of stationary structs., role of eye movements, theoretical model 0-81594
- difference thresholds modelling, appl. of ordered topological vector spaces 0-104587
- direction-specific adaptation, 2D anal. 0-61555
- dishabituation in visual aftereffect adapting to two orientations 0-97921
- EEG, event-related potential changes in chronic alcoholics 0-67076
- effect of vibration on reading numeric displays 0-104582
- electronic eye for blind people, implementation through the optical nerve (*Croatian*) 0-109060
- epileptic subjects, background illumination effect obs., intermittent stimulation 0-98009
- evoked cortical potential meas., signal optimisation using Kalman filter (*Japanese*) 0-72348
- evoked electrocortical response rel. to microwave-induced hyperthermia, guinea pig 0-61627
- evoked potential, microsecond sensitivity of human system to irregular flicker 0-81586
- evoked potential, N1-P2 correls. of reaction time at the single trial level 0-85389
- evoked potentials, appl. in brain mechanism studies and diagnosis (*German*) 0-61535
- evoked potentials, event-related, in normal, mentally retarded and autistic children 0-85388
- evoked potentials, latency and wave form obs. 0-97907
- evoked potentials, single-trial classification using stepwise discriminant anal. 0-85387
- evoked potentials, spectral band analysis, contrib. to attentional processes study (*French*) 0-61721
- evoked potentials and sensory dimensions 0-61548
- evoked potentials in the first 6 years of life 0-97905
- evoked potentials to electronic pattern reversal, latency variations 0-94202
- evoked potentials to stimulus trains, normative data and photosensitive seizures appl. 0-94204
- evoked response, central visual field contris. 0-108881
- evoked response, simultaneous recording to flashes at different retinal locations. 0-72279
- evoked responses, peripheral versus foveal, multiple sclerosis early diagnosis appl. 0-67276
- external geniculate body, cat, geometric props. of space of description of images 0-94203

## vision continued

- eye motion kinetics in moving target pursuit, oculomotor abnormalities in neurological disorders detect. 0-108888  
 filter performance, inhomogeneous and anisotropic 0-76738  
 fixation distance changes, ocular translation and cyclotorsion obs. 0-89752  
 flash evoked potentials following unilateral electroconvulsive therapy 0-97906  
 flicker, vel. specificity to pattern sensitivity ratio, human vision 0-101181  
 foveal fixation, functional test based on differential cone directional sensitivity 0-85399  
 functional visual field 0-81578  
 giant neuron of fly, performance, spike generation 0-108886  
 glasses, prescription meas. 0-67981  
 glial smooth endoplasmic reticulum acid phosphatase transport into damaged axons, role of microtubules 0-85381  
 grating induction, a new type of aftereffect 0-72175  
 gratings moving in opposite directions, summation and discrimination 0-72169  
 head movements of mealworm beetle, props. and role 0-76772  
 head movements of mealworm beetle, responses to rotating panoramas 0-76773  
 historical paper by Jean Mery written in 1704 0-57050  
 human retinal image processing, two-channel model 0-94215  
 illumination and reflection edges, recognition by human visual system 0-94209  
 information processing, multi-input system representation, polynomial algorithm properties 0-101145  
 instrument focusing to take account of eye accommodation 0-101811  
 intensity discrimination capacity of tree shrew retinal ganglion cells 0-61556  
 LED true checkerboard pattern reversal stimulator for visually evoked pots. study 0-61658  
 luminance changes, discrimination and detect. 0-101171  
 luminance edge thresholds under stabilised viewing conditions, eye movement role 0-81589  
 lumirhodopsin, photoconversion at 77K, quantum efficiency estimation 0-67081  
 Macular pigment, role in polarised light detect., meas. technique 0-61560  
 magnetophosphenes, quantitative anal. of thresholds 0-72184  
 magnetophosphenes, quantitative determ. of thresholds 0-61620  
 metarhodopsin transition, triggering of light-induced change in Ca binding, rod disk membranes 0-94211  
 microsaccades, role in high acuity observational tasks 0-108893  
 microtubules in optic nerves of temperature acclimated goldfish, electron microscopy 0-85395  
 microwave exposed monkeys, skilled visual-motor performance obs. 0-61634  
 midbrain, similarities between overlapping visual and tactile maps in mammals and reptiles 0-61550  
 molecular basis of vision 0-108876  
 monocular deprivation, unequal, alternating, cause of asymmetric visual fields in cats 0-104584  
 monocular light exclusion, reduction of retinal directional sensitivity obs. 0-81592  
 monocular vergence movements produced by external visual feedback 0-108883  
 motion flow perception, conditions for in dynamic visual noise 0-72174  
 motor systems of eye and hand, optimal response in pointing at a visual target 0-61567  
 movement detection mechanism spatial characts., achromatic vision 0-89753  
 movement-detecting neurons, fly, contrast sensitivity obs. 0-72163  
 moving objects localisation, cats 0-76736  
 neocognitron, self-organising neural network model, pattern recognition mechanism unaffected by shift in position 0-76745  
 nerve signals derivation from contrast flash data 0-108885  
 nervous mechanism for visual information processing (*Japanese*) 0-97908  
 nonlinear visual processing in cat's retina, model 0-85385  
 nonlinearity, analytical derivation 0-67082  
 optic tectum, goldfish, fine struct. 0-85396  
 optic tract fibres, physiologically characterised, projection patterns, cat obs. 0-101167  
 optics conference, Madrid, Spain (Sept. 1978) 0-77547  
 optometry conference, Anaheim, USA (Dec. 1979) 0-90602  
 outer isopter perimetric response variability obs. in old subjects 0-108894  
 parallel visual pathways review 0-89751  
 pattern rotation system for a visual stimulator 0-98061  
 pattern visual evoked pots., age-dependent latency change obs. 0-85390  
 pattern-evoked cortical pots., human infants, spatial and temporal interaction 0-101169  
 patterns having the same coordinates pre- and post-saccades, interaction 0-61551  
 peripheral, size and luminance discrimination obs. 0-101172  
 peripheral contrast sensitivity for sine-wave gratings and single periods 0-61562  
 peripheral luminance gratings, lateral effect of oscill. 0-108903  
 phosphenes, X-ray induced, mech. of formation, electrophysiological obs. on albino rats 0-104675  
 photoreceptor, invertebrate., basic mechanisms of excitation and adaptation 0-81593  
 photoreceptor membrane interfacial pots., light-induced 0-72161  
 photoreceptor optics, angular sensitivity 0-61541  
 photoreceptor optics, formalism and excitation 0-61540  
 photostimulator, LED fibre optic, for research on visual nervous integration 0-67302  
 physiology and psychology, development, contrib. of Joseph LeConte 0-86063  
 picture distortions compensation of moving patterns typical for time filters 0-76731  
 reading without a fovea 0-76748  
 receptive fields in area 17 of cat visual cortex, linear and nonlinear properties 0-104583  
 recognition system with thinking, model for humans 0-76744  
 reduced eye, expts. in life science labs. 0-82617  
 research and future trends (*Japanese*) 0-97899  
 retinal ganglion cell layer, cat, newly identified presumptive microneurons population 0-67077  
 retinal ganglion cells, orientation bias, cat expts. 0-94206  
 retinal ganglion cells in the galago, size and topographic arrangement 0-67078

## vision continued

- retinal photoreceptors, response increase and noise decrease by circadian clock in *Limulus* brain 0-94210  
 retinotectal projection in goldfish to an inappropriate region with a reversal in polarity 0-72153  
 rhodopsin and thermal intermediates, fast struct. fluctuations in protein component 0-72137  
 rods, toad, spontaneous quantal events induced by pigment bleaching 0-108895  
 saccades, small, lack of useful purpose considerations 0-61553  
 screening-pigment migration in retinula cells of crayfish, spectral sensitivity 0-72165  
 search, effects of target, background and observer variables 0-101187  
 sensitivity, resolution and Rayleigh matches following monocular occlusion for one week 0-104585  
 simulator of human visual system (*Russian*) 0-76877  
 smallest channel in early human vision 0-101178  
 spatial frequency channels, inhibition between, complex gratings adaptation 0-72160  
 spatial frequency psychometric discrimination thresholds in different orientations 0-81590  
 spatial frequency tuning studies, psychometric curves description by probability summation 0-61576  
 spatial summation for complex bar patterns 0-61557  
 spectral eye fatigue, school lighting effects 0-76732  
 spectral luminous efficiency of human eyes, approximate representation by Gauss-function (*German*) 0-81591  
 stabilisation of visual world rel. to voluntary nystagmus and saccadic suppression 0-101184  
 stereopsis clinical test 0-61566  
 striate cortex, cat, differential responses of 'simple' and 'complex' cells during saccades 0-85394  
 striate cortex, cat, inhibitory sidebands of complex receptive fields 0-67079  
 striate cortex, cat, movement direction detect. and contrast reversal effects, cell response obs. 0-72155  
 tapetum lucidum, cat, morphology obs. 0-108878  
 target tracking, eye movement evaluation using EOG 0-109057  
 transient mechanism in the human system, spatiotemporal characterisation 0-72159  
 transient sensitisation by a contrast flash 0-72162  
 two eyes constituting separate visual channels, expts. 0-97923  
 veiling reflections and reflected glare from glossy paper, lighting conditions for visual comfort 0-76733  
 vergence control, role of spatial freq. tuned channels 0-101170  
 vertebrate retinas, outer segment layer, light-induced Ca fluxes 0-94207  
 visual pattern recognition, models (*Japanese*) 0-97920  
 visual-vestibular interaction during body rotation in man, nonlinear model 0-76735  
 X-ray phosphenes, mech. of formation, photochem. investigations 0-108877
- vision defects**  
*see also contact lenses*  
 albino humans, asymm. of visual evoked response, brain abnormality 0-94208  
 amblyopia, human, differences in neural basis, effect of mean luminance 0-72156  
 amblyopia, lack of normalcy of dominant eye 0-97898  
 amblyopia, monocular, prevalence among anisometropes 0-67071  
 amblyopia, neural function and dysfunction, activity within an amblyopic channel 0-108890  
 amblyopia, neural function and dysfunction, co-operative activity of amblyopic channels 0-108891  
 amblyopia, speedy evoked pot. methods for vision assessment 0-61661  
 aniseikonia, artificial, geometrical explanation of induced size effect, binocular vision 0-72173  
 aphakia, best retinal focus for various fixation distances 0-108882  
 astigmatism and orientation preference in human infants 0-61542  
 binocularity affected by sectioning of corpus callosum, of cat 0-97922  
 blind aid, image conversion to a tactile presentation 0-94414  
 chromatic aberration meas. with chromoretinoscopy 0-81581  
 chromatic aberration rel. to accommodation, meas. using dynamic laser speckle pattern 0-81582  
 comitancy testing, new method 0-94305  
 dichromats, large-field substitution Rayleigh matches 0-101173  
 disc vasculature in Down's Syndrome 0-67069  
 divergence excess strabismus, optometric therapy 0-97902  
 hemianopia, new mirror design for detect. 0-108892  
 heterophoria, prism-induced, oculomotor adaption 0-108880  
 jerk nystagmus, some new findings 0-67074  
 keratoconus, position of corneal apex 0-94200  
 myopia, supernormal visual capacity 0-81612  
 myopia in developing chicks following monocular and binocular lid closure 0-61543  
 night convergence and presbyopia (*Spanish*) 0-89746  
 ophthalmic correcting cylinder axis, ophthalmometric prediction 0-98174  
 refractive error meas. using dynamic laser speckle pattern 0-81583  
 retinal images, defocused and spatially filtered, stereoscopic acuity 0-101177  
 retinal research and study, selected review 0-108874  
 retrolental fibroplasia, A-mode ultrasonography and oculometry 0-89816  
 senile macular degeneration, colour discrimination rel. to visual acuity 0-108897  
 signal transmission by visual pathways, distortions of retinal images 0-85400  
 stereoblind humans, residual binocular interaction 0-89764  
 strabismus, fusional convergence ranges using random dot stereograms, operant conditioning 0-108900  
 vertical fixation disparity, correction by horizontal prism 0-67281
- visual auras** *see aurora*
- visual perception**  
 bandwidth compression effect on military target observers' detection and recognition performance 0-106484  
 binocular vision, artificial aniseikonia, geometrical explanation of induced size effect 0-72173  
 binocular vision, frog ipsilateral retino-tectal pathways 0-85401  
 binocularity affected by sectioning of corpus callosum, of cat 0-97922  
 biphasic optokinetic response in crab, anal. 0-101175  
 brightness perception and retinal rivalry in binocular vision, integrated model 0-101180



**visual perception continued**

- colour vision model 0-81604  
 colour vision zone fluctuation model, nonlinear processing at receptor level 0-81601  
 Craik-O'Brien effect in human visual system, temporal depend. 0-81608  
 depth perception and size constancy (*Japanese*) 0-97918  
 depth perception in young cats, effect of neonatal section of corpus callosum 0-61572  
 displacement thresholds, foveal and peripheral, rel. to stimulus luminance, line length, movement duration 0-101183  
 egomotion and relative depth map from optical flow 0-76743  
 emmetropic observers, perceptual effects of low-power plus lenses 0-67084  
 evoked potentials, luminosity and chromatic responses in man, subjective hue estimates 0-97903  
 figure perception, role of eye movements 0-101186  
 flicker-induced asymmetries in border enhancement, brightness and darkness perception 0-67083  
 gloss perception, model using binocular cells in lateral geniculate body 0-72167  
 grating perception at threshold, noise masking expt. technique 0-72171  
 interference in peripheral recognition of embedded letters (*Japanese*) 0-61569  
 kinetic depth effect, amplitude, freq. and phase determinants of perceived rotations and rigidity 0-76746  
 motion flow perception, conditions for in dynamic visual noise 0-72174  
 motion in depth, binocular and monocular stimuli, review 0-61570  
 motion perception, functional difference between central and peripheral vision (*Japanese*) 0-61568  
 movement detection, performance of a wide-field element in the blowfly visual system 0-89763  
 movement detection by foveal and parafoveal retina, effects of background struct. and target size 0-85403  
 myopia, supernormal visual capacity 0-81612  
 orientation discrimination by young infants 0-61573  
 orientation sensitivity of visual movement detection system activating landing response of blowflies 0-101176  
 pattern recognition from psychological view-point (*Japanese*) 0-97919  
 pattern recognition functional mechanisms in humans 0-81609  
 polarized light incident on cornea, transient adaptation 0-81596  
 psychometric measures for specifying colour appearance 0-76747  
 psychophysical analysis of the 'sensation of reality' induced by a visual wide-field display 0-108901  
 remoteness of point light source in space with no optical reference, visual estimate accuracy 0-104590  
 retinal images, defocused and spatially filtered, stereoscopic acuity 0-101177  
 retinex systems' role in colour perception 0-81598  
 saccadic eye movements, small, perceptual function 0-61577  
 signal transmission by visual pathways, distortions of retinal images 0-85400  
 single stroke figures, influence of visual field size on perception 0-101179  
 size, shifts after adaptation to gratings 0-85398  
 size of one object among many, expt. obs. 0-81607  
 size of perceptive fields fovea and periphery, light- and dark-adapted obs. 0-61574  
 spatial freq. responses and multi-channel theory (*Japanese*) 0-97916  
 spatial phase, sensitivity obs. 0-72172  
 spatio-temporal stimulation in lightness and colour (*Japanese*) 0-97917  
 spatiotemporal contrast detection invariances, humans 0-85402  
 stereopsis in human infants 0-89762  
 stereovision in SEM 0-73532  
 Stiles Crawford I effect using polarized light 0-81595  
 striate cortex, spatial mapping approach to perceptual coding 0-101168  
 striate cortex functional architecture quantitative model 0-89747  
 stroboscopically illuminated moving noise patterns, movement and spatial periodicity dual percept 0-81605  
 Talbot's law failure, foveal vision of discontinuous test 0-81611  
 temporal sensitivity of human visual system to sinusoidal gratings 0-97915  
 threshold conditions, quantum coincidence theory 0-81610  
 tilt illusion magnitude, influence of colour and contour rivalry 0-61575  
 US imaging light intensity perception charact., stochastic noise influence 0-98053  
 vestibular nuclei visual-vestibular convergence in cat 0-85420

**visualisation, particle track** *see particle track visualisation***vitreous state**

- see also electron energy states of amorphous solids; glass; glass transition*  
 abietic acid, transverse US wave propag., glass and liquid transition region 0-79883  
 alkali glasses, rapidly quenched, alkali ion cond. 0-107559  
 ceramics, vitreous, slow neutron irradiation effect (*Spanish*) 0-57816  
 EBBA, orientational order in glassy and nematic phases, IR dichroism meas. 0-64891  
 ethanol, polymorphic forms, mol. motion, NMR obs. 0-88885  
 ethanol-d<sub>2</sub>(d<sub>1</sub>), glassy state, solvated electron geometry, electron spin echo modulation obs. 0-66009  
 glassy C electrodes for photogalvanovoltaic and photovoltaic cells 0-89630  
 glassy-C, irradiation induced dimensional changes 0-65052  
 ill-condensed matter, summer school, Les Houches, France (July-Aug. 1978) 0-82561  
 induced crystallisation in glass-forming systems, heterogeneous nucleation 0-64903  
 liquid-glass transition, glass transition depend. on heating and cooling rates 0-79920  
 local motions, dielec. losses and relax. phenomena 0-108154  
 MBBA, frozen nematic glass, EPR spectra of copper and cobalt triazene-1-oxide complexes 0-88871  
 MBBA, orientational order in glassy and nematic phases, IR dichroism meas. 0-64891  
 MBBA, Raman spectra in cryst., frozen glassy, and liq. cryst. states 0-60601  
 obsidian, *Japanese*, <sup>57</sup>Fe Mossbauer spectra of naturally occurring glasses 0-67364  
 organic glasses, low temp. mol. mobility, NMR T<sub>1</sub> meas. 0-60439  
 PMMA based plastics, specific fracture energy depend. on crack growth rate, mol. struct. effect 0-66639

**vitreous state continued**

- poly(spiro[2.4]hepta-4,6-diene) molecular characterisation, glassy state props. 0-64928  
 polycarbonate, glassy state, enthalpy relax., thermal density fluctuations 0-59678  
 polymer, glassy state, <sup>13</sup>C NMR (*German*) 0-93188  
 polymer glasses, enthalpy relax., scanning calorimetry technique 0-90851  
 polymers, glassy, craze surface displacements, model 0-93651  
 N-p-propoxybenzylidene-p-pentylaniline, orientational order in glassy and nematic phases, IR dichroism meas. 0-64891  
 quartzite, vitrified, and quartzite based refractory concretes, prep. and props. 0-89188  
 rheology of glassy state and highly viscous liq. 0-70130  
 solid electrolytes, conductance mechanism cc AgI/Ag oxysalt system, vitreous solid electrolytes, conductance mechanism 0-107560  
 structure, isobaric variation, phenomenological theory (*French*) 0-59393  
 As-S-Ti, glass, viscosity and elastic props. 0-100180  
 As<sub>2</sub>O<sub>3</sub>, vitreous, X-ray diffr. study of struct. 0-92464  
 B<sub>2</sub>O<sub>3</sub>, vitreous, struct. study using small-angle X-ray scatt. 0-84071  
 B<sub>2</sub>O<sub>3</sub>, vitreous, struct. study using <sup>11</sup>B NMR 0-84658  
 BeF<sub>2</sub>, glass, glass transition temp. and thermal expansion 0-64902  
 BeF<sub>2</sub>, ionic transport and defect struct. 0-107472  
 C, directional O ion beam etching, compared with reactive ion etching 0-71781  
 C, glassy, electrolytic durability 0-66809  
 CaCl<sub>2</sub>(Br<sub>2</sub>)(I<sub>2</sub>), glassy aqueous soln., LF region Raman spectra 0-84729  
 GeO<sub>2</sub>, vitreous, struct., contrasted with EXAFS obs. of ZnCl<sub>2</sub> liq. and glass struct. 0-70133  
 GeO<sub>2</sub>, vitreous, struct. study using small-angle X-ray scatt. 0-84071  
 Li salt based solid electrolyte, synthesis and characterisation, secondary cell appl. (*French*) 0-72034  
 (Li<sub>2</sub>B<sub>2</sub>O<sub>7</sub>)<sub>1-x</sub>(WO<sub>3</sub>), dipolar glass, space charge injection, thermally stimulated depolarisation currents 0-66103  
 LiCl-Li<sub>2</sub>O-P<sub>2</sub>O<sub>5</sub>, glass system, vitreous domain, struct., elec. cond. (*French*) 0-70135  
 LiCl(Br)(I), glassy aqueous soln., LF region Raman spectra 0-84729  
 Li<sub>2</sub>O-Al<sub>2</sub>O<sub>3</sub>-SiO<sub>2</sub>, study of elastic props. 0-104205  
 xMnO<sub>2</sub>(100-x)[19TeO<sub>2</sub>PbO], EPR studies of Mn<sup>2+</sup> ion distribution 0-71167  
 NaF-SrF<sub>2</sub>-CrF<sub>3</sub>, glass transition, crystn. and melting temps., optical transmission (*French*) 0-64910  
 PbMnFeF<sub>7</sub> and Pb<sub>2</sub>MnFeF<sub>9</sub>, vitreous, insulating, evidence of spin-glass transition 0-97112  
 PbO-SiO<sub>2</sub>, glasses, high temp. ESR of Fe(III) 0-60410  
 Sb-O-CH(Br)(I), glass-forming regions 0-88057  
 Se, glassy, structural excitation energies of defects, pseudopot. approach 0-107061  
 Se, trigonal and vitreous, sp. ht. and thermal cond., 3 to 300K 0-59676  
 SiC fibre, development from organosilicon polymers by heat treatment 0-81014  
 Si<sub>3</sub>-H<sub>2</sub>, noncrystalline film, struct., interatomic distances, SRO 0-107053  
 SiO<sub>2</sub>, charged defect centres 0-107745  
 SiO<sub>2</sub> films, growth on Si, role of defect structure 0-65403  
 SiO<sub>2</sub>, fused, broken bond defect generation mechanisms 0-88044  
 SiO<sub>2</sub>, paramag. centres associated with bonding defects 0-80609  
 SiO<sub>2</sub>, pure and Ge doped, luminescence centres at 396 and 280 nm 0-103996  
 SiO<sub>2</sub>, transient electrical transport, general and unified treatment 0-59977  
 SiO<sub>2</sub>, viscosity meas., review 0-103513  
 SiO<sub>2</sub>, vitreous, hydroxyl free, reaction with H<sub>2</sub>, diffusion, absorpt. spectra 0-85210  
 SiO<sub>2</sub>, vitreous, laser-annealed surface, characterisation by ellipsometry 0-103544  
 SiO<sub>2</sub>, vitreous, low temperature heat capacity enhancement model 0-75369  
 SiO<sub>2</sub>, vitreous, quant. X-ray anal. of cristobalite 0-88049  
 SiO<sub>2</sub>, vitreous layers, thermal growth on Si 0-93675  
 SiO<sub>2</sub>, X-ray compaction efficiency 0-65044  
 SiO<sub>2</sub>/Ag, X-ray induced EPR and luminesc. centre 0-65043  
 TlAs<sub>2</sub>(Se<sub>2</sub>)(Te<sub>2</sub>), vitreous, crystn. kinetics 0-64918  
 YIG, vitreous electric-field-gradient distrib., Mossbauer quadrupole splitting meas. 0-75901  
 ZnCl<sub>2</sub> glass, glass transition temp. and thermal expansion 0-64902  
 ZnCl<sub>2</sub>, glassy and liq. EXAFS obs. of struct., comparison with vitreous GeO<sub>2</sub> 0-70133  
 ZrF<sub>4</sub> based glasses, solid electrolyte, conductivity and activation energy 0-70464  
 ZrF<sub>4</sub>-BaF<sub>2</sub>-MF<sub>n</sub> (M=Na, Ca, Ln, Th, n=1, 2, 3, 4), vitreous phases, network formers, modifiers and stabilisers (*French*) 0-64909

**vitrification**

- acoustic emission obs. during heating through glass temp. 0-84253  
 alkali silicate glasses, struct. and thermal props. 0-84075  
 commercial glasses, viscosity and stress relax. in glass transition region 0-93589  
 communal entropy and glass transition, theory 0-70131  
 critical cooling rate for glass form., crystn. and nucleation 0-84078  
 glass, electrothermal props. in structural transform. zones (*French*) 0-88047  
 metal metal system, glass formation 0-64921  
 metallic glasses, formation, stabilities, and props. 0-64912  
 metallic glasses, formation and rapid quenching techniques 0-76214  
 phosphate system, containing halogens glass formation 0-103254  
 quartz, dislocations, electron irradi. induced vitrification 0-107252  
 radioactive waste, vitrification using in-can melting process 0-83204  
 radioactive waste immobilisation using continuous glass melter 0-83199  
 X-ray scattering at small angles study of glasses containing no modifying oxides 0-84071  
 AgX-Ag<sub>2</sub>O-P<sub>2</sub>O<sub>5</sub> (X=I, Br, Cl), glass formation and ionic conductivity 0-65290  
 As-Te-In, glass-forming, density and microhardness 0-103257  
 As<sub>2</sub>S<sub>3</sub>, thermal capacity, 300 to 600K 0-103492  
 As<sub>2</sub>Se<sub>3</sub>, thermal capacity, 300 to 600K 0-103492  
 As<sub>2</sub>Te<sub>3</sub>, thermal capacity, 300 to 600K 0-103492  
 BaB<sub>2</sub>O<sub>7</sub>-RF<sub>2</sub>, R=Mg, Ca, Sr, Ba, glass form., struct. and props. 0-84077  
 Ba(PO<sub>3</sub>)<sub>2</sub>-AlF<sub>3</sub>-CaF<sub>2</sub>, elec. cond. and IR spectra 0-89005  
 Ba(PO<sub>3</sub>)<sub>2</sub>-AlF<sub>3</sub>-MgF<sub>2</sub>, elec. cond. and IR spectra 0-89005  
 BeF<sub>2</sub> glass, glass transition temp. and thermal expansion 0-64902

**vitrification** continued

- Ca<sub>0.65</sub>M<sub>0.35</sub>, glass transition temp., comp. depend. 0-79702  
 CdAs<sub>2</sub>, cryst. struct. and vitrification capacity 0-88126  
 Cu-Ag-Ge, Hume-Rothery glass form. 0-96449  
 Cu-Sb-I system, glass form., struct. and IR spectra 0-64915  
 Fe-C-X, glasses and metastable cryst. phases, third element effect 0-75171  
 Fe<sub>83-1</sub>M<sub>17</sub> and Fe<sub>78-1</sub>M<sub>22</sub>Si<sub>10</sub>B<sub>12</sub> (M=refractory metal), glass form. and thermal stability 0-79703  
 Fe<sub>72</sub>Ni<sub>28</sub>Cr<sub>10</sub>P<sub>10</sub>B<sub>2</sub>, metallic glass, effect of pre-ageing on glass transition temp. 0-100326  
 Ge-S-Se, glass formation 0-103251  
 Ge-Si-S system, glass formation, transition temp., crystallisation and melting 0-100178  
 Ge<sub>2</sub>S<sub>3</sub>, glass form. and characterisation (*German*) 0-64913  
 Ge<sub>2</sub>Se<sub>3</sub>, glass form. and characterisation (*German*) 0-64913  
 3KNO<sub>3</sub>-2Ca(NO<sub>3</sub>)<sub>2</sub>, glass form. from liq., struct. transform., Raman spectrum obs. 0-64916  
 3KNO<sub>3</sub>-2ZnCl<sub>2</sub>, glass form. from liq., struct. transform., Raman spectrum obs. 0-64916  
 Na-A zeolite, struct. obs. by high-resolution electron microscopy 0-84175  
 NaF-SrF<sub>2</sub>-CrF<sub>3</sub>, glass transition, crystn. and melting temps., optical transmission (*French*) 0-64910  
 Na<sub>2</sub>O-B<sub>2</sub>O<sub>3</sub>-SiO<sub>2</sub>, containing halogens glass formation 0-103254  
 Na<sub>2</sub>O-P<sub>2</sub>O<sub>5</sub>-SiO<sub>2</sub> glass, metastable liquid immiscibility 0-100331  
 Na<sub>2</sub>O-PbO-SiO<sub>2</sub> glass-ceramic composite, directionally crystallised 0-107058  
 Na<sub>2</sub>O-SiO<sub>2</sub> glass containing halogens glass formation 0-103254  
 Nb-Ir(Rh) system glasses, form., crystn. and microhardness, resist. obs. 0-89178  
 Nb-Ni amorphous alloys, glass transition and ductility, O additions effect 0-75168  
 Ni<sub>78-1</sub>M<sub>22</sub>Si<sub>10</sub>B<sub>12</sub> (M=refractory metal), glass form. and thermal stability 0-79703  
 PbO-B<sub>2</sub>O<sub>3</sub> glass-forming melt, specific volume and viscosity, temp. depend. 0-84073  
 Pd-Cu-Si, glass form., crit. cooling rate 0-75169  
 Pd<sub>77</sub>Cu<sub>6.0</sub>Si<sub>16.5</sub> metallic glass, glass transition temp., cooling rate depend. 0-75181  
 3RbNO<sub>3</sub>-2Ca(NO<sub>3</sub>)<sub>2</sub>, glass form. from liq., struct. transform., Raman spectrum obs. 0-64916  
 Sb-O-Cl(Br)(I), glass-forming regions 0-88057  
 SbSbR glass, IR reflectivity spectra 0-71403  
 SiO<sub>2</sub>-NaAlSiO<sub>4</sub> glasses and devitrification, prep. and vibr. spectroscopy study (*Polish*) 0-93530  
 Ta-Ir(Rh) system glasses, form., crystn. and microhardness, resist. obs. 0-89178  
 Te<sub>80</sub>Ge<sub>20-x</sub>A<sub>x</sub> glasses, rapid melt cooled, glass transition and stability range 0-75170  
 Ti-Ni amorphous alloys, glass transition and ductility, O additions effect 0-75168  
 TiO<sub>2</sub>-SiO<sub>2</sub> glass form. by low temp. chem. polymerisation 0-84899  
 Tl-Ge-Te, glass formation 0-103255  
 U-Co(Ce)(Fe)(Mn)(Ni)(V) metallic glasses, glass form. and thermal stability 0-75183  
 ZnB<sub>2</sub>O<sub>4</sub>-RF<sub>2</sub>, R=Mg, Ca, Sr, Ba, glass form., struct. and props. 0-84077  
 ZnCl<sub>2</sub> glass, glass transition temp. and thermal expansion 0-64902  
 Zr-Cu amorphous alloys, glass transition and ductility, O additions effect 0-75168  
 Zr-Cu(Ni)(Co)(Fe) metallic glasses, glass form. and thermal stability 0-75177  
 Zr<sub>0.475</sub>Cu<sub>0.475</sub>M<sub>0.05</sub>, glass transition temp., comp. depend. 0-79702

**Vlasov equation**

- Chirikov-Taylor model, turbulent diffusion calc. 0-79469  
 cylindrical shells, boundary conditions in Vlasov theory 0-69660  
 ion acoustic wave, self excited, in hot plasma, dispersion theory 0-92283  
 ion-acoustic wave, phase velocity 0-103147  
 Langmuir system, kinetic theory of mag. field generation 0-69974  
 Langmuir waves in Vlasov plasma, nonlinear theory, wave-particle interaction 0-64701  
 Langmuir waves in Vlasov plasma, nonlinear theory, wave-wave interaction 0-64700  
 laser radiation, nonlinear scatt. by fast ion waves in plasma 0-106916  
 magnetised plasma, Vlasov theory coherent state approach 0-64675  
 Maxwellian local velocity distribution, Vlasov equilb. 0-87928

**V<sub>2</sub>O<sub>5</sub>-P<sub>2</sub>O<sub>5</sub> semiconducting glasses** see amorphous semiconductors**vocoders**

see also speech synthesis

- 32 channel multiplex audio response system based on formant vocoder principle (*German*) 0-96133  
 Bengali vowels format struct., tracking loop formant extraction system 0-106673  
 formant representations of parameters for channel vocoder 0-83709  
 linear predictive coded speech digitisers, background noise spectral subtraction 0-96140  
 log likelihood ratio interpretation as measure of waveform code performance 0-83706  
 multimicroprocessor implementation of all-digital speech synthesizer 0-96143  
 pole-zero modelling of speech 0-83716  
 real-time speech high-performance processor design 0-96144  
 signal models for low bit-rate coding of speech 0-106674  
 speech noise suppression filter for narrowband vocoder 0-91977  
 speech waveform coders, objective quality meas. equipment and method 0-91981

voice see speech

voice coders see vocoders

**voice communication**

- Bengali vowels format struct., tracking loop formant extraction system 0-106673  
 digital multiplex system, acquisition performance of frame synchronisation system 0-99901  
 digital speech interpolation system called adaptive DPCM with time assignment speech interpolation 0-99903  
 feedback suppression during acoustic irradiation, adaptive method (*German*) 0-106676  
 forward and backward prediction in adaptive differential PCM over nonideal channels 0-99902

**voice communication** continued

- loudness function of artificial speech, for reference equivalent meas. 0-79068  
 man-machine voice communication, speech production mechanisms and models (*Spanish*) 0-87665  
 parametric coding of speech spectra, computer studies 0-96137  
 parametric coding of speech spectra 0-96136  
 signal models for low bit-rate coding of speech 0-106674

**voids (solid)**

- benzil cored fibres, void-free cryst. growth, X-ray diffr. and optical microscopy study 0-71586  
 brass, soft 70/30, density changes, void growth in biaxial stress fields, plastic deformation 0-71692  
 brass wire, US inspection, immersion method 0-66757  
 cavity growth diagram, for high temp. creep 0-65140  
 coated, capture efficiency 0-96515  
 creep, swelling and growth, radiation induced, bias factors estimated from self-consistent model 0-88249  
 creep crack growth, diffusion and deformation controlled 0-79867  
 creep damage and the remaining life concept 0-59574  
 detection, thermal NDT of delamination and inclusion flaws, ID anal. 0-71820  
 m-dinitrobenzene cored fibres, void-free cryst. growth, X-ray diffr. and optical microscopy study 0-71586  
 ductile fracture, strain hardening and damage relationship 0-108564  
 elastic wave scatt., appl. of matrix method of optimal truncation 0-62480  
 evolution, of void and interstitial loop evolution in pulsed fusion reactors 0-84217  
 FBR fuel pin failure, fuel porosity and crack effects on transient over-power analysis 0-71760  
 Fokker-Planck eqn. describing evolution of interstitial loop microstruct. during irradiation 0-107215  
 fusion reactors, inertial confinement, first walls, void growth, analytical model 0-63377  
 IR crystals, optical imaging of growth defects 0-64988  
 metal, heavy ion bombard., void conc., effect of implanted He (*Russian*) 0-88213  
 metal, irradi., containing pre-existing dislocations, interstitial loop form. kinetics 0-65040  
 metals, compensated and uncompensated, effect of spherical voids on electrical magnetoresistivity 0-65531  
 metals, void growth and time-lag, statistical theory 0-88208  
 Metglas 2826 ribbon, voids formation during crystallisation 0-108428  
 Nimonic, irradiated, void nucleation, numerical evaluation 0-70252  
 Nimonic 80A superalloy, contrast from cavities in HVEM 0-79780  
 Nimonic PE-16, electron irradi. in HVEM, void growth, vacuum environment influence 0-107323  
 plastic deformation, necked bar, void growth, finite element anal. 0-64383  
 polymers, filled, cumulative internal damage, US assessment 0-97653  
 porous metals, plasticity, stress-strain curves, yield stresses, strain vectors 0-83738  
 sapphire ribbon crystals, EFG growth and charact., voids, grain boundaries and dislocations 0-103283  
 sapphire ribbon EFG prod., substrate for heteroepitaxial Si, sheet and distrib. microvoids 0-108342  
 spherical, annular crack initiation, stress intensity factor estimates 0-106757  
 steel, Al killed, density changes, void growth in biaxial stress fields, plastic deformation 0-71692  
 steel, Cr-Mo-P (2.25, 1 wt.%), stress relief cracking, effect of P segregation 0-89324  
 steel, low-C, kinetics of void development in fracturing A533B tensile bars 0-76357  
 steel, low-C, S10C and 520C, tensile fracture at low temps. (*Japanese*) 0-81163  
 steel, Ni-Cr-Mo and Cr-Cu-Mo and sintered, ductile fracture, microvoid effects (*Japanese*) 0-108542  
 steel, pearlitic, creep-induced micropore healing kinetics of 12MKh and 15Kh1M1F, TEM obs. (*Russian*) 0-71690  
 steel, stainless, irradiated, void nucleation, numerical evaluation 0-70252  
 steel, stainless, voids, TEM, diff. contrast 0-75218  
 steel, stainless 316, Fokker-Planck eqn. describing evolution of interstitial loop microstruct. during irradiation 0-107215  
 steel, stainless 316, soln. annealed, cavity alignment and precipitation during dual ion bombardment 0-70273  
 steel, types 60G, ShKh15, structural changes near holes and inclusions due to pulsed currents (*Russian*) 0-108459  
 steel welds, bead-on-plate, H<sub>2</sub> diffusion and trapping 0-96697  
 steel wire, US inspection, immersion method 0-66757  
 superconductors, multifilamentary, voids growth obs., via hot stage SEM 0-70089  
 superplastic alloys, cavity growth 0-93627  
 superplasticity, cavity growth anal. 0-60923  
 swelling, nucleation theory 0-65038  
 swelling, volume, errors in determ. by TEM 0-84208  
 TEM contrast, aid void vol. determ. 0-75217  
 Van der Waals energy between voids and particles, from asymptotic to close contact 0-80351  
 Ag film, void growth, TEM obs. 0-59833  
 Al, Al ion irradiated, void swelling and annealing of voids, electron microscopy study 0-88216  
 Al alloy 2024-T4, ductile fracture, microvoid effects (*Japanese*) 0-108542  
 Al, commercial purity, density changes, void growth in biaxial stress fields, plastic deformation 0-71692  
 Al, neutron damage, positron annihilation 0-65056  
 Al-Cu-Mg/mica particulate composite mech. props. 0-100919  
 Al-Mg, Si alloy, void form. under different precip. conditions, after Al ion irradi. 0-59529  
 Al-Mg (0.1 at.%), neutron damage, positron annihilation 0-65056  
 Al-Mg-Si alloys, ductile intergranular fracture mechanisms, void formation and nucleation 0-108578  
 Al-Zn-Mg superplastic alloy, cavity growth under creep conditions 0-60940  
 Au, optical props., dielec. function, void model, sample effects 0-76048  
 B fibre, US inspection, immersion method 0-66757  
 B<sub>2</sub>O<sub>3</sub>-SiO<sub>2</sub>-Na<sub>2</sub>O phase-separated glass, creep fracture morphology 0-81151  
 C fibre derived from mesophase-pitch, Young's modulus and tensile strength, struct. flow elimination 0-80995



**voids (solid) continued**

- CaF<sub>2</sub>, electron irradi. defect aggregates, ordering, U and Th impurity effects 0-75216  
 CdS single cryst., vaporization and form. of negative whiskers 0-92659  
 Cu, polycryst., creep and fracture behaviour, effects of prestrain and O 0-97544  
 Cu-Fe (1.5 wt.%), precipitation-effect on void formation during electron irradiation 0-84211  
 Cu-Fe (1.5 wt.%) alloy, void form. during irradi. in HVEM, reactor irradi. simulation and ageing effects 0-107327  
 Fe, pure, hydrogen-charged, initial cracking obs. 0-108580  
 $\alpha$ -Fe whiskers, pure, ductile fracture, microscopic obs. of initiation mechanism 0-85044  
 Fe-Cr-Ni (12, 15 wt.%) austenitic alloy, Ni<sup>6+</sup> irradiated, void swelling and phase stability, Si and Ti effects 0-65055  
 Fe-Cr-Ti-Mo-TiO<sub>2</sub> (13, 3.5, 1.5, 2 wt.%) dispersion hardened, void swelling 0-65046  
 Fe<sub>80</sub>B<sub>20</sub>, metallic glass, Doppler broadening of positron annihilation  $\gamma$ -radiation and elec. resist. 0-66321  
 Fe<sub>70</sub>Mo<sub>30</sub>, metallic glass, Doppler broadening of positron annihilation  $\gamma$ -radiation and elec. resist. 0-66321  
 Fe<sub>3</sub>Ni<sub>13</sub>Cr<sub>14</sub>P<sub>12</sub>B<sub>6</sub>, metallic glass, Doppler broadening of positron annihilation  $\gamma$ -radiation and elec. resist. 0-66321  
 IrO<sub>2</sub>, electrochromic, oxidation state changes and struct. 0-100950  
 KCl crystals, Eu<sup>2+</sup> concentration effect on lattice parameter and density of crystals 0-88169  
 Li ferrites, porous, porosity effect on saturation of magnetisation 0-108036  
 Mo, neutron irradi., radiation anneal hardening mechanism 0-71678  
 Mo, void containing, positron annihilation characts. 0-80898  
 Mo wire, US inspection, immersion method 0-66757  
 Na<sub>2</sub>O-B<sub>2</sub>O<sub>3</sub>-SiO<sub>2</sub> glass-Ni compact, indented, strength and fracture toughness 0-93636  
 Na<sub>2</sub>O-CaO glass, shear deform. under pyramidal indentations 0-84989  
 Nb, TEM, elastic side band imaging 0-75219  
 Nb-Ge, compounds with A15 structure, films, TEM study (*French*) 0-80135  
 Nb-Ge-Si, compounds with A15 structure, films, TEM study (*French*) 0-80135  
 Nb-Si, compounds with A15 structure, films, TEM study (*French*) 0-80135  
 Nb<sub>3</sub>Sn, thin film, TEM microanalysis 0-104491  
 Ni, cavity coalescence following <sup>4</sup>He<sup>+</sup> irradi. 0-70272  
 Ni, ion irradi. with 20 and 500 keV <sup>4</sup>He<sup>+</sup>, depth distrib. of cavities and dislocation damage 0-107346  
 PbTe thermoelectric materials, microstructure anal. using SEM X-ray microanalysis 0-107211  
 Pt, neutron damage, positron annihilation 0-65056  
 Si:Ar, ion-implanted, epitaxial regrowth by laser annealing, microstruct. 0-84404  
 Si-Al-O-N ceramic, grain boundary desegregation and intergranular cohesion 0-100872  
 Sn/Au thin film diffusion couples, Kirkendall void form. 0-96698  
 Ti-Al-V (6.4 wt.%), ion irradiated, microstruct. study using TEM 0-96572  
 Ti-Al-V (6.4 wt.%), microstruct. effect of base metals on diffusion welding (*Japanese*) 0-89296  
 Ti-Fe-C-N, ion irradiated, microstruct. study using TEM 0-96572  
 TiC, electron irradi. damage, electron microsc. study 0-84210  
 $\alpha$ -U, strain rate effect on flow and fracture 0-100887  
 W fibre reinforced Cu composites, correl. between thermal cycling-induced microstructural changes at interphase boundaries and tensile behaviour (*Japanese*) 0-71674  
 W wire, AKS-doped, second phase particle obs. by TEM, SEM and atom probe microanalysis 0-108457  
 W wire, US inspection, immersion method 0-66757  
 WC-Ni hard alloy composite, sintered, void healing 0-60821  
 Zn, electron momentum distrib., neutron-induced defects, positron annihilation study, for single cryst. 0-71508  
 Zr, void swelling during electron irradi., HVEM study 0-92559

**Voigt effect** see *magneto-optical effects*

**volatilisation** see *vaporisation*

**volcanology**

- airborne particles in stratosphere, effect on radiation reaching Earth surface 0-82035  
 SWAlaksa, episodic accretion and plutonism 0-101346  
 central Arizona, reversal chronology from volcanic sequence rel. to ocean floor polarity record 0-72419  
 Asama Volcano, spectral studies of explosion earthquakes assoc. with 1973 eruptions (*Japanese*) 0-67340  
 ash, SEM examination, examples of devitrification and early diagenesis 0-81860  
 atmosphere temp. drop due to airborne volcanic dust 0-85726  
 Australia, tectonic, igneous and metallogenic provinces rel. to mantle convection and subcrustal stresses 0-72484  
 Azores, volcanism controlled by earthquake rupture direction 0-104911  
 basalt glasses from Mid-Cayman Rise spreading centre, geochemical var. and petrogenesis 0-101364  
 Bataan Peninsula, volcanoes exhibiting no seismicity 0-81827  
 Cerro Galan, NW.Argentina, Sr isotope evidence for crustal contamination of calc-alkaline volcanic rocks 0-98318  
 cinder cone fields, struct. and emplacement 0-76949  
 climate change acting as trigger to volcanism 0-81858  
 climate change due to climate activity, <sup>14</sup>C and historical records 0-98442  
 Coso Range, California, Late Cainozoic volcanism 0-90049  
 Dellwood knolls, volcanic activity age rel. to role in triple junction tectonics off northern Vancouver Island 0-90067  
 Diablo Plateau region, W.Texas, intracrustal magmatic activity rel. to tectonic uplift 0-72481  
 dust veil index, correl. with N.Hemisphere average temps. during Little Ice Age 0-82050  
 episodic plutonism in magmatic arcs, rel. to arc-trench gap accretion 0-76956  
 eruptions beneath glaciers, landforms rel. to Mars 0-67616  
 explosive eruption column behaviour; magma props. and conduit geom. influence 0-109128  
 Fuego eruption, aerosol emission, density, temp. and particle content determ. 0-90050  
 fumarole B isotope composition, Satsuma Iwo-Jima, Japan 0-67358

**volcanology continued**

- Galapagos Rift hydrothermal fields, struct. and morphology of seafloor 0-72489  
 greenstone belts, numerical models of vertical Archaean tectonism 0-81861  
 Hawaii Geothermal Project, groundwater geochem. study 0-72567  
 Hawaiian volcanoes, rift zones as expressions of plume generated radial stress fields 0-90051  
 hypersthenic magmas, water contents 0-72507  
 NE Iceland, dyke swarms rel. to geomag. anomalies ( $\Delta Z$ ) 0-89951  
 Iceland, sea floor morphology to south and west rel. to recent volcanic activity 0-90068  
 Iceland, statistical anal. of damaging earthquakes and volcanic eruptions, (1550 to 1978) 0-89975  
 SW Iceland, stratigraphy and palaeomagnetism of Esja, Eyrafjall and Akrafjall mountains 0-89950  
 Iceland, Tertiary lava pile struct. props. rel. to continuum model of crustal generation 0-90059  
 N Iceland, volcanic activity rel. to height meas., (1965 to 1977) 0-89931  
 N.Iceland fissures, relative movements and tile changes 0-90062  
 NE Iceland neovolcanic zone, geotect. meas. and horizontal crustal movements 0-89930  
 Icelandic subglacial volcanisms, thermal and physical studies 0-101350  
 Icelandic volcanism, rift zones as expressions of plume generated radial stress fields 0-90051  
 intra-plate volcanism during Cainozoic, rel. to mantle convection 0-98293  
 island arc development, obs. expts. and speculations 0-98298  
 Kerguelen Islands igneous rocks, Nd isotopic study rel. to enriched oceanic mantle sources 0-98319  
 Kilauea, Hawaii, ground Rn survey of Puna geothermal area is lower east rift 0-85657  
 Kilauea, Hawaii, heat transfer meas. in 1977 lava flow 0-85632  
 Kirishima volcanoes, Japan, geothermal survey (*Japanese*) 0-67357  
 Klyuchevskaya Sopka volcano (1974), volcanic bombs and lava, chem. anal. 0-101351  
 Krafla, Iceland, 1978 July deflation, magma intrusion rel. to seismic activity 0-90054  
 Krafla caldera, N Iceland, gravity and height vars. during present rifting episode 0-90060  
 Krafla Caldera, NE Iceland, gravity and elevation changes caused by magma movement 0-90052  
 Krafla fissure swarm, Iceland, surface deform. in rifting events 0-90061  
 Krafla volcano area, N. Iceland, subsidence events, (1975 to 1979) 0-90053  
 La Soufriere, Guadeloupe, seismic profiles of superficial structs. (*French*) 0-76932  
 lava flow terrain, radar imaged by satellite 0-98285  
 lava flows, Quaternary, age determ. via thermoluminescence dating of volcanic plagioclases 0-98475  
 Longonot volcano, Central Kenya, geology, question of volumes of volcanic products 0-85633  
 magma chamber, fluid dynamics model of differentiation and layering 0-76939  
 Mauna Loa, air quality obs. as meas. of volcanic activity 0-76950  
 mid-ocean ridges, obs. and implications of ridge crest hot springs 0-98304  
 midocean ridge basalts, source evolution from Bay of Islands ophiolite complex Nd and Sr isotopic study 0-85651  
 Nauru Basin, basalt composition rel. to Cretaceous intra-plate eruptions 0-94499  
 Oshima Volcano (W.Hokkaido), eruptions at time of 1741 tsunami (*Japanese*) 0-67345  
 Philippine Islands, tectonic struct. revealed by seismicity and volcanicity 0-94511  
 piezomagnetic field, assoc. with Mogi model of surface displacements around volcanoes 0-67334  
 Pleistocene explosive eruptions in NW.America, surface albedo increase 0-61789  
 Quaternary basaltic volcanism in Coso Range, California, rel. to geothermal anomaly 0-90002  
 Quaternary volcanic rocks across NE.Japan, trace element contents, lateral variation 0-104926  
 rare gases in volcanic rocks, isotopes mass fractionation as indicator of gas transport to or from magma 0-98292  
 Reykjanes Ridge crest, morphology near 62°N 0-90070  
 Santorini (Thera), tephra from 1450 BC eruption discovered at Rhodes 0-109129  
 South Noto-Tolbachinsky volcano, flowing lava elec. cond. 0-72498  
 St. Lucia, Sulphur Springs geothermal field model 0-94494  
 Takayama volcanic area, Japan, upper mantle S-wave anisotropy 0-90024  
 Thetford Mines ophiolites, Quebec, palaeomagnetism 0-61757  
 Yellowstone caldera, Wyoming, USA, vertical crust movement 0-81859
- volt-ampere meters**  
 see also *power measurement; wattmeters*  
 No entries
- Volta effect** see *contact potential*
- voltage** see *electric potential*
- voltage comparators** see *comparators (circuits)*
- voltage control**  
 dual slide projector fader control cct., using a triac dimmer 0-69489  
 fusion reactors, Wendelstein VII and ASDEX, neutral beam injectors, HV power supply system, thyristor control 0-99332  
 steel, mild, corrosion rate meas. in H<sub>2</sub>SO<sub>4</sub> using microprocessor controlled potentiostat 0-71798
- voltage drop** see *electric potential*
- voltage measurement**  
 see also *potentiometers; voltmeters*  
 AC, by analogue transducers, checking and calibration methods in USSR 0-98872  
 contact potential, at Hg-polymer surface, charge exchange obs. 0-75642  
 cyclotron dee voltage calibration using an intrinsic Ge X-ray detector 0-99359  
 gas adsorption on metal film, cct. for surface potential changes meas. by static capacitor 0-62691  
 intramembrane potential jump meas. by potentiodynamic method 0-81778  
 Josephson element principles, applications to precision meas. of electric potential and magnetic flux at high freq. (*Norwegian*) 0-80447  
 laser light measuring techniques (*Japanese*) 0-86342

**voltage measurement continued**

- moving-coil expt. for meas. of current and EMF, vel. control technique 0-98939
- multilayer Ni deposits, simultaneous thickness and electrochemical potential determination for individual layers 0-71813
- penetrator cassette, multiple exposure, for meas. of effective kilovoltage of diagnostic X-ray beams 0-61662
- reproduction of volt at German ASMW 0-98944
- RMS measurement errors quantified 0-57274
- standard cells combination with low temp. coeff. for Josephson voltage standard maintenance 0-101788
- standard cells with low temp. coeff., characts. 0-101090
- surface potentials visualisation and meas., using SEM 0-68307
- transients, fast digital technique (*Polish*) 0-86340
- volt dissemination method and standard cell enclosure design 0-98876
- volt realization, method and equipment based on fundamental physical const., and superconductivity phenomenon 0-98943
- voltage standards, using Si reference diodes 0-62619
- $O_2^-$  low partial press., thermogalvanic meas. using  $O_2^-$  ion conductors 0-73389

**voltage reference diodes** see *avalanche diodes; Zener diodes*

**voltage regulation** see *voltage control*

**voltage regulator diodes** see *avalanche diodes; Zener diodes*

**voltage transformers** see *potential transformers*

**voltage transients** see *transients*

**voltammetry (chemical analysis)**

see also *polarography*

- automatic controller for voltammetric anal., design, operational sequence 0-71968
- digital signal generator for rapid scan differential pulse voltammetry 0-61182
- staircase voltammetry, microcomputer-controlled polarograph appls. 0-66895
- static mercury drop electrode 0-97740
- thionine-coated electrode for photogalvanic cells, electrochem. and XPS anal. 0-72071
- p-tricyanovinylphenyldicyanomethide ion, donor props., cyclic voltammetry and  $\pi$ -complex form. 0-88520
- CdTe electrode, redox reaction due to complex  $M(CN)_6^{3/4-}$  (*French*) 0-89482
- Zn, electrode in alkaline soln., exam. of surface state by potentiodynamic voltammetry 0-85187
- $ZnSO_4$  electrolytes containing Ge and Co, polarisation charact., exam. by cyclic voltammetry 0-104444
- ZnTe electrode, redox reaction due to complex  $M(CN)_6^{3/4-}$  (*French*) 0-89482

**voltmeters**

see also *digital voltmeters; potentiometers*

No entries

**volume control (gain)** see *gain control*

**volume diffusion** see *diffusion in solids*

**volume measurement**

- anatomical feature or lesion volume estimation algorithm 0-98080
- biomedical volume estimation, computer algorithm 0-98043
- bubbles, acoustical meas. of gas bubble volumes and gas flow rates 0-62633
- calibration of nuclear materials accountability tanks 0-68829
- capacitance sensors for phase percentage determ. in multiphase pipelines 0-62625
- cardiology, radioisotope sequential meas. of ventricular vols. and cardiac output 0-94319
- dilatometer, meas. thermal dilatation of metallic amorphous ribbons 0-86258
- dilatometer for PVT meas. of liquids and plastic crystals at low temperature 0-68208
- lung volume, online calc. by digital computer 0-72351
- lung volume estimation method, constant inflation pressure 0-67306
- lung volume measurement from supine portable chest radiographs 0-81703
- medical, algorithm based on polyhedral approx., using US or CT data 0-104790
- nuclear materials accountability, tank volume calibration algorithm 0-83159
- nuclear materials accountability tanks, automated calibrator 0-83158
- sensor for conductive liquids using array of point sensors 0-68177
- timber volumetric meter (*Russian*) 0-57253
- US renal volumetry in children, accuracy and simplicity of the method 0-98044
- Ar, compressed gas, PVT meas. at high press. 0-98927

**vortex flow** see *vortices*

**vortex flow (superconductivity)** see *flux flow*

**vortex lattice pinning** see *flux pinning*

**vortex state (superconductivity)** see *mixed state*

**vortex structure (superconductivity)** see *flux-line lattice*

**vortexes** see *vortices*

**vortices**

see also *cavitation; turbulence*

- acoustic radiation from bodies in unsteady flows 0-69799
- acoustically excited jet, discrete noise spectrum, vortex pairing 0-74847
- aerodynamic sound generation by unsteady subsonic flows around rigid bodies 0-69798
- air, damp, working characteristics of vortex tubes (*Russian*) 0-74903
- airfoil trailing edge noise, near-wake struct. and unsteady pressures at trailing edge 0-69794
- annular fluid jets, small inner diameter, investigation of vortices by schlieren photography 0-74935
- atmosphere, effect of subjectively enhancing initial vorticity field in short-range numerical forecast 0-82008
- Atmospheric Cloud Physics Laboratory simulation, vorticity transport eqn. solns. 0-94690
- backwash vortex under waves running up sloping bed 0-100001
- Bianchi universes, magnetic fields and fluids with conductivity 0-83864
- biphase liquid cylindrical vortex, mass force effect on dispersion phase distrib. (*Russian*) 0-79388
- blades, three-dimens. annular array, aerodynamic forces with nonsteady flow 0-99991
- body of revolution, tail region flow vorticity calcs. 0-69845
- Bose systems, free, infinite, condensation region 0-73259

**vortices continued**

- breaking gravity-wave flow near tip, time-dependent free-surface flows 0-83808
- centrifugal instabilities in finite containers, periodic model 0-106783
- channel, curved rectangular, secondary flow, Taylor-Gortler vortex pattern 0-106849
- channel, laminar boundary layer, Gortler vortices 0-64572
- chaotic flows of autonomous dissipative systems 0-73176
- circular cylinder flows, coherence function method 0-96068
- combined free and forced convection, periodic vortex formation 0-74878
- conditional eddies in isotropic turbulence, higher order estimates 0-92119
- convection currents in axisymmetric cyclone 0-77084
- Couette-Taylor flow, laser Doppler velocimetry obs. of transition to turbulence 0-92163
- crossflow developing in boundary layer during longit. flow around right dihedral angle 0-59049
- curved semicircular duct laminar flow, secondary vortex flow 0-106847
- curved wall power fluidics characts. 0-103053
- cyclone development along weak thermal fronts, model soln. 0-81994
- cylinder, axisymmetric, with slanted base, near-wake flow 0-74886
- cylindrical annulus, rotating, transition to Taylor vortices, Ekman layers 0-87776
- detached flow around bodies with local vortex sheets 0-87778
- discrete frequency sound generation by fluid flows 0-69812
- divergent duct, vortex flow breakdown, group vel. criterion 0-87807
- drop deformation, shear and vorticity effects 0-87795
- elliptic cylinder about axis perpendicular to flow, autorotation 0-103033
- energetics of a linear array of hollow vortices of finite cross-section 0-92157
- ferromagnetic superconductors, self-induced vortices, magnetisation, Gibbs free energy 0-70916
- flame advection and propagation in fluid 0-59097
- flow measurement, plane mixing layer vortex digital image processing 0-103095
- flow separation, unsteady, behind normal plate, discrete-vortex model, velocity-point scheme (*Japanese*) 0-79330
- flow separation, unsteady, behind normal plate, discrete-vortex model, modified velocity-point scheme (*Japanese*) 0-79331
- four-vortex integrable and chaotic motions 0-103035
- gas, perfect, vortex sheet, separation from smooth body at large Reynolds number (*French*) 0-74908
- gas, turbulent boundary layer vel. distrib., probabilistic statistical approach, vortices 0-92123
- gas flow meas. with vortex meter and microcomputer (*German*) 0-92241
- Gortler stability at rigid and elastic plane plates (*Russian*) 0-79261
- Gortler vortex type perturbation profiles in boundary layers problem on curved surface (*Russian*) 0-74834
- Gulf Stream, anticyclonic eddy obs. in slope water aboard CGC Evergreen 0-72546
- hurricane formation, tropical storm control by cloud seeding (*German*) 0-90207
- Hurricane Gladys (1975), subcloud layer energy transformations 0-77089
- hydraulic resistance in vortex, tangential self-oscills. effects 0-87775
- hydroacoustics, role of surface shear stress fluctuations 0-69808
- hydrodynamic instabilities and turbulence, flow states, examples and meas. methods 0-92116
- incompressible flows, 2-D, potential flow past aerodynamic body, subsurface panel method 0-74901
- incompressible laminar planar flow between parallel plates, ang. vorticity formulation 0-64643
- inviscid flow, 2-D, weakly sheared, past circular cylinder 0-74893
- inviscid fluid, accelerating flow horizontal divergence, turning vorticity eqn. anal. 0-77013
- isolated nonlinear vortex evolution 0-81910
- isotropic vorticity theory, appl. to adverse pressure gradient flow 0-59047
- jet noise generation, role of vortex pairing 0-69807
- jets, axisymmetric, large eddies, numerical model 0-79375
- Josephson tunnel junction, nonresonant vortex motion 0-97037
- Kelvin-Helmholtz instability in supersonic and super-Alvenic fluids 0-87816
- Maxwell fluid, diffusion of vortex line in stagnation point flow 0-74892
- mixing layer, free, axisymmetric, turbulent spot, vorticity and Reynolds stress 0-79281
- NDT, thermal, vortex tube appl. 0-89453
- neutron stars, rotating, form of quantum vortex filaments 0-67770
- nozzles, convergent, swirl effects on mass flux and thrust 0-74936
- ocean, wind driven, new class of steady solns. to wind-driven ocean problem 0-85667
- open pipe exits, flow during acoustic resonance, vortices and boundary layers 0-92224
- ovalling oscillations of cylindrical shells in cross flow, comments 0-59045
- perforated screen, sound diffraction, vortex shedding influence 0-69849
- piston-cylinder assembly with open annular port, unsteady flows 0-79329
- planar magnets, quasi-two-dimensional, dynamics of vortices 0-71066
- plasma, ion vortex from baroclinic vector 0-79501
- plate, Kirchhoff-Rayleigh flow, separation, wakes and vortices 0-69839
- potential vorticity in jet stream-frontal systems role of turbulence 0-77044
- protogalactic medium, vortex generation 0-62360
- quantum, dynamics 0-59758
- quasi-standing-wave phenomenon due to oscillating internal flow, vortices in shear layer 0-106809
- rectangular elbow, 3-dimens. turbulent compressible duct flow, stagnation pressure losses, vortices 0-64640
- rotating disc boundary layer transition regime, spiral vortices 0-59040
- semi-infinite porous medium bounded by horizontal surface, mixed convective flow, vortex instability 0-79304
- shedding, influence of grazing flow on the acoustic impedance of a cylindrical wall cavity 0-69784
- shedding, interaction of induced sound with flow past a square leading edged plate in a duct 0-69783
- shedding flowmeter, stabilisation in low Reynolds number range 0-83865
- shedding of vortices, flow meas. (*German*) 0-79419
- simulation of flow, vortex methods, review 0-106801
- small particles suspended in turbulent fluid, convection, mass transfer 0-87793
- sound generation and simulated emission by vortex flows 0-69797
- sound generation by flow-acoustic coupling 0-69793
- sound generation by head-on collision of two vortex rings 0-69801
- sphere in current carrying liq., convection mass transfer, num. anal. 0-83851



**vortices continued**

- spiral vortex flow stability, experimental investigation 0-79327
- stable flow past a wing, appl. of method of discrete vortices 0-74889
- stably stratified medium, plane free convection from local heat source 0-96253
- stagnation flow turbulence about circular cylinder, visual study 0-96248
- standing vortices behind cylinder in glycerin-water solns., visualization 0-59151
- standing waves on hollow core vortices 0-106807
- statistical dynamics of chaotic flows 0-106786
- steady translating vortex pair family with distributed vorticity 0-92158
- steady viscous flow past circular cylinder, numerical study, vortices and separation 0-92108
- Stokeslets and eddies in creeping flow, review, book contrib. 0-96265
- stratosphere, potential vorticity rel. to polar stratosphere-troposphere exchange in summer 0-72599
- streaklines in a shear layer perturbed by two waves 0-59055
- superconductors, type II, vortex pinning at edge dislocations, electrostatic mechanism 0-103802
- superfluid, rotating, continuous model of vortex oscills. 0-70490
- swirling convective boundary layer, vorticity dynamics 0-59048
- Taylor 0-59044
- Taylor cells hydrodynamics instability and vortex currents in Couette flow 0-64571
- Taylor vortex flow with imposed laminar axial flow and isothermal surface heat transfer, velocity profiles 0-103031
- Taylor vortices near oscillating cylinder, subharmonic destabilisation 0-92162
- Taylor-vortex flow, mathematics in finite length cylinders 0-100002
- temperature gradient effect on stability of flow between concentric rotating cylinders 0-79263
- three-dimensional flow over wings with leading-edge vortex separation 0-74927
- tornado-like vortex, laboratory expt. of swirl ratio effect 0-61862
- tropical cyclones, preferred mode of Ekman conditional instability of second kind (CISK) 0-72617
- tube, round, vortex streams, radius of separation (*Russian*) 0-69841
- tube input parameters, effect on rate of rotation of flows (*Russian*) 0-96264
- turbulence, 2-D, hydrodynamic and plasma applications, dynamical eqns., diffusion, MHD, superfluidity, review 0-69769
- turbulence caused by slender bodies, high angles of attack to medium of travel (*French*) 0-59041
- turbulent flow noise generation, role of tornado-like vortices 0-69811
- turbulent free convection in mag. field, statistical characts., vortices 0-79310
- turbulent horseshoe vortex 0-103016
- turbulent vortex flow meas. by laser Doppler anemometer, meas. of turbulent vortex flow 0-79412
- two dimensional turbulent mixing layer, spanwise struct., vortices 0-69771
- unstable flow past cavity, three-dimens. nature, obs. 0-59053
- unsteady airfoil, Kutta condition (*Japanese*) 0-92155
- vertical axis wind turbine, flow field exam. using vortex model 0-61267
- vibrations of several obstacles within the two dimensional flow of an incompressible fluid (*French*) 0-69846
- viscous flow, unsteady, around elliptic cylinder, heat transfer, finite difference method (*Japanese*) 0-69831
- vortex-induced wake buffeting and its suppression 0-103030
- vortical momentum of bounded ideal incompressible fluid flows 0-59051
- vorticity vector, rot. theory 0-82604
- wedge like sharp edge starting vortex, flow visualisation expts. 0-59046
- wing-tip vortex cavitation, vapour core characteristics eval. by asymptotic expansion 0-106825
- <sup>4</sup>He films, vortices and superfluid decay 0-96710
- <sup>4</sup>He film, superfluid, dynamics 0-59748
- <sup>4</sup>He, superfluid, fluctuations in turbulent counterflow, vortex line density fluctuation power spectra 0-84335
- <sup>4</sup>He, superfluid, freely suspended, rot. vel. nonregular variation (*Russian*) 0-88376
- <sup>4</sup>He, superfluid, isotopically pure, roton-driven mech. for nucleation of negatively charged vortex rings 0-59746
- <sup>4</sup>He, superfluid, rotating, vortex position photography technique 0-96708
- <sup>4</sup>He, superfluid, spherically confined, quantised vortices (*Russian*) 0-70487
- <sup>4</sup>He, superfluid, vortex form., crit. vel. depend. on oscill. period (*Russian*) 0-92732
- <sup>4</sup>He, superfluid, vortex lattice form. relax. times in two-valued vessel subjected to ang. accelerations (*Russian*) 0-92731
- <sup>4</sup>He, superfluid, vortex nucleation inhibition by strong electric fields 0-92735
- <sup>4</sup>He, superfluid, vortex pinning, surface roughening effects 0-88381
- <sup>4</sup>He, superfluid film, superflow decay, vortex pinning effects 0-84332
- A<sub>70</sub>Nb<sub>30</sub>, Abrikosov vortex formation kinetics (*Russian*) 0-93055
- unsaturated films, decay of persistent currents obs. <sup>4</sup>He superfluid, 0-75397

**vulcanisation**

- epoxy resin, plastic deform. mechanism 0-97534
- fibre reinforced polymer, soaking, wetting and compounding of materials during production (*German*) 0-93535
- mixtures in range of reversion, vulcanetry, cross-linking model (*German*) 0-104113
- natural rubber vulcanisate, network changes during physical testing 0-60936
- rubber-metal facings, vulcanisation degree determ.,  $\gamma$ -ray method 0-61043

**waiting line theory** *see queueing theory***wakes**

- airfoil trailing edge noise, near-wake struct. and unsteady pressures at trailing edge 0-69794
- axisymmetric afterbodies, separated turbulent flows, wakes, exhaust plume effects 0-74885
- bird flight, wake behind finch 0-81629
- chlorobenzene drops falling freely through water, breakup 0-69899
- circular cylinder flows, coherence function method 0-96068
- cylinder, axisymmetric, with slanted base, near-wake flow 0-74886
- Darrieus rotor windmill arrays, wake interaction, wind tunnel simulation 0-61245
- Darrieus rotor, aerodynamic analyses comparison 0-61264
- dichloroethane drops falling freely through water, breakup 0-69899

**wakes continued**

- disc wake, cavitating flows with perturbations 0-92190
- discrete frequency sound generation by fluid flows 0-69812
- flow separation, unsteady, behind normal plate, discrete-vortex model, velocity-point scheme (*Japanese*) 0-79330
- flow separation, unsteady, behind normal plate, discrete-vortex model, modified velocity-point scheme (*Japanese*) 0-79331
- free turbulent mixing in streamwise press. gradients, linearised k- $\epsilon$  anal., wakes 0-59039
- ionosphere satellite wake, assessment ion current distrib. 0-101527
- nonequilibrium turbulent flows near wall, matching problem 0-96250
- nozzle in different jet regimes, internal and external flows, separation and wakes 0-100023
- perforated plate generators in wind tunnels, wake, shear flow and isotropic turbulence prod. 0-69770
- plate, Kirchhoff-Rayleigh flow, separation, wakes and vortices 0-69839
- propane flame, wake stabilized, response to sudden accel. or deceleration of free stream 0-61096
- reacting particle in fluid, convective diffusion, nonlinear surface reaction kinetics 0-106854
- rectangular cylinders, 2-dimens., drag coeff., correction method comparison 0-64568
- slightly heated small perturbation jets and wakes in press. grad., self-preservation 0-96290
- steady viscous flow past circular cylinder, numerical study, vortices and separation 0-92108
- Stokes flow, effect of separation on drag and torque 0-106818
- tube, cylindrical, coaxial, effect of array of spheres on mass transfer rate to tube wall 0-74884
- two circular discs in tandem, drag reduction, wakes 0-106795
- vehicle hypersonic wake, radiation from injected small particles, free molecular regime 0-64650
- vibrations of several obstacles within the two dimensional flow of an incompressible fluid (*French*) 0-69846
- viscous drag of two-dimensional contours moving in a weak polymer solution 0-100014
- viscous flow, unsteady, around elliptic cylinder, heat transfer, finite difference method (*Japanese*) 0-69831
- vortex-induced wake buffeting and its suppression 0-103030
- wedges, high Reynolds number flow, base pressure in near wake 0-59038
- windmill arrays, wake interaction, theory and preliminary results 0-61246
- wings near ground, nonlinear unsteady one dimensional theory 0-79344

**Wannier functions**

- Coulombic interaction summation in Gaussian basis 0-70575
- cubic crystals, perfect, nonBloch electron state density 0-75487
- excitons, Wannier, electronic spectrum, in quasi-two-dimensional structures 0-65460
- metal, doubly occupied Wannier functions, constructive definition 0-75492
- semiconductor, dielectric liq. of Wannier-Mott excitons 0-65458
- surface bands, lattice and symmetrical description 0-70785
- transition metal-H systems, energy and electron density of states, improvements to theory 0-70636
- Be, X-ray scattering, Wannier function calcs. 0-87988
- Ge-Si, electronic structure, short-range order effects, calc. 0-92861
- Na, BCC, doubly occupied Wannier functions, constructive definition 0-75492
- Si, total energy calcs. by r-space method, Wannier functions 0-88503
- TiCl<sub>3</sub>, ground-state props., Wannier functions, and electronic struct., ab initio self-consistent calc. 0-80178

**warning systems** *see alarm systems***waste disposal**

- see also radioactive waste*
- Atlantic nuclear waste disposal site, radionuclide redistrib. 0-85309
- Biblis nuclear power station, waste production, storage and disposal 0-68903
- cellulosic, municipal, ethanol production 0-61502
- cemented radioactive wastes, stability improvement method 0-57869
- fuel production, refuse derived fuels, pyrolysis, hydrolysis, fluidised beds 0-66920
- irradiated fuel elements recycling plant design modifications and safety of used nuclear fuel during storage and disposal (*German*) 0-99219
- irradiated nuclear reactor fuel rod components, EM separation, feasibility 0-99224
- Lac du Bonnet batholith, Canada, geological reconnaissance for nuclear waste disposal 0-73977
- LWR spent fuel elements, disposal in geologic isolation, feasibility study report 0-106140
- municipal refuse, utilisation of heat energy 0-66919
- nuclear generating station, waste disposal and licensing (*German*) 0-99222
- nuclear power stations, licensing procedure, public participation under Atomic Energy Act (*German*) 0-102256
- nuclear power stations, waste management principles modifications (*German*) 0-102255
- polychlorinated biphenyls waste disposal by pyrolysis, plasma torch appl. 0-76487
- radioactive, Czechoslovak Research Institute activities (*Slovak*) 0-83188
- radioactive waste, site selection and eqpt. planning at Gorleben, FRG (*German*) 0-68855
- radioactive waste, transceramic, from nuclear power plants, storage vessels and methods (*Dutch*) 0-68845
- radioactive waste disposal, popular assumptions, critical examination 0-106141
- radioactive waste disposal by solidification and burial, geological aspects 0-63316
- radioactive waste disposal in geologic formations, site selection criteria 0-106142
- radioactive waste geologic disposal, safety anal., functional relations of risk to input data uncertainties 0-83189
- radioactive waste storage in salt domes, conceptual design 0-106143
- radioactive waste study, groundwater vel. estimation 0-82111
- radioactive waste treatment and disposal (*French*) 0-99221
- radioactive waste underground disposal, solutes movement through aqueous fissures in porous rocks 0-94553
- spent fuel storage and disposal and plant building and operating legislation (*German*) 0-99223
- spent nuclear fuel stored in basalt, chances of reintroduction into biosphere, analysis 0-106144

**waste disposal continued**

- storage and shipment of spent fuel elements INFCE Working Group 6 (German) 0-102257  
 underground repository of high-level radwaste, water intrusion scenario studies, anal. and re-eval. 0-73950  
 Rn emanation from  $\alpha$ -emitting waste, expts. 0-98314

**water**

- see also groundwater; heavy water; hydroxonium ion; ice; moisture; seawater; steam  
 absorption on  $\text{Na}_3\text{AlF}_6$  film on Si, fused quartz substrates, IR anal. 0-75446  
 absorption on ZnS film on Si, fused quartz substrates, IR anal. 0-75446  
 acoustic relaxation in critical region (Russian) 0-92609  
 adsorbed on  $\text{Al}_2\text{O}_3$ , Raman spectroscopy study 0-65358  
 adsorbed vapour, effect on liq. water flow in Pyrex glass capillary tubes 0-92759  
 adsorption on  $\beta$ -AgI surface, effective pair pot. model 0-100394  
 adsorption on amorphous, porous, hydrophilic P-doped  $\text{SiO}_2$  0-80061  
 adsorption on Pt (111), thermal desorption, UPS, and XPS study 0-80088  
 adsorption on Re(0001), XPS, UPS and temp. programmed desorption 0-71574  
 affinity for  $\text{Li}^+(\text{Na}^+)(\text{K}^+)$ , ab initio SCF calcs. 0-58125  
 alkaline electrolysis using inorganic-membrane-electrolyte for  $\text{H}_2$  prod. 0-72092  
 annular mist flow in tube, wall film mass flow rate 0-69905  
 asteroids, search for water of hydration from IR reflectance spectra 0-77318  
 atmosphere, dimer conc. in  $\text{H}_2\text{O}$  vapour at different temps. and vapour press. (Chinese) 0-109237  
 atmosphere, weak spectral absorpt. of vap. in visible and near IR 0-82062  
 atmosphere  $\text{H}_2\text{O}$ , vibrationally excited, collisional emission rel. to new diffuse bands in twilight 0-72662  
 atmosphere vapour, transport between troposphere and stratosphere implications for pollutant transport 0-105034  
 atmospheres of Uranus and Neptune, estimation of ammonia and water vapour contents 0-90366  
 backscatter and absorption coeffs., simultaneous determ. 0-82074  
 biological samples, PMR, fast-exchange model interpretation via differential kinetics clarified 0-67033  
 biophotolysis, living electrode of algae as long-lived photoconverter 0-104510  
 bladder, toad, temp. dependence of ADH-induced water flow and intramembranous particle aggregates 0-61520  
 boiling and heat transfer on horizontal pipes with annular fins 0-74855  
 boiling at subatmospheric press., heat transfer rate, heating surface effects 0-69630  
 boiling superheat, maximum, of drop submerged under immiscible liquid layer 0-79928  
 Brillouin light scatt., temp. gradient induced 0-100663  
 bubble growth in superheated water at reduced pressures, finite difference anal. (Japanese) 0-92150  
 calorimeter for absorbed dose meas. 0-76836  
 cavitation expts. in steel Berthelot tube 0-87788  
 cavitation expts. using shock tube 0-87789  
 cellulose, mobility of adsorbed water, NMR pulse obs. 0-108835  
 channel blockage and turbulence influence on water transverse flow past cylinder (Russian) 0-79401  
 chemical attack on float glass, behaviour of Al tracer (French) 0-89378  
 chemical processes induced radiolytically in well defined aqueous systems 0-66823  
 chemisorbed on metal surface, molecule struct., interband angle 0-59787  
 chemisorbed on Pt (111), EELS spectra, vibr. freqs. 0-80920  
 chemisorption, on Ni catalysts, dynamics, neutron spectrosc. obs. 0-59778  
 chemisorption on reduced and stoichiometric  $\text{SrTiO}_3(111)$ , UPS and XPS studies, illum. effects 0-71572  
 chemisorption on Rh (111), effect of adsorbed O, H, or CO, LEED and thermal desorption meas. 0-75435  
 coadsorption with Br, on Cu(100), Helmholtz layer model system 0-92777  
 coherent Raman ellipsometry, vibr. stretching region and liq. struct. obs. 0-93341  
 compressed, thermodynamic props., evaluation by statistical error anal. 0-92685  
 concentration in stratosphere, simultaneous inference using inversion algorithm 0-82000  
 condensation on AgI aerosol particles, implications for ice-forming activity 0-101406  
 critical mixture with 2,6-lutidine, spinodal decomposition, Rayleigh scatt. 0-70416  
 CW and flash photoelectrolysis using ferroelectric photoanodes 0-81339  
 decomposition by solar energy conversion for  $\text{H}_2$  production 0-97813  
 detection of bacteria and algae by resonance Raman spectroscopy 0-94418  
 determination in rocks and minerals by inorganic gas chromatography 0-85767  
 dielectric breakdown with picosecond laser pulses, SHG sharp increase 0-102769  
 dielectric relaxation of compressed liquid at 17.613 GHz using microwave refl. meas. method (German) 0-71306  
 dielectric relaxation spectroscopy of polar fluids in microwave region, double beam interferometry method (German) 0-71309  
 dimer, difference electrostatic mol. pot. contour maps, basis set superposition effect 0-102462  
 dimer, partially deuterated, microwave spectra and struct. 0-74212  
 dimer, struct. studied by CNDO/2 method 0-69081  
 DNA, water localisation in a DNA mol. by differential Fourier synthesis 0-94164  
 drinking water, Finland, internal radiation doses due to radioactivity 0-109029  
 drinking water, Finland, natural radioactivity 0-108819  
 droplet size distrib. spectra in cumulus clouds (Russian) 0-81991  
 droplets, ebullition under steady-state superheated conditions 0-74928  
 droplets, ebullition under transient superheated conditions 0-74929  
 droplets, subcooled, nucleation in  $\text{Ar-H}_2\text{O}$  vapour mixture, rate const. 0-61131  
 electric breakdown for applied electric fields in range 200-500 kV/cm in the 2-10 microsecond time domain 0-71316

**water continued**

- electrolysis, design and operation of advanced  $\text{H}_2\text{O}$  electrolyzers for  $\text{H}_2$  prod., review 0-61449  
 electrolysis,  $\text{H}_2$  production, module design, geometry, capacity, operating temps., pressures, electrode types 0-72098  
 electrolysis, nucleate boiling, vapour bubble behaviour, heat and mass diffusion 0-67013  
 electrolysis, solid polymer electrolyte,  $\text{H}_2$  technology 0-67012  
 electrolysis  $\text{H}_2$  production, onsite, for electric generator cooling 0-72097  
 electrolysis in fused NaOH for  $\text{H}_2$  prod. 0-76660  
 electrolysis with solid polymer electrolyte, for  $\text{H}_2$  production 0-61442  
 evaporation through monolayer free and monolayer covered surfaces, temp. gradients meas. 0-88402  
 films, subcooled, flowing down vertical tube, heat transfer 0-79318  
 fission reactor coolant, water chemistry (Japanese) 0-68737  
 flow in heated tubes, with near critical parameters, turbulent flow, heat transfer 0-59022  
 formation on  $\text{O}_2$  exposure of hydrides of intermetallic cpds. 0-97727  
 free energy calcs. by random network model 0-92688  
 gamma-ray buildup factors for  $\text{Pb/H}_2\text{O}$  stratified radiation shields 0-86994  
 gravitational wave absorption by water mols. 0-82189  
 heat emission of a rough-surfaced tube in turbulent water flow (Russian) 0-74837  
 heating at microwave freqs. and complex permittivity meas. for specific purities and salt. soln. 0-60480  
 high pressure steam/water mixture flow through cylindrical channels, obs. 0-79404  
 hypersthenic magmas, water contents 0-72507  
 ice, crystalline, localised excess electrons yield studied as function of dose rate 0-97712  
 injection of gases through porous plate, squeezing out of liq. 0-64622  
 interface with  $\text{Al}_2\text{O}_3$  layer on stainless steel, leaky wave generation 0-75419  
 interstellar  $\text{H}_2\text{O}$ , synthesis in interstellar clouds by radiative association reaction  $\text{H} + \text{OH} \rightarrow \text{H}_2\text{O} + \text{h}\nu$  0-90509  
 interstellar  $\text{H}_2\text{O}$  maser emission, new sources detect. 0-62298  
 interstellar  $\text{H}_2\text{O}$  maser source in Orion A, obs. of outburst (Russian) 0-105320  
 interstellar  $\text{H}_2\text{O}$  masers in NGC 6334, positions and spectra rel. to star form. 0-73025  
 irradiated by photons up to 2 MeV, initial energies of Compton electrons and photoelectrons 0-108320  
 isobutyril acid-water critical mixtures, US and hypersonic study 0-88268  
 isobutyril acid-water near-critical liquid mixture, nucleation 0-92664  
 liquid, diamagnetism, temp. dependence, NMR chemical shift calcs., molecular interactions data 0-75707  
 liquid, electrical breakdown in  $\mu\text{s}$  regime with Cu, brass, steel and Al electrodes 0-103917  
 liquid, electron solvation dynamics 0-85205  
 liquid, equations for mag. susceptibility, electric polarisability 0-75708  
 liquid, physical props., two-state model approach 0-75144  
 liquid, proton spin-lattice relax. by slow proton exchange 0-60437  
 liquid, Raman and IR spectrum in overtone OH stretching region 0-58263  
 liquid, relax. compressibility and heat capacity 0-92580  
 liquid, thermal conductivity at high pressures, meas. with Ag co-axial cylinder cell (Japanese) 0-80007  
 liquid, UV absorpt. spectra 0-76043  
 2,6-lutidine-water, anomalous supercooling near critical point 0-70384  
 2,6-lutidine-water thick films, interferometric obs. of crit. behaviour 0-93266  
 lysozyme hydration, correl. of diverse types of meas. 0-61507  
 maser sources near Herbig-Haro objects 7-11, 22 GHz obs. 0-73019  
 mass spectrometric chem. anal. of  $\text{D}_2\text{O}$  and  $^{18}\text{O}$  from natural waters of Mt. Everest (Chinese) 0-77016  
 metastable state, fundamental equation 0-103447  
 metastable superheated water, specific vols. and P-V-T props. 0-92032  
 mixture with toluene-sodium dodecyl sulphate-butanol 1, interface light scatt., interface tension meas. 0-76039  
 modified droplet model, mean droplet interaction below  $T_c$  0-70363  
 molecular energy quantities from localised charge densities, dependence on geometry and basis set 0-63525  
 molecular static polarisability, ab initio SCF wave functions 0-74106  
 molecule, bond bending, bond orbitals rel. to nucl. motion 0-95513  
 molecule, CI calcs. using modified virtual orbitals 0-58163  
 molecule, core 1s shakeup study, XPS and Xalpha calcs. 0-69064  
 molecule, correl. energy, fourth order diagrammatic, many body Rayleigh Schrodinger perturbation theory 0-63556  
 molecule, electron impact, vibr. excitation, effective range theory 0-83485  
 molecule, electron impact dissociation,  $\text{OH}(\text{A}^2\Sigma^+ \rightarrow \text{X}^2\Pi)$  emission spectra, crossed-beam investigations 0-83504  
 molecule, excited stretching vibrs., quantum mechanics. 0-91535  
 molecule, ground state, CI calcs. on triply and quadruply excited configs., basis set effects 0-95549  
 molecule, ground state, cond. energies, higher-order excitation contribs. 0-58166  
 molecule, harmonic and anharmonic matrix elements comparison, appl. to vibrational energy transfer 0-63760  
 molecule, harmonic force consts., vibr. freqs., integrated intensities, MINDO/3 method 0-58411  
 molecule, intermolecular interaction energies calcs. using minimal basis sets 0-78681  
 molecule, many electron Green's function calcs. optical pot. 0-58126  
 molecule, mol. Rydberg S-S and S-T transitions, semi-empirical SCF MO calc. 0-91453  
 molecule, multi-root config. interaction calcs. 0-102451  
 molecule, multiphoton absorpt. and dissociation 0-99530  
 molecule, multiplet states, SCF theory 0-69062  
 molecule, nucl. elec. shielding tensor calcs. 0-83296  
 molecule, orbital relax. energy for single and double ionis. from valence shells 0-106253  
 molecule, photoassisted decomposition at  $\text{SrTiO}_3$  surface 0-85202  
 molecule, photodissoc. resonances, converged 3-dimens. quantum mech. calcs. 0-106366  
 molecule, photoionisation cross sections and asymmetry parameters, SCF Xa scatt. wave calcs. 0-63542  
 molecule, polarisability and mag. susceptibility calc. by SCF and CI method 0-99443  
 molecule, quenching of laser-excited  $\text{O}_2$  0-99515



## water continued

- molecule, relative ionisation energies, Tamm-Dancoff approx. calcs. 0-83243  
 molecule, SCF calcs. using cusped Gaussian basis sets, polarisation effects 0-74118  
 molecule, semiempirical CNDO/2 wave functions, pair density anal., environmental effects 0-91451  
 molecule, separated electron pair theory, numerical calcs. 0-87049  
 molecule, threshold PES,  $\text{OH}^+$  fragment obs. 0-78647  
 molecule, vertical valence ionis. pot. calc. by perturbation, CI and CPA techniques 0-69263  
 molecule, VUV photodissoc., vibr. and rot. distrib. 0-87191  
 molecule +  $\text{N}_2^* \rightarrow \text{N}_2 + \text{H}_2\text{O}^*$  0-87212  
 molecule bond distribution functions, anharmonicity effects on electron diff. pattern 0-69234  
 molecule core 1s and 1b, photoelectron bands, vibr. excitations, ab initio calc. 0-63543  
 molecule in  $\alpha$ -oxalic acid dihydrate,  $\text{H}_2\text{O}$  proton shielding tensor, multiple pulse proton NMR obs. 0-63655  
 molecules, charged, model for form. and stabilisation of clathrate 0-91714  
 molecules, isotopic, vibr. intensities, ab initio and empirical calcs., band strengths 0-78593  
 molecules, isotopic vibr. intensities, ab initio and empirical calcs. 0-78592  
 Monte Carlo simulation of struct. and thermodynamic props. 0-88017  
 neutron activation analysis for determ. of selected elements and heavy metals 0-76580  
 pair pot. near H bonded equil. config., amorphous and crystalline solid and liq. 0-64946  
 permittivity at mm wavelengths 0-66098  
 photochemical dissociation utilising solar energy for  $\text{H}_2$  prod., review 0-61452  
 photodecomposition of gaseous  $\text{H}_2\text{O}$  over  $\text{TiO}_2$  and  $\text{TiO}_2\text{-RuO}_2$  surfaces 0-85194  
 photodecomposition over Pt/ $\text{TiO}_2$  catalysts 0-81337  
 photoelectrolysis, using  $\text{Fe}_x\text{O}_y$ -coated n-Si heterostruct. photoanode 0-61384  
 photoelectrolysis with  $\text{TiO}_2$  catalyst 0-60755  
 photolysis, for  $\text{H}_2$  prod. using chlorophyll photocatalysts 0-61458  
 photolysis, Si catalyst, I-V model 0-108721  
 photolysis, using solar energy for  $\text{H}_2$  prod., feasibility of large scale generation 0-72095  
 photolysis using biological and artificial catalysts for H prod. 0-61444  
 photolysis using Pt/(chlorophyll a.2 $\text{H}_2\text{O}$ ) reaction for  $\text{H}_2$  production 0-89663  
 $\beta$ -picoline-water solution, light scatt. spectra, ultra- and hypersonic absorpt. (Russian) 0-93353  
 plane-parallel convective flow instability near 4°C 0-92137  
 plasma impurity in  $\text{N}_2$  RF capacitive discharge, effect on heating 0-59312  
 plasma water shifts during thermal dehydration 0-67044  
 plasmochemical decomposition using nuclear energy source for thermochem.  $\text{H}_2$  production 0-61436  
 positronium formation, isotope effects 0-93432  
 pulsed opto-acoustic spectroscopy 0-62743  
 pyridine-water soln., reorientational relax. and activation energy of pyridine, depolarised Rayleigh scattering 0-76037  
 pyrolysis, thermodynamics, solar- $\text{H}_2$  energy systems 0-61448  
 pyrolysis, utilising solar energy for  $\text{H}_2$  prod., thermodynamics, review 0-61450  
 pyrolysis using Fe-Cl thermochem. cycle for  $\text{H}_2$  prod., chem. engineering anal. 0-97811  
 radiolysis of  $\text{H}_2\text{O}$  vapour,  $\text{H}_2$  production by thermoradiation dehydrogenation using nuclear power, kinetic anal. 0-67010  
 random network model, entropy calc. 0-64870  
 random network model, liq. and ice polymorphs enthalpy and heat content 0-64869  
 renography, comparative study in hydration and dehydration (Japanese) 0-81726  
 sapphire- $\text{H}_2\text{O}$  interface,  $\text{SiO}_2$  sputtered film performance as acoustic antireflection coating 0-106686  
 self-diffusion, pressure and temp. depend., NMR spin-echo obs. 0-65266  
 serine, neutral and zwitterion, water solvation, Monte Carlo simulation 0-76707  
 shock compression at high press. (Russian) 0-92608  
 shock compression at press. approaching 1 Mbar (Russian) 0-79851  
 snow, liq. water content investigation by radiometry in 3 to 60 mm wavelength region 0-72561  
 snow, water equiv. of dry snowpack, active and passive microwave response 0-72563  
 snow wetness, active and passive microwave response 0-67382  
 solubility and transport behaviour, dissolution during oxidation of Si 0-93801  
 ST2 discrepancy between Monte Carlo and mol. dynamics calc. using truncated pot. anal., internal energy determ. 0-95702  
 stellar  $\text{H}_2\text{O}$  maser emission, new sources detect. 0-62298  
 stratosphere,  $\text{H}_2\text{O}$  mixing ratio, in-situ obs. using NOAA UV fluoresc. instrument 0-90137  
 stratosphere composition, mixing ratio profiles from IR solar spectra obs. 0-105015  
 stratospheric composition, in situ obs. of  $\text{H}_2\text{O}$  0-105077  
 stratospheric  $\text{H}_2\text{O}$ , maintenance of extreme aridity, review 0-105028  
 structuring and protein adsorpt. on surface of hydrophilic polymers, ESCA evaluation 0-108758  
 supercooled, sound vel. dispersion, struct. relax. effect, Brillouin scatt. obs. 0-107375  
 supercooled to  $-33^\circ\text{C}$ , sound vel. determ. by acoustic levitation method 0-88269  
 superheated water, Brillouin scatt., sound velocity meas. 0-95631  
 superheated water, flashing kinetics,  $\gamma$ -radiation effects 0-92025  
 surface tension from Skeleton table (German) 0-75407  
 tension effects, Berthelot-Bourdon tube method 0-88238  
 thermochemical decomposition utilising solar heat for  $\text{H}_2$  prod. 0-61451  
 transport in biomembrane, NME determ. methods (Rumanian) 0-94435  
 transport phenomena in cellulose diacetate membranes, hydration and dialysis coeffs. 0-76556  
 trimer, geometric config. energies, SCF LCAO MO calcs. 0-63551  
 triple point as temp. fixed point 0-59626  
 turbid natural waters, spectral scatt. props. 0-72560  
 US vel. and adiabatic compressibility determination, 25 to  $80^\circ\text{C}$  0-88265

## water continued

- US velocities in superheated ordinary and heavy water, thermodynamic props. 0-65156  
 US velocity in crit. region 0-59582  
 vapourisation and thermoelastic press. due to  $\text{CO}_2$  laser pulse 0-84227  
 vapour, adsorption on  $\text{NiO}$ , prepared by thermal decomp. of  $\text{Ni}(\text{OH})_2$ , effect on microporosity 0-80060  
 vapour, attenuation of HF/ $\text{CO}_2$  laser beam 0-61905  
 vapour, initial reaction probability with Ba getter film, AES obs. 0-61153  
 vapour, IR bands transmission functions 0-106324  
 vapour, perturbed-hard-sphere eqn. of state 0-96331  
 vapour, Raman linear meas., daytime atmosphere 0-85718  
 vapour, visible absorpt. spectrum, fine struct. acoustooptical determ. 0-86450  
 vapour absorpt. bands, long distance meas. of cloudy atm. by radiometry 0-90196  
 vapour and liquid far IR spectroscopy 0-60610  
 vapour continuum absorption (3.5 to 4  $\mu$ ) temp. dependence obs. 0-61903  
 vapour ionised by  $\text{He}^+$  and  $\text{He}^{2+}$ , secondary electron emission yield obs. 0-102562  
 vapour IR continuum absorpt., appl. to aerosol IR spectrometry theory 0-101428  
 vapour laser, CW 28  $\mu\text{m}$ , operating characts. and discharge conditions 0-69369  
 vapour plasma, electron energy distrib. function, electron sink and plasma resist. effect (Russian) 0-106987  
 vapour submillimetric-wave absorption obs. with photoacoustic cell 0-61901  
 vapour vertical profile in stratosphere (French) 0-77033  
 water mobility in blood plasma, NMR determ., viscosity correl. to  $1/T_2$  0-67176  
 water photoelectrolysis, rel. to charge transfer via surface states of semiconductor 0-75636  
 water-air plug-train system, press. wave propag. characts. 0-59058  
 water-alcohol mixtures, US attenuation meas., method of streaming 0-88272  
 water-dye solution, light scatt. effects on photoacoustic spectroscopy 0-95144  
 water-imidazole, H bond interrupted chain, cooperative effects, STO-3G ab initio calcs. 0-63535  
 water-methanol mixtures, viscosity at  $25^\circ\text{C}$ , isotope substitution effects 0-92700  
 water-oil microemulsions, optical matching 0-61157  
 water-p-dioxane at 11 and  $25^\circ\text{C}$ , US absorption 0-65171  
 water-petroleum emulsions, mean particle diameter and conc. determ. by light scatt. 0-89538  
 $\text{CO}_2\text{-H}_2\text{O-NH}_3$ -methanol, solid mixture vibr. modes, IR spectra 0-90504  
 $\text{CO}_2\text{-N}_2\text{-H}_2\text{O}$  fast flow discharge laser, output power time depend. 0-99697  
 $\text{CO}_2$ -water, saturated two phase flow system, non-equilib. state transient process 0-59096  
 DOD, vibr. intensities, ab initio and empirical calcs. 0-78592  
 DOD, vibr. intensities, ab initio and empirical calcs., band strengths 0-78593  
 $\text{D}_2\text{O}^+(\text{H}_2\text{O})_{0.12} + \text{H}_2\text{O}$  reactions, SIFT studies, review 0-58435  
 ethanol-water system, complex dielec. permitt. in UHF region and NMR spectra (Japanese) 0-100620  
 $\text{H}_2$  and  $\text{O}_2$  production from  $\text{H}_2\text{O}$  using solar energy, eval. of a hybrid process 0-104519  
 $\text{H}^+(\text{D}^+)$  exchange rates,  $^{17}\text{O}$  NMR linewidths, pH depend. 0-91661  
 $\text{H}^+(\text{H}_2\text{O})_n$  ion-induced water clusters, mass spectra, IR continuum absorpt. 0-87257  
 $\text{H}_2\text{O}$  dimer, continuum absorpt. spectra in 8-13  $\mu\text{m}$  range (Chinese) 0-109237  
 $\text{H}_2\text{O}$  photodissociation,  $\text{OH}(\text{A}^2\Sigma^+ \rightarrow \text{X}^2\Pi)$  yields 0-71927  
 $\text{H}_2\text{O}$  vapour under point corona discharge, microprocessor control for vapour generator and EHD phenomena 0-106852  
 $\text{H}_2\text{O}^+$ , ab initio potential energy surface study by CI techniques, equilibrium conform. determ., mol. dissociation pathways 0-78550  
 $\text{H}_2\text{O}^+$  in cometary tails, surface brightness rel. to  $\text{CO}^+$  0-72880  
 $\text{H}_2^{18}\text{O}$ , chemisorption on  $\text{SrTiO}_3$ , oxidation and reduction, isotope exchange study 0-104461  
 $\text{H}_2^{18}\text{O}$ , self-diffusion, pressure and temp. depend., NMR spin-echo obs. 0-65266  
 $\text{H}_2\text{O}$ -air, two phase upflow across horizontal tube bundles, void fraction and flow pattern 0-92201  
 $\text{H}_2\text{O}$ - $\text{H}_2$ , isolation of singular component for heat capacities of supercooled  $\text{H}_2\text{O}$  0-107437  
 $\text{H}_2\text{O}$ -HF heterodimer, H bonding, microwave rot. spectrum, mol. geometry and moment 0-99501  
 $\text{H}_2\text{O-Li}^+$  complex, charge transfer theory, Mulliken population, ab initio calc., multiconfiguration scheme 0-106392  
 $\text{H}_2\text{O}$ -liquid metal stratified flow, horizontal co-current, interface heat transfer, turbulence model 0-92131  
 $\text{H}_2\text{O-N}_2\text{-H}_2$ , isolation of singular component for heat capacities of supercooled  $\text{H}_2\text{O}$  0-107437  
 $\text{H}_2\text{O} + \text{D}_2\text{O}^+(\text{D}_2\text{O})_n$  binary reactions, rate coeffs. and product ion distributions determ. 0-81305  
 $\text{H}_2\text{O} + \text{H}_2\text{O}(\text{He})(\text{Ar})(\text{N}_2)(\text{O}_2)(\text{CO}_2)$ , vibr. energy transfer temp. depend. 0-63763  
 $\text{H}_2\text{O} + \text{He}$ , collisional excitation of interstellar molecules, rate consts. 0-67816  
 $\text{H}_2\text{O} + \text{methyl ion}$ , ternary association reaction in energy range 0.04-0.1 eV 0-71896  
 $\text{H}_2\text{O} + \text{N}_2^*$ , deactivation, from laser-induced  $\text{CO}_2$  fluoresc. obs. 0-63776  
 $\text{H}_2\text{O} + \text{Ne}^+$ , pot. energy surfaces, MO and CI calcs., Penning ionisation electron spectra 0-106376  
 $\text{H}_2\text{O}^+ + \text{NO}_2(\text{O}_2)(\text{NO})(\text{CO})(\text{H}_2)(\text{ethylene})(\text{methane})$ , rate constants determ. as function of relative kinetic energy 0-81292  
 HOD, HOT, vibr. intensities, ab initio and empirical calcs. 0-78592  
 HOH, HOD, HOT, vibr. intensities, ab initio and empirical calcs., band strengths 0-78593  
 $\text{H}_2\text{SO}_4\text{-H}_2\text{O}$  aerosols nucleation rate in presence of ionisation source 0-104464  
 $\text{H}_2\text{SO}_4\text{-H}_2\text{O}$ -ion aerosol particles, ultrafine, stratospheric form., ion-induced nucleation 0-72608  
 $^3\text{H}$  measurement, deep electrolytical enrichment, behaviour of phosphate pickled mild steel cathodes 0-93764  
 $\text{Na}_2^{2-}(\text{H}_2\text{O})_n$  clusters, gas phase, high press. mass spectrometry, atmospheric implications 0-58436

**water continued**

- Na<sub>2</sub>O-B<sub>2</sub>O<sub>3</sub>-SiO<sub>2</sub>, optical waveguide glass, molar absorptivity of water 0-80066  
 Na<sub>2</sub>O-SiO<sub>2</sub> glasses, water reactions at elevated temps. and press. 0-81312  
 Na<sub>2</sub>SO<sub>4</sub>-CoSO<sub>4</sub>-H<sub>2</sub>O, phase equilib., activities, Pitzer eqn. calcs. (*Russian*) 0-65190  
 OH+H<sub>2</sub>O, OH linewidth rot. depend. on UV transitions 0-91606  
 TOT, vibr. intensities, ab initio and empirical calcs. 0-78592  
 TOT, vibr. intensities, ab initio and empirical calcs., band strengths 0-78593  
 ZnAs<sub>2</sub>-H<sub>2</sub>O, Schottky diodes, elec. and photoelec. props., excitons 0-65653  
 ZnP<sub>2</sub>-H<sub>2</sub>O Schottky diodes, elec. and photoelec. props., excitons 0-65653  
 ZnSe/water, interface, laser-induced damage in ZnSe 0-102746

**water boilers** *see* **boilers****water conditioning** *see* **water treatment****water cooling towers** *see* **cooling towers****water pollution**

- see also* **water pollution detection and control**  
 acidification of headwater stream, New Jersey Pinelands 0-81945  
 NW.Africa, snowfield acidity (1977-79) 0-98370  
 Bedford Ouse River, systems model of stream flow and water quality 0-81956  
 benzo(a)pyrene in lake sediment, western USA 0-61476  
 biological waste water treatment by activated sludge at Haguenau City water treatment plant (*French*) 0-61473  
 Bombay, coastal pollution physicochemical studies 0-104522  
 coal-fired power station, heavy metal fallout to nearby pond 0-76667  
 coastal marine environment, pollutant dispersal and deposition, Th isotope analogue expts. 0-81927  
 coastal marine sediments, <sup>14</sup>C ages rel. to pollution, fossil C effect 0-98308  
 Cochín backwaters, industrial pollution, impact on water quality and hydrographic features 0-76668  
 conference, Rochester, NY, USA (May 1979), polluted rain 0-82585  
 drinking water, Finland, internal radiation doses due to radioactivity 0-109029  
 estuary, chlorination of drinking water affecting organic colloids 0-97824  
 estuary sediment containing lead pollution, rel. to flood control measures, California 0-76670  
 estuary sediment heavy metals, Mosquito Lagoon, Florida 0-76671  
 fallout in sediments, mixing and accumulation study 0-81864  
 gas-oil mixtures trapped under ice, stable config. obs., energy meas. 0-108818  
 Greck Lakes water quality, remote sensing data interpretation 0-98364  
 heavy metals in non-industrial river, baseline study of northern New England, USA 0-61477  
 humic acid and fulvic acids chemistry as pollution indicator 0-76688  
 N.Indian Ocean, dissolved petroleum content 0-98361  
 Laccadive Sea, absence of Hg pollution determ. from total Hg concs. meas. 0-104996  
 Lake Michigan, sulphate deposition in stable atmos. conditions 0-81494  
 Lake Michigan, trace element input by aerosol deposition 0-76672  
 Lake Naini Tal, India, metal pollution in water and sediment 0-97828  
 Lake Ontario water quality near Port Granby radioactive waste storage site 0-97829  
 lake sediment records in New York State 0-85311  
 Mediterranean, floating plastic debris obs. 0-104999  
 E.Mediterranean sediments, heavy metal content, off Lebanon coast 0-97830  
 nuclear industry, radiation doses, health risks from various power sources 0-57899  
 nuclear waste ponds and streams, Hanford, ecological search for radiation effects 0-89804  
 oil film on sea, retardation of O<sub>2</sub> exchange with atmos. 0-109175  
 oil on sea surface, thermal radioemission spectral characts. 0-85686  
 Persian Gulf and approaches, oil pollution, 1978 obs. 0-105000  
 pesticides in USSR rivers, 1973-1976 period 0-81495  
 radioactive pollution consequences from liquid pathways due to reactor core meltdown accident 0-104778  
 radioactive transport in the aquatic ecosystem, foodweb model 0-104777  
 radionuclide redistrib. at Atlantic nuclear waste disposal site 0-85309  
 runoff from land receiving animal wastes, pollutant transport, review 0-97831  
 stream sediment trace metals, downstream of Pb smelter 0-61475  
 surfactants affecting temp. of skin-layer, for oil slick studies (*Russian*) 0-109172  
 Tolo Harbour, Hong Kong, untreated waste entering via streams 0-89685  
 underground repository of high-level radwaste, water intrusion scenario studies, anal. and re-eval. 0-73950  
<sup>14</sup>C in Atlantic from nucl. weapons tests 0-89683  
<sup>112</sup>Cd<sup>111</sup>, in marine organisms and sediment around Marshall Island nucl. test site 0-109174  
 Hg loss rate from contaminated estuarine sediments 0-85310  
 P in streams draining from agricultural watershed 0-61474  
 Pb in lakes, rel. to boating activities and sediment interaction 0-104523  
 Pb in subalpine pond sediments, anthropogenic source var. 0-85315  
 Pu from fallout in alkaline, saline lakes 0-97826  
<sup>226</sup>Ra, A=226, 228, content in groundwater of Fall Line aquifers 0-89682  
 T in deep N.Atlantic current, from weapons tests 0-101380

**water pollution detection and control**

- see also* **water treatment**  
 arsenic in freshwater fish traced to fly ash leachate using neutron activation analysis 0-97827  
 automatic water monitoring system, Finland 0-67026  
 borehole vertical groundwater flow as aid in pollution study 0-81938  
 diatom recognition and counting, matched-filter and statistical method 0-101304  
 dielectric props. and determ. of microwave emissivity 0-101142  
 dissolved forms of trace elements in streams, dialysis cell meas. 0-97851  
 environmental chemistry, anal. techniques, conf., Barcelona, Spain, (Nov. 1978) 0-88038  
 Finnish river water pollution monitoring network 0-89686  
 humic acid and fulvic acids chemistry as pollution indicator 0-76688  
 laser image printer for IR scans of ocean surface (*French*) 0-72119  
 marine chlorophyll a analysis, using aircraft multispectral scanners 0-77164

**water pollution detection and control continued**

- marine oil pollution surveillance, microwave remote sensing technology (*Japanese*) 0-76685  
 matrix isolation Raman spectroscopy, water pollution detect. appl. 0-108829  
 nuclear power plants, hydrobiological studies, conception and data obtained (*French*) 0-76665  
 oil fractional analysis by high-performance liquid chromatography (*Japanese*) 0-81936  
 oil recovery, polymer additives in reservoir flooding 0-72100  
 oil spill, extinction coefficient meas. using coaxial dual channel laser system 0-73425  
 oil spill detection by airborne laser fluorosensor 0-67024  
 oil traces, on water surface, continuous detect. system (*German*) 0-72115  
 optical methods of water quality determ., turbid waters spectral scatt. props. 0-72560  
 Par River estuary, India, pollution transport and abatement methods 0-104521  
 petroleum spills on water, control using gellants 0-61496  
 phosphorus removal system, automation 0-76669  
 portable computerised laboratory for water quality monitoring 0-61472  
 radioactive waste, liquid effluents, aquatic radiological impact anal., radio-caesium transport in sediment 0-95486  
 remote sensing appls. (*Japanese*) 0-94122  
 river pollution distribution determination by remote sensing, study 0-81512  
 River Tiber, physical processes related to discharge into sea, aerospatial obs. 0-108831  
 rivers downstream pollution, one-dimensional transient model for short-term prediction 0-81496  
 RWE environment protection organisation outline and functions (*German*) 0-101552  
 sea and beach persistent oil spill identification methods 0-90101  
 surface water continuous analysis by NH<sub>4</sub><sup>+</sup>-sensitive plastic membrane electrode 0-89701  
 ultrapure water, trace metal determ. 0-81394  
 USSR environmental pollution obs. and monitoring system 0-85322  
 Cs in marine sediments, determination method 0-104543  
<sup>137</sup>Cs/<sup>134</sup>Cs radioisotopes in seawater, Cs-selective resin determ. 0-94137  
 N<sub>2</sub>O, determ. in water using electron capture detection gas chromatography, multiple equilib. 0-76566  
 P determination, automated procedure 0-81517  
<sup>210</sup>Pb determination in sediment core from ocean floor off Californian coast 0-72101  
 Pu and Am inventory of ecosystem near a nuclear facility 0-97820  
<sup>226</sup>Ra in public water supplies, conc. determ. (*German*) 0-94138

**water purification** *see* **water treatment****water supply**

- see also* **dams**  
 centralized management systems for Kagawa Prefecture irrigation-water system (*Japanese*) 0-89684  
 Finnish river water pollution monitoring network 0-89686  
 groundwater recharge in Ganges Basin, alternative methods for water supply 0-81952  
 horizontal-axis wind-turbine system for pumping duties in Third World agriculture, design 0-61259  
 seasonal forecasting models, Akaike's information criterion 0-67386  
 solar plant for hot water supply (*Rumanian*) 0-97766  
 Turkey, karst water resource development 0-61821  
<sup>226</sup>Ra in public water supplies, conc. determ. (*German*) 0-94138

**water treatment**

- see also* **desalination**  
 biological waste water treatment by activated sludge at Haguenau City water treatment plant (*French*) 0-61473  
 phosphorus removal system, automation 0-76669  
 primary and secondary water chemistry of PWR power stations, European experience 0-106110  
 PWR power station secondary water chemistry study, progress report 0-106108  
 P reduction in sewage effluent by electrochemical process 0-104445

**watthour meters***see also* **power measurement**

No entries

**wattless power** *see* **reactive power****wattmeters**

- see also* **power measurement**; **volt-ampere meters**  
 errors, systematic and random, in wattmeter apparatus for measuring unit losses in electrical steel sheet 0-71858

**wave analysers***see also* **spectral analysers**

- seismic microvibration frequency analysis by 50 m interferometer 0-109276

**wave digital filters**

- eEG transient detection by matched inverse digital filtering 0-85506

**wave equations**

- see also* **Dirac equation**; **Schrodinger equation**  
 anharmonic oscillator system, hierarchy of evolution eqns. 0-68053  
 atomic resonant states, wavefunctions of complex order. method 0-106282  
 Benjamin-Ono equation, higher order, solns. 0-62482  
 Bernoulli equation, wave motion in relaxing gas 0-90681  
 Bossinesq equation, similarity solutions and Backlund transformation 0-68056  
 causality of a wave equation and invariance of its hyperbolicity conditions 0-91000  
 circular duct with hyperbolic horn, sound radiation modes 0-96096  
 conserved densities, Hamiltonian systems 0-90682  
 coupled bilinear eqns., exact one- and two-periodic wave soln. 0-68050  
 curved space-time, compact and noncompact sources 0-73571  
 cylindrical KdV equations, soln. asymptotic behaviour (in t), Cauchy problem 0-98803  
 diatomic molecule, vibr.-rot. states, high accuracy wave functions and energies 0-74159  
 diffracted wave fronts 0-82652  
 energy loss of a modified Korteweg-de Vries solitary wave in a varying medium 0-90683  
 evolution equations, impulse and distributed control (*French*) 0-68049  
 evolution equations, nonlinear, inverse spectral transform, generalisation of Klein-Gordon problem 0-68055



## wave equations continued

evolution equations, unknown control dates, periods and type, optimal control, existence theorem (*French*) 0-62478  
 evolution systems and convection-diffusion, stiffness and stability, Gershgorin theory 0-77626  
 extension of nonlinear evolution equations of the K-dV (mK-dV) type to higher orders 0-105508  
 Field-Koros-Noyes chemical wave equation, asymptotic solutions 0-66857  
 gravity waves, interfacial and internal long, dissipation, Korteweg-de Vries eqns. 0-90686  
 gyrotropic absorbing crystals, nonorthogonal eigenwave refl. 0-99624  
 gyrotropic medium, Green's function and field of moving charges 0-58445  
 higher order Korteweg de Vries eqn., Backlund transform 0-105510  
 higher order modified KdV eqns., bilinearisation 0-105509  
 hypergeometric functions, two-variable, Lie theory and separation of variables 0-73189  
 incompressible irrot. flow, water waves and Korteweg-de Vries eqns. 0-69850  
 initial value problem, several space dimensions, Rothe method 0-82651  
 integrable nonlinear evolution equation, soliton soln. from inverse scatt. method 0-73186  
 inverse scattering method, commutator representation of Painleve type ordinary differential eqns. 0-68052  
 KdV equation, perturbative expansion and initial value problem 0-62487  
 Klein-Gordon eqn., asymptotic growth of  $L^p$  norm (*French*) 0-73178  
 Klein-Gordon eqn., nonlinear interactions of counter-travelling waves 0-77627  
 Klein-Gordon equation, inverse spectral transform 0-68055  
 Klein-Gordon equation, Lie-Backlund transformation group 0-68371  
 Klein-Gordon equation, potential interaction using a metric space 0-82879  
 Klein-Gordon equation, spinor and scalar fields in 4-D non-Euclidean momentum space, eqns. of motion, vacuum momentum 0-68379  
 Klein-Gordon equation, time-independent, relativistic Stark effect, resonances 0-62890  
 Korteweg de Vries eqn., second modified, exact multi-soliton soln. 0-73180  
 Korteweg-de Vries eqn., generalised, conserved quantities 0-68054  
 Korteweg-de Vries eqn. and 2nd Painleve transcendent, boundary value problem in plasma theory 0-69971  
 Korteweg-de Vries equation, higher-order, Backlund transforms. 0-77631  
 Korteweg-de Vries equation prolongation Lie algebra 0-62501  
 Korteweg-de Vries solitary wave, energy loss 0-62489  
 Korteweg-de Vries soliton solutions, perturbations 0-105511  
 Korteweg-de Vries type eqns., group-theoretical interp. 0-77624  
 Lagrangian-Hamiltonian systems, partial quantisation (*Portuguese*) 0-77653  
 Laplace eqn., axisymmetrical Koshi problem (*Russian*) 0-101713  
 linearization of relativistic nonlinear wave equations 0-62837  
 long waves in dispersive media, solitary wave interaction 0-59062  
 massive particles with any spin, consistent eqns., Klein-Gordon divisor, review 0-73577  
 Miura transformation of Kaup and Mikhailov eqns. 0-57103  
 molecules resonant states, wavefunctions of complex coord. method 0-106282  
 Moller wave operators, existence and completeness 0-82649  
 monodromy- and spectrum-preserving deformations. I, soln. of nonlinear differential eqns. 0-98802  
 nonlinear, constrained harmonic motion 0-77625  
 nonlinear evolution equations, connection with Painleve type ordinary differential eqns., inverse scatt. transform 0-62486  
 nonlinear evolution equations, reverse scattering method, Hamilton's structure and Beklund's transformations (*Russian*) 0-86090  
 nonlinear evolution equations and conservation laws, spectral transform method 0-62488  
 nonlinear evolution of waves in free shear layers, effects of critical layer structure 0-83809  
 nonlinear wave equation, periodic solutions 0-73188  
 optical fibre, graded index, wave eqn. for propag. fields 0-58757  
 optically thin phase grating, comparison of optical path and differential eqn. methods 0-102823  
 Poisson relation for the wave equation in an unbounded open set (*French*) 0-73179  
 quantised many-body problem, dissipative system wave eqn. 0-86104  
 reduced wave equation, fixed incident field, inverse problem 0-62484  
 relativistic, coupled to external fields, constraints problems 0-86549  
 relativistic three-body wave equation for Dirac particle+two Klein-Gordon particles, preon model 0-73574  
 shallow water waves with quasi-periodic boundary conditions, eigensolutions of elliptic problem 0-83804  
 sine-Gordon eqn., inverse method for solving differential-difference and difference-difference eqns. 0-105513  
 sine-Gordon eqn. and Laplacian invariant, separable solns., complex solitons 0-90680  
 sine-Gordon equation, 3 and 4 dimens., exact solns. 0-86091  
 sine-Gordon equation, Backlund transform., physical space-time solitons 0-77629  
 sine-Gordon equation, Backlund transformations and Dirac factorisation 0-73185  
 sine-Gordon equation, double, multidimensional multisoliton kink solutions 0-73184  
 sine-Gordon equation, nonlinear, constrained harmonic motion 0-77625  
 sine-Gordon equation, nonlinear field equations, quantum inverse scattering transform method, 2-D ice and ferroelectric lattices 0-68348  
 sine-Gordon equation, separability, variable transforms 0-57102  
 solitons, review of concepts and methods in theory (*Polish*) 0-68057  
 sound generation and propagation in flows, inhomogeneous convected wave equation 0-69813  
 special relativity, transport equation for discontinuity wave amplitude (*French*) 0-90667  
 stability of wave fronts defined by eikonal equations, elementary catastrophes 0-73187  
 stochastic medium, propagation of mean field 0-73177  
 SU(3) wave eqns. for quarks 0-57571  
 symmetry approach to exactly solvable evolution equations 0-82648  
 symplectic operators and hereditary symmetries, applic. to soliton eqns. 0-82650  
 Toda lattice, wave behaviour in nonlinear LC equivalent circuit 0-105577  
 Toda lattice equation, nonlinear, constrained harmonic motion 0-77625  
 triloccal structures, secular eqn. 0-90776

## wave equations continued

vector product formulation of special relativity and electromagnetism 0-105496  
 $Ca_2$ , vibr.-rot. states, high accuracy wave functions and energies 0-74159  
 H atom, Dirac and Klein-Gordon relativistic eqns., energy level splitting 0-77938  
 H, low density atomic gas calculation, for dilute hard-sphere Bose-gas model 0-87194

wave functions  
*see also orbital calculation methods*  
 atom+diatom, energy correction of infinite order sudden approx., improved phase shift approach 0-95710  
 atom+polyatom systems, rotation-vibration symmetry. correlation 0-61074  
 atomic eigenfunctions, nodal structure 0-57122  
 atomic resonant states, wavefunctions of complex coord. method 0-106282  
 charge exchange, quantum mechanical and impact parameter capture amplitude 0-87226  
 closed-shell atoms, Jastrow wave functions, var. calcs. 0-83249  
 correlated wave functions anal. gradients from two particle density matrix and unitary group 0-78548  
 correlation coefficient and electron correlation 0-78552  
 diatomic molecule, electron scatt., low energy, multichannel variational calcs., static exchange approx. 0-83483  
 diatomic molecule, vibr.-rot. states, high accuracy wave functions and energies 0-74159  
 diatomic systems, nonadiabatic coupling matrix elements by Hellmann-Feynman theory and HF 0-83263  
 disordered system, one-dimens., density of states and wavefunction shape, periodic boundary condition influence 0-80223  
 education, nonspeading wave packets, physical interpretation of Berry Balazs wave function 0-57040  
 electron+ion scattering, Schwinger's variational principle, Rydberg states 0-78713  
 excited states, oscill. strengths calcs., influence of wave function determ. method 0-99478  
 excited states, perturbation and SCF calcs. 0-102455  
 exponential potential and mass dependence 0-73199  
 fermions, quantum mechanics of ground state 0-82713  
 free electron in external field, wavefunctions, nonrelativistic treatment 0-99611  
 free relativistic electron in external field 0-99612  
 harmonic oscillator wavefunctions, asymptotic behaviour 0-67979  
 high-Z elements subshells, photoelectron angular distribution 0-99487  
 hypervirial scaling iterative method 0-73196  
 integrated spatial electron populations, evaluations for simple mol. 0-78524  
 ion+polar molecule collision, low-energy, rot. state approach 0-74224  
 isoelectronic sequence, E1 and E2 oscillator strengths, MCHF calcs. 0-106292  
 lipid hydrocarbon chain, biomembrane, rot. motion and fluidity 0-76714  
 local scaled Schrodinger relations and the virial theorem, kinetic energy operator 0-78527  
 MCSCF and CI wave functions, two-particle density matrix and graphical unitary group approach 0-63558  
 methane, harmonic and anharmonic matrix elements comparison, appl. to vibrational energy transfer 0-63760  
 molecular quantum mechanically calculated observables, reliability determ. 0-63505  
 molecular static polarisability, ab initio SCF wave functions 0-74106  
 molecules, transition probability evaluation in double asymmetric pot. well 0-69120  
 molecules resonant states, wavefunctions of complex coord. method 0-106282  
 momentum eigenfunctions in complex momentum plane, Hartree Fock functions 0-63517  
 nodeless wave function quantum theory 0-57119  
 nuclear octupole vibration, collective, wave functions, spherical harmonics 0-68532  
 orbital-optimised, instability, rel. to positive orbital energies 0-58109  
 perturbed ladder operator method, wavefunctions, matrix elements, closed form expressions 0-73203  
 phase, relationship with Green's function 0-105543  
 planar defect 'on edge', electron wave function in vicinity 0-88002  
 Politzer-Parr partitioning, electron correl., isoelectronic, isonuclear, spin and excitation aspects 0-78522  
 positive ions, electron impact ionisation, Coulomb-Born approx. 0-74249  
 primitive wave function in theory of intermolecular interactions 0-95703  
 pseudopotentials from self-consistent atomic calcs., appl. to band struct. determ. 0-59846  
 pseudostates wave functions determ. in modified close-coupling calcs. 0-99572  
 quantum field theory, multilocal, Fock-space technique, particle creation effects 0-77945  
 rare earth atoms, Gaussian basis sets calcs. 0-63541  
 relativistic wavefunctions, approx. near turning point, WKB calcs. for  $Z > 137$  0-86598  
 Schrodinger equation, exactly soluble with bistable pot. 0-67950  
 self consistent electron pair theory, perfect pairing valence bond generalisation 0-63532  
 superposition state in regular and irregular spectrum, time evolution, intramolecular dynamics 0-83335  
 three-body problem in one dimension 0-82655  
 two electron atoms, three-body problem 0-83286  
 two-body corals., variational approach 0-91455  
 two-electron atom, trial wave function for ground state 0-78510  
 two-electron wave functions with monopole interaction, asymptotic forms 0-78528  
 unified theory of atoms and atomic aggregates, self consistent theory 0-102418  
 unrestricted Hartree Fock wave function, spatial symmetry recovery by spin projection 0-58150  
 BH<sub>2</sub>-ethylene complex, semiorthogonalised orbitals, integral approx. scheme 0-83262  
 Be isoelectronic series, excited states, oscill. strengths calcs., influence of wave function determ. method 0-99478  
 CO, one-electron props., corrections, Moller-Plesset perturbation theory calc. 0-95519  
 Ca<sub>2</sub>, vibr.-rot. states, high accuracy wave functions and energies 0-74159

**wave functions continued**

- $\text{Cs}_2^{2+}$ , low-lying states, MC SCF+CI 0-69053  
 Eu, electron impact excitation cross section, Born and Ochur approx. 0-87230  
 EuO, cryst. field parameters due to  $4f^{N-1}5D$  configs. 0-80230  
 H, elastic electron scatt., pseudostates wave functions determ. in modified close-coupling calcs. 0-99572  
 H, in static multipole field, logarithmic perturbation expansion 0-91431  
 H, Stark and photoabsorption spectrum, density of oscillator strengths, atom c.f. semiconductor spectra 0-83318  
 H, Stark spectrum and field ionisation, density of continuum states, normalised wavefunctions 0-83317  
 H+H<sub>2</sub>, scatt. wave function modal struct. and global behaviour 0-81307  
 H+methane, abstraction and exchange reaction, barrier height calc. using POL-CI wave functions 0-81304  
 H<sub>2</sub>, four-body system, adiabatic representation 0-91530  
 H<sub>2</sub><sup>+</sup>, exchange perturbation theory 0-63518  
 HCN, Fermi and Coulomb correl. holes, SCF and CI wave functions 0-69085  
 HCl, electrostatically interacting mols., CI multipole function calcs. convergence 0-91458  
 HCl, one-electron props., corrections, Moller-Plesset perturbation theory calc. 0-95519  
 HF, electrostatically interacting mols., CI multipole function calcs. convergence 0-91458  
 H<sub>2</sub>O, excited stretching vibrs., quantum mechanics. 0-91535  
 H<sub>2</sub>O, harmonic and anharmonic matrix elements comparison, appl. to vibrational energy transfer 0-63760  
 H<sub>2</sub>O, multiplet states, SCF theory 0-69062  
 H<sub>2</sub>O, semiempirical CNDO/2 wave functions, pair density anal., environmental effects 0-91451  
 He isoelectronic sequence,  $\delta(r_1)$  matrix elements using spatially distrib. operators 0-102445  
 He metastable state, two- and three-photon ionisation 0-91518  
 He-He, Born Oppenheimer pot. using Hylleraas-type electronic wave functions 0-91442  
 He-He, energy and interaction potential of two ground-state atoms 0-63740  
 He+H<sub>2</sub>, adiabatic distorted-wave infinite order sudden approx. 0-99558  
 Hg, positron scatt. at low energy 0-91670  
 p-Hz, quantum diffusion of O-H<sub>2</sub> impurities 0-96719  
 Li ground state, HFS 0-91699  
 Li isoelectronic sequence of three electron atoms, pair correlation study 0-74096  
 Li, optical oscill. strengths calcs. 0-91495  
 Na, molecular electronic struct. for lowest  $^3\Sigma_u^+$ ,  $^3\Sigma_u^+$ ,  $^3\Sigma_g^+$ ,  $^1\Pi_u$ ,  $^1\Pi_g$ ,  $^1\Sigma_u^+$  and  $^1\Sigma_g^+$  states 0-63738  
 O isoelectronic sequence, optical oscillator strengths 0-63589  
 SO<sub>2</sub>, harmonic and anharmonic matrix elements comparison, appl. to vibrational energy transfer 0-63760  
 Sc I, oscill. strength calc. 0-78571  
 Si<sub>2</sub>, electronic struct. and bonding, atomic effective pot. appl. 0-95745  
 SmO, cryst. field parameters due to  $4f^{N-1}5D$  configs. 0-80230  
 Yb, electron impact excitation cross section, Born and Ochur approx. 0-87230  
 YbO, cryst. field parameters due to  $4f^{N-1}5D$  configs. 0-80230  
 Zn, isoelectronic sequence, oscill. strength and MCHF wavefunctions, outer correl. 0-91505

**wave mechanics**

- see also wave equations; wave functions  
 -ZZ 0-67949  
 Einstein-Podolsky-Rosen paradox, de Broglie's physical waves, solitons 0-90710  
 electron atom collision, radial wave packets, appl. to target distortion 0-87234  
 gauge invariant wave mechanics and the Power-Zienau-Woolley transformation 0-99073  
 nonlinear-wave mechanics and particulate self-focusing 0-105520  
 quantum numbers as hidden parameters, in causal interpretation of wave mechanics (French) 0-68062  
 resonant interaction, three-wave, separable initial-value problem of initially nonoverlapping envelopes 0-68058  
 thermoelectric materials, heat conducting, relativistic theory of wave propagation 0-83748

**wave power generation**

- energy accounting study 0-76589  
 inexhaustible energy resources, research and development in Britain (German) 0-72000  
 Kaime, air-turbine coupled to AC generator 0-72010  
 materials aspects of wave energy converters, review 0-85262  
 ocean current power plant, vertical axis turbine, design and anal. 0-61272  
 pneumatic wave-energy convertor, performance study (Russian) 0-76600  
 Sweden, review of possible developments (Swedish) 0-93847  
 utilisation prospects 0-61269

**wave propagation**

- see also acoustic wave propagation; electromagnetic wave propagation  
 barrier theory based on half-barrier penetration, reflection and transmission coeffs. 0-98801  
 boundedness and periodicity criteria for wave motion in the Eulerian formulation 0-101720  
 degenerative dispersion laws, motion invariants and kinetic equations 0-90684  
 dissipative and nonequilibrium media, pulse spreading 0-94961  
 EHD flow, nonstationary, with charge diffusion, nonlinear and linear wave processes 0-59124  
 elastic half-space over circular pressure zone with non-uniformly changing radius 0-92080  
 elastic waves in anisotropic media, asymptotic equipartition of kinetic and strain energy 0-92081  
 excitation and propagation of elastic waves, book 0-94937  
 fluctuations of intensity at two wavelengths in turbulent medium 0-87318  
 gas, dissociating, relativistic flows, growth and decay of weak waves, shock wave formation 0-69949  
 gas, relaxing, in thermodynamical state of weak equilib., Bernoulli equation 0-90681  
 Helmholtz eqn. integral formulation for inhomogeneous media 0-81919  
 high strain rate processes, review 0-84864  
 hyperbolic systems, high-order methods, dynamic problems 0-68033

**wave propagation continued**

- ideal string, extremal solutions of inverse eigenvalue problems with finite spectral data 0-101712  
 impacted solids, compression and shear wave propag., modelling 0-83755  
 inhomogeneous media, determ. of structure from plane wave reflection response, numerical approx. 0-73183  
 inhomogeneous media, determ. of structure from plane wave reflection response, direct problem 0-77628  
 linear propagation in rotating fluid, critical level absorption and valve effects 0-106805  
 linear wave motions study using FFT, NDT appl. 0-92038  
 long internal Rossby waves, nonlinear propag. 0-81896  
 paraboloids of revolution, internal fractures due to stress wave focusing 0-83762  
 perforated screen, sound diffraction, vortex shedding influence 0-69849  
 plane elastic wave diffraction by wedge, three dimensional nonstationary problem 0-69723  
 plane periodic waves, nonlinear propagation in relaxing gas, numerical anal. 0-92170  
 plastic wave theory, comparison of predictions with impact expts. 0-83742  
 pseudostationary wave, anal. 0-82605  
 pulse propag. in media with freq. dependent Q, theory 0-72438  
 quasilinear elastic strip, modulated propagating normal wave transform. 0-74800  
 radiating gases, sonic wave propag., wave front curvature effects, shocks 0-87784  
 randomly inhomogeneous layer, statistical moments of wave field, strong fluctuations of wave intensity 0-57107  
 rectilinear rarefaction waves, systems of first-order quasi-linear hyperbolic equations 0-90679  
 relativistic fluid with vibrational relaxation, growth and decay of weak discontinuities 0-69948  
 rotating fluid of spherical configuration 0-106804  
 scalar-wave propag. in random elastic layer 0-83754  
 self-focusing of waves on deep water surface (Russian) 0-94536  
 shoaling of finite-amplitude surface waves on water of slowly-varying depth 0-69853  
 shock waves, plane, relativistic, propag. in slowly moving medium 0-62005  
 slowly varying wavetrains, dissipation and dispersion effects 0-64573  
 solid particle suspension in compressible fluid, wave propag. 0-69858  
 spectral broadening of waves propagating in a random medium 0-94960  
 stable baroclinic Rossby wave propag. through mean shear flow 0-81895  
 stationary waves, teaching 0-67999  
 stochastic medium, propagation of mean field 0-73177  
 strain wave propagation in viscoelastic bars due to longitudinal impacts anal. (Japanese) 0-96223  
 surface waves propagation over liquid and crystalline layers, elastic consts. of crystals. 0-76924  
 surface waves propagation over liquid and crystalline layers, theory 0-76925  
 temperature compensation and travel times of waves 0-69731  
 thermal wave propagation in nonlinear absorbing medium 0-96183  
 thermoviscoelastic media, non-homogeneous, discontinuity propagation 0-102972  
 translational relaxation at shock wave front in gas mixture 0-74917  
 travelling pressure induced over a stepped depth change (Russian) 0-79335  
 unidirectional wave propagation in one-dimensional first order Hamiltonian systems 0-86092  
 Van der Pol diffusion coupled oscillators, wave self-focusing and self modulation 0-90685  
 viscoelastic bar, transient wave propag. 0-106745  
 viscoelastic layered composites, wave propag., dispersion and dissipation effects 0-102982  
 viscoelastic wave propagation, integration contour deform. for Laplace transform inversion 0-74801  
 water-air plug-train system, press. wave propag. characts. 0-59058  
 weakly nonlinear wave propagation due to dispersion and dissipation. long wave approx. 0-57104
- wave scattering see scattering**  
**waveform analysis**  
 see also spectral analysis  
 analog signal processing, book 0-86047  
 earthquake foreshocks, waveform anal. rel. to differentiation from earthquake swarms (Japanese) 0-67342  
 earthquake swarms, seismic waveform anal. rel. to differentiation from foreshocks (Japanese) 0-67342  
 human scalp, olfactory evoked brain pot., correl. anal. of recorded waveforms (Japanese) 0-97946  
 seismic waves, multi-segment traces deconvolution and synthesis 0-77162
- wavefront-reconstruction imaging see holography**  
**waveguide antennas**  
 far IR antennas for 0.1 to 3.0 mm range, review 0-69553  
 focused spot-size controlled Gaussian-beam launcher for microwave exposure studies 0-89920  
**waveguide attenuators**  
 Helmholtz resonator array for attenuation of zeroth normal mode in tubes 0-87602  
**waveguide connectors see waveguide couplers**  
**waveguide couplers**  
 see also directional couplers  
 planar waveguide structure for integrated optics, props. (Czech) 0-96018  
 SAW multistrip coupler, superposition model 0-74674  
**waveguide joints see waveguide couplers**  
**waveguide junctions see waveguide couplers**  
**waveguide theory**  
 see also guided electromagnetic wave propagation; optical waveguide theory  
 cylindrical waveguide filled with uniaxial, collisional, hot and moving plasma, dispersion for TE and TM modes 0-106934  
 electrodynamic boundary problems, method for solving 0-95773  
 electrodynamics, projection methods, applicability limit 0-91734  
 EM transmission structures, relativistic foundation and network formalisms 0-58446  
 inhomogeneous dielectric filled uniform waveguides, EM wave propag. 0-83666  
 low-loss dielectric tube leaky waveguide, transmission characts. 0-95999



**waveguide theory continued**

- plasma heating, lower hybrid waves, backscatter, effect of waveguide boundary conditions 0-64709  
 radially inhomogeneous waveguide modes, vector wave characts. 0-78960  
 relativistic electron beam in waveguide, slow cyclotron waves 0-106983  
 relativistic free-electron wave generators, electrically pumped 0-91742

**waveguides**

- see also *acoustic waveguides; circular waveguides; dielectric-loaded waveguides; dielectric waveguides; optical waveguides; plasma filled waveguides; rectangular waveguides*  
 conference, IR and MM waves and appls., Miami Beach, USA (Dec. 1979) 0-57009  
 fibre reinforced composite waveguides, axisymm. elastic vibrs. 0-102995  
 X-ray, planar, self-imaging 0-57443  
 Cr, film, trivalent, cathodic deposition, as bonding interface between Cu and polyethylene, dielec. lined mm waveguide appl. 0-76201

**WAVES**

- see also *charge density waves; elastic waves; electromagnetic waves; gravitational waves; gravity waves; liquid waves; magnetohydrodynamic waves; magnetostatic waves; ocean waves; oscillations; plasma waves; spin density waves; spin waves; surface waves (fluid); wave propagation*  
 annual review of fluid dynamic, book 0-94927  
 approximate solution in gasdynamics 0-92174  
 atmosphere, large-scale wave transport of stratospheric O<sub>3</sub> to Pacific Ocean 0-72600  
 atmosphere, mean motion induced by transient inertio-gravity waves 0-105029  
 atmosphere, planetary wave heat and momentum fluxes rel. to stratosphere and mesosphere meridional circulations 0-109219  
 atmosphere, upper westerly waves interaction with intertropical convergence zone rel. to Zambian weather during rainy season 0-90175  
 atmosphere features of topographic wave clouds in central and northern Urals 0-101413  
 atmosphere general circulation, eqns. of kinetic and available pot. energy evolution in wave-number freq. space 0-109227  
 autowave processes in distributed kinetic systems, review 0-101721  
 backwash vortex under waves running up sloping bed 0-100001  
 bubble collapse in liquid, pressure wave, nonequilib. vapour condensation effects 0-59060  
 channel, constant depth, wave field from uniform movement bidimensional source (French) 0-79332  
 closed tube, nonlinear resonant acoustic oscillators, finite rate theory 0-92171  
 combined convection flow along vertical surface, fluctuating boundary layers 0-96254  
 conduit with variable gradient, rapidly flowing incompressible liquid, short waves 0-92219  
 deep water waves, instabilities, review, book contrib. 0-96274  
 density waves in galaxies, energy and lifetime rel. to galaxies classification and spiral struct. 0-98715  
 divergent duct, vortex flow breakdown, group vel. criterion 0-87807  
 ducts, one-dimensional models for transient gas-liquid flows 0-64614  
 finite amplitude wave propagation in nearly parallel flow 0-74899  
 finite depth stratified fluids, internal wave solitons, infinite depth limit 0-64574  
 galaxies, spiral, non-linear corrugation waves numerical computations 0-67859  
 galaxies discs, spiral waves nonlinear interaction with stars near corotation radius (Russian) 0-62289  
 geophysical fluid dynamics theory, book 0-105443  
 head on collisions between two solitary waves 0-87780  
 hydrodynamic wave excitation at tangential discontinuity by high-intensity US beams 0-58851  
 ice-water interface, wave formation, heat transfer in presence of turbulent flow 0-103015  
 inclined surfaces, wave instability of laminar mixed convection flow 0-69837  
 incompressible stably stratified fluid, internal waves, Brunt-Vaisala freq. 0-79343  
 interstellar medium, wave-wave interactions in rotating gravitating gas cloud 0-105154  
 inverse scattering solution for three dimens. three-wave resonant interaction 0-77633  
 Kelvin-Helmholtz wave, large amplitude, in atmosphere, struct. determ. from altocumulus billows 0-72621  
 Mach reflection of solitary wave 0-79340  
 Mandel'shtam and nonlinear oscillations and wave theory, review 0-105515  
 mesosphere, Southern hemisphere, wind speed quasi 2-day wave obs. 0-109207  
 MHD, generalised polar diagrams of plane-parallel stationary similarity flows, waves 0-96314  
 multistable self-wave media 0-86094  
 nonlinear interaction of two waves in boundary-layer flows 0-59016  
 nonlinear wave resistance theories for 2-dimens. press. distrib. 0-87781  
 normal mode linear initialisation on sphere 0-77042  
 periodic solution above level bottom 0-57099  
 plane periodic waves, nonlinear propagation in relaxing gas, numerical anal. 0-92170  
 plane wave-plane shock interaction in magnetofluidynamics 0-69931  
 planetary wave, radiatively damped, in middle atmosphere, interaction with zonally averaged circulation 0-109217  
 pneumatic wave-energy convertor, performance study (Russian) 0-76600  
 quasi-standing-wave phenomenon due to oscillating internal flow, vortices in shear layer 0-106809  
 rectilinear rarefaction waves, systems of first-order quasi-linear hyperbolic equations 0-90679  
 self-gravitating fluid column, modulational instability 0-85848  
 semi-infinite body, two-dimensional linear and nonlinear stern waves, separation point 0-69852  
 solar five-minute oscillations, horizontal energy flows struct. 0-62103  
 solar photosphere, waves and convective motions determ. from spectral lines asymmetry (Russian) 0-72901  
 solar wind, long-period waves upstream from Earth bow shock rel. to wind deceleration 0-98528  
 standing waves on hollow core vortices 0-106807  
 steady rotating flow over topography, steady  $\beta$ -plane channel, quasi-linear theory 0-92159  
 steam generator tubes, forced and natural circulation, inception condition correlations 0-74868

**waves continued**

- stratosphere, effect of planetary waves on Lagrangian motion of air parcels 0-109215  
 stratosphere, travelling planetary waves 0-105030  
 stratosphere, zonal mean winds vars. rel. to planetary wave props. and links with troposphere 0-109225  
 thermosphere, winter, evidence for long wavelength propagating tidal modes in S. hemisphere meteor region 0-109287  
 three-wave decay interaction, steady-state turbulence spectrum 0-96249  
 tropical middle atmosphere, wave/zonal flow interaction rel. to semiannual oscillation 0-109216  
 two-phase stratified horizontal flow, averaged and local instantaneous formulations, stability 0-64613  
 viscous fluids with hidden variables and hyperbolic systems, exceptional waves 0-103037  
 weak nonlinear waves in compressible fluid, higher order approx. 0-92165  
 Weddell Sea, planetary wave modes rel. to bottom water variability 0-67366
- waxes**  
 blooming of rubber 0-104109  
 Parowax, thermal energy storage, phase change material, time variation of storage and release 0-67008  
 polyethylene-paraffin wax, blends, rapid cooling processing techniques 0-84905
- waxing** see *polishing*
- weak ferromagnetism**  
 see also *canted spin arrangements; Morin temperature*  
 antiferromagnet, rhombohedral, spin-reorientation phase transition (Russian) 0-93122  
 collective excitations in transverse mag. field, AFMR spectrum 0-93100  
 copper formate tetrahydrate, antiferromag. phase, neutron diff. study 0-93085  
 dipropylammonium manganese tetrachloride, two-dimens. weak ferromagnet, AC susceptibility 0-65823  
 domain wall dynamics, nonlinear waves, mag. solitons (Russian) 0-75793  
 Landau-Lifshitz eqn. solutions, moving domain walls, struct. (Russian) 0-100596  
 manganese stearate, two-dimensional mag. struct. 0-108040  
 uniaxial ferromagnet, with easy plane anisotropy correl. functions and magnetisation, temp. depend. (Russian) 0-84581  
 BaMn<sub>0.99</sub>Co<sub>0.01</sub>F<sub>4</sub>, magnetoelec. phenomena, dielec. behaviour near Neel temp. 0-71151  
 BaO-Mn<sub>2</sub>O<sub>3</sub>-B<sub>2</sub>O<sub>3</sub>, amorphous mag. oxide, field-cooling effect (Japanese) 0-84615  
 CoCO<sub>3</sub>, weakly ferromag., light absorpt. dichroism and mag. config. 0-66223  
 Cu<sub>2</sub>S,  $1 \leq x \leq 2$ , quantum temp. size effect and magnetism (Russian) 0-103764  
 DyFeO<sub>3</sub>, spin reorientation transitions induced by magnetic fields, Mossbauer study 0-71246  
 DyFeO<sub>3</sub>, weak ferromagnet,  $\mu$ SR study 0-93226  
 ErFeO<sub>3</sub>, weak ferromagnet,  $\mu$ SR study 0-93226  
 FeBO<sub>3</sub>, spin-reorientation phase transition (Russian) 0-93122  
 Fe<sub>2</sub>BO<sub>6</sub>, Faraday rotation and birefringence 0-100650  
 Fe<sub>2</sub>Pd<sub>82-x</sub>Si<sub>18</sub> metallic glass, mag. transitions, weak ferromagnetism 0-100583  
 FeTh<sub>2</sub>S<sub>8</sub>, mag. struct. and props., neutron diff. and mag. meas. 0-60201  
 MnB<sub>2</sub>, polycryst., magnetoresist. and mag. props. (Russian) 0-92907  
 $\alpha$ -Na<sub>3</sub>Fe<sub>2</sub>(PO<sub>4</sub>)<sub>3</sub> orthophosphate, cryst. and vitreous, Mossbauer spectroscopy and mag. susceptibility (French) 0-80657  
 NiS<sub>2</sub>, weak ferro- and antiferromag., magnetisation and neutron diff. meas. 0-65794  
 TiBe<sub>1.8</sub>Cu<sub>0.2</sub>, ferromag., magnetisation density 0-103817  
 TiFe<sub>2</sub>Co<sub>1-x</sub>, thermal expansion and magnetoelastic effects 0-80585
- weak interactions, elementary particle** see *elementary particle weak interactions*
- weapons**  
 LMFBR fuel cycles that reduce nuclear weapon material proliferation 0-106105  
<sup>235</sup>U, recovery from enrichment plant tailings by laser isotope separation, non-proliferation of nuclear weapons aspects 0-83212
- WEAR**  
 see also *abrasion; hardness*  
 abraded surfaces, topography rel. to contact area and abrasion mechanism 0-58986  
 brass,  $\alpha$ - $\beta$  phase transformation caused by friction 0-76378  
 brass, comparison of liquid impact erosion and cavitation erosion 0-104302  
 built-up edge form., direct SEM obs. 0-104303  
 cast Fe (3% C), erosion in cavitating venturi 0-108602  
 cavitation corrosion of materials in molten metals on const. mag. field appl. (Russian) 0-60987  
 ceramics and brittle solids, abrasive wear, role of plastic deform. and fracture 0-108594  
 composite friction and bearing materials, development, friction and wear theory, review 0-60979  
 composite materials, water lubrication, wear studies 0-60984  
 conference, Dearborn, MI, USA (April 1979) 0-105426  
 contact, frictionally heated, thermoelastic deform. 0-83764  
 contact platform effect, roughness, friction and wear 0-64497  
 cutting tools, diffusive wear, mag. field effect 0-60985  
 dry sliding wear, role of dynamic recrystallisation 0-108599  
 elastic half-space, with crack inside, determ. of stress intensification factors 0-99964  
 elastomeric bearings, high-capacity, laminated, finite-element anal. 0-96197  
 elastomeric materials, friction testing using reciprocating friction and wear tester 0-76451  
 entropy production model 0-74815  
 epoxy resin, stresses arising during high-speed droplet impact 0-71764  
 fluorocarbon polymer thin films for lubrication of Au contact surfaces 0-89157  
 fretting wear, slip amplitude effects (Japanese) 0-96237  
 friction and wear, material aspects in manufacturing processes 0-81210  
 glasses, high vol. low cost, as solar reflectors, compositions and weathering effects 0-106589  
 graphite, sliding against C, dusting wear regime 0-97595  
 graphite dispersed Al-Si, wear characts. (Korean) 0-93658  
 grinding wheel life modelling, group method of data handling 0-58987

## wear continued

hard alloy insert jig brushes, wear resist. (*Russian*) 0-60977  
 holographic technique with computer aided anal. for wear meas. 0-87345  
 hydraulic liquids, cavitation-erosion props. assessment using ultrasonic dis-  
 pergator 0-71832  
 ion-implanted alloys, surface props. effects and appls. 0-79824  
 lubricant wear debris examination, oil anal. techniques, appl. to plain  
 bearing materials study 0-97596  
 lubricated, contrib. to theory 0-88257  
 magnesite-dolomite refractories, tar bound, fracture and wear 0-104287  
 materials under melting, intensity calc. 0-103416  
 metal, ductile, jet-impingement solid-particle erosion testing, halo effect  
 0-76376  
 metal surfaces, factors influencing contact behaviour 0-92092  
 metallic wear debris, morphological anal. 0-76453  
 noble metals (Ru, Rh, Pd, A, Re, Os, Ir, Pt, Au), wear coefficients  
 determ. using pin-on-disc apparatus 0-76366  
 non-magnetic material wear in presence of magnetic field 0-60982  
 periclase refractories, props. after testing at over 2000°C 0-104317  
 polyethylene-glass fibre composites, gamma-irradiated filler 0-66840  
 polymer-metal sliding, wear eqn. in terms of fatigue and topography of  
 sliding surfaces 0-108597  
 prosthesis wear, holographic studies using optical contouring 0-67288  
 PTFE, wear, sliding speed, contact press. and rubbing surface temp.  
 0-76372  
 rolls in hot strip mills, contact fatigue failure 0-60950  
 sliding contact, friction, wear, temp. anal. 0-93659  
 spark gap electrodes, erosion characts. 0-103204  
 spark switches, high repetition rate, with Al and brass electrodes, surface  
 ageing 0-106997  
 sputtered refractory carbides, adhesion to metal substrates, improved  
 0-76481  
 steel, alloy, rolling wear study of misaligned cylindrical contacts  
 0-108590  
 steel, alloy, surface quality improvement, thermomech. treatment  
 0-61020  
 steel, austenitic, friction in vacuum of type U8 steel under microshock  
 loading (*Russian*) 0-108583  
 steel, austenitic stainless, unlubricated, friction, wear and microstruct. of  
 types 304, 316 and Nitronic 60 0-108589  
 steel, C, rolling wear study of misaligned cylindrical contacts 0-108590  
 steel, Cr, carburising with high-activity carburiser 0-76412  
 steel, Cr plated, factors influencing durability 0-108643  
 steel, Cr with metastable austenite, wear resist., temp. effect 0-76370  
 steel, friction and wear during hot forging 0-89358  
 steel, high speed tool, wear, effect of magnetisation on tool life 0-89361  
 steel, pearlitic, wear behaviour rel. to basic material props. 0-108592  
 steel, stainless, 316, erosion in cavitating venturi 0-108602  
 steel, stainless, type EP838 ion irradiated, surface structure changes dur-  
 ing post-irradiation heating (*Russian*) 0-75272  
 steel, type Kh12M, rel. between structural inhomogeneity and wear resist.  
 (*Russian*) 0-66672  
 steel, wear characts. of burnished machined surfaces 0-108595  
 steel, wear resistance of low temp. nitriding treatment 0-89357  
 steel (alloy)-TiC (70, 30 wt.%) composite, sintered, wear resist. 0-100815  
 steel jig brushes, wear resist. (*Russian*) 0-60977  
 styli of electrical surface roughness meas. instrums., electron microscopic  
 examination of wear (*German*) 0-101782  
 synthetic diamond drills, improved durability 0-87573  
 systems analysis, and description of wear processes (*German*) 0-103417  
 testing device, cyclic load and temp. var., to 800°C 0-66718  
 thermoelastic transition from line to point contact 0-83768  
 three-body abrasive wear classification, design of new tester 0-108682  
 white cast Fe, abrasive wear 0-108587  
 zinc dialkylidiphosphate surface film, prep. and nature 0-104300  
 Ag, wear under reversed friction, temp. effect 0-108588  
 Ag-Zn, internally oxidized, elec. contact characts., alloying additions effect  
 (*Japanese*) 0-88619  
 Al and Al-Cu(Mg), comparison of liquid impact erosion and cavitation  
 erosion 0-104302  
 Al, erosion by solid particle impingement at normal incidence, SEM obs.  
 0-104304  
 Al, surface deformation and wear track obs. using analytical electron  
 microscope 0-108687  
 Al, wear under reversed friction, temp. effect 0-108588  
 Al-Cu type 2024 alloy, erosion in cavitating venturi 0-108602  
 Al-Cu-Mg (4, 1.5 wt.%), mica dispersed, wear characts. and bearing  
 performance 0-108591  
 Al-Cu(Mg), liquid impact erosion 0-108598  
 Au-plating, additive-free, electronic appls. props. 0-108718  
 C, hard, surface wear characts. 0-108596  
 Cd film, dry lubrication on C steel, tribological behaviour 0-89364  
 Cd, wear under reversed friction, temp. effect 0-108588  
 Co base alloys, unlubricated, adhesive wear study 0-108593  
 Co, single crystal, cavitation erosion, role of twinning 0-107272  
 Cu, erosive wear mechanisms, combined TEM and SEM obs. 0-108601  
 Cu pin against steel ring, dry sliding wear, role of dynamic recrystallisa-  
 tion 0-108599  
 Cu pin-on-disc friction and wear under boundary lubrication, dissolved O<sub>2</sub>  
 effect 0-76365  
 Cu, wear under reversed friction, temp. effect 0-108588  
 Fe, cast, surface temperature effect on dry sliding wear 0-60983  
 Fe, comparison of liquid impact erosion and cavitation erosion 0-104302  
 MgF, polycryst., quartz particle impacts no. effect on erosion in elastic-  
 plastic response regime 0-81209  
 MgO single cryst., impact wear characts. 0-76374  
 MgO single cryst., impact wear damage 0-76375  
 MgO, sintered, refractories, props. after testing at over 2000°C 0-104317  
 Mo-Zr-Ti (0.5, 0.1%), adhesive wear polishing of 25 mm spheres  
 0-89397  
 MoS<sub>2</sub>, solid lubricant, antifriction and elec. props. depend. on oxidation  
 temp., dopant influence 0-108584  
 Na<sub>2</sub>O-CaO-SiO<sub>2</sub> glass, high-vel. liq. impact, oblique impact anomaly  
 0-89329  
 Na<sub>2</sub>O-CaO-SiO<sub>2</sub> glass, hot erosion plastic flow and fracture 0-89354  
 NbSe<sub>2</sub>, solid lubricant, antifriction and elec. props. depend. on oxidation  
 temp., dopant influence 0-108584  
 Ni base alloys, unlubricated, adhesive wear study 0-108593  
 Ni, erosive wear mechanisms, combined TEM and SEM obs. 0-108601  
 SiC, reaction-bonded, impact erosion by ang. Al<sub>2</sub>O<sub>3</sub> particles 0-89362  
 SiC-Si, wear resist., props. under abrasion and corrosion 0-100927

## wear continued

Ti alloys, lubrication by chloroparaffins, friction and wear (*Russian*)  
 0-93657  
 Ti electrodes, RuO<sub>2</sub> coated, corrosion during O evolution rel. to electrode  
 prep. (*French*) 0-76420  
 Ti metal-metal interface, adhesion energy, surface treatment and ion  
 implantation effects 0-107660  
 Ti-Al-V alloy, friction coeff. reduction on injection with TiC particles  
 0-85086  
 TiC, frictional characts. and contact-zone deform. in homogeneity range  
 0-66673  
 (W, Mo)C, hard-facing applications, effect of Mo on struct and hardness  
 of WC 0-108474  
 WS<sub>2</sub>, solid lubricant, antifriction and elec. props. depend. on oxidation  
 temp., dopant influence 0-108584  
 Zn, wear under reversed friction, temp. effect 0-108588

**wear, abrasive** *see abrasion*

**wear resistant coatings**  
 bronze powders, electric-pressure sintering onto cylindrical parts in flu-  
 idised bed 0-100960  
 brush plating, for wear resist. appls. 0-66443  
 diamond coatings, for increased wear resist. 0-76371  
 hard metal powders, electric-pressure sintering onto cylindrical parts in  
 fluidised bed 0-100960  
 Ioncoating process, using field emission systems for corrosion and  
 abrasion protection (*German*) 0-76205  
 IR segmented composite window design 0-106621  
 plasma arc spraying, operating principles and applications (*French*)  
 0-76418  
 plasma sprayed coating consolidation by laser remelting 0-93697  
 Al powders, electric-pressure sintering onto cylindrical parts in fluidised  
 bed 0-100960  
 C diamondlike layers, RF plasma deposited, frictional props. 0-71762  
 Cr plated steel, factors influencing durability 0-108643  
 Cu-Sn industrial bronzes, Sn diffusion in deform. zone influence on wear  
 resistance, friction (*Russian*) 0-108582  
 Fe<sub>2</sub>O<sub>3</sub> films, DC reactively sputtered, for selectively semitransparent pho-  
 to masks, struct., mech. and chem. props. 0-59835  
 TiC coated WC-Co cemented carbides, fracture toughness 0-85046  
 TiC, laser CVD, coating characterisation 0-93494  
 TiN, hard coating on soft Al alloy, tribological anal. 0-108600

**weather** *see meteorology*

**webs (membranes)** *see membranes*

**weighers** *see balances*

**weighing**  
 automatic, application in ceramics industry 0-95074  
 balances with weight and cost read-out (*Polish*) 0-90820  
 electronic weighing system, digital transducer instruments 0-95076  
 free-piston manometer comparison, weight relocation method 0-90831  
 hydrostatic, for porosity determ. of coatings 0-66714  
 hydrostatic, solid density standards 0-77758  
 LPE source materials, weighing method 0-66439  
 mass comparator, high precision, using bonded strain gauge load cell  
 0-57261  
 microweighing in vacuum and controlled environments and use of beam  
 microbalance, book 0-62401  
 SI units fundamentals (*French*) 0-95059  
 thermogravimetry, balance inclination and specimen temp. error sources  
 0-98887

**weighing machines** *see balances*

**weight, atomic** *see atomic mass*

**weight, molecular** *see molecular weight*

**weight indicators** *see balances*

**weight measurement** *see weighing*

**weightlessness experiments** *see zero gravity experiments*

**Weinberg model**  
 Cabibbo angle calcs., mass matrices in Weinberg-Salam model 0-86674  
 D<sub>3</sub> group, 2 values of Cabibbo angle, 4 quark flavours 0-68405  
 electro-weak interactions, neutral currents, W and Z-bosons 0-73638  
 electroweak mixing angle, sequential triplets scheme of fermions 0-86650  
 fermion asymmetry of the Universe and the W condensate, Weinberg  
 Salam model (*Russian*) 0-73087  
 flavor-changing effective neutral-current couplings in the Weinberg-Salam  
 model 0-86649  
 gauge theory, renormalisation of ghost and Goldstone fields and ghost  
 symmetries 0-90987  
 Glashow-Weinberg-Salam model, one-loop corrections to vector boson  
 masses 0-57548  
 heavy Higgs boson decay in Weinberg-Salam model 0-95241  
 Higgs doublets, massless, particle masses, perturbation constraint  
 0-57541  
 Higgs mechanism, unification of weak and EM interactions (*French*)  
 0-77999  
 Higgs-induced neutral processes, natural-flavour conservation, K-  
 symmetries 0-57539  
 high energy lepton pair prod. with pol. hadrons, P and C violations  
 0-99068  
 left-right symmetry and quark-lepton unification extension 0-78002  
 neutrino pair bremsstrahlung and number of lepton generations 0-101978  
 nonleptonic decays, Weinberg-Salam and harmonic oscillator quark model  
 0-102048  
 parity nonconservation in heavy atoms and weak magnetism in neutral  
 currents (*Russian*) 0-82932  
 sin<sup>2</sup>θ<sub>w</sub>, grand unified gauge theories and proton decay 0-73634  
 SU<sub>2</sub>×U<sub>1</sub>×U<sub>1</sub> electroweak model, Weinberg-Salam intermediate bosons  
 0-105831  
 SU(2)<sub>c</sub>×U(1) gauge model, mixing angles and CP violation 0-73648  
 SU(2)<sub>c</sub>×U(1) theory, radiative corrections, simple renormalisation frame-  
 work 0-101973  
 SU(2)<sub>c</sub>×U(1) gauge Weinberg Salam model, lepton number bound  
 0-82927  
 SU(2)<sub>c</sub>×U(1) Weinberg-Salam model, possible classical solns. 0-86644  
 supersymmetric, Lagrangian, invariant under SU(2/1) gauge group and  
 rotations, in 6-D graded space 0-57537  
 torsion potential, coupling strength, experimental bounds 0-73249  
 twistor theory in Weinberg-Salam and Georgi-Glashow SU(5) model  
 0-73651  
 vacuum instability, cosmology and particle mass constraints for Wein-  
 berg-Salam model 0-78007



**Weinberg model continued**

- weak neutral currents unveiled 0-73658  
 $e^+e^-$ ,  $SU_L(2) \times U(1)$  and  $SU_L(2) \times SU_R(2) \times U(1)$  predictions at high  $Q^2$ , neutral currents, Z-bosons 0-63029  
 $e^+e^-$  annihilation, charged Higgs boson prod. signatures, Weinberg-Salam parametrisation 0-57620  
 $e^+e^- \rightarrow b\bar{b}$ , heavy quark masses and C- and P-odd asymmetries, Weinberg-Salam model (Russian) 0-102060  
 $e^+e^- \rightarrow \mu^+\mu^-$ , radiative corrections around  $Z^0$ , Weinberg-Salam model 0-99103  
 $e^+e^- \rightarrow q\bar{q}g$ , gluon bremsstrahlung, neutral current and beam polarisation effects 0-99106  
eN, deep inelastic scatt., heavy lepton mixings, Weinberg-Salam model 0-82992  
eN  $\rightarrow eX$ ,  $SU_L(2) \times U(1)$  gauge theory distinguished from  $SU_L(2) \times SU_R(2) \times U(1)$ , neutral currents, z-bosons 0-62908  
eN elastic scatt., pol. e, nucleon form factors, P violating symmetry, Weinberg-Salam calcs. 0-68461  
 $\gamma$  circular polarisation, neutral current effect in bremsstrahlung and pair production 0-73655  
 $\gamma \rightarrow$  lepton pair, P violating asymmetry 0-105901  
 $K \rightarrow \pi\mu\mu$ ,  $\mu$  polarisation and T-odd correlations, Weinberg model of CP violation (Russian) 0-62969  
 $\mu$ -e mass quotient, modified Weinberg-Salam model calcs. (French) 0-82926  
 $\mu$ N, deep inelastic scatt., heavy lepton mixings, Weinberg-Salam model 0-62992  
NNp couplings, parity-violating, QCD and MIT bag model,  $1/2^-$  resonance contribs.,  $SU(6)_s$  symmetry 0-57540  
 $\nu$  EM form factors and mag. moments, neutral currents, astrophysics applies. (German) 0-62904  
 $\bar{z}$ e annihilation in Weinberg-Salam model, number of quarks and leptons (Russian) 0-102041  
 $\nu \rightarrow \mu^+\mu^-$ , Higgs boson exchange effects on second-class currents 0-91075  
 $\nu \rightarrow \mu^+\mu^-$ ,  $SU_L(2) \times U(1)$  gauge theory distinguished from  $SU_L(2) \times SU_R(2) \times U(1)$ , neutral currents, z-bosons 0-62908  
 $\bar{\nu}p \rightarrow \mu^+n$ , Higgs boson exchange effects on second-class currents 0-91075  
 $\bar{\nu}p$ ,  $\bar{\nu}p$ ,  $SU_L(2) \times U(1)$  and  $SU_L(2) \times SU_R(2) \times U(1)$  predictions at high  $Q^2$ , neutral currents, Z-bosons 0-63029  
 $\bar{\nu}p \rightarrow e^+e^-$  annihilation, weak neutral current effects (Russian) 0-105837  
 $\bar{\nu}p$  scatt.,  $<300$  MeV P-odd asymmetry for pol.  $\rho$  (Russian) 0-102063  
 $\Sigma^+ \rightarrow p\gamma$ ,  $1/2^-$  resonance poles to parity-violating amplitude, two-quark weak transitions 0-78062  
 $W$ -production via Z-decay in Weinberg-Salam model 0-101979  
 $^2H(\gamma,n)p$ , parity violation expts. review, weak NN interaction 0-73792  
 $^4He$  production, nonzero neutrino rest mass effects 0-105413

**Weissenberg cameras** see cameras; X-ray crystallography apparatus**welding**

- see also electric welding; electron beam welding; laser beam welding; lead bonding; ultrasonic welding  
austenitic welds, US inspection 0-71821  
cellular and cellular dendritic growth, general microsegregation eqn. 0-84921  
Colmonoy, self-weldability in high temp Na (Japanese) 0-89392  
fusion reactor vacuum vessel welds, ultrasonic scanner 0-99288  
impact welding, wavy interface characts. and formation 0-97680  
impact welding process, fundamental parameters 0-97679  
inspection system for Space Shuttle external fuel tank, automatic, interim report 0-76463  
joints, radiographic inspection, real flaws detectability evaluation 0-81266  
metal, diffusion welding, migration of oriented intergranular boundary with pores (Russian) 0-84943  
metal strips, welded, aged, reduction of deformations (Russian) 0-97508  
multipass welds, high temp. internal deformations development and effects on crack formation 0-81082  
permanent joining techniques 0-82782  
pipes, welded branch, stresses calc. 0-108493  
residual stresses, evaluation by Barkhausen noise meas. 0-76436  
steel, alloy, sheet, crack-propag. resist. in heat-affected zone in presence of  $H_2$ , rolling direction and preliminary plastic tensile strain effects 0-60971  
steel, alloy 10G2S1 welds, fracture, subjected to low-temp. fatigue 0-89350  
steel, austenitic stainless, liquation cracking during welding, comp. influence 0-66645  
steel, Cr-Mo weld metal, reheat cracking, residual elements and microstruct. influence 0-66553  
steel, Cr-Mo weld metal, trace element embrittlement suppression by creep strength effects 0-66656  
steel, Cr-Mo-V low-alloy, mech. props. and stress relief cracking, effects of impurities and deoxidation practice 0-66599  
steel, low alloy, high strength, fatigue crack growth, in presence of welding residual stresses (Russian) 0-71739  
steel, low alloy-high strength, deforms. during cold crack developments in welded joints 0-81142  
steel, stainless, austenitic, explosively welded, orientation relationship in martensitic transform. 0-104158  
steel, stainless, Cr-(Mo)-(Ni), self-weldability in high temp Na (Japanese) 0-89392  
Stellite, self-weldability in high temp Na (Japanese) 0-89392  
stress measuring device design and application 0-68194  
TEM, welded crystals, grain boundaries in Si 0-103364  
ultrasonic and eddy current testing of welded titanium tubes (Japanese) 0-108651  
ultrasonic inspection, welded joints in sugar extraction diffusion apparatus 0-93703  
US testing of austenitic welds, metallurgical noise reduction 0-76466  
US weld inspections with freq. scanned SH waves 0-76465  
Zircaloy-4, resistance-welded, microstruct. of weld region 0-66549  
Al-Mg (2.5wt.%) sheet, surface oxide state and weldability 0-59769  
Cu-mild steel explosively welded interface, SEM examination (German, English) 0-96746  
Ni alloys, liquation cracking during welding, comp. influence 0-66645  
Ni, diffusion welding, migration of oriented intergranular boundary with pores (Russian) 0-84943  
Ni-Cr, self-weldability in high temp Na (Japanese) 0-89392  
Ti-Al-V (6.4 wt.%), microstruct. effect of base metals on diffusion welding (Japanese) 0-89296

**welding electrodes**

- coated arc electrodes, identification of types and brands using SEM with energy-dispersive X-ray detector 0-81400  
manual metal arc electrode constitution effect on AISI 316 weld metal mech. props. 0-66601

**Wentzel-Kramers-Brillouin calculations** see WKB calculations**Wertheim effect** see Wiedemann effect**wetting**

- capillary flow, initial stage analysis, relax. model 0-74977  
cemented carbides, physical and chem. nature 0-76265  
drop spreading on solid surface, initial stage charact. 0-59761  
E-glass textile filaments, wetting characts. 0-80030  
fibre reinforced polymer, soaking, wetting and compounding of materials during production (German) 0-93535  
film boiling, effect of adsorption characts. on minimum temp. 0-79114  
horizontal crystal ribbon growth, meniscus stability 0-103281  
manometers, liq., sensitivity, wetting hysteresis effect 0-98926  
periodic capillary tube, two phase fluid flow and hysteresis 0-107615  
periodic capillary tube, two phase fluid flow and hysteresis 0-107616  
quartz, dynamic wetting angle of dry lyophilic surface 0-88405  
solid-liquid interface, wetting and adhesion, thermodynamic aspects 0-89525  
 $Al_2O_3$ , wetting by Cu-Ti ternary alloys 0-107617  
 $B_4C$ , reaction kinetics with liq. Al, Si, Ni and Fe 0-84344  
Cu-Sn binary system, wettability and interaction between solids and liqs. (Japanese) 0-92760  
GaAs, surface wetting with Hg, doping degree influence 0-92762  
 $LaB_6$ -Cu, form. by wetting of  $LaB_6$  with Cu 0-100813  
 $Na_2O$ -CaO glass, wettability, effect of cleaning procedures 0-65336  
Sn-Pb solder, wettability on Cu and mild steel plates (Japanese) 0-89244  
TiC, wetting by Cr-Ni-Mo-Mn alloy steel, expt. planning investigation 0-60822

**whiskers (crystal)**

- film, thermal strain, strain relax. above room temp. 0-59841  
mass transport and assoc. failures 0-59694  
single crystals under large loads, theoretical elastic behaviour, review and appl. 0-71681  
vapour-liquid-solid growth mechanism (Russian) 0-107074  
whisker crystal growth, radial periodic instability mechanism (Russian) 0-107682  
Al, stability and strength of FCC metal using Morse pot. 0-59430  
Bi, excess 1/f noise, 50 to 350K 0-92951  
Bi, persistent metallic behaviour, elec. resist. meas. 0-75544  
Bi-Sb (6 at.%), persistent metallic behaviour, elec. resist. meas. 0-75544  
CdS single cryst., vaporization and form. of negative whiskers 0-92659  
Fe,  $90^\circ$  walls, stable orientations, theory and X-ray observations (Japanese) 0-60359  
Fe, ferromag. domain theory, quasi-dislocation theory appl. (Japanese) 0-60358  
Fe, inverse Wiedemann effect, torsional strain and azimuthal mag. field influence 0-108045  
Fe, magnetoresistance, deviations from Kohler's rule 0-70673  
Fe whisker, magnetisation curve meas. using SQUID system 0-86347  
Fe, whisker single crystals, ferromag. reson. and surface anisotropy 0-71187  
Fe, whiskers,  $H_2$  effect on mech. props. 0-108556  
 $\alpha$ -Fe whiskers, pure, ductile fracture initiation, macroscopic obs. of deform. history and failure 0-85043  
 $\alpha$ -Fe whiskers, pure, ductile fracture, microscopic obs. of initiation mechanism 0-85044  
Ga whisker growth from GaN/Ga layered films 0-92800  
GaAs ribbon whiskers, photopumped, laser action 0-91801  
GaAs, vapor-phase etching, mechanisms and kinetics 0-100934  
GaAs:Zn optically pumped ribbon-whisker laser, picosecond pulses 0-99771  
GaN, photoluminesc. spectra, energy distrib. 0-97339  
GaP, vapor-phase etching, mechanisms and kinetics 0-100934  
In whiskers from Sn-In alloys, current carrying, superconductivity breakdown 0-60133  
Pb, third-order elastic const. combinations 0-92585  
PbTe single crystals, growth from vapour phase under micro-gravity conditions 0-80957  
SiC microtubes, formation by carburisation of Si whiskers 0-81011  
TiC, TF electron emitters props. obs. 0-66403  
TiN(C) whisker growth in CVD 0-59843  
W needle crystal growth, discharge-induced decomp. of hexacarbonyltungsten mols. 0-84414  
ZrN(C) whisker growth in CVD 0-59843

**whistlers**

- see also ionospheric electromagnetic wave propagation; magnetospheric electromagnetic wave propagation  
Alfven wave turbulence, interaction with whistler wave turbulence 0-64728  
auroral hiss, nearly reson. whistler amplified Cherenkov radiation, limitations 0-101482  
banded struct. origin, on refl. from ionosphere 0-101476  
coherent nonlinear interaction dependent on wave amplitude 0-72715  
coherent VLF signal injection into magnetosphere, threshold power for growth 0-101496  
deuteron trans-equatorial whistlers, in topside ionosphere 0-77203  
dipole antenna in magnetoactive plasma EM field distrib. 0-100079  
ducting in plasmasphere, ray-trace study 0-72704  
electron plasma oscillation bursts correl. with whistlers 0-72703  
equator obs. confirming that whistlers do not propagate to Earth surface 0-77216  
low latitude whistlers, lower and upper freq. cut-off explanation 0-82131  
low-latitude coordinate observation system using direction finder and real-time analyser 0-67479  
low-latitude propagation limit 0-82152  
lower oblique whistler resonance cone, interference struct. in Maxwellian magnetoplasma 0-59219  
magnetic storm low-latitude whistlers, for magnetosphere elec. field 0-85817  
magnetosphere, whistler duct struct. and formation 0-94659  
magnetospheric plasma, whistler propagation 0-90294  
pararesonance (PR) whistlers, features 0-67455  
precursor emissions, newly observed monochromatic precursor starts 0-85809  
propagation in magnetoplasma, interpretation of 6-component measurements 0-83921

**whistlers continued**

- rays and foci in a magneto-ionic medium with linearly varying magnetic field, theory 0-105135
- side-band mutual interaction of whistler-mode waves 0-82148
- VLF radiation during simultaneous magnetospheric substorm and thunderstorm, rel. to elec. fields and electron precip. 0-67392
- VLF waves triggered by natural whistlers 0-98521
- VLF whistler obs. of radial plasma drift and coupling to ionosphere 0-77239

**white dwarfs**

- 2A 0311-227, AM Herculis type binary star, IR photometry and polarimetry 0-77517
- 2A 0311-227, AM Herculis type X-ray binary, optical counterpart, radial vel. obs. 0-94890
- 2A 0311-227, optical counterpart, AM Herculis type eclipsing binary, V-band obs. 0-101617
- 2A 0311-227 optical counterpart, binary star, light curve Fourier anal. 0-82549
- 2A 0311-227 optical counterpart, simultaneous photometric and spectroscopic obs. 0-90572
- 2A 0526-328, optical counterpart, eclipsing binary, visible emission line variability 0-73075
- Abell 46, planetary nebula, eclipsing binary nucleus, hot component UV continuum obs. by IUE 0-98693
- R Aquarii (M7+pec), white dwarf component identification from IUE obs. of circumstellar emission 0-82370
- atmosphere structure rel. to composition in hot stars 0-98658
- binary star, white dwarf outer layer C and O enrichment from companion 0-109465
- binary stars, rapid mass accretion on to white dwarfs and extended envelope form. 0-67723
- in binary systems, accretion disk flux distrib. and colours 0-94778
- in binary systems, surface nucl. reactions and origin of mag. fields 0-101616
- $\zeta$  Capricorni, Ba star, white dwarf+giant, UV spectra obs. 0-105284
- OY Carinae, white dwarf cataclysmic, eclipsing binary, parameter determ. 0-82385
- ZZ Ceti stars, constraints on possible long-term variability 0-90428
- Z Chamaeleontis, eruptive binary, model from photoelectric data anal. 0-72961
- conservation of energy equation from scale covariant gravitation theory 0-73216
- coronae, low-temperature, contrib. to EUV background 0-62324
- SS Cygni, dwarf nova, white dwarf mass from rapid optical oscils. obs. 0-85947
- DA stars, H I Balmer  $\gamma$  line profiles and masses 0-77399
- degenerate cores, thermomagnetic instability conditions 0-77395
- degenerate relativistic electron gas, electron collisions, thermal conductivity 0-109355
- degenerate star surface, slow deflagration front stability 0-67729
- degenerate star-red giant interacting binary stars, compressible fluid flow, accretion 0-67779
- 40 Eridani B, no X-ray or 4885 MHz image 0-105282
- faint blue stars, southern, UVB photometry 0-82349
- formation, effects of stellar mass loss 0-77281
- G128-7, cool DA white dwarf, atmospheric parameters and evolutionary consequences 0-62126
- G 165-7, metallic line white dwarf, model atm. code anal. of spectrum 0-85940
- H 2252-035, spectrophotometry, no periodic linear polarization (1980 Sept.) 0-105401
- H 2252-035, X-ray flux modulation, compact star rotation 0-101652
- H 2252-035 cataclysmic variable, white dwarf rot. period from photometry and spectrum 0-101651
- $\phi$  Herculis, Hg-Mn star, corona search, UV obs. 0-72986
- AM Herculis, visual magnitude estimates (1980 March-June) 0-82428
- AM Herculis (3U 1809+50), polarimetry and spectrophotometry rel. to mag. field 0-94835
- AM Herculis (3U 1809+50), UV spectrum obs. 0-67782
- AM Herculis (4U 1814+50), X-ray emitting mag. white dwarf binary, review of props. 0-105403
- DQ Herculis (Nova 1934), white dwarf rot. period rel. to nova remnant shape 0-105244
- hot white dwarfs, luminosity function, spectral type anal. 0-90418
- HR-diagram and luminosity function determ. (Chinese) 0-77403
- HZ 43, He abundance and stellar struct. from soft X-ray spectra 0-72944
- LP 145-141, C<sub>2</sub> white dwarf, spectrum, strong UV absorpt. obs. by IUE 0-67715
- luminosity function, of Population I white dwarfs in SA 51, SA 57 and (SA 68) 0-98648
- magnetic DA white dwarfs, spectral line and circular polarisation profiles 0-62123
- magnetic white dwarfs, unexplained spectral features theory 0-82187
- magnetised, accretion, role of electron conduction 0-82358
- mass, main sequence star max. mass for white dwarf evolutionary stage 0-105237
- mass-accreting white dwarfs, evolution 0-77281
- novae, effect of binary companion on outburst 0-82394
- novae, effects of white dwarf rot. on remnants shapes 0-105244
- one-component plasma, crystallized, dynamics and energy, self-consistent-phonon theory 0-107384
- oscillations, junction conditions across perturbed contact discontinuities 0-94787
- planetary nebulae nuclei, temps. rel. to masses and nebulae evolution 0-82344
- VV Puppis, AM Herculis type binary, optical absorpt. spectrum, cyclotron interpretation and models 0-73003
- radial oscill. mode of hot white dwarf, nonlinear calc. 0-67713
- review, structure and evolution, luminosities, spectra and non-radial oscils. 0-82356
- Ross 640, He-rich star, C, Mg, S and Fe abundances from UV spectra 0-94790
- WZ Sagittae, eruptive binary, model from hot spot eclipses anal. 0-72962
- spectra of magnetic dense stars, theoretical anal. of atomic spectra 0-105160
- stability, of white dwarfs undergoing spherically symmetric steady-state accretion 0-77402

**white dwarfs continued**

- supernova, type I, explosions, contrary evidence from radial distrib. in spiral and elliptical galaxies 0-62163
- surface accretion, C enhancement mechanism for fast nova occurrence 0-85936
- symbiotic stars, accretion rates rel. to subclasses 0-62144
- XUV emission, possibility of detect. (German) 0-109372
- C-O white dwarfs, C-O eutectic model 0-77405
- He flash and nova evolution 0-72938
- He rich stars, intermediate and extreme, spectral atlas in 3700 to 4600 Å range 0-94806

**white noise**

- function, distorted by noise, resolution into sum of exponentials 0-77707
- Markov fields and local operators, difference between Gaussian and Poisson white noise 0-57186
- nematics, EHD instabilities, white noise effect 0-70115
- nonlinear second order system, eigenfunction expansion solutions of Fokker-Planck eqn. 0-73172
- stellar spectroscopy, linear filtering theory for case of white noise (Italian) 0-90340
- stochastic stability of dynamic multi-nonlinearity systems, action of white noise 0-68135

**wideband amplifiers**

- stochastic beam cooling expts., low-noise wide-band power amplifier system 0-58011

**Widmanstätten structure**

- stability principle for plate growth 0-84939
- steel, alloy type, photoemission electron microscope obs. of high temp. precip. behaviour 0-108456
- steel, medium C, Ni-Cr-Mo, overheated, fractographic study (Chinese) 0-66616
- steel, V, precip. and transform. kinetics, effect of N 0-97485
- Zircaloy-2, hot-pressed, influence of diffused C on structure and oxidation 0-61016
- Zircaloy-4, resistance-welded, microstruct. of weld region 0-66549
- Fe-Ni meteorite, STEM/X-ray microanalysis across  $\alpha/\gamma$  interface 0-105212
- $\alpha$ - $\beta$  Ti alloy interfaces, elastic interact. stresses, effect on plastic flow onset 0-104218
- Ti-Al-Mo-V (8, 1, 1 wt.%), Widmanstätten colonies, fracture toughness 0-85031
- Ti-Al-V (6.4 wt.%) cast alloy, with improved microstruct., mech. props. (Japanese) 0-71701
- Zr-Al (8.6 wt.%), dimensional stability struct. and mech. props, effects of neutron irradi. 0-92563

**Wiedemann effect**

- Fe whiskers, inverse Wiedemann effect, torsional strain and azimuthal mag. field influence 0-108045

**Wiedemann-Franz law** *see* Lorenz number**Wien effect**

- No entries

**Wigner coefficients** *see* Clebsch-Gordan coefficients**Wigner crystal**

- electron gas, diamagnetism and surface currents 0-88496
- electron gas, Wigner distribution for cylindrically symmetric system 0-65475
- electrostatic energy, Fuchs calc. 0-79743
- electrostatic energy, Fuchs method, Wigner solids and Coulomb lattices, theory 0-79745
- electrostatic energy, Fuchs method 0-79744
- one-component plasma model, crystallised, dynamics 0-107384
- two-dimensional, melting temp., quantum effects 0-88491
- two-dimensional, melting temp. in strong mag. fields, quantum effects 0-88492
- two-dimensional, phonon coupling with second surface sound in liq. He (Russian) 0-92756
- EuTe, magnetic impurity states, mag. and transport props. 0-96913
- GaAs-Al<sub>0.1</sub>Ga<sub>0.9</sub>As multilayers, two-dimens. transport at high mag. fields 0-65724
- Gd<sub>3-x</sub>□<sub>x</sub>S<sub>4</sub>, transport and mag. props., mag. Wigner localisation 0-97069
- He, liq., surface, two-dimens. Wigner cryst., electron-ripplon reson. anomalies (Russian) 0-92754
- Si inversion layers, phase diagram in strong mag. fields 0-88492

**Wigner effect** *see* radiation effects**Wigner lattice** *see* Wigner crystal**Wilson cloud chambers** *see* cloud chambers**wind**

- acoustic noise, wind-generated noise produced by implant of spray with ocean surface 0-106655
- air composition at Barrow, Alaska, influenced by wind direction 0-85704
- airflow over bell-shaped mountain, cloud model 0-77049
- airflow turbulent kinetic energy, budgets in mountainous terrain 0-105022
- Antarctica, wind struct. up to 80 km altitude 0-81992
- N.Atlantic easterly gales, 1881-1970 period 0-77101
- atmosphere surface layer, features of organised motion rel. to local wind vel. 0-72602
- auroral oval, dayside, neutral wind profiles obs. between 115 and 175 km altitude 0-98494
- baroclinic waves, influence of static stability and wind shear time changes 0-109226
- W.Bay of Bengal, 1978 southwest monsoon effects. on wave characts. 0-109152
- Bear River Range, north-central Utah, wind direction rel. to cirque characts. 0-72510
- Beaufort Sea, winds and surface temps. rel. to August ice cover vars. 0-101366
- S.Benguela Current, upwelling site, wind effects and biology 0-104987
- blocking of mid latitude westerly winds by planetary waves 0-105036
- boundary layer, bulk model for wind and pot. temp. 0-77030
- boundary layer, lateral coherence of isotropic turbulence and wind 0-72575
- boundary layer at nighttime, vertical struct. obs. 0-61848
- boundary layer jetlike wind over open coast, mesoscale nocturnal phenomena 0-81971
- boundary layer measurement system, for wind and temp. struct. (German) 0-94616
- boundary layer wind shear hazard, radar detection feasibility 0-90256



## wind continued

- breeze characteristics, statistical model 0-85737
- cloud motion fully automated method, Meteostat data comparison with gradient winds 0-109244
- cloud winds over oceans, satellite obs. technique 0-85764
- Coningsby, Lincolnshire, surface wind assoc. with snow rollers form. (1979 January 2) 0-72568
- cumulus cloud motion as indication of air flow vel. 0-98418
- cumulus congestus cloud unmixed updraught cores, ice initiation 0-81997
- diabatic surface layer, wind prediction model 0-77032
- direction determ. from rime deposits 0-98428
- direction meas., wind vane motion 0-90264
- direction meas. with vane, graphic recording and averaging 0-82098
- dispersing plume, crosswind geometry, second-order reaction 0-61480
- dispersion expts. in Sydney region using SF<sub>6</sub> as tracer 0-67389
- double theodolite measurement of wind speed and direction, control of inherent uncertainties 0-77160
- dry snow and bare ice surface, interaction with wind 0-109181
- dual Doppler radar and vel. azimuth display of subsynoptic-scale vertical wind 0-109263
- dual-Doppler radar measurement, coverage area as function of meas. accuracy and spatial resolution 0-82093
- dust haze of African Harmattan wind, 1962-1973 visibility obs. 0-61900
- energy, prospecting in Prince Edward Island, programme overview and status report 0-61243
- energy potential in Karnataka State, in India 0-108782
- equatorial mesosphere and stratosphere, vertical vel. determ. from Diurnal Experiment 0-77047
- equatorial stationary zonal circulation, numerical calcs. 0-85732
- equatorial westerlies over E.Africa and Lake Naivasha level changes 0-61819
- F-region, neutral wind during dayside aurora 0-90273
- F-region, neutral zonal winds rel. to interhemispheric ion transport 0-98509
- F-region height neutral air wind, servo model of ionosphere 0-101486
- F-region wind affecting O<sup>+</sup> and H<sup>+</sup> equal ionisation level 0-90280
- geostrophic flow over shallow topography 0-90120
- Gulf Coast, USA, boundary layer speed and direction 0-101404
- Gulf of Alaska, Seasat comparison data set 0-94570
- gust front of thunderstorm, wind shear meas. using pulsed lidar 0-67415
- Harmattan dust deposition, N.Nigeria, rel. to wind speed 0-94578
- hill affecting airflow, in boundary layer, overspeed effect 0-72577
- Himalaya, wind and storms during summer 0-72620
- hurricane dection by Doppler radar for coast of U.S.A. 0-67414
- hurricane season activity analysis, N.Atlantic (1886-1974) 0-101427
- hurricanes in the USA, speed determ. by Monte Carlo method 0-90209
- ionosphere, lower, wind obs. by Kyoto meteor radar 0-67444
- ionosphere vertical wind causing equatorial counter electrojet 0-85795
- jet stream, VHF radar obs. 0-90187
- jet stream and associated O<sub>3</sub> enhancement (*Russian*) 0-94568
- jet stream generation of Kelvin-Helmholtz instability 0-90165
- Lagrangian wind and current vectors very close to short-fetch windswept sea surface 0-72553
- lake circulation models, wind driving 0-85688
- Ligurian Sea continental shelf, wind and current autumnal data series anal. 0-85675
- local climatic wind, use of trees as indicator 0-82007
- longshore pressure gradients caused by offshore wind 0-67370
- lower thermosphere gravity wave obs., 5-90 minute period 0-61930
- mapping for windpower development programme in Sweden 0-61237
- marine atmosphere, climatic comparisons of estimated and measured winds from ships 0-105020
- marine atmosphere, mean wind speeds and turbulence 0-98406
- marine atmosphere, wind vel. rel. to oceanic whitecaps and sea state 0-72554
- mean zonal wind in middle atmosphere, calc. from numerical model of zonal mean circulation 0-109218
- meridional geostrophic wind along 50°N 0-101399
- mesosphere, mag. storm effects at mid-latitudes 0-61970
- mesoscale wind fields, satellite-derived, covariance anal. 0-82013
- mesosphere, Southern hemisphere, wind speed quasi 2-day wave obs. 0-109207
- mesosphere, wind variance rel. to eddy diffusion models 0-109198
- mesosphere zonal wind obs., long-period waves at 60-90 km altitude 0-77056
- meteor region winds, periodic fluctuations of recurrent nature 0-90266
- meteor trail distortion studies 0-85870
- middle atmosphere, VHF radar obs. 0-105032
- Mohliner Feld (east of Basle), influence of wind on topoclimate (*German*) 0-61890
- Mount Kenya, wind speed rel. to condensation nuclei concs. 0-82012
- mountain in airflow, 2-D numerical simulation (*Russian*) 0-81986
- nonuniform shear effect on mountain waves refl. and intensification 0-90127
- North Sea, winds rel. to sea surface temp. year to year changes, (1948 to 1974) 0-67367
- ocean, wind driven currents in inshore region deep water 0-81925
- ocean, wind speed meas. 200 km from land rel. to air-sea heat transfer coeffs. 0-72552
- ocean, wind stress and buoyancy flux effects on continental shelf circulation 0-72540
- ocean, wind vel. rel. to distrib. and steepness of ripples on carrier waves 0-72548
- ocean, wind-induced turbulence energy distrib. rel. to mixed layer evolution (*Russian*) 0-94529
- ocean boundary layer wind flow, determ. from phase speeds of upwind and downwind travelling waves 0-98332
- ocean currents driven by large scale atmos. disturbances 0-109159
- ocean forcing, mixing mechanism in upper ocean, Langmuir circulation instability 0-104970
- ocean interaction, wind-driven equilib. Langmuir circulation model 0-101381
- ocean wave radar monitoring, ground wave and sky wave sensing techniques 0-109256
- offshore wind power model estimates 0-61244
- Orange Lake, Florida, wind vel. fluctuations rel. to lake latent and sensible heat fluxes prediction 0-72562
- orography, influence on atmospheric movement with Coriolis force included (*Russian*) 0-94565
- Pacific Ocean, equatorial, easterly wind stress rel. to 14°C isotherm slope annual var. 0-72537

## wind continued

- Pacific Ocean, wind forcing rel. to oceanic circulation around New Zealand 0-72538
- Peruvian oceanic upwelling system near 15°S, wind obs. 0-101377
- planetary boundary layer, 3-D field obs. width radar 0-90183
- pollutant dispersal, Gaussian plume model parameters for ground-level and elevated sources 0-82010
- pollutants long distance transport, time-averaged wind field for analytical diffusion model 0-94125
- pollution of industrial area, occurrence affected by wind direction 0-89691
- pollution transport, air quality models development for limited wind fetch 0-104533
- pressure field, use in solenoidal wind velocity component, forecast 0-82034
- radar observation of vertical component of lower atmos. wind 0-72642
- radar technique for tropo- and stratosphere wind measurement 0-90257
- Rome, effect of urban heat island on wind flow during summer season 0-85717
- rough terrain mass-consistent flow fields, derivation method using wind obs. 0-105013
- runner's forward motion, effects of wind assistance and resistance 0-101204
- Santorini (Thera) eruption, 1450 BC, evidence for northwesterly winds from tephra discovery at Rhodes 0-109129
- Scotian shelf (N.Atlantic Ocean), wind-induced sea level changes 0-72531
- sea surface drift induced by wind and waves 0-81914
- sea surface reflection of radar signal, spatial intensity fluctuations 0-109170
- sea surface wind speed, retrieval from scanning multichannel microwave radiometer obs. 0-90261
- shear, effect on acoustic backscatter in GATE 0-85709
- shoreline escarpment affecting boundary layer turbulence, wind profile etc. 0-109243
- solenoidal wind velocity component, forecast from known press. field 0-82034
- Somali jet, planetary boundary layer model 0-72591
- speed, freq. distrib. of hourly meas. 0-94554
- speed and direction from automated environmental monitoring system 0-81513
- speed and direction meas., review of cup, propeller and laser anemometers 0-90264
- speed and direction meas., using digital anemograph (*Czech*) 0-77174
- speed in cloudy atm., long distance meas. by radiometry 0-90196
- stochastic predictors of site wind, AR and ARMA models 0-67400
- stratosphere, diurnal variation of wind and temp. in equatorial region 0-82022
- stratosphere, vertical wind shear from Lagrangian wind field obs. 0-82032
- stratosphere, zonal mean winds vars. rel. to planetary wave props. and links with troposphere 0-109225
- stratosphere, zonal wind speed oscils., solar cycle influence 0-94562
- stratosphere, zonal winds effect on Earth rot. 0-81804
- stratosphere wind phenomena affecting troposphere circulation pattern 0-82021
- surface layer wind profile curvature rel. to Richardson number 0-81974
- surface stress estimation, mathematics of vel. scaling parameter 0-61849
- surface wind of Arizona cold season, correl. to press. gradients 0-98379
- surface winds of Alaska, mountain barrier baroclinity effects 0-90118
- symmetric instability of stratified geostrophic flow 0-98425
- thermosphere, lower, wind variance field rel. to eddy diffusion models 0-109198
- thermosphere, N Polar Cap winds 0-67445
- thermosphere, winter, prevailing winds in S.hemisphere meteor region 0-109287
- thermosphere temperature and wind measurement Fabry-Perot-interferometer imaging system appl. 0-101441
- thermosphere wind influences on F-region TIDs 0-109305
- tornado activity rel. to precipitation, assessment 0-61882
- tornado in Cheyenne, USA, 16th July 1979, storm damage 0-77029
- tornado interpretation of 1646 East Anglian meteorite 0-68009
- tornado outbreaks, automated 12 to 36 hour probability forecasts 0-77062
- tornado over Delhi, of 1978 March 17, sodar obs. 0-109188
- tornado simulation, core radii and peak vels. in modeled vortices 0-90130
- tornado-like vortex, laboratory expt. of swirl ratio effect 0-61862
- tornadoes in UK, rel. to solar mag. sector crossing, 1957-77 period 0-77094
- tropical cyclone, model of ocean-atmos. boundary layer interaction 0-109231
- tropical cyclones, radius and frequency of 15 m s<sup>-1</sup> (30 kt) winds 0-105025
- tropical E.Atlantic, press. and wind fields from TROPEX data 0-82040
- tropical region, wind roses of freq. and stability appl. to pollutant dispersal 0-97846
- troposphere wind at 300 mb, scale-interaction study with horiz. filtering method 0-98423
- troposphere winds, evidence for solar cycle signal 0-72604
- troposphere winds, radar obs. made at Kwajalein Atoll, equatorial Pacific 0-90188
- troposphere-stratosphere wind profile, using Poker Flat MST radar 0-72579
- upper troposphere/lower stratosphere winds, rel. to satellite-derived radiance gradient 0-98447
- turbulent wind structure on hill crest 0-85722
- typhoon tracks near Taiwan, forecasting using simulations 0-90200
- typhoons anomalous tracks, over East China Sea, mechanism (*Chinese*) 0-82043
- upper mesopause, diurnal variation of zonal and meridional components 0-109284
- urban-scale wind fields, three-dimensional, construction, objective anal. technique 0-101407
- US Federal wind energy programme, wind charact. programme element, overview 0-61242
- velocity meas. near wind power plant in Sweden 0-61883
- Venetian region, advection-diffusion model for for real-time forecasting of air pollution episodes 0-77096
- vertical air velocity, airborne meas. system 0-77159
- warm frontal region, wind and precipitation struct., Doppler radar study 0-81995

**wind continued**

- water surfaces, new evaluation of wind stress coeff. 0-72603
- water waves generation, spatial correl. rel. to freq. independent phase vels. 0-98333
- wind-field analysis methods 0-105038
- windchill maps of lowland Britain, calc. from instantaneous data 0-61893
- zonal wind in tropical middle atmosphere, observational evidence of semiannual oscillation 0-109216

**wind energy** *see* **wind power****wind power**

- AEROSOLEC, combined solar-wind power station for telecommunication appls. 0-61306
- alternative versus conventional energy sources, economic comparison (*German*) 0-72002
- assessment, wind energy resource survey methodology 0-76594
- conference, Amsterdam, Netherlands (Oct. 78) 0-61235
- Cycloturbine, straight-bladed vertical axis wind turbine with cyclically pitched blades 0-61263
- Darrieus rotor, aerodynamic analyses comparison 0-61264
- Darrieus vertical axis wind turbines 0-76599
- development, availability, and storage possibilities (*French*) 0-89587
- development programme in Sweden 0-61237
- electricity production, windmill construction (*French*) 0-66925
- energy accounting study 0-76589
- energy conversion system, electricity storage using batteries 0-72008
- energy resources, review of alternatives to fossil fuel (*Italian*) 0-66917
- exploitation, programmes in Tanzania 0-61240
- exploitation on large scale, physical planning aspects in Holland 0-61241
- flexible blade windmills 0-66930
- flow over complex terrain, wind tunnel simulation 0-76596
- horizontal axis wind turbines, 100 to 2500 kW, development status 0-76597
- horizontal-axis wind-turbine system for pumping duties in Third World agriculture 0-61259
- industrial utilisation of energy, book 0-61222
- mean wind isowind maps for many parts of the world showing sites suitable for wind power plants (*Italian*) 0-89586
- meteorological aspects, resource assessment, site selection, US R and D program 0-76593
- New Zealand, wind energy prospects in Otago region 0-76595
- North Sea windmill deployment for 20% of UK's needs 0-97759
- off-shore based wind turbine systems for Sweden, systems concept study 0-61261
- offshore wind power model estimates 0-61244
- potential in Karnataka State, in India 0-108782
- power plants, experimental projects in progress, design problems and results achieved (*Italian*) 0-72007
- prospecting in Prince Edward Island, programme overview and status report 0-61243
- recent developments aid economic aspects 0-61238
- research and developments, future trends as to viability as energy source 0-66924
- research programme, in Holland 0-61236
- Savonius rotors, wind-tunnel air-speed corrections 0-61255
- seawater desalination by wind power, anal. 0-108781
- shrouded wind turbine, pilot plant construction 0-66931
- site evaluation, estimation of wind characteristics using COMPLEX model 0-101075
- small wind energy conversion systems, commercialisation, R and D program 0-76598
- systems technology, R and D review 0-76592
- US Federal wind energy programme, wind charact. programme element, overview 0-61242
- utilisation prospects 0-61269
- vertical axis wind turbine, flow field exam. using vortex model 0-61267
- vertical axis wind turbines, design, construction, testing and manufacturing 0-66929
- vertical axis windmill with variable geometry, development 0-61254
- wind heat system utilising wind turbine driven heat pump 0-66926
- windmill arrays, wake interaction, theory and preliminary results 0-61246

**wind power plants**

- 60 kW experimental wind power plant in Sweden, test results 0-61253
- 60 m diameter wind turbine generator, design concept 0-61262
- 200 kW Gedser windmill in Denmark, performance and structural response meas. 0-61431
- 200 kW generator, design features and details of parallel operation with diesel engine driven plant (*Italian*) 0-101074
- 200 kW vertical axis wind turbine, preliminary test results 0-66928
- AEROSOLEC, combined solar-wind power station for telecommunication appls. 0-61306
- control strategy for variable speed wind power generator (*French*) 0-76591
- desalination plant utilising reverse osmosis, 6 kW convertor 0-61282
- design, atmospheric turbulence structural influences 0-61247
- development, safety, reliability and quality assurance, low cost approach 0-61268
- developments in Japan 0-61239
- experimental projects in progress, design problems and results achieved (*Italian*) 0-72007
- fixed-pitch propeller, water heating appl. 0-61260
- integration into existing power systems, implications 0-61258
- Magdalen Islands wind turbine, nine months operating experience report 0-66927
- parameters for rational and economic installation (*Italian*) 0-89586
- performance evaluation method 0-61248
- power system that includes wind energy generators, model based regulation 0-61256
- power transmission, epicyclic gear design 0-61252
- research and developments, future trends as to viability as energy source 0-66924
- small wind energy conversion systems, commercialisation, R and D program 0-76598
- value to electric utility, economic model 0-61257
- velocity meas. near wind power plant in Sweden 0-61883

**wind tunnels**

- low density wind tunnel for rarefied gas dynamics 0-96285
- reflected-beam laser anemometry using photon correlator 0-106861
- Savonius rotor, aerodynamic performance testing in wind tunnel 0-61266
- Savonius rotors, wind-tunnel air-speed corrections 0-61255

**wind tunnels continued**

- turbulent boundary layers on rough surfaces, simple roughness elements, natural wind simulation 0-69774
- unsteady pressure coefficients digital measuring unit (*French*) 0-68169

**wind turbines**

- 200 kW vertical axis wind turbine, preliminary test results 0-66928
- aerodynamics, machine performance and rotor aerodynamics 0-74904
- aeroelastic behaviour, large Darrieus rotors derived from behaviour of 5.5 m rotor 0-61251
- Cycloturbine, straight-bladed vertical axis wind turbine with cyclically pitched blades 0-61263
- Darrieus rotor windmill arrays, wake interaction, wind tunnel simulation 0-61245
- Darrieus rotor, aerodynamic analyses comparison 0-61264
- Darrieus vertical axis wind turbines 0-76599
- efficiency, Lanchester-Betz limit 0-97758
- energy effectiveness of arbitrary arrays of wind turbines, calc. 0-97755
- flexible blade windmills 0-66930
- horizontal axis wind turbine blades, aeroelastic stability and response 0-61250
- horizontal axis wind turbines, 100 to 2500 kW, development status 0-76597
- horizontal-axis wind-turbine system for pumping duties in Third World agriculture, design 0-61259
- large, aeroelastic stability 0-61249
- Magdalen Islands wind turbine, nine months operating experience report 0-66927
- off-shore based wind turbine systems for Sweden, systems concept study 0-61261
- Savonius rotor, aerodynamic performance testing in wind tunnel 0-61266
- Savonius rotors, wind-tunnel air-speed corrections 0-61255
- shrouded wind turbine, pilot plant design and construction 0-66931
- variable geometry vertical axis windmill development 0-61254
- variable pitch vertical axis, investigation 0-61265
- vertical axis wind turbine, flow field exam. using vortex model 0-61267
- vertical axis wind turbines, design, construction, testing and manufacturing 0-66929
- vertical axis, tilting using overspeed control 0-97757
- vortex augmentor to increase power, test model results 0-97756
- wind heat system utilising wind turbine driven heat pump 0-66926
- windmill arrays, wake interaction, theory and preliminary results 0-61246

**winding (process)**

- fusion reactor, Large Coil Program, coil winding development support 0-106190

**WKB calculations**

- (2+1) dimensional compact QED, combined WKB-variational method, vacuum tunnelling 0-101960
- accretion onto compact gravitating object, travelling sound wave behaviour WKB anal. 0-67551
- defective dielectrics, EM heating with time depend. param., WKB calcs. 0-71367
- four term WKB approx., appl. to Varshni V and Lennard-Jones pot. 0-58113
- free boson gas in weak external pot. 0-86203
- free particle propagator covariant WKB expansion in Riemannian space 0-68100
- graded index fibre, error estimates for first order WKB calc. method 0-87488
- Helmholtz eqn., 1-dimens., refined Maslov-WKB technique appl. 0-90795
- JWKB phase integrals, higher order, evaluation 0-87195
- magnetosonic and Alfvén waves, transfer by solar wind 0-67490
- multidimensional bistable potential, diffusion, WKB calc. 0-101770
- multimode fibre bandwidth computation from measured index profiles 0-58740
- neutron dynamical diffraction, gravitational and mag. field effects 0-59345
- numerical integration leading to Bohr-Sommerfeld formula, alternative to JWKB calcs. 0-86119
- phase integral approximations, advantages over JWKB approx. 0-87027
- plasma, one dimens. screening 0-65478
- potential problems, non-local, Perey effect, WKB method 0-68077
- radial wave functions, JWKB connection with bound-state/free-state duality 0-62950
- radio wave propagation in critical coupling media, comparison of generalised WKB and Katsenelenbaum's methods 0-91728
- ray and wave optics of integrable and stochastic systems, WKB method 0-59244
- relativistic wavefunctions, approx. near turning point, WKB calcs. for  $Z \geq 137$  0-86598
- step-index fibres, pulse responses investig. using WKB approx. 0-91898
- WKB method for systems of integral equations 0-98787
- $\text{Ar} + \text{HCl}$ , inelastic scatt. exponential perturbation theories 0-74217
- $\text{Ar} + \text{N}_2$ , inelastic scatt. exponential perturbation theories 0-74217
- Ba I, quasi-Landau spectrum, semiclassical strong field mixing models 0-63847
- $\text{Ba}^{2+}$ , very long lived vibr. states, lifetimes, WKB calc. 0-78560
- $\text{He} + \text{H}_2$ , inelastic scatt. exponential perturbation theories 0-74217
- Sr I, quasi-Landau spectrum, semiclassical strong field mixing models 0-63847

**wolfram** *see* **tungsten****wood**

- energy in W. Virginia 0-72006
- fibre reinforced Portland cement composite, strength 0-100822
- flash pyrolysis, in cyclone, solar gas-solid chemical reactor (*French*) 0-61296
- fracture toughness variations with specimen size, statistical approach 0-100889
- gasification of wood wastes using flash pyrolysis and concentrated solar energy (*French*) 0-61226
- trees, US pulse echo method for flaw detection 0-66731
- urea-formaldehyde resin/wood materials, book 0-73114

**work function**

- see also* **electron emission**; **Schottky effect**
- adsorbed layers, order-disorder transition, effect on work function 0-59791
- caesiated surface, negative ion emission (*French*) 0-108314
- cathode material choice methodology to obtain low work function 0-100500



## work function continued

- DC method for continuous meas. of work function changes 0-84503  
 insulators, XPS, binding energy, surface pot. and work function calcs. 0-89113  
 metal, contrib. of John Bardeen 0-57057  
 metal, electronic work function under tension, 20 to 1200°C 0-76448  
 metal, surface dipole barrier, calc. 0-96958  
 metal, work function, pseudopot. calc. 0-96970  
 metal oxides, nonstoichiometric, work function and near-surface chem. diffusion 0-80034  
 metallic surface, self-consistent electron theory, review 0-88616  
 mirror electron microscopy, appl. to work function variation meas. 0-86505  
 MIS negative barrier contact for induced back surface field solar cell 0-101101  
 nontransition metals, electron density, bulk and surface props. relation 0-103609  
 p 0-80072  
 porous metal cathodes, emission props., work function 0-100502  
 rare gas, crystal, quasi-atomic and quasi-molecular exciton states (*Russian*) 0-103628  
 semiconductor, electron emission from surface subband, reduced work function 0-60757  
 silicide Schottky barriers, elemental description 0-60085  
 single crystals with lowered work function, secondary and Auger electron emission anisotropy 0-100716  
 stainless steel, austenitic, surface, interaction with O<sub>2</sub>, AES and work function obs. 0-65364  
 surface microstructure determ. and microanalysis by ultrahigh vacuum field emission gun SEM 0-96423  
 surface potential and work function meas. from secondary electron emission energy in SEM 0-66343  
 surface-atom polarisability derivation from field-ion energy deficits 0-76155  
 Ag, thin film deposited on Si, work function (*French*) 0-80353  
 Ag-O-Cs surface, oxidation, role of Cs suboxides in low work function surface layers, XPS 0-76131  
 Al, initial interaction of O with single cryst. faces, LEED, AES and work function study 0-84392  
 Al, thin film deposited on Si, work function (*French*) 0-80353  
 Au, surface dipole moment calc. 0-60060  
 BaO, film, emission props. in relation to struct. 0-100501  
 BaO, monolayer on W (110), film struct. and electron state 0-100498  
 BaTiO<sub>3</sub>, electron exoemission unipolarity associated with phase transitions 0-97415  
 Be film, on W (110), growth mode, work function, thermal desorption, and struct. 0-75477  
 CdGa<sub>2</sub>S<sub>4</sub> double surface-barrier diodes, current-voltage characts. 0-92972  
 CeB<sub>6</sub>, crystal preparation, elec. resistance, phase transitions 0-97427  
 Cs ion source, thermionic emission in SF<sub>6</sub> mol. gas 0-71557  
 Cs/W, work function measurement in SEM 0-80918  
 Cu (100), electronic struct., self-consistent local-orbital calc. 0-80348  
 Cu adsorption of O<sub>2</sub>, N<sub>2</sub>O on (100) surface, reaction with CO 0-103583  
 Fe, polycrystalline, H<sub>2</sub> adsorpt. and embrittlement, work function changes 0-96741  
 GaAs epitaxial thin films with neg. electron affinity, photoelectron energy distrib. 0-100755  
 p-GaAs/rare earth metal contacts, surface pot. barrier 0-60086  
 GdB<sub>6</sub>, crystal preparation, elec. resistance, phase transitions 0-97427  
 Ge (111) surface, clean, O<sub>2</sub> adsorption rate and electron work function 0-59779  
 Ge strain-confined large electron-hole drop characteristics 0-65469  
 Ir, field emission spectrosc. from (111) flat and stepped planes 0-76157  
 LaB<sub>6</sub> (100), (110), and (111), surface structs. and work functions 0-70512  
 LaB<sub>6</sub> (210) surface, work function, struct. and chemisorpt. stability, XPS, UPS and LEED 0-65344  
 LaB<sub>6</sub> cathodes, single crystal, of <100> and <110> orientations, brightness meas. from 1500 to 1950K 0-62808  
 LaB<sub>6</sub> single cryst. tips with [100], [110], [111] and [210] orientations, thermionic emission patterns 0-66379  
 LaCrO<sub>3</sub>-MgO, LC20M electrode material in open cycle MHD systems, thermionic emission characts. 0-97394  
 Mo (111), work function temp. coeff. 0-100499  
 Mo, coadsorption of O<sub>2</sub> and Cs, electron emission props., thermal stability 0-66878  
 Ni (100), dissociative chemisorption and mol. adsorption of NO 0-65373  
 Ni film, interaction with O<sub>2</sub>, AES, EELS, work function, and gravimetric meas. 0-75433  
 Ni surface, (111), chemisorbed CO, bond energies 0-100398  
 Ni-H, ferromag., H impurities and  $\mu$ SR, self-consistent calc. 0-84447  
 NiO, nonstoichiometric, near-surface and bulk chem. diffusion 0-80035  
 Pb, electron field emission, temp. effect 0-60756  
 Pd (111), chemisorption of Cl<sub>2</sub>, LEED, AES, thermal desorption, and work function meas. 0-75444  
 Pd film, work function changes due to adsorbed H<sub>2</sub>, surface and interface dipoles 0-96972  
 Pd ribbon, H<sub>2</sub> adsorption, thermal desorption and work function meas. 0-70538  
 Pt (111), chemisorption of Cl<sub>2</sub>, LEED, AES, thermal desorption, and work function meas. 0-75444  
 Pt (111), chemisorption of mol. O<sub>2</sub>, XPS, UPS, EELS, and work function meas. 0-76139  
 Pt, surface dipole moment calc. 0-60060  
 Re:C, work function, graphitic layer formation 0-96966  
 p-Si/rare earth metal contacts, surface pot. barrier 0-60086  
 SmB<sub>6</sub>, crystal preparation, elec. resistance, phase transitions 0-97427  
 W (100), condensation of Cu and Ag, early stage comparison with Mi(100) 0-80072  
 W (100), surface reconstruction kinetics in presence of O half-monolayer 0-65375  
 W (110) surface, adsorbed Pd, growth, struct., stability, desorption 0-59794  
 W, coadsorption of La and B, field emission and field ion microscopy 0-104049  
 W epitaxy on W(110) substrate, work function meas., LEED investigation 0-80103  
 W faces, simultaneous adsorption of Ba and Cu atoms, work function changes 0-65378  
 W, joint adsorption of Ba and Ti, work function meas. 0-100411

## work function continued

- W single cryst., dislocation effects on thermionic emission and work function 0-76129  
 W, surface dipole moment calc. 0-60060  
 W, work function measurement in SEM 0-80918  
 W(001), surface states and surface resonances, self-consistent electronic struct. 0-96960  
 Zr, adsorption and absorpt. of CO, NO, N<sub>2</sub>, O<sub>2</sub>, and D<sub>2</sub>, dissociation and diffusion 0-80085
- work hardening**  
*see also cold working*  
 alloy, dispersion hardened, work hardening due to Orowan loops, temp. depend. (*Japanese*) 0-66534  
 alloys, single cryst., work hardening phenomena and screw dislocation dipole clusters 0-100845  
 brass, cold rolling, inhomogeneous texture 0-89251  
 $\alpha$ -brass, fatigue crack propag., role of dislocation substruct. 0-60963  
 $\beta$ -brass, uniaxial tension and compression, cyclic stress-strain behaviour 0-97551  
 brass (37%Zn), workhardened thin specimens, fracture, anisotropy coeff. role (*French*) 0-104276  
 cell wall and lattice misorientation origin during deform. 0-71712  
 composite superconductor, flux jumps and training 0-70911  
 cracktip under incipient creep deform., stress field and modified J-integral (*Japanese*) 0-103411  
 crystalline materials, in situ deform. by high voltage electron microscopy 0-103352  
 deformation broaching of difficult-to-form metals 0-108473  
 discrete structures under dynamic loading, work hardening adaptation 0-74726  
 dislocation train, moving through dislocation forest, loop formation 0-107238  
 ductile fracture, strain hardening and damage relationship 0-108564  
 elastic-viscoplastic frames, dynamic responses, strain hardening effects 0-79178  
 fatigue crack propagation, crack closure, effective stress range factors 0-100924  
 fracture stress obtained from the elastic crack tip enclave model 0-71730  
 galvanic coatings, adhesion after strain hardening, test device 0-71837  
 metal, polycrystalline, strain hardening, dislocation link length model 0-84953  
 metal sheet, circular, impulsive press. by underwater wire explosions, dynamic plastic deform. 0-84866  
 metals, porous, plastic flows, microscopic frictional effects, J<sub>2</sub>-flow potential and yield function 0-64384  
 metals, research at Birmingham, (1945-55) 0-62444  
 plane-strain work hardening, meas. and anal. 0-81073  
 sheet material, method for strength meas. under biaxial tension 0-66717  
 soil, plastic flows, microscopic frictional effects, J<sub>2</sub>-flow potential and yield function 0-64384  
 steel, austenite, carbide strain hardened, strength and plasticity, effect of Mn content (*Russian*) 0-97500  
 steel, C, low temperature strength, preliminary plastic deform. effect 0-81128  
 steel, Cr-Mn, strain hardening, 4.2 to 293K 0-81076  
 steel, Cr-Mo (2.25, 1 wt.%), creep and high temp. low-cycle fatigue tests 0-85061  
 steel, Cr-Ni, strain hardening, 4.2 to 293K 0-81076  
 steel, ferritic, cleavage fracture toughness, temp. and strain rate depend. 0-85028  
 steel, high-strength, low cycle fatigue, hysteresis loops, cyclic strain curves, fatigue diagrams (*Polish*) 0-66638  
 steel, low C, initial stages of plastic deform. (*Japanese*) 0-93618  
 steel, low C, type En3, high strain deform., struct. and props. 0-89301  
 steel, low-alloy, bearing, mech. props., carbide behaviour effect (*Korean*) 0-93615  
 steel, medium C, microflow and strain hardening under cyclic loading 0-104182  
 steel, stainless, type 304, viscoplastic behaviour, strain rate sensitivity, creep, relaxation, tensile tests 0-66727  
 steel, stainless, wire, axial texture after electroplastic drawing, X-ray struct. investigation (*Russian*) 0-104177  
 steel, stainless 304 sol. of annealed and thermally-aged, high-cycle fatigue behaviour 0-100923  
 steel, strain-hardened subsurface layer, residual stress change in fatigue 0-81185  
 steel, type 20Kh deformed, austenite grain size, inheritance effect with quenching and tempering 0-60881  
 steel 1Kh17N2Sh, fatigue failure, surface finishing influence 0-60972  
 stretch zone width and striation spacing. The comparison of theories and experiments 0-85051  
 viscoplastic materials, dynamic convergence theorem for strain and work hardening 0-96199  
 Zircaloy, annealed, neutron irradiated, inhomogeneous deform. behaviour 0-85014  
 Zircaloy-2 fuel tubes, low cycle fatigue studies at room temp., 300 and 350°C 0-93637  
 Ag, cold rolling, inhomogeneous texture 0-89251  
 Al alloy RR58, low cycle fatigue at 423K, prior treatment effect 0-104254  
 Al bicrystal, plastically deformed, slip heterogeneities 0-79858  
 Al, cold rolling, inhomogeneous texture 0-89251  
 Al, commercially pure, stress-strain curves, cyclic loading initial stage (*Japanese*) 0-93617  
 Al, initial stages of plastic deform. (*Japanese*) 0-93618  
 Al, workhardened thin specimens, fracture, anisotropy coeff. role (*French*) 0-104276  
 Al-(Mg)(Fe), pure (dilute), large wire drawing plastic deform. 0-108508  
 Al-Cu, type 2036-T4, plane-strain work hardening, meas. and anal. 0-81073  
 Al-Cu (4 wt.%), supersaturated and aged conditions, high strain deform. 0-60907  
 Al-Mg (2 wt.%), hardening and fracture characts.,  $\beta$ -phase dissolution role 0-81178  
 Al-Mg-Si, type 6010, microstruct. characts. influence on formability, heat treatment 0-81090  
 Al-Ni (6 wt.%), fine-grained, deform. in tension and torsion 0-85008  
 Al-Ni(Cd)(Fe)(Si), cold worked, struct. and props. 0-71666  
 Al-Si (1.2 wt.%), dispersion hardened, work hardening due to Orowan loops, temp. depend. (*Japanese*) 0-66534

**work hardening continued**

- Al-Ti alloy for use in aircraft, mechanical props. improvement (*French*) 0-97502
- Bi, strain hardening curve correlation with slip band nucleation stress spectra 0-70217
- CoO single crystals, strain rate deform. characts., yield stresses and work hardening 77 to 1400K 0-60939
- Cu, fatigue crack propag., role of dislocation substruct. 0-60963
- Cu, polycryst., surface layer hardening by multiple impact 0-108469
- Cu, swaged, inhomogeneous work hardening (*German*) 0-76267
- Cu, wire, axial texture after electroplastic drawing, X-ray struct. investigation (*Russian*) 0-104177
- Cu-Al<sub>2</sub>O<sub>3</sub>(SiO<sub>2</sub>)(TiO<sub>2</sub>) alloys, internally oxidised, plastically deformed, influence of particle form on primary loop nature (*French*) 0-103344
- Cu-Be (2 at.%), plastic deform. and dislocation substruct. 0-76307
- Cu-Nb multifilamentary composite, dislocation resistivity 0-70671
- Cu-Ni (10 at.%), hardening, recovery, and struct. changes during high temp. creep (*Russian*) 0-89288
- Cu<sub>3</sub>Au, disordered [001]-orientated single crystals, plastic deform., TEM and slip line studies 0-97541
- Fe, Armcro, microflow and strain hardening under cyclic loading 0-104182
- Fe, cast, contact deformation, reverse slipping effect (*Russian*) 0-97591
- Fe-Mn (1 at.%), strain age hardening 0-108472
- Fe-Ni-Cr-Ti-Al, with thermoelastic control coeff., comp. and heat treatment influence on props. (*French*) 0-81074
- Fe-Si, microflow and strain hardening under cyclic loading 0-104182
- LiF, strain hardening curve correlation with slip band nucleation stress spectra 0-70217
- Mo fibre reinforced Cu, rule of mixtures of deform. parameters in stage III 0-97532
- Mo fibre reinforced Cu with weak interfaces, stability of tensile deform. 0-97533
- Mo, single and polycryst., struct. change during work softening, HVEM 0-103336
- Mo-Cr-V-P, load curves, structure states boundaries and strain hardening (*Russian*) 0-89241
- Mo-Ti (3.5 wt.%), load curves, structure states boundaries and strain hardening (*Russian*) 0-89241
- Ni, polycrystalline, strain hardening, dislocation link length model 0-84953
- Ni single crystal, compressed, strengthening and dislocation cells (*German*) 0-66536
- Ni<sub>2</sub>Fe, mono- and polycryst., strain hardening, test temp. effects (*Russian*) 0-66531
- Ti alloy VT-3-1, fatigue failure, surface finishing influence 0-60972
- Ti-Al-V (6.4 wt.%) superplastic alloy, maximum attainable ductility 0-60919
- $\beta$ -Ti-Mo, thermal instability, hardness and tensile deform. (*Japanese*) 0-71703
- Zn crystal, {11 $\bar{2}$ 2}{11 $\bar{2}$ 3} slip system, deform. stress, dislocation density depend. (*Russian*) 0-103353
- Zn-Al-Cu casting alloys, mech. props. and dendritic morphology, Al content effect (*Korean*) 0-93612

workers see personnel

wrapping see packaging

Written filters see optical filters

X<sup>0</sup> meson resonances see eta meson resonances**X-ray absorption**

see also X-ray absorption spectra

- attenuation measurements on Y tong shielding material (*German*) 0-98145
- benzyl mercury chloride, cryst. struct. and absorpt. calcs. 0-84166
- brain, experimental oedema, serial meas. of specific gravity and computerised tomography attenuation 0-98005
- diffraction expt., incident beam intensity meas. by absorpt. method 0-68333
- half-value layer determ., analytic method 0-66747
- sample cell for extended X-ray absorption fine structure meas. up to 1000°C 0-57454
- spectral distribution, evaluation of method of estimation from attenuation data (*Japanese*) 0-95207
- water irradiated by photons up to 2 MeV, initial energies of Compton electrons and photoelectrons 0-108320
- Al, K X-ray absorption, K-emission spectrum, band struct. using APW method 0-97380
- MgO-NiO, STEM microanal., absorpt. effects 0-80902

**X-ray absorption spectra**

- amorphous materials, X-ray K-absorption edge chemical shifts 0-80904
- amorphous solids, Raman intensities, connection with EXAFS Debye-Waller factors 0-108214
- CO<sub>2</sub> ferrite, crystal structure, X-ray absorpt. spectra, chemical shifts 0-88118
- continuous X-ray radiation due to picosecond ruby laser plasma heating (*Russian*) 0-75079
- disordered alloys, interatomic distances, coord. numbers, and mean relative displacements, EXAFS anal. 0-89087
- EXAFS, determ. of struct. of disordered regions (*French*) 0-80905
- EXAFS amplitudes, many-body effects 0-97379
- EXAFS and surface EXAFS from X-ray refl. meas 0-71512
- filter assembly for fluorescence EXAFS meas. 0-90971
- glass local structure exam. by EXAFS 0-108301
- graphite, C K-edge fine struct. 0-66325
- graphite-Br<sub>2</sub> intercalation cpds., EXAFS study 0-71515
- K-emission satellites, low and high freq. origin 0-80900
- metals, exciton effects on X-ray absorption edges 0-108298
- optical fibre preforms, refractive index distribution measurement using X-ray absorption measurements (*Japanese*) 0-87506
- polyacetylene, AsF<sub>5</sub> doped, X-ray absorpt. meas., 5K to room temp. 0-71516
- (rare-earth)Al<sub>2</sub>Ga<sub>3</sub>, synthesis, NMR and X-ray absorpt. studies 0-108083
- silicate glasses, local order around Fe, exam. using X-ray absorpt. spectrometry 0-79701
- soft, meas. by photoelectron anal. 0-73557
- superionic conductor, EXAFS investigation of struct. and ion motion 0-108302
- surface atomic and electronic struct. studied with synchrotron radiation 0-80945
- surface reactions, EXAFS obs. 0-108735

**X-ray absorption spectra continued**

- transition elements, first-group, K-emission satellites, quasi-stationary states and origin 0-80903
- Ag and Ag<sub>2</sub>O, X-ray absorption, discontinuities and limits, chem. combination effects 0-93435
- AgI, EXAFS investigation of struct. and ion motion 0-108302
- $\alpha$ -AgI, superionic, anal. of Ag K-EXAFS data 0-97377
- Al, (111) surface, adsorbed O, surface struct., LEED and SEXAFS data 0-92782
- Al-Cu (1.9 at.%), solute fluctuations, EXAFS study 0-79949
- Au and Au<sub>2</sub>O<sub>3</sub>, X-ray absorption, discontinuities and limits, chem. combination effects 0-93435
- Au, core-electron excitation edges 0-66345
- Au, thin foil, enhanced electron energy deposition heated, soft X-ray vacuum UV spectra 0-80901
- Ba<sub>1-x</sub>Sm<sub>x</sub>, electron config. of Sm ions, X-ray L-absorpt. spectroscopy 0-60715
- BaTiO<sub>3</sub>, K-edge X-ray absorpt., cond. band states 0-97382
- Bi and Bi<sub>2</sub>O<sub>3</sub>, X-ray absorption, discontinuities and limits, chem. combination effects 0-93435
- Ca<sub>1-x</sub>Sm<sub>x</sub>, electron config. of Sm ions, X-ray L-absorpt. spectroscopy 0-60715
- CdSiP<sub>2</sub>, electronic struct., X-ray spectroscopic investigation 0-108300
- Cl<sub>2</sub>, inner shell excited states, X-ray absorpt. spectra, HF calcs. 0-78536
- Co, X-ray K-absorption spectrum 0-97378
- Co, X-ray refl. near L<sub>2,3</sub> absorpt. edge 0-71513
- Co-Al, X-ray K-absorption spectrum 0-97378
- Cu and Cu oxides, X-ray absorption, discontinuities and limits, chem. combination effects 0-93435
- Cu, and Cu-Al disordered alloys, interatomic distances, coord. numbers, and mean relative displacements, EXAFS anal. 0-89087
- Cu complexes, N ligands, X-ray K-absorpt. edge, expt. 0-89084
- Cu, core-electron excitation edges 0-66345
- Cu extended X-ray fine struct., lattice consts. 0-89085
- Cu, film, partially oxidised, EXAFS studies on superficial regions 0-75474
- Cu II complex, extended X-ray absorpt. fine struct. study 0-104011
- Cu, orbital energies and X-ray K-absorpt. spectra 0-69060
- Cu, oxidation, EXAFS obs. 0-71808
- CuBr, superionic behaviour at high temp., EXAFS study 0-107496
- CuCl, band struct., OPW calc. and X-ray spectra meas. 0-75506
- CuCl, superionic behaviour at high temp., EXAFS study 0-107496
- CuCl<sub>2</sub>(Br<sub>2</sub>), aq. solns., EXAFS meas. 0-60714
- CuI, EXAFS investigation of struct. and ion motion 0-108302
- CuO, mol. orbital energies and X-ray K-absorpt. spectra 0-69060
- Cu<sub>2</sub>O, mol. orbital energies and X-ray K-absorpt. spectra 0-69060
- CuSO<sub>4</sub>·5H<sub>2</sub>O, EXAFS, rel. between Debye-Waller factor and thermal parameters meas. by neutron diff. 0-84803
- Eu solid solutions with lanthanides, monosulfides, and oxides, vacant d states, X-ray absorpt. 0-103623
- EuB<sub>6</sub>, valence state of Eu, X-ray line displacement meas. 0-70633
- EuCu<sub>2</sub>Si<sub>2</sub>, mixed valence system, X-ray absorption spectroscopic study 0-80906
- Eu<sub>1-x</sub>Sm<sub>x</sub>, electron config. of Sm ions, X-ray L-absorpt. spectroscopy 0-60715
- Fe monomers and dimens. in solid Ar, EXADS study 0-97381
- Fe rich micas, X-ray absorpt., heat treatment effects, chem. and struct. interpretation 0-84806
- Fe, X-ray absorpt. spectra, effective co-ordination charges 0-84805
- Fe<sub>3</sub>Cr<sub>3</sub>Ni<sub>4</sub>B<sub>12</sub>B<sub>6</sub>, amorphous X-ray absorpt. spectra, effective co-ordination charges 0-84805
- Fe<sub>40</sub>Ni<sub>60</sub>P<sub>20</sub>, metallic glasses, local struct. and dynamic disorder of Fe and Ni, EXAFS obs. 0-89088
- Fe<sub>2</sub>O<sub>3</sub>, X-ray absorpt. spectra, effective co-ordination charges 0-84805
- Fe<sub>2</sub>O<sub>4</sub>, X-ray absorpt. spectra, effective co-ordination charges 0-84805
- Fe<sub>2</sub>O, X-ray absorpt. spectra, effective co-ordination charges 0-84805
- Ga, anisotropy of white line in K-absorption spectrum, EXAFS mechanism 0-89086
- Ge, EXAFS at high press. 0-97376
- GeS, anisotropic EXAFS, cryst. struct. determ. 0-66323
- KCl, fine structure of X-ray absorption spectra 0-71514
- La-Sm-Au, amorphous, surface effects on Sm valence, XPS and X-ray absorption meas. 0-108325
- LiNbO<sub>3</sub>:Fe<sup>(3+)</sup>, X-ray absorpt. 0-108299
- MgSiP<sub>2</sub>, electronic struct., X-ray spectroscopic investigation 0-108300
- Mn and Mn oxides, K X-ray absorpt. discontinuity, shape and extended fine struct. 0-66324
- Mn compounds, single and complex, X-ray absorption near edge structs. 0-104013
- NaBr, EXAFS at high press. 0-97376
- NaF, quasimolecular struct. characts. of NaL<sub>II,III</sub> absorpt. edge 0-93436
- Na<sub>2</sub>O-SiO<sub>2</sub>-Fe<sub>2</sub>O<sub>3</sub>, glass, X-ray absorpt. spectra, effective co-ordination charges 0-84805
- Ni, core-electron excitation edges 0-66345
- Ni, L<sub>II</sub>-binding energy, absolute determ. from self-absorpt. meas. 0-71519
- NiCl<sub>2</sub>(Br<sub>2</sub>), aq. solns., EXAFS meas. 0-60714
- Pb and Pb oxides, X-ray absorption, discontinuities and limits, chem. combination effects 0-93435
- Pt, core-electron excitation edges 0-66345
- Ru-Cu clusters, EXAFS study 0-84804
- (SN)<sub>2</sub>, brominated, X-ray absorpt. meas., 5K to room temp. 0-71516
- SbCu<sub>2</sub>Si<sub>3</sub>, mixed valence system, X-ray absorption spectroscopic study 0-80906
- SiH<sub>4</sub>, L<sub>II,III</sub> continuous absorpt. spectrum of Si 0-95645
- Sm-Au, amorphous, surface effects on Sm valence, XPS and X-ray absorption meas. 0-108325
- Sm<sub>4</sub>Bi<sub>3</sub>, mixed valence system, X-ray absorption spectroscopic study 0-80906
- Sm<sub>0.75</sub>Y<sub>0.25</sub>S, mixed-valence, electron-lattice correlations, EXAFS studies 0-76103
- SrBr<sub>2</sub>, aq. solns., EXAFS meas. 0-60714
- Sr<sub>1-x</sub>Sm<sub>x</sub>, electron config. of Sm ions, X-ray L-absorpt. spectroscopy 0-60715
- SrTiO<sub>3</sub>, K-edge X-ray absorpt., cond. band states 0-97382
- Ti, X-ray refl. near L<sub>2,3</sub> absorpt. edge 0-71513
- TiO<sub>2</sub>, rutile, K-edge X-ray absorpt., cond. band states 0-97382
- TmSe, mixed valence, X-ray absorption study 0-76102
- UO<sub>2</sub>, electronic distributions by X-ray spectroscopy 0-97407
- Xe like ions (I<sup>+</sup>, Cs<sup>+</sup>, Ba<sup>2+</sup>, La<sup>3+</sup>) 3d<sup>4f</sup> config., collapse of 4f electron, X-ray spectral obs. (*Russian*) 0-58204



**X-ray absorption spectra continued**

- Yb<sub>1-3</sub>, Sm<sub>5</sub>, electron config. of Sm ions, X-ray L-absorpt. spectroscopy 0-60715  
 ZnBr<sub>2</sub>, aq. solns., EXAFS meas. 0-60714  
 ZnCl<sub>2</sub>, glassy and liq. EXAFS obs. of struct., comparison with vitreous GeO<sub>2</sub> 0-70133  
 ZnF<sub>2</sub>, X-ray absorpt. spectrum polarisation depend. 0-104012  
 ZnSiP<sub>2</sub>, electronic struct., X-ray spectroscopic investigation 0-108300

**X-ray analysis**

- see also *electron probe analysis; X-ray chemical analysis; X-ray crystallography; X-ray diffraction examination of materials; X-ray spectroscopy*  
 analytical electron microscope optimization of X-ray microanalysis, instrum. problems 0-73540  
 biological X-ray microanalysis, principles 0-73566  
 electron probe microanalysis for calcification studies of bone and cartilage 0-76885  
 energy selective, appls. in TEM 0-84036  
 environmental particulate exposure in humans, documentation 0-76886  
 industrial X-ray installation, spectroscopic anal. (German) 0-97668  
 NDT, X-ray flash methods and equipment (German) 0-97669  
 peak-to-background method for quantitative anal. of single particles, with electron probe, developmental progress 0-73541  
 plasma diagnostics, PLT and PDX Tokamaks 0-75104  
 prevention of losses and damage 0-73567  
 scanning electron microscopy; pellet mould for bulk specimen anal. 0-95191  
 spatial resolution in STEM 0-84039

**X-ray apparatus**

- see also *biomedical equipment; X-ray crystallography apparatus; X-ray monochromators; X-ray spectrometers; X-ray tubes*  
 biomedical, motor-tilted diagnostic examination device Model UV-5B 0-85479  
 biomedical collimators, semi-automatic and automatic, manufactured by Medcor Works 0-85475  
 biomedical equipment, state of the art 0-81688  
 biomedical image storing equipment of Medcor Works 0-85476  
 biomedical spot-camera of Medcor Works 0-85477  
 camera, 5-frame, for charged particle, inertial confinement fusion studies 0-57453  
 camera, attachment for aimed investigation of fractures 0-85102  
 catoptrical crossed-mirror imaging at grazing incidence 0-77923  
 corrosion study apparatus, cell for in-situ corrosion in high temp. water 0-90936  
 cryostat for low-temp. X-irradiation of solid samples 0-86321  
 Debye-Scherrer camera conversion to back reflection camera 0-99024  
 EXAFS system, tunable 0-57452  
 filter assembly for fluorescence EXAFS meas. 0-90971  
 flash X-ray machine, distributed pulse power system anal. using SCEP-TRE circuit code techniques 0-68336  
 focusing mirror for synchrotron radiation 0-90961  
 generators, meas. of peak voltage with PIN-photodiodes 0-105754  
 image intensifier noise evaluation, digital method 0-98097  
 image receptor, large area, with electrophoretic display 0-98091  
 imaging system, surface roughness and scatt. effects 0-77921  
 Kratky compact small-angle X-ray collimation system 0-105757  
 LLL type interferometer, interfering beam phase rels. 0-90973  
 mirror profile meas. machine 0-69496  
 penetrometer cassette, multiple exposure, for meas. of effective kilovoltage of diagnostic X-ray beams 0-61662  
 plasma diagnostics, soft X-ray imaging instrument for the Alcator A Tokamak 0-73563  
 quantimeter, ETL-type for angular distribution measurement 0-91367  
 radiographic testing equipment, device characts. (German) 0-76438  
 radiography, computed, low-dose X-ray imaging system 0-98092  
 radiotherapy hard X-ray machine, RT 305, phys. aspects and appl. 0-81709  
 random array grid collimators 0-62817  
 resonator based on successive refls. of surface wave 0-99021  
 rotating disk device for slit radiography of the chest 0-98116  
 stereoscopic X-ray unit for medical diagnostic sets 0-85467  
 storage ring, soft X-ray microscopy/lithography branch line at SSRL 0-91344  
 tissue-equivalent compensators for 4-MV X-rays, basic data 0-98069  
 tomography, computerized, NDT appls. (German) 0-76439  
 waveguide, planar, self-imaging 0-57443  
 XUV mirror reflectivities from 50-150 eV 0-90966  
 zone plates, fabrication using electron beam and X-ray lithography 0-68335  
 Xe-filled MWPC for hard X-ray imaging with sub-mm spatial resolution 0-99418

**X-ray applications**

- see also *radiation therapy; radiography*  
 Buddha sculpture survey using X-ray computed tomography (Japanese) 0-101915  
 crack inspection in foam insulation 0-76440  
 CW X-ray preioniser for high-repetition-rate gas lasers, appl. to HF pulsed laser 0-64037  
 lithography for microfabrication for guided-wave optical devices 0-58812  
 NDT, X-ray flash methods and equipment (German) 0-97669  
 photolithography, fabrication of submicrometer period gratings with precisely defined profiles for integrated optics applications 0-58814  
 plasma diagnostics, emission spectrum of plasma focus, use of Ross filters and Si detectors 0-59273  
 scattered radiation characteristics, local approach to determination of the coordinates of an interface with air 0-86540

**X-ray astronomical observations**

- see also *X-ray sources (astronomical)*  
 1732-303, 1745-248, new X-ray burst sources, discovery and identifications with globular clusters (Terzan 1, 5) 0-98739  
 2A 0251+413, identification as AWM 7 galaxy cluster by HEAO 1 0-90573  
 2A 0311-227, X-ray flux modulation period from HEAO obs. 0-77516  
 A 0538-66, X-ray burster position and optical candidate in LMC 0-73076  
 Abell 1060 galaxy cluster, X-ray spectrum obs. by (HEAO A-2) 0-82518  
 Abell 2029 galaxy cluster, radio and SAS 3 X-ray obs. 0-82519  
 Aigol, eclipsing binary, spectral obs., description and interpretation 0-105283

**X-ray astronomical observations continued**

- Aquila X-1 (4U 1908+00), 1978 summer X-ray and optical outburst 0-73068  
 Aquila X-1 (4U 1908+00), X-ray outburst obs. 0-77514  
 Centaurus galaxy cluster, X-ray spectrum obs. by (HEAO A-2) 0-82518  
 Centaurus X-3, neutron star characts. from correlated spin-up and X-ray luminosity meas. 0-101648  
 Circinus X-1, binary model, orbital eccentricity from X-ray and radio obs. 0-98735  
 clusters of galaxies, large-scale struct. 0-82524  
 cosmological objects, Einstein X-ray observatory appl. 0-105171  
 Cygnus Loop, ANS obs. of SNR 0-82455  
 Cygnus Loop, SNR, soft X-ray spectra emission line features obs. 0-94849  
 Cygnus X-1, accretion disk round black hole, temp. var. 0-109561  
 Cygnus X-1, obs. during high state (1980 June 11 to 27) 0-86017  
 Cygnus X-1, transition from high X-ray state to low X-ray state, 1980 June to July 0-98738  
 Cygnus X-1 (X-2, X-3), X-ray polarisation obs. from OSO 8 0-90571  
 Cygnus X-3, 34.1 day period, 2-12 keV obs. by COS-B 0-94897  
 Cygnus X-3, period derivative and asymmetric X-ray light curve from HEAO 2 obs. 0-105394  
 Cygnus X-ray superbubble 0-90575  
 diffuse X-ray flux in 2 to 7 keV range, galactic component obs. 0-98745  
 early type stars, luminosity determ. X-ray obs. 0-105241  
 40 Eridani A (=e<sup>2</sup> Eridani), evidence of corona on X-ray image 0-105282  
 40 Eridani C, X-ray image of dM4e flare star 0-105282  
 ESO 012-G21, type I Seyfert galaxy, Ariel V X-ray spectra 0-90539  
 FXP 0520-66, flaring X-ray pulsar, nature and optical identification (Russian) 0-77521  
 galactic centre, Prognoz-6 obs. of X-ray fluxes and energy spectra (Russian) 0-109562  
 galactic centre region, high-energy X-ray detection 0-67854  
 galactic X-ray sources, unidentified, positions with HEAO-1 scanning modulation collimator 0-105395  
 galaxies compact groups, X-ray emission obs. 0-90574  
 GX 3+1, X-ray bursts obs., (1980 July 19 to August 18) 0-98739  
 H0118-067, identification with RS Canum Venaticorum star UV Piscium, X-ray obs. 0-101654  
 H0630+82, identification with RS Canum Venaticorum star SV Camelopardalis, X-ray obs. 0-101654  
 H2027+19, Delphinus soft X-ray source, model 0-90576  
 H 2252-035, X-ray flux modulation, compact star rotation 0-101652  
 HDE 226868 (Cygnus X-1), X-ray and UV spectra from HEAO 2 and IUE 0-82543  
 Hercules X-1, eclipsing binary, X-ray spectra from Ariel V satellite 0-90580  
 Kepler's supernova remnant; X-ray obs. from Einstein Observatory 0-82465  
 late-type main-sequence and subgiant stars, HEAO 1 obs. of active cor- nae 0-72925  
 LMC bar, soft X-ray source identification 0-82491  
 LS I+61°303, variable binary radio star (BI Ib), X-ray emission detect. 0-105400  
 Lupus Loop, X-ray spatial extent and spectrum of SNR 0-82457  
 M86, elliptical galaxy, X-ray evidence for hot gas retention 0-90535  
 Markarian 464, type I Seyfert galaxy, Ariel V X-ray spectra 0-90539  
 MCG -6-30-15, type I Seyfert galaxy, X-ray and optical obs. 0-82479  
 MCG 8-11-11, X-ray obs. of Seyfert 1 galaxy 0-105344  
 MSH 11-54 (H1122-59), supernova remnant, X-ray obs. 0-82463  
 MXB 1636-536, binary nature from simultaneous X-ray and optical obs. 0-82548  
 MXB 1730-333, no burst activity in 1980 July-Sept. period 0-105402  
 NGC 4151, Seyfert galaxy, repeated X-ray flaring obs. 0-90534  
 North Polar Spur, SNR, soft X-ray spectra emission line features obs. 0-94849  
 North Polar Spur (Radio Loop 1), X-ray obs. 0-105370  
 OAO 1653-40 38 s pulsating X-ray source position and optical search 0-73072  
 observational test of cosmological particle production theories 0-109574  
 X Persei (A 0535+26), Prognoz-6 obs. of X-ray fluxes and energy spectra (Russian) 0-109562  
 PKS 2155-304, BL Lacertae object, rapid X-ray variability obs. 0-73035  
 PSR 0833-45, Vela pulsar, pulsed soft X-ray flux, upper limits 0-105268  
 V861 Scorpii, upper limit on X-ray emission, and non-coincidence with (OAO 1653-40) 0-73072  
 Scorpius X-1, binary star, X-ray spectrum 20-75 keV, high sensitivity determ. 0-98741  
 Scorpius X-1, binary star X-ray obs. from 20 to 250 keV 0-94893  
 Scorpius X-1, high energy X-ray and SHF radio obs. 0-73067  
 Scorpius X-1, mag. field determ. via linear polarisation spectrum (Russian) 0-90344  
 Scorpius X-1, Prognoz-6 obs. of X-ray fluxes and energy spectra (Russian) 0-109562  
 Scorpius X-1, rapid variability simultaneous X-ray and optical obs. 0-62322  
 Serpens X-1, no IR bursts assoc. with Type I X-ray burst 0-98742  
 SN 1006 remnant, X-ray spectrum 0-82457  
 solar flare, electron density determ. from X-ray spectra obs. 0-82326  
 solar spectrum, Ni IX to Ni XII transitions identifications from laboratory wavelengths 0-99474  
 Sun, 1979 March 25 flare 0-85915  
 Sun, active region McMath 12628, EUV and X-ray obs. 0-67692  
 Sun, coronal loops in an active region, physical props. XUV obs. 0-90376  
 Sun, flares, X-ray emission (50-100 keV) directivity 0-105218  
 Sun, flaring X-ray bright points, assoc. with type III bursts 0-67681  
 Sun, gamma-ray lines from flare, HEAO 1 obs. 0-67682  
 Sun, young active regions, filaments, and flares 0-72910  
 4U 1608-52, burst activity since Hakucho launch (1980 April) 0-62321  
 4U 1700-37 (=HD 153919), eclipsing binary, X-ray obs. 0-86016  
 4U 1700-37 (HD 153919), X-ray binary, high-energy X-ray obs. 0-86014  
 4U 1822-37, 2129+42, X-ray fluxes modulation periods from HEAO obs. 0-77516  
 4U 1907+09, optical identification using HEAO-1 scanning modulation collimator position 0-82542  
 SU Ursae Majoris, soft X-ray halo around dwarf nova 0-98677



**X-ray astronomical observations continued**

- Vela X-1 (HD 77581), binary source, spectral obs. 0-94892  
 WRA 977 (4U 1223-62, GX 301-2), binary star orbit determ., SAS 3  
 obs. 0-90570

**X-ray astronomy**

- see also *X-ray sources astronomical*  
 80 cm X-ray telescope, facilities and observational possibilities (German)  
 0-109358  
 Advanced X-ray Astrophysics Facility, results obtained 0-109366  
 automodulation collimator telescope, for point X-ray source imaging (Russian)  
 0-62018  
 background emission from quasars and clusters of galaxies 0-105405  
 diffuse X-ray background, rel. to intergalactic matter 0-109543  
 diffuse X-ray background intensity, implications of uniformity of quasars  
 radial distrib. in chronometric cosmology 0-105409  
 Einstein X-ray observatory and obs. of cosmological objects 0-105171  
 Hadamard transform X-ray telescope, characts. (Japanese) 0-94714  
 HEAO-2 Observatory, protective design considerations, system reliability  
 0-61983  
 HEAO-B, high-energy astrophysical satellite lab., X-ray observ. facilities  
 (Dutch) 0-61986  
 high pressure gas scintillation spectrometers for X-ray astronomy  
 0-105166  
 imaging gas scintillation counter for X-ray astronomy 0-98551  
 intergalactic C model abundance, X-ray absorpt. effects 0-62270  
 Lixoscope, X-ray and gamma-ray telescope system 0-62020  
 sky survey project EXUV 10-1000 Å waveband, proposed mission  
 0-82165  
 solar flare, transient plasma X-ray spectra, electron density and temp.  
 diagnostics 0-77363  
 solar flare plasma, Langmuir turbulence spectrum estimate from X-ray  
 obs. 0-82329  
 solar flares, transient plasma X-ray lines, rate coeff. determ. 0-72903  
 solar flares, X-ray line spectra from transient plasma 0-98626  
 space optics, imaging X-ray optics workshop, Huntsville, Alabama (1979  
 May 22 to 24) 0-62384  
 Space Shuttle, instrums. and expts. 0-109363  
 spectra, direct deconvolution method 0-85867  
 spectrometer-telescope system for solar corona studies 0-105168  
 transmission gratings for 7-304 Å operation, efficiency and resolution  
 0-82195  
 wide field camera, design, sensitivity and performance 0-85863  
 XUV astronomy, review (German) 0-109372  
 XUV solar telescope and white light coronagraph, CCD camera systems  
 and support electronics 0-62023  
 XUV telescope/white light coronagraph expt., quadratic A/D converter  
 0-62024

**X-ray characteristic temperature** see Debye temperature**X-ray chemical analysis**

- see also *electron probe analysis; X-ray diffraction examination of materials; X-ray fluorescence analysis*  
 air pollution monitoring, PIXE and NRA studies using lichen indicator  
 0-61744  
 alkali borosilicate glasses, observation of phase separation using SEM-  
 EDX technique 0-76224  
 alloys, thin foils, data correction for absorpt. effects 0-85255  
 alloys, X-ray fluorescence correction in thin foil analysis 0-85256  
 applications, conf., Denver, CO, USA, July-Aug. 1979 0-90613  
 atmospheric aerosols, chem. characterisation by X-ray absorpt. spectrosc.  
 0-61501  
 atmospheric aerosols, chem. characterisation by X-ray absorpt. spectrosc.  
 0-72121  
 coal, computer controlled technique 0-71994  
 coated arc electrodes, identification of types and brands using energy-  
 dispersive X-ray anal. 0-81400  
 corrosion in H<sub>2</sub>SO<sub>4</sub>, estimated from weight loss meas. at 270°C and 56  
 bar (French) 0-85080  
 electron probe analysis, spatial resolution in thin foils 0-101065  
 electron probe dispersion influence on spatial resolution in STEM  
 0-85257  
 electron probe X-ray microanalysis, quantitative investigation of thin spec-  
 imens 0-101068  
 elemental analysis, quantitative, using energy-dispersive X-ray spec-  
 trometer 0-104840  
 energy dispersive, STEM microanalysis of precipitates in Ni-base superal-  
 loy 0-104492  
 energy dispersive spectral analysis, using semicond. detectors, review  
 0-85237  
 energy dispersive X-ray spectrometry, qualitative and quantitative analysis  
 problems 0-85249  
 field emission gun STEM 0-85260  
 films, orientation effects in quantitative X-ray microanal. 0-85259  
 gas atmosphere quantitative analysis adsorption chamber 0-85234  
 Ge-Si sandwich struct., sputter profiling, combined Auger-X-ray anal.  
 0-66909  
 hair, human, PIXE analysis, correction factor, rel. to pollution monitoring  
 0-61743  
 k-shell ionizations in proton induced X-ray emission analysis 0-101054  
 light elements, ultrasoft X-ray spectroscopy, local anal., electron-  
 microprobe excited radiation 0-99027  
 microanalysis, in TEM up to 1000 kV 0-101063  
 microchemical analysis, optimising conditions, analytical electron micro-  
 scopy 0-101067  
 microscopy, high resolution, with synchrotron radiation, for chem.  
 microanal. 0-81416  
 mineral fibre characterisation using energy dispersive X-ray spectrometry  
 in TEM (French) 0-82857  
 mineralogical use of energy dispersive X-ray spectrometry with Si(Li)  
 diodes (French) 0-85251  
 ore dressing X-ray spectrometric analysis centre 0-86541  
 phosphosilicate glass coatings, measurement of P content using SEM and  
 energy-dispersive X-ray analyser 0-76588  
 phosphosilicate glasses, P content determ. by Rutherford backscatt., PIXE,  
 and activation anal. (Hungarian) 0-85233  
 PIXE, appl. to primate trace element retention 0-81792  
 PIXE, use of liposomes to reduce enhancement-absorption effects  
 0-101053  
 PIXE appl. to design and evaluation of catalysts 0-61201  
 polynuclear aromatic hydrocarbons, analysis by X-ray excited optical  
 luminescence technique 0-66891

**X-ray chemical analysis continued**

- precipitate free zones, X-ray microanal. 0-108768  
 pulmonary fibrosis disease diagnosis, histological section SEM and  
 energy-dispersive X-ray microanalysis 0-72314  
 quartz glass, Ge and B dopants, OH impurities, preform material and  
 fibre optic waveguide struct. 0-64173  
 radiometric analyser, appl. of expt. planning 0-61186  
 research and quality assurance appl. 0-73556  
 scanning microprobe microscopy, conf., Paris, France (Oct. 1979)  
 0-82569  
 solid, backscattering coeff. meas. of 15 to 60 keV electrons at various  
 angles of incidence, rel. to X-ray microanal. 0-80919  
 spatial resolution, for SEM and STEM specimens, Monte Carlo methods  
 0-101066  
 spatial resolution, use of STEM 0-104490  
 specimen particles dimensions effect on X-ray intensity excited by protons  
 0-85238  
 spectral line superpositioning, calc. 0-85240  
 steel, Al-Cr, FeO(Al,Cr...),O<sub>2</sub> inclusions, thermodynamics 0-60831  
 steel, Cr-Mo-P (2.25, 1 wt.%), stress relief cracking, effect of P segrega-  
 tion 0-89324  
 steel, ferritic stainless, Cr-Mo (12.1 wt.%) microstructure influence on  
 localised corrosion behaviour 0-61018  
 steels, obs. and anal. of sulphides, using non-aqueous electrolyte-  
 potentiostatic etching method (Japanese) 0-89433  
 STEM, appl. to materials science 0-103228  
 STEM, structural and chemical analysis, appls. 0-88003  
 STEM appl., statistical variation limitation 0-61208  
 surface anal. tools review 0-103540  
 surfaces and interfaces, analysis by combined Auger, X-ray and SEM  
 studies 0-81413  
 surfaces and thin film studies by combined system of SIMS, AES and  
 XPS 0-86536  
 TEM, exptl. and theoretical X-ray prod. 0-85258  
 thin film, sputter profiling, combined Auger-X-ray anal. 0-66909  
 thin foil, X-ray microanalysis in electron microscope (French) 0-61191  
 thin samples, mass thickness and chem. composition determ., by TEM and  
 X-ray anal. 0-103227  
 tubes, for diff. anal., spectral purity, quantitative determ. (Chinese)  
 0-57444  
 Al, sputter deposit PIXE expt. 0-61196  
 Al<sub>2</sub>O<sub>3</sub>, sintering temperature effect of titanate additions 0-60808  
 Al<sub>2</sub>O<sub>3</sub> thin film used in inelastic electron tunnelling spectroscopy, X-ray  
 photoelectron spectrum 0-108319  
 Al<sub>2</sub>O<sub>3</sub>:MgO, grain boundary segregation of Ca and Mg X-ray spectrosc.  
 and STEM study 0-107269  
 BaTiO<sub>3</sub>:BaTiO<sub>3</sub>, dielec. props. and microstruct. 0-60481  
 (CaO):SiO<sub>2</sub> cement pastes, electron microsc. anal. 0-108761  
 Cu, sputter deposit PIXE expt. 0-61196  
 Cu-metal thin film couples, room temperature interactions 0-96699  
 Cu-Ni-Nb (30, 0.9 at %), precipitate free zones, X-ray microanal.  
 0-108768  
 Eu-B-C ternary and binary boundary systems, preparation techniques,  
 X-ray analysis 0-60840  
 Ga<sub>2</sub>As<sub>2</sub> based layer structures, optimum growth conditions, comp. and  
 struct. perfection 0-104069  
 Hg lamps, RF-excited, dark film anal. 0-92789  
 InP, Zn diffused single-crystal, substitutional dopant and hole conc. meas.  
 0-75260  
 MgO-NiO, STEM microanal., absorpt. effects 0-80902  
 Mn-Zn ferrites, grain boundary exam. using TEM and AES 0-107268  
 Sn<sub>2</sub>, Pb,Se(Te) films, oxidation rel. to annealing temp. and time, Moss-  
 bauer spectra, X-ray and microstruct. obs. 0-104311  
 Ti<sub>2</sub>O<sub>3</sub>-Al<sub>2</sub>O<sub>3</sub> (MgTi<sub>2</sub>O<sub>7</sub>), solid solubility, X-ray phase and optical micro-  
 scopic exam. 0-59657  
 ZrO<sub>2</sub>, partially stabilized, processing defects 0-97558

**X-ray crystallography**

- For results of structure analysis see crystal atomic structure  
 see also *X-ray crystallography apparatus; X-ray crystallography calcula-  
 tion methods; X-ray crystallography technique*  
 anomalous dispersion correction determ., use of photoelec. attenuation  
 meas. 0-84026  
 conference, Crystal XII, Canberra, Australia (Jan.-Feb. 1980) 0-62388  
 defects classification according to influence on radiative diffraction (Russian)  
 0-70189  
 electron and magnetisation densities in molecules and crystals, Arles,  
 France (Aug. 1978) 0-105428  
 HCP lattice, Huang diffuse scatt. from interstitials 0-88142  
 indexing reliability, of X-ray diffraction powder patterns 0-87990  
 lattice dynamics and X-ray diff., early work by I. Waller 0-62439  
 standard X-ray diffraction powder patterns 0-64839  
 standing waves obs. at Si crystal surface 0-96417  
 structure amplitude phases, statistical-thermodynamic determ. 0-84028  
 texturised materials, orientation distrib., demonstration of ghost effect  
 0-70080

**X-ray crystallography apparatus**

- see also *goniometers; X-ray diffractometers; X-ray monochromators*  
 acid phthalate curved crystal spectrograph, diffraction efficiency calc.  
 method 0-79630  
 Bonse-Hart X-ray diffractometer, asymmetrically cut, comparison with  
 Kratky camera 0-77917  
 camera, topographic 0-84029  
 colour display of Laue patterns with scanning X-ray beam 0-87991  
 comparator for meas. cutoff angle of piezoelec. quartz wafers 0-105755  
 diamond-anvil press, cell for X-ray diff. obs. with solid-state or propor-  
 tional counter 0-75119  
 filament lifetimes, in rotating-anode X-ray machines, increasing using  
 beam-deflecting magnet 0-77918  
 focal site lengthening, in Elliott rotating-anode X-ray sets 0-77919  
 goniometer, for precise X-ray powder diffraction with temp. control  
 (French) 0-79631  
 goniometer, for stress measurement in single crystals, and coarse-grained  
 specimens 0-64837  
 goniometer for cutting single crystals 0-86275  
 monochromator for synchrotron radiation using three wave Bragg diff.  
 0-87993  
 MWPC, flat area detector data acquisition system for X-ray crystallogra-  
 phy 0-91381  
 position-sensitive detector, appl. to high pressure X-ray diff. using diam-  
 ond-anvil cell 0-79632



**X-ray crystallography apparatus continued**

- powder-film calibration device 0-84030  
 semiconductor detector uses and problems (*French*) 0-84031  
 topographic camera, high-sensitivity double-crystal, lattice parameter meas. 0-77915  
 topography, new on-line system 0-79638  
 tubes, for diff. anal., spectral purity, quantitative determ. (*Chinese*) 0-57444  
 LiF cell, for X-ray struct. investigations 0-64829  
 LiF curved crystal spectrograph, diffraction efficiency calc. method 0-79630

**X-ray crystallography calculation methods**

- acid phthalate curved crystal spectrograph, diffraction efficiency calc. method 0-79630  
 Bragg reflection in case of multiple X-ray scatt. 0-100127  
 Bragg reflection in case of multiple X-ray scatt. 0-100128  
 Bragg reflections, ratio of integral intensities, determ. struct. perfection of single crystals 0-87987  
 close-packed crystals, with chaotic subtraction packing defects, general soln. of diff. problem 0-92422  
 close-packed structures, with faults, anal. soln. for X-ray diff. integrated intensities 0-100256  
 composite multidimensional function decomposition into its components 0-79625  
 crystal setting, and data reduction, on a PW 1100 diffractometer, program using simple method based on real space 0-59342  
 crystal structure determ., optimal selection method on starting reflexion set (*Chinese*) 0-84025  
 crystallites, needle shaped, X-ray powder reflection profiles calc., principles 0-100124  
 cube, correlation function, intersect distrib. and scattering 0-59338  
 deformed crystal, theory of X-ray scatt. (*Russian*) 0-70077  
 drift and lattice const. determ., graphic method (*Chinese*) 0-87985  
 dynamic scattering, crystal with equidistantly bent reflecting planes, eqns. (*Russian*) 0-70079  
 dynamic theory of scattering, crystal with equidistantly bent reflecting planes (*Russian*) 0-70078  
 elastic X-ray scattering, by thermodynamic average electron-charge density 0-100123  
 energy dispersive diagrams, eval. using small computer on-line techniques 0-92423  
 equivalent reflections averaging, using small computers 0-79634  
 extinction correction, in white X-ray and neutron diff. 0-100120  
 Frevel ZRD-SEARCH-MATCH program, for powder diff. anal., generalisation 0-59341  
 integration method, extension of  $\sin^2\psi$  method (*German*) 0-92420  
 intensity distrib., and integrated intensity in topography of crystals, Laue cases, statistical dynamic theory 0-107014  
 interbranch scattering fringes, contrast (*Russian*) 0-64835  
 interference pattern, influence of medium inhomogeneities on nature and intensity (*Russian*) 0-64834  
 isovector structure, relationship between basic and vector point systems 0-79626  
 Laue photograph indexing and monocrystal orientation determination by computer, new approach (*Chinese*) 0-79636  
 layer structures, intensity calcs. of diff. product bands (*French*) 0-59339  
 metals, cubic, crystallographic orientations distribution function, computer calc. 0-64827  
 misfit boundary crystals, reflection curves 0-92421  
 multi-beam dynamical diff. of X-rays, permitted models of propag. 0-107015  
 multi-solution general form in Patterson method for low symm. system (*Chinese*) 0-107016  
 needle crystals, very small, X-ray powder reflection profiles calc., principles 0-100124  
 one-phase semiinvariants, practical aspects and appls. of probabilistic formulae 0-100119  
 one-phase structure semiinvariants, of first rank, estimation by generalised second representations 0-107013  
 orientation distribution function analysis from incomplete pole figures normalised by iterative method 0-59344  
 P2 space group, compensation of excess intensity 0-107088  
 partial Patterson function, use for superlattice reflection phase determ. 0-79627  
 particle dimension determination, by direct Fourier cosine transformation, of expt. SAXS data 0-79624  
 Patterson method, multiple solutions for low symm. systems (*Chinese*) 0-87986  
 perfect crystals, X-ray diff. for finite duration (*Russian*) 0-64825  
 $\beta$ -phycocerythrin crystals, twinned by merohedry, diff. data treatment 0-108845  
 polarisation factor, for cryst.-monochromated radiation, weighted scheme for products 0-100122  
 polarisation factor errors, for cryst.-monochromated X-radiation 0-100121  
 powder samples, peak positions determ. from step-scanned X-ray powder diff. data 0-103217  
 satellite tobacco necrosis virus struct., detect. and idealisation procedures of non-crystallographic symmetry with phase refinement appl. 0-108840  
 shift-type packing defects, involving dislocation representations, influence on diff. pattern 0-107239  
 slit correction functions, exact soln. of slit-height correction problem in small angle X-ray scattering 0-79622  
 small-angle scattering, information content and error anal., Shannon sampling 0-59340  
 small-angle scattering problems, multiple scattering treatment 0-100125  
 spot broadening, resolution, X-ray and electron beam diff. patterns (*German*) 0-84033  
 structural fragment, automatic construction, taking account of attainable chem. bond lengths 0-92419  
 structure amplitude phases, statistical-thermodynamic determ. 0-84028  
 structure semi-invariants, representations method 0-79724  
 texture of materials, data acquisition and processing 0-64828  
 thermal factor refinement procedure, restrained-parameter 0-79628  
 valence electron distribution, in crystals, diff. data processing 0-92418  
 wave packet polarisation, in X-ray monochromators, dynamic theory (*Russian*) 0-64826  
 Al {111}, X-ray Huang diffuse scatt. from dislocation loops 0-79797

**X-ray crystallography calculation methods continued**

- Be, X-ray scattering, Wannier function calcs. 0-87988  
 LiF curved crystal spectrograph, diffraction efficiency calc. method 0-79630

**X-ray crystallography technique**

- amorphism, techniques for determ. very short room temp. lifetimes 0-84981  
 broadly divergent X-ray beam method, possibility of obtaining diff. patterns from polycryst. specimens 0-107020  
 crystal monochromators, determ. of polarisation ratio 0-99018  
 crystal setting, and data reduction, on a PW 1100 diffractometer, program using simple method based on real space 0-59342  
 diffractometry and tomography for observation of semiconductor crystal growth and defects 0-73546  
 elastically vibrating single crystal, simultaneous diff. effect on rocking curve 0-107019  
 energy dispersive diffractometry, semicond. detector uses and problems (*French*) 0-84031  
 energy dispersive X-ray diffraction, determ. struct. of amorphous alloys 0-84063  
 focusing, with (n,m)-positioning of crystals 0-87989  
 high-pressure X-ray diff. patterns, nonuniform line broadening 0-79629  
 incident beam intensity meas. by absorpt. method 0-68333  
 interbranch scattering fringes, contrast (*Russian*) 0-64835  
 isomorphous derivative data collection, strategy with oscillation method 0-79633  
 large monocrystal X-ray reflection/scanning and transmission topographic methods 0-96415  
 Laue reflections splitting and defects image contrast form. (*Russian*) 0-64833  
 optical filtration methods, processing of X-ray images 0-87992  
 $\beta$ -phycocerythrin crystals, twinned by merohedry, diff. data treatment 0-108845  
 polymers, non-crystalline, experimental separation of coherent component of X-ray scattering prior to RDF anal. 0-64838  
 powder camera films, calibration method 0-79635  
 powder diffraction technique appl., in research and quality assurance, impact of computerised data handling 0-73556  
 powder samples, peak positions determ. from step-scanned X-ray powder diff. data 0-103217  
 ring Laue diff., X-ray struct. anal. method (*Russian*) 0-96416  
 section topograph technique, high resolution, applicable to synchrotron radiation sources 0-57449  
 specular reflection coefficient, influence of X-ray beam parameters on meas. accuracy 0-107022  
 synchrotron radiation from electron storage rings, appl. to X-ray topography 0-64830  
 topographic patterns, spectral sensitivity of TV system for visualisation (*Russian*) 0-62814  
 topography, new on-line system 0-79638  
 topography developments, review 0-64836

**X-ray detection and measurement**

- see also X-ray spectrometers  
 angular distribution measurement by ETL quantameter for X-ray emission from thick targets 0-91367  
 autoradiographic inventory methods for nondestructive assay of reactor fuels and fuel assemblies 0-71875  
 collective heavy ion electron ring accelerators, X-ray particle beam diagnostics 0-102358  
 computerised tomography, expt. dual XE detectors for quantitative CT and spectral artifact correct. 0-76825  
 computerized tomography field measurement utilising the partial vol. effect 0-89865  
 cyclotron dee voltage calibration using an intrinsic Ge X-ray detector 0-99359  
 diamond-anvil press. cell for X-ray diff. obs. with solid-state or proportional counter 0-75119  
 drift chamber based detector for X-ray scatt. expts. 0-58045  
 dual proportional counter for recording transition radiation 0-63458  
 Geiger coordinate counters for UV and X-ray photons 0-69026  
 high resolution gas scintillation proportional counter for studying low energy cosmic X-ray sources 0-58052  
 industrial X-ray installation, spectroscopic anal. (*German*) 0-97668  
 ionisation chamber, parallel-plate, collection efficiency in pulsed X-ray field 0-99407  
 molecular biology, time resolved X-ray scatt. expts., rapid data collection systems 0-61740  
 multichannel semiconductor detectors for X-ray transmission computed tomography 0-58058  
 parallel grid imaging proportional counter optimized for detection of low brightness stellar XUV-sources 0-58049  
 position sensitive gas scintillation proportional counter for X-ray astronomy 0-58053  
 position-sensitive detector, appl. to high pressure X-ray diff. using diamond-anvil cell 0-79632  
 quantum counters, dead time determ., accuracy estimation 0-99022  
 semiconductor detectors for energy dispersive X-ray spectral analysis, review 0-85237  
 $^{252}\text{Cf}$  fission fragment  $\beta$ -decay, X-ray- $\beta$  particle coincidence technique 0-74094  
 CsI photocathodes, efficiency evaluation for soft X-ray diagnostics 0-57442  
 CuI photocathodes, efficiency evaluation for soft X-ray diagnostics 0-57442  
 Ge X-ray detector, Au contact layer thickness meas. 0-62627  
 HgI<sub>2</sub> detectors for X-ray, computerized tomography, evaluation 0-89837  
 Kr photo-ionization proportional scintillation chamber 0-58056  
 $^{92}\text{Nb}^m$ , production and impregnation in polystyrene microspheres for X-ray detector calibration 0-74065  
 Si photodiode array, position-sensitive photon detector for the UV or X-ray range 0-90970  
 p-Si semiconductor detector in radiometric inspection problems 0-62819  
 Si(Li) X-ray detector, Au contact layer thickness meas. 0-62627  
 Xe high pressure proportional, scintillation camera for X- and  $\gamma$ -ray imaging 0-99412

**X-ray diffraction**

- see also X-ray crystallography; X-ray diffraction examination of materials; X-ray diffractometers; X-ray scattering  
 applications, conf., Denver, CO, USA, July-Aug. 1979 0-90613

**X-ray diffraction continued**

cyclic X-ray monochromators, with perpendicular dispersion planes, emission coherence 0-90974  
flash X-ray tube for diffraction studies on 2-stage light gas gun 0-86537  
generalities and classical methods (*Italian*) 0-87984  
grating optimal blazing configuration calc. 0-105762

**X-ray diffraction examination of liquids**

see also *liquid structure*  
butyloxylbenzylidene octylaniline, two- and three-dimensional smectic B liq. cryst. film, long range order 0-96442  
CBOOA, smectic-A reentrant nematic transition under press., X-ray obs. 0-59637  
colloidal particles, in a flowing solution, SAXS 0-61163  
cyanooctylbiphenyl, smectic A phase, X-ray diff. study 0-79690  
dextrins, branched, in soln., cross-section factor correction in small-angle X-ray scatt. data 0-84048  
dipalmitoyl lecithin bilayer, mol. tilt, X-ray diffraction obs. in gel phase 0-84059  
ferrofluids, conc. depend. mag. grain correls., small angle X-ray scatt. study 0-61160  
liquid crystal, high resolution X-ray and light scatt. obs. 0-92460  
liquid crystals, X-ray diff. studies, review 0-100166  
mesogenic materials, tails or smear effects in X-ray diff. photographs 0-96438  
mesophase pitch, magnetically-oriented, phys. props., mol. struct. 0-64885  
n-pentyl 4-(4-n-dodecyloxybenzylidene-amino)-cinnamate, X-ray studies in smectic I phase 0-70119  
4-n-pentyl-phenylthiol-4'-n-octyloxybenzoate, smectic A-smectic C phase transition, high-resolution X-ray study 0-79921  
polybutadiene-poly- $\alpha$ -methylstyrene copolymers, struct. obs., prep. (*French*) 0-59401  
sodium undecanoate/water system, lyotropic liq. cryst. struct. change due to polymerisation of amphiphilic component 0-59386  
TBBA, mesophase identification by X-ray diff., review 0-100166  
TBBA liquid crystal, monoclinic cell parameters of solid, smectic and metastable phases, temp. dependence 0-70122  
Ar, liq., critical exponent,  $\eta$ , X-ray scatt. 0-92660  
EuCl<sub>3</sub>, coord. in aq. Cl<sup>-</sup> soln., X-ray diff. obs. 0-92445  
He, fluid struct. factor meas. in range 5.5 to 7.0K 0-80011  
N<sub>2</sub>, liq., atom pair pots., X-ray diff. 0-100158  
Na-K liquid alloys, struct., X-ray and neutron diff. meas. 0-107041  
NaNO<sub>3</sub>, aqueous soln., X-ray diffraction, radial functions and positional correl. 0-79665  
R<sup>3+</sup> ions, coord. in aq. Cl<sup>-</sup> soln., X-ray diff. obs. 0-92445  
SmCl<sub>3</sub>, coord. in aq. Cl<sup>-</sup> soln., X-ray diff. obs. 0-92445

**X-ray diffraction examination of materials**

for results of crystal structural analysis see *crystal atomic structure*  
see also *X-ray chemical analysis*; *X-ray diffraction examination of liquids*; *X-ray diffraction examination of microstructure*; *X-ray diffraction examination of molecular structure*  
Agave cantala natural fibre, small-angle X-ray scatt. of densely packed colloidal system, scatt. inhomogeneities 0-76565  
alloys, machining damage, depth of surface layers determ. 0-85094  
amylopectin, glycerin impregnated, dynamic viscoelasticity (*Japanese*) 0-104203  
amylose, glycerin impregnated, dynamic viscoelasticity (*Japanese*) 0-104203  
benzene, phase transform. process, energy-dispersive X-ray diffractometry 0-96631  
benzil cored fibres, void-free cryst. growth, X-ray diff. and optical microscopy study 0-71586  
2-benzyl-5-benzylidenecyclopentanone, and substituted form, topochem. single-cryst.-to-single-cryst. photodimerisation 0-66819  
bis-(p-toluene-sulphonate) of 2,4-hexadiyne 1,6-diol, X-ray scattering obs. of polymerisation mechanism and phase transition (*French*) 0-70399  
bis-p-toluene sulphonate of 2,4-hexadiyne-1,6-diol, X-ray scatt., incommensurate modulated struct. obs. 0-70185  
7CaO-V<sub>2</sub>O<sub>5</sub>-2SiO<sub>2</sub>, X-ray diff. data 0-81037  
carbon tetrachloride, phase transform. process, energy-dispersive X-ray diffractometry 0-96631  
[CC] Ag-(100)InP, metal-semicond.cathode contact, metallurgical, physical, chemical processes 0-107911  
ceramic building materials, breakdown kinetics by X-ray diff. 0-108526  
clay sample preparation for X-ray diff. anal. 0-97647  
colloidal particles, in a flowing solution, SAXS 0-61163  
composite materials, crack growth, conc. criterion 0-65146  
computer-aided system of X-ray stress meas. (*Japanese*) 0-104366  
crystalline materials, struct. of grain boundaries using diff. techniques 0-59478  
cyano compounds, liq. cryst. phases, incommensurate coexistent density fluctuations 0-79691  
cybotactic nematic mesophase 0-92454  
cyclohexanol, glassy cryst., diffuse X-ray scatt. study 0-100171  
diacetylmonocarboxylic acids, multilayers, struct. phase transitions and polymerisability 0-80129  
diamond, synthetic monocrystals, inclusions phase comp., radiographic method 0-100978  
diamond, ultradisperse, ESR, particle size and lattice microdistortions 0-97140  
diamond anvill cell, high press. diff., pseudo-Kossel lines 0-79623  
diamond powders, Mo coated, X-ray diff. study 0-100936  
diamond synthesis by graphitisation of carbon materials at high press. and temp., Ni influence 0-60795  
dickite, unusual crystal habit, structural disorder 0-59445  
m-dinitrobenzene cored fibres, void-free cryst. growth, X-ray diff. and optical microscopy study 0-71586  
dioctadecyl hydrogen maleate crystals, X-ray spectroscopic true 2d<sub>h</sub> value, 'effective' 2d value concept of Bragg spectrometer crystals 0-70081  
divalent Sr, Ba, Ca, Zn, Cd iodates, complex salts, phase transitions, cryst. struct. (*Chinese*) 0-70171  
emerald, artificial single crystal, distrib. of Cr<sup>3+</sup> impurity 0-59505  
esters, long-chain, X- and Y-type multilayers, form. conditions and struct. characterisation 0-80127  
F 0-100329  
ferroelectric tetragonal ceramics, 90° domain-rot. fraction after polarisation, X-ray determ. 0-75992  
film, thermal strain, strain relax. above room temp. 0-59841  
glass fragments, classification into window and non-window types 0-81401

**X-ray diffraction examination of materials continued**

glass struct. study using small-angle X-ray scatt. 0-84071  
glasses, inorganic, struct. by X-ray scatt. diff. obs. 0-84069  
graphite fluorides, (CF)<sub>n</sub> and (C<sub>2</sub>F)<sub>n</sub>, prep., struct., discharge charact., electrode props. 0-89502  
graphite salts, C<sub>8</sub><sup>+</sup>MF<sub>6</sub><sup>-</sup>, (M=Os,Ir,As), struct. and elec. props. 0-70183  
graphite-AsF<sub>5</sub> intercalated species, fractional ionisation and identification 0-97397  
Hastelloy-X, Ni-Cr-Fe-Mo, cyclic oxidation resist. improvement by high temp. etching treatment 0-97627  
hollandites, cryst. growth and structural props. 0-89129  
II-VI semiconductors, thin epitaxial layer, direct synthesis (*German*) 0-104070  
Invar, Fe-Ni (36 wt.%), alloy 36N, effect of melting conditions on thermal expansion coeff. 0-65256  
lipid thermotropic clustering in Tetrahymena endoplasmic reticulum membranes 0-85363  
lunar regolith samples from Lunar-24, X-ray diff. and thermogravimetric obs. 0-67598  
manganese stearate, Langmuir-Blodgett layers, high resolution X-ray diff. 0-80126  
metal, textured cubic, residual stress evaluation 0-89435  
metallomacrocycles, mixed valent, cofacial assembly, cond. polymeric material 0-70143  
5-methyl-1-thia-5-azacyclooctane-1-oxide perchlorate, single cryst. transform., evidence for intermediate state 0-88078  
4,4'-methylenebis(1,3,5-trimethyl-4-imidazolin-2-one), cryst. and mol. struct. 0-107201  
muscle contraction process, 10 ms time resolution X-ray diff. 0-61741  
neutron-bombarded, diffuse X-ray scattering (*Russian*) 0-92560  
nosean identification, in sodalite and conversion of nosean sodalite 0-84907  
Nylon 6 film, prior high-press. treatment effects, weight swelling, density, IR crystallinity, X-ray and viscosity obs. 0-81025  
Nylon-12 film, casting conditions effect on polymorphism 0-84903  
octadecylacrylamide films, oriented ultrathin, radiation-induced solid state polymerisation 0-80128  
para-polyamide based fibres, struct. deform. props. 0-60928  
PET, amorphous, intrinsic birefringence calc. from wide angle X-ray scatt. 0-108178  
trans-polyacetylene, bulk crystallinity, small-angle X-ray diff. study 0-103263  
polyalkane imides, crystallisability, supermol. and crystalline structures 0-84100  
polyamide, aromatic, fibre, high modulus, mol. and supramol. struct. 0-79710  
polyaryloxyphosphazene copolymers, thermal, morphological and rheological props. 0-103265  
polybutadiene-poly- $\alpha$ -methylstyrene copolymers, struct. obs., prep. (*French*) 0-59401  
polybutylene terephthalate, melt crystallised, solvent crystallised films and moulded bars, morphological obs. 0-84101  
polycapraamide, oriented filaments, mech. props. 0-66550  
polycarbonate, bisphenol A, WAXS pattern, temp. effect and thermal history 0-93583  
polyethylene,  $\gamma$ -irrad., asymmetric 002 X-ray line profiles, analysis 0-96567  
polyethylene, high press. phase, US, DTA, and X-ray diff. study 0-75188  
polyethylene, melt-crystallised fractions, surface and full-strand melting, small-angle X-ray scatt. obs. 0-84279  
polyethylene fibre, high-strength high-modulus, morphology and tensile prop. relations 0-103264  
polyethylene oxide, nascent and annealed, X-ray study of crystal structure 0-64922  
polyethylene oxide-polystyrene-polyethylene oxide triblock copolymer, surface and full-strand melting, small-angle X-ray scatt. obs. 0-84279  
polyethylene terephthalate, oriented, amorphous, stress-induced crystn., shrinkage meas. 0-92466  
polyethylene terephthalate, shear compliances meas. of oriented sheet 0-104363  
trans-1,4-polyisoprene crystals, press. effect on melting temp. and lamellar thickness, press. crystn. 0-88302  
polymer concretes, hydrothermally stable, hydraulic cement-type fillers 0-85144  
polymer liquid-crystalline solns., struct. 0-103235  
polymer spherulite, cryst. lattice strains, mech. behaviour, X-ray diff. detect. 0-59558  
polyoxymethylenes, dielectric relaxation, molecular mechanism (*Russian*) 0-88923  
portland cement, doped with ZnO, struct. and props. 0-60914  
PVC, oriented mouldings, struct. order 0-60896  
 $\alpha$ -quartz, Renninger effect, forbidden X-ray reflections 0-64980  
rare earth chalcobismuthites, RBiTe<sub>3</sub>, prep., elec. props., and crystallographic date 0-59981  
rare earth hydrides, form. by rare earth reaction with H<sub>2</sub>O vapour 0-76504  
rare earth metal silicide thin film formation on (100), (111)Si substrates, backscattering study 0-70542  
sapphire ribbon crystals, EFG growth and charact., voids, grain boundaries and dislocations 0-103283  
seed materials subjected to mag. field, X-ray diff. patterns. 0-89721  
Si, ion implanted by high energy C ions structural and optical props. 0-107292  
silicate glasses, polishing, surface charact. using grazing X-ray reflection (*French*) 0-65353  
spacecraft materials failure, metallurgical exam. 0-71868  
starch, glycerin impregnated, dynamic viscoelasticity (*Japanese*) 0-104203  
stearic acid, vacuum evaporated film, for low-loss capacitors 0-71317  
steel, austenitic stainless, phosphide analysis using nonaqueous electrolyte potentiostatic etching method (*Japanese*) 0-89221  
steel, austenitic stainless, unlubricated, friction, wear and microstruct. of types 304, 316 and Nitronic 60 0-108589  
steel, austenitic stainless, welded explosively, induced martensites morphology 0-104153  
steel, austenitic stainless, X-ray stress meas., accuracy and method of data treatment (*Japanese*) 0-104365  
steel, C, phosphide analysis using nonaqueous electrolyte potentiostatic etching method (*Japanese*) 0-89221



**X-ray diffraction examination of materials continued**

- steel, Cr-C, structural, struct.-prop. rel., high strength and toughness design criteria 0-97491
- steel, Cr-Mo (10-14, 2-6 wt.%), heat-resist., creep-rupture strengths 0-104271
- steel, Cr-Mo (2.25, 1.0 wt.%), temper embrittlement, effect of P, Sn, comp. and carbide precip. 0-85036
- steel, Cr-Mo (2.25, 1.0 wt.%), temper embrittlement, effect of Mn, Si, comp. and carbide precip. 0-85037
- steel, fatigue crack tip plastic deform., X-ray diffr. investigation (*Russian*) 0-104251
- steel, ferritic stainless, phosphide analysis using nonaqueous electrolyte potentiostatic etching method (*Japanese*) 0-89221
- steel, high C, type 7KhFNSh, plastic deform. influence of X-ray interference line breadth (*Russian*) 0-93599
- steel, high-speed tool, splat quenching, props. and struct. 0-76294
- steel, low C, electroboronising by superimposed cyclic current,  $\text{Na}_2\text{CO}_3$ ,  $\text{B}_2\text{C}$ ,  $\text{NaCl}$ ,  $\text{NaOH}$  activator studies 0-85081
- steel, low C, initial stages of plastic deform. (*Japanese*) 0-93618
- steel, low C structural, fracture toughness and X-ray diffr. obs. of surface (*Japanese*) 0-66634
- steel, maraging stainless, phase transformation and mech. props. rel. to heat treatment (*Chinese*) 0-66501
- steel, medium C, ground, residual stresses, X-ray evaluation 0-79863
- steel, Ni, 11.6%, quenched cylinder residual stresses, boring/turning and X-ray diffr. obs. (*German*) 0-93586
- steel, powder forged, fatigue, surface treatment effect 0-85048
- steel, Si-Mn-P-S-Ni-Cr, residual stress meas. by X-ray diffr. 0-71688
- steel, stainless, fixing pins for fractured bones, strength, ultrasound effect 0-71710
- steel, stainless, wire, axial texture after electroplastic drawing, X-ray struct. investigation (*Russian*) 0-104177
- steel, surface Si reinforced type U8, metastable phase, composition, struct. (*Russian*) 0-92599
- steel, type Kh13N9D2MT martensitic aged, struct. and mech. props. (*Russian*) 0-93600
- tetramethylammonium tetrachlorozincate, X-ray study of incommensurate phase 0-71351
- thiourea, incommensurate phase transition, X-ray and neutron scatt. study 0-75963
- transition metal-metalloid glasses, struct. and plastic flow, review 0-84090
- transition metal-nonmetal glasses, with defined local coordination, struct. model 0-84092
- tridymite, thermal expansion meas. 0-59682
- triglycine fluoberyllate, deuterated, dislocation line defect X-ray topographic analysis 0-59465
- $\text{TTF}_0\text{TSCF}_6\text{-TCNQ}$ ,  $2\text{K}_\text{F}$  and  $4\text{K}_\text{F}$  CDWs, X-ray study 0-65474
- (TTF)Cl<sub>2</sub>, disorder transition, cond. decrease and commensurate charge density waves 0-70153
- vanadocene, order-disorder phase transition, sp. ht. and crystallographic study (*French*) 0-84131
- wrought metals, plastic deform. testing, X-ray line profile anal. (*Hungarian*) 0-97663
- Ag, Debye temp., X-ray diffr. determ., anharmonic parameters of pot. function 0-100320
- Ag electrodeposition, on (100) face of single crystal Ag in presence of sulphadiazine 0-89161
- Ag halide film physical props., effect of gelatin structure 0-97715
- Ag powder, ultrafine, sintering, coalescence growth stage 0-89174
- Ag-Bi-S, ternary phase diagram, DTA and X-ray diffr. investigation 0-84917
- Ag-Cu metastable solid soln., form. by ion-beam mixing 0-75244
- $\alpha$ -Ag-In solid solutions, lattice dynamics parameters (*Russian*) 0-96477
- Ag-InP interface,  $\text{AgP}_2$  formation during sintering 0-65309
- AgBr-NaBr, phase diagram, miscibility, binodal curve and demixing kinetics, X-ray meas. 0-96659
- AgGaS<sub>2</sub>-AgGaSe<sub>2</sub> system, phase diagram, lattice consts., and IR spectra 0-60841
- $\text{Ag}_2\text{S}+\text{Ln}_2\text{S}_3$ , powdered mixtures, reaction rate, production of ionic semiconductors 0-93741
- $\text{Ag}_2\text{SBr}$ , ionic conductivity in temp. range 93-573K, X-ray diffr. and DTA 0-79988
- $\beta\text{Ag}_2\text{SI}$ , anharmonic thermal vibr. of cations 0-65214
- $\text{Ag}_2\text{SI}$ , ionic conductivity in temp. range 93-573K, X-ray diffr. and DTA 0-79988
- Al anodising, porous films formed in chromic acid 0-100966
- Al binary alloys, rapid quenching, struct. and decomp. 0-76244
- Al, Debye temp., X-ray diffr. determ., anharmonic parameters of pot. function 0-100320
- Al, initial stages of plastic deform. (*Japanese*) 0-93618
- Al single crystals, relation between axial orientation rotating and deform. banding 0-104206
- Al/Pd thin film couples, thermal reactions 0-59830
- Al-Al<sub>2</sub>Pt<sub>3</sub> eutectic alloys, unidirectionally solidified, struct. study 0-108394
- Al-Cu, type 1100, synchrotron radiation microradiography 0-85121
- Al-Cu-Mg/mica particulate composite mech. props. 0-100919
- Al-Cu-Mn, type 2219, synchrotron radiation microradiography 0-85121
- Al-Ge(001) interface, struct., total-reflected X-ray diffr. 0-88441
- Al-Si-N-O system, comps. corresponding to  $\beta$ -sialon phase reaction hot-pressing 0-84891
- Al-Zn-Mg, age-hardenable, precipitation and dissolution processes, positron annihilation and X-ray small-angle scattering comparison 0-89238
- AlF<sub>3</sub> based glasses, chem., thermal and optical props. (*French*) 0-70139
- AlGaAsSb LPE growth, lattice-matched to GaSb, characterisation 0-60794
- Al<sub>2</sub>Ga<sub>1-x</sub>P, LPE, crystallographic obs. and electrochem. 0-88445
- Al<sub>2</sub>Mg<sub>3</sub>, diffusionless phase transformation 0-104150
- AlN film, oriented c-axis, low temp. deposition by reactive magnetron sputtering 0-76180
- $\beta\text{-AlO}_2\text{-(Na,Li)}_2\text{O}$ , NMR, Raman and IR spectra, and X-ray diffr., heat treatment induced changes 0-107508
- $\alpha\text{-Al}_2\text{O}_3$ , grain boundary segregation, electron microscopy 0-103361
- $\beta\text{-Al}_2\text{O}_3\text{-Ag}_2\text{O}$ , stoichiometric and nonstoichiometric, structure comparison, phase transitions in stoichiometric compound (*French*) 0-60856
- $\beta\text{-Al}_2\text{O}_3\text{-NH}_4^+$ , single cryst. characts. and AC cond. obs. 0-107514
- Al(OH)<sub>3</sub>, precip. from solns. containing Li ions, X-ray diffr. patterns and comp. determ. 0-76502
- 3.5Al<sub>2</sub>O<sub>3</sub>.2SiO<sub>2</sub>, mullite, decomposition by SiO<sub>2</sub> volatilisation 0-61082
- Am, phase transformation at high press. 0-107422

**X-ray diffraction examination of materials continued**

- As<sub>2</sub>O<sub>3</sub>, vitreous, X-ray diffr. study of struct. 0-92464
- As<sub>2</sub>S<sub>3</sub>, amorphous, struct., vibr. and electronic spectra 0-64908
- (As<sub>0.45</sub>Se<sub>0.55</sub>)<sub>100-x</sub>Cu<sub>x</sub>, glassy, struct. and elec. cond. study 0-59399
- Au, electrodeposited and sputtered, hard, reactive softening, X-ray diffr. studies 0-100414
- Au, fine particles, gas evaporation technique for prep., X-ray diffr. study 0-75327
- Au, fine particles, gas evaporation technique of prep., X-ray diffr. study, charact. temp. 0-75328
- Au powder, ultrafine, sintering, coalescence growth stage 0-89174
- Au, thin foil, spatial resolution of X-ray microanalysis 0-101065
- Au-Ge system, struct. of metastable phases (*German*) 0-108430
- AuCu-Al thin film bilayer system, phase formation, backscattering spectra 0-96728
- Au<sub>2</sub>Si<sub>3</sub>m, metastable phase, substruct. unit cell (*German*) 0-88091
- B-Si, (0 to 14.3 at.%), phase charact., regions of existence (*French*) 0-104117
- BN, contact reactions with Ti and WC-Co at high pressures 0-61029
- BN, conversion of wurtzite into cubic form, stress state effect 0-64943
- BaFe<sub>2</sub>O<sub>9</sub>, Ca<sup>2+</sup> substitution effect on hexaferrite lattice and mag. props. 0-60243
- BaFe<sub>2</sub>O<sub>9</sub>, powder, milled and annealed, phase composition, lattice consts. and crystallite size 0-71677
- BaFe<sub>2</sub>O<sub>9</sub>, powders, fast reaction presintering 0-97445
- BaFe<sub>2</sub>O<sub>4</sub> amorphous film, prep. by RF sputtering, crystallisation 0-76183
- $\beta\text{-BaFe}_2\text{S}_4$ , cryst. struct., X-ray diffr. obs. 0-84153
- Ba<sub>3</sub>FeTa<sub>2</sub>O<sub>9</sub>, Mossbauer and X-ray diffr. studies 0-103905
- BaGd<sub>2</sub>X<sub>2</sub>O<sub>17</sub> (X=Si,Ge), cell consts., luminesc. of various rare-earth activators 0-93376
- BaMnF<sub>4</sub>, spectroscopy near ferroelec. transition, dielec. anomalies near mag. ordering temp. 0-75965
- Ba(NO<sub>3</sub>)<sub>2</sub>, isomorphous crystals, growth defects, X-ray topography 0-70188
- Ba<sub>2</sub>NaNb<sub>2</sub>O<sub>7</sub>, incommensurate refls. near ferroelastic transition, neutron and X-ray precession obs. 0-70395
- BaO-B<sub>2</sub>O<sub>3</sub>-V<sub>2</sub>O<sub>5</sub> glass, oxidation-reduction of V, thermodynamics 0-85169
- BaO-TiO<sub>2</sub>-Al<sub>2</sub>O<sub>3</sub> system, subsolidus equilibria, X-ray powder diffr. 0-108413
- BaO.6Fe<sub>2</sub>O<sub>3</sub>, solubility of CaO 0-100333
- BaSi<sub>2</sub>, trimorphic, transform. of three-connected Si nets, press.-temp. phase diagram, 40 kbar and 1000°C 0-75198
- Ba<sub>2</sub>Sr<sub>1-x</sub>Nb<sub>2</sub>O<sub>6</sub> crystals, defects and their characteristic features 0-88138
- BaTiO<sub>3</sub>, polycryst., phase transition obs. in -170 to 220°C range (*Russian*) 0-103474
- BaTiO<sub>3</sub>Co, tricritical point, X-ray diffr. meas. 0-71341
- Ba(Ti<sub>1-x</sub>Sn<sub>x</sub>)<sub>2</sub>O<sub>7</sub> thick film, ferroelec., phase transitions and dielec. props. 0-97215
- BaY<sub>4</sub>X<sub>2</sub>O<sub>17</sub> (X=Si,Ge), cell consts., luminesc. of various rare-earth activators 0-93376
- Be, thick film, amorphous, RF magnetron sputtering 0-80971
- Bi film, structure and electronic props. 0-70562
- C, nongraphitizable, catalytic graphitization by Cr<sub>2</sub>O<sub>3</sub>, MnO<sub>2</sub> 0-97440
- C<sub>12</sub><sup>2+</sup>PtF<sub>6</sub><sup>-</sup>, struct. and elec. props. 0-70183
- CaF<sub>2</sub>-AlF<sub>3</sub>-Na<sub>3</sub>AlF<sub>6</sub>(-Al<sub>2</sub>O<sub>3</sub>), phase equilibria, X-ray diffr. and DTA meas. 0-108409
- CaO-SrO-Fe<sub>2</sub>O<sub>3</sub> system, phase relations, Sr hexaferrite field occurrence 0-93545
- CaO.6Al<sub>2</sub>O<sub>3</sub>, thermodynamic stability, reaction with Ti, Cr and Zr oxides 0-92687
- Ca<sub>2</sub>SiO<sub>4</sub>, structurally related phases, high-temp. X-ray powder diffr. 0-81050
- Cd films, struct. and props., X-ray diffr. spectra anal. 0-80119
- Cd<sub>2</sub> polytypes, vapour growth mechanism 0-84124
- CdS:Mn, vacuum deposited film, Mn migration, EPR and X-ray study 0-65411
- CdTe-In system, equilib. phase diagram and liq. phase epitaxial growth of CdTe from In soln. (*Japanese*) 0-71634
- Ce-M intermetallic cpds., M=3d transition metal, sorption of H<sub>2</sub>, structural charges 0-88429
- CeCo<sub>5-x</sub>Cu<sub>x</sub>, 0≤x≤1 internal oxidation kinetics, oxide struct., X-ray study 0-104329
- CeNH<sub>4</sub>P<sub>2</sub>O<sub>12</sub> and Ce(NH<sub>4</sub>)<sub>2</sub>(PO<sub>3</sub>)<sub>3</sub>, synthesis by solid-phase reaction, characts. 0-60778
- CePd<sub>3</sub>, single crystal Czochralski growth and characterisation 0-60767
- Co complex, [Co(NH<sub>3</sub>)<sub>6</sub>]<sup>3+</sup>, enantiotropic phase transition obs. 0-107412
- Co-Al alloy, multilayer martensite phases, illustration of polytype structures 0-84932
- Co-Ge binary system, phase diagram rel. to that of Ni-Ge (*French*) 0-97463
- Co-P, electrodeposited alloys, heat-induced structural changes (*Japanese*) 0-89263
- Co<sub>9</sub>Er<sub>13</sub> amorphous alloy, sputtered, local order and amorphous struct. 0-88061
- CoFe<sub>2</sub>O<sub>4</sub> mag. fluid particles, comp., struct., and mag. props. 0-60374
- Co<sub>9</sub>Fe<sub>10</sub> noncrystalline ferromagnet, electroless deposited, struct. and microscopic mag. props. 0-88063
- Co<sub>90</sub>Zr<sub>10</sub>, ferromag. amorphous alloy, crystn. and domain struct. study 0-107056
- Cr, corrosion in SO<sub>2</sub>, 700-1000°C 0-97642
- Cr film, preparation by decomp. of bis-arene cpds., struct. and phys. props 0-60785
- Cr-Ge system, phase diagram, thermal anal., X-ray diffr., microhardness, and electron probe anal. (*French*) 0-97462
- Cr-Ge system, XPS, X-ray and neutron diffr. and mag. meas. to study chem. bonding and electronic struct. 0-60749
- Cr<sub>2</sub>Fe<sub>3</sub>O<sub>8</sub>.Fe<sub>3</sub>C<sub>3</sub>, stacking fault study, morphology, comp. and struct. 0-84190
- Cs-SiO<sub>2</sub>-Al<sub>2</sub>O<sub>3</sub> system interactions, getter development for radiocaesium 0-83208
- CsH<sub>2</sub>PO<sub>4</sub>, ferroelec., X-ray struct. study at room temp. 0-88113
- CsI:TI, precipitation of TI solid solns. 0-70419
- Cs<sub>2</sub>NaM<sup>3+</sup>Cl<sub>6</sub> (M<sup>3+</sup>=Bi, Nd, Pr), ferroelastic phase transitions, thermal expansion, elasticity, and X-ray anal. 0-70399
- Cs<sub>2</sub>PbCu(NO<sub>2</sub>)<sub>6</sub>, incommensurate Jahn-Teller transition, Huang scatt. 0-70401
- Cu, plastically deformed, lattice strain distrib. (*German*) 0-85012
- Cu, wire, axial texture after electroplastic drawing, X-ray struct. investigation (*Russian*) 0-104177

## X-ray diffraction examination of materials continued

- Cu-Ag (3 at.%), plastically deformed, lattice strain distrib. (*German*) 0-85012
- Cu-Ag-Ge, Hume-Rothery glass form. 0-96449
- Cu-Ag-P(6-14, 11-14 wt%) amorphous, crystn. and elec. props., X-ray diff., elec. resist. and DTA meas. (*Japanese*) 0-84088
- $\alpha$ -Cu-Al (6 to 17 at.%), short-range order investigated by diffuse X-ray scatt. (*Russian*) 0-104187
- Cu-Be-Co, discontinuous reaction, analytical TEM 0-100842
- Cu-Ni-Ti system, phase equilibria in Cu rich region and Cu-T quasi-binary constitution (*Japanese*) 0-89203
- Cu-Ni-Ti system, reactions with melt in Cu-rich region (*Japanese*) 0-89202
- Cu-Sn-Al, deform at high temps. (*Polish*) 0-89284
- Cu-Zr amorphous alloy, splat cooled, local order and amorphous struct. 0-88061
- Cu, Ag,  $\gamma$ -I crystals, layer strucs., X-ray diff. studies 0-96457
- CuGaSe<sub>2</sub>, thermal expansion obs. 0-70432
- CuInS<sub>2</sub> films, RF sputtered, growth and props. 0-80124
- CuInSe<sub>2</sub>, amorphous thin film, flash evaporation, struct., stoichiometry 0-89150
- Cu<sub>2</sub>MnIn<sub>1-x</sub>Sn<sub>x</sub> alloys compositional SRO, hyperfine interactions 0-71065
- Cu<sub>40</sub>Nb<sub>30</sub>X<sub>30</sub> (X=Ti, Zr, Hf), superconductors with metastable ordered strucs. 0-108484
- Cu<sub>2</sub>S+Ln<sub>2</sub>S<sub>3</sub>, powdered mixtures, reaction rate, production of ionic semiconductors 0-93741
- Cu<sub>2</sub>-S, digenite, X-ray determ. of structural transitions 0-92474
- DyRh<sub>1-x</sub>Sn<sub>3.6x</sub>, new supercond./mag. cpds., X-ray powder diff. data 0-100215
- ErRh<sub>1-x</sub>Sn<sub>3.6x</sub>, new supercond./mag. cpds., X-ray powder diff. data 0-100215
- ErRh<sub>1-x</sub>Sn<sub>3.6x</sub>, synthesis, supercond. and mag. props. 0-100547
- EuB<sub>6</sub>, thermal expansion, X-ray method, room temp. to 1300 C 0-96670
- $\beta$ -FeOOH, Mossbauer spectra obs., chemical and thermal anal., X-ray diff., saturation magnetisation 0-88896
- Fe, Armc, ground, residual stresses, X-ray evaluation 0-79863
- Fe, cast, graphite content determ. by X-ray diff. method 0-100977
- Fe-B, amorphous alloy, mag. props. 0-84618
- Fe-B, amorphous alloys, compositional study on short-range struct. 0-84095
- Fe-B metallic glass, X-ray diff. meas., semi-empirical struct. model 0-107059
- Fe-Cu (4.54 wt.%) alloy, scaling behaviour, 700-1000°C, 1 atm. O<sub>2</sub> 0-93679
- Fe-Ni alloy, fluorination kinetics and fluoride film form., chem. nature obs. 0-101035
- Fe-Ni meteorite, STEM/X-ray microanalysis across  $\alpha/\gamma$  interface 0-105212
- Fe-Ni-B metallic glass, X-ray diff. meas., semi-empirical struct. model 0-107059
- Fe-Ni-C (30, 0.5 wt.%) single cryst., stress induced martensitic transform. 0-60860
- Fe-Ni-Ti, preaged martensite, shear strain magnitude, X-ray diff. method 0-93592
- Fe-Pd Invar, low temp. FCT phase obs. 0-93538
- Fe-Sb-Ti(V)(Cr)(Mn)(Co)(Ni), interactions and segregations, Mossbauer and X-ray diff. study 0-70415
- Fe-Si, single cryst., mag. domain wall motion, X-ray topography study 0-65953
- Fe-Si (2-8 wt.%), single crystals, growth striations, X-ray studies 0-79774
- Fe-Ti-C, rapidly quenched by splat-cooling 0-84923
- Fe-W-Cr-Mo system, mag. and mech. props. rel. to production methods (*Japanese*) 0-71107
- Fe<sub>80</sub>B<sub>20</sub> amorphous wire, crystn. by annealing at 780°C 0-100177
- Fe<sub>80</sub>B<sub>20</sub>, Metglas 2605, Young's modulus meas. using piezoelectric US composite oscillator technique 0-108656
- Fe<sub>1-x</sub>Mg<sub>1-x</sub>Zn<sub>1-x</sub>Ti<sub>0.3</sub>O<sub>4</sub> spinel system, X-ray diffraction, Fe Mossbauer effect 0-88900
- Fe<sub>1-x</sub>Mn<sub>x</sub>Al, ordering of Fe atoms, X-ray diff. meas. and mid gamma reson. anal. (*Russian*) 0-96469
- (Fe<sub>0.45</sub>Nb<sub>0.55</sub>)O<sub>2</sub>, rutile, cation distrib. and mag. ordering (*German*) 0-107116
- (Fe<sub>0.6</sub>Ni<sub>0.4</sub>)<sub>100-x</sub>B<sub>x</sub> and (Fe<sub>100-x</sub>Ni<sub>x</sub>)<sub>80</sub>B<sub>20</sub> amorphous alloys, X-ray diff. struct. determ. 0-64906
- Fe<sub>40</sub>Ni<sub>38</sub>Mo<sub>4</sub>B<sub>18</sub>, amorphous, mag. anisotropy, Mossbauer study 0-65864
- Fe<sub>2</sub>O<sub>3</sub> films, DC reactively sputtered, for selectively semitransparent photomasks, struct., mech. and chem. props. 0-59835
- Fe<sub>2</sub>O<sub>3</sub> mag. fluid particles, comp., struct., and mag. props. 0-60374
- Fe<sub>2</sub>O<sub>3</sub>, substituted magnetite, correl. between IR spectra, X-ray diff., and struct. vacancy distrib. 0-84753
- Fe(OH)<sub>3</sub> thin films, Mossbauer spectra obs., chemical and thermal anal., X-ray diff., saturation magnetisation 0-88896
- $\delta$ -Fe(OH), study of thermal decomp. by X-ray diff., electron diff. and TEM 0-66790
- Fe<sub>2</sub>O(OH)<sub>3</sub>, Mossbauer spectra obs., chemical and thermal anal., X-ray diff., saturation magnetisation 0-88896
- Fe<sub>80</sub>P<sub>13</sub>C<sub>7</sub>, amorphous and crystalline, electrochemical and semicond. behaviour (*Russian*) 0-101021
- Fe<sub>2</sub>Pt, atomic thermal vibr. anisotropy, martensitic transform. model (*French*) 0-70355
- (Fe<sub>0.5</sub>Ta<sub>0.5</sub>)O<sub>2</sub>, rutile, cation distrib. and mag. ordering (*German*) 0-107116
- Fe<sub>2</sub>VS<sub>2</sub> (0.20 < x < 1.00), phase diagram and order-disorder transition of vacancies 0-81039
- Ga whisker growth from GaN/Ga layered films 0-92800
- Ga, Al<sub>1-x</sub>As<sub>x</sub> heteroepitaxial layer distortion characterisation by X-ray multiple diff. 0-96754
- GaAs, chem. bond, modulation X-ray diff. obs. 0-96464
- GaAs thin films, reactively sputtered, ESCA/XPS study 0-97430
- GaAs-GaIn<sub>1-x</sub>P heterostructure, elastic stresses and substrate/epitaxial film mismatch, X-ray diff. method 0-92794
- (GaAs)<sub>x</sub>(AlAs)<sub>1-x</sub> multilayers, MBE, interdiffusion, X-ray diff. study 0-70474
- Ga, In<sub>1-x</sub>As<sub>x</sub>P<sub>1-x</sub>/GaAs structure, LPE growth and lattice const. matching conditions 0-59822
- Ga, In<sub>1-x</sub>P MBE layers, comp., Rutherford scatt. and X-ray diff. meas. 0-75457
- GaNbO<sub>4</sub>, polymorphic transition under high press. 0-100835
- $\alpha(\beta)$ -Ga<sub>2</sub>Se<sub>3</sub>, cryst. growth, optical, X-ray diff. and SEM study 0-71587
- Ga<sub>2</sub>Se<sub>3</sub>-FeSe, phase diagram, elec. cond., mag. susceptibility 0-88301

## X-ray diffraction examination of materials continued

- Gd-C-N system, isothermal section at 1200°C, X-ray investigation (*German*) 0-93543
- Ge, Pendellosung fringe shape depend. on specimen-film distance (*Russian*) 0-87994
- GeO<sub>2</sub> particles used for optical fibre fabrication, struct. props. 0-89167
- HUO<sub>2</sub>AsO<sub>4</sub>·4H<sub>2</sub>O and HUO<sub>2</sub>PO<sub>4</sub>·4H<sub>2</sub>O layered cpds., struct. investigations, below antiferroelec. transition temps., H bond ordered strucs. 0-107416
- Hf-Al-C, phase diagram and lattice constants, X-ray diff. method 0-89207
- Hf<sub>1-x</sub>Fe<sub>x</sub> amorphous alloys, formation, crystallisation and electrical resistivity 0-96838
- Hg<sub>1-x</sub>AsF<sub>6</sub>, one-dimens. lattice dynamics, X-ray scatt. study 0-75317
- InAs-CdTe quasi-binary system, temp.-comp. diagram, physicochem. and thermodynamic analysis 0-104127
- In<sub>1-x</sub>Ga<sub>x</sub>P<sub>1-y</sub>As<sub>y</sub> lattice-matched epitaxial layers, LPE growth on GaAs(100), characterisation 0-75465
- InN film growth by reactive sputtering in Ar-N<sub>2</sub> discharge, mechanism 0-89107
- In<sub>2</sub>O<sub>3</sub>, thermally evaporated film, struct. and elec. props. 0-104066
- In<sub>2</sub>O<sub>3</sub>, thin film, sputter deposition form., optical and elec. props. 0-60123
- In<sub>2</sub>O<sub>3</sub>-InN film growth by reactive sputtering in N<sub>2</sub>-O<sub>2</sub> discharge, mechanism 0-89108
- In<sub>2</sub>Si<sub>2</sub>O<sub>7</sub>, thin film, sputter deposition form., optical and elec. props. 0-60123
- INVO<sub>4</sub>, synthesis and thermal props. (*French*) 0-97443
- (K<sub>3/4</sub>Bi<sub>1/4</sub>)(Zn<sub>1/6</sub>Nb<sub>5/6</sub>)O<sub>3</sub>, cation disordered perovskite, elastic const. and thermal expansion 0-96587
- KC<sub>24</sub>, press. induced staging transition 0-79938
- KCl, pure and Ba doped, symm. of elastic fields due to defect displacements, diffuse X-ray scatt. 0-70256
- KCoF<sub>3</sub>, antiferromag. domain wall motion under external stress 0-80583
- KD<sub>2</sub>PO<sub>4</sub>, transparent dielec., thermal analysis of laser-induced damage 0-66336
- KF-ErF<sub>3</sub>, phase diagram 0-92645
- K<sub>2</sub>(M<sub>1</sub>Ti<sub>2-x</sub>)O<sub>4</sub>, (M=Mg, Zn, Ni, Cu, Fe<sup>III</sup>, Mn<sup>III</sup>), (0.7 ≤ x ≤ 0.9), new layer struct. (*French*) 0-84149
- KNbO<sub>3</sub>, cubic, temp. depend. of intensity of X-ray interference 0-59613
- KNiF<sub>3</sub>, magnetostriction, X-ray diffractometry and strain gauge meas. 0-65997
- KOH-KO<sub>2</sub>, phase diagram (*French*) 0-107177
- K<sub>2</sub>PbCu(NO<sub>3</sub>)<sub>6</sub>, incommensurate Jahn-Teller transition, Huang scatt. 0-70401
- KYbHP<sub>2</sub>O<sub>10</sub>, thermal decomp., thermogravimetric and X-ray obs. 0-101013
- La-Al amorphous alloys, internal friction, relaxation process 0-92607
- La-Au, splat-quenched, Mossbauer effect and elec. resist., amorphous struct. 0-84676
- LaB<sub>6</sub>, thermal expansion, X-ray method, room temp. to 1300 C 0-96670
- LaFe<sub>2</sub>P<sub>2</sub>-type structure ternary arsenides, synthesis and cryst. struct. 0-84154
- LaLi<sub>0.5</sub>Ir<sub>0.5</sub>O<sub>3</sub>, perovskite, prep. and mag. study 0-80486
- LaNi<sub>4</sub>B<sub>0.6</sub>, H<sub>2</sub> absorpt. props. 0-88432
- La<sub>2</sub>Si<sub>2</sub>O<sub>7</sub>N<sub>2</sub> single cryst. growth by floating zone method with SiO<sub>2</sub>-Si<sub>3</sub>N<sub>4</sub> additions 0-93481
- Li, X-ray scatt. factor, solid state effect 0-70163
- Li-Co ferrite, mag. anisotropy induced by thermomag. treatment, ionic order effect, magnetostriction meas. 0-103830
- Li-Pt, phase diagram for comp. range 0-40 at.% Pt, mag. and elec. props. (*German*) 0-84912
- LiNbO<sub>3</sub>, cleaved, crystallographic and electrooptic props. 0-59575
- Li<sub>2</sub>O-Al<sub>2</sub>O<sub>3</sub>-SiO<sub>2</sub> glass containing ZrO<sub>2</sub>, cryst. process 0-103253
- Li<sub>2</sub>O-Al<sub>2</sub>O<sub>3</sub>-SiO<sub>2</sub> glass, crystallised, grain size and internal strain 0-103259
- Li<sub>2</sub>O-LiX-B<sub>2</sub>O<sub>3</sub> glass, X=halogen, high anionic cond. of new solid electrolytes 0-107546
- Li<sub>2</sub>O-MgO-Al<sub>2</sub>O<sub>3</sub> system, subsolidus phase equilibria 0-81036
- Li<sub>2</sub>O-TiO<sub>2</sub>, pseudobinary phase rotations, DTA and X-ray anal. 0-108411
- Li<sub>3+x</sub>P<sub>2</sub>O<sub>3x+1</sub>, polyphosphate, melting and crystallisation 0-70376
- Li<sub>2</sub>SO<sub>4</sub> based solid electrolytes, FCC phase transport mechanism studies and uses 0-107525
- Li<sub>2</sub>SO<sub>4</sub>, fast ion conductors, X-ray diff., neutron diff., and Brillouin scatt. study 0-107170
- Li<sub>1-x</sub>Ti<sub>2-x</sub>O<sub>4</sub>, high temp. spinel-Ramsdellite transform. 0-70407
- Lu<sub>2</sub>Si<sub>2</sub>O<sub>7</sub>, charact., synthesis and spectroscopic study 0-84846
- Mg films, struct. and props., X-ray diff. spectra anal. 0-80119
- Mg-Zn alloy, aged, one dimensional transition phase  $\beta_2$ , crystallographic obs. (*Chinese*) 0-60865
- MgCa(CO<sub>3</sub>)<sub>2</sub>, dolomite, partial thermal decomp. into MgO and CaCO<sub>3</sub>, product cryst. growth 0-108706
- MgCr<sub>2</sub>O<sub>4</sub>-TiO<sub>2</sub>, porous ceramics, humidity-sensitive electrical conduction 0-107782
- Mg<sub>2</sub>GeO<sub>4</sub>-Mg<sub>2</sub>SiO<sub>4</sub> system, struct. similar solid soln. obs. and characts. 0-108403
- Mg(OH)<sub>2</sub>, sintering, IR spectra, X-ray anal. 0-66452
- Mn<sub>1-x</sub>Mg<sub>x</sub>Se, mag. and struct. phase transitions, mag. susceptibility and X-ray diff. study 0-71022
- Mn<sub>2</sub>O<sub>4</sub>, hausmannite, tetragonal-cubic transform., X-ray anal. 0-103288
- $\alpha$ -MnSe, mag. and struct. phase transitions, mag. susceptibility and X-ray diff. study 0-71022
- MnSi-Si system, striations and cryst. struct. of matrix 0-103292
- MnSi<sub>1-1.73</sub> crystal growth and characterisation 0-93474
- Mo, dislocation structure evolution near electro-eroded crater (*Russian*) 0-100237
- Mo oxides, low-grade, soda roasting study (*Korean*) 0-93508
- Mo-Al-Ge, phase equilibria, X-ray and microstructural anal. 0-93536
- Mo-Si film-substrate interface, reaction on heat treatment, silicide formation 0-79999
- MoO<sub>3</sub> topotactic transform into MoO<sub>2</sub>, electron microscopy, X-ray anal. 0-107417
- MoS<sub>2</sub>, prep. and mag. props. (*French*) 0-93072
- MoSi<sub>2</sub>, refractory formation by As<sup>+</sup> ion beam bombardment 0-107286
- MoSi<sub>3</sub> films, magnetron DC reactive sputtering, struct. and props. 0-80966
- <sup>15</sup>N<sub>2</sub>, solid struct., and thermodynamic props. (*Russian*) 0-88083
- NaCl, dislocation ordering influence on integrated X-ray coeff. 0-103357
- NaF, isothermal compression at 673K, up to 10 GPa, X-ray diff. study 0-59565
- NaFeF<sub>2</sub>, Mossbauer and low-temp. dilatometry study (*French*) 0-80662



## X-ray diffraction examination of materials continued

- (Na,Ky).CO<sub>3</sub>, non-stoichiometric, cryst. struct. (*French*) 0-79761  
 Na<sub>2</sub>O-Ag<sub>2</sub>O-B<sub>2</sub>O<sub>3</sub> glass, Ag<sup>+</sup> ion distrib., X-ray diff. study 0-84076  
 Na<sub>2</sub>O-SiO<sub>2</sub> glass, internal and surface struct. by X-ray scatt. 0-84074  
 Na<sub>2</sub>PO<sub>4</sub>-Ni<sub>3</sub>(PO<sub>4</sub>)<sub>2</sub> system, phase equilibrium diagrams, crystallographic study, double orthophosphates (*French*) 0-93546  
 Na<sub>2</sub>Sc<sub>2</sub>P<sub>2</sub>O<sub>12</sub>, fast-ion conductor, struct. phase transition 0-88362  
 Nb/Cu layered ultrathin coherent struct. 0-80122  
 Nb-Al-C, phase diagram and lattice constants, X-ray diff. method 0-89207  
 Nb-H(D), H ordering, review 0-60850  
 Nb-N, superconducting layers, sputtering in high vacuum apparatus (*German*) 0-89147  
 NbC, diffuse, superconductive props. obs. (*Bulgarian*) 0-80467  
 Nb<sub>2</sub>Ge, supercond. film, amorphous content, X-ray diff. study, rel. to transition temp. 0-75668  
 Nb<sub>2</sub>Ge(Si), RF sputtered films, amorphous atomic scale struct. 0-84064  
 NbH<sub>3</sub>, coherent  $\alpha$ - $\alpha'$  phase transition 0-71641  
 NbH<sub>3</sub>, structural transform. rel. to order-disorder transform. 0-60858  
 NbN, diffuse, superconductive props. obs. (*Bulgarian*) 0-80467  
 NbN single crystal preparation, zone melting and nitriding techniques 0-60776  
 NbN, supercond. RF reactively sputtered films, deposition parameter effects on props. 0-80972  
 Nb<sub>2</sub>N, supercond. props. and structural phase transform. induced by C<sup>+</sup> and N<sup>+</sup> implantation 0-107942  
 Nd, magnetic-structure, neutron and X-ray diff. study 0-60197  
 NdP<sub>2</sub>O<sub>14</sub>, ferroelastic, hydrostatic press. effect on phase transition temp. 0-70293  
 NdRh<sub>2</sub>Sn<sub>4</sub>, new supercond./mag. cpds., X-ray powder diff. data 0-100215  
 Nd<sub>2</sub>Y<sub>1-x</sub>Zn system, solid soln., mag. susceptibility, 77 to 600K (*Russian*) 0-65776  
 Ni, cold-rolled, anomalous effects during X-ray stress meas. (*German*) 0-104184  
 Ni, corrosion, high temp., SO<sub>4</sub> induced, studied at 900°C in O<sub>2</sub>+4.2% SO<sub>2</sub> 0-97639  
 Ni precipitates, isothermal annealing influence on structural state, X-ray diff. anal. (*Russian*) 0-100849  
 Ni superalloy, STEM microanal. of precipitates and their nuclei 0-81067  
 Ni-Co-Al alloys, continuous precip., SEM, TEM, X-ray diff. study 0-89220  
 Ni-Co-W, electrodeposition, surface morphology and cryst. struct. 0-71602  
 Ni-Cr-Ta system, phase equil. of Ni rich region at 1523- and 1273K 0-93541  
 Ni-ferrite powders, form. in presence of Li<sub>2</sub>SO<sub>4</sub>-Na<sub>2</sub>SO<sub>4</sub> molten salts, prep. and characts. 0-84869  
 Ni-Ge binary system, phase diagram rel. to that of Co-Ge (*French*) 0-97463  
 Ni-Ni<sub>3</sub>B eutectic, high temp. X-ray anal. 0-71639  
 Ni-P, amorphous, low P, struct. study using high-angle X-ray diff. 0-107055  
 Ni-Pd-Mn ternary alloys, mag. characts., use for thermoseed 0-107995  
 Ni-Ta (70, 30 wt.%) metallic glass, struct. and crystn. (*Russian*) 0-70136  
 NiFe<sub>2</sub> film preparation and characterisation 0-59815  
 NiFe<sub>2</sub>O<sub>4</sub> mag. fluid particles, comp., struct., and mag. props. 0-60374  
 NiH<sub>2</sub>, formation and decomp. studies 0-71626  
 Ni<sub>2</sub>Mo<sub>2</sub>S<sub>2</sub>O<sub>2</sub>, O-containing Chevrel phases, synthesis and props. 0-108368  
 NiO samples, colour difference, X-ray line broadening study 0-100206  
 NiTi, premartensitic transformation of B2 phase, shape memory 0-84931  
 Ni<sub>40</sub>Ti<sub>60</sub>, amorphous, chem. short-range-order, X-ray and neutron scatt. obs. 0-96447  
 Ni<sub>0.25</sub>Zn<sub>0.75</sub>Fe<sub>2</sub>O<sub>4</sub>, structural phase transition, X-ray and neutron diff. study 0-79735  
 NpO<sub>3</sub> single crystal growth, gas phase chemical transport method (*French*) 0-60760  
 P, amorphous, prepared by chem. transport in low-pressure H<sub>2</sub> plasma, radial distrib. function 0-64899  
 PCl<sub>5</sub>, sublimed phase studied by <sup>31</sup>P NMR, Raman spectra and X-ray diff. 0-100209  
 PLZT ferroelectric thin films, epitaxial growth and optical props. 0-70543  
 PbO, thin film, microstruct. and thermal stress, doping effects 0-88458  
 Pb<sub>2</sub>Ge<sub>2</sub>O<sub>11</sub>, lattice dynamics parameters anisotropy, X-ray diff. study 0-59612  
 Pb<sub>2</sub>Ge<sub>2</sub>O<sub>11</sub>, sputtered ferroelec. films, prep. struct. and dielec. props. 0-75452  
 PbO, reactively evaporated, photocond., H<sub>2</sub>O induced phase transform. 0-60122  
 PbS films, polycryst. and epitaxial, small-angle X-ray scatt. and electron density inhomogeneities 0-96758  
 PbS-Si heterojunction, PbS film growth and struct. 0-96762  
 PbSc<sub>2/3</sub>Te<sub>1/3</sub>O<sub>3</sub>-PbSc<sub>2/3</sub>W<sub>1/3</sub>O<sub>3</sub>(PbFe<sub>2/3</sub>Te<sub>1/3</sub>O<sub>3</sub>) ferroelec. props. and lattice const. 0-60520  
 PbSnF<sub>4</sub>, allotropic transformations 0-84926  
 PbTe-Ga<sub>2</sub>Te<sub>3</sub>, phase interaction, DTA, XPA and microstructural anal. 0-96625  
 PbTe-InTe system, phase interactions and solid soln. form., physicochem. and elec. characteris. 0-104129  
 Pb(Zr,Ti)O<sub>3</sub>, tetragonal ferroelec. ceramic, 90° domain-rot. fraction after polarisation, X-ray determ. 0-75992  
 Pb(Zr,Ti)O<sub>3</sub>-Cr<sub>2</sub>O<sub>3</sub> ceramics, reson. freq. comp. and temp. depend. 0-70413  
 PbZrTi<sub>1-x</sub>O<sub>3</sub> ceramics, morphotropic phase boundary 0-81035  
 Pd-D, crystallite size effects, simultaneous sorption and X-ray study 0-65237  
 Pd-Ni-Si amorphous alloys, crystn. process during isothermal ageing 0-89275  
 Pd-Si, amorphous, compositional study on short-range struct. 0-84095  
 Pd-Si, amorphous metallic glass, with defined local coordination, struct. model 0-84092  
 (Pd<sub>80</sub>Au<sub>20</sub>)<sub>13</sub>/Fe<sub>30</sub>, compositionally modulated amorphous film, diffusion, struct. relax. 0-103518  
 Pd<sub>2</sub>MnIn<sub>1-x</sub>Sn, and Pd<sub>2</sub>MnIn<sub>1-x</sub>Sb, Heusler alloys, mag. order, disorder effects 0-88723  
 Pd<sub>2-x</sub>MnSb, struct., appl. as improved neutron polariser 0-60199  
 Pd<sub>2</sub>Si and PdSi films, on Si, stress obs. 0-80145

## X-ray diffraction examination of materials continued

- Pd<sub>80</sub>Si<sub>20</sub>, amorphous alloy, partial struct. functions, X-ray, electron and neutron diff. studies (*Japanese*) 0-88050  
 (Pd<sub>85</sub>Si<sub>15</sub>)<sub>61</sub>/(Fe<sub>85</sub>B<sub>15</sub>)<sub>39</sub>, compositionally modulated amorphous film, diffusion, struct. relax. 0-103518  
 Pr<sub>1-x</sub>Ca<sub>x</sub>MnO<sub>3</sub>, struct. and magnetisation study 0-65804  
 PrRh<sub>2</sub>Sn<sub>2</sub>, crystallography X-ray powder diff. study 0-100217  
 Pt-Ni vacuum condensates on Si and SiO<sub>2</sub>, thermally treated, X-ray anal. (*Russian*) 0-70559  
 PtSi films, on Si, stress obs. 0-80145  
 RbNbWO<sub>6</sub>, pyrochlore struct., tetragonal to cubic phase transition 0-75355  
 Rb<sub>2</sub>PbCu(NO<sub>3</sub>)<sub>6</sub>, incommensurate Jahn-Teller transition, Huang scatt. 0-70401  
 Sb-O-Cl(Br)(I), glass-forming regions 0-88057  
 Se powder compacts, sintered, electrical cond. 0-70693  
 Si, amorphous film, RF plasma deposition from SiCl<sub>4</sub>-H<sub>2</sub>, characterisation 0-66435  
 Si crystal, Czochralski grown, enhanced Borrmann effect 0-70191  
 Si crystal surface, adsorbed Br, X-ray standing waves obs. 0-96417  
 Si, elastically bent, strain conc. determ. by microfluorescent densitometry of X-ray topography 0-79245  
 Si film, low press. CVD prep., struct., elec. and optical props. 0-70548  
 Si, oxide scale microstruct. of oxidised single cryst. 0-108613  
 Si surface electron beam deposited silicide formation using scanning CW laser beam 0-66862  
 Si, X-ray section topography in the Bragg case 0-79637  
 Si:B, implanted laser annealed, lattice strain, X-ray study 0-96554  
 Si:B ion implanted, strain profiles from X-ray rocking curves 0-107290  
 Si:H film, amorphous, plasma-deposited, small angle X-ray and neutron scatt. studies 0-59826  
 Si-B system, DTA, X-ray diff. and metallographic study (*German*) 0-66484  
 Si-Cr interfaces, metallurgical and electrical props. 0-60081  
 Si-Na-B-O-N glass, synthesis and characterisation 0-108381  
 Si-Pd-Ti, silicide form. in evaporated films 0-80006  
 SiAlON, prepared from siliceous sand and Al powder, hot pressing, staeite contamination effects (*Japanese*) 0-93528  
 SiC, oxide scale microstruct. of oxidised single cryst. 0-108613  
 Si-Cr, sintering, B transport and lattice parameter change 0-108370  
 B-SiC, X-ray diff. study of anisotropic layers in twinned seams 0-107274  
 Si<sub>3</sub>N<sub>4</sub>, hot-pressed, strength anisotropy origins 0-89330  
 Si<sub>3</sub>N<sub>4</sub>CeO<sub>2</sub> additive, hot-pressing and oxidation behaviour 0-71618  
 SiO<sub>2</sub>, amorphous, very small angle X-ray scatt. before and after thermal neutron irradi. 0-75270  
 SiO<sub>2</sub> fabric, structural stability rel. to brittleness, X-ray diff. and IR spectrosc. studies 0-96634  
 SiO<sub>2</sub> gel, internal and surface struct. by X-ray scatt. 0-84074  
 SiO<sub>2</sub> vitreous, quant. X-ray anal. of cristobalite 0-88049  
 SmCo<sub>5</sub>, high coercivity isotropic plasma-sprayed magnet, eutectoid decomp. 0-80568  
 SmCo<sub>5</sub>, isotropic plasma-sprayed high coercivity magnet, eutectoid decomp. 0-75810  
 Sm<sub>6</sub>Mn<sub>23-x</sub>Fe<sub>x</sub>, magnetic behaviour, temp. and comp. depend. 0-93090  
 Sn ternary intermetallic systems, new supercond./mag. cpds., X-ray powder diff. data 0-100215  
 Sn/Cu electroplated bimetallic films, interfacial reaction 0-96765  
 SnO<sub>2</sub> films, non-stoichiometric, DC reactively sputtered, elec. props. 0-80415  
 Sr Nb<sub>2</sub>O<sub>6</sub>, crystallography, polymorphism and isomerism, X-ray diff. and DTA study 0-100216  
 SrFe<sub>2</sub>O<sub>9</sub>, Ca<sup>2+</sup> additives effect on hexaferrite lattice and mag. props. 0-60243  
 Sr<sub>2</sub>FeTa<sub>2</sub>O<sub>9</sub>, Mossbauer and X-ray diff. studies 0-103905  
 Sr(NO<sub>3</sub>)<sub>2</sub>, amorphous crystals, growth defects, X-ray topography 0-70188  
 SrTiO<sub>3</sub>, cubic, temp. depend. of X-ray reflection intensities 0-107021  
 Ta-Al-C, phase diagram and lattice constants, X-ray diff. method 0-89207  
 Ta-H(D), H ordering, review 0-60850  
 TaSe<sub>2</sub> (2H), broken hexagonal symm., incommensurate charge-density wave struct. 0-96646  
 TaSe<sub>2</sub> (2H) CDW, reentrant lock in transition at high press. 0-88320  
 TaSi<sub>2</sub>, refractory formation by As<sup>+</sup> ion beam bombardment 0-107286  
 TbRh<sub>2</sub>Sn<sub>2</sub>, crystallography X-ray powder diff. study 0-100217  
 TeO<sub>2</sub>-MoO<sub>3</sub>-V<sub>2</sub>O<sub>5</sub>, phase comp. determ. using X-ray diff., electron microscopy and DTA (*German*) 0-88046  
 Th-C-N system, existence of new  $\beta'$ 'ThCn' phase, struct. and thermodynamic study (*French*) 0-92499  
 $\alpha$ -Ti alloys VT1 and VT5, struct. and phys. props., H<sub>2</sub> effect 0-108576  
 Ti, fatigue damage, SEM, X-ray diff. and surface trace anal. 0-85040  
 Ti/Cu(Au) thin films thermocompression bonds degradation by thermal ageing 0-66546  
 Ti-Al-Mo, type BT22, phase transformations under step-by-step heat treatment (*Russian*) 0-108436  
 Ti-Mo (20 at.%), incommensurate struct., stacking soliton 0-107109  
 Ti-Mo alloys, structural stability under high-pressure soaking 0-104151  
 Ti-Mo-Zr-Sn (11.5, 6, 4.5 wt.%),  $\beta$  III, mech. props. rel. to heat treatment 0-84961  
 Ti-Mo-Zr-Sn (11.5, 6.0, 4.5 wt.%) alloy, struct. as affected by processing history 0-84972  
 Ti-Nb (4.32 wt.%), high temp. oxidation kinetics under 1 bar pressure, 1255-1471K 0-89410  
 Ti-Nb-Zr-Ta, superconducting props. comp. depend., stress effects and precipitation behaviour, X-ray scatt. 0-93059  
 Ti-Ta (4.37 wt.%), oxidation kinetics, 1258-1473K, and at pressure of 0.013, 0.133 and 1.0 bar 0-89411  
 TiC, frictional characts. and contact-zone deform. in homogeneity range 0-66673  
 TiC<sub>N</sub>, powder preparation, physical, chemical props. (*Russian*) 0-76212  
 TiCr<sub>1.8</sub>H and D soln., enthalpy, solubility and mol. vibr. determ., comparison with soln. in metals and binary alloys 0-79951  
 Ti-Bi-Sb-Te system, peritectic reactions in TiBiTe<sub>2</sub>-TiSbTe<sub>2</sub> cross section, crystn. character 0-108406  
 Ti-Sn system equilibria, polythermal and isothermal cross sections obs., ternary comp. form. 0-104128  
 Ti<sub>2</sub>PbCu(NO<sub>3</sub>)<sub>6</sub>, incommensurate Jahn-Teller transition, Huang scatt. 0-70401  
 Ti<sub>2</sub>Te<sub>3</sub>-Ti<sub>4</sub>SnTe<sub>3</sub>-Ti<sub>4</sub>PbTe<sub>3</sub>, phase equil., DTA, SPA and microhardness meas. 0-96628



**X-ray diffraction examination of materials continued**

- TiVO<sub>4</sub>, synthesis and thermal props. (French) 0-97443  
 U-Y-C FBR nuclear fuels, phase anal., 1400°C 0-66485  
 UAs, search for lattice distortions at low temps. 0-79759  
 UC, miscibility with rare earth nitrides (German) 0-96654  
 UN, search for lattice distortions at low temps. 0-79759  
 U<sub>1-x</sub>Nd<sub>x</sub>S, mag. phase diagram 0-71027  
 U<sub>1-x</sub>Pr<sub>x</sub>S, mag. phase diagram 0-71027  
 USb, search for lattice distortions at low temps. 0-79759  
 V, oxidation in low press. O<sub>2</sub> at high temp. (Japanese) 0-71807  
 V-H(D), hydrogen ordering, review 0-60850  
 V<sub>2</sub>O<sub>3</sub>, impurity doping effects, elec. props. obs. 0-75609  
 V<sub>2</sub>O<sub>3</sub>, amorphous semicond., solubility and fibrous texture 0-75162  
 V<sub>2</sub>O<sub>5</sub>-Ti<sub>2</sub>O<sub>5</sub>, DTA, mag. susceptibility and X-ray diffr. study 0-70970  
 VSe<sub>2</sub> (1T), incommensurate periodic lattice distortion, X-ray diffraction study 0-107414  
 WC-Co DC and RF sputtered coatings, bias effect, struct., X-ray-Auger study 0-70565  
 W<sub>50</sub>Fe<sub>50</sub> glassy alloy, refractory, triode sputtered 0-75185  
 WO<sub>3</sub>, acoustic instability near monoclinic orthorhombic phase transition, X-ray scatt. 0-65215  
 WSi<sub>2</sub>, refractory formation by As<sup>+</sup> ion beam bombardment 0-107286  
 Y-M intermetallic cpds., M=3d transition metal, sorption of H<sub>2</sub>, structural charges 0-88429  
 Y<sub>2</sub>(CO<sub>3</sub>)<sub>3</sub>·nH<sub>2</sub>O, tengerite, single cryst. hydrothermal growth 0-97417  
 Y(OH)CO<sub>3</sub>, ancylite like phase, hydrothermal cryst. growth (French) 0-108340  
 Zn-As system, homogeneity range of ZnAs<sub>2</sub> and electrophys. props. 0-60833  
 ZnO film, RF sputtered, characterization for SAW transducers 0-80138  
 ZnO piezoelectric films, RF planar-magnetron sputtered, characterisation 0-96751  
 ZnO powder, effect of dry grinding in EPR and catalytic activity (Japanese) 0-84640  
 ZnO RF sputtered films, post deposition annealing behaviour 0-100416  
 ZnS film, RF sputtered, characterization for SAW transducers 0-80138  
 ZnSiP<sub>2</sub>(As<sub>2</sub>), thermal expansion coeffs. meas. (Russian) 0-65258  
 ZnTe-Cu films, high cond., elec. and optical props. 0-88651  
 Zr-Al-C, phase diagram and lattice constants, X-ray diffr. method 0-89207  
 ZrB<sub>2</sub>-Nb, reactions between components 0-100812  
 Zr(Ca,Y)O<sub>2-x</sub>, local ionic arrangement, X-ray diffr. study 0-100203  
 Zr<sub>70</sub>Co<sub>30</sub>, Zr<sub>70</sub>Fe<sub>30</sub>, Zr<sub>70</sub>Ni<sub>30</sub> and Zr<sub>70</sub>Pd<sub>30</sub> amorphous alloys, struct. factors and radial distrib. functions 0-84096  
 ZrI<sub>4</sub>, high-temp. enthalpy, X-ray powder diffr. data 0-107446  
 ZrO<sub>2</sub>, porous, sintered stabilised microspheres, strength and fracture studies 0-85019  
 ZrO<sub>2</sub> thin film, optical props. rel. to cryst. struct. 0-97357  
 ZrO<sub>2</sub>-Sc<sub>2</sub>O<sub>3</sub>-Y<sub>2</sub>O<sub>3</sub> system, order-disorder phenomena, Raman spectra study 0-97254

**X-ray diffraction examination of microstructure**

- see also crystal microstructure  
 absorbing crystals, dislocation contrast in the case of anomalous X-ray transmission 0-100240  
 borosilicate glass, birefringent, X-ray small-angle scatt. study 0-103937  
 Burgers vector sign determ. for nearly screw dislocations, X-ray dynamical theory applic. 0-59467  
 dislocation velocity, thermal activation exam. of applied stress and temp. depend., expt. methods (French) 0-59474  
 grain boundary sliding model 0-75237  
 lattice distortion, X-ray moiré pattern fine struct. study 0-79775  
 metal-C system, spheroidal graphite formation, role of high angle boundaries (Russian) 0-81065  
 nonisothermal devitrification kinetics 0-92465  
 Nylon 6 gut yarn, fine struct. change in twisting, annealing and untwisting, microbeam X-ray obs. 0-81026  
 Nylon 6 gut yarn, fine struct. change in twisting, annealing and untwisting, X-ray and electron microscopy obs. 0-84904  
 petroleum feedstocks and cokes, graphitizability 0-93580  
 polyethylene-polypropylene blend, extruded, thermal swelling and mech. characterisation 0-81110  
 α-quartz, synthetic, growth, defects induced by seed orientation 0-96454  
 rare earth germanes, flux-grown, X-ray topography 0-64939  
 siloxane, temp. transitions, linear dilatometry and X-ray diffr. obs. (Russian) 0-59404  
 solid-solid interface chemistry, characterisation, theory 0-75448  
 steel, cold strained, defects interaction with carbide strengthening phases, carbide decomp. degree (Russian) 0-84955  
 steel, Cr-Mn type, martensite struct. after quenching and HTMT 0-84975  
 steel, high C, investigation of transformations during tempering by nuclear gamma resonance method (Russian) 0-76256  
 steel, maraging, ageing kinetics and struct. of N12K7M5TYu, effect of high temp. deform. of austenite (Russian) 0-84960  
 steel, Ni (17 wt.%), martensitic deform. temp., cryst. struct. effect (Russian) 0-66576  
 steel, Ni-P plated, electroless, fatigue strength and plated layer microstruct. (Japanese) 0-93645  
 steel, stainless, carbide and intermetallic phases, quantitative anal. by X-ray diffr. 0-66514  
 steel, structural, strained in tension after tempering, compression effects on struct. changes (Russian) 0-66577  
 steel, W-Co-Mo-Cr-V-C (8.5, 8.1, 4.5, 3.5, 2.2, 1.02 wt.%), phase composition, struct. and props. 0-104163  
 steel fine structure after heat treatment, X-ray diffr. exam. 0-60890  
 steel Ni-Cr-Ti-C (2.8, 0.9, 0.2, 0.73 wt.%), ferrite, orientation in pearlite, rel. to austenite (Russian) 0-81072  
 TBBA liquid crystal, monoclinic cell parameters of solid, smectic and metastable phases, temp. dependence 0-70122  
 TTF-TCNQ crystals, X-ray topographic study of cryst. perfection 0-96525  
 Ag-In-Sn, internal oxidation, precipitation behaviour of oxide (Japanese) 0-66515  
 Ag-Sn system, phase diagram, eutectic temps., microstruct. (German) 0-104119  
 Ag-Sn, splat-quenched, X-ray diffr. study 0-81094  
 Ag<sub>3</sub>Au<sub>1-x</sub>Cu<sub>x</sub>, phase relations, X-ray diffr. and differential thermal anal. 0-108395  
 AgZn, β'→γ transformation, effect of additional elements 0-66507

**X-ray diffraction examination of microstructure continued**

- Al-Cu (3 wt.%), stress aged, GP zone struct. by X-ray diffuse scatt. meas. (Japanese) 0-71653  
 Al-Zn, X-ray diffr. after omnidirectional compression (Russian) 0-88262  
 Al-Zn-Mg (3.6, 1.95 wt.%), ageing and plastic deform., effect on structure, electron microsc. and X-ray diffr. study (Russian) 0-81108  
 Al<sub>2</sub>O<sub>3</sub> substrates, tape-casted, fracture strength analysis 0-60948  
 Au-Pt-Pd-Ag-Cu, commercial dental alloy, age-hardening characts. 0-89235  
 Au<sub>3</sub>Cu<sub>1-x</sub>Ag<sub>x</sub>, phase relations, X-ray diffr. and differential thermal anal. 0-108395  
 Be<sub>2</sub>SiO<sub>4</sub>, phenakite, flux grown single crystals, twinning study by hydrothermal etching and X-ray diffr. 0-107271  
 Co-mischmetall system, phase relations, microstruct., mag. props. 0-104118  
 Co-Pt, mag. annealing, form. of ordered phase, study using X-ray scatt. (Russian) 0-81052  
 Co-Ti-C, secondary precipitation and allotropic transform., TEM obs. 0-108453  
 Cr foil, laser irradiated, low-angle X-ray scatt., angular block misalignment and hardness (Russian) 0-103413  
 Cr-W-O, phase relations, thermodynamic props. of CrWO<sub>4</sub> and Cr<sub>2</sub>WO<sub>6</sub> 0-104120  
 Cu foil, laser irradiated, low-angle X-ray scatt., angular block misalignment and hardness (Russian) 0-103413  
 Cu, single crystals, cyclically and unidirectionally deform. X-ray diffr. study 0-89319  
 Cu-Bi (0.02 wt.%) alloy, intergranular fracture, Kossel X-ray diffr. in SEM obs. 0-108579  
 Cu-Ni-Sn (10, 6 wt.%), spinodal decomposition, X-ray and electron diffr. study 0-81063  
 Cu-Ni-Sn (15, 8 wt.%), prior deform. effect on spinodal age hardening 0-108465  
 Cu<sub>3</sub>Ag<sub>1-x</sub>Au<sub>x</sub>, phase relations, X-ray diffr. and differential thermal anal. 0-108395  
 Fe, 90° walls, stable orientations, theory and X-ray observations (Japanese) 0-60359  
 Fe, cast, white, high Cr, phase composition, B effect 0-104172  
 Fe, creep at 77, 295K, formation of five struct. 0-60926  
 Fe, high-purity single crystals, X-ray topography and double-crystal diffraction 0-92534  
 α-Fe, nitrated, aged at room temp. 0-71679  
 Fe-Al, single crystals, deform. at high temps. 0-81125  
 Fe-Co-V-(Ni), annealing effect on microstruct. rel. to mag. and mech. props. 0-89267  
 Fe-Cr-O system, phase relations at 1200°C using diffusion couple technique 0-89205  
 Fe-Mn, ε-martensite, preferred orientation and constitution, reverse pole figures (Russian) 0-104178  
 Fe-Mo (13-20 at.%) binary alloys, spinodal decomp. on ageing, TEM and X-ray diffr. study 0-97503  
 Fe-Ni-C austenitic alloy, banded struct. formed by deform. 0-71713  
 Fe-Si (3 wt.%), mag. domain wall contrast in synchrotron X-ray topographs 0-75792  
 β-Fe<sub>2</sub>Ge<sub>3</sub>, formation in isothermal sintering, phase transition kinetics 0-89197  
 Fe<sub>2</sub>O<sub>3</sub>, haematite platelets, growth and cross-connection in consolidation of haematite pellet (Chinese) 0-104186  
 α-Fe<sub>2</sub>O<sub>3</sub>, single cryst., hematite, X-ray topographic obs. of domain struct. changes in external mag. field 0-88785  
 Fe<sub>2</sub>O<sub>3</sub>-Al<sub>2</sub>O<sub>3</sub> mixed oxide, X-ray diffr. and elec. cond. 0-79954  
 Fe<sub>3</sub>Pt austenite, long range order parameter, temp. depend. discussion 0-97481  
 GaAs:Si, stacking fault prod. during heat treatment in As vapour 0-96547  
 Gd-Co based amorphous sputtered films, microstruct. variability and mag. anisotropy, implanted ion effects 0-88459  
 Gd<sub>3</sub>Ga<sub>5</sub>O<sub>12</sub>, X-ray topography and double-crystal diffraction 0-92534  
 Ge single crystals, constitutional supercooling growth conditions, structural and chem. inhomogeneities 0-93473  
 GeO<sub>2</sub> glass, nonisothermal devitrification kinetics 0-92465  
 Hg<sub>1-x</sub>Cd<sub>x</sub>Te, segregation, compositional characterisation 0-107434  
 Hg<sub>1-x</sub>Fe<sub>x</sub>Te, struct. invest. using X-ray diffr. and electron microscopy 0-75365  
 In-Sn alloy crystals, phase changes and shape memory effect (Japanese) 0-108502  
 In-Tl, single crystal containing Li, X-ray study of FCC⇌FCT transform. (Japanese) 0-108435  
 InSb, X-ray topographic evidence of asymmetrical pre-yield behaviour 0-75229  
 β-In<sub>3</sub>Sn, decomposition, X-ray powder diffr. study 0-89196  
 KH<sub>2</sub>PO<sub>4</sub>, Burgers vector sign determ. for nearly screw dislocations, X-ray obs. 0-59467  
 La-Si-As ternary cpd., synthesis, stoichiometry 0-104083  
 Mg, HCP lattice, Huang diffuse scatt. from interstitials 0-88142  
 Mg-Zn (5 wt.%), age hardening, X-ray diffr. anal. (Chinese) 0-104173  
 Mn-Al-C, ferromag. alloy, transform. kinetics 0-76229  
 Mo, dislocation structure of diffusional welding zone (Russian) 0-96531  
 Mo-(Zr+Y+C) (1.1 wt.%) alloy, phase composition, carbide phase microhardness (Russian) 0-60834  
 NaClO<sub>3</sub>, dislocations rel. to growth mechanism from aq. soln., X-ray topography 0-59464  
 Na<sub>2</sub>O-CaO-Al<sub>2</sub>O<sub>3</sub>-SiO<sub>2</sub> glass, crystn. for the purpose of obtaining vitroceramics (French) 0-75163  
 Nb-Pd constitution diagram, metallographic and X-ray diffr. anal. 0-89204  
 Nb<sub>2</sub>Sn, powder metallurgically produced, microstruct. characts. 0-89233  
 Ni, 109° and 71° walls, stable orientations, theory and X-ray observations (Japanese) 0-60359  
 Ni, carbonyl powder, dislocation density sintering 0-108372  
 Ni, creep at 77, 295K, formation of five struct. 0-60926  
 Ni, dislocation structure evolution after hydroextrusion (Russian) 0-96530  
 Ni, variation in dislocation density during creep, determ. by X-ray diffr. analysis (Russian) 0-76302  
 Ni-Cr, high temp. thermomech. treatment effect on tensile diagrams of KhN77TYuR (Russian) 0-60884  
 Ni-Fe-Nb-Al (11.2, 8.09, 79.66 wt.%), modulated struct. growth process rel. to ageing (Chinese) 0-66541  
 NiPt, quenched, ordering kinetics and domain struct. form. during isothermal tempering (Russian) 0-66502



**X-ray diffraction examination of microstructure continued**

- Pb film, monocryst., heteroepitaxial growth, struct. defects, and elec. props. (*Russian*) 0-84403  
 $\text{Pb}_{0.5}\text{Sn}_{0.5}\text{Te}$  crystals, Bridgman grown, X-ray perfection study 0-107018  
 Si, crack-tip dislocation pattern, X-ray topography (*French*) 0-107253  
 Si, epitaxial, on sapphire, characterisation, X-ray rocking curves 0-75458  
 Si, high-dose Ar implantation, X-ray topographic obs. of strains and damage 0-59496  
 Si  $n^+p$  solar cells, degradation mechanisms associated with Ti impurities 0-81465  
 Si, oxidation-induced Frank sessile dislocation loops, struct. change 0-75228  
 Si, precipitation of O, 650°C, IR absorpt. and X-ray diff. 0-76258  
 Si, X-ray topography and double-crystal diffraction 0-92534  
 Si-P polycrystalline layer, role in lattice defect reduction assoc. with P predeposition 0-70229  
 $\text{SmCo}_5$  sintered magnets, eutectoid decomp. 0-89219  
 $\text{Tb}_2\text{Ge}_2\text{O}_7$ , flux-grown, X-ray topography 0-64939  
 $(\text{Th,U})\text{O}_2$ , burnup simulated, high O<sub>2</sub> pot., chem. state 0-91220  
 Ti-Al(Mo), phase relations 0-108398  
 Ti-Mo, structure associated with BCC to omega transform. (*Russian*) 0-108432  
 Ti-Si amorphous alloy, melt-quenched, transform. studies and mech. props. 0-100838  
 $\text{V}_2\text{O}_5$  and lower oxides, defect structures and related props. 0-59454  
 W, deformed, surface layer struct. effect on polygonisation and recryst., X-ray diff. anal. and metallographic exam. (*Russian*) 0-84948  
 W, vapour deposited, dislocation struct., rel. to texture (*Russian*) 0-65394  
 Zn, HCP lattice, Huang diffuse scatt. from interstitials 0-88142  
 $\text{ZrO}_2\text{-CaO}$ , stabilised microspheres, structure, mechanical props. (*Russian*) 0-100379  
 $\text{ZrO}_2\text{-Y}_2\text{O}_3$ , stabilised microspheres, structure, mechanical props. (*Russian*) 0-100379

**X-ray diffraction examination of molecular structure**

- see also molecular configurations  
 cholesteryl ethyl carbonate, long periods in sol. state, X-ray diff. study 0-96503  
 chromatin, low-angle X-ray and neutron diff., interparticle effects 0-72134  
 copolymer, semicryst. random, characterisation by small angle neutron and X-ray scatt. 0-75189  
 DNA compact form, tertiary struct., small angle X-ray scatt. 0-72129  
 ferredoxin, *S. platensis* [2Fe-2S], struct. and evolution of chloroplast-type ferredoxins 0-94165  
 heart, review of studies, book contrib. 0-109079  
 muscle, contracting, dynamic structure, X-ray scatt., time resolved, rapid data collection systems 0-61740  
 muscle contraction, single, high-time resolution X-ray investigation method 0-81777  
 polyethylene, chlorinated, semicryst. random, characterisation by small angle neutron and X-ray scatt. 0-75189  
 polymer surface, supramol. struct. characterisation, use of C X-radiation 0-79705  
 polymers, structure elucidation, model construction and X-ray methods (*German*) 0-103267  
 polystyrene, atactic, structure elucidation, model construction and X-ray methods (*German*) 0-103267  
 polystyrene, conform. and near all-trans extended-chain model relevant in gels, X-ray diff. patterns interpret. 0-79707  
 retinal photoreceptors, small angle X-ray data processing 0-81536  
 sarcoplasmic reticulum membranes, small angle X-ray data processing 0-81536  
 solution X-ray scattering, review of recent developments, book contrib. 0-109077  
 1,3,5-trioxane-1, 3-dioxolane copolymer, semicryst. random, characterisation by small angle neutron and X-ray scatt. 0-75189  
 Cu complex,  $[\text{Cu}(1,4,7,10\text{-tetrabenzyl-1,4,7-10-tetraazacyclododecane})\text{Cl}]\text{NO}_3$ , cryst., struct. 0-64966

**X-ray diffractometers**

- APD 3600 automatic X-ray powder diffractometer, sophisticated derivative method appls., JCPDS data base 0-107017  
 Bonse-Hart X-ray diffractometer, asymmetrically cut, comparison with Kratky camera 0-77917  
 Bonse-Hart X-ray diffractometer, asymmetrically cut, for SAXS, design and performance 0-77916  
 Bragg X-ray intensities, collected on single cryst. diffractometer with graphite monochromator, assessment 0-57448  
 fast X-ray diffractometer based on a spherical drift multiwire proportional chamber with digital position encoder 0-90969  
 four-circle single-crystal diffractometer, mechanical devices for aiding alignment 0-99029  
 microprocessor-based, features 0-70082  
 residual stress measurement, X-ray diff. equipment, comparison 0-82858

**X-ray effects**

- see also biological effects of X-rays  
 actomyosin, X-irradiated ENDOR and ELDOR obs. 0-63689  
 alkali metal halides, X-ray induced colour centre and halogen aggregate form. 0-96565  
 cryostat for low temperature X-irradiation and electron paramagnetic resonance 0-86321  
 dipotassium glucose-1-phosphate, X-irrad., ESR-ENDOR obs 0-60419  
 5-halouracils, solid, radiation damage, free radicals in 5-fluorouracil single crystals. 0-71926  
 s-halouracils, solid, radiation damage obs., deoxyribose ring opening in single crystals. 0-71929  
 MOST, short channel, output conductance, effect of ionising radiation 0-70836  
 myosin, X-irradiated ENDOR and ELDOR obs. 0-63689  
 poly-p-xylylene films, carrier traps, X-ray induced TSC, thermolum. and dielec. loss study 0-88570  
 polycrystalline dipeptides, X-irradiated ENDOR and ELDOR obs. 0-63689  
 polyvinylidene fluoride, X-ray induced TSC 0-75578  
 quartz, surface damage by X-rays,  $\gamma$ -rays, neutrons, SEM study 0-79837  
 solid-electron and X-ray interaction (*Chinese*) 0-70253  
 solids, interaction with electrons and X-rays (*Chinese*) 0-80896  
 TGS, internal field prod. in layer periodical domain struct. by X-ray irradi. 0-71359  
 TTF-TCNQ, anisotropic cond., X-ray effects 0-96855

**X-ray effects continued**

- $\beta\text{-Al}_2\text{O}_3\text{-Na}_2\text{O}$ , X-ray induced defects, EPR and ENDOR study 0-60456  
 Ar, solid, X-ray induced point defects 0-59514  
 Ca fluorapatites, carbonated, B-type, EPR of  $\text{F}^{+}$ -centre after X-irrad. (*French*) 0-108065  
 $\text{CaCO}_3\text{:Li}$ , synthetic calcite,  $(\text{CO}_3\text{Li})^{2-}\text{-Li}^{+}$  defect after X-irrad., EPR study 0-75852  
 $\text{CaF}_2$ :Ni crystals, X-irradiated, EPR study of  $\text{Ni}^{+}$  and  $\text{Ni}^{3+}$  0-75849  
 $\text{CaF}_2\text{:M}$ ,  $\text{M}=\text{Mn, Fe, Co, Ni}$ , X-irrad., impurity effects on defect prod. 0-92525  
 $\text{CaF}_2\text{:Mn}$ , EPR and optical absorpt. spectra 0-93171  
 $\text{CaF}_2\text{:Mn}$ , low temp. X-irrad., Mn centres, optical absorpt. and emission props. 0-60635  
 $\text{CaF}_2\text{:Mn}(\text{Co})(\text{Ni})$ , X-irrad., thermolum. 0-60686  
 $\text{CaF}_2\text{:Ni}$ , X-irrad., optical absorpt. spectra and dichroism meas. 0-108239  
 $\text{CaF}_2\text{:Ni}$ , X-irradiated, optical and EPR meas. 0-108235  
 $\text{CaSO}_4\text{:Sm}$  phosphors, X-irrad., thermoluminesc., charge compensation effects 0-97351  
 $\text{CsCdBr}_3\text{:Cr}^{3+}(\text{Cr}^{+})$ , EPR of impurities, charge compensation, X-ray effects 0-60407  
 $\text{CsI:Na}$ , X-ray irradiated, optical and ESR studies in IR absorption band 0-80828  
 $\text{CsMgCl}_3(\text{Br}_3)\text{:Cr}^{3+}(\text{Cr}^{+})$ , EPR of impurities, charge compensation, X-ray effects 0-60407  
 $\text{Fe}_{0.5}\text{Co}_{0.5-x}\text{Cr}_x$  films, vacuum-deposited cryst. and mag. struct. (*Russian*) 0-93081  
 KBr, cation defects creation mechanism 0-75224  
 KBr, X-irrad. crystals, halogen aggregation, absorpt. spectra obs. (*Russian*) 0-66234  
 $\text{KBr}(\text{Cl})\text{:Sr}^{2+}\text{Cu}^{+}$ , thermolum. response, extension of two-step reaction model 0-89075  
 KCl, X-ray irradiated, first-stage F-centre prod. 0-107231  
 KCl, X-ray irradiated, vacancy conc. determ., thermal expansion meas. 0-79782  
 $\text{KCl:Ag}$ , X-irrad., thermoluminesc. study of Ag centres 0-80874  
 $\text{KCl:Ca}^{2+}$ , Z-centre thermolum. 0-80879  
 $\text{KCl:Li}$ , X-irrad.,  $\text{F}_A$  centres, thermolum. studies 0-80878  
 $\text{KCl:Pb}^{2+}$ , X-ray irradi., electron-trapped centres,  $\text{Pb}^{+}$  and  $\text{Pb}^0$ , optical absorpt. spectra 0-71461  
 $\text{KCl:SnCl}_3$ , photostimulated hole recombination luminesc. (*Russian*) 0-80833  
 $\text{KMg}_3[\text{AlSi}_2\text{O}_{10}]\text{F}_2$  with excess Al, synthetic fluorophlogopite, radiation-induced paramag.  $\text{O}^{-}$  centres 0-60417  
 $\text{LiF:Mg}$ , dependence of optical absorpt. on temp. during X-ray irradi. 0-66237  
 $\text{LiF:Mg}$ , X-irrad., colour centres, ESR and UV absorpt. meas. 0-108069  
 $\text{LiF:Mg}$ , X-irrad. induced sensitisation mechanism, optical absorpt. spectra 0-60637  
 LiH, defect form. at low temp., EPR, thermolum. and TSC study 0-107222  
 LiH, formation and annihilation of Li colloids and H bubbles 0-107228  
 $\text{MgO}$ , thermally stimulated exoelectron emission (*German*) 0-66404  
 $(\text{NH}_4)_2\text{SO}_4\text{:MnO}_4^{-}$ , X-ray irradi. damage, optical absorpt. spectra study 0-66246  
 $\text{Na}_3\text{Al}_6\text{Si}_6\text{O}_{24}\text{:Cl}(\text{Br})(\text{I})$ , cathodochromic sodalites, coloured crystals, tunnel and recomb. luminesc., temp. depend. (*Russian*) 0-66261  
 $\text{Na}_3\text{Al}_6\text{Si}_6\text{O}_{24}\text{:NaX}(\text{X}=\text{Cl, Br, I})$ , X-ray irradi., thermal-erase cathodochromism and dihalide mol. centres (*Russian*) 0-66236  
 NaCl, pure and doped, 20K X-ray irradiation, thermolum. and recovery processes 0-93412  
 $\text{NaCl}(\text{Br})$ , X-ray or UV irradiated, cation defects creation mechanism 0-75224  
 NaF, X-irrad., colour centres and thermolum. 0-84790  
 $\text{NaMgF}_3$ , defects induced by X- and vacuum UV irradi., optical and elec. study 0-107319  
 $\text{Na}_2\text{O-SiO}_2\text{:Au+CeO}_2$ , Au particle nucleation 0-81066  
 $\text{RbCl}(\text{Br})$ , cation defects creation mechanism 0-75224  
 S, polycryst., photoelectret state following X-irrad. 0-60485  
 SiC, radiation resistant substrate materials, for X-ray gratings 0-90960  
 $\text{SiO}_2$ , vitreous, X-ray compaction efficiency 0-65044  
 $\text{SiO}_2\text{:Ag}$ , cryst. and glassy, X-ray induced EPR and luminesc. centre 0-65043  
 $\text{SrF}_2\text{:Ni}$ , X-irrad., optical absorpt. spectra and dichroism meas. 0-108239  
 $\text{SrFCl}$ , thermolum. and optical absorption spectra 0-66309  
 $\text{Tb}_2\text{O}_3\text{-P}_2\text{O}_5\text{-MO}$  system glasses, ( $\text{M}=\text{Mg, Ca, Sr, Ba or Pb}$ ), photoluminesc. under X-ray excitation 0-89060  
 $\text{TiO}_2$ , thermally stimulated exoelectron emission (*German*) 0-66404  
 $\text{V}_2\text{O}_5$ , thermally stimulated exoelectron emission (*German*) 0-66404  
 $\text{Y}_2\text{O}_3\text{:Zr}^{3+}$ , F-centre charge state, ESR and thermally stimulated luminesc. obs. 0-60418  
 $\text{ZnO}$ , thermally stimulated exoelectron emission (*German*) 0-66404  
 $\text{ZrSiO}_4$ , X-irrad., trapping and emission centres,  $\text{OH}^{-}$  ion contribution 0-80876

**X-ray emission spectra**

- see also appearance potential spectra; conversion electron spectra  
 alkali halide, irradi. stability obs. using X-ray emission meas. (*Russian*) 0-66326  
 alkali silicate glasses, struct. and thermal props. 0-84075  
 alkaline earth oxide, irradi. stability obs. using X-ray emission meas. (*Russian*) 0-66326  
 chemical shifts of hard X-ray lines, applicability of Koopmans' theorem, HF calcs. 0-74145  
 electron probe X-ray microanalysis, quantitative investigation of thin specimens 0-101068  
 heavy ion collisions, electron EM field interaction, quantised field formalism 0-83478  
 inert gas binary mixture,  $\mu$ -capture, near 5 atm., X-ray yield 0-58419  
 interband transition probabilities calc. based on muffin tin potential 0-104014  
 lutetium diphthalocyanine, solid-state anion migration in anodic oxidation 0-60994  
 meson transfer reactions in solids, surface struct. effects 0-104015  
 metal, soft X-ray emission spectra and Fermi surface, contrib. of John Bardeen 0-57057  
 metal film, thickness meas., using nondestructive radioisotopic technique 0-68179  
 metallic film, single layer and multilayer, thickness determ. by X-ray fluoresc. 0-68180

## X-ray emission spectra continued

- microchemical analysis, optimising conditions, analytical electron microscopy 0-101067  
 molecular X-ray fluorescence spectra, observation using 5 m grating spectrograph 0-86538  
 muonic atoms, X-ray emission polarisation (*German*) 0-69268  
 muonic X-rays, circular polarisation (*German*) 0-69266  
 plasma, laser-produced, X-ray spectra 0-75075  
 plasma dielectronic satellite spectra, electron collisions, corona model theory 0-59188  
 protonium, atomic X-ray yields 1s and 2p level shifts and widths, cascades, calc. 0-78730  
 rare earth metals, X-ray 5p emission bands, valence energy band 0-104016  
 soft X-ray transition radiation observation from medium energy electrons 0-76104  
 spectrometer for soft X-ray emission studies of liquid metals and metallic vapours 0-73564  
 superheavy and intermediate atomic collision systems, UNILAC expts. 0-63751  
 thin film, sputter profiling, combined Auger-X-ray anal. 0-66909  
 third-row elements, at. K-shell X-ray prod. by  $^{14}\text{N}^+$  bombardment 0-91482  
 time-resolved X-ray spectroscopy of laser-produced plasmas 0-84004  
 transition elements, first-group, K-emission satellites, quasi-stationary states and origin 0-80903  
 X-ray intensity ratio  $L\beta/L\alpha$ , atomic number dependence 0-62818  
 Ag+H $^+$  excited X-ray polarisation, Born approx. calcs. (*Russian*) 0-78566  
 Al, K X-ray absorption, K-emission spectrum, band struct. using APW method 0-97380  
 Al laser plasma, high-Z, temp. meas. from bremsstrahlung emission 0-87914  
 Al, soft X-ray emission edge, temp. depend. 0-89090  
 Al $^{2+}$  foil-excited ion, X-ray spectra and satellite classification 0-95567  
 Al+He(C)(N)(O), inner-shell multiple ionisation systematics, X-ray obs. 0-63790  
 AlIX-XII, plasma, X-ray line radiation, radiation transport eqns., calc. method 0-64777  
 Al $_2\text{O}_3$ , irradi. stability obs. using X-ray emission meas. (*Russian*) 0-66326  
 Ar, electron impact, L X-ray spectrum, radiative Auger transitions 0-58227  
 Au, energy band structure, X-ray N-emission spectra, relativistic APW calcs. 0-70596  
 Au, energy band structure, X-ray emission spectra, APW calc. 0-92811  
 Au single cryst., thin films and bulk, anisotropic X-ray emission 0-108303  
 B, evaporated, electronic struct., XPS, SXS and isochromat investig. 0-76143  
 B, muonic X-ray transitions, nuclear charge radii 0-99589  
 Be muonic X-ray transitions, nuclear charge radii 0-99589  
 Be, soft X-ray emission edge, temp. depend. 0-89090  
 C, muonic X-ray transitions, nuclear charge radii 0-99589  
 Cd, proton-induced L-shell ionisation cross-sections 0-100707  
 CdSiP $_2$ , electronic struct., X-ray spectroscopic investigation 0-108300  
 Cl X-ray emission spectra, detect. from Alcator-A Tokamak 0-92389  
 Cu, 15-33 MeV electron bombardment, X-ray ang. distrib. meas. using ETL quantimeters 0-91367  
 Cu (111), final state band gap effects in UPS 0-89120  
 Cu, polycryst., X-ray intensity, microfocus source, non-linear rise studies 0-77927  
 Cu, XX 0-100707  
 Cu+Cu collisions, K $\alpha$  X-ray energy shifts, target thickness depend. 0-83311  
 CuCl, band struct., OPW calc. and X-ray spectra meas. 0-75506  
 Er, L-line emission spectrum diagram line 0-84808  
 F, isoelectronic sequence, X-ray spectra 0-87071  
 F K $\alpha$ , X-ray satellite struct. and KLL Auger electron spectra, solid-state effects 0-89089  
 F, K-shell X-ray spectra from light ion bombard. studies 0-71518  
 Fe, inner-shell vacancies, cascade decay, multiple ionisation and X-ray emission calcs. 0-87072  
 Fe, K $\alpha$  satellite lines following electron bombardment 0-69097  
 Fe $_2$ Si(Al), electronic structure, X-ray spectra comparison with band struct. calcs. 0-97383  
 $^{155}\text{Gd}$  L $_{2,3}$  subshell X-ray fluorescence and Coster-Kronig yields from  $^{155}\text{Er}$  decay 0-69102  
 H, mesic, atomic X-ray yields 1s and 2p level shifts and widths, cascades, calc. 0-78730  
 $^3\text{He}$ , liquid, pionic K X-ray transition energies and Lorentzian widths 0-78727  
 $^{155}\text{Ho}$  L $_{2,3}$  subshell X-ray fluorescence and Coster-Kronig yields from  $^{155}\text{Er}$  decay 0-69102  
 Ir, energy band structure, X-ray emission spectra, APW calc. 0-92811  
 K, soft X-ray emission edge, temp. depend. 0-89090  
 K $_2$ Pt(CN) $_4$ , muonic X-ray radiation anisotropy (*German*) 0-69267  
 Mg, soft X-ray emission edge, temp. depend. 0-89090  
 Mg $^{2+}$ , foil-excited ion, X-ray spectra and satellite classification 0-95567  
 MgAl $_2\text{O}_4$ , irradi. stability obs. using X-ray emission meas. (*Russian*) 0-66326  
 Mn $_2$ Si, electronic structure, X-ray spectra comparison with band struct. calcs. 0-97383  
 Mo, proton-induced L-shell ionisation cross-sections 0-100707  
 Mo X-ray emission spectra, detect. from Alcator-A Tokamak 0-92389  
 N, muonic X-ray transitions, nuclear charge radii 0-99589  
 NH $_3$ , vibr. excitation in soft X-ray emission and core ESCA spectra 0-69163  
 Na K $\alpha$ , X-ray satellite struct. and KLL Auger electron spectra, solid-state effects 0-89089  
 Na $_2\text{O}$ -TiO $_2$ -SiO $_2$  glass, co-ordination of Ti, X-ray emission spectra study 0-84072  
 NaV $_2\text{O}_5$ , monocrystal, electronic struct. and X-ray emission spectra anisotropy 0-84807  
 Nb, L-spectra, influence of temp., liq. N $_2$  temps. (*Russian*) 0-80907  
 NbC, band struct. and X-ray emission spectra, APW and X $\alpha$  calc. 0-70605  
 Ne, isoelectronic sequence, X-ray spectra 0-87071  
 Ne recoil ion, highly charged, K X-ray emission 0-91649  
 Ne, X-ray line shift for high density laser produced plasma diagnostics 0-64778

## X-ray emission spectra continued

- Ni, L $_{2,3}$ -binding energy, absolute determ. from self-absorpt. meas. 0-71519  
 Ni, proton-induced L-shell ionisation cross-sections 0-100707  
 Ni, X-ray intensity reson. near 2p threshold 0-60717  
 O I, isoelectronic sequence, X-ray spectra 0-87071  
 Pb, 15-33 MeV electron bombardment, X-ray ang. distrib. meas. using ETL quantimeters 0-91367  
 Pd, L-spectra, influence of temp., liq. N $_2$  temps. (*Russian*) 0-80907  
 Pd, proton-induced L-shell ionisation cross-sections 0-100707  
 Pt, energy band structure, X-ray emission spectra, APW calc. 0-92811  
 Rh, L-spectra, influence of temp., liq. N $_2$  temps. (*Russian*) 0-80907  
 Rh, proton-induced L-shell ionisation cross-sections 0-100707  
 S $^{2+}$ , travelling in solids, K $\alpha$  X-ray spectra 0-100706  
 Si, solid, electron rearrangement after inner shell ionisation by heavy charge particle impact 0-87043  
 SiH $_4$ (SiF $_4$ ), electron rearrangement after inner shell ionisation by heavy charge particle impact 0-87043  
 SiO $_2$ , proton induced ionisation, energy dependence of K $\alpha$ /K $\beta$  intensity ratio 0-60716  
 Sn+He(C)(N)(O), inner-shell multiple ionisation systematics, X-ray obs. 0-63790  
 Th, L and M X-ray emission following H and O ion impact, parameter depend. 0-66327  
 TiO $_2$ , core levels, cryst.-field splitting, X-ray emission study 0-66328  
 Ti $_2$ V $_2$ C, electronic struct. and X-ray emission spectra, cluster MO calc. 0-5444  
 UO $_2$ , electronic distributions by X-ray spectroscopy 0-97407  
 V $_2\text{O}_5$ , core levels, cryst.-field splitting, X-ray emission study 0-66328  
 V $_2\text{O}_5$ , energy band struct. rel. to expt. studies 0-70603  
 W, proton-induced L-shell ionisation cross-sections 0-100707  
 Xe like ions (I $^-$ , Cs $^+$ , Ba $^{2+}$ , La $^{3+}$ ) 3d $^{24f}$  config., collapse of 4f electron, X-ray spectral obs. (*Russian*) 0-58204  
 YS, band struct. and X-ray emission spectra, APW and X $\alpha$  calc. 0-70605  
 Zn, core levels, cryst.-field splitting, X-ray emission study 0-66328  
 Zn, proton-induced L-shell ionisation cross-sections 0-100707  
 ZnSiP $_2$ , electronic struct., X-ray spectroscopic investigation 0-108300  
 $^{68}\text{Zn}$ , 2s-2p muonic X-ray transition obs. 0-74264  
 $^{68}\text{Zn}$  muonic atom, dynamical E0 excitation, E0 resonances, muonic X-rays 0-95749  
 ZrAl $_3$ , X-ray energy spectrum of valence electrons (*Russian*) 0-108304  
 Zr $_2$ Al, X-ray energy spectrum of valence electrons (*Russian*) 0-108304  
 Zr $_4$ Al $_3$ , X-ray energy spectrum of valence electrons (*Russian*) 0-108304  
 ZrX $_2$  alloy, Laves phases with MgZn $_2$ , MgCu $_2$  structs., X-ray emission spectra (*Russian*) 0-71517

## X-ray fluorescence analysis

- absolute determinations and matrix corrections, high con. method 0-81379  
 airborne mineralogical dusts, metallic elements determ. by energy dispersive X-ray fluorescence anal. 0-76569  
 applications, conf., Denver, CO, USA, July-Aug. 1979 0-90613  
 bauxites, analysis, comparison of atomic absorpt., X-ray fluoresc. and other classical methods 0-89551  
 blood presence on Shroud of Turin, spectroscopic and chem. tests 0-102875  
 crystalline solids, electronic industry, chem. anal. instrumental methods progress 0-66903  
 energy selective X-ray anal. in TEM 0-84036  
 equations of bond, review 0-66898  
 erythrocytes labelled with stable Rb, survival determ. by fluoresc. excitation anal., rabbits 0-81788  
 filter assembly for fluorescence EXAFS meas. 0-90971  
 flexible scanning industrial X-ray/fluorescopic inspection 0-89459  
 fracture surfaces, quantitative analysis problems in energy dispersive X-ray spectrometry with Si(Li) diodes (*French*) 0-89571  
 glass fragments, classification into window and non-window types 0-81401  
 glasses, high vol. low cost, as solar reflectors, compositions and weathering effects 0-106589  
 K X-ray fluorescent multi-strip probe for accelerator beam studies 0-102362  
 laterites, Venezuelan, analysis, comparison of atomic absorpt., X-ray fluoresc. and other classical methods 0-89551  
 method with corrections for absorption 0-85239  
 monazite, from South Indian beach sand, superheavy element search, K X-ray fluoresc. anal. 0-61801  
 nuclear fuels, nondestructive measurement of U and Th conc. and quantities using XFA and gamma spectrometry 0-71877  
 nuclear materials, nondestructive element and isotope assay of Pu and U 0-71870  
 nuclear materials safeguards, assay of dissolver solns. by totally sampled wavelength dispersive X-ray fluorescence 0-83160  
 nuclear materials safeguards, nondestructive, energy-dispersive, X-ray fluorescence analysis of product-stream concentrations from reprocessed nuclear fuels 0-83163  
 optical emission and X-ray spectrometry developments (*French*) 0-68263  
 particle induced X-ray fluorescence emission, moving target mechanism 0-73562  
 Shroud of Turin, scientific investigation 0-87576  
 steel, dual phase HSLA, compositional anal., TEM 0-85253  
 steel, tool and high-speed, high freq. induction melting and centrifugal casting in instrumental anal. 0-84886  
 steel foil, microanalysis by energy dispersive X-ray spectrometry (*French*) 0-85250  
 surface chemical anal. using RHEED-solid state detector method 0-108760  
 tomography, X-ray fluorescence techniques, I distrib. in thyroid gland 0-61664  
 wavelength and energy dispersive X-ray fluorescence spectrometers compared 0-89573  
 Ag thin film, X-ray fluoresc. spectroscopy of surface using RHEED-solid state detector method 0-108760  
 Al $_2$ Ga $_{1-x}$ P, proportional ingredient content determ. by X-ray fluoroscopy 0-97747  
 Au artifacts from Sarawak, X-ray fluorescence and at. absorpt. analysis 0-85229  
 Au coins, surface anal. by X-ray fluoresc., SEM and scanning Auger spectroscopy 0-89552



**X-ray fluorescence analysis continued**

- Co/Ni zeolite, -A and -Y type, local coordination of Co(II) ions studied by X-ray absorpt. fine struct. spectroscopy 0-93434  
 Cu-Ga, binary alloy constituent EDS anal., secondary fluorescence, SEM study (*Chinese*) 0-85231  
 ErD<sub>2</sub> thin film, degradation during film processing, investigation 0-101047  
 Fe-Si (3wt.%), grain-oriented, secondary recryst., grain growth inhibition 0-89245  
 Ga-As, binary alloy constituent EDS anal., secondary fluorescence, SEM study (*Chinese*) 0-85231  
 Hf and Zr, trace elements, simultaneous determ. in soln. using X-ray fluorescence anal. 0-97752  
 In, Al<sub>1-x</sub>P, proportional ingredient content determ. by X-ray fluoroscopy 0-97747  
 In, Ga<sub>1-x</sub>P, proportional ingredient content determ. by X-ray fluoroscopy 0-97747  
 InSb, films, X-ray fluoresc. anal. method, long-term stability 0-61212  
 LiF focusing array for fluoresc. EXAFS in dilute samples 0-99028  
 Mg, inclusions, types and size distrib. (*German, English*) 0-97492  
 YIG:La,Ga, film, LPE-grown, Ga incorporation, depend. of magnetisation on growth rate 0-84627  
 Zr and Hf, trace elements, simultaneous determ. in soln. using X-ray fluorescence anal. 0-97752

**X-ray fluorimetry see X-ray fluorescence analysis****X-ray lasers**

- atomic collision processes and X-ray and UV lasers 0-64787  
 confined plasma column, soft X-ray lasing action conditions 0-74346  
 relativistic ion beam laser, continuously IR to X-ray tunable, in negative temp. state (*Chinese*) 0-87373  
 resonator based on successive refls. of surface wave 0-99021  
 short-wave emission, initial plasma parameters 0-99692  
 soft X-ray population inversion in laser plasmas, reson. photoexcitation, photon-assisted processes 0-87378  
 Ge complanar X-ray resonator circulating beam, high symm. multiple wave configurations (*Russian*) 0-78875  
 He<sup>2+</sup> + Li collisions, soft X-ray emission obs. 0-83591  
 KrF\* laser, generation of high-spectral-brightness tunable XUV radiation at 83 nm 0-91846  
 Li I laser, 207 Å, oscillator strengths 0-83598

**X-ray monochromators**

- BESSY SX/700: a monochromator system covering the spectral range 3 eV ≤ hν ≤ 700 eV 0-90952  
 channel-cut, identification of spurious reflections 0-90959  
 crystal monochromators, determ. of polarisation ratio 0-99018  
 cyclic X-ray monochromators, with perpendicular dispersion planes, emission coherence 0-90974  
 Daresbury SRS, VUV and soft X-ray 0-90942  
 development for synchrotron radiation facilities 0-91351  
 diffracted-beam monochromator, in single-cryst. diffractometry, a performance assessment 0-57448  
 (n,m) focusing position, to create monochromator for synchrotron radiation 0-87989  
 geometry for focusing synchrotron radiation above 10 keV 0-90958  
 grasshopper monochromator, improved high resolution, 10 to 1000 eV 0-90939  
 grazing incidence for UV monochromators using toroidal holographic gratings 0-90946  
 grazing incidence monochromators, optimisation for synchrotron radiation 0-90943  
 grazing incidence monochromators with holographic toroidal gratings, 10 to 150 eV 0-90947  
 holographic transmission diffraction gratings for soft X-rays 0-90965  
 LURE Rowland circle grazing incidence monochromator, performance 110 to 280 eV 0-90945  
 monolithic monochromators for synchrotron radiation, 1 to 4 Å, order sorting, focusing and polarising 0-90955  
 scattering at grazing incidence from optical surfaces, effect of surface topography 0-90968  
 section topography, high resolution, using asymmetrically reflecting plane crystal monochromator 0-57449  
 straight groove toroidal grating monochromators, 10 to 500 Å, design optimisation for synchrotron radiation 0-90944  
 transmission diffraction gratings for synchrotron rad. sources, modelling 0-90964  
 ultra-high-vacuum double crystal monochromator beam line for studies in the spectral range 500-4000 eV 0-90957  
 wave packet polarisation, in X-ray monochromators, dynamic theory (*Russian*) 0-64826  
 XUV monochromator design for use with synchrotron radiation sources 0-90940  
 LiF focusing array for fluoresc. EXAFS in dilute samples 0-99028  
 Si impurity-doped cryst. plate, as an X-ray monochromator, strain distrib. for 220 reflection 0-100126

**X-ray photoeffect see X-ray photoelectron spectra****X-ray photoelectron spectra**

- acetylene adsorbed on Fe containing segregated C, hydrogenation, C-1s XPS spectra obs. 0-84366  
 adhesion, surface anal. techniques appl. 0-65381  
 adsorbed molecules, core ionisation, negative shake-up energy 0-100749  
 alkali metaborates, vapour over heated solid, XPS, obs. 0-87171  
 alkaline earth fluorides, orbital binding energy and ionicity relations, XPS meas. 0-97399  
 Auger lines, generation by bremsstrahlung 0-87174  
 cobalt stearate, monomolecular multilayers, XPS escape length depend. on emission angle, elastic scatt. role (*Japanese*) 0-84833  
 electronic material and device characterisation using surface-sensitive analytical techniques 0-65341  
 ESCA shifts and effective charges 0-78648  
 glasses and ceramics, characterisation with analytical electron microscope 0-84068  
 grain boundary segregation, critical assessment 0-75362  
 graphite fibre, surface anal. by XPS and polar/dispersive free energy anal. 0-65340  
 graphite-AsF<sub>3</sub> intercalated species, fractional ionisation and identification 0-97397  
 Inconel 600, nuclear reactor boiler corrosion, XPS 0-66709  
 Inconel 600, nuclear reactor boiler corrosion, XPS 0-71816  
 insulators, XPS, binding energy, surface pot. and work function calcs. 0-89113

**X-ray photoelectron spectra continued**

- lifetime broadening in electron spectroscopy of core levels in solids 0-80938  
 metal, independent electron, soln. of X-ray edge problem, recoil spectrum of suddenly perturbed Fermi sea 0-80932  
 metals, X-ray photoemission spectroscopy, anomalous, frequency dependence of exponents 0-71563  
 methane, core 1s shakeup study, XPS and Xalpha calcs. 0-69064  
 MIS solar cells, interface problems, AES, SIMS and XPS study 0-89627  
 molecules containing 1st row atoms, K-shell binding energy shifts, NDDO MO calcs. 0-58413  
 p-nitroanilines, intramol. charge transfer satellites, XPS 0-78650  
 PDX vacuum vessel, glow discharge conditioning 0-79607  
 phthalocyanine compounds, XPS and charge transfer 0-95681  
 polyacetylene:AsF<sub>3</sub>, AES, XPS, UPS, and X-ray induced 0-66400  
 polyacetylene:I, electronic structure, XPS and UPS meas. 0-66385  
 polyphenylene oxide thin films, electrochem. prep., impurity effects on cond., electroforming 0-88655  
 PVC surfaces, natural and stabilised, composition, ageing, oxidation and weathering, ESCA obs. (*French*) 0-61139  
 quantitative, rel. to subshell photoionis. cross-sections and electron mean free path 0-81389  
 α-quartz, electronic struct., local disorder influence 0-59870  
 α-quartz surface, XPS study 0-93451  
 rare earth alloys, RBe<sub>13</sub>, XPS, resist. and susceptibility study 0-71565  
 rare earth metals, 3d core electron XPS spectra, low-binding-energy satellites, exception of Eu 0-104040  
 rare earth metals, density of 4f states below and above Fermi level, XPS and bremsstrahlung isochromat spectroscopy 0-76140  
 rubber-metal interface, adhesion mechanism, XPS study 0-65382  
 self-consistent charge calcs. of core-electron binding energy shifts 0-69084  
 silicate minerals, X-ray photoelectron diffr., quantitative anal. 0-66912  
 soft X-ray spectra, meas. by photoelectron anal. 0-73557  
 sputtered refractory carbides, adhesion to metal substrates, improved 0-76481  
 steel, austenitic, Cr-Ni, ion-implanted N, chem. state study by AES and XPS 0-79825  
 steel, cold-rolled sheet, surface chemistry 0-61146  
 steel, industrial, surface chem. characterisation by SIMS, glow discharge spectrometry and other techniques 0-66907  
 steels, stainless, surface characterisation rel. to adhesive bonding chem. etching, SEM, AES, XPS and electron probe microanal. 0-88416  
 Stellite-6, XPS obs. of aqueous oxidation, surface comp. and gaseous oxidation effect 0-81238  
 surface analytical techniques, quantification, review 0-65342  
 surface segregation, effect on metallurgical props, SIMS, XPS and AES (*French*) 0-80045  
 synchrotron radiation techniques for studying atomic physics 0-63583  
 thionine-coated electrode for photogalvanic cells, electrochem. and XPS anal. 0-72071  
 transition metal elements of fifth period, core level binding energies 0-71564  
 transition metal oxides, second and third-row, XPES 0-87170  
 transition metal sulphides, ion bombardment damage, XPS obs. 0-97404  
 transition metals, alloys, and cpds., XPS asymmetry of core electrons and electronic struct. parameters 0-93460  
 1,3,5-trinitro 1,3,5-triazacyclohexane, shock-induced intramol. bond breaking, XPS and EPR study 0-76512  
 trinitrotoluene, shock-induced intramol. bond breaking, XPS and EPR study 0-76512  
 Y-type zeolites, rare earth ion exchanged, XPES obs. 0-83421  
 Ag (111) surface, ethylene adsorption, XPS and UPS investigation 0-103573  
 Ag, Auger spectra, 4d bandwidth effect 0-89093  
 Ag, core level binding energies 0-71564  
 Ag surface, CO chemisorption, SIMS, XPS study 0-84382  
 Ag-Mn, dil., valence and core level spectra, XPS study 0-84838  
 Ag-O-Cs surface, oxidation, role of Cs suboxides in low work function surface layers, XPS 0-76131  
 Ag<sub>2</sub>S-K<sub>2</sub>SO<sub>4</sub> mixtures, surface comp., AES and XPS obs. 0-81386  
 Al, adsorption and decomp. of NH<sub>3</sub> and hydrazine, XPS obs. 0-92783  
 Al sheet surfaces, chem. characterisation by SIMS, glow discharge spectrometry and other techniques 0-66907  
 Al-Mn(Ni)(Cu), dil., core and valence band spectra, XPS study 0-84837  
 AlAg, Auger spectra, 4d bandwidth effect 0-89093  
 Al<sub>2</sub>O<sub>3</sub> thin film used in inelastic electron tunnelling spectroscopy, X-ray photoelectron spectrum 0-108319  
 Au clusters on alkali halide surface, size depend. of valence bands, XPS study 0-65647  
 Au/GaSb (110) interface, heat-treated, struct. and chem. state, angle-resolved XPS 0-97400  
 Au-Al/GaAs interfaces, atomic interdiffusion, soft XPS studies 0-65302  
 Au-Fe(Co)(Ni), dil., valence and core level spectra, XPS study 0-84838  
 B, evaporated, electronic struct., XPS, SXS and isochromat investig. 0-76143  
 BaO, XPS valence bandstruct. 0-89117  
 BaTiO<sub>3</sub>, band struct. calc., interpretation of XPS and UPS spectra 0-70597  
 BaTiO<sub>3</sub>, photoelectron and optical spectra derived from self-consistent charge MO and band calcs. 0-96785  
 BaTiO<sub>3</sub>, XPS and UPS from surface defects 0-76136  
 C, adsorbed on Fe(100), adsorbate coverage determ. by LEED, AES and XPS 0-103566  
 C bonding to Tokamak walls, XPS studies 0-80942  
 C:Ni, X-ray photoemission studies 0-76138  
 Ca, photoelectric cross sections at 52.4, 60, 72.2 and 84.4 keV 0-69187  
 CaO, XPS valence bandstruct. 0-89117  
 Cd, core level binding energies 0-71564  
 Cd, electron binding energy and shift, core level XPS 0-87088  
 Cd, photoelectric cross sections at 52.4, 60, 72.2 and 84.4 keV 0-69187  
 CdF<sub>2</sub>, UPS and XPS spectra, rel. to optical props. 0-66386  
 CdS, XPS, secondary illumination effects, band bending, level shifts 0-108324  
 CdS-Al(Au) interfaces, bonding and interdiffusion, XPS obs. 0-80000  
 CdSe photoanodes, S substitution during operation and mech. of surface protection XPS study 0-107906  
 CdTe surface, sputter cleaning and dry oxidation, XPS and LEED study 0-108618  
 CeBe<sub>3</sub>, intermediate valence state, XPS, resist. and susceptibility study 0-71565

## X-ray photoelectron spectra continued

- CePd<sub>3</sub>, mixed-valence, 3d and 4d core levels, XPS study 0-89111  
 Co base amorphous alloys, alloying elements influence on corrosion behaviour, XPS obs. 0-89422  
 Co II acetylacetonate, XPS 0-74196  
 Co, oxidation, XPS obs. of epitaxial CoO form. 0-66396  
 CoSe<sub>2</sub>(Se<sub>2</sub>), core-level and valence-band XPS 0-93450  
 CoSe<sub>2</sub>(Se<sub>2</sub>), electronic struct., UPS and XPS study 0-80935  
 Cr<sup>6+</sup>/Cr<sup>3+</sup> colloidal SiO<sub>2</sub> surface films on Al, TEM/XPS study 0-85090  
 Cr-Ge system, XPS, X-ray and neutron diff., and mag. meas. to study chem. bonding and electronic struct. 0-60749  
 Cr(NO)<sub>3</sub>, bonding, shake-up intensities and shake-up energies, SCF X $\alpha$  multiple scatt. calc. 0-74121  
 Cr(NO)<sub>3</sub>, XPS and UV photoelectron spectra, compared to NO data 0-58317  
 CrO<sub>2</sub>, particulate, proton donor adsorption effect on mag. moment, XPS anal. 0-71117  
 CsBO<sub>2</sub>, vapour over heated solid, XPS, obs. 0-87171  
 Cs<sub>3</sub>Sb vacuum deposited photoemitter, XPS study 0-89122  
 Cu surface, (110), methanol adsorption, XPS, UPS and thermal desorpt. study 0-84388  
 Cu-Fe(Co)(Ni), dil., valence and core level spectra, XPS study 0-84838  
 CuAl<sub>2</sub>O<sub>4</sub>, pure and NiO promoted catalysts, surface oxidation state and comp., XPS study 0-76134  
 CuCl<sub>2</sub>, ESCA satellite intensity, ab initio SCF calcs. 0-74103  
 CuFeS<sub>2</sub>, superficial degradation in air and water, XPS obs. (French) 0-89110  
 CuSe<sub>2</sub>(Se<sub>2</sub>), electronic struct., UPS and XPS study 0-80935  
 CuZr, photoemission study 0-104046  
 Fe (110), coadsorption of K and O<sub>2</sub>, XPS, UPS, AES, and LEED study 0-80084  
 Fe, adsorption of acetic acid and ethylenediamine, XPS study 0-76132  
 Fe, evaporated, adsorbed acetylacetonate, XPS study 0-76133  
 FeB and Fe<sub>2</sub>B, ESCA and mag. spin data, electronic struct., isomer shifts, valence bands and chemical bonding 0-75489  
 Fe<sub>1-x</sub>(P,B)<sub>x</sub>, amorphous and crystalline, photoemission and band structure 0-60754  
 FeS<sub>2</sub>, core-level and valence-band XPS 0-93450  
 FeS<sub>2</sub>, superficial degradation in air and water, XPS obs. (French) 0-89110  
 FeTi, surface and mag. props., heat treatment and hydrogenation effects 0-75447  
 Fe(100), CO and H<sub>2</sub> adsorption and desorption, C, O, S and K adlayer effects 0-71573  
 GaAs anodic films, XPS study 0-71562  
 GaAs, polycryst., wet and dry oxides, comparative study by AES, SIMS and XPS 0-80116  
 GaAs, shallow core level spectra 0-104037  
 GaAs solar cell, polycryst., grain boundary passivation by oxidation, AES, SIMS and XPS obs. 0-81467  
 GaAs, surface cryst. regularity by X-ray photoelectron diff. 0-89112  
 GaAs thin films, reactively sputtered, ESCA/XPS study 0-97430  
 GaAs, XPS, secondary illumination effects, band bending, level shifts 0-108324  
 GaAs-Au(Ag) Schottky barrier solar cells, interface problems, AES, SIMS and XPS study 0-89627  
 GaN, electron struct., ESCA study 0-89116  
 GaS, shallow core level spectra 0-104037  
 GaSe, shallow core level spectra 0-104037  
 Ge/GaAs (110) heterojunction, valence band discontinuity in XPS spectra, precise determ. 0-84834  
 H<sub>16</sub>MoO<sub>3</sub>, electronic props., mag. susceptibility and spectra 0-80266  
 H<sub>2</sub>O, core 1s shakeup study, XPS and X $\alpha$  calcs. 0-69064  
 H<sub>2</sub>WO<sub>3</sub>, bronzes, Anderson transition, XPS 0-107705  
 He(I), 0-63599  
 He(II), 0-63599  
 HfC<sub>2</sub>N<sub>1-x</sub>, X-ray valence photoelectron spectrum, 4f signal calc. 0-66391  
 Hg, electron binding energy and shift, core level XPS 0-87088  
 Hg<sub>0.8</sub>Cd<sub>0.2</sub>Te surface, sputter cleaning and dry oxidation, XPS and LEED study 0-108618  
 HgTe surface, sputter cleaning and dry oxidation, XPS and LEED study 0-108618  
 In, chemisorption of O<sub>2</sub>, XPS and static SIM spectral study 0-80055  
 In, core level binding energies 0-71564  
 In, photoelectric cross sections at 52.4, 60, 72.2 and 84.4 keV 0-69187  
 InN film growth by reactive sputtering in Ar-N<sub>2</sub> discharge, mechanism 0-89107  
 In<sub>2</sub>O<sub>3</sub>-InN film growth by reactive sputtering in N<sub>2</sub>-O<sub>2</sub> discharge, mechanism 0-89108  
 InSb, single crystal, chem. and ion etching, surface changes (French) 0-108614  
 InSe thin film, sputter growth and chem. anal. by XPS/ESCA 0-80976  
 K, adsorbed on Fe(100), adsorbate coverage determ. by LEED, AES and XPS 0-103566  
 K adsorbed on Fe(110), UPS and XPS meas. 0-95675  
 K adsorbed on Pt(111), UPS and XPS meas. 0-95675  
 KBO<sub>2</sub>, vapour over heated solid, XPS, obs. 0-87171  
 K<sub>2</sub>SO<sub>3</sub>-Ag<sub>2</sub>SO<sub>4</sub> mixtures, surface comp., AES and XPS obs. 0-81386  
 La-Sm-Au, amorphous, surface effects on Sm valence, XPS and X-ray adsorption meas. 0-108325  
 LaB<sub>6</sub> (100), (110), and (111), surface structs. and work functions 0-70512  
 LaB<sub>6</sub> (210) surface, work function, struct. and chemisorpt. stability, XPS, UPS and LEED 0-65344  
 Li, surface characterization of film growth 0-81240  
 LiC<sub>6</sub>, intercalation compound, electronic struct., XPS meas. 0-59850  
 LiNbO<sub>3</sub> surfaces, ion and electron bombard., photoelectron spectroscopy and electronic props. 0-71559  
 LiNbO<sub>3</sub>, XPS and UPS from surface defects 0-76136  
 Mg, XPS, plasmon gains as monitor of incomplete relax., interference effects and sudden to adiabatic limits transition 0-66390  
 MgAg, Auger spectra, 4d bandwidth effect 0-89093  
 Mg<sub>2</sub>Cu polycrystals, surface study by AES, XPS and X-ray induced AES 0-65346  
 MgO, XPS valence bandstruct. 0-89117  
 Mn-Ag, XPS meas., Fermi level to 1000 eV below it 0-66389  
 MnAg alloys, XPS meas. 0-60751  
 MnO<sub>2</sub>, UV irradiated, XPS rel. to Viking gas exchange reaction on Mars 0-72831  
 MnS<sub>2</sub>(Se<sub>2</sub>), core-level and valence-band XPS 0-93450

## X-ray photoelectron spectra continued

- NH<sub>3</sub>, core 1s shakeup study, XPS and X $\alpha$  calcs. 0-69064  
 NH<sub>3</sub>, vibr. excitation in soft X-ray emission and core ESCA spectra 0-69163  
 NH<sub>4</sub>NO<sub>3</sub>, shock-induced intramol. bond breaking, XPS and EPR study 0-76512  
 N<sub>2</sub>O, photoelectron spectrum, vibronic interaction and autoionis. effects 0-95680  
 Na, XPS, plasmon gains as monitor of incomplete relax., interference effects and sudden to adiabatic limits transition 0-66390  
 NaNCO, val. band electronic struct., XPS meas., MOC and INDO calc. 0-95520  
 Na<sub>2</sub>O-SiO<sub>2</sub> glass, bridging to non-bridging ratio and correl. to glass density and refr. index, ESCA study 0-84832  
 Nb films, oxidation, XPS study 0-80944  
 Nb-NbO<sub>2</sub>-Pb superconductive tunnel junctions, oxide tunnelling barriers, ESCA characterisation 0-65745  
 Nd, photoelectric cross sections at 52.4, 60, 72.2 and 84.4 keV 0-69187  
 Ni (001), photoelectron diff., effects in core-level photoemission 0-76144  
 Ni, adsorption of acetic acid and ethylenediamine, XPS study 0-76132  
 Ni, band struct. and multielectron excitations, angle-resolved photoemission determ. 0-76147  
 Ni, electronic structure, photoelectron spectra, theory 0-80168  
 Ni, evaporated, adsorbed acetylacetonate, XPS study 0-76133  
 Ni halides, XPS, multiplet struct. and multielectron excitations, in 3p and 2p shells 0-78649  
 Ni II acetylacetonate, XPS 0-74196  
 Ni, M<sub>1,III</sub> spectrum, ab initio calculation 0-83276  
 Ni, photoelectric cross sections at 52.4, 60, 72.2 and 84.4 keV 0-69187  
 Ni, quasi-particle energies, two-hole XPS satellite 0-66399  
 Ni/Al<sub>2</sub>O<sub>3</sub> catalysts, coprecipitated methanation type, metal-support interaction, XPS obs. 0-80936  
 Ni-Cr(Fe)(Cu) alloy, matrix effect in SIMS anal. using O<sub>2</sub><sup>+</sup> primary beam 0-76576  
 Ni-P amorphous alloys, electrodeposited and melt-quenched atomic and electronic structures 0-88062  
 NiO film, formed by Ni galvanic oxidation in borate buffer soln., struct. 0-100948  
 NiO-MgO solid solns., surface comp. study by XPS 0-104035  
 NiS<sub>2</sub>(Se<sub>2</sub>), core-level and valence-band XPS 0-93450  
 NiS<sub>2</sub>(Se<sub>2</sub>), electronic struct., UPS and XPS study 0-80935  
 Ni<sub>3</sub>Sn<sub>2</sub>Sn<sub>0.04</sub>, surface segregation, XPS and AES obs. 0-76135  
 O, adsorbed on Fe(100), adsorbate coverage determ. by LEED, AES and XPS 0-103566  
 O bonding to Tokamak walls, XPS studies 0-80942  
 Pb-In-(Au) base electrode film Josephson junctions, tunnel barrier oxide struct. 0-65750  
 PbS, superficial degradation in air and water, XPS obs. (French) 0-89110  
 Pd surface, CO chemisorption, SIMS, XPS study 0-84382  
 Pd surface, segregated S state, AES, EELS, UPS and XPS study 0-93452  
 PdAg surface, CO chemisorption, SIMS, XPS study 0-84382  
 PdZr, photoemission study 0-104046  
 Pt (111), chemisorption of mol. O<sub>2</sub>, XPS, UPS, EELS, and work function meas. 0-76139  
 Pt (111), interaction with water, thermal desorption, UPS, and XPS study 0-80088  
 Pt (111) and Pt (S)-12(111)X(111)surfaces, adsorption of O, thermal desorption, AES, XPS, and LEED study 0-70534  
 Pu, oxidation, binding energies, Auger and X-ray photoelectron spectra study 0-76550  
 rare earth oxides, XPS 0-87170  
 RbBO<sub>2</sub>, vapour over heated solid, XPS, obs. 0-87171  
 Re, electronic struct. and CO adsorption characts., XPS, UPS, and thermal desorption study 0-71571  
 Re surface, interaction with N<sub>2</sub><sup>+</sup> beam, reaction dynamics studied by XPS and thermal desorpt. spectrometry 0-93797  
 Re(0001), adsorption of O<sub>2</sub>, CO, NO, and H<sub>2</sub>O, XPS, UPS and temp. programmed desorption 0-71574  
 S, adsorbed on Fe(100), adsorbate coverage determ. by LEED, AES and XPS 0-103566  
 S-N system, inorganic, electronic struct. obs. by photoemission XPS and UPS, CNDO calcs. 0-78653  
 S<sub>2</sub>N<sub>2</sub>, gas phase and solid state core level XPS 0-66401  
 S<sub>2</sub>N<sub>4</sub>, solid state core level XPS 0-66401  
 (SNBr<sub>0.04</sub>)<sub>x</sub> and (SNBr<sub>0.25</sub>)<sub>x</sub>, solid state core level XPS 0-66401  
 Sb, core level binding energies 0-71564  
 Si (111), intermediate oxidation state, core photoelectron absorpt. vs. chemical shifts 0-81220  
 Si, chemisorption of XeF<sub>2</sub> and SiF<sub>4</sub>, XPS and Auger spectra, surface chemistry 0-81358  
 Si layer, on buried SiO<sub>2</sub> layer formed by high-dose, O ion implantation, TEM, AES, and XPS obs. 0-88172  
 Si:H, amorphous, 2p level shift, XPS obs. 0-97401  
 Si<sub>1-x</sub>C<sub>x</sub>H glow discharge films, local atomic struct., XPS and AES study 0-93448  
 SiO<sub>2</sub>:Au(Ag)(Cu), XPS line broadening and extra-atomic relax. energies 0-71561  
 SiO<sub>2</sub>-Na<sub>2</sub>O-CaO-MgO float glass, surface SnO<sub>2</sub> distrib., ellipsometry and XPS study 0-84346  
 Sm metal, valence transition at surface of Sm 0-70652  
 Sm, surface mixed valence, XPS study 0-60753  
 Sm-Au, amorphous, surface effects on Sm valence, XPS and X-ray adsorption meas. 0-108325  
 SmB<sub>6</sub>, surface mixed valence, XPS study 0-60753  
 SmS<sub>1-x</sub>P<sub>x</sub>, valence changes, XPS and UPS study 0-97402  
 Sn, core level binding energies 0-71564  
 SnO<sub>2</sub>-NiO(ZnO)(Nb<sub>2</sub>O<sub>5</sub>), activated sintering mechanism 0-60810  
 SrF<sub>2</sub>, UPS and XPS spectra, rel. to optical props. 0-66386  
 SrO, XPS valence bandstruct. 0-89117  
 SrTiO<sub>3</sub> (111), O<sub>2</sub>, H<sub>2</sub> and H<sub>2</sub>O chemisorption, UPS and XPS studies, illum. effects 0-71572  
 Te, core level binding energies 0-71564  
 Th, valence and 5f states, XPS and bremsstrahlung isochromat spectroscopy 0-66393  
 TiH<sub>2</sub> and TiD<sub>0.9</sub>, surface characts., AES, EELS, SIMS, and XPS study 0-65343  
 TiO<sub>2</sub>, sputtering defects, associated surface electron states, UPS, XPS and AES obs. 0-60755



**X-ray photoelectron spectra continued**

- TiO<sub>2</sub>-Ni (100) interface, electronic props., struct., comp., chemical bonding 0-84499  
 TiBr, polymorphism, XPS obs. 0-97398  
 TiCl, polymorphism, XPS obs. 0-97398  
 TmTe, f<sup>12</sup> and f<sup>13</sup> config. photoemission fractional parentage coeffs., intermediate and LS coupling calc. 0-84829  
 U, valence and 5f states, XPS and bremsstrahlung isochromat spectroscopy 0-66393  
 UAl<sub>2</sub>(Co)<sub>2</sub>, surface comp. and electronic struct., photoemission study 0-66382  
 UO<sub>2</sub>, electronic distributions by X-ray spectroscopy 0-97407  
 UO<sub>2</sub>, electronic transitions, crystal field effects and phonons, phase transition 0-97303  
 UO<sub>2</sub>, Mg K $\alpha$  and He(II) photoelectron spectra, origin from multi-configurational Dirac-Fock calcs. 0-66387  
 V, photoelectric cross sections at 52.4, 60, 72.2 and 84.4 keV 0-69187  
 V<sub>2</sub>O<sub>3</sub> and lower oxides, defect structures and related props. 0-59454  
 V<sub>2</sub>O<sub>3</sub> and lower oxides, electronic, optical, structural and surface props., review 0-88120  
 V<sub>2</sub>O<sub>3</sub> energy band struct. rel. to expt. studies 0-70603  
 W, XPS, angle-resolved, from valence bands, obs. of strong temp. depend. and direct-transition effects 0-60752  
 Y, photoelectric cross sections at 52.4, 60, 72.2 and 84.4 keV 0-69187  
 Y, XPS relative intensity and photoionisation cross-section 0-63599  
 Yb-Al mixed valent film form., XPS study 0-80943  
 YbAu<sub>2</sub>, valence transition at surface of Yb 0-70652  
 Zn, electron binding energy and shift, core level XPS 0-87088  
 Zn, photoelectric cross sections at 52.4, 60, 72.2 and 84.4 keV 0-69187  
 ZnS, superficial degradation in air and water, XPS obs. (French) 0-89110  
 Zr, XPS relative intensity and photoionisation cross-section 0-63599  
 Zr-Co, amorphous and crystalline, d-band struct., alloying effects 0-59862  
 Zr-Ni, amorphous and crystalline, d-band struct., alloying effects 0-59862  
 ZrB<sub>3</sub>, self-consistent band struct., XPS, reflectance, NQR, Hall effect and density of states meas. 0-107689  
 ZrS, electronic struct., bonding effects, photoelectron spectroscopic and low temp. heat capacity cal. 0-96780

**X-ray production**

- see also X-ray tubes*  
 betatron 5 MeV, design and performance, X-ray prod. 0-63421  
 CHESS synchrotron radiation facility, high energy tunable X-ray source 0-68984  
 coherent X-ray emission from relativistic electron beam 0-91739  
 flash X-ray machine, distributed pulse power system anal. using SCEP-TRE circuit code techniques 0-68336  
 generator design, with thyristor based power supply, bell shape pulses generation 0-57446  
 TEM, analytical, sources of background X-radiation 0-101908  
 transition radiation source 0-69303  
 Ag, electron (positron), impact, K- and L-shell ionisation, K $\alpha$  and L X-rays meas. 0-99575  
 Au, X-ray production cross sections for protons, fluoresc. obs. 0-102476  
 Au+light and heavy ions, L-shell X-ray production and subshell ionisation cross sections meas. 0-91637  
 C<sup>19+</sup>+Cu, K X-ray production and radiative electron capture, fluoresc. yield determ. 0-99553  
 Pb, X-ray production cross sections for protons, fluoresc. obs. 0-102476

**X-ray protection** *see radiation protection***X-ray reflection**

- catoptrical crossed-mirror imaging at grazing incidence 0-77923  
 EXAFS and surface EXAFS from X-ray refl. meas 0-71512  
 intensifying screen, role of reflective layer 0-62816  
 interface co-ordinate determ. by X-ray backscatt., signal-noise ratio 0-77925  
 metal density measurement, using X-ray total external reflect. and double crystal spectrometer 0-64831  
 mirror profile meas. machine 0-69496  
 monochromatic images of X-ray emitting sources, hot plasma diagnostics appl. 0-64772  
 resonator based on successive refls. of surface wave 0-99021  
 Co, X-ray refl. near L<sub>2,3</sub> absorpt. edge 0-71513  
 Ti, X-ray refl. near L<sub>2,3</sub> absorpt. edge 0-71513

**X-ray scattering**

- see also Compton effect; X-ray diffraction*  
 atomic systems, elastic X-ray scatt. intensity, rel. to average electron density, isoelectronic changes 0-91424  
 critical angles in total reflection of, Compton, X-ray and fluoresc. scatt. 0-59343  
 DNA compact form, tertiary struct., small angle X-ray scatt. 0-72129  
 elastic X-ray scattering, by thermodynamic average electron-charge density 0-100123  
 EM radiation in media with spatial dispersion, spatial coherence formation and polarisation increase 0-106442  
 film adsorbed on graphite, two-dimensional phase transitions 0-107653  
 grazing incidence scattering, from optical surfaces, effect of surface topography 0-90968  
 Guinier-Preston zones, X-ray small angle scattering, for extra-resist. calcs. 0-92873  
 imaging system, surface roughness and scatt. effects 0-77921  
 plasmon excitation during X-ray scatt. 0-108297  
 reverberation and time-dependent Comptonisation in X-ray sources, rel. to rapid time variability 0-86013  
 synchrotron radiation camera and data acquisition system for time resolved X-ray scattering studies 0-99023  
 tissue equivalent phantom, scatt. obs. 0-94279  
 Al alloys, age-hardenable, precipitation and dissolution processes, positron annihilation and X-ray small-angle scattering comparison 0-89238  
 Al, incoherent scatt. factors calc. by direct integration over impulse approx. Compton profiles 0-102475  
 Ar, incoherent scatt. factors calc. by direct integration over impulse approx. Compton profiles 0-102475  
 Be, X-ray scattering, Wannier function calcs. 0-87988  
 Cu extended X-ray fine struct., lattice consts. 0-89085  
 InAs, intensity of 3-phonon diffuse scattering of X-rays 0-84027

**X-ray scattering continued**

- Kr, incoherent scatt. factors calc. by direct integration over impulse approx. Compton profiles 0-102475  
 Na, incoherent scatt. factors calc. by direct integration over impulse approx. Compton profiles 0-102475

**X-ray sources (astronomical)**

- see also X-ray astronomical observations*  
 1732-303, 1745-248, new X-ray burst sources, discovery and identifications with globular clusters (Terzan 1, 5) 0-98739  
 HR 1099, RS Canum Venaticorum type binary, light and colour curve meas. 0-73004  
 A0620-00, transient source, optical counterpart, visible and IR obs. 0-101653  
 A1742-28, transient source, optical counterpart, visible and IR obs. 0-101653  
 2A 0251+413, identification as AWM 7 galaxy cluster by HEAO 1 0-90573  
 2A 0311-227, AM Herculis type binary star, IR photometry and polarimetry 0-77517  
 2A 0311-227, AM Herculis type X-ray binary, optical counterpart, radial vel. obs. 0-94890  
 2A 0311-227, optical counterpart, AM Herculis type eclipsing binary, V-band obs. 0-101617  
 2A 0311-227, optical counterpart high speed photometry 0-82547  
 2A 0311-227, simultaneous optical photometric and spectroscopic obs. 0-90572  
 2A 0311-227, X-ray flux modulation period from HEAO obs. 0-77516  
 2A 0311-227 optical counterpart, binary star, light curve Fourier anal. 0-82549  
 2A 0335+096, identification with galaxy cluster Zw 0335.1+0956 0-90574  
 2A 0526-328, optical counterpart, eclipsing binary, visible emission line variability 0-73075  
 2A 0526-328, optical counterpart radial vel. meas. and orbital period 0-90579  
 2A 0526-328, spectroscopic obs. of optical counterpart 0-77515  
 A 0535+26, X-ray pulsar, optical counterpart HDE 245770 spectral type and luminosity 0-72976  
 A 0538-66, X-ray burster position and optical candidate in LMC 0-73076  
 2A 2151-316, BL Lacertae object, optical counterpart, spectral slope from far UV obs. 0-82509  
 2A 2251-179, X-ray quasar,  $\overline{\text{UBV}}$  photometry 0-82349  
 3A 2252-035, optical counterpart, proper motion and radial vel. determ. 0-82395  
 2A 2315-428 (NGC 7582), narrow emission line X-ray emitting nucleus, UV spectra 0-101640  
 Abell 1060 galaxy cluster, X-ray spectrum obs. by (HEAO A-2) 0-82518  
 Abell 2029 galaxy cluster, radio and SAS 3 X-ray obs. 0-82519  
 Abell 399/Abell 401, X-ray binary galaxy cluster, mass 0-90546  
 Abell 401, X-ray cluster of galaxies, radio emission distrib. 0-98731  
 Abell 401 cluster, lunar occultation obs. at 327 MHz, survey 0-73052  
 accretion column of X-ray pulsar, cyclotron line formation 0-67901  
 accretion disk model, gas flow above alpha disk 0-62161  
 Aquila X-1 (4U 1908+00), 1978 summer X-ray and optical outburst 0-73068  
 Aquila X-1 (4U 1908+00), optical outburst obs. 0-67909  
 Aquila X-1 (4U 1908+00), X-ray outburst obs. 0-77514  
 KR Aurigae, X-ray source nearby, X-ray, IR and visible obs. 0-67742  
 background, hot clumpy intergalactic medium emission contrib. 0-62335  
 background contribution from young galaxies 0-82550  
 background data from Ariel V, universal large scale shearing 0-62352  
 background irregularities 0-62331  
 background radiation, detection of quasar contrib. 0-62323  
 binaries, Fe line emission from Alfvén shell 0-98737  
 binary pulsating X-ray sources, spin-up due to accretion from Keplerian disc 0-67904  
 binary stars, cyclotron line feature identification 0-90577  
 binary X-ray sources, accretion of plasma onto neutron stars 0-109452  
 binary X-ray sources, cyclotron emissivity in accreting neutron stars 0-90463  
 binary X-ray sources, models of supercritical accretion discs around black holes 0-105272  
 binary X-ray sources, recurrent transients model 0-109565  
 binary X-ray sources, review of types and props. 0-109564  
 black hole, massive, radiation spectrum of gas debris from tidally disrupted star 0-90467  
 burst sources, radiation spectrum rel. to neutron stars mass-radius relation 0-77444  
 burst sources, radiative heat transfer in mag. neutron stars surface layers 0-94826  
 burst sources, thermonuclear flashes in envelope of accreting neutron star 0-109455  
 RS Canum Venaticorum stars, H $\alpha$  line variability, visible spectra obs. 0-105277  
 Centaurus galaxy cluster, X-ray spectrum obs. by (HEAO A-2) 0-82518  
 Centaurus X-3, binary star, cyclotron line feature identification 0-90577  
 Centaurus X-3, neutron star characts. from correlated spin-up and X-ray luminosity meas. 0-101648  
 Centaurus X-4, spectroscopic obs. of visual counterpart, companion type 0-82545  
 Centaurus X-4, transient X-ray burster, optical counterpart discovered 0-67906  
 Circinus X-1, binary model, orbital eccentricity from X-ray and radio obs. 0-98735  
 Circinus X-1, binary model, radio emission 0-98736  
 Circinus X-1, changes in optical, IR and radio emission 0-67910  
 clusters of galaxies, intergalactic matter rel. to X-ray emission interpretation 0-109543  
 clusters of galaxies, large-scale struct. 0-82524  
 clusters of galaxies, rich X-ray emitting clusters, VHF obs. 0-62294  
 compact X-ray sources, as cosmic laboratories for study of neutron stars and hadron matter 0-77442  
 compact X-ray sources, form. from evolution of mass-accreting white dwarfs 0-77281  
 Crab nebula, model for pulsed  $\gamma$ -ray and X-ray emission 0-62230  
 Cygnus Loop, supernova remnant, X-ray spectra var. with position 0-82472  
 Cygnus superbubble 0-105323

**X-ray sources (astronomical) continued**

- Cygnus X-1, accretion disk round black hole, temp. var., X-ray obs. 0-109561
- Cygnus X-1, critique of polarimetric evidence on physical parameters and orbital inclination 0-109486
- Cygnus X-1, neutron star model from bi-metric theory of gravitation 0-90466
- Cygnus X-1, obs. during high state (1980 June 11 to 27) 0-86017
- Cygnus X-1, radio source, variable binary system, SHF obs. 0-73071
- Cygnus X-1, transition from high X-ray state to low X-ray state, 1980 June to July 0-98738
- Cygnus X-1, X-ray and UV spectra from HEAO 2 and IUE 0-82543
- Cygnus X-1 (V1357 Cygni), optical light curve vars. rel. to X-ray vars. 0-109560
- Cygnus X-1 (V1357 Cygni), optical photometry (1980 May 25 to July 7) 0-90578
- Cygnus X-1 (X-2, X-3), X-ray polarisation obs. from OSO 8 0-90571
- Cygnus X-1 and X-3, search for 1-20 MeV gamma rays, balloon-borne obs. 0-67912
- Cygnus X-2, binary, radial vel. and orbital elements from visible spectra obs. 0-77519
- Cygnus X-3, 34.1 day period, 2-12 keV obs. by COS-B 0-94897
- Cygnus X-3, period derivative and asymmetric X-ray light curve from HEAO 2 obs. 0-105394
- Cygnus X-6, X-7, part of large X-ray superbubble, X-ray obs. 0-90575
- Cygnus X-1, main energy release region, plasma temp. determ. 0-85850
- Cygnus X-ray superbubble, existence and power source, X-ray obs. 0-90575
- HR Delphini (Nova 1967), simultaneous X-ray, UV and optical obs. 0-109440
- detection of cosmological objects 0-62323
- Einstein Observatory sources fields, RI photometry with CCD camera 0-62315
- emission mechanism involving accretion onto compact bodies 0-90459
- 40 Eridani A ( $\alpha^2$  Eridani), evidence of corona on X-ray image 0-105282
- 40 Eridani C, X-ray image of dM4e flare star 0-105282
- extragalactic sources, positional and spectral data, HF obs. 0-86019
- FXP 0520-66, flaring X-ray pulsar, nature and optical identification (*Russian*) 0-77521
- galactic, anticorrelation with radio sources, plasma cloud interpretation 0-82514
- galactic bulge sources, radio continuum obs. at 2.7, 4.8 and 10.7 GHz 0-101619
- galactic centre, Prognoz-6 obs. of X-ray fluxes and energy spectra (*Russian*) 0-109562
- galactic centre, X-ray point source flux rel. to central black hole mass 0-90467
- galactic centre region, high-energy X-ray detection 0-67854
- galactic distrib. 0-67905
- galactic hard and soft X-ray sources, space distrib. and physical nature 0-62316
- galactic sources, unidentified, positions with HEAO-1 scanning modulation collimator 0-105395
- galaxies compact groups, X-ray emission obs. 0-90574
- galaxies in MKW-AWM poor clusters, optical props. 0-94878
- galaxy cluster X-ray sources, luminosity function evolution 0-62314
- Galaxy contrib. to diffuse X-ray flux in 2 to 7 keV range 0-98745
- galaxy coronae, hot gas dynamics simulation 0-82481
- GX 1+4, galactic centre source, X-ray obs. periodicity 0-105399
- GX 301-2, binary star, cyclotron line feature identification 0-90577
- GX 3+1, X-ray bursts obs. (1980 July 19 to August 18) 0-98739
- H0118-067, identification with RS Canum Venaticorum star UV Piscium, X-ray obs. 0-101654
- H0630+82, identification with RS Canum Venaticorum star SV Camelopardalis, X-ray obs. 0-101654
- H2027+19, extended soft X-ray source in Delphinus, discovery 0-90576
- H 0523-00 assoc. with Arakelian 120, X-ray obs. of Seyfert 1 galaxy 0-105344
- H 2252-035, optical counterpart photometry and spectrum 0-101651
- H 2252-035, spectrophotometry, no periodic linear polarization (1980 Sept.) 0-105401
- H 2252-035, X-ray flux modulation, compact star rotation 0-101652
- Hercules X-1, (HZ Herculis), optical and UV obs. 0-109487
- Hercules X-1, accretion disc viscosity determ. using slaved disc model 0-62110
- Hercules X-1, binary star, cyclotron line feature identification 0-90577
- Hercules X-1, eclipsing binary, X-ray spectra from Ariel V satellite 0-90580
- Hercules X-1, implications of cyclotron features in X-ray spectrum 0-86015
- Hercules X-1 (HZ Herculis), 1978 UBVR photometry of active state 0-62189
- Hercules X-1 (HZ Herculis), 35 day clock mechanism 0-73070
- Hercules X-1 (HZ Herculis), IUE Obs., spectrum and light var. 0-73069
- Hercules X-1 (HZ Herculis), light curve, radiation pressure effects 0-105280
- Hercules X-1 (HZ Herculis), X-ray continuum and Fe line emission during X-ray low state 0-105393
- Hercules X-1 (HZ Herculis) binary system, pre-supernova parameters 0-62318
- AM Herculis, visual magnitude estimates (1980 March-June) 0-82428
- hot white dwarf, radial oscill. mode nonlinear calc. 0-67713
- HR 1099 (V711 Tauri), RS Canum Venaticorum star, H $\alpha$  line variability, visible spectra obs. 0-105277
- HR 5110, Algol type RS Canum Venaticorum star, H $\alpha$ , yu photometry obs. 0-105276
- EX Hydrae, spectra of dwarf nova 0-98670
- intergalactic collapsed objects, gas accretion, source of cosmic X-ray background 0-90581
- Kepler's supernova remnant, X-ray obs. from Einstein Observatory 0-82465
- Kerr black hole, low-freq. radiation from infalling particle 0-62176
- late-type main-sequence and subgiant stars, HEAO 1 obs. of active cor-  
nae 0-72925
- LMC bar, soft X-ray source identification 0-82491
- LMC X-1, optical candidate spectrum and semi-accurate position 0-67908
- LS 1+61°303, variable binary radio star (B1 Ib), X-ray emission detect.  
0-105400

**X-ray sources (astronomical) continued**

- lunar occultations of X-ray sources, first and last dates (1980 to 1985)  
0-77513
- M86, elliptical galaxy, X-ray evidence for hot gas retention 0-90535
- M87, Faraday rot. in radio/X-ray halo 0-67844
- massive binaries, evolution review 0-82343
- massive binary stars, X-ray induced shocks in stellar winds 0-94784
- MCG-6-30-15, type I Seyfert galaxy, X-ray and optical obs. 0-82479
- MSH 11-54 (H1122-59), supernova remnant, X-ray obs. 0-82463
- MXB 1636-536, binary nature from simultaneous X-ray and optical obs.  
0-82548
- MXB 1730-333, no burst activity in 1980 July-Sept. period 0-105402
- MXB 1730-333 (Liller 1), unusual burst in K-band (2.2  $\mu$ m) 0-62319
- MXB 1730-335, X-ray rapid burster, unsuccessful search for IR bursts  
0-98740
- MXB 1730-335 (Rapid Burster), microwave bursts obs. 0-62320
- neutron star models 0-62175
- neutron stars, burst source from He burning shell 0-85968
- neutron stars, Eddington luminosity limit and supercritical accretion,  
time-independ. calcs. 0-67768
- neutron stars, effects of superfluidity on X-ray emission 0-77441
- neutron stars, electrodynamics of disk accretion, magnetic field structure  
0-85973
- neutron stars, nonequilibrium shells, role in X-ray emission and nucleosyn-  
thesis, review 0-67774
- neutron stars, thermonuclear flashes in envelopes of accreting objects  
0-67772
- neutron stars, X-ray emission assoc. with supercritical time-dependent  
accretion 0-85967
- neutron stars, X-ray spectra from accretion column, optically thick region  
inc. 0-67767
- NGC 1851, X-ray globular cluster, UV energy distrib. from OAO pho-  
tometry 0-73009
- NGC 4151, Seyfert galaxy, repeated X-ray flaring obs. 0-90534
- NGC 6440 (MX 1746-20), globular cluster, surface photometry of  
cluster core 0-82436
- NGC 6624, optical counterparts of X-ray burster in core of globular  
cluster 0-67801
- North Polar Spur (Radio Loop 1), X-ray obs. 0-105370
- OAO 1653-40 38 s pulsating X-ray source position and optical search  
0-73072
- of giant black holes (*French*) 0-94828
- optical counterparts, appl. of simultaneous fast double head UBVR pho-  
tometer 0-72775
- optical spectral line emission bursts in X-ray heated medium (*Russian*)  
0-77286
- periodicity investigation at 21 cm 0-82529
- X Persei (A 0535+26), Prognoz-6 obs. of X-ray fluxes and energy spec-  
tra (*Russian*) 0-109562
- Perseus X-ray cluster, form. of optical filaments in cooling gas round  
NGC 1275 galaxy 0-67862
- PKS 2155-304, BL Lacertae object, rapid X-ray variability obs.  
0-73035
- plasma clouds, comptonisation of X-rays, radiation spectra 0-85850
- point X-ray source, imaging via automodulation collimator telescope (*Rus-  
sian*) 0-62018
- polarized radiation transfer in X-ray pulsars, analytical solns. 0-94894
- PSR 1913+16, X-ray and timing meas. correlations, grav. radiation, gas  
cloud friction 0-62171
- pulsating X-ray sources, accretion disc mag. field calc. for oblique mag.  
dipole configuration 0-94895
- pulsating X-ray sources, neutron stars accretion disc and rot. mag. field  
interaction 0-62173
- Puppis A supernova remnant, X-ray spectra var. with position 0-82472
- quasars, Comptonised spectrum, Monte Carlo simulation 0-90566
- quasars, discrete evolving sources contrib. to X-ray background 0-82551
- quasars, low redshift X-ray selected, visible spectra and UBVR phot-  
ometry 0-105397
- quasars, possible source for X-ray background 0-94898
- quasars, uniformity of radial distrib. in chromometric cosmology rel. to  
X-ray background 0-105409
- radio emission from point X-ray sources, origin 0-62317
- rapid time variability, role of time-dependent Comptonisation and X-ray  
reverberations 0-86013
- relativistic electron spectra, inference from meas. of inverse Compton  
radiation 0-90339
- 2S 1702-363, optical counterpart UBVR photometry 0-82349
- Scorpius X-1, binary star, X-ray spectrum 20-75 keV, high sensitivity  
determ. 0-98741
- Scorpius X-1, binary star X-ray obs. from 20 to 250 keV 0-94893
- Scorpius X-1, high energy X-ray and SHF radio obs. 0-73067
- Scorpius X-1, mag. field determ. via linear polarisation spectrum (*Rus-  
sian*) 0-90344
- Scorpius X-1, Prognoz-6 obs. of X-ray fluxes and energy spectra (*Russian*)  
0-109562
- Scorpius X-1, rapid variability simultaneous X-ray and optical obs.  
0-62322
- Scorpius X-1, UV, visible, IR and X-ray obs., X-ray obs. 0-82541
- Serpens X-1, no IR bursts assoc. with Type I X-ray burst 0-98742
- Serpens X-1 (4U 1837+04), burster optical binary counterpart visible  
spectra and photometry 0-94891
- Seyfert 2 X-ray galaxies, nucleus spectra and photometry obs. 0-98712
- solar flares, acceleration mechanisms, implications for hard X-ray burst  
models 0-72912
- spherical accretion, luminosity thermal limit 0-82546
- SS 433, 164° period as precessional motion, massive black hole and pulsar  
models 0-62138
- SS 433, 180 mm interferometric obs. of triple structure 0-105259
- SS 433, accreting black hole model 0-85958
- SS 433, accretion disc viscosity determ. using slaved disc model 0-62110
- SS 433, beam acceleration, radiation and precession theory 0-72971
- SS 433, beam models, energetics anal., possible triple system 0-90433
- SS 433, change in radio strct., 1980 January to June, from VLBI obs.  
0-109557
- SS 433, deviations from standard model 0-98669
- SS 433, disk-driven precession 0-94803
- SS 433, dissipative infall model 0-67749
- SS 433, emission regions and black hole accretion disk 0-67746
- SS 433, general spectral features 0-77421
- SS 433, IR variability obs. 0-98676



**X-ray sources (astronomical) continued**

- SS 433, light curves, double peak and binary-like period, photometry 0-94804  
 SS 433, magnetic X-ray binary model 0-109447  
 SS 433, models of supercritical accretion discs around black holes 0-105272  
 SS 433, nearby faint, highly-contorted nebular filament discovery 0-94855  
 SS 433, no 6-day periodicity in 1978 June-1980 Feb. obs. period 0-62150  
 SS 433, radial vel. curve low amplitude section, visible spectra anal. 0-67737  
 SS 433, reality of 6-day periodicity in spectral lines wavelengths var. 0-67743  
 SS 433, relativistic beam interaction with interstellar matter, mass loss rate, visible obs. 0-101629  
 SS 433, review of obs. and theories 0-72987  
 SS 433, search for radio spectral lines in UHF 0-109556  
 SS 433, spectral features interpreted a precessing neutron star with jets, possible binary 0-90447  
 SS 433, V band photometry and broad min. prediction (1980 April-May) 0-82390  
 SS 433 inside SNR, unique spectrum 0-82381  
 supernova remnants, adiabatic phase, thermal X-ray spectra 0-82475  
 supernovae remnants, parameter determ. from X-ray data and known age, blast model (*Chinese*) 0-77471  
 young supernovae remnants, X-ray props. rel. to neutron stars cooling 0-77443  
 4U 0115+634, X-ray binary, 1980 Aug. photometry and spectroscopy 0-101650  
 4U 0352+30 (X Persei), Be star, evidence for 6-year photometric periodicity 0-109446  
 4U 0833-45, X- and gamma-ray emission from Vela SNR and pulsar (*Russian*) 0-94861  
 4U 0900-40 and 1700-37, polarimetric obs. of massive X-ray binaries 0-98688  
 4U 1145-61, optical counterpart HD 102567, atm. model from UV obs. 0-105396  
 4U 1145-61 (Henize 715), Be-type star, colour and luminosity vars. (1976-1980) 0-72979  
 4U 1223-62, binary X-ray pulsar, optical counterpart Wray 977, spectra 0-72984  
 4U 1223-62 (GX 301-2, WRA 977), binary star orbit determ. from X-ray obs. 0-90570  
 4U 1322-42 (Centaurus A, NGC 5128) nucleus, radio and X-ray variability model 0-90522  
 4U 1326+11, identification with galaxy cluster MKW 11 0-90574  
 4U 1608-52, burst activity since Hakucho launch (1980 April) 0-62321  
 4U 1700-37 (=HD 153919), eclipsing binary, X-ray obs. 0-86016  
 4U 1700-37 (=HD 153919) eclipsing binary, supergiant-neutron star, optical variability 0-82419  
 4U 1700-37 (HD 153919), X-ray binary, high-energy X-ray obs. 0-86014  
 3U 1805+50 (AM Herculis) eclipsing binary, UV and visible spectra anal. 0-109563  
 3U 1809+50 (AM Herculis), polar, IR photometric obs. 0-98687  
 3U 1809+50 (AM Herculis), polarimetry and spectrophotometry rel. to mag. field 0-94835  
 3U 1809+50 (AM Herculis), simultaneous three-channel photometry rel. to optical flickering mechanism 0-82411  
 3U 1809+50 (AM Herculis), spectrophotometric obs. at min. light 0-98692  
 3U 1809+50 (AM Herculis), UV spectrum obs. 0-67782  
 4U 1814+50 (AM Herculis), X-ray emitting mag. white dwarf binary, review of props. 0-105403  
 4U 1822-37, 2129+42, X-ray fluxes modulation periods from HEAO obs. 0-77516  
 4U 1907+09, optical identification using HEAO-I scanning modulation collimator position 0-82542  
 4U 2129+12, in M 15, nature of emission-line variable in cluster core 0-77458  
 UKS 1751-241, globular cluster near galactic centre, IR studies 0-82434  
 SU Ursae Majoris, soft X-ray halo around dwarf nova 0-98677  
 Vela X-1 (HD 77581), binary source, spectral obs., UV, visible and X-ray 0-94892

**X-ray spectra**

- see also *X-ray absorption spectra; X-ray chemical analysis; X-ray emission spectra*  
 acid phthalate curved crystal spectrograph, diffraction efficiency calc. method 0-79630  
 atomic line shape broadening anal., least squares method 0-63588  
 mammography, simulation of X-ray spectra 0-76826  
 measurement standards, National Bureau of Standards (USA) 0-90807  
 Moseley's expts.:  $K\alpha$  line freqs., rel. to at. number, reinterpretation 0-82616  
 plasma diagnostics appl., using Ross filters and Si detectors 0-59273  
 spectral distribution, evaluation of method of estimation from attenuation data (*Japanese*) 0-95207  
 spin doublets in X-ray satellite spectra 0-58203  
 Ba, X-ray spectra, high energy  $L\gamma$  satellites 0-102474  
 Eu<sub>1-2</sub>, La<sub>2</sub>S, electron struct., lattice const., X-ray spectral study (*Russian*) 0-100432  
 LiF curved crystal spectrograph, diffraction efficiency calc. method 0-79630  
 Mg XI resonance lines, dielectronic satellite lines atomic parameters calcs. 0-78567  
 Mo, X-ray spectra,  $K\alpha$  hypersatellites 0-63576  
 Ni IX to Ni XII, wavelengths of transitions between lower configurations 0-99474  
 NaI, isoelectronic sequence, X-ray spectra 0-87071  
 Se, meas. of K-edge dispersion anomalies using X-ray interferometry 0-90956  
 Sm<sub>1-2</sub>, La<sub>2</sub>S, electron struct., lattice const., X-ray spectral study (*Russian*) 0-100432  
 TiN<sub>1-x</sub>, substoichiometric, electronic density of states, CPA method calcs., X-ray spectra calc. 0-88464  
 V-Ti-C, high temp. carbide form., electron microscopy study 0-89228

**X-ray spectrometers**

see also *X-ray crystallography apparatus*

- 5 m grating spectrograph for studying molecular X-ray fluorescence spectra 0-86538  
 control system, automatic control of pitch motion 0-69012  
 curved crystal spectrometer for pionic X-ray measurements 0-78487  
 curved-cryst. spectrometer, principle and performance 0-99026  
 double crystal, appl. in density meas. of metals using X-ray total external reflect. 0-64831  
 double-beam triple-crystal X-ray spectrometer, high sensitivity, for lattice parameter and topographic meas. 0-77915  
 electron probe microanal. in SEM by means of X-ray spectrometers, review 0-95194  
 energy dispersive, quantitative elemental anal. 0-104840  
 excitation-potential spectrometer for excitation potentials of soft X-rays 0-101912  
 fluorescence spectrometer with sample loader, meas. sequence flexibility increase, electronic modification 0-77926  
 high pressure gas scintillation spectrometers for X-ray astronomy 0-105166  
 Lixoscope with good energy resolution 20 to 200 keV 0-99401  
 multicrystal with independent standard sample, for internal stresses determ. in single crystals. 0-64832  
 ore dressing X-ray spectrometric analysis centre 0-86541  
 plasma diagnostics using multichannel high-speed spectrometer, bremsstrahlung of hot electron component obs. 0-57445  
 position sensitive gas scintillation proportional counter for X-ray astronomy 0-58053  
 position-sensitive low-intensity X-ray imaging scope 0-86539  
 soft X-ray emission studies of liquid metals and metallic vapours 0-73564  
 soft X-ray spectra, meas. by photoelectron anal. 0-73557  
 synchrotron radiation spectrometer for 100 to 130 nm 0-90953  
 telescope-X-ray spectrometer system for solar corona studies 0-105168  
 toroidal grating spectrometer for soft X-ray region, 16 to 625 Å 0-90948  
 transmission gratings for 7-304 Å operation, efficiency and resolution 0-82195  
 wavelength and energy dispersive X-ray fluorescence spectrometers compared 0-89573  
 XRF, for classification of small glass fragments into window and non-window types 0-81401  
 Hg<sub>L</sub> detectors,  $\gamma$ - and X-ray detection, solution grown crystals 0-63452  
 Si(Li) detectors, operational possibilities from -90°C to -60°C 0-73555  
 Si(Li)-NaI spectrometer, L X-rays, meas. of trace radionuclides in soil 0-58020

**X-ray spectroscopy**

- see also *appearance potential spectroscopy; X-ray crystallography; X-ray diffraction; X-ray spectra*  
 analytical and quality control techniques, review 0-98989  
 astronomy, spectroscopic and photometric facilities of 80 cm X-ray telescope (*German*) 0-109358  
 Bragg mode analyser potassium acid phthalate, Bragg refl. coeff. obs. 0-85204  
 calibration materials for X and  $\gamma$ -ray spectrometers, decay data 0-106221  
 curved cryst. X-ray diffr. spectrometry, image formation 0-99025  
 DESY absorption spectroscopy set-up 0-74069  
 energy dispersive, technique, appls. (*Japanese*) 0-57450  
 energy dispersive microanalysis, in SEM, artifacts (*German*) 0-73561  
 excitation potentials of soft X-rays, meas. using spectrometer with channel electron multiplier 0-101912  
 failure analysis tools comparison and selection 0-71865  
 fracture surfaces, quantitative analysis problems in energy dispersive X-ray spectrometry with Si(Li) diodes (*French*) 0-89571  
 high-pressure and low-temp. cell for X-ray diffuse scattering studies 0-86336  
 inhomogeneities analysis in metals and ceramics, use of STEM field emission gun 0-59354  
 light elements, ultrashort X-ray spectroscopy, local anal., electron-microprobe excited radiation 0-99027  
 microscopic equipment, methods, appls. and related topics, bibliography 0-73124  
 microscopy, high resolution, with synchrotron radiation, for chem. microanal. 0-81416  
 multichannel analysers (*Hungarian*) 0-95205  
 optical emission and X-ray spectrometry developments (*French*) 0-68263  
 polynuclear aromatic hydrocarbons, analysis by X-ray excited optical luminescence technique 0-66891  
 SEM imaging techniques, and X-ray microanal. 0-57432  
 SEM microanalysis techniques, review 0-71995  
 steel foil, microanalysis by energy dispersive X-ray spectrometry (*French*) 0-85250  
 surfaces and thin film studies by combined system of SIMS, AES and XPS 0-86536  
 synchrotron radiation, application to EXAFS and angle resolved photoemission spectrosc. (*Korean*) 0-74453  
 Bi-MnBi eutectic region, of Bi-Mn phase diagram 0-81034  
 Cu-Ga, binary alloy constituent EDS anal., secondary fluorescence, SEM study (*Chinese*) 0-85231  
 Fe-Si (3wt.%), grain-oriented, secondary recryst., grain growth inhibition 0-89245  
 GaAs, binary alloy constituent EDS anal., secondary fluorescence, SEM study (*Chinese*) 0-85231  
 Mg<sub>1.86</sub>Al<sub>1.67</sub>Si<sub>2.47</sub>O<sub>3.19</sub>N<sub>3.81</sub>, 12H polytype, intergranular phases and compositional variations 0-79645  
 Si  $K\alpha$  source, sensitivity factors, cross-section and resolution data 0-77920

**X-ray transport** see *photon transport theory***X-ray tubes**

- diagnostic tubes, meas. of focal spot size 0-89831  
 education, Poisson statistics demonstration using X-ray tube, electronic 'shot noise' 0-73129  
 filament lifetimes, in rotating-anode X-ray machines, increasing using beam-deflecting magnet 0-77918  
 flash, for diffraction studies on 2-stage light gas gun 0-86537  
 focal spot lengthening, in Elliott rotating-anode X-ray sets 0-77919  
 heavy-duty rotating anode X-ray tubes 0-73568  
 image intensifier, magnetic interferences (*German*) 0-105761  
 microfocus source, non-linear intensity rise studies 0-77927

**X-ray tubes continued**

- modulation effectiveness, electron gun considerations 0-73554  
 pulsed high-power subnanosec. X-ray source 0-73565  
 radiographic testing equipment, device characts. (*German*) 0-76438  
 rotary anode, C by transition metal carbides (*German*) 0-105759  
 rotary anode, HV insulation, discharges due to back scattered electrons elimination (*German*) 0-105758  
 rotary anodes, high continuous power, with Rh-W disc bonded to graphite (*German*) 0-105760  
 spectral purity, for diffr. anal. appls., quantitative determ. (*Chinese*) 0-57444  
 Super Rotalix Ceramic, new type of X-ray tube 0-104749  
 X-ray source, industrial, use for electronic component radiation effects work, calibration 0-63402

**X-rays**

- see also cosmic ray X-rays; photons  
 80 years progress in techniques (*Dutch*) 0-82859  
 linear accelerator beam energy at off-axis points, calc. technique for correct. 0-81742  
 linear accelerator X-ray beams, off-axis beam quality change 0-78461

**X-Y model**

- antiferromagnet, one-dimens., nonlinear dynamics 0-80521  
 biquadratic, spin one, variation of Curie temp. 0-97102  
 classical, comparison of plane rotor with Ising ferromag. 0-60348  
 dialkylammonium iron tetrachloride, antiferromag., mag. susceptibility meas. 0-60220  
 dimethylamine iron tetrachloride, antiferromag., mag. susceptibility meas. 0-60220  
 duality props. and phase diagrams of general discrete planar models 0-60286  
 ferromagnet, anisotropic, in external mag. field, continuous phase transition existence 0-108011  
 ferromagnet,  $S=1/2$ , on triangular lattice, ground state props. 0-60165  
 Heisenberg-Ising spin chain quantum inverse scatt. method, Jordan-Wigner transformation 0-93068  
 interactions, spirals and phase transitions with and without long range order 0-60350  
 Josephson junction array, granular supercond., phase transition 0-88684  
 Lifshitz point region, crit. exponents 0-65898  
 mean-field theory of Peierls and spin-Peierls instabilities—commensurability, harmonics and dimerized-state pinning 0-108014  
 noncollinear magnetic order and spin wave spectrum in presence of competing exchange interactions 0-65834  
 one-dimensional isotropic, dynamics 0-71057  
 praseodymium ethylsulphate:Sm, one-dimens. X-Y system, spin dynamics, electron spin echo meas. 0-66031  
 quantum,  $S=1/2$ , zero temp. renormalisation group method in transverse field 0-108025  
 quantum effects and dynamics at low temps., path integral approach 0-84584  
 quantum spin system, two-dimens., frustration, renormalisation group study 0-80535  
 solid-on-solid representation, planar model Monte Carlo simulation 0-96727  
 spin  $1/2$ , phase transitions at  $T=0$ , z-field renormalisation group method 0-71051  
 spin glass, X-Y and Heisenberg, below four dimensions, vanishing of Edwards-Anderson order parameter 0-60347  
 spin glasses, time translation, spatial scaling and nonexponential relaxation 0-97110  
 spin XY one dimensional system containing impurities, static mag. props. (*Russian*) 0-65826  
 susceptibilities of  $S=1/2$  XY model on the square lattice at  $T=0$  0-88732  
 thermal excitations in Heisenberg-xy systems 0-97047  
 TMMC, linear antiferromag., mag. phase diagram, expt. and theoretical study 0-71038  
 transverse correlations, eqns. of motion of finite temp. 0-105581  
 Co complex,  $\text{Co}(\text{II})(1,2,4\text{-triazole})_2(\text{NCS})_2$  quasi two-dimens. canted  $S=1/2$  antiferromag. 0-70976  
 $\text{Co}(\text{C}_2\text{H}_5\text{NO})_2(\text{ClO}_4)_2 [(\text{BF}_4)_2]$ , X-Y antiferromagnet, Neel temp., spin correlation functions 0-60345  
 $\text{CsNiF}_3$ , one-dimensional ferromagnet, optical absorpt. and static spin correlation functions 0-71415

**Xalpha calculations**

- alkali dithioferrates (III), electronic struct. and hyperfine interactions, X $\alpha$  calcs. 0-100448  
 all electron pseudopotential method 0-83282  
 diatomic mols., one electron props., SCF-Xalpha scattered wave method 0-83279  
 ethane, rot. barriers, MS-SCF-X $\alpha$  calcs. 0-106267  
 exchange potential, elimination in multiple scatt. method 0-103652  
 first-row atoms, atomic X $\alpha$  calcs. 0-83280  
 Hartree-Fock formalism, fractional occupation, local X $\alpha$  pot. calcs. 0-95538  
 hexafluoroethane, rot. barriers, MS-SCF-X $\alpha$  calcs. 0-106267  
 metal atom cluster compounds, bonding calc. using d-orbital overlap model, SCF-X $\alpha$ -SW calc. 0-102595  
 methane, core 1s shakeup study, XPS and Xalpha calcs. 0-69064  
 metal potential X $\alpha$  method for electronic struct. calcs. 0-102446  
 dimolybdenum tetraformate, metal-metal bond energy, SCF-X $\alpha$ -SW calcs. 0-78538  
 SCF-X $\alpha$ -scatt. wave calcs. for photoionisation cross sections and asymmetry parameters 0-63542  
 second-row atoms, atomic X $\alpha$  calcs. 0-83280  
 self-consistent charge X $\alpha$  method, appl. to small mols. 0-91449  
 self-consistent charge X $\alpha$  method, theory 0-91448  
 stable negative ions instability, Xalpha calcs. 0-99452  
 TC, internal conversion, scattered-wave cluster technique 0-107696  
 tetrabromomethane, electronic struct., X $\alpha$  SW calcs. 0-102447  
 tetrafluoromethane, electronic struct., X $\alpha$  SW calcs. 0-102447  
 3d-transition metal ions, s-doublet struct., appl. of exchange correlation mass operator approx. 0-102666  
 AgBr, vapour, photoelectron spectrosc., interpretation 0-95679  
 AgCl, vapour, photoelectron spectrosc., interpretation 0-95679  
 AgI, vapour, photoelectron spectrosc., interpretation 0-95679  
 $\beta\text{-Al}_2\text{O}_3\text{-Na}_2\text{O}$ , adsorption of Na, surface electronic struct. calcs. 0-75431  
 Ar, Compton profiles, Xalpha wavefunctions 0-106265  
 Be $_2$ , ground state, multiple scatt. X $\alpha$  calcs. 0-58149

**Xalpha calculations continued**

- BrF $_3$ , electronic struct. and ionisation pot., SCF DV Xalpha method 0-69057  
 BrF $_5$ , electronic struct. and ionisation pot., SCF DV Xalpha method 0-69057  
 CO, LCAO-X $\alpha$  method calcs., comparison with Hartree Fock and MS X $\alpha$  methods 0-95539  
 Ca $_2$ , ground state, multiple scatt. X $\alpha$  calcs. 0-58149  
 ClO $_4^-$ , dummy spheres in SCF Xalpha calcs. 0-69056  
 ClO $_4^-$ , ionisation energies, SCF-X $\alpha$  transition state calcs. 0-74115  
 Cr(NO) $_4$ , bonding, shake-up intensities and shake-up energies, SCF X $\alpha$  multiple scatt. calc. 0-74121  
 Cr(NO) $_4$ , XPS and UV photoelectron spectra, compared to NO data 0-58317  
 Cu $_4$  clusters, electronic structures, SCF-X $\alpha$ -SW method 0-88468  
 CuCl $_2(\text{Cl}_4^{2-})(\text{Cl}_4^{4-})$ , electronic struct. studies by SCF, MSX $\alpha$  and INDO method 0-74119  
 CuF $_2(\text{F}_4^{4-})$ , electronic struct. studies by SCF, MSX $\alpha$  and INDO method 0-74119  
 Cu $_2$ Zn clusters, electronic structures, SCF-X $\alpha$ -SW method 0-88468  
 GeBr $_4$ , electronic struct., X $\alpha$  SW calcs. 0-102447  
 GeF $_4$ , electronic struct., X $\alpha$  SW calcs. 0-102447  
 Ge $_2$ H $_6$ , rot. barriers, MS-SCF-X $\alpha$  calcs. 0-106267  
 H $_2$ O, core 1s shakeup study, XPS and Xalpha calcs. 0-69064  
 inert gases, solid, Compton profiles, APW-X $\alpha$  calc. 0-80894  
 MnNbO $_3$ , orthorhombic, electronic struct., SCF-MS-X $\alpha$  calc. 0-70600  
 Mg $_2$ , ground state, multiple scatt. X $\alpha$  calcs. 0-58149  
 Mo $_2$ , metal-metal bond energy, SCF-X $\alpha$ -SW calcs. 0-78538  
 Mo $_2\text{Cl}_8^{4-}$ , metal-metal bond energy, SCF-X $\alpha$ -SW calcs. 0-78538  
 Mo $_2\text{Cl}_8^{4-}$  complexes, cluster exchange coupling consts. SCF-X $\alpha$ -SW calcs. 0-74120  
 Mo $_2\text{X}_8^{4+}$  cluster cpds. (X=F, Cl, Br, I), SCF-SW-X $\alpha$  calcs. 0-74276  
 NH $_3$ , core 1s shakeup study, XPS and Xalpha calcs. 0-69064  
 NbC, band struct. and X-ray emission spectra, APW and X $\alpha$  calc. 0-70605  
 Ne, Compton profiles, Xalpha wavefunctions 0-106265  
 Ni clusters local densities of states 0-88466  
 Ni(001), adsorbed  $\text{C}(2\times 2)\text{-CO}$ , struct. by LEED, self-consistent scatt. pot. 0-70536  
 PO $_3^{3-}$ , ionisation energies, SCF-X $\alpha$  transition state calcs. 0-74115  
 Pt, chemisorption of O $_2$  and CO, SCF-X $\alpha$  cluster calcs. 0-65365  
 SMS, band struct. and semicond. metal phase transition 0-80180  
 SO $_2^{2-}$ , ionisation energies, SCF-X $\alpha$  transition state calcs. 0-74115  
 Si, solid, electron rearrangement after inner shell ionisation by heavy charge particle impact 0-87043  
 Si:O, A centre, theoretical study 0-75521  
 SiBr $_4$ , electronic struct., X $\alpha$  SW calcs. 0-102447  
 SiF $_4$ , electronic struct., X $\alpha$  SW calcs. 0-102447  
 SiH $_4$ , L $_{11111}$  continuous absorpt. spectrum of Si 0-95645  
 Si $_2$ H $_6$ , rot. barriers, MS-SCF-X $\alpha$  calcs. 0-106267  
 SiH $_4(\text{SiF}_4)$ , electron rearrangement after inner shell ionisation by heavy charge particle impact 0-87043  
 ThF $_4(\text{Cl}_4)$ , electronic struct., MS-SCF-X $\alpha$  calcs. and VUV photoelectron spectra 0-63710  
 UC, electronic struct., comparison with photoemission spectra 0-91450  
 UF $_4(\text{Cl}_4)$ , electronic struct., MS-SCF-X $\alpha$  calcs. and VUV photoelectron spectra 0-63710  
 UN, electronic struct., comparison with photoemission spectra 0-91450  
 XeCl $_2$ , electronic structure, MSW-SCF-X $\alpha$  method 0-78539  
 XeF $_n$ ,  $x=2, 4, 6$ , electronic structure, MSW-SCF-X $\alpha$  method 0-78539  
 YS, band struct. and X-ray emission spectra, APW and X $\alpha$  calc. 0-70605  
 Zn $_4$  clusters, electronic structures, SCF-X $\alpha$ -SW method 0-88468

**xenon**

- see also nuclei with .....  
 adsorbed on (0001) surface of graphite, monolayer liquid and solid struct. 0-65400  
 adsorbed on Cu, NaCl, stepped and disordered surfaces, two-dimens. phase transformations 0-103580  
 adsorbed on Pd (110), anomalous 5p photoemission, electron binding energies 0-100750  
 adsorbed on W (110), mobility and two-dimens. compressibility, field emission current fluctuation method 0-80089  
 Allende mineral grain inclusion, excess  $^{129}\text{Xe}$  meas., chronological information 0-67675  
 atom, 4d $^{10}$  shell, photoionisation cross sections, electron shell alterations determ. (*Russian*) 0-58144  
 atom, 5s $^2$  shell, oscillator strength determ. (*Russian*) 0-58144  
 atom, approximate relativistic Hartree-Fock eqns., soln. using Slater-type functions 0-58168  
 atom, autoionising reson., Stark effect 0-58198  
 atom, first excited config., intermediate coupling coeff. 0-83450  
 atom, photoelectron asymmetry parameters 0-95684  
 atom, photoionisation, spin-polarised photoelectrons angular distrib. 0-106306  
 atom, recently enhanced multiphoton ionisation and third harmonic generation 0-91526  
 atom, resonantly enhanced multiphoton ionis., photoelectron energy anal. 0-63597  
 atom, subshell photoionisation, multichannel k-matrix calc., spin orbit interactions 0-63600  
 atom, visible lines, absolute transition probabilities 0-69108  
 atom+H(D), ion pair formation, curve crossing model 0-87216  
 atoms, inner-shell level energies, absorpt. spectroscopy with synchrotron radiation 0-99583  
 atoms in Ne matrix, radiative and nonradiative lifetimes in excited states 0-69106  
 brain, Xe regional kinetics meas., imaging methods in transmission computerised tomography 0-98131  
 chloropentafluoroethane-Xe, multiphoton dissoci.,  $^{13}\text{C}$  enrichment factor, CO, laser wavelength and fluence depend. 0-58331  
 computerised tomography, expt. dual XE detectors for quantitative CT and spectral artifact correct. 0-76825  
 condensed at high press., electron-band theory and fluid theory calcs. 0-59875  
 crystalline, lattice constant at insulator-metal transition 0-107706  
 DC arcs, with and without focal spot, electric behaviour (*German*) 0-64800  
 desorption, on Pt (111), gas surface interactions, 3-D generalised Langevin model appl. 0-107637



## xenon continued

- diffusion coefficients and mobilities of  $F^-$  ions in Kr and Xe 0-100048  
 dilute gas, transport props., simple pair pot. model 0-87835  
 excimer laser, atm. press. and low e-beam excitation rates, expt. studies 0-78863  
 excimer laser, VUV fluoresc. study, electron beam excitation 0-87379  
 fission gas release from (U,Pu) $C_{1-x}N_x$  LMFBR MX-type fuels 0-73921  
 fission gas release from  $UO_2$ -Zr high burnup nuclear fuel rods 0-57846  
 fission reactor mixed carbide fuels, radial distrib. of bonded fission gas 0-57844  
 flash lamp for pumping Nd:glass Mikron laser system 0-91815  
 fluid, high density behaviour, extrapolated  $P\rho T$  surfaces and critical density 0-87834  
 fluid, near crit. point, correl. range and Rayleigh linewidth 0-93352  
 gas, atoms, electron thermalization time and position distribution meas. 0-93771  
 gas, ion mobility and longit. diffusion coeff. of  $Na^+$  0-106866  
 gas, liquid, solid, refractive index, density and dielectric const. 0-66138  
 gas, two-body time correl., Van Hove scatt. function meas. 0-100053  
 gas mixtures for gas-filled particle detectors 0-74089  
 high pressure lamp for polymer spectral sensitivity determ. (German) 0-61119  
 HTR, Xe dynamics, 2D reactor models, axially collapsing methods (German) 0-68731  
 ion implantation defect introduction in ZnTe, cathodolum. studies 0-75250  
 ion source, HF, proton yield increase, influence of various admixtures to  $H_2$  obs. 0-57422  
 isoelectronic series,  $3d^9 4f$  config., collapse of  $4f$  electron, X-ray spectral obs. (Russian) 0-58204  
 laser, new IR laser transitions, 3.725 to 17.233  $\mu m$  0-87374  
 laser amplifiers, spectral narrowing and saturation induced rebroadening optical heterodyne obs. 0-63976  
 Lennard Jones (12,6) pot. distance parameter, transport props. calc. 0-79423  
 light scattering, multiple scattering contribs. to depolarisation 0-87842  
 liquid,  $\alpha$ -particle and electron excited luminesc., time depend., specific ionisation density effect 0-71495  
 liquid, comparison on interaction induced light scatt. and IR absorption 0-60561  
 mass spectroscopic chemical anal. using quadrupole mass spectrometer for fissile material accounting 0-63300  
 Murray (C-2) carbonaceous chondrite, I-Xe age and trapped Xe components 0-98618  
 organ blood flow measurements, effect of instantaneous partition coeff. of Xe 0-101256  
 outer  $p_{1/2}$  subshell photoionisation, polarised electrons, relativistic RPA calcs. 0-83331  
 photoabsorption, local field effects 0-74151  
 plasma, dense, shock-heating, calc. of equilibrium props. (Japanese) 0-79513  
 plasma, emission and absorption coeff. at high electron density 0-103121  
 plasma, high-pressure arc discharge, elec. cond. 0-59181  
 plasma jet, radiating, bulk energy distrib. 0-75107  
 rarefied plasma, emission characts. 0-103122  
 secondary scintillation under mag. fields, effect in gas proportional counters 0-58055  
 short-arc lamp, current modulated, arc forms and instability 0-96399  
 solid, two-phonon difference scatt. 0-60588  
 St. Severin chondrite, fission Xe rel. to U and Pu distrib. 0-72889  
 thermal conductivity, at high press. 0-103099  
 valence orbital, electron impact ionisation, absolute cross-section 0-69241  
 whole-body counting and dose determs. 0-89853  
 Ar-Xe high press. transverse discharge laser using Xe IR transitions 0-63978  
 Ar-Xe IR laser pumped by electron beam stabilised discharge, lasing parameters 0-102698  
 Cs-Xe solar-pumped MHD excimer laser, modelling 0-95873  
 HCl-Xe, liq., enthalpy of mixing, calorimetric meas. 0-59661  
 He-Ne-Xe ion lasers, hollow cathode, CW operation and excitation mechanism 0-69363  
 He-Xe, eqn. of state, Monte Carlo calcs. 0-59158  
 He-Xe, Xe I TEA lasers, energy characteristics 0-63977  
 He-Xe 3.51  $\mu m$  laser mode competition in axial mag. field 0-63974  
 He $^+$  + Xe, internal energy distrib. at 100 eV 0-99564  
 $^3He$ -Xe, nucl. lasing, population inversion mechanism 0-63980  
 $^3He$ -Xe nuclear pumped laser, small signal gain coeff. and power output, theory comparison with expt. 0-63983  
 $^3He$ -Xe nuclear pumped laser, electron distrib. function role 0-63984  
 $^3He$ -Xe volume pumped nuclear laser survey of lasing 0-63979  
 Hg-Xe vapour deposited films, cond. transitions, effect of disorder on supercond. 0-88659  
 Kr-Xe, phase matched, generation of Lyman- $\alpha$  radiation 0-91845  
 Na-Xe excimer lasers, high-power discharges, models 0-69373  
 Na + Xe + hw, collisions in presence of nonresonant lasers 0-99567  
 Se $^{2+}$  + inert gas, low energy reactions, SIFT and drift tube obs. 0-97705  
 Tl-Xe, excimer band emission from electron beam initiated discharge in TlI-Xe 0-78840  
 $^{133}X$  calibration of environmental and personal dosimeters 0-86992  
 Xe are discharge, radiative characts. computational model requirements 0-64812  
 Xe fission gas release and microscopic swelling in LMFBR highly-rated MX-type fuels 0-57848  
 Xe I three-level system, level splitting within natural width, saturation spectrum 0-106291  
 Xe VI, emission spectral lines, classification 0-95563  
 Xe $^+$ , absolute electron impact ionisation cross section 0-83496  
 Xe $^{3+}$ , molecular electron impact ionisation 0-102582  
 Xe $^{4+}$ , molecular electron impact ionisation 0-102582  
 Xe $^{5+}$ , molecular electron impact ionisation 0-102582  
 Xe-F two module discharge laser, gain and temporal characts. 0-87385  
 Xe-He, 3.51  $\mu m$  laser amplifiers, spectral narrowing and saturation induced rebroadening optical heterodyne obs. 0-63976  
 Xe-Mg discharge and MgXe excimer band, emission intensities and excited-state densities meas. 0-92413  
 Xe-Ne, equilibrium of coexisting phases 0-87197  
 Xe + He $^{2+}$ , optical transition excitation function and cross sections 0-63787  
 Xe + acetylene, vibr. relax. study using laser-induced fluoresc. 0-74219  
 Xe + Ar $^{2+}$  (Ne $^{2+}$ ), single electron capture excitation, photon emission, VUV spectroscopy 0-58379

## xenon continued

- Xe + Ar(Kr), collision induced microwave absorpt. spectra 0-74216  
 Xe + Br $_2$ (CCl $_4$ ), excitation functions and rotational polarisation, chemiluminesc., crossed beam study 0-76491  
 Xe + Ca collision-induced dipole transition due to long range interaction, absorpt. obs. 0-63779  
 Xe + Cl $_2$ , classical trajectory calcs., energy threshold for collision induced dissoci. determ. 0-95709  
 Xe + Cl $_2$ (F $_2$ ), XeCl(XeF) form., relax. and quenching 0-81314  
 Xe + ClF, thermal and photochem. reactions investig. 0-61117  
 Xe + Li( $2^2P_{1/2}$ ), collision induced fine struct. transition rate coefficients determ. 0-74220  
 Xe + Na,  $3^3P-3^3D$  line broadening obs. 0-78684  
 Xe + Na, non-Lorentzian spectral line shape 0-106297  
 Xe + Na $_2^+$ , rot. energy transfer, vel. depend. 0-95715  
 Xe + Ne, quenching of excited Xe\*( $^3P_2$ ,  $^3P_1$ ,  $^3P_0$ ) states 0-63578  
 Xe + Ne $^{2+}$ , electron capture collisions, 15 to 50 keV, excitation 0-102566  
 Xe + N $_2$ , rate const., energy corrected scaling laws 0-69225  
 Xe + O, magnetically selected O( $^3P$ ) state scatt. 0-99543  
 Xe + Xe $^+$ , XeI reson. line excitation 0-87220  
 Xe + XeF\* + F $_2$  temp. dependent quenching rate constants 0-63701  
 Xe $^+$  + Ar, XeAr $^+$  form., dissoci. energy, reaction equilib. and rate const. 0-61071  
 Xe $^+$  + Cl + Ne, three body ion-ion recombination probability, Monte Carlo simulation 0-85160  
 Xe $^+$  + molecules,  $^2P_{3/2}$ ( $^2P_{1/2}$ ) doublet ground state reactions at 300K 0-108702  
 Xe $^+$  + Xe, XeI reson. line excitation 0-87220  
 Xe $^+$  + Xe $^+$ , charge transfer and ionisation Xe $^{2+}$  prod. 0-91659  
 Xe $^{24+}$  + Ne, highly charged very slow Ne recoil ions, K X-ray transition 0-91649  
 Xe $^{n+}$  + H, (H $_2$ ), electron capture by heavy multicharged ions at low velocities total cross sections meas. 0-99548  
 Xe $_2$ , dispersion damping functions and interaction energy calcs. 0-78673  
 Xe $^{2+}$ (Xe $^{4+}$ )(Xe $^{6+}$ ), molecular electron impact ionisation 0-102582  
 $^A X$ , A = 133, 135, interference with low-energy meas. systems 0-89872  
 $^{129}Xe$ , health physics, dose calcs. 0-98142  
 $^{129}Xe$ , in mineral grains from Allende inclusions, chronological information 0-67675  
 $^{133}Xe$  charcoal traps, simple leak tests, nuclear medicine appl. 0-104734  
 $^{133}Xe$  clearance, meas. of pig cerebral blood flow 0-94421  
 $^{133}Xe$  in a plastic catheter, diffusion dynamics obs. 0-79973  
 $^{133}Xe$ , myocardial blood flow studies, theoretical, technical and practical aspects 0-94355  
 $^{133}Xe$ , use in quantitative meas. of skin perfusion 0-81707  
 $^{133}Xe$  washout method for meas. of bone blood flow and obs. 0-72288  
 Xe\*, synchrotron radiation excited, time resolved spectroscopy 0-69092  
 Xe(nf) + SF $_6$ , l-changing collisions obs. 0-91633  
 Xe(nf Rydberg state) + NH $_3$ , n- and l-changing and ionising collisions 0-58360
- xenon compounds**
- XeAr $^+$ , dissoci. energy, reaction equilib. and rate const. 0-61071  
 XeBr, B and C states, energy ordering from temp. depend. of emission spectra 0-78837  
 XeBr electric discharge pumped laser (Chinese) 0-102701  
 XeCl, B and C states, energy ordering from temp. depend. of emission spectra 0-78837  
 XeCl discharge, KrF laser induced preionization 0-84020  
 XeCl, electric discharge excimer laser with intense preionisation 0-63991  
 XeCl electroionisation laser, energetic, threshold and spectral characts. 0-99705  
 XeCl excimer laser, excited by discharge stabilised by electron beam 0-63992  
 XeCl, form., relax. and quenching 0-81314  
 XeCl frequency-tuned laser, coherent tunable vacuum UV near H Ly- $\beta$  transition 0-99798  
 XeCl, high-energy subnanosecond pulse amplification 0-99770  
 XeCl laser, B-X, form. and quenching kinetics 0-74341  
 XeCl laser, lifetime extension by H addition 0-91773  
 XeCl laser, UV picosecond pulse amplification 0-74372  
 XeCl mini-laser operation at high repetition rate 0-74396  
 XeCl + HCl (inert gas atom), ground state destruction, quenching rate const., meas. 0-63758  
 XeCl $_2$ , electronic structure, MSW-SCF-Xa method 0-78539  
 XeCl $_2$ , triatomic excimer, transient gain meas. at 488.0, 497.6, 514.5 nm 0-58511  
 XeCl triatomic excimer laser in visible 0-64048  
 XeCl(B) formation in electron beam assisted Xe/HCl laser discharge 0-63988  
 XeCl(F), inert gas halide lasers, 60-ns electron beam excitation 0-74340  
 XeF, direct pumping by electron beam pulses, gain and laser oscill. obs. in blue-green 0-102699  
 XeF, electric discharge excimer laser with intense preionisation 0-63991  
 XeF electroionisation laser, energetic, threshold and spectral characts. 0-99705  
 XeF electron-beam-pumped laser, characts., 300-600K 0-78839  
 XeF excimer laser, excited by discharge stabilised by electron beam 0-63992  
 XeF, form., relax. and quenching 0-81314  
 XeF, ground state kinetics, multilevel model of energy transfer 0-99707  
 XeF laser, output control by injection locking 0-74405  
 XeF laser performance, ground state population effect 0-63987  
 $^{136}Xe$  in polycrystalline XeF $_2$  or XeF $_4$ , ESR spectra, struct. and dynamic parameters of radical sites determ. 0-84652  
 XeF $_2$ , chemisorption of Si surface, chemistry, XPS and Auger spectra 0-81358  
 XeF $_2$ , pseudopotential SCF-MO studies, equilib. struct., stretch-stretch interaction force const. 0-95525  
 XeF $_4$ , pseudopotential SCF-MO studies, equilib. struct., stretch-stretch interaction force const. 0-95525  
 XeF $_4^+$ , pseudopot. SCF MO studies, steric aspects of struct. and force fields, Jahn-Teller effect 0-99444  
 XeF $_4$  molecules with Jahn-Teller pseudo-effect, ang. depend. of inelastic scatt. of electrons 0-69246  
 XeF $_4$ , pseudopot. SCF MO studies, steric aspects of struct. and force fields, Jahn-Teller effect 0-99444  
 XeF $_6$  seeded mol. beam, transverse ionisation, space charge, mass spectra and vel. 0-78725



**xenon compounds** continued

- XeF<sub>2</sub>(C) state lifetime, quenching rate consts., photolysis in inert gas atmospheres 0-66816  
 XeF(CI)(Br), discharge pumped multiwavelength lasers (*Chinese*) 0-102703  
 XeF\*, B<sup>2</sup>Σ<sup>+</sup> and C<sup>2</sup>II<sub>1/2</sub> states, fluoresc. decay dynamics, collisional quenching and radiative lifetimes 0-58306  
 XeF\*, electron impact excitation, temp. depend. quenching rate consts. 0-63701  
 XeF\* nuclear pumped laser obs. 0-63996  
 XeF\* + F<sub>2</sub> + Xe, temp. dependent quenching rate constants 0-63701  
 XeI\*, production via laser absorpt. processes at 193 nm, quenching kinetics 0-91466  
 XeO, low lying state characterisation 0-99543

**xerography** see *electrophotography; reproduction (copying)*

**xeroradiography** see *electrophotography*

**XPS** see *X-ray photoelectron spectra*

**Yang-Mills theory**

- $\nu$ -dimensional Yang-Mills and ( $\nu$ -1)-dimens. nonlinear  $\sigma$ -model connection, quark confinement, dual strings 0-90978  
 $\sigma$ -model supersymmetric dynamics on pre-QCD level with elementary quarks and composite gluons 0-82886  
 't Hooft electromagnetic tensor for Higgs fields of arbitrary isospin 0-68364  
 bifurcation solutions of cylindrically symmetric Yang-Mills equations 0-99034  
 bounded solutions 0-105764  
 broken symmetry soln., Higgs fields' and Einstein gravity action 0-101746  
 caloron importance in high-temp. Yang-Mills gas 0-95221  
 classical Yang-Mills eqns., soln. method 0-77970  
 configuration constraint 0-82903  
 confinement and the consistency of Yang-Mills theory 0-62852  
 conformally flat spaces and solutions to Yang-Mills equations 0-57481  
 conservation-law violation at high energy by anomalies 0-62855  
 cosmic matter-antimatter asymmetry and gravitational force 0-90586  
 Coulomb gauge vacua of (2+1) dimensional Yang-Mills theory 0-90997  
 CP<sup>n-1</sup> model, embeddings of classical solns. of O(2p+1) nonlinear  $\sigma$ -models, instantons 0-86562  
 defect dynamics, field equations, four dimensional space-time setting 0-96521  
 dyons, mag. charge and Pontryagin index equality in SU(2) 0-57562  
 dyons, spatial volume integral of Tr F(tilde) F, Yang-Mills theory 0-77943  
 Einstein-Yang-Mills equations, canonical connections on Riemannian symmetric spaces 0-95004  
 equations of motion finite range classical solns., confinement 0-57474  
 Euclidean, vanishing of energy-momentum tensor 0-77961  
 Euclidean self-dual Yang-Mills field configurations, set of linear algebraic eqns. 0-73587  
 extended supersymmetric Yang-Mills theories, superfield formulation, auxiliary component fields 0-90995  
 Faddeev-Popov ghost field, explicit classical construction, Yang-Mills field 0-82874  
 fermion-fermion high energy scatt., transverse momentum cut-off hypothesis, Yang-Mills theory 0-86575  
 gauge ambiguities and nonlinear  $\sigma$ -model relations in Yang-Mills vacuum sector 0-105767  
 gauge invariant gluons, Hamiltonian operator 0-105843  
 gauge theory, renormalisation of ghost and Goldstone fields and ghost symmetries 0-90987  
 gauge zero modes, treatment methods 0-62840  
 gravitational and strong interactions, unified gauge theory 0-95016  
 gravitational field, compact internal symmetry groups 0-95022  
 gravitational instantons, self-dual soln. to Euclidean gravity 0-68118  
 Higgs field zeros for axially symmetric multi-monopole configurations 0-82887  
 Higgs Kibble model on basis of canonical Yang-Mills field theory 0-105781  
 instanton gas, first order phase transition existence conditions (*Russian*) 0-62866  
 instanton sector renormalisation, zeroth sector comparison, pure Yang-Mills perturbation theory 0-105775  
 instanton solutions, Penrose twistor transform and methods of algebraic geometry 0-73612  
 instanton statistical mechanics in QCD 0-57567  
 instantons, multi-, quantum fluctuations, Seelye coeffs. 0-77934  
 instantons and monopoles in Yang-Mills gauge field theories 0-91003  
 integral formulation divergence elimination, connecting const. renormalisation (*Russian*) 0-68369  
 Lagrangian in winding number space, kinetic and potential energy, band structure of  $\theta$ -vacuum (*Chinese*) 0-62860  
 magnetic fields, flux string and monopole, geometric configuration, compared to O(3) nonlinear  $\sigma$ -model 0-57527  
 manifestly gauge invariant gluon eqns. from Yang-Mills fields 0-86681  
 massless propagator, IR bound 0-73581  
 meron pair, introduction, motivation and formalism 0-82861  
 meron pairs, bare activity 0-82862  
 N=4 supersymmetric Yang-mills theory, 3-loop  $\beta$  function zero value 0-105783  
 non-Abelian gauge theories in external electromagnetic fields (*Russian*) 0-57533  
 non-Abelian gauge theories, high energy behaviour, reggeon field theory, QCD 0-62822  
 non-Abelian gauge theory, Yang-Mills phase factor renormalisability 0-95211  
 non-Abelian phase factors, Yang-Mills Hamiltonian 0-73575  
 non-relativistic scattering by stationary external metrics and Yang-Mills potentials 0-101938  
 O(3)-symmetric merons in SU(N) gauge theory 0-82904  
 operator ordering and Feynman rules in gauge theories 0-101926  
 perturbation Feynman rule, gauge-nonfixing method 0-57462  
 planar diagrams, SU(N) asymmetric model, semiclassical approach 0-77957  
 QCD and Weinberg-Salam model for strong and electro-weak interactions 0-73638  
 QCD vacuum in strong external gauge fields, spontaneously, broken chiral symmetries 0-57555  
 quantisation, without fixing gauge, functional technique 0-57471

**Yang-Mills theory** continued

- quantum collective field method, planar limit appl., SU(N) theory and harmonic oscillators 0-57468  
 quantum string representation, SU<sub>2</sub> gauge group 0-57465  
 quark confinement, absence of localised coloured/charged physical states, coherent photon states 0-57573  
 relativity, seven-dimensional, 4-D gravity coupled to Yang-Mills fields 0-82699  
 renormalisation theory, perturbative, general features, quantum action principles, pure Yang-Mills theory 0-105794  
 scattering amplitudes, sixth-order, Yang-Mills fields, finite-diagram theory 0-73585  
 Schrodinger particle as the source of a Yang-Mills field 0-57494  
 self dual SU(2) fields in multicentre spaces 0-73600  
 SO (1,3) gravity, post-Newtonian, strong equivalence principle 0-68113  
 spinning solutions of classical Yang-Mills theory 0-101937  
 static magnetic SU(2) Yang-Mills-Higgs system, static axial and mirror symmetric monopoles 0-90992  
 static solutions of 4-dimens. eqns. of Yang-Mills gauge fields with mass 0-82872  
 SU(2) classical Yang-Mills eqn., multimeron solns. 0-57477  
 SU(2) gauge theory, external charges, topological classification for Yang-Mills eqns. 0-90977  
 SU(2) supergroups, Yang-Mills, Lie groups, chiral coeffs., Baker-Campbell-Hausdorff formula 0-68355  
 SU(2) theory, 1<sup>st</sup> and 2<sup>nd</sup> order eqn. equivalence 0-90979  
 SU(2) Yang Mills theory, field-strength description of non-Abelian gauge theories 0-62856  
 SU(2) Yang-Mills eqns., elliptic generalization of the one-meron configuration 0-62854  
 SU(2) Yang-Mills theory, finite field eqn. 0-62830  
 SU(2) Yang-Mills theory, ground state 0-101939  
 SU(2) Yang-Mills theory, vacuum struct. 0-57501  
 SU(N) Yang-Mills field eqns., constant classical solns. for N=∞ 0-73589  
 super Yang-Mills theory, anomalies and supersymmetric regularisation by dimensional reduction 0-82916  
 superspace gauge theories, superspace Maxwell and Yang-Mills actions 0-86582  
 superspace geometry in supergravity, Riemannian theory reduction, Yang-Mills connections 0-57156  
 supersymmetric, Ward identity, one-loop level, renormalisation 0-73597  
 supersymmetric extension, OSp(1,4), superfield formulation in anti-de Sitter space 0-57508  
 supersymmetric Yang-Mills field theory, point splitting regularisation, superformal anomaly 0-91014  
 supersymmetric Yang-Mills theory in Wess-Zumino gauge, supersymmetric regulators and supercurrent anomalies 0-86614  
 transverse lattice QCD, hadron mass spectrum 0-57568  
 UV infinity suppression in gravity modified field theories 0-105787  
 Yang equations, invariance props. 0-62836  
 e<sup>+</sup>e<sup>-</sup> → W<sup>+</sup>W<sup>-</sup>γ(e<sup>+</sup>e<sup>-</sup> W<sup>+</sup>W<sup>-</sup>), Yang-Mills coupling 0-68443

**yield point**

- see also *yield strength; yield stress*  
 composite superconductor, flux jumps and training 0-70911  
 orthorhombic symmetry, yield surface characts. 0-64405  
 plate, simply supported circular, transverse shear and rot. inertia, dynamic plastic response 0-79175  
 plate weakened by equal-armed cross-shaped crack, plastic strain and fracture 0-69740  
 PMMA, plastic deform. by crazing (*Japanese*) 0-93619  
 polycarbonate, amorphous, yield behaviour in oriented and unoriented condition, effect of temp. 0-97537  
 polycarbonate, rigid plastic, yield behaviour (*Japanese*) 0-93620  
 polypropylene, crystalline, yield behaviour in oriented and unoriented condition, effect of temp. 0-97537  
 PVC, rigid plastic, yield behaviour (*Japanese*) 0-93620  
 shell, rectangular flexible elastoplastic, yield theory and deformation theory appl. 0-74773  
 steel, austenitic, ageing and plastic deform. effect on struct. and mech. props. of N15Kh5G3T3 (*Russian*) 0-71691  
 steel, C, tensile props. in high press. H<sub>2</sub> at room temp. (*Japanese*) 0-108501  
 steel, comp. and ferrite grain size influence on Ludwik eqn. constants (*German*) 0-81107  
 steel, low-alloy, plastic deform. mechanisms under dynamic loading 0-100883  
 steel, research of Cottrell and Bilby, (1945-55) 0-62444  
 steel, structural, wide plate tensile testing eval. (*German*) 0-100969  
 steel, toughness, review of joint tests (*German*) 0-65142  
 steel plates, explosively clad, fatigue crack propagation behaviour (*Japanese*) 0-104262  
 steels, austenitic stainless, stress corrosion cracking, correl. between electrochem. and mech. parameters 0-97613  
 steels, wide plate and V-notch bending tests evaluation on basis of materials mechanics (*German*) 0-66571  
 steels, with yield pt. of about 420 to 720 N/mm<sup>2</sup>, correlation between yield pt./tensile strength ratio and toughness (*German*) 0-66615  
 viscoplastic kinematic hardening model, cyclic loading appl., yield surface 0-79162  
 Zircaloy-2, yield pts. obtained by ageing at two stresses 0-81091  
 Ag-Ni (10 wt.%) wire, plastically deformed, fracture struct. (*German*) 0-71744  
 Cu, plastically deformed, lattice strain distrib. (*German*) 0-85012  
 Cu-Ag (3 at.%), plastically deformed, lattice strain distrib. (*German*) 0-85012  
 Cu-Cd (1.0 wt.%), yield stress and flow stress 0-97524  
 Fe, Arcco, Bauschinger effect, computerised evaluation method 0-93625  
 Fe-Si (2.6 wt.%) single cryst., crack propag., controlled plastic crack tip opening rate 0-60943  
 InP single crystals, uniaxial compression deform. characts. 0-84991  
 InSb, X-ray topographic evidence of asymmetrical pre-yield behaviour 0-75229  
 Nb, Sn, hot isostatically pressed, plastic deform. 0-108510  
 Ti, yield pts. obtained by ageing at two stresses 0-81091  
 Zn single cryst., dislocation velocity and plastic deform. 0-64998  
 Zr, yield pts. obtained by ageing at two stresses 0-81091  
 Zr-Nb (2.5 wt.%), nuclear fuel channels, neutron effects on ultimate fracture strength, 293 to 573K 0-85054



## yield strength

- brass, cold rolling, inhomogeneous texture 0-89251  
 elastomers, rel. between relax. behaviour and tensile strength (*German*) 0-66604  
 fatigue crack propagation, crack closure, effective stress range factors 0-100924  
 metallic glasses, friction coeff. determ. using sliding friction rig 0-89355  
 metals, constitutive model at high strain-rate, shear modulus, yield strength 0-75292  
 metals, plastic yield criteria, interpolation scheme 0-64400  
 1-nylon polymers, stress-strain curve 0-60938  
 plastic deform., generalised constitutive eqns. 0-104219  
 polyethylene, photodegradation mechanism, from yield strength, elongation and mol. wt. studies (*Japanese*) 0-76311  
 polyethylene ribbons, flow-induced crystn. from melt, in dies fed by single screw extruder 0-84110  
 polypropylene, flow-induced crystn. from melt, in dies fed by single screw extruder 0-84110  
 sheet material, method for strength meas. under biaxial tension 0-66717  
 steel, austenitic, tensile strength, elec. current impulse effect down to 4.2K 0-81131  
 steel, austenitic stainless, supercond. magnets, mech. and phys. props. at 4K 0-86976  
 steel, austenitic stainless SUS 301, stress corrosion cracking susceptibility, effect of strain-induced  $\alpha'$ -martensite (*Japanese*) 0-104335  
 steel, austenitic stainless types 304 and 316, environment effect on crack growth, under creep and fatigue conditions 0-85035  
 steel, C-Mn-V-Cb-N, high strength low alloy, controlled-rolled 0-100803  
 steel, cast automatic couplings, yield strength, crack propag. resistance and ductile-brittle transition temp. 0-104281  
 steel, Cr-Mo, effect of Mo on high-temp. props. 0-85005  
 steel, Cr-Mo (10-14, 2-6 wt.%), heat-resist., creep-rupture strengths 0-104271  
 steel, Cr-Mo-V pressure vessel, microstruct. parameters and yielding rel. to plastic deform. 0-89318  
 steel, effect of H<sub>2</sub> on phys. and mech. props. 0-101657  
 steel, eutectoid, mech. behaviour, thermomech. treatment effects 0-84970  
 steel, fatigue and cyclic plasticity rel. to struct. inhomogeneity 0-81184  
 steel, ferritic stainless, embrittlement 0-85041  
 steel, ferritic-martensitic, fatigue crack tip plastic zone (*Japanese*) 0-71738  
 steel, high alloy Cr-Mo-W, splat quenched, formation of metastable austenite 0-84974  
 steel, high-strength, dynamic yield strengths, phase transition press. and Hugoniot parameters 0-75331  
 steel, low alloy, ferritic-pearlitic, carbonitride hardening 0-104174  
 steel, microalloyed, types V1599, V1600, V1286, NbCN precipitation in undeformed austenite 0-89230  
 steel, Mn-V reinforcing type, strain ageing characts. rel. to mech. props. 0-84969  
 steel, Ni, welded joints on LNG carriers mech. props. and fracture toughness 0-85017  
 steel, rail, toughness, effect of Sn, SEM exam. 0-97569  
 steel, stainless, type 316, modelling effects of fast neutron irradiation in mech. behaviour 0-84234  
 steel, type 10G2SAF, yield strength, influence of deform. rate (*Bulgarian*) 0-89315  
 steel, type IN-787, for use in Arctic, low temp. effects on mech. props. 0-76310  
 steels, wide plate and V-notch bending tests evaluation on basis of materials mechanics (*German*) 0-66571  
 TZM-Mo alloy, mech. props., effect of exposure to high temp. He containing O<sub>2</sub>, room temp. study 0-93639  
 Ag, cold rolling, inhomogeneous texture 0-89251  
 Al alloys, (5083, 6061, 2219), supercond. magnets, mech. and phys. props. at 4K 0-86976  
 Al, cold rolling, inhomogeneous texture 0-89251  
 Al foils, high strength, vapour deposited on curved surfaces, quantitative characterisation 0-80144  
 Al-(Mg)(Fe), pure (dilute), large wire drawing plastic deform. 0-108508  
 Al-Cu (4.6 wt.%), cold work and ageing influence on ductility and fracture behaviour (*Japanese*) 0-89295  
 Al-Cu-Mn (1-5.2, 0-0.6 wt.%), N alloying and comp. effect on mech. props. (*Bulgarian*) 0-71719  
 Al-Li-Mn (2.8, 0.3 wt.%), recrystallised sheet, fracture behaviour, SEM and TEM study 0-97566  
 Al-Mg-Si, type 6061-T6, 6063-T6, effective stress range factor in fatigue 0-100924  
 Al-Ni (6 wt.%), fine-grained, deform. in tension and torsion 0-85008  
 Al-Si(9.3, 12) with graphite particles seizure resistance study using Hohn wear tester 0-89360  
 Al-Zn-Mg-Cu alloys, heat treatment optimisation 0-60888  
 Al<sub>2</sub>O<sub>3</sub>, vacuum condensate, struct. and mech. props., second phase effect (*Russian*) 0-71705  
 Cd, warm rolled, texture and grain size depend. of tensile props. 0-71720  
 Co-Fe-V-Ni, mag. and mech. props., heat treatment and stress effects 0-60363  
 Co-Ti-Fe (3, 1 to 2 wt.%), spinodal decomposition 0-100839  
 Cu, cold rolled sheet, anisotropy of elastic and strength props. 0-81077  
 Cu powder compacts, yield curve comparison, different loading paths (*Japanese*) 0-93621  
 Cu-Be (2 at.%), plastic deform. and dislocation substruct. 0-76307  
 Cu-Cd (1.0 wt.%), yield stress and flow stress 0-97524  
 Cu-Cr (0.75 wt.%), deformation characts., fully reversed cyclic strain with fatigue cracks and dislocation struct. 0-81148  
 Fe-Cr-Al (7, 5 wt.%), expt. stainless alloys, phys. and mech. props. 0-97637  
 Fe-Ni-Al-(Cu) (12, 0.5, 0.5 to 3 wt.%), Cu addition strengthening at 77K, mech. props. 0-60875  
 Fe-Ni-Ti-(Cu) (12, 0.25, 2 wt.%), Cu addition strengthening at 77K, mech. props. 0-60875  
 Fe-Ni-V-(Cu) (12, 2, 2 wt.%), Cu addition strengthening at 77K, mech. props. 0-60875  
 Fe-Ni-(Cu) (12, 0.5 to 3 wt.%), Cu addition strengthening at 77K, mech. props. 0-60875  
 Fe-Si (3 wt.%), electron irradiated, yield strength and elongation 0-76325  
 MgO crystal, yield strength and dislocation mobility 0-93601  
 Mo, mech. props., effect of exposure to high temp. He containing O<sub>2</sub>, room temp. study 0-93639

## yield strength continued

- NbC, vacuum condensate, struct. and mech. props., second phase effect (*Russian*) 0-71705  
 Ni alloy, fatigue and cyclic plasticity rel. to struct. inhomogeneity 0-81184  
 Ni-H, thermally charged, serrated yielding 0-85007  
 Pb(Ag) alloys, effect of Ag content on yield strength 0-76322  
 Ti-Mo-Zr-Sn (11.5, 6, 4.5 wt.%),  $\beta$  III, mech. props. rel. to heat treatment 0-84961  
 TiB<sub>2</sub>, TiC, vacuum condensate, struct. and mech. props., second phase effect (*Russian*) 0-71705  
 Zn, nitrided, yield strength, influence of deform. rate (*Bulgarian*) 0-89315  
 Zr-Nb (2.5 wt.%), nuclear fuel channels, neutron effects on ultimate fracture strength, 293 to 573K 0-85054  
 Zr-Nb (2.5 wt.%) pipe, fracture resistance, hydrogenation effect 0-104279  
 ZrO<sub>2</sub>, ZrB<sub>2</sub>, vacuum condensate, struct. and mech. props., second phase effect (*Russian*) 0-71705
- yield stress**  
 see also yield point; yield strength  
 alloys, with ordered domains and disordered regions, critical shear stress (*Russian*) 0-107237  
 brass, single cryst., yielding behaviour rel. to low temp. annealing treatment (*Japanese*) 0-93582  
 concretes, further development of 2 point test for workability and extension of its range 0-66728  
 crack tips, blunt, elastic-plastic stress field, plane stress and plane strain (*Chinese*) 0-64469  
 cracks, penny-shaped, ductile, dynamic effects in propagation, Hankel and Laplace transform methods 0-87741  
 disperse system, plastoviscous, cone plastometer for strength props. determ. 0-76426  
 epoxy resin, plastic deform. mechanism 0-97534  
 eutectics, single grained, directionally solidified, anisotropic yielding behaviour 0-103412  
 FCC alloy, hardening by spinodal modulated structure 0-60874  
 fracture stress obtained from the elastic crack tip enclave model 0-71730  
 hot metal, dynamic yield characts. during multistage deform., plastometer design 0-85135  
 plastic deformation, inhomogeneous, reference degree of deform. definition (*German*) 0-99936  
 polycarbonate, rigid plastic, yield behaviour (*Japanese*) 0-93620  
 porous metals, plasticity, stress-strain curves, yield stresses, strain vectors 0-83738  
 PVC, oriented mouldings, struct. order 0-60896  
 PVC, rigid plastic, yield behaviour (*Japanese*) 0-93620  
 rod of rate-sensitive material, elastic-plastic tension-torsion analysis 0-83741  
 stability of thin-walled pressure vessels of elastic-plastic linear hardening material 0-92075  
 steel, eutectoid, mech. behaviour, thermomech. treatment effects 0-84970  
 steel, ferritic, cleavage fracture toughness, temp. and strain rate depend. 0-85028  
 steel, lamellar pearlite, containing proeutectoid cementite, brittle fracture study (*Japanese*) 0-93648  
 steel, low and medium C, dynamic and static strength, strain rate and temp. depend. of flow stress 0-85139  
 steel, microalloyed, types V1599, V1600, V1286, NbCN precipitation in undeformed austenite 0-89230  
 steel, Ni, welded joints on LNG carriers mech. props. and fracture toughness 0-85017  
 tensile tests, standardization from metal physics viewpoint (*German*) 0-93711  
 Al, polycrystalline, movement of 3-fold nodes of boundaries in high temp. creep 0-89317  
 Al-Bi(Cd)(Pb)-Ti, containing low-melting pt. inclusions, mech. props. 0-93632  
 Al-Mg (2 wt.%), hardening and fracture characts.,  $\beta$ -phase dissolution role 0-81178  
 Al-Ni (6 wt.%), fine-grained, deform. in tension and torsion 0-85008  
 Al-Ni(Cd)(Fe)(Si), cold worked, struct. and props. 0-71666  
 Co single crystals, strain rate deform. characts., yield stresses and work hardening 77 to 1400K 0-60939  
 Cu powder compacts, yield curve comparison, different loading paths (*Japanese*) 0-93621  
 Cu-Cd (1.0 wt.%), yield stress and flow stress 0-97524  
 Cu-Cr-(SiO<sub>2</sub>), single crystals, yield and pre-yield behaviour rel. to aging time 0-81103  
 Fe-Al-Si (6.22, 9.63 wt.%), bending test under high press., high temp. 0-85057  
 Fe-Ni, single cryst., solid soln. softening, effect of interstitial N 0-97496  
 Fe-Ni, dilute, irradiation softening effect on yield stress 0-76319  
 Fe-Si, dilute, irradiation softening effect on yield stress 0-76319  
 Fe-V, dilute, irradiation softening effect on yield stress 0-76319  
 GeTe, stoichiometry deviations influence on mech. props., 25-500°C 0-103410  
 LiF, dislocation structure, influence of variable deform. temp. 0-70211  
 MgO crystal, yield strength and dislocation mobility 0-93601  
 MgO crystals, plastic deform. activation parameters, rel. between macroscopic and in-situ HVEM expts. 0-103355  
 Mo, neutron irradi., radiation anneal hardening mechanism 0-71678  
 Nb-O system, solid soln. hardening and softening 0-71665  
 Ni<sub>3</sub>(Al, Nb) single crystal, yield stress, orientation and temp. depend. 0-108511  
 $\gamma$ -Ni<sub>3</sub>(Al,Ti), single crystal, dislocation movement, HVEM obs. (*Japanese*) 0-108503  
 Pb, film, hillock formation by grain boundary sliding 0-107673  
 Pb(Ag) alloys, effect of Ag content on yield strength 0-76322  
 Pd<sub>3</sub>Si<sub>2</sub> amorphous alloy, skip deform. and crit. shear stress, using tensile testing machine 0-89321  
 Pd<sub>3</sub>Si<sub>2</sub>, glass, deform. localisation, plastic instabilities and fracture 0-89320  
 239PuO<sub>2</sub>, stoichiometric, high-temp. deformation 0-81111  
 Si thin ribbon grown at high speed, thermal stresses, reduced thermal buckling 0-107078  
 $\alpha$ -Ti, determination of microflow parameters from compression tests 0-66584  
 Ti-Er(Y), effects of Er and Y additives on deformation behaviour 0-81121

## yield stress continued

- Zr-Al (8.6 wt.%), dimensional stability struct. and mech. props, effects of neutron irradi. 0-92563  
 Zr-Nb (2.5 wt.%), cold-worked, pressure tubing, metallography and mech. props. 0-89269

## yielding see plastic deformation

## Young's modulus

- acrylourethane coatings, radiation curable, tensile, elongation and modulus props. appl. techniques 0-66847  
 bagasse fibre reinforced phenol formaldehyde, tensile strength and Young's modulus, SEM study 0-60952  
 $\beta$ -brass bicrystals, shear-incompatible, grain boundary contrib. to Bauschinger effect 0-97550  
 ceramic layers on metallic substrates, mech. props. meas. (French) 0-104375  
 eddy current determination 0-65116  
 education, Young's modulus meas. using audio generator amplifier and speaker 0-62427  
 epoxy resin, plastic deform. mechanism 0-97534  
 fibre-reinforced materials, slender, non-dilute, thermal and mechanical props. 0-103524  
 glass fibre reinforced cement, durability in wet and dry conditions, fibre length and content effect 0-71726  
 glass fibre reinforced plastics, exposed to liq. media, dynamic high-speed Young's modulus determ. (German) 0-85123  
 glass-ceramic, machinable, elastic const. temp. depend. 0-79852  
 Jahn-Teller system, thermodynamic properties, internal stress effects 0-59679  
 laminates, exposed to liq. media, dynamic high-speed Young's modulus determ. (German) 0-85123  
 metals, polycryst., relations between shear modulus, bulk modulus and Young's modulus 0-97540  
 piezoelectric transducer automatic setup, for continuous meas. of internal friction and elastic moduli of solids 0-108652  
 polyethylene-polypropylene blend, extruded, thermal swelling and mech. characterisation 0-81110  
 polyester polymer concrete, longitudinal deform. modulus study is creep conditions (Bulgarian) 0-71685  
 polyethylene, linear, draw temp. and mol. wt. effect on draw ratio and Young's modulus 0-84998  
 polyethylene fibre, high-strength high-modulus, morphology and tensile prop. relations 0-103264  
 polyethylenes, ultra-high modulus, manufacture by drawing through conical die 0-66583  
 polypropylene, ultrahigh modulus, tensile drawing, mol. wt. effect 0-104211  
 polyvinylidene fluoride, piezoelec., nonlinear dynamic response 0-75946  
 raw kaolin, acoustical investigations of the effect of additives on elastic props. 0-66559  
 steel, austenitic stainless, N-alloyed 0-108490  
 steel, Cr-Mn (13, 19 wt.%), elastic const. behaviour, anomalous, low temp. 0-97521  
 stretch zone width and striation spacing. The comparison of theories and experiments 0-85051  
 Stycast-1266, mechanical props. at low temps. 0-57286  
 wire reinforced Al, stress-deformed state, elastic, strength props. (Russian) 0-76303  
 Ag, Young's modulus depend. on temp. and mech. action (Russian) 0-92584  
 Al-Cu (2-5 wt.%), precipitation total surface influence on resistivity (French) 0-71650  
 Al-SiC cermet elasticity, porosity meas. by US means 0-81101  
 $\alpha$ -Al<sub>2</sub>O<sub>3</sub> fibre FP, manufacture, strength and modulus 0-81013  
 Al<sub>2</sub>O<sub>3</sub> refractories, fracture, J-integral meas. 0-108537  
 a-As, second and third order elastic const., ultrasonic velocity meas. 0-103408  
 Bi, Young's modulus and internal friction, 20°C to melting point (Russian) 0-89278  
 C fibre derived from mesophase-pitch, Young's modulus and tensile strength, struct. flow elimination 0-80995  
 C fibres, mech. props., thermal stability up to 2000°C 0-60929  
 Cd, Young's modulus and internal friction, 20°C to melting point (Russian) 0-89278  
 Cr-Fe, elastic moduli, electron conc., pulse echo overlap meas. 0-59550  
 Cu, cold rolled sheet, anisotropy of elastic and strength props. 0-81077  
 Cu, dislocation pinning rate, neutron and electron irradi., meas. by internal friction method 0-96570  
 Cu, Young's modulus depend. on temp. and mech. action (Russian) 0-92584  
 Fe, and its alloys, Young's modulus of Fe<sub>3</sub>C phase (Russian) 0-76297  
 Fe-B phase ferromag. amorphous alloys, stiffening below Curie temp., pole effect (Japanese) 0-84632  
 Fe-B(P) amorphous alloys, anomalous thermal expansion,  $\Delta E$  effect, Invar and Elinvar characts., delay time 0-80589  
 Fe-Cr-Co, elastic props. anisotropy at room temp. (Russian) 0-89279  
 Fe-Pd Invar alloy, Young's modulus, magnetostriction, Curie temp. 0-65988  
 Fe-Si (3 wt.%), magnetisation variation during bending oscills., rel. to  $\Delta E$  effect (Russian) 0-65983  
 Fe<sub>80</sub>B<sub>20</sub>, Metglas 2605, Young's modulus meas. using piezoelectric US composite oscillator technique 0-108656  
 (Fe<sub>2</sub>Co<sub>1-x</sub>)<sub>70</sub>Si<sub>8</sub>B<sub>14</sub>, amorphous, saturation magnetostriction, strain modulated FMR obs. 0-75863  
 Fe<sub>20</sub>Ni<sub>80</sub>Mo<sub>4</sub>B<sub>18</sub> and Fe<sub>70</sub>Mo<sub>30</sub>B<sub>20</sub> amorphous ribbons, magnetoelastic effects in as-quenched and stress-relieved states 0-80588  
 Fe<sub>40</sub>Ni<sub>60</sub>P<sub>14</sub>B<sub>6</sub>, bending tests, evidence of ideal elastic-plastic deform. 0-97543  
 GaS, elastic prop. anisotropy, Debye temp. (Russian) 0-88244  
 GaS(Se), elastic characteristics, Debye temp., ultrasonic study (Russian) 0-79872  
 Li<sub>2</sub>O-Na<sub>2</sub>O-B<sub>2</sub>O<sub>3</sub>-Al<sub>2</sub>O<sub>3</sub>-SiO<sub>2</sub> glass, Young's modulus and density, ion exchange effects 0-84982  
 Mn-Bi mictomagnetic alloy, mag., elec. and elastic props. (Russian) 0-108028  
 $\gamma$ -MnAu, antiferromag., phase diagram, X-ray diffraction and Young's modulus meas. 0-71024  
 Nb<sub>3</sub>Sn, Young's modulus, 4.2-300K, behaviour near martensitic transition 0-66564  
 Ni<sub>36</sub>Fe<sub>32</sub>Cr<sub>14</sub>P<sub>12</sub>B<sub>6</sub> metallic glass, mech. props. and thermal stability 0-76362

## Young's modulus continued

- Pb, Young's modulus and internal friction, 20°C to melting point (Russian) 0-89278  
 Sn, Young's modulus and internal friction, 20°C to melting point (Russian) 0-89278  
 Ti-Mo-V-Al-Cr-Fe (4.8, 4.7, 5.2, 1.1, 1.0 wt.%), structural changes during heating up to 1000°C, DTA study (Russian) 0-93552  
 Ti-V, elastic moduli, electron conc., pulse echo overlap meas. 0-59550  
 TiC, frictional characts. and contact-zone deform. in homogeneity range 0-66673  
 UFe<sub>2</sub>, giant magnetoelastic deform. of cryst. struct. mag. props. (Russian) 0-93159  
 UN-ZrN, antiferromagnetic anomaly 0-92583  
 V-H single crystals., elastic const., temp. depend., H effects 0-66563  
 ZrO<sub>2</sub>, partially stabilized, props. and appl. to extrusion dies 0-97507

## ytterbium

see also nuclei with .....

- 4f<sup>14</sup>6s6p <sup>3</sup>P<sub>1</sub> and <sup>1</sup>P<sub>1</sub> levels, Stark effect, tensor polarisabilities 0-87080  
 amorphous metal films, crystallisation with and without mag. field 0-70570  
 atom, electron impact excitation cross section, Born and Ochkur approx. 0-87230  
 atom, highly excited levels, odd and even parity spectra, multichannel quantum defect anal. 0-58133  
 atom, highly excited levels, reson., visible two photon absorpt. spectra obs. 0-58228  
 electrical resistivity of solid and liquid phases, thermopower, melting temp. 0-59955  
 electron radiation damage, elec. resistivity change rates 0-59954  
 metaphosphate glass: Nd<sup>3+</sup>, Yb<sup>3+</sup> luminesc., energy transmission and migration between Nd<sup>3+</sup> and Yb<sup>3+</sup> 0-66297  
 phosphate glass: Yb<sup>3+</sup>, luminesc. band struct., chronoscopic study at 4.2K 0-60663  
 piezoresistance gauge, lateral compressive stresses meas. in shock-loaded PMMA 0-103007  
 KCl:Yb, Z<sub>2</sub> and Z<sub>2</sub><sup>+</sup> centres, excited state, magneto-optical spectra 0-108233  
 KMgF<sub>3</sub>:Yb<sup>3+</sup>, perovskite type cryst., ENDOR meas. 0-80638  
 KZnF<sub>3</sub>:Yb<sup>3+</sup>, perovskite type cryst., ENDOR meas. 0-80638  
 Y<sub>2</sub>SiO<sub>5</sub>:Yb<sup>3+</sup>, EPR and spin-lattice relax. 0-108063  
 Yb I, high Rydberg levels of 4f<sup>14</sup> 6snd configs., very high resolution obs. 0-106300  
 Yb I isotope shift studies in 3900 to 6500 Å region 0-74144  
 Yb II, 6s <sup>2</sup>S<sub>1/2</sub>-6p <sup>2</sup>P<sub>3/2</sub> transition, relativistic oscillator strengths, influence of core polarisation 0-58132  
 ZnO:Yb, electrolum. brightness, field strength and freq. depend. 0-100696

## ytterbium alloys

- Au-Yb, dil., EPR at 100 mK to 1K 0-66028  
 Au-Yb thin films, ESR spectra, strain effects 0-71172  
 Gd-Yb, magnetocrystalline anisotropy, magnetisation and torque curve meas. 0-65859  
 Yb-Al mixed valent film form., XPS study 0-80943  
 YbAl<sub>2</sub>Ga<sub>2</sub>, synthesis, NMR and X-ray absorpt. studies 0-108083  
 YbAu<sub>2</sub>, valence transition at surface of Yb 0-70652  
 YbCuAl, mixed valence cpd., dynamic susceptibility, neutron inelastic scatt. 0-65807  
 YbCuAl, mixed-valent cpd., thermal expansion and magneto-volume effects 0-66005  
 YbCu<sub>2</sub>Si<sub>2</sub>, interconfiguration fluctuation, NMR expts. 0-66069  
 YbFe<sub>2</sub>, cryst. elec. field and exchange interac., <sup>170</sup>Yb Mossbauer obs., magnetostriction contrib. 0-108124  
 YbFe<sub>2</sub>, high field Mossbauer study 0-75893  
 YbSn<sub>3</sub>, powdered, de Haas-van Alphen effect 0-59857  
 Yb<sub>1-x</sub>Y<sub>x</sub>CuAl, disordered extended Anderson model, CPA-alloy analogue treatment 0-65506

## ytterbium compounds

see also ytterbium alloys

- ethyl sulphate, crystal field effects on mag. and hyperfine props. of Yb<sup>3+</sup> 0-97101  
 silicate: Yb<sub>2</sub>O<sub>3</sub> glassy film, Yb laser spectral microanalysis 0-76585  
 CaYb intercalation compounds, three dimensional continuous melting 0-59631  
 Eu<sub>1-x</sub>Yb<sub>x</sub>Te, (0 < x < 1), mag. semicond., elec., mag. and optical props. 0-97070  
 KYbHP<sub>2</sub>O<sub>10</sub>, thermal decomp., thermogravimetric and X-ray obs. 0-101013  
 SbCu<sub>2</sub>Si<sub>2</sub>, mixed valence system, X-ray absorption spectroscopic study 0-80906  
 Sm<sub>1-x</sub>Yb<sub>x</sub>B<sub>6</sub>, valence transition, lattice parameter and mag. susceptibility meas. 0-59929  
 YFe<sub>2</sub>O<sub>4</sub>, extra electron reflections 0-100139  
 (YGdYbBi)<sub>2</sub>(FeAl)<sub>2</sub>O<sub>12</sub> ferrite-garnet films, effect of in-plane field on dynamics of domain walls 0-65979  
 (YGdYbBi)<sub>2</sub>(FeAl)<sub>2</sub>O<sub>12</sub> epitaxial garnet film, uniaxial ferromagnet domain struct., phase transition (Russian) 0-108044  
 (YYbBi)<sub>3</sub>(FeAl)<sub>2</sub>O<sub>12</sub> films, Faraday effect in transverse mag. field, orientation depend. 0-88971  
 Y<sub>1-x-y</sub>Yb<sub>x</sub>Er<sub>y</sub>OCr, Er ion excited state decay and population (Russian) 0-100694  
 YbAG, electrostatic model of cryst. field 0-59945  
 YbAsO<sub>4</sub>, ferroelectricity, dielec. meas. 0-60515  
 YbB<sub>6</sub>, resistivity press. variation, lattice const. 0-100456  
 YbCl<sub>3</sub>·6H<sub>2</sub>O·Gd<sup>3+</sup>, EPR, temp. depend., spin-lattice relax. time 0-93173  
 Yb<sub>0.5</sub>Eu<sub>0.5</sub>Fe<sub>2</sub>O<sub>4</sub>, rhombohedral oxides, symmetry group (French) 0-84157  
 YbF<sub>2</sub>, thermal props. (German) 0-81355  
 YbFe(CN)<sub>6</sub>·5H<sub>2</sub>O, powder, elec. transport props. obs. 0-70701  
 YbFe<sub>2</sub>O<sub>4</sub>, rhombohedral oxides, symmetry group (French) 0-84157  
 Yb<sub>2</sub>Fe<sub>2</sub>O<sub>7</sub>, extra electron reflections 0-100139  
 Yb<sub>2</sub>Fe<sub>2</sub>O<sub>10</sub>, extra electron reflections 0-100139  
 YbGaG, mag. props. between 44-600 mK 0-80517  
 YbGa<sub>2</sub>O<sub>12</sub>, dipolar magnet, sp. th. and magnetisation meas. 0-60344  
 YbMo<sub>2</sub>S<sub>8</sub>, low temp. Mossbauer study and mag. susceptibility 0-80656  
 YbO, cryst. field parameters due to 4f<sup>14</sup>-5d configs. 0-80230  
 Yb<sub>2</sub>O<sub>3</sub>, electronic cond. rel. to partial press. of O<sub>2</sub> of high temp. (French) 0-59979  
 Yb<sub>2</sub>O<sub>3</sub> thin film on Cr substrate, refr. index depend. on thin film thickness 0-108290  
 Yb<sub>2</sub>O<sub>4</sub>, extra electron reflections 0-100139



**yttrium compounds continued**

- $\gamma$ -Yb<sub>2</sub>Se<sub>3</sub>, mag. susceptibility and cryst. field parameters 0-65510  
 Yb<sub>1-x</sub>Sm<sub>x</sub>S, electron config. of Sm ions, X-ray L-absorpt. spectroscopy 0-60715  
 YbTe, high-temperature evaporation and reactivity 0-103469

**yttrium**

- see also nuclei with .....*  
 addition to Cr<sub>3</sub>C<sub>2</sub> fibre reinforced Ni-based composite, effect on oxidation and creep 0-66685  
 atom, XPS relative intensity and photoionisation cross-section 0-63599  
 core level binding energies 0-71564  
 electron radiation damage, elec. resistivity change rates 0-59954  
 electronic excitations, charact. energy loss meas. up to 50 eV 0-60723  
 implantation on Cr-Ni Nb stabilized austenitic stainless steel surface, effect on oxidation behaviour 0-71791  
 implementation of Fe-Cr-Al FeCrAlloy stainless steel surface, effect on oxidation behaviour 0-71790  
 interband, collective and atomic (p,d) excitations, Z-160 eV, fast EELS 0-93443  
 photoelectric cross sections at 52.4, 60, 72.2 and 84.4 keV 0-69187  
 plastic deformation, at different deform. speeds, dislocation glide (*Russian*) 0-93598  
 plastic deformation props., deformation ageing, plastic flow, dislocation-impurity interactions (*Russian*) 0-66582  
 silicite thin film formation on (100) and (111)Si substrate, backscattering study 0-70542  
 sorption of T from liq. Li fusion reactor blanket 0-95434  
 spin-spin relaxation times, pH depend. 0-66059  
 BaF<sub>2</sub>:Y<sup>3+</sup>, phonon reson. and IR absorpt. 0-84752  
 CaF<sub>2</sub>:Y<sup>3+</sup>, ionic cond. and thermal depolarisation obs. of defect clustering 0-71298  
 CaF<sub>2</sub>:Y<sup>3+</sup>, O<sup>2-</sup>, thermal depolarisation obs. of defect clusters 0-71299  
 CeO<sub>2</sub>:Y, slow transient phenomenon 0-107550  
 Fe:Y, ion implanted, deep D traps due to Y-vacancy complex 0-103372  
 Si:Y, photoelectric props. 0-107860  
 Y+H<sub>2</sub>(D<sub>2</sub>)(T<sub>2</sub>), high temp. equilib. meas. 0-66780  
 Y<sub>2</sub>O<sub>3</sub> plasma, eqn. of state investig. 0-75027

**yttrium alloys**

- see also yttrium compounds*  
 steel, stainless, FeCrAlloy, creep-rupture props., 650-800°C 0-97535  
 Ag-Y, dil., virtual bound states, transport props. obs. 0-70667  
 Al-Si-Y alloy, phase equilibria in Al rich region (*Russian*) 0-93537  
 Al-Y, specific elec. resist., variation with Y conc. 0-84455  
 Au-Y, dil., conduction electron-local moment exchange interaction meas. 0-60191  
 Au-Y, dil., virtual bound states, transport props. obs. 0-70667  
 Be-Y, plastic deform., flow stresses, fracture (*Russian*) 0-108496  
 (Ce,Y)Al<sub>2</sub>, collective phenomena 0-65933  
 (Ce,Y<sub>1-x</sub>)Fe<sub>2</sub>, mag. susceptibility and Mossbauer meas., lattice parameters 0-97068  
 Cu-Cu<sub>2</sub>Y eutectic alloy, cast and directionally solidified, struct. and props. (*Russian*) 0-104138  
 Fe-Cr-Al-Y, oxidation resistance, heat treatment and Al<sup>+</sup> ion implantation 0-71785  
 Fe-Cr-Al-Y, scales,  $\alpha$ -Al<sub>2</sub>O<sub>3</sub>, early stages development at high temp. 0-89413  
 Fe-Ni-Cr-Al-Y, oxidation mechanism, Y addition effect on kinetics and oxide adherence 0-97623  
 Fe-Ni-Cr-Y, Y addition effect on selective oxidation/diffusion phenomena relationship (*French*) 0-108623  
 Gd-Y alloys, mag. crit. temp. gap 0-60260  
 (Gd,Y<sub>1-x</sub>)Al<sub>2</sub>, ferromag. and spin glass like behaviour, magnetisation meas. 0-75734  
 (Gd,Y<sub>1-x</sub>)Al<sub>2</sub>Co<sub>3</sub>, Curie temp. and resist.-temp. curves, comp. depend. 0-71020  
 Gd<sub>1-x</sub>Y<sub>x</sub>Ni, FeB-CrB type stacking variations, cryst. struct. 0-64952  
 Gd<sub>1-x</sub>Y<sub>x</sub>Zn, ferromag., mag. susceptibility and magnetisation, temp. depend. 0-70975  
 Ho<sub>1-x</sub>Y<sub>x</sub>Sb system, magnetisation, elec. resist., and sp. ht. meas. 0-60213  
 Ir-Y eutectic alloy, supercond. transition enhancement due to lattice softening 0-103775  
 (La,Y)Ce, dil., Kondo supercond., transition temp., susceptibility and resist. 0-65733  
 La-Y/AlO<sub>x</sub>/Al tunnel junctions, cond. meas., cryst. field effects 0-88694  
 Nd<sub>1-x</sub>Y<sub>x</sub>Zn system, solid soln., mag. susceptibility, 77 to 600K (*Russian*) 0-65776  
 Ni-Al-Cr<sub>3</sub>C<sub>2</sub>-Y, eutectic alloy, directionally solidified, oxidation resistance, influence of Y 0-89409  
 Ni-based superalloys, hot workability, effect of S, Ca, Mg, Y and Zr minor elements 0-66552  
 Ni-Y, amorphous, elec. resist., press. depend. 0-96841  
 Sn-Y system, heats of form. 0-89517  
 Ti-Er(Y), effects of Er and Y additives on deformation behaviour 0-81121  
 Y-B, amorphous, B-rich, low freq. modes, Raman scatt. obs. 0-108202  
 Y-Co, amorphous, thermal stability, crystn., DSC and elec. resist. study 0-107060  
 Y-Fe, amorphous, thermal stability, crystn., DSC and elec. resist. study 0-107060  
 Y-Gd, dil., reverse resist. anomaly and negative magnetoresist. 0-84459  
 Y-Gd, spin glasses, low temp. sp. ht. and magnetisation 0-65913  
 Y-Ir, dil., elec. field gradient at <sup>193</sup>Ir, Mossbauer meas. 0-66090  
 Y-M intermetallic cpds., M=3d transition metal, sorption of H<sub>2</sub>, structural charges 0-88429  
 Y-Ru, elec. field gradient and temp. depend. TDPAC meas. 0-60477  
 YBe<sub>13</sub> lattice spacings and susceptibilities 0-65778  
 YCo<sub>3</sub> amorphous films, <sup>59</sup>Co spin echo study 0-80636  
 YCo<sub>3</sub>, hydride phase synthesis, thermal stability and struct. 0-59438  
 YCo<sub>3</sub>, uniaxial intermetallic, large magnetisation anisotropy 0-71011  
 Y<sub>1-x</sub>Co<sub>x</sub>, amorphous, mag. props. 0-84590  
 Y<sub>2</sub>Co<sub>7</sub>, NMR spin echo meas., dipolar field anisotropy 0-71236  
 Y(Co<sub>1-x</sub>Ni<sub>x</sub>), distrib. of Co and Ni atoms, neutron diffr. obs. (*Russian*) 0-64954  
 YFe<sub>2</sub>, ErFe<sub>2</sub>-YFe<sub>2</sub> (30, 70 wt.%), mag. props., 80-1300K (*Russian*) 0-75750  
 Y<sub>2</sub>Fe<sub>23</sub>, magnetostriction, temp. depend., 20 to 350K 0-65994  
 Y(Fe<sub>1-x</sub>Co<sub>x</sub>)<sub>2</sub>, NMR study 0-75882  
 Y(Fe<sub>1-x</sub>Co<sub>x</sub>)<sub>2</sub>, x $\leq$ 0.2, mag. props. and Mossbauer meas. 0-75798  
 Y<sub>6</sub>(Fe<sub>1-x</sub>Mn<sub>x</sub>)<sub>23</sub>, Mn-rich compounds, Mossbauer effect study 0-71276

**yttrium alloys continued**

- Y<sub>1-x</sub>Gd<sub>x</sub>Co<sub>5</sub>, ferrimag., magnetisation, exchange interactions, mag. anisotropy 0-80565  
 Y<sub>2</sub>Ir<sub>2</sub>, cryst. struct. 0-96473  
 YM<sub>2</sub>-Gd, M=transition metal, correl. between g-shift and stability, EPR study 0-88874  
 YMg, Pauli paramagnet, mag. susceptibility, nonlinear band behaviour 0-75706  
 Y<sub>6</sub>Mn<sub>23</sub>, low temp. specific heat determ. 0-65896  
 YMn<sub>23</sub>Fe<sub>2</sub>H<sub>22</sub>, mag. props., ordering temps. 0-71028  
 Y<sub>1-x</sub>Nd<sub>x</sub>Co<sub>5</sub>, ferrimag., magnetisation, exchange interactions, mag. anisotropy 0-80565  
 YNi<sub>3</sub>, magnetism resurgence, neutron diffr. and mag. props. study 0-65819  
 YNi<sub>5</sub>, Hauke compounds, low temp. heat capacity, Debye temp. 0-96663  
 Y<sub>2</sub>Os, cryst. struct. 0-96474  
 Y<sub>2</sub>Os, cryst. struct. 0-96475  
 Y<sub>2</sub>Pd, cryst. struct. 0-96474  
 Y<sub>2</sub>Ru, cryst. struct. 0-96474  
 Y<sub>1-x</sub>Tb<sub>x</sub>Co<sub>5+0.1x</sub>, ferrimag., magnetisation, exchange interactions, mag. anisotropy 0-80565  
 Y<sub>1-x</sub>Tb<sub>x</sub>Pd<sub>3</sub>, magnetisation, magnetostriction, and inelastic neutron spectra 0-65998  
 Yb<sub>1-x</sub>Y<sub>x</sub>CuAl, disordered extended Anderson model, CPA-alloy analogue treatment 0-65506

**yttrium compounds**

- see also yttrium alloys*  
 crystal growth from fused oxides, flow method, simple and economical apparatus (*Italian*) 0-80960  
 dihydrides, structs. and stabilities 0-107146  
 garnet, inhomogeneous collective magnon oscill. excited by RF field (*Russian*) 0-100582  
 large growth-induced anisotropy to preferential occupation of Fe sites 0-75754  
 perovskite-like oxides, synthesis, struct., elec. props. 0-65554  
 tetrabutylammonium europium yttrium isothiocyanate, conc.-depend. electron-phonon coupling, and self-quenching 0-60657  
 Al<sub>2</sub>O<sub>3</sub>-Y<sub>2</sub>O<sub>3</sub>, melting behaviour and metastability determ. by optical DTA 0-92648  
 Al<sub>2</sub>O<sub>3</sub>-Y<sub>2</sub>O<sub>3</sub>, sintering kinetics, influence of minor additions of Y<sub>2</sub>O<sub>3</sub> 0-84868  
 BaY<sub>2</sub>X<sub>2</sub>O<sub>7</sub> (X=Si,Ge), cell const., luminesc. of various rare-earth activators 0-93376  
 $\delta$ -(Bi<sub>2</sub>O<sub>3</sub>)<sub>1-x</sub>(Y<sub>2</sub>O<sub>3</sub>)<sub>x</sub>, thermoelectric power rel. to fast ionic conduction 0-107549  
 CdF<sub>2</sub>-YF<sub>3</sub>, thermal ionisation energy of monovalent centres 0-80207  
 CeO<sub>2</sub>-Y<sub>2</sub>O<sub>3</sub>, O ion cond. and defect struct. 0-107553  
 CeO<sub>2</sub>-Y<sub>2</sub>O<sub>3</sub> solid soln. phases, synthesis 0-104132  
 Ce<sub>0.08</sub>Y<sub>0.92</sub>Sb, dilute f-electron system in cluster regime, crystal field and exchange splittings 0-97062  
 Er<sub>2</sub>Y<sub>1-x</sub>Rh<sub>x</sub>B<sub>4</sub>, mag. and supercond. transitions 0-70874  
 Eu<sub>2</sub>O<sub>3</sub>-Y<sub>2</sub>O<sub>3</sub> solid soln. phases, synthesis 0-104132  
 (Gd,Tm,Y)<sub>3</sub>(Fe,Ga)<sub>5</sub>O<sub>12</sub> LPE garnet thin films, magnetocrystalline anisotropy 0-93147  
 KY(WO<sub>4</sub>)<sub>2</sub>:Ho<sup>3+</sup>, stimulated emission at low temps. 0-106526  
 LiTb<sub>0.5</sub>Y<sub>0.5</sub>F<sub>4</sub>, uniaxial dipolar ferromag., critical behaviour, mag. susceptibility meas., effect of Y<sup>3+</sup> dilution 0-80528  
 LiYF<sub>4</sub>:Ho laser, TEM<sub>00</sub> mode and Q-switched operation 0-74395  
 Na<sub>2</sub>O-P<sub>2</sub>O<sub>5</sub>-Y<sub>2</sub>O<sub>3</sub>-Tb<sub>2</sub>O<sub>3</sub> glass, conc. quenching of luminesc. in disordered system with dipolar interaction 0-89059  
 Na<sub>2</sub>YSc(SiO<sub>3</sub>)<sub>2</sub>, crystal struct., atom coordinates, X-ray study 0-59446  
 Na<sub>2</sub>YSiO<sub>4</sub>, crystal structure refinement, X-ray anal. 0-79764  
 NaY<sub>1-x</sub>Sm<sub>x</sub>F<sub>4</sub>, luminesc. expt. suggesting Sm<sup>3+</sup> ion pairing 0-76065  
 Na<sub>2</sub>Y<sub>2</sub>Zr<sub>2</sub>O<sub>7</sub>, ionic cond. and NMR mobility obs., comp. depend. (*French*) 0-70459  
 Nd<sub>2</sub>O<sub>3</sub>-Y<sub>2</sub>O<sub>3</sub> film, segregation obs. by EELS 0-79953  
 Nd<sub>2</sub>Y<sub>1-x</sub>P<sub>x</sub>O<sub>4</sub>:Nd<sup>3+</sup>, radiationless decay processes, laser photoacoustic spectroscopy meas. 0-84766  
 Se<sub>2</sub>O<sub>3</sub> solid and liq. phases, thermophysical and electrophysical props. 0-103495  
 Si<sub>3</sub>N<sub>4</sub>-SiO<sub>2</sub>-Y<sub>2</sub>O<sub>3</sub>, subsolidus phase relations 0-60845  
 Si<sub>3</sub>N<sub>4</sub>-Y<sub>2</sub>O<sub>3</sub>-Al<sub>2</sub>O<sub>3</sub> (4-17, 4 wt.%), sintering 0-81009  
 SiO<sub>2</sub>-Al<sub>2</sub>O<sub>3</sub>-Y<sub>2</sub>O<sub>3</sub>-La<sub>2</sub>O<sub>3</sub>-TiO<sub>2</sub> glasses with high elastic moduli, alkaline durability 0-85071  
 SmO<sub>2</sub>Y<sub>2</sub>Fe<sub>3</sub>Ga<sub>12</sub>O<sub>12</sub> epitaxial films, uniaxial mag. anisotropy, ferrimag. reson. study 0-80577  
 Sm<sub>0.75</sub>Y<sub>0.25</sub>S, mixed-valence, electron-lattice correlations, EXAFS studies 0-76103  
 Sm<sub>1-x</sub>Y<sub>x</sub>S, magnetoresist. in semicond. and metallic phases 0-96914  
 Sm<sub>1-x</sub>Y<sub>x</sub>S, mixed valence system, electron-phonon coupling, theory 0-70343  
 Sm<sub>1-x</sub>Y<sub>x</sub>S, mixed valence, phonon softening and linewidths, calc. 0-75319  
 Tb<sub>0.26</sub>Y<sub>0.74</sub>Fe<sub>2</sub>O<sub>7</sub>, garnet, mag. transition, mag. props. anomaly 0-93120  
 ThO<sub>2</sub>-YO<sub>3</sub>, solid solns., defective oxides, ionic cond. 0-107548  
 (U,Y)C, U self-diffusion 0-92711  
 U-Y-C FBR nuclear fuels, phase anal., 1400°C 0-66485  
 (Y,Sm,Ca)<sub>3</sub>(Fe,Ge)<sub>5</sub>O<sub>12</sub> epitaxial films, mag. props., growth condition effects 0-97124  
 Y-Si-Al-O-N ceramic, phase assemblages, relationships with props. 0-60848  
 Y-Sm ferrogarnet (*Russian*) 0-71140  
 YAG, as substrate for Er<sub>3</sub>Al<sub>3</sub>Ga<sub>3</sub>O<sub>12</sub> LPE film for solid laser 0-93419  
 YAG crystals, dislocations and inclusions, birefringence topography obs. 0-107248  
 YAG, electrostatic model of cryst. field 0-59945  
 YAG, melting behaviour and metastability determ. by optical DTA 0-92648  
 YAG, optical absorption of hole centres, polaron model 0-97314  
 YAG, simulated mol. images, point models and kinematical struct. amplitudes 0-103223  
 YAG:Cr, optical detection of phonons 0-92630  
 YAG:Er, elastic wave damping, 300 to 1500 MHz, impurity effects 0-92602  
 YAG:Ho<sup>3+</sup>, spectroscopy, stimulated emission 0-93374  
 YAG:Ho<sup>3+</sup>, stimulated emission at low temps. 0-106526  
 YAG:Nd crystal, orientation influence on thermally induced birefringence (*Chinese*) 0-88958

## yttrium compounds continued

- YAG:Nd<sup>3+</sup>, radiationless decay processes, laser photoacoustic spectroscopy meas. 0-84766  
 YAl<sub>3</sub>(BO<sub>3</sub>)<sub>4</sub> solubility in K<sub>2</sub>Mo<sub>3</sub>O<sub>10</sub> melt 0-65211  
 Y<sub>3</sub>(AlO<sub>3</sub>Ga<sub>0.5</sub>O<sub>12</sub>)<sub>2</sub>Nd<sup>3+</sup>, radiationless decay processes, laser photoacoustic spectroscopy meas. 0-84766  
 YAlO<sub>3</sub>, melting behaviour and metastability determ. by optical DTA 0-92648  
 YAlO<sub>3</sub>:Ce, fast decay UV phosphor 0-71471  
 YAlO<sub>3</sub>:Ho<sup>3+</sup>, stimulated emission at low temps. 0-106526  
 Y<sub>3</sub>Al<sub>2</sub>O<sub>12</sub> crystal growth from melt, gas bubble capture theory 0-64941  
 YBiTe<sub>3</sub>, prep., elec. props., and crystallographic data 0-59981  
 Y<sub>2</sub>(CO<sub>3</sub>)<sub>3</sub>·nH<sub>2</sub>O, tengerite, single cryst. hydrothermal growth 0-97417  
 YC<sub>4</sub> (n=2, 3, 4, 5, 6), atomisation energies, Knudsen cell mass spectrometric obs. 0-58409  
 YCo<sub>2</sub>Si<sub>2</sub>, mag. props. 0-107988  
 YCrO<sub>3</sub>, bubble domain struct. temp. depend. 0-71137  
 YCrO<sub>3</sub>-W(Mo)(Cr) eutectics, prep. and microstruct. 0-108380  
 YCu<sub>2</sub>Mn<sub>2</sub>O<sub>12</sub>, synthesis and mag. props. 0-75717  
 YD<sub>96</sub>, cryst. struct. by neutron diff. 0-70179  
 (YErCa)<sub>3</sub>(FeGeSi)<sub>2</sub>O<sub>12</sub>, mag. loss and domain wall mobility 0-65980  
 (YEuCa)<sub>3</sub>(FeGeSi)<sub>2</sub>O<sub>12</sub>, mag. loss and domain wall mobility 0-65980  
 (YEuTm)<sub>3</sub>(GaFe)<sub>2</sub>O<sub>12</sub> ferrite garnet films, mag. bubbles, translational motion, mechanism for inertial effects 0-100606  
 Y<sub>2</sub>F<sub>2</sub>O<sub>12</sub>, amorphous, magnetic props. (*French*) 0-80490  
 YFe<sub>2</sub>-Al<sub>2</sub>O<sub>12</sub>, impurity redistrib. kinetics, temp. depend., vacancy effects 0-75263  
 Y<sub>3</sub>Fe<sub>2</sub>-xAl<sub>2</sub>O<sub>12</sub>, permeability spectra rel. to microstruct. 0-71100  
 Y<sub>3</sub>Fe<sub>2</sub>-xAl<sub>2</sub>O<sub>12</sub>, mixed garnet, cation distrib., temp. depend., magnetisation study 0-79831  
 Y<sub>3</sub>Fe<sub>2</sub>-xCo<sub>2</sub>/ySi<sub>2</sub>O<sub>12</sub>, spin reorientation, NMR and ferromag. reson. meas. 0-65890  
 YFe<sub>4</sub>Ga<sub>0.5</sub>O<sub>12</sub> domains, neutron polarisation and Faraday rotation study 0-93137  
 YFe<sub>2</sub>-Ga<sub>2</sub>O<sub>12</sub>, impurity redistrib. kinetics, temp. depend., vacancy effects 0-75263  
 Y<sub>3</sub>Fe<sub>4</sub>Ga<sub>0.5</sub>O<sub>12</sub>, domain struct., neutron depolarisation and Faraday rot. 0-71084  
 Y<sub>3</sub>Fe<sub>2</sub>-xGa<sub>2</sub>O<sub>12</sub>, mag. domains and cryst. defects 0-75789  
 Y<sub>3</sub>Fe<sub>2</sub>-xGa<sub>2</sub>O<sub>12</sub>, mixed garnet, cation distrib., temp. depend., magnetisation study 0-79831  
 Y<sub>3</sub>Fe<sub>2</sub>-xGd<sub>2</sub>O<sub>12</sub>, permeability spectra rel. to microstruct. 0-71100  
 YFeO<sub>3</sub>, domain boundary inertia during mag. reversals (*Russian*) 0-88776  
 YFeO<sub>3</sub>, floating zone method growth, interface shapes 0-60775  
 YFeO<sub>3</sub>, mag. anisotropy in cryst. field approx. 0-60241  
 YFeO<sub>3</sub>, orthoferrite, crit. domain wall vel. 0-71135  
 YFeO<sub>3</sub>, Raman scatt. from magnons, anisotropy consts. determ. 0-66178  
 Y<sub>2</sub>Fe<sub>2</sub>O<sub>12</sub> LPE growth on Gd<sub>2</sub>Ga<sub>2</sub>O<sub>12</sub> substrates, substrate orientation effect 0-66438  
 YGaG, magnetoelastic wave propagation time dispersion reduction 0-75836  
 Y<sub>3</sub>Ga<sub>2</sub>O<sub>12</sub>:Nd<sup>3+</sup>, radiationless decay processes, laser photoacoustic spectroscopy meas. 0-84766  
 Y<sub>2.55</sub>Gd<sub>0.45</sub>GaFe<sub>2</sub>O<sub>12</sub>, garnet thin films, magnetisation orientation, temp. depend. 0-71125  
 YGdIG, with various domain wall orientations, natural spin reson. 0-66040  
 Y<sub>2</sub>GdIG film, amorphous, mag. bubbles obs. and structural transformation 0-75824  
 YGdTmFe<sub>3</sub>Ga<sub>0.7</sub>O<sub>12</sub> epitaxial films, bubble-domain lattices with specified parameters 0-60386  
 (YGdTm)<sub>3</sub>(FeGa)<sub>2</sub>O<sub>12</sub> epitaxial film, formation of lattice of cylindrical mag. domains from stripe domains (*Russian*) 0-80579  
 (YGdYbBi)<sub>3</sub>(FeAl)<sub>2</sub>O<sub>12</sub> ferrite-garnet films, effect of in-plane field on dynamics of domain walls 0-65979  
 (YGdYbBi)<sub>3</sub>(FeAl)<sub>2</sub>O<sub>12</sub> epitaxial garnet film, uniaxial ferromagnet domain struct., phase transition (*Russian*) 0-108044  
 YH<sub>98</sub>, cryst. struct. by neutron diff. 0-70179  
 YH<sub>3</sub>, location of H, PMR rigid-lattice second moment meas. 0-71198  
 YH<sub>2</sub>Er, proton distrib. and site energies, ESR meas. 0-59509  
 YH<sub>2</sub>Ir II<sup>+</sup> system, Fourier spectrometry, rovibrational anal. 0-83360  
 YIG, Bi-substituted, LPE, domain wall reson. 0-60387  
 YIG, Bloch line mass and mobility in a domain boundary (*Russian*) 0-93138  
 YIG, Brillouin-Mandelstam scattering from thermal and excited magnons 0-70980  
 YIG crystals, bulk growth from high temp. solns., props. 0-66413  
 YIG, cylindrical mag. domains, translational motion 0-108043  
 YIG, domain wall mobility and mass meas. method (*Russian*) 0-108033  
 YIG, electron and γ-irrad., photomagnetic effect 0-103877  
 YIG, electrostatic model of cryst. field 0-59945  
 YIG, Faraday effect, influence of mag. field on sublattice contributions 0-88975  
 YIG film, magnetostatic surface wave propag. in nonuniform mag. field 0-80574  
 YIG film, periodically corrugated, insertion loss, reson. linewidth effect 0-80614  
 YIG, floating zone method growth, interface shapes 0-60775  
 YIG, MW dielectric losses, causes and reduction (*Chinese*) 0-75930  
 YIG, magnetic domain wall motion in high drive fields 0-65955  
 YIG, magneto-optical Kerr effect, reflectivity spectra 0-66157  
 YIG, magnetoelastic wave propagation time dispersion reduction 0-75836  
 YIG, multiple mag. layer structures, magnetostatic surface wave propag. 0-88839  
 YIG, Neel point behaviour in stoichiometry vicinity 0-88750  
 YIG, nonreciprocal attenuation of magnetoelastic Rayleigh waves 0-60399  
 YIG, one-magnon Raman scatt., Faraday rot. 0-66156  
 YIG, open die hot pressing, spin wave and FMR line width 0-89170  
 YIG, permeability, domain rot. and wall displacement contrib. 0-80564  
 YIG, permeability spectra rel. to microstruct. 0-71100  
 YIG, polycryst., initial and reversible parallel suceptibilities, hydrostatic press. effects 0-75835  
 YIG sandwiched between grounded dielectric layers, magnetostatic bulk wave propagation 0-60380  
 YIG single crystals, liq. flux growth, obs. 0-66416  
 YIG, sound vel., temp. depend., phonon scatt. processes 0-96598  
 YIG, spin wave parametric excitation threshold at low temp. 0-97084  
 YIG, substituted, magnetite nucleation in transitional zone, ionic process, lattice imaging 0-107424

## yttrium compounds continued

- YIG, thermomag. anal. by electron diff. 0-108035  
 YIG, thin film, Brillouin scattering from spin waves 0-65843  
 YIG thin film gyromag. waveguide, on GGG substrate, optical propag. props. Faraday effect 0-74513  
 YIG, thin films, magnetostatic modes at Q-band freq. 0-65828  
 YIG, vitreous electric-field-gradient distrib., Mossbauer quadrupole splitting meas. 0-75901  
 YIG:Si single crystals, mag. props. 0-107981  
 YIG-Ca, oxidising effects of high temp. annealing in reducing atmosphere 0-66696  
 YIG-Co film, influence of stress induced anisotropy on domain struct. 0-100605  
 YIG:Ga(Se), magneto-optical Kerr effect, reflectivity spectra 0-66157  
 YIG:La,Ga, film, LPE-grown, Ga incorporation, depend. of magnetisation on growth rate 0-84627  
 YIG:La(Ga) films, ferromagnetic resonance, ion implantation effect 0-97145  
 YIG:Ru, optical absorpt. and MCD obs. of Ru<sup>4+</sup> site occupancy 0-71456  
 YIG:Si single crystals, liq. flux growth, obs. 0-66416  
 YIG:Si(Ge), effects of nonrigid crystal. field on spectroscopic props. of Fe<sup>3+</sup> ions 0-92864  
 YIG:Sm<sup>3+</sup>, mag. anisotropy, effect of Sm<sup>3+</sup> ferromag. reson. study 0-80615  
 YIG:Tb garnet, Faraday effect in strong mag. field (*Russian*) 0-100651  
 YIG:Zr, near IR absorpt. and magnetic circular dichroism 0-60580  
 Y<sub>2.85</sub>La<sub>0.15</sub>Fe<sub>3.75</sub>Ga<sub>1.25</sub>O<sub>12</sub> LPE films, ion implantation effect on spin waves 0-71124  
 Y<sub>2.85</sub>La<sub>0.15</sub>Fe<sub>3.85</sub>Ga<sub>1.15</sub>O<sub>12</sub> garnet, mag. props., ion implantation effect, Mossbauer study 0-97166  
 Y<sub>3</sub>-La<sub>2</sub>Fe<sub>2</sub>O<sub>12</sub>, mag. props. rel. to ionic struct. 0-75756  
 (YLuSmCa)<sub>3</sub>(FeGe)<sub>2</sub>O<sub>12</sub> garnet film, bubble domain expansion, fuzzy wall struct. 0-71128  
 (YLuSmCa)<sub>3</sub>(GeFe)<sub>2</sub>O<sub>12</sub> garnet films, bubble expansion saturation vel., sampling optical photography 0-75820  
 Y<sub>2</sub>Mo<sub>2</sub>O<sub>7</sub>, pyrochlore compounds, sp. heat meas. 0-107438  
 Y<sub>2</sub>O<sub>3</sub> and double oxides, photon multiplication and secondary electron-hole pairs generation (*Russian*) 0-66262  
 Y<sub>2</sub>O<sub>3</sub> capillary discharge plasma, temp., radiation screening elimination 0-64682  
 Y<sub>2</sub>O<sub>3</sub> ceramics, strength under mech. and thermal actions 0-97554  
 Y<sub>2</sub>O<sub>3</sub> coated Ag mirror for the 0.5 to 14 μm region 0-87456  
 Y<sub>2</sub>O<sub>3</sub>, crucible material, Cu-Nb alloy prep. 0-84879  
 Y<sub>2</sub>O<sub>3</sub>, dislocation and plasticity dissociation 0-107247  
 Y<sub>2</sub>O<sub>3</sub>, electronic excitations, charact. energy loss meas. up to 50 eV 0-60723  
 Y<sub>2</sub>O<sub>3</sub>, in MIM struct., electroforming props. 0-65705  
 Y<sub>2</sub>O<sub>3</sub>, interband, collective and atomic (p,d) excitations, Z-160 eV, fast EELS 0-93443  
 Y<sub>2</sub>O<sub>3</sub>, liq. and solid phase elec. cond., high temp. meas. 0-84468  
 Y<sub>2</sub>O<sub>3</sub>, nonstoichiometry study, thermal emission of electrons 0-108317  
 Y<sub>2</sub>O<sub>3</sub> sintered-ceramic separator plate development, LiAl/LiCl-KCl/FeS battery applications 0-61321  
 Y<sub>2</sub>O<sub>3</sub> sintering activator, effect on α-Al<sub>2</sub>O<sub>3</sub> mineralisation, alumina heat treatment 0-89186  
 Y<sub>2</sub>O<sub>3</sub>, strength-controlling fracture energy depend. on flaw-size to grain-size ratio 0-81152  
 Y<sub>2</sub>O<sub>3</sub>:Eu, cathodoluminesc. investig., appl. to cathode ray tube screening 0-108282  
 Y<sub>2</sub>O<sub>3</sub>:Nd<sup>3+</sup>, absorpt. spectra, hypersensitivity of <sup>4</sup>I<sub>9/2</sub> to <sup>4</sup>G<sub>5/2</sub> <sup>2</sup>G<sub>7/2</sub> transition 0-97309  
 Y<sub>2</sub>O<sub>3</sub>:Zr<sup>3+</sup>, F-centre charge state, ESR and thermally stimulated luminesc. obs. 0-60418  
 Y<sub>2</sub>O<sub>3</sub>-AlN-SiO<sub>2</sub> oxy-nitride glasses, elec. props. 0-80267  
 Y<sub>2</sub>O<sub>3</sub>-P<sub>2</sub>O<sub>5</sub>-M<sub>2</sub>O(M'O), (M=alkali metal, M'=alkaline earth), metaphosphate glass phosphors, fluoresc. props., activation conc. effect 0-89058  
 Y<sub>2</sub>O<sub>3</sub>(Nd) single crystal growth, floating zone method with Xe arc lamp imaging furnace 0-60777  
 Y(OH)<sub>3</sub>, dynamical effects of interaction between 4f electrons and optical phonons 0-108196  
 Y(OH)CO<sub>3</sub>, anclite like phase, hydrothermal cryst. growth (*French*) 0-108340  
 Y<sub>2</sub>O<sub>3</sub>:S:Eu, high press. effect on luminesc. efficiency and lifetime, charge transfer absorpt. 0-66266  
 YPO<sub>4</sub>:Gd<sup>3+</sup>, zircon struct. EPR investig., rel. to radiation resistance 0-97138  
 YPO<sub>4</sub>:Pb<sup>3+</sup>, EPR, hyperfine interactions 0-108050  
 (YRb)<sub>3</sub>(FeAl)<sub>2</sub>O<sub>12</sub> films, R=Gd, Yb, Faraday effect in transverse mag. field, orientation depend. 0-88971  
 YRh, gaseous, dissociation energies, high temp. mass spectrometric determ. 0-93790  
 Y<sub>2</sub>Ru<sub>2</sub>, Mn<sub>2</sub>C<sub>2</sub>-type struct., X-ray cryst. struct. determ. 0-96483  
 Y<sub>2</sub>Ru<sub>2</sub>O<sub>7</sub>, pyrochlore compounds, sp. heat meas. 0-107438  
 YS, band struct. and X-ray emission spectra, APW and Xα calc. 0-70605  
 YSeF, orthorhombic polytype 140, struct. study (*French*) 0-88102  
 Y<sub>2</sub>SiO<sub>5</sub>:Ce<sup>3+</sup>(Nd<sup>3+</sup>)(Er<sup>3+</sup>)(Yb<sup>3+</sup>), EPR and spin-lattice relax. 0-108063  
 Y<sub>1-x</sub>Sm<sub>x</sub>Fe<sub>0.5</sub>Fe<sub>0.5</sub> film, ion implanted, Mossbauer conversion spectra study 0-80663  
 (YSmLuCa)<sub>3</sub>(FeGe)<sub>2</sub>O<sub>12</sub>, mag. loss and domain wall mobility 0-65980  
 (YSmLuCa)<sub>3</sub>(FeGe)<sub>2</sub>O<sub>12</sub> epitaxial films, LPE grown, annealing effects on mag. anisotropy 0-66348  
 Y<sub>2</sub>Sn<sub>2</sub>Mo<sub>2</sub>S<sub>8</sub>, supercond. props. 0-97023  
 Y<sub>1.5</sub>Tb<sub>0.5</sub>Al<sub>0.65</sub>Fe<sub>4.35</sub>O<sub>12</sub> garnet thin films, magnetisation orientation, temp. depend. 0-71125  
 Y<sub>2</sub>Ti<sub>2</sub>O<sub>7</sub>, ferroelec., layer type struct., cryst. growth 0-108348  
 Y<sub>2</sub>gTm<sub>0.2</sub>Se, sp. ht. meas., 1.6 to 20K, mag. contrib. 0-65934  
 Y<sub>2</sub>UO<sub>12</sub>, energy transfer, cryst. struct. and chemical composition effect 0-108248  
 YVO<sub>4</sub>:Eu, cathodoluminesc. investig., appl. to cathode ray tube screening 0-108282  
 YVO<sub>4</sub>:Nd<sup>3+</sup>, energy transfer processes, laser-excited time-resolved spectroscopy 0-84765  
 YVO<sub>4</sub>:Nd<sup>3+</sup>, radiationless decay processes, laser photoacoustic spectroscopy meas. 0-84766  
 YVO<sub>4</sub>:Nd<sup>3+</sup>, zircon struct., cryst. field analysis 0-80232  
 Y<sub>1-x-y</sub>Yb<sub>x</sub>Er<sub>y</sub>OCl, Er ion excited state decay and population (*Russian*) 0-100694



**yttrium compounds continued**

- ZrO<sub>2</sub>-Y<sub>2</sub>O<sub>3</sub>, stabilised microspheres, structure, mechanical props. (*Russian*) 0-100379  
 ZrO<sub>2</sub>-Y<sub>2</sub>O<sub>3</sub> ceramic with graining structure, props., effect of heating to 2000°C 0-104194  
 ZrO<sub>2</sub>-YO<sub>1.5</sub>, solid solns., defective oxides, ionic cond. 0-107548  
 ZrO<sub>2</sub>-YO<sub>1.5</sub>-TaO<sub>2.5</sub>, cubic fluorite phase, elec. cond. 0-107551  
 ZrO<sub>2</sub> (0.9(Y<sub>2</sub>O<sub>3</sub>)<sub>0.1</sub>:Cr, Mn, stabilised single crystal, EPR of Mn<sup>2+</sup> and Cr<sup>3+</sup> obs. 0-66024

**Yukawa potential** *see meson field theory; nuclear forces***Z-centres**

- alkali halides, irradiated, formation of Z centre 0-103326  
 alkali halides, Z<sub>1</sub>-centres, peculiarities of thermolum. 0-103999  
 KCl, Z<sub>2</sub> centres in triplet state, EPR study 0-108068  
 KCl:Ca<sup>2+</sup>, Z-centre thermolum. 0-80879  
 KCl:Ca(Yb), Z<sub>2</sub> and Z<sub>2</sub><sup>+</sup> centres, excited state, magneto-optical spectra 0-108233  
 KCl:Sr crystal, Z<sub>4</sub> colour centre, luminesc. study 0-64993  
 LiF, thermolum., trapping mechanism based on Z-centres 0-76089  
 LiF:Mg, dependence of optical absorpt. on temp. during X-ray irradi. 0-66237  
 LiF:Mg, X-irrad. induced sensitisation mechanism, optical absorpt. spectra 0-60637  
 LiF:Mg, Z<sub>2</sub><sup>+</sup> and associated Z-centres, elec. cond., ionic thermocurrent, and optical absorpt. meas. 0-107229  
 RbCl:Ca<sup>2+</sup>, thermolum. and optical absorption studies 0-104002

**Z pinch** *see pinch effect***Z transforms**

- TeO<sub>2</sub>, time-integrating acousto-optical correlator for chirp spectrum analyses 0-106474

**Zeeman effect**

- see also atomic spectra; Hanle effect; spectral line breadth*  
 application to atomic absorption spectroscopy 0-76567  
 atom+atom collisional intense-field fluoresc., Zeeman degeneracy effects 0-99477  
 atomic absorption analysis, Zeeman effect appls. 0-85245  
 backward Raman amplifier for excimer laser pulse compression, parasitic superfluoresc. suppression 0-69453  
 caesium perfluoro-octanoate/D<sub>2</sub>O system, <sup>2</sup>H NMR quantum orders, RF pulses 0-103892  
 diatomic molecules, laser-induced predissoc., surface mag. field effect 0-106365  
 1,8-dichlorooctane, quadrupolar relax. centres, limited spin diffusion 0-100649  
 energy interval measurement by obs. Zeeman transition in microwave spectra 0-69274  
 free-base porphyrin, Zeeman shift meas. by photochem. hole-burning 0-83416  
 gas superluminescence in high-current discharge, polarisation due to Zeeman splitting 0-100060  
 glyoxal, singlet-triplet radiationless processes in mag. field 0-106347  
 AM Herculis (3U 1809+50), polarimetry and spectrophotometry rel. to mag. field 0-94835  
 interdoublet EPR spectrum ang. depend. for ions with arbitrary electron and nuclear spins in strong axial cryst. field 0-93164  
 isothiazole, rot. Zeeman effect, localised susceptibilities 0-91600  
 line profile, mag. field determ., appl. of radiative transfer problem soln. 0-82221  
 methane, rotational state, avoided-crossing molecular beam spectroscopy 0-63730  
 methyl-d groups, reorienting or tunnelling spin-lattice relax. 0-97156  
 monochloroacetic acid single crystal, Zeeman and <sup>35</sup>Cl NQR investig. 0-66066  
 NQR, electronics appls. 0-63668  
 paramagnetic system with quadrupole splitting, magneto-optical effects, magnetic resonance saturation 0-60404  
 relativistic correction to the linear Zeeman effect in a Coulomb field 0-102484  
 Rydberg spectra, Landau standing wave form. 0-102466  
 spectrophotometer, Zeeman effect appl., development of spectral-line sources 0-76583  
 tetramethyl pyrazine in durene, phosphorescent mols., quantum beats in triplet states 0-58312  
 tetramethylgermanium, Zeeman spin-lattice relaxation rate maxima 0-84666  
 thiazole, rot. Zeeman effect, localised susceptibilities 0-91600  
 trinuclear exchange clusters, Dzyaloshinsky coupling effects in Mossbauer spectra (*Russian*) 0-108142  
 two step reson. photoionisation, multimode and level degeneracy effects 0-78583  
 xanthione, large zero-field splitting of lowest triplet state 0-58171  
 Zeeman atomic absorpt. spectroscopy, absorpt. max. in analytical curves 0-86442  
 AgBr, photoluminesc. study of excitons in high mag. fields 0-80843  
 Al particles, small supercond. nuclear spin-lattice relax. meas. 0-88681  
 As I, level identification and Zeeman effect obs. 0-95571  
 C II, Zeeman splitting of high-n recomb. lines 0-58210  
 CdBr<sub>2</sub>:Co<sup>2+</sup>, exchange-coupled Co<sup>2+</sup> pairs, optical absorpt. and Zeeman studies 0-66242  
 CdS:Ni<sup>2+</sup>, Zeeman effect at Ni impurities 0-60633  
 CdTe, exciton magnetoreflectance spectra, multicomponent polaritons, Zeeman splitting 0-88974  
 Cs<sub>2</sub>TiF<sub>6</sub>:Mn<sup>2+</sup>, spin-orbit and field splitting, Jahn-Teller effect, Zeeman meas. 0-80234  
 Cu complex, Cu(H<sub>2</sub>O)<sub>6</sub><sup>2+</sup>, ligand hyperfine interactions, orbital angular momentum contrib. 0-96833  
 Dy<sub>2</sub>O<sub>3</sub>SO<sub>4</sub>, mag. ordering, magnetisation, AC susceptibility and Zeeman effect meas. 0-60205  
 GaAs, conduction band effective mass, influence of high uniaxial stress 0-80162  
 GaAs:Cr, semi-insulating, Zeeman studies of 0.839 eV emission 0-103987  
 GaP:Co, optical spectra and Zeeman anal. of Co 3d<sup>7</sup> state 0-66247  
 Ge, impurity spectral linewidth meas., free electron effects 0-71463  
 Ge:Sb, excited donor states, double optical transitions, reson. absorpt. meas. 0-93371  
 H II, Zeeman splitting of high-n recomb. lines 0-58210  
 H<sub>2</sub>, Bender-Wu formula, SO(4,2) dynamical group and Zeeman effect, perturbation coeffs. determ. 0-95674

**Zeeman effect continued**

- H<sub>2</sub> and H<sub>3</sub> spectral profiles from neutral beams and plasmas in high mag. fields 0-83999  
 He II, Zeeman splitting of high-n recomb. lines 0-58210  
 He-Xe 3.51 μ laser mode competition in axial mag. field 0-63974  
 Hg, two photon excitation, time resolved spectroscopy 0-87075  
 Ho<sub>2</sub>O<sub>3</sub>SO<sub>4</sub>, mag. ordering, magnetisation, AC susceptibility and Zeeman effect meas. 0-60205  
 K+He, 4<sup>2</sup>P state j<sub>1</sub>m<sub>1</sub>-j<sub>2</sub>m<sub>2</sub> Zeeman transition, total cross section energy depend. 0-83475  
 LaF<sub>3</sub>:Er<sup>3+</sup>, optically excited, direct-process spin-lattice relaxation 0-93378  
 LaF<sub>3</sub>:Pr<sup>3+</sup>, ultraslow optical dephasing 0-58648  
 LaF<sub>3</sub>:Pr<sup>3+</sup>, ultraslow opt. dephasing at 2K 0-91864  
 NH<sub>2</sub>, ν<sub>2</sub> band, laser mag. reson. 0-83523  
 NO, Zeeman modulation spectroscopy, line shape analysis 0-74197  
 NO, Zeeman spectrum, mol. beam elec. reson. spectrosc. 0-91621  
 Na, <sup>3</sup>S<sub>1/2</sub>-<sup>3</sup>P<sub>3/2</sub>, spectral distrib. and collisional depolarisation of laser light, D<sub>2</sub>-fluorescence 0-58209  
 Na vapour, laser induced population grating 0-69466  
 Na vapour, Zeeman coherence, transient and stationary, polarisation spectroscopy 0-58212  
 Na<sub>2</sub>Pr(C<sub>6</sub>H<sub>5</sub>O<sub>2</sub>)<sub>3</sub>.2NaClO<sub>4</sub>.6H<sub>2</sub>O, absorpt., circular dichroism, and mag. circular dichroism spectra 0-97243  
 O 2.53 mm line, Zeeman splitting rel. to geomagnetic field vars. 0-77124  
 OH, isotope effects, Zeeman effect, far IR laser mag-reson. spectra obs. 0-63674  
 ONF, J transitions, rot. Zeeman effect 0-63707  
 Pb traces in human blood plasma, atomic absorpt. anal., nonspecific absorpt. correction using Zeeman effect 0-76881  
 Pt porphyrin in n-alkane single cryst. <sup>2</sup>E<sub>g</sub>-<sup>1</sup>A<sub>1g</sub> transition, Zeeman expts. at 4.2K 0-78645  
 Si:Al, localised exciton bound to isoelectronic trap 0-66283  
 Si:Au, EPR spectrum, strong nucl. quadrupole effect 0-93172  
 Si:K, bound exciton luminescence in mag. field (*Russian*) 0-108278  
 Si:Li, photolum. of bound exciton and bound multiexciton complex, Zeeman effect 0-108265  
 Sml, Zeeman coherence, transient and stationary, polarisation spectroscopy 0-58212  
 SnCl<sub>2</sub>.1.5H<sub>2</sub>O single cryst., <sup>35</sup>Cl NQR, cryst. struct. 0-60449  
 UFe<sub>2</sub>B<sub>2</sub>(B<sub>2</sub>), Mossbauer effect of <sup>57</sup>Fe nuclei, mag. props. 0-103907  
 Xe I three-level system, level splitting within natural width, saturation spectrum 0-106291  
 YIG:Si(Ge), effects of nonrigonal cryst. field on spectroscopic props. of Fe<sup>2+</sup> ions 0-92864  
 ZnO:Ni<sup>2+</sup>, Zeeman effect at Ni impurities 0-60633  
 ZnS:Ni<sup>2+</sup>, Zeeman effect at Ni impurities 0-60633  
 ZnTe:Li, Zeeman splitting of ground and excited acceptor states, selective pair luminesc. 0-84780
- Zener breakdown** *see Zener effect*
- Zener diodes**  
 No entries
- Zener effect**  
*see also Zener diodes*  
 Ga<sub>0.47</sub>In<sub>0.53</sub>As p-n junctions, band-to-band tunnelling current 0-107895  
 InGaAsP avalanche photodiodes, breakdown mechanism, donor conc. effect 0-70710
- Zener relaxation**  
 Pd-Ag-H(D), elastic energy dissipation peak 0-60905  
 Pd-H system, α and α+β phases, annealed and deformed, anelastic effects 0-66567  
 Pd-H(D), elastic energy dissipation peak 0-60905  
 Pd-Pt-H(D), elastic energy dissipation peak 0-60905
- zero gravity experiments**  
 acoustic levitation and manipulation method for controlling liquid samples 0-74666  
 biosatellite Cosmos-782, biological expts. 0-61710  
 blood viscosity and red cell aggregation at zero and 1G, instrumentation for Space Lab 3 0-61716  
 body fluid volume changes induced by spaceflight 0-61715  
 exercise response to simulated weightlessness 0-61713  
 floating zone, under reduced gravity, Marangoni convection 0-66425  
 human, haematological response, math. and expl. simulation 0-61714  
 liquid metal thermal conductivity meas. in Spacelab (*German*) 0-57303  
 low gravity solidification expts., use of metallic analogue materials 0-71635  
 lung, human, radiographic comparison of shape during normal gravity and weightlessness 0-67260  
 material charging in space environment 0-109327  
 optical glass, melting, fining, surface tension, diffusion, nucleation in microgravity 0-81016  
 sled programme, Spacelab, weightlessness expts. on man 0-94381  
 Al-Cu (33 wt.%) eutectic, solidification under reduced gravity, behaviour of suspended Al<sub>2</sub>O<sub>3</sub> particles (*German*) 0-60853  
 NH<sub>4</sub>Cl-H<sub>2</sub>O, solidification microstructs., effect of reduced gravity 0-96632  
 PbTe single crystals, growth from vapour phase under micro-gravity conditions 0-80957
- zero sound**  
*see also liquid helium sound propagation*  
 ferromagnet, excitonic, zero-sound excitations, Fermi liq. model 0-93101  
<sup>3</sup>He, liq. interface with nonmag. solid, Kapitza resist., quantum perturbation treatment 0-88385  
<sup>3</sup>He liquid, zero sound lifetime, neutron inelastic scatt. study 0-65329  
<sup>3</sup>He, liquid, zero sound with velocity less than Fermi velocity (*Russian*) 0-92747  
<sup>3</sup>He, normal liquid, elementary excitations, density and spin density, zero sound mode, press. depend. RPA model calcs. 0-59749  
<sup>3</sup>He, superfluid A-phase, spin relax. and zero sound attenuation at low temp. 0-107595  
<sup>3</sup>He, superfluid B-phase, HF sound propag. meas. 0-88391  
<sup>3</sup>He, superfluid B-phase, zero sound attenuation peak obs. 0-88390  
<sup>3</sup>He/solid interface, refl. of transverse zero sound (*Russian*) 0-70492
- zeros** *see poles and zeros*
- zeta-potential** *see electrokinetic effects*
- zinc**  
*see also nuclei with .....*  
 atom, <sup>1</sup>S, <sup>3</sup>P, <sup>1</sup>P states, dipole polarisabilities from compact variational trial functions 0-63568

## zinc continued

- atom +  $H^+$  ( $D^+$ ), K shell ionisation, nuclear Coulomb effect 0-91650  
 atomic vibrations, mean square displacements in cryst. lattice, rel. to sp. ht. (*German*) 0-79902  
 atoms, electron binding energy and shift, core level XPS 0-87088  
 basal screw dislocation, exptl. determ. of line energy 0-88154  
 black Zn-dust pigmented solar selective coatings for solar photothermal conversion 0-66997  
 core levels, cryst.-field splitting, X-ray emission study 0-66328  
 crack form. at grain and twin boundaries at low temp. (*Russian*) 0-66620  
 creep, low-temp., thermal heating and quantum mechanisms 0-79868  
 deforming stress and dislocation density depend. in slip system {112}(112) (*Russian*) 0-103353  
 diffusion in GaAs under open tube conditions 0-84326  
 dislocation structure, high press. effects, plastic deform. (*Russian*) 0-88159  
 dislocation velocity and plastic deform., single crystals. 0-64998  
 electrocrystallisation, reaction mechanism, appl. of impedance meas. (*French*) 0-103597  
 electrode, dispersed, for primary and secondary cells, electric vehicles appl. (*French*) 0-72023  
 electrode in alkaline soln., exam. of surface state by potentiodynamic voltammetry 0-85187  
 electrolytic deposition, on Pt single crystal spheres, critical overvoltage 0-104080  
 electron emission depend. on surface mechanical treatment (*Russian*) 0-100945  
 electron momentum distrib., neutron-induced defects, positron annihilation study, for single cryst. 0-71508  
 evaporation rate, effect of inert gas 0-84285  
 film, thickness meas., using nondestructive radioisotopic technique 0-68179  
 film deposition on Al, TEM and electron diffr. obs. 0-75460  
 fine powder, electrodeposition 0-60802  
 fracture stress of single crystals. 0-104269  
 galvanisation, hot, production components, installation and power supply (*French*) 0-66686  
 grain boundary nonactivated motion vel., orientation depend. (*Russian*) 0-84180  
 growth from melt, conditions influencing dislocation struct. (*Russian*) 0-97424  
 HCP lattice, Huang diffuse scatt. from interstitials 0-88142  
 internal friction anomalies in temp. initiated brittle-plastic transition (*Russian*) 0-96648  
 isoelectronic sequence, electron impact excitation of reson. transitions 0-63825  
 isoelectronic sequence, oscill. strength and MCHF wavefunctions, outer correl. 0-91505  
 K-shell X-ray prod. by  $^{14}N^+$  bombardment 0-91482  
 lattice Hg location and quadrupole interaction, gamma-spectral study 0-80227  
 liquid, thermal conductivity meas. in Spacelab, measuring cell design and testing (*German*) 0-57303  
 liquid, thermoelectric power, pseudopotential calc. 0-59959  
 liquid, viscosity determination by oscillating vessel method (*Japanese*) 0-70439  
 microcrack propagation and plastic strain 0-81187  
 microplastic deformation, basal dislocation generation, glide and locking, X-ray topography study 0-88156  
 nitrated, yield strength, influence of deform. rate (*Bulgarian*) 0-89315  
 N.Pacific, trace metal vertical profiles 0-67381  
 photoelectric cross sections at 52.4, 60, 72.2 and 84.4 keV 0-69187  
 plasma arc spraying, chem. reaction with plasma gases 0-66427  
 plating C steel nails, barrel plating efficiency 0-100964  
 proton-induced L-shell ionisation cross-sections 0-100707  
 recycling, effect on comp. 0-66455  
 residual electrical resistance of single crystals., contrib. of basal dislocations (*Russian*) 0-75539  
 resonant two hole bound state at 3p core threshold 0-60750  
 secondary batteries, props. of alternate electrolytes 0-104502  
 serum, human, trace elements determ. by proton activation 0-81731  
 solar photosphere abundance, discrepancy with meteorite abundance 0-72897  
 sputtered excited states, secondary photon emission, role of transition probability 0-102483  
 sputtering, binding energies 0-108312  
 steels, types SS41, SB42, SM50A, STK55, liq. Zn embrittlement (*Japanese*) 0-81164  
 superconducting film for energy selective phonon detection 0-92621  
 surface layer of Ge, heterodiffusion due to H atom surface recombination stimulation (*Russian*) 0-59726  
 surface oxidation, Auger spectrosc. obs. 0-97388  
 thermal expansion, temp. depend., vacancy effects 0-79962  
 twinning, influence of dislocation drag, mag. field effects 0-59472  
 wear under reversed friction, temp. effect 0-108588  
 Z dependence of thick target  $\beta$ -ray backscattering 0-76118  
 (Al,Ga)As:Zn planar stripe lasers with deep Zn diffusion, guiding mechanisms controlled by impurity concs. 0-78853  
 Al:Zn, ion implanted, electron beam annealing 0-59500  
 Al<sub>0.51</sub>Ga<sub>0.47</sub>As:Zn solar cells by LPE, open circuit voltage, fill factor 0-101108  
 BP:Zn, epitaxial layers, ion implantation, defects and lattice locations, channelling obs. 0-88179  
 Bi-Zn, light ion large angle scatt. in weakly screened Rutherford region 0-84823  
 Cu-Zn thin film couples, room temperature interactions 0-96699  
 GaAlAs/GaAs solar cells, Be and Zn behaviour 0-101111  
 Ga<sub>1-x</sub>Al<sub>x</sub>As:Zn, acceptor energy level and elec. props. 0-65482  
 GaAs:Zn, implanted, furnace annealed, electrical, Rutherford backscattering and TEM meas. 0-100272  
 GaAs:Zn, implanted, laser annealing, elect., Rutherford backscattering and SEM meas. 0-100273  
 GaAs:Zn, ion implanted, TEM study after laser and furnace annealing 0-70234  
 GaAs:Zn, sign inversion of the linear photogalvanic effect (*Russian*) 0-80321  
 GaAs:Zn optically pumped ribbon-whisker laser, picosecond pulses 0-99771  
 GaAs:Zn polycrystalline film, Hall effect, resistivity meas. 0-96911  
 GaN:Zn, n-i struct., anomalous luminesc. 0-80865

## zinc continued

- GaP:Zn, O, influence of impurity-absorbed illumination on luminesc. 0-93395  
 p-GaP:Zn:S, spin polarisation of donors and acceptors in mag. field, optical and microwave study 0-93393  
 pGaP:Zn-electrolyte interface, electrochemical LED, luminescence obs. 0-84507  
 Ge:Zn, Sb, photoelec. props., 70 to 300K 0-65621  
 p-Ge:Zn,Au,Sb, radiation-defect form., Au influence 0-92911  
 Ge:Zn photoresistor, current responsivity rel. to nonequilib. hole lifetime 0-60035  
 Ge:Zn<sup>11</sup>, G and D lines, stress induced components 0-71447  
 Ge:Zn<sup>11</sup> carrier lifetime, nonequilibrium, phase method for determ. 0-65629  
 He-Zn hollow cathode laser discharge, radiative cascade excitation effect on upper laser levels 0-102697  
 p-In<sub>0.51</sub>Ga<sub>0.47</sub>As:Zn on InP, elec. and optical props. 0-75662  
 In<sub>0.51</sub>Ga<sub>0.47</sub>As:Zn, lattice matching to InP, LPE growth conditions 0-70541  
 InP:Zn, avalanche photodiode characts., impurity diffusion effects 0-70709  
 InP:Zn, substitutional dopant and hole conc. meas. 0-75260  
 p-InP:Zn, ohmic contact formation on InP by laser photochemical doping 0-80369  
 InSb:Zn, impurity centre behaviour, impurity conc. and Hall coeff. meas. 0-65490  
 InSb:Zn, ion-irrad., p-n conversion during heat treatment 0-96558  
 KCl(Br)(I):Zn<sup>2+</sup>, optical absorpt. bands rel. to charge transfer 0-66245  
 K<sub>2</sub>MnF<sub>6</sub>:Zn, mag. effects of impurities 0-65869  
 K<sub>2</sub>MnF<sub>6</sub>:Zn(Mg)(Ni), local magnetisation, NMR and Green's function study 0-65870  
 Sb, optical phonon anharmonicity and melting, light scatt. study 0-60621  
 Si:Zn, impurity states, localised orbital approach 0-92851  
 Si:Zn, minority carrier lifetime investigation 0-80292  
 Zn electrodeposition, on Zn and Al single crystals., from H<sub>2</sub>SO<sub>4</sub> bath, SEM obs. (*Japanese*) 0-93502  
 Zn XX, energy levels and one electron transitions, relativistic calculations 0-87051  
 Zn<sup>2+</sup> ions, adsorpt. by doped MnO<sub>2</sub>, <sup>65</sup>Zn  $\gamma$ -ray scintillation investig. 0-70529  
 Zn:Al, ion implantation, temp. and time depend. 0-65013  
 Zn-like ions, 4s-4p reson. lines and transitions obs. by means of laser prod. plasma, appl. to Tokamaks 0-99468  
 Zn+He, Penning ionisation cross section of target atom, for He(2<sup>3</sup>S<sub>1</sub>) 0-63777  
 Zn+O<sub>2</sub>, matrix reactions, IR, Raman and visible spectra in Ar and N<sub>2</sub> matrices 0-87110  
 Zn<sub>4</sub> clusters, electronic structures, SCF-X $\alpha$ -SW method 0-88468  
<sup>62</sup>Zn/<sup>62</sup>Cu generator, source of <sup>62</sup>Cu for radiopharmaceuticals 0-67248  
<sup>68</sup>Zn, 2s-2p muonic X-ray transition obs. 0-74264  
<sup>68</sup>Zn muonic atom, dynamical E0 excitation, E0 resonances, muonic X-rays 0-95749

## zinc alloys

see also brass; zinc compounds

- Admiralty Metal, transgranular stress corrosion crack propag. 0-89402  
 Al-Zn-Mg (5.1 wt.%), decomp. process, TEM study 0-71660  
 Cu-Zn-Mn, de-alloying props. 0-104332  
 precipitate free zones, X-ray microanal. 0-108768  
 rare earth alloys, ferromag., parastriction and magnetoelastic coeffs. 0-65996  
 rolled and press. die-cast, creep and deformation behaviour (*German*) 0-66611  
 Ag-Zn, internally oxidized, elec. contact characts., alloying additions effect (*Japanese*) 0-88619  
 Ag-Zn, molten, EMF meas. of activities using ZnO<sub>2</sub> solid electrolytes (*Japanese*) 0-88339  
 Ag-Zn-Te-(Sn)-(In), internally oxidised, oxide particle size control (*Japanese*) 0-89480  
 AgZn, B2 intermediate phase, slip system, ordering energy and atomic size ratio depend. 0-59471  
 AgZn,  $\beta'$ - $\gamma$  transformation, effect of additional elements 0-66507  
 $\gamma$ -Ag<sub>2</sub>Zn<sub>3</sub>, high pressure effect on brass struct. 0-107108  
 Al-Ca-Zn (5.5 wt.%) superplastic sheet alloy, mechanical properties, superplastic forming behaviour 0-60920  
 Al-Mg-Zn alloys, Al-rich, weld metal comp. effect on microsegregation and eutectic phase segregation (*German*) 0-108455  
 Al-Mg-Zn alloys, evaporation effect of alloying elements Mg and Zn in in-situ EM studies 0-103388  
 Al-Mg-Zn-Cu, type 7050, calorimetric study of fatigue induced microstructural changes 0-85034  
 Al-Ni(Pt)(Zn), rapidly solidified, twinned dendrites 0-70572  
 Al-Zn, dil., magnetoresist., temp. depend. 0-70682  
 Al-Zn, grain boundary reaction sites, determ. of struct. aspects, by electron microscopy 0-103359  
 Al-Zn, rapid quenching, struct. and decomp. 0-76244  
 Al-Zn, spinodally decomposing, main wavelength of conc. fluctuations calc. 0-97459  
 Al-Zn, type 7075-T6, coldworked hole specimens, residual stresses, fracture mech. anal. 0-97587  
 Al-Zn, X-ray diffr. after omnidirectional compression (*Russian*) 0-88262  
 Al-Zn (10 wt.%), ageing at low temp., effects of fluctuation of solute conc. 0-76287  
 Al-Zn (10 wt.%), ageing at low temp., effects of fluctuation of solute conc. 0-76288  
 Al-Zn (38 at.%), alloy, TEM study of precipitation processes or different microstructures during ageing 0-93561  
 Al-Zn (6.8 wt.%), Guinier Preston zones internal struct., study by X-ray diffraction,  $\alpha_R$  phase comparison (*French*) 0-66472  
 Al-Zn (70, 30 wt.%), decomp. study, 25-160°C (*Czech*) 0-89225  
 Al-Zn (8-25 wt.%), solid solns., residual resist. during clustering 0-97483  
 Al-Zn alloys, interfacial stability of planar solid-liq. interface during solidification 0-104145  
 Al-Zn alloys, interfacial holes distrib. at beginning of interfacial instability in solidification 0-104146  
 Al-Zn thin film, prep. using Sn-Zn evaporant source 0-100789  
 Al-Zn-Mg, age-hardenable, precipitation and dissolution processes, positron annihilation and X-ray small-angle scattering comparison 0-89238  
 Al-Zn-Mg, atmosphere effect on fatigue crack propag. (*Japanese*) 0-81161  
 Al-Zn-Mg, crack-arrest markings on intergranular stress corrosion fracture surfaces 0-89405



## zinc alloys continued

- Al-Zn-Mg, long term strength and creep 0-60925  
 Al-Zn-Mg, oriented growth of precipitates on dislocations, model 0-108448  
 Al-Zn-Mg, TEM and calorimetric study 0-76290  
 Al-Zn-Mg, TEM character. of precipitates 0-104166  
 Al-Zn-Mg, type 7075-T651 plate, thickness direction inhomogeneity of mech. props. and fracture toughness 0-100892  
 Al-Zn-Mg, type V-95, ultimate tensile strength for brief impact 0-70309  
 Al-Zn-Mg (3.6, 1.95 wt.%), ageing and plastic deform. effect on structure, electron microsc. and X-ray diff. study (*Russian*) 0-81108  
 Al-Zn-Mg (3.87, 1.79 wt.%), oriented growth of precipitates on dislocations, TEM obs. 0-108447  
 Al-Zn-Mg (91, 6, 3, wt.%), H embrittlement and trapping, HVEM obs. 0-76364  
 Al-Zn-Mg alloy, Ag addition and pre-precipitation treatment, influence on GP zone growth 0-71658  
 Al-Zn-Mg alloy AA-7039, stress corrosion cracking, SEM obs. 0-104323  
 Al-Zn-Mg alloys, grain boundary segregation, implications to stress corrosion cracking 0-84936  
 Al-Zn-Mg granules and bands rolled from them, heat treatment 0-100862  
 Al-Zn-Mg superplastic alloy, cavity growth under creep conditions 0-60940  
 Al-Zn-Mg type 7N01-T4, weld, SCC in NaCl-H<sub>2</sub>O<sub>2</sub> soln. (*Japanese*) 0-108631  
 Al-Zn-Mg-Cu (6, 2.5, 1.5 wt.%), deform. simulation using torsional test, elastoplastic constitutive eqn. 0-93594  
 Al-Zn-Mg-Cu (6.2, xwt.%) type alloy, fatigue crack propag., Cu content and recryst. effect 0-60960  
 Al-Zn-Mg-Cu type 7075, heat treatment optimisation 0-60888  
 Al-Zn-Ti(Mn), mech. props., Ti or Mn addition effect (*Korean*) 0-93613  
 AlZn, disordered, residual resistivity due to clustering, ageing effects 0-65521  
 Au-Zn, molten, EMF meas. of activities using ZrO<sub>2</sub> solid electrolytes (*Japanese*) 0-88339  
 Au-Zn/p-Ga<sub>1-x</sub>In<sub>1-x</sub>/PyAs<sub>1-y</sub>, specific contact resist. 0-84509  
 Au<sub>50</sub>-Pd<sub>50</sub>Zn<sub>50</sub> (0 ≤ x ≤ 15.02) β'-phase, Hall effect and elec. cond. 0-107768  
 Au<sub>100-x</sub>Zn<sub>x</sub> (47 ≤ x ≤ 52), β'-phase, Hall effect and elec. cond. 0-107768  
 CdZn<sub>3</sub>, struct. with mixed BaLi<sub>2</sub> and CeCu<sub>2</sub>-like ordering 0-107106  
 Cd-Zn binary systems, melts, elec. resist., 0-700°C 0-65517  
 Cd-Zn eutectics, microstruct. after solidification, heat pipe influence 0-76243  
 Co-Ni-Zn, diagram of state, crystalline lattice constns., microhardness (*Russian*) 0-66479  
 Co-Zn, physical-chemical metallurgy (*German*) 0-108390  
 Co-Ni-Zn (18, 27 wt.%), surface comp., Auger electron spectroscopy study, manufacture and storage influence 0-65348  
 Cu-Ni-Zn alloy, surface comp., outdoor exposure influence 0-59770  
 Cu-Ni-Zn-Mn fine grained precipitation-hardenable alloy, high strength and ductility 0-100805  
 Cu-Sn alloy, surface comp., outdoor exposure influence 0-59770  
 Cu-Zn, de-alloying props. 0-104332  
 Cu-Zn, interface sliding of FCC and BCC boundaries 0-104240  
 Cu-Zn, solid soln., rheological study of crystallographic order on creep (*French*) 0-97548  
 Cu-Zn (30 wt.%), single crystals, quantitative anal. of stress relax., obstacle strength and athermal stress variation 0-89277  
 Cu-Zn (4 at.%), anneal hardening mechanism 0-60879  
 Cu-Zn alloy, α-phase, lattice sp. ht. calcs. 0-65246  
 Cu-Zn alloys, surface comp., outdoor exposure influence 0-59770  
 Cu-Zn-Al, β<sub>1</sub>' martensite crystal crossing rel. to reversible shape memory effect (*Japanese*) 0-108499  
 Cu-Zn-Al, reversible shape memory effect (*Japanese*) 0-108500  
 Cu-Zn-Al martensite, lattice dynamics, neutron scatt. meas. 0-88286  
 Cu-Zn-Mn, steady-state diffusion of Zn and Mn 0-70445  
 Cu, Zn<sub>1-x</sub>, sputtering, binding energies 0-108312  
 Cu<sub>2</sub>NiZn, comparison between different theories predicting stacking fault energy from extended nodes 0-75240  
 Cu<sub>2</sub>NiZn, stacking fault energy determ. from extended nodes 0-107280  
 β-CuZn, acoustic emission rel. to stress induced martensitic transformation 0-81061  
 CuZn, planar faults, faint electron microscopic image contrast obs. 0-107283  
 Cu<sub>2</sub>Zn clusters, electronic structures, SCF-Xα-SW method 0-88468  
 Cu<sub>66</sub>Zn<sub>34</sub>, amorphous metallic glass, differences caused by preparation technique (*French*) 0-103247  
 Fe-Zn, prep. and phase diagrams (*French*) 0-76231  
 Fe-Cu-Zn, high-temperature phase diagrams (*German*) 0-108390  
 Fe-Mn-Zn, high-temperature phase diagram (*German*) 0-108390  
 Fe-Si-Zn, influence of trace elements on morphology (*German*) 0-108390  
 Fe-Zn, coercive force anisotropy after cold plastic deform. (*Bulgarian*) 0-75809  
 Fe-Zn, galvanization study (*French*) 0-66447  
 Fe-Zn, homogeneous phases, Gibbs free energies of form., Knudsen effusion method 0-66481  
 Fe-Zn, physical-chemical metallurgy (*German*) 0-108390  
 Fe-Zn, quenched, martensite struct. and hardness, electron microscope exam. (*Russian*) 0-66619  
 Ga-Ge-Zn ternary alloys, thermodynamic props., EMF meas. 0-81033  
 Ga-Zn, eutectic system, diffusion coeff. depend. on composition (*Russian*) 0-59695  
 Gd<sub>2</sub>Nd<sub>1-x</sub>Zn, ferromag., mag. susceptibility and magnetisation, temp. depend. 0-70975  
 Gd<sub>2</sub>Y<sub>1-x</sub>Zn, ferromag., mag. susceptibility and magnetisation, temp. depend. 0-70975  
 Hg<sub>1-x</sub>Zn<sub>x</sub>Cr<sub>2</sub>Se<sub>4</sub>, magnetic struct., neutrographic and mag. investigation (*Russian*) 0-88726  
 In-Zn binary system, melts, elec. resist., 0-700°C 0-65517  
 Mg-Al-Zn (94.3, 3.9, 1.8 wt.%), precip. on dislocations, weak-beam TEM 0-76264  
 Mg-Al-Zn-Mn (8, 0.5, 0.3 wt.%) casting alloy, penetration resistance 0-100901  
 Mg-MgNi<sub>2</sub>-Zn, diagram of state, Zn solubility, initial phase precipitation (*Russian*) 0-66478  
 Mg-Nd-Zn dilute alloy, metallography and precip. kinetics 0-71655  
 Mg-Zn (5 wt.%), age hardening, X-ray diff. anal. (*Chinese*) 0-104173  
 Mg-Zn alloy, aged, one dimensional transition phase β<sub>2</sub>', crystallographic obs. (*Chinese*) 0-60865  
 MgZn<sub>2</sub>, two-layer, Friedel-Laves phases, stacking variants 0-96468

## zinc alloys continued

- Mn<sub>2</sub>ZnN, sp. ht., 6 to 350K, mag. and crystallographic phase transitions 0-71060  
 Nd<sub>2</sub>Y<sub>1-x</sub>Zn system, solid soln., mag. susceptibility, 77 to 600K (*Russian*) 0-65776  
 Ni-Zn, dil., ferromagnetic, hyperfine field and relax. time obs. of impurity heavy nuclei 0-75533  
 Ni-Zn, implantation damaged, crit. behaviour, perturbed ang. distrib. meas. anal. 0-60476  
 Ni-Zn, physical-chemical metallurgy (*German*) 0-108390  
 NiZn with γ-brass struct., superstructures and defect obs. 0-107284  
 Pb-Zn, unmixed alloys, mathematical model for solidification process (*Russian*) 0-81047  
 SmZn, ferromag., cond. band antiparallel polarisation exceeding 4f moment 0-60207  
 TbZn, elec. resist., behaviour at mag. crit. points 0-65901  
 TbZn, ferromag., thermoelec. power, temp. depend. and crit. behaviour 0-96852  
 TbZn, mag. excitations meas. 0-70979  
 Tm-Zn, paramagnetism, mag. excitations, exchanges interactions 0-88718  
 TmZn<sub>2</sub>, Mossbauer effect meas. in antiferromag. and paramag. states 0-71265  
 Zn-Al, electroless plating of Ni, baths and activating solns. (*Japanese*) 0-71604  
 Zn-Al (0.4 wt.%), intergranular slip during in situ superplastic deform. 0-96538  
 Zn-Al (1.1 wt.%) superplastic alloy, grain size determ. (*Czech*) 0-81118  
 Zn-Al (22 wt.%), eutectoid, low stress and superplastic creep behaviour 0-81120  
 Zn-Al (22 wt.%) superplastic alloy, grain growth texture 0-81075  
 Zn-Al-Cu casting alloys, mech. props. and dendritic morphology, Al content effect (*Korean*) 0-93612  
 Zn-Al(Cu), mech. and technological props. (*Polish*) 0-89286  
 Zn-Al(22 wt.%), alloy sheet, superplastic, cold-rolling effects on mech. props. and microstructure (*Japanese*) 0-71671  
 Zn-As system, homogeneity range of ZnAs<sub>2</sub> and electrophys. props. 0-60833  
 Zn-Bi, liquid, inconsistent conjugated liquidus 0-76232  
 Zn-Cd alloys, liq. and solid, ultrasound speed and compressibility meas. 0-102941  
 Zn-Ga, temp. regime of crystn. on rapid cooling (*Russian*) 0-66495  
 Zn-In alloy, solid-liq. equilib. roughening transition 0-96630  
 Zn-Mn, Kondo-system, ion implantation as method for study 0-70241  
 Zn-Sn-Bi, ternary phase diagrams, interactive computer program 0-71629  
 ZnMn, dil., magnetoresist. meas., temp. depend. anisotropy 0-65532  
 ZrZn<sub>2</sub>, de Haas-van Alphen effect, Fermi surface, theory 0-103614  
 ZrZn<sub>2</sub>, high press. study of Curie temp. and mag. susceptibility 0-84600  
 ZrZn<sub>2</sub>, itinerant electron ferromagnet, magnetovolume effects 0-60397

## zinc compounds

## see also zinc alloys

- chalcogenides, thin films, VPE, needle-like cryst. growth 0-80148  
 dialkylammonium zinc dichlorobromides, long chain cpds., phase transitions, calorimetric study 0-70390  
 dialkylidithiophosphate surface film, prep. and nature 0-104300  
 ferrite, hexagonal, with M, W and Y structures containing Fe<sup>2+</sup> and Fe<sup>3+</sup> mag. ions, saturation moment and anisotropy 0-71009  
 formate dihydrate:Co, spin lattice relax. of Co<sup>2+</sup> ions 0-75847  
 methylzinc methoxide, tetrameric, X-ray cryst. struct. determ. 0-107197  
 oxalate, isothermal crystallisation from soln. 0-108336  
 phthalocyanine, electrochromism and oxidation 0-93768  
 polyphosphinate, bulk compressibility meas. to 30 kbar 0-76306  
 portland cement, doped with ZnO, struct. and props. 0-60914  
 pyrochlorophyllide in nematic liq. cryst., oriented photoexcited triplets, EPR study 0-84636  
 sphalerite, hydrothermal single crystals, feasibility of optical methods for quality control 0-89065  
 stearate, additive to UO<sub>2</sub> green pellet fuel, effect on sintering 0-68908  
 tetramethylammonium tetrachlorozincate, incommensurate phase study, ferroelectric-paraelectric phases (*French*) 0-88318  
 tetramethylammonium zinc tetrachloride, incommensurate phase transitions, <sup>13</sup>C NMR study 0-75968  
 tetramethylammonium zinc tetrachloride, Raman spectra near incommensurate phase transitions 0-76013  
 zinc octaethyl porphyrin, soln., photochem. ionogenesis 0-61116  
 zinc phthalocyanine, resonant two hole bound state at 3p core threshold 0-60750  
 Zn<sub>3</sub>B<sub>2</sub>O<sub>7</sub>Br, ferroelec. 43m-mm2 phase transition, molar heat capacity meas. 0-93249  
 ZnO/Si acoustoelectric devices 0-80332  
 ZnS:V<sup>2+</sup>, impurity states by Green's function method 0-92855  
 Ba<sub>2</sub>Zn<sub>2-7(x+y)</sub>Cd<sub>2y</sub>Fe<sub>12</sub>O<sub>22</sub>, mag. props. and Mossbauer spectrum 0-75765  
 BaZn<sub>2</sub>Fe<sub>12</sub>-M<sub>2</sub>O<sub>27</sub> (M=Al, Ga, In, Sc), mag. props. and Mossbauer effect 0-75766  
 Ba<sub>2</sub>Zn<sub>2</sub>Fe<sub>12</sub>O<sub>27</sub>, ferromag. reson., low power nonlinear effects 0-75861  
 n-CdS/p-ZnIn<sub>2</sub>Se<sub>4</sub> thin film solar cell, photovoltaic props. 0-89628  
 CdTe-ZnS(Se) solid solns., optimal synthesis conditions for single cryst. growth 0-100776  
 CdZnS thin films, growth and evaluation for fabrication of high performance photovoltaic solar cells 0-93501  
 Cd<sub>1-x</sub>Zn<sub>x</sub>S films, thermal evaporation prep., phys. props. 0-84410  
 Cd<sub>1-x</sub>Zn<sub>x</sub> heteroepitaxial single-cryst. layers, photoluminesc. props. 0-100692  
 Cd<sub>1-x</sub>Zn<sub>x</sub> solar cell thin films, microprobe characterisation (*French*) 0-61349  
 Cd<sub>2</sub>Zn<sub>1-x</sub>S films, chem. sprayed, carrier density and mobility 0-60121  
 Co<sub>0</sub>-ZnO-MgO ternary systems, solid solns., struct. charact. 0-60629  
 Co<sub>1-x</sub>Zn<sub>x</sub>F<sub>2</sub>, antiferromag. crit. props., neutron scatt. obs. 0-88749  
 Co<sub>2</sub>Zn<sub>1-x</sub>Fe<sub>2</sub>O<sub>4</sub>, ferrite, DC cond., dielec. props., lattice constns. 0-80272  
 Co<sub>2</sub>Zn<sub>1-x</sub>Rh<sub>x</sub>O<sub>4</sub>, mag. props., EPR spectra, antiferromag. order 0-75736  
 (Cu<sub>2</sub>Zn)Cs<sub>2</sub>(SO<sub>4</sub>)<sub>2</sub>·6(H<sub>2</sub>O)·Tutton salt, proton spin-lattice relax. time, proton cond. depend. and spin diffusion role 0-71221  
 Cu<sub>2</sub>Fe<sub>2</sub>O<sub>7</sub>-ZnFe<sub>2</sub>O<sub>7</sub>, cation distrib., mag. moment, Mossbauer spectra, chem. anal. 0-75210  
 CuGa<sub>0.5</sub>In<sub>0.5</sub>Se<sub>2</sub>/Zn<sub>0.29</sub>Cd<sub>0.71</sub>S heterojunction solar cell, preparation and props. 0-101110  
 Cu<sub>2</sub>S-Zn<sub>2</sub>Cd<sub>1-x</sub>S and Cu<sub>2</sub>S-CdS thin film solar cells by solid state reaction, comparison 0-101109

## zinc compounds continued

- $\text{Cu}_2\text{S}-\text{Zn}_2\text{Cd}_{1-x}\text{S}$  heterojunction, improved model of electro-optic behavior 0-94023  
 $\text{Fe}_{1-x}\text{Zn}_x\text{F}_2$ , dil. antiferromag., electronic and mag. props., Raman scatt. and optical absorpt. study 0-108207  
 $\text{Fe}_{1-x}\text{Zn}_x\text{F}_2$ , electronic Raman scatt., mag. anisotropy 0-66184  
 $\text{Fe}_2\text{Zn}_{1-x}\text{F}_2$ , Neel point and short range order, dilution effects, mag. birefr. obs. 0-71019  
 $\text{K}_2\text{CuZn}_{1-x}\text{F}_4$ , Curie temp., Cu conc. depend. 0-60255  
 $3\text{KNO}_3-2\text{ZnCl}_2$ , glass form. from liq., struct. transform., Raman spectrum obs. 0-64916  
 $\text{K}_2\text{Zn}_2\text{Be}_2(\text{SiO}_4)(\text{Si}_2\text{O}_7)$ , cryst. struct. determ. 0-88121  
 $\text{K}_2\text{Zn}(\text{CN})_6$ , third order elastic consts. 0-84231  
 $\text{K}_2\text{ZnCl}_4$ ,  $^{35}\text{Cl}$  NQR study of incommensurate phase transition 0-60450  
 $\text{K}_2\text{ZnF}_6$ , exchange interactions of transition metal ions in orbitally degenerated excited states 0-65512  
 $\text{Li}-\text{Zn}$  ferrites, (Li, Zn, Ti, Cr substituted), Mossbauer spectrometry, effect of supertransferred hyperfine fields and relaxation (French) 0-80654  
 $\text{Li}_2\text{GeO}_4-\text{Zn}_2\text{GeO}_4$ , solid electrolyte system, phase diagram 0-66489  
 $\text{LiZn}$  ferrosilicates, mol. field, coeff. conc. depend. 0-97114  
 $\text{Li}_2\text{Zn}_2(\text{GeO}_4)_4$  LISICON system, Li ionic conductivity (Chinese) 0-88350  
 $\text{Li}_4\text{Zn}(\text{GeO}_4)_4$ , LISICON, AC meas. of ionic cond., 298 to 573K 0-107526  
 $\text{Mn}_{0.75}\text{Zn}_{0.75}\text{Fe}_2\text{O}_4$ , ferrite, DC cond., dielec. props., lattice consts. 0-80272  
 $\text{Mg}_2\text{Zn}_{1-x}\text{Te}$ , band struct. refl. spectra meas. 0-80813  
 $\text{Mg}_2\text{Zn}_{1-x}\text{Te}$ , comp. profile, second derivative wavelength modulation 0-103967  
 $(\text{Mn},\text{Zn})\text{Fe}_2\text{O}_4\text{:Si}$ , Ca, Ti, second phase effect on elec. and mag. props. 0-60986  
 $\text{Mn}-\text{Zn}$  ferrites, grain boundary exam. using TEM and AES 0-107268  
 $\text{MnZn}$  ferrite, initial mag. permeability rel. to mag. anisotropy 0-80557  
 $\text{MnZn}$  ferrite powder prep., wet method 0-89180  
 $\text{MnZn}$  ferrite powders, reactive, mag. materials obtained by compaction 0-89182  
 $\text{MnZn}$  ferrites, form. of comp. heterogeneity during high-temp. sintering 0-60818  
 $\text{MnZn}$  ferrites, internal friction and  $\Delta E$  effect depend. on demagnetisation method 0-80584  
 $\text{MnZn}$  ferrites, post sinter-cooling rates effects 0-89369  
 $\text{MnZn}$  ferrous ferrite, initial mag. permeability second-order magnetocrystalline anisotropy influence 0-88820  
 $\text{MnZn}$  ferrous ferrites, mag. permeability stress depend. 0-88822  
 $\text{Mn}_2\text{Zn}_{1-x}\text{F}_2$ , Neel point and short range order, dilution effects, mag. birefr. obs. 0-71019  
 $\text{Mn}_{1-x}\text{Zn}_x\text{Fe}_2\text{O}_4$ , prepared by wet method, neutron diff. and high field Mossbauer expts. 0-75719  
 $(\text{NH}_4)_2\text{ZnCl}_4$ , ferroelectricity and incommensurate-commensurate phase transitions 0-60523  
 $\text{NaBaZn}$  glass,  $\text{Eu}^{2+}$  centre symm. 0-100447  
 $\text{Ni}-\text{Zn}-\text{Co}$  ferrites, synthesis from solid solns. of schoenite-type salts 0-93511  
 $\text{NiZn}$  ferrite, dielec. props., Jahn-Teller ion effects 0-97181  
 $\text{NiZn}$  ferrite, prep. of single crystal by chem. transport with  $\text{TeCl}_4$  0-104051  
 $\text{NiZn}$  ferrite,  $\text{ZrO}_2$  additions influence on sintering and physicochem. props. 0-108369  
 $\text{NiZn}$  ferrites, internal friction and  $\Delta E$  effect depend. on demagnetisation method 0-80584  
 $\text{NiZn}$  ferrites, mag. head props., technical possibilities and limitations 0-88803  
 $\text{NiZn}$  ferrites, nonstoichiometric, initial susceptibility and microstruct. 0-84591  
 $\text{NiZn}$  ferrites,  $\text{V}_2\text{O}_5$  induced mag. aftereffects 0-60379  
 $\text{NiZnCo}$  ferrites, switching time and coeff., hydrostatic press. effect 0-88802  
 $\text{NiZnCo}$  ferrites, voltage response under sinusoidal and pulse magnetisation effected by hydrostatic press. 0-88846  
 $\text{Ni}_{0.2}\text{Zn}_{0.75}\text{Fe}_2\text{O}_4$ , Mossbauer study, spin fluctuations 0-60471  
 $\text{Ni}_{0.2}\text{Zn}_{0.75}\text{Fe}_2\text{O}_4$ , Mossbauer study, noncollinear spin struct. 0-60472  
 $\text{Ni}_{0.2}\text{Zn}_{0.75}\text{Fe}_2\text{O}_4$ , structural phase transition, X-ray and neutron diff. study 0-79735  
 $\text{Ni}_{0.2}\text{Zn}_{0.4}\text{Fe}_2\text{O}_4$  coarse grain polycryst. ferrite, diffusional creep (Japanese) 0-104238  
 $\text{Ni}_{0.8}\text{Zn}_{0.15}\text{Fe}_2\text{O}_4$ , ferrite, mag. anisotropy compensation under neutron irradi. 0-75807  
 $\text{Ni}_{1-x}\text{Zn}_x\text{Fe}_2\text{O}_4$ , polycryst., domain wall energy rel. to anisotropy 0-71090  
 $\text{PbF}_2-\text{ZnSe}$  multilayer  $16\text{ }\mu\text{m}$  dichroic mirror,  $16\text{ }\mu\text{m}$  region, mech. stress compensation 0-74465  
 $\text{Rb}_2\text{ZnCl}_4$ , phase transitions, thermal expansion coeff. 0-100638  
 $\text{SiO}_2-\text{Al}_2\text{O}_3-\text{CaO}-\text{BaO}-\text{SrO}-\text{ZnO}-\text{Na}_2\text{O}-\text{K}_2\text{O}-\text{B}_2\text{O}_3$ , glaze effect of  $\text{P}_2\text{O}_5$  additions 0-60824  
 $\text{SnO}_2-\text{Cu}_2\text{S}-\text{ZnS}-\text{Mn}-\text{Cu}-\text{Al}_2\text{O}_3-\text{Al}$ , light-emitting struct., cond. and electrolum., heat treatment 0-97345  
 $\text{ZnO}-\text{ZnO}$ , activated sintering mechanism 0-60810  
 $\text{V}_2\text{O}_5-\text{V}_2\text{O}_4-\text{BaZnO}_3$  glass, V ion states, mag. and elec. props. 0-88556  
 $(\text{Zn},\text{Mg})_3(\text{PO}_4)_2\text{:Mn}^{2+}$ , cathodoluminescence obs. 0-71492  
 $\text{Zn}$  complex,  $\text{Zn}(1,2,4\text{-triazole})_2(\text{NCS})_2\text{:Co}$ , quasi two-dimens. canted  $S=1/2$  antiferromag. 0-70976  
 $\text{Zn}-\text{S}-\text{CdS:Ag}(\text{Cu})$ , cathodoluminesc. investig., appl. to cathode ray tube screening 0-108282  
 $\text{Zn-In-S}$  thin layers, ternary phases, optical props. near long-wavelength intrinsic absorpt. edge 0-80887  
 $\text{ZnAs}_2$ , homogeneity region and electrophys. props. 0-60833  
 $\text{ZnAs}_2$ , Schottky diodes, elec. and photoelec. props., excitons 0-65653  
 $\text{ZnAs}_2$  and  $\text{ZnAs}_2$ , molten, thermal expansion and atomic bond strength parameters 0-65257  
 $\text{Zn}_3\text{As}_2$ , oxidation, hardness and electromechanical polishing response 0-71776  
 $\text{Zn}_2(\text{AsO}_4)(\text{OH})$ , paramadite, crystal struct., anisotropic temp. factors 0-84145  
 $\text{Zn}(\text{BF}_4)\cdot 6\text{H}_2\text{O}:\text{Ni}$ , phase transition study, EPR of diluted  $\text{Ni}^{2+}$ , 98-298K 0-75846  
 $\text{ZnB}_2\text{O}_7\text{-RF}_2$ ,  $\text{R}=\text{Mg}, \text{Ca}, \text{Sr}, \text{Ba}$ , glass form., struct. and props. 0-84077  
 $\text{Zn}_3\text{B}_{10}\text{Cl}$ , boracite, single cryst. prep. and phys. props. 0-100763  
 $\text{ZnBr}_2$ , aq. solns., EXAFS meas. 0-60714

## zinc compounds continued

- $\text{Zn}_2\text{Cd}_{1-x}\text{S}$  film, optimal synthesis conditions for single cryst. growth 0-100776  
 $\text{Zn}_2\text{Cd}_{1-x}\text{S}$  films, spray pyrolysis, elec. props. 0-75657  
 $\text{Zn}_2\text{Cd}_{1-x}\text{S}$  monocrysal petal lasers, single-photon excitation (Russian) 0-99736  
 $\text{Zn}_2\text{Cd}_{1-x}\text{S}$ , thin solid soln. films, vapour deposited, elec. and optical characts. 0-60110  
 $\text{Zn}_2\text{Cd}_{1-x}\text{S}-\text{Cu}_2\text{S}$  heterojunction solar cells, props., comp. meas. of interfacial region 0-81472  
 $\text{Zn}_2\text{Cd}_{1-x}\text{S}_2\text{Se}_{1-y}$ , energy bandgap and lattice constant contours 0-103622  
 $\text{Zn}_2\text{Cd}_{1-x}\text{S}_2\text{Te}_{1-y}$ , energy bandgap and lattice constant contours 0-103622  
 $p\text{-ZnO}-\text{Cd}_{0.9}\text{Sb}$ , thermoelec. anisotropic semicond., carrier kinetics at low temps. 0-92893  
 $\text{ZnO}-\text{Cd}_{0.9}\text{Sb}$ , thermoelectrically isotropic semicond., carrier kinetics in intrinsic cond. range 0-92894  
 $\text{Zn}_1-x\text{Cd}_x\text{Se}$ , mixed crystals, antireson. in phonon spectrum, Raman spectroscopy 0-88992  
 $\text{Zn}_2\text{Cd}_{1-x}\text{S}_2$ , exciton reflection spectra anomalies (Russian) 0-97304  
 $\text{Zn}_2\text{Cd}_{1-x}\text{S}_2\text{Te}_{1-y}$ , energy bandgap and lattice constant contours 0-103622  
 $\text{ZnCl}_2$ ,  $^{35}\text{Cl}$  NQR freqs. meas. 0-58285  
 $\text{ZnCl}_2$ , aq. soln., structural transition, neutron diff. study 0-64872  
 $\text{ZnCl}_2$  glass, glass transition temp. and thermal expansion 0-64902  
 $\text{ZnCl}_2$ , glassy and liq. EXAFS obs. of struct., comparison with vitreous  $\text{GeO}_2$  0-70133  
 $\text{ZnCl}_2\text{-KCl-NaCl}$ , molten system, containing  $\text{Ni}^{2+}$  ions, appl. to electrorefining, polarographic study 0-66810  
 $\text{ZnCl}_2\text{-LiCl}(\text{NaCl})(\text{KCl})(\text{CsCl})$ , molten, US velocity, thermodynamic quantities and struct. (Japanese) 0-88270  
 $\text{ZnCl}_2\text{-LiCl}(\text{NaCl})(\text{KCl})(\text{CsCl})$ , molten, US absorption coeffs. and bulk viscosity coeffs. (Japanese) 0-88271  
 $\text{ZnCl}_2\text{-PbCl}_2$ , molten, US velocity and absorpt., thermodynamic quantities and bulk viscosity (Japanese) 0-84249  
 $\text{ZnCl}_2(\text{Br}_2)(\text{I}_2)$  glassy aqueous solutions, Raman spectral study 0-84738  
 $\text{ZnCl}_2(\text{NCR})_2$ ,  $\text{R}=\text{CH}_3$  or  $\text{C}_2\text{H}_5$ , thermal decomp., thermogravimetric and differential thermal anal. (Chinese) 0-81291  
 $(\text{Zn}_{0.5}\text{Co}_{0.5}(\text{Ni}_{0.8}\text{O}_{0.8}))_2\text{O}_3$ , ZnO evaporation in vac. 0-59640  
 $\text{ZnCr}_2\text{Fe}_{1-x}\text{O}_4$ , Mossbauer spectra, quadrupole splitting, Debye temp. 0-93218  
 $\text{ZnCr}_2\text{O}_4$ , antiferromag. spinel, absorpt. and luminesc. spectra 0-66225  
 $\text{ZnCr}_2\text{Se}_4$ , electroconductivity, thermoelectromotive force, Hall effect (Russian) 0-70694  
 $\text{ZnCr}_2\text{Se}_4$ , screw spin structure, method of controlling the sense, polarised neutron diff. study 0-70944  
 $\text{ZnCr}_2\text{Se}_4$ , screw spin structure, magnetoelectric effect 0-75827  
 $\text{ZnCr}_2\text{Se}_4\text{-In}$ , magnetoresist. and elec. resist. above and below Neel temp. (Russian) 0-88576  
 $\text{Zn},\text{Cu}_{0.1}\text{Fe}_{2.9-x}\text{O}_4$ , ferromag. relax. 0-60422  
 $\text{Zn},\text{Cu}_{0.1}\text{Fe}_{2.9-x}\text{O}_4$ , ferromag. reson., g-factors, Jahn-Teller ion effects 0-66043  
 $\text{ZnF}_2$ ,  $^{67}\text{Zn}$  Mossbauer spectroscopy with 93 keV reson. 0-66095  
 $\text{ZnF}_2$ , high temp. polymorphism and thermal props. 0-75199  
 $\text{ZnF}_2$ , X-ray absorpt. spectrum polarisation depend. 0-104012  
 $\text{ZnF}_2\text{:Co}^{2+}$ , Raman tensor calcs. of isolated impurity in diamagnetic matrix 0-76025  
 $\text{ZnF}_2(\text{FCl})(\text{FBr})$ , matrix isolated IR and Raman spectra, assignments, force consts., isotope effects and thermodynamic props. 0-63631  
 $\text{Zn}_2\text{Fe}_{3-x}\text{O}_4$  ferrite, mag. struct., Mossbauer spectra and magnetisation study, 4.2K 0-103818  
 $\text{Zn}_2\text{Fe}_{3-x}\text{O}_4$ , ferromag. reson., g-factors, Jahn-Teller ion effects 0-66043  
 $\text{ZnGa}_2\text{O}_4\text{:Cr}^{3+}$ , weak exchange interaction determ., ESR study 0-93107  
 $\text{ZnGa}_2\text{S}_4$ , band struct., pseudopot. method 0-92816  
 $\text{Zn}_{1-x}\text{Ge}_x\text{Fe}_{2-x}\text{Fe}_{2x}\text{O}_4$ , double exchange magnetism, Mossbauer study 0-66087  
 $\text{ZnGeP}_2$ , bandgap absorption edge, spectra, electron transitions (Russian) 0-97305  
 $\text{ZnGeP}_2$ , p-n homodiode, polarisation photosensitivity and photopleochroism spectra 0-107866  
 $\text{ZnGeP}_2$ , temp. depend. phase-matched nonlinear optical devices 0-99794  
 $\text{ZnGeP}_2$ , thermo-optic coefficient, dispersion 0-71396  
 $\text{Zn,Hg}_{1-x}\text{Se}$ , current carrier scattering mechanism 0-65546  
 $\text{Zn,Hg}_{1-x}\text{Te}$ , vacancy electron states, acceptor behaviour, electron mobility 0-70193  
 $\text{ZnI}_2$ ,  $^{127}\text{I}$  NQR freqs. meas. 0-58285  
 $\text{Zn}(\text{IO}_3)_2$ , complex salts, phase transitions, cryst. struct. (Chinese) 0-70171  
 $\text{ZnIn}_2\text{S}_4$  crystals, switching effect, electric field distribution 0-107872  
 $\text{ZnIn}_2\text{S}_4$ , Raman scatt., hydrostatic press. effect 0-84745  
 $\text{ZnIn}_2\text{S}_4$ , S-type negative resist. and switching effects 0-65581  
 $\text{ZnIn}_2\text{S}_4$ , vibr. spectrum, Raman study 0-97278  
 $\text{Zn}^{2+}\text{Mo}^{6+}\text{O}_4$ , defect spinel struct., elec. and mag. props. 0-70176  
 $\text{ZnNH}_4\text{H}_3(\text{PO}_4)_2\cdot\text{H}_2\text{O}$ , X-ray cryst. struct. determ. (French) 0-88104  
 $\text{Zn}(\text{NH}_4)_2(\text{SeO}_4)_2\cdot 6\text{H}_2\text{O}:\text{Mn}^{2+}$ , EPR spectra 0-100608  
 $\text{ZnNb}_2\text{O}_6$ , force fields rel. to cryst. struct. (French) 0-107104  
 $\text{ZnO}$ ,  $^{67}\text{Zn}$  Mossbauer spectroscopy with 93 keV reson. 0-66095  
 $\text{ZnO}$ , adhesion deterioration between Ni-SiC coating and Al alloy (Russian) 0-66697  
 $\text{ZnO}$ , adsorbing p- and n-type dyes, surfaces pot., UV light illum. effect 0-75624  
 $\text{ZnO}$ , adsorption of isopropyl alcohol, (acetone), decomp., IR and kinetic obs. 0-59780  
 $\text{ZnO}$ , aqueous-deposited films, struct. and electronic props. for solar cell appls. 0-100797  
 $\text{ZnO}$ , CVD of epitaxial films on sapphire, SAW interdigital transducer fabrication 0-66430  
 $\text{ZnO}$  ceramic varistors, thermal breakdown 0-88928  
 $\text{ZnO}$ , charged dislocations, flow of charge with plastic deform. 0-85010  
 $\text{ZnO}$ , cryst. growth using  $\text{K}_2\text{S}_2\text{O}_7$  as flux material 0-71582  
 $\text{ZnO}$ , defect struct. calc., doping effects 0-107218  
 $\text{ZnO}$ , elastic, piezoelec. and dielec. props. 0-108157  
 $\text{ZnO}$ , elec. cond. at high fields 0-80287  
 $\text{ZnO}$ , electron-hole plasma, gain and refl. spectra study 0-66227  
 $\text{ZnO}$  epitaxial film, nonuniform cond. due to H chemisorption (Russian) 0-65723  
 $\text{ZnO}$ , exciton luminesc., 16 to 77K 0-97329  
 $\text{ZnO}$  film, optical measure of acoustic quality 0-80893  
 $\text{ZnO}$  film concave transducers for scanning acoustic microscopes 0-74663



## zinc compounds continued

- ZnO film on glass substrate, high-rate deposition using DC reactive magnetron sputtering 0-80978  
 ZnO films, RF sputtered single-cryst., on sapphire, struct. and SAW props. 0-80105  
 ZnO films preparation using spray pyrolysis 0-96985  
 ZnO, fully dense, grain growth 0-93526  
 ZnO, in silicate glass, thermal capacity 0-88335  
 ZnO, influence on frequency-temp. coeff. of SAW devices 0-79066  
 ZnO, irradiation in high voltage electron microscope dislocation loops study 0-88157  
 ZnO, isoelectric point meas. 0-88609  
 ZnO low-loss optical waveguides on amorphous substrates 0-58793  
 ZnO non-ohmic ceramic, degradation props. under AC and DC bias 0-80262  
 ZnO nonohmic ceramic, formation mechanism 0-60813  
 ZnO phosphor fired with Zn, luminesc. in green and red region 0-66265  
 ZnO piezoelectric films, RF planar-magnetron sputtered, characterisation 0-96751  
 ZnO polar surfaces, H and O<sub>2</sub> exposed, ion irradi., and heat treated, cond., EELS study 0-71525  
 ZnO powder, effect of dry grinding in EPR and catalytic activity (*Japanese*) 0-84640  
 ZnO RF sputtered films for SAW transducers, X-ray characterisation 0-80138  
 ZnO RF sputtered films, post deposition annealing behaviour 0-100416  
 ZnO, single cryst., photo- and thermoluminescence 0-66311  
 ZnO, single crystals, photocond. lifetimes, Zn<sup>2+</sup> hole traps 0-75581  
 ZnO, spacecraft thermal control material, low-energy proton effects 0-70288  
 ZnO sputtered films, undoped and Ga doped, props. rel. to deposition conditions 0-107935  
 ZnO, thermally stimulated exoelectron emission (*German*) 0-66404  
 ZnO thin film opt. waveguide, collinear acousto-optic interaction and appl. to tunable opt. filter 0-74509  
 ZnO thin-film loading of LiNbO<sub>3</sub>, suppression of SAW harmonic generation 0-84355  
 ZnO transparent films for conductor-insulator-semiconductor (CIS) solar cells 0-93947  
 ZnO UV laser, electron-beam pumped 0-99753  
 ZnO varistor ceramics, current-voltage characts., inhomogeneities and single barriers 0-80273  
 ZnO:Ba, Co, rare earth metal varistors, microstructure-prop. relations 0-100249  
 ZnO:Bi, Sb, Co, second phase effect on elec. and mag. props. 0-60986  
 ZnO:Ce(Tb) phosphors, electrolum. brightness, voltage and freq. depend. 0-60681  
 ZnO:Dy(Yb)(Nd)(Sm)(Pr)(Gd)(La)(Er), electrolum. brightness, field strength and freq. depend. 0-100696  
 ZnO:Ni<sup>2+</sup>, Zeeman effect at Ni impurities 0-60633  
 ZnO/quartz for SAW device appls., expt. study of props. 0-80050  
 ZnO/Si SAW structs., anal. of charge injection 0-80049  
 ZnO-Al<sub>2</sub>O<sub>3</sub>, isoelectric point meas. 0-88609  
 ZnO-B<sub>2</sub>O<sub>3</sub>, glass, refraction, refractive index from 0.365 to 2.50  $\mu$ m 0-88953  
 ZnO-B<sub>2</sub>O<sub>3</sub> glass, structure toughness-composition relationship 0-104257  
 ZnO-CdTe heterojunctions preparation using spray pyrolysis 0-96985  
 ZnO-Cu<sub>2</sub>O heterojunction solar cells, prop. by RF sputtering 0-93945  
 ZnO-Fe<sub>2</sub>O<sub>3</sub>, isoelectric point meas. 0-88609  
 ZnO-glass layered system, characts. of phase-velocity dispersion and struct. of surface waves 0-59775  
 ZnO-grainboundary-ZnO junction in ceramic varistor, capacitance-voltage characts. 0-65689  
 ZnO-La<sub>2</sub>O<sub>3</sub>-B<sub>2</sub>O<sub>3</sub>, glass, refraction, refractive index from 0.365 to 2.50  $\mu$ m 0-88953  
 ZnO-P<sub>2</sub>O<sub>5</sub> glass, ESR of VO<sup>2+</sup> ions 0-100610  
 ZnO-SiO<sub>2</sub> layered system, characts. of phase-velocity dispersion and struct. of surface waves 0-59775  
 ZnO-SiO<sub>2</sub>-Si SAW device, interface transduction 0-102949  
 ZnO-WO<sub>3</sub>, phase rels. and cryst. struct. 0-108410  
 (Zn(OH)(NH<sub>3</sub>))<sub>2</sub>, model for biological active sites, ab initio calcs., comparison with Be complex 0-104551  
 ZnP glass heavy-ion track detectors 3 to 120 MeV 0-91389  
 ZnP<sub>2</sub>, 442 class gyrotropic crystals., self-induced rot. of light polarisation plane 0-99810  
 ZnP<sub>2</sub>, Brillouin scattering and optical props. meas. 0-76041  
 ZnP<sub>2</sub>, cryst., tetragonal, 2-phonon IR absorpt. 0-66176  
 $\alpha$ -ZnP<sub>2</sub>, doped, single crystal, electrical properties 0-92892  
 $\alpha$ -ZnP<sub>2</sub>, lattice parameters and thermal expansion, 80-320K, X-ray obs. 0-75373  
 ZnP<sub>2</sub>, resonance Raman scatt. singularities (*Russian*) 0-89007  
 $\alpha$ -ZnP<sub>2</sub>, resonant Brillouin scatt. near indirect band gap 0-93350  
 ZnP<sub>2</sub> Schottky diodes, elec. and photoelec. props., excitons 0-65653  
 ZnP<sub>2</sub> tetragonal crystals, polarisation study of photocond. 0-96942  
 ZnP<sub>2</sub>:In(Ga)(Ge)(S)(Se), doped and undoped, optical absorpt. spectra in range 0.5 to 2.2 eV 0-66250  
 Zn<sub>3</sub>P<sub>2</sub>, elec. cond., Hall effect, P interstitial effects 0-84465  
 Zn<sub>3</sub>P<sub>2</sub>, evaporated metal contact barrier heights 0-80375  
 Zn<sub>3</sub>P<sub>2</sub> large crystal growth, vapour transport perforated capsule technique, prototype solar cell appls. 0-93464  
 Zn<sub>3</sub>P<sub>2</sub>, optical props., transition energies from transmission and refl. meas. 0-60532  
 Zn<sub>3</sub>P<sub>2</sub>, polycryst. thin film photovoltaic materials, photon loss anal., expt. determ. 0-93888  
 Zn<sub>3</sub>P<sub>2</sub>, thermoluminescence glow curve method for radiation induced traps 0-60689  
 Zn<sub>3</sub>P<sub>2</sub> thin polycrystalline films for solar photovoltaic cells 0-97797  
 Zn<sub>3</sub>P<sub>2</sub>-metal contacts, photoelectric props. 0-92930  
 Zn<sub>3</sub>(PO<sub>4</sub>)<sub>2</sub>, thermoluminescence glow curve method for radiation induced traps 0-60689  
 ZnRb<sub>2</sub>(SeO<sub>4</sub>)<sub>2</sub>·6H<sub>2</sub>O:Mn<sup>2+</sup>, EPR spectra 0-100608  
 ZnS, <sup>67</sup>Zn and <sup>35</sup>S nuclear magnetic shielding, chemical shifts and linewidths 0-60434  
 ZnS, <sup>67</sup>Zn Mossbauer spectroscopy with 93 keV reson. 0-66095  
 ZnS CVD IR window, optical and physical characteristics 0-106620  
 ZnS, cathodolum. emission spectra, exciton lines 0-76084  
 ZnS, charged dislocations, flow of charge with plastic deform. 0-85010  
 ZnS crystals, structural change under plastic deform., partial dislocation movement 0-79736  
 ZnS crystals in electrolyte, electrolum. and elec. props. 0-93407  
 ZnS, cubic, compression 0-107358

## zinc compounds continued

- ZnS, cubic, thermal vibr. temp. depend., anharmonic models 0-92618  
 ZnS evaporated film, refl. loss on UV irradi., ZnO form. 0-99813  
 ZnS film, defect form. and development 0-96759  
 ZnS film, intrinsic stress meas. 0-71696  
 ZnS film deposition using radiation-heated tubular-type evaporator 0-76191  
 ZnS film on Si, fused quartz substrates, H<sub>2</sub>O absorpt., IR anal. 0-75446  
 ZnS films, electrolum., bistable excitation 0-93406  
 ZnS, four-photon transitions, perturbation theory calc. 0-96786  
 ZnS, high purity, prep. from ZnO (*Rumanian*) 0-76206  
 ZnS ion beam etching, topographic changes, amorphisation, luminescence study 0-76078  
 ZnS, ion implantation effects on luminesc., thermo-EMF 0-88178  
 ZnS, lattice dynamics, phonon freq., bond bending force model calcs. 0-70335  
 ZnS, linear electrooptic coeff. dispersion 0-71380  
 ZnS, low-temp. trap anal. thermally stimulated luminesc. model extension 0-80877  
 ZnS monocrystalline substrate, influence of struct. on CdS epitaxial growth and nucleation 0-88455  
 ZnS, ODMR of Zn vacancy obs. 0-108121  
 ZnS, oxidation, hardness and electromechanical polishing response 0-71776  
 ZnS, phonon spectra calc. by recursion method 0-59596  
 ZnS phosphor, powdered, in host material, solar cells wavelength shifting 0-85286  
 ZnS photoconductors, spectral sensitisation, role of local centres (*Russian*) 0-90924  
 ZnS, polytype relative stabilities, entropy contribs. 0-100197  
 ZnS, post field recomb. in pulsed electrolum. 0-71488  
 ZnS powder phosphors electroluminescent cells, AC electrolum. characts. (*Japanese*) 0-71489  
 ZnS, prebreakdown electrolum., domain form. and negative resist. effects 0-84788  
 ZnS RF sputtered films for SAW transducers, X-ray characterisation 0-80138  
 ZnS, Raman scatt. by phonon polaritons 0-103959  
 ZnS, reson. Brillouin scatt. and piezobirefringence 0-93348  
 ZnS single crystal, linear electro-optical props., temp. depend. 0-71376  
 ZnS, single electron excitation study, cathodoluminescence image contrast using STEM 0-89072  
 ZnS structure, evaluation of finite strain eqns. of state using lattice models 0-96620  
 ZnS, superficial degradation in air and water, XPS obs. (*French*) 0-89110  
 ZnS, thermal expansion and lattice dynamics under press. 0-100316  
 ZnS, thermoluminescence at different excitation levels 0-93413  
 ZnS thin films, effect of fabrication parameters on electroluminescence and related props. (*Japanese*) 0-76083  
 ZnS, twist boundary struct., atomic scale electron microscopy obs. 0-107276  
 ZnS UV laser, electron-beam pumped 0-99753  
 ZnS:<sup>57</sup>Co Mossbauer sources, Fe<sup>2+</sup> transient charge state 0-108128  
 ZnS:Ag, cathodoluminesc. investig., appl. to cathode ray tube screening 0-108282  
 ZnS:Co, impurity luminescence, no phonon line depend. on temp., Debye temp. 0-66273  
 ZnS:Cu, Cl, Mn film, AC electrolum. 0-60680  
 ZnS:Cu, deep transition metal impurity states, SCF CNDO cluster calcs. 0-100442  
 ZnS:Cu, Mn DC electroluminescent powder panels, bulk and junction effects 0-89068  
 ZnS:Cu, spectral distrib., rise and decay behaviour (*German*) 0-60625  
 ZnS:Cu crystal, powder, epitaxial film, luminescence anomalous thermal 0-76077  
 ZnS:Fe<sup>2+</sup>, reson. relax. time for impurity electrons and localised phonons interaction, appl. to thermal cond. 0-59590  
 ZnS:In, recombination emission by optically detected magnetic resonance 0-66272  
 ZnS:Mn, Cu, Cl films, AC electrolum. 0-60679  
 ZnS:Mn AC thin film devices, domain electrolum. 0-66303  
 ZnS:Ni, IR luminesc. and absorpt. spectroscopy 0-108261  
 ZnS:Ni, optical absorpt., impurity ionisation, optical phonon coupling 0-88505  
 ZnS:Ni<sup>2+</sup>, Zeeman effect at Ni impurities 0-60633  
 ZnS:Pb, blue luminesc., photoexcited EPR spectrum 0-108070  
 ZnS:Tb, Cu(Ag) phosphors, luminesc. props. 0-100690  
 ZnS:Tm<sup>3+</sup>, charge compensation and polytypism influences on fluorescence 0-89051  
 ZnS-Au electrolum. Schottky barrier diode, S<sup>+</sup>-implanted, blue emission 0-76082  
 ZnS-MgF<sub>2</sub> mirror, dielectric, Rayleigh scatt. at 441.6 nm 0-97367  
 ZnS-SiO<sub>2</sub>, multilayer reflector, reflectance under slight absorpt. conditions 0-83655  
 ZnSO<sub>4</sub> electrolytes containing Ge and Co, polarisation charact., exam. by cyclic voltammetry 0-104444  
 ZnS<sub>1-x</sub>Se<sub>x</sub>, electron trap associated with anion vacancy, DLTS study 0-80210  
 ZnS<sub>1-x</sub>Se<sub>x</sub>, phonon spectra calculations by recursion method, mixed crystals 0-103430  
 ZnS<sub>1-x</sub>Se<sub>x</sub>, VPE on CaF<sub>2</sub> substrate, in flowing H<sub>2</sub>, growth and characterisation (*French*) 0-107678  
 ZnSb, orientated crystn. conditions during reaction diffusion (*Russian*) 0-70558  
 ZnSb, thermoelec. anisotropic semicond., carrier kinetics at low temps. 0-92893  
 ZnSb<sub>2</sub>O<sub>6</sub>, force fields rel. to cryst. struct. (*French*) 0-107104  
 ZnSe, <sup>67</sup>Zn Mossbauer spectroscopy with 93 keV reson. 0-66095  
 ZnSe, <sup>67</sup>Zn nuclear magnetic shielding, chemical shifts and linewidths 0-60434  
 ZnSe, band-edge photoluminesc., far-below band-gap excitation 0-76063  
 ZnSe, blue photoluminesc. excited with strong laser radiation 0-93391  
 ZnSe, charged dislocations, flow of charge with plastic deform. 0-85010  
 ZnSe cryst., IR absorpt., annealing effect 0-80774  
 ZnSe crystals, degenerate four-wave interaction, nonlinear optics effects 0-91856  
 ZnSe crystals, doped and undoped, optical absorption edge 0-60626  
 ZnSe, donor-acceptor pair emissions characts. (*French*) 0-108249  
 ZnSe, EXAFS amplitudes, many-body effects 0-97379  
 ZnSe, electric charge transport by dislocations 0-103709

## zinc compounds continued

- ZnSe, electron beam induced current study of grain boundaries by SEM 0-59479  
 ZnSe, electron trap associated with anion vacancy, DLTS study 0-80210  
 ZnSe, epitaxial growth on Ge substrate 0-75469  
 ZnSe etalon, temp. controlled, multiline oscillation characts. of TEA CO<sub>2</sub> laser 0-74334  
 ZnSe, exciton emission, halfwidths, thermal and optical activation energies obs. (*French*) 0-66268  
 ZnSe, exciton refl. spectra, temp. depend. 0-59886  
 ZnSe films, long wavelength IR polariton emission band thermal shift and broadening 0-92833  
 ZnSe films, reson. Raman spectra 0-80888  
 ZnSe, heat-treated in controlled partial press. of Zn or Se, TSC 0-59910  
 ZnSe laser windows, AR coated, photoacoustic chopping freq. studies using CO<sub>2</sub> laser 0-83629  
 ZnSe laser windows, photoacoustic signal var. with chopping freq. 0-75309  
 ZnSe layers, cond. type determ. by pot. profiling 0-73387  
 ZnSe, low resistance ohmic contacts using In-Ga liquid alloy, LED fabrication appl. 0-70823  
 ZnSe, luminesc., hot electron effects 0-66277  
 ZnSe, MBE growth, elec. and optical props. 0-75462  
 ZnSe, minority carriers diffusion length by surface photovoltage method 0-60003  
 ZnSe, multiphonon ionisation of deep point centres in a charged dislocation field (*Russian*) 0-100281  
 ZnSe, near band edge photoluminescence, electron-hole recombination 0-80835  
 ZnSe, phonon dispersion relations, eight-parameter bond-bending forces model 0-70334  
 ZnSe, photolum. excitation spectra of tightly bound holes, valence band contrib. 0-60658  
 ZnSe, piezobirefringence in opaque region 0-60541  
 ZnSe, positron annihilation study 0-60713  
 ZnSe, residual cond., recomb. of photoexcited carriers, Hall coeff. 0-75605  
 ZnSe, resonance Raman scatt., exciton-polariton luminescence (*Russian*) 0-97287  
 ZnSe, self-compensation, role of impurities 0-92850  
 ZnSe single cryst., lasing action excited by ruby laser picosecond pulses 0-64035  
 ZnSe single cryst., linear electro-optical props., temp. depend. 0-71376  
 ZnSe solar spectrum converter for GaAs solar cells 0-10117  
 ZnSe, thermal expansion and lattice dynamics under press. 0-100316  
 ZnSe, thermally treated crystals, photoluminesc. 0-60661  
 ZnSe:Co, impurity luminescence no phonon line depend. on temp., Debye temp. 0-66273  
 ZnSe:In, highly compensated single crystals, thermally initiated current breakdown, current-voltage characts. 0-65579  
 ZnSe:Mn/n-GaAs low threshold thin film DC electrolum. cell, pulse-excited characts. 0-76081  
 ZnSe:Mn<sup>2+</sup>-n-Ge thin film electrolum. cell with low-threshold voltage 0-84786  
 ZnSe:Ni, optical absorpt., impurity ionisation, optical phonon coupling 0-88505  
 ZnSe:Ni, photolum. excitation spectroscopy 0-80841  
 ZnSe:Ti<sup>2+</sup>, EPR meas. 0-80594  
 ZnSe/water, interface, laser-induced damage in ZnSe 0-102746  
 ZnSe-Si, IR segmented composite window design 0-106621  
 ZnSe-Si heterojunctions, IR quenching of photocapacitance 0-92968  
 ZnSe(Te), fine structure of lowest exciton state (*Russian*) 0-96801  
 p-ZnSiAs<sub>2</sub>, electron irradi. elec. props. annealing, lattice defects 0-100465  
 ZnSiAs<sub>2</sub>, thermal expansion coeffs. meas. (*Russian*) 0-65258  
 Zn<sub>2</sub>SiO<sub>4</sub>:Mn, energy storage effect and retrieval 0-100684  
 ZnSiP<sub>2</sub>, electronic struct., X-ray spectroscopic investigation 0-108300  
 ZnSiP<sub>2</sub>, thermal expansion coeffs. meas. (*Russian*) 0-65258  
 p-ZnSnAs, LPE, electronic struct. obs. by laser excited photolum. 0-60654  
 ZnTe, MBE growth, elec. and optical props. 0-75462  
 ZnTe, <sup>67</sup>Zn Mossbauer spectroscopy with 93 keV reson. 0-66095  
 ZnTe, <sup>67</sup>Zn nuclear magnetic shielding, chemical shifts and linewidths 0-60434  
 ZnTe, 1.5 to 30K, thermal expansion and Gruneisen parameter meas. 0-59681  
 ZnTe, charged dislocations, flow of charge with plastic deform. 0-85010  
 ZnTe clean and adsorbed O<sub>2</sub> (110) surfaces, UV photoemission spectra (*Japanese*) 0-93456  
 ZnTe crystals, polariton effects in luminesc. 0-103988  
 ZnTe, doping and intrinsic stoichiometric defects, self-compensation 0-59918  
 ZnTe, edge luminesc. excited by electron bombard. 0-66308  
 ZnTe, elec. field and impurity conc. effects on ionisation energy of impurities, appl. to acceptors 0-88514  
 ZnTe electrode, redox reaction due to complex M(CN)<sub>6</sub><sup>3-/4-</sup> (*French*) 0-89482  
 ZnTe film, exciton spectra, press. and temp. depend. 0-80886  
 ZnTe films, internal stress effect on fund. refl. spectra 0-60701  
 ZnTe films, simple and modified Poole-Frenkel cond. 0-97017  
 ZnTe growth from vapour, growth interruption 0-97416  
 ZnTe, ion implantation defect introduction, cathodolum. studies 0-75250  
 ZnTe, irradiation induced radiative centers obs. 0-66290  
 ZnTe, lattice dynamics and phonon parameters, bond bending force model lattice dynamics and phonon parameters bond bending force model 0-59595  
 ZnTe, low voltage green LED, struct. double diffusion procedure 0-100697  
 ZnTe, photolum. excitation spectra of tightly bound holes, valence band contrib. 0-60658  
 ZnTe, pure and P(As) doped, shallow-acceptor, donor, free-exciton, and bound-exciton states 0-60667  
 ZnTe, secondary emission, transient behaviour under band-to-band excitation 0-108266  
 ZnTe, self-diffusion profile and trapping of Zn 0-75381  
 ZnTe single cryst., lasing action excited by ruby laser picosecond pulses 0-64035  
 ZnTe single crystal, Schottky-barrier diodes and ohmic contacts props. 0-96987  
 p-ZnTe, spin-flip Raman scattering, review 0-108209  
 ZnTe, thermal expansion and lattice dynamics under press. 0-100316

## zinc compounds continued

- ZnTe:As, impurity identification and characterisation, capacitance, luminescence and IR absorption 0-60639  
 ZnTe:Bi, laser annealing, channelling, reflectivity spectra 0-66215  
 ZnTe:Co, impurity luminescence no phonon line depend. on temp., Debye temp. 0-66273  
 ZnTe:Cu films, high cond., elec. and optical props. 0-88651  
 ZnTe:Li, electron-phonon interactions in Raman scatt. 0-60594  
 ZnTe:Li, O, Hagemark theory, O modification isoelectronic trap 0-75517  
 ZnTe:Li, Zeeman splitting of ground and excited acceptor states, selective pair luminesc. 0-84780  
 ZnTe:Mn, spin-lattice coeffs. of Mn<sup>2+</sup> 0-84646  
 ZnTe:Mn<sup>2+</sup>, forbidden transitions of Mn<sup>2+</sup> induced by hyperfine interactions 0-60458  
 ZnTe:P(As), ion implanted, cathodoluminescence emission spectrum 0-108281  
 ZnTe(S), semiconductor-metal transition, press. calibration above 100 kbars fixed points 0-77808  
 ZnTe,Se<sub>1-x</sub>, phonon spectra calculations by recursion method, mixed crystals 0-103430  
 ZnWO<sub>4</sub>, scintillation characts. 0-66256  
 ZnY<sub>2</sub>O<sub>4</sub>, cryst. struct. 0-100207

## zirconium

- see also nuclei with .....  
 adsorption and absorpt. of CO, NO, N<sub>2</sub>, O<sub>2</sub>, and D<sub>2</sub>, dissoc. and diffusion 0-80085  
 atom, XPS relative intensity and photoionisation cross-section 0-63599  
 breakaway oxidation kinetics at 623K, SEM study 0-97633  
 core level binding energies 0-71564  
 creep and growth, radiation induced, fundamental mechanisms 0-92596  
 diffusion of H, NMR study 0-108088  
 electron irradiation damage, direct obs. 0-84212  
 electronic excitations, charact. energy loss meas. up to 50 eV 0-60723  
 foil, dislocation loop nucleation and growth during 1 MeV electron irradi. 0-88152  
 foil bending by in situ ion irradi., neutron damage simulation, room temp. oxide growth 0-107342  
 foils, dehydrogenation of V by annealing 0-96736  
 gettering of H, mass spectrometry and microgravimetry study, rel. to HTGR gas purification 0-73374  
 hydride precipitation and growth at crack tips, electron optical obs. 0-108449  
 ion-implanted polycryst., thermal oxidation 0-71786  
 irradiation growth, influence of microstructure and test conditions 0-92561  
 irradiation growth, reaction rate theory calcs. 0-88212  
 liquid, viscosity at melting point, free energy (*Russian*) 0-92699  
 magnetic susceptibility, plastic deform. effect (*Russian*) 0-65984  
 neutron irradiated at 573 to 923K, damage struct. 0-107334  
 oxidation, in O<sub>2</sub>-N<sub>2</sub> atmospheres 0-104353  
 phonon dispersion, modified Sharma-Joshi model 0-100311  
 phonon dispersion relations, d-electron contrib. to Cauchy discrepancy 0-92628  
 photon emission due to Ar<sup>+</sup> ion bombard., adsorbed and recoil-implanted O effect 0-80872  
 plasma arc spraying, chem. reaction with plasma gases 0-66427  
 range distributions for 25-200 keV <sup>14</sup>N<sup>+</sup> ions 0-103405  
 ribbon filament lamp, calibrated source for IR radiometer 0-83653  
 sputtered ion fraction meas. using matrix isolation spectroscopy 0-60738  
 superconductivity enhancement obs. after H(D) implantation 0-70884  
 thin film, TEM, sources of background X-radiation 0-101908  
 twin interfaces {1012}, serrated 0-84182  
 void swelling during electron irradi., HVEM study 0-92559  
 X-ray fluorescence analysis, simultaneous determ. of Zr and Hf trace elements in soln. 0-97752  
 yield points, obtained by ageing at two stresses 0-81091  
 Al<sub>2</sub>O<sub>3</sub>:Zr ceramic, elec. props., additives effect, and interaction with steel melt 0-104305  
 LiNbO<sub>3</sub>:Co<sup>2+</sup>, Zr<sup>4+</sup> film, improvement in temp. stability and SAW device apps. 0-75939  
 SrS:Mn, Zr phosphor, photodiode effect 0-107848  
 W-Zr field emitter, time-of-flight atom-probe study 0-80949  
 W(100) coating, TF electron emitters props. obs. 0-66403  
 YIG:Zr, near IR absorpt. and magnetic circular dichroism 0-60580  
 Y<sub>2</sub>O<sub>3</sub>:Zr<sup>3+</sup>, f-centre charge state, ESR and thermally stimulated luminesc. obs. 0-60418  
 Zr IV, energy levels, spectrum obs. 440 to 2670 Å 0-99470  
 Zr IX, 4s<sup>2</sup>4p<sup>2</sup>-4s4p<sup>2</sup> transitions, in VUV 0-91480  
 Zr VIII, reson. transitions in UV 0-91479  
 Zr/Al, getter for TFTR Flexibility Modification, in-torus surface pumping 0-95451  
 Zr-O-W (100) thermal field emitters, operational experience 0-71576  
 Zr+H<sup>+</sup>, K-shell ionisation cross-section, 85 to 790 keV 0-106390  
<sup>94</sup>Zr(n,α)<sup>91</sup>Sr, fast n, fission spectrum averaged cross section 0-63177

## zirconium alloys

## see also zirconium compounds

- creep and growth, irradiation induced, microstruct. depend. 0-93602  
 creep and growth, irradiation induced, rate theory approach 0-89294  
 diffusion of H, NMR study 0-108088  
 foil, dislocation loop nucleation and growth during 1 MeV electron irradi. 0-88152  
 pseudo-binary alloys, Zr(A<sub>1</sub>B<sub>1-x</sub>)<sub>2</sub> (A=V, Cr, Mn; B=Fe, Co), H<sub>2</sub> absorpt. capacity 0-88433  
 stress relaxation, in-reactor study at low temps. 0-93588  
 TZM-Mo alloy, mech. props., effect of exposure to high temp. He containing O<sub>2</sub>, room temp. study 0-93639  
 Zircaloy, annealed, neutron irradiated, inhomogeneous deform. behaviour 0-85014  
 Zircaloy, breakaway mechanism, corrosion kinetics in steam 0-61030  
 Zircaloy, creep and growth, radiation induced, fundamental mechanisms 0-92596  
 Zircaloy, foil, dislocation loop nucleation and growth during 1 MeV electron irradi. 0-88152  
 Zircaloy, LWR fuel rod cladding, damage accumulation during I<sub>2</sub>-induced stress corrosion cracking 0-71810  
 zircaloy, nuclear microprobe methods for investigating oxidative corrosion 0-71787  
 Zircaloy, PWR fuel induced cladding deformation, creep correl., in-pile meas. 0-97547



## zirconium alloys continued

- Zircaloy, textured, interactive creep and growth, upper-bound evaluation 0-89293
- Zircaloy, unirrad., stress corrosion cracking, I<sub>2</sub>-induced, effect of test temp., alloy comp. and heat treatment 0-97632
- Zircaloy cladding, enhanced steam oxidation by deformation under LWR LOCA 0-73917
- Zircaloy cladding, stress corrosion cracking, inner surface texture effect 0-66695
- Zircaloy cladding stress corrosion cracking due to I (Japanese) 0-78361
- Zircaloy fuel cladding, irradiation-induced in-reactor corrosion in CANDU reactors 0-104352
- Zircaloy PWR fuel cladding deformation tests under mainly convective cooling conditions 0-57862
- Zircaloy sheath, fission gas absorpt. following irradi., power history effects 0-78395
- Zircaloy sheaths, oxidation rate calc. method 0-78394
- Zircaloy-2, anodic oxidation kinetics, in 0.05M oxalic acid (aq. and alcoholic) 0-104331
- Zircaloy-2, hot-pressed, influence of diffused C on structure and oxidation 0-61016
- Zircaloy-2, hydride precipitation and growth at crack tips, electron optical obs. 0-108449
- Zircaloy-2, irradiation growth, influence of microstructure and test conditions 0-92561
- Zircaloy-2, irradiation growth, reaction rate theory calcs. 0-88212
- Zircaloy-2, irradiation growth, shape and volume changes 0-92562
- Zircaloy-2, mech. props. after exposure to I<sub>2</sub>-methanol solutions, SEM study 0-93689
- Zircaloy-2, neutron irradi. at 573 to 923K damage struct. 0-107334
- Zircaloy-2, neutron irradi. damage, TEM characts. 0-107332
- Zircaloy-2, oxide coating thermal cond. meas. 0-80009
- Zircaloy-2, plastic deform. generalised constitutive eqns. 0-104219
- Zircaloy-2, pressure tubes, irradi. creep and growth, anisotropy factors 0-97536
- Zircaloy-2, yield pts. obtained by ageing at two stresses 0-81091
- Zircaloy-2 fuel tubes, cumulative damage fatigue tests at room temp. and 300°C 0-93638
- Zircaloy-2 fuel tubes, low cycle fatigue studies at room temp., 300 and 350°C 0-93637
- Zircaloy-2 pressure tube, elongation in Douglas Point CANDU reactor 0-78398
- Zircaloy-2 pressure tube elongation, neutron induced creep and growth, meas. and anal. 0-93628
- Zircaloy-4, creep rupture at superimposed non-stationary stress and temp. loading 0-66630
- Zircaloy-4, elastic props., O additions effect 0-66565
- Zircaloy-4, failure strain prediction under non-stationary loading conditions 0-93640
- Zircaloy-4, fuel cladding, burst criteria under LOCA conditions 0-73931
- Zircaloy-4, resistance-welded, microstruct. of weld region 0-66549
- Zircaloy-4, stress-relieved and cold-worked, stress relaxation in bending at 673K 0-93609
- Zircaloy-4 BWR channels, corrosion resistance 0-104351
- Zircaloy-4 cladding deformation under LOCA transient heating conditions, analytical modelling 0-104236
- Al-Si-Cu-Zr, ageing kinetics (Russian) 0-76274
- Al-Zr (1-13 wt.%), rapidly quenched, extended solid solubility, grain refinement and age-hardening 0-76266
- Al<sub>20</sub>Cu<sub>25</sub>Zr<sub>55</sub> metallic glass, inelastic deform., free energy spectra 0-71699
- Co-Zr, amorphous phase form. in Zr-poor region, hardness and fracture strength (Japanese) 0-84914
- Co-Zr, dendritic segregation 0-76260
- Co<sub>90</sub>Zr<sub>10</sub>, ferromag. amorphous alloy, crystn. and domain struct. study 0-107056
- Cr-Zr evaporation source improvement, diffusion barrier layer deposition for IC metallurgy 0-76163
- Cu-Zr amorphous alloy, splat cooled, local order and amorphous struct. 0-88061
- Cu<sub>40</sub>Nb<sub>30</sub>X<sub>30</sub> (X=Ti, Zr, Hf), superconductors with metastable ordered structs. 0-108484
- Cu<sub>40</sub>Zr<sub>60</sub>, Cu<sub>56</sub>Zr<sub>44</sub>, and Cu<sub>60</sub>Zr<sub>40</sub> metallic glass, inelastic deform., free energy spectra 0-71699
- CuZr, photoemission study 0-104046
- Cu<sub>57</sub>Zr<sub>43</sub>, amorphous alloy, neutron diff. obs. of struct. 0-88060
- Cu<sub>40</sub>Zr<sub>60</sub>, amorphous alloys, supercond. transition temp., press. depend. 0-84524
- Cu<sub>57</sub>Zr<sub>43</sub>, amorphous alloy, computer simulation of atomic structure 0-70125
- Cu<sub>60</sub>Zr<sub>40</sub>, amorphous, ductility and stress relief, low-temp. annealing effects 0-76296
- Fe-Zr, amorphous phase form. in Zr-poor region, hardness and fracture strength (Japanese) 0-84914
- GdZrFe<sub>3</sub>, hyperfine field at Gd, TDPAC meas. 0-93214
- Mo-(Zr+V+C) (1.1 wt.%) alloy, phase composition, carbide phase micro-hardness (Russian) 0-60834
- Mo-Ti-Zr, TZM, corrosion behaviour in high temp. impure He gas 0-76402
- Mo-Zr, nucleation conditions, effect on formation of oxide phase during internal oxidation (Russian) 0-81064
- Mo-Zr (0.15 wt.%), wrought, fracture, characteristic features 0-104278
- Mo-ZrC, eutectic formation of regular struct., crystn. (Russian) 0-66496
- Nb-Ti-Zr ternary system, high-field supercond. 0-97045
- Nb-W-Mo-Zr (5, 2.1, 0.92 wt.%), creep resist., high temp. ageing in vacuum 0-71716
- Nb-W-Zr-N alloy, with dispersed second phase, ductile-brittle transition 0-93653
- Nb-W-Zr-Ta (90, 4.5, 3.5, 2 wt.%) creep and creep limit in super vac. at 1100°C, heat treatment effect 0-81133
- Nb-Zr, crit. current, flow-flow resist. depend., allowance for superheating (Russian) 0-93061
- Nb-Zr, thermoelec. power, 4.2 to 300K 0-70683
- Nb-Zr (1 wt.%), corrosion behaviour in high temp. impure He gas 0-76402
- Nb-Zr (3 wt.%), neutron-irradiated, positron annihilation ang. correl. meas. 0-93430
- Nb-Zr alloy, BCC- $\omega$  phase transition, electronically driven nature 0-103433
- Nb-Zr-C welding solid solutions, ageing kinetics, influence of inclusion elements (Russian) 0-100853
- zirconium alloys continued
- Nb-Zr-N biphase alloy, recrystallization annealing 0-104180
- Nb-Zr-Si, ductile amorphous, superconductivity 0-60131
- Nb<sub>70</sub>Zr<sub>30</sub>, supercond. and normal, sp. ht. meas., 2-20K 0-70893
- (Nb<sub>99.99</sub>Zr<sub>0.01</sub>)<sub>3</sub>Sn, AC power losses in parallel AC and DC mag. fields 0-97041
- Ni-based superalloys, hot workability, effect of S, Ca, Mg, Y and Zr minor elements 0-66552
- Ni-Cr-Zr, degradation after exposure to 1% H<sub>2</sub>S/H<sub>2</sub> gas mixture at 1000°C 0-89408
- Ni-Zr, amorphous phase form. in Zr-poor region, hardness and fracture strength (Japanese) 0-84914
- Ni<sub>2</sub>Zr<sub>1-3</sub>, metallic glass, crystallisation kinetics, elec. resist. and mag. susceptibility meas. 0-103659
- PdZr, photoemission study 0-104046
- Pd<sub>30</sub>Zr<sub>70</sub>, amorphous alloys, supercond. transition temp., press. depend. 0-84524
- Pd<sub>35</sub>Zr<sub>65</sub>, mag. susceptibility meas. 0-75740
- Sc-Zr, low-temp. heat capacity 0-75370
- Sm<sub>91</sub>Zr<sub>9</sub>(Co<sub>65</sub>Cu<sub>10</sub>Fe<sub>0.22</sub>)<sub>6.7</sub> alloy permanent magnet, coercive force (Russian) 0-65966
- Sr<sub>2</sub>(Co<sub>1-x</sub>Ti<sub>x</sub>)<sub>17</sub>, powders, influence of substitutes on mag. props. 0-100601
- Th-Pu-U-Zr (20, 4, 8 wt.%) metal fuels, compatibility with cladding alloys for FBR appls. 0-102242
- Ti-Al-Mo-Zr, compressor disk, surface plastic deform., optimal method 0-60924
- Ti-Al-Sn-Zr, Ti-680, O contamination under high temp. (Chinese) 0-66688
- Ti-Al-Sn-Zr-Mo (6,2,4,6 wt.%) fusion weldment, substruct. characts. 0-84183
- Ti-Al-Zr-Mo-Si (6, 5, 0.5, 0.25 wt.%),  $\beta$ -processed, fatigue props., hold time effect 0-60961
- Ti-Mo-Zr-Sn (11.5, 6.0, 4.5 wt.%), mech. property, microstruct. relationships 0-84961
- Ti-Mo-Zr-Sn (11.5, 6.0, 4.5 wt.%) alloy, struct. as affected by processing history 0-84972
- $\beta$ -Ti-Mo-Zr-Sn(11.5, 6, 4.5 wt.%), metastable phase III, microstruct. and age hardening response 0-84945
- Ti-Mo-Zr-(Al) (15, 5 (3) wt.%), quenched and aged metastable  $\beta$ -phase, crystallography, morphology and decomposition 0-76262
- Ti-Nb-Zr-Fe, supercond. and paramag. props., effect of Fe additions (Russian) 0-65730
- Ti-Nb-Zr-Ta, superconducting props. comp. depend., stress effects and precipitation behaviour, X-ray scatt. 0-93059
- Ti<sub>90</sub>Be<sub>10</sub>Zr<sub>10</sub>, amorphous, crystn. temp., press. and heating rate depend. 0-70132
- Ti<sub>1-x</sub>Zr<sub>x</sub>Mn<sub>2-x-3</sub>Cr<sub>3-x</sub>V<sub>x</sub>, hydrogen storage appl. (Japanese) 0-61443
- U-Pu-Zr-(Th) LMFBR metal fuel elements, development and performance 0-75856
- V<sub>2</sub>(Hf<sub>1-x</sub>Zr<sub>x</sub>), NMR and mag. susceptibility, density of states determ. (Russian) 0-66053
- V<sub>2</sub>Hf<sub>1-x</sub>Zr<sub>x</sub>, normal and supercond. state, transition temps., mag. susceptibility and specific heat determ. (Russian) 0-60132
- Zircaloy-2, effect of simulated fission products on mech. props. 0-73922
- Zircaloy-2, electron irradiation damage, direct obs. 0-84212
- Zircaloy-4, deformation behaviour between 77 and 900K 0-71686
- Zr-Al (8.6 wt.%), dimensional stability struct. and mech. props, effects of neutron irradi. 0-92563
- Zr-Al (8.6 wt.%), fast neutron irradiated, tensile props. and fracture toughness 0-84994
- Zr-Al getter modules, transient getter scheme for Tokamak fusion test reactor 0-79584
- Zr-Al-C, phase diagram and lattice constants, X-ray diff. method 0-89207
- Zr-Co, amorphous and crystalline, d-band struct., alloying effects 0-59862
- Zr-Cu amorphous alloys, glass transition and ductility, O additions effect 0-75168
- Zr-Cu(Ni)(Co)(Fe) metallic glasses, glass form. and thermal stability 0-75177
- Zr-H, precip. of  $\gamma$ -ZrH, shear mechanism 0-104170
- Zr-H formation, of  $\delta$ - $\gamma$  transformation 0-84929
- Zr-H formation, the  $\delta$ - $\epsilon$  transformation 0-84930
- Zr-Hf (2.2 wt.%), high temp. oxidation in flowing O<sub>2</sub>, 873-1173K 0-93687
- Zr-Ir, dil., elec. field gradient at <sup>193</sup>Ir, Mossbauer meas. 0-66090
- Zr-Nb, structure associated with BCC to omega transform. (Russian) 0-108432
- Zr-Nb (0.1, 2.5 wt.%), foil, dislocation loop nucleation and growth during 1 MeV electron irradi. 0-88152
- Zr-Nb (2.5 wt.%), channel tubes, in-reactor creep and irradi. growth 0-93604
- Zr-Nb (2.5 wt.%), cold-worked, pressure tubing, metallography and mech. props. 0-89269
- Zr-Nb (2.5 wt.%), high temp. oxidation in flowing O<sub>2</sub>, 873-1173K 0-93687
- Zr-Nb (2.5 wt.%), hydride precipitation and growth at crack tips, electron optical obs. 0-108449
- Zr-Nb (2.5 wt.%), neutron irradi. at 573 to 923K, damage struct. 0-107334
- Zr-Nb (2.5 wt.%), nuclear fuel channels, neutron effects on ultimate fracture strength, 293 to 573K 0-85054
- Zr-Nb (2.5 wt.%), pressure tubes, irradi. creep and growth, anisotropy factors 0-97536
- Zr-Nb (2.5 wt.%) pipe, fracture resistance, hydrogenation effect 0-104279
- Zr-Nb (2.5 wt.%) pressure type rel. between stress intensity factor, crack opening displacement and J-integral 0-100920
- Zr-Nb (97.5, 2.5 wt.%) nuclear reactor pressure tube material, H embrittlement study by TEM 0-76363
- Zr-Nb-Sn (3.0, 1.0 wt.%), high temp. oxidation in flowing O<sub>2</sub>, 873-1173K 0-93687
- Zr-Nb(2.5 wt.%), irradiation growth, influence of microstructure and test conditions 0-92561
- Zr-Ni, amorphous and crystalline, d-band struct., alloying effects 0-59862
- Zr-Rh-H(D), superconducting transition temp., effect of H(D) conc. 0-84532
- Zr-Ru, alloy Zr rich, Ru solubility, eutectic decay,  $\alpha$ - $\beta$  transform., struct. (Russian) 0-65227



## zirconium alloys continued

- Zr-Sn (1.5 wt.%), electron irradiation damage, direct obs. 0-84212  
 Zr-Sn-Fe-Ni (1.5, 0.1, 0.15 wt.%), electron irradiation damage, direct obs. 0-84212  
 Zr-Sn(Fe)(Ni) (0.15 wt.%), electron irradiation damage, direct obs. 0-84212  
 $\alpha$ -Zr-Sn(Mo), creep charact., influence of Sn and Mo (*Czech*) 0-81119  
 Zr-Ti-Be metallic glass, phase separation 0-97464  
 Zr-ZrC, eutectic formation of regular struct., crystn. (*Russian*) 0-66496  
 ZrAl<sub>3</sub>, X-ray energy spectrum of valence electrons (*Russian*) 0-108304  
 Zr<sub>2</sub>Al<sub>3</sub>, X-ray energy spectrum of valence electrons (*Russian*) 0-108304  
 Zr<sub>3</sub>Al, deformed and irradiated, lattice defects obs., superlattice dislocations and defect clusters 0-107261  
 Zr<sub>3</sub>Al, ordered, oxidation, weight gain and metallography 0-89398  
 Zr<sub>3</sub>Al ordered alloy, ion bombardment damage, TEM 0-100287  
 Zr<sub>4</sub>Al<sub>3</sub>, X-ray energy spectrum of valence electrons (*Russian*) 0-108304  
 ZrAlC<sub>2-x</sub>, lattice constants, X-ray powder diff. method 0-89207  
 Zr<sub>2</sub>Al<sub>3</sub>C<sub>5-x</sub>, lattice constants, X-ray powder diff. method 0-89207  
 Zr<sub>2</sub>Al<sub>3</sub>C, lattice constants, X-ray powder diff. method 0-89207  
 ZrB<sub>2</sub>-Nb, reactions between components 0-100812  
 Zr<sub>1-x</sub>Co<sub>x</sub>, amorphous alloys, thermal stability, elec. cond. enthalpy 0-100172  
 Zr<sub>70</sub>Co<sub>30</sub> amorphous alloys, struct. factors and radial distrib. functions 0-84096  
 ZrCr<sub>2</sub>, mag. props. H absorpt. effect 0-88821  
 Zr(Cr<sub>1-x</sub>Co<sub>x</sub>)<sub>2</sub>, mag. props. H absorpt. effect 0-88821  
 ZrCr<sub>2</sub>D<sub>2</sub>, site occupation modes and cryst. struct., neutron diff. study 0-59440  
 Zr(Cr<sub>1-x</sub>Fe<sub>x</sub>)<sub>2</sub>, mag. props. H absorpt. effect 0-88821  
 ZrCu, constitutional and struct. studies, by mag. susceptibility, metallography and X-ray diff. 0-70166  
 Zr<sub>0.475</sub>Cu<sub>0.475</sub>Mo<sub>0.05</sub>, glass transition temp., comp. depend. 0-79702  
 Zr<sub>70</sub>Fe<sub>30</sub> amorphous alloys, struct. factors and radial distrib. functions 0-84096  
 Zr(Fe-Co)<sub>2</sub>, itinerant electron ferromagnet, magnetovolume effects 0-60397  
 Zr(Fe<sub>1-x</sub>Al<sub>x</sub>)<sub>2</sub>, Curie temp., magnetisation, and cryst. struct., conc. depend. 0-75730  
 Zr(Fe<sub>1-x</sub>Co<sub>x</sub>)<sub>2</sub>, ferromag. and micromag., thermal expansion and forced volume magnetostriction 0-75830  
 Zr(Fe<sub>1-x</sub>Co<sub>x</sub>)<sub>2</sub>, NMR study 0-75882  
 Zr<sub>3</sub>In, Li<sub>2</sub> ordered alloy, positive temp. depend. on strength, phase destabilization 0-81203  
 ZrMn<sub>2</sub>, mag. props. H absorpt. effect 0-88821  
 ZrMn<sub>2</sub>H<sub>x</sub>, proton NMR relax. time and Knight shifts, diffusional activation energies meas., sorption props. 0-75871  
 (Zr<sub>1-x</sub>Nb<sub>x</sub>)Fe<sub>2</sub>, antiferromag. spin struct., Mossbauer effect study 0-66086  
 Zr<sub>70</sub>Ni<sub>30</sub> amorphous alloys, struct. factors and radial distrib. functions 0-84096  
 Zr<sub>70</sub>Pd<sub>30</sub> amorphous alloys, struct. factors and radial distrib. functions 0-84096  
 ZrV<sub>2</sub>, anomalous softening at martensitic transform. 0-93630  
 ZrV<sub>2</sub>, Knight shift vs. susceptibility plot 0-75712  
 Zr(V<sub>1-x</sub>Co<sub>x</sub>)<sub>2</sub>, relation between electronic struct. and H<sub>2</sub> storing props. 0-76662  
 ZrV<sub>2</sub>D<sub>2</sub>(H<sub>x</sub>), site occupation modes and cryst. struct., neutron diff. study 0-59440  
 ZrX<sub>2</sub> alloy, Laves phases with MgZn<sub>2</sub>, MgCu<sub>2</sub> structs., X-ray emission Zr spectra (*Russian*) 0-71517  
 ZrZn<sub>2</sub>, de Haas-van Alphen effect, Fermi surface, theory 0-103614  
 ZrZn<sub>2</sub>, high press. study of Curie temp. and mag. susceptibility 0-84600  
 ZrZn<sub>2</sub>, itinerant electron ferromagnet, magnetovolume effects 0-60397

## zirconium compounds

- see also *zirconium alloys*  
 ceramics containing metastable tetragonal ZrO<sub>2</sub>, grinding induced tempering 0-89260  
 gels, thermal and related studies 0-71937  
 halides, XY<sub>4</sub> molecules, force consts. by modified Redington and Aljibury method 0-69261  
 polymer filled ceramic, ZrO<sub>2</sub> stabilised, fracture mechanism (*Russian*) 0-100895  
 Ag-Zn, molten, EMF meas. of activities using ZrO<sub>2</sub> solid electrolytes (*Japanese*) 0-88339  
 Al<sub>2</sub>O<sub>3</sub>-SiO<sub>2</sub>-ZrO<sub>2</sub>, refractories, corrosion behaviour in glassmelting furnaces (*Polish*) 0-71783  
 Al<sub>2</sub>O<sub>3</sub>-ZrSiO<sub>4</sub>, granular corundum-zircon refractory, development 0-66462  
 3Al<sub>2</sub>O<sub>3</sub>·2SiO<sub>2</sub>-ZrO<sub>2</sub> composites, sintered, in situ-reacted, fracture props. 0-81158  
 Au-Zn, molten, EMF meas. of activities using ZrO<sub>2</sub> solid electrolytes (*Japanese*) 0-88339  
 CC ZrS<sub>2</sub>O<sub>4</sub>, X-irradiated, trapping and emission centres, thermolum. meas. 0-89076  
 CaO-MgO-Cr<sub>2</sub>O<sub>3</sub>-Al<sub>2</sub>O<sub>3</sub>-ZrO<sub>2</sub>-SiO<sub>2</sub> system, subsolidus region charact. 0-97466  
 Cr<sub>2</sub>O<sub>3</sub>-ZrO<sub>2</sub> granules, from spray drying of suspensions 0-104100  
 Cu<sub>2</sub>In<sub>2</sub>Zr<sub>1-x</sub>S<sub>2</sub> system, struct. and cond. meas. (*French*) 0-88354  
 Dy<sub>2</sub>O<sub>3</sub>-ZrO<sub>2</sub> phase diagram and long range ordering 0-93542  
 GdF<sub>3</sub>-BaF<sub>2</sub>-ZrF<sub>4</sub> glass fibres, IR transmission, losses, fabrication 0-87516  
 Gd<sub>2</sub>Zr<sub>1-x</sub>O<sub>2-x/2</sub>, elec. cond. of ceramic solid solutions 0-107554  
 Gd<sub>2</sub>Zr<sub>1-x</sub>O<sub>2-x/2</sub>, fluorite and pyrochlore solid solutions, electrical conductivity meas. 0-65287  
 HfF<sub>4</sub>-BaF<sub>2</sub>-ThF<sub>4</sub>-(ZrF<sub>4</sub>) glass system, IR transmitting, synthesis and props. 0-71623  
 Na<sub>2</sub>Y<sub>2</sub>Zr<sub>1-x</sub>S<sub>2</sub>, ionic cond. and NMR mobility obs., comp. depend. (*French*) 0-70459  
 Na<sub>4</sub>Zr<sub>2</sub>Si<sub>2</sub>O<sub>12</sub>, struct. analysis at 300 and 600°C, rel. to ionic cond. 0-107189  
 Na<sub>1-x</sub>Zr<sub>2</sub>Si<sub>2</sub>P<sub>3-x</sub>O<sub>12</sub>, press. and comp. effect on fast Na<sup>+</sup> ion transport 0-107516  
 Na<sub>2</sub>Zr<sub>2</sub>Si<sub>2</sub>PO<sub>12</sub>, NASICON, ionic cond. temp. depend., comparison with  $\beta$ -Al<sub>2</sub>O<sub>3</sub>-Na<sub>2</sub>O 0-107520  
 Nd<sub>2</sub>Zr<sub>1-x</sub>O<sub>2-x/2</sub>, elec. cond. of ceramic solid solutions 0-107554  
 Nd<sub>2</sub>Zr<sub>1-x</sub>O<sub>2-x/2</sub>, fluorite and pyrochlore solid solutions, electrical conductivity meas. 0-65287  
 Pb(Zr,Ti)O<sub>3</sub> fibre arrays in epoxy cement, ferroelectric ceramic-plastic composites 0-81015  
 Pb(ZrTi)O<sub>3</sub> ceramic transducer for generation and detection of unipolar stress pulses 0-64328

## zirconium compounds continued

- Si<sub>3</sub>N<sub>4</sub>/ZrO<sub>2</sub>, hot-pressed, compressive surface stresses developed by oxidation induced phase change 0-60992  
 (U,Zr)C, U self-diffusion 0-92711  
 UN-ZrN, Young's modulus antiferromagnetic anomaly 0-92583  
 U,Zr<sub>1-x</sub>Fe<sub>x</sub>, Curie temp. and saturation moment at 4.2K 0-70966  
 ZrB<sub>2</sub>, abrasive, effect on machinability of Ti alloys (*Russian*) 0-97593  
 Zr<sub>2</sub>C, abrasive, effect on machinability of Ti alloys (*Russian*) 0-97593  
 Zr-N<sub>2</sub>, condensate formed by plasma flow precipitation in vacuum, cryst. and surface props. (*Russian*) 0-100788  
 ZrB<sub>2</sub>, self-consistent band struct., XPS, reflectance, NQR, Hall effect and density of states meas. 0-107689  
 ZrB<sub>2</sub>, vacuum condensate, struct. and mech. props., second phase effect (*Russian*) 0-71705  
 Zr(BH<sub>4</sub>)<sub>4</sub> catalytic reactions on Al<sub>2</sub>O<sub>3</sub>, inelastic electron tunnelling spectra 0-75425  
 ZrC-C composite system, negative magnetoresist. 0-60008  
 ZrC-C composites, hot pressed, thermophys. props. at high temps. 0-59675  
 Zr(Ca,Y)O<sub>2-x</sub>, local ionic arrangement, X-ray diff. study 0-100203  
 ZrF<sub>4</sub> based glasses, solid electrolyte, conductivity and activation energy 0-70464  
 ZrF<sub>4</sub>:Eu<sup>3+</sup> glass, luminesc. of Eu<sup>3+</sup>, transition probabilities 0-80845  
 ZrF<sub>4</sub>-BaF<sub>2</sub>-MF<sub>n</sub> (M=Na, Ca, Ln, Th, n=1, 2, 3, 4), vitreous phases, network formers, modifiers and stabilisers (*French*) 0-64909  
 ZrF<sub>4</sub>-BaF<sub>2</sub>-ThF<sub>4</sub>-NaF(RF<sub>3</sub>) (R=rare-earth) glass system, anion cond. 0-70460  
 ZrF<sub>4</sub>-BaF<sub>2</sub>-ThF<sub>4</sub>(LaF<sub>3</sub>)(NdF<sub>3</sub>)(PrF<sub>3</sub>), F<sup>-</sup> ion cond. glasses, cond. process 0-107477  
 ZrF<sub>4</sub>-based glasses, elec. transport props. 0-79983  
 ZrF<sub>4</sub>-THF<sub>4</sub>-BaF<sub>2</sub> glass, IR-transparent, synthesis using reactive atm. processing technique 0-100826  
 Zr(HPO<sub>4</sub>)<sub>2</sub>·H<sub>2</sub>O, Na<sup>+</sup> transport, gas-solid and solid-solid reaction kinetics 0-61086  
 ZrI<sub>4</sub>, high-temp. enthalpy, X-ray powder diff. data 0-107446  
 Zr<sub>1-x</sub>In<sub>2x</sub>O<sub>2-x</sub>, ionic conductivity, lattice const. 0-96688  
 Zr(KPO<sub>4</sub>)<sub>2</sub>, cryst., ionic cond., layered struct. 0-92710  
 Zr(LiPO<sub>4</sub>)<sub>2</sub>, cryst., ionic cond., layered struct. 0-92710  
 ZrN, whisker growth in CVD 0-59843  
 ZrN-Al<sub>2</sub>O<sub>3</sub> composites, strength rel. to solid-, liquid-phase sintering 0-100823  
 Zr(NaPO<sub>4</sub>)<sub>2</sub>, cryst., ionic cond., layered struct. 0-92710  
 ZrO, Franck-Condon factors rot. depend. 0-58319  
 ZrO, predicted IR spectrum and possible presence in S-type stars 0-62124  
 ZrO, singlet-triplet separation meas. 0-78623  
<sup>90,92,94</sup>ZrO<sup>+</sup>, rot. anal. in near IR 0-74162  
 ZrO<sub>2</sub> additions in NiZn ferrite, influence on sintering and physicochem. props. 0-108369  
 ZrO<sub>2</sub> based solid electrolyte, use for study of O<sub>2</sub> solubility and diffusivity in liq. metals 0-59669  
 ZrO<sub>2</sub>, CaO stabilised, preferred slip system 0-66585  
 ZrO<sub>2</sub> ceramic, dense nonstabilized, fabrication by hydrothermal reaction sintering 0-97451  
 ZrO<sub>2</sub> coating on Zircaloy-2, thermal cond. meas. 0-80009  
 ZrO<sub>2</sub>, crystallite growth from oxide plasmas, growth morphology 0-59417  
 ZrO<sub>2</sub>, decomp. of CaO·6Al<sub>2</sub>O<sub>3</sub> 0-92687  
 ZrO<sub>2</sub>, doped, ionic cond., theoretical model 0-107552  
 ZrO<sub>2</sub>, electronic excitations, charact. energy loss meas. up to 50 eV 0-60723  
 ZrO<sub>2</sub>, enthalpy and heat capacity at 1100-2500K 0-103472  
 ZrO<sub>2</sub> glass, melting depend. on minute components, surface crystallisation 0-84278  
 ZrO<sub>2</sub>, glaze, liq. phase separation rel. to cryst. in glassy phase 0-103252  
 ZrO<sub>2</sub>, high pressure polymorphism 0-59429  
 ZrO<sub>2</sub>, in Li<sub>2</sub>O-Al<sub>2</sub>O<sub>3</sub>-SiO<sub>2</sub> glass, cryst. process 0-103253  
 ZrO<sub>2</sub>, metastable, tetragonal, strengthening by surface grinding 0-71777  
 ZrO<sub>2</sub> microsphere stabilised ceramic, fracture charact., thermal stability (*Russian*) 0-76335  
 ZrO<sub>2</sub>, partially stabilised ceramics, strengthening, post-sintering heat treatment 0-97518  
 ZrO<sub>2</sub>, partially stabilised, props. and appl. to extrusion dies 0-97507  
 ZrO<sub>2</sub>, partially stabilised, processing defects 0-97558  
 ZrO<sub>2</sub>, porous, sintered stabilised microspheres, strength and fracture studies 0-85019  
 ZrO<sub>2</sub>, semisintered, shear strength at high press. 0-76308  
 ZrO<sub>2</sub> solid electrolyte, electrochem. reduced, electrocatalytic decomp. of NO 0-61113  
 ZrO<sub>2</sub> stabilised with lime, electrical conductivity at high temp. (*Rumanian*) 0-65575  
 ZrO<sub>2</sub>, synthesis by solid state reaction 0-100821  
 ZrO<sub>2</sub> thin film, optical props. rel. to cryst. struct. 0-97357  
 ZrO<sub>2</sub>, vacuum condensate, struct. and mech. props., second phase effect (*Russian*) 0-71705  
 ZrO<sub>2</sub>/Pt solid electrolyte/porous electrode system, interface polarisation effects 0-61114  
 ZrO<sub>2</sub>/SnF<sub>3</sub> mirror coatings, light scatt. and optical strength in UV range 0-106595  
 ZrO<sub>2</sub>-CaO, and ZrO<sub>2</sub>-YO<sub>1.5</sub>, solid solns., defective oxides, ionic cond. 0-107548  
 ZrO<sub>2</sub>-CaO, stabilised microspheres, structure, mechanical props. (*Russian*) 0-100379  
 ZrO<sub>2</sub>-CaO solid electrolyte, for O<sub>2</sub> flow regulator 0-57301  
 ZrO<sub>2</sub>-CaO(Y<sub>2</sub>O<sub>3</sub>) ceramics with grainy structure, props., effect of heating to 2000°C 0-104194  
 ZrO<sub>2</sub>-Sc<sub>2</sub>O<sub>3</sub>-Y<sub>2</sub>O<sub>3</sub> system, order-disorder phenomena, Raman spectra study 0-97254  
 ZrO<sub>2</sub>-SiO<sub>2</sub>, liquid immiscibility, microstruct. of plasma dissociated ZrSiO<sub>4</sub> 0-107429  
 ZrO<sub>2</sub>-SiO<sub>2</sub>(-Na<sub>2</sub>O) glass fibres, prep. from metal alkoxides, resistance to NaOH soln. 0-97454  
 ZrO<sub>2</sub>-Y<sub>2</sub>O<sub>3</sub>, stabilised microspheres, structure, mechanical props. (*Russian*) 0-100379  
 ZrO<sub>2</sub>-YO<sub>1.5</sub>-Ta<sub>2</sub>O<sub>5</sub>, cubic fluorite phase, elec. cond. 0-107551  
 (ZrO<sub>2</sub>)<sub>0.9</sub>(Y<sub>2</sub>O<sub>3</sub>)<sub>0.1</sub>:Cr, Mn, stabilised single crystal, EPR of Mn<sup>2+</sup> and Cr<sup>3+</sup> obs. 0-66024  
 4.26ZrO<sub>2</sub>·Nb<sub>2</sub>O<sub>5</sub>, elec. cond. meas. 0-100463  
 6.14ZrO<sub>2</sub>·Ta<sub>2</sub>O<sub>5</sub>, elec. cond. meas. 0-100463  
 ZrO<sub>2</sub>-x(cubic)-ZrO<sub>2</sub>-x(cubic+tetragonal), phase boundary 0-81038  
 ZrS, electronic struct., bonding effects, photoelectron spectroscopic and low temp. heat capacity cal. 0-96780



**zirconium compounds continued**

- ZrS<sub>2</sub>, valence density of states, Gilat-Raubenheimer method 0-88465  
 ZrS<sub>3</sub>, excitonic transition, reson. Raman spectra, Franck-Condon factors 0-97252  
 ZrS<sub>3</sub>, paired-anion ligand effects in valence band, photoemission spectrosc. obs. 0-87173  
 ZrS<sub>3</sub>, photolum. from excitons 0-66274  
 ZrS<sub>3</sub>, quasi one-dimens. semicond., elec. transport props. 0-107790  
 ZrSe<sub>2</sub>, photo-intercalation: possible application in solar energy devices 0-108803  
 ZrSe<sub>3</sub>, valence density of states, Gilat-Raubenheimer method 0-88465  
 ZrSe<sub>3</sub>, paired-anion ligand effects in valence band, photoemission spectrosc. obs. 0-87173  
 ZrSiO<sub>4</sub>, body centered matrix basis 0-79765  
 ZrSiO<sub>4</sub>, natural, radiation defect centre, EPR obs. 0-75853  
 ZrSiO<sub>4</sub>, X-irrad., trapping and emission centres, OH<sup>-</sup> ion contribution 0-80876  
 ZrSiO<sub>4</sub> zircon ceramic with glass-forming additives, sintering and mech. props. 0-60814  
 ZrSiO<sub>4</sub>, zircon yellow pigment, synthesis (*Polish*) 0-66466  
 ZrSiO<sub>4</sub>-Al<sub>2</sub>O<sub>3</sub> (SiO<sub>2</sub>) suspensions for slip casting, prep. and props. 0-104103  
 ZrTe<sub>5</sub>, giant resistivity anomaly 0-107794  
 Zrc, whisker growth in CVD 0-59843

**zodiacal light**

- see also sky brightness  
 brightness, depend. on heliocentric coords. 0-72878  
 dust, light scatt. intensity, theory 0-109324  
 dust cloud, thermal emission at 11 and 20 microns 0-90367  
 meteor streams, sunlight scatt. rel. to meteor shower assoc. nightglow 0-94761  
 scattering by irregular absorbing particles, new model 0-67543  
 UV brightness excess from interplanetary dust motion obs. 0-101555

**zonal heating** see atmospheric thermodynamics**zone melting**

- control for floating-zone melting with viscous torque 0-89140  
 float glass, Sn penetration in bottom surface, synthesis 0-79993  
 floating zone method growth, interface shapes 0-60775  
 II-VI semiconductors, optimal synthesis methods for single cryst. growth 0-100764  
 Marangoni convection, floating zone, under reduced gravity 0-66425  
 optical fibre crystals floating zone growth, for IR optical waveguides 0-79019  
 (rare-earth), Ti<sub>2</sub>O<sub>7</sub>, (RE=La-Nd, Sm, Gd, Y), ferroelec., layer type struct., cryst. growth 0-108348  
 refining, theory, mathematical treatments, current state-of-the-art, and possible developments (*Spanish*) 0-76172  
 rotating container melt growth, crystallisation parameters calcs. 0-103285  
 sapphire constant diameter crystal., laser heated float zone growth, meniscus angle meas. 0-108347  
 shaped crystal growth from melt, meniscus-controlled process 0-107075  
 B-Si alloys, B-rich, prep., anal. and cryst. growth (*French*) 0-104091  
 Bi-Sb (1 at.%) alloy single cryst. growth solid-liq. interface study 0-107073  
 CeB<sub>6</sub>, crystal preparation, elec. resistance, phase transitions 0-97427  
 Fe, purification, recrystn. temp. and elec. resistivity (*Japanese*) 0-100780  
 GdBr<sub>3</sub>, crystal preparation, elec. resistance, phase transitions 0-97427  
 KBr(Cl), prep. of crystals containing impurities of specified amounts (*Russian*) 0-66424  
 La<sub>2</sub>Si<sub>2</sub>O<sub>7</sub>N<sub>3</sub>, single cryst. growth by floating zone method with SiO<sub>2</sub>-Si<sub>3</sub>N<sub>4</sub> additions 0-93481  
 Lu<sub>2</sub>-Si<sub>2</sub>O<sub>7</sub>/Eu<sub>2</sub>, synthesis and spectroscopic study 0-84846  
 NbN,  $\gamma$ - and  $\delta$ -forms, cryst. growth and supercond. transition temp. 0-107946  
 NbN single crystal preparation, zone melting and nitriding techniques 0-60776  
 NbN<sub>0.7</sub>C<sub>0.3</sub>, cryst. growth and supercond. transition temp. 0-107946  
 Nd<sub>2</sub>Ga<sub>2</sub>O<sub>12</sub>, floating zone method growth, interface shapes 0-60775  
 Si, float zone crystal, dislocation creation and elimination 0-107072  
 Si multicrystalline solar cell material prep., fast-pulled float zone, CZ and cast ingot and foil methods 0-93483  
 Si purification, plasma melting zone technique (*French*) 0-89141  
 Si purification, plasma melting zone technique, optimisation (*French*) 0-89142  
 Si ribbon growth by laser zone melting 0-93482  
 Si solar cells, capacitance transient spectra of processing- and radiation-induced defects 0-61340  
 Si:In extrinsic IR detector material with high responsivity compensated by neutron transmutation, float-zone growth 0-75597  
 SmB<sub>6</sub>, crystal preparation, elec. resistance, phase transitions 0-97427  
 YFeO<sub>3</sub>, floating zone method growth, interface shapes 0-60775  
 YIG, floating zone method growth, interface shapes 0-60775  
 Y<sub>2</sub>O<sub>3</sub>:(Nd) single crystal growth, floating zone method with Xe arc lamp imaging furnace 0-60777

**zone plates (optical)** see optical zone plates**zone refining**

- semiconductor, doping reduction using zone recrystn. with temp. gradient 0-104062  
 theory, mathematical treatments, current state-of-the-art, and possible developments (*Spanish*) 0-76172  
 Fe, free surface and grain boundary O<sub>2</sub> and S chemistry 0-75410  
 LaB<sub>6</sub> crystals, zone refined, chem. characterisation 0-93821  
 Nb-Th, eutectic composition 0-100828  
 Si:Pt, implanted and laser annealed, segregation and increased dopant solubility 0-65016  
 Te-(Bi,Sb<sub>1-x</sub>)<sub>2</sub>Te<sub>3</sub> eutectic, electrophys. props., directed crystn. conditions influence and comp. depend. 0-107827  
 Te-based eutectics, crystn. rate effect on electrophys. props. mutual solubility effect 0-60774  
 Ti-Th, eutectic composition 0-100828

**zoology**

- anthozoans, pennatulacea, colonial coordination 0-94197  
 auditory primary neurons, comparative physiology 0-94224  
 bee, thermoregulation by evaporative cooling of head (honeybee) 0-61515  
 behaviour patterns in cod released by elec. stimulation of olfactory tract bundles 0-97951  
 coral reef epifauna, susceptibility to UV irrad. 0-98037  
 dolphin, lung collapse and intramuscular circulation during diving 0-81643

**zoology continued**

- dolphin swimming, leaping for efficiency at high speed 0-61619  
 elephant, hearing freq. range 0-104596  
 firefly larva, bioluminesc. exhibiting circular polarisation 0-94441  
 forces in animal joints 0-94251  
 gastropod photosynthesis with incorporated algal chloroplast, Placobranchus sp. 0-61522  
 gastropod locomotion, role of pedal mucus 0-76780  
 geomagnetic field sensitivity in animals, ferromag. coupling to muscle receptors as basis 0-72185  
 hummingbird colour vision to near UV light 0-97914  
 insect colour vision, effected by one visual pigment and filters 0-94212  
 marine cephalopods, radioactive trace elements obs. 0-94379  
 Peracarida, burrowing, temp. effects on emergence rhythms (*French*) 0-94174  
 rat thermoregulatory behaviour when subject to microwave irrad. 0-81547  
 ratfish, electroreception, obs. 0-94442  
 reptile epidermis, water permeability rel. to lipid content 0-97875  
 spider, web vibr. sensed by Argyrodes elavatus kleptoparasite 0-61595  
 turtle, sex determination during embryo development, temp. depend. 0-81546  
 whales, southern right, sound playback expts. 0-89772

**zoosemantics** see biocommunications**Zr** see zirconium



ABSTRACTS AND CURRENT PAPERS JOURNALS

SUBSCRIPTION PRICES

	USA \$	UK £	ROW £	JAPAN ¥
<b>PHYSICS ABSTRACTS</b>				
Paper or Microfiche.....	1105	440	565	452,000
Paper and Microfiche.....	1658	660	848	678,000
2nd and subsequent copies.....	480	250	250	200,000
<b>ELECTRICAL &amp; ELECTRONICS ABSTRACTS</b>				
Paper or Microfiche.....	820	375	450	360,000
Paper and Microfiche.....	1230	562	675	540,000
<b>COMPUTER &amp; CONTROL ABSTRACTS</b>				
Paper or Microfiche.....	495	230	290	232,000
Paper and Microfiche.....	742	345	435	348,000
<b>PA/EEA/CCA COMBINED SUBSCRIPTION</b>				
Paper or Microfiche.....	2150	915	1165	932,000
Paper and Microfiche.....	3225	1372	1748	1,398,000
<b>EEA/CCA COMBINED SUBSCRIPTION</b>				
Paper or Microfiche.....	1200	535	675	540,000
Paper and Microfiche.....	1800	802	1012	810,000
<b>CURRENT PAPERS IN PHYSICS</b>				
Member rate.....	60	30	30	—
Non-Member rate.....	140	80	80	64,000
<b>CURRENT PAPERS IN ELECTRICAL &amp; ELECTRONICS ENGINEERING</b>				
Member rate.....	55	30	30	—
Non-Member rate.....	118	65	65	52,000
<b>CURRENT PAPERS ON COMPUTERS &amp; CONTROL</b>				
Member rate.....	55	30	30	—
Non-Member rate.....	118	65	65	52,000
<b>KEY ABSTRACTS</b>				
Member rate *.....	30	15	15	—
Non-Member rate.....	65	30	30	24,000
<b>KEY ABSTRACTS EMI/PMI COMBINED</b>				
.....	—	50	50	40,000

\*The Key Abstracts Member rate is available to Members of the IEE and IEEE only.

CUMULATIVE INDEXES

Cumulative indexes are available for *Physics Abstracts*, *Electrical & Electronics Abstracts* and *Computer & Control Abstracts*, for both

authors and subjects. These cumulations generally cover a period of four years, with the exception of *Computer & Control Abstracts*

where the initial volume covered the period 1966-68. The table below shows the prices and periods for the two types of cumulative index.

	PHYSICS ABSTRACTS		ELECTRICAL & ELECTRONICS ABSTRACTS		COMPUTER & CONTROL ABSTRACTS	
	Subject	Author	Subject	Author	Subject	Author
	£	£	£	£	£	£
1955-59	20	20	15	20	—	—
1960-64	40	17	20	12	—	—
1965-68	63	25	35	20	—	—
1969-72	—	—	72	64	48	30
1973-76	600	300	250	150	150	75
1966-68	—	—	—	—	15	

For US\$ and Yen prices please contact the appropriate address below

ORDERING PROCEDURE

THE AMERICAS

North (including Canada), Central and South

All orders from the above areas, and orders from members of Institute of Electrical and Electronics Engineers Inc. anywhere in the world, should be sent to Fulfillment Manager, Institute of Electrical & Electronics Engineers Inc., 445 Hoes Lane, Piscataway, N.J. 08854, USA.

日本のお客様にご案内申し上げます

日本国内に於ける INSPEC の購入価格はすべて円建てとなっております。また刊行物はすべて航空便で配達されます。INSPEC 刊行物の価格、その他についてのお問い合わせは最寄りの洋書取扱専門店または輸入総代理店㈱ユー・エス・エシオテック・カンパニー 〒105 東京都港区新橋1-13-12、TEL 03 (502) 6471 までご連絡ください。

REMAINDER OF THE WORLD

All remaining subscriptions should be sent to INSPEC Marketing Department, P.O. Box 26, Hitchin, Herts SG5 7RS, England. Telephone Hitchin 53331, Telex 825962, Telegrams IEE G.

OTHER INSPEC SERVICES

SDI

(Selective Dissemination of Information.) This is a service individually tailored to the requirements and interests of the engineer or research worker. Details of information relevant to the interest profile of the individual subscriber are selected from the data being processed for the INSPEC database. Information is dispatched weekly on 150 mm x 100 mm (6" x 4") cards.

TOPICS

This is an SDI service based on standard profiles. There are over 70 subjects covering high-activity areas of research and development. This is an inexpensive card service designed to alert engineers and researchers to the availability of literature within their subject area.

MAGNETIC TAPES

Tapes containing all the information included in the INSPEC publications are issued twice monthly. They enable the larger research and development organisations to produce their own internal information and current-awareness services.



articles from  
literature you  
do not hold ?

# **BOSTON SPA**

**Can help you**

**Over 43000 current periodicals available\***

Most of the papers listed in INSPEC services  
are held at the British Library Lending Division (BLLD)

**REQUESTS DEALT WITH IN 48 HOURS\***

Write for further information to:

The Director General  
The British Library Lending Division  
Boston Spa  
Wetherby  
West Yorkshire LS23 7BQ  
England

\*Photocopies of papers are available for research or private study to organisations in the UK registered as users of the BLLD. Where individuals in the UK do not belong to an organisation registered with the BLLD they should apply via their public library. In case of difficulty please contact the BLLD.

All requests from outside the UK should be made via the BLLD Overseas Photocopy Service.